SPRINGER REFERENCE

Wei-Yin Chen
Toshio Suzuki
Maximilian Lackner
Editors

Handbook of Climate Change Mitigation and Adaptation

Second Edition

Springer

Wei-Yin Chen • Toshio Suzuki
Maximilian Lackner
Editors

Handbook of Climate Change Mitigation and Adaptation

Second Edition

2017

With 1108 Figures and 352 Tables

Springer

Foreword

Scientific evidence is mounting that human activities have begun to change global climate. As a consequence, attention is increasingly turning in the public, private, and nonprofit sectors to the options available for dealing with that change. As we gradually begin to realize, actually only three options are available to us: mitigation, adaptation, and suffering. Mitigating climate change means cutting and sequestering emissions of greenhouse gases to prevent further increases in their atmospheric concentrations and perhaps even reducing concentrations to levels deemed less unsafe than the ones to which they have been driven since the start of the industrial revolution. Adaptation means finding ways that can help reduce the impacts of climate change on society, the various sectors of its economy, and the places in which we live – be those small rural villages or the cities and towns that by now house the majority of the human population, that account for the bulk of infrastructure investments, and that contribute most to energy consumption and carbon emissions. To the extent that mitigation and adaptation efforts are too timid, suffering will inevitably result.

What are safe concentrations of greenhouse gases is a topic of vigorous debate because we do not yet fully understand the coupled earth system and human system dynamics that will play themselves out in a world of unprecedented greenhouse gas concentrations. How high is too high will be known well after the point of no return has been reached, that is when developments in the global biogeochemical system are kicked off to move in a direction and rate that cannot be undone. Ice sheets may melt and free the methane and carbon dioxide long locked up in the soils underneath, thus further accelerating climate change. Major ocean currents, which move waters and nutrients to support the biological activity in the seas, may abruptly change direction or entirely cease. The established precipitation and temperature patterns, which are so central to agriculture, may be altered in ways that further challenge our abilities to feed a growing human population. And so, the extent to which we embrace mitigation, in part, reflects our aversion – or desire – to take risks in matters pertaining not just to the stability of global climate conditions but the global human condition and that of other species more broadly.

It is against this backdrop that this volume illuminates humanity's mitigation options. From its coverage it is quite obvious that there is no magic knife with which to cut emissions, because the sources of emissions are varied and intricately woven

into the very fabric of our society and economy. Movement from oil, coal, and natural gas, for example, to biological feedstocks for the production of fuels and chemicals is an essential strategy to decarbonize our economies, but the effect of this strategy hinges on the extent to which production of biomass can decouple itself from fossil-based generation of fertilizers and pesticides, minimize land conversation, and prevent the associated release of carbon from soils and impacts on biodiversity. Other, at least equally daunting, challenges surround the conversion of syngas to fuel; the deployment of geothermal, solar, and fusion technology; and the various means to sequester greenhouse gases. Policy and investment decision makers who wish to navigate and shape the resultant dynamics are further challenged in their abilities to understand and project resource and emissions trends into the future because of the rapid changes in technologies and markets, as well as the emergence of new, major players in the game, such as has happened in recent years with the proliferation of shale oil and shale gas developments.

Even if the production of new sources of energy and materials can occur with lower emissions, the end use technologies and infrastructures need to be in place to take full advantage of these improvements. This will require changes in our built environment – from houses to transportation networks to energy storage to power grids and beyond. These changes, in turn, will, at least for the foreseeable future, require continued use of existing infrastructures that have developed around the use of conventional fuels and land use practices.

Decarbonization at the process level, even when combined with the most aggressive efficiency improvements in the end uses of materials and energy, however only translates to net reductions in emissions if "other influences" do not overwhelm the rates at which these improvements are realized. Among these other influences are economic growth that comes from generating ever larger production of output, population growth that leads to ever more demand for goods and services, and climate change itself that is triggering a need for surplus production to built up our safety nets – from personal insurance to large-scale flood control systems – that can help us weather adverse climate conditions.

In the final analysis, it is the interplay of technology change, behavioral change, institutional change, and environmental change that must be managed for mitigation to become effective. How well that interplay is orchestrated will in large part depend on our ability to provide the right incentives for climate mitigation – be it through international agreements or through unilateral action, through market-based approaches, direct government intervention, or a mix of them all. Our success will be indicative not just of the technological prowess of our age, but also of the values and institutions that guide our actions.

Despite all efforts to stabilize and perhaps even reduce, in the long run, atmospheric greenhouse gas concentrations, humans have already committed themselves to decades of temperature changes and centuries of sea level rise. And, to worsen the outlook, rising global temperatures and sea levels will be accompanied by many other changes in our biophysical and socioeconomic environment. Since the heat budget of the globe will be disturbed, the frequency and severity of extreme weather events will likely increase. Disruptions in biophysical conditions will trigger, and be

triggered by, changes in ecosystems – including changes in the productivity of managed forests and croplands, as well as changes in the distribution of pests and diseases. The associated tightening of resource constraints will undermine the livelihoods of people, displace populations, and inflict pain and death.

There are unlikely to be long-term winners from climate change. None of the places already suffering from shortages in water and food, for example, or flooding and crumbling infrastructures will, in the long run, be better off because of climate change. Even if they do feel like "winners" temporarily – perhaps because the length of growing seasons increases with rising temperatures or a melting of sea ice improves shipping and boosts their economy – those benefits are fleeting. Climate will not stop changing once optimal conditions are reached, and benefits in one sector may already be overwhelmed by costs imposed on other parts of the economy and society. Clearly, some form of adaptation will need to take place.

Ideally, adaptation strategies are implemented not just as climate change unfolds, but in anticipation of any further climate change so that people, economic sectors, cities and their infrastructures, as well as natural systems such as wetlands and forests, are better prepared for, and perhaps even protected from, further disruptions. But even if there were no further climate change, there already is considerable variability in the weather conditions with which people, economic sectors, cities, and natural systems must cope. Maintaining vital wetlands well before flooding events will help provide natural buffers for coastal communities. Creating redundancies in lifeline infrastructures, such as the different ways of powering businesses and homes from centralized power plants and small-scale generators, will allow for switching across electricity sources during extreme weather events, for example. And promoting more efficient energy use in the first place will reduce the reliance on some of that energy. To the extent that adaptation helps reduce already existing inefficiencies, it can make good social, economic, and environmental sense irrespective of the details with which future climate conditions manifest themselves.

The conclusion one may draw that "less mitigation today can be balanced by more adaptation in the future," however, is misleading. It suggests that the two strategies are, at some abstract level, substitutable. In reality, though, less mitigation today means not just a need for more adaptation in the future. Rather, less mitigation today means more adaptation over more of our future, because even reduced emissions continue to add to atmospheric greenhouse gas concentrations, *and* because the damages that result will be cumulative in nature – heat waves, droughts, and flooding events, for example, will continuously undermine our wealth and welfare and require ever larger diversion of resources to address the causes and effects of climate change. Understanding the role of mitigation and choosing the proper mitigation strategies is, therefore, an essential forebear to anything else we may be doing about climate change. Recognizing the urgency for preparedness, given the extent to which humanity has already committed itself to a changing climate, is central to motivating investment in new technologies, changes in behaviors, and deployment of infrastructures that can better withstand the vagaries of the climate.

A worldview that is consistent with this understanding sees mitigation and adaptation as complements, offers them as strategies to address persistent and nascent inefficiencies, and treats them as a package that substitutes for the only other option available, namely suffering. It is in this sense that this *Handbook of Climate Change Mitigation and Adaptation* provides valuable insights into the preconditions for a prosperous future.

School of Public Policy and Urban Affairs
Northeastern University
Boston, MA, USA

Matthias Ruth
Director and Professor

Contents

Volume 1

Volume 2

Volume 3

About the Editors

Wei-Yin Chen is a Chemical Engineering professor with degrees in Chemical Engineering and Applied Mathematics and Statistics. He initiated the Sustainable Energy and Environment (SEE) group, which was formed at the University of Mississippi in 2007 and now has over 200 collaborators around the world. The SEE group has been offering new courses on climate change and sustainable energy, edited this Handbook, been developing experimental modules for outreach with several nationally recognized awards, and been developing a multidisciplinary research program leading to efficient power generation, CO_2 utilization, CO_2 capture, and carbon activation. He has served as a panelist, reviewer, or advisor for research organization in the USA, China, Romania, India, Jordan, Malaysia, etc. He is an adjunct or visiting faculty of five universities in China and Taiwan. He is currently on the editorial board of five journals. He has reviewed manuscripts and book proposals for over 50 journals and publishers. He has received the outstanding research, teaching, and service awards from the School of Engineering of the University of Mississippi. His publications on pedagogy have been cited as the "Best Practice" by a review of *Chemical Engineering Education* in both the thermodynamics and chemical reaction engineering areas.

Toshio Suzuki is Group Leader of Functional Integration Technology Group, at Japan's National Institute of Advanced Industrial Science and Technology (AIST), working in the fields of materials science, electrochemistry, and nanotechnology, especially on the development of next generation electrochemical devices such as solid oxide fuel cells (SOFCs). He is specializing in the design of advanced materials for energy conversion, with R&D experience in electrical, structural, and optical properties of novel ion conducting materials, correlating with microstructure. Dr. Suzuki received his

Ph.D. in Ceramic Engineering from University of Missouri-Rolla, USA, in 2001 and has published over 140 research articles, book chapters, and patents.

Maximilian Lackner received his Ph.D. in Technical Chemistry from Vienna University of Technology, Austria, in 2003, and his habilitation in Chemical Engineering in 2009. His research interests include: climate change mitigation, material science, lasers in chemistry, combustion, biofuels, and biobased plastics. Dr. Lackner was visiting researcher at Munich University of Technology (Germany), Darmstadt University (Germany), and Lund Institute of Technology (Sweden). He held several senior leadership positions in the petrochemical industry in Austria and China and founded five companies. Dr. Lackner has published over 100 research articles, book chapters, and patents. He is lecturer at Vienna University of Technology, the University of Applied Sciences FH Technikum Wien, and Johannes Kepler University (Austria).

Contributors

Javier Abanades School of Marine Science and Engineering, University of Plymouth, Plymouth, UK

Aishetu Abdulkadir Centre for Disaster Risk Reduction and Development Studies (CDRM & DS), Federal University of Technology, Minna, Nigeria

Dawood Al Abri Department of Electrical and Computer Engineering, Sultan Qaboos University, Muscat, Oman

Arun S. Agarwal Materials Program, Strategic Research and Innovation, DNV GL, Dublin, OH, USA

Sonia Akter Social Sciences Division, International Rice Research Institute, Los Baños, Laguna, Philippines

Mohammed Albadi Department of Electrical and Computer Engineering, Sultan Qaboos University, Muscat, Oman

Martin Altemeyer-Bartscher Faculty of Law and Economics, Martin-Luther University Halle-Wittenberg, Halle Institute for Economic Research, Halle (Saale), Germany

Edward John (Ben) Anthony CanmetENERGY, Natural Resources Canada, Ottawa, ON, USA

Masanobu Awano National Institute of Advanced Industrial Science and Technology (AIST), Nagoya, Japan

David A. Baah Department of Chemical Engineering, Tuskegee University, Tuskegee, AL, USA

Olivier Baboulet ISA, School of Physics-A28, The University of Sydney, Sydney, NSW, Australia

James Bennett U. S. Department of Energy, National Energy Technology Laboratory, Morgantown, WV, USA

Simon J. Bennett Imperial Centre for Energy Policy and Technology, Imperial College, London, UK

International Energy Agency, Paris, France

Ronald W. Breault U. S. Department of Energy, National Energy Technology Laboratory, Morgantown, WV, USA

Gabriele Centi Dip. Ingegneria Elettronica, Chimica ed Ingegneria Industriale (DIECII), University of Messina, ERIC aisbl and CASPE-INSTM, Messina, Italy

Yassine Charabi Department of Geography, Sultan Qaboos University, Muscat, Oman

Wei-Yin Chen Department of Chemical Engineering, The University of Mississippi, Oxford, MS, USA

Steven S. C. Chuang First Energy Advanced Energy Research Center, Department of Chemical and Biomolecular Engineering, The University of Akron, Akron, OH, USA

Whitney Colella Sandia National Laboratories, Albuquerque, NM, USA

Paula Coussy Economics and Environmental Evaluation Department, CO2 Market Expert, IFP Energies nouvelles, Rueil-Malmaison, France

Jennifer Cox Alabama Science in Motion Program, Alabama State University, Montgomery, AL, USA

Douglas Crawford-Brown Cambridge Centre for Climate Change Mitigation Research, Department of Land Economy, University of Cambridge, Cambridge, UK

Belén del Río Chair in International Studies, University of the Basque Country (UPV/EHU), Bilbao, Spain

Jared Delcamp Department of Chemistry and Biochemistry, The University of Mississippi University, Oxford, MS, USA

Qi Deng Department of Biological Sciences, Tennessee State University, Nashville, TN, USA

Yan Ding National Center for Computational Hydroscience and Engineering, The University of Mississippi, Oxford, MS, USA

Shuhong Duan Research Institute of Innovative Technology for the Earth (RITE), Kizugawa-shi, Kyoto, Japan

Greg Easson Mississippi Mineral Resources Institute, The University of Mississippi, Oxford, MS, USA

Nosa O. Egiebor Department of Chemical Engineering and Division of Global Engagement, The University of Mississippi, Oxford, MS, USA

Sandra Einloft FAQUI – Faculty of Chemistry, Pontifical Catholic University of Rio Grande do Sul, Porto Alegre, Brazil

Gamal El Afandi Department of Agricultural and Environmental Sciences, College of Agriculture, Environment and Nutrition Sciences, Tuskegee University, Tuskegee, AL, USA

Department of Astronomy and Meteorology, Faculty of Science, Al Azhar University, Cairo, Egypt

Mengxiang Fang Institute for Thermal Power Engineering, Zhejiang University, Hangzhou, Zhejiang, China

Xing Fang Department of Civil Engineering, Auburn University, Auburn, AL, USA

Herminia A. Francisco Economy and Environment Program for Southeast Asia (EEPSEA), Los Baños, Laguna, Philippines

Carla Freeman School of Advanced International Studies, Johns Hopkins University, Washington, DC, USA

Yoshihiro Fujii Graduate School of Global Environmental Studies, Sophia University, Tokyo, Japan

Kevin Galloway Department of Metallurgical and Materials Engineering, Colorado School of Mines, Golden, CO, USA

Scott A. Gold Department of Chemical and Materials Engineering, University of Dayton, Dayton, OH, USA

Jacob D. Graham Johns Hopkins University, Baltimore, MD, USA

Brenton Greska Cameron International, Houston, TX, USA

Nathan I. Hammer Department of Chemistry and Biochemistry, The University of Mississippi University, Oxford, MS, USA

Timothy G. Harrison Bristol ChemLabS, School of Chemistry, University of Bristol, Bristol, UK

Yi He Department of Chemical and Biological Engineering, Institute of Industrial Ecology and Environment, College of Chemical and Biological Engineering, Zhejiang University, Hangzhou, Zhejiang, People's Republic of China

Elizabeth Hickman Alabama Mathematics and Science Technology Initiative, Auburn University, Auburn, AL, USA

Katsuya Hihara Graduate School of Public Policy, the University of Tokyo, Hongo Bunkyo-ku, Tokyo, Japan

Davion Hill Energy and Materials, DNV GL, Dublin, OH, USA

Satoshi Hirano Thermal and Fluids Systems Group, Energy Technology Research Institute, National Institute of Advanced Industrial Science and Technology (AIST), Tsukuba, Japan

Damon Honnery Department of Mechanical and Aerospace Engineering, Monash University, Melbourne, VIC, Australia

A. K. M. Azad Hossain National Center for Computational Hydroscience and Engineering (NCCHE), The University of Mississippi, Oxford, MS, USA

Nasser Hosseinzadeh Department of Electrical and Computer Engineering, Sultan Qaboos University, Muscat, Oman

John C. P. Huang Focus Capital Group, Cupertino, CA, USA

Yinlun Huang Lab for Multiscale Complex Systems Science and Engineering, Department of Chemical Engineering and Materials Science, Wayne State University, Detroit, MI, USA

Dafeng Hui Department of Biological Sciences, Tennessee State University, Nashville, TN, USA

Gregorio Iglesias School of Marine Science and Engineering, University of Plymouth, Plymouth, UK

Rodrigo S. Iglesias FENG – Engineering Faculty, Pontifical Catholic University of Rio Grande do Sul, Porto Alegre, Brazil

Tsuneo Ishido National Institute of Advanced Industrial Science and Technology (AIST), Geological Survey of Japan, Tsukuba, Ibaraki, Japan

Sudha Iyer Cerebronics, LLC, Hoboken, NJ, USA

Peter C. Jacobson Minnesota Department of Natural Resources, Park Rapids, MN, USA

Jingsheng Jia International Commission on Large Dams (ICOLD), Paris, France

Liping Jiang Department of Civil Engineering, Auburn University, Auburn, AL, USA

Teruhiko Kai Research Institute of Innovative Technology for the Earth (RITE), Kizugawa-shi, Kyoto, Japan

Akila G. Karunanayake Department of Chemistry, Mississippi State University, Starkville, MS, USA

Asadullah Kazi Isra University, Hyderabad, Sindh, Pakistan

J. Marcelo Ketzer IPR – Institute of Petroleum and Natural Resources, Pontifical Catholic University of Rio Grande do Sul, Porto Alegre, Brazil

H. Komakech Department of Water and Environmental Sciences and Engineering, Nelson Mandela Institution of Science and Technology-Tengeru, Tengeru, Arusha, Tanzania

Anna Krenz Nordic Folkecenter for Renewable Energy, Hurup Thy, Denmark

Anjaneyulu Krothapalli Department of Mechanical Engineering, Florida State University, Tallahassee, FL, USA

Maximilian Lackner Institute of Advanced Engineering Technologies, University of Applied Sciences FH Technikum Wien, Vienna, Austria

Ming-Kuo Lee Department of Geology and Geography, Auburn University, Auburn, AL, USA

Susannah Lee Department of Chemical and Metallurgical Engineering, Chemical and Materials Engineering Department, LME 310, MS 388, University of Nevada, Reno, NV, USA

Xing Lei National Institute of Advanced Industrial Science and Technology (AIST), Geological Survey of Japan, Tsukuba, Ibaraki, Japan

Manfred Lenzen ISA, School of Physics-A28, The University of Sydney, Sydney, NSW, Australia

Qing Liu Department of Chemical and Biological Engineering, Institute of Industrial Ecology and Environment, College of Chemical and Biological Engineering, Zhejiang University, Hangzhou, Zhejiang, People's Republic of China

Shaomin Liu Department of Chemical Engineering, Curtin University, Perth, WA, Australia

Helen H. Lou Dan F. Smith Department of Chemical Engineering, Lamar University, Beaumont, TX, USA

Jenny Lovell Environmental Studies Department, University of California Santa Cruz, Santa Cruz, CA, USA

Tyaunnaka Lucy Alabama Mathematics and Science Technology Initiative, Auburn University, Auburn, AL, USA

Yiqi Luo Department of Microbiology and Plant Sciences, University of Oklahoma, Norman, OK, USA

Zhongyang Luo State Key Laboratory of Clean Energy Utilization, College of Energy Engineering, Zhejiang University, Hangzhou, Zhejiang, People's Republic of China

Jing Ma China Institute of Water Resources and Hydropower Research, Beijing, China

Preben Maegaard Nordic Folkecenter for Renewable Energy, Hurup Thy, Denmark

Swetha Mahalaxmi Department of Chemical Engineering, The University of Mississippi, Oxford, MS, USA

Trinh Van Mai Institute for Agricultural Environment, Vietnam Academy of Agricultural Sciences, Phudo, South Tu Liem, Hanoi, Vietnam

Arif S. Malik Department of Electrical and Computer Engineering, College of Engineering, Sultan Qaboos University, Muscat, Oman

Itziar Martínez de Alegría Engineering School of Bilbao, University of the Basque Country (UPV/EHU), Bilbao, Spain

L. Martz Department of Geography, University of Saskatchewan, Saskatoon, SK, Canada

Linta M. Mathew Social Sciences Division, International Rice Research Institute, Los Baños, Laguna, Philippines

Jonathan Mbah Department of Chemical Engineering, Florida Institute of Technology, Melbourne, FL, USA

Qingmin Meng Department of Geosciences, Mississippi State University, Starkville, MS, USA

M. Misra Department of Metallurgical Engineering, University of Utah, Salt Lake City, UT, USA

Chandana Mitra Department of Geology and Geography, Auburn University, Auburn, AL, USA

Todd E. Mlsna Department of Chemistry, Mississippi State University, Starkville, MS, USA

Gonzalo Molina University of the Basque Country (UPV/EHU), Bilbao, Spain

Cristian Moore Alcoa Inc., Alcoa, TN, USA

Patrick Moriarty Department of Design, Monash University, Melbourne, VIC, Australia

K. C. Mukwana Energy and Environment Engineering Department, Quaid-E-Awam University of Engineering, Science and Technology (QUEST), Nawabshah, Sindh, Pakistan

Vanisree Mulabagal Department of Chemical Engineering, Tuskegee University, Tuskegee, AL, USA

Hirofumi Muraoka North Japan Research Institute for Sustainable Energy, Hirosaki University, Aomori, Japan

A. N. N. Muzuka Department of Water and Environmental Sciences and Engineering, Nelson Mandela Institution of Science and Technology-Tengeru, Tengeru, Arusha, Tanzania

Shinsuke Nakao National Institute of Advanced Industrial Science and Technology (AIST), Geological Survey of Japan, Tsukuba, Ibaraki, Japan

Yuji Nishi National Institute of Advanced Industrial Science and Technology (AIST), Geological Survey of Japan, Tsukuba, Ibaraki, Japan

Tatsuya Oki National Institute of Advanced Industrial Science and Technology (AIST), Onogawa Tsukuba, Ibaragi, Japan

Anne Nyatichi Omambia National Environment Management Authority, Nairobi, Kenya

Sebastian Otte Technische Universität Bergakademie Freiberg, Freiberg, Germany

Holly A. Page Imperial College, London, UK

Siglinda Perathoner Dip. Ingegneria Elettronica, Chimica ed Ingegneria Industriale (DIECII), University of Messina, ERIC aisbl and CASPE-INSTM, Messina, Italy

Donald L. Pereira Minnesota Department of Natural Resources, St. Paul, MN, USA

B. Pesic Chemical and Materials Engineering, University of Idaho, Moscow, ID, USA

Ralph W. Pike Minerals Processing Research Institute, Louisiana State University, Baton Rouge, LA, USA

Karen Pittel Ifo Institute – Leibniz Institute for Economic Research and University of Munich, Munich, Germany

Charles U. Pittman Department of Chemistry, Mississippi State University, Starkville, MS, USA

Matthew E. Poese Applied Research Laboratory, State College, PA, USA

Damion Proctor Department of Chemistry, Mississippi State University, Starkville, MS, USA

Petras Punys Water Management Department, Water and Land Management Faculty, Lithuanian University of Agriculture, Kaunas-Akademija, Lithuania

Dirk Rübbelke Technische Universität Bergakademie Freiberg, Freiberg, Germany

K. S. Raja Chemical and Materials Engineering, University of Idaho, Moscow, ID, USA

Roger Raufer Hopkins Nanjing Center, Nanjing University, Nanjing, Jiangsu Province, China

David H. Reed Department of Biology, University of Louisville, Louisville, KY, USA

L. Reijnders Institute for Biodiversity and Ecosystem Dynamics, University of Amsterdam, Amsterdam, The Netherlands

Alison C. Rivett Bristol ChemLabS, School of Chemistry, University of Bristol, Bristol, UK

Edward Rode Materials Program, Strategic Research and Innovation, DNV GL, Dublin, OH, USA

Chris Rodger Department of Mathematics and Statistics, Auburn University, Auburn, AL, USA

David J. Rutherford Department of Public Policy Leadership, The University of Mississippi, Oxford, MS, USA

Nigel M. Sammes Department of Metallurgical and Materials Engineering, Colorado School of Mines, Golden, CO, USA

S. R. Samo Quaid-E-Awam University of Engineering, Science and Technology (QUEST), Nawabshah, Sindh, Pakistan

Ivonne Andrea Sanchez Hernandez Sustainability Development, AB Origen Fundación, Armenia, Quindio, Colombia

John M. Seiner

Debalina Sengupta Texas A&M University, College Station, TX, USA

Mustafa F. Serincan Department of Mechanical Engineering, University of Connecticut, Storrs, CT, USA

Lawrence J. Shadle U. S. Department of Energy, National Energy Technology Laboratory, Morgantown, WV, USA

Dudley E. Shallcross Bristol ChemLabS, School of Chemistry, University of Bristol, Bristol, UK

Ceven Shemsanga Department of Water and Environmental Sciences and Engineering, Nelson Mandela Institution of Science and Technology-Tengeru, Tengeru, Arusha, Tanzania

Department of Environmental Engineering and Management, University of Dodoma, Dodoma, Tanzania

---

David H. Reed: deceased.

John M. Seiner: deceased.

Yao Shi Department of Chemical and Biological Engineering, Institute of Industrial Ecology and Environment, College of Chemical and Biological Engineering, Zhejiang University, Hangzhou, Zhejiang, People's Republic of China

Sofie Waage Skjeflo UMB School of Economics and Business, Norwegian University of Life Sciences, Ås, Norway

A. A. Sohu Mechanical Engineering Department, QUCEST, Larkano, Sindh, Pakistan

Masao Sorai National Institute of Advanced Industrial Science and Technology (AIST), Geological Survey of Japan, Tsukuba, Ibaraki, Japan

Narasi Sridhar Materials Program, Strategic Research and Innovation, DNV GL, Dublin, OH, USA

Heinz G. Stefan St. Anthony Falls Laboratory, Department of Civil Engineering, University of Minnesota, Minneapolis, MN, USA

Michael Sterner Forschungsstelle Energienetze und Energiespeicher (FENES), Fakultät für Elektro- und Informationstechnik, OTH Regensburg, Regensburg, Germany

Vaidyanathan (Ravi) Subramanian Department of Chemical and Metallurgical Engineering, Chemical and Materials Engineering Department, LME 310, MS 388, University of Nevada, Reno, NV, USA

Jaka Sunarso Department of Chemistry, University of Waterloo, Waterloo, ON, Canada

Sarah Sutton Department of Chemistry and Biochemistry, The University of Mississippi University, Oxford, MS, USA

Toshio Suzuki National Institute of Advanced Industrial Science and Technology (AIST), Nagoya, Japan

Kristen Alley Swain Meek School of Journalism and New Media, The University of Mississippi, Oxford, MS, USA

Pal Szentannai Department of Energy Engineering, Budapest University of Technology and Economics, Budapest, Hungary

Amy Thomas Outreach Program, College of Sciences and Mathematics, Auburn University, Auburn, AL, USA

Hanqin Tian International Center for Climate and Global Change Research, School of Forestry and Wildlife Sciences, Auburn University, Auburn, AL, USA

Jauyah Tuah Secretariat of Brunei Darussalam Technical and Vocational Education Council, Permanent Secretary Office (Higher Education), Ministry of Education, Bandar Seri Begawan, Brunei Darussalam

Waheed Uddin Department of Civil Engineering, The University of Mississippi, Oxford, MS, USA

Melissa Vandiver Department of Chemical and Metallurgical Engineering, Chemical and Materials Engineering Department, LME 310, MS 388, University of Nevada, Reno, NV, USA

María-Azucena Vicente-Molina Economics and Business Administration College, University of the Basque Country, Bilbao, Spain

Balasubramanian Viswanathan National Center for Catalysis Research, Indian Institute of Technology Madras, Chennai, Tamil Nadu, India

Qinhui Wang Institute for Thermal Power Engineering, Zhejiang University, Hangzhou, Zhejiang, China

Takao Watanabe Central Research Institute of Electric Power Industry, Yokosuka, Kanagawa, Japan

Eric Thomas Weber Department of Public Policy Leadership, University of Mississippi, Oxford, MS, USA

Rangana Wijayapala Department of Chemistry, Mississippi State University, Starkville, MS, USA

Clint Williford Department of Chemical Engineering, The University of Mississippi, Oxford, MS, USA

Aishuang Xiang Chemical Engineering Department, Massachusetts Institute of Technology, Cambridge, MA, USA

Hiroshi Yamada Department of Helical Plasma Research, National Institute for Fusion Science, Toki, Gifu, Japan

Toshiaki Yamaguchi National Institute of Advanced Industrial Science and Technology (AIST), Nagoya, Japan

David W. Yarbrough R&D Services, Inc., Cookeville, TN, USA

Fei Yu Agricultural and Biological Engineering, Mississippi State University, Starkville, MS, USA

Noor Aini Zakaria Economy and Environment Program for Southeast Asia (EEPSEA), Los Baños, Laguna, Philippines

Kun Zhang Department of Chemical Engineering, Curtin University, Perth, WA, Australia

Long Zhang Department of Polymer Science, The University of Akron, Akron, OH, USA

Kailiang Zheng Dan F. Smith Department of Chemical Engineering, Lamar University, Beaumont, TX, USA

Jingsong Zhou State Key Laboratory of Clean Energy Utilization, College of Energy Engineering, Zhejiang University, Hangzhou, Zhejiang, People's Republic of China

Dechen Zhu Institute for Thermal Power Engineering, Zhejiang University, Hangzhou, Zhejiang, China

Part I

Scientific Evidences of Climate Change and Societal Issues

Introduction to Climate Change Mitigation

Maximilian Lackner, Wei-Yin Chen, and Toshio Suzuki

Contents

Abstract

Since the first edition of the Handbook, important new research findings on climate change have been gathered. The handbook was extended to also cover, apart from climate change mitigation, climate change adaptation as one can witness increasing initiatives to cope with the phenomenon. Instrumental

M. Lackner (✉)
Institute of Advanced Engineering Technologies, University of Applied Sciences FH Technikum Wien, Vienna, Austria
e-mail: maximilian.lackner@tuwien.ac.at

W.-Y. Chen
Department of Chemical Engineering, The University of Mississippi, Oxford, MS, USA
e-mail: cmchengs@olemiss.edu

T. Suzuki
National Institute of Advanced Industrial Science and Technology (AIST), Nagoya, Japan
e-mail: toshio.suzuki@aist.go.jp

W.-Y. Chen et al. (eds.), *Handbook of Climate Change Mitigation and Adaptation*,
DOI 10.1007/978-3-319-14409-2_1

recording shows a temperature increase of 0.5 °C Le Houérou (J Arid Environ 34:133–185, 1996) with rather different regional patterns and trends (Folland CK, Karl TR, Nicholls N, Nyenzi BS, Parker DE, Vinnikov KYA (1992) Observed climate variability and change. In: Houghton JT, Callander BA, Varney SDK (eds) Climate change, the supplementary report to the IPCC scientific assessment. Cambridge University Press, Cambridge, pp 135–170). Over the last several million years, there have been warmer and colder periods on Earth, and the climate fluctuates for a variety of natural reasons as data from tree rings, pollen, and ice core samples have shown. However, human activities on Earth have reached an extent that they impact the globe in potentially catastrophic ways. This chapter is an introduction to climate change.

Climate Change

There has been a heated discussion on climate change in recent years, with a particular focus on global warming. Over the last several million years, there have been warmer and colder periods on Earth, and the climate fluctuates for a variety of natural reasons as data from tree rings, pollen, and ice core samples have shown. For instance, in the Pleistocene, the geological epoch which lasted from about 2,588,000 to 11,700 years ago, the world saw repeated glaciations ("ice age"). More recently, "Little Ice Age" and the "Medieval Warm Period" (IPCC) occurred. Several causes have been suggested such as cyclical lows in solar radiation, heightened volcanic activity, changes in the ocean circulation, and an inherent variability in global climate. Also on Mars, climate change was inferred from orbiting spacecraft images of fluvial landforms on its ancient surfaces and layered terrains in its polar regions (Haberle et al. 2012). Spin axis/orbital variations, which are more pronounced on Mars compared to Earth, are seen as main reasons. As to recent climate change on Earth, there is evidence that it is brought about by human activity and that its magnitude and effects are of strong concern.

Instrumental recording of temperatures has been available for less than 200 years. Over the last 100 years, a temperature increase of 0.5 °C could be measured (Le Houérou 1996) with rather different regional patterns and trends (Folland et al. 1992). In (Ehrlich 2000), Bruce D. Smith is quoted as saying, *"The changes brought over the past 10,000 years as agricultural landscapes replaced wild plant and animal communities, while not so abrupt as those caused by the impact of an asteroid as the Cretaceous-Tertiary boundary some 65 Ma ago or so massive as those caused by advancing glacial ice in the Pleistocene, are nonetheless comparable to these other forces of global change."* At the Earth Summit in Rio de Janeiro in 1992, over 159 countries signed the United Nations Framework Convention on Climate Change (FCCC, also called "Climate Convention") in order to achieve "stabilization of greenhouse gas concentrations in the atmosphere at a level that would prevent dangerous anthropogenic interference with the climate system" (United Nations (UN) 1992). In 2001, the Intergovernmental Panel on Climate Change (IPCC) (Intergovernmental Panel on Climate Change (IPCC) 2007) wrote, *"An increasing body of*

observations gives a collective picture of a warming world and other changes in the climate system… There is new and stronger evidence that most of the warming observed over the last 50 years is attributable to human activities."

In its fourth assessment report of 2007, the IPCC stated that human actions are "very likely" the cause of global warming. More specifically, there is a 90 % probability that the burning of fossil fuels and other anthropogenic factors such as deforestation and the use of certain chemicals have already led to an increase of 0.75° in average global temperatures over the last 100 years and that the increase in hurricane and tropical cyclone strength since 1970 also results from man-made climate change.

In its fifth assessment report of 2013, the IPCC confirms their findings as *"Warming of the climate system is unequivocal, and since the 1950s, many of the observed changes are unprecedented over decades to millennia. The atmosphere and ocean have warmed, the amounts of snow and ice have diminished, sea level has risen, and the concentrations of greenhouse gases have increased"* (IPCC 2013).

Figures 1 and 2 show some details of IPCC's findings.

In Fig. 2, natural and man-made (anthropogenic) radiative forcings (RF) are depicted. RF, or climate forcing, expressed in W/m^2, is a change in energy flux, viz., the difference of incoming energy (sunlight) absorbed by Earth and outgoing energy (that radiated back into space). A positive forcing warms up the system, while negative forcing cools it down.

(Anthropogenic) CO_2 emissions, which have been accumulating in the atmosphere at an increasing rate since the Industrial Revolution, were identified as the main driver.

The position of the IPCC has been adopted by several renowned scientific societies, and a consensus has emerged on the causes and partially on the consequences of climate change. The history of climate change science is reviewed in (Miller et al. 2009). There are researchers who oppose the scientific mainstream's assessment of global warming (Linden 1993). However, the public seems to be unaware of the high degree of consensus that has been achieved in the scientific community, as elaborated in a 2009 World Bank report (Worldbank 2009). In (Antilla 2005), there is a treatment of the mass media's coverage of the climate change discussion with a focus on rhetoric that emphasizes uncertainty, controversy, and climate scepticism. Climate change skeptic films were found to have a strong influence on the general public's environmental concern (Greitemeyer 2013).

The Greenhouse Effect

A greenhouse, also called a glass house, is a structure enclosed by glass or plastic which allows the penetration of radiation to warm it. Gases capable of absorbing the radiant energy are called the greenhouse gases (GHG). Greenhouses are used to grow flowers, vegetables, fruits, and tobacco throughout the year in a warm, agreeable climate. On Earth, there is a phenomenon called the "natural greenhouse" effect, or the Milankovitch cycles.

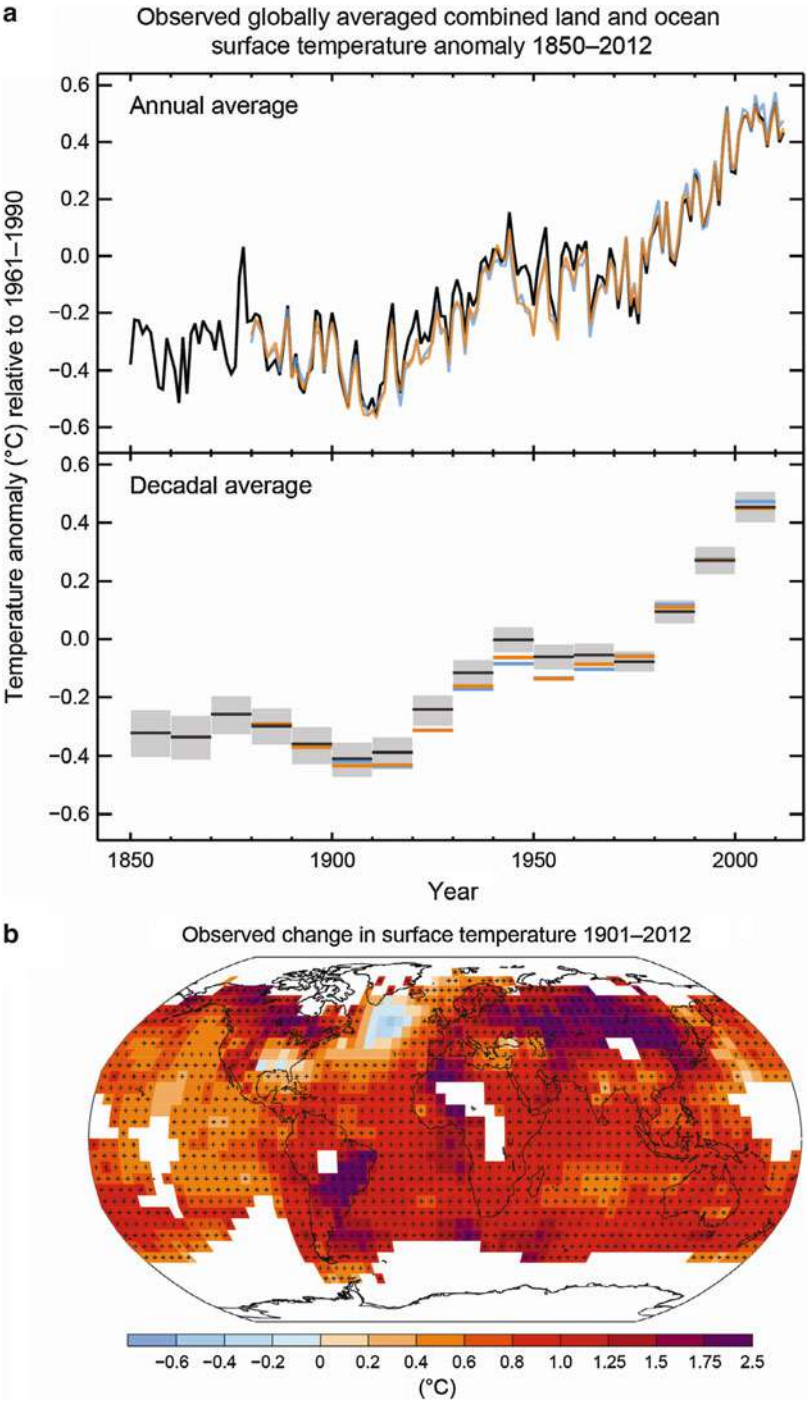

Fig. 1 (continued)

Without the greenhouse gas effect, which is chiefly based on water vapor in the atmosphere (Linden 2005) (i.e., clouds that trap infrared radiation), the average surface temperature on Earth would be 33 °C colder (Karl and Trenberth 2003). The natural greenhouse effect renders Earth habitable since the temperature which would be expected from the thermal equilibrium of the irradiation from the sun and radiative losses into space (radiation balance in the blackbody model) is approximately −18 °C.

On the moon, for instance, where there is hardly any atmosphere, extreme surface temperatures range from −233 °C to 133 °C (Winter 1967). On Venus, by contrast, the greenhouse effect in the dense CO_2− laden atmosphere results in an average surface temperature in excess of 450 °C (Sonnabend et al. 2008; Zasova et al. 2007).

The current discussion about global warming and climate change is centered on the anthropogenic greenhouse effect. This is caused by the emission and accumulation of greenhouse gases in the atmosphere. These gases (water vapor, CO_2, CH_4, N_2O, O_3, and others) act by absorbing and emitting infrared radiation. The combustion of fossil fuels (oil, coal, and natural gas) has led mainly to an increase in the CO_2 concentration in the atmosphere. Preindustrial levels of CO_2 (i.e., before the start of the Industrial Revolution) were approximately 280 ppm, whereas today, they are above 380 ppm with an annual increase of approximately 2 ppm. According to the IPCC Special Report on Emission Scenarios (SRES) (IPCC 2010a), by the end of the twenty-first century, the CO_2 concentration could reach levels between 490 and 1,260 ppm, which are between 75 % and 350 % above the preindustrial levels, respectively.

CO_2 is the most important anthropogenic greenhouse gas because of its comparatively high concentration in the atmosphere. The effect of other greenhouse-active gases depends on their molecular structure and their lifetime in the atmosphere, which can be expressed by their greenhouse warming potential (GWP). GWP is a relative measure of how much heat a greenhouse gas traps in the atmosphere. It compares the amount of heat trapped by a certain mass of the gas in question to the amount of heat trapped by a similar mass of CO_2. With a time horizon of 100 years, the GWP of CH_4, N_2O, and SF_6 with respect to CO_2 is 25, 298, and 22,800, respectively (IPCC 2010b). But CO_2 has a much higher concentration than other GHGs, and it is increasing at a higher rate due to burning of fossil fuels. Thus, while the major mitigating emphasis has mainly been placed on CO_2, efforts on mitigating CH_4, N_2O, and SF_6 have also been active.

Fig. 1 (**a**) Observed global mean combined land and ocean surface temperature anomalies, from 1850 to 2012 from three data sets. *Top panel*: annual mean values. *Bottom panel*: decadal mean values including the estimate of uncertainty for one dataset (*black*). Anomalies are relative to the mean of 1961–1990. (**b**) Map of the observed surface temperature change from 1901 to 2012 derived from temperature trends determined by linear regression from one dataset (*orange line* in panel a). Trends have been calculated where data availability permits a robust estimate (i.e., only for grid boxes with greater than 70 % complete records and more than 20 % data availability in the first and last 10 % of the time period). Other areas are white. Grid boxes where the trend is significant at the 10 % level are indicated by a + sign (Source: IPCC (IPCC 2013))

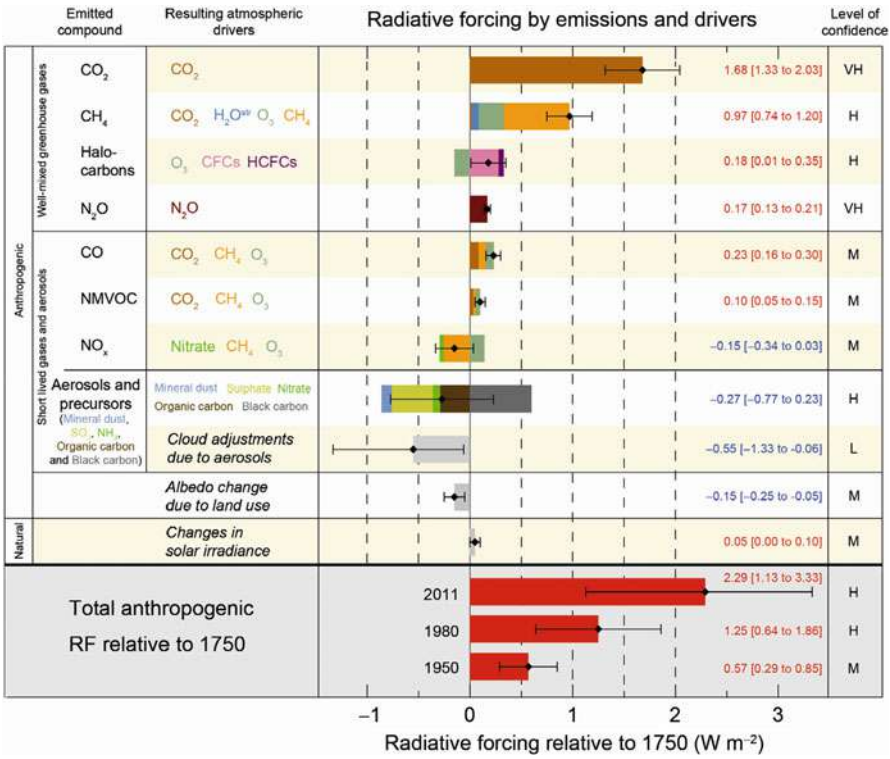

Fig. 2 Radiative forcing estimates in 2011 relative to 1750 and aggregated uncertainties for the main drivers of climate change. Values are global average radiative forcing (*RF*), partitioned according to the emitted compounds or processes that result in a combination of drivers. The best estimates of the net radiative forcing are shown as *black diamonds* with corresponding uncertainty intervals; the numerical values are provided on the *right* of the figure, together with the confidence level in the net forcing (*VH* very high, *H* high, *M* medium, *L* low, *VL* very low). Albedo forcing due to black carbon on snow and ice is included in the black carbon aerosol bar. Small forcings due to contrails (0.05 W m^{-2}, including contrail induced cirrus), and HFCs, PFCs and SF6 (total 0.03 W m^{-2}) are not shown. Concentration-based RFs for gases can be obtained by summing the like-coloured bars. Volcanic forcing is not included as its episodic nature makes is difficult to compare to other forcing mechanisms. Total anthropogenic radiative forcing is provided for three different years relative to 1750 (Source: IPCC (IPCC 2013))

Anthropogenic Climate Change

The climate is governed by natural influences, yet human activities have an impact on it as well. The main impact that humans exert on the climate is via the emission of greenhouse gases. Deforestation is another example of an activity that influences the climate (McMichael et al. 2007). Figure 3 shows the share of greenhouse gas emissions from various sectors taken from (Quadrelli and Peterson 2007). The energy sector is the dominant source of GHG emissions.

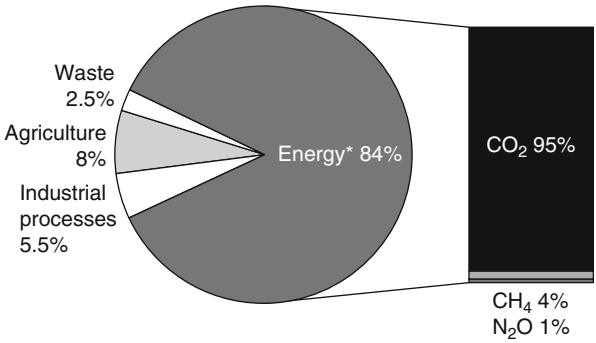

Fig. 3 Shares of global anthropogenic greenhouse gas emissions (Reprinted with permission from (Quadrelli and Peterson 2007))

According to the International Energy Agency (IEA), if no action toward climate change mitigation is taken, global warming could reach an increase of up to 6° in average temperature (International Energy Association IEA 2009). This temperature rise could cause devastating consequences on Earth, which will be discussed briefly below.

Effects of Climate Change

Paleoclimatological data show that 100–200 Ma ago, almost all carbon was in the atmosphere as CO_2, with global temperatures being 10 °C warmer and sea levels 50–100 m higher than today. Photosynthesis and CO_2 uptake into the oceans took almost 200 Ma. Since the Industrial Revolution, i.e., during the last 200 years, this carbon is being put back into the atmosphere to a significant extent. This is a rate which is 10^7 times faster, so there is a risk of a possible "runaway" reaction greenhouse effect.

Figure 4 shows the timescales of several different effects of climate change for the future.

Due to the long lifetime of CO_2 in the atmosphere, the effects of climate change until a new equilibrium has been reached will prove long term. A global temperature increase of 6 °C would be severe, so the IEA has developed a scenario which would limit the temperature increase to 2 °C (International Energy Association IEA 2009) to minimize the effects.

Sea level rise will indeed be the most direct impact. Other impacts including those on weather, flooding, biodiversity, water resources, and diseases are discussed here.

Climate Change: What Will Change?

An overall higher temperature on Earth, depending on the magnitude of the effect and the rate at which it manifests itself, will change the sea level, local climatic conditions, and the proliferation of animal and plant species, to name but a few of the most obvious examples. The debate on the actual consequences of global warming is the most heated part of the climate change discussion.

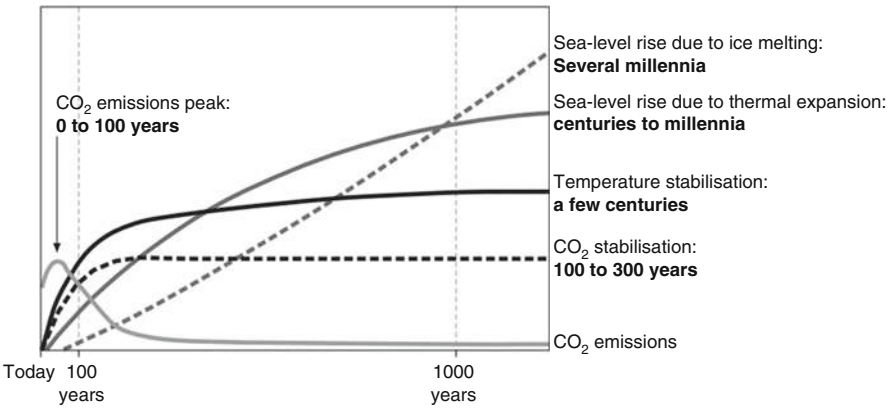

Fig. 4 Time scales of climate change effects based on a stabilization of CO_2 concentration levels between 450 and 1,000 ppm after today's emissions (Reprinted with permission from (Quadrelli and Peterson 2007))

Apart from changes in the environment, there will be various impacts on human activity. One example is the threats to tourism revenue in winter ski resorts (Hoffmann et al. 2009) and low-elevation tropical islands (Becken 2005). Insurance companies will need to devise completely new business models, to cite just one example of businesses being forced to react to climate change.

Impact of Climate Change Mitigation Actions

The purpose of climate change mitigation is to enact measures to limit the extent of climate change. Climate change mitigation can make a difference. In the IEA reference scenario (International Energy Association IEA 2009), the world is headed for a CO_2 concentration in the atmosphere above 1,000 ppm, whereas that level is limited to 450 ppm in the proposed "mitigation action" scenario. In the first case, the global temperature increase will be 6 °C, whereas it is limited to 2 °C in the latter (International Energy Association IEA 2009).

The Intergovernmental Panel on Climate Change has projected that the financial effect of compliance through trading within the Kyoto commitment period will be limited at between 0.1 % and 1.1 % of GDP. By comparison, the Stern report estimated that the cost of mitigating climate change would be 1 % of global GDP and the costs of doing nothing would be 5–20 times higher (IPCC 2010b; Stern 2007).

Climate Change Adaptation Versus Climate Change Mitigation

Individuals (Grothmann and Patt 2005), municipalities (Laukkonen et al. 2009; van Aalst et al. 2008), businesses (Hoffmann et al. 2009), and nations (Næss et al. 2005; Stringer et al. 2009) have started to adapt to the ongoing and expected state of

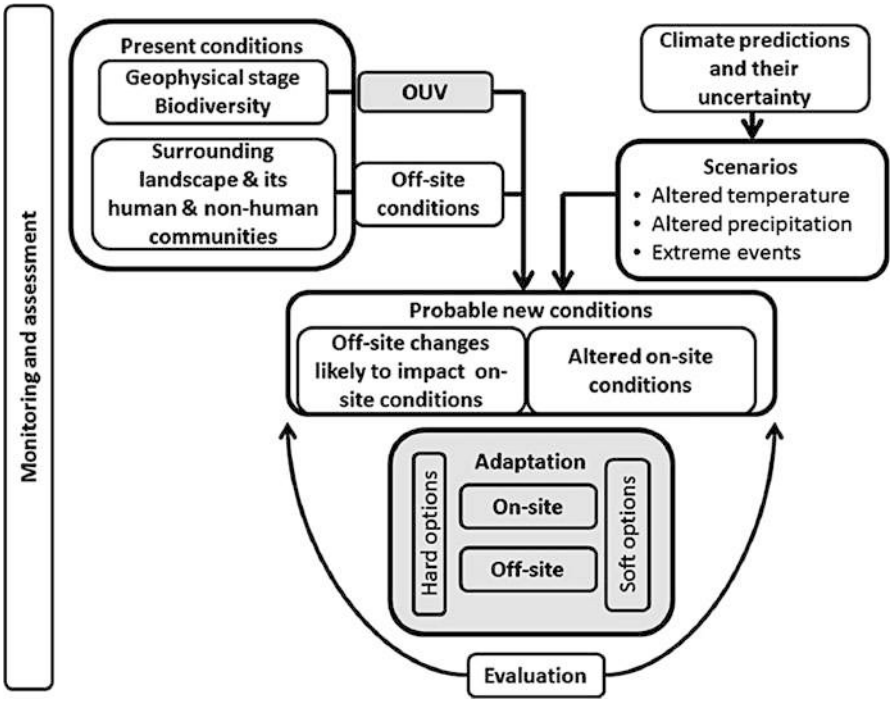

Fig. 5 Conceptual framework for developing a climate change adaptation strategy. *OUV* Outstanding Universal Values (each World Heritage (*WH*) site has one or more such OUV. According to UNESCO, WH represent society's highest conservation designation (Source: Jim Perry (2015))

climate change. Climate change adaptation and climate change mitigation face similar barriers (Hamin and Gurran 2009). To best deal with the situation, there needs to be a balanced approach between climate change mitigation and climate change adaptation (Becken 2005; Laukkonen et al. 2009; Hamin and Gurran 2009). This will prove to be one of mankind's largest modern challenges. Figure 5 shows a conceptual framework for developing a climate change adaptation strategy. Details are presented in this Handbook.

Handbook of Climate Change Mitigation and Adaption

Motivation

The struggle in mitigating climate change is not only to create a sustainable environment but also to build a sustainable economy through renewable energy resources. "Sustainability" has turned into a household phrase as people become increasingly aware of the severity and scope of future climate change. A survey of

the current literature on climate change suggests that there is an urgent need for a comprehensive handbook introducing the mitigation of climate change to a broad audience.

The burning of fossil fuels such as coal, oil, and gas and the clearing of forests has been identified as the major source of greenhouse gas emissions. Reducing the 24 billion metric tons of carbon dioxide emissions per year generated from stationary and mobile sources is an enormous task that involves both technological challenges and monumental financial and societal costs with benefits that will only surface decades later. The Stern Report (2007) provided a detailed analysis of the economic impacts of climate change and the ethical ground of policy responses for mitigation and adaptation.

The decline in the supply of high-quality crude oil has further increased the urgency to identify alternative energy resources and develop energy conversion technologies that are both environmentally sound and economically viable. Various routes for converting renewable energies have emerged – including energy conservation and energy-efficient technologies.

The energy industry currently lacks an infrastructure that can completely replace fossil fuels in the near future. At the same time, energy consumption in developing countries like China and India is rapidly increasing as a result of their economic growth. It is generally recognized that the burning of fossil fuels will continue until an infrastructure for sustainable energy is established. Therefore, there is now a high demand for reducing greenhouse gas emissions from fossil fuel–based power plants.

Adaptation is a pragmatic approach to deal with the facts of climate change so that life, property, and income of individuals can be protected.

The pursuit of sustainable energy resources has become a complex issue across the globe. The *Handbook on Climate Change Mitigation and Adaptation* is a valuable resource for a wide audience who would like to quickly and comprehensively learn the issues surrounding climate change mitigation.

Why This Book Is Needed

There is a mounting consensus that human behaviors are changing the global climate and that its consequence, if left unchecked, could be catastrophic. The fourth climate change report by the Intergovernmental Panel on Climate Change (IPCC 2007) has provided the most detailed assessment ever on climate change's causes, impacts, and solutions. A consortium of experts from 13 US government science agencies, universities, and research institutions released the report *Global Climate Change Impacts in the United States* (2009), which verifies that global warming is primarily human induced and climate changes are underway in the USA and are only expected to worsen.

From its causes and impacts to its solutions, the issues surrounding climate change involve multidisciplinary sciences and technologies. The complexity and scope of these issues warrants a single comprehensive survey of a broad array of topics, something which the *Handbook on Climate Change Mitigation and Adaptation* achieves by providing readers with all the necessary background information on

the mitigation of climate change. The handbook introduces the fundamental issues of climate change mitigation in independent chapters rather than directly giving the detailed advanced analysis presented by the IPCC and others. Therefore, the handbook will be an indispensable companion reference to the complex analysis presented in the IPCC reports. For instance, while the IPCC reports give large amounts of data concerning the impacts of different greenhouse gases, they contain little discussion about the science behind the analysis. Similarly, while the IPCC reports present large amounts of information concerning the impacts of different alternative energies, the reports rarely discuss the science behind the technology. There is currently not a single comprehensive source that enables the readers to learn the science and technology associated with climate change mitigation.

Audience of the Handbook

Since the handbook covers a wide range of topics, it will find broad use as a major reference book in environmental, industrial, and analytical chemistry. Scientists, engineers, and technical managers in the energy and environmental fields are expected to be the primary users. They are likely to have an undergraduate degree in science or engineering with an interest in understanding the science and technology used in addressing climate change and its mitigation.

Scope

This multivolume handbook offers a comprehensive collection of information on climate change and how to minimize its impact. The chapters in this handbook were written by internationally renowned experts from industry and academia. The purpose of this book is to provide the reader with an authoritative reference work toward the goal of understanding climate change, its effects, and the available mitigation *and adaptation* strategies with which it may be tackled:

- Scientific evidence of climate change and related societal issues
- The impact of climate change
- Energy conservation
- Alternative energy sources
- Advanced combustion techniques
- Advanced technologies
- Education and outreach

This handbook presents information on how climate change is intimately involved with two critical issues: available energy resources and environmental policy. Readers will learn that these issues may not be viewed in isolation but are mediated by global economics, politics, and media attention. The focus of these presentations will be current scientific technological development although societal impacts will not be neglected.

References

Antilla L (2005) Climate of scepticism: US newspaper coverage of the science of climate change. Global Environ Change Part A 15(4):338–352

Becken S (2005) Harmonising climate change adaptation and mitigation: the case of tourist resorts in Fiji. Global Environ Change Part A 15(4):381–393

Ehrlich PR (2000) Human natures: genes cultures and the human prospect B&T. Island Press, Washington, DC. ISBN 978-1559637794

Folland CK, Karl TR, Nicholls N, Nyenzi BS, Parker DE, Vinnikov KYA (1992) Observed climate variability and change. In: Houghton JT, Callander BA, Varney SDK (eds) Climate change, the supplementary report to the IPCC scientific assessment. Cambridge University Press, Cambridge, pp 135–170

Greitemeyer T (2013) Beware of climate change skeptic films. J Environ Psychol 35:105–109

Grothmann T, Patt A (2005) Adaptive capacity and human cognition: the process of individual adaptation to climate change. Global Environ Change Part A 15(3):199–213

Haberle RM, Forget F, Head J, Kahre MA, Kreslavsky M, Owen SJ (2012) Summary of the Mars recent climate change workshop NASA/Ames Research Center. Icarus 222(1):415–418

Hamin EM, Gurran N (2009) Urban form and climate change: balancing adaptation and mitigation in the U.S. and Australia. Habitat Int 33(3):238–245

Hoffmann VH, Sprengel DC, Ziegler A, Kolb M, Abegg B (2009) Determinants of corporate adaptation to climate change in winter tourism: an econometric analysis. Global Environ Change 19(2):256–264

Intergovernmental Panel on Climate Change (IPCC) (2007) IPCC fourth assessment report: climate change 2007 (AR4), vol 3. Cambridge University Press, Cambridge

International Energy Association IEA (2009) World energy outlook 2009. International Energy Association (IEA), Paris. ISBN 9789264061309

IPCC (2010) Special Report on Emission Scenarios (SRES). http://www.grida.no/climate/ipcc/emission/

IPCC (2010) Intergovernmental panel on climate change. http://www.ipcc.ch/

IPCC (2013) Climate change 2013: the physical science basis, summary for policymakers. http://www.ipcc.ch/report/ar5/wg1/

IPCC IPCC third assessment report, chap 2.3.3 was there a “Little ice age” and a “Medieval warm period”? http://www.grida.no/publications/other/ipcc_tar/?src=/climate/ipcc_tar/wg1/070.htm

Jim Perry (2015) Climate change adaptation in the world’s best places: A wicked problem in need of immediate attention, Landscape and Urban Planning, 133:1–11

Karl TR, Trenberth KE (2003) Modern global climate change. Science 302(5651):1719–1723

Laukkonen J, Blanco PK, Lenhart J, Keiner M, Cavric B, Kinuthia-Njenga C (2009) Combining climate change adaptation and mitigation measures at the local level. Habitat Int 33(3):287–292

Le Houérou HN (1996) Climate change, drought and desertification. J Arid Environ 34:133–185

Linden HR (1993) A dissenting view on global climate change. Electron J 6(6):62–69

Linden HR (2005) How to justify a pragmatic position on anthropogenic climate change. Ind Eng Chem Res 44(5):1209–1219

McMichael AJ, Powles JW, Butler CD, Uauy R (2007) Food, livestock production, energy, climate change, and health. Lancet 370:1253–1263

Miller FP, Vandome AF, McBrewster J (eds) (2009) History of climate change science. Alphascript, Mauritius. ISBN 978-6130229597

Næss LO, Bang G, Eriksen S, Vevatne J (2005) Institutional adaptation to climate change: flood responses at the municipal level in Norway. Global Environ Change Part A 15(2):125–138

Quadrelli R, Peterson S (2007) The energy-climate challenge: recent trends in CO_2 emissions from fuel combustion. Energy Policy 35(11):5938–5952

Sonnabend G, Sornig M, Schieder R, Kostiuk T, Delgado J (2008) Temperatures in Venus upper atmosphere from mid-infrared heterodyne spectroscopy of CO_2 around 10 μm wavelength. Planet Space Sci 56(10):1407–1413

Stern N (2007) The economics of climate change: the stern review. Cambridge University Press, Cambridge. ISBN 978-0521700801

Stringer LC, Dyer JC, Reed MS, Dougill AJ, Twyman C, Mkwambisi D (2009) Adaptations to climate change, drought and desertification: local insights to enhance policy in southern Africa. Environ Sci Policy 12(7):748–765

United Nations (UN) (1992) United framework convention on climate change. United Nations, Geneva

van Aalst MK, Cannon T, Burton I (2008) Community level adaptation to climate change: the potential role of participatory community risk assessment. Global Environ Change 18(1): 165–179

Winter DF (1967) Transient radiative heat exchange at the surface of the moon. Icarus 6 (1–3):229–235

Worldbank (2009) Attitudes toward climate change: findings from a multi-country poll. http://siteresources.worldbank.org/INTWDR2010/Resources/Background-report.pdf

Zasova LV, Ignatiev N, Khatuntsev I, Linkin V (2007) Structure of the Venus atmosphere. Planet Space Sci 55(12):1712–1728

Loss and Damage Associated with Climate Change Impacts

Linta M. Mathew and Sonia Akter

Contents

Abstract

The impacts of climate change that are not mitigated, or appropriately adapted or coped with, are referred to as "loss and damage." The global community has recently recognized that addressing and financing the "residual" loss and damage from climate change requires a different approach as such costs cannot or have not been appropriately mitigated or adapted to. Although international pressures to weigh a country's contribution to climate change financing against their contribution to climate change has been proposed, no such legally binding climate change

L.M. Mathew • S. Akter (✉)
Social Sciences Division, International Rice Research Institute, Los Baños, Laguna, Philippines
e-mail: l.matthew@irri.org; linta_merinmathew@hotmail.com; s.akter@irri.org; soniakter@yahoo.com

W.-Y. Chen et al. (eds.), *Handbook of Climate Change Mitigation and Adaptation*,
DOI 10.1007/978-3-319-14409-2_55

deals have been fashioned. Most parties have only agreed to nonbinding actions to either reduce emissions or finance loss and damage in low-income, vulnerable countries. This is because the concept of loss and damage and the approaches to address the concept have been widely contested and debated. Additionally, the lack of a global consensus on an appropriate mechanism to attribute gradual and extreme natural calamities to climate change has further intensified the debate. Given this background, this chapter seeks to synthesize the key issues surrounding this debate. The objectives of this chapter are to review the definitions of loss and damage, examine the evolution of its significance in the international climate politics, present a comparative analysis of the approaches to address climate change-induced loss and damage, and outline empirical evidence of loss and damage in geographically and economically vulnerable nations.

Introduction

In its effort to combat climate change, the global community focused on rapid reduction of greenhouse gases (GHGs) by implementing enhanced mitigation efforts from the early 1990s to the mid-2000s. By the mid-2000s, scientific evidence indicated the likelihood of global temperature rising between 3 °C and 4 °C above the preindustrial level within this century (IPCC 2007a). This evidence suggested that mitigation efforts alone will not be sufficient to avoid climate change as some of the climate change impacts may already have started to take effect. Although steep cuts in global GHGs could stabilize atmospheric GHG concentrations at lower levels than under the status quo, they likely would be above the current levels, thus resulting in further rises in global temperatures. The projected impacts of a 3–4 °C temperature rise would lead to serious consequences for humans and ecosystems due to dangerous sea-level rise, unprecedented heat waves, severe drought, and major floods in many parts of the world (IPCC 2007a).

Once it became clear that mitigation efforts would be insufficient to avoid all climate change impacts, adaptation became a necessary complement to mitigation (Ott et al. 2008). Adaptation was defined by the Intergovernmental Panel for Climate Change (IPCC) (2007b) as "adjustment in natural or human systems in response to actual or expected climatic stimuli or their effects, which moderates harm or exploits beneficial opportunities." As of 2007, global adaptation cost estimates ranged from $4 billion to well over $100 billion a year (Parry et al. 2009). These estimates led to the establishment of the Green Climate Fund (GFC) in Durban, South Africa, in 2011 during the 16th session of the Conference of Parties (COP), with the objective of raising a minimum of $100 billion/year by 2020 to support sustainable and climate-resilient development (Institute for Policy Studies 2014; Green Climate Fund 2014). This came to be known as the "adaptation fund."

However, adaptation also appeared to have its limit. It became increasingly apparent that adaptation cannot successfully contain all the adversities invoked by climate change. Such remnants of the adverse effects of climate change came to be

known as "residual loss and damage." Widespread international understanding and agreement on the distinction between adaptation and loss and damage was deemed essential in recognizing that not all adversities of climate change can be successfully mitigated or adapted to. Such remnants of the ill effects of climate change impacts were forecasted to account for two-thirds of all potential impacts across all sectors over the longer term (Parry et al. 2009). This recognition highlighted the need to allocate adequate compensation and relief efforts, above and beyond the GCF, to help the victims of loss and damage in geographically and economically vulnerable countries.

The term loss and damage appeared in the United Nations Framework Convention on Climate Change (UNFCCC) negotiations in 2007 at COP 13, where the Bali Action Plan called for enhanced action on adaptation including the consideration of "disaster risk reduction strategies and means to address loss and damage associated with climate change impacts in vulnerable countries" (Roberts 2012). Loss and damage was recognized as a separate concept from adaptation in 2008, when the Alliance of Small Island States (AOSIS) proposed a Multi-Window Mechanism to address and finance the distinct concept of loss and damage due to climate change impacts. This was followed by the establishment of the UNFCCC Work Program on Loss and Damage in 2010 and the Warsaw International Mechanism on Loss and Damage in 2013. In addition, the Loss and Damage in Vulnerable Countries Initiative was formed in 2012, with the aim of understanding both the national context and the range of accessible implementation options for addressing loss and damage (Roberts 2012). However, no official lifetime commitment by developed countries to provide funds to the vulnerable communities has been undertaken as yet. Hence, the initiatives could be seen as weak attempts by the rich countries to admit liability for their contributions to climate change.

In this chapter, we synthesize the debates surrounding the classification of loss and damage and also uncover the issues around an appropriate compensation mechanism. The purpose of the chapter is to not add to the already substantive literature on loss and damage but to provide a review of the concept, historical treaties and conventions that finally led up to increased international focus on the issue, and the empirical heterogeneity in its estimate and impact across a multi-country sample. The remainder of this chapter is structured as follows: section "Definition of Loss and Damage" provides an in-depth examination of the definition and debates surrounding the concept of loss and damage. Section "History" accommodates a study of the international conventions and treaties on climate change and examines the gradual recognition of the need to address loss and damage in the international climate politics. This is followed by a discussion in section "Approaches to Address Loss and Damage" of the different approaches in addressing loss and damage such as monetary versus nonmonetary costs and insurance versus compensation. Finally, section "Empirical Evidence of Loss and Damage" provides empirical evidence of the global and international estimates of loss and damage as well as multi-country evidence of loss and damage experienced by some of the most geographically and economically vulnerable countries in the world.

Definition of Loss and Damage

A widely accepted definition of loss and damage does not exist. The framing of the definition and its conceptual discussion continue to evolve within the UNFCCC and the academic literature with different groups displaying heterogeneous understanding of the terminology and concept. The UNFCCC defined the concept as one of the "impacts associated with climate change in developing countries that negatively affects human and natural systems" (UNFCCC 2012).

However, the definition offered by the UNFCCC was found to be at its nascent stages and was therefore found to lack much clarity. This led to the formation of the Loss and Damage for Vulnerable Countries Initiative in 2012, headed by the Government of Bangladesh, to understand the meaning of the concept and how it can be approached in vulnerable countries (Roberts 2012). The UNFCCC and Warsaw International Mechanism for Loss and Damage act as guides to the initiative. Loss was defined by the Loss and Damage in Vulnerable Countries Initiative, as the "negative impacts that cannot be repaired or restored (such as loss of geological freshwater sources related to glacial melt or desertification)," whereas damage was defined as the "negative impacts that can be repaired or restored (such as windstorm damage to the roof of a building)." Therefore, the Loss and Damage in Vulnerable Countries Initiative views loss and damage as the avoidable and the unavoidable costs associated with climate change impacts.

The Loss and Damage in Vulnerable Countries Initiative definition also identified the need to include "the full range of climate change related impacts from (changes in) extreme events to slow onset process and combinations thereof." This definition included a continuum of climate change events and not only the extreme calamities resulting from climate change. The UNFCCC's Working Program on Loss and Damage called for a similar attempt to investigate a range of tools and approaches to address all forms of loss and damage resulting from climate change, ranging from slow onset to extreme weather conditions (UNFCCC 2012). However, the convention itself does not define loss and damage as the Work Program, which again indicates the lack of consistency and clarity of the concept.

Another working definition of loss and damage, compiled by Action Aid (2010), characterized loss and damage as consequences of the adverse effects of climate change that cannot be (or have not been) adapted to. This gave rise to the ideology of "residual" loss, i.e., unavoidable and unavoided loss and damage and recognized that certain aspects of climate change cannot be appropriately adapted to, given the limited resources available by many of the vulnerable nations affected by climate change. Action Aid (2010) summarized different categories of loss and damage, of which unavoided and unavoidable loss and damage were regarded as residual loss and damage (Table 1).

Unavoided costs can also be classified as the "avoidable costs of loss and damage," i.e., the costs of climate change impacts that can be avoided through appropriate mitigation and/or adaptation. However, such costs are not always avoided due to limited capacity or resource. It is very important to regionally and internationally allocate appropriate resources, such that the resulting loss and

Table 1 Avoided, unavoided, and unavoidable damage

Avoided damage	Unavoided damage	Unavoidable damage
Avoidable damage avoided	Avoidable damage and loss not avoided	Unavoidable damage and loss
Damage prevented through mitigation and/or adaptation measures	Where the avoidance of further damage was possible through adequate mitigation and/or adaptation, but where adaptation measures were not implemented due to financial or technical constraints	Damage that could not be avoided through mitigation and/or adaptation measures, e.g., coral bleaching, sea-level rise, damage due to extreme events where no adaptation efforts would have helped prevent physical damage

Source: Action Aid (2010)

damage can be reduced or mitigated completely. In least developed countries (LDCs), this often implies that such resulting loss and damage will only be adapted to if national benefits from adaptation exceed national losses and damages. Therefore, the loss and damage resulting from slow onset events and its victims events are often ignored[1]. This remains to be one of the major, but often sidelined, issues in the international climate change debate. Additionally, even in the case of unavoidable loss and damage, appropriate financing/funding still remains to be a problem. This is due to the "attribution problem" in climate change science, which can be briefly described as the inability to completely underpin the loss and damage due to weather-related events to climate change[2].

A technical representation of residual (unavoidable and unavoided) loss and damage was compiled by Rothman et al. (2003). This is represented in Fig. 1, where residual unavoidable and unavoided impacts of climate change with adaptation are demonstrated by the dotted line.

Unavoidable and unavoided residual loss and damage reflects ill effects that have not been mitigated and which cannot/have not been adapted to. One must also note that for stakeholders to undertake adaptation measure, the benefits from adaptation ("effect of adaptation") must be greater than adaptation costs. Although the diagram above seems straightforward enough, the effects of adaptation and the impact of climate change (its cost) are quite hard to calculate and reproduce in such a simple two-dimensional linear frame. Another schematic representation of the residual damage as compiled by Parry et al. (2009) is presented in Fig. 2.

Figure 2a represents the short-term nonlinearity of climate change impacts. Lower adaptation costs are associated with higher avoided damage, therefore giving it a low incremental adaptation cost to avoided damage ratio. This curve is estimated to fluctuate greatly across sectors and gives one a clearer picture of the variability and nonlinearity of such a concept. Figure 2b represents a longer time period of adaptation to damage, which illustrates that over the longer term, all damages will

[1]For more information on this, refer to section "Empirical Evidence of Loss and Damage."

[2]This "attribution problem" and the resulting financing issue will be examined in greater detail in section "Approaches to Address Loss and Damage."

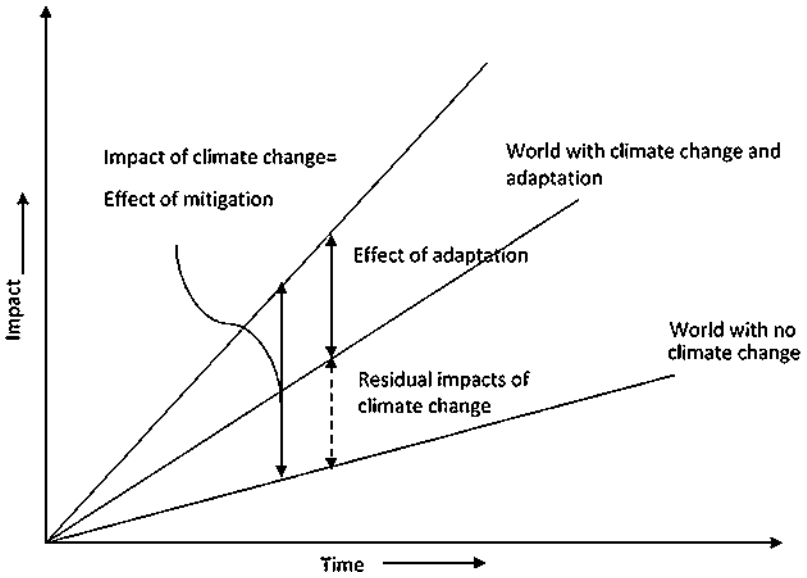

Fig. 1 Traditional representation of climate impacts and adaptation (Source: Rothman et al. (2003))

not be adapted to, due to its lack of economic viability or structural feasibility (Parry et al. 2009). The above representation also considers the trend in damage due to asset growth, therefore normalizing asset damage, such that the increase in damage is not associated with an asset growth.

The impact of loss and damage should be narrowed down to the ones that can be attributed to climate change. This can be accomplished by attempting to distinguish between bad weather and natural calamities that can be attributed to climate change. However, the lack of traceability of such events to climate change has induced reluctances by many stakeholders to officially commit to any binding financial agreements. This is commonly referred to as the "attribution problem" in climate science. Various methods of calculating the odds of relating extreme natural calamities to climate change have been devised to aid the allocation of climate change-related funds (Hulme et al. 2011). One such event attribution, termed as the probabilistic event attribution, compiled by Stone and Allen (2005), seeks to differentiate between weather changes caused as a result of human interference and "bad luck" (Hulme et al. 2011).

History

This section presents a history of evolution of the concept of loss and damage including the formation of the Loss and Damage in Vulnerable Countries Initiative and the Warsaw International Mechanism for Loss and Damage.

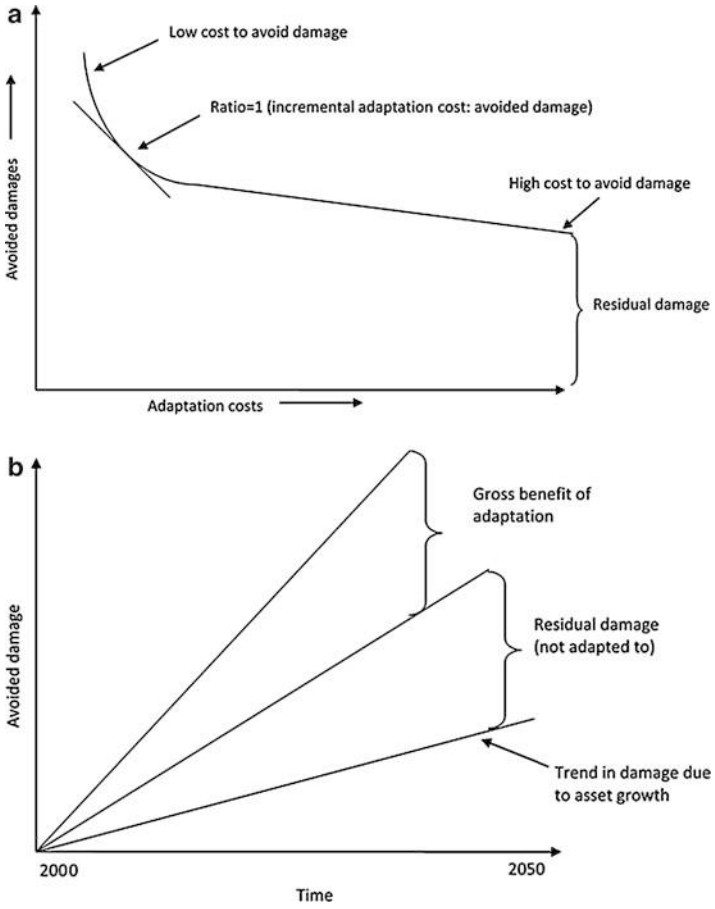

Fig. 2 Avoided damages and residual costs over the short term and long term (Source: Parry et al. (2009))

Conventions and Treaties

Various conventions and treaties were established over the years starting from 1979, which led up to the formation of the IPCC in 1988, followed by the creation of the UNFCCC in 1992. The role of the IPCC is to "assess on a comprehensive, objective, open and transparent basis the scientific, technical and socio-economic information relevant to understanding the scientific basis of risk of human-induced climate change, its potential impacts and options for adaptation and migration" (IPCC 2007b). The scientific evidence on climate change, gathered by the IPCC, underlined the severity of the issue and played a major role in the creation of the UNFCCC (IPCC 1995). The UNFCCC was formed to work to limit average global temperature increases and the resulting climate change and to cope with the unavoidable loss and

damage (UNFCCC 2014e). A summary of the major climate change conventions and treaties, post the initiation of the UNFCCC, is presented in Table 2.

Loss and Damage in Vulnerable Countries Initiative

The Loss and Damage in Vulnerable Countries Initiative was commenced by the Government of Bangladesh and expanded with the help of the Climate and Development Knowledge Network (CDKN), which appointed a consortium of specialists including Germanwatch, United Nations University – Institute for Environmental and Human security (UNU – EHS), International Centre for Climate Change and Development (ICCAD), and Munich Climate Insurance Initiative (MCII) and was implemented from 2012 (Loss and Damage in Vulnerable Countries Initiative 2014).

The Loss and Damage in Vulnerable Countries Initiatives are to:

Understand the scope and significance of loss and damage associated with the adverse impacts of climate change;
Developing and cocreating an approach and vision for loss and damage among decision makers and relevant stakeholders;
Assisting least developed countries and other vulnerable countries to develop a coherent approach to the loss and damage debate;
Identifying and beginning to take necessary steps to support a paradigm shift on loss and damage in the coming years;

Source: Loss and Damage in Vulnerable Countries Initiative (2014)

The activities of the UNFCCC and Warsaw International Mechanism for Loss and Damage guide the initiative. The initiative follows four main activity areas to support less developed nations in their plight to reduce and mitigate loss and damage due to climate change impact and to "create momentum in the climate change debate" (Loss and Damage in Vulnerable Countries Initiative 2014). These activities include supporting and strengthening the position of LDCs in loss and damage negotiations in the UNFCCC Work Program on loss and damage, conceptually framing loss and damage and providing policy assistance, providing country-specific insights on the adverse effects of loss and damage, and imparting the cumulative results of mitigation and adaptation efforts in Bangladesh as an analytical tool for other vulnerable countries.

Warsaw International Mechanism for Loss and Damage

The Warsaw International Mechanism for Loss and Damage was established to address the loss and damage due to climate change, including "extreme and slow onset events" in economically and geographically vulnerable countries (UNFCCC 2013). Two-year work plans were drawn up for the initiative during the resumed initial meeting in September 2014, which involved understanding the concept of loss and damage of extreme and slow onset events, risk management, comprehending the

Table 2 Precedent conventions and treaties

Year	Key event(s)	Description
1992	**AOSIS proposal for an insurance scheme**	Proposal for an insurance scheme was put forward by the members of the Alliance of Small Island States (AOSIS), the principle objective of which was to create an International Climate Fund and an International Insurance Pool to finance measures and to provide appropriate financial insurance respectively to counter the adverse effects of climate change.
		However, the parties only agreed to the insurance pool 10 years onward, provided that over the 10-year period, the "rate of global mean sea-level rise will have reached an agreed figure" (Hayes and Smith 1993).
1995	**The first Conference of Parties (COP 1): Berlin Mandate**	The COP1 held in Germany, where the Berlin mandate established the need for developed countries to "take the lead in combating climate change" and for developing countries to achieve sustainable economic growth (UNFCCC 1995).
1997	**COP 3**: **Kyoto Protocol Adoption**	Adoption of the Kyoto Protocol is undertaken in Kyoto, Japan, setting legally binding emission reduction targets.
		The summit recognized the greater role of developed countries in having historically contributed significantly to greenhouse emissions (through their previously active roles in industrial activity), and therefore placed a'heavier burden'(UNFCCC 2014) on developed nations under the notion of'common but differentiated responsibilities'(UNFCCC 1998).
2001	**COP 7**: **Marrakesh Accords**	Formation of the Marrakesh Accords, which laid out the rules and details for the implementation of the Kyoto Protocol, set up adaptation methodologies, and formed a technology transfer framework (UNFCCC 2014a).
2005	**Meeting of the Parties to the Kyoto Protocol** (**MOP 1**)	The Kyoto Protocol entered into force as the Russian Federation submitted its compliance (United Nations 2014).
		Negotiations for the next phase of the protocol under the Ad Hoc Working Group on Further Commitments for Annex Parties under the Kyoto Protocol (AWG-KP), later known as the "Nairobi Work Program," were also agreed upon.

(*continued*)

Table 2 (continued)

Year	Key event(s)	Description
2007	**COP 13**: **Bali Road Map**	Introduction of the Bali Road Map in Bali, Indonesia, which included the "Bali Action Plan." This plan was envisioned to charter the way toward a post-2012 outcome (UNFCCC 2014e).
		The Bali Action Plan is divided into categories such as shared vision, mitigation, adaptation, technology, and financing.
		However, it is to be noted that no significant effort was made to differentiate between adaptation and loss and damage in this stage.
2008	**COP 14**: **Joint Implementation Mechanism for the Kyoto Protocol**	A joint Implementation Mechanism for the Kyoto Protocol was initiated.
		This was described by UNFCCC (2014d) as an initiative that "allows a country with an emission reduction or limitation commitment under the Protocol to earn emission reduction units from an emission reduction or emission removal project in another country with similar commitments".
	AOSIS proposal of a Multi-Window Mechanism	The Alliance of Small Island States (AOSIS) proposed a Multi-Window Mechanism to address and finance loss and damage from climate change impacts (Alliance of Small Island States 2008).
2009	**COP 15**: **Copenhagen Accord**	The Copenhagen Accord was developed at COP15 in Copenhagen, Denmark, where developed countries undertook emission reduction and mitigation and adaptation action plan for the period of 2010–2012, pledging $30 billion as start-up finance (UNFCCC 2014e; United Nations 2014).
2010	**COP 16**: **Cancun Adaptation Framework**	The Cancun Adaptation Framework was formed at COP16, where governments of developed countries pledged comprehensive packages to assist developing countries to deal with climate change (UNFCCC 2014e).
		The agreements also made the reduction pledges of the countries official, which formed the "largest collective effort to reduce emission in a manually accountable way" (United Nations 2014).
	UNFCCC Work program to address loss and damage	The Cancun Adaptation Framework also established a work program to address the loss and damage impacts of climate change in LDCs vulnerable to the adverse effects of climate change (Roberts 2012).

(*continued*)

Table 2 (continued)

Year	Key event(s)	Description
2011	**COP 17: Durban Platform for Enhanced Action**	Plans to draw up a new universal climate change agreement by 2015, to deal with the adverse effects of climate change beyond 2020, were formed in Durban, South Africa. This led to the formation of the Durban Platform for Enhanced Action or the Ad Hoc Working Group on the Durban Platform for Enhanced Action (ADP) (UNFCCC 2014e).
	Green Climate Fund	COP 17 also led to the formation of the Green Climate Fund (GCF), with an aim of raising $100 billion per year in climate financing by 2020 (Institute for Policy Studies 2014).
2012	**COP 18: Doha Amendments to the Kyoto Protocol**	The Doha Amendments to the Kyoto Protocol commenced.
		This includes new commitments for a second commitment period from January 2010 until December 2020, a revised list of greenhouse gases to be reported by the Parties, and amendments to several articles of the Kyoto Protocol to issues pertaining to the first commitment period (UNFCCC 2014b).
		Governments also agreed to work speedily toward drafting a universal climate change agreement by 2015 (UNFCCC 2014b).
		The Doha Convention further addressed international efforts and strengthened international cooperation on loss and damage as a result of climate change (European Commission 2013).
	Loss and Damage Initiative in Vulnerable Countries Initiative	Loss and Damage Initiative was implemented in February 2012, with the objective of partnering with vulnerable LDCs and other parties to better understand loss and damage (Roberts 2012).
2013	**COP 19: Warsaw Outcomes**	The Decision to progress on the ADP Platform was agreed upon.
		A rulebook for reducing emissions from deforestation and forest degradation, enhancing the conservation and sustainable management of forests and forest carbon stocks in developing countries (REDD+), establishing a mechanism to address loss and damage from long-term climate change impact, and agreeing on capitalizing the GCF in the second half of 2014, as part of the Warsaw Outcome was undertaken (UNFCCC 2014g).

current coping and adaptation mechanisms, and drawing up socioeconomically appropriate policies to adapt to monetary and nonmonetary residual losses as a result of climate change (UNFCCC 2014f). The introduction of the mechanism was seen as a "notable step forward" as it allowed to address and implement socioeconomically appropriate policies to deal with the adversities of climate change in vulnerable communities (Warner 2013).

The primary roles of the Warsaw International Mechanism are to:

Facilitate support of actions to address loss and damage;
Improve coordination of the relevant work of existing bodies under the Convention;
Convene meetings of relevant experts and stakeholders;
Promote the development of, and compile, analyze, synthesize, and review information;
Provide technical guidance and support;
Make recommendations, as appropriate, on how to enhance engagement, actions, and coherence under and outside the Convention, including on how to mobilize resources and expertise at different levels.

Source: UNFCCC (2014f)

Approaches to Address Loss and Damage

This section summarizes the different approaches and their challenges for assessing and addressing loss and damage. Monetary and nonmonetary nature of loss and damage is discussed first followed by a range of economic instruments that can be used to address these costs. Finally, the attribution problem which lies at the center of the loss and damage debate is discussed in detail.

Monetary Versus Nonmonetary Costs

Climate change invokes both monetary and nonmonetary loss and damage in vulnerable countries. These categories are also known as economic and noneconomic loss and damage. Monetary or economic loss and damage refer to the costs for which economic or monetary estimates are readily available, such as structural damage and crop failure due to flooding[3]. Nonmonetary losses are those that cannot be measured in monetary or economic terms, such as loss of biodiversity, loss of livelihoods, or number of deaths caused by flooding. As these goods are not traded in the market, the monetary estimates of loss and damage caused to these goods are not readily available, and hence, these items are generally ignored by the loss and damage accounting (Morrissey and Smith 2013). The concept of nonmonetary

[3]A wide range of the estimates of the monetary costs from climate change have been estimated in previous studies, the details of which have been covered in section "Global Estimate of Loss and Damage."

costs was also highlighted in COP16 in Copenhagen where the parties recognized that all social and environmental loss and damage cannot be adequately captured by monetary measures. However, as such costs are difficult to quantify and monetize, it can be quite problematic to analyze the costs for inaction for such costs.

Nonmarket valuation techniques are often used to assign monetary values to the goods and services that are not traded in the market. Many studies, such as "valuing the ocean" study by the Stockholm Environment Institute (SEI), instead of employing market values to decipher loss and damage, monetized the costs of climate change to the ocean by focusing on five areas, namely, fisheries, sea-level rise, storms, tourism, and the ocean carbon sink (Stockholm Environmental Institute 2012). They pinned monetary values on such components by employing two scenarios: low climate change impact scenario, where emissions are reduced quickly, and a high climate change impact scenario, where the global emissions continue to rise for the next few decades (Stockholm Environmental Institute 2012). However, the results of the study were criticized as it only considers variables that can be "realistically altered by humans and can be monetized" (The Guardian 2012). Thus, the study only took into account the avoidable costs of loss and damage from climate change. Therefore, even though some studies have tried to monetize the marketed and nonmarketed goods affected by climate change, not all nonmarketed costs were effectively captured.

Insurance Versus Compensation

The concrete proposal put forth by the AOSIS in 2008 highlighting the need to finance a "Multi-Window Mechanism to Address Loss and Damage from Climate Change Impacts" placed the issue of financing loss and damage under the limelight. The proposed mechanism suggested three interdependent components for compensation: (1) insurance, (2) rehabilitation/compensation, and (3) risk management (AOSIS 2008). The insurance component was proposed to manage financial risk from extreme weather events and to provide insurance to countries who cannot find access to insurance. The rehabilitation/compensatory component addressed the progressive unavoidable climate change impacts, such as sea-level rise and ocean acidification. Finally, the risk management component was incorporated for risk assessment and management and to inform the insurance and the rehabilitation/compensatory component (AOSIS 2008).

The insurance option is one where regular payment by an individual to a private or public insurance entity subsists, such that the entity insures against any loss and damage that may be accidentally incurred by the individual. Munich Climate Insurance Initiative (MCII) (2012) stated that "insurance options can support adaptation and risk resilience for extreme weather, but are not appropriate for many, usually slower-onset, climate-induced impacts." Therefore, insurance was suggested to be an appropriate adaptation measure against unpredictable extreme events and not for predictable, slow onset events (Warner et al. 2012). This is because insurance companies will only be prepared to provide insurance payouts if the loss and damage

is entirely uncontrolled for and unforeseen. Insurance was suggested to be an adaptation, as opposed to a coping measure, as it reduces the impact of loss and damage and helps a timely recovery in the aftermath of extreme unforeseen calamities (Warner et al. 2012).

Insurance policies were found to be an unpopular method of financing loss and damage among the poorer households in geographically and economically vulnerable countries (Gine et al. 2008; Akter 2012). This was attributed to the lack of knowledge and affordability of insurance premiums in such countries. In some cases, coupling microcredit with insurance schemes was seen as a viable option to extend insurance services to low-income households. For instance, in a study conducted by OECD (2005), the Grameen Bima insurance programs in Bangladesh were found to offer insurance with microcredit, where no premiums were required to be a member of the fund, but payments to the fund were bundled with the interest paid on loans. However, the program was seen to be taken up by the middle class, as opposed to the low-income households, as the poor could not afford the premium (OECD 2005).

Compensation schemes in the context of loss and damage financing are funds provided by states or institutions to reduce the impact of loss and damage. The compensation option is perceived to be more appropriate than insurance schemes in funding the loss and damage from the gradual and predictable impacts of climate change. Therefore, the loss and damage from gradually occurring predictable events such as rising sea levels and desertification are best funded by states or institutions. However, individuals not insured against unpredictable extreme calamities should be considered for compensation schemes. This includes individuals in the poorer counterpart of the society, who are not able to afford the insurance premiums. Additionally, the lack of sufficient resources in low-income vulnerable countries does not enable appropriate compensation for all. The effectiveness in reducing the impact of loss and damage of such compensation packages depends on the efficiency of state policies and their outreach approach.

Attribution

Attributing weather-related range of slow set to extreme calamities to climate change was found to be quite difficult and operates as one of the major limitations in climate change financing. The lack of good traceability measures also provides a good justification for many developed countries to reject liability and therefore fail to make any firm commitments to financing loss and damage in low-income countries. Hence, the following paragraphs examine the effectiveness and limitations of such attribution mechanisms and their potential role in aiding the global community with financing loss and damage from negative climate change impacts.

The most popular method in climate change attribution is the examination of another related variable, which is linked to the characteristics of the extreme natural event. This is done as it is difficult to gain insights from examining trends of extremely rare natural calamities (Huggel et al. 2013). However, such studies have

confirmed the link between some natural calamities and climate change, but not all. Increasingly, studies have identified that the increase in economic damages from extreme events has been attributed to increased "exposed asset values" rather than an increased intensity of extreme natural calamities (Huggel et al. 2013). To this end, Neumayer and Barthel (2011) calculated an actual-to-potential-loss ratio (APLR), which provided a normalization method to measure the economic loss after the onset of a severe natural disaster. Even though no upward trend in normalized loss and damage was found, the authors did not account for mitigation measures, which may have compromised the findings. Additionally, even if the increased loss and damage is accounted to increased asset value, this does not imply that the resulting loss and damage must not be compensated for. Such a finding, if anything, calls for increased insurance or compensation schemes to be implemented by regional and international bodies.

However, many limitations in relying on such attribution methods to allocate any loss and damage funds were found such as the unreliability of such methodologies as they are based on climate estimates without climate change, which cannot be logically verified; the inability to accurately predict the percentage of overall risk attributable to human actions; and the undesirable shift in international climate change initiative from adaptation to compensation, if such methodologies are extensively used to allocate the international adaptation finance (Hulme et al. 2011). The lack of good quality data may also affect the accuracy of such measures. However, even though many such objections to attribution measures exist, formulating attribution mechanisms should be encouraged by the international community as it helps to reduce (to some extent) the moral hazard related to adverse events, where individuals will take greater risks (for instance, building houses in flood-prone areas) in the hope of being compensated. However, care must be taken in order to not get carried away by such measures. Successfully implemented techniques can help eradicate such uncertainty, which can aid the international community to identify the victims of climate change and to allocate funds to communities who are essentially negatively affected from climate change.

The global community should allocate sufficient funds such that until a clear measure of attribution is found, the civilians experiencing loss and damage, especially in geographically and economically vulnerable countries, as a result of climate change impacts, do not suffer substantially. This was highlighted by the Philippines Senate Present Juan Ponce Enrile who stated that "developing countries like the Philippines should be receiving compensation… Instead, however, we are accepting, or worse, being "forced" to avail of loans that are, in the long run, more disadvantageous for the country" (Climate Justice Now 2010).

Empirical Evidence of Loss and Damage

This section presents monetary estimates of loss and damage due to climate change impacts both at the global and local level. The first subsection summarizes the global estimates of loss and damage available in the literature. The second subsection

presents country-specific local estimates of loss and damage from eleven most economically and geographically vulnerable countries in the world. It also outlines the existing loss and damage-coping strategies used by the households in these countries.

Global Estimate of Loss and Damage

Various global estimates of loss and damage have been produced over the years. Global monetary estimates of loss and damage can be measured in terms of the social costs of carbon, which is defined as the "net economic costs of damages from climate change aggregated across the globe and discounted to the present" (IPCC 2007). IPCC's *Fourth Assessment Report* (AR4) disclosed that the peer-reviewed estimate of the social cost of carbon in 2005 has an average value of US$12/t of carbon dioxide. However, the range from 100 estimates was found to be large ($3–$95/t of carbon dioxide), which demonstrates a substantial degree of disagreement on its measurement (IPCC 2007). Natural disasters are estimated to have doubled from an average of 200/year in 1998 to an average of 400/year in 2008, whereas costs of natural disasters in monetary terms have increased sevenfold (United Nations 2009; cited in Action Aid 2010). Therefore, future estimates of climate change have painted a dull portrait of an impending catastrophe.

Monetary values of loss and damage can also be calculated from the overall loss and damage caused by climate change after accounting for certain scenarios of mitigation and adaptation (Action Aid 2010). One such probabilistic estimation method, known as the Policy Analysis for the Greenhouse Effect (PAGE), calculates the regional and global impacts of climate change, social costs of greenhouse gases, and also the cost of abatement and adaptation (UNFCCC 2014d). This model helps one to calculate the economic loss from such climate change adversities. Action Aid (2010) put together a table for global loss and damage under a scenario of no mitigation and the lowest emission scenario proposed by UNFCCC. Adaptation costs were also derived from UNFCCC reports. The costs are accrued over the years 2000–2200 and presented in discounted net present values (NPV).

From the analysis presented in Table 3, it was inferred that with respect to the cost of impact, the optimal action is to combine mitigation and adaptation. However, even with successful mitigation, a residual loss of US$275 trillion was found. However, this method of calculation was found to be more appropriate to predict global, as opposed to regional, loss and damage. Regional calculations of loss and damage are mostly obtainable from local insurance estimates. However, such estimates in low-income developing countries may only adumbrate monetary loss and damage to important sectors such as energy and infrastructure and neglect or overlook the loss and damage to most households. In such circumstances, national statistics are ones' best gamble in obtaining regional loss and damage statistics.

Although the calculation of residual loss and damage has been highly debated, as demonstrated by the noteworthy range of the formulated estimates, a common underlying theme of globally increasing loss and damage was found. Additionally, the calculations of monetary loss and damage also suggested that if appropriate

Table 3 Monetary estimates under "no mitigation" and "mitigation and lowest emission" scenarios

	Trillion US$					
	No mitigation			Lowest emission scenario		
	Lower end	Mean	Higher end	Lower end	Mean	Higher end
Cost of impact (without adaptation)	270	1,240	3,290	100	410	1,070
Cost of impacts (with adaptation)	170	890	2,340	60	275	760
Adaptation costs	4	6	9	4	6	9
Mitigation costs				50	110	170

Source: Action Aid (2010)

measures are not taken to constantly curb global emissions, loss and damage, particularly to low-income vulnerable countries, would only increase exponentially over time. Therefore, communities with a higher exposure to the risks of climate change and with lower adaptive capacity would experience a greater burden of loss and damage in comparison to others. Such vulnerable countries include the Alliance of Small Island States (AOSIS), threatened by the rise in sea level, and low-income developing countries, where a large proportion of the population relies on agricultural income, particularly susceptible to climatic fluctuations. Although developed rich nations may experience greater monetary losses from extreme events due to a higher proportion of exposed assets, the loss and damage as a percentage of GDP is peripheral in comparison to the low-income vulnerable nations. This is demonstrated in the figure below which compares the monetary damage to the monetary damage as a *percentage of GDP* in both developing and developed countries.

Figure 3 shows the damages as a percentage of GDP are higher for low-income developing countries than for the developed rich nations. On average, the agricultural sector contributes substantially to a poor developing nations' GDP, which is particularly vulnerable to the weather changes that have resulted from climate change. Additionally, poorly built infrastructure and households in low-income developing countries are often unable to withstand extreme weather disruptions, causing greater damage as a proportion of GDP in such countries.

Country-Specific Evidence of Loss and Damage

Country-level evidence of loss and damage occurring due to climate change impacts in vulnerable countries is crucial in assessing the future risks of climate change in such countries. Table 4 summarizes the environmental and economic vulnerability facing eleven low-income countries due to climate change impacts. The specific nature of the vulnerability, monetary estimate of loss, and damage resulting from unavoidable climate change impacts and coping strategies are summarized in the following paragraphs.

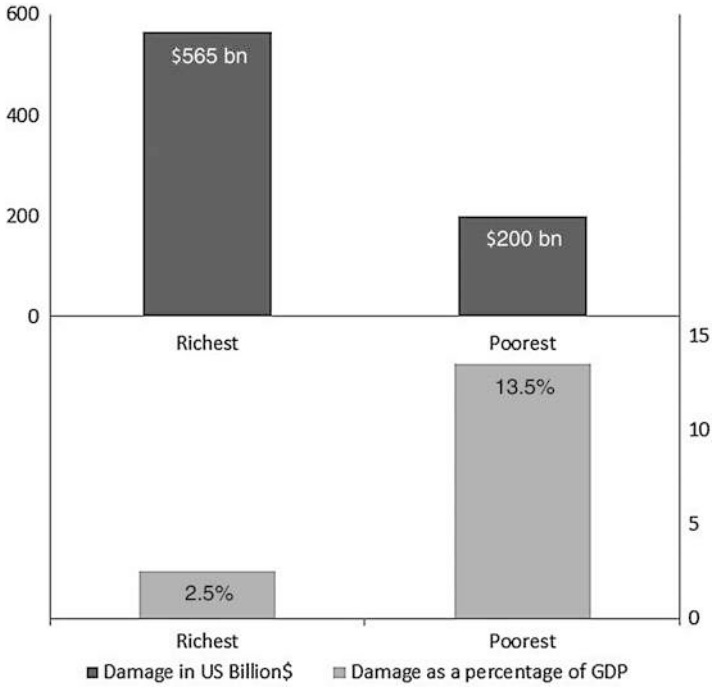

Fig. 3 Disaster losses, total and as a share of GDP, in the richest and poorest nations, 1985–1999 (Source: United Nations Inter-Agency Secretariat for the International Strategy for Disaster Risk Reduction (2003))

Bangladesh

In the case of Bangladesh, it was found that climatic susceptibility along with increased climate change has adverse consequences, especially in the coastal region. Frequent cyclones, such as Sidr in 2007 and Aila in 2009, caused massive loss and damage to the coastal population. Cyclone Sidr claimed 4,234 lives, injured 55,282 people, and damaged 8.9 million people's livelihood (Ministry of Disaster Management and Relief 2014). The economic damage caused by Cyclone Sidr was equivalent to US$1.67 billion (Ministry of Disaster Management and Relief 2014). Eleven out of the 19 coastal districts were severely affected by Cyclone Aila. It claimed 190 lives, injured 7,000 people, killed 100,000 livestock, and caused US$170 million worth of economic damage (United Nations Development Fund 2010 cited in Akter and Mallick 2013). The loss and damage experienced by a cyclone as powerful as Cyclone Sidr are expected to rise nearly fivefold to over $9 billion by 2050, accounting for 0.6 % of GDP (World Bank 2010).

These cyclones forced saline water into the agricultural lands (Rabbani et al. 2013). The rise in sea level, also attributed to global climate change, is expected to push saline water further inland, therefore severely affecting the agricultural productivity and the quality of drinking water in the coastal districts of

Table 4 Climatic susceptibility, long-term climate change threat, and livelihood impact in the nine disaster-prone areas

Country	Region	Climatic susceptibility	Long-term threats	Impacts
Bangladesh	Sathkira	Cyclones	Sea-level rise, salinity intrusion	Rice, drinking water
Bhutan	Punakha	Glacial lake outburst floods	Changing monsoon	Rice
Burkina Faso	Sahel	Drought	Changing rainfall patterns	Livestock, crops
Ethiopia	Gambella	Floods	Changing rainfall patterns	Habitability, crops, livestock
Gambia	North Bank	Drought	Changing rainfall patterns	Agriculture
Kenya	Budalangi	Floods	Changing rainfall patterns	Livestock, crops, property, disruption of social and economic activities
Micronesia	Kosrae	Storms	Sea-level rise, coastal erosion	Crops, livestock, fish
Mozambique	South/ Central	Floods/ droughts	Changing rainfall patterns	Housing, livelihood
Nepal	Udayapur	Floods	Changing rainfall patterns	Staple crops
Pakistan	Baluchistan	Flood, glacial lake outbursts	Changing rainfall patterns	Agriculture, transport and communication
Philippines	Tacloban	Cyclones	Changing storm intensity	Lives, agriculture, livestock, and property

Source: Warner and van der Geest (2013) and (Roberts et al. 2014)

Bangladesh (Rabbani et al. 2013). High yielding rice varieties were unable to withstand the increase in soil salinity (Rabbani et al. 2013). New varieties, such as BINA 8 and BRRI 47, henceforth developed after 2009, to resist high-salinity levels, were however found to be inappropriate for the chosen region (Rabbani et al. 2013). It is also estimated that the region incurred a decrease in its rice production by 0.1 million tons between 2008 and 2010. The total cost of loss to rice production due to salinity was estimated to be US $1.9 million from 2009 to 2011. The dangers of massive rural–urban and coastal-central migration looms in the near future if the region continues to experience such frequent calamities.

Bhutan

The district of Punakha is referred to as Bhutan's "rice bowl," where a substantial proportion of the population engages in small-scale farming (Kusters and Wangdi 2013). Kusters and Wangdi (2013) conducted a study on this region. A large proportion of the research participants recognized a pattern of unreliable monsoon and overall annual precipitation. This observation was confirmed by rainfall data collected over 1990–2008. This changing water availability was reported to have a negative effect on crop production. Coping measures adopted by the households include ritual performance (costing households between US$700 and US$900 per year), developing or modifying water-sharing arrangements, maintaining irrigation channels, changing cropping pattern, buying irrigation water from upstream villages, and using water pumps. Improved availability of fertilizers and modern technology was found to greatly enhance agricultural productivity for many farmers. Nevertheless, most adaptation measures were not without costs, some of which are monetary and some are nonmonetary. For instance, unsuccessful water-sharing arrangements led to local conflicts, disrupting social cohesion. Maintenance of irrigation canals required a substantial contribution, which was typically found to be unaffordable by the poor households, and therefore they were excluded from such water-sharing arrangements. Some farmers changed the cropping pattern from rice to maize resulted in an economic loss equivalent to US$2,000/acre.

Even though improved seed varieties and the availability of fertilizers and pesticides led to an overall increase in rice production in the district between 2002 and 2010, this improvement was not uniform across the whole region as poorer households failed to access these inputs. Therefore, the need to promote equal access to agricultural inputs is identified in the study. Additionally, the local officials often perceive the issue of glacial lake outburst floods due to the melting of glaciers and the threat of destabilizing ice-cored dams as a policy priority in comparison to changes in precipitation levels. This allowed them to overlook the problem of gradual changes in water availability, as the effects were less visible and less severe in relation to the impact of floods.

Burkina Faso

Burkina Faso is a semiarid, landlocked country in western Africa. Ninety percent of its population is engaged in agriculture and livestock sectors (Traore and Owiyo 2013). The high reliance on the agricultural and livestock by a large proportion of the population in the Sahel region of Burkina Faso implied that a substantial proportion of the population is engaged in activities that are weather sensitive. Therefore, their livelihoods depend significantly on climatic conditions. Traore and Owiyo (2013) found draught to be the main climatic stressor in the region. The occurrence of draught was confirmed by rainfall data, which indicated a high variation of rainfall and also a recent history of draught in the Sahel region. Severe negative impact on crop and livestock rearing was reported by a large percentage of the sampled households. Coping measures included reducing food consumption, selling property and livestock, cutting expenditure, receiving external support, migrating, earning extra income, transhumance, and a small proportion of the sample reported resorting

to begging. Modifying food consumption and selling property were found to be the most popular coping mechanisms. However, from the households that reported to undertake coping mechanism, 71 % indicated that they were still experiencing negative effects of the drought. The destruction caused by the onset of draughts, such as the lack of water for crop yields, led to the unavailability of water for the local people and their livestock, which further limited their future coping and adaptation ability. The range of average crop production loss was reported to be between US$577 and US$636 per household, whereas the range of average livestock loss was found to be between US$1,922 and US$8,759 per herder in the region.

Ethiopia

Ethiopia is heavily dependent on rain-fed agriculture. Historically, the country is prone to extreme weather events mostly characterized by highly variable rainfall pattern. Using spatially explicit analyses of climate change effects on selected key sectors of Ethiopia's economy, Robinson et al. (2013) found that the residual loss and damage might cost an annual average of US$0.4–3.0 billion. A case study was conducted by Haile et al. (2013) in the lowlands of Gambella, Ethiopia. The area experienced frequent river flooding that severely affected its people and their livelihoods. The main source of livelihood of the participants was crop cultivation and livestock rearing. The 2007 extreme flooding severely damaged the crops of three quarters of the respondents of the study and damaged the household properties of a quarter of the respondents. Most of the participants described the effect of the flood as either "very severe" or "disastrous" (Haile et al. 2013).

However, unlike in the case of Sahel in Burkina Faso, the ability to relocate livestock ensured a better source of livelihood for the livestock owners as opposed to the farmers, most of who reported that the yield of their next cropping season severely suffered as a result of the floods. Coping mechanisms included relying on assistance from NGOs, social networks, government support, and religious organizations. NGOs and social networks provided support to the largest proportion of the affected households. Nevertheless, the erosive quality of some coping measures is highlighted, where the respondents believed that the goodwill and resources of their reliable contacts will gradually diminish, inhibiting their future coping ability. Hence, the reliance on social networks was not perceived to ensure a long-term adaptation solution. Moreover, a majority of the households who had undertaken preventive measures such as increasing the floor height, harvesting premature crops, and constructing a high stage for livestock were unable to fully evade the negative effects of the 2007 flood. Additionally, as voluntary government resettlement plans are underway, the villagers are questioning its habitability as the new villages are lacking essential services such as health services and potential security.

Gambia

A study by Njie et al. (2007) estimated the residual damages from climate change in Gambia to range between US$123 million and US$130 million/year in the near term. For the more distant 2070–2099 period, residual damage cost estimated to

range from US$955 million to US$1.0 billion (Njie et al. 2007). A case study conducted by Yaffa (2013) in severely drought-prone regions of Gambia found that the varying level of rainfall and shorter duration of the rainy season along with rising temperatures implied severe calamity for its community that was mostly reliant on agriculture for their livelihoods. The prominent ill effects incurred by the community included food shortage, rise in food prices and reduction in crop production, and livestock ownership. Similar coping measures, as seen in the previous case studies, were adopted, where most of the measures were seen to aid short-term relief.

Kenya

Climate change poses a serious threat to Kenya's economy. Currently climate change accounts for an approximate monetary loss of approximately US$0.5 billion/year which is equivalent to 2 % of the country's GDP (Stockholm Environment Institute 2009). This cost is expected to rise and eventually claim 3 % of Kenya's GDP by 2030 (Stockholm Environment Institute 2009). A forecasted increase in rainfall in Kenya, due to climate change, along with human activities such as deforestation and overgrazing, is speculated to have increased the severity of flooding in the low-lying coastal regions of Kenya (Opondo 2013). The main sources of livelihood in the flood-prone regions are crop cultivation, livestock rearing, and other nonagricultural activities such as fishing, small-scale trade, and manual labor. It was found that more than three fourths of the farmers in the affected region reported that their livelihood had been severely affected by the flooding. Additionally, almost three fourths of all participants from all the occupational and income categories had reported that they were severely affected. The most common coping strategies included reducing food consumption and receiving help from local governments, NGOs, and religious organizations. However, most coping strategies, as in the case of the previous case studies, were found to be short-term solutions and most of such coping mechanisms implied "long term negative effects on the household economy" (Van der Geest and Dietz 2004 cited in Opondo 2013). For instance, undertaking the sale of property implied a reduced household asset base, unfavorable for a longer-term sustainable means of adaptation.

Micronesia

The case study examined below demonstrates a principal environmental concern of Micronesia as well as other small island states of the Pacific Ocean. Monnereau and Abraham (2013) confirmed that the rising sea level (attributed to climate change) has led to severe coastal erosion in the coastal region of Kosrae and has threatened the livelihood and habitability of many of its inhabitants. A rise in the sea level and coastal erosion is particularly dangerous to such island territories as it leads to a reduction in island size. The study revealed that the households who had adopted coping measures such as building seawalls, reinforcing their homes, and planting trees provided only temporary protection for the local inhabitants and had adverse long-term environmental effects. For instance, the building of sea walls and the

planting of trees only provided short-term solutions and only protected small sections of coastline. This highlighted the requirement of a large-scale or even state-level investment to provide sufficient barriers for the coastline. However, no initiatives have been successfully implemented to date as previous studies had indicated that the building of sea walls was found to have caused current changes and beach loss. The majority of the participants had indicated that they suffered from the effect of coastal erosion and that the coping strategies pursued was not sufficient to counter its adverse effects.

Mozambique

With a large coastline, Mozambique was found to experience severe floods in the lowlands (central), which adversely affected the livelihood of the rural farmers. In the year 2007 itself, Mozambique experienced a total economic loss and damage of $71 million from severe flooding (United Nations Office for Disaster Risk Reduction 2014). Brida et al. (2013) provided an account of the struggle of the community and the coping and adoption measures adopted and their effectiveness. The government of the country undertook resettlement projects, relocating communities to the uplands (south). However, this turned out to be as disastrous to the community as the uplands experienced frequent draughts, forcing many to go back to the lowlands and endure the negative effects of the floods. Crop cultivation, livestock rearing, and fishing were the most prominent sources of income in decreasing order of importance. Overall, a "double blow" from both the floods and the droughts was found to affect the entire sample interviewed, where the greatest ill effect was experienced by the farmers (Brida et al. 2013). As a result of food shortage, food prices increased, therefore further intensifying the adversity. The most prominent coping mechanisms included looking for other sources of income that includes laboring for the better-off households and selling property. However, as seen in previous case studies, such measures did not provide any long-term solutions. Moreover, the government resettlement initiative was found to worsen the situation for many.

Nepal

Frequent floods are one of the recurrent natural disasters that affect Nepal. Between 1971 and 2007, a staggering amount of 2,500 floods were recorded, which claimed more than 3,000 lives and damaged at least 150,000 buildings. The region of Udayapur in Nepal was found to be particularly susceptible to increasingly severe floods and vulnerable to the impact of climate change (Bauer 2013). The two main rivers in Udaypur reported increased rate of flooding. This was worsened by man-made obstructions such as roads and bridge piers, along with other activities such as deforestation which made the rivers shallower and accelerated sedimentation. Agriculture constituted the largest source of livelihood for many. More than 4/5 of all households reported that their agricultural output has decreased over the past years. Prevention and coping mechanisms undertaken by the farmers such as constructing stonewalls and seeking help from institutions such as NGOs was inadequate to avoid the recurrent loss and damage. Another frequent coping

mechanism was labor migration to cities and overseas. The relatives of the migrants often relied on their remittances as an extra source of income, but often male migration was associated with increased work load for the women.

Pakistan

Flooding and overflowing rivers caused substantial damage to 14 districts, particularly to the southern and northern parts of the district in 2010. It directly affected an estimated 14-20 million people, and killed over 1,700 (Kirsch et al. 2012). The floods also severely affected crops and livestock, where the crops were either partially or completely submerged and the livestock suffered from a lack of fodder availability. A total country-wide loss of US$9.7 billion was expected to have occurred in the agricultural sector (Kirsch et al. 2012). Food insecurity and malnutrition were also reported to have occurred in poorer societies. The average reported household monthly income of the affected community decreased by 50% (Kirsch et al. 2012). National response mechanisms included the use of military-affiliated rescue and aid operations, civil society relief operations included aid and establishment of social welfare infrastructure, and international donor aid and assistance was provided to affected areas (Asian Development Bank 2011). Rebuilding projects are being undertaken with the aim of constructing a flood-resilient society. However, the lack of proper pre-disaster awareness techniques prevents adequate preparation procedures. Therefore, loss and damage due to extreme flooding can almost be perceived as an unavoidable consequence. Additionally, even though civilians were requested to not reside in low-lying areas or near rivers, such a request is unfeasible as most of the rural poor reside in such vulnerable areas.

Philippines

According to National Disaster Reduction and Management Council (NDRRMC) (2014) 6,201 persons were killed, 28,626 were injured and 1,785 are missing over the entire Philippines in the aftermath of Typhoon Haiyan. The typhoon was the most powerful typhoon to make landfall to date which also caused significant economic damage to infrastructure and property. The damage to infrastructure and agriculture damages were estimated at US$802 million (Mori et al. 2014). Most of the residents were recorded to have taken sufficient coping and adopting mechanisms to frequent storms that hit the country. Local residents were reported to have never experienced a typhoon even remotely as brutal as Haiyan and were therefore defenseless. National and international relief efforts were mobilized post disaster, although the collapse of the local airport slowed down the process. Local inhabitants, with little or no socioeconomic assets and connections, are still known to be suffering from the adversities of the typhoon and were soon after subject to the adversities. After the onset of such a calamity, the Philippines hosted the Conference of United Nations Risk Reduction and Management in Manila to emphasize the importance of an available, accessible, and affordable disaster risk information system as part of the "Post-Haiyan Tacloban Declaration" (The United Nations Office for Disaster Risk Reduction 2014). During the 2013 Warsaw Conference, the Philippine Climate Change Commissioner, Naderev Yeb Sano, fought back tears while warning the

international community that his country is particularly suffering as a result of climate change, reflecting on the recently acquired news of his family's safe residence after Typhoon Haiyan (Galarraga and Roman 2013).

Conclusions

Loss and damage was recognized as a separate concept from adaptation in 2008, when the AOSIS proposed a Multi-Window Mechanism to address and finance the distinct concept of loss and damage arising due to climate change impacts. This was followed by the establishment of the UNFCCC Work Program on Loss and Damage in 2010 and the Warsaw International Mechanism on Loss and Damage in 2013 to further comprehend and address the issue. The Loss and Damage in Vulnerable Countries Initiative, formed in 2012, was the largest independent entity solely dedicated to building a common understanding of loss and damage. However, despite current global efforts in understanding the concept of loss and damage, the exact definition is still as elusive as ever and is still widely contested among the stakeholders.

Additional issues such as distinguishing between avoidable and unavoidable loss and damage, slow onset and extreme events, and monetary and nonmonetary loss and damage were also highlighted in this chapter. Discriminating between such categories of loss and damage from climate change adversities is essential as each category would require a different approach. For instance, in the case of avoidable and unavoidable loss and damage, it was pointed out previously that institutions and individuals must dedicate resources such that avoidable losses and damages can be successfully mitigated or adapted to and unavoidable losses and damages can be appropriately financed. Additionally, the debate regarding the constituents of loss and damage impacts from climate change makes it quite difficult to converge on a global estimate, therefore impeding a concrete commitment to tackle such an adversity. However, a global climate deal is being furnished and will be executed in 2015, where parties have agreed to adhere to a legally binding international climate change deal. Nevertheless, this agreement was only concurred by the EU, some other European nations, and Australia. Although this can be seen as a significant step forward, the lack of commitment by all developed countries still poses a great obstacle in obtaining an ideal climate change deal.

The biggest limitation in forming a concrete deal to address loss and damage was found to be the attribution problem. This can be described as lack of solid traceability of adverse weather impacts to climate change, which was found to impede any solid commitments by countries. To resolve the attribution problem, many studies have devised mechanisms to examine the extent to which adverse weather impacts can be attributed to climate change. However, as of now, no globally agreed upon mechanism has been fashioned. Additionally, the degree of impact of loss and damage due to climate change on livelihoods differed substantially across developing and developed countries. On the one hand, civilians in developed countries were mostly insured against the loss and damage from natural calamities or their losses and damages were mostly compensated for, where insurance or compensation policies

depended on country-specific requirements and regional policies. On the other hand, the poor farmers and livestock owners in vulnerable low-income countries were found to suffer substantially as a result of such climatic changes.

Country-specific loss and damage estimates and coping strategies from some of the most economically vulnerable countries have been analyzed in this chapter. The degree to which such adversities affected households depended on their socioeconomic status and geographical location. The livelihood of the poorer farmers and livestock owners was generally seen to be affected the most due to their restricted mobility and limited livelihood options (after a partial/complete destruction of their farms and livestock from extreme natural calamities). Common coping measures for predictable events included modifying food consumption, selling property and livestock, cutting expenditure, receiving external support, and finding extra income sources. However, many of the coping strategies adopted by the locals were seen as temporary and some measures even eroded their long-term coping capacity. Additionally, extreme and unexpected events, such as typhoon Haiyan in the Philippines, addressed the need to identify disaster identification technologies to reduce the loss and damage from such natural calamities. Overall, the case studies of economically and geographically vulnerable countries highlighted the need to identify and implement long-term measures to mitigate loss and damage and the need for active collaboration between international organizations, NGOs, and local governments to draw up cost-effective and feasible policies to combat such residual loss and damage.

Future Directions

Future directions for research include extended research work on regional- or country-specific insurance or compensation schemes for low-income countries, such that financing options that are best suited to address the environmental and social vulnerability of the region can be devised. Additionally, it was found that one of the biggest limitations in the climate change debate was the "attribution problem." Therefore, such a problem must be appropriately conceptualized and addressed, where better attribution techniques should be thoroughly examined and critiqued, and its applicability to the entire range of slow on set to extreme climatic conditions should be studied.

References

Action Aid (2010) Loss and damage from climate change: the cost for poor people in developing countries. Action Aid, Johannesburg

Akter S (2012) The role of microinsurance as a safety net against environmental risks in Bangladesh. J Environ Dev 21:263–280

Akter S, Mallick B (2013) The poverty–vulnerability–resilience nexus: evidence from Bangladesh. Ecol Econ 96:114–124

Alliance of Small Island States (2008) Proposal to the AWG-LCA: multi-window mechanism to address loss and damage from climate change impacts. UNFCCC, Bonn

Asian Development Bank (2011) Pakistan floods 2010: preliminary damage and needs assessment. Asian Development Bank, Islamabad
Bauer K (2013) Are preventive and coping measures enough to avoid loss and damage from flooding in Udayapur district, Nepal? Int J Glob Warm 5:433–451
Brida AB, Owiyo T, Sokona Y (2013) Loss and damage from the double blow of flood and drought in Mozambique. Int J Glob Warm 5:514–531
Climate Justice Now (2010) Philippines' senate leader calls for climate "compensation". [Online] Available at: http://www.climate-justice-now.org/philippines-senate-leader-calls-for-climate-compensation/
European Commission (2013) The 2015 International Climate Change Agreement: Shaping international Policy beyond 2020. European Commission, Brussels
Galarraga I, Roman M V (2013) Warsaw conference: small steps forward while awaiting major decisions at the 2015 Paris conference. Basque Centre for Climate Change, Policy Briefings PB 2013/Special Issue-01, Bilbao Bizkaia
Gine X, Townsend R, Vickery J (2008) Patterns of rainfall insurance participation in rural India. World Bank Econ Rev 22:539–566
Green Climate Fund (2014) Background. [Online] Available at: http://www.gcfund.org/about/the-fund.html
Haile AT, Kusters K, Wagesho N (2013) Loss and damage from flooding the Gambela region, Ethiopia. Int J Glob Warm 5:483–497
Hayes P, Smith K (1993) The global greenhouse regime: who pays? United Nations University Press,Tokyo
Huggel C, Stone D, Auffhammer M, Hansen G (2013) Loss and damage attribution. Nat Clim Chang 3:694–696
Hulme M, O'Neill SJ, Dessai S (2011) Climate change: is weather event attribution necessary for adaptation funding? Science 334:764–765
Institute for Policy Studies (2014) Green climate fund. [Online] Available at: http://climatemarkets.org/glossary/green-climate-fund.html
Intergovernmental Panel on Climate Change (2005) IPCC second assessment: climate change 1995. A report of the Intergovernmental Panel on Climate Change. WMO, Geneva
Intergovernmental Panel on Climate Change (2007a) An Assessment of the Intergovernmental Panel on Climate Change. Synthesis Report. IPCC, Valencia
IPCC (2007b) Climate change 2007: impacts, adaptation and vulnerability. In: Parry ML, Canziani OF, Palutikof JP, van der Linden PJ, Hanson CE (eds) Contribution of Working Group II to the fourth assessment report of the Intergovernmental Panel on Climate Change. Cambridge University Press, Cambridge
Kirsch TD, Wadhwani C, Sauer L, Doocy S, Catlett C (2012) Impact of the 2010 Pakistan floods on rural and urban populations at six months. PLoS currents 4
Kusters K, Wangdi N (2013) The costs of adaptation: changes in water availability and farmers' responses in Punakha district, Bhutan. Int J Glob Warm 5:387–399
Roberts E (2012) Bangladesh leading the way on loss and damage. Loss and Damage in Vulnerable Countries Initiative, Bonn
Loss and Damage in Vulnerable Countries Initiative (2014) Adverse impacts of climate change. Loss and Damage in Vulnerable Countries Initiative, Bonn
Ministry of Disaster Management and Relief, Government of People's Republic of Bangladesh (2014) Hazard profile: cyclone and storm surges, http://www.ddm.gov.bd/cyclone.php. Accessed 3 Dec 2014
Monnereau I, Abraham S (2013) Limits to autonomous adaptation in response to coastal erosion in Kosrae, Micronesia. Int J Glob Warm 5:416–432
Mori N, Kato M, Kim S, Mase H, Shibutani Y, Takemi T, Tsuboki K, Yasuda T (2014) Local amplification of storm surge by Super Typhoon Haiyan in Leyte Gulf. Geophys Res Lett 41 (14):5106–5113

Morrissey J, Oliver-Smith A (2013) Perspectives on non-economic loss and damage: understanding values at risk from climate change. Loss and Damage in Vulnerable Countries Initiative, Bonn
Munich Climate Insurance Initiative (2012) Insurance solutions in the context of climate change-related loss and damage: needs, gaps, and roles of the Convention in addressing loss and damage. Subsidiary Body for Implementation (SBI) Work Program on Loss and Damage, Bonn
National Disaster Risk Reduction and Management Council (NDRRMC) (2014) Effects of Typhoon "Yolanda". SitRep. #92. http://www.ndrrmc.gov.ph
Neumayer E, Barthel F (2011) Normalizing economic loss from natural disasters: a global analysis. Glob Environ Chang 21:13–24
Njie M, Gomez BE, Hellmuth ME, Callaway JM, Jallow BP, Droogers P (2007) Making economic sense of adaptation in upland cereal production in the Gambia. In: Leary N, Conde C, Kulkarni J, Nyong A, Pulhin J (eds) Climate change and vulnerability and adaptation. Earthscan, London, pp 131–146
OECD (2005) Catastrophic risks and insurance. Policy Issues in Insurance 8 OECD, Paris
Opondo DO (2013) Erosive coping after the 2011 floods in Kenya. Int J Glob Warm 5:452–466
Ott H, Sterk W, Watanabe R (2008) The Bali roadmap: new horizons for global climate policy. Climate Policy 8:91–95
Parry M, Arnell N, Berry P, Dodman D, Fankhauser S, Hope C, Kovats S, Nicholls R, Satterthwaite D, Tiffin R, Wheeler T (2009) Assessing the costs of adaptation to climate change. International Institute for Environment and Development, London
Rabbani G, Rahman A, Mainuddin K (2013) Salinity-induced loss and damage to farming households in coastal Bangladesh. Int J Glob Warm 5:400–415
Roberts E, van der Geest K, Warner K, Andrei S (2014) Loss and damage: when adaptation is not enough. [Online] Available at: lossanddamage.net
Robinson S, Strzepek K, Cervigni R (2013) The cost of adapting to climate change in Ethiopia: sector-wise and macro-economic estimates. International Food Policy Research Institute, Addis Ababa
Rothman DS, Amelung B, Polome P (2003) Estimating non-market impacts of climate change and climate policy. OECD, Paris
Stockholm Environment Institute (2009) Economics of Climate Change in Kenya. Project Report - 2009, Stockholm Environment Institute, Oxford
Stockholm Environmental Institute (2012) Valuing the ocean: draft executive summary. Stockholm Environmental Institute, Stockholm
Stone DA, Allen MR (2005) The end-to-end attribution problem: from emissions to impacts. Climatic Change 71:303–318
The Guardian (2012) What is the cost of climate change to our oceans? [Online] Available at: http://www.theguardian.com/environment/datablog/2012/mar/26/climate-change-oceans
The United Nations Office for Disaster Risk Reduction (2014) The Tacloban declaration. [Online] Available at: http://www.unisdr.org/archive/37912
Traore S, Owiyo T (2013) Dirty droughts causing loss and damage in Northern Burkina Faso. Int J Global Warm 5:498–513
UNFCCC (1995) Framework convention on climate change. [Online] Available at: http://unfccc.int/resource/docs/cop1/07a01.pdf
UNFCCC (1998) Kyoto protocol to the United Nations framework convention on climate change. [Online] Available at: http://unfccc.int/resource/docs/convkp/kpeng.pdf
UNFCCC (2012) Slow onset events. [Online] Available at: http://unfccc.int/resource/docs/2012/tp/07.pdf
UNFCCC (2013) Warsaw international mechanism for loss and damage associated with climage change impacts. [Online] Available at: http://unfccc.int/files/meetings/warsaw_nov_2013/in-session/application/pdf/fccc.cp.2013.l.15.pdf
UNFCCC (2014a) Background on the UNFCC: the international response to climate change [Online]. http://unfccc.int/essential_background/items/6031.php
UNFCCC (2014b) Kyoto protocol [Online]. http://unfccc.int/kyoto_protocol/items/2830.php

UNFCCC (2014c) Making those first steps count: an introduction to the Kyoto protocol [Online]. http://unfccc.int/essential_background/kyoto_protocol/items/6034.php
UNFCCC (2014d) Policy Analysis for the Greenhouse Effect (PAGE 2002) [Online]. http://unfccc.int/adaptation/nairobi_work_programme/knowledge_resources_and_publications/items/5447.php
UNFCCC (2014e) Timeline [Online]. http://unfccc.int/timeline/
UNFCCC (2014f) Two-year workplan-18 September 2014 [Online]. http://unfccc.int/files/adaptation/cancun_adaptation_framework/loss_and_damage/application/pdf/workplan_18sept_11am.pdf
UNFCCC (2014g) Warsaw outcomes [Online]. http://unfccc.int/key_steps/warsaw_outcomes/items/8006.php
United Nations (2010) International cooperation on humanitarian assistance in the field of natural disasters, from relief to development [Online]. http://www.preventionweb.net/english/professional/resolutions/index.php?o=scat_title&o2=ASC&ps=50&pg=9
United Nations (2014) UN and climate change: towards a climate agreement [Online]. www.un.org/climatechange/towards-a-climate-agreement/
United Nations Development Fund (2010) Cyclone Aila: UN joint multi-sector assessment & response framework. United Nations Development Fund, Dhaka
United Nations Office for Disaster Risk Reduction (2014) Prevention Web. [Online] Available at: http://www.preventionweb.net/english/countries/statistics/?cid=117
United Nations Inter-Agency Secretariat for the International Strategy for Disaster Reduction (2003) Linking disaster risk reduction and climate change adaptation. Presentation. Bonn
Van der Geest K, Dietz T (2004) A literature survey about risk and vulnerability in drylands with a focus on the Sahel. In: Dietz AJ, Ruben R, Verhagen A (eds). The impact of climate change on drylands: with a focus on West Africa. Springer Netherlands, pp 117–146
Warner K (2013) The warsaw international mechanism: a legitimate policy space for loss and damage widens and deepens. United Nations University Institute for Environment and Human Security, Tokyo
Warner K, van der Geest K (2013) Loss and damage from climate change: local-level evidence from nine vulnerable countries. Int J Glob Warm 5:367–386
Warner K, Kreft S, Zissener M, Hoppe P, Bals C, Loster T, Linnerooth-Bayer J, Tschudi S, Gurenko E, Haas A, Young S, Kovacs P, Dlugolecki A, Oxley A (2012) Insurance solutions in the context of climate change-related loss and damage. Munich
World Bank (2010) Economics of adaptation to climate change, synthesis report. World Bank, Washington, DC
Yaffa S (2013) Loss and damage from drought in the North Bank Region of The Gambia. United Nations University Institute for Environment and Human Security, Bonn

Paleoclimate Changes and Significance of Present Global Warming

Asadullah Kazi

Contents

Abstract

Earth's climate has been changing since the conceivable beginning of the geological history of Earth. This is reflected by paleoclimate occurrences of ice ages, followed by consequent warmer interglacial episodes. The most recent ice age has been tentatively traced back to some three million years ago. However, the onslaught of industrial revolution has greatly affected the framework of climate change. Atmospheric carbon dioxide levels are now 40 % higher than before the industrial revolution. This, in turn, has given rise to increase in temperature during the past couple of centuries. Glaciers have recently started melting, and the global average sea level has risen by more than 25 cm. Study of core records from Antarctica and Greenland disclose that paleoclimate ice cores dating back to 800,000 years revealed that the current concentrations of greenhouse gases exceeded the concentration of these gases, preserved in those

A. Kazi (✉)
Isra University, Hyderabad, Sindh, Pakistan
e-mail: asadkazi@isra.edu.pk; asadkazi1943@gmail.com

W.-Y. Chen et al. (eds.), *Handbook of Climate Change Mitigation and Adaptation*,
DOI 10.1007/978-3-319-14409-2_56

ice cores. Currently, global warming has emerged as the most serious environmental threat to mankind, and unless a drastic cut is made in the emission of greenhouse gases, the world would be heading toward an unretractable disaster. Consequently, this requires a global approach for development to combat the situation. To start with, there has to be awareness and preparedness, followed by capacity building through community education and training, as well as enforcement of regulations. This approach supports strategy of adaptation to vulnerability reduction and readiness to policy-supporting development, as the future course of action.

Introduction

Earth's climate is a global challenge. It is an ever-changing long-term phenomenon, whose incidence is manifested by repeated ice ages and the corresponding warmer interglacial periods, during paleoclimate episodes, in the geological history of Earth. Incidentally, such glacial and interglacial events occur in a cyclic pattern in conformity with average global temperature. A number of ice ages have occurred throughout Earth's history; the earliest was over two billion years ago, and the most recent one began approximately three million years ago and is followed by an interglacial stage of events. Earth was warmer than at present for most of this time interrupted by sporadic ice ages (Fig. 1).

Carbon dioxide is the primary greenhouse gas resulting from human activities (such as burning fossil fuels for energy and transportation). Incidentally, human activity-derived greenhouse gases are the largest potential cause of global warming.

It is reported that there is a direct relationship between the concentration of greenhouse gases, particularly carbon dioxide (CO_2) in the atmosphere, and the temperature of Earth, during the past 400,000 years (NOAA 2008) (Fig. 2).

It is also important to recognize that CO_2, CH_4, and NO_2 show high concentration during interglacial times and lower concentrations during the glacial episode. The atmosphere already contains over 25 % more CO_2 than it had done for the last 160,000 years (Leggett 1990).

In his lecture, "Changing Planet: Past, Present, Future – Earth's Climate back to the Future," Schrag (2012) portrayed a history of how the Earth's climate changed over since its birth.

Table 1 shades light on sources and buildup of common greenhouse gases and their relative contribution in the atmosphere. Currently, we are in a warm interglacial episode that began about 11,000 years ago. The main question that worries us is what if the continuing buildup of greenhouse gases in the atmosphere, resulting in the warm-up of Earth, would lead to abundant melting of ice? And if so, what needs to be done to circumvent this impending devastation?

NASA (2014) is preparing to launch a satellite to measure atmospheric concentrations of CO_2, a greenhouse gas that contributes almost 55 % to global warming (Table 1). It is stated that CO_2 levels have reached their highest concentration in the

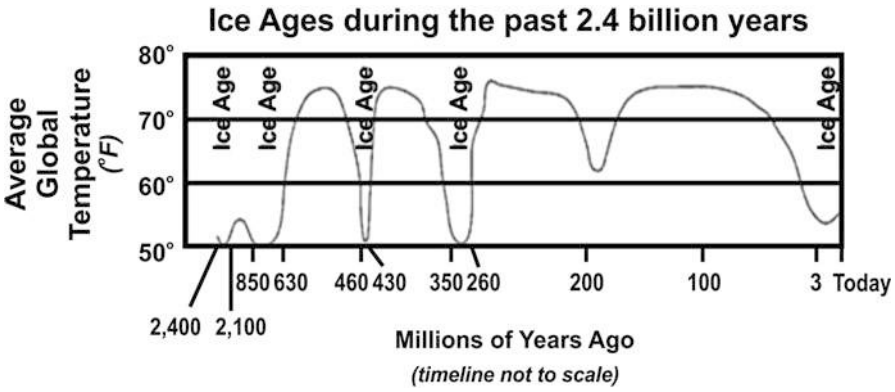

Fig. 1 Time history of five major ice ages of Earth's history (Adapted from Saltzman (2002), and Eldredge and Biely (2010))

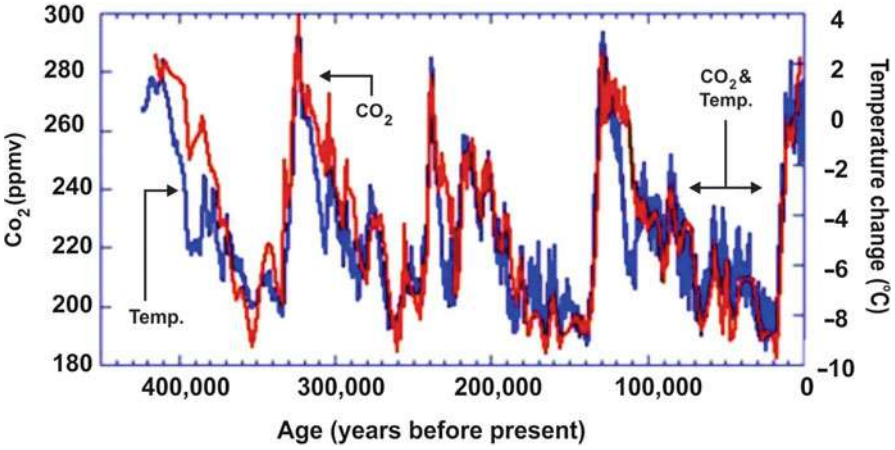

Fig. 2 Temperature change and carbon dioxide change observed, in ice core records (Adapted from NOAA (2008))

past 800,000 years or so. In the northern hemisphere, it has reached 400 parts per million by volume (ppmv), for the first time in human history. This level is 40 % up since the wide use of fossil fuels began with the industrial revolution. The World Meteorological Organization expects the global average concentration to be above 400 ppmv in 2015–2016. Rising concentration of this heat-trapping gas raises risks of more heat waves, droughts, and rising sea level. It may be mentioned that during the last 800,000 years, the level of atmospheric CO_2 fluctuated between 180 and 280 ppmv and has probably not been above 400 ppmv. The UN panel of experts, on greenhouse gas, suggested that the concentration of CO_2 gas would have to be kept below 450 ppmv to give a good chance of achieving less than 2 °C increase in global temperature, before the end of this century.

Table 1 The common greenhouse gases, their origins, rates of buildup in the atmosphere, and their contribution to global warming in the 1980s (Source: Leggett 1990)

Gas	Principal sources	Current rate of annual increase and concentration[a]	Contribution to global warming (%)
Carbon dioxide (CO_2)	Fossil fuel burning (77 %), deforestation (23 %)	0.5 % (353 ppmv)	55
Chlorofluorocarbons (CFCs) and related gases (HFCs and HCFCs)	Various industrial uses: refrigerants, foam-blowing solvents	4 % (764 pptv)	24
Methane (CH_4)	Rice paddies, enteric fermentation, gas leakage	0.9 % (1.72 ppmv)	15
Nitrous oxide (N_2O)	Biomass burning, fertilizer use, fossil fuel combustion	0.8 % (310 ppbv)	6

[a]*ppmv* parts per million by volume, *ppbv* parts per billion by volume, *pptv* parts per trillion by volume

Human activities are altering the carbon cycle, both by adding more CO_2 to the atmosphere and by influencing the ability of natural sinks, like forests and oceans, which absorb and trap (capture) CO_2 and keep the temperature rise within permissible limits.

Slightly different values of greenhouse gas contribution to global warming are quoted by the UN Framework Convention on Climate change (UNFCCC) (1992). Nevertheless, estimated contribution of greenhouse gases to global warming, during the last 100 years, as reported by the UNFCCC is as follows:

$$CO_2 - 66\%;\ CH_4 - 23\%;\ \text{CFC's} - 8\%;\ N_2O - 3\%.$$

Comparing these concentrations with those in 1980s, by UNFCCC, reveals that in terms of contributions to global warming, CO_2 has increased by 17 %, CH_4 has decreased by 5 %, HCFCs increased by 6 %, and NO_2 increased by 3 %. The increase in the magnitude of CO_2 can obviously be attributed to higher consumption of fossil fuels in the energy mix; United States, China, and India, among others, are the countries that make the maximum use of fossil fuels in the energy sector of their strong economies.

Paleoclimate Perspective

Carbon dioxide, as described above, is a major greenhouse gas, which contributes to Earth's global warming leading to climate change. Paleoclimate sources of information, leading to an assessment of conditions that prevailed during the life history of Earth, are important in predicting likely climatic changes in the future (Fig. 3).

Research in the study of ice cores drilled in Greenland and Antarctica provides much-needed information about variations in past temperatures and composition of

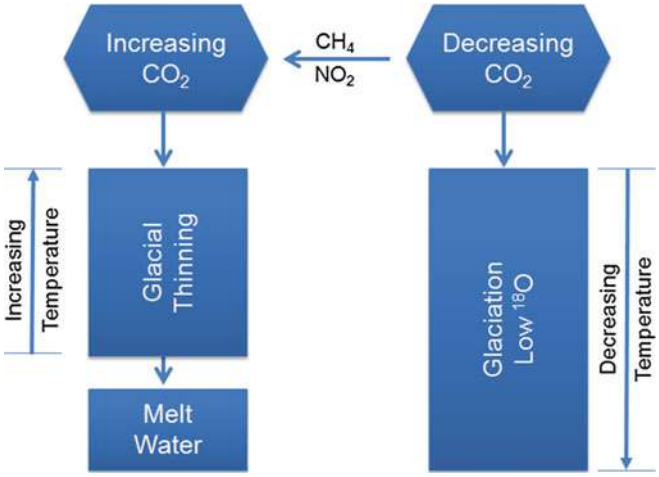

Fig. 3 Climatic changes during glacial and interglacial episodes of the history of Earth

atmospheric gases such as CO_2, NO_2, and CH_4, as well as many other aspects of the global environment.

It is also understood that, among other things, the warming of glacial periods is essentially synchronized by gradual shift in Earth's rotation (USEPA 2014a; Hansen and Sato 2011). However, changes in climate change are accompanied mainly by changes in CO_2, NO_2 and CH_4, leading to changes in the temperature.

Ice Core Records of Temperature

Crucially, the ice cores enclose small bubbles of air in the atmosphere, and from these, it is possible to measure the past concentration of gases. According to briefings of British Antarctic Survey (BAS), pertaining to "ice cores and climate change," the oldest ice core records extend to 123,000 years in Greenland and 800,000 years in Antarctica. The longest ice cores lengthen to 3 km in depth. Analysis of these ice core records reveals details of Earth's past climate and is, therefore, useful in recreating long-term records of temperature as well as other environmental counterparts that allow us to explore the past climate. It may be pointed out that in the instance of temperature, no direct measurement of temperature is available (www.climatedata.info, 2010). However, the ratio of heavy oxygen (^{18}O) to light oxygen (^{16}O) is helpful in elucidating climate changes, which occurred in the past.

Water molecules, containing light oxygen, evaporate easily as compared to water molecules containing heavy oxygen atom. At the same time, water vapor molecules, containing the heavy oxygen, condense more easily. Furthermore, the concentration of ^{18}O in precipitation decreases with temperature. As shown in Fig. 4, the difference in ^{18}O concentrations in annual precipitation, compared to

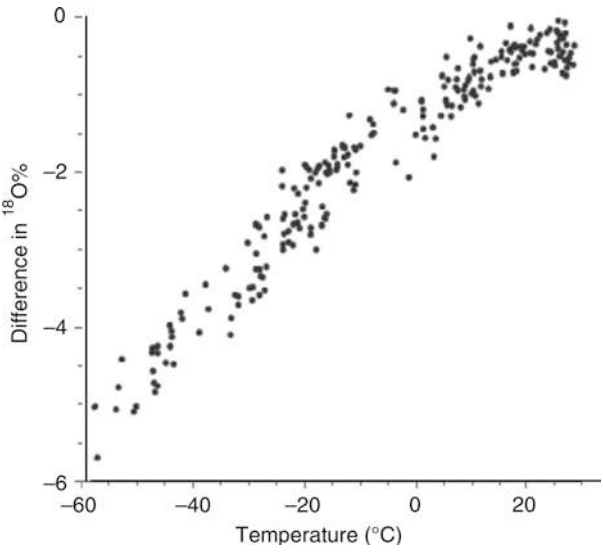

Fig. 4 Concentration of ^{18}O decreases with temperature (Adapted from Jonzel et al. (1994))

the average annual temperature, at the present-day ice-capped locations is fairly obvious.

As explained in the feature articles of NASA (paleontology: the oxygen balance), air cools by moving toward the poles, and the moisture begins to condense and falls as precipitation. Initially, the rain contains a higher ratio of water made of heavy oxygen molecules, which condense more easily than water vapor containing light oxygen. The remaining moisture in the air becomes depleted in of heavy oxygen, as the air continues to move toward colder upper latitudes. Consequently, the falling rain or snow now is made up of more water-containing light oxygen. Less heavy oxygen in the frozen water means that temperatures were cooler.

According to NASA (2010), the Earth moved out of ice ages, over the past millions of years; the glacial temperature rose by a total of 4–7 °C, over approximately 5,000 years. The stage of changes in temperature and CO_2 across glacial–interglacial episodes in the past is consistent with the proposition that CO_2 acts as an important amplifier of climate changes in the natural system (Wolff 2011). In the past century alone, the temperature in response to increase in CO_2 has climbed 0.7 °C, which is roughly 10 times faster than the average rate of ice age recovery warming. This leaves many questions to answers in the context of the present global warming.

Changing Atmospheric Chemical Composition

Unlike temperature, the ice cores allow direct measurements of atmospheric gases, like carbon dioxide and methane. The fastest natural increase in carbon dioxide (CO_2) and methane (CH_4), measured in older ice cores, is 20 parts per million by

volume, in 1000 years. This is seen as the order of magnitude during Earth's emergence from the last ice age, around 12,000 years ago. The concentration of carbon dioxide (CO_2) increased in the last two centuries by the same amount. Similarly, methane (CH_4) also shows unprecedented increase in concentration over the last 200 years. Its concentration is now much more than double its preindustrial levels. Nitrous oxide (NO_2) is yet another constituent which increased from a preindustrial concentration of about 265 ppb to the present-day value of 319 ppb (Forster et al. 2007). Atmospheric CO_2 levels are now 40 % higher than before the industrial revolution (British Antarctic Survey 2014).

The increase in the magnitude of global temperature is crucially important as it is proportional to increase in CO_2. UN Secretary-General, Ban Ki-moon (2013), pointed out, "We must limit global temperature rise to 2°. We are far from there, and even that is enough to cause dire consequences. If we continue along current path, we are close to 6° increase." At the end of most interglacial episodes, NO_2 remains considerably longer on interglacial levels than methane. This is substantiated by studies on glacial–interglacial and millennial scale variations in the atmospheric NO_2 concentrations during the last 800,000 years (Schilt et al. 2010). Furthermore, it is noted that increase in the nitrous (NO_2) concentration starts before the onset of the warming period (Flückiger et al. 2004).

Current Climate Change and Global Warming Perspective

Global warming, resulting from climate change, has emerged as the most serious environmental threat, suggesting that the mankind is heading for deep trouble unless a drastic cut is made in emission of greenhouse gases into the atmosphere. In a report by the Intergovernmental Panel on Climate (IPCC), a body set by the UN General Assembly in 1988, emissions resulting from human activities are substantially increasing the atmospheric concentration of greenhouse gases. If this increase in the greenhouse gas continued at the present rates, the world average temperature will rise by one degree centigrade or thereabouts within just 30 years.

Counteracting Present-Day Climate Change

From the human point of view, "if you change climate, you change everything." It is, therefore, pertinent to build a future in which humans live in harmony with nature. Table 2 presents a summary of the potential of greenhouse gases and the effects that occur over a period of about 100 years, after a particular mass of a gas is emitted (USEPA 2014c).

Some gases stay longer in the atmosphere than others. Indeed, there is no doubt that there is a climate change, and part of this change is caused by human activities (Cook et al 2013). But, is the part played by humans significant enough to bring about change in the natural glacial–interglacial cycle of episodes, prior to the existence of humans on the Earth?

Table 2 Major long-lived greenhouse gases and their characteristics (USEPA 2014b)

Greenhouse gas	How it is produced	Average lifetime in the atmosphere	100-year global warming potential
Carbon dioxide	Emitted primarily through the burning of fossil fuels (oil, natural gas, and coal), solid waste, and trees and wood products. Changes in land use also play a role. Deforestation and soil degradation add carbon dioxide to the atmosphere, while forest regrowth takes it out of the atmosphere		1
Methane	Emitted during the production and transport of coal, natural gas, and oil. Methane emissions also result from livestock and agricultural practices and from the anaerobic decay of organic waste in municipal solid waste landfills	12 years	28
Nitrous oxide	Emitted during agricultural and industrial activities, as well as during combustion of fossil fuels and solid waste	121 years	265
Fluorinated gases	A group of gases that contain fluorine, including hydrofluorocarbons, perfluorocarbons, and sulfur hexafluoride, among other chemicals. These gases are emitted from a variety of industrial processes and commercial and household uses and do not occur naturally. Sometimes used as substitutes for ozone-depleting substances such as chlorofluorocarbons (CFCs)	A few weeks to thousands of years	Varies (the highest is sulfur hexafluoride at 23,500)

Figure 5 shows the impact of climate change in terms of projected increase in temperature by the year 2100. Five types of risk factors are identified together with the likely future temperature. There is a range of scenarios and uncertainties accompanied with each risk factor. Under worst conditions, if the future temperature rises above 3 °C, there will be a risk of irreversible large-scale and abrupt transition.

Knowing that the present-day anthropological factors have accelerated the climate change, efforts must be to stop, or adapt or mitigate, the arrival of the advent of the natural cycle of events, which can be nothing less than disastrous. It may not be humanly possible to stop; nevertheless, efforts must be made to adapt or mitigate and continue to make developments in the fast-moving socioeconomic setup of knowledge-based society.

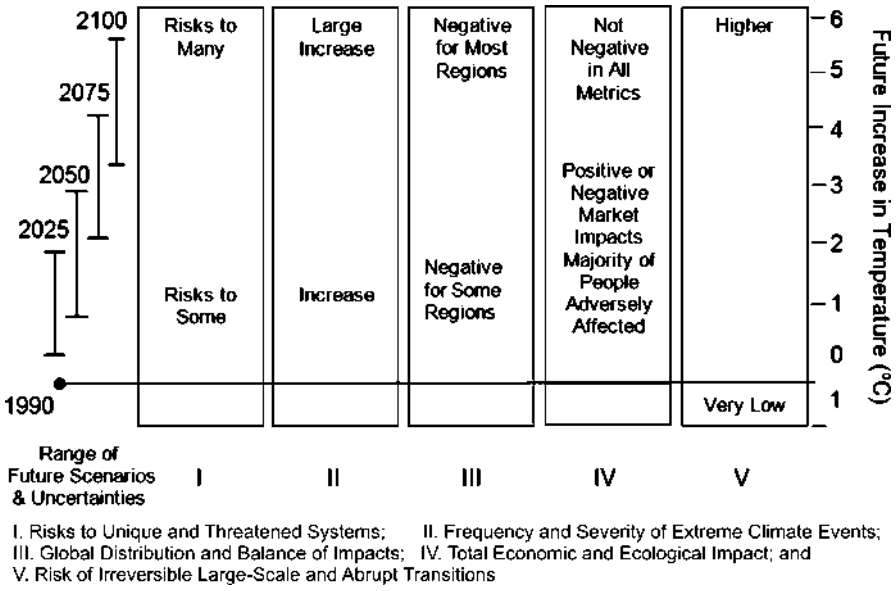

Fig. 5 Risks and impact of climate change (Source: Smith et al. 2009)

For a sustainable development, holistic approach integrating climate change in policy making for resource development is presented, in a guideline entitled "Training Manual on Climate Change Adaptation and Development," compiled by Geene et al. (2010). In 1997, the Kyoto Protocol was concluded and established legally binding obligations for developed countries to reduce their greenhouse gas emissions. Furthermore, Millennium Development Goals (MDG) of the United Nations (2014) also put emphasis on efforts to ensure environmental sustainability (goal number 7) and to develop a global partnership for development (goal number 8). Figure 5 shows the impact of climate change in terms of projected increase in temperature by the year 2100.

In order to control and reverse the process of global warming, it is essential to look into adaption and development together with awareness and mitigation measures.

Awareness and Mitigation

Climate change is a global challenge. This challenge will continue to affect all forms of life. Apparently, there was little awareness of this calamity prior to preindustrial period (prior to 1760 AD), but at the present time, if nothing is done to curb this menace, irreparable damage may jeopardize the entire ecosystem and the human development process.

Management of greenhouse gases includes measures, which are necessary before a catastrophic situation appears. Emphasis is placed on awareness and

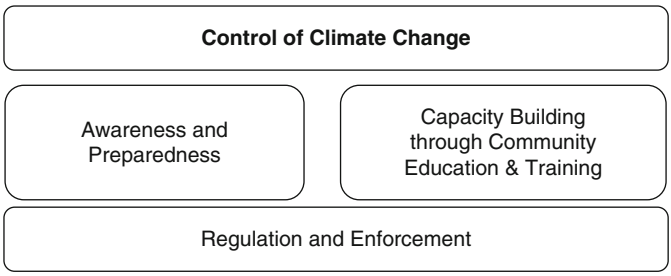

Fig. 6 Steps to control climate change

preparedness, capacity building through community education and training, as well as enforcement of regulations (Fig. 6), meant to reduce or capture emissions. This requires a global partnership, for development to combat the situation.

The principal cause of climate change as noted in Fig. 3 is attributed to three principal greenhouse houses, namely, CO_2, NO_2, and CH_4. The former is the utmost contributor of change in temperature, which has affected the climate, both in the paleoclimate and the present scenario. The IPCC (2001, 2007) has clearly spelled out that "adaptation will be necessary to address impacts resulting from warming, which is already unavoidable due to past emissions." This supports the idea that adaptation and development should be treated as a complimentary response strategy to awareness and mitigation.

Adaption and Development

Adaption to climate change can either be planned or automatic. Plants and animals have no plan to control over environment. For them, adaptation in response to environmental changes is necessary for their survival else they will disappear. For humans, in spite of being aware of the effects of climate change, it is necessary to take measures which may not stop but at least reduce the impact of environmental changes through specific policy framework (Füssel and Klein 2006). Adaption can, therefore, be taken as an option after mitigation. It implies reduction of impacts rather than vulnerability for development (Fig. 7).

Indeed, climate change is a reality, and there is a general agreement that "we must stop and reverse this process now or face a devastating cascade of natural disasters that will change life on earth, as we know it."

Reversal of Climate Change

Climate change can be looked into paleoclimate and preindustrial perspectives. It is only in the postindustrial period that the effects of climate change were noticed. Nevertheless, there is growing and convincing evidence that climate change has

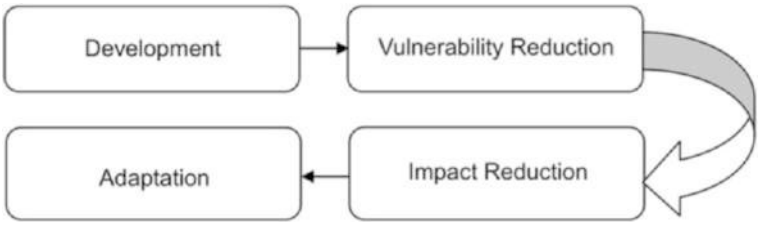

Fig. 7 Development preceded by adaptation

been occurring throughout the geological history of Earth due to natural causes. However, the anthropogenic activities have added to causes of climate change manifested by a growing increase in temperature in the postindustrial instance. It is, therefore, pertinent to control as well as reverse the process of global warming by awareness, mitigation, and adaptation to bring about the much-needed development (Fig. 8).

Reducing deforestation and encouraging reforestation can reduce emission from fossil fuels by trapping CO_2 and thus play a significant role in the long run to curtail global warming (Union of Concerned Scientists 2013). But, this may not be the only solution. At the global community level, it may be useful to reverse the global warming process and follow adaptation and development together with awareness and mitigation.

This is well and good, but research is being conducted to curb the release of CO_2, which acts as cover to stop it from escaping into the upper layers of atmosphere and as a result raises the temperature of Earth. Today, the power sector alone represents global CO_2 emissions approximating 40 %. As reported by Curry (2004), researchers in the MIT Laboratory for Energy and the Environment have been studying a global climate change mitigation technology called "carbon dioxide capture and storage," since 1989, under the auspices of a program currently called the "Carbon Capture and Sequestration Technologies Program." Similar research is being conducted at centers and institutes of research and development elsewhere.

Basically, there are three steps involved in this venture. The first step is to trap and separate CO_2 from other gases. In the second step, this gas is taken to a far-flung storage location, away from the atmosphere, and lastly, the gas is carefully stored deep inside the Earth's crust or deep in oceans. Furthermore, there are three methods of capture, namely, post-combustion carbon capture, pre-combustion capture, and oxyfuel carbon capture (GreenFacts 2014).

Future Directions

Paleoclimate sources of information, leading to an assessment of conditions that prevailed during the life history of Earth, are important in predicting likely climatic changes in the future. The Earth's climate is constantly changing. There are a number of processes that can influence this fluctuation. Increase in CO_2, among

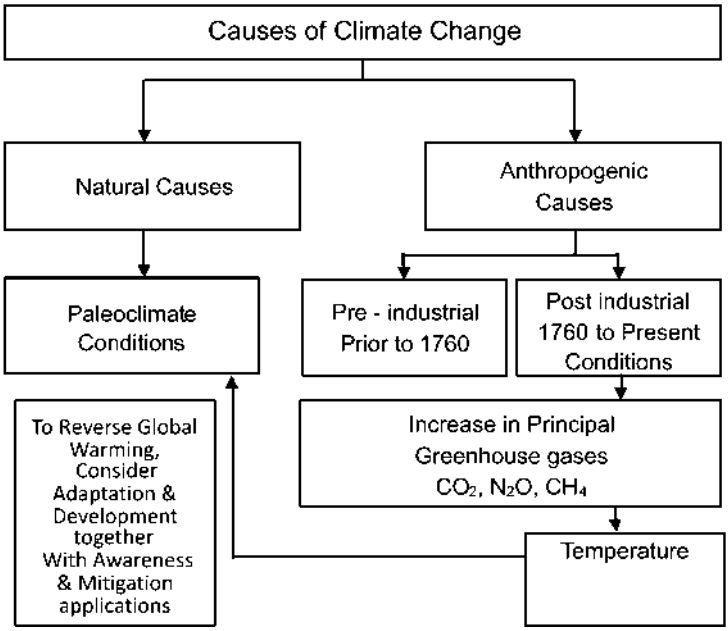

Fig. 8 Historic perspective of climate change and reversal approach of combating climate change

other variables, is the main ingredient of this variation. Comparison with prehistoric records reveals that the concentration of CO_2 has been on the rise since postindustrial times. This has led to fears that the consequent rise in the temperature of atmosphere may be extraordinarily difficult to handle.

The UN panel of experts on greenhouse gases, led by CO_2, suggested that the concentration of this gas would have to be kept below 450 ppmv to give a good chance of achieving less than 2 °C increase (2014) in global temperature, before the end of this century. Failure to control the rising concentration of CO_2 can be nothing less than disastrous in this regard. The best way of control would be to reduce emission from the fossil fuel (oil, gas, and coal)-based power plants, industrial units, or the transport sector in this situation. Reducing deforestation and encouraging reforestation can reduce emission from fossil fuels by trapping CO_2 and thus play a significant role in the long run to curtail global warming. The concern is that anthropogenic emissions of greenhouse gases may be driving average global temperature higher than previously recorded or estimated.

At the global community level, it may be useful to reverse the global warming process and follow adaptation and development together with awareness and mitigation. Research is being conducted in some developed countries to find a technically feasible and economically affordable solution to capture CO_2 at source and store the same at depth either in the sea or in the Earth's crust.

References

British Antarctic Survey (2014) Ice cores and climate change. www.antarctica.ac.uk/bas-research/science-briefings/icecorebriefing.php

Climate Data Information (2010) www.Climatedata.info

Cook J, Nuccitelli D, Green SA, Richardson M, Winkler B, Pointing R, Way R, Jacobs G, Skuce A (2013) Quantifying the consensus on anthropogenic global warming in the scientific literature. Environ Res Lett 8(2):024024, 7pp

Curry TE (2004) Public awareness of carbon capture and storage: a survey of attitudes towards climate change mitigation: a thesis submitted to the Engineering Systems Division in partial fulfillment of the requirements for the degree of Master of Science in Technology & Policy at the Massachusetts Institute of Technology

Eldredge S, Biely B (2010) Ice Ages- what are they and what causes them? Utah Geological survey. Surv Notes 42(3):2

Flückiger J, Blunier T, Stauffer B, Chappellaz J, Spahni KR, Schwander J, Stocker TF, Jensen D (2004) N_2O and CH_4 variations during the last glacial epoch: insight into global processes. Global Biogeochem Cycles 18:GB1020

Forster P, Ramaswamy V, Artaxo P, Berntsen T, Betts R, Fahey DW, Haywood J, Lean J, Lowe DC, Myhre G, Nganga J, Prinn R, Raga G, Schulz M, Van Dorland R (2007) Changes in atmospheric constituents and in radiative forcing. In: Solomon S, Qin D, Manning M, Chen Z, Marquis M, Averyt KB, Tignor M, Miller HL (eds) Climate change 2007: the physical science basis. Contribution of Working Group 1 to the Fourth Assessment Report of the Intergovernmental Panel on Climate Change. Cambridge University Press, Cambridge, UK/New York

Füssel H-M, Klein RJT (2006) Climate change vulnerability assessments: an evolution of conceptual thinking. Clim Change 75(3):301–329

Geene J. van, Terwisscha Van Scheltinga CTHM, Gordijn F, Jaspers AMJ, Argaw M (2010) Trainer's manual on climate change adaptation and development: integrating climate change in policy making for sustainable development in agriculture and natural resources management. Wageningen UR

GreenFacts (2014) CO_2 capture and storage. www.greenfacts.org/en/co2-capture-storage/

Hansen J, Sato M (2011) Paleoclimate implications for human-made climate change. In Climate Change at the Eve of the Second Decade of the Century: Inferences from Paleoclimate and Regional Aspects: Proceedings of the Milutin Milankovitch 130th Anniversary Symposium. In: Berger A, Mesinger F, Šijaci D (eds). Springer, (in press)

IPCC (2001) Third assessment report of the IPCC. Cambridge University Press, Cambridge

IPCC (2007) Working Group II, summary for policy makers. Cambridge University Press, Cambridge

Jonzel J, Koster RD, Snozzo RJ (1994) Stable Water isotope behavior during the last glacial maximum: a general circulation model analysis. J Geophys Res 99:25791–25802

Leggett J (1990) The nature of the greenhouse threat, Chapter 1, pp 14–43. In: Global warming, the greenpeace report, Introduction. Oxford University Press, Oxford, pp 1–9

NASA (2014) NASA readies satellite to measure atmosphere CO_2. The Necos International, 20 June 2014

NASA Earth Observation (2010) Global Warming Goddard Space Flight Center, USA

NOAA (2008) A Paleo perspective on global warming. Temperature change and carbon dioxide, National Oceanic and Atmospheric Administration, paleo@ hoaa.gov

Saltzman B (2002) Dynamical paleoclimatology: generalized theory of climate change. Academic/Elsevier Science, Santiago, 354 p

Schilt A, Baumgartner M, Blunier T, Schwander J, Spahni R, Fischer H, Stocker TF (2010) Glacial–interglacial and millennial-scale variations in the atmospheric nitrous oxide concentration during the last 800,000 years. Quat Sci Rev 29(1-2): 182–192

Schrag D (2012) Changing planet: past, present, future – earth's climate back to the future, Lecture 3. Harvard University

Smith, JB, Schneider, SH, Oppenheimer M, Yohe GW, Hare W, Mastrandrea MD, Patwardhan A, Burton I, Corfee-Morlot J, Magadza CHD, Fussel HM, Pittock AB, Rahman A, Suarez A, van Ypersele JP (2009) Assessing dangerous climate change through an update of the Intergovernmental Panel on Climate Change (IPCC) 'reasons for concern'. In: Proceedings of the National Academy of Sciences 106(11):4133–4137. doi:10.1073/pnas.0812355106. PMC 2648893.

UN Secretary General Ban Ki-moon (2013) United Nations global issues: climate change. www.un.org/en/globalissues/climatechange/. 3p

UNFCCC (1992) United Nation framework convention on climate change. United Nations Publisher, New York.

Union of Concerned Scientists (2013) Global warming. www.ucsusa.org/gobal_warming/solutions/stop-deforestation/

United Nations (2014) United Nations Millennium Development Goals. Last retrieved: 01 July 2014. http://www.un.org/millenniumgoals/bkgd.shtml

USEPA (2014a) Climate change indicators in the United States. United States Environment Protection Agency. EPA Headquarters, Washington, DC, 99p

USEPA (2014b) A student's guide to climate change, United States Environmental Agency. EPA Headquarters, Washington, DC

USEPA (2014c) Climate change indicators in the United States. Green House Gases. United Agency, EPA's Office of Research and Development, EPA Headquarters, Washington, DC, 4pp

Wolff EW (2011) Greenhouse gases in the earth system: a paleoclimate perspective. Philos Trans R Soc A Math Phys Eng Sci 369(1943):2133–2147

Life Cycle Assessment of Greenhouse Gas Emissions

L. Reijnders

Contents

L. Reijnders (✉)
Institute for Biodiversity and Ecosystem Dynamics, University of Amsterdam, Amsterdam, The Netherlands
e-mail: l.reijnders@uva.nl

W.-Y. Chen et al. (eds.), *Handbook of Climate Change Mitigation and Adaptation*,
DOI 10.1007/978-3-319-14409-2_2

Abstract

Life cycle assessments of greenhouse gas emissions have been developed for analyzing products "from cradle to grave": from resource extraction to waste disposal. Life cycle assessment methodology has also been applied to economies, trade between countries, aspects of production, and waste management, including CO_2 capture and sequestration. Life cycle assessments of greenhouse gas emissions are often part of wider environmental assessments, which also cover other environmental impacts. Such wider-ranging assessments allow for considering "trade-offs" between (reduction of) greenhouse gas emissions and other environmental impacts and co-benefits of reduced greenhouse gas emissions. Databases exist which contain estimates of current greenhouse gas emissions linked to fossil fuel use and to many current agricultural and industrial activities. However, these databases do allow for substantial uncertainties in emission estimates. Assessments of greenhouse gas emissions linked to new processes and products are subject to even greater data-linked uncertainty. Variability in outcomes of life cycle assessments of greenhouse gas emissions may furthermore originate in different choices regarding functional units, system boundaries, time horizons, and the allocation of greenhouse gas emissions to outputs in multi-output processes.

Life cycle assessments may be useful in the identification of life cycle stages that are major contributors to greenhouse gas emissions and of major reduction options, in the verification of alleged climate benefits, and to establish major differences between competing products. They may also be helpful in the analysis and development of options, policies, and innovations aimed at mitigation of climate change.

The main findings from available life cycle assessments of greenhouse gas emissions are summarized, offering guidance in mitigating climate change. Future directions in developing life cycle assessment and its application are indicated. These include better handling of indirect effects, of uncertainty, and of changes in carbon stock of recent biogenic origin and improved comprehensiveness in dealing with climate warming.

Introduction

This handbook is about climate change mitigation. In decision-making about climate change mitigation, question marks about proper choices regularly emerge. Is going for electric cars a good thing, when power production is largely coal based? Do the extra inputs in car production invalidate the energy efficiency gains of

hybrid cars? Should a company focus its greenhouse gas management on its own operations or on those of raw material suppliers? Is material recycling better or worse for climate change mitigation than incineration in the case of milk cartons? And what about biofuels: should their use be encouraged or not? Regarding all these questions, assessment of the life cycle emission of greenhouse gases, or more in general the environmental burden, is important for giving proper answers.

Life cycle assessments may lead to anti-intuitive results. This can be illustrated by the case of liquid biofuels (Hertwich 2009). It has been argued that biofuels are "climate neutral" (e.g., Sann et al. 2006; De Gorter and Just 2010). The CO_2 which emerges from burning biofuels has been recently fixed by photosynthesis, so, it has been argued, there should be no net effect of burning biofuels on the atmospheric concentration of CO_2. However, if one looks at the "seed-to-wheel" life cycle of biofuels, a different picture may emerge. Consider, e.g., corn ethanol used as a transport biofuel in the USA. In the actual production thereof, there are substantial inputs of fossil fuels (Fargione et al. 2008; Searchinger et al. 2008). Corn cultivation also leads to emissions of the major greenhouse gas N_2O (Crutzen et al. 2007). And corn cultivation is associated with changes in carbon stocks of agroecosystems (Searchinger et al. 2008). Considering the life cycle emissions of greenhouse gases leads to the conclusion that bioethanol from the US corn is far from "climate neutral" but is rather associated with larger greenhouse gas emissions than conventional gasoline (Searchinger et al. 2008; Reijnders and Huijbregts 2009). This has clearly implications for making good decisions about mitigating climate change linked to fuel choice (Hertwich 2009).

Against this background, this chapter will consider current life cycle assessment, with a focus on the life cycle emission of greenhouse gases. First, it will be discussed what life cycle assessment is and how it is done. It will appear that such assessment may give rise to substantial uncertainty. Notwithstanding such uncertainty, life cycle assessments can be helpful in making proper choices about climate change mitigation. To illustrate this, main findings from available peer-reviewed life cycle assessments of greenhouse gas emissions will be summarized.

What Is Life Cycle Assessment and How Does It Work?

Life cycle assessment has been developed for analyzing current products from resource extraction to final waste disposal, or from cradle to grave. Apart from analyzing the status quo, life cycle assessments may also deal with changes in demand for, and supply of, products and with novel products. The latter type of assessment has been called *consequential*, as distinguished from the analysis of status quo products, which has been called *attributional* (Sanden and Kalström 2007; Frischknecht et al. 2009). The assessment of novel products has also occasionally been called: *prospective attributional* (Hospido et al. 2010; Song and Lee 2010).

Different data may be needed in attributional and consequential life cycle assessment. Whereas in attributional life cycle assessment one, e.g., uses electricity data reflecting current power production, in consequential life, one needs data regarding

changes in electricity supply. For the short term, assessing a marginal change in capacity of current electricity supply may suffice to deal with changes in electricity supply. When the longer term is at stake, major changes in energy supply, including complex sets of energy supply technologies, should be assessed (Lund et al. 2010).

When novel products go beyond existing components, materials, and processes, knowledge often partly or fully relates to the research and development stage or to the limited production stage. These stages reflect immature technologies. Comparing these with products of much more mature technologies may be unfair, as maturing technologies are optimized and tend to allow for better resource efficiency and a lower environmental impact (Wernet et al. 2010; Mohr et al. 2009). Also, novel products may be subject to currently uncommon environmental improvement options and may have to operate under conditions that diverge from those that are currently common (Sanden and Kalström 2007; Frischknecht et al. 2009). The latter conditions may, e.g., include constraints on resource availability which currently do not exist, new infrastructures, budget constraints, higher resource costs which are conducive to resource efficiency, and strict caps on greenhouse gas emissions. A solution to such divergence from "business as usual" may be found in assuming technological trajectories and/or constructing scenarios which include assumptions about the environmental performance of future mature technologies under particular conditions (Frischknecht et al. 2009; Mohr et al. 2009; Jorquera et al. 2010; Spatari et al. 2010).

It should be realized that the assumptions involved lead to considerable uncertainty regarding the outcomes of consequential life cycle assessments, as these assumptions may be at variance with "real life" in the future.

Life cycle assessment is generally divided in four stages (Guinee 2002; Rebitzer et al. 2004):

- Goal and scope definition
- Inventory analysis
- Impact assessment
- Interpretation

Goal and Scope Definition

In the *goal and scope definition* stage, the aim and the subject of life cycle assessment are determined. This implies the establishment of "system boundaries" and usually the definition of a "functional unit."

A functional unit is a quantitative description of service performance of the product(s) under investigation. It may, for instance, be the production of a megawatt hour (MWh) of electricity. This allows for comparing different products having the same output: e.g., photovoltaic cells, a coal-fired power plant, a gas-fired power plant, and a wind turbine. It should be noted though that the functional unit may cover only a part of the service performance, because products may have special properties. For instance, in the case of power generation, the production of a MWh of electricity as a functional unit does not take account of the

phenomenon that a coal-fired power plant is most suitable for base load and a gas-fired power plant for peak load.

In the *goal and scope definition* stage, a number of questions have to be answered. For instance, the life cycle of products usually includes a transport stage. As to transport the question arises what to include into the assessment: production of the transport vehicle? road building? building storage facilities for products? Similarly, in the life cycle assessment of fishery products, questions arise such as: should one include the bycatch of fish which is currently discarded? the energy input in shipbuilding and ship maintenance? and/or the energy input in building harbor facilities?

In the *goal and scope definition* stage, one should also consider the matter of significant indirect effects of products. A well-known example thereof is the rebound effect in the case of more energy-efficient products with lowered costs of ownership. Such products may, for instance, increase use of the product and may lead to spending of money saved by the energy-efficient product, which in turn may impact energy consumption, and associated greenhouse gas emissions (Schipper and Grubb 2000; Thiesen et al. 2008; Greene 2011). Another case in point concerns biofuels from crops that currently serve as source for food or feed. When carbohydrates or lipids from such crops are diverted to biofuel production, this diversion may give rise to additional food and/or feed production elsewhere, because demand for food and feed is highly inelastic (Searchinger et al. 2008). This, in turn, may have a substantial impact on estimated greenhouse gas emissions. Similarly, the use of waste fat for biodiesel production may have the indirect effect of reducing the amount of fat available for feed production, which in turn might lead to an increased use of virgin fat, which will impact land use and may thus change carbon stocks of recent biogenic origin. However, indirect effects of decisions about biofuels do not end with the consideration of indirect effects on land use. It may, for instance, be argued that not expanding biofuel production may increase dependency on mineral oil and that this may increase military activities to safeguard oil installations and shipping and associated emissions of greenhouse gases (De Gorter and Just 2010). Still another example of indirect effects regards wood products. These may have the indirect effect of substituting for non-wood products, and including such substitution has a significant effect on estimated greenhouse gas emissions (Sathre and O'Connor 2010). Decision-making about significant indirect effects is not straightforward. This has led some to the conclusion that including indirect effects is futile (e.g., De Gorter and Just 2010), whereas others have argued that including at least some indirect effects is conducive to good decision-making (e.g., Searchinger et al. 2008; Sathre and O'Connor 2010).

System boundaries refer to what is included in life cycle assessment. In general, system boundaries are drawn between technical systems and the environment, between relevant and irrelevant processes, between significant and insignificant processes, and between technological systems. An example of the latter is, for instance, a boundary between the motorcar life cycle and the life cycle of the building in which the car is produced. The choice of system boundaries may have a substantial effect on the outcomes of life cycle assessments (also: Finnveden et al. 2009; Gandreault et al. 2010).

Inventory Analysis

The *inventory analysis* gathers the necessary data for all processes involved in the product life cycle. This is a difficult matter when one is very specific about a product: for instance, the apples which I bought last Saturday in my local supermarket. However, databases have been developed, such as Ecoinvent (Frischknecht et al. 2005), the Chinese National Database (Gong et al. 2008), Spine (www.globalspine.com), JEMAI (Narita et al. 2004), and the European Reference Life Cycle Data System (ELCD 2008), which give estimates about resource extraction and emissions that are common in Europe, China, the USA, and Japan for specified processes (for instance, the production and use of phosphate fertilizer). Also, there are databases which extend to economic input–output analyses and give resource extraction and emission data at a higher level of aggregation than the process level (Tukker et al. 2006). A study of De Eicker et al. (2010), which also gives a fuller survey of available databases, suggests that among available databases the Ecoinvent database is preferable for relatively demanding LCA studies. If only greenhouse gas emissions are considered, the 2006 guidelines for national greenhouse gas inventories of the IPCC (Intergovernmental Panel on Climate Change; www.ipcc.ch/) were found to be useful (De Eicker et al. 2010).

Available databases do not always give the same emissions for the same functional units. For instance, according to a study of Fruergaard et al. (2009), data about the average emission of greenhouse gases linked to 1 kWh electricity production in 25 EU countries varied between databases by up to 20 %. For similar estimates in the USA, an even greater between-database uncertainty (on average 40 %) was found (Weber et al. 2010). Though such uncertainties are substantial, they should not detract from using databases such as Ecoinvent, Spine, and JEMAI, if only because between-process differences often exceed uncertainty. This may be illustrated by the geographical variability in greenhouse gas emissions linked to electricity production. For instance, country-specific average emissions of greenhouse gases per kWh of electricity in such databases vary by a factor of 160 (Fruergaard et al. 2009). For marginal emissions of greenhouse gases per kWh of electricity (which are used to assess changes in supply or demand as needed for consequential life cycle assessment), variations were even larger: up to 400–750 times (Fruergaard et al. 2009).

In the *inventory* stage of life cycle assessments of greenhouse gas emissions, the focus is evidently on the latter emissions. In wider-ranging life cycle assessments, the inventory may comprise all extractions of resources and emissions of substances causally linked to the functional unit for each product under consideration, within the system boundaries that were established in the stage of goal and scope definition. Such wider-ranging life cycle assessments have a benefit over life cycle assessments, which only focus on greenhouse gas emissions. First, they give a better picture of the overall environmental impact, for which life cycle greenhouse gas emissions may well be a poor indicator (Huijbregts et al. 2006, 2010; Laurent et al. 2010). Also, such wider-ranging LCAs allow for considering “trade-offs”

between environmental impacts and the occurrence of co-benefits linked to reducing greenhouse gas emissions (Nishioka et al. 2006; Haines et al. 2009; Markandya et al. 2009; Chester and Horvath 2010; Walmsley and Godbold 2010). For instance, Walmsley and Godbold (2010) concluded that stump harvesting for bioenergy may not only impact greenhouse gas emissions but may have the co-benefit of reducing fungal infections and may have negative co-impacts linked to erosion, nutrient depletion and loss, increased soil compaction, increased herbicide use, and loss of valuable habitat for a variety of (non-pest) species. Many current transport biofuels have larger life cycle greenhouse gas emissions than the fossil fuel which they replace but have the benefit that dependence on mineral oil is reduced (Reijnders and Huijbregts 2009).

A large part of the impacts which go beyond climate change can be covered by standard wider-ranging LCAs. Aspects of environmental impact which are, apart from the emission of greenhouse gases, often covered by such wider-ranging life cycle assessments are summarized in Box 1.

In evaluating buildings, the indoor environment may also be a matter to consider (Demou et al. 2009; Hellweg et al. 2009). New operationalizations of some of the aspects of environmental impact mentioned in Box 1 and additions to the list of Box 1 are under development. The latter include ecosystem services (Koellner and de Baan 2013) and the impacts of freshwater use (Boulay et al. 2011; Verones et al. 2013). Adding to the aspects often covered in wide ranging LCAs, a proposal has been published for the inclusion into life cycle assessment of change in albedo which is relevant to climate, characterized in terms of CO_2 equivalents (Munoz et al. 2010). An estimate of the contribution inclusion of black carbon emissions to climate change has also become available (IPPC Working Group I 2013).

In life cycle assessments, the problem arises that many production systems have more than one output. For instance, rapeseed processing not only leads to the output oil, which may be used for biodiesel production, but also to rapeseed cake, which may be used as feed. Similarly, mineral oil refinery processes may not only generate gasoline but also kerosene, heavy fuel oil, and bitumen, and biorefineries produce a variety of product outputs too (Brehmer et al. 2009). In the case of multi-output processes, extractions of resources and emissions have to be allocated to the different outputs. There are several ways to do so. Major ways to allocate are based on physical units (e.g., energy content or weight of outputs) or on monetary value (price). There may also be allocation on the basis of substitution. In the latter case, the environmental burden of a coproduct is established on the basis of another, similar product. Different kinds of allocation may lead to different outcomes of life cycle assessment (Reijnders and Huijbregts 2009; Finnveden et al. 2009; Fruergaard et al. 2009; Sayagh et al. 2009).

The usual outcome of the *inventory analysis* of a wide ranging life cycle assessment is a list with all extractions of resources and emissions of substances causally linked to the functional unit for the product considered and, apart from the case of nuisance, commonly disregarding place and time of the extractions and emissions.

Box 1: Aspects of Environmental Impact Which Are Often Considered in Wide Ranging Life Cycle Assessments
Resource depletion (abiotic, biotic)
Effect of land use on ecosystems and landscape
Desiccation
Impact on the ozone layer
Acidification
Photooxidant formation
Eutrophication or nitrification
Human toxicity
Ecotoxicity
Nuisance (odor, noise)
Radiation
Casualties
Waste heat
Water footprint

Impact Assessment

The next stage in life cycle assessment is *impact assessment*. This firstly implies a step called characterization. In this step, extractions of resources and emissions are aggregated for a number of impact categories. When only greenhouse gas emissions are considered, the aggregation aims at establishing the emission of other greenhouse gases in terms of CO_2 equivalents (CO_2eq), which means that the emission of greenhouse gases like N_2O, CH_4, and CF_4 are recalculated in terms of CO_2 emissions. To do so, one needs to choose a time horizon (e.g., 25 years, 100 years, 10^4 years), because the greenhouse gas effect of emitted greenhouse gases may be different dependent on the time horizon chosen (see Table 1). The time-dependent differences in Table 1 reflect differences in atmospheric fate of greenhouse gases. For instance, the removal of CH_4 from the atmosphere is much faster than the removal of CO_2 (Myrhe et al. 2013).

In practice, often a time horizon of 100 years is chosen and the global warming potentials (GWP) from the corresponding column of Table 1 are commonly used in life cycle assessments.

Table 1 considers only direct impacts or effects of the greenhouse gases. There are however also indirect impacts. For instance, the emission of CH_4 may affect the presence of ozone, which is also a greenhouse gas. There have been proposals for including such indirect effects in global warming potentials. Using a 100-year time horizon and assuming the GWP of CO_2 to be 1, Brakkee et al. (2008) proposed, for instance, a GWP for CH_4 of 28 and for non-methane volatile organic compounds, a GWP of 8. The latter have a direct GWP of 0. A number of estimated examples of global warming potentials calculated with and without indirect effects are in Table 2.

Table 1 Estimated global warming potentials (GWP) in CO_2eq of CH_4 and N_2O for time horizons of 20 and 100 years as proposed by the Intergovernmental Panel on Climate Change (IPCC) (Myrhe et al. 2013). Apart from climate–carbon interactions, only direct effects are considered

Gas/time horizon	20 years	100 years
CO_2	1	1
CH_4	86	34
N_2O	268	298

Table 2 Estimated global warming potentials (GWP) with a time horizon of 100 years relative to the GWP of CO_2 for a number of gases as calculated by Brakkee et al. (2008)

Gas/type of GWP	GWP, direct effect only; time horizon 100 years	GWP, including indirect effects; time horizon 100 years
CH_4	18	28
CO	0	3
Non-methane volatile organic compounds (NMVOC)	0	8
Chlorofluorocarbon (CFC) 11	4,800	3,300
Chlorofluorocarbon (CFC) 12	11,000	6,100
Chlorofluorocarbon (CFC) 113	6,200	4,700
CF_4	6,100	6,100
CO_2	1	1

Table 3 Global warming potentials in CO_2eq for a number of gases

Gas/global warming potential	GWP assuming 70 % removal from atmosphere (direct effect only) (Sekiya and Omamoto 2010)	GWP as in Table 1 with a time horizon of 100 years as calculated by IPCC (Myrhe et al. 2013)
CH_4	10.6	34
Chlorofluorocarbon (CFC) 11	2,249	5,350
CF4	1,560,558	7,350
CO_2	1	1

One may note that Brakkee et al. (2008) give an estimate for the GWP of CH_4 (direct effect only), which is different from the value in Table 1.

Still another possibility is to calculate GWPs on the basis of a similar percentage of greenhouse gas remaining in, or lost from, the atmosphere. This is exemplified by Table 3, with values as calculated by Sekiya and Okamoto (2010).

In the case of life cycle assessment of greenhouse gas emissions, calculating the emission in terms of CO_2eq is where the impact assessment stage often ends, though there is also the option to quantify the impact in terms of damage to public

health (e.g., Haines et al. 2009), human health, and ecosystems (De Schryver et al. 2009) and in terms of negative effects on the economy (e.g., Stern 2006). Such damage-based characterizations facilitate weighing of trade-offs and co-benefits, when a variety of environmental impacts (cf. Box 1) are included in life cycle assessment.

Having CO_2eq emissions as an outcome of life cycle assessment is often sufficient to guide the selection of product life cycle options, policies, and innovations aimed at mitigation of climate change, because the emission of greenhouse gases is in a first approximation directly causally linked with environmental impact (climate change).

Still, it should be noted that the temporal pattern of greenhouse emissions may affect the rate of climate change, which in turn is, e.g., a major determinant of impact on ecosystems. When the temporal pattern of the emissions is important, as, for instance, in the case of land use change or capital investments in production systems, it is possible to adapt life cycle assessment by including the estimated temporal pattern of greenhouse gas emissions linked to the object of life cycle assessment (cf. Reijnders and Huijbregts 2003; Kendall et al. 2009).

Also, one may note that effect of activities on climate may go beyond the emission of greenhouse gases. For instance, agricultural activities may change albedo, evaporation, and wind speed, which may in turn affect climate (Reijnders and Huijbregts 2009). Also, the greenhouse effect of air traffic may be different than expected solely on the basis of CO_2, N_2O, and CH_4 emissions, because air traffic triggers formation of contrails and cirrus clouds (Lee et al. 2010a).

A direct causal link between emission and impact for greenhouse gas emissions may be at variance with other environmental impact categories. For instance, lead emissions which do not lead to exceeding a no-effect level for exposure of organisms will have no direct environmental impact. Also, specificity as to time and place can be very important for other impacts than climate change caused by greenhouse gases, such as the impacts of the emissions of hazardous and acidifying substances (Schöpp et al. 1998; Hellweg et al. 2005; Pottimg and Hauschild 2005; Basset-Mens et al. 2006). It may be noted, however, that in such cases time and place specificity may be introduced by adaptation of life cycle assessment or combining life cycle assessment with other tools (e.g., Hellweg et al. 2005; Huijbregts et al. 2000; Rehr et al. 2010).

Interpretation

The *interpretation* stage connects the outcome of the impact assessment to the real world.

Much of the practical usefulness of life cycle assessments of greenhouse gas emissions in this respect depends upon the uncertainty of outcomes, which has a variety of sources (e.g., Finnveden et al. 2009; Huijbregts et al. 2001, 2003; Geisler et al. 2005; De Koning et al. 2010; Williams et al. 2009). These can be categorized as uncertainties due to choices, uncertainties due to modeling, and parameter

uncertainty (Huijbregts et al. 2001, 2003). Parameter uncertainty and uncertainty due to choice (e.g., regarding time horizon, type of allocation, system boundaries, and functional unit) would seem to be the most important types of uncertainty in the case of estimating life cycle greenhouse gas emissions.

Uncertainty in the outcomes of life cycle assessments of greenhouse gas emissions partly depends on the reliability of input data (categorized as parameter uncertainty). As pointed out above, databases regarding fossil fuel use in industrialized countries such as the USA, China, and Japan and EU countries allow for substantial uncertainties in this respect (Sann et al. 2006; Fruergaard et al. 2009). Similar data regarding other countries tend to be still more uncertain. Greenhouse gas emissions linked to land use, N_2O emissions, and animal husbandry are also characterized by a relatively large uncertainty (Reijnders and Huijbregts 2009; Röös et al. 2010).

Additional variability in outcomes of life cycle assessments of greenhouse gas emissions may originate in different choices regarding system boundaries. This has, for instance, been shown by Christensen et al. (2009) and Gandreault et al. (2010), who analyzed life cycle greenhouse gas emissions of forestry products. They found that different assumptions about the boundary to the forestry industry and interactions between the forestry industry on one hand and on the other hand the energy industry and the recycled paper market might lead to substantial differences in outcomes of life cycle assessments. Choices regarding time horizons and the allocation of greenhouse gas emissions to outputs in multi-output processes may also have major consequences for such outcomes (Reijnders and Huijbregts 2009).

Sensitivity analysis may be part of the *interpretation* stage and, for instance, consider the dependence on different assumptions regarding allocation and time horizon. Similarly, uncertainty analysis may be part of the *interpretation* stage. Several approaches to uncertainty analysis have been proposed, using Monte Carlo techniques (Huijbregts et al. 2003; Hertwich et al. 2000), matrix perturbation (Heijungs and Suh 2002), or Taylor series expansion (Hong et al. 2010). In practice, uncertainty analysis has been applied in a limited way.

Also, in the interpretation stage, conclusions can be drawn. For instance, stages or elements of the product life cycle can be identified, which are linked to relatively high greenhouse gas emissions. These can be prioritized for emission reduction options and policies. Also, it may be established that, given a functional unit and specified assumptions, one product has lower greenhouse gas emissions (in CO_2eq) than another. Examples of conclusions which can be drawn from life cycle assessments are given in section "Main Findings from Life Cycle Studies of Greenhouse Gas Emissions."

Though life cycle assessment has been developed for products, in practice the methodology has been applied more widely (cf. "Published Life Cycle Assessments"). To the extent that life cycle assessment methodology, which does not focus on products, essentially assesses parts of product life cycles (e.g., the nickel industry, waste incineration, and CO_2 capture and sequestration), the usefulness of assessment may be similar to the assessment of products: one may find, prioritize, and validate emission reduction options.

Some of the applications of life cycle assessments, which go beyond products, give rise to additional problems. For instance, applying life cycle assessments to state economies and trade may give rise to double counting of emissions (Lenzen 2008). On the other hand, e.g., expansion of life cycle assessments to trade between states may give useful insights about the actual environmental impacts of imports and exports. This is a useful addition to climate regimes such as the Kyoto protocol, which focus on greenhouse gas emissions within state borders. Also, economy-wide LCAs may help in prioritizing product categories or economic sectors for policy development (Jansen and Thollier 2006).

Life Cycle Assessments Focusing on Greenhouse Gas Emissions or a Part Thereof

The emergence of climate change as a major environmental concern has led to a rapid increase in life cycle assessments focusing on the emission of greenhouse gases. However, it should be pointed out that there are also life cycle assessments which cover only a part of the greenhouse gases. In this context, one may note the growing popularity of "carbon footprinting" (e.g., De Koning et al. 2010; Barber 2009; Johnson 2008; Weber and Matthews 2008; Schmidt 2009). There is no generally agreed upon definition of carbon footprinting. In practice, the focus of carbon footprinting is often on the emission of carbonaceous greenhouse gases, if the footprinting is not being "slimlined" to covering CO_2 only (e.g., Schmidt 2009). Also, there is an increasing interest in life cycle assessments focusing on the cumulative input of fossil fuels, which in turn is closely related to the life cycle emission of the major greenhouse gas CO_2 (Laurent et al. 2010; Nishioka et al. 2006).

The focus on carbonaceous greenhouse gases may lead to outcomes which substantially deviate from overall greenhouse gas emissions. As several authors (Crutzen et al. 2007; Reijnders and Huijbregts 2009; Laurent et al. 2010; Nishioka et al. 2006) have pointed out, cumulative energy demand may be substantially at variance with overall environmental performance and life cycle emissions of greenhouse gases, in the case of agricultural commodities and in other cases in which life cycles impact land use. The same will hold in the case of a number of compounds, such as adipic acid, caprolactam, and nitric acid, when syntheses are used which generate N_2O in a poorly controlled way (Fehnann 2000; Perez-Ramirez et al. 2003). Also, there can be a major divergence of "carbon footprinting" from overall life cycle greenhouse gas emissions when there are substantial emissions of halogenated greenhouse gases. The latter, e.g., applies to the case of halogenated refrigerant use (Ciantar and Hadfield 2000), the use of halogenated blowing agents for the production of insulation (Johnson 2004), to primary aluminum production, which is associated with the emission of potent fluorinated greenhouse gases such as CF_4 (Fehnann 2000; Weston 1996), and to circuit breakers using SF_6 and magnesium foundries (Fehnann 2000; Harrison et al. 2010). In the following, only assessments will be used which give an estimate of all greenhouse gas emissions, recalculated as CO_2eq emissions.

Simplified Life Cycle Assessments

Full life cycle assessments require extensive data acquisition, which tends to be laborious and time-consuming, and this may well be beyond what practice in industry and policy requires (Bala et al. 2010). This has led to the emergence of simplified tools for the life cycle assessment of greenhouse gas emissions, such as screening LCAs. These tend to focus on major causes of life cycle greenhouse gas emissions ("hotspots") and are often useful in identifying and prioritizing emission reduction options (Andersson et al. 1998; Rehbitzer and Buxmann 2005).

Published Life Cycle Assessments

A wide variety of products has been the object of life cycle assessments of greenhouse gas emissions. Examples range from teddy bears to power generators, from pesticides to motorcars, from tomato ketchup to buildings, and from a cup of coffee to tablet e-newspapers. Products have not been the only objects of life cycle assessments of greenhouse gas emissions. Life cycle assessment has also been used for state economies, trade between countries, branches of industry, industrial symbiosis, aspects of production and product technologies, networks, soil and groundwater remediation, and waste management options, including CO_2 capture and sequestration.

Main Findings from Life Cycle Studies of Greenhouse Gas Emissions

Though, as pointed out in section "Goal and Scope Definition," there are substantial uncertainties in assessments of life cycle greenhouse gas emissions, some outcomes of such assessments are robust to such an extent that they provide a sufficiently firm basis for conclusions. The latter are summarized here, assuming a time horizon of 100 years, using the values for global warming potentials as given by IPCC (Myrhe et al. 2013) (see Table 1), and focusing on direct effects only, unless indicated otherwise. After this summary, options for life cycle greenhouse gas emission reduction which commonly emerge from life cycle assessments will be briefly discussed.

Energy Conversion Efficiency

Improvements in efficiency of the conversion of primary energy to energy services, including reduction of heat loss, often lead to lower life cycle greenhouse gas emissions for energy services (e.g., Erlandsson et al. 1997; Citherlet et al. 2000; Nakamura and Kondo 2006; Citherlet and Defaux 2007;

Boyd et al. 2009) when only direct effects are considered. There are some exceptions. Phase change materials, which may be used in buildings to improve energy conversion efficiency, have been shown to not significantly reduce the life cycle greenhouse gas emission of buildings in a Mediterranean climate (De Gracia et al. 2010). Electric heat pumps, though generally giving rise to lower life cycle greenhouse gas emissions for space heating, may increase life cycle greenhouse gas emissions when electricity generation is coal based (Saner et al. 2010). Also, the III/V solar cells, which contain, e.g., In (indium) and Ga (gallium) and have higher conversion efficiencies for solar energy into electricity than Si (silicium)-based photovoltaic cells, do not appear to have lower life cycle greenhouse gas emissions per kWh than multicrystalline Si solar cells (Mohr et al. 2009).

Noteworthy is the potential for indirect effects linked to improvements of energy efficiency. As noted before: in the case that improvements in energy conversion lead to lower costs of ownership, there may be a rebound effect on energy use because money linked to such lower costs tends to be spend on increased use of the product or elsewhere, which in turn entails additional energy consumption and emission of greenhouse gases (Schipper and Grubb 2000; Thiesen et al. 2008; Greene 2011). Lower costs may also be conducive to economic growth (Thiesen et al. 2008). When only microeconomic effects of improved energy efficiency are considered, life cycle greenhouse gas emissions tend to be still lowered, though less so than when only the effect of energy efficiency by itself is considered (Schipper and Grubb 2000; Greene 2011). Including economy-wide rebound effects in life cycle assessments of improved energy conversion efficiency has as yet no firm empirical basis (Thiesen et al. 2008).

Products Consuming Energy

Life cycle greenhouse gas emissions of products which consume energy are often dominated by emissions during the use stage of the life cycle, when shares of fossil fuels in the production and consumption stages are similar (Nakamura and Kondo 2006; Boyd et al. 2009, 2010; Finkbeiner et al. 2006; Kofoworola and Gheewala 2008; Yung et al. 2008; Cullen and Allwood 2009; Duan et al. 2009; Ortiz et al. 2010; Rossello-Batle et al. 2010). There are exceptions, however, such as, for instance, a personal computer for limited household use (Choi et al. 2006), mobile phones (Andrae and Andersen 2010), and very energy-efficient dwellings (Citherlet and Defaux 2007). The latter illustrates a more general point. To the extent that energy conversion efficiency in the use stage improves, energy embodied in the product (e.g., Kakudate et al. 2002; Blengini and di Carlo 2010) and in the case of transport also energy embodied in infrastructure (e.g., Frederici et al. 2009) often become a more important factor in life cycle greenhouse gas emissions. It may be noted, though, that there are exceptions as to the growing importance of energy embodied in the product, such as CMOS chips for personal computers and other electronics (Boyd et al. 2009, 2010).

Transport

At continental distances in the order of <500 km, where train transport and air transport can be competitors, train transport tends to be associated with relatively low life cycle greenhouse gas emissions per person kilometer when occupancy rates are high (Chester and Horvath 2010; Blengini and di Carlo 2010; Frederici et al. 2009).

In freight transport, ships tend to do relatively well per ton kilometer regarding life cycle greenhouse gas emissions if compared with truck transport (Chapman 2007). Ceteris paribus, the diesel personal car has a lower life cycle greenhouse gas emission than the gasoline-powered car, whereas lighter cars tend to have lower greenhouse gas emissions than heavier cars, even when highly energy-intensive materials such as aluminum are used for weight reduction (Kakudate et al. 2002; Spielman and Althaus 2007; Bertram et al. 2009). The electric car might do better as to life cycle greenhouse gas emissions than the conventional car, unless electricity supply is heavily dependent on coal (Granovskii et al. 2006).

Conventional and Unconventional Fossil Fuels

Among current fossil fuels, the life cycles of conventional natural gas tend to give rise to the lowest greenhouse gas emissions and lignite to the highest. Burning (hard) coal leads to somewhat lower life cycle greenhouse gas emissions than burning lignite, whereas the life cycle emissions for burning conventional mineral oil and its derivative fuels tend to be between those of conventional natural gas and coal. Fuels derived from fossil carbonaceous stocks remaining beyond the peaks of conventional natural gas and conventional mineral oil supply are likely to be associated with higher life cycle greenhouse gas emissions than current conventional gas and mineral oil-derived fuels, with greenhouse gas emissions for tight gas and shale gas dependent on methane leakage from casing and cement impairment and soil layers subject to fracking (Ingraffea et al. 2014; Lave et al. 2000; Petron et al. 2012; Jaramillo et al. 2009; Reijnders 2009a).

Green Energy Supply

Among the options for expanding "green energy supply," solar boilers; solar cells; solar-assisted heating, ventilating, and air conditioning (HVAC) systems; marine current turbines; and wind turbines do relatively well if compared with fossil fuel-based alternatives (Mohr et al. 2009; Jorquera et al. 2010; Rebitzer et al. 2004; Schipper and Grubb 2000; Thiesen et al. 2008; Greene 2011; Sathre and O'Connor 2010; Finnveden et al. 2009; Gandreault et al. 2010; Frischknecht et al. 2005; Gong et al. 2008; Narita et al. 2004; ELCD 2008; Tukker et al. 2006; De Eicker et al. 2010; Fruergaard et al. 2009; Weber et al. 2010; Huijbregts et al. 2000, 2001, 2003, 2006, 2010; Laurent et al. 2010; Nishioka et al. 2006; Haines et al. 2009;

Markandya et al. 2009; Chester and Horvath 2010; Walmsley and Godbold 2010; Demou et al. 2009; Hellweg et al. 2005, 2009; Koellner and de Baan 2013; Boulay et al. 2011; Verones et al. 2013; Munoz et al. 2010; IPPC Working Group I 2013; Brehmer et al. 2009; Sayagh et al. 2009; Myrhe et al. 2013; Brakkee et al. 2008; Sekiya and Omamoto 2010; De Schryver et al. 2009; Stern 2006; Reijnders and Huijbregts 2003; Kendall et al. 2009; Lee et al. 2010a, b; Schöpp et al. 1998; Pottimg and Hauschild 2005; Basset-Mens et al. 2006; Rehr et al. 2010; Geisler et al. 2005; De Koning et al. 2010; Williams et al. 2009; Röös et al. 2010; Christensen et al. 2009; Hertwich et al. 2000; Heijungs and Suh 2002; Hong et al. 2010; Lenzen 2008; Jansen and Thollier 2006; Barber 2009; Johnson 2004, 2008; Weber and Matthews 2008; Schmidt 2009; Fehnann 2000; Perez-Ramirez et al. 2003; Ciantar and Hadfield 2000; Weston 1996; Harrison et al. 2010; Bala et al. 2010; Andersson et al. 1998; Rehbitzer and Buxmann 2005; Erlandsson et al. 1997; Citherlet et al. 2000; Nakamura and Kondo 2006; Citherlet and Defaux 2007; Boyd et al. 2009, 2010; De Gracia et al. 2010; Saner et al. 2010; Finkbeiner et al. 2006; Kofoworola and Gheewala 2008; Yung et al. 2008; Cullen and Allwood 2009; Duan et al. 2009; Ortiz et al. 2010; Rossello-Batle et al. 2010; Choi et al. 2006; Andrae and Andersen 2010; Kakudate et al. 2002; Blengini and di Carlo 2010; Frederici et al. 2009; Chapman 2007; Spielman and Althaus 2007; Bertram et al. 2009; Granovskii et al. 2006; Ingraffea et al. 2014; Lave et al. 2000; Petron et al. 2012; Jaramillo et al. 2009; Reijnders 2009a; Martinez et al. 2009; Ardente et al. 2005; Douglas et al. 2008; Nugent and Sovakool 2014; Batlles et al. 2010). When intermittent forms of energy supply increase their share in energy supply, energy storage systems may be needed. These have also been evaluated regarding their life cycle greenhouse gas emissions (e.g., Lee et al. 2010b; Froese et al. 2010). It would seem that energy storage systems do not invalidate the climate benefits from the intermittent energy supply options considered here. Greenhouse gas emissions of hydropower facilities strongly depend on submerged carbon stocks and their anaerobic conversion, and low greenhouse gas emissions are correlated by low land use per unit of electricity generated (Hertwich 2013).

Biofuels

Greenhouse gas emissions associated with the life cycle of biofuels vary widely, dependent on fossil fuel inputs, changes in soil and aboveground carbon stocks, and N_2O emissions (Reijnders and Huijbregts 2009; Kloverpris et al. 2010). Burning woody residues from forests with (at least) constant carbon stocks in power plants tend to do relatively well in this respect, if compared with its main fossil fuel-based competitor: burning coal (Reijnders and Huijbregts 2009; Zhang et al. 2010; Denholm and Kulcinski 2004). However, with a few exceptions such as ethanol from sugarcane in the Brazilian Cerrado region, current liquid biofuels from crops which compete with food crops for good soils compare unfavorably with conventional gasoline and diesel when indirect effects on land use are included, when

biofuel production expands rapidly and when allocation of life cycle emissions is on the basis of monetary value of outputs (Searchinger et al. 2008; Reijnders and Huijbregts 2009; Hertel et al. 2010). Such liquid biofuels would have much lower life cycle greenhouse gas emissions when the crops from which they are derived would be grown on abandoned agricultural soils which have sequestered little carbon, but use of such abandoned soils is unattractive under market conditions (Reijnders and Huijbregts 2009). Still, a policy decision restricting feedstock generation for biofuels to abandoned soils which have sequestered little carbon would lead to life cycle greenhouse gas emissions for liquid biofuels that will usually be lower than those linked to fossil fuels.

A relatively poor performance will probably also apply to the life cycle greenhouse gas emissions linked to methane for injection into the gas grid originating in the anaerobic conversion of energy crops in temperate climates if compared (fossil) with natural gas. The reason for this is that, without taking into consideration the indirect effect of expanding the cultivation of energy crops on land use, the life cycle emission of (cleaned-up) biogas is only slightly lower than the corresponding emission of natural gas (Jury et al. 2010). Fossil fuel inputs to achieve an elevated optimum temperature are an important contributor to the relatively poor performance of anaerobic conversion in temperate climates (Jury et al. 2010). In warmer climates, anaerobic conversion may well do better. Microbial fuel cells producing electricity have been reported to have a lifetime environmental performance and a life cycle CO_2 emission, similar to anaerobic conversion (Foley et al. 2010).

The actual greenhouse gas emissions linked to the life cycle of future biofuels, such as ethanol, produced from lignocellulosic crops and algal biodiesel are highly uncertain. Relatively poor yields and/or high fossil fuel inputs, which are characteristic for current lignocellulosic ethanol and algal biodiesel production technology, are associated with relatively high life cycle greenhouse gas emissions (Reijnders and Huijbregts 2009; Havlik et al. 2011; Reijnders 2010). Predictions of relatively low life cycle greenhouse gas emissions in the future are typically linked to large increases in biofuel yield and reductions in fossil fuel input (e.g., Jorquera et al. 2010; Spatari et al. 2010), to the use of abandoned soils for lignocellulosic crops (Havlik et al. 2011; Reijnders 2010), or, in the case of algae, the use of "wastes" conducive to growth (Clarens et al. 2010; Reijnders 2013). In the latter case, it is assumed that there is no allocation to the wastes of greenhouse gas emissions associated with the process from which they are derived. Ultimately, life cycle greenhouse gas emissions associated with liquid biofuels produced from part of the lignocellulosic harvest residues from no-till agriculture may be more favorable than the use of mineral oil-derived products (Reijnders and Huijbregts 2009; Spatari et al. 2010).

Food

Food consumption by relatively rich people in industrialized countries is often linked to a higher life cycle greenhouse gas emission than food consumption by relatively poor people (e.g., Weber and Matthews 2008). However, food consumption by (poor)

swidden ("slash-and-burn") agriculturalists practicing short fallow periods may be associated with relatively high life cycle greenhouse gas emissions, as it is linked with a large reduction of the carbon stock in agroecosystems (Reijnders 2006; Bruun et al. 2009). Diets do matter: plant protein-based foods tend to have lower life cycle greenhouse gas emissions than meat, and the same tends to hold for vegetarian diets versus diets with much produce for animal husbandry, unless vegetarian foods are frozen, flown in by airplanes, or produced in greenhouses intensively heated by fossil fuels (Weber and Matthews 2008; Reijnders and Soret 2003; Carlsson-Kanyama and Gonzalez 2009). One kilogram of beef protein is usually linked to greater life cycle greenhouse gas emissions than 1 kg chicken or pork protein (Carlsson-Kanyama and Gonzalez 2009; De Vries and de Boer 2010; Gössling et al. 2010). Per unit of food energy, pelagic fishes (e.g., mackerel, herring) tend to be associated with lower life cycle greenhouse gas emissions linked to fossil fuel use than deep-sea fishes (e.g., cod), shrimps, or lobster (Gössling et al. 2010).

Per unit of cereal-based food energy, rice is on average associated with relatively high greenhouse gas emissions, if compared with wheat and rye. A major cause thereof is the relatively high CH_4 emission during rice cultivation (Gössling et al. 2010). When transport distances are similar, produce from greenhouses seems on average linked with higher greenhouse gas emissions per unit of food energy than cultivation in the open field (Gössling et al. 2010). Canning and commercial freezing for food conservation do much increase the life cycle greenhouse gas emissions of foods (Reijnders and Soret 2003; Iribarren et al. 2010).

Current expansion of arable land for food production is linked with high greenhouse gas emissions because it mainly replaces forests and wooded lands with much larger carbon stocks than arable land (Reijnders and Huijbregts 2009; Hertel et al. 2010).

Chemicals

Complex "fine chemicals" synthesized in a relatively large number of "steps" tend to be associated with relatively high life cycle greenhouse gas emissions per kg (Wernet et al. 2010). A study comparing a range of synthetic chemicals with biobased equivalents (Weiss et al. 2012) suggested lower greenhouse gas emissions for biobased substances excepting acetic acid. Changes in ecosystem carbon stocks were not included, but the conclusion that biobased caprolactam does better than its synthetic equivalent seems robust.

Polymeric Materials

In a number of cases, it is possible to replace the plastic PVC by other materials, having a lower life cycle greenhouse gas emission (Kleijn et al. 2008). However, large-scale substitution of PVC might have indirect effects, originating in impacts on caustic soda production, which might lead to a net increase of greenhouse gas

emissions (Kleijn et al. 2008). LCA studies (van der Velden et al. 2014) suggest that when polymeric textiles are compared, acryl and polyester do relatively well if compared with cotton and nylon. The bioplastic PLA and PHB derived from starch crops, such as corn, by current technology (Searchinger et al. 2008; Khoo et al. 2010; Kim and Dale 2008; Tabone et al. 2010), and the production of PHB by genetically modified plants (Kurdikar et al. 2000) might well do worse than their petrochemical competitors, when indirect effects and land use are included and non-food applications of starch crops rapidly expand. This may be changed by future changes in bioplastic production.

Using sugarcane bagasse fibers instead of talc to reinforce polypropylene composites was found to lower life cycle greenhouse gas emissions (Luz et al. 2010).

Crop-Based Lubricants and Solvents

There is marketing of crop-based lubricant oils and solvents for general purpose cleaning (Curran 2003). There are few LCAs of such products (Curran 2003). These do not take account of direct and indirect changes in ecosystem carbon sequestration linked to crop cultivation. To the extent that LCA studies of crop-based lubricants and solvents are available (Curran 2003), it would seem unlikely that such lubricant oils and solvents are better than their fossil fuel-based competitors regarding life cycle greenhouse gas emissions. They may, however, have other benefits, such as reduced dependence on mineral oil or lower toxicity.

Recycling

Provided that transport distances and inputs in recycling and remanufacturing processes remain modest, product reuse, remanufacturing, and recycling of materials used in products tend to be associated with lower life cycle greenhouse gas emissions than the use of virgin virtually nonrenewable resources (such as metal ores and fossil carbon) (e.g., Björklund and Finnveden 2005; Lankey and McMichael 2000; Nakinawa and Graedel 2002; Rydh and Karlström 2002; Huang et al. 2009). Supposed that the same provision regarding modest transport distances and inputs in recycling holds, recycling can also be associated with relatively low greenhouse gas emissions in the case of renewable resources such as wood (Björklund and Finnveden 2005; Hoglmeier et al. 2014). Use of recycled concrete does well regarding greenhouse gas emissions (Wu et al. 2014).

Nanotechnology

Outcomes of LCAs regarding engineered nanomaterials tend to be uncertain but suggest that the alleged advantage of nanotechnology ("less is better") does not necessarily materialize (Kushnir and Sanden 2008; Meyer et al. 2009; Hischier and

Walser 2012). This can be traced back to factors such as limited durability and efficiency, relatively high inputs in producing nanoparticulate materials, and relatively low recyclability (Kushnir and Sanden 2008; Meyer et al. 2009; Hischier and Walser 2012). Further maturing and upscaling of nanotechnology may improve the outcomes of LCAs regarding greenhouse gas emissions.

Reduction of Life Cycle Greenhouse Gas Emissions

In previous sections, the use of life cycle assessments in the reduction of life cycle greenhouse gas emissions has already been briefly referred to. In practice, life cycle assessments are often used in identifying elements of the life cycle, which are linked to relatively high greenhouse gas emissions. Also, life cycle assessments can be used to evaluate the impact of improvement options on life cycle greenhouse gas emissions. There is some evidence that communicating about programs for the reduction of product-related life cycle greenhouse gas emissions does provide a better fit to consumer perceptions than expecting producers to choose between products on the basis of the lowest life cycle greenhouse gas emissions (Upham et al. 2010).

Elements which are often included in programs for the reduction of product-related life cycle greenhouse gas emissions are briefly summarized in Box 2.

Many of these elements mentioned in Box 2 are uncontroversial and often also serve the reduction of other environmental problems, but some may give rise to discussion about the net benefit, including the reduction of life cycle greenhouse gas emissions. Controversies about the use of "biobased" products, such as biofuels, have been referred to earlier in this section. There is also controversy about the net effect of climate compensation. For instance, planting trees has been argued to not properly provide climate compensation for the use of fossil fuels, because the lifetime of trees is limited, if compared with the 30,000–35,000 years needed for the complete removal of CO_2 emitted by burning fossil fuels, because ongoing existence of forests over this period cannot be guaranteed and because tree planting projects often give rise to "leakage": land use changes in which trees are cut (Reijnders 2009b).

Box 2: Elements That Are Often Included in Programs for the Reduction of Product-Related Life Cycle Greenhouse Gas Emissions

- Reduced life cycle fossil energy use
- Use of energy supply with low greenhouse gas emissions per joule
- Reduction of land use change
- Lower non-energy inputs in production
- Lowering non-product outputs ("wastes" and emissions) of production processes, especially emissions with a relatively large "greenhouse effect" (e.g., of halogenated compounds, CH_4, N_2O)
- Dematerialization of products

(continued)

- Increased recycling
- Reduced "downstream" greenhouse gas emissions linked to improved energy efficiency, e.g., using means of transport that have relatively low greenhouse gas emissions per ton kilometer, by increasing electronic retailing, or improving energy efficiency of products which consume energy
- Reduction of transport distances, more efficient logistics
- Increased carbon sequestration and/or "climate compensation"

Future Directions

There is a growing societal interest in life cycle assessments of greenhouse gas emissions and related assessments, such as life cycle carbon footprinting (e.g., Fava et al. 2009). This seems to be paralleled by a trend to simplification (see, e.g., section "Simplified Life Cycle Assessments"). However, one should be aware that there are several methodological issues that have substantial relevance to the correspondence of the outcomes of life cycle assessments and impact on climate change in the real world. These issues will be briefly addressed. They are partly in the domain of those involved in methodology development and partly in the domain of those applying life cycle assessment.

Change in Carbon Stocks of Recent Biogenic Origin

Changes in carbon stocks of recent biogenic origin have turned out to be very important to life cycle greenhouse gas emissions of food and biofuels. However, their inclusion in life cycle assessments of food and biofuels is so far patchy. Also, one might expect such changes to be important in other "biobased" products, such as "bioplastics" and crop-based lubricants, solvents, and other chemicals. However, their inclusion of life cycle assessments of such products is rare. Buildings, roads, hydroelectric dams, and other infrastructural works might also be expected to impact carbon stocks of recent biogenic origin, but again their inclusion in life cycle assessments is very rare. Studies thoroughly evaluating impacts of changes in carbon stocks of recent biogenic origin on life cycle greenhouse emissions would be welcome. These might provide better knowledge regarding the cases that such changes have at least a substantial impact on life cycle greenhouse gas emissions.

Indirect Effects

Product life cycles may have indirect effects which are substantial when evaluating their life cycle greenhouse gas emissions. Indirect effects of biofuels on land use

change, linked to the inelasticity of demand for food and feed (see section "Published Life Cycle Assessments"), are a case in point. The same holds for the rebound effect linked to lowered costs by improved energy (see section "Published Life Cycle Assessments"). Relations between economic activities as reflected in input–output tables constructed by economists may also be important (Lifset and Anes 2009). A more thorough study and discussion of the question when which indirect effects should be within the system boundaries drawn for life cycle assessment would seem appropriate.

Uncertainty

As pointed out in section "Interpretation," there is substantial uncertainty regarding the outcome of life cycle assessments of greenhouse gas emissions, largely originating in parameter uncertainty and uncertainty due to choices. Transparency about the actual uncertainties regarding the outcome of life cycle assessments of greenhouse gas emissions is in practice very limited. Comprehensive uncertainty and sensitivity analyses are rare. However, it is important that societal stakeholders get at least a rough indication of the uncertainties in the outcomes of life cycle assessments presented to them.

Comprehensives of Dealing with Climate Warming

As noted in section "Inventory Analysis," a proposal has been made to include changes in albedo linked to land use change into life cycle assessment (Munoz et al. 2010). Also, there have been proposals for the quantitative inclusion of the climate effects linked to contrails and cirrus clouds in the climate impact estimates for air traffic (Lee et al. 2010a). However, there is still some way to go for a comprehensive coverage of climate warming in life cycle assessment. On a time scale of centuries, there are changes in albedo, which will probably contribute to further warming, following from climate change (e.g., due to loss of ice and desertification) (Hansen et al. 2008). These changes in albedo are as yet not covered by life cycle assessments. A contributor to climate change currently absent from life cycle assessment of climate impact is black carbon (carbonaceous aerosol, soot) (Highwood and Kinnersly 2006; McConnell et al. 2007; Ming et al. 2009; Andreae and Gelenesér 2006). Black carbon has a variety of effects which are relevant to climate (Highwood and Kinnersly 2006; McConnell et al. 2007; Ming et al. 2009; Andreae and Gelenesér 2006). When emitted, black carbon absorbs and scatters solar radiation and may affect humidity profiles (cloud formation) and droplet size in clouds. When deposited, black carbon may have an effect on surface albedo. It is currently estimated that the net effect of black carbon emissions on climate is warming (Andreae and Gelenesér 2006). For comprehensiveness in dealing with life cycle impacts on climate, it would seem proper to include both black carbon emissions and long-term changes in albedo in life cycle assessment.

Consequential Life Cycle Assessment

In mitigating climate change, changes in products and technologies are much more important than studies of existing products and technologies. Such changes are the object of consequential life cycle assessment. As pointed out in section "What is Life Cycle Assessment and How Does It Work?," consequential life cycle assessment is a relatively recent development. The methodological approach, such as constructing scenarios and technological trajectories, deserves substantial attention, if only to provide a more solid basis for more widespread application in the development of new products and technologies.

Concluding Remarks

Life cycle assessments of greenhouse gas emissions may be helpful in the analysis and development of options, policies, and innovations aimed at mitigation of climate change. The main findings from available life cycle assessments summarized in section "Main Findings from Life Cycle Studies of Greenhouse Gas Emissions" provide for guidance in that respect. It can be noted that in several cases, indirect effects have significant effects on the overall climate impact of products, and including those effects in considering options, policies and innovations aimed at mitigation of climate change would seem important.

For any product, or part of the product life cycle, life cycle assessment can be useful in identifying the aspects of production which are main contributors to life cycle greenhouse gas emissions. This can provide a focus for trying to identify or develop options which might reduce such emissions and for life cycle management. Furthermore, life cycle assessments may help in providing guidance for future research and development work, though it should be noted that such guidance may be characterized by relatively large uncertainties.

References

Andersson K, Ohlsson T, Olsson P (1998) Screening life cycle assessment (LCA) of tomato ketchup: a case study. J Cleaner Prod 6:277–288

Andrae ASG, Andersen O (2010) Life cycle assessments of consumer electronics – are they consistent? Int J Life Cycle Assess 15:827–836

Andreae MO, Gelenesér A (2006) Black carbon or brown carbon? The nature of light-absorbing carbonaceous aerosols. Atmos Chem Phys 6:3131–3148

Ardente F, Beccali G, Cellura M, Lo Brano V (2005) Life cycle assessment of a solar thermal collector. Renew Energy 30:1031–1054

Bala A, Raugei M, Benviste G, Gazulla C, Fullana-i-Palmer P (2010) Simplified tools for global warming potential evaluation: when 'good enough' is best. Int J Life Cycle Assess 15:489–498

Barber WPF (2009) Influence of anaerobic digestion on the carbon footprint of various sewage sludge treatment options. Water Environ J 25:170–179

Basset-Mens C, Anibar L, Durand P, van der Werf HMG (2006) Spatialised fate factors for nitrate in catchments: modeling approach and implication for LCA results. Sci Total Environ 367:367–382

Batlles FI, Rosiek S, Munoz I, Fernandez-Alba AB (2010) Environmental assessment of the CIESOL solar building after two years of operation. Environ Sci Technol 44:3587–3593
Bertram M, Buxmann K, Furrer P (2009) Analysis of greenhouse gas emissions related to aluminum transport applications. Int J Life Cycle Assess 14:S62–S69
Björklund A, Finnveden G (2005) Recycling revisited: life cycle comparisons of global warming impact and total energy use of waste management strategies. Resour Conserv Recycl 44:309–317
Blengini GA, di Carlo T (2010) The changing role of life cycle phases, subsystems and materials in the LCA of low energy buildings. Energy Build 42:869–880
Boulay A, Bulle C, Bayart B (2011) Regional characterization of fresh water use in LCA: modeling direct impacts on human health. Environ Sci Technol 45:8948–8957
Boyd SB, Horvath A, Dornfeld D (2009) Lifecycle energy demand and global warming potential of computational logic. Environ Sci Technol 43:7303–7309
Boyd SB, Horvath A, Dornfeld DA (2010) Life-cycle assessment of computational logic produced from 1995 through 2010. Environ Res Lett 5:014011 (8 pp)
Brakkee KW, Huijbregts MAJ, Eickhout B, Hendriks AJ, van de Meent D (2008) Characterisation factors for greenhouse gases at a midpoint level including indirect effects based on calculations with the IMAGE model. Int J Life Cycle Assess 13:191–201
Brehmer B, Boom RM, Sanders J (2009) Maximum fossil fuel feedstock replacement potential of petrochemicals via biorefineries. Chem Eng Des 87:1103–1119
Bruun TB, de Neergaard A, Lawrence D, Ziegler AD (2009) Environmental consequences of the demise in swidden cultivation in southeast Asia: carbon storage and soil quality. Hum Ecol 37:375–388
Carlsson-Kanyama A, Gonzalez AD (2009) Potential contributions of food consumption patterns to climate change. Am J Clin Nutr 89:1704S–1709S
Chapman L (2007) Transport and climate change: a review. J Transp Geogr 15:354–367
Chester M, Horvath A (2010) Life-cycle assessment of high-speed rail: the case of California. Environ Res Lett 5:014003
Choi B, Shin H, Lee S, Hur T (2006) Life cycle assessment of a personal computer and its effective recycling rate. Int J Life Cycle Assess 11:122–128
Christensen TH, Gentil E, Boldrin A, Larsen AW, Weidema BP, Hauschild M (2009) C balance, carbon dioxide emissions and global warming potentials in LCA-modelling of waste management systems. Waste Manage Res 27:707–715
Ciantar C, Hadfield M (2000) An environmental evaluation of mechanical systems using environmentally acceptable refrigerants. Int J Life Cycle Assess 5:209–220
Citherlet S, Defaux T (2007) Energy and environmental comparison of three variants of a family house during its whole life span. Build Environ 42:591–598
Citherlet S, Di Guglielmo F, Gay J (2000) Window and advanced glazing systems in life cycle assessment. Energy Build 32:225–234
Clarens AF, Resurreccion EP, White MA, Colosi LM (2010) Environmental life cycle comparison of algae to other bioenergy feedstocks. Environ Sci Technol 44:1813–1819
Crutzen PJ, Mosier AR, Smith KA, Winiwater W (2007) N_2O release from agro-biofuel production negates global warming reduction by replacing fossil fuels. Atmos Chem Phys Discuss 7:11191–11205
Cullen JM, Allwood JM (2009) The role of washing machines in life cycle assessment studies. J Ind Ecol 13(1):27–37
Curran MA (2003) Do bio-based products move us towards sustainability? A look at three USEPA case studies. Environ Prog 22:277–292
De Eicker MO, Hischier R, Hurni H, Zah R (2010) Using non local databases for the environmental assessment of industrial activities: the case of Latin America. Environ Impact Assess Rev 30:145–157
De Gorter H, Just DR (2010) The social costs and benefits of biofuels: the intersection of environmental, energy and agricultural policy. Appl Econ Perspect Policy 32:4–32

De Gracia A, Rincón L, Castell A, Jiménez M, Boer D, Medrano M, Cabeza LG (2010) Life cycle assessment of the inclusion of phase change materials in experimental buildings. Energy Build 42:1517–1523

De Koning A, Schowanek D, Dewaele J, Weisbrod A, Guinee J (2010) Uncertainties in a carbon footprint model for detergents: quantifying the confidence in a comparative result. Int J Life Cycle Assess 15:79–89

De Schryver AM, Brakkee KW, Goedkoop MJ, Huijbregts MAJ (2009) Characterization factors for global warming in life cycle assessment based on damages to humans and ecosystems. Environ Sci Technol 43:1689–1695

De Vries M, de Boer IJM (2010) Comparing environmental impacts for livestock products: a review of life cycle assessments. Livest Sci 128:1–11

Demou E, Hellweg S, Wilson P, Hammond SK, McKone TE (2009) Evaluating indoor exposure modeling alternatives for LCA: a case study in the vehicle repair industry. Environ Sci Technol 43:5804–5810

Denholm P, Kulcinski GL (2004) Life cycle energy requirements and greenhouse gas emissions from large scale energy storage systems. Energy Convers Manage 45:2153–2172

Douglas GA, Harrison GF, Chick JP (2008) Life cycle assessment of Seagen marine current turbine. J Eng Marit Environ 222M:1–12

Duan H, Eugster M, Hischier R, Streicher-Porte Li J (2009) Life cycle assessment study of a Chinese desktop personal computer. Sci Total Environ 407:1755–1764

ELCD (2008) European commission joint research centre – European reference life cycle data system. http://lct.jrc.ec.europa.eu/lcanfohub/dataset

Erlandsson M, Levin P, Myhre L (1997) Energy and environmental consequences of an additional wall insulation of a dwelling. Build Environ 32:129–136

Fargione J, Hill J, Tilman D, Polasky S, Hawthorne P (2008) Land clearing and the biofuel carbon debt. Science 319:1235–1238

Fava J, Baer S, Cooper J (2009) Increasing demands for life cycle assessments in North America. J Ind Ecol 13:491–494

Fehnann J (2000) Industrial non-energy, non-CO_2 greenhouse gas emissions. Technol Forecast Soc 63:313–334

Finkbeiner M, Hoffmann R, Ruhland K, Liebhart D, Stark B (2006) Application of life cycle assessment for the environmental certificate of the Mercedes-Benz S class. Int J Life Cycle Assess 11:240–246

Finnveden G, Hauschild MZ, Ekvall T, Guine J, Heijungs R, Hellweg S, Koehler A, Pennington D, Suh S (2009) Recent developments in life cycle assessment. J Environ Manage 91:1–21

Foley JM, Rozendal RA, Hertle CK, Lant PA, Rabaey K (2010) Life cycle assessment of high rate anaerobic treatment, microbial fuel cell, and microbial electrolysis cells. Environ Sci Technol 44:3629–3637

Frederici M, Ulgati S, Basosi R (2009) Air versus terrestrial transport modalities: an energy and environmental comparison. Energy 24:1493–1503

Frischknecht R, Jungbluth N, Althaus H, Doka G, Dones R, Heck T, Hellweg S, Hischier R, Nemecek T, Rebitzer G, Spielmann M (2005) The ecoinvent database; overview and methodological framework. Int J Life Cycle Assess 10:3–9

Frischknecht R, Büsser S, Krewitt W (2009) Environmental assessment of future technologies: how to trim LCA to fit this goal? Int J Life Cycle Assess 14:584–588

Froese RL, Shonnard DR, Miller CA, Koers KP, Johnson DM (2010) An evaluation of greenhouse gas mitigation options for coal-fired power plants in the US Great Lakes States. Bio-mass Bioenergy 34:251–262

Fruergaard T, Astrup T, Ekvall T (2009) Energy use and recovery in waste management and implications for accounting greenhouse gases and global warming contributions. Waste Manage Res 27:724–737

Gandreault C, Samson R, Stuart PR (2010) Energy decision making in a pulp and paper mill: selection of LCA system boundary. Int J Life Cycle Assess 15:198–211

Geisler G, Hellweg S, Hungerbühler K (2005) Uncertainty analysis in life cycle assessment (LCA): case study on plant-protection products and implications for decision making. Int J Life Cycle Assess 10:184–192

Gong X, Nie Z, Wang Z, Zuo T (2008) Research and development of Chinese LCA database and LCA software. Rare Met 25(6):101–104

Gössling S, Garrod B, Aall C, Hille J, Peeters P (2010) Food management in tourism: reducing tourism's carbon 'footprint'. Tourism Manage 32:534–543

Granovskii M, Dincer I, Rosen MA (2006) Economic and environmental comparison of conventional, hybrid, electric and hydrogen fuel cell vehicles. J Power Sources 159:1186–1193

Greene DL (2011) Rebound 2007: analysis of U.S. light duty vehicle travel statistics. Energy Policy. doi:10.1016/j.enpol.2010.03.083

Guinee JB (ed) (2002) Handbook on life cycle assessment. Kluwer, Dordrecht

Haines A, McMichael AJ, Smith KR, Roberts I, Woodcock J, Markandya A, Armstoing BG, Campbell-Lendrum D, Dangour AD, Davies M, Bruce N, Tonne C, Barrett M, Wilkinson P (2009) Public health benefits of strategies to reduce greenhouse-gas emissions: overview and implications for policy makers. Lancet 374:2104–2114

Hansen J, Sato M, Kharecha P, Beerling D, Berner R, Masson-Delmotte V, Pagani M, Raymao M, Royer DL, Zachos JC (2008) Target atmospheric CO_2: where should humanity aim. Open Atmos Sci J 2:217–231

Harrison GP, Maclean EJ, Karamanlis S, Ochoa LF (2010) Life cycle assessment of the transmission network in Great Britain. Energy Policy 38:3622–3631

Havlik P, Schneider UA, Schmid E, Böttcher H, Fritz S, Skalsky R, Aoki K, de Cara S, Kinderman G, Kraxner F, Leduc S, McCallum I, Mosnier A, Sauer T, Obersteiner M (2011) Global land-use implications of first and second generation biofuel targets. Energ Policy. doi:10.1016/j.enpol.2010.03.030

Heijungs R, Suh S (2002) The computational structure of life cycle assessment. Kluwer, Dordrecht

Hellweg S, Fischer U, Hofstetter TB, Hungerbühler K (2005) Site-dependent fate assessment in LCA: transport of heavy metals in soil. J Cleaner Prod 13:341–361

Hellweg S, Demou E, Bruzzi R, Meijer A, Rosenbaum RK, Huijbregts MA, McKone TE (2009) Integrating human indoor air pollutant exposure within life cycle impact assessment. Environ Sci Technol 43:1670–1679

Hertel TW, Golub AA, Jones AD, O'Hare M, Plevin RJ, Kammen DM (2010) Effects of US maize ethanol on global land use and greenhouse gas emissions: estimating market-mediated responses. Bioscience 60:223–231

Hertwich E (2009) A concise guide to the biofuels environmental conundrum. J Ind Ecol 13:990–991

Hertwich EG (2013) Addressing biogenic greenhouse gas emissions from hydropower in LCA. Environ Sci Technol 47:9604–9611

Hertwich EG, McKone TE, Pease WS (2000) A systematic uncertainty analysis of an evaluative fate and exposure model. Risk Anal 20:439–454

Highwood EJ, Kinnersly R (2006) When smoke gets in your eyes. The multiple impacts of atmospheric black carbon on climate, air quality and health. Environ Int 32:560–566

Hischier R, Walser T (2012) Life cycle assessment of engineered nanomaterials: state of the art and strategies to overcome existing gaps. Sci Total Environ 425:271–282

Hoglmeier K, Weber-Blaschke G, Richter K (2014) Utilization of recovered wood in cascades versus utilization of primary wood- a comparison with life cycle assessment using system expansion. Int J Life Cycle Assess. doi:10.1007/s11367-014-0774-6

Hong J, Shaked S, Rosenbaum RK, Jolliet O (2010) Analytical uncertainty propagation in life cycle inventory and impact assessment: application to an automobile front panel. Int J Life Cycle Assess 15:499–510

Hospido A, Davis J, Berlin J, Sonesson U (2010) A review of methodological issues affecting LCA of novel food products. Int J Life Cycle Assess 15:44–52

Huang Y, Bird R, Heidrich O (2009) Development of the life cycle assessment tool for construction and maintenance of asphalt pavements. J Cleaner Prod 17:283–296

Huijbregts MAJ, Thissen UMJ, Guinee JB, Jager T, Kalf D, van der Meent D, Ragas AMJ, Wegener Sleeswijk A, Reijnders L (2000) Priority assessment of toxic substances in life cycle assessment. Part I: calculation of toxicity potentials for 181 substances with the nested multi-media fate exposure and effects model USES-LCA. Chemosphere 41:541–573

Huijbregts MAJ, Norris G, Bretz K, Giroth A, Maurice B, von Bahr B, Weidema B, de Beaufort ASH (2001) Framework for modeling data uncertainty in life cycle inventories. Int J Life Cycle Assess 6:127–132

Huijbregts MAJ, Gilijamse W, Ragas AMJ, Reijders L (2003) Evaluating uncertainty in environmental life cycle assessment. A case study comparing two insulation options for a Dutch one family dwelling. Environ Sci Technol 37:2600–2608

Huijbregts MAJ, Rombouts LJA, Hellweg S, Frischknecht R, Hendriks J, van de Meent D, Ragas AJM, Reijnders L, Struijs J (2006) Is cumulative fossil energy demand a useful indicator for the environmental performance of products? Environ Sci Technol 40:641–648

Huijbregts MAJ, Hellweg S, Hendriks HWM, Hungerbühler K, Hendriks AJ (2010) Cumulative energy demand as predictor for the environmental burden of commodity production. Environ Sci Technol 44:2189–2196

Ingraffea AR, Wells MT, Santoro RL, Shonkoff SBC (2014) Assessment and risk analysis of casing and cement impairment in oil and gas wells in Pennsylvania, 2000–2012. Proc Natl Acad Sci U S A 111:10955–10960

IPPC Working Group I (2013) Climate change 2013: the physical science basis. Cambridge University Press, Cambridge, UK/New York

Iribarren D, Hospido A, Moreira MT, Feijoo G (2010) Carbon footprint of canned mussels from a business-to-consumer approach. A starting point for mussel processors and policy makers. Environ Sci Policy. doi:10.1016/j.envsci.2010.05.003

Jansen B, Thollier K (2006) Bottom-up life cycle assessment of product consumption in Belgium. J Ind Ecol 10(3):41–55

Jaramillo P, Samaras C, Wakeley H, Meisterling K (2009) Greenhouse gas implications of using coal for transportation: life cycle assessment of coal-to-liquids, plug-in hybrids, and hydrogen pathways. Energ Policy 37:2689–2695

Johnson RW (2004) The effect of blowing agent choice on energy use and global warming impact of refrigerator. Int J Refrig 27:794–799

Johnson E (2008) Disagreement over carbon footprints: a comparison of electric and LPG forklifts. Energ Policy 36:1569–1573

Jorquera O, Kiperstock A, Sales EA, Embirucu M, Ghirardi ML (2010) Comparative energy life cycle-analyses of microalgal biomass production in open ponds and photobioreactors. Bioresour Technol 101:1406–1413

Jury C, Benetto E, Koster D, Schmitt B, Welfring J (2010) Life cycle assessment of biogas production by monofermentation of energy crops and injection into the natural gas grid. Biomass Bioenergy 34:54–66

Kakudate K, Kajikawa Y, Adachi Y, Suzuki T (2002) Calculation model of CO_2 emissions for Japanese passenger cars. Int J Life Cycle Assess 7:85–93

Kendall A, Chang B, Sharpe B (2009) Accounting for time-dependent effects in biofuel life cycle greenhouse gas emissions calculations. Environ Sci Technol 43:7142–7147

Khoo HH, Tan RBH, Chng KWL (2010) Environmental impacts of conventional plastic and bio-based carrier bags. Int J Life Cycle Assess 15:284–293

Kim S, Dale BE (2008) Energy and greenhouse gas profiles of polyhydroxybutyrates derived from corn grain: a life cycle perspective. Environ Sci Technol 42:7690–7695

Kleijn R, van der Voet E, Udo de Haes HA (2008) The need for combining IEA and IE tools: the potential effects of a global ban on PVC on climate change. Ecol Econ 65:266–281

Kloverpris JH, Baltzer K, Nielsen PH (2010) Life cycle inventory modeling of land use induced by crop consumption. Part 2: example of wheat consumption in Brazil, China, Denmark and the USA. Int J Life Cycle Assess 15:90–103

Koellner T, de Baan L (2013) UNEP-SETAC guideline on global land use impact assessment on biodiversity and ecosystem services in LCA. Int J Life Cycl Assess 18:1188–1202

Kofoworola OF, Gheewala SH (2008) Environmental life cycle assessment of a commercial office building in Thailand. Int J Life Cycle Assess 13:498–511

Kurdikar D, Fourner L, Slate SC, Pater M, Gruys KJ, Gerngross TU, Coulon R (2000) Greenhouse gas profile of a plastic material from a genetically modified plant. J Ind Ecol 4(3):107–122

Kushnir D, Sanden BA (2008) Energy requirements of carbon nanoparticle production. J Ind Ecol 12:360–375

Lankey RL, McMichael FC (2000) Life-cycle methods for comparing primary and rechargeable batteries. Environ Sci Technol 34:2299–2304

Laurent A, Olsen SI, Hauschild MZ (2010) Carbon footprint as environmental performance indicator for the manufacturing industry. CIRP Ann Manuf Technol 59:37–40

Lave L, McLean H, Hendrickson C, Lankey R (2000) Life-cycle analysis of alternative fuel/propulsion technologies. Environ Sci Technol 34:3598–3605

Lee DS, Pitari G, Grewe V, Gierens K, Penner JE, Petzold A, Prather MJ, Schumann U, Bais A, Berntsen T, Iachetti D, Lim LL, Sausen R (2010a) Transport impacts on atmosphere and climate: aviation. Atmos Environ 44:4678–4734

Lee J, An S, Cha K, Hur T (2010b) Life cycle environmental and economic analyses of a hydrogen station with wind energy. Int J Hydrogen Energy 35:2213–2225

Lenzen M (2008) Double counting in life cycle calculations. J Ind Ecol 12:583–599

Lifset R, Anes R (2009) The indirect effects of industrial ecology. J Ind Ecol 13:347–349

Lund H, Mathiesen BV, Christensen P, Schmidt JH (2010) Energy system analysis of marginal electricity supply in consequential LCA. Int J Life Cycle Assess 15:260–271

Luz SM, Caldeira-Pires A, Ferrao PMC (2010) Environmental benefits of substituting talc by sugarcane bagasse fibers as reinforcement in polypropylene composites: ecodesign and LCA strategy for automotive components. Resour Conserv Recycl 54:1135–1141

Markandya A, Armstrong BG, Hales S, Chiabai A, Criqui P, Mima S, Tonne C, Wilkinson P (2009) Public health benefits of strategies to reduce greenhouse-gas emissions: low carbon electricity generation. Lancet 374:2006–2015

Martinez E, Sanz F, Pellegrini S, Jimenez E, Blanco J (2009) Life cycle assessment of a multi-megawatt wind turbine. Renew Energy 34:667–673

McConnell JR, Edwards R, Kok GL, Flanner MG, Zender CS, Salzman ES, Banta JR, Pasteris DR, Carter MM, Kahl JDW (2007) 20th-century industrial black carbon emissions altered Arctic climate forcing. Science 317:1381–1384

Meyer DE, Curran MA, Gonzalez MA (2009) An examination of existing data for the industrial manufacture and use of nanocomponents and their role in life cycle impact of nanoproducts. Environ Sci Technol 43:1256–1263

Ming J, Xiao C, Cachier H, Qin D, Qin X, Li Z, Pu J (2009) Black carbon (BC) in the snow and glaciers in west China and its potential effects on albedo. Atmos Res 92:114–123

Mohr N, Meijer A, Huijbregts MAJ, Reijnders L (2009) Environmental impact of thin-film GaInP/GaAs and multicrystalline silicon solar modules produces with solar energy. Int J Life Cycle Assess 14:225–235

Munoz I, Campra F, Fernandez-Alba AR (2010) Including CO_2-emission equivalence of changes in land surface albedo in life cycle assessment. Methodology and case study on greenhouse agriculture. Int J Life Cycle Assess 15:672–681

Myrhe G, Shindell D, Bréon F, Fuglestvedt J, Huang J, Koch D, Lamarque J, Lee D, Mendoza B, Nakajima T, Robock A, Stephens G, Takemura T, Zhang H (2013) Anthropogenic and natural radiative forcing. In: Climate change 2013: the physical science basis. Contribution of Working Group I to the fifth assessment report on the Intergovernmental Panel on Climate Change. Cambridge University Press, Cambridge, United Kingdom and New York

Nakamura S, Kondo Y (2006) Hybrid LCC of appliances with different energy efficiencies. Int J Life Cycle Assess 11:305–314
Nakinawa C, Graedel TE (2002) Life cycle and matrix analyses for re-refined oil in Japan. Int J Life Cycle Assess 7:95–102
Narita N, Nakahara Y, Morimoto M, Aoki R, Suda S (2004) Current LCA database development in Japan – results of the LCA project. Int J Life Cycle Assess 9:355–359
Nishioka Y, Levy JI, Norris GA (2006) Integrating air pollution, climate change, and economics in a risk based life-cycle analysis. A case study of residential insulation. J Hum Ecol Risk Assess 12:552–571
Nugent D, Sovakool BK (2014) Assessing the lifecycle greenhouse gas emissions from solar PV and wind energy: a critical meta-survey. Energy Policy 65:229–244
Ortiz O, Castells F, Sonnemann G (2010) Operational energy in the life cycle of residential dwellings: the experience of Spain and Colombia. Appl Energy 87:673–680
Perez-Ramirez J, Kapteijn F, Schöffel K, Moulijn JA (2003) Formation and control of N_2O in nitric acid production. Where do we stand today? Appl Catal B Environ 44:117–151
Petron G, Frost G, Miller BR, Hirsch AI (2012) Hydrocarbon emissions characterization in the Colorado Front Range: a pilot study. J Geophys Res 117, D04304
Pottimg J, Hauschild M (2005) Background for spatial differentiation in LCA impact assessment – the EDIP2003 methodology. Danish Ministry of the Environment. www.mst.dk/Udgiv/publications/2005/87-7614-581-6/pdf
Rebitzer G, Ekvall T, Frischknecht R, Hunkeler D, Norris G, Rydberg T, Suh S, Schmidt W, Pennington DW, Weidema B (2004) Life cycle assessment. Part I: framework, goal and scope definition, inventory analysis and applications. Environ Int 30:701–720
Rehbitzer G, Buxmann K (2005) The role and implementation of LCA within life cycle management at Alcan. J Cleaner Prod 13:1327–1335
Rehr AP, Small MJ, Matthews HS, Hendrickson CT (2010) Economic sources and spatial distribution of airborne chromium risks in the US. Environ Sci Technol 44:2131–2137
Reijnders L (2006) Is increased energy utilization linked to greater cultural complexity? Energy utilization by Australian aboriginals and traditional swidden agriculturalists. Environ Sci 3:207–220
Reijnders L (2009a) Fuels for the future. J Integr Environ Sci 6:279–294
Reijnders L (2009b) Are forestation, biochar and landfilled biomass adequate offsets for the climate effect of burning fossil fuels. Energy Policy 37:2839–2841
Reijnders L (2010) Transport biofuel yields from food and lignocellulosic C_4 crops. Biomass Bioenergy 34:152–155
Reijnders L (2013) Lipid-based liquid biofuels from autotrophic microalgae: energetic and environmental performance. WIREs Energy Environ 2:73–85
Reijnders L, Huijbregts MAJ (2003) Choices in calculating life cycle emissions of carbon containing gases associated with forest derived biofuels. J Cleaner Prod 11:527–532
Reijnders L, Huijbregts MAJ (2009) Biofuels for road transport. A seed to wheel perspective. Springer, London
Reijnders L, Soret S (2003) Quantification of the environmental impact of different dietary protein choices. Am J Clin Nutr 78:664S–668S
Röös E, Sundberg C, Hansson P (2010) Uncertainties in the carbon footprint of food products: a case study on table potatoes. Int J Life Cycle Assess 15:478–488
Rossello-Batle B, Moia A, Cladera A, Martinez V (2010) The energy use, CO_2 emissions and waste throughout the life cycle of a sample of hotels in the Balearic Islands. Energy Build 42:547–558
Rydh CJ, Karlström M (2002) Life cycle inventory of recycling portable nickel-cadmium batteries. Resour Conserv Recycl 34:289–309
Sanden B, Kalström M (2007) Positive and negative feedback in consequential life cycle assessment. J Cleaner Prod 15:1469–1481

Saner D, Juraske R, Kubert M, Blum P, Hellweg S, Bayer P (2010) Is it only CO_2 that matters? A life cycle perspective on shallow geothermal systems. Renewable Sustainable Energy Rev 14:1798–1813
Sann TE, Palanisamy K, Nazrain M, Ani FN (2006) Study of carbon dioxide emission during combustion of biodiesel. In: International conference on energy and environment 2006, Kajang, pp 65–70
Sathre R, O'Connor JO (2010) Meta-analysis of greenhouse gas displacement factors of wood product substitution. Environ Sci Policy 13:104–114
Sayagh S, Ventura A, Hoang T, Francois D, Jullien A (2009) Sensitivity of the LCA allocation procedure for BFS recycled into pavement structures. Resour Conserv Recycl 54:348–358
Schipper L, Grubb M (2000) On the rebound? Feedback between energy intensities and energy uses in IEA countries. Energy Policy 28:367–388
Schmidt H (2009) Carbon footprinting, labelling and life cycle assessment. Int J Life Cycle Assess 14:S6–S9
Schöpp W, Potting J, Hauschild M, Blok K (1998) Site-dependent life cycle impact assessment of acidification. J Ind Ecol 8(2):63–87
Searchinger T, Heimlich R, Houghton RA, Dong F, Elobeid A, Fabiosa J, Tokgoz S, Hayes D, Yu T (2008) Use of US croplands for biofuels increases greenhouse gases through emissions from land use change. Science 319:1238–1240
Sekiya A, Omamoto S (2010) Evaluation of carbon dioxide equivalent values for greenhouse gases: CEWN as a new indicator replacing GWP. J Fluorine Chem 131:384–386
Song J, Lee K (2010) Development of a low carbon product design system based on embedded GHG emissions. Resour Conserv Recycl 54:547–556
Spatari S, Bagley DM, McLean HL (2010) Life cycle evaluation of emerging lignocellulosic ethanol conversion technologies. Bioresour Technol 101:654–667
Spielman M, Althaus H (2007) Can a prolonged use of a passenger car reduce environmental burdens? Life cycle analysis of Swiss passenger cars. J Cleaner Prod 15:1122–1134
Stern N (2006) Stern review on the economics of climate change. HM Treasury, London. http://apo.org.au/
Tabone MD, Gregg JJ, Beckman EJ, Landis AE (2010) Sustainability metrics: life cycle assessment and green design in polymers. Environ Sci Technol 44:82-64–82-69
Thiesen J, Christensen TS, Kristensen TC, Andersen RD, Brunoe B, Gregersen TK, Thrane M, Weidema BP (2008) Rebound effect of price differences. Int J Life Cycle Assess 13:104–114
Tukker A, Eder P, Duh S (2006) Environmental impact of products. J Ind Ecol 10(3):183–198
Upham P, Dendier L, Bleda M (2010) Carbon labeling of grocery products: public perceptions and potential emissions reductions. J Cleaner Prod 19:348–355
van der Velden NM, Patel MK, Vogtländer JG (2014) LCA benchmarking study on textiles made of cotton, polyester, nylon, acryl or elastane. Int J Life Cycle Assess 19:331–356
Verones F, Pfister S, Hellweg S (2013) Quantifying area changes of internationally important wetlands due to water consumption in LCA. Environ Sci Technol 47:9799–9807
Walmsley JD, Godbold DL (2010) Stump harvesting for bioenergy – a review of the environmental impacts. Forestry 83:17–38
Weber CL, Matthews HS (2008) Quantifying the global and distributional aspects of the American household carbon footprint. Ecol Econ 66:379–391
Weber CL, Jaramillo P, Marriott J, Samaras C (2010) Life cycle assessment and grid electricity; what do we know and what can we know. Environ Sci Technol 44:1895–1901
Weiss M, Haufe J, Carus M, Brandao M, Bringezu S, Hermann B, Patel MK (2012) A review of environmental impacts of biobased materials. J Ind Ecol 16:S169–S181
Wernet G, Conradt S, Isenring HP, Jimenez-Gonzales C, Hungerbühler K (2010) Life cycle assessment of fine chemical production: a case study of pharmaceutical synthesis. Int J Life Cycle Assess 15:294–303
Weston RE (1996) Possible greenhouse effects of tetrafluoromethane and carbon dioxide emitted from aluminum production. Atmos Environ 30:2901–2910

Williams ED, Weber CL, Hawkins TR (2009) Hybrid framework for managing uncertainty in life cycle inventories. J Ind Ecol 13:928–944

Wu P, Xia B, Zhao X (2014) The importance of use and end-of -life phases to the life cycle greenhouse gas (GHG) emissions of concrete – a review. Renew Sustain Energy Rev 37:360–369

Yung WKC, Chan HK, Choi ACK, Yue TM, Mahzar MI (2008) An environmental assessment framework with respect to the requirements of energy using products directive. Proc Inst Mech Eng 222B:643–651

Zhang Y, McKechnie J, Cormier D, Lyng R, Mabee W, Ogino A, Maclean HR (2010) Life cycle emissions and cost of producing electricity from coal, natural gas and wood pellets in Ontario, Canada. Environ Sci Technol 44:538–544

Some Economics of International Climate Policy

Karen Pittel, Dirk Rübbelke, Martin Altemeyer-Bartscher, and Sebastian Otte

Contents

K. Pittel (✉)
Ifo Institute – Leibniz Institute for Economic Research and University of Munich, Munich, Germany
e-mail: pittel@ifo.de

D. Rübbelke • S. Otte
Technische Universität Bergakademie Freiberg, Freiberg, Germany
e-mail: dirk.ruebbelke@vwl.tu-freiberg.de; sebastian.otte@vwl.tu-freiberg.de

M. Altemeyer-Bartscher
Faculty of Law and Economics, Martin-Luther University Halle-Wittenberg, Halle Institute for Economic Research, Halle (Saale), Germany
e-mail: martin.altemeyer-bartscher@iwh-halle.de; martin.altemeyer-bartscher@wirtschaft.tu-chemnitz.de

W.-Y. Chen et al. (eds.), *Handbook of Climate Change Mitigation and Adaptation*,
DOI 10.1007/978-3-319-14409-2_4

Abstract

This chapter discusses economic aspects of international efforts to curb the global warming threat. The first commitment period of the Kyoto Protocol expired in 2012, which has until then been the dominant climate agreement although competing – or allegedly complement – international climate protection schemes like the Asia-Pacific Partnership on Clean Development and Climate also existed. While as of 5 April 2011, the Asia-Pacific Partnership on Clean Development and Climate (APP) formally concluded its joint work, tangible preparations for a second commitment period of the Kyoto Protocol started at the climate conference in Montreal (comprising MOP and COP-11) in 2005. In Montreal, a new working group was established for the discussion of future commitments (after 2012). And at the COP-18 in Doha in 2012, an agreement on a second commitment period of the Kyoto Protocol for 2013–2020 could be reached.

In this chapter, we describe the main features of Kyoto and APP schemes and their failure to establish an efficient global climate protection regime, and we elaborate on the disincentives for countries to commit to efficient climate protection efforts in an international agreement. In doing so we also take into account the growing importance of adaptation to climate change in the international climate policy arena.

The situation in international negotiations on climate change mitigation faced by national governments is depicted in game theoretic settings, and private ancillary benefits of climate policy are identified to raise the likelihood for countries joining an international agreement. Yet, it remains quite disputable to which extent ancillary benefits can be an impetus for more action in international climate policy. Finally, after dedicating a large part of the chapter to agreements, like the Kyoto Protocol, stipulating abatement quantities, alternative schemes are presented which were coined "price ducks" since they influence the effective prices of climate protection. By manipulating prices, e.g., via an international carbon tax, incentives are generated for producing higher climate protection levels. Recently, the so-called matching schemes influencing effective prices of climate protection raised much attention in the scientific literature. Such schemes may attenuate free- or easy-rider incentives in international climate policy and may even induce a globally efficient climate protection level.

Introduction

Global environmental threats have gained much attention in the political as well as the scientific arena during recent decades. Among the most prominent examples of such environmental problems are climate change, the destruction of the ozone layer, the pollution of international waters, and the loss of biodiversity. These problems are likely to have an important impact on the quality of life on earth: "Traditionally, the next generation's well-being improves compared with that of preceding generations

as knowledge, capital, and other assets are passed down. If environmental deterioration continues to destroy the earth's assets, this tradition will end" (Sandler 1997, Preface). By the time the Brundtland Commission presented its report "Our Common Future" (WCED 1987) at the latest, the necessity to stop international environmental deterioration had become largely undisputed. Nevertheless, the way to achieve this is subject to an extremely controversial discussion.

A main cause of this dispute lies in the fact that, in contrast to local environmental problems, international challenges cannot be counteracted by regulations invented by a coercive central authority. Because of this lack of a coercive authority that can force sovereign nations to take protective actions, international environmental policy crucially depends on the decisions made by the individual countries. These decisions are unlikely to produce a globally efficient level of protection efforts, because countries have incentives to take an easy ride with respect to the protection of global commons like the atmospheric system.

International environmental problems have been regularly addressed by international negotiations aiming at agreements on protection efforts. With respect to climate change, the central global challenge to be addressed in this book chapter, the Framework Convention on Climate Change constituted an important a landmark in this respect. It was ultimately signed by more than 150 countries at the Rio "Earth Summit" in 1992. However, the convention only stipulates strategies for protecting the climate, as well as general principles; it does not specify targets for greenhouse gas emission reductions. The following meetings of the Conference of Parties (COP) to the Framework Convention on Climate Change were assigned to make decisions on specific obligations for climate protection.

Outstanding was the third meeting in Kyoto 1997 where the so-called "Kyoto Protocol" was agreed upon. The protocol stipulates that the parties included in Annex I to the Framework Convention (industrialized countries and European economies in transition) have to reduce their greenhouse gas emission levels within a specified time frame. At the COP-13 in Bali in 2007, a 2-year process was launched in order to already promote a post-Kyoto agreement (Gupta 2010).

As Edenhofer et al. (2010) point out: "achieving deep emission reductions requires a comprehensive global effort which includes both a complete change in the energy supply of industrialized countries and the establishment of low-carbon systems in developing countries and emerging markets – in essence, nothing short of a full-scale transformation towards a carbon-free economic system." Hence, international negotiations pursuing an efficient global agreement on climate change are an immense challenge.

This book chapter will describe past international efforts to curb the global warming threat, and it will also outline why the past efforts have failed to yield an efficient global climate protection scheme. Finally, "price ducks" are presented which are international policy regimes targeting the rise in international climate protection efforts by manipulating the effective prices of such efforts. These schemes represent an interesting alternative to "quantity ducks" like the Kyoto scheme which primarily focus on the agreement of greenhouse gas abatement quantities.

This chapter is organized as follows. In section "International Climate Policy," it provides an overview of past international agreements on climate change. It does not consider national agreements like the British Climate Change Agreements and largely disregards other national instruments like the British emission trading scheme, although it was launched even before the European Emissions Trading Scheme started. For a discussion of the British Climate Change Agreements, see, e.g., Glachant and de Muizon (2006) and Dijkstra and Rübbelke (2013), and for an analysis of the UK Emissions Trading Scheme, see, e.g., Smith and Swierzbinski (2007). Policies like carbon taxes, matching grants, or side payments are only discussed in an international context. In section "Why Efficient Climate Protection is so Difficult to Achieve," the public good properties of climate protection are outlined, and the conditions and interplays which lead to a suboptimal low level of climate protection efforts on a global scale are explained. Due to these conditions and interplays and the lack of a global coercive authority, the attainment of an efficient global agreement on climate change is a very difficult task. Alternative negotiation schemes, which differ from the Kyoto concept of negotiating emission-reduction quantities, are described. These schemes, the so-called price ducks, draw on manipulating prices in such a way that it becomes rational for the individual countries to raise their climate protection efforts up to a globally efficient level. Section "Future Directions" concludes.

International Climate Policy

Global Challenges

After the UN Conference on the Human Environment took place in Stockholm in 1972, research gradually found alarming facts about the development of the earth's state. One among the several hints of the deterioration of the earth's condition was given by the chemists Mario Molina and Sherwood Rowland from the University of California who published a scientific paper (Molina and Rowland 1974) in 1974 which stresses that the emission of chlorofluorocarbons (CFCs) might deplete the stratospheric ozone layer. CFCs are very stable artificially generated gases whose production is rather inexpensive. They were used as, e.g., propellants in spray cans, refrigerants in air-conditioning systems, and solvents in cleaning processes. Stratospheric ozone, which is indeed destroyed by CFCs, absorbs a large part of hostile ultraviolet radiation of the sun and thereby renders possible human life on earth. The depletion of stratospheric ozone causes the so-called ozone holes which are areas in the stratosphere where the concentration of ozone declines below 200 Dobson units and where damaging ultraviolet radiation can advance to a larger extent toward the earth's surface. Among the negative impacts of the penetration of short-wave ultraviolet radiation is the more frequent occurrence of skin cancer and eye impairments.

The problem of the ozone layer depletion was already addressed in 1987, when the Montreal Protocol was opened for signature. In the Montreal Protocol, which

entered into force in 1989, and its amendments, reductions and bans of CFCs were agreed upon on an international level. These international environmental agreements have been the first in whose negotiation process multinational companies (like the globally largest producer of CFCs in 1988, i.e., Du Pont) have been involved (Smith 1998, p. 557). The international efforts to curb CFC emissions were complemented by a reinforcement of the CFC-producing companies' efforts in researching and developing environmentally friendly substitutes for CFCs.

While the problem of ozone layer depletion is largely regarded to be solved, there are many other international environmental problems which are still threatening the earth. These threats have been addressed by the United Nations Conference on Environment and Development (UNCED) which took place in Rio de Janeiro, Brazil, on June 2–14, 1992. Five major agreements are associated with this conference: (1) Rio Declaration on Environment and Development, (2) Agenda 21, (3) Statement of Principles for the Sustainable Management of Forests, (4) United Nations Convention on Biological Diversity, and (5) United Nations Framework Convention on Climate Change.

The Rio Declaration on Environment and Development contains a set of 27 legally nonbinding principles which are designed to commit governments to ensure environmental protection and responsible development. The Agenda 21 is an international plan of action to sustainable development which outlines key policies for achieving sustainable development that meets the needs of the poor and recognizes the limits of development to meet global needs. The Statement of Forest Principles is the first global agreement concerning sustainability of forest management, and the United Nations Convention on Biological Diversity stipulates the aims of the conservation of biological diversity, the sustainable use of its components, and the fair and equitable sharing of the benefits arising out of the utilization of genetic resources.

Since the United Nations Framework Convention on Climate Change (UNFCCC) is the document of the UNCED which is most important for the analysis in this chapter, the UNFCCC and its offspring agreement, i.e., the Kyoto Protocol, will be discussed in more detail.

The UNFCC and the Kyoto Protocol

The United Nations Framework Convention on Climate Change stipulates general strategies for protecting the climate as well as general principles, but it does not specify concrete targets for greenhouse gas emission reductions. The following meetings of the Conference of Parties to the Framework Convention on Climate Change were assigned to make decisions on specific obligations for climate protection. At the third meeting in Kyoto 1997, the so-called "Kyoto Protocol" was agreed upon. The protocol stipulates that the parties included in Annex I to the Framework Convention (industrialized countries and European economies in transition) have to reduce their greenhouse gas emission levels within a specified time frame. The EU-15, for example, has agreed to cut its emissions by 8 % between 1990 and

2008–12, but reduction obligations vary among individual EU countries as well as among Annex-I parties in general (as stipulated in Annex B to the protocol). The EU-15 has agreed to share the burden of its overall Kyoto target as depicted in Fig. 1 (the so-called burden sharing agreement).

If the sub-targets of the individual countries are compared with the GDP per capita in these countries in 1998 (see Fig. 2), when the burden sharing was negotiated, it is conspicuous that the poorest countries (Spain, Portugal, and Greece) have

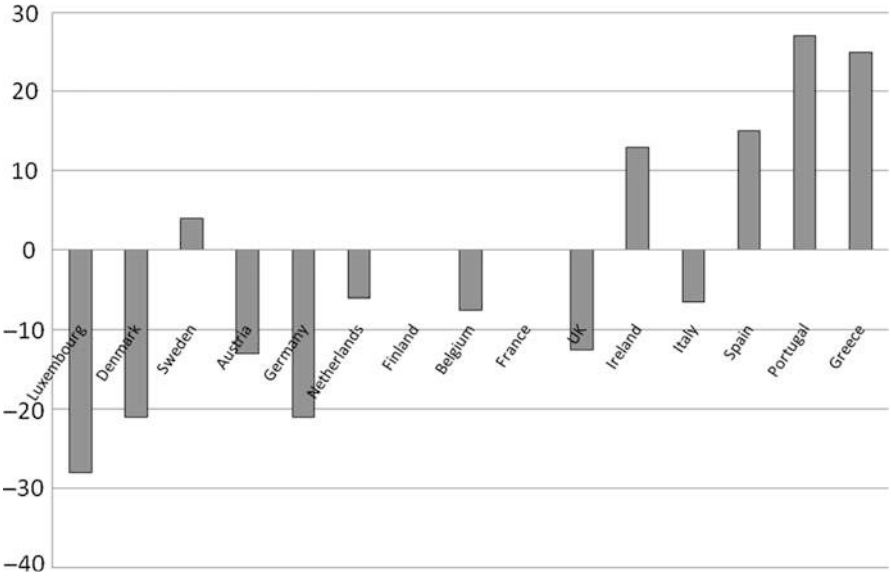

Fig. 1 National commitments under the EU burden sharing agreement in percentage change of GHG emissions between 1990 and 2008–12

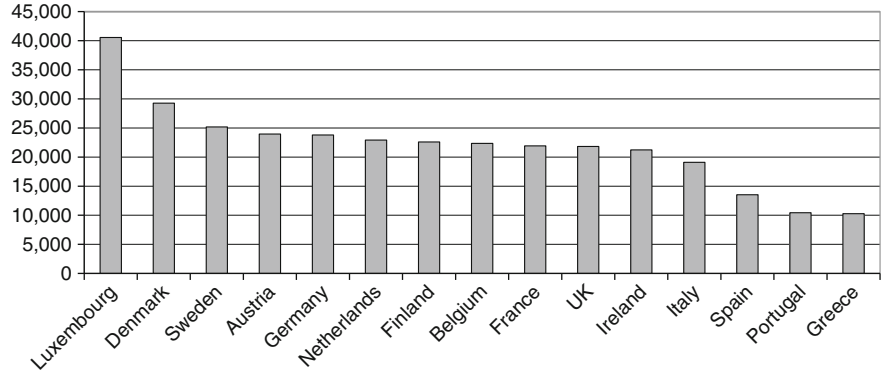

Fig. 2 GDP per capita in the EU-15 in 1998 (data from Eurostat 2006) in Euro

the largest tolerance for emission changes. And indeed the political decision about reduction loads within the EU-15 was made taking into account different country-specific characteristics among which was the economic development of the individual EU countries: "The −8 % target for the EU as a whole has been shared out amongst Member States so as to allow for different economic development patterns" (EC 2000, p. 2). Dessai and Michaelowa (2001), p. 329, point out regarding the climate policy process at the EU level that it tends to prefer less-stringent emission targets for countries *with lower per capita income*.

The aim was for the overall emissions of the Annex-I parties to be at least 5.2 % below the 1990 levels in the commitment period 2008–2012. However, for the protocol to come into effect, at least 55 parties had to sign it. Among these, there had to be Annex-I countries that together account for at least 55 % of the 1990 CO_2 emissions of the whole group of Annex-I parties. At the sixth session of the Conference of Parties in Bonn 2001, most industrialized countries, not the USA though, agreed upon the ratification of an undermined version of the protocol which then entered into force on 16 February 2005.

The Kyoto Protocol limits emissions of the greenhouse gases carbon dioxide (CO_2), methane (CH_4), nitrous oxide (N_2O), hydrofluorocarbons (HFCs), perfluorocarbons (PFCs), and sulfur hexafluoride (SF6). Of these gases, CO_2 is the most important contributor to climate change. Estimates of its contribution to the anthropogenic greenhouse effect vary, however, widely, predominantly in the range of 50–80 %. Since CO_2 represents the most important greenhouse gas, environmental policies that induce reductions of CO_2 emissions and concentrations are attractive means for mitigating climate change. Therefore, the main focus in this chapter will be on these policies. Regarding the properties of greenhouse gases (illustrated for the examples of carbon dioxide, methane, and nitrous oxides) and the determinants of their importance to climate change, see the short overview in Box 1.

Anthropogenic CO_2 emissions are – except for emissions by deforestation and to a lower extent by cement production – almost entirely generated by the burning of fossil fuels. With it, many other pollutants like sulfur dioxide (SO_2) and nitrogen oxides (NO_X) are emitted. In contrast to the local/regional pollutants SO_2 and NO_2, the emissions of CO_2 can still not be removed from post-combustion exhaust in a cost-effective way. Thus major remaining reasonable approaches to mitigate CO_2 concentrations are the reduction of the combustion of substances or the shift to fuels or energies with lower CO_2 content. Sequestration of carbon is another option. As Lal (2004) explains, soil carbon sequestration is not only an option for mitigating climate change, but it is also a strategy to achieve food security through improvement in soil quality.

Box 1: Greenhouse Gases and their Contribution to Climate Change

The gas mainly responsible for the anthropogenic greenhouse effect is CO_2. Other pollutants contributing to the anthropogenic greenhouse effect are

(continued)

Box 1: (continued)
especially CH_4, N_2O, and CFCs (Enquete-Kommission 1995, pp. 35–75; Houghton 1997, p. 22). The contribution of CFCs to the anthropogenic greenhouse effect will decline in the future, since their reduction and phasing out were agreed on in the Montreal Protocol and its amendments. Tropospheric ozone (O_3) also plays an important role in aggravating global warming (Enquete-Kommission 1990, p. 216, 1995, pp. 33–36), yet its importance is difficult to quantify because of the strong variability in its concentration as a consequence of its short lifetime (Bauer 1993, pp. 23–24). Dickinson and Cicerone (1986, p. 122), explain that the ozone "is of considerable interest because of its important roles, its complex behavior, and its susceptibility to human-induced global change."

The importance of the respective greenhouse gases, i.e., their contribution to the anthropogenic greenhouse effect, depends on the following three "properties":

Global Warming Potential

The IPCC (1996, p. 21) defines the global warming potential (GWP) "as the cumulative radiative forcing between the present and some chosen time horizon caused by a unit mass of gas emitted now, expressed relative to that for some reference gas." The radiative forcing is defined as "the change in average net radiation at the top of the troposphere . . . which occurs because of a change in the concentration of a greenhouse gas" (Houghton 1997, pp. 22–23). With CO_2 representing the reference gas and for a time horizon of 100 years, the GWPs of CH_4 and N_2O are 21 and 310 respectively (IPCC 1996, p. 22); of course, from the definition it follows that the GWP of CO_2 equals unity. Yet, as Smith and Wigley (2000) point out, global warming potentials are accurate only for short time horizons.

Concentration in the Atmosphere

The atmospheric concentration of CO_2 has grown significantly from about 280 ppmv in preindustrial times (about 1,750 AD) to 391 ppmv in 2011 (IPCC 2013b); ppmv stands for parts per million by volume. The IPCC (2013b) reports a CH_4 concentration of 1.803 ppmv and a N_2O concentration of 0.324 ppmv in 2011. Thus, the preindustrial concentrations of CO_2, CH_4, and N_2O are already exceeded by about 40 %, 150 %, and 20 % (IPCC 2013b).

Lifetime

CO_2 prevails for 50–200 years in the atmosphere, CH_4 only for 12 ± 3 years, and N_2O for about 120 years (IPCC 1996, pp. 15–19). Thus the importance of the single greenhouse gases varies depending on the time horizon of

(continued)

Box 1: (continued)
investigations. Short horizons tend to understate the importance of greenhouse gases which prevail for a long time in the atmosphere.

Since CO_2 represents the most important anthropogenic greenhouse gas,[1] environmental policies that induce reductions of CO_2 emissions and concentrations are attractive means for mitigating climate change. Therefore, the main focus in this chapter will be on these policies. Anthropogenic CO_2 emissions are – except for emissions by deforestation and to a lower extent by cement production – almost entirely generated by the burning of fossil fuels. With it, many other pollutants like sulfur dioxide (SO_2) and nitrogen oxides (NO_X) are emitted. In contrast to the local/regional pollutants SO_2 and NO_2, the emissions of CO_2 can still not be removed from post-combustion exhaust in a cost-effective way. Thus major remaining reasonable approaches to mitigate CO_2 concentrations are the reduction of the combustion of substances or the shift to fuels or energies with lower CO_2 content. Sequestration of carbon is another option. As Lal (2004) explains, soil carbon sequestration is not only an option for mitigating climate change, but it is also a strategy to achieve food security through improvement in soil quality.

Assessment of the Kyoto Protocol/UNFCCC Scheme and Flexible Mechanisms

There have been intense disputes about whether the Kyoto Protocol leads a good way to protect the world's climate. Nordhaus (1998, p. 1) criticizes the Kyoto Protocol: "Given the lack of political support, the Kyoto Protocol is a dead duck. Given its inefficiency, it probably deserves to be a dead duck. We need to go back to the duck drawing board."

The Kyoto Protocol does not prescribe greenhouse gas (GHG) reductions to developing countries, and this fact is employed by opponents to the Kyoto Protocol to stress its inefficiency, since GHG emission mitigation options can regularly be exploited more cheaply in the developing world. The USA which refused to join the Protocol demands participation of developing countries in international GHG emission-reduction efforts. This demand is rejected by the developing world because of the economic burden which such efforts would imply. Furthermore, developing countries argue that the industrialized world is mainly responsible for the current dimension of the global warming threat. "North America and Europe have produced around 70 % of CO_2 emissions from energy production since 1850, while developing countries – non-Annex 1 parties under the Kyoto Protocol – account for less than

[1]Water vapor is of course the overall most important greenhouse gas, yet anthropogenic emissions of water vapor contribute very little to climate change (see IPCC 2013a, Chap. 8). For this reason, we do not discuss the role of water vapor in detail but rather refer the interested reader to IPCC (2013a) and references within.

one quarter of cumulative emissions" (Stern 2007, Chap. 7). Therefore, from the developing world's perspective, it is mainly the industrialized world's responsibility to combat global warming.

Yet, the Kyoto Protocol integrates a mechanism which addresses both opponent views. This mechanism, the Clean Development Mechanism (CDM), allows industrialized countries to fulfill their GHG abatement obligations partly by mitigating GHG emissions in developing countries, where mitigation options can be exploited in a cheaper way. The CDM-associated costs of climate protection are borne by the industrialized world. "With the already huge and growing amount of greenhouse gas emissions and a great deal of low-cost abatement options available, China is widely expected as the world's number one host country of CDM projects" (Zhang 2006). According to UNFCCC (2014a), about 60 % of the expected Certified Emission Reduction (CER)[2] units from registered projects in the year 2014 will be earned by China. As Rive and Rübbelke (2010) show for CDM transfers from Europe to China, this mechanism may not only help to improve the efficiency and to raise the level of international climate protection, but it may also support development in poor countries. Yet, as they find out, the level of success of the mechanism in supporting development depends to a large extent on the domestic environmental regulations in the host country of CDM projects.

The CDM is only one of the three flexible mechanisms comprised in the Kyoto scheme, the other two being joint implementation and emission permit trading (or for short: emissions trading). ("The Kyoto mechanisms include international emissions trading, Joint Implementation (JI), the Clean Development Mechanism (CDM), and some would argue joint fulfilment" (Dessai and Schipper 2003, p. 150). Hence, some would also regard the burden sharing agreement within the EU-15 as an application of a flexible Kyoto mechanism (joint fulfillment)).

Joint implementation (JI) allows Annex-I countries to fulfill their GHG abatement obligations partly by mitigating GHG emissions in other Annex-I countries (industrialized countries and European economies in transition). Laroui, Tellegen, and Tourilova (2004, p. 901) describe the mutual benefits arising for JI investor countries and for host countries of JI projects. For investing countries, JI means a contribution to meeting the emission-reduction targets at lower cost than this could be achieved by own national measures. Furthermore, they argue that it creates new business opportunities for renewables, efficiency technologies, management tools, products, and consultants. According to Laroui, Tellegen, and Tourilova (2004, p. 901), JI provides opportunities for the host country, e.g., to attract foreign investments, to create incentives for starting new businesses in the sectors for renewable and efficiency technologies, and to enhance energy security and independence by lessening demand for energy use.

[2]A CER is a unit issued for emission reductions from CDM project activities in accordance with the CDM rules and requirements, and it is equal to one metric ton of carbon dioxide equivalent (UNFCCC 2014b).

The key idea of emission permit trading is to stipulate an allowed amount of GHG emissions, to partition this amount, and to allocate the parts on tradable emission permits. By allowing transferability of these permits, an emission permit market is constituted. The owners of permits can relinquish their permits and sell them to other agents. Hence, while the total amount of emission permits is preassigned, the permit price is formed in the market. In environmental economics, permit schemes are known as options to cost efficiently internalize externalities. In the EU, the CO_2 emissions trading system (EU-ETS) started on the first of January 2005.

At the COP-18 in Doha in 2012, an agreement on a second commitment period of the Kyoto Protocol for 2013–2020 was reached. Yet, several Annex-I countries (e.g., Canada, Japan, Russia, and the USA) decided not to participate in the second commitment period. The remaining Annex-I countries (e.g., Australia, the EU, and its member states) committed to quantified emission reductions. At the COP-17 in Durban, it was agreed "to launch a process to develop a protocol, another legal instrument or an agreed outcome with legal force under the Convention applicable to all Parties" (UNFCCC 2011), and this process should bring about a protocol, another legal instrument, or an agreed outcome with legal force that enters into force in 2020.

One important issue regarding a post-Kyoto agreement is the question of whether and how to integrate climate policy's second pillar besides mitigation: adaptation to climate change. As the IPCC stresses "Societies can respond to climate change by adapting to its impacts and by reducing GHG emissions (mitigation), thereby reducing the rate and magnitude of change" (IPCC 2007, p. 56). However, in the early years of the UNFCCC's operation, adaptation issues hardly played a role in international negotiations (Yamin and Depledge 2004; Pickering and Rübbelke 2014). Then, at the COP-7 in Marrakesh in 2001, it was agreed to establish three funds (Least Developed Countries Fund, Special Climate Change Fund, and the Adaptation Fund) that are dedicated to international adaptation support which was a strong sign of the – meanwhile – increased importance of the adaptation pillar in international climate policy. Also a large share of the 100 billion USD annually that developed countries formally pledged (at the COP-16 in Cancun in 2010) to mobilize by 2020 in order to support climate policies in developing countries will be channeled toward adaptation projects in developing countries. As Rübbelke (2011) and Pittel and Rübbelke (2013) argue, this adaptation support for developing countries might raise fairness perception in international negotiations on climate change mitigation and with it increase developing countries' willingness to contribute to international mitigation efforts. Then, successful negotiations within the Kyoto scheme might become more likely.

Despite the flexible mechanisms and current as well as planned international transfers, the Kyoto mechanism is unlikely to generate an efficient global climate protection level. Before reasons for the difficulties in reaching an efficient international environmental agreement are discussed, an alternative international scheme to protect the environment, i.e., the Asia-Pacific Partnership on Clean Development and Climate, is shortly described.

Asia-Pacific Partnership on Clean Development and Climate

The Asia-Pacific Partnership on Clean Development and Climate (APP) was announced in July 2005 and formally launched in January 2006. In fact, Australia and the USA were the driving forces behind the APP and convinced China, India, Japan, and South Korea to join the partnership; Canada joined in 2007. The APP partners agreed to work together and with private sector partners to meet goals for energy security, national air pollution reduction, and climate change in ways that promote sustainable economic growth and poverty reduction. Hence, according to McGee and Taplin (2006, p. 191): "No longer is Kyoto the "only game in town" in terms of national participation in international climate-change initiatives." For a discussion of further non-UN climate change initiatives, see McGee and Taplin (2009).

The APP focused on expanding investment and trade in cleaner energy technologies, goods, and services in key market sectors. Projects supported by the APP typically involved small amounts of government funding in conjunction with private investment (Lawrence 2009, p. 282). The APP was remarkable not only because it constituted an additional "game in town" but also because of the fact that the involved seven partner countries collectively account for more than half of the world's economy, population, and energy use. They produce about 65 % of the world's coal, 62 % of the world's cement, 52 % of world's aluminum, and more than 60 % of the world's steel (see: http://www.asiapacificpartnership.org/english/default.aspx). Hence, the APP succeeded in gathering countries without which no solution to the global warming threat is attainable, since their economies cause climate change to a large extent. The question, however, remained how effective their cooperation in APP would be with respect to lowering emissions.

The partnership established eight public-private task forces to develop and implement action plans as depicted in Fig. 3. The Policy and Implementation Committee oversaw the APP as a whole, guided the task forces, and reviewed their work. The Administrative Support Group coordinated the APP's communications and activities and supported the Policy and Implementation Committee as well as the partnership more broadly (APP 2008, p. 3).

In contrast to the Kyoto Protocol, the APP formulated no legally binding commitments on greenhouse gas reduction or the placing of a price upon greenhouse gas emissions. Instead, the individual members of the APP were free to set their own targets based upon individual national circumstances; there were no compulsory contributions to funding climate protection projects. The voluntary national targets were aiming at reductions of greenhouse gas intensities, rather than committing to emission reductions in absolute terms. As Pezzey, Jotzo, and Quiggin (2008, p. 107) point out: "Unrealistic assumptions were made about how much innovation can be achieved by voluntarism and cooperation supported by only paltry funding, in the absence of either market price incentives or mandatory measures."

McGee and Taplin (2006) saw the real problem posed by the APP in the diversion of attention away from absolute GHG reduction targets. If the partnership "takes hold as a fully-fledged alternative climate-change regime, or as a modifier of the

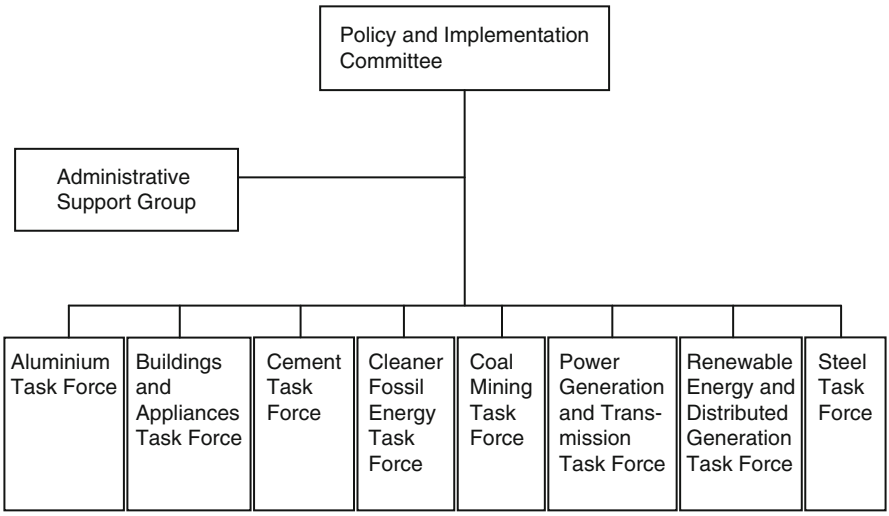

Fig. 3 Organizational structure of the partnership (Figure adopted from APP 2008, p. 3)

future shape of Kyoto, there will be no absolute global emissions reduction and hence a greater risk of dangerous climate change" (McGee and Taplin 2006, p. 192).

The motivation behind launching a scheme – which was described by its founders as a complement to the Kyoto Protocol – was questioned by many researchers. McGee and Taplin (2006, p. 191) drew the conclusion from their analysis that the regime interaction between APP and Kyoto scheme was most likely to be obstructive and competitive and that the claims of complementarity between both regimes would consequently not be justified. As Lawrence (2009, p. 282) argued, "Australia's strong advocacy of the APP in this early period was linked to coal and energy-intensive industry interests." And Karlsson-Vinkhuyzen and van Asselt (2009, p. 202) pointed out that in February 2005, when the world was celebrating the entry of the Kyoto Protocol "into force in a sort of defiant support of multilateralism after the US rejection, it is quite natural that the US wanted to improve their reputation and show some initiative. It seems logical that the US sought the support of the other Kyoto 'defector' in the enterprise." Yet, although the initial motivations to launch the APP may have been dubious, this does not mean that the scheme could not have had positive effects.

However, as Heggelund and Buan (2009, p. 314) argued, given the enormous challenge of global warming, the relatively low number of APP projects set up since its inception "makes us question the likelihood of the APP significantly contributing to climate change mitigation, even if it could make a contribution to technology transfer." Furthermore, as Karlsson-Vinkhuyzen and van Asselt (2009, p. 206) argued, there were political signs which could be interpreted as unequivocal support for the UN climate regime. Indeed, as of 5 April 2011, the APP formally concluded its joint work.

Why Efficient Climate Protection Is So Difficult to Achieve

Despite all the efforts going into international negotiations and despite the international cooperation within the Kyoto Protocol and the APP, global climate protection still remains on a suboptimal low level. To a large extent, the reason for this dismal result is a global-scale market failure. Climate protection has global public good properties, i.e., climate protection exerts positive externalities which are not compensated via markets. This in turn causes a suboptimal low provision of the public good "climate protection."

In the economics discipline, a pure public good is considered to have two distinguishing properties: (1) non-excludability of consumption and (2) non-rivalry in consumption; in contrast, a private good has none of these two properties (see Cornes and Sandler 1996, p. 3).

Non-excludability with respect to climate protection means that every country in the world benefits from climate protection activities, regardless where these activities have been accomplished. Hence, for a country it does not make a difference whether GHGs are abated in Australia, China, the UK, or the USA; the abatement will positively affect the global climate, and no country can be excluded from the respective benefits.

Non-rivalry in the consumption of climate protection means that one country enjoying the benefits of the mitigation of global warming does not affect the benefits received by another country from this mitigation.

Welfare Optimum

If countries individually decide about the provision of public goods like climate protection, they will provide a – from a global perspective – suboptimally low amount since they face the so-called free-rider incentives. Since non-excludability of benefits from climate protection prevails (country A cannot force country B "not to enjoy" the benefits of the climate protection produced by country A), no price can be charged on a market for these benefits. Since production of climate protection is costly, while its consumption is free of charge, countries prefer that others produce more climate protection, while they themselves prefer to contribute less and to enjoy the benefits from the others' efforts for free.

In general the notion of "free riding" is employed in the scientific literature in order to characterize such a situation. But in contrast to, e.g., agreements on climate change where countries may take a "free ride" from participation, the problem regarded here is one of degree. As can be shown, it is rational for each single country to provide the public good up to a level where its own marginal abatement benefits coincide with its own marginal abatement costs. Hence, it might be more appropriate to employ the expression "easy riding," since this is not equivalent to "not providing anything to the public good." Therefore, Cornes and Sandler (1996, p. 30) suggest using the notion "easy riding" in such contexts.

In the economics discipline, efficiency or optimality describes a situation where welfare is maximized. In a next step, the maximization problem which the government of an individual country i faces is illustrated, or put differently, the case where the national government intends to act in a way that maximizes the welfare of the country's residents is regarded. The national welfare function characterizes the preferences of the residents, and the government can enhance the residents' welfare by allocating the country's resources in such a way that the respective function is maximized subject to the national income constraint. Let us for simplicity assume that income can be spent on two different groups of commodities: the first commodity is a private good y_i, and the second is the public good climate protection x_i.

Due to the public good property of climate protection, the total level X of climate protection consumable by country i can be expressed as the sum of all countries' or regions' individual contributions to climate protection. In a world of n countries (with $i = 1,\ldots, n$), the total level of climate protection is this given by

$$X = x_i + \sum\nolimits_{i \neq j} x_j = x_i + \tilde{X}_i, \tag{1}$$

where $\tilde{X}_i$ is the sum of climate protection by all countries except for the climate protection x_i provided by the regarded country i.

The preferences of country i concerning both goods are represented by the utility function which is continuous, strictly increasing, strictly quasi-concave, and everywhere twice differentiable.

The individual country i maximizes its welfare U_i

$$\max_{y_i, x_i} U_i\left(y_i, x_i + \tilde{X}_i\right) = U_i(y_i, X) \tag{2}$$

s.t.

$$y_i + x_i c = I_i, \tag{3}$$

where I_i is the monetary income of country i. For all countries, the unit price of the private commodity is set equal to unity, and the unit price of climate protection is set equal to c (with c being constant and strictly positive, i.e., $c > 0$). In the maximization the Nash assumption is employed, i.e., the welfare-maximizing country supposes that its choices do not affect the behavior of the other countries, i.e., it takes $\tilde{X}_i$ to be exogenous.

From the first-order conditions for the welfare maximum, we get

$$MRS_i = \frac{\partial U_i / \partial X}{\partial U_i / \partial y_i} = c. \tag{4}$$

Consequently, it is optimal for the individual country to provide climate protection up to the level where the marginal rate of substitution (left-hand side of Eq. 4)

between public good and private good becomes equal to the unit price ratio (right-hand side of Eq. 4) between public and private good (i.e., $\frac{c}{1}$). To put it plainly, when deciding about allocating its income between private goods and climate protection, a country fares best when it invests in climate protection until the benefit from spending another dollar on the climate compared to the benefits from spending another dollar on private goods is equal to the relative costs of buying the two goods.

While this provision level is optimal from an individual country's point of view, it is not optimal from a global perspective. Global welfare could be raised by deviating from the provision levels associated with condition (4). In order to illustrate this, global welfare is maximized in a next step.

It seems reasonable to assume that global welfare is a function of the individual countries' welfare levels. The global welfare level attainable from the consumption of private goods and climate protection is, however, restricted by the aggregate income that the countries can spend on private goods and climate protection. Thus the global welfare maximization problem reads

$$\max_{y_1,\ldots,y_n,X} U(U_1(y_1,X),U_2(y_2,X),\ldots,U_n(y_n,X)) \tag{5}$$

s.t.

$$\sum_{i=1}^{n} y_i + cX = \sum_{i=1}^{n} I_i. \tag{6}$$

Let us – for simplicity – assume that each individual country's welfare has an equal weight with respect to global welfare, i.e., $U(U_1(y_1,X),U_2(y_2,X),\ldots,U_n(y_n,X)) = U_1(y_1,X)+U_2(y_2,X)+\ldots+U_n(y_n,X)$. Then, optimization yields the so-called Samuelson condition (see Samuelson 1954, 1955)

$$\sum_{i=1}^{n} MRS_i = \sum_{i=1}^{n} \frac{\partial U_i/\partial X}{\partial U_i/\partial y_i} = c. \tag{7}$$

Therefore, in order to maximize global welfare, an individual country should provide climate protection up to a level where the sum of all countries' marginal rates of substitution between public and private good becomes equal to the unit price ratio between public and private good. Such outcomes, where no country can improve its welfare without harming another one, are called Pareto optima.

Condition (7) deviates from condition (4), since – without international coordination – an individual country would only take into account its own marginal rate of substitution between public and private goods (i.e., its own benefits from the two goods) when deciding about its climate protection efforts, while Pareto efficiency requires that countries also take into account spillovers exerted on other countries (i.e., the global benefits generated by its climate protection efforts). Therefore also the other countries' marginal rates of substitution between the public and private good have to be included in the efficiency condition.

Fig. 4 Prisoner's dilemma game

B's strategy / A's strategy	no participation	participation
no participation	0, –1	6, –3
participation	–4, 7	5, 6

On a national level, efficient public good provision can be enforced by the government, but on the global scale there is no central coercive authority which can enforce an efficient global climate protection level. Therefore, the only option is for countries to voluntarily negotiate a climate protection agreement in order to get closer to the globally efficient protection level.

International Negotiations in Normal Form Games

Such international negotiations on climate change can be comfortably depicted in a game-theoretical setting. Regularly, such negotiations are described as a prisoner's dilemma game which captures the free-rider incentives associated with the provision of public goods. A normal form game in the shape of a prisoner's dilemma (PD) situation with two agents or countries is presented in Fig. 4.

Both considered countries have the choice between "participation" in an international climate protection agreement (or climate protection efforts) and "no participation" in international climate protection efforts. In the matrix, the numbers in front of the commas represent the payoffs for country A, while the numbers behind the commas stand for the payoffs received by country B. In the prisoner's dilemma case of Fig. 4, the dominant strategy for each agent is to choose "no participation" in an international climate protection agreement (a dominant strategy is a strategy which always yields the highest payoff for the agent choosing this strategy, regardless of the choice of the opponents. For a more detailed discussion of these and related game theoretic concepts, see, e.g., Fudenberg and Tirole (1991)).

This outcome is the so-called Nash equilibrium where no country has anything to gain by changing only its own strategy unilaterally. While this equilibrium is stable, the payoffs of countries A and B are merely 0 and −1, respectively. However, "From an economic viewpoint an ideal state of cooperation has two features: It is a Pareto-optimum and it is stable" (Buchholz and Peters 2003, p. 82). The Nash equilibrium in the depicted PD situation is of course not Pareto optimal. Both agents would obtain a higher payoff if they would both participate in the international agreement.

Fig. 5 Chicken game

B's strategy / A's strategy	no participation	participation	
no participation	–6, –6	6, –3	$1-p$
participation	–3, 6	3, 3	p
	$1-q$	q	

Alternatively, a "Chicken" game setting can be employed in order to illustrate the negotiation situation. Lipnowski and Maital (1983) provide an analysis of voluntary provision of a pure public good in general as the game of Chicken. In fact, a Chicken game tends to describe international negotiations on the provision of the specific public good "climate protection" in a more adequate way than the prisoner's dilemma game (see Carraro and Siniscalco 1993). The case of a Chicken game, which belongs to the group of coordination games, is depicted in Fig. 5. In contrast to the PD situation, there exists no dominant strategy.

There are a couple of papers investigating the differences associated with the two, PD and Chicken, games. Ecchia and Mariotti (1998) investigate coalition formation in international environmental agreements and compare different versions of the two game types using simple three-country examples. In their paper, Rapoport and Chammah (1966) stress the difference between both games with respect to the attractiveness of retaliation decisions. Snyder (1971) examines differences in the logic and social implications of PD and Chicken games in the context of international politics. Lipman (1986) and Hauert and Doebeli (2004) analyze how the evolution of cooperation differs in the two games. Rabin (1993), Rübbelke (2011), and Pittel and Rübbelke (2013) investigate fairness in these settings. Pittel and Rübbelke (2012) depict negotiations on climate change in (3×3) matrices in which they integrate both Chicken and PD settings simultaneously. Hence, in their study they allow for a broader range of choices for the involved countries.

The main difference between both games, i.e., between PD and Chicken games, is that the agents in the PD situation obtain the lowest payoffs when they play unilateral "participation," while in the Chicken game, they face the lowest payoffs if they mutually play "no participation." This outcome is the reason why the Chicken game is said to represent international negotiations better: in case of mutual non-participation, the whole world is threatened by a global warming catastrophe. This catastrophe can be prevented in the best way by means of mutual cooperation in international climate protection. However, if the other agent refuses to cooperate, then unilateral participation in international climate protection efforts would be the best choice since this is the only remaining way to prevent the global warming

catastrophe. Yet, if the other agent provides climate protection (and thus chooses "participation"), it would be best to choose "no participation" and thus to take a free ride.

Each agent hopes that the other agent provides climate protection, such that he himself can take a free ride in climate protection. As can be observed from Fig. 5, there exist multiple Nash equilibria, which are associated with pure and mixed strategies. The Nash equilibria in connection with pure strategies prevail where the payoffs (−3,6) and (6,−3) arise.

Given possible uncertainties regarding the countries' behavior, mixed strategies become germane. Agents form probabilities about the other agent's behavior. Country A assesses the likelihood with which country B will participate (q) or not participate ($1 - q$) and vice versa for country B (p and $1 - p$). In order to determine the mixed strategies in the Chicken game situation in Fig. 5, the likelihood q^* (resp. p^*) of participation by country B (country A) has to be calculated that makes country A (country B) indifferent between playing "participation" and "no participation." Probability q^* is determined by calculating the level of q, for which the expected payoffs of both strategies of A ("participation" and "no participation") are equal. This is the case if

$$-3(1-q)+3q=-6(1-q)+6q. \tag{8}$$

The left-hand side represents A's expected payoff from participation, and the right-hand side reflects A's expected payoff from defection. Analogously p^* can be determined from solving

$$-3(1-p)+3p=-6(1-p)+6p \tag{9}$$

for p. In this case, the mixed-strategy equilibrium requires

$$q^*=p^*=½. \tag{10}$$

If country A or country B is uncertain whether the other country participates or defects, then it should cooperate (participate) provided it expects the antagonist to play "participation" with a probability of less than ½.

Integration of Ancillary Benefits into the Negotiations

Climate policies regularly generate side effects. Afforestation and reforestation, for example, do not only mitigate CO_2-induced global warming by sequestering carbon; these measures also increase the habitat for endangered species. Furthermore, forests can serve as recreational areas and reduce soil erosion. As Ojea, Nunes, and Loureiro (2010) stress, forests' "provision of goods and services plays an important role in the overall health of the planet and is of fundamental importance to human economy and welfare." Furthermore, Sandler and Sargent (1995, p. 160) point out that tropical

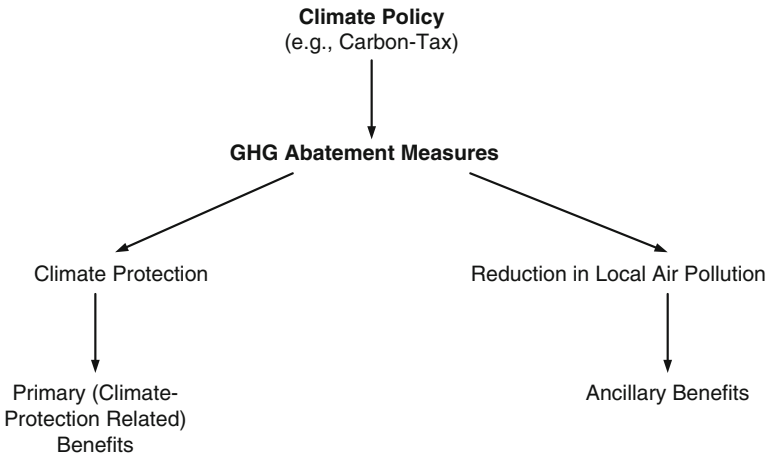

Fig. 6 Climate policy generating primary and ancillary benefits, see Rübbelke (2002, p. 36)

forests provide a bequest value which the current generation derives from passing on the forests to future generations. Concerning the case of Brazil, Fearnside (2001, p. 180) stresses: "The environmental and social impacts of mitigation options such as large hydropower projects, mega-plantations or nuclear energy, contrast with the "ancillary" benefits of forest maintenance." An overview of studies assessing the co-effects of afforestation is provided by Elbakidze and McCarl (2007, p. 565).

Similarly, side effects arise from the implementation of more efficient technologies, the reduction of road traffic, and the substitution of carbon-intensive fuels. Ancillary or secondary benefits induced by these CO_2-emission-reducing activities accrue, for example, when the emissions of other pollutants like particulate matter are reduced simultaneously (see Fig. 6). There are a number of terms which convey the idea of ancillary or secondary benefits. The others are co-benefits and spillover benefits (see IPCC 2001). The main difference is the relative emphasis given to the climate change mitigation benefits versus the other benefits (Markandya and Rübbelke 2004, p. 489).

In fuel combustion processes, CO_2 emissions are accompanied by emissions of, e.g., NO_X, SO_2, N_2O, and others. Therefore, fuel combustion reductions do not only cause a decrease in CO_2 emissions but also diminish the emissions of other pollutants. In general, positive health effects of air pollution reduction that accompany climate protection measures are assessed to represent the most important category of secondary benefits. (However, Aunan et al. (2003, p. 289) annotate that "some particulate air pollution has a cooling effect on the atmosphere, reducing it may exacerbate global warming.") Further negative impacts of air pollution, like accelerated surface corrosion, weathering of materials, and impaired visibility are mitigated by fuel combustion reductions, too. But, road traffic mitigation does not only produce ancillary benefits by reducing the emission of air pollutants, but it is also accompanied by lower noise levels and reduced frequency of accidents, less traffic congestion, and less road surface damage.

While primary benefits accrue globally from the prevention of climate change-induced damages, ancillary benefits are mostly local or regional (IPCC 1996, p. 217; Pearce 1992, p. 5). They represent domestic public goods for individual countries. (However, regarding the abatement of the greenhouse gases chlorofluorocarbons (CFCs), the ancillary effect of ozone layer protection and the respective ancillary benefits can be enjoyed globally.) Local air pollution mitigation generated by climate policy, for example, can be exclusively enjoyed by the protecting country. Therefore, ancillary effects can be considered to be private to the host country of a climate policy. Consequently, they differ from climate protection-related primary benefits which exhibit global publicness. Global damages arise, e.g., in the form of droughts caused by global warming. Rübbelke and Vögele (2011, 2013) recently analyzed the effects of such droughts on the power sector.

Several studies ascertaining the level of ancillary benefits found that such benefits even represent a multiple of climate protection-related primary benefits, as Pearce (2000, p. 523) illustrates in an overview.

In the next stage, ancillary benefits will be explicitly introduced into our normal form game. It will be taken into account that ancillary benefits are enjoyed (mainly) privately by the host country of the climate protection activity. Ancillary benefits arise regardless of the behavior of the antagonist. In Fig. 7, ancillary benefits (AB_A, AB_B) are explicitly included into the matrix of the Chicken game, where it is assumed that $AB_A < AB_B$.

Analogously to the procedure concerning the Chicken game situation without ancillary benefits, the mixed strategies can be investigated here. Again, probability q^* is determined by identifying the level of q, where the expected payoffs of both strategies of A ("participation" and "no participation") balance. This is the case if

$$(-3 + AB_A)\ (1 - q) + (3 + AB_A)q = -6\ (1 - q) + 6q. \tag{11}$$

Analogously p^* can be specified

$$(-3 + AB_B)\ (1 - p) + (3 + AB_B)p = -6\,(1 - p) + 6p. \tag{12}$$

Fig. 7 Chicken game with ancillary benefits

B's strategy / A's strategy	no participation	participation	
no participation	–6, –6	6, –3 + AB_B	1–p
participation	–3 + AB_A, 6	3 + AB_A, 3 + AB_B	p
	1–q	q	

From Eqs. 11 and 12, q^* and p^* can be derived. Scientific studies largely assess that there are especially important co-benefits of local/regional air pollution reduction in developing countries; an overview of a selection of studies investigating ancillary benefits in developing countries can be found in Appendix 1. Neglecting potential differences in the primary benefits and supposing that A represents the group of industrialized countries, while B represents the developing world, we obtain:

$$q^* = ½ + AB_A/6 < p^* = ½ + AB_B/6. \tag{13}$$

If country A (resp. country B) is uncertain whether the antagonist participates or defects, then it should participate provided it expects the antagonist to play "participation" with a probability of less than $½ + AB_A/6$ (resp. $½ + AB_B/6$).

Comparison of Eqs. 10 and 13 shows that q^* and p^* rise due to the inclusion of ancillary benefits into the analysis. Consequently, for the Chicken game example illustrated above, it is found that taking ancillary benefits into account will increase the likelihood of cooperative behavior in international negotiations on climate change. According to Eq. 13, the inclusion of ancillary benefits into the reasoning brings about especially an increase in the likelihood that developing countries will participate in international climate protection efforts (for a more general analysis of the influence of ancillary benefits in international negotiations on climate change, see Pittel and Rübbelke 2008). Consequently, these results confirm Halsnæs and Olhoff (2005, p. 2324) who stress that "the inclusion of local benefits in developing countries in GHG emission reduction efforts will [...] create stronger incentives for the countries to participate in international climate change policies."

Yet, in their analysis of qualitative and strategic implications associated with ancillary benefits, Finus and Rübbelke (2013) find a more moderate influence of co-benefits on the participation in international climate agreements and on the success of these treaties in welfare terms. They employ a setting of noncooperative coalition formation in the context of climate change. According to their results, ancillary benefits will not raise the likelihood of an efficient global agreement on climate change to come about although ancillary benefits provide additional incentives to protect the climate. The rationale behind this result is that countries taking the private ancillary benefits to a greater extent into account will undertake more emission reduction, irrespective of an international agreement.

However, if we consider the high local/regional pollution levels in developing countries, it remains at least highly disputable whether developing countries conduct efficient local/regional environmental policies. Hence, the commitment in an international climate protection agreement will most likely help to raise the efficiency in local/regional environmental protection in these countries. Consequently, ancillary benefits – although not being the major impetus for immediate action – may take the role of a catalyst to climate policy (rather than that of a direct driver). Joining international climate protection efforts may become politically more feasible for

developing countries (like China and India) which face serious local/regional pollution problems, when ancillary benefits are included in the political reasoning.

Price Ducks: An Approach to Break the Deadlock?

Due to the inefficiency of the Kyoto Protocol scheme, which is a quantity duck since it stipulates emission-reduction quantity targets, there arose an intense discussion about general alternatives to such quantity ducks (which are more than just technology-focused climate policy partnerships like the APP). Nordhaus (2006, p. 31) points out: "Unless there is a dramatic breakthrough or a new design the Protocol threatens to be seen as a monument to institutional overreach."

- Price-influencing international climate protection schemes have been proposed by Nordhaus (2006) as a proper successor of the quantity approach of the Kyoto type. "This is essentially a dynamic Pigovian pollution tax for a global public good" (Nordhaus 2006, p. 32). An international carbon tax scheme where no international emission limits are dictated is considered to have several significant advantages over the Kyoto mechanism. This scheme could also contain side payments in order to motivate countries to participate: "Additionally, poor countries might receive transfers to encourage early participation," Nordhaus (2006, p. 32).
- Such a scheme is a price duck, because via the taxes, the prices of polluting activities are increased, such that there are additional incentives to mitigate the level of such polluting activities.
- In contrast to taxing polluting activities in order to protect the climate, of course, prices can be influenced by subsidizing climate-protecting activities (e.g., energy-efficient appliances or carbon sequestration measures could be subsidized). The subsidy will reduce the effective price of climate-protecting activities, and hence the agents receiving the subsidy will raise their provision level of climate protection.
- Recently, Altemeyer-Bartscher, Rübbelke, and Sheshinski (2010) elaborated Nordhaus' proposal of an international carbon tax scheme. They analyze how individual countries or regions could negotiate the design of such a tax scheme in a decentralized way. In the scheme they suggest countries offer side payments to their opponents that are conditional on the level of the environmental tax rates implemented in the transfer-receiving opponent country. As can be shown, such a side-payment scheme might yield the first-best optimal tax policy and hence an efficient global climate protection regime. The scheme does not require the coercive power of a central global authority as the individual countries implement carbon taxes voluntarily. Altemeyer-Bartscher, Markandya, and Rübbelke (2014) investigate the effects of ancillary benefits on the outcomes of this scheme.

- Other price-influencing schemes which work in a similar way and do not require an international coercive authority are matching schemes which were first developed by Guttman (1978, 1987). Danziger and Schnytzer (1991) provide a general formulation of Guttman's matching idea which allows for income effects, non-identical players, and nonsymmetric equilibria. Guttman's matching approach has been applied to the sphere of international environmental agreements by Rübbelke (2006) and Boadway, Song, and Tremblay (2007, 2011).

Guttman's basic scheme consists of two stages. Each agent i's contribution x_i to the public good can be written as:

$$x_i = a_i + b_i \sum_{j=1}^{n} a_j \qquad (j \neq i), \tag{14}$$

where a_i is the agent's unconditional or flat contribution to the public good (in our case "climate protection") and b_i is his matching rate, which he provides for each unit of flat public good contributions by other agents. Therefore, the agent's matching contribution is $b_i \sum_{j=1}^{n} a_j \; (j \neq i)$. The unit costs of the goods are supposed to be equal to unity. The budget constraint of the agent in the shape of the income restriction is:

$$y_i + a_i + b_i \sum_{j=1}^{n} a_j = I_i \qquad (j \neq i). \tag{15}$$

I_i is again the monetary income of the considered agent i.

In the first stage of the game, each agent makes a decision on the level of the matching rates he wants to offer to the other agents. It could be assumed that this decision is stipulated in an international agreement on matching rates, where all negotiating agents or decision makers – as representatives of their nations – agree on the matching rates their countries will provide (see Rübbelke 2006). All the agents' actions in both stages of the game are guided by welfare-maximizing behavior, i.e., the agents aim to maximize their individual countries' welfare as represented by the function in Eq. 2.

In the second stage, all agents will make decisions about their flat contributions. Total public good contribution of all agents then becomes equal to:

$$X = \sum_{i=1}^{n} \left(a_i + b_i \sum_{j=1}^{n} a_j \right) \qquad (j \neq i). \tag{16}$$

Given the matching rates of the other agents, the considered agent will contribute flat contributions to the public good up to the level where the marginal rate of

substitution between public and private good is equal to the effective price of the public good, i.e., where

$$MRS_i = \frac{1}{1 + \sum_{j=1}^{n} b_j} \qquad (j \neq i). \tag{17}$$

The decline in the effective price, from unity to the level specified on the right-hand side of Eq. 17, induces an increase in the private provision of the public good. Comparison of the right-hand sides of Eq. 4 (for which it is assumed that $c = 1$) and of Eq. 17 shows that in the matching scheme the considered agent or country faces a decline in the effective price of the public good "climate protection" as long as at least one other agent provides a positive matching rate b_j. As Bergstrom (1989) illustrates, there are indeed incentives to announce positive matching rates.

Consequently, the matching scheme has a price-influencing effect (similar to that of a subsidy) which the quantity targets stipulated by the Kyoto Protocol do not exert. Due to the decline in the effective price, the agent tends to raise the level of his public good provision. Put differently, within the matching scheme, individual countries manipulate (via their matching commitments) the effective price of climate protection from other countries' point of view in order to influence these opponent countries to raise their public good provision levels. And as Boadway, Song, and Tremblay (2007, p. 682) point out: "the notion that countries might attempt to influence other countries' contributions by preemptive matching commitments is not far-fetched in light of recent examples of disaster relief or international campaigns to combat the effects of infectious diseases."

In the case of identical agents, Summing (Eq.17) up over all i generates

$$\sum_{i=1}^{n} MRS_i = n \frac{1}{1 + (n-1)b_j} (j \neq i) \tag{18}$$

Hence, a Pareto optimum is attainable if each agent would choose $b_i = 1$. As Buchholz, Cornes, and Rübbelke (2009) demonstrate, matching may work better if there is a large number of agents/countries (than when there is a small number of agents), which is an important result if it is taken into account that international negotiations involve many countries.

Future Directions

The Kyoto Protocol has been an inefficient agreement, although its flexible mechanisms (CDM, Joint Implementation, ETS) helped to mitigate this inefficiency. Efficiency would require that the cheapest GHG abatement options are abated first, which is not generally the case under the Kyoto Protocol. Furthermore, the

emissions of large greenhouse gas emitters in the industrialized world, e.g., Russia and the USA, are not restricted under the protocol in the second commitment period.

The immense threat of global warming necessitates an improved global climate protection regime, since otherwise the world might experience dramatic and life-threatening consequences. Among the possible negative effects are the melting of glaciers, a decline in crop yields (especially in Africa), rising sea levels, sudden shifts in regional weather patterns, and an increase in worldwide deaths from malnutrition and heat stress (Stern 2007, Chap. 3).

An improved future international climate protection regime has to organize climate protection more effectively, and it has to stipulate significant GHG emission reductions for all major polluters. Developing countries like China and India belong to the group of major emitter countries. Consequently, if international climate policy is to succeed in combating global warming, developing countries will also have to commit to emission reductions under an international agreement.

Since there is no global coercive authority which could enforce countries to conduct an efficient climate protection in the future, mutual voluntary negotiations are the only means by which international coordination in climate protection can be accomplished. Put differently, "international treaties have to rely on voluntary participation and must be designed in a self-enforcing way" (Eyckmans and Finus 2007, p. 74). Yet, international easy- or free-rider incentives which are due to the global public good property of climate protection make the agreement on such an international treaty a difficult task.

Another way to protect the global climate, which deviates from the Kyoto concept of stipulating GHG emission-reduction quantities, is the negotiation of international price-influencing regimes. These regimes manipulate effective prices via taxes, subsidies, or matching grants in order to influence the behavior of individual countries in such a way that globally efficient climate protection levels are reached.

An international carbon tax, as suggested by Nordhaus (2006), might indeed yield a more efficient outcome, but due to the lack of will in the political arena to launch such a tax, it might be more promising to base the future global climate protection architecture on the already established structures associated with the Kyoto scheme. Yet, the advantages of price ducks like matching schemes are remarkable, and international price-influencing concepts like the global carbon tax or matching schemes should not be dismissed with levity.

Private ancillary benefits may take the role of a catalyst to climate policy rather than a direct driver to international climate negotiations. Joining international climate protection efforts may become politically more feasible for developing countries (like China and India) which face serious local/regional pollution problems when ancillary benefits are included in the political reasoning. Not only co-effects in terms of reduced local/regional air pollution are relevant but also co-benefits in the shape of, e.g., economic development, energy security, and employment.

Appendix 1

See Table 1

Table 1 Ancillary benefit studies regarding developing countries

Study	Country	Pollutants (local/regional)	Model/approach
Aunan et al. (2003)	China	PM, SO_2, TSP	Comparison of studies that comprise a bottom-up study, a semi-bottom-up study, and a top-down study using a CGE model
Aunan et al. (2004)	China	SO_2, particles	Analysis and comparison of six different CO_2-abating options
Aunan et al. (2007)	China	NO_X, TSP	CGE model
Bussolo and O'Connor (2001)	India	NO_X, particulates, SO_2	CGE model
Cao (2004)	China	SO_2, TSP	Technology assessment, sensitivity to discount rate
Cao et al. (2008)	China	NO_X, particulates, SO_2	Integrated modeling approach combining a top-down recursive dynamic CGE model with a bottom-up electricity sector model
Chen et al. (2007)	China		Comparison of partial and general equilibrium MARKAL models
Cifuentes et al. (2000)	Chile	CO, PM, NO_X, SO_2	No economic modeling
Cifuentes et al. (2001)	Brazil, Chile, Mexico	Ozone, particulates	Development of scenarios that estimate the cumulative public health impacts of reducing GHG emissions
Dadi et al. (2000)	China	SO_2	Linear programming model
Dessus and O'Connor (2003)	Chile	CO, lead, NO_2, ozone, PM, SO_2	CGE model
Dhakal (2003)	Nepal	CO, HC, NO_X, SO_2, particles, lead	Analysis of long-range energy system scenarios
Eskeland and Xie (1998)	Chile, Mexico	NO_X, particulates, SO_2, VOCs	Technology and cost-curve assessment
Garbaccio et al. (2000)	China	PM, SO_2	CGE model
Garg (2011)	India	PM_{10}	Health impacts (mortality and morbidity) quantified for different socioeconomic groups in Delhi
Gielen and Chen (2001)	China	NO_X, SO_2	MARKAL, technology assessment, and alternative policy scenarios

(*continued*)

Table 1 (continued)

Study	Country	Pollutants (local/regional)	Model/approach
Ho and Nielsen (2007)	China	SO_2, TSP	CGE model
Kan et al. (2004)	China	Particulates	Shanghai MARKAL model
Larson et al. (2003)	China	SO_2	MARKAL of energy sector; base vs. advanced technology scenarios for controlling CO_2 and SO_2
Li (2006)	Thailand	Particulates	Dynamic recursive CGE model
Markandya et al. (2009)	China, India	Particles	Use of the POLES and GAINS models as well as of a model to estimate the effect of $PM_{2.5}$ on mortality on the basis of the WHO's comparative risk assessment methodology
McKinley et al. (2005)	Mexico	CO, HC, NO_X, particulates, SO_2	Analysis of five pollution control options in Mexico City
Mestl et al. (2005)	China	PM, SO_2	Project-by-project analysis
Morgenstern et al. (2004)	China	SO_2	Survey of recent banning of coal burning in small boilers in downtown area of Taiyuan
O'Connor et al. (2003)	China	NO_X, SO_2, TSP	CGE model
Peng (2000)	China	Particulates, SO_2	RAINS-Asia for local and GTAP for economy-wide effects
Rive and Rübbelke (2010)	China	SO_2, development benefits	CGE model
Shrestha et al. (2007)	Thailand	NO_X, SO_2	Four scenarios, use of end-use-based Asia-Pacific Integrated Assessment Model (AIM/Enduse)
Smith and Haigler (2008)	China		Sample calculations regarding interventions in the household energy sector
Van Vuuren et al. (2003)	China	SO_2	Simulation model
Vennemo et al. (2006)	China	SO_2, TSP	Synthesis of a significant body of research on co-benefits of climate policy in China
Wang and Smith (1999a, b)	China	Particulates, SO_2	No economic modeling
West et al. (2004)	Mexico	CO, HC, NO_X, particulates, SO_2	Linear programming model
Zheng et al. (2011)	China	SO_2	Using a panel of 29 Chinese provinces over the period 1995–2007, application of panel cointegration techniques

References

Altemeyer-Bartscher M, Rübbelke DTG, Sheshinski E (2010) Environmental protection and the private provision of international public goods. Economica 77:775–784

Altemeyer-Bartscher M, Markandya A, Rübbelke DTG (2014) International side-payments to improve global public good provision when transfers are refinanced through a tax on local and global externalities. Int Econ J 28:71–93

APP (2008) Asia-Pacific Partnership on clean development and climate. Department of State Publication # 11468 (Brochure)

Aunan K, Fang J, Mestl HE, O'Connor D, Seip HM, Vennemo H, Zhai F (2003) Co-benefits of CO_2-reducing policies in China – a matter of scale? Int J Global Environ Issues 3:287–304

Aunan K, Fang J, Vennemo H, Oye K, Seip HM (2004) Co-benefits of climate policy lessons learned from a study in Shanxi, China. Energy Policy 32:567–581

Aunan K, Berntsen T, O'Connor D, Hindman Persson T, Vennemo H, Zhai F (2007) Benefits and costs to China of a climate policy. Environ Dev Econ 12:471–497

Bauer A (1993) Der Treibhauseffekt. J.C.B Mohr, Tübingen

Bergstrom T (1989) Puzzles – love and spaghetti, the opportunity cost of virtue. J Econ Perspect 3:165–173

Boadway R, Song Z, Tremblay J-F (2007) Commitment and matching contributions to public goods. J Public Econ 91:1664–1683

Boadway R, Song Z, Tremblay J-F (2011) The efficiency of voluntary pollution abatement when countries can commit. Eur J Polit Econ 27:352–68

Buchholz W, Peters W (2003) International environmental agreements reconsidered – stability of coalitions in a one-shot game. In: Marsiliani L, Rauscher M, Withagen C (eds) Environmental policy in an international perspective. Kluwer Academic, Dordrecht

Buchholz W, Cornes RC, Rübbelke DTG (2009) Existence and warr neutrality for matching equilibria in a public good economy: an aggregative game approach, CESifo working paper no. 2884, Munich

Bussolo M, O'Connor D (2001) Clearing the air in India: the economics of climate policy with ancillary benefits, working paper no. 182, OECD Development Centre, Paris

Cao J (2004) Options for mitigating greenhouse gas emissions in Guiyang, China: a cost-ancillary benefit analysis, 2004-RR2. Economy and Environment Program for Southeast Asia (EEPSEA), Singapore

Cao J, Ho MS, Jorgenson DW (2008) "Co-benefits" of greenhouse gas mitigation policies in China – an integrated top-down and bottom-up modeling analysis, Environment for development discussion paper series, DP 08–10

Carraro C, Siniscalco D (1993) Strategies for the international protection of the environment. J Public Econ 52:309–328

Chen W, Wu Z, He J, Gao P, Xu S (2007) Carbon emission control strategies for China: a comparative study with partial and general equilibrium versions of the China MARKAL model. Energy 32:59–72

Cifuentes LA, Sauma E, Jorquera H, Soto F (2000) Preliminary estimation of the potential ancillary benefits for Chile. In: OECD (ed) Ancillary benefits and costs of greenhouse gas mitigation. OECD, Paris, pp 237–261

Cifuentes L, Borja-Aburto VH, Gouveia N, Thurston G, Davis DL (2001) Assessing the health benefits of Urban air pollution reductions associated with climate change mitigation (2000–2020): Santiago, São Paulo, México City, and New York City. Environ Health Perspect 109:419–425

Cornes RC, Sandler T (1996) The theory of externalities, public goods and club goods. Cambridge University Press, Cambridge

Dadi Z, Yingyi S, Yuan G, Chandler W, Logan J (2000) Developing countries and global climate change: electric power options in China. Pew Center on Global Climate Change, Arlington

Danziger L, Schnytzer A (1991) Implementing the Lindahl voluntary-exchange mechanism. Eur J Polit Econ 7:55–64
Dessai S, Michaelowa A (2001) Burden sharing and cohesion countries in European climate policy: the Portuguese example. Clim Pol 1:327–341
Dessai S, Schipper EL (2003) The Marrakech Accords to the Kyoto Protocol: analysis and future prospects. Glob Environ Chang 13:149–153
Dessus S, O'Connor D (2003) Climate policy without tears: CGE-based ancillary benefits estimates for Chile. Environ Resour Econ 25:287–317
Dhakal S (2003) Implications of transportation policies on energy and environment in Kathmandu Valley, Nepal. Energy Policy 31:1493–1507
Dickinson RE, Cicerone RJ (1986) Future global warming from atmospheric trace gases. Nature 319:109–115
Dijkstra B, Rübbelke DTG (2013) Group rewards and individual sanctions in environmental policy. Resour Energy Econ 35:38–59
EC (2000) Communication from the Commission to the Council and the European Parliament on EU policies and measures to reduce greenhouse gas emissions: towards a European Climate Change Programme (ECCP), COM(2000) 88 final, Brussels
Ecchia G, Mariotti M (1998) Coalition formation in international agreements and the role of institutions. Eur Econ Rev 42:573–582
Edenhofer O, Knopf B, Luderer G, Steckel J, Bruckner T (2010) More heat than light? On the economics of decarbonisation. In: John KD, Rübbelke DTG (eds) Sustainable energy. Routledge, London/New York
Elbakidze L, McCarl BA (2007) Sequestration offsets versus direct emission reductions: consideration of environmental co-effects. Ecol Econ 60:564–571
Enquete-Kommission (1990) Schutz der Erde – Eine Bestandsaufnahme mit Vorschlägen zu einer neuen Energiepolitik, Dritter Bericht der Enquete-Kommission "Vorsorge zum Schutz der Erdatmosphäre" des 11. Deutschen Bundestages, Teilband 1, Bonn
Enquete-Kommission (1995) Mehr Zukunft für die Erde – Nachhaltige Energiepolitik für dauerhaften Klimaschutz, Schlußbericht der Enquete-Kommission "Schutz der Erdatmosphäre" des 12. Deutschen Bundestages, Bonn
Eskeland GS, Xie J (1998) Acting globally while thinking locally: is the global environment protected by transport emission control programs? J Appl Econ 1:385–411
Eyckmans J, Finus M (2007) Measures to enhance the success of global climate treaties. Int Environ Agreements 7:73–97
Fearnside PM (2001) Saving tropical forests as a global warming countermeasure: an issue that divides the environmental movement. Ecol Econ 39:167–184
Finus M, Rübbelke DTG (2013) Public good provision and ancillary benefits: the case of climate agreements. Environ Resour Econ 56:211–226
Fudenberg D, Tirole J (1991) Game theory. MIT Press, Cambridge
Garbaccio RF, Ho MS, Jorgenson DW (2000) The health benefits of controlling carbon emissions in China. In: OECD (ed) Ancillary benefits and costs of greenhouse gas mitigation. OECD, Paris, pp 343–376
Garg A (2011) Pro-equity effects of ancillary benefits of climate change policies: a case study of human health impacts of outdoor air pollution in New Delhi. World Dev 39:1002–1025
Gielen D, Chen C (2001) The CO_2 emission reduction benefits of Chinese energy policies and environmental policies: a case study for Shanghai, period 1995–2020. Ecol Econ 39:257–270
Glachant M, de Muizon G (2006) Climate change agreements in the UK: a successful policy experience? In: Morgenstern RA, Pizer WD (eds) Reality check: the nature and performance of voluntary environmental programs in the United States, Europe and Japan. Resources for the Future, Washington, DC, pp 64–85
Gupta J (2010) A history of international climate change policy. WIREs Clim Change 1:636–653

Guttman JM (1978) Understanding collective action: matching behavior. Am Econ Rev 68:251–255
Guttman JM (1987) A non-cournot model of voluntary collective action. Economica 54:1–19
Halsnæs K, Olhoff A (2005) International markets for greenhouse gas emission reduction policies – possibilities for integrating developing countries. Energy Policy 33:2313–2325
Hauert C, Doebeli M (2004) Spatial structure often inhibits the evolution of cooperation in the snowdrift game. Nature 428:643–646
Heggelund GM, Buan IF (2009) China in the Asia–Pacific partnership: consequences for UN climate change mitigation efforts? Int Environ Agreements 9:301–317
Ho MS, Nielsen CP (2007) Clearing the air: the health and economic damages of air pollution in China. MIT Press, London
Houghton JT (1997) Global warming: the complete briefing. Cambridge University Press, Cambridge
IPCC (1996) Climate change 1995 – the science of climate change. Cambridge University Press, Cambridge
IPCC (2001) Climate change 2001 – mitigation. Cambridge University Press, Cambridge
IPCC (2007) Climate change 2007: synthesis report. Cambridge University Press, Cambridge
IPCC (2013a) Climate Change 2013: The Physical Science Basis. Contribution of Working Group I to the Fifth Assessment Report of the Intergovernmental Panel on Climate Change [Stocker, T. F., D. Qin, G.-K. Plattner, M. Tignor, S. K. Allen, J. Boschung, A. Nauels, Y. Xia, V. Bex and P. M. Midgley (eds.)]. Cambridge University Press, Cambridge, United Kingdom and New York, NY, USA
IPCC (2013b) Climate change: the physical science basis, summary for policymakers. Cambridge University Press. http://www.ipcc.ch/pdf/assessment-report/ar5/wg1/WGIAR5_SPM_brochure_en.pdf
Kan H, Chen B, Chen C, Fu Q, Chen M (2004) An evaluation of public health impact of ambient air pollution under various energy scenarios in Shanghai, China. Atmos Environ 38:95–102
Karlsson-Vinkhuyzen SI, van Asselt H (2009) Introduction: exploring and explaining the Asia-Pacific partnership on clean development and climate. Int Environ Agreements 9:195–211
Lal R (2004) Soil carbon sequestration impacts on global change and food security. Science 304:1623–1627
Laroui F, Tellegen E, Tourilova K (2004) Joint implementation in energy between the EU and Russia: outlook and potential. Energy Policy 32:899–914
Larson ED, Wu Z, DeLaquil P, Chen W, Gao P (2003) Future implications of China's energy-technology choices. Energy Policy 31:1189–1204
Lawrence P (2009) Australian climate policy and the Asia Pacific partnership on clean development and climate (APP). From howard to rudd: continuity or change? Int Environ Agreements 9:281–299
Li JC (2006) A multi-period analysis of a carbon tax including local health feedback: an application to Thailand. Environ Dev Econ 11:317–342
Lipman BL (1986) Cooperation among egoists in prisoners' dilemma and chicken games. Public Choice 51:315–331
Lipnowski I, Maital S (1983) Voluntary provision of a pure public good as the game of "chicken". J Public Econ 20:381–386
Markandya A, Rübbelke DTG (2004) Ancillary benefits of climate policy. Jahrbücher für Nationalökonomie und Statistik 224:488–503
Markandya A, Armstrong BG, Hales S, Chiabai A, Criqui P, Mima S, Tonne C, Wilkinson P (2009) Public health benefits of strategies to reduce greenhouse-gas emissions: low-carbon electricity generation. Lancet 374:2006–2015
McGee J, Taplin R (2006) The Asia–Pacific partnership on clean development and climate: a complement or competitor to the Kyoto Protocol? Glob Chang Peace Secur 18:173–192

McGee J, Taplin R (2009) The role of the Asia Pacific partnership in discursive contestation of the international climate regime. Int Environ Agreements 9:213–238
McKinley G, Zuk M, Höjer M, Avalos M, González I, Iniestra R, Laguna I, Martínez MA, Osnaya P, Reynales LM, Valdés R, Martínez J (2005) Quantification of local and global benefits from air pollution control in Mexico city. Environ Sci Technol 39:1954–1961
Mestl HES, Aunan K, Fang J, Seip HM, Skjelvik JM, Vennemo H (2005) Cleaner production as climate investment: integrated assessment in Taiyuan city, China. J Clean Prod 13:57–70
Molina MJ, Rowland FS (1974) Stratospheric sink for chlorofluoromethanes: chlorine atom-catalysed destruction of ozone. Nature 249:810–812
Morgenstern R, Krupnick A, Zhang X (2004) The ancillary carbon benefits of SO_2 reductions from a small-boiler policy in Taiyuan, PRC. J Environ Dev 13:140–155
Nordhaus WD (1998) Is the Kyoto Protocol a dead duck? Are there any live ducks around? Comparison of alternative global tradable emission regimes, preliminary version of the paper presented at the Snowmass workshop on architectural issues in the design of climate change policy instruments and institutions, Yale University, New Haven
Nordhaus WD (2006) After Kyoto: alternative mechanisms to control global warming. Am Econ Rev 96:31–34
O'Connor D, Zhai F, Aunan K, Berntsen T, Vennemo H (2003) Agricultural and human health impacts of climate policy in China: a general equilibrium analysis with special reference to Guangdong, technical papers no. 206, OECD
Ojea E, Nunes PALD, Loureiro ML (2010) Mapping biodiversity indicators and assessing biodiversity values in global forests. Environ Resour Econ 47:329–347
Pearce D (1992) Secondary benefits of greenhouse gas control, CSERGE working paper no. 92-12, London
Pearce D (2000) Policy framework for the ancillary benefits of climate change policies. In: OECD (ed) Ancillary benefits and costs of greenhouse gas mitigation. OECD, Paris, pp 517–560
Peng CY (2000) Integrating local, regional and global assessment in China's air pollution control policy, CIES working paper no. 23
Pezzey JCV, Jotzo F, Quiggin J (2008) Fiddling while carbon burns: why climate policy needs pervasive emission pricing as well as technology promotion. Aust J Agric Resour Econ 52:97–110
Pickering J, Rübbelke DTG (2014) International cooperation on adaptation. In: Markandya A, Galarraga I, de Sainz Murieta E (eds) Routledge handbook of the economics of climate change adaptation. Routledge, Oxon/New York
Pittel K, Rübbelke DTG (2008) Climate policy and ancillary benefits – a survey and integration into the modelling of international negotiations on climate change. Ecol Econ 68:210–220
Pittel K, Rübbelke DTG (2012) Transitions in the negotiations on climate change: from prisoners' dilemma to chicken and beyond. Int Environ Agreements 12:23–39
Pittel K, Rübbelke D (2013) International climate finance and its influence on fairness and policy. World Econ 36:419–436
Rabin M (1993) Incorporating fairness into game theory and economics. Am Econ Rev 83:1281–1302
Rapoport A, Chammah AM (1966) The game of chicken. Am Behav Sci 10:10–28
Rive N, Rübbelke DTG (2010) International environmental policy and poverty alleviation. Rev World Econ 146:515–543
Rübbelke DTG (2002) International climate policy to combat global warming – an analysis of the ancillary benefits of reducing carbon emissions. Edward Elgar, Cheltenham/Northampton
Rübbelke DTG (2006) An analysis of an international environmental matching agreement. Environ Econ Policy Stud 8:1–31
Rübbelke DTG (2011) International support of climate change policies in developing countries: strategic, moral and fairness aspects. Ecol Econ 70:1470–80
Rübbelke DTG, Vögele S (2011) Impacts of climate change on European critical infrastructures: the case of the power sector. Environ Sci Pol 14:53–63

Rübbelke DTG, Vögele S (2013) Short-term distributional consequences of climate change impacts on the power sector: who gains and who loses? Clim Chang 116:191–206
Samuelson PA (1954) The pure theory of public expenditure. Review of Economics and Statistics 36:387–389
Samuelson PA (1955) Diagrammatic exposition of a theory of public expenditure. Review of Economics and Statistics 37:350–356
Sandler T (1997) Global challenges – an approach to environmental, political, and economic problems. Cambridge University Press, Cambridge
Sandler T, Sargent K (1995) Management of transnational commons: coordination, publicness, and treaty formation. Land Econ 71:145–162
Shrestha RM, Malla S, Liyanage MH (2007) Scenario-based analyses of energy system development and its environmental implications in Thailand. Energy Policy 35:3179–3193
Smith B (1998) Ethics of Du Pont's CFC strategy 1975–1995. J Bus Ethics 17:557–568
Smith KR, Haigler E (2008) Co-benefits of climate mitigation and health protection in energy systems: scoping methods. Annu Rev Public Health 29:11–25
Smith S, Swierzbinski J (2007) Assessing the performance of the UK Emissions Trading Scheme. Environ Resour Econ 37:131–158
Smith SJ, Wigley TML (2000) Global warming potentials: 1. Climatic implications of emissions reductions. Clim Chang 44:445–457
Snyder GH (1971) "Prisoner's dilemma" and "chicken" models in international politics. Int Stud Q 15:66–103
Stern N (2007) The economics of climate change – the stern review. Cambridge University Press, Cambridge
UNFCCC (2011) Decision 1/CP.17: establishment of an Ad Hoc Working Group on the Durban platform for enhanced action. United Nations Framework Convention on Climate Change, Bonn
UNFCCC (2014a) Distribution of expected CERs from registered projects by Host Party. https://cdm.unfccc.int/Statistics/Public/files/201407/ExpRed_reg_byHost.pdf. Last viewed 19 Aug 2014
UNFCCC (2014b) Glossary: CDM terms. https://cdm.unfccc.int/Reference/Guidclarif/glos_CDM.pdf. Last viewed 19 Aug 2014
Van Vuuren DP, Fengqi Z, de Vries B, Kejun J, Graveland C, Yun L (2003) Energy and emission scenarios for China in the 21st century – exploration of baseline development and mitigation options. Energy Policy 31:369–387
Vennemo H, Aunan K, Jinghua F, Holtedahl P, Tao H, Seip HM (2006) Domestic environmental benefits of China's energy-related CDM potential. Clim Chang 75:215–239
Wang X, Smith KR (1999a) Near-term health benefits of greenhouse gas reductions: a proposed assessment method and application in two energy sectors of China, WHO/PHE/99.1. World Health Organization, Geneva
Wang X, Smith KR (1999b) Secondary benefits of greenhouse gas control: health impacts in China. Environ Sci Technol 33:3056–3061
WCED (1987) Our common future. Oxford University Press, Oxford
West JJ, Osnaya P, Laguna I, Martínez J, Fernández A (2004) Co-control of Urban air pollutants and greenhouse gases in Mexico city. Environ Sci Technol 38:3474–3481
Yamin F, Depledge J (2004) The international climate change regime: a guide to rules, institutions and procedures. Cambridge University Press, Cambridge
Zhang ZX (2006) Towards an effective implementation of CDM projects in China. Energy Policy 34:3691–3701
Zheng X, Zhang L, Yu Y, Lin S (2011) On the nexus of SO_2 and CO_2 emissions in China: the ancillary benefits of CO_2 emission reductions. Reg Environ Chang 11:883–891

Ethics and Environmental Policy

David J. Rutherford and Eric Thomas Weber

Contents

Abstract

This chapter offers a survey of important factors for the consideration of the moral obligations involved in confronting the challenges of climate change. The first step is to identify as carefully as possible what is known about climate change science, predictions, concerns, models, and both mitigation and adaptation efforts. While the present volume is focused primarily on the mitigation side of reactions to climate change, these mitigation efforts ought to be planned in part with reference to what options and actions are available, likely, and desirable for adaptation. Section "Understanding Climate Change," therefore, provides an

D.J. Rutherford (✉) • E.T. Weber
Department of Public Policy Leadership, The University of Mississippi, Oxford, MS, USA
e-mail: druther@olemiss.edu; etweber@olemiss.edu

W.-Y. Chen et al. (eds.), *Handbook of Climate Change Mitigation and Adaptation*,
DOI 10.1007/978-3-319-14409-2_5

overview of the current understanding of climate change with careful definitions of terminology and concepts along with the presentation of the increasingly strong evidence that validates growing concern about climate change and its probable consequences. Section "Uncertainties and Moral Obligations Despite Them" addresses the kinds of uncertainty at issue when it comes to climate science. The fact that there are uncertainties involved in the understanding of climate change will be shown to be consistent with there being moral obligations to address climate change, obligations that include expanding the knowledge of the subject, developing plans for a variety of possible adaptation needs, and studying further the various options for mitigation and their myriad costs. Section "Traditions and New Developments in Environmental Ethics" covers a number of moral considerations for climate change mitigation, opening with an examination of the traditional approaches to environmental ethics and then presenting three pressing areas of concern for mitigation efforts: differential levels of responsibility for action that affects the whole globe, the dangers of causing greater harm than is resolved, and the motivating force of diminishing and increasingly expensive fossil fuels that will necessitate and likely speed up innovation in energy production and consumption that will be required for human beings to survive once fossil fuels are exhausted.

Introduction

Few subjects are as complex and as frequently oversimplified as climate change. After big snowfalls in winters past, news outlets have featured various observers of these local events, who dismiss the idea of global warming with statements such as "so much for the global warming theory" (LaHay 2000). On the other hand, climate scientists note that Earth's average temperature has risen over time, and as a result, they predict increases in temperature extremes and vaporization of water that, in turn, lead to an expectation of increased snowfall in some years. Problems of understanding and misunderstanding such as these are important causes of confusion in discussions about climate change, and those problems and that confusion combined with the complexity of the issues at stake add considerable challenge to addressing the topic of focus in this chapter: the ethics of climate change mitigation.

This chapter will argue that despite limitations to knowledge about the complexities of the climate system, certain efforts must be undertaken to prepare for and address the developments in climate change. The science on the subject is growing increasingly compelling, showing that there is need to work toward mitigating the causal forces that are bringing about climate change along with preparing adaptations to changes in climate, some of which have already begun (Walther et al. 2002). Furthermore, the existence of uncertainties with respect to climate science calls for more study of the subject of climate change, with greater collaboration than is already at work. Calling for further study of the subject, however, does not imply the postponement of all or any particular measure of precaution and potential action. This chapter will examine the current knowledge about climate change as well as the

moral dimensions at issue in both seeking to minimize those changes and working to prepare for the changes and their effects.

When the term "mitigation" arises in this chapter, it is important to keep in mind a consistent meaning. To mitigate something generally means to make it less harsh and less severe, but in relation to climate change, mitigation carries a more precise meaning. The term refers to human actions taken to reduce the forces that are believed responsible for the increase of the average temperature of the Earth. The primary concern with climate change is the increase of global average temperature, and mitigation is aimed at decreasing the rate of growth of this global temperature and stabilizing it or even decreasing it should it rise too high. Mitigation is sometimes referred to as abatement. Generally, the idea of abatement is either to reduce the rate of growth that is or will likely be problematic or to actually reverse the trend and reduce global average temperature. In contrast to mitigation, a second category of response to climate change is to find ways of adapting life to new conditions, the method of adaptation. Adaptation refers to adjustments made in response to changing climates that moderate harm or exploit beneficial opportunities (Intergovernmental Panel on Climate Change 2007a). The interesting issue that arises in focusing on climate change mitigation – the efforts to decrease the causal forces of rising global temperatures – is that subtle changes in temperature might be the kind to which some or even many people will be able to adapt relatively easily. For instance, if people live on coastal lands that are increasingly inundated, there are ways of reclaiming land from water or places to which people can move in adaptation to the climate changes. Other adaptations might include systems of planned agricultural crop changes prepared to avoid problems that could arise in growing food for the world's increasing population. An important consideration about adaptation is that while humans may be able to change and adjust to changing climates, natural ecosystems and habitats may not, a point that will also be addressed in this chapter.

There are certainly reasons to worry about sudden, great changes, but more gradual and less severe changes raise a host of ethical issues. For instance, it is reasonable to ask whether a farmer has the moral right to grow a certain crop. If so, then it may be that people have a responsibility to avoid changing the climate. Belief in such a right, however, could be considered highly controversial. What if farmers could reasonably expect some help in adapting the crops that they raise to new conditions? This idea would lessen the moral concern over the ability to grow a certain crop in a particular region, and thus a matter of adaptation would have bearing on the moral dimensions of climate change mitigation.

It is likely that the best solution to address the ill effects of climate change will require a combination of mitigation and adaptation strategies. A central claim of this chapter, therefore, is that the ethics of climate change mitigation must not be considered in isolation from the options available for adaptation. Of the two, however, the more controversial, morally speaking, are abatement efforts or mitigation. This is because when climate conditions change, there will be no choice for people but to adapt to new circumstances if presented with serious challenges for survival, at least until humans are able to exert control in a desirable way on the trends in global climate. But abatement efforts, on the other hand, require sacrifices

early, before certainty exists about the exact nature and extent of the problems to come and whom the problems, benefits, and mitigating efforts will most affect and how.

Accompanying the problem of complexity that exists in climate change is a necessary challenge of uncertainty. The approach of addressing change through adaptive measures can be started early and is also possible as some more gradual changes occur, such as in the evacuation of islands that slowly disappear under the rising level of the sea. Other problems, however, are predicted to occur swiftly, such as in the potential disruption of the ocean conveyor, a "major threshold phenomenon" that could bring "significant climatic consequences," such as severe droughts (Gardiner 2004, pp. 562–563). The problem of knowledge, of the limits to human abilities to identify where suffering or benefits will occur, under what form, by which mechanisms, implies that preventive adaptations may be impossible in the face of sudden changes in global climates. Furthermore, if there existed no idea of changes that might occur, this limited knowledge might render the effects of changing conditions less troubling morally speaking. But the fact is that today many scientists have devised models that suggest potential outcomes of climate change and so undercut the option of ignorant dismissal or avoidance of moral obligation. Limited knowledge about climate change first and foremost calls for increasing the knowledge and study of the subject, but it also demands consideration of the kinds of problems that can be expected, weighed against the anticipated costs of alleviating the worst of the threats.

This chapter will offer a survey of a number of important factors for the consideration of the moral obligations involved in confronting the challenges of climate change. The first step is to identify as carefully as possible what is known about climate change science, predictions, concerns, models, and both mitigation and adaptation efforts. While the present volume is focused primarily on the mitigation side of reactions to climate change, these mitigation efforts ought to be planned in part with reference to what options and actions are available, likely, and desirable for adaptation. Section "Understanding Climate Change," therefore, provides an overview of current understanding of climate change with careful definitions of terminology and concepts along with the presentation of the increasingly strong evidence that validates growing concern about climate change and its probable consequences. Next, section "Uncertainties and Moral Obligations Despite Them" will address the kinds of uncertainty at issue when it comes to climate science. The fact that there are uncertainties involved in human understanding of climate change will be shown to be consistent with there being moral obligations to address climate change. As mentioned above, these are obligations to know more than is currently known, to develop plans for a variety of possible adaptation needs, and to study further the various options for mitigation and their myriad costs. Plus, Gardiner (2004) presented a convincing case for the weighing of options that concludes in accepting the consequences of a small decrease in GNP from setting limits on global greenhouse gas emissions. Gardiner's argument is compelling even in the face of uncertainty. After all, the uncertainties involved in climate change resemble uncertainties that motivate moral precaution in so many other spheres of human conduct. Finally,

section "Traditions and New Developments in Environmental Ethics" covers a number of moral considerations for climate change mitigation. This section opens with an examination of the traditional approaches to environmental ethics and then presents three pressing areas of concern for mitigation efforts: differential levels of responsibility for action that affects the whole globe, the dangers of causing greater harm than is resolved (with geoengineering efforts, among others), and the motivating forces of diminishing and increasingly expensive fossil fuels that will necessitate and likely speed up innovation in energy production and consumption that will be required for human beings to survive once fossil fuels are exhausted.

Understanding Climate Change

Given the complexity of addressing global climate change, it is crucial to clarify the meaning of a number of key terms, forces, and strategies for mitigation, so this first section will begin with a description of central terms and concepts at issue. The section then covers perceptions and methods for describing climate change because ideologies and affective influences on discourse about climate change can be used to mislead the public about the nature and the state of climate science. After that, the section examines the state of scientific knowledge and the predictions that the scientific community has presented about the future of climate change. This is important in order to grasp the extent of concern that world leaders and publics ought to feel about the future of the world's climates. Finally, this section will close with a brief description of the various proposals that have been considered for mitigating climate change.

Terminology and Concepts

Uncertainty, confusion, and misunderstanding result from poorly or ambiguously defined terminology and concepts, and this is especially the case with the topic of climate change. Climate change is complex and often elicits heated and impassioned public discourse. To reduce such problems, this section provides definitions for terms and concepts that are essential for both an explanation of what is known about climate change and for consideration of the broader topic of ethics and climate change mitigation. Some of these definitions are contested, and in such cases, the preferred definitions presented here will be contrasted with other definitions found in the literature, along with provision of an explanation for the selections made.

Weather and Climate

The term "weather" refers to short-term atmospheric conditions occurring in a specific time and place and identified by the sum of selected defining variables that can include temperature, precipitation, humidity, cloudiness, air pressure, wind (velocity and direction), storminess, and more. Weather is measured and reported at the scale of moments, hours, days, and weeks. Climate, on the other hand, is defined

(in a narrow sense) as the aggregate of day-to-day weather conditions that have been averaged over longer periods of time such as a month, a season, a year, decades, or thousands to millions of years. Climate is a statistical description that includes not just the average or mean values of the relevant variables but also the variability of those values and the extremes (McKnight and Hess 2000; Intergovernmental Panel on Climate Change 2007b).

The Climate System

Understanding climate entails more than consideration of just the aggregated day-to-day weather conditions averaged over longer periods of time. Those average atmospheric conditions operate within the wider context of what is called the climate system that includes not just the atmosphere but also the hydrosphere, the cryosphere, the Earth's land surface, and the biosphere.

- The *atmosphere* is a mixture of gasses that lie in a relatively thin envelope that surrounds the Earth and is held in place by gravity. The atmosphere also contains suspended liquid and solid particles that "can vary considerably in type and concentration and from time to time and place to place" (Kemp 2004, p. 37). On average, 50 % of the atmospheric mass lies between sea level and 5.6 km (3.48 miles or 18,372 ft) of altitude. To highlight how thin this is, consider that the peak of Mt. McKinley in Alaska is 6.19 km (20,320 ft) above sea level and, as a result, the density of air is less than 50 % of that available at sea level or that the peak of Mt. Everest at 8.85 km (29,029 ft) has less than 32 % of the air density that is available at sea level. Commercial jet airliners generally fly at about 10.5 km (35,000 ft) above sea level, and humans would lapse into unconsciousness very quickly if cabin pressure were to decrease suddenly at this altitude (Strahler and Strahler 1978).
- The *hydrosphere* consists of liquid surface water such as the ocean, seas, lakes, and rivers, along with groundwater, soil water, and, importantly, water vapor in the atmosphere.
- The *cryosphere* consists of all snow, ice (glaciers and ice sheets), and frozen ground (including permafrost) that lie on and beneath the surface of the Earth.
- Earth's *land surface* consists of the naturally occurring rock and soil along with the structures (buildings, roads, etc.) that humans have constructed.
- The *biosphere* consists of all living organisms, both plant and animal, on land, in fresh water, and in the ocean, including derived dead organic matter such as litter, soil organic matter, and ocean detritus.

The climate system functions by means of complex interactions among these five components in which flows and fluxes of energy and matter take place through myriad processes such as radiation, convection, evaporation, transpiration, chemical exchanges, and many more (Climate Change 2007c). Given this complexity, climate science is an interdisciplinary endeavor that necessarily involves the interactions and contributions of a wide range of the physical sciences such as physics, chemistry, biology, ecology, oceanography, and the atmospheric sciences. Moreover, because

human existence involves interactions with climate, the social sciences such as psychology, political science, and sociology also play important roles in human understanding. In addition, climate operates over time and space, so the synthesizing disciplines of history and geography have much to contribute as well. Furthermore, as shown later in this chapter, the humanities contribute to the understanding of the social dimensions of climate systems when it comes to considering the moral implications of various situations and actions in response to climate change.

Climate Change

The most recent definition of climate change developed by the Intergovernmental Panel on Climate Change (IPCC) will be used in this chapter:

> Climate change refers to a change in the state of the climate that can be identified (e.g., by using statistical tests) by changes in the mean and/or the variability of its properties, and that persists for an extended period, typically decades or longer (Climate Change 2007c, p. 78; see also USCCSP (United States Climate Change Science Program) 2007).

Importantly, this definition is solely descriptive and includes no reference to causation, particularly no indication of the extent to which any changes in climate result from natural or human (anthropogenic) causes. Other definitions of climate change include causation, such as the United Nations Framework Convention on Climate Change:

> "Climate change" means a change of climate which is attributed directly or indirectly to human activity that alters the composition of the global atmosphere and which is in addition to natural climate variability observed over comparable time periods (UNFCCC (United Nations Framework Convention on Climate Change) 1992, p. 3).

The first definition was selected for use in this chapter because it focuses on identifying and describing observed changes in climate and specifically refrains from assigning causation to either natural or anthropogenic processes. As a result, it draws attention to the distinction between two aspects of inquiry: (1) questions related to the presence, extent, and direction of changes in climate and (2) questions about causation of any observed changes, especially determinations of natural or anthropogenic causes. Views about (2) are often disconnected from questions about presence, extent, and direction of change and also tend to generate more contentious debate, especially in public and political discourse. As means to reduce contention, it is helpful to make the clear distinction between these two aspects of inquiry, and such clarity is especially important in this chapter, considering issues of ethics, mitigation, and adaptation. Additionally, and importantly, the selected definition implies no specific type of change(s) but instead fosters recognition that changes can occur in all manner of the variables that constitute climate such as temperature, precipitation, humidity, cloud cover, etc. (this point is further elaborated below with respect to the terms "climate change" and "global warming").

An additional reason to clarify the difference between (1) and (2) is that consideration of (1) generally engenders less controversy, while the task of determining

who should act in addressing any needs that arise from climate change will depend in part on how one addresses issue (2). As such, (2) is not to be ignored in addressing the ethics of climate change, but after untangling (1) from (2), the problems to be addressed can be recognized for what they are more easily.

Climate Variability

Most definitions of climate variability found in the literature differ little from the above definitions of climate change. For example, as defined in the Synthesis Report for the IPCC Fourth Assessment (Climate Change 2007c, pp. 78–79), the two terms actually seem synonymous in that they both refer to changes occurring on timescales of multiple decades or longer and they both allow for natural and anthropogenic causes. Other definitions of climate variability retain the focus on timescales of multiple decades or longer but limit climate variability to only natural causes (Batterbee and Binney 2008; Climate Research Program 2010). In this chapter, however, the term will refer to something different from either of these uses.

The term "climate variability" is used in this chapter in recognition that the long-term, statistical averages of the variables that define climates can contain substantial variation around the mean. Droughts, rainy periods, El Niño events, etc., occur in time periods of a year to as much as three decades within climates that are considered to be stable as well as within climates that are experiencing changes in the longer term. This variability is different from extreme weather events such as floods and heat waves that occur on timescales of hours, days, and weeks, and it is also different from the long-term climate changes that occur on scales that span multiple decades to millions of years (which have already been defined above as "climate change").

The reasons to differentiate climate variability from climate change in this way are twofold. First, climate variability can generate considerable "noise" in the data that can lead to erroneous conclusions about climate change. For example, Fig. 1 shows two levels of variability – interannual and multi-decadal – that are present in the observed global temperature record that extends from 1880 to 2009. Interannual

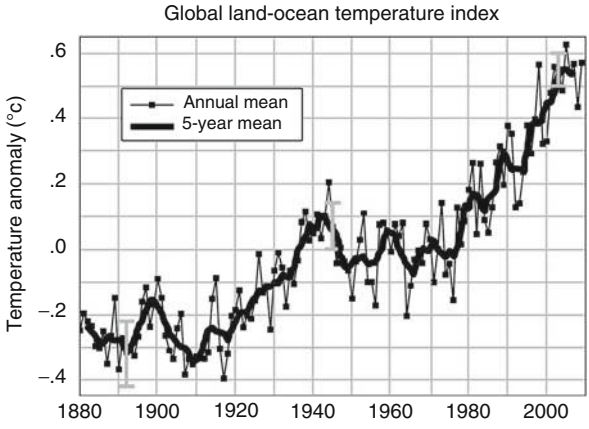

Fig. 1 A *line plot* of the global land-ocean temperature index from 1880 to 2009, with the base period 1951–1980. The *dotted black line* is the annual mean and the *solid black line* is the 5-year mean. The *gray bars* show uncertainty estimates (GISS (Goddard Institute for Space Studies) 2010a)

variability (variability from year to year) is as much as 0.3 °C (0.54 °F), a range that could be expressed as 1 year with a very hot summer and a mild winter followed by a second year with a mild summer and a very cold winter. The conditions present in either of these years could lead people to make poor judgments about climate. In particular, the long-term warming trend that the graph shows occurring across the full 119-year period is sometimes dismissed because people generally give greater weight in decision making and opinion formation to immediate affective sensory input over cognitive consideration of statistics (Weber 2010) (more will be said below about human decision making that is affect based compared to a basis on statistical description). The variability over several decades is exhibited in Fig. 1 for the time period 1940–1980, which shows a plateau within the longer-term, 119-year warming trend. During this shorter time period, media reports and even a few researchers erroneously forecast "global cooling" based on the observational record at the time that included inadequate and uncertain data from years earlier than this time period and, obviously, no data beyond 1980 (de Blij 2005, p. 85).

The second important reason for distinguishing between climate variability and climate change in the way defined in this chapter is related to dynamic equilibrium in ecosystems. Dynamic equilibrium results as ecosystems adapt to dynamic, ongoing forces that are not so extreme as to produce catastrophic changes. This dynamic equilibrium occurs because the change forces are not dramatic enough (or they cancel each other out), so that relative stability in the ecosystem can be perpetuated as the organisms (plants and animals) and the physical environment respond with adjustments that are within their adaptive capacities. In general, ecosystem adaptive capacity is not exceeded (and dynamic equilibrium is maintained) as a result of climate variability as defined here, but climate change, on the other hand, often exceeds this capacity and leads to fundamental alterations of the ecosystems. Such fundamental alterations occurring in natural ecosystems include processes such as species extinction, changes in community compositions, changes in ecological interactions, changes in geographical distributions, etc. Fundamental alterations can also occur within ecosystems upon which humans depend, leading to such changes as increases/decreases in agricultural productivity and the availability of water, changes in storm patterns, etc. (Intergovernmental Panel on Climate Change 2007a). These effects on both natural and human ecosystems will be discussed in more detail in what follows, but the important point here is that climate variability rarely produces such fundamental alterations, whereas climate change frequently can.

Global Warming and Global Average Temperature

Global warming is defined as an increase in the average temperature of Earth's surface NASA (National Aeronautics and Space Administration) 2007. As Fig. 1 illustrates, this average surface temperature has increased by 0.75 °C ± 0.3 °C (1.35 °F ± 0.54 °F) between 1880 and 2009. While this change might seem small, the paleoclimate record demonstrates that even "mild heating can have dramatic consequences" such as advancing or retreating glaciers, sea level changes, and changes in precipitation patterns that can all force considerable changes in human activity and

push natural ecosystems beyond dynamic equilibrium (Hansen 2009). The graph in Fig. 1 comes from NASA's Goddard Institute for Space Studies Surface Temperature Analysis (GISTEMP) database which contains temperature observations from land and sea from 1880 to the present (GISS (Goddard Institute for Space Studies) 2010b). It is one of the three such large databases of Earth surface atmospheric observations that all begin in the mid- to late nineteenth century and extend to the present. The National Oceanic and Atmospheric Administration (NOAA) maintains the second database that is titled the Global Historical Climatology Network (GHCN), and while this database contains observations from land stations only, it includes precipitation and air pressure data as well as temperature (National Climatic Data Center 2008). The third database is abbreviated HadCRUT3 which reflects the source of the dataset being a collaborative project of the Met Office Hadley Center of the UK National Weather Service ("Had") and the Climate Research Unit ("CRU") at the University of East Anglia. The Hadley Center provides marine surface temperature data, and the Climate Research Unit provides the land surface temperature data. These three databases are not completely independent because they share some of the same observation stations, but nevertheless, some differences in the raw data exist, and the three centers work independently using different approaches to the compilation and analysis done on the datasets. As such, the comparisons of results from the different databases allow for verification. Considerable consistency is apparent across the databases, especially in the overall trend of global warming since 1880. The different centers "work independently and use different methods in the way they collect and process data to calculate the global average temperature. Despite this, the results of each are similar from month to month and year to year, and there is definite agreement on temperature trends from decade to decade. Most importantly, they all agree that global average temperature has increased over the past century and this warming has been particularly rapid since the 1970s" (Stott 2011).

Figure 2 shows the temperature record for each of the three datasets superimposed upon one another, and the consistency among them is clear. In addition, research has been done to identify and quantify uncertainty in the data, and good estimates of the uncertainty indicate that the data are valid. As one such study stated:

> Since the mid twentieth century, the uncertainties in global and hemispheric mean temperatures are small, and the temperature increase greatly exceeds its uncertainty. In earlier periods the uncertainties are larger, but the temperature increase over the twentieth century is still significantly larger than its uncertainty (Brohan et al. 2006, p. 1).

The temperature records shown in Fig. 2 for each of the three centers are developed as each center uses its dataset to calculate a "global average temperature," both for the past and for monthly updates, and it is these values that are displayed on the graphs in the figure. While these calculations are done differently at the three centers, all three use the following general procedure. First, they expend considerable efforts to obtain the most accurate data possible and define the uncertainty that remains in those data. Then, the monthly average temperature value for each

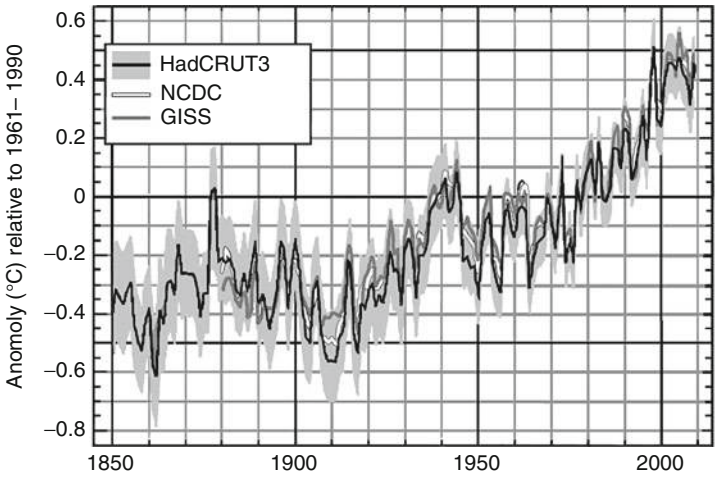

Fig. 2 Correlation between the three global average temperature records. All three datasets show clear correlation and a marked warming trend, particularly over the past three decades. The *HadCRUT3 graph* shows uncertainty bands which tighten up considerably after 1945 (WMO (World Meteorological Organization) 2010)

reporting station is converted into what is called an "anomaly." The anomaly of each reporting station is calculated by subtracting the monthly average value from the average value that the station has maintained over some relatively long-term "base period" (e.g., the HadCRUT3 uses the period 1961–1990 as its base period). The reason for using anomalies is stated as follows:

> For example, if the 1961–1990 average September temperature for Edinburgh in Scotland is 12 °C and the recorded average temperature for that month in 2009 is 13 °C, the difference of 1 °C is the anomaly and this would be used in the calculation of the global average (Stott 2011).

One of the main reasons for using anomalies is that they remain fairly constant over large areas. So, for example, an anomaly in Edinburgh is likely to be the same as the anomaly further north in Fort William and at the top of Ben Nevis, the UK's highest mountain. This is even though there may be large differences in absolute temperature at each of these locations.

The anomaly method also helps to avoid biases. For example, if actual temperatures were used and information from an Arctic observation station was missing for that month, it would mean the global temperature record would seem warmer. Using anomalies means missing data such as this will not bias the temperature record (Stott 2011; see National Climatic Data Center 2010a for additional explanation of the calculation and use of anomalies as used for the National Climate Data Center's GHCN system).

Even though using anomalies produces the most accurate record of Earth's global average temperature, it is still interesting to calculate one single absolute "global

average temperature." Using the GHCN dataset (National Climatic Data Center 2010b), the average value for the last 10 years, the warmest decade on record (GISS (Goddard Institute for Space Studies) 2010a; Atmospheric Administration 2009; WMO (World Meteorological Organization) 2009), produces a global average temperature for planet Earth of 14.4 °C or 58 °F.

Climate Forcing and Climate Feedback

Climate forcing refers to the processes that produce changes in the climate. The word force is generally defined as "strength or energy that is exerted or brought to bear [and that often] causes motion or change" (Merriam-Webster 2003). With respect to Earth's climate system, a variety of forces cause climates to change. These are called "climate forcings," and they are all related to Earth's "energy balance," that is, the balance between incoming energy from the Sun and outgoing energy from the Earth. The forcings can be internal or external. "Internal forcings" occur within the climate system and include processes such as changes in atmospheric composition or changes in ice cover that cause different rates of absorption/reflection of solar radiation. "External forcings" originate from outside the climate system and include processes such as changes in Earth's orbit around the Sun and volcanic eruptions. Forcings can be naturally occurring, such as those resulting from solar activity or volcanic eruptions, or anthropogenic in origin, for example, the emission of greenhouse gases or deforestation (Intergovernmental Panel on Climate Change 2007a, p. 9).

A feedback is defined as a change that occurs within the climate system in response to a forcing mechanism. A feedback is called "positive" when it augments or intensifies the effects of the forcing mechanism or "negative" when it diminishes or reduces the effects caused by that original forcing mechanism (Intergovernmental Panel on Climate Change 2007a, p. 875).

Forcing and feedback mechanisms often interact in complex ways that make it difficult to decipher the processes and dynamics of climate change. This difficulty also frequently frustrates policymakers, the media, and the public, and it can result in the dissemination of misinformation, both intentional and unintentional, into the public discourse. One example of this relates to the relationship between carbon dioxide (CO_2) and temperature. While it is relatively easy to understand that increasing concentrations of atmospheric CO_2 can increase the naturally occurring greenhouse effect thereby causing global warming, confusion and misinformation result when research brings to light a climate record in which changes in the atmospheric CO_2 level lag behind changes in temperature by 800–1,000 years. The legitimate question arises as to how it could be possible that CO_2 causes global warming if the rise in temperature occurs before the increase in the atmospheric concentration of CO_2. While the question is legitimate, unfortunately, some who are disposed to doubt claims of global warming neither seek answers to the question nor pursue additional investigation. Instead, they simply assert the premise that because CO_2 lags temperature, it cannot possibly be the cause of global warming. However, a more objective review of the scientific literature emphasizes the importance of distinguishing between forcings and feedbacks.

The initial, external forcing that begins the temperature changes observed in the climate record stems from fluctuations in the orbital relations between the Sun and Earth, and these fluctuations produce rather small changes in the amount of solar radiation reaching Earth (Hays et al. 1976). This relatively weak forcing action causes small temperature changes that are then amplified by other processes (Lorius et al. 1990). One such amplifying process that appears to be quite significant occurs because ocean temperature changes also change the ocean's capacity to retain soluble CO_2. As this capacity changes, it causes CO_2 to either be released from the oceans into the atmosphere (during times of warming temperatures) or removed from the atmosphere and dissolved into the oceans (during times of cooling temperatures). Consequently, CO_2 operates in these situations as a *positive feedback* mechanism that augments the temperature change. In other words, it enhances the greenhouse effect and amplifies temperature increases during times of warming and reduces the greenhouse effect and reinforces temperature decreases during times of cooling (Martin et al. 2005). Careful analysis therefore suggests that a climate record which shows CO_2 operating as a feedback mechanism neither negates nor renders less likely the potential that CO_2 could operate as an initial forcing mechanism as well. Considering that the atmospheric concentration of CO_2 has increased by 25 % in the last 50 years (Atmospheric Administration 2010), it is entirely possible that this increasing CO_2 concentration is functioning as the forcing agent for contemporary global warming. Simply put, it is a false premise to claim that CO_2 could not be causing contemporary global warming because CO_2 has been observed to lag behind temperature changes in the past. This false premise has been lampooned by the analogous statement that "Chickens do not lay eggs, because they have been observed to hatch from them" (Bruno 2009).

Global Warming Versus Climate Change

The terms "global warming" and "climate change" have been defined above, and those definitions will not be repeated here. But it is important to emphasize the difference between the two terms and the significance of exercising precision in use of them. While "global warming" is a useful way to refer to the increase of global average temperature that strong scientific evidence shows has occurred over the last 130 years (Fig. 2), for some people, the term carries the automatic connotation that human activity is the cause of this observed temperature increase. As stated earlier, a clear distinction should be made between questions that, on the one hand, relate to the changes in climate, if any, that are occurring and, on the other hand, the causes of any identified changes, specifically, naturally occurring or anthropogenic. Because the term "global warming" carries the more polemical and politicized connotation, it poses a higher probability of conflating the two questions than does the term "climate change" which has not yet attracted such politicized interpretations. Consequently, in general, the term "climate change" is preferable.

A second deficiency with the term "global warming" is the one-dimensional and totalizing change that it implies. Although the average temperature of planet Earth is increasing, the temperature change that any particular place on the Earth might

experience could be cooling instead of warming, or perhaps that place might be experiencing no change in temperature at all. But the term "global warming" is easily, and perhaps most naturally, understood to mean that all places on the Earth will experience warming. Moreover, even if the term is explained, it does not readily lend itself to the broader understanding that although the global average temperature is increasing, it is not necessarily the case that temperature is increasing at any given place on Earth. The term "climate change," on the other hand, does not imply this uniform nature of change and thus possesses greater capacity to communicate the potential for different changes occurring in different places and regions. In addition, the term "global warming" implies a narrow view of the nature of changes that can occur in the climate system, namely, an exclusive focus on temperature. But the possible changes to climate are not restricted to just the climate variable of temperature, and the observed increase in global average temperature has been associated with changes in a range of other climate variables that include precipitation amounts, timing and patterns, cloudiness, humidity, wind direction and velocity, storminess, and more. While the term "global warming" places the focus on temperature, the term "climate change" offers a much richer capacity to incorporate these other types of changes as well and, as a result, is generally emerging as the preferred term.

Thresholds and Tipping Points

The term "threshold" in ecology and environmental science means "a fixed value at which an abrupt change in the behavior of a system is observed" (Park 2008, p. 450). In climate science, the term "climate threshold" means the point at which some forcing of the climate system "triggers a significant climatic or environmental event which is considered unalterable, or recoverable only on very long time-scales, such as widespread bleaching of corals or a collapse of oceanic circulation systems" (Intergovernmental Panel on Climate Change 2007a, p. 872). Substantial research indicates that climate changes are prone to such thresholds, or "tipping points," at which climate on a global scale or climates at regional scales can suddenly experience major change (Committee on Abrupt Climate Change 2002; Lenton et al. 2008). A wide number of complex systems exhibit similar threshold events – financial markets, ecosystems, and even epileptic seizures and asthma attacks – in which the system seems stable right up until the time when the sudden change occurs (Scheffer et al. 2009). Research has provided general ideas on where these thresholds or tipping points might operate with respect to climate – the loss of Arctic sea ice or Antarctic ice shelves, the release of methane into the atmosphere from the melting of Siberian permafrost, or the disruption of the "oceanic conveyor belt" – but this knowledge is rudimentary at best. Scheffer and colleagues (2009) report tentative efforts to identify "early warning signs" that precede threshold events, and with respect to climate, they state that "flickering," "rapid alterations," or increased weather and climate "variability" seem to have preceded sudden changes observed in the climate record. But at present, predicting these climatic thresholds is vague at best. One of the authors explained the idea of thresholds and the uncertainty about them in an interview with *Time* magazine, "Managing the environment is like

driving [on] a foggy road at night by a cliff. . . .You know it's there, but you don't know where exactly" (Walsh 2009).

Defining and Communicating Uncertainty

Clearly, climate science contains uncertainties that are endemic to the data sources used, to the understanding of processes involved, and to predictions of future trends, impacts, and outcomes. Consequently, it is essential to accompany any study of climate change with careful, explicit, and candid assessments of the levels of certainty or confidence associated with the findings or claims made. Indeed, reports or studies are suspect if they fail to include such information and/or if they make unequivocal statements about "proving" their points. To some extent, the same can be said about commentaries, news reports, or various information sources. While the politicized environment in which climate change is debated might encourage strong and definite affirmations, such statements can prove counterproductive if they are perceived or exposed as exaggerated (Weber 2010; Hodder and Martin 2009).

Numerous approaches exist for defining and communicating uncertainty, and this brief discussion here does not attempt a comprehensive overview. Instead, it focuses on the approach that the IPCC has developed for its assessment reports. The main function of the IPCC is to "assess the state of our understanding and to judge the *confidence* with which we can make projections of climate change, its impacts, and costs and efficacy of options," but in its first and second assessments (1990 and 1995, respectively), the IPCC gave inadequate attention to "systematizing the process of reaching collective judgments about uncertainties and levels of confidence or standardizing the terms used to convey uncertainties and levels of confidence to the decision-maker audience" (Moss 2006, p. 5 emphasis added). Consequently, the IPCC conducted a comprehensive project to rectify these inadequacies (Moss and Schneider 2000; Manning et al. 2004), and the result was the following system for defining and communicating uncertainties in the Fourth Assessment Report published in 2007.

The first step is to present a general summary of the state of knowledge related to the topic being presented. This summary should include (1) the amount of evidence available in support of the findings and (2) the degree of consensus among experts on the interpretation of the evidence (Climate Change 2005). Figure 3 illustrates how these two factors form interacting continua that produce qualitative categories.

The IPCC guidance notes for addressing uncertainty (Climate Change 2005, p. 3 emphasis in original) state that in cases where the level of knowledge is determined to be "*high agreement*, *much evidence*, or where otherwise appropriate," additional information about uncertainty should be provided through specification of a level of confidence scale and a likelihood scale. The level of confidence scale addresses the degree of certainty that the results are correct, while the likelihood scale specifies a probability that the occurrence or outcome is taking place or will take place. The IPCC guidelines state that the level of confidence scale "can be used to characterize uncertainty that is based on expert judgment as to the correctness of a model, an analysis or a statement. The last two terms in the scale should be reserved for areas of major concern that need to be considered from a risk or opportunity perspective, and

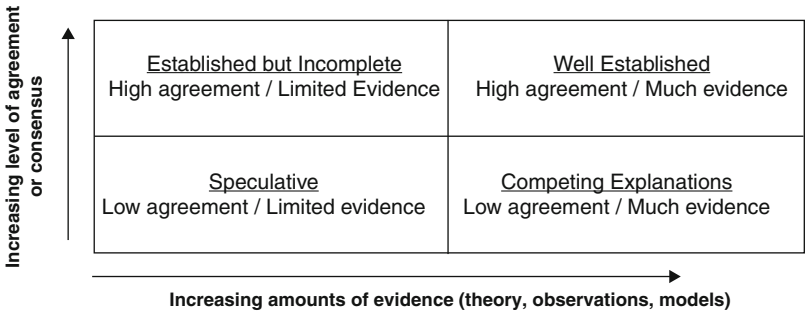

Fig. 3 Conceptual framework for assessing the current level of understanding (Moss 2006; Climate Change 2005)

the reason for their use should be carefully explained" (Climate Change 2005, p. 4). Table 1 shows the scale. The likelihood scale is used to refer to "a probabilistic assessment of some well defined outcome having occurred or occurring in the future" (Climate Change 2005, p. 4).

Adaptation and Mitigation

The terms "adaptation" and "mitigation" were briefly discussed in the introduction of this chapter, but the more detailed definition and explanation in Table 2 outline important distinctions that will be helpful for the sections of the chapter that follow.

Perceptions, Communication, and Language of Climate Change

Moser (Moser 2010, p. 33) writes that "a number of challenging traits make climate change a tough issue to engage with," and she implies that something in the nature of climate change itself makes it more challenging for people to perceive and communicate about than many other, even related issues (environmental, hazards, health). She lists the following characteristics of climate change that produce this substantial challenge:

- Invisible causes: Greenhouse gasses are not visible and have no direct or immediate health implications. The same is true for other forcing agents such as Earth/Sun relations.
- Distant impacts: The lack of immediacy in temporal and geographic distance.
- Insulation of modern humans from their environment: This diminishes the perception of any changes in the climate or their significance.
- Delayed or absent gratification for taking action: Action taken today is not likely to reduce global average temperature within the lifetime of the person taking the action.
- The lack of recognition that humans have of their technological power: This produces disbelief that humans have the capacity to alter the global climate.

Table 1 Scales of uncertainty used in the IPCC Fourth Assessment Report, 2007. None of these are statistically significant because no tests are conducted to determine the values. Instead, they are based on expert judgment

Qualitatively calibrated levels of confidence (Climate Change2005)	
Terminology	Degree of confidence in being correct
Very high confidence	At least 9 out of 10 chances of being correct
High confidence	About 8 out of 10 chances of being correct
Medium confidence	About 5 out of 10 chances of being correct
Low confidence	About 2 out of 10 chances of being correct
Very low confidence	Less than 1 out of 10 chances of being correct
Likelihood scale (Intergovernmental Panel on Climate Change2007b)	
Terminology	Likelihood of the occurrence or outcome (%)
Virtually certain	>99
Extremely likely	>95
Very likely	>90
Likely	>66
More likely than not	>50
About as likely as not	33–66
Unlikely	<33
Very unlikely	<10
Extremely unlikely	<5
Exceptionally unlikely	<1

- Complexity and uncertainty: This leads to considerations of climate change taking on less importance than immediate needs such as family and job responsibilities.
- Inadequate signals indicating the need for change: Inertia in the climate system and lack of observable economic or social costs or benefits reduce incentives for action.
- Self-interest: Not only are many powerful forces in society interested in maintaining the status quo, but also the majority of people in developed countries defend the comforts of their modern lifestyles, even if unintentionally and unconsciously.

Weber (2010) adds additional factors that make the perception and communication of climate change difficult. First is the difference between *affect-based* and *analysis-based* processing of environmental information. The general public relies heavily on affect-based processing, that is, relying on personal experience. However, climate change is not easily detected in this manner. Climate, defined above as the aggregate of day-to-day weather conditions that have been averaged over longer periods of time, requires analysis-based processing of statistical information that includes averages, trends, and uncertainty estimates, among others. The majority of people are simply ill equipped to process this type of information, and they have little patience in attempting to decipher it. Compounding the difficulty is that "People's fundamental values and worldviews influence which phenomena and risks they attend to and

Table 2 Definitions and explanations of the terms adaptation and mitigation from the IPCC Fourth Assessment Report 2007

Adaptation	"Adjustment in natural or human systems in response to actual or expected climatic stimuli or their effects, which moderates harm or exploits beneficial opportunities: Various types of adaptation can be distinguished including anticipatory, autonomous, and planned adaptation
Anticipatory adaptation	Adaptation that takes place before impacts of climate change are observed. Also referred to as proactive adaptation
Autonomous adaptation	Adaptation that does not constitute a conscious response to climatic stimuli but is triggered by ecological changes in natural systems and by market or welfare changes in human systems. Also referred to as spontaneous adaptation
Planned adaptation	Adaptation that is the result of a deliberate policy decision, based on an awareness that conditions have changed or are about to change and that action is required to return to, maintain, or achieve a desired state" (Intergovernmental Panel on Climate Change 2007a, p. 869)
Mitigation	"An anthropogenic intervention to reduce the anthropogenic forcing of the climate system; it includes strategies to reduce greenhouse gas sources and emissions and enhancing greenhouse gas sinks"
Mitigative capacity	"This is a country's ability to reduce anthropogenic greenhouse gas emissions or to enhance natural sinks, where ability refers to skills, competencies, fitness and proficiencies that a country has attained and depends on technology, institutions, wealth, equity, infrastructure and information. Mitigative capacity is rooted in a country's sustainable development path" (Intergovernmental Panel on Climate Change 2007a, p. 84)
Mitigation potential	"In the context of climate change mitigation, the mitigation potential is the amount of mitigation that could be – but is not yet – realised over time
	Market potential is the mitigation potential based on private costs and private discount rates, which might be expected to occur under forecast market conditions, including policies and measures currently in place, noting that barriers limit actual uptake. Private costs and discount rates reflect the perspective of private consumers and companies
	Economic potential is the mitigation potential that takes into account social costs and benefits and social discount rates, assuming that market efficiency is improved by policies and measures and barriers are removed. Social costs and discount rates reflect the perspective of society. Social discount rates are lower than those used by private investors
	Studies of market potential can be used to inform policy makers about mitigation potential with existing policies and barriers, while studies of economic potential show what might be achieved if appropriate new and additional policies were put into place to remove barriers and include social costs and benefits. The economic potential is therefore generally greater than the market potential
	Technical potential is the amount by which it is possible to reduce greenhouse gas emissions or improve energy efficiency by implementing a technology or practice that has already been demonstrated. No explicit reference to costs is made but adopting 'practical constraints' may take implicit economic considerations into account" (Intergovernmental Panel on Climate Change 2007a, p. 84)

Table 3 "Repertories" employed by people in response to information about climate change (Ereaut and Segnit 2006)

Alarmism	Climate change is constructed as "awesome, terrible, immense, and beyond human control. . . an inflated or exaggerated rhetoric. . . urgent tone. . . quasi-religious register of death and doom. . . language of acceleration and irreversibility. . . sensationalism [and that it] undermines its ability to help bring about action"
Settlerdom	". . . named after 'settlers'. . . people with sustenance-driven needs. . . optimistic but non-pragmatic. . . rejects and mocks the alarmist. . . invoking 'common sense' on behalf of the 'sane majority'. . . dismisses climate change as a thing so fantastic that it cannot be true. . . a refusal to engage in the debate. . . broadly right-wing. . . immune to scientific argument"
British comic nihilism	". . . an evasive rhetorical repertoire. . . rejection of climate change is whimsical, unserious, blithely irresponsible. . . a sunny refusal to engage in the debate. . . comic musings on the positive possibilities of a future with climate change. . . dealing with adversity and threat by use of humour"
Small actions	". . . the eminent 'pragmatic' optimist. . . asking a large number of people to do small things. . . language of ease, convenience and effortless agency. . . easily lapses into 'wallpaper' – the domestic, the routine, the boring and too easily ignorable. . . lacking in energy. . . may not feel compelling. . . the unspoken but obvious question: how can small actions really make a difference to things happening on this epic scale?"

which they ignore or deny" (Weber 2010, p. 335). When limited processing capacity and patience wane, people default to reliance on their fundamental values and worldviews, which generate a wide range of responses that are generally politicized and deeply held. Several typologies exist for categorizing these responses, but Ereaut and Segnit (2006, p. 7) have developed a very useful one from empirical studies conducted in the UK that contain the four "repertoires" presented in Table 3.

Future Directions: The State of Climate Change Knowledge and Future Predictions

As stated earlier, consideration of human knowledge of climate change and future predictions must differentiate two questions: What is the direction and rate of change, if any, in Earth's climate? What is the cause, natural or anthropogenic, of any observed climate change? It is almost universally accepted across the scientific community that global average temperature is increasing in accordance with the data presented in the graph in Fig. 1. This is summarized as follows:

> Since the mid twentieth century, the uncertainties in global and hemispheric mean temperatures are small, and the temperature increase greatly exceeds its uncertainty. In earlier periods the uncertainties are larger, but the temperature increase over the twentieth century is still significantly larger than its uncertainty (Brohan et al. 2006, p. 1).

With respect to differentiating natural from anthropogenic causes of this observed warming, although broad consensus of scientific judgment suggests anthropogenic

Table 4 Statements from the various IPCC Assessment Reports showing the increasing levels of certainty regarding the causes of the observed increase in global average temperature spanning the period 1990–2007

1990. First assessment report (Climate Change 1990, emphasis added)	"The size of this warming is broadly consistent with prediction of climate models, but it is also of the same magnitude as natural climate variability. Thus the observed increase *could be largely due* to this natural variability; alternatively this variability and other human factors could have offset a still larger human-induced greenhouse warming. The unequivocal detection of the enhanced greenhouse effect is not likely for a decade or more"
1995. Second assessment report (Climate Change 1995, p. 22 emphasis added)	"Since the 1990 IPCC Report, considerable progress has been made in attempts to distinguish between natural and anthropogenic influences on climate. The balance of evidence *suggests* a discernible human influence on global climate"
2001. Third assessment report (Climate Change 2001, p. 31 emphasis added)	"There is new and stronger evidence that most of the warming observed over the last 50 years is attributable to human activities (p. 5). Most of observed warming over last 50 years is *likely* due to increases in greenhouse gas concentrations due to human activities"
2007. Fourth assessment report (Climate Change 2007d, p. 39 emphasis added)	"Most of the observed increase in global average temperatures since the mid-twentieth century is *very likely* due to the observed increase in anthropogenic GHG concentrations. This is an advance since the TAR's [Third Assessment Report] conclusion that 'most of the observed warming over the last 50 years is likely to have been due to the increase in GHG concentrations'"

causes, a substantial minority remains less convinced. The IPCC represents the former group that assigns causation to anthropogenic causes. But it has taken almost 20 years for the IPCC to reach this conclusion. Table 4 outlines relevant statements from the various IPCC Assessment Reports spanning the period 1990–2007.

Types of Mitigation Strategies

Because the focus of this handbook is climate change mitigation, various mitigation strategies are detailed elsewhere. Consequently, this section will not attempt thorough explanation of them, but will briefly list and outline the major types of mitigation strategies as a foundation for considering the ethical issues associated with them.

The most often discussed category of strategies for mitigating climate change is to reduce the emission of CO_2 that results from the combustion of fossil fuels. Public policy actions serve as the primary driver for effecting these mitigation strategies.

One policy action is to simply *set limits on the CO_2emissions* from the various sources (electrical generation plants, cars, etc.) as the impetus to develop cleaner technologies. Another is the well-known *cap and trade system* in which a government body limits the amount of CO_2 that can be emitted and then issues (allocates or sells) permits to private firms to emit specified amounts of CO_2. Firms can then sell or buy permits as needed depending on their amount of emissions. Cap and trade has been criticized on a number of counts, most notably (1) that it increases the cost of fuel and so disproportionally affects the poor rather than the wealthy and (2) that in the places where it has been tried, for a variety of reasons, it has not reduced CO_2 emissions and has resulted in volatile emissions trading market. A proposed alternative to "cap and trade" is known as the *fee and dividend system*, described as follows:

> . . . a fee is collected at the mine or port of entry for each fossil fuel (coal, oil, and gas), i.e., at its first sale in the country. The fee is uniform, a single number, in dollars per ton of carbon dioxide in the fuel. The public does not directly pay any fee or tax, but the price of the goods they buy increases in proportion to how much fossil fuel is used in their production. . .The carbon fee will rise gradually so that the public will have time to adjust their lifestyle, choice of vehicle, home insulation, etc., so as to minimize their carbon footprint. . .100 percent of the money collected from the fossil fuel companies at the mine or well is distributed uniformly to the public. Thus those who do better than average in reducing their carbon footprint will receive more of the dividend than they will pay in the added costs of the products they buy. (Hansen 2009, p. 209)

Proponents of the fee and dividend system list some of its additional benefits as (1) it is revenue neutral in that it does not raise taxes; (2) only a very small government bureaucracy is needed; (3) it "internalizes" the incentives to reduce the use of fossil energy (e.g., cost savings) across "billions of decisions ranging from commuting behavior to the design of vehicles, aircraft, cities, and so forth" (Hansen 2009, p. 211); and (4) it raises the cost of fossil energy sources to reflect their cost to society and the environment (pollution, climate change, health impacts, etc.) and to improve the competitiveness of renewables that do not carry these costs. Another climate change mitigation strategy focused on reducing production of CO_2 is *population control*, though it is highly controversial. Proponents argue that increasing human population causes increasing emissions of CO_2, and as a result, stabilization of human population is necessary to stabilize or reduce concentrations of atmospheric CO_2. Opponents respond that people are not pollution, but rather, the blame lies on the system that depends on fossil fuels for economic development. Instead of reducing population, they argue, policy should focus on changing that system. Further controversy has to do with the issues of liberty and family values, which can be said to conflict with policies limiting family size. A final strategy for reducing emissions of CO_2 involves *improving energy efficiency and conservation*. As efficiency increases, less fuel will be used, and as a result, less CO_2 will be emitted. This readily achievable and cost-effective strategy could not only reduce CO_2 emissions substantially but could also significantly reduce the world's energy demand (IEA (International Energy Agency) 2006).

In contrast to strategies that reduce the emission of CO_2, the second category of mitigation strategies removes CO_2 from the atmosphere once it has been produced. There are a number of such strategies. *Reforestation* involves the planting of forests, either new forests or the restocking of existing forests that have experienced deforestation, as means to sequestrate more CO_2 from the atmosphere. The process is explained as follows:

> Carbon dioxide is constantly exchanged between the atmosphere, the oceans and terrestrial ecosystems. Vegetation and soils can accumulate carbon, thus reducing the rate of CO_2 build-up in the atmosphere that is responsible for climate change… Forest ecosystems contain the majority (approximately 60 per cent) of the carbon stored in terrestrial ecosystems. Thus the world's forests sequester and conserve more carbon than all other terrestrial ecosystems and account for 90 per cent of the annual carbon flux between the atmosphere and the earth's land surface. (Strech and Scholz 2006, p. 861)

While reforestation efforts have potential to sequester CO_2, the effect is less than envisioned in virtually all such measures. The predominant means of reforestation is the "forest plantation" where a single species of tree is planted. The amount of carbon sequestration has been found to be 28 % less in forest plantations than in naturally occurring primary or secondary forests (Liao et al. 2010). Consequently, while not diminishing the importance of reforestation, it seems that the most efficient efforts involving forests would be to preserve existing ones. This provides good rationale to pursue a related strategy of *preventingdeforestation* which retains the natural, primary, and secondary forests.

Another strategy to remove CO_2 from the atmosphere is called *carbon capture and storage* (or sometimes carbon capture and sequestration). Other chapters in this handbook provide considerable detail on this topic, so it will only be briefly defined here. Carbon capture entails trapping the CO_2 at its emission source and then transporting it to a location where it can be stored so that it does not escape into the atmosphere (usually in underground rock formations).

A final suite of strategies to mitigate the effects of CO_2 is called *geoengineering*, defined as a "large-scale engineering of the environment in order to combat or counteract the effects of changes in atmospheric chemistry" (Committee on Science, Engineering, and Public Policy 1992, p. 433). They take the form of either shielding Earth from incoming solar radiation or facilitating the transport of heat energy from Earth to space, primarily by reducing the concentration of atmospheric CO_2. One of the most talked-about is to inject sulfur dioxide (several million tons per year) into the stratosphere (Kunzig 2008), where it would undergo various chemical reactions to produce sulfate particles that would scatter incoming sunlight and thereby cool the planet. It is known that this works because of observations of the effects of volcanoes that produce sulfur dioxide (SO_2), most recently, the Pinatubo volcano that injected over 20 million tons of SO_2 into the stratosphere in 1991, which resulted in a decrease of global average temperature by about 0.5 °C (1 °F) for about 1 year. The delivery of SO_2 into the stratosphere is proposed using either balloons or with planes burning high sulfur fuel, at an estimated cost of $25–$50 billion annually (Kunzig 2008). While studies indicate it would reduce global average temperature, it

would not address problems associated with increasing CO_2 levels, most notably, acidification of the ocean which causes negative impacts on organisms that make calcareous structures, such as shells and corals, along with the ecosystems of which they are a part. Another strategy that promises to reduce global average temperature by reducing atmospheric CO_2 is called *artificial iron fertilization* of the ocean. Such fertilization occurs naturally when dust storms carry iron into the ocean and cause blooms of the photosynthesizing organisms known as phytoplankton. By artificially spreading powdered iron into the ocean, the idea is to promote the phytoplankton blooms that would absorb CO_2 through the photosynthesis process. A commercial firm named Planktos explored this idea and conducted some small-scale tests. However, they failed to gain adequate investor funding to scale up the project, primarily as a result of questions about various and potentially negative unintended consequences of the project that included adverse effects on marine organisms and ecosystems (Courtland 2008). This highlights a serious drawback to these and the various other geoengineering strategies and possible unintended consequences that would be global in scale and sometimes unstoppable.

Uncertainties and Moral Obligations Despite Them

The previous section introduced the kinds of uncertainties involved in human understanding of climate change. The first point to address concerning moral obligations in the face of uncertainty is that it is wrong to overstate the uncertainties involved. This is the case because, in large part, consequences for denying what has been well established include delaying and softening the response to problems that are likely to require significant effort and collaboration to address. Democratically, furthermore, obfuscations of the kinds that the previous section sought to undo, such as in the conflation of the issues of warming global temperatures with the causal forces bringing the warming about, only get in the way of making intelligent progress in addressing either of these concerns.

Three issues are worth covering in this section given their bearing on uncertainties and moral obligations despite them. The first concerns the ethics of news reporting about scientific developments regarding uncertainties with respect to climate change. The second regards a fallacy of reason that is committed all too often about climate change. The third one concerns caution and collective obligations in the face of uncertainty.

Ethics and Reporting About Climate Science

One important development in news reporting has been the recognition that news outlets often exhibit biases. A traditional way of thinking suggested that reporting should only be considered the relaying of facts. This outlook is generally ascribed to modernism and has inspired a reaction that has been called postmodern, a view that holds that no outlook in news reporting can be considered perfectly objective or

absolutely without bias. While the postmodern movement has its flaws and excesses, it is not wrong in seeing that the long-held ideal of a "view from nowhere," a point of view without bias, may be unachievable and imaginary.

Building upon postmodern thinking, more pragmatic approaches to knowledge have come to see biases as things to be recognized and controlled. What has come about as a result of this shift is an effort in countless news outlets always to demonstrate balance about issues that get reported. A problem that emerges is that news outlets sometimes make use of commentators, explicitly holding a point of view, but then contrast them with people whose points of view are minimally relevant to the topic being reported.

One troubling consequence of this effort to appear more credible, to issue news that is more purposefully and intentionally balanced from a political point of view, is the fact that some people want to deny the findings of science. Examples of this problem include detractors of climate science along with other examples such as those who believe that the age of the Earth should be determined by reading religious texts rather than with the scientific method. In short, when a vocal minority of people speaks up, they can make it appear as though there is balance, a 50–50 way of reporting the facts about scientific developments. When it comes to matters such as climate science, however, this development is pernicious because it promotes the idea that genuine controversies exist within the sciences when no fundamental disagreement exists among scientists. There is a moral problem at issue here in which some people use the idea of media balance to "spin" a point of view that makes uncertainties appear far greater than they are.

The motivations for misinformation or for the propagation of claims unjustified or even contradicted by science are varied. While people certainly have a right to beliefs from religious or other sources, this fact produces tension wherever such beliefs conflict with the findings of science. In many cases, these tensions are dealt with in constructive ways, but in other cases, some persons may think that their interests would be best served if scientific developments were stalled or obfuscated. Efforts of this kind surely produce troubling manipulations of the democratic need for carefully evaluated and verified political as well as scientific information.

Avoiding the Fallacy of Appealing to Ignorance

Uncertainties about climate change precipitate a common challenge to the idea that action should be taken to address it. There is an important fallacy at play in such arguments, beyond the fact that often obfuscations are made about what uncertainties there are exactly involved in climate change. It is the fallacy of appealing to ignorance.

An appeal to ignorance is a fallacy of reason that occurs when one makes a strong conclusion about the state of some subject matter on the grounds that knowledge is lacking about it. Take an example of Jack, who is a serial killer. Mindy and Alex do not know that Jack is a killer, but Mindy has a bad feeling about him, and she says so to Alex. Alex defends Jack by stating "you don't actually know that Jack's a bad guy,

so he's a good guy, really." Alex holds a kind assumption that people are nice unless proven otherwise, but in this case, it is clearly wrong. Alex moves from the fact that someone lacks knowledge to some other substantive fact that the lack of knowledge clearly cannot substantiate. This fallacy of reason is called an appeal to ignorance.

The appeal to ignorance seems to be one of the most common responses to climate change efforts. People tend to imagine or pretend that the science is inconclusive, but in a way that in fact may be insufficient a challenge to the idea that people ought perhaps to take precautions. Beside this precautionary motivation, known as the Precautionary Principle, the fact is that the science is stronger than it has been in many cases portrayed, as shown in the previous sections in this chapter.

The Limits of Challenges About Uncertainty

The first thing to say here is that the uncertainty people claim is involved in scientists' understanding of climate change is frequently overstated or misstated. In this section, let us imagine that some of the bolder claims about uncertainty with respect to climate change were true. There is still reason, nonetheless, to think that moral obligations could and do exist for people despite such a hypothetically strong uncertainty.

The common response in the environmental ethics literature to the challenge of uncertainty is that the potential harm that can come from problems such as climate change can be catastrophic (Manson 1999). Thus, even if there is uncertainty about a problem or a very small likelihood of trouble, it is typically wise and a moral obligation to avoid that catastrophic scenario. This is general practice in medical situations. When a set of possible medical courses of action are generally safe and yield little risk of adverse effects, they are almost always what one should do before other options whose effects could be catastrophic. The reason for the moral obligation to choose the less risky option is known as the Precautionary Principle. The Precautionary Principle in the context of climate change resembles what in the history of philosophy has been called Pascal's Wager.

Pascal's Wager is about belief in God. He argued that four options exist:

- If one does not believe in God and God exists, then a devastating outcome could ensue – eternal damnation for one's disbelief.
- If one does not believe in God and there is no God, no problem.
- If one believes in God and there is none, then one has lost some time and effort.
- If one believes in God and there is a God, then one could receive great rewards.

This set of options, Pascal believed, is excellent reason to believe in God. Of course, religious arguments can analyze whether or not such motivations are enough for genuine belief, but the point of relation to the subject here, climate change mitigation, concerns especially the one similar circumstance that could arise for the environment. In other words, what if people do not concern themselves about the environment and in fact allow or increase the chances of catastrophic circumstances

as a result? The worry involved there is something akin to that involved in risky medical practices that are not accepted in all but the rarest of cases.

The response to the wager for the environmental context is to say that there are costs of mitigation and adaptation to climate change. Of course, if there is no choice but to adapt, then those costs cannot be avoided, though they can be distributed more or less justly. When it comes to efforts to mitigate climate change, however, things like caps on greenhouse gas emissions can have profound effects on the ways in which businesses work. In short, a challenge to the Precautionary Principle emerges related to the cost-benefit analysis of action to address climate change. Neil Manson (1999) estimates that the costs of inaction could be seen as enormous, which is why people should not be afraid to enter into discussions about precautions and valuations of climate change. Environmentalists are often wary of entering into cost-benefit analyses, since it is difficult to value things like the survival of species. However, Manson also argues that environmentalists could devise strategies for valuing the costs of changes to climate. In short, there are a number of important elements that can factor into moral obligation even if there are uncertainties about climate change. There is a whole industry in the insurance business that practices the process of putting monetary value on things that average persons would have an extraordinarily difficult time valuing, since people in general do not think of the world as do those who manage risk for a living. It is important to note here in concluding this section that none of these responses to challenges of uncertainty about climate change should be construed as reason to doubt the increasingly strong evidence that suggests human beings have a significant impact on the environments on a large scale or the even more strongly defended judgment that global temperatures are increasing over the long run, occurrences for which the Precautionary Principle would prescribe that humanity to prepare (see Gardiner 2006 for an explanation of the Precautionary Principle).

Traditions and New Developments in Environmental Ethics

The study of environmental ethics has grown substantially in the last 30 years. In the background of developments in this study lie cultural beliefs about the world and humankind's place in it. Often, the Earth is conceived as God's gift to mankind, to be used for human purposes. At the same time, things that are gifts from God could also be considered important targets for stewardship. Stewardship refers to the duties one has to objects or property bestowed on oneself in some honored fashion, like a family heirloom or in this case a divine gift. Whether one approaches environmental ethics with a religious motivation or a secular one, a tension arises often between the idea that the Earth is property, a mere tool for human ends, and the opposing belief that human beings have a duty to take the best care they can of shared resources. This tension arises in the study of environmental ethics in the form of arguments that address human interests primarily, the anthropocentric approach, and arguments that give moral weight to things like places, animals, ecosystems, etc. The present section will cover a number of the approaches that environmental ethicists have taken for

considering the moral duties human beings have to care for the environments on which they depend. The section will begin with a discussion on the tradition of environmental ethics, focusing on theories about the source of value in ethics. Next, the matter of who is affected in problems of environmental ethics is important to consider. Finally, some recent developments will be discussed, which suggest that a cultural shift is noticeably growing public acceptance for environmental values and precautions.

Sources of Value in Environmental Ethics

The traditional way of thinking about land and environments has largely been religious. In 2010, founder of southern Indiana's Corydon Tea Party Norman Dennison explained a traditional outlook on religiously motivated opposition to understanding about climate change. Dennison explained that human-induced climate change "is a flat out lie." According to a *New York Times* article, Dennison explained that "he had based his view on the preaching of Rush Limbaugh and the teaching of scripture. 'I read my Bible,' Mr. Dennison said. 'He [God] made this earth for us to utilize'" (Broder 2010). Here, Dennison illustrates contempt for the findings of climate science, to be sure, but he also demonstrates the central background for thinking about environmental concern as uniquely anthropocentric and based on God's purported decision that the Earth is intended to be used up. Rachel Carson has argued that the tradition treats the Earth as an object to be exploited and conquered, without consideration for its well-being (Carson 1962/1987).

Religious outlooks on environmental policy do not exclusively follow Dennison's orientation to deny climate science. Matthew Hay Brown in *The Baltimore Sun*, for instance, asks "Where would Jesus drill?" in his article "Religious Environmentalists Hope Spill Wins Converts" (Brown 2010). What is noticeable, therefore, is that although traditional views may suggest that humankind ought to have great powers over God's gift of the Earth, even in religious discussions, the source of environmental value and what ought to be done is neither settled nor determined for all. In particular, a central challenge to such traditional views concerns the idea that environmental ethics ought to be anthropocentric.

One of the most influential thinkers to challenge solely anthropocentric values in environmental ethics was Aldo Leopold. In *A Sand County Almanac*, he called for an expansive view of the source of value in ethics (Leopold 1968). He named a new kind of ethic the Land Ethic. Although Leopold was a hunter and enjoyed nature very much, he saw in nature a source of value that is independent of his enjoyment of it. In this section, it should become clear that there is common ground to be found between the different views that are presented here. Whether value is inherent in nature or not, ultimately anyone concerned must convince others to share that concern. Therefore, the anthropocentrism or the inherent value theorist like Leopold needs not only to attend significantly to human interests but to expand people's understandings of what those interests could more intelligently appreciate.

The common tendency in debates about ethics and environmental issues is to have human beings pitted against something like an endangered animal. Some people wonder why they must be terribly concerned about rarefied fish, for example, especially when countless species have gone extinct in the past. Plus, in biology, students are taught that animals survive when they are fit for their environments. Thus, one might argue that any animal that is in danger of becoming extinct is simply showing its unfitness for present conditions, whether those conditions are man-made or not. If they become unfit for the environment by accident or by purposeful human action, what is the moral difference?

Environmentalist responses have varied to such challenges, and Leopold's answer is straightforward. He said that inasmuch as you and he have rights and worth and deserve respect in efforts to live, so do other animals and environments. He believed that the problem fundamentally has to do with the fact that people think they simply have no obligation to the things and other forms of life in this world. As such, it follows that the right of things to live and to be can in many circumstances trump human claims on freedom to change the environments in ways that harm the natural habitats of animals, thought Leopold. In this sense, Leopold believed in the importance of human stewardship of land. He saw not only animals and plants as living things but ecosystems and natural environments as having lives as well. The reason people generally do not think about mountains as alive comes from not seeing the place of mountains in an overall living system and also not looking at them on the right scale. After all, mountains, streams, and grasslands all change and grow, erode, and serve as homes for countless animal and plant species. If people care about their own lives, it is life ultimately that counts, Leopold argued. He saw the history of ethics as a growth in consideration for people and groups and then pets and other cared-for things in an expanding circle of consideration. He believed the next step was for humans to broaden consideration even further, to include the environment. The most important element that Leopold brought to the attention of moral thought had to do with this broadening of moral consideration beyond the simply anthropocentric view. Today, the existence of laws about the treatment of animals is one form of outgrowth of theories like Leopold's.

Two matters are important to note at this point about global climate change and the ethics involved in efforts to mitigate it and its effects. First, the idea of speaking for the Earth as a whole is one strategy that has been appealed to in ethics. Environmental ethics scholar J. Baird Callicott (1994) has on several occasions argued, however, that it is quite certain that the Earth itself will be here whatever human beings do to it. Thus, the strategy of arguing for the Earth's sake, an approach that Callicott claims to be too diffuse to be practical in inspiring people, is also misguided in a greater sense. The people who would argue for human-centered values in ethics are not taking the wrong track. It is life on Earth, including human life, which will be affected substantially by things like climate change. Thus, it is not problematic to focus on the values of environmental efforts that are based on the quality of human life and the cares of human beings.

Following Callicott's advice, whether one believes in the independent theory of environmental value or only the anthropocentric theory, it seems most rhetorically

powerful not only to argue according to human interests but to expand how people think of these. Philosopher Andrew Light has taken this approach, for example (Light 2002). One might differ from Leopold in how to defend things like unique fish in a river that could be destroyed due to some construction change or industrial practice and might instead consider the possible effects of such changes for human beings. One way to think of human interest with regard to generally unfamiliar animals or environments has been studied under the category of "ecosystem services" (Ecosystem Assessment 2005). Among the effects that have been considered in arguing for the defense of ecosystems are the kinds of benefits that come from biological diversity. The first among these is the fact that animals serve as food for other animals. As such, then, when one species is wiped out, it almost invariably has a rippling effect on other species, who either have to change their diets substantially, sometimes failing and thus dying out also, or to bring a substantial shift in effect on other animals that then become prey, potentially wiping them out. The number of animals and species affected can be enormous, then, from one simple change in biodiversity in a particular environment. When one realizes the breadth of possible effects from climate change, the results could be truly catastrophic (Gardiner 2004). The idea of "ecosystem services" points out the fact that humans get things like clean drinking water from a whole ecosystem. When people affect a significant element of an ecosystem, a great chain of events can mean danger for human beings as well as the animals and environments initially altered.

The skeptic could ask, however, what it matters if an ecosystem changes substantially, beyond the occasional cases in which things like drinking water are affected. What practical consequences are there for human beings in other cases? The first answer here would be that human beings enjoy their environments. Change to those environments could easily affect human beings negatively, therefore. Examples include changes for simple appreciation of beautiful environments that become less beautiful – the element of aesthetics in ethics. When one's landscape is beautiful and valuable as such, one's property values decrease significantly if the environments become less beautiful and desirable, which is a financial aspect of an aesthetic change. Another aesthetic change similarly can occur for hunters, who are no longer able to enjoy either their hunting environments or the animals that they hunt because of effects on populations due to environmental changes. As mentioned above, Leopold was a hunter too, who enjoyed environments as he respected their inherent value at the same time.

A second consequence could be agricultural. When an animal is eliminated that would otherwise keep insects in check, crops can be devastated all of a sudden because the insects are more able to multiply in huge numbers. Famines can result from such changes, if crops become devastated. The costs of shifts in agriculture are more immediately obvious for human interests. They can also be direr for human beings than aesthetic changes. In relation to issues of climate change, whatever the cause of changes in climates, farmers have begun to report the need to change the kinds of crops that they farm because of environmental changes. According to Mendelsohn,

> The largest known economic impact of climate change is upon agriculture because of the size and sensitivity of the sector. Warming causes the greatest harm to agriculture in

> developing countries primarily because many farms in the low latitudes already endure climates that are too hot. . . Even though adaptation will blunt some of the worst predicted outcomes, warming is expected to cause large damages to agriculture in developing countries over the next century. (Mendelsohn 2009, p. 5)

Agriculture, economies, and food supplies are each threatened by changes in climate, therefore. So, when confronting problems in ethics for climate change, cost and benefit analyses of action surely bear weighty elements for consideration. At the same time, the people who are affected by these costs are important to consider. The point here at first, however, has simply been to show that one does not abandon consideration of environmental problems when one takes the impacts on human beings of things like climate change as essential sources of value for decision making. After all, those who care deeply about the value of a certain species alone need to make their cases in ethical debates with human beings, who bring their interests to the table. The strength for such persons, however, in the process is the profound impact on people that changes in environments can have.

Persons Who Experience Benefits and Costs

The subject of who is affected by changes in climate is important to consider. There is an intensely complex set of conflicting interests involved in considerations of who is affected by climate change and by efforts to mitigate it. The tradition in ethics has nearly always been to consider first and foremost the values and effects on persons who are presently living when debating the costs and benefits of action or of constraints on freedom. In the case of climate change, there certainly are people who are affected in the present through changes in things like aesthetics, hunting, and agriculture, as outlined in the previous section. For example, rivers that are drying up and that had attracted animals in some countries now no longer bring them, which affects agriculture and a vast number of organisms, in turn affecting food supply and economies for human beings (Mendelsohn 2009).

At the same time, some of the greatest potential worries about climate change are expected to come in the next few generations, not in the present. Thus, when it comes to ethics, an important question arises concerning the nature of present human beings' responsibilities to future generations. After all, the people to whom some say living human beings have obligations are not even here today. They have not yet been born. How can people alive today have moral obligations to nonexistent people? The Stern Review (Stern 2007) has generated fairly profound impact on this subject, and the basic arguments have been summarized by the editors of *Scientific American*:

- Future generations will suffer most of the harmful effects of global climate change. Yet if the world economy grows, they will be richer than we are.
- The present generation must decide, with the help of expert advice from economists, whether to aggressively reduce the chances of future harm or to let our richer descendants largely fend for themselves.

- Economists cannot avoid making ethical choices in formulating their advices.
- Even the small chance of utter catastrophe from global warming raises special problems for ethical discussion (Broome 2008, p. 97).

There are a number of practices already observable that offer examples to follow regarding these questions of responsibilities to generations that are not present. First, when persons die, in most societies, people honor obligations to persons who have passed away. Part of the reason for this has to do with legal codes, and part of it has to do with resolving conflict among the living about those who die. But there are ways in which people honor those who have died in various ways, such as with memorials.

What is more interesting for the present issue of debate has to do with future generations. With regard to them, politicians in recent years, such as Senator John McCain, have argued for clear obligations to children and grandchildren in the United States. McCain argues that accruing debt today is wrong because of the negative effect it will have on future generations, who will be "saddled" with debt (McCain 2009). In these instances, politicians like McCain raise problems about the national debt and the deficits that cause it to grow. What deficits do is to increase the country's future financial obligations to pay back loans incurred for the purpose of present spending. Those who defend such spending argue that there are long-term effects of such spending, such as in rebuilding an economy that can pay back the debts and avoid greater recessions or another depression. At the same time, then, both sides of the debate about rising deficits are making claims about moral obligations both to present *and future* citizens. The claim some detractors make about government spending is that it is irresponsible, it is wrong, to create negative future financial circumstances for future generations – children, their children, and their children after that. The argument goes that people have obligations to their children's grandchildren. Such ideas are not farfetched, and they can be seen clearly to apply to matters of environmental ethics.

Those who would reject obligations to future generations make quite a controversial claim. The more common line would be by analogy to the idea of proximity. In some ethical circumstances, it seems quite clear, for instance, that people have obligations to help someone if they can when that person is close and is in great pain. If people can help and choose not to do so, they allow greater suffering to continue than would occur if they were to intervene. Thus, in the view of some moral philosophers, people are partly responsible for the outcome that ensues from inaction. Even inaction has effects, in other words. The key point here is that one may have an obligation to help someone drowning 15 f. away, but the person who is drowning a mile away is someone either who cannot be helped or who is not sufficiently proximal. A better example is starvation, since it is not quite as immediate a problem. If someone nearby is starving and so someone is far away, people have a tendency to think that either the person close to them is the one for whom they have the greater obligation or it is the person with the greater pain. When all things are equal regarding the extent of the suffering, people perhaps naturally feel a greater obligation to those who are closest to them. Translate this trend that is here described spatially to the temporal level and the same pattern seems to hold. If people are

starving today, human beings seem to have a far greater moral obligation to them than to address the starvation of possible people who may or may not come to be born tomorrow or in several generations. This at least is the set of options for considering obligations to people present and in the future. The common motivation for taking present and close persons to be more important is understandable, therefore, all things equal, compared with people who are not present or close. The trouble is, however, that the future which is put on hold in moral consideration could be deeply affected by choices that provide only small benefits or pose only small costs today. In fiscal terms, consider the US Congress throwing an incredible national party at enormous expense to future generations. It may be fun, but the benefits would be short-lived and appear incredibly thoughtless to future generations who then have to suffer the burdens of an inconsiderate earlier society. When it comes to ethics and climate change, it is hard to think that people have no obligation to future generations. There are also long-term predictions that appear quite worrisome given the apparent increase in the rates of temperature rise and other factors relevant to climate change. Thus, policymakers must think about the environmental crisis that future generations might have to face, much as they already consider the problem of passing on debt to future generations of children and grandchildren.

Beyond the problems of obligations for present and future persons is the fact that the costs and benefits of constraints on freedom and of positive action regarding climate change mitigation are disconnected. In other words, the persons who are affected by costs are rarely the same people who reap benefits. The following are three important examples of this idea.

The first example concerns persons currently affected by climate change. Consider the farmers who presently have to change their crops or who have lost their crops and the potential to raise them. Whether climate change can be attributed clearly to the production of greenhouse gases or not, the persons who are benefiting from greenhouse gas consumption the most, especially the recipients of wealth that come as a result, or at least the persons most likely to pay the costs of action about climate change, typically the wealthier nations, are either going to lose some of the benefits they get or incur some of the costs of the response to climate change mitigation when they themselves are to a far less devastating extent affected by the change in climate. In this sense, then, climate change is something unlikely to be addressed in profound ways by individuals acting only in their own self-interest, at least until sufficient problems occur to bring about a serious threat for the wealthier nations and persons. In this sense, then, the disconnection in present time is a real problem for bringing about one kind of response to climate change mitigation. It makes it far more likely that any real effort to address climate change will take place primarily at the state (national) level or through channels for which there is private benefit for making changes, which might include, for instance, the development of energy-efficient technologies that get sold for profit.

Another similar disconnect occurs at the level of present and future people. While future consequences can only be addressed by present people at any given time, benefits in equations of cost and benefit can seem less weighty because future people are not present. As such, then, the people who will make the sacrifice for future

generations are present and feel less the impulse to help those whom they cannot see. This entails the idea of discounting the future. The problem occurs in many spheres. When roads are unsafe but are costly to change, it often takes catastrophe in terms of loss of life for people to feel sufficiently motivated to bring about change. The same problem occurs for issues of fiscal discipline. Also, the arguments against present action in favor, for instance, of allowing present businesses to continue unhampered in their practices that promote climate change see importance in the effects of changes to economic success as ripples. In other words, greater constraint on economic growth now can have negative effects on future generations also. The matter of who is affected by climate change and efforts to mitigate it is quite complicated, therefore, and is most likely to occur at the larger, state level or at the level of vast agreements for changes that are established with cooperation between government and industry.

A further disconnect is important to notice in considering who will be affected by constraints on the production of greenhouse gases or other efforts to mitigate climate change. Poor nations argue that limitations on their industries are limitations on their development. In other words, when burning fuels like coal is the cheaper energy route that makes places like China and India grow, they argue that to push them not to use such fuels is unfair in terms of market competition. They argue that the United States and other such wealthy nations that industrialized first would perpetuate poverty in poor nations for the sake of environmental concerns, when poor countries' development needs are great. Therefore, the people affected by efforts to change industries, practices, and efforts that mitigate climate change not only concern poor farmers and wealthy nations but also those nations seeking economic growth out of poverty. They wish for the freedom to develop in ways that will bring masses of people out of poverty, raising the standard of living for human beings in poor places. The result of making allowances for such cases, however, is that those nations who accept responsibility to act for the sake of mitigating climate change may argue, with debatable merit, that double standards are hypocritical. These kinds of problems and arguments demonstrate how difficult it is and will be to create significant coalitions in efforts to mitigate climate change. The web of conflicting interests involved renders the problem of laying out a simple ethic of environmental action enormously difficult. The motivation for clarifying these issues, however, is powerful nonetheless, since the potential harm to humanity of inaction could be catastrophic. Incredibly complex circumstances have been resolved before, but only with great effort and time. The effort and time spent to date in climate change have yet to resolve these issues.

New Developments

With still so much to be developed about the future of climate change, adaptation options, and potential methods of mitigation, the ethical responsibilities involved may take shape in a variety of ways. An important shift has occurred since the start of the environmental movement. That shift is cultural. A movement has taken hold to

consider future steps for addressing environmental problems. Early on in the environmental movement, there was far less study of environmental science than is available today. Cultural elements like the development of recycling systems have become commonplace in countless population centers worldwide. Plus, what started as an apparently politically polarized concern for the environment has grown to be recognized in many spheres. Just one example of this is in sanitation. It is clear to people that the faster landfills fill up, for instance, the sooner new costs will come for more land, farther carrying of trash at greater fuel expenses, etc. Also, in communities with well-run recycling efforts, municipalities can see financial benefit from the materials recycled that would otherwise just fill up landfills. These elements I call cultural because they are not measures that address climate change directly. Rather, they are elements of a culture of consideration for what it means to be a part of an ecosystem today.

At one level, something like a cultural shift is necessary, since no one solution is likely to resolve the problems of climate change. Andrew Light's environmental pragmatism suggests an effort to move beyond traditional philosophical debates about the nature of environmental value. He argued that "the important thing to impress upon environmental philosophers [is] the need to take up the largely empirical question of what morally motivates human to change their attitudes, behaviors, and policy preferences toward those more supportive of long-term environmental sustainability" (Light 2002, p. 446). What is most likely is that a variety of efforts combined will be necessary to bring about both the will for change and the consequent support for public policy that addresses environmental concern adequately. Those efforts should include both adaptation and some potential measures of mitigation, and these will inescapably have to be joined with developments in new technologies whose benefits should bring about a decrease in harmful emissions, a decrease in demand for finite energy resources, and an increase in sustainable practices. These joint goals do not yet have a singular solution for achieving them all, but together they embody the various important elements that will enable cultural shifts in energy use and thus emissions to take hold in wealthier nations and abroad. But the problems of climate change may require drastic action in some regions, and with any drastic action, costs arise, both in carrying out the action and in dealing with its new effects. The most effective outcomes will likely occur with the help of interdisciplinary teams working in concert to bring about maximally beneficial environmental results, such as are starting to arise with projects like architectural planning for new buildings. Even if changes come, yielding a culture of concern for the environment, however, some new developments in ethics and in climate change considerations will grow increasingly important and complex and will continue to challenge cultural beliefs and practices. These include the following:

- The need for new technologies, such as trapping of GHG's, and energy efficiencies
- The possible need for population controls and the conflicts that will likely arise regarding fairness and freedom in relation to such controls
- Policies and plans for the future migrations of people who have no other choice

- Challenges of dividing up responsibilities when changes require costs
- The offset of cost involved in choosing practices that are sustainable over ones that are simpler and cheaper, but at greater environmental cost

A final consideration is worth noting. There are regions in which people do not yet live. In those places, there are natural resources that could be gathered. Among these circumstances is the Arctic National Wildlife Refuge (ANWR) in the United States, which has been at the center of controversy about drilling for oil in new locations. People argue that America ought to exploit this location since no one uses it. A few considerations already mentioned combine in rendering such cases more complex. For instance, it could be claimed that such areas will not have future benefit for people because people do not travel there. As climate changes, however, it is altogether possible that uninhabitable places become inhabitable. In that process, places like refuges near the poles will become more frequented as a result of the thawing of cold regions, but it is uncertain whether or not future generations will make use of such refuges. In this instance, then, the problem of uncertainty for the future returns, while not directing specific action – since people must not commit the fallacy of appealing to ignorance – it is important nevertheless to raise the question about whether it is true that the ANWR will not be used in the future. Also, it appears that climate change, while potentially devastating in some regions, may bring benefit to colder regions to some degree. Finally, the matter of responsibilities to future generations arises, when coupled with these first two considerations, showing concern for children and grandchildren, who may 1 day frequent places like the Arctic National Wildlife Refuge. Nevertheless, the people of today need to be concerned about sources of energy, as well as their economic well-being, for without the necessary financial and energy resources, expensive efforts to mitigate climate change will be impossible.

Conclusion

Changes in climate are of the immensely complex sort that will require consideration about a vast array of responsibilities and inputs. This fact has slowed the development of a culture of environmental concern, but today that culture is building and appears to recognize more than ever before the need for concerted efforts to get ready for the greater changes and costs that climate change will bring about. For the present volume on climate change mitigation, the focus has been on terminology, options for mitigation, as well as the various ways of thinking and the considerations that should be taken into account for ethical approaches to human conduct about climate change. At the same time, in the cost and benefit analyses to be used in evaluation of the various methods that are and will become available for responding to new problems, it is important to factor in options for adaptation to new circumstances, remaining as open as possible to intelligent deliberation about the ideal resolution of the problems of climate change. People must also take into account the fact that measures to mitigate climate change always come with costs of their own, both direct and

indirect. The fact that there are costs to the work of addressing climate change, however, ought not to be seen as implying that the world would lose equally from action as from inaction. Climate science, mitigation strategies, and projections of adaptation options, all are becoming better understood as further inquiry develops into these areas. Skepticism is often a healthy force in inspiring further study and justification for public action. Past skepticism has inspired more and more study over time, which appears to be converging on the conclusion that the need for action must be taken seriously and proposals weighed. This chapter has been aimed at exposing readers to a number of issues related to a broad understanding of climate change, mitigation, and the moral norms that ought to be taken into account as international efforts are shaped to address the future of the global climate.

References

Batterbee R, Binney H (2008) Natural climate variability and global warming. Blackwell, Oxford

Broder J (2010) Climate change doubt is tea party article of faith. The New York Times, 20 Oct. http://www.nytimes.com/2010/10/21/us/politics/21climate.html. Accessed 22 Dec 2010

Brohan P, Kennedy JJ, Harris I, Tett SFB, Jones PD (2006) Uncertainty estimates in regional and global observed temperature changes: a new data set from 1850. J Geophys Res 111, D12106

Broome J (2008) The ethics of climate change. Sci Am 298(6):97–102

Brown MH (2010) Religious environmentalists hope spill wins converts. Baltimore Sun, 8 July. http://weblogs.baltimoresun.com/news/faith/2010/07/religious_environmentalists_ho.html. Accessed 22 Dec 2010

Bruno J (2009) Climate denial crock of the week: "temp leads carbon." http://www.climateshifts.org/?p=3362&cpage=1. Accessed 14 July 2010

Callicott JB (1994) Earth's insights: a survey of ecological ethics from the Mediterranean basin to the Australian outback. University of California Press, Los Angeles

Carson R (1962/1987) Silent spring. Houghton Mifflin, Boston

Committee on Abrupt Climate Change (2002) Abrupt climate change: inevitable surprises. National Academy Press, Washington, DC

Committee on Science, Engineering, and Public Policy (1992) Policy implications of greenhouse warming: mitigation, adaptation, and the science base. National Academies Press, Washington, DC

Courtland R (2008) Planktos dead in the water. NAT News. doi:10.1038/news.2008.604. http://www.nature.com/news/2008/080215/full/news.2008.604.html. Accessed 7 Jan 2011

de Blij H (2005) Why geography matters. Oxford University Press, Oxford/New York

Ereaut G, Segnit N (2006) Warm words: how are we telling the climate story and can we tell it better? Institute for Public Policy Research, London. http://www.ippr.org/members/download.asp?f=/ecomm/files/warm_words.pdf&a=skip. Accessed 6 Jan 2011

Gardiner SM (2004) Ethics and global climate change. Ethics 114:555–600

Gardiner SM (2006) A core precautionary principle. J Polit Philos 14(1):33–60

GISS (Goddard Institute for Space Studies) (2010a) 2009: second warmest year on record; End of warmest decade. GISS (Goddard Institute for Space Studies), New York. http://www.giss.nasa.gov/research/news/20100121/. Accessed 25 Feb 2011

GISS (Goddard Institute for Space Studies) (2010b) GISS surface temperature analysis (GISTEMP). GISS. http://data.giss.nasa.gov/gistemp/. Accessed 14 July 2010

Hansen J (2009) Storms of my grandchildren. Bloombury, New York

Hays JD, Imbrie J, Shackleton NJ (1976) Variations in Earth's orbit: pacemaker of the ice ages. Science 197(4270):1121–1132

Hodder P, Martin B (2009) Climate crisis? The politics of energy framing. Econ Polit Wkly 44 (36):53–60

IEA (International Energy Agency) (2006) Energy technology perspectives 2006. IEA (International Energy Agency), Paris

IPCC (Intergovernmental Panel on Climate Change) (1990) IPCC first assessment report working group I: scientific assessment of climate change. IPCC (Intergovernmental Panel on Climate Change), Geneva

IPCC (Intergovernmental Panel on Climate Change) (1995) IPCC second assessment: climate change 1995. IPCC (Intergovernmental Panel on Climate Change), Geneva. http://www.ipcc.ch/pdf/climate-changes-1995/ipcc-2nd-assessment/2nd-assessment-en.pdf. Accessed 23 Apr 2010

IPCC (Intergovernmental Panel on Climate Change) (2001) Climate change 2001: synthesis report (third assessment report). Summary for policymakers. IPCC (Intergovernmental Panel on Climate Change), Geneva. http://www.grida.no/climate/ipcc_tar/vol4/english/pdf/spm.pdf. Accessed 23 Apr 2010

IPCC (Intergovernmental Panel on Climate Change) (2005) Guidance notes for lead authors of the IPCC fourth assessment report on addressing uncertainties. IPCC (Intergovernmental Panel on Climate Change), Geneva. http://www.ipcc.ch/pdf/supporting-material/uncertainty-guidance-note.pdf. Accessed 19 July 2010

IPCC (Intergovernmental Panel on Climate Change) (2007a) Contribution of working group II to the fourth assessment report of the Intergovernmental Panel on Climate Change: impacts, adaptation, and vulnerability. In: Parry ML, Canziani OF, Palutikof JP, van der Linden PJ, Hanson CE (eds) Cambridge University Press, Cambridge. http://www.ipcc.ch/publications_and_data/publications_ipcc_fourth_assessment_report_wg2_report_impacts_adaptation_and_vulnerability.htm. Accessed 14 July 2010

IPCC (Intergovernmental Panel on Climate Change) (2007b) Climate change 2007: the physical science base, contribution of working group I to the fourth assessment report of the Intergovernmental Panel on Climate Change, 2007. In: Solomon S, Qin D, Manning M, Chen Z, Marquis M, Averyt KB, Tignor M, Miller HL (eds) Cambridge University Press, Cambridge/New York. http://www.ipcc.ch/publications_and_data/ar4/wg1/en/contents.html. Accessed 13 July 2010

IPCC (Intergovernmental Panel on Climate Change) (2007c) Climate change 2007: synthesis report. Contribution of working groups I, II and III to the fourth assessment report of the Intergovernmental Panel on Climate Change. In: Core Writing Team, Pachauri RK, Reisinger A (eds) IPCC, Geneva. http://www.ipcc.ch/publications_and_data/ar4/syr/en/contents.html. Accessed 13 July 2010

IPCC (Intergovernmental Panel on Climate Change) (2007d) Climate change 2007: synthesis report (fourth assessment report). IPCC (Intergovernmental Panel on Climate Change), Geneva. http://www.ipcc.ch/pdf/assessment-report/ar4/syr/ar4_syr.pdf. Accessed 23 Apr 2010

Kemp DD (2004) Exploring environmental issues: an integrated approach. Routledge, London, p 37

Kunzig R (2008) A sunshade for planet Earth. Geoengineering: how to cool Earth – at a price. Sci Am 299(5):46–55. http://www.scientificamerican.com/article.cfm?id=geoengineering-how-to-cool-earth. Accessed 6 Jan 2011

LaHay PM (2000) Storm crawls across southeast. Associated Press, New York

Lenton TM, Held H, Kriegler E, Hall JW, Lucht W, Rahmstorf S, Schellnhuber HJ (2008) Tipping elements in the Earth's climate system. Proc Natl Acad Sci 105(6):1786–1793

Leopold A (1968) A sand county Almanac. Oxford University Press, New York

Liao C, Luo Y, Fang C, Li B (2010) Ecosystem carbon stock influenced by plantation practice: implications for planting forests as a measure of climate change mitigation. PLoS One 5(5): e10867. doi:10.1371/journal.pone.0010867. http://www.plosone.org/article/info%3Adoi%2F10.1371%2Fjournal.pone.0010867. Accessed 5 Jan 2011

Light A (2002) Contemporary environmental ethics from metaethics to public philosophy. Metaphilosophy 33(4):426–449

Lorius C, Jouzel J, Raynaud D, Hansen J, Le Treut H (1990) The ice-core record: climate sensitivity and future greenhouse warming. Nature 347:139–145

Manning MR, Petit M, Easterling D, Murphy J, Patwardhan A, Rogner H-H, Swart R, Yohe G (eds) (2004) IPCC workshop on describing scientific uncertainties in climate change to support analysis of risk and of options. Intergovernmental Panel on Climate Change, Geneva. http://www.ipcc.ch/pdf/supporting-material/ipcc-workshop-2004-may.pdf. Accessed 17 July 2010

Manson N (1999) The precautionary principle, the catastrophe argument, and Pascal's Wager. Ends Means 4(1):12–16. http://www.abdn.ac.uk/philosophy/endsandmeans/vol4no1/manson.shtml. Accessed 22 Dec 2010

Martin P, Archer D, Lea DW (2005) Role of deep sea temperature in the carbon cycle during the last glacial. Paleoceanography 20:PA2012. http://www.geol.ucsb.edu/faculty/lea/pdfs/Martin%202005%20Paleo.pdf. Accessed 14 Mar 2011

McCain J (2009) Interview on State of the Union with John King. CNN, 15 Feb. http://edition.cnn.com/TRANSCRIPTS/0902/15/sotu.01.html. Accessed 22 Dec 2010

McKnight TL, Hess D (2000) Physical geography, 6th edn. Prentice Hall, Upper Saddle River

MEA (Millennium Ecosystem Assessment) (2005) Ecosystems and human well-being: health synthesis. World Health Organization, Geneva. http://www.who.int/globalchange/ecosystems/ecosys.pdf. Accessed 22 Dec 2010

Mendelsohn R (2009) The impact of climate change on agriculture in developing countries. J Nat Resour Policy Res 1(1):5–19

Merriam-Webster (2003) Merriam-Webster's Collegiate dictionary, 11th edn. Merriam-Webster, Springfield

Moser SC (2010) Communicating climate change: history, challenges, processes and future directions. Wiley Interdiscip Rev Clim Chang 1(1):31–53

Moss RH (2006) Improving information for managing an uncertain future climate. Glob Environ Chang 17:4–7

Moss RH, Schneider SH (2000) Uncertainties in the IPCC TAR: recommendations to lead authors for more consistent assessment and reporting. In: Pachauri R, Taniguchi T, Tanaka K (eds) Guidance papers on the cross cutting issues of the third assessment report of the IPCC. Intergovernmental Panel on Climate Change, Geneva, pp 33–51. http://www.ipcc.ch/pdf/supporting-material/guidance-papers-3rd-assessment.pdf. Accessed 17 July 2010

NASA (National Aeronautics and Space Administration) (2007) Global warming. NASA. http://www.nasa.gov/worldbook/global_warming_worldbook.html. Accessed 14 July 2010

NCDC (National Climatic Data Center) (2008) GHCN monthly Version 2. NOAA. http://www.ncdc.noaa.gov/oa/climate/ghcn-monthly/index.php. Accessed 14 July 2010

NCDC (National Climatic Data Center) (2010a) Global surface temperature anomalies. NOAA. http://www.ncdc.noaa.gov/cmb-faq/anomalies.html#mean. Accessed 14 July 2010

NCDC (National Climatic Data Center) (2010b) State of the climate report. NOAA. http://www.ncdc.noaa.gov/bams-state-of-the-climate/. Accessed 14 July 2010

NOAA (National Oceanic and Atmospheric Administration) (2009) Global temperatures well above average; slightly above average for U.S. http://www.noaanews.noaa.gov/stories2009/20091208_globalstats.html. Accessed 17 July 2010

NOAA (National Oceanic and Atmospheric Administration) (2010) http://ftp.cmdl.noaa.gov/ccg/co2/trends/co2_mm_mlo.txt. Accessed 14 July 2010

Park C (2008) Oxford dictionary of environment and conservation. Oxford University Press, Oxford

Scheffer MJ, Bascompte WA, Brock V, Brovkin SR, Carpenter V, Dakos H, Held EH, van Nes MR, Sugihara G (2009) Early-warning signals for critical transitions. Nature 461(7260):53–59

Stern N (2007) The economics of climate change: the stern review. Cambridge University Press, Cambridge

Stott P (2011) Global average temperature records. Met Office, Exeter. http://www.metoffice.gov.uk/climate-guide/science/temp-records. Accessed 18 Mar 2016

Strahler AN, Strahler AH (1978) Modern physical geography. Wiley, New York

Strech C, Scholz SM (2006) The role of forests in global climate change: whence we come and where we go. Int Aff 82(5):861–879

UNFCCC (United Nations Framework Convention on Climate Change) (1992) United Nations framework convention on climate change. UNFCCC (United Nations Framework Convention on Climate Change), Bonn. http://unfccc.int/resource/docs/convkp/conveng.pdf. Accessed 13 July 2010

USCCSP (United States Climate Change Science Program) (2007) Our changing planet: the U.S. climate change science program for fiscal year 2007. USCCSP (United States Climate Change Science Program), Washington, DC. http://www.usgcrp.gov/usgcrp/Library/ocp2007/ocp2007.pdf. Accessed 13 July 2010

Walsh B (2009) Is there a climate-change tipping point? Time, 4 Sept. http://www.time.com/time/health/article/0,8599,1920168,00.html. Accessed 16 July 2010

Walther G, Post E, Convey P, Menzel A et al (2002) Ecological responses to recent climate change. Nature 416:389–395

WCRP (World Climate Research Program) (2010) Climate variability and predictability project. International CLIVAR Project, Southampton. http://www.clivar.org/index.php. Accessed 13 July 2010

Weber EU (2010) What shapes perceptions of climate change? Wiley Interdiscip Rev Clim Chang 1(3):305–474. http://www3.interscience.wiley.com/cgi-bin/fulltext/123325177/PDFSTART. Accessed 16 July 2010

WMO (World Meteorological Organization) (2009) Press release No. 869: 2000–2009 the warmest decade. http://www.wmo.int/pages/mediacentre/press_releases/pr_869_en.html. Accessed 17 July 2010

WMO (World Meteorological Organization) (2010) WMO statement on the status of the climate in 2009. WMO (World Meteorological Organization), Geneva. http://www.wmo.int/pages/publications/showcase/documents/1055_en.pdf. Accessed 26 Feb 2010

Mass Media Roles in Climate Change Mitigation

Kristen Alley Swain

Contents

Abstract

News media portrayals of climate change have strongly influenced personal and global efforts to mitigate it through news production, individual media consumption, and personal engagement. This chapter explores the media framing of climate change mitigation and adaptation strategies, including the effects of media routines, factors that drive news coverage, the influences of claims-makers, scientists, and other information sources, the role of scientific literacy in interpreting climate change stories, and specific messages that mobilize action or paralysis. It also examines how journalists often explain complex climate science and legitimize sources, how audiences process competing messages

K.A. Swain (✉)
Meek School of Journalism and New Media, The University of Mississippi, Oxford, MS, USA
e-mail: kaswain@olemiss.edu

W.-Y. Chen et al. (eds.), *Handbook of Climate Change Mitigation and Adaptation*,
DOI 10.1007/978-3-319-14409-2_6

about scientific uncertainty, how climate stories compete with other issues for public attention, how large-scale economic and political factors shape news production, and how the media can engage public audiences in climate change issues.

Introduction

By the end of the twenty-first century, global climate change is predicted to raise sea levels and increase the frequency and severity of storms. Rising temperatures would create heat waves, drought, and disease pandemics. Hundreds of thousands of square miles of coastal wetlands and lowlands could be inundated. Flooding from excessive rain and sea-level rise would threaten lives, agriculture, livestock, buildings, and infrastructures. Salt water advancing into aquifers and estuaries would threaten water supplies, ecosystems, and agriculture.

The effectiveness of climate change mitigation and adaptation is linked to public understanding of climate change issues, which people gain through daily media consumption. News is ubiquitous in everyday life, "a sort of instant historical record of the pace, progress, problems, and hopes of society." It also can influence the outcomes of the events it describes. However, mainstream U.S. news media have failed to adequately report on climate change.[1]

Public awareness of climate change issues continues to rise worldwide, but in most nations, coverage of sports, celebrities, politics, the economy, and crime dwarfs that of climate change. The news media often represent climate change mitigation and adaptation as dynamic and contested issues within the intersecting realms of policy, science, and the public. Although science has confirmed that human activities are heavily implicated in climate change, the global phenomenon has been increasingly framed as catastrophic as though it must be considered dreaded and irreversible to warrant public attention. Social scares that accelerate political demands can spark broad social change.[2]

Media framing can strongly influence audience motivations to act or to become fatalistic. The cost of inaction could be severe in the case of climate change. The predicted consequences of inaction include ozone depletion, melting of the polar ice caps, destruction of wildlife habitats, catastrophic sea level rise, extreme weather patterns, flooding and drought, increase in average temperatures, and other irreversible climatic changes. Even if all greenhouse gas emissions could stop immediately, more major climate changes still would occur because of lags in the Earth-atmosphere system.

Rapidly shifting attitudes among nongovernmental groups on the issue of global climate change can affect the public debate and the international negotiating process. Climate and adaptation leadership involves a struggle for meaning that can rapidly shift over time. Leaders must guide deliberation about whether to aim at emission

[1] Bennett (2002), Kenix (2008)

[2] Shanahan (2007), Boykoff and Roberts (2007), Hulme (2006), Ungar (1992)

reduction targets that would be stringent enough to effectively fight climate change and to evaluate methods to reach the emission reduction targets in light of the ends that are reached.[3]

David King, the UK government's chief scientific advisor, asserts that climate change is a greater threat than global terrorism, while former U.S. vice-president Al Gore has equated the need for collective action to that posed by the rise of fascism in the twentieth century. According to the 700-page *Stern Review on the Economics of Climate Change*, climate change could shrink the global economy by 20 %, but acting now to address climate change would cost only 1 % of global GDP.[4]

Since 2006, adaptation has emerged as a newsworthy focus of climate change coverage in the global news media. A review of 75 studies from across the world revealed that increasing numbers of people (between 25 % and 65 % in most nations) perceive changes in the environment or believe they have already experienced the impacts of climate change. Others still place climate change in the distant future.[5]

This chapter explores the media framing of mitigation and adaptation strategies, including the effects of media routines, the factors that drive news coverage, the influences of claims-makers, scientists, and other information sources, the role of scientific literacy in interpreting climate change stories, and specific messages that mobilize action or paralysis. It also examines how journalists often explain complex climate science and legitimize sources, how audiences process competing messages about scientific uncertainty, how climate stories compete with other issues for public attention, how large-scale economic and political factors shape news production, and how the media can engage public audiences in climate change issues.

History of Climate Change Coverage

Global climate change has been a major issue on the U.S. political agenda since 1988. The conjecture that humanity might change the climate of the entire planet first appeared in 1896 in a prediction that carbon dioxide from fossil fuel combustion could gradually warm the globe. Climate change was first reported in the U.S. press in the 1930s, but coverage of human contributions to climate change did not clearly appear until the 1950s. For example, in 1957, the International Geophysical Year, a *Christian Science Monitor* article posed the question, "Are men changing the Earth's weather?" In the subsequent three decades, climate coverage remained sparse.[6]

During the 1960s, research suggested that small perturbations might lead to an abrupt change in the climate system. Some began to frame global warming as an environmental risk, a security risk, a practical policy question, an international relations issue, and even a moral problem. By the late 1970s, a scientific consensus

[3]Carpenter (2002), Uusi-Rauva (2010)

[4]Shanahan (2007), Stern (2006)

[5]Moser (2014a)

[6]Gushee (2004), Weart (2009)

began to take shape. Three media-science-policy spheres intersected in the mid-1980s, when coverage of climate change began to increase dramatically.[7]

When the issue of global warming first rose to prominence in the U.S.A. and UK in the late 1980s, it focused on mitigation. This coverage was fueled by public interest about chlorofluorocarbons, the ozone hole, and the U.S. presidential election. Coverage in the late 1980s and early 1990 was dominated by discussions of nuclear energy as a potential alternative to carbon-based consumption, as well as U.S. Senate bills to reduce anthropogenic emissions. Boykoff and Roberts explored newspaper coverage of climate change in 40 English-language newspapers in 17 countries, across five continents. Among 40 of the most influential English-language world newspapers, climate coverage increased globally when the Intergovernmental Panel on Climate Change reports were released in 1990, 1995, and 2001, during the UN Framework Convention on Climate Change in 1992, and during the Kyoto Protocol convention in 1997.[8]

Distinct phases in climate science policy have been reflected in media attention over time. The 1990s were characterized by a complex politicization of climate science, media, and policy. A small group of skeptical spokesmen and scientists, many of whom received funding from carbon-based industry interests, gained prominence in the news in the early 1990s by refuting scientific findings about human contributions to climate change.[9]

Since 1995, a strong scientific consensus of more than 2,000 researchers has asserted that humans influence the global climate. By the end of the 1990s, increasing media warnings of peril made most of the literate world public aware of the issue, but skepticism and aversion to regulation persisted. Most people in the world were now concerned but not motivated to take action. Between 2003 and 2006, coverage of climate change adaptation increased substantially. In developing countries and rural areas, climate change news is communicated primarily through radio.[10]

News coverage of climate change in the aftermath of Hurricane Katrina in 2005 emphasized conflict and immediacy frames, which could have inhibited public understanding of climate issues. Climate change news coverage between 2006 and 2010 sparked a surge in public interest in articles about the environment, energy, and pollution. This coverage coincided with the greatest turmoil in the history of the news industry, a time when journalism jobs were drastically reduced, news outlets had extremely limited print space and airtime, and editors were often disinterested in climate issues. As public interest in "going green" increased during the first decade of the twenty-first century, editors and reporters became more attentive to the ethical line between writing about the environment and writing on behalf of the environment (Thompson 2009; Brainerd 2007a).[11]

[7]Boykoff and Roberts (2007), Weart (2009)

[8]Ungar (1992), Weisskopf (1988), Boykoff and Roberts (2007)

[9]Trumbo (1996), Boykoff and Boykoff (2004), Gelbspan (1998), Schneider (2001)

[10]Weart (2009), Boykoff and Roberts (2007), Luganda (2005)

[11]Thompson (2009), Brainard (2007a)

The Intergovernmental Panel on Climate Change consensus report in 2007 asserted that human activities are more than 90 % likely to be the cause of climate change and that impacts could be abrupt and irreversible. It added that if urgent steps are taken, climate change could be addressed at a reasonable cost. Nearly 200 nations endorsed the IPCC findings in 2007, which were based on thousands of published, peer-reviewed studies. In the same year, China suddenly and quickly overtook the U.S.A. as the world's worst in greenhouse gas emissions because of its rapid economic expansion. Most special reports on climate change in news publications mentioned China because global efforts to make the planet greener hinge on China's politics, emissions, and actions. In 2007, Patrick Symmes said in *Outside* magazine, "China is the asterisk at the end of every conversation about the environment." In this piece, he related his own story of whitewater rafting down the Yangtze River, whose valleys may soon be flooded from the construction of hydroelectric dams. The best U.S. print news coverage of China's economic growth has used visual storytelling to highlight its extreme pollution and environmental degradation. Many stories emphasized China's reliance on coal, inefficient use of energy, pollution-related death toll, and preference for growth over environmental protection.[12]

In 2007, Andrew Revkin, former environment reporter for *The New York Times*, started Dot Earth, an innovative blog where he posts and exchanges ideas about climate and sustainability issues. In the same year, CBS's Katie Couric asked each presidential candidate to answer a single question during a 7-minute segment: "Is the threat of climate change overblown?" Some critics felt Couric's pointed question was posed irresponsibly within a skeptical and meaningless frame and that it only allowed for candidates to spout talking points. In any case, CBS was the first network to draw voter attention to a new and underrepresented campaign issue on national, prime-time television.[13] By 2008, news coverage moved beyond climate change science into the broader arena of action – what governments, entrepreneurs, and ordinary citizens are doing about it. As of 2010, Abu Dhabi announced it will have the first city in the world with zero carbon emissions by 2018. In addition, developers plan to build a desert city for 50,000 residents relying completely on solar power and other renewable energy, and the Dutch are developing ways to protect vulnerable coastlines against rising sea levels.[14]

The IPCC defines adaptation as any "*adjustment in natural or human systems in response to actual or expected climatic stimuli or their effects, which moderates harm or exploits beneficial opportunities*"[15] Although the news media rarely mentions "adaptation," the climate science community frequently uses the term in both scholarship and policy. For instance, the UN Framework Convention on Climate Change clearly identified adaptation as the complementary approach to mitigation (emission reductions).

[12]Brainard (2007b)

[13]Brainard (2007c)

[14]Russell (2008)

[15]Goidel et al. (2012)

Adaptation measures needed to protect human life and property fall into three categories: retreat, accommodation, and protection. Retreat involves migration or abandoning the coastal zone, while accommodation measures include flood shelters, elevating buildings, converting agriculture to fish farming, innovative irrigation, reforestation, drought-tolerant crops, rainwater storage, or growing flood/salt-tolerant crops. Protection includes more permanent and expensive measures such as geoengineering, weather control, damming glacial lakes, hard structures such as sea walls and dikes, as well as soft solutions such as dunes and vegetation, to protect the land from the sea so that existing land uses can continue.

Between 1988 and 2006, adaptation represented less than 1 % of all climate-related news coverage in major news outlets within the U.S.A. and Great Britain. However, between 2003 and 2007, coverage of this topic rose dramatically. Moser (2014)[16] observed a multifold spike in newspaper coverage of adaptation in 2006 and 2007. Adaptation coverage peaked in 2007 in the U.S.A. and India, coinciding with the release of the IPCC Fourth Assessment Report, and again in 2009 in covering the Copenhagen Conference of the Parties.[17]

Media Framing of Climate Change

As a news topic, climate change has potential narrative elements that include the oil industry and the earth's climatic balance. The world's leading scientists now insist that the story should shift from whether climate change is happening to what will be done about it. While newspapers in the U.S.A. might be avoiding the issue, all regions hesitated to frame climate change in light of extreme weather consequences or oil reduction solutions.[18]

Individuals "frame" an issue by mentally organizing and discussing with others an issue's central ideas. This framing can greatly influence how they understand the nature of the problem, who or what they see as being responsible for the problem, and what they feel should be done to address the problem.[19] Similarly, news framing is the process of organizing and packaging information. It involves selecting aspects of a perceived reality to make them more salient. It promotes a particular problem definition, assignment of responsibility, causal interpretation, ethical or moral interpretation, or recommended solution. News frames are embodied in key words and concepts emphasized in stories. Most news content is either framed episodically in terms of specific events or thematically to emphasize broad or abstract concepts. For example, describing the impact of climate change on polar bears with an episodic or thematic frame in a news story does not prompt individual behavior change.

[16]Moser (2014)

[17]Boykoff et al. (2013)

[18]Good (2008), Herman and Chomsky (1988)

[19]Gamson et al. (1992), Price et al. (2005)

However, the use of a thematic frame promotes greater support for policies that address climate change than the use of an episodic frame.[20]

The media tend to reframe a major scientific debate when they increase attention to ethical issues, more prominent public discourse, or scientific-economic issues. Gamson and Modigliani identified eight frames that consistently appear across science-related policy debates: social progress, economic development/competitiveness, morality/ethics, scientific/technical uncertainty, Pandora's box/runaway science, public accountability/governance, middle way/alternative path, and conflict/strategy. Claims-makers compete for legitimacy through the news media, while the news media construct, interpret, and frame the claims-makers and their issues.[21]

Solutions and effect frames dominated Peruvian coverage of an international climate conference, while policy and science frames were limited. In a cross-national comparison of Dutch and French newspaper framing of climate change during the annual United Nations Conferences of the Parties between 2001 and 2007, Dirikx and Gelders identified five dominant frames in the coverage: nonpursuit, consequences, responsibility, conflict, and human interest. Most stories referred to the consequences of not pursuing a certain course of action and of possible losses and gains, a consequences frame. The responsibility frame included the need for urgent actions and possible solutions, as well as the responsibility of governments for alleviating climate change problems. The conflict frame appeared less frequently than the other four frames but more regularly than the human interest frame.[22]

The growing enormity of challenges created by climate change has redefined international security in global media coverage since 2007. This new norm has defined climate change as a security threat, in light of authoritative scientific evidence. It emerged in the wake of an international legal framework constituted through the 1992 United Nations Framework Convention on Climate Change, the 1997 Kyoto Protocol, and the 2009 Copenhagen Accord. However, internalizing the security threat norm within treaties was not sufficient to crystallize the norm. A dramatic and complex position shift in U.S. domestic policy was required, as well as the participation of many local and state governments and the private sector. The shift eventually led to greater media attention to the security aspects of climate change, which afforded this dimension of the debate enormous prominence.[23]

In the broadest sense, the media tend to frame climate change problems in light of underlying concerns, such as the character of capitalism, the relationship between nature and culture, the social process of defining problems, and societal transformation in response to climate change. Progress, conflict, generic risk, and the interplay between market incentives and regulation are the most common frames used in controversial science stories. These frames imply responsibility for societal outcomes from science and technology. Citizens also are more likely to dissociate

[20]Entman (1993), Hart (2010)

[21]Listerman (2010), Gamson and Modigliani (1989)

[22]Takahashi (2010), Dirikx and Gelders (2010)

[23]Garcia (2010)

themselves from the causes, impacts, and responsibility for tackling climate change when news media use the term "climate change" instead of "global warming."[24]

Lakoff argues that people unconsciously reject facts that appear to fall outside the frame they use to see the world. A person's frame, often created by values instilled in childhood, leads him to see only the world that agrees with his values, while blocking out conflicting facts and arguments.[25] British newspaper stories that use a religious metaphor to denigrate anthropogenic climate change undermine the scientific status of climate change by presenting it as irrational faith-based religion and its proponents as religious extremists intolerant of criticism. Some stories mock climate change using notions of sin such as describing "green" behaviors as atonement or sacrifice. The religious metaphor damages constructive debate by emphasizing morality and how climate change is discussed and by detracting attention from the content of scientific data and theories. News framing of controversial science also can affect perceived ethics of research when it includes a political conflict frame but not when it uses a scientific progress frame. People who believe that science is morally neutral perceive greater usefulness of research. Individuals with higher self-reported science interest and exposure tend to rate the research as more credible.[26]

To convince a skeptic that climate change is an emergency worthy of attention, a message must tailor its arguments to fit within the person's existing framework. To communicate climate change ideas and policies to political conservatives, the term "climate change" could be replaced with "climate security" to better explain how the changing climate adversely affects America's economic health, national security, and prosperity. Highlighting clean "energy advancement" could avoid negative connotations associated with reducing emissions and economic growth, and the objective of cap-and-trade policies could be emphasized, to "harness the power of the market."[27]

The news plays a major role in informing the public about the science and policy of climate change. The framing of climate change coverage involves interview source selection, presentation and evaluation of conflicting arguments, and scientific uncertainty interpretations. Climate stories shape and influence public opinion, politics, public understanding, and action in complex, dynamic, and nonlinear ways. For many journalists, the climate change topic is new, extremely complex, and easy to get wrong. BBC's Richard Black and Roger Harrabin warned fellow journalists how critical it was for them to catch up: "If we do not have a strong grasp of the fundamentals of the climate debate, we risk presenting our audiences with a set of opinions which is outdated, driven by spin, or simply wrong."[28]

Over time, various leaders have framed climate change stories about social, political, and cultural issues according to their political agendas. Carvalho and

[24]Shove (2010), Weaver et al. (2009), Whitmarsh (2009)

[25]Lakoff (2004)

[26]Woods et al. (2010), Stewart et al. (2009)

[27]Lakoff (2004), Schottland (2010)

[28]Boykoff and Roberts (2007), Herrmann (2007)

Burgess identified three major themes in this coverage: power mobilization, the public sphere, and personal engagement. The most frequent frames in climate change coverage have been political, consequences, and scientific frames. Elite Western media tend to frame emissions as global, without challenging or differentiating available data, and often frame climate change in terms of regulatory frameworks, political constraints, and economic drivers. The media frames in this coverage are created through complex relationships between scientists, policy actors, and the public. Wire service stories strongly influence how climate change science is framed to the public. Three clusters of "carbon compounds," common catchphrases that focus on finance, lifestyle, and attitudes include "carbon footprint" and "carbon finance." These phrases serve as tools of communication about climate change mitigation.[29]

Worldwide news coverage of climate change sharply declined after it spiked around the 2009 United Nations Climate Change Conference meetings in Copenhagen. This decline may have occurred because news organizations had to devote coverage to many other critical issues competing for news attention. According to public arena theory, the public, political actors, and news organizations each can only pay attention to a few problems at any given time. As one issue rises in prominence, attention to other issues declines. The number of public arenas available for coverage in a given day is limited by the carrying capacity of individual media outlets.[30]

Climate coverage is more attention getting when it focuses on one specific aspect of the story. For instance, the scientific uncertainty frame appeals to people who do not want to change, but the national security frame could inspire action from the same individuals. The polar bear frame appeals most to animal lovers, but few people have ever seen a polar bear or would miss it if it went extinct. The money frame presents climate change as a business opportunity or outlines the costs and benefits of mitigation or inaction. However, messages framed in terms of economics and losses do no better than messages framed in terms of environment and gains in encouraging the adoption of sustainable behaviors. While the catastrophe frame may leave people feeling helpless, a justice or equity frame could be empowering.[31]

Two dominant themes, weather and renewable energy, often appear in both fear-laden and inspirational representations of climate change. Much of the climate change coverage in the U.S.A. has been tied to specific events, such as severe weather, rather than ongoing issues. In a content analysis of a decade of evening news programs about energy and environmental news topics, news in both Canada and the U.S.A. tend to focus on severe weather, with a somewhat greater focus on severe weather events in the U.S.A. The tone of climate change coverage in Canada has been more critical than comparable climate change coverage in the

[29]Carvalho and Burgess (2005), Weintraub (2007), Agarwal and Narain (1991), Boykoff and Roberts (2007), Antilla (2010), Koteyko (2010)

[30]Boykoff (2008), Nisbet (2011), Hilgartner and Bosk (1988)

[31]Shanahan (2007), Walton (2007)

U.S.A. Granger causality tests reveal that coverage of climate change, pollution, and related issues depends on coverage of disasters and other weather events. Journalists are more likely to discuss climate during unusually warm periods. For example, local temperatures in New York and Washington, DC have been positively related to frequency of attention to climate issues.[32]

Positive frames are more likely to prompt active engagement with climate change issues than negative frames, which can lead people to disengage or become fatalistic. For example, an April 2008 headline on *Time* magazine's cover, "How to win the war on global warming" showed the famous image of the Iwo Jima soldiers planting a tree instead of a flag. *Time*'s framing of climate change in that issue "marks a major departure from a past emphasis on doom and impending disaster, offering a new focus on national unity around a common challenge similar in nature to the Great Depression, the Space Race, or World War II." Some media critics felt the *Time* story crossed over the line of objectivity into advocacy, while others argued that the coverage provided more analysis and depth than most climate change stories do. Negative frames, including predicted climate change impacts and frightening statistics, have been covered by more TV stations and in more detail than the more positive frames of solutions, adaptation, or mitigating greenhouse gas emissions. Only 25 % of climate change stories in UK newspapers focused more on solutions than problems. Alarmism and small actions are the most common media frames in climate change coverage, but these narratives can be confusing, contradictory, and disempower the public.[33]

One example of negative framing appeared in the Australian news coverage of climate change–related sea level rise in the tiny island of Tuvalu. The stories often framed Tuvalu inhabitants as the tragic victims of environmental displacement, marginalized discourses of adaptation for Tuvaluans and other inhabitants of low-lying islands, and silenced alternative constructions of Tuvaluan identity that could emphasize resilience and resourcefulness. A recent British Medical Journal editorial asserted that failure of the world's nations to successfully curtail emissions will likely lead to a global health catastrophe, yet most Americans are only dimly aware of the health implications of climate change. However, most people respond more positively to information about the potential health benefits associated with specific climate mitigation–related policy actions than to basic information about health risks of climate change. Thus, emphasizing the health benefits of mitigation could make the overall climate change problem more personally relevant, significant, and understandable to members of the public.[34]

News framing of climate change affects how and whether audiences respond to the problem. Recent coverage has been characterized by a catastrophe narrative that disempowers people, as well as lack of relevance to audiences, little attention

[32]Manzo (2010), Soroka et al. (2009), Shanahan and Good (2000)

[33]Carvalho (2010), Nisbet (2008), Painter (2007), Futerra Sustainability Communications (2006), Institute for Public Policy Research (2006)

[34]Farbotko (2005), Jay and Marmot (2009), Leiserowitz (2005), Maibach et al. (2010)

devoted to adaptation and the perspectives of the poor, and lack of reporting on ways to address climate change that bring benefits. Climate problem indicators, high-profile international events, and climate science feedback are all attention-grabbing factors that influence media and congressional attention to climate change. These factors promote issue salience, focus attention on climate change, and promote interagenda interaction and partisan advantage on agenda setting.

For individual citizens, media representations can construct particular positions, cultivate their dispositions to action or inaction, or constrain their political engagement with climate change issues. Policymakers, however, often view climate change coverage in terms of singular concerns about security or economic interests. For example, policymakers tend to view natural disasters abetted by the man-made effects of climate change as simple emergencies requiring a straightforward response in terms of providing food, shelter, and medical supplies. They rarely talk about climate-driven emergencies as man-made, complex emergencies where humans are self-evidently at fault.[35]

The media are more likely to reinforce rather than change existing attitudes about climate change. Sometimes, the media reflect a cultural anxiety or perspective as much as they create it. Over time, coverage may progressively cultivate a particular way of looking at the world or how society should set priorities. Media interest in science issues often is triggered by the release of articles in major journals, policy decisions, political controversies, or public protest. Coverage of these topics may contain sensationalism or scaremongering because of the inherent dramatic value of these stories. The visuals and narrative structure of a story tend to be more compelling than the logic or explanations within a media text. When media attention, framing, and sourcing shift across key stages of scientific, political, and policy development, forces can combine to emphasize certain dimensions of a science controversy over others. The issue then gains, maintains, or loses political and media attention.[36]

Effective policymaking involves the ability to control media attention to an issue, while framing an issue in favorable terms. These two characteristics of media coverage both reflect and shape where an issue is decided, by whom, and with what outcomes. Over time, cyclical waves in media attention and historical shifts determine how an issue is framed and link it to policy decisions. The mediated issue development model accounts for the type of policy arena where debate takes place, the media lobbying activities of strategic actors, the journalistic need for narrative structure, and the competition from other issues for attention across policy and media environments. Related factors include the type of journalist-assigned coverage and the level of attention from opinion pages.[37]

Climate change reporting in the elite U.S. press has reflected issue attention cycles sparked by dramatic events. Over time, climate change lost much of its

[35]Shanahan (2007), Liu et al. (2009), Carvalho (2010), Moeller (2008)

[36]Kitzinger (2006), Nisbet et al. (2003)

[37]Nisbet and Huge (2006)

perceived dramatic storytelling value, which previously had driven journalists' coverage. In the past, open political conflict, personality clashes, and contested claims over risks had allowed journalists to develop news sagas they could track over time. The up and down cycles of attention hinge mainly on dramatic political events. Audience response also depends to some extent on how the current phase of the problem is framed.[38]

Public attention to environmental issues moves through five sequential stages in an issue attention cycle: preproblem, alarmed discovery and euphoric enthusiasm, gradual realization of the cost, gradual decline of intense public interest, and postproblem. In the preproblem stage, an ecological problem exists but has not yet captured public attention. Expert communities are aware of the risks, but the information is not widely disseminated. Climate change coverage was in the preproblem stage prior to 1988. In the second stage, alarmed discovery and euphoric enthusiasm, dramatic events make the public aware of the problem and alarmed about it. In the late 1980s, when more news hooks for climate change stories emerged, the public became increasingly alarmed. In the third stage, gradual realization of the cost, various claims-makers acknowledge the costs of dealing with the problem.

When a cohesive group of climate skeptics emerged in the early 1990s, they began to challenge scientific findings about anthropogenic climate change. In the fourth stage, gradual decline of intense public interest, key actors become discouraged at the prospect of appropriately dealing with the problem, and crises are normalized through suppression or boredom. This may have prompted the decline in climate change coverage in the mid-1990s. In the postproblem stage, the formerly "hot" issue "moves into a prolonged limbo – a twilight realm of lesser attention or spasmodic reoccurrences of interest… [and the issue] once elevated to national prominence may sporadically recapture public interest."[39]

Climate change and other environmental issues may not conform to Downs' issue attention cycle, since these problems have worsened, new problems have arisen, and social movement organizations have emerged to keep them alive. Cycles may have sped up in recent years and become less apparent. While the Downs model offers useful explanations about public attention, it cannot explain how media representations of climate change are constructed.[40]

Media Framing of Adaptation

Most adaptation news coverage has originated from Western European and North American newspapers and to a lesser extent from English-speaking newspapers in Australia, New Zealand, the Middle East, Asia, Eastern Europe, and South Africa.[41]

[38]McComas and Shanahan (1999), Downs (1972)

[39]Boykoff and Roberts (2007), Downs (1972, pp. 39–41)

[40]Dunlap (1992), Brossard et al. (2004), Jordan and O'Riordan (2000), Boykoff and Roberts (2007)

[41]Boykoff and Roberts (2007)

Early-stage adaptation measures, which tend to be agency internal thus less visible to the public, are needed to plan and build capacity but are perceived as not newsworthy.[42] News media often rely on a limited cast list in telling climate change stories because of journalistic training, traditions of the craft, deadlines, competition, as well as limited resources including staff, time, and money. These routines often produce distorted or cramped representations of climate change risks and prevent regular and in-depth treatment of adaptation.[43] Identifying trends and widely applicable insights is challenging for journalists, not only because of the language used to explain adaptation but also by the fact that adaptation language is often not used at all.[44]

Moser (2014)[45] notes that tracking media coverage of adaptation is challenging because often the word "adaptation" is not explicitly mentioned in stories. For instance, in coastal areas, stories may discuss adaptation plans or measures such as beach nourishment, building shoreline protection, residents retreating from the coast, or relocation of roads, airports, or water-related infrastructure. The number of small local newspapers and qualified journalists that could report on adaptation is in decline. Many media scholars examine coverage in leading national newspapers and magazines, so their analyses often do not reflect adaptation efforts at the local level. Adaptation coverage in national elite newspapers typically depicts international climate policy debates and how countries should position themselves. However, the more locally based adaptation news coverage tends to focus on concrete impacts and specific needs for adaptive actions.[46]

Takahashi and Meisner[47] found a predominance of the "effects frame" (a focus on impacts) in their study of Peruvian news coverage of climate change. This emphasis also appeared in specialized farming magazines in Sweden,[48] as well as on websites of U.S. NGOs and government agencies.[49] Major news outlets tend to cover developed nations,[50] while underrepresenting less wealthy parts of the world. Developing nations cannot afford the large-scale infrastructure adaptation projects seen in richer countries, the projects that attract most of the media attention. Therefore, smaller-scale projects and innovations may receive little or no attention.[51]

Although the term "adaptation" has been widely taken up in discussions in Europe, Canada, Australia, and Asia, it has not been easily accepted in

[42]Moser (2014)
[43]Smith (2005)
[44]Moser (2014)
[45]Moser (2014)
[46]Boykoff et al. (2013)
[47]Takahashi and Meisner (2013)
[48]Asplund et al. (2013)
[49]Pike et al. (2012)
[50]Boykoff and Roberts (2007)
[51]Moser (2014)

U.S. discourse. The resistance to "adaptation" in the U.S.A. is rooted in the challenge of communicating climate change more generally to American audiences.[52] In conservative political contexts where climate change or sea level rise are considered ideological positions rather than real phenomena,[53] early adaptation efforts are frequently not named but rather hidden in disaster preparedness or hazard mitigation plans, general land use plans, or redevelopment strategies.[54]

Funfgeld and McEvoy[55] identified four common adaptation frames: hazards (natural disasters), risk management, vulnerability (who/what will be affected and how), and resilience (a community's ability to cope with external stressors). Effort to make the abstract concept of "adaptation" more meaningful and acceptable to decision-makers and public audiences has led to the use of many catchphrases such as climate-smart, climate-resistant, climate-resilient, and climate-ready. In media coverage and other public communications, the word "adaptation" is often replaced with more familiar terms such as "preparation," "preparedness," "readiness," "adjustments," "planning," "coping," "triage," "climate risk management," or "mitigating the impacts of climate change."[56]

Some introduce adaptation via more familiar, concrete actions, such as installing irrigation, building a sea wall, managing fuel to prevent wildfires, wetland restoration, reforestation, increasing urban forest cover, ensuring food security, or establishing heat-health warning systems. For example, in announcing New York City's adaptation plan in 2013, Mayor Bloomberg never mentioned the word "adaptation." Instead, he described specific plans to build a "stronger, more resilient city" in the face of climate change and extreme events.[57]

Moser[58] identified several challenges in using the term "adaptation" in public communications. It is still a relatively new term, allowing a variety of alternate terms to be field tested before one becomes widely accepted and a common understanding of it stabilizes. "Adaptation" is an abstract jargon term, which does not allow for simple, intuitive interpretation. Journalists and other local professionals rarely follow peer-reviewed adaptation literature,[59] so they may lack both scientific understanding and access to experts who can effectively translate that science. How adaptation is framed often depends on the lead actors involved. The word "adaptation" often carries connotations that are unacceptable or not motivational to different audiences.

Adaptation language is often used to achieve a certain effect within a specific audience, such as to be alarming, provocative, appeasing, inclusive, or

[52]Ruddell et al. (2012)
[53]Capstick et al. (2013)
[54]Reser et al. (2012)
[55]Funfgeld and McEvoy (2011)
[56]Moser (2014)
[57]Moser (2014)
[58]Moser (2014)
[59]Tribbia and Moser (2008)

encouraging.[60] Adaptation must be translated from a global problem into a specific national or local problem.[61] Finally, adaptation is colored by historical legacies of communicating climate change science and mitigation,[62] including the deeply polarized political context in the U.S.A. Depending on the local context, there may be value in avoiding using the term or avoid naming causes.[63]

One study found the "preparedness" frame 15 % more compelling than "adaptation," while 100 climate and sustainability leaders and social science and communication experts judged the word "adaptation" to be "negative and demobilizing."[64] A more recent study identified two common adaptation frames in public communications: those emphasizing climate change impacts, disruptions, and extremes and the need to prepare for them, as well as by frames that introduced and explained the notion of adaptation for species, landscapes, and the built environment.[65] Discussion about economic impacts of extreme events in the U.S.A. has drawn in influential actors and helped to break the climate change and adaptation impasse in many locations.[66]

Extreme events like fire and floods – or resource scarcity issues like water and drought – are typically local (or at most regional) stories. Even so, in light of how climate change has been reported for years, adaptation is still largely a global story, as well.[67]Global climate stories often include science and policy debates about whether global warming is real, human caused, and what to do about its causes.[68] However, as common sources of information on environmental news stories, scientists often are reluctant to link local extreme events to global warming.[69] Although stories often do not link individual events to climate change, recently more coverage has emphasized the consistency of patterns of the more extreme events with global warming theory.[70]

In many areas of the world, extreme weather events are part of normal life, sometimes seen as cyclical[71] or just the wrath of Mother Nature. Where these perceptions prevail, they may hinder adaptation discussions outside of the usual "getting back to normal" postdisaster responses.[72] For some intractable climate

[60]Spence and Pidgeon (2010)
[61]Brown et al. (2011)
[62]Moser (2012)
[63]Mellman (2011)
[64]ecoAmerica (2012)
[65]Pike et al. (2012)
[66]Smith and Jenkins (2013)
[67]Resource Media (2009)
[68]Australian Department of Climate Change (2009)
[69]Shearer and Rood (2011)
[70]Gavin et al. (2010), Resource Media (2012)
[71]Connor and Higginbotham (2013)
[72]Moser (2014)

change challenges like drought or sea level rise, socially acceptable adaptation solutions are rare.[73]

Since adaptation researchers assume lower vulnerability and greater adaptive capacity in developed countries than in developing countries, they have focused more research in the latter.[74] Climate vulnerability is determined by many factors, including variations in wealth, social equality, food availability, health and education status, physical and institutional infrastructure, and access to natural resources and technology.[75]

Although vulnerability is an important dimension of adaptation coverage, the media in developed nations often portray people in developing countries as victims.[76] For instance, Australian news reporting on the impacts of sea level rise on the small island nation of Tuvalu constructed Tuvaluans as tragic victims of environmental displacement, reducing their identity to individuals lacking resilience and resourcefulness.[77] Some scholars argue that framing poor people as climate change victims can be demoralizing and paralyzing[78] and promote a false sense of safety in developed nations.[79]

Audiences often turn to local television news for information about weather extremes. However, since many TV meteorologists are skeptical about the human causation of climate change, they are reluctant to link local extreme events with global trends.[80]Trust in weather forecasters is a key factor in making climate change information acceptable to TV viewers.[81] Extreme weather events can increase the amount of climate change media coverage when journalists link these extremes to climate change.[82] But journalists rarely do this. For instance, British news coverage of flood events between 2001 and 2007 was linked to climate change infrequently, and whenever a possible connection was discussed, the message was mixed and inconsistent.[83]

Similarly, news coverage of drought in the U.S. Southeast between 1997 and 2007 included details about the dynamics of vulnerability and higher-order impacts of water shortage and drought responses but provided no discussion of climate change.[84] TV and print coverage of wildfires in the Western U.S.A. in 2012 and 2013 found the stories linked wildfires to climate change in only 3 % and 6 % of

[73]Resource Media (2012)
[74]Adger et al. (2007)
[75]Brooks et al. (2005)
[76]Doultona and Brown (2009)
[77]Farbotko (2005)
[78]Barnett et al. (2013)
[79]O'Brien et al. (2006)
[80]Maibach et al. (2011a, b)
[81]Anderson et al. (2013)
[82]Corfee-Morlot et al. (2007)
[83]Gavin et al. (2010)
[84]Dow (2010)

cases, respectively,[85] with an increase to 14 % during the summer wildfire season.[86] Resource Media[87] observed that the water/climate connection is nearly invisible in U.S. news coverage,and innovative adaptation solutions are hardly discussed at all.

Risk Perception

Most news stories about environmental issues do not mention environmental risks, and the stories that do discuss risks tend to be dramatic and ambiguous and provide little information that would help the public understand the risks. Climate stories also frequently fail to highlight the most significant facts, as defined by scientists or risk assessments. Political debate obfuscates risk assessments in news coverage. For example, when Sen. James Inhofe railed against the climate research "hoax" and the "alarmist" scientific press in 2006, journalists struggled to untangle his arguments about bad science and bad reporting. Mainly, Inhofe criticized overblown predictions of doom in news coverage that alternated scientific predictions of global warming and cooling over the last 100 years. Many journalists have pegged stories about climate change to disasters like hurricane intensity, drought, wildfires, crop failure, and other hazards, without discussing how greenhouse gases spur climate change or including a skeptic's viewpoint. Public opinion turned against climate reporters whose stories were "balanced" to a fault.[88]

In Britain, climate change coverage has reframed nuclear power as part of the solution to the need for low-carbon energy options. Framing of nuclear power in Britain often centers on risk trade-off scenarios. Citizens express reluctant acceptance of nuclear power but renegotiate their position on nuclear energy when it is positioned alongside climate change. Various countries have tried to calculate the most rational global economic response to climate change threats in different ways. The social sciences, including economics, have had a limited role in projections about climate change impacts and about societies' responses to changing climates. In light of the dimensions of risk description and prescription in the media, environmentalists and scientific media tend to feature more proactive discourse, while industry and political media feature more reactive discourse. The way the news media frame a story about environmental issues also can influence audience perceptions of risk. In light of a guard-dog perspective of the media, social change or status quo news frames can affect individual risk perceptions about environmental issues. People who read news stories that use a social change frame report higher risk awareness than those who read stories containing a status quo frame. The risk information seeking and processing model has been used to isolate predictors of public knowledge of global warming. The number of media sources used, individual

[85]Fitzsimmons et al. (2012), Greenberg (2013)

[86]Fitzsimmons (2012)

[87]Resource Media (2012)

[88]Major and Atwood (2004), Kitzinger (2006), Brainard (2006a)

information seeking effort, and general education about climate change are relatively strong predictors of climate change knowledge.[89]

Most people realize the benefits of a future centered on sustainable resource use and societal welfare, but individual considerations about the future are not largely influenced by scenarios. The credibility of climate change projections depends on individuals' prior beliefs and trust in the science portrayed. In light of spatial data that maps individual physical risk associated with expected climate change, the relationship between actual and perceived risk is driven by specific physical conditions and experiences. Mutually reinforcing processes of media influence and selective attention to the media can elicit individual fear or anxiety about climate change, which in turn can enhance information seeking. The reinforcing spirals model has shown mutual influence between individual media use and global warming perceptions. Analysis of data from the 2006 General Social Survey showed that media use mediates the effects of age, race, and education on perceived knowledge about global warming. Perceived knowledge and concern over global warming also predict future information seeking about the polar regions.[90]

Climate change issues in general, and mitigation technologies specifically, are often poorly understood among public audiences. A 2007 Nielsen survey found that Latin Americans and Europeans were the most aware and concerned about climate change, while North Americans were the least aware and concerned. People in their teens and 20s appeared to be the least informed but among the most concerned about climate change, highlighting the need to reach younger people with accurate information on climate change. Many climate stories are fraught with overstatement, overcertainty, and confusion. These reporting problems can lead people to greatly overestimate scientific scenarios for temperature and sea level rises to confuse the greenhouse effect and ozone depletion. There is often a considerable mismatch between reporting of scientific information and the public's understanding of causes of the greenhouse effect. Ultimately, ignorance about climate change science leads the public away from dealing with the consumption of fossil fuels.[91]

Even those most concerned about climate change are less concerned about it than other daily issues. However, people are more likely to take action if they feel they can and should make a difference and if they trust government and other institutions to mitigate risks and achieve change. Most do not support adaptation measures when they perceive the costs as concentrated and the benefits as diffuse, relative to other daily concerns. According to the Gallup Organization's annual survey on environmental issues, Americans have become increasingly concerned about environmental quality over the last decade. More than a third typically express a great deal of worry about the quality of the environment, even though the issue ranks in the middle among a dozen different issues. Americans typically worry more about global

[89]Bickerstaff et al. (2008), Yearley (2009), Sonnett (2010), Durfee (2006), Kahlor and Rosenthal (2009)

[90]Lorenzoni and Hulme (2009), Brody et al. (2008), Zhao (2009)

[91]Herzog et al. (2005), Bell (1994a)

warming than any other environmental issue, and most believe global warming is mostly the result of human activities rather than natural changes. On climate change policy, Americans believe that science leaders, compared with leaders in other sectors, are relatively knowledgeable and impartial and should be relatively influential. However, they also perceive a significant lack of consensus among scientists on this issue.[92]

Many people are demobilized by feelings of isolation, hopelessness, powerlessness, and lack of public trust in government to effectively address climate issues. As public concern about the global economy rises, concern about the environment drops. This may represent a shift to public concern about an immediate rather than potential catastrophe. A large international survey identified three limitations that can make responses unrepresentative of larger public understanding: levels of acquiescence, different cultural interpretations of "global warming," and varying socioeconomic and educational levels of Internet users. U.S. audiences labeled "alarmists" tend to be younger, while those who believe anthropogenic global warming is negligible and overhyped tend to be white males who are Republican, individualist, religious, and rely on radio as their main source of news.[93]

Political ideology and partisanship are critical factors in credibility assessments and perceived bias in climate news. Climate change stories that use moderate sources or that suggest solutions or compromise are often seen as less biased and more credible than articles that use confrontational language and sources with intense viewpoints. The hostile media phenomenon holds that highly partisan individuals judge media to be biased against their side and favorable to their opponent's. This effect has been strongest among Republicans and conservatives, in opposing environmental protection.

A hostile media phenomenon often occurs in consumption of climate change news when highly partisan individuals judge media to be biased against their side and favorable to their opponent's. However, climate change stories that use moderate sources and suggestions of compromise are seen as lower in bias and higher in credibility than articles using confrontational language and sources with intense viewpoints. Hostile media perception is a major audience barrier to stimulating urgent concern about climate change. Partisanship can play a significant role in perceived media bias about climate change news coverage. News consumers' anger can mediate hostile media perception, which in turn predicts individual trust in climate change coverage and selective media use.[94]

When news reports don't favor preferred policy positions, whether it is election politics or scientific topics like global warming, conservatives attack the messenger. The public has been split on whether the media exaggerate climate change threats, although more Americans believe the media downplays them. The most common

[92]Lorenzoni and Pidgeon (2006), The Nielsen Company (2007), Leiserowitz (2005), National Science Board (2008)

[93]Boykoff and Roberts (2007), Will (2009), Leiserowitz (2005)

[94]Marlowe (2005), Kim (2010)

risk categories in international newspaper coverage of climate change, in light of Slovic's risk perception framework, were no risk, severe risk, future risk, immediate risk, catastrophic risk, and risk to nonhuman life. Beliefs about the severity of climate change are a function of personal experiences such as exposure to weather disasters, perceived consequences or vulnerability to climate change, and messages from informants such as scientists. Knowledge reduces uncertainty, which can increase assessments of national seriousness. In turn, these assessments increase policy support when attitudes and beliefs about human responsibility facilitate necessary reasoning. Public perception of global climate change has been strongly influenced by media constructions of scientific knowledge. Non-U.S. news organizations, especially in Britain, are at the forefront of discourse on climate feedback loops and climate thresholds. However, U.S. coverage of these topics generally has been poor because of self-censorship.[95]

To some extent, media coverage of climate change reflects the U.S. risk management system, which tries to create pockets of insulated expertise in an effort to neutralize unfounded public fears through rationality, efficiency, and authority. However, this leaves little room or reason for lay inputs. Putting too little faith in people and too much in the objectivity of formal analysis can lead to a breakdown in civic dialogue. When an event involves controversial science, citizens and public institutions can experience a communication breakdown, when a mismatch exists between what governmental institutions are supposed to do for the public and what they actually do.

In the U.S.A., citizen trust often rests in formal processes and styles of reasoning designed to ensure the transparency and objectivity of governmental decisions. But when citizens do lose trust in government, they look elsewhere for information and advice. In a situation involving pervasive uncertainty, the distance between citizens and experts is reduced, so that the lay public is almost as well positioned as experts to make sensible decisions about risk reduction. People tend to perceive climate change as a moderate risk, and melting glaciers and polar ice were the most prominent images associated with climate change and with bipartisan support for emission reduction policies at the international and national levels.

Broad support for policy action often is not linked to support for specific policies, such as raising gas prices, which could curb behaviors related to global emissions. However, climate change messages are effective when they are tailored to the needs and predispositions of particular audiences to either directly challenge fundamental misconceptions or to resonate with strongly held values. Most people prefer mitigation of emissions over adaptation measures such as providing economic assistance and also prefer to help people in one's own country before people in other countries.[96]

Research on intertemporal discounting suggests that individuals tend to believe future costs are much steeper than upfront costs[97] and thus might see the future costs of adaptation as lower than the current costs of mitigation. However, negative image

[95]Nisbet (2006), Slovic (1987), Weintraub (2007), Krosnick and Holbrook (2006), Antilla (2010)
[96]Jasanoff (1997), Leiserowitz (2006), Baron (2006)
[97]Soman et al. (2005)

associations can increase risk perceptions of global warming.[98] Thus, news coverage of adaptation options could help audiences visualize the impacts of climate change by considering adjustments needed to adapt to a warmer climate. For example, Evans and colleagues[99] found that individuals who answered questions about sea level rise and climate change adaptation measures in their local community reported a greater willingness to perform emission-reducing behaviors, compared to those who had not received the questions.

Conversely, the risk compensation hypothesis suggests that remedies to reduce the impacts of risky behaviors can unintentionally reinforce and increase those risky behaviors. For example, drivers who feel more secure when wearing seatbelts may compensate by driving more recklessly, leading to more traffic accidents. This phenomenon is known as an "offsetting effect" or "compensatory behavior."[100] Adaptation news coverage could contribute to this lulling effect, if audiences see adaptation as a remedy to a problem that can be paid for in the distant future and that costly preventative mitigation actions are no longer needed.[101] The other extreme can occur when news coverage promotes fatalism. When the media frames climate change impacts as a pending apocalypse or irreversible tipping point, in an effort to convey urgency and mobilize communities to act, this reporting may have the opposite effect by demoralizing its audiences .[102]

Media Routines

Media representations shape and affect international climate science policy and the translation of scientific uncertainty through the routines, norms, and pressures that guide daily journalistic decision-making. Most climate coverage reflects news pressures, values, and norms. Press coverage of climate science is shaped by both macro-level and micro-level factors. Macro-level factors include media ownership and cultural values, while micro-level factors include journalistic routines, professional values, and organizational norms. News reporting on climate science occurs within the wider context of the growing concentration and globalization of news media ownership. When scientific projections call for revolutionary mitigation efforts, media outlets in a capitalist society must try to report on this while appeasing advertisers who pay their salaries and other expenses. The greatest amount of advertising promotes automobiles, real estate, airlines, fast food, and home furnishings, the consumption of which may increase climate change emissions and prohibit effective mitigation.[103]

[98]Smith and Leiserowitz (2012)
[99]Evans et al. (2014)
[100]Calkins and Zlatoper (2001)
[101]Carrico et al. (2014)
[102]Foust and O'Shannon (2009)
[103]Boykoff (2008), Hansen (1994), Anderson (2009), Boykoff and Roberts (2007)

In Canadian newspapers, science stories are typically event-oriented, nonlocal wire reports that have a positive tone but are not prominent in terms of frequency and placement. These newspapers publish more medical stories than environmental items, and the environmental stories more often highlight negative consequences. Few science stories include information on science processes. Canadian journalists often cover environmental issues as hard news and less frequently and more negatively than other topics because of organizational constraints on media workers and the perceived marketability of science as a news product. Although the percentage of U.S. science stories has steadily increased over the last three decades, the range of topics covered did not change nor has comprehensiveness of accounts. Science stories still frequently omit methodological and contextual information.[104]

Many climate stories lack easy, event-driven news pegs, moments on which a front-page or top-of-the-news story can be hung. These stories demand that the media devote significant resources of time, labor, and money, with little perceived bang for the buck. Journalists must focus on events and have difficulty reporting "creeping" stories about chronic problems and their contexts, especially stories that do not culminate in obvious events. Tight deadlines limit journalists' ability to comprehend and communicate complex climate science concepts. The bottom line also can limit climate coverage. In many countries, editors cite insufficient financial resources as a key reason they do not cover climate change adaptation issues, including migration to the cities, renewable energy, recycling, irrigation, seed saving, fuel changes, and tree planting. Although drama can give social problems life and sustain their growth, dramatized or alarmist news can downplay detailed analysis of long-term problems. Sensationalism in climate coverage also can trivialize content, block out facts that do not hold an immediate sense of excitement or controversy, or preclude a constructive message. Reporters often overlook underlying causes and long-term consequences in their day-to-day pursuit of new angles on deadline.[105]

Although the public relies primarily on television news as a source of climate change information, few environment and/or science reporters cover the topic for broadcast stations. The attitudes and values the weathercasters hold about climate change influences their knowledge of the scientific consensus on climate change and their cognitive understanding of the topic. Reporters who primarily use scientists as sources and who work the environmental beat full time have the most accurate climate change knowledge. Scientists often rate overall climate coverage as worse than their own story evaluations of accuracy. Specific accuracy problems include overstating the progression of climate change and confusing ozone depletion and the greenhouse effect. Experts have a higher level of

[104]Einsiedel (1992), Pellechia (1997)

[105]Fedler and Bender (1997), Dunwoody and Griffin (1993), Boykoff and Roberts (2007), Harbinson et al. (2006), Hilgartner and Bosk (1988, p. 62), Wilkins and Patterson (1987), Ereaut and Segnit (2006), Wilson (2000a)

knowledge about current climate state, causes, and consequences of climate change than environmental journalists, politicians, and laypersons. Most people know more about climate change causes than the current state or future consequences, and most also know more about weather and sea/glacier consequences than health consequences. Experts express more confidence in their own knowledge than journalists, politicians, and laypersons. Journalists are more likely than experts to adjust confidence in their own knowledge when confronted with actual knowledge.[106]

Journalists often lack the space or time to report complex detail. They must simplify for a general audience and use familiar and emotive terms in place of scientific ones. Journalists avoid some issues because they are too complex or lack attention-getting images. Media accounts that do provide more explanatory content about climate change can boost reader interest and understanding of the issue. Explanatory news text can significantly enhance reader interest and understanding of the content, compared with the traditional inverted pyramid news stories, even among readers who lack science expertise. Most journalists strive to write at a sixth-grade level to improve readability, but this can lead to the oversimplification of climate news and the omission of the complexities and consequences of energy choices.

Peak oil, the theory that oil production has or soon will reach its zenith and then enter into a terminal decline, is a complex story that gained prominence after 2005 but remained underreported and lacked clear, nuanced explanation. Newsrooms often avoid covering peak oil because it is not an event-based story and involves gradual accumulation of data that do not provide easy answers. They feel the story lacks good visuals and is not lucrative enough to justify the newsroom resources required to report on it properly.[107]

Surveys of print, radio, and television journalists from Honduras, Jamaica, Sri Lanka, and Zambia found that editors and journalists had little interest in covering adaptation because of low levels of knowledge on the issue, insufficient financial resources, and different priorities for news coverage.[108]

Sourcing

Most American reporters have autonomy in deciding how to cover a story and which sources to use. Sources are perceived to be more credible when they have established credentials, understand news production norms, are known to the public, and have the resources to continually meet the media's information needs. A source's assertiveness and quotability, as well as understanding of daily media routines, ability to provide credible information on a timely basis, and availability to produce

[106]Wilson (2002), Wilson (2000b), Bell (1994b), Sundblad et al. (2009)
[107]Kitzinger (2006), Yaros (2006), Plate (2009)
[108]Harbinson et al. (2006)

commentary or analysis also can affect his or her prominence in news coverage. Similarly, Meyer's credibility index uses five variables to assess the credibility of a communication source: fairness, bias, completeness, accuracy, and trust. News media organizations often fail to follow up on sources when covering climate change.[109]

Matthew Nisbet identified three groups of public intellectuals arguing for action on climate change, the elites who are frequently quoted in media coverage: ecological activists, smart growth reformers, and ecomodernists. Ecological activists like American writer and activist Bill McKibben "argue that climate change is a symptom of a capitalist society that has dangerously exceeded the carrying capacity of the planet. They are skeptical of technological or market-based solutions to the problem, urging the need for a global movement that dramatically re-organizes society." Smart growth reformers like former U.S. vice president Al Gore "agree that climate change poses catastrophic risks but argue that those risks can be avoided if political leaders adopt the right market-based mechanisms, enabling sustainable economic growth to continue." Ecomodernists like *New York Times* writer Andrew Revkin "argue for recognizing the biases in how we have conventionally defined climate change as a social problem."[110]

The specialist journalists who cover climate science in the British national press value journalistic professionalism and skill more highly than formal training in their area of specialization, apply conventional news values but emphasize relevance to the reader in selecting science news, and use elaborate routines for obtaining credibility, including actively cultivating mutual trust with sources and seeking more sources that are institutionally based and authoritative. Prospective interview sources representing different interests and agendas competitively try to influence the flow of information through media gatekeepers. Source credibility influences how environmental journalists choose interview sources from environmental groups in covering climate change. For example, in news coverage of an international climate conference, the Peruvian media relied mainly on government sources and gave limited access to dissenting voices such as environmentalists.[111]

Interview sources have a substantial influence over how news about climate change is framed, and politicians and government officials are big winners when it comes to the competition for public attention through the media. Journalists often rely on interviews with a small set of "authorities" without identifying a wider range of perspectives, especially when climate change coverage appears because of a looming or unfolding crisis. The public assigns the most credibility to political and expert sources in news coverage of climate change, and this public trust in authority figures can, in turn, influence climate policy decision-making.

[109]Detjen et al. (2000), Ryan et al. (1998), Stempel and Culberston (1984), Roscho (1975), Meyer (1988), Mooney (2009)

[110]Nisbet (2015)

[111]Hansen (1994), Flynn (2002)

Contrarians, environmental groups, and other nongovernmental claims-makers can gain traction for their ideas and shift public discourse through media coverage and thus can have a strong impact on public understanding. Over time, these claims-makers have increasingly replaced scientists as dominant interview sources. Those with the power to define the terms of the debate can determine the outcomes. In speaking out against consensus in climate science and through privileged media access, contrarians and other skeptics amplify perceived uncertainty about human contributions to climate change and construct the argument that human's role is negligible. Contrarians who can gain embedded power and leverage public legitimacy through the media can broadly convey the counterclaim that climate change is not problematic.[112]

In 2007, Fox News Corporation became "carbon neutral" and generally endorsed scientific warnings about global warming. Its CEO, Rupert Murdoch, announced not only that the media group held a corporate view about climate change but that its editorial coverage would change. From 1997 to 2007, opinion pieces produced by newspapers and television stations owned by News Corporation largely denied the science of climate change and dismissed those who were concerned about it. While the intensity of commentary about climate change varied across media outlets owned by News Corporation, its corporate view framed the issue as one of political correctness rather than science. Scientific knowledge was portrayed as an orthodoxy and climate skepticism as courageous dissent. In recent decades, corporate and special interests have developed numerous methods to manufacture doubt about climate science because it threatens their economic interests. When reporters cover rhetorical claims about scientific ignorance and uncertainty that actors use to discredit threatening science, they contribute to the social construction of ignorance in scientific controversies. Trade associations have issued rhetorical claims intended to sow public confusion about university studies that had threatened to undermine their industries' activities. Journalists' use of these claims appears to vary as a function of their perceptions of their journalistic roles and of their audiences, even though their knowledge of science also plays a role.[113]

Michael Mann, the scientist who helped author the well-known "hockey stick" climate change temperature graph, claimed that climate change denial groups stole his emails from servers at Britain's University of East Anglia, in an effort to discredit him. Deniers claimed the emails showed unethical conduct, while scientific organizations and academic panels defended Mann and the credibility of climate science. Mann believes news coverage about the campaign against him ultimately led the U.S. Senate to refuse to take action on carbon dioxide emission controls, even though the incident apparently did not compromise public belief in climate science.

[112]Boykoff (2007), Plate (2009), Miller and Riechert (2000), McManus (2000), Pidgeon and Gregory (2004), Lorenzoni and Pidgeon (2006), Trumbo (1996), McCright and Dunlap (2003), Leiserowitz (2005), McCright and Dunlap (2000), Freudenburg (2000)

[113]McKnight (2010), Stocking and Holstein (2009)

Scholars have identified three major counterclaims in media coverage of climate change: that the evidentiary basis of global warming is weak, uncertain, or flawed, that global warming will have substantial long-term benefits, and that climate policy action will do more harm than good. They found that dissenters collaborate with conservative think tanks, antienvironment movements, and carbon-based industry to disseminate messages that disempower top climate science in national and international discourse about the causes of climate change. Throughout the 1990s, the government officials who cited skeptics became the most frequently quoted interview source in elite press articles, surpassing scientists, who had been the most cited source in 1988.[114]

Environmental pressure groups such as Greenpeace, World Wildlife Fund, and Environmental Defense help to overcome social inertia and bureaucratic resistance to policy action but also can push media discourse beyond the parameters of what science can currently claim and frame issues as overly catastrophic or alarmist. Media coverage of climate change outcomes is necessarily speculative. If interview sources for these stories followed Gregg Easterbrook's "law of doom saying," they would predict catastrophe no sooner than 5 years from now but no later than 10 years away, soon enough to terrify but distant enough that people will forget if they are wrong.[115]

Attitudes about global warming generally are not strongly influenced by scientific evidence. However, the news media increasingly are important sources of scientific information about climate change. Scientists can be influential in shaping attitudes on a wide range of issues when they are quoted in news coverage, especially where scientific opinions are central to policy debates. Media coverage influences scientific opinion about climate change and its consequences. The vast majority of climate scientists in a variety of fields believe that human-induced global warming is occurring and that it poses a significant threat to the planet in the future. Scientists who foresee the most severe future global consequences are younger scientists, those who work in colleges and universities, and those most likely to believe that researchers understand the process of climate change relatively well.[116]

Science has autonomy from other social institutions in its pursuit of long-term questions that build knowledge incrementally, within a society that is basically impatient and pragmatic. While scientists are generally respected in the U.S.A., their voices are often marginalized in the arena of public policy, and they fail to engage the public directly. Scientists share a worldview that presupposes rationality and orderliness and believe answers to most empirical problems are eventually obtainable by posing the right questions and approaching them systematically. Most Americans are not comfortable with risk probabilities or long-term problems. Scientists' input on climate policy has been problematic.

[114]Bulletin of the Atomic Scientists (2010), McCright and Dunlap (2000, 2003), Wilkins (1993)

[115]Newell (2000), Hulme (2006), Ereaut and Segnit (2006), Will (2009)

[116]Brittle and Muthuswamy (2009), Wilson (2000), Farnsworth and Lichter (2009)

Scientists often fail to frame policy options, assign weight to them, make their input less technical, or take political considerations into account when serving as technical advisors to policymakers. When scientists do disagree with policy decisions, they must risk their professionalism and credibility by resorting to advocacy or silence. When news stories do frame policy options, they often do not assign proper weight to relevant science. Media accounts often refer to theory as something not proven, often give equal voice to scientific consensus and contrarians, and have difficulty putting risk and other uncertainties into an easily understood frame of reference. Science operates in a framework of decades or longer, while political pressures push resources toward popular or expedient solutions, not necessarily those with the greatest chance for long-term success.[117]

Scientific expertise has played an important role in media coverage of the policy process regarding climate change and ozone layer protection. Contrary to the IPCC's assumptions, scientific consensus is not necessary to achieve political goals. A climate of expectation, along with pressure from leader countries, can be more important than consensus in achieving change. While ambitious political regulations in the ozone case were achieved under greater scientific uncertainty, negotiations on climate change have been much more modest but based on a large scientific consensus.

Public opinion tends to move in the direction of elite consensus but polarize when citizens perceive that elites are divided. Perceived consensus among scientists has not prompted public engagement or individual action. There are variations in the strength of scientific evidence in media portrayals of scientific consensus and in the presence of political cues in news coverage of climate change. Specifically, the presence of political cues in newspaper articles about climate change activated ideological beliefs and made such beliefs a stronger predictor of concern, regardless of whether scientific elites were portrayed as agreeing or disagreeing. However, scientific agreement and evidence strength were not related to concern. British media reconstructions of scientific claims are strongly entangled with ideological viewpoints. Journalists use these ideas and values as a powerful selection device for deciding what is scientific news, what the relevant "facts" are, who is authorized as "agents of definition" of scientific matters, and which program of action has greatest legitimacy.[118]

Scientists often find themselves enveloped in furies triggered by skepticism about the global warming consensus. Historically, a scientific consensus will prevail until a diametrically different consensus comes along. For example, in the 1970s, a scientific consensus and media coverage predicted that the world faced potentially catastrophic cooling. In 1975, the New York Times reported that a major cooling of the climate was widely considered inevitable because the Northern Hemisphere's climate had been getting cooler since about 1950. While some media accounts at the time did hype a cooling scare, others suggested more reasons to be concerned about

[117] Yankelovich (2003)

[118] Grundmann (2006), Boykoff and Roberts (2007), Brittle (2005), Carvalho (2007)

global warming. During that time, between 1965 and 1979, the scientific literature emphasized greenhouse warming. Mooney also argued that it is misleading to draw a parallel between global cooling concerns articulated in the 1970s, when the field of climate research was relatively new, and climate change concerns today, when hundreds of scientists worldwide repeatedly ratify the conclusion that human activities are driving global warming.[119]

In general, people are no more concerned about climate change, even when the evidence is strong and scientists agree. They tend to ignore scientific evidence, which implies that scientists may have little influence in shaping public concern. People who already have high environmental concern are more likely to incorporate evidence into their attitudes, especially when scientists agree. Also, political cues in the news coverage seem to activate additional message processing among these individuals, perhaps by making them more anxious and attentive to evidence strength.[120]

International media coverage of the IPCC's work has greatly influenced the construction, global mobilization, and consumption of climate change knowledge around the world. However, the U.S. media continue to suggest that scientific consensus estimates of global climate disruption, such as those from the IPCC, are exaggerated and overly pessimistic. By contrast, the Asymmetry of Scientific Challenge suggests that such consensus assessments probably understate climate disruptions. Science tends to be self-correcting over time. U.S. climate change coverage generally appeared during two major periods: when the papers were overstating challenges to the then-prevailing scientific consensus and in 2008 after the IPCC and former Vice-President Gore shared the Nobel Prize for their work on climate disruption and before opinion polls showed the U.S. public to be growing more skeptical toward climate science again. During both periods, new scientific findings were more than 20 times as likely to support the ASC perspective than the usual framing of the issue in the U.S. media. Supposed challenges to the scientific consensus on global warming should be subjected to greater scrutiny and that journalistic balance should account for the scientifically legitimate view that global climate disruption may be significantly worse than has been suggested in scientific consensus estimates to date.[121]

Scientists use excessive jargon in communicating about climate change. When journalists interview scientists, they often qualify their findings in light of uncertainties in their research. Since uncertainties are difficult to translate into the clear language needed in policy decisions, journalists often omit discussion of uncertainties or translate hypotheses into certainties. Although scientific insights evolve over years, media only can take snapshots of this knowledge, which in turn provide limited interpretations. Sometimes, the finer points of a climate story are lost when a journalist tries to translate science into public information. Even a small reporting

[119]Will (2009), Mooney (2009)

[120]Brittle (2005)

[121]Hulme and Mahony (2010), Freudenburg and Musellia (2010)

mistake can discredit both scientists and the media organization that covers their work, and the consequences of the misinformation are difficult to roll back.

In 2006, reporters misinterpreted a scientist's point about melting Arctic ice. An Associated Press wire story and the *San Francisco Chronicle* sounded a false alarm when they claimed that sea ice was actually melting during both the winter and summer. Most previous AP and *Chronicle* stories had accurately reported the risks associated with sea ice melt, including global warming feedback effects and threats to polar bears. But an early press release from NASA had misconstrued a scientist's findings, which then led to misleading statements in the earliest news stories. The scientist also claimed he was misquoted. Some newspapers did provide spot-on reporting. For instance, the *Washington Post* lead stated, "The amount of ice being formed in the Arctic winter has declined sharply in the past 2 years, a finding that NASA climate researchers say significantly increases their confidence that greenhouse gases created by autos and industry are warming the Arctic and the globe."[122]

Sometimes, reporters unintentionally dramatize scientific findings. An example of recent news that sensationalized research was the coverage of ice sheet collapses. The IPCC deemed both the potential collapse in the Thermohaline Circulation (THC) and the collapse of the West Antarctic Ice Sheet (WAIS) to be equally unlikely events. However, the THC issue received more than three times more coverage than the WAIS issue. Representation of the THC as the "Gulf Stream" caused adverse reactions from some scientists. More than 80 % of newspaper articles covering the THC issue did not indicate the probability of collapse or contain contradictory probabilities. The relatively large amount of coverage about the THC issue, the absence of accompanying probabilistic statements, and the use of sensationalist headlines had a significant influence on public perceptions of the climate future.[123]

Scientists often struggle to translate uncertainties inherent in their research into ordinary language. When scientific uncertainty enters into public debate, it can inspire inaction. When elite U.S. print coverage of climate change emphasizes uncertainty, this serves as a boundary between the public and scientists. This emphasis has led to a deferential citizen acceptance of the need for more research. Coverage of climate contrarians amplified this uncertainty but did not explain that the counterclaims were marginalized within the climate science community. Greater contextualization in climate stories can help mitigate controversy stirred up through uncertainty.[124]

Climate scientists sometimes comment on the technical merits of proposed policy responses. Political cues in a news article can activate ideological beliefs and make such beliefs a stronger predictor of concern about climate change, regardless of whether the story portrays scientific elites as agreeing or disagreeing. People are no

[122]Harbinson et al. (2006), Weingart et al. (2000), Carvalho and Burgess (2005), Brainard (2006b)

[123]Jennings and Hulme (2010)

[124]Pollack (2003), Demeritt (2001), Zehr (2000), Wilkins (1993), Zehr (1999), McCright (2007), Schneider (1993), Dunwoody (1999), Corbett and Durfee (2004)

more concerned about global warming even when evidence is strong and scientists agree, because people tend to ignore scientific evidence when shaping concern about scientific topics. However, those high in environmental concern incorporate evidence into their attitudes when scientists agreed and political cues were present.[125]

Conflict and Balance

Journalists are expected to create "balance" by devoting equal attention to two sides of a given story, and this routine practice also can help reporters who lack requisite scientific knowledge or who are facing a tight deadline to produce a credible story. Journalists typically feel a story is balanced if it gives equal attention to scientific opinion and the opposite opinion in story about risk. Many news media organizations have been accused of cherry picking misleading bits of information, to provide the appearance of artificial balance, and failing to apply critical thinking to the weighing of evidence.[126]

The U.S. news media have consistently represented conflict and contentions, despite an emergent consensus view regarding anthropogenic climate science. Journalists often create a conflict frame in a story by pitting authorities against one another or by seeking sources to contest dominant opinions. This illusion of conflict leads to dramatization, personalization, as well as the pretense of balance needed to boost the story's credibility and objectivity. British coverage of controversial science issues often represents the government as undemocratic and beholden to powerful political and economic interests. As the science becomes a contested issue, coverage increasingly emphasizes the importance of deliberative and inclusive forms of science policy decision-making.[127]

In the U.S.A., political ideology plays a larger role in shaping adaptation concerns than any risk perception effects. American liberals tend to support mitigation and adaptation policies, while conservatives oppose them regardless of the framing used.[128] Many conservatives live in southern states and other areas that may experience more severe climate impacts.

In contrast, non-Western news coverage of climate change often emphasizes international relations while de-emphasizing conflicts and controversies. In the Mexican newspaper Reforma, the ecology/science and consequences frames have been the most intensely reported frames, while scientific conflict and U.S. conflict frames have received the least attention. International relations were the most frequently presented solution to global warming, and story frequencies peaked during international conferences. Scientists were the most frequent source of conflicting statements in broadcast news coverage of the continuous rise in

[125]Gushee (2004), Brittle (2005)

[126]Entman (1989), Dunwoody and Peters (1992), Kitzinger (2006), Mooney (2009)

[127]Boykoff and Roberts (2007), Cunningham (2003), Augoustinos et al. (2010)

[128]Moser (2014)

greenhouse gases between 2000 and 2005, but these stories more often quoted political or governmental sources. Most stories in U.S. elite newspapers give equal attention to the view that humans contribute to global warming and to the view that exclusively natural fluctuations explain the earth's temperature increase. Coverage significantly diverged from the scientific consensus from 1990 through 2002.[129]

Before 2005, most climate coverage tried to balance the view that humans cause climate change with the opposite viewpoint. Policy debate about mitigation has been framed as a conflict between skeptics and supporters. Artificial balance, most prevalent in the U.S.A., often arises from journalists' need to appear unbiased and tell a story from two sides. Critics contend that since conflict sells more than consensus, journalists have "balanced" the overwhelming scientific consensus with skepticism. This has confused and misinformed the public and delayed mitigation. Some critics have characterized the debate as a disingenuous pseudocontroversy because of inequitable resources, motives, authority behind the scenes, and extensive commercial and political interests trying to manipulate public information and mislead the public. Political polarization in the climate change debate has been amplified through the rapid rise of the public relations industry in recent years, as well as through claims-makers who use increasingly sophisticated media strategies.[130]

The U.S. news media have moved from an earlier era of false balance to a new phase of overdramatization, which skeptics can easily exploit to dismiss climate change as a problem. Audiences, in turn, filter such critiques through their preferred partisan lens and assumptions about liberal media bias. Although contradictory information about climate change can confuse audiences, it also can boost perceived issue importance. Conflict and immediacy in news stories can impart a sense of fleetingness to climate change issues, which in turn may inhibit public understanding.

By 2005, most British journalists stopped reporting on climate change by balancing expert vs. skeptic voices and by knocking the human-induced climate change argument through prominent coverage of an alternative theory. These changes in media treatment of climate change, which appeared in the British press but not the U.S. media, helped lay the groundwork for a dramatic shift in the depth and regularity of coverage, as well as in the quality of public debate on the issue. British journalists discovered the center of gravity of informed opinion on climate change after providing a decade of polarized coverage, even though the basics of the science had changed little since the mid-1990s. This delay may have occurred, in part, because of a well-intentioned preference for skeptical opinion, but this earlier reporting routine may have impeded public debate about the next political and economic steps to take.[131]

[129]Gordon et al. (2010), Kuban (2007), Boykoff and Boykoff (2004)

[130]Boykoff (2007), Shanahan (2007), Banning (2009), Anderson (2009)

[131]Revkin (2007), Boykoff and Rajan (2007), Lee and Yoo (2004), Andreadis and Smith (2007)

Investigative reporting has exposed vested financial interests among companies and politicians who tried to undermine science and subvert journalism. Financial conflicts of interest have been exposed among major media outlets, as well. For example, from 2007 to 2009, *Newsweek* sold advertising packages to the American Petroleum Institute – the oil and gas industry's largest trade group – to cohost forums on energy issues. *Newsweek*'s parent, The Washington Post Company, also planned but cancelled a series of closed-door "salons" in 2009 where lobbyists and interest groups would have paid for access to public officials and journalists. Atlantic Media, *The Wall Street Journal*, and *Fortune* also accepted corporate funding for conferences and other events, many focusing on energy issues. These events have served as important moneymakers for news outlets in a time of rapidly declining revenues but present potential conflicts of interest that can erode media credibility.[132]

The news media may have underreported several key climate issues, including the urgency of adaptation, costs of acting and failing to act, views of the poor, vested interests that resist change, and potential for action to address climate change to bring substantial benefits. One possible reason for inattention to critical issues may be the financial pressure for climate news to complement the advertising that supports it. In the U.S.A., car and fuel companies have threatened to withdraw advertising from radio stations after they reported on climate change. For many reporters, investigating American climate policy has proven more difficult than translating climate science for the public. Unraveling the Bush administration's approach on climate change policy was challenging for reporters, and some persevered for several years before discovering key paper trails. In 2007, *Rolling Stone* ran a 16-page report on "The Climate Crisis," following a long line of national magazines that published special sections about climate change. The report included an investigative piece, "Six Years of Deceit," about the Bush administration's campaign to deny global warming, cast aspersions on climate science, and allow polluters to shape climate policy. Similarly, *The New York Times* scrutinized oil and coal industry influence on Bush climate policy and unearthed evidence that the Bush administration had tampered with scientific reports about climate change shortly after the president's first inauguration. In 2005, the *Times* also exposed Philip Cooney, a top deputy of the federal Council on Environmental Quality, for heavily editing government climate reports to play up scientific uncertainties about climate change.[133]

Public Understanding of Climate Change

Polls show that public understanding of climate change is low and public action lower still. Maintaining public interest in global climate change through news coverage is necessary for the survival of the issue. Not only is the climate change

[132]Shanahan (2007), Columbia Journalism Review editors (2009)

[133]Shanahan (2007), Brainard (2007d)

issue widely perceived as diffuse and nonpersonal, it also has been framed in terms of false inferences. Most Americans do not understand the difference between weather and climate, and some news coverage, commentary, and media-sponsored polls have led people to believe they can draw inferences about climate change just by looking out their windows. Climate science has important things to say about the prevalence, distribution, and dangers of rainfall and flooding. However, the connection between reporting about high-profile flooding events and scientific understanding of climate change is often tenuous. Responsible climate coverage elucidates scientific details to promote intelligent debate and explains that climate change is a long-term threat with impacts that may not be seen immediately or discernibly.[134]

Public engagement with climate change issues may be required to spark climate change mitigation on any level. The public engagement model proposed by Collins and Evans consists of three waves of public engagement with a science issue over time: knowledge deficits, democratization of science and practice, and authorized expertise. In the first wave, poor choices and actions are attributed to a dearth of knowledge, reliance on "sound" science, and the need to eliminate uncertainty before taking action. In the second wave, democratic public engagement mitigates common "bads" and "goods" in a risk society. In the third wave, some groups and institutions are authorized to speak about climate change while others are not.[135]

People show the greatest concern, commitment, and optimism in the developing economies and the greatest indifference, reluctance, and fatalism in developed nations, even though global climate change coverage does not reach all people equally. Prime-time evening news on the main TV stations in China, India, Mexico, Russia, and South Africa made no mention of the IPCC report on mitigation when it was released in 2007. Meanwhile, the poorest, most vulnerable people in the world, those who have contributed least to the problem and have the least access to climate information, will suffer the most from its impacts. Climate change is a media-driven issue, in the sense that the media can easily make the issue salient in the public's thinking through news reporting. However, because climate change is an intangible issue, is difficult to explain to the average citizen, and is framed as a debate, the public is generally misinformed about the issue despite volumes of information and data generated over the last 30 years. Although the global energy crisis may have become too large and complex for the media to handle on its own, public apathy about the future energy economy is not solely the media's fault. Since news originates and disseminates into the public sphere before entering the private sphere of individual engagement, personal responsibility is diffuse. Although all humans contribute to greenhouse gas emissions through daily activities, some vulnerable human groups suffer concentrated impacts.[136]

[134]Miller (2004), Gavin et al. (2010)

[135]Shanahan (2007), McComas and Shanahan (1999), Brainard (2007e), Collins and Evans (2002), Beck (1992)

[136]HSBC (2007), Painter (2007), Shanahan (2007), Soroka (2002), Trumbo (1996), Plate (2009), Lowi (1972)

In working through science issues, the public opinion climate is complex, and the development of consensus policy can be problematic. In a science controversy such as the climate change debate, a spiral of silence can develop when visible dissent decreases, even as public opinion begins to appear hegemonic, because personal fear of social isolation inhibits people from expressing opinions perceived to be in the minority. A spiral of silence in public opinion about controversial science is more likely to develop when skeptical citizens are willing to speak among those who believe themselves to be more knowledgeable about science or among those who apply moral reasoning besides consequentialist and utilitarian arguments. Canadians are more likely than Americans to be ethical populists in a science controversy, in the sense that they believe ordinary people should make personal decisions about science issues based on ethical considerations. The most common group in each country is made up of utilitarians who believe risks or costs and benefits should be weighed in developing policy and this should be done by experts. Two other cluster groups, moral authoritarians and democratic pragmatists, exist in equivalent proportions in both countries. Most media coverage of climate politics emphasizes expert and elitist discourse while neglecting the interests, views, and voices of citizens. One reason citizens are left out of the deliberation is the ignorant assumption that "the environment" does not involve human action and society. The assumption that greater understanding leads to more positive attitudes has informed many practical initiatives in the public understanding of climate change. The media provide an important part of the social context through which citizens judge controversial science issues such as climate change.[137]

Learning about climate change through newspapers and television leads to increased understanding about the connections between fossil fuel use and climate change. In turn, increased understanding increases people's stated intentions to take action. However, climate change issues often lack the day-to-day relevance needed to motivate people to actually take action. As their specialized knowledge and concern increases, so does their compartmentalization of understanding. Climate change knowledge then can become relegated to an arena where "appropriate" action is seen as too problematic. Public perceptions of science are generally shaped by value predispositions, schema, and media use rather than scientific knowledge. Value predispositions related to social ideology, along with reservations about science, often serve as primary influences on citizen evaluations of controversial science issues. Ideology can have a strong effect on citizen understanding of climate science, and ideology can interact with other factors, such as college education that affect comprehension of information. As citizens' ideology shifts from liberal to conservative, concern for global warming decreases, and college education does not increase global warming concern among conservative ideologues. However, citizens with a college education and higher general science literacy do not tend to have higher concern for global warming. It is difficult for any media consumer to ever know how to recognize the real conclusions of climate science and how to

[137]Priest (2006), Beck (2010)

distinguish them from scientific-sounding spin or misinformation. When partisans wield vastly different facts, finding truth and common ground is difficult. Science journalist Chris Mooney argues that journalism should be constrained by standards of evidence, rigor, and reproducibility similar to the canons of modern science itself.[138]

Attention to newspaper coverage and certain entertainment television genres can influence citizen evaluations of science. Trust in university scientists, exposure to national television news, and familiarity affect perception of research benefits. When individuals read science or environment news, this attention predicts heightened global warming risk perceptions and stronger policy support, while attention to political news predicts lower risk perceptions and less support for climate policies. The internal consistency of individual attitudes toward science tends to be poor, and the links between attitudes toward science in general and attitudes toward specific areas of scientific research are weak. Understanding of science is weakly related to more positive attitudes in general, but it is also associated with more coherent and discriminating attitudes. Knowledgeable citizens tend to be more favorably disposed toward science in general but are less supportive of morally contentious areas of research such as climate change than those who are less knowledgeable. Ultimately, informed public opinion can actually constrain climate change research.[139]

Lack of public support for climate change mitigation may be linked to poor science literacy. Although the rate of civic scientific literacy in the U.S.A. has long hovered around 20 %, a strong and continuing public belief in the value of scientific research for economic prosperity and quality of life existed before 1999. Before that time, some concerns lingered about the pace of change caused by science and technology and the relationship between science and faith, but the public consistently reconciled these differing perceptions in favor of science.[140]

The "deficit model" of public attitudes toward science asserts that scientific knowledge predicts and explains citizen attitudes toward science. Knowledge is a strong determinant of attitudes toward science. Although the success of environmental policymaking depends on public participation, the scientific construction of environmental issues often means that such participation is difficult when the public lacks scientific expertise. Lay ideas are typically discounted as nonscientific, and educating citizens about environmental science does not guarantee that they can constructively participate in policymaking. The dominant assumption is that science literacy in climate change discourse is both the problem and the solution to societal conflicts. However, science communication initiatives can facilitate conversations with the public that recognize, respect, and incorporate differences in knowledge, values, perspectives, and goals.

[138]Stamm et al. (2000), Bord et al. (2000), Ungar (2000), Nisbet and Goidel (2007), Zia and Todd (2010), Mooney (2009)

[139]Evans and Durant (1995)

[140]Miller (2004)

The benefits of public engagement initiatives about risk-related policy issues are difficult to establish without a rigorous evaluation of engagement processes. These initiatives often are not evaluated at all, even though they are advocated as an antidote to deficits in lay knowledge and other policymaking problems. Participatory action research can be used to evaluate climate change campaigns. A grassroots organization can be transformed through personal and collective political power, through a process of double-loop learning. From inception to widespread grassroots endorsement and political awareness of a proposed bill, activist groups can contribute to legislative outcomes on climate change. Public concern about the impacts of climate change and the federal government's weak response was more pronounced because of increased media coverage.[141]

When citizens draw the line in a science controversy, they often discuss regulation and which conditions should be the subject of research. Ambiguities and tensions in lay accounts can enable, rather than stifle, greater democratization of science policy. Beyond the deficit model of science ignorance, lay people may hold technical, methodological, institutional, and cultural knowledge. When citizens do mobilize a stock of knowledge, it is influenced by their own social context and perceptions of relevancy. Identifying lay people as expert in, rather than ignorant of, the way science may shape their lives is a fundamental first step in moving toward greater citizen participation in policy discussions. When attributing responsibility for collective action, the media often avoid discussing scientific uncertainty, in the belief that it might undermine the demand for collective action. Reporters are typically responsive to the political setting in which they operate and tend to link local, national, and transnational risks. Many British governmental publications have advocated greater public dialogue and engagement in science issues. Moving beyond mere sloganizing about science and democracy requires strategic message development. Opinion-leader campaigns can catalyze wider political engagement on climate change and sustainable consumer choices and behaviors. Combining the recruitment of digital opinion leaders with traditional media strategies leads to significant trade-offs, in comparison with face-to-face initiatives. However, only in specific conditions are digital opinion leaders effective in strengthening online interactions and real-world connections.[142]

Effective public communication can engage audiences in low-carbon lifestyles by facilitating top-down public acceptance of regulation and by stimulating bottom-up, grassroots action through affective and rational engagement with climate change. Using communication to stimulate demand for regulation may reconcile these top-down and bottom-up approaches. Climate communication campaigns often require significant resources to promote attitudinal change, but research suggests that encouraging attitude change alone is not likely to be effective. The link between individual attitudes and subsequent behavior is mediated by social norms and other

[141]Sturgis and Allum (2004), Eden (1996), Nisbet and Scheufele (2009), Rowe et al. (2005), Hall et al. (2010)

[142]Kerr et al. (1998), Olausson (2009), Irwin (2001), Nisbet and Kotcher (2009)

influences. Introducing regulation that forces green behavior can promote mitigative behaviors, but government fears the loss of political capital. Conversely, communication approaches that advocate individual, voluntary action ignore the social and structural impediments to behavior change.[143]

The threat that global climate change poses to the health and well-being of human and nonhuman species has received relatively little attention in the press. Relatively few people hold clear top-of-mind associations between climate change and human health risks. Although international polls reflect that climate change lacks salience as a health issue, a survey of U.S. residents found that framing climate change in terms of public health can make climate change more personally relevant and emotionally engaging to segments of the public who are currently disengaged or even dismissive of the issue.[144]

Most people in the U.S.A., Canada, and Malta believe climate change poses significant health risks, and about a third believe people are already being harmed. More than a third of Americans and Canadians see themselves, their family, and people in their community as vulnerable to at least moderate harm from climate change. Many Canadians believe the elderly and children are at heightened risk of harm, while Americans see people in developing countries as being at greater risk than people in their own nation. When prompted, most Canadians and Maltese say climate change could cause respiratory problems, heat-related problems, cancer, and infectious diseases. Canadians also named sunburn and injuries from extreme weather events.

Substantive news attention to health threats associated with climate change can increase the capacity of communities to pursue mitigation and adaptation actions, but much of the current news coverage is not substantive. Health impacts such as extreme heat, disease, and respiratory problems and threats such as hurricanes are rarely mentioned, and most stories that do mention health threats simply react to heat waves, storms, and other naturally occurring events. Few stories include enterprise or explanatory reporting. News agenda–building strategies might be useful for generating substantive reporting about regional climate studies, regional public health meetings, and other localized topics.[145]

If the mass media could promote individual behavior change, this in turn could boost public engagement with climate change issues and contribute to health-related climate change mitigation and adaptation goals. Intersections between health communication and public health scholarship underlie an emergent research framework known as public health communication. Effective public health communication about climate change requires transdisciplinary theory and methodology. Communication interventions have considerable potential to promote population behavior change consistent with climate change prevention and adaptation objectives. Communication interventions can promote beneficial changes in behavior, either by

[143]Ockwell et al. (2009)

[144]Myers et al. (2012)

[145]Akerlof et al. (2010), Nisbet et al. (2010a)

directly targeting people already concerned about climate change and the people who influence them or by indirectly creating changes in the environments where people live and work. To optimize the influence of a climate change communication intervention, planners should identify opportunities to use media to target both people and places in ways that complement and extend existing programs. Although Americans are only dimly aware of the health implications of climate change, providing a human health frame of reference in news coverage could enhance public engagement with climate change.[146]

The success of proposed climate policy reforms such as cap and trade, carbon tax, and international climate treaties may depend on generating widespread public support and mobilization while countering partisan gridlock and the communication efforts of opponents. Public engagement is necessary for policy action but hinges on whether the media can reframe the relevance of climate change in ways that can reach more Americans. High-quality news coverage often reaches only a small audience of already informed and engaged citizens, while the rest of the public either ignores the coverage or reinterprets competing claims based on partisanship or self-interest.[147]

Fear-inducing representations of climate change are widely used in news stories and effectively attract attention to climate change. The popular film "The Day After Tomorrow" caused viewers to become more anxious about climate change and motivated to take action on it. It also made them less concerned about extreme events as a result of climate change, such as a possible shutdown of the North Atlantic thermohaline circulation, also known as the Gulf Stream. Fear is generally not an effective tool for motivating genuine personal engagement. Nonthreatening visual imagery and icons that link to individuals' everyday emotions and concerns in the context of climate change issues tend to be more engaging. In light of anchoring and objectification in social representations, verbal and visual representations often are attached to fear, hope, guilt, compassion, and nostalgia. Thus, emotional representations of climate change can enhance public engagement in the issue but also may draw attention away from climate change as an abstract, long-term phenomenon.[148]

Nisbet and colleagues argue that the global community will not take meaningful action on climate change until four cultures can collaboratively engage audiences through rigorous and accessible science, shared values, and personal relevance. The four cultures are (1) environmental sciences, which provide environmental data and predictive models; (2) philosophy and religion, which ground a society's discourse about what is good, right, and valuable; (3) social sciences, which provide theories and data about mental models, narratives, and frames of reference public audiences need to understand and make decisions about climate change; and (4) creative arts and professions, including nature and poetry writing, documentary filmmaking,

[146]Kreps and Maibach (2008), Maibach et al. (2008), Abroms and Maibach (2008)

[147]Nisbet (2009), Ho et al. (2008)

[148]O'Neill and Nicholson-Cole (2009), Lowe et al. (2006), Höijer (2010)

multimedia design, and journalism, because they tell inspiring and emotional stories that shape human actions, provide different forms of learning, sponsor deliberation, and provoke action.[149]

Public Understanding and Engagement About Adaptation

Until recently, U.S. policymakers and scholars avoided discussing adaptation, out of concern that public awareness of adaptation could reduce policy support for mitigation.[150] Victor and colleagues[151] noted that "until just a few years ago, even discussing adaptation to climate change was taboo" (p. 119). The consequences of framing climate change as mitigation or adaptation could have important effects on public support for policy adoption and implementation.[152]

Learning about adaptation may "spill over" into attitudes toward mitigation. Negative spillover effects occur when adoption of one proenvironmental behavior reduces the likelihood of adopting another proenvironmental action.[153] This often happens when individuals feel morally "off the hook"[154] or believe the problem already has been dealt with.[155] Weber's work on single action bias found that farmers who adapted their cultivation practices, such as crop selection, or adopted off-farm adaptations such as investing in futures were less supportive of government intervention to mitigate climate change.[156]

Discussing adaptation does not necessarily reduce support for mitigation or concern about climate change. For instance, Carrico and colleagues[157] found that politically moderate individuals exposed to adaptation information rated climate change as a higher political priority and were more supportive of policy to subsidize mitigation technology than those who did not view any adaptation information. This may be explained by applying the risk salience hypothesis, which suggests that information about climate change adaptation may increase the salience of impacts and therefore increase mitigation support.

Even when individuals do support mitigation and adaptation policies, they consistently prefer mitigation actions (such as reducing energy use or using sustainable energy sources) over adaptation actions such as purchasing flood insurance,

[149] Nisbet et al. (2010b)
[150] Pielke et al. (2007), Ruhl (2010)
[151] Victor et al. (2012)
[152] Carrico et al. (2014)
[153] Bratt (1999), Thøgersen (1999), Tiefenbeck et al. (2013), Truelove et al. (2015)
[154] Zhong et al. (2009)
[155] Weber (1997)
[156] Weber (1997, 2006)
[157] Carrico et al. (2014)

preparing homes against flooding, or moving to another home. They feel others should take adaptation actions but are not willing to do these things personally.[158]

Research about place attachment and place identity provide useful implications for improving public engagement on adaptation issues.[159] Places are understood through the personal meanings instilled in them, as well as through the emotional experiences, learning and growth, family and other social ties, occupational and recreational practices, and spiritual practices enacted there. Ties to place help people develop a sense of belonging.[160] Adaptation actions that impact places can affect person–place intimacy. Disruption of these relationships or displacements can cause grief,[161] as well as resistance and defensiveness to change, such as reactions to a recommendation that residents retreat from a shoreline or floodplain.[162]

As values become anchored in places,[163] they give meaning to events, motivate behavior, influence perceptions of adaptation options, and guide interpretation of situations as they unfold.[164] For example, in coastal Louisiana researchers noted how the slow process of coastal land loss due to relative sea level rise forced a constant and heightened awareness of place attachment. The perceived fragility of the place was reinforced through political alienation from decision-making processes.[165] Place attachment evokes visible impacts on the places people hold dear.[166] Proactive adaptation could be enhanced when place identity is embedded in news coverage[167] because place identity motivates publics to act personally and civically.[168] Engaging place, place attachment, and place identity could improve adaptation messaging and reduce unproductive political disputes.[169]

Among public audiences, knowledge about how to prepare for or protect against climate impacts is often limited and socially conditioned.[170] However, past experience with extreme weather events is an important teacher.[171] Issue publics tend to be better informed and more willing to engage in discussions about adaptation.[172]

When the media invokes global risks or frames local impacts as unknown, overwhelming, or beyond individual control, audiences are more likely to want

[158]Chilvers et al. (2014)
[159]Moser (2014)
[160]Lawrence (2009)
[161]Fried (2000)
[162]Agyeman et al. (2009)
[163]van der Werff et al. (2013)
[164]Wolf et al. (2013)
[165]Burley et al. (2007)
[166]Moser (2014)
[167]Whitmarsh (2008)
[168]Schweizer et al. (2013)
[169]Carbaugh and Cerulli (2013)
[170]Moser (2013)
[171]Ogalleh et al. (2012)
[172]Moser (2013)

national and local governments to take adaptation measures.[173] At least in principle, most people favor proactive government planning and preparation, as opposed to "wait and see" or merely cleaning up after disasters.[174] In reality, however, initial adaptation planning efforts at the local level often focus only on disaster preparedness and recovery, without addressing the changing climate. To communicate more effectively about adaptation, news organizations should help audiences appraise the risks they face from climate change and how they can alleviate the threat. Journalists also should present different scenarios and explain the uncertainties in understandable ways and with clear relevance to the implications for actions at different times.[175]

Moser recommends that news reports point to past experience or experience in other locations with similar adaptation approaches, such as relocation of communities out of floodplains, significant shifts in policy or regulatory environments, or creative financing and compensatory mechanisms. This coverage can familiarize audiences with the idea of adaptation and create a sense of continuity and stability in the midst of change.[176]

To justify proposed adaptation measures, stories can explain how long a given behavior or management approach will work in light of climate change (and other stressors) and identify points at which an objective can no longer be achieved with "business as usual." Then, the story can show how well adaptation alternatives may achieve the objective. For example, the Climate Vulnerability Monitor evaluates climate change impacts for a particular location, to produce a vulnerability factor for the year 2030.[177] Solid reporting should communicate the costs and benefits of adaptation options and outline different ways to reach each intended outcome. Media organizations ultimately can use news coverage to facilitate public deliberation about risks, adaptation goals, and the adaptation options needed to achieve them.[178]

Conclusions

Dominant framing of public understanding of climate science reflects the assumption that laypeople are defensive, risk averse, uncertainty averse, and unreflexive, while science is assumed to be the epitome of reflexive self-criticism. Although awareness of global warming is growing, the public has resisted coming to terms with the trade-offs involved in any serious solution such as an international regulatory treaty, investment in alternative fuels, or control of carbon dioxide emissions. Public engagement must transcend science literacy, because people do not need to become

[173]Harvatt et al. (2011)
[174]Bray and Martinez (2011)
[175]Moser (2014)
[176]Moser (2014)
[177]DARA (2012)
[178]Moser (2014)

amateur scientists to deliberate about policy choices. Moving people beyond awareness to judgment and resolution requires the public to actively deliberate and reconcile possible actions with their own beliefs and habits.[179]

Coverage reached a historic peak in 2007, and limited attention to Climategate in 2009 was followed by a quick return to relative nonattention. Climate change coverage may not return to 2007 levels again, unless a novel storyline emerges that defines the problem in ways that are more localized and personally relevant than long-term catastrophic environmental impacts, regulatory actions, and politics. Human health risks, economic growth from energy innovation, or energy insecurity might provide this news hook, if journalists could convey these risks using noncatastrophic frames. Local angles might play best in small and medium-sized newspapers, which in the past have typically provided only national wire stories that lacked details about regional impacts of climate change and regional policy initiatives.[180]

The future of climate change mitigation and adaptation likely will depend in part upon the effectiveness of news media content to motivate audiences to take action and support proactive policies. Media routines, including framing, balance, and sourcing, can in turn mitigate the flow of complex and politicized content about climate change science and policy. Scientists and policymakers should identify specific frames that can help journalists present climate change problems in ways that are more personally relevant, significant, and understandable to public audiences.

References

Abroms L, Maibach E (2008) The effectiveness of mass communication to change public behavior. Annu Rev Public Health 29:1–16

Adger WN et al (2007) Climate change 2007: impacts, adaptation and vulnerability. In: Parry M, Canziani O, Palutikof J, van der Linden P, Hanson C (eds) Contribution of Working Group II to the fourth assessment report of the Intergovernmental Panel on Climate Change. Cambridge University Press, Cambridge, pp 717–743

Agarwal A, Narain S (1991) Global warming in an unequal world: a case of environmental colonialism. Center for Science and Environment, New Delhi

Agyeman J, Devine-Wright P, Prange J (2009) Close to the edge, down by the river? Joining up managed retreat and place attachment in a climate changed world. Environ Plan 41:509–513

Akerlof K, DeBono R, Berry P, Leiserowitz A, Roser-Renouf C, Clarke KL, Rogaeva A, Nisbet MC, Weathers MR, Miabach EW (2010) Public perceptions of climate change as a human health risk: surveys of the United States, Canada and Malta. Int J Environ Res Public Health 7 (6):2559–2606

Anderson A (2009) Media, politics and climate change: towards a new research agenda. Sociol Compass 3(2):166–182

Anderson AA, Myers TA, Maiback E, Cullen H, Gandy J, Witte J, Stenhouse N, Leiserowitz A (2013) If they like you, they learn from you: how a brief weathercaster-delivered climate

[179]Wynne (1993), Yankelovich (2003)

[180]Nisbet (2011)

education segment is moderated by viewer evaluations of the weathercaster. Weather Clim Soc 5:367–377
Andreadis E, Smith J (2007) Beyond the ozone layer. Br Journal Rev 18(1):50–56
Antilla L (2010) Self-censorship and science: a geographical review of media coverage of climate tipping points. Public Underst Sci 19:240–256
Asplund T, Hjerpe M, Wibeck V (2013) Framings and coverage of climate change in Swedish specialized farming magazines. Clim Chang 117:197–209
Augoustinos M, Crabb S, Shepherd R (2010) Genetically modified food in the news: media representations of the GM debate in the UK. Public Underst Sci 19:98–114
Australian Department of Climate Change (2009) Climate change adaptation actions for local government. Department of Climate Change, Government of Australia, Canberra
Banning ME (2009) When poststructural theory and contemporary politics collide: the vexed case of global warming. Commun Crit/Cult Stud 6(3):285–304
Barnett J, O'Neill S, Waller S, Rogers S (2013) Reducing the risk of maladaptation in response to sea-level rise and urban water scarcity. In: Moser SC, Boykoff MT (eds) Successful adaptation to climate change: linking science and policy in a rapidly changing world. Routledge, London, pp 37–49
Baron J (2006) Thinking about global warming. Climatic Change 77(1):137–150
Beck U (1992) Risk society: towards a new modernity. Sage, London
Beck U (2010) Climate for change, or how to create a green modernity? Theory Cult Soc 27 (2–3):254–266
Bell A (1994a) Climate of opinion: public and media discourse on the global environment. Discourse Soc 5(1):33–64
Bell A (1994b) Media (mis)communication on the science of climate change. Public Underst Sci 3 (3):259–275
Bennett WL (2002) News: the politics of illusion. Longman, New York, p 10
Bickerstaff K, Lorenzoni I, Pidgeon NF, Poortinga W, Simmons P (2008) Reframing nuclear power in the UK energy debate: nuclear power, climate change mitigation and radioactive waste. Public Underst Sci 17(2):145–169
Bord RJ, O'Connor RE, Fisher A (2000) In what sense does the public need to understand global climate change? Public Underst Sci 9:205–218
Boykoff MT (2007) Flogging a dead norm? Newspaper coverage of anthropogenic climate change in the United States and United Kingdom from 2003–2006. Area 39(4):470–481
Boykoff MT (2008) Media and scientific communication: a case of climate change. Geol Soc Lond Spec Publ 305:11–18
Boykoff MT, Boykoff JM (2004) Bias as balance: global warming and the U.S. prestige press. Glob Environ Chang 14(2):125–136
Boykoff MT, Rajan SR (2007) Signals and noise: mass-media coverage of climate change in the USA and the UK. Eur Mol Biol Organ Rep 8(3):1–5
Boykoff MT, Roberts JT (2007) Media coverage of climate change: current trends, strengths, weaknesses. United Nations Development Programme. http://hdr.undp.org/fr/rapports/mondial/rmdh2007-2008/documents/Boykoff,%20Maxwell%20and%20Roberts,%20J.%20Timmons.pdf
Boykoff MT, Ghosh A, Venkateswaran K (2013) Media coverage on adaptation: competing visions of "success" in the Indian context. In: Moser SC, Boykoff MT (eds) Successful adaptation to climate change: linking science and practice in a rapidly changing world. Routledge, London, pp 237–252
Brainard C (2006a) Inhofe, climate change and those alarmist reporters. Columbia Journalism Review. www.cjr.org/behind_the_news/inhofe_climate_change_and_thos.php
Brainard C (2006b) A reporting error frozen in time? Columbia Journalism Review, Sept. www.cjr.org/behind_the_news/a_reporting_error_frozen_in_ti.php
Brainard C (2007a) Environmental journalism? Environmentalism? Columbia Journalism Review, Sept. www.cjr.org/behind_the_news/environmental_journalism_envir.php
Brainard C (2007b) Chinese pollution in words, pictures and more. Columbia Journalism Review. http://www.cjr.org/behind_the_news/chinese_pollution_in_words_pic.php

Brainard C (2007c) Climate goes prime-time with Couric. Columbia Journalism Review. www.cjr.org/campaign_desk/climate_goes_primetime_with_co.php
Brainard C (2007d) Rolling Stone breaks climate news! Well, sort of. . .. Columbia Journalism Review, July. www.cjr.org/behind_the_news/rolling_stone_breaks_climate_n.php
Brainard C (2007e) For ABC, weather equals climate change. Columbia Journalism Review, Feb. www.cjr.org/behind_the_news/for_abc_weather_equals_climate.php
Bratt C (1999) Consumers' environmental behavior: generalized, sector-based, or compensatory? Environ Behav 31(1):28–44
Bray D, Martinez G (2011) A survey of the perceptions of regional political decision makers concerning climate change and adaptation in the German Baltic Sea region, vol 50. International BALTEX Secretariat, Helmholtz-Zentrum Geesthacht, Centre for Materials and Coastal Research, Geesthacht
Brittle C (2005) Global warnings! The impact of scientific elite disagreement on public opinion. Doctoral dissertation, University of Michigan
Brittle C, Muthuswamy N (2009) Scientific elites and concern for global warming: the impact of disagreement, evidence strength, partisan cues, and exposure to news content on concern for global warming. Int J Sustain Commun 4:23–44
Brody SD, Zahran S, Vedlitz A, Grover H (2008) Examining the relationship between physical vulnerability and public perceptions of global climate change in the United States. Environ Behav 40(1):72–95
Brooks N, Adger WN, Kelly PM (2005) The determinants of vulnerability and adaptive capacity at the national level and the implications for adaptation. Glob Environ Chang 15:151–163
Brossard D, Shanahan J, McComas K (2004) Are issue-cycles culturally constructed? A comparison of French and American coverage of global climate change. Mass Commun Soc 7(3):359–377
Brown T, Budd L, Bell M, Rendell H (2011) The local impact of global climate change: reporting on landscape transformation and threatened identity in the English regional newspaper press. Public Underst Sci 20:658–673
Bulletin of the Atomic Scientists (2010) Michael E. Mann: a scientist in the crosshairs of climate-change denial. Bull At Sci 66(6):1–7
Burley D, Jenkins P, Laska S, Davis T (2007) Place attachment and environmental change in coastal Louisiana. Organ Environ 20:347–366
Calkins LN, Zlatoper TJ (2001) The effects of mandatory seat belt laws on motor vehicle fatalities in the United States. Soc Sci Q 82(4):716–732
Capstick S, Pidgeon N, Whitehead M (2013) Public perceptions of climate change in Wales: summary findings of a survey of the Welsh public conducted during November and December 2012. Climate Change Consortium of Wales, Cardiff
Carbaugh D, Cerulli T (2013) Cultural discourses of dwelling: investigating environmental communication as a place-based practice. Environ Commun 7:4–23
Carpenter C (2002) Businesses, green groups and the media: the role of non-governmental organizations in the climate change debate. Int Aff 77(2):313–328
Carrico AR, Truelove HB, Vandenbergh MP, Dana D (2014) Does learning about climate change adaptation change support for mitigation? J Environ Psychol 41:19–29
Carvalho A (2007) Ideological cultures and media discourses on scientific knowledge: re-reading news on climate change. Public Underst Sci 16:223–243
Carvalho A (2010) Media(ted)discourses and climate change: a focus on political subjectivity and (dis)engagement. Wiley Interdiscip Rev Clim Chang 1(2):172–179
Carvalho A, Burgess J (2005) Cultural circuits of climate change in UK broadsheet newspapers, 1985–2003. Risk Anal 25(6):1457–1469
Chilvers J, Lorenzoni I, Terry G, Buckley P, Pinnegar JK, Gelcich S (2014) Public engagement with marine climate change issues: (Re)framings, understandings and responses. Glob Environ Chang 29:165–179
Collins HM, Evans R (2002) The third wave of science studies: studies of expertise and experience. Soc Stud Sci 32(2):235–296

Columbia Journalism Review editors (2009) Newsweek, API, and ethics. Columbia Journalism Review, Nov. http://www.cjr.org/news_meeting/newsweek_api_and_ethics.php
Connor LH, Higginbotham N (2013) "Natural cycles" in lay understandings of climate change. Global Environ Change 23(6):1852
Corbett JB, Durfee JL (2004) Testing public (un)certainty of science: media coverage of new and controversial science. In: Friedman SM, Dunwoody S, Rogers CL (eds) Communicating uncertainty: media coverage of new and controversial science. Erlbaum, Mahwah, pp 3–22
Corfee-Morlot J, Maslin M, Burgess J (2007) Global warming in the public sphere. Philos Trans R Soc A Math Phys Eng Sci 365:2741–2776
Cunningham B (2003) Re-thinking objectivity. Columbia Journal Rev 42(2):24–32
DARA (2012) Climate vulnerability monitor: a guide to the cold calculus of a hot planet. DARA and the Climate Vulnerable Forum. http://daraint.org/climate-vulnerability-monitor/climate-vulnerability-monitor-2012/
Demeritt D (2001) The construction of global warming and the politics of science. Ann Assoc Am Geogr 91(2):307–337
Detjen J, Fico F, Li X, Kim Y (2000) Changing work environment of environmental reporters. Newsp Res J 21:2–25
Dirikx A, Gelders D (2010) To frame is to explain: a deductive frame-analysis of Dutch and French climate change coverage during the annual UN Conferences of the Parties. Public Underst Sci 19:732–742
Doultona H, Brown K (2009) Ten years to prevent catastrophe? Discourses of climate change and international development in the UK press. Glob Environ Chang 19:191–202
Dow K (2010) News coverage of drought impacts and vulnerability in the U.S. Carolinas, 1998–2007. Nat Hazards 54:497–518
Downs A (1972) Up and down with ecology: the issue-attention cycle. Public Interest 28:38–50
Dunlap RE (1992) Trends in public opinion toward environmental issues: 1965–1992. Soc Nat Resour 4(3):285–312
Dunwoody S (1999) Scientists, journalists, and the meaning of uncertainty. In: Friedman SM, Dunwoody S, Rogers CL (eds) Communicating uncertainty: Media coverage of new and controversial science. Mahwah, NJ: Lawrence Erlbaum Associates
Dunwoody S, Griffin RJ (1993) Journalistic strategies for reporting long-term environmental issues: a case study of three superfund sites. In: Hansen A (ed) The mass media and environmental issues. Leicester University Press, Leicester, pp 22–50
Dunwoody S, Peters HP (1992) Mass media coverage of technological and environmental risks. Public Underst Sci 1(2):199–230
Durfee JL (2006) "Social change" and "status quo" framing effects on risk perception: an exploratory experiment. Sci Commun 27(4):459–495
ecoAmerica (2012) Changing season, changing lives: new realities, new opportunities. Leadership summit report. ecoAmerica, Washington, DC
Eden S (1996) Public participation in environmental policy: considering scientific, counter-scientific and non-scientific contributions. Public Underst Sci 5:183–204
Einsiedel EF (1992) Framing science and technology in the Canadian press. Public Underst Sci 1:89–101
Entman RM (1989) Democracy without citizens: media and the decay of American politics. Oxford University Press, New York
Entman RM (1993) Framing: toward clarification of a fractured paradigm. J Commun 43:51–58
Ereaut G, Segnit N (2006) Warm words: how are we telling the climate story and can we tell it better. Institute for Public Policy Research. London, England
Evans G, Durant J (1995) The relationship between knowledge and attitudes in the public understanding of science in Britain. Public Underst Sci 4:57–74
Evans L, Milfont TL, Lawrence J (2014) Considering local adaptation increases willingness to mitigate. Glob Environ Chang 25:69–75

Farbotko C (2005) Tuvalu and climate change: constructions of environmental displacement in the Sydney Morning Herald. Geografiska Annaler Ser B Hum Geogr 87(4):279–293
Farnsworth SJ, Lichter SR (2009) The structure of evolving U.S. scientific opinion on climate change and its potential consequences. American Political Science Association, Toronto
Fedler F, Bender JR (1997) Reporting for the media. Harcourt Brace, Fort Worth
Fitzsimmons J (2012) Media begin to connect the dots between climate change and wildfires. Media Matters for America, Washington, DC
Fitzsimmons J, Fong J, Johnson M, Theel S (2012) Media avoid climate context in wildfire coverage. Media Matters for America, Washington, DC
Flynn T (2002) Source credibility and global warming: a content analysis of environmental groups. Paper presented to the Association for Education in Journalism and Mass Communication convention. Miami Beach, FL
Foust CR, O'Shannon MW (2009) Revealing and reframing apocalyptic tragedy in global warming discourse. Environ Commun 3:151–167
Freudenburg WR (2000) Social construction and social constrictions: toward analyzing the social construction of 'The Naturalized' and well as 'The Natural'. In: Spaargaren G, Mol APJ, Buttel FH (eds) Environment and global modernity. Sage, London, pp 103–119
Freudenburg WR, Musellia V (2010) Global warming estimates, media expectations, and the asymmetry of scientific challenge. Glob Environ Chang 20(3):483–491
Fried M (2000) Continuities and discontinuities of place. J Environ Psychol 20:193–205
Funfgeld H, McEvoy D (2011) Framing climate change adaptation in policy and practice. Victorian Centre for Climate Change Adaptation Research, Victoria, Australia
Futerra Sustainability Communications (2006) Climate fear vs. climate hope: are the UK's national newspapers helping tackle climate change? Futerra report. http://www.docstoc.com/docs/28404782/Fear-or-hope
Gamson WA, Modigliani A (1989) Media discourse and public opinion on nuclear power: a constructionist approach. Am J Sociol 95(1):1–37
Gamson WA, Croteau D, Hoynes W, Sasson T (1992) Media images and the social construction of reality. Annu Rev Sociol 18:373–393
Garcia D (2010) Warming to a redefinition of international security: the consolidation of a norm concerning climate change. Int Relat 24(3):271–292
Gavin NT, Leonard-Milsom L, Montgomery J (2010) Climate change, flooding and the media in Britain. Public Underst Sci 20:422–438
Gelbspan R (1998) The heat is on: the climate crisis, the cover-up, the prescription. New York, NY: Perseus Press
Goidel K, Kenny C, Climek M, Means M, Swann L, Sempier T, Schneider M (2012) 2012 Gulf coast climate change survey: Norman, OK: Southern Climate Impacts Planning Program
Good JE (2008) The framing of climate change in Canadian, American and international newspapers: a media propaganda model analysis. Can J Commun 33(2)
Gordon JC, Deines T, Havice J (2010) Global warming coverage in the media: trends in a Mexico City newspaper. Sci Commun 32:143–170
Greenberg M (2013) Media still largely fail to put wildfires in climate context. Media Matters for America, Washington, DC
Grundmann R (2006) Ozone and climate: scientific consensus and leadership. Sci Technol Human Values 31(1):73–101
Gushee DE (2004) CAIChE offers technological insights to the public policy debate on global climate change. Environ Prog 19(3):F2–F4
Hall NL, Taplin R, Goldstein W (2010) Empowerment of individuals and realization of community agency: applying action research to climate change responses in Australia. Action Res 8 (1):71–91
Hansen A (1994) Journalistic practices and science reporting in the British press. Public Underst Sci 3:111–134

Harbinson R, Mugara R, Chawla A (2006) Whatever the weather: media attitudes to reporting on climate change. Panos Institute, London
Hart PS (2010) One or many? The influence of episodic and thematic climate change frames on policy preferences and individual behavior change. Sci Commun 33(1):28–51
Harvatt J, Petts J, Chilvers J (2011) Understanding householder responses to natural hazards: flooding and sea-level rise comparisons. J Risk Res 14:63–83
Herman ES, Chomsky N (1988) Manufacturing consent: the political economy of the mass media. Pantheon Books, New York
Herrmann S (2007) Climate sceptics. BBC News. www.tinyurl.com/2fd54u.
Herzog HJ, Curry TE et al (2005) Climate change survey. Massachusetts Institute of Technology, Boston
Hilgartner S, Bosk CL (1988) The rise and fall of social problems: a public arenas model. Am J Sociol 94(1):53–78
Ho SS, Brossard D, Scheufele DA (2008) Effects of value predispositions, mass media use, and knowledge on public attitudes toward embryonic stem cell research. Int J Public Opin Res 20 (2):171–192
Höijer B (2010) Emotional anchoring and objectification in the media reporting on climate change. Public Underst Sci 19(6):717–731
HSBC (2007) HSBC climate confidence index. HSBC Holdings, London, http://www.hsbc.com/1/PA_1_1_S5/content/assets/newsroom/hsbc_ccindex_p8.pdf
Hulme M (November 4, 2006) Chaotic world of climate truth. BBC News. Available at: http://news.bbc.co.uk/2/hi/science/nature/6115644.stm
Hulme M, Mahony M (2010) Climate change: what do we know about the IPCC? Prog Phys Geogr 34(5):705–718
Institute for Public Policy Research (2006) Warm words: how are we telling the climate story and can we tell it better? IPPR, London, http://www.ippr.org.uk/ecomm/files/warm_words.pdf
Irwin A (2001) Constructing the scientific citizen: science and democracy in the biosciences. Public Underst Sci 10:1–18
Jasanoff S (1997) Civilization and madness: the great BSE scare of 1996. Public Underst Sci 6:221–232
Jay M, Marmot MG (2009) Health and climate change: will a global commitment be made at the UN climate change conference in December? Br Med J 339:645–646
Jennings N, Hulme M (2010) UK newspaper (mis)representations of the potential for a collapse of the Thermohaline Circulation. Area 42(4):444–456
Jordan A, O'Riordan T (2000) Environmental politics and policy processes. In: O'Riordan T (ed) Environmental science for environmental management. Prentice Hall. New York, NY: Routledge
Kahlor L, Rosenthal S (2009) If we seek, do we learn? Predicting knowledge of global warming. Sci Commun 30:380–414
Kenix LJ (2008) Framing science: climate change in the mainstream and alternative news of New Zealand. Polit Sci 60(1):117–132
Kerr A, Cunningham-Burley S, Amos A (1998) The new genetics and health: mobilizing lay expertise. Public Underst Sci 7:41–60
Kim KS (2010) Public understanding of the politics of global warming in the news media: the hostile media approach. Public Underst Sci 20(5):690–705
Kitzinger J (2006) The role of media in public engagement. In: Turney J (ed) Engaging science: thoughts, deeds, analysis and action. Wellcome Trust, London, pp 44–49, http://www.nsf.gov/statistics/seind08/pdf/c07.pdf
Koteyko N (2010) From carbon markets to carbon morality: creative compounds as framing devices in online discourses on climate change mitigation. Sci Commun 32(1):25–54
Kreps G, Maibach E (2008) Transdisciplinary science: the nexus between communication and public health. J Commun 58:732–748

Krosnick JA, Holbrook AL (2006) The origins and consequences of democratic citizens' policy agendas: a study of popular concern about global warming. Clim Chang 77(1):7–43
Kuban A (2007) The U.S. broadcast news media as a social arena in the global climate change debate. Master's thesis, Iowa State University
Lakoff G (2004) Don't think of an elephant: know your values and frame the debate. Chelsea Green, White River Junction
Lawrence A (2009) The first cuckoo in winter: phenology, recording, credibility and meaning in Britain. Glob Environ Chang 19:173–179
Lee G, Yoo CY (2004) Attribute salience transfer of global warming issue from online papers to the public. Paper presented to the Association for Education in Journalism and Mass Communication convention, Toronto
Leiserowitz A (2005) American risk perceptions: is climate change dangerous? Risk Anal 25 (6):1433–1442
Leiserowitz A (2006) Climate change risk perception and policy preferences: the role of affect, imagery, and values. Clim Chang 77(1):45–72
Listerman T (2010) Framing of science issues in opinion-leading news: international comparison of biotechnology issue coverage. Public Underst Sci 19(1):5–15
Liu X, Lindquist E, Vedlitz A (2009) Explaining media and congressional attention to global climate change, 1969–2005: an empirical test of agenda-setting theory. Polit Res Q 64 (2):405–419
Lorenzoni I, Hulme M (2009) Believing is seeing: laypeople's views of future socio-economic and climate change in England and in Italy. Public Underst Sci 18:383–400
Lorenzoni I, Pidgeon NF (2006) Public views on climate change: European and USA perspectives. Clim Chang 77(1):73–95
Lowe T, Brown K, Dessai S, de França Doria M, Haynes K, Vincent K (2006) Does tomorrow ever come? Disaster narrative and public perceptions of climate change. Public Underst Sci 15 (4):435–457
Lowi TJ (1972) Four systems of policy, politics, and choice. Public Adm Rev 32(4):298–310
Luganda P (2005) Communication critical in mitigating climate change in Africa. Open meeting of the International Human Dimensions Programme, Bonn
Maibach E, Roser-Renouf C, Leiserowitz A (2008) Communication and marketing as climate change intervention assets: a public health perspective. Am J Prev Med 35(5):488–500
Maibach EW, Nisbet M, Baldwin MP, Akerlof K, Diao G (2010) Reframing climate change as a public health issue: an exploratory study of public reactions. Biomed Central Public Health 10:299
Maibach E, Cobb S, Leiserowitz A, Peters E, Schweizer V, Mandryk C, Witte J, Bonney R, Cullen H, Straus D et al (2011a) A national survey of television meteorologists about climate change education. Center for Climate Change Communication, George Mason University, Fairfax
Maibach E, Witte J, Wilson K (2011b) "Climategate" undermined belief in global warming among many American TV meteorologists. Bull Am Meteorol Soc 92:31–37
Major AM, Atwood LE (2004) Environmental risks in the news: issues, sources, problems, and values. Public Underst Sci 13:295–308
Manzo K (2010) Beyond polar bears? Re-envisioning climate change. Meteorol Appl 17 (2):196–208
Marlowe E (2005) Seeing red in green news: credibility and perceived bias in environmental news articles. Master's thesis, University of Missouri
McComas K, Shanahan J (1999) Telling stories about global climate change: measuring the impact of narratives on issue cycles. Commun Res 26(1):30–57
McCright AM (2007) Dealing with climate contrarians. In: Moser SC, Dilling L (eds) Creating a climate for change: communicating climate change and facilitating social change. Cambridge University Press, Cambridge, MA
McCright AM, Dunlap RE (2000) Challenging global warming as a social problem: an analysis of the conservative movement's counter-claims. Soc Probl 47(4):499–522

McCright AM, Dunlap RE (2003) Defeating Kyoto: the conservative movement's impact on U.S. climate change policy. Soc Probl 50(3):348–373
McKnight D (2010) A change in the climate? The journalism of opinion at News Corporation. Journalism 11(6):693–706
McManus PA (2000) Beyond Kyoto? Media representation of an environmental issue. Aust Geogr Stud 38(3):306–319
Mellman M (2011) Preparing for a changing climate: observations from focus groups and interviews. The Mellman Group, Washington, DC
Meyer P (1988) Defining and measuring credibility of newspapers: developing an index. Journal Q 65(567–574):588
Miller JD (2004) Public understanding of, and attitudes toward, scientific research: what we know and what we need to know. Public Underst Sci 13:273–294
Miller MM, Riechert BP (2000) Interest group strategies and journalistic norms: news media framing of environmental issues. In: Allan S, Adam B, Carter C (eds) Environmental risks and the media. Routledge, London, pp 45–54
Moeller SD (2008) Considering the media's framing and agenda-setting roles in states' responsiveness to natural crises and disasters. Joan Shorenstein Center on the Press, Politics and Public Policy, Cambridge, MA, http://www.hks.harvard.edu/fs/pnorris/Conference/Conference%20papers/Moeller.pdf
Mooney C (2009) Climate change myths and facts. Washington Post, 21 Mar
Moser SC (2012) Adaptation, mitigation, and their disharmonious discontents. Clim Chang 111:165–175
Moser SC (2013) Navigating the political and emotional terrain of adaptation: community engagement when climate change comes home. In: Moser SC, Boykoff MT (eds) Successful adaptation to climate change: linking science and policy in a rapidly changing world. Routledge, London, pp 289–305
Moser SC (2014) Communicating adaptation to climate change: the art and science of public engagement when climate change comes home. WIREs Clim Change 5(3):337–358
Myers TA, Nisbet MC, Maibach EW, Anthony A, Leiserowitz AA (2012) A public health frame arouses hopeful emotions about climate change. Clim Chang 113(3–4):1105
National Science Board (2008) Science and technology: public attitudes and understanding. In: Science and Engineering Indicators 2008. National Science Board, Arlington, http://www.nsf.gov/statistics/seind08/pdf/c07.pdf
Newell P (2000) Climate for change: non-state actors and the global politics of the greenhouse. Cambridge University Press, Cambridge, MA, p 152
Nielsen Company (2007) Global Omnibus Survey. New York: AC Nielsen
Nisbet MC (2006) Does the public believe Inhofe's hype? Framing Science blog, Sept. http://scienceblogs.com/framing-science/2006/09/does_the_public_believe_inhofe.php
Nisbet MC (2008) Time magazine's "reported analysis" of global warming. Framing Science. http://scienceblogs.com/framing-science/2008/04/time_magazines_reported_analys.php
Nisbet MC (2009) Communicating climate change: why frames matter for public engagement. Environment. http://www.environmentmagazine.org/Archives/Back%20Issues/March-April%202009/Nisbet-full.html
Nisbet MC (2011) Climate change enters downward cycle in news attention as dramatic storytelling potential wanes. Big Think. http://bigthink.com/ideas/26410
Nisbet MC (2015) Disruptive ideas: public intellectuals and their arguments for action on climate change. Wiley Interdiscip Rev Clim Chang 5(6):809–823
Nisbet MC, Goidel RK (2007) Understanding citizen perceptions of science controversy: bridging the ethnographic-survey research divide. Public Underst Sci 16(4):421–440
Nisbet MC, Huge M (2006) Attention cycles and frames in the plant biotechnology debate: managing power and participation through the press/policy connection. Int J Press/Polit 11(2):3–40
Nisbet MC, Kotcher JE (2009) A two-step flow of influence? Opinion-leader campaigns on climate change. Sci Commun 30(3):328–354

Nisbet MC, Scheufele DA (2009) What's next for science communication? Promising directions and lingering distractions. Am J Bot 96:1767–1778
Nisbet MC, Brossard D, Kroepsch A (2003) Framing science: the stem cell controversy in an age of press/politics. Int J Press/Polit 8(2):36–70
Nisbet MC, Price S, Pascual-Ferra P, Maibach E (2010a) Communicating the public health relevance of climate change: a news agenda building analysis. Working paper. American University, Washington, DC. http://scienceblogs.com/framing-science/Nisbet_etal_(2010)_NewsCoverageClimateChangePublicHealth_WorkingPaper.pdf
Nisbet MC, Hixon M, Moore KD, Nelson M (2010b) The four cultures: new synergies for engaging society on climate change. Front Ecol Environ 8:329–331
O'Brien K, Eriksen S, Sygna L, Naess LO (2006) Questioning complacency: climate change impacts, vulnerability, and adaptation in Norway. Ambio 35:50–56
O'Neill S, Nicholson-Cole S (2009) "Fear won't do it": promoting positive engagement with climate change through visual and iconic representations. Sci Commun 30(3):355–379
Ockwell D, Whitmarsh L, O'Neill S (2009) Reorienting climate change communication for effective mitigation: forcing people to be green or fostering grass-roots engagement? Sci Commun 30(3):305–327
Ogalleh S, Vogl C, Eitzinger J, Hauser M (2012) Local perceptions and responses to climate change and variability: the case of Laikipia District, Kenya. Sustainability 4:3302–3325
Olausson U (2009) Global warming: global responsibility? Media frames of collective action and scientific certainty. Public Underst Sci 18:421–436
Painter J (2007) All doom and gloom? International TV coverage of the April and May 2007 IPCC reports. http://www.tinyurl.com/2qd7ky
Pellechia MG (1997) Trends in science coverage: a content analysis of three U.S. newspapers. Public Underst Sci 6:49–68
Pidgeon N, Gregory R (2004) Judgment, decision-making and public policy. In: Handbook of judgment and decision making. Blackwell, Oxford, UK, pp 604–623
Pielke R, Prins G, Rayner S, Sarewitz D (2007) Climate change 2007: lifting the taboo on adaptation. Nature 445:597–598
Pike C, Hyde K, Herr M, Minkow D, Doppelt B (2012) Climate communication and engagement efforts: the landscape of approaches and strategies. A Report to the Skoll Global Threats Fund. The Resource Innovation Group's Social Capital Project, Eugene
Plate T (2009) An (oil) peak too high. Columbia Journalism Review, Oct. www.cjr.org/the_kicker/when_newsweek_met_oil_lobby.php
Pollack H (2003) Can the media help science? Skeptic 10(2):73–80
Price V, Nir L, Capella JN (2005) Framing public discussion of gay civil unions. Public Opin Q 69 (2):179–212
Priest SH (2006) Public discourse and scientific controversy: a spiral-of-silence analysis of biotechnology opinion in the United States. Sci Commun 28(2):195–215
Reser JP, Bradley GL, Glendon AI, Ellul MC, Callaghan R (2012) Public risk perceptions, understandings and responses to climate change and natural disasters in Australia and Great Britain: final report. Griffith University, Australia: National Climate Change Adaptation Research Facility
Resource Media (2009). Communicating Climate Change and Water Linkages in the West — Guidelines and Toolkit. Available at: http://www.carpediemwest.org/wp-content/uploads/Western_Water_and_Climate_Change_Communications_Guidelines-WEB.pdf
Revkin A (2007) Climate change as news: challenges in communicating environmental science. In: DiMento JC, Doughman PM (eds) Climate change: what it means for us, our children, and our grandchildren. MIT Press, Boston, pp 139–160
Roscho B (1975) Newsmaking. University of Chicago Press, Chicago
Rowe G, Horlick-Jones T, Walls J, Pidgeon N (2005) Difficulties in evaluating public engagement initiatives: reflections on an evaluation of the UK GM Nation? Public debate about transgenic crops. Public Underst Sci 14:331–352

Ruddell D, Harlan S, Grossman-Clarke S, Chowell G (2012) Scales of perception: public awareness of regional and neighborhood climates. Clim Chang 111:581–607
Ruhl J (2010) Climate change adaptation and the structural transformation of environmental law. Environ Law 363:365–375
Russell C (2008) Climate change: now what? Columbia Journalism Review. www.cjr.org/feature/climate_change_now_what.php
Ryan C, Carrage KM, Schwerner C (1998) Media movements and the quest for social justice. J Appl Commun Res 26:165–181
Schneider SH (1993) Degrees of certainty. Res Explor 9(2):173–181
Schneider SS (2001) A constructive deconstruction of deconstructionists: a response to Demeritt. Ann Assoc Am Geogr 91(2):338–344
Schottland T (2010) Climate security: how to frame a winning argument. It's Getting Hot in Here (blog). http://itsgettinghotinhere.org/2010/02/20/climate-security-how-to-frame-a-winning-argument/
Schweizer S, Davis S, Thompson JL (2013) Changing the conversation about climate change: a theoretical framework for place-based climate change engagement. Environ Commun 7:42–62
Shanahan M (2007) Talking about a revolution: climate change and the media. International Institute for Environment and Development. http://www.iied.org/pubs/pdfs/17029IIED.pdf
Shanahan J, Good J (2000) Heat and hot air: influence of local temperature on journalists' coverage of global warming. Public Underst Sci 9:285–295
Shearer C, Rood RB (2011) Changing the media discussion on climate and extreme. Weather. earthzine (blog). http://www.earthzine.org/2011/04/17/changing-the-media-discussion-on-climate-and-extreme-weather/
Shove E (2010) Social theory and climate change: questions often, sometimes and not yet asked. Theory Cult Soc 27(2–3):277–288
Slovic P (1987) Perceptions of risk. Science 236:280–285
Smith J (2005) Dangerous news: media decision making about climate change risk. Risk Anal 25 (6):1471–1482
Smith A, Jenkins K (2013) Climate change and extreme weather in the USA: discourse analysis and strategies for an emerging "public". J Environ Stud Sci 3:259–268
Smith N, Leiserowitz A (2012) The rise of global warming skepticism: exploring affective image associations in the United States over time. Risk Anal 32(6):1021–1032
Soman D, Ainslie G, Frederick S, Li X, Lynch J, Moreau P et al (2005) The psychology of intertemporal discounting: why are distant events valued differently from proximal ones? Mark Lett 16(3–4):347–360
Sonnett J (2010) Climates of risk: a field analysis of global climate change in U.S. media discourse, 1997–2004. Public Underst Sci 19(6):698–716
Soroka SN (2002) Agenda-setting dynamics in Canada. UBC Press, Vancouver
Soroka S, Farnsworth SJ, Young L, Lawlor A (2009) Environment and energy policy: comparing reports from U.S. and Canadian network news. American Political Science Association, Toronto
Spence A, Pidgeon N (2010) Framing and communicating climate change: the effects of distance and outcome frame manipulations. Glob Environ Chang 20:656–667
Stamm KR, Clark F, Eblacas PR (2000) Mass communication and public understanding of environmental problems: the case of global warming. Public Understanding of Science 9:219–237
Stempel G, Culberston H (1984) The prominence and dominance of news sources in newspaper medical coverage. Journal Q 61:671–676
Stern N (2006) Stern review on the economics of climate change. HM Treasury, London, http://www.webcitation.org/5nCeyEYJr
Stewart CO, Dickerson DL, Hotchkiss R (2009) Beliefs about science and news frames in audience evaluations of embryonic and adult stem cell research. Sci Commun 30:427–452
Stocking SH, Holstein LW (2009) Manufacturing doubt: journalists' roles and the construction of ignorance in a scientific controversy. Public Underst Sci 18:23–42

Sturgis P, Allum N (2004) Science in society: re-evaluating the deficit model of public attitudes. Public Underst Sci 13:55–74
Sundblad E, Biel A, Garling T (2009) Knowledge and confidence in knowledge about climate change among experts, journalists, politicians, and laypersons. Environ Behav 41:281–302
Takahashi B (2010) Framing and sources: a study of mass media coverage of climate change in Peru during the V ALCUE. Public Underst Sci 20(4):543–557
Takahashi B, Meisner M (2013) Climate change in Peruvian newspapers: the role of foreign voices in a context of vulnerability. Public Underst Sci 22:427–442
Thøgersen J (1999) Spillover processes in the development of a sustainable consumption pattern. J Econ Psychol 20(1):53–81
Thompson M (2009) Do it for the polar bears: an examination of global warming discussion after Hurricane Katrina. Paper presented at the annual meeting of the Association for Education in Journalism and Mass Communication, Boston. http://www.allacademic.com/meta/p375724_index.html
Tiefenbeck V, Staake T, Roth S (2013) For better or for worse? Empirical evidence of moral licensing in a behavioral energy conservation campaign. Energy Policy 57:160–171
Tribbia J, Moser SC (2008) More than information: what coastal managers need to plan for climate change. Environ Sci Pol 11:315–328
Truelove H, Carrico A, Weber E, Raimi K, Vandenbergh M (2015) Positive and negative spillover of pro-environmental behavior: an integrative review and theoretical framework. Global Environ Change 29:127–138
Trumbo C (1996) Constructing climate change: claims and frames in U.S. news coverage of an environmental issue. Public Underst Sci 5:269–283
Ungar S (1992) The rise and (relative) decline of global warming as a social problem. Sociol Q 33(4):483–501
Ungar S (2000) Knowledge, ignorance and the popular culture: Climate change versus the ozone hole. Public Understanding of Science 9:297–312
Uusi-Rauva C (2010) The EU energy and climate package: a showcase for European environmental leadership? Environ Policy Gov 20(2):73–88
van der Werff E, Steg L, Keizer K (2013) The value of environmental self-identity: the relationship between biospheric values, environmental self-identity and environmental preferences, intentions and behavior. J Environ Psychol 34:55–63
Victor D, Kennell CF, Ramanathan V (2012) The climate threat we can beat. Foreign Aff 119:112–121
Walton J (2007) Making sustainability matter: the effect of message framing on inclination to act. Master's thesis, Colorado State University
Weart SR (2009) The idea of anthropogenic global climate change in the 20th century. Wiley Interdiscip Rev Clim Chang 1(1):67–81
Weaver DA, Lively E, Bimber B (2009) Searching for a frame: news media tell the story of technological progress, risk, and regulation. Sci Commun 31(2):139–166
Weber E (1997) Perception and expectation of climate change: precondition for economic and technological adaptation. In: Bazerman MH, Messick DM, Tensbrunsel A, Wade-Benzoni K (eds) Psychological perspectives to environmental and ethical issues in management. Jossey-Bass, San Francisco, pp 314–341
Weber E (2006) Experience-based and description-based perceptions of long-term risk: why global warming does not scare us (yet). Clim Chang 77(1–2):103–120
Weingart P, Engels A et al (2000) Risks of communication: discourses on climate change in science, politics, and the mass media. Public Underst Sci 9:261–283
Weintraub D (2007) Newspaper coverage of global climate change: risk, frames and sources. Master's thesis, University of South Carolina
Weisskopf M (1988) Two senate bills take aim at 'greenhouse effect'. Washington Post, p A17

Whitmarsh L (2008) Are flood victims more concerned about climate change than other people? The role of direct experience in risk perception and behavioural response. J Risk Res 11:351–374
Whitmarsh L (2009) What's in a name? Commonalities and differences in public understanding of "climate change" and "global warming". Public Underst Sci 18(4):401–420
Wilkins L (1993) Between facts and values: print media coverage of the greenhouse effect, 1987–1990. Public Underst Sci 2:71–84
Wilkins L, Patterson P (1987) Risk analysis and the construction of news. J Commun 37(3):80–92
Will GF (2009) Climate science in a tornado. Washington Post, 27 Feb
Wilson KM (2000a) Communicating climate change through the media: predictions, politics, and perceptions of risk. In: Allan S, Adam B, Carter C (eds) Environmental risks and the media. Taylor and Francis, London, pp 201–217
Wilson KM (2000b) Drought, debate, and uncertainty: measuring reporters' knowledge and ignorance about climate change. Public Underst Sci 9:1–13
Wilson KM (2002) Forecasting the future: how television weathercasters–attitudes and beliefs about climate change affect their cognitive knowledge on the science. Sci Commun 24:246–268
Wolf J, Allice I, Bell T (2013) Values, climate change, and implications for adaptation: evidence from two communities in Labrador, Canada. Glob Environ Chang 23:548–562
Woods R, Fernandez A, Coen S (2010) The use of religious metaphors by UK newspapers to describe and denigrate climate change. Public Underst Sci 21:323–339
Wynne B (1993) Public uptake of science: a case for institutional reflexivity. Public Underst Sci 2:321–337
Yankelovich D (2003) Winning greater influence for science. Issues Sci Technol 19(4). http://www.issues.org/19.4/yankelovich.html
Yaros RA (2006) Is it the medium or the message? Structuring complex news to enhance engagement and situational understanding by non-experts. Commun Res 33(4):285–309
Yearley S (2009) Sociology and climate change after Kyoto: what roles for social science in understanding climate change? Curr Sociol 57(3):389–405
Zehr S (1999) Scientists' representations of uncertainty. Communicating uncertainty: media representations of global warming. Sci Commun 26(2):129
Zehr SC (2000) Public representations of scientific uncertainty about global climate change. Public Underst Sci 9:85–103
Zhao X (2009) Media use and global warming perceptions: a snapshot of the reinforcing spirals. Commun Res 36(5):698–723
Zhong CB, Liljenquist K, Cain D (2009) Moral self-regulation: licensing and compensation. In: de Cremer D (ed) Psychological perspectives on ethical behavior and decision making. Information Age, Charlotte, pp 75–89
Zia A, Todd AM (2010) Evaluating the effects of ideology on public understanding of climate change science: how to improve communication across ideological divides? Public Underst Sci 19(6):743–761

Economics for a Sustainable Planet

Arif S. Malik

Contents

Abstract

Sustainable development endorses the idea that social, environmental, and economic progress is possible within the limits of earth's natural resources. Sustainable development acknowledges that everything in the world is connected through space and time; hence, environmental pollution created in one part of

A.S. Malik (✉)
Department of Electrical and Computer Engineering, College of Engineering, Sultan Qaboos University, Muscat, Oman
e-mail: asmalik@squ.edu.om

W.-Y. Chen et al. (eds.), *Handbook of Climate Change Mitigation and Adaptation*,
DOI 10.1007/978-3-319-14409-2_7

the globe disturbs the other part of the globe or decisions made by the present generation will affect the future generations. Sustainable development is the route to world's sustainable future. Therefore, to achieve true sustainability there is a need to harmoniously balance economic, social, and environmental sustainability factors. Environmental sustainability means that world's ecological limits are not transgressed. Economic sustainability requires that existing resources are used optimally so that a responsible and beneficial balance can be achieved over the longer term. Social sustainability is the ability of society, or any social system, to continually achieve a good social wellbeing. Yet there are policies and practices in social, political, and economic milieu that constantly promote unsustainability or are fundamentally in tension with the sustainable development notion. For example, sustainability and economic growth are fundamentally incompatible because the contemporary global economic system, which promote economic growth, assumes continuous expansion in consumption of material goods and resources, a phenomenon that conflicts with the environmental notion of a finite planet with limited resources. Similarly, the unfair economic structures in the economic system create great wealth inequalities, which could lead to social unsustainability and social unrest. Likewise, the solutions to world's political problems if enforced without considering the will and aspirations of the affected local population create social unrest and affect the global peace.

This chapter emphasizes on the need for a fair and just economic system to achieve sustainability. It shows that climate change, ecological degradation, population growth, poverty and the resource scarcity, the problems of failing financial markets, and economic recession are all intertwined with the present economic system, which has been responsible for transgressing the balance of nature. The chapter then reviews reforms and alternatives, proposed in literature, to the present economic system to promote sustainability such as steady-state economics; environmental economics, ecological economics; restorative economics; local self-reliance/alternative currency, etc. Existence of interest and discount rates, which are a given necessity of the world economic system, means that the future costs and benefits are less valuable than those in the present – a clear case of intergenerational inequity and injustice. The chapter, using the concepts of systems thinking, make a case against discounting the future and shows that the discounting practice is in conflict with the holistic approach to the environment. The chapter shows that all the reforms or alternatives to contemporary economic system proposed in the literature do not really address the root cause of all the problems, which is the built-in interest-based system, made possible with the paper currency, in the economy that creates great injustices. The chapter argues that solutions of science and technology to ecological problems are limited because of ecological shortsightedness and corporate greed. Finally, in the future directions a broad framework of "fair and just" economic system is laid out which if realized can lead to an ecologically sustainable future for the planet.

Introduction

How serious is the global threat to sustainability and the environment? This is the question one has to ponder if one truly cares about the planet he lives in. One way to judge is by carefully considering the present world predicament – by bearing in mind the present state of humanity as a whole – and where it is heading.

Human civilization as a whole is on a path to increasing world population pressure; rising poverty and hunger; an increasing gap between rich and poor among the nations and within nations; growing potential for social and political conflicts; escalating violence or terrorism in response to injustices (Milne 2001), or in the very least, to call attention to perceived wrongs or injustices; huge world military spending; accelerating climate change; food, water, and energy shortages; worsening industrial, urban, and agricultural pollution; nonstop destruction of the ozone layer (Environmental Protection Agency 2015); accelerating reduction of biodiversity; and continued loss of atmospheric oxygen (Bardi 2013). Humankind also runs the risk of global destruction through nuclear war, risk of mega disasters caused by nuclear accidents and leaking nuclear waste, devastating floods, storms, and cyclones due to climate change; and widespread health problems owing to natural catastrophes due to the accumulation of toxins, in soil, air, and water (Milne 2001; Environmental Protection Agency 2015; Bardi 2013; Capra 1983; Laszlo 2006). This, then, in brief is the dire state of the world humanity is in and if human civilization continues on the same trajectory, it is on a collision course with nature. How did it come to be as it is and how can the human race avoid this imminent disaster?

Unless this sickness is thoroughly understood, no cure is possible. This chapter will delve into the fundamental contributing factors that led to this pathetic situation and then suggest a future remedy to emerge from this state. After providing a brief introduction to ecology, economy and economic growth, and ecosystem concepts, the effect of economic activities on the global ecological situation is examined. Poverty and population growth are discussed as drivers of social unsustainability. The concept of sustainable development is then introduced and the compatibility of a market-based capitalist economic system with sustainability is reviewed. Several reforms/alternatives, proposed in literature, to the present economic system are reviewed to promote sustainability. The case of intergenerational equity and discounting the future is critically discussed in light of systems thinking. Recent advances in hierarchical systems approach concepts in systems theory are employed to argue against the economic growth imperative of capitalist economic system. Next, the cause of all the ills – the interest-bearing system of the capitalist economy – is discussed in rather detail. Before giving a prescription, the role of technology is critically reviewed. Finally, the concept of a "fair and just" economic system is introduced for sustainable development of humanity and future guidelines are provided for its realization.

Ecology and Ecosystem

Ecology is the science of relationships between living organisms and their environment. Ecology is also the study of ecosystems. An ecosystem is everything in a specified area – the air, soil, water, living organisms, and physical structures, including everything built or devised by humans. The living parts of an ecosystem – microorganisms, plants, humans, and animals are its biological community. Ecosystems can be of any size. A small pond in a forest is an ecosystem, and the entire forest is an ecosystem. A single farm is an ecosystem, and a rural landscape is an ecosystem. Villages, towns, and large cities are ecosystems. A region of thousands of square kilometers is an ecosystem, and the planet earth is an ecosystem. People affect ecosystems when they use resources such as water, fish, timber, and livestock grazing pasture. After using materials from ecosystems, people return the materials to ecosystems as waste (Marten 2001). The main driver behind the changes in ecosystems is human economic activity and the related economic growth.

Economic Growth

Economics is defined as the discipline dealing with the production, distribution, and consumption of wealth. Economic growth is then an increase in production and consumption of goods and services. It is a function of increasing population and per capita consumption and is typically expressed in Gross Domestic Product (GDP) or Gross National Product (GNP). When the economy grows, natural capital is either consumed as a nonrenewable resource or reallocated to humans as a man-made capital. Natural capital, in this context, is the stock of all environmental and natural resource assets, from oil in the ground to the quality of soil and groundwater, from the stock of fish in the oceans to the capacity of the globe to recycle and absorb carbon (Pearce et al. 1990). One fascinating character of natural capital is that, unlike man-made capital, it has the capability to maintain itself provided its "health" is not critically deteriorated. If critical ecological thresholds are crossed, ecosystems may not only lose their capacity to maintain, renew, and replenish themselves, but may also begin to deteriorate spontaneously (Blignaut and Aronson 2008).

Economic Growth and the Environment

The vast expansion of economic activity that occurred in the twentieth century and continues today is the predominant cause of the environmental decline that has occurred to date. This activity is consuming vast quantities of resources from the environment and returning to the environment vast quantities of waste products. The damages are already huge and are on a path to be ruinous in the future. Yet the world economy, now increasingly integrated and globalized, is poised for unprecedented growth. The engine of this growth is modern capitalism or, better, a variety of capitalisms (Speth 2008). Capitalism includes competitive markets, the price

mechanism, the modern corporation as its principal institution, the consumer society and the materialistic values that sustain it, and the administrative state actively promoting economic strength and growth for a variety of reasons. Inherent in the dynamics of capitalism is a powerful drive to earn profits, invest them, innovate, and thus grow the economy. The capitalist era has in fact been characterized by a remarkable exponential expansion of the world economy (Speth 2008).

However, these features of capitalism, as they are constituted today, work together to produce an economic and political reality that is highly destructive to the environment (Speth 2010). The worldwide commitment to economic growth at almost any cost; enormous investment in technologies designed with little regard for the environment; powerful corporate interests whose overriding objective is to grow by generating profit, including profit from avoiding the environmental costs they create; markets that systematically fail to recognize environmental costs unless corrected by governments; governments that are subservient to corporate interests and the growth imperative; rampant consumerism spurred by a worshipping of novelty and by sophisticated advertising; economic activity is so large in scale that its impacts alter the fundamental biophysical operations of the planet – all combing to deliver an ever-growing world economy that is undermining the planet's ability to sustain human life (Speth 2010).

The current ecological situation is radically different from anything humanity has ever been confronted with in its history. This is due to the fact that the dangerous transformation of the environment has become global. These changes have affected all the subsystems and components of the environment over the entire surface of the planet, extending as far as its poles, leaving untouched perhaps only the ocean depths, as has been confirmed by various scientific studies (Speth 2008; Danilov-Danil'yan et al. 2009). Below are some points summarized from (Laszlo 2006; Speth 2008, 2010; Danilov-Danil'yan et al. 2009) elaborating the current global ecological crisis that has occurred due to the economic activity of mankind:

- Sudden rise in the CO_2 in the twentieth century due to emissions from human economic activity (burning fossil fuels and land clearing). Anthropogenic carbon emissions in 2008 are estimated at nearly nine billion tons per year. Models for CO_2 indicate that the earth is only absorbing about half of the CO_2 generated by human activity and the remainder accumulates in the atmosphere.
- Increasing average global temperature predicted to rise in the range 1.5–4.5 °C in the twenty-first century.
- Destruction of ecosystems. At the turn of the twentieth century, territories with ecosystems completely destroyed or depleted by humans comprised only 20 % of the dry landmass, but by the end of the twentieth century they had increased to 63.8 %.
- Decrease in forest reserves. In the preindustrial period alone, according to various estimates, 30–50 % of forests were destroyed all over the Earth. Another 9 %, of which tropical forests comprised the majority, were eliminated in the last 200–300 years. Unfortunately, there is no indication that this process has declined in any manner today but increasing at alarming rate. Because of difficulties in estimating

tropical forest loss, yearly estimates of global tropical deforestation vary widely from 50,000 km^2 – roughly the size of Costa Rica or the U.S. state of West Virginia – to 170,000 km^2 – about the size of the South American country of Uruguay or the U.S. state of Florida. At such rates, half of the world's remaining tropical forests will be gone in 35–117 years, resulting in a dramatic loss and degradation of biodiversity and the ecosystem services it provides (Miller and Spoolman 2009).

- Quality of soil degradation. Soil mantle loss from erosion and degradation due to modern agricultural practices amounts to 60,000 km^2 per year. In addition, thousands of square kilometers are neutralized every year through the salinization and erosion of soils, which no longer remain available for the Earth's biosphere (Danilov-Danil'yan et al. 2009).
- Increased desertification. The rate of desertification is also increased through anthropogenic pressure on semiarid ecosystems, especially as a result of massive water diversion for irrigation.
- Degradation of quality of fresh water in rivers. Increased scale of water regulation (river canalization as well as the construction of dams and water reservoirs, etc.) is undermining the self-rejuvenating capacity of river water.
- Water environment degradation due to acidification and salinization of freshwater reservoirs. The direct cause of acidification is acid rain brought about by the emission into the atmosphere of sulfur and nitrogen oxides formed through the process of fossil fuel combustion. As they become absorbed by raindrops, these compounds settle on water and soil surfaces, often poisoning organisms.
- Depletion of underground water-bearing strata. This could lead to palpable fresh water shortages in certain world regions as early as the next 10–15 years. According to estimates from the International Water Management Institute, by 2025 a billion people will be living in countries with an absolute fresh water deficiency (less than 1,700 m^3 per person per year). These would include parts of the Near East and South Asia, almost all of Africa, as well as the North of China. As a result, there will be even more acute water shortages for agricultural needs in these regions.
- Biodiversity loss. The rate of biodiversity loss (biodiversity is the variation of life forms within a given ecosystem, or on the entire Earth) amounts on average to at least one species per day. And in case of vertebrates, since the early 1600s, the Earth has lost an estimated 23 species of fish, 2 species of amphibians, 113 bird species, and 83 mammalian species. Each extinct species constitutes a final and irreparable loss for the biosphere, and a far greater number of species is in danger of extinction.
- Rapid accumulation in the environment of waste from human economic activity, including the products of chemical synthesis with pronounced toxic characteristics, some of which are discussed below:
  (i) Most of the waste, especially its solid forms is generated through the relentlessly growing process of mineral raw material production. The volume of waste generated by economic activity is indeed truly daunting and defies the imagination. Thus, for every inhabitant of the Earth, 50 t of raw

materials are extracted and transported from mining to processing per year. However, only 2 t of this is transformed into finished products but even the 2 t of final product are essentially a form of waste generation, merely postponed into the future. Therefore, from an ecological perspective, almost everything produced by humanity in the material sphere is sooner or later bound to become waste.

(ii) Aerosols, minute suspended particles, containing both solid (dust, ashes, soot) and liquid components (dissolved sulfur and nitrogen oxides, ammonia as well as airborne hydrocarbons), with a diameter of 0.1 to hundreds of microns, are typical atmospheric contaminants caused by anthropogenic activities. These aerosols, also absorb many metals, lead in particular, and high molecular toxic compounds, which upon reaching human respiratory channels, act as direct irritants and allergens. Other compounds penetrate the blood stream and can provoke a generally toxic effect.

(iii) Dangerous waste and supertoxicants constitute a special category of pollutants, 90 % of which originate in industrialized countries. Less than seven drops of supertoxic chemical if given in a liquid form to a 70 kg human could be lethal (Miller and Spoolman 2009). These include dioxins, biphenyl, furans, etc., and are quite stable in the environment and are not subject to easy chemical and biological decomposition. In this manner, for example, dioxins, formed as a byproduct of many technological processes, have been found not only in the atmosphere, water, and soil, but also in food, including human and animal mothers' milk. The truly global extent of these pollutants is evident in their significant presence even beyond the Arctic Circle (Danilov-Danil'yan et al. 2009). Some of them affect the hormonal, neural, and reproductive systems, hence the term "supertoxicants."

(iv) The role of pesticides in the pollution of the soil and water environments is well known. In particular, it turns out that many pesticides, starting with previously banned DDT (dichlorodiphenyltrichloroethane), as well as polychlorinated biphenyls, dioxins, furans, and finally an entire series of metals (cadmium, lead, mercury), are responsible for disruptions in the human endocrine system, hormonally determined breast cancer and cancer of the prostate, lower sperm counts, infertility, congenital defects, and neurological anomalies in children (Miller and Spoolman 2009). Furthermore, substances in this category are very slow to decompose or to be excreted by the body and therefore tend to accumulate in the body. Thus, lead concentrates in bone tissue; resulting in nearly 1,000 times higher concentrations in bones of modern humans than in bones of those living 1,500 years ago. Chlorinated pesticides and biphenyls accumulate in fat tissue and penetrate into breast milk in fat droplets.

(v) As many as 100,000–200,000 (including synthesized) substances are circulating on the world market; 80 % of these are unknown (Danilov-Danil'yan et al. 2009) and are unlikely to ever be known completely nor how they act upon living organisms. All foreign chemicals can easily enter human body because these are present in the air, water, or food used on daily basis.

As seen from the above, the ecological crisis is immense and the past century witnessed unprecedented destruction mainly due to the economic activity of humankind. Another important factor contributing to the ecological crisis is poverty, which is largely a result of the growing inequity in distribution of wealth (Human Development 2014; Shah 2010a).

Poverty and Population Growth

Global poverty statistics are dismal. According to income-based measures of poverty, 1.2 billion people live with $1.25 or less a day. However, according to the UNDP Multidimensional Poverty Index, almost 1.5 billion people in 91 developing countries are living in poverty with overlapping deprivations in health, education, and living standards (Human Development 2014). Those living in extreme poverty and deprivation are among the most vulnerable. About more than 15 % of the world's people remain vulnerable to multidimensional poverty. Large disparities in income, wealth, education, health, and other dimensions of human development persist across the world, heightening the vulnerability of marginalized groups and undermining their ability to recover from shocks. At the same time, nearly 80 % of the global population lack comprehensive social protection. About 12 % (842 million) suffer from chronic hunger, and nearly half of all workers – more than 1.5 billion – are in informal or precarious employment (Human Development 2014).

Poverty and environmental degradation are inextricably linked (Danilov-Danil'yan et al. 2009). Due to the lack of sufficient income, people begin using and in turn overuse every resource available to them when their survival is at stake. As desperate hunger leads to desperate strategies for survival, many trees are harvested for firewood, timber, and arts and crafts. Most of the poor use this firewood as their source of income by selling it, and arts and crafts products are also used to generate income. The struggle of the poor to survive creates a range of environmental impacts where the poor themselves are often the primary victims. For example, Nepal and Bangladesh have suffered from various environmental problems such as increasingly devastating floods, often believed to be resulting from large-scale deforestation (Shah 2010a). Deforestation also causes the erosion of the soil, and the land the poor farmers cultivate becomes of low quality, thus reducing the overall yield. The high level of pollution in Developing World cities is also amplified by the inability of the urban poor to pay for environmental cleanup. As a result, a large portion of solid household waste is not taken away; therefore, it is in such locations that the world's highest level of water and air pollution is found. Consequently, in the Developing World, intestinal disease alone (caused by dirty water) brings about the deaths of around two million children per year (Danilov-Danil'yan et al. 2009).

Poverty encourages high birthrates because children help subsistence-level families garner the resources needed for survival. Population growth creates more poverty, and more people destroy more of the environment. Without eradicating poverty it is difficult to control the population growth.

As seen from the discussion above, the two main causes for the ecological crises are economic growth based on the economic system that supports it, and the abject poverty related to it is the population growth. In fact, poverty is largely the effect of a world economic system that creates great inequity in the distribution of wealth. As Pope Francis once said, "Human rights are not only violated by terrorism, repression or assassination, but also by unfair economic structures that creates huge inequalities" (The Guardian 2013). The link between poverty and economic system shall be discussed in the later part of the chapter but before that the world response to the growing ecological damage is reviewed.

The industrialized nations having destroyed their own natural ecosystems some time ago were the first to realize the ecological consequences for the rest of the world attempting to emulate their policies. By the 1970s, the ground had been laid for new perspectives on global development. In *Limits to Growth* (1972), Meadows and other MIT researchers modeled trends in global population, resource consumption, and pollution, and found that without policy changes of a drastic kind, they projected population collapse somewhere in the mid twenty-first century (Meadows et al. 1972). They advocated for an end to ever expanding growth, holding population at present levels, and maintaining the per capita industrial output (that is, the average amount of industrial products produced by each person) at the 1975 level; with goods recycled and pollution controlled, soil restored and consumer goods made more durable. After this, alarmist report a tide of literature on sustainability followed. Some even strongly criticized the industrial way of life and its ethos of continuous expansion. It is largely through the Report of the Brundtland Commission in the 1980s the term "sustainable development" entered the wider scientific vocabulary (Danilov-Danil'yan et al. 2009).

Sustainable Development

Among the several definitions of sustainable development, the most frequently quoted definition is from *Our Common Future*, also known as the *Brundtland Report*, which proposes (World Commission on Environment and Development 1987):

> Sustainable development is development that meets the needs of the present without compromising the ability of future generations to meet their own needs.

It contains the concept of needs, in particular the essential needs of the world's poor, to which overriding priority should be given; and the needs of future generations. Taking care of the needs of the future generations or as it is called "intergenerational justice" would be impossible to achieve in the absence of present-day social justice, if the economic activities of some group of individuals continue to jeopardize the well-being of individuals belonging to other groups or living in other parts of the world (The World Bank 2004). What this suggests is the interconnected nature of the world.

All definitions of sustainable development require that the world should be seen as a system – a system that connects in space and time. When the world is considered as a system connected in space, one becomes conscious that greenhouse gases emitted mainly by industrialized countries can lead to global warming and flooding of certain low-lying islands – resulting in the displacement and impoverishment of entire nations. When the world is considered as a system connected in time, one can understand that the economic, social, or environmental decisions taken now will affect the future generations.

The concept of sustainable development is rooted in this sort of systems thinking, which helps understand humanity better and gives humans a higher purpose of life in this world. After more than two decades, there seems to be consensus that sustainability assessments ought to (Gasparatos et al. 2008):

- Integrate economic, environmental, social, and increasingly institutional issues as well as to consider their interdependencies;
- Consider the consequences of present actions well into the future;
- Acknowledge the existence of uncertainties concerning the result of society's present actions and act with a precautionary bias;
- Engage the public;
- Include equity considerations (intragenerational and intergenerational).

Although writers on sustainability share the same basic concerns about the directions of global development, there are also several recurrent debates between them. One main rift is between those who maintain a faith in technology, scientific rationality, and economic growth and those who do not (Wheeler 2004). The former approach is advocated by a large body of economists and sits well with the politicians continuously beating the drum of economic growth. This approach also sits well with the mainstream conservation movement within industrialized nations and with large international development agencies and research institutes that are used to engaging in detailed scientific, economic, and policy-related analysis. They aim to achieve ecological goals by quantifying environmental impacts, analyzing economic policy options, fine-tuning regulation of private industry, and adjusting market incentives. In contrast, others believe that sustainable development is fundamentally incompatible with current capitalist economic structures, attitudes, and lifestyles (Capra 1983; Laszlo 2006; Danilov-Danil'yan et al. 2009; Czech 2000). These advocates are either environmentalists, or equity activists, or spiritually and ethically oriented writers. Environmentalists tend to be motivated by the threat of ecological crises. The ecological worldview, in contrast, acknowledges cultural diversity but seeks to ground the development of society in fundamental values that are shared by virtue of being human and sharing a small planet. This perspective emphasizes interdependence and views the world in terms of overlapping complex systems and organic unity, rather than as an atomistic collection of people and material things, as in positivistic science and neoclassical economics (Capra 1983). Equity advocates often focus on inequality, exploitation, and developed world overconsumption, and develop detailed analyses of how concentrations of

political and economic power lead to exploitation. Such individuals and groups often mobilize politically against economic globalization and to regain local control over economic activity. Spiritual writers and ethicists dwell on the need for a transformation of values and mindsets as a precondition to sustainable development. By reconnecting with the earth, each other, and human relations to the universe, this viewpoint suggests, humans will become better able to coexist with one another and the planet. Ecofeminist critiques of development follow a similar path, arguing that specifically male values, mindsets, and institutions are much of the problem (Milne 2001; Meadows et al. 1972).

David Orr, a distinguished professor on Environmental Studies and Politics, writes (Orr 2010) "The conversation arising now from the concern for the sustainability of humankind on Earth in many ways resembles that of the eighteenth century Enlightenment, which aimed to free humanity from superstition and tyranny in their many guises. The global conversation about sustainability, similarly, aims to free humankind from the superstition that we are separate and isolated from each other and nature and the tyranny arising from those who would exploit our ignorance of our deep interdependence." Sustainability then can be seen as one of the core values and goals of an emerging ecological worldview that weaves together recent developments in physics, ecology, psychology, and many other fields along with core elements of many of the world's great spiritual traditions (which support the importance of ethical action within an interdependent world). This cognitive outlook sees the world in terms of interdependence and coevolving complex systems, and supports values, ethics, and actions that likewise emphasize interdependence (Wheeler 2004). Environmental, equity, and spiritual or ethical perspectives on sustainability can all fit well with this worldview with the exception of the dominant economic worldview.

Sustainability and the Current Economics System

The prevailing market-based capitalist economic system is very good at regulating supply and demand, allocating resources, and providing incentives for entrepreneurship and innovation. It is also clearly good at generating wealth and a high level of material comfort for a minority (Wheeler 2004). However, the current capitalist economic system – both in theory and practice – has many flaws from a sustainability perspective, as listed below (Wheeler 2004; Chang 2012):

- Interest fees in capitalism cause equity disparities with the effect that the rich become richer and the poor become poorer. Less efficient small businesses cannot survive resulting in unemployment and large corporations are formed with concentration of wealth and monopoly of power, resulting in a new wealth and monumental increases in the material standard of living for a minority, but for the growing masses it brings deepening poverty and seemingly hopeless marginalization.

- Existence of interest and discount rates means that the future costs and benefits are less valuable than those in the present – a clear case of intergenerational inequity and injustice.
- Capitalist economics assumes continuous expansion in consumption of material goods and resources, a phenomenon that conflicts with the environmental notion of a finite planet with limited resources.
- Difficulty in placing a price on social and environmental goods (such as human health, equity, and environmental quality), with the problem of externalities, those enormous social and environmental impacts of production and consumption that are generally not incorporated into economic decision making.
- Demand and human "needs" are manipulated by corporations and advertising to increase the level of material consumption.
- Global trade distances consumers from the true costs of their economic decisions, making it difficult for them to understand these costs, while displacing social and environmental harm onto far-distant people and ecosystems.
- Economic power tends to subvert democratic institutions and shape cultures to meet its own ends, meaning that economic objectives constantly threaten to overwhelm environmental and equity goals (Perkins 2011).

These deficiencies of capitalist economics – and of economic analysis generally – undermine sustainability.

Unfortunately, sustainability is not currently the burning issue for most world leaders, whether politicians or business executives. Their immediate concern is to keep the global casino afloat. Issues of justice, equity or environmental degradation, or stories about unstoppable global ecological change are backstage to the everyday business of firing the boilers of the world economy (Adams and Jeanrenaud 2008). However, a number of alternative strategies have been proposed over the years to restructure capitalist economics to meet environmental, equity, and economic goals.

Alternative Economic Approaches to Promote Sustainability

Steady-State Economics: John Stuart Mill, a classical economist, first raised this issue in the mid-nineteenth century but the main advocate of this position since the 1970s has been US economist Herman Daly (Daly 2010). Under steady-state economics, human population and consumption are held at constant levels with a minimum throughput of resources, while qualitative, technological, and moral evolution occurs instead of quantitative increases in material production. The endless growth in material consumption, in other words, is brought to a halt. Daly has proposed progressive resource depletion quotas as a mechanism to push the economy toward this steady level of consumption. In this scenario, the government would set a maximum quantity of nonrenewable resources that could be consumed each year and then adjust the level downwards annually. From this point market mechanisms would do the rest. Prices would rise correspondingly, promoting

conservation and substitution of alternative materials. Some policy measures are discussed in (Daly 2010) to achieve a steady-state economy.

Environmental Economics: This approach first appeared in 1970s with the ambition to reconcile environmental and economic goals (Pearce et al. 1989). The focus of this approach is to include the externality costs of production and resource depletion into economic equations and a framework to reduce pollution. The approach does not fundamentally challenge any of the basic assumptions of capitalist economics.

Ecological Economics: It is distinguished from environmental economics, which is the mainstream economic analysis of the environment, by its treatment of the economy as a subsystem of the ecosystem and its emphasis upon preserving natural capital. The identity of ecological economics as a field has been described as fragile, with no generally accepted theoretical framework and a knowledge structure that is not clearly defined. According to ecological economist Malte Faber, ecological economics is defined by its focus on nature, justice, and time. Issues of intergenerational equity, irreversibility of environmental change, uncertainty of long-term outcomes, and sustainable development guide ecological economic analysis and valuation (Faber 2008). Ecological economists have questioned fundamental mainstream economic approaches such as cost-benefit analysis, and the separation of economic values from scientific research, contending that economics is unavoidably normative rather than positive (empirical) (Victor 2008).

Restorative Economics: In the book Natural Capitalism (Hawken et al. 1999), the authors argue for a restorative economics that uses the enormous power of markets to bring about environmental restoration rather than exploitation. Mechanisms to assist in this process might include higher prices for nonrenewable resources and waste disposal and green taxes to internalize the environmental externalities of productions (examples for such externalities are. . .). Problems such as pollution and social injustice may then be seen as failures to properly account for all forms of capital including human, manufactured, financial, and natural. This approach might be seen as an extended version of ecological economics, in which specific policy mechanisms are used to integrate economics into a broader framework including equity and the environment.

Local Self-Reliance/Alternative Currency Networks: There have been efforts toward local self-reliance since the 1960s. For example, India sought import substitution policies in the 1960s to promote locally produced goods and restricted imports from abroad (Wheeler 2004). These efforts were undermined by advocates of export-oriented countries and often did not work well because of the difficulty of producing a wide spectrum of goods locally in the face of international competition and political pressure. In the USA, there have been proponents of self-reliance who advocated local development strategies that promote locally owned businesses rather than large multinational companies (Morris 1983). More recently in his bestselling book *Deep Economy*, Bill McKibben has made a compelling case for moving beyond "growth" as the paramount economic ideal and pursuing prosperity in a more local direction, with regions producing more of their own food, generating more of their own energy, and even creating more of their own culture and

entertainment (McKibben 2007). He argues that attention should be redirected toward more traditional means of pursuing prosperity within communities, such as farmers' markets, community-supported agriculture farms, community-based radio stations, and mercantile cooperatives. Alternative currency networks such as Ithaca Hours have also attempted to promote local self-reliance through the dramatic strategy of introducing a new currency that can be used locally, with notes representing hours of labor instead of dollars (Wheeler 2004). Anyone receiving such a note as payment can then redeem it at other local businesses for other products or services. A similar suggestion is proposed by Thomas Greco, in his book *The End of Money and the Future of Civilization* (Greco 2009). The suggestion is about individuals, groups, and communities taking control of the monetary system at the grassroots level and creating an entirely new basis for trade than bank-owed debt. Greco discusses the large and growing worldwide "LETS" movement – Local Exchange Trading Systems, like the Ithaca Hours system in Ithaca, New York. The LET Systems that have proliferated in communities around the world use the credit clearing process, as do commercial trade exchanges. Credit clearing systems are, in essence, clearing houses – but their members are businesses and individuals instead of banks. Greco writes about national and international barter exchanges that involve over 400,000 businesses trading at an annual level of $10 billion.

Sustainability: Intergenerational Equity and Discounting

The emphasis on sustainability implies a greater concern for the future and for future generations. The past models of the development process have tended to assume that the "future will look after itself," whereas the sustainable development approach acknowledges that the ability of the future to do this can be seriously impaired by actions taken now. Discounting has been subject to numerous critiques due to its present bias, especially as the time period under consideration becomes longer. Because of climate change, the debate on discounting and discount rates has recently become vigorous.

Discounting

Discounting is a standard technique used for making intertemporal decisions in which the future is given less weight than the present; thus the process of converting monetary values backward in time to an equivalent amount is called discounting. Discounting procedures are fundamental to the theory and practice of cost-benefit analysis for evaluating proposed projects and public policies (Howarth 1996). When weighing the costs and benefits of large public projects, the selection of a discount rate on which to discount the future is a key consideration and often a source of controversy. A simple example demonstrates the general point. At a discount rate of 10 %, typically used for cost-benefit analysis, the value of $1 million 100 years from

now is the same as a mere $73 today. Thus it would apparently be justifiable to impose costs of up to $1 million on people 100 years from now in order to enjoy $73 worth of consumption today. By this logic, much resource depletion and environmental damage could be considered acceptable, and even optimal, according to a criterion of economic efficiency. It is because of this, the practice of discounting the future, a standard feature of the economic approach to inter-temporal decision making, is discussed critically in the following few sections here.

Discount Rate and its Effect on Project Selection

What is a social discount rate? The social discount rate is the rate at which society as a whole is willing to trade off present for future benefits (Atmospheric Administration 2007). When weighing the decision to undertake a project with long-term benefits versus one with short-term benefits and high capital cost versus low capital costs, the discount rate plays an extremely important role in determining the outcome of the analysis. Indeed, a number of project evaluation measures based on present worth criteria (e.g., net present value, discounted benefit-cost ratio, discounted payback period, return on investment) depend critically on the chosen discount rate.

All present worth criteria involves ranking alternatives according to their discounted profits and costs. For example, net present value (NPV) is calculated according to the difference between the present value of benefits and the present value of costs. Mathematically,

$$\text{Net present value} = \sum_{t=0}^{N} \frac{B_t - C_t}{(1+i)^t} \tag{1}$$

Where, B_t and C_t are benefits and costs streams in years $t = 0,1,..,N$ and i is the discount rate.

To illustrate the effect of the discount rate on project selection, let us assume that there are two projects, A and B, with annual costs and benefits streams as shown in Table 1. By using the streams of costs and benefits in Table 1 in Eq. 1, the net present value for each project is calculated for different discount rates. Figure 1 shows the effect, of changing the discount rate from 0 % onward, on the net present value of the two projects. It can be seen that Project A is more economical when the discount rate is below 8 %, whereas Project B has a better NPV beyond an 8 % discount rate. At a 20 % discount rate none of the projects, however, is economically feasible.

Rationale For and Against Discounting

Why is there a need to discount the future values? The usual and most common argument given is because a dollar received today is more valuable than one received in the future. There are generally three main reasons used for applying discounting.

Table 1 Cost and benefit streams

	Project A		Project B	
Year	Costs ($)	Benefits($)	Costs($)	Benefits($)
1	15,000	0	10,000	0
2	5,000	0	0	5,000
3	0	6,000	0	4,000
4	0	6,000	0	3,000
5	0	6,000	0	2,000
6	0	6,000	0	1,000
7	0	6,000	0	0
8 and beyond	0	0	0	0

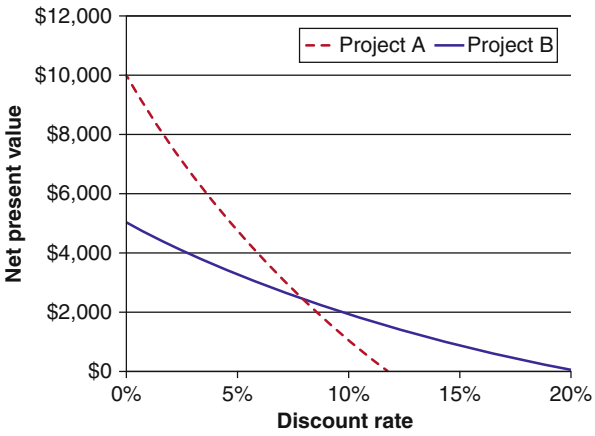

Fig. 1 Effect of discount rate on project selection

1. *Pure Time Preference*: humans are generally impatient and prefer instant gratification to waiting for long-term benefits.
2. *Opportunity Cost or Marginal Productivity of Capital*: money can be invested today, earning a positive rate of return.
3. *Risk*: there is uncertainty surrounding the ability to obtain promised future income. That is, there is the risk that a future benefit will never be realized.

All the three arguments are critically analyzed in the following paragraphs.

Pure Time Preference

Arguments in Favor: Empirical evidence suggests that humans value immediate or near-term resources at higher levels than those acquired in the distant future (Atmospheric Administration 2007). It is further argued that society, which consists of the sum of its living individuals, also prefers the present to the future. Furthermore, the dominant underlying value judgment of Western economic philosophy is that people's preference should count (Pearce et al. 1990). Hence it is difficult to argue with

the proposition that if people prefer the present over the future, then pure time preference indicates that discount rates are positive. Thus, discounting has been introduced to address the issues raised by the existence of this phenomenon, which is known as time preference.

Counterarguments: There have been arguments against the use of time preference to influence social discount rates. Firstly, that the individual time preference is not necessarily consistent with individual lifetime welfare maximization (Strotz 1956). There is a more general view shared by many economists that there seems to be no "ethical" justification for putting a utility discount into the social welfare function (Ramsey 1928; Pigou 1932). Secondly, the value judgment is improperly expressed. The argument is that it is tomorrow's satisfaction that matters, not today's assessment of tomorrow's satisfaction (Goodin 1986). Atleast this much is established in the literature.

But the question is whether any positive social discount rate used in a project that creates costs and benefits that are separated over a long period of time will discriminate the future generations and that is against the very spirit of sustainability; the definition of which says "meeting today's needs of development without compromising future generations' ability to develop."

Opportunity Cost or Marginal Productivity of Capital

Arguments in Favor: The opportunity cost of capital is the expected financial return foregone by investing in a project rather than in comparable financial securities. Theoretically, firms invest up to a point where the rate of return on marginal projects is equal to the interest rate. Consumer plans to save are brought to equality with producers' plans to invest and the ruling interest rate reflects both the time preference of consumers and the rate of return on capital (Kula 1997).

Counterarguments: There have been attempts to discredit the rationale of discounting based on the opportunity cost concept (Goodin 1986; Parfit 1983; Cowen and Parfit 1992). For example, Cowen and Parfit (1992) argue that the opportunity costs of consumption are determined by the marginal return to capital, which, in turn, depends on investment levels, which depend upon how high future benefits are weighted. If society as a whole valued all future periods equally, it would continue to invest until the rate of return on those investments (and, thus, the opportunity cost) was driven to zero. That opportunity costs are the result of valuing future outcomes less, not a reason for doing so. In other words, if the interest is removed from the society, the opportunity cost of capital will automatically fall to zero. But there is an argument against using a low or zero discount rate so that it will encourage more investment overall, and this will increase the demand for resources and environmental services. In the author's view, this argument is not valid as can be seen that in the case of national economic development, the investment portfolio would consist of all projects to be carried out within the capital budget constraint as determined by the availability of foreign exchange and local currency so the investment will only take place within the budget constraints and only those projects will be carried out that are economically justified and environmentally less harmful. As far as the private firms and businesses are concerned, the government can impose

resource taxes to discourage those projects that may harm the environment excessively.

On the contrary, it can be observed that high discount rates used in developing countries under the "prescription" of the World Bank and other lending agencies are a cause of much environmental degradation as the selection of such rates includes opting for short-term measures designed to satisfy immediate wants and at the expense of sustainable practices (Perkins 2011). In turn, poor prospects arising from environmental degradation actually assist in generating the poverty that causes high discount rates (poverty trap).

Risk

Arguments in Favor: Public projects involve uncertainty and risk. When public projects are undertaken there is a chance that future benefits will not be fully realized or realized at a higher level than estimated (there are also uncertainties associated with costs). The further out into the future these benefits are expected to be realized, the greater the risk that some unexpected event or factor will occur and diminish the value of the future benefit. This uncertainty is handled by adding a risk premium to the discount rate. For example, a 2 % "premium" attached to the officially recommended 5 % "test discount rate" has been used in the past in the UK (Treasury 1980).

Counterarguments: While adding risk premium to the discount rates it is assumed that the scale of the risk increases exponentially in time. There is no reason to believe that the risk factor takes this particular form and so the allowance for it through a single discount rate adjustment is invalid. This argument is widely accepted by economists (Dasgupta and Pearce 1972; Stiglitz 1986). Usually, the preferred method for dealing with uncertainty is to directly adjust benefits and costs (or to perform the analysis quantifying the uncertainty and explicitly considering it in the estimates of benefits and costs) and not to change the discount rate (Pearce et al. 1990; Atmospheric Administration 2007).

Controversy Over Social Discount Rates

As seen from the discussion above, debate already exists on the rationale for discounting but still a greater debate exists as to what the appropriate social discount rate should be. Various conceptual foundations have been proposed for the social discount rate, including the market rate of interest, the social opportunity cost of investment, and the consumption rate of interest (Guo et al. 2006). In an interest-based economy under ideal conditions, where there are no externalities, taxes or market imperfections of any description, these various rates will be identical and in equilibrium. However, no real economy satisfies these assumptions, so the debate exists on the conceptual foundations of the social discount rate. But there is a general consensus that the social discount rate should be based on the "social time preference rate" (STPR), which is the value society attaches to present consumption relative to future consumption. The Ramsey formula (Ramsey 1928) gives the expression for

the "socially efficient" discount rate to use for cost-benefit analysis (CBA). Letting i denote the social discount rate, the Ramsey formula gives the relation:

$$i = \rho + \mu g \tag{2}$$

where ρ is the "pure time preference rate" (PTPR), g is the growth rate of the economy, and μ is the income elasticity of marginal utility. The PTPR is the utility discount rate, which reflects society's preference for utility. The growth rate of per capita consumption, g, varies from country to country. The income elasticity of marginal utility, μ, measures the rate of change of the utility derived from an extra unit of income as society's income level increases. The literature suggests that this value is around unity (Guo et al. 2006). This implies that an extra dollar to a generation that has twice the consumption of the current one will only bring half as much utility to that generation. From a practical point of view, one only needs to specify values for the ρ, μ, and g to derive the discount rate. For instance, the UK government recommends a discount rate of 3.5 % for CBA (for use across all departments and all projects) based upon the following figures: $\rho = 1$ %, $\mu = 1$, and $g = 2.5$ % (Guo et al. 2006). The Stern Review (Stern 2007), another important UK government document on the economics of climate change, proposes a discount rate of 1.4 % using $\rho = 0.1$ %, $\mu = 1$, and $g = 1.3$ %. This low discount rate has already been criticized as being low in (Nordhaus 2007; Weitzman 2007).

It is clear from above that there is a lack of consensus on the value of the time preference rate and on the value of the growth rate of consumption. As stated in Jouini et al. (2010), there has never been consensus even among the experts on this subject. Different possible values for the parameters lead to very different values for the discount rate, which in turn lead to very different conclusions, as illustrated in Fig. 1 and shown by the following example. For instance, the present value of \$100 in 100 years' time is \$37 at a 1 % discount rate, \$5.2 at 3 %, 76¢ at 5 %, and only 0.007¢ at 10 %. This shows a small change in the discount rate has a large impact on policy outcomes, meaning that arguments about the "correct" number become weightier. Second, exponential discounting at even moderate discount rates implies that costs and benefits in the far future are almost irrelevant to decisions made today.

Moreover, this lack of consensus among experts about the right values for the growth rate and the time preference rate reveals another more fundamental problem, namely the fact that agents differ in their time preference rates as well as in their anticipation about the future of the economy. The Ramsey formula has been derived under the assumption of homogeneous agents (same time preference rate ρ and same anticipated growth rate of the economy g). This raises the question as to what extent the Ramsey formula remains valid once heterogeneity in time preference rates and heterogeneity in anticipation about the future are taken into account.

As far as the pure time preference is concerned estimates for individual rates are almost always positive for the simple reason that humans prefer good things to come earlier rather than later. Given the inevitability of death for individuals, a preference for benefits to accrue earlier rather than later is entirely sensible. However, at

individual level PTPR may reflect different levels of impatience. In a setting with long-lived agents that represent present and future generations, these rates reflect divergence of opinion about the importance granted to the welfare of future generations relative to the present. At the social level, the distinction is drawn and even it has been argued to use zero PTPR by philosophers and economists for decades. A positive PTPR involves placing a lower weight on the welfare of future generations, which is impartial and contrary to intergenerational equity. Cline (2004), for example, proposes to use a zero PTPR in evaluating climate change policies.

As far as the heterogeneity in anticipation about the future is concerned, agents (or experts) currently do not have a complete understanding of the determinants of long-term economic evolution. Long-term forecasts are subject to great errors, and forecasts for the next century or millennium are subject to potentially enormous divergence. The debate on the notion of sustainable growth is an illustration of the degree of possible divergence of opinion about the future of society. Some will argue that the effects of improvement in information technology have yet to be realized and the world faces a period of more rapid growth. On the other hand, those who emphasize the effects of natural resource scarcity will argue for lower growth rates in the future. Some even suggest a negative growth in per capita GDP in the future, due to the deterioration of the environment, population growth, and decreasing returns to scale (see for example (Wegner and Pascual 2011)). The debate among economists (and also among philosophers) on the notion of intergenerational equity, prompted by the challenges of climate change, biodiversity losses, and nuclear waste management, is an illustration of this possible divergence. These issues have spurred economists and policy makers to think more carefully about long-term intergenerational trade-offs. Some economists have advocated abandoning discounting altogether, proposing alternative methods to value the future (Wegner and Pascual 2011). Other economists conclude that although discounting (and cost-benefit analysis) is still very useful, it must be employed in a framework that guarantees intergenerational equity. A third view is that although conventional discounting is satisfactory for short-term decisions, it needs refinement before it can be legitimately used for long-term decisions (Cline 2004; Arrow et al. 2013). Yet another view is for zero discounting meaning that the future counts for as much as the present.

Heterogeneity in time preference rates and in anticipations about the future of the economy and issues coupled with intergenerational equity are critical features that render the debate on discounting and discount rates with virtually no consensus at all.

Cartesian Paradigm

Essentially all these approaches of finding an appropriate discount rate are based on reductionist philosophy. Reductionism is an approach to understanding the nature of complex things by reducing them to the interactions of their parts, or to simpler or

more fundamental things. Reductionist thinking and methods form the basis for many of the well-developed areas of modern science, including much of physics, chemistry, and cell biology. Classical mechanics in particular is seen as a reductionist framework. The atomic physicist Fritjof Capra has expressed this in a particularly lucid and eloquent way in his best-selling book entitled "*The turning point*," saying (Capra 1983):

> The triumph of Newtonian mechanics in the eighteenth and nineteenth centuries established physics as the prototype of a 'hard' science against which all other sciences were measured. . . . this tendency to model scientific concepts and theories after those of Newtonian physics has become a severe handicap in many fields, but more than anywhere else, perhaps, in the social sciences. (The social sciences deal with the social and cultural aspects of human behavior. They include the disciplines of economics, political science, sociology, social anthropology, and – in the view of many of its practitioners – history). The social sciences have been traditionally regarded as the 'softest' among the sciences, and social scientists have tried very hard to gain respectability by adopting the Cartesian paradigm (after Descartes, his mathematical methods, or his philosophy, especially with regard to its emphasis on logical analysis and its mechanistic interpretation of physical nature) and the methods of Newtonian physics. However, the Cartesian framework is often quite inappropriate for the phenomena they are describing, and consequently their models have become increasingly unrealistic. This is now especially apparent in economics. Present-day economics is characterized by the fragmentary and reductionist approach that typifies most social sciences. Economists generally fail to recognize that the economy is merely one aspect of the whole ecological and social fabric; a living system composed of human beings in continual interaction with one another and with their natural resources, most of which are, in turn, living organisms.

The author believes that with a fragmented worldview, there will never be a satisfactory solution to the problem of discounting which is essentially by nature a systemic issue (Malik 2011).

Systems Thinking and Discounting

McLaughlin and Davidson (1994) describe systems thinking as: "Seeing Whole Patterns. . . . It's time for us to make the next leap in consciousness to holistic thinking – to seeing whole patterns. In contrast with the prevailing linear paradigm, the New Paradigm sees everything as interconnected and interdependent . . . . Thus it is critical to keep the large picture – the whole system – in mind in order to create any kind of lasting solution and to avoid undue focus on effects, rather than dealing with causes that may be part of another system altogether.

Holistic thinking or ecological thinking – seeing how everything affects everything else – is finally beginning to influence other national policies, such as economics, where piecemeal solutions never work, since all sectors of a nation's economy are interrelated and interdependent with the world economy. The systems view sees the world in terms of relationships and integrated wholes whose properties cannot be reduced to those of smaller units."

It is challenging to find a clearer or more complete exposition of pure "Systems Thinking" than that contained in the above few lines. The depletion of the ozone layer or the increase in greenhouse gas emissions or the pollution of oceans is no more a concern of a single society presently living in any country. Similarly, society is no more a collection of living individuals whose preferences should count. The case of discounting based on "pure time preference" and "opportunity cost of capital" concepts should be investigated from the holistic viewpoint.

When the pure time preference argument is considered from a holistic viewpoint, a question can be asked: whose time preference is under consideration? Whose capital and wealth are linking whose time? Is it the present society living in USA or Canada or is it in some African country, for instance? And what about the generations to come? Who will take care of their time preferences? Therefore, from a holistic viewpoint, a pure time preference argument is ethically and morally indefensible in the selection of a discount rate.

Before analyzing the opportunity cost of the capital concept from a holistic viewpoint, first the practical implication of this concept for selecting discount rates in different countries is examined. Since the opportunity cost is linked to the prevailing conditions within a given country, the discount rate tends to vary, often significantly, from country to country. For developing countries, the discount rate used is much higher than for industrialized countries to reflect the scarcity of capital and the much larger profitability of new investment projects that compete for limited financial resources. Since there are different discount rates for different countries, a project considered "good" in the USA may not be "economically justified" in India. For example, a large-scale coal-fired power plant that generates millions of tons of greenhouse gases in its lifetime may be economically justified in one country but may not be a good project in another country because of the use of different discount rates for selection of the project. By considering the holistic approach, it becomes clear that the harm to the environment is the same whether such a project is carried out in the USA or India. So in this regard the discount rate should not be linked to opportunity costs of capital in a country but in the sustainability context to the environment.

It is clear from above that both the time preference and the opportunity cost concepts cannot override systems thinking. Both these concepts are also used as tools to support the institution of interest (Ahmad 1991), and the practice of discounting is just one of its obnoxious fruits. The practice of treating interest as an item of cost and ascribing it to the productivity of capital is based on the particular institutional setup of the capitalist society. In fact, it is the institution of interest that makes it possible for capitalist economists to ascribe a positive return to capital that is its value productivity, and not the other way round (Siddiqi 2001). The next section, using the hierarchical systems approach, emphasizes the need to change the present economic system so that renewable natural capital keeps functioning and maintaining itself and the global ecosystem may survive.

Renewal Cycle in Systems Theory and Capitalist Economic System

According to systems theory, the systems are not static, but evolve (more specifically economic, ecological, and social systems) as a combination of dynamically occurring renewals in their components (Voinov and Farley 2007). The renewal cycle has been observed in many natural and man-made systems. The renewal cycle assumes that a system goes through a series of stages, starting from growth, followed by conservation, then release or collapse and finally renewal. The phase of release does not necessarily mean loss or extinction of all components or species that make the system, but it implies that the systemic function that they perform is modified, at least temporarily. The released components may recombine to perform again as a similar system but the system itself will be different (Holling 2001). Examples of release phase can be observed in man-made and natural systems, e.g., bankruptcy of a company or forest fires. In bankruptcy of a company when employees are laid off, and assets are sold. It is the release phase and is the end of the company. It comes when the business as a socioeconomic system is no longer sustainable and can no longer extend the conservation stage. The components (human and material resources) may recombine in the form of another company (renewal), but that will be a different system. Similarly forest fires release organic material and nutrients thus ending a system. Forests may grow afterward in the same place, but these will be different forests: they may have a different spatial and species organization.

Any effort to sustain a system beyond its natural conservation phase, to avoid the release phase, has harmful effects on its next higher hierarchical system of which it is a subsystem. For example, efforts to sustain failing industries and even sectors would prevent capital from being reallocated to other or more dynamic ones in their growth stages. Inefficient enterprises if kept afloat by huge subsidies keeping human and material resources unavailable for recombination decreases the overall adaptive capacity of the socioeconomic system by making it vulnerable to disturbances that lead to its collapse. The Soviet Union is a societal example of accumulated rigidities that became vulnerable to societal discontentment and revolt against it, which ultimately resulted in a sudden collapse. Similarly in studying managed ecosystems, it has been observed that any attempt to manage a target variable for sustained production of food and fiber has resulted in less resilient and more vulnerable ecosystems (Holling 1996). The collapse in these cases is usually observed at the next higher hierarchical level, i.e., over landscapes.

The economic system itself is a managed sub-ecosystem of the sustaining and continuing global ecosystem (Voinov and Farley 2007). Human society is currently engaged in a global effort to sustain the growth phase of this subsystem. The integral feature of the economic system obsessed with growth and expansion is technological progress in an attempt to increase productivity.

The combined effect of technological and economic growth is that it has created an environment in which life has become physically and mentally unhealthy. Polluted air, irritating noise, traffic congestion, chemical contaminants, radiation

hazards, and many other sources of physical and psychological stress have become part of almost everyone's life. Obsessed with expansion, increasing profits, and raising productivity, the industrialized world has developed societies of competitive consumers who have been induced to buy, use, and throw away ever increasing quantities of products of marginal utility (Capra 1983). For example, in this consumption cycle, the total material flow still remaining in products or use 6 months after their sale in North America is just one percent. In other words, 99 % of the stuff that is harvested, mined, processed, transported and that runs through this system is trashed within 6 months (Leonard 2010). (This statement is not saying that 99 % of the stuff being bought is trashed. Think beyond one's household to the upstream waste created in the extraction, production, packaging, transportation, and selling of all the stuff he/she bought. For example, the No Dirty Gold campaign explains that there is nearly two million tons of mining waste for every 1 t of gold produced; that translates into about 20 t of mine waste created to make one gold wedding ring.) Excessive consumption and strong emphasis on high technology not only create massive quantities of waste but also require huge amounts of energy. Most of the world energy comes from nonrenewable fossil fuels that are declining with the passage of time resulting in an increase in energy prices. In their attempt to maintain, and even increase, their current levels of production, the world's industrialized countries have ferociously exploited the available resources of fossil fuels. Some industrialized countries have even used their military might by either directly to procure world natural resources or installing or supporting undemocratic regimes in some countries to dictate policies that suit their own economic and strategic objectives (Perkins 2011). The repercussions of these actions have created restlessness in the local populations and deep resentment against those industrialized countries involved in exploiting their resources directly or indirectly.

Economic growth conceived in terms of higher production not only ignores the ecological and social costs of development such as pollution and depletion of nonrenewable resources but also results in stresses and strains on individuals and families (Siddiqi 2001). The capitalist concept of development also ignores the fair distribution of wealth. How can the development of human society be conceived of in terms of amassing of wealth only, irrespective of whether this wealth is available to the bulk of its members or not. The enormous expansion of economic output throughout the industrial era has provided material benefits and more comfortable lives for a minority. Yet billions of others have been excluded and exploited in the process (Greco 2009). This distributive injustice condemns most of the world population to live in debt. The effect of debt is like a blood transfusion from sick to healthy. Each person born in Latin America owes already $1,600 in foreign debt; each child born in Sub-Saharan Africa carries the burden of a $336 debt interest, for something that their ancestors have long ago paid-off. In 1980, the debt of Southern countries amounted to $567 billion; since then, they have paid $3,450 billion in interests and write-offs, six times the original amount. Despite this, this debt had quadrupled by the year 2000 reaching $2,070 billion (http://www.henciclopedia.org.uy/autores/Laguiadelmundo/Usury.htm. Accessed 14 Dec 2014). The huge debt in under-developed and disadvantaged countries has made a poverty trap. For example,

in Pakistan and Tunisia, International Monetary Fund (IMF) bailout loans are being used entirely to repay old debts – in Pakistan's case, to pay previous IMF loans. In Portugal, the IMF and EU loans are simply paying off the reckless banks (Jubilee Debt Campaign 2013). There is more than abundant evidence that the repayment of loans of these poor countries is achieved at the cost of consumption of natural capital and the degradation of the environment (Shah 2010a; Perkins 2011; Jubilee Debt Campaign 2013).

Thus the present setup of the economic system is maintained only at the cost of higher hierarchical levels. Simply sustaining the present economic system will certainly threaten the global ecosystems. Collapse of these higher hierarchical levels is something that the human species, and indeed, many, many other species, cannot afford. In order to save the super hierarchical system (humanity as a whole and biosphere as a whole), the capitalist economic system compounded and nurtured by a system of interest must undergo the release phase to allow renewal through the emergence of a fair and just economic system so that humanity and global ecosystem may persist.

High Interest Rate: The Engine of Destruction and the Root Cause of Unsustainability

High interest rate causes injustice and major financial inequality in the society. It breeds greed and is the opposite of charity. The practice of high interest rates – lending money and accumulating financial gains on a loan – can be traced back 4,000 years (http://www.henciclopedia.org.uy/autores/Laguiadelmundo/Usury.htm. Accessed 14 Dec 2014). But it has always been despised, condemned, restricted, or banned by moral, ethical, legal, or religious entities. High interest rates in the modern banking system are made possible through the current paper money system in circulation. Money as has been claimed is not only a medium of exchange but a means of control. This is not the place to trace the development of all the changes which occurred in forming the present banking system but suffice it to say that the power has become rapidly concentrated into the hands of fewer and fewer financiers who control political affairs from behind the scenes, holding no social responsibility whatsoever for the millions of human beings who in ever greater numbers fall under their control (Bewley 2014a). One of the great studies of this process is described in *Religion and the Rise of Capitalism* by the English historian R.H. Tawney (Tawney 2000). Some brief history of formation of banking system can also be traced in (Greco 2009; Brown 2007).

The monetary and financial regimes that are spread around the world have the legal privilege to create virtually the entire nation's money by making a few bookkeeping entries and lending it out at interest (debt-money system). The imposition of interest on the debt by which the money is created causes debt to grow exponentially with the passage of time, if not paid back in timely fashion. Exponential growth can be observed by a simple example. Imagine a poor country has borrowed $1 at 10 % interest rate and is not able to pay it back, then after 50 years

the amount would grow to $117.4, after 100 years it would be $113,780.6 and after 200 years it would be $189,905,276, i.e., almost 190 million dollars. This is a ridiculous amount but true and that is the magic of compound interest.

Professor Thomas Greco in his book *The End of Money and the Future of Civilization* (Greco 2009) summarizes the money problem as: "the way in which money is created by the banking system today causes a debt imperative, which derives a growth imperative – this forces destructive competition for the available supply of money, which is never sufficient to enable all debtors to pay what they owe." As the debt grows in time, the money needed to pay this debt does not. Additional money comes into circulation only as the banks make additional loans. He describes three primary ways in which bank-created debt-money malfunctions. The first is artificial scarcity: there is never enough money to allow every debtor to pay what is owed to the banks, so someone must fail. Thus, debt continually mounts, and businesses and individuals are forced to compete for markets and scarce money in a futile attempt to avoid defaulting on their debts. Businesses must take measures to enhance revenues by increasing production, sales, and profits and reduce costs. This not only causes gross inequities and social strife, but it also promotes the destruction of the planet because the corporations do not internalize the externalities to cut their cost of production. A major reason corporations merge and consolidate and increase in size is so that they can gain synergies and also exercise both greater political influence and greater market dominance. Of the 100 largest economies in the world, 53 are now global corporations, larger than countries like Sweden and Norway, South Africa and Mexico, Belgium and Egypt, etc. The 200 largest global corporations now control nearly 30 % of global economic activity, but they employ only one half of 1 % of the global workforce, as monopoly and efficiencies of scale reduce employment and keep salaries down (Mander 2003). Capital wealth becomes even more concentrated in corporate conglomerates that must seek higher returns on their investments. They are driven to expand their markets and dominate economies, using support of governments to apply military power both overtly and covertly to ensure the continued flow of low-priced raw materials, the availability of low-cost labor, and access to markets in which to sell their products (Perkins 2011; Greco 2009).

The second factor of malfunction is the requirement that interest be paid, which causes a net transfer of wealth from the debtor class to the moneyed class or from producers to nonproducers. Those who must earn their livelihood by selling their labor and talents in the market are kept at a disadvantage relative to those who live off returns from their capital.

The third aspect of malfunction is that money created as bank credit is misallocated at its source. Much of it goes to finance government deficit spending for weapons, military interventions, and transfer payments to corporate clients. This money added to the existing supply enters the banking system where it becomes additional "reserves" that enable the banks collectively to lend many times that amount of money into circulation thus causing creeping inflation. This is the cruelest form of taxation as it eats away at the assets or wealth of all, particularly the moneyed class.

This entire system favors authoritarian governments, increasing concentrations of power and wealth, short-range planning, and the production of short-lived disposable junk over durable consumer products (Greco 2009). How long this system will continue is just a matter of time.

There is no person on the earth who does not now live and die in debt whether they know it or not and an ever increasing number know it only too well as their personal debts to banks and credit agencies mount and mount, causing terrible anxiety and stress and not infrequently leading to crime and sometimes suicide. The situation of national debt is notorious. Even the wealthiest countries in terms of natural resources are hopelessly in debt to supranational finance. For example by 2006, combined personal, corporate, and federal debt in the United States had reached a staggering 44 trillion dollars – four times the collective national income, or $147,312 for every man, woman and child in the country (Brown 2007). The United States is legally bankrupt, defined conventionally as being unable to pay one's debts, being insolvent, or having liabilities in excess of a reasonable market value of assets held. Local, state, and national governments are all so heavily in debt that they have been forced to sell off public assets to satisfy creditors (Brown 2007). The total national income of many poorer countries does not even cover the interest payments on the money they owe, much of which has been borrowed to finance vast megaprojects whose incalculable environmental damage to the earth's increasingly fragile ecosystem is becoming more and more evident day by day. This is just the tip of the iceberg of the detrimental effects of the world financial system. And it is all so that an infinitesimal percentage of the world's population, who are virtually unknown but who know all too well how to manipulate the situation, can skim billions off the top of the money mountain, and wield wealth and power to an extent never conceived of before in the whole of human history (Bewley 2014a).

One element in the elite plan is to further reduce the amount of control that national governments, particularly in the developing world, have over their economies and finances (Greco 2009). When a country cannot meet its debt obligation, the International Monetary Fund (IMF) imposes "structural adjustment" programs that favor western banks, wrest away control of national resources, and create hardships for local population. As detailed further below, the IMF and World Bank provide financial assistance to countries seeking it, but apply conditions such as (Shah 2010b):

- "Liberalization" of the economy and resource extraction/export-oriented open markets as part of their structural adjustment
- Minimizing the state role
- Encouraging privatization as well as reducing protection of domestic industries
- Currency devaluation, increased interest rates, "flexibility" of the labor market, and the elimination of subsidies such as food subsidies (Perkins 2004, 2011)
- Reduce or remove various regulations and standards to attract foreign investors

The impact of these preconditions on poorer countries can be devastating. This process leads to further misery for the developing nations and keeps them dependent

on developed nations. Poor countries must export more in order to raise enough money to pay off their debts in a timely manner but because there are so many nations being asked or forced into the global market place and told to concentrate on similar cash crops and commodities as others, the situation becomes like a large-scale price war. Then, the resources from the poorer regions become even cheaper, which favors consumers in the West. Governments of poor countries then need to increase exports just to keep their currencies stable (which may not be sustainable, either) and earn foreign exchange with which to help pay off debts. They must spend less, reduce consumption, remove or decrease financial regulations, and so on. Over time then the value of labor decreases, capital flows become more volatile, a spiraling race to the bottom then begins, which generates social unrest, which in turn leads to "IMF riots" and protests around the world (Shah 2010b).

These nations are then told to peg their currencies to the dollar. But keeping the exchange rate stable is costly due to measures such as increased interest rates. Investors obviously concerned about their assets and interests can then pull out very easily if things get tough, and in the worst cases, capital flight can lead to economic collapse, such as it is seen in the Asian/global financial crises of 1997/98/99, or in Mexico, Brazil, and many other places. When IMF donors keep the exchange rates in their favor, it often means that the poor nations remain poor or get even poorer (Shah 2010b).

While describing his job in World Bank of evaluating projects John Perkins writes in *Confessions of an Economic Hit Man* (Perkins 2004):

> The unspoken aspect of every one of these projects was that they were intended to create large profits for the contractors and to make a handful of wealthy and influential families in the receiving countries very happy, while assuring the long-term financial dependence and therefore the political loyalty of governments around the world. The larger the loan, the better. The fact that the debt burden placed on a country would deprive its poorest citizens of health, education, and other social services for decades to come was not taken into consideration.

Shaykh Abdalqadir As-Sufi, graphically sums up the present situation in his book, *Technique of the Coup de Banque* (As-Sufi 2000):

> We are tyrannized, enslaved, and indebted to entirely unelected elites whose names we do not even know. With hereditary titles abolished and with hereditary wealth made impossible for the masses through powerful taxation, the case of this elite remains an anomaly. Their wealth and their lands spiral up into almost incalculable statistics, beyond the dreams of Alexander. They have no racial loyalty. They have no class loyalty. They certainly have no national loyalty. Upholding humanism, it could be said that they have no human loyalty. Insisting on their compassion they uphold the Rights of Man, sure in the certainty that the upholding of that empty rhetoric will distract you from ever attempting to refrain from their monetary system and live without banking. They are an oligarchy. This is not to say they are oligarchic in the platonic sense, for it is in the nature of the modern social nexus that there is a dysfunction between them and the human species rather than that they are at the summit of human society as in the primitive model. All the crimes of all the criminals in the world added together do not amount to the enormity of this crime that they daily commit through their continued application of the [. . .] system. The pollution of the ocean is their

> achievement. The poisoning of the earth is the result of their programs. The toxic air of the world's megacities is the direct result of their existence. The millions of dead caused by the sporadic uprising across the globe of the poor driven from their land, who in abject misery turn on their neighbors, the world's poor scavenging on rubbish tips are to them an unfortunate side-effect of their monetary policies.

The current debt situation, with the major role that interest is playing in it, is potentially very devastating for the world as a whole. In 2000, the CIA made a prediction which reads more like a statement of the bleeding obvious (National Intelligence Council 2000):

> The rising tide of the global economy will create many economic winners, but it will not lift all boats. . . ...[It will] spawn conflicts at home and abroad ensuring an ever-wider gap between regional winners and losers than exists today. . . ...[Globalization's] evolution will be rocky, marked by chronic financial volatility and a widening economic divide. . . ... Regions, countries and groups feeling left behind will face deepening economic stagnation, political instability and cultural alienation. They will foster political, ethnic, ideological and religious extremism, along with the violence that often accompanies it.

So much for sustainability! The money in anyone's pocket is not the medium of exchange it pretends to be; it is precisely the financial instrument which has enabled the present situation to come about and which allow it to continue to proliferate. Societies' willing participation in the process is what keeps it going. Before discussing the alternative choice to out of control capitalism it would be worthwhile to ponder whether technology has the ability to solve the environmental problems without fundamentally changing or challenging the present economic setup.

Sustainability and Technology

World models have shown that if the world continues on its present course, i.e., business-as-usual, then disaster is imminent (Meadows et al. 1972, 1992; Bardi 2011). Although a general consciousness is emerging especially in the industrialized world that a lifestyle of consumption and squandering is part of the problem. Nevertheless, generally speaking, the belief in science remains that "science can save the future," that it has the ability to provide humanity with the knowledge to understand and manage earth's natural resources and that the effects of new technologies can be managed by doing proper cost/benefit analysis to maximize the benefits and minimize the costs that environmental damage from human activity can be minimized by doing environmental assessments, etc. The reason for this faith in science can be seen in the dazzling effusion of technological expertise which is put forward as the justification of the scientific method and as proof that present society is more advanced than any which has preceded it. The manifestations of technology tend to be viewed by people with awe, i.e., the airplane, the computer, the heart-transplant, the television, the neutron bomb, the credit card, the internet, the social media, and so on and so on. Optimistic materialism remains a powerful force in the

western way of thinking. People believe that technology is, on balance, beneficial. People define happiness in terms of their ability to accumulate new gadgets; the business community, anxious to sell merchandise, spares no expense in promoting a gleeful consumerism. Thus on the whole the belief in science and technology remains that it can solve the environmental problems and address sustainability issues.

It should be cautioned, however, that there are two problems with the way the technology is employed which limits its ability to attend to the issue of sustainability in a satisfactory manner. First, the essence of the technological process which has produced all these offspring is that it views the rest of existence as a standing reserve, as something that is there for no other reason than to be exploited for its own ends (Bewley 2014b). Everything else is seen as something to be brought under control and used. Nothing is seen as existing in its own right but only as a resource to be used up. The trouble is that man himself has become ensnared in the process (Bewley 2014b). Humans are seen as a workforce, as consumers, as a market, as human potential, etc.. People are no longer respected in their own right. The terrible end-result is that individuals then come to see themselves as a standing reserve. The second problem with technology is that it is difficult to anticipate all of the environmental consequences of technologies, however, beneficial they may seem; for example, consider the unanticipated scourge of DDT, plastics, and even cars. Who could foresee the real costs of even the most apparently benign innovations and inventions, such as antibiotics and television? For example, a journal article (Baker and George 2010) discussing the role of television in household debt concludes ". . . the empirical results suggest that greater access to television is associated with a greater tendency to maintain household debt and to borrow for durable goods, especially automobiles. Results also suggest that greater access to television is associated with higher levels of debt for durable goods. . ." This is just one side-effect of apparently benign technology.

Having understood the technological imperative and human limitations to understanding the environmental consequences of technology, it should be emphasized, however, that technology should not be rejected out of hand. One of the characteristics of technology is that once it is there, it is almost impossible to do without it; it makes itself indispensable. There is, therefore, a need for more research on cleaner fuels, alternative technologies that are more environmentally friendly and in harmony with the environment, and more public awareness. Those technologies whose environmental consequences are not fully known should not be adopted or adopted with caution with continued review of environmental assessment because there is a danger that instead of solving the problem of environment the future is mortgaged by opting for the immediate benefits of new inventions.

It should be reemphasized that science has been limited by its ecological short-sightedness and corporate greed. The question to be asked is if science is so full of promise to improve the welfare of society then why is the world beset with species extinction, poverty and starvation, atmospheric degradation, global pollution, desertification and deforestation? It may be remembered that the solutions to the

environmental crisis will not come from science and technology but will be political and socioeconomic.

Future Directions: Toward a Fair and Just Economic System

To summarize what has been said earlier. Neither "safe and benign" technology nor environmental regulations nor any amount of recycling alone can solve the sustainability problem as long as the present world economic system with its philosophy of economic growth compounded and nurtured by interest which creates greed and gross injustice is in place. The focus on increasing wealth has driven the planet's ecological system to the brink of failure, without making people happier (McKibben 2007). If Chinese ate the way Americans do they would use two-thirds of the world's grain harvest; if they drove as many cars as Americans do, they would use all the oil in the world currently produces plus 15 million extra barrels a day (Brown 2006). The economic model of fossil-fuel based, auto-centered, throwaway economy is not going to work in the medium and long term. Humanity has to dispel many old conceptions and beliefs such as: economic rationality; market distributes benefits; wealth and happiness are connected; economic ends justify military means; the cult of efficiency; technology is the answer; new is always better; jingoistic allegiance to one's country whether it is right or wrong; and future will look after itself (Laszlo 2006). People need to live more simply and not contributing more to the ecological and social worldwide catastrophe. In the short-term, local self-reliance and alternative currency networks mentioned in section "Alternative Economic Approaches to Promote Sustainability" seems to be part of the answer to limit the harmful effects of the current doing. However, the struggle should continue to challenge the system in place. Only a fair and just economic system can guarantee sustainability. ***Justice is the key to the future of sustainability.*** Humanity must devise an economic system:

- That takes on a holistic view and does not exploit the weak and oppressed;
- In which high interest rates are forbidden which focuses on distribution of wealth instead of growth;
- In which the distinction is drawn between public property and private property. The basic necessities of life especially water, air, and energy should be under public control (Owning a deep mine of minerals or petroleum fields is not the same as owning a house or a piece of land; neither is owning petro-chemical plants or various large energy generating units or a weapons manufacturing facility the same as owning a garment factory or a candy shop; and neither is owning a railway network similar to owning a car. On the recent Deepwater Horizon oil spill in the Gulf of Mexico, Costanza et al. in Solution Journal commented (Costanza et al. 2010): "The continuing oil spill from the Deepwater Horizon is causing enormous economic and ecological damage. Estimates of the size and duration continue to escalate, but it is now the largest in U.S. history and clearly among the largest oil spills on record. *One major lesson is that our natural*

capital assets and other public goods are far too valuable to continue to put them at such high risk from private interests." In (Wheeler 2004) the author writes: "*Developers, corporations, and ordinary citizens have maximized private benefit at the expense of shared public goods – including the quality of our cities and towns, not to mention the environment.* Individualism has triumphed over collective well-being. In a conservative era dominated by free market philosophies, there has been little political interest in recognizing that someone, usually the public sector, must stand up for the common good. Government, which exists in large part to protect and advocate for public interests, is routinely attacked by those who would like to privatize everything. Individualistic attitudes have been institutionalized through law, government policies, corporate practice, advertising, the media, and many other structural elements of our society. These structural forces also reinforce individualistic, consumption-oriented values, types of behavior, and modes of thought within individuals."); [emphasis added]

- In which big corporations do not exploit the world resources in poor and disadvantaged countries;
- Based on mutual welfare, trust and partnership in which both the supplier of capital and the user of capital become partners in profit and loss (equity financing instead of debt financing);
- In which business dealings are fair, free from speculations and not tied up to any particular currency. Any crisis in the dollar badly affects the currencies of other countries. Also paper currency is a form of exploitation and is part and parcel of present economic structure. To avoid such fiscal crises and be fair and just to all bimetallic coins of gold and silver medium of exchange should be adopted which have their own intrinsic value (Maloney 2008);
- In which businesses that exploit society in harmful ways should be banned.

What is clear from this is that that there is a need for a paradigm shift – a complete change in perspective. Awareness of sustainability has opened up discussion on many fronts and that necessarily includes economical and financial system in place. There is a need to engage meaningfully in understanding the harmful effects of current economic and financial system on the environment and indeed on the sustainability of the planet. While the full implications of the quantum change in perspective have yet to filter down to the level of general consciousness the forest has been cleared and the path is open. No doubt there may be reluctance due to powerful vested interests related to both cognitive belief systems and to the institutional position. But with courage and commitment the present growth-based economic system of exploitation can be challenged.

Remember by introducing a fair and just economic system in society the world is (Malik 2012):

- Reducing the environmental risk
- Reducing poverty in the developing world
- Reducing the gap between rich and poor
- Reducing the unemployment problem

- Reducing the problem of inflation
- Promoting a culture of charity and sacrifice and condemning the culture of greed and selfishness
- Doing justice to nature
- Increasing the economic efficiency

Safeguarding the interest of future generations; and so on.

References

Adams W, Jeanrenaud S (2008) Transition to sustainability: towards a humane and diverse world. IUCN, The World Conservation Union, Gland

Ahmad S (1991) Towards interest-free banking. Institute of Islamic Culture, Lahore

Arrow K et al (2013) Determining benefits and costs for future generations. Science 341:349–350

As-Sufi S (2000) Technique of the coup de banque. Kutubia Mayurqa, Palma

National Oceanic and Atmospheric Administration (2007) Discounting and time preference. NOAA Coastal Services Center, Charleston. http://coast.noaa.gov/archived/coastal/economics/discounting.htm. Accessed 11 Dec 2014

Baker M, George L (2010) The role of television in household debt: evidence from the 1950s. BE J Econ Anal Policy 10 (online). http://www.degruyter.com/view/j/bejeap.2010.10.1/bejeap.2010.10.1.2393/bejeap.2010.10.1.2393.xml?rskey=ow8ghL&result=1. Accessed 14 Dec 2014

Bardi U (2011) The limits to growth revisited. Springer, New York

Bardi U (2013) The great suffocation – will we have enough oxygen to breathe? http://cassandralegacy.blogspot.com/2013/12/the-great-suffocation-will-we-have.html. Accessed 29 Jan 2015

Bewley A (2014a) Islam and the real money. http://bewley.virtualave.net/index.html. Accessed 14 Dec 2014

Bewley A (2014b) The decline and fall of the human being. http://bewley.virtualave.net/index.html. Accessed 14 Dec 2014

Blignaut J, Aronson J (2008) Getting serious about biodiversity. Conserv Lett 1:12–17

Brown L (2006) China forcing world to rethink its economic future. Earth Policy News – 5 Jan. Earth Policy Institute

Brown E (2007) Web of debt – the shocking truth about our money system – the sleight of hand that has trapped us in debt and how can we break free. Third Millennium Press, Baton Rouge

Capra F (1983) The turning point – science, society and the rising culture. Bantam Books, New York

Chang H (2012) 23 things they don't tell you about capitalism. Bloomsbury Press, New York

Cline W (2004) Meeting the challenge of global warming. In: Lomborg B (ed) Global crises, global solutions. Cambridge University Press, Cambridge

Costanza R, Batker D, Day J et al (2010) The perfect spill: solutions for averting the next deepwater horizon. Solutions. Available at: http://www.thesolutionsjournal.com/node/629. Accessed on 14 Dec 2014

Cowen T, Parfit D (1992) Against the social discount rate. In: Laslett P, Fishkin J (eds) Justice between age groups and generations. Yale University Press, New Haven

Czech B (2000) Shoveling fuel for a runaway train – errant economists, shameful spenders, and a plan to stop them all. University of California Press, Berkeley

Daly H (2010) From a failed-growth economy to a steady-state economy. Solutions. http://www.thesolutionsjournal.com/node/556. Accessed 14 Dec 2014

Danilov-Danil'yan V, Losev K, Reyf I (2009) Sustainable development and the limitation of growth – future prospects for world civilization. Springer/Praxis, Berlin

Dasgupta A, Pearce D (1972) Cost-benefit analysis: theory and practice. Macmillan, London
Faber M (2008) How to be an ecological economist. Ecol Econ 66:1–7
Gasparatos A, El-Haram M, Horner M (2008) A critical review of reductionist approaches for assessing the progress towards sustainability. Environ Impact Assess Rev 28:286–311
Goodin R (1986) Protecting the vulnerable. University of Chicago Press, Chicago
Greco T (2009) The end of money and the future of civilization. Chelsea Green Publishing, Vermont
Guo J, Hepburn C, Tol R, Anthoff D (2006) Discounting and the social cost of carbon: a closer look at uncertainty. Environ Sci Policy 9:205–216
Hawken P, Lovins A, Lovins L (1999) Natural capitalism: creating the next industrial revolution. Little Brown, Boston
Holling C (1996) What barriers? What bridges? In: Gunderson L, Holling C, Light S (eds) Barriers and bridges to the renewal of ecosystems and institutions. Columbia University Press, New York
Holling C (2001) Understanding the complexity of economic, ecological, and social systems. Ecosystems 4:390–405
Howarth R (1996) Discount rates and sustainable development. Ecol Model 92:263–270
Human Development Report (2014) Sustaining human progress: reducing vulnerabilities and building resilience. http://hdr.undp.org/sites/default/files/hdr14-report-en-1.pdf. Accessed 30 Jan 2015
Jouini E, Marin J, Napp C (2010) Discounting and divergence of opinion. J Econ Theory 145:830–859
Jubilee Debt Campaign (2013) Life and debt: global studies of debt and resistance. http://jubileedebt.org.uk/wp-content/uploads/2013/10/Life-and-debt_Final-version_10.13.pdf. Accessed 14 Dec 2014
Kula E (1997) Time discounting and future generations: the harmful effects of an untrue economic theory. Quorum Books, London
Laszlo E (2006) The chaos point – the world at the crossroads. Hamptons Road Publishing, Charlottesville
Leonard A (2010) Story of stuff. www.storyofstuff.com. Accessed 14 Dec 2014
Malik A (2011) Justice to nature and to the disadvantaged. World Futures 67:106–114
Malik A (2012) Sustainable development: ecology and economic growth. In: Chen W, Seiner J, Suzuki T, Lackner M (eds) Handbook of climate change mitigation. Springer, New York
Maloney M (2008) Guide to investing in gold and silver: protect your financial future. Business Plus, New York
Mander J (2003) Alternatives to globalization: a better world is possible. Speech at World Affairs Council on 4/02/03, San Francisco. Available at: http://www.ifg.org/jerrywac.htm
Marten G (2001) Human ecology – basic concepts for sustainable development. Earthscan Publication, London
McKibben B (2007) Deep economy: the wealth of communities and the durable future. Henry Holt and Company LLC, New York
McLaughlin C, Davidson G (1994) Spiritual politics: changing the world from the inside out. Random House, New York
Meadows D, Meadows D, Randers J, Behrens W (1972) The limits to growth. Universe Books, New York
Meadows D, Meadows D, Randers J (1992) Beyond the limits: confronting global collapse, envisioning a sustainable future. Chelsea Green, Post Mills
Miller G Jr, Spoolman S (2009) Living in the environment: concepts, connections, and solutions. Cengage Learning, Belmont
Milne S (2001) What powerful states call terrorism may be an inevitable response to injustice, The guardian. http://www.theguardian.com/world/2001/oct/25/afghanistan.terrorism9. Accessed 29 Jan 2015
Morris D (1983) Self-reliant cities: energy and the transformation of urban America. Sierra Club, San Francisco
National Intelligence Council (2000) Global trends 2015: a dialogue about the future with nongovernment experts. Central Intelligence Agency, Washington, DC

Nordhaus W (2007) Critical assumptions in the Stern Review on climate change. Science 317:202–210
Orr D (2010) The hour glass. Solutions. http://www.thesolutionsjournal.com/node/577. Accessed 14 Dec 2014
Parfit D (1983) Energy policy and the further future: the social discount rate. In: MacLean D, Brown P (eds) Energy and the future. Rowman and Littlefield, Totowa
Pearce D, Barbier E, Markandya A (1989) Blueprint for a green economy. Earthscan, London
Pearce D, Barbier E, Makandya A (1990) Sustainable development: economics and environment in the third world. Earthscan Publications, London
Perkins J (2004) Confessions of an economic hit man. Berrett-Koehler Publishers, San Francisco
Perkins J (2011) Hoodwinked: an economic hit man reveals why the global economy imploded – and how to fix it. Crown Publishing, New York
Pigou A (1932) The economics of welfare. Macmillan, London
Ramsey F (1928) A mathematical theory of saving. Econ J 38:543–559
Shah A (2010a) Poverty and the environment. Global issues. http://www.globalissues.org/article/425/poverty-and-the-environment#IntroductionLinkingtheEnvironmentandPoverty. Accessed 14 Dec 2014
Shah A (2010b) Structural adjustment – a major cause of poverty. Global issues. http://www.globalissues.org/article/3/structural-adjustment-a-major-cause-of-poverty. Accessed 14 Dec 2014
Siddiqi M (2001) Economics – an Islamic approach. Institute of Policy Studies, Islamabad
Speth G (2008) The bridge at the edge of the world – capitalism, the environment, and the crossing from crisis to sustainability. Yale University Press, New Haven/London
Speth G (2010) Towards a new economy and a new politics. Solutions. http://www.thesolutionsjournal.com/node/619. Accessed 14 Dec 2014
Stern N (2007) The economics of climate change: the Stern review. Cambridge University Press, Cambridge, UK. Online at http://webarchive.nationalarchives.gov.uk/+/http:/www.hm-treasury.gov.uk/media/4/3/executive_summary.pdf. Accessed 14 Dec 2014
Stiglitz J (1986) Economics of the public sector. Norton, New York
Strotz R (1956) Myopia and inconsistency in dynamic utility maximization. Rev Econ Stud 23:165–180
Tawney R (2000) Religion and the rise of capitalism. Transaction, London
The Guardian (2013) Pope Francis: the humble pontiff with practical approach to poverty. http://www.theguardian.com/world/2013/mar/13/jorge-mario-bergoglio-pope-poverty. Accessed 11 Dec 2014
The World Bank (2004) Responsible Growth for the new millennium integrating society, ecology, and the economy. The World Bank, Washington, DC
Treasury UK (1980) Investment appraisal and discounting techniques and the use of the test discount rate in the public sector. UK Treasury, London
U.S. Environmental Protection Agency (2015) http://www.epa.gov/ozone/science/q_a.html. Accessed 29 Jan 2015
Victor P (2008) Book review: frontiers in ecological economic theory and application. Ecol Econ 66:2–3
Voinov A, Farley J (2007) Reconciling sustainability, systems theory and discounting. Ecol Econ 63:104–113
Wegner G, Pascual U (2011) Cost-benefit analysis in the context of ecosystem services for human wellbeing: a multidisciplinary critique. Glob Environ Chang 21:492–504
Weitzman M (2007) A review of the Stern Review of the economics of climate change. J Econ Lit 45:703–724
Wheeler S (2004) Planning for sustainability – creating livable, equitable, and ecological communities. Taylor & Francis e-Library, New York
World Commission on Environment and Development (1987) Our common future (The 'Brundtland Report'). Oxford University Press, Oxford, UK

Emissions Trading

Roger Raufer, Paula Coussy, Carla Freeman, and Sudha Iyer

Contents

R. Raufer (✉)
Hopkins Nanjing Center, Nanjing University, Nanjing, Jiangsu Province, China
e-mail: rr@rogerraufer.com; rraufer1@jhu.edu

P. Coussy
Economics and Environmental Evaluation Department, CO2 Market Expert, IFP Energies nouvelles, Rueil-Malmaison, France
e-mail: paula.coussy@ifpen.fr

C. Freeman
School of Advanced International Studies, Johns Hopkins University, Washington, DC, USA
e-mail: cfreeman5@jhu.edu

S. Iyer
Cerebronics, LLC, Hoboken, NJ, USA
e-mail: iyersu@gmail.com

W.-Y. Chen et al. (eds.), *Handbook of Climate Change Mitigation and Adaptation*,
DOI 10.1007/978-3-319-14409-2_8

Abstract

Climate change is being exacerbated by the emissions of globe-warming greenhouse gases (GHGs) as a consequence of economic activities associated with energy, industry, transportation, and land use. From an economic viewpoint, the Earth's climate is a *public good*, and pollution a *negative externality*; such change therefore constitutes *market failure*. Controlling air pollution by utilizing economic mechanisms represents an important change in environmental thinking – literally a paradigm shift away from historical command-and-control engineering systems. Today, this approach is being utilized to mitigate the emissions of GHGs, addressing the pollution externality by putting a price on carbon. The international carbon market, largely developed as a result of the Kyoto Protocol, had a total value of $176 billion in 2011, but it has decreased significantly in recent years. With the addition of China and other national and subnational programs, however, it is expected that it will once again increase, as a larger and larger portion of emitted GHGs come under such regulatory purview. Historically, the largest component of that market has been the European Union's Emission Trading Scheme (EU ETS), which represents a regional market designed first to assist Europe in achieving compliance with the Protocol's requirements, and now is a cornerstone of the EU's policy to combat climate change. It also has links to the Protocol's project-based mechanisms, the Clean Development Mechanism (CDM), and Joint Implementation (JI), which help minimize compliance costs. China's nascent market – currently seven pilot schemes, but expected to become a national program in 2016 – should ultimately become twice as large as the EU ETS. Other carbon markets created in numerous countries (e.g., the U.S., Japan, South Korea, etc.) as well as a voluntary market are also expected to make significant contributions. This chapter discusses the structure of these emissions trading carbon markets, the theory behind their development, their historical evolution, ongoing governance challenges, and future prospects.

Introduction

The issue of global climate change is as much an economic conundrum as it is one of science and regulatory policy. Climate change is exacerbated by the emissions of globe-warming greenhouse gases (GHGs) as a consequence of economic activities associated with energy, industry, transportation, and land use. Historically, polluters have not had to directly bear the social costs of emitting substances into the atmosphere – and therefore they have had no incentive to reduce such emissions.

In economics, the Earth's climate is considered a "public good," that is, a good that can be consumed by everybody in a society, where those who fail to pay for the good cannot be excluded from enjoying its benefits. An "externality" is the impact of an economic transaction on a party that is not a direct participant of the transaction, and the price therefore does not reflect the full cost of a certain good. Human-induced climate change, then, is a "negative externality," since the emitter of

GHGs does not pay the cost of detrimentally altering a public good (i.e., the Earth's climate). This means that climate change, from an economic viewpoint, is a market failure; in fact, the British government's *Stern Review*, a well-known economic analysis of climate change, called it a "market failure on the greatest scale the world has seen" (Stern 2006).

While the fundamental theory of public goods and externalities forms the basis of any economic approach, there are a few facets of global warming that make a market solution to the problem of climate change even more challenging: the climate change externality is global; the impacts are persistent and develop over time because some GHGs remain in the atmosphere for hundreds of years; since there is no accurate way of predicting the change in the climate system due to increases in atmospheric GHGs, there are considerable uncertainties and risks in developing a mitigation strategy based upon economic theory.

In standard economic theory, the marginal abatement cost (MAC) of pollution control should equal the marginal social benefit (MSB) of such abatement. This means that the goal of the economic control program should be to set a control level such that the next dollar spent on pollution control purchases exactly one dollar's worth of environmental amenities. Figure 1 illustrates the marginal abatement cost (MAC) and marginal social benefit curves (MSB).

Economists then offer two approaches to arrive at that point:

- A price-based mechanism also called a Pigouvian tax
- A quantity-based mechanism commonly referred to as emissions trading

The Pigouvian tax approach was first developed by Arthur Cecil Pigou (1877–1959), a British economist who was a professor at Cambridge. Pigou discussed the concept of externalities in his book *The Economics of Welfare* (Pigou 1920) and argued that a tax should be imposed on negative externalities such as pollution in order to discourage them. In the case of climate change, a

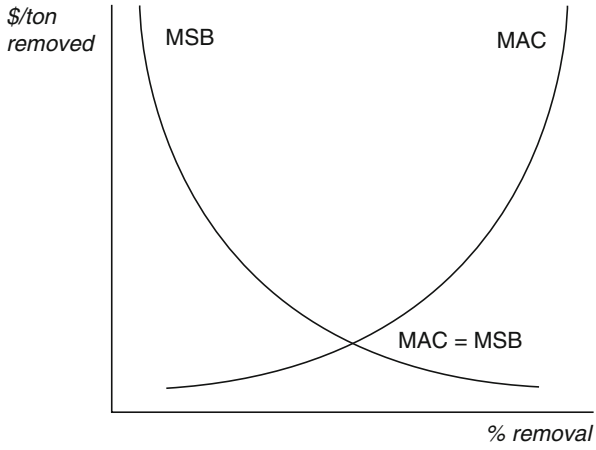

Fig. 1 The economists' idea of abating pollution

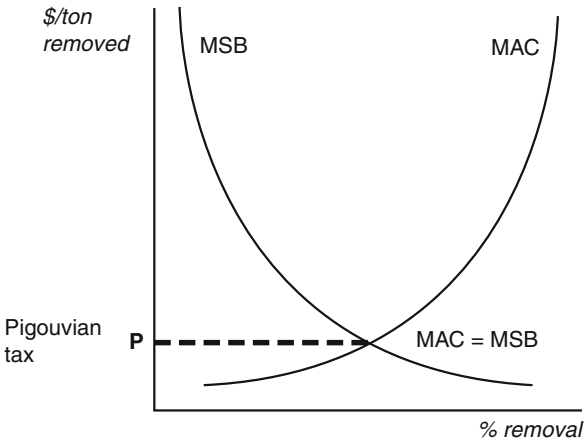

Fig. 2 A price-based approach to abate pollution: Pigouvian taxation

Pigouvian solution would introduce a tax on GHG emissions. If the MAC of a polluter is higher than the tax, the polluter will find it more cost effective to pay the tax and continue emitting. If the MAC is lower than the tax, then the polluter will try to abate the pollution as opposed to paying the tax (Fig. 2).

A Pigouvian tax is now considered a well-known and traditional means of bringing a modicum of market forces and therefore better market *efficiency* to economic situations where externalities exist. Such a tax will make it more expensive to pollute and will ensure a change in behavior by the polluting entity – forcing the polluter to either pay the tax or implement technologies to reduce pollution, whatever is more cost effective. Despite being an efficient solution to controlling pollution, taxes introduce a political dynamic that raises questions about wealth transfer from industry to government, the distribution of this revenue, lobbying of the government by special interest groups, polluters, etc. Economists have attempted to address this wealth transfer by linking the tax with subsidies (and utilizing the revenue generated by the tax to fund such efforts); by removing other taxes (so that there is tax neutrality); and similar schemes.

The quantity-based market approach, on the other hand, has an extensive background in the economics literature, but is perhaps most often associated with the work of John Dales, Professor of Economics at the University of Toronto, and his classic 1968 book *Pollution, Property and Prices* (Dales 1968). In that work, Dales proposed a new market-oriented policy instrument for tackling pollution problems. Dales' idea was to have an environmental authority issue a limited number of rights (or permits) to emit a specified pollutant and then leave the determination of the price of these permits to emitters within a market. Today, transactions in such markets are commonly called "emissions trading." A regulator sets an overall emission limit ("cap"), which is the total quantity of a pollutant that the participants in the scheme are allowed to emit. That quantity is then divided into a number of "allowances," and polluters are allowed to trade (i.e., buy and sell) such allowances in a market. Such "cap-and-trade" schemes have become quite popular over recent decades, and

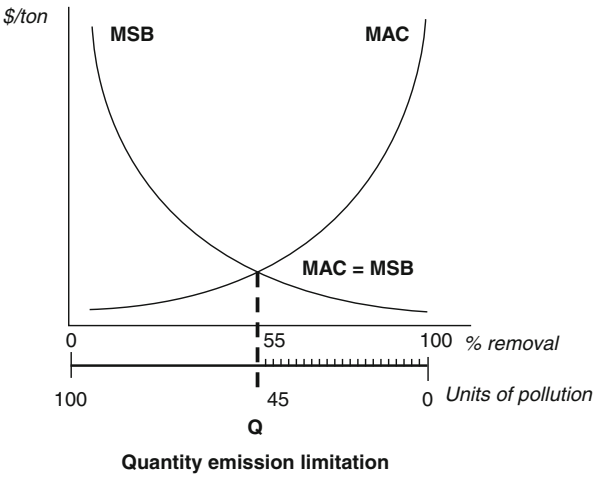

Fig. 3 A quantity-based mechanism to control pollution: Emissions trading

their success has led to the development of carbon markets under the Kyoto Protocol. In the figure above, a cap is set at the point where MAC = MSB, which is at the point where 55 % of the pollution is controlled. The "cap" of 45 units of pollution could be divided into 45 allowances, which could be bought and sold by polluters. Note that those with low marginal costs of control will put on control, rather than purchase such an allowance, and society will ultimately end up at the point where MAC = MSB; the figure also indicates that those with higher marginal costs should ultimately end up holding the allowances (Fig. 3).

There are several advantages to such "cap-and-trade" programs, the most obvious being that it is an economically efficient way to control pollution without the government having to worry about setting prices. It also has considerable flexibility in addressing the political issues associated with the wealth transfer noted above – allowance allocation schemes can call for 100 % auctioning (creating a transfer similar to that of a Pigouvian tax); or distribute the allowances for free to existing polluters (typically called 'grandfathering'); or utilize any combination in between. This gives the government considerable political leverage in addressing distributional concerns, and politicians can utilize, and have utilized, this to minimize political resistance to the pollution control program. Importantly, such quantity-based systems also limit the total amount of pollution, shifting the burden of dealing with growth on polluters. Under the "cap," individual emitters participating in the scheme have the flexibility of determining how best and where to deliver emission reductions.

A significant cap-and-trade program was introduced in the USA in the early 1990s for acid rain control, but this was not the first emissions trading program. Earlier, in the 1970s, a *baseline-and-credit trading* emissions trading system had been established. In baseline-and-credit trading, the regulator defines a specific set of acceptable conditions (the baseline) for an emission source. Depending upon preset

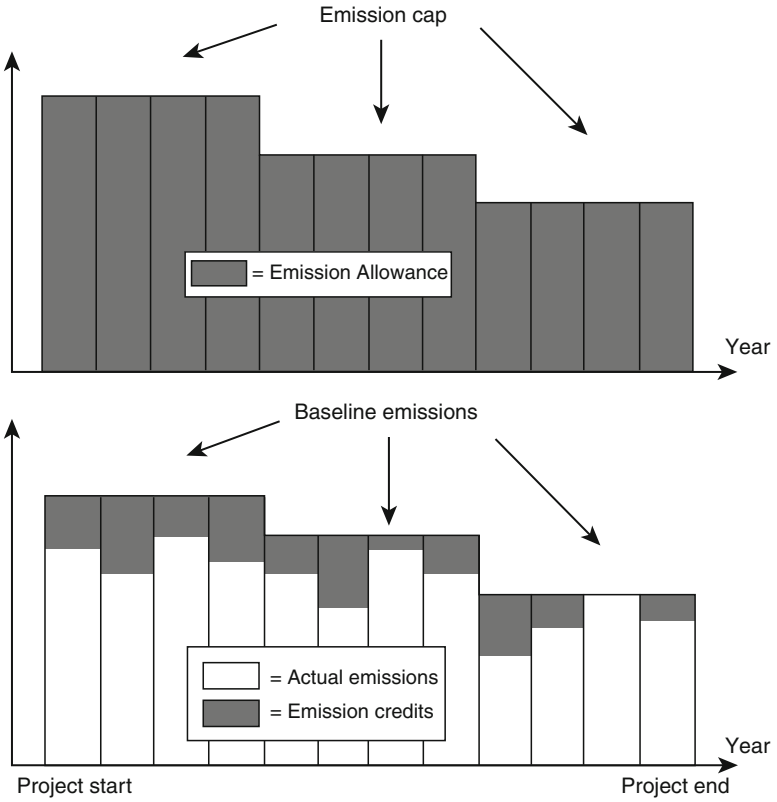

Fig. 4 Allowances versus Credit Trading (Source: Adapted from OECD 1997)

rules, improvements to this situation may qualify for "credits" (called Emission Reduction Credits [ERCs] in the US program) which could then be used for various purposes – to either offset new emissions, to reduce the control requirement on other units or be sold to others who might have trouble meeting their own baseline requirements. Figure 4 illustrates the difference between cap-and-trade and baseline-and-credit trading schemes. Later sections will make clear that both of these emissions trading approaches play an important role in the international carbon market.

The key aim of market-based approaches toward climate change policy is to ensure that those generating GHGs face cost for emissions that reflects the damage they cause (i.e., what economists call "internalizing the externality"). In ideal market conditions, both price and quantity-based mechanisms, if designed correctly, can be used to create such a price for carbon, and both approaches have the potential to deliver emission reductions efficiently.

This chapter seeks to analyze the role that quantity-based approaches play in mitigating climate change, and the resulting compliance and voluntary carbon markets that have been developed and are in operation around the world. The chapter

is organized in such a manner as to provide the reader a historical framework for the development of such market approaches – beginning first with traditional engineering approaches to pollution control, and then moving towards implementation of the economists' ideal, in order to see how carbon markets obtained their current structure. It then profiles the compliance carbon markets and the complementary, but increasingly important, secondary and related markets in operation today.

The Evolution of Emissions Trading

The development of markets to address environmental issues represents a strategic shift in the thinking behind environmental management. Pollution control has a long evolutionary history, beginning with traditional engineering approaches and subsequently developing into the economic realm with market-based approaches.

Historically, most governments have utilized "command-and-control" (CAC) types of regulations to address pollution problems. As the name suggests, the government would issue some form of "command" – typically a mandate for a pollution source to use some type of technology, or meet some specific pollution level. The government then faced the problem of ensuring that the command was actually followed out – and this required active "control." "Control" typically includes the monitoring, reporting, and verification (MRV) of emissions, as well as punishment for a failure to meet "commands." The absolute form of "command" is prohibition, which is used if the potential damage to the environment is severe and difficult to remediate. More frequently, however, technology-based requirements are employed, typically requiring polluters to meet some emission limit or performance standard for their equipment. Monetary fines, or perhaps imprisonment for egregious cases, are now the norms for "control."

In an 1874 amendment to Britain's Alkali Act of 1863, polluters faced a requirement to utilize the "best practicable means" (BPM) of pollution control. From an engineer's perspective, if everyone was utilizing BPM, then whatever happened to the environment simply happened – after all, everyone was doing the best they could with technology. An alternative regulatory approach was adopted in the USA in the 1960s, however. This alternative suggested that the goal of pollution control systems was not simply to use the best technology, but rather, to focus on achieving environmental quality. Technology was just a means of accomplishing such an end, not the goal itself. Environmental goals were thus developed in terms of *environmental quality standards*, and the technology-oriented requirements became recognized as the means to accomplish such goals. The resulting CAC programs developed in the 1970s therefore adopted the "traditional" (i.e., engineering) approach outlined on the left side of Fig. 5.

Economists had a different idea, however, as discussed earlier and as noted on the right side of Fig. 5. From their theoretical perspective, the goal is to develop a program where marginal costs of pollution abatement is equal to the marginal social benefit (i.e., MAC = MSB). All of the information used by the regulators to set environmental quality standards in the traditional approach would somehow have to

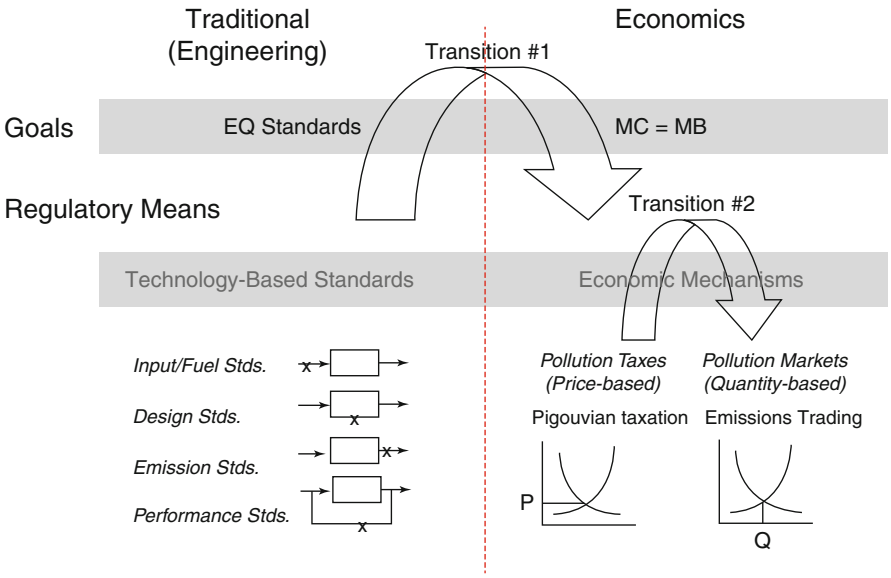

Fig. 5 Engineering versus Economic worldviews

be incorporated into the marginal social benefit curves outlined in the right side of that figure. This obviously would be a very difficult task.

Figure 5 suggests that two transitions are occurring today – a shift from an engineering to an economic worldview in environmental management and a secondary shift from price-to-quantity-based mechanisms. There are important caveats associated with both transitions, however. For the first, the transition is only occurring in the bottom portion of the figure – i.e., within the regulatory means, not environmental goal setting. Governments fully recognize the difficulties associated with developing accurate MSB curves, and thus tend to stay with environmental quality standards or depend upon political compromise to set goals. However, they increasingly recognize the strength of using the economic regulatory means (i.e., Pigouvian taxation and emissions trading) as tools to help accomplish such goals.

Any portend of a price-to-quantity shift within economic instruments must similarly be heavily qualified. Economists make choices about the appropriate price or quantity instruments to use based upon numerous factors, including the slopes of the MAC and MSB curves; confidence in the data used to estimate them; administrative simplicity (including the means of future adjustments); their visibility (explicit vs. hidden); second-best considerations; and a host of similar concerns. Certainly many governments – and economists – are more comfortable using price-based instruments, and it has frequently been suggested that these are a more appropriate tool for dealing with climate change. Nordhaus (2009, 2013), for example, has been a major proponent of carbon taxation, and notes that:

- The damages associated with GHGs strongly favor price-based policies, since GHGs are a stock pollutant, while control costs are related to the flow
- Quantity-based targets are difficult to set, and "are particularly troublesome where targets must adopt to growing economies, differential economic growth, uncertain technological change, and evolving science"
- A tax approach "may add less to the distortion caused by existing taxes" (i.e., second-best considerations), and is less susceptible to corruption and rent seeking behavior

Despite such efficiency considerations, the political economy and flexibility of quantity-based systems noted above, as well as the increasing difficulty faced by many governments in imposing taxation schemes, has led to such a longer-term shift over recent decades. Further, many believe that it is more appropriate for the government to focus on the physical goal (i.e., the quantity) and have prices respond than the converse. The EU has made cap-and-trade the predominant policy mechanism for dealing with its largest emission sources, and China has similarly chosen it as a key tool for reducing the carbon intensity of its economy. Prospective US regulation is likely following a similar path, as discussed below.

While this chapter focuses on the emissions trading (i.e., quantity) mechanism, the World Bank tracks both price and quantity instruments in its annual survey. It notes that "about 40 national and over 20 subnational jurisdictions are putting a price on carbon. Together these carbon pricing instruments cover almost 6 Gt CO_2e or about 12 % of the annual GHG emissions" (World Bank 2014).

Emissions Trading Programs

The US Environmental Protection Agency (EPA) introduced the concept of emission markets in 1976, as a means for new emission sources to locate in areas with unhealthy air quality (i.e., areas that did not meet the National Ambient Air Quality Standards). The new sources were required to use stringent control technology (i.e., Lowest Achievable Emission Rate), but were also required to "offset" the additional pollution they created by a ratio greater than 1:1. Thus, the new source would help clean up the nonattainment area even though it was adding new pollution. Some economists realized that this created a new asset: emission reduction "credits" from an existing source were now worth something to a new source hoping to locate within a nonattainment area (such as Los Angeles). This emissions trading scheme was expanded in 1979 to include existing sources as well as new ones through the "bubble" policy, which allowed sources to put an imaginary bubble over their facility, and then meet CAC requirements in the most cost-effective manner under the bubble (i.e., based upon their own determination of MAC rather than the government's embedded within the CAC requirements). Other mechanisms added that same year included "netting," a simplified-permit strategy which allowed sources to "trade" their old emissions for new emissions when replacing equipment and "banking," which provided firms the flexibility of storing their emission

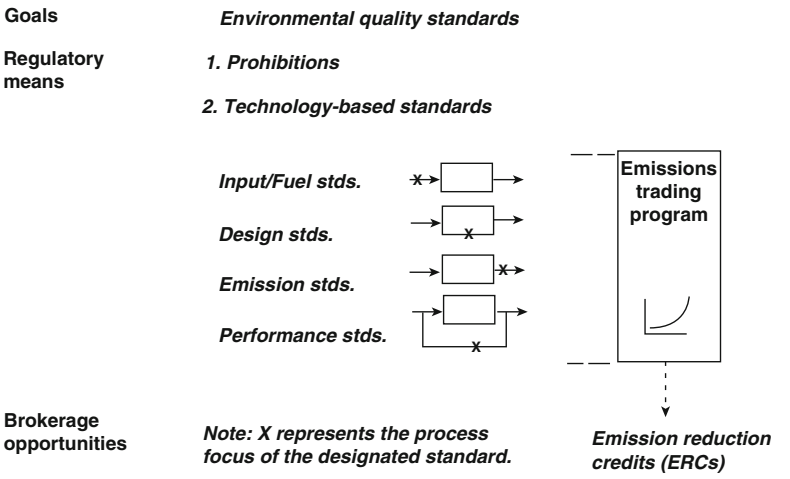

Fig. 6 The US EPA's Initial Emission Trading Program

reduction credits over time. These four regulatory provisions were collectively brought together in a draft Emissions Trading Program (ETP) in 1982, and finalized in 1986. The US EPA's ETP did not change the CAC requirements – it merely introduced a new and more flexible means for emission sources to meet them. The time and costs associated with completing a specific ERC transaction have been high, however, and while thousands of ERC trades have occurred, high transaction costs have hobbled this market. The resulting baseline-and-credit ETP is shown in Fig. 6, and remains in effect today.

The US Acid Rain Program (ARP)

The ETP laid the groundwork for a pioneering acid rain allowance trading program that is the predecessor of quantity-based trading programs in operation today. In 1980, rising concern about the extensive environmental impacts of acid rain (i.e., acid deposition) prompted the US Congress to establish the National Acid Precipitation Assessment Program, an interagency organization designed to study the causes, effects, and potential control of this environmental concern. With the Clean Air Act amendments in 1990, Congress addressed the control issue and sought to achieve major reductions of the primary components of acid rain: 10 million tons of sulfur dioxide (SO_2) and 2 million tons of oxides of nitrogen (NO_x) below 1980 levels by the year 2000. In doing so, the legislation established a new paradigm for environmental protection, since the resulting emissions control program was the first significant one utilizing the economists' idea of a quantity-based emissions trading mechanism.

The centerpiece of the Acid Rain Program (ARP) was a cap-and-trade system for SO_2. The NO_x reduction program initially took a command-and-control approach,

but in 1999 a cap-and-trade NO_x program was developed in the US Northeast (primarily for ozone-control purposes). A two-phased tightening of restrictions on fossil fuel-fired power plants was adopted: total emissions in 1995 (under Phase I) were 25 % below 1990 levels, and more than 35 % below 1980 levels (Burtaw et al. 2005). Phase II, which began in 2000, represented a significant 50 % cut from 1980 SO_2 levels (US EPA 2002).

A 2010 governmental analysis of the ARP estimated annual benefits of the program to be $122 billion, and costs to be only $3 billion (50 % of the figure estimated by the EPA in 1990) – a 40-to-1 benefit/cost ratio (US EPA 2010). Such numbers illustrate why *The Economist* (July 6, 2002) called it "probably the greatest green success story of the past decade."

Lately, however, the SO_2 market price has collapsed, and the clearing price in US EPA's March 2014 spot auction was only $0.35/t (and $0.04/t in the 7-year advance auction) (USEPA, 2014 Allowance Auction Results 2014a). The reason for this is that other regulatory initiatives (such as the 2005s Clean Air Interstate Rule, and its replacement, the Cross State Air Pollution Rule) have instituted further SO_2 reductions designed to tackle environmental concerns such as PM-2.5. Accordingly, as one prominent environmental economist noted, "the emissions constraint under the 1990 Clean Air Act amendment has become irrelevant, and the price of those tradable emissions allowances has fallen from several hundred dollars a ton to near zero." In that economist's view, this was indicative of an "institutional blind spot" in environmental economics – legislative actors were simply not capable of readily amending a statute to correspond to changing scientific information (Burtraw 2013).

While the current SO_2 market is essentially moribund, the ARP market design kept the existing ETP (with emission reduction credits) to protect local air quality and public health near the power plants, while superimposing a cap-and-trade scheme (with emission allowances) to deal with total loading of the pollutant. This dual 'baseline-and-credit' and 'cap-and-trade' market scheme was a forerunner of the international carbon market, which would similarly use both types of instruments to accomplish desired environmental goals.

Carbon Markets

The foundation for the international carbon market began at the "Earth Summit," in Rio de Janeiro, Brazil in 1992. The Earth Summit, formally called the UN Conference on Environment and Development, addressed a wide range of environmental and governance issues, including biodiversity, the management of toxic chemicals, and similar issues – but it is perhaps best remembered today for establishing the United Nations Framework Convention on Climate Change (UNFCCC). The UNFCCC committed the signatory governments to a voluntary, nonbinding effort to reduce GHGs with the goal of "preventing dangerous anthropogenic interference with the earth's climate system." The UNFCCC came into force in 1994, after 50 countries had ratified it, in accordance with the terms of the treaty.

Signatory countries of the UNFCCC agreed to "common but differentiated responsibilities" for addressing emissions, recognizing that the largest share of historical and current emissions was generated from developed countries (i.e., as a result of more than 150 years of industrial activity), and that the share of emissions from developing countries would need to grow to meet their social and developmental needs. This resulted in a division amongst the signatory countries into two principal groupings: Annex I countries, which are industrialized nations and nations with economies in transition such as Russia and Ukraine and Non-Annex I countries, which are the remaining (mostly developing) nations. [NB: There is also an Annex II grouping, consisting of OECD members and the European Union, which have a "special obligation" to provide financial resources and facilitate technology transfer to developing countries.]

The Kyoto Protocol was adopted on 11 December 1997 in Kyoto, Japan, during the third meeting of the UNFCCC (called the Conference of Parties [COP]), and, while it opened for signature on 14 March 1998, the Protocol only came into force on 16 February 2005. As of 2014, 192 countries and one regional economic integration organization (the European Community) are parties to the treaty. A major feature of the Kyoto Protocol was that it set binding GHG emission constraints for the Annex I countries (in Article 3 and Annex B). These were equivalent to an average 5.2 % emissions reduction from a 1990 baseline over the first 5-year commitment period (2008–2012). Thus, while the UNFCCC encouraged industrialized nations to reduce GHG emissions, the Kyoto Protocol committed them to doing so.

Even though the USA initially introduced the idea of emissions trading and was an ardent proponent of market-based mechanisms to address climate change (based upon its successful experience with the ARP), it never ratified the Kyoto Protocol. As a participant, the US would have been required to reduce GHG emissions by 7 % below 1990 levels. The USA experienced rapid economic growth during the late 1990s, however, and that 7 % reduction would have amounted to approximately 30 % in real terms for the 2008–2012 commitment period, as growth continued. The US disagreed with other parties about how the market-based "flexibility mechanisms" should be implemented, as well as other policy issues (e.g., the role of forestry "sinks") and subsequently withdrew from the process completely in March, 2001. The US did pursue a number of limited domestic initiatives to reduce emissions, but never joined the emissions trading markets created by the Kyoto Protocol.

Flexible Mechanisms of the Kyoto Protocol

The Kyoto Protocol remains a binding agreement today, in its second commitment period (2013–2020). In the first commitment period (2008–2012), it regulated six GHGs: carbon dioxide (CO_2), methane (CH_4), nitrous oxide (N_2O), perfluorocarbons (PFCs), hexafluorocarbons (HFCs), and sulfur hexafluoride (SF_6). Emissions of these GHGs are primarily associated with the generation and use of energy, chemical and industrial processes, municipal wastes, and land-use activities such as

deforestation. A seventh chemical, nitrogen trifluoride (NF_3), used primarily in the electronics industry, was added in the second commitment period. For reporting and tracking purposes, the Global Warming Potential (GWP) in the atmosphere of each gas is expressed in terms of a CO_2 equivalent (CO_2e). Methane for example, has a GWP that is 25 times that of CO_2 (although the carbon market has employed an earlier estimate of 21). The Protocol set individual GHG emission-reduction targets for Annex I countries under the UNFCCC. These targets were specified in Annex B of the Kyoto Protocol. For the Annex I countries that ratified the Protocol, their assigned GHG emission amounts acted as a legally binding cap on emissions between 2008 and 2012.

Annex B countries could meet their emission reduction targets either through national measures (e.g., regulations, taxes or environmental markets), or through the use of three flexible market mechanisms incorporated into the Protocol. Described in Articles 6, 12, and 17 of the Protocol, these flexible mechanisms allowed Annex B countries to pursue opportunities to cut emissions or sequester carbon more cheaply in other countries than within their own domestic market.

Article 6 of the Protocol defines a mechanism known as *Joint Implementation* (JI), which allowed emission-reduction or removal projects in Annex I countries to generate *Emission Reduction Units (ERUs)*, which could then be used to meet the emission reduction or limitation commitments of other Annex B countries. Each ERU is equivalent to one ton of CO_2, and could be counted towards Kyoto target requirements. Article 12 defined the *Clean Development Mechanism* (CDM), which allowed similar carbon credits known as *Certified Emission Reductions (CERs)* to be generated from projects in developing (i.e., Non-Annex I) countries. The *International Emissions Trading (IET)* mechanism was outlined in Article 17 of the Protocol, and allowed Annex B parties to trade *Assigned Amount Units (AAUs)* in order to meet their commitments. Countries in Annex B that have spare (i.e., permitted but not used) AAUs could thus sell them to countries that exceeded their targets. As discussed below, these flexible mechanisms evolved over time. The CDM was the first to be implemented, since projects under the mechanism could start generating credits relatively quickly (i.e., before the first commitment period began). This was followed by the JI, and thirdly, IET. These latter mechanisms did not fully commence until the start of the first commitment period in 2008.

Thus, an Annex B country had several options to reduce emissions in order to comply with its Kyoto Protocol targets. Annex B nations could:

- Limit emissions through domestic policy, such as implementing direct regulation, Pigouvian taxation, or setting up domestic emissions markets (note: the role of regional markets such as the EU ETS is discussed below)
- Set up eligible projects in non-Annex I countries under CDM, and use the CER carbon credits generated from these projects
- Set up eligible projects in Annex I countries under JI, and use the ERU carbon credits from these projects and/or
- Utilize the IET program to buy/sell AAUs

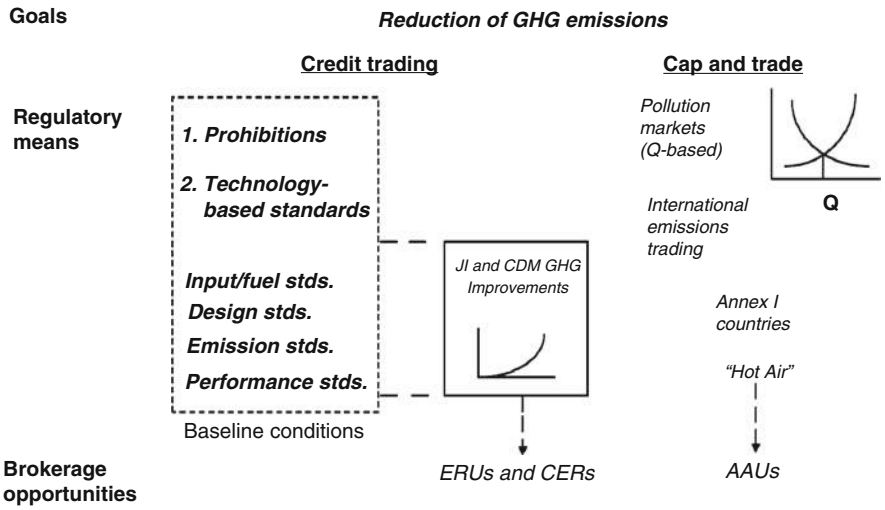

Fig. 7 The Kyoto Protocol flexibility mechanisms

As an example, Britain, which had a relatively high reduction target of 12.5 %, during the first commitment period could achieve this target by implementing a portfolio of domestic regulatory policies, such as improving building codes; employing price instruments such as a petrol taxes to reduce emissions from the transportation sector; and using emissions markets (in this case, the EU ETS) to reduce pollution from the power sector. Over and above such domestic efforts, the country could purchase AAUs from Russia or Ukraine, or invest in CDM or JI projects abroad (either through the EU ETS, or separately). The overall market framework for the Kyoto Protocol flexibility mechanisms is shown in Fig. 7. These mechanisms were indeed flexible, and countries were at liberty to employ one or all of these mechanisms, in any combination, depending upon their emissions constraints and economic situation.

Clean Development Mechanism (CDM)

Since climate change is a global problem and the physical nature of the pollutant makes the location of emissions reductions irrelevant, CO_2 emission reductions could be obtained anywhere – and usually at lower cost in the developing world. Article 12 of the Kyoto Protocol provides for such reductions, and the Clean Development Mechanism outlined in that article has two goals: to reduce GHG emissions and to foster sustainable development.

CDM is a project-based mechanism that allows public or private entities to invest in GHG-mitigating activities within developing countries, and to earn abatement credits for those projects. These credits, called CERs and equivalent to one ton of CO_2, can then be applied against their own emissions or sold in the marketplace. Buyers in other Annex I countries, for example, might purchase them to assist in meeting their own GHG reduction goals.

Prior to the generation of CERs from a CDM project, the developers of the project are required to go through a formal and rather complex process. They interact with three institutions: the CDM Executive Board (EB), which implements and supervises the mechanism; the Designated National Authority (DNA) of the host country which reviews and approves CDM projects, and provides country-specific guidance (e.g., for sustainable development criteria); and Designated Operational Entities (DOEs), which are independent private companies serving as auditors.

In order to qualify to receive CERs, projects have to have begun after January 1, 2000, and must submit a Project Design Document (PDD) which includes at least the following information:

- General description of the project activity (including location, technology, ownership, etc.)
- Application of a UN-approved baseline methodology for that specific activity. Baseline methodologies have now been approved for most standard renewable energy and energy efficiency applications, but any novel technology or application would first require such an approval
- Selection of a crediting period. Project developers can select either a fixed 10-year baseline period, or three 7-year baselines with adjustments at the end of the first and second periods (with the exception of afforestation and reforestation sink projects)
- Monitoring methodology and plan
- Estimation of GHG emissions and reductions
- Assessment and demonstration of "additionality" (i.e., that emissions reductions are above and beyond those that would have happened anyway – i.e., they are "additional" or "surplus"). Additionality is important because developing countries are not required to reduce emissions under the Kyoto Protocol and Annex I countries utilizing CERs from these countries will take credit for such reductions. This is usually the most difficult criterion for CDM projects to meet and document
- Documentation that the project meets the DNA's sustainability criteria for projects within that host country
- Other relevant data (e.g., contact information for project participants, stakeholder comments, information on the use of public financing, etc.)

The CDM project process is outlined in Fig. 8. Note that after the PDD is completed in the design stage, it is validated by the DOE, which will make a recommendation to the EB to register the project. Later, a second DOE will verify that the project has performed as expected, based upon the monitoring plan submitted as part of the PDD – and will recommend that the appropriate number of CERs be issued. Only if all of these criteria are met will the project then be issued CERs, which can be sold in the international carbon market.

As of October 1, 2014, 12,253 projects had submitted PDDs, and 7,562 of them had reached the registration stage. During the first commitment period, 1,491 million CERs (MCERs) were issued, and it was expected that 5,081 MCERs would be issued in the second commitment period. Seventy one percent of the CDM projects

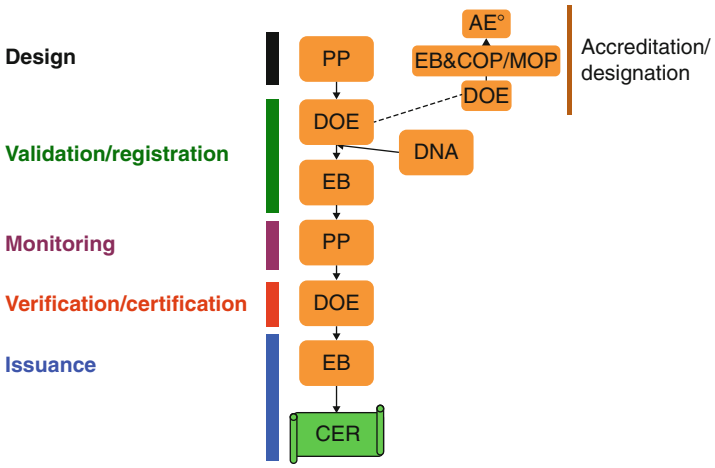

Fig. 8 Carbon credits from the Clean Development Mechanism of the Kyoto Protocol (Source: UNFCCC n.d.)

were associated with renewables in the first commitment period, but these represented only 34 % of the CERs. China has captured 59.9 % of the CERs issued to date, with the top five countries (China, India, South Korea, Brazil and Mexico) representing almost 90 % of the CDM market. Less than 3 % of the CDM projects were located in Africa (UNEP DTU Partnership 2014).

These figures do not make clear, however, the significant contraction which has taken place in the CDM (and Kyoto Protocol) marketplace in recent years. Prices for CERs have collapsed by 98 % over a 5-year period, to less than $0.50 per ton. Such prices do not even cover the transaction costs of issuance, let alone any project investment. As the World Bank noted, "since the second half of 2012 there has been a growing feeling in the CDM market that demand is saturated. With little prospect of a significant recovery, the biggest players have begun to leave the market, along with their skills and expertise"(World Bank 2014). One estimate suggests that the demise of CDM will require a write-down of $66 billion in asset value – over 40 % of owner's equity on average – primarily for developing country investors (CO_2 Spain 2013).

There are a number of reasons for the collapse in CERs prices, beginning with the fact that most demand was associated with the EU ETS – which saw its own significant price declines. As discussed below, the EU's "Linking Directive" created the largest demand for CERs, but the recession and economic contraction in Europe lessened demand significantly. Perhaps more importantly, however, Europe revised the rules of the EU ETS for CER usage in the second commitment period in a manner which had a profound effect upon the CER market.

There had already been considerable displeasure in Europe over the role that industrial gases had played in early stages of the carbon market. HFC-23 is a highly-potent and long-lived GHG that was one of the six gases originally included in the

Kyoto Protocol. With a global warming potential 11,700 times that of CO_2, every ton of HFC-23 destroyed produced 11,700 CERs for sale in the CDM market. The destruction of HFC-23 (a by-product of HCFC-22 [chlorodifluoromethane] production, which is used as a refrigerant) saw windfall profits created in several projects (especially in China). The NY Times reported that industrialized nations could end up paying $800 million a year to buy CERs, even though the cost of building and operating incinerators would only be approximately $31 million per year (NY Times 2006). In response to such windfall profits, China imposed a 65 % tax on CER revenue generated by HFC-23 projects (as well as a 35 % tax on N_2O projects), and set up a CDM Fund to utilize such revenues. So much potential revenue distorted the economics of new refrigerant facilities (Wara 2006), but when Europe tried to modify the approach for new facilities under Kyoto Protocol processes, it was blocked. It therefore unilaterally determined to eliminate the use of such CERs in Phase III of the EU ETS.

Given the magnitude of CDM revenue streams to China and other middle-income countries, the EU ETS also determined to purchase new-project CERs in Phase III solely from Least Developed Countries (LDCs). Thus, only projects registered before January 1, 2013 could provide CERs in Phase III (other than new projects from the LDCs). It put in another timing constraint as well: after March 31, 2015, only CERs generated in the second commitment period (i.e., after 2012) could be employed. These constraints on demand contributed to the price collapse noted earlier, and it is not clear whether the CDM can be resurrected in future COP negotiations– particularly given concerns about certain aspects of its design.

One such fundamental concern (or, as discussed below, what some consider a fundamental flaw) has been the determination of the "additionality" of a CDM project. Defined in paragraph 5c, Article 12 of the UNFCCC, emissions from a CDM project should be ". . .additional to any that would occur in the absence of such activities." This statement, however, is vague and has been subject to many different interpretations. The idea behind additionality is that the project should owe its existence to the prospective earnings from carbon credits sold in the CDM market, i.e., the emission reductions should go beyond what they would be in the absence of the CDM. In general, determining additionality has proven not only cumbersome, but has resulted in increased transaction costs, as well as liability and risk for investors. Friends of the Earth has estimated, for instance, that 75 % of all approved CDM projects were already up and running at the time they were approved by the CDM EB (Friends of the Earth and International Rivers 2009). David Victor, formerly head of Stanford's Energy and Sustainable Development Program, estimated that between a third and two-thirds of CDM offsets may not represent actual emission cuts (International Rivers 2008). In mid-2009, the CDM EB ordered an unprecedented review of a number of Chinese wind projects, to determine whether they satisfied additionality requirements. Now referred to as the "Chinese wind controversy," ten projects were rejected outright just before COP15 in Copenhagen, sending shockwaves through the CDM investment community. The resulting imbroglio was indicative of what He and Morse (2013) have termed the "Offsetters' Paradox": "On one hand, including domestic subsidies in the additionality

calculation creates perverse incentives for the host country by making projects less eligible for CDM and therefore discouraging policies that would jeopardize CDM revenues. On the other hand, ignoring these subsidies assures crediting for business as usual projects, which reduces the integrity of global emissions caps."

While CDM has thus suffered a number of critical blows in recent years, it has nonetheless served as the template for all baseline-and-credit trading schemes in the international carbon market. The procedures developed under CDM for generating, validating and verifying carbon reductions are now routinely employed in both compliance and voluntary markets around the world. As an example, China now issues Chinese CERs (CCERs) for use in its domestic carbon trading programs, utilizing procedures it learned under CDM.

Joint Implementation (JI)

Joint Implementation is a project-based mechanism under the Kyoto Protocol that assists Annex I countries in meeting their Kyoto commitments by participating in projects in other Annex I countries. Entities may partake in JI projects to generate emission credits, known as ERUs, in order to use them for compliance with their emissions targets or to sell in the international carbon market. Similar to the CDM, JI offers parties a flexible and cost-effective means of fulfilling part of their Kyoto commitment, while the host party benefits from foreign investment and technology transfer. Unlike CDM, however, projects could only begin generating ERUs in 2008.

To be eligible to qualify as a JI activity and to receive ERUs, projects must be undertaken between Annex 1 countries; must provide a reduction that is additional to any that would otherwise occur in the absence of the project; and must be supplemental to domestic actions to reduce greenhouse gas emissions. The lifecycle for projects to be eligible for JI ERUs similarly begins with the preparation of a PDD, following JI guidance established by the JI Supervisory Committee (SC). Then, an Accredited Independent Entity (AIE) determines if the emission reductions were correctly estimated, and if necessary procedures were established to monitor the project performance during its implementation. At this stage, the JI Supervisory Committee will consider the quality of the project and, after 45 days, the project automatically acquires a status of JI project. As with CDM, most countries involved in JI establish their own national Designated Focal Points (DFP) in charge of JI project approval. There are two main tracks by which projects qualify for generating ERUs: Track 1, where a host party meets all eligibility requirements and verifies that emission reductions from the project are additional to a baseline scenario (i.e., the project implementation is largely left up to the participating states); and Track 2, where a host party meets only a limited set of eligibility requirements (verified by an accredited independent entity) and verification of the emission reduction as being additional has to be done by the JI SC.

Ukraine (321 projects) and Russia (96 projects) have been the biggest JI suppliers, while countries such as The Netherlands, Denmark and Austria have been the most active buyers, through governmental purchase programs or participation in carbon funds. As of October 1, 2014, Track 1 has a total of 574 registered projects and Track 2 has 206 projects registered in the JI pipeline (UNEP DTU Partnership 2014).

Like CDM, the JI market has contracted severely in recent years, and is complicated by the fact that post-2012 ERUs cannot be created until AAUs for the second commitment period are assigned – an issue still under debate in COP negotiations. Further, even though Russia had a significant number of JI projects, it refused to accept any constraints during the second commitment period, and thus is not eligible to register new projects.

International Emissions Trading (IET)

The Kyoto Protocol provides for a quantity-based cap-and-trade scheme called International Emissions Trading that is limited to Annex B countries. The national allocations used in the emissions trading are expressed as levels of allowed emissions, or assigned amount units (AAUs). Although these are national allocations and commitments, in practice, individual countries devolve their emissions targets and requirements down to major industrial entities such as power plants and large emitters. Therefore, the ultimate market participants may be individual companies that expect their emissions to exceed their quotas. Russia, Ukraine, and the Central and Eastern European countries have an estimated 8–12 billion tons surplus of AAUs for the 2008–2012 Kyoto commitment period associated with the collapse of the former Soviet Union, which occurred after the Kyoto Protocol's 1990 base year. This surplus is often pejoratively referred to as "hot air." Annex I countries could theoretically achieve compliance by purchasing "hot air," but many buyers were reluctant to do so since that would merely represent payment for economic collapse which occurred nearly 20 years ago, with little ongoing environmental benefits. Green Investment Schemes (GIS) were introduced to address this "hot air" situation. Under GIS, revenues from the sale of surplus AAUs were invested in environmental improvements (or "green" activities) in the selling nation, even though such activities might not strictly qualify for carbon credits (e.g., training energy auditors, etc.). This way, purchased AAUs were linked to GHG mitigation efforts, and many GIS schemes began to mirror CDM and JI carbon credit mechanisms, paying detailed attention to additionality, sustainable development criteria, etc. (Tuerk et al. 2010). The total amount of "hot air" sold is estimated to be 453 million AAUs. ((UNEP DTU Partnership 2014). Negotiators addressed the "hot air" issue for the second commitment period at COP 18 (in Doha), removing the ability of countries to profit from the sale of such AAUs in that period. This primarily focused on Ukraine, since Russia declined to accept a second period constraint (Morel 2013).

International Cap-and-Trade Programs

As noted earlier, the 2014 World Bank survey indicated that there were 40 national and more than 20 subnational carbon pricing mechanisms in place around the world. That report (World Bank 2014) and a number of other documents (see, for example, (ICAP 2014a; IETA 2013; ICIS 2014); etc.) provide detailed information about the characteristics of individual programs around the world, and this chapter does not

attempt to duplicate such information. Instead, it outlines below some of the salient features of the largest existing international carbon market (i.e., the EU ETS), as well as emissions trading efforts underway within the two largest GHG-emitting countries (i.e., China and the US).

The European Union Emissions Trading Scheme (EU ETS)

Although the EU was initially skeptical about emissions trading, it has become a driving force behind its implementation on a worldwide basis. In January 2005, the EU ETS commenced operation as the largest multicountry, multisector GHG trading scheme worldwide. There are four phases in the Scheme: Phase I from 2005 to 2007, also called the trial period; Phase II from 2008 to 2012, coinciding with the first commitment period of the Kyoto Protocol; Phase III from 2013 to 2020, currently in progress; and Phase IV, from 2021 to 2028, which has not yet been clearly defined. Furthermore, a 2030 policy framework for climate and energy was adopted by the European Commission in October 2014. The center piece of this framework is a target to reduce EU domestic greenhouse gas emissions by 40 % below 1990 levels by 2030, and sectors covered by the EU ETS would have to reduce their emissions by 43 % compared to 2005 (EC 2014).

The EU ETS established a mandatory CO_2 cap-and-trade system, which addressed emissions from major sources throughout the EU; it covers about 45 % of the CO_2e emissions, from more than 11,000 heavy energy-using installations in power generation and manufacturing industry. Sources were first allocated a certain number of emission allowances, based on historic performance and other parameters. Specific national targets were established in Phase I and II by national governments in what were called National Allocation Plans (NAPs), which specified how many allowances would be awarded to emitters in each regulated industry, and the distribution of such allowances. As is characteristic of a cap-and-trade market, participants who reduced their emissions below their allocation could sell the resulting excess allowances. Those companies who found that reducing their emissions internally was cost-prohibitive could purchase allowances in the open market. Those who did not hold sufficient allowances to match their actual emissions at the reconciliation date were fined 40€ per ton of CO_2 emitted in Phase I, which rose to 100€ per ton of CO_2 in Phase II and III.

It is important to note that while the EU ETS was designed to meet the goals of the Kyoto Protocol, it is operated by the EU, and is independent of the UN. The EU has announced that it will proceed with Phase III and IV of the ETS, regardless of the actions of other countries in post-2012 and 2015 climate negotiations.

EU ETS Phase I

Phase I of the EU ETS (2005–2007) was established as a "trial" or "learning" phase, before the Kyoto Protocol's targets came into effect. It was designed to provide companies and governments with experience in developing, operating, and participating in carbon markets. Phase I covered CO_2 emissions from more than 11,000 installations in several major emission sectors across the 28 European Union Member States. The sectors included energy (combustion installations >20 MW, mineral

oil refineries, coke ovens); ferrous metals; factories making cement, brick, glass, ceramics, and pulp and paper. Tradable "European Union Allowances" (EUAs) were distributed to these installations (typically for free), with the sum of distributed allowances equal to the total cap. The amount of emissions allowed by the cap itself was determined on a country-by-country basis; each member state proposed a quantity of EUAs, which was reviewed and approved by the EU commission (Ellerman and Joskow 2008).

The transportation, chemistry and building sectors were excluded in Phase I. In cases of *force majeure*, such as exceptionally low winter temperatures, additional emission allowances could be issued by national authorities. Member states also had the flexibility of opting out individual facilities. A notable feature of Phase I of the EU ETS was that there was effectively no restriction on banking or borrowing of allowances within any given multiyear period, but this did not hold between trading periods. While each member state maintained its own registry to record the creation, transfer and surrender of allowances, a central registry, called the Community Independent Transaction Log (CITL) recorded transfers of EUAs among installations in different member states – in this way, the EU Commission would be able to block transfers from any member state that failed to gain approval of its NAP.

The Linking Directive

Another important design feature of the Emissions Trading Scheme is the *Linking Directive*, which was formally adopted in 2004. Up to a certain limit, it allows entities to comply with emission caps by submitting qualifying credits for emission reductions accomplished outside of the EU through the CDM (since 2005) and JI mechanisms (since 2008). Credits generated from certain CDM activities such as those from projects associated with nuclear power or CO_2 sinks were not allowed. Figure 9 illustrates the role of the Linking Directive.

The Linking Directive provided a strong stimulus for the development of CDM projects, and made their use an important means of compliance in the EU ETS. It helped to accelerate the carbon marketplace, i.e., the EU ETS provided demand in 2005, and the Linking Directive allowed the Kyoto Protocol's flexible mechanisms to provide supply. Thus, the carbon market was up in 2005–2006 and running well before the Kyoto Protocol's first commitment period.

As the EU ETS Phase I went into effect on January 1, 2005, a price between 8€ and 12€ a ton emerged for EUAs in the EU ETS market. Prices then climbed to over 30€ a ton for several reasons, including a cold winter spell in early 2005, a dry summer in southern Europe, and high natural gas and oil prices that made coal more attractive. Another reason was that companies with installations that were short allowances and needed to cover their emissions were disproportionately greater in number than those that held long positions (Ellerman and Joskow 2008).

In April 2006, however, within a span of a week, EUA prices fell sharply from over 30€ a ton to 20€ for Phase II EUAs and 15€ for Phase I EUAs. The precipitating event was the very first reporting of 2005 emissions by several member states, with emission levels that were significantly less than expected. For the trial period, allowances had been distributed based on an *estimate* of aggregate emissions, rather

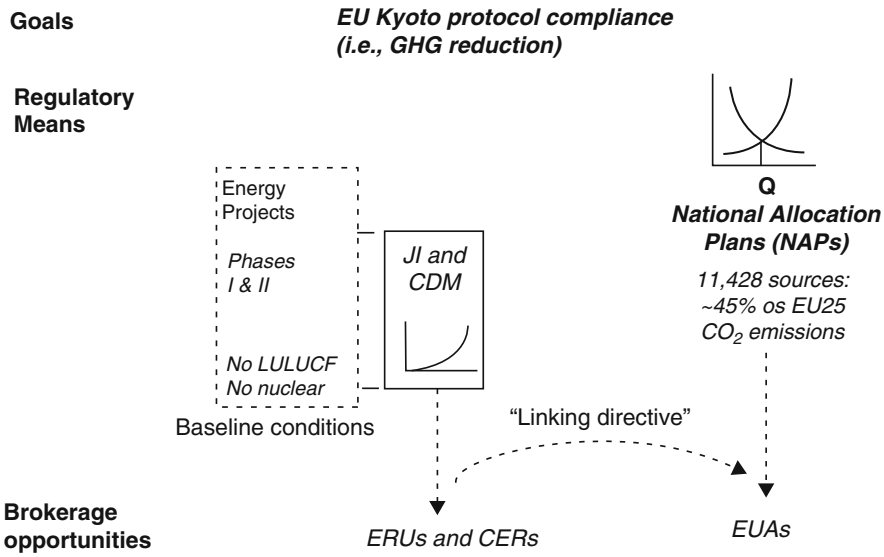

Fig. 9 The EU ETS linking directive

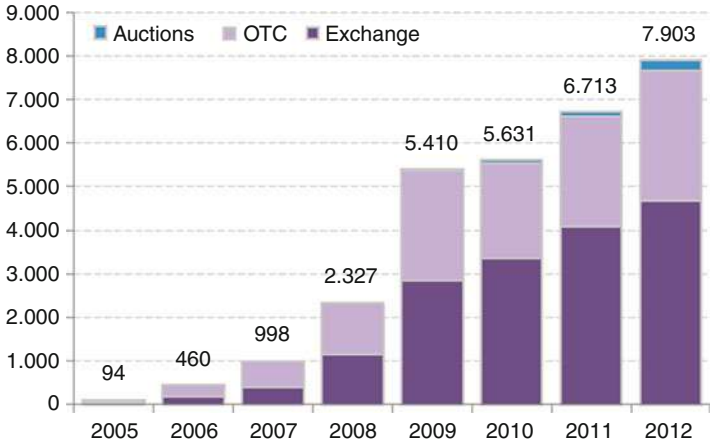

Fig. 10 Trading volumes in EU emission allowances (in millions of tons) (Source: EC 2013; Prepared by Bloomberg New Energy Finance, with data from Bloomberg, ICE, BlueNext, EEX, GreenX, Climex, CCX, Greenmarket, Nordpool; other sources include UNFCCC and Bloomberg New Energy Finance estimations)

than actual emissions. In addition, the restriction on trading between Phases I and II caused prices to decline sharply after September 2006, effectively making trading during the trial period self-contained. OTC markets were the dominant form of trading during the first years. However, trading in organized exchanges has gained popularity over time, and in 2012 it supported greater than three-fifths of trades (see Fig. 10).

From 2013, auctioning is the default method of allocating allowances within the EU ETS, and more than 40 % of allowances were auctioned in that year. Two auction platforms are in place: the European Energy Exchange (EEX) is the common platform for the large majority of countries participating in the EU ETS; a second auction platform is ICE Futures Europe (ICE) in London, which acts as the United Kingdom's platform.

Ultimately, the "learning by doing" phase did exactly what it was expected to do – it established the necessary infrastructure and created a carbon market for the free trade of emission allowances across the EU. There were several lessons learned from the exercise: the lack of verified emissions data caused difficulties in setting compliance targets; the free distribution of allowances resulted in windfall profits for several power companies, who received allowances for free, yet charged electricity consumers based upon their market price; and the haphazard release of emissions data by individual governments was problematical, since market positions could be affected by such information. The process for setting the cap made it difficult to ensure scarcity in the market, given the uncertainty about the emissions data, as well as the fact that national governments were under considerable pressure from companies not to be too stringent – after all, their competitors in the US, China, and other major economies were not operating under such constraints. The total EU-wide allocation in Phase I was estimated to be only 1 % below projected "business as usual" scenarios. In fact, during 2005, 2,088 million allowances were issued, but actual emissions were only 2,007 million tons resulting in 80 million surplus allowances (Baker and McKenzie International 2008). These issues were addressed in the design of subsequent phases of the EU ETS.

EU ETS Phases II and III

The EU ETS Phase II was in operation in 2008–2012 and coincided with the Kyoto Protocol's first commitment period. Phase II had a number of changes from Phase I; one of them was the inclusion of Norway, Iceland and Lichtenstein (1.1.2008).

Phase II removed the *force majeure* provisions, and raised the auctioning limit from 5 % to 10 %. The penalty for noncompliance increased from 40€ to 100€/t CO_2e. More installations were covered in Phase II, including hydrocarbon cracking units, carbon black, flaring, furnaces, and integrated steel works. Importantly, targets specified in the NAPs reflected actual 2005 reported emissions, as opposed to estimates (i.e., the case in Phase I). Moreover, in order to ensure that a significant portion of the expected emission reductions occurred within each country, the use of CERs and ERUs for meeting compliance requirements was limited within the ETS Phase II as a percentage of the allocation to an installation.

Despite the fact that the number of allowances was reduced by 6.5 % for Phase II, the economic downturn cut emissions (and thus demand) by an even greater amount. This led to a surplus of unused allowances and credits, which continues to weigh upon the carbon price (see Fig. 11).

Phase III of the EU ETS contained reforms designed to make it a more efficient, harmonized and a fairer trading system. Among the major changes in Phase III, NAPs were abolished in favor of an EU-wide cap, and a progressive shift towards

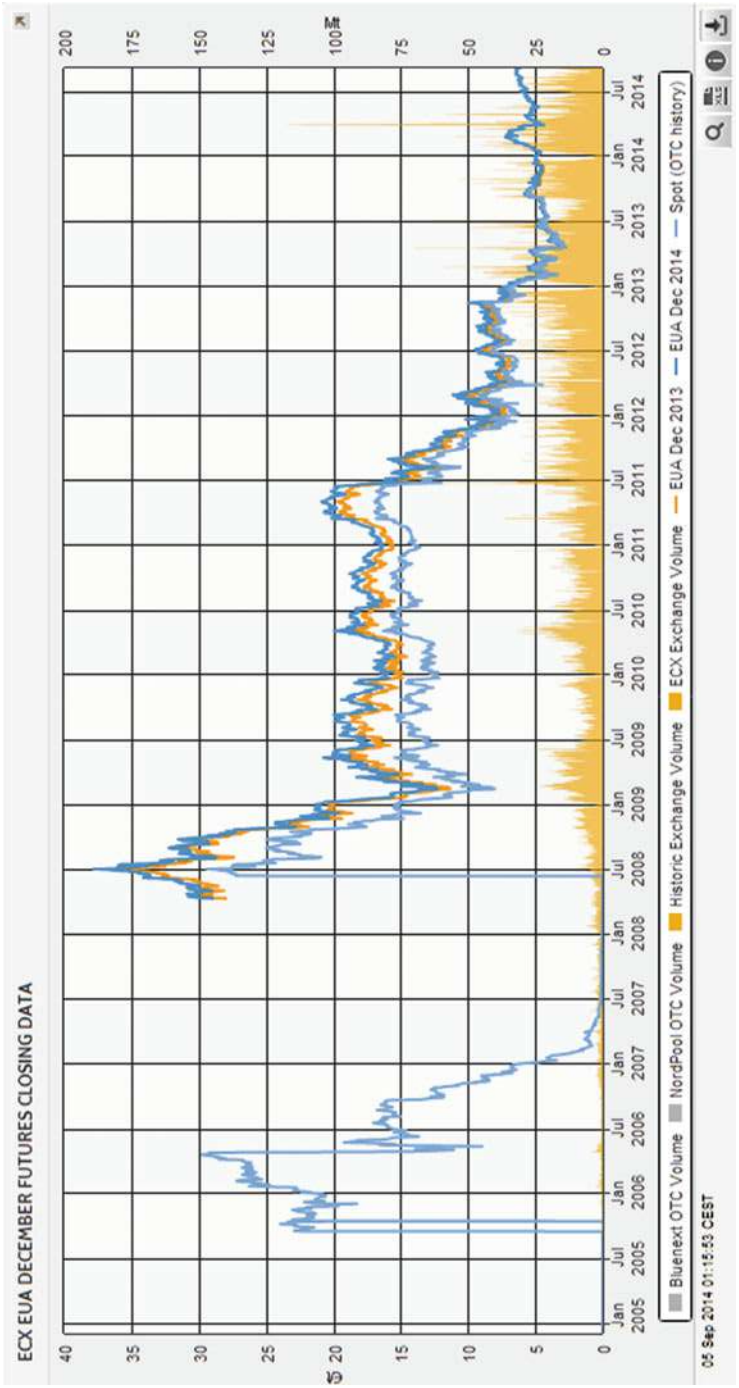

Fig. 11 ECX EUA December Futures Closing Data (Source: Point Carbon – Europe 2014)

auctioning of allowances has replaced cost-free allocation. In 2013 more than 40 % of all allowances in the system were auctioned. The EU legislation set the goal of phasing out free allocation completely by 2027. The cap currently decreases every year by 1.74 % of the average total quantity of allowances issued annually in 2008–2012. Thanks to this decreasing cap, in 2020 emissions from fixed installations will be 21 % lower than in 2005. Croatia joined the EU ETS in 2013, and, in addition to CO_2, nitrous oxide emissions from the production of nitric, adipic, glyoxylic acid, and perfluorocarbons from the aluminum sector were included in the scheme. Allowances for these sectors were given free in the same manner as other sectors already covered. Carbon capture and geological storage was also added. The power sector is subject to full auctioning, but may receive free allowances for district heating and high-efficiency cogeneration activities. For auctioning purposes, 88 % of the allowances are distributed on the basis of the member state's share of historic emissions under the EU ETS – but for purposes of solidarity and growth, 12 % of the total quantity is also distributed in a manner that takes into account GDP per capita and the achievements under the Kyoto-Protocol.

The EU ETS faced considerable problems when it tried to add the aviation sector, a sector not addressed until 2012. Initially all flights from and to EU-28 airports and Norway, Liechtenstein and Iceland (European Economic Area; EEA) were to be included in the EU ETS after January 2012, but this was met with fierce opposition from other countries. In November 2012, the EC therefore issued a "Stop the Clock" amendment, which exempted international flights to and from all EEA countries for a period of 1 year. This allowed time for the International Civil Aviation Organization (ICAO) to develop a global market-based mechanism, and present it to the General Assembly in October 2013. No agreement was reached in the ICAO meetings, however, and after further negotiations the European Council and Parliament decided in March 2014 to extend "Stop to Clock" until 2016. This limited aviation emissions covered within the EU ETS to flights operated solely within the EU for the period from 2013 to 2016. The European Parliament voted in favor of this extension on April 3, 2014, and it was published April 30, 2014 in the Official Journal of the European Union.

The overall use of CDM and JI credits was capped at 50 % of the EU-wide emission reductions over the period 2008–2012, and 50 % of the EU-wide reductions below 2005 levels of new sectors and aviation for the period 2013–2020. In November 2013 the EC set the maximum permitted use of international credits equal to 1,600 to 1,700 million international credits for 2008–2020. Facility operators used 1,059 million Kyoto credits in Phase II, and swapped 133 million Kyoto credits in 2013, leaving room for the use of 400–500 million international credits to meet their compliance obligations up to 2020. Given the low CER prices and the CER–EUA spread, most of the limit for international credits is expected to be used up in the beginning of Phase III. Since 2009 the EU ETS has experienced a growing surplus of allowances and international credits compared to emissions. By the end 2013, there was a surplus of 2.1 billion allowances in the market. This surplus significantly weakened the carbon price signal. EUA prices remained depressed, in the range of about US $5-9 (4–7€) in 2013, contrasting with US$18 (13€) in 2009–2010 (World Bank 2014).

The European Commission has undertaken an initiative to postpone (or 'back-load') the auctioning of 900 million allowances until 2019–2020 as an immediate first step. Back-loading does not reduce the overall number of allowances to be auctioned during Phase III, only the distribution over the period.

Phase IV and the 2030 Framework for Climate and Energy Policy

The 2030 policy framework for climate and energy proposed by the European Commission in January 2014 targets a reduction of EU domestic greenhouse gas emissions by 40 % below the 1990 level by 2030. This target is in line with European objective of cutting emissions by at least 80 % by 2050. EU leaders agreed on this 2030 policy framework in October 2014.

To achieve the overall 40 % target, the sectors covered by the EU ETS would have to reduce their emissions by 43 % compared to 2005. A sustainable solution to the imbalance between supply and demand requires structural changes to the EU ETS. The Commission proposes to establish a market stability reserve (MSR) at the beginning of Phase IV in 2021. This reserve would address both the surplus of emission allowances and the supply of allowances to be auctioned. To address the market imbalance a faster reduction in the EU ETS cap was proposed. The cap will need to be lowered by 2.2 % per year from 2021, compared with 1.74 % currently.

The EU ETS remains the largest carbon market compared to other markets (e.g., China's ETS) or market segments (such as the CDM and JI), accounting for over three-quarters of international carbon trading in 2013. In the EU ETS market, 7.9 billion allowances were traded in 2012 with a total value of 56€ billion (EC 2013). The economic recession in Europe and elsewhere in 2008 and 2009 led to lower demand for housing, cement, automobiles, steel, etc. As demand and commodity prices collapsed, cement and steel companies substantially cut back their production and power consumption. Emissions were therefore lower, as was the need to purchase carbon allowances. Higher supply and lower demand for allowances brought substantially lower prices for EUAs, and although there has been some rebound in 2010, prices remain well below pre-recession ones.

The EU ETS was the very first emission trading regulatory scheme for GHG emissions in the world. Today there are numerous other emission trading systems in place, learning from the EU ETS experience. It is clear that the difficult economic period faced in Europe after 2008 affected both quantities of allowances within the market, and the resulting low prices. Even as the EU ETS became more informed about emissions from the regulated entities (thanks to the registries), it was not able to respond quickly enough to changes brought about by shifts in the global economy. With the new back loading provisions, the CO_2 price should be stabilized during Phase III but at a relatively low price (below 10€/t CO_2). This price will not provide for important decarbonization investments necessary within the economy. With the proposed MSR mechanism, the hope (or fear, to some) is that higher CO_2e prices will become real – perhaps in the range of 48.3€/t CO_2 in 2030 (in nominal terms), according to one forecast (see Fig. 12) (Thomson Reuters Eikon 2014). One recent review of the EU ETS evaluated both the backloading and MSR mechanisms, and viewed both as positive contributions; but it noted that while incentives to abate

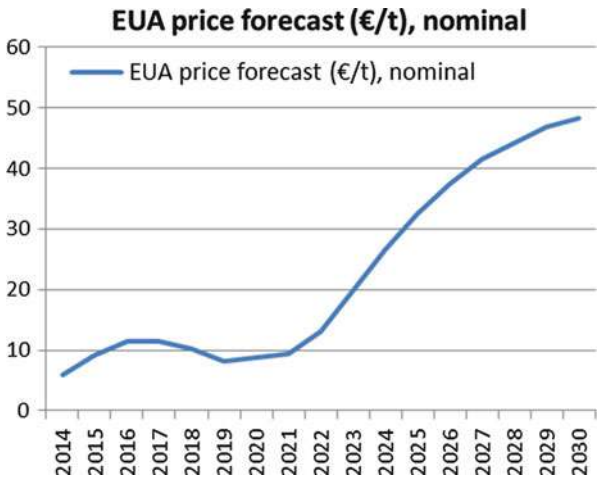

Fig. 12 2014–2030 EUA price forecast (€/t) (Source: IFPEN from Thomson Reuters Eikon 2014)

carbon are growing, they remain very weak. "The one over-riding, inescapably dominant feature of the ETS is its surplus" (Sandbag 2014).

China's ETS

Energy-intensive high-speed growth fueled by a coal-dominated energy mix has made China the world's biggest emitter of greenhouse gases. China has ratified the Kyoto Protocol; however, as a non-Annex I, developing country it is not obligated under the terms of the Protocol to set a specific carbon reduction target. Nonetheless, concerned about runaway emissions and already grappling with the effects of climate change (only projected to intensify), China has sought to take climate action by constraining its carbon emissions. China's 12th Five Year Plan (FYP) (2011–2015) set a carbon intensity reduction target of 17 % from 2010 levels by 2015. Under the leadership of the country's most powerful central government ministry, the National Development and Reform Commission (i.e., NDRC), which is responsible for leading national climate policy, China has begun developing a national market for carbon trading. The country has experience with emissions trading, having experimented with SO_2 trading in the 1980s and 1990s with US support. It has also been the world's leading supplier of CERs under the CDM. Nonetheless, the challenges involved in establishing a national carbon market within a still-developing country, in a rapidly growing economy still undergoing a transition from centralized planning towards a market-based approach cannot be overstated.

Rather than designing a carbon market from the top down through a unified national scheme, carbon market development in China has been initiated as a bottom-up and incremental process. To draw a parallel with the European ETS, China similarly began development of its carbon market with a trial process. Unlike Europe, however, carbon market development has centered on the implementation of experimental local markets, with trading to be scaled up nationwide only after all pilot markets have started accumulated experience (Kong and Freeman 2013).

The NDRC launched the development of carbon markets in China with its "Notice on Carbon Emissions Trading Pilots," announcing in October 2011 that it had selected seven diverse geographic locations across China. The seven pilot regions included two provinces and five cities. The goal of this first phase of China's carbon market development was to have trading underway in all seven pilot markets within approximately 2 years. Only after all pilot markets had begun trading in mid-2014 did the Chinese government commit to having a national carbon market in place by 2016 (Chen and Reklev 2014b). At the time of writing, China's ultimate national carbon trading scheme is still in the design process. There is limited information about what the national carbon market's design will look like, how it will be implemented, and what role the pilot projects will play in a scaled-up trading system. Certainly, the lessons learned during the pilot phases, and the effects of alternate designs, will influence the national program.

With NDRC encouragement, other regions have already begun the process of establishing their own local carbon markets (China Carbon 2014). One of the pilots, Guangdong, is considering linking to other regions, with the goal of designing an interprovincial market (Munnings et al. 2014). This suggests that China may opt for a national trading system that gives local governments the primary responsibility for administering and managing trading within their regions, with the central government setting national standards, including a national legal framework and exercising final authority over local allocation plans (Swartz 2013). Before a national trading system can be successfully established, however, a number of significant structural and policy factors will need to be addressed. If optimistic scenarios prevail, China's carbon market will be the largest in the world, with coverage estimated at 4 billion $MTCO_2$ and an aggregate value of USD 65 billion by 2020, according to NDRC projections (Bifera 2014).

China's ETS Phase I

The NDRC's pilot approach to developing a carbon market in China followed a tried and true approach associated with other significant reform initiatives in the country, as it has "marketized" its one-time command economy by beginning with local experiments. The seven pilots selected by the NDRC and announced in 2011 comprised the cities of Beijing, Shanghai, Tianjin, Chongqing, and Shenzhen, and the provinces of Guangdong and Hubei – locations representative of China's geographic and economic diversity. Estimates vary, but most indicate that the pilot regions cover roughly 1.3 billion $MTCO_2$ in aggregate. In accordance with a local decomposition of the national carbon intensity reduction goal, each pilot region set a different emission intensity reduction target for 2015 compared to 2010, ranging from 15 % of CO_2 for Tianjin and Shenzhen to 17 % for the same period for Hubei, 17 % for Chongqing, 19 % for Shanghai, and 19.5 % for Guangdong (Mao 2014). Local authorities in pilot regions were made responsible for undertaking all aspects of carbon market development, including distributing emissions allowances, creating registries for tracking allowances and emissions, and developing the monitoring and verification standards and procedures integral to a functioning market.

Absent a national standard, every pilot has followed its own path to establishing its market, with the result that each trading scheme has discrete features (see Table 1). Some of these differences reflect the diverse economies of the regional economies represented by the pilots, which vary significantly both in terms of economic structure and by level of development (see Table 2). For example, the share of the tertiary sector in the GDP of the coastal city of Shenzhen, the first of China's special economic zone (SEZs) opened in 1979, was about 52 % in 2012, but only around 36 % for the inland city of Chongqing. It is notable that the order in which trading got underway loosely mirrored the level of economic development of the regions. Shenzhen, with the highest per capita GDP of the group (at approximately USD 22,000 in 2013), launched trading in June 2013; the western province of Hubei and city of Chongqing, with per capita GDPs around USD 7,000 (Statistical Communiqué 2013), were the last two regions to begin trading in April and June 2014 respectively.

The diversity of market design across the seven regions was also reinforced by limited information sharing among them, as each competed to roll out a design that might potentially be selected as a national model or win designation as the central trading platform for a national scheme. There are differences among the local schemes along multiple dimensions. The percentage of emissions covered differs across regions, ranging from 60 % of total estimated regional emissions in Tianjin at the upper end, down to 35 % in Hubei. In addition, some pilots (Beijing and Shenzhen) have passed legislation to structure local cap-and-trade, while others rely on various types of administrative guidelines. There is also considerable variation in the way that the emissions caps are set and in the quantity and structure of offsets (which may be a percentage of emissions or allowances). Regions with relatively small industrial economies and substantial service sectors, like Beijing and Shenzhen, require some companies in the service sector to take part in carbon trading. Beijing includes major public buildings, for example; Shenzhen includes 197 large buildings. Compliance is also enforced by both penalties and incentives that vary across the pilots. Penalties may involve fines and or reductions in the number of free permits in the subsequent year. Incentives include such benefits to firms in compliance as priority access to national funding for low-carbon development, a strategy deployed in Guangdong, for example (Munnings et al. 2014).

The scope of "nonregulated" players able to take part in trading also varies across regions. Most pilot markets do not allow investors and other entities that are not covered by the trading scheme to engage in trading. However, this is not the case for Shenzhen and Tianjin, which do permit financial institutions and other entities not mandated to participate in the trading scheme to take part (Song and Lei 2014). Finally, most pilots do not mandate absolute emission reductions. Beijing is the exception, requiring absolute annual emission reductions for existing facilities in both the manufacturing and service sectors. Other pilots set other types of targets: firms in Shenzhen, for example, are required to reduce their carbon intensity per unit of Industrial Added Value (gross domestic product GDP due to industry) by 32 % below 2010 levels by 2016, keeping their absolute annual emissions growth to less than 10 %, with 2013 as the baseline (Song and Lei 2014).

Table 1 China's seven carbon pilots compared

Pilots		Beijing	Chongqing	Guangdong	Hubei	Shanghai	Shenzhen	Tianjin
ETS Structure	**Start Date**	November 28, 2013	June 19, 2014	December 19, 2013	April 2, 2014	November 26, 2013	June 18, 2013	December 26, 2013
	Total GHG Emissions	103 MtCO_2e (2010)	125 MtCO_2e (2010)	510 Mt CO_2e (2010)	320 Mt CO_2e (2010)	211/240 Mt CO_2e (2010)	83.4 Mt CO_2e (2010)	134 Mt CO_2e (2010)
	Allowances	78 Mt	130 Mt	388 Mt	324 Mt	160 Mt	30 Mt	160 Mt
	Trading center	CBEEX	CCEEX	CEEX in Guangzhou	HCEEX	SEEEX	CEEX in Shenzhen	CTEEX
	Allowance name	BEA	x	GDEA	HBA	SHEA	SZA	TJEA
	Guidance regulation	Decision on carrying out pilot ETS under the strict control of carbon emissions in Beijing	Interim Measures for the Admin. of Carbon Emissions of Chongqing	Interim Measures for the Admin. of Carbon Emissions of Guangdong	Interim Measures of Hubei carbon emissions trading	Interim Measures for the Admin. of Carbon Emissions of Shanghai	Draft Measures on Emissions Trading Pilot	Interim Measures for the Admin. of Carbon Emissions of Tianjin
Coverage	GHG covered	CO_2 (direct and indirect)	6 GHGs (direct and indirect)	CO_2 (direct and indirect)	CO_2 (direct and indirect)	CO_2 (direct and indirect)	CO_2 (direct and indirect)	CO_2 (direct and indirect)
	Coverage	49 %	39.50 %	40 %	35 %	57 %	54 %	60 %
	Sectors	Electricity providers, heating sector, manufacturers (automobile, cement, and petrochemicals), major public buildings (health,	Production of electrolytic aluminum, ferroalloys, calcium carbide, cement, caustic soda, iron and steel. (Could target emissions from forests.)	Power, cement, steel, iron, petrochemicals, (Textile, nonferrous metals, plastic, paper may be included.) Transport and buildings (public,	13 sectors: power plants and industrial companies (iron and steel, cement, chemicals, automobile, manufacturing, nonferrous	16 sectors: industrial sectors (electricity, iron and steel, petrochems., nonferrous metal, chems., building materials, textile, pulp	26 sectors for now Including industrial companies, building sector and electricity generators. Transport	Iron and steel producers, chemical facilities, power and heat generators, oil and gas exploitation,

		education, banking)		commercial) construction.	metals, glass and paper)	and paper, rubber, chem. fiber); other sectors (aviat., ports, rail., comm.,etc.)	under consideration.	civil buildings.
	Liable entities and mandatory reporting	About 490 entities Threshold: 10 $ktCO_2$/year (average of 09-11) Mandatory reporting and voluntary participation. Threshold: 2 ktce/year energy consumption.	About 240 Threshold: 20,000 tCO_2/year (any year of 2008–2010), and new installation after 2010: 20,000 tCO_2/year	Now: 242 liable entities with >20 $ktCO_2$/year (any year of 2011–2014) New regulation: Industry >10 $ktCO_2$/year, mandatory reporting when >5 $ktCO_2$/year, Non industrial sectors: with > 5 $ktCO_2$/year Transport: threshold TBD	Province's 138 biggest emitters Threshold: 120,000 tCO_2e/year (any year of 2010–2011). Mandatory reporting Threshold: 8 ktce of energy consumed/year	191 companies Threshold: 20 $ktCO_2$/year (any year of 2010 or 2011) for industrial companies; 10 $ktCO_2e$/year for other sectors. Mandatory emissions reporting for about 600 firms. Threshold: 10 $ktCO_2$/year	832 companies Threshold: 5 $ktCO_2e$/year 197 large buildings. Threshold: 20,000 m^2 for public buildings and 10,000 m^2 for state office buildings. Mandatory reporting. Threshold: emissions btw. 3-5 $ktCO_2e$/year +	114 entities Threshold: 20 $ktCO_2$/year (any year since 2009) Mandatory reporting for carbon intensive industries and civil buildings with >10 $ktCO_2e$/year (steel, iron, power, heating, (petro) chemicals).
	New entrants and activity change	Entities with emission change of >5 $ktCO_2$/year or >20 % are liable to request	x	New entrants reserve (20 Mt). New project (including capacity extension or	x	In case of closure or displacement of activity, compliance obligation is	Reserve (2 % of total cap). New fixed-asset projects with over ¥ 200 million	Compliance obligation in case of closure.

(*continued*)

Table 1 (continued)

Pilots		Beijing	Chongqing	Guangdong	Hubei	Shanghai	Shenzhen	Tianjin
		allowance change.		reconstruction) with >10 $ktCO_2$/year should purchase all quotas prior to operation. Quota reallocation for activity change, reduction and closure.		due and 50 % of following-year allowances after obligation shall be taken back.	invest. should submit emission eval. report. In case of closure or displacement of activity, compliance due and 50 % of following-year allowances shall be taken back.	
	Allocation	Grandfather method (2009–2011)	Grandfather (2008–2012)	Grandfather method (2010–2012)	Comprehensive method; grandfather	Grandfather (2009–2011) Benchmarking	Carbon Emission per Industrial Value Added	Grandfather (base year not specific)

Sources: Zhong (2014), Wu et al. (2014), Quemin and Wang (2014)

Table 2 Economic structure of the seven carbon market pilot regions (% share of GDP, 2012)

Pilots	Primary sector	Secondary sector	Tertiary sector	Energy mix (coal)
Beijing	0.9 %	24 %	75.1 %	43 %
Chongqing	8.6 %	55 %	36.4 %	50 %
Guangdong	5 %	50 %	45 %	22 %
Hubei	13.4 %	48.7 %	37.9 %	72.5 %
Shanghai	0.7 %	42.1 %	57.2 %	30 %
Shenzhen	0.1	47.5 %	52.4 %	59 %
Tianjin	1.6	52.4 %	46.0 %	71 %

Sources: PMR (2014), Liu and Xu (2012), UNDP China and Institute for Urban and Environmental Studies, CASS (2013)

Despite the variation among them, the seven pilots also share many fundamental features. All pilots include both indirect and direct emissions of carbon dioxide (ICAP 2014b). Most pilots use grandfathering as the principal method by which to allocate initial allowances (PMR 2014). Nearly all pilots distribute allowances for entities mandated to participate in the cap-and-trade system at the beginning of a compliance year without a charge. (In Shenzhen and Guangdong, however, a small number of allowances are also allocated via fixed-price sale or auction (King and Wood Mallesons 2014).) The majority of pilots allow offsets that may or may not include CCERs and other offset types (such as Hubei, which includes forest offsets from within the Province; Chongqing is also considering doing so). Finally, most, with the exception of Shenzhen, which bases its cap on a set of criteria, set their cap based on a minimum quantitative level of carbon emissions.

Carbon trading transactions reached approximately USD 140 million by September 2014 (Carbon Eight Group 2014). Every pilot region has its own carbon exchange; membership in the exchange is a prerequisite for trading. Allowances are tradable only in the regional exchanges. During the first year in which trading took place, price volatility was a feature of most of the pilot regions. Prices also varied considerably from one region to the next, not surprisingly, given the variation in design and economic structures among the pilot markets (see Fig. 13). Trading volumes have also been quite low. As one study points out, Shenzhen, which has been the most active of the pilot markets, traded just 4 % of the total allowances available in its market during his first compliance year (Munnings et al. 2014). Pilots have been experimenting with ways to boost liquidity. To date, Chinese authorities have prohibited futures contracts in carbon trading out of concerns that doing so would invite destabilizing speculation in its financial markets. However, Guangdong, Tianjin, and Hubei have allowed some investors to trade permits with entities bound by emissions limits. Shanghai allows registered institutional investors to trade permits; Shenzhen plans to allow foreign investors to do so, reportedly allowing trading in foreign currency (Chen and Reklev 2014b).

Fig. 13 Prices for Chinese ETSs, July 2013–October 2014 (Source: Bifera 2014)

China ETS Phase II

The announcement by a senior climate policy official from the NDRC in late August 2014 that China would launch a national carbon market by 2016, with regulations for a national market to be sent to the State Council for approval by the end of the year, was an unequivocal commitment by China's central authorities to scale up carbon market development (Chen and Reklev 2014b). Launching a national carbon market would be an ambitious undertaking for even the most developed economy; to implement cap-and-trade on a nationwide scale for a transitional economy the size and complexity of China's requires authorities to tackle numerous challenges. They must not only arrive at a functional design but also construct the institutions necessary to create a national market for buying and selling carbon. Doing so requires substantial numbers of technically capable trained personnel along with regulatory institutions that can set emissions caps, support an emissions trading registry, and monitor trading and enforce compliance. Pilots have taken on these challenges at the local level. However, as will be discussed below, the development of regional schemes has also revealed the challenges of designing an effective market in a political-economy in which transparency is limited. For a market to function, an accurate accounting of carbon emissions must be made in order for legitimate transactions to take place. China's official data collections systems are highly opaque, a feature that must be adjusted for cap-and-trade to work. Specifically, a national MRV system capable of inspiring confidence in trade for an intangible commodity must be developed (Kong and Freeman 2013). In short, on the institutional front, as China's proposal for market readiness observes, what is required is a "reliable statistical system, effective program management system and necessary laws and/ or regulations." (PMR 2013). The latter includes the passing by the National People's Congress of a national environmental law that defines carbon as a commodity and explicitly enables enforcement of compliance by regulated firms (Munnings et al. 2014).

In addition to institutional development and implementation, it is also necessary that the central government determine which specific sectors will be covered by the national carbon market, with an eye to future emissions trends, mitigation potential, and other factors such as international linkages (PMR 2013). China has already published monitoring and reporting guidelines for the national level, covering ten sectors: power generation, power transmission and distribution, aviation, cement, ceramics, flat glass, electrolytic aluminum, magnesium smelting, chemicals, and iron and steel. Among the considerations to be addressed are the development of policies to mitigate potential constrains on firm competitiveness and leakage from cap-and-trade; ways of encouraging liquidity without excessive risk to China's fragile financial system; and management of potential new entrants to ensure that increased participation does not add to carbon emissions (Munnings et al. 2014).

China ETS Challenges and Opportunities Ahead

China's bottom-up approach to carbon market development offers numerous lessons for the NDRC as it moves forward. However, the differences among the protocols established for measuring emissions among pilots alone reflects a heterogeneity which will pose challenges to future efforts at harmonization. The seven pilots applied different rules for monitoring, reporting, and verifying emissions; however, a national market requires a single set of enforceable procedures (Kong and Freeman 2013). Chinese authorities, led by the NDRC, are in the process of drafting a National Climate Change law that could provide a legal foundation for a national trading system. The NDRC has also published guidelines for some industries to date but a national registry for greenhouse gas emissions is still under development (Song and Lei 2014). Moreover, for a cap-and-trade system to function, China must develop a system for data reporting, and for collecting greenhouse gas emissions data about industrial sources that is transparent. In addition, China's lack of a well-developed legal system means that compliance by individual firms is heavily dependent on administrative enforcement, which in turn relies on the capacity and will of local authorities to do so. Currently, local officials' (cadres') promotion opportunities are closely linked to economic growth. China's central authorities will have to complete the retooling of China's "cadre evaluation system" to increase the effectiveness of local implementation, as they move ahead with legal development in the country.

Other key systems structuring China's economy also require reform and development for a national cap-and-trade system in China to function effectively. First, reforms are needed in how China manages power pricing. Currently, there are centrally-determined price caps on electricity in place that prevent power producers from passing on the cost of carbon to consumers. This explains why local pilots exclude the power sector or limit coverage to implied (i.e., emissions divided by activity) rather than direct emissions from power consumption. To fully bring the power sector– among the largest sources of carbon emissions in China – into the carbon trading system, difficult national policy changes in this area will be required (Kong and Freeman 2013). Second, China's financial system remains undeveloped and fragile. Concerned about risk, China's NDRC took futures trading off the table

of options for local carbon trading pilots' design. However, most experts see trading in derivative products as necessary for China's carbon market to have the liquidity to be an effective tool in reducing the cost of cuts to emissions (Song and Lei 2014). China's authorities are actively engaged in pushing reforms in the financial sector that will bring it into line with more mature economies; however, this process is a delicate one that will take time. Finally, national tools must be developed to mitigate against the potential for carbon leakage. This requires the ability to assess the risks of leakage accurately so that provisions can be made for regulated enterprises subject to this risk – something the European cap-and-trade system does through rebates in the form of allocations (Munnings et al. 2014). These are just some of the tasks ahead for China as it develops carbon trading on a national scale. Thus, while China's pilot markets mark significant progress toward the development of cap-and-trade, the country still has a long way to go to build an effective national carbon trading system.

US Carbon Trading Programs

While the US played a key role in introducing emissions trading through its ETP and acid rain regulatory programs, and also introduced the market-oriented approach into the Kyoto Protocol, the Bush Administration's withdrawal from the Kyoto process in early 2001 led to a significantly diminished role for the country. European countries, initially quite skeptical about emissions trading, assumed the lead with the launch of the EU ETS in January 2005.

The US did not pursue national carbon trading during the Bush administration, but expectations grew as the 2008 elections approached, because all three major candidates – Hillary Clinton and Barack Obama on the Democratic side and John McCain on the Republican one – espoused support for cap-and-trade legislation during the Presidential campaign. The build-up to the Copenhagen meeting thus assumed that the US would rejoin international efforts, and perhaps link its own national carbon market to ongoing EU ETS and Kyoto Protocol efforts.

Such enthusiasm was enhanced when the American Clean Energy and Security Act (ACES) passed the US House of Representatives less than 6 months after Obama's inauguration in January 2009. It contained an allowance-based program that required a 17 % CO_2 reduction by 2020 (from a 2005 base year) and an 83 % reduction by 2050. Often referred to as the Waxman-Markey bill (after its two principal sponsors), ACES provided for the use of international offsets and also included an allowance price floor. Very similar legislation, entitled the American Power Act (APA), was submitted to the US Senate by Senators Kerry and Lieberman in May of 2010 – but a special election in the State Of Massachusetts earlier that year meant that the Democrats no longer had a "filibuster-proof" Senate (i.e., a Senate able to pass legislation over the objections of Republicans).

The overwhelming Republican victory in mid-term elections later in 2010 ensured that such cap-and-trade legislation would not be enacted at the national level, and that party's efforts have since then focused on rolling back existing environmental legislation (and US EPA's budget) rather than passing new mandates. Prospects for new emissions trading legislation thus appear quite bleak; as one recent

article in *Foreign Policy* noted: "Congress will never pass cap-and-trade, at least until Miami starts flooding" (Galbraith 2014).

Despite such problems, market-oriented GHG control efforts continued at the state level (in California); at the regional level (in the Northeast's Regional Greenhouse Gas Initiative [RGGI]); and even at the national level, through previous legislation initially designed for CAC regulation. These three levels of programs in the US are described below:

California's Emissions Trading Program

California's cap-and-trade program is a result of the California Global Warming Solutions Act of 2006 (AB 32), which required the state's Air Resources Board to develop regulations and market mechanisms to cut the state's GHG emissions back to 1990 levels by 2020 – a reduction of approximately 25 %. Its emissions trading program is thus part of a larger regulatory effort (including a Low Carbon Fuel Standard as well as other energy efficiency standards) to achieve that target.

The market-oriented program went into effect in January, 2012, with compliance obligations beginning 1 year later. The first two compliance years focus solely on electricity and industrial sectors, but the program will expand after that to include transportation and heating fuels (see Fig. 14). It is thus the first multisector carbon trading plan in the US, and given its emissions coverage, is second in size only to the EU ETS.

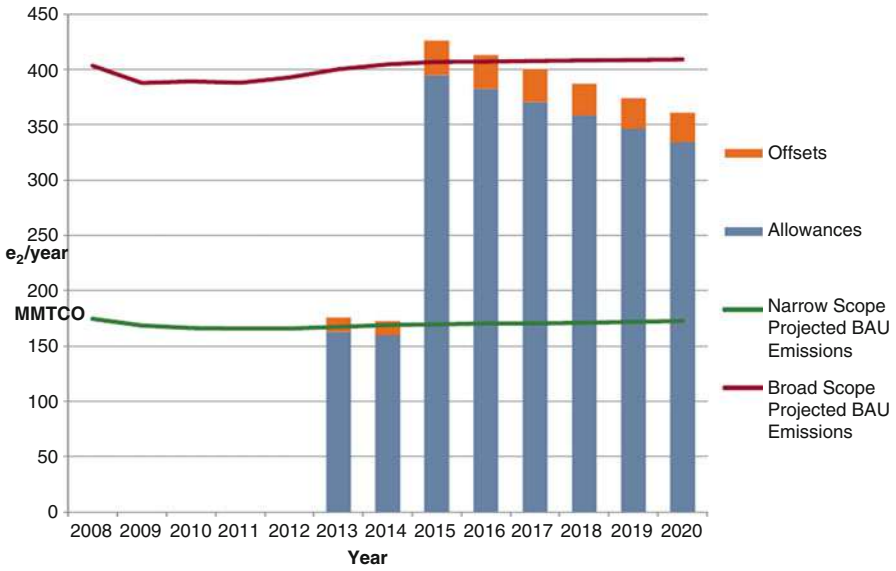

Fig. 14 California's GHG Cap compared with BAU projections (Source: Center for Climate and Energy Solutions 2014; adapted from CARB 2010)

The market covers the same six pollutants as the first commitment period of the Kyoto Protocol, as well as NF3 and other fluoridated gases. It covers approximately 350 business (with 600 facilities), and has been designed to link with similar trading programs in other states and regions.

The California market has several notable features, including both cost containment and market flexibility mechanisms. There is an auction floor price (starting at $10 per allowance in 2012, rising at 5 % above inflation annually) and a strategic reserve (rising from 1 % to 7 % over time, with higher tiered prices similarly rising at 5 % above inflation). There are thus both floor and ceiling mechanisms in place to contain prices (as long as there are sufficient allowances in the reserve).

There are three compliance periods: (a 2-year period [2013–2014]), followed by two 3-year periods [2015–2017 and 2018–2020]). At the end of every year, a source must provide allowances and offsets to cover 30 % of its previous year's emissions. Then, at the end of each compliance period, it must provide the remaining allowances and offsets. This provides sources with the ability to cover any annual variation in product output. If the source does not do so and is not in compliance, then four allowances must be surrendered for every ton not covered within the compliance period.

Offsets are allowed in the California program, but were initially restricted to US emission reduction projects from four targeted types: forestry; urban forestry; dairy digesters; and the destruction of ozone depleting substances. A linkage with Quebec's emissions trading scheme began in January 2014, and linkages with other systems are ultimately expected to occur as well.

Regional Greenhouse Gas Initiative

The Regional Greenhouse Gas Initiative (RGGI) was the first regulatory US cap-and-trade scheme addressing GHGs. It was designed to reduce CO_2 emissions from power plants in ten Northeastern US states – although this was subsequently reduced to nine states when the Republican Governor of New Jersey withdrew his state from the program in 2011.

RGGI is a regional program, but it is implemented through legislation adopted by each individual state. A "Model Rule" was drafted in 2006 and finalized in 2008, with requirements for individual facilities (i.e., fossil-fueled power plants greater than 25 MW generating capacity) beginning on January 1, 2009. RGGI initially sought to cap CO_2 emissions at a steady rate through 2014, and then drop them annually by 2.5 % – and thus achieve a 10 % reduction one decade later. A significant fuel shift towards natural gas at power plants in the region, however, coupled with lower electricity demand and increased levels of both nuclear power and renewables led to an overallocation of allowances. Prices reflected that, and the clearing price for allowances at RGGI auctions was often less than $2.

RGGI's target was revised when New Jersey left, and was then significantly changed as a result of a 2012 Program Review. The new cap called for a reduction of 45 % by 2020 (from 2005 levels), with a 2.5 % reduction occurring annually from the revised 2014 cap levels. This new Model Rule also introduced other provisions, including a Cost Containment Reserve (CCR), and an interim compliance period requiring sources to hold specific allowance levels in time periods before final

compliance dates (Bifera 2013). Most of the allowances in RGGI are sold through auctions, and the collected funds are dedicated for energy efficiency, renewable and clean energy, as well as bill support for low-income energy consumers.

RGGI allows offsets to achieve compliance, but only from five categories: (1) Landfill methane capture and destruction; (2) Reduction in emissions of sulfur hexafluoride (SF_6) in the electric power sector; (3) Sequestration of carbon due to US forest projects (reforestation, improved forest management, avoided conversion) or afforestation (for CT and NY only); (4) Reduction or avoidance of CO_2 emissions from natural gas, oil, or propane end-use combustion due to end-use energy efficiency in the building sector; and (5) Avoided methane emissions from agricultural manure management operations (RGGI n.d.).

Despite the significant drop in target levels in 2014, Fig. 15 shows that the actual emissions in recent years were not significantly above the new cap (i.e., 92 million short tons in 2012, just above the 91 million ton target in 2014). The cap will tighten in coming years, however, and it is not clear that the fuel shifts and other downward trends evident in recent years will continue. Thus, it is anticipated that the RGGI cap could become more binding in the future (EIA 2014).

The US EPA's Clean Power Plan

President George Bush promised to address CO_2 emissions during the 2000 Presidential campaign, but reneged on this shortly after taking office. In 2003, his Administration's EPA overturned a previous Clinton Administration decision, and declared that it did not have the authority to regulate CO_2 under the Clean Air Act – and further noted that it would refrain from doing so, even if it did have the authority. The State of Massachusetts and others filed suit against EPA for its failure to act, a suit which was subsequently decided in their favor in 2007 by the US Supreme Court. The Court ruled that EPA did have such authority, but the law required EPA to determine whether or not such emissions could reasonably be anticipated to endanger public health or welfare. In 2009, under the Obama Administration, US EPA issued such an "Endangerment Finding," and proceeded to issue new standards for light, medium and heavy duty vehicles in the following years. The Agency also proposed GHG standards for new power plants in 2012 and then revised and proposed them once again in September 2013.

On June 2, 2014, it proposed standards for existing power plants, under a program called the Clean Power Plan. Utility emissions are the largest source of carbon pollution in the US, accounting for roughly one-third of all domestic GHGs (EPA 2014b). The Clean Power Plan tackled this in two ways: (1) It set state-specific goals, which were based on achieving a level of carbon intensity in the state by 2030. This would have the effect of reducing CO_2 emissions from the power sector by 30 % (from a 2005 base) and (2) The EPA provided guidelines for the states in how they might achieve such goals.

Under the Clean Power Plan, states would have until June 2016 to submit plans to achieve these goals, with the possibility of a 1-year extension – or 2 years if states join together in a multistate plan. The states were also required to make "reasonable progress" in achieving such goals by 2020.

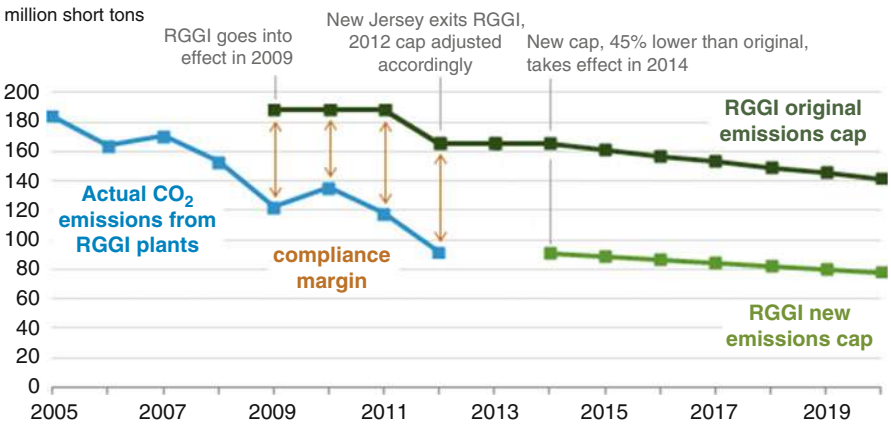

Fig. 15 Regional Greenhouse Gas Initiative CO_2 emissions cap vs. actual emissions (Source: EIA 2014)

Section 111(d) of the Clean Air Act requires US EPA to issue "standards of performance" reflecting the "best system of emission reduction" (BSER), and the Agency has used four "building blocks" of BSER to set the state-by-state goals: (1) heat rate improvements; (2) dispatch changes among affected units (e.g., coal to natural gas units); (3) expanded low- or zero-carbon generation (e.g., renewables and nuclear); and (4) use of demand-side energy efficiency, thereby reducing generation requirements.

US EPA has offered the states considerable flexibility in determining how they might meet their goals. They are able, for example, to:

- Look broadly across the power sector for strategies that get reductions
- Invest in existing energy efficiency programs – or create new ones
- Consider market trends toward improved energy efficiency and a greater reliance on lower-emitting power sources
- Expand renewable energy generation capacity
- Tap into investments already being made to upgrade aging infrastructure
- Integrate their plans into existing power sector planning processes
- Design plans that use innovative, cost-effective regulatory strategies
- Develop a state-only plan or collaborate with each other to develop plans on a multistate basis (USEPA 2014c)

Note that these last two options allow individual states to team up with other states if they choose – and also to employ market-based mechanisms to achieve their goals. Not only would this would allow them to accomplish their reductions in the most cost efficient manner – they will also get an extension on the time required to develop such an approach.

The Clean Air Act of 1970 is a piece of legislation now almost 45 years old, and its principal architecture was developed within the CAC framework. It was never

intended to tackle a problem as complicated and as comprehensive as GHG control. The failure of the political system to pass legislation (such as ACES or APA) means that it must now serve as the foundation for such control, given the fact that the problem is real (as indicated in the Endangerment Finding) and the courts have indicated that US EPA has the authority (and, indeed, the responsibility) to address it.

The US EPA has developed a creative regulatory approach that will allow states to utilize emissions trading, if they so choose – and to do so on a multistate basis. This plan will surely be modified in response to public comment, and must also survive the inevitable lawsuits when it is promulgated. Opponents have already attacked the Plan, based upon media reports that environmentalists played a key role in its development (Davenport 2014; Chait 2014). The final 111(d) rule is due to be released in June 2015, and while states must begin to make reductions by 2020, full compliance with the CO_2 emission performance level in the state plan must be achieved by no later than 2030.

Voluntary Carbon Market

In addition to the "compliance" markets discussed above, a corollary, voluntary market has developed that provides carbon trading opportunities for companies, individuals, and other entities not subject to mandatory limitations, but still wishing to offset their GHG emissions. As the name implies, the voluntary carbon market includes all carbon offset trades that are not required by regulation. Over the past several years, this market has not only provided an opportunity for consumers to alleviate their carbon footprint, but also provided an alternative source of carbon finance. The instrument of trading is called a Voluntary Emission Reduction (VER), although it should be noted that some market participants consider this acronym to mean "Verified Emission Reduction." While still very much smaller than the compliance market (<1 % in value), this voluntary carbon market has gained traction in recent years – although there was a downturn in 2013 in both market size and average price (World Bank 2014). Importantly, however, the voluntary market provided an outlet for forestry and land use–type projects that were excluded by the EU ETS.

The voluntary carbon market is not new – in fact, the world's first carbon offset deal was brokered in 1989, well before regulated carbon markets. AES Corp., an American electric company, invested in an agroforestry project in Guatemala to offset the GHG emitted by electricity production at one of their facilities in Connecticut. AES paid Guatemalan farmers to plant 50 million pine and eucalyptus trees on their land. The deal was voluntary and marked the beginning of this new type of carbon market (Bayon et al. 2007). Another early example was a program established in the late 1990s in Costa Rica to provide funds for reforestation and forest protection on private lands. This program sold carbon certificates called "Certifiable Tradable Offsets" (CTOs) to industrialized countries, and Costa Rica was able to pay thousands of private landowners to establish, protect, and manage

forest plantations on their lands. Nations such as Norway were invited to voluntarily purchase such CTOs for use in meeting their own compliance targets.

These programs were precursors to the provisions for afforestation and reforestation within the CDM. Two types of credits may be generated by Land Use Land Use Change and Forestry (LULUCF) within the CDM, specifically, afforestation and reforestation (A&R) projects. *Temporary credits (tCERs)* from such projects expire at the end of the commitment period following that in which they were issued, and must be replaced by the holder to ensure continuing carbon storage. *Long-term credits (lCERs)* expire at the end of the project's *crediting period*, as opposed to a tCER that expires at the end of the *commitment* period. The crediting period for an afforestation/reforestation project is the period for which net anthropogenic GHG removals by sinks are verified and certified by a DOE (CDM Rulebook 2008). Accordingly, the amount of tCERs issued equals the carbon stock of the whole project, whereas lCERs are only issued for incremental gains in the carbon stock. However, as noted above, the EU ETS' Linking Directive excluded CERs generated from forestry projects for use as offset credits within the Scheme. This is the primary reason that much of the forestry credits have been handled in the voluntary marketplace, rather than the compliance market. Offset credits from "Reduced Emissions from Deforestation and Degradation" (REDD) projects (and also REDD+ projects, which also include sustainable forestry management practices) have also found a home in the voluntary marketplace because they were not included in the Kyoto Protocol's first commitment period. There was a strong push for REDD and REDD+ projects to be included in the post-2012 agreement during COP15 in Copenhagen, but the prospect of a flood of credits from such sources has worried many carbon market proponents (see, for example, (KEA3 2009)). This issue remains as yet unresolved.

Buyers in the voluntary market are motivated by various reasons that are vastly different from those in the compliance market. Not having any binding emission reductions to comply with, companies in the voluntary market purchase credits to offset their carbon footprint for either Corporate Social Responsibility (CSR) reasons or for establishing better public relations with the community. Of the 100 largest economic entities in the world, 40 are corporations, not countries (Global Trends 2013), so voluntary commitments on their part are welcome. Firms in the retail or banking industry, for example, typically do not have a large carbon footprint, but have a high interest in demonstrating that they are socially responsible and "green." They are therefore major purchasers of voluntary carbon credits. Buyers also include individuals who are interested in being environmentally conscientious, and offsetting the carbon footprint of their lifestyles (including homes, cars, travel, etc.).

Voluntary markets initially had a "wild west" quality, and they experienced rapid growth that is now being tamed by verification/standardization. The verification and certification process is often the most important aspect of a product, since it determines the price that the VER from the project commands in the market. The generation of VERs for an offset project mimics the generation of CERs closely, and the quality of an offset project is usually evaluated based on the characteristics of

additionality, permanence (the project generates GHG emissions over a stated period of time), leakage (ensuring that the project does not transfer emissions to another location outside the project area), and co-benefits (benefits derived from the project over and above GHG reductions, such as habitat for biodiversity, contributions to local communities, etc.). In general, consumers prefer third-party verification to in-house verification for reasons of credibility. Major standards and certification programs used in the voluntary carbon markets are listed in the Carbon Offset Research and Education (CORE) website, a joint effort of the Stockholm Environment Institute and the GGH Management Institute (CORE 2011). Each standard has a slightly different focus in terms of project goals and addresses each of the above characteristics according to those goals.

The Verified Carbon Standard (VCS) is the most popular standard (VCS 2014), while premium carbon verification standards such as the Gold Standard tend to attract the highest prices for VERs accredited to them. VERs have typically sold at a discount to CERs or other compliance market project-based carbon credits, although the low prices across all instruments in the carbon market have led buyers to place additional focus on the co-benefits associated with their generation – a situation particularly relevant within the CSR-oriented voluntary market.

Voluntary carbon credits may be traded bilaterally, OTC, or in organized exchanges. Several exchanges throughout the world began with a focus on voluntary carbon trading, with the earliest one being the Chicago Climate Exchange (CCX). CCX was the world's first legally binding, rules-based GHG emissions trading system (Sandor 2012). It was important for several reasons, including the fact its owners spread the GHG carbon exchange approach to Europe (through its sister company, the European Climate Exchange [ECX]) and China (through a partnership with the municipal government of Tianjin and PetroChina in the Tianjin Climate Exchange). Members voluntarily joined the CCX, and agreed to a legally binding carbon reduction policy. It grew to include some 300 members, including 11 % of the Fortune 100 companies in the US, and 20 % of the country's largest CO_2 emitters. The CCX's unit of trade was the Carbon Financial Instrument (CFI), which represented 100 tCO_2e. CCX represented a significant fraction of the voluntary carbon market after the company's founding in 2003, representing more than 50 % of voluntary carbon trading volume in 2008. Its parent company (Climate Exchange Plc) was acquired by Intercontinental Exchange Inc. in mid-2010, however, and its emission reduction program closed at the end of that year. The CCX's offsets registry program has continued, however.

Many exchanges in developing countries began in the voluntary carbon market, with plans to become established and then play a much larger role in future compliance regimes. The China Beijing Environment Exchange (CBEEX), for example, is an environmental equity transaction institution authorized by the Beijing Municipal Government. In 2009, the CBEEX signed a deal with BlueNext to build a trading platform for carbon credits, and at the Copenhagen COP announced the Panda Standard, the first voluntary standard created specifically for the Chinese VER market. The CBEEX also traded the first VER transaction in China in August 2009. Today, as noted above, it is playing a key role in the country's compliance market.

Carbon Financial Derivatives

In anticipation of a price on carbon emissions and the associated market growth created by a cap-and-trade scheme, a number of financial instruments and derivatives based on carbon as a commodity have been developed. These have led to increased carbon trading activity in financial markets. While government officials are responsible for designing effective cap-and-trade systems, and polluters participate in the resulting market to comply with emissions constraints, carbon derivatives trading brings commodities traders, speculators, hedge funds, financial firms, and exchanges into the fray.

Derivatives are financial instruments whose cash flow is *derived* from an underlying instrument. There are several types of derivatives, including *future and forward contracts*, which are fundamental derivatives that represent an agreement to sell a certain commodity in the future at a fixed price; *options*, which are slightly more complicated derivatives where the buyer is given the right (but not the obligation) of purchasing the commodity depending on the price of the commodity in the future at a price (agreed upon at the present time), and *swaps*, in which two counterparties exchange certain benefits of one party's financial instrument for those of the other party's instrument.

Derivatives can be used for a variety of purposes. They can be used to hedge a transaction, (i.e., reduce risk exposure), and derivatives markets are thus risk transfer mechanisms. They facilitate the transfer of risk from those exposed to it but who do not wish to bear the risk (i.e., hedgers) to others not naturally exposed to it, but willing to bear the risk (i.e., speculators). Derivatives also contribute to price discovery; since individuals with information can buy or sell derivatives, their trades affect prices and these prices reflect their information. Derivatives may be traded bilaterally, or in the OTC market through brokers, or in organized exchanges such as the New York Mercantile Exchange (NYMEX).

Compliance carbon markets can also support the trading of such derivative products, including futures, options, and swaps. Currently, most carbon is sold in futures or forward contracts. These contracts contain promises to deliver carbon allowances or credits in a certain quantity, at a certain price, by a specified date. In the case of the EU ETS, the forward and futures markets have developed faster than the spot market. Approximately 95 % of the total volume in the European carbon market is seen in derivatives trades, with the remaining in spot trades. According to the ECX, this may partly be explained by the initial delay of national registries and final allocations in many of the EU member states, which prevented the execution of instant delivery for spot contracts. Another reason may be that in such a new and volatile market, derivative instruments are crucial tools to optimize the value of an emissions portfolio.

Carbon derivatives trading was severely affected by several factors in 2009. The economic recession slowed down manufacturing and other industries, causing reduced economic output, and hence lower emissions and a surplus of allowances. A large sell-off of EUAs started in September 2008, as companies realized that the allowances they had received at no charge could help provide liquidity, particularly

in the midst of a financial credit crunch. The EUA sell-off, mostly on the spot market, was followed by a discernible increase in trading of EUA options (more calls than puts, on average), showing the intent of some installations to hedge any anticipated 2008–2012 compliance exposure (World Bank 2010). Failure by governments to achieve a solid agreement on climate change negotiations in Copenhagen in December 2009 added to the downward trend of carbon markets, with carbon prices falling nearly 10 % (the biggest decline in 2009) immediately after the summit. The uncertainty about the future of emissions trading after the Kyoto Protocol's first commitment period expired in 2012, and the continued absence of a national cap-and-trade program in countries such as US, depressed prices even further. Reuters reported that the global carbon market would have reached $2 trillion by 2020 if nations had agreed to a new climate pact curbing greenhouse gas emissions and if the United States introduced its own federal cap-and-trade scheme (Reuters 2009). However, because neither case seemed probable, banks and investors started pulling out of the carbon market and emptying their carbon trading desks in early 2010 (Guardian 2010).

To make matters worse, the EU ETS was hit by a number of other significant controversies in Phase II. In December 2009, Europol announced that the EU ETS had been the victim of fraudulent traders over a period of 18 months, resulting in losses of approximately 5€ billion for several nations (Europol 2009). Traders would collect Value Added Tax (VAT) on carbon market transactions, but then not submit the collected revenue to national governments. They would then disappear without a trace, leading to the phrase "missing trader fraud" to describe the crime.

In early 2010, there were market disruptions because of the resale of two million surrendered CERs by the Hungarian Government. The Hungarian government first covered the CERs (which had been surrendered by Hungarian companies to comply with the emissions cap under the EU ETS) with AAUs because the CER price exceeded that of an AAU. They then signed a deal to sell those same CERs to a trading firm, and some of these "recycled CERs" eventually came back into the European market. A number of exchanges were thus forced to shut down, until the integrity of their CERs could be fully established and this loophole closed.

In 2010, there were also reports of "boiler room operations" that were selling emissions reduction credits (i.e., carbon offsets) as investments in the U.K. These are organizations that tend to target vulnerable or unsophisticated individuals with (often worthless) investment products using deceptive or especially aggressive sales tactics. The US-based Center for Resource Solutions has prepared a manual addressing such practices in the carbon market (Jones 2014).

The 2008 financial crisis caused by subprime mortgages and financial derivatives such as credit default swaps based on questionable risk profiles also raised other questions about carbon derivatives trading. For example, the potential for "subprime carbon" credits, i.e., relatively high-risk contracts to deliver carbon that might not mature to fruition (Chan 2009), was noted by some analysts. Carbon offset aggregators bundle small offset projects for buyers, and increased demand might give rise to exotic derivatives and structured products, similar to the situation in mortgage-backed securities. In November 2008, Credit Suisse announced just such a

securitized carbon deal in which credits from 25 offset projects were bundled. These were then securitized into three tranches of different risk levels and sold to investors. The 25 projects were at various stages of UN approval, and were spread across three different countries and five project developers (Chan 2009). Such off-balance sheet products, albeit profitable in the short-term, are highly risky and require close regulatory oversight. As the carbon market has contracted, banks and other financial institutions have withdrawn – and such arcane financial engineering has similarly declined. Regulators are also more diligent. China, for example, has limited its pilot projects to spot market transactions only in initial phases, in part to gain regulatory experience.

In May 2014, however, China General Nuclear Power Group announced that it would launch the first carbon-linked financial product, a debt note linked to the performance of carbon offsets on the Shenzhen Emissions Exchange (Chen and Reklev 2014a). The Shenzhen Emissions Exchange announced just a few months later (in August) that it would allow foreigners to trade on its exchange, although a date has not yet been set. Regulators thus face a challenge as carbon markets become increasingly sophisticated in emerging nations, to ensure that they offer stable and consistent financial systems, as well as ultimately satisfy the environmental objectives they are designed to accomplish.

Renewable Energy and Energy Efficiency Markets

While pollution presents policy makers with a *negative externality*, some energy technologies might be thought of as generating *positive externalities* because they are easily replenished and nonpolluting in nature, are decentralized, and can increase system resiliency, etc. While not the principal focus of this chapter, those interested in emissions trading should nonetheless be aware that a mirror image exists in the form of "positive externality" instruments. These typically provide support for renewable energy systems and energy efficiency and are growing in popularity.

Renewable Energy Certificates (RECs)

The market-based instrument employed in renewable energy markets is the Renewable Energy Certificate (REC), also called a *green tag* or *greencertificate*. It typically represents 1 MWh of electricity generated from a renewable energy source. A REC is an environmental commodity, and may be sold separately from the underlying electricity generated. Buyers can select RECs based on the generation source (e.g., wind, solar, geothermal), as well as the location of the renewable generator.

RECs may be used in both compliance and voluntary markets. In the US, compliance markets have been established by state Renewable Portfolio Standards (RPS), which require utilities to meet a certain quota of their electricity from renewable sources by a certain date. This quota is often increased over time, the converse of an emissions cap being lowered to reduce GHG emissions. An RPS

provides states with a mechanism to increase renewable energy generation using a cost-effective, market-based approach that is administratively and economically efficient. The goal of an RPS is to stimulate market and technology development so that, ultimately, renewable energy will be economically competitive with conventional forms of electric power.

Currently, 29 US states, the District of Columbia, and two US territories (i.e., Guam and the Northern Mariana Islands) have RPS policies in place, covering more than half of the electricity sales in the country. California, for instance, requires 33 % of its electricity to be generated from eligible renewable sources by the year 2020. Another nine states and two territories have nonbinding RPS goals (DSIRE 2014a). It is important to note that not all states permit REC trading for compliance with their RPS. An important feature of the REC compliance market in the US is that the goals differ from state to state; therefore, prices of RECs also differ. Compliance buyers are generally indifferent to the type of resource that created the REC, but are limited to the geographical area where the REC can be produced. The US Department of Energy's National Renewable Energy Laboratory (NREL) expects demand in the RPS market for renewable energies to grow from 22,296 GWh in 2008 to 156,527 GWh in 2015 (Bird et al. 2009).

European Union nations have established similar schemes to comply with an EU target of 20 % energy from renewable sources by 2020. In the UK, a scheme similar to the RPS has been set up where *Renewable Obligation Certificates (ROCs)*, each representing one MWh, are tradable green certificates issued to an accredited generator for eligible renewable electricity generated and supplied to customers within the country. Similarly, since January 2012 Sweden and Norway have had a common market for RECs. It was based on Sweden's "Electricity Certificate System" (established in 2003), and is designed to increase renewable energy production by a total of 26.4 TWh in the two countries between 2012 and 2020. The market is designed to be in place until 2035 (Energimyndigheten and NVE 2013).

There is also an active voluntary REC market, spurred by companies, government agencies and private consumers who have opted to support "green power" either by buying renewable energy directly, or through a variety of retail programs. In many cases, buyers purchase the "green attributes" of the REC associated with energy generation. Several factors motivate demand in the voluntary renewable energy market, including corporations seeking to differentiate themselves from competitors by environmental means, as well as environmentally-minded consumers of electricity. Although much smaller than RPS compliance markets, voluntary REC markets have been growing in the United States and in Europe.

The advantage of RECs in voluntary markets is that they can be sold unbundled from electricity, and so their market is national, while green power markets tend to be tied to local providers.

Prices of certificates from eligible renewable facilities under an RPS scheme (compliance RECs, or C-RECS) differ from RECS generated in the voluntary market (V-RECs) because the drivers of demand differ (Gillenwater 2008a, b), and prices can be considerably different (e.g., between $50 and $60 per MWh in the Northeastern US in 2011, versus less than $5 in Ohio and Texas). Prices for voluntary

RECs were below $1 per MWh for this same period, although RECs from wind projects in the West were somewhat higher (NREL 2012). Voluntary market purchases rely on certification programs to verify that the RECs were indeed generated by the renewable resource that is claimed, and that a REC is not sold to more than one buyer. The *Green-e* program is a nationally recognized standard that helps consumers identify environmentally qualified RECs.

The dynamics of linking renewable energy markets with emissions trading schemes brings up interesting questions and controversies. Because RES emit little-to-no pollutants, they are economically advantaged by any policy that puts a cost on emitting pollutants within the power sector. The issue of converting RECs to carbon offsets has produced heated debates in the voluntary carbon markets, especially in the US (Ecosystem Marketplace 2009). While the REC market essentially operates independently of the carbon market, RECs are sometimes viewed as tons of carbon dioxide avoided, and are sold into the voluntary carbon market as a carbon offset. The controversy in this practice revolves around the accuracy of carbon calculations, the additionality and ownership terms operating in different markets, and the potential for double counting in two markets with different (but often complementary) policy goals. Voluntary green power and GHG offset markets are not regulatory markets (by definition) and lack standardized commodities, resulting in a great deal of confusion for consumers wishing to offset their emissions associated with energy consumption. Because RECs are typically less expensive (mostly due to differences in additionality requirements) than offset credits, they are generally favored for purchase.

Renewable energy now represents more than 20 % of electricity production worldwide, and its share has been growing faster than conventional sources. RECs markets are therefore likely to play an increasingly important role.

Energy Efficiency Certificates (EECs)

Energy Efficiency Certificates (sometimes called *white tags*, or *whitecertificates*) are similar to RECs, except that they represent a unit of energy *not used*. White tags are usually created through energy conservation projects such as equipment upgrades, retrofits, combined heat and power (CHP), or cogeneration and demand-side management. A market for energy efficiency is created by setting an energy-saving obligation on entities in the energy supply chain, with preset rules for trading, monitoring, and verification. EECs are awarded to entities that create more energy savings than the target (typically in terms of electricity or oil equivalent energy units), and these EECs may then be sold or traded in the marketplace to those entities that are unable to meet their obligations.

Energy savings are usually cost-effective and efficient ways to reduce GHG emissions, in addition to providing energy security and independence. The process of measuring the energy efficiency savings requires establishing a baseline for energy use and/or demand before and after the implementation of an efficiency project. The approach to doing this depends on the specific market design rules, and can include “deemed savings” figures (i.e., standard figures for projects where the

expected savings are well understood), engineering calculations, and direct measurement. Many compliance markets require third party verification using a MRV protocol. The protocol may vary depending on policy decisions about program implementation cost, ease of compliance, and other factors. White tags are a type of offset credit instrument because they require the application of project-based accounting rules, with baseline, additionality, leakage, and ownership constraints. Currently, EEC markets exist in Italy, the UK, France, and several other nations in Europe. As of February, 2013, 20 US states have energy efficiency targets, typically through Energy Efficiency Resource Standards (EERS), and another seven have nonbinding goals (DSIRE 2014b).

India, now the third largest GHG emitter (after China and the US) launched the "Perform, Achieve and Trade" (PAT) scheme in July 2012, to comply with the National Mission for Enhanced Energy Efficiency (NMEEE), a part of the country's National Action Plan on Climate Change. PAT affects eight energy-intensive sectors (including thermal power plants, iron and steel facilities, cement plants, etc.). These eight sectors account for 25 % of the country's GDP and about 45 % of its primary energy consumption. PAT addresses the energy use of 478 industrial consumers, and creates a market in tradable white certificates called Energy Saving Certificates (ESCerts). One ESCert is equivalent to 1 MTOE (Metric Ton of Oil Equivalent), and PAT is expected to save the country approximately 6.6 million MTOE by the end of 2015. In addition to its PAT program, India also began a RECs green certificate market the previous year (i.e., 2011), and analysts have been studying whether a coordinated program (i.e., with fungible certificates) is feasible and/or appropriate (Ministry of Power and Government of India 2012; EDF and IETA 2012).

Such questions obviously arise as RECs and EEC markets are superimposed or run in parallel with emissions trading schemes. In 2008, the EU explored the potential for establishing a pan-European market in "Guarantees of Origin" to help meet its 20 % renewable energy goal by 2020, but ultimately decided that conflicts and interactions with the EU ETS warranted the more conservative approach of national indicative targets rather than binding quotas and trading. The Greenhouse Gas Protocol (the most widely used accounting tool for quantifying and managing GHG emissions) and carbon registries around the world face an exceedingly difficult task as the complexity of instruments, the potential for "double counting," and potential interactions increase.

Future Directions

The world now has almost four decades of experience with emissions trading, and much has changed during that period. It was introduced almost inadvertently in the US, as a means of dealing with problems associated with CAC regulation, and employed a baseline-and-credit scheme to deal with localized air quality. The resulting markets were very small, and – while offering some economic relief – were not designed to change environmental conditions (relying upon the CAC to do so).

There was considerably more success, however, when the US employed the economists' ideal of a quantity-based approach (called "cap-and-trade") in 1990 to cut sulfur dioxide emissions from the power sector in half. This success led to the subsequent adoption of such emissions trading mechanisms – both baseline-and-credit and cap-and-trade – within the Kyoto Protocol.

Today, SO_2 trading has collapsed within the US power sector, primarily because further controls were deemed necessary (to address PM-2.5, mercury, regional haze, etc.); the spatial characteristics of the control were recognized as significant (i.e., as opposed to the simpler "total loading" goals of the acid rain control program); and further economic analyses have made clear that essentially full controls for pollutants such as SO_2, particulate, and NOx are readily available and appropriate.

Carbon dioxide is a different matter, however. The technological options for pollution control (e.g., amine stripping, carbon capture and storage techniques, etc.) tend to be energy intensive and very expensive. The physical characteristics and impacts of the pollutant are also notably different. Humans exhale carbon dioxide, and toxic impacts only occur at extremely high concentrations – well above those normally occurring in natural systems. The pollutant mixes uniformly throughout the atmosphere, and the spatial characteristics are thus not significant (i.e., it doesn't matter where emissions occur, or where control takes place). Carbon dioxide is thus almost the perfect pollutant for an international market-based emissions trading approach.

Carbon trading in the real world, however, has similarly suffered its own downturns over recent years. The driving force behind the carbon market was the EU, not the US. The EU ETS was established to help European countries meet their Kyoto Protocol targets in an efficient manner, but that market was soon awash in allowances as economic contraction rather than new technology reduced emissions. Prices fell dramatically. The weak economy, lingering unemployment and the financial crisis, linked with real and perceived abuses in the financial markets, caused great suspicion in peoples' minds about the role of markets in general and trading in particular. Neither the USA nor China, the two largest GHG emitters, faced any comparable carbon constraints, and while China was able to receive considerable sums by selling carbon credits to Europeans, it continued to build coal-fired power plants at a rate which negated much of the impact of Kyoto. The 2009 COP was widely seen by Europeans as a failure, since the Copenhagen Accord, drawn up in the meeting's final hours by the US, India, China, Brazil, and South Africa (but not the EU), was viewed by many as a repudiation of Europe's strong, rules-based, global carbon market approach. Europe changed the rules for its own market after the first commitment period of the Kyoto Protocol ended, and demand for Kyoto's instruments (i.e., CERs, ERUs, and AAUs) plummeted and their prices similarly collapsed.

Today, there is some reason to be a bit more optimistic. China has developed seven pilot carbon emissions trading schemes, and is scheduled to develop a national program in 2016. Its success is by no means assured, but the country faces a severe environmental problem, and is devoting considerable resources and managerial attention to the issue. The USA has similarly decided to tackle GHG emissions

from its power plants, albeit in a rather circuitous manner, designed to circumvent strong political resistance by one of its major political parties. It relies on an environmental statute now nearly 45 years old, designed to provide CAC directives. However, the newly proposed regulations have been crafted in a manner that will allow emissions trading to flourish if individual states choose such an approach. There will be numerous lawsuits challenging these proposed regulations, and they will still face considerable political opposition – but nonetheless offer a progressive step forward from the current regulatory stasis in the country. Europe is also addressing some of the current concerns about the EU ETS, through its actions on backloading, its proposal for a market stability reserve system, and focus on more aggressive caps post 2020.

Just as in the buildup before Copenhagen, expectations are currently running high about the 2015 COP meeting in Paris, which is expected to lay down a framework for international post-2020 GHG control efforts. While many hope to see a world-wide emissions trading system like Kyoto, it seems much more likely that there will be numerous country-based efforts, coordinated in some manner by the UNFCCC. Negotiations are already well underway, and countries have been submitting their thinking about "New Market Mechanisms" (NMM) and the "Framework for Various Approaches" (FVA) to the UNFCCC. There seems to be relative agreement about such components as the registries infrastructure and the international transactions log, and the fact that only the international aspects of domestic trading programs would be addressed by the UNFCCC. However, significant issues concerning the role of the UN, the future of Kyoto-based mechanisms such as the CDM, and the linkage to the Nationally Appropriate Mitigation Actions (NAMAs) remain unclear.

As discussed earlier, there are essentially three means of controlling pollution: (1) command and control measures; (2) price-based economic instruments such as Pigouvian taxation; and (3) quantity-based economic instruments such as emissions trading. Given the scale of the environmental problem associated with GHGs, all three will be necessary in the future. They are likely to address different sectors of the economy, and each country is likely to employ a different mix.

Emissions trading's role in that future will continue to evolve. The possibility of linking up a diverse, robust mixture of "bottom-up" trading systems has appeal, even if the "top-down" post-Kyoto system sought by Europe cannot be developed over coming years. From an economic perspective, cost saving opportunities will be greatest in a situation where participants face very different marginal abatement costs. Linking emissions trading systems will tend to equalize abatement costs faced by companies around the world, thus significantly reducing costs as well as competitiveness concerns. There will be numerous difficulties associated with linking up emissions trading programs, however, including MRV concerns, enforcement, and the potential for fraud (such as that already seen in the world's largest carbon market, the EU ETS). In emissions trading, the integrity of these factors is magnified because the commodity being traded owes its very existence to governmental mandates.

The efficiency and distributive aspects of quantity-based schemes offer some very real appeal – and they have already been successfully implemented to tackle

environmental problems. The churning, volatility, self-interest of participants, and seeming chaos of dynamic markets can be uncomfortable, and can pose considerable regulatory challenges – particularly in externality markets specifically constructed by governments. But such markets are ultimately crucial in harnessing entrepreneurial skills for an energy technology revolution, and for delivering the scale of behavioral, technological, and social change being sought.

Climate change presents a unique challenge on a global scale to humanity in general and to economics in particular: the problem is global; it deals with long time horizons, has major risk and uncertainty at its core and requires unprecedented, immediate, collective action. Economics can provide a strong foundation for developing policies to guide action and reducing costs by providing flexibility on how, where, and when emissions are reduced. But pricing the pollution externality and developing robust carbon markets represent only part of the economic task involved in mitigating climate change. Policy frameworks that promote the development and deployment of new, cleaner technologies (i.e., what economists refer to as "induced technological change") and changing behavior in energy consumption (perhaps utilizing "behavioral economics" techniques) will be needed as well. One thing is for certain, the costs of reducing emissions enough to limit global warming to 2 °C may be high but doing so will provide certain obvious benefits that will clearly outweigh the costs. And the cost of not acting is likely to be very high indeed.

References

Baker and McKenzie International (2008) Overseas emissions trading experience. Sydney

Bayon R, Hawn A, Hamilton K (2007) Voluntary carbon markets. Earthscan, London

Bifera L (2013) Regional greenhouse gas initiative. Retrieved from Center for Climate and Energy Solutions

Bifera L (2014) Charting China's carbon horizon. Retrieved 14 Oct 2014, from The Energy Collective. http://theenergycollective.com/lucas-bifera/2139716/charting-chinas-carbon-horizon

Bird L, Hurlbut D, Donohoo P, Cory K, Kreycik C (2009) An examination of the regional supply and demand balance for renewable electricity in the United States through 2015. National Renewable Energy Laboratory, Golden, Colorado

Burtaw D, Evans D, Krupnick A, Palmer K, Toth R (2005) Economics of pollution trading for SO_2 and NOx. Resources for the Future, Washington, DC

Burtraw D (2013) An institutional blind spot in environmental economics. Daedalus 142:110–118

CARB (2010) California cap and trade regulation initial statement of reasons, appendix E: setting the program emissions cap. California Air Resources Board. Retrieved 12 Oct 2014, from http://www.arb.ca.gov/regact/2010/capandtrade10/capv3appe.pdf

Carbon Eight Group (2014) Charting China's carbon horizon. Retrieved from http://carboneightgroup.com/uploads/3/4/2/0/3420632/carboneightgroup_chinacarbondownload_8.8.14.pdf

CDM Rulebook (2008) Clean development mechanism rules, practice and procedures. Retrieved 2010, from http://cdmrulebook.org/715

Center for Climate and Energy Solutions (2014) California cap and trade program summary. Retrieved 12 Oct 2014, from Center for Climate and Energy Solutions: http://www.c2es.org/us-states-regions/key-legislation/california-cap-trade

Chait J (2014) Obama environmental plan tainted by association with environmentalists. Retrieved 19 Oct 2014, from http://nymag.com/daily/intelligencer/2014/10/environmentalists-taint-obama-environment-plan.html
Chan M (2009) Subprime carbon? Rethinking the world's largest new derivatives market. Friends of the Earth, Washington, DC
Chen K, Reklev S (2014a) China to launch first carbon-linked financial product on Thursday. Retrieved 7 May 2014, from Reuters: http://www.reuters.com/article/2014/05/06/china-carbon-idUSL3N0NS0FI20140506
Chen K, Reklev S (2014b) China's national carbon market to start in 2016 – official. Retrieved 7 Oct 2014, from Reuters: http://uk.reuters.com/article/2014/08/31/china-carbontrading-idUKL3N0R107420140831
ChinaCarbon (2014) Qingdao progresses towards launching 8th pilot carbon market in China. Retrieved 14 Oct 2014, from http://ChinaCarbon.net.cn/qingdao-progresses-towards-launching-8th-pilot-carbon-market-in-china/
CO_2 Spain (2013) Stranded costs from the Demise of the CDM: summary. Retrieved 4 Oct 2014, from CO_2 Spain: http://www.co2spain.com/strandedcosts.php
CORE (2011) Voluntary offset standards & programs. Retrieved from Carbon Offset Research and Education : http://www.co2offsetresearch.org/policy/VoluntaryStd.html
Dales J (1968) Pollution, property and prices. University of Toronto Press, Toronto
Davenport C (2014) Taking oil industry cue, environmentalists drew emissions blueprint. New York Times. Retrieved from http://www.nytimes.com/2014/07/07/us/how-environmentalists-drew-blueprint-for-obama-emissions-rule.html
DSIRE (2014a) Database of state incentives for renewables & efficiency. Retrieved 5 Oct 2014, from http://www.dsireusa.org/documents/summarymaps/RPS_map.pdf
DSIRE (2014b) Database of state incentives for renewables & efficiency. Retrieved from http://www.dsireusa.org/documents/summarymaps/EERS_map.pdf
EC (2013) The EU Emissions Trading System (EU ETS). Retrieved 19 Oct 2014, from European Commission: http://ec.europa.eu/clima/publications/docs/factsheet_ets_en.pdf
EC (2014) 2030 framework for climate and energy policies. Retrieved 14 Oct 2014, from European Commission: http://ec.europa.eu/clima/policies/2030/index_en.htm
Ecosystem Marketplace (2009) Fortifying the foundation: state of the voluntary carbon markets 2009. Forest Trends Association, Washington, DC
EDF and IETA (2012) India: a case study. Retrieved 5 Oct 2014, from http://www.ieta.org/assets/EDFCaseStudyMarch2014/india%20ets%20case%20study%20march%202014.pdf
EIA (2014) Lower emissions cap for regional greenhouse gas initiative takes effect in 2014. Energy Information Agency. Retrieved from http://www.eia.gov/todayinenergy/detail.cfm?id=14851
Ellerman AD, Joskow PL (2008) The European Union's emissions trading system in perspective. Massachusetts Institute of Technology. Pew Center for Global Climate Change, Arlington, Virginia
Energimyndigheten and NVE (2013) The Swedish-Norwegian electricity certificate market; annual report 2012. Retrieved 5 Oct 2014, from http://www.nve.no/Global/Elsertifikater/Elcertifikat2013_Eng_TA%20(2).pdf
European Climate Exchange (n.d.) EUA futures. Retrieved 30 Mar 2010
Europol (2009) Carbon credit fraud causes more than 5 billion euros damage for European Taxpayer. Retrieved 30 Mar 2010, from http://www.europol.europa.eu/index.asp?page=news&news=pr091209.htm
Friends of the Earth and International Rivers (2009) Trading in fake carbon credits: problems with the Clean Development Mechanism (CDM) Friends of the Earth, Washington, DC
Galbraith K (2014) Environmentalism is dead. Foreign Policy. Retrieved 19 Oct 2014, from http://www.foreignpolicy.com/articles/2014/09/25/environmentalism_is_dead_climate_change_united_nations_united_states
Gillenwater M (2008a) Redefining RECs – Part 1: untangling attributes and offsets. Energy Policy 36:2109–2119

Gillenwater M (2008b) Redefining RECs – Part 2: untangling certificates and emissions markets. Energy Policy 36:2120–2129
Global Trends (2013) Corporate Clout 2013: time for responsible capitalism. Retrieved 2 Apr 2010, from http://www.globaltrends.com/knowledge-center/features/shapers-and-influencers/190-corporate-clout-2013-time-for-responsible-capitalism
Guardian (2009a) European taxpayers lose €5bn in carbon trading fraud. Retrieved 7 May 2010, from http://www.guardian.co.uk/business/2009/dec/14/eu-carbon-trading-fraud
Guardian (2009b) Low targets, goals dropped: Copenhagen ends in failure. Retrieved 17 Apr 2010, from http://www.guardian.co.uk/environment/2009/dec/18/copenhagen-deal
Guardian (2010) Copenhagen dampens banks' green commitments. Retrieved 30 Mar 2010, from http://www.guardian.co.uk/environment/2010/jan/24/carbon-emissions-green-copenhagen-banks
He G, Morse R (2013) Addressing carbon offsetters' paradox: lessons from Chinese wind CDM. Energy Policy 63:1051–1055
ICAP (2014a) Emissions trading worldwide, status report 2014. International Carbon Action Partnership. Berlin
ICAP (2014b) Emissions Trading Schemes (ETS) around the World. Retrieved 15 Oct 2014, from International Carbon Action Partnership: https://icapcarbonaction.com/newsletter-archive/mailing/view/listid-0/mailingid-2/listype-1
ICIS (2014) Carbon markets almanac 2014: global developments and outlook. Reed Business Information Ltd., Sutton, Surrey
IETA (2013) Greenhouse gas market 2013. International Emissions Trading Association. Retrieved 6 Feb 2014, from http://www.ieta.org/ghgmarket2013
International Rivers (2008) Rip-Offsets: the failure of the Kyoto protocol's clean development mechanism. International Rivers, Berkeley, California
Jones T (2014) Protecting carbon markets from boiler room activities. Center for Resource Solutions, San Francisco, California
KEA3 (2009) REDD and the effort to limit global warming to 2oC: implications for including REDD credits in the international carbon market, NZ, March 9. Report prepared for Greenpeace International
King & Wood Mallesons (2014) China's pilot carbon markets at a glance. Retrieved 14 Oct 2014, from Lexology: http://www.lexology.com/library/detail.aspx?g=53db13c6-cdd6-4b77-8a18-12431b2d7122
Kong B, Freeman C (2013) Making sense of carbon market development in China. Carbon Climate Law Rev 7:194–212
Liu S, Xu N (2012) Data gaps hobble carbon trading. Retrieved from chinadialogue: https://www.chinadialogue.net/article/show/single/en/5093-Data-gaps-hobble-carbon-trading
Mao R (2014) China carbon market research report. Environomist Ltd., Beijing
Ministry of Power, Government of India (2012) Union Power Minister Launches "PAT" Scheme. Press Information Bureau. Retrieved 5 Oct 2014, from http://www.pib.nic.in/newsite/PrintRelease.aspx
Morel R (2013) Analysis: how the negotiators handled the 'hot air' issue for the second commitment period of the Kyoto Protocol. Retrieved 4 Oct 2014, from CDC Climate Research: http://www.cdcclimat.com/IMG//pdf/13-02-12_analysis_-_ukraine-3.pdf
Munnings C et al (2014) Assessing the design of three pilot programs for carbon trading in China. Resources for the Future, Washington, DC
New York Times (2010) Energy & environment. Retrieved 17 Apr 2010 from Cantwell-Collins Bill Generates Lobbying Frenzy: http://www.nytimes.com/cwire/2010/02/15/15climatewire-cantwell-collins-bill-generates-lobbying-fre-54450.html
Nordhaus W (2009) Economic issues in a designing a global agreement on global warming. Yale University, New Haven, Connecticut
Nordhaus W (2013) The climate casino: risk, uncertainty, and economics for a warming world. Yale University Press, New Haven, Connecticut

NREL (2012) Market brief: status of the voluntary renewable energy certificate market (2011 Data) National Renewable Energy Laboratory, Golden, Colorado
NY Times (2006) Outsize profits, and questions, in effort to cut warming gases. Retrieved 20 Apr 2010, from http://www.nytimes.com/2006/12/21/business/21pollute.html?pagewanted=2&_r=1
OECD (1997) Greenhouse gas emissions trading annex I expert group on the UNFCCC, working paper no. 9. OECD/GD(97)76
Pigou A (1920) The economics of welfare. Macmillan, London
PMR (2013) Partnership for market readiness. Retrieved from http://www.thepmr.org/system/files/documents/China_MRP_final_19-02-2013rev_0.pdf
PMR (2014) Survey of the MRV systems for China's ETS pilots. Partnership for Market Readiness. Retrieved from https://www.thepmr.org/system/files/documents/Technical%20Note%208_proper%20covers.pdf
Point Carbon – Europe (2014) Commodities research & forecast. Retrieved from Thomson Reuters
Quemin S, Wang W (2014) Overview of climate change policies and development of emissions trading in China. Retrieved from Les Cahiers de la Chaire Economie du Climat : http://www.chaireeconomieduclimat.org/wp-content/uploads/2014/03/14-03-18-Cahier-ID30-Quemin-and-Wang.pdf
Reuters (2009) Carbon trade on brink of boom – or backwater. Retrieved 30 Mar 2010, from http://www.reuters.com/article/idUSTRE5AH2U420091118?sp=true
RGGI (n.d.) Retrieved 17 Oct 2014, from http://www.rggi.org/market/offsets/categories
Sandbag (2014) Slaying the Dragon: vanquish the surplus and rescue the ETS. Sandbag Climate Campaign, London, UK
Sandor R (2012) Good derivatives: a story of financial and environmental innovation. Wiley, New York
Song R, Lei H (2014). Emissions trading in China: first reports from the field. Retrieved 14 Sep 2014 from World Resources Institute: http://www.wri.org/blog/2014/01/emissions-trading-china-first-reports-field
Statistical Communiqué (2013) Retrieved from GDP data re: National Economic and Social Development: http://www.tjcn.org/help/27489.html
Stern N (2006) The economics of climate change: the stern review. Cambridge University Press, Cambridge
Swartz J (2013) A user's guide to emissions trading in China. International Emissions Trading Association, Geneva
Thomson Reuters Eikon (2014) Retrieved from Price Forecasts data 10 June 2014 Thomson Reuters, New York
Tuerk A, Frieden D, Sharmina M, Schreiber H, Urge-Vorsatz D (2010) Green investment schemes: first experiences and lessons learned. Joanneum Research, Graz
UNDP China and Institute for Urban and Environmental Studies, CASS (2013) China National Human Development Report 2013; Sustainable and liveable cities: toward ecological civilization. Retrieved from http://www.cn.undp.org/content/dam/china/docs/Publications/UNDP-CH-HD-Publication-NHDR_2013_EN_final.pdf
UNEP DTU Partnership (2014) UNEP Risoe CDM/JI pipeline analysis and database. Retrieved from http://www.cdmpipeline.org/overview.htm
UNFCCC (n.d.) CDM project activity cycle. Retrieved 2010, from http://cdm.unfccc.int/CommonImages/ProjectCycleSlide.jpg
US EPA (2002) Clearing the air: the facts about capping and trading emissions. US EPA, Washington, DC
US EPA (2010) Acid rain program benefits exceeds expectations. US EPA, Washington, DC
USEPA (2014a) 2014 allowance auction results. Retrieved 3 Oct 2014, from http://www.epa.gov/airmarkets/trading/2014/index.html
USEPA (2014b) Fact sheet: clean power plan overview. Retrieved 18 Oct 2014, from US Environmental Protection Agency: http://www2.epa.gov/carbon-pollution-standards/fact-sheet-clean-power-plan-overview

USEPA (2014c) Fact sheet: clean power plan flexibility. Retrieved 18 Oct 2014, from US Environmental Protection Agency: http://www2.epa.gov/carbon-pollution-standards/fact-sheet-clean-power-plan-flexibility

VCS (2014) Retrieved 5 Oct 2014, from http://www.v-c-s.org/how-it-works/why-vcs

Wara M (2006) Measuring the clean development mechanism's performance and potential. Center for Environmental Science and Policy, Stanford University, Stanford, California

World Bank (2010) State and trends of the carbon market 2010. Washington, DC

World Bank (2014) State and trends of the carbon market 2014. Retrieved May 2014 from http://www-wds.worldbank.org/external/default/WDSContentServer/WDSP/IB/2014/05/27/000456286_20140527095323/Rendered/PDF/882840AR0REPLA00EPI2102680Box385232.pdf

Wu Q, Neelis M, Casanova C (2014) Chinese emission trading schemes: initial assessment of allocation. Ecofys. Retrieved from http://www.ecofys.com/files/files/ecofys-2014-industry-view-chinese-ets-allocations-english.pdf

Zhong Q (2014) China carbon market report 2014. Retrieved from IETA-IEA-EPRI Workshop, Paris: http://www.iea.org/media/workshops/2014/21ZHONGQINGChinaCarbonMarketReport2014.pdf

Carbon Markets: Linking the International Emission Trading Under the United Nations Framework Convention on Climate Change (UNFCCC) and the European Union Emission Trading Scheme (EU ETS)

Itziar Martínez de Alegría, Gonzalo Molina, and Belén del Río

Contents

Abstract

The trading of carbon emission permits is an instrument created recently to tackle the climate change problem. From 2005 onward, in particular, the volume and significance of different carbon emission trading schemes have increased spectacularly; despite the fact that new emission trading schemes are appearing, the

I. Martínez de Alegría (✉)
Engineering School of Bilbao, University of the Basque Country (UPV/EHU), Bilbao, Spain
e-mail: itziar.martinezdealegria@ehu.es

G. Molina
University of the Basque Country (UPV/EHU), Bilbao, Spain
e-mail: g.molina.igartua@gmail.com

B. del Río
Chair in International Studies, University of the Basque Country (UPV/EHU), Bilbao, Spain
e-mail: rosabelen.delrio@ehu.es

W.-Y. Chen et al. (eds.), *Handbook of Climate Change Mitigation and Adaptation*,
DOI 10.1007/978-3-319-14409-2_57

value of the market had fallen by the end of the Kyoto Protocol's first commitment period in 2012. One fundamental reason for this was the uncertainty as to whether a new global agreement or protocol would be reached in 2015. The main goal of this chapter is to offer an overview of International Emission Trading under the Kyoto Protocol together with the European Union Emission Trading Scheme (EU ETS), as the schemes at the core of today's carbon markets, exploring their basic structure, their main links, and their differences, including a carbon price analysis underlining their fundamental weaknesses and strengths.

Introduction

Broadly similar global carbon prices are considered to be an essential element of international collective action to reduce greenhouse gas (GHG) emissions. That price can, in theory, be created through internationally harmonized taxation or intergovernmental emissions trading, but neither is straightforward in practice (Stern 2007). Within the European Union (EU), a proposal for a harmonized carbon tax failed due to the concerns of some European industries about their competitiveness and to a lack of unanimity between Member States for its adoption (Martínez de Alegría et al. 2009; Brohé et al. 2009). This is a sign of the difficulties of adopting a carbon tax at the international level. On the other hand, as a result of pressure by the USA and some of its allies, emission trading in the form of carbon permits was included as a flexibility mechanism in the Kyoto Protocol to help the concerned parties to meet their commitments (Babiker et al. 2002; Walsh and Whalley 2008; Brohé et al. 2009). From then on, it has remained the main international policy instrument for addressing the climate change problem.

Trading in emission permits is a relatively recent instrument for dealing with environmental problems. The theory underlying such permits was first stated by Coase in 1960 (Coase 1960; Ellerman 2005; Brohé et al. 2009). A decade later, they were applied specifically to environmental problems (Ellerman 2005). Trading emission permits began to be applied on a large scale in the USA from 1974 onward, and by the end of 1997, six types of emission trading initiatives had been implemented there (Solomon 1999; Tietemberg et al. 1999; Ellerman 2005). There are currently a number of carbon emission trading schemes or low-carbon initiatives that generate emission permits. Each permit corresponds to the right to emit GHG into the atmosphere. All the emission permits generated under the Kyoto Protocol's International Emission Trading system (henceforth referred to as Kyoto Units) and from European Union Allowances (EUAs), i.e., the allowances generated under the European Union Emission Trading Scheme (EU ETS), are measured in units of one metric ton of carbon dioxide equivalent or $CO_{2eq.}$ The definition of CO_{2eq} is the amount of CO_2 emission that would cause the same radioactive forcing as an emitted amount of a well-mixed greenhouse gas or a mixture of well-mixed greenhouse gases, all multiplied with their respective global warming potentials (GWPs) to take into account the differing times they remain in the atmosphere (IPCC 2007).

According to the *State and Trends of the Carbon Market* reports, especially that of 2005, there has been impressive growth in the overall value of the global carbon market to the tune of around $159 by 2010 and $176 billion by 2011 (Linacre et al. 2011; Kossoy and Guigon 2012). EUAs increased their market share from 71 % of the global carbon market in terms of value in 2005 to 84 % in 2011 (Linacre et al. 2011; Kossoy and Guigon 2012). The sum of all emission permits generated by the Kyoto Protocol's International Emission Trading system (the so-called Kyoto Units) accounted for around 15 % of the total carbon market value in 2011. According to the data offered by Kossoy and Guigon, Certified Emission Reductions (CERs), i.e., the credits generated by the Clean Development Mechanisms (CDM), accounted for around 14 % of the market value in that year, while emission permit transactions outside the International Emission Trading under the umbrella of the Kyoto Protocol accounted for less than 1 % (Kossoy and Guigon 2012). The *Mapping Carbon Pricing Initiatives* report follows the same path as the aforesaid *State and Trends of the Carbon Market* reports but represents a fundamental change of scope in comparison to the previous reports. Instead of providing a quantitative, transaction-based analysis of the international carbon market (adducing that "current market conditions invalidate any attempt to undertake such an analysis"), it presents an overview of different carbon price initiatives around the world (including not only emission trading schemes but also carbon taxes). It asserts that "with limited support, prices reached historical lows and at the same time, several national and sub-national carbon pricing initiatives are emerging" (Kossoy et al. 2013). The *State and Trend of Carbon Pricing* report published in 2014 illustrates that 39 national and 23 subnational jurisdictions around the world have implemented or are scheduled to implement carbon pricing instruments (including emissions trading systems and taxes) (World Bank and Ecofys 2014). A total of eight new carbon markets opened in 2012 and another early in 2014. In total, the world's emissions trading schemes "are valued at about $30 billion" (World Bank and Ecofys 2014). This represents a remarkable reduction in scale compared to the figure estimated in 2011. In 2013, the cap for installations under the EU ETS was 2,084 million allowances, while the cap for the six pilot projects in China was 1,115 Mt CO_{2eq}, making the country the second largest carbon market in the world, after the EU ETS (World Bank and Ecofys 2014).

Based on a review of the most relevant literature and main legislative documents on the matter, this chapter gives an overview of the functioning of the Kyoto Protocol's International Emission Trading and the EU ETS, which represent the core of carbon markets between 2008 and 2012, as they were the main international emission trading schemes in that period. Section "Overview of International Emission Trading under the Kyoto Protocol" explores the basic elements of the International Trading Scheme under the Kyoto Protocol and its critical concerns. Section "Overview of the European Union Emission Trading Scheme (EU ETS)" focuses on the EU ETS, analyzing its basic structure and underlining its critical concerns. Section "Linking and Comparing the Two Trading Schemes" presents a comparative analysis of the two schemes, focusing on their main links and differences, including a supply–demand balance between different carbon emission

permits (subsection "A Supply–Demand Balance of Emission Permits and the Level of Ambition in the Trading Schemes") and a carbon price comparison (subsection "A Carbon Price Analysis"). Section "Conclusions" concludes.

Overview of International Emission Trading Under the Kyoto Protocol

This section provides an overview of International Emission Trading under the Kyoto Protocol. Firstly, its basic structure is analyzed; secondly, the main critical questions concerning its present and future as a carbon trading instrument are examined.

Basic Structure of International Emission Trading Under the Kyoto Protocol

The United Nations Framework Convention on Climate Change (UNFCCC) is a statement of aspirations, principles, goals, and the means to meet the commitment (IPCCC 2014) which seeks to achieve the "stabilisation of greenhouse gas concentrations (GHG) in the atmosphere at a level that would prevent dangerous anthropogenic interference with the climate system" (UNFCCC 1992). The Kyoto Protocol (KP) was adopted in 1997 and came into force in February 2005, establishing individual, legally binding GHG emission limitation or reduction commitments for the 38 ratifying parties (ratification means formal approval, often by a Parliament or other national legislature, of a convention, protocol, or treaty, enabling a country to become a party; it is a separate process that occurs after a country has signed an agreement; UNFCCC 2015b) listed in its Annex B (henceforth called "Annex B countries;" see Table 2 in Annex). The protocol called on these parties, individually or jointly, to reduce their overall GHG emission level by 5.2 % below the 1990 levels in the first commitment period, i.e., from 2008 to 2012 (UNFCCC 1998). The main goal of the Kyoto Protocol is to contain or reduce emissions of the main GHGs in ways that reflect the underlying national differences in emissions, wealth, and capacity, according to the main principles agreed in the United Nations Framework Convention on Climate Change (UNFCCC) (1992), including the principle of "common but differentiated responsibilities" with the corresponding leadership by the richer and higher-emitting industrialized countries.

The Kyoto Protocol established the following Flexibility Mechanisms to help the Annex B countries to meet their commitments:

- The so-called bubble concept, which allowed European Union (EU) Member States to redistribute their joint 8 % reduction commitment between them as illustrated in Annex B to the Protocol (see Table 2 in Annex). This redistribution was stated by the Burden Sharing Agreement (BSA), which resulted, for instance, in 15 % emission growth for Spain, a 21 % reduction for Germany, etc. (Council of the European Union 2002).

- The so-called Kyoto Mechanisms or Flexibility Mechanisms, i.e., the International Emission Trading system, the Joint Implementation (JI) Mechanism, and the Clean Development Mechanism (CDM). These last two mechanisms are project-based mechanisms and have become the focal point for direct private sector involvement in the Kyoto Protocol. They state that a ton of GHG emissions saved, thanks to the development of a project or program, gives the right to emit a ton of GHG elsewhere. For the purpose of meeting their commitments, Annex B countries may transfer to, or acquire from, any other such party Emission Reduction Units (ERUs) which result from Joint Implementation projects, while the joint objective of the Clean Development Mechanisms is to assist developing country parties in achieving sustainable development and reducing GHG through the development of Clean Development Mechanism projects and to help Annex B countries in achieving compliance with their commitments. This last point is to be facilitated through the use of the aforesaid Certified Emission Reductions (CERs) generated by the cited projects. All Joint Implementation and Clean Development Mechanism projects must necessarily comply with the additionality rule. Using these two project-based mechanisms, any legal entity can participate in a Joint Implementation or a Clean Development Mechanism project to acquire Emission Reduction Units (ERUs) or Certified Emission Reductions (CERs), acting directly as a project developer or indirectly, for example, acquiring credits through the existing Carbon Funds. The objective of a Carbon Fund is to collect financial contributions from public and private sector entities and then use those funds to promote projects that reduce GHG emissions, in turn redistributing the Emission Reduction Units generated to the financing contributors according to their respective contributions (Carr and Rosembuj 2007).
- When Annex B countries have negative net emissions derived from land use, land use change, and forestry (LULUCF) activities (Art. 3.4 KP), those countries can receive Removal Units (RMUs). This type of carbon sink activities, i.e., activities that absorb CO_2, is expected to represent a relevant percentage of the different countries' commitments. The first Removal Units were issued in 2011 to those national registries that opted to print them annually (such as France and Australia, which received at least 23 million RMUs each; Russia, which held 4 million in 2011 and 462 million in February 2012; Hungary, which has received at least 3.9 million (Kossoy and Guigon 2012), but also Denmark, Monaco, Liechtenstein, and Switzerland. The rest of the Annex I countries opted to print their Removal Units after the "true-up period" (the "true-up period" or "additional period for fulfilling commitments" is the specific period of 100 days after provided by the Protocol that is to occur after the completion of the review of the final annual report for the commitment period in order for parties to continue making transactions for the purpose of "truing up" any remaining differences between the parties' total emissions during the commitment period and units retired for compliance; so during this period, each party is allowed to continue to undertake transactions of Kyoto Units) (UNFCCC 2008a, b).
- The possibility of carrying over (or banking) unused permits from the 2008–2012 period to the 2013–2020 period may be another relevant cause of flexibility in this

second period; however, that possibility is expected to be very limited (see subsection "Critical Concerns").

The Kyoto Protocol's accounting system is based on two parallel information streams: GHG inventories and the information regarding the operations linked to Kyoto Units. To manage this last information, a registration system has been developed which includes three types of registry: (i) the national registries of each of the Annex B parties which have ratified the Kyoto Protocol (including the EU) registry, i.e., the Community Independent Transaction Log (CITL) was replaced in 2013 by the European Union Transaction Log (EUTL) (see Table 1 in section "Linking and Comparing the Two Trading Schemes"); (ii) the Clean Development Mechanism (CDM) registry; and (iii) the International Transaction Log (ITL), which has been put in place and administered by the UNFCCC secretariat to verify the validity of transactions. Each of these registries is to operate through a link established with the ITL, which verifies the operations registered in real time to ensure that they are consistent with the rules agreed under the Kyoto Protocol.

According to the GHG emissions cap (established in Annex B to the Kyoto Protocol), an initial amount of Assigned Amount Units (AAUs) is allocated free of charge (this is known as grandfathering) to the Annex B countries at the beginning of 2008 (UNFCCC 2008b). Apart from these free allowances, the following Kyoto Units also give the right to emit one ton of CO_{2eq} to the atmosphere and may also be transacted under the International Emission Trading without restrictions, with the exception of the commitment period reserve (UNFCCC 2008a): Removal Units (RMUs); Emission Reduction Unit (ERU) credits (which are units converted from Assigned Amount Units or Removal Units on the basis of Joint Implementation projects (Art. 6 KP)); Certified Emission Reduction (CER) credits (given for emission reductions certified for a CDM project (Art. 12 KP)); and finally, tCER and lCER credits (derived from forestation and afforestation activities also developed under Art. 12). All the cited Kyoto Units represent the same compliance value in dealing with Kyoto commitments.

The Annex B countries have the following options to comply with their respective commitments under the Kyoto Protocol:

- To carry on internal abatement measures and obtain domestic GHG emission reductions
- To remove GHG from the atmosphere by increasing carbon sinks (LULUCF activities as mentioned above)
- To use the Kyoto Mechanisms mentioned above

The decision depends on the relative costs of each option at each moment, on the legislation in place, and, as explained by Grubb (2003), on the political objectives of each country.

Thanks to the aforesaid registry system, Annex B countries may add and subtract Kyoto Units from their corresponding national registries, reducing or increasing their level of Kyoto Units compared to their initial assigned amount (their total AAUs at

Table 1 Fundamental characteristics, links, and differences between the Kyoto Protocol's IET and the EU ETS

Period: 2008–2020	Kyoto Protocol's ET first commitment period (2008–2012); second commitment period (2013–2020)	EU ETS Phase I (2005–2007); Phase II (2008–2012); Phase III (2013–2020)
Parties involved	*FCP: 38 parties = 37 ratifying industrialized countries included in the Kyoto Protocol's Annex B + the EU **SCP: 34 (Russia, Canada, and Japan, which ratified the Kyoto Protocol and stayed out in the post-Kyoto 2012); the "Doha Amendment" still not ratified (status December 2014)	Operates in the 28 EU countries and the three EEA-EFTA states (Iceland, Liechtenstein, and Norway)
Sectors of the economy affected	Country focused	Company focused: European big industrial emitters of GHGs ***Phase II: the energy sector, iron and steel production and processing, mineral industry, and paper and board industry *[v]Phase III: new sectors (e.g., aviation, ammonia, and aluminum (EU 2009))
Type of GHG affected	FCP: CO_2; CH_4; N_2O; HFCs; PFCs; SF_6 (included in Annex A to the KP) SCP: NF_3 is included	Phase II: mainly CO_2 Phase III: new GHGs affected, N_2O and PCF
% of GHG emissions covered	FCP: with the ratification of Russia in 2005, at least 55 % of the world's GHGs were covered SCP: Japan, Canada, and Russia are out of the "Doha Amendment to the Kyoto Protocol," so only around 15 % of the world's GHGs are covered (see Table 2)	*2005–2012 period: around 40 % of EU emissions *2013–2020: around 45 % of EU emissions
Emission permits involved and their links	Kyoto Units: AAU; RMU; ERU; CER; lCER and tCER	Phase II: EUAs (which are converted from AAUs) + a limited quantity of CERs and ERUs that can also be used for accomplishment Phase III: EUAAs included
Registry system	Three types of registry: the 37 national registries; the CITL and the ITL (from 2013 the EUTL superseded the CITL; see next column). There is a direct link between the EU ETS registry system and the ITL as established by European Commission Regulation (EC) No 2216/2004	Between 2005 and 2012: 30 electronic registries + the CITL Phase III[i] the European Union Transaction Log (EUTL) is the successor of the CITL and is now the only registry operated by the European Commission
Targets	FCP: added together parties must reduce 5.2 % below the 1990 levels SCP: 18 % between 1990 and 2020	2005–2020: 21 % reduction target as stated by Directive 2009/29/EC; the Commission proposes 43 % lower by 2030

(*continued*)

Table 1 (continued)

Period: 2008–2020	Kyoto Protocol's ET first commitment period (2008–2012); second commitment period (2013–2020)	EU ETS Phase I (2005–2007); Phase II (2008–2012); Phase III (2013–2020)
Consequences of noncompliance	Disqualification from participating in the Kyoto Mechanism and a penalization by deduction from allowed emissions in subsequent rounds with a 30 % penalty factor (Grubb 2003)	Any operator that does not surrender sufficient annual emission permits to cover its verified emissions must pay a penalty of EUR 100 for each ton of $CO_{2\text{-eq.}}$ for which the operator has not submitted an emission permit and in addition must surrender the corresponding amount of emission permits
Flexibility to reach commitments	To help them reach their targets, Annex B parties can use (a) the bubble concept; (b) emission trading; (c) unlimited amounts of UREs, CERs, tCERs, and lCERs; (d) carbon sinks (with certain limits); and (e) the limited possibility of banking AAUs (as stated by EU, Australia, Norway, and Switzerland)	To help them reach their targets, EU ETS firms can (a) use emission trading; (b) use a limited amount of CERs and UREs; and (c) bank or carry over EUAs for 2013–2020

Source: Own work; *first commitment period (FCP), from 2008 to 2012; **second commitment period (SCP), from 2013 to 2020; ***Phase II of the EU ETS from 2008 to 2012; *^{v}Phase III of the EU ETS from 2013 to 2020

the beginning of 2008). To comply with the Kyoto commitments at the end of the first commitment period, these countries must send to their respective retirement accounts a number of Kyoto Units equivalent to their total GHG emissions in those 5 years. It must be taken into account that, due to the complexity of data collection, final GHG data are reported with a time lag of at least 2 years on their actual emission. This is why the period known as the "true-up period" is instated. The "true-up period" is a 100-day period after the final GHG emission data have been reported when parties have the opportunity to undertake any final transactions necessary to achieve compliance with their Article 3, paragraph 1 commitment (UNFCCC 2008a). 2014 is the year of the "true-up period."

Critical Concerns

The commitments between 2008 and 2012 were never intended to provide the definitive solution to climate change and "second and subsequent periods are likely to require more stringent emission commitments" (Grubb 2003). With a view to the 2013–2020 period, in order to maintain GHG concentration at a level of below 450 ppm CO_{2eq}, the Intergovernmental Panel on Climate Change (IPCC) highlights that the Annex I countries need to cut their GHG emissions by 25–40 % by 2020 compared to the 1990 levels and also that developing countries need to significantly

reduce their emissions (Gupta et al. 2007). As part of the Copenhagen Accord reached at the Copenhagen Conference of Parties (the COP-15), most Annex I parties formally submitted voluntary GHG emission reduction pledges. In addition, seven major emerging economies (China, India, Brazil, Indonesia, Mexico, South Africa, and South Korea) also sent in mitigation action plans (UNFCCC 2015a). Various studies indicate that the said pledges will not suffice to bring about the reductions needed to limit the increase in global warming to 2 °C, especially if the lowest-ambition pledges are implemented at a time when LULUCF accounting rules and the use of surplus emission units result in a net increase of emissions (Den Elzen et al. 2010a, 2011; Kartha and Erikson 2011). As stated in 2011 at the Durban Conference of Parties (the COP-17), Annex I parties must start the process for the development of a new protocol or another instrument with legal force under the UNFCCC, applicable to all parties, which should be adopted by the COP-21 (i.e., by 2015 in Paris), in order for it to come into effect and be implemented from 2020 (UNFCCC 2012a). Due to the need to increase the level of ambition with regard to GHG emission reductions, the Warsaw UNFCCC Conference of Parties agreed that there was a need to set more comparable targets together with a calendar from Warsaw to Paris (UNFCCC 2014a).

In the framework of the Kyoto Protocol, the possibility of using all the Flexibility Mechanisms and the corresponding Kyoto Units for the second commitment period, that is, from 2013 to 2020, is allowed by the 2011 Durban Conference of the Parties, serving as the meeting of the parties to the Kyoto Protocol (the CMP-7) (UNFCCC 2012b). The following year, the Doha Agreement (the CMP-8) stated that those Annex B parties taking commitments in the 2013–2020 period should reduce their overall emissions by at least 18 % below the 1990 levels in this second period (UNFCCC 2013a). CMP-8 includes an Annex called the "Doha Amendment to the Kyoto Protocol" (Annex A to CMP-8), which comprises a new list of limitation or reduction commitments for the Annex B countries of the Kyoto Protocol. However, apart from the United States (USA), a number of Annex I countries (notably Canada, Japan, Russia, but also Belarus, New Zealand, Norway, Switzerland, and Ukraine) decided not to participate in the second commitment period (UNFCCC 2015c), so the small proportion of world GHG emissions affected (around 12 %: see subsection "A Supply–Demand Balance of Emission Permits and the Level of Ambition in the Trading Schemes") is the main weakness of the post-Kyoto 2012 period.

Other relevant questions that determine the level of ambition as regards the 2013–2020 period within the Kyoto framework are linked to whether or not surplus Kyoto Units can be banked. Of course, mitigation efforts to 2020 could be reduced considerably if the total surplus of Kyoto Units is used and transacted with no limits. Although the "Doha Amendment" did not agree on any additional restrictions on the banking of AAUs for the next commitment period, major GHG emitters included in the amended Annex B (notably the EU, Australia, Norway, and Switzerland) have confirmed that they will not purchase or use carried-over AAUs transferred from other parties for compliance in the second commitment period (UNFCCC 2013a).

In regard to project-based mechanisms, between 2004 and 2013, over 7,300 project activities were registered under the Clean Development Mechanism in over

90 countries, over 1,500 component project activities were included in over 230 programs of activities registered in over 60 countries, over 1.4 billion Certified Emission Reductions were issued, and over USD 215 billion was invested; under the Joint Implementation Mechanism, 547 Track 1 projects and 52 Track 2 projects were implemented and 840 million Emission Reduction Units were issued for emission reductions generated before the end of 2012 (UNFCCC 2014b). For the 2013–2020 period, Warsaw decisions 3 and 5 by CMP-9 express concern regarding the difficult market situation currently faced by participants in Joint Implementation and the Clean Development Mechanism and the consequent loss of institutional capacity related to the mechanisms, which is threatening their value as a tool for parties to collaborate in achieving the objective of the Convention and its Kyoto Protocol (UNFCCC 2014b). Indeed, 2012 saw a dramatic increase in registrations, while 2013 saw a dramatic decline in the number of Clean Development Mechanism projects registered and a dramatic decline in the number of projects entering the Clean Development Mechanism pipeline as a result of diminished demand for CERs, tied ultimately to the level of ambition of parties to reduce GHG emissions (UNFCCC 2013b). According to the Joint Implementation Supervisory Committee (JISC), this mechanism is virtually at a standstill, while countries turn their attention to negotiating a new climate deal, due to be agreed in Paris at the end of 2015 and take effect in 2020. The Joint Implementation Mechanism is facing difficulty due mainly to low demand, ultimately tied to the countries' level of ambition to reduce greenhouse gas emissions. The JISC is also challenged critically by the fact that JI units are created by converting a portion of a country's total allowable emissions, the so-called Assigned Amount Units, which for the current commitment period of the Protocol have yet to be issued (Joint Implementation Supervisory Committee (JISC), 2014).

Scientific literature has detected the following critical concerns, which may have led to a decrease in the degree of confidence in Clean Development Mechanisms:

- *There are various methodological problems in determining baselines and the additionality* of Clean Development Mechanism projects (Gupta et al. 2007), such as the problem that although the Clean Development Mechanism's additionality toll is well respected, it does not guarantee that only additional projects are approved (Kollmuss et al. 2008). On the other hand, as stated by the Warsaw CMP-9 conference, work may be done on the simplification and streamlining of methodologies, with the aim of reducing transaction costs for all project activities and programs of activities, especially those in regions underrepresented in the Clean Development Mechanism (UNFCCC 2014b).
- As mentioned, the *coverage of forestry and forest-related projects* is another cause of uncertainty due to the problems linked to the impermanence of forests and leakage to other regions (Gupta et al. 2007).
- *The sustainability of the projects*. The Marrakech Accord, where the main rules for the implementation of the Kyoto Mechanism are provided, states the host party's prerogative in confirming whether a Joint Implementation or a Clean Development Mechanism project activity assists it in achieving sustainable

development (UNFCCC 2002). A number of publications can be found which deal with the question of the sustainability of Clean Development Mechanism projects, highlighting mainly the lack of guarantees concerning the sustainability of the projects carried out and the need to establish adequate indicators for their evaluation (Holm Olsen and Fenhann 2006; Kollmuss et al. 2008; Watson and Fankhauser 2009). Some significant initiatives implemented in an attempt to deal with these problems can be outlined, such as that of BlueNext, an emission trading exchange company which divides spot CER contracts into two: spot CERs (involving N_2O from adipic acid and nitric acid production and HFC-23 from HFC-22 production) and spot green CERs (involving wind, solar, energy efficiency, and other project types) (Bluenext 2012), and the Gold Standard certification, which is a standard for creating high-quality emission reduction projects mainly in the Clean Development Mechanism (CDM). It is designed to ensure that carbon credits are not only real and verifiable but that they make measurable contributions to sustainable development so some of the issued credits are called CER Gold Standard (Gupta et al. 2007; Kollmuss et al. 2008). Within the EU ETS, credits from all types of projects are accepted except nuclear energy projects (European Commission 2014a) and CERs from projects starting from 2013 involving the destruction of industrial gases (trifluoromethane (HFC-23) and nitrous oxide (N_2O)) (EU 2011).

Finally, the existence of an adequate, transparent accounting system that guarantees the correct functioning of Kyoto Unit transactions is fundamental for the proper functioning of International Emission Trading under the Kyoto Protocol. In this regard, several authors have pointed out the potential for double accounting of offsets as a major source of uncertainty and have estimated that this could account for 0 to +1.3 Gt CO_{2eq} (den Elzen et al. 2010a, b). In regard to Removal Units, tCERs and lCERs, as explained by Grubb, carbon sinks were one of most technically complex issues in the Kyoto Protocol's entire negotiations (Grubb 2003). The main criticisms related to the inclusion of carbon sinks have to do with the accounting of GHG fluxes and the risk of impermanence. Indeed, major criticisms regarding forestry-based compliance methods are linked to uncertainties regarding the net emissions from forests (IPCC 2007; LeBlanc 1999). According to IPCC estimates, uncertainties regarding the annual carbon flux in the 1990s may account for 5500 $MtCO_{2eq}$/year (IPCC 2007).

Overview of the European Union Emission Trading Scheme (EU ETS)

Basic Structure of the EU ETS

All parties to the UNFCCC (including developing countries) have a general commitment to adopt climate change mitigation policies that includes submitting reports on the actions that they are taking. In 2007, the European Council established the

"20/20/20 mandate" (i.e., to achieve by 2020 a reduction of GHG emissions by 20 % on the 1990 levels, to save 20 % of primary energy consumption compared to the forecasts for 2020, and to increase the level of renewable energy sources in the EU's overall mix of final energy consumption to 20 % (European Council 2007)). To achieve this mandate, a wide range of measures (legislative, technological, etc.) have been developed (Martínez de Alegría et al. 2009, 2012), offering an ambitious, integrated pack of measures. It is worth noting that EU legislation distinguishes between the following economic sectors:

- The so-called *diffuse sectors*, such as agriculture, services, buildings, and transport, which are affected by Decision 406/2009/EC, which sets a 10 % GHG reduction (average) for them below the 2005 levels for the whole of the EU by 2020, with different targets established for different Member States
- Big *industrial emitters (or EU ETS firms)*, which are included in the EU ETS

According to Directive 2003/87/EC, the EU ETS started functioning in January 2005 (EU 2003) and was inspired and generated under the umbrella of the Kyoto Protocol's International Emission Trading. "The EU emissions trading system (EU ETS) is a cornerstone of the European Union's policy to combat climate change and its key tool for reducing industrial greenhouse gas emissions cost-effectively. The first – and still by far the biggest – international system for trading greenhouse gas emission allowances, the EU ETS covers more than 11,000 power stations and industrial plants in 31 countries, as well as airlines" (European Commission 2014a).

The main source of information on the EU ETS is the Community Independent Transaction Log (CITL) (known as the European Union Transaction Log (EUTL) from 2013 onward), which is administered by the European Commission and has the task of checking and reporting all transactions taking place within this trading system. As mentioned above, European Union Allowances (EUAs) are specific allowances created within the EU ETS. Each EUA entitles its owner to emit one metric ton of CO_{2eq} into the atmosphere. The following types of account can be distinguished in the scheme: *the party account*, which corresponds to those Annex B parties which are included in the EU ETS, that is, the EU countries; *the operator account*, which is comprised by the EU ETS firms that hold allowances that correspond to AAUs previously converted into EUAs; and *the person account*, which corresponds to any natural or legal person that wishes to participate in the EU ETS (EU 2004).

- Directive 2003/87/CE distinguished between Phase I (2005–2007) and Phase II (2008–2012), when each Member State must develop a National Allocation Plan (NAP) (which must be approved by the European Commission), establishing the overall and individual cap for the affected EU ETS firms for each phase. According to the National Allocation Plans, EUAs were distributed mainly for free (grandfathering) among EU ETS firms (in Phase I and Phase II, at least 95 % and 90 %, respectively, of the allowances were distributed for free, while the rest went through auctioning). After each year, those firms must surrender enough

allowances to cover all their emissions; otherwise, different fines would be imposed. If a firm reduced its emissions, it could keep the spare allowances to cover its future needs or sell them to another EU ETS firm that needed allowances. During Phase II, the 30 participating countries (27 EU Member States, Iceland, Lichtenstein, and Norway) emitted on average around 40 % of the total emissions of the EU (European Environment Agency (EEA) 2012). In 2009, Directive 2009/29/EC was adopted, to be applied from 2013 (i.e., Phase III), establishing new rules and relevant changes such as the possibility of banking EUAs between Phase I and II. Other relevant new features in Phase III are: different national caps are replaced by an EU-wide cap system, to be established by the European Commission.

- *New relevant sectors and gases are included*. Initially, the focus was on CO_2 emitters (such as the electricity sector, the mineral industry, etc.). From 2013 the EU ETS scope was to be further extended to include new sectors as the ammonia and aluminum sectors (EU 2009) and the aviation sector (EU 2008) and gases, such as CO_2 emissions from petrochemicals, as well as N_2O emissions from the production of nitric and adipic acids and perfluorocarbon (PCF) emissions from aluminum production (EU 2009).
- The inclusion of the target of a 21 % reduction in GHG on the 2005 levels by 2020 for the EU ETS-covered sectors.
- An *auctioning system* was set in place.

Some critical factors in regard to these novelties are analyzed in more depth in the next subsection ("Critical Concerns").

Critical Concerns

According to various authors, within these types of emission trading scheme, an auction system is preferred to grandfathering because it tends to generate less market distortion (Grubb and Neuhoff 2006; Hentrich et al. 2009). However, other authors affirm that, considering the past experiences of auctioning, the sophisticated allocation rules applied, which are highly influenced by lobbying groups, are not in line with the desire for simplicity and transparency (Benz et al. 2010). The current experience in regard to the auctioning system established in the EU ETS will determine whether market distortion is weakened or reinforced.

As stated by Directive 2009/29/EC, in 2013 more than 40 % of allowances should have been auctioned and this share should rise progressively each year. Indeed, the Directive states that full auctioning should be the rule from 2013 onward for the power sector and only when the risk of "carbon leakage" is high will some allowances be allocated for free for a period of time. On the other hand, the Directive envisages a transitional system for those sectors deemed to be at risk of carbon leakage, for which free allocation will initially account for 80 % of the amount. Thereafter, free allocation should decrease each year by equal amounts resulting in 30 % free allocation in 2020 and no free allocation in 2027 (EU 2009). Sectors

deemed to be at risk of carbon leakage are those that may suffer a material competitive disadvantage against competitors located in areas outside the EU which do not have similar emission reduction commitments, which could in turn lead to an increase in GHG emissions. The Directive also states that allowances in the EU ETS must decrease by a linear factor of 1.74 % per annum, compared to the average annual total quantity for 2008–2012, leading to a reduction of just over 70 % in the ETS cap by 2050 (European Commission 2011). However, that linear factor seems not to be balanced by the necessary level of ambition within the EU (see subsection "A Supply–Demand Balance of Emission Permits and the Level of Ambition in the Trading Schemes"). In 2014, "in the light of the evidence and the experience of current policies the European Commission proposes a new reduction target for domestic GHG emissions of 40 % compared to 1990, to be shared between the ETS and the non-ETS sector (. . .) the ETS sector would have to deliver a reduction of 43 % in GHG in 2030 and the non-ETS sector a reduction of 30 % both compared to 2005. In order to bring about the required emission reductions in the ETS sector, the annual factor by which the cap on the maximum permitted emissions within the ETS will have to be increased from 1.74 % currently to 2.2 % after 2020" (European Commission 2014b).

According to Directive 2008/101/EC, the aviation sector is included in the EU ETS from 2012 onward. This entails the creation of European Union Aviation Allowances (EUAAs): special emission allowances that can only be used by airline companies for compliance purpose. From 2012 emissions from all flights from, to, and within the European Economic Area (EEA) (the 28 EU Member States plus Iceland, Liechtenstein, and Norway) were included in the EU ETS. However, in 2013, the International Civil Aviation Organization (ICAO) Assembly agreed to adopt a definitive agenda for a global agreement to tackle emissions in the aviation sector, and pending the possible adoption of international rules, the EU limited the coverage of the EU ETS to flights within the EEA for the period from 2013 to 2016 (European Commission 2014a).

Without doubt, the frauds detected within the EU ETS (e.g., VAT fraud and double accounting) (EU 2010; Linacre et al. 2011) have helped undermine the confidence in different agents in the scheme.

Linking and Comparing the Two Trading Schemes

This section presents a comparative analysis between the two trading schemes, focusing on their main links and differences and including a demand–supply analysis (subsection "A Supply–Demand Balance of Emission Permits and the Level of Ambition in the Trading Schemes") and a price analysis (subsection "A Carbon Price Analysis").

An emission trading scheme may be established as a climate policy instrument at both domestic and regional levels. Various national schemes (e.g., New Zealand (NZ ETS) and Australia) and regional schemes (e.g., the EU ETS) have been established under the umbrella of the Kyoto Protocol's ET. Any transfer of emission

permits between entities in different Annex B parties under such domestic or regional schemes is also subject to the Kyoto Protocol's rules (UNFCCC 2008a). In a major step toward the first full intercontinental linking of emission trading systems, the European Commission and Australia announced an agreement in August 2012 on a pathway for linking the EU ETS and the Australian emission trading scheme (European Commission 2012a).

There are two direct links between the emission permits allowed in the EU ETS, i.e., EUAs, and Kyoto Units. On the one hand, a link between the EU ETS and project-based mechanisms is established through Directive 2004/101/EC, which allows EU ETS firms to use a limited number of ERU and CER credits to meet their targets during Phase II (2008–2012). These firms used 1.058 billion international credits (European Commission 2014a). On the other hand, even though the EU ETS started functioning in 2005 and operated independently from the Kyoto Protocol's accounting system, in 2008 the two trading schemes were linked through the International Transaction Log (ITL), and between 2008 and 2012 Assigned Amount Units (AAUs) were converted into European Union Allowances (EUAs) before being allocated to different EU ETS firms. Later, once these firms had surrendered an amount of EUAs equivalent to their verified emissions to their corresponding national registry (within the Community Independent Transaction Log (CITL)), the EUAs were again converted and transferred to the retirement account within the International Transaction Log (ITL). The retirement account is the special account were each party must ensure that it has transferred a quantity of units equal to its total Annex A emissions for the commitment period by the end of the true-up period, so the compliance of an Annex B country at the end of 2012 is assessed by comparing the total amount of Kyoto Units in its retirement account to its total verified emissions for the commitment period (UNFCCC 2014c).

There are different ways of acquiring Kyoto Units. It has been common for different buying countries to acquire carbon credits (mainly CERs) through the participation in the aforementioned Carbon Funds and carbon allowances (especially AAUs) through bilateral agreements using Green Investment Schemes (GIS). In a Green Investment Scheme, revenues from emission trading are used to support investments in climate-friendly projects – that is, in projects that reduce emissions. These investments can be made in project reductions that are measurable and quantifiable ("hard greening") or in capacity building, such as emissions inventory development in the seller country, which is nonmeasurable ("soft greening") (Kossoy and Guigon 2012; Point Carbon 2009; Grubb 2003). It is estimated that the total Annex B government demand for Kyoto Units for the first commitment period was 547 Mt CO_{2eq} with the EU-15 accounting for around 75 % of the total and Japan for about 17 %. The main sellers of AAUs linked to these Green Investment Schemes were the governments of Ukraine, with more than one third of the total; the Russian Federation, with around 13 %; the Czech Republic with 8 %; and other EU-10 countries with 40 % of the total. Gross demand for private entities was expected to be around 1070 $MtCO_{2eq}$, while the demand of EU ETS firms, mainly for CERs and ERUs, accounted for 81 % of the total. However, these numbers correspond to the amount of AAUs that governments intend to sell,

which is much lower than the whole amount of excess AAUs, now estimated at more than 10 $GtCO_{2eq}$ over the first commitment period, with Russia accounting for half, Ukraine one quarter, and Poland one fifth (Kossoy and Guigon 2012). According to Point Carbon, there are also private sector entities and intermediaries engaged in the trading of AAUs. By 2009, approximately 147 million AAUs had been transacted. A further 50–60 million AAUs were reported to be under negotiation, with the Czech Republic and Ukraine as the largest sellers, with 68.5 and 44 million AAUs, respectively. The Japanese government and private companies appear to be the largest buyers, having bought most of the volume transacted by those two countries (Point Carbon 2009). 57.81 million tons of AAUs were transacted in 2010 and 47 million in 2011, with Estonia being the biggest seller and Lithuania the second biggest in 2011 (Kossoy and Guigon 2012).

Table 1 summarizes some fundamental characteristics, links, and differences between the Kyoto Protocol's International Emission Trading system and the EU ETS in the 2008–2012 and the 2013–2020 commitment periods. Apart from the number of countries, the GHG, and the economic sectors affected, which are of course much more significant in the case of the Kyoto Protocol's IET, there are other relevant differences to be remarked, such as the targets set, the level of ambition, the consequences of noncompliance, and the instrument of flexibility for reaching the targets.

Apart from those shown in Table 1, there are also other relevant similarities between these two trading schemes, such as the negative trend observed in the different carbon emission prices, which is closely linked with the number of GHGs affected and the caps established, and consequently the over-allocation of emission permits observed in the 2008–2012 period. These issues are analyzed in greater depth below.

A Supply–Demand Balance of Emission Permits and the Level of Ambition in the Trading Schemes

An overview of the supply–demand balance for different emission permits is fundamental in understanding the trends in their corresponding prices. When analyzing the demand and supply of Kyoto Units (especially AAUs) in the first commitment period, two types of countries can be distinguished: *Kyoto Unit seller countries*, that is, those countries that emit less than their "assigned amount," thus generating a surplus of Kyoto Units, and *Kyoto Units buyer countries*, such as Japan, Canada, Australia, and some EU countries (Grubb 2003; Kossoy and Guigon 2012).

As stated on the Kyoto Protocol, parties that represent at least 55 % of the total carbon dioxide emissions for 1990 included in Annex I of the UNFCCC must deposit their instruments of ratification, acceptance, approval, or accession (UNFCCC 1998). Accordingly, when Russia joined the Protocol, it came into force in February 2005. In regard to the level of ambition for 2008–2012, as affirmed by Grubb, the aggregate emissions of Annex I countries in the year 2000 were already below the aggregate Kyoto cap of 5.2 %, but with a huge east–west

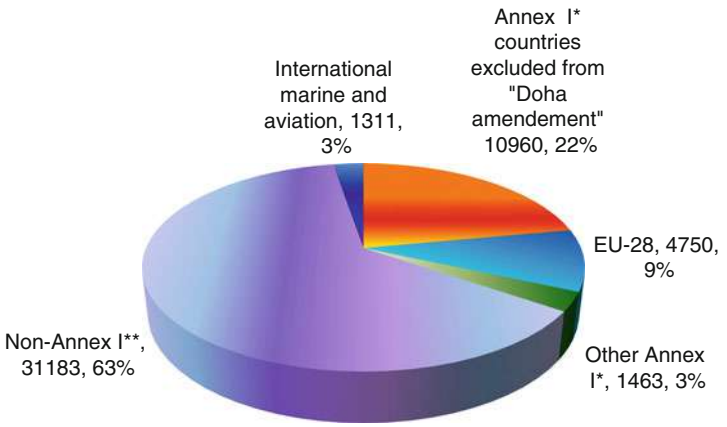

Fig. 1 GHG emissions in 2010 per group of countries (%). Annex I* excluding Turkey and excluding LULUCF. Non-Annex I** including LULUCF for the countries with a high share of LULUCFs, i.e., Brazil, Indonesia, Mexico, Chile, Colombia, Costa Rica, Papua New Guinea, and Peru (Own work using data from Hof et al. (2013))

discrepancy in distribution (Grubb 2003). As explained by this author, the three tumultuous events of 2001 were expected to have as a result a large potential supply against a radically reduced demand of emission permits: the withdrawal of the USA (by far the largest source of potential demand of permits), the expected surplus of AAUs from Russia, and the Bonn/Marrakech deal on carbon sinks (the named LULUCF activities). As a result, the modeling projections of the price plummeted after 2001 (Grubb 2003). It is estimated that most AAU surplus originate from the economic downturn in the "economies in transition" of Central and Eastern Europe and the former Soviet Union due to the so-called hot air problem. This "hot air problem" occurs when some governments are able to meet their targets with minimal effort and can then flood the market with emission rights, reducing the incentive for other countries to cut their own domestic emissions (UNFCCC 2015b). The total surplus of emission units at the end of the first commitment period was estimated to be between 9 and 13 $GtCO_{2eq}$ (Point Carbon 2009; Den Elzen et al. 2010a, b).

Figure 1 illustrates the percentage of GHG emissions by different groups of countries in 2010. As aforesaid, Canada, Japan, and Russia opt out of the "Doha Amendment to the Kyoto Protocol" and so do the USA, all together accounting for around 10,960 Gt CO_{2eq} in 2020. With the world's total emissions of around 60,627 Gt CO_{2eq}, the aforesaid countries amount to around 22 % of the total emissions. Non-Annex I countries emitted a total of 31,191 Gt CO_{2eq} in that year so as illustrated in Fig. 1; they account for around 62.8 % of total emissions worldwide. Finally, the commitment acquired by the countries which are involved in the "Doha Amendment to the Kyoto Protocol" represents only around 12 % the total emissions worldwide with around 6, 2013 Gt CO_{2eq} (Fig. 1).

In the EU-28, the total GHG emissions (not counting international aviation and LULUCF) in 2012 are already 19.2 % below the 1990 levels and 21.6 % below the

Kyoto base year levels. According to preliminary estimates, total emissions decreased by a further 1.8 % in 2013. This means that the EU-28 overachieves its targets by a total of 4.2 Gt CO_{2eq} in the first commitment period, and its emissions over the second commitment period are expected to be 23 % down from the 1990 levels (excluding international aviation and LULUCF) (European Commission 2014c). This means that unless a new accord is reached by the Paris Conference in 2015 a very low level of ambition is envisaged for the 2013–2020 period. However, it must be outlined that there are differences in regard to the potential level of fulfillment by the different Member States of their corresponding commitments to 2020. The European Commission Progress Report estimates that around half of Member States will need additional efforts to meet their 2020 targets domestically for non-ETS sectors, while the rest are forecast to reach these commitments with existing policies and measures (European Commission 2014c).

Within the EU ETS framework, GHG emissions by the firms involved are 5 % below their allocated allowances for the first commitment period, i.e., 5 % below their corresponding caps (EEA 2012). In any case, the over-allocation indicated may vary considerably depending on the sector analyzed, so the following distinction should be made within the EU ETS: on the one hand, *seller EU ETS subsectors* (e.g., Spanish EU ETS firms other than power generation firms) and, on the other, *buyer EU ETS subsectors*. According to the European Commission, the EU ETS has helped to deliver real GHG emission reductions in line with EU targets for 2020. However, partly due to the estimated surplus of almost two billion allowances at the start of Phase III and to record the use of international credits, serious imbalances are expected to emerge in the short term between supply and demand with potentially long-term repercussions which may profoundly affect the ability to meet the ETS target in future phases in a cost-effective manner (European Commission 2014a). This surplus of two billion allowances is due to several factors: auctioning of Phase II allowances and remaining allowances in the new entrant reserve, early auctioning of Phase III allowances, and sales of Phase III allowances to generate funds for the NER300 program (300 million allowances set aside in the New Entrants' Reserve (NER) to fund the deployment of renewable energy technology innovations as well as carbon capture and storage through the NER 300 program) (European Commission 2014a). In regard to the use of international credits, as indicated above, operators used 1.058 billion international credits in Phase II (2008–2012), and based on an earlier draft of the regulation on international credit entitlements, market analysts expect that a total of around 1.6–1.7 billion credits will be available for use in Phases II and III combined (European Commission 2014a).

In a 2012 report by the European Commission to the European Parliament, addressing the European Union Allowance (EUA) surplus problem for Phase III (2013–2020), two types of action are proposed (European Commission 2012b): (a) a review of the auction timetable as a short-term measure, postponing auctions of a certain amount of allowances (so-called back-loading), and (b) more *structural measures*, such as increasing the EU GHG target to 30 % by 2020, retiring a number of allowances, bringing more sectors into the EU ETS, access rules to international

credits and discretionary price management, and an early revision of the linear reduction factor. In regard to short-term measures, on 25 February 2014, the Auctioning Regulation was amended with the back-loading of 900 million allowances to the end of the trading period, i.e., 2020. However, as far as we know, no structural measures have yet been adopted. Moreover, in regard to the aforesaid reduction factor, Directive 2009/29/EC states that the total amount of allowances must decrease by a linear factor of 1.74 % per annum, leading to a reduction of just over 70 % in the ETS cap by 2050, but to be consistent with the EU's agreed long-term objective of 80–90 reduction by 2050 on the 1990 levels as set out in the 2050 Low-Carbon Roadmap (European Commission 2012c) and to achieve the target of a 40 % reduction from 1990 to 2030 as stated by the European Council in 2014 (European Council 2014), the European Commission affirms that this linear factor would need to be revised and lowered to 2.2 % per year (European Commission 2014a, b).

A Carbon Price Analysis

According to Kossoy and Guigon, in 2011 the average price reported per Assigned Amount Unit (AAU) is €5.1/tCO_{2eq}, while at the end of 2010, prices are in the range of €5–7/$tCO_{2\text{-}eq}$. This downward trend coincides with the overall trajectory for all carbon assets and is motivated mainly by lower than expected emissions and length in allowance supplies. However, there were also other contributing factors to explain this downward trend (i) the regulatory uncertainty surrounding surplus AAUs face to the second commitment period, and (ii) the fact that some Japanese private entities (who had been key AAU buyers since 2009), shifted their priorities elsewhere after the Fukushima incident (Kossoy and Guigon 2012). Meanwhile, the EU ETS showed significant price volatility during its start-up period (i.e., Phase I from 2005 to 2007). In late April 2006, prices were over €30, but they fell dramatically when the first EU ETS plant-level emissions data from different Member States were released (Ellerman and Buchner 2007; Ellerman 2009).

Figure 2 illustrates that the European Union Allowance (EUA) spot market price is higher than the Certified Emission Reduction (CER) spot market price throughout the first commitment period, and both prices show the same downward trend, from more than €23/tCO_{2eq} and €18/tCO_{2eq} in August 2008 to €7/$tCO_{2\text{-}eq}$ and €3.5/tCO_{2eq}, respectively, in May 2012. However, the difference between the EUA and CER spot prices increases especially since the end of 2010. Indeed, on 14 November 2012, the EUA spot price is €7.91 (with 421,000 allowances transacted), while the CER spot price is €0.78 (with 87,000 credits transacted) (so the difference was €7.13). Note that the price per tCO_{2eq} of the *green CER* is €1.03 (with 218,000 credits transacted), so the difference with the EUA totals €6.88. Finally, the Emission Reduction Unit (ERU) price at that time is as low as €0.54 (with 200,000 emission rights transacted) (Bluenext 2012).

This downward tendency in all the emission permit prices observed is linked to the aforesaid oversupply of emission permits in both emission trading schemes

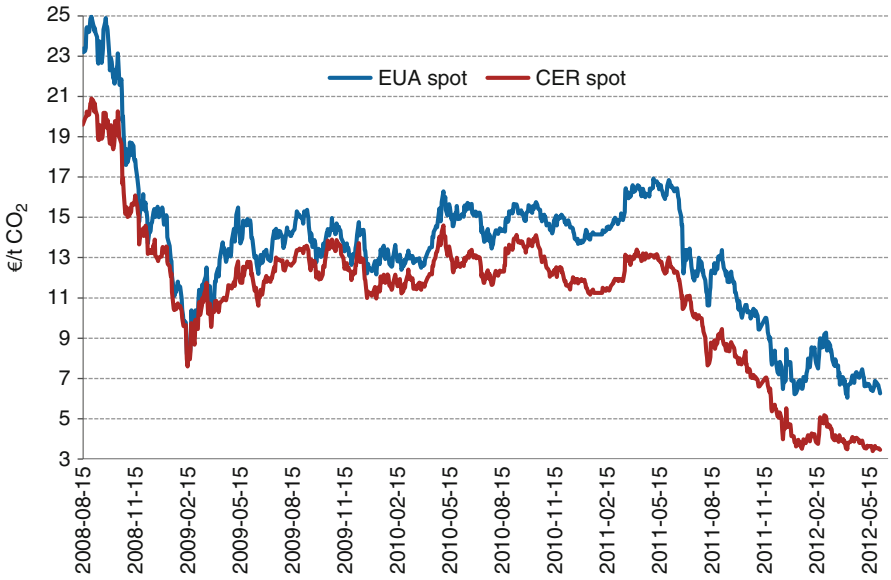

Fig. 2 Trend in EUA and CER spot prices in the 2008–2012 period (Source: Wind to Market, 2012)

(see subsection "A Supply–Demand Balance of Emission Permits and the Level of Ambition in the Trading Schemes"), and as illustrated, major differences exist between the different emission permits. In regard to the EU ETS, the European Commission affirms that from 2009 onward, a growing surplus of allowances and international credits became available on the carbon market, leading to a fall in the carbon price (European Commission 2014a). However, Ellerman affirms that a uniform price for CO_2 exists across the EU ETS system and is taken into account in operating and investment decisions by most owners of EU ETS firms. He also concludes that the EU ETS has shown itself to be an effective mechanism for limiting GHG emissions in the sectors covered and that it is being used to effect progressively more significant emission reduction (Ellerman 2009). By contrast, as shown, notable differences exist between the prices of the different Kyoto Units. According to Grubb (Grubb 2003), some of this discrimination may come directly from the private sector. Especially in this formative stage, the value accorded to emission units by the private sector is strongly affected by both reputational considerations (which make companies averse to large-scale and potentially controversial projects) and political risk considerations (which include the risks associated with uncertainty about what kind of units governments will ultimately accept). In this sense this author affirms that credits from project mechanisms may attract a premium over AAUs from trading, because they can be associated with actual project investment and also that direct trading of national emission allowances appears to be

subject to the greatest political risks and subsequently the greatest discounting (Grubb 2003). However, the trend in emission permit prices illustrates that the average estimated AAU price has been higher than the average CER spot price. This could be due to several reasons: on the one hand, there may be a problem linked to the delay of certain CER credits issued from different Clean Development Mechanism projects, which may have pushed some Annex B buyer countries to buy AAU allowances instead of CERs in order to reduce their degree of uncertainty; on the other hand, it is possible that what the author quoted has overestimated the political risk associated with the direct trading of AAUs, especially because a relevant amount of AAUs are probably being transferred through Green Investment Schemes, which means that the trading of AAUs could be associated with real project investments. Reputational risks may not be such a relevant factor, moreover, as the controversies in regard to the contribution to sustainable development of certain Clean Development Mechanism projects (see subsection "Critical Concerns"), which may have acted as a disincentive to demand for CER credits. Finally, as the transfer of AAUs occurs between countries that are both subject to legally binding constraints, it does not carry many of the political and technical complexities associated with the Clean Development Mechanism. This may be another cause for their lower demand. Indeed, it is probable that problems related to transaction costs due to the complexity of the methodologies established have also discouraged demand for CERs.

Conclusions

This chapter underlines the close relationship between the EU ETS and International Emission Trading under the Kyoto Protocol in the 2008–2012 period. The future of this International Emission Trading is now being called into question. Despite the fact that the countries signed up to the "Doha Amendment to the Kyoto Protocol" are able to use the Flexible Mechanism for the 2013–2020 period, the main weakness in regard to the future of the post-Kyoto 2012 period can be summed up as follows:

- The small proportion of GHGs included in the Doha Amendment, which accounts for only around 12 % of the worldwide total
- The low level of ambition of the countries involved, especially considering that the EU-28 group (which accounts for around 9 % of world emissions) had by 2012 achieved a 19.2 % GHG reduction below the 1990 levels

These weaknesses are robbing this trading instrument of relevance in tackling the worldwide climate change problem. The next UNFCCC 2015 meeting in Paris may be critical for the future of the International Emission Trading and also for the international policy against the climate change problem as a whole. It must also be underlined that, although the EU-28 has already overachieved the 18 % reduction target set by the Doha Agreement, major differences exist between Member States,

which means that there may be some Kyoto Unit buyer countries that will need to buy emission permits to reach their respective comments. However, considering current conditions, the most likely outcome is that they will have to pay a very low price for the units that they acquire.

Despite the critical situation faced by the International Emission Trading under the Kyoto Protocol and their links, the EU ETS still represents one of the most significant instruments for reducing GHG emissions in the EU. However, the problem of surplus allowances for 2013–2020 may also undermine its effectiveness as a trading instrument. It is still necessary to verify whether the EU will adopt the necessary measures to solve the surplus problem, whether the short-term measures adopted (the back-loading of 900 million allowances) will be effective, and whether more structural measures are still needed.

The downward trend observed in emission prices is closely linked to the oversupply of emission permits in both emission trading schemes. However, future expectations may be also fundamental to understanding different carbon price trends, especially at the end of the first commitment period, when the prices observed collapsed. The fall in Kyoto Unit prices is probably also directly linked to uncertainties regarding a possible future agreement in 2015 for an ambitious engagement of countries to face the climate change problem and the low level of significance of the Doha Agreement. These reasons are also relevant in understanding the current critical situation observed in the Clean Development Mechanisms and the virtual standstill of the Joint Implementation mechanism. Present chapter also outlines several reasons that may explain why the Certified Emission Reduction Prices are lower than Assigned Amount Unit prices, such as the delay of certain credits issued from some Clean Development Mechanisms projects.

Although a uniform price existed between 2008 and 2012 for European Union Allowances, notable differences were observed between the prices of different Kyoto Units, especially between Assigned Amount Unit (AAU) and Certified Emission Reduction (CER) credits. Questions linked with the existence of methodological problems when determining baselines and additionality, the coverage of forestry-related projects, the sustainability of the projects implemented, and other factors may have discouraged the demand for Certified Emission Reduction (CER) credits from certain Clean Development Mechanism projects, and that could largely explain the fall observed in average CER spot prices compared to average AAU estimated prices.

As illustrated, there are in addition other relevant factors to be considered, such as the necessity for robust, transparent regulations regarding the different emission permit transaction and accounting systems. Without doubt the frauds detected in the EU and the high level of complexity inherent in such trading systems (as may occur in regard to the recent complex auctioning system set up in the EU ETS) have probably increased the level of skepticism toward them as policy instruments.

Acknowledgment This work has been possible thanks to the collaboration of the Energy Working Group, which belongs to the Chair of International Relations (Social Sciences Faculty) of the University of the Basque Country (UPV–EHU).

Annex

See Table 2.

Table 2 Annex B parties to the Kyoto Protocol

Party	Quantified emission limitation or reduction commitment (percentage of base year or period)
Australia	108
Austria	92
Belgium	92
Bulgaria[a]	92
Canada	94
Croatia[a]	95
Czech Republic[a]	92
Denmark	92
Estonia[a]	92
European Community	92
Finland	92
France	92
Germany	92
Greece	92
Hungary[a]	94
Iceland	110
Ireland	92
Italy	92
Japan	94
Latvia[a]	92
Liechtenstein	92
Lithuania[a]	92
Luxembourg	92
Monaco	92
Netherlands	92
New Zealand	100
Norway	101
Poland[a]	94
Portugal	92
Romania[a]	92
Russian Federation	100
Slovakia[a]	92
Slovenia[a]	92
Spain	92
Sweden	92
Switzerland	92
Ukraine[a]	100
United Kingdom of Great Britain and Northern Ireland	92 93
USA[b]	

Source: UNFCCC (1998)

[a]Countries that are undergoing the process of transition to a market economy

[b]The USA has not ratified the Kyoto Protocol

References

Babiker MH, Jacoby HD, Reilly JM, Reiner DM (2002) The evolution of a climate regime: Kyoto to Marrakech and beyond. Environ Sci Pol 5:195–206

Benz E, Löschel A, Sturm B (2010) Auctioning of CO2 emission allowances in Phase 3 of the EU emission trading scheme. Clim Pol 10(6):705–718

Bluenext (2012) The Earth's exchange. http://www.bluenext.eu/. Accessed Nov 2012

Brohé A, Eyre N, Howarth N (2009) Carbon markets. An international business guide. Earthscan, London

Carr C, Rosembuj F (2007) World Bank experiences in contracting for emission reductions. Environment Liability Published by Lawtext Publishing Limited. http://www.lawtext.com

Coase RH (1960) The problem of social cost. J Law Econ 3(1):1–44

Council of the European Union (2002) Council Decision of 25 April 2002 concerning the approval, on behalf of the European Community, of the Kyoto Protocol to the United Nations Framework Convention on Climate Change and the joint fulfillment of commitments there under. 25 Apr 2002. http://eur-lex.europa.eu/legal-content/EN/TXT/PDF/?uri=OJ:JOL_2002_130_R_0001_01&from=EN

de Martínez Alegría I, Vicente A, Larrea M (2012) Promotion of renewables and energy efficiency by politics: case study of the European Union. In: Chen W-Y, Seiner J, Suzuki TS, Laeckner M (eds) Handbook of climate change mitigation. Part 2. Springer, New York/Dordrecht/Heidelberg/London, pp 277–318. doi:10.1007/978-1-4419-7991-9_9, e-ISBN 978-1-4419-7991-9. ISBN 978-1-4419-7990-2

Den Elzen M, Hare W, Höhne N, Levin K, Lowe J, Riahi K, Rogelj J, Sawin E, Taylor C, van Vuuren D, Ward M (2010a) The emissions gap report. Are the Copenhagen Accord pledges sufficient to limit global warming to 2o or 1.5o? A preliminary assessment. United Nations Environment Programme (UNEP), Nairobi

Den Elzen M, Roelfsema M, Slingerland S (2010b) Dealing with surplus emissions in the climate negotiations after Copenhagen: what are the option for compromise? Energy Policy 38:6615–6628

Den Elzen MGJ, Hof AF, Mendoza Beltran A, Grassi G, Roelfsema M, van Ruijven B, van Vliet J, van Vuuren DP (2011) The Copenhagen Accord: abatement costs and carbon prices resulting from the submissions. Environ Sci Pol 14:28–39

Ellerman AD (2005) A note on tradeable permits. Environ Resour Econ 31:123–131, Springer

Ellerman AD (2009) The EU's emissions trading scheme: a prototype global system? MIT joint program on the science and policy of global change, report no. 170

Ellerman AD, Buchner BK (2007) The European Union Emission Trading Scheme: origins, allocation and early results. Rev Environ Econ Policy 1:66–86

EU (2003) Directive 2003/87/EC of the European Parliament and of the Council of 13 October 2003 establishing a scheme for greenhouse gas emission allowance trading within the Community and amending Council Directive 96/61/EC. Official Journal. L 275/32

EU (2004) Commission Regulation (EC) N° 2216/2004 of 21 December 2004 for a standardised and secured system of registries pursuant to Directive 2003/87/EC of the European Parliament and of the Council and Decision N° 280/2004/EC of the European Parliament and of the Council

EU (2008) Directive 2008/101/EC of the European Parliament and of the Council of 19 November 2008 amending Directive 2003/87/EC so as to include aviation activities in the scheme for greenhouse gas emission allowance trading within the Community. Official Journal L 8/3

EU (2009) Directive 2009/29/EC of the European Parliament and of the Council of 23 April 2009 amending Directive 2003/87/EC so as to improve and extend the greenhouse gas emission allowance trading scheme of the community. Official Journal L 140/63, 5 June 2009

EU (2010) Commission regulation EU (2010) Commission regulation (EU) No 920/2010 of 7 October 2010 for a standardised and secured system of registries pursuant to Directive 2003/87/EC of the European Parliament and of the Council and Decision No 280/2004/EC of the European Parliament and of the Council. Official Journal of the European Union. L 270/1, 14. Oct 2010

EU (2011) Commission Regulation (EU) No 550/2011 of 7 June 2011 on determining, pursuant to Directive 2003/87/EC of the European Parliament and of the Council, certain restrictions applicable to the use of international credits from projects involving industrial gases. Official Journal of the European Union. L 149/1

European Commission (2011) Guidance Document n°5 on the harmonized free allocation methodology for the EU-ETS post 2012. Guidance on carbon leakage. European Commission Directorate-General Climate Action Directorate B – European & International Carbon Markets. Final version issued on 14 Apr 2011

European Commission (2012a) Australia and European Commission agree on pathway towards fully linking emissions trading systems, 28 Aug 2012. http://ec.europa.eu/clima/news/articles/news_2012082801_en.htm. Accessed Nov 2012

European Commission (2012b) Report from the Commission to the European Parliament and the Council: The estate of the European Carbon Market in 2012. Brussels, 14 Nov 2012: COM (2012) 652 final

European Commission (2012c) A Roadmap for moving to a competitive low carbon economy in 2050. COM(2011) 112 final

European Commission (2014a) Climate action: the EU emissions trading system (EU ETS). http://ec.europa.eu/clima/. Accessed Nov 2014

European Commission (2014b) Communication from the Commission to the European Parliament, the Council, the European economic and social committee and the committee of the Regions, a policy framework for climate and energy in the period from 2020 to 2030. Brussels, 22 Jan 2014, COM (2014) 15 final

European Commission (2014c) Report from the Commission to the European Parliament and the Council: progress toward achieving the Kyoto and EU 2020 objectives. Brussels. 28 Oct 24, COM (2014) 689 final

European Council (2007) Brussels European Council, 8 and 9 Mar 2007. Presidency conclusions. Brussels. 2 May 2007, COM (2007) 7224/1/02 Rev 1

European Council (2014) Brussels European Council, 23–24 Oct 2014. EUCO 169/14

European Environment Agency (EEA) (2012) Greenhouse gas emission trends and projections in Europe 2012: tracking progress towards Kyoto and 2020 targets, EEA report no. 6/2012

Grubb M (2003) The economics of the Kyoto Protocol. World Econ 4(3):143–189

Grubb M, Neuhoff K (2006) Allocation and competitiveness in the EU emissions trading scheme: policy overview. Clim Pol 6:7–30

Gupta S, Tirpak DA, Burger N, Höhne J, Boncheva AI, Kanoan GM, Kolstad C, Kruger JA, Michaelowa A, Murase S, Pershing J, Saijo T, Sari A (2007) Policies, instruments and co-operative arrangements. In: Metz B, Davidson OR, Bosch PR, Dave R, Meyer LA (eds) Climate change 2007: mitigation. Contribution of Working Group III for the fourth assessment report to the Intergovernmental Panel on Climate Change. Cambridge University Press, Cambridge/New York

Hentrich S, Matschoss P, Michaelis P (2009) Emissions trading and competitiveness: lessons from Germany. Clim Pol 9:316–329

Hof AF, den Elzen MGJ, Roelfsema M (2013) The effect of updated pledges and business-as-usual projections, and new agreed rules on expected global greenhouse gas emissions in 2020. Environ Sci Pol 33(11):308–319

Holm Olsen, K, Fenhann J (2006) Sustainable development benefits of clean development mechanism projects: development for a new methodology for text analysis of the project design documents submitted for validation. http://cd4cdm.org/Publications/SustainableDevelopmentBenefitsCDM.pdf. Accessed Nov 2014

IPCC (2007) Summary for policymakers. In: Metz B, Bosch OR, Dave R, Meyer LA (eds) Climate change 2007: mitigation. Contribution of Working Group III to the fourth assessment report of the Intergovernmental Panel on Climate Change. Cambridge University Press, Cambridge/New York

Joint Implementation supervisory Committee (JISC) (2014) Joint implementation supervisory committee thirty-fifth meeting (Meeting Report No. version 01.1). 16-17 September 2014, Bonn

Kartha S, Erikson P (2011) Comparison of Annex 1 and non-Annex 1 pledges under the Cancun Agreements. Stockholm Environment Institute (SEI). http://www.sei-international.org/mediamanager/documents/Publications/Climate/sei-workingpaperus-1107.pdf. Accessed Nov 2012

Kollmuss A, Zink H, Policarp C (2008) Making sense of the voluntary carbon market: a comparison of Carbon Offset Standards. Stockholm Environment Institute (SEI-US), Tricorona, WWF Germany. http://assets.panda.org/downloads/vcm_report_final.pdf. Accessed Nov 2012

Kossoy A, Guigon P (2012) State & trends of the carbon market 2012. Carbon Finance at the Word Bank, Washington, DC

Kossoy A, Oppermann K, Reddy RC, Bosi M, Boukerche S, Höhne N, Klein N, Gilbert A, Jung M, Borkent B, Lam L, Röser F, Braun N, Hänsel G, Warnecke C (2013) Mapping carbon pricing initiatives : developments and prospects 2013. World Bank, Washington, DC. © World Bank. https://openknowledge.worldbank.com/handle/10986/15771 License: CC BY 3.0 IGO

LeBlanc A (1999) Issues related to including forestry based offsets in a GHG emission trading system. Environmental Science & Policy 2:199–206

Linacre NK, Kossoy A, Ambrosi P (2011) State & trends of the carbon market 2011. World Bank, Washington, DC

Martínez de Alegría I, Díaz de Basurto P, Martínez de Alegría I, Ruíz de Arbulo P (2009) European Union's renewable energy sources and energy efficiency policy review. The Spanish perspective. Renew Sust Energ Rev (RSER) 13:100–114

Point Carbon (2009) Assigned Amount Unit: Seller/buyer analysis and impact on post-2012 climate regime. http://www.pointcarbon.com

Solomon BD (1999) New directions in emission trading: the potential contribution of new institutional economics. Ecol Econ 30(3):371–387

Stern N (2007) The economics of climate change. The Stern review. Part VI: international collective action. 22 creating a global price for carbon. Cabinet Office – HM Treasury Government, Cambridge, UK. http://www.hmtreasury.gov.uk/sternreview_index.htm

Tietemberg T, Grubb M, Michelowa A, Swift B, Zhang ZX (1999) International rules for greenhouse gas emission trading: defining the principles, modalities, rules and guidelines for verification, reporting and accountability. United Nations conference on trade and development. UNCTAD, Geneva

UNFCCC (1992) United Nations Framework Convention on Climate Change. FCCC/Informal/84. GE.05-62220 (E) 200705

UNFCCC (1998) Kyoto Protocol to the United Nations Framework Convention on Climate Change. United Nations 1998. FCCC/Informal/83*. GE.05-61702 (S) 130605 130605

UNFCCC (2002) Report of the conference of the parties on its seventh session, held at Marrakesh from 29 Oct to 10 Nov 2001. FCCC/CP/2001/13/add.2. 21 Jan 2002

UNFCCC (2008a) Kyoto Protocol reference manual on accounting of emissions and assigned amount. Nov 2008. http://unfccc.int

UNFCCC (2008b) Conference of the parties serving as the meeting of the parties to the Kyoto Protocol. Fourth session Poznan, 1–12 Dec 2008. Item 12 of the provisional agenda Annual compilation and accounting report for Annex B Parties under the Kyoto Protocol. FCCC/KP/CMP/2008/9/Add.1. 17 Nov 2008

UNFCCC (2012a) Report of the conference of the parties on its seventeenth session, held in Durban from 28 Nov to 11 Dec 2011. Addendum Part Two: Action taken by the Conference of the Parties at its seventeenth session. FCCC/CP/2011/9/Add.1. 15 Mar 2012

UNFCCC (2012b) Report of the conference of the parties serving as the meeting of the parties to the Kyoto Protocol on its seventh session, held in Durban from 28 Nov to 11 Dec 2011, FCCC/KP/CMP/2011/10/Add.1. 15 Mar 2012

UNFCCC (2013a) Report of the Conference of the parties serving as the meeting of the parties to the Kyoto Protocol on its eighth session, held in Doha from 26 Nov to 8 Dec 2012 Addendum Part Two: Action taken by the Conference of the Parties serving as the meeting of the Parties to

the Kyoto Protocol at its eighth session. Decision 1/CMP-8. FCCC/KP/CMP/2012/13/Add1. 28 Feb 2013

UNFCCC (2013b) Annual report of the Executive Board of the Clean Development Mechanism to the conference of the parties serving as the meeting of the parties to the Kyoto Protocol. FCCC/KP/CMP/2013/5 (Part I). 24 Oct 2013

UNFCCC (2014a) Report of the conference of the parties serving as the meeting of the parties to the Kyoto Protocol at its ninth session, held in Warsaw from 11 to 23 Nov 2013, Addendum. Part two: action taken by the Conference of the Parties serving as the meeting of the Parties to the Kyoto Protocol at its ninth session FCCC/KP/CMP/2013/9/Add.1. 31 Jan 2014

UNFCCC (2014b) National greenhouse gas inventory data for the period 1990–2012. Note by the secretariat. United Nations Office at Geneva, Geneva, 17 Nov 2014. http://unfccc.int/documentation/documents/advanced_search/items/6911.php?priref=600008149#beg

UNFCCC (2015a) Information provided by Annex I relating to Appendix I of the Copenhagen Accord (quantified economy-wide emission targets for 2020) can be consulted at: http://unfccc.int/meetings/copenhagen_dec_2009/items/5264.php: While information provided by Non Annex I relating to Appendix I of the Copenhagen Accord (nationally appropriate mitigation actions of developing country Parties) can be consulted at: http://unfccc.int/meetings/cop_15/copenhagen_accord/items/5265.php. Accessed Jan 2015

UNFCCC (2015b) The glossary of the UNFCCC. http://unfccc.int/essential_background/glossary/items/3666.php#H. Accessed Jan 2015

UNFCCC (2015c) http://unfccc.int/meetings/cop_15/copenhagen_accord/items/5265.php. Accessed Jan 2015

Walsh J, Whalley S (2008) Bringing the Copenhagen global climate change negotiations to conclusion. In CESifo working paper no. 2458, category 1: trade policy, pp 1–43

Watson C, Fankhauser S (2009) The clean development mechanism: too flexible to produce sustainable development benefits?, Centre for Climate Change Economics and Policy and Grantham Research Institute on Climate Change and the Environment, 2. Centre for Climate Change Economics and Policy and Grantham Research Institute on Climate Change and the Environment, London, working paper no. 3. http://eprints.lse.ac.uk/37605/. Accessed Mar 2013

World Bank, Ecofys (2014) State and trends of carbon pricing 2014. State and trends of carbon pricing. World Bank Group, Washington, DC. http://documents.worldbank.org/curated/en/2014/05/19572833/state-trends-carbon-pricing-2014

York IPCC (2014) Climate change 2014: mitigation of climate change, contribution of Working Group III to AR5, final draft, accepted but not approved in detail by the 12th session of Working Group III and the 39th session of the IPCC, 12 Apr 2014, Berlin

European Union (EU) Strategy to Face the Climate Change Challenge in the Framework of the International Commitments

Itziar Martínez de Alegría, María-Azucena Vicente-Molina, and Cristian Moore

Contents

Abstract

Since climate change has become an international concern, most of the developed countries have attempted to adopt policies to mitigate global warming and its side effects in the last years. In this chapter, firstly the climate change framework for international action and policy development is analyzed. Likewise, due to the strategic importance of the European Union (EU) leadership in developing and

I. Martínez de Alegría (✉)
Engineering School of Bilbao, University of the Basque Country (UPV/EHU), Bilbao, Spain
e-mail: Itziar.martinezdealegria@ehu.es

M.-A. Vicente-Molina
Economics and Business Administration College, University of the Basque Country, Bilbao, Spain
e-mail: azucena.vicente@ehu.es

C. Moore
Alcoa Inc., Alcoa, TN, USA
e-mail: chris.moore@alcoa.com

W.-Y. Chen et al. (eds.), *Handbook of Climate Change Mitigation and Adaptation*,
DOI 10.1007/978-3-319-14409-2_95

implementing new instruments and policies to mitigate climate change through energy efficiency and renewable energy sources, this work is mainly focused on its energy legislative instruments to face the climate change. The present energy model of the EU, which supports its economic growth and prosperity, is nearly 80 % dependent on fossils fuels and increasingly dependent on energy imported from non-EU member countries, creating economic, social, political, and other risks for the EU. From the 1990s, the key objectives of the EU have been energy security of supply, competitiveness, and environmental protection, making renewable energy sources and energy efficiency the basis for EU's new energy strategy. Accordingly, the EU has recently adopted new legislative instruments with the aim to become the world leader in the impulse of climate change mitigation through the employment of renewable energy sources and energy efficiency technologies. Therefore, this chapter presents and discusses the main legislative measures adopted recently, as well as their potential incidence on the EU's objectives to comply with climate change amendments under the Kyoto Protocol.

Introduction

In recent years, various local, state, federal, and international programs have been introduced, proposed, and adopted with the intent to implement measures to reduce the levels of carbon dioxide (CO_2) and other greenhouse gas (GHG) pollutants emitted into the atmosphere (See Annex 1), which are considered the main cause of climate change. Due to the need for consistent international evaluation of GHG emissions and to enable a universal standard of measurement for climate change impacts, GHG emissions are commonly referred to in terms of "carbon dioxide equivalents" or CO_{2eq}, because CO_2 is the most abundant among the mentioned GHGs (e.g., it represents around 80 % of the European Union's GHG). The definition of carbon dioxide equivalent (CO_{2eq}) is the amount of CO_2 emission that would cause the same radioactive forcing as an emitted amount of a well-mixed greenhouse gas or a mixture of well-mixed greenhouse gases, all multiplied with their respective global-warming potentials (GWPs) to take into account the differing times they remain in the atmosphere (IPCC 2007). Around 78 % of the total GHG emission increase in the period 1970–2010 has been due to CO_2 emissions from industrial processes and fossil fuel combustion (IPCC 2014). A specific global-warming potential (GWP) has been developed for each identified GHG. The global-warming potential is a measure of the impact of the emissions of the specific GHG's climate change influence relative to a similar amount of CO_2 over a consistent time frame (see Annex 1). The type of pollutant and its specific GWP is an important aspect in the planning of legislative and regulatory approaches to mitigate climate change.

As shown in Fig. 1, despite a growing number of climate change mitigation policies in place, from 1970 to 2010, total anthropogenic GHG emissions kept on growing continuously, with larger absolute increases toward the end of this period.

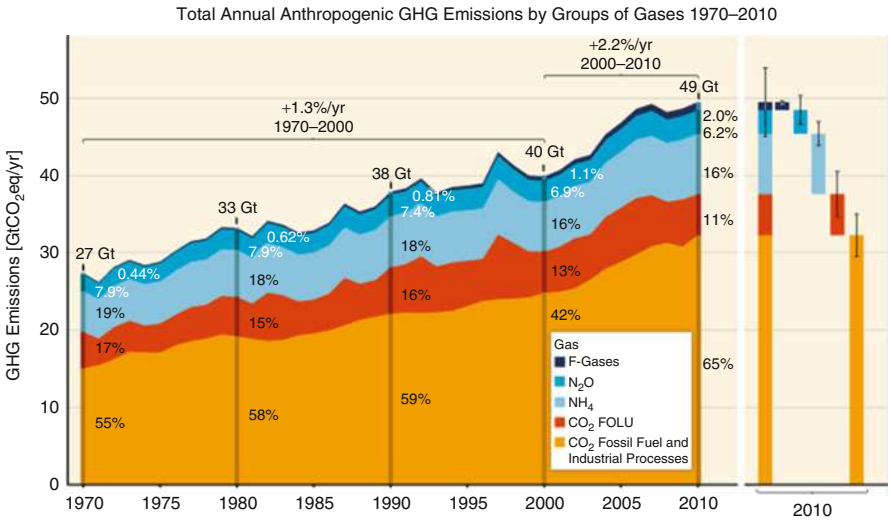

Fig. 1 GHG emissions by group of gases. *F-Gases* Fluorinated gases, *FOLU* Forestry and other land use (Source: IPCC 2014)

The most important drivers of increases in CO_2 emissions from fossil fuel combustion continue to be economic and population growth. Both drivers offset emission reduction due to energy efficiency. Accordingly, the International Panel on Climate Change (IPCC) prevents that emission growth is expected to persist driven by growth in global population and economic activities, unless additional efforts are taken to reduce GHG emissions (IPCC 2014). Figure 2 illustrates the main CO_2 emitter countries in 1995 and 2010.

Since fossil fuels are the first source of CO_2 emissions in the EU (IPCC 2014), which are, at the same time, the most common gases among the GHGs contributing to climate change, the EU has decided to reduce the use of these energy sources betting for this purpose on a strategy focused on renewable energy sources and energy efficiency increase. According to the European Council, the EU is committed to reducing GHG emissions to 80–95 % below 1990 levels by 2050 in the context of necessary reductions by developed countries as a group (European Council 2009). The EU's energy and climate strategy includes, on one hand, the implementation of an Emission Trading Scheme (the EU ETS from now) that focuses on the EU great CO_2 emitters (the EU ETS firms from now) and covers around half of the total GHG and, on the other hand, a wide number of policy measures that affect at the same time the aforesaid EU ETS firms and also the rest of sectors (referred as the diffuse sectors). The main objective of the present work is to offer an overview of the current climate change policy strategy carried out by the EU focusing on the legislation affecting the generation and use of energy. This is why a relevant amount of policies and regulation, which may have a fundamental impact on the future evolution of the GHG in the EU, have been kept out from the present analysis (specially that linked to

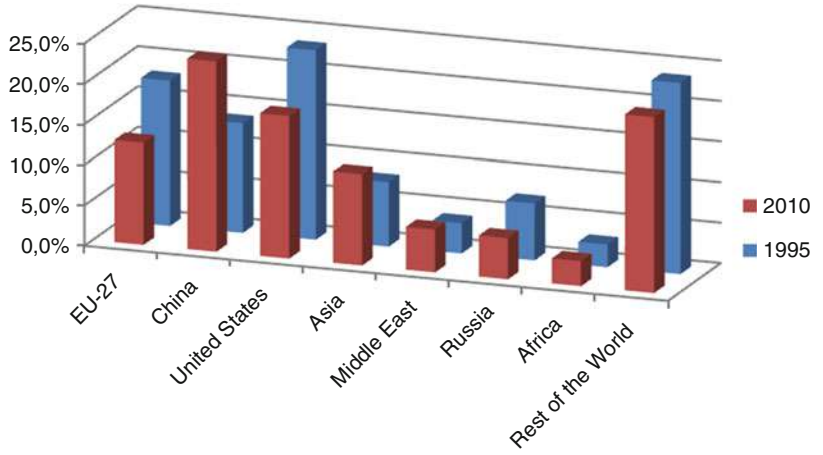

Fig. 2 Contribution to the world CO_2 emissions (%) by emitter countries or regions (Source: Elaborated with data from European Commission 2013a)

the agriculture sector that aimed at promoting carbon sinks or that linked with the nuclear energy). The legislation related with the fluorinated gases ("F-gases") (which are a family of GHG manmade gases used in a range of industrial applications whose global warming effects are up to 23,000 times greater than carbon dioxide (CO_2) and which are rising strongly and affect the sector of cars and vans (the MAC directive), the buildings' air conditioning, etc.), the legislation related with the completion of the internal energy market, and the financial measures destined to promote the climate change policy within the EU (such as the different R + D Frameworks Programs, the Intelligent Energy Europe Programme 2007–2013, etc.) are also kept out from the present study.

Figure 3 shows a synopsis of the most relevant binding targets established recently by the EU to face the climate change through GHG emission reduction and the main pillars of its "Climate Change Policy."

As illustrated in Fig. 3, under the UNFCCC framework, the EU committed to reducing its GHG emissions by 8 % (on average) compared to 1990 emissions by 2012 (as stated by the Kyoto Protocol in 1997). In 2012, the Doha Agreement included the objective to reduce GHG emissions by 18 % from 1990 to 2020 (UNFCCC 2013). In 2007, the EU committed to reduce GHG emissions by 20 % by 2020 (30 % in the case of an international agreement being reached) (European Council 2007). Unfortunately, no agreement has been reached in this regard till now. To reach this target, the EU established the so-called 20/20/20 mandate, upon which the EU has lately articulated its strategy against climate change, which is supported by three fundamental pillars: increasing energy efficiency (+20 %), use of renewable energy sources (20 %), and reducing GHG emissions (−20 %). Along this line, the EU distinguishes between big emitters (industrial and power sectors) and small emitters or diffuse sectors (e.g., citizens in their daily life activities, such as heating

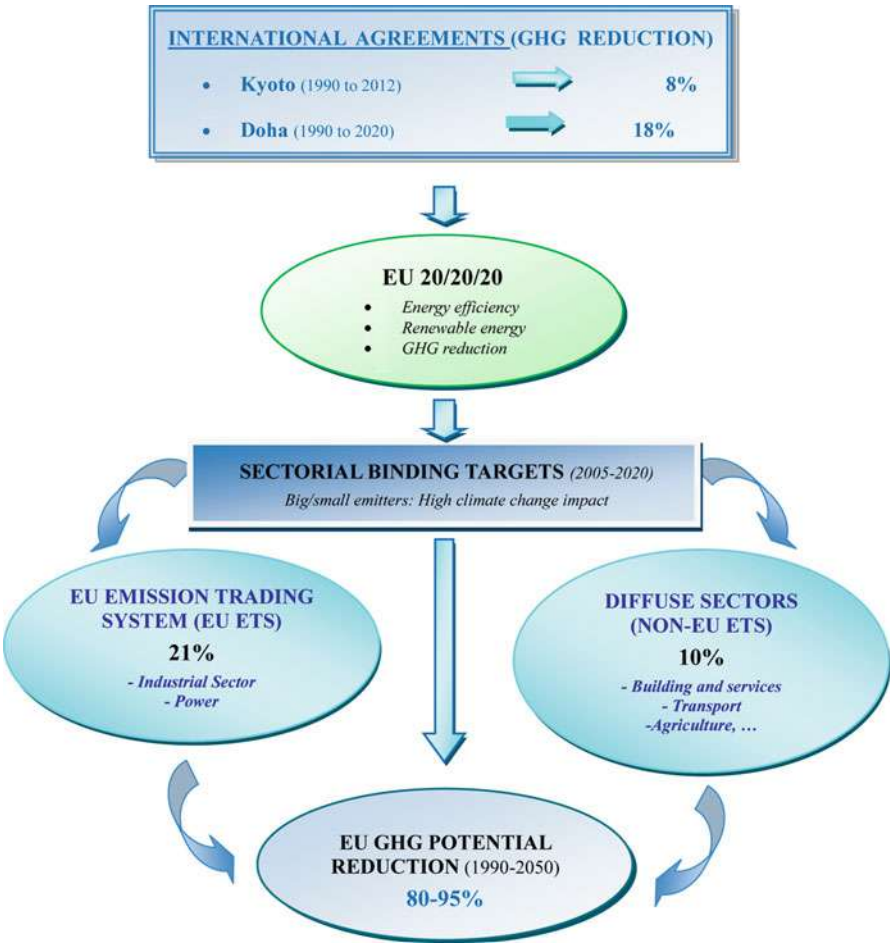

Fig. 3 Binding targets of European Union for climate change mitigation, GHG emission reduction

of buildings, etc.), whose GHG emissions have individually or in the whole an important impact on climate change. This classification serves as a guide in the development of a wide amount of EU legislative instruments, being the great emitters included in the EU Emission Trading System (EU ETS) in order to control their large individual impact on climate change. The rest of the emitters, who are not included in the aforesaid system, form the diffuse sectors and comprise building, services, transport, and agriculture (although only building and transport sectors are analyzed).

Following the scheme represented in Fig. 3, the present chapter is organized as follows: First, the international framework to face climate change and main accords reached (section "International Framework for Action and Policy Development

Toward Climate Change Mitigation") are briefly shown. Second, the EU policy strategy to face climate change is analyzed focusing on main legislative instruments, roadmaps, and policy guides adopted (section "European Union Strategy to Face Climate Change"). Section "European Union Strategy to Face Climate Change" is divided into two parts, which comprise a historical perspective of the EU's energy and climate strategy (section "Historical Perspective") and a sectorial analysis of the aforesaid strategy (section "Analysis of Climate Change Legislative Instruments from a Sectorial Perspective") including the analysis of the EU ETS sector (section "The EU ETS Sector"), the residential sector (section "The Diffuse Residential Sector"), and the transport sector (section "The Transport Sector"). Finally, section "Conclusions" concludes with a summary and an outlook.

International Framework for Action and Policy Development Toward Climate Change Mitigation

In the early 1980s, the United States directed the completion of a study of worldwide environmental challenges that included a detailed analysis of climate change impacts. Although no specific actions resulted from this study of climate change and related issues, in 1988, "because of the need of broad and balanced information about climate change" and "to provide the governments of the world with a clear scientific view of what is happening to the world's climate," the Intergovernmental Panel on Climate Change (IPCC) was established in order to (IPCC 2010)

- Prepare a comprehensive review and recommendations with respect to the current state of knowledge of the science of climate change
- Evaluate the current and projected social and economic impacts of climate change
- Determine possible response strategies and elements for inclusion in a potential future international convention on climate

The scientific evidence produced in the first IPCC Assessment Reports in the 1990s revealed the importance of climate change as a future topic of interest for environmental policy and planning. In the years following, the IPCC's work has been and continues to be a key work in developing policies to address climate change mitigation.

In 1992, the United States and 153 other countries signed the United Nations Framework Convention on Climate Change (UNFCCC), in Rio de Janeiro (Brazil), which committed all parties to voluntarily reduce GHG emissions to reasonable levels in future years, becoming the main multilateral forum focused on addressing climate change, with nearly universal participation. Following ratification of the UNFCCC, annual meetings of all included parties have been conducted in meetings generally referred to as Conferences of the Parties (COP). Major COP meetings to date are briefly summarized in Table 1.

Table 1 Summary of major UNFCCC Conference of Parties (COP) meetings

COP -No / Year Location	Main objectives and/or amendments
COP-1 / 1995 Berlin, Germany	This was the first meeting of UNFCCC COP. It established an assessment phase known as the Berlin Mandate to develop control options for countries and implemented a 2 year analytical and assessment phase to define specific climate change mitigation options for countries.
COP-3 / 1997 Kyoto, Japan	The Kyoto Protocol was adopted and specific emission reduction or limitation targets for developed countries (with an overall GHG emission levels reduction commitment of 5.2 % below 1990) were established. The United States signed the protocol; however, United States Senate resolutions blocked further action. Note that the Bush administration openly rejected the Kyoto Protocol in 2001.
COP-7 / 2001 Marrakech, Morocco	The rules for the implementation of the Kyoto Protocol were detailed, especially in regard to the Clean Development Mechanism and the Joint Implementation Mechanism. The United States continued as observers only and declined to be active in the negotiations amid hope that the United States would re-engage in the process.
COP-11 / 2005 Montreal, Canada	One of the largest climate change meetings ever held. Entry into force of the Kyoto Protocol. Discussion of the ratified Kyoto Protocol including discussion of emissions trading systems and other aspects of global emissions policy development. The meeting resulted in the Montreal Action Plan that extended the life of the Kyoto Protocol beyond the original 2012 expiration date with deeper GHG emission cuts planned.
COP-13 / 2007 Bali, Indonesia	Parties agreed on the Bali Road Map on implementation timelines and structured negotiation on post Kyoto 2012 timeframe.
COP-14 / 2008 Poznan, Poland	Agreements reached on financing to help poor nations cope with climate issues through adaptation and financial assistance. Approval of forest protection mechanism to combat climate change impacts in heavily impacted forest areas.
COP-15 /2009/ Copenhagen, Denmark	The original goal of COP-15 was to reach a global climate agreement for the period after the Kyoto Protocol expiration in 2012. The COP-15 expressed the environmental objective in terms of limiting increases in average global temperature of 2 °C above pre-industrial levels. It was agreed that developed countries should raise funds of $30 billion from 2010 to 2012 and a goal to raise $100 billion per year by 2020. After the summit, parties sent their corresponding GHG emission limitation or reduction pledges referred as the "Copenhagen pledges." These Accords were later ratified by the Cancun Agreement (COP-16).
COP-17 / 2011 Durban, South Africa	Annex I parties decided to start the process for the development of a new Protocol, or another instrument with legal force under the UNFCCC, which should be adopted by 2015 (to come to effect and be implemented from 2020). To this aim the Durban Platform for Enhanced Action was established.
COP-18 / 2012 Doha, Qatar	Adoption of the "Doha amendment to the Kyoto Protocol" to enable the continuing with the Kyoto Protocol through a second commitment period from 2013 to 2020.
COP-19 / 2013 Warsaw, Poland	An accord to establish more comparable targets face to the future Paris Agreement in 2015 and a calendar in order to establish more ambitious objectives were agreed.

(*continued*)

Table 1 (continued)

COP -No / Year Location	Main objectives and/or amendments
COP-20 / 2014 Lima, Peru	Nations concluded by elaborating the elements of the new agreement, scheduled to be agreed in Paris in late 2015, while also agreeing the ground rules on how all countries can submit contributions to the new agreement during the first quarter of 2015. These Intended Nationally Determined Contributions (INDCs) will form the foundation for climate action post 2020 when the new agreement is set to come into effect.

Source: UNFCCC (2015a) and Moore (2012)

The Major Steps in International Climate Change Mitigation: From Kyoto to Paris

The most significant development resulting from all of the COP meetings since the inception of the UNFCCC (1992) was likely the Kyoto Protocol adopted in Kyoto, Japan, in 1997. The Kyoto Protocol required that "at least 55 % of the total carbon dioxide emissions for 1990 of the Parties included in Annex I" of the UNFCCC (see Annex 2) must deposit their instruments of ratification, acceptance, approval, or accession (UNFCCC 1998). Accordingly, with the adhesion of Russia, it entered into effect on February 16, 2005. The Kyoto Protocol is generally seen as an important first step toward a complete international GHG emission reduction program that will stabilize GHG emissions, provide the essential architecture for any future international agreement on climate change, and enable efficient mitigation and adaptation programs to be developed and implemented. The major achievement of the Kyoto Protocol is that it established binding GHG emission reduction targets for 37 industrialized nations and the European Community. These reductions amount to an average of 5.2 % against 1990 emission levels over the 5 year period from 2008 to 2012. The Kyoto Protocol places a larger burden on more developed nations under the principle of "common but differentiated responsibilities" based on the belief that developed countries are "principally responsible" for the levels of GHG emissions in the atmosphere and should assume a greater burden for mitigation of emissions (UNFCCC 2010a).

Under the Kyoto Protocol, countries are required to meet their GHG emission reduction targets primarily through federal and regional measures. However, the Kyoto Protocol offers them additional means of meeting their reduction targets by way of three market-based mechanisms (also referred to as three flexible mechanisms):

- GHG emission trading or international emission trading
- Clean development mechanisms
- Joint implementation

These three market-based mechanisms were established to help stimulate significant green investment and technology advancement while also helping all countries

meet their GHG emission reduction targets in an efficient and cost-effective manner. Each of the market-based mechanisms is defined in more detail below.

International Emission Trading

As noted previously, countries that are party to the Kyoto Protocol have agreed to targets for reducing their GHG emissions during the 2008–2012 initial commitment period (UNFCCC 2010b). Emissions trading, as established in Article 17 of the Kyoto Protocol, allows countries to sell excess GHG emission credits to other countries that exceed their committed target level of GHG emissions. Beyond actual GHG emission reduction credits, other units are available for trading under the program including

- A removal unit on the basis of land use, land use change, and forestry activities (LULUCF) (e.g., reforestation)
- An emission reduction credit generated by a joint implementation project
- A certified emission reduction generated from a clean development mechanism project

Under the Kyoto Protocol, each country's actual GHG emissions have to be accurately monitored and detailed records maintained of carbon market activity through carbon registries and other means. GHG emission trading schemes may be established in regional or national markets under the guidelines established in the Kyoto Protocol.

Clean Development Mechanism and Joint Implementation Mechanism

The clean development mechanism is essentially a global clearinghouse of acceptable GHG emission offset programs or projects that have been successfully implemented and are thereby certifiable for GHG emission credits. Designed to stimulate sustainable development and GHG emission reductions, this mechanism provides a means of added flexibility for industrialized countries to meet their GHG emission reduction targets and comply with associated limitations. This mechanism also allows emission reduction projects in developing countries to earn certified emission reduction (CER) credits. Each CER credit is equivalent to 1 ton of CO_{2eq}. These CERs can be traded and sold on the international market and utilized by industrialized nations to meet their GHG emission reduction targets under the Kyoto Protocol (UNFCCC 1998). Joint implementation, as defined in Article 6 of the Kyoto Protocol, allows a country with a GHG emission reduction or limitation commitment to earn emission reduction units from an emission reduction project in another country that is party to the Kyoto Protocol and to be counted toward the specific country's GHG emission reduction target. Joint implementation, thus, allows countries under the Kyoto Protocol the flexibility to invest in other countries through capital projects and technology transfer.

Country Classifications Under the Kyoto Protocol and UNFCCC

An important aspect of implementation of the Kyoto Protocol and planning under the UNFCCC is how each country is classified. On the one hand, the UNFCCC set the following classification: *The Annex I parties*, comprising industrialized countries that signed the UNFCCC (it includes the 24 original OECD members, the European Union, and 14 countries with economies in transition) (see Annex 2). *The Annex II* parties is a subgroup of Annex I parties with a special obligation to provide financial resources and facilitate technology transfer to developing countries (Annex II parties include the 24 original OECD members plus the European Union). The rest of countries are referred to as non-Annex I countries (see Annex 2). On the other hand, the Kyoto Protocol included two other new Annexes: *the Annex A*, which includes the GHG affected by the cited Protocol*, and the Annex B*, which includes a list of countries with their respective emission reduction or limitation commitments compared to their 1990 levels (see Annex 2). It must be noted that the United States, being comprised in the Annex B of the Kyoto Protocol and being currently the second biggest GHG emitter country after China (see Fig. 4), did not ratify the Kyoto Protocol for its first commitment period.

According to the UNFCCC, developing countries are not required to reduce GHG emissions unless developed countries in Annex II provide sufficient funding and technological investment. Developing countries may volunteer to become Annex I countries when they are sufficiently developed.

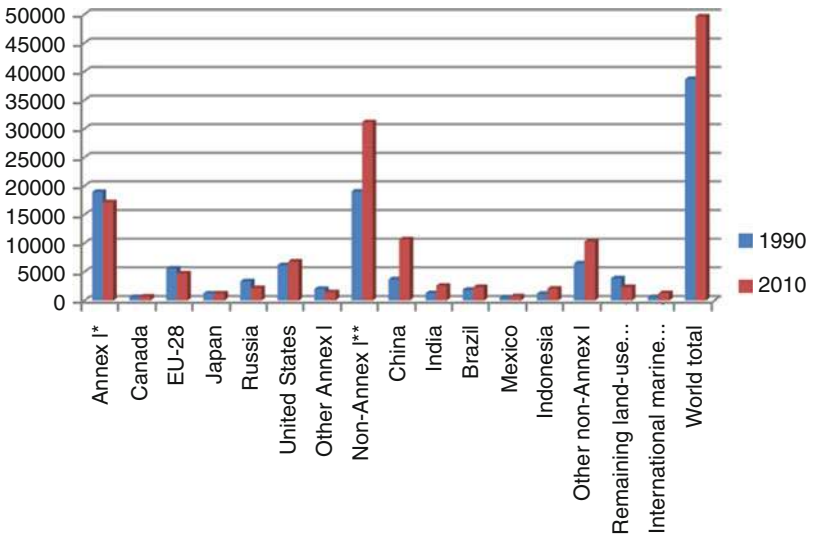

Fig. 4 GHG emissions 1990 and 2010, by Annex I, Non-Annex I and other main GHG country or regions emitters ($GtCO_{2eq}$). Annex I* excluding Turkey and LULUCF. Non-Annex I** including LULUCF for the countries with a high share of LULUCFs, i.e., Brazil, Indonesia, Mexico, Chile, Colombia, Costa Rica, Papua New Guinea and Peru (Source: Adapted from Hof et al. (2013) data)

Current Developments in the International Negotiations

As negotiated in the Bali Conference in 2007 (COP-13), by the end of the first commitment period of the Kyoto Protocol in 2012, an updated international framework that would deliver the GHG emission reductions that the IPCC had deemed necessary must have been developed, negotiated, and ratified. As explained by the UNFCCC, ratification means formal approval (often by the country Parliament or other national institution), of a convention, protocol, or treaty, enabling a country to become a party, so ratification is a separate process that occurs after a country has signed an agreement and must be deposited with a "depositary" (in the case of the Climate Change Convention, the UN Secretary-General) to start the countdown to becoming a party (UNFCCC 2015c). The UNFCCC meeting took place in Copenhagen (Denmark), during December 2009, became the focal point for the development of this new international framework. Although prospects looked dim early in the meeting for any type of agreement, near the conclusion of the meetings government leaders negotiated with focused intensity to reach a global agreement on climate change. In describing the newly touted Copenhagen Accord, United States President Obama commented that there was "a meaningful and unprecedented breakthrough here in Copenhagen." President Obama went on to comment that while the international community has come a long way, there is still a long way to go to reach consensus on climate change mitigation policy. Despite no "new legal agreement" being made, after the Copenhagen Conference, most of Annex I parties formally submitted their GHG emission reduction pledges. In addition, seven major emerging economies (China, India, Brazil, Indonesia, Mexico, South Africa, and South Korea) sent their mitigation action plans (UNFCCC 2015b). However, as most individual targets include high and low estimates, contain assumptions and conditions attached (which depend in many cases on future agreements), use differing base years and GHG gases, and include distinct approaches to the account of offsets and sequestration methods, it is a difficult task to compare various pledges. According to some studies, the cited pledges will not be sufficient to reach the necessary reductions to obtain a max. 2 °C temperature increase reduction objective, especially if the lowest-ambition pledges are implemented at the same time that the aforesaid land use and land use change accounting rules and the use of surplus emission units result in a net increase of emissions (Den Elzen et al. 2010, 2011; Kartha and Erikson 2011).

Later, in the Conference of Parties that took place in Durban in 2011, Annex I parties highlighted the significant gap existing between the aggregate effect of a party's mitigation pledges, in terms of global annual emissions of GHG by 2020, and aggregate emission pathways, likely to have a chance of holding the increase in a global average temperature below 2 °C or 1.5 °C above preindustrial levels. It was also decided to start the process for the development of a new protocol, or another "instrument with legal force" under the UNFCCC, applicable to all parties by 2015 (in order for it to come to effect and be implemented from 2020). To prepare this new Protocol or "instrument with legal force" face to 2015, the Ad Hoc Working Group on the Durban Platform for Enhanced Action was established also at the COP-17 (UNFCCC, 2011). Another major decision adopted in the Durban Conference of

Parties, as meeting of the Parties to the Protocol (UNFCCC 2012) and ratified later by the eighth Conference of the Parties held in Doha in 2012, was the "Doha Amendment to the Kyoto Protocol," which enabled the continuing with the Kyoto Protocol through a second commitment period from 2013 to 2020 (according to which parties may provisionally apply the aforesaid amendment pending its entry into force). The "Doha Amendment" meant the creation of a new Annex B of the Kyoto Protocol, converting the "Copenhagen Pledges" into new quantified emission limitations or reduction commitments for the affected Annex B countries (UNFCCC 2013). However, apart from the United States (USA), a number of Annex I countries (notably Canada, Japan, and Russia but also Belarus, New Zealand, Norway, Switzerland, and Ukraine) decided not to participate in the second commitment period (UNFCCC 2015d). As illustrated in Fig. 5, the world total GHG emissions in 2020 are estimated at around 60,626 $GtCO_{2eq;}$ therefore, the aforesaid countries plus the USA GHG emissions (that will amount to around 6,802 $GtCO_{2eq}$ in 2020) all together account for around 22 % of the world emission in 2020. Meanwhile, countries inside the Doha Amendment only amount to around 12 % of the total emissions worldwide.

In the Conference of Parties held in Warsaw (Poland), in 2013, it was agreed to set more comparative targets together with a calendar from Warsaw (the COP-19) to Paris (the future COP-21), in order to establish more ambitious objectives (UNFCCC 2014). However, in spite of the existing advances in regard to the international policy to face the climate change, the key question to be kept in mind is the level of ambition in relation to the new Agreement to be adopted in 2015. Not only, the final number of countries agreed, should a binding target be taken into account but also the real, absolute level of reduction or limitation of their corresponding GHG emissions, considering the potential flexibility offered by the market-based mechanisms and the land use and land use change activities.

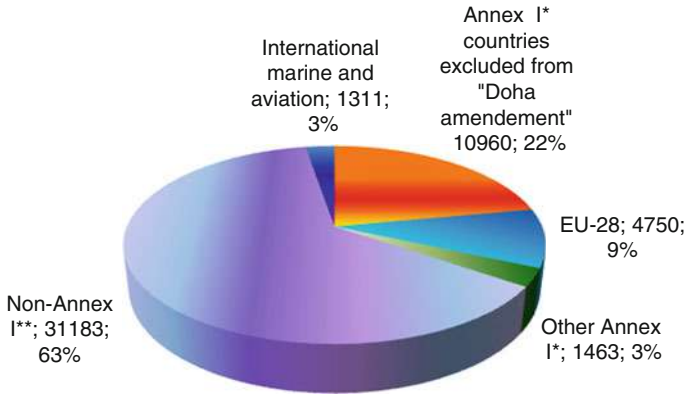

Fig. 5 GHG emissions (in $GtCO_{2eq}$ and %) by different groups of countries in 2010. Annex I* excluding Turkey and LULUCF. Non-Annex I** including LULUCF for the countries with a high share of LULUCFs, i.e., Brazil, Indonesia, Mexico, Chile, Colombia, Costa Rica, Papua New Guinea and Peru (Source: Hof et al. 2013)

As stated by the IPCC, under regime designs for low concentration stabilization levels (450 ppm CO_{2eq}), Annex I countries would need to reduce their emissions substantially during this century by 2020 (−25 % to −40 % below 1990 levels) and to still lower levels by 2050 (−40 % to −95 %), even if developing countries make substantial reductions. It was estimated that 450 ppm CO_{2eq} limit the temperature increase to 2 °C (IPCC 2007). The European Council and the Parliament endorsed these calls for emission reductions as an EU objective, in the context of necessary reductions according to the IPCC by developed countries as a group (COM 2011a).

European Union Strategy to Face Climate Change

In this section, the strategy of the EU to fight against climate change alongside to face the problem of security of energy supply and the increase of the European competitiveness is analyzed.

The EU objective to face the Kyoto Protocol was to reduce by 8 % its GHG emissions between 1990 and 2012. According to the European Environment Agency, a reduction of 19.2 % in GHG emissions was achieved by the EU-28 (without LULUCF), from 1990 to 2012 (EEA 2014). In the following paragraphs, the strategy chosen by the EU to achieve these positive results is shown.

Historical Perspective

The present European Union's model of economic growth and prosperity is around 53.8 % dependent on foreign fuels (European Commission 2013a). Since fossil fuels are the main source of CO_2, which is, at the same time, the most common gas among the GHG (IPCC 2014), this economic model is not environmentally sustainable. In addition, the EU economic model is increasingly dependent on energy imported from non-EU member countries (see Table 2), which creates economic, social, political, and other risks for the Union. Therefore, in the last decade, the Union has attempted to focus its growth on a low-carbon economy through legislative

Table 2 Gross Inland (GI) energy consumption, external dependence and GHG emissions for EU-27

Variable	1995	2005	2010
Energy consumption (Mtoe/year)	1,668	1,824	1,759
Variation rate compared to 1995	–	9.3 %	5.4 %
External energy dependence (All fuels)	43.2 %	52.5 %	52.7 %
GHG emissions (Mio ton CO_{2eq}/year)	5,429	5,445	4,907
Variation rate compared to 1995	–	0.29 %	−9.6 %

Source: Authors' own elaboration from data of European Commission 2012, 2013a

measures, where the increase of renewable energy sources and energy efficiency are key factors not only for energy security of supply but also for climate change mitigation.

As shown in Table 2, the EU Gross Inland energy consumption increased in the period 1995–2010 nearly 5.5 %, and the energy external dependence increased from 43.2 % in 1995 to 52.7 % in 2010. With regard to GHG emissions, from 1995 to 2005 there was an average increase of 0.29 %, while from 2005 to 2010 the trend changed and a reduction of 9.8 % was reached in these last 5 years. There was a 9.6 % reduction for the whole period, 1995–2010, which is a considerable reduction.

The need of promoting energy efficiency was already present in the European energy programs adopted during the 1980s, and in the 1990s the environmental aspects of energy gained importance. Since 1995, the following three key objectives are pursued by the European Energy Strategy: security of supply, environmental protection, and improvement of competitiveness. In 1997, the European Commission (from now on Commission) published a White Paper on Renewable Energy (COM 1997), which announced a target to double the European Union's renewable energy share to 12 % by 2010. The White Paper also announced a renewable energy strategy and action plan, highlighting the need to develop all renewable energy resources, create stable policy frameworks, and improve planning regimes and electricity grid access for renewable energy. A key element of the action plan was the establishment of European legislation to provide a stable policy framework and clarify the expected development of renewable energy in each Member State. In this regard, Directive 2001/77/EC (EU 2001) and Directive 2003/30/EC (EU 2003a) set indicative targets for 2010 for all Member States and require actions to improve the growth, development, and access of renewable energy. A Biomass Action Plan was also adopted in 2005 paying attention to the specific need for Member States to develop Europe's biomass resources (COM 2005). The objective of the EU was to change the increasing dependency on fossil fuels and energy import through the promotion of energy efficiency and the use of renewable energy sources.

In the domestic framework, in response to a request formulated by the 2005 Autumn European Council, the Commission worked on the following important tasks:

- The establishment of the basis for a **Common Energy Policy** that should be based on the following three pillars: sustainable development, increase of competitiveness, and security of supply (COM 2007). The three of them are directly related to renewable energy sources and energy efficiency.
- The elaboration of the **"European Strategic Plan for Energy Technology"** for the consecution of the three pillars. The final objective is the restructuring of the European full energy system, starting with competitiveness and passing through to technological processes. The Commission also highlighted that to reach this objective, and compared with the current situation, a higher quantity of resources (human and financial) would be needed.

In order to overcome the Kyoto Commitment of 8 % GHG emission reduction target, the commonly named "20/20/20" mandate was established, with the following ambitious targets for 2020 compared to 1990 levels (European Council 2007):

- Reduction in greenhouse gas (GHG) emissions by 20 % (and by 30 % in the event of a new global climate change agreement being reached and other developed countries committing themselves to comparable emission reductions and economically more advanced developing countries contributing adequately according to their responsibilities and respective capabilities)
- Saving 20 % of total primary energy consumption compared to projections
- Increasing the level of renewable energy in the EU's overall energy mix to 20 % (with a minimum target for biofuels of 10 % in transport consumption for each Member State)

The first of these targets was a clear sign of engagement and the "ethic leadership" of the European Union to face the Kyoto Protocol commitment, while the following two were internal objectives and constitute the best complement to reach the first one.

In 2008, the European Commission proposed what is being referred to as "Climate and Energy Package," which is a set of different legislative measures destined to reach the 20/20/20 mandate. It comprises four pieces of complementary legislation (adopted all along in 2009) regarding

(a) Carbon Capture and Storage Directive
(b) Measures destined to the big industrial GHG emitters or EU ETS sectors
(c) National targets and measures for non-EU ETS or diffuse sectors
(d) National renewable energy binding targets

(a) The Carbon Capture and Storage Directive (EU 2009a) creates a legal framework for the environmentally safe use of carbon capture and storage technologies. It involves capturing CO_2 emitted by industrial processes and storing it underground geological formations so it does not contribute to the global warming.

(b and c) The EU establishes a gradual and foreseeable trajectory of GHG emission reduction. The total effort for GHG reduction is divided between the sectors affected by the European Union Emission Trading Scheme, which covers around 45 % of the total EU's GHG emissions (European Commission 2014a), and the rest of sectors also referred to as the non-EU ETS sectors or "diffuse sectors." These diffuse sectors are a wide range of sectors that are made up of many small-scale GHG emitters, such as transport (cars and trucks), buildings (especially heat consumption), services, small industrial facilities, agriculture, and waste, that together represent large amounts of emissions. Each Member State must achieve a different objective of emission reduction from 2005 to 2020 *"based on the principle of solidarity between Member States and the need for sustainable economic growth across the Community, taking into account the relative per capita GDP of Member State"* (European Parliament and Council 2009a). As illustrated in Fig. 6, this

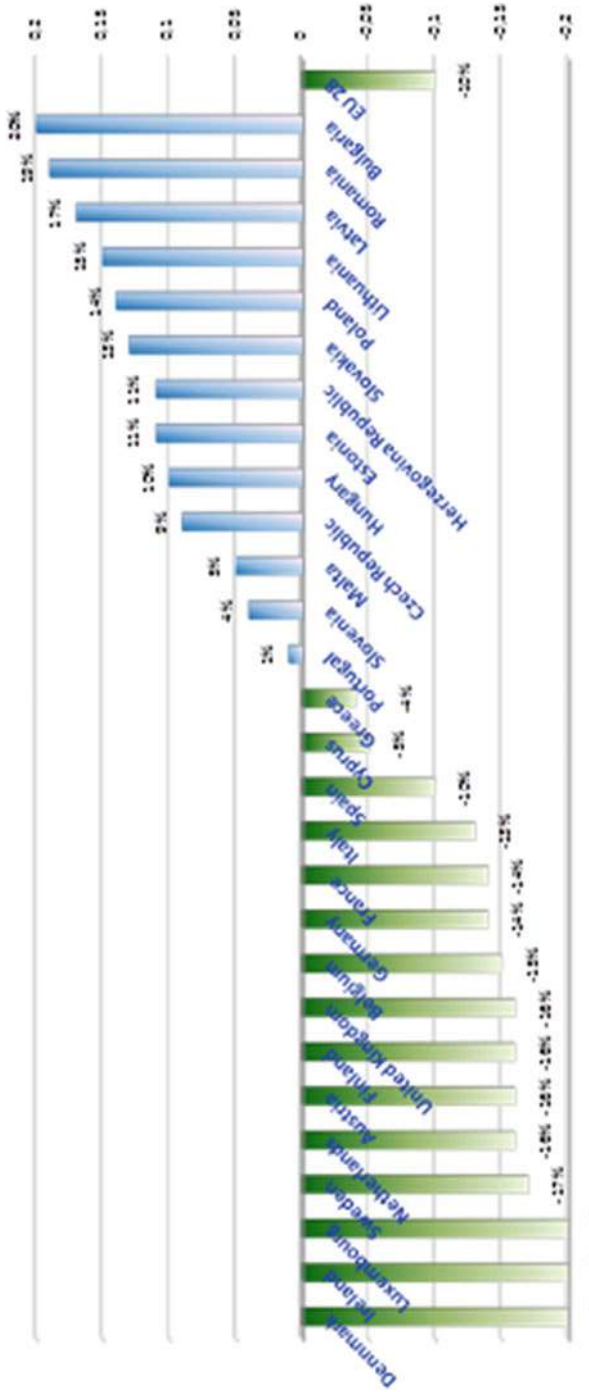

Fig. 6 Member State GHG emission limits in 2020 compared to 2005 levels (Source: European Commission 2014a)

objective represents on average an overall reduction of 10 %. The limits between Member States vary from −20 % to +20 % (e.g., −20 % for Luxembourg, + 20 % for Bulgaria, and −10 % for Spain) (European Parliament and Council 2009a). However, there are differences in regard to the potential level of fulfillment by the different Member States of their corresponding commitments to 2020. Member States are responsible for the fulfillment of this objective through the implementation of national measures. The most profitable way for both the EU ETS sectors and non-EU ETS sectors to perform their GHG reduction objectives (21 % and 10 %, respectively) is basically through the promotion of energy efficiency and the use of renewable energy sources (COM 2008; EU 2009a).

(d) The EU adopted in 2009 the new Directive on the Promotion of the Use of Energy from Renewable Energy Sources (EU 2009b), which does not distinguish between conventional and nonconventional renewable energy sources. A novelty of this Directive compared to previous Directives on the matter is that it establishes different nationally binding objectives for the Member States (from 8.5 % to 20 %), with an overall target of increasing the level of renewable energy in the EU's energy overall mix to 20 % (with a minimum target for biofuels of 10 % for all Member States). According to the Directive, all Member States had to notify the Commission by June 2010 about their national renewable energy action plans. These plans should include not only the share of renewable energy sources but also the information on policy measures (including public aid) adopted to fulfill their national objectives. The increased use of energy from renewable sources, together with energy savings and increased energy efficiency, constitute important tools to comply with the Kyoto Protocol, promoting at the same time the security of energy supply and the technological development and providing opportunities for employment and regional development, especially in rural and isolated areas.

It should be outlined that all the aforesaid legislation was adopted without a common legislative basis (Martínez de Alegría et al. 2009) until the entry in force of the Treaty on the Functioning of the European Union that contained for the first time the Article 194 (EU 2010a). This Article 194 established the framework and the objectives for the development of the EU's common energy policy; however, it must be taken into account that the Member States are still very active in regard to the development of their own energy sector and they still keep a great scope to develop their own energy policy strategy that may affect the trend in future GHG emissions (e.g., the type of energy infrastructures to be promoted in order to guarantee the security of energy supply, the type of incentives – or the lack of them – that are being set up to promote the renewable energy sources). Another element to be kept in mind is that the "Energy and Climate Package" does not address the energy efficiency target directly. As stated in 2011 by the Emissions Roadmap 2050, the EU was on track to meet two of the 20/20/20 targets, *"but with current policies, only half of the 20 % energy efficiency target would be met by 2020"* (COM 2011a). Instead, with full implementation of the 2011 Energy Efficiency Plan, the 20 % of GHG reduction objective could be surpassed in 2020 (European Commission 2011a). The 2011 Energy Efficiency Plan affirms that the energy efficiency is at the heart of the 20/20/20 mandate and declares that energy

efficiency is one of the most cost-effective ways to enhance security of energy supply and to reduce GHG emissions and could be considered Europe's biggest energy resource (COM 2011b).

In December 2012, the new Directive on Energy Efficiency (EU 2012) entered into force, its main objective being to ensure the achievement of the aforesaid 20 % of energy saving objective and to establish the path for further energy efficiency improvements beyond that date, helping to remove barriers and overcome market failures that impede efficiency in the supply and use of energy. It quantifies the EU energy efficiency target as the *"Union's 2020 energy consumption of no more than 1,483 Mtoe primary energy,"* which, compared to the EU-28's primary energy consumption in 1990 (of 1,667 Mtoe) (Eurostat 2014), would mean an energy consumption average reduction of around 11 % between 1990 and 2020. Such reduction is more or less equivalent to the aforesaid 20 % of energy consumption reduction target compared to projections by 2020. However, the directive does not establish individual binding objectives for different Member States; instead they had the obligation to set, by 30 April 2013, an absolute level of primary energy consumption and final energy consumption in 2020.

On the other hand, it is clear that technology and the efficient use of resources are also fundamental to reach the EU 20/20/20 challenge (COM 2009a). Indeed, the EU aspires to gain world leadership in the renewable energy sector (EU 2007). The European Strategic Energy Technology Plan (SET Plan) considers that the key factors to reach the mentioned leadership are to accelerate the availability of energy technologies into the market and, at the same time, to engage industry in the process. In other words, these targets are achievable if adequate technological strides are taken, but it is also necessary that these technologies are well introduced into the market. This is why the Council gave to the Commission two new mandates: on the one hand, the elaboration of the aforementioned "Climate and Energy package" of proposals linking the two areas; on the other hand, to elaborate a specific proposal for the development and execution of the aforesaid SET Plan. According to the Commission, "*the achievement of the goals of the European energy and climate change policy necessitates the development and deployment of a diverse portfolio of low carbon energy technologies (. . .) However (. . .) the EU will continue to rely on conventional energy technologies unless there is a radical change in our attitude and investment priorities for the energy system. In response, the EU has endorsed the European Strategic Energy Technology Plan (SET-Plan) as a vehicle to accelerate the development and large scale deployment of low carbon technologies"* (COM 2009a).

As affirmed by the European Commission in 2014, much has been changed from 2008. On the one hand, the economic downturn has negatively affected the EU Member States' capacity to invest. On the other hand, the fossil fuel prices remain high, which negatively affects their balance of payments, and based of current policies it proposes a new reduction target for domestic reductions of 40 % compared to 1990 by 2030 (COM 2014a). In line with this position, the European Council held in October 2014 adopts the following three targets (European Council 2014):

- A binding EU target of 40 % less GHG emissions by 2030, compared to 1990
- A target of at least 27 % renewable energy consumption
- A 27 % energy efficiency increase

Analysis of Climate Change Legislative Instruments from a Sectorial Perspective

The Energy and Transport sectors play a large role in climate change, as they are the two biggest emission sources (Eurostat 2009). The buildings account for around 40 % of total European Union's final energy consumption, and the sector is expanding (EU 2010b). Energy-related emissions represented approximately 80 % of total emissions in the EU, with the Energy Industry being the largest emitting source (40 % of energy-related emissions), followed by the transport sector (further 24 % of energy-related emissions) (Eurostat 2009). The potential CO_2 reductions for the different economic sectors are illustrated in Table 3.

The Energy Roadmap 2050 points out different scenarios that explore routes toward decarbonization of the energy system. Improvement of the energy efficiency and political commitment to very high energy savings is a priority in all decarbonization scenarios. The diversification of energy supply technologies is also fundamental (including high renewable energy sources' share of gross final energy consumption of 30 % by 2030 but also the use of Carbon Capture and Storage as well as the nuclear technology). The development of storage technologies is also crucial, as well as the development of the smart grids and infrastructures that improve interconnection which could reduce the need of energy storage. All scenarios show that electricity will have to play a much greater role than now (almost doubling its share in final energy demand to 36–39 % in 2050) and that it will have to contribute to the decarbonization of transport and heating/cooling, but to reach this last target, a structural change of the power generation system is needed. Decarbonization will also require, among other measures, a large quantity of biomass for heat, electricity, and transport (COM 2011a, c).

Table 3 Sectorial GHG reductions (%) from 1990 to 2005 (real), and potential to 2030 and 2050

Sector	2005	2030	2050
Electricity (CO_2)	−7	−54 to −68	−93 to −99
Industry (CO_2)	−20	−34 to −40	−83 to −87
Transport (incl. aviation excl. maritime)	+30	+20 to −9	−54 to −67
Residential & services	−12	−37 to −53	−88 to −91
Agriculture (non CO_2)	−20	−36 to −37	−42 to −49
Other non CO_2 emissions	−30	−72 to −73	−70 to −78
Total	−7	−40 to −44	−79 to −82

Source: COM 2011a

In the following section, the most recent and relevant regulation adopted by the EU toward the "low carbon energy model" is analyzed. The section offers a legislative analysis of most relevant CO_2 emitters distinguishing between the following economic subsectors: on the one hand, the big industrial GHG emitters or EU ETS sector; on the other hand, the non-EU ETS or diffuse sectors, including the Transport and the Residential and Services sectors. These last two sectors (Transport and Residential/Services) are the most important CO_2 emitters among the aforesaid diffuse sectors.

The EU ETS Sector

As mentioned, the Power and Industry sectors will play a fundamental role toward the decarbonization of the European economy. The Emissions Roadmap 2050 shows that these sectors reduced their emissions of 7 % and 20 % between 1990 and 2005 and a GHG reduction potential between 1990 and 2050 of around 99 % and 87 % has been estimated, respectively, by 2050 (COM 2011a) (see Table 3). As it is shown, the Power sector is the one with the highest reduction potential; however, as explained, the decarbonization scenario requires the higher penetration of renewable energy sources and the increase of the energy efficiency, but the development and penetration of a wide range of low-carbon technologies (e.g., smart grids, nuclear, carbon capture and storage, etc. after 2020), is also needed (COM 2011c).

Table 4 illustrates main legislative and policy instruments destined to reach the 20 % emission reduction objective by 2020 within these sectors. The first part of the Table 4 shows the specific legislative measures that establish the EU ETS framework focused on these big industrial emitters. The objective as stated by the directive 2009/29/EC is that these EU ETS firms meet their 21 % of GHG reduction objective from 2005 to 2020 (see below) mainly through the increase of their energy efficiency and the higher penetration of the renewable energy sources but also by the use of the EU ETS, which allow to these sectors that in the case that they do not reach their corresponding objectives, they can buy emission permits to balance out their excess of emissions.

The lower part of the Table 4 contains the transversal instruments affecting these big industrial emitters including (a) the main legislation destined to push the higher penetration of renewable energies alongside of promoting the increase of the energy efficiency within these sectors; (b) the fundamental roadmaps that set the pathways to reach the EU's GHG emission reduction objectives (see Fig. 3 and Table 3) including other policy instruments, such as information concerning public aids (which establish exceptions for enabling the promotion of renewable energy sources and energy efficiency).

The EU ETS is a cap-and-trade system that started functioning in January 2005 following the requirements established by the Directive 2003/87/EC (EU 2003b). Initially, the corresponding emission rights (The European Union Allowances) were allocated via grandfathering (for free). The mentioned Directive drew a distinction between Phase I (2005–2007) and Phase II (2008–2012) of the EU ETS when each Member State needed to draw up a National Allocation Plan for each phase setting up the total cap and allocating the individual caps for the EU ETS firms.

Table 4 Energy-climate legislative instruments to support the GHG reduction of big industrial emitters (or the EU ETS sector)

Specific and transversal legislative instruments for EU ETS sector *Goal: −21 % GHG emissions reduction target affecting the industrial emitters*
Specific legislation: emission trading
EU ETS Directive 2009/29/EC (Auctions) (EU 2009c)
Directive 2008/101/EC (includes the aviation sector from 2012) (EU 2008)
Directive 2004/101/EC connects the Kyoto Flexibility Mechanisms (the Clean Develop Mechanism and the Joint Implementation Mechanism) (EU 2004)
EU ETS Directive 2003/87/EC (establishes the EU ETS framework) (EU 2003b)
Transversal instruments
New Energy Efficiency Directive (DIR 2012/27/EU) (EU 2012)
Emissions 2050 Roadmap (COM (2011) 112 final) (COM 2011a)
Energy Efficiency 2011 Action Plan (COM (2011) 109 final) (COM 2011b)
Energy 2050 Roadmap (COM (2011) 885/2) (COM 2011c)
Carbon Capture and Storage (DIR 2009/31/CE) (EU 2009a)
Renewable Energy Directive (DIR 2009/28/CE) (EU 2009b)
Ecodesign Directive (DIR 2009/125/CE) (EU 2009d)
Policy framework for climate and energy 2020–2030 (COM 2014a)
Financing measures: State Aids (IP/08/80), Structural /Cohesion Funds ...

Source: Authors' own elaboration

Accordingly, the EU allowances were distributed among the different firms. At least 90 % of allowances should be freely assigned in Phase II. As stated by Directive 2008/101/EC, the aviation sector is also included in the EU ETS from 2012, which involves the creation of European Union Aviation Allowances – that is, the special emission allowances that can only be used by airline companies for compliance purposes (EU 2008).

The new Directive 2009/29/EC (adopted in 2009 and which amended the previous Directive 2003/87/EC) establishes a gradual application of an auctioning system for the allocation of European Union Allowances (EUAs) for the Power sector from 2013, while there is a transition period for the rest of the sectors affected by the Directive. This Directive has improved and extended the GHG emission allowance trading scheme of the Community and regulates the allowance trade from 1st January 2013. The regime established by this Directive encompassed several important novelties with regard to the previous one (EU 2009c):

- It established an objective of a 21 % reduction of GHG below 2005 for the affected industries.
- In the previous Directive, the focus was on large CO_2 industrial emitters (such as the power sector, the mineral industry, etc.), which all together represented approximately 42.9 % of the EU-27 overall emissions (EEA 2009). However, from 2013 new relevant sectors such as fertilizers and aluminum industries emitting other GHGs (perfluorocarbons and nitrous oxide) are also included in the EU ETS. According to the European Commission, the EU ETS firms represent around half of the EU's GHG emissions (European Commission 2014a).

- The auctioning of allowances becomes the basic principle for allocation from 2013 (apart from exceptions and transitional provisions which will be applied in those sectors with a relevant risk of "carbon leakage," that is, with risk of delocalization).

The Commission establishes the overall emission volume to allocate among all Member States, which means that a Community view was established opposite to the national approach set by the former Directive. This system requires for the affected firms that for each tonne of CO_2 emitted, the emitting entity should present the necessary allowances that will have been previously acquired through auction (EU 2009c).

In order to address the European Union Allowance (EUA) surplus problem for Phase III (from 2013 to 2020), two types of action are proposed (COM 2012a): (a) a review of the auction timetable as a short-term measure, postponing auctions of a certain amount of allowances (so-called back-loading); (b) *structural measures*, such as increasing the EU GHG target to 30 % by 2020; retiring a number of allowances; bringing more sectors into the EU ETS; access rules to international credits and discretionary price management; and an early revision of the linear reduction factor. On 25 February 2014, the Auctioning Regulation is amended with the back-loading of 900 million allowances to the end of the trading period, i.e., 2020. However, no structural measures have yet been adopted. According to Directive 2009/29/EC, the total amount of allowances must decrease by a linear factor of 1.74 % per annum, leading to a reduction of just over 70 % in the ETS cap by 2050; however, to be consistent with the EU's agreed long-term objective of 80 % – 90 % reduction by 2050 on 1990 levels (as set out in the 2050 Low-Carbon Roadmap (COM 2011a)) at the same time that the target of a 40 % reduction from 1990 to 2030 as stated by the European Council in 2014 (European Council 2014) is achieved, the European Commission affirms that this linear factor should be revised and lowered by 2.2 % per year (European Commission 2014a; COM 2014a).

The Diffuse Residential Sector

As shown previously in Table 3, a 12 % GHG reduction was reached from 1990 to 2005, and there is a potential of GHG reductions from 88 % to 91 % by 2050, being the second sector with highest GHG emission reduction potential. Being responsible for around the 40 % of the energy consumption, and considering that the sector is expanding, the 2011 Energy Efficiency Plan states that the greatest saving potential lies in buildings. The key drivers for these reductions should be got through improved insulation in buildings, more use of (low-carbon) electricity, and renewable as well as more energy-efficient appliances (COM 2011b). As stated by the Energy Roadmap 2050, Renewable heating and cooling are vital to decarbonization. A shift in energy consumption toward low-carbon and locally produced energy sources (including heat pumps and storage heaters) and renewable energy (e.g., solar heating, geothermal, biogas, biomass), including through district heating systems, is needed (COM 2011a).

Table 5 Energy-climate policy instrument to support the reduction of GHG on the residential sector

Specific and transversal legislative instruments *Goal: 10 % GHG emissions reduction target affecting the residential sector*
Specific legislative instruments: buildings
Recast-Energy Performance of Buildings Directive (EPBD) (2010/31/EU) (EU 2010b)
Transversal instruments
New Energy Efficiency Directive (DIR 2012/27/EU) (EU 2012) Emissions 2050 Roadmap (COM(2011) 112 final) (COM 2011a) Energy Efficiency 2011 Action Plan (COM (2011) 109 final) (COM 2011b) Energy 2050 Roadmap (COM(2011) 885/2) (COM 2011c) Renewable Energy Directive (DIR 2009/28/CE) (EU 2009b) Ecodesign Directive (DIR 2009/125/EC) (EU 2009d) Energy Efficiency: Delivering the 20 % target COM(2008) 772 final (COM 2008) Lighting Initiatives, "EC Energy Star," and others Policy framework for climate and energy 2020–2030 (COM 2014a) Financial (State Aids (IP/08/80) Structural / Cohesion Funds...) and Socio-Economic Initiatives (e.g., Concerts, Smart Cities, Covenant of Mayors...)

Source: Authors' own elaboration

As well as previous Table 4, Table 5 makes a resume of the current existing legislation destined to promote the energy efficiency together with the renewable energy sources in the Residential/Services sectors. Besides, the fundamental roadmaps that set the pathways to reach the EU's GHG emission reduction objectives (see Fig. 2 and Table 3) including other policy instruments, such as information concerning public aids (which establish exceptions for enabling the promotion of renewable energy sources and energy efficiency), are also included in this Table 5.

In regard to the energy efficiency of buildings, on 19 May 2010 a recast of the Directive on Energy Performance of Buildings is adopted (Directive 2010/31/EU) in order to strengthen the energy performance requirements and to clarify and streamline some of its provisions (EU 2010b). The recast Directive maintains the objective of the previous Directive which states that *"Member States must apply some minimum requirements as regard the energy performance of new and existing buildings, ensure the certification of their energy performance and require the regular inspection of boilers and air conditioning system."* However, the recast Directive includes the following novelties: (a) it requires that by December 2020, Member States shall ensure that all new buildings are nearly zero-energy buildings (NZEB) (and by December 2018 for public buildings) and (b) it states a set of minimum requirements for Member States to support the accomplishment of the cited NZEF objective.

Moreover, a large part of the Energy Efficiency legislation is oriented to establish minimum energy efficiency requirements or design standards and labeling systems to promote a more efficient consumption, especially in the residential and building sectors. These questions are addressed by the new Energy Efficiency Directive (Directive 2012/27/EC) and the aforesaid recast Energy Performance of Buildings Directive (EPBD) (Directive 2010/31/EC). However, as illustrated in Table 5, there

are also other legislation measures, such as the Ecodesign Directive (EU 2009d) or other instruments to promote these aspects (e.g., Lighting initiatives, see Martínez de Alegría et al. 2009) that specifically address this question and may be relevant to understand the improvements of the energy efficiency in this sector, including to reach the aforesaid objective that by December 2020, Member States shall ensure that all new buildings are NZEB. The new energy efficiency Directive 2012/27/EU, from January 2014, sets the obligation to renovate 3 % of buildings owned and occupied by the central governments and by including energy efficiency considerations in public procurement, so as to purchase energy efficient buildings, products, and services (EU 2012).

The financial aids (e.g., through the Structural Funds or the R + D Framework programs) may be determinant to promote the energy efficiency within the building sector. Without doubt, the social collective behaviors of citizens and public authorities in the choice of energy options in regard to streetlights, the cooling and heating of buildings, etc. are fundamental to reduce GHG emissions in the building sector. Some educational measures to improve these behaviors have been developed through the following initiatives:

- The Energy Star Program
- Smart Cities
- Covenant of Mayors
- Others

Finally, as aforesaid, heating and cooling is the most significant component of household energy demand, and for the first time, Directive 2009/28/EC promotes remarkably the use of renewable energies for heating and cooling.

The Transport Sector

In the last years, numerous specific legislatives have been adopted by the European Union for the transport sector, in order to achieve its GHG emission targets at the Union (COM 2008) and national level (European Parliament and Council 2009b), by 2020 and onward (COM 2014b). Those measures affect the transport sector in general, and the road transport particularly, vehicles and fuels being the main targets of these new legislative measures developed (see Table 6).

The transport sector should reduce its CO2 emissions by around 60 % of its 1990 level by 2050 to support the targets set out by the European Union Roadmap to a Low-Carbon Economy (COM 2011a) and the White Paper on Transport (COM 2011d). Recently, the Commission has proposed the 2030 Climate Policy Framework indicating that the objective for transport will be to reduce GHG emissions to around 20 % below their 2008 level by 2030 (COM 2014a).

Transport is a highly emitting diffuse sector associated with the economy and the users' habits, which are to be changed. Around a quarter of EU GHG emissions are generated by transport sector, making it the second biggest GHG emitting sector after energy (European Commission 2014b).

Table 6 Energy-climate legislative instruments to support the GHG reduction of the transport sector

Specific and transversal legislative instruments
Specific legislative instruments: vehicles, fuels, transport and mobility
Goal: Each Member State shall limit its GHG emissions by 2020, at least by the percentage set for that Member State, in relation to its emissions in 2005 (Decision 406/2009/EC) (European Parliament and Council 2009a)
Vehicles
Strategy for reducing Heavy-Duty Vehicles' fuel consumption and CO_2 Emissions (COM(2014) 285 final) (COM 2014b)
Amending regulation (R 443/2009) to Reduce CO_2 Emissions from New Passenger Cars (European Parliament and Council 2014)
Guidelines on Financial Incentives for Clean and Energy Efficient Vehicles (SWD(2013) 27 final) (European Commission 2013b)
Emission Performance Standards for New Light Commercial Vehicles (R(EU)510/2011) (European Parliament and Council 2011)
European Strategy on Clean and Energy Efficient Vehicles (COM(2010)186 final) (COM 2010a)
Regulation on Emission Performance Standards for New Passenger Cars (R(EC)443/2009) (European Parliament and Council 2009b)
Directive on the Promotion of Clean and Energy Efficient Road Transport Vehicles (DIR 2009/33/EC) (EU 2009e)
Fuel
Directive on the Deployment of Alternative Fuels (2014/94/EU) (EU 2014)
Clean Power for Transport: European Alternative Fuels Strategy (COM(2013) 17) (COM 2013a)
Proposal for a Directive amending Directive 98/70/EC Relating to the Quality of Petrol and Diesel Fuels (COM(2012) 595) (COM 2012)
Directive on Environmental Quality Standards for Fuel (DIR 2009/30/EC) (EU 2009f)
Transport and Mobility
Urban Mobility Package (COM(2013) 913 final) (COM 2013b)
White Paper. Roadmap to a Single European Transport (COM(2011)144 final) (COM 2011d)
Transversal instruments
A policy framework for climate and energy in the period from 2020 to 2030 (COM 2014a)
New Energy Efficiency Directive (DIR 2012/27/EU) (EU 2012)
Roadmap for moving to a low-carbon economy in 2050 Emissions 2050 Roadmap (COM(2011) 112 final) (COM 2011a)
Energy 2050 Roadmap (COM(2011) 885/2) (COM 2011c)
Energy Efficiency 2011 Action Plan (COM (2011) 109 final) (COM 2011b)
Europe 2020: A Strategy for Smart, Sustainable and Inclusive Growth (COM(2010) 2020 final) (COM 2010b)
Renewable Energy Directive (DIR 2009/28/CE) (EU 2009b)
Ecodesign Directive (DIR 2009/125/EC) (EU 2009d)
Delivering the 20 % target COM(2008) 772 final (COM 2008)
Financial (e.g.,: State Aids (IP/08/80) Structural & Cohesion Funds...) and Socio-Economic Initiatives (e.g., Concerts, Smart Cities, Covenant of Mayors...)

Source: Authors' own elaboration

European Union faces two key challenges regarding transport:

1. Transport system is heavily dependent on imported oil (COM 2013a). In 2010, transport was 94 % dependent on oil, and 84 % of it was imported, which represents an important problem for the Union trade balance (deficit of around 2.5 % of GDP) (COM 2013a).

2. GHG emissions, especially CO_2, have been increasing for most modes of transport in the last two decades despite the measures adopted by the European Union. While emissions from other sectors have been falling (around 15 % in some sectors), those from transport have increased more than 30 % between 1990 and 2007 (COM 2011c; European Commission 2014b). Changing habits in road transport is a real challenge for the EU, since road transport alone contributes about one-fifth of the EU's total emissions of carbon dioxide (CO_2) (European Commission 2014b).

The EU has so far put a wide range of policies to lower emissions from the transport sector and for breaking the oil dependence of transport. The Commission recognized in 2008 that measures adopted in transport were insufficient to reach both objectives, and since 2009 the transport sector has become the focus of new legislative measures. Some of the new specific legislative measures are

- A strategy for clean and energy-efficient vehicles
- A strategy for light-duty vehicles (cars and vans), including emission targets for new vehicles
- A strategy for high-duty vehicles (trucks, coaches, etc.) to measure and reduce GHG emissions
- A sustainable alternative fuels strategy to reduce the GHG intensity from fuels, as well as to develop the appropriate infrastructure
- The White Paper on Transport: a key specific legislative instrument that sets out the route for the transport sector
- Other measures, such as directives, regulations, etc.

Road transport is a complex sector, among diffuse sectors, because many small emitters (i.e., cars, vans, trucks, etc.) contribute to generate a large amount of GHG emissions, and individual behaviors of emitters are not easy to control and change. The level of complexity of transport, as diffuse sector, demands to deal with a plural view, in which social and economic aspects play an important role. Therefore, the transition to a more efficient and sustainable European transport system includes acting jointly on four main factors:

(a) Technology of vehicles and associated legislation
(b) Fuel technology and associated legislation
(c) Social collective behaviors of citizens in the rational and sustainable use of vehicles and transport means
(d) Integrating general political direction of all the previous factors

These factors are analyzed in depth in the following paragraphs.

(a) **Technology of vehicles and associated legislation**

From 1990 to 2007, GHG emissions of road transport increased by 33 %, but they have since fallen due to economic downturn growth (during the period 1990 to 2010,

GHG emissions from road transport increased by nearly 23 % (European Commission 2014b, c). That is, the whole increase during this period is lower than that from 1990 to 2007 (23 % and 33 %, respectively), what has been possible thanks to high oil prices, increased efficiency of passenger cars, and slower growth in mobility. This trend is expected to continue up until 2020 (COM 2014a, b).

Likely due to the fact of the high contribution of road transport to the EU's total emissions of CO_2 (around 20 %) (European Commission 2014b), many legislative instruments have been developed in the last years (2009–2014) for reducing their GHG emissions. It must be noted that the European Union's transport policy has also included some new legislative measures for maritime and aviation subsectors, although they are not the objective of this analysis for the aforesaid reasons.

One of the first decisions to change trends observed in road transport is the adoption of a Directive on the Promotion of Clean and Energy-Efficient Road Transport Vehicles (EU 2009e), aiming at a broad market introduction of environmentally friendly vehicles. This Directive is addressed to influence the market for standardized vehicles produced in large quantities such as passenger cars, buses, coaches, and trucks. Considering that clean and energy-efficient vehicles initially have a higher price than conventional ones, this directive attempts to create sufficient demand for such vehicles to ensure that economies of scale lead to cost reductions (EU 2009e). It also highlights that ensuring a sufficiently substantial level of demand for clean and energy-efficient road transport will encourage manufacturers to invest in and further develop vehicles with low energy consumption, CO_2 emissions, and pollutant emissions (EU 2009e). This Directive requires that environmental and energy impacts linked to the vehicles over their whole lifetime are taken into account in all purchases of road transport vehicles, as covered by the public procurement directives and the public service regulation.

Taking into account that reduction of consumption of energy in 2020, to comply with the so-called 20/20/20 mandate, might be achieved with more efficient and less emitting new vehicles that gradually replaced the old ones, Regulation of New Passenger Cars is adopted in 2009 as well (European Parliament and Council 2009b). The regulation objective is to set emission performance standards in order to reduce CO_2 emissions from light-duty vehicles (passenger cars) while ensuring the adequate functioning of the internal market. Therefore, it sets standards (average cap) to frame the CO_2 emissions of new cars sold in EU and also establishes the formulae for calculating average CO_2 emission target by manufacturer. The limit set by this Regulation is 130 g of CO_2/km from 2012, which is to be reduced gradually to reach 95 g of CO_2 by 2020. This means that the fleet average of CO_2 emissions to be achieved by each manufacturer of cars registered in the EU should be 130 g of CO_2/km, or less, from 2012 onward. Manufacturers that exceed their specific emissions target must pay an additional premium from 2012 (the penalty amount for light-duty vehicles is determined by different levels of violation over the minimum CO_2 emission target. For the period 2012–2018, the penalty settings are 5€ for the first g/km over the target; 15€ for the second g/km over the target; 25€ for the third g/km over the target; 95€ for the fourth g/km and subsequent. After 2019, violation per g/km will be 95€). However, in order not to introduce distortions in the

market for small manufacturers of cars, those manufactures that register fewer than 10,000 new cars in the EU could be excluded for accomplishing this emissions target, although they should apply for their exclusion to the Commission.

This regulation also attempts to encourage car industry to technological diversification for the development of new types of vehicles, such as the electric car (powered by batteries) or the hybrid and the plug-in hybrid cars. It sets out incentives for the development of new cars and investment in new technologies. To this aim, regulation determines how each new passenger car with emissions of CO_2 of less than 50 g CO_2/km should be counted in the average CO_2 emissions target, indicating that these cars count as 3.5 cars in 2012 and 2013 and as 1 car from 2016 in the calculation of the fleet average CO_2 emission of each car manufacturer.

In 2010, the European Strategy on Clean and Energy-Efficient Vehicles (COM 2010a) is presented by the European Commission as an integrating instrument for encouraging the development and uptake of vehicles with low environmental impact. Among other measures, it contains a commitment to present a set of technological rules which should be taken into consideration while preparing financial schemes for incentivizing the deployment of the clean and fuel-efficient vehicles.

As part of the strategy to reduce CO_2 emissions from light-duty vehicles (cars and vans), in 2011 the EU adopts the Regulation for New Light Commercial Vehicles (vans), which establishes similar rules to that for new passenger cars. Regulation establishes CO_2 emissions performance requirements for new light commercial vehicles that are registered in the Union for the first time. CO_2 emissions from these vehicles must not exceed the average level of 175 g of CO_2/km as from 2017 (the requirement will be introduced gradually as from 2014). From 2020, the level is not to exceed 147 g of CO_2/km, and manufacturers of light commercial vehicles shall ensure that its average specific emissions of CO_2 do not exceed its specific emissions target. These CO_2 emission levels represent a reduction of 3 % and 19 %, respectively, compared with the 2012 average (European Parliament and Council 2011). This Regulation actively promotes ecoinnovation and indicates that CO_2 savings can be achieved notably through improvements in vehicle motor technology and the use of innovative technologies in light commercial vehicles, including as well fuel efficiency progress.

In 2013, Guidelines are provided as a practical reference for the Member States on the implantation of demand-side measures (European Commission 2013b). Guidelines also identify best practices and encourage Member States to avoid unnecessary distortion of the internal market and maximize their supportive effect on the market uptake of clean vehicles.

Despite the economic importance of CO_2 emissions from high-duty vehicles (HDVs) – trucks, buses, and coaches – those emissions have been neither measured nor reported (COM 2014b). In this sense, the High-Duty Vehicles Strategy, adopted in May 2014, is a relevant step toward curbing such emissions and represents the EU's first initiative to tackle them. A key issue hampering action to reduce these emissions is the knowledge gap resulting from the fact that HDV CO_2 emissions are not measured and recorded when new vehicles are registered. However, there is a

significant potential, through employing existing technologies, to improve HDV performance and cut CO_2 emissions in a cost-efficient way. Therefore, the Commission intends to propose legislation in 2015 which would require CO_2 emissions from new HDVs to be certified, reported, and monitored with the help of a simulation tool developed ad hoc. This initiative will contribute to the adoption of more energy-efficient technologies, with effective reductions of at least 30 % in CO_2 emissions from new HDVs as suggested by studies carried out by EU (COM 2014b). The proposed strategy consists of short-term actions, such as filling the identified knowledge gap by measuring HDV fuel consumption and CO_2 emissions in order to provide the Commission and other stakeholders with righter information. Findings from short-term actions would serve as basis for medium-term actions, including the setting of mandatory CO_2 emission limits for new HDVs in order to support the implementation of the EU 2030 climate and energy policy framework (COM 2014a).

In April 2014, the Commission has reviewed the modalities of achieving CO_2 emission reduction targets for passenger cars in a cost-effective manner and has developed a new Regulation (European Parliament and Council 2014), amending some rules and articles of previous one. While this new Regulation holds on to the target of 95 g CO_2/km for the average emissions of the fleet (new cars) from 2020 onward, it establishes as main amendments to previous regulation the following (COM 2014a):

- Manufacturers responsible for fewer than 1,000 new passenger cars registered in the EU annually are directly excluded from the scope of the specific emissions target and the excess emissions premium, from 1 January 2012. This exclusion is due to the disproportionate impact on the smallest manufacturers resulting from the high administrative burden of the derogation procedure and the marginal benefit in terms of CO_2 emissions reduction from the vehicles sold by these manufacturers.
- Each new car with less than 50 g CO_2/km shall be counted as two passenger cars to calculate the fleet average of CO_2 emissions in 2020 (it must be remembered that the previous regulation set out that it should be counted as one car from 2016).

(b) **Technology of fuels and legislation associated**

The urgent need to break the overdependence of EU transport on oil has led to research of alternative fuel solutions. Although there are successful technological developments in alternative fuels, additional policy action is still required for their market acceptance.

It is broadly accepted that fuel quality rules are a key element in reducing GHG emissions from transport, since the quality of fuels affects the emissions. In this regard, the Fuel Quality Directive regulates the characteristics that the fuels must fulfill for the transport sector, and it sets a low carbon fuel standard in order to reduce the GHG intensity of fuels used in vehicles by up to 10 % renewables by 2020 (EU 2009f). Under this Directive, a notable reduction in the sulfur content of fuels

has been achieved, enabling the deployment of vehicle technologies to reduce greenhouse gas and air pollutant emissions.

According to the Directive for renewable energies, a binding 10 % minimum target for renewable energy in transport must be achieved by each Member State in 2020 (2009c). Biofuels might play a key role in this target, as they could be used as an alternative fuel, especially in heavy-duty trucks. However, an increasing demand of biofuels could also increase pressure on biodiversity and water management, and their production could contribute to the conversion of land (e.g., forests and wetlands) into agricultural land, leading to increase GHG emissions. Therefore, the EU considers that the introduction of criteria of sustainability for the biofuels destined to the transport is of great importance, in order to avoid the lateral environmental damages that the production and use of such fuels might produce. Thus, in 2012 the European Commission makes a Proposal amending the Fuel Quality Directive to include emissions from *indirect land use change* in the reporting of the GHG emission savings from biofuels under that Directive (COM 2012b). The Commission also proposes limiting the amount of food-based biofuels to 5 %, in the EU's target of reaching a 10 % share of renewable energy in the transport sector by 2020. This limit will allow non-food-based biofuels, as second- and third-generation biofuels produced from materials (e.g., lignocellulose, algae, straw, and various types of waste), which do not create an additional demand for land, to make a greater contribution to meeting the 10 % target. Moreover, the raw materials for biofuels cannot be sourced from land with high biodiversity or high carbon stock, what reinforces the need to advance in second- and third-generation biofuels (COM 2012b).

The Clean Power for Transport Package aims to facilitate the development of a single market for alternative fuels through two new legislative tools:

- The European Alternative Fuels Strategy (COM 2013a) provides a framework for the long-term substitution of oil as energy source in all modes of transport. It pursues to guide technological development and give confidence to consumers on the market development. The current high cost of innovative alternative fuel applications is largely a consequence of the insufficient market development of alternative fuels due to technological and commercial shortcomings, lack of consumer acceptance, and missing adequate infrastructure. Therefore, a coherent and stable overarching strategy was required in order to overcome these shortcomings and to show the paths for the deployment of alternative fuels.
- The Directive on the Deployment of Alternative Fuels (EU 2014) establishes a common framework of measures for the deployment of alternative fuels infrastructure in the Union in order to mitigate environmental impact of transport and its dependence on oil. This Directive sets out minimum requirements for the building-up of alternative fuels infrastructure, including recharging points for electric vehicles and refueling points for natural gas and hydrogen, to be implemented by means of Member States' national policy frameworks. Moreover, it provides common technical specifications for such recharging and refueling points as well as the way of fuel labeling at refueling points and on vehicles to ensure clarity in the consumer information on vehicle/fuel compatibility.

(a) **Social collective behaviors of citizens in the use of vehicles and transport means**

Some initiatives have been developed in the EU to educate people in a more responsible driving and a more environmental friendly use of transport means, such as initiatives related to road safety education, environmentally respectful driving behaviors, and behaviors of sustainability of municipalities and regions in terms of transport, etc.

In this regard, the Urban Mobility Package presents a basis for moving together toward competitive and resource-efficient urban mobility. Urban mobility in the Union is still heavily dependent on the use of conventionally fueled private cars and accounts for a high share (some 23 %) of all CO_2 emissions from transport (COM 2013b). This Package emphasizes that there is still a large potential for cities to move toward a low-carbon transport through the development of walking, cycling, public transport, and vehicles powered by alternative fuels. The Commission recommends a concrete set of measures to be taken on several relevant issues like urban logistics, urban access regulations, deployment of urban intelligent transport system solutions, and road safety and encourages cities to participate in specific actions that will be carefully monitored to measure results.

The Europe 2020 Strategy for Smart, Inclusive, and Sustainable Growth (COM 2010b) highlights the importance of a modernized and sustainable European transport system for the future development of the Union and stresses the need to address the urban dimension of transport. This Strategy aims to reinforce the support to European cities for tackling urban mobility challenges and ensure that goals for a competitive and resource-efficient European transport system are met. It also points out the need to overcome fragmented approaches and develop the single market for innovative urban mobility solutions by addressing issues like common standards and specifications.

Other European initiatives related to transport and mobility are

- Ecodriving program
- CIVITAS
- Smart Cities
- Covenant of mayors
- Others

(b) **Integrating general political direction of all the previous factors**

There have been several legislative pieces that have attempted to integrate – partially or totally – the diverse factors that affect the GHG emissions of transport and the dependence on oil of EU's transport system. However, the most important legislative instrument to integrate political direction of all aforesaid factors is likely the White Paper on Transport.

In 2011, the European Commission launches the White Paper on Transport, which establishes the EU's general policy in transport and the route toward 2020

and later. The White Paper not only provides a combined set of measures to increase the sustainability of the transport system but also highlights that technological innovation can help the transition to a more efficient transport system by acting on three main factors: vehicle efficiency through new engines, materials, and design; a cleaner energy use through new fuels and propulsion systems; and initiatives to educate citizens in the responsible and environmental use of vehicles and transport means and infrastructure (COM 2011d).

The main goal of transport legislation adopted during the period 2009–2014 is to ensure that CO_2 emissions from vehicles continue to be reduced, while giving the automotive industry the certainty it needs to carry out long-term investments and develop innovative technologies. The sector-specific state aid adds incentives which include the use of structural funds in order to devote a greater part to finance investments in a more efficient and sustainable transport system. Other economic incentives are reduction of tax registration and circulation for fuel-efficient vehicles and low emitters, reduction in VAT, especially for products and fuel-efficient vehicles and low emitters, aids to encourage consumers to purchase fuel-efficient vehicles, etc.

Summarizing the main driver for reversing the trend of increasing GHG emissions in the transport sector is likely to remain improved efficiency of both fuels and engines. Securing affordable mobility and reducing emissions from roads below 1990 levels in 2020–2030 can be possible in combination with measures such as refueling and charging infrastructure, improving public transport, pricing schemes to tackle congestion and air pollution, and intelligent city planning. Better demand-side management, fostered through CO_2 standards and smart taxation systems, should also facilitate the gradual transition toward large-scale penetration of cleaner vehicles in all transport modes, including plug-in hybrids and electric vehicles. The synergies with other sustainability objectives such as the reduction of oil dependence, the competitiveness of Europe's automotive industry, as well as benefits for health are enough reasons for the EU to step up its efforts to accelerate the development and early deployment of alternative fuels and propulsion methods for the whole transport system. In this respect, it is not surprising to see automotive industries in the USA, Japan, Korea, and China, making efforts to develop and/or improve electric, hybrids and fuel-eficient vehicles in order to lead this market.

The Union aviation sector should collaborate with the International Civil Aviation Organisation (ICAO) in order to create by 2016 a global market-based mechanism that will operate from 2020. The maritime sector will be integrated in the EU's GHG reduction strategy while the Commission works with the International Maritime Organisation (IMO) on a global approach to achieve the necessary emission reductions through the most appropriate measures (COM 2014b).

Conclusions

Although the Doha Agreement makes it possible to use the Flexible Mechanisms (i.e., the International Emissions Trading, the Clean Development Mechanism, and the Joint Implementation Mechanism) to face the 20013–2020 period, there are two

main factors that undermine the level of ambition of the aforesaid Agreement: first, only around 12 % of the world GHG emissions are concerned; second, the EU-28 has already reached around a 19 % GHG emission reduction by 2012. By 2015, a new Protocol (or other legal instrument) should be adopted by the Annex I Parties in order to face the climate change problem; however, more comparable targets are needed to face the aforesaid 2015 Agreement, and apparently, most Parties are waiting for this 2015 Conference to reveal their respective positions. Meanwhile, all the UNFCCC process to reach real and effective measures to face the climate change problem is suffering a period of real uncertainty.

In the EU framework, the threats of the conventional energy model (environmental problems, exhaustion of fossil sources, possible inflation process and loss of competitiveness, dependency toward energy export countries, etc.) have forced a change in its traditional energy strategy where the key objectives include also the increase of the European competitiveness and the environmental protection, making Renewable Energy Sources and Energy Efficiency its fundamental basis. The "Energy/Climate Change Package" complements the previous existing legislation on climate change and Renewable Energy Sources and Energy Efficiency and constitutes a fundamental set of tools for achieving the 20/20/20 mandate.

An important novelty of the new Directive 2009/28/EC for the promotion of Renewable Energies comparing with previous legislation is the establishment of different nationally binding targets, with an overall target of 20 % in the EU's energy overall mix by 2020; however, differences in regard to the level of consecution of their corresponding targets may be obtained between the EU-28 members. In regard to the energy efficiency, a notable improvement on the energy consumption patterns has been observed within the EU, with an average reduction of 9.8 % of the total primary consumption between 2005 and 2010. However, considering that this reduction has occurred in a period of economic downward development, in the case of the recovery of the European economy, the 20 % energy efficiency objective may be under question, which could put at risk the consecution of the two other 20/20 mandates (specially the objective of 20 % of renewable energy by 2020).

The most relevant measure adopted for the nondiffuse sector is the establishment of the EU ETS. Though this emission trading scheme may have contributed to delivering real GHG emission reductions for this sector in the past, the estimated surplus of emission permits may generate serious imbalances in the future. It is feared that these imbalances may profoundly affect the ability to meet the EU ETS targets by 2020.

In regard to the promotion of the Energy Efficiency in the building sector, the recast of the Energy Performance of Buildings Directive (EPBD) and the new Energy Efficiency Directive (Directive 2012/27/EU) follow the path of previous legislation, reinforcing the existing market-based instruments, especially the energy labeling instruments. The most relevant novelty of the aforesaid new Energy Efficiency Directive is that it establishes a quantitative target to reach an EU-28 gross energy consumption reduction target (of around 11 % between 1990 and 2020, which is more or less equivalent to the target established by the mandate 20/20/20), however without

establishing individual binding targets for each Member State, which could have as a consequence a different level of consecution between Member States. The recast of the Energy Performance of Buildings Directive (EPBD) requires that by December 2020, Member States shall ensure that all new buildings are nearly zero-energy buildings (NZEB) (and by December 2018 for public buildings). However, the real consecution of the cited target for different Member States is also uncertain.

In the transport sector, numerous legislative measures have been adopted to achieve 2020 objectives, although some more legislative instruments are still needed to address the challenges of the sector in a 2030 perspective and beyond. In line with the White Paper on Transport and the Alternative Fuels Strategy, efforts have been made on improving the efficiency of the transport system, further development and deployment of electric vehicles, second- and third-generation biofuels, and other alternative sustainable fuels as part of a more holistic and integrated approach. The improvements observed in passenger vehicles in recent years will have to continue; while in other transport modes there will be a need for a significant acceleration of current efforts to tap the significant unexploited potential. Additional reduction of emissions from transport will require a gradual transformation of the transport system toward a better integration among modes, greater exploitation of the nonroad alternatives, improved management of traffic flows through intelligent transport systems, and extensive innovation in and deployment of new propulsion and navigation technologies and alternative fuels (COM 2014b). Moreover, Member States should consider how fuel and vehicle taxation can be used to support GHG reductions in the transport sector.

Acknowledgments This work has been possible thanks to the collaboration of the Energy Working Group, which belongs to the Chair of International Relations (Social Sciences Faculty) of the University of the Basque Country (UPV-EHU). Special thanks must be given to Gonzalo Molina Igartua for his inestimable help and collaboration.

Annexes

Annex 1

The key GHGs under consideration in the most common legislative strategies are

- Carbon dioxide (CO_2) from fossil fuel burning, wood and other fuel burning, chemical manufacturing, and mobile source fuel combustion
- Methane (CH_4) from the production and transport of coal, natural gas, and oil; livestock and other agricultural practices; and decay of organic waste in municipal solid waste landfills
- Nitrous oxide (N_2O) from agricultural and industrial activities and combustion of fossil fuels and solid waste

Table 7 Global warming potentials of key GHGs

Type of GHG	Global warming potential
Carbon dioxide (CO_2)	1
Methane (CH_4)	21
Nitrous oxide (N_2O)	310
Hydrofluorocarbons (HFCs) and Perfluorocarbons (PFCs)	140 to 11,700
Sulfur Hexafluoride (SF_6)	23,900

Source: IPCC 2007

- Hydrofluorocarbons (HFCs) from industrial processes
- Perfluorocarbons (PFCs) from industrial processes
- Sulfur hexafluoride (SF_6) from industrial processes

In what is being referred to as the "Doha amendment" of the Kyoto Protocol, the following GHG was included in the Amended Annex A of the Kyoto Protocol:

- Nitrogen trifluoride (NF_3).

The GWPs for the key GHGs (assuming a 100 year time frame) are summarized in Table 7 below.

For example, in a 100 year time frame, 1 ton of nitrous oxide will impact climate change 310 times more significantly than 1 ton of carbon dioxide.

Annex 2

List of Annex I parties to the UNFCCC

Australia	European Union	Liechtenstein[a]	Russian Federation[a]
Austria	Finland	Lithuania	Slovakia[a]
Belarus[a]	France	Luxembourg	Slovenia[a]
Belgium	Germany	Malta	Spain
Bulgaria	Greece	Monaco[a]	Sweden
Canada	Hungary	Netherlands	Switzerland
Croatia[a]	Iceland	New Zealand	Turkey[a]
Cyprus	Ireland	Norway	Ukraine[a]
Czech Republic[a]	Italy[a]	Poland	United Kingdom of Great Britain and Northern Ireland
Denmark	Japan	Portugal	United States of America
Estonia	Latvia	Romania	

[a]Party for which there is a specific (COP) and/or Conference of Parties as Meeting of the Parties to the Kyoto Protocol (CMP) decision
Source: UNFCCC 2014

List of Non- Annex I Parties to the UNFCCC

Afghanistan	Comoros	Iran (Islamic Republic of)	Nauru	Sierra Leone
Albania[b]	Congo	Iraq	Nepal	Singapore
Algeria	Cook Islands	Israel	Nicaragua	Solomon Islands
Andorra	Costa Rica	Jamaica	Niger	Somalia
Angola	Cuba	Jordan	Nigeria	South Africa
Antigua and Barbuda	Côte d'Ivoire	Kazakhstan[b]	Niue	South Sudan
Argentina	Democratic People's Republic of Korea	Kenya	Oman	Sri Lanka
Armenia[b]	Democratic Republic of the Congo	Kiribati	Pakistan	Sudan
Azerbaijan	Djibouti	Kuwait	Palau	Suriname
Bahamas	Dominica	Kyrgyzstan	Palestine[a]	Swaziland
Bahrain	Dominican Republic	Lao People's Democratic Republic	Panama	Syrian Arab Republic
Bangladesh	Ecuador	Lebanon	Papua New Guinea	Tajikistan
Barbados	Egypt	Lesotho	Paraguay	Thailand
Belize	El Salvador	Liberia	Peru	The former Yugoslav Republic of Macedonia
Benin	Equatorial Guinea	Libya	Philippines	Timor-Leste
Bhutan	Eritrea	Madagascar	Qatar	Togo
Bolivia	Ethiopia	Malawi	Republic of Korea	Tonga
Bosnia and Herzegovina	Fiji	Malaysia	Republic of Moldova[b]	Trinidad and Tobago
Botswana	Gabon	Maldives	Rwanda	Tunisia
Brazil	Gambia	Mali	Saint Kitts and Nevis	Turkmenistan[b]
Brunei Darussalam	Georgia	Marshall Islands	Saint Lucia	Tuvalu
Burkina Faso	Ghana	Mauritania	Saint Vincent and the Grenadines	Uganda
Burundi	Grenada	Mauritius	Samoa	United Arab Emirates
Cambodia	Guatemala	Mexico	San Marino	United Republic of Tanzania
Cabo Verde	Guinea	Micronesia (Federated States of)	Sao Tome and Principe	Uruguay

(*continued*)

Cameroon	Guinea-Bissau	Mongolia	Saudi Arabia	Uzbekistan[b]
Central African Republic	Guyana	Montenegro	Senegal	Vanuatu
Chad	Haiti	Morocco	Serbia	Venezuela (Bolivarian Republic of)
Chile	Honduras	Mozambique	Seychelles	Viet Nam
China	India	Myanmar	Saint Vincent and the Grenadines	Yemen
Colombia	Indonesia	Namibia	Samoa	Zambia
				Zimbabwe

[a]Observer State
[b]Party for which there is a specific Conference of Parties (COP) and/or Conference of Parties as Meeting of the Parties (CMP) to the Kyoto Protocol decision
Source: UNFCCC 2012

Annex B parties of the Kyoto Protocol

Party	Quantified emission limitation or reduction commitment (Percentage of base year or period)
Australia	108
Austria	92
Belgium	92
Bulgaria[a]	92
Canada	94
Croatia[a]	95
Czech Republic[a]	92
Denmark	92
Estonia[a]	92
European Community	92
Finland	92
France	92
Germany	92
Greece	92
Hungary[a]	94
Iceland	110
Ireland	92
Italy	92
Japan	94
Latvia[a]	92
Liechtenstein	92
Lithuania[a]	92
Luxembourg	92
Monaco	92

(*continued*)

Netherlands	92
New Zealand	100
Norway	101
Poland[a]	94
Portugal	92
Romania[a]	92
Russian Federation	100
Slovakia[a]	92
Slovenia[a]	92
Spain	92
Sweden	92
Switzerland	92
Ukraine[a]	100
United Kingdom of Great Britain and Northern Ireland	92
United States of America	93

[a]Countries that are undergoing the process of transition to a market economy
Source: UNFCCC 1998

References

COM (1997) Communication from the Commission. Energy for the future: renewable sources of energy. White Paper for a Community Strategy. COM(97) 599 final, Brussels, 26 Nov 1997

COM (2005) Communication from the Commission of 7 December 2005 on Biomass Action Plan; COM(2005) 628 final. Official Journal of the European Union of the European Union C 49, 28 Feb 2005

COM (2007) Communication from the Commission to the Council and the European Parliament, An Energy Policy for Europe. SEC (2007) 12, COM (2007) 1 final. Brussels, 10 Jan 2007

COM (2008) Commission Communication. Energy Efficiency: Delivering the 20% target. COM (2008) 772 final. Brussels, 13 Nov 2008

COM (2009a) Communication from the Commission to the European Parliament, the Council, the European Economic and Social Committee and the Committee of the Regions: Investing in the Development of Low Carbon Technologies. (SET-Plan): A Technology Roadmap. SEC(2009) 1295, Brussels, 7 Oct 2009

COM (2010a) Communication from the Commission to the European Parliament, the Council, the European Economic and Social Committee: A European strategy on clean and energy efficient vehicles. COM(2010) 186 final, Brussels, 28 Apr 2010

COM (2010b) Communication from the Commission. Europe 2020: A Strategy for Smart, Sustainable and Inclusive Growth, COM(2010) 2020 final, Brussels, 3 Mar 2010

COM (2011a) Communication from the Commission to the European Parliament, the Council, the European Economic and Social Committee and the Committee of the Regions. A Roadmap for Moving to a Competitive Low Carbon Economy in 2050. COM(2011) 112 final

COM (2011b) Communication from the Commission to the European Parliament, the Council, the European Economic and Social Committee and the Committee of the Regions of 8 March 2011. Energy Efficiency Plan 2011. COM (2011) 109 final, not published in the Official Journal

COM (2011c) Communication from the Commission to the European Parliament, the Council, the European Economic and Social Committee and the Committee of the Regions. Energy Roadmap 2050. COM (2011) 885 final, Brussels 15 Dec 2011

COM (2011d) White Paper: Roadmap to a Single European Transport Area – Towards a Competitive and Resource Efficient Transport System, COM(2011) 144 final, Brussels, 28 Mar 2011 COM (2012a) Report from the Commission to the European Parliament and the Council: The State of the European Carbon Market in 2012, Brussels, 14 Nov 2012: COM (2012) 652 final

COM (2012) Proposal for a Directive of the European Parliament and of the Council amending Directive 98/70/EC relating to the quality of petrol and diesel fuels and amending Directive 2009/28/EC on the promotion of the use of energy from renewable sources, COM(2012) 595 final, 2012/0288 (COD), Brussels, 17 Oct 2012

COM (2013a) Communication from the Commission to the European Parliament, the Council, the European Economic and Social Committee and the Committee of the Regions. Clean Power for Transport: A European alternative fuels strategy, COM(2013) 17 final, Brussels, 24 Jan 2013

COM (2013b) Communication from the Commission to the European Parliament, the Council, the European Economic and Social Committee and the Committee of the Regions. Together towards competitive and resource-efficient urban mobility. COM(2013) 913 final, Brussels 17 Dec 2013

COM (2014a) Communication from the Commission to the European Parliament, the Council, the European Economic and Social Committee and the Committee of the Regions A policy framework for climate and energy in the period from 2020 to 2030, COM(2014) 15 final, Brussels, 22 Jan 2014

COM (2014b) Communication from the Commission to the Council and the European Parliament. Strategy for reducing Heavy-Duty Vehicles' fuel consumption and CO_2 Emissions, COM(2014) 285 final, Brussels, 21 May 2014

Den Elzen M, Hare W et al (2010) The Emissions Gap Report. Are the Copenhagen Accord Pledges Sufficient to Limit Global Warming to 2° or 1.5°? A preliminary Assessment, United Nations Environment Programme (UNEP)

Den Elzen M, Hof AF et al (2011) The Copenhagen Accord: abatement costs and carbon prices resulting from the submissions. Environ Sci Policy 14:28–39

EEA (2009) Annual European Community greenhouse gas inventory 1990–2007 and inventory report 2009. Submission to the UNFCCC Secretariat, European Environment Agency (EEA) Version. Technical Report 4/2009. 27 May 2009

EEA (2014) Annual European Union greenhouse gas inventory 1990–2012 and inventory report 2014 Submission to the UNFCCC Secretariat, European Environment Agency (EEA). Technical Report 9/2014

EU (2001) Directive 2001/77/EC of the European Parliament and of the Council of 27 September 2001 on the promotion of electricity produced from renewable energy sources in the internal electricity market. Official Journal of the European Communities, L 283/33, 27 Oct 2001

EU (2003a) Directive 2003/30/EC the European Parliament and of the Council of 8 May 2003 on the promotion of the use of biofuels or other renewable fuels for transport. Official Journal of the European Union L 123/42, 17 May 2003

EU (2003b) Directive 2003/87/EC of the European Parliament and of the Council of 13 October 2003 establishing a scheme for greenhouse gas emission allowance trading within the Community and amending Council Directive 96/61/EC. Official Journal of European Union L 275/32, 25 Oct 2003

EU (2004) Directive 2004/101/EC of the European Parliament and of the Council of 27 October 2004 amending Directive 2003/87/EC establishing a scheme for greenhouse gas emission allowance trading within the Community, in respect of the Kyoto Protocol's project mechanisms. Official Journal of the European Union L 338/18, 13 Nov 2004

EU (2007) Why Europe needs a strategic energy technology plan; MEMO/07/469; Brussels, 19 Nov 2007

EU (2008) Directive 2008/101/EC of the European Parliament and of the Council of 19 November 2008 amending Directive 2003/87/EC so as to Include Aviation Activities in the Scheme for Greenhouse Gas Emission Allowance Trading within the Community. Official Journal of European Union L 8/3, 13 Jan 2009

EU (2009a) Directive 2009/31/EC of the European Parliament and of the Council of 23 April 2009 on the promotion on the geological storage of carbon dioxide. Official Journal of the European Union L 140/114, 23 Apr 2009
EU (2009b) Directive 2009/28/EC of the European Parliament and of the Council of 23 April 2009 on the promotion of the use of energy from renewable sources and amending and subsequently repealing Directives 2001/77/EC and 2003/30/EC. Official Journal of the European Union L 140/16, 5 June 2009
EU (2009c) Directive 2009/29/EC of the European Parliament and of the Council of 23 April 2009 amending Directive 2003/87/EC so as to improve and extend the greenhouse gas emission allowance trading scheme of the Community, Official Journal of the European Union L 140/63, 5 June 2009
EU (2009d) Directive 2009/125/EC of the European Parliament and of the Council of 21 October 2009 Establishing a Framework for the Setting of Ecodesign Requirements for Energy-Related Products (Recast). Official Journal of the European Union L 285/10, 31 Oct 2009
EU (2009e) Directive 2009/33/EC of the European Parliament and of the Council of 23 April 2009 on the promotion of clean and energy-efficient road transport vehicles. Official Journal of the European Union L 120, 15 June 2009
EU (2009f) Directive 2009/30/EC of the European Parliament and of the Council of 23 April 2009 amending Directive 98/70/EC as regards the specification of petrol, diesel and gas-oil and introducing a mechanism to monitor and reduce greenhouse gas emissions and amending Council Directive 1999/32/EC as regards the specification of fuel used by inland waterway vessels and repealing Directive 93/12/EEC. Official Journal of the European Union L 140/88, 5 June 2009
EU (2010a) Consolidated Versions of the Treaty on European Union and the Treaty on the Functioning of the European Union. Official Journal of the European Union C83, vol 53. 30 Mar 2010
EU (2010b) Directive 2010/31/EU of the European Parliament and of the Council of 19 May 2010 on the energy performance of buildings, (recast). Official Journal of the European Union L 153/13, 18 June 2010
EU (2012) Directive 2012/27/EU of the European Parliament and of the Council of 25 October 2012 on Energy Efficiency, amending Directives 2009/125/EC and 2010/30/EU and repealing Directives 2004/8/EC and 2006/32/EC. Official Journal of the European Union L 315/1, 14 Nov 2012
EU (2014) Directive 2014/94/EU of the European Parliament and of the Council of 22 October 2014 on the deployment of alternative fuels infrastructure. Official Journal of the European Union L 307/1, 28 Oct 2014
European Commission (2012) EU energy in figures statistical pocketbook 2012. Publications Office of the European Union, Luxembourg
European Commission (2013a) EU energy in figures statistical pocketbook 2013. Publications Office of the European Union, Luxembourg
European Commission (2013b) Commission Staff Working Document. Guidelines on Financial Incentives for Clean and Energy Efficient Vehicles, SWD(2013) 27 final. Brussels, 28 Feb 2013
European Commission (2014a) Climate action: the EU Emissions Trading System (EU ETS), Last update: 23 Sep 2014, http://ec.europa.eu/clima/
European Commission (2014b) Climate action: reducing emissions from transport, Last update: 8 Nov 2014. Available at: http://ec.europa.eu/clima/policies/transport/index_en.htm
European Council (2007) Brussels European Council, 8 and 9 March 2007 Presidency Conclusions COM (2007) 7224/1/02 Rev 1, Brussels, 2 May 2007
European Council (2009) Brussels European Council, 29/30 October 2009, Presidency Conclusions 15265/1/09 REV 1, Brussels, 1 Dec 2009
European Council (2014) Brussels European Council 23/24 October 2014. EUCO 169/14, Brussels 24 Oct 2014
European Parliament and Council (2009a), Decision 406/2009/EC of 23 April 2009 on the effort of Member States to reduce their greenhouse gas emissions to meet the Community's greenhouse

gas emission reduction commitments up to 2020, Official Journal of the European Union L 140/136, 5 June 2009

European Parliament and Council (2009b) (EC) No 443/2009 of the European Parliament and of the Council of 23 April 2009, Setting emission performance standards for new passenger cars as part of the Community's integrated approach to reduce CO_2 emissions from light-duty vehicles. Official Journal of the European Union L 140/1, 5 June 2009

European Parliament and Council (2011) Regulation (EU) No 510/2011 of the European Parliament and of the Council of 11 May 2011, Setting emission performance standards for new light commercial vehicles as part of the Union's integrated approach to reduce CO_2 emissions from light-duty vehicles. Official Journal of the European Union L 145/1, 31 May 2011

European Parliament and Council (2014) Regulation (EU) No 333/2014 of the European Parliament and of the Council of 11 March 2014 amending Regulation (EC) No 443/2009 to define the modalities for reaching the 2020 target to reduce CO_2 emissions from new passenger cars. Official Journal of the European Union, L 103/15, 5 Apr 2014

Eurostat (2009) Sustainable development in the European Union. 2009 monitoring report of the EU sustainable development strategy. Office for Official Publications of the European Union, Luxembourg

Eurostat (2014) Gross inland energy consumption by fuel type. Available at: http://epp.eurostat.ec.europa.eu/portal/page/portal/energy/data/main_tables

Hof AF, Den Elzen M et al (2013) The effect of updated pledges and business-as-usual projections, and new agreed rules on expected global greenhouse gas emissions in 2020. Environ Sci Policy 33 (0) (11):308–319

IPCC (2007) In: Metz B, Davidson OR, Bosch PR, Dave R, Meyer LA (eds) Climate change 2007: mitigation of climate change. Contribution of working group III to the fourth assessment report of the Intergovernmental Panel on Climate Change (IPCC), 2007. Cambridge University Press, Cambridge, UK/New York

IPCC (2010) History of intergovernmental panel on climate change. Panel on Climate Change (IPCC). http://www.ipcc.ch/organiza-tion/organization_history.htm. Accessed June 2010

IPCC (2014) Summary for policymakers. In: Edenhofer O, Pichs-Madruga R, Sokona Y, Farahani E, Kadner S, Seyboth K, Adler A, Baum I, Brunner S, Eickemeier P, Kriemann B, Savolainen J, Schlömer S, von Stechow C, Zwickel T, Minx JC (eds) Climate change 2014, mitigation of climate change. Contribution of working group III to the fifth assessment report of the Intergovernmental Panel on Climate Change (IPCC). Cambridge University Press, Cambridge, UK/New York

Kartha S, Erikson P (2011) Comparison of Annex 1 and non-Annex 1 pledges under the Cancun Agreements. Stockholm Environment Institute (SEI). 11 June 2011. Available at: http://www.seiinternational.org/mediamanager/documents/Publications/Climate/sei-workingpaperus-1107.pdf. Accessed Nov 2012

Martínez de Alegría I, Diaz de Basurto P, Martínez de Alegría I, Ruiz de Arbulo P (2009) European Union's renewable energy sources and energy efficiency policy review: the Spanish perspective. Renew Sustain Energy Rev (RSER) 13:100–114

Moore C (2012) Climate change legislation: current developments and emerging trends. In: Chen W-Y, Seiner J, Suzuki TS, Laeckner M (eds) Handbook of climate change mitigation. Springer, New York, pp 43–87

UNFCCC (1992) United Nations framework on climate change. Available at: http://unfccc.int/

UNFCCC (1998) Kyoto Protocol to the United Nations framework convention on climate change. United Nations Framework Convention on Climate Change, Bonn. Available at: http://unfccc.int/resource/docs/convkp/kpeng.pdf

UNFCCC (2010a) Kyoto Protocol background. Available at: http://unfccc.int/kyoto_protocol/items/2830.php

UNFCCC (2010b) Background on the emissions trading. Available at: http://unfccc.int/kyoto_protocol/mechanisms/emissions_trading/items/2731.php

UNFCCC (2012) Report of the Conference of the Parties serving as the Meeting of the Parties to the Kyoto Protocol on its seventh session, held in Durban from 28 November to 11 December 2011, FCCC/KP/CMP/2011/10/Add.1, 15 Mar 2012
UNFCCC (2013) Report of the Conference of the Parties serving as the meeting of the Parties to the Kyoto Protocol on its eighth session, held in Doha from 26 November to 8 December 2012 Addendum Part Two: action taken by the conference of the Parties serving as the meeting of the Parties to the Kyoto Protocol at its eighth session FCCC/KP/CMP/2012/13/Add1, 28 Feb 2013
UNFCCC (2014) Report of the Conference of the Parties on its nineteenth session, held in Warsaw from 11 to 23 November 2001, Addendum. Part two: action taken by the conference of the parties at its nineteenth session. FCCC/CP/2013/10/Add.1, 31 Jan 2014
UNFCCC (2015a) Essential background. http://unfccc.int/essential_background/items/6031.php. Accessed Jan 2015
UNFCCC (2015b) Information provided by Parties relating to Appendix I of the Copenhagen Accord (Annex I- Quantified economy-wide emissions targets for 2020) Available at: http://unfccc.int/meetings/copenhagen_dec_2009/items/5264.php. Accessed Jan 2015
UNFCCC (2015c) Glossary. Accessed Jan 2015
UNFCCC (2015d) http://unfccc.int/meetings/cop_15/copenhagen_accord/items/5265.php. Accessed Jan 2015

Implications of Climate Change for the Petrochemical Industry: Mitigation Measures and Feedstock Transitions

Simon J. Bennett and Holly A. Page

Contents

S.J. Bennett (✉)
Imperial Centre for Energy Policy and Technology, Imperial College, London, UK

International Energy Agency, Paris, France
e-mail: simon.bennett04@imperial.ac.uk

H.A. Page
Imperial College, London, UK
e-mail: holly.page12@imperial.ac.uk

W.-Y. Chen et al. (eds.), *Handbook of Climate Change Mitigation and Adaptation*,
DOI 10.1007/978-3-319-14409-2_10

Abstract

For over half a century, society has relied on the products of the organic chemical industry to supply the clothes we wear, the food we eat, our health, housing, transportation, security, and other commodities. Approximately 92 % of organic chemical products are derived from oil and gas. In addition, these same resources are generally used to provide the large quantities of process heat and power needed by the industry. In the modern petrochemical industry, oil and gas inputs for both raw material and process energy compose around 50 % of the operating costs.

Not only is the chemical industry (including petrochemicals) the industrial sector with the highest emissions worldwide, it is also very vulnerable to variations in fossil fuel prices and, potentially, climate policies. Efficiency has long been a major factor in determining competitiveness in petrochemicals, and the sector has a high success rate in reducing its energy intensity. Yet, while global use of oil for energy grew globally by 12 % between 2002 and 2012, the use of oil for chemical feedstocks grew 21 %. It now represents 9 % of total global oil use and 6 % of total global gas use. Reducing greenhouse gas (GHG) emissions in an industry that is so dependent on fossil fuels presents a significant challenge.

This chapter introduces the history of the modern chemical industry and the establishment of its close relationship with the oil industry. This relationship has recently come under strain as new sources of oil and gas are increasingly exploited, and growth in hydrocarbon demand for chemical products outpaces that for energy from these sources. It goes on to describe some of the major chemical processes, their GHG emissions, and their geographical variations. The benefits and challenges of several technological mitigation options are discussed. These are recycling, efficiency gains through cogeneration, CO_2 capture and storage (CCS), and feedstock switching via biorefining.

Introduction

Many of the chapters in this book describe the potential for renewable and low-carbon technologies to reduce the rate of emissions of greenhouse gases from human activity. Other chapters address key components in these efforts, recognizing the energy sector as the major source of greenhouse gases (GHG) worldwide, the crucial role of energy efficiency and carbon capture technologies, and the importance of individual consumption patterns. However, all of these components impact (and are impacted by) the petrochemical industry. It permeates our daily lives and is one of the global economy's most important industrial sectors. Moreover, it faces implications from climate change not only in terms of its energy consumption and greenhouse gas emissions but also in terms of its very feedstock. The petrochemical industry's complex integration with fossil fuels is uniquely challenging in the climate change landscape and must be understood in its own right.

The chemical industry has for many decades been highly integrated with the prevailing energy system. In general, the organic chemical industry derives both its

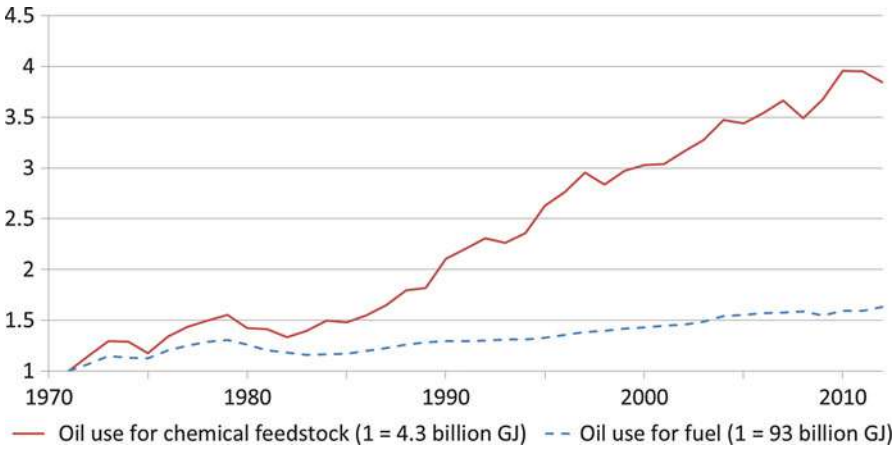

Fig. 1 Global growth in oil use for chemical feedstocks and energy, indexed to 1971 (IEA 2014b)

energy requirements and its raw materials from petroleum, making it both a heavy emitter of GHG and also highly dependent on fossil fuels: in the modern petrochemical industry, around 50 % of the operating costs are due to oil and gas inputs for both raw materials and process energy.

Overall, approximately 97 % of chemical products are produced from petroleum (including natural gas), while coal delivers 0.4 % of chemical feedstock globally, by energy content (IEA 2014b). The amount of oil used for chemical feedstocks continues to grow globally, at a rate of 4 % per year, representing an increasing proportion of growing global oil (total global oil use has grown at a rate of 1.4 % per year) (Fig. 1). The primary product from the petrochemical industry is plastics, and as plastics consumption has increased with gross domestic product (GDP) per capita, worldwide demand for plastics is expected to rise rapidly as the average wealth increases, particularly in emerging economies with very large populations (De Vries et al. 2006; Andre et al. 2014). Demand for petrochemical products has not yet reached saturation point, and the industry is expected to grow for some time yet.

Indeed, the diversity and high functionality of petrochemical products have resulted in their use across our daily lives. Some have simply replaced existing materials in society, taking the place of wood or metal. Others have created new opportunities, now essential to our modern lives. Over the last 50 years, society has become reliant on the products of the organic chemical industry to supply not only plastics but the clothes we wear, the food we eat, health products and pharmaceuticals, secure housing, transportation, security, and numerous other commodities (Wittcoff and Reuben 1980).

In addition, derivative products from petrochemical feedstocks are also pervasive throughout the industrial economy. Products generally undergo numerous stages of processing and are each transferred between firms within the value chain for further processing, such that the industry as a whole consumes more than a quarter of its own production. Petrochemical products can be divided into categories of “bulk”

and "speciality." Bulk organic chemicals are generally commodity products that are produced in large volumes and compete with one another on price. They include the major platform chemicals such as ethylene, propylene, and benzene and each of their immediate derivatives. Methanol, ethanol, and commodity polymers (including many fabrics and plastics) are also considered bulk products. Meanwhile speciality chemicals cater to specific custom markets and generally compete on the basis of technological expertise that can provide a greater added-value to their products. These end products typically include speciality high-performance plastics, fabrics, paints, pigments, and cosmetics.

While chemical production does not dominate the fossil industries, it does account for a significant share of the fossil resources. In the United States, approximately 3.4 % of a barrel of oil is used for chemical products, while nearly 20 times that amount (70.6 %) goes to fuel uses (Marshall 2007). This ratio is slightly higher for Europe, where 9 % is used for chemical feedstocks, as oil (naphtha) dominates natural gas for bulk chemical production in this region (IEA 2014b). Despite the differences in production volumes, the values of the two industries are comparable, due to the higher retail value of petrochemical products relative to oil-derived fuels.

However, the industry is changing. High oil prices at the beginning of the twenty-first century have combined with the shifts in the global economy to accelerate the petrochemical industry's migration eastward, from Europe and North America toward the Middle East and Asia Pacific. The former, in particular, offers opportunities to exploit low-cost liquefied petroleum gas (LPG) feedstocks, which are an associated by-product of oil refining and therefore widely available where oil production costs are low. Recent economic growth in Asia Pacific meanwhile has seen rapidly changing ownership structures of petrochemical companies and investment in new plants, with this region rapidly increasing its global share of the petrochemical sector (Lewe et al. 2012). Additionally, the shale gas "revolution" in the United States has seen North American natural gas prices decouple from global oil prices, leaving European naphtha-based chemical production increasingly exposed. Such changes are not entirely without precedent, and concern about volatile feedstock costs and potential oil supply constraints instigated a debate about the sustainability of petroleum-based products years ago (Hodges 2009; Koopmans 2006). Furthermore, growing concern about climate change and increasingly stringent GHG regulations are now driving the organic chemical industry to revise its energy use for the future and assess its process routes. Economic motivation, greenhouse gas reduction, and supply security are all acting as drivers toward greater energy efficiency and renewed interest in use of alternative feedstocks.

This chapter introduces the history of the modern chemical industry and the establishment of its close relationship with the oil industry – a relationship that has recently come under strain. It goes on to describe some of the major chemical processes, their GHG emissions, and their geographical variations. The main focus of the chapter is a discussion of the benefits and challenges of three main technological mitigation options: efficiency gains, CO_2 capture and storage, and feedstock switching. The interaction of these options with the main climate policy instruments in Europe, and worldwide, is considered.

The concept of "biorefining" for bio-based chemicals is given particular prominence for its potential to deliver renewability, low CO_2, and energy/feedstock security in the long term. However, establishing new production routes based on biomass in Europe is shown to face considerable social, technical, and economic obstacles to reaching a scale that can contribute valuable emission reductions.

The Chemical Industry Value Chain: From Feedstocks to Final Users

Organic chemicals are those that contain a structure based on carbon, usually in combination with hydrogen. Although there is no official definition, organic chemicals are widely understood to be the carbon-containing compounds associated with life (such as sugars and proteins) or the hydrocarbons present in fossil fuels. Oil, gas, and coal contain largely pure hydrocarbons with a carbon backbone of varying length, dependent on the source, and without a high prevalence of heteroatoms, such as oxygen, nitrogen, or metals. This gives them high energy densities and also makes them particularly suitable for chemical production.

Extracted hydrocarbon feedstocks first undergo pretreatment or fractionation, before being processed to produce targeted chemicals and products. Overall, the seven organic chemicals with the largest production volumes can be divided into three groups: olefins (e.g., ethylene, propylene, butadiene); aromatics, based on a six-carbon ring (e.g., benzene, toluene, xylene); and methanol, being the most basic alcohol. Global production of benzene alone in 2012 was 43 million tons (Mt) with current aromatics production amounting to 115 Mt each year; 2012 saw ethylene and propylene production reach 220 Mt, and methanol production in 2012 (most of which was used to make other chemicals) was around 58 million Mt (IEA 2013a). Some of the petrochemical industry's key molecular structures are shown in Table 1. Each of these can then be processed again and sold on, either to final consumers or to new industries for further processing.

Production of one chemical, such as acrylonitrile butadiene styrene (ABS) rubber, can be used to exemplify the complexity of such a value chain and highlights the many stages between fossil fuel and final product (Fig. 2). The fundamental building block for this material is 1–3-butadiene, which is used to make polybutadiene. Hydrocarbon feedstock (such as LPG or naphtha) is first cracked to provide the unsaturated olefin platform chemicals: ethylene, propylene, and butadiene. This production of bulk chemicals will typically occur at an integrated petrochemical and refining site. The crude butadiene is then separated using solvent extraction. This can take place remotely, in which case the crude butadiene is shipped or piped to an extraction unit; however, most extraction units are located close to the olefin cracker since butadiene is gaseous, meaning that significant energy is required to liquefy and transport it. Butadiene monomer is then polymerized to polybutadiene, which is subsequently copolymerized with styrene and acrylonitrile to make ABS resin. ABS resin is then sold to manufacturers who wish to take advantage of the thermoplastic's lightness, rigidity, insulating properties, and recyclability. These properties are

Table 1 Formulae and structures of the main hydrocarbons used in fuel and chemical production (with the exception of methane, only carbon–carbon bonds are shown as lines. Hydrogen atoms are omitted)

Group	Example hydrocarbons	Formulae	Structures
Natural gas	Methane	CH_4	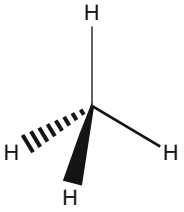
Olefins	Ethylene, propylene, butadiene	C_2H_2, C_3H_6, C_4H_6	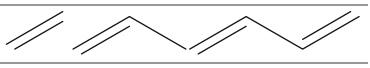
LPG	Ethane, propane, butane	C_2H_4, C_3H_8, C_4H_{10}	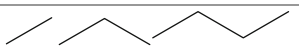
BTX	Benzene, toluene, xylenes	C_6H_6, C_7H_8, C_8H_{10}	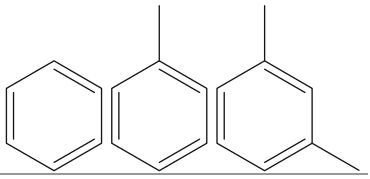
Gasoline	Octane, plus a variety of saturated and unsaturated hydrocarbons	C_8H_{18}, other C_4 to C_{12}	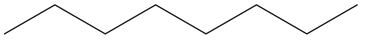
Diesel	Cetane, plus a variety of saturated and unsaturated hydrocarbons	$C_{16}H_{18}$, other C_8 to C_{21}	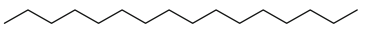
Coal	60–90 % carbon	Approximately $C_{135}H_{96}O_9NS$	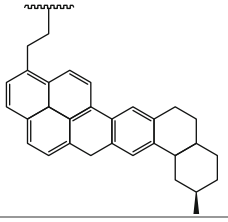

valued across many sectors, and ABS is used for a wide range of final products for sale to end users: from car parts, drain pipes, and electronic products to Lego bricks and even tattoo inks.

From this example, it is clear that the industry's supply chains are varied and complex. Firstly, the downstream users of butadiene, polybutadiene, and ABS are usually very different firms to the major petrochemical companies that extract fossil resources and produce the primary bulk chemicals (Morrow 1990). Secondly, it should be noted that styrene and acrylonitrile are both produced from olefins: styrene from ethylene and acrylonitrile from propylene. Each of the value chain steps is

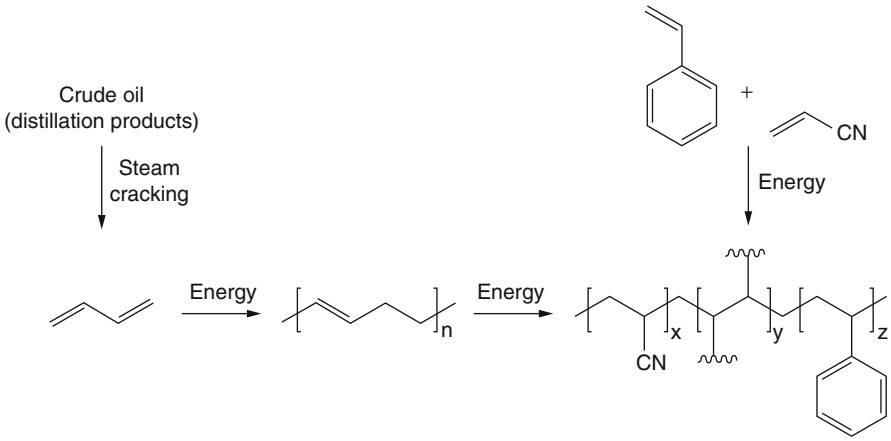

Fig. 2 Synthesis of ABS

highly integrated with one another, and as such there are inherent complexities in influencing change in any one step: they cannot be treated in isolation. This also indicates the large amount of process energy required for petrochemical production, most of which also comes from petroleum sources. Overall, one kilogram of ABS requires approximately two kilograms of petroleum in both feedstock and energy. Petrochemicals are doubly connected to the petroleum industry, and while this chapter deals with each of these relationships in turn, it is important to note that they are very closely integrated.

Feedstocks: Fossil History and Biomass Contenders

Oil

Oil is a relatively easily handled liquid comprised of a number of different lengths of hydrocarbon chain, and it is the main feedstock used for petrochemical production. In 2012, 396 million tons (Mt) of oil products were used for chemical feedstock worldwide, representing 9.4 % of the oil used for energy (IEA 2014b). A similar amount was also used by the petrochemical industry for processing energy, although exact figures are unavailable, due in large part to the integrated nature of refinery and petrochemical processes, and the difficulties in allocating energy balances between the various processes. However, all these numbers are projected to increase significantly. The World Energy Outlook 2014 considers that chemical feedstocks will be the fastest growing use of oil until 2040, at which point oil use for chemicals will reach a quarter of that used for transport (WEO 2014d). As this chapter will describe, the history of petrochemicals is closely linked to oil, and this relationship is expected to continue for some time.

After crude oil is extracted, it is distilled to separate the major components, most of which are further processed to deliver liquid transportation fuels. In terms of tonnage, the primary energy products are diesel (31 %), gasoline (25 %), jet fuel (6 %), and residual fuel oil which is often used in power generation (15 %). The proportions of the different products are determined by the nature of the oil – whether it contains mostly short or long chain molecules – which varies between locations and between oil wells. However, refinery operators have some flexibility to manipulate these values to meet demand, as is evident from a brief consideration of the history of oil demand and supply.

History

In 1850, when James "Paraffin" Young first patented his method of oil distillation, it was the illuminating properties of the kerosene product that ensured his technology a bright future (Redwood 2009). The early US oil-refining business continued to target the production of lighting, and throughout the supremacy of Standard Oil, liquid kerosene lamp fuel determined how refineries were designed. Kerosene was the only valuable product of otherwise dirty and unpleasant crude. The development of the internal combustion engine had demonstrated a use for one of the other distillates, but motoring did not take off until the 1920s and 1930s at which point there was not enough by-product to meet the demand (Levingston 2006). The story of the oil refinery is one adjustment to new technologies that maximizes output of products for the most attractive markets. The development of thermal cracking increased the petrol yield, and its replacement with catalytic cracking then opened the way for selling higher purity coproducts to the chemical and electricity industries, among others (Nguyen et al. 2005).

The use of oil for chemical production began in the United States with the manufacture of ethylene derivatives for solvents, in particular ethylene glycol and tetraethyl lead, whose functions as antifreeze and antiknocking additives went hand-in-hand with the manufacture of gasoline during the huge expansion in automobile ownership through the 1920s. The feedstock for this was primarily refinery off-gases, which were in plentiful supply adjacent to the oil refineries on the Gulf Coast of the United States (Spitz 1988). Since that point, the history of petrochemicals has been one of close interaction with the oil refining industry. At each turn, innovative chemists have found ways of tailoring fuel products to meet the needs of new engine technologies, such as production of high-octane fuel for military aircraft in the 1930s (Ogston 1997), and they have increasingly found new outlets for unused distillation fractions as chemical products. Early ethylene-based products built on existing acetylene lighting technology and targeted existing product families like solvents, surfactants, and lubricants. These product families were expanded to integrate other olefin raw materials and were based predominantly on small reactive molecular entities. For example, isopropyl alcohol from olefinic propylene was Standard Oil's first petroleum-based chemical product in 1920 (Mann 1966).

The mid-1930s saw major breakthroughs in the field of polymer science, causing a major revolution in organic chemical production. The theory developed by Hermann Staudinger revealed that small, reactive chemicals could be purposefully

joined together to synthesize products with known, useful properties. Indeed he suggested that it "is not improbable, that sooner or later a way will be discovered to prepare artificial fibres from synthetic high-molecular products" (Staudinger 1936, p 99). Confirmation of this theory was then delivered by DuPont's commercialization of nylon in 1938. Nylon (aliphatic polyamides) and polyethylene played highly significant roles in driving petrochemicals into markets where they could displace natural products, such as rubber, wood, and metal. The demonstrated effectiveness of these materials during World War II opened up the prospect of an almost limitless demand for olefins and fundamentally altered the economics of refining, ensuring that petrochemical complexes would be built alongside refineries in the United States from the 1940s onward.

However, the experience in Europe was markedly different, and European petrochemicals production did not catch up with the United States until the 1950s. Before North Sea oil and gas were discovered in the 1960s, Europe did not produce oil to fuel its vehicles but imported gasoline from North America, Russia, and the Middle East, meaning that there was not a ready supply of olefin by-products available. Furthermore, the two major energy-using European nations, Germany and the UK, had well-developed technology based on their coal reserves and were reluctant to exchange their leadership in coal-based technologies for reliance on imported fuel and feedstocks (Reader 1977). Decisions to support coal-to-oil conversion, alcohol motor fuel, and overseas oil exploration were influenced heavily by governmental attempts to steer technology change toward particular policy priorities: securing energy supplies, supporting troubled industries, and addressing unemployment. This was accompanied by industrialists' attempts to steer policy priorities toward maintaining or developing their own preferred technologies (Bennett and Pearson 2009). In 1927, Alfred Mond, the Chairman of the UK's Imperial Chemical Industries (ICI), expressed his belief that "not only oil, but the whole field of organic products will be based upon coal as a raw material in the near future" (Reader 1975, p. 84). Consequently, when ICI decided to invest in petrochemicals after the War, they did not do so in collaboration with BP – the major British oil company that was simultaneously moving some refining operations from Iran to Scotland – but as a stand-alone chemical plant near their existing coal-based operations. For cracking to olefins, ICI instead chose to import naphtha, a liquid by-product of oil refining that can be transported by ship. This was a novel approach and reflected the value that ICI and the British government placed on maintaining independent industrial enterprises. This allowed the UK to continue to lead Europe in petrochemicals, especially as Germany remained committed to its indigenous coal reserves as it rebuilt its economy after the War. European crackers continue to operate on naphtha today, a configuration that partly reflects this history.

Now

The story is different still for the Middle East, in particular Saudi Arabia, where the exploitation of abundant sources of LPG (liquefied petroleum gas: propane and butane) for chemicals has been a relatively recent development. This is because petrochemicals production requires sizeable investment in local infrastructure, requiring a more complex industrial strategy than the rapid returns delivered by

investment in oil production and export. Combined with a lack of local demand for high-value chemical products, this led to delays in investment. Today, the continued shift of refineries eastwards is threatening to relegate European naphtha crackers to become marginal suppliers of ethylene and propylene, and as long-term projections of oil prices indicate an increase over the coming decades, the dominance of LPG in the Middle East is expected to become further entrenched (Hodges et al. 2008).

In summary, the current utilization of petroleum as the major organic chemical feedstock and its options for greater sustainability must be understood in the context of the petrochemicals industry's codevelopment with fuel-orientated oil refining. The close integration of these two industries has resulted in highly efficient manufacturing complexes, with designs that have evolved over five decades. It is generally expected that this relationship will continue to determine the technologies, product mixes, and the economics of organic chemical production for some time to come.

Gas

Natural gas is an increasingly important feedstock and energy source for the petrochemical industry, with 183 Mt of natural gas used for chemical feedstocks in 2012, representing 6.4 % of that used for energy (IEA 2014b). The primary component of natural gas is methane, though ethane, propane, and heavier hydrocarbons may also be present in much smaller quantities. The carbon-hydrogen covalent bond in methane is exceptionally strong and requires a lot of energy to break, which to some extent limits its use as a building block for organic chemicals. However, natural gas is the primary source of hydrogen worldwide, through the steam reforming processing of methane to yield hydrogen and carbon dioxide. Hydrogen produced by this method is widely used in the chemical industry, in particular for the production of ammonia via the Haber process. Indeed, of the 50 Mt of hydrogen produced each year, approximately half goes to ammonia production, of which 80 % is then further processed to fertilizers (Da Rosa 2009; DOE 2013). Steam reforming of methane in this way releases large quantities of CO_2, which means that ammonia production is a significant emitter of CO_2, especially when the energy intensity of the Haber process is also considered. Depending on feedstock and process, CO_2 emissions have been estimated to vary from around 1.1 t of CO_2 per ton of ammonia in Spain to 1.3 t in the United States and 3.4 t in Belgium (Bosch and Kuenen 2009).

Due to the costs of transporting gases, the use of gas has historically been limited by local availability. However, natural gas is seen to occupy a different market niche to oil, and where it is readily available, natural gas can be an attractive source of carbon for organic chemical feedstocks. When compared to LPG or naphtha feedstocks, its use is often associated with lower CO_2, and it benefits from being relatively independent of the markets for other petroleum refinery products. Research into chemical conversion of natural gas is ongoing, and the advent of shale gas (discussed later in this chapter) has renewed interest into the economic conversion of methane to useful longer chain hydrocarbon building blocks, such as olefins (Ren and Patel 2009; Barteau and Kota 2014).

History

Gas has had a very different history to oil, since the cost of compression or pipeline construction for transportation historically precluded international trade. This has led to innovation in gas to chemical production in certain remote locations with abundant gas but little local demand for energy. In New Zealand, for example, following the discovery of natural gas, two plants were established in the early 1980s to convert methane to methanol. The first step of this process used steam reforming of methane to give carbon monoxide and hydrogen. Up to 6,700 t crude methanol was produced each day. Part of this was upgraded to gasoline via the Mobil process, and part was exported as chemical grade methanol for further processing in the main foreign petrochemical facilities (Dry 1988; NZIC 1988). At the time, this represented the world's largest methanol production capacity, and the two plants found a crucial market niche for chemical production from natural gas in an area with relatively low energy demand.

In addition to use as a feedstock, the petrochemical industry also uses natural gas to provide the process heat and electricity that power petrochemical facilities (Table 2). Heat is used in nearly all petrochemical processes, and there has been considerable interest in replacing the fuels used to heat petrochemical plants and refineries – typically crude oil and waste petroleum products from the conversion processes – with more efficient natural gas, which can reduce process costs and energy-related carbon emissions. Petroleum fuel products can then instead be used for feedstock or for higher-quality energy products.

Table 2 Fossil fuel consumption figures for the world and OECD in 2012 (IEA 2014b)

	Total primary energy supply (billion GJ)	Energy used by chemical industry (incl. petrochemicals) (billion GJ)	Used as organic chemical feedstock (billion GJ)	Percentage of total primary energy supply used by chemical industry (incl. petrochemicals)	Percentage of total primary energy supply used as petrochemical feedstock
World					
Oil and oil products	176.2	2.0	16.6	10.5 %	9.4 %
Natural gas	119.1	4.0	7.7	9.8 %	6.4 %
Coal	162.1	2.9	0.1	1.9 %	0.06 %
OECD					
Oil and oil products	79.8	0.8	8.9	12.2 %	11.1 %
Natural gas	56.3	2.4	1.4	6.8 %	2.5 %
Coal	42.4	0.5	0.04	1.2 %	0.09 %

Now

Use of natural gas has grown steadily over the last few decades. In part this is due to the increase in economically viable transport and use of liquefied natural gas (LNG), which has allowed much wider use of the fuel without the need for pipelines. Construction of LNG terminals has grown at a rapid rate in recent decades: from a capacity of around 55 million tons per annum (mtpa) in 1990 to more than 220 mtpa in 2010, with a slower rate of growth in recent years as 2013 saw LNG trade of around 240 mtpa (Wood 2013). The shipping of LNG has opened up new markets for natural gas and facilitated its use in regions without natural gas resources. Nevertheless, there still remains considerable interest in conversion of natural gas to methanol, dimethyl ether (DME), and especially gasoline for export. Perhaps the most notorious case is that of Qatar, where methanol production is proceeding alongside LNG and gasoline production from natural gas.

In addition to the new opportunities from LNG, the shale "revolution" in the United States has helped to trigger new interest in the use of this feedstock for chemical production. The boom of shale gas discoveries has lowered the price of natural gas in the United States, and there has been significant investment in optimizing olefin production from readily available, low-cost shale gas sources. Use of shale gas for ethylene production in particular is lowering prices and reinvigorating North American chemicals production (Platts 2013).

Switching from oil or coal to gas for heat and power provision can be particularly attractive in the petrochemical industry due to the sector's consistent demand for heat and power in numerous processes requiring a higher energy quality, including pumps, instruments, and motors. In addition, there has been increasing attention paid to the concept of heat integration in recent years. Provision of heat and power via heat cogeneration, or "combined heat and power" (CHP), plants (IEA 2014c) offers a particular opportunity for cost and carbon reduction: through heat integration, CHP can be 50 % more efficient than supplying steam and electricity separately. Thus, as a consequence of higher fuel costs and ever more stringent environmental legislation, CHP is increasingly being incorporated into petrochemical sites. At present, Europe's largest gas-fuelled CHP plant is capable of generating 1,240 MW with a thermal efficiency over 70 % while providing steam and power to the petrochemical and refining processes at Immingham in the UK. The role of CHP is addressed in more detail toward the end of this chapter.

Coal

Coal is typically higher in oxygen content and has a lower H/C atomic ratio than petroleum or gas. Additionally, unlike oil or gas, solid coal must undergo conversion through gasification or other processes before it can be used for further chemical manufacture (Speight 2012). However, this processing can be justified when there are abundant local resources or when access to oil and gas is limited. Particularly in coal-rich countries, such as China and Indonesia, coal feedstock continues to play an important role in the petrochemical industry.

History

Coal was the original energy source and feedstock for the organic chemical industry when it evolved from the early British coal tar pigment industry in the late nineteenth century. Indeed, it has been remarked that the synthetic dye industry became the "synthetic-everything-else-industry" (Belt 1987, p. 136). In addition to the aromatic chromophores (naphthalene, anthracene, and benzene derivatives) that were obtained from coal tar, coal was gasified to yield acetylene and synthesis gas (syngas) which could be upgraded to produce some basic synthetic chemicals. By the end of the 1930s, German and US coal-based chemistry had developed to a stage where liquid fuel, rubber, plastics, solvents, lubricants, and many other chemical products were commercially manufactured from coal. Coal-based chemistry laid the foundations for the modern petrochemical industry, often via carbon monoxide as an intermediate. In 1938, DuPont claimed that "in the field of carbon monoxide chemistry," they had "an answer to anything the oil companies can do from hydrocarbon gases" (Reader 1975, p. 321). However, by this time, coal had already been replaced by petroleum as the primary organic chemical feedstock in the United States and was about to be overtaken in the UK. Figure 3 shows the transition from coal to oil-based chemicals in the UK. This mirrors the substitution of coal by oil and gas in primary energy use, and although starting later, the overturn of the raw material base was even more rapid, reaching 50 % penetration 20 years earlier than as energy source. Coal was finally displaced by oil in the 1960s, when technologies for producing aromatic chemicals, such as benzene, from petroleum were

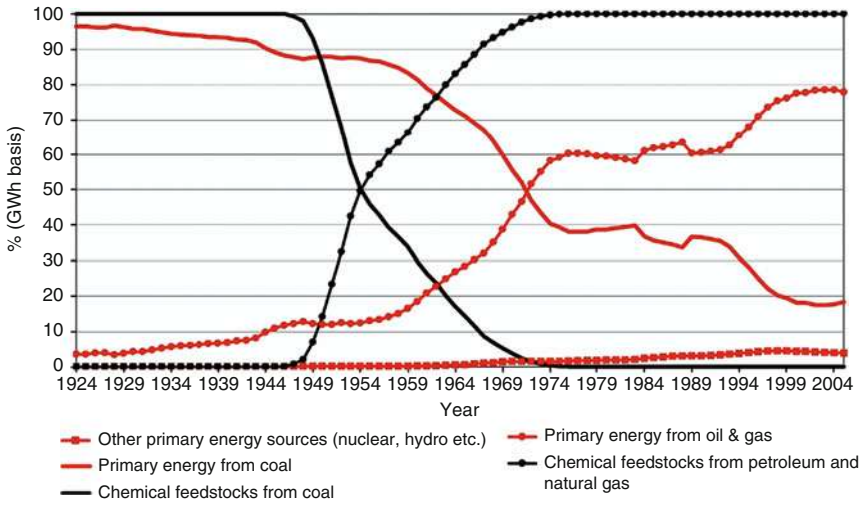

Fig. 3 Transitions from coal to oil and gas in UK primary energy (*red*) and chemical feedstocks (*black*) 1924–2005 (5-year rolling averages from UK official energy statistics. Nonfossil feedstocks are excluded from this diagram due to a lack of reliable data. They are thought to account for a shrinking proportion (from a high of up to 15 % in the 1930s to less than 3 % today.) (Bennett and Pearson 2009)

commercialized. Until that point, aromatics – crucial for so many applications – had remained the preserve of the coal-based chemical industry.

Petroleum-based processes began to out compete coal-based chemistry in 1940, and since then coal feedstocks have thrived only under severe resource pressures. This was seen in Germany during World War II, where, deprived of access to reliable oil supplies, chemists focused their energies on products from syngas: in particular gasoline and synthetic rubber. This technology was subsequently applied by the South African oil and chemical giant Sasol, who had restricted access to international oil markets but allowed access to large domestic coal deposits. By 1974, Sasol was operating its first integrated fuel and chemical plant based on coal gasification, and by 1982 (just before a significant drop in the global oil price), it was producing 80 different chemicals for about 700 clients, with its sales of chemicals representing 16 % of total sales (Hodge 2000). Most of this was produced from olefins, which were generated by cracking the naphtha fraction of the Fischer–Tropsch liquid fuel manufactured from syngas. Still today, Sasol produces around 2 Mt of olefins from coal each year for the South African chemical industry.

Now

Of all the sources of chemical feedstock or process energy, coal gives rise to the largest amount of CO_2 emissions, estimated at between 8 and 11 t of CO_2 per ton of high-value chemical produced (Ren and Patel 2009). By comparison, oil-derived process routes emit around 4 t CO_2 per ton of product, and natural gas routes are slightly higher at 4–5 t (due to the additional energy requirements of producing syngas from methane). However, despite these high CO_2 emissions and an increasingly stringent greenhouse gas regime, coal-based chemistry continues to be favored in certain locations. In large part, this stems from local availability: most notably in China, where indigenous coal is far more abundant than other fossil fuels, about 20 % of the domestic chemical industry is based on coal as a feedstock (Yang and Jackson 2012). This chemical production is largely based on traditional "low-tech" processes such as coking, processing of coke and coal tar, and carbide chemistry. Future developments in China are likely to see growth in coal-to-liquids, coal-to-methanol, and C1 chemistry based on syngas, such as is used by Sasol (Xie et al. 2010). Indeed, significant investments into research of coal to olefins technology have been made in recent years, with a target in the 12th five-year plan to have 20 % of China's olefin consumption to come from coal, and it is expected that by 2020, China will be 62 % self-sufficient in ethylene production, most of which could come from coal (Horncastle et al. 2011). As technology improves and learning effects lower plant costs, coal-derived chemicals are expected to become increasingly competitive with imported petroleum-based routes. Multiple plants are already in operation, and there are a number of international collaborations underway, which share expertise and finance for new technological ventures. There have been a number of collaborations between South Africa's Sasol and China's Shenhua group, and recently Shenhua also partnered with Dow Chemicals for the Yulin Integrated Chemicals project: a US $3.9 billion coal to many chemical plants, scheduled to launch in 2016 (Zhao 2013).

Biomass

Concern about climate change and sustainability of fossil resources has driven renewed recent interest in biomass. While it is not a petrochemical in the same way as oil, gas, or coal, biomass also consists of hydrocarbon chains, which can be extracted and processed in very similar ways to fossil feedstocks.

Biomass refers to vegetation or other plant material that can be converted industrially into useful energy, fuel, or materials. At present it is estimated that around 5 % of current global chemical sales are produced from biomass, with biomass additionally supplying about 10 % of global primary energy (IEA 2013b). Most of the biomass that enters the chemical industry's value chain is either in traditional bulk processes that have never been fully displaced by petrochemicals or in smaller quantities of speciality products that harness specific natural properties of biomass. The former category includes products such as cellophane, produced from wood cellulose, vegetable oil components in soap, pine resins in paint, and use of castor oil to produce polyurethane. The latter category, meanwhile, includes speciality products such as cosmetics, food additives, dyes, and medical products, including specialist materials that can biodegrade in the body. Companies such as Croda, a UK company founded in 1925 to manufacture lanolin from sheep's wool, is today a speciality chemicals firm that obtains 70 % of its raw materials (and 24 % of its energy) from renewable resources (Croda 2014). The company produces personal care products, as well as crop care, polymers, and coatings, and achieved a revenue of £1.08 billion in 2013. In addition, there are other firms, not historically linked to biomass utilization, who are now looking to biomaterials to diversify their feedstock dependence and increase resilience. With new technological developments and increasing environmental awareness among consumers, bio-based chemicals may be entering a new era of technological and economical competitivity.

History

In many ways, the history of the petrochemical industry is one of replacement of biomass by synthetic products. Wood, for example, has been replaced in a wide variety of furniture applications by plastics, while synthetic fibers such as nylon have now superseded cotton for certain fabric products. In addition, there are now numerous more sophisticated synthetic materials from bio-based chemical feedstocks, which have a more complex relationship with fossil-based chemicals.

While fossil chemicals have dominated in recent years, use of biomass for chemicals has a history at least as long. Indeed, the early stages of the chemical industry's development saw strong competition between biomass and fossil feedstock-derived pathways. Between World War I and World War II, Europe and America showed great interest in industrial use of fermentation ethanol, with support schemes operating in Germany, France, Italy, the UK, and the United States, among others (Bernton et al. 1982). There were various reasons for these policies, in particular relating to concerns about the security of supply of oil for motor cars, the need to provide farm support during and after the depression, and, particularly in the European context, a lack of convincing evidence that petrochemistry was truly

superior or cheaper than biomass routes. In the UK, the added incentive of adding value to the molasses obtained from sugar plantations in the British Empire led to significant tax relief for industrial alcohol production, known as the inconvenience allowance (Reader 1975). As a result of the inconvenience allowance, and the partly related lack of UK refineries, British chemical companies first deployed the ethylene-based chemistry that was being developed in the United States by dehydrating ethanol produced by ex-whisky producers such as the Distiller's Company (Weir 1995). As such, in 1938 when the first polyethylene plant was developed, it was based on bioethanol, not fossil feedstock.

Around this time in the United States, a movement based around the Farm "Chemurgic" Council advocated harnessing agricultural production for soybean plastics, corn-based rubber, and Agrol (gasoline–ethanol blends) to relieve farm poverty and dependence on powerful oil companies (Finlay 2004; Hale 1930). In 1941, Henry Ford unveiled a car that ran on Agrol and had a soybean plastic body. The notion of separating plastics production from the oil industry was revisited following the oil shocks in the 1970s when ICI began the development of Biopol, a polymer made from fermented glucose (Bennett 2008). As oil prices dropped, the prospect of commercially competitive Biopol production receded, but the development work undertaken by ICI provided the foundations for a new generation of bio-based chemicals.

While petrochemical feedstocks have dominated the latter part of the twentieth century, biomass has not been forgotten, and ongoing research into this feedstock has been driven by interest, circumstance, and economics. For example, one of the first demonstrations of aviation biofuels came in 1979 when a group of amateur flying enthusiasts developed alcohol fuels in an attempt to mitigate the impacts of the gasoline crisis (Bernton et al. 1982).

Now

Recently, climate change is one of the concerns that have generated renewed interest in using biomass as a chemical feedstock. Biomass is a renewable resource that has the advantage of sequestering CO_2 from the atmosphere as it grows. If the biomass is then used as a chemical feedstock, then atmospheric CO_2 is incorporated into products. Depending on the end-of-life disposal of the product, the carbon is either locked up indefinitely and kept out of the atmosphere or returned to the atmosphere upon degradation or incineration, but still creating lower net emissions than the equivalent fossil-based product. A lower carbon footprint has been calculated for a number of synthetic materials from bio-based feedstocks, such as for polylactic acid (PLA) and Mater-Bi plastics, and fibers made from corn starch by NatureWorks in Nebraska, United States, and by Novamont in Terni, Italy (Madival et al. 2009; Murphy et al. 2008; Uihlein et al. 2008).

Most bio-based plastics are still more expensive than their petrochemical counterparts, and so commercial production is generally limited to those with specialist properties (such as biodegradability) where niche markets can be accessed.

However, the landscape is changing. Increasingly, "green" product premiums are growing the market for bio-based goods, as consumers become more aware of the

environmental footprint of their products and the marketability of (and willingness to pay for) green credentials increases. In addition, continued research and technological progress are lowering the costs, and bioplastics in particular are becoming increasingly competitive (Golden and Handfield 2014).

Major companies are increasingly investing in biomass-derived routes, for economic and technical reasons as much as environmental motivation. The Lego company, large-scale consumers of ABS, have instigated research into alternative, biomass-based plastics to replace this petroleum component of their children's toys with a target of achieving full feedstock switching by 2030 (Miel 2014). Focusing on the technical and potential economic advantages, the Toyota car company have set a target of replacing 20 % by weigh of all fossil-based plastics with bioplastics by 2015, with many of their cars already making use of bio-based polyesters, PET, and PLA-blends (FNR 2014). Several other investments have been triggered by concerns about resource availability. Projections of butadiene shortages in the coming decades led the tire company Michelin to initiate the Bio Butterfly project, a €52 million research program, to develop butadiene production from biomass. Additionally chemical companies such as Mitsui, DuPont, Dow Chemicals, and Braskem have all invested in new bio-based polymer routes, with a wide variety of applications. As biochemical markets develop, the output and diversity of bio-based facilities is scaling up and further reducing costs. One such plant is the BioAmber plant in Sarnia, Canada, due to commence operation in 2015, which will see production of 50,000 t of bio-based succinic acid per annum.

For details on bio-based plastics, see the respective chapter in this handbook.

However, as with fossil feedstocks, the full environmental impact of biomass is not entirely straightforward. While carbon is captured during plant growth, crop cultivation and biomass processing still has impacts on water use, gaseous emissions, and uses resources, including fossil resources. A life cycle assessment (LCA) approach has been developed to take these impacts into account and to compare the benefits of different process routes. Full LCA analysis is particularly important for biomass, as at present it is a more limited resource than oil, gas, or coal. It is frequently advocated that its use should be directed to those functions with the greatest environmental gain, which does not currently match the greatest economic gain. Resource availability is discussed in more detail in the context of biorefineries, toward the end of this chapter.

Future Trends

Concerns About Resource Sustainability

Because of the reliance of the organic chemical industry on fossil fuels, especially oil, for both feedstock and energy, the sustainability of oil supply is of utmost importance. If the global oil market becomes disrupted or tight, competition for available oil supplies raises the production costs of petrochemicals more than for other commodities. This could benefit other feedstocks if they can be deployed

rapidly enough to take advantage of the imbalance between demand and supply of oil. Alternatively, total demand for organic chemicals could be reduced. While there are numerous political and economic factors that can lead to volatility in oil prices, long-term oil prices could be influenced by geological supply constraints. This notion that such constraints could lead to a peak in oil supply is commonly referred to as "peak oil."

The two men most associated with the ideas behind peak oil concerns are William Stanley Jevons and M. King Hubbert. Both looked at a finite fossil fuel resource and noted that the production rate of that resource, which had initially risen exponentially, would reach a maximum point long before the resource became exhausted. Jevons correctly predicted that UK coal supply would be unable to keep up with demand in the early twentieth century. Hubbert correctly predicted a peak in US oil production in the mid-twentieth century. For both resources, the growth rate of supply was checked at approximately half of the total reserve. Although British coal and American oil could subsequently be replaced by alternative fossil energy sources, mainly through imports, what was recognized by these theorists was that if there is no alternative supply source that can be used as a substitute at similar cost, then the inevitable decline in production will cause intense competition between consumers if their levels of demand are inflexible due to existing infrastructure and expectations. Peak oil proponents predict that after the global peak in the rate of production, price rises would accompany sharp declines in production rates unless demand were rapidly reduced, thus the key date would be the extraction of half the conventional oil resource and not the date of total exhaustion.[1] While concern was high in the early 2000s that rapid price rises could mean an end to decades of economic growth based on cheap access to oil, the addition of substantial oil production from unconventional sources has relieved many of these concerns in the last few years.

Conventional oil refers to crude oil, condensate, and natural gas liquids, which are usually relatively easily extracted from subsurface oil fields and require relatively little upgrading to liquid fuels. By contrast, unconventional oil refers to tight oil sands, shale oil, and extra-heavy oil, which are not found in a usable form and require more treatment to yield liquid fuels. To unconventional oil can be added synfuels (coal-to-liquids, gas-to-liquids, and biofuels) (IEA 2013c). Unconventional liquids are generally more expensive to produce than conventional oil, but their production is nevertheless increasing, partly due to higher than historical oil prices.

The date and severity of peak oil remains unresolved. It not only depends on the total remaining conventional oil resource but also the costs of extraction, the elasticity of oil demand, the availability of substitutes, and the rate at which demand is suppressed by market saturation and efficiency policies in various countries. Figures 4 and 5 show the global trends in oil reserves and production. It can be seen that oil reserves are increasing, reflecting a mixture of technological progress

[1]Studies suggest that most of the world's major fields have peaked at between 30 % and 40 % of their total resource (Hökök et al. 2009).

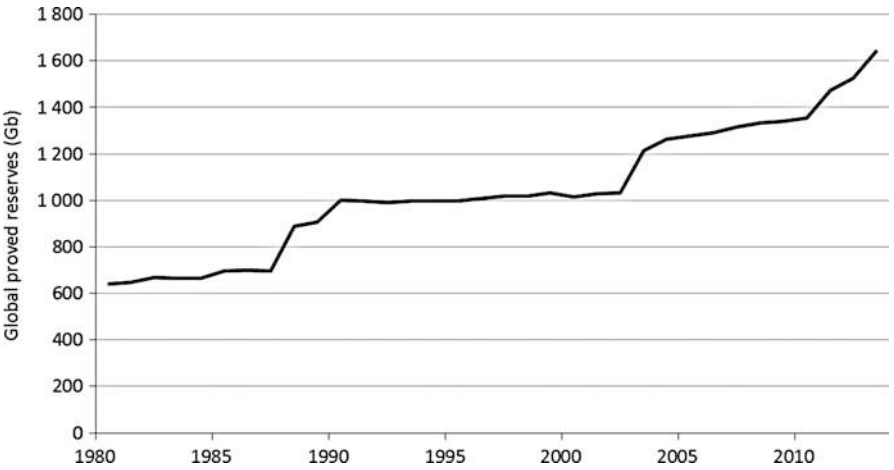

Fig. 4 Global trends in proved conventional oil reserves (EIA 2014a) (Proved reserves of crude oil are the estimated quantities of all liquids defined as crude oil, which geological and engineering data demonstrate with reasonable certainty to be recoverable in future years from reservoirs under existing economic and operating conditions. They are thus subject to changes in technology and oil price) Gb = gigabarrel

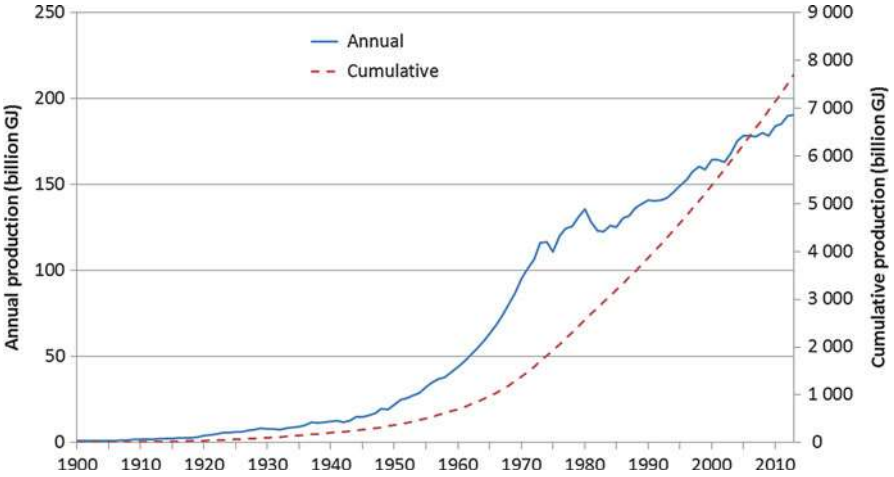

Fig. 5 Global trends in oil production (EIA 2014b; Emetad and Luciani 1991)

that reduces extraction costs of resources that are more difficult to access and oil prices above the long-term average that make higher-cost oil economic. Production growth has slowed, reflecting some consumer response to higher oil prices but also changes in consumption patterns in major economies such as the United States, Europe, and China. Fuel efficiency standards and fuel switching to less polluting fuels are having an impact. Yet, despite these trends, reserve additions are not

keeping pace with production. Recent years have seen relatively strong rates of exploration drilling; however, the discovered volumes have dropped since 2013, and the total number of discoveries per annum has fallen by 50 % between 2008 and 2014 (IHS 2014).

In a review of the evidence for a peak in conventional oil by 2030 by Sorrell et al. (2009), it is noted that although there are around 70,000 oil fields in the world, 100 fields account for half of production and up to 500 fields account for two-thirds of cumulative discoveries. Most of these giant fields are well past their peak of production or will begin to decline in the next decade. Their analysis indicates that just to maintain production at current levels, three million barrels per day of new capacity must be added each year – equivalent to a new Saudi Arabia coming on stream every 3 years. This means that in order to prevent production from falling, more than two-thirds of current crude oil production capacity may need to be replaced by 2030. Yet there appears little chance that new giant fields will be discovered and discoveries of new smaller fields are not currently at the levels needed.

While the likelihood of high future oil prices may have positive outcomes in terms of demand reduction and CO_2 emissions reduction, this needs to be balanced against the implications for economic activities such as petrochemical production, which is currently configured to take advantage of available and conventional oil at prices that have historically made production profitable. In a world that takes strong action to mitigate climate change, unconventional oil sources might comfortably substitute for declining conventional oil production. If demand does not decline due to climate action, however, the availability of synfuels and biofuels, including their public acceptance, will be more important.

For details on bio-based fuels, see the respective chapter in this handbook.

Unconventional Oil

Global oil production is expected to increase from 89 million barrels per day in 2013 to more than 104 million barrels per day in 2040 (IEA 2014d). The proportion of conventional oil will fall, with the proportion of natural gas liquids and unconventional oil increasing. It is also notable that OPEC's share of production is expected to increase somewhat, as well as increasing production from Brazil, Canada, Kazakhstan, and the United States. The increasing share of unconventional substitute fuels will also determine what resources are available for use in the chemical industry. This is already being seen in the United States, where the availability of shale gas is leading to its increased use as chemical feedstock.

Unconventional fuels primarily consist of oil sands, shale oil, and other heavy oils, shale gas, gas-to-liquids, coal-to-liquids, and biofuels. Each of these unconventional resources is itself a limited resource of differing proportions, and none is anticipated to offer a sole solution. Unlike for crude oil, production of liquid fuels from these resources do not generally produce by-products – such as LPG or naphtha – that are highly suitable as chemical feedstocks. Olefins, aromatics, or syngas can all be produced from unconventional liquids, but they would compete for the raw

material with fuel users, who may be willing to bid high prices if the available resource is constrained. Integrating unconventional feedstocks into the petrochemical industry could also require costly changes to the upstream infrastructure, which could be very costly.

Moreover, in terms of emissions, unconventional feedstocks often require more energy-intensive processing methods to yield fuels and feedstocks, such as gasification, hydroconversion, or steam injection. This additional energy consumption adds cost and will leave the chemical industry even more exposed to volatile energy prices than it already is. Furthermore, an increase in process energy will increase the carbon footprint of the industry, a factor which is becoming increasingly pertinent. Extraction of unconventional oil is predicated on the condition of economic as well as technical viability – it must be possible to make money from the process. However, the global economy is increasingly taking note of the concept of a "carbon budget": a finite, maximum total amount of CO_2 that can be released into the atmosphere if the planet is to stay within globally agreed temperature limits. To stay below a 2 °C increase, it is currently estimated that between 60 % and 80 % of proven fossil fuel reserves will need to remain in the ground. This has led organizations such as the Carbon Tracker Initiative to monitor and highlight the potential risk of investing in fossil fuel assets, some of which could become unexploitable if demand is curtailed by carbon pricing or regulation (CTI 2013). In such a situation, unconventional oil could be the most severely affected if its production cost (including any carbon price) were more expensive than the marginal oil price. Use of unconventional oil for chemical feedstock may therefore be more vulnerable to climate mitigation policy than other feedstock options and suffer from any reduced investment in unconventional oil production for fuel purposes.

Impacts of Energy Use by the Petrochemical Industry

The previous section explored the dependence of the petrochemical industry on fossil feedstocks. However, the sector is doubly dependent on fossil fuels, as it is also a massive consumer of process energy for heat and electricity. Many chemical processes are highly energy intensive, and the volumes of production mean that the petrochemical sector is one of the major consumers in the global energy landscape. Most of this energy is supplied through combustion of fossil fuels; as has been described, the modern petrochemical industry largely emerged as a corollary of primary fuel refining, and most petrochemical facilities continue to be located in close proximity to these sites if not integrated within the same complex and ownership structure. As a consequence, the fossil source for feedstock is often used for energy production too, supplying some of the 15 billion GJ/year used by the chemical and petrochemical industry for processing, not including the additional energy required to produce the feedstock (IEA 2012). While the many processes, products, and feedstocks make this a complex landscape, this section explores the main implications of climate change for the petrochemical industry as an energy consumer.

Primary Sources of Greenhouse Gases

The global industrial sector accounts for 21 % of direct greenhouse gas emissions. When indirect emissions (including those from electricity consumption) are included, industry's share rises to 32 % of global total GHG emissions, making it the primary source of GHG, above even the combined emissions from agriculture, forestry, and land use (IPCC 2013). The vast majority of this comes from energy use, and the chemical and petrochemical industry uses more than 30 % of the total industrial energy use worldwide, giving rise to very high volumes of GHG emissions. Overall, CO_2 emissions are found to account for the majority of these, accounting for around 99 % of greenhouse gas emissions from the petrochemical industry (Benchaita 2013), and while emissions of chlorofluorocarbons, methane, and nitrous oxides should be reduced wherever possible, the biggest implications are for CO_2, which is the focus of this section.

Data on the energy efficiency and GHG emissions from the global petrochemical sector are not readily available, for a number of reasons. Firstly, the diversity and complexity of the sector mean that there are a vast number of processes, products, and feedstocks that must be accounted for. This also leads to difficulties in allocating emissions between the heavily integrated processes on site, and without a global obligation to record and report CO_2 emissions, there are serious limitations to and discrepancies within the data that is available. Lastly, intellectual property and antitrust issues can prevent full disclosure of CO_2 figures. The world total GHG emissions attributed to chemical and petrochemical processes amounts to 1,240 MtCO2 equivalent annually. GHG emissions of the 18 largest volume chemicals are 960 MtCO2 equivalent per year, or more than 75 % of the total (IEA 2013a). This does not account for all emissions from power generation or energy recovery from petrochemical products during disposal, but does include both inorganic and organic chemicals production.

However, the situation is particularly complex for the petrochemical industry as compared to other industrial sectors. Much of the energy is used as feedstock, which then is locked up in products until the end of their lifetime and in many cases for a long time after their disposal. This makes the industry an effective "store" of fossil carbon in chemical products – carbon that would otherwise have been burnt for fuel and released to the atmosphere. It is estimated that carbon storage in plastics worldwide is around 477 Mt of CO_2 equivalent per year, and growing as plastic consumption rises (IEA 2007). With only 30 Mt of plastics incinerated annually at the end of their lifetime, the rest of the carbon continues to be locked into the plastic product. Furthermore, when considering the full lifecycle of the product, chemical industry representatives note that not only should end-of-life disposal be taken into account but also the contributions that use of the product made during its active product life. Carbon-containing products can contribute significant efficiency gains during their life: for example, the replacement of metal panels with carbon fiber reduces the weight (and therefore fuel consumption) of vehicles, and the use of polymers for insulation saves more in carbon dioxide via reduction in energy consumption than was generated during their production (Cefic 2006). Indeed, it

Table 3 Energy requirements for steam cracking for three different feedstocks (IEA 2007)

Feedstock	GJ/t ethylene
Ethane	15–25
Naphtha	25–40
Gas oil	40–50

has been estimated that in the food packaging industry, the replacement of materials such as metals, glass, or cardboard with petrochemically derived plastics has resulted in GHG reductions, as the plastics require fewer raw materials and less energy, as well as transport emission savings resulting from lighter weight plastics (IEA 2013a). However, it is difficult to create transferable metrics for the different stages of the product life, and it is likely that a robust carbon price, applied to all CO_2 emissions throughout the economy, would be the only way to effectively do this.

The vast majority of CO_2 emissions from the petrochemical industry stem from its energy consumption, which is used to power energy-intensive production processes. A typical petrochemical plant includes three types of energy consumption: about 60 % is due to fuel consumption, 35 % due to steam energy consumption, and 5 % fuel to power consumption (Benchaita 2013). Steam cracking to produce olefins is highly energy intensive, and it is used extensively, making it the major energy-consuming process worldwide. The energy used in steam cracking depends on both the technology used, and the choice of feedstock, with lighter feedstocks such as ethane cracked at lower temperatures, and the final ethylene yield decreasing (and so per-product emissions increasing) as the molecular weight of feedstock increases. One ton of ethylene can be produced from 1.25 t of ethane, 2.2 t of propane, or as much as 3.2 t of naphtha (Table 3).

In addition to the previously mentioned challenges for securing energy data, it must also be noted that the petrochemical industry is highly diverse, and it would be extremely challenging to develop separate indicators for each product. In response to this challenge, the IEA proposed an aggregate product indicator, composed of 49 products, which together account for more than 95 % of the total energy consumed by the industry (Tam and Gielen 2006). The five most energy-intensive processes are production of acetic acid (34 GJ/t), production of benzene via steam cracking (27 GJ/t), production of xylene by steam cracking (26 GJ/t), production of toluene by steam cracking (24 GJ/t), and production of toluene diisocyanate (22 GJ/t). Accounting for production volumes, it becomes clear that the three largest energy uses are for the processes that yield ethylene (1.3 million GJ per annum), propylene (0.7 million GJ per annum), and benzene (0.6 million GJ per annum). Considering the aggregate product indicator for the 49 products, it is found that efficiency savings just from implementing the best available practices and technologies in the core chemical processes could save around 14 % of this energy each year (excluding electricity), or more than 21 % when including electricity (IEA 2014a). However, the magnitude of the emissions from the top energy consumers clearly shows that targeting savings from these processes alone would yield significant climate change mitigation benefits.

Emissions also arise from the transport of chemical products, for further processing and for final sale. While many processing units are integrated with or sited near each other and near the refineries themselves, this is not always the case, and large volumes of chemicals (often gaseous or unstable, thereby requiring liquefaction or compression) must be transported to other locations. As with all industries, greater transportation leads to higher costs and GHG emissions from transport. Therefore, the economies of scale associated with large-scale petrochemical sites must be balanced with the increased demand for transport to sites of product consumption.

Calculations of the impact on the climate from organic chemicals should be undertaken with an understanding of the life cycle impact of a particular product or application. Such an approach could place appropriate emphasis on downstream users of chemical products to demand chemical commodities and synthetic materials that have a lower carbon footprint.

There is no space in this chapter to look in depth at particular products. Instead, the later sections on climate change mitigation options consider the potential for improvement of some of the most energy-intensive petrochemical processes.

Geographical Variations

The main petrochemical-producing regions are Europe, the Middle East, and the United States, although there has been significant growth in China during the last decade. Each of these regions relies to a large extent on different raw materials, meaning that their GHG emissions vary. Ethylene is one of the most important olefins, with production growing at an annual rate of 4.5 % each year (Benchaita 2013). Figure 4 shows the percentages of ethylene production capacity in different regions that are based on the six main feedstocks. This shows that while ethane dominates in the Middle East, naphtha and heavier fractions dominate in Europe. The United States is mainly reliant on LPG and some naphtha, while Asia Pacific is dominated by naphtha: indeed in 2013, 80 % of ethylene production facilities in China were naphtha based (Kalkman and Keller 2012). While the capacities vary between regions, the core technology designs are similar and are based on the steam cracking process developed in the United States in the early 1940s. The steam cracking process is energy intensive and globally accounts for more than 39 % of the chemical and petrochemical industry's final energy use. The energy used by each facility however depends on a number of factors, with feedstock being a key element since lighter feedstocks (such as ethane) are cracked at lower temperatures (IEA 2007) (Fig. 6).

The distribution of CO_2 emissions in Table 4 reflects these regional differences and also the emission intensities of the processes. Thus, the top countries in the table are those with high energy costs and therefore incentives to operate highly efficient, integrated plants and those that use lighter "cleaner" feedstocks.

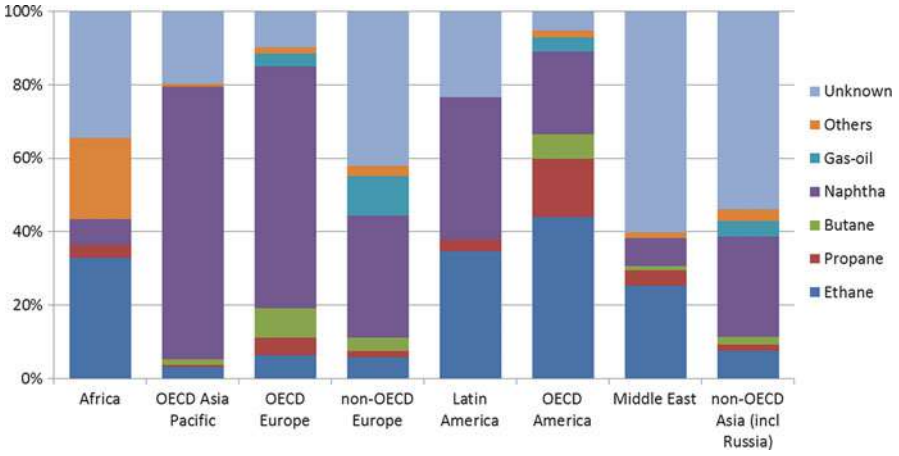

Fig. 6 Ethylene plants by feedstock and region (Oil and Gas Journal 2014)

Table 4 Total CO_2 emissions from national chemical industries, in reverse order of their estimated emissions intensity (IEA 2007)

Country	Million tons of CO_2 per year in 2004 (Mt CO_2/year)
Netherlands	22.7
Saudi Arabia	53.1
Japan	120.1
United Kingdom	19.4
France	24.3
India	51.0
Germany	46.8
Italy	10.1
United States	275.0
Brazil	13.6
China	51.0
Chinese Taipei	13.4

Future Trends in Geographical Variations

The main influences on GHG emissions from the organic chemical industry are feedstock costs and climate change regulation.

The high oil prices experienced in 2007–2008 gave an indication of how the industry could develop if investment decisions are made in the belief that oil supplies will be tight in the next decades. Middle East producers of olefins from ethane were the most advantaged under these conditions due to the low cost of both feedstock and manufacture from this feedstock. European naphtha-based crackers became the marginal producers and were able to continue operation only due to continued

integration with local refineries. However, prices of both naphtha feedstock and process energy increased sharply for these producers and caused a delayed downturn in demand. This was compounded by the greater damage done to demand for petrochemicals by the credit crunch and ensuing global recession.

Long-term increases in oil prices would be likely to cause a marked shift in basic petrochemical production to locations where light crude oil is plentiful, especially Saudi Arabia and the Middle East. Although the use of LPG as a basic feedstock is accompanied by lower CO_2 emissions, the increasing exploitation of LPG as a chemical feedstock in affluent oil-producing nations means that the carbon intensity of olefin production has decreased; this is more than offset by the rise in production and the use of heavier feedstocks elsewhere in the industry.

Nevertheless the nature of the industry is such that minimizing energy costs (for feedstock, heat, steam, and power) is a major factor in plant design worldwide. The development of shale gas in the United States has led to renewed investment in the nation's chemical sector. Through exploitation of relatively cheap shale gas, US organic chemical companies have been able to compete internationally for capital and markets. European companies, meanwhile, may find it necessary to return to a level of vertical integration that allows them to absorb price volatility in the value chain and focus on high-value-added products. Large plants and multinational companies have always been the status quo in the petrochemical industry, and this is not foreseen to change.

Another outcome of the oil price spike in 2007–2008 was the growth in interest in coal and biomass feedstocks. Coal has most interest in China, the United States, Australia, and South Africa for reasons of indigenous supplies and technological expertise. However, it must be noted that increased use of coal as a feedstock for ammonia and methanol production would lead to higher CO_2 emissions.

Overall, an eastward shift in chemical production appears to be an inescapable trend for the near future. Aside from raw materials costs, this relates to lower capital and operating costs in China, India, and Brazil, less costly regulatory environments, and the higher rates of demand growth in these regions. In the OECD, the main markets for bulk chemical products are largely saturated. Investment in new capacity in Europe is likely to continue to focus on speciality products and infrastructure considered to be of strategic importance.

Chemical plants in regions subject to GHG emission regulations have a very strong incentive to implement mitigation technologies. Although the timetable is unclear, there is a broad expectation that GHG emissions will be costly for chemical producers in most regions of the world in the coming decades. Investments today will therefore consider measures such as extensive heat integration and CHP as competitive advantages, as well as the use of biomass to provide a proportion of the heat and power requirements of a chemical site, perhaps through co-firing.

Another macroeconomic trend with possible impacts on the petrochemical industry's emission intensity is that of changes to refinery output. Modern refineries are capable of adjusting their output to meet demand by cracking and upgrading the different distillation fractions to meet fuel requirements. For example, heavier fractions can be cracked and reformed to produce more high-octane gasoline. As a

consequence, because of the high levels of integration between the fuels and chemical industries, changes in the – much larger by volume – fuel industry could impact on the fractions of crude oil that is available for chemical feedstocks. In the near-to-medium term, most of these changes to the current balance of products would most probably lead to a larger amount of processing in order to continue to supply the existing infrastructure. More processing generally indicates more CO_2. Plausible changes in refinery configurations could result from, among other things, a global trend toward diesel-powered cars; the emergence of a highly competitive market for LPG fuel; a substantial increase in the proportion of electric, hybrid, and biofuel-powered cars worldwide; and a trend toward "heavier" crude oils. This last change appears unavoidable: oil sands, coal-to-liquids, and other unconventional and difficult-to-access sources of liquid fuels will be needed to replace the depleted supplies of conventional light crude oil. Moreover, if demand continues to increase, these unconventional fuels will become increasingly cost competitive (assuming no carbon price). It should be borne in mind, however, that complex industries that have evolved together over many decades will only reorient their supply chains to radically new technologies on the scale of decades, as the inertia in the infrastructure is very great.

It is worth considering these future trends as they could all impact negatively on the ease with which the organic chemical industry can mitigate its impact on the climate. In the next section on mitigation options, the main focus will be on long-term options that offer serious emission cuts. Incremental efficiency improvements will also have a role to play, but they may be insufficient to offset trends that lead to higher emission intensities.

Implications of and Response to Climate Change

The previous parts of this chapter have described the extent to which the petrochemical industry is closely integrated with fossil resources. This section looks specifically at the climate mitigation options that have the potential to increase the sustainability of the chemical industry.

It must be acknowledged that the most obvious route would be to reduce consumption of petrochemical products or at least to slow the rate of growth. This would benefit both resource sustainability and climate mitigation impacts. However, the continued rate of growth in demand for chemicals, fibers, and plastics in particular appears unlikely to slow in the near future: indeed it has been suggested that it would only plateau once average wealth is in excess of USD 15,000 per capita, which is a long way from the current global economic reality (Andre et al. 2014). In addition, if reduced production were enforced, it may withhold many of the lifecycle benefits associated with use of some petrochemical-derived products. The transition to a climate conscious regime will require the technical qualities of specialist plastics, lightweight carbon fiber structures, and a multitude of other petrochemical products. Chemical products can thus contribute to GHG savings in downstream markets, something that demands a life cycle approach to understanding costs and

benefits. However, this section assumes that the products of the petrochemical industry will continue to be produced globally on a similar scale today to meet the material demands of a modern society with a growing population, and therefore, its emissions from chemicals manufacture will require attention.

The second most impactful route would be to decarbonize the electricity supply and electrify existing chemical processes. However, the challenges of moving domestic electricity networks to renewable energy have proven considerable, even without expanding electricity demand to include vehicular transport and industrial manufacturing. Nevertheless, even if it is unlikely that the fossil fuel-dependent petrochemical industry will shift to low-carbon electricity for heat and power in the near future, there will be many instances where installing local renewable energy sources to power certain processes may be economic. The extent of this switch will depend on local conditions and available government support.

However, there are a number of impactful technical measures that the chemical industry can take to reduce its emissions. This section considers a number of routes for the chemical industry to adjust moving forward: efficiency gains, focusing on combined heat and power (CHP), plastics recycling, carbon capture and storage (CCS), and feedstock switching, which focuses on the concept of the biorefinery. Each of these options and technologies has their own merits and opportunities, and they can complement one another. Indeed, a carbon-conscious future is likely to see the implementation of several of these technologies together.

Efficiency Gains and CHP

Efficiency Gains

Efficiency gains in energy and resource consumption can both reduce climate impact and costs for the petrochemical industry, as it both mitigates the economic impacts of climate regulation and reduces vulnerability to volatile fossil resource prices. These two drivers have been effective in provoking significant improvements in energy and resource efficiency within the petrochemical industry, and there is a long track record of such improvement.

High efficiency is a natural pursuit of any business that is highly exposed to the cost of energy, and consequently many of the key industrial processes in the chemical industry have improved their performance year on year. The oil price shocks of the 1970s offered a notable impetus to this efficiency focus: while early naphtha crackers consumed approximately 38 GJ per ton of ethylene produced, the 1970s saw extensive process redesign, which lowered the energy requirements by 40–50 % (Gielen et al. 2006). Today, furnace and product separation at new plants operate at around 18–25 GJ per ton as a norm. Continued improvements have been seen and are most apparent in Europe, where the energy efficiency of steam crackers improved by 10 % between 1999 and 2003 alone, with improvement in North America of just 3 % during the same time period. This stems in large part from the differential pressures from using imported naphtha in Europe, where other regions utilize local LPG resources which require less furnace and separation energy in

cracking. In the future, the battle for efficiency is likely to be due to both the costs of GHG emissions and energy.

There remain improvements that could be made to crackers in developed and developing countries alike. Higher-temperature furnaces, gas turbine integration, advanced distillation columns, and combined refrigeration plants are possibilities that have been identified as potentially leading to savings of up to 3 GJ per ton of ethylene. Other options, such as fluidized catalytic crackers (FCC) and new deep catalytic cracking processes, have milder temperature and separation requirements, although they are limited either by feedstock availability – FFC generally uses refinery gases – or by the impact on other integrated processes. For instance, deep catalytic cracking yields are generally achieved at the expense of gasoline yields. With rapid growth in production capacity occurring in areas heavily dependent on naphtha feedstocks, reduction of the energy intensity of the steam cracking process in particular (steam cracking currently accounts for 30 % of all chemical industry energy consumption (Ren and Patel 2009) will be necessary to reduce GHG emissions, potentially contributing a 143 Mt CO_2 equivalent saving, and research is ongoing into catalytic cracking approaches.

Efficiency improvements can offer the major petrochemical firms an important competitive edge, as well as leading to GHG savings, and they are expected to be realized wherever they are profitable. Where there is a shift to lower-cost regions of production, the savings may be realized faster than the expected 30-year infrastructure replacement cycle. After all, many of the plants built in the Middle East and Asia are made to cutting-edge designs, for example, the methyl methacrylate plant commissioned in 2008 by British firm Lucite in Singapore.[2]

Overall, improvements to the environmental performance of existing processes are encapsulated by the 12 principles of Green Chemistry (Table 5). Green chemistry is an approach to chemical production that stresses the environmental impacts of all process steps and encourages a holistic view of all processes, inputs, and outputs. It encourages industrial producers to use processes that meet as many of the 12 aims as possible, with "increase energy efficiency" as principle 9. The Presidential Green Chemistry Challenge Awards have been awarded annually since 1996 by the American Chemical Society, supported by the US Environmental Protection Agency (EPA). In 2009, the Greener Synthetic Pathways Award was won by Eastman Chemical Company for a novel route to the production of esters. The old process used strong acid catalysts at high temperatures; using enzymes eliminates the need for harsh conditions and thus significantly reduces energy use. It reduces the overall requirements for feedstock and solvents. It is also a cheaper process, which was only made possible by taking a holistic approach to the industrial process.

The European Chemical Industry Council (Cefic) considers that energy efficiency improvements will continue to contribute the greatest GHG reductions from the chemical industry (Cefic 2013). As an industry body, they also note that unlike other options, such an approach would reduce the costs of the industry in the near term,

[2]Lucite was subsequently subject to acquisition by Mitsubishi of Japan.

Table 5 The 12 principles of green chemistry (Anastas and Warner 1998)

1	Prevent waste
2	Design safer chemicals and products
3	Design less-hazardous chemical syntheses
4	Use renewable feedstocks
5	Use catalysts, not stoichiometric reagents
6	Avoid chemical derivatives
7	Maximize atom economy
8	Use safer solvents and reaction conditions
9	Increase energy efficiency
10	Design chemicals and products to degrade after use
11	Analyze in real time to prevent pollution
12	Minimize the potential for accidents

making it particularly appealing for the European context where recent years have seen stiff competition from production in regions where energy costs are much lower. This is also highly promising in terms of climate mitigation: implementation of best practice and best available technologies, in particular – increased development and use of catalysts – could reduce energy intensity for key products by up to 40 % by 2050, saving around 1,000 $MtCO_2$ equivalent per year in 2050, as compared to a "business-as-usual" scenario (IEA 2013a). This is particularly important in European and North American plants, where the majority of apparatus was designed and built more than two decades ago and efficiency is often considerably lower than plants built more recently (Benchaita 2013). However, currently available technologies can only go so far, and to achieve deeper energy and emission cuts, larger technological changes will also be needed.

Combined Heat and Power (CHP)

At present, there still remain efficiency gains that have not yet been realized (Fig. 7). As well as implementation of best practice technology and process intensification, CHP is particularly important to consider across all regions due to the massive demand for process heat in the chemical industry. Because heat is a low-grade energy product, its dedicated production can be considered to be a low-value use of resources anywhere where it could be recovered from other processes that generate excess heat, e.g., the production of electricity or even chemicals themselves.

Thus, by making use of the "waste" heat produced as steam in electricity production, CHP increases the overall efficiency of a power plant. A petrochemical facility has a high demand for both power and high-temperature steam, for processes such as steam cracking.

Industry is already one of the largest users of CHP. In 2011, industrial CHP facilities generated 26 % total global electricity generation from CHP (IEA 2014c). In the United States, 23 of the total 82 GW of installed CHP capacity was in the chemical sector in 2013, with estimates suggesting a technical potential for a further

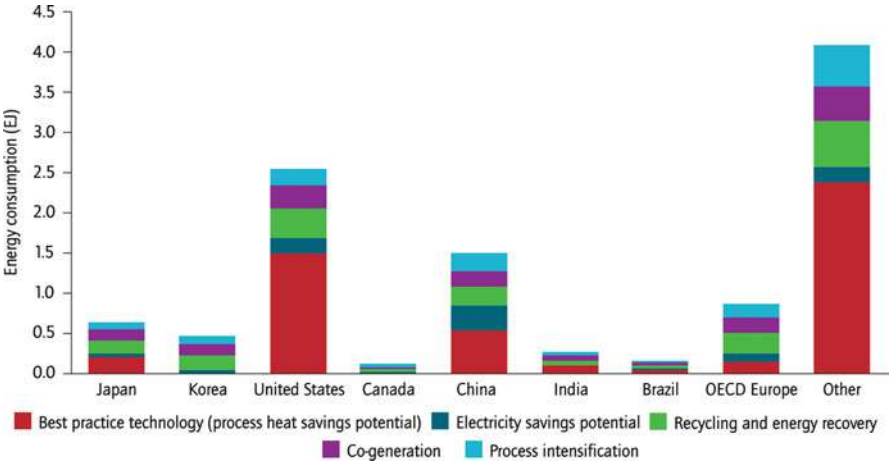

Fig. 7 Energy efficiency potential in the chemical and petrochemical industry (IEA 2013a)

25 GW capacity in chemical production alone (Gowrishankar et al. 2013). The EU meanwhile has specifically incorporated cogeneration into its energy policy through the CHP Directive and the Energy Efficiency Directive. Numerous refineries and chemicals sites have already installed CHP systems – including Immingham in the UK (1,240 MW), which is one of the largest CHP installations in Europe and operates with approximately 70 % thermally efficiency.

CHP is a technology that could be applied at nearly all chemical sites worldwide and could realize considerable GHG emission savings. It has the advantage of being possible to retrofit without redesigning and investing in new process infrastructure, unlike the huge theoretical energy savings that are actually distributed among many different process improvements. GHG emissions can be reduced still further by using sustainably produced biomass fuel. Two challenges face the expansion of CHP for the organic chemical industry, however. Firstly, the technology needs to become more economically viable at smaller scales than it is at present (e.g., below 50 MW). Secondly, policies for supporting renewable energy need to be aligned with those for CHP to incentivize the use of biomass with CHP and realize the maximum benefit from this technology.

Recycling and Waste Management

Another aspect of resource sustainability that must be considered is that of waste management and recycling. Waste management is important for managing the environmental impact of organic chemical products at the end of their life, including the GHG emissions. As well as a solution to the waste management problem, recycling also has major benefits in terms of reducing the need for fossil raw materials.

Taking plastics as an example, global production of plastics was around 288 million metric tons in 2012, of which only around 10 % was recycled. There are large geographical variations in recycling rates, however, and in the United States, Japan, and Europe, the proportion is much higher than this. In addition, post-consumer plastic waste is also increasingly being incinerated for energy recovery. Most plastics have relatively high energy contents, comparable to other hydrocarbon energy sources. Polypropylene, for example, contains 46 MJ per kg, which is equivalent to that of kerosene. On average household-mixed plastic waste contains around 32 MJ per kg, which is favorable compared to coal (approximately 25 MJ per kg). Hence, energy recovery from plastics can partially substitute fossil fuels in heat or power production, offering a sizable, secure, and competitive energy source. If even half of the global waste plastic resource was used for energy recovery, this would be a significant resource. With landfill taxes being employed in many countries for reasons of space constraints and waste management, this resource is increasingly attractive.

The climate story around energy recovery is slightly different. As mentioned earlier, the use of fossil fuels as plastics feedstocks effectively locks up the carbon, which breaks down only very slowly in landfills. (It should be noted that where it does break down, it may yield methane, a much more potent GHG, although this can be partially dealt with by landfill gas collection for energy use.) Use of plastics as an energy source creates CO_2 emissions that can be considered as deriving from fossil carbon. If this displaces coal combustion, then the climate benefit would be small but useful. If it replaces natural gas combustion, then the climate impact would be unfavorable. Therefore, while energy recovery is attractive in terms of conservation of fossil fuels, it is unlikely to be attractive for reduction of GHG emissions. Recycling, on the other hand, offers both energy security and climate benefits.

Reducing the amount of fossil (or bio-based) feedstock necessary for chemical production can have a positive effect on the available energy supplies. Perhaps, more importantly, recycling can reduce the energy demand, and therefore the GHG emissions, of plastic manufacture by about 0.6 t of CO_2 equivalent per ton of plastic recycled compared to landfilling (Wrap 2010). Maximizing recycling is therefore a vital tool in the pursuit of sustainability in the chemical industry from economic, social, and environmental perspectives.

To conclude this short overview of recycling, it is necessary to briefly distinguish between thermoplastic recycling and so-called feedstock recycling. Thermoplastics are polymers that become liquid when heated and can be reset as plastics when cooled and put to a new use, and most recycling today is thermoplastic recycling. Meanwhile feedstock recycling generally refers to the use of plastic waste as a raw material for thermochemical conversion to new feedstocks. This can either be achieved by pyrolysis to liquid fuel or, as is more usually promoted, by gasification to syngas and then use in similar chemical processes to those fed by natural gas or coal; this could be, for instance, production of ammonia, liquid fuels, methanol, Fischer–Tropsch olefins, or dimethyl ether. Because feedstock recycling to chemicals requires energy-intensive conversion of the plastic waste to syngas, it offers a solution primarily to the problem of resource sustainability, but is less

favorable as a climate mitigation tool. It may only yield GHG emission reductions when compared to coal gasification processes or if it provides exceptional savings in downstream uses of the resulting products.

However, one potential advantage of feedstock recycling is the hydrogen-rich syngas produced in comparison to that from coal. This could be advantageous in the future in which syngas is widely used for production of hydrogen, fuel, or chemicals, suggesting a possible role for "co-gasification" of plastic, coal, and biomass.

Carbon Capture and Storage (CCS)

CCS offers the unique ability to separate fossil fuel use from climate harm. By capturing CO_2 at source, transporting it, and sequestering securely underground, it could be a powerful tool in the fight against climate change. Without CCS, few climate scenarios are able to achieve the carbon reduction targets compliant with 2 °C warming, and the latest IPCC projections assume CCS to contribute a sixth of the CO_2 emission reductions required by 2050 (IPCC 2013). While other chapters of this book consider the technical details and policy context of CCS in more detail, this section explores the applicability and potential importance of CCS for the chemical industry.

CCS is really a collection of technologies rather than a single procedure. At each stage of the process, there are several technological options: CO_2 separation can take place pre-combustion, post-combustion, or via oxy-fuel combustion; transport can occur through pipelines or potentially through shipping; and there are a range of geological storage options, including depleted fossil fuel reservoirs, saline aquifers, and even coal seams. The different choices of technology will depend on the particular context. Post-combustion capture can be retrofitted to existing industrial facilities or power stations, whereas integrating pre-combustion capture can increase the efficiency of the overall process. Similarly, the captured CO_2 can be stored locally if a suitable aquifer or depleted hydrocarbon reservoir is nearby, or it can be piped (or potentially shipped) offshore for underground injection.

Each of the individual technological components is well demonstrated. CO_2 capture from flue gases was first commercialized in the 1970s for sale of CO_2 to the chemical and food industries, and for decades CO_2 has been transported over many hundreds of kilometers by the American oil industry for the purposes of enhanced oil or gas recovery (EOR/EGR). On the storage side, plants such as Sleipner in the North Sea have seen over a million tons of CO_2 per year stored since 1996.

However, the full chain of CCS, with capture from industry or the power sector, and geological storage with monitoring to verify storage permanence has never been integrated at a commercial scale. This is primarily due to the absence of markets that can absorb the capital costs. CCS plants generally have costs in the range of hundreds of millions, or even a billion, of dollars. In addition, the cost of investment in pipeline infrastructure, upfront storage identification, and long-term monitoring and verification to satisfy untested regulatory procedures all add upfront financial risks.

A strong business case is needed for CCS implementation, which in the longer term may be based on strong climate policy, but in the early stages has been dependent on the use of CCS for EOR/EGR.[3] At present, the majority of operational large-scale CO_2 capture plants use the captured CO_2 for enhanced oil or gas recovery (EOR/EGR), which has been a driver of technology development for CCS. Where these sites are able to demonstrably store CO_2 permanently and not raise overall oil and gas demand, they could also demonstrate CO_2 emission reductions.

CCS is often discussed in terms of its ability to decarbonize the power sector. However, dependent on the pace of climate policy development, the roll out of CCS in the power sector has been slow: with the first large-scale-integrated CCS project in the power sector only coming online in October 2014 (Boundary Dam, Canada). However, CCS is also particularly relevant for non-power applications such as gas processing, refining, cement and steel industries, and, in particular, chemical production.

The production of hydrogen, methanol, and ammonia offer significant promise for reduction of CO_2 via CCS. Many of these industrial applications generate CO_2 streams with higher purity than are seen from the power sector, and so could offer lower-cost abatement options. Capture from natural gas processing is already used in large-scale commercial projects, such as Sleipner in Norway and the upcoming Gorgon plant in Western Australia. Production of chemicals such as ammonia, hydrogen, methanol, and coal-to-chemicals has also been used to source CO_2. The Air Products Port Arthur project in the United States has captured CO_2 from hydrogen production since 2013, as will the Quest project in Canada, due to commence operation in 2015. These projects demonstrate the cost competitiveness of CO_2 capture from chemical processes and are together gradually building a base of demonstration projects from which future projects will learn.

Where coal is used a chemical feedstock, CCS offers relatively low-cost mitigation options to avoid emissions from highly carbon-intensive processes. Coal gasification to syngas is usually followed by separation of hydrogen and carbon monoxide (syngas) from carbon dioxide as a normal part of the process. This is a similar principle to integrated gasification-combined cycle (IGCC) power plants, which can be integrated with hydrogen production. Syngas is already widely used in the chemical industry. Integration of CCS with industrial syngas "hubs" could enable these alternative feedstocks to be utilized in a manner that is compatible with a low-carbon economy. With a strong carbon price or climate regulation, syngas, electricity, hydrogen, and CO_2 could all have value in a single, large industrial site similar to those that have been proposed in China (Fig. 7) (Fig. 8).

[3]It may seem incongruous that CCS, a climate change mitigation technology, be used to enhance the production of oil, yet while CCS passes through its technology development stages, this link with oil revenue can reduce the cost of project financing, a cost that otherwise often falls on the public purse. This use of CCS for EOR/EGR, combined with increasing climate change awareness have driven CO_2 capture technology toward reducing costs, potentially allowing application in larger (and lower margin) markets.

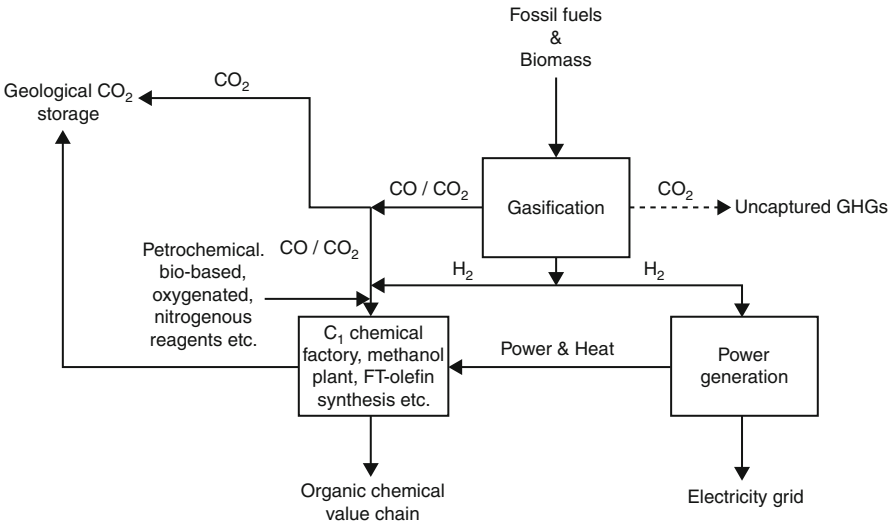

Fig. 8 Schematic representation of a gasification-based chemical complex with CCS

For some highly emitting processes, such as coal-to-chemical production, CCS may offer the only route to continue operation in a carbon-constrained future. However, for most petrochemical sites, the marginal costs of capture from all CO_2 sources will be similar to the power sector, and the smaller source sizes from the chemical industry (often less than 1MtCO_2 per year) mean that integrating transport and storage could be more complex and not benefit from economies of scale. Coordination with other emitters will help overcome this challenge through the development of industrial CCS hubs or clusters. CCS could this be well suited to the chemical industry. GHG emissions from petrochemical manufacture tend to be concentrated upstream in coastal areas of heavy industry, refining, and oil and gas production. These factors offer potential for linking emission sources together and accessing suitable offshore, or onshore, storage sites.

The White Rose CCS project in Yorkshire, UK, has been proposed as part of such a configuration. The proposed plant will capture CO_2 from a 426 MW coal power plant, with the concurrent construction of the "Yorkshire Humber CCS Trunkline," an oversized transportation system that will be able to accommodate local industrial emissions at a later date. This will then enable the next, much larger, tranche of CCS plants to plug into the already existing pipeline networks and utilize the same storage sites. This will greatly reduce costs. However, it should be noted that government intervention may be vital here to coordinate the development of such industrial hubs or clusters.

Above all, the chemical industry is particularly vulnerable to the pressures of international trade. Unlike the power sector, it does not have captive domestic markets: trade of chemicals and goods is global and increased costs from CCS will

disadvantage chemical industrial producers. This trade exposure of the chemical industry makes the costs of deep decarbonization highly risky and unattractive (ZEP 2013). Charting a policy course in this area will be extremely challenging, and certainly in the near term, carbon pricing is unlikely to be sufficient to facilitate this. In the absence of a global CO_2 price, asymmetric carbon pricing between regions will be compensated for by mechanisms such as free allowances that can reduce a sector's incentive to mitigate (Bennett and Heidug 2015).

Captured CO_2 from flue gases in the chemicals and power sectors has been used for chemical production since the late 1970s, primarily for soda ash and urea manufacture. Recycling CO_2 within the chemical industry could potentially reduce emissions and generate economic value.[4] Unfortunately, these remain limited. Due to the strength of the chemical bonds in CO_2 molecules, it often requires more energy and generates more CO_2 to convert a quantity of CO_2 into useful products than can be saved, even if the energy is derived from renewable energy (Ademe 2014; Bennett et al. 2015). Research into lower energy routes and potential uses of CO_2 remains an active area. Furthermore, to help mitigate climate change, potential uses of CO_2 will need to demonstrate a life cycle benefit compared to other value chains. CO_2 locked up in products can in some cases act as a carbon store, but incineration or decomposition of the products will release CO_2 at the end of life. If uses can be found whose life cycles can demonstrably prevent the emission of significant volumes of CO_2, both upstream and downstream, then chemical utilization of CO_2 may yet have a role to play in climate change mitigation.

Realizing widespread CCS requires governments and companies to develop shared visions of how the future chemical industry might look in a carbon-constrained world. The IEA has indicated that 18.5 Mt per year of CO_2, or 11 % of all captured CO_2, could be from the chemical industry in 2020 as part of a lowest-cost path to stabilizing CO_2 levels at 450 ppm. Plants capturing CO_2 from sources such as ammonia and fertilizer production offer near-term, low-cost opportunities. At present, climate policies do appear likely to be strong enough to support such a rollout of CCS this decade, and its future post-2020 will depend not only on climate policy but also any public opposition to CCS. Public opposition has already been observed in Europe where CCS has been connected to coal use in the power sector.

This chapter has mentioned numerous technologies that can partly address the fossil fuel dependency and climate impact of the global organic chemical industry. CCS on its own can do very little about the former, but could be a very potent weapon against the latter.

[4] CO_2 is today used in the agriculture industry to enhance crop growth and in the food industry to carbonate drinks and decaffeinate coffee (among other uses), but these also suffer from short-term net storage and limited markets.

Biorefineries

As described earlier in this chapter, the coevolutionary history of the organic chemical industry and the petroleum fuels industry has led to a highly integrated modern production system. While the majority of each barrel of oil is used for fuel, certain fractions are used to make higher-value chemicals such as plastics, thereby contributing to the economic advantage of oil in the energy mix. Worldwide there are only about 700 oil refineries, but their products underpin almost every aspect of modern society, and their integrated business models continue to dominate the fuel and chemicals sector. Indeed the synergies of this by-product relationship make it more difficult for either sector – fuels or chemicals – to individually make the switch to alternative, cleaner resources. However, there is an emerging alternative, based on the same refinery model, but with a renewable resource for fuel and feedstock: the biorefinery. This concept aims to maximize biomass raw material utilization and potentially offers a way to harness integration as a means of improving cost-effectiveness.

The term "biorefinery" covers a wide range of concepts, with various combinations of potential feedstocks, processes, and end products that can be targeted by an individual system. There is not a clear definition of a biorefinery, but it is generally considered to include the processing of various biomass sources to produce a "spectrum" of products, such as value-added chemicals, fuels, and agricultural products (Peck et al. 2009; Koutinas et al. 2007), just as a petrochemical refinery yields different fractions for different purposes. By also utilizing renewable biomass energy to power its chemical and biochemical processes, a biorefinery can reduce the overall consumption of fossil fuels and GHG emissions in the production of organic chemicals. Feedstocks range from cane or beet sugars, to oilseeds, to lignocellulosic materials from woods and grasses. An olive factory in Spain is even pursuing the route of chemical production from olive stones, to make the most of the available resource. Conversion technologies meanwhile can be thermal (such as gasification), chemical catalytic (including Fischer–Tropsch synthesis), enzymatic, or biochemical fermentation. The relatively low energy density of biomass means that large volumes are needed, and this can increase the costs of chemical processing significantly.

As with a petroleum refinery, the composition of the feedstock will determine the products and process routes to an extent, but adjustments to the chemical processing can target different production routes. This can add resilience to the system, by providing the flexibility to respond to feedstock changes and market signals.

Many biorefineries produce both lower-value bulk fuels and platform chemicals in combination with some higher value speciality chemicals. Platform petrochemicals are the olefins and aromatic BTX (benzene, toluene, and xylenes) that form the basic building blocks for most derivative chemicals in all organic chemical market segments. One approach for a biorefinery is to simply replicate these with bio-based products. For example, ethylene from bioethanol is chemically identical to that from fossil feedstocks, and its production is already economically competitive with ethylene from conventional routes. However, while Braskem produces 200,000 t ethylene each year from cheap Brazilian cane sugar-based ethanol (Braskem 2007),

and bio-ethylene capacity in India is rapidly expanding, overall bio-ethylene still only accounts for about 0.3 % of total global ethylene capacity (IRENA 2013). The disadvantage of producing bulk platform chemicals is the immediate exposure to competition with established fossil fuel routes. However, as consumers become increasingly interested in the environmental credentials of their goods, a market niche for bio-based platform chemicals is beginning to emerge. Companies such as Coca-Cola are seeking to source bio-ethylene for their product bottles, and long-term contracts on a multinational scale could help develop the competitiveness of this industry. Already, DuPont commercially produces 1,3-PDO from corn feedstock, and myriad routes to other platform chemicals are being widely explored.

There is also particular interest in the development of aromatic platform chemicals from lignocellulosic feedstocks, which could potentially be used to complement the development of chemicals from shorter-chain shale gas (Chemweek 2014; Golden and Handfield 2014). Global demand for aromatics is increasing by 5–10 % each year, and while the old joke that lignin can be used "to make anything but money" still has some truth, developments in lignocellulose enzyme technology (Teter et al. 2014) suggest that it may yet become a valuable source of aromatic platform chemicals. 2013 saw the opening of the largest cellulosic ethanol project in the world in Crescentino, Italy. Using local straw residues, this plant will produce up to 40,000 MT of ethanol per year and potentially marks a step change in the lignocellulosic material use. Indeed, plans have already been announced for a similar plant in Fuyang, China, which will target a capacity four times this size by the end of 2015.

However, not all bio-based platform chemicals are able to replace their fossil counterparts so easily. Biomass-derived platform chemicals tend to be more oxygenated than their petrochemical counterparts, and thus require more processing to yield materials of equal performance. In addition to the increased climate impact associated with more processing, this can lead to greater complexity in developing product lines for their derivatives, and overall leads to cost increases and lower competitively.

An alternative approach is for biorefineries to target new products, which could be accessed more directly from the complex molecules present in biomass. This strategy is often adopted by smaller chemical firms, keen to exploit the market insulation afforded by occupying a "green" product niche. Bioplastics and in particular biodegradable polymers are good examples of this (Harmsen and Hackmann 2013). The bioplastic polylactic acid (PLA) was discovered more than 80 years ago, but even though it has only been produced commercially since 2002, it is currently the most common bioplastic in use. PLA is used for medical implants and compostable mulch films for agriculture, and as research improves the ability to tailor the rate of biodegradability, it is increasingly being used for a broad portfolio of packaging applications. One of the things people generally find convenient about plastics is that they do not degrade during the time that people are actively using them, and accommodating these properties has been a challenge for some bio-based routes.

As with CO_2 utilization, calculation of the environmental impact of biorefineries is rather more complicated than simply subtracting the emissions of a comparative fossil fuel product. Where biomass is cultivated for a biorefinery (e.g., as opposed to agricultural waste), significant land use change will occur. Agriculture is a major emitter of GHGs, with high energy demand associated with fertilizer production, irrigation, and crop transportation. It is vital to conduct a full life cycle analyses for each new biorefinery configuration in order to ensure that there is a net environmental gain associated with the production route. Otherwise, while development of biorefineries can improve resource security, the climate impact can potentially be worse than fossil fuel production routes, and local environmental impacts (such as local biodiversity) can create negative impacts on a large scale. PLA is a case in point: while LCAs confirm that there is a net environmental gain from this production route, much of the carbon reduction relative to fossil fuel analogues is in fact offset by the energy intensity of the corn feedstock cultivation. Due to high capital costs and risk associated with the early stage of technological development, biorefineries are likely to require public financial support as the industry develops. It will therefore be important to consider the full LCA and target those concepts that can deliver the greatest carbon reduction overall.

There are also important scaling issues that need to be considered. Biomass offers the potential to replace both fossil fuels and petrochemicals with low-carbon, renewable alternatives, but the scale at which this can be achieved must be approached with caution. Biomass material is less carbon dense than oil or coal and requires both space and time to grow. While estimates for the size of the total resource volume vary (Slade et al. 2011), replenishment of the resource is unlikely to be able to match the rate at which mankind has been able to produce petroleum during the last 50 years, unless yields can be improved dramatically. In current circumstances, however, cultivation of biomass for biorefineries is highly likely to compete with forestry and other uses of agricultural land. The "food-versus-fuel" debate that has emerged from this prospect has led bodies such as the European Commission to revise subsidy regimes and research objectives such that they now overwhelmingly focus on second- and third-generation biorefinery concepts, which use biomass feedstocks such as forest residue or food waste and do not directly compete with food production. While in depth analyses by Ecofys, among others (Hamelinck 2013), indicate that increased biofuel production need not impact on food security (and the lower production volumes of the chemical industry mean that biofuels for chemicals will have even less impact), the debate remains controversial and will influence policy and exclude some options.

In summary, it is clear that while many of the products may be the same, biorefining is a different prospect to oil refining. Oil refineries are based on a fixed set of principles and a relatively fixed set of hydrocarbon distillation products. Biorefineries, because of the diversity of designs, raw materials, products, and scales will not be able to benefit from "by-product" relationships to the same extent. Thus, it may take a lot longer to approach the kind of standardized biorefinery designs that can be licensed and propagated worldwide.

The climate mitigation benefits of biorefining will be determined by individual biorefinery configurations and could potentially be improved by innovations in industrial arrangements. These could perhaps include gasification processes or localized processing of biomass before shipping the lighter, more valuable components for further processing; however, these opportunities will only become known as the industry develops. In any case, continued research into the effects of land use changes and the overall biorefinery LCA will be crucial to securing the optimum climate benefit. Limitations around feedstock production and techno-economic viability are likely to limit the rate at which the industry can grow. The technological development needed combined with the land use requirements mean that this industry will not radically arrive in a fully developed form. Biorefineries are beginning to emerge where there are feedstock opportunities or market niches that can be monetized, but the scale of biomaterials production remains extremely low. Long-term visions of a "bioeconomy" where biorefineries supply all consumer chemicals in all their forms are still a long way off. While mandates and policy support encourage production of biofuels worldwide, there is no similar subsidy for biomaterials. Without financial support, early applications will rely on one off subsidies and downstream demand for green products. Though this demand is observed at present, the historical overview of the petrochemical industry offered in this chapter clearly shows that current attitudes are not always indicative of future trends.

Future Directions

This chapter has sought to introduce the organic chemical industry as a highly energy-dependent sector of the economy. Presently, the industry is dominated by petrochemicals and a manufacturing system that is almost entirely reliant on fossil fuels, especially oil, for both raw materials and large amounts of process energy. This situation can be understood as the consequence of almost 80 years of "coevolution" of organic chemical production with liquid fuel production, based around the oil refinery and the platform chemicals that are produced in the refining process. This process of close integration was especially pronounced during the periods of very rapid expansion during the 1950s and 1960s in Europe and North America. It has bequeathed a network of petrochemical clusters that feed the world's manufacture of plastics, synthetic fibers, solvents, lubricants, medical products, and cosmetics. The efficiency of large-scale, integrated production continues to drive growth and innovation among the small number of multinational firms. As a result, this pattern of fossil fuel use, and thus GHG emissions, can be perceived to be somewhat "locked in," making it potentially more difficult for new low-carbon technologies to break into the chemical value chain.

The chemical industry continues to be responsible for 30 % of industrial energy use and about 5 % of global CO_2 emissions. This chapter proposes that to seriously address climate change, GHG emissions from the chemical industry need to be severely reduced and that to do so will require a thorough understanding of the

integration between the oil and chemical industries and the ambiguous nature of fossil carbon storage in chemical products. Truly sustainable solutions will therefore need to address the future trends in petroleum resource availability and overcome the barriers to market entry raised by the economics of the by-product relationship of olefins production and oil refining.

In addition to greatly increased global recycling, three options have been introduced that could have the potential to either "green" the existing production paradigm or disrupt it through radical innovation based on biotechnology. These three technology areas – efficiency savings through CHP, carbon capture and storage, and biorefining – could furthermore be combined to enable long-term organic chemical production that is compatible with deep GHG emission cuts. In addition, demand reduction and green chemistry are clearly identified as vital complements to the introduction of new technologies. However, as the industry moves closer to a world in which its use of carbon is tightly regulated, new tools that are able to account for the full lifecycle impacts of organic chemicals will need to be developed and established as international standards. For instance, there can be environmental benefits to locking up carbon in nondegradable plastics but only if they are not subsequently burned for energy recovery without CCS. Likewise, if biomass resources are limited, then there could be an argument for directing them to where they can have the greatest impact on GHG emission reductions. This calls for a major role for lifecycle assessment or policies that fully integrate carbon prices into the world economy. The challenge appears to be immense and one that requires committed and enduring action from industry and government.

References

Ademe (2014) Valorisation chimique du CO_2: état des lieux. Quantification des bénéfices énergétiques et environnementaux et évaluation économique de trois voies chimiques. Ademe, Angers

Anastas PT, Warner J (1998) Green chemistry: theory and practice. Oxford University Press, London

Andre S, Chan V, Greenberg E (2014) Climbing the curve quickly in petrochemicals, McKinsey Quarterly http://www.mckinsey.com/Insights/Winning_in_Emerging_Markets/Climbing_the_curve_quickly_in_petrochemicals?cid=mckq50-eml-alt-mkq-mck-oth-1410, Accessed 22 Feb 2015

Barteau M, Kota S (2014) Shale gas: a game-changer for U.S. manufacturing? University of Michigan, Michigan

Belt HVD (1987) The Nelson-Winter-Dosi model and synthetic dye chemistry. In: Bijker WE et al (eds) The social construction of technological systems. MIT Press, Cambridge

Benchaita T (2013) Greenhouse gas emissions from new petrochemical plants. Inter-American Development Bank, Washington, DC

Bennett SJ (2008) Greener past years: the history of Biopol. Cleantech Magazine 2(10):20–22

Bennett SJ, Heidug W (2015) CCS for trade-exposed sectors: an evaluation of incentive policies. Energy Procedia (forthcoming)

Bennett SJ, Pearson PJG (2009) From petrochemical complexes to biorefineries? The past and prospective co-evolution of liquid fuels and chemicals production in the UK. Chem Eng Res Des (ChERD) 87(9):1120–1139

Bennett SJ, Schroeder DJ, McCoy ST (2015) Towards a framework for discussing and assessing CO_2 utilisation in a climate context. Energy Procedia (forthcoming)
Bernton H, Kovarik W, Sklar S (1982) The forbidden fuel. Power alcohol in the twentieth century. Boyd Griffin, New York
Bosch P, Kuenen J (2009) Greenhouse gas efficiency of industrial activities in EU and Non-EU. TNO report TNO-034-UT-2009-01420_RPT-ML for the European Commission. TNO, Utrecht
Braskem (2007) Braskem has the first certified green polyethylene in the world. Press release. http://www.braskem.com.br/site/portal_braskem/en/sala_de_imprensa/sala_de_imprensa_detalhes_6062.aspx, Accessed 22 Feb 2015
Cefic (2006) The chemical industry helps to protect the climate. The European Chemical Industry Council, Brussels
Cefic (2013) European chemistry for growth. The European Chemical Industry Council, Brussels
Chemweek (2014) Petrochemicals: Huge midstream investments underpin rebirth of US industry, http://www.chemweek.com/sections/cover_story/59746.html, Accessed 10 September 2014
Croda (2014) Environmental impact http://www.croda.com/home.aspx?s=1&r=79&p=1808 Accessed 22 Feb 2015
CTI (2013) Unburnable carbon 2013: wasted capital and stranded assets. Carbon Tracker Initiative, London
Da Rosa AV (2009) Hydrogen production. In: Fundamentals of renewable energy processes, 2nd edn. Academic, Boston
De Vries HJM, Blok K, Patel M, Weiss M, Joosen S, Visser ED, Sijm J, Wilde HD (2006) Assessment of the interaction between economic and physical growth. Dutch Ministry of the Environment (VROM), The Hague
DOE (2013) Report of the hydrogen production expert panel: a subcommittee of the hydrogen fuel cell technical advisory committee. US Department of Energy, Washington, DC
Dry RJ (1988) Possibilities for the development of large-capacity methanol synthesis reactors for synfuel production. Ind Eng Chem Res 27(4):616–624
EIA (2014a) US Energy Information Administration, International Energy Statistics, 2014 http://www.eia.gov/cfapps/ipdbproject/iedindex3.cfm?tid=5&pid=57&aid=6&cid=ww,&syid=1980&eyid=2014&unit=BB. Accessed 22 Feb 2015
EIA (2014b) US EIA Historical Statistics for 1981–2013. U.S. Energy Information Administration, via: www.tsp-data-portal.org. Accessed 22 Feb 2015
Emetad B, Luciani, J (1991) World energy production, 1800–1985, via: www.tsp-data-portal.org. Accessed 22 Feb 2015
Finlay MR (2004) Old efforts at new uses: a brief history of chemurgy and the American search for biobased materials. J Ind Ecol 7(3–4):33–46
FNR (2014) Bioplastics, Fachagentur Nachwachsende Rohstoffe e.V. (FNR) Agency for Renewable Resources, Gülzow-Prüzen
Gielen D, Bennaceur K, Tam C (2006) IEA petro- chemical scenarios for 2030–2050: energy technology perspectives. International Energy Agency, Paris
Golden JS, Handfield RB (2014) Why biobased? Opportunities in the emerging bioeconomy. US Department of Agriculture, Washington, DC
Gowrishankar V, Angelides C, Druckenmiller H (2013) Combined heat and power systems. NRDC, New York
Hale WJ (1930) When agriculture enters the chemical industry. Ind Eng Chem 22(12):1311–1315
Hamelinck C (2013) Biofuels and food security: risks and opportunities, Utrecht
Harmsen P, Hackmann M (2013) Green building blocks for biobased plastics. Wageningen UR Food & Biobased Research, Wageningen
Hodge J (2000) An overview of the role of producer services in the petrochemicals industry in south Africa: a case study of sasol. Development policy research unit working paper 9686. University of Cape Town, Cape Town
Hodges P (2009) Coping with oil price volatility: chemical companies would be wise to assume that recent oil price volatility will continue in 2009. Chem Ind 2:17–19

Hodges P, Keeley J, Townsend B (2008) Feedstocks for profit. International eChem, London
Hökök M, Söderbergh B, Jakobsson K, Aleklett K (2009) The evolution of giant oil field production behavior. Nat Resource Res 18(1):39–56
Horncastle A, Sastry A, Corrigan J, Branson D (2011) Future of chemicals Part VI: global feedstock developments and implications for GCC players, Booz & co. http://www.strategyand.pwc.com/media/file/Strategyand-Future-of-Chemicals-Global-Feedstock-Developments-Implications-GCC.pdf. Accessed 22 Feb 2015
IEA (2007) Tracking industrial energy efficiency and CO_2 emissions. In support of the G8 plan of action. International Energy Agency, OECD, Paris
IEA (2012) Energy technology perspectives 2012. OECD/IEA, Paris
IEA (2013a) Technology roadmap: energy and GHG reductions in the chemical industry via catalytic processes, International Energy Agency, 2014
IEA (2013b) Key World energy statistics 2013. OECD/IEA, Paris
IEA (2013c) Resources to reserves 2013. OECD/IEA, Paris
IEA (2014a) Energy efficiency indicators: essentials for policy making. OECD/IEA, Paris
IEA (2014b) IEA World energy statistics and balances database. OECD/IEA, Paris
IEA (2014c) Linking heat and electricity systems. OECD/IEA, Paris
IEA (2014d) World energy outlook 2014. OECD/IEA, Paris
IHS (2014) Trends in global exploration: what's happening to conventional oil and gas discoveries? IHS, Colorado
IPCC (2013) Fifth assessment report working group III summary for policymakers. Cambridge University Press, Cambridge, UK
IRENA (2013) Production of bio-ethylene, http://www.irena.org/DocumentDownloads/Publications/IRENA-ETSAP%20Tech%20Brief%20I13%20Production_of_Bio-ethylene.pdf. Accessed 22 Feb 2015
Kalkman J, Keller A (2012) Global petrochemicals – who is really benefitting from the growth in the new world? Roland Berger Strategy Consultants, Germany
Koopmans RJ (2006) R&D challenges for the 21st century. Soft Matter 2(7):537–543
Koutinas AA, Arifeen N, Wang R, Webb C (2007) Cereal-based biorefinery development: integrated enzyme production for cereal flour hydrolysis. Biotechnol Bioeng 97(1):61–72
Levingston S (2006) As the auto age dawned, gasoline wasn't king. Washington Post, August 13 F01
Lewe T, Doerler J, Alberich J, Smith G, Walters N, Kaushal V, Corak T, Gaspar D, Forrest R (2012) Refining 2021: who will be in the game? AT Kearney
Madival S, Auras R, Singh SP, Narayan R (2009) Assessment of the environmental profile of pla, pet and ps clamshell containers using LCA methodology. J Clean Prod 17(13):1183–1194
Mann SA (1966) Feedstocks for the chemical industry. Chemistry in Britain (Jan)
Marshall J (2007) Biorefineries: curing our addiction to oil. New Sci 2611:28–31
Miel R (2014) Lego looking for a sustainable replacement for ABS. Plastics News http://www.plasticsnews.com/article/20140218/NEWS/140219915/lego-looking-for-a-sustainable-replacement-for-abs. Accessed 22 Feb 2015
Morrow NL (1990) The industrial production and use of 1, 3-butadiene. Environ Health Perspect 86:7–8
Murphy RJ, Davis G, Payne M (2008) Life cycle assessment (LCA) of biopolymers for single-use carrier bags. National Non-Food Crops Centre, Imperial College, London
Nguyen P, Saviotti P-P, Trommetter M, Bourgeois B (2005) Variety and the evolution of refinery processing. Ind Corp Change 14(3):469–500
NZIC (1988) The production of methanol and gasoline. In: NZIC (ed) Chemical processes in New Zealand. New Zealand Institute of Chemistry, Christchurch
Ogston AR (1997) A short history of aviation gasoline development. In: SAE (ed) History of aircraft lubricants. SAE, Warrendale
Oil & Gas Journal (2014) International survey of ethylene from steam crackers – 2014. Penwell Corporation, Tulsa

Peck P, Bennett SJ, Lenhart J, Bissett-Amess R, Mozaffarian H (2009) Understanding, acceptance, and support for the biorefinery concept among policy-makers. Biofuels Bioprod Bioref 3 (3):361–383
Platts (2013) The shale revolution and its impacts on aromatics supply, pricing and trade flows, November 2013, Platts Special report, Platts McGraw Hill Financial
Reader WJ (1975) Imperial chemical industries: a history, vol 2 the first quarter-century 1926–1952. Oxford University Press, Oxford
Reader WJ (1977) Imperial chemical industries and the state. In: Supple B (ed) Essays in British business history. Oxford University Press, Oxford
Redwood B (2009) Petroleum: its production and use. BiblioBazaar, Charleston
Ren T, Patel MK (2009) Basic petrochemicals from natural gas, coal and biomass: energy use and CO_2 emissions. Resource Conserv Recycling 53(9):513–528
Slade R, Saunders R, Gross R, Bauen A (2011) Energy from biomass: the size of the global resource. Imperial College Centre for Energy Policy and Technology and UK Energy Research Centre, London
Sorrell S, Speirs J, Bentley R, Brandt A, Miller R (2009) Global oil depletion. An assessment of the evidence for a near-term peak in global oil production. UK Energy Research Centre, London
Speight JG (2012) The chemistry and technology of coal, 3rd edn. Taylor and Francis, Hoboken
Spitz PH (1988) Petrochemicals: the rise of an industry. Wiley, New York
Staudinger H (1936) The formation of high polymers of unsaturated substances. Trans Faraday Soc 32:97–115
Tam C, Gielen DJ (2006) Petrochemical indicators. In: IEA/CEFIC workshop: feedstock substitutes, energy efficient technology and CO_2 reduction for petrochemical products, 12–13 Dec 2006, Paris
Teter SA, Brandon Sutton K, Emme B (2014) Enzyme processes and enzyme development in biorefining. In: Watson KW (ed) Advances in biorefineries, biomass and waste supply chain exploitation. Elsevier, Cambridge, UK
Uihlein A, Ehrenberger S, Schebek L (2008) Utilisation options of renewable resources: a life cycle assessment of selected products. J Clean Prod 16(12):1306–1320
Weir RB (1995) The history of the distillers company 1877–1939. Oxford University Press, New York
Wittcoff HA, Reuben BG (1980) Industrial organic chemicals in perspective. Part 1: raw materials and manufacture. Wiley, New York
Wood DA (2013) A review and outlook for the global LNG trade. J Nat Gas Sci Eng 9:16–27
Wrap (2010) Environmental benefits of recycling – 2010 update. Wrap, London
Xie K, Li W, Zhao W (2010) Coal chemical industry and its sustainable development in china. Energy 35(11):4349–4355
Yang C-J, Jackson RB (2012) China's growing methanol economy and its implications for energy and the environment. Energy Policy 41:878–884
ZEP (2013) CO_2 capture and storage (CCS) in energy-intensive industries. European Technology Platform for Zero Emission Fossil Fuel Power Plants
Zhao R (2013) China coal gets nod for Yulin coal chemicals project, China Coal Resource. http://en.sxcoal.com/86632/NewsShow.html. Accessed 22 Feb 2015

Venture Capital Investment and Trend in Clean Technologies

John C. P. Huang

Contents

J.C.P. Huang (✉)
Focus Capital Group, Cupertino, CA, USA
e-mail: JCHuang99@yahoo.com; jch@focusventure.com

W.-Y. Chen et al. (eds.), *Handbook of Climate Change Mitigation and Adaptation*,
DOI 10.1007/978-3-319-14409-2_11

Abstract

"Cleantech" is being widely used to replace "Green Technology." It describes a group of emerging technologies and industries, based on principles of physics, chemistry, biology, and resource efficiency, new paradigms in energy, and water conservation. The scope of this field includes large-scale infrastructure projects as well as innovative technologies. The term Cleantech is also often associated with venture capital (VC) investment. A goal of this chapter is to provide readers with an overview of the scope and trends in venture capital-funded innovation in Cleantech, where and how to seek VC funding, and Cleantech implications on world climate change.

This chapter addresses the basics of venture capital and the dynamic field of Cleantech. Subjects covered are as follows: **(1) VC investment trend** based on the volume of funds invested and the number of projects funded; **(2) the scope of Cleantech** encompassing renewable energy, energy efficiency, green building, transportation, smart power, smart grid and energy storage, air, water, and waste; **(3) Cleantech technology trend** detailing 2014 Cleantech top 100 companies – a barometer of the changing face of global Cleantech innovation; **(4) Cleantech investment in Silicon Valley** assumed a leading role in the global competition to develop renewable energy and other clean, green technologies; and **(5) Cleantech investment in emerging nations** addressing the status in China and other developing nations.

The **Concluding Remark***discusses* multidiscipline for Cleantech and the key to the deployment of Cleantech innovations. The **Appendix** provides a brief introduction of how and where to find information and seek for VC funding.

Introduction

In recent years, the term "Cleantech" is being widely used to replace "Clean Technologies" and "Green Technology." It describes a group of emerging technologies and industries, based on principles of physics, chemistry, biology, and resource efficiency, new paradigms in energy, and water conservation. The scope of this field includes large-scale infrastructure projects as well as innovative technologies.

The term Cleantech is also often associated with venture capital (VC) investment. In 2002, the Global Cleantech VC investment was US $0.9 billion and grew to the peak of $9.3 billion in 2008. After the financial crisis of 2009, its investments were gradually reduced, fluctuated, and then recovered to around $9 billion in 2013. This chapter addresses the dynamic field of Cleantech in the following four sections:

1.0 **Venture Capital Investment Trend** addresses the basics of venture capital and provides an analysis of the historical venture capital investment trend in terms of funds invested and the number of projects funded.
2.0 **The Scope of Cleantech** lists the scope of Cleantech encompassing renewable energy, energy efficiency, green building, transportation, smart power, smart grid and energy storage, air, water and waste, big data, and resource sharing.
3.0 **Cleantech Technology Trend** provides an overview of the key technologies that received venture capital or corporate investment. This is accomplished through a detailed discussion of 2014 Cleantech 100 – a barometer of the changing face of global Cleantech innovation and knowing where venture capitalists and corporate investors are interested to invest. These 100 Cleantech companies are selected from 5,995 companies across 17 countries and 17 technology sectors.
4.0 **Cleantech in Silicon Valley** has assumed a leading role in the global competition to develop renewable energy and other clean, green technologies. Cleantech is poised to be the valley's next great wave of innovation after semiconductor, information technology, biotechnology, and Internet-related technology.
5.0 **Cleantech in Emerging Markets** discusses Cleantech investment in development countries and gives examples of VC investment and start up in the fast-growing emerging markets.
Concluding Remark discusses the integration and deployment of VC-funded innovation in Cleantech and its implications on world climate change.

Venture Capital Investment Trend

Venture Capital

Venture capital (also known as VC or venture) (Venture Capitalist 2014) is provided as seed funding to early-stage, high-potential, growth companies and more often after the seed funding round as growth funding round (also referred as series A round) in the interest of generating a return through an eventual realization event

such as an IPO (initial public offering) or trade sale of the company. To put it simply, an investment firm will give money to a start-up and growing company. The growing company will then use this money to do research, build infrastructure, develop products, advertise, etc. The investment firm is called a venture capital firm or company, and the money that it gives is called venture capital.

The venture capital firm makes money by owning a stake in the firm it invests in. The start-up company that a venture capital firm will invest in usually has a novel technology or creates a business model. Venture capital investments are generally made in cash in exchange for shares in the invested company. It is typical for venture capital investors to identify and back companies in high-technology industries such as semiconductor, biotechnology, IT (information technology), Internet, and now Cleantech.

The source of funding of venture capital typically comes from institutional investors, endowment funds, and high-net-worth individuals and is pooled together by dedicated investment firms. Venture capital firms typically comprise small teams with technology backgrounds (scientists, researchers) or those with business training, financial management, or deep industry experience.

A core skill within VC is the ability to identify novel technologies or business models that have the potential to generate high commercial returns at an early stage. By definition, VCs also take a role in managing entrepreneurial companies at an early stage, thus adding skills as well as capital (thereby differentiating VC from buyout private equity which typically invests in companies with proven revenue) and thereby potentially realizing much higher rates of returns.

Inherent in realizing abnormally high rates of returns is the risk of losing all of one's investment in a given start-up company. As a consequence, most venture capital investments are done in a pool format where several investors combine their investments into one large fund that invests in many different start-up companies. By investing in the pool format, the investors are spreading out their risk to many different investments versus taking the chance of putting all of their money in one start-up firm.

Venture Capitalist

A venture capitalist (2014) is a person or investment firm that makes venture investments, and these venture capitalists are expected to bring managerial and technical expertise as well as capital to their investments. A venture capital fund refers to a pooled investment vehicle, often an LP (limited partner) or LLC (limited liability corporation), that primarily invests the financial capital of third-party investors in enterprises that are too risky for the standard capital markets or bank loans.

Venture capital is attractive for new companies with limited operating history that are too small to raise capital in the public markets and have not reached the point where they are able to secure a bank loan or government small business loan. In exchange for the high risk that venture capitalists assume by investing in smaller and less mature companies, venture capitalists usually get significant control over company decisions, in addition to a significant portion of the company's ownership.

Young companies wishing to raise venture capital require a combination of extremely rare yet sought-after qualities, such as innovative technology, potential for rapid growth, a well-developed business model, and an impressive management team. VCs typically reject 90–98 % of opportunities presented to them, reflecting the rarity of this combination. The general rule of thumb for the success rate of VC-invested start-up is about 60 % start-up failed and 30 % existed for 5 or more years with little or no profit; only about 10 % start-ups go to IPO or acquired by larger corporations as a separation business unit or merge into an existing operation of a larger corporation.

Venture Capital Investment Review

Traditionally, the venture capital industry has been focused on information technology, Internet, wireless and broadband communications, and biotechnology. All projects related to innovation of energy generation, energy saving, waste management, and environmental impact were grouped into a general industry category, and the investment funds were relatively small. In recent years, however, Cleantech investment has become a separate category and played a major role in the VC portfolio.

In 2014, venture capital funding (VC 2014) hit its highest annual mark since 2001 as venture investors participated in $47.3 billion across 3,617 deals. Even versus 2013, the past year was huge as venture capital skyrocketed 62 % year over year due to multiple $500 M+ mega-rounds, while deal growth was more modest, climbing 8 %.

A mix of traditional VC money coupled with corporate VCs, hedge funds, private equity investors, and even sovereign wealth funds created a potent cocktail in 2014 lifting funding levels to the highs seen during the dot-com boom. 2014 ended with a bang on the funding front as VC-backed deals hit $7.1B in the final month of the year. The massive funding figure was largely driven by mega tech deals to companies including Uber and Snapchat.

Although there were 738 VC-backed exits in 2014, the IPO picture was a bit mixed. The healthcare IPO market continued its momentum from 2013 with 64 US companies going public in 2014, up to 68 % year over year. Venture-backed tech IPO activity stalled a bit after Alibaba's IPO in September but did finish up versus 2013 and closed out with a strong December.

California and Massachusetts took 62 % of the US-headquartered venture-backed IPOs in 2014. California saw a whopping 45 % jump in venture-backed IPOs on a year-over-year basis. New York grew its number of IPOs significantly versus 2013 but remains a distant third to Massachusetts.

New Enterprise Associates is 2014's most active VC firm. As it targets a new $2.5B fund, New Enterprise Associates topped all venture investors by unique company deals in 2014. Andreessen Horowitz, which ranked first by deal count in 2013, again ranked in the top 2, followed by fellow mega-fund Kleiner Perkins Caufield & Byers. A list of the top 100 most active venture capital investors in 2014 by unique company deals is at appendix.

Global Venture Capital Investment in Cleantech

The following table lists venture capital investment in Cleantech from 2002 to 2014.

Year	Investment (billion US$)	Deals
2002	0.9	164
2003	1.3	301
2004	1.3	333
2005	2.0	381
2006	4.4	458
2007	6.42	564
2008	9.27	653
2009	6.23–7.5	557–691
2010	8.28–9.45	715–823
2011	9.61–10.8	243–829
2012	6.46–8.25	236–704
2013	6.75–7.35	175–1007
2014	3.98 (US only)	316 (US only)

From 2002 to 2005, Source: Cleantech Group (Global Cleantech Innovation 2014)
From 2006 to 2013, Source: Cleantech Group (Global Cleantech Innovation 2014) and San Jose Mercury News (MoneyTreeTM Report-Q3 2014) dated 03 Jan 2013
2014, Source: Cleantech Group (Global Cleantech Innovation 2014): San Jose Mercury News (MoneyTreeTM Report-Q3 2014)

Concurrent with the apparent decline in share of Cleantech venture capital in North America, the US government has invested around $16 billion a year and plans to increase investment to $50 billion annually by 2020. Part of the funding, about $15 billion, will come from tax credits and other fiscal measures. The rest will be derived from rate-payer increases for electricity and other energy. This spending should lead to very large investments in wind, solar, and carbon capture. In addition, the bill would bring into existence the first nationwide system of building codes, which would be further tightened every year through 2030. These codes will lead to considerable demand for green building technologies.

We can see venture capital investment in Cleantech is a smaller portion of the total investments by including government funding, but these VC-supported projects are often the most creative and full of scientific innovations.

The Scope of Cleantech

The scope of Cleantech encompasses a broad range of technology categories, including renewable energy, energy efficiency, green building, transportation, smart power, smart grid and energy storage, and air, water, and waste. The following lists (Clean Tech Open Defines Clean Technology) provide examples of technologies within each of the major categories:

Renewable Energy

The *renewable energy* category includes innovations that use, enable, and accelerate the migration to renewable energy. Renewable energy encompasses technologies that use waste streams to directly produce energy. Examples include low-emission power sources, such as solar, biofuel, wind, wave and tidal energy, and hydropower. Example technologies include:

- Solar for energy production
- CIGS
- Thin film solar manufacture
- Concentrating solar PV
- Coatings for solar panels
- Polysilicon supply and manufacture
- Residential-scale solar deployment
- Ethanol
- Bio-based fuels
- Tidal energy
- Wave energy capture
- Landfill gas to energy systems
- Agricultural waste to energy systems
- Hydropower
- Turbine blade design
- Advanced fluid flow designs
- Wind power aerodynamics
- Wind power conversion efficiency

Energy Efficiency

The *energy efficiency* category comprises technology that can significantly reduce wasted energy (including natural gas), driving toward the common goal of saving the equivalent of "a power plant a year." Examples include advanced light sources and controls, smart/user-friendly energy management systems, energy-efficient water heaters and other appliances, high-efficiency industrial process systems, motors, pumps, and advanced space heating and cooling systems. Example technologies include:

- Pumps for water/material
- Industrial process improvements
- Natural gas monitoring and control (industrial or residential)
- LED lighting
- Advanced lighting controls
- Water heating
- HVAC solutions

- Heat pumps
- Waste heat management
- Efficient heat transfer
- Utility-scale natural gas controls
- Display systems for energy management
- Materials used in microelectronics manufacturing
- Deposition and sputtering processes
- Alternatives to heat-intensive processes
- Cooling solutions
- Glass material production
- Pure manufacture techniques for fuel cells

Green Building

The *greenbuilding* category focuses on reducing the environmental impact of building construction or operation through improved design or construction practices, new or innovative use of building materials, or new hardware or software applications. Technologies are applied directly to the built environment. (Building energy efficiency submissions will be considered in the energy efficiency category).

Examples include improved site planning, water management systems, reduction of hazardous materials in building construction or operation, use of new environmentally friendly or recycled materials, systems to improve indoor environmental quality, and systems for improved waste reduction or disposal. Example technologies include:

- Insulation materials
- Cement alternatives
- Cement production techniques
- Building-integrated PV (BIPV)
- Indoor air filtration systems
- Modular housing
- Disaster relief housing
- Architectural designs for thermal management
- Office environment
- Low VOC carpeting and flooring
- Water-saving toilets, showers, and plumbing
- Residential heat pumps
- Recycled materials for use in building material
- Design improvements to commercial environment

Transportation

The *transportation* category encompasses transportation and mobile technology applications that improve fuel efficiency, reduce air pollution, reduce oil consumption, or reduce vehicle travel (not limited to automobiles). Technologies are applied

directly to transportation systems or vehicles. Examples include new vehicles and new types of transport services and infrastructure, efficient batteries, fuel cells, bio-based transportation fuels, and use of information technologies.

Example technologies include:

- Fleet management hardware and software systems
- Routing and data solutions for public transportation operators
- Logistics management
- Carpooling solutions
- Hybrid motor systems
- Storage of energy specifically applied to vehicles
- Plug-in hybrid vehicles
- All electric vehicles
- Fuel cell vehicles
- Biodiesel applications
- Intermodal tracking and monitoring
- NOX/SOX reductions for ocean-going vessels
- Cold-ironing systems
- Diesel particulate matter filters for locomotives
- Combustion designs
- Fuel blends
- Flex fuel engines and applications
- Drive train conversion kits
- Route management via GPS networks
- Exploiting GPS and location information
- Monitoring and control of driver behavior

Smart Power, Green Grid, and Energy Storage

The *smart power*, *green grid*, *and energy storage* category promotes links between information technologies and electricity delivery that give industrial, commercial, and residential consumers greater control over when and how their energy is delivered and used. It includes improvements in all forms of energy storage, from battery technology for consumer-scale products to large chemical, metal, biological, or other approaches to storage of utility-scale energy, as well as methods for controlling or increasing the efficiency of energy storage or energy transmission.

Examples include wireless metering and use of real-time pricing information, intelligent sensors, batteries, fuel cells, flywheels, and advanced materials or systems for energy transmission, such as hardware and software controls. Example technologies include:

- Advanced metering
- Network architecture for power management
- Cloud computing, applied to grid

- Batteries
- Novel battery chemistry
- Nickel-metal hydride improvements
- Hydrogen storage
- Li-ion cells
- Form factor improvements
- Improved cycle life for batteries
- Depth of discharge for batteries
- Solid oxide fuel cells
- Novel catalysts in batteries and fuel cells
- Advanced fuel cell membranes
- Methanol fuel cells
- PEM fuel cells
- Flywheels
- Grid-scale hardware and infrastructure
- Power storage for intermittent, renewable resources
- Monitoring and deploying power generated from renewables
- Transmission efficiency
- Electrical engineering and controls for power distribution
- Novel metals and alloys for power transmission
- Superconducting power transmission
- Real-time power monitoring

Air, Water, and Waste

Entries in the *air*, *water*, and *waste* category focus on improving resource availability, conservation, and pollution control. With respect to waste, the category focuses on cradle-to-cradle approaches to reduction, reuse, and recycling technologies, as well as innovative business models and approaches to material usage.

Air examples include services, instruments, and equipment related to emission control, treatment, or reduction technologies. Also included are creative approaches to greenhouse gas reduction, including carbon conversion and sequestration. **Water** examples include treatment, storage and monitoring, recycling, and conservation technologies. **Waste** examples include waste management equipment; sorting; resource recovery processes; pollution prevention, control, and treatment technology; as well as waste reduction through innovative recycling processes and new recyclable materials, such as bio-based plastics. Example technologies include:

- Water monitoring – on-site in situ real-time water monitoring for pathogens
- Cooling solution
- On-site wastewater recycling – industrial and commercial applications
- Advanced water metering
- Storm-water and flood control and rainwater harvesting
- Smart irrigation

- On-site water disinfection
- Membranes for water treatment
- Advanced filtration without membranes
- Produced water (from oil exploration and drilling)
- Energy-efficient water pumping
- Reverse osmosis
- Advanced filters and filtration (air or water)
- Emission controls
- Scrubber technology
- Carbon and GHG monitoring and control
- Carbon sequestration
- Carbon capture and storage
- Technology enablers for carbon markets
- Reduction and remediation of VOCs
- Waste cleanup and remediation
- DI water supply
- Agricultural waste treatment
- Recycling
- Microbial water treatment
- Bio-based packaging solutions
- Methane capture and storage
- Soil technology
- Natural pesticides
- Clean coal

Big Data, Communication, and Resource Sharing

Innovation in smart grid 5 years ago was much more concentrated around effective communication with the grid. The wireless was the hottest examples of the "communication network" investment theme. Now that those types of companies are maturing, the new crop of hot companies is trending around the "big data" theme. While "data" was always a focal area for utilities, whether for digitally optimizing grid infrastructure or monitoring "loads" for large customers, a new bucket of businesses are targeting, like never before, the streamlining of large quantities of data. The other area is in resource sharing where many applications are being launched. Examples (CleanTech 100 2014) are:

- Software to help utilities manage complexities in order to provide easily visualized options for decision-making and to address operational challenges
- Software to manage big data in buildings with their behavior and the behavior of their commercial customers through providing them with tailored data to evaluate where real energy savings can be made
- Software for Internet resource sharing of vehicle use and sharing of extra rooms in a home

The scope of Cleantech is extremely broad and involves many scientific and academic disciplines. It is a good field for today's science and engineering students to pursue as a career for the next decade.

Cleantech Technology Trend

This chapter will report the trend by way of detailing **2014 Cleantech 100** – a barometer of the changing face of global Cleantech innovation. In recent years, **CleantechGroup.com** (CleanTech 100 2014) began a process of identifying key 100 Cleantech companies that present the potential of becoming big in the near future.

For **2014 Cleantech 100**, a total of 5,995 companies were nominated with the end result of 100 companies across 17 countries and 17 subsectors. The 84 external panelists active in helping Cleantech Group reach the final list of 100 were drawn from 41 corporations (responsible for Cleantech-related investment) and 43 financial investors (venture capitalist) located in Asia, Europe, and North America. The selection criteria are:

1. Innovation (the problem it solves, uniqueness, sustainability of advantage, etc.)
2. Market (accessibility, size, growth dynamics, barriers to entry, etc.)
3. Ability to execute (finances, team competencies, connections and networks, etc.)

The corporate expert panelists tended to vote more strongly for companies with long-term market potential, whereas financial investors focused more on track record and strength of team. In comparison with previous year, 2014 had a majority of retentions (52 %) compared to new entrants (37 %) on the Global Cleantech 100 list.

Now in its sixth edition, 67 % of the Global Cleantech 100 companies are from the North America region and 28 % from the Europe and Israel region – led by the UK (7), Germany (6), and the Nordics (6). M-KOPA (Kenya) is the first company from the Africa region to make it to the Global Cleantech 100.

There are many B2C models trending among the Global Cleantech 100, testament to the idea that the consumer's mind-set is the most open to disruptive change. Over 15 % of the Global Cleantech 100 companies are providing services to oil and gas companies, representing the mounting case to clean up the industry's operations.

At least 25 % of 2014 Global Cleantech 100 companies are already focusing, or will soon focus, on growing their business into Asia and other emerging and highly populated markets. There were more solar companies in 2014 (9) compared to 2013 (6), suggesting a renaissance of new business models that will continue to help raise deployment figures. A big data service for utilities is a big emergent theme in this year's 100, as companies are continuing to innovate on ways to address ongoing energy challenges.

The Global Cleantech 100 List

See Fig. 1.

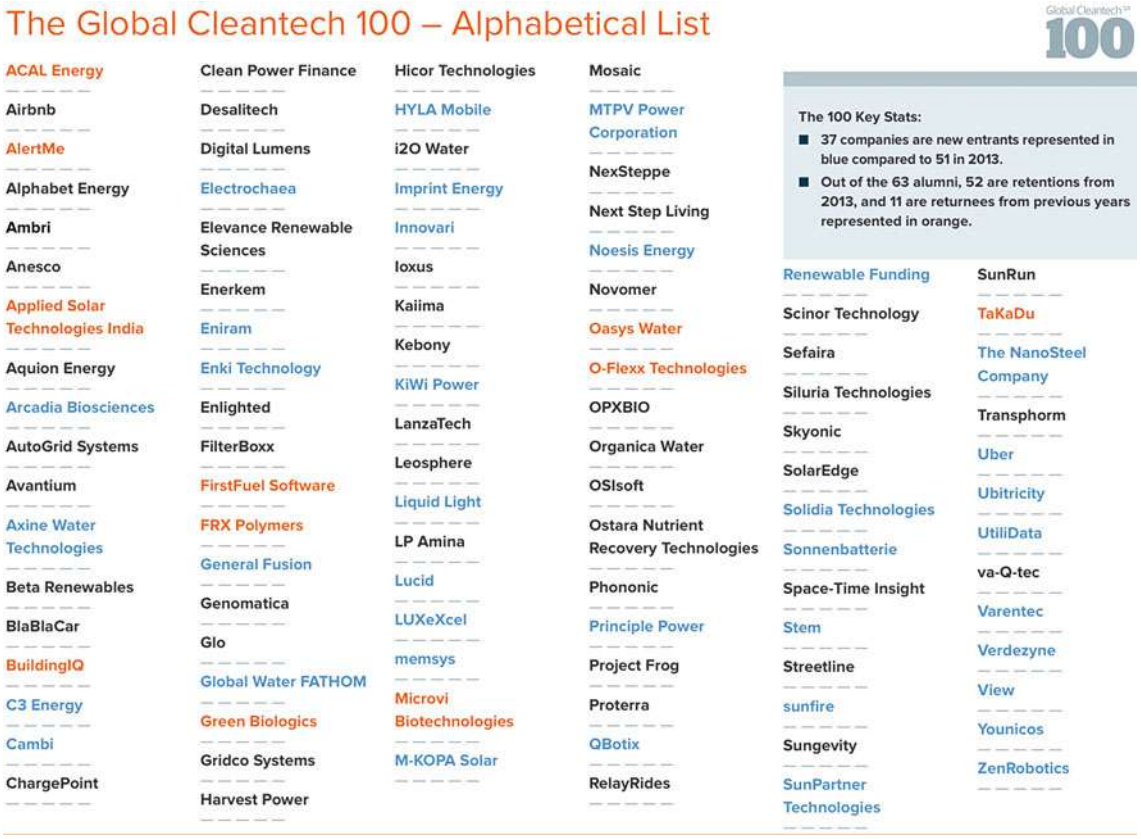

The Global Cleantech 100 – Alphabetical List

Global Cleantech 100

ACAL Energy
Airbnb
AlertMe
Alphabet Energy
Ambri
Anesco
Applied Solar Technologies India
Aquion Energy
Arcadia Biosciences
AutoGrid Systems
Avantium
Axine Water Technologies
Beta Renewables
BlaBlaCar
BuildingIQ
C3 Energy
Cambi
ChargePoint
Clean Power Finance
Desalitech
Digital Lumens
Electrochaea
Elevance Renewable Sciences
Enerkem
Eniram
Enki Technology
Enlighted
FilterBoxx
FirstFuel Software
FRX Polymers
General Fusion
Genomatica
Glo
Global Water FATHOM
Green Biologics
Gridco Systems
Harvest Power
Hicor Technologies
HYLA Mobile
i2O Water
Imprint Energy
Innovari
Ioxus
Kaiima
Kebony
KiWi Power
LanzaTech
Leosphere
Liquid Light
LP Amina
Lucid
LUXeXcel
memsys
Microvi Biotechnologies
M-KOPA Solar
Mosaic
MTPV Power Corporation
NexSteppe
Next Step Living
Noesis Energy
Novomer
Oasys Water
O-Flexx Technologies
OPXBIO
Organica Water
OSIsoft
Ostara Nutrient Recovery Technologies
Phononic
Principle Power
Project Frog
Proterra
QBotix
RelayRides
Renewable Funding
Scinor Technology
Sefaira
Siluria Technologies
Skyonic
SolarEdge
Solidia Technologies
Sonnenbatterie
Space-Time Insight
Stem
Streetline
sunfire
Sungevity
SunPartner Technologies
SunRun
TaKaDu
The NanoSteel Company
Transphorm
Uber
Ubitricity
UtiliData
va-Q-tec
Varentec
Verdezyne
View
Younicos
ZenRobotics

The 100 Key Stats:

- 37 companies are new entrants represented in blue compared to 51 in 2013.
- Out of the 63 alumni, 52 are retentions from 2013, and 11 are returnees from previous years represented in orange.

Figure 1

The Global Cleantech 100 by Sector

Seventeen sectors are represented, showing a diversity of interests and a continued focus on water and wastewater, advanced materials, and other areas of sustainable innovation that take us well beyond the narrower confines of just energy (Fig. 2).

1. Energy efficiency (24)
2. Water and wastewater (12)
3. Biofuels and biochemicals (10)
4. Solar (9)
5. Smart grid (7)
6. Energy storage (7)
7. Transportation (7)
8. Advanced materials (6)
9. Conventional fuels (4)
10. Air (3)
11. Recycling and Waste (3)
12. Agriculture and Food (2)
13. Fuel cells and hydrogen (2)
14. Biomass generation (1)
15. Nuclear (1)
16. Resource sharing (1)
17. Wind (1)

Global Cleantech 100 by Geography

See Fig. 3.

1. Sixty-seven percent from the North America region, with 62 companies from the USA
2. Twenty-eight percent from the Europe and Israel region – led by the UK (7), Germany (6), and the Nordics (6)
3. Four percent from the Asia-Pacific
4. One percent from the Africa region (Kenya) (Fig. 4)

Assessment of Global Cleantech 100 by Expert Panelists

The 2014 Expert Panel was comprised of representatives from 43 financial investors and 41 corporations (or corporate venture units) from all over the world. The most common reasons that all expert panelists gave for positive comments of selected companies are:

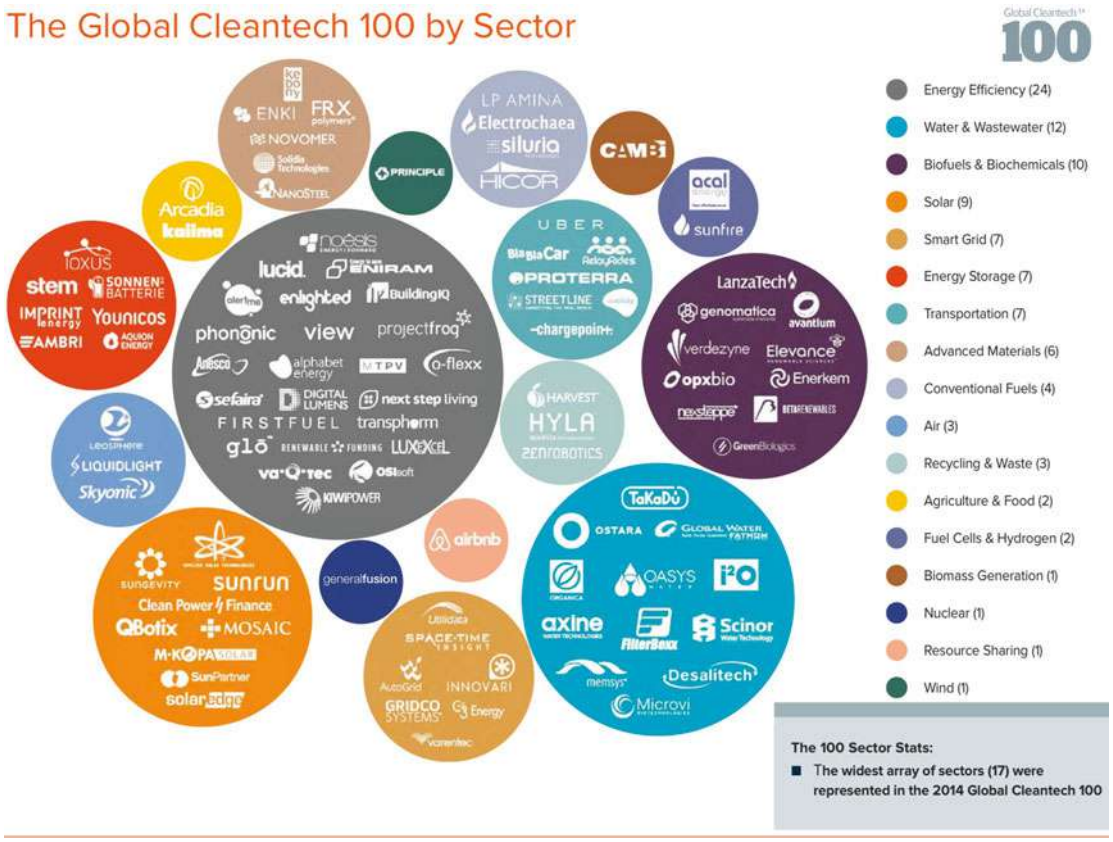
The Global Cleantech 100 by Sector
Global Cleantech 100
Energy Efficiency (24)
Water & Wastewater (12)
Biofuels & Biochemicals (10)
Solar (9)
Smart Grid (7)
Energy Storage (7)
Transportation (7)
Advanced Materials (6)
Conventional Fuels (4)
Air (3)
Recycling & Waste (3)
Agriculture & Food (2)
Fuel Cells & Hydrogen (2)
Biomass Generation (1)
Nuclear (1)
Resource Sharing (1)
Wind (1)
The 100 Sector Stats:
The widest array of sectors (17) were represented in the 2014 Global Cleantech 100

Figure 2

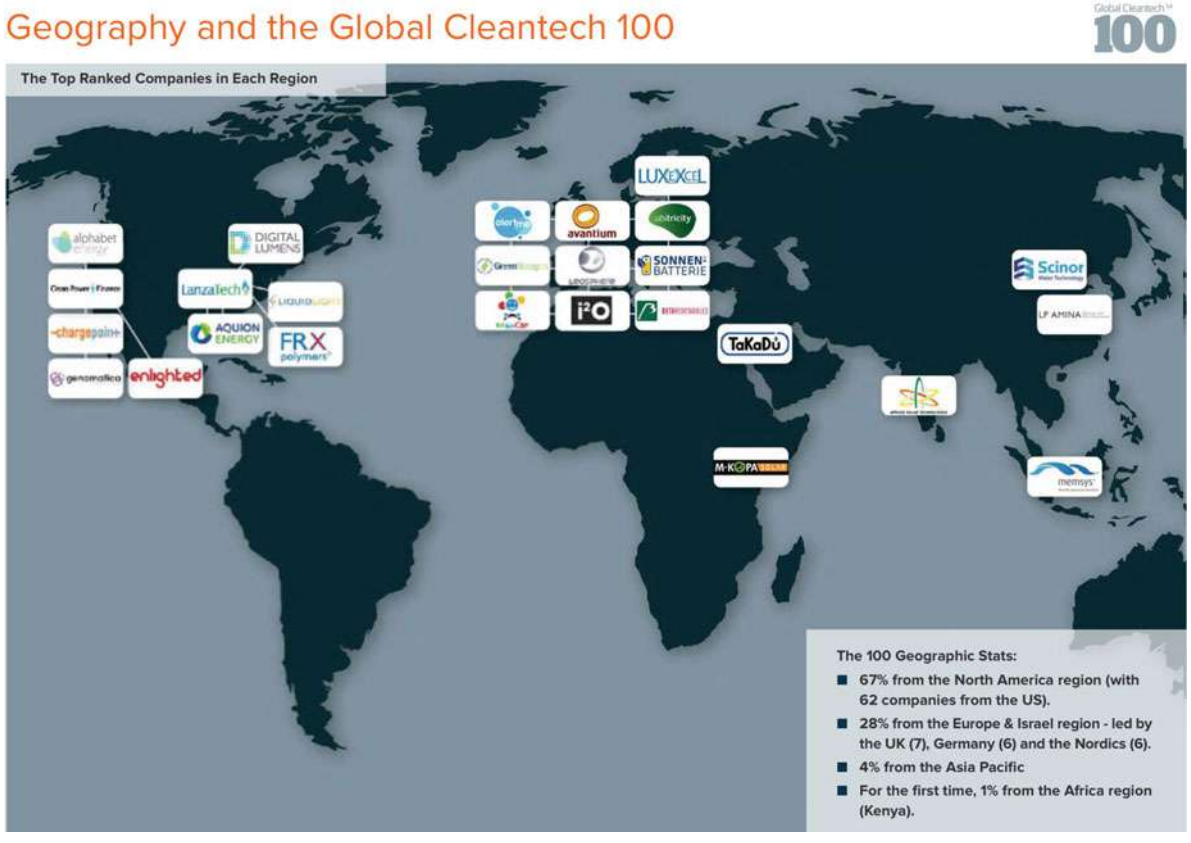
Geography and the Global Cleantech 100
Global Cleantech 100
The Top Ranked Companies in Each Region
alphabet energy
DIGITAL LUMENS
LanzaTech
LIQUIDLIGHT
AQUION ENERGY
FRX polymers
chargepoint
genomatica
enlighted
LUXeXCEL
avantium
SONNEN BATTERIE
i2O
TaKaDu
Scinor
LF AMINA
M-KOPA
memsys
The 100 Geographic Stats:
67% from the North America region (with 62 companies from the US).
28% from the Europe & Israel region - led by the UK (7), Germany (6) and the Nordics (6).
4% from the Asia Pacific
For the first time, 1% from the Africa region (Kenya).

Figure 3

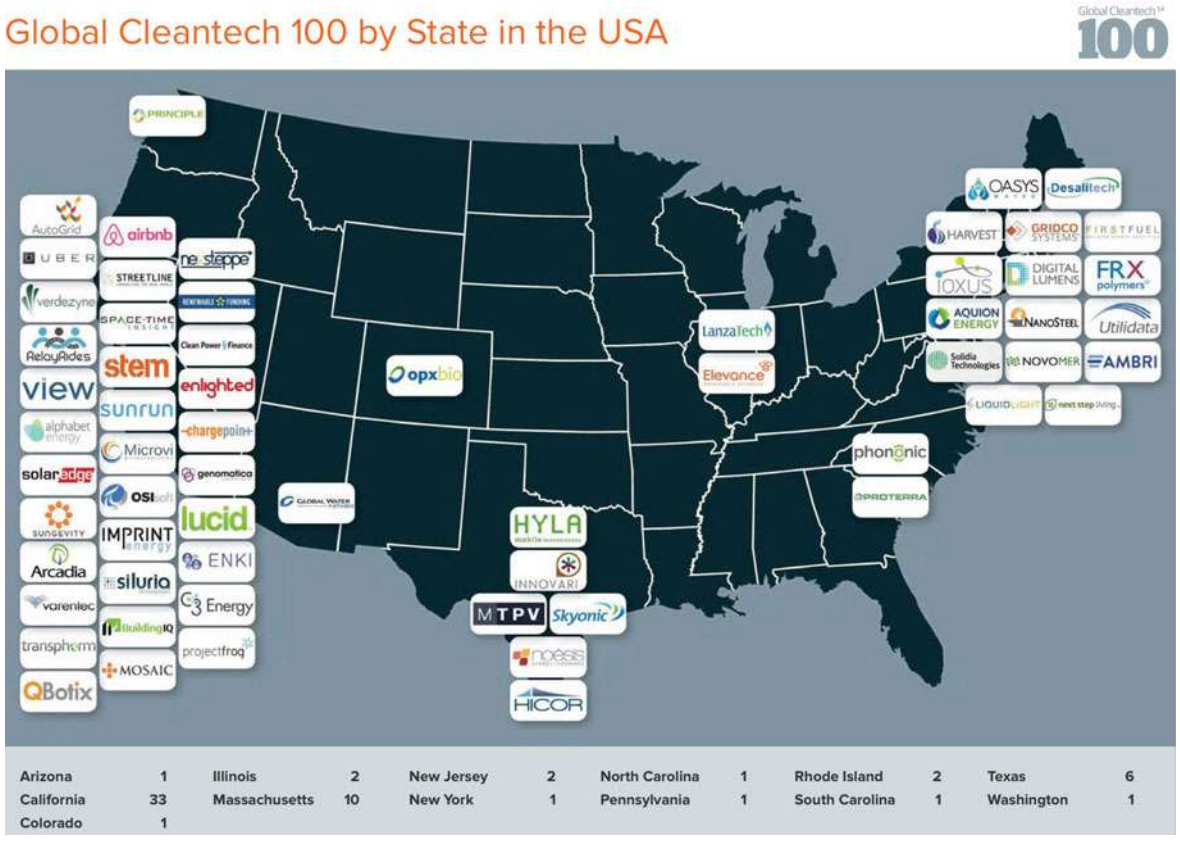
Global Cleantech 100 by State in the USA
Global Cleantech 100
PRINCIPLE
AutoGrid
airbnb
UBER
STREETLINE
ne steppe
verdezyne
SPACE-TIME INSIGHT
RelayRides
stem
enlighted
view
SUNRUN
chargepoint
alphabet energy
Microvi
solarEdge
genomatica
OSIsoft
SUNGEVITY
IMPRINT Energy
lucid
Arcadia
ENKI
silurio
varentec
C3 Energy
BuildingIQ
transphorm
projectfrog
MOSAIC
QBotix
opxbio
GLOBAL WATER
HYLA
INNOVARI
MTPV
Skyonic
HICOR
LanzaTech
Elevance
OASYS
Desalitech
HARVEST
GRIDCO SYSTEMS
FIRSTFUEL
IOXUS
DIGITAL LUMENS
FRX polymers
AQUION ENERGY
NANOSTEEL
Utilidata
Solidia Technologies
NOVOMER
AMBRI
LIQUIDLIGHT
next step living
phononic
PROTERRA
Arizona 1
California 33
Colorado 1
Illinois 2
Massachusetts 10
New Jersey 2
New York 1
North Carolina 1
Pennsylvania 1
Rhode Island 2
South Carolina 1
Texas 6
Washington 1

Figure 4

- Companies with an impressive CEO or management team, with the right background and leadership to take the company to the next stage.
- Companies have the longer-term market potential, such as the potential demand size for the product or service.
- Companies have breakthrough technology, evidence of traction, and competitive cost structure importance in the minds of investor and corporate panelists.

At the top of the 2014 List – as measured by companies that received the most peer validations in the expert panel assessments without any negative cases made against them – are the following three companies:

1. **Avantium**, a specialist in advanced catalytic research, has developed a sugar-to-furanics technology that allows for the production of bio-based PEF plastics which has the potential to replace many petrochemical materials (bottles, films, fibers) "if cost and performance goals are met." Avantium is "not only leading the way with renewable chemicals, but the R&D specialization offering they provide is very relevant," said one expert panelist. The company has achieved impressive financing rounds, including a recent $50 million infusion to build its first commercial PEF scale plant. With strategic backers and partners like Coca-Cola, Danone, and ALPLA, Avantium continues to gain traction "with some of the biggest consumers within the plastics industry."
2. **Clean Power Finance** is acting as a key enabler of distributed generation by expanding third-party financing of rooftop solar – a field that is poised to grow tremendously in many countries. The company connects solar professionals with institutional investors through its CPF Market, an online business-to-business marketplace for solar finance products by loans or leases. Although it has several competitors, the company's innovative business model, impressive list of project finance backers, and new channel partners (Kilowatt Financial and North American Power) make revenue growth and traction real.
3. **FRX Polymers** has developed non-migrating, phosphorus-based polymer additives for use in halogen-free flame retardants. The company's patented plastic products – Nofia – have multiple market applications to consumer electronics, building and construction, and transportation markets. This new halogen-free flame retardant will change the plastics industry and is very important for security reasons.

   The company recently received funding from a strong syndicate of investors including the Flemish government and chemical corporations BASF and Evonik – closing a $20 million Series C financing round in May 2014. FRX Polymers is now entering an accelerated growth phase, following the launch of its first commercial plant in Antwerp, Belgium, in 2013.

   The companies in the final 100 that attracted the strongest split of opinions across the expert panel, a mix of positive and negative votes, in significant volumes were:
4. **Ambri**, the liquid metal battery technology company, has a disruptive, high-power energy storage technology and offers a new take on the battery with its

liquid metal technology by using inexpensive, earth-abundant materials. Can it get beyond being a science project and prove itself against Li-ion evolving systems? If it works, it will be disruptive.

5. **General Fusion** has made significant progress in building fusion energy subsystems at scale. Many panelists admire the company for "attempting something so audacious." Will it be commercial in the next 10 years? Is it too dependent on fickle government regulations? The company has the potential to revolutionize power generation if it can succeed with its technical milestones.
6. **Siluria Technologies**, with its proprietary catalysts to convert methane to drop-in fuels and chemicals, could change the way we think about fuels. However, Siluria has to show the cost of capital and the ease of operation.

Top Picks by Corporations with Its Own Venture Unit

Diversified Industrials: Energy efficiency start-ups generally tend to be popular among corporations in the Diversified Industrials vertical, who see a variety of applications for these technologies. This year, building energy management system companies **BuildingIQ** and **Enlighted** are the running favorites. BuildingIQ is a specialist in HVAC for commercial buildings. Enlighted specializes in lighting efficiency along with extended building services such as real estate analytics. Both are entering a phase of accelerated growth in the USA and rapidly expanding into Asia too.

Materials and Chemicals: Avantium and **LanzaTech** appeal particularly strongly to the materials and chemicals corporations. They recently received $50 and $60 million, respectively, from prestigious investors. "Avantium has the potential to replace many petrochemical materials with renewable feedstock," which is why it emerges as a natural winner among materials and chemicals corporations. Similarly, LanzaTech converts carbon-rich wastes and gases into valuable fuel and chemical products. A "fascinating technology" with a "large addressable market," said one of the panelists.

Oil and Gas: Faced with ever-higher operational costs and more stringent environmental standards, oil and gas corporations focused their attention on solutions that may improve the performance and safety of their operations.

Liquid Light, which develops an electro-catalytic technology enabling the conversion of CO_2 into high-value chemicals, was remarked upon for its potential impact on the oil and gas industry, a large emitter of carbon dioxide.

Houston-based **Hicor Technologies** offers a system of trailers that carry natural gas from compression sites to the customer's door at a cost lower than traditional transit infrastructure. Hicor promises to "make it easy for customers to switch to natural gas as a primary energy source."

Environmental Services: Corporations are showing interest in water and wastewater treatment solutions that align with their business operations and help them address a variety of markets. **Cambi** is a supplier of thermal hydrolysis systems for treatment of biowaste prior to anaerobic digestion. The company has "impressive

growth in sludge pretreatment" and "enjoys unrivaled domination of the market for large-scale municipal installations."

Global Water FATHOM provides a geospatial platform that helps water utilities optimize their back operations.

FATHOM's AMS service allows utilities to repair aging water networks and is "the only vehicle available that allows customers to track their own consumption in real time."

Utilities: Utilities remain interested in start-ups that offer solutions to enhance the viability and economics of existing technologies in which they have a vested interest. **Ioxus** has developed ultra-capacitors that prolong the lifespan of batteries used for various alternative energy applications, including micro-hybrid for electric vehicles. "Wait til Elon Musk figures that out to improve his Teslas!" said one panelist. **QBotix** creates rugged and intelligent solar tracking robots that deliver significant project cost savings and high-system-level reliability and flexibility of installation in the commercial- and utility-scale solar power plant sectors.

The Consumer-Centric Business Models

With the endless number of energy-saving tools on the market, a number of companies are seeking to make it simpler and easier for the everyday consumer to make energy efficiency changes in their home.

1. Smart Homes: Users of **AlertMe's** smart home monitoring system can connect to their home's broadband and remotely control household appliances, thereby cutting domestic energy consumption and costs. UK-based AlertMe is "leading the trend towards an ever more connected world on the consumer level – it is a company to watch," said one panelist.

   Anesco provides comprehensive energy efficiency solutions to homeowners (from audits to recommendations, installations, maintenance, and capital funding plans). Anesco's success has impressed panelists, who praised its "strong growth," its "impressive financial performance," and "excellent execution of strategy."
2. **Mobile Devices**: HYLA Mobile collects used mobile devices and refurbishes them to meet certification standards – and subsequently sells them to consumers in developing countries at an affordable price. This consumer-centric recycling solution improves resource efficiency rates in the USA while enlarging access to affordable technology in the developing world.
3. **Consumer Products –** A New Level of Energy Saving: **Phononic** commercializes solid-state heat pumps that displace compressors for home refrigeration, cooling, and heating, thus making home appliances quieter and more efficient. According to Phononic's CEO Anthony Atti, the company aspires to become the "Intel Inside" of refrigerators and air conditioners. "This area of materials has the best chance to impact energy efficiency in the future," commented an expert panel member.

   Germany's **Sonnenbatterie** manufactures battery systems that allow homeowners to store energy generated from residential solar installations.

Sonnenbatterie's customers can avoid peak demand prices and optimize their energy consumption.

4. **Car Sharing – The New Norm in Transportation:** In the age of the "sharing economy," consumers are more interested in gaining access to various modes of transportation, without the burden of owning a car. Next-generation mobility solutions are reducing both congestion and pollution while providing tremendous consumer convenience and operational efficiencies.

   BlaBlaCar has established itself as the leading carpooling platform in Europe, with more than 2.9 million members and 500,000 monthly ride shares to its credit. Building on this success, the company is starting to noticeably reduce congestion and decrease CO_2 emissions. **RelayRides** allows car owners to rent out their vehicles via an online interface. A market leader in peer-to-peer car sharing in the North America, RelayRides has aggressively grown its customer base and has expanded its reach into airport parking. RelayRides' service results in "increased resource efficiency rates."

   Through its mobile app, Uber allows users to book and pay for on-demand private car service and also enables passengers to share rides. The company's success and high valuation "signal the market's acceptance of the changing nature of mobility."

Emerging Market Demand

1. **Feeding the Developing World with Agronomics: Arcadia Biosciences**, a California-based developer of enhanced agronomic products, works with agricultural organizations across the emerging world. Alongside Argentina-based agricultural cooperative Bioceres, it formed Verdeca, a JV specializing in biotech-enhanced soybean varieties. It works with Indian agronomic research companies Advanta and Bioseed Research to develop next-generation products such as salt-tolerant and nitrogen-use-efficient sorghum. Arcadia also has partnerships with research center CIMMYT (Mexico) and the African Agricultural Technology Foundation (Kenya).

   In just 7 years, Israeli seed technology start-up Kaiima has expanded its activities well into emerging markets, with customers in China, Niger, Madagascar, Brazil, Peru, or Mongolia – to name a few. It is working with Philippine-based International Rice Research Institute (IRRI) to bring to the developing world new-generation high-yielding crops. Kaiima's solutions are "critical for water-constrained agricultural regions – there is a huge market opportunity" said a panelist.
2. **Modernizing Wastewater Treatment Systems:** UK-based **i2O** is supplying its water pressure management technology to leading utilities across the emerging world. It boasts Malaysia-based Syabas and Philippine-based Manila Water, two of Southeast Asia's largest water utilities, as customers. i2O works with JOAT Group, one of South Africa's leading water management organizations, to implement its solutions in some of the country's major metropolitan areas. i2O is also active in South and Central America, where it has partnerships with Chile's

Glemans and Aguas de Antofagasta, Peru's Esboña Corporation, and Mexico's Grupo SCR Mexico.

Organica Water, a Hungary-based developer of biological wastewater treatment plants, has gained multiple customers across China, India, and Indonesia. Organica boasts partnerships with India's engineering conglomerate Larsen & Toubro and China's famous Foxconn Group. It delivered a commercial wastewater treatment plant for the latter's industrial park in Shenzhen, China. "The company is thriving in rapidly urbanizing Asian countries, where the sewage networks are not keeping pace with new-build," said one panelist.

3. **Sustainably Fueling Growth in the Emerging World:** Italy's **Beta Renewables** transforms nonfood, cellulosic biomass into biofuels through a conversion technology marketed as Proesa. Beta Renewables has established development partnerships with Malaysia-based chemical companies MyBiomass and Hock Lee Group. It is also active in Brazil and will license its Proesa technology to the world's next largest cellulosic ethanol biorefinery, located in Fuyang, China, and partially owned by one of Beta Renewables' shareholders, the chemical company Gruppo Mossi and Ghisolfi.

   LanzaTech has gained remarkable traction across Asia, establishing partnerships with big players such as steel companies Baosteel, Jindal Steel, and POSCO, with oil giants Petronas and Indian Oil, and in the near term with global industrial multinational Mitsui. LanzaTech has established itself as an industry leader in China, where it has forged solid relationships with the government, steel mills, and other state-owned companies.

4. **Reducing the Cost of Electricity Consumption: Innovari**, a provider of a load duration management platform, is connecting utilities with commercial energy partners to incorporate demand-side management into the grid. The Texas-based start-up is now exporting its solution in the emerging world, for example, by helping Colombian utility EMCALI to implement a demand-side management platform for its local distribution system. And it announced it would deploy its Interactive Energy Solution to the customers of Reliance Infrastructure, India's largest power utility, in Mumbai.

   Utilidata, a Rhode Island-based supplier of voltage optimization products, already caters to multiple utilities across North America, but it is now going global with partnerships in Saudi Arabia, Russia, South Korea, and China. Utilidata's main partner is Saudi Aramco, the largest oil and natural gas company in the world. "We see a big opportunity to scale in Asia, where the benefits of increased efficiency and intelligent control could significantly reduce the cost of electricity, enabling sustainable growth," said one of Utilidata's recent investors.

Cleantech Goes Inside the Oil and Gas Industry

Many promising Cleantech start-ups are working with oil and gas corporations to help them address the growing technical, financial, and environmental challenges

facing both upstream and downstream operations. Here are four ways in which Cleantech start-ups in this year's list are potentially shaping changes in the oil and gas industry.

1. **Converting oil and gas by-products and waste heat into resources**: **Alphabet Energy** manufactures easy-to-install thermoelectric products that transform waste heat in exhaust gas into electricity.

   MTPV Power Corporation develops thermo-photovoltaic technologies for converting waste heat to electricity. It enables oil and gas companies to reduce their operating costs by reusing the exhaust heat.

   Skyonic uses a thermolytic process to capture carbon dioxide at the source of emission and transform it into valuable chemicals. Oil and gas companies, one of the largest industrial emitters of GHGs, could use this technology to curb carbon dioxide emissions generated during the production process.
2. **Facilitating the treatment of oil and gas process water: Axine Water's** chemical-free, scalable system treats high concentrations of recalcitrant toxic materials in oil and gas process water. Axine's solution has huge potential in water treatment of offshore production. FilterBoxx's wide experience in treating process water from enhanced oil recovery operations and unconventional drilling methods makes it a natural partner of the oil and gas industry.

   Memsys develops thermal separation processes based on membrane distillation. The technology is geared toward the unconventional gas marketplace, which faces complex wastewater treatment challenges. **Oasys Water** works with oilfield engineering firms to deliver forward osmosis water reuse solutions into the global oil and gas produced water market. As heavy industries like oil and gas and mining seek to be more sustainable, important treatment components like dewater technology will be increasingly relevant in these markets.

   The **NanoSteel Company** delivers nanostructured steel alloys with a unique combination of high strength, ductility, and wear resistance. With these properties, NanoSteel's metallic coatings meet demand for next-generation material technologies that hold up to the challenge of drilling in high-pressure, high-temperature environments.
3. **Improving the overall performance of oil and gas through software and data analytics**: **OSIsoft's** real-time data analytics help oil and gas companies maximize asset performance, optimize production flows, and centralize enterprise expertise. **Space-Time Insight's** solutions for oil and gas leverage geospatial and visual analytics software to enable pipeline integrity monitoring, crisis mitigation, hydrocarbon supply chain management, risk monitoring, situational awareness, and condition-based maintenance.
4. **Disrupting the downstream segment: Electrochaea** is the developer of a power-to-gas energy storage technology that converts excess electricity from wind and solar into renewable gas. This gas can then be injected into the existing natural gas infrastructure.

Hicor Technologies' compressed natural gas solution allows energy corporations to deliver natural gas to any customer who doesn't have access to a physical pipeline. **Siluria Technologies** develops a methane conversion technology for creating fuels and chemicals from natural gas.

Toward Downstream Solar and Decentralized Energy Services

In the past, most companies were innovating on the "hardware" side of solar (i.e., photovoltaic equipment suppliers, or solar module builders). In 2014, they demonstrate a 180° shift in investor appetite away from such semiconductor-style businesses, and a resulting slowdown in new innovation aimed at higher efficiency upgrades of solar equipment and components. The second trend includes business models that favor decentralization over centralization of solar provision. Consumers are no longer going to their local utility as a one-stop shop to obtain their energy plan. Instead, they are decentralizing decisions and processes by using smaller players with advantageous services.

Clean Power Finance operates an online platform that connects the distributed generation (DG) solar industry with institutional investors who want to own residential solar assets. CPF is a good example of "transactional innovation effectively lowering the cost and accelerating the adoption of rooftop solar."

Mosaic, the organizer of community solar financing projects, has democratized solar investment by allowing the public to elect centers, schools, libraries, etc. to go solar. The company is also making smart alliances with equipment manufacturers to accelerate the pace of deployment.

M-KOPA, the provider of pay-per-use solar charging systems in Kenya, will "revolutionize asset financing in emerging markets," according to one panelist. The company has developed a technology platform that combines embedded GSM and mobile payments to make it affordable for Kenyans to purchase solar energy solutions.

Renewable Funding helps residential and commercial property owners to finance renewable energy and energy efficiency projects. The company provides low-cost financing for home improvements via a secondary market for clean energy loans.

Sungevity, the solar system integrator, has a "strong IT platform" targeting the residential rooftop market and provides its customers with services to secure financing and rebates. The company is "scaling well and has teamed up with E.ON Benelux, to expand solar into the European market."

Sunrun engages customers through PPAs, by owning, insuring, and monitoring the solar panels on a homeowner's roof, while families pay a low rate for clean energy and fix their electric costs for 20 years. "With a good market trend and growing size," the company is bound to lower the cost barrier to residential solar and increase adoption rates.

"From Waste to Wealth": Recovery of a Trillion-Dollar Market

Key innovators today are designing new business models that allow for the recovery of usable materials, chemicals, or gas out of disposed goods, products, and waste. The companies below are pioneering the way forward to bring solutions to the questions: How can we reuse and remanufacture waste in current industrial processes to create economic value and less resource dependence? How can we develop a restorative society, which thrives even when the price of commodities surges? How can we use emerging technologies to help emerging markets to resolve their health and environmental challenges?

1. **Energy Efficiency – Alphabet Energy**, Hayward, CA, USA: More than 60 % of the chemical energy from fossil or renewable fuels today is lost during combustion processes, primarily as waste heat. **Alphabet Energy** solves this problem by developing a thermoelectric technology which can convert heat to electricity with target markets including energy generators and automobiles, and the company is working on military applications for the US Army and US Air Force.
2. **Recycling and Waste – Harvest Power**, Waltham, MA, USA: **Harvest Power** converts organic food waste into renewable energy and soil enhancement products (i.e., mulch and fertilizer). The company's technology "enables value add to organic waste stream" and the "fertilizer angle is an attractive side of the recycling market," according to several panelists. Its largest anaerobic digester site in Vancouver supplies power to over 900 homes.
3. **Biofuels and Biochemicals** – **LanzaTech**, Skokie, IL, USA: LanzaTech is a "pioneer in (syn)gas fermentations." The company's thermochemical technology is based on proprietary microbes that are able to transform industrial waste gases into usable chemicals. The company has established strong global partnerships with multinational corporations (e.g., Baosteel, Shougang Group, POSCO, Boeing, Virgin Atlantic).
4. **Air – Liquid Light**, Monmouth Junction, NJ, USA: Liquid Light develops a waste-to-resource technology that captures carbon dioxide gases directly at the point of emission and uses electrocatalysts to convert them into useful industrial chemicals. The company has generated enthusiasm among the corporate panelists who believe it is "strongly positioned to become the first CO_2-to-chemical technology" and "is very likely to be a long-term winner."
5. **Water and Wastewater – Ostara**, Vancouver, BC, Canada: Expert panelists praised Ostara Nutrient Recovery Technologies for "cleverly combining wastewater treatment with the production of a revenue-generating, green fertilizer." Ostara's proprietary technology recovers otherwise polluting chemicals, such as phosphorus and nitrogen, from municipal and industrial water streams and transforms them into an ecofriendly fertilizer that can increase food production.
6. **Recycling and Waste – ZenRobotics**, Helsinki, Finland: ZenRobotics provides a waste processing recycling system which is able to identify and extract valuable

materials and improves the efficiency of excavator sorting. The company is "linking the worlds of robotics, artificial intelligence, and sorting waste" and claims to be "the most promising cure to the waste and raw material crisis."

The Big Data Solution Providers for Utilities

New businesses are targeting the streamlining of large quantities of data. These companies are seeking to help utilities manage complexities in order to provide easily visualized options for decision making and to address operational challenges. Other companies are helping utilities manage big data in buildings, with the focus on serving their clients' needs for greater energy efficiency and better insights into energy management systems.

1. **Forecast and Management Tools for Distributed Generation: AutoGrid**'s software system runs complex optimization algorithms that enables electricity providers to forecast generation. **C3 Energy**'s software applies big data, smart grid analytics, social networking, and cloud computing to all aspects of power delivery. **Gridco Systems'** products enable utilities to actively manage voltage and other key parameters of the distribution system with precision in real time. Space-Time Insight gives utilities access to data about the power grid to help them to solve challenges around distributed generation, reliability, and security.
2. **Platforms for Better Energy and Building Analytics: FirstFuel Software** has developed a platform that uses advanced meter data analytics to track energy efficiency savings behind the meter in commercial buildings. **KiWi Power** is the developer of demand response software which can track customers' activities and generate automated performance reports.

   OSIsoft has developed a data infrastructure and event management software platform with applications to utilities' operations optimization and real-time situational awareness. **Stem** offers customer-sited, battery energy storage-enabled energy management systems to reduce electricity costs.

The Global Cleantech 100 Mini-Profiles

Advanced Materials
Enki Technology (United States)
Developer and marketer of functionalized coatings for the solar photovoltaic industry, optimizing the way solar modules interface with their environments
FRX Polymers (United States)
Developer of a patent protected, non-halogen, non-burning family of transparent high-flow thermoplastics in the global flame retardant plastics market
Kebony (Norway)
Manufacturer of sustainable hard wood created by modifying sustainably sourced soft wood

(*continued*)

Novomer (United States)
Producer of sustainable polymers and chemicals that use CO_2 as feedstocks via proprietary catalysts
Solidia Technologies (United States)
Developer of proprietary technology used in building and construction materials that can reduce CO_2 emissions up to 70 % while needing less water and lower temperatures
The NanoSteel Company (United States)
Developer of advanced nanostructured material solutions for the oil and gas, mining, power, and automotive industries
Agriculture and Food
Arcadia Biosciences (United States)
Developer of agricultural technologies such as low-water and nitrogen-consuming plants, salt-tolerant plants, and extended shelf-life produce
Kaiima (Israel)
Pioneer of a non-GMO technology platform and advanced breeding program that boosts the inherent productivity and resource usage efficiency of high-impact food and energy crops
Air
Leosphere (France)
Developer of ground-based and nacelle-mounted LIDAR (Light Detection and Ranging) for remote-sensing instruments and atmospheric observation
Liquid Light (United States)
Developer and licensor of process technologies to convert carbon dioxide into high-value major chemicals
Skyonic (United States)
Developer of a carbon dioxide mineralization technology for industrial use in capturing, converting, and sequestering carbon emissions as valuable by-products
Biofuels and Biochemicals
Avantium (Netherlands)
Developer of a process to convert biomass into bio-based materials and fuels
Beta Renewables (Italy)
Developer of cost-effective nonfood cellulosic biomass for biofuel production
Elevance Renewable Sciences (United States)
Creator of specialty chemicals derived from natural oils for use in personal care products, detergents, additives, engineered polymers, and specialty chemicals
Enerkem (Canada)
Producer of biofuels and chemicals from waste with proprietary thermochemical technology
Genomatica (United States)
Developer of green chemicals from renewable feedstocks such as sugar and garbage
Green Biologics (United Kingdom)
Developer of microbial, fermentation, and process technology to turn readily available waste and agricultural byproducts into high-value chemicals and fuels
Energy Efficiency
LanzaTech (United States)
Developer of a carbon capture and reuse technology that transforms abundant waste and low-cost resources into low-carbon fuels and chemicals

(*continued*)

NexSteppe (United States)
Developer of sustainable feedstock solutions for the biofuels, biopower, and bio-based products' industries
OPXBIO (United States)
Manufacturer of renewable bio-based chemicals and fuels including BioAcrylic from sugar feedstocks
Verdezyne (United States)
Producer of bio-based chemicals from renewable, nonfood sources
Biomass Generation
Cambi (Norway)
Provider of a technology to convert biodegradable material to renewable energy
Conventional Fuels
Electrochaea (Denmark)
Developer of a power-to-gas energy storage technology that converts excess electricity from wind and solar into renewable gas for direct injection into the existing natural gas infrastructure
Hicor Technologies (United States)
Developer of compression technology that decreases the energy required to compress and transport natural gas
LP Amina (China)
Provider of products and services that improve the efficiency and reduce emissions of power plants
Siluria Technologies (United States)
Developer of methane conversion technology for creating fuels and chemicals from natural gas
Energy Efficiency
AlertMe (United Kingdom)
Developer of a smart energy and home monitoring system that allows users to control energy usage in all appliances
Alphabet Energy (United States)
Developer of low-cost thermoelectric technology for waste heat recovery
Anesco (United Kingdom)
Provider of energy efficiency and carbon reduction solutions for homeowners, local authorities, and businesses
BuildingIQ (United States)
Provider of a Software as a Service (SaaS) solution to optimize energy use in commercial buildings that can reduce HVAC energy costs by as much as 25 %
Digital Lumens (United States)
Developer of intelligent LED-based lighting systems for industrial facilities that reduce lighting energy use and provide fully integrated controls and reporting capabilities
Eniram (Finland)
Developer of maritime energy management technologies that reduce fuel consumption and emissions in the shipping sector
Enlighted (United States)
Provider of lighting control systems for energy management applications

(*continued*)

FirstFuel Software (United States)
Provider of commercial energy analytics platform to help utilities and government agencies achieve efficiency targets
Glo (Sweden)
Developer of nanowire light-emitting diodes (nLED)
KiWi Power (United Kingdom)
Developer of demand response hardware and software used by large industrial and commercial consumers of electricity as well as government regulators
Lucid (United States)
Provider of cloud-based, real-time performance monitoring software for commercial buildings
LUXeXceL (Netherlands)
Manufacturer of optical solutions for the global LED lighting industry with digital printing, optical and lighting technology
MTPV Power Corporation (United States)
Developer of Micron-Gap Thermal Photovoltaic (MTPV) semiconductors that convert heat to energy with high efficiency
Next Step Living (United States)
Provider of full-service home energy efficiency and environmental impact assessments
Noesis Energy (United States)
Provider of analytical tools and data to help end users make more informed energy management decisions; formerly known as Brazos Software
O-Flexx Technologies (Germany)
Developer of thermoelectric products that convert heat into electricity
OSIsoft (United States)
Provider of enterprise software infrastructure for real-time data
Phononic (United States)
Producer of solid-state heat pumps and fully integrated systems that displace compressors for residential and commercial refrigeration, room air conditioning, and heating
Project Frog (United States)
Designer and manufacturer of resource-efficient and zero-net-energy modular buildings
Renewable Funding (United States)
Developer of innovative solutions for renewable energy and energy efficiency financing
Sefaira (United Kingdom)
Developer of cloud software for high-performance building design
Transphorm (United States)
Developer of technology to eliminate electric conversion losses when converting power from one form to another: AC/DC, AC/AC, DC/AC, and DC/DC
va-Q-tec (Germany)
Provider of customized vacuum insulation panels (VIPs) and heat and cool storage elements containing phase-change materials (PCMs)
View (United States)
Developer of energy-efficient glass technologies for use in buildings

(*continued*)

Energy Storage
Ambri (United States)
Developer of an all-liquid metal battery technology for grid-scale energy storage
Aquion Energy (United States)
Developer of batteries based on ambient-temperature sodium-ion technology; formerly known as 44 Tech
Imprint Energy (United States)
Developer of thin, flexible, print-based, non-lithium rechargeable batteries that use high-conductivity polymer electrolytes
Ioxus (United States)
Developer of ultra-capacitors and hybrid capacitors that can be made into individual cells, prepackaged modules, or complete systems
Sonnenbatterie (Germany)
Provider of battery systems specifically designed to support distributed solar photovoltaic arrays
Stem (United States)
Provider of energy optimization services that combines big data, predictive analytics, and energy storage to reduce electricity costs for businesses
Younicos (Germany)
Younicos is a leading global provider of intelligent energy storage solutions that make grids smarter, more flexible, and more resilient and thus able to accommodate greater amounts of renewable energy
Fuel Cells and Hydrogen
ACAL Energy (United Kingdom)
Developer of chemicals and systems used to power fuel cells both for automotive power trains and stationary power source
Sunfire (Germany)
Provider of energy conversion technologies including solid oxide fuel cells as well as solutions that produce renewable synthetic fuels based on solid oxide electrolyzers
Nuclear
General Fusion (Canada)
Developer of magnetized target fusion energy generation with a new compression system to collapse the plasma
Recycling and Waste
Harvest Power (United States)
Developer of systems that maximize the value of organic materials through the production of renewable energy and soils, mulches, and natural fertilizers
HYLA Mobile (United States)
Provider of mobile phone recycling services (formally known as eRecyclingCorps)
ZenRobotics (Finland)
Developer of robotic recycling systems that use artificial intelligence-enabled waste sorting for construction and demolition waste
Resource Sharing
Airbnb (United States)
Developer of online marketplace that allows people to list and book private accommodations, improving resource utilization and decreasing idle capacity and urban sprawl

(*continued*)

Smart Grid
AutoGrid Systems (United States)
Provider of software and cloud-based services for utilities, grid operators, and end users
C3 Energy (United States)
Developer of smart grid analytics software with applications such as transmission, distribution, and advanced metering
Gridco Systems (United States)
Leader in active grid infrastructure solutions, enabling utilities to more effectively integrate renewable and distributed generation, increase energy efficiency, manage peak capacity, and improve system reliability
Innovari (United States)
Platform provider connecting utility companies with commercial energy partners to incorporate demand-side technology into the grid
Space-Time Insight (United States)
Developer of situational intelligence solutions that transform disparate information into intuitive visual displays that businesses can use to analyze their resources across location and time
Utilidata (United States)
Supplier of voltage optimization products for the electric utilities
Varentec (United States)
Developer of next-generation digital power electronics
Solar
Applied Solar Technologies India (India)
Developer of solar PV off-grid power solutions for telecom towers
Clean Power Finance (United States)
Developer of an online business-to-business marketplace to connect the solar industry with capital markets
M-KOPA Solar (Kenya)
Provider of pay-per-use solar charging systems
Mosaic (United States)
Organizer of community solar financing projects
QBotix (United States)
Developer of robotic technology to improve the operation and management of solar plants
SolarEdge (United States)
Provider of distributed DC systems that maximize power generation of residential and large-scale photovoltaic solar sites
Sungevity (United States)
Solar system integrator targeting the residential rooftop market
Sunpartner Technologies (France)
Developer of thin photovoltaic surface materials
Sunrun (United States)
Developer of solar systems that engage customers through PPAs to eliminate the cost barrier to residential solar adoption
Transportation
BlaBlaCar (France)
Provider of a carpooling online marketplace

(*continued*)

ChargePoint (United States)
Provider of electric vehicle (EV) charging solutions
Proterra (United States)
Developer of battery-powered buses and other clean commercial transit solutions
RelayRides (United States)
Developer of a peer-to-peer car sharing platform that connects car owners willing to rent their cars that are not in use, with drivers who need short-term vehicle access
Streetline (United States)
Provider of smart parking solutions through wireless sensors located in parking spots and managed through a wireless mesh network
Uber (United States)
Provider of an integrated, mobile-based car booking and payment system
Ubitricity (Germany)
Developer and provider of a mobile metering technology and billing platform for EV smart charging infrastructure
Water and Wastewater
Axine Water Technologies (Canada)
Developer of a low-cost, chemical-free solution for treating toxic organic pollutants in industrial wastewater
Desalitech (United States)
Developer of reverse osmosis water desalination projects
FilterBoxx (Canada)
Supplier of containerized water treatment systems to industrial, municipal, resort, and aboriginal clients
Global Water FATHOM (United States)
Provider of cloud-based utility-to-utility solutions for municipalities to manage water systems
i2O Water (United Kingdom)
Developing the world's leading technology solutions for optimizing the performance of water distribution networks
Memsys (Singapore)
Developer of thermal process modules for various water and wastewater applications
Microvi Biotechnologies (United States)
Developer and manufacturer of innovative biocatalytic technologies in water, wastewater, and chemical sectors
Oasys Water (United States)
Developer of a forward osmosis platform for desalination, water treatment, and waste heat recovery
Organica Water (Hungary)
Provider of Fixed-Bed Biofilm Activated Sludge (FBAS) wastewater treatment plants in urban and residential population centers
Ostara Nutrient Recovery Technologies (Canada)
Provider of solutions recovering phosphorus and nitrogen from used water streams and transforming them into environmentally responsible, slow-release fertilizer

(*continued*)

Scinor Technology (China)
Provider of membrane-based water treatment technology
TaKaDu (Israel)
Provider of a Web-based platform that monitors water distribution networks and alerts in real time on inefficiencies, water loss, faults, and other network problems
Wind
Principle Power (United States)
Supplier of WindFloat foundations and design services to offshore wind project developers and utilities

Cleantech in Silicon Valley

USA has been a leader in venture capital financing for Cleantech, which has been particularly vibrant in California where strong Cleantech investment continues. Silicon Valley earned its name and first great fortune as the cradle of the computer age. Then it built a launching pad for the Internet age. Now the valley has assumed a leading role in the global competition to develop renewable energy and other clean, green technologies. Cleantech is poised to be the valley's third great wave of innovation (Harris 2010) – not just the next big thing, but perhaps the biggest thing ever. Confronting the peril of greenhouse gases and climate change happens to be a multi-trillion-dollar business opportunity.

Silicon Valley Could Be Called Solar Valley

Leading venture capitalist suggests that Silicon Valley may someday be called Solar Valley, given that dozens of solar companies have sprung up in recent years. But solar represents just one aspect of the Cleantech revolution. Around the valley, technologists are now busy trying to electrify the automobile industry, driverless cars, while other technologists are developing energy-efficient glass, drywall, and cement. Still others are introducing cutting-edge information technology to the twentieth-century electricity grid, working on biofuels and fuel cells, and pioneering new methods to recycle waste, protect air and water quality, and enhance agriculture and aquaculture.

Cleantech may seem like a radical departure from Silicon Valley's semiconductor roots. But solar photovoltaic cells are a simple form of semiconductor, and smart grid innovators are essentially integrating twenty-first-century software efficiencies into a wasteful twentieth-century electrical infrastructure. The valley's expertise in biotechnology is vital to biofuels, and its work in nanotechnology is critical to new materials that might find their way into nuclear reactors or a suburban home.

However, Silicon Valley does not have a natural advantage in talent – like chemical engineers, fermentation experts, engine designers, and physicists. But Silicon Valley does have a support culture for entrepreneurship and a culture of risk-taking and risk-funding.

Goldman Sachs' Investment in Silicon Valley

Investment banking giant Goldman Sachs (Parkinson 2014) has declared the renewable energy sector to be one of the most compelling and attractive markets and is backing up its talk with $US40 billion of made and planned investments.

Goldman Sachs is not the first big bank to talk up the renewable energy sector, or even "sustainable" investment. But it is one of the first to put real money behind it. In 2012, the bank made a commitment to invest $US40 billion in renewable energy, and it has made a number of large equity investments, over and above the normal advisory and fundraising work that is the usual bread-and-butter revenue for investment banks such as Goldman Sachs.

Among Goldman Sachs' key investments are the recently approved $1.5 billion investments for a near 20 % stake in Danish offshore wind energy developer Dong Energy. It has also a substantial investment in BrightSource Energy, which is about to bring its huge Ivanpah solar power project (pictured) into full production; it will be the largest in the world.

Goldman Sachs also provided $500 million of finance to SolarCity, to allow the biggest solar installer in the USA to expand its solar leasing business. Goldman is one of a number of banks to do that; the latest was Bank of America/Merrill Lynch.

0.01w?>It has also been an early investor in First Solar, the largest solar PV manufacturer in the USA, and SunEdison and made big money from the sale of Horizon Wind Energy to Portugal's EDP for $2.15 billion in 2007. Goldman's commitment of $40 billion is based around a number of assumptions: that costs will continue to decline as efficiency improves, that solar and wind will reach grid parity without subsidies in the nottoodistant future, and that energy storage issues will also be solved.

Google Makes Huge Investment in Clean Energy

When we conduct a search on Google, our query goes across the Internet, hits a server, gets processed, and is sent back to us in microseconds. One would be surprised how much energy is consumed in that process.

In the fourth quarter of 2013, Google (Berniker 2014) spent $2.25 billion on data centers and infrastructure spending, a huge area of costs for the company. That's one of the reasons the company is aggressively moving to solar, wind, and other alternative energies to power its data centers and banks of servers scattered around the world (Fig. 5).

If you ask the executives of Google, Apple, Facebook, or Microsoft, they will all tell you they are gigantic consumers of energy. And it's for this reason that top companies in Silicon Valley are in a race to be the leader of clean and renewable energies. But more than any other, Google is the most aggressive in advancing a clean energy agenda. Google has made 15 wind and solar investments totaling more than $1 billion in 15 projects that have the capacity to produce two gigawatts of

Figure 5 The Google campus has numerous green buildings designed for minimum power usage that helps reduce the company's carbon footprint. (Source: Nickelsberg, Getty Images)

power around the world, mostly in the USA, but that's the equivalent of Hoover Dam's worth of power generation.

In Feb 2014, one of the Google's solar investments kicked into operation. Google and several partners flipped the switch on the world's largest solar thermal project in Ivanpah, near the California-Nevada line. The project uses 347,000 sun-facing mirrors to produce 392 MW of electricity. Ivanpah's clear energy will power electricity for more than 140,000 California homes.

And while Google isn't alone among Silicon Valley's top tech companies to embrace alternative energy usage, no other company is looking at solar and wind as integrated in fueling its internal operations and also making sizable external investments.

Cleantech in Emerging Markets

The Pew Environment Group has released a report which shows that China's investments in clean energy have overcome the US figures. According to Pew, China now leads the way with $34.6 billion invested in 2009 across all investment types – nearly double the US figure of $18.6 billion (Berger 2010).

Top 10 Developing Nations Investing in Clean Energy

The history of clean energy in leading countries like Denmark, Spain, or Germany is well known: big investments, subsidies, and an energy matrix that is much greener than that of other developed nations like the USA or Japan. However, developing nations represent a large and rapidly growing share of the world's clean energy investment, according to Climatescope 2014 (Climatescope 2014), a

country-by-country assessment, interactive report, and index that offers the clearest picture yet of clean energy in 55 emerging markets in Africa, Asia, and Latin America and the Caribbean.

The results of this study suggest that renewable technologies can be just as cost-competitive in emerging parts of the world as they are in richer nations and show how clean energy capacity added in these nations grew at a faster pace than in developed countries, more than doubling in the past 5 years and totaling 142 GW, more than France's current capacity. According to Climatescope, these are the top 10 developing countries in clean energy investments:

1. China
2. Brazil
3. South Africa
4. India
5. Chile
6. Uruguay
7. Kenya
8. Mexico
9. Indonesia
10. Uganda

China's Cleantech has primarily been a project of government initiative and funding and ranks #1 and received the highest ranking as the largest manufacturer of wind and solar equipment in the world and the largest demand market for said equipment, followed closely by Brazil, Latin America's biggest economy. While Brazil still dominates, Latin America and the Caribbean as a whole are emerging as a destination for clean energy investment with Chile, Uruguay, and Mexico making it to the top 10.

Demand for clean energy is growing faster in these countries than in more developed nations. From 2008 to 2013, Climatescope nations added 142 GW of new, non-large hydro-renewable capacity. That represented a 143 % growth rate. By comparison, wealthier OECD nations added 213 GW, posting a clean energy capacity growth rate of 84 %. At a regional level, clean energy provided more than 92 TWh in 2013 to the Latin American and Caribbean's 600 m population, representing 6.4 % of total energy generation. Adding large hydro-generation, which is not included in the Climatescope survey, the region met more than half of its power demand through zero-CO_2 emitting power sources.

Goldman Sachs' Investments in Emerging Markets

In the past two years, Goldman Sachs' investments are focus on the emerging economies of Brazil, China, India, and Mexico – along with developed economies such as Japan and South Korea that have also made a large commitment to renewables and are reliant on expensive fossil fuel imports.

In Japan, Goldman Sachs has established a new independent power producer called Japan Renewable Energy (JRE) – to develop, build, and operate solar, wind, and other renewable projects. It is backed by the bank's $3.1 billion GS Infrastructure Partners II fund (GSIP). It has already committed to a 250 MW solar project in Okayama and a 40 MW PV plant near Tokyo.

Goldman has paid more than $3400 million for a majority stake in an Indian wind energy business called Renew Wind Power, which plans to build 1 GW of facilities within 2 years, and it is looking to build solar energy plants to supply mining operations in Chile, where even companies such as BHP Billiton are looking at alternatives. Other investments include the FloDesign Wind Turbine, a startup that was developing an experimental high-efficiency shrouded wind turbine, and South Korean wind turbine manufacturer CS Wind, which plans an IPO this year.

Hong Kong as a Launchpad for Overseas Green Tech Start-ups

The limelight has long been shed on Hong Kong as a start-up-friendly destination (2015). Besides efficient business setup, a robust legal system, easygoing regulatory environment, and a simple tax system, one of the Hong Kong's greatest advantages is its proximity to the largest economy in the world.

China, a massive but notoriously challenging market to navigate, is the ultimate expansion destination for many foreign start-ups – especially those in the green energy space. Besides overtaking Germany as the world's biggest market for solar power in 2013, China has also exceeded the USA in energy-efficient investments – spending $4.3 billion on smart grids in the same year. According to the Global Status report 2014, China has also dropped a whopping $56.3 billion on projects within the wind, solar, and renewable arena. The following is an example of a start-up story reported by Asia on 04 Jan 2015.

A Canadian hardware start-up Nanoleaf, which makes the world's most efficient LED lightbulb **(photo on the right)**, used Hong Kong to grow the Asia side of their

business. Cofounder and COO Christian Yan said: "Electronics-wise, Shenzhen, Guangzhou and the Dongguan area is your epicenter for everything that is made, and Hong Kong being so close to Taiwan as well – that makes it the perfect place to be. Plus the English transparency, almost zero corruption, fast company registration, small accounting firms, co-working spaces and trademark registration."

On their road to IP protection, Nanoleaf needed to register a trademark in China, Hong Kong, Europe, and the USA, and Yan noted the vast differences in efficiency. He revealed that while the registration process in Hong Kong was completed within 6 months, with the USA and Europe finishing soon after, Nanoleaf is still waiting on China's approval. As for entrepreneurs looking to apply for a design or utility patent in China, Yan said they should expect more than 3 year's wait.

Staying close has contributed to Nanoleaf's success. Besides piquing the interest of Li Ka-shing – one of the richest men in Asian, who has invested an undisclosed sum via his VC firm Horizons Ventures – Nanoleaf raised almost $500,000 through two Kickstarter campaigns and has also launched into Hong Kong retail stores. With distribution partners in the USA, Canada, Germany, Scandinavia, and Dubai, Yan said that Nanoleaf has 50,000 units in the pipeline ready to be sold globally and will be moving into Australia and China by 2015.

For other start-ups in the green tech space seeking a launchpad for Asia-Pacific, they should look no further than Hong Kong.

Why Greentech Will Be Huge in India

Compared to the difficult market that technologies like clean power and water desalination face in many states in the USA, because of India's rapidly growing GDP, the country is quickly building out its infrastructure – including power generation and water systems (2011). That means green technologies have the potential for a vibrant and growing market within the country. The Indian government has also taken a large role in setting mandates to push clean power from the top down.

Because of the desire for more energy, Indian plans to add 100 GW of power generation over the next 5 years, and that will be made up by mostly coal and clean power. The rapidly growing Indian middle class will soon want to consume similar amounts of power to the USA and Europe, and that will require these massive power infrastructure projects.

GE is focusing to develop technology and people in renewable energy and smart grid. Wind is currently cheaper than solar on a per kWh basis and is an even bigger market than solar in India right now. GE, which is one of the world's largest wind blade makers, is also working on how to use energy storage to make the grid more reliable, as well as smart grid technology in the country.

Clean power growth – Indian is installing 3 GW of solar by 2016, compared with the 54 MW of solar installed in 2010. The government has a top-down plan to hit

20 GW of solar by 2020, and big power companies and start-ups alike are developing solar project development businesses.

Smart grid and clean water – The power grid is a major bottleneck for adding on 100 GW to India's power grid, and the power companies will need to invest in making the grid much more efficient than it currently is. GE has been researching and testing smart grid technologies for the domestic market in its labs, and other companies like IBM have a strong presence in India.

India's utilities are also looking to build out clean water infrastructure, as clean running water has been notoriously poor to date. Desalination projects that can't get funding in markets like the USA – where clean water pipelines reach almost 100 % of the population – are far more economic in India. And there is a lot of money to be made in clean water. A desalination company VA Tech Wabag, based in Chennai, India, went public in 2010.

Israel Crowned World's Top Innovator in Cleantech Field

Israel is the country with the most potential to produce and commercialize entrepreneurial Cleantech start-up companies according to the 2014 Global Cleantech Innovation Index (2014). "Israel topped the 2014 index, with its relative outperformance on the measure of start-up companies per capita being a key reason that it did so," the report, released Tuesday, said. "The country generates the culture, education and 'chutzpah' necessary to breed innovation, plus it has the survival instincts."

The annual report, compiled by the Cleantech Group and World Wildlife Foundation, compiled data on 40 countries reflecting their level of innovation, government support, infrastructure, and existing Cleantech companies in fields such as alternative or renewable energy, water technology, and other environmental technology.

Israel scored a 4.34 on the index, followed by Finland with 4.04, the USA with 3.67, Sweden with 3.55, and Denmark with 3.45. In the past 3 years, Israel had 19 Cleantech companies voted onto the shortlist of the Global Cleantech 100 index.

Yet while Israel's overall score put it on top, other countries bested it in the individual categories. Israel pulled ahead with a particularly strong score on its Emerging Cleantech Innovation score: 8.92. Only three other countries scored above a five on the measure, which included data on early-stage investment, high-impact companies, and environmental patents. Most scored between zero and two.

"No one country excelled in all four indicators," the report stated. "Israel, for example, far exceeded others in the emerging cleantech innovation factor, however dropped to eighth place in the 'evidence of commercialized innovation' factor – confirming that there is room for improvement in even the most inspiring countries."

Avi Feldman, who leads the Cleantech forum at the umbrella group Israel Advanced Technology Industries, says that while the government is generally

helpful, it could play a stronger role in helping Cleantech companies develop beyond their early stages. Like biotechnology, he says, Cleantech companies take longer than others to get from early development to marketing their products and producing revenues. “The support has to be divided into the different stages of company growth. I think that most of the government support is directed at the very early stages, leaving the companies to die later on,” he said.

Even though most Cleantech companies look toward a global market, he believes that Israel could do more to encourage companies by adopting more renewable technology into its energy plans. While German energy is about 27 % renewable and American energy about 13 %, Israel lags far behind. Israel has the best conditions for solar [energy production] but gets only 1 % of its energy resources from it.

Concluding Remark: Integration and Deployment of Cleantech

The following four phases are essential to implement a Cleantech innovation:

(a) A concept development through academic approach from multidiscipline field
(b) A prototype development
(c) A small-scale infrastructural project
(d) A larger-scale infrastructural implementation

This sequence involved multidiscipline, integration of Cleantech individual partners, venture capital investment, and multinational corporations.

Deployment of Cleantech – Modern society is counting on Cleantech to meet growing energy and other resource demands while reducing environmental impacts and generating new opportunities for the economy. However, it is important to remember that ultimate success will depend on the coordination of technology development and technology deployment, two separate endeavors, each with requisite incubation characteristics and catalysts.

Deployment often depends on the scalability and price parity of new technologies, which often takes years beyond the time of the initial innovation for it to reach the mainstream. New technologies have the potential to continue to improve the world but also require planning and long-term commitment to its application – indeed, a different skill set than the work of innovation itself.

Therefore, it is important that individuals, engineering and science graduates, participating in Cleantech maintain a balanced perspective, based on creativity on the one hand and pragmatism on the other hand, while focusing on the goal of advancement. Through this chapter, readers should gain an overview of the trends in venture capital-funded innovation in Cleantech, the broad scope of the basic science and technology, and Cleantech implications that affect world climate change.

Appendix

Venture Capital Firms in the USA

USA has more than 2000 VC firms. The best way for an entrepreneur to seek VC funding is first look at the local or regional VC firms to begin with. The following is the list of 100 of the most active venture capital firms funding US start-ups in 2014. It is critical to find a firm that fits your journey. A true venture partner provides more than money but mentorship and strategic advice that can elevate your business to new heights (100 of the most active venture capital firms).

Ranking	Firm names	US $million invested	No. of deals
1.	Andreessen Horowitz	1,020.23	50
2.	Khosla Ventures	808.63	45
3.	SV Angel	736.74	47
4.	Accel Partners	721.59	29
5.	New Enterprise Asso.	690.65	44
6.	Sequoia Capital	650.34	30
7.	Venrock	620.26	15
8.	First Round Capital	606.17	34
9.	Spark Capital	542.33	18
10.	Triangle Peak Partners	535.03	3
11.	Franklin Square Cap	505.00	1
12.	Kleiner Perkins Cauf	489.25	33
13.	Google Ventures	461.89	35
14.	Founders Fund	450.41	21
15.	ARCH Venture Parts	445.61	9
16.	Bezos Expeditions	425.50	6
17.	Lightspeed Venture	414.91	21
18.	Thrive Capital	390.70	18
19.	General Catalyst	373.22	24
20.	Redpoint Ventures	363.98	24
21.	Atlas Venture	359.45	35
22.	QED Investors	353.82	1
23.	Greylock Partners	336.41	20
24.	Formation 8	321.26	18
25.	Bain Capital VC	274.79	12
26.	Iridium Communica	270.00	1
27.	Lerer Hippeau VC	269.48	30
28.	Collaborative Fund	266.20	19
29.	Bessemer Venture	255.24	19
30.	Flagship Ventures	248.38	6

(*continued*)

Ranking	Firm names	US $million invested	No. of deals
31.	OrbiMed Advisors	247.99	8
32.	SherpaVentures	241.37	15
33.	Insight Venture	230.00	5
34.	Institutional Venture	220.28	6
35.	True Ventures	217.26	33
36.	Greycroft Partners	214.55	22
37.	Menlo Ventures	211.77	13
38.	Intel Capital	210.69	22
39.	Battery Ventures	206.51	14
40.	Tiger Global Mgmt	206.08	7
41.	Deerfield Mgmet	202.31	4
42.	Charles River VC	199.96	17
43.	WRF Capital	199.86	7
44.	Benchmark Capital	198.90	7
45.	FirstMark Capital	196.51	11
46.	CrunchFund	196.51	20
47.	Canaan Partners	195.36	15
48.	Polaris Partners	195.19	12
49.	Sofinnova Ventures	194.51	5
50.	InterWest Partners	189.12	9
51.	Crestline Investors	176.00	1
52.	Third Rock Ventures	174.65	5
53.	Slow Ventures	169.83	14
54.	VegasTechFund	167.83	20
55.	Comcast Ventures	166.54	12
56.	Felicis Ventures	164.30	16
57.	Draper Fisher Jurve	162.85	11
58.	ff Venture Capital	162.63	11
59.	Norwest Venture	160.74	10
60.	Silicon Valley Bank	159.06	10
61.	5 AM Ventures	157.85	5
62.	Rock Springs Capital	157.75	3
63.	GGV Capital	157.40	8
64.	Social + Capital Partnr$153.39	13	
65.	Correlation Ventures	152.43	19
66.	Qualcomm Ventures	149.74	16
67.	AME Cloud VC	149.41	14
68.	DCM	149.07	10
69.	Madrona Venture	149.00	15
70.	MPM Capital	146.62	8
71.	Harrison Metal Capital$146.58	9	
72.	500 Start-ups	143.19	29

(*continued*)

Ranking	Firm names	US $million invested	No. of deals
73.	RRE Ventures	142.41	14
74.	Shasta Ventures	141.06	17
75.	Alexandria Venture	140.88	4
76.	The Data Collective	139.02	18
77.	SV Life Sciences	138.05	4
78.	Alexion Pharma	135.00	1
79.	Foundation Capital	134.05	8
80.	Fidelity Investments	134.00	1
81.	RA Capital Managem	130.50	3
82.	BoxGroup	130.41	17
83.	Laboratory Corp America$130	1	
84.	Crosslink Capital	128.49	16
85.	e.ventures	128.14	11
86.	Revolution	126.28	4
87.	SoftBank Capital	125.11	16
88.	Fidelity Biosciences	124.00	5
89.	T. Rowe Price	122.75	2
90.	IA Ventures	119.48	7
91.	Western Technology	119.20	8
92.	Matrix Partners	116.61	12
93.	Summit Partners	116.39	2
94.	Wellington Mgmt	113.75	3
95.	Trinity Ventures	113.58	12
96.	Aisling Capital	112.68	6
97.	FLOODGATE Fund	112.32	16
98.	Cisco Investments	112.05	6
99.	Forerunner Ventures	110.38	8
100.	Mousse Partners	104.21	4

Venture Capital Firms in Europe

Europe historically did not have many VC firms. In recent years, the VC industry has flourished. Here is a directory as provided by Directory (2010):

3i	Investment focus: European and South-East Asian start-ups
Add Partners Limited	Focus: early- to late-stage European start-ups in information technology
AltAssets	Focus: news service for global venture capital and private equity professionals

Ariadne Capital	Focus: part of a new European model, helping manage investor exits, drive consolidation, and leverage entrepreneurialism
Athena	Focus: international, for-profit, high-technology, business incubator
Baring Communications Equity	Focus: media and communications focused fund for Central and Eastern Europe and the CIS
Business Angels Connect	Focus: global services package to young entrepreneurs
CGS Management	Focus: medium-sized technology-based European companies with an emphasis on Switzerland
Cobblestone Private Equity	Focus: venture-oriented direct investments in emerging European technology companies seeking expansion and US market penetration
Copan	Focus: leading European technology executives and investors
Delta Partners	Focus: venture capital and private equity early-stage funding to high-technology companies in Europe and Ireland
DeMinds	A pan-European investment group focused on the global Internet market
European Equity Partners	Investment focus: Euro one-half to three million initially and up to Euro five to eight million based on meeting key milestones and criteria
Financier Natexis Banques Populaires	Focus: private equity investment holding company active in all segments of the business including venture capital
Hunter Lovec	Focus: consultants helping Central European companies solve their financial problems and achieve their financial goals
IDEA Network	Focus: network of international experts and consultants working under donor-funded projects
Innova Capital	Focus: advises private equity funds with more than Euro 300 million for investments into profitable companies in the EU accession countries of Central Europe
Internet Ventures Scandinavia	Focus: adds capital and partner experience to unique Internet ventures

Invest Mezzanin	Investment focus: later-stage private equity investing in companies in Austria, Switzerland, and Germany
Investindustrial Holdings Limited	Specializes in medium-sized companies, principally in Italy and Spain
Kildare European Leader Teoranta	Focus: rural development company for County Kildare, Ireland, with funding to distribute to innovative rural projects
Mericom	Focus: venture capital financing and investment services for telecommunication projects, start-up companies, and new businesses in the telecom industry
Michelsen-Partners	Focus: European cross-border mergers and acquisitions advisory services, structured finance advice, and international fund management
Net Partners	Investment focus: European start-up and early-stage initiatives related to the Internet
Northzone Ventures	Offers early-stage venture capital investments and focusing on technology companies
ORAH Investments	Swiss-based venture capital holding financing businesses in Southeast Europe
Permira	Investment focus: formerly known as Schroder Ventures Europe, a leading private equity group and advising funds
Pino Venture Partners	Investment focus: Italian company for operations in information technology, communications, and media
PrivateEquityOnline.com	Focus: tracks private equity activity across Europe, delivering daily news on funds, deals, and exits
PROPHETES	Focus: providing and investing venture capital into innovative companies and projects and providing support to investors who invest capital in the countries of Southeastern Europe
Seven Summits Capital	Focus: active in the international private equity market participating in buyouts as an investor, initiator, or catalyst
Start-up Avenue	Paris-based B2B incubator funding Internet start-ups that focus on Europe

Stratos Ventures	Investment focus: wireless information and communications technology companies with substantial global growth potential
Triago	Focus: private equity fund-raising, limited partnerships, and joint ventures
Trust Capital Partners	Focus: Belgian venture capital investment fund
VCG.dk	Focus: lists all Danish venture companies and a profile on them
Venture Capital in Europe	Discussion of the state of venture capital in Europe and its trends
Venture Consulting	Focus: professional business consultancy and services based on extensive international experience
ViewPoint Capital Partners	Specializes in software technology companies in early-, expansion-, and late-stage situations. Offices in Frankfurt, Amsterdam, and Zurich
West Private Equity	Focus: provides capital for management buyouts and buy-ins and the expansion or refinancing of companies headquartered in Western Europe

Venture Capital Firms in India, China, Japan, and Israel

India's venture capital industry has about 25 VC films. Wekpedia.com has a listing.

China's venture capital industry has more than 150 VC firms, which altogether manage over US$100 billion in venture capital and private equity funds. China Venture Capital Association (CVCA) provides details of its VC services at www.cvca.com.cn (China Venture Capital 2010).

Japan's venture capital industry has about 100 active funds. A list could be found at www.irasia.com/venture/jp (2010).

Israel's venture capital industry has about 70 active venture capital funds, of which 14 international VCs with Israeli offices. For more information, refer www.investinisrael.gov.il (2010).

Australia's venture capital industry has very limited VC films. It is mainly supported by the government. For detail, see www.avcal.com.au (2010).

How to Secure Venture Capital Money?

Venture capitalists invest money in start-ups in exchange for an equity ownership in the company. VCs receive hundreds of business plan from entrepreneurs each year. There are more than 1,000 venture capital funds around the world. Here are few tips to gain the attention of VC:

Step 1: Prepare a comprehensive **business plan**. VCs will expect you to clearly define the purpose of your business, disclose pertinent financial information (including revenue streams and projections), and provide information on your executive management team.

Step 2: Do research on venture funds to find the appropriate fit for your company. Look in Pratt's Guide to Venture Capital Sources, available in many bookstores and libraries, to see what fields each firm is likely to fund. Some focus on retail and service companies, while others look specifically for technology start-ups.

Step 3: Get an introduction to the venture capital firm. You'll have a much better chance if you've been personally introduced to the VC rather than blindly sending your business plan. These introductions can be made by executives of companies already being funded by the VC or by lawyers and accountants who work with the firm. Try to contact four to five VCs.

Step 4: Arrange a meeting with the VC. Consider bringing key members of the management team to the meeting.

Step 5: Follow up your visit with a thank-you note and additional information.

Step 6: Be persistent and polite; wait for VC evaluations.

How a Business Plan Is Evaluated?

When a business plan (BP) arrived at VC office, venture capitalists tend to give a quick review. If they decide a BP deserves a further study, the entrepreneur is invited to VC office for a power point presentation. In the process, one venture capitalist categorized BP into four types (2010): *a Home-run*, *a Struggle*, *a Joy-ride*, *or a Time-waster*. A Joy-ride project will get many media publicity, but investors would not make much return. The objective of VC is to sponsor a real winner – a Home-run. A project that is not too obvious or too easy to implement; otherwise, others will launch the identical or similar one. When great minds think alike, most of them don't make much money. So a good BP needs:

- High market potential – customers will buy it.
- Technology novelty – nonobvious innovation.
- An entrance barrier – a valid patent protection.
- A cohesive and complementary team – technology skill plus management professional.
- A complementary business alliance.
- Reasonable funding requirement.
- Reasonable timing to realize a high return.

Cleantech Expert Panel for Global Cleantech 100

A valuable reference for those who seek investment and sponsorship from venture capitalists and corporate sponsors (CleanTech 100 2014):

Laura Nereng, Business Development Manager, 3 M
Andre Loesekrug-Pietri, Managing Partner, A Capital
Grant Allen, Senior Vice President, ABB Technology Ventures
Rhea Hamilton, Managing Director, Aeris Capital
Greg Fleming, Investment Director, ALIAD (Air Liquide)

Jean-Pascal Tranie, President, Aloe Private Equity
Paul Gagliardo, Manager – Innovation Development, American Water
Tae Jun Park, Senior Investment Associate – Applied Ventures, Applied Materials
Pascal Siegwart, Partner, Aster Capital
Rob Day, Partner, Black Coral Capital

Eric Landais, Managing Director, Blue Orange (Suez Environment)
Ulrich Quay, Partner, BMW iVentures
Meghan Sharp, US Director, BP Ventures
Sulkhan Davitadze, Investment Director, Bright Capital
Dr. Paul Decraemer, Senior Investment Manager, Capricorn Venture Partners

Ian Cooke, Director, Head of New Ventures, Carbon Trust
Dr. Wal van Lierop, President and CEO, Chrysalix Energy Venture Capital
Paul Straub, Partner, Claremont Creek Ventures
Stefan Brand, Senior Manager, New Business Development, Clariant
Troy Ault, Director of Research, Cleantech Group

Sheeraz Haji, CEO, Cleantech Group
Michele Parad, Senior Analyst, Cleantech Group
Richard Youngman, Managing Director, Europe and Asia, Cleantech Group
Alex Betts, Partner, Climate Change Capital
Peter Kennedy, Managing Director, CLSA Capital Partners

Nancy Pfund, Managing Partner, DBL Investors
Olivier Dupont, Chairman of the Board, Demeter Partners
Rodrigo Navarro, New Business Creation Manager, DSM Innovation Center
Konrad Augustin, Principal, Strategic Co-Investment Group, E.ON
Valery Prunier, Director, Innovation North America, EDF

Luis Manuel, Executive Director, EDP Ventures
Gina Domanig, Managing Partner, Emerald Technology Ventures
Carlo Papa, Chief Innovation Officer, Enel Green Power
Sumit Sarkar, Director – Venture Investments, Energy Technology Ventures
Wally Hunter, Managing Director, EnerTech Capital

Fabrice Bienfait, Principal, Environmental Technologies Fund
Dr. Bernhard Mohr, Managing Director – Corporate Venturing, Evonik Industries
Dr. Dirk De Boever, Head of Investments, Finindus

Ignacio Martinez, Partner, Flagship Ventures
Chris Thomas, Founder and Partner, Fontinalis Partners

Iyad Omari, Partner, Frog Capital
Hendrik Van Asbroeck, Director Corporate Venture Capital, GDF Suez
Andrew Lackner, Senior Director, Investments, GE Ventures
Colin Le Duc, Partner, Generation Investment Management LLP
Nicholas Atkins, Partner, Georgieff Capital

Sherwin Prior, Corporate Strategy and Business Development, GM Ventures
Eric Wang, Partner, GRC Chrysalix
Thorbjorn Machholm, Business Development Director, Grundfos New Business
Tony Pandjiris, Managing Director, Hercules Technology Growth Capital
Diego Diaz Pilas, Head of New Ventures, Iberdrola

Nicolas Chaudron, Partner, Idinvest Partners
Kelsey Lynn, Director, Technology Ventures, Imperial Innovations
Sean Petersen, Senior Investment Officer – Venture Capital, International Finance Corporation (IFC)
Glen Schwaber, Partner, Israel Cleantech Ventures
Joe McGee, Executive Vice President – Strategic Planning and Development, Jabil

Kevin Self, Vice President, Strategy and Corporate Development, Johnson Controls
Eric Tao, Partner, Keytone Ventures
Guido Ketteler, Innovation and Technology Manager, Lanxess
Kai Engelhardt, Head of Corporate Venture Capital, Mahle
Yossi Yaacoby, Director of WaTech Division, Mekorot

Kevin Kuhn, General Manager, Mitsubishi Corporation (Americas)
Martin Kröner, Managing Partner, Munich Venture Partners
Ravi Viswanathan, Partner, New Enterprise Associates
Keith Gillard, General Partner, Pangaea Ventures
Iñigo Palacio, Director, Repsol Energy Ventures

Keimpe Keuning, Investment Director, Robeco SAM Private Equity
Dhiraj Malkani, Partner, Rockport Capital Partners
Fabien Mondini, Senior Investment Manager, Sabic Ventures
Chris Brown, Partner and Chief Scientist, SAIL Capital Partners
Delphine Geny-Stephann, Director of NOVA External Venturing, Saint Gobain

MJ Maloof, Investment Director, Saudi Aramco Energy Ventures
Xavier Datin, Senior Vice President – EcoBusiness, Schneider Electric
Gerd Goette, Investment Partner, Siemens Venture Capital
Joshua Raffaelli, Partner, Silver Lake Kraftwerk
Thierry Piret, Head of Corporate Venturing, Solvay

Mark Bonnar, Investment Director, Southern Cross Venture Partners
Kurt Faulhaber, Investment Director, Stafford Capital Partners
Vicky Sharpe, Strategic Advisor to the Board, Sustainable Development Technology Canada (SDTC)
Peleg Chevion, Global Head of Abiotic Stress Management/Crop Enhancement, Syngenta
Astorre Modena, Partner, Terra Venture Partners

Nick Cizek, Sensor Strategist, The Climate Corporation
Mike Jackson, Managing Partner, The Westly Group
Steve Kloos, Partner, True North Venture Partners
Don Ye, Partner, Tsing Capital
Stephan Dolezalek, Managing Director, VantagePoint Capital Partners
Mia Javier, Senior Open Innovation Officer – Americas, Veolia Environnement
Joseph Vaillancourt, Vice President – Corporate Venturing, Waste Management
Samer Salty, CEO, Zouk Capital

References

(2010) Japan venture capital industry. www.irasia.com/venture/jp
(2010) Israel venture capital industry. www.investinisrael.gov.il
(2010) Australian Private Equity & Venture Capital Guide 2010. www.vcjournal.com.au
(2011) Why Greentech will be huge in India. www.gigaom.com. 19 Dec 2011
Berger E (2010) China's clean energy investments surpass the United States. www.blogs.chron.com/sciguy/archives/2010/03/. 25 Mar 2010
Berniker M (2014) Google makes huge investment in clean energy. ETCNBC.com. 16 Feb 2014
China Venture Capital Association (2010) China venture capital industry. www.cvca.com.cn
Clean Tech Open Defines Clean Technology (2015) www.cleantechopen.com
CleanTech 100 (2014) www.CleantechGroup.com
Climatescope (2014) Global study shows clean energy activity surges in developing world. Bloomberg – New Energy Finance. 28 Oct 2014
Directory Investment (2010) Venture Capital in Europe.www.directoryinvestment.com
Global Cleantech Innovation Index (2014) www.CleantechGroup.com
Harris SD (2010), Cleantech: Silicon Valley's next great wave of Innovation. www.MercuryNews.com. 11 May 2010
How to Evaluate a Business Idea. www.Gaebler.com
Iris L (2015) Hong Kong: "The Perfect Launchpad for Overseas Green Tech Startups" Forbes Asia www.forbes.com. 4 Jan 2015
MoneyTreeTM Report- Q3 (2014) San Jose Mercury News
Parkinson G (2014) Goldman Sachs sees 'transformational moment' in renewables investment. http://www.greentechmedia.com/. 5 Feb 2014
Tanya BK (2015) 100 of the most active venture capital firms. www.entrepreneur.com/vc100
Venture Capital & Venture Capitalist (2014) www.wikipedia.org
VC (2014) CBInsights.com

Analysis of the Co-benefits of Climate Change Mitigation

Douglas Crawford-Brown

Contents

Abstract

Economic development of the poorer nations brings competing influences on public health. On the one hand, the increase in per capita wealth reduces susceptibility to environmental pollutants. On the other hand, industrialization may increase the emissions of those same pollutants. Global climate policy negotiations have recognized this conflict, striving to identify a pathway to decarbonize the global economy while allowing growth in world regions at the bottom of the economic pyramid. This chapter explores the conflict by developing a quantitative methodology for calculating the economic growth's net impact on public health and the co-benefits of greenhouse gas reductions associated with exposure to particulate matter. The chapter shows that co-benefits of decarbonization are significant; GDP growth in non-Annex I nations carries its own health benefit; the co-benefits are in part reduced through the increase in GDP by between 12 % and 17 %; and failure to include economic growth projections into co-benefit calculations produces greater errors in co-benefit estimates as the stringency of climate policies is increased.

D. Crawford-Brown (✉)
Cambridge Centre for Climate Change Mitigation Research, Department of Land Economy, University of Cambridge, Cambridge, UK
e-mail: djc77@cam.ac.uk

W.-Y. Chen et al. (eds.), *Handbook of Climate Change Mitigation and Adaptation*,
DOI 10.1007/978-3-319-14409-2_59

Introduction

Justifications for decarbonizing the global economy usually focus on the reduction in greenhouse gas (GHG) emissions and the resulting change in climate risks (Markandya and Chiabai 2009). The political will to carry out ambitious mitigation policies then rests on a belief in the reliability of the science of climate change, the effectiveness of policies at reducing GHG emissions, and the economic costs of the policy actions. Since impacts from climate change can be in areas of the world and for periods of time outside the time and geographic scope of a single nation, political will to act is often reduced.

There are, however, many other reasons why a nation might move along a trajectory of decarbonization. There might be concern for reducing risks of damage to human health from co-pollutants of GHG emissions. There might be concern for energy security. There might be a desire for lower energy bills through reduced energy consumption, reducing energy poverty. There might be a government target for economic development, with investment in low-carbon buildings or infrastructure providing a stimulus for this development. Experience shows that moving a policy such as decarbonization forward is most viable when there are multiple reasons for doing so and where the impacts are local and immediate, ensuring the widest range of participating actors and protection against deep regrets should any one policy justification prove in hindsight to be unwarranted.

It is therefore natural to ask whether decarbonization might bring with it impacts that affect the ability of a nation to reach other economic, energy, and/or environmental aims. These impacts might be beneficial, helping to reach these other policy goals, or they might present new problems that impede reaching climate change goals (a process of maladaptation). Consideration of these co-impacts is important for several reasons:

- If they are co-benefits, they can be used to marshal additional political support for policies of decarbonization.
- Inclusion of co-impacts provides a more complete understanding of the multiple effects of a policy, improving the ability to inform multi-attribute decisions.
- Assessment of co-impacts potentially provides a more balanced perspective on the net costs and benefits of a policy to and within society.
- Co-impacts may reveal a multiplier effect of policies in the economy, better characterizing the beneficiaries of those policies.
- Identification of co-impacts provides insights into where hurdles might be encountered in implementing policies of decarbonization and how they might be overcome.
- Early recognition of adverse co-impacts can avoid situations of backlash if the impacts become evident in the future.

This chapter assesses co-impacts in regard to climate change and decarbonization policies using the example of global public health.

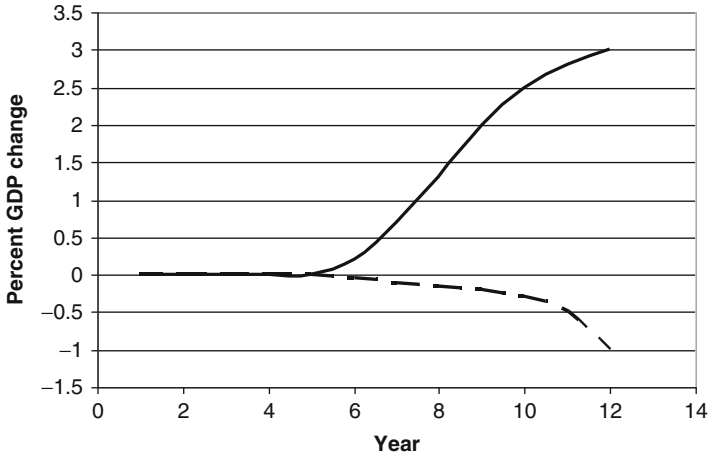

Fig. 1 Predicted impact of a carbon tax on the economy of Bangkok, Thailand, without considering co-benefits of PM reduction (*dashed line*) and with co-benefits (*solid line*). The *y*-axis is a cumulative percent change in GDP relative to the baseline projection with no carbon tax

Since the assessment of co-impacts can add appreciably to the effort involved in policy assessment, it is natural to ask whether the additional information brings significant new insights to the overall societal effect of a policy. As a partial answer to that, consider the case of a study of the impact of carbon taxes on the economy of Bangkok, Thailand (Li 2002). In that study, the impact of a carbon tax on GHG emissions and national GDP was first assessed using an economic model without co-benefits associated with public health. The policy was reassessed taking into account the co-reduction of emissions of particulate matter (PM) when strategies that reduce GHGs through reduced energy consumption driven by a carbon tax are introduced.

The results are shown in Fig. 1, indicating that consideration of co-benefits of reduced PM emissions not only changed the magnitude of predicted GDP impacts but reversed the sign of those impacts. What appeared to be a climate change policy creating a loss of GDP without considering the co-benefits of PM reduction became an impact that was positive on GDP growth when these co-benefits were considered.

Figure 1 concerns only the influence of PM reductions. There are, however, many more co-benefits than from PM reduction, including a variety of environmental and ecological indicators of sustainability. A good review of the literature on these has been provided by Bollen et al. (2009). Their review draws several key conclusions:

- Mitigation policies yield long-term benefits, but effects from co-benefits often are much more immediate and reliable. In the short-to-medium term, it will be largely the co-benefits that will be realized by a nation rather than the direct impacts related to climate change.

- Co-benefits could be achieved by other, more direct policies than climate change mitigation. A key issue is the cost-effectiveness of producing the same improvements in the environment and/or health through GHG reduction policies or through policies targeting benefits directly.
- Climate change and local air pollution policies can at times be in conflict. It is crucial that these interactions be taken into account to ensure the net effect of a co-impact is truly beneficial.
- The health-care cost savings of these co-benefits range between $10 and $60 per ton of carbon dioxide abated. As shown in a study by the OECD (Bollen et al. 2009), the cost savings from the health co-benefits alone will be higher than the cost of abatement for a ton of carbon dioxide equivalent for five of the 15 regions they studied in the global economy.
- The same OECD study (Bollen et al. 2009) estimated that the percentage reduction in premature mortality of all air pollutants combined was slightly below the percentage reduction in GHG emissions; an 80 % reduction in GHG emissions produced approximately a 50 % reduction in annual premature mortality (attributable to air pollution) as of 2050.
- Depending on existing concentrations of pollutants in ambient air, the co-reduction of non-GHG pollutants can bring about savings in air pollution control costs, since a reduction in PM and other pollutants by GHG mitigation equates with a savings in reduction by other methods such as investments in scrubbers, baghouses, etc.

The most significant co-pollutants are black carbon, PM, SOx, NOx and N_2O, CH, O_3, and NH_3. As just one example, a study by International Institute for Applied Systems Analysis (IIASA) and the EC Joint Research Centre (IIASA 2004) indicates that a pathway to decarbonization would produce a reduction of 10–25 % for ozone, which is significant given the estimated cumulative loss globally of $580B (2,000 USD) as a result of increased mortality and morbidity associated with tropospheric ozone (Selin et al. 2009).

Co-benefits to Human Health

The human health co-benefits considered here are those of the air toxic that is of primary concern globally in regard to human health as this relates to a co-benefit of GHG reduction: particulate matter (PM). These co-benefits are a function not only of decarbonization policies but also of economic change. Various studies have established a relationship between a country's health variables and economic growth (Barro 1996; Bloom and Canning 2003; Bloom et al. 2004; Weil 2005). Both the susceptibility and sensitivity of populations to environmental change such as ambient PM are functions of socioeconomic status. Significant links between income and general health conditions have been demonstrated in sociology and epidemiology literatures. The change in GDP in many of the poorer nations in the recent past, as those nations simultaneously improve their economic condition and increase GHG

emissions, will therefore change the susceptibility and sensitivity of the populations to PM exposures, in turn changing the co-benefits of decarbonization. It is necessary to include within co-benefit calculations, therefore, the impact of GDP change under decarbonization scenarios on the susceptibility and sensitivity of populations.

The methodology used in this chapter is similar to that used in regulatory assessments of policies aimed at other reductions in air or water toxics. Calculations of the relationship between health and emissions of an air toxic such as PM are often executed at refined levels of spatial and temporal resolution for regulatory assessments (Li and Crawford-Brown 2011). This involves (i) creating the emission inventory for each pollutant for each source category (e.g., mobile, stationary, nonpoint); (ii) gridding the geographic area, often into census blocks or census tracts of several thousand people each; (iii) assigning each source a pollutant emission rate into the relevant geographic gridblock; (iv) using atmospheric dispersion and chemistry models to calculate ambient air concentration; (v) applying "microenvironment" factors to account for differences between ambient air concentration and the concentration indoors, near roadways, etc.; (vi) assigning individuals to specific gridblocks; (vii) developing activity patterns that move people between grid blocks (e.g., through travel) and that determine metabolic rates due to physical activities (e.g., breathing rates); (viii) calculating exposures in each gridblock based on air concentration and activity; (ix) applying age-specific risk coefficients in each grid block to convert exposures to probability, frequency, and/or severity of effect; (x) multiplying per capita incidence by population size to obtain estimates of annual or lifetime disease incidence; and (xi) applying cost of illness (COI) values to convert incidence of morbidity and mortality into annual costs of health impacts.

This level of spatial and temporal detail is not feasible for the global models of coupled energy-economy-environment policies because the computational resources required are quite high and because the data required are insufficient for the majority of nations and regions. As a result, the present analysis uses an approximation employed elsewhere in the literature (Li 2002; Li and Crawford-Brown 2011) in which:

1. An economic model is used to estimate economic activity, energy demand, and energy provision due to a policy scenario. This is repeated for all regions of the global economy. The same is done for the baseline (no policy) scenario.
2. The material and energy use from Step 1 is utilized to estimate emissions of air toxics such as PM. By running these first two steps both with and without a climate change policy, the difference in emissions resulting from the policy can be calculated.
3. Empirical factors are developed to convert fractional changes in emissions (Step 2) into fractional changes in ambient air concentration. For PM, the empirical factor is approximately 0.5 (a 50 % change in ambient air concentration associated with a 100 % change in emissions) based on available global data. This empirical factor varies between regions depending on degree of industrialization, density of vehicular traffic, mix of petrol and diesel use in vehicles, and existing air pollution control measures. For example, in Hyderabad, India, it is estimated

to be 0.5 (Guttikunda and Aggarwal 2009). The values are approximately 0.53 in several regions of China (Zhang et al. 2004) and 0.4 in Korea (Heo et al. 2009). Roughly similar results have been obtained in the Southeastern US (Lee et al. 2007). This chapter uses a central tendency value of 0.5.

4. The result of Step 3 is multiplied by region-specific estimates of ambient air concentration to calculate the change in ambient air concentration resulting from a policy, in units of $\mu g/m^3$. For PM, the assumption used here is that the contribution of a given source to ambient air concentration in a particular region is proportional to the contribution of that source to the total rate of PM emissions in that region, following a process of Source Apportionment (Lee et al. 2007). This is repeated for all regions in the global economy.
5. Changes in ambient air concentration (Step 4) are converted to estimates of change in incidence of disease (number of cases annually or over a lifetime of a policy) through application of risk coefficients taken from meta-analyses performed on the global literature concerning population sensitivities. This is repeated for all regions in the global economy.
6. Finally, changes in cost of illness are determined through application of cost of illness (COI) factors for each illness, multiplying these by the results of Step 5 on the number of cases avoided by the policy. For mortality, cost of illness is not applied.

The illnesses considered here are respiratory and cardiovascular, as the majority of epidemiological studies conducted worldwide have focused on these effects for exposures to air toxics (USEPA 2010).

The analysis in this chapter uses a multivariate regression equation estimated by Philip Chen of the Cambridge Centre for Climate Change Mitigation Research (4CMR) using ordinary least squares regression to explicitly account for country-specific socioeconomic status (SES) characteristics using the Global Burden of Disease study (Lim et al. 2013; Murray et al. 2013). The specific illness categories measured are "lower respiratory infections"; "trachea, bronchus, and lung cancers"; "ischemic heart disease"; "cerebrovascular disease"; and "chronic obstructive pulmonary disease (COPD)."

Considering first mortality, the estimated regression equation using an excess relative risk (ERR) model is

$$Ln(\mathrm{ERR}) = -0.3916 + 0.0139^{*}\mathrm{PM2.5} - 0.0000232^{*}\mathrm{GDP\ perCap} + 0.889^{*}\mathrm{UrbRate} - 6.617^{*}\mathrm{Gini}$$

And so the incidence, y (deaths per year), as a function of PM exposure (E), per capita GDP (GDPperCap), urbanization rate (UrbRate), and measure of economic inequality (Gini coefficient, which is a method for calculating the degree of variance – between individuals – in access to wealth within a nation) is

$$y(\mathrm{E}) = \mathrm{BM}^{*}\exp(-0.3916 + 0.0139^{*}\mathrm{PM2.5} - 0.0000232^{*}\mathrm{GDP\ perCap} + 0.889^{*}\mathrm{UrbRate} - 6.617^{*}\mathrm{Gini})$$

The coefficient in the term associated with PM2.5 is similar to that found in meta-analyses of epidemiological studies, which report an increase of 0.5–1 % in daily respiratory and cardiovascular mortality per 10 μg/m^3 increase in daily average PM10 (divide approximately by 2 for PM2.5) among exposed adults (USEPA 1996, 2008).

Studies on the association of morbidity and air pollution exposure are less comprehensive (Wang and Mauzerall 2006), but indicate a relative risk ratio for chronic obstructive pulmonary disease and pneumonia of between 1.06 and 1.25 for a 50 μg/m^3 increase in daily PM10. This translates into a relative risk coefficient for acute morbidity effects of approximately 1–5 % per 10 μg/m^3 increase in daily PM10 or 2–10 % per 10 μg/m^3 increase in daily PM2.5. Studies in developing countries produce approximately the same range of values (Chen et al. 2002; Hagler Bailly 1998; Xu et al. 1995; Ostro 1987).

For morbidity, the economic value associated with a change in health outcome (V_i), is given by:

$$V_i = A_i \times COI_i \times SF$$

where, A_i is the change in the incidence (annual number of cases) of a specific health endpoint i, COI_i is the cost of illness per case of effect i (for morbidity), and SF is the scaling factor equal to the ratio of per capita GDP in the region divided by per capita GDP in the reference developed nation (here, the US), with a minimum ratio of 0.2.

The specific values for COI are taken from the USEPA Benefits Assessment (USEPA 2008), using the 2020 values provided in that report. All are given as 2020 USD per statistical case of the effect. They are equal to: $90,000 for nonfatal heart attack, $16,600 for hospital admissions for chronic obstructive pulmonary disease, $8,900 for hospital admissions for asthma, $24,700 for hospital admissions for all cardiovascular effects combined, $24,600 for hospital admissions for all respiratory effects combined, and $130 for work loss days.

The risk coefficients for morbidity effects specify only the increase in PM-related effects overall and are not tied directly to these specific categories of health care expenditure. In Deck et al. (2001), the summary of studies examined produces a ratio of all respiratory effects over hospital admissions and extended health-care (including cardiovascular and respiratory admissions) – as a result of PM exposures – equal to 0.018/0.0016 or approximately 10:1. From the cost information above, the average cost per case of hospital admission and/or significant health-care is $27,000. Since only 10 % of effects are assumed to result in such health care costs, the average cost per effect used here is $2,700 (alternatively, the COI value is left at $27,000 and the number of effects multiplied by 0.1).

Co-benefit Calculations for Decarbonization Policies

This chapter considers policies that focus solely on reducing energy consumption from fossil fuels, in which a percentage change in GHG emissions is accompanied by the same percentage change in PM emissions. This is equivalent to assuming that

the climate policy changes the total consumption of fuels by changing demand, but not the mix of fuels or the technologies in which they are used.

The first calculations consider percentage change in GHG emissions that vary between 0 % and 100 %, with no associated change in GDP within nations. Fractional reductions in GHG and hence PM emissions are assumed uniform in all nations globally (which differs from many of the results reported elsewhere in this book). Published values of the ratio of percentage PM reduction to percentage carbon dioxide reduction vary from 0.77 (Cifuentes et al. 2001) to 1.0 in transport resulting from fuel efficiency improvements (Caton and Constable 2000) and as high as 140 % (Changhong et al. 2004). Policies that cause a switch to biomass fuel, carrying carbon dioxide emission reductions (by up to 80 %), result in reductions of up to 75 % when the switch is from coal-fired plants, but can increase PM emissions when the switch is from fuel oil, gas oil or natural gas (AEA 2008). Hence the assumption in the current study that a percentage reduction in PM emissions equals that of the carbon dioxide emissions reduction appears valid.

Figures 2, 3, and 4 show the reduced annual costs and number of cases of morbidity (all PM-related causes combined) and mortality (number of cases only) globally as a function of the fractional reduction in GHG emissions.

When socioeconomic change (per capita GDP) is included in the calculations, the results change, although not dramatically. For this analysis with socioeconomic change (i.e., economic growth both increases GHG emissions and decreases sensitivity to co-pollutants), results for mortality only are considered to determine whether inclusion of economic growth significantly alters conclusions from above.

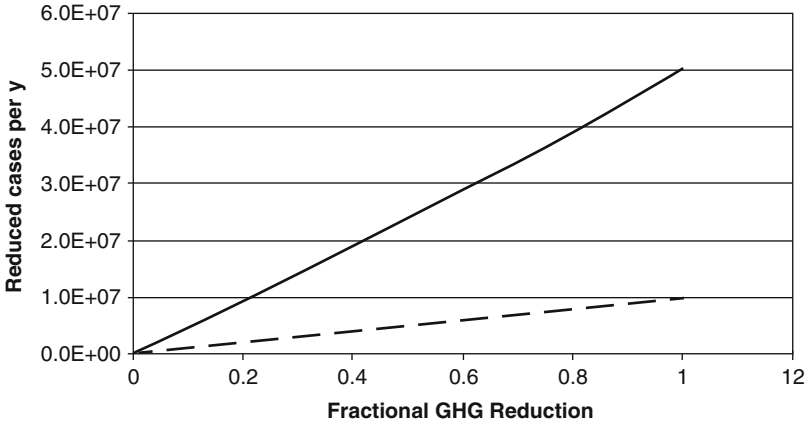

Fig. 2 Reduction in annual PM-induced morbidity (respiratory and cardiovascular combined) globally for different levels of GHG emission reductions shown on the *x*-axis. The results shown as *solid lines* assume that climate policies cause emission reductions uniformly across all nations, with no distinction between Annex I and non-Annex I nations (and hence no distinction between developed and developing economies). The results shown as *dashed lines* assume that reduction policies are in place only in the Annex I, developed, nations

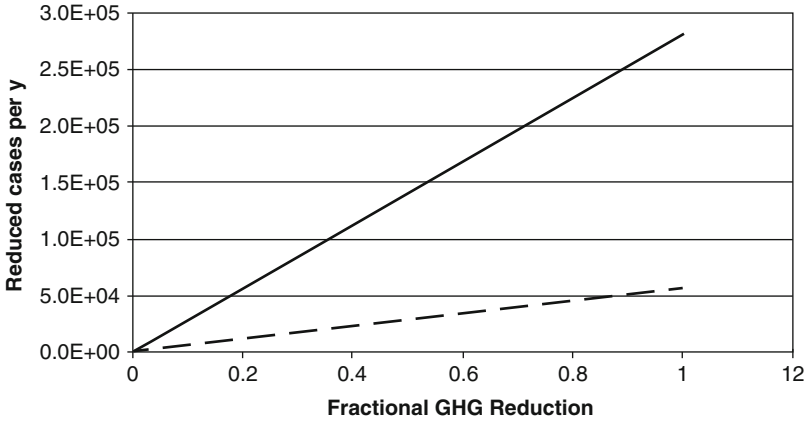

Fig. 3 Reduction in annual PM-induced mortality (respiratory and cardiovascular combined) globally for different levels of GHG emission reductions shown on the *x*-axis. The results shown as *solid lines* assume that climate policies cause emission reductions uniformly across all nations, with no distinction between Annex I and non-Annex I nations (and hence no distinction between developed and developing economies). The results shown as *dashed lines* assume that reduction policies are in place only in the Annex I, developed, nations

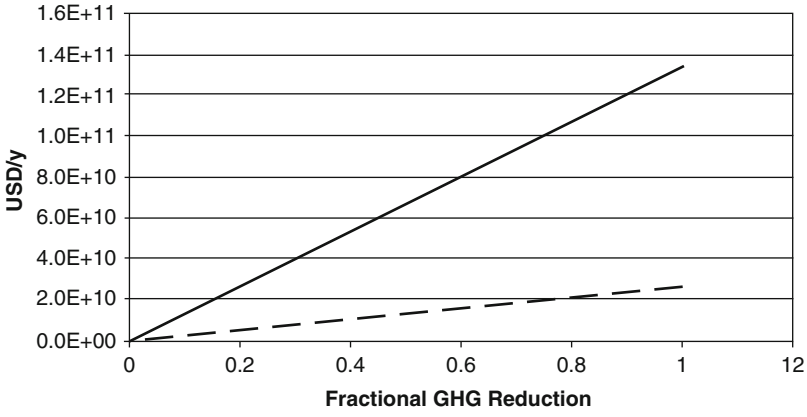

Fig. 4 Reduction in annual cost of PM-induced illness from morbidity (respiratory and cardiovascular combined) globally for different levels of GHG emission reductions shown on the *x*-axis. The results shown as *solid lines* assume that climate policies cause emission reductions uniformly across all nations, with no distinction between Annex I and non-Annex I nations (and hence no distinction between developed and developing economies). The results shown as *dashed lines* assume that reduction policies are in place only in the Annex I, developed, nations

In this analysis, a baseline scenario of very little decarbonization prior to 2050 is used as a baseline and compared against the results from three scenarios where decarbonization is more significant. Scenario 1 is a moderate level of decarbonization needed to remain below approximately 600 ppm CO_2; Scenario

2 is a weakly decarbonizing scenario equivalent to only current, pledged mitigation policies being implemented; and Scenario 3 is a more ambitious decarbonization trajectory needed to remain below a target of 550 ppm.

Future Directions

The co-benefit estimates in section "Co-benefits Calculations for Decarbonisation Polices" support the contention that co-impacts of climate change mitigation strategies can be a significant adjunct to policies focused solely on climate change itself and will provide the basis for justifying transitions of the energy system in both the near and long-term future. The reduction in lives lost (mortality) associated with an 80 % reduction in carbon dioxide emissions globally is approximately 220,000 per year across these nations. With a global population of seven billion, this corresponds to a reduction in mean annual probability of death equal to 3.1×10^{-5}, or about three chances per year per 100,000 people. Over the course of a lifetime of 70 years, the reduction in mean lifetime probability of death is 2.2×10^{-3}, above the "fuzzy bright line" level of excess mortality (10^{-4}) usually considered a level requiring corrective action.

Short-term action on climate change is restricted to the Annex I nations under the UN Framework Convention on Climate Change (UNFCCC). If attention is focused solely on these nations, arguing that they are the ones that must marshal the will to political action first, the results are not dissimilar to the global results above. The reduction in lives lost (mortality) associated with an 80 % reduction in carbon dioxide emissions in only the Annex I nations is approximately 50,000 per year across these nations. With a population of 1.3 billion in the Annex I nations, this corresponds to a reduction in mean annual probability of death equal to 3.9×10^{-5}, or about four chances per year per 100,000 people. Over the course of a lifetime of 70 years, the reduction in mean lifetime probability of death is 2.7×10^{-3}. Again, these co-benefits would usually be considered adequate justification for regulation under risk-based approaches in the Annex I nations.

Note also that inclusion of economic growth in co-benefit calculations makes a significant but not dramatic difference in the results of those calculations. Under all four scenarios, there is a decrease in both the cumulative and average annual mortalities induced by PM2.5 exposures as a result of increasing per capita GDP over the simulation period (2010–2050), as seen in the first four rows of Table 1. This decrease is approximately 13 %, 12 %, 13 %, and 11 % for scenarios 0 (baseline), 1, 2, and 3, respectively. Similar percentage reductions are noted for annual average mortality rate (excess deaths per year due to PM2.5 exposures). These changes indicate that allowing for continuing increases in per capita GDP while designing global climate policies can have a health benefit by itself, not necessarily in relative terms but in absolute terms.

Given these findings, it is likely that decarbonization of the global energy system will be increasingly allied with issues of improvement in public health. Both national

Table 1 Summary of findings on PM-related mortality co-benefits with and without consideration of GDP change, given for the baseline of no policy (0), policy Scenario 1, policy Scenario 2, and policy Scenario 3. The differences between Scenarios 1, 2, and 3 and the baseline are shown as (0-1), (0-2), and (0-3), respectively

	No GDP change		With GDP change		Fractional difference	
	Total Cumulative	Annual average	Total Cumulative	Annual average	Total Cumulative	Annual average
0	1.35E + 08	3.38E + 06	1.18E + 08	2.96E + 06	1.26E − 01	1.26E − 01
1	1.09E + 08	2.72E + 06	9.63E + 07	2.41E + 06	1.16E − 01	1.16E − 01
2	1.33E + 08	3.33E + 06	1.16E + 08	2.91E + 06	1.26E − 01	1.26E − 01
3	9.68E + 07	2.42E + 06	8.61E + 07	2.15E + 06	1.10E − 01	1.10E − 01
0-1	2.64E + 07	6.61E + 05	2.21E + 07	5.52E + 05	1.65E − 01	1.65E − 01
0-2	2.14E + 06	5.36E + 04	1.91E + 06	4.77E + 04	1.10E − 01	1.10E − 01
0-3	3.86E + 07	9.66E + 05	3.22E + 07	8.06E + 05	1.65E − 01	1.65E − 01

and international environmental laws have demonstrated the role of public health in creating binding legislation, even when reference to climate change alone has proven ineffective.

References

AEA (2008) Measurement and modelling of fine particulate emissions (PM10 & PM2.5) from Wood-burning Biomass Boilers. Report to the Scottish Government, 26 Sept

Barro R (1996) Health and economic growth. Organización Panamericana de la Salud. Anexo I de la convocatoria para propuestas de investigación sobre inversión en salud y crecimiento económico de la Organización Panamericana de la Salud. OPS, Washington, DC

Bloom D, Canning D (2003) Health as human capital and its impact on economic performance. Geneva Pap R I – Iss P 28:304–315

Bloom DE, Canning D, Sevilla J (2004) The effect of health on economic growth: a production function approach. World Dev 32:1–13

Bollen J, Guay B, Jamet S, Corfee-Morlot J (2009) Co-benefits of climate change mitigation policies: literature review and new results. OECD Economics Department, Working paper 693

Caton R, Constable S (2000) Clearing the air: a preliminary analysis of air quality co-benefits from reduced greenhouse gas emissions in Canada. David Suzuki Foundation, Vancouver, BC

Changhong C, Bingyan W, Qingyang F, Green C, Streets D (2004) Reductions in emissions of local air pollutants and co-benefits of Chinese energy policy: a Shanghai case study. Energy Policy 34:754–762

Chen C, Chen D, Green C, Wu C (2002) Benefits of expanded use of natural gas for pollutant reduction and health improvement in Shanghai. Sinosphere J 5:58–64

Cifuentes L, Borja-Aburto VH, Gouveia N, Thurston G, Davis DL (2001) Assessing the Health benefits of urban air pollution reductions associated with climate change mitigation (2000–2020): Santiago, Sao Paulo, Mexico City, and New York City. Environ Health Perspect 109(Suppl 3):419–425

Deck LB, Post ES, Smith E, Wiener M, Cunningham K, Richmond H (2001) Estimates of the health risk reductions associated with attainment of alternative particulate matter standards in two U.S. cities. Risk Anal 21:821–836

Guttikunda S, Aggarwal R (2009) Contribution of vehicular activity to air pollution in Hyderabad, India. Ind J Air Pollut Control 9:37–46

Hagler Bailly Inc (1998) Final report: health effects of particulate matter air pollution in Bangkok. A report prepared for air quality and noise management, pollution control department, Bangkok, Mar 1998

Heo J, Hopke P, Yi S-M (2009) Source apportionment of PM2.5 in Seoul, Korea. Atmos Chem Phys 9:4957–4971

IIASA (2004) Medium-term mitigation for long-term stabilization: National mitigation potentials, costs and co-benefits. Presentation at the COP10, 8 Dec 2004

Lee S, Russell A, Baumann K (2007) Source apportionment of fine particulate matter in the Southeastern United States. J Air Waste Manage Assoc 57:1123–1135

Li J (2002) Including the feedback of local health improvement in assessing costs and benefits of GHG reduction. Rev Urban Reg Dev Stud 14:282–304

Li Y, Crawford-Brown DJ (2011) Assessing the co-benefits of greenhouse gas reduction: health benefits of particulate matter related inspection and maintenance programs in Bangkok, Thailand. Sci Total Environ 409:1774–1785

Lim SS, Vos T, Flaxman AD, Danaei G, Shibuya K, Adair-Rohani H, ... Davis A (2013) A comparative risk assessment of burden of disease and injury attributable to 67 risk factors and risk factor clusters in 21 regions, 1990–2010: a systematic analysis for the Global Burden of Disease Study 2010. Lancet 380(9859):2224–2260

Markandya A, Chiabai A (2009) Valuing climate change impacts on human health: empirical evidence from the literature. Int J Environ Res Public Health 6:759–786

Murray CJ, Vos T, Lozano R, Naghavi M, Flaxman AD, Michaud C, ... Bridgett L (2013) Disability-adjusted life years (DALYs) for 291 diseases and injuries in 21 regions, 1990–2010: a systematic analysis for the Global Burden of Disease Study 2010. Lancet 380 (9859):2197–2223

Ostro BD (1987) Air pollution and morbidity revisited: a specification test. J Environ Econom Manage 14:87–98

Selin N, Wu S, Nam K, Reilly J, Paltsev S, Prinn R, Webster M (2009) Global health and economic impacts of future ozone pollution. Environ Res Lett 4:1–9

USEPA (1996) Air quality criteria for particulate matter. Office of Research and Development, Office of Health and Environmental Assessment. EPA report no. EPA/600/P-95/001aF

USEPA (2008) Integrated science assessment for particulate matter. Office of Research and Development, Washington, DC

USEPA (2010) Environmental benefits mapping and analysis program user's manual. Office of Air Quality Planning and Standards, Research Triangle Park, NC

Wang X, Mauzerall DL (2006) Evaluating impacts of air pollution in China on public health: implications for future air pollution and energy policies. Atmos Environ 40:1706–1721

Weil DN (2005) Accounting for the effect of health on economic growth. Report no. w11455, National Bureau of Economic Research, Cambridge, MA

Xu X, Li B, Huang H (1995) Air pollution and unscheduled hospital outpatient and emergency room visits. Environ Health Perspect 103:286–289

Zhang Y, Zhu X, Slanina S, Shao M, Zeng L, Hu M, Bergin M, Salmon L (2004) Aerosol pollution in some Chinese cities. J Pure Appl Chem 76:1227–1239

The Role of Aviation in Climate Change Mitigation

Katsuya Hihara

Contents

Abstract

This chapter summarizes the recent policy and research development of the aviation emission reduction and its mechanism. First we trace the policy process surrounding UNFCCC, Kyoto Protocol, and Post-Kyoto Protocol negotiations, mostly focusing on the activities in the ICAO. Key factors in the policy process are (1) the disparities in the field of international aviation among the nations, such as income level and preferences between environment and growth. Such disparities could be interpreted as the notion of "common but differentiated responsibilities and capabilities (CBDR)" in the Kyoto Protocol. The second key factor is (2) uncertainties surrounding the impact of GHG emission on utilities of nations. Then we look into the theoretical developments in the field of

K. Hihara (✉)
Graduate School of Public Policy, the University of Tokyo, Hongo Bunkyo-ku, Tokyo, Japan
e-mail: hihara@pp.u-tokyo.ac.jp

W.-Y. Chen et al. (eds.), *Handbook of Climate Change Mitigation and Adaptation*,
DOI 10.1007/978-3-319-14409-2_60

international aviation from the economics viewpoint. Main objectives are to illustrate the impact of market-based mechanism (MBM), such as the emission allowance trading, and the inherent difficulties to reach social optimal allocations through the bargaining among nations in the presence of nations' disparities and uncertainties of GHG emission's impact on nations' utilities.

Policy Developments

Introduction

The scientific researches about the impact of aviation on climate change are still underway. The aviation is the total complex system comprising various subsystems such as the process of fuel burning in an engine of an aircraft to the accumulation of thousands of flights of many aircrafts. The scientific impact on the climate of simple phenomenon, such as contrail entailing aircraft in the sky for a while, is still very much the main research topic from the pioneering work of the IPCC special report (1999) and ICAO (2010). The schematic illustration of aviation and its climate impact are shown in Fig. 1.

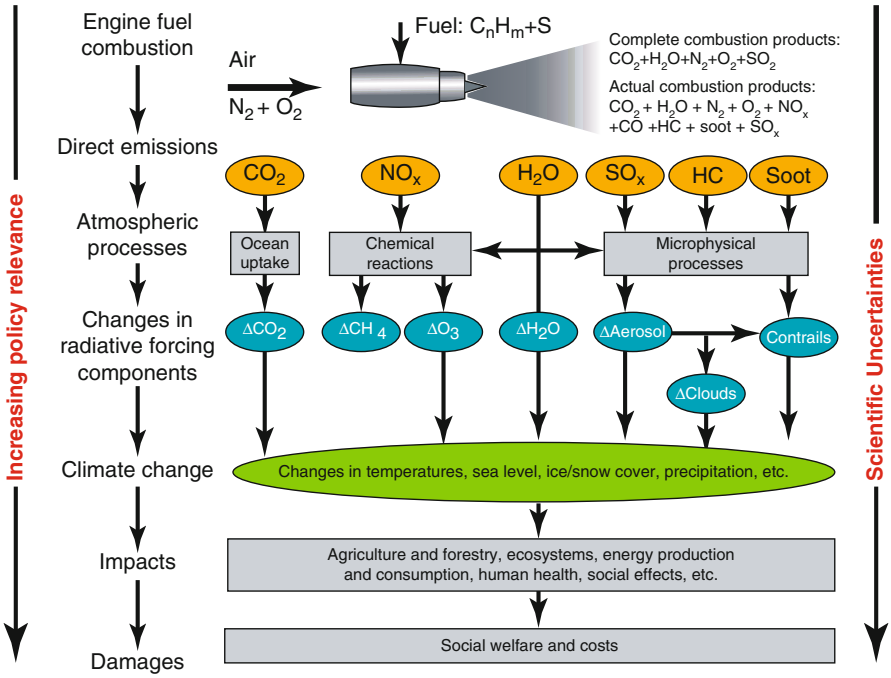

Fig. 1 Schematic representation of aircraft emissions and their causal linkage with potential climate and social welfare impacts (ICAO 2010)

Out of many greenhouse gases (GHGs), CO_2 have politically special importance, since it is not toxic in itself, and its effects probably is larger than other GHGs. UNFCCC sets aside the international aviation and maritime sector, and the GHG reductions' matters of both sectors are to be tackled by the ICAO (International Civil Aviation Organization) of the UN[1].

According to the ICAO, the share of aviation in total emission is about 2 % of the total anthropogenic CO_2 emission. Out of the emission, the international aviation emission accounts for about 60 % of the total emission of the aviation. But the growth rate is rather large, and emission level is expected to be double around the next two decades or so. Especially around Asia-Pacific region is the high growth area.

Aviation Sector Growth

According to the ICAO forecast (ICAO (2013)), the world passenger traffic, expressed in terms of revenue passenger kilometers (RPKs), is expected to grow from 5 billion to more than 13 billion RTKs over the 2010–2030 periods, at an average annual growth rate of 4.9 %. The international traffic section would grow at 5.1 % per year, and the domestic traffic section would grow at a slower rate of 4.4 % per year.

During the next 10 years, 2030–2040, growth is estimated to moderate to an average of 4.0 % per year with international and domestic air traffic growing at the rate of 4.1 % and 3.8 % per annum, respectively.

Geographical distribution of the passenger traffic and its growth from 2010 to 2040 is shown in Fig. 2. The Domestic North America is the highest traffic volume in 2010. Intra Europe and North Atlantic are the second and the third. The Intra Asia and Pacific routes are the most expected to grow, while Domestic China/Mongolia and Domestic North America are following. So in 2040, Intra Asia is the highest traffic volume, and Domestic China/Mongolia and Domestic North America are the second and the third, respectively.

Under such demand forecast, Fig. 3 shows the fuel burn from the international aviation from 2005 to 2050. Some of the emission mitigation technologies are taken into account, but the global aspirational goal of 2 % annual fuel efficiency improvement, which will be discussed later in this section, is very hard to achieve as the graphs show.

Uncertainties: Large Impacts

A lot of uncertainties are involved in the environmental issues. The aviation is the total system of a lot of human activities and mechanical functions in addition to natural/climatological/meteorological phenomena. The aircraft movements,

[1]Kyoto Protocol Article 2.2. "The parties shall pursue limitation or reduction of emissions of greenhouse gases… from aviation …, working through the International Civil Aviation Organization…."

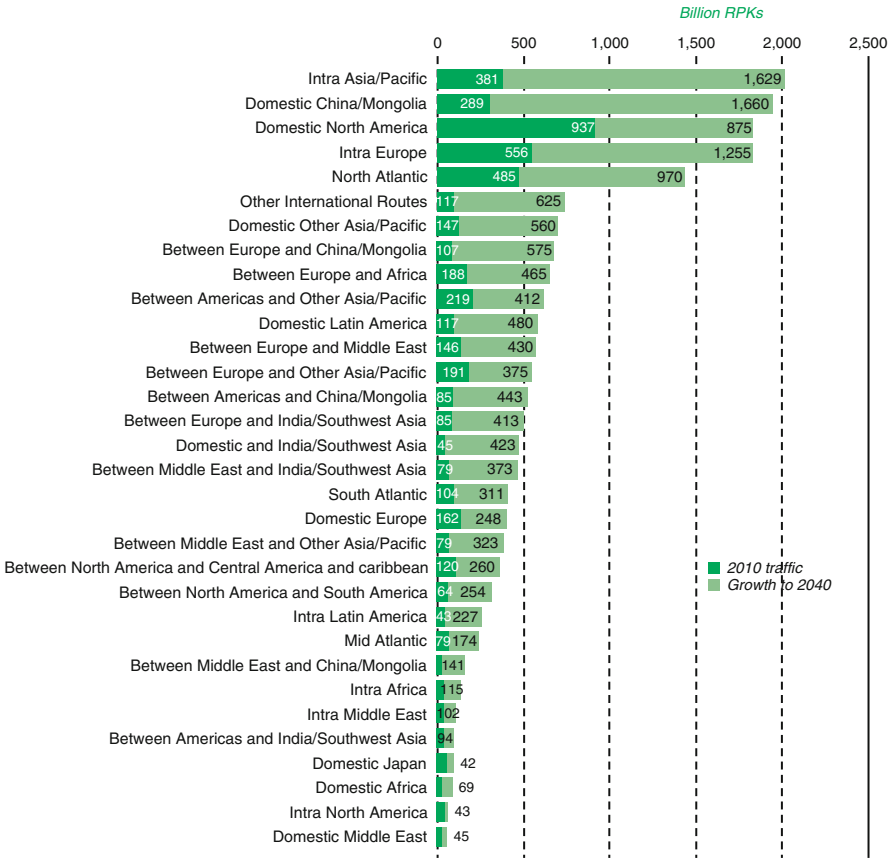

Fig. 2 ICAO/CAEP passenger traffic forecast (*central*) by Route Group (ICAO (2013))

including maintenance/repair, are both human and mechanical, so is air traffic control service with human judgment and ICT system combined. Fuel composition and selection are also very important in the impact alleviation front.

The impact of aviation on climate change through the natural system is far more complicated and yet to assess accurately than that of human activities. Contrails that aircraft entail in sky, for example, stay for a while and seem to have certain level of impacts on climate system, but the accurate assessment is still in the early stage of research according to the UNFCCC report.

So uncertainties in the field of international aviation and their impact on climate change come from all fronts, either from human activities or from natural/ecosystem. From human fronts comes all the uncertainty involving human activities like demand uncertainty, as well as more trivial problem such as measurements inconsistencies, counting errors, and reporting inaccuracies. But the uncertainties involving the global ecosystem through which CO_2 emission has impacts on the climate are at least as complicated and hard to analyze as those involving human activities.

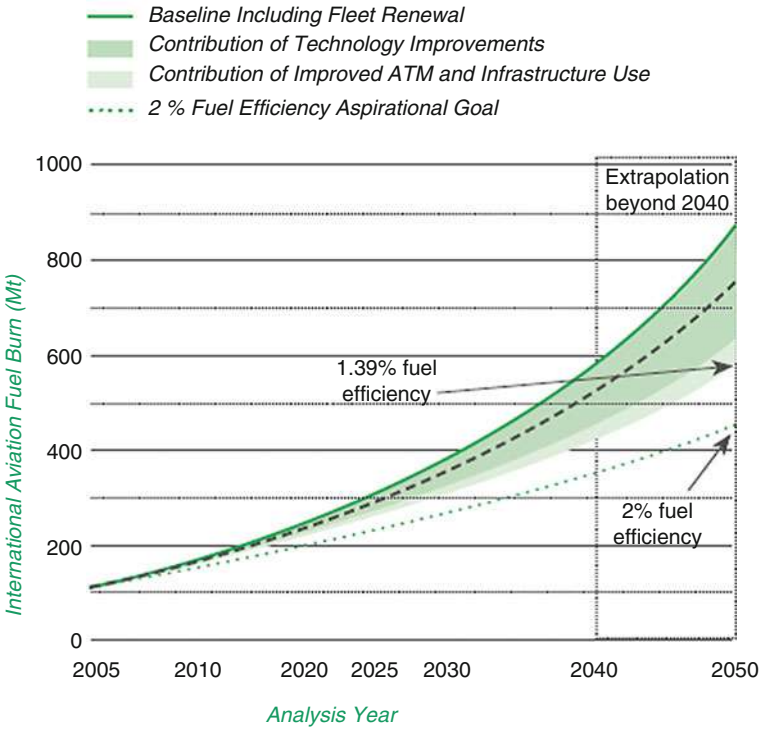

*Dashed line in technology contribution range represents the "Low Aircraft Technology Scenario".

Note: Results were modelled for 2005, 2006, 2010, 2020, 2025, 2030, and 2040 then extrapolated to 2050.

Fig. 3 ICAO/CAEP fuel burn trends from international aviation, 2005–2050 (ICAO (2013))

As we can see in Fig. 4, the uncertainty involving mainly human factors, about the demand forecast for future aviation passengers roughly based on population and income level forecasts, has a very wide range, as much as 50 % of central forecast in 45 years of forecast time.

Under the fuel burn estimations, the ICAO calculated the CO_2 emission from international aviation. Figure 5 is the projection of CO_2 emission by the ICAO from the international aviation from 2005 to 2050.

The Total Approach

As we discussed, the aviation is the complex system of many airplanes/airlines, airports, air traffic controlling service providers, various ground service providers, and local and central government authorities, which are in charge of many matters

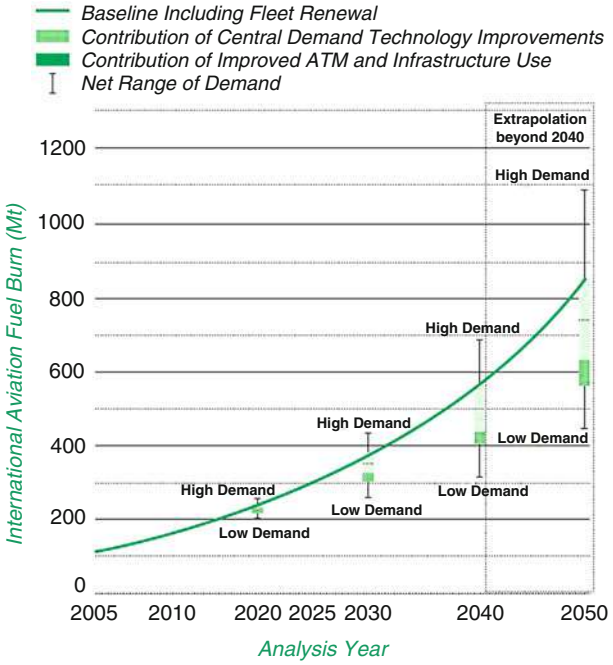

Fig. 4 Range of uncertainties associated with demand forecast, 2005–2050 (ICAO (2013))

including local air quality control and global environmental constraints as well as the safety and human or mechanical issues.

Fuel selection is a major front in the reduction technological challenge in the international aviation. Fuel burn reduction directly contributes to the CO_2 emission reduction. Fuel burn efficiency has improved about 70 % since 1950s, mainly thanks to the improvement of the engine and aircraft body[2].

On the technical fronts of emission reduction, here we introduce briefly the two major environmental technological projects in the EU and USA. In the EU front, the Advisory Council for Aeronautics Research in Europe (ACARE) published a report, "ACARE 2020," in which they set goals for 2020, such as 50 % noise reduction, 80 % NOx emission reduction, and 50 % CO_2 emission reduction from the levels of 2000. They are projected based on active wing design project to actively control streamline flow and its connected projects. Also more recent and long-term vision after 2020 is announced.

[2]This section relies on the contents of Hihara and Okano (2012).

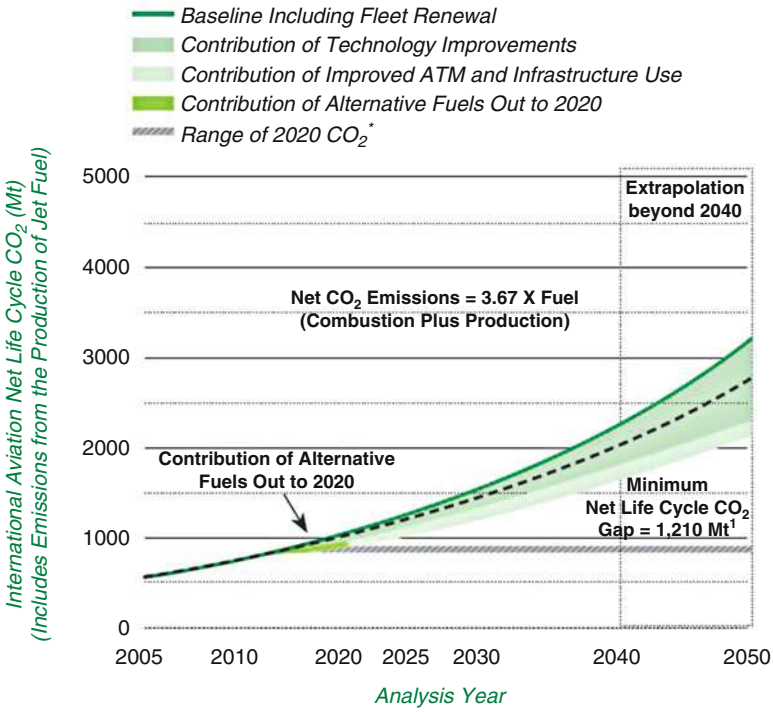

1 **Potential Alternative Fuels Contribution in 2050**[2]
State targets could close up to 25% of gap
Maximum potential contribution could close in excess of 100% of gap

2 if all alternative fuels in 2050 were zero net carbon

*Actual carbon neutral line is within this range. Dashed line in technology contribution range represents the "Low Aircraft Technlogy Scenario."
Note: Results were modelled for 2005, 2006, 2010, 2020, 2025, 2030, and 2040 then extrapoled to 2050.

Fig. 5 Net life cycle CO_2 emission trends from international aviation, 2005–2050 (ICAO (2013))

In the US front, the National Aeronautics Research and Development Plan was announced in 2007. Based on the plan, the goals were set to 50 % reduction of CO_2 from 2005 level and 75 % reduction of NOx from CAEP 6 level, for example, through the development of subsonic transportation system. For that goal, ERA (Environmentally Responsible Action) project was also deployed to develop the necessary technologies for the plan, such as wing-body integrated design and laminarization technology.

In addition to these projects, we still have several fronts for the reduction of gas emissions. First is the reduction of body weight of aircrafts. Now, more and more part of aircrafts is made of CFRP (carbon-fiber-reinforced plastics) instead of aluminum alloy. 50 % of the weight of the recent B-787 is made of CFRP, while in the case of B-777, just 11 % of its weight is made of CFRP.

The second is the research of BWB (blended wing body) to decrease airflow resistance. In a proposed concept of BWB, wings are integrated with the main body, which results in increased aerodynamic characteristics.

Third is the increase of fuel efficiency of jet engines. We still have quite a few challenges in this front. Improving thrust efficiency and heat efficiency is the main way of increasing fuel efficiency. Open-rotor engines are still under research, for example, for improving thrust efficiency. Also ceramic-composite materials are under development for improving heat efficiency.

Aviation is one big system, which combines human activities and natural/ecosystems. So the system optimization is another source of emission reduction. One is the flight path optimization. The dynamic flight path adjustment based on the most up-to-the-minute meteorological conditions and measures is the example. Also the smooth descent approach, called CDA (continuous descent approach), is being tested for real implementations.

As we can see so far, the approaches taken to curve the emission from aviation are the total strategies that involve all of the major players mentioned above.[3] According to their document_1, the industries' reduction strategies into the future include various approaches from fleet renewal/mechanical technology developments and better air traffic managements to low carbon fuel usage.

UNFCCC and Aviation: Disparities Among Nations

Under the UNFCCC (UN Framework Convention on Climate Change), contracting parties of the convention agreed to the Kyoto Protocol in 1997. One of the key elements of the Kyoto Protocol is the principle of CBDR (common but differentiated responsibilities and respective capabilities). The principle basically means that the industrialized countries which have mainly provided emissions so far should bear more responsibilities of future reductions than developing countries that provided emissions less thus far.

Annex I of the Kyoto Protocol lists up mainly the developed countries, and such countries are to bear the responsibility of GHG reduction target during the commitment period (2008–2012) for each county, based on CBDR. So the Kyoto Protocol clearly distinguishes the role of developed countries from that of developing ones.

In the aviation, the Kyoto Protocol allocated the responsibilities of emission reduction from aviation in two ways. First, reduction of the domestic aviation emission is under the national reduction target stipulated in Annex I. Second, the reduction of international aviation emission is stipulated to be worked through international organization, namely, the ICAO, since the international nature of international aviation is very hard to allocate among relevant countries.

[3]Material presented to ICAO GIACC/3 February 2009 by Paul Steele on behalf of ACI, CANSO, IATA, and ICCAIA.

In 2012, COP (congress of parties) 18 of UNFCCC decided the extension of the Kyoto Protocol and made another commitment period (the second commitment period, 2013–2020) beyond the previous period (the first commitment period, 2008–2012). In addition to the USA, which never ratified the Kyoto Protocol, industrialized countries, such as Japan, Canada, New Zealand, and Russia, had announced that they would not take on reduction target for the second period. The contracting parties are discussing the framework beyond 2020, and they are scheduled to agree on the new framework by the end of COP 21 in 2015.

Works at the ICAO

Entrusted with the reduction of international aviation emission by the Kyoto Protocol, the ICAO convened GIACC (Group on International Aviation and Climate Change) in 2008. The main cause of difficulties comes from the ICAO principle set by the Chicago Convention of nondiscrimination and equal and fair opportunities to develop international aviation, which is in conflict with CBDR of the Kyoto Protocol.

European countries pursue the nondiscrimination principle, and developing countries, including China and India, support CBDR over nondiscrimination principle. To overcome this conflict, GIACC came up with the target index based on the fuel burn efficiency[4]. The index is fuel liter/RTK (revenue ton kilometer). Both developed countries and developing countries have almost the same level of index of fuel burn efficiency, since the efficiency mainly depends on the manufacturing date of each airplane irrespective of the country of airline that owns the airplane.

In 2009, the ICAO decided the world global aspirational goal for the international aviation sector, namely, improving fuel efficiency (fuel liter/RTK) by 2 % per year. This global aspirational goal is, unlike the Kyoto Protocol, shared by all of the main aviation countries, such as the USA and China in addition to the EU and other industrialized countries.

Also the ICAO agreed on the carbon-neutral growth from 2020, which means keeping net CO_2 emissions from international aviation at the same levels from 2020 onward.

In addition, the ICAO is taking the total approach for the international aviation GHG emission reduction. This means that the aviation authorities and industries will seek to establish the measurement/methodology of GHG emission level from individual aircrafts, industries will seek to diffuse the use of biofuel, air service provider bodies will seek to efficiently use air traffic management, and the ICAO and other public authorities will seek to establish the scheme of global market-based mechanism (MBM).

[4]The negotiations process among major member states and relevant papers in the process can be found in GIACC (2008), GIACC (2009), and ICAO (2009).

The Resolution A38-18 in 2013 builds upon the series of the ICAO's recent achievements and incorporates a number of important key elements. The following is the main points of the resolution.

The ICAO General Assembly Resolution A38-18 in 2013

1. Reaffirmation of collective global aspirational goals for the international aviation sector, namely, improving fuel efficiency by 2 % per year and keeping net CO_2 emissions at the same levels from 2020 onward
2. Further work to explore the feasibility of a long-term global aspirational goal for international aviation
3. Maintenance and enhancement of appropriate standard, methodologies, and a mechanism to measure/estimate, monitor, and verify global greenhouse gas (GHG) emissions from international aviation
4. Development of a global CO_2 Emissions Standard for aircraft, aiming for adoption by the ICAO Council in 2016
5. Maintenance and update of guidance on air traffic management (ATM) improvements and other operational measures to reduce international aviation emissions and continue development of tools to assess their benefit
6. Development of coordinated national policy actions to accelerate the appropriate development, deployment, and use of sustainable alternative fuels for aviation with measures to ensure the sustainability of alternative fuels for aviation
7. Development of a global market-based mechanism (MBM) scheme for international aviation, which addresses key design elements, including means to take into account the special circumstances and respective capabilities of states, in particular developing states, as well as the implementation mechanisms from 2020, for decision by the 39th Assembly in 2016
8. Voluntary preparation and update of states' action plans on CO_2 emissions reduction activities, for submission to the ICAO by June 2015, and to be made publically available
9. Enhancement of the ICAO's strategy for capacity building and assistance, including support for the development and update of states' action plans, as the mechanisms to facilitate access to financial resources[1]

The interesting point is the market-based mechanism (MBM) from the economical point of view. To tackle the emission reduction, there are mainly two ways. The first is the reduction by regulation, such as the forced emission reduction by law. The second is using the market and pricing mechanism, such as cap and trade.

By cap-and-trade approach, first the total emission amount is set, and emission allowance is allocated for each emitter. The emission allowance can be tradable for cash or other remunerations. If the emitter exceeds its allocated allowances, then the one can buy the necessary amount of allowances for the difference of actual emission levels and the allocated emission level, which allocated allowance indicates.

The ICAO's MBM could be the example of the second approach. For cap-and-trade approach, we have some examples already implemented, for example, the EU-wide emission trading mechanism, called EU-ETS, which is cap-and-trade system.

Originally, the EU unilaterally proposed its own emission allowance trading mechanism for international aviation in/out of the EU region using EU-ETS. In the EU's application to international aviation[5], total amount of CO_2 emission is set for each airline of each county, whether they are EU member state or not, and if an airline emit more than the allocated free allowance, it should buy the allowance for the extra emission allowance from EU-ETS.

This proposal was vehemently opposed by the USA, China, and other industrialized/newly developing countries. Despite these oppositions, in 2008, the EU again unilaterally announced to begin its scheme in 2012. Because of the strong opposition from the USA, China, India, and other countries, the EU finally decided to "stop the clock," meaning that the EU suspends the procedure to introduce international aviation into EU-ETS until the end of 2016. Meanwhile, the ICAO has time to contemplate the framework of global MBM to curve the GHG emission reduction and to consult it with the member nations. If the ICAO delivers the MBM, the inclusion of aviation to EU-ETS will never happen. If the ICAO fails to deliver it, however, the inclusion enforcement will "automatically" revive.

The main difficulty lies with the structural disparities. The Kyoto Protocol, with the legal obligation, sets only on the industrial nations but not on developing nations. The concept of CBDR (common but differentiated responsibilities and capabilities) in the Kyoto Protocol clearly reflects this uneven burden sharing of the Kyoto Protocol. As it is often pointed out, the environmental issues are very difficult, since they entail long-term effects, generationally unequal impacts, and various uncertainties from scientific mechanism of cause and effects to economic and social impacts, for which accurate, objective, or plausible assessments are usually very difficult.

It is a challenge to cope with the conflicting contents of CBRD, based on the disparities among nations, and ICAO's equal and fair treatment among them, in the field of GHG issues of international aviation in a constructive way. Some level of ingenuity in the policy process, such as coming up with the inclusive target of fuel efficiency in the global aspirational goal in ICAO, instead of zero-sum-type emission allowance allocation, is very important in order to attain meaningful policy progress.

Theoretical Illustrations

Introduction

Understanding the basic interaction mechanism among nations surrounding CO_2 emissions is critically important for the policy formulation analysis in aviation sector at present, especially for market-based measures such as emission allowance

[5]The EU's inclusion of international aviation into the EU-ETS is documented in EU (2009).

trading. Also we would like to incorporate the large impacts uncertainties entail into our analysis.

Here, we show, based on Hihara (2012), some emission trading simulations and two theoretic analyses of the global welfare in the field of international aviation emission reduction.

First, this study performed simulation analyses on the hypothetical emission allowance trading if China and the USA joined the Kyoto Protocol and participated in the global trading at the time in 1990 and showed the numerical effects based on the conditions.

Second, the study analyzed the socially efficient allocation condition with the presence of negative public goods, namely, CO_2, and the uncertainty of such impact that CO_2 emission has on our utility levels through the ecosystem.

Third, the study constructed the theoretical model and illustrated the effects of asymmetric structures of difference of initial conditions and risk aversion among countries and uncertainty level increase.

With all the analyses, the study showed under the asymmetric structures, including the difference of the initial conditions (income level, consumption, and production level) and the preference (pro-environment or pro-development) of player countries, that the bargaining among the countries on the emission allowances is inherently difficult to reach social optimum. The study's main points are as follows.

So it is necessary and relevant to study the effects of these typical uncertainties on the welfare level with or without emission allowance trading in order to understand deeper into the negotiation dynamics and to possibly reach long-run agreement.

The first key question for the policy formulation on emission allowance trading is, "how will the trading market work, and how will prices result after trading?" The second key question is, "what is the impact of uncertainties, other than uncertainties of CO_2 production or bunker fuel consumption in the international aviation sector, on the global social welfare level with emission allowance trading or without such trading (e.g., game-theoretic emission allowance allocation without trading)?"

In this study, we first illustrate how emission allowance trading works in the hypothetical global trading market based on the past game-theoretic study with other relevant research results for the first key question. Secondly, we look into more general and theoretic framework as to how the uncertainties affect the global welfare level with or without emission allowance trading for the second key question.

Emission Allowance Allocation Process Simulations

Past Literature

A lot of analyses were performed about the emission allowance allocation process, like that of the Kyoto Protocol Negotiation process. Okada (2004), for example, analyzed the bargaining mechanism for the initial allowance and reduction costs by the method of noncooperative game theory based on the empirical work done by Nordhaus (1991) and Bohm and Larsen (1994).

Also a lot of cooperative game-theoretic analyses were done about the allowance distribution bargaining. The work done by Tadenuma in Imai and Okada (2005) shows there is a stable coalition set (von Neumann-Morgenstern solution) even though, according to Okada (2003), the core of the voting game on distributions of a fixed total amount of emission allowances is empty.

Here, we focus on noncooperative game framework and make some simulation of including new members into the bargaining.

Base Model

According to the work by Nordhaus (1991), Bohm and Larsen (1994), and Okada (2004), we have the formulae for the competitive price of carbon emission allowances under the framework of noncooperative game approach, indicated below. The following equations and notations are from Okada (2004).[6] Okada (2004) assumes marginal cost pricing of emission allowance in the trading market after the reduction level or emission allowance allocation is attained by asymmetric Nash bargaining solution among nations.[7] Data for the estimated parameters of the following equations are from Nordhaus (1991) and Bohm and Larsen (1994).

Let $N = 1,\ldots, n$ be the set of counties. For every $i \in N$, we denote by E_i country i's current level of carbon emission. The total level of carbon emitted by n countries is given by $E = \sum_{i \in N} E_i$. x_i denotes the country i's reduction of carbon emission. ω_i is the emission allowance allocation for country i $\overline{\omega} = \sum_{i \in N} \omega_i$.

$$p^* = -185.2 \ln\left(1 - \frac{E - \overline{\omega}}{\sum_{i \in N} E_i (1 - r_i)}\right) \tag{1}$$

$$x^* = \frac{E(1 - r_i)}{\sum_{i \in N} E_i (1 - r_i)} (E - \overline{\omega}) \tag{2}$$

$$c_i^e = 185.2 x_i^* + p^* (E_i r_i - \omega_i) \tag{3}$$

$$r_i = \begin{cases} 1 - \dfrac{e_i}{e_{USA}} (e_i \leq e_{USA}) \\ \dfrac{e_{USA}}{e_i} - 1 (e_{USA} \leq e_i) \end{cases} \tag{4}$$

$$e_i = \frac{E_i}{GDP_i} \tag{5}$$

e_i is the carbon intensity of country i, which is emission level E_i over GDP. p^* is the competitive equilibrium price of this negotiation.

[6] They are specifically from proposition 3 in Sect. 4, "Numerical Results" of Okada (2004).

[7] They are specifically from line 14 of page 9 and Theorem in page 19 in Sect. 3, "Noncooperative Bargaining Process of Emission Reduction" of Okada (2004).

x_i^* is the equilibrium reduction of CO_2 emissions for country i.
c_i^e is the cost of country i with the initial allocation ω_i, competitive equilibrium price p^*, and reduction amount x_i^*.
r_i is the marginal cost index of country i in relation with that of the USA.

This model is about the mechanism of global emission allowance trading across countries based on the relative reduction cost of each nation compared with that of the USA.

By Eqs. 1–5, we can simulate any number of countries with any type of initial allowances or any type of emission intensity.

These equilibrium equations loosely states that if the countries anticipate competitive equilibrium market for emission allowance trading in the second stage, they can attain a bargaining solution on emission reduction level or emission allowance allocation in the first stage. Although the emission allowance trading market could be oligopolistic, here we use these setting of competitive market, as a start, to illustrate the price effect of new entrants into the hypothetical global trading market.

However, since these numbers are available, based on empirical works, only for 1990, we can only perform the simulation about 1990 and cannot do about other years like 2005, for example.

Simulation

What would have happened if major players such as China and India were included in the Kyoto Protocol and the hypothetical global emission trading in 1990?

Table 1 below is the basic real data for the carbon emission level (million ton carbon, GDP in US dollars, carbon intensity for the15 EU nations (EU15), Former Soviet Union nations, Japan, the USA, China (including Hong Kong and Macau), Korea (not including DPRK), and India from the UN and IPCC database.

If the hypothetical emission trading had been done in 1990 among the original contracting developed countries of 15 EU nations, Former Soviet Union nations, Japan, and the USA, what would have happened? The simulation result is indicated in Table 2. The reduction rate are based on the Kyoto Protocol, and initial permits are calculated by subtracting a reduction ton based on reduction rate from carbon emission level of 1990 for each country.

The equilibrium price and equilibrium cost are derived from 1 to 5 by inputting the relevant numbers for each country and summations of those for all countries into variables of these equations. The resulting equilibrium price is about 9.65 US dollars per ton carbon.[8]

[8]Notice that the price here is US$ per ton carbon, not US$ per ton CO_2. External cost from car gasoline consumption is about 5,000–50,000 yen per ton carbon, and 30,000 yen per ton carbon is the medium estimate according to Kanemoto et al. (2006). According to IPCC (2007a), the average social cost of CO_2 based on 100 estimates is about 12 US$ per ton of CO_2 for 2005, although the estimation range is from −3 to 95 US$. The external cost of aviation is from 0.16 to1.09 euro per aircraft-km for CO_2 and H_2O for average technology if price of CO_2 ton is 30 euro according to Ding et al. (2003).

Table 1 Basic real numbers of the players

Country or area	Carbon emission in 90 (mil. ton)	GDP in 90 (Bil. US$)	Carbon intensity[c]
EU 15	915	6,961	0.13
FSU 22	989	1,535	0.64
Japan	292	2,970	0.10
USA	1,315	5,794	0.23
China[a]	662	484	1.37
Korea[b]	66	264	0.25
India	186	327	0.57

Source: UN and IPCC web data base
[a]China includes Hong Kong and Macau
[b]Korea excludes DPRK
[c]Carbon intensity is the carbon emission level per GDP (ei = Ei/GDPi)

Table 2 Results of hypothetical emission trade among four players

Country	Reduction rate	Reduction (mil. ton)	Initial permits (mil. ton)	P* (US$)[a]	Equilibrium cost (mil. US$)
EU 15	0.08	73	841	9.65	575
FSU 22	0	0	989	9.65	−402
Japan	0.06	18	275	9.65	138
USA	0.07	92	1223	9.65	563

[a]P^* is the equilibrium price of carbon emission allowance

Table 3 Results of hypothetical emission trade among seven players

Countries	Reduction rate	Reduction (mil. ton)	Initial permits (mil. ton)	P* (US$)	Equilibrium cost (Mil. US$)
EU 15	0.08	73	841	6.65	424
FSU 22	0	0	989	6.65	−192
Japan	0.06	18	275	6.65	102
USA	0.07	92	1223	6.65	457
China[a]	0	0	662	6.65	−143
Korea[b]	0	0	66	6.65	−8
India	0	0	186	6.65	−35

[a]China includes Hong Kong and Macau
[b]Korea excludes DPRK

If the major emission countries such as China, Korea, and India also had participated in the hypothetical emission trading with the obligation of zero reduction like Former Soviet Union nations, the results would have been those in Table 3.

The equilibrium price is about 6.65 US dollars, since the new entrants are not obliged to reduce the emission level and they can sell emission allowances to the USA, EU15, and Japan.

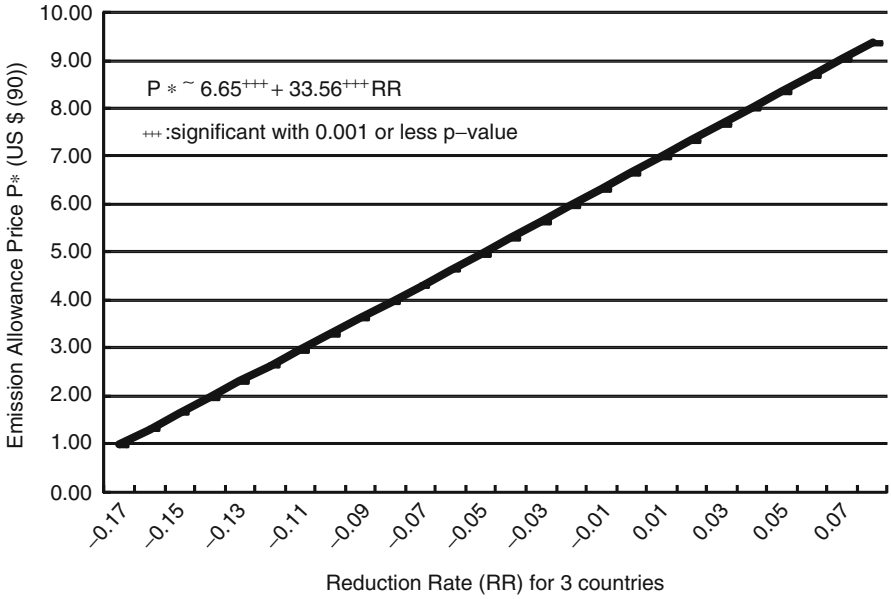

Fig. 6 Sensitivity of reduction rate for three countries

What happens if the reduction obligation increases commonly for all the three countries from zero percent to higher percentages is in Fig. 6.

According to our basic model, 1 % increase (+0.01) of reduction obligation among these three nations lead to about 33 cents increase of the emission allowance price, which is indicated by the slope 33.56 of our estimated line in Fig. 6. 0.33 is the effect of 0.01 increase of reduction obligation.

The price and its slope are common to all countries participating in the emission allowance trading, since the equilibrium price is determined uniquely by Eq. 1 in the market. Therefore, the slope of estimated price change is also common to all countries. If reduction obligation increases for these countries, the needs for emission allowance go up and so does the price of emission allowance.

If carbon intensity (= emission level over GDP) of these three countries commonly improves by 1 % (−0.01), the emission allowance price would go up by about 2 cent. This relationship is depicted in Fig. 7. The slope of the estimated line is about –2.40, and 0.024 is the effect for −0.01 change in carbon intensity variation.

With these simulations, more players' participation can reduce the price of emission allowance, but the situation depends on the factors such as the reduction obligation of the new players and carbon intensity variations.

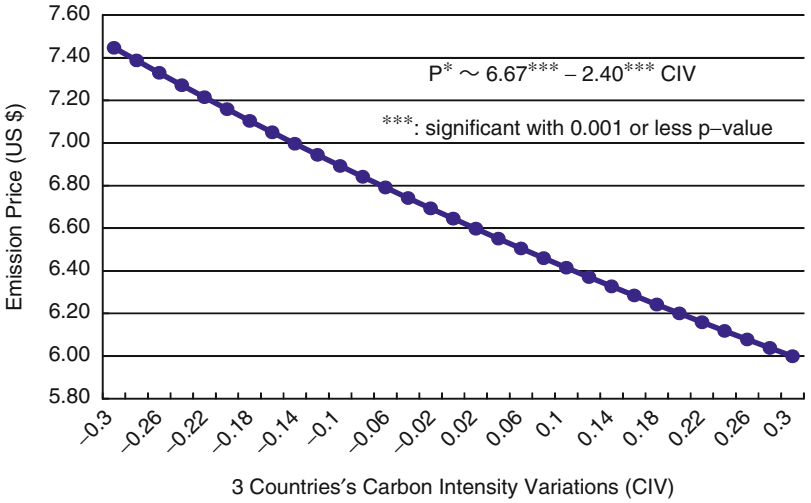

Fig. 7 Sensitivity of three countries' carbon intensity variation to emission price

Welfare Analysis with a Negative Public Good

Past Literature

Emission charge on airlines is studied by several authors on the effect on airfares, service quality, and aircraft design as shown by Brueckner and Zhang (2009).

In more general context, including other sectors in addition to international transportation, a lot of literature on the climate change policy is published. The standard book on environmental economics is by Kolstad (2000), for example. Roger Guesnerie (2008) and Yang (2008) are among the most recent publications.

But a limited number of literatures are on the welfare impact analysis using the characteristics of CO_2 as negative public goods and further limited number of literatures are based on the game theory or bargaining theory analysis in addition to the characteristic as negative public goods. This study explores the welfare implication analysis, using the characteristic of negative public goods, by game theory and bargaining theory in order to depict more general situation than competitive market of emission allowance trading in addition to reduction level or emission allowance allocation stage.

Lindahl-Bowen-Samuelson Condition

Lindahl-Bowen-Samuelson Condition

The condition for the allocation in the economy with a public good to be Pareto efficient is that the sum of all members' marginal rate of substitution of private

goods for the public good is equal to the marginal rate of transformation of private goods for the public good.

$$\sum_{i=1}^{n} \frac{u_{s+j}^{i}}{u_{r}^{i}} = \frac{F_{s+j}}{F_{r}} (i = 1, 2, \ldots, n; r = 1, 2, \ldots, s; j = 1, 2, \ldots m) \tag{6}$$

n is the number of the players. s is the number of private goods and r is their index. m is the number of public goods and j is their index. u is the utility function. F is the production function.

This is the condition of Lindahl-Bowen-Samuelson (=LBS condition) based on Samuelson (1954). The CO_2 emission quantity is the negative public good. So in the case of the CO_2 emission, we could directly use the LBS condition for the Pareto efficient allocation of the CO_2 emission.

Extension of LBS Condition to Consumption Externalities

In the presence of external effect from the consumption as well as that from production, we can use the extension of the Lindahl-Bowen-Samuelson according to the work of Tadenuma (2003, 2005), which extended the LBS condition to the cases where consumption activities also generate greenhouse gases. The following derivation of the extension of LBS condition to consumption externalities is in Tadenuma (2003, 2005). Here, we introduce them so that we can later extend them further to include uncertainty.

There are n countries, $N = 1, \ldots, n$. Let $y_i \in R_+$ denote the gross domestic product (GDP) of country $i \in N$, $c_i \in R_+$ the consumption of country i. Both production and consumption are accompanied by emissions of greenhouse gases. Let $x_i^p \in R_+$ denote the emission of greenhouse gases from production.

The relation of x_i^p and y_i is represented by the function $x_i^p = f_i(y_i)$, where $f_i' > 0$, $f_i'' > 0$.

Let $x_i^c \in R_+$ denote the emission of greenhouse gases from consumption. The relation of x_i^c and c_i is represented by the function $x_i^c = g_i(c_i)$, where $g_i' > 0$, $g_i'' \geq 0$.

Here, we assume, just as in Tadenuma (2003, 2005), $f_i'' > 0$and $g_i'' \geq 0$ so that the values of the CO_2 emission functions from production and consumption are increasing or nondecreasing to the right similar to the standard assumption of production cost function.

Let $x_i \equiv x_i^p + x_i^c$ be the total emission of greenhouse gases of country i, and let $X \equiv \sum_{i \in N} x_i$ be the global emission of greenhouse gases.

We assume that there is an amount $\widehat{X}$ of global emission of greenhouse gases such that the human beings cannot survive if the emission exceeds $\widehat{X}$. Each country i has the preferences over pairs $(c_i, X) \in R_+ \times \left[0\widehat{X}\right]$ of its own consumption and a global amount of emissions of greenhouse gases. The preferences are represented

by a continuously differentiable and strictly quasi-concave function $V_i : R_+ \times \left[0\widehat{X}\right] \to R$. We call the function V_i the welfare function of country i.

Problem A

$$\max_{(\mathrm{y},\mathrm{c},x)\in R_+^{3n}} V_i\left(c_i, \sum_{h\in N} x_h\right) \tag{7}$$

subject to

$$x_j = f\left(y_j\right) + g\left(c_j\right)(\forall j \in N) \tag{8}$$

$$\sum_{h\in N} y_h = \sum_{h\in N} c_h \tag{9}$$

$$V_j\left(c_j, \sum_{h\in N} x_h\right) = \breve{V}_j(\forall j \in N, j \neq i) \tag{10}$$

The condition (10) means that other players are at the optimal level of utility at $\breve{V}_j \equiv V_j\left(c_j^*, \sum_{h\in N} x_j^*\right) \in R$.

Solving this problem, we can get the extended condition of LBS to include the external effect from consumption. The Lagrangian for the problem A is as follows;

$$\begin{aligned} &L\left(\left(c_h\right)_{h\in N}, \left(x_h\right)_{h\in N}, \left(y_h\right)_{h\in N}, \left(\lambda_h\right)_{h\in N}, \left(\gamma_h\right)_{h\in N}, \delta\right) \\ &\equiv V_i\left(c_i, \sum_{i\in N} x_h\right) - \sum_{j\neq i} \lambda_j \left(V_j\left(c_j, \sum_{h\in N} x_h\right) - \breve{V}_j\right) \\ &\quad - \sum_{j\in N} \gamma_j \left(x_j - f_j(y_i) - g_j\left(c_j\right)\right) - \delta\left(\sum_{h\in N} y_h - \sum_{h\in N} c_h\right) \end{aligned} \tag{11}$$

From the first-order condition,

$$\frac{\partial V_i\left(c_i^*, \sum_{h\in N} x_h^*\right)}{\partial c_i} + \gamma_i g_i{}'\left(c_i^*\right) + \delta = 0 \tag{12}$$

$$\frac{\partial V_i\left(c_i^*, \sum_{h\in N} x_h^*\right)}{\partial X} - \sum_{j\neq i} \lambda_j \frac{\partial V_j\left(c_j^*, \sum_{h\in N} x_h^*\right)}{\partial X} - \gamma_i = 0 \tag{13}$$

$$\gamma_i f_i'\left(y_i^*\right) - \delta = 0 \tag{14}$$

and for each $j \neq i$,

$$-\lambda_j \frac{\partial V_i\left(c_i^*, \sum_{h \in N} x_h^*\right)}{\partial c_j} + \gamma_j g_j'\left(c_j^*\right) + \delta = 0 \tag{15}$$

$$\frac{\partial V_i\left(c_i^*, \sum_{h \in N} x_h^*\right)}{\partial X} - \sum_{j \neq i} \lambda_j \frac{\partial V_j\left(c_j^*, \sum_{h \in N} x_h^*\right)}{\partial X} - \gamma_j = 0 \tag{16}$$

$$\gamma_j f_j'\left(y_j^*\right) - \delta = 0 \tag{17}$$

Solving these equations, we get the following extended condition of LBS including the consumption externality, which is exactly the same as in Tadenuma (2003, 2005).

Extended Condition of LBS for Consumption Externalities
The allocation (y^*, c^*, x^*) is Pareto efficient, if the following is satisfied.

$$\sum_{i \in N} \nu_i \left(c_i^*, \sum_{h \in N} x_h^* \right) \left(f_i'\left(y_i^*\right) + g_i'\left(c_i^*\right) \right) = 1 \tag{18}$$

$$\nu_i\left(c_i^*, X\right) \equiv \left| \frac{\dfrac{\partial V_i\left(c_i^*, X\right)}{\partial X}}{\dfrac{\partial V_i\left(c_i^*, X\right)}{\partial c_i}} \right|$$

This is the extension of Lindahl-Bowen-Samuelson condition in a sense that the impacts of CO_2 emission from consumption as well as that of production are considered. Specifically, at Pareto optimal allocation, the weighted sum of the marginal rate of substitution of consumption for global emission of GHGs over all the countries is equal to one, where each weight is the sum of the marginal emission from production and the marginal emission from consumption in each country.

Extension of LBS Condition to Utility with Uncertainty
So far, we deal with the Pareto optimal condition with a negative public good. This setting has no uncertainty. In other words, the setting is based on perfect information.

Now we try to extend the LBS condition further to uncertain world. If we add the uncertainty to utility function, then **Problem** A becomes the new maximization problem with the uncertainty. But in order to track the utility function and

constraints, we need to set the structure of the relationship between the uncertainty and the other factors in utility function, namely, consumption c_i, production y_i, and their emission levels $f_i(y_i)$ and $g_i(c_i)$.

In order to set the structure, we introduce the following assumption.

Assumption 1

The uncertainty is linearly separable from production, consumption, and their emission functions. In other words, the uncertainty does not exist in production y_i, consumption c_i, their emission function $f_i(y_i)$ or $g_i(c_i)$, or their relationship in the utility function.

This means that the uncertainty is not about observation accuracy or accounting consistency, but is purely the remaining category other than human activities, i.e., consumption expenditures, or the emission amount of CO_2 from each country's human activities.

So this uncertainty could be the other type of uncertainty after we know the exact amount of CO_2 emission. This could be, for example, such uncertainty about the net ultimate effect of CO_2 emission through the earth ecology system on our utility level even if we know the exact level of consumption expenditures and the entailing exact emission level of CO_2 in each country.

In the aviation sector, the best estimate still have ± 30 % uncertainties about the effect of CO_2 even if we know the exact amount of fuel burn or CO_2 concentration in the atmosphere.[9] These scientific uncertainties are typical and persistent in the discussion of policy formulation about global climate change. What kinds of effect these uncertainties have on the negotiation by countries and organizations are very much central to the analysis of the study of bargaining mechanism of climate change policy. These uncertainties can be separable from fuel burn activity itself and CO_2 concentration in the atmosphere from the international aviation sector, since they are the uncertainties that remain even if we know the exact amount of emission level.

(continued)

[9]According to"6 Potential Climate Change from Aviation" in IPCC (1999), CO_2 is, unlike ozone and water vapor perturbations, one of well-mixed gases, and there is small uncertainty in calculating radiative forcing (RF, a single measure of climate change defined by IPCC, which calculates the global annual average of radiative imbalance ($W/m2$) to the atmosphere-land-ocean system caused by anthropogenic perturbations and sets the RF of preindustrial atmosphere to be zero). Still the RF for aviation CO_2 in 1992 based on NASA-1992 aviation scenario, for example, is estimated to be +0.018($W/m2$) with a likely range of ± 30 % that includes uncertainties in the carbon cycle and in radiative calculations for a fixed amount of fuel burn (160.3(*million tons/year*)) and a fixed CO_2 concentration level (1.0 ppmv). Also, while the persistent linear contrails have relatively small impact on the environment, other spreading types of contrail from global aviation have no best estimates of their effects on cirrus cloudiness. Global effect of aviation aerosol on background cloudiness remains unknown according to IPCC report (IPCC 2007b).

As we already mentioned earlier, the ICAO agreed to collect CO_2 emission data from its member countries. This measure will significantly reduce the uncertainties about level of CO_2 emission from production or consumption in the international aviation sector. Also that measure makes the typical scientific uncertainties relatively more relevant in the welfare analysis on climate change from the international aviation sector. So it is necessary and relevant, in our view, to include such scientific uncertainties in welfare analysis. Here, we are capturing these kinds of uncertainties.

Based on **Assumption 1**, the uncertainty is a rather limited structure in the welfare function. To include uncertainties around production, consumption, or their emission functions and to combine them with the typical scientific uncertainties are very much desirable for the deeper analysis. This, however, could drastically enhance the requirement of mathematical treatment, resulting in the complexity.

Here, we start with the very simple structure but with relevant kind of uncertainties in utility function as the beginning to be able to capture the situation in the real world where the information is not always perfect and there remain uncertainties.

By **Assumption 1**, our uncertainty is linearly separated from production y_i, consumption c_i, or their emission function $f_i'(y_i)$ and $g_i(c_i)$.

With this assumption of the linear separability of uncertainty, **Problem** A now becomes **Problem** B below. By solving **Problem** B, Lindahl-Bowen-Samuelson condition can be extended further to the situation where uncertainty exists.

Problem B

$$\max_{(y,c,x)\in R_+^{3n}} E\left[V_i\left(c_i, \sum_{h\in N} x_h, \varepsilon\right)\right] \tag{19}$$

subject to

$$x_j = f\left(y_j\right) + g\left(c_j\right)(\forall j \in N) \tag{20}$$

$$\sum_{h\in N} y_h = \sum_{h\in N} c_h \tag{21}$$

$$E\left[V_j\left(c_j, \sum_{h\in N} x_h, \varepsilon\right)\right] = \breve{V}(\forall j \in N, j \neq i) \tag{22}$$

ε could be a random variable according to any probability distribution. In this sense, since we do not know the probability distribution of ε yet, what ε represents is not "risk" but "uncertainty" in the meaning of Frank Knight's terminology.

Also notice that ε is introduced to all the countries, is common to all, and is not varying from one county to another. In this sense, all the countries share the common uncertainty, which is very much the characteristic of typical scientific uncertainties surrounding climate change.

Because of **Assumption 1**, we can describe the equality constrains without quoting ε.[10]

But solving **Problem** B is not simple. Here, we introduce additional assumption.

First, we define $\overline{V}_i$ as the expected value of $V_i\left(c_i, \sum_{h\in N} x_h, \varepsilon\right)$;

$$\overline{V}_i\left(c_i, \sum_{h\in N} x_h\right) \equiv E\left[V_i\left(c_i, \sum_{h\in N} x_h, \varepsilon\right)\right] \tag{23}$$

Assumption 2
ε is from normal distribution, $N(\mu, \sigma^2)$ and utility function is CARA (constant absolute risk aversion) utility function.[11]

Under **Assumption 1** and **Assumption 2**, Eq. 23 becomes

$$\begin{aligned}\overline{V}_i\left(c_i, \sum_{h\in N} x_h\right) &= E\left[V_i\left(c_i, \sum_{h\in N} x_h, \varepsilon\right)\right] \\ &= E\left[-\exp\left\{-\eta_i\left(H_i\left(c_i, \sum_{h\in N} x_h\right) + \varepsilon\right)\right\}\right]\end{aligned} \tag{24}$$

where $H_i\left(c_i, \sum_{h\in N} x_h\right)$ is the relationship function between c_i and $\sum_{h\in N} x_h$

[10]The uncertainty here is only one dimension. The structure, however, can be extended to multidimension uncertainties without loss of generality.

[11]CARA utility function has the general form $V = A1 + A2\exp\{-\eta c\}$, with η indicating coefficient of absolute risk aversion, i.e., degree of risk aversion. We can arbitrarily set the value $A1$ and $A2$. In the following case, we use $A1 = 0$ and $A2 = -1$ for simplicity.

Although, in this case, the welfare function returns a negative value, we can interpret this negative welfare value as the difference from the highest welfare value, for example.

$A1$ and $A2$ could be considered as the location adjusting parameter and scale parameter, respectively, for the CARA utility function.

without any uncertainty. This can be possible because of the linear separability of uncertainty from other economic activities under **Assumption 1** and the CARA utility function's characteristics form **Assumption 2**.

So we get,

$$\begin{aligned}\overline{V}_i\left(c_i, \sum_{h\in N} x_h\right) &= -\exp\left\{-\eta_i\left(H_i\left(c_i, \sum_{h\in N} x_h\right)\right)\right\} E[\exp\{\eta_i(\varepsilon)\}] \\ &= -\exp\left\{-\eta_i\left(H_i\left(c_i, \sum_{h\in N} x_h\right)\right) - \mu\eta_i + \frac{\eta_i^2\sigma^2}{2}\right\}\end{aligned} \tag{25}$$

Notice that under **Assumption 2**, $\varepsilon \sim N(\mu, \sigma^2)$;

$$\begin{aligned}&E[\exp\{-\eta(\varepsilon)\}] \\ &= \int_{-\infty}^{\infty} e^{-\eta\varepsilon} \frac{1}{\sqrt{2\pi}\sigma} e^{\frac{-(\varepsilon-\mu)^2}{2\sigma^2}} d\varepsilon \\ &= e^{-\eta\mu+\frac{\eta^2\sigma^2}{2}} \frac{1}{\sqrt{2\pi}\sigma} \int_{-\infty}^{\infty} e^{\frac{-\left(\varepsilon-\left(\mu-\sigma^2\eta\right)\right)^2}{2\sigma^2}} d\varepsilon \\ &= e^{-\eta\mu+\frac{\eta^2\sigma^2}{2}} \cdot 1.\end{aligned}$$

Now we can derive the extension of LBS condition to include the uncertainty described above. Equations 19–22 become as follows.

Problem B ⋆

$$\max_{(y,c,x)\in R_+^{3n}} \overline{V}_i\left(c_i, \sum_{h\in N} x_h\right) \tag{26}$$

subject to

$$x_j = f\left(y_j\right) + g\left(c_j\right) (\forall j \in N) \tag{27}$$

$$\sum_{h\in N} y_h = \sum_{h\in N} c_h \tag{28}$$

$$\overline{V}_j\left(c_j, \sum_{h\in N} x_h\right) = \breve{V}\,(\forall j \in N, j \neq i) \tag{29}$$

By Eq. 25, we can treat Eqs. 26–29 without any random variables. These equations in **Problem B** ⋆ can be solved by the usual maximization problem just as in **Problem** A.

Define the Lagrangian as follows:

$$\begin{aligned} &L\left((c_h)_{h\in N},(x_h)_{h\in N},(y_h)_{h\in N},(\lambda_h)_{h\in N},(\gamma_h)_{h\in N},\delta\right) \\ &\equiv \overline{V}_i\left(c_i,\sum_{i\in N}x_h\right)-\sum_{j\neq i}\lambda_j\left(\overline{V}_j\left(c_j,\sum_{h\in N}x_h\right)-\breve{V}_j\right) \\ &-\sum_{j\in N}\gamma_j\left(x_j-f_j(y_i)-g_j(c_j)\right)-\delta\left(\sum_{h\in N}y_h-\sum_{h\in N}c_h\right). \end{aligned} \tag{30}$$

Notice that the term $V_i\left(c_i,\sum_{h\in N}x_h\right)$ in the Lagrangian (11) in **Problem** A now becomes $\overline{V}_i\left(c_i,\sum_{h\in N}x_h\right)$ in the Lagrangian (30) in **Problem B** $\star$.

Other than this, the Lagrangian is the same as in solving **Problem** A.

Thus, we can get the following familiar condition.

As the first-order condition,

$$\frac{\partial\overline{V}_i\left(c_i^*,\sum_{h\in N}x_h^*\right)}{\partial c_i}+\gamma_i g_i{}'\left(c_i^*\right)+\delta=0 \tag{31}$$

$$\frac{\partial\overline{V}_i\left(c_i^*,\sum_{h\in N}x_h^*\right)}{\partial X}-\sum_{j\neq i}\lambda_j\frac{\partial\overline{V}_j\left(c_j^*,\sum_{h\in N}x_h^*\right)}{\partial X}-\gamma_i=0 \tag{32}$$

$$\gamma_i f_i{}'\left(y_i^*\right)-\delta=0 \tag{33}$$

and for each $j\neq i$,

$$-\lambda_j\frac{\partial\overline{V}_i\left(c_i^*,\sum_{h\in N}x_h^*\right)}{\partial c_j}+\gamma_j g_j{}'\left(c_j^*\right)+\delta=0 \tag{34}$$

$$\frac{\partial\overline{V}_i\left(c_i^*,\sum_{h\in N}x_h^*\right)}{\partial X}-\sum_{j\neq i}\lambda_j\frac{\partial\overline{V}_j\left(c_j^*,\sum_{h\in N}x_h^*\right)}{\partial X}-\gamma_j=0 \tag{35}$$

$$\gamma_j f_j{}'\left(y_j^*\right)-\delta=0 \tag{36}$$

Notice also that

$$\frac{\partial\overline{V}_i}{\partial X}=\overline{V}_i(-\eta_i)\frac{\partial H_i}{\partial X},\ \frac{\partial\overline{V}_i}{\partial c_i}=\overline{V}_i(-\eta_i)\frac{\partial H_i}{\partial c_i}$$

We get the following result:

$$\nu_i(c_i, X) \equiv \left| \frac{\dfrac{\partial \overline{V}_i(c_i, X)}{\partial X}}{\dfrac{\partial \overline{V}_i(c_i, X)}{\partial c_i}} \right| = \left| \frac{\overline{V}_i(\eta_i) \dfrac{\partial H_i}{\partial X}}{\overline{V}_i(\eta_i) \dfrac{\partial H_i}{\partial c_i}} \right| = \left| \frac{\dfrac{\partial H_i(c_i, X)}{\partial X}}{\dfrac{\partial H_i(c_i, X)}{\partial c_i}} \right| \tag{37}$$

By solving Eqs. 31–36 and Eq. 37, we can describe the extended condition of LBS for uncertainty.

Proposition 1: Extended Condition of LBS for Uncertainty
Under **Assumption 1** and **Assumption2**, at Pareto optimal allocation, the weighted sum, over all the countries, of the marginal rate of substitution of consumption for global emission of GHGs, which is composed only of the certain part of the utility function with uncertainty, is equal to one, where each weight is the sum of the marginal emission from production and the marginal emission from consumption in each country.

$$\sum_{i \in N} \nu_i \left(c_i^*, \sum_{h \in N} x_h^* \right) \left(f_i'(y_i^*) + g_i'(c_i^*) \right) = 1 \tag{38}$$

$$\nu_i(c_i^*, X) \equiv \left| \frac{\dfrac{\partial H_i(c_i^*, X)}{\partial X}}{\dfrac{\partial H_i(c_i^*, X)}{\partial c_i}} \right|$$

This is the extended condition of LBS to include the uncertainty under **Assumption 1** and **Assumption 2**. Notice that in $\nu_i(c_i^*, X)$, we have $H_i(c_i^*, X)$, instead of $V_i(c_i^*, X)$. $H_i(c_i^*, X)$ is the certain (= without any uncertainty) part of the utility function V_i $\left(c_i^*, \sum_{h \in N} x_h, \varepsilon \right)$ with uncertainty ε under **Assumption 1** and **Assumption 2**.

Welfare Implication with Numerical Examples

Basic Model

Let $N = 1, 2$. The emission functions are defined as follows: for every $i \in N$,

$$f_i(y_i) = y_i^2 \tag{39}$$

$$g_i(c_i) = c_i \tag{40}$$

For each $i \in N$, the welfare function $V_i : \in {R_+}^3 \rightarrow R$ is expressed with the assumption of CARA utility function as follows:

$$E[V_i(c_i, X, \varepsilon)] = E[-\exp\{-\eta_i(H_i + \varepsilon)\}] \tag{41}$$

$$H_i = c_i^{a_i}(10 - X)^{1-a_i} (0 \le a_i \le 1) \tag{42}$$

Under the assumption of the normal distribution for ε, we can get the following:

$$\overline{V}_i(c_i, X) = -\exp\left\{-\eta_i\left(c_i^{a_i}(10 - X)^{1-a_i}\right) - \mu\eta_i + \frac{\eta_i^2\sigma^2}{2}\right\} \tag{43}$$

If we pick the specific numbers for parameters $a_1 = 0.8$, $a_2 = 0.2$, then we have the following equations:

$$\overline{V}_1(c_1, X) = -\exp\left\{-\eta_1\left(c_1^{0.8}(10 - X)^{0.2}\right) - \mu\eta_1 + \frac{\eta_1^2\sigma^2}{2}\right\} \tag{44}$$

$$\overline{V}_2(c_2, X) = -\exp\left\{-\eta_2\left(c_2^{0.2}(10 - X)^{0.8}\right) - \mu\eta_2 + \frac{\eta_2^2\sigma^2}{2}\right\} \tag{45}$$

Notice that parameters $a1$ and $a2$ represent the weights on consumption and on climate change effect in their utility functions. If $a_1 > a_2$, country 1 puts more weight on consumption than country 2, and country 1 puts less weight on climate change effect than country 2.[12]

With Eqs. 44 and 45 as well as the extended condition of LBS for uncertainty, we can derive the Pareto frontier, bargaining frontier, disagreement point, and Nash product[13] based on Tadenuma (2003, 2005), which is the model for no uncertainty.

Here, we do not go into the details for these frontiers and points, which are explained in Tadenuma (2003, 2005). But the gist of them is as follows.

Pareto frontier is the locus of the welfare vectors of the two countries under our study that can be attained by satisfying the extended condition of LBS depicted in Eqs. 18 and 38. Namely, the vectors(V_1, V_2) must satisfy the following relationships in our numerical example:

$$V_1 = \overline{V}_1(c_1(c_2), X(c_2))$$

$$V_2 = \overline{V}_2(c_2, X(c_2))$$

$$(c_1 + c_2 + 1)\left(\frac{c_1}{4} + 4c_2\right) - 10 + \frac{(c_1 + c_2)^2}{2} + c_1 + c_2 = 0$$

[12]According to sensitivity analysis, the more a_1 and a_2 are different, the more bargaining frontier spread. This means more room for the two countries to bargain. If these parameters are closer, the bargaining frontier is getting tighter. This means less room for the two countries to bargain.

[13]The bargaining model is theoretically founded in Nash (1950).

$$X(c_2) = \frac{(c_1 + c_2)^2}{2} + c_1(c_2) + c_2$$

The last two equations can be derived from the extended condition of LBS in (18) or (38). The locus welfare vectors (V_1, V_2) are drawn for the relevant value for c_2.

Bargaining frontier is the locus of the welfare vectors that are attained at various levels of the total emission X with a given proportional rule, i.e., the share of initial emission allowances, (θ_1, θ_2) in our case, and emission allowance trading, entailing the trade price $q(X)$. Namely, the vectors (V_1, V_2) in the locus are those that satisfy the following relationships:

$$V_i = \overline{V}_i(c_i(X), X)$$

$$c_i = \frac{1}{4q(X)(1 + q(X))} + \frac{q(X)\theta_i X}{1 + q(X)}$$

$$X = \frac{1}{4q^2} + \frac{1}{4q^2} + \frac{1}{q}$$

In these settings, $q(X)$ is the inverse function of the last equation. Over the relevant range of X, we have the locus of (V_1, V_2), which is the bargaining frontier. Notice that the bargaining frontier depends on the initial allocation, (θ_1, θ_2). The bargaining frontier changes its shape according to the value of the initial allocation.

Disagreement point of the Nash bargaining theory is the Nash equilibrium welfare levels of the two countries in the emission game without any regulation. Specifically, we have the two players who do not bargain with each other and take the other's emission level as given. Their utility function is as follows:

$$V_1 = \overline{V}_1 = -\exp\left\{-\eta_1\left(c_1^{0.8}\left(10 - x_2 - c_1^2 - c_1\right)^{0.2}\right) - \eta_1\mu + \frac{\eta_1^2\sigma^2}{2}\right\}$$

$$V_2 = \overline{V}_2 = -\exp\left\{-\eta_2\left(c_2^{0.2}\left(10 - x_1 - c_2^2 - c_2\right)^{0.8}\right) - \eta_2\mu + \frac{\eta_2^2\sigma^2}{2}\right\}$$

The best response functions are obtained by differentiating the functions with respect to c_i and setting the value to zero. Then, by solving these response function equations, the Nash equilibrium consumption, emissions, and welfare levels are derived. This vector of the derived welfare, which could be thought as what you get if you fail to bargain, is the disagreement point (d_1, d_2).

Nash product is defined by

$$(V_1 - d_1)(V_2 - d_2)$$

Before we go further, we first set the parameters as follows:

$$\mu = 0$$

$$\sigma = 1$$

$$\eta_1 = \eta_2 = 0.2$$

Also the initial allocations for the emission allowances for player 1 and player 2 are θ_1 and θ_2, respectively. We set these as follows:

$$\theta_1 = 0.925$$

$$\theta_2 = 0.075$$

Fig. 8 is the result loci for these frontiers and points.

Since our CARA utility function is the monotone transformation of the utility function in Tadenuma (2003, 2005), the shape of the frontiers are quite similar except for their location and scale. The same comparison can be derived about the disagreement points. As in Tadenuma (2003, 2005), Pareto frontier and bargaining frontier touch at one point, where each player's emission levels are equal, i.e., $x_1^* = x_2^*$. In these settings, disagreement point is within the bargaining frontier. So it could be possible that starting from disagreement point both players can reach higher utility level by bargaining. But as Fig. 8 shows, limit of bargaining is not as

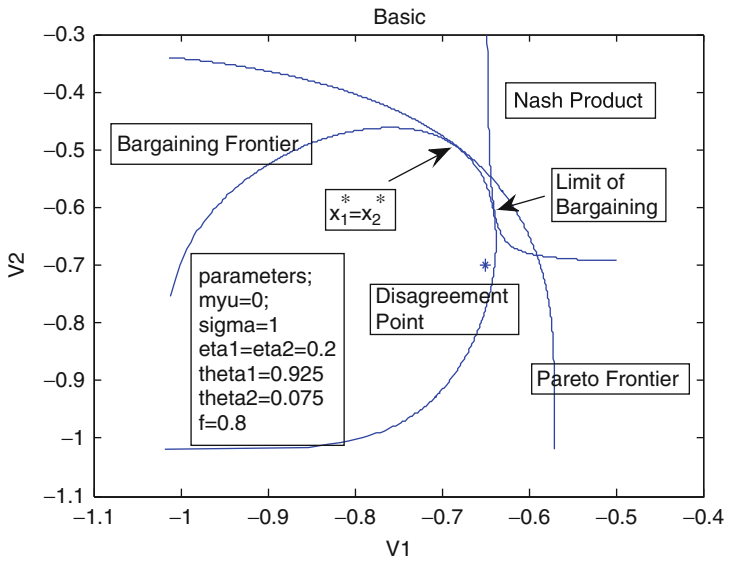

Fig. 8 Frontiers and limits of asymmetric world

high as the Pareto frontier, of which is the point where each player's emission is the same, namely, $x_1^* = x_2^*$.

Symmetric Structure World

If both players' H_i function is the same function (their degree of risk averse was already set to be the same, i.e., $\eta_1 = \eta_2 = 0.2$), then both players' Vi functions are as follows:

$$\overline{V}_1(c_1, X) = -\exp\left\{-\eta(c_1(10 - X)) - \mu\eta + \frac{\eta^2\sigma^2}{2}\right\} \tag{46}$$

$$\overline{V}_2(c_2, X) = -\exp\left\{-\eta(c_2(10 - X)) - \mu\eta + \frac{\eta^2\sigma^2}{2}\right\} \tag{47}$$

Furthermore, the initial allocation is even, namely,

$$\theta_1 = 0.5$$

$$\theta_2 = 0.5$$

Under the setting, the bargaining frontier collapses as in Fig. 9. In this world, everything is symmetric. So both players can start with the disagreement point

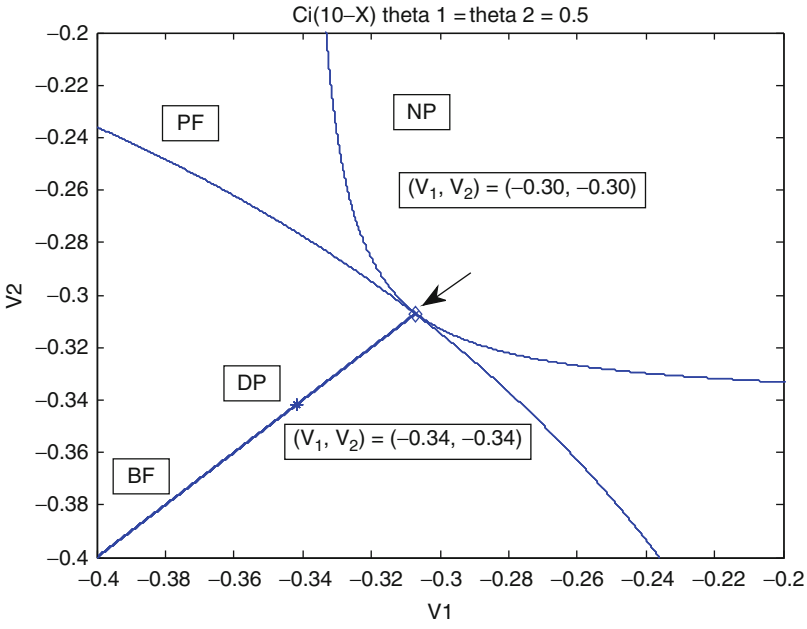

Fig. 9 Frontiers and limits of symmetric world

(DP), moving along the bargaining frontier, now a line, and the two can reach the Pareto frontier and realize the social efficiency.

If the real world is symmetric as in Fig. 9, then the bargaining could lead to social efficiency.

Impact of Uncertainty Increase

Back in the basic case, which is in Fig. 8, if the uncertainty increases, the σ would increase. In Fig. 10, we depict the world as σ increases, namely, $\sigma = 1, 2, 3, 4, 5, 6$. As the uncertainty, namely, σ, increases, the world shrinks to the lower left corner.

This means you have to settle for smaller level of utility. Under uncertainty increase settings, bargaining is almost surely more difficult than otherwise.

Asymmetric Risk Aversion

If player 1's risk aversion level is more than that of player 2, player 1's utility function changes like in Fig. 11.

The utility function is getting more skewed into the upper left as the risk aversion parameter η increases, namely, $\eta = 0.2, 0.4, \ldots, 1.8, 2.0$.

Under these settings, player 1 evaluates more in the upper side of income, namely, higher x in Fig. 11, to compensate the lower evaluation for lower side of income. This is the content of risk aversion. As a result, under our parameter setting, player 1 needs more than player 2. So the world in Fig. 8 is skewed to the right to allocate more to player 1 just as in Fig. 12.

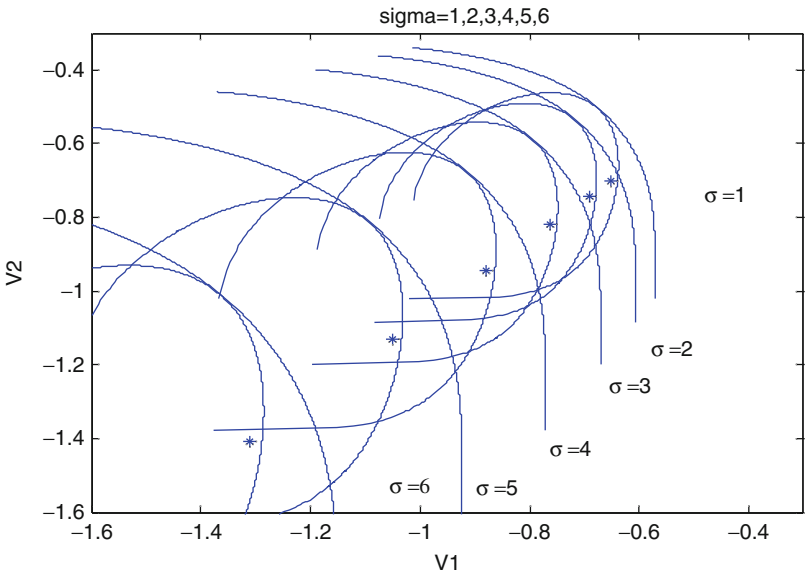

Fig. 10 As uncertainty increases, world shrinks

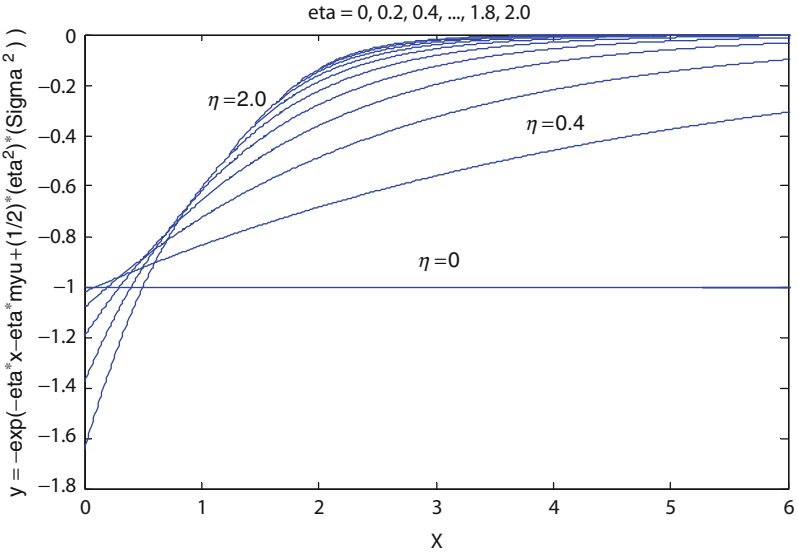

Fig. 11 CARA utility function skews as risk aversion increases

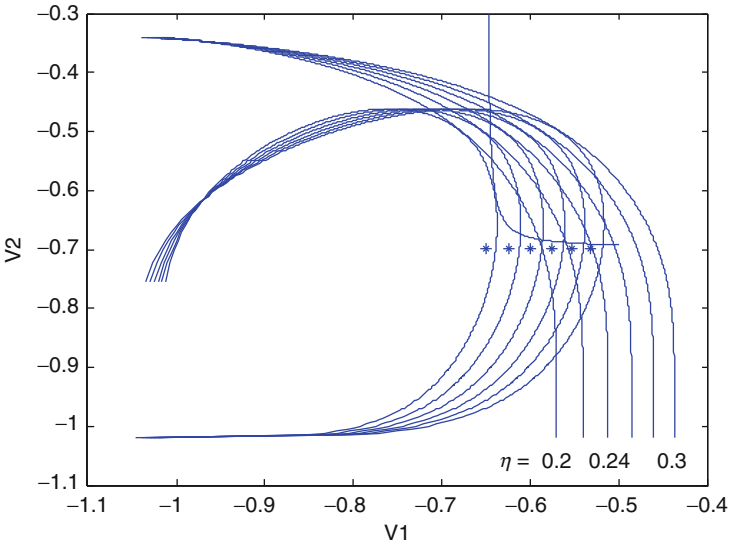

Fig. 12 Player 1 is getting more risk averse than player 2

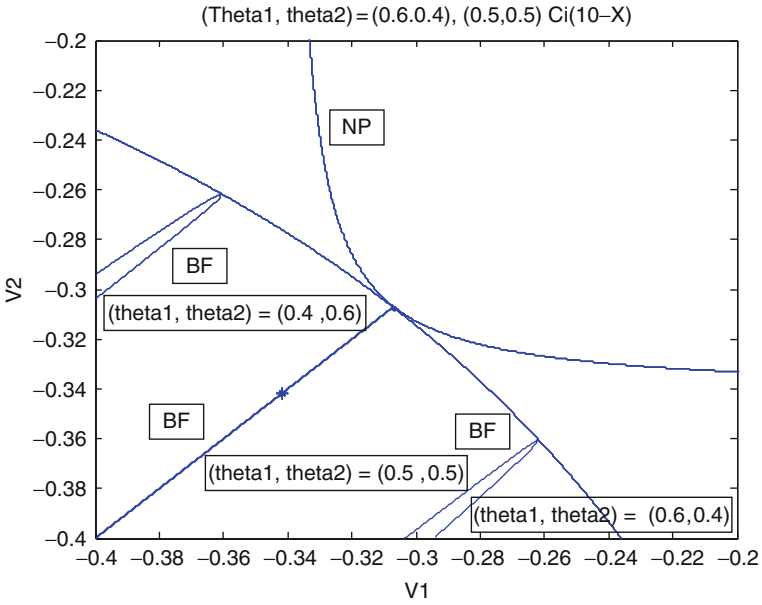

Fig. 13 Initial allocation perturbation in symmetric world

All things equal, if the risk aversion of one of the players is more than the other, the player could ask for more in bargaining, and this could lead to more difficult bargaining process since in the real bargaining process, you cannot see the other players' risk aversion parameter.

Initial Allocation Perturbation

To make the comparison easier, we go back to the even world in Fig. 9.

The initial allocation for each player is even in Fig. 9, namely,

$$\theta_1 = 0.5$$

$$\theta_2 = 0.5.$$

The disagreement point is on the bargaining frontier.

If the allocation is off from the even about 0.1 in our setting in Fig. 9, the bargaining frontier dislocates from the original collapsed bargaining frontier (line) to the upper side or lower side depending on the plus or minus of the deviation from the original allocation as in Fig. 13.

In these cases, the disagreement point, which does not move, is out of the bargaining frontier in either upper or lower case. Getting to the higher welfare level through bargaining starting from the disagreement point is not feasible, let alone attaining the social efficiency frontier.

Conclusion of the Theoretical Study

We performed simulation analysis on the international CO_2 emission allowances trading, especially on the effects on pricing of CO_2 emission allowances by including major players such as China, India, and Korea into the hypothetical global trading scheme according to noncooperative game-theoretic framework. As the three countries enter into the trading and their reduction obligation increases by 1 %, the emission allowance price goes up by about 33 cents. Also if the three countries improve their carbon intensity variation by 1 % (−1 %), then the emission allowance price goes up by 2 cents.

In the presence of negative public goods, i.e., CO_2 emission into the earth atmosphere, we extended the Lindahl-Bowen-Samuelson condition so as to include at least some class of the uncertainty into the utility. That is, under **Assumption 1** and **Assumption 2**, we introduce the CARA utility function and linearly separable uncertainty from consumption, production, and their emission functions. This kind of scientific uncertainty is typical in climate change policy.

If such uncertainty increases, then both Pareto frontier and bargaining frontier shrink and make the negotiation harder, since the players have to settle for less than before. If the risk preferences are different between the players, then the Pareto frontier and bargaining frontier skew. So the simple allocation rule, like the same percentage reduction for different countries, could be difficult to be agreed upon. Moreover, under the condition of asymmetric risk aversion levels and asymmetric utility structure, with uneven initial allocations of CO_2 allowances, it is shown that reaching the bargaining frontier, let alone Pareto frontier, by bargaining could be extremely difficult.

The policy implications from these results could be that if typical scientific uncertainties become large due to, for example, discovery of contradicting observations or people's losing confidence in the scientific researches by noticing some mistakes in the researches, then the negotiation process becomes very difficult. IPCC scientific research effort and keeping its research integrity are very important in the highly complex problems with large uncertainties like global climate change.

Also if the negotiating countries' preferences are very different (due to the difference of how much to put weight on climate change in their utility structure, for example), the adjusting efforts to decrease the differences (by transferring fund or technology so that the countries seeking development more than environment can get development cheaply or environmentally friendly) are more important.

References

Bohm P, Larsen B (1994) Fairness in a tradable-permit treaty for carbon emission reduction in Europe and the former Soviet Union. Environ Resour Econ 4:219–239

Brueckner JK, Zhang A (2009) Airline emission charges: effects on airfares, service quality, and aircraft design. Working paper

Ding J, Wit RCN, Leurs BA, Davidson M (2003) External cost of aviation. Federal Environmental Agency (UBA), Berlin

EU (2009) Directive 2008/101/ec of European parliament and of the council of 19 November 2008 (amending directive 2003/87/ec so as to include aviation activities in the scheme for green-house gas emission allowance trading within the community). Off J Eur Union, L8/3-L8/21
GIACC (2008) Giacc/2-wp/4. working paper
GIACC I (2009) GIACC report 1 June 2009. ICAO
Guesnerie HTR (ed) (2008) The design of climate policy. The MIT Press, Cambridge, MA
Hihara K (2012) An analysis of airport-airline relationship with a risk sharing contract. Transp Res E 48:978–992
Hihara K, Okano M (2012) Chapter 6 the environmental issues. In: Suzuki S, Okano M (eds) Modern aviation – from technologies to industry & policy. The University of Tokyo Press, Tokyo, pp 191–207
ICAO (2013) 2013 environmental report, destination green. ICAO, Montreal
ICAO (2009) High-level meeting on international aviation and climate change summary of discussions-revised. ICAO, Montreal
ICAO general assembly resolution (A38-18) in 2013. ICAO, Montreal
ICAO environmental report 2010 Aviation and Climate Change. ICAO, Montreal
Imai H, Okada A (2005) Application of game theory (in Japanese). Keiso Shobo, Tokyo
IPCC (1999) Aviation and the global atmosphere. Cambridge University Press, Cambridge
IPCC (2007a) Climate change 2007: synthesis report (the fourth assessment report). IPCC, Geneva
IPCC (2007b) Report of working group i technical summary. WG 1 report, 30
Kanemoto Y, Hasuike K, Fujiwara T (2006) Microeconomic modeling for policy analysis (in Japanese). Toyo Keizai Shimpo Sha, Tokyo
Kolstad CD (2000) Environmental economics. Oxford University Press, Oxford
Nash JF (1950) The bargaining problem. Econometrica 28:155–162
Nordhaus W (1991) The cost of slowing climate change: a survey. Energy J 12:37–65
Okada A (2003) A market game analysis of international CO_2 emissions trading: evaluating initial allocation rules. Springer, Tokyo
Okada A (2004) International negotiations on climate change: a non-cooperative game analysis of the Kyoto protocol. Discussion paper 2004-2, Graduate School of Economics, Hitotsubashi University
Samuelson PA (1954) The pure theory of public expenditure. Rev Econ Stat 84:387–389
Tadenuma K (2003) International negotiations for reduction of green-house gases with emission permits trading. Project on International Equity (PIE) Discussion Paper Series, Hitotsubashi University
Tadenuma K (2005) Possibility and optimality of agreements in international negotiations on climate change. Project on International Equity (PIE) Discussion Paper Series, Hitotsubashi University
Yang Z (2008) Strategic bargaining and cooperation in greenhouse gas mitigation. The MIT Press, Cambridge, MA

Part II

Impact of Climate Change and Adaptation

Carbon Liability

Yoshihiro Fujii

Contents

Abstract

By the term "carbon liability," we mean a calculation of values approximating to the economic externalities of carbon emissions in the global economy, in relation to the totality of global economic activity. As a consequence of over two centuries of industrialization, the global carbon budget and its associated global carbon balance sheet have clearly diverged from a state of natural equilibrium. Deterioration of carbon budget has affected on asset value of energy intensive companies which have huge fossil fuel reserves, called as stranded assets. Three material identifiable, types of carbon risks, "cap-and-trade" schemes are important economic mechanism aiding both the rectification of these imbalances and restoration of natural carbon cycle disrupted by emissions of anthropogenic greenhouse gas (GHG) in both developed and emerging countries. Such schemes establish an economic value to carbon through open market trading. They serve to quantify and to reduce carbon risk, in accordance with appropriate and efficient economic regulation. Monetizing carbon liabilities through these market mechanisms is a

Y. Fujii (✉)
Graduate School of Global Environmental Studies, Sophia University, Tokyo, Japan
e-mail: fujii@genv.sophia.ac.jp

W.-Y. Chen et al. (eds.), *Handbook of Climate Change Mitigation and Adaptation*,
DOI 10.1007/978-3-319-14409-2_12

means to place boundaries on, and thus to mitigate, the uncertainties of carbon liability. This process of monetization may also transform market risk into an opportunity for economic exploitation.

Introduction

The Fifth Assessment Report of the Intergovernmental Panel on Climate Change (IPCC 2014, AR5 (The Fifth Assessment Report of the Intergovernmental Panel on Climate Change 2014)) concluded that "human influence on the climate system is clear, and recent anthropogenic emissions of greenhouse gases are highest in history" and that "warming of the climate system is unequivocal, and since the 1950s." The certainty of the relation between increase in global average temperatures since the mid-twentieth century and increase in anthropogenic greenhouse gas(GHG) concentrations is defined as "extremely likely" rather than "very likely" in previous report (AR4, 2007) which means probability of causality increase 95 ~ 100 % in AR4 to 95 ~ 100 % in AR5. The report said "Climate change will amplify existing risks and create new risks for natural and human systems. Risks are unevenly distributed and are generally greater for disadvantaged people and communities in countries at all level of development." This means managing carbon balance sheets both in global economy and individual economic entities would be emerged critical issues.

Carbon Liability as a Concept in Accounting and in Ecology

Carbon Liability

This chapter focuses on the importance of these findings, in relation to the concept of "carbon liability" and its implications. By this term, it means a calculation of values related to the economic externalities of carbon emissions in the global economy and the process of apportioning those values, both in macroeconomic terms within the global economy and microeconomically, to achieve a more true economic value for each individual emitting entity. It can be referred to these processes as "carbon management."

What is a "carbon liability"? Liability is a concept which arises in accounting and in law. It means a legally enforceable obligation, whether imposed contractually or unilaterally or by civil society. The obligation on a citizen to pay tax is an example of a unilateral liability imposed by a government. From an accounting point of view, liability means a present obligation arising from past events. Its settlement is expected to result in an outflow of resources. The International Accounting Standards Board (IASB) sets out the accounting and disclosure requirements for provisions, contingent liabilities, and contingent assets as International Accounting Standards (IAS) 37. This chapter discusses the current definition.

Carbon liability has its roots in this environment of civil obligation. In recent years, governments have introduced regulations to restrict quantified volumes of

GHG (greenhouse gas) emissions by incorporated entities, a measure directed toward the public goods of controlling the unequivocal danger – an economic "bads" – of which is global warming. Thus "carbon liability" arises from an established tradition of state-initiated regulation.

Entities addressed by governments are required to meet the costs of their obligations using their own resources in order to comply with the demands of regulation. Liability in relation to carbon emissions differs in kind, however, from other forms of liability, in that it includes a lot of messy uncertainties about its causality and its composition. The IASB's International Financial Reporting Standards (IFRS) categorizes such instances as a "contingent liability," in the IFRS' words, "a possible obligation depending on whether some uncertain future event occurs" and "a present obligation but payment is not probable or the amount cannot be measured reliably." These characteristics correspond to the nature of carbon liability, which encompass the past, present, and future responsibilities for GHG emissions.

Carbon liability belongs in addition to a broader definition of environmental liability. This field has already been defined legally and in accounting terms in both the USA and the European Union. The US Environmental Protection Agency (EPA) has defined "environmental liability" as an obligation in environmental law to make a future expenditure to remedy the past or ongoing manufacture, use, release, or threatened release of a particular substance, or other activities that adversely affect the environment (Environmental Protection Agency 1996). This regulatory stance arose from a succession of environmental disasters in the USA during the 1970s and 1980s, which resulted in asbestos exposure and soil contamination and damage to people, property, and the natural environment. To prevent and remedy such damages, US legislators enacted the Comprehensive Environmental Responses, Compensation, and Liability Act (CERCLA), otherwise known as the "Superfund Act." It was enacted in 1980 then was amended as Superfund Amendment and Reauthorization Act (SARA) in 1986. Small Business Liability Relief and Brownfields Revitalization Act in 2002, respectively.

Drawing on this American legislation, the European Union constructed its own legal framework for the prevention and remediation of damages to the human and natural environment. In 2004, the EU Commission published its Directive on Environmental Liability (ELD), and it came into effect in all EU states in 2008. These legal frameworks on either sides of the Atlantic share common characteristics.

Drawing on these models, the US Federal Accounting Standards Board (FASB) and the IASB have developed an accounting framework on environmental liability. The FASB issued EITF 93-5, "Accounting for Environmental Liabilities," in 1993; in 1996, it was included in the Statement of Position (SOP 96-1, Environmental Remediation Liabilities) in the American Institute of Certified Public Accountants (AICPA). As noted earlier, the IASB has referred to environmental liabilities in its IAS 37 standard.

What definitions of "the environment" are used in these legal and accounting frameworks? The concept in those frameworks is very broad. For example, the Lugano Convention (Convention on Civil Liability for Damage Resulting from Activities Dangerous to the Environment, June 1993) which laid down fundamental

concepts of strict liability for environmental damages caused in EU territories considers environment to be the realm of all natural resources, both abiotic and biotic, such as air, water, soil, fauna and flora, and the interaction between the same factors, property which forms part of the cultural heritage and the characteristic aspects of the landscape.

Similarities and Differences Between the Concepts of Carbon Liability and Environmental Liability

It is clear that any concept of "carbon liability" should be considered in the context of an established corpus of environmental liabilities. Carbon emitted by corporations shares characteristics with other forms of environmental damage including, as already noted, cost of damages attributable to past or present commercial activities, including production of GHGs and/or their release into the atmosphere. To discharge these obligations, entities must pay the expenses of remediation or reparation from their own resources. In other words, this discharge of legal responsibilities under regulation entails for corporate entities an internalization of a type of cost control of carbon emissions – which was previously considered as an economic externality. What these similarities in definitions demonstrate is that they can be constructed the same kind of legal and accounting framework for carbon liabilities in order to manage resulting marginal costs to the environment and to society as a whole.

Similarities notwithstanding, the concept of carbon liability also has several differences from general environmental liability. Most importantly, GHGs are not in themselves toxic. This contrasts directly with the toxic or noxious characteristics of most general pollutants specified or implicated in legislation on environmental liability, such as asbestos, sulfur dioxide, heavy metals, etc. Directly and indirectly, the latter harm human health and the ecosystem. Carbon dioxide, the most common GHG and a primary factor in most cases of carbon liability, is not toxic in itself. It is merely one component in the atmosphere, a natural chemical by-product of all plant and animal life. Of course carbon monoxide (CO), which is chemically related to CO_2, is clearly toxic. In theory, CO_2 itself can be poisonous in high volumes; such a danger is however never likely in naturally occurring concentrations.

In this context, concentrations of CO_2, even in the most dangerous scenario simulated in the IPCC's AR5 toward the end of this century, will cause only *indirect* loss and damages, as part of the indirect consequences resulting from climate change. This indirect attenuated chain of causality presents serious difficulties in the calculation of carbon liability in society.

Cows' Belch Can Be Tradable Commodities

The planet is populated with very many agents of GHG emissions, whether animal, corporate, or human. Corporations contribute GHGs by their activities in resource consumption, in production and distribution, and in demand stimulation. Nature's emission processes include deforestation, volcanic eruptions, swamps, and wetlands. Even ruminant livestock in agriculture add to the emissions of animals: the human population, now on the cusp of 7.0 billion, is of course the most highly polluting species of fauna. A belch from a cow or other ruminant emits methane, a GHG with

28 times the warming power of CO_2. Estimates of global warming potential by methane have increased from 21 in AR4 to 28 in AR5.

The Worldwatch Institution, an independent research organization, has estimated that GHG emissions from ruminants contribute between 10 % and 15 % of the planet's annual GHG total from all sources (Goodland and Anhang 2009). The legal implication is clear: the belch of a cow might be regarded as a carbon liability for its owner. A rancher might compensate by participating in carbon trading, offsetting the wider economic cost of methane from his livestock. If he can find a way of reducing methane from his cows, he trade a carbon credit on the free market linked to his animals thereby earning additional income besides selling milk or meat. Actually, Idemitsu Kosan, a Japanese petroleum company, with Hokkaido University has developed a new food for cattle to reduce output of methane gas bovine eructation in 2007.

Besides biology, GHGs are emitted through innumerable economic and industrial processes in manufacturing, power generation, farming, logging, transportation, and so on. These are in addition to the emissions of individual humans, of course. Consequently, it is very difficult to restrict GHG emissions from all sources. This near-universal emission by billions of agents and processes, of gases which are very often essential to life itself, presents a completely different, universally pervasive causality which is more complex than with other recognized pollutants. This difference presents a major obstacle in forming policies to reduce emissions and to manage carbon, both in macroeconomic policy and in the carbon management strategies of individual corporations.

Different Legal Treatments of Carbon Liability

As noted above, the concept of carbon liability can be seen as an obligation like others in environmental law. Its treatment and remedies differ from jurisdiction to jurisdiction, however. Developed countries which ratified the Kyoto Protocol recognized a duty to reduce their GHG emissions from 1990 levels. On the other hand, developing countries including even major emitters such as China, India, and Brazil face only a voluntary, nonbinding commitment to reduce their own emissions. These differences are called "common but differentiated responsibilities."

Some additional differences remained between developed countries. Targets in GHG reductions to be achieved before 2012 under the Kyoto Protocol range from 6 % for Japan, 7 % for the EU, and 8 % for the USA. After promising quantified reductions, the USA failed to ratify the agreement and left for domestic political reasons. As a result, even in developed countries, there have been different types of legal measures for reducing GHG emissions. These have affected the respective impact of carbon liabilities under different jurisdictions, both in terms of global macroeconomic policy and in relation to the responses and obligations of individual corporations.

In consequence, discussions on the post-Kyoto framework focused as much on the differences between the commitment and stances of developing countries as on the importance of emerging economies such as China, India, and Brazil. Through a series of COP (Conference of the Parties of UNFCCC) meetings, developed and

developing countries have agreed to fill up these differences in the climate change negotiations beyond 2020. At COP17 in Durban of South Africa in 2011, they all agreed to play their part to the best of their ability and all will be able to reap the benefits of success together based on "common responsibility" and some kinds of "burden sharing."

Contents of the new framework would be discussed and expected to reach the legal agreement at COP 21 in Paris at the end of 2015, although there will be still many things remained unclear.

Invisible to Visible

Impact of Potential Carbon Cost

What consequences do carbon liabilities carry for carbon-emitting corporations? There are a lot of works for this subjects, and one of them is a renown study by Trucost, which is a UK-based environmental consulting firm published under the auspices of the UN's Principles for Responsible Investment and the United Nations Environment Program (UNEP), which reveals some interesting answers. It calculates that the full cost to the world's biggest companies of GHG emissions, pollution, and other environmental damage was almost $6.6 trillion in 2008. This figure is 20 % larger than the $5.4 trillion decline in the value of pension funds in developed countries caused by the global financial crisis in 2007/2008 and equivalent to 11 % of world's GDP (UNEP FI and PRI 2010).

IPCC also estimates macroeconomic impact by carbon liability in AR5, as the aggregate economic costs of mitigation. It's mitigation scenarios that are likely to limit warming to below 2 °C through the twenty-first century relative to preindustrial levels entail losses in global consumption – not including benefits of reduced climate change as well as co-benefits in global consumption – of 1–4 % (median, 1.7 %) in 2030 and 2–6 % (median, 3.4 %) in 2050 and 3–11 % (median, 4.8 %) in 2100 relative to consumption in baseline scenarios (BAU) that grow anywhere from 300 % to more than 900 % over the century. Monetary value of world's GDP (equivalent to global consumption) in 2012 is $72.7 trillion, which means carbon liability for mitigating cost below 2 °C would be $1.2 trillion in 2030 and $2.5 trillion in 2050 and $3.5 trillion. These figures would be manageable for global economy. On the contrary, carbon liability will expand from $220 trillion to $650 trillion over the century in BAU scenarios. It couldn't be manageable for all of us. This means that carbon liability is quite variable depending on policy selection.

In addition to this huge mitigation cost, we have to count adaptation cost as carbon liability. United Nations Environment Program (UNEP) estimates that the cost of adapting to climate change in developing countries is likely to reach as high as $150 billion by 2025/2030 and $250–500 billion per year by 2050 (UNEP 2014a). These figures are two to three times higher than estimate in AR5 because UNEP uses the latest figures.

In calculating carbon impacts over the entire global economy, it must consider the tasks both of quantifying carbon impacts on the planet's ecosystem and, secondly, of

monetizing these carbon liabilities. The first task, an impact assessment of GHG volumes, can be focused on.

Quantifying Carbon Impacts

The fast developing science of climate change obliges all countries on this planet to cut very quickly the GHG concentrations in the atmosphere back toward sustainable levels. Based on the IPCC's AR5, although it has been already well known in the world, concentrations of CO_2 in the planet's atmosphere were approximately 390 ppm in 2011, an increase of about 100 ppm – or 40 % – from levels before the Industrial Revolution began in Europe in the late eighteenth century. Over the past two centuries, the growth in GHG concentrations has averaged 1.9 ppm per year. The long-term rise in GHGs is calculated to have pushed up average global temperatures by 0.85 °C during 1880–2012 and to have caused sea levels to rise almost 19 cm across all oceans, according to IPCC AR5.

IPCC said anthropogenic greenhouse gas emissions are mainly driven by population size, economic activities, lifestyle energy use, land use patterns, technologies, and climate policy. They have introduced new estimate methods called the "Representative Concentration Pathways (RCP)" divided into four pathways to the end of this century, which are used for making projections based on these various factors. Desirable scenario, RCP2.6 aims to keep global warming likely below 2 °C, above preindustrial temperatures. Two intermediate scenarios (RCP4.5 and RCP6.0) and worst scenario with very high greenhouse gas emissions is RCP8.5. Scenarios without additional efforts to constrain emissions (baseline scenarios) lead to pathways ranging between RCP6.0 and RCP8.5.

Assuming an unchanged global dependence on fossil fuels, the IPCC AR5's worst-case scenario (RCP8.5) predicts a 3.7° rise in average temperatures by 2100 compared to 1986–2005, resulting in an 82 cm rise in sea levels. Such a worst-case scenario is anticipated to result in near-cataclysmic damage, affecting all life on the planet. In order to avoid such cataclysm and to discharge the intergenerational liability to children and to theirs, action is imperative to decrease concentrations of GHGs in the planet's atmosphere.

Global Carbon Budget

The concentrations of GHGs which have built up through human economic activities, due primarily to more than two centuries' use of fossil fuels, have clearly harmed the earth's natural ability to sustain life. In nonscientific terms, "Mother Nature" has for billions of years supported plant, animal, and human life through her generosity and tolerance. But now, emissions of carbon dioxide have combined with other GHGs and sources of man-made pollution, waste, and other detritus of postindustrial economies. The effect is to exceed the planet's inherent capacity to absorb the shocks imposed on it by humanity's weight of life, as much as by its way of life.

UNEPreport (UNEP 2014b) pointed out that IPCC's estimated a total carbon dioxide budget of about 3,670 Gt CO_2 for a likely chance of staying within the 2 °C limit. But since emissions began rapidly growing in the late nineteenth century, the

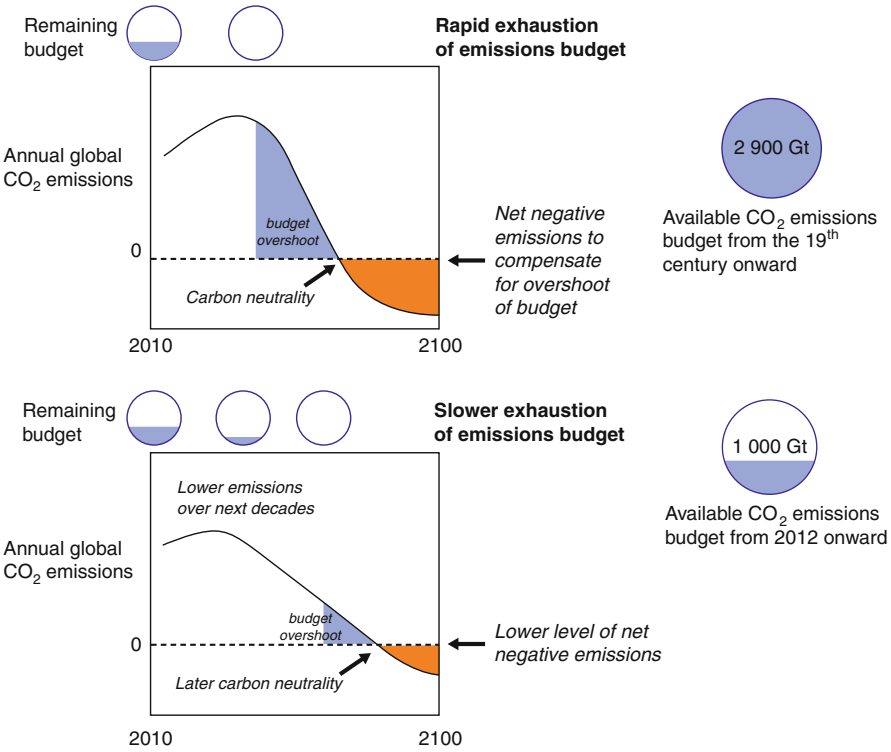

Fig. 1 Carbon neutrality (Notes: The Emissions Gap Report 2014. A UNEP Synthesis Report. November 2014)

world has already emitted around 1,900 Gt CO_2 and so has used up a large part of this budget. Moreover, human activities also result in emissions of a variety of other substances including methane from our cows' belches that have an impact on global warming, and these substances also reduce the total available budget to about 2,900 Gt CO_2. This means there are less than about 1,000 Gt CO_2 to "spend" in the future as Fig. 1 explains. (AR5 mentioned CO_2 budget between 2011 and 2100 of about 630–1,180 Gt CO_2.)

Since 1990, global emissions have grown by more than 45 % and were approximately 54 Gt CO_2-e in 2012. About 40 % of these emissions have remained in the atmosphere and the rests have been removed from the atmosphere and stored on land and in the ocean by the earth. The ocean has absorbed about 30 % of the emitted anthropogenic, causing ocean acidification which means another carbon liability.

According to BAU scenarios like RCP8.5, GHG emissions would rise to about 59 Gt CO_2-e in 2020, 68 Gt CO_2-e in 2030, and 87 Gt CO_2-e in 2050. It is clear that global emissions are not expected to peak unless additional international emission reduction policies are introduced. Based on the CO_2 budget approach, the levels of annual global emissions consistent with the 2 °C limit have been estimated. GHGs in

2050 are around 55 % below 2010 level. This means that by 2030, global emissions have already turned the corner and are more than 10 % below 2010 levels after earlier peaking. It also estimates the global carbon neutrality which means staying within the 2 °C limit, or net zero emissions on the global scale which implies some remaining CO_2 emissions could be compensated by the same amount of CO_2 uptake (negative emissions) so long as the net input of CO_2 to the atmosphere due to human activities is zero. The best estimate by AR5 is that global carbon neutrality is reached between 2055 and 2070 in order to have a likely chance of staying within the 2 °C limit.

If we fail to follow these carbon neutrality scenarios and shift to BAU ones, the resultant rises in global temperatures will not only continue but will speed up, following the well-established principle of positive and exponential feedback in complex natural systems. In other words, the absorptive or "uptake" functions of the Earth have fallen into environmental near bankruptcy in terms of their capability to adjust to the changes humanity has made to the makeup of the atmosphere.

Before the Industrial Revolution, man-made concentrations of GHGs could be contained safely within the earth's natural capacity to absorb them. This historical fact clearly compels human beings to recover as quickly as they can the earlier successful balance of consumption and of nurture in which humans must coexist with the planet. In economic terms, people must respect the planet's natural "uptake capacity." More broadly, they must restore the relationship between the earth and human activities. This means that they have to mitigate and decrease unabsorbed GHG concentrations.

Annual imbalance in emissions toward neutrality might be referred to it as a global "income statement of emissions," as a "profit and loss statement," for anthropogenic GHGs. Any year's excess of GHG adds to a huge GHG accumulation in the atmosphere, built-up over two centuries' use of fossil fuels.

Excess Cost of Carbon Imbalance

How can monetary values be assigned to these quantities of emissions? In the previous section, global CO_2 emissions volume estimated approximately 54 Gt CO_2-e in 2012. Then a monetary value can be derived for these quantities by referring to market prices for carbon in the EU's Emission Trading Scheme (EU-ETS), the world's first mandatory GHG emission trading market. But a value of EUA (European Union Allowances) has been fluctuated by supply and demand since its inception in 2005, roughly nearly €30 to below €5 per tonnes (Fig. 2).

In 2012, it has been traded as many as 40 million allowances per day and 7.9 billion allowances were traded yearly. The total value of carbon under the system in 2012 was €56 billion (European Union 2013). Carbon price traded in RGGI (Regional Greenhouse Gas Initiative) which is an initiative of the Northeast and Mid-Atlantic States of the USA has traded quite steady around $4–6 per tonnes during 2014 (RGGI Inc 2014). Another regional carbon trading scheme in the USA is California's Cap-and-Trade Program that took effect in early 2012. The price of carbon under their quarterly auction of GHG allowances for sale in 2014 was $11.34, almost double of the other side of the continent (California Environmental Protection

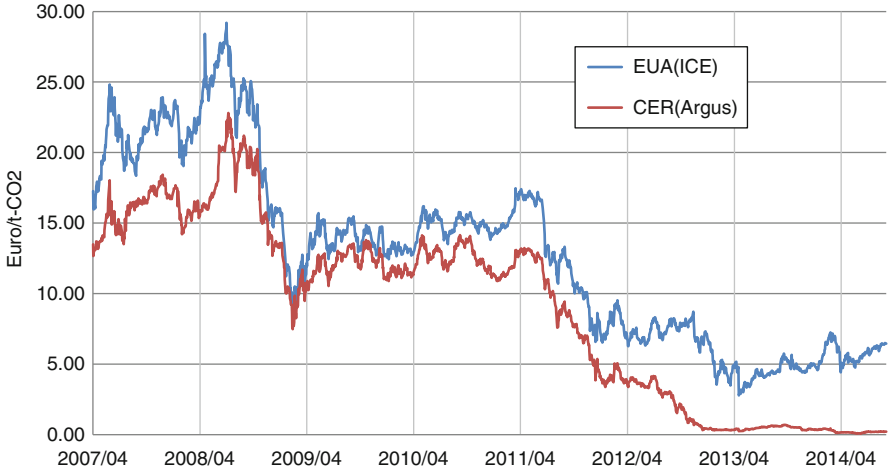

Fig. 2 Price differences between EUA and CER (Note: Argus Media, ICE (2014))

Agency, auction and reserve sale information 2014). If we use €30 per tonnes as historically highest price of EUA to calculate total global carbon deficit, it would monetize to €1.6 trillion and €5 as the lowest price of that would be €270 billion annually.

The annual buildup of CO_2 in the atmosphere represents the net increase of carbon liabilities across the planet – or rather, it represents the liabilities of the human race. Huge though these carbon deficits are, they show only one side of the picture. As already mentioned, these trends in accumulation have continued for almost 200 years, since the start of the Industrial Revolution in the eighteenth century. What are the continuing impacts on the earth of those early and long-lasting carbon burdens? They can be considered not only as yearly increments but also on a fully amortized, "total cost of ownership" basis, as might be used in calculating a "global carbon balance sheet" of the planet. Sadly, these calculations are not easy, due not least to major gaps in the knowledge and in available data sets.

For example, it cannot be reconciled as the total assets and liabilities of the earth in both monetary sense and in a nonmonetary one. It is very difficult to calculate the remaining periods of atmospheric carbon in the earth. Much recent debate in economics has focused on this topic; estimates vary from 15 years to as much as 200 years. Using 15 years as the hypothesis for the remaining period of atmospheric carbon, it must be increased by 15 times AR5's "per year" assessment of excess liability and monetized to €24 trillion as a total price of carbon liabilities.

On any basis of calculation, this number will be huge. In accounting terms, it has to be concluded that, if the earth was an enterprise, she should go bankruptcy, owing to her children's persistent ecological trashing of the family home, sustained over a score of decades.

Recent studies in the economics of climate change have attempted to set fair value (market value) on human centuries of ecological vandalism. Among the varying

estimates produced, the safest conclusion is that the differences between the balance sheets of man-made carbon production of the earth would be huge even in comparison to the previously mentioned annual income statements of carbon. This much is true, not least because account has to be taken of 200 years of anthropogenic CO_2 accumulation. Huge liabilities remain, in the form of excess, unabsorbed carbon. That is the reason why it is not enough merely to stabilize the human beings' consumption of fossil fuels at current levels. People should be aggressively cutting consumption if they are to stand any chance of achieving 80 % cuts in GHG emissions by 2050.

Stranded Assets

To examine on carbon budget of the earth, we should see an asset side of carbon balance sheet as well as the liability one. As Fig. 1 explained, we could spend less than about 1,000 Gt CO_2 toward 2100 in order to achieve 2 °C scenario. What does it mean on asset side of our carbon balance sheet?

According to Carbon Tracker[1], that expected CO_2 emissions from world fossil fuel reserves, total of oil, gas, and coal, are estimated 2,860 Gt CO_2. It means nearly three times larger than 2 °C limits. They calculate that only 20 % of total fuel reserves can be burnt by 2050. In the absence of negative emissions technologies like CCS, the carbon budget for the second half of the century would be only 74 Gt CO_2 to have an 80 % probability of hitting 2 °C target. This is equivalent to just over 2 years of emissions at current levels. Carbon Tracker has named these impacts of the asset side of the balance sheet of the earth as "unburnable carbon" or "stranded assets" (Carbon Tracker).

Stranded assets are assets that have suffered from unanticipated or premature write-downs, devaluations, or conversion to liabilities, and therefore they can be caused by not only carbon risk but also other environment-related risks. Smith School of University of Oxford pointed out these risk factors as follows (Smith School of Enterprise and the Environment 2014):

- Environmental challenges (e.g., climate change, natural capital degradation)
- Changing resource landscape (e.g., shale gas abundance, phosphate scarcity)
- New government regulations (e.g., carbon pricing, air pollution regulation)
- Falling clean technology costs (e.g., solar PV, onshore wind, electric vehicle, carbon capture, and storage)
- Evolving social norms (e.g., fossil fuel divestment campaign) and consumer behavior (e.g., certification scheme)
- Litigation (e.g., carbon liability) and changing statutory interpretations (e.g., fiduciary duty, disclosure requirements)

In their definition, the meaning of the carbon liability is limited narrowly for individual entities which have emitted CO_2 or will emit in the future. Based on their

[1]Carbon Tracker is a team of financial, energy, and legal experts in the UK.

definition, stranded assets mean that 60–80 % of coal, oil, and gas reserves of listed energy companies are unburnable. These carbon budget deficits pose a major risk for investors. Therefore listed energy companies face the litigation risk from investors.

The net lost impact of stranded assets by carbon budget was estimated to amount $3 trillion including governments, producers, and consumers during transition periods (New Climate Economy 2014). But, if innovation could spark during the transition, we could get net profit from lower fuel expenses, new business return related to the innovation, some estimate $7 trillion.

Avoiding Carbon Insolvency

Continuing the "balance sheet" analogy, people must conclude that after two centuries of mass industrialization, they in mankind remain terrible managers of carbon factors of production, of carbon assets, and of carbon liabilities. Judged on such universally accepted principles of accounting as "true and honest valuation" and "prudence," the history of economic activity amounts to a disaster tantamount to "carbon insolvency" or, at the very best, a staggering profligacy with nonrenewable carbon assets.

AR5 presents a simple benchmark for assessing the short- and long-term effects of CO_2 increase. This is the "airborne fraction" – in other words, the increase in CO_2 concentrations in the atmosphere, as a share of all fossil fuel emissions. From 1960 to 2010, with remarkably little variation, the airborne fraction has averaged 0.44 ($\pm$0.06). That means the absorptive capacity of the earth's biosphere has consistently removed the remaining 56 % of fossil-derived CO_2 from the atmosphere (but there is no consensus on the trend). So the recent accelerating rate of increase in atmospheric CO_2 reflects an increased level of emissions from burning fossil fuels.

The Carbon Break-Even Point

Correcting and rewriting the global balance sheet of carbon places us in a series of double binds, in multiple tensions between growth and the ecology, between developing and developed countries, between uncertainty and certainty, and between present and future. Reconciling these oppositions is far from easy, but it has to be done. The labor of finding balancing points on each continuum depends on how resources distribution can be improved. In short, it must be identified by the level of resources people should provide, appropriate both to achieving cuts in carbon emissions and to securing economic growth.

Any honest or prudent management of the planet's carbon balance sheet to keep 2 °C would oblige people to allocate to responsible agents €1.6 trillion (maximum) or €270 billion (minimum) worth of costs of GHG reductions. If we consider future strengthening of regulation to curve GHG emissions, these monetized estimates should be increased more on how would these amounts of money impact on world economic balance sheet? There are famous analyses produced by Sir Nicholas Stern in his 2006 book, *The Economics of Climate Change* (2006). It might be defined as the classical theory of the environmental finance like Adam Smith of conventional economics.

At that time Stern wrote that

> If a wider range of risks and impacts [of climate change] is taken into account, the estimates of damage could rise to 20 % of GDP or more. In contrast, the costs of action can be limited to around 1 % of global GDP each year. (Stern 2007)

The latest estimate of world GDP in 2013 amounted to $87.25 trillion (purchasing power parity) (CIA. The world fact book). Under this analysis in consequence, estimates of the damage due to climate change could vary as high as $17.57 trillion and as low as $0.87 trillion. Comparing Stern's figures to the carbon balance sheet for staying within the 2 °C limit, both of our €1.6 trillion ($1.95 trillion[2]) and €270 billion ($330 billion) estimates are regarded as the cost of action by Stern and almost medium in between his lower figure. But Stern's estimates are approximately 10 years before; after that, lots of works have been done. The latest one by the International Energy Agency (IEA) showed that figure is almost similar to our estimate, $1.9 trillion. So it can be safely concluded that securing this value of resources for measures to cut carbon would represent the break-even point. In other words, such a resource base would constitute a "sweet spot," a point of balance favoring continued economic growth while at the same time preventing further global warming.

Besides monetizing and valuing carbon emissions into carbon liabilities, it also has to be accounted for the effects of feedbacks and positive reinforcement in the climate-carbon cycle. These feedback effects mean that global warming tends to slow down absorption of carbon dioxide by the planet's landmasses and oceans, thus increasing the fraction of emissions remaining in the atmosphere. According to one estimate, the phenomenon of positive feedback will be responsible by itself for a rise in corresponding global average warming of more than 1 °C by 2100.

This assumption suggests that people might reach a sustainable point of equilibrium, merely by establishing break-even points of GHG emissions. But this action would be only one step. They need to move very far and very quickly, if people are to achieve meaningful reductions in emissions and stabilize the climate by the middle of this century.

Measuring the Valuation Materiality of Corporate Carbon

SEC Guidance

The next task is clear. It must be allocated and distributed in calculable amounts of cash toward reducing global GHG emissions. The most cost-effective way of achieving this allocation would be by considering both macroeconomic and microeconomic issues. The issues could affect more closely human beings' own destinies and that of the earth. Nobody can escape and survive from the implications of climate change.

[2] €/$ = 1.22 (as of December 2014).

The microeconomic agenda including compelling corporations has emerged to apportion sufficient resources to cover climate-related carbon liabilities. The US Securities and Exchange Commission (SEC) published a guidance to companies facing responsibilities to disclose to investors the materiality of their carbon-related activities in 2010[3].

The SEC issued its guidance in answer to requests from members of United States Climate Action Partnership (USCAP)[4] and other. An urgent need is being felt for a policy framework on climate change, in order to make coherent disclosures of material relevant to carbon-related liabilities, for the purposes of valuing companies. The SEC guidelines stress the necessity of carbon disclosure to investors, as defined in regulations from the US Environmental Protection Authority (EPA), especially as the rules on GHG data affect reporting by the large emitter entities as well as the disclosure regulations contained in the EU-ETS. Currently, based on EPA rule, as of 2013, over 8,000 facilities in nine industry sectors reported direct GHG emissions to the GHG Reporting Program(GHGRP) totaled 3.18 billion metric tons CO_2, which were about half of the total US GHG. Reporting entities are 965 suppliers, and 92 facilities reported injecting CO_2 underground.

Regulation Risk

The SEC's guidance examines the materiality of carbon-emitting activities under three categories:

1. Regulatory risk
2. Physical risk
3. Market risk

This scheme seems to be recognized generally by businesses as acceptable and workable. The SEC document begins by explaining the impact of regulatory risk on three types of companies. For some, the regulatory, legislative, and other developments could have a significant effect on operating and financial decisions, chiefly decisions involving capital expenditure needed to reduce GHG emissions.

Secondly, for companies subject to "cap-and-trade" legislation (not yet introduced in Japan, in the USA it has been introduced only to several states under RGGI and AB32[5]), the SEC note sets out the expenses permissible to purchase emissions allowances, where reduction targets cannot be met. Thirdly, the notes describe how firms not directly affected by emissions regulation could still be affected indirectly, through higher prices, charged by directly affected companies who need to pass on their own increased costs of compliance. One consequence is that even in jurisdictions still without a mandatory "cap-and-trade" regime, companies may yet face

[3]SEC, Commission Guidance Regarding Disclosure Related to Climate Change, February 2010.

[4]http://www.us-cap.org/

[5]The State of California introduced their own cap-and-trade system from November 2012 under the California Global Warming Solutions Act called as Assembly Bill No.32, AB32).

some regulatory risk, as a consequence of international trade or cross-border procurement and supply chains.

These new regulations on emissions reduction may also present new opportunities for investment. This has been the lesson from the EU-ETS and its associated carbon markets, although carbon prices have been volatile in the markets. Companies with more allowances than they need, or who are eager to earn offset credits, can raise capital by selling these instruments on the markets. Companies must thus manage both sides of their own carbon balance sheets to balance their carbon assets and liabilities.

Just as important in assessing regulatory risk associated with carbon liabilities is the necessity for companies to understand cycles of trading and regulation. Even in the EU-ETS, which was initially based on the Kyoto Protocol, trading was limited to a defined period. But then EU decided to extend the trading period to the end of 2020 under the third phase of the ETS. Also beyond 2020, EU has showed further extension of the trading period toward 2030. These practical reform concerning trading period have been welcomed in the markets, but what the trading periods are decided by the political will mean there are always regulatory risks potentially; as a result, companies face uncertainty and unclarity. The SEC's guidelines are equally unclear on this point.

Physical and Market Risk

Climate change presents corporations with increased physical risk. Extreme weather events such as fiercer storms, hurricanes, more frequent flooding, deeper erosion of coastlines, melting of permafrost, and higher temperatures will all affect enterprises' facilities and operations. Changes in the availability or quality of water and other factors of production are among innumerable physical challenges about to confront to businesses.

Physical changes associated with climate change may depress consumer demand for products or services. Warmer winters may cut demand for heating fuels, servicing, and equipment. These effects could affect companies' operations and the value of their assets.

Market risk due to climate change may be defined as companies confronting the risk of reductions or eliminations in business opportunities, consequent upon changes in consumer demands and in society's needs. If companies have not reacted astutely in response to regulatory and physical risks, they could lose consumers' or investor's confidence. This risk is reputational and can be considered a type of market risk.

The SEC's guidance advises that, depending on a registrant company's business and its reputation with the public, it may need to consider whether public perception of its published data on GHG emissions could expose it to potential adverse consequences to its business operations or financial condition.

The SEC emphasizes the importance of disclosing risk factors linked to climate change in companies' financial reports, even where the data's materiality may be hard to assess. The SEC notes fail to give methods for evaluating such data, neither do they provide any criteria to measure the materiality of nonfinancial factors.

The sole quantified threshold shown is the SEC's explanation on Instruction 5 to Item 103 of Regulation S-K. This recommends citing any current or outstanding environmental litigation related to governmental regulation.

Notwithstanding the SEC's guidance on climate change, familiar questions remain. How can corporations and other carbon-emitting organizations calculate the materiality of their own carbon liability? How should this be measured? There are several efforts and trials to solve these questions. Let's explain and describe them one by one.

Quantitative Carbon Disclosure

Companies are left to their own devices in deciding how to measure the materiality of their carbon exposure and to disclose this in financial reports. With this realization the next problem, namely, measuring a corporation's carbon liability, must be focused.

Research in corporate reporting reveals several different approaches to climate-related risk. Examples include the disclosure of a company's carbon budget, as described above, and its philosophy for carbon management. Firms in such carbon-intensive sectors such as oil exploration, electricity, chemicals, steel, and cement have been quick to adopt such approaches. This is because they have hitherto faced the three types of carbon risks already mentioned.

Firms can no longer tuck such data away in financial reports. In its latest corporate citizenship report, Exxon Mobil explains that it emitted 126 million metrics tonnes on a CO_2 equivalent from upstream, downstream, and chemical divisions in 2013. The US oil giant publishes detailed information on its gas flaring and on its cogeneration capacity, two factors with major impacts on carbon liabilities in its sector.

Exxon's peers Shell, Chevron, and BP also disclose their quantified data of carbon emissions. Besides, BP has faced another hugely expensive environmental liability, stemming from the huge oil spill in the Gulf Coast in April 2010. In its disclosures of quantified carbon emissions, BP emitted 64.9 million tonnes on a CO_2 equivalent in 2010. But it reduced to 49.2 million tonnes in 2013, 24 % reduction than 3 years before, due to the result of the sale of two refineries, Texas City and Carson in the USA, as part of our divestment program. A huge volume of environmental liabilities, as well as carbon ones, continues to disclose in BP's basic report, as it meets claims arising from the Gulf Coast accident, which is now rated as America's worst ever oil disaster.

Shell emitted 73 million tonnes on a CO_2 equivalent in 2013, which is slightly higher than 72 million tonnes in 2012. The main reasons for this increase were the ramp-up of production in Qatar and the restart of production in Iraq and so on. These increases were partially offset by reduced flaring and lower production in other places.

Those figures show that Exxon has almost double weight of carbon liabilities than other two competitors in absolute quantity. But monetary burdens by the carbon liability are not calculated only by absolute quantity but amount of their assets and provisions to be able to offset. In addition, assets would be stranded as we have already checked (Figs. 3, 4, and 5).

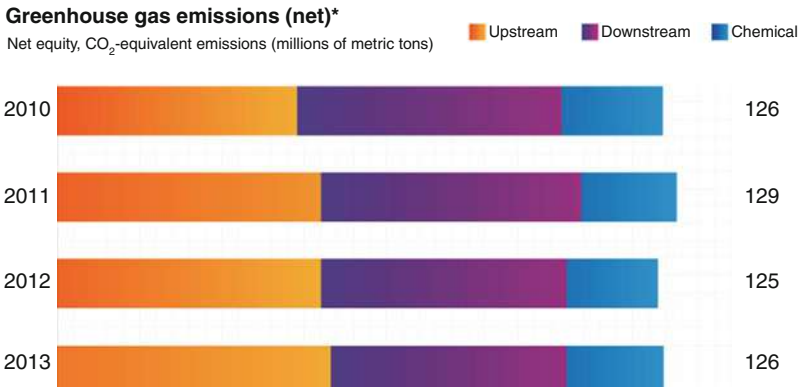

Fig. 3 Direct GHG emissions of Exxon Mobil (Exxon Mobil Corporate Citizenship Report 2013)

Fig. 4 Direct GHG emissions of BP (BP corporate citizenship report 2013)

The Movement for Quantitative Carbon Disclosure

Years of pressure by environmental movements have given strength to regulators seeking quantitative disclosure of CO_2 emissions by companies. Prominent among them are the UK's Carbon Disclosure Project (CDP)[6] and the Climate Disclosure Standards Board (CDSB)[7]. The CDP is a voluntary, nonprofit organization which, through force of argument and through a tailored questionnaire, works to persuade

[6] https://www.cdp.net/en-US/WhatWeDo/Pages/investors.aspx
[7] http://cdsb.net/

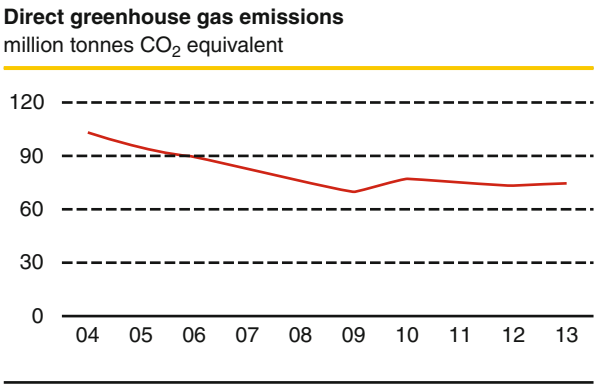

Fig. 5 Direct GHG emissions of Shell

global companies to measure and disclose CO_2 emissions and strategies in relation to climate change. CDP coordinates research on behalf of 767 institutional investors, with combined holdings worth in the region of $92 trillion in 2014. CDP reports include statistics on carbon emissions from its respondent companies plus other analysis. Open to public scrutiny, this information yields important trends and developments in corporate management of carbon emissions.

The Climate Disclosure Standards Board is composed of a pro-environment consortium of global companies, accountancy firms and accounting organizations, and nonprofit lobby groups. CDSB's mission is to develop a global framework for corporate reporting on GHG emissions, with the aim of supporting, strengthening, and harmonizing existing initiatives in climate-related reporting. The board seeks to enhance best practice in the form of a single consistent global framework.

Both the CDP and the CDSB claim that their activities continue to raise standards of corporate accountability toward the environment; neither would claim that their work is complete. Information in companies' financial reports may be useful for investors seeking to select environment-friendly companies for ESG portfolios. But quantified information in financial reports does not necessarily reflect the precise cash values associated with liabilities in relation to carbon emissions, nor the resources which companies must dedicate to meet them.

Quantified disclosure of climate- and carbon-related liabilities is gradually becoming obligation under company law. Participating companies in the EU-ETS are obliged to provide their emission data on a site-by-site basis to EU national governments. Since 2005, enterprises in Japan consuming 1,500 kl per year in fossil fuels must submit emissions data, the legislation stipulates reporting of all six main greenhouse gases.

The Japanese government has published company names over a certain level of quantitative CO_2 emission, in recalculating sum of sites emission data to company basis. Companies who fail to report face fines. In January 2012, US EPA had the first year of GHG Reporting Program (GHGRP) which data can be available to the public.

Carbon Materiality in the Sustainable Accounting Reporting

There are several activities to integrate environmental factors including GHG from economic entities with their conventional financial reporting processes, called as an Integrated Reporting, such as Global Reporting Initiative (GRI), International Integrated Reporting Council (IIRC)[8], Sustainability Accounting Standard (SASB)[9], and so on.

Among them, we would like to focus the SASB's activities, because they are going to set out disclosure guidance and accounting standards on sustainability issues to be included into companies' mandatory financial annual filings. GRI, IIRC, and others are mainly based on voluntary reporting which accompany with mandatory filings but separate from it. SASB is an independent nonprofit organization in the USA and is developing sustainability accounting standards for more than 80 industries in 10 sectors. Their standards are designed for the disclosure of material sustainability issues in mandatory SEC filings, such as the Form 10-K and 20-F.

As we have already seen about SEC's guidance on climate change which recommends on instruction of Regulation S-K, which sets forth certain disclosure requirements associated with SEC filings, SASB has attempted to identify these sustainable information including carbon liability that may be material for all companies based on Regulation S-K and required to describe them in the Management's Discussion and Analysis of Financial Condition and Results of Operations (MD&A) section of Form 10-K.

According to SASB (Sustainable Accounting Standards Board 2013), in determining whether a trend or uncertainty should be disclosed, the SEC has stated that management should use a two-part assessment based on probability and magnitude. The one is a reasonable likelihood that the known trend, demand, commitment, event, or uncertainty will occur. The second part is a reasonable likelihood that occurrence will have a material effect on the registrant's financial condition or results of operation. This approach is consistent with FASB's approach to entity-specific materiality determination.

When companies consider making disclosure on carbon liability including stranded assets in their mandatory financial reports, they should describe them in the MD&A, in a subsection titled "Sustainability Accounting Standards Disclosures." In addition to the MD&A section, companies should consider disclosing sustainability information in other sections of 10-K, as relevant, such as description of business (Item 101 of S-K), legal proceedings (Item 103 of S-K), and risk factors (Item 503(c) of S-K).

SASB's approach to describe sustainable material factors on the mandatory reports is quite pragmatical. They set out and evolve fundamental concepts and procedures by themselves, but for tools for reporting, they recommend existing measurement or guidance developed by other standardizer entities. For instance, in

[8]International Integrated Reporting Council; http://www.theiirc.org/

[9]Sustainable Accounting Standard Board, a 501(c)3 registered nonprofit organization based at San Francisco http://www.sasb.org/

the case of oil and gas exploration and production sector, SASB says companies should disclose their significant direct GHG emissions based on SASB's description, but it recommends to use various tools for accounting metrics to describe their quantitative or narrative information from other standardizer entities (SASB 2014a).

In the case of GHG emissions from companies, they describe GHG emissions should be disclosed Scope 1 level, six GHGs covered under the Kyoto Protocol, calculated them in metric tons of CO_2 equivalent (CO_2-e), and which facilities and equipment should be included as emission sources and so on. To disclose those quantitative and qualitative information, they select relevant tools to disclose, for instance, the Greenhouse Gas Protocol[10] as GHG Scope 1, CDP Guidance and IPIECA GHG Guidelines[11] as financial control approach, and CDSB's Climate Change Reporting Framework (CCRF) as organizational boundary setting.

Sectorial Disclosure Approach

SASB is developing sustainability accounting standards at the industry level, focusing on intractable issues that are closely tied to resource use and business models and other factors at play in the industry that can result in unsustainable outcomes. But traditional industry classification systems do not always group together industries with common sustainability characteristics, making the determination of common sustainability issues difficult. Therefore SASB developed the Sustainable Industry Classification System (SICS), which builds on traditional ones and categorizes 10 sectors and 88 industries in accordance with their resource intensity and sustainability impact as well as their sustainability innovation potential.

One of such industry-specific area is nonrenewable resources sector. We can pick out oil and gas exploration and production industry as an example in the sector. Material impacts of global warming of the activities of this industry are mainly two topics, GHG emissions and reserve valuation and capital expenditures.

Many of the companies' normal operations in the industry involve the combustion of fossil fuels to produce energy and then emit GHG. They are required to report their GHG emissions annually to the EPA under GHGRP at the facility level when emissions of GHG exceed 25,000 metric tons. The sources of these emissions vary based on the activities in which they are engaged and the type of fuel they are using. Therefore they should monitor and disclose their use of energy input as well as their emissions of GHGs, both in accordance with applicable laws and regulations and to improve their overall balance sheets to reduce carbon liabilities.

On GHG emissions, companies should disclose gross amount of GHG Scope 1 emissions of all six gases in metric tons of CO_2-e. These emissions include direct emissions of GHGs from stationary or mobile sources that include, but are not limited to, equipment at well sites, production facilities, refineries, chemical plants,

[10]Developed by the World Resources Institute and the World Business Council on Sustainable Development(WRI/WBCSD): http://www.ghgprotocol.org/

[11]Petroleum Industry Guidelines for Reporting Greenhouse Gas Emissions; http://www.ipieca.org/publication/petroleum-industry-guidelines-reporting-greenhouse-gas-emissions-2nd-edition

Table 1 Example of integrated disclosure. Gross Scope 1 emissions (mock data)

Year-end December 31	2012	2013	2014
Gross global Scope 1 emissions (in thousands of metric tons CO_2-e)	6,525	7,765	7,762
Conventional oil operations (%)	63 %	47 %	45 %
Unconventional oil operations	2 %	9 %	11 %
Conventional gas operations	35 %	32 %	31 %
Unconventional gas operations	0 %	12 %	13 %
Percentage covered under a regulatory program	3 %	3 %	3 %

SASB Standard for Oil and Gas Exploration and Production; Example of Integrated Disclosure in Form 10-K

Table 2 Main sources of GHG emissions (mock data)

Thousands of metric tons CO_2-e	2012	2013	2014
Combustion	5,546	6.591	6.598
Flared hydrocarbons	326	388	388
Process emissions	457	543	543
Directly vented releases	326	388	388
Fugitive emissions and leaks	196	233	237

SASB, same as the above

terminals, fixed site drilling rigs, office buildings, marine vessels transporting products, tank truck fleets, mobile drilling rigs, and movable equipment at drilling production facilities.

In addition to those gross figures, they shall provide a breakdown of its emissions by four classifications of hydrocarbon resources: (1) conventional oil, (2) unconventional oil, (3) conventional gas, and (4) unconventional gas. Unconventional oil includes oil shale, oil sands, heavy oil, etc. Unconventional gas includes coal seam gas, shale gas, etc. (SASB 2014b).

The bottom line of the Table 1 shows regulated emission ratio (emission covered under mandatory regulated scheme to the gross emissions they emit). The ratio increases operating cost may also increase.

Their emissions come from various sources as a normal by-product of necessary operational practices. They are involved in diverse exploration and production operations. Therefore they should disclose main sources of emissions among their activities in the mandatory financial report (Table 2).

Oil and gas exploration and production industry also should disclose stranded assets due to acceleration of global warming. Because they usually have huge reserve assets of oil and gas reserves and make significant investments in new reserves. Their activities generate significant direct GHG emissions, contributing to climate change and creating additional regulatory compliance costs and risks for them due to climate change mitigation policies. Also improved competitiveness of renewable energy technologies including policy supports to them through tax breaks and subsidies that have the potential to significantly alter the economic value of reserves, particularly those of oil. The price and cost impacts from climate

Table 3 Sensitivity of reserve levels to future scenarios in which a price is charged on carbon (mock data)

Price case	Proved reserves		Probable reserves	
Scenario	Oil MMbbls	Gas MMsf	Oil MMbbls	Gas MMscf
Current (base)	435	5,828	757	7,200
New policies scenario	415	5,400	723	6,900
450 scenario	378	4,800	701	6,430

SASB, same as the above

regulations and development of alternative energy can affect the net present value of proven reserves that we have already seen as stranded assets.

SASB asks companies belonging to this industry how long they have those assets under several future scenarios, such as BAU, International Energy Agency's New Policies Scenario, and 450 ppm (2 °C) Scenario (Table 3).

In this case, E&P companies have conducted a sensitivity analysis of its proved and probable reserves based on price scenarios outlined by IEA in its World Energy Outlook publication (International Energy Agency, World Energy Outlook 2014). Under this price outlined in IEA's New Policies Scenario, company may see a small reduction in the size of its proved and probable reserves. Under the 450 Scenario, it should reduce its reserves significantly than the former case. Investor can distinguish their targeting companies to compare with these disclosed figures among peer industrial group.

Assets value of E&P companies would be damaged not only by carbon liability but also by social factors, such as security, human rights, and rights of indigenous peoples. Companies face heightened community-related risks when operating in conflict zones with weak or absent governance institutions, rule of law, and legislation to protect human rights or with vulnerable communities such as indigenous peoples. SASB points out that without corresponding enhanced diligence measures to protect human rights and the rights of indigenous peoples in such area, companies could encounter difficulties in accessing reserves or significant operational disruptions with impacts on costs and liabilities (SASB 2014c). We can call these assets as socially stranded assets.

Putting a Price on Carbon

Difficulties in Monetizing a Price for Carbon

Methods are evolving quickly to collect quantified data on carbon emissions from various types and sizes of corporations under various jurisdictions around the world. What are the next steps?

Measuring a corporation's carbon liability means putting a price on it, in other words, monetization. How should this be done? Carbon markets already provide an important tool to measure current prices for carbon in a free market. The emission

trading schemes like the EU's exist to link sellers with buyers, in the process setting of a market-clearing price. Two types of environmental trading systems exist, "cap and trade" and "baseline and credit."

In the EU's cap-and-trade system, carbon emission credits such as the European Union Allowance (EUA) have been traded (the abovementioned Fig. 2). A closing price for this security is reported after every day's trading. The process is identical to that for trading currencies, stocks commodities, or any other form of financial instrument.

As the biggest trading mechanism for corporate carbon credits, the EU-ETS is highly influential in setting a global price for carbon. In consequence, the prices of Certified Emission Reduction (CER) which are issued by the Clean Development Mechanism (CDM) projects in developing countries admitted as one of the emission reduction tools that started under the Kyoto Protocol and have settled on arbitrage trading with EUA markets, although both of them have been struggling with keeping suitable carbon prices due to European economic turbulence after 2010. The effect of such price-setting markets has been that, in general, the more emissions a company causes through its activities, the more it must pay to cover its carbon liabilities.

Complete understanding of techniques to value carbon liabilities will be lacking, however, if they are considered merely as a mean to the end of trading of carbon credits in the market. Three types of carbon risk exist, each presenting its own valuation issues, namely, regulatory risk, physical risk, and market risk. Regrettably, a market mechanism such as trading cannot monetize all three types of risks. Let's consider why.

Firstly, regulation risks are not shared equally between all types of carbon emitters. Proof of this emerges, when it can be examined the composition of the current EU-ETS. Now in its third phase of operations, the EU-ETS expands its targeted eligible sectors in chemicals, aluminum, and aviation, in addition to have been covered heavy-emitting industries including power utilities, energy generation, iron smelting, cement, and oil refining. But it has not yet covered all of CO_2 emitting sectors.

Besides, EU-ETS has faced significant problem which they should solve to put price on carbon. Due to economic downtown during 2010–2013, the so-called European sovereign crisis, demand for carbon credit was fallen sharply as Fig. 2 showed clearly. This means carbon credit is as same economic goods as other goods and services which value goes up and down. But without functional price setting mechanism, we can't rate carbon liability. We need to improve C&T system's more functional ways and integrate fragmented C&T markets in several regions or states into wider ones.

Needs for Integrated Accounting Standards of Carbon Value

We have already seen SASB's attempt to make sectorial disclosure approach on carbon value. We respect their efforts, but at present it is not a mandatory scheme but voluntary one, although there is some possibility that most of listed companies in the USA would use SASB's disclosure standards in their financial statements as de facto standards to describe their own carbon liabilities. To create common accounting

standards to calculate carbon liabilities and carbon vales, there has been repeated trial and error.

The International Financial Reporting Interpretations Committee (IFRIC) is the interpretative body of the IASB (International Accounting Standards Board). In December 2004, just as the EU launched its ETS, the IFRIC committee issued IFRIC3, its formal accounting interpretation on Emission Rights or carbon credits. At that time, it was decided that EU-ETS came into effect from 1 March 2005. In practice, the IFRIC3 thus became the new accounting tool of choice for EU-ETS. But it was withdrawn by the committee themselves after only a month, the victim of wrangles between accounting regulators and business leaders.

The allowances granted by national governments to companies participating in the ETS were at issue. According to IASB, IFRIC3 specified the following (International Accounting Standards Board 2010):

1. Rights (allowances) are intangible assets that should be recognized in the financial statements in accordance with IAS 38.
2. When allowances are issued to a participant by government (or government agency) for less than their fair values, the difference between the amount paid (if any) and their fair value is a government grant that is accounted for in accordance with IAS 20.
3. As a participant produces emissions, it recognizes a provision for its obligation to deliver allowances in accordance with IAS 37. This provision is normally measured at the market value of the allowances needed to settle it.

The issue was how to treat such an allowance on the balance sheet. A consensus among businesses held that an allowance is an asset, because it is acquired at a cost, in the same way as any other factors of production such as raw materials and equipments. IFRIC agreed; however, not all business leaders did so. As the IFRS is an interpretative body of the IASB, it is bound by the IASB Framework on the Preparation and Presentation of Financial Statements ("Framework"). This framework does not assess an asset from the cost evaluation viewpoint. It defines an asset as a "resource controlled by the entity as a result of past events and from which future economic benefits are expected to flow to the entity" (Cook 2009).

As the EU-ETS began trading, the IFRIC standard recognized as an asset the allocation by EU governments of allowances to companies in their own territory. However, IASs set by IASB require assets to be measured at fair value at each reporting date. In consequence, the IFRIC interpreted allowances in an undifferentiated manner, failing to discriminate between allowances purchased from the market or granted by governments. In contrast at that time, the IASB had a long-standing proposal to amend recognition of government-allocated granting of rights in the IAS 20 (Accounting for Government Grants and Disclosure of Government Assistance), and this stipulated that any grant from a government could no longer be considered as income.

The dispute's implication was that any free emission allowances granted by governments would have to be recognized immediately as income. Business leaders

protested that it was impractical for them to recognize fair value at the onset of the trading. Then, IASB withdraw IFRIC3.

Further accounting disputes have followed, concerning the structures of the emission trading schemes and in particular how to establish a scale of values for initial allowances and allocate them among the scheme's members. At question have been competing methods of rights allocation such as the so-called grandfathering approach as used in the first phase of the EU-ETS; alternative methods also considered have included benchmarking approaches, and allocation based on auctions of emission rights. IFRIC3's failure was a direct consequence of the "grandfathering" approach favored by the EU.

In a statement, the Board of the IASB justified its withdrawal of IFRIC3 claiming that "the Board decided to take the time to conduct a broader assessment of the nature of the various volatilities resulting from the application of IFRIC3 to a cap-and-trade scheme and to consider whether and how it might be appropriate to amend existing standards to reduce or eliminate some of those volatilities." The decision was taken by an overwhelmingly vote of 12 in favor, 1 against, and 1 abstention.

After several years, the IASB restarted the debate on limiting free issues in emissions trading schemes. But it chose not to address the controversy surrounding accounting standards for all government grants at December 2007. In May 2008, IASB started joint discussions with the USA counterpart, FASB. But after piled up discussions between them, in December 2012, IASB announced and formally reactivated this project as an IASB-only research project. They didn't explain why the joint discussions met with failure. New IASB-only research project is expected to result in the publication of a discussion paper considering the financial reporting consequences of government-developed schemes designed to encourage reductions in the production of GHGs, which will include an inventory of trading schemes, an analysis of common economic characteristics of those schemes, and an initial assessment of the potential reporting solutions (IFRS).

Calculating Physical Risk to Price

Despite long-standing discussions on setting up comprehensive and intelligible rules in carbon accounting, markets seem to provide the simplest method for setting a carbon price. Companies trading under mandatory emission trading schemes like the EU-ETS can compare carbon prices in the market with their own carbon management on issues such as raw materials purchase, investment in production equipment, identifying a development site, or in decision about production of a new product or service. As described above, accounting standards for reporting carbon values have not been decided, and none will be accepted until the new draft of' "IFRICα" emerges.

Carbon pricing in free markets serves well as one measurement of carbon liability. It is limited, however, in relation to regulatory risk. As described above, the concept of carbon liability comes not only from regulation but also from physical and market risk types. Physical risk may increase carbon damage to the asset side of a company's balance sheet such as stranded assets described above, as opposed to its liabilities.

Some simple examples illustrate the point. Rising sea levels pointed out by AR5 may halt or impede operation of an enterprise's factories and facilities located along coastlines. Companies face operational interruption or damage, due to fiercer storms, heavier rain, more frequent typhoons, or land erosion caused by drought. Firms will be well advised to introduce a climate contingent Business Continuity Plans (BCPs) to prevent deterioration of their fixed assets and operational interruptions caused by climate change. Introducing climate contingent BCPs could work as a form of environmental insurance against carbon impacts.

Applying ARO Method

As companies struggle to calculate climate-related physical risks to their asset base, both now and in future, they have available useful accounting technique. This is the accounting rule for asset retirement obligations (AROs). AROs are legal obligations associated with the retirement of a tangible long-term asset. Such obligations result from the acquisition, construction, development, or normal operation of a long-term tangible asset, as defined in the FAS 143 standard issued in 2002 by the FASB. This accounting rule applies a "fair value" measure of fixed assets which includes environmental damage or other future removable obligations.

For example, the owner of an asset that is subject to environmental laws such as CERCLA is required to recognize their liability as an ARO on their balance sheet in the period in which it is incurred, based on a reasonable estimate of its fair value. Even if it is not possible to estimate with precision, the liability must be recognized whenever a reasonable estimate of fair value can be made.

An ARO is not quite the same as a carbon liability associated with any fixed asset. But it can be said that the nature of the uncertainty surrounding any carbon liability might be quite similar to the processing of evaluating an ARO. Companies have to estimate fair value of a carbon obligation, against the uncertainty of future regulation framework and possibility of physical risk. FIN47 is the FASB's interpretation of FAS 143 issued in March 2005. The US-based environmental accounting consultant C Gregory Rogers (2006) specifies that the fair value of an ARO may be determined based on any of the following methods:

1. The amount of the obligation embedded in the acquisition price of the asset
2. A market quote in an active market for transfer of the obligation (or if neither of these two situations applies)
3. Application of an expected present value technique to estimate fair value

Changing Market Risk to Opportunity

Setting a price on carbon liabilities associated with market risk can be very difficult, not least because this type of risk may be influenced by customers' changes in taste or in buying behavior. One solution may be to apply marketing method such as Customer Related Marketing (CRM). If companies use these carbon marketing techniques, they may persuade their customers that their products are differentiated by virtue of low impact on the environment. Perceptions can be altered by careful marketing.

It is not yet clear how many customers will value, or will react to, perceptions of low carbon positioning, rather than to traditional lower prices and higher quality. But more easily than with the other carbon risk types, market risk can be turned from a liability to into an asset and a source of competitive advantage.

Carbon management entails the full realization and declaration of all costs and liabilities arising from man-made carbon and allocating these costs to appropriate activities both in their production and to the final retail value of a product. In discharging this management obligation more efficiently, corporations must establish a well-planned architecture of mandatory carbon trading which minimizes regulatory risk. Equally desirable and necessary is an agreement on more accurate accounting methods, capable of producing coherent and usable valuations of carbon liabilities, as they effect materially a company's base of fixed assets and related liabilities.

In addition, companies should apply across all key audiences – customers, investors, and other stakeholders – a comprehensive, appropriately designed strategy of carbon marketing. The goal should be to request and to achieve collective changes in patterns of consumption as well production in order to safeguard the interests of future generations.

References

California Environmental Protection Agency, auction and reserve sale information. Sept 2014. http://www.arb.ca.gov/cc/capandtrade/auction/2014_annual_reserve_price_notice_joint_auction_update.pdf

Carbon Tracker (2013). Unburnable carbon 2013. The Grantham Research Institute, LSE, London

CIA. The world fact book. Dec 2014. https://www.cia.gov/library/publications/the-world-factbook/geos/xx.html

Cook A (2009) Accounting for emissions: from costless activity to market operations. In: Freestone D, Streck C (eds) Legal aspects of carbon trading. Oxford University Press, Oxford

European Union (2013) The EU emissions trading system (EU ETS). European Commission, Brussel, Belgium

Goodland R, Anhang J (2009) What if the key actors in climate change are cows, pigs, and chickens? World Watch Institute, Washington DC

IFRS. Emissions trading schemes (Research Project). http://www.ifrs.org/Current-Projects/IASB-Projects/Emission-Trading-Schemes/Pages/Emissions-Trading-Schemes-research-project.aspx

International Accounting Standards Board (2010) Explanation on emission trading schemes

International Energy Agency, World Energy Outlook 2014. Nov 2014

New Climate Economy (2014) Better growth better climate. The Global Commission on the Economy and Climate, London, UK

RGGI Inc (2014) Report on the secondary market for RGGI CO_2 allowances: third quarter 2014

Rogers CG (2006) Financial reporting of environmental liabilities and risks after Sarbanes-Oxley. Wiley, Hoboken, NJ, USA

SASB (2014a) Sustainability accounting standard for oil & gas exploration & production SASB, California, USA

SASB (2014b) Example of integrated disclosure in form10-K SASB California, USA

SASB (2014c) Oil & gas exploration & production research brief SASB California, USA

Smith School of Enterprise and the Environment (2014) Financial dynamics of the environment: risks, impacts, and barriers to resilience, Oxford University, Oxford, UK

Stern N (2007) The economics of climate change. Cambridge University Press, Cambridge, UK
Sustainable Accounting Standards Board (2013) Conceptual framework. SASB, California, USA
The fifth assessment report of the Intergovernmental Panel on Climate Change, 2014
UNEP (2014a) The adaptation gap report. SASB, California, USA
UNEP (2014b) The emissions gap report 2014. SASB, California, USA
UNEP FI, PRI (2010) Universal ownership. Contributed by Trucost, Trucost, London UK
US Environmental Protection Agency (1996) Valuing potential environmental liabilities for managerial decision-making:a review of available techniques. EPA Washington, USA

Climate Change and Carbon Sequestration in Forest Ecosystems

Dafeng Hui, Qi Deng, Hanqin Tian, and Yiqi Luo

Contents

D. Hui (✉) • Q. Deng
Department of Biological Sciences, Tennessee State University, Nashville, TN, USA
e-mail: dhui@tnstate.edu; qdeng@tnstate.edu

H. Tian
International Center for Climate and Global Change Research, School of Forestry and Wildlife Sciences, Auburn University, Auburn, AL, USA
e-mail: tianhan@auburn.edu

Y. Luo
Department of Microbiology and Plant Sciences, University of Oklahoma, Norman, OK, USA
e-mail: yluo@ou.edu

W.-Y. Chen et al. (eds.), *Handbook of Climate Change Mitigation and Adaptation*,
DOI 10.1007/978-3-319-14409-2_13

Abstract

Forest ecosystems have been identified to be the largest land carbon sink and account for more than half of carbon stored in the terrestrial ecosystems. The influences of climate change on forest ecosystems could have significant implications on global carbon cycling. In this chapter, we reviewed research progresses about climate change impacts on forest ecosystem carbon cycling in the past 20 years. Our review is mostly on field experiments and modeling studies. This chapter starts with a brief description of climate change and forest ecosystems. Different experimental studies are then presented. The impacts of global change such as elevated CO_2, global warming, and changes in precipitation and O_3 on carbon cycling in forest ecosystems are synthesized. Next, we present some modeling studies of forest ecosystem carbon cycling at ecosystem, regional, and global scales. At the end of the chapter, we make some recommendations for future studies.

Introduction: Global Climate Change and Forest Ecosystem Carbon Cycling

As a major terrestrial ecosystem, forests occupy 30–43 % of the world's land surface. Forests are an important source for fiber and fuel, for human consumption, and of vital importance for the economy of many regions in the world (Dixon et al. 1994; Pan et al. 2013). In addition, forests provide a suite of services, including habitats for wildlife, clean water and carbon storage, and climate mitigation (Lindquist et al. 2012). Forest biomass is the major pool of vegetation carbon. The total amount of carbon sequestered in forest vegetation is approximately 359 billion tons (Allen et al. 2010). Forest soil is another carbon pool that stores large amount of carbon. Overall, the amount of carbon stored in the forest ecosystems is twice that in the atmosphere (Lal 2005). As forests play an important role in the global carbon cycling and curbing climate change, understanding the types and distribution and assessing the present and future forest ecosystem carbon balance have been of both scientific and policy interest (Nabuurs et al. 2010).

Climate change has been considered as one of the great threatens to the world. Due to fossil fuel burning and deforestation, concentration of atmospheric carbon dioxide (CO_2) has increased from 280 ppm at preindustrial revolution to 394 ppm presently (Peñuelas et al. 2013). As a result, average global surface temperature is

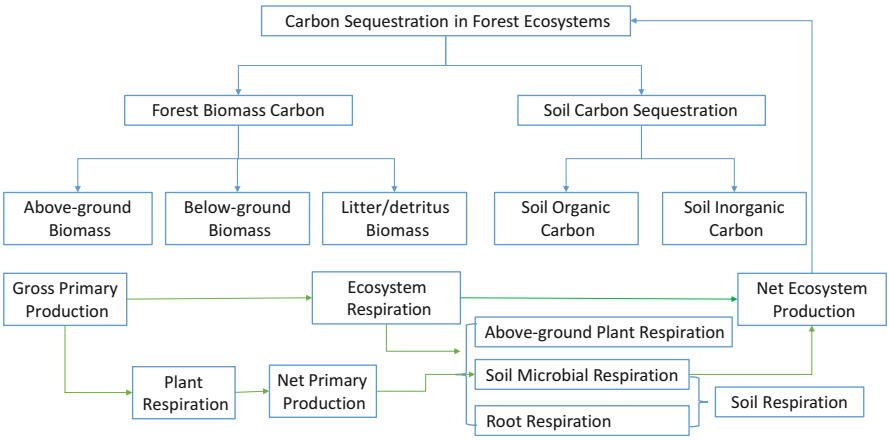

Fig. 1 Carbon sequestration in forest ecosystems, including major carbon pools and fluxes (Lal 2005)

increasing at an unprecedented rate. These changes as well as changes in precipitation, nitrogen deposition are likely to have significant effects on tree growth and forest dynamics, and eventually, carbon accumulation in forest ecosystems (Zuidema et al. 2013). Understanding the accumulated impacts of these climate changes (e.g., global warming, elevated CO_2, precipitation change, and nitrogen deposition) is crucial for predicting ecosystem carbon dynamics in forest ecosystems.

Climate change affects forest ecosystem carbon cycling both directly and indirectly (Hui and Luo 2004). Whether forest ecosystems sequestrate more carbon into ecosystems (carbon sinks) or release more carbon from ecosystems (carbon sources) depends on the net ecosystem carbon exchange, the difference between gross ecosystem primary productivity and ecosystem respiration (Fig. 1). When climate change stimulates photosynthesis process by elevated atmospheric CO_2 or improved growing conditions (i.e., warmer temperatures, more favorable moisture balance, improved nutrient availability, or decreased pollutants such as tropospheric O_3) or decreases plant or microbial respiration process as a result of altered chemical or physical composition of the plants and soil organic matter, the ecosystems act as carbon sinks (Field et al. 2007). Otherwise, the converse processes can make ecosystems act as carbon sources.

Many experimental and modeling studies have been conducted in order to better understand the potential effects of global warming, elevated atmospheric CO_2, and changing precipitation regimes on these forest ecosystem processes (Peters et al. 2013). The effects of climate change on forests have been found to be both positive (e.g., increases in forest growth and water use efficiency under elevated CO_2) and negative effects (e.g., reduced growth due to the combined impacts of

climate change and O_3) and may vary with other factors (Allen et al. 2010; Tian et al. 2012). Increased atmospheric CO_2 concentrations may enhance tree growth, increase NPP, but the effects vary with plant nitrogen conditions and plant species or change over time (Peters et al. 2013). Atmospheric nitrogen deposition is a major factor influencing forest growth under natural conditions (Lu et al. 2011). Both CO_2 and nitrogen deposition may interact with other climate factors such as warming and precipitation to affect tree physiology, carbon allocation, and ecosystem carbon sequestrations (Allen et al. 2010; Tian et al. 2012; Norby and Luo 2004).

Due to the importance of forest ecosystems, many scientific papers have been published on the impacts of climate change on forest ecosystems during the past several decades (Norby and Luo 2004; Deng et al. 2012). Several studies have also reviewed the effects of climate change on forest ecosystems at large spatial scales, such as in Europe and USA, and for specific forest ecosystems such as tropic forests and boreal forests (Lindner et al. 2010). Forest carbon sequestrations have been quantified at small and large scales (Allen et al. 2010), but there are very large uncertainties in the distribution of carbon stocks and carbon exchange in forest ecosystems (Le Toan et al. 2011). Future observations, research, and tool development are needed to further understand the interactions between climate change and forest ecosystems.

In this chapter, we reviewed the existing knowledge about forest ecosystem carbon stocks and dynamics under potential climate change. The following two questions were addressed: (1) What are the estimated carbon stocks in forest ecosystems? (2) What are the main impacts of climate change on forest ecosystem carbon dynamics? We first synthesized the estimations of global forest ecosystem carbon stocks in forest biomass and soil and then presented some typical research studies of climate change on forest ecosystem carbon stocks and fluxes. Two approaches are summarized here. One is the experimental studies considering increased CO_2, global warming, precipitation changes, and nitrogen deposition. Another is a modeling study of forest ecosystem carbon dynamics from past to present and future. We also identify some of the remaining questions warranting further research for better understanding the capacity of forest ecosystems to adapt to climate change, including the interactions with other drivers of global change, and for better understanding the possible feedbacks on climate of these changes in forest ecosystems.

Forest Ecosystems

Forests are the dominant terrestrial ecosystems on the Earth with a total area of more than 4.1×10^9 ha (Dixon et al. 1994; Pan et al. 2013). Forests provide habitats for the majority of species on Earth and produce valuable ecosystem resources and services to human beings, such as food, fiber, timber, clean water, carbon storage, and climate mitigation (Allen et al. 2010).

Forest Types

Forests are dominated by trees and other woody vegetation. At large scale, the major types of forests can be classified by biomes (Dixon et al. 1994). Three major biomes of forests are tropical forests, temperate forests, and boreal forests (Fig. 2).

Tropical forests are characterized by the greatest diversity of species and productivity of trees. They are located between 23° north and south of the Equator, respectively. Temperature is 20–25 °C on average and varies little in a year. Precipitation is high (with annual rainfall exceeding 2000 mm) and evenly distributed throughout the year. Plants can grow during the whole year. Trees are usually 25–35 m tall. Canopy in tropical forests is multilayered and continuous. Tropical forests contain an enormous diversity of hardwood tree species and are important for carbon sequestration. About half of the carbon in rainforests is contained in the vegetation. The remaining carbon is in tropical forest soils: tropical forest soils have only modest carbon levels, because the dead biomass rapidly decomposes in the warm, humid conditions, and the minerals rapidly leach out of tropical forest soils (Table 1) (Gorte 2007).

Temperate forests typically occur in the mid-latitudes, generally ranged between 50° north and south of the Equator. Temperature varies greatly from −30 ° C to 30 ° C, but precipitation (750–1500 mm) is distributed evenly throughout the year. There are a large variety of temperate forests, including hardwood, softwood, and a few mixed forests. Trees are distinguished by broad leaves that are lost annually. Species include oak, hickory, beech, hemlock, maple, etc. Temperate forests have much lower tree species diversity than tropical forests and generally contain less carbon averaging about 1.57×10^5 kg ha^{-1} (Table 1). More than one-third of the carbon is stored in the vegetation and nearly two-thirds in the soil (Gorte 2007).

Boreal forests represent the largest terrestrial biome occurring between 50° and 60° north latitudes. Temperatures are very low and precipitation (400–1000 mm annually) is primarily in the form of snow. Seasons are divided into short, moist, and moderately warm summers and long, cold, and dry winters. Boreal forests are dominated by conifers, including pine, fir, and spruce, with scattered birch and aspen stands. Boreal forests generally contain more carbon than temperate or tropical forests, averaging more than 4.04×10^5 kg ha^{-1} (Table 1), due to very slow decomposition rates owing to short summers and the high acidity of conifer forest soils. Less than one-sixth of boreal forest carbon is in vegetation. The rest 84 % is in boreal forest soils. The high boreal forest soil carbon level is important for carbon cycling, because many believe that management activities and climate change that disturb boreal forest soils can increase their release of carbon (Gorte 2007)

Forest Distributions

The global distributions of forests are mostly determined by the climatic factors, particularly temperature and precipitation. At the regional and local scales, soil type, topography, and other local environmental factors could influence the distributions

Fig. 2 Examples of different forests around the world. (**a**) Temperate Oak forest in Tennessee, USA, photo credit: Brain Stansberry. (**b**) Amazon tropical rainforest, Brazil, photo credit: Caterdral Verde. (**c**) Alaska coastal temperate rainforest, USA, photo credit: Nick Bonzey. (**d**) Spruce forest (boreal forest) in Sweden, photo credit: Nick Lott. (**e**) Great Smoky Mountain forest, USA, photo credit: Miguel V. (**f**) Gallatin National Forest, Montana, USA

(Pan et al. 2013). Mapping forest distribution usually involves a combination of two or more of the following methods: field observations and measurements, remote sensing and geographic information system (GIS), and ecosystem modeling (Pan et al. 2013). Global and regional mapping of forest distribution increasingly relies on satellite remote sensing due to the advantages of consistency and automated image processing (Pan et al. 2013). Facilitated by remotely sensed land-cover data (e.g., SPOT and AVHRR) and geographic information system (GIS), various global classifications and maps have been developed (Pan et al. 2013; FAO 2001). At the global scale, MODIS-based observations can currently identify only four physiognomic classes of trees (evergreen needle-leaved, evergreen broad-leaved, deciduous

Table 1 Carbon stock in selected biomes of the world (Dixon et al. 1994; Lal 2005; Fang et al. 2007). Multiple numbers in one cell are estimates from different sources

Biome	Area (Mha)	Carbon density (Mg/ha)		Carbon stock (Pg)	
		Vegetation	Soil	Vegetation	Soil
Tropical	1755	121, 133, 157	123, 136, 122	212, 234, 340	216, 238, 213
Temperate	1038	57, 62, 96	96, 106, 122	59, 64, 139	100, 110, 153
Boreal	1372	64, 72, 53	343, 378, 296	88, 98, 57	471, 519, 338
High latitudinal belt	1372	64	343	88	471
Russia	884	36.1, 83	281	28, 74	249
Canada	436	28, 37.4	484	12, 15.2	211
Alaska	52	39	212	2	11
Mid latitudinal belt	1038	57	96	59	100
Continental USA	241	61, 62	108	12, 15	26
Europe	283	32	90	9	25
China	118	42.1, 114	136	4.3, 17	16
Australia	396	45	83	18	33
Low latitudinal belt	1755	121	123	212	216
Asia	310	132–174	139	41–54	43
Africa	527	99	120	52	63
Americas	918	130	120	119	110
Total	4165	66	189	359	787

needle-leaved, and deciduous broad-leaved trees) and seven relatively coarse woody biome types based on trees and shrubs (Fig. 3) (Pan et al. 2013).

Forest Ecosystem Functioning and Carbon Cycling in Forest Ecosystems

As we mentioned before, forests are vital to our quality of life and society, as they provide many resources and services including mitigation of climate change (IPCC et al. 2013). Trees take up CO_2 in the atmosphere and release oxygen (O_2) through photosynthesis. The sum of photosynthesis over a year is termed gross primary productivity (GPP) (Nowak and Crane 2002; Pan et al. 2011). The fixed carbon is then transferred to their stems, roots, and leaves for growth. The actual carbon fixed into plants, the net primary productivity (NPP) of an ecosystem, is the balance between GPP and the carbon lost through plant respiration (i.e., the construction and maintenance cost). When leaves and branches fall and decompose, the stored

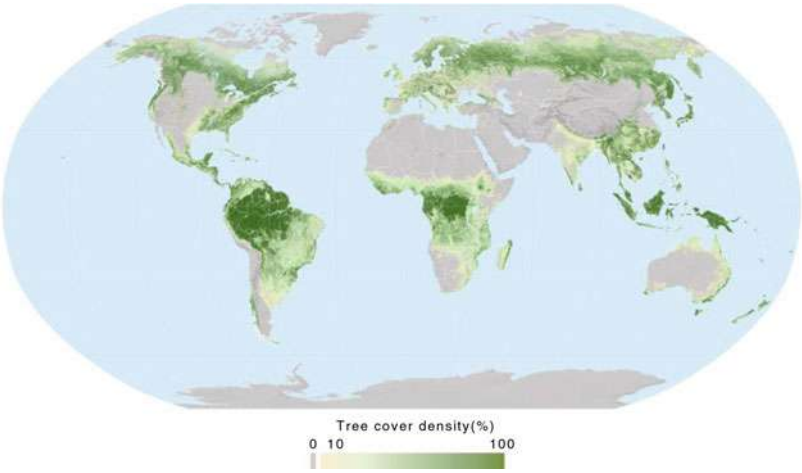

Fig. 3 Global forest cover map (FAO 2010. Forests of the World. http://data.fao.org)

carbon will be released back to atmosphere through respiration. Part of dead organic matter will be transferred to the soil. When carbon losses by microbial respiration (heterotrophic respiration, Rh) in litter and soil are accounted for, we obtain the net carbon balance of an ecosystem. This net balance is termed net ecosystem productivity (NEP). Forest ecosystems play a major role in the global carbon cycle by storing large amount of carbon in live plant biomass, dead plant material, and the soils and are considered as carbon sinks. In order to understand how forest ecosystems respond and feedback to climate change, we need to quantify carbon stocks in vegetation and soil in forest ecosystems.

There are several methods currently used for estimation of forest biomass carbon (Pan et al. 2011, 2013; Brown 2002; Yu et al. 2014): (1) Field measurement-based estimation using forest inventory data (Yu et al. 2014). These methods include (a) the mean biomass density method [MBM] that directly measures biomass in sample plots and uses the average of total plot biomass for each forest type to get biomass for that type, requiring only inventory data on forest area. A biomass expansion factor (BEF) is used to convert stem volume to biomass to account for all components of trees; (b) the continuous biomass expansion factor method [CBM] expands on the MBM by treating BEF not as a constant but as a function of forest age, stand density, and type of site; and (c) continuous BEF method (CBM). Fang et al. (2007) derived an equation that accommodates changing BEF values over time from inventory data on forest area and volume. (2) Remote sensing-based techniques. Remote sensing data such as satellite imagery to aerial photo-imagery from low-flying airplanes may provide a useful means for measuring carbon stocks in forests (Brown 2002). (3) Micrometeorological techniques such as Eddy covariance technique and their

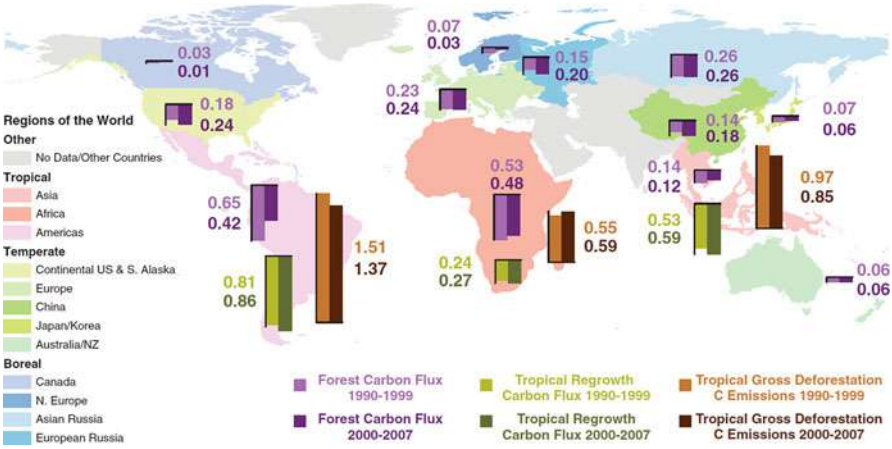

Fig. 4 Carbon sinks and sources (Pg C year^{-1}) in the world's forests. Colored bars in the down-facing direction represent C sinks, whereas bars in the upward-facing direction represent C sources (Adapted from Pan et al. (2011))

upscaling (Nabuurs et al. 2010). (4) Large-scale ecosystem models as BIOME-BGC, LPJ, ORCHIDEE, or DLEM (Tian et al. 2012; Hui et al. 2012).

Each of these methods has its strengths and weaknesses (Nabuurs et al. 2010; Karjalainen et al. 2003). For example, field measurement-based method provides estimates of both the carbon stock changes and the size of the stocks but has limited capability to forecast future changes. Ecosystem models can explore the importance of ecosystem physiological responses to climate variability or increasing CO_2, but most of them do not yet consider natural or human-induced disturbances (Karjalainen et al. 2003). So far, the estimates of the contemporary carbon balance still vary a lot (Nabuurs et al. 2010).

Globally forests store over half of the carbon residing in terrestrial ecosystems (FAO 2001). The total biosphere carbon pool is estimated at 2.19×10^{18} kg C. Of this, approximately 1.0×10^{18} kg is in forests, about 50 % more carbon than now resides in the atmospheric pool. Forests account for 75 % of GPP in terrestrial ecosystems and 80 % of the total plant biomass on the Earth. Forests store about 2.4×10^{12} kg of carbon per year (Pan et al. 2011) and account for almost all of world's land-based carbon uptake (Fig. 4).

In the USA, approximately 33 % (3.03×10^{8} ha) of the land base is forested (Karjalainen et al. 2003). US forests and long-lived wood products accounted for a net sink of 2.51×10^{11} kg of carbon (Karjalainen et al. 2003). Estimates for the European terrestrial biosphere net sink, based on inversion for forest and agricultural lands, vary from 300 to 7.0×10^{11} kg C year^{-1} with large uncertainties (Karjalainen et al. 2003). Estimates based on forest inventories suggest much smaller net sink for European forests, between 1.0 and 1.1×10^{11} kg C year^{-1} (Nabuurs et al. 2010).

Climate Change: From Historical Change to Current and Future

Recent changes in global and regional climate have been well documented and generally show an increase in mean annual temperature, with more extreme events such as hot days and droughts (Peters et al. 2013). Increasing emissions of greenhouse gases such as carbon dioxide (CO_2) are now widely acknowledged by the scientific community as a major cause of current global warming and climate change (Allen et al. 2010). Due to fossil fuel combustion and deforestation, atmospheric carbon is estimated to be increasing by approximately 2.6×10^{12} kg annually (Nowak and Crane 2002). As a result, the concentration of atmospheric CO_2 has risen from 280 ppm at the beginning of the industrial revolution to the current 394 ppm (Peñuelas et al. 2013). An increase in 2.36 ppm of CO_2 in 2010 was reported as one of the largest annual increases in recent decades (Peñuelas et al. 2013; Peters et al. 2013). Atmospheric CO_2 concentration in 2100 is projected to increase to at least 486 ppm or as high as 1000 ppm, depending on different models or model scenarios (Lindner et al. 2010). This rapid increase in the atmospheric CO_2 concentration and other greenhouse gases has the potential to drive current climatic changes more quickly than all previous climatic changes (Peñuelas et al. 2013; IPCC et al. 2013).

Climate observations have demonstrated the existence of a global warming trend: global average air temperature at the Earth's surface has increased by 0.8 °C since 1900 (IPCC et al. 2013) and the 12 hottest years observed globally since 1880 all occurred between 1990 and 2005 (Lindner et al. 2010). Globally, a rapid increase in air temperature was observed. For example, the period of 2001–2010 was 0.477 °C above the 1961–1990 mean annual temperature and was 0.217 °C warmer than the 1991–2000 decade (Morice et al. 2012). Global mean air temperature is expected to increase by 1.0–3.7 °C by the end of this century, with concurrent changes in global and regional precipitation regimes (IPCC et al. 2013). Latest climate change scenario projections for Europe suggest that by 2100 temperatures will increase between about 2–5 °C and by 1.4–5.8 °C globally, depending on the quantity of future greenhouse gas emissions (Peters et al. 2013). Extreme weather events such as heat waves and frequency and severity of extreme droughts are predicted to increase, with spatial differences (IPCC et al. 2013).

These rapid changes in climate may exceed the capacities of trees and forest ecosystems to assimilate them (Peñuelas et al. 2013). Understanding and predicting the consequences of these climatic changes on forest ecosystems is one of the grand challenges for global change scientists, particularly on forest carbon cycling (Allen et al. 2010).

Experimental Studies

Overview

Experimental study is one of the most powerful tools to evaluate the responses of climate change on terrestrial ecosystems and to understand the mechanisms underlying these responses (Rustad 2008). The results from experimental studies can also

be used to parameterize and validate terrestrial ecosystem models (Hui et al. 2012). In the past several decades, numerous manipulative experiments have been conducted on tree seedlings and forests in the laboratory and under field conditions (Rustad 2008; Norby et al. 2010). These experimental studies often use perturbation approaches that create different treatment levels (i.e., magnitudes in changes of treatment factors) to evaluate the effects of climate change in the past, current, and future conditions (Hui et al. 2012). While earlier studies mostly focused on a single climatic factor, now more experiments considered two or more climatic factors in the same studies, which can quantify not only the main effects of climatic factors but also the interactive effects of them (Deng et al. 2010). Some international networks of experimental studies have also been established over the past decade. For example, an international research coordination network – Terrestrial Ecosystem Response to Atmospheric and Climatic Change (TERRAC) – includes 135 field experimental sites of different ecosystems in 25 countries (Rustad 2008). Ecosystems include deciduous forests and coniferous forests, among others. These experimental studies and others have generated large amounts of high-quality data and greatly improved our understanding of the response of terrestrial ecosystems to climate change. In this section, we mainly summarize the findings from experimental studies examining the effects of climate change on carbon sequestration in forest ecosystems.

Effects of CO_2

The effects of rising atmospheric CO_2 concentrations on carbon sequestration in forest ecosystems have been studied for decades. In the early years, researchers used closed chambers such as glasshouse and growth chamber to grow tree seedling or small trees in pots under control and elevated CO_2 levels. These studies were criticized as glasshouse and growth chamber cannot really mimic the real world environment, thus generated responses that are different to these under natural conditions. Open-top chambers provide natural light and precipitation for trees to grow but may modify air and soil temperature inside the chambers. More recently, trees have been exposed to elevated CO_2 using free-air CO_2 enrichment (FACE) technology, which allows the fumigation of intact forest ecosystems with air enriched in CO_2 in large-diameter plots without walls (Norby et al. 2005; Drake et al. 2011).

Experimental studies provide direct evidences of increased vegetation carbon accumulation and ecosystem productivity in forest ecosystems under elevated CO_2. The enhancement of aboveground biomass for trees under elevated CO_2 range from 0 % to 50 %, with the higher values observed in young trees and little to no response observed in the few experiments conducted to date in mature natural forests (de Graaff et al. 2006). For the belowground biomass, the maximum increases by elevated CO_2 can exceed 50 %, hence usually resulting in lower shoot:root ratio (de Graaff et al. 2006). Early results from an open-air CO_2 enrichment experiment in a young North Carolina forest also showed increased ecosystem net primary

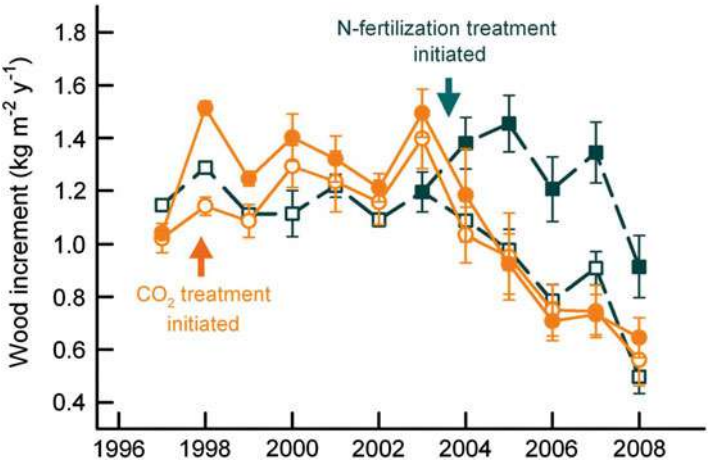

Fig. 5 Growth responses in the FACE and nitrogen addition experiments. Elevated CO_2 (*solid circles*) caused a significant increase in wood increment in the first year after treatment initiation (1998), but the response diminished in subsequent years and in later years was not statistically different from FACE controls (*open circles*). N fertilization (*shaded squares*) caused an immediate and sustained increase in wood increment compared with unfertilized plots (*open squares*) ($p < 0.001$) (Adapted from Norby et al. (2010))

productivity during the first 2 years of exposure, but later findings indicated that this productivity declined with time (Finzi et al. 2002). Experimental studies using FACE technology also indicated that CO_2 enrichment of 550 ppm increased NPP by about 20–25 % across a range of temperate forest sites (Norby et al. 2005), but the long-term outcome was diminishing (Fig. 5) (Norby et al. 2010). Furthermore, some FACE experiments showed lack of CO_2 fertilization effect (Liu et al. 2010). Nutrient limitation is hypothesized as primary cause for reduced or lack of CO_2 fertilization effect observed on NPP (Norby et al. 2010; Luo et al. 2004). For example, experimental studies have shown that elevated CO_2 could stimulate plant nitrogen uptake and enhance tissue carbon:nitrogen ratio (Luo et al. 2006), resulting in progressive nitrogen limitation (PNL) (Luo et al. 2004). In addition, nutrients other than nitrogen may also influence forest NPP responses to elevated CO_2. Some forest ecosystems are limited or co-limited by phosphorus availability, and other nutrients (e.g., potassium), which has received even less attention in experimental study. Thus, carbon accumulated in forest vegetation by the CO_2 fertilization is still uncertain. Interactions between forest vegetation carbon sequestration and nutrient limitation under elevated CO_2 levels should be a focus of future studies. Long-term FACE experiment in old-grown tropical forests will be required, because plant growth in these forest ecosystems is generally limited by phosphorus availability.

Elevated CO_2 should also potentially enhance carbon sequestration in forest soils due to increased aboveground litter, altered C allocation between shoots and roots, enhanced coarse roots production and fine roots turnover, and root exudation.

However, experimental studies of elevated CO_2 suggested a small C sequestration of only average 5.8 % increase in forest soils (Luo et al. 2006), and the magnitudes, sometimes even the direction of the change, vary among different tree species, CO_2 experimental facilities, and length of experiments. This is rather surprising. The newly increased soil C input under elevated CO_2 may stimulate microbial degradation of soil organic matter decomposition, a phenomenon known as a "priming effect" (Bader and Cheng 2007). It has been shown that CO_2-induced priming effect can override environmental effects (such as soil temperature, soil moisture, or soil properties) to accelerate soil organic matter decomposition rates, and hence resulting in expanded soil respiration to offset the extra soil C input due to increased plant growth, and a decrease in soil C content (Bader and Cheng 2007). Several studies have detected priming effects in temperate forests (Bader and Cheng 2007; Carney et al. 2007). Carney et al. (2007) reported that despite higher plant growth, the CO_2-induced priming effect enhanced soil microbial activity and resulted in a double reduction in soil C in scrub-oak ecosystem. Drake et al. (2011) also reported that total quantity of C entering the soil via litter fall and all belowground C inputs increased 17 % from c. 1.50 kg C m^{-2} $year^{-1}$ under ambient CO_2 to c. 1.75 kg C m^{-2} $year^{-1}$ under elevated CO_2. However, these increases in C entering the soil under elevated CO_2 was matched by increased C loss attributable to significant increases in fine and coarse root respiratory fluxes (i.e., autotrophic respiration) and a significant increase in heterotrophic respiration (Fig. 6) (Drake et al. 2011). Furthermore, a recent laboratory study found that shift of soil microbial community by elevated CO_2 could increase soil organic matter decomposition, resulting in a decrease of 9 % in soil carbon (Cheng et al. 2012). These experimental studies have added to the uncertainty about whether the soil C pool would act as a net sink for atmospheric CO_2 under future increasing atmospheric CO_2 concentrations.

Effects of Temperature

Experimental study of warming impacts on forest carbon sequestration is critical for determining the terrestrial carbon feedback to climate change. A number of warming experiments have been conducted in forest ecosystems busing greenhouses, electrical surface soil warming, passive heating, overhead infrared lamps, and closed- and open-top chambers (Hui et al. 2012; Rustad et al. 2001). Since 2001, several of these studies have been completed, new studies have been initiated, and several are ongoing. Of the ongoing studies, the soil warming experiment at the Harvard Forest in Petersham, MA, USA, is one of the longest running. Initiated in 1991, electric heat resistance cables buried at 10 cm depth in the soil warm surface soils to 5 °C above ambient in a mixed northern hardwood forest. Next Generation Ecosystem Experiments-Tropics, or NGEE-Tropics, was initiated to investigate how rising temperatures, shifting precipitation patterns, increasing greenhouse gas levels, and other natural and human-induced changes affect tropical forests' influence on Earth's climate (http://esd1.lbl.gov/research/projects/ngee_tropics/index.html, Accessed June 1, 2015).

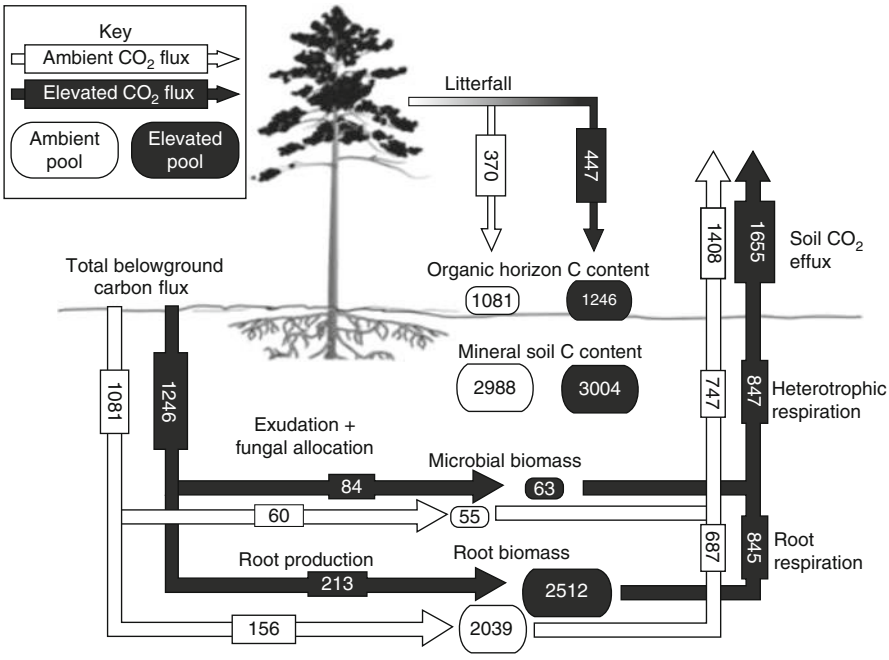

Fig. 6 Belowground carbon budgets for a warm-temperate forest exposed to elevated atmospheric CO_2 at the Duke free-air CO_2 enrichment (*FACE*) site. Ambient CO_2 is shown in white, while elevated CO_2 is shown in black. Ovals reflect pools and have units of g C m^{-2}; squares within arrows reflect fluxes of C and have units of g C m^{-2} $year^{-1}$ (Adapted from Drake et al. (2011), with permission from John Wiley and Sons)

The effects of experimental warming on vegetation carbon accumulation in forest ecosystems are highly variable. Regional environmental factors such as temperature, precipitation, and availability of soil nitrogen may contribute to diverse changes observed in global forest warming experiments. For example, soil warming in a Norway spruce forest at Flakaliden in northern Sweden increased the stem-wood growth of trees in heated plots by 50 % relative to controls after 5 years (Jarvis and Linder 2000). In relatively warmer region, however, the aboveground biomass of sugar maples decreased in response to warming in the open-top chambers. Furthermore, Cunningham and Read (2002) found that Australian tropical trees demonstrate higher physiological temperature optima but narrower photosynthetic temperature tolerances than temperate tree species. Observed growth declines in tropical forests have been attributed to temperature-induced increases in plant respiration and decreased net photosynthesis as a result of increasing temperature beyond the thermal optimum (Doughty 2011). In some environments with pronounced dry spells, the effect of warming may also lead to significantly enhanced moisture limitation, in turn reducing carbon inputs into plant biomass by reduced NPP. Further evidence of warming increasing mortality rates was revealed in several forests

around the world during strong El Niño Southern Oscillation (ENSO) years, which exhibit higher temperatures and lower rainfall than normal years. In addition, Melillo et al. (2002) reported the results from a decade long warming experiment conducted in a hardwood forest. They observed that soil warming also increased the availability of mineral N to plants, which in an N-limited forest may further stimulate carbon storage in plant biomass. Over the 7-year study of warming in a deciduous forest in New England, subsequently, Melillo et al. (2011) found that plant carbon storage increased by up to 7.0×10^6 kg C ha^{-1} in the heated areas relative to control areas (Fig. 7). Increases in vegetation carbon storage in the heated area are likely due, for the most part, to the warming-induced increase in net nitrogen mineralization of about 27 kg N ha^{-1} $year^{-1}$. This represents a 45 % increase relative to the nitrogen mineralization rate in the control area.

The experimental warming studies published to date have suggested significant decrease in carbon from forest soils, although warming-induced increases in plant-derived carbon input (Lu et al. 2013). Warming-induced decrease in forest soil carbon storage should be attributed to a larger carbon loss via soil respiration. As temperature increases, soil respiration generally increases (Melillo et al. 2002), because warming generally directly increases both autotrophic and heterotrophic soil respiration. For example, with 5 °C soil temperature increase above ambient temperature using buried heating cables, Peterjohn et al. (1994) reported an additional C release of 538 g m^{-2} $year^{-1}$ from soil in Harvard Forest. Similarly, Melillo et al. (2011) found that soil warming has resulted in a cumulative net loss of carbon (1.3×10^7 kg C ha^{-1}) from a New England forest relative to a control area over the 7-year study. However, the magnitude of response in soil respiration to soil warming is greater in cold, high-latitude ecosystems than in warm, temperate areas (Lu et al. 2013). Thus, warming has likely caused a great loss of C in boreal forest soils. It is also commonly observed that the magnitude of response in soil respiration to warming decreases over time (Rustad et al. 2001). The experimental warming at the Harvard Forest showed a dramatic 26–75 % increase in soil respiration at the first 4 years (Peterjohn et al. 1994), while 10 years after the initiation of treatments, soil respiration in the warmed plots in 2000 was no longer significantly different from the control, a trend that has continued through the latest period of record. The unchanged soil respiration under warmed treatment can be attributable to acclimatization and/or depletion of substrates (Rustad et al. 2001). In addition, warming caused a shift in the soil microbial community toward more fungi, which are more tolerant to high soil temperature and dry environments than bacteria owing to their filamentous nature. Shifted microbial community structure may partially explain observed decreases in the temperature sensitivity of soil respiration.

Effects of Precipitation

Experiments in which precipitation was manipulated in the field span a wide range of experimental treatments and use a variety of methodologies. Precipitation has been manipulated in a wide range of forest ecosystems through both decreases and

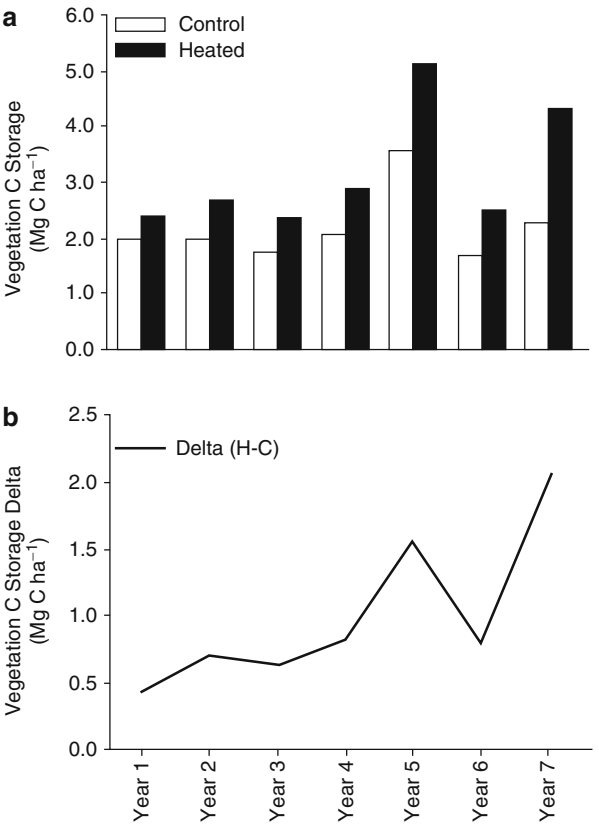

Fig. 7 (**a**) Annual vegetation carbon storage in the heated and control areas (in Mg C ha^{-1}) in a deciduous forest in New England. (**b**) Annual vegetation in carbon storage delta (heated minus control) (in Mg C ha^{-1}) in a deciduous forest in New England (Adapted from Melillo et al. (2011))

increases in rainfall amount and changes in rainfall seasonality. Drought has been often simulated using rainout shelters, while increases in precipitation have been simulated using a combination of rainout shelters and irrigation. Studies at both small and large scales have been conducted. The throughfall exclusion experiment conducted in a mature evergreen forest near Santarém, Brazil, is the largest in scale, reaching 1 ha (Davidson et al. 2008). Because confidence in both historic reconstructions and future global trends in precipitation has lagged behind that for atmospheric CO_2 and temperature, there are fewer precipitation manipulation experiments that have been initiated over the past several decades, and to date, no global synthesis of existing results has been undertaken.

In general, plant production responded positively to experimental increases in precipitation and negatively to experimental decreases in precipitation. However, the magnitude of response in plant to change of precipitation patterns depend on whether water availability is limiting to plant growth and whether the plant community is adapted to drought conditions. In the largest scale throughfall exclusion experiment, Brando et al. (2008) reported that wood production in an Amazon forest was the most sensitive component of aboveground net primary productivity to drought,

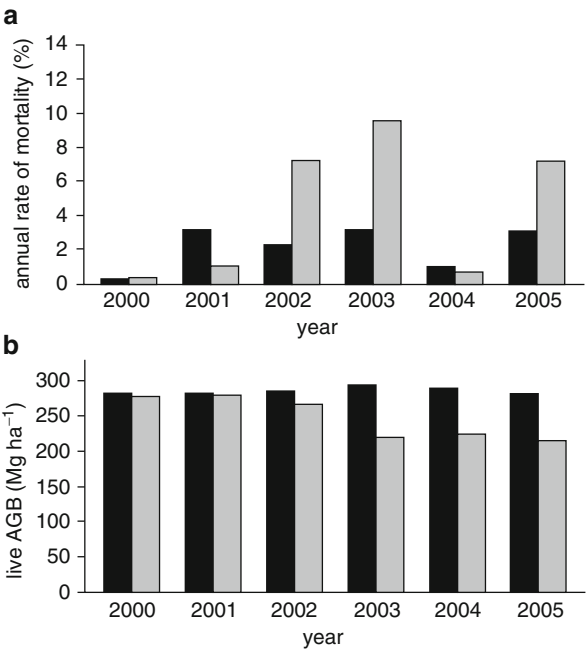

Fig. 8 (**a**) Annual percent of mortality measured on an individual basis for all individuals ≥10 cm dbh in the throughfall exclusion and control plots from Dec. 2000 to Dec. 2005. (**b**) Aboveground standing live biomass of all individuals ≥10 cm dbh from throughfall exclusion and control plots during the same period. *Black bars*, control; *grey bars*, exclusion (Adapted from Brando et al. (2008) with permission)

declining by 13 % the first year and up to 62 % thereafter. Live aboveground carbon declined by 3.25×10^7 kg ha^{-1} through the effects of drought on tree growth and mortality (Fig. 8). In addition, a long-term manipulation of precipitation inputs in a forested ecosystem showed that saplings of *C. florida* and *A. rubrum* grew faster and mortality was less on the wet plot compared with the dry and control plots (Hanson et al. 2001). Conversely, diameter growth of large trees was unaffected by the treatments. However, tree diameter growth averaged across treatments was affected by year-to-year changes in soil water status. Growth in wet years was as much as two to three times greater than in dry years (Hanson et al. 2001). These field growth data also suggest that intra- and interannual variability in precipitation were more important in determining tree growth than large directional changes in the amount of precipitation falling at any given time (Hanson et al. 2001).

There were only a few experimental studies attempted to directly assess the effect of precipitation change on soil carbon storage in forest ecosystems. Meier and Leuschner (2010) observed that soil carbon decreased by approximately 25 % in beech forests with annual precipitation >900 mm year^{-1} compared to those with precipitation <600 mm year^{-1}. However, an experimental study in Mediterranean woodland suggests that minor changes (around 10 % reduction) in precipitation amount are not likely to significantly affect or soil carbon stocks, although enhanced soil moisture during summer significantly accelerates C cycling through stimulated annual stem primary production, litter fall, soil respiration, and net annual plant-

derived C input to soil. Numerous experimental studies of precipitation change impact on soil carbon storage often focus on its impacts on forest soil respiration. Rainfall-manipulation experiments generally showed increased soil respiration following experimental water additions and decreased soil respiration following rain exclusion. However, the response of soil respiration to precipitation change differed according to moisture conditions. In a mixed deciduous forest at the Harvard Forest, Massachusetts, throughfall exclusion significantly decreased soil respiration by 53 mg C m^{-2} h^{-1} over 84 days in 2001 and by 68 mg C m^{-2} h^{-1} over 126 days in 2002, representing 10–30 % of annual soil respiration in this forest and 35–75 % of annual net ecosystem exchange of C (Borken et al. 2006). However, Deng et al. (2012) reported that soil respiration in two of three subtropical forests showed little response to precipitation increase, even when the precipitation was doubled. The precipitation increase treatment only slightly increased soil respiration in the pine forest (15.4 %), where ambient soil moisture level is relatively lower than those in the other two subtropical forests in southern China (Deng et al. 2012). The effect of precipitation on soil respiration is more complex in tropical forests. For example, drought could drive increases in plant root mortality, declines in decomposer activity (or both), and hence lower soil CO_2 emissions in eastern Amazonian rainforest, Brazil (Sotta et al. 2007). Alternatively, increased decomposition of dead roots may more than offset root mortality-related declines in soil respiration, resulting in unchanged soil respiration under throughfall exclusion plots in a mature evergreen forest near Santarém, Brazil (Davidson et al. 2008). However, results from a recent experimental study indicated that experimental drought in a humid tropical rain forest may also increase soil carbon losses to the atmosphere due to higher concentrations in litter dissolved organic matter (Fig. 9) (Cleveland et al. 2010).

Effects of O_3

There has been increased understanding of the effects of O_3 on plants since 1864, particularly during the last half of the twentieth century. Similar to elevated CO_2, ecologists usually use double O_3 concentration or increase it at a specific level in the onset of experiments conducted in greenhouses, growth chambers, open-top chambers, and FACE facilities.

Experimental studies indicated that elevated O_3 generally decreased biomass production, with greater sensitivity of root biomass to elevated O_3. Wittig et al. (2009) using a meta-analysis reported that current ambient O_3 (40 ppb on average) significantly reduced the total biomass of trees by 7 % compared with trees grown in charcoal-filtered (CF) controls, which approximate preindustrial O_3. Elevated O_3 of 64 ppb reduced total biomass by 11 % compared with trees grown at ambient O_3, while elevated O_3 of 97 ppb reduced total biomass of trees by 17 % compared with CF controls (Fig. 10). Similarly, King et al. (2013) found that the mean decrease in biomass production in young trees relative to the control was −12.5 %, with the most responsive parameter being total belowground biomass (−19.1 %) and

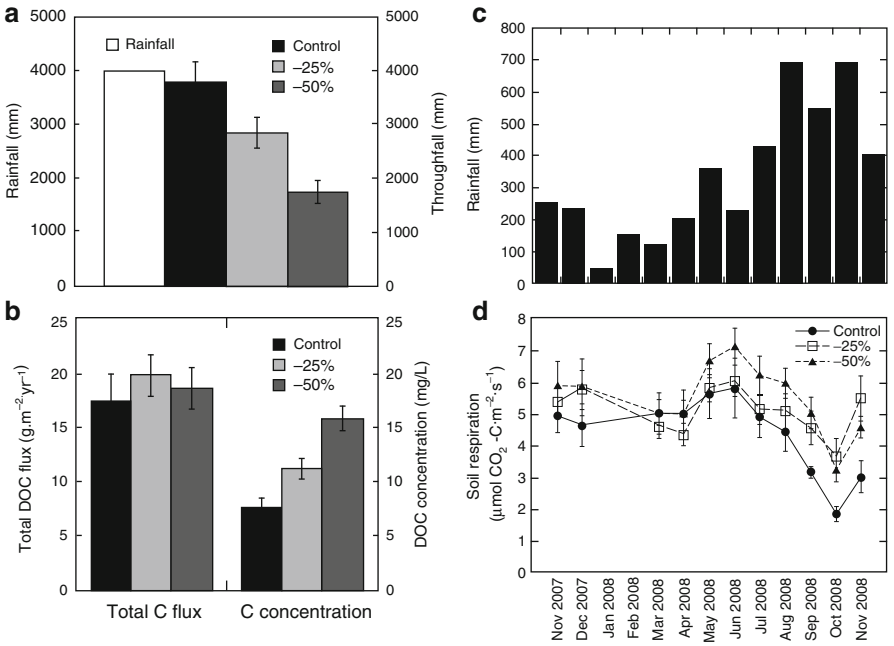

Fig. 9 (**a**) Annual rainfall (*open histogram bar*) and throughfall fluxes and (**b**) total annual dissolved organic carbon (*DOC*) fluxes and concentrations in the control and rainfall reduction (−25 % and −50 %) exclosure plots. (**c**) Monthly rainfall and (**d**) mean monthly surface soil CO_2 fluxes (respiration) from the control and rainfall reduction (−25 % and −50 %) exclosure plots. Values are means ± SD (Adapted from Cleveland et al. (2010))

the least being coarse roots (−2.7 %). For intermediate-age trees, the decrease in biomass production due to elevated O_3 relative to the control averaged −15.0 %.

Decreased allocation to roots under elevated O_3 should potentially reduce soil carbon stock in forest ecosystem. However, the trend of elevated O_3 impacts on soil carbon is poorly characterized. Unlike the total plant production, for example, King et al. (2013) reviewed that fine root biomass in intermediate-age trees (6–12 years) showed a mean stimulation due to elevated O_3 of 1.82 % relative to the control. The extremely large variance occurred because of the 11 observations, six were negative (average of −20.4 %) and five were positive (average of 28.5 %). At the Aspen FACE project, the pure aspen community showed a consistent stimulation in fine root biomass under elevated O_3 over time, whereas the aspen-birch and aspen-maple communities did not, suggesting a strong genetic effect on ecosystem function. Accordingly, soil respiration showed contrasting responses to elevated O_3 in different forest ecosystems. For example, soil respiration decreased from loblolly pine pots exposed to ozone (Edwards 1991). Soil respiration increased in response to elevated O_3 in ponderosa pine seedlings (Scagel and Andersen 1997). A later analysis (Zak et al. 2011) incorporated estimates of turnover with the fine root

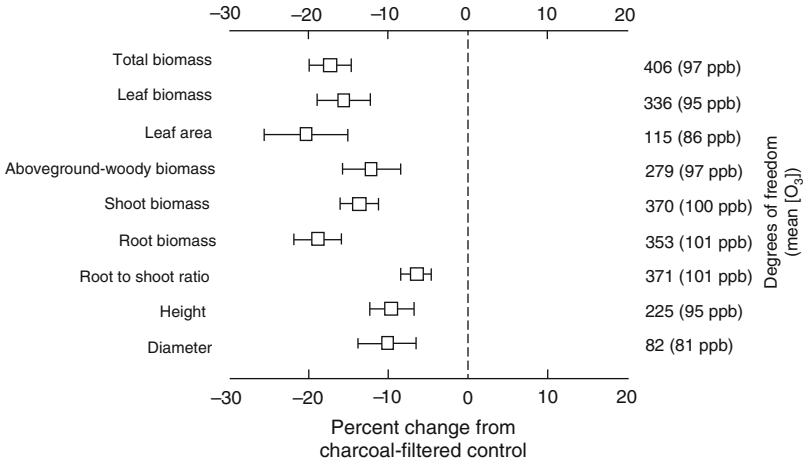

Fig. 10 Percent change in biomass, leaf area, root-to-shoot ratio, height, and diameter of all trees exposed to elevated ozone concentrations relative to charcoal-filtered controls. Symbols are bracketed by 95 % bootstrapped confidence intervals; degrees of freedom and mean O_3 are given along the y-axis (Adapted from Wittig et al. (2009), with permission from John Wiley and Sons)

biomass and estimated a nonsignificant 8 % increase in total NPP in the aspen community in the 12th year of the experiment. The fine root dynamics can have such a large impact on total NPP, and potentially net ecosystem productivity (NEP), in response to air pollution illustrates the continuing need for a much better understanding of belowground processes.

Effects of N Deposition

Atmospheric deposition of reactive nitrogen compounds (i.e., forms of nitrogen that interact with the biosphere and atmosphere) is a byproduct of human activity that can have large impacts on carbon sequestration in forest ecosystems. Since 1980s, numerous experiments of nitrogen addition have been conducted in forest ecosystems using solid or liquid nitrogen fertilization. The types of nitrogen fertilization include NH_4^+, NO_3^-, NH_4NO_3, and urea. Nitrogen fertilization studies usually provide the nitrogen in a single or a few applications, in contrast to atmospheric deposition, which is essentially continuous in the dry form (NOx, HNO_3 vapor) and in small, frequent pulses as wet deposition (NH_4^+ and NO_3^-) in precipitation. Furthermore, in contrast to fertilizer additions where nitrogen inputs are retained primarily in soil, vegetation accounts for most of the retention of nitrogen deposited from the atmosphere.

Experimental evidences in forest ecosystems indicated that plant biomass generally increases with nitrogen additions, and aboveground growth increases more than belowground growth, leading to decreased root/shoot ratios. Using a meta-analysis, Lu et al. (2011) reported that experimental nitrogen addition in forest ecosystems increased aboveground and belowground biomass by about 35 % and 30 %, respectively. However, responses tend to vary depending on tree species and the level of nitrogen availability in soil. In the Harvard Forest Long-Term Ecological Research system, for example, plant productivity increased by 50 % in broadleaf forest after 9 years of nitrogen fertilizer, while it decreased by about 30 % in pine forest at the high nitrogen fertilizer of 30 kg N ha^{-1} $year^{-1}$ (McNulty et al. 1996). In Europe NITREX network, forest NPP increased by 50 % when high nitrogen deposition was removed (Magill et al. 2000). This indicated that excess nitrogen inputs have led to a reduction in plant productivity in Europe NITREX forests. Nitrogen deposition is likely to stimulate fine root production but also increase fine root turnover, resulting in a decrease in fine root biomass. However, fine root production could decrease if chronically elevated nitrogen deposition leads to tree mortality (Nadelhoffer 2000).

Most of nitrogen fertilizer studies suggest a significant increase in soil carbon in forest ecosystems. In 15 long-term (14–30 years) experiments in *Picea abies* and *Pinus sylvestris* stands in Sweden and Finland, for example, Hyvönen et al. (2008) reported that addition of a cumulative amount of N of 600–1800 kg N ha^{-1} resulted in a mean increase in soil C stock of 11 kg (C sequestered) kg^{-1} (N added) ("N-use efficiency"). Nave et al. (2009) conducted a meta-analysis of the responses of soil C storage on north temperate forest and found that N inputs increased soil carbon by 7.7 %, with largest increase in the western conifers forests (Fig. 11). Using isotope technology, Nadelhoffer et al. (1999) reported that nitrogen deposition accounts for 20 % of the annual 1.5 $\pm$ 1.9 Pg CO_2-carbon uptake attributed to forest growth in north temperate forests. Nevertheless, Lu et al. (2011) found that soil carbon did not significantly change in forest ecosystems in response to N addition. They explained that in forest ecosystems, the input of increased plant carbon to the soil was mainly via the aboveground litter fall. Both litter and organic horizon C:N ratios significantly decreased in response to N addition. Unprotected surface litter and organic horizon soil with high substrate quality decomposed quickly. The regression analyses also showed that N-induced variations in soil carbon pools were not significantly correlated with changes in aboveground plant growth but were positively correlated with changes in soil respiration. This is rather surprising. In most of the temperate forests, soil microbial activity is often and also limited by nitrogen; increasing N input can significantly enhance soil respiration (Zhou et al. 2014). However, in some forests such as subtropical forests in southern China where ambient nitrogen deposition is relatively high, increasing N input can significantly reduce soil respiration but still stimulate plant growth (Deng et al. 2010). Nitrogen addition in these forests caused a large increase of about 30 % in soil carbon in subtropical forest in southern China (Chen et al. 2012).

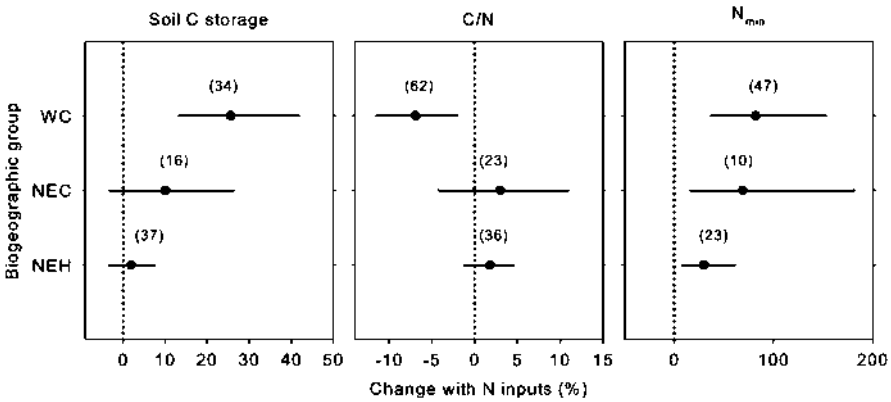

Fig. 11 The effects of N inputs on mineral soils, by biogeographic group. Points are means ± bootstrapped 95 % confidence intervals, with number of studies (k) in parentheses. Soil C storage response ratios include pool sizes only. Biogeographic groups are western conifers (*WC*), northeast conifers (*NEC*), and northeast hardwoods (*NEH*) (Reprinted from Geoderma, Vol. 153, Nave et al., Impacts of elevated N inputs on north temperate forest soil C storage, C/N, and net N-mineralization, 231–240, Copyright (2009), with permission from Elsevier)

Multiple Factors Studies

Unlike common single-factor experiments, global change involves simultaneous changes in multiple factors, which could potentially have complex interactive influences on carbon sequestration in forest ecosystems. Currently, more and more experiments now consider more than one climatic factor of elevated CO_2, temperature, precipitation, O_3, and nitrogen. In experimental studies with CO_2 and N manipulations, for example, trees often had greater aboveground growth stimulation by elevated CO_2 at high rather than at low N supply (Norby et al. 2010; Liu et al. 2010). Even in southern China where nitrogen is not the limited factor for tree growth, Liu et al. (2010) reported greater tree growth stimulation by elevated CO_2 at high rather than at low N supply (Table 2). Similarly, the CO_2-induced soil carbon accumulation was larger at high rather than at low N supply (Chen et al. 2012). Deng et al. (2010) also reported that both CO_2 and N treatments significantly affected soil respiration in this subtropical forest in southern China, and there was significant interaction between elevated CO_2 and N addition ($p < 0.001$, $p = 0.003$, and $p = 0.006$, respectively). Deng et al. (2013) further revealed the seasonal importance of environmental controls under elevated CO_2 and N deposition in the assessment of soil C sequestration potential in subtropical forest ecosystems in southern China. Climate warming and elevated CO_2 could interactively alter plant and soil N cycling, which in turn could influence the response of forest carbon sequestration to elevated CO_2. Experimental studies found altered elevated CO_2 fertilization response due to temperature only at temperatures substantially different than typical or optimal thermal environments. For instance, warming increased soil N availability and thereby enhanced relative responses of

Table 2 Tree aboveground biomass and belowground biomass (means ± standard errors) under different CO_2 and N treatments (Liu et al. (2010)). Treatments with the same letter are not significantly different from each other ($p > 0.05$). The treatments were: CK control, N+ high N, C+ high CO_2, and CN high CO_2+high N (Liu et al. 2010)

Sampling month	CN	C+	N+	CK
Aboveground biomass (kg m^{-2})				
Aug 05	0.22 ± 0.01	0.15 ± 0.00	0.18 ± 0.01	0.21 ± 0.00
Jan 06	0.48 ± 0.00a	0.31 ± 0.01b	0.36 ± 0.04b	0.37 ± 0.01b
May 06	0.75 ± 0.03	0.51 ± 0.04	0.57 ± 0.07	0.53 ± 0.01
Jan 08	4.38 ± 0.18a	3.11 ± 0.29b	3.42 ± 0.42ab	2.62 ± 0.15b
Sep 08	6.59 ± 0.15b	4.77 ± 0.20bc	6.00 ± 0.10ab	4.07 ± 0.08c
Jan 09	7.98 ± 0.21a	5.55 ± 0.09b	7.94 ± 1.26a	4.82 ± 0.02b
Belowground biomass (kg m^{-2})				
Aug 05	0.07 ± 0.00	0.06 ± 0.00	0.06 ± 0.01	0.07 ± 0.00
Jan 06	0.15 ± 0.00	0.13 ± 0.00	0.13 ± 0.02	0.13 ± 0.00
May 06	0.23 ± 0.01	0.22 ± 0.02	0.19 ± 0.03	0.20 ± 0.00
Jan 08	1.30 ± 0.04a	1.08 ± 0.07b	1.08 ± 0.11b	0.93 ± 0.03b
Sep 08	1.93 ± 0.04a	1.59 ± 0.11b	1.88 ± 0.28ab	1.39 ± 0.12b
Jan 09	2.39 + 0.12a	1.85 ± 0.10b	2.37 ± 0.15a	1.62 ± 0.09b

photosynthesis to elevated CO_2 (Shaw and Harte 2001), which in turn could enhance NPP responses to elevated CO_2.

The interaction of elevated CO_2 and O_3 was generally not statistically significant and resulted in positive stimulation of all biomass production parameters in both young and intermediate-age trees relative to the control. This suggests that the effects of elevated CO_2 and O_3, when occurring together, are generally additive and that the positive effects of elevated CO_2 more than offset the negative effects of elevated O_3 on biomass production (King et al. 2013). All data on changes in soil C were from only two studies conducted at the Aspen FACE Project at different stages of stand development (Loya et al. 2003; Talhelm et al. 2009). Although the mean responses showed elevated CO_2 and O_3 altered total soil carbon in forest ecosystems, the changes were not statistically significant (Talhelm et al. 2009). The 11-year study at Aspen FACE indicated that the effects of elevated CO_2 and O_3 on soil C varied with stand development (King et al. 2013). After the first 4 years of fumigation at the Aspen FACE, Loya et al. (2003) found that the formation of new soil carbon under elevated CO_2 and O_3 treatment was 51 % less than that under elevated CO_2-only treatment. However, a later study by Talhelm et al. (2009) suggested that the initial reduction in new C accumulation in elevated O_3 under elevated CO_2 was only a temporary effect. After 11 years of fumigation, neither elevated CO_2 nor elevated O_3 induced significant impacts on new soil carbon accumulation or total soil carbon content (Table 3).

Thus, evaluating multifactor interactions in influencing carbon sequestration in forest ecosystems is critical to understanding their response to global change in the

Table 3 Pretreatment (1997) of soil carbon (C) traits (means ± SE) and ANOVA P-values (Talhelm et al. (2009)). Carbon dioxide (CO_2) is not a factor in the analyses of $\delta^{13}C$ because only elevated CO_2 plots ($+CO_2$, $+CO_2+O_3$) were later fumigated with $\delta^{13}C$-depleted CO_2. Community is not a factor in this analysis because this sampling predated the establishment of the model communities and did not distinguish between soils in the various parts of the rings. Effects with $P < 0.1$ are in bold whereas those with $P < 0.05$ are in bold and italics (Talhelm et al. 2009)

	Bulk density ($g\ cm^{-3}$)	Carbon ($mg\ g^{-1}$)	Carbon ($Mg\ ha^{-1}$)	Soil $\delta^{13}C$ (%)
Treatment				
Ambient	1.2 ± 0.0	15.4 ± 1.5	37.2 ± 4.1	–
$+CO_2$	1.3 ± 0.1	15.2 ± 0.5	39.5 ± 0.9	−26.4 ± 0.0
$+O_3$	1.3 ± 0.0	15.0 ± 1.5	37.8 ± 4.0	–
$+CO_2 + O_3$	1.4 ± 0.0	13.0 ± 1.1	37.2 ± 3.6	−26.1 ± 0.2
Source				
CO_2	***0.018***	0.453	0.831	–
O_3	**0.071**	0.381	0.835	0.251
$CO_2 \times O_3$	0.394	0.550	0.736	–

real world. Indeed, when interactive effects dominate over the main effects of individual factors, results from single-factor experiments become less useful for understanding ecosystem changes. In the case that interactive effects are minor relative to main effects, results from single-factor experiments may become useful in informing us of potential changes of ecosystems in response to multifactor global change.

Conclusion

Responses of forest carbon sequestration to climate change play an important role in regulating future climate change. The current experimental studies, to certain extent, reveal true forest carbon sequestration responses to climate change and help understand mechanisms of these responses. However, the magnitude and direction of these responses may vary with time. Long-term experiments are needed to resolve ecosystem responses to changing climate that occur on decadal or greater time scales. Nutrient limitation is hypothesized as one of the primary causes for the contrasting responses of forest carbon sequestration to climate change (not limited to CO_2). Experimental examples validate this concern (Norby et al. 2010; Melillo et al. 2011), indicating not only plant growth but also soil carbon decomposition can be limited by the nutrient availability under climate change (Cheng et al. 2012). Thus, interactions between forest carbon sequestration and nutrient limitation under climate change should be a focus of future studies. Unlike atmospheric CO_2 concentration and temperature, changes in precipitation include quantity, timing, intensity, and interval of precipitation. However, current precipitation manipulation experiments in forest ecosystems often consider the change in precipitation amount only, and the

response showed relatively complex (Cleveland et al. 2010), highlighting the need to support more types of precipitation manipulation experiments in forest ecosystems particularly in tropical forests. New precipitation manipulation experiments will continue to increase our understanding of the current contrasting results we have seen to date and our ability to quantify the response of large-scale forest ecosystems to realistic precipitation change scenarios. Similarly, technological advances such as large-scale air warming (including ecosystem level) and improved infrared heating can improve our understanding of understudied processes not only belowground but also aboveground vegetation. In addition, multifactor climate change experiments have shown that forest carbon sequestration responses to multiple interacting factors of global change can be nonlinear and nonadditive. It is therefore imperative to continue to initiate and support multifactor experiments to explore these interactions at different locations.

Modeling Studies

Overview

Modeling is an important approach to investigate the effects of global change on forest ecosystems. Ecosystem models can be used to estimate dynamics of forest ecosystem functions, explain the observed changes and the underlying mechanism, and forecast ecosystem carbon cycling in the future climatic conditions (Tian et al. 2012; Hui et al. 2012; Dale and Rauscher 1994; Pan et al. 2014). Ecological models are also useful for assessing the relative importance and the impacts of different environmental change factors on forest ecosystems (Tian et al. 2012).

Ecological models have been developed at different scales, from leaf to plant canopy, ecosystem, regional, and global scales. Most of the models simulate the processes of plant photosynthesis and respiration, stomatal conductance, evapotranspiration, nitrogen uptake, carbon allocation among plant organs, litter production, nitrogen mineralization, and soil organic carbon decomposition and use these processes to calculate the carbon fluxes between vegetation, soils, and the atmosphere (Hanson et al. 2004). At leaf and canopy levels, Farquhar model is widely used to simulate leaf photosynthesis (Tian et al. 2012; Luo et al. 2001). This model considers several key process of CO_2 assimilation including CO_2 diffusion into leaf through leaf stomata and CO_2 uptake by rubisco enzyme. At regional or global scales, some biogeochemical models include Farquhar model while others use a simplified light use efficient model to simulate photosynthesis and ecosystem productivity (Tian et al. 2012; Pan et al. 2014).

At the larger spatial scales, dynamic global vegetation models (DGVMs) have also been developed to simulate carbon dynamics at regional and global scales (Tian et al. 2012; Potter et al. 1993). These models also consider the species composition changes with time under climate change. Several multiple model comparison studies have been conducted to compare model structures, ecological processes, and model performances compared with experimental/observational data. In this section, we

will present a few models as case studies and use several examples to illustrate the climatic effects on ecosystem carbon dynamics as model applications.

Ecological Models at Leaf, Stand, Ecosystem, Regional, and Global Levels

Leaf and Stand Models

Leaf and tree physiology are directly affected by atmospheric CO_2 concentration, temperature and precipitation, particularly leaf photosynthesis, respiration, tree growth, and water use (Galik and Jackson 2009). Photosynthesis is the most important biochemical process that green plants use to incorporate atmospheric CO_2 for plant growth. At the leaf level, Farquhar model can simulate photosynthesis and tree growth (Tian et al. 2012; Luo et al. 2001). Tree growth models are often used to predict the impacts of climate change on tree growth and development, physiology, and forest ecosystem fluxes (Galik and Jackson 2009). These models are often based on a mass balance approach and consider forest ecosystem fluxes, organic matter decomposition, and water balance. As a result, the models can be used to estimate above- and belowground biomass and production, explain decomposition processes, and quantify carbon dynamics and budget for specific sites.

Many models at stand and ecosystem levels have been developed, mostly with similar model structures but different complexity and model parameters (Table 4) (Hanson et al. 2004). For example, Hanson et al. (2004) compared 13 stand level ecosystem models and found that most models use Farquhar equation for photosynthesis calculation but vary greatly in growth cost setting, carbohydrate feedbacks, and soil organic pools, as well as in their spatial, mechanistic, and temporal complexity.

In addition to process-based models, some statistical models are also used to assess the forest carbon fluxes with climatic factors (Hui and Luo 2004; Hui et al. 2012; Dale and Rauscher 1994). These models usually require large calibration data sets and are generally derived from extensive growth records using regression analysis. The models may simulate observations and forecast ecosystem changes in the future with no basis in biological processes. Such statistical models usually work well under given site and stand conditions.

Regional and Global Ecosystem Models

Several ecosystem models have been developed at regional and global scales, such as Carnegie-Ames-Stanford Approach (CASA)-Biosphere (Potter et al. 1993), Terrestrial Ecosystem Model (TEM) (McGuire et al. 1992), and Dynamics Land Ecosystem Model (DLEM) (Tian et al. 2012). Most of the terrestrial ecosystem carbon cycling models start with a leaf-level photosynthesis model, often employing a modified version of the Farquhar et al. (1980) photosynthesis model. Here we used DLEM as an example to illustrate model structure, processes involved, and model functions.

DLEM is a highly integrated process-based ecosystem model that simulates the fluxes and storage of carbon, water, and nitrogen among/within the terrestrial

Table 4 Physiological characteristics of the 13 models used in a multiple model comparison (Hanson et al. 2004)

Model	BGC++	BIOME-BGC	CANOAK	EALCO	Ecosys	INTRASTAND	LaRS	LINKAGES	LoTEC	MAESTRA	NuCM	PnET-II	SPA
Photosynthesis	Farquhar	Farquhar	Farquhar	Farquhar	Farquhar	Farquhar	Biophysics iochemistry	N/A	Farquhar	Farquhar	N/A	Empirical	Farquhar
Leaf conductance	[a]Multi-Regression	[a]Multi-Regression	Ball-Berry	Ball-Berry	Ball-Berry	Ball-Berry	[a]Multi-Regression	[a]Multi-Regression	Ball-Berry	Ball-Berry	N/A	N/A	f[SWP]
Maintenance resp leaves[b]	f[M,T]	f[M,N,T]	??	f(N,T)	f[M,N,T]	f[M, N,T]	f[M,N,T, abs. PAR]	N/A	f[M,N, T]		N/A	f [M,T]	F[M,N, T]
Maintenance resp stems[c]	f[T, W]	f[T, N, W]	f[T]	f[T,N]		f [T, W]	f[T,W]	N/A	f[T, N. W]		N/A	f [T, W]	N/A
Growth cost (gCcost/ gCbuilt)													
Leaves	0.3	1.2	N/A	0.29	0.49	0.277	f [T, mass]	N/A	0.22	N/A	N/A	dynamic	N/A
Stems	0.2	2	N/A	0.29	0.32	0.22	f [T, mass]	N/A	0.28	N/A	N/A	dynamic	N/A
Roots	0.25	1.2	N/A	0.29	0.49	0.23	f [T, mass]	N/A	0.22	N/A	N/A	dynamic	N/A
Coarse roots	0.2	2	N/A	0.29	N/A	na	f [T, mass]	N/A	0.28	N/A	N/A	N/A	N/A
Carbohydrate feedbacks	No	Yes	No	Yes	No	No	Yes	No	Yes	No	N/A	Yes	N/A
Soil N/plant C feedbacks	Yes	Yes	No	Yes	Yes	No	No	Yes	No	No	N/A	Yes	N/A
ET approach	Pen/Mon	Pen/Mon	Energy balance	Energy balance	Leaf/soil	Leaf/litter	Leaf/soil	Pen/Mon	Big leaf	Pen/Mon	Calibrated	Big leaf	Pen/ Mon
Canopy interception	yes	yes	No	yes	yes	yes	Yes	Yes	yes	No	N/A	Yes	Yes
Litter evaporation	No	No	No	No	No	yes	No	No	No	No	N/A	No	Yes
Soil evaporation	yes	Yes	No	Yes	No	No	Yes	No	No	No	N/A	No	Yes
Hydraulic lift	No	No	No	off	No	No	yes	No	No	No	N/A	No	No
Stem capacitance	No	No	No	Yes	No	Yes	No	No	No	No	No	No	No

(*continued*)

Table 4 (continued)

Model	BGC++	BIOME-BGC	CANOAK	EALCO	Ecosys	INTRASTAND	LaRS	LINKAGES	LoTEC	MAESTRA	NuCM	PnET-II	SPA
Soil organic matter pools	1	4	N/A	3	2	N/A	N/A	N/A	2active 1 passive	N/A	N/A	0	N/A
Litter pools	1	3	N/A	3	2	1	0	N/A	2	N/A	N/A	0	N/A
Soil/ heterotrophic respiration[d]	f [T, SW, C]	f [T, SW, C]	f [T, SWP]	F[T, SWP, C]	f[T, WFPS, C]	f [T, SWP]	f [T, SW]		f [T, SWD, C]			f [T, SW]	
Rate dynamics	first order	first order	first order	first order	microbial kinetics	first order	–	??	first order	??	??	exponential	N/A
Temp depth	N/A	0–10 cm	N/A	N/A	N/A	N/A	5 cm	N/A	10 cm	N/A	N/A	N/A	N/A
Ratio of root/ hetero	N/A	N/A	N/A	N/A	N/A	0.5	dynamic	??	predicted	??	??	N/A	N/A
Coarse wood decomposition	Yes	Yes	No	No	No	No	Yes	N/A	N/A	N/A	N/A	No	N/A

[a]BGC++ = f[T, VPD, PAR, CO_2, SWP, minimum night temp]; BIOME-BGC = f[T, VPD, PAR, CO_2, SWP]; LaRS = f[T, VPD, PAR, SWP]; LINKAGES = f[T, VPD, PAR, ext soil water]
[b]*M* leaf mass, *T* temperature, *N* nitrogen, *abs.PAR* absorbed photosynthetically active radiation
[c]*T* temperature, *W* wood or sapwood mass
[d]*T* temperature, *SW* soil water content, *SWP* soil water potential, *WFPS* water-filled pore space, *C* carbon

ecosystem components with consideration of multiple natural and anthropogenic perturbations (e.g., climate change, CO_2 concentration, atmospheric composition, land use and management practices), working at multiple scales in time from daily to yearly and space from meters to kilometers, from region to globe.

The DLEM includes five core components (Fig. 12): (1) biophysics, (2) plant physiology, (3) soil biogeochemistry, (4) dynamic vegetation, and (5) disturbance, land use, and management. Briefly, the biophysics component simulates the instantaneous fluxes of energy, water, and momentum within land ecosystems and their exchanges with the surrounding environment. The plant physiology component simulates major physiological processes, such as plant phenology, C and N assimilation, respiration, allocation, and turnover. The soil biogeochemistry component simulates the dynamics of nutrient compositions and major microbial processes. The biogeochemical processes including the mineralization/immobilization, nitrification/denitrification, decomposition, and methane production/oxidation are considered in this component. The dynamic vegetation component simulates the structural dynamics of vegetation caused by natural and human disturbances. Two processes are considered: the biogeography redistribution when climate change occurs and the recovery and succession of vegetation after disturbances. Like most dynamic global vegetation models, the DLEM builds on the concept of plant functional types (PFT) to describe vegetation distributions. The disturbances, land use, and management component simulates cropland conversion, reforestation after cropland abandonment, and forest management practices such as harvest, thinning, fertilization and prescribed fires. The DLEM has been extensively used to study the terrestrial carbon, water, and nitrogen cycles around the world in response to global change.

Model Applications

Leaf and Stand Models

Effects of climate change on photosynthesis, growth, respiration, and decomposition have been investigated by many studies over the past several decades. Some ecological models specifically simulate the impacts of elevated CO_2 on terrestrial ecosystem carbon processes, while most of the biogeochemical models consider multiple factor impacts and have the capability to simulate the effects of multiple climatic factors on forest ecosystem carbon cycling. Several intermodel comparison studies also compared the features, ecological processes built in the models, and model simulation results among some ecosystem models (Hanson et al. 2004). Due to different model structures and processes implemented, multimodel comparisons typically reveal divergent responses across models. These modeling excises not only quantify model uncertainty but also provide insight to the underlying processes causing the divergent model responses. Below, we summarize some modeling results of climate change impacts on forest ecosystem carbon processes, including elevated CO_2, global warming, precipitation, and nitrogen deposition.

Effects of CO_2 on leaf photosynthesis are very well simulated. Increase in CO_2 concentration generally increases leaf photosynthesis and decrease photorespiration

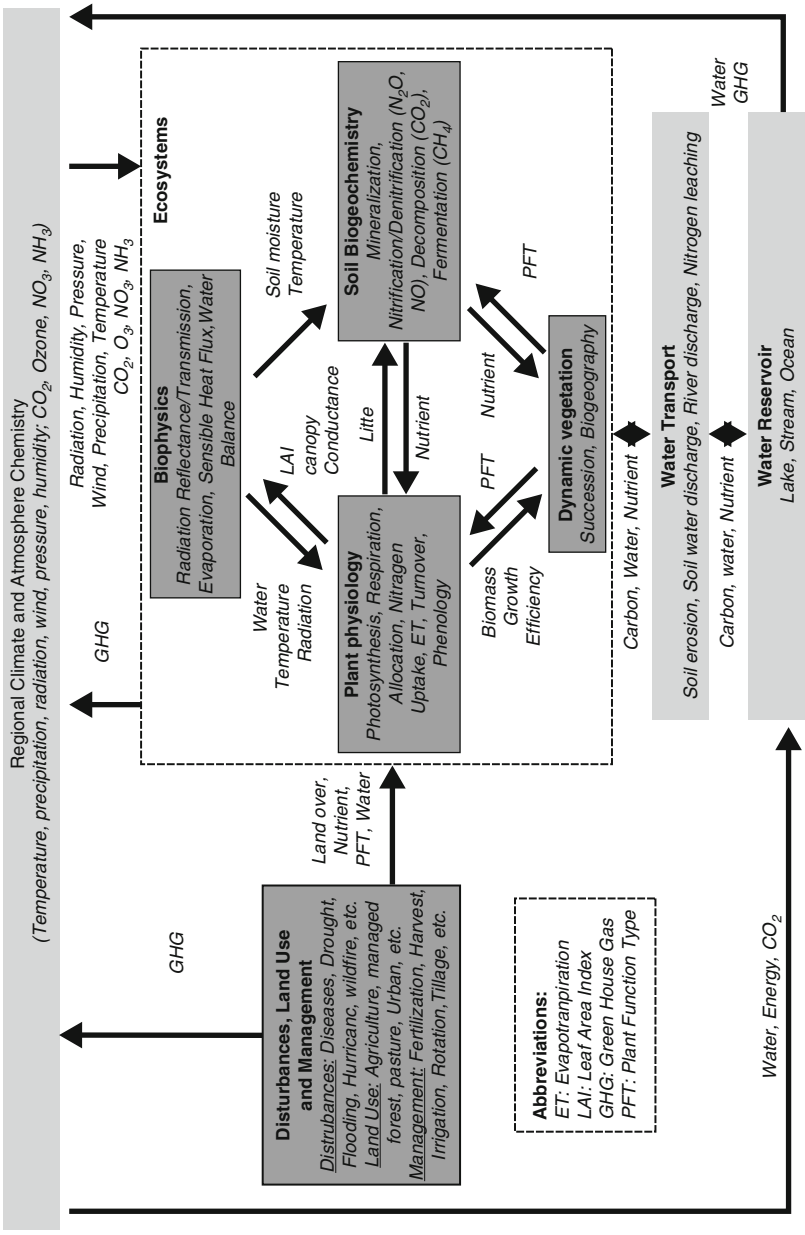

Fig. 12 Framework of the Dynamic Land Ecosystem Model (*DLEM*) (Adapted from Tian et al. (2012) with permission)

(Lloyd and Farquhar 1996), as a result, increases growth of trees and leaf area (Curtis and Wang 1998). Elevated CO_2 also reduces stomatal conductance to water vapor due to partial stomatal closure (Ainsworth and Rogers 2007). Using physiologically based canopy model, MAESTRA, Luo et al. (2001) simulated gross primary productivity of loblolly pine in the Duke Forest and found that elevated CO_2 significantly increased canopy carbon fixation by 35–43 %. At the same forest site, Hui & Luo (Allen et al. 2010) simulated the effects of CO_2 on soil respiration using a process-based model and found that soil respiration was enhanced by 18–26 % by elevated CO_2. In a multiple model evaluation of the response of climate-carbon cycle models to future CO_2 emissions, they applied 11 ecosystem models and found that all models showed an increase in carbon storage with higher atmospheric CO_2, driven by a 12–76 % increase in NPP with CO_2 doubling (Friedlingstein et al. 2006). Bonan (2014) used a process-based model to simulate the biomass production of Norway spruce under both current climate and climate change scenarios. Doubling current ambient CO_2 concentration was projected to increase NPP by 36 %. These modeling studies and many others demonstrated that NPP and GPP will increase under elevated CO_2 conditions but differ in the magnitudes of the enhancement from different stands.

Precipitation is another important factor regulating photosynthesis, respiration, and ecosystem carbon sequestration. For the effects of precipitation, Gerten et al. (2008) used four process-based ecosystem models (TECO, LPJ, ORCHIDEE, and DayCent) to simulate ecosystem carbon and water responses. They found that NPP response to precipitation changes differed not only among different sites/ecosystems but also within a year at a given site. Plants grown at humid sites were least responsive to precipitation change as compared to dry sites. Solomon (1986) simulated the effects of precipitation and temperature on forests across eastern North America using FORENA, an individual-based forest stand model. The model predicted slower growth rates of most deciduous tree species and a universal dieback of the original forest, up to 1000 years from the initial change in climate. Climate-induced drought and heat stress have affected some temperate forests, particularly those in arid regions such as the western United States. Precipitation change has increased tree mortality, suppressed forest productivity, and reduced forest biomass and total carbon stocks (Allen et al. 2010).

Nitrogen availability is often the limiting factor in net primary productivity (Bonan 2014). Nitrogen deposition is one of the major anthropogenic nitrogen inputs to forest ecosystems. Photosynthetic rate is often well correlated with leaf nitrogen content, as photosynthesis is driven by the nitrogen-rich enzyme rubisco. The potential of ecosystems to take up carbon is constrained by the availability of nitrogen (Luo et al. 2004). Without supplemental N additions or decreases in N losses, the availability of mineral N declines with time in ecosystems exposed to elevated atmospheric CO_2 in comparison with N availability at low CO_2 levels (i.e., progressive N limitation) (Luo et al. 2004). Simulation models linking nutrient cycling to plant production and C sequestration consistently predict less terrestrial CO_2 uptake and storage than models that do not incorporate N regulation of carbon-related processes (Wang and Houlton 2009). Zaehle et al. (Lloyd and Farquhar 2008)

used 11 ecosystem models to investigate the effects of N availability on the response of forest productivity to elevated CO_2 at two FACE sites – a deciduous broadleaf forest at Oak Ridge National Laboratory (ORNL) and the evergreen needleleaf (i.e., loblolly pine) Duke Forest. They found that most of the models can reproduce the observed initial enhancement of net primary production (NPP) at both sites, but none can simulate NPP changes in the long term (Fig. 13). Most models showed signs of progressive N limitation.

Warming temperature has proved to have direct physiological effects on photosynthesis and indirect stomatal effects (Meir et al. 2006). Many models included temperature influence on photosynthetic machinery (Doughty 2011). Bonan (2014) simulated the biomass production of Norway spruce in southeastern Norway and reported that NPP was projected to increase by 7 % over the current 1.01×10^4 kg ha^{-1} $year^{-1}$ under a mean annual air temperature elevated by 4 °C over current levels.

Overall, climate change, elevated CO_2, and nitrogen deposition have affected forest productivity and biomass stocks. Nitrogen deposition has a more positive effect on NPP than on other factors, although the positive effect from elevated atmospheric CO_2 is also significant. Climate changes have less obvious effects on average productivity but increased the interannual variability.

Regional and Global Models

At regional and global scales, climate models (general circulation models (GCMs)) have been coupled to terrestrial ecosystem models, dynamic global vegetation models (DGVMs), during the past decade (Smith et al. 1992). Smith et al. (Sitch et al. 2008) compared potential impacts on vegetation distribution of climate change projections from four GCMs. Forest areas increase toward the poles with all scenarios having an increase in the extent of tropical forests into areas that are now occupied by subtropical or warm temperate forests and a shift of the boreal forest zone into area now occupied by tundra. All scenarios suggest an increase in terrestrial carbon storage ranging from 8.5 to 180.5×10^{12} kg.

DGVMs are useful tools for diagnosing the potential responses of forest NPP and biomass to changing climate and atmospheric composition, such as rising CO_2 concentration. Model results have showed that the efficiency of forest carbon uptake under future climate change will decrease, with forests becoming less capable of mitigating the growth in atmospheric CO_2 concentrations (Pan et al. 2014; Friedlingstein et al. 2006). Carbon cycle predictions of different DGVMs are generally consistent with global land carbon budgets but if used to forecast future change, the results diverge considerably. But most models agree that effects of elevated CO_2 counteracts carbon losses caused by climate change, resulting in the forests being a net sink for carbon (Hickler et al. 2008). For example, LPJ model predicted a 35 % increase in NPP for tropical forests under elevated CO_2 at 550 ppm compared to 370 ppm (Galbraith et al. 2010). Galbraith et al. (Fernández-Martínez et al. 2014) tested the importance of precipitation changes relative to other environmental drivers, including CO_2 using three DGVMs (HyLand, LPJ, and TRIFFID) and found that modeled responses to increased temperature are as important, or more

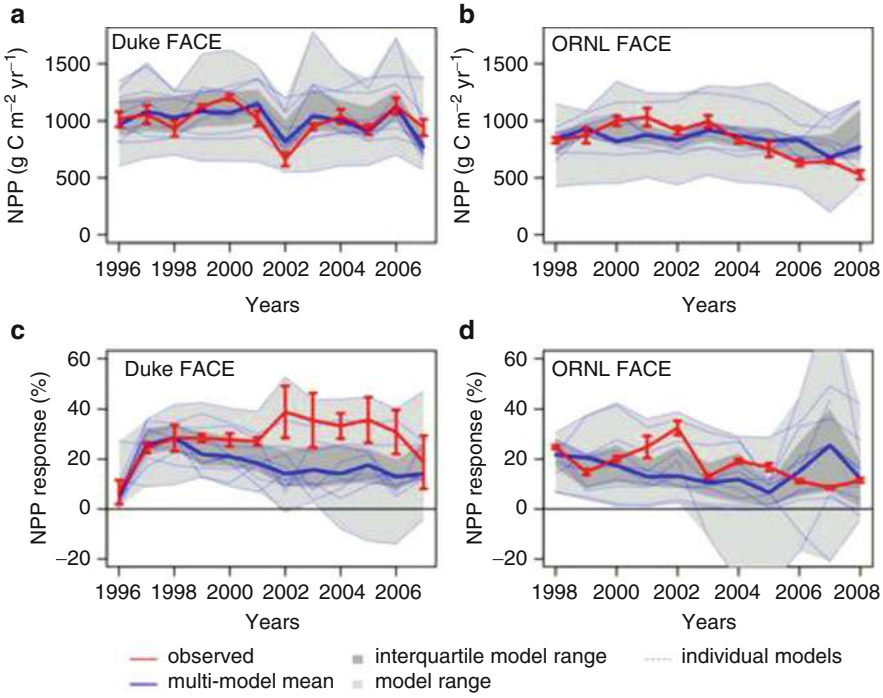

Fig. 13 Ambient net primary production (*NPP*; **a**, **b**) and its response to elevated CO_2 (**c**, **d**) at the Duke (**a**, **c**) and Oak Ridge National Laboratory (*ORNL*) (**b**, **d**) Free-air CO_2 enrichment (*FACE*) experiments. The observations are across-plot averages, and the error bars denote ± 1SE (Adapted from Zaehle et al. (2014), with permission from John Wiley and Sons)

important, than reduced precipitation in causing loss of plant biomass carbon. Model simulated responses of forests to climate change often vary with soil nutrient conditions. Fernández-Martínez et al. (Song et al. 2013) found that forests growing in fertile soils are able to sequester about 30 % of the carbon that they take up during photosynthesis but only 6 % of that carbon if growing in nutrient-poor soils.

Tian et al. (2012) quantified ecosystem NPP in the Southern USA by employing the integrated process-based ecosystem model, DLEM. They found that elevated CO_2 stimulated more carbon uptake in forests than in other land-cover types. Forest NPP was stimulated by 12 % and C storage was stimulated by 6 % from 1895 to 2007. The mean regional total NPP was 1.18×10^{15} g C $year^{-1}$ (525.2 g C m^{-2} $year^{-1}$) during 1895–2007. NPP increased consistently from 1895 to 2007 with a rate of 2.5×10^{12} g C $year^{-1}$ or 1.10 g C m^{-2} $year^{-1}$. Elevated CO2 played an important role in both deciduous broadleaf and evergreen needleleaf forests (Fig. 14). Song et al. (Zaehle et al. 2014) projected terrestrial carbon sequestration of the southeastern USA in the twenty-first century using DLEM model and found that carbon storage will increase from 13.5 kg C m^{-2} in the 2000s to 16.8 kg C m^{-2}

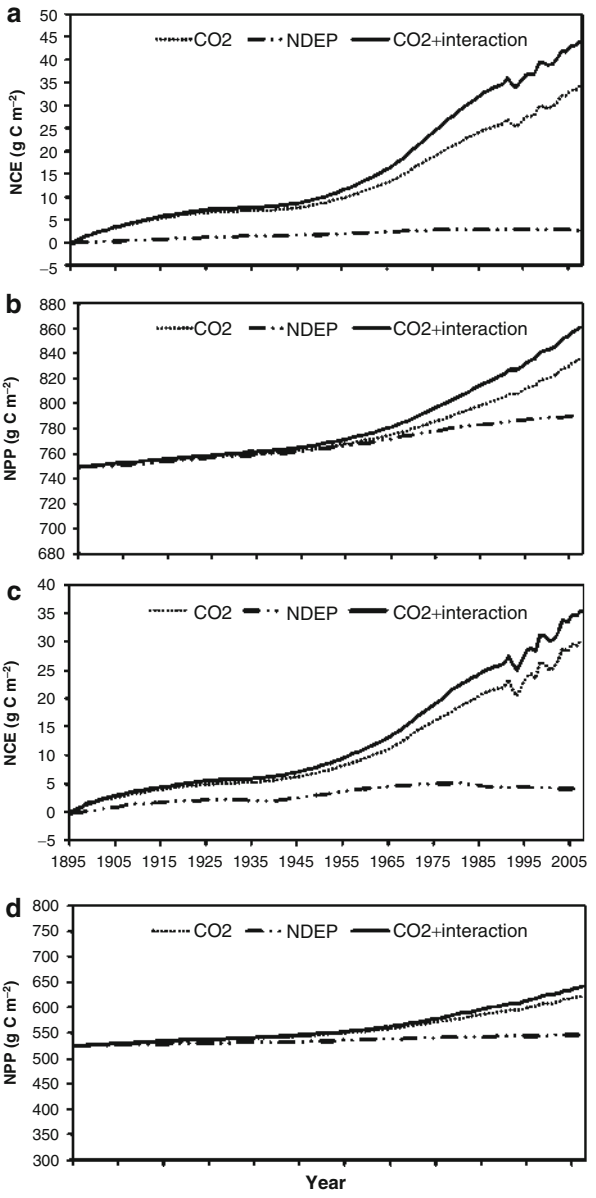

Fig. 14 Interactive effects of CO_2 and N deposition on NCE, NPP for different biomes in the Southeastern USA. (**a**, **b**), deciduous broadleaf forest; (**c**, **d**) evergreen needleleaf forest. CO_2: CO_2 only; NDEP: N deposition only (With kind permission from Springer Science+Business Media: Ecosystems, 15, 2012, Tian et al., Fig. 11. ©2012, Springer Science+Business Media, LLC)

in the 2090s. Both deciduous and evergreen forests show large increases. In the 2000s, the carbon storage in the deciduous forest shows a 42.4 % increase from 14.7 to 20.9 kg C m^{-2} , and the evergreen forests shows a 23.2 % increase from 22.0 to 27.1 kg C m^{-2}. The carbon sequestration is primarily caused by elevated

atmospheric CO_2 and nitrogen deposition. Forests are major contributor to the carbon sink in terrestrial ecosystems.

Conclusion

The forest carbon cycle exerts a large and significant influence over the physical and chemical aspects of the Earth system, but we still have limited understanding of this influence (Smith et al. 1992). Until now, most ecological models to predict forest carbon sequestration at large scales had only considered the effect of nitrogen but did not take into account other constraints such as phosphorus or the pH of the soil, which is related to the availability of nutrients. The frontiers of global terrestrial biosphere modeling, such as phosphorus cycling, microbial models of decomposition, and photosynthetic and respiratory temperature acclimation, should be included in these models (Lloyd and Farquhar 2008). New measurements as well as new modeling studies are needed to assess fully the importance of forest ecosystem–climate interactions for future climatic change. Greater attention must be given to understanding processes, rather than model projections of the future (Lloyd and Farquhar 2008). Better-constrained predictions of future changes in forest ecosystems and climate will also require improved links between data and models, perhaps through the application of formal data assimilation techniques (Meir et al. 2006; Smith et al. 1992).

Closing Remarks and Future Research

Considerable progresses have been made during the past several decades to better understand forest ecosystem responses to climate change using both experimental and modeling approaches. While the manipulative field studies provide useful insight into how forests respond to individual climate change factors, logistical constraints often prevent the examination of some climatic factors, and more importantly, the complex interactions between multiple and changing climatic factors (Norby et al. 2010; Deng et al. 2010; Shaw and Harte 2001; Fisichelli et al. 2012). Due to the facility limitation, the early studies on the elevated CO_2 effects mostly used growth chamber or open-top chamber on tree seedlings. Only after the FACE facility is constructed, the effect of CO_2 on mature trees can be investigated. Due to the cost of construction and fire concerns, warming studies in forests are often limited to soil warming (Rustad 2008; Melillo et al. 2002; Lu et al. 2013). The whole ecosystem warming studies have seldom been done. Temperature and precipitation forcings are also codependent, requiring a complex systems approach to understand the impact on forest ecosystem carbon dynamics and their feedbacks. Increases in productivity under elevated CO_2 can be partially offset by reductions in productivity from warming-induced drought stress (Rustad et al. 2001; Lu et al. 2013), and experimental studies incorporating more climatic factors are needed. Additionally, experimental studies typically conducted at plot or stand scales

and over relatively short time scales leave gaps in our understanding about the long-term effects of climate change at landscape and regional scales. The long-term and multifactor experiments should be conducted. For ecosystem biogeochemical modeling study, data model need to be better integrated. Inverse modeling techniques need to be applied to better parameterize the models. Uncertainty analysis in term of measurement error, model structures, model parameters, and parameter combinations need to be conducted to improve confidence of model estimation and prediction (Tian et al. 2012; Reyer et al. 2013). As more data are accumulating in long-term manipulative experiments, inverse modeling and data assimilation will play a more important role in global change ecology. Besides climate variability, climate disturbances such as drought, cold spell, heat wave, and fire and biological disturbances such as disease, insect outbreak need to be built into biogeochemical models. At large scale and for long-term prediction, dynamic changes of vegetation need to be considered in the models (Tian et al. 2012). Thus, great effort will be required to integrate previous and new data from experimental results and process knowledge into ecosystem models. Further development of data-model assimilation tools, analytical methods, and ecosystem models to improve understanding of climate change effects on forests will be needed in order to actually predict the carbon sequestration in forest ecosystems, inform policy makers, and provide guidelines for conservation and forest management (Zuidema et al. 2013).

Acknowledgments Our work has been supported by grants from the Office of Science (BER), US Department of Energy, grant DE-FG03-99ER62800, National Science Foundation (1504886), National Natural Science Foundation of China (31428001), and the United State Department of Agriculture (USDA) Evans-Allen and CBG projects.

References

Ainsworth EA, Rogers A (2007) The response of photosynthesis and stomatal conductance to rising CO_2: mechanisms and environmental interactions. Plant Cell Environ 30:258–270

Allen CD, Macalady AK, Chenchouni H et al (2010) A global overview of drought and heat-induced tree mortality reveals emerging climate change risks for forests. For Ecol Manag 259:660–684

Bader N, Cheng W (2007) Rhizosphere priming effect of *Populus fremontii* obscures the temperature sensitivity of soil organic carbon respiration. Soil Biol Biochem 39:600–606

Bonan GB (2014) Connecting mathematical ecosystems, real-world ecosystems, and climate science. New Phytol 202:731–733

Borken W, Savage K, Davidson EA et al (2006) Effects of experimental drought on soil respiration and radiocarbon efflux from a temperate forest soil. Glob Chang Biol 12:177–193

Brando PM, Nepstad DC, Davidson EA et al (2008) Drought effects on litterfall, wood production, and belowground carbon cycling in an Amazon forest: results of a throughfall reduction experiment. Philos Trans R Soc B 363:1839–1848

Brown S (2002) Measuring carbon in forests: current status and future challenges. Environ Pollut 116:363–372

Carney KM, Hungate BA, Drake BG et al (2007) Altered soil microbial community at elevated CO_2 leads to loss of soil carbon. Proc Natl Acad Sci U S A 104:4990–4995

Chen XM, Liu JX, Deng Q et al (2012) Effects of elevated CO_2 and nitrogen addition on soil organic carbon fractions in a subtropical forest. Plant Soil 357:25–34
Cheng L, Booker FL, Tu C et al (2012) Arbuscular mycorrhizal fungi increase organic carbon decomposition under elevated CO_2. Science 337:1084–1087
Cleveland CC, Wieder WR, Reed SC et al (2010) Experimental drought in a tropical rain forest increases soil carbon dioxide losses to the atmosphere. Ecology 91:2313–2323
Cunningham SC, Read J (2002) Comparison of temperate and tropical rainforest tree species: photosynthetic responses to growth temperature. Oecologia 133:112–119
Curtis PS, Wang X (1998) A meta-analysis of elevated CO_2 effects on woody plant mass, form and physiology. Oecologia 113:299–313
Dale VH, Rauscher HM (1994) Assessing impacts of climate change on forests: the state of biological modeling. Clim Chang 28:65–90
Davidson EA, Nepstad DC, Ishida FY et al (2008) Effects of an experimental drought and recovery on soil emissions of carbon dioxide, methane, nitrous oxide, and nitric oxide in a moist tropical forest. Glob Chang Biol 14:2582–2590
de Graaff MA, van Groeningen KJ, Six J et al (2006) Interactions between plant growth and nutrient dynamics under elevated CO_2: a meta-analysis. Glob Chang Biol 12:1–15
Deng Q, Zhou GY, Liu JX et al (2010) Responses of soil respiration to elevated carbon dioxide and nitrogen addition in young subtropical forest ecosystems in China. Biogeosciences 7:315–328
Deng Q, Hui D, Zhang D et al (2012) Effects of precipitation increase on soil respiration: a three-year field experiment in subtropical forests in China. PLoS One 7(7):e41493. doi:10.1371/journal.pone.0041493
Deng Q, Cheng XL, Zhou GY et al (2013) Seasonal responses of soil respiration to elevated CO_2 and N addition in young subtropical forest ecosystems in southern China. Ecol Eng 61:65–73
Dixon RK, Solomon AM, Brown S et al (1994) Carbon pools and flux of global forest ecosystems. Science 263:185–191
Doughty CE (2011) An in situ leaf and branch warming experiment in the Amazon. Biotropica 43:658–665
Drake JE, Gallet-Budynek A, Hofmockel KS et al (2011) Increases in the flux of carbon below-ground stimulate nitrogen uptake and sustain the longterm enhancement of forest productivity under elevated CO_2. Ecol Lett 14:349–357
Edwards NT (1991) Root and soil respiration responses to ozone in *Pinus taeda* L, seedlings. New Phytol 118:315–321
Fang JY, Guo ZD, Piao SL et al (2007) Terrestrial vegetation carbon sinks in China, 1981–2000. Sci China Ser D Earth Sci 50(9):1341–1350
FAO (2001) Smallholder irrigation technology: prospects for Sub-Saharan Africa. IPTRID Secretariat food and agriculture organization of the United Nations Paper No. 3 – March 2001, FAO, Rome
Farquhar GD, von Caemmerer S, Berry JA (1980) A biochemical model of photosynthetic CO_2 assimilation in leaves of C3 species. Planta 149:79–90
Fernández-Martínez M, Vicca S, Janssens IA et al (2014) Nutrient availability as the key regulator of global forest carbon balance. Nat Clim Chang 4:471–476
Field CB, Lobell DB, Peters HA et al (2007) Feedbacks of terrestrial ecosystems to climate change. Annu Rev Environ Resour 32:1–29
Finzi AC, DeLucia EH, Hamilton JG et al (2002) The nitrogen budget of a pine forest under free air CO2 enrichment. Oecologia 132:567–578
Fisichelli N, Frelich LE, Reich PB (2012) Sapling growth responses to warmer temperatures "cooled" by browse pressure. Glob Chang Biol 8:3455–3463
Friedlingstein P, Cox P, Betts R et al (2006) Climate–carbon cycle feedback analysis: results from the C4MIP model intercomparison. J Clim 19:3337–3353
Galbraith D, Levy PE, Sitch S et al (2010) Multiple mechanisms of Amazonian forest biomass losses in three dynamic global vegetation models under climate change. New Phytol 187:647–665

Galik CS, Jackson RB (2009) Risks to forest carbon offset projects in a changing climate. For Ecol Manag 257:2209–2216

Gerten D, Luo Y, Le Maire G et al (2008) Modelled effects of precipitation on ecosystem carbon and water dynamics in different climatic zones. Glob Chang Biol 14:2365–2379

Gorte RW (2007) Carbon sequestration in forests. CRS report for congress RL31432. congressional research service

Hanson PJ, Todd DE Jr, Amthor JS (2001) A six-year study of sapling and large-tree growth and mortality responses to natural and induced variability in precipitation and throughfall. Tree Physiol 21(6):345–358

Hanson PJ, Amthor JS, Wullschleger SD et al (2004) Oak forest carbon and water simulations: model intercomparisons and evaluations against independent data. Ecol Monogr 74:443–489

Hickler T, Smith B, Prentice IC et al (2008) CO_2 fertilization in temperate FACE experiments not representative of boreal and tropical forests. Glob Chang Biol 14:1531–1542

Hui D, Luo YQ (2004) Evaluation of soil CO_2 production and transport in Duke forest using a process-based modeling approach. Glob Biogeochem Cycles 18:GB4029. doi:10.1029/2004GB002297

Hui D, Tian H, Luo Y (2012) Impacts of climatic changes on biogeochemical cycling in terrestrial ecosystems. In: Chen W-Y, Seiner J, Suzuki T, Lackner M (eds) Handbook of climate change mitigation. Springer, New York

Hyvönen R, Persson T, Andersson S et al (2008) Impact of long-term nitrogen addition on carbon stocks in trees and soils in northern Europe. Biogeochemistry 89:121–137

IPCC, Stocker TF, Qin D, Plattner G-K, Tignor M, Allen SK, Boschung J, Nauels A, Xia Y, Bex V, Midgley PM (eds) (2013) Climate change 2013: the physical science basis: contribution of working group I to the fifth assessment report of the intergovernmental panel on climate change. Cambridge University Press, Cambridge

Jarvis PG, Linder S (2000) Constraints to growth of boreal forests. Nature 405:904–905

Karjalainen T, Pussinen A, Liski J et al (2003) Scenario analysis of the impacts of forest management and climate change on the European forest sector carbon budget. For Policy Econ 5:141–155

King J, Liu LL, Aspinwall M (2013) Tree and forest responses to interacting elevated atmospheric CO_2 and tropospheric O_3: a synthesis of experimental evidence. Dev Environ Sci 13:179. doi:10.1016/B978-0-08-098349-3.00009-8

Lal R (2005) Forest soils and carbon sequestration. For Ecol Manag 220:242–258

Le Toan T, Quegan S, Davidson MWJ et al (2011) The BIOMASS mission: mapping global forest biomass to better understand the terrestrial carbon cycle. Remote Sens Environ 115:2850–2860

Lindner M, Maroschek M, Netherer S et al (2010) Climate change impacts, adaptive capacity, and vulnerability of European forest ecosystems. For Ecol Manag 259:698–709

Lindquist EJ, D'Annunzio R, Gerrand A et al (2012) Global forest land-use change 1990–2005. FAO forestry paper no. 169. In: Food and agriculture organization of the United Nations and European Commission Joint Research Centre. FAO, Rome

Liu JX, Zhou GY, Zhang DQ et al (2010) Carbon dynamics in subtropical forest soil: effects of atmospheric carbon dioxide enrichment and nitrogen addition. J Soils Sediments 10:730–738

Lloyd J, Farquhar GD (1996) The CO_2 dependence of photosynthesis, plant growth and response to elevated CO_2 concentrations and their interaction with soil nutrient status. I. General principles and forest ecosystems. Funct Ecol 10:4–32

Lloyd J, Farquhar GD (2008) Effects of rising temperatures and [CO_2] on the physiology of tropical forest trees. Philos Trans R Soc B 363:1811–1817

Loya WM, Pregitzer KS, Karberg NJ et al (2003) Reduction of soil carbon formation by tropospheric ozone under increased carbon dioxide levels. Nature 425:705–707

Lu M, Zhou XH, Luo Y et al (2011) Minor stimulation of soil carbon storage by nitrogen addition: a meta-analysis. Agric Ecosyst Environ 140:234–244

Lu M, Zhou XH, Luo Y et al (2013) Responses of ecosystem carbon cycle to experimental warming: a meta-analysis. Ecology 94:726–738

Luo Y, Medlyn B, Hui D et al (2001) Gross primary productivity in Duke forest: modeling synthesis of CO_2 experiment and eddy-flux data. Ecol Appl 11:239–252
Luo Y, Su B, Currie WS et al (2004) Progressive nitrogen limitation of ecosystem responses to rising atmospheric carbon dioxide. Bioscience 54:731–739
Luo Y, Hui D, Zhang D (2006) Elevated carbon dioxide stimulates net accumulations of carbon and nitrogen in terrestrial ecosystems: a meta-analysis. Ecology 87:53–63
Magill A, Aber J, Berntson G et al (2000) Long-term nitrogen additions and nitrogen saturation in two temperate forests. Ecosystems 3:238–253
McGuire AD, Melillo JM, Joyce LA (1992) Interactions between carbon and nitrogen dynamics in estimating net primary productivity for potential vegetation in North America. Glob Biogeochem Cycles 6:101–124
McNulty SG, Aber JD, Newman SD (1996) Nitrogen saturation in a high elevation New England spruce-fir stand. For Ecol Manag 84:109–121
Meier IC, Leuschner C (2010) Variation of soil and biomass carbon pools in beech forests across a precipitation gradient. Glob Chang Biol 16:1035–1045
Meir P, Cox P, Grace J (2006) The influence of terrestrial ecosystems on climate. Trends Ecol Evol 21:254–260
Melillo JM, Steudler PA, Aber JD et al (2002) Soil warming and carbon-cycle feedbacks to the climate system. Science 298:2173–2176
Melillo JM, Butler S, Johnson J et al (2011) Soil warming, carbon, nitrogen interactions, and forest carbon budgets. Proc Natl Acad Sci U S A 108:9508–9512
Morice C, Kennedy J, Rayner N et al (2012) Quantifying uncertainties in global and regional temperature change using an ensemble of observational estimates: the hadcrut4 data set. J Geophys Res 117:D08101. doi:10.1029/2011JD017187
Nabuurs GJ, Hengeveld GM, Werf DC et al (2010) European forest carbon balance assessed with inventory based methods – an introduction to a special section. For Ecol Manag 260:239–240
Nadelhoffer KJ (2000) The potential effects of nitrogen deposition on fine-root production in forest ecosystems. New Phytol 147:131–139
Nadelhoffer KJ, Emmett BA, Gundersen P et al (1999) Nitrogen deposition makes a minor contribution to carbon sequestration in temperate forests. Nature 398:145–148
Nave LE, Vance ED, Swanston CW et al (2009) Impacts of elevated N inputs on north temperate forest soil C storage, C/N, and net N-mineralization. Geoderma 153:231–240
Norby RJ, Luo Y (2004) Evaluating ecosystem responses to rising atmospheric CO_2 and global warming in a multi-factor world. New Phytol 162:281–294
Norby RJ, DeLucia EH, Gielen B et al (2005) Forest response to elevated CO_2 is conserved across a broad range of productivity. Proc Natl Acad Sci U S A 102:18052–18056. doi:10.1073/pnas.0509478102
Norby RJ, Warren JM, Iversen CM et al (2010) CO_2 enhancement of forest productivity constrained by limited nitrogen availability. Proc Natl Acad Sci U S A 107:19368–19373
Nowak DJ, Crane DE (2002) Carbon storage and sequestration by urban trees in the USA. Environ Pollut 116:381–389
Pan YD, Birdsey RA, Fang JY et al (2011) A large and persistent carbon sink in the world's forests. Science 333:988–993
Pan YD, Birdsey RA, Phillips OL et al (2013) The structure, distribution, and biomass of the world's forests. Annu Rev Ecol Evol Syst 44:593–622
Pan S, Tian H, Dangal SRS (2014) Modeling and monitoring terrestrial primary production in a changing global environment: toward a multiscale synthesis of observation and simulation. Adv Meteorol. 17. doi:10.1155/2014/965936
Peñuelas J, Sardans J, Estiarte M et al (2013) Evidence of current impact of climate change on life: a walk from genes to the biosphere. Glob Chang Biol 19:2303–2338
Peterjohn WT, Melillo JM, Steudler PA (1994) Responses of trace gas fluxes and N availability to experimentally elevated soil temperature. Ecol Appl 4:617–625

Peters EB, Wythers KR, Zhang SX et al (2013) Potential climate change impacts on temperate forest ecosystem processes. Can J For Res 43:939–950

Potter CS, Randerson JT, Field CB et al (1993) Terrestrial ecosystem production: a process model based on global satellite and surface data. Glob Biogeochem Cycles 7:811–841

Reyer CPO, Leuzinger S, Rammig A et al (2013) A plant's perspective of extremes: terrestrial plant responses to changing climatic variability. Glob Chang Biol 19:75–89

Rustad LE (2008) The response of terrestrial ecosystems to global climate change: towards an integrated approach. Sci Total Environ 404:222–235

Rustad LE, Campbell JL, Marion GM et al (2001) A meta-analysis of the response of soil respiration, net nitrogen mineralization, and aboveground plant growth to experimental ecosystem warming. Oecologia 126:543–562

Scagel CF, Andersen CP (1997) Seasonal changes in root and soil respiration of ozone-exposed ponderosa pine (*Pinus ponderosa*) grown in different substrates. New Phytol 136:627–643

Shaw MR, Harte J (2001) Response of nitrogen cycling to simulated climate change: differential responses along a subalpine ecotone. Glob Chang Biol 7:193–210

Sitch S, Huntingford C, Gedney N et al (2008) Evaluation of the terrestrial carbon cycle, future plant geography and climate-carbon cycle feedbacks using five dynamic global vegetation models (DGVMs). Glob Chang Biol 14:2015–2039

Smith TM, Leemans R, Shugart HH (1992) Sensitivity of terrestrial carbon storage to CO_2-induced climate change: comparison of four scenarios based on general circulation models. Clim Chang 21:367–384

Solomon AM (1986) Transient response of forests to CO_2-induced climate change: simulation modeling experiments in eastern North America. Oecologia 68:567–579

Song X, Tian H, Xu X et al (2013) Projecting terrestrial carbon sequestration of the southeastern United States in the 21st century. Ecosphere 4, art88. doi:10.1890/ES12-00398.1

Sotta ED, Veldkamp E, Schwendenmann L et al (2007) Effects of an induced drought on soil carbon dioxide (CO_2) efflux and soil CO_2 production in an Eastern Amazonian rainforest, Brazil. Glob Chang Biol 13:2218–2229

Talhelm AF, Pregitzer KS, Zak DR (2009) Species-specific responses to atmospheric carbon dioxide and tropospheric ozone mediate changes in soil carbon. Ecol Lett 12:1219–1228

Tian HQ, Chen G, Zhang C et al (2012) Century-scale response of ecosystem carbon storage and flux to multifactorial global change in the Southern United States. Ecosystems 15:674–694

Wang YP, Houlton BZ (2009) Nitrogen constraints on terrestrial carbon uptake: implications for the global carbon-climate feedback. Geophys Res Lett 36:L24403. doi:10.1029/2009GL041009

Wittig VE, Ainsworth EA, Naidu SL et al (2009) Quantifying the impact of current and future tropospheric ozone on tree biomass, growth, physiology and biochemistry: a quantitative meta-analysis. Glob Chang Biol 10:396–424

Yu D, Wang X, Yin Y et al (2014) Estimates of forest biomass carbon storage in Liaoning province of northeast China: a review and assessment. PLoS ONE 9(2):e89572. doi:10.1371/journal.pone.0089572

Zaehle S, Medlyn BE, De Kauwe MG et al (2014) Evaluation of 11 terrestrial carbon–nitrogen cycle models against observations from two temperate free-air CO_2 enrichment studies. New Phytol 202:803–822

Zak DR, Pregitzer KS, Kubiske ME et al (2011) Forest productivity under elevated CO_2 and O_3: positive feedbacks to soil N cycling sustain decade-long net primary productivity enhancement by CO_2. Ecol Lett 14:1220–1226

Zhou L, Zhou X, Zhang B et al (2014) Different responses of soil respiration and its components to nitrogen addition among biomes: a meta-analysis. Glob Chang Biol 20:2332–2343

Zuidema PA, Baker PJ, Groenendijk P et al (2013) Tropical forests and global change: filling knowledge gaps. Trends Plant Sci 18:413–419

Impact of Climate Change on Biodiversity

David H. Reed

Contents

Abstract

Biodiversity, the diversity of living things on Earth, is a critical measure of the Earth's health. Biodiversity provides immense direct benefits to humans, with at least 40 % of the world's economy being derived from biological resources. Maintaining biodiversity provides greater food security, opportunities for economic development, and provides a foundation for new pharmaceuticals and other medical advances. Ironically, maintaining biodiversity levels and functioning ecosystems is critical to ameliorating climate change; yet, climate change is expected to cause serious disruptions to Earth's ecological systems, resulting in an overall loss of biodiversity and a reduction in the goods and services provided

David H. Reed: deceased.

D.H. Reed (✉)
Department of Biology, University of Louisville, Louisville, KY, USA

W.-Y. Chen et al. (eds.), *Handbook of Climate Change Mitigation and Adaptation*,
DOI 10.1007/978-3-319-14409-2_15

to humans. Extinction rates in the future are very difficult to predict. However, with immediate and decisive action to mitigate climate change, losses of biodiversity can be minimized and humans can continue to reap many of the benefits nature provides; business as usual scenarios will likely lead to the loss of >50 % of all plant and animal species on Earth and the collapse of many ecosystems worldwide. Such losses will drastically lower the quality of life for humans and will take millions of years to reverse.

Introduction

Biodiversity refers to the sum variation of all living organisms (animal, plant, fungal, and microbial) on Earth, including their genetic diversity, species diversity, and the diversity in the ecosystems (e.g., rainforests, coral reefs, estuaries) they help build and regulate. There is a hierarchical structure to biodiversity. Genetic diversity is the most fundamental level of diversity and the one on which all other levels of biodiversity depend, and all levels of biodiversity contribute to the amount and diverse types of ecosystem services provided and the utilitarian and aesthetic value of biodiversity (Reed 2010).

Biodiversity contributes to human welfare in innumerable ways. Examples of ecosystem services include the regulation of climate from a local to global level, purification of the fresh water supplies necessary for human survival, the storage and recycling of the nutrients on which all life depends, and the formation of soil necessary for agriculture. Biodiversity also provides resources such as foods, medicines, and wood products. At least 40 % of the world's economy, and 80 % of the economy of less-industrialized nations, is derived directly from biological resources (1992). Biodiversity enriches the lives of humans in very tangible and utilitarian ways, but also provides us with emotional gratification and inspiration.

Given the importance of biodiversity to human well-being and the irreversibility of its loss, the depletion of biodiversity is one of the most important environmental threats that humanity faces (Millennium Ecosystem Assessment (MEA) 2005). The golden toad (*Bufo periglenes*) is thought to be the first species to go extinct due primarily to global warming (Pounds and Crump 1994), and climate change has already been implicated in numerous population extinctions and at least one other species extinction (Pounds et al. 2006). However, this is just the tip of the iceberg. Examination of past extinction events and current warming predictions suggests that global climate change alone could drive more than half of the known species on Earth to extinction (Fig. 1).

This chapter will cover some of the many reasons why biodiversity is vital to human life and well-being, briefly describe global warming scenarios, present the results of data and models suggesting how many species are likely to go extinct in the near future if steps are not taken to sharply decrease greenhouse gases, and conclude with suggestions for what needs to be done to ameliorate global climate change in a way that is compatible with minimizing biodiversity loss and maintaining the critical ecosystem functions that nature provides.

Fig. 1 The golden toad vanished from Costa Rica's Pacific coastal-mountain cloud forest in the late 1980s. Several researchers have linked outbreaks of the chytrid fungus that drove the golden toad to extinction, and threatens dozens of other species of frogs and toads in the same region, to climate change (Pounds et al. 2006)

Importance of Biodiversity: Ecosystem Services

Biodiversity and healthy ecosystems are vital to life and to human well-being. Biodiversity underlies everything from food production to medical advances. Humans, the world over, use at least 40,000 species of plants and animals on a daily basis (Primack 2002). Many people still depend on wild species for some or all of their food, shelter, and clothing. All of our domesticated plants and animals, including our closest companion the dog, came from wild-living ancestral species.

Ecosystem services are the services provided for humans by natural ecosystems (Daily 1997). These ecosystem services can be divided into four major categories: supporting, regulating, provisioning, and cultural (Millennium Ecosystem Assessment (MEA) 2005). As an example, mature forests help regulate local and regional climates by contributing to rainfall and temperature in the areas they occupy. They do this in part by extracting carbon dioxide from the air and producing oxygen as a byproduct of photosynthesis. The health of ecosystems depends on having viable populations of the species that make up those ecosystems (Reed et al. 2003a) and maintaining viable populations of plants and animals will require immediate and strong actions to limit global climate change and a commitment to biodiversity friendly land use changes and conservation efforts.

Supporting Ecosystem Services

These are the biogeochemical and biological processes underlying all other ecosystem processes, such as nutrient cycling, oxygen production, pollination, seed dispersal, primary productivity, and soil formation. Three of these are elaborated on in more detail below.

Net primary productivity (NPP) is the amount of organic material generated through the process of photosynthesis. This underlies the capacity of all ecosystems to provide ecosystem services, as well as provisioning and regulating much of what humans use. Humans currently consume or forego about 35 % of global terrestrial NPP (see Fig. 2 for one example) (Vitousek et al. 1986; Rojstaczer et al. 2001; Imhoff et al. 2004; Helmut et al. 2007). Forego means that our altering of the natural environment diminishes the potential NPP of the planet, for example, by covering potentially productive land with asphalt and concrete, overgrazing and overfarming many formerly productive areas of the Earth's surface until they become desert, and polluting many rivers and lakes. Thus, because we have already exceeded the carrying capacity of the planet the foundational productivity of the planet is slowly being eroded.

Nitrogen is the single largest component of the Earth's atmosphere. However, atmospheric nitrogen is unavailable for biological use, leading to a scarcity of usable nitrogen in many types of ecosystems. The nitrogen cycle is crucial for life on Earth and affects the rate of key ecosystem processes, including primary production and decomposition. Alteration of the nitrogen cycle by human activities is global and pervasive (Galloway and Cowling 2002; Gruber and Galloway 2008; Duce et al. 2008; Galloway et al. 2008). Human activities now convert more N_2 from the atmosphere into reactive forms than all of the Earth's terrestrial processes combined, mostly via the creation and use of fertilizers to enhance food production. Agricultural runoff and the burning of fossil fuels have boosted the supply of reactive nitrogen in the open oceans 50 % above preindustrial levels. This excess nitrogen causes great harm to marine and freshwater ecosystems, contributes to global warming, and harms human health (Galloway and Cowling 2002; Gruber and Galloway 2008; Duce et al. 2008; Galloway et al. 2008).

Pollination and seed dispersal of both domestic and wild plants is another essential ecosystem service provided free of charge by many diverse animal species. Approximately 80 % of wild plants, and about 35 % of the agricultural crop species that feed the world, require animal pollination for successful reproduction (Fig. 3) (Klein et al. 2007; Ricketts et al. 2008). Similarly, without animal species acting as seed dispersers, many plants would fail to reproduce successfully. Animal seed dispersers, such as bears, birds, elephants, and monkeys play a central role in the structure and regeneration of forests (Lanner 1996; Nathan and Muller-Landau 2000; Seidler and Plotkin 2007). Disruption of these complex services may leave large areas of forest devoid of seedlings and younger age classes of trees, and are thus unable to recover swiftly from human impacts such as land clearing. The great importance of forests will be expounded upon at several points in the chapter (Fig. 4).

In the USA alone, the agricultural value of wild pollinators is estimated in billions of dollars per year. Meanwhile, the diversity of natural pollinators available to both wild and domesticated plants is diminishing and negative effects on plants clearly visible (Buchmann and Nabhan 1996; Rodríguez-Cabal et al. 2007; Anderson et al. 2011). As an example of the value of pollinators, experiments preserving tropical forest fragments around coffee farms boosted crop yields roughly by 7 %, as coffee plants near forested areas received twice as many visits from bees and produced 20 % more coffee beans (Ricketts et al. 2004a, b).

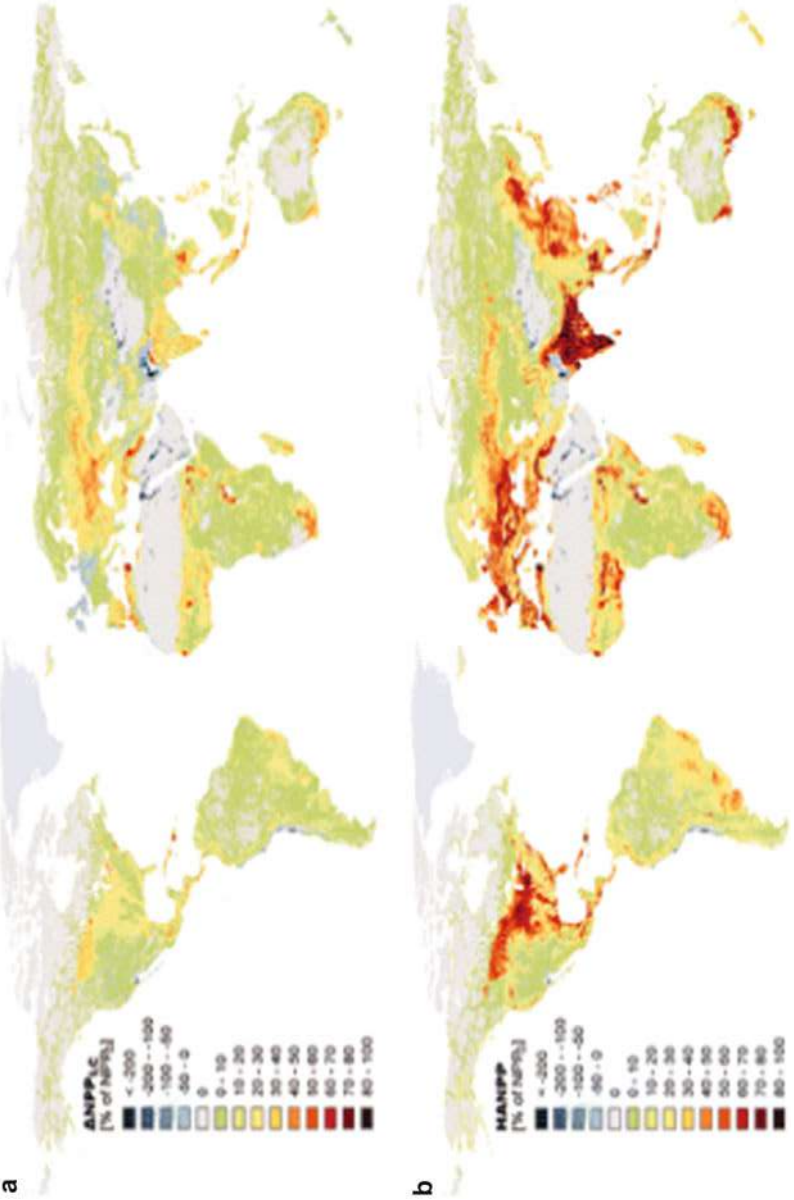

Fig. 2 Maps of the human appropriation of net primary production (*NPP*), excluding human-induced fires. (**a**) Land-use-induced reductions in NPP as a percentage of NPP_0. (**b**) Total NPP as a percentage of NPP_0. *Blue* (negative values) indicates increases of NPP_{act} (**a**) or NPP_t (**b**) over NPP_0, *green* and *yellow* indicate low HANPP, and *red* to *dark* colors indicate medium to high HANPP (Reprinted from Fig. 1 of Helmut et al. (2007))

Fig. 3 Iridescent green sweat bee (*Agapostemon* sp.) covered in pollen. Bees are the best known pollinators. Pollination by bees and other animals increases the quality and/or yield of harvests for 70 % of leading global crops (Jackson and Overpeck 2000) (Photo courtesy of Jon Sullivan, pdphoto.org)

Fig. 4 Old-growth forests, such as the tropical rainforest around San Rafael Falls in Yasuni National Park (Ecuador) pictured below, provide a vast array of ecosystem services such as carbon storage and mitigation of climate change, micro- and macro-climate control, oxygen production, water purification, regeneration of nutrients, and maintenance of soils. They also provide food, fibers, timber, and other renewable resources for humans. Old-growth forests also contain a vast array of plants, animals, fungi species, along with their almost infinite variety of genes, which provide huge benefits to humans. The forests are also spectacularly beautiful

Regulating Ecosystem Services

Examples of regulating ecosystem services include climate regulation, flood regulation, nutrient retention, pest control, protection from soil erosion, and purification of both air and water. A few of these examples are elaborated on in greater detail below.

Plants, trees in particular, have a major influence on local, regional, and even global climate. Approximately half of the annual rainfall in the Amazon basin is recycled by the forest itself. Extensive deforestation can dramatically reduce rainfall in a region, raise temperatures (via loss of shade and reduced evapotranspiration), increase fire frequency, and negatively affect agriculture and access to clean potable water (Webb et al. 2005; Werth and Avissar 2004; Lavelle et al. 2006; Foley et al. 2007). According to the Intergovernmental Panel on Climate Change, and others, deforestation probably accounts for more than 20 % of total anthropogenic carbon dioxide emissions (IPCC 2007a). Living trees extract carbon dioxide and other pollutants from the air, slowing the buildup of carbon dioxide in the atmosphere, while the burning of forests to clear land for agriculture releases large amounts of CO_2 into the atmosphere, which contributes to global warming (Korner 2000; Fearnside and Laurance 2004).

The conversion of wetlands increases flooding rates, and deforestation of uplands and flood plains also increases the frequency and severity of flooding events, at least in some areas (Hey and Philippi 1995; Bradshaw et al. 2007; Ward et al. 2008; Chang et al. 2009). Wetlands store and slowly release surface water, rain, snowmelt, groundwater, and flood waters. Trees and other vegetation impede the movement of flood waters and distribute them more slowly over floodplains. This combined water storage and slowing action lowers flood heights and reduces soil erosion downstream and on adjacent lands. Preserving and restoring wetlands typically provides flood protection at a lower cost than dredging operations and levees and also serves as excellent wildlife habitat and carbon sinks. Flooding in Asia, Europe, and North America over the past several decades has claimed thousands of lives, destroyed hundreds of thousands of homes, and damaged more than 13 million hectares of farmland (Fig. 5). Increased flooding rates along the Mississippi River are due to drainage of floodplain wetlands, the construction of levees, and the loss of beaver dams (Fearnside and Laurance 2004). Though there are a number of factors impacting flooding severity and economic losses, it is worth noting that Missouri, Illinois, and Iowa suffered the most damage from the 1993 floods and all three have less than 15 % of their original wetlands left (Ward et al. 2008). Europe has seen a number of devastating floods over the past 15 years. For the River Meuse, an analysis suggests that landscape changes brought on by humans, especially deforestation and draining of wetlands are the primary causative agents for the increase in flooding, along with increased variability in rainfall (Chang et al. 2009). Recent catastrophic flooding in Korea has been determined to be due to increased frequency of severe rainfall events with deforestation also contributing (US Geological Survey 1999). Note that the increases in severe rainfall events is a prediction of climate change models and their implication in recent flooding events is foreshadowing even more severe events in the future.

Fig. 5 Flooding in Thailand (2010) killed 232 people (*top photo*), flooding in Brazil (2011) killed 702 people (*center photo*), and flooding of the Mississippi River in the U.S. (2011) has killed at least 400 people (*bottom photo* is from Mississippi River flooding of 1993). Draining of wetlands, deforestation, and deleterious changes in rainfall patterns due to climate change will make floods like these more common in the future (*Center photo* courtesy of Agência Brasil, permission does not imply that Agência Brasil endorses this use of their photo)

In addition to inland flooding from rivers, coastal areas are also prone to flooding. Mangrove forests and coral reefs buffer the coast against ocean storm surges and prevent coastal erosion. The building of levees, along with the destruction of freshwater wetlands, contributed to the massive flooding of New Orleans following Hurricane Katrina (Stokstad 2005). Evidence suggests that mangrove forests are more effective than concrete sea walls in controlling floodwaters from tropical storms (Raven and McNeely 1998) and that areas with intact mangrove forests and/or coral reefs were less damaged during the Southeast Asian Tsunami of 2004 than areas without them (Marris 2005; Kunkel et al. 2006; Wells and Kapos 2006). However, both salt marshes and mangrove forests are rapidly being destroyed and coral reefs may be functionally extinct by 2050 due to climate change (Carpenter et al. 2008; Veron et al. 2009). Besides buffering from storms, coral reefs and mangrove forests harbor vast amounts of biodiversity and are among the most productive breeding grounds for commercially important fish.

Studies have confirmed intense periods of soil erosion associated with the rise and subsequent decline of civilizations in the Middle East, Greece, Rome, Central and South America, as well as other regions around the world (Judson 1968; Pope and van Andel 1984; Beach 1998; Van Andel et al. 1990; Beach et al. 2006). The high

rates of soil erosion are due both to deforestation and agriculture (Ponting 1993; Williams 2003; Montgomery 2007). When vegetation is removed, the rates of soil erosion increase rapidly. Clear cutting slopes lead to landslides that have killed tens of thousands of people across the world over the past few decades. Soil runoff into rivers and oceans kills freshwater and marine animals. Erosion and flooding can make the water supplies along rivers undrinkable. The UN Food and Agricultural Organization estimated that from 1990 to 1999, erosion damaged or destroyed more than 600,000 km (1992) of the world's cropland. In China, erosion has forced the abandonment of one third of all formerly arable land. China's Loess Plateau was cleared of trees about 1,000 years ago, since then it has been eroding, causing 40 % declines in agricultural output and flooding and landslides in the lower reaches of the river that killed thousands in 2010. Data from studies worldwide strongly suggest that erosion rates from conventionally plowed agricultural fields are 10–100 times greater than rates of soil production (Montgomery 2007).

Provisioning Ecosystem Services

Provisioning ecosystem services consist primarily of food, pharmaceuticals, and wood, but also include a number of other services such as use in biofuels, bioremediation of pollution, natural insecticides, and providing materials for building shelters and producing clothing. The focus of this section will be on food security and pharmaceuticals.

It is obvious that humans rely on plants and other animals for food. For example, the world's aquatic ecosystems are the leading source of animal protein for human consumption (Kareiva and Marvier 2011). Three species of plant, wheat, corn, and rice provide about 60 % of the calories humans consume. However, few realize the importance of biodiversity (both at the genetic and species level) for food security.

The dangers of relying on genetically depauperate crops are illustrated by the Great Irish Potato Famine. Potatoes were introduced into Ireland from the New World and eventually most of the Irish people became dependent on this one crop. In 1845, the windborne Potato blight (*Phytophthora infestans*) spread throughout the country and caused almost complete failure of the potato crop over the next 3 years. It is estimated that at least one million people died of starvation and another million emigrated out of the country, reducing the population by 20–25 %. The severity of the famine was greatly exacerbated by the lack of genetic variation in the potatoes, which made them particularly vulnerable to disease. More than a century later a wild relative of the potato would be discovered in Peru, that when hybridized with the standard crop plant, produces a variety of potato resistant to potato blight. Another wild potato species, *Solanum fendleri*, is used in breeding for resistance to a nematode species that attacks cultivated potatoes. A potato species from Mexico, *Solanum bulbocastanum*, has been used to genetically engineer the potato to resist new strains of the potato blight (Song et al. 2003).

Despite evolutionary theory and history, much agriculture continues to depend on genetically uniform crops. For example, in most less-industrialized nations, more

than half of the rice varieties come from a single mother plant. In the past century, about 75 % of the genetic diversity of our most important domestic crops has been lost (Fowler and Mooney 1990). The widespread planting of a single corn variety contributed to the loss of over a billion dollars worth of corn in 1970, when the US crop was overwhelmed by a fungus (*Bipolaris maydis*). In 1991, the genetic similarity of Brazil's orange trees made them easy targets for the worst outbreak of a citrus disease in the country's history.

And wild relatives of our domestic crops continue to come to the rescue of current food production. Agriculture and genetic resources are critically interdependent and agricultural production relies on continuing infusions of genetic resources from wild relatives for maintaining or increasing yield. A wild barley plant from Ethiopia (*Hordeum bulbosum*) provided a novel gene conferring complete resistance to the yellow dwarf virus that causes huge losses in barley, oats, wheat, maize, and rice worldwide. In the 1970s, an outbreak of grassy stunt virus decimated rice harvests across Asia. Scientists from the International Rice Research Institute screened 6,273 samples of rice plants looking for genetic resistance to the disease. They found it in a wild relative, *Oryza nivara*, which grows in India. The gene has been incorporated into most new rice varieties since the discovery. In fact, rice is protected from most major rice diseases and much more by genes brought in from at least a dozen wild species (Table 1). The list of examples of wild species improving domesticated crops is very long, wild species genes contribute more than US$100 billion per year to profits from agriculture.

Historically, agricultural varieties of cereals have had a life expectancy of only 5–10 years before diseases or insect pests evolve to take advantage of them and the crop must be replaced with a different genetic variety because the old one is no longer productive. With global climate change, increasing water shortages, increasing pollution, decreasing amounts of arable land, and increasing dispersal of insect pests and diseases, we need these wild species now more than ever. Unfortunately many of them have likely already gone extinct and thousands more face imminent extinction. In fact, not only have we tapped only a small amount of the genetic diversity within species already cultivated, we also only use a very small proportion of the edible species. About 30,000 species of plants are thought to be edible, but only about 150 are used as human food (Wilson 1992). Of those species, only 15 species make up more than 90 % of the food we eat. Genetic diversity is most important when environments are changing rapidly (Reed 2008) and the environment may never have changed more rapidly during the history of life on Earth than it is changing right now.

The pharmaceutical industry is very dependent on natural products (Fig. 6). About a quarter of all prescription drugs in the USA (and up to 80 % of pharmaceuticals in developing nations) are taken directly from plants and 73 % of them are modeled on natural compounds (Farnsworth et al. 1988; Grifo et al. 1997; Newman et al. 2003). These include artemisinin (antimalarial and a potential treatment for cancer), aspirin, atropine, codeine, cyclosporine (the immunosuppressive which transformed the field of human organ transplantation), digitalis, morphine, penicillin, pilocarpine (used to treat glaucoma), quinine (model for modern antimalarial drugs),

Table 1 Introgression of genes from wild *Oryza* species into cultivated rice (*Oryza sativa*)

Trait improved	Wild (donor) species
Grassy stunt resistance	*O. nivara*
Bacterial blight resistance	*O. longistaminata*
	O. officinalis
	O. minuta
	O. latifolia
	O. australiensis
	O. brachyantha
Blast resistance	*O. minuta*
Brown planthopper resistance	*O. officinalis*
	O. minuta
	O. latifolia
	O. australiensis
Whitebacked planthopper resistance	*O. officinalis*
Cytoplasmic male sterility	*O. sativa* f. *spontanea*
	O. perennis
	O. glumaepatula
Tungro tolerance	*O. rufipogon*
	O. rufipogon

Modified from Khush and Brar (2002)

Fig. 6 Poison Dart Frogs, such as *Dendrobates tinctorius* and *D. azureus* shown above, may hold the key to improved pain-relief drugs and other medications. However, their habitat is rapidly disappearing

and warfarin. Most of these come from tropical forests, but less than 1 % of rainforest plants have been tested for medicinal uses and at current rates of deforestation almost all rainforest will be gone within 40 years (Wilson 2002).

Several examples of potential cures, for diseases that kill hundreds of thousands of people, being lost or nearly lost due to the extinction of the plant or animal

supplying it are available. In 1987, leaves were collected from *Callophylum lanigerum* in Malaysian Borneo. Years later, the National Cancer Institute determined that extract from the leaves completely stopped the replication of HIV-I (Wilson 1992). A return trip was made to find the original tree, but the area had been clear cut and leaf samples from other *C. lanigerum* in the region failed to yield any of the original compound (calanolide). Luckily, a related species (*C. teysmannii*) also produced a slightly less potent anti-HIV drug called calanolide B. Calanolide B is currently in preclinical trials in the United States and seems to have low potential for cross-resistance with other therapies (Newman et al. 2008; Currens et al. 1996).

The gastric-brooding frogs consisted of only two species (*Rheobatrachus vitellinus* and *R. silus*), both native to Australia. The genus was unique because it contained the only known frog species that incubated tadpoles inside the stomach of the mother. Preliminary studies with gastric-brooding tadpoles demonstrated that the tadpoles secreted a substance, or substances, that both inhibits the secretion of stomach acids and prevents stomach emptying so that the tadpoles do not end up being digested by the mother. In the 1980s, both species became extinct, terminating studies which might have led to important new insights for treating human peptic ulcers (Newman et al. 2008).

The Pacific Yew tree (*Taxus brevifolia*) is a rare and slow-growing tree found only in old-growth forests of the Pacific Northwest, an area that is currently being logged under generous concessions to logging companies at US tax-payer's expense. The tree also used to be the only source of a drug called paclitaxel, which appears to be very effective in treating ovarian cancer and has great promise for treating lung, prostrate, and breast cancer as well. Clinical trials were delayed for this drug as it takes six Pacific yew trees to extract enough paclitaxel to treat one patient and there were not that many trees. Fortunately, paclitaxel is now being produced by semi-synthetic conversion of precursor compounds found in a variety of yew trees (Newman et al. 2008).

Gastric-brooding frogs are not the only amphibians that produce(d) compounds of potential medical benefit to humans. The skin secretions of the phantasmal poison frog (*Epipedobates tricolor*), listed by the IUCN as endangered, yield a nonaddictive painkiller (epibatidine) that is 200 times stronger than opium and does not lead to tolerance (Newman et al. 2008). Because of the very small difference between a therapeutic dose and a lethal dose, epibatidine has never been used in humans. However, research is under way to invent derivatives of epibatidine that are less toxic, but still have the desired qualities of being an extremely powerful and nonaddictive analgesic (Donnelly-Roberts et al. 1998; Drisdel et al. 2008; Sun et al. 2008). Epibatidine and other derivatives from the poisonous secretions of the frog are also being investigated for a number of other medical uses. In fact, 50 species within the family Dendrobatidae, many of which are critically endangered, have yielded 500 structurally complex compounds new to science and of medical interest (Newman et al. 2008; Daly et al. 2002). One drug investigated in clinical trials and a subject of much further research (Daly et al. 2002; Decker et al. 2001; Baraznenok et al. 2005; Zhang et al. 2006; Bunnelle et al. 2007; Arneric et al. 2007), tebanycline, was almost lost when one of the two sites of Ecuadorian forest from which the frog

was originally collected were cleared for a banana plantation (Plotkin 2000). Amphibians as a whole are more endangered than any other group of vertebrates and more than 200 antimicrobial and antifungal compounds from the skin of frogs and toads have been discovered (Wilson 2002). Given that the world now faces a severe problem due to the widespread resistance of pathogenic bacteria to multiple antibiotics, amphibian compounds can serve as powerful models for drug invention because they have novel forms of function.

There has never been a comprehensive assessment of the risk of extinction for cone snail (*Conus*) species. However, 50 % of the Earth's coral reefs are close to collapse and at least 33 % of mangrove habitat is already destroyed. These two habitats are the primary centers for cone snail diversity. Warming ocean temperatures, acidification of the ocean, coastal development, and direct exploitation of snails for their shells are all threats to this group. The species *Conus magus* produces a peptide that the commercial medication ziconotide is based on. It is about 1,000 times more powerful than morphine and relieves pain in 50 % of advanced cancer and AIDS patients whose pain is unresponsive to opiates, and results in neither addiction nor tolerance (Newman et al. 2008). At least seven other medicines derived from cone snail poisons are in clinical trials and others show promise for treatment of neurodegenerative diseases and epilepsy (Newman et al. 2008). However, only about 100 of the estimated 70,000 cone snail toxins have been characterized (Herndon and Butler 2010).

Six species of bear are threatened with extinction, including a species I study, the Asian Black Bear (*Ursus thibetanus*) (Fig. 7). The threats to bears are habitat destruction and fragmentation, direct harvesting, and global climate change. Several medical benefits have already arisen from the study of bears and others are being investigated (Newman et al. 2008). For example, denning bears appear to produce a substance that inhibits cells that break down bone and promote substances that encourage bone and cartilage production; determining the mode of action of these substances could lead to breakthroughs in treating osteoporosis and cartilage damage. Denning bears can survive for a period of 5 months or more without excreting their urinary wastes, whereas humans would die from the buildup of these toxic substances after only a few days. An estimated 1.5 million people worldwide are receiving treatment for end-stage renal disease, and the hope is that by studying bears, we may be able to learn how to treat them more effectively (Herndon and Butler 2010).

Cultural Services

Biodiversity is worth conserving because it is beautiful, interesting, and provides inspiration to inventers, artists, and people all over the globe. Wild animals, plants, and natural areas contribute to our emotional and physical well-being (Louv 2005). Hundreds of millions of people visit natural areas or zoos each year and billions of dollars are spent on hunting, fishing, and nature tourism. Other living things have also contributed greatly to human progress by providing scientific and educational

Fig. 7 The Asiatic black bear (*Ursus thibetanus*) is one of six bear species threatened with extinction from sources as varied as habitat destruction, poaching, and climate change. Bears not only serve as important models for medical uses, but Asian black bears are important seed dispersers and polar bears (*Ursus maritimus*) are top carnivores helping to structure their ecosystems. The photo is of mother Asiatic black bear and her cub. The photograph was taken by remote camera in Khao Yai National Park, Thailand (Photo courtesy of Dusit Ngoprasert)

services that are usually overlooked. For example, most of what we know about genetic diseases in humans comes from studies on the fruit fly (*Drosophila melanogaster*) or the laboratory mouse/rat. Rats (*Rattus norvegicus*) have been used in many experimental studies, which have added to our understanding of disease processes, the effects of drugs, physiology, psychology, and genetics, and other topics in health and medicine.

Summary

By this point you should be convinced that if all ecosystem services provided by Earth's biodiversity were to stop, life on Earth would be impossible. Also, by this time it should be obvious that biodiversity makes a huge and undervalued contribution to the quality of life that humans enjoy. However, you might well say to yourself, *We have already identified the organisms most valuable to humans and the species we rely on for food, and the ones that perform many of the more important ecosystem functions are in no danger of becoming extinct.*

This statement has some element of truth to it. However, it has two major weaknesses. First, we never know what species will turn out to be valuable in the future. Could you have predicted that discovery of a fluorescent protein from a bioluminescent species of jellyfish (*Aequorea victoria*) would be worthy of a 2008 Nobel Prize, a fungus (*Amycolatopsis orientalis*) found in soil samples from the rainforests of Borneo would yield the powerful antibiotic vancomycin, saliva from the canine hookworm (*Ancylostoma caninum*) would provide an anticoagulant (NAP_{c2}) that has potential use in heart attack victims and the treatment of Ebola (Newman et al. 2008), ingredients from the venom of a pit viper *Bothrops jaracara* would yield a model for hypertension drugs, vincristine and vinblastine would be isolated from the rosy periwinkle plant (*Catharanthus roseus*) and increase the chances of remission to 99 % in childhood leukemia and to 70 % in Hodgkin's disease, leech (*Hirudo medicinalis*) saliva would yield a powerful blood anticoagulant, the silk of a spider (*Nephila clavipes*) would prove useful in regenerating neurons (Allmeling et al. 2006), a bread mold (*Penicillium notatum*) would be the source of one of the most useful antibiotics and that other molds in the same genus would have statins isolated from them that may potentially reduce the risk of having a heart attack or stroke by 25 % (Wilson 2002), the synthesis of the first effective antiretroviral drug AZT would be guided by compounds isolated from a sponge (*Tethya crypta*) (Newman et al. 2000), or that a revolution in the field of molecular biology would be achieved through isolation of a DNA polymerase from a bacterium (*Thermus aquaticus*) collected out of a Yellowstone hot spring? Thus, uncertainty surrounding the value of millions of yet undescribed species suggests that we should be cautious in our destruction of habitats and the short-sighted extirpation of species that have taken millions of years to evolve their specific characteristics.

We also do not know how many species can be removed from an ecosystem before it collapses, though there is good evidence that such collapses will occur and the concomitant loss of ecosystem services (May et al. 1995; Carpenter et al. 2011).

Impact of Global Climate Change on Biodiversity

Current Rates and Causes of Extinction

In the fossil record, an individual vertebrate (amphibian, bird, fish, mammal, or reptile) species lasts on average at least one million years before it becomes extinct. Thus, in an average year, no more than one out of one million species should go extinct. The current observed extinction rate since 1,600, for vertebrates, is 2.6 per 10,000 species per year. That is at least 260 times the background rate of extinction. At this rate, it would take less than 15,000 years to equal the extinction event that killed the dinosaurs over several million years. Further, because we know that the primary cause of modern extinctions is the loss, degradation, and fragmentation of habitat, and because we know the response to habitat loss is not linear, we expect that background rate to continue to increase and probably become an order of magnitude greater than it is currently (Whiteside and Ward 2011; Pimm and Raven 2000).

The reason for this increased and increasing rate of extinction is not difficult to fathom. Humans have been strongly implicated in global extinctions for tens of thousands of years (Jetz et al. 2007; Brook et al. 2008), but the current mass extinction is due to the fact that in the last 50 years we have used more of Earth's resources than we have for the entire history of humanity before that point. We are losing topsoil at least ten times faster than it can be replaced (Montgomery 2007), about 10 % of the Earth's agricultural land has become unfit for agriculture in the past 40 years while the population continues to expand, 80 % of the world's fish stocks for which assessment information is available are reported as fully exploited or overexploited, we are using more than 20 % of the world's renewable fresh water just for irrigation (Cassman and Wood 2005), and about 40 % of the world's rainforests have been lost in the past 50 years. The human population has increased from 3.0 to 6.9 billion during those same 50 years and we are expecting another two billion over the next 40 years.

However, the current rate of extinction might pale compared to what anthropogenic climate change threatens (Pimm and Raven 2000; Jetz et al. 2007). If we do not do something about climate change then all the money and the effort that has gone into saving species from extinction will likely be lost. This is particularly true because the current threat from habitat destruction and fragmentation interacts with climate change in a nonlinear way so that the negative impacts are greater than expected by looking at the threats independently.

Current and Future Rates of Global Climate Change

Over the past century the Earth has warmed approximately 0.74 °C, averaged over all land and ocean surfaces (IPCC 2007a). This warming of the Earth has clear effects on the species that live there. By the 1990s data started being published showing that 1,700 species had shifted their ranges an average of 6.1 km per decade toward the poles and that the timing of spring activities (e.g., breeding, migration, egg laying, flowering of plants) were occurring several days earlier each decade over the past 50 years. There is now a vast amount of data showing changes in the biology of plants and animals which are in accordance with expectations under a warming climate (Cassman and Wood 2005; Walther et al. 2002; Parmesan and Yohe 2003; Root et al. 2003; Hickling et al. 2006; Parmesan 2006; IPCC 2007b). Predictions for the next century are for increases in average global temperature of anywhere from 1.1 °C to 6.4 °C (Hickling et al. 2006), due mostly to unprecedented increases in the atmospheric concentrations of the three most important greenhouse gases, carbon dioxide, methane, and nitrous oxide. However, growth in emissions continues to far exceed expectations and it is possible that predicted increases in temperature are conservative. Further, temperatures are expected to increase for at least several centuries beyond this one, because of the half-life of CO_2 in the atmosphere, loss of polar ice which reflects rather than absorbs the sun's energy (Albedo effect), release of energy from the ocean into the atmosphere, and interactions between atmospheric warming and release of CO_2 from sources such as melting permafrost.

Another major impact of climate change includes effects on rainfall patterns and water storage. Rainfall is expected to become more variable with longer droughts and more flooding. Drought areas have more than doubled over the past 40 years (Leadley et al. 2010). In many parts of the world more precipitation will fall as rain instead of snow, snows at higher elevations will melt earlier, and this will cause deleterious changes in river flow. These changes are already causing a looming water crisis in the western USA (Dai et al. 2004). Similarly, the Tibetan plateau and the Himalayas are sources for the five major rivers of Asia, all of which are vitally important to already threatened biodiversity and to 1.4 billion people. Changes in temperature and precipitation are expected to drastically alter snow melt patterns over the next 40 years, so that the Indus, Brahmaputra, and Mekong basins are likely to experience severe negative effects owing to the dependence on irrigated agriculture and meltwater in these areas (Barnett et al. 2008; Immerzeel et al. 2010).

In terms of temperature, sea levels, and other climatic factors, we are headed towards conditions that have not existed for millions or probably tens of millions of years. Even the most rapid changes in the Earth's climate that led to those conditions in the past took at least 100,000 years to occur, not a couple of centuries or less.

Climate Change and Biodiversity

There are three possible fates for populations and species making up the current biodiversity of Earth, in a rapidly changing environment: (1) Plants and animals can migrate in order to leave unfavorable environmental conditions in one area and take up residence in an area with environmental conditions that are more conducive to survival and reproduction. The evidence that plants and animals have migrated long distances during past warming and cooling periods over the past 250,000 years is irrefutable. We already see such movement in extant species and can expect to see much more in the future. (2) Adapt to changing conditions through selection on genetic diversity present or arising in the population during the period of climatic change. (3) Go extinct when some combination of the first two are not sufficient to keep the population or species extant. Over hundreds of millions of years, the Earth has experienced innumerable cooling and heating periods of different magnitudes and rates. Periods of rapid change are usually accompanied by increases in extinction rates.

Projections of species extinction rates during the current period of global climate change are controversial because of uncertainty concerning how much the climate will change and how fast, because of methodological challenges especially concerning species ability to migrate through a human-dominated habitat matrix, and because of imperfect data from past extinctions. However, much is known and reasonable estimates can be made by looking at past extinctions under global climate change. An analysis of the fossil record over the past 520 million years provides a consistent relationship between global temperatures and biodiversity levels. During warm phases, extinction rates have been relatively high in both terrestrial and marine environments (Fig. 8) (Västilä et al. 2010). Extinction rates may increase

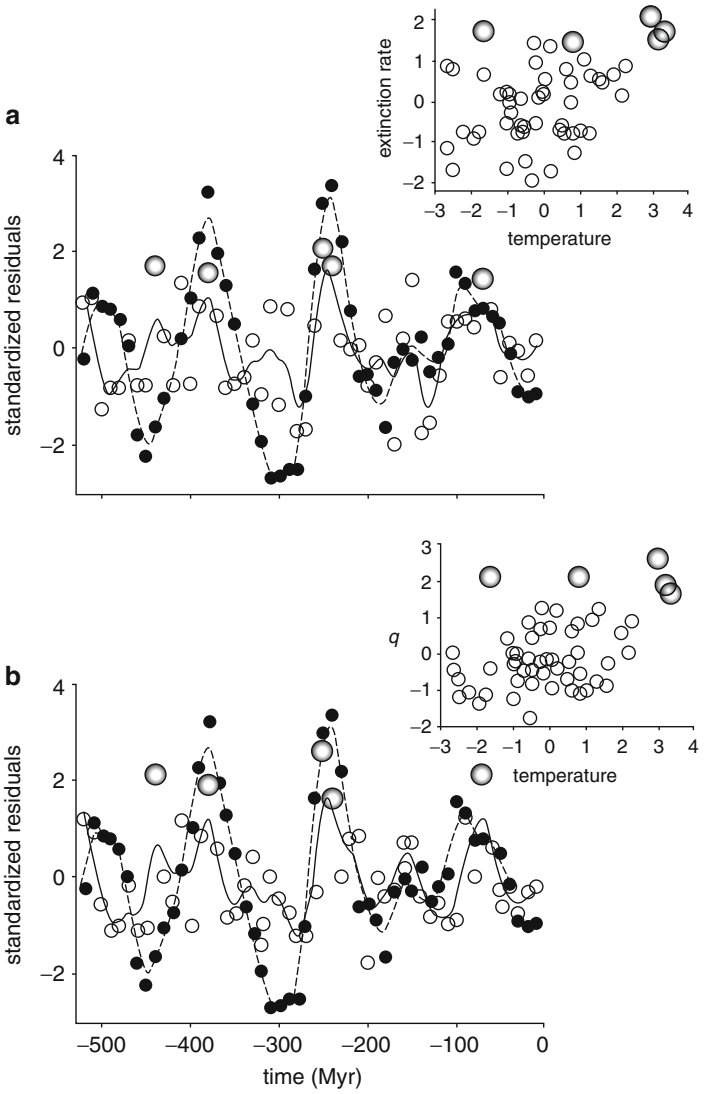

Fig. 8 Increase in extinction rates, over the past 520 million years, with increases in temperature. (**a**) the per-taxon rate of extinction for families (Myr^{-1}) using the maximum dating assumption and (**b**) the estimated *per capita* rate, *q*, of extinction (Myr^{-1}) for marine animal genera. Rates and temperature were transformed, detrended and mean standardized. Closed circles and dashed lines represent temperature and open circles and continuous lines extinction rates. Large double open symbols represent periods of mass extinction, defined as the five largest positive extinction residuals (in order of decreasing age: end Ordovician; Late Devonian; end Permian; Early Triassic, end Cretaceous). Insets show the positive association between extinction rate and temperature residuals across the time series (Reprinted with permission of the Proceedings of the Royal Society B. Fig. 3 from Mayhew et al. (2008))

approximately 10 % for every 1 °C increase in temperature. The end-Permian event that caused the extinction of approximately 95 % of all species on Earth was accompanied by a 6 °C increase in global temperatures over a few million years (Mayhew et al. 2008; Benton and Twitchett 2003). An increase in temperature of approximately 5 °C over several million years caused a great loss of plant biodiversity in Greenland (Västilä et al. 2010).

The biodiversity currently extant on Earth faces a much more difficult situation than does biodiversity during past periods of rapid climate change. There are two major reasons for this: (1) Species habitats are smaller than in the past. Smaller habitats support smaller populations which harbor less genetic diversity and have less evolutionary potential (Reed 2008). This evolutionary potential is critical for species' ability to adapt to the changing environmental conditions. (2) Species habitats are more fragmented than in the past. The fragmentation prevents individuals from being able to shift their distribution in response to climate-related impacts as easily as in the past. Recall, these are the two fates available to species other than going extinct: adapt to climate change or migrate in response to climate change in order to track environmental conditions favorable to survival. The current rate of climate change is probably unprecedented and would present extreme challenges to the biota of the planet under normal circumstances (McElwain et al. 2009). However, the combination of the magnitude of change, the extreme fragmentation of habitats, and the fact that there are 6.9 billion people using a very large proportion of the Earth's resources means that neither evolution nor migration will be sufficient to allow many species to cope with current rates of global climate change. They will go extinct and their value to humans and their beauty lost.

Many of the extinction may not be due directly to global climate change alone. The interactions between climate change and other factors will likely be extremely important. Habitat destruction and conversion continues in Southeast Asia and the Amazon, both places where I have done research and both areas rich in biodiversity. The continued fragmentation and loss of these forested areas alone is cause for grave concern. However, when you factor in that destruction of forests in these areas further limits movement of species trying to track a changing environment and that this continues to fuel further climate change by dumping more CO_2 into the atmosphere, it starts to appear catastrophic. Warmer temperatures will cause novel diseases to spread into naïve populations and will act as a general stress causing species to be susceptible to diseases their immune systems once were able to fight. The interaction between global climate change and diseases is already manifest in the widespread extinction of amphibians (Primack 2002). Increases in the frequency of drought and the introduction of novel diseases form an almost perfect combination for driving populations extinct, as these are the two biggest causes for population collapse among vertebrates (Reed et al. 2003b). Temperature stress, and other forms of environmental stress incurred through climate change, will interact with declining population size and loss of genetic diversity in a way that makes populations more vulnerable than either factor independently (Reed et al. 2007; Liao and Reed 2009; Fox and Reed 2011).

Table 2 Several million species of plant and animals face extinction due to global climate change, perhaps as early as 2050. Species most affected would be poor dispersers or those for which anthropogenic habitat fragmentation prevents dispersal and those with very narrow thermal tolerances and/or low genetic variation that prevent(s) evolution of new tolerances. The table below is based on the results of Thomas et al. (2007), who predicted extinction under different warming and movement scenarios. Migration rates are certainly somewhere between the extreme of no movement and the ability to track moving habitats perfectly, and current data suggests that warming trends will be close to the warmest predictions of Thomas et al. (2007). Consequently, ≥33 % of known species may be doomed to extinction by 2050

Warming level	No movement (%)	Perfect movement (%)
Low	34 extinction	11 extinction
Medium	45 extinction	19 extinction
High	58 extinction	33 extinction

Exactly how bad will it get? The prediction from a team of experts is that if temperatures increase by >3.5 °C, 40–70 % of plant and animal species will face extinction (Rosenzweig et al. 2008). One prominent study suggests that about 25 % of known plant and animal species will be committed to extinction by 2050 under current warming predictions (Table 2) (Thomas et al. 2004). A recent study suggests that 20 % of lizards may be extinct by 2080 as a direct result of increasing global temperatures (Sinervo et al. 2010). Exact predictions are of course impossible, but the combination of extremely rapid climate change, reduced population sizes, and fragmented habitats suggest that a very large proportion of Earth's biodiversity (>50 % of plants and animals) suffers a very high risk of extinction, particularly if definitive measures are not taken rapidly to ameliorate climate change. This level of species extinctions will be associated with an even larger percentage loss of populations and genetic diversity. This represents a very large proportion of the biodiversity and biological resources that humans need now more than ever.

Future Directions

In order to stave off huge losses in biodiversity and to save vast amounts of human suffering, humans will have to change the way they live and use their boundless innovation to produce a high quality of life in a way that does not endanger the planet. The following are some urgent and important general suggestions for directions human societies need to head in to mitigate climate change:

- Limit land-use change and make intelligent choices in land-use changes that balance agriculture against biodiversity loss (Koh and Ghazoul 2010; Lambin and Meyfroidt 2011). This is especially urgent in tropical and subtropical regions, but also in boreal and temperate forests (Bradshaw et al. 2009). Zero-loss of old-growth forests must be the immediate goal and this be combined with reforestation. Manage forests more efficiently and create/enforce laws that protect

forests from illegal logging and pillaging from corporations at the expense of the general populace.

- Aggressive climate change mitigation, including immediate implementation of existing cleaner energy technologies (Pacala and Socolow 2004), increased research to develop cleaner energy sources, and immediate legislation to increase fuel efficiency for motor vehicles.
- Place a global cap on greenhouse gas emissions and sell permits up to that cap in a global auction. Use the profits to finance the other mitigation measures discussed. Include the economic price for land-use emissions (Thomson et al. 2010). Economic models must begin to include all costs associated with production of goods, governments must regulate rather than subsidize corporations and their impacts on the public, and people must hold their governments accountable for lack of enforcement or collusion with corporations.
- Stabilize and eventually reduce human population size through intense family planning, education, and a change in societal norms.
- Make human-dominated landscapes more hospitable to biodiversity. Reclamation of degraded lands and reintroduction of extirpated species.
- Education of people, especially in the rural tropics, concerning biodiversity and the value of nature. Shift in the education and reward systems of developed nations away from short-term profiteering and financial markets toward science, engineering, innovation, and longer-term good to society.
- Create space and opportunities for ecosystems to self-adapt and reorganize because novel climates without current analogs will appear (Williams et al. 2007).

References

Allmeling C, Jokuszies A, Reimers K, Kall S, Vogt PM (2006) Use of spider silk fibers as an innovative material in a biocompatible artificial nerve conduit. J Cell Mol Med 10:770–778

Anderson SH, Kelly D, Ladley JJ, Molloy S, Terry J (2011) Cascading effects of bird functional extinction reduce pollination and plant density. Science 331:1068–1071

Arneric S, Holladay M, Williams M (2007) Neuronal nicotinic receptors: a perspective on two decades of drug discovery research. Biochem Pharmacol 74:1092–1101

Baraznenok I, Jonsson E, Claesson A (2005) 3-(2,5-Dihydro-1H-pyrrol-2-ylmethoxy)pyridines: synthesis and analgesic activity. Bioorg Med Chem Lett 15:1637–1640

Barnett TP, Pierce DW, Hidalgo HG, Bonfils C, Santer BD, Das T, Bala G, Wood AW, Nozawa T, Mirin AA, Cayan DR, Dettinger MD (2008) Human-induced changes in the hydrology of the western united states. Science 319:1080–1083

Beach T (1998) Soil catenas, tropical deforestation, and ancient and contemporary soil erosion in the Peten, Guatemala. Phys Geogr 19:378–404

Beach T, Dunning N, Luzzadder-Beach S, Cook DE, Lohse J (2006) Impacts of the ancient Maya on soils and soil erosion in the central Maya Lowlands. Catena 65:166–178

Benton MJ, Twitchett RJ (2003) How to kill (almost) all life: the end-Permian extinction event. Trends Ecol Evol 18:358–365

Bradshaw CJA, Sodi NS, Peh KSH, Brook BW (2007) Global evidence that deforestation amplifies flood risk and severity in the developing world. Glob Chang Biol 13:2379–2395

Bradshaw CJA, Warhentin IG, Sodhi NS (2009) Urgent preservation of boreal carbon stocks and biodiversity. Trends Ecol Evol 24:541–548

Brook BW, Sodhi NS, Bradshaw CJA (2008) Synergies among extinction drivers under global change. Trends Ecol Evol 23:453–460

Buchmann SL, Nabhan GP (1996) The forgotten pollinators. Island Press, Washington, DC

Bunnelle W, Daanen J, Ryther K, Schrimpf M, Dart M, Gelain A, Meyer M, Frost J et al (2007) Structure-activity studies and analgesic efficacy of *N*-(3-pyridinyl)-bridged bicyclic diamines, exceptionally potent agonists at nicotinic acetylcholine receptors. J Med Chem 50:3627–3644

Carpenter KE et al (2008) One-third of reef-building corals face elevated extinction risk from climate change and local impacts. Science 321:560–563

Carpenter SR, Cole JJ, Pace ML, Batt R, Brock WA, Cline T, Coloso J, Hodgson JR, Kitchell JF, Seekell DA, Smith L, Weidel B (2011) Early warnings of regime shifts: a whole-ecosystem experiment. Science 332(6033):1079–1082

Cassman KG, Wood S (2005) Cultivated systems. In: Hassan R et al (eds) Ecosystems and human well-being: current state and trends. Island Press, Washington, DC, pp 745–794

Chang H, Franczyk J, Kim C (2009) What is responsible for increasing flood risks? The case of Gangwon Province, Korea. Nat Hazards 48:339–354

Convention on biological diversity. (1992) United Nations.

Currens M, Gulakowski R, Mariner J, Moran R, Buckheit RJ, Gustafson K, McMahon J, Boyd M (1996) Antiviral activity and mechanism of action of calanolide A against the human immunodeficiency virus type-1. J Pharmacol Exp Ther 279:645–651

Dai A, Trenberth KE, Qian T (2004) A global dataset of Palmer drought severity index for 1870–2002: relationship with soil moisture and effects of surface warming. J Hydrometeorol 5(6):1117–1130

Daily GC (1997) Nature's services: societal dependence on natural ecosystems. Island Press, Washington, DC

Daly J, Kaneko T, Wilham J, Garraffo H, Spande T, Espinosa A, Donnelly M (2002) Bioactive alkaloids of frog skin: combinatorial bioprospecting reveals that pumiliotoxins have an arthropod source. Proc Natl Acad Sci U S A 99:13996–14001

Decker M, Meyer M, Sullivan J (2001) The therapeutic potential of nicotinic acetylcholine receptor agonists for pain control. Expert Opin Investig Drugs 10:1819–1830

Donnelly-Roberts DL, Puttfarcken PS, Kuntzweiler TA, Briggs CA, Anderson DJ, Campbell JE, Piattoni-Kaplan M, Mckenna DG, Wasicak JT, Holladay MW, Williams M, Arneric SP (1998) ABT-594 [(*R*)-5-(2-azetidinylmethoxy)-2-chloropyridine]: a novel. Orally effective analgesic acting via neuronal nicotinic acetylcholine receptors: I. In vitro characterization. J Pharmacol Exp Ther 285:777–786

Drisdel RC, Sharp D, Henderson T, Hales TG, Green WN (2008) High affinity binding of epibatidine to serotonin type 3 receptors. J Biol Chem 282:9659–9665

Duce RA et al (2008) Impacts of atmospheric anthropogenic nitrogen on the open ocean. Science 320(5878):893–897

Farnsworth NR et al (1988) Screening plants for new medicines. In: Wilson EO (ed) Biodiversity. National Academy Press, Washington, DC

Fearnside PM, Laurance WF (2004) Tropical deforestation and greenhouse-gas emissions. Ecol Appl 14:982–986

Foley JA, Asner GP, Costa MH, Coe MT, DeFries R, Gibbs HK, Howard EA, Olson S, Patz J, Ramankutty N, Snyder P (2007) Amazonia revealed: forest degradation and loss of ecosystem goods and services in the Amazon Basin. Frontiers Ecol Environ 5:25–32

Fowler C, Mooney P (1990) Shattering: food, politics, and the loss of genetic diversity. University of Arizona Press, Tucson

Fox CW, Reed DH (2011) Inbreeding depression increases with environmental stress: an experimental study and meta-analysis. Evolution 65:246–258

Galloway JN, Cowling EB (2002) Reactive nitrogen and the world: two hundred years of change. Ambio 31:64–71

Galloway JN et al (2008) Transformation of the nitrogen cycle: recent trends, questions, and potential solutions. Science 320(5878):889–892

Grifo F et al (1997) The origin of prescription drugs. In: Grifo F, Rosenthal J (eds) Biodiversity and human health. Island Press, Washington, DC
Gruber N, Galloway JN (2008) An earth system perspective of the global nitrogen cycle. Nature 451:293–296
Helmut H, Erb KH, Krausmann F, Gaube V, Bondeau A, Plutzar C, Gingrich S, Lucht W, Fischer-Kowalski M (2007) Quantifying and mapping the human appropriation of net primary production in earth's terrestrial ecosystems. Proc Natl Acad Sci U S A 104:12942–12947
Herndon CN, Butler RA (2010) Significance of biodiversity to health. Biotropica 42:558–560
Hey DL, Philippi NS (1995) Flood reduction through wetland restoration – the upper Mississippi River basin as a case history. Restor Ecol 3:4–17
Hickling R, Roy DB, Hill JK, Fox R, Thomas CD (2006) The distributions of a wide range of taxonomic groups are expanding polewards. Glob Chang Biol 12:450–455
Imhoff ML, Bounoua L, Ricketts T, Loucks C, Harriss R, Lawrence WT (2004) Global patterns in human consumption of net primary production. Nature 429:870–873
Immerzeel WW, van Beek LPH, Bierkens MFP (2010) Climate change will affect the Asian water towers. Science 328:1382–1385
IPCC (2007a) Climate change 2007: the physical science basis. Contribution of working group I to the fourth assessment report of the intergovernmental panel on climate change. Cambridge University Press, Cambridge. http://www.ipcc.ch/pdf/assessment-report/ar4/wg1/ar4-wg1-chapter7.pdf
IPCC (2007b) Climate Change 2007: impacts, adaptation and vulnerability. Contribution of working group II to the fourth assessment report of the intergovernmental panel on climate change. Cambridge University Press, Cambridge
Jackson ST, Overpeck JT (2000) Responses of plant populations and communities to environmental changes of the late quaternary. Paleobiology 26:194–220
Jetz W, Wilcove DS, Dobson AP (2007) Projected impacts of climate and land-use change on the global diversity of birds. PLoS Biol 5:e157
Judson S (1968) Erosion rates near Rome, Italy. Science 160:1444–1446
Kareiva P, Marvier M (2011) Conservation science: balancing the needs of people and nature. Roberts, Greenwood Village
Khush GS, Brar DS (2002) Biotechnology for rice breeding: progress and potential impact. International Rice Commission, UN Food and Agriculture Organization, Rome
Klein AM, Vaissiére B, Cane JH, Steffan-Dewenter I, Cunningham SA, Kremen C et al (2007) Importance of crop pollinators in changing landscapes for world crops. Proc R Soc Lond B Biol Sci 274:303–313
Koh LP, Ghazoul J (2010) Spatially explicit scenario analysis for reconciling agricultural expansion, forest protection, and carbon conservation in Indonesia. Proc Natl Acad Sci U S A 107:11140–11144
Korner C (2000) Biosphere responses to CO_2 enrichment. Ecol Appl 10:1590–1619
Kunkel CM, Hallberg RW, Oppenheimer M (2006) Coral reefs reduce tsunami impact in model simulations. Geophys Res Lett 33:23
Lambin EF, Meyfroidt P (2011) Global land use change, economic globalization, and the looming land scarcity. Proc Natl Acad Sci U S A 108:3465–3472
Lanner RM (1996) Made for each other: a symbiosis of birds and pines. Oxford University Press, New York
Lavelle P et al (2006) Nutrient cycling. In: Ecosystems and human well-being. Island Press, Washington, DC
Leadley P et al (2010) Biodiversity scenarios: projections of 21st century change in biodiversity and associated ecosystem services. In: Secretariat of the convention on biological diversity, Montreal
Liao W, Reed DH (2009) Inbreeding-environment interactions increase extinction risk. Anim Conserv 12:54–61

Louv R (2005) Last child in the woods: saving our children from nature-deficit disorder. Algonquin Books, Chapel Hill
Marris E (2005) Tsunami damage was enhanced by coral reef theft. Nature 436:1071
May EM, Lawton JH, Stork NE (1995) Assessing extinction rates. In: Lawton JH, May RM (eds) Extinction rates. Oxford University Press, Oxford
Mayhew PJ, Jenkins GB, Benton TG (2008) A long-term association between global temperature and biodiversity, origination and extinction in the fossil record. Proc R Soc B 275:47–53
McElwain JC, Wagner PJ, Hesselbo SP (2009) Fossil plant relative abundances indicate sudden loss of late Triassic biodiversity in east Greenland. Science 324:1554–1556
Millennium Ecosystem Assessment (MEA) (2005) Ecosystems and human well-being: synthesis. Island Press, Washington, DC, 155 pp
Montgomery DR (2007) Soil erosion and agricultural sustainability. Proc Natl Acad Sci U S A 104:13269–13272
Nathan R, Muller-Landau HC (2000) Spatial patterns of seed dispersal, their determinants and consequences for recruitment. Trends Ecol Evol 15:278–285
Newman D, Cragg G, Snader K (2000) The influence of natural products upon drug discovery. Nat Prod Rep 17:215–234
Newman DJ, Cragg GM, Snader KM (2003) Natural products as sources of new drugs over the period 1981–2002. J Nat Prod 66:1022–1037
Newman DJ, Kilama J, Bernstein A, Chivian E (2008) Medicines from nature. In: Bernstein A, Chivian E (eds) Sustaining life: how human health depends on biodiversity. Oxford University Press, New York, pp 117–161
Pacala S, Socolow R (2004) Stabilization wedges: solving the climate problem for the next 50 years with current technologies. Science 305:968–972
Parmesan C (2006) Ecological and evolutionary responses to recent climate change. Annu Rev Ecol Evol Syst 37:637–669
Parmesan C, Yohe G (2003) A globally coherent fingerprint of climate change impacts across natural systems. Nature 421:37–42
Pimm SL, Raven P (2000) Biodiversity – extinction by numbers. Nature 403:843–845
Plotkin M (2000) Medicine quest: in search of nature's healing secrets. Viking, New York
Ponting C (1993) A green history of the world: the environment and the collapse of great civilizations. Penguin, New York
Pope KO, van Andel TH (1984) Late quaternary alluviation and soil formation in the southern Argolid: its history, causes and archaeological implications. J Archaeol Sci 11:281–306
Pounds JA, Crump ML (1994) Amphibian declines and climate disturbance: the case of the golden toad and harlequin frog. Conserv Biol 8:72–85
Pounds JA, Bustamante MR, Coloma LA, Consuegra JA, Fogden MPL, Foster PN, La Marca E, Masters KL, Merino-Viteri A, Puschendorf R, Ron SR, Sánchez-Azofeifa GA, Still CJ, Young BE (2006) Widespread amphibian extinctions from epidemic disease driven by global warming. Nature 439:161–167
Primack RB (2002) Essentials of conservation biology, 3rd edn. Sinauer, Sunderland
Raven P, McNeely J (1998) Biological extinction: its scope and its meaning for us. In: Guruswamy L, McNeely J (eds) Protection of global biodiversity: converging strategies. Duke University Press, Durham
Reed DH (2008) The effects of population size on population viability: from mutation to environmental catastrophes. In: Carroll SP, Fox CW (eds) Conservation biology: evolution in action. Oxford University Press, New York, pp 16–34
Reed DH (2010) Albatrosses, eagles, and newts, Oh My!: exceptions to the prevailing paradigm concerning genetic diversity and population viability? Anim Conserv 13:448–457
Reed DH, O'Grady JJ, Brook BW, Ballou JD, Frankham R (2003a) Estimates of minimum viable population sizes for vertebrates and factors influencing those estimates. Biol Conserv 113:23–34
Reed DH, O'Grady JJ, Ballou JD, Frankham R (2003b) Frequency and severity of catastrophic die-offs in vertebrates. Anim Conserv 6:109–114

Reed DH, Nicholas AC, Stratton GE (2007) The genetic quality of individuals directly impacts population dynamics. Anim Conserv 10:275–283

Ricketts TH et al (2004a) Economic value of tropical forest coffee production. Proc Natl Acad Sci U S A 101:12579–12582

Ricketts TH et al (2004b) Tropical forest fragments enhance pollinator activity in nearby coffee crops. Conserv Biol 18:1262–1271

Ricketts TH, Regetz J, Steffan-Dewenter I, Cunningham SA, Kremen C, Bogdanski A, Gemmill-Herren B, Greenleaf SS, Klein AM, Mayfield MM, Morandin LA, Ochiengâ A, Viana BF (2008) Landscape effects on crop pollination services: are there general patterns? Ecol Lett 11:499–515

Rodríguez-Cabal MA, Aizen MA, Novaro AJ (2007) Habitat fragmentation disrupts a plant-disperser mutualism in the temperate forest of South America. Biol Conserv 139:195–202

Rojstaczer S, Sterling SM, Moore NJ (2001) Human appropriation of photosynthesis products. Science 294:2549–2552

Root TL, Price JT, Hall KR, Schneider SH, Rosenzweig C et al (2003) Fingerprints of global warming on wild animals and plants. Nature 421:57–60

Rosenzweig C, Karoly D, Vicarelli M, Neofotis P, Wu Q, Casassa G, Menzel A, Root TL, Estrella N, Seguin B, Tryjanowski P, Liu C, Rawlins S, Imeson A (2008) Attributing physical and biological impacts to anthropogenic climate change. Nature 453:353–357

Seidler TG, Plotkin JB (2007) Seed dispersal and spatial pattern in tropical trees. PLoS Biol 4(11): e344. doi:10.1371/journal.pbio.0040344

Sinervo B, Méndez-de-la-Cruz F, Miles DB, Heulin B, Bastiaans E, Villagrán-Santa Cruz M, Lara-Resendiz R, Martínez-Méndez N, Lucía Calderón-Espinosa M, Meza-Lázaro RN, Gadsden H, Avila LJ, Morando M, De la Riva IJ, Sepulveda PV, Rocha CFD, Ibargüengoytía N, Puntriano CA, Massot M, Lepetz V, Oksanen TA, Chapple DG, Bauer AM, Branch WR, Clobert J, Sites JW Jr (2010) Erosion of lizard diversity by climate change and altered thermal niches. Science 328:894–899

Song J, Bradeen JM, Naess SK, Raasch JA, Wielgus SM, Haberlach GT, Liu J, Kuang H, Austin-Phillips S, Buell CR, Helgeson JP, Jiang J (2003) Gene RB cloned from *Solanum bulbocastanum* confers broad spectrum resistance to potato late blight. Proc Natl Acad Sci U S A 100:9128–9133

Stokstad E (2005) After Katrina: Louisiana's wetlands struggle for survival. Science 310:1264–1266

Sun C, Speer CM, Wang G-Y, Chapman B, Chalupa LM (2008) Epibatidine application in vitro blocks retinal waves without silencing all retinal ganglion cell action potentials in developing retina of the mouse and ferret. J Neurophysiol 30:5404–5414

Thomas CD, Cameron A, Green RE, Bakkenes M, Beaumont LJ, Collingham YC, Erasmus BFN, Siqueira MFD, Grainger A, Hannah L (2004) Extinction risk from climate change. Nature 427:145–148

Thomson AM, Calvin KV, Chini LP, Hartt G, Edmonds JA, Bond-Lamberty B, Frolking S, Wise MA, Janetos AC (2010) Climate mitigation and the future of tropical landscapes. Proc Natl Acad Sci U S A 107:19633–19638

U.S. Geological Survey (1999) National water summary on wetland resources, vol 2425, United States Geological Survey water supply paper. USGS, Reston

Van Andel TH, Zangger E, Demitrack A (1990) Land use and soil erosion in prehistoric and historical Greece. J Field Archaeol 17:379–396

Västilä K, Kummu M, Sangmanee C, Chinvanno S (2010) Modelling climate change impacts on the flood pulse in the lower mekong floodplains. J Water Clim Change 1:67–86

Veron JEN, Hoegh-Guldberg O, Lenton TM, Lough JM, Obura DO, Pearce-Kelly P, Sheppard CRC, Spalding M, Stafford-Smith MG, Rogers AD (2009) The coral reef crisis: the critical importance of <350 ppm CO_2. Mar Pollut Bull 58:1428–1436

Vitousek PM, Ehrlich PR, Ehrlich AH, Matson PA (1986) Human appropriation of the products of photosynthesis. Bioscience 36:368–373

Walther G-R, Post E, Convey P, Menzel A, Parmesan C, Beebee TJC, Fromentin J-M, Heogh-Guldberg O, Bairlein F (2002) Ecological response to recent climate change. Nature 416:389–395

Ward PJ, Renssen H, Aerts JCJH, van Balen RT, Vandenberghe J (2008) Strong increases in flood frequency and discharge of the River Meuse over the late Holocene: impacts of long-term anthropogenic land use change and climate variability. Hydrol Earth Syst Sci 12(1):159–175

Webb TJ et al (2005) Forest cover-rainfall relationships in a biodiversity hotspot: the Atlantic forest of Brazil. Ecol Appl 15:1968–1983

Wells S, Kapos V (2006) Coral reefs and mangroves: implications from the tsunami one year on. Oryx 40:123–124

Werth D, Avissar R (2004) The regional evapotranspiration of the Amazon. J Hydrometeorol 5:100–109

Whiteside JH, Ward PD (2011) Ammonoid diversity and disparity track episodes of chaotic carbon cycling during the early Mesozoic. Geology 39:99–102

Williams M (2003) Deforesting the earth: from prehistory to global crisis. University of Chicago Press, Chicago

Williams JW, Jackson ST, Kutzbach JE (2007) Projected distributions of novel and disappearing climates by 2100 AD. Proc Natl Acad Sci U S A 104:5738–5742

Wilson EO (1992) The diversity of life. Norton, New York

Wilson EO (2002) The future of life. Vintage, New York

Zhang C, Ge Z, Cheng T, Li R (2006) Synthesis and analgesic activity of secondary amine analogues of pyridylmethylamine and positional isomeric analogues of ABT-594. Bioorg Med Chem Lett 16:2013–2016

Sea-Level Rise and Hazardous Storms: Impact Assessment on Coasts and Estuaries

Yan Ding

Contents

Abstract

Sea-level changes in coasts and estuaries may differ substantially from global mean sea-level variations, showing complex spatial patterns which result from coastal-ocean dynamic processes, movements of the sea floor, and changes in gravity due to water mass redistribution. Because dominant hydrodynamic and

Y. Ding (✉)
National Center for Computational Hydroscience and Engineering, The University of Mississippi, Oxford, MS, USA
e-mail: ding@ncche.olemiss.edu

W.-Y. Chen et al. (eds.), *Handbook of Climate Change Mitigation and Adaptation*,
DOI 10.1007/978-3-319-14409-2_14

morphodynamic processes in coastal and estuarine zones are unsteady and of multi-scale, assessment of hazardous storms under the future sea-level rise heavily relies on numerical simulations of dynamic responses to sea-level rise and storm conditions. Thus, this chapter focuses on the following three objectives: (1) investigation of the impacts of hazardous storms/hurricanes and sea-level rise on coasts and estuaries, (2) review of impact assessment approaches by using numerical simulation models, and (3) demonstration of impact assessment of coastal floods and erosions under the combined conditions of hazardous storms (extreme events) and the future sea-level rise scenarios. It emphasizes a systematic approach for the impact assessment of sea-level rise by using integrated coastal process models which are widely used to simulate coastal/estuarine hydrodynamic and morphodynamic processes to predict flooding/inundation and coastline erosion/deposition under complex hydrological, morphological, oceanographic, and meteorological conditions. It also demonstrates an application of an integrated coastal model, CCHE2D-Coast, to simulate waves, tides, sediment transport, and morphological changes in an estuary and to predict the hydrodynamic and morphodynamic impacts of hazardous storms and five hypothetical sea-level rise scenarios. It shows that the integrated physical process modeling technique is the most effective method to predict the impact of spatially varying mean sea-level changes in coasts and estuaries and to facilitate coastal flood management, erosion protection, and infrastructure designing/planning against extreme hydrological conditions and climate changes.

Introduction

The increasing trend of atmospheric concentrations of carbon dioxide and other gases in the past decades, especially due to anthropogenic greenhouse gas emissions, leads to increase in the Earth's temperature, thermal expansion of the upper ocean, and the melting of small ice caps (Church et al. 2001). Consequentially, a primary effect of global warming is an increase in the global volume of the ocean and accelerated global mean sea-level (GMSL) rise, which will speed up permanent inundation, shoreline erosion and retreat, and land loss of low-lying coastal/estuarine areas. Historically, global mean sea level has risen over 120 m at some locations from the low stand of the last glacial maximum 20,000 years ago when temperatures were between 5 °C and 10 °C cooler than today (Jouzel et al. 1989; Church et al. 2001). Geologic evidence suggests a global mean sea-level rise rate of 0.1 to 0.2 mm/year over last 3,000 years with a significant acceleration that may have occurred around the mid-nineteenth century (Church et al. 2001). Based on global tide-gauge data, global mean sea levels are estimated to have risen 10–20 cm during the twentieth century (or 1.0–2.0 mm/year) (Douglas 1991, 1997; Church et al. 2001). It has since been argued that an estimated average of a 20-cm rise during the past century is most consistent with the available data (Douglas and Peltier 2002). Thus, a significant sea-level rise during the twentieth century occurred,

which has been arguably one stress factor contributing to many of the existing coastal problems. Predictions from the Fourth Assessment Report (AR4) by Intergovernmental Panel on Climate Change (IPCC) suggest that sea level may rise by as much as 60 cm by 2100 (IPCC 2007). The Fifth Assessment Report (AR5) of IPCC presented the latest results on the GMSL rise that may rise 74 cm of a median value by 2100 with a likely range from 52 to 98 cm (Church et al. 2013). Uncertainty, however, remains about how projected melting of the Greenland and Antarctic ice sheets will contribute to sea-level rise.

Based on the selected long-term tide gauges on the East Coast of the United States, it has been found that along the US Atlantic coast, over the last century, relative sea-level rise rates have ranged from 1.8 mm/year to as much as 4.4 mm/year (US-CCSP 2008). The lowest rates (1.75–2.00 mm/year) are close to the present global rate of 2.0 mm/year and occur along coastal New England and from Georgia to northern Florida. The highest rates (4.42 ± 0.16 mm/year) have been observed in the mid-Atlantic region between northern New Jersey and southern Virginia. It is also found that subsidence of the land surface due to a range of factors contributes to the high rates of relative sea-level rise observed in this region.

GMSL rise does not translate into a uniform rise in sea level around the world. Considerable variation often exists between global and local changes over a range of time/spatial scales. For example, based on available tide-gauge data collected by the National Oceanic and Atmospheric Administration (NOAA) on the mid-Atlantic coast (NOAA 2011), Cooper et al. (2005) obtained an approximate relative sea-level rise trend of 3.53 mm/year during the twentieth century, which is almost double the global mean value of sea-level rise. In general, the local sea-level change at any coast location can be determined by the sum of GMSL rise, regional sea-level change due to meteo-oceanographic factors (i.e., atmospheric pressure, storm surge, wave setup, and ocean circulations), and vertical land movement (i.e., subsidence and/or uplift) due to various geological processes such as tectonics, glacial isostatic adjustment, sediment consolidation, groundwater withdrawal, etc. (Nicholls 2003).

The development of a coastal zone management plan considering a local/relative sea-level rise and its impact area is of utmost importance. Due to existing multi-scale and unsteady physical processes driven by waves, tides, storm surge, sediment transport (erosion and deposition), and tectonic movement (subsidence and rise), a local sea-level rise is not equal to the estimate by the IPCC and generally varying with time and locations from coast to coast. For coastal hazard management and coastal defense planning in a specific coastal/estuarine zone, it is essential to predict the dynamic impacts of the local/relative sea level under local hydrological conditions such as waves, storm surges, and morphology, especially generated by hazardous weather.

The surface water motion in coasts and estuaries encompasses various hydrodynamic processes driven by astronomical tides, waves, river flows, wind-induced currents, turbulence, etc. Morphodynamic processes include the evolutions of landscapes and seascapes (erosion and deposition) due to sediment transport. Because unsteady and multi-scale hydrodynamic and morphodynamic processes are dominant in coastal/estuarine zones, numerical simulation of dynamic responses to

sea-level rise and storms, in fact, becomes the only effective approach to systematically assess the impacts of storms under the future sea-level rise scenario conditions. Thus, the objectives of this chapter are (1) to investigate the impacts of sea-level rise due to climate change on coasts and estuaries; (2) to review impact assessment approaches for flood water management, coastal erosion protection, and infrastructure designing/planning against extreme hydrological conditions; and (3) to demonstrate impact assessment of coastal floods and erosions under the combined conditions of hazardous storms and the future sea-level rise scenarios. It focuses on the regional-scale assessment of the dynamic impacts of hazardous storms (i.e., extreme events in ocean) including hurricanes and typhoons under the conditions of sea-level changes, using numerical simulation techniques, which are applicable to directly predict flooding/inundation and morphological changes in coastal zones and estuarine regions. By employing an integrated coastal process modeling system, CCHE2D-Coast, simulations of waves, tides, sediment transport, and morphological changes in an estuary are demonstrated under these natural physical conditions and sea-level rise scenarios. Assessment of impacts of a hazardous storm combined with sea-level rise scenarios in the estuary is discussed accordingly.

This chapter in the following context is organized as follows: At first, the GMSL scenarios, as well as some regional relative sea-level rise projections in the United States, are briefly reviewed. Second, the relationship between regional/local sea-level rise and hydrological, meteorological, and oceanographic conditions is discussed; accordingly, geophysical and socioeconomic impacts of local sea-level rise on coasts and estuaries are summarized. For coastal zone management, general impact assessment approaches under sea-level rise scenarios are discussed. Then, a more detailed review on numerical modeling, using global circulation models (GCM), coastal process models (or inundation models), and downscaling techniques, for predicting coastal hazards under sea-level rise conditions in the future is given. By applying an integrated coastal process simulation model, a case study on the assessment of sea-level rise impacts in an estuary located at the west coast of Taiwan is demonstrated. Finally, concluding remarks and discussions on the future research directions are presented.

Future Global Main Sea-Level Projection/Scenarios

In the IPCC Third Assessment Report, the projected sea-level rise from 1990 to 2100 was between 9 and 88 cm with a mid estimate of 48 cm (Church et al. 2001), which however does not include the contribution from Antarctica. Based on the emission scenarios in the twenty-first century, the Fourth Assessment Report (AR4) of IPCC on Emission Scenarios (SRES) has projected the six SRES marker scenarios (IPCC 2007), i.e., the SRES B1, A1T, B2, A1B, A2, and A1FI, as shown in Table 1. The SRES scenarios represent mutually consistent characterizations of how the world might evolve during the twenty-first century. Each scenario is a short narrative of a possible pathway of future development from the current world. They explore what might happen if political, economic, technical, and social developments take specific

Table 1 Projected global surface warming and sea-level rise at the end of the twenty-first century by the IPCC AR4 (IPCC 2007)

Scenario	Approximate carbon dioxide CO_2-equivalent concentration (ppm)	Likely range of temperature change (°C at 2090–2099 relative to 1980–1999)	Sea-level rise (m at 2090–2099 relative to 1980–1999)
B1	600	1.1–2.9	0.18–0.38
A1T	700	1.4–3.8	0.20–0.45
B2	800	1.4–3.8	0.20–0.43
A1B	850	1.7–4.4	0.21–0.48
A2	1,250	2.0–5.4	0.23–0.51
A1FI	1,550	2.4–6.4	0.26–0.59

alterative directions at the global level, including consideration of potential differences and interactions. Approximate CO_2-equivalent concentrations corresponding to the computed radiative forcing due to anthropogenic greenhouse gases (GHGs) and aerosols in 2100 for the six SRES scenarios are about 600, 700, 800, 850, 1,250, and 1,550 ppm, respectively. (Radiative forcing is a measure of the influence a factor has in altering the balance of incoming and outgoing energy in the Earth-atmosphere system and is an index of the importance of the factor as a potential climate change mechanism (IPCC 2007, p. 36). In the IPCC AR4 report, radiative forcing values are for changes relative to preindustrial conditions defined at 1750 and are expressed in watts per square meter [W/m^2].) Based on these GHG emission scenarios, estimates about temperature change and sea-level rise are assessed from a hierarchy of models that encompass a simple climate model, several Earth models of intermediate complexity, and a large number of atmosphere-ocean general circulation models (AOGCMs) as well as observation constraints (IPCC 2007). The model-based results of sea-level rise, excluding future rapid dynamic changes in ice flow, show that the bottom line of GHG emission (i.e., 600 ppm) will cause a global mean sea-level rise at 2090–2099 within a range from 18 to 38 cm. The top line (1,550 ppm), however, will give the sea-level rise about 26–59 cm, relative to 1980–1999. Following the SRES scenarios, Nicholls (2004) has investigated coastal flooding and wetland loss in the twenty-first century corresponding to only four SRES scenarios (i.e., A1FI, A2, B1, and B2) with a GMSL rise range from 22 to 34 cm by the 2080s, relative to 1990. The conclusion is that sea-level rise increases the flood impacts in all cases, and coastal wetland will be lost due to sea-level rise in all scenarios with 5–20 % losses by the 2080s in the A1FI scenario.

For the Fifth Assessment Report (AR5) of IPCC, instead of the six scenarios used the IPCC AR4 report (IPCC 2007), the IPCC work group has defined a set of four new scenarios, which are denoted Representative Concentration Pathways (RCPs) (IPCC 2013). As given in Table 2, for the Coupled Model Intercomparison Project Phase 5 (CMIP5), the four new scenarios reflect by their approximate total radiative forcing in year 2100 relative to 1750: 2.6 W/ m^2 for RCP2.6, 4.5 W/ m^2 for RCP4.5, 6.0 W/ m^2 for RCP6.0, and 8.5 W/ m^2 for RCP8.5. These four RCPs include one mitigation scenario leading to a very low forcing level (RCP2.6), two stabilization

Table 2 Projected global surface warming and sea-level rise for the late twenty-first century (2081–2100) relative to the reference period of 1986–2005 by the IPCC AR5 (IPCC 2013)

Scenario	Radiative forcing in year 2100 relative to 1750 (W/m^2)	Approximate carbon dioxide (CO_2)-equivalent concentration (ppm)	Median value and likely range of temperature change (°C)	Median value and likely range of sea-level rise (m)
RCP2.6	2.6	475	1.0 [0.3–1.7]	0.40 [0.26–0.55]
RCP4.5	4.5	630	1.8 [1.1–2.6]	0.47 [0.32–0.63]
RCP6.0	6.0	800	2.2 [1.4–3.1]	0.48 [0.33–0.63]
RCP8.5	8.5	1,313	3.7 [2.6–4.8]	0.63 [0.45–0.82]

scenarios (RCP4.5 and RCP6), and one scenario with very high greenhouse gas emissions (RCP8.5). The RCPs can thus represent a range of twenty-first-century climate policies, as compared with the no-climate policy of the Special Report on Emissions Scenarios (SRES) used in the Third Assessment Report and the Fourth Assessment Report. Including the prescribed concentrations of CH_4 and N_2O, the combined CO_2-equivalent concentrations are 475 ppm (RCP2.6), 630 ppm (RCP4.5), 800 ppm (RCP6.0), and 1,313 ppm (RCP8.5). Those scenarios represent a possible range of the mean global mean surface temperature from 1.0 °C to 3.7 °C. The peak value of this surface temperature may reach 4.8 °C in the case of RCP8.5.

Projections of GMSL rise in the IPCC AR5 are larger than in the AR4, primarily because of improved modeling land-ice contributions (Church et al. 2013). As shown in Table 2, for the period of the late twenty-first century (2081–2100), compared to 1986–2005, GMSL rise is likely (medium confidence) to be in the 5–95 % range of projections from process-based models, which give 0.26–0.55 m for RCP2.6, 0.32–0.63 m for RCP4.5, 0.33–0.63 m for RCP6.0, and 0.45–0.82 m for RCP8.5. At 2100, the median and likely ranges of GMSL rise are 0.44 [0.28–0.61] m (RCP2.6), 0.53 [0.36–0.71] m (RCP4.5), 0.55 [0.38–0.73] m (RCP6.0), and 0.74 [0.52–0.98] m (RCP8.5) (Church et al. 2013, p.1182).

In all scenarios, the rate of GMSL rise at the start of the RCP projections (2007–2013) is about 3.7 mm/year, slightly above the observational range of 3.2 [2.8–3.6] mm/year for 1993–2010. In RCP2.6, it becomes roughly constant (central projection 4.5 mm/year) before the middle of the century and subsequently declines slightly. The rate of rise becomes roughly constant in RCP4.5 and RCP6.0 by the end of the century, whereas acceleration continues throughout the century in RCP8.5, reaching 8.0–16.0 mm/year in 2081–2100.

In all scenarios, thermal expansion is the largest contribution, accounting for about 30–55 % of the projections. Glaciers are the next largest, accounting for 15−35 % of the projections. By 2100, 15–55 % of the present volume of glaciers outside Antarctica is projected to be eliminated under RCP2.6 and 35–85 % under RCP8.5.

Local/Regional Sea-Level Rise Scenarios

Local/regional sea-level changes may differ substantially from a GMSL average, showing complex spatial patterns which result from ocean dynamical processes, movements of the sea floor, and changes in gravity due to water mass redistribution (land ice and other terrestrial water storage) in the climate system (IPCC 2013). The local/regional distribution is associated with a dynamical redistribution of water masses and a change of sea water properties caused by spatiotemporal variations of winds and air pressure, air-sea heat, and freshwater fluxes and ocean currents.

IPCC AR5 (IPCC 2013) concludes that it is very likely that in the twenty-first century and beyond, sea-level change will have a strong regional pattern, with some places experiencing significant deviations of local and regional sea-level change from the global mean change. Over decadal periods, the rates of regional sea-level change as a result of climate variability can differ from the global average rate by more than 100 % of the global average rate. By the end of the twenty-first century, it is very likely that over about 95 % of the world ocean, regional sea-level rise will be positive, and most regions that will experience a sea-level fall are located near current and former glaciers and ice sheets. About 70 % of the global coastlines are projected to experience a relative sea-level change within 20 % of the global mean sea-level change.

Local/regional sea-level change can be estimated from long-term tide-gauge data measured at tide gauges over a century. Tide gauges, usually placed on piers, measure the mean sea-level change relative to a nearby geodetic benchmark. Therefore, the local sea-level rise trends usually do not follow the abovementioned IPCC SRES or RCP storylines. Due to tectonic uplift or subsidence, tide gauges may also move vertically with the region. These vertical crustal movements greatly complicate the problems of determining local/regional sea-level change from tide-gauge data.

For instance, using available tide-gauge data in the New Jersey coast (NOAA 2011), Cooper et al. (2005) estimated that the New Jersey coast may have a local component of sea-level rise of 2 mm/year attributed to land subsidence and sediment compaction. Based on the range of GMSL rise from 9 to 88 cm between 1990 and 2100 (Church et al. 2001), adding the local estimation of subsidence and consolidation (2 mm/year), they suggested a local/relative sea-level rise for the New Jersey coast will be between 31 and 110 cm, giving a central value of approximately 71 cm. Furthermore, in the study of the sea-level rise and land use using 7.5 min digital elevation models (DEMs) with 10-m horizontal resolution, they provided the assessment results on two specific (median-projected) sea levels, 61 cm (2 ft) and 122 cm (4 ft), for 2050 and 2100, respectively, by means of the so-called contour-line projection approach. On the other hand, some studies of sea-level rise only evaluated the impact of hypothetical sea-level rise. For example, the US-CCSP (2008) used three assumed sea-level rise scenarios (30, 50, and 100 m of sea-level rise by 2100) to evaluate several aspects of their impacts for the Mid-Atlantic US coast using a range of elevation data sets which have large variations in vertical resolution and horizontal accuracy.

In the New Orleans region, land-surface altitude data collected in the leveed areas of the New Orleans metropolitan region during five survey epochs between 1951 and 1995 indicated mean annual subsidence of 5 mm per year (Burkett et al. 2003). By considering this rate of land subsidence and the IPCC mid-range estimate of sea-level rise (48 cm), Burkett et al. (2003) suggested a net 1.0-m decline in elevation during the next 100 years relative to present mean sea level in the New Orleans region. They estimated accordingly that the areas of New Orleans and vicinity that are presently 1.5–3.0 m below mean sea level will likely be 2.5–4.0 m or more below mean sea level by 2100.

Global Warming, Sea-Level Rise, Hurricanes, and Storm Surges

Climate variability and any resulting change in the characteristics of tropical cyclones (tropical storms, subtropical storms, and hurricanes) have become topics of great interest and research within the past years. An emerging focus is how the frequency of tropical cyclones has changed over time, and whether any changes could be linked to anthropogenic global warming. A special attention to Atlantic hurricane activity and its relation with tropical Atlantic warmth has been paid, because the Atlantic is the one tropical cyclone basin that has quantitative records back to the mid-nineteenth century for the whole basin (i.e., North Atlantic Ocean, Caribbean Sea, and Gulf of Mexico) (Landsea 2007). Mann and Emanuel (2006) analyzed those data to conclude that there is a strong historical relationship between tropical Atlantic sea surface temperature (SST) and tropical cyclone frequency for the period of 1871–2005. Similarly, Holland and Webster (2007) investigated Atlantic tropical cyclone frequency and found a doubling of the number of tropical cyclones over the past 100 years. With no conclusions about the existence of the Atlantic Multidecadal Oscillation (AMO) which is a natural climate cycle, both papers linked these changes of Atlantic tropical cyclone frequency to anthropogenic greenhouse warming. However, Landsea (2007) pointed out that both analyses, with no indication of uncertainty or error bars, presumed that tropical cyclone counts are complete or nearly complete for the entire basin going back in time for at least a century. And this presumption is not reasonable and that improved monitoring in recent years is responsible for most, if not all, of the observed trend in increasing frequency of tropical cyclones. Through reanalyzing the historical data of Atlantic basin storms, Landsea (2007) indicated that large, long-term "trends" in tropical cyclone frequency are primarily manifestations of increased monitoring capabilities and likely not related to any real change in the climate in which they develop.

From the point of view of coastal hazard (flooding and erosion) management, increasing tropical storm and hurricane activity may cause more frequent flooding and inundation in the current coastal floodplains. Even if it is assumed that the strength of storms shows no change in the future, under the future conditions of sea-level rise, current flood levels and inundation areas will be exceeded, and low-lying lands will still be permanently inundated. For example, Cooper et al. (2005) studied the future sea-level rise in the New Jersey coast by introducing

only two sea-level rise scenarios, i.e., 0.61 m (1 ft) and 1.22 m (2 ft). By comparing with the US Federal Emergency Management Agency (FEMA) tidal surge frequency for 5-, 10-, 20-, 30-, 50-, and 100-year flood water levels for Atlantic City, New Jersey, they found that sea-level rise will allow current flood levels to be exceeded and low-lying lands to be flooded with increase frequency. In the case of 0.61 m rise in sea level, the current 30-year storm will produce a flood water elevation of 2.96 m, which exceeds the current 100-year FEMA flood level (2.90 m at Atlantic City). After a 1.22 m rise in sea level, the current 5-year storm will cause water levels above the current 100-year flood level. In other words, provided that other factors being equal, New Jersey's current 100-year flood levels could become the 30-year flood level after a 0.61 m sea-level rise and the 5-year flood level after a 1.22 m rise. Cooper et al. (2005) further estimated that 6.5 % of the state's total land area will be inundated in the case of the current FEMA 100-year flood level due to storm; the inundation area due to the same storm after 0.61 m rise in sea level will increase up to 9 % of the state's total land area.

In low-lying areas, subsidence and uplift play an important role in flood management. As mentioned above, an average 5-mm per year land subsidence in the New Orleans region and IPCC mid-range estimate of sea-level rise (480 mm) suggests a net 1.0-m decline in elevation during the next 100 years relative to present mean sea level (Burkett et al. 2003). A storm surge from a category 3 hurricane (estimated at 3–4 m without waves) at the end of this century, combined with global mean sea-level rise and land subsidence, would place storm surge at 4–5 m above the city's present altitude. The effect of such a storm on flooding in the New Orleans Metropolitan Statistical Area (MSA) will depend upon the height and integrity of the regional levees and other flood-protection projects at that time (Burkett et al. 2003).

The US-CCSP (2008) examined the effects of sea-level rise on coastal floodplains and on coastal flooding management issues confronting the US FEMA, the floodplain management community, the coastal zone management community, and the public, including private industry. From the analysis of historical tide station records for the highest storm tides in the Mid-Atlantic Coast, this report shows that storms today with slightly lesser storm surge than historical storms have had slightly higher storm tide elevations relative to the land due to sea-level rise. This suggests that any given storm could have higher flooding potential in the future due to higher sea levels than it would if it occurred today.

During storm events, local water elevations at coastal zones will significantly increase due to nonlinear physical processes such as storm surges, high tides, wave setup, and their combinations. These combinations largely determine temporally/spatially varying flooding/inundation, coastal erosion, and overwash in barrier islands in coastal regions. Additionally, sea-level rise will lift up flood levels by providing a higher base for a storm surge to build upon. Even if the frequency and strength of storms will keep no change in the future, sea-level rise undoubtedly will cause flooding/inundation over a wider coastal area due to shoreline retreat, higher wave setup, and storm surges. Because of the nonlinear and unsteady behavior of storms, the linear contour-line project approach can lead to poor depiction of reality of sea-level rise impacts. It is, therefore, essential to assess the dynamic, interactive,

and nonlinear impacts of hazardous storms under conditions of sea-level rise for the purpose of better coastal protection management in a local or regional area.

Coupled coastal and ocean process models have been applied to assess the impacts of local/regional sea-level rise and storm/hurricane events. Using a numerical storm surge model, Smith et al. (2010) investigated potential impacts of 0.5 and 1.0 m of local sea-level rise on hurricane surges waves in southeast Louisiana. They found that in the regions of large surges, the effect of mean sea-level (MSL) rise added linearly to the simulated surges. However, in the regions of moderate surges (2–3 m), particularly in wetland-fronted areas, the increase in surge height was 1–3 m larger than the increase in mean sea-level rise. They showed that sea-level rise alters the speed of propagation of surges and their amplification in different regions of the coast. For lower Texas coast bays in the Gulf of Mexico, Mousavi et al. (2011) developed a simple relationship between storm surges, sea-level rise, and hurricane intensification for three major historical hurricanes, concluding that the dynamic interaction of surge and sea-level rise lowered or amplified the surge at different points within a shallow coastal bay. For the Mississippi and Alabama coast, Bilskie et al. (2014) introduced a modeling procedure to simulate the response of storm surges to changes in sea level, land use and land cover, and land-surface elevations for past (1960), present (2005), and future (2050) conditions. The results show that the storm surge response to SLR is dynamic and sensitive to changes in the landscape.

Geophysical and Socioeconomic Impacts of Sea-Level Rise on Coast and Estuary

Human populations have a tremendous impact on the quality of coastal and estuarine environments. The ultimate goal of assessment of sea-level rise and climate change is to quantify these impacts on coastal communities as human society. In 2001 just over half the world's population – around 3.2 billion people – lived within 200 km of a coastline (Hinrichsen 2009). The rate of population growth in coastal areas is accelerating and increasing tourism adds to the pressure on the environment. In the United States, around 37 % of the total US population lives in the 364 "coastal counties," including the Great Lakes, which contains V zones (a coastal hazard zone defined by FEMA (2009)) (Crowell et al. 2007). In their recent publication (Crowell et al. 2010), it is shown that about 8.2 % of the coastal population (86,541,000 people) live in 1 % annual chance (or 100-year) coastal flood hazard areas as defined by FEMA. Therefore, the impacts of sea-level rise on coastal and estuarine area are, in principle, closely related to its geophysical and socioeconomic effects to the natural habitat of human being in the areas. In general, there are four primary geophysical impacts of sea-level rise, i.e.:

- Permanent inundation and displacement of coastal lowlands, including loss of wetland
- Increased flood and storm damage

Table 3 The physical impacts of sea-level rise and other relevant factors

Impact of sea-level rise	Other relevant interacting factors			
	Meteorology	Oceanography	Hydrology	Geomorphology
Permanent inundation and displacement of coastal lowlands	Wind, temperature, storm, hurricane, rainfall	Wave, storm surge, tide, ocean current	Runoff, river flood, backwater effect	Sediment supply, morphological changes, land claim, subsidence
Increased flood and storm damage	Wind setup, rainfall	Wave setup, storm surge, strong surge, tide current	Runoff, river flood, backwater effect	Morphological changes
Increased erosion	Rainfall	Wave, storm surge, tide, current	River flood	Sediment supply, subsidence, land claim
Salinization of surface and increased waters	Temperature, storm, hurricane, rainfall	Tide, surge, ocean current	Runoff, groundwater table change, catchment management	Morphological change, subsidence

- Increased erosion
- Salinization of surface and increased waters

In Table 3, the geophysical impacts of sea-level rise and relevant interacting factors are summarized. This table indicates that the relevant interacting factors of the impacts of sea-level rise are related to multi-scale physical processes including meteorology, oceanography, hydrology, and geomorphology. Assessment of the impacts of sea-level rise strongly depends on the understanding of nonlinear behavior of the integrated coastal system driven by these multi-scale physical processes. Considering specific coastal regions, more detailed categories on the geophysical impacts of sea-level rise can be identified as follows:

- Increased wave energy in the nearshore area (shoreline erosion and land erosion)
- Upward and landward migration of beaches (shoreline retreats)
- Accelerated coastal retreat and erosion
- Saltwater intrusion into coastal freshwater aquifers and rivers (upstream)
- Damage to coastal infrastructure due to increased wave energy
- Broad impact on coastal economy of coastal communities (coastal resilience)

Assessment of socioeconomic impacts of sea-level rise is an ultimate goal for building resilient coastal communities to alleviate coastal hazards generated from severe storms together with sea-level rise. Readers may find a large number of publications such as government reports and academic papers on the assessment of socioeconomic impacts and management policies on this issue, e.g., IPCC report

(IPCC 2007), US-Climate Change report (US-CCSP 2008), and Nicholls et al. (2007). Although discussions of the socioeconomic impacts are out of this chapter's range, potential socioeconomic impacts of sea-level rise summarized by Nicholls (2003) are listed as follows:

- Increased loss of property and coastal habitats
- Increased flood risk and potential loss of life
- Damage to coastal protection works and other infrastructure
- Loss of renewable and subsistence resources
- Loss of tourism, recreation, and transportation functions
- Loss of nonmonetary cultural resources and values
- Impacts on agriculture and aquaculture through decline in soil and water quality

In the following contents, the impact of sea-level rise means its geophysical impact if there is no special explanation.

Assessment of Impact of Local Sea-Level Rise for Coastal Zone Management

The impacts of sea-level rise can be assessed in different ranges of spatial scales, i.e., global, regional, and local scales, in which some case studies are driven by policy making (e.g., Nicholls et al. 1999; Nicholls 2004; Schleupner 2007), and some are more science orientated to examine the methodologies that can transfer scientific knowledge into decision-making tools (e.g., Cooper et al. 2005; Capobianco et al. 1999). Sea-level rise may significantly change the areas of coastal hazard maps in a specific coast. Therefore, coastal hazard management in coastal zones requires local assessment of impacts of sea-level rise. Figure 1 presents a general procedure for assessment of impacts of sea-level rise from global scale to local scale. As for the sea-level rise assessment methodologies, since the contour-line projection approaches to assess sea-level rise only can give an average estimation (most likely underestimation) of the impacts, further accurate numerical simulations are needed to include the nonlinear variations of other physical factors such as storm surge, wave, tide, etc., along with sea-level rise. In fact, direct numerical modeling plays an important role on predicting multi-scale physical processes including storm track, weather change, ocean volume increase, surge, tide, wave, and inland flood in atmosphere, ocean, and coast, as well as quantitative evaluation of sea-level rise impacts in time and space. It also has to point out that the reliability of the sea-level rise assessment results strongly depend on the accuracy of the coupled physical models.

In order to assess the impacts of sea-level rise in a specific coast, coastal zone management is usually practiced through defining coastal flood plain and coastal flood hazard zones based on coastal processes. In general terms, a floodplain is any normally dry land surrounding a natural water body that holds the overflow of water during a flood. The US federal regulations governing FEMA (2009) define

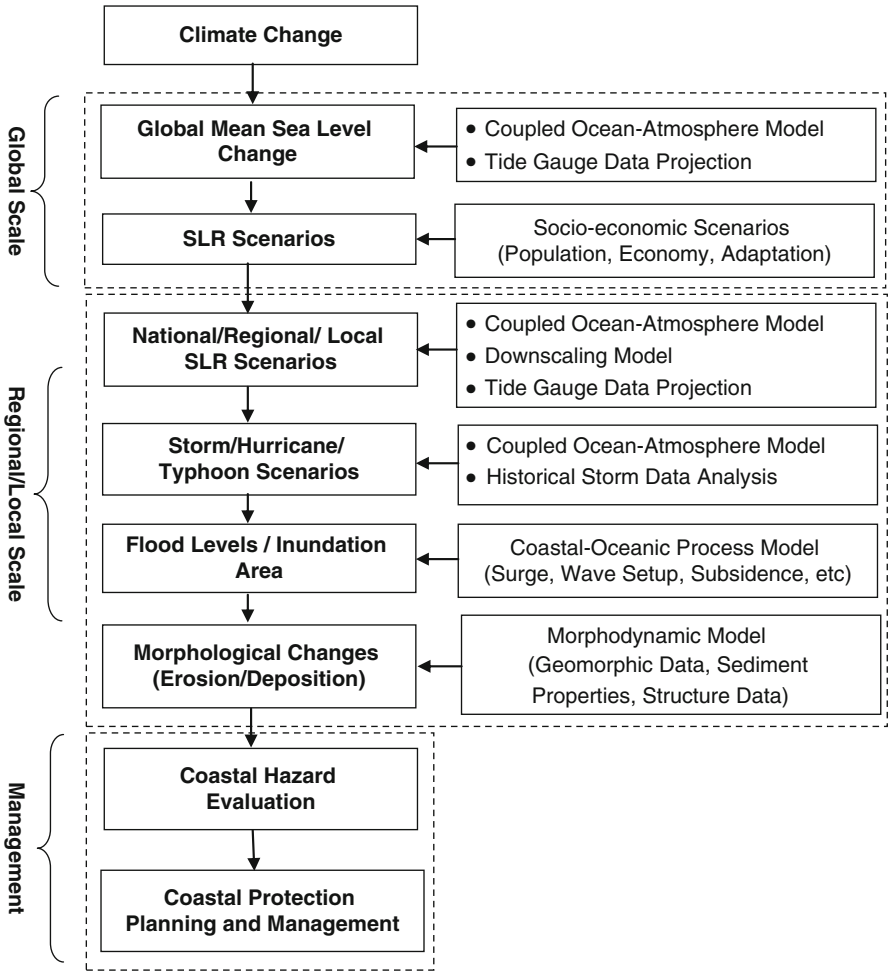

Fig. 1 Assessment of sea-level rise in global/regional/local scale

floodplains as "any land area susceptible to being inundated by flood waters from any source." The National Oceanic and Atmospheric Administration (NOAA) National Weather Service (NWS) defines a floodplain more specifically as the portion of a river valley that has been inundated by the river during historic floods. None of the formal definitions of floodplains include the word "coastal." However, as river systems approach coastal regions, river base levels approach sea level, and the rivers become influenced not only by stream flow but also by coastal processes such as tides, waves, and storm surges (Ding and Wang 2008b). Coastal areas are periodically inundated by tides, waves, and surges. The slope and width of the coastal plain determine the size and inland extent of coastal influences on river systems. The US-CCSP (2008) has given a good working definition of a coastal

floodplain, borrowing from the river floodplain definition, which is any normally dry land area in coastal areas that is susceptible to being inundated by water from any natural source, including oceans (e.g., tsunami run-up, coastal storm surge, relative sea-level rise) in addition to rivers, streams, and lakes. (Tsunami run-up occurs when a peak in the tsunami wave travels from the nearshore region onto shore. Run-up is a measurement of the height of the water onshore observed above a reference sea level. For more information, one may refer to USGS (2011).)

FEMA (2009) has defined four coastal zones in cross shore for management of coastal flood hazards: *Offshore zone* is the area, usually in the deep water, influenced by waves and water levels that are not substantially influenced by bathymetry (i.e., the water depth relative to sea level) or topography (i.e., the elevations above sea level). Dominant processes in this zone include swell, seas, astronomical tides, storm surge, and large-scale climate perturbations such as El Niño. *Shoaling zone* is the area outside the surf zone where offshore conditions (mainly waves) are transformed by interaction with bathymetry or topography. This transformation of wave in the shoaling zone includes refraction, diffraction, dissipation, and generation of waves by wind. *Surf zone* is defined as the area where waves break as they interact with the bottom. Dominant processes in the surf zone include wave setup, run-up, overtopping, erosion/deposition, and interaction with structures. *Backshore zone* represents the area that is outside the normal surf zone but may be subject to inundation during coastal flooding events. This area is subject to development and is the critical area for determination of flood hazards. As for coastal hazard management, on the other hand, FEMA generally divided coastal flood hazard zones into three categories: (1) *VE zone*: the coastal high hazard area where wave action and/or high-velocity water can cause structural damage during the 1 % annual chance flood including wave run-up zone, wave overtopping splash zone, high-velocity flow zone, breaking wave zone, and primary frontal dune zone; (2) *AE zone*: where flood hazards are not as severe as in VE zones; and (3) *X zone*: which is only subject to flooding by flood more severe than the 1 % annual chance flood.

Numerical Modeling for Assessing Dynamic Impacts of Local Sea-Level Rise and Hazardous Storms

Numerical modeling plays a decisive role in assessing various impacts of sea-level rise in different spatial scales. Since climate change is a global-scale phenomenon, a global circulation model (GCM) is the first choice to predict the thermodynamic motion of atmosphere layers due to greenhouse gas emission. By coupling with ocean models which represent oceanographic processes, a coupled ocean-atmosphere model (OAM) is able to predict the variation of ocean water volume in response to the changes of atmospheric temperature. Usually, GCMs and OAMs can predict global-scale temporal-spatial variations of various physical variables such as air temperature, precipitation, concentration of greenhouse gases, sea-level change, etc. However, the spatial resolution of the numerical results is in general

several hundred kilometers on the Earth's surface. So far, there is not a numerical model capable of directly simulating sea-level changes under local hydrological conditions with a local coastal scale (which can be several meters to several kilometers). As shown in Fig. 1, a number of numerical models for different spatial scales are usually employed to obtain the sea-level rise scenarios in response to greenhouse gas concentrations on the global scale, to downscale the GCM model results to a local/regional scale, and then to use a coastal-ocean process model to predict the impacts of the sea-level rise scenarios together with a hazardous storm condition in a specific local coast/estuary.

Projection Approach and Numerical Simulation

Other than numerical simulation modeling based on physical principles, projection approach (e.g., Cooper et al. 2005) is a simple but quick way to delineate flood hazard areas due to mean sea-level scenarios by projecting the corresponding contour lines on terrain maps within GIS models. But its demerit is the underestimation of the impacts of sea-level rise such as area of inundation and erosion. The only way to predict the day-to-day weather and changes to the climate over longer timescales is to use numerical simulation models, such as a GCM or OAM. These models solve complex mathematical equations that are based on well-established physical laws that define the nonlinear and unsteady behavior of weather and climate. According to the 2001 IPCC Third Assessment Report, a total of seven GCMs were used for assessing the global climate change. In the 2007 IPCC Fourth Assessment Report, as many as 23 GCMs were adopted to predict the global climate change including sea-level variations in response to eight greenhouse gas emission scenarios (IPCC Data Distribution Centre 2010).

Owing to computer capacity limitations, it is highly impossible to represent all the detail in the real world in a computer model, so approximations have to be made. The models are tried and tested in a number of ways: (1) They are used to reproduce the climate of the recent past, both in terms of the average and variations in space and time (John et al. 1997). (2) They are used to reproduce ancient climates that have been known (which are more limited) (John et al. 2003). These climate models typically have three-dimensional representation of the ocean and sea ice, an interactive carbon cycle, interactive atmospheric chemistry models, and the coupled atmosphere-ocean-carbon-cycle-chemistry model (White and Bromley 1995; Gordon et al. 2000). The global-scale climate simulations are extensive and usually carried out in high-performance parallel computers.

In a regional/local scale, 2D or/and 3D coastal/estuarine models are used to simulate and to predict physical processes under a set of given conditions which typically represent storm/hurricane events and sea-level rise scenarios (e.g., Ding et al. 2013). Coastal/estuarine models are to compute coastal and estuarine processes such as wave transformation, storm surge, tide, sediment movement, erosion/deposition, water quality, etc., so as to predict hydrological variables, e.g., water levels, velocities, bed changes, biomass properties, etc. Those process-based models can

predict complex unsteady physical processes to provide a set of dynamic results (basic databases) for engineering assessment and coastal hazard mapping. They enable to handle various data inputs such as hydrological data (wave, wind, tide, runoff, river inflow, storm track, etc.), bathymetry/topography (e.g., DEM data from GIS application), boundary condition data, etc. So far, coastal/estuarine numerical modeling is the most accurate methodology to predict/plan coastal hazards and sea-level rise impacts on coasts and estuaries. They have been extensively adopted in coastal storm water management.

Downscaling Techniques

GCMs are in general three-dimensional climate models which are based on physical principles and take into account as many physical variables as possible that could affect global climate. They are the only capable tools for predicting global-scale climate patterns in response to the increase of greenhouse gas emission. They are therefore widely applied to assess climate change impacts for various climate change scenarios. IPCC has provided all the output results generated by the selected IPCC GCMs in the online site of IPCC Data Distribution Centre at www.ipcc-data.org for public data download service. However, the horizontal resolution of the GCM model results is very coarse, up to several hundred kilometers in grid. For a regional assessment of climate change, a downscaling technique is needed to nest a higher-resolution local/regional climate model within a coarse resolution GCM. Wilby et al. (2002) categorized downscaling methodologies into four main types: (1) dynamic climate modeling, (2) synoptic weather typing, (3) stochastic weather generation, and (4) regression-based approaches. They give a detailed description and review on the downscaling techniques. Among them, dynamic downscaling together with a regional climate change model can resolve smaller-scale atmospheric features such as orographic precipitation (i.e., rain, snow, or other precipitation produced when moist air is lifted as it moves over a mountain range) or low-level jets better than the host GCM. Regression-based downscaling methods, which are relatively simpler, rely on empirical relationships between local-scale predictands and regional-scale predictors. Individual downscaling schemes differ according to the choice of mathematical transfer function, predictor variables, or statistical fitting procedure.

Challenges to Planning and Management of Coastal Zone Under Conditions of Sea-Level Rise and Hazardous Storms

Planning and management of coastal zone are facing more new challenges due to sea-level rise and increasingly frequent storms and hurricanes in order to alleviate the damage of flooding, inundation, and erosion. Under the conditions of climate change and sea-level rise, these difficulties could happen to coastal zone management and planning to:

- Find new design criteria of coastal infrastructure, e.g., design parameters for storm, wave, surge, and tide
- Redefine extreme storm events, e.g., the 1 % annual chance storm (i.e., 100-year storms due to global climate change)
- Update out-of-date flooding/inundation maps for most of coastal communities
- Redefine storm surge zones, evacuation route and evacuation zones, emergency shelter, etc.
- Reevaluate coastal resiliency, hazard preparedness, coastal emergency management, first responding planning, coastal infrastructure planning, etc.
- Establish and maintain a premier data collection and delivery system such as a GIS- and Internet-based system.

Brief Review on Coastal and Estuarine Process Modeling

Understanding the nonlinear and unsteady features of coastal and estuarine processes driven by astronomical tides, storm surge, wind-generated waves, and river flows is essential to quantify the impacts of sea-level rise with hazardous storms for the purposes of coastal flood prevention, sediment management, shoreline erosion control, navigation channel maintenance, and designing coastal infrastructure. Sediment transport, consisting of longshore and cross-shore sediment movements and river sediment supply into coasts and estuaries, leads to complex morphological changes such as shoreline erosion/accretion, levee/barrier breaching, river bank erosion, variations of river mouth bar, navigation channel refilling, migration of offshore bar, etc. (A levee breach or levee failure is a situation where a levee fails and the water that was retained by that levee is allowed to flood the land behind the levee. A barrier breach happens in barrier islands in a coast when storm surges and/or high waves breached barrier.) Under increase of sea levels and shoreline retreat, some bathymetrical changes during storm and flood period may aggravate the problem of coastal flood and inundation.

Numerical modeling is the only way to predict the temporal-spatial variations of sea-level rise impacts in a specific coast under naturally complex hydrological conditions. In the past decades, significant progress has been made in the studies of coastal and estuarine processes by means of physical experiments and computational simulations. Due to the complexities of physical processes, direct simulation of long-term (daily to yearly) hydrodynamic and morphodynamic responses to sea-level changes and storm events in a large-scale coast driven by astronomical tides, unsteady irregular waves, storm surges, wave-induced currents, and sediment transport has been a challenging goal. In recent years, with the process-based approach having been employed to the development of the coastal and estuarine process model, the long-term simulation of multi-scale hydrodynamic and morphodynamic changes has become feasible (e.g., Shimizu et al. 1996; Zyserman and Johnson 2002). In general, this multi-scale simulation is accomplished by computing sequentially the wave field, the current field, and the seabed changes under the given boundary conditions and sea-level changes. Then a new bathymetry

will be fed back to affect the computations of the wave and current fields in the next time step. By this iterative procedure going through the wave-current-morphological models, it is possible to simulate the morphodynamic process by using an empirical sediment transport model for the time-scale morphological process (e.g., Ding and Wang 2008a).

According to the existence of different spatial scales, the practical numerical model for simulating hydrodynamic and morphodynamic processes in coasts and estuaries has the following four types: (1) one-dimensional (1D) longshore coastline models, (2) two-dimensional (2D) cross-shore coastal profile models, (3) 2D horizontal coastal/estuarine/oceanic process models, and (4) fully three-dimensional (3D) models. 1D coastline models can only describe behaviors of the longshore sediment transport and shoreline evolutions by using the sand budget approach; 2D cross-shore coastal profile models are able to predict the vertical variations of coastal profiles, but not the variations of the longshore sediment transport; 2D horizontal coast/estuary/ocean models can simulate hydrological and morphological variations over a coastal area with a rather wide range of spatial scales (e.g., 100 m^2 to 100 km^2) with the vertical variations of waves and currents ignored. Nevertheless, only fully 3D morphological models are expected to take into account both the vertical and horizontal variations of wave and current (e.g., Lesser et al. 2004; Warner et al. 2008). However, due to the time-consuming nature for practical problems, 3D models are restricted generally to predict the temporal-spatial hydrological and morphological changes in a relatively small near-field and in a short duration. On the other hand, the horizontal 2D models have the potential to assess the impacts of storms and sea-level rise in local/regional/global scales. Therefore, a quasi-3D model with the efficiency of the 2D depth-averaged model and better accuracy than 2D models would be a feasible tool for the long-term morphodynamic simulations in large-scale coastal engineering problems. Zyserman and Johnson (2002) and Ding et al. (2006b) have presented, respectively, two quasi-3D coastal process models in which an empirical 3D shear stress distribution was used to take into account a quasi-3D effect of sediment transport. They concluded that quasi-3D coastal/estuarine process models enable to compute accurately free-surface water motions, cross-shore sediment transport, and morphological changes under natural hydrological conditions with high computing efficiency.

Recently, semi-empirical numerical approaches were presented by means of tide-averaging currents to assess long-term morphological changes on both the meso- and macro-scale in coastal inlets and tidal lagoons in estuaries, e.g., rapid assessment of morphology (RAM) by Roelvink (2006). But these tidal-phase-averaging approaches are not able to simulate nonlinear and highly unsteady hydrodynamic and morphodynamic processes during a short-term storm, as they cannot capture the peak surge and maximum flood inundation in storms/hurricanes. Nevertheless, due to the concern of computing time for assessing long-term impacts of sea-level rise over a few decades in the future, a similar approach based on tide-averaging hydrodynamic variables for rapid assessment of impacts of sea-level rise may be needed.

Table 4 Summary of computer codes of phase-averaged wave models

Models	Wave processes included	Steady or unsteady	Mesh coordinates	References
CCHE2D-Coast	Refraction, shoaling, breaking, diffraction, wave-current interaction, friction, transmission through obstacles	Steady or quasi-steady	Non-orthogonal	Ding et al. (2006b)
SWAN 40.41	Refraction, shoaling, breaking, whitecapping*, wave-wave interaction, reflection, diffraction	Steady or optionally unsteady	Cartesian or spherical	SWAN (2011)
WAM	Refraction, shoaling, breaking, whitecapping, wave-wave interaction	Steady or optionally unsteady	Cartesian	WAMDI (1988)
MIKE21 NSW	Refraction, shoaling, breaking	Steady	Cartesian	Holthuijsen et al. (1989)
STWAVE	Refraction, shoaling, breaking, whitecapping	Steady	Cartesian	Smith and Cialone (2000)
CMS-WAVE	Refraction, shoaling, breaking, diffraction, wave-current interaction, friction, wind-induced waves	Steady	Cartesian	Lin et al. (2008)

[a]Note: Wave whitecapping is a situation that wave is blown by the wind so its crest is broken and appears white

As an example of quasi-3D coastal and estuarine process models, CCHE2D-Coast is capable of simulating tides, waves, currents, sediment transport, and morphological changes in various coasts and estuaries (Ding et al. 2006b; Ding and Wang 2008a). It has been applied to assess the impacts of hazardous hydrological forcings including sea-level changes during storms and hurricanes (or typhoon) on coastal flood inundation, erosion and deposition, and navigation maintenance (Ding et al. 2007, 2013; Ding and Wang 2008b). This model has systematically integrated three major submodels for simulating irregular wave deformations, astronomical tides, river inflows, wave-induced currents, sediment transport due to combined waves and currents, and morphological changes in coasts and estuaries. A validated algorithm in the CCHE2D (Jia et al. 2002) for the treatment of wetting/drying was directly used for predicting tidal flat variations and coastal inundations. This process-based model has been extensively validated by simulating waves, wave-induced currents, and morphological changes in coastal applications in various laboratory and field scales (Ding et al. 2004, 2006a, b; Ding and Wang 2005, 2008a).

Some other commercial and in-house numerical models capable of modeling coastal and estuarine processes are briefly reviewed as follows: Table 4 gives a short list of computer codes of phase-averaged irregular wave models, in which the wave transformation and deformation processes and mesh coordinates are evaluated. In Table 5, some 2D hydrodynamic models have been compared with each other in respect to their numerical methods, grid systems, wetting/drying modeling capability, consideration of irregular waves, modeling capability for complex quasi-3D flow structures, and the

Table 5 Some existing 2D coastal/estuarine hydrodynamic models

Models	Num. method	Irregular waves	Undertow flow	Wetting and drying	Description of structures	Mesh system	References/developers
MIKE2D HD	FD	√	N/A	Unstable(1)	Not good(1)	SCG	MIKE 21 (2008)/DHI
DELFT3D-FLOW	FD	√	N/A	√	Unclear	SCG	Roelvink and Van Banning (1994)/WL Delft Hydraulics
TELEMAC 2D	FE	N/A	N/A	No validation	√	Unstructured	TELEMAC-2D (1995)/EDF-DER, France
CCHE2D-Coast	EE	√	√	√	√	NOG	Ding et al. (2006b)/NCCHE
TRIM 2D	FD	N/A	N/A	No validation	Unclear	RG	Casulli and Cheng (1992)/USGS, USA
ADCIRC-2D	FE	√	N/A	√	√	Unstructured	Westerink et al. (1993)

Note: for (1) please refer to the report of CHL-ERDC by Scott (2003)
FD finite difference, *FE* finite elemental, *EE* efficient element, FV finite volume, *RG* rectangular grid, *SCG* staggered curvilinear grid, *NOG* non-orthogonal grid, *DHI* Danish Hydraulic Institute, *EDF-DER Laboratoire National d'Hydraulique* in France

Table 6 Some models available for modeling morphological processes in coasts and estuaries

Model	Spatial dimension	Flow	Salinity	Sediment transport modeling	
				Stochastic process	Non-equilibrium
MIKE 21	2	SWE	√	Uni.	Equi.
CCHE2D	2	SWE	N/A	Non-uni.	Non-uni.
CCHE2D-Coast	2	SWE	√	Uni.	Equi.
CCHE3D	3	RAE + HS	N/A	Non-uni.	Non-uni.
MIKE 3	3	RAE	√	Uni.	Equi.
TELEMAC3D	3	RAE-HS	√	Uni.	Equi.

Note: *SWE* shallow water equations, *RAE* 3D Reynolds averaged equations, *HS* hydrostatic assumption, *Uni*. uniform sediment size, *Non-uni*. nonuniform sediment sizes, *Equi*. equilibrium transport, *Non-equi*. nonequilibrium transport

effects of coastal structures. The different capabilities of the models available for modeling sediment transport and morphological changes are shown in Table 6. In addition, there are some other storm surge models which can be used to predict storm surge and coastal inundation due to sea-level rise and storms, but incapable of simulating sediment transport and morphological change together with coastal hydrodynamic simulation, e.g., POM model (Blumberg and Mellor 1987), SLOSH model (Jelesnianski et al. 1992), and SHORECIRC model (Svendsen et al. 2003).

A Case Study: Assessment of Impacts of Sea-Level Rise and Hazardous Storm in an Estuary

This case study is to demonstrate the assessment of impacts of sea-level rise and hazardous storms by simulating hydrodynamic variations and morphological changes in an estuary located in the west coast of Taiwan by using CCHE2D-Coast. This study did not estimate how much the sea-level rise will be; instead, it used several sea-level rise scenarios which are broadly based on recent sea-level rise forecasting studies and combined with historical storms as hydrological forcings. In this study, four scenarios, i.e., 0.5, 1.0, 1.5, and 2.0 m sea-level rise by 2100, were adopted to assess the impacts of sea-level rise in the estuary. CCHE2D-Coast was used to predict hydrodynamic processes (water elevations and velocities) and morphological changes under the conditions of the four scenarios and a storm flood event.

Information of the Study Estuary and Model Validations

The estuary of study site is located at the west coast of Taiwan called Touchien Estuary, facing to Taiwan Strait. As shown in Fig. 2, this estuary has a 2.0-km wide river mouth, a river mouth bar, two islands inside the bay, and two rivers (Touchien

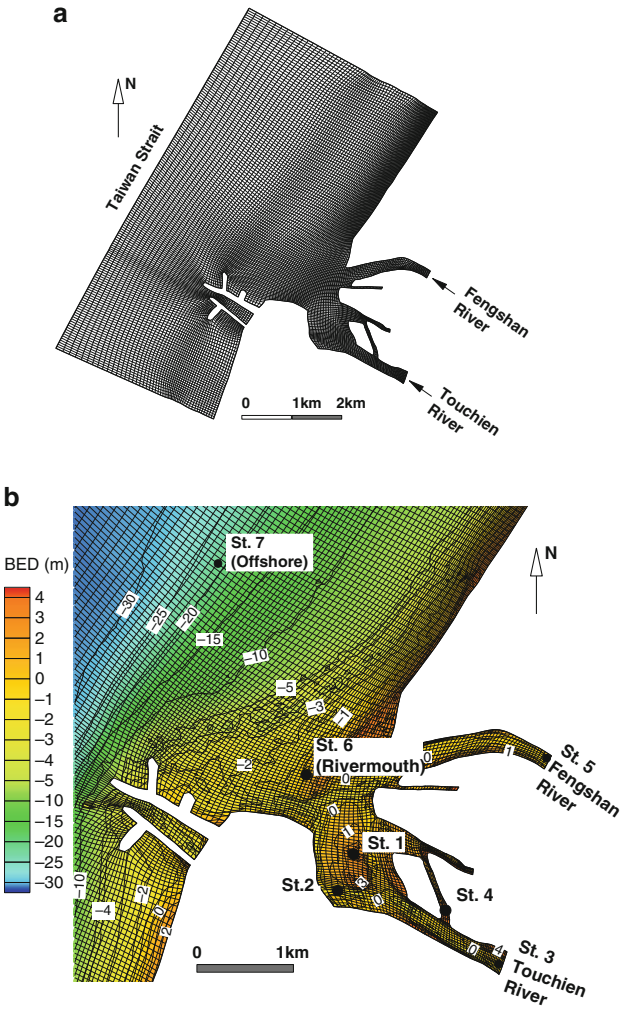

Fig. 2 Grid and bathymetry in Touchien Estuary. (**a**) Overview of the computational domain. (**b**) Close-up view of the estuary

and Fengshan Rivers). A highly dense population lives in the coastal communities very close to the beaches. And the coastal zone is vulnerable facing storm (typhoon) attack and river floods and meanwhile is sensitive to sea-level rise. During storms or typhoons, this small estuary has equally important hydrodynamic and morphodynamic processes driven by tides, storm waves, surges, and river floods. The morphodynamic processes are therefore driven by multi-scale physical forcing such as river flows, tidal currents, nearshore currents, and wave breaking across the surf zone. Morphological changes in the estuary are generally complex. To investigate floods and morphological changes in the estuary, a computational domain, as

shown in Fig. 2a, was used in the simulations. A non-orthogonal structural grid was generated by the CCHE2D mesh generator (Zhang and Jia 2005) to cover this entire estuarine and its adjacent coastal area. Figure 2b shows a close-up view of the estuarine area in which several stations are marked for output of model results. Through simulating morphological changes during a 3-year period from 2004 to 2006 in which nine typhoon events (i.e., Mindulle, Aere, Haima, Haitang, Matsa, Talim, Longwang, Bilis, and Kaemi) were included, the CCHE2D coastal model has been validated in this study area (Ding et al. 2008). The boundary conditions of tidal elevations and wave properties at offshore in the 3-year simulation were prepared beforehand using a regional storm surge model (a POM model) (POM 2011; Blumberg and Mellor 1987) and the SWAN wave model (SWAN 2011). (The Princeton Ocean Model (POM) is an ocean model that is able to simulate hydrodynamic processes of free-surface flows such as circulation and mixing processes in rivers, estuaries, shelf and slope, lakes, seas, and ocean. SWAN is a wave model that computes random, short-crested wind-generated waves in coastal regions and inland waters. For more information, one may refer to SWAN (2011).) The offshore incident wave properties, i.e., the significant wave heights, the periods, and the mean directions, were provided by field observations and the extracted results from the simulations by the SWAN model. The significant wave heights were usually lower than 2.0 m in most typhoons landed at the east coast and flood events in the coast. According to the grain size measurements, a uniform grain size, $d_{50} =$ 0.2 mm, was used for representing the coastal sediments in the domain. A total load sediment transport formulation was used to calculate sediment fluxes and morphodynamic process from river to coast. Ding et al. (2008) have shown that the computed morphological changes induced by all the storms during the 3-year validation period are in good agreement with the observations. As a result, CCHE2D-Coast was validated in the estuary using the field observation data. For the details on this site-specific model validation, one may refer to Ding et al. (2008).

Hydrodynamic and Morphodynamic Responses to Sea-Level Rise and Storm

As mentioned above, sea-level rise may cause disastrous flooding and inundation during storm periods in the low-lying areas of coasts and estuaries. In order to examine the impacts of sea-level rise together with a storm event, a real storm (typhoon Talim which occurred in August 2005), which attacked the Touchien Estuary from 8/31/2005 to 9/2/2005, was used as the extreme event for this case study. As shown in Fig. 3, two hydrographs, which represent respectively time series of flood flow discharges from the two rivers caused by rainfall of the typhoon, were applied to the two river inlets as the river inflow boundary conditions. These two hydrographs at the inlets of the two river upstreams were obtained beforehand by simulating respectively the storm flood flows in the two rivers from far upstream down to the estuary using a one-dimensional river flow model. The peak discharge was 2,013.67 m^3/s in the Touchien River and 992.66 m^3/s in the Fengshan River, respectively.

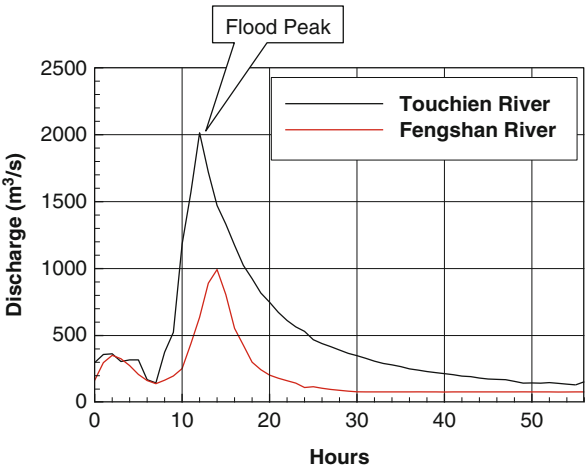

Fig. 3 Hydrographs at two river upstream inlets during a storm flood event

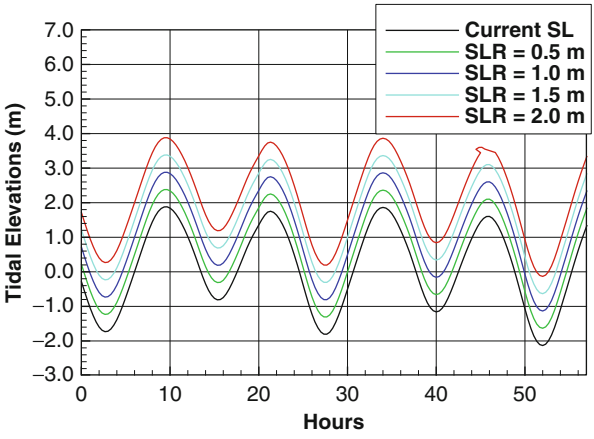

Fig. 4 Tidal elevations boundary conditions at the offshore

Then, the site-specifically validated CCHE2D-Coast was applied to simulate flood flows and sediment transport driven by this selected storm combined with the five sea-level rise scenarios (i.e., 0.5, 1.0, 1.5, 2.0 m sea-level rise, and a case without mean sea-level change). The mean sea-level changes were considered as the different scenarios of tidal elevations at the open sea. So the sea-level changes were added into the tidal elevations during the storm event to create new tidal elevation time series with the mean sea-level rise. Figure 4 shows the five time series of tidal elevations at the offshore which represent the tides under the conditions of the five sea-level rise scenarios. As the boundary conditions of a wave action model at offshore of the estuary, the wave properties (i.e., significant heights, averaged periods, and mean directions) at the offshore were specified on the offshore boundary for simulation of wave transformation from the offshore to the coast zone and the estuarine area. The offshore incident significant wave heights varied in the range

from 0.5 to 1.6 m during the storm event (Ding et al. 2013). In addition, the time series of prevailing wind speed and direction observed during the storm event were used in this study as the surface wind forcing over the estuary, in which the wind speed varies from 0.3 to 16.4 m/s.

Under these boundary conditions of tides and waves with the combined sea-level rise and storm, hydrodynamic and morphodynamic processes in the estuary were simulated using the site-specifically validated CCHE2D-Coast. The numerical simulations were performed by sequentially computing waves, currents, sediment fluxes, and morphological changes driven by the given hydrological conditions such as tides, waves, and river inflows at the five sea-level rise scenarios. To do so, the wave fields were updated every 1 h to reflect the changes of the offshore incident wave climate. And the sediment fluxes in the alluvial river reaches, the estuary, and the coastal area were calculated by an empirical sediment transport formulation which has taken into account the variations of sediment transport due to waves and currents over the entire estuarine region from the river-flow-dominant upstream to the wave-dominant coast (Ding and Wang 2008a).

Figure 5 shows the spatial distributions of computed significant wave heights and mean wave directions at the flood peak under the different conditions of sea-level rise. Along with the increase of the flooding area in the estuary from the current sea level (i.e., no sea-level rise) to 2-m rise, numerical results show that the offshore waves could invade the estuarine area from the river mouth toward the upstream river reaches. In comparison with the case for the current sea level (Fig. 5a), sea-level rises from 0.5 to 2.0 m would promote the invasion of offshore waves inside the estuary and could further change the morphological features in the bay area.

Figure 6 shows the comparisons of the computed currents and water elevations at the flood peak in the five cases over a range from the current sea level to 2.0 m rise. The results indicate that significant increases in water elevations, offshore surge water invasion inside the estuary, and widening inundation areas occur when the sea-level rise is more than (and equal to) 1.0 m.

In order to investigate the water elevation increases in the estuary which respond to the sea-level rise and the storm event, the time series of water elevations at seven selected monitoring stations are plotted in Fig. 7. As the locations of the stations are shown in Fig. 2b, these stations represent respectively the offshore, river mouth, cross sections inside the estuary, and two rivers upstream. Intercomparisons of these water elevation changes clearly show that the tidal variations will affect the two river upstreams if sea-level rises up to 1.0 m. With the sea-level rise up to 2.0 m, the entire river reaches will become tidal reaches and therefore possibly receive the saline water from ocean. Furthermore, the differences of water elevations at a same station generated by the five sea-level scenarios are shown in Fig. 8. It also can be concluded that all the computational area could become tide-influenced estuary if there is 2.0-m sea-level rise, and most of the coastal community will be exposed to the attack of high tides, storm waves, and river floods. As it can be seen from Fig. 8a, there is an increasing inundation area at the river mouth bar due to the sea-level rise, and the river mouth area behaves like the offshore after the rise is equal to and higher than 1.5 m. And the upstream river area is more susceptible to the tidal effect as it is

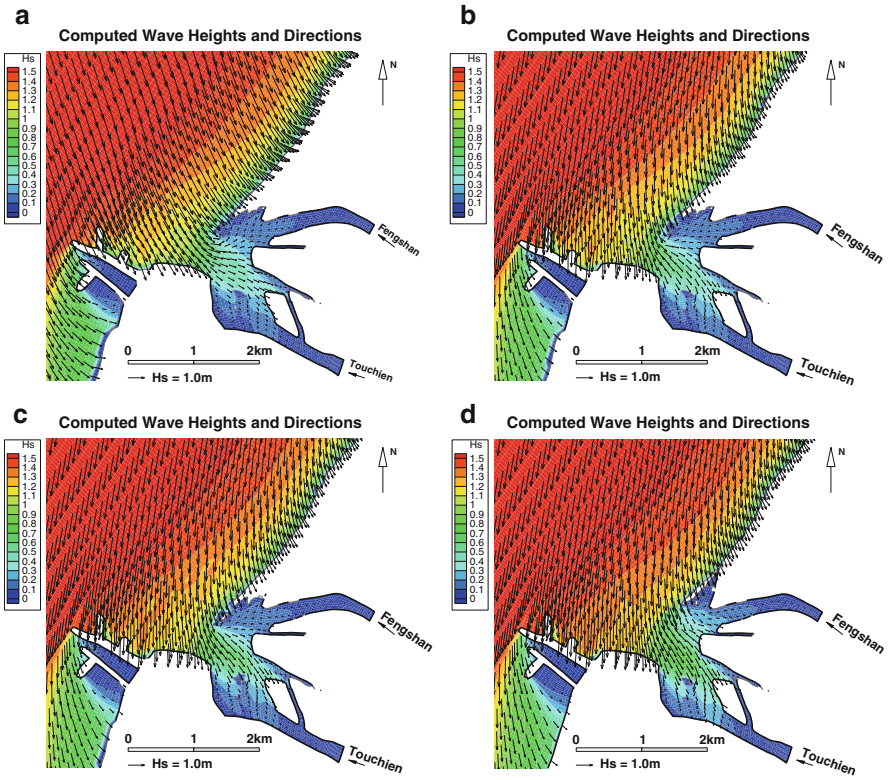

Fig. 5 Comparison of computed wave height (unit: m) and directions at the flood peak for different sea-level rise scenarios. (**a**) Current sea level, (**b**) 0.5-m rise, (**c**) 1.0-m rise, and (**d**) 2.0-m rise

shown in Fig. 8d. The increase of sea level promotes the invasion of tidal waves inside the rivers and elevates the water levels in river reaches, and the tidal effect may even influence farther upstream.

The morphodynamic processes are complicated in the estuary due to the highly irregular bathymetry and hydrological conditions. In particular, the existence of the two interior islands affects river courses and sediment transport. As depicted in Fig. 9, the simulated morphological changes indicate erosion/deposition areas in the estuary, river mouth, and the adjacent coasts due to the storm and the sea-level changes. They show the gradually reducing areas of deposition in the offshore when sea-level rise increasing from current sea level to 2.0 m mean sea level. This is because the increased water depth causes wave-breaking zone (or the surf zone) shifting to upstream (or landward), and the current surf zones turn to be shoaling zones where wave breaking may no longer occur. Therefore, sediment transport at the offshore becomes less active. Figure 9 also shows that with the increasing of sea levels, the river mouth bar is increasingly eroded, which consequently will cause a

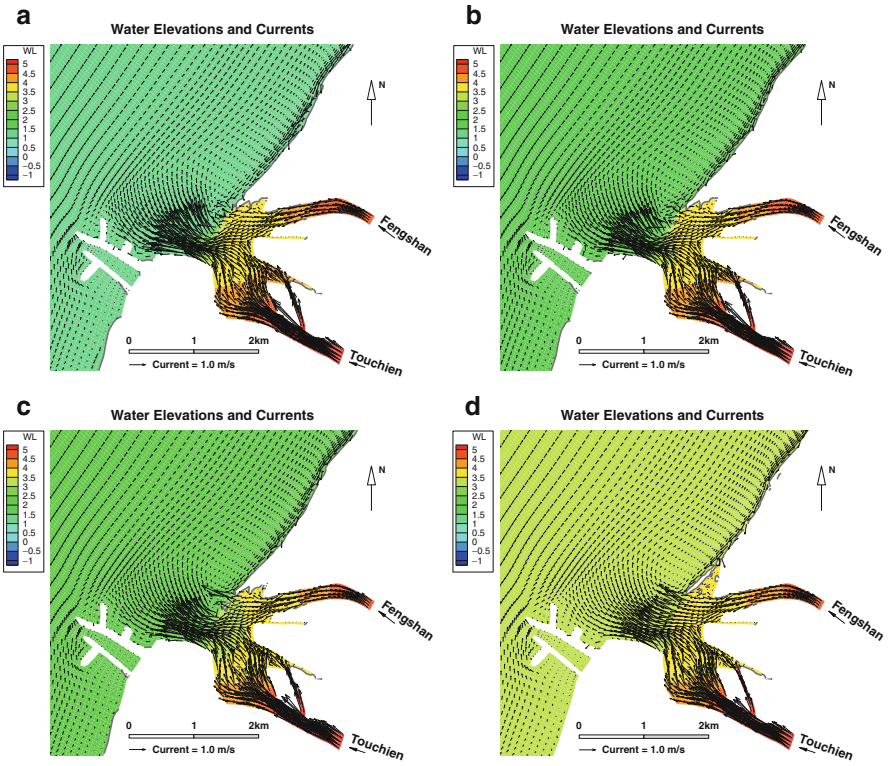

Fig. 6 Comparison of computed water elevations and currents at the flood peak due to sea-level rise scenarios. (**a**) Current sea level, (**b**) 0.5-m rise, (**c**) 1.0-m rise, and (**d**) 2.0-m rise

landward displacement of the shoreline. And the river mouth bar may migrate to the junction area of the two rivers in the estuary. Figure 10 presents the profiles of computed bed elevations and bed changes at the river mouth along with the transect A-A', of which the location is shown in Fig. 9d, after the storm flood with the conditions of the sea-level rise scenarios. The profiles clearly show that the erosion process in the river mouth is not linearly increasing, but typically nonlinearly varying with the sea-level changes; in fact, 1.0-m sea-level rise will cause a river mouth to be narrowed (turning to close), and the river mouth widening process could be accelerated only after the sea-level rises up to 2.0 m.

Discussions on the Impacts of Sea-Level Rise in Touchien Estuary

In this case study, the site-specifically validated coastal process model, CCHE2D-Coast, was applied to compute hydrodynamic and morphodynamic responses to a set of hypothetical sea-level rise scenarios combining with a real storm event happened

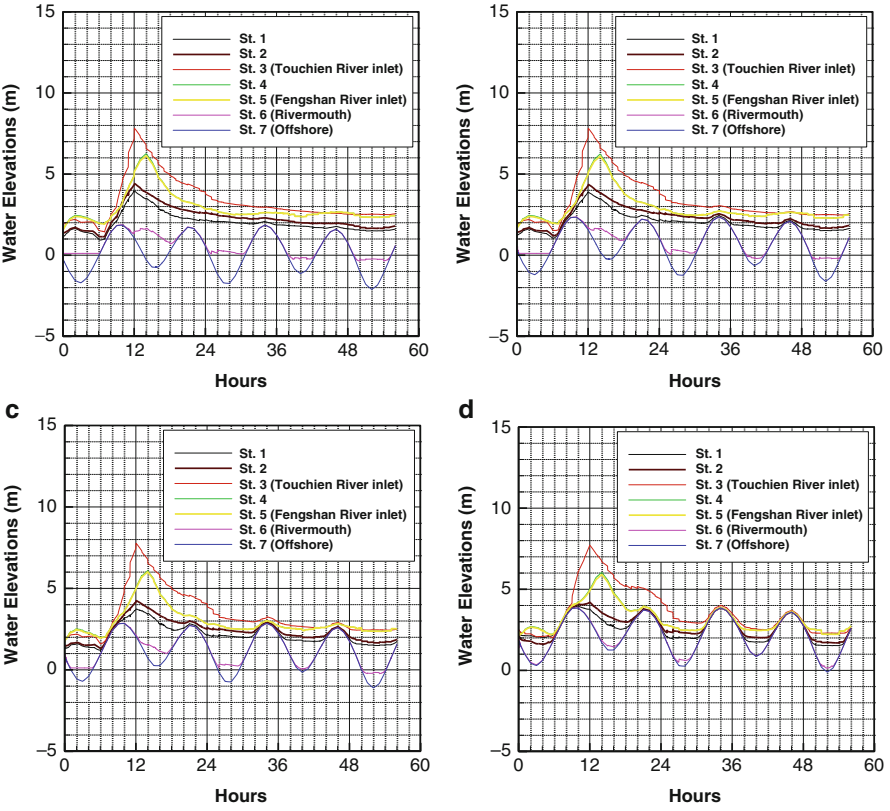

Fig. 7 Comparison of computed water elevation time series at seven stations under the same sea-level rise scenarios. (**a**) Current sea level, (**b**) 0.5-m rise, (**c**) 1.0-m rise, and (**d**) 2.0-m rise

in Touchien Estuary located in the west coast of Taiwan. The hydrodynamic results show that there are obvious wet/dry cycle changes at all the upstream monitoring stations. And there is an increasing inundation effect at the river mouth bar in case of the mean sea level higher than 1.5 m. The river area is more susceptible to the tidal effect at the 1.5-m mean sea-level rise. In addition, the morphodynamic results show that there is apparent change in erosion/deposition areas due to sea-level rise. Especially, the river mouth bar is more exposed to be eroded, which consequently could cause landward retreat of shoreline and displacement of rivermouth bar due to inundation and waves approaching inland. The preliminary test results in the case study demonstrate that the CCHE2D-Coast model is able to effectively simulate the nonlinear and unsteady hydrodynamic and morphodynamic processes in the coastal and estuarine area under different mean sea-level scenarios. Therefore, this model can be used for coastal/estuarine planning and management to assess the impacts of sea-level rise and storm events under naturally temporal-spatial varying hydrological conditions.

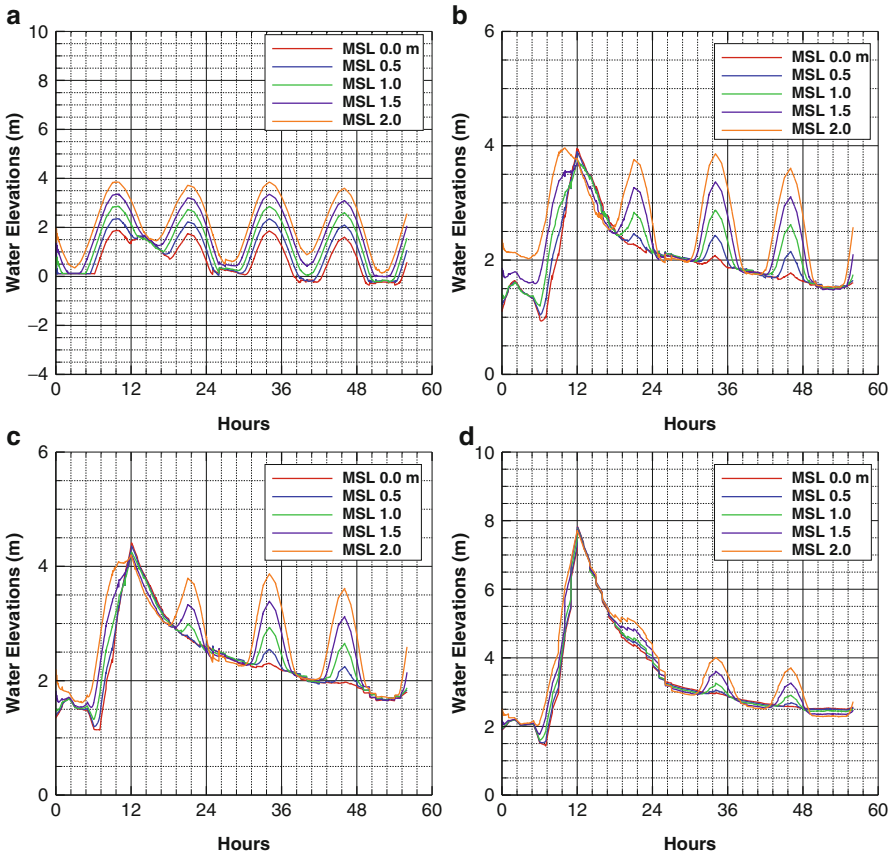

Fig. 8 Comparisons of computed water elevations at different stations according to different sea-level rise scenarios. (**a**) River mouth (St. 6), (**b**) Island (St. 1), (**c**) South Bank (St. 2), and (**d**) Touchien River inlet (St. 3)

Concluding Remarks and Future Research Topics

This chapter investigates the dynamic impacts of sea-level rise by assessing hydrodynamic and morphodynamic responses to storms (hurricanes or typhoons) under natural physical conditions of coastal and estuarine processes which are induced by astronomical tides, waves, storm surges, river inflows (floods), sediment transport, and morphological changes in coasts and estuaries. It also presents a review on the impact assessment approaches such as projection and numerical modeling to assess the impacts of sea-level rise in local/regional/global scales. A special attention in the chapter has been paid to emphasize the importance and applicability of numerical modeling to quantify the dynamic impacts of hazardous storms after sea-level rise occurs, since simulated results on flooding/inundation areas and erosion are the

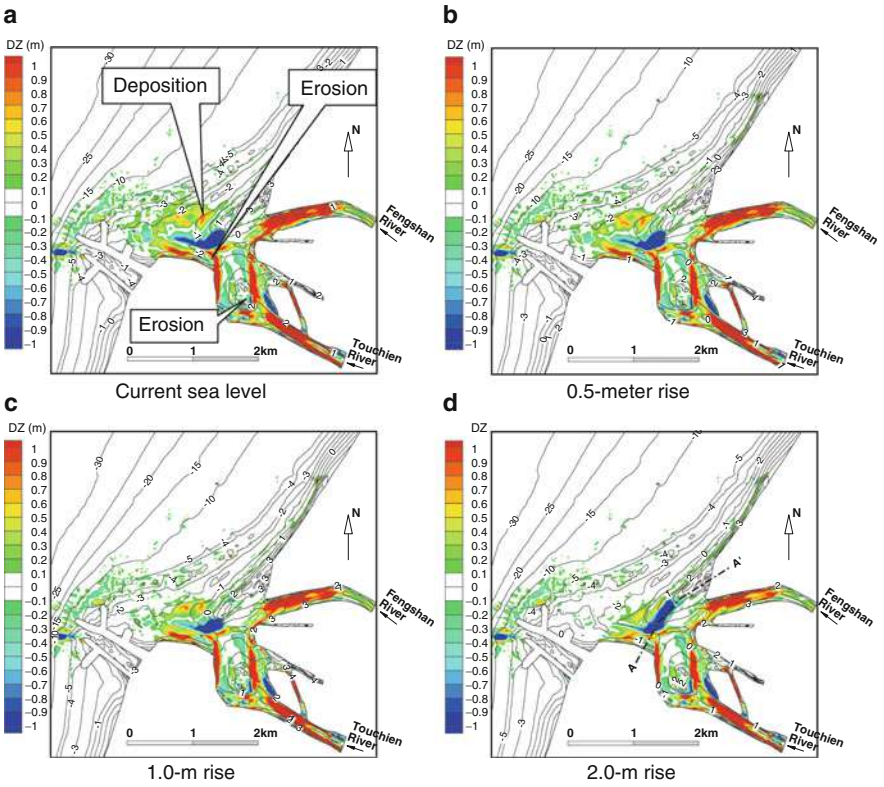

Fig. 9 Comparisons of computed bed changes after the storm flood under the conditions of different sea-level rise scenarios. (DZ is bed change. The contour lines are computed bed elevations.) (**a**) Current sea level, (**b**) 0.5-m rise, (**c**) 1.0-m rise, and (**d**) 2.0-m rise

firsthand data base to engineers, managers, and decision makers to practice flood water management, shoreline erosion protection, and design/planning of coastal infrastructure against hazardous storms.

It also gives a brief review on the existing coastal/estuarine process models which are applicable to simulate/predict hydrodynamic and morphodynamic responses to the complex hydrological conditions in coasts and estuaries. Finally, using an integrated coastal/estuarine process model called CCHE2D-Coast, the simulations of flows and morphological changes in an estuary located in the west coast of Taiwan under the conditions of several sea-level rise scenarios and a selected extreme storm are demonstrated. It shows that numerical modeling of coastal/estuarine processes can predict temporal-spatial variations of flows (water elevations and current velocities), sediment transport, and morphological changes due to the combined physical conditions from waves, tides, surges, and river floods. These numerical simulation results indicate that this integrated process model is capable of predicting the dynamic impacts of sea-level rise with storm events such as inundation of

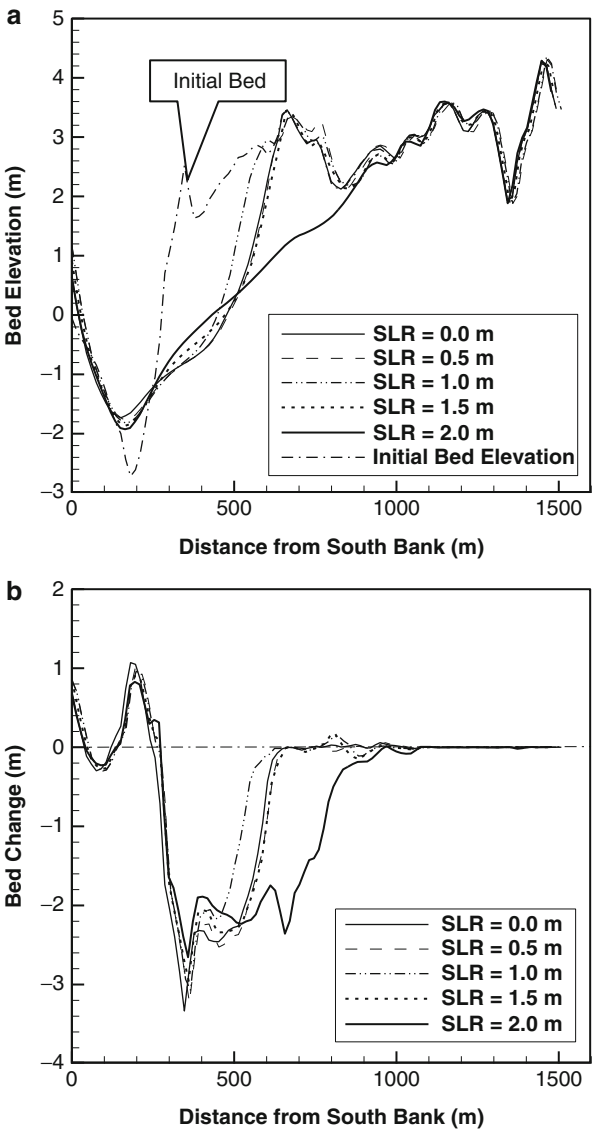

Fig. 10 Comparisons of profiles of computed bed elevations and bed changes after the storm flood at the river mouth along with the transect A-A' shown in Fig. 9d. (**a**) Bed elevations and (**b**) bed elevation changes

low-lying area, shoreline retreat, changes of coastal zones, tidal water intrusion, etc. These models enable to facilitate the assessment of dynamic impacts of sea-level rise and storms in different time and spatial scales (local/regional scales) for various practical engineering application purposes such as flood management, coastal erosion protection, and coastal community development/planning. By integrating with other numerical models for prediction of water quality and ecological processes in the future, this kind of integrated physical process model will also be applied for

assessment of the environmental impacts of sea-level rise such as saline water intrusion and pollutant transport in coasts and estuaries.

As for the potential future research topics for better assessment of impacts of sea-level rise and hazardous storms (extreme events), basically, there are three aspects that need to be enhanced in the future:

1. Improve understanding of sea-level rise and coastal hazardous events or extreme events including other extreme events such as tsunami and large-scale oil spill.
2. Improve assessment tools by advancing all scale-level numerical modeling techniques with more accurate, efficient, and higher-resolution numerical simulations.
3. Develop mitigation and adaptation to sea-level rise and extreme storms with increasing storm strength and frequency.

Nicholls et al. (2007) pointed out that the level of knowledge and understanding on sea-level rise, storms/hurricanes, and their interactions is not consistent with the potential severity of the problem of climate change and coastal zones. Key uncertainties in the climate drivers and responses of coasts and oceans increase with the largest uncertainties concerning in their interactions. It is vital to establish better baselines of actual sea-level changes and coastal changes in morphology and ecology through observations and expanded monitoring. In addition to traditional tide-gauge measurements, there is a need to collect more accurate data from altimetric satellites, such as TOPEX/Poseidon (launched in 1992 and still operating), which observe almost the entire planet and determine the absolute, not relative, sea level because they make measurements with respect to Earth's center of mass (without uncertainty of subsidence existing in some tide-gauge data) (Douglas and Peltier 2002). For a better assessment of impact of sea-level rise and storms, it is also of vital importance to improve understanding of extreme tropical storms/hurricanes, particularly their strength and frequency increasing with global climate change. Better knowledge about occurrence of coastal extreme events will definitely facilitate a more accurate impact assessment and building a stronger coastal defense community. Assessment of human vulnerability in coastal and low-lying areas is an ultimate goal to build a sustainable coastal community, which though is out of the scope of this chapter; one may refer to Nicholls et al. (2007) for detailed assessment of socioeconomic impacts of sea-level rise due to climate changes.

Numerical modeling is the only assessment tool to evaluate impact of sea-level rise with various spatial scales and to predict time-dependent variation patterns of physical variables including climate driving factors and coastal/oceanographic factors. It is essential to continue to develop numerical models with higher accuracy by including improved knowledge on climate changes and coastal/ocean processes so that uncertainties from natural processes can be reduced as much as possible. Detailed model validation/verification is always requested to control the quality of numerical simulations before a model can be applied to a real-world problem. The models with different scales should be validated by the observation data sets obtained from relevant field measurements. To make the multi-scale assessment more effective, multi-scale modeling techniques have to be developed to meet the

increasing demand for assessing local/regional impact of sea-level rise with the conditions of storms and hurricanes. Development of high-performance computing techniques is critical to improve the computing efficiency of climate models and local assessment models, especially due to multidimensional and unsteady physical problems in the interactions of climate changes and coastal/ocean processes. It is undoubted that an integrated modeling system with better accuracy and efficiency will be a unique powerhouse to help scientists, engineers, and policy/decision makers to better assess coastal vulnerability and provide the cost-effective plan for mitigation and adaptation against the impacts of sea-level rise and extreme coastal events, as well as their interactive impacts.

Acknowledgment This work was a product of the research partially sponsored by the National Center for Computational Hydroscience and Engineering in the University of Mississippi. The authors would like to thank Dr. Keh-Chia Yeh in National Chiao Tung University, Hsinchu, Taiwan, for his help to provide the boundary conditions for the case study. Special thanks are given to Mr. Moustafa Elgohry for his research assistance.

References

Bilskie MV, Hagen SC, Medeiros SC, Passeri DL (2014) Dynamics of sea level rise and coastal flooding on a changing landscape. Geophys Res Lett 41(3):927–934. doi:10.1002/2013GL058759

Blumberg AF, Mellor GL (1987) A description of a three coastal ocean circulation model. In: Heaps N (ed) Three dimensional coastal ocean models, vol 4. American Geophysical Union, Washington, DC

Burkett VR, Zilkoski DB, Hart DA (2003) Sea-level rise and subsidence: implications for flooding in New Orleans, Louisiana. In: Prince KR, Galloway DL (eds) Subsidence interest group conference, proceedings of the technical meeting, Galveston, 27–29 November 2001. USGS water resources division open-file report series 03-308. U.S. Geo-logical Survey, Austin. http://www.nwrc.usgs.gov/hurricane/Sea-Level-Rise.pdf. Assessed 16 Sept 2009

Capobianco M, DeVriend HJ, Nicholls RJ, Stive MJF (1999) Coastal area impact and vulnerability assessment: a morphodynamic modeller's point of view. J Coast Res 15(3):701–716

Casulli V, Cheng RT (1992) Semi-implicit finite difference methods for three-dimensional shallow water flow. Int J Numer Methods Fluids 15:629–648

Church JA, Gregory JM, Huybrechts P, Kuhn M, Lambeck K, Nhuan MT, Qin D, Woodworth PL (2001) Changes in sea level. In: Houghton JT, Ding Y, Griggs DJ, Noguer M, van der Linden PJ, Xiaosu D (eds) Climate change 2001. The scientific basis. Cambridge University Press, Cambridge, pp 639–693

Church JA, Clark PU, Cazenave A, Gregory JM, Jevrejeva S, Levermann A, Merrifield MA, Milne GA, Nerem RS, Nunn PD, Payne AJ, Pfeffer WT, Stammer D, Unnikrishnan AS (2013) Sea level change. In: Stocker TF, Qin D, Plattner G-K, Tignor M, Allen SK, Boschung J, Nauels A, Xia Y, Bex V, Midgley PM (eds) Climate change 2013: the physical science basis. Contribution of Working Group I to the fifth assessment report of the intergovernmental panel on climate change. Cambridge University Press, Cambridge, UK\New York

Cooper MJP, Beevers MD, Oppenheimer M (2005) Future sea level rise and the New Jersey coast – Assessing potential impacts and opportunities, science, technology and environmental policy program. Woodrow wilson school of public and international affairs, Princeton University. http://www.environmentnewjersey.org/uploads/sR/9N/sR9N-sL9cXyA7pGI_ODVlw/Future_Sea_Level_Rise.pdf. Accessed 3 Dec 2009

Crowell M, Edelman S, Coulton K, McAfee S (2007) How many people live in coastal areas? J Coast Res 23(4):iii–vi
Crowell M, Coulton K, Johnson C, Westcott J, Bellomo D, Edelman S, Hirsch E (2010) An estimate of the U.S. population living in 100-year coastal flood hazard areas. J Coast Res 26(2):201–211
Ding Y, Wang SSY (2005) Tests of capability and reliability of a model simulating coastal processes. In: Walton R (ed) World water congress 2005: impacts of global climate change, proceedings of the 2005 World Water and Environmental Resources Congress. ASCE, Anchorage
Ding Y, Wang SSY (2008a) Development and application of coastal and estuarine morphological process modeling system. J Coast Res Spec Issue 52:127–140
Ding Y, Wang SSY (2008b). Numerical simulations of coastal flood and morphological change due to hazardous hydrological conditions at coast and estuary. In: Louise Wallendorf et al (ed) Solutions to coastal disasters 2008. ASCE, Proceeding of solutions to coastal disasters 2008 conference, Oahu, 13–16 Apr 2008, pp 349–360
Ding Y, Wang SSY, Jia Y (2004) Development and validation of nearshore morphodynamic area model in coastal zone. In: Altinakar MS, Wang SSY, Holz KP, Kawahara M (eds) Advances in hydro-science and engineering. Proceedings of the sixth international conference on hydroscience and engineering, vol VI, Brisbane, 30 May–June 3 2004
Ding Y, Jia Y, Wang SSY (2006a) Numerical modeling of morphological processes around coastal structures. In: Proceedings of ASCE-EWRI congress 2006, Omaha, 21–25 May 2006
Ding Y, Wang SSY, Jia YF (2006b) Development and validation of a quasi three-dimensional coastal are morphological model. J Waterw Port Coast Ocean Eng ASCE 132(6):462–476
Ding Y, Yeh K-C, Chen H-K, Wang SSY (2007) Simulations of morphodynamic changes due to waves and tides in an estuary using CCHE2D-coast model. In: Proceedings of ASCE-EWRI congress 2007, Tampa, 15–19 May 2007
Ding Y, Yeh K-C, Chen H-K, Wang SSY (2008) Validation of a coastal and estuarine model for long-term morphodynamic simulations driven by tides, storms, and river floods. In: Babcock RW Jr, Walton R (eds) World environmental and water resources congress 2008 – Ahupua'A. ASCE, Proceedings of ASCE-EWRI congress 2008, Honolulu, 12–16 May 2008 (CD-ROM, ISBN: 978-0-7844-0976-3)
Ding Y, Kuiry SN, Elgohry M, Jia Y, Altinakar MS, Yeh K-C (2013) Impact assessment of sea-level rise and hazardous storms on coasts and estuaries using integrated processes model. Ocean Eng 71:74–95
Douglas BC (1991) Global sea level rise. J Geophys Res 96(C4):6981–6992
Douglas BC (1997) Global sea level acceleration. J Geophys Res 97(C8):12699–12706
Douglas BC, Peltier WR (2002) The puzzle of global sea-level rise. Phys Today 55(2):35–40
FEMA (2009) Federal Emergency Management Agency, Federal Insurance Administration, National Flood Insurance Program definitions home page. http://www.fema.gov/business/nfip/19def2.shtm#F. Accessed 3 Oct 2009
Gordon C, Cooper C, Senior CA, Banks HT, Gregory JM, Johns TC, Mitchell JFB, Wood RA (2000) The simulation of SST, sea ice extents and ocean heat transports in a version of the Hadley Centre coupled model without flux adjustments. Clim Dyn 16:147–168
Hinrichsen D (2009) Ocean planet in decline. http://www.peopleandplanet.net/doc.php?id=429&section=6. Accessed 26 Sept 2009
Holland GJ, Webster PJ (2007) Heightened tropical cyclone activity in the North Atlantic: natural variability or climate trend? Philos Trans R Soc Lond Ser A. doi:10.1098/rsta.2007.2083. http://www.nationalwildlife.org/hurricanes/pdfs/HollandandWebster2007.pdf. Assessed 20 Sept 2009
Holthuijsen LH et al (1989) A prediction model for stationary, short-crested waves in shallow water with ambient currents. Coast Eng 13(1):23–54
IPCC (2007) Climate change 2007: synthesis report. Intergovernmental Panel on Climate Change. http://www.ipcc.ch/pdf/assessment-report/ar4/syr/ar4_syr.pdf. Accessed 31 Mar 2008
IPCC Data Distribution Centre (2010) http://www.ipcc-data.org/ddc_about.html. Accessed 11 July 2010

IPCC (2013) Climate change 2013: the physical science basis. In: Stocker TF, Qin D, Plattner G-K, Tignor M, Allen SK, Boschung J, Nauels A, Xia Y, Bex V, Midgley PM (eds) Contribution of Working Group I to the fifth assessment report of the intergovernmental panel on climate change. Cambridge University Press, Cambridge, UK\New York, 1535 pp

Jelesnianski C, Chen J, Shaffer W (1992) SLOSH: sea, lake, and overland surges from hurricanes. NOAA technical report NWS 48, Silver Spring

Jia YF, Wang SSY, Xu YC (2002) Validation and application of a 2D model to channel with complex geometry. Int J Comput Eng Sci 3(1):57–71

Johns TC, Carnell RE, Crossley JF, Gregory JM, Mitchell JFB, Senior CA, Tett SFB, Wood RA (1997) The second hadley centre coupled ocean–atmosphere GCM: model description, spinup and validation. Clim Dyn 13:103–134

Johns TC, Gregory JM, Ingram WJ, Johnson CE, Jones A, Lowe JA, Mitchell JFB, Roberts DL, Sexton DMH, Stevenson DS, Tett SFB, Woodage MJ (2003) Anthropogenic climate change from 1860 to 2100 simulated with the HadCM3 model under updated emissions scenarios. Climate Dynam 20:583–612

Jouzel J, Raisbeck G, Benoist JP, Yiou F, Lorius C, Raynaud D, Petit JR, Barkov NI, Korotkevitch YS, Kotlyakov VM (1989) A comparison of deep antarctic cores and their implications for climate between 65,000 and 15,000 year ago. Quatern Res 31(2):135–150

Landsea CW (2007) Counting atlantic tropical cyclones back to 1900. Eos Trans AGU 88 (18):197–208

Lesser GR, Roelvinka JA, van Kester JATM, Stelling GS (2004) Development and validation of a three-dimensional morphological model. Coast Eng 51(8–9):883–915

Lin L, Demirbilek Z, Mase H, Zheng J, Yamada F (2008) CMS-wave: a nearshore spectral wave processes model for coastal inlets and navigation projects. Technical report ERDC/CHL TR-08-13. U S Army Engineer Research and Development Center, Vicksburg

Mann M, Emanuel K (2006) Atlantic hurricane trends linked to climate change. Eos Trans AGU 24:233, 238, and 241

MIKE 21 (2008) MIKE 21 – Inland, coastal waters and seas in 2D. http://www.dhigroup.com/Software/Marine/MIKE21.aspx. Accessed 16 Jan 2008

Mousavi M, Irish JL, Frey AE, Olivera F, Edge BL (2011) Global warming and hurricanes: the potential impact of hurricane intensification and sea level rise on coastal flooding. Clim Change 104(3–4):575–597. doi:10.1007/s10584-009-9790-0

Nicholls RJ (2003) Case study on sea-level rise impacts. In: OECD workshop on the benefits of climate policy: improving information for policy makers. http://www.oecd.org/dataoecd/7/15/2483213.pdf. Accessed 12 Sept 2009

Nicholls RJ (2004) Coastal flooding and wetland loss in the 21st century: changes under the SRES climate and socio-economic scenarios. Glob Environ Chang 14:69–86

Nicholls RJ, Hoozemans FMJ, Marchand M (1999) Increasing flood risk and wetland losses due to global sea-level rise: regional and global analyses. Glob Environ Chang 9:S69–S87

Nicholls RJ, Wong PP, Burkett VR, Codignotto JO, Hay JE, McLean RF, Ragoonaden S, Woodroffe CD (2007) Coastal systems and low-lying areas. In: Parry ML, Canziani OF, Palutikof JP, van der Linden PJ, Hanson CE (eds) Climate change 2007: impacts, adaptation and vulnerability. Contribution of Working Group II to the fourth assessment report of the intergovernmental panel on climate change. Cambridge University Press, Cambridge, UK, pp 315–356

NOAA (2011) NOAA tides and currents. http://tidesandcurrents.noaa.gov/. Accessed 13 Feb 2011

POM (2011) The princeton ocean model. http://www.aos.princeton.edu/WWWPUBLIC/htdocs.pom/. Accessed 13 Feb 2011

Roelvink JA (2006) Coastal morphodynamic evolution techniques. Coast Eng 53:277–287

Roelvink JA, Van Banning GKFM (1994) Design and development of Delft3D and application to coastal morphodynamics. In: Proceedings hydroinformatics'94 conference, Delft

Schleupner C (2007) Spatial assessment of sea level rise on Martinique's coastal zone and analysis of planning frame works for adaptation. J Coast Conserv 11:91–103. doi:10.1007/s11852-008-0010-2

Scott S (2003) Evaluation of selected two-dimensional hydrodynamic and sediment transport numerical models for simulation of channel morphology change, Coastal and Hydraulics Laboratory. U.S.Army Engineer Research and Development Center, Vicksburg

Shimizu T, Kumagai T, Watanabe A (1996) Improved 3-D beach evolution model coupled with the shoreline model (3D-SHORE). In: Proceedings 25th conference on coastal Engineering, ASCE, vol 3, pp 2843–2856

Smith JM, Cialone MA (2000) Waves and currents: STWAVE, technology-transfer workshop, Hilton airport Melbourne, Florida. http://cirp.wes.army.mil/cirp/presentations/ws2000/stwave/. Accessed 1–2 Feb 2000

Smith JM, Cialone MA, Wamsley TV, McAlpin TO (2010) Potential impact of sea level rise on coastal surges in southeast Louisiana. Ocean Eng 37:37–47. doi:10.1016/j.oceaneng.2009.07.008

Svendsen IA, Haas K, Zhao Q (2003) Quasi-3D nearshore circulation model SHORECIRC – Version 2.0. Technical report, center for applied coastal research. University of Delaware, Newark, DE19716

SWAN (2011) Simulating waves nearshores. http://swanmodel.sourceforge.net/. Accessed 13 Feb 2011

TELEMAC-2D (1995) TELEMAC-2D modelling system: TELEMAC-2D hydrodynamic computation software version 3.0, principal note, direction des Etudes et Recherches

US-CCSP (U.S. Climate Change Science Program) (2008) Coastal sensitivity to sea level rise: a focus on the mid-atlantic region for synthesis and assessment product 4.1. http://www.climatescience.gov/Library/sap/sap4-1/public-review-draft/. Accessed 16 May 2008

USGS (2011) Tsunamis and earthquakes – Basics- USGS WCMG. http://walrus.wr.usgs.gov/tsunami/basics.html. Accessed 12 Feb 2011

WAMDI (1988) The WAM model – a third generation ocean wave prediction model. J Phys Oceanogr 18:1775–1810

Warner JC, Sherwood CR, Signell RP, Harris CK, Arango HG (2008) Development of a three-dimensional, regional, coupled wave, current, and sediment-transport model. Comput Geosci 34 (10):1284–1306

Westerink JJ, Luettich RA Jr, Scheffner NW (1993) ADCIRC: an advanced three-dimensional circulation model for shelves coasts and estuaries, report 3: development of a tidal constituent data base for the Western North Atlantic and Gulf of Mexico. Dredging research program technical report DRP-92-6. U.S. Army Engineers Waterways Experiment Station, Vicksburg, 154 pp

White AA, Bromley RA (1995) Dynamically consistent, quasi-hydrostatic equations for global models with a complete representation of the Coriolis force. Q J Roy Meteorol Soc 121:399–418

Wilby RL, Dawson CW, Barrow EM (2002) SDSM- A decision support tool for the assessment of regional climate change impacts. Environ Model Software 17:147–159

Zhang YX, Jia YF (2005) CCHE2D mesh generator, user's manual – version 2.6, national center for computational hydroscience and engineering technical report, no. NCCHE-TR-2005-05. http://www.ncche.olemiss.edu/software/meshgenerator. Accessed 13 Feb 2011

Zyserman JA, Johnson HK (2002) Modelling morphological processes in the vicinity of shore-parallel breakwaters. Coast Eng 45(3):261–284

Projected Impacts of Climatic Changes on Cisco Oxythermal Habitat in Minnesota Lakes and Management Strategies

Xing Fang, Heinz G. Stefan, Liping Jiang, Peter C. Jacobson, and Donald L. Pereira

Contents

X. Fang (✉) • L. Jiang
Department of Civil Engineering, Auburn University, Auburn, AL, USA
e-mail: xing.fang@auburn.edu; lzj0012@tigermail.auburn.edu

H.G. Stefan
St. Anthony Falls Laboratory, Department of Civil Engineering, University of Minnesota, Minneapolis, MN, USA
e-mail: stefa001@umn.edu

P.C. Jacobson
Minnesota Department of Natural Resources, Park Rapids, MN, USA
e-mail: peter.jacobson@state.mn.us

D.L. Pereira
Minnesota Department of Natural Resources, St. Paul, MN, USA
e-mail: don.pereira@state.mn.us

W.-Y. Chen et al. (eds.), *Handbook of Climate Change Mitigation and Adaptation*,
DOI 10.1007/978-3-319-14409-2_16

Abstract

Water quality and fish habitat models were developed and applied to investigate impacts of future climate change on cisco oxythermal habitat in Minnesota lakes. Long-term daily water temperature (T) and dissolved oxygen (DO) profiles were simulated for different types of representative lakes (surface area from 0.05 to 50 km^2) in Minnesota under the past climate conditions (1961–2008) and projected future climate scenarios. A process-oriented, dynamic, and one-dimensional year-round lake water quality model was developed and applied for the temperature and DO simulations, which were run in daily time steps over a 48-year simulation period. The lake parameters required as model input were surface area (A_s), maximum depth (H_{max}), and Secchi depth (as a measure of radiation attenuation and trophic state). Weather records from eight stations in Minnesota and North Dakota were used for model simulations. Two projected future climate scenarios were based on the output of the third-generation Canadian Centre for Climate Modeling and Analysis coupled general circulation model (CCCma CGCM 3.0) and the Model for Interdisciplinary Research on Climate (MIROC 3.2). The climate scenarios lead to a longer period of hypoxic hypolimnetic conditions in stratified lakes that will result in various negative environmental and ecological impacts in lakes. The study has identified potential refuge lakes important for sustaining cisco habitat under climate warming scenarios. Cisco *Coregonus artedi* is the most common cold-water stenothermal fish species in lakes over the several northern states in the USA such as Minnesota. To project its chances of survival under future warmer climate conditions, using simulated daily T and DO profiles in 44 representative and 30 virtual lake types, three oxythermal habitat modeling options were used: (1) constant lethal T and DO limits, (2) lethal-niche-boundary curve, and (3) an oxythermal habitat variable, TDO3, i.e., water temperature at DO = 3 mg/L. The fish habitat models using constant and variable lethal limits were validated in the 23 Minnesota lakes of which 18 had cisco mortality while five had no cisco mortality in the unusually warm summer of 2006. Cisco lethal and habitable conditions in the 23 lakes simulated by the models had overall good agreement with observations in 2006. Cisco lethal days were simulated in the 44 representative lake types. Polymictic shallow lakes with lake geometry ratio $A_s^{0.25}/H_{max} > 5.2\ m^{-0.5}$ (A_s in m^2 and H_{max} in m) were simulated to typically not support cisco oxythermal habitat under past climate conditions and the future climate scenario (MIROC 3.2). Medium-depth lakes are projected to be most vulnerable to climate warming with most

increase in the number of years with cisco kill. The mean daily TDO3 values over a 31-day fixed and variable benchmark periods were calculated for each of simulated years and then averaged over the simulation period for each lake type. Projected increases of the multiyear average TDO3 (called AvgATD3) under the two future climate scenarios and relative to the 47-year simulation period from 1962 to 2008 had averages from 2.6 °C to 3.4 °C. Isopleths of AvgATD3 were interpolated for the 30 simulated virtual lakes on a plot of Secchi depth versus lake geometry ratio used as indicators of trophic state and summer mixing conditions, respectively. Marking the 620 Minnesota lakes with identified cisco populations on the plot of AvgATD3 allowed to partition the 620 lakes into three tiers depending on where they fell between the isopleths: lakes with AvgATD3 $\leq$ 11 °C (tier 1 lakes) were selected to be most suitable for cisco; lakes with 11 °C $<$ AvgATD3 $\leq$ 17 °C (tier 2 lakes) had suitable habitat for cisco; and non-refuge lakes with AvgATD3 $>$ 17 °C (tier 3 lakes) would support cisco only at a reduced probability of occurrence or not at all. About 208 (one third) and 160 (one fourth) of the 620 lakes that are known to have cisco populations are projected to maintain viable cisco habitat under the two projected future climate scenarios using the fixed and variable benchmark periods, respectively. These selective lakes have a Secchi depth greater than 2.3 m (mesotrophic and oligotrophic lakes) and are seasonally stratified (geometry ratio less than 2.7 $m^{-0.5}$). Management strategies were developed and implemented for some of the refuge lakes.

Introduction

The potential significance of climate change for inland aquatic ecosystems (e.g., streams, lakes, reservoirs) caught the attention of water resource professionals and scientists in the early 1990s. An increase of carbon dioxide (CO_2) and/or other greenhouse gases in the atmosphere is projected to cause climate warming (NRC 1983; IPCC 2007), which would alter water temperature (T), ice/snow cover, and dissolved oxygen (DO) characteristics in lakes (Blumberg and Di Toro 1990; Stefan et al. 1996). These changes are in turn expected to have an effect on indigenous fish populations: cold-water, cool-water, and warmwater fish species (Coutant 1990; Magnuson et al. 1990; Chang et al. 1992; Stefan et al. 1995; De Stasio et al. 1996). Chapter 16 in the previous edition of the handbook has summarized some basic information on effects of climate change on water quality (water temperature, dissolved oxygen, snow and ice covers) and fish habitat for three fish guilds (8, 7, and 14 species of cold-water, cool-water, and warmwater fish guilds, respectively) in lakes in Minnesota and the contiguous USA (Fang and Stefan 2012). This chapter summarizes simulation results and model validation of cisco oxythermal habitat in Minnesota lakes that were used to identify cisco "refuge lakes" under future climate scenarios and develop management strategies for them. A "refuge lake" is a cisco lake that is projected to provide suitable cold-water habitat under future climate scenarios.

Cisco *Coregonus artedi* is the most common cold-water stenothermal fish in northern lakes in Minnesota, Wisconsin, and other northern states, and it is a common forage fish for walleye *Sander vitreus* and northern pike *Esox lucius* among other prized sport fishes. The Minnesota (MN) Department of Natural Resources (DNR) has sampled cisco from 648 lakes in netting assessments since 1946 (MN DNR files). These lakes are typically deeper and more transparent than average lakes in Minnesota (Fang et al. 2009). The lakes are scattered throughout much of the central and northern portions of the state (Fig. 1) and cross several land uses (agricultural, urban, and forested). The wide distribution suggests that ciscoes are somewhat more eurythermal than other native, lentic cold-water stenotherms such as lake whitefish *Coregonus clupeaformis* (sampled in 155 Minnesota lakes), lake trout *Salvelinus namaycush* (124 Minnesota lakes), and burbot *Lota* (233 Minnesota lakes). Cisco physiologically requires cold, well-oxygenated water to survive, grow, and reproduce (Cahn 1927; Frey 1955). The combination of a wide distribution (Fig. 1) and a requirement for cold, oxygenated water (Frey 1955) make cisco an excellent "canary in a mineshaft" species that is a sensitive indicator of ecological stresses such as eutrophication and climate warming. For example, 18 lakes in north-central Minnesota experienced cisco mortality in the unusually hot summer of 2006 (Jacobson et al. 2008), and one example of cisco mortality is given in Fig. 2.

The climate warming is projected to warm the water and increase hypolimnetic oxygen depletion during periods of stratification in lakes (Blumberg and Di Toro 1990; Fang and Stefan 1999, 2000, 2009). Fish habitat is constrained by water temperature, available DO, food supply, human interference, and other environmental factors (Frey 1955; Fry 1971). In lakes, water temperature and DO are the two important water quality parameters that affect survival and growth of cold-water fishes (Magnuson et al. 1979; Coutant 1985, 1990; Christie and Regier 1988; Jacobson et al. 2010; Fang et al. 2012a, b; Jiang et al. 2012). Therefore, projected changes of water temperature and DO characteristics due to climate warming have the potential to reduce cold-water fish habitat (such as cisco) in lakes (Magnuson et al. 1990; Schindler et al. 1996; Stefan et al. 1996; Fang et al. 2004b). Ciscoes have been declining in recent years in Minnesota lakes, likely because of climate warming (Jacobson et al. 2012). Recently, Sharma et al. (2011) estimated that 30–70 % of the cisco population in about 170 of Wisconsin's deepest and coldest lakes could become a climate change casualty and disappear from most of the Wisconsin cisco lakes by the year 2100.

The goal of the study was to simulate daily water temperature and DO profiles in different cisco lakes to project the quality of cold-water fish habitat in 620 known cisco lakes in Minnesota under future climate scenarios and to identify potential cisco refuge lakes and impacts of climate change on cisco habitat. To make projections of water quality and fish habitat in lakes under future climate scenarios, numerical simulation models of daily temperature and DO profiles are useful. It is infeasible to simulate 620 cisco lakes in Minnesota using MINLAKE2010/MINLAKE2012 (Fang et al. 2012a). In this study, simulations of daily water temperature and DO profiles were made for the 30 virtual lakes

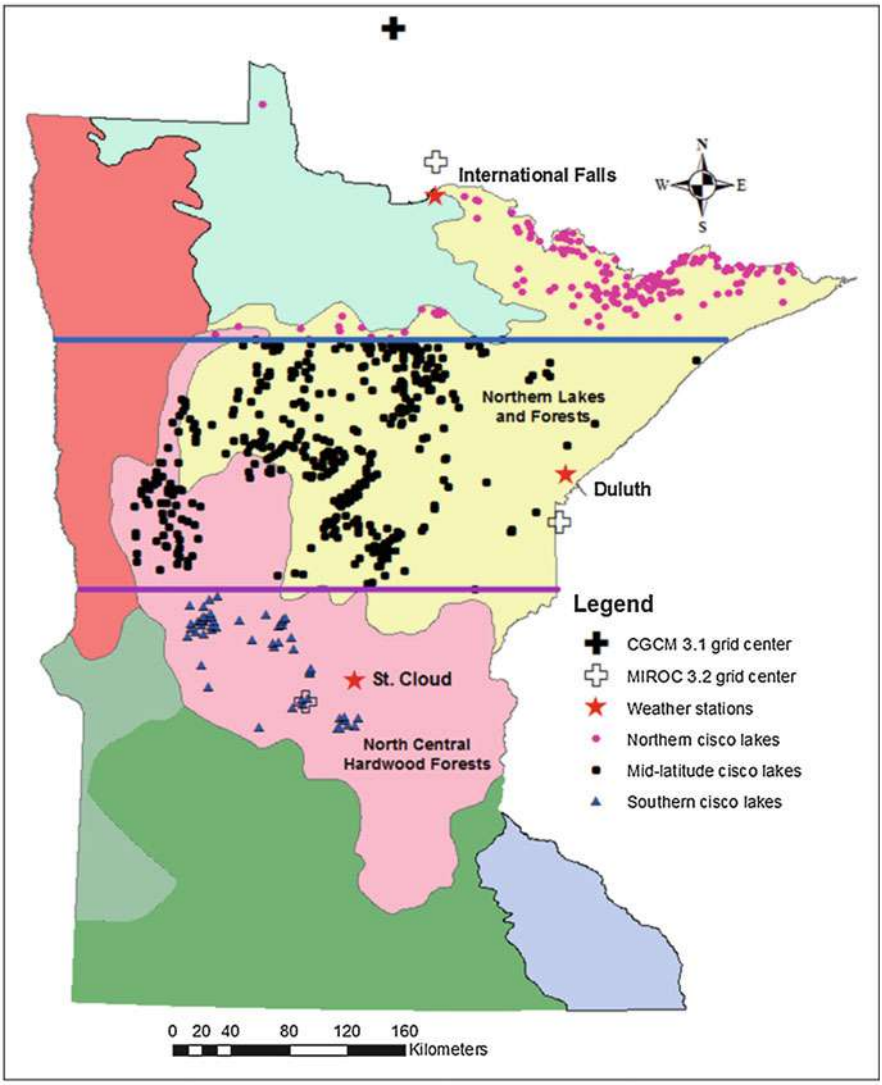

Fig. 1 Geographic distribution of 620 cisco lakes grouped by latitude, three weather stations (stars), and associated grid center points (crosses) of CGCM 3.1 and MIROC 3.2 used for model simulations. Background shades identify ecoregions of Minnesota. Cisco lakes are essentially in two ecoregions: (1) Northern Lakes and Forests and (2) North Central Hardwood Forests (modified from Jiang et al. 2012)

(Fang et al. 2012b; Jiang et al. 2012) and 44 representative lakes (Fang et al. 2014) in Minnesota before cisco oxythermal habitat and lethal conditions were examined in these lakes. The overall modeling methodology for the study is discussed in detail in the next section (Fig. 3).

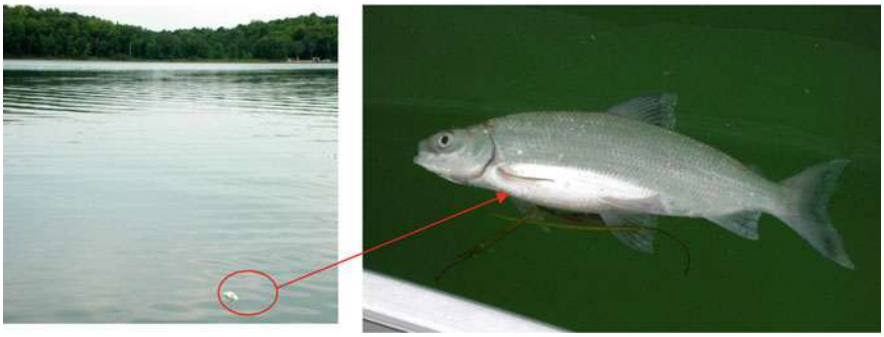

Fig. 2 Lake Andrusia in Minnesota had cisco mortality in July 2006 (Photo: Peter C. Jacobson, Minnesota Department of Natural Resources)

In this study, cold-water oxythermal fish habitat was identified using three different methods (Fig. 3): (1) constant lethal limits (lethal temperature, LT and DO survival limit), (2) lethal-niche-boundary curve (Jacobson et al. 2008) (also called variable lethal limits), and (3) a single oxythermal habitat variable TDO3, temperature at 3 mg/L of DO (Jacobson et al. 2010). Depths at the good-growth temperatures and lethal limits and TDO3 values were calculated day by day from simulated daily lake water temperature and DO profiles obtained from the process-oriented, one-dimensional year-round water quality model MINLAKE2010/MINLAKE2012 (Fang et al. 2012a). The model was run in daily time steps over a continuous 48-year simulation period for past (1961–2008) climate conditions and for two projected future climate scenarios (CGCM 3.1 and MIROC 3.2). Monthly (31-day) fixed and variable benchmark periods (Fang et al. 2012b; Jiang et al. 2012; Jacobson et al. 2010) were used to identify future cold-water fish habitat in lakes based on projected future temperature and DO profiles.

Overall Modeling Methodology

Figure 3 shows a flowchart of the study to project impacts of climate changes on cisco oxythermal habitat in Minnesota. Past climate conditions (1961–2008, 48 years) and two future climate scenarios at different weather stations were assembled and used as model inputs (atmospheric boundary conditions) to the deterministic, unsteady, one-dimensional (vertical) lake water quality model MINLAKE2010/MINLAKE2012 which can simulate T and DO profiles in cisco lakes continuously for 48 years over the open-water seasons and winter ice-cover periods.

A cisco habitat model with three different modeling options were developed, validated, and used for the study. The first option is to use the constant lethal limits to model cisco habitat in Minnesota lakes. The constant limits for fish survival (lethal) and good growth do not change with time, and the method was previously used to

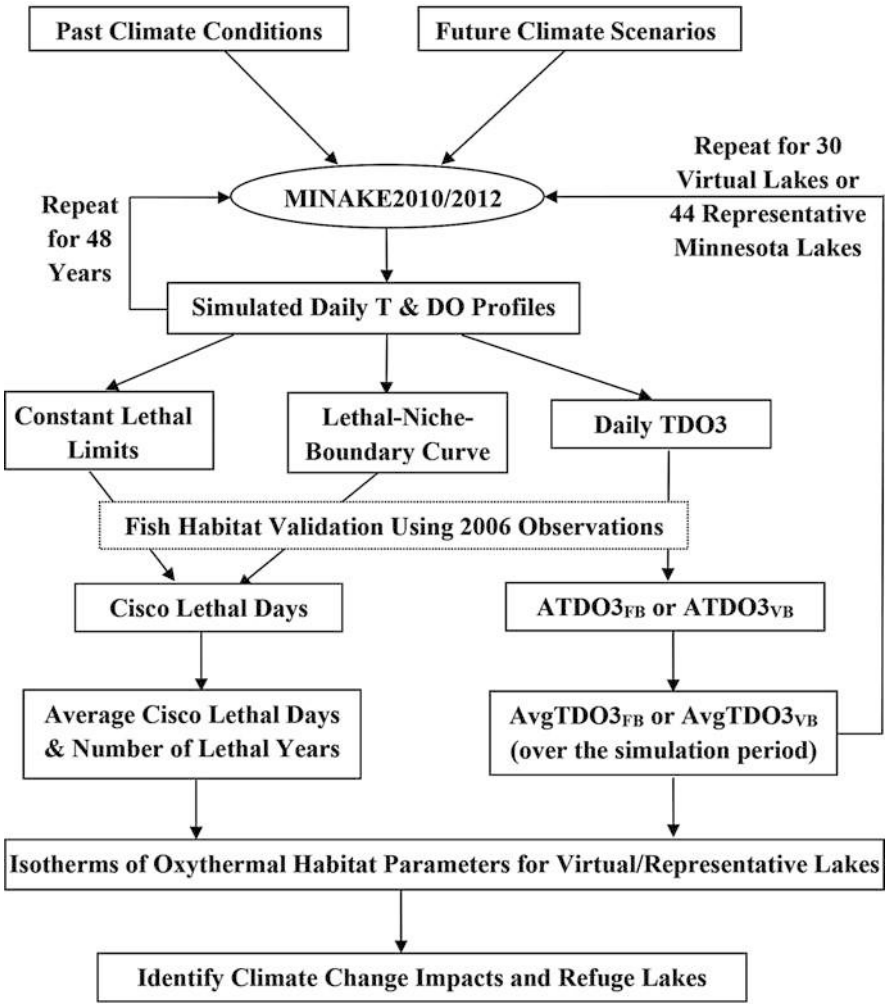

Fig. 3 Flowchart of the study to project impacts of climate changes on cisco oxythermal habitat in Minnesota lakes

project cold-water, cool-water, and warmwater fish habitat in small lakes in Minnesota and over the contiguous USA (Stefan et al. 2001). The constant lethal limits of cisco were calculated from the lethal-niche-boundary curve of adult cisco (Jacobson et al. 2008) and then determined through model validation in 23 Minnesota lakes using cisco mortality and survival data in the summer of 2006. The second option is to use a fitted regression equation as the lethal niche boundary of adult cisco. The equation was developed by Jacobson et al. (2008) and gives DO survival limits at different temperatures, which are temperature-varying lethal limits. The third option is to use a single oxythermal variable TDO3 to identify cisco refuge lakes

(Fang et al. 2012b; Jiang et al. 2012). TDO3 has been a useful parameter for quantifying the oxythermal niche of cold-water fish (Jacobson et al. 2010). TDO3 was calculated from simulated daily T and DO profiles for every simulated day except days in 1961 to avoid effects of initial conditions. In the third option of cisco oxythermal habitat modeling, the daily TDO3 values were averaged over either the fixed benchmark (FB) period ($ATDO3_{FB}$) (Fang et al. 2012b) or the variable benchmark (VB) period ($ATDO3_{VB}$) (Jiang et al. 2012) for each simulated lake and year. Using the variable benchmark periods for each simulated year gave the maximum average TDO3 over a 31-day period in different years and different lake types (Jiang et al. 2012).

The oxythermal habitat options 1 and 2 determine which day lethal conditions can occur. In the first option, when the LT isotherm and the DO limit isopleth for cisco intersect in a particular day (Stefan et al. 2001; Fang et al. 2004a; Fang and Stefan 2012), the entire depth of a stratified lake is under lethal conditions on that day. The lethal conditions are because water temperature is higher than LT from the water surface to or below the intersecting depth and DO is lower than the DO limit from the lake bottom to or above the intersecting depth. In the second option, lethal conditions for cisco are assumed to occur if the simulated DO is less than the DO_{lethal} value in all water layers (from the lake water surface to the lake bottom) on that day when DO_{lethal} is calculated from simulated water temperature using the lethal-niche-boundary curve (Jacobson et al. 2008).

To understand climatic variability, the water quality model and fish habitat model were run using the weather data from 1961 to 2008 for the past climate conditions in 30 virtual deep lakes and 44 representative lakes (Table 1) in Minnesota (Fig. 3). A number of years with cisco kill and number of cisco lethal days were determined during the simulation period for the habitat modeling options 1 and 2. The cisco kill was assumed to occur when the continuous lethal days of cisco last 3 or 7 days (Fang et al. 2014). To assess the quality of cisco habitat in a lake and identify refuge lakes, the 47-year averages of annual $ATDO3_{FB}$ and $ATDO3_{VB}$ values in the 1962–2008 simulation period (i.e., $AvgATD3_{FB}$ and $AvgATD3_{VB}$) were calculated in 30 virtual deep lakes (Table 2) and compared to TDO3 limits (11 °C and 17 °C determined by the analysis of field data) to divide cisco lakes into three tiers: tiers 1 and 2 refuge lakes and tier 3 non-refuge lakes (Fang et al. 2012b; Jiang et al. 2012).

To implement the above modeling approach, 44 "representative" Minnesota lake types (Table 1 and Fig. 3) and 30 "virtual" cisco lake types (Table 2 and Fig. 3) were chosen as representative of the entire set of Minnesota lakes in general and 620 cisco lakes, respectively; a similar approach using 27 "generic" lake types had been used to study climate warming impact on fish habitat in small lakes in Minnesota (Stefan et al. 1996) and in the contiguous USA (Stefan et al. 2001; Fang et al. 2004a, b), because it was not viable to run the deterministic model for all 620 cisco lakes over 47 years. To apply the oxythermal habitat results to the hundreds of cisco lakes that could not all be simulated, the virtual and representative simulated lakes had to be characterized in a generic way. Following previous practice (Stefan et al. 2001; Fang et al. 2004a, b), two parameters were chosen for this purpose: a lake geometry ratio (GR) as an indicator of a lake's potential for strong or weak summer stratification (Gorham and Boyce 1989) and mean summer Secchi depth (SD) as an indicator of

Table 1 Morphometric characteristics and "names" of the 44 representative or regional lake types in Minnesota simulated with the MINLAKE2010/MINLAKE2012 model

Maximum depth (m)	Surface area A_S (km^2)	Secchi depth, *SD* (m)				Geometry ratio (GR)
		1.2	2.5	4.5	7.0	$A_s^{0.25}/H_{max}$
H_{max} = 4 m (shallow)	0.2	LakeR01[a]	LakeR02	LakeR03	LakeR28	5.29 m$^{-0.5}$
	1.7	LakeR04	LakeR05	LakeR06	LakeR29	9.03 m$^{-0.5}$
	10	LakeR07	LakeR08	LakeR09	LakeR30	14.06 m$^{-0.5}$
H_{max} = 13 m (medium depth)	0.05	LakeR37	LakeR38	LakeR39	LakeR40	1.15 m$^{-0.5}$
	0.2	LakeR10	LakeR11	LakeR12	LakeR31	1.63 m$^{-0.5}$
	1.7	LakeR13	LakeR14	LakeR15	LakeR32	2.78 m$^{-0.5}$
	10	LakeR16	LakeR17	LakeR18	LakeR33	4.33 m$^{-0.5}$
H_{max} = 24 m (deep)	0.2	LakeR19	**LakeR20**[b]	**LakeR21**	**LakeR34**	0.88 m$^{-0.5}$
	1.7	LakeR22	**LakeR23**	**LakeR24**	**LakeR35**	1.50 m$^{-0.5}$
	10	LakeR25	**LakeR26**	**LakeR27**	**LakeR36**	2.34 m$^{-0.5}$
	2.32	LakeR41[c]	LakeR42	LakeR43	LakeR44	1.63 m$^{-0.5}$

Note:
[a]The first 28 shallow and medium-depth lakes were used for fish habitat modeling of the constant lethal limits method
[b]These highlighted lakes are strongly stratified mesotrophic and oligotrophic deep lakes used for fish habitat modeling of the lethal-niche-boundary curve method
[c]These four deep lakes (LakeR41–LakeR44) have the same geometry ratio but different surface areas as four medium-depth lakes LakeR10–LakeR12 and LakeR31 for comparison study

Table 2 Morphometric characteristics and "names" of the 30 virtual cisco lakes simulated with the MINLAKE2010/MINLAKE2012 model (maximum lake depth $H_{max} = 24$ m)

Surface area A_S (km^2)	Secchi depth *SD* (m)					Geometry ratio, $GR = A_s^{0.25}/H_{max}$
	1.2	2.5	4.5	7.0	8.5	
0.1	LakeC01	LakeC02	LakeC03	LakeC04	LakeC05	0.74
0.5	LakeC06	LakeC07	LakeC08	LakeC09	LakeC10	1.11
1.5	LakeC11	LakeC12	LakeC13	LakeC14	LakeC15	1.46
5.0	LakeC16	LakeC17	LakeC18	LakeC19	LakeC20	1.97
13.0	LakeC21	LakeC22	LakeC23	LakeC24	LakeC25	2.50
50.0	LakeC26	LakeC27	LakeC28	LakeC29	LakeC30	3.50

lake trophic state and transparency. These virtual and representative lakes are described in detail in a separate section.

Simulation Models for Year-Round Water Quality

To make projections of water quality and fish habitat in small lakes under future climate scenarios, numerical simulation models of daily temperature and DO profiles are indispensable. The one-dimensional (vertical) year-round lake water quality model MINLAKE2010 was developed to run continuously over many simulation years for both the open-water season and the ice-cover period (Fang and Stefan 1996a). The model uses a stacked layer system (Fig. 4); the layers consist of lake water and lake sediments during the open-water season and additional ice cover and snow cover during the winter ice-cover period (Fang and Stefan 2009). It simulates daily water temperature profiles in a lake using daily weather data as input. Figure 4 is a schematic of a stratified lake including heat transfer components, oxygen sources and sinks for the year-round water temperature and DO models, and typical temperature and DO profiles in the summer and winter (Fang and Stefan 1996a, b, c). MINLAKE2010 uses a mixed layer approach (Chapra 1997), which considers a mechanical energy balance (kinetic and potential energy), to predict the thickness of the mixed layer (epilimnion) after the heat diffusion equation is solved and convective mixing is considered (Ford and Stefan 1980).

A lake is divided into a series of well-mixed horizontal water layers (Fig. 4) because the horizontal variations of water quality parameters are typically much smaller than the vertical variations in a small stratified lake. The one-dimensional, unsteady heat transfer equation in a lake is solved for daily vertical water temperature profiles (Hondzo and Stefan 1993):

$$\frac{\partial T}{\partial t} = \frac{1}{A}\frac{\partial}{\partial z}\left(K_{zT} A \frac{\partial T}{\partial z}\right) + \frac{H_w}{\rho C_p} \tag{1}$$

where $T(z, t)$ is the water temperature (°C) in a horizontal layer, t is the time (day), $A(z)$ is the horizontal area (m^2) as a function of depth z (m) based on lake bathymetry

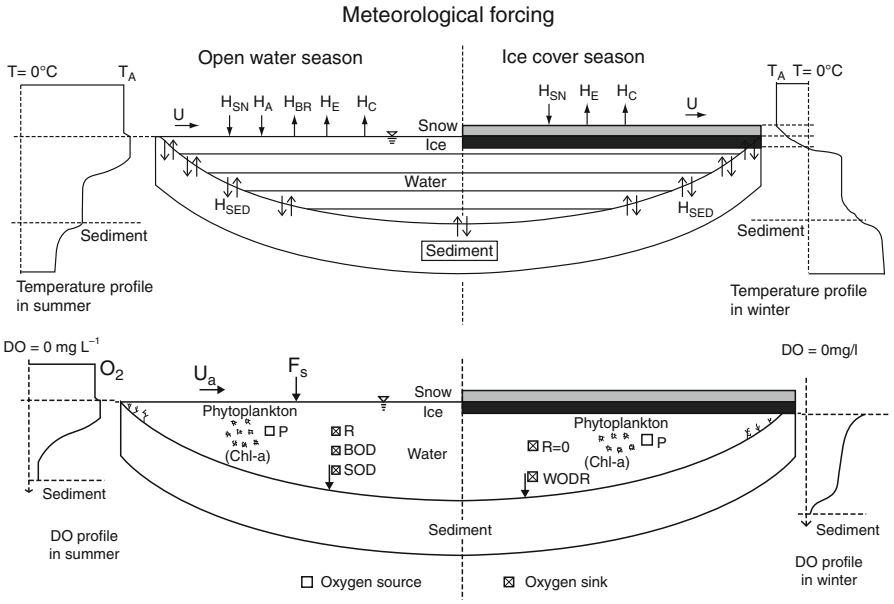

Fig. 4 Schematic of a stratified lake showing heat transfer components, oxygen sources and sinks for the year-round water temperature and DO model MINLAKE96/MINLAKE2010/MINLAKE2012, and typical temperature and DO profiles in summer open-water season (*left*) and winter ice-cover period (*right*) including sediment, water, ice, and snow layers (Fang and Stefan 2009)

input data, K_{zT} is the vertical turbulent heat diffusion coefficient ($m^2\ day^{-1}$), ρC_p is the density of water (ρ) times heat capacity of water (C_p) and represents heat capacity per unit volume ($J\ m^{-3}\ °C^{-1}$), and H_w is the internal heat source strength per unit volume of water ($J\ m^{-3}\ day^{-1}$). Solar radiation absorption in the water column is the main contributor to the heat source term during the open-water season (Stefan and Ford 1975). Heat exchange with the bottom sediment layer included in MINLAKE2010 can be important in the shallow water layers and during the winter ice-cover periods (Fang and Stefan 1996b).

Heat exchange between the lake and the atmosphere is treated as a source or sink term (Fig. 4) for the topmost water layer of a lake during the open-water season due to the surface wind mixing, i.e., $H_w(1)$ in Eq. 1 $= A_s/V(1) \times (H_{SN} + H_A - H_{BR} - H_E - H_C)$, where A_s is the lake surface area and $V(1)$ is the volume of the topmost/first water layer. It includes surface heat fluxes in $J\ m^{-2}\ day^{-1}$ such as net incoming heat from shortwave solar radiation (H_{SN}), long-wave radiation (H_A), outgoing heat from back radiation (H_{BR}), evaporation/condensation (H_E), and conduction/convection (H_C) related to wind speed (U, Fig. 4). The computation of above surface heat fluxes and the internal heat source term (H_w) using daily weather input data has been discussed by Hondzo and Stefan (1993), among others. During the ice-cover period (Fang and Stefan 1996b, c), the model first simulates snow/ice thicknesses

and sediment temperature profiles (heat conduction equation), then determines the heat source/sink terms, and finally solves the heat transfer equation to obtain water temperature profiles below the ice. The heat budget components through the water surface are directly linked to climate parameters that are related to future climate changes.

Dissolved oxygen concentration is viewed as one of the most important lake water quality parameters which indicate a lake's overall ecological health. The vertical DO profiles in the lake are computed from a balance between oxygen sources (surface reaeration and photosynthesis, Fig. 4) and oxygen sinks (sedimentary oxygen demand (SOD), biochemical oxygen demand (BOD), and plant respiration (R)). The numerical simulation model for daily DO profiles in a lake solves the one-dimensional, unsteady transport equation:

$$\begin{aligned}\frac{\partial C}{\partial t} &= \frac{1}{A}\frac{\partial}{\partial A}\left(AK_Z\frac{\partial C}{\partial z}\right) - \frac{S_b}{A}\frac{\partial A}{\partial z}\,\theta_s^{T-20} + P_{\mathrm{MAX}}\,\theta_p^{T-20}\mathrm{Min}[L]\;\;\mathrm{Chla} \\ &- \frac{1}{YCHO2}\,k_r\theta_r{}^{T-20}\,\mathrm{Chla} - k_b\,\theta_b{}^{T-20}\mathrm{BOD}\end{aligned} \tag{2}$$

In Eq. 2, $C(z, t)$ is the DO concentration in mg/L as a function of depth (z) and time (t), $K_z(z, t)$ is the DO vertical turbulent diffusion coefficient in $m^2\ day^{-1}$, and S_b is the coefficient for SOD at 20 °C in mg $O_2\ m^{-2}\ day^{-1}$. P_{MAX} is the maximum specific oxygen production rate by aquatic plants at 20 °C under saturating light conditions in mg O_2 (mg Chla)$^{-1}$ day^{-1}. Min[L] is the light limitation determined by Haldane kinetics (Megard et al. 1984). Chla is the chlorophyll-*a* concentration in mg/L to represent the biomass of aquatic plants in a lake. *YCHO2* is the yield coefficient, i.e., the ratio of mg chlorophyll-*a* to mg oxygen. The first-order decay rate coefficients are k_b and k_r for BOD and plant respiration (day^{-1}), respectively. The temperature adjustment coefficients for SOD, photosynthesis, BOD, and plant respiration are θ_s, θ_p, θ_b, and θ_r, respectively. Typical values and ranges of temperature and DO model parameters have been summarized elsewhere (Fang and Stefan 2012).

Oxygen production is related to chlorophyll-*a* concentration and limitation of available light determined by Haldane kinetics. In the DO model, chlorophyll-*a* is specified by a mean annual value which depends on the specified trophic state of a lake and a function that calculates typical seasonal chlorophyll-*a* cycles (Stefan and Fang 1994a) based on observational data from 56 lakes and reservoirs in Europe and North America (Marshall and Peters 1989). Annual mean chlorophyll-*a* concentration that represents biomass or phytoplankton in the MINLAKE2010 model was calculated from the relationship between chlorophyll-*a* and Secchi depth used in the Carlson trophic index (Carlson 1977) for virtual and representative lakes in Minnesota (Tables 1 and 2) or measured data for calibration lakes.

In the model, the oxygen transfers through the water surface (reaeration) during the open-water season is used as an oxygen source or sink term in the topmost water (surface) layer of the lake after the reaeration is multiplied by the surface area and divided by the layer volume, and the surface oxygen transfer coefficient is calculated as a function of wind speed. SOD is treated as a sink term for each water layer

because each water layer is in contact with lake sediments. BOD occurs in the water column along all water depths, and plant respiration for all water layers is a function of chlorophyll-*a* concentration. BOD (mg/L) is used to reflect biodegradable detritus in lake water column. Diffusive oxygen flux at the lake bottom is set equal to zero as a boundary condition (the flux is not explicitly modeled, but SOD is used as surrogate of the flux).

For the DO simulations in a lake during the ice-cover period (Fig. 4), modifications must be made to account for the presence of an ice cover and low temperatures. For example, reaeration is zero because the lake ice cover prevents any significant gas exchange between the atmosphere and the water body. The water column oxygen demand (WOD in Fig. 4) is set at 0.01 g O^2 m^{-3} per day after model calibration. DO concentrations are simulated after water temperature and snow/ice covers have been simulated. Equations 1 and 2 are solved numerically for time steps of 1 day and layer thicknesses from 0.02 m (near the water surface and the ice-water interface) to 1.0 m (when $z > 1.0$ m) for small lakes using an implicit finite difference scheme and a Gaussian elimination method. Model parameters and detailed formulations of the year-round DO model (Eq. 2) have been described elsewhere (Stefan and Fang 1994a; Fang and Stefan 1997).

Several modifications and refinements were made to develop MINLAKE2010 from MINLAKE96 for relative deep cisco lakes in Minnesota and have been reported by Fang et al. (2012a). Most recent version MINLAKE2012 (Fang et al. 2014) used in a part of the study is a spreadsheet model developed from MINLAKE2010. The most important upgrades of MINLAKE2012 compared to MINLAKE2010 are the conversion to a user-friendly Excel spreadsheet (for data input and displaying basic graphic results) and the introduction of variable temporal resolution, allowing the model to run at hourly and daily time steps.

The MINLAKE model was calibrated and validated against extensive Minnesota lake data: first, using 5,378 water temperature and DO measurements for 48 lake years in 9 lakes for MINLAKE96 (Fang and Stefan 1996) and then using 7,384 water temperature and DO measurements for 439 lake years in 28 lakes for MINLAKE2010 (Fang et al. 2012a). Twenty-one cisco lakes and seven non-cisco lakes were selected for model calibration of MINLAKE2010 based on multiyear data availability; more than half of these 28 lakes had maximum depths greater than 24.0 m, which is H_{max} used for the 30 virtual lakes in Table 2, and 23 of the 28 lakes were either mesotrophic or oligotrophic lakes (Fang et al. 2012a). After calibration, the average standard error of estimates against measured data for all 28 lakes was 1.47 °C for water temperature (range from 0.8 °C to 2.06 °C) and 1.50 mg/L for DO (range from 0.88 to 2.76 mg/L) (Fang et al. 2012a).

Cisco Lakes in Minnesota

The modeling analysis was conducted for 620 known cisco lakes in Minnesota (Fig. 1); the MN DNR had netting assessments for these lakes since 1946. On average, Minnesota cisco lakes are deeper and more transparent (larger Secchi

depth) and have lower chlorophyll-*a* concentrations than other lakes in Minnesota (Fang et al. 2009). The 620 cisco lakes vary in mean Secchi depth (SD) and lake geometry ratio (GR) as shown in Fig. 5. The lake GR is defined as $A_s^{0.25}/H_{max}$ in $m^{-0.5}$ when surface area A_s is in m^2 and maximum depth H_{max} in m. The strength of the seasonal lake stratification is related to the GR (Gorham and Boyce 1989). Polymictic lakes such as large shallow lakes have the highest GR numbers, while strongly stratified lakes have the lowest GR numbers; the transition from weakly to strongly stratified lakes occurs when GR is between 3 and 5 (Gorham and Boyce 1989). Lake geometry ratios of Minnesota cisco lakes range from 0.47 to 22.7 $m^{-0.5}$ (Fig. 4), and about 73 % of these lakes have GR less than 3.0 $m^{-0.5}$ (Fang et al. 2009). Only 6 % or 39 of these lakes have GR greater than 5.0 $m^{-0.5}$; these are very weakly stratified or unstratified lakes during the summer. Lake of the Woods is located at the border of the USA and Canada and has the largest surface area (3847.8 km^2) with the largest GR = 22.7 $m^{-0.5}$ and a maximum depth of 10.97 m. Mille Lacs Lake has the second largest GR = 11.9 $m^{-0.5}$ with a maximum depth of 12.8 m and surface area of 536.5 km^2.

Maximum depths of the 620 cisco lakes range from 3.0 to 64.9 m, and 25 % of these lakes have maximum depth greater than 24 m (Fang et al. 2009). For these 620 cisco lakes in Minnesota, there are 14 shallow lakes with $H_{max} < 5.0$ m, 385 medium-depth lakes (Fig. 5 top) with 5.0 m $\leq H_{max} <$ 20.0 m, and 221 deep lakes with $H_{max} > 20.0$ m (Fig. 5 bottom) based on regional lake classifications in Minnesota (Stefan et al. 1996). Surface areas of these lakes range from 0.04 to 3,847.8 km^2 (Fang et al. 2009) and mean summer Secchi depths from 0.7 to 9.5 m. Nineteen percent and 81 % of the 620 cisco lakes (Fang et al. 2009) have mean summer Secchi depth greater than 4.5 m (oligotrophic lakes) and 2.5 m (mesotrophic lakes), respectively, based on regional lake classifications in Minnesota (Stefan et al. 1993).

For modeling purposes, the 620 Minnesota cisco lakes were grouped by either shortest distance or latitude to associate with three Class I National Weather Service (NWS) weather stations in Minnesota (International Falls, Duluth, and St. Cloud; Fig. 1). Weather data from only these three Class I NWS weather stations were useful and available for cisco lake long-term simulations for the period from 1961 to 2008. Three options (methods) were used to associate each lake with one of the three weather stations: (1) association by shortest distance (Fang et al. 2012b), (2) association by latitude (Jiang et al. 2012), and (3) association of one single weather station with all lakes simulated (Fang et al. 2010b). Refuge lakes were determined using each of the three options (Fang et al. 2010b), but results were similar; simulation results by methods (1) and (2) are presented here.

Representative Lake Types in Minnesota

Simulations of daily water temperature and DO profiles and oxythermal habitat parameters were made for 30 virtual cisco lakes and 44 representative lakes (lake types or classes) in Minnesota before fish habitat was examined in 620 cisco lakes. The 44 representative lake types in Table 1 were expanded from the 27 lake types

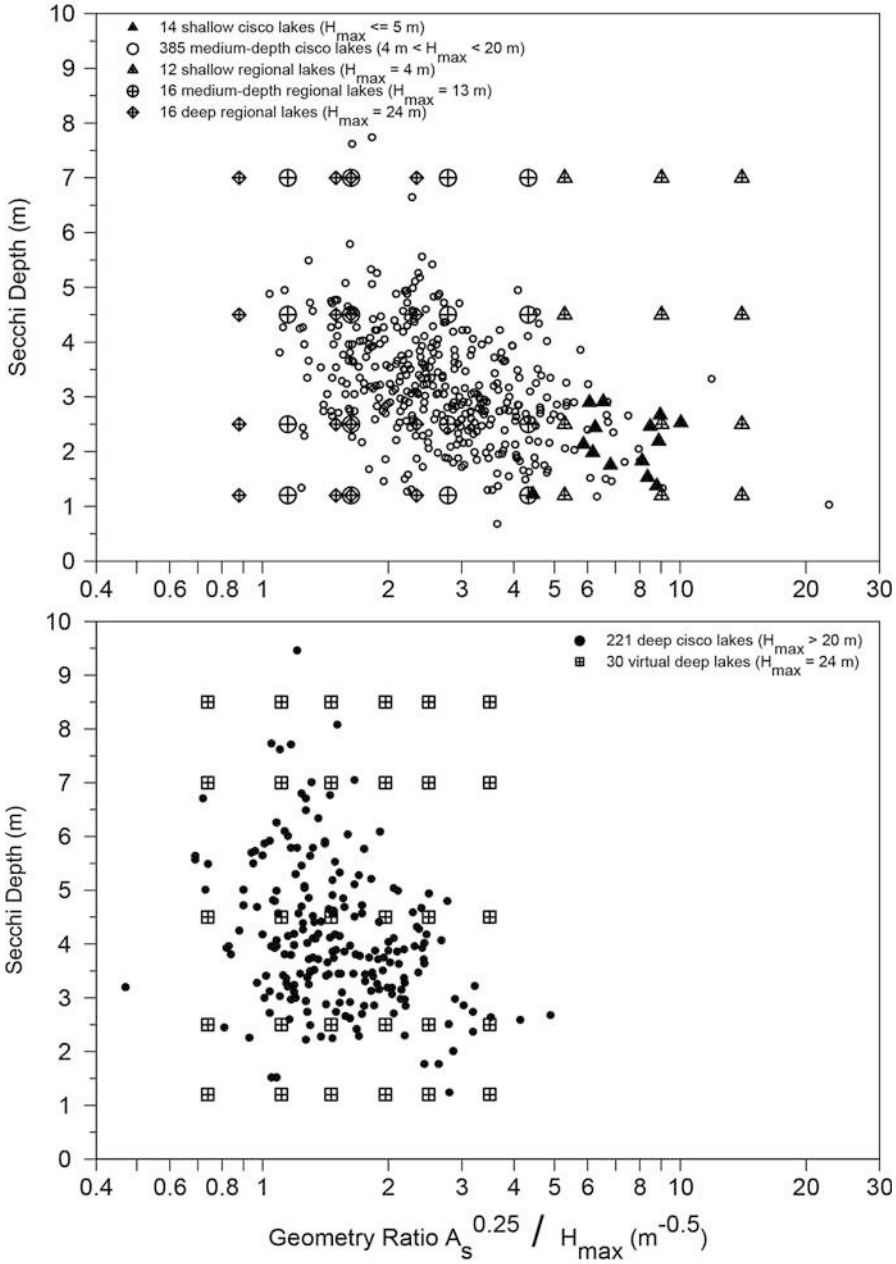

Fig. 5 Distribution of 14 shallow and 385 medium-depth cisco lakes (*top*) and 221 deep cisco lakes (*bottom*) from 620 cisco lakes in Minnesota including 44 regional or representative lakes (Table 1) and 30 virtual deep lakes (Table 2) plotted using Secchi depth and lake geometry ratio as axes

used to study fish habitat in Minnesota (Stefan et al. 1996) and in the contiguous USA (Fang et al. 2004a). Lakes were classified by lake geometry (surface area A_s and maximum depth H_{max}) and trophic state as related to Secchi depth (SD in Tables 1 and 2). The representative surface areas chosen for the 27 lake types were 0.2, 1.7, and 10.0 km^2 for small, medium-size, and large lakes (Stefan et al. 1996; Fang et al. 2004a), respectively. The representative maximum depths chosen were 4, 13, and 24 m for shallow, medium-depth, and deep lakes (Stefan et al. 1996; Fang et al. 2004a), respectively. With these numbers for A_s and H_{max}, nine lake types were obtained ranging from relatively large and shallow lakes to relatively small and deep lakes.

Secchi (disk) depth (SD) is a common limnological parameter to measure transparency of a lake (Hutchinson 1957; Horne and Goldman 1994). It was used in previous fish habitat studies (Stefan et al. 1996; Fang et al. 2004a) to represent both trophic state (primary productivity of biomass or photosynthesis of plants) and solar radiation attenuation in a lake, which is used to quantify how much solar energy reaching the water surface can penetrate through a water column to heat water and to support photosynthesis of aquatic plants (Fig. 4). Lake turbidity from suspended inorganic sediment is relatively rare in Minnesota, and total phosphorus or chlorophyll-*a* in most Minnesota lakes is well correlated with SD (Stefan and Fang 1994b). Therefore, SD is a representative parameter to characterize trophic state of each of the 620 cisco lakes in the database. Contours (isotherms or isopleths) on plots with SD versus GR as axes have been previously used successfully by the authors to give/present generic, but regional, patterns or variations of different characteristic parameters in lakes, e.g., maximum surface water temperatures, maximum lake bottom temperatures, minimum DO at the sediment/water interface, and various fish habitat parameters in lakes (Stefan et al. 1996; Fang and Stefan 1997, 1999).

The representative Secchi depths of 1.2, 2.5, and 4.5 m were previously selected for eutrophic, mesotrophic, and oligotrophic Minnesota lakes (Stefan et al. 1996; Fang et al. 2004a), respectively, using Carlson's trophic state index (Carlson 1977). Ten percent or 62 lakes of 620 cisco lakes have mean summer Secchi depths of 5.0–9.5 m. Therefore, the fourth Secchi depth of 7.0 m was added creating nine new representative lake types for the study. A set of virtual cisco lakes (Table 2) with SD = 7.0 m was first used before to study cisco refuge lakes in Minnesota (Jiang et al. 2012). Therefore, the first 36 representative lake types (Table 1) were characterized by a 3 × 3 × 4 matrix consisting of (a) three different lake surface areas, (b) three lake maximum depths, and (c) four Secchi depths.

The first 28 shallow and medium-depth lakes in Table 1 were used for fish habitat modeling of the constant lethal limits method (Fang et al. 2014). Four medium-depth lakes LakeR37–LakeR40 were added to have a lake geometry ratio of 1.15 to reflect some of the medium-depth cisco lakes with smaller GR (Fig. 5). Four deep lakes (LakeR41–LakeR44) were added to have the same geometry ratio but different surface areas as four medium-depth lakes LakeR10–LakeR12 and LakeR31 to compare fish habitat parameters in these two groups of lakes (Fang et al. 2014). With above eight additional regional lakes, there

are a total of 44 representative lakes (Table 1 and Fig. 5 top) used for cisco habitat modeling in Minnesota. These representative or regional values for each parameter (As, Hmax, and SD in Table 1) were selected from the data analysis of these parameters in the Minnesota Lakes Fisheries Database containing lake survey data for 3,002 lakes (Hondzo and Stefan 1993) and 620 cisco lakes (Fang et al. 2009). The lake bathymetry of these 44 lakes (the shape of the lake basin as part of model input data) is characterized by three functions $A(z)/A_s$ versus $z/H_{\max}$ for small, medium-size, and large lakes, which are regression equations developed from 122 Minnesota lakes by Hondzo and Stefan (1993). More important than the geometric characteristics of each lake type is the likelihood of relating a strong or weak stratification in a lake to the lake's geometry ratio $\mathrm{GR} = {A_s}^{0.25}/H_{\max}$ (Gorham and Boyce 1989). The above 44 lake types cover geometry ratios from 0.88 to 14.06 $\mathrm{m}^{-0.5}$ (Table 1). Polymictic lakes, i.e., large shallow lakes, have the highest geometric ratio, while strongly stratified lakes, i.e., small deep lakes, have the lowest geometry ratio. Hence, these 44 lake types selected for the study include the full range of stratification behavior.

The set of 30 virtual cisco lakes (Fig. 5 bottom) comprised lakes with five different SD values (1.2, 2.5, 4.5, 7.0, and 8.5 m) and six different surface areas (0.1, 0.5, 1.5, 5.0, 13.0, and 50 km^2). The maximum depth of all 30 virtual lakes was set at 24 m (Fang et al. 2009, 2012; Jiang et al. 2012). Combinations of the maximum depth and surface areas gave six different geometry ratios for the 30 virtual lakes, i.e., 0.74, 1.11, 1.46, 1.97, 2.50, and 3.50 $\mathrm{m}^{-0.5}$ (Table 2). Twenty of the 30 virtual cisco lake types were strongly stratified with $\mathrm{GR} < 2\ \mathrm{m}^{-0.5}$; the other ten lake types were weakly stratified (Table 2). The 30 virtual cisco lakes (Table 2) did not include any polymictic lakes because they likely would not provide suitable cold-water habitat in Minnesota after climate warming. For example, Fang et al. (2012a) studied the oxythermal habitat variable TDO3 in 21 study cisco lakes in Minnesota and found that two cisco lakes with $\mathrm{GR} > 4.0\ \mathrm{m}^{-0.5}$ (White Iron Lake and South Twin Lake) had high annual maximum TDO3 values indicating unfavorable conditions for cisco survival and growth. Values of TDO3 extracted from observed temperature and DO profiles were lowest in lakes with small geometry ratios ($\mathrm{GR} < 2\ \mathrm{m}^{-0.5}$); a geometry ratio of 4 $\mathrm{m}^{-0.5}$ effectively marked the transition between stratified and unstratified lakes (Jacobson et al. 2010).

Even though the lake bathymetry (surface area and maximum depth) and Secchi depth of the 30 virtual cisco lakes were subjective, the selected values were representative of most of the 620 Minnesota cisco lake database (Fang et al. 2009). The 30 virtual cisco lakes were all stratified lakes based on geometry ratio and included eutrophic to oligotrophic lakes (Table 2). The 30 virtual cisco lakes were more or less uniformly distributed on the plot of SD vs. GR (Fig. 5 bottom) (Fang et al. 2012b). None of the 30 virtual cisco lakes in Table 2 have the same lake surface areas as 44 representative Minnesota lakes in Table 1. These two groups of generic lake classes (types) were used in the different fish habitat modeling options (Fig. 3): 44 representative lakes for the oxythermal model options 1 and 2 using lethal limits (Fig. 5) and 30 virtual lakes for the model option 1 (constant lethal limits) and the model option 3 using TDO3 (Fig. 3) during different study periods.

Past Climate and Future Climate Scenarios

Climate conditions control water temperature and DO distribution in a lake. Climate scenarios are model inputs of MINLAKE2010/MINLAKE2012 for producing water temperature and DO concentration scenarios for the simulated lakes (Tables 1 and 2), which are used to assess potential changes in cisco habitats in these lakes. To identify refuge lakes, we need to project whether a lake that currently has a cisco population can support cisco habitat under future climate scenarios, i.e., after climate warming. To make the projection, the model outputs from two coupled general circulation models (CGCMs) of the earth's atmosphere and oceans (i.e., CGCM 3.1 and MIROC 3.2) were used as input to the MINLAKE2010 model to calculate a range of future water quality conditions.

Forty-eight years (1961–2008) of recorded daily weather data, which were obtained from the Solar and Meteorological Surface Observation Network (SAMSON) and Midwestern Regional Climate Center, were used to describe past climate conditions for the study lakes. Weather data used for lake modeling consist of daily air temperature, dew point temperature, wind speed, solar radiation, percent sunshine, and precipitation (both rainfall and snowfall).

The CGCM 3.1 (Kim et al. 2002, 2003) is the third generation of CGCMs from the Canadian Centre for Climate Modeling and Analysis (CCCma). The CCCma CGCM 3.1 uses the ocean component from the earlier second-generation CGCM (McFarlane et al. 1992) and applies a substantially updated atmospheric component – the third-generation atmospheric general circulation model. Output of the CGCM 3.1 model with a coarse global surface grid resolution of roughly 3.75° latitude and longitude or approximately 410 km in Minnesota was used for the study because it was available to be downloaded from the Intergovernmental Panel on Climate Change (IPCC) data center in 2008. When CGCM 3.1 is used for the study, there is one grid center point within Minnesota and another grid center point in Canada that is the closest grid point to International Falls weather station (Fig. 1).

The MIROC 3.2 (Hasumi and Emori 2004) was developed by the Center for Climate System Research, University of Tokyo; the National Institute for Environmental Studies; and the Frontier Research Center for Global Change – Japan Agency for Marine-Earth Science and Technology. Output of the MIROC 3.2 model with a high spatial surface grid resolution of roughly 1.12° latitude and longitude or approximately 120 km in Minnesota was used. The MIROC 3.2 model has 17 grid center points in Minnesota, and Fig. 1 shows three grid center points from MIROC 3.2 that are the closest to three weather stations (St. Cloud, Duluth, and International Falls) used for the model study.

At all CGCM grid center points, the differences or ratios known as "change fields" were produced and reported at a monthly interval. The 2070–2099 change field data, 30-year averages compatible with the Third Assessment Report of the IPCC (2007), were downloaded from the IPCC's website and used in the study. These monthly climate parameter differences or ratios predicted by CGCM models were then applied to measured daily climate conditions (1961–2008) month by month to produce the projected daily future climate scenario. Monthly increments

Table 3 Monthly changes of air temperature (°C) and solar radiation (Langley/day) projected by MIROC 3.2 and CGCM 3.1 for the three principal Minnesota weather stations

Station	International Falls		Duluth		St. Cloud	
Month	T_{air}[a]	S_{RAD}[b]	T_{air}	S_{RAD}	T_{air}	S_{RAD}
January	5.15/ 6.89[c]	−20.34/ −5.69	4.67/ 4.84	−15.92/ −7.49	4.35/ 4.84	−4.60/ −7.49
February	4.70/ 5.07	−25.36/ −9.51	4.67/ 8.09	−23.42/ −38.21	4.17/ 8.09	−9.13/ −38.21
March	4.64/ 3.90	−24.84/1.83	4.53/ 6.25	−15.75/ −55.05	4.08/ 6.25	0.35/−55.05
April	4.52/ 4.31	−3.32/ −18.77	3.89/ 3.60	0.78/−25.99	3.88/ 3.60	9.80/−25.99
May	4.37/ 4.12	−4.43/ −29.39	4.21/ 3.47	−15.22/ −19.96	4.33/ 3.47	2.45/−19.96
June	3.62/ 4.59	−3.82/9.63	3.59/ 3.28	−3.92/2.28	3.67/ 3.28	0.36/2.28
July	3.53/ 3.80	−5.38/14.43	3.68/ 3.25	10.36/14.78	3.67/ 3.25	17.08/14.78
August	3.75/ 3.30	−0.49/7.63	3.82/ 3.32	0.52/3.66	3.92/ 3.32	3.64/3.66
September	3.80/ 3.49	16.57/10.69	3.81/ 3.34	19.27/0.34	3.87/ 3.34	24.14/0.34
October	4.46/ 3.19	−2.76/3.94	4.29/ 3.39	3.03/−1.18	4.30/ 3.39	9.87/−1.18
November	4.10/ 2.89	−4.22/ −1.82	3.89/ 3.06	3.03/−2.16	3.87/ 3.06	5.79/−2.16
December	4.18/ 4.14	−12.80/ −4.86	3.99/ 2.91	−9.24/−1.32	3.92/ 2.91	−3.16/ −1.32
Average	4.24/ 4.14	−7.60/ −1.82	4.09/ 4.07	−3.87/ −10.86	4.00/ 4.07	4.71/−10.86

[a]Conversion of temperature changes, 1.0 °C = 1.8 °F
[b]Stands for solar radiation, 1.0 Langley/day = 0.484 W/m^2
[c]The first value is for MIROC 3.2 and the second value is for CGCM 3.1

from the grid center point closest to a weather station were used to specify the future climate. For the MIROC 3.2 future climate scenario, each of the three Class I NWS weather stations (International Falls, Duluth, and St. Cloud) used for the study had a closest grid center point (Fig. 1); for the CGCM 3.1 future climate scenario, Duluth and St. Cloud used the grid center point in Minnesota (Fig. 1), and International Falls used a grid center point in Canada (Fig. 1).

Monthly air temperature increases projected by MIROC 3.2 range from 3.53 °C to 4.70 °C with annual averages of 4.00–4.24 °C for the three weather stations (Table 3); CGCM 3.1 projection has a range from 2.89 °C to 8.09 °C with annual averages of 4.07–4.14 °C for the three weather stations (Fang et al. 2010b). The average monthly increases in air temperature range from 3.6 °C to 4.7 °C (3.6–3.8 °C from July to September) in Bemidji, Minnesota, which was also used for the oxythermal habitat option 2 (lethal-niche-boundary curve).

Simulation and Validation of Cisco Oxythermal Habitat Using the Constant Lethal Limits

The physiological response of adult populations of different fish species to T and DO levels has been the subject of numerous laboratory and field studies, e.g., by Coutant (1970), McCormick et al. (1972), and Hokanson et al. (1977). These studies correlated fish survival, growth, reproduction, and other responses to chronic levels of T and DO exposure. Simulation of oxythermal fish habitat in lakes was conducted in small lakes (up to 10 km^2 surface area) in Minnesota and the contiguous USA using constant survival limits (Stefan et al. 1996; Fang et al. 2004a, b). The oxythermal habitat approach commonly used in cold-water fish niche modeling (Dillon et al. 2003) defines an upper boundary for T and a lower boundary for DO, which are lethal temperature (*LT*) and DO survival limit (DO_{lethal}). These oxythermal habitat models determine the water volume or layer thickness in a stratified lake between the upper temperature and lower DO bound that represent either optimal thermal habitat (Dillon et al. 2003) or nonlethal/useable habitat (Stefan et al. 2001). The "uninhabitable spaces" or "lethal conditions" for a fish species in a lake are where temperature is above or DO is below the survival limits (Stefan et al. 2001). This study uses the oxythermal habitat approach to investigate the lethal conditions and fish kill in summer for a cold-water fish species – cisco *Coregonus artedi* in Minnesota lakes. The goals of the study were to first validate cisco survival and lethal conditions in 23 Minnesota lakes (Tables 4 and 5) under 2006 weather conditions and then simulate daily T and DO profiles in 58 lake types (28 shallow and medium-depth lakes in Table 1 and 30 virtual lakes in Table 2) to project cisco survival and potential lethal conditions in 620 cisco lakes in Minnesota under future climate scenarios. The 28 shallow and medium-depth lakes include LakeR01–LakeR18, LakeR28–LakeR33, and LakeR37–LakeR40 in Table 1.

Prediction of Cisco Lethal Conditions Using Constant Lethal Limits

Cisco habitat (survival) and lethal conditions were determined using simulated daily T and DO profiles in lakes, similar to the approach by Christie and Regier (1988). Temperature and DO limits of lethal conditions for adult cisco were applied to simulated water temperature and DO profiles day by day to examine whether lethal conditions occur or not in each specific day, as shown in Fig. 6 for Pine Mountain Lake. Simulated T and DO profiles were not averaged during the simulation period as was done in previous studies (Stefan et al. 1996; Fang et al. 2004a, b). When the *LT* isotherm and the DO_{lethal} isopleth for cisco intersect in a particular day, the entire depth of a stratified lake is under lethal conditions on that day. The lethal conditions are because water temperature is higher than *LT* from the water surface to or below the intersecting depth and DO is lower than the DO_{lethal} from the lake bottom to or above the intersecting depth. When the maximum daily water temperature is lower than the *LT*, the *LT* isotherm does not show up in the plot of depth-time contours of cold-water habitat (the upper and lower good-growth temperature contours used in previous

Table 4 Lethal days simulated in the 23 Minnesota lakes using the constant value method with eight different lethal temperatures (LT) and DO survival limits

	Number of days with lethal conditions							
	LT = 23.4 °C			**22.0 °C**			21.2 °C	22.6 °C
Lake name	DO = 2 mg/L	3 mg/L	4 mg/L	2 mg/L	**3 mg/L**	4 mg/L	2 mg/L	4 mg/L
Little Turtle	27	29	29	58	**62**	63	71	48
Andrusia	19	25	29	55	**60**	66	62	51
Little Pine (Otter Tail)	1	3	5	5	**15**	21	15	15
Cotton	37	37	37	57	**58**	59	72	52
Pine Mountain	12	23	35	35	**56**	72	56	55
Leech	24	24	24	36	**36**	36	56	28
Itasca	26	27	28	48	**53**	55	59	41
Gull	0	0	17	4	**22**	54	29	28
Woman	27	28	29	55	**59**	61	67	46
Little Pine (Crow Wing)	18	50	68	39	**54**	106	59	45
Eighth Crow Wing	28	29	30	53	**55**	47	67	47
Straight	0	0	5	0	**5**	20	2	9
Mille Lacs	36	36	36	49	**49**	49	56	43
Star	0	0	6	9	**15**	29	16	20
Bemidji	0	0	0	0	**7**	16	6	8
Seventh Crow Wing	3	10	19	17	**20**	23	22	20
Long	0	0	0	0	**4**	12	1	7
Carlos	0	0	0	0	**0**	0	0	0
Reference lakes without cisco kills in 2006								
Big Trout	0	0	0	0	**0**	0	0	0
Kabekona	0	0	0	0	**0**	0	0	0
Scalp	0	0	0	0	**0**	0	0	0
Ten Mile	0	0	0	0	**0**	0	0	0
Rose	0	0	0	0	**0**	0	0	0

studies were not used/shown in Fig. 6). Therefore, the DO lethal/survival limit becomes the only lethal criterion during the early spring, late fall, and winter ice-cover period, but the study only deals with lethal conditions of cisco during the summer months. Figure 6 shows cisco habitat results from April 15 to October 31, i.e., the day of year (DOY) 105–304, which is during the typical open-water season in Minnesota.

The *LT* is the water temperature to which fish cannot be acclimated without causing death. In early publications by authors, it was called as the upper survival temperature limit (Stefan et al. 1996), which was the 95th percentile of the weekly mean temperatures from an updated national fish/temperature database (Stefan

Table 5 Maximum depth (H_{max}), lake geometry ratio (GR), and fish habitat validation results using constant lethal limits ($LT = 22.0$ °C and $DO_{lethal} = 3$ mg/L) for 23 Minnesota lakes. Simulated and observed days with lethal conditions or mortality for cisco are given

Lake name (H_{max} in m, GR in $m^{-0.5}$)	Lethal conditions			Simulated lethal days in 2006	Observed mortality day in 2006	Model agreement
	First day	Last day	No. of days			
Little Turtle (9.1, 4.02)	180	241	62	180 (62)[a]	200 (7/19)[b]	Yes (Yes)[c]
Andrusia (18.3, 2.75)	192	251	60	192 (59)	202 (7/21)	Yes (Yes)
Little Pine (Otter Tail) (23.8, 2.26)	202	216	15	202 (15)	203 (7/22)	Yes (Yes)
Cotton (8.5, 6.07)	184	241	58	184 (58)	205 (7/24)	Yes (Yes)
Pine Mountain (23.8, 2.11)	193	250	56	193 (36); 232 (20)	207 (7/26)	Yes (Yes)
Leech (13.0, 10.91)	188	225	36	188 (3); 193 (31); 224 (2)	211 (7/30)	Yes (Yes)
Itasca (13.7, 3.32)	188	241	53	188 (38); 227(15)	209 (7/28)	Yes (Yes)
Gull (24.4, 3.26)	206	227	22	206 (22)	210 (7/29)	Yes (Yes)
Woman (16.5, 4.02)	183	241	59	183 (59)	210 (7/29)	Yes (Yes)
Little Pine (Crow Wing) (11.0, 2.90)	186	250	54	186 (2); 192 (34); 227 (2); 230 (7); 238 (4); 246 (5)	214 (8/2)	Yes (Yes)
Eighth Crow Wing (9.1, 4.11)	187	241	55	188 (55)	216 (8/4)	Yes (Yes)
Straight (19.2, 1.94)	211	215	5	211 (5)	213 (8/1)	Yes (Yes)
Mille Lacs (10.7, 14.14)	203	251	49	203 (49)	204 (7/23)	Yes (Yes)
Star (28.7, 2.26)	203	217	15	203 (15)	200 (7/19)	Yes (No)
Bemidji (23.2, 3.13)	211	217	7	211 (7)	208 (7/27)	Yes (No)
Seventh Crow Wing (12.2, 2.61)	196	215	20	196 (20)	216 (8/4)	Yes (No)
Long (39.0, 1.22)	213	216	4	214 (4)	218 (8/6)	Yes (No)
Carlos (49.7, 1.15)			0	No kill	239 (8/27)	No

(*continued*)

Table 5 (continued)

Lake name (H_{max} in m, GR in $m^{-0.5}$)	Lethal conditions			Simulated lethal days in 2006	Observed mortality day in 2006	Model agreement
	First day	Last day	No. of days			
Reference lakes without cisco kill in 2006						
Big Trout (39.0, 1.24)			0	No kill	No kill	Yes
Kabekona (40.5, 1.38)			0	No kill	No kill	Yes
Scalp (27.4, 1.15)			0	No kill	No kill	Yes
Ten Mile (63.4, 1.06)			0	No kill	No kill	Yes
Rose (41.8, 1.12)			0	No kill	No kill	Yes

Note:
[a]Stands for a DOY in 2006 and the number of continuous cisco lethal days from the lethal day predicted by the fish habitat model
[b]DOY followed by month and date in 2006 inside brackets
[c]The first Yes/No gives the agreement of cisco lethal prediction and reported cisco mortality in 2006, and Yes/No inside brackets gives the agreement whether or not cisco lethal days from the model include reported date with cisco mortality

et al. 1996) that includes observed stream temperature and fish observations. The LT values compared favorably with laboratory test results involving exposures of fish in several days (Stefan et al. 1992). The $LT = 23.4$ °C used for the cold-water fish guild in previous studies (Stefan et al. 1996, 2001) was the mean value of LT values for nine cold-water fish species (pink salmon, sockeye salmon, chinook salmon, chum salmon, coho salmon, brown trout, rainbow trout, brook trout, and mountain whitefish), which do not include cisco. The LT of cold-water fish species ranged from 22.1 °C (brook trout) to 26.6 °C (brown trout) in the 1992 study (Stefan et al. 1996). Eaton et al. (1995) updated the LT values that ranged from 19.8 °C (chum salmon) to 24.1 °C (brown trout) with guild mean of 22.9 °C. The DO concentration of 3.0 mg/L requirement for the cold-water fish guild, below which mortality is more likely to occur or growth is impaired (US EPA 1976), was developed from an available US EPA database (Chapman 1986). Jacobson et al. (2010) selected a benchmark oxygen concentration of 3 mg/L which is probably lethal or nearly so for many cold-water species. Frey (1955) also used an oxygen concentration of 3 mg/L in his definition of cisco habitat. Several benchmark DO concentrations (2, 3, 4, and 5 mg/L) were considered by Jacobson et al. (2010), and they were highly correlated (Table 4).

Before appropriate LT and DO limits for adult cisco were determined/used for cisco oxythermal modeling, a sensitivity analysis using 22.0 °C and 23.4 °C as LT and 2, 3, and 4 mg/L as DO survival limit was performed. The lethal temperature of 22.0 °C used for the sensitivity analysis was determined from the lethal-niche-boundary curve (Jacobson et al. 2008) (Eq. 3) at $DO_{lethal} = 3$ mg/L. The 22.0 °C

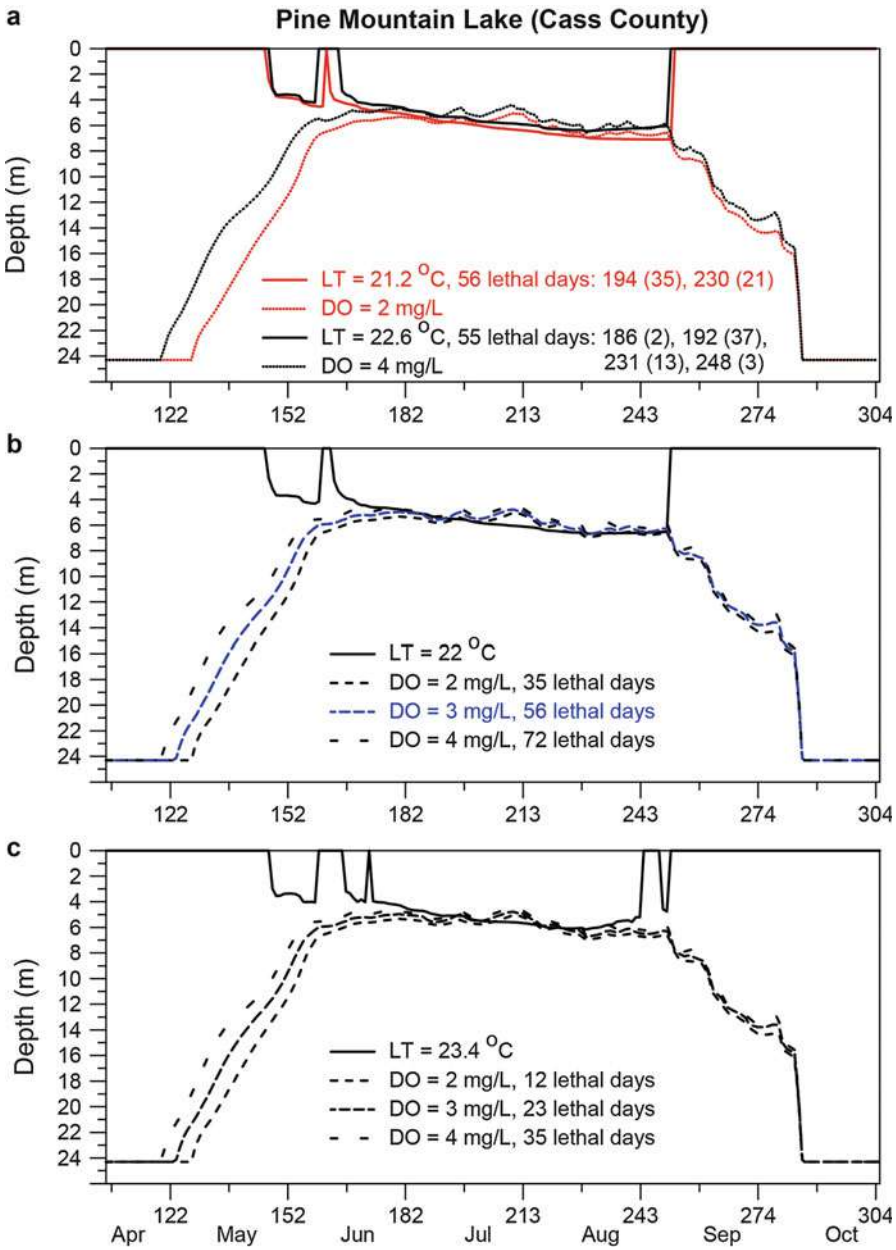

Fig. 6 Simulated isopleths of lethal temperatures (*LT*) and DO_{lethal} limits in 2006 for Pine Mountain Lake for eight LT-DO limit combinations. Selected LT are 21.2 and 22.6 °C (*top*) 22.0 °C (*middle*) and 23.4 °C (*bottom*), and selected DO survival limits are 2, 3, and 4 mg/L

LT compares favorably with lower LT values for other cold-water fish species in previous studies (Stefan et al. 1992, 1996; Eaton et al. 1995). Using the lethal-niche-boundary curve (Jacobson et al. 2008), the lethal temperatures were 21.2 °C and 22.6 °C for $DO_{\text{lethal}} = 2$ and 4 mg/L, respectively, and these two LT-DO combinations were also used for the sensitivity analysis (Table 4). The combinations of four LTs and three DO limits resulted in eight constant LT-DO criteria for the sensitivity analysis of the fish habitat model. The final LT-DO criteria, $LT = 22.0$ °C and $DO_{\text{lethal}} = 3$ mg/L, were chosen according to fish habitat model validation based on the cisco mortality field data in 2006 (Table 5) as discussed below.

Fish Habitat Model Validation in 23 Lakes Against 2006 Observations

The fish habitat model uses simulated daily temperature and DO profiles in a lake to check day by day whether cisco habitable or lethal conditions occur. When the LT isotherm and the DO limit isopleth for cisco do not intersect in a day, cisco is survivable in that day; otherwise, the entire depth of a stratified lake is under lethal conditions (too warm temperature or lower DO) in that day. A number of days with cisco lethal conditions in 2006 under eight different criteria are given in Fig. 5 for Pine Mountain Lake as an example. Pine Mountain Lake located in Cass County, Minnesota, has a maximum depth of 23.8 m (deep lake) and a surface area of 6.36 km^2. Pine Mountain Lake is a mesotrophic stratified lake because of its mean Secchi depth 2.4 m, mean chlorophyll-a concentration 6.5 μg/L, and GR = 2.11.

The total number of lethal days in 2006 increases from 35 to 72 days (Fig. 5b and Table 4) when LT = 22.0 °C and the DO survival limit changes from 2 to 4 mg/L. The 35 lethal days were not continuous as shown in Fig. 5b and were 2 days from DOY 196 (July 15–16, 2006), 26 days from 199 (July 18–August 12), 1 day from 227 (August 15), 2 days from 235 (August 23–24), and 4 days from 238 (August 26–29). When LT increases to 23.4 °C (mean LT for cold-water fish species not including cisco), the total number of lethal days in 2006 decreases to 12–35 days (Fig. 5c), respectively, when DO survival limits are 2–4 mg/L.

With $LT = 21.2$ °C and $DO_{\text{lethal}} = 2$ mg/L limits (Fig. 5a) from the lethal-niche-boundary curve, Pine Mountain Lake was simulated to have 56 lethal days: 196 (37 continuous lethal days) and 230 (21); with $LT = 22.6$ °C and $DO_{\text{lethal}} = 4$ mg/L limits, Pine Mountain Lake was simulated to have 55 lethal days: 186 (2), 192 (37), 231 (13), and 248 (3). With $DO_{\text{lethal}} = 4$ mg/L, lethal days started 10 days early, but prevalent lethal conditions occurred after DOY 196 (July 15) for all three LT-DO limit combinations from the lethal-niche-boundary curve.

Results of the sensitivity analysis using eight *LT* and DO survival limits in all 23 lakes are summarized in Table 4. The period of lethal conditions (lethal days) simulated using $LT = 22.0$ °C is typically longer than the lethal days using $LT = 23.4$ °C. When DO survival limits increase from 2 to 4 mg/L, cisco lethal days increase also (Fig. 5 and Table 4) when *LT* is fixed. Using $LT = 23.4$ °C, Star, Little Pine (Otter Tail County), Bemidji, Gull, Straight, Long, and Carlos lakes were simulated to have zero or a few days with lethal conditions in 2006, which indicates

that $LT = 23.4$ °C used in previous studies for the cold-water guild is little too high for cisco. Three LT-DO combinations, where LT was computed using DO_{lethal} and the cisco lethal-niche-boundary curve, resulted very similar values on lethal days in 23 lakes (Table 4), but starting days of lethal conditions could be somewhat different as shown in Fig. 5 for Pine Mountain Lake. Detailed simulation results of $LT = 22.0$ and $DO_{\text{lethal}} = 3$ mg/L are given in Table 5 for 23 Minnesota lakes for model validation against cisco mortality observations in 2006.

Table 5 lists the first DOY, the last DOY, and the total number of days with cisco lethal conditions predicted by the model (using constant lethal limits) in 2006 (hindcast or backtesting). It also lists the DOYs and the number of continuous days from DOYs with cisco lethal conditions predicted in 2006. For example, Little Turtle Lake has "180(62)" under "simulated lethal days in 2006" in Table 5 that means lethal conditions were simulated on DOY 180 (June 29, 2006) and the number of continuous cisco lethal days is 62 (DOYs 180–241). The DOY and month/day in 2006 inside brackets when cisco mortality was reported in each lake is listed under "observed mortality date in 2006" in Table 5 and used to examine model agreement. In the last column of Table 5, the first Yes/No gives the agreement of cisco lethal prediction and reported cisco mortality in 2006, and the second Yes/No inside brackets gives the agreement whether or not cisco lethal days from the model include reported date with cisco mortality. For example, for Mille Lacs Lake, the fish habitat model predicted a total of 49 days from July 22 (DOY 203) to September 8 (DOY 251) having cisco lethal conditions, which agree with reported cisco mortality in 2006, and the period of predicted cisco lethal conditions includes the reported day with cisco mortality, i.e., July 23 or DOY 204. Therefore, the model agreement with mortality observation is "Yes (Yes)" as listed in Table 5. The fish habitat model predicted the "Yes (Yes)" agreement in 13 of the 18 lakes that experienced cisco mortality in 2006 (Table 5).

For four lakes (Bemidji, Star, Seventh Crow Wing, and Long), the model predicted cisco lethal conditions, but the predicted lethal periods did not include corresponding reported cisco mortality days in 2006; these lakes have the "Yes (No)" agreement (Table 5). For two lakes (Bemidji and Star), cisco lethal conditions were predicted to occur after the reported cisco mortality days in 2006. For Seventh Crow Wing Lake, cisco lethal conditions were predicted to occur from DOY 196 to 215 (August 3) in 2006, and the cisco mortality was reported on August 4. For Long Lake, cisco lethal conditions were predicted to occur from DOY 213 to 216 (August 4) in 2006, and the cisco mortality was reported on August 6. These two cases can be considered as "Yes (Yes)" agreement because cisco mortality might be reported one or a few days after cisco mortality occurred when study lakes were not constantly monitored and observed. Long Lake was predicted with only 4 days of lethal conditions. Long Lake located in Otter Tail County, Minnesota, has a maximum depth of 39.0 m (deep lake) and a surface area of 5.1 km^2. Long Lake is a mesotrophic strongly stratified lake because of its mean Secchi depth 3.0 m, mean chlorophyll-a concentration 7.2 μg/L, and GR = 1.22. There was only 1 day in 2006 with observed temperature and DO profiles in Long Lake for model calibration.

For Lake Carlos, the model did not predict cisco lethal conditions, but they had cisco mortality in 2006; the model has the No agreement with mortality observation (Table 5). Lake Carlos located in Douglas County, Minnesota, has a maximum depth of 49.7 m and a surface area of 10.5 km^2. Lake Carlos is a mesotrophic strongly stratified lake because of its mean Secchi depth 3.0 m, mean chlorophyll-*a* concentration 5.0 μg/L, and GR = 1.15. The late summer cisco mortality event that occurred on August 27 (DOY 239) in Lake Carlos did not fit the lethal-niche-boundary curve developed from the midsummer events in 16 lakes (Jacobson et al. 2008). Based on the lethal-niche-boundary curve and measured profiles on September 1, 2006 (Jacobson et al. 2008), cisco could exist in some surface layers with low temperatures and high DO, but could not exist in the hypolimnion with anoxic conditions.

Jacobson et al. (2008) also studied the five reference lakes that did not experience cisco mortality in 2006. These five reference lakes are all deep strongly stratified lakes (GR < 1.4). The fish habitat model using constant LT and DO_{lethal} limits predicted no lethal conditions for cisco in all five reference lakes (Table 5). Therefore, the fish habitat model has an overall good agreement in the 23 study lakes with and without cisco mortality reported in 2006.

With $LT = 21.2$ °C and $DO_{\text{lethal}} = 2$ mg/L limits, Straight Lake changed the agreement from "Yes (Yes)" to "Yes (No)" and Seventh Crow Wing from "Yes (No)" to "Yes (Yes)"; with $LT = 22.6$ °C and $DO_{\text{lethal}} = 4$ mg/L limits, Star Lake changed the agreement from "Yes (No)" to "Yes (Yes)" when comparing with cisco mortality observations in 2006. Therefore, three LT and DO_{lethal} limit combinations derived from the lethal-niche-boundary curve (Jacobson et al. 2008) had similar overall agreement with cisco mortality observations in 2006, and all of them could be used for constant lethal limits for adult cisco when there is no additional laboratory and field data support on survival limits. To be consistent with previous studies with DO survival limit (Stefan et al. 1996, 2001; Fang et al. 2004a, b) or benchmark DO (Jacobson et al. 2010; Fang et al. 2012b; Jiang et al. 2012) of 3 mg/L, $LT = 22.0$ °C and $DO_{\text{lethal}} = 3$ mg/L limits were used for remaining of the oxythermal habitat modeling with constant lethal limits.

Simulation Results of 28 Regional Lakes and 30 Virtual Lakes

Both 28 regional lakes (LakeR01–LakeR18, LakeR28–LakeR33, and LakeR37–LakeR39 in Table 1) and 30 virtual lakes (Table 2) were first simulated using MINLAKE2010 to generate daily temperature and DO profiles over 48 simulation years (1962–2008 under the past climate conditions) and then simulated using the fish habitat model to determine number of days with cisco lethal conditions year by year (excluding the first year 1961) using constant lethal limits. Results for shallow or medium-depth lakes and deep lakes were grouped and analyzed separately as recommended by Fang et al. (2014).

Figure 7 shows contour plots of total number of years with cisco lethal days and average cisco kill days for the years with lethal conditions under past (left frames)

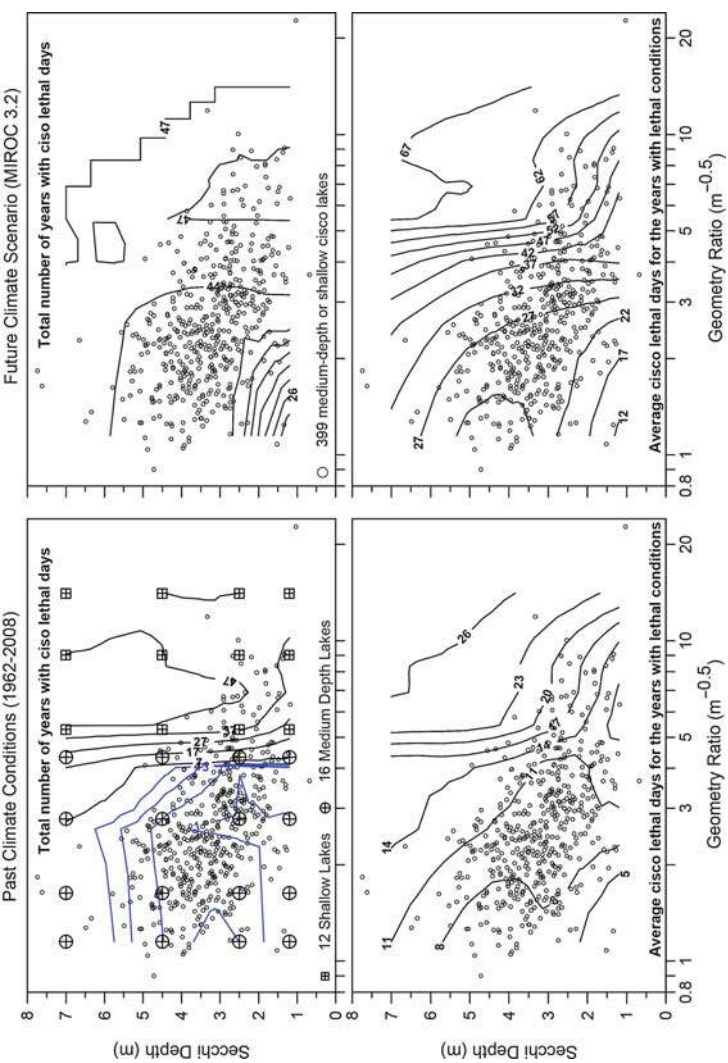

Fig. 7 Contour plots of total number of years with cisco lethal days (*top*) and average cisco lethal days for the years with lethal conditions (*bottom*) under past (1962–2008) and future (MIROC 3.2) climate scenarios. Duluth weather data were used for model simulations. Contours were derived by interpolation from simulated points for 28 regional lakes

and future (right frames for MIROC 3.2) climate scenarios. Duluth weather data over 47 years were used for model simulation results presented in Fig. 7. Contours were derived by interpolation from simulated points for 28 regional/representative lakes (Fig. 7). Under the past climate conditions, shallow lakes with a geometry ratio >5.2 $m^{-0.5}$ had 23–47 years with lethal conditions and are projected to have all 47 years with lethal days under MIROC 3.2 (Fig. 7). Average cisco lethal days for the years with lethal conditions under the past climate conditions ranged from 11 to 26 days and are projected to range from 38 to 65 days in shallow lakes under MIROC 3.2 climate scenario. Therefore, 12 shallow regional lakes simulated (Fig. 7) and 14 shallow lakes in the 620 cisco lake database (Fig. 5) do not provide suitable habitat conditions to support cisco.

For 16 medium-depth lakes simulated under the past climate conditions, there were 0 (GR = 1.63 $m^{-0.5}$) to 8 (GR = 4.33 $m^{-0.5}$) years with lethal conditions with average lethal days ranging from 0 to 14 days (Fig. 7). Under future climate scenario (MIROC 3.2), they are projected to have 20–47 years with lethal conditions with average lethal days ranging from 12 to 52 days (Fig. 7). It seems medium-depth lakes are most vulnerable to climate change with largest increases in lethal days and the number of years with lethal conditions.

When simulated under past climate conditions, none of the 30 virtual deep lakes (H_{max} = 24 m) have cisco lethal conditions; therefore, deep lakes provided relatively good fish habitats compared with shallow and medium-depth lakes. The results for virtual deep lakes under past climate conditions seem to have certain disagreement with cisco mortality observations (Table 5). Minnesota lakes with H_{max} < 20.0 m were classified as deep lakes (Stefan et al. 1996), and 7 of the 18 study lakes with cisco mortality in 2006 are deep lakes with GR ranging from 1.15 to 3.26 $m^{-0.5}$ (Table 5). Generalized model parameters (Fang et al. 2010a) were used for simulations in the 30 virtual lake types, but for the 23 lakes (Table 5), model parameters were first calibrated against measured profiles before the cisco habitat model was applied. Differences in model parameters are one of the major reasons for disagreement in habitat projections and suggest that other oxythermal habitat parameters, e.g., TDO3 (Jacobson et al. 2010), should be used for studying cisco fish habitat in relatively deep lakes.

Under the future climate scenario (MIROC 3.2), projected number of years with lethal conditions are up to 20 years with average lethal days up to 23 days (Fig. 8). Distributions of total number of years with cisco lethal days and average cisco kill days for the years with lethal conditions under MIROC 3.2 are given in Fig. 8, which shows eutrophic deep lakes are projected with more lethal days. Figure 8 was not used to divide 221 deep cisco lakes into tier 1 to tier 3 refuge lakes as it was done using TDO3 (Fang et al. 2012; Jiang et al. 2012). Under MIROC 3.2 climate scenario, those lakes with 0–2 years (Fig. 8 top) and 0–3 days (Fig. 8 bottom) with lethal conditions provide most suitable habitat for cisco, and lakes with 2–5 years (Fig. 8 top) and 3–6 days (Fig. 8 bottom) with lethal conditions also provide suitable habitat for cisco. Good-growth habitat areas and volumes used in previous studies (Stefan et al. 1996, 2001; Fang et al. 2004a, b) may be used to classify refuge lakes in the future.

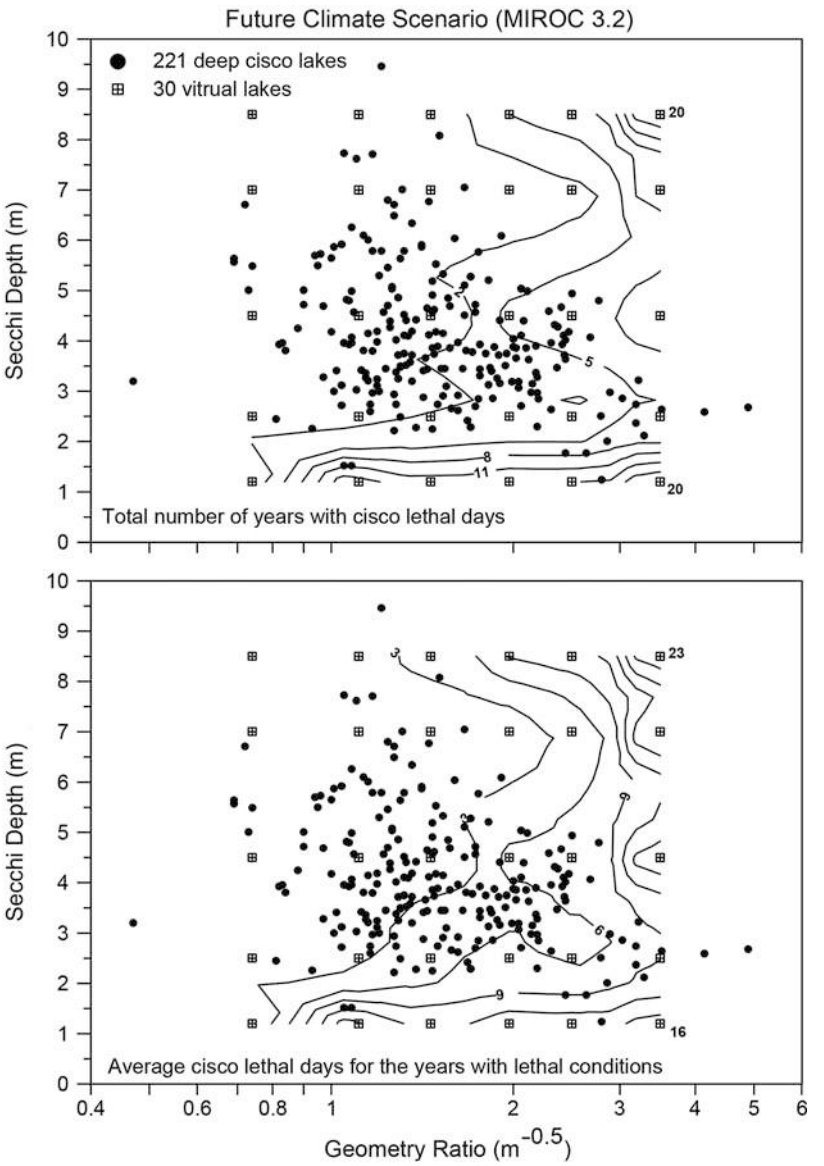

Fig. 8 Contour plots of total number of years with cisco lethal days (*top*) and average cisco lethal days for the years with lethal conditions (*bottom*) in deep lakes under future (MIROC 3.2) climate scenarios. Duluth weather data were used for model simulations. Contours were derived by interpolation from simulated points for 30 virtual lakes ($H_{max} = 24$ m)

Simulation and Validation of Cisco Oxythermal Habitat Using the Lethal-Niche-Boundary Curve

For oxythermal habitat modeling of cisco, the second option is to use temperature-varying lethal DO limits. The fish habitat model uses a fitted regression equation as the lethal niche boundary of adult cisco developed by Jacobson et al. (2008). The equation mapped the DO concentrations and water temperatures from the profiles measured in 16 Minnesota lakes that experienced cisco mortality in 2006 (Table 6). One profile was measured in each of the 16 lakes on the same day or a few days after reported mortality. The shifted exponential function given in Eq. 3 is a fit of the 99th quartile nonparametric regression line bracketed the lethal combinations of observed oxygen and temperature in 16 lakes with midsummer (July 19 to August 6) mortality events in 2006 (Jacobson et al. 2008). First, the fish habitat model (the option 2) was validated in 23 Minnesota lakes (Table 6) and then used to project cisco lethal conditions in 36 representative lake types under past (1992–2008) climate conditions and a future climate scenario (MIROC 3.2) at Bemidji, Minnesota. Based on the number of years with cisco kill and the number of annual cisco lethal days, lake types that most likely could not support cisco were identified, and lake types that can support cisco under both the past climate and the future climate scenarios were identified as potential cisco refuge lakes.

Fish Habitat Projection Model

There were 18 Minnesota lakes with reported cisco mortality in 2006, but no temperature and DO profiles were measured in Mille Lacs Lake, which had automated temperature recorder data at 2 m below the surface (Jacobson et al. 2008). Measured temperature and DO profiles in Lake Carlos, which had late summer cisco mortality event occurred on August 27, were not used to fit the lethal-niche-boundary curve (Jacobson et al. 2008). The lethal-niche-boundary curve of adult cisco developed from measured temperature and DO profiles in 16 Minnesota lakes is given as

$$DO_{\text{lethal}} = 0.40 + 0.0000060 \ e^{0.59T} \tag{3}$$

where DO_{lethal} and T are the DO concentrations (in mg/L) and the water temperatures (in °C), respectively, which define the lethal niche boundary (Jacobson et al. 2008). The computed DO_{lethal} is the required minimum DO concentration at a given water temperature T for cisco to survive. For the regression Eq. 3, the coefficients 0.40 and 0.0000060 are in mg/L, and the coefficient 0.59 for the exponent is in $^{\circ}C^{-1}$.

Equation 3 indicates the DO survival limit for adult cisco is not constant but depends on water temperature. The lethal-niche-boundary curve for cisco (Eq. 3)

Table 6 Fish habitat validation results using the lethal-niche-boundary curve for 23 Minnesota lakes. Simulated and observed days with lethal conditions for cisco are given as DOYs

Lake name	Lethal conditions			Simulated lethal days in 2006	Observed mortality day in 2006	Model agreement
	First day	Last day	No. of days			
Little Turtle	181	222	38	182(4)[a], 187(4), 193(30)	200 (7/19)[b]	Yes (Yes)[c]
Andrusia	192	234	39	192(37), 233(2)	202 (7/21)	Yes (Yes)
Little Pine (Otter Tail)	199	216	17	199(1), 201(16)	203 (7/22)	Yes (Yes)
Cotton	188	225	36	188(1), 190(1), 192(34)	205 (7/24)	Yes (Yes)
Pine Mountain	192	241	49	192(45), 238(4)	207 (7/26)	Yes (Yes)
Leech	189	217	22	189(1), 195(6), 203(15)	211 (7/30)	Yes (Yes)
Itasca	189	222	31	189(1), 193(30)	209 (7/28)	Yes (Yes)
Gull	209	227	19	209(19)	210 (7/29)	Yes (Yes)
Woman	183	224	36	183(2), 187(1), 190(1), 193(32)	210 (7/29)	Yes (Yes)
Little Pine (Crow Wing)	183	240	48	183(5), 190(39), 233(3), 240(1)	214 (8/2)	Yes (Yes)
Eighth Crow Wing	195	222	28	195(28)	216 (8/4)	Yes (Yes)
Bemidji	212	217	6	212(6)	208 (7/27)	Yes (No)
Mille Lacs	216	241	26	216(26)	204 (7/23)	Yes (No)
Star	212	216	5	212(5)	200 (7/19)	Yes (No)
Seventh Crow Wing	196	215	20	196(20)	216 (8/4)	Yes (No)
Long	216	216	1	216(1)	218 (8/6)	Yes (No)
Carlos			0	No kill	239 (8/27)	No
Straight			0	No kill	213 (8/1)	No
Reference lakes without cisco kill in 2006						
Big Trout			0	No kill	No kill	Yes
Kabekona			0	No kill	No kill	Yes
Scalp			0	No kill	No kill	Yes
Ten Mile			0	No kill	No kill	Yes
Rose			0	No kill	No kill	Yes

Note:
[a]Stands for a DOY in 2006 and the number of continuous cisco lethal days from the lethal day predicted by the fish habitat model
[b]DOY followed by month and date in 2006 inside brackets
[c]The first Yes/No gives the agreement of cisco lethal prediction and reported cisco mortality in 2006, and Yes/No inside brackets gives the agreement whether or not cisco lethal days from the model include reported date with cisco mortality

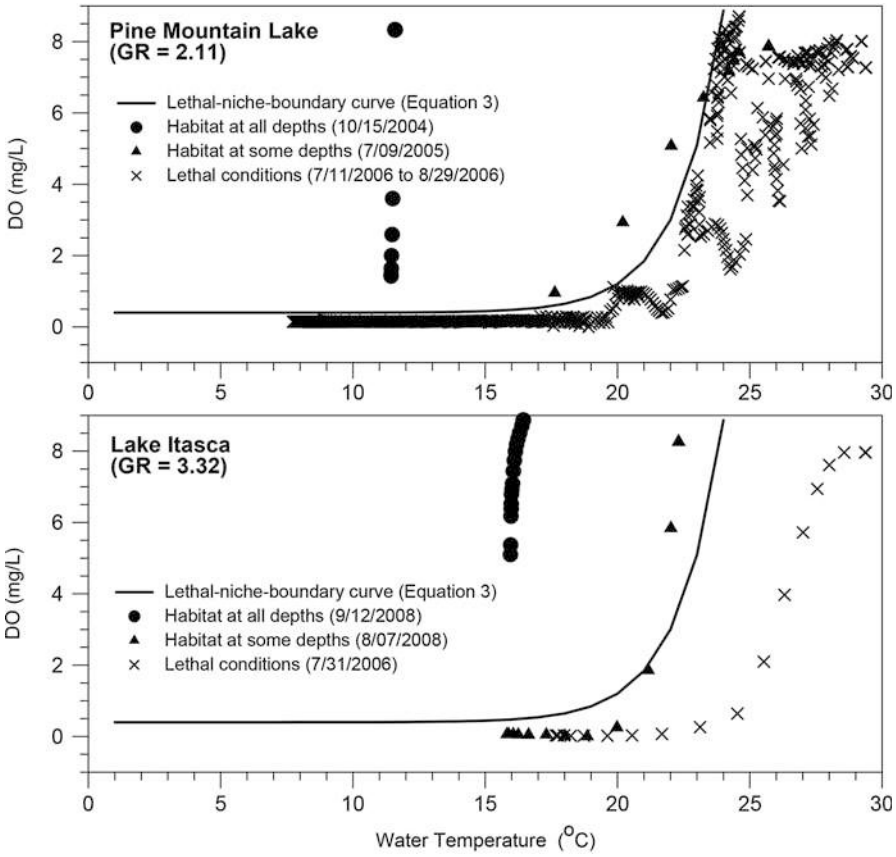

Fig. 9 Simulated DO versus simulated temperature for selected days to show three different types of fish habitat in Pine Mountain Lake and Lake Itasca (Table 6) and the lethal-niche-boundary curve of adult cisco (Eq. 3)

was plotted in Fig. 9 for two Minnesota lakes (Pine Mountain Lake and Lake Itasca). In comparison with the previous constant lethal temperature for cold-water fish species, i.e., 23.4 °C (Eaton et al. 1995), the lethal temperature from Eq. 3 is only 22.0 °C when 3.0 mg/L is used as the DO survival limit (Jacobson et al. 2008). In this study, the required DO concentration DO_{lethal} was computed from the simulated water temperature in each water layer of a lake for each simulated day using Eq. 3. The computed DO_{lethal} value was then compared with the simulated DO concentration in the same layer; lethal conditions for cisco were assumed to occur if the simulated DO concentrations were less than the DO_{lethal} values in all water layers (from the lake water surface to the lake bottom) on that day. In Fig. 9, simulated DO was plotted against simulated temperature for selected days in the two lakes. In Pine Mountain

Lake, from July 11, 2006 (DOY 192 in Table 6) to August 29, 2006 (DOY 241), there were 49 days (Table 6, one discontinuous lethal day) that all simulated T-DO data points (shown by the crosses) are located at the right side of or below the lethal-niche-boundary curve when simulated DO concentrations were below computed DO_{lethal} values at simulated temperatures at all water depths. The same situation of cisco lethal conditions was predicted to occur on July 31, 2006 in Lake Itasca.

If simulated DO concentrations are less than the DO_{lethal} values in only some of the water layers, lethal conditions for cisco are not assumed to occur on that day because cisco can swim to other water layers having suitable T and DO condition. These days with habitat at some depths are shown as filled triangles in Fig. 9. Pine Mountain Lake on July 9, 2005 had lower DO at higher temperatures near the surface and near anoxic DO (0.2 mg/L) in the hypolimnion. Therefore, layers near the surface and in the hypolimnion could not support cisco habitat, but some intermediate layers had high enough DO at simulated temperatures to support cisco habitat. Lake Itasca on August 7, 2008 had suitable cisco habitat in the surface layers and no cisco habitat in the bottom layers (Fig. 9). Lake Itasca located in Clearwater County, Minnesota, has a maximum depth of 13.7 m and a surface area of 4.3 km^2. Lake Itasca is mesotrophic due to its mean Secchi depth 2.8 m and mean chlorophyll-a concentration 10.4 μg/L and has relatively weak stratifications because of its GR = 3.32 (Gorham and Boyce 1989; Stefan et al. 1996).

When simulated DO concentrations are greater than the DO_{lethal} values in all water layers, fish can live in any depth of the lake, i.e., filled circles in Fig. 9 (e.g., October 15, 2004 in Pine Mountain Lake and September 12, 2008 in Lake Itasca).

Validation of Fish Habitat Model

Figure 9 shows simulated DO versus simulated temperature during two periods (July 11, 2006–August 24, 2006 and August 26–29, 2006) in Pine Mountain Lake when cisco lethal conditions were predicted by the fish habitat model using the cisco lethal-niche-boundary curve. Surface water temperatures in Pine Mountain Lake ($A_s = 6.36$ km^2, $H_{\max} = 23.77$ m, and $GR = 2.11$ $m^{-0.5}$) reached 29.4 °C on July 31, 2006. When the lethal temperature of 22.0 °C for adult cisco was used, for the 49 days in Pine Mountain Lake (Fig. 9), 43 % of water depths had temperatures greater than 22.0 °C, and 58 % of water depths had DO < 3 mg/L. The cisco mortality in Pine Mountain Lake was reported on July 26, 2006 (Jacobson et al. 2008) when the fish habitat model predicted continuous 16 days of lethal conditions starting from July 11, 2006.

The fish habitat modeling using the cisco lethal-niche-boundary curve was validated in the 23 Minnesota lakes that Jacobson et al. (2008) studied first in 2006. Validation results are summarized in Table 6 for each lake, which shows similar information as Table 5 does but using different oxythermal lethal limits. For example, Lake Andrusia has "192(37), 233(2)" under "simulated lethal days in 2006" in Table 6 that means lethal conditions were simulated on DOY 192 (July 11, 2006) with the number of continuous cisco lethal days of 37 (DOYs 192–228)

and on DOYs 233–234 (August 21–22, 2006). Lethal conditions were not simulated for DOYs 229–232 (August 17–20, 2006) in Lake Andrusia. In comparison to "Observed mortality day in 2006" in Table 6, the model agreement with mortality observation is "Yes (Yes)" for Lake Andrusia (Table 6).

Using the lethal-niche-boundary curve, for five lakes (Bemidji, Mille Lacs, Star, Seventh Crow Wing, and Long), the model predicted cisco lethal conditions, but the predicted lethal periods did not include corresponding reported cisco mortality days in 2006; these lakes have the "Yes (No)" agreement (Table 6). For three lakes (Bemidji, Mille Lacs, and Star), cisco lethal conditions were predicted to occur after the reported cisco mortality days in 2006. In the Seventh Crow Wing Lake, cisco lethal conditions were predicted to occur from DOY 196 to 215 (August 3) in 2006, and the cisco mortality was reported on August 4. This case can be considered as "Yes (Yes)" agreement because cisco mortality might be reported one or a few days after cisco mortality occurred when study lakes were not constantly monitored and observed. Long Lake was predicted with only 1 day of lethal conditions.

There are two lakes (Straight Lake and Lake Carlos) that the model did not predict cisco lethal conditions, but they had cisco mortality in 2006; the model has the No agreement with mortality observation (Table 6). Lake Carlos had a late summer cisco mortality event occurred on August 27, which might be due to the formation of the metalimnetic oxygen minimum during part of the summer (Smith et al. 2014).

The five reference lakes (deep strongly stratified) that Jacobson et al. (2008) studied did not experience cisco mortality in 2006. The fish habitat model using simulated temperature and DO profiles predicted no lethal conditions for cisco in all five reference lakes (Table 6). Therefore, the fish habitat model using the lethal-niche-boundary curve has overall good agreement in the 23 study lakes with and without cisco mortality reported in 2006. The overall good agreement is very similar but not exactly the same as the agreement using the constant lethal limits ($LT = 22.0$ °C and $DO_{\text{lethal}} = 3$ mg/L, Table 5).

Fish Habitat Simulations in 36 Representative Lake Types

To understand cisco habitat and to determine cisco kill in 36 different lake types (LakeR01–LakeR36 in Table 1), daily water temperature and DO profiles were simulated using MINLAKE2012 under past (1991–2008) climate conditions from Bemidji weather station and the corresponding future climate scenario (MIROC 3.2). Bemidji weather station is close to most of the 23 study lakes (Tables 5 and 6) and has 18 years of weather data. The fish habitat model for cisco was applied every day year by year from 1992 to 2008 using simulated daily water temperature and DO profiles. Results for the first simulation year (1991) were not used for cisco modeling in order to remove the possible effect of initial conditions.

Total Days of Cisco Lethal Conditions in Each Year

Total days of lethal conditions for cisco in each year over 17 simulation years were used to create box plots showing the maximum and minimum and 25 %, 50 %, and

75 % quartile values simulated for each of the 36 representative lake types in Minnesota under past climate conditions and MIROC 3.2 future climate scenario (Fang et al. 2014). Lethal conditions may be continuous for many days or discontinuous for some days (Fig. 9 and Table 6). For the 12 shallow lakes with GR $\geq$ 5.29 $m^{-0.5}$, median annual days of cisco lethal conditions ranged from 13 to 22 days under past climate conditions and are projected to range from 47 to 55 days under the future climate scenario (Fang et al. 2014). These results indicate again that shallow lakes typically cannot support cisco habitat. In the MN DNR cisco lake database, there are a total of 620 cisco lakes, of which 37 lakes have GR $\geq$ 5.29 $m^{-0.5}$ and maximum depths less than 11.0 m. There are 14 lakes with $H_{max} < 5.0$ m that are classified as shallow lakes in Minnesota (Stefan et al. 1996), of which 13 lakes have GR $>$ 5.29 $m^{-0.5}$ and one lake has GR $=$ 4.4 $m^{-0.5}$. These lakes had cisco observed in the past, but, most likely, they cannot sustain cisco habitat.

For the 12 medium-depth lakes with $H_{max} = 13.0$ m (LakeR10–LakeR18 and LakeR31–LakeR33), GR values are 1.63, 2.78, and 4.33 $m^{-0.5}$ (Table 1). Median annual days of cisco lethal conditions ranged from 0 to 1 day under past climate conditions and are projected to range from 19 to 49 days under the future climate scenario. Under past climate conditions, cisco lethal conditions reached a maximum of 30 days for medium-depth lakes during the unusual hot summer in 2006. These lakes are vulnerable to climate warming because lethal conditions are projected up to 80 days (Fang et al. 2014).

For the 12 deep lakes with $H_{max} = 24$ m (LakeR19–LakeR27 and LakeR34–LakeR36), eutrophic deep lakes (LakeR19, LakeR22, and LakeR25) and mesotrophic large deep lake (LakeR26 with GR $=$ 2.34 $m^{-0.5}$) are projected to have some cisco lethal days under the future climate scenario (Fang et al. 2014). Cisco lethal conditions, however, were not simulated to occur under past climate conditions (1992–2008). Large deep lakes with GR $=$ 2.34 $m^{-0.5}$ seem to require Secchi depth more than 2.5 m to have nonlethal conditions under the future climate scenario. Other strongly stratified mesotrophic and oligotrophic deep lakes (LakeR20, LakeR21, and LakeR34 with GR $=$ 0.88; LakeR23, LakeR24, and LakeR35 with GR $=$ 1.50; and LakeR27 and LakeR36 with GR $=$ 2.34 in Table 1) are possible to support cisco habitat under both past and future climate conditions. These deep lakes are good candidates of cisco refuge lakes (Fang et al. 2012b; Jiang et al. 2012).

Annual cisco lethal days are strongly dependent on lake stratification characteristics (i.e., GR) but vary relatively weakly with trophic status (i.e., SD). The four lakes with the same GR but different Secchi depths were grouped together to compute mean and standard deviation of annual cisco lethal days under past climate conditions and the future climate scenario (Fig. 10). There are consistent patterns of average annual lethal days for each group of lakes with the same maximum depth (shallow, medium-depth, and deep). Shallow lakes (GR $>$ 5.2 $m^{-0.5}$) have large numbers of cisco lethal days, medium-depth lakes (GR $=$ 1.63, 2.78, and 4.33 $m^{-0.5}$) have cisco lethal days increasing with geometry ratio (Fig. 10), and deep lakes (GR $=$ 0.88, 1.50, and 2.34 $m^{-0.5}$) have little or no cisco lethal days.

The four lakes with GR $=$ 1.63 $m^{-0.5}$ (LakeR10–LakeR12 and LakeR31) are small medium-depth lakes ($A_s = 0.2$ km^2 and $H_{max} = 13.0$ m). Cisco lethal days

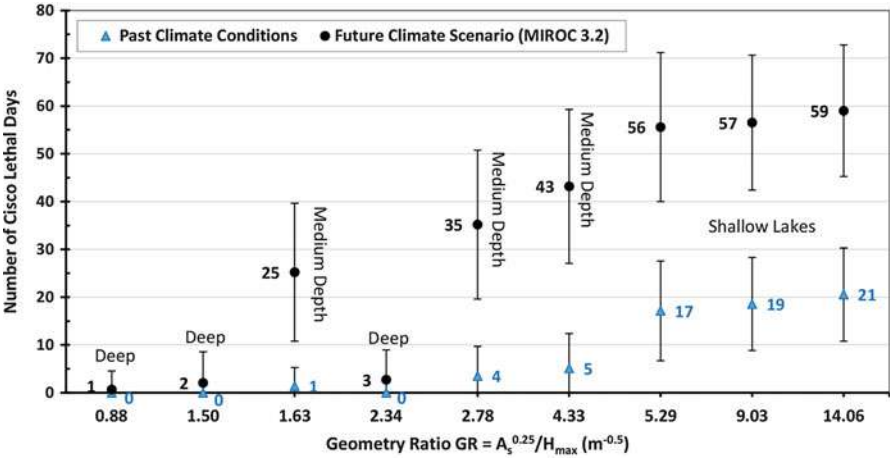

Fig. 10 Number of annual cisco lethal days (mean ± standard deviation) simulated for the 36 representative lake types with nine GR values under past climate conditions and the future climate scenario (Fang et al. 2014)

projected for these four lakes (especially under the future climate scenario) are different from deep lakes with GR just less or greater than 1.63 $m^{-0.5}$ (Fig. 10). These results may indicate that fish habitat modeling for deep lakes should be separated from the modeling for medium-depth lakes. To further prove the point, four deep lakes (LakeR41–LakeR44, Table 1) having GR = 1.63 $m^{-0.5}$ with larger A_s = 2.32 km^2 and deeper H_{max} = 24.0 m were created, and daily temperature and DO profiles were simulated using MINLAKE2012 under past climate conditions and the future climate scenario. The simulated number of annual cisco lethal days in these four deep lakes is zero for all years (1992–2008) under past climate conditions and is projected to be zero under the future climate scenario except for LakeR41, which is an eutrophic deep lake having 1 year with 4 days of cisco lethal projection. Therefore, simulations of cisco lethal days in these deep lakes (LakeR41–LakeR44) are consistent with other deep lakes but different from medium-depth lakes with the same geometry ratio. Other fish habitat parameters, e.g., good-growth period for cold-water fish in 27 Minnesota lake types, had similar discontinuous patterns in some medium-depth and deep lakes in a previous study (Fang et al. 2004b). In the MN DNR cisco lake database, there are 385 medium-depth lakes with 5 m $\leq H_{max} <$ 20 m and 221 deep lakes with $H_{max} \geq$ 20 m. Therefore, it is recommended to model cisco habitat and survival separately for medium-depth lakes and deep lakes in the future.

Number of Years with Cisco Kill

It is still uncertain how many days that exceed non-survival or lethal niche limits are necessary to result fish mortality. In previous regional fish habitat projections (Stefan et al. 1996) when daily water temperature and DO concentration profiles used for fish habitat simulations were long-term (30-year) averages, fish kill was assumed to occur when the number of non-survival days (either consecutive or discontinuous) totaled at

least seven. In this study, a sensitivity analysis on the number of continuous lethal days for determining cisco kill was performed when daily profiles were not averaged over 17 years (1992–2008), but cisco lethal conditions were checked in each day year by year. A cisco kill was assumed to occur if the number of continuous lethal days was greater than 3, 7, and 14 days for the sensitivity analysis. The 3 days are the half of 7 days used before, and 14 days are the double of 7 days. For the 11 Minnesota lakes (Table 6) in which the simulated lethal days included the reported cisco mortality days in 2006, the number of continuous lethal days to the mortality day was calculated and ranged from 2 (Gull Lake) to 25 (Little Pine Lake in Crow Wing County) days. Median value of the number of continuous lethal days to the mortality day was 14 days (mean value 13 days with a standard deviation 7 days). This result provides another reason to use 14 days for the sensitivity analysis.

When 3, 7, and 14 continuous lethal days were used for determining cisco kill, Fig. 11 shows the numbers of years with cisco kill simulated for the 36 representative lake types in Minnesota for 17 simulation years under past (1992–2008) climate conditions (blue triangles) and the future climate scenario (red circles). The x axis gives lake's geometry ratio, and the four lake types with the same geometry ratio (Table 1) were grouped together to compute mean and standard deviation of the number of years with cisco kill. Under past climate conditions, the 12 shallow lakes (LakeR01–LakeR09, LakeR28–LakeR30, GR = 5.29, 9.03, and 14.06 $m^{-0.5}$) were simulated to have cisco kills on average in 14–15 years when 3 continuous lethal days were used to determine whether cisco kill happens or not. Under the future climate scenario (MIROC 3.2), the 12 shallow lakes are projected to have cisco kills in all 17 simulation years. These results provide strong evidence to indicate that shallow lakes cannot sustain cisco habitat under future warmer weather. The shallow lakes in MN cisco database are weakly stratified or polymictic with relatively high temperatures from surface to bottom during the summer which caused summer cisco kill almost every year from 1992 to 2008. Although cisco was observed in these 14 lakes in the past, whether cisco still exists in them is unknown. The projection under the future climate scenario shows they are not favorable to support cisco habitat every year.

When 7 continuous lethal days were used to determine whether cisco kill happens, the 12 shallow lakes were simulated to have cisco kills on average in 11–12 years (range from 9 to 13 years) under past climate conditions and are projected to have 17 years of cisco kills under the future climate scenario. When 14 continuous lethal days were used to determine whether cisco kill happens, the 12 shallow lakes were simulated to have only 1 year (2006) with cisco kill under past climate conditions and are projected to have 11–12 years of cisco kills under the future climate scenario. It projects there are more years with cisco kills in some medium-depth lakes than in the 12 shallow lakes under the future climate scenario (Fig. 11). This finding may indicate that 14 continuous lethal days for determining cisco kill may be longer than how many lethal days would be needed for cisco mortality to occur because it gives inconsistent results on fish habitat projections.

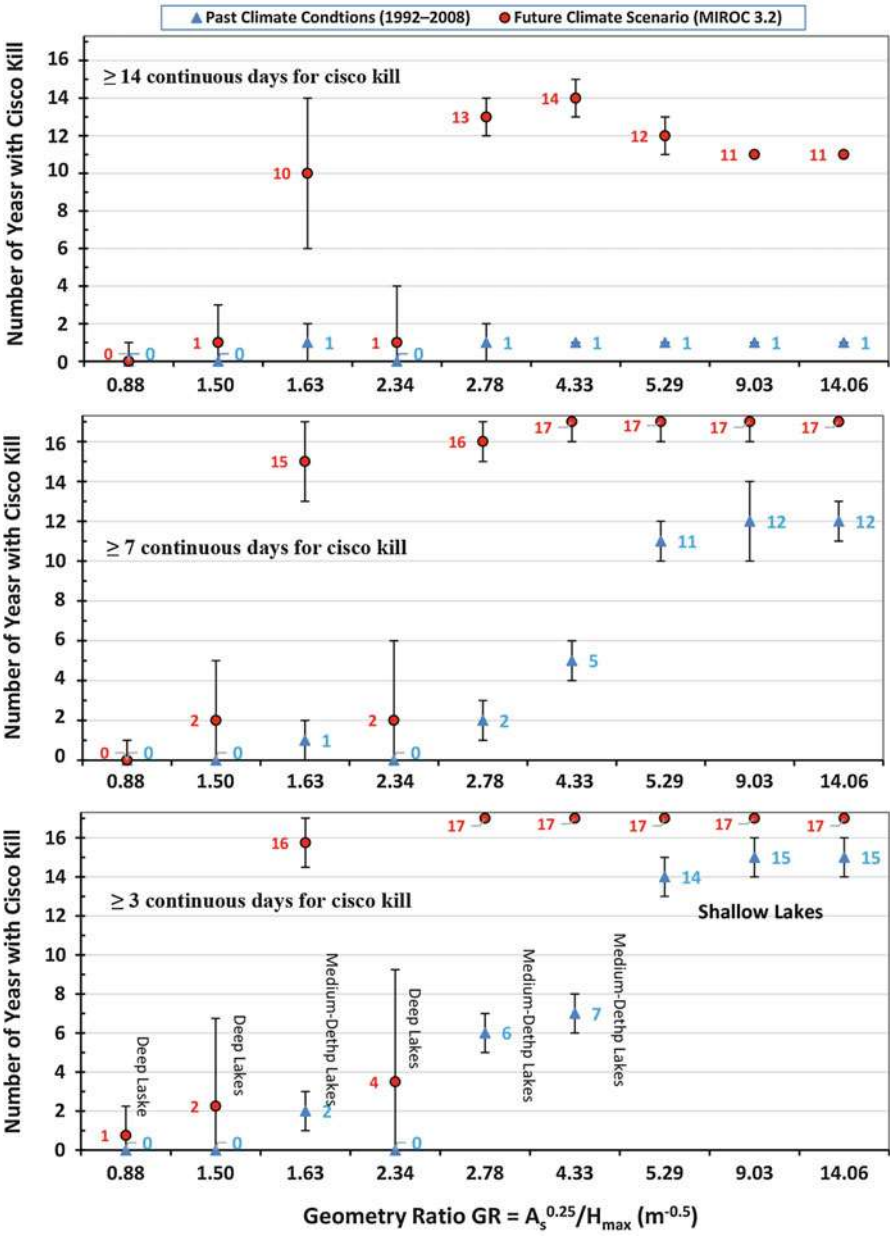

Fig. 11 Numbers of years with cisco kill simulated for the 36 representative lake types in Minnesota under past climate conditions (*triangles*) and the future climate scenario (*circles*) using 3, 7, and 14 continuous lethal days for determining cisco kill (Fang et al. 2014)

Therefore, the 14 continuous lethal days for determining cisco kill are not recommended for further fish habitat study.

Using 3 continuous lethal days for determining cisco kill, the 12 medium-depth lakes were simulated to have cisco kills on average in 2–7 years (range from 1 to 8 years) under past climate conditions and are projected to have 16–17 years of cisco kills under the future climate scenario. Using 7 continuous days for determining cisco kill, the 12 medium-depth lakes were simulated to have cisco kills on average in 1–5 years (range from 0 to 6 years) under past climate conditions and are projected to have 15–17 years (range from 13 to 17 years) of cisco kills under the future climate scenario. Figure 11 shows medium-depth lakes are most vulnerable to climate warming with average increase of 13 years with cisco kill (range from 9 to 15 years).

The 12 deep lakes (LakeR19–LakeR27, LakeR34–LakeR36) were simulated to have no cisco kill under past climate conditions using either 3, 7, or 14 continuous lethal days for determining cisco kill (Fig. 11). The 12 deep lakes are projected to have on average 1–4 years (range from 0 to 9 years) or 0–2 years (range from 0 to 6 years) of cisco kills under the future climate scenario when 3 and 7 continuous lethal days were used for determining cisco kill, respectively. Only eutrophic deep lakes ($SD = 1.2$ m, LakeR19, LakeR22, and LakeR25) and large mesotrophic deep lake ($A_s = 10$ km^2, $SD = 2.5$ m, LakeR26) are projected to have a few years with cisco kill under the future climate scenario. Figure 11 shows most mesotrophic and oligotrophic deep lakes can support cisco habitat under both past climate conditions and the future climate scenario and are good candidates for cisco refuge lakes, as supported by previous studies (Fang et al. 2012b; Jiang et al. 2012). It seems that 3 or 7 continuous lethal days for determining cisco kill provide quite reasonable results for cisco kill simulations in shallow, medium-depth, and deep lakes in Minnesota.

The box plots of the numbers of annual continuous lethal days greater than or equal to 3 and 7 days simulated for the 36 lake types in Minnesota under past climate conditions (1992–2008) and the future climate scenario (MIROC 3.2) were presented elsewhere (Fang et al. 2014). Those lethal days that are not continuous for 3 or 7 days were excluded. Under past climate conditions, 1 to a few years with cooler summers did not result in cisco kills in the 12 shallow lakes, but most other years had cisco kills with annual continuous lethal days up to 36 days (Fang et al. 2014). Under the future climate scenario, projected annual continuous lethal days are up to 94 days and 40 days in shallow lakes and eutrophic deep lakes, respectively. Medium-depth lakes are projected to have relatively large change in annual continuous lethal days.

Identification of Cisco Refuge Lakes Using the Fixed Benchmark Period

Cisco Habitat Criteria and Selection of Cisco Refuge Lakes

The oxythermal habitat approach used in the oxythermal fish niche modeling options 1 and 2 (Fig. 3) uses lethal limits for temperature and oxygen. In the third option, the quality of oxythermal habitat for cisco was determined using a single variable,

TDO3, i.e., water temperature at 3 mg/L of DO, proposed by Jacobson et al. (2010). A higher TDO3 value represents higher oxythermal stress for the cold-water fish. For example, if TDO3 is high, then fish must choose between well-oxygenated water that is too warm and live in hypoxic water that is of a proper temperature. The oxygen concentration of 3 mg/L is probably lethal or nearly so for many cold-water species (Frey 1955; US EPA 1986; Evans 2007) and therefore represents a desirable benchmark for a presence/absence niche model.

Oxythermal habitat niche relationships developed for several cold-water fish (including cisco) by Jacobson et al. (2010) were used to identify potential refuge lakes for cisco under future climate scenarios. Niche breadth measures, i.e., central response borders used by Heegaard (2002), were used by Jacobson et al. (2010) to identify values of TDO3 measured in the period of greatest oxythermal stress in late summer ($maxT_{DO3}$) useful for describing the quality of cold-water habitat for cisco. Central response borders essentially bracket the core range of a habitat variable required for a species to thrive (Heegaard 2002). The central species response borders for cisco ranged from $maxT_{DO3}$ of 4.0 °C to 16.9 °C (Jacobson et al. 2010).

TDO3 can be determined by interpolation from measured or simulated (vertical) temperature and DO profiles in a stratified lake. When non-monotonic profiles generate low oxygen concentrations with more than one TDO3 value, the coldest TDO3 was used (Jacobson et al. 2010). Temperature and DO profiles simulated for the first year (1961) were not used to compute TDO3 in order to avoid possible effects of assumed initial conditions. Figure 12 illustrates the procedure how TDO3 can be extracted from either measured or simulated temperature and DO profiles. Elk Lake (Fig. 12) has a maximum depth of 27 m and mean summer Secchi depth of 3.6 m (mesotrophic lake). Elk Lake has a lake geometry ratio of 1.16 and is a strongly stratified (dimictic) lake; it has excellent cold-water oxythermal habitat with TDO3 = 5.8 °C on June 24, 2008 (using observed temperature and DO profiles) and is projected to have a TDO3 value of 6.3 °C on June 24 under the future climate scenario MIROC 3.2. There were 99 measured T and DO profiles that had adequate data to extract TDO3 values for the 21 cisco lakes (Fang et al. 2010b). The standard error of TDO3 determined from simulated profiles against TDO3 from 99 measured profiles was 2.19 °C with correlation coefficient R = 0.88 (Fang et al. 2010b).

Through cisco habitat modeling, cisco refuge lakes were selected and identified in two categories: tier 1 refuge lakes and tier 2 refuge lakes. Tier 1 refuge lakes have TDO3 less than or equal to 11 °C, and tier 2 refuge lakes have TDO3 less than or equal to 17 °C but greater than 11 °C. Lakes having TDO3 greater than 17 °C are classified as tier 3 or non-refuge lakes. The limit of 17 °C corresponds to the upper cisco central response border of TDO3, and the limit of 11 °C is near the midpoint of the cisco central response borders of TDO3, as well as the upper central response border of TDO3 for lake whitefish *Coregonus clupeaformis* (Jacobson et al. 2010). Therefore, tier 1 refuge lakes identified for cisco in this study are also useful to the management of lake whitefish in Minnesota.

The multiyear average TDO3 over a fixed benchmark (FB) period was used to identify cisco refuge lakes in Minnesota. The benchmark period is the period of greatest oxythermal stress for cold-water fish. It is defined as the month (31-day

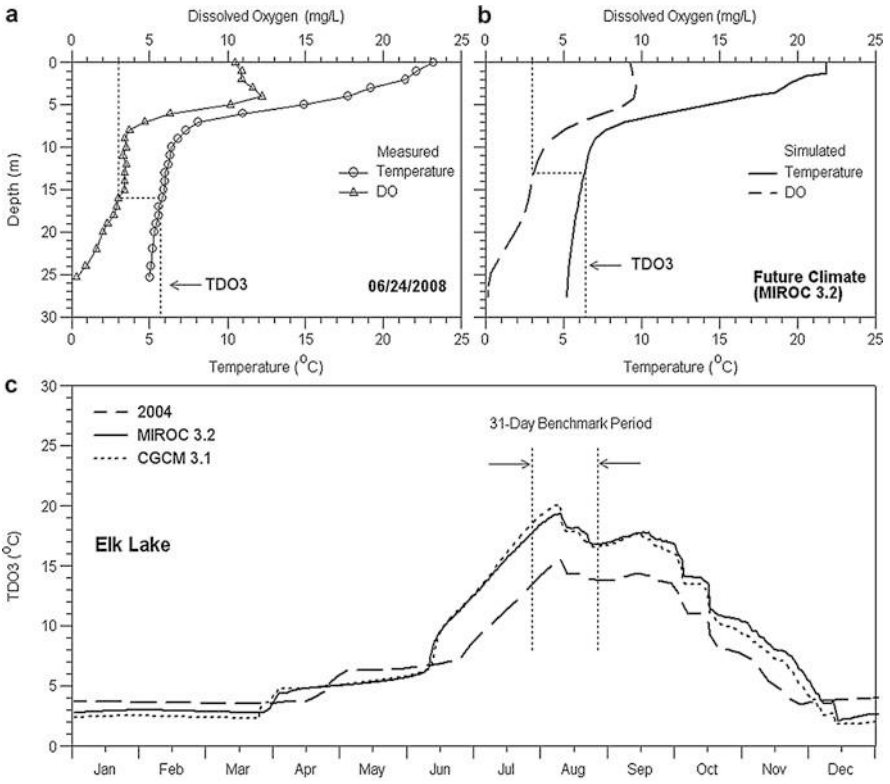

Fig. 12 Examples of measured (**a**) and simulated (**b**) temperature and DO profiles in Elk Lake for past (**a**) and a future (**b**) climate to show the determination of TDO3 (temperature at 3 mg/L DO) and (**c**) time series of simulated daily TDO3 values for Elk Lake in 2004 and for future climate scenarios CGCM 3.1 and MIROC 3.2. The fixed benchmark periods for stratified lakes are between the vertical dashed lines (Fang et al. 2012b)

period) with the highest value of TDO3 and typically occurs in late summer (Jacobson et al. 2010). From a total of 9,521 T and DO profiles measured in 1,623 Minnesota lakes in the years 1993 through 2005, associated maximum TDO3 values were computed in summer periods, and then Jacobson et al. (2010) determined that the period of greatest oxythermal stress for cold-water fish differed by stratification status of a lake. The stress occurred earlier in unstratified lakes. In this study, the fixed benchmark (FB) period from July 28 through August 27 proposed by Jacobson et al. (2010) was chosen to calculate the monthly (31-day) average of daily TDO3, called $ATDO3_{FB}$, in each simulated year over the 47-year simulation period because the 30 simulated virtual cisco lakes (Table 2) are strongly stratified lakes.

The overall modeling approach of the option 3 was depicted in Fig. 3 and discussed in detail by Fang et al. (2012b). To pursue the overall objective, we had to (1) review how the T and DO habitat constraints on cold-water fishes in lakes can be quantified (oxythermal fish habitat criteria), (2) develop a method to quantify

oxythermal fish habitat under past climate and by how much climate warming will change it in existing cisco lakes, (3) validate that the methods under (1) and (2) would give results for past climate conditions that would match actual cisco observations in lakes, (4) apply the method to make projections for a representative number of lakes in the future, and (5) extrapolate those results to 620 cisco lakes of Minnesota. To implement the above modeling approach, 30 "virtual" cisco lake types (Table 2) were chosen as representative of the entire set of 620 lakes. For step (4), to assess the quality of cisco habitat in 30 virtual cisco lakes and to identify refuge lakes, the 47-year average of annual $ATDO3_{FB}$ values in the 1962–2008 simulation period (i.e., $AvgATD3_{FB}$, Fig. 3) was calculated and compared to TDO3 limits (11 °C and 17 °C determined by the analysis of field data) to divide 620 Minnesota cisco lakes into three tiers.

It is impossible to validate the projected number of refuge lakes for future climate scenarios, but a model validation on 23 cisco study lakes was performed (Table 7). Adult cisco mortality was reported in 18 lakes in Minnesota during the unusually hot summer of 2006, and no cisco mortality was reported in five reference lakes (Jacobson et al. 2008), which is shown in the last column "Reported 2006 cisco mortality" of Table 7. Water temperature and DO profiles in all 23 lakes were simulated under 2006 weather data from the closest weather station after necessary model calibration (Fang et al. 2014). $ATDO3_{FB}$ in 2006 was calculated for each lake and used to classify the lake into tier 1 and tier 2 refuge lakes or tier 3 non-refuge lake. The $ATDO3_{FB}$ values in 2006 range from 13.2 °C (Lake Carlos) to 25.3 °C (Little Turtle Lake) for 18 Minnesota lakes with cisco mortality (Table 7). Except Lake Carlos (tier 2 refuge lake), all other 17 cisco lakes with 2006 cisco mortality are classified as tier 3 non-refuge lakes because their $ATDO3_{FB}$ values in 2006 are greater than 17 °C. The $ATDO3_{FB}$ values in 2006 for five reference lakes range from 6.4 °C (Big Trout Lake) to 14.3 °C (Rose Lake): four references are classified as tier 1 refuge lake, and only Rose Lake is classified as tier 2 non-refuge lake in 2006 (Table 7). Rose Lake has one profile for model calibration. Out of 23 cisco study lakes, there are two lakes (Lake Carlos and Rose Lake) having sort of disagreement with 2006 observations. Overall, there is a remarkable agreement between model predictions of refuge lake classification using $ATDO3_{FB}$ and observed adult cisco mortality and survival lakes in 2006 (Table 7).

This study was to develop a method to rank the quality of fish habitat for cisco in Minnesota lakes and the identification of potential refuge lakes if and when projected future (warmer) climate scenarios become reality. When a fish species is eliminated by changes in water temperature, it is not only a loss but also opens the habitat for other, exotic invasive species. For these reasons, a method to identify potential refuge lakes is important.

Multiyear Average of Oxythermal Stress ($AvgATDO3_{FB}$)

From the time series of daily TDO3 for each year in the 47-year (1962 to 2008) simulation period, different TDO3 statistics can be extracted, e.g., the annual

Table 7 Simulated habitat parameters in 23 Minnesota lakes that had cisco mortality or habitat observations in 2006

Lake name	Stratified or not[a]	$ATDO3_{FB}$ (°C)[b]	$ATDO3_{VB}$ (°C)	Tier of refuge lake[c]	$AvgTDO3_{FB}$ (°C)[d]	$AvgTDO3_{VB}$ (°C)	Tier of refuge lake[e]	$TDO3_{AM}$ (°C)	Having lethal days[f]	Reported 2006 cisco mortality
Little Turtle	No	25.28	25.31	3	21.88	22.18	3	27.04	Yes	Yes
Star	Yes	22.63	23.15	3	20.02	20.69	3	24.82	Yes	Yes
Mille Lacs	No	22.75	24.20	3	20.76	22.09	3	24.83	Yes	Yes
Andrusia	Yes	24.08	24.62	3	21.10	21.52	3	25.80	Yes	Yes
Little Pine (Otter Tail)	Yes	21.09	22.44	3	19.49	20.20	3	24.56	Yes	Yes
Cotton	No	25.25	25.25	3	22.00	22.30	3	26.62	Yes	Yes
Pine Mountain	Yes	24.21	24.99	3	21.83	22.45	3	26.77	Yes	Yes
Leech	No	23.91	23.92	3	20.77	21.10	3	26.15	Yes	Yes
Bemidji	Yes	21.82	22.04	3	19.37	19.75	3	23.25	Yes	Yes
Itasca	Yes	23.66	24.55	3	20.71	21.43	3	26.33	Yes	Yes
Gull	Yes	23.23	23.43	3	20.45	20.68	3	24.41	Yes	Yes
Woman	No	25.23	25.32	3	21.36	21.90	3	27.13	Yes	Yes
Straight	Yes	21.55	22.34	3	16.69	17.08	2 or 3	24.06	Yes	Yes

Little Pine (Crow Wing)	Yes	24.07	25.29	3	21.39	22.10	3	27.15	Yes	Yes
Seventh Crow Wing	Yes	21.50	23.06	3	19.71	20.68	3	24.72	Yes	Yes
Eighth Crow Wing	No	24.46	24.50	3	21.57	21.89	3	25.78	Yes	Yes
Long	Yes	21.84	22.01	3	19.23	19.57	3	23.38	Yes	Yes
Carlos	Yes	13.21	16.54	2	9.14	14.41	2	17.27	**No**	**Yes**
Big Trout	Yes	6.43	9.31	1	6.20	8.85	1	10.04	No	No
Kabekona	Yes	9.60	13.48	1 or 2	8.57	12.25	1 or 2	14.43	No	No
Scalp	Yes	7.06	8.61	1	8.60	12.32	1 or 2	9.31	No	No
Ten Mile	Yes	8.99	10.86	1	8.40	10.30	1	11.19	No	No
Rose	Yes	14.26	16.33	2	11.87	14.40	2	17.25	No	No

Note:
[a]Stratification classification based on Jacobson et al. (2008)
[b]$ATDO3_{FB}$ and $ATDO3_{VB}$ are 31-day average TDO3 for 2006
[c]Tier classification of refuge lakes based on $ATDO3_{FB}$ and $ATDO3_{VB}$
[d]$AvgTDO3_{FB}$ and $AvgTDO3_{VB}$ are averaged ATDO3 over the simulation period based on available weather data (e.g., 1962–2012 or 1992–2008), 2006
[e]Tier classification of refuge lakes based on $AvgTDO3_{FB}$ and $AvgTDO3_{VB}$
[f]Lethal condition predicted from the constant lethal limits ($LT = 22\ ^{\circ}C$ and $DO_{lethal} = 3$ mg/L) and $TDO3_{AM}$

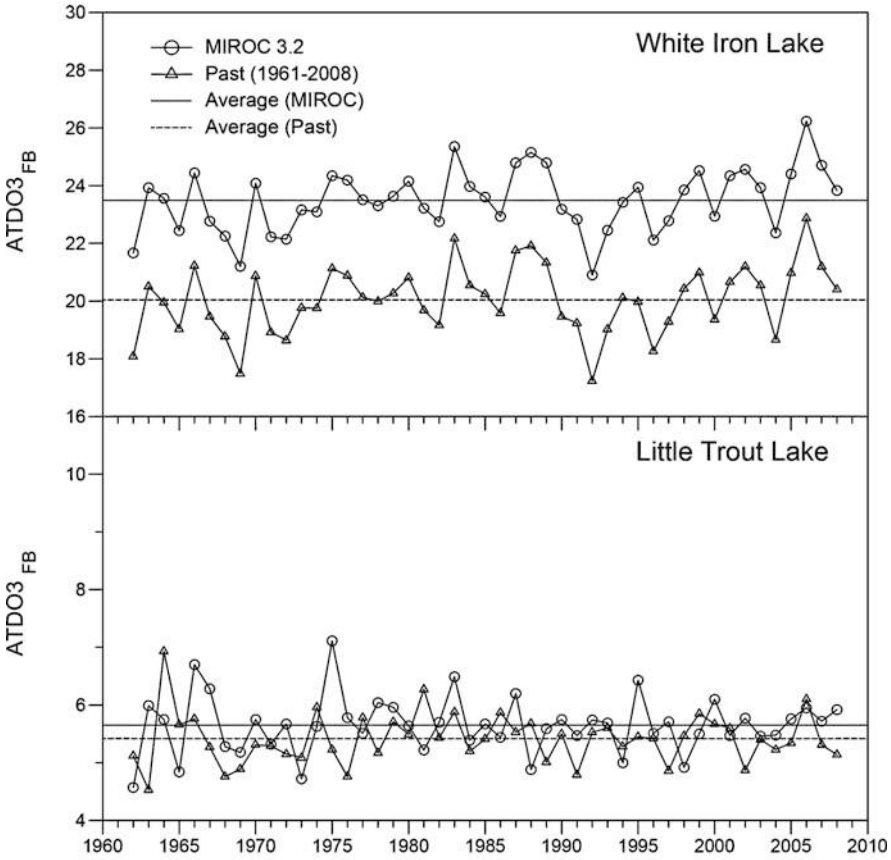

Fig. 13 Examples of annual time series of mean daily TDO3 values for the fixed benchmark periods for past climate (1962–2008) and for the future climate scenario MIROC 3.2. Averages ($AvgATDO3_{FB}$) over the 47-year simulation period are presented as dashed horizontal lines. Weather data from the closest Class I NWS weather station were used for the model simulations (Duluth for White Iron Lake and International Falls for Little Trout Lake)

maximum of daily TDO3 ($TDO3_{AM}$), monthly (31-day) averages over fixed benchmark periods ($ATDO3_{FB}$), multiyear averages of the above, etc. Twelve options of TDO3 characteristic values or statistics were calculated and explored (Fang et al. 2010b). Examples of daily TDO3 time series for Elk Lake are given in Fig. 12. The $TDO3_{AM}$ value was 15.5 °C in 2004 for Elk Lake (bottom of Fig. 12); the day of occurrence of $TDO3_{AM}$ was DOY = 222 (August 10). The $TDO3_{AM}$ value is projected to increase by 3.8 or 4.3 °C in Elk Lake under the future climate CGCM 3.1 and MIROC 3.2 scenarios, respectively (Fig. 12).

Two of the 21 cisco study lakes (Fang et al. 2012a, b), White Iron Lake and Little Trout Lake, were selected to illustrate examples of time series of mean daily TDO3 in the 31-day FB periods, $ATDO3_{FB}$ (Fig. 13). Lake geometry ratios for White Iron

Lake and Little Trout Lake are 4.27 and 1.08 $m^{-0.5}$, respectively. White Iron Lake is a weakly stratified lake or a relatively shallow, large, and eutrophic lake (maximum depth $H_{max} = 14.3$ m, surface area $A_s = 13.9$ km^2, Secchi depth SD = 1.4 m). Little Trout Lake ($H_{max} = 29.0$ m and SD = 6.3 m) is a strongly stratified and oligotrophic lake. Values of $ATDO3_{FB}$ ranged from 17.2 °C to 22.9 °C for White Iron Lake (using fixed benchmark period for unstratified lakes) and from 4.5 °C to 6.9 °C for Little Trout Lake under past climate conditions. $ATDO3_{FB}$ values in weakly stratified eutrophic White Iron Lake are much larger than $ATDO3_{FB}$ in strongly stratified oligotrophic Little Trout Lake. Under the future climate scenario MIROC 3.2, values of $ATDO3_{FB}$ are projected to range from 20.9 °C to 26.2 °C for White Iron Lake and from 4.6 °C to 7.1 °C for Little Trout Lake (Fig. 13).

Mean daily TDO3 values over the fixed benchmark ($ATDO3_{FB}$) period for each simulated year were averaged over the simulation period to obtain the parameter value $AvgATDO3_{FB}$, which had been chosen as the TDO3 characteristic parameter for the selection of cisco refuge lakes (Fang et al. 2010b, 2012b). The $AvgATDO3_{FB}$ value is one value for the 47-year simulation period (1962–2008) for each lake and each climate scenario, whereas $ATDO3_{FB}$ has one value for each simulated year and 47 values in the simulation period. The $AvgATDO3_{FB}$ values were 20.0 °C (standard deviation STD = 1.19 °C) for White Iron Lake and 5.4 °C (STD = 0.44 °C) for Little Trout Lake under past climate conditions (1962–2008). $AvgATDO3_{FB}$ is typically higher for weakly stratified lakes (e.g., White Iron Lake) than for stratified lakes (Little Trout lakes, Fig. 13). Values of $AvgATDO3_{FB}$ for the future climate scenario MIROC 3.2 are projected to be 23.5 °C for White Iron Lake and 5.7 °C for Little Trout Lake; the projected increases of $AvgATDO3_{FB}$ are 3.5 °C and 0.2 °C for these two lakes, respectively.

Simulated $AvgATDO3_{FB}$ values in 23 Minnesota lakes using available climate data (ranging 17–50 years) from a closest weather station are listed in Table 7. Based on $AvgATDO3_{FB}$, the tier of the refuge lake is signed for each lake. Results of the refuge lake classification based on $ATDO3_{FB}$ and $AvgATDO3_{FB}$ are almost the same except Straight Lake. Straight Lake has $AvgATDO3_{FB}$ of 16.7 °C, which is slightly less than 17 °C, and is classified as tier 2 refuge lake based on $AvgATDO3_{FB}$ instead of tier 3 non-refuge lake based on $ATDO3_{FB}$ in the warmer summer of 2006. Overall agreement between refuge lake classification using $AvgATDO3_{FB}$ and observation of cisco mortality and suitable habitat in 2006 is very good. Table 7 also lists the maximum TDO3 in 2006 ($TDO3_{AM}$) for each lake that was used to determine whether lethal days could occur or not based on the constant lethal limits ($LT = 22$ °C and $DO_{lethal} = 3$ mg/L). The projection of having lethal days based on $TDO3_{AM}$ in 2006 has almost perfect agreement with 2006 cisco mortality observation except Lake Carlos (Table 7).

Simulated $AvgATDO3_{FB}$ values are affected by lake bathymetry and trophic state (Fig. 14) for stratified lakes, but they are less dependent on Secchi depth (trophic status) when a lake is weakly stratified, e.g., GR > 4. This is very similar to the findings by Jacobson et al. (2010) that lake productivity did not significantly affect TDO3 in the unstratified lakes. Simulated $AvgATDO3_{FB}$ values are lower in northern Minnesota (International Falls, Fig. 14) than in north-central and central

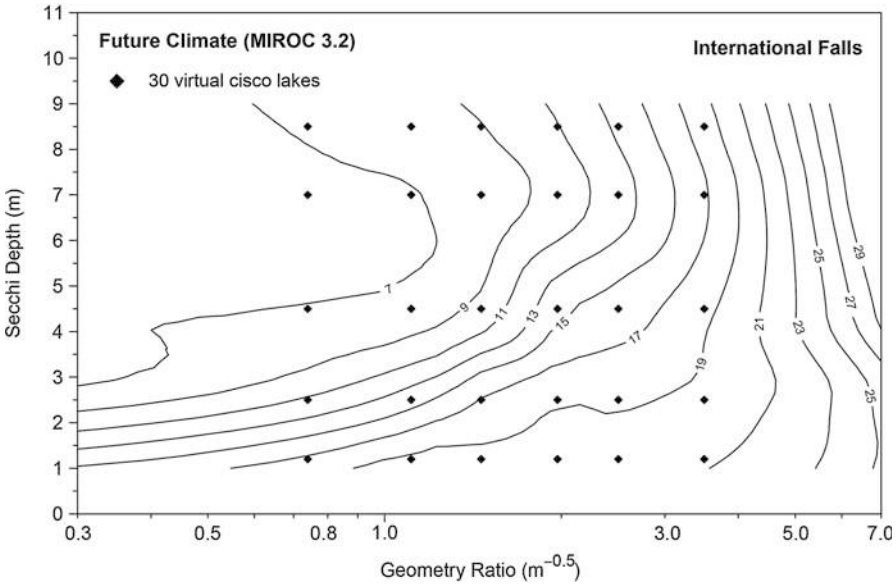

Fig. 14 Contour plots of AvgATDO3$_{FB}$ values under the future climate scenario MIROC 3.2 at International Falls, Minnesota. Contours were derived by interpolation from simulated data points for 30 virtual cisco lakes

Minnesota (Duluth and St. Cloud), but they have similar relationships (patterns) as function of GR and SD at all three locations (Fang et al. 2012b).

The AvgATDO3$_{FB}$ values ranged from 6.1 °C to 19.6 °C under past climate conditions and from 6.3 °C to 23.3 °C under two future climate scenarios at three weather stations for the 30 virtual cisco lakes (Fang et al. 2012). The projected increases of AvgATDO3$_{FB}$ values from past climate to future scenarios were from 0.0 °C to 6.5 °C in the 30 virtual lakes, and average increases are projected to be from 2.6 °C to 2.9 °C (Fang et al. 2012b), which is about 1.0–1.5 °C less than projected annual air temperature increases under the climate scenarios MIROC 3.2 and CGCM 3.1 (Table 3), respectively.

Identified Cisco Refuge Lakes in Minnesota

The selection of cisco refuge lakes was based on TDO3 parameters projected under the CGCM 3.1 and MIROC 3.2 future climate scenarios using the temperature boundaries derived from 30 simulated lakes (e.g., AvgATDO3$_{FB}$ in Fig. 14). Cisco refuge lakes were also determined by simulations for past climate conditions (1962–2008) because the results would be expected to match actual cisco lakes in Minnesota and would be a useful reference to gage both the reliability of the selection procedure and the impact of climate warming on cisco lakes in Minnesota.

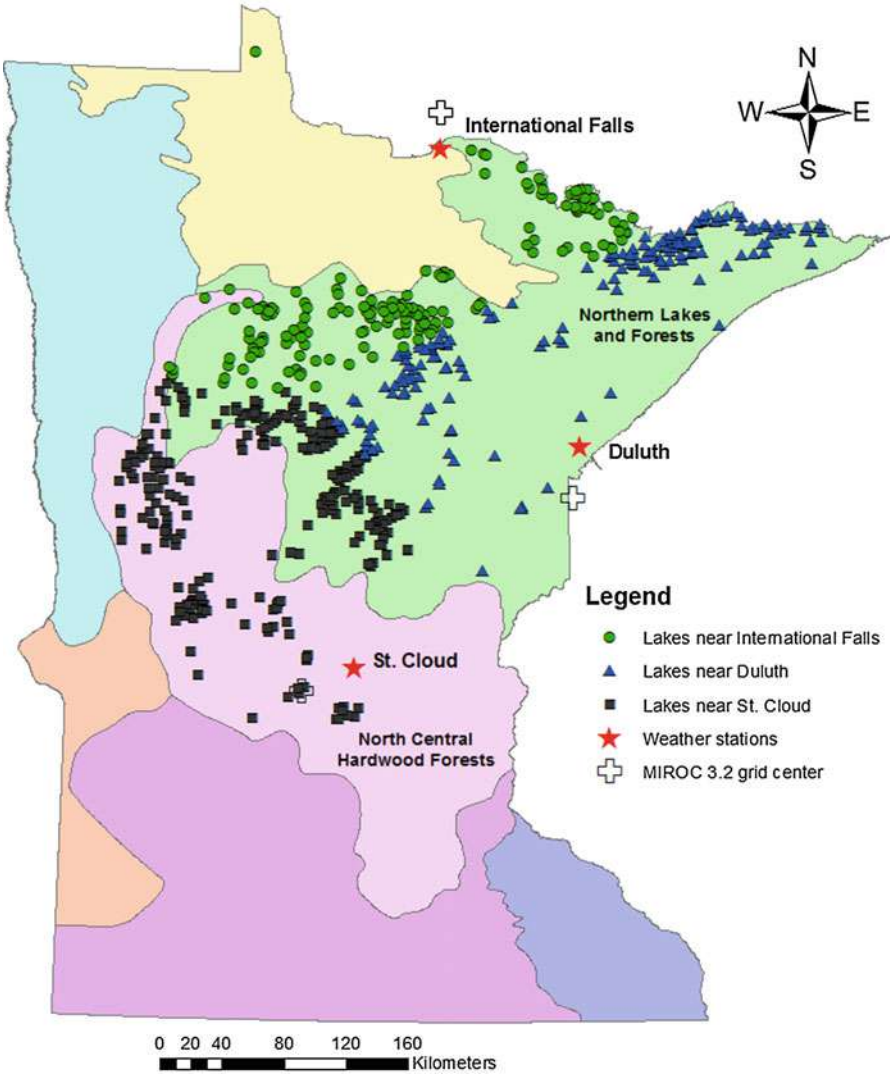

Fig. 15 Geographic distribution of 620 cisco lakes in Minnesota assigned by shortest distance to one of the three weather stations (International Falls, Duluth, and St. Cloud). The three weather stations (stars) and the grid center points (crosses) of MIROC 3.2 GCM are shown. Background shades identify ecoregions of Minnesota. Cisco lakes are found in two ecoregions: (1) Northern Lakes and Forests and (2) North Central Hardwood Forests

For the 620 cisco lakes, lakes were grouped by the shortest distance to one of the three Class I NWS weather stations in Minnesota; 169, 189, and 262 lakes were associated with International Falls, Duluth, and St. Cloud, respectively (shown by different symbols, Fig. 15).

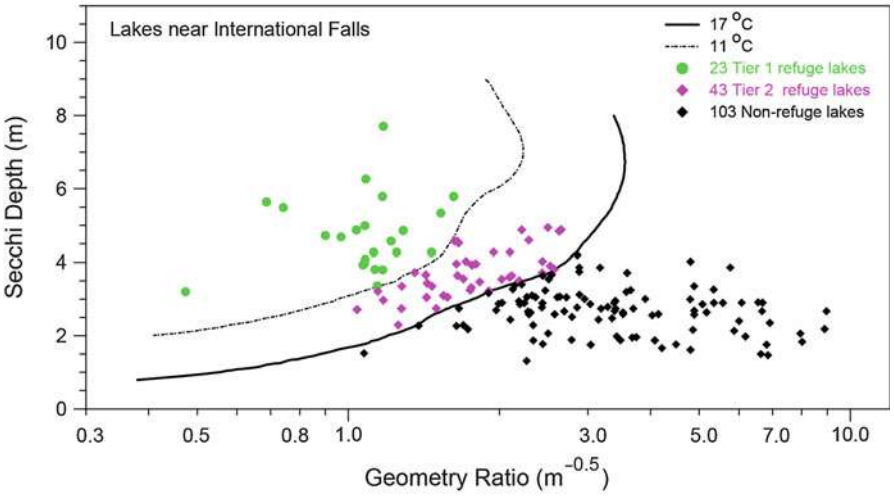

Fig. 16 Distribution of tier 1 and tier 2 refuge lakes and tier 3 non-refuge lakes on a plot of Secchi depth versus lake geometry ratio for 169 cisco lakes close to International Falls. The boundary contour lines between tiers 1, 2, and 3 are for $AvgATDO3_{FB} = 11$ °C and 17 °C, respectively, and were determined by the fixed benchmark method for the future climate scenario MIROC 3.2

The cisco lakes assigned to International Falls, Duluth, and St. Cloud weather stations were divided into tier 1 and tier 2 refuge lakes and tier 3 non-refuge lakes by the 11 °C and 17 °C isotherms of $AvgATDO3_{FB}$ simulated using corresponding climate input. The selection of refuge lakes shown in Fig. 16 was based on contour lines of $AvgATDO3_{FB}$ for the fixed benchmark period simulated under the future climate scenario MIROC 3.2. It was projected that 66 (23 + 43 in Fig. 16), 89, and 56 lakes associated with International Falls, Duluth, and St. Cloud, respectively, would be tier 1 plus tier 2 refuge lakes. A total of 211 or 205 lakes of 620 cisco lakes were identified as refuge lakes (tier 1 plus tier 2) under the future climate scenarios MIROC 3.2 and CGCM 3.1, respectively (Fang et al. 2012b). It means that about one third of the 620 lakes that currently have cisco populations are projected to maintain cisco habitat under future projected warmer climate scenarios.

Under past climate conditions (1962–2008), 483 lakes or 78 % of the 620 lakes with documented cisco populations were classified as refuge lakes (tier 1 plus tier 2) (Fang et al. 2012b). Mean values of gillnet catch per unit effort (CPUE, number of cisco gillnet) were determined from standard MN DNR netting assessments of cisco in 474 lakes. The CPUE is used as a measure of relative abundance. Mean CPUE values were 5.1, 4.1, and 3.6 for 49 tier 1 (out of total 474 lakes MN DNR studied), 97 tier 2, and 328 tier 3 refuge lakes, respectively. The netting assessment data show that there is a correlation between the tier and relative abundance, i.e., cisco abundance diminishes from tier 1 to tier 3 lakes.

The geographic distribution or a division of the 620 Minnesota cisco lakes into 84 tier 1 refuge lakes (large green circles), 127 tier 2 refuge lakes (medium-size pink pentagons), and 409 non-refuge cisco lakes (small black hexagons) is projected for

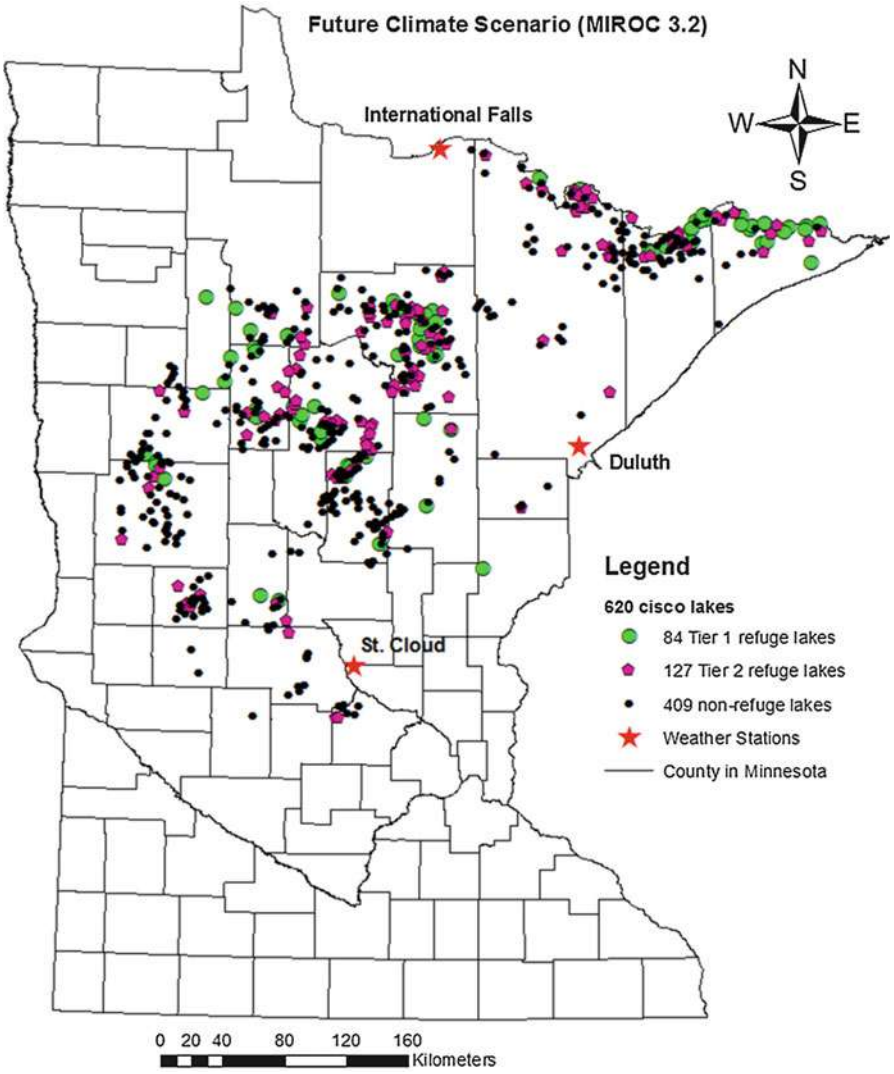

Fig. 17 Geographic distribution of tier 1 and tier 2 cisco refuge lakes and tier 3 non-refuge cisco lakes obtained from simulations for the future climate scenario MIROC 3.2. The boundary limits for tier 1 and tier 2 refuge lakes were contour lines of $\mathrm{AvgATDO3_{FB}} = 11\ ^{\circ}\mathrm{C}$ and 17 °C, respectively. The fixed benchmark method and weather data from principal weather stations in International Falls, Duluth, and St. Cloud, Minnesota, were used

the future climate scenario MIROC 3.2 (Fig. 17). Twenty-three (23) tier 1 and 43 tier 2 cisco refuge lakes (Fig. 16 and Table 8) are associated with International Falls where there is little urban or agricultural development (protected by the Superior National Forest); 39 tier 1 and 50 tier 2 refuge lakes (Table 8) are near Duluth where more development pressure exists and more protection may be necessary; and there

Table 8 Number (%) of lakes selected as tier 1 and tier 2 refuge lakes and tier 3 non-refuge lakes from cisco lakes partitioned by shortest distance to weather stations in International Falls, Duluth, and St. Cloud, Minnesota. The total number of lakes considered is 620

Closest weather station	Climate scenario	Tier 1 refuge lakes	Tier 2 refuge lakes	Total number of refuge lakes	Non-refuge lakes	Total number of lakes
International Falls	Past	49 (8)	88 (14)	137 (22)	31 (5)	169 (27.2)
	CGCM 3.1	23 (4)	39 (6)	62 (10)	106 (17)	169 (27.2)
	MIROC 3.2	23 (4)	43 (7)	66 (11)	103 (17)	169 (27.2)
Duluth	Past	78 (13)	91 (15)	169 (27)	20 (3)	189 (30.5)
	CGCM 3.1	36 (6)	51 (8)	87 (14)	102 (16)	189 (30.5)
	MIROC 3.2	39 (6)	50 (8)	89 (14)	100 (16)	189 (30.5)
St. Cloud	Past	49 (8)	128 (21)	177 (29)	85 (14)	262 (42.3)
	CGCM 3.1	19 (3)	37 (6)	56 (9)	206 (33)	262 (42.3)
	MIROC 3.2	22 (4)	34 (5)	56 (9)	206 (33)	262 (42.3)
All three stations	Past	176 (28)	307 (50)	483 (78)	137 (22)	620 (100)
	CGCM 3.1	78 (13)	127 (20)	205 (33)	415 (67)	620 (100)
	MIROC 3.2	84 (14)	127 (20)	211 (34)	409 (66)	620 (100)

are 22 tier 1 and 34 tier 2 refuge lakes (Table 8) associated with the St. Cloud area and its moderate development pressure.

It was found that 84 tier 1 refuge lakes have mean summer Secchi depths from 3.20 to 9.46 m (oligotrophic lakes), lake geometry ratios from 0.47 to 1.83 $m^{-0.5}$ (strongly stratified lakes), maximum depths from 13.7 to 64.9 m, and surface areas from 0.08 to 21.27 km^2 (Fang et al. 2012b). The upper 50 % of the 127 tier 2 refuge cisco lakes have a mean summer Secchi depth greater than 3.89 m, a geometry ratio from 1.56 to 2.66 $m^{-0.5}$, and a maximum depth greater than 21.3 m (Fang et al. 2012b). On the other hand, the lower 50 % of the 409 tier 3 non-refuge lakes have a mean summer Secchi depth less than 2.9 m, a geometry ratio from 2.72 to 11.89 $m^{-0.5}$, and a maximum depth less than 13.4 m.

Tier 1 plus tier 2 refuge lakes selected under the MIROC 3.2 climate scenario have a Secchi depth greater than 2.3 m, a lake geometry ratio less than 2.7 m, and a maximum depth greater than 11.6 m (Fang et al. 2012b). The geographic distribution of the projected cisco refuge lakes in Minnesota was surprisingly uniform (Fig. 16). Refuge lakes are not exclusively found in the northern and colder region; in fact, many non-refuge lakes are in the north, and a few refuge lakes are near St. Cloud in the south. This is because stratification characteristics related to lake geometry ratio

and trophic status play an important role in determining cold-water habitat for cisco in addition to climate conditions.

Identification of Cisco Refuge Lakes Using the Variable Benchmark Periods

In the third option of the oxythermal habitat modeling for cisco, single variable TDO3 can be determined by interpolation from simulated temperature and DO profiles in a stratified lake such as Elk Lake shown in Fig. 12. To determine refuge cisco lakes, average TDO3 in each simulation year can be quantified in two different periods, i.e., fixed benchmark period (Fang et al. 2012b) and variable benchmark periods (Jiang et al. 2012). Jacobson et al. (2010) determined that the period of greatest oxythermal stress for cold-water fish differed by stratification status of a lake. The 31-day fixed benchmark period of greatest oxythermal stress went from July 13 through August 12 (DOY 194 to DOY 224) for unstratified lakes and from July 28 through August 27 (DOY 209 to DOY 239) for stratified lakes; these benchmark periods explained 65 % of the deviance in TDO3 for the stratified lakes and 68 % for the unstratified lakes (Jacobson et al. 2010). However, fixing the benchmark period in time may introduce a bias for some lakes (Jiang et al. 2012). The highest average daily TDO3 value in any 31-day sliding (variable) benchmark (VB) period, called $ATDO3_{VB}$ (Fig. 3), was calculated for each simulated lake and year. Multiyear average of annual maximum oxythermal stress $ATDO3_{VB}$, i.e., $AveATDO3_{VB}$ (Fig. 3), was then used to compare with the TDO3 limits of 11 °C and 17 °C to identify cisco refuge lakes.

Figure 18 shows time series of daily TDO3 values in Big Trout Lake under 2006 and future climate scenarios (CGCM 3.1 and MIROC 3.2). The annual maximum daily TDO3 ($TDO3_{AM}$) was 9.8 °C, and the day of its occurrence was at DOY = 283 (October 10) in 2006 in Big Trout Lake. The $TDO3_{AM}$ value is projected to increase by 1.2–1.8 °C in Big Trout Lake under the future climate CGCM 3.1 and MIROC 3.2 scenarios, respectively (Fig. 18). Big Trout Lake, with a maximum depth of 39.0 m and a lake geometry ratio of 1.24, is a seasonally stratified (dimictic) lake and is projected to have a smaller increase in TDO3 under the future climate scenarios than White Iron Lake which has a maximum depth of 14.3 m and a geometry ratio of 4.27 and is a weakly stratified lake (Jiang et al. 2012).

The variable benchmark periods were determined using sliding window of 31 days to find the highest average daily TDO3 (called $ATDO3_{VB}$) over any 31-day period in each simulated year. The variable (sliding) 31-day benchmark period retained for each simulation year must not only have the highest mean daily $ATDO3_{VB}$ but must also contain the maximum daily TDO3 in that year (i.e., $TDO3_{AM}$). Using time series of daily TDO3 in each simulated year, the mean daily TDO3 over each sliding benchmark period of 31 days was calculated, and only the highest mean value in any of the sliding benchmark periods of a year (i.e., $ATDO3_{VB}$) was retained in the fish habitat program. For example, the beginning date of the VB period in Big Trout Lake was DOY 262 (September 19) in 2006 (Fig. 18),

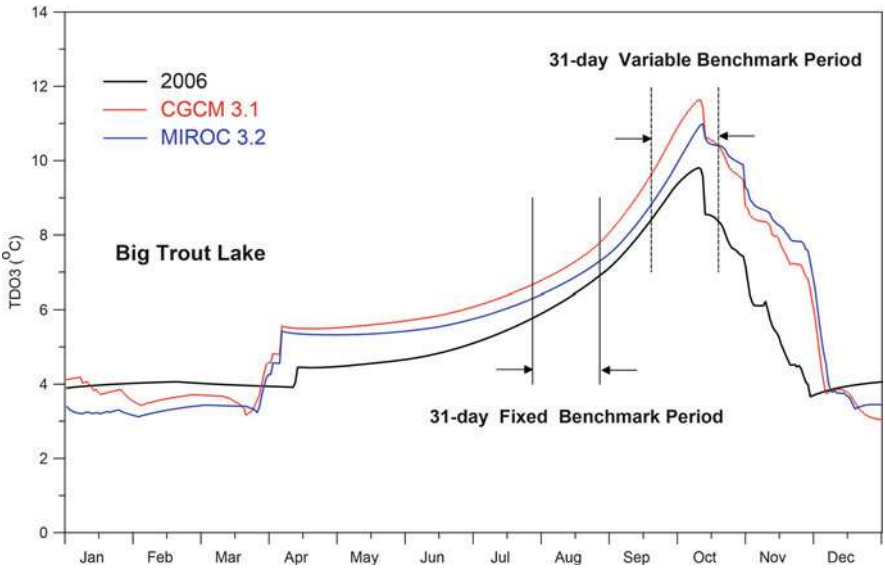

Fig. 18 Time series of simulated daily TDO3 for Big Trout Lake in 2006 and for future climate scenarios CGCM 3.1 and MIROC 3.2. The beginning dates of variable benchmark periods of highest mean daily TDO3 in 2006 for Big Trout Lake are DOY 262 (September 19)

which was quite different from the fixed benchmark period (DOYs 209 to 239). Under the future climate scenarios MIROC 3.2 and CGCM 3.1, the beginning dates for the $ATDO3_{VB}$ period are projected (simulated) to be DOYs 273 and 265 in Big Trout Lake, respectively; these dates are not much different from the beginning dates of the $ATDO3_{VB}$ for the past climate conditions. The VB period in White Iron Lake was DOY 199 (July 18) in 2006, which was about 2 months earlier than the VB period in Big Trout Lake.

To further illustrate the variability of the VB periods that give the annual $ATDO3_{VB}$ values, the beginning dates of these VB periods for virtual cisco LakeC06 and LakeC08 were determined for past climate (1962–2008) and for the future climate scenario MIROC 3.2 (Jiang et al. 2012). Duluth weather data were used as model simulation input. The beginning dates of these VB periods ranged from DOY 192 to 226 for LakeC06 and from DOY 241 to 271 for LakeC08 under past climate conditions. Average beginning dates were DOY 210 (July 29) for LakeC06 and DOY 253 (September 10) for LakeC08 under past climate conditions (1962–2008). These two small virtual lakes have the same lake geometry but different Secchi depths (Table 2); LakeC06 is an eutrophic lake with SD = 1.2 m, and LakeC08 is an oligotrophic lake with SD = 4.5 m. Isolines that give simulated average beginning dates of the VB periods of greatest oxythermal stress over the 47-year simulation period as a function of Secchi depth and lake geometry ratio were developed and studied (Jiang et al. 2012). Averages of the beginning dates of the VB periods for $ATDO3_{VB}$ ranged from DOY 207 (July 26) to DOY 269 (September 26)

for the 30 virtual lakes under past climate conditions (1962–2008). It was found that the beginning date of greatest oxythermal stress for cisco can vary considerably from year to year depending on weather, but it can also vary by lake type, i.e., stratification characteristics and trophic status (Jiang et al. 2012). Later dates occur in lakes with lower geometry ratio and higher Secchi depth, i.e., stratified oligotrophic lakes produce oxythermal stress for cisco later in the season than other lakes. The differences between the latest and earliest average beginning dates of the greatest oxythermal stress period for cold-water fish in Minnesota lakes were ranged from 59 to 89 days under past and future climates using weather data from three Class I weather stations. Therefore, variable (sliding) benchmark periods ($ATDO3_{VB}$) performed better than fixed benchmark periods to quantify the maximum oxythermal stress to cisco. The differences in average beginning dates of VB periods are much smaller (nearly negligible) between projected future climate and past climate than the differences between different lake types and the differences from year to year (Jiang et al. 2012).

Oxythermal Parameters ($ATDO3_{VB}$ and $AveATDO3_{VB}$) for VB Periods

To evaluate oxythermal stress for cisco in different lake types and under different climate scenarios, the $AvgATDO3_{VB}$ was chosen as the TDO3 parameter to identify and select cisco refuge lakes for the study (Fang et al. 2010b). The time series of $ATDO3_{VB}$ for virtual cisco LakeC06 and LakeC08 (Table 2) were analyzed under past climate (1962–2008 at Duluth) and the future climate scenario MIROC 3.2 (Jiang et al. 2012). Over the simulation period (1962–2008), $ATDO3_{VB}$ values ranged from 7.3 °C to 12.1 °C for LakeC06 and from 11.8 °C to 19.9 °C for LakeC08 under past climate conditions. Averages of $ATDO3_{VB}$ over the 47-year simulation period (i.e., $AvgATDO3_{VB}$) were 9.3 °C with standard deviation of 1.0 °C for LakeC06 and 15.6 °C with standard deviation of 1.5 °C for LakeC08 under past climate conditions (1962–2008). Values of $AvgATDO3_{VB}$ for the MIROC 3.2 future climate scenario are projected to be 12.6 °C for LakeC06 and 20.7 °C for LakeC08; the projected increases are 3.3 °C and 5.1 °C, respectively (Jiang et al. 2012).

Figure 19 shows contour plots of $AvgATDO3_{VB}$ under the past climate conditions and the CGCM 3.1 and MIROC 3.2 future climate scenarios using Duluth weather data. Contours were derived by interpolation from simulated $AvgATDO3_{VB}$ data points for the 30 virtual cisco lakes (dots in top frame of Fig. 19). Statistics of $AvgATDO3_{VB}$ values under past climate and future scenarios for three weather stations (International Falls, Duluth, and St. Cloud) were summarized by Jiang et al. (2012). The $AvgATDO3_{VB}$ values ranged from 7.48 °C to 19.91 °C under past climate conditions and from 8.02 °C to 23.28 °C under two future climate scenarios for the 30 virtual cisco lakes (Jiang et al. 2012). The projected increases of $AvgATDO3_{VB}$ values from past climate to future scenarios are from 0.30 °C to 5.11 °C, and average increases are projected to be from 2.79 °C to 3.40 °C. These increases are crucial, when cisco refuge lakes for future climate scenarios are identified and selected. Values of $AvgATDO3_{VB}$ vary by lake type depending on

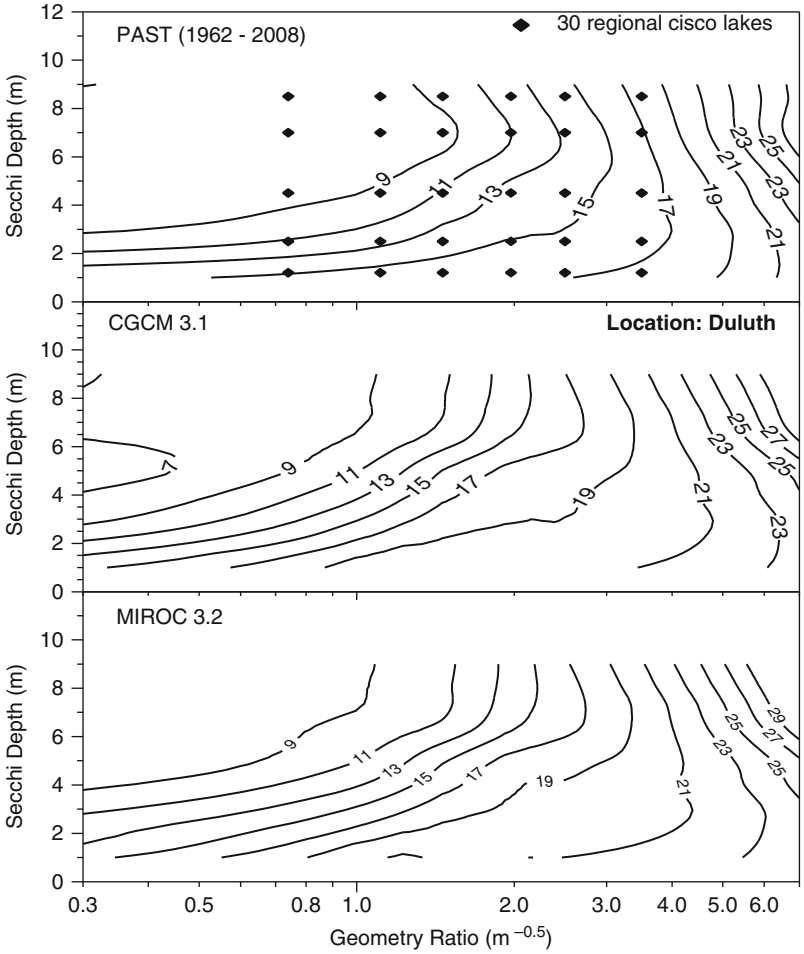

Fig. 19 Contour plots of averages of mean TDO3 over variable benchmark periods ($AvgATDO3_{VB}$) under past (1962–2008), CGCM 3.1, and MIROC 3.2 future climate scenarios. Duluth weather data was used for past climate condition. Contours were derived by interpolation from simulated data points for 30 virtual lakes

stratification characteristics and trophic status (Fig. 19); stratified oligotrophic lakes produce lower $AvgATDO3_{VB}$ values or lower oxythermal stress for cisco.

Cisco Refuge Lakes in Minnesota

Contour lines of 11 °C and 17 °C in the contour plots of $AvgTDO3_{VB}$ in Fig. 19 were used to identify cisco refuge lakes in the database of 620 Minnesota cisco lakes. The final selection of cisco refuge lakes was based on $AvgTDO3_{VB}$ projected under

Table 9 Number (%) of lakes selected as tier 1 and tier 2 refuge lakes and tier 3 non-refuge lakes from cisco lakes grouped by latitude (Fig. 1). Weather input data from three principal weather stations (International Falls, Duluth, and St. Cloud) are each assigned to a different range of latitudes for use in the simulations (Jiang et al. 2012)

Weather station by latitude	Climate scenario	Tier 1 refuge lakes	Tier 2 refuge lakes	Total number of refuge lakes	Tier 3 non-refuge lakes	Total number of lakes
Northern (International Falls)	Past	41 (7)	96 (15)	137 (22)	29 (5)	166 (27)
	CGCM 3.1	24 (4)	43 (7)	67 (11)	99 (16)	166 (27)
	MIROC 3.2	19 (3)	43 (7)	62 (10)	104 (17)	166 (27)
Mid-latitude (Duluth)	Past	52 (8)	285 (46)	337 (54)	62 (10)	399 (64)
	CGCM 3.1	10 (2)	83 (13)	93 (15)	306 (49)	399 (64)
	MIROC 3.2	10 (2)	84 (14)	94 (15)	305 (49)	399 (64)
Southern (St. Cloud)	Past	1 (<1)	31 (5)	32 (5)	23 (4)	55 (9)
	CGCM 3.1	0	4 (1)	4 (1)	51 (8)	55 (9)
	MIROC 3.2	0	4 (1)	4 (1)	51 (8)	55 (9)
All three latitudes	Past	94 (15)	412 (66)	506 (82)	114 (18)	620 (100)
	CGCM 3.1	34 (5)	130 (21)	164 (26)	456 (74)	620 (100)
	MIROC 3.2	29 (5)	131 (21)	160 (26)	460 (74)	620 (100)

the CGCM 3.1 and MIROC 3.2 future climate scenarios. Under past climate conditions (1962–2008), 506 lakes or 82 % were classified as "refuge" lakes (tier 1 plus tier 2). It means that the proposed methodology using VB periods identified current cisco lakes with an 82 % success ratio (Jiang et al. 2012).

The results of refuge lake selection using $AvgATDO3_{VB}$ are summarized in Table 9. Figure 20 shows the division of the 166 northern cisco lakes (Fig. 1) into tier 1 and tier 2 refuge lakes and tier 3 non-refuge lakes based on contour lines of 11 °C and 17 °C for $AvgATDO3_{VB}$ under the future climate scenario MIROC 3.2. It is projected that 19, 43, and 104 lakes out of 166 northern cisco lakes would be tier 1, tier 2, and tier 3 refuge lakes (Table 9 and Fig. 20) under MIROC 3.2. A total of 164 and 160 lakes or about 25 % of 620 cisco lakes were identified as tier 1 plus tier 2 refuge lakes under the future climate scenarios MIROC 3.2 and CGCM 3.1, respectively (Table 9). Thus, under fairly stringent selection criteria ($AvgATDO3_{VB} \leq 17$ °C), about one fourth of the 620 lakes that currently have cisco populations are projected to maintain viable cisco habitat (tier 1 plus tier 2) under projected future climate scenarios. In other words, climate warming under the MIROC 3.2 future

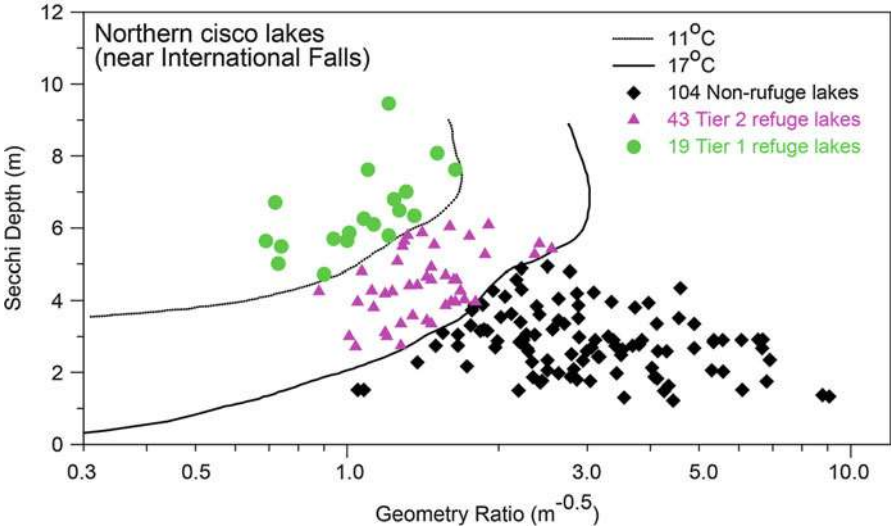

Fig. 20 Distribution of tier 1 and tier 2 refuge lakes and tier 3 non-refuge lakes on a plot of Secchi depth versus lake geometry ratio for 166 northern lakes using $AvgATDO3_{VB} = 11\ °C$ and 17 °C, as boundary lines

climate scenario is projected to potentially decrease the number of Minnesota cisco refuge lakes (tier 1 plus tier 2) by 346 (= 506 − 160) from past climate conditions (Table 9).

Table 7 summarizes the refuge lake classification in 23 Minnesota lakes based on $ATDO3_{VB}$ and $AvgTDO3_{VB}$. Except Lake Carlos, all lakes with cisco mortality in 2006 are classified as tier 3 non-refuge lakes. For five reference lakes, Kabekona and Scalp were classified as tier 2 refuge lakes using $AvgTDO3_{VB}$ (Table 7). Using VB period, $TDO3_{VB}$ does represent better actual oxythermal stress that occurs at different time periods in different lakes. Overall, there is a good agreement between refuge lake classifications using $ATDO3_{VB}$ or $AvgTDO3_{VB}$ and observed adult cisco mortality and suitable habitats in 2006 (Table 7).

The projected geographic distribution of refuge lakes and non-refuge lakes in Minnesota based on results in Fig. 20 and Table 9 is shown in Fig. 21. A division of the 620 Minnesota cisco lakes into 29 tier 1 refuge lakes (large green squares), 131 tier 2 refuge lakes (medium-size red triangles), and 460 non-refuge cisco lakes (small dark circles) is projected for the MIROC 3.2 future climate scenario when 11 °C and 17 °C contour lines of $AvgATDO3_{VB}$ were used as boundary limits (Fig. 20), and refuge lakes were selected separately from the three groups divided by latitude.

The statistics of four physical lake parameters that appear important for tier 1, 2, and 3 cisco lakes were developed (Jiang et al. 2012). For 29 tier 1 refuge lakes, the mean Secchi depths are from 4.72 to 9.46 m (oligotrophic lakes), lake geometry ratios from 0.69 to 1.64 $m^{-0.5}$ (strongly stratified lakes), maximum depths from 18.0

to 63.4 m, and surface areas from 0.19 to 21.27 km^2. The 50 % of the 460 non-refuge lakes have a mean summer Secchi depth less than 3.0 m (eutrophic to mesotrophic lakes), a maximum depth less than 14.3 m (relatively shallow lakes), and a geometry ratio greater than 2.52 $m^{-0.5}$. Tier 1 plus tier 2 refuge lakes selected under the MIROC 3.2 climate scenario have a Secchi depth greater than 2.3 m, a lake geometry ratio less than 2.6 m, and a maximum depth greater than 13.1 m (Jiang et al. 2012).

Discussion of Refuge Lake Selections

The fish habitat model simulated cisco oxythermal habitat similar to Jacobson et al. (2010), who developed an empirical model to predict TDO3 as a function of lake productivity, climate, and lake geometry ratio. Summer total phosphorus concentration was selected to represent primary productivity of each lake (Jacobson et al. 2010). In our study, phosphorus was not used to characterize any of the cisco lakes. Instead, Secchi depth, a measure of lake transparency, was used to represent trophic state. The trophic state expresses primary productivity and is directly related to DO production by photosynthesis in the MINLAKE2010 model. Chlorophyll-*a* concentration in cisco lake was calculated from Secchi depth using the Carlson trophic index (Carlson 1977) and generic seasonal growth patterns (Marshall and Peters 1989). Therefore, SD and GR are representative parameters to characterize each of the 620 cisco lakes in the database. Contour plots using GR and SD as axes were previously and successfully used to present characteristics of water temperature, DO, and fish habitat parameters in lakes (Fang and Stefan 1997, 1999, 2009; Fang et al. 2004a, b).

The effects of dissolved organic carbon (DOC), e.g., in the form of humic acids, were not modeled explicitly in MINLAKE2010, although DOC can contribute to water color and light attenuation in Minnesota lakes; this effect is captured by Secchi depth, but it also weakens the relationship between SD and primary productivity, chlorophyll-*a* concentrations, and DO production by photosynthesis. MINLAKE2010 did not directly include nutrient input from the surrounding watershed into a lake or groundwater inflow. Simulation results obtained with MINLAKE2010 are, nevertheless, representative of the nutrient input from the watershed which is reflected in the trophic state and therefore the Secchi depth (SD) of the lake; but groundwater inflow and its effect on stratification are not accounted for in SD or GR.

$AvgATDO3_{VB}$ values derived from 30 virtual lakes are presented as isolines on a coordinate system of lake geometry ratio GR versus Secchi depth (SD) (Figs. 14 and 19). GR and SD appear to be sufficient to represent essential features of different lake types, GR characterizes the potential for stratification and mixing dynamics, and SD characterizes transparency, but also trophic state as a surrogate, at least in most Minnesota lakes. Lake turbidity from suspended inorganic sediment is relatively rare in Minnesota, and total phosphorus or chlorophyll-*a* in most Minnesota lakes are well correlated with SD. Monthly variations in these parameters follow well-established generic patterns in Minnesota lakes.

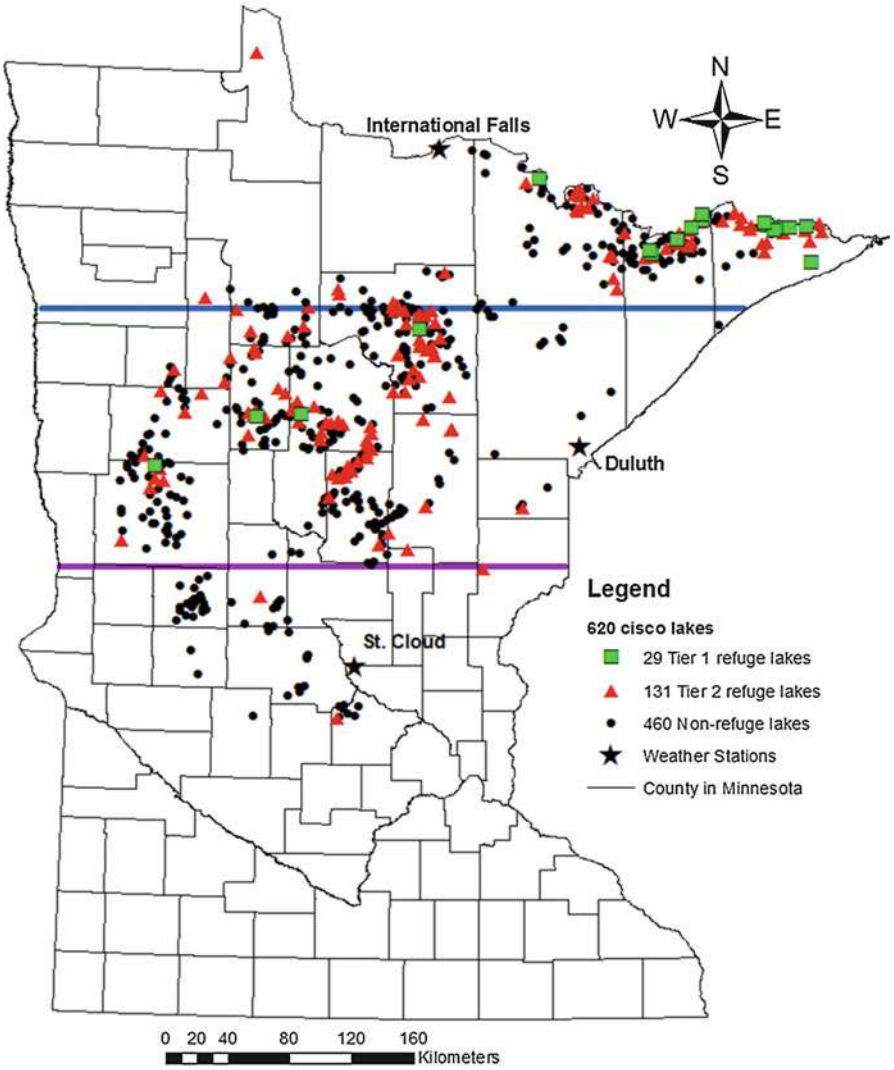

Fig. 21 Geographic distribution of tier 1 and tier 2 cisco refuge lakes and tier 3 non-refuge cisco lakes simulated for the future climate scenario MIROC 3.2. Lakes are grouped by latitude into 166 northern, 399 mid-latitude, and 55 southern cisco lakes. The boundary limits for tier 1 and tier 2 refuge lakes were contour lines of $\text{AvgATDO3}_{\text{VB}} = 11\ ^{\circ}\text{C}$ and 17 °C, respectively. Variable benchmark periods were used, and principal weather stations (International Falls, Duluth, and St. Cloud) were associated by latitude with each lake group (modified from Jiang et al. 2012)

The partitioning of cisco lakes into tiers was useful for distinguishing potential refuge value for cisco and possibly other species after climate warming. Because the TDO3 limit of 11 °C corresponds to the upper central niche border for lake whitefish (Jacobson et al. 2010), the tier 1 refuge lakes selected from the study are useful for

the management of lake whitefish. The partitioning of the cisco lakes into tiers 1, 2, and 3 was guided by TDO3 temperatures of 11 °C and 17 °C. These boundary lines are considered fairly stringent because the upper ultimate lethal temperature of young ciscoes was determined in a laboratory study by Edsall and Colby (1970) to be 26 °C, and mortality of adults begins at 22 °C at 3 mg/l of oxygen based on the analysis of observed temperature and DO profiles in 23 Minnesota lakes (Jacobson et al. 2008). Median values of $\max T_{DO3}$ were 18.2 °C for lakes with cisco populations (Jacobson et al. 2010).

Tier 1 and tier 2 cisco lakes identified for past climate conditions (1961–2008) may be called viable cisco lakes where cisco is capable of living, growing, and reproducing under favorable conditions. Using fixed and variable benchmark methods, 137 (22 %, Table 8) and 114 (18 %, Table 9), respectively, of the current 620 lakes with known cisco populations were identified by the simulations as non-refuge lakes under past climate conditions (1962–2008) and represent marginal cisco habitat. This does not mean that these 137 or 114 cisco lakes cannot support cisco habitat at all. Cisco can still persist in lakes with TDO3 values greater than 17 °C but at a reduced probability of occurrence in this marginal habitat (Jacobson et al. 2010). Frey (1955) postulated that young ciscoes are more tolerant of high temperatures and low DO concentrations than the larger and older ciscoes; they can survive through hot summers in a thin stratum above the thermocline in stratified deep lakes. Therefore, summer mortality events primarily affect adult cisco (see Fig. 2). Cisco populations can persist in lakes with multiple years of mortality as long as some juveniles remain in the lakes. Recruitment of juveniles is therefore as important to cisco's survival as the duration of exposure to lethal conditions, but recruitment is not included in current simulations and projections. At the same time, the shallow lakes that are projected to have cisco kill every year with continuous lethal conditions up to 94 days (Fig. 11) under the future climate scenario are most likely not able to sustain cisco habitat at any life stage.

For the selection of refuge lakes, lakes were divided into three categories (tiers) using only two TDO3 isotherms (11 °C and 17 °C) as contour lines (Figs. 16 and 20). Another approach would be to use more isotherms at finer increments to rank each lake according to where it is located between TDO3 contour lines. To do this, 620 cisco lakes in Minnesota were assembled in narrow (2 °C and 1 °C) bands of TDO3 values (Fang et al. 2010b). Names and locations of lakes in each band were tabulated, and lakes with the lowest TDO3 values were placed on top of the list and were presumed to be the best candidates for cisco refuge lakes, because low TDO3 values are presumed to reflect the least stress on adult cisco.

Projected changes in the multiyear average TDO3 (i.e., AvgATDO3_{FB}) between future (CGCM 3.1 and MIRCO 3.2) and past climate conditions have mean values ranging from 2.58 °C to 2.93 °C with model input from three weather stations in Minnesota (maximum differences up to 6.51 °C). The potential impact of climate change on fish habitat is inevitable. Using fixed and variable benchmark period methods (Fang et al. 2012b; Jiang et al. 2012), 67 % and 74 % of cisco lakes projected to be non-refuge lakes are similar to those of a study (using a different methodology) of about 170 cisco lakes in Wisconsin (Sharma et al. 2011) which was

summarized as "By 2100, 30–70 % of Cisco populations could be extirpated in Wisconsin due to climate change, Cisco are much more at risk due to climate change rather than interactions with exotic species."

The fixed benchmark (FB) period is a very good average for many lakes, but may not fit some individual lakes. In a given year, ATDO3 in the FB period can be different from the highest ATDO3 over the VB period. There were moderate differences in the number of refuge lakes obtained using FB and VB periods with identical TDO3 isotherms (11 °C and 17 °C) as boundary lines. When VB periods were used, 34 (past), 64 (CGCM 3.1), and 74 (MIROC 3.2) fewer refuge lakes were identified than with an FB period by comparing results between Tables 8 and 9.

Management Strategies of Cisco Refuge Lakes

The identification of cisco refuge lakes (Fang et al. 2010b) has formed the basis of a significant conservation effort in Minnesota directed at protecting these important lakes (Jacobson et al. 2013). Specifically, the good water quality that is critical for the ability of these lakes to provide cold, oxygenated water in the future will need to be protected. Threats to water quality include urban development and conversion of forest lands to agriculture in the watersheds of these lakes. Jacobson et al. (2013) identified catchments most at risk to some of these land-use changes and developed a prioritization system for targeting protection efforts toward those catchments. Since these lakes lie primarily in the forested region of Minnesota, the primary goal of these lake protection efforts is to keep forested lands in the watersheds of these lakes forested. Conservation tools such as private forest conservation easements, forest land acquisition, and zoning regulations are being used or considered in those targeted watersheds. These efforts will use watershed protection goals suggested by Cross and Jacobson (2013) of maintaining at least 75 % of a lake's watershed in a forested state. Protection of these watersheds will be critical for the lakes to operate as refuges in climate-warmed Minnesota.

Future Directions

Distributions of total number of years with cisco lethal days and average cisco kill days for the years with lethal conditions under MIROC 3.2 (Figs. 7 and 8) were not used to divide 385 medium-depth and 221 deep cisco lakes into tier 1 to tier 3 refuge lakes as it was done using TDO3 (Fang et al. 2012b; Jiang et al. 2012). Several good-growth parameters, e.g., the good-growth period, good-growth habitat area (GGHA), and good-growth habitat volume fraction (GGHVF), were derived when the fish model was run for these lakes but have not been analyzed. These good-growth habitat parameters used in previous studies (Stefan et al. 1996, 2001; Fang et al. 2004a, b) may be used to classify cisco lakes into tiered refuge lakes in a future study.

Jacobson et al. (2010) developed central species response borders of TDO3 derived from measured T and DO profiles for lake trout, lake whitefish, and burbot. The method developed to rank the quality of fish habitat for cisco in Minnesota lakes was presented as a flowchart in Fig. 3 and can be applied for other cold-water fish species and at other geographic locations. The next future study could be to use the same methodology developed in this study to identify refuge lakes for lake trout in Minnesota. Lake trout was present in lakes with the lowest values of $maxT_{DO3}$ and represented by central species response borders of $maxT_{DO3}$ from 4.0 °C to 5.1 °C (Jacobson et al. 2010). It will be interesting and valuable to use the method to identify cisco refuge lakes in Wisconsin, which can be directly compared with results by Sharma et al. (2011). Requirements for the study include a database of cisco lakes in Wisconsin, observed T and DO profiles in several cisco lakes for further model validation, and historical weather data at representative locations in Wisconsin.

Although variable benchmarks perform better to quantify the maximum oxythermal stress to a fish species, fixed benchmarks are still valuable because the niche model developed by Jacobson et al. (2010), which was used to identify refuge lakes, was based on them (including the 11 and 17° tier thresholds). To fully use a variable benchmark model, it is necessary to redo the niche model with variable benchmark periods in the future research.

The increase in the number of annual lethal days in different lake types is projected under one future climate scenario (MIROC 3.2), and the selection of refuge lakes was performed under two future climate scenarios (CGCM 3.1 and MIROC 3.2). Many hydrologic studies conducted on the impacts of climate warming or climate change on watersheds and aquatic systems used an assemblage of GCMs. Future studies on cisco habitat projections should include more GCM future climate scenarios from most recent IPCC studies. Overall, the projection of fish kill and fish growth in lakes is still a challenging and growing research area and needs further model validation with more field observations of fish species in different lakes.

References

Blumberg AF, Di Toro DM (1990) Effects of climate warming on dissolved oxygen concentrations in Lake Erie. Trans Am Fish Soc 119(2):210–223

Cahn AR (1927) An ecological study of southern Wisconsin fishes, the brook silverside and the cisco, in their relation to the region. Ill Biol Monogr 11(1):1–151

Carlson RE (1977) A trophic state index for lakes. Limnol Oceanogr 22(2):361–369

Chang LH, Railsback SF, Brown RT (1992) Use of a reservoir water quality model to simulate global climate change effects on fish habitat. Clim Change 20(4):277–296

Chapman G (1986) Ambient aquatic life criteria for dissolved oxygen. US Environmental Protection Agency, Washington, DC

Chapra SC (1997) Surface water-quality modeling. McGraw-Hill, New York

Christie CG, Regier HA (1988) Measurements of optimal habitat and their relationship to yields for four commercial fish species. Can J Fish Aquat Sci 45:301–314

Coutant CC (1970) Thermal resistance of adult Coho (*Oncorhynchus kisutch*) and jack Chinook (*O. tshawytscha*) salmon and the adult steelhead trout (*Salmo gairdneri*) from the Columbia River. Batelle-Northwest, SEC, BNWL-1508, Richland, Washington

Coutant CC (1985) Striped bass, temperature, and dissolved oxygen: a speculative hypothesis for environmental risk. Trans Am Fish Soc 14:31–61

Coutant CC (1990) Temperature-oxygen habitat for freshwater and coastal striped bass in a changing climate. Trans Am Fish Soc 2:240–253

Cross TK, Jacobson PC (2013) Landscape factors influencing lake phosphorus concentrations across Minnesota. Lake Reservoir Manage 29:1–12

De Stasio JBT, Hill DK, Kleinhans JM, Nibbelink NP, Magnuson JJ (1996) Potential effects of global climate changes on small north-temperate lakes: physics, fish, and plankton. Limnol Oceanogr 41(5):1136–1149

Dillon PJ, Clark BJ, Molot LA, Evans HE (2003) Predicting the location of optimal habitat boundaries for lake trout (*Salvelinus namaycush*) in Canadian Shield lakes. Can J Fish Aquat Sci 60(8):959–970

Eaton JG, McCormick JH, Goodno BE, O'Brien DG, Stefan HG, Hondzo M (1995) A field information based system for estimating fish temperature requirements. Fisheries 20(4):10–18

Edsall T, Colby P (1970) Temperature tolerance of young-ofthe-year cisco, Coregonus artedii. Trans. Amer. Fish. Soc, 99(3):526–531

Evans DO (2007) Effects of hypoxia on scope-for-activity and power capacity of lake trout (*Salvelinus namaycush*). Can J Fish Aquat Sci 64(2):345–361

Fang X, Stefan HG (1996a). Development and validation of the water quality model MINLAKE96 with winter data. Project report 390. St. Anthony Falls Laboratory, University of Minnesota, Minneapolis

Fang X, Stefan HG (1996b) Dynamics of heat exchange between sediment and water in a lake. Water Resour Res 32(6):1719–1727

Fang X, Stefan HG (1996c) Long-term lake water temperature and ice cover simulations/measurements. Cold Reg Sci Technol 24(3):289–304

Fang X, Stefan HG (1997) Simulated climate change effects on dissolved oxygen characteristics in ice-covered lakes. Ecol Model 103(2–3):209–229

Fang X, Stefan HG (1999) Projection of climate change effects on water temperature characteristics of small lakes in the contiguous U.S. Clim Change 42:377–412

Fang X, Stefan HG (2000) Projected climate change effects on winterkill in shallow lakes in the northern U.S. Environ Manage 25:291–304

Fang X, Stefan HG (2009) Simulations of climate effects on water temperature, dissolved oxygen, and ice and snow covers in lakes of the contiguous United States under past and future climate scenarios. Limnol Oceangr 54(6):2359–2370

Fang X, Stefan HG (2012) Chapter 16 Impacts of climatic changes on water quality and fish habitat in aquatic systems. In: Chen W-Y, Seiner J, Suzuki T, Lackner M (eds) Handbook of climate change mitigation, vol 1. Springer, New York/Dordrecht/Heidelberg/Berlin, pp 531–570

Fang X, Stefan HG, Eaton JG, McCormick JH, Alam SR (2004a) Simulation of thermal/dissolved oxygen habitat for fishes in lakes under different climate scenarios: part 1. Cool-water fish in the contiguous US. Ecol Model 172(1):13–37

Fang X, Stefan HG, Eaton JG, McCormick JH, Alam SR (2004b) Simulation of thermal/dissolved oxygen habitat for fishes in lakes under different climate scenarios: part 2. Cold-water fish in the contiguous US. Ecol Model 172(1):39–54

Fang X, Alam SR, Jacobson P, Pereira D, Stefan HG (2009). Characteristics of Minnesota's cisco lakes. Project report no. 532. Minneapolis, MN, St. Anthony Falls Laboratory, University of Minnesota

Fang X, Alam SR, Jacobson P, Pereira D, Stefan HG (2010a). Simulations of water quality in cisco lakes in Minnesota. Project report no. 544. Minneapolis, St. Anthony Falls laboratory, University of Minnesota, Minneapolis

Fang X, Alam SR, Jiang LP, Jacobson P, Pereira D, Stefan HG (2010b). Simulations of cisco fish habitat in Minnesota lakes under future climate scenarios. Project report no. 547. St. Anthony Falls laboratory, University of Minnesota, Minneapoli

Fang X, Alam SR, Stefan HG, Jiang L, Jacobson PC, Pereira DL (2012a) Simulations of water quality and oxythermal cisco habitat in Minnesota lakes under past and future climate scenarios. Water Qual Res J Can 47(3–4):375–388

Fang X, Jiang L, Jacobson PC, Stefan HG, Alam SR, Pereira DL (2012b) Identifying cisco refuge lakes in Minnesota under future climate scenarios. Trans Am Fish Soc 141(6):1608–1621

Fang X, Jiang L, Jacobson PC, Fang NZ (2014) Simulation and validation of cisco habitat in Minnesota lakes using the lethal-niche-boundary curve. Br J Environ Clim Change 4 (4):444–470

Ford DE, Stefan HG (1980) Thermal prediction using internal energy model. J Hyd Div ASCE 106 (1):39–55

Frey DG (1955) Distributional ecology of the cisco, *Coregonus artedi*, in Indiana. Invest Indiana Lakes Streams 4:177–228

Fry EFJ (1971) The effect of environmental factors on the physiology of fish. Academic, New York

Gorham E, Boyce FM (1989) Influence of lake surface area and depth upon thermal stratification and the depth of the summer thermocline. J Great Lakes Res 15(2):233–245

Hasumi H, Emori S (eds) (2004) K-1 coupled GCM (MIROC) description. Center for Climate System Research, University of Tokyo, Tokyo

Heegaard E (2002) The outer border and central border for species-environmental relationships estimated by non-parametric generalised additive models. Ecol Model 157(2–3):131–139

Hokanson KE, Kleiner CF, Thorslund TW (1977) Effects of constant temperatures and diel temperatures fluctuations on specific growth and mortality rates and yield of juvenile rainbow trout, *Salmo gairdneri*. J Fish Res Board Can 34:639–648

Hondzo M, Stefan HG (1993a) Lake water temperature simulation model. J Hydraul Eng 119 (11):1251–1273

Hondzo M, Stefan HG (1993b) Regional water temperature characteristics of lakes subjected to climate change. Clim Change 24:187–211

Horne A, Goldman C (1994) Limnology. McGraw-Hill, New York

Hutchinson GE (1957) A treatise on limnology. Wiley, New York

IPCC (2007) Climate change 2007 – synthesis report. The fourth assessment report of the inter-governmental panel on climate change (IPCC). Cambridge University Press, Cambridge/New York

Jacobson PC, Jones TS, Rivers P, Pereira DL (2008) Field estimation of a lethal oxythermal niche boundary for adult ciscoes in Minnesota lakes. Trans Am Fish Soc 137(5):1464–1474

Jacobson PC, Stefan HG, Pereira DL (2010) Coldwater fish oxythermal habitat in Minnesota lakes: influence of total phosphorus, July air temperature, and relative depth. Can J Fish Aquat Sci 67 (12):2003–2013

Jacobson PC, Cross TK, Zandlo J, Carlson BN, Pereira DL (2012) The effects of climate change and eutrophication on cisco *Coregonus artedi* abundance in Minnesota lakes. Adv Limnol 63:417–427

Jacobson PC, Fang X, Stefan HG, Pereira DL (2013) Protecting cisco (*Coregonus artedi* Lesueur) oxythermal habitat from climate change: building resilience in deep lakes using a landscape approach. Adv Limnol 64:323–332

Jiang L, Fang X, Stefan HG, Jacobson PC, Pereira DL (2012) Oxythermal habitat parameters and identifying cisco refuge lakes in Minnesota under future climate scenarios using variable benchmark periods. Ecol Model 232:14–27

Kim S-J, Flato GM, Boer GJ, McFarlane NA (2002) A coupled climate model simulation of the last glacial maximum, part 1: transient multi-decadal response. Climate Dynam 19:515–537

Kim S-J, Flato GM, Boer GJ (2003) A coupled climate model simulation of the last glacial maximum, part 2: approach to equilibrium. Climate Dynam 20:635–661

Magnuson JJ, Crowder IB, Medvick PA (1979) Temperature as an ecological resource. Am Zool 19:331–343

Magnuson JJ, Meisner JD, Hill DK (1990) Potential changes in thermal habitat of Great Lakes fish after global climate warming. Trans Am Fish Soc 119(2):254–264

Marshall CT, Peters RH (1989) General patterns in the seasonal development of chlorophyll a for temperate lakes. Limnol Oceanogr 34(5):856–867

McCormick JH, Hokanson KE, Jones BR (1972) Effects of temperature on growth and survival of young brook trout (*Salvelinus fontinalis*). J Fish Res Board Can 29:1107–1112

McFarlane NA, Boer GJ, Blanchet J-P, Lazare M (1992) The Canadian Climate Centre second-generation general circulation model and its equilibrium climate. J Climate 5(10):1013–1044

Megard RO, Tonkyn DW, Senft WH (1984) Kinetics of oxygenic photosynthesis in planktonic algae. J Plankton Res 6(2):325–337

NRC (1983) Changing climate: report of the carbon dioxide assessment committee. National Research Council (NRC), National Academy Press, Washington, DC

Schindler DW, Bayley SE, Parker BR, Beaty KG, Cruikshank DR, Fee EJ, Schindler EU, Stainton MP (1996) The effects of climate warming on the properties of boreal lakes and streams at the experimental lakes area, northwestern Ontario. Limnol Oceanogr 41(5):1004–1017

Sharma S, Zanden MJV, Magnuson JJ, Lyons J (2011) Comparing climate change and species invasions as drivers of coldwater fish population extirpations. PLoS One 6(8), e22906

Smith EA, Kiesling RL, Galloway JM, Ziegeweid JR (2014) Water quality and algal community dynamics of three deepwater lakes in Minnesota utilizing CE-QUAL-W2 models, U.S. Geological Survey Scientific Investigations report 2014–5066, 73 p. doi:10.3133/sir20145066

Stefan HG, Fang X (1994a) Dissolved oxygen model for regional lake analysis. Ecol Model 71:37–68

Stefan HG, Fang X (1994b) Model simulations of dissolved oxygen characteristics of Minnesota lakes: past and future. Environ Manage 18(1):73–92

Stefan H, Ford DE (1975) Temperature dynamics in dimictic lakes. J Hydraul Div ASCE 101 (HY1):97–114

Stefan HG, Hondzo M, Sinokrot B, Fang X, Eaton JG, Goodno BE, Hokanson KEF, McCormick JH, O'Brien DG, Wisniewski JA (1992). A methodology to estimate global climate change impacts on lake and stream environmental conditions and fishery resources with application to Minnesota. Project report 323. St Anthony Falls Hydraulic Laboratory, University of Minnesota, Minneapolis, 141 pp

Stefan HG, Hondzo M, Fang X (1993) Lake water quality modeling for projected future climate scenarios. J Environ Qual 22(3):417–431

Stefan HG, Hondzo M, Eaton JG, McCormick JH (1995) Validation of a fish habitat model for lakes. Ecol Model 82(3):211–224

Stefan HG, Hondzo M, Fang X, Eaton JG, McCormick JH (1996) Simulated long-term temperature and dissolved oxygen characteristics of lakes in the north-central United States and associated fish habitat limits. Limnol Oceanogr 41(5):1124–1135

Stefan HG, Fang X, Eaton JG (2001) Simulated fish habitat changes in North American lakes in response to projected climate warming. Trans Am Fish Soc 130:459–477

US EPA (1976) Quality criteria for water. United States Environmental Protection Agency (US EPA), Washington, DC

US EPA (1986) Ambient water quality criteria for dissolved oxygen. United States Environmental Protection Agency (US EPA), Washington, DC. Report 440/5-86-003

Impact of Climate Change on Crop Production

Gamal El Afandi

Contents

G. El Afandi (✉)
Department of Agricultural and Environmental Sciences, College of Agriculture, Environment and Nutrition Sciences, Tuskegee University, Tuskegee, AL, USA

Department of Astronomy and Meteorology, Faculty of Science, Al Azhar University, Cairo, Egypt
e-mail: gelafandi@mytu.tuskegee.edu; gamalafandy@yahoo.com

W.-Y. Chen et al. (eds.), *Handbook of Climate Change Mitigation and Adaptation*,
DOI 10.1007/978-3-319-14409-2_64

Abstract

Changes in the atmospheric composition due to anthropogenic increase in greenhouse gases lead to changes in the radiative balance of the earth and consequent alterations in temperature, general wind circulation pattern, and weather patterns. The aftereffects of these changes are likely to manifest as major climate changes over the surface of the earth. Numerical models of the atmosphere have proved to be a very good tool in the assessment of the effect of increasing greenhouse gases on the earth's climate. These models predicted an increase in the earth's surface temperature during this century because of accumulation of greenhouse gases in the atmosphere. The effect of buildup of the sulfate aerosols in the atmosphere and its ability to increase the albedo of the atmospheric system, thereby cooling the atmosphere, has been recognized recently by the Intergovernmental Panel on Climate Change.

Agricultural activities are very sensitive to climate conditions. Agricultural decision-makers either are at the mercy of these natural factors or try to be benefit from them. The following decisions should not be made without knowing the elements of climate change.

Through the Decision Support System for Agrotechnology Transfer (DSSAT), the study for rice crop was carried out in order to define the impact of climate change on yield production in addition to flowering date, physiological maturity, and biomass at harvest.

The current work contains detailed analysis and investigation of possible changes up to 2017 (Egyptian strategy planning year). The results imply quiet remarkable changes in all agriculture parameters for this period, and sensitivity to climate variations was fairly detected.

Introduction

The Earth has warmed by 0.7 °C on average since 1900 (Jones and Moberg 2003). Most of the warming since 1950 is due to human activities that have increased greenhouse gases (IPCC 2001). There has been an increase in heat waves, fewer frosts, warming of the lower atmosphere and upper ocean, retreat of glaciers and sea ice, an average rise in global sea level of approximately 17 cm, and increased heavy rainfall in many regions (IPCC 2001; Alexander et al. 2006). Many species of plants and animals have changed their location or behavior in ways that provide further evidence of global warming (Hughes et al. 2003). To estimate future climate change, scientists have developed greenhouse gas and aerosol emission scenarios for the twenty-first century. These are not predictions of what will actually happen. They allow analysis of "what if?" questions based on various assumptions about human behavior, economic growth, and technological change (Church and White 2006). Computer models of the climate system are the best tools available for

simulating climate variability and change. These models include representations of the atmosphere, oceans, biosphere, and polar regions (Vinnikov et al. 2006). Confidence in the reliability of these models for climate projections has also improved (IPCC 2001), based on tests of the ability to simulate the present average climate, including the annual cycle of seasonal changes, year-to-year variability, extreme events such as storms and heat waves, climates from thousands of years ago, and observed climate trends in the recent past. The Intergovernmental Panel on Climate Change (IPCC) attributes most of the global warming observed over the last 50 years to greenhouse gases released by human activities. To estimate future climate change, the IPCC prepared 40 greenhouse gas and sulfate aerosol emission scenarios for the twenty- first century that combine a variety of assumptions about demographic, economic, and technological driving forces likely to influence such emissions in the future.

Crop simulation models can be used to assess the likely impact of climate change on grain yield and yield variability. These crop models must accurately predict several key characteristics over a wide range of climatic conditions, such as timing of flowering and physiological maturity, through correct descriptions of phenological responses to temperature and day length. Furthermore, accumulation of yield needs to be predicted by accurately predicting the development and loss of leaf area and, therefore, a crop's ability to intercept radiation, accumulate biomass, and partition it to harvestable parts such as grain.

Climate change urgently needs to be assessed at the level of the farm so that poor and vulnerable farmers dependent on agriculture can be appropriately targeted in research and development activities to alleviate poverty (Jones and Throntonb 2003). Assessing the possible impact of climate change on production risks is therefore necessary to help decision-makers and stakeholders to identify and implement suitable measures of adaptation (Torriani et al. 2007).

Climate Change Scenarios

In this work, the HadCM3 which is a coupled Atmosphere-Ocean General Circulation Model (AOGCM) developed at the Hadley Centre for Climate Prediction and Research (United Kingdom) was used (Gordon et al. 2000; Pope et al. 2000) and considered as significant and more sophisticated than earlier versions (Hulme and Jenkins 1998). This model has a spatial resolution of 2.50 × 3.75 (latitude by longitude). HadCM3 provides information about climate change over the entire world during the twenty-first century and presents information about three times slices: 2020s, 2050s, and 2080s. In order to provide information on possible changes in the world climate, the climate change models are forced to consider future scenarios. The IPCC (Nakicenovic et al. 2000) has developed emission scenarios known as Special Report on Emission Scenarios (SRES). The four

SRES scenarios combined two sets of divergent tendencies: one set varying between strong economic values and strong environmental values and the other set between increasing globalization and increasing regionalization (IPCC-TGCIA 1999). Two climate change scenarios were considered in this study: A2 and B2. These selected two scenarios consider a rise in global mean temperature by 3.09 °C and 2.16 °C, respectively; CO_2 concentration will be 834 and 601 ppm, respectively; and global mean sea level will rise by 62 and 52 cm, respectively. As the resolution of the model is too big, simple interpolation techniques of these percentages have been applied to fit the station site. Data were downloaded in GRIB format (GRIdded Binary is an international, public, binary format for the efficient storage of meteorological/oceanographic variables) from the Intergovernmental Panel on Climate Change (IPCC) Data Distribution Centre Web site. The GRBCONV program was used to convert the data files from GRIB format to the more conventional ASCII (American Standard Code for Information Interchange). The download site does not offer the option to subset the data based on an area of interest, so a custom program was used to extract the data for the region of interest. HadCM3 model (Hadley Centre for Climate Prediction and Research, UK) variables were monthly precipitation, solar radiation, and minimum and maximum temperatures. A2 and B2 climate change scenarios were used to run the CropSyst model to predict wheat yield for the chosen climate period. The simplest method of downscaling is to interpolate the change fields to the site or region of interest by using Cartesian geometry and geostatistics.

Crop Environment Resource Synthesis (CERES-RICE) Model

The CERES-RICE is one of the family members of the Decision Support System for Agrotechnology Transfer (DSSAT) system. The DSSAT system is a set of crop models, utility programs, and data sets for facilitating technology testing through simulation. The CERES-RICE simulates the growth, development, and yield of a component crop growing on a uniform area of land under prescribed or simulated management as well as the changes in soil water, carbon (C), and nitrate (N) that take place under the cropping system over time. The model considers the effects of weather, genetics, soil water, soil C and N, and management in single or multiple seasons and in crop rotations at any location where minimum inputs are provided. Hunt and Boote (1994) provided the minimum data sets for operation, calibration, and validation either of rice model, grown singly or in sequence.

Rice Production in Egypt

Rice production occurs mostly in the lower valley of the Nile River in about 10 % of the agricultural area of Egypt. Egypt is the largest rice producer in the Near East region (Sabaa and Sharaf 2000).

According to the Egyptian agriculture calendar, rice is a summer crop that is mainly grown in the Nile Delta. Rice areas have gradually increased since the construction of the countrywide irrigation network in the nineteenth century. Almost 50 % of the amount of water diverted to rice fields is consumed in terms of evapotranspiration, and the rest is lost via percolation (EWUP 1983).

Farmers like planting rice because it brings high profits. Since rice cannot be grown in all areas of Egypt, some areas have a rice surplus and others have a rice deficit. Today Egypt is a rice exporter too (FAO 2004).

Effect of Climate Change on Rice Production

The impact of climate change on rice yields differs from scientist to scientist because of the model and the scenario used. Leemans and Solomon (1993) predicted an 11 % increase using simple crop models. On the other hand, Rosenzweig and Parry (1994) found that rice yields would reduce by 2–4 %.

Boote et al. (1994), Horie et al. (1996, 1997), and Matthews et al. (1995) have assessed the impacts of high temperature and carbon dioxide on both growth and rice production. They have found that adoption of high-temperature-tolerant cultivars is considered as one of the most effective way to counteract a danger or threat of climate change to keep high productivity and stability of rice under the anticipated climate in temperate regions.

Conroy et al. (1994) proved that crop responses to a change in temperature depend on the temperature optima of photosynthesis, growth, and yield, all of which may differ. Baker and Allen (1993) found that small increase in temperature can dramatically reduce grain yield of rice. Increasing temperature reduced photosynthetic water use efficiency of rice canopy by increasing water loss (Jones et al. 1985; Baker and Allen 1993).

Kimball et al. (2002) found that rice (*Oryza sativa* L.) is generally less responsive to elevated CO_2 compared to other crop species, while variation exists in the degree of enhancement by elevated CO_2 among previous studies of rice, ranging from 4 % up to 44 % (Baker and Allen 1993; Nakagawa and Horie 2000; Kim et al. 2003).

Baker (2004) reported that at the 28 °C temperature treatment, CO_2 enrichment increased grain yield by 46–71 % among the three cultivars. Yamakawa et al. (2004) found that the dry matter of rice has increased by an elevated CO_2.

Data and Methodology

This experiment has been carried out at Sakha, latitude 31.12° and longitude 30.95°, Kafr el-Sheikh Governorate, Egypt, during two growing seasons of 1998 and 1999 and published by Sedeek (2001). Eleven rice cultivars (Giza 171, Giza 172, Giza 176, Giza 177, Giza 178, Giza 181, Sakha 101, Sakha 102, Sakha 103, Sakha 104, and Egyptian Yasmin) have been used in this experiment.

Table 1 Pedigree of the different cultivars of rice used in this study (Field Crops Research Institute, ARC, Giza, Egypt)

Cultivars	Pedigree
Giza 171	Nahda/Calady40
Giza 172	Nahda/Kinmaze
Giza 176	Calrose 76/Giza 172//GZ 242-5
Giza 177	Giza171/Yomji No. 1//Pi No. 4
Giza 178	Giza 175/Milyang 49
Giza 181	IR 24/IR 22
Sakha101	Giza 176/Milyang 79
Sakha102	GZ 4096-7-1/GZ 4120 – 205-2
Sakha103	GZ 4120 – 205- 2/Suweon 349
Sakha104	GZ 4096-8-1/GZ4100-9
Egyptian Yasmin	IR 262-43-8- 11/KDML 105

The genotypes used in this investigation have been obtained from the Agricultural Research Center (ARC), Giza, Egypt. Pedigree of genotypes of these rice cultivars has been shown in Table 1.

The minimum data set required to run the CERES-RICE model and validate its outputs has been obtained from the previously mentioned experiment in addition to other sites like Central Laboratory for Agricultural Climate (CLAC), ARC, Egypt. All these data have been converted to fit the CERES-RICE model format. These data are site weather data for the duration of the growing season, site soil data, and management and experimental data for the experiment.

The root mean square error (RMSE) is a good overall measure of model performance. The weighting of (prediction-observation) by its square tends to inflate RMSE, particularly when extreme values are present. With respect to a good model, the root mean square error should approach zero.

The mean bias (MB) is the degree of correspondence between the mean prediction and the mean observation. Lower numbers are the best, and values less than zero indicate underprediction.

The equations for RMSE, MB, and its percentages are given by Eqs. 1, 2, 3, and 4:

$$\mathrm{RMSE} = \left(\sum_{i=1}^{n} \left(X_p - X_o \right)^2 / n \right)^{0.5} \tag{1}$$

$$\mathrm{RMSE}\% = \left(\mathrm{RMSE} / \overline{X_o} \right)^{*} 100 \tag{2}$$

$$\mathrm{MB} = \sum_{i=1}^{n} X_p - X_o / n \tag{3}$$

$$\mathrm{MB}\% = \left(\mathrm{MB} / \overline{X_o} \right)^{*} 100 \tag{4}$$

where n is the number of observations, X_p and X_o are predicted and observed values, respectively, and $\overline{X_o}$ is the average of observed values.

Weather Data

The weather data includes latitude and longitude of the weather station, daily values of incoming solar radiation (MJ/m^2-day), maximum and minimum air temperature (°C), and rainfall (mm). The length of weather records for validation must, at minimum, cover the duration of the experiment and preferably should begin a few weeks before planting and continue a few weeks after harvest so that "what-if" type analyses may be performed.

Soil Data

Rice is cultivated and concentrated mainly in the Nile Delta region north of Egypt, because of its soil fertility and suitability. Soil data includes soil classification, surface slope, color, permeability, and drainage class.

Delta and the flood plain of the River Nile are stratified loams or clays (calcaric fluvisols) which represent the most essential soils in this area. They are moderately calcareous with pH values ranging from 8.1 to 8.3; in saline-sodic patches, the pH value is greater than 8.5. These soils have high potential especially for irrigated crops such as rice. In the narrow coastal belt of the Delta region about 40 km wide, very strongly, saline soils (solonchaks) are found. In the eastern Mediterranean coastal strip, other soils of semi-arid Mediterranean climates (xerosols and yermosols) occur and extending from Alexandria in the east to the Libyan borders in the west. They are deep clay soils near the northwestern tip of the Nile Delta and sandy, loamy, and gravelly in other parts. However, for the limitations of climate, these soils have a medium to high potential for rice. The rest of the country consists mainly of stony, mountainous, and sandy desert areas with little potential for improvement except as poor rangelands (FAO database).

Management and Experiment Data

Management data includes information on planting date, dates when soil conditions were measured prior to planting, planting density, row spacing, planting depth, crop variety, irrigation, and fertilizer practices.

The strategy of the Ministry of Agriculture in Egypt is to study the impacts of climate change on the potential crops such as rice and wheat until year 2017. Therefore, we will stress ourselves to study the impacts of climate change on rice from 2010 to 2017.

The data of climate change of two emission scenarios SRES A2 and SRES B2 of HadCM3 model outputs are used as inputs for CERES-RICE model. These two emission scenarios have been interpolated to apply for the desired station at Sakha. Interpolation belongs to a very useful branch of mathematics, called approximation theory. Statistical interpolation considers fields having random fluctuations.

Various interpolation methods have been invented to solve interpolation problems in practical applications.

The output of two emission scenarios SRES A2 and SRES B2 was monthly values, and the CERES-RICE model needs a daily climate data; therefore, we used the weather generator embedded in DSSAT 3.5 to generate daily climate data. Stochastic weather generators are widely used to generate synthetic weather data, which can be arbitrarily long for input into impact models, such as crop models and hydrological models that are used for making long-term risk assessments. These weather generators may be used for predicting crop yields based on seasonal climate forecasts (Hansen and Indeje 2004) and interpolating between stations, e. g., to create gridded daily meteorological time series data sets (e.g., Kittel et al. 2004).

Validation of CERES-RICE Model

The model has been validated at Sakha through flowering date (number of days from sowing to flowering), physiological maturity date (number of days from sowing to physiological maturity), biomass at harvest or biological yield (kg/ha), and grain yield (kg/ha).

Flowering Date

Table 2 shows comparison between measured and predicted flowering date for rice cultivars at Sakha and its percentage difference. The percentage difference is the difference between predicted and measured values divided by measured value and multiplied by 100.

One may notice that the measured and predicted values of the cultivar Giza 171 have the maximum flowering date compared to other rice cultivars. However,

Table 2 Comparison between measured and predicted flowering date for rice cultivars at Sakha

Cultivar	Measured	Predicted	Difference %
Giza 171	105	107	1.90
Giza 172	103	103	0.00
Giza 176	95	94	−1.05
Giza 177	81	80	−1.23
Giza 178	86	88	2.33
Giza 181	96	98	2.08
Sakha 101	89	88	−1.12
Sakha 102	79	79	0.00
Sakha 103	82	80	−2.44
Sakha 104	87	87	0.00
Egyptian Yasmin	96	95	−1.04
Average	90.82	90.82	0.00

the cultivar Sakha 102 has the minimum measured and predicted values for flowering date. The measured and predicted values of the cultivars Giza 172, Sakha 102, and Sakha 104 have equal values and their percentage difference equals zero. Therefore, the CERES-RICE model gave an equal prediction compared to the measured values for these cultivars. The percentage differences for the cultivars Giza 171, Giza 178, and Giza 181 are positive with maximum value for Giza 178. This means the predicted flowering date for these rice cultivars using the CERES-RICE model are overestimated but within the acceptable range. The percentage differences for the cultivars Giza 176, Giza 177, Sakha 101, Sakha 103, and Egyptian Yasmin are negative values; Sakha 103 has the maximum negative value, but all negative percentages are acceptable. Thus, the predicted flowering date using the CERES-RICE model is underprediction for these rice cultivars. The average measured and predicted flowering dates for all rice cultivars have the same value of 90.82, so their percentage difference equals zero. The root mean square error (RMSE) for all rice cultivars equals 1.35 with percentage of 1.48, and its mean bias (MB) and percentage equal zero. Therefore, the CERES-RICE model successes to predict the flowering date for all rice cultivars with very high performance.

Physiological Maturity

Table 3 gives comparison between measured and predicted physiological maturity for rice cultivars at Sakha and its percentage difference. From it, one can deduce that the measured and predicted physiological maturity date of the cultivar Giza 171 has the maximum value compared to other rice cultivars. However, the cultivar Sakha 102 has the minimum value for both measured and predicted physiological maturity date, while the cultivar Giza 181 has an equal value for measured and predicted, so the percentage difference equals zero; therefore, CERES-RICE model gave an equal prediction compared to measurements for this cultivar. The

Table 3 Comparison between measured and predicted physiological maturity for rice cultivars at Sakha

Cultivar	Measured	Predicted	Difference %
Giza 171	150	152	1.33
Giza 172	140	143	2.14
Giza 176	140	138	−1.43
Giza 177	115	117	1.74
Giza 178	125	128	2.40
Giza 181	140	140	0
Sakha 101	130	129	−0.77
Sakha 102	115	116	0.87
Sakha 103	110	113	2.73
Sakha 104	130	129	−0.77
Egyptian Yasmin	140	139	−0.71
Average	130.45	131.27	0.63

percentage differences for the cultivars Giza 171, Giza 172, Giza 177, Giza 178, Sakha 102, and Sakha 103 are positive values with maximum value for Sakha 103. Hence, the CERES-RICE model can overpredict the physiological maturity date for these rice cultivars but within the acceptable range. The percentage differences for the cultivars Giza 176, Sakha 101, Sakha 104, and Egyptian Yasmin are negative values. Giza 176 has the maximum negative value, but all negative percentages are acceptable. Therefore, the predicted physiological maturity date using the CERES-RICE model is underprediction for these rice cultivars.

The average measured and predicted physiological maturity dates for all rice cultivars are 130.45 and 131.27 and have close values to each other, so its percentage difference equals 0.63. The RMSE for all rice cultivars equals 1.98 with percentage of 1.52, MB equals 0.82, and its percentage equals 0.63. Therefore, the CERES-RICE model successes to predict the physiological maturity date for all rice cultivars with very high performance.

Biomass at Harvest

Table 4 reports a comparison between measured and predicted biomass at harvest for rice cultivars at Sakha. It is obvious that the Egyptian Yasmin has the maximum value of measured biomass at harvest compared to other rice cultivars. On the other hand, the maximum predicted one has been recorded for the Giza 172. The minimum measured biomass at harvest has been reported for Sakha 103, while the minimum predicted one has been reported for Sakha 102. At the same time, there are no cultivars having equal values for both measured and predicted biomass at harvest. The percentage differences for the cultivars Giza 172, Giza 176, Giza 177, Giza 181, and Sakha 103 are positive values with maximum value for Giza 181. Therefore, CERES-RICE model gave an overestimation prediction for biomass at harvest for these cultivars but within the acceptable range except for Giza 181. The percentage differences for Giza 171, Giza 178, Sakha 101, Sakha

Table 4 Comparison between measured and predicted biomass at harvest for rice cultivars at Sakha

Cultivar	Measured	Predicted	Difference %
Giza 171	15,000	14,607	−2.62
Giza 172	14,280	14,801	3.65
Giza 176	13,620	14,116	3.64
Giza 177	12,180	12,435	2.09
Giza 178	13,560	13,414	−1.08
Giza 181	12,000	14,275	18.96
Sakha 101	14,220	13,749	−3.31
Sakha 102	14,220	11,956	−15.92
Sakha 103	12,000	12,308	2.57
Sakha 104	16,800	13,494	−19.68
Egyptian Yasmin	15,300	14,316	−6.43
Average	13,925.45	13,588.27	−2.42

102, Sakha 104, and Egyptian Yasmin are negative values. At the same time, Sakha 104 has the maximum negative value; all negative percentages are acceptable except for Sakha 104 and Sakha 102. It can be deduced that the CERES-RICE model gave an underestimated prediction for biomass at harvest for these cultivars.

The average measured and predicted biomass at harvest for all rice cultivars are 13925.45 and 13588.27, respectively, so its percentage difference equals −2.42. The RMSE for all rice cultivars equals 1454.59 with percentage of 10.45 and MB equals −337.18 with percentage equals −2.42. Therefore, the CERES-RICE model successes to predict biomass at harvest for all rice cultivars except for some of them with very high performance.

Grain Yield

Table 5 gives a comparison between measured and predicted grain yield for rice cultivars at Sakha.

It is obvious that Sakha 101 has the maximum measured grain yield compared to other rice cultivars, while the maximum predicted one has been reported for Giza 178. On the other hand, Giza 171 has the minimum measured grain yield but the minimum predicted value has been reported for Giza 172. In addition, comparison has revealed that there are no equal values for the measured and predicted grain yield for all cultivars. The percentage differences for the cultivars Giza 171, Giza 181, Sakha 102, Sakha 103, and Sakha 104 are positive values with maximum value for Sakha 102. This means the predicted grain yield using the CERES-RICE model is overestimated for these cultivars but within the acceptable range except for Sakha 102. At the same time, the percentage differences for the cultivars Giza 172, Giza 176, Giza 177, Giza 178, Sakha 101, and Egyptian Yasmin are negative. Sakha 101 has the maximum negative value, but all negative percentages are acceptable with some exception for some cultivars. Therefore, the predicted grain yield values

Table 5 Comparison between measured and predicted grain yield for rice cultivars at Sakha

Cultivar	Measured	Predicted	Difference %
Giza 171	7500	7686	2.48
Giza 172	8000	7604	−4.95
Giza 176	9000	8653	−3.86
Giza 177	7700	7665	−0.45
Giza 178	9900	9480	−4.24
Giza 181	8500	8647	1.73
Sakha 101	10,000	9288	−7.12
Sakha 102	7600	8260	8.68
Sakha 103	8100	8177	0.95
Sakha 104	8800	8949	1.69
Egyptian Yasmin	8500	8029	−5.54
Average	8509.09	8403.45	−1.24

using the CERES-RICE model were underestimated for the previous cultivars. The average measured and predicted grain yields for all rice cultivars are 8509.09 and 8403.45, respectively, so its percentage difference equals −1.24. The RMSE for all rice cultivars equals 393.54 with percentage of 4.62, and MB equals −105.64 with percentage equals −1.24. Therefore, the CERES-RICE model successes to predict grain yield for all rice cultivars with very high performance except for some cultivars.

From all previous discussions, one may conclude that CERES-RICE model has high performance percentage to predict flowering date and physiological maturity, while this performance decreases a little bit for grain yield and biomass at harvest predictions.

Simulation of the Impact of Climate Change on Rice

The impact of climate change on rice at Sakha will be measured through flowering date, physiological maturity, biomass at harvest or biological yield (kg/ha), and grain yield (kg/ha).

Flowering Date

Figure 1 report the comparison between measured and predicted flowering date using SRES A2 and SRES B2 emission scenarios of HadCM3. In addition, Table 6 represents the percentages of root mean square error and mean bias for rice cultivars at Sakha for the period 2010 to 2017.

It is noticed that there is a small difference between the two emission scenarios in predicting flowering date. In most rice cultivars, the predicted flowering date by SRES A2 scenario is greater than the one predicted by SRES B2 except for a few years. However, the predicted values by the two emission scenarios are small compared to the measured one. This is approximately true for all rice cultivars in all years except for Giza 171 and Giza 178 predicted by SRES A2 in 2014. Hence, it is easy to conclude that the flowering date of all rice cultivars will be smaller than the measured one during the period 2010 to 2017. From Table 6 one may notice that the maximum percentage ratio of root mean square error and the maximum negative percentage ratio of mean bias have been recorded for Sakha 102, while the minimum percentage ratio of root mean square error and the minimum negative percentage ratio of mean bias have been registered for the cultivar Giza 178. Therefore, the maximum decrease in flowering date will occur for Sakha 102 and the minimum decrease will happen in Giza 178.

Generally, one may conclude that the flowering date of all rice cultivars will be decreased compared to the measured one during the period 2010 to 2017 as a whole.

Physiological Maturity

Figure 2 show the comparison between measured and predicted physiological maturity by using SRES A2 and SRES B2 emission scenarios of HadCM3. In addition, Table 7 reports percentages of root mean square error and mean bias for rice cultivars at Sakha for the period 2010–2017.

It is noticed that there is a small difference between the two emission scenarios for predicting physiological maturity in most rice cultivars. At the same time, the

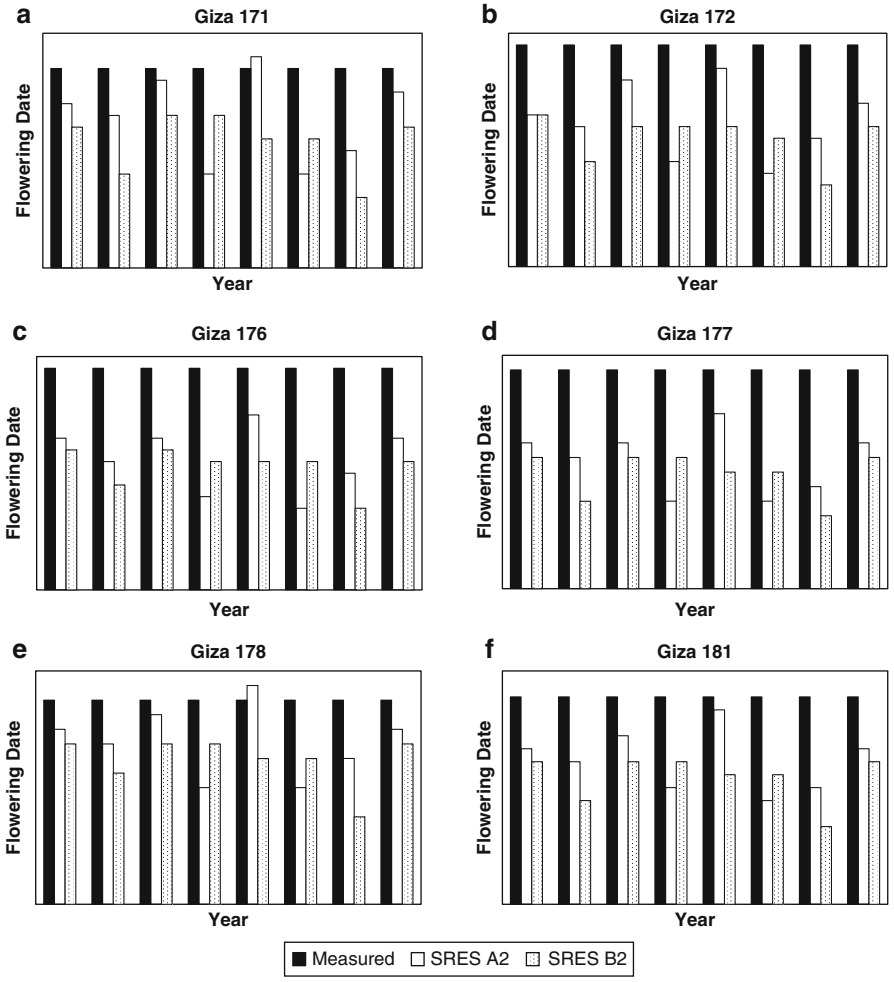

Fig. 1 (continued)

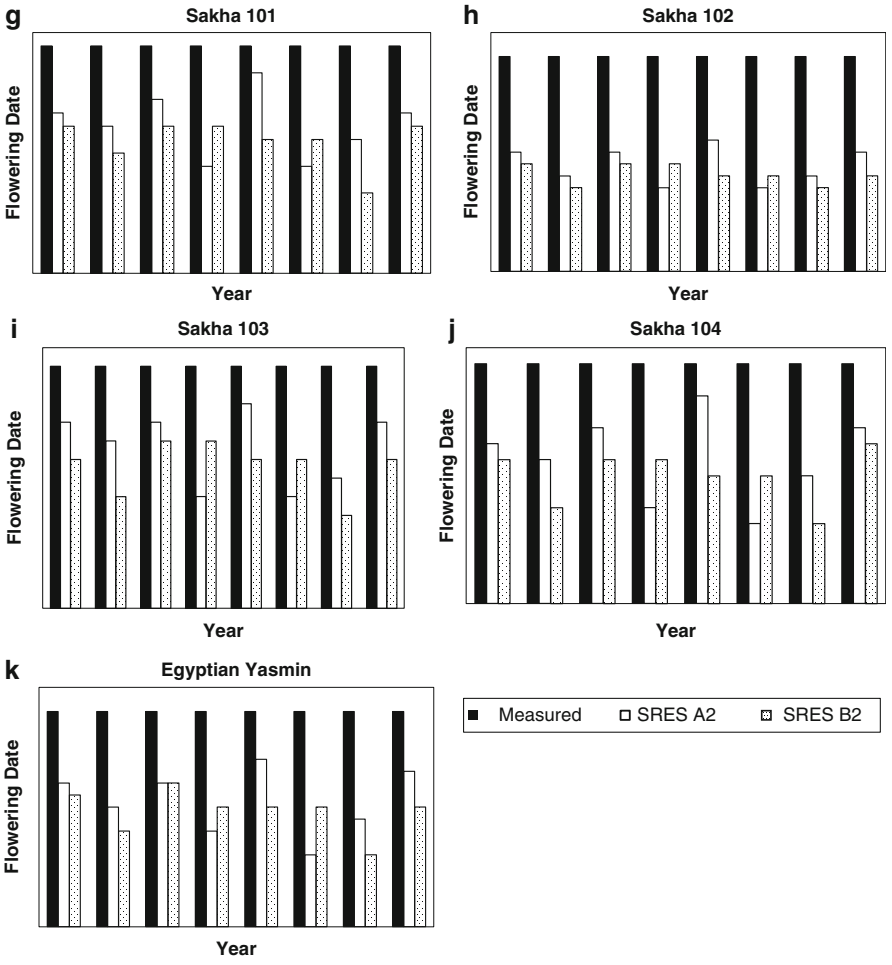

Fig. 1 (**a**–**k**) Comparison between measured and predicted flowering date by using SRES A2 and SRES B2 emission scenarios for rice cultivars at Sakha

values predicted by SRES A2 scenario are greater than the one predicted by SRES B2 except for a few years. In addition, the predicted values by the two emission scenarios for physiological maturity are small compared to the measured one for all rice cultivars in all years without any exception. Hence, one can say that the physiological maturity of all rice cultivars will be decreased compared to the measured one during the period 2010 to 2017. It can be noticed in Table 7 that the cultivar Giza 176 has the maximum percentage ratio of root mean square error and the maximum negative percentage ratio mean bias in the two scenarios, while the minimum percentage ratio of root mean square error and the minimum negative percentage ratio mean bias have been recorded for the Sakha 103. Hence, the

Table 6 Comparison between measured and predicted flowering date and percentages of root mean square error and mean bias by using SRES A2 and SRES B2 emission scenarios for rice cultivars at Sakha

Cultivar	Measured	SRES A2	SRES B2
Giza 171	105	101	99
Giza 172	103	97	96
Giza 176	95	87	87
Giza 177	81	75	74
Giza 178	86	83	81
Giza 181	96	91	90
Sakha 101	89	83	82
Sakha 102	82	73	72
Sakha 103	79	75	74
Sakha 104	87	81	80
Egyptian Yasmin	96	89	88

	RMSE %		MB %	
Cultivar	SRES A2	SRES B2	SRES A2	SRES B2
Giza 171	5.24	6.35	−4.05	−5.95
Giza 172	6.93	7.98	−6.31	−7.77
Giza 176	8.60	9.10	−8.16	−8.95
Giza 177	8.12	8.98	−7.72	−7.13
Giza 178	4.25	5.15	−3.34	−4.80
Giza 181	5.57	6.75	−5.08	−6.51
Sakha 101	7.07	8.21	−6.60	−8.01
Sakha 102	11.27	12.08	−11.13	−12.04
Sakha 103	6.02	7.01	−5.54	−6.80
Sakha 104	7.35	8.25	−6.75	−8.05
Egyptian Yasmin	8.25	8.91	−7.81	−8.72

maximum decrease in physiological maturity will occur for the cultivar Giza 176 and the minimum decrease will be for the cultivar Sakha 103. It is obvious that the physiological maturity of all rice cultivars will be decreased compared to the measured one during the period 2010 to 2017.

Biomass at Harvest

Figure 3 show a comparison between measured and predicted biomass at harvest by using SRES A2 and SRES B2 emission scenarios of HadCM3. In addition, Table 8 reports the percentages of root mean square error and mean bias for rice cultivars at Sakha for the period 2010–2017.

One may notice that there is a noticeable difference between the predicted biomass at harvest using the two emission scenarios. This difference is not small

compared to the prediction of both flowering date and physiological maturity. At the same time, not in most rice cultivars, the values predicted by SRES A2 scenario are greater than the ones predicted by SRES B2 except for a few years.

In addition, the predicted biomass at harvest using the two emission scenarios is smaller than the measured one for all rice cultivars except for Giza 172, Giza 176, and Giza 181. Hence, the biomass at harvest of rice cultivars, except for the previous three cultivars, will decrease compared to the measured one during the period of study. Table 8 showed that Sakha 104 has the maximum percentage ratio of root mean square error and maximum negative percentage ratio of mean bias in the two scenarios.

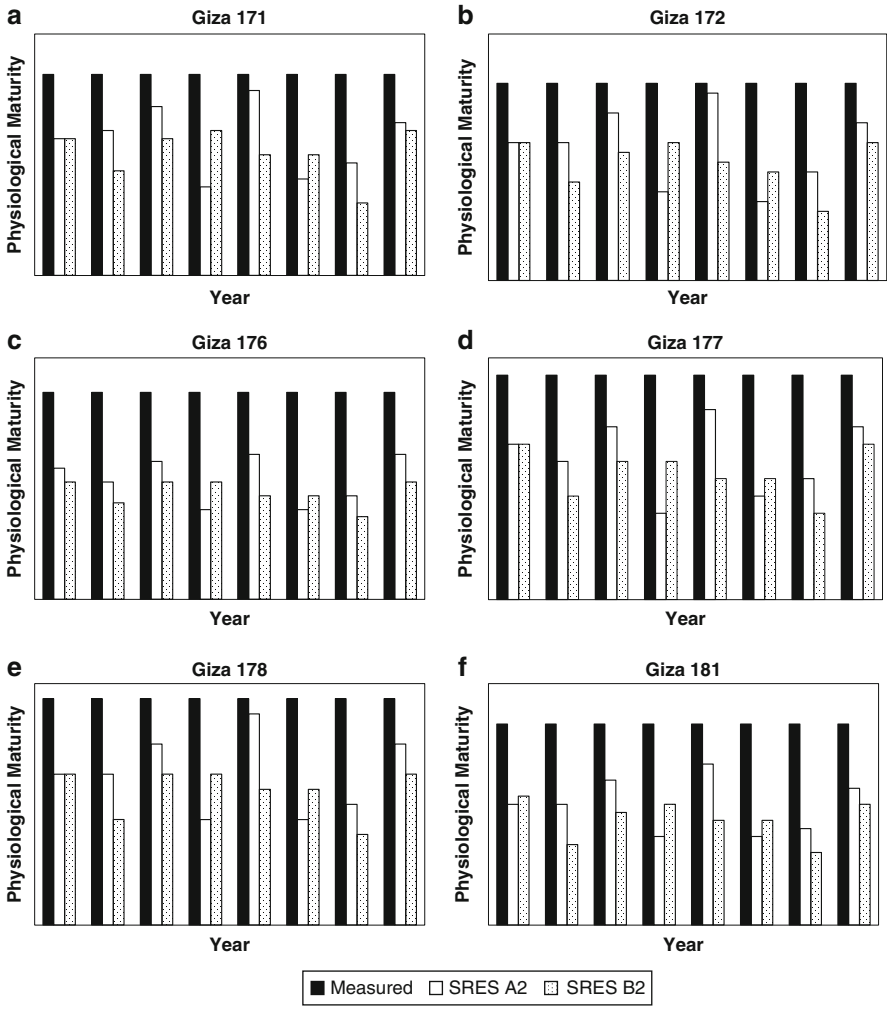

Fig. 2 (continued)

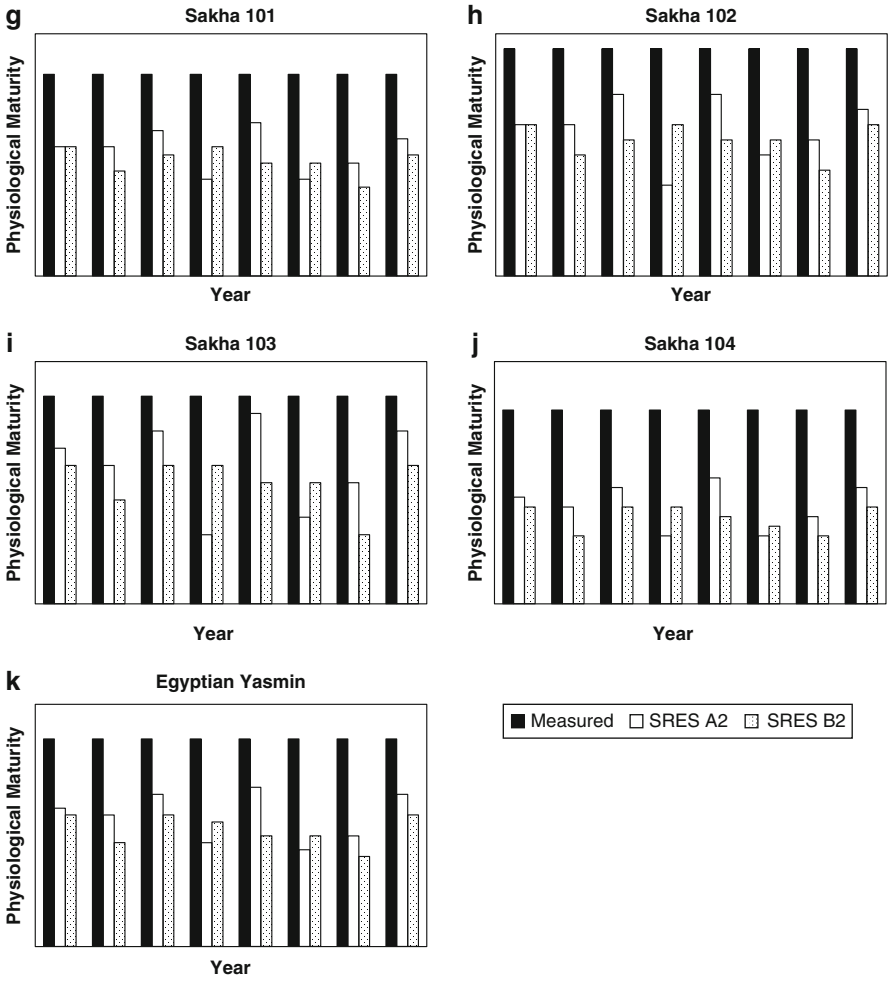

Fig. 2 (**a**–**k**) Comparison between measured and predicted physiological maturity by using SRES A2 and SRES B2 emission scenarios for rice cultivars at Sakha

However, the minimum percentage ratio of root mean square error is reported for Giza 172 and the minimum negative percentage ratio mean bias is for Giza 171. Therefore, the maximum decrease in biomass at harvest will be for the cultivar Sakha 104, while the minimum increase will be for the cultivars Giza 172, Giza 176, and Giza 181 and the minimum decrease will be for the cultivar Giza 171.

It is obvious that the biomass at harvest for all rice cultivars will be decreased comparable to the measured one during the period 2010–2017 except for Giza 172, Giza 176, and Giza 181.

Table 7 Comparison between measured and predicted physiological maturity and percentages of root mean square error and mean bias by using SRES A2 and SRES B2 emission scenarios for rice cultivars at Sakha

Cultivar	Measured	SRES A2	SRES B2
Giza 171	150	142	140
Giza 172	140	134	132
Giza 176	140	127	126
Giza 177	115	110	109
Giza 178	125	120	119
Giza 181	140	130	128
Sakha 101	130	121	119
Sakha 102	115	110	109
Sakha 103	110	106	105
Sakha 104	130	120	119
Egyptian Yasmin	140	129	127

	RMSE %		MB %	
Cultivar	SRES A2	SRES B2	SRES A2	SRES B2
Giza 171	6.03	6.77	−5.42	−6.50
Giza 172	5.32	6.03	−4.64	−5.80
Giza 176	9.30	10.43	−9.02	−10.36
Giza 177	4.48	5.02	−4.13	−4.89
Giza 178	4.44	5.04	−4.00	−4.90
Giza 181	7.57	8.64	−7.23	−8.48
Sakha 101	7.55	8.36	−7.31	−8.27
Sakha 102	4.86	5.29	−4.57	−5.22
Sakha 103	4.22	4.70	−3.64	−4.55
Sakha 104	7.77	8.61	−7.60	−8.56
Egyptian Yasmin	8.28	9.49	−7.95	−9.38

Grain Yield

Figure 4 show the comparison between measured and predicted grain yield using SRES A2 and SRES B2 emission scenarios of HadCM3. In addition, Table 9 reports the percentages of root mean square error and mean bias for rice cultivars at Sakha for the period 2010–2017.

One may notice that there is a small difference between the two emission scenarios in predicting grain yield. At the same time, the predicted values using SRES A2 scenario were greater than the one using SRES B2 except for a few years.

The predicted grain yield using the two emission scenarios was smaller than the measured ones for all rice cultivars in all years, except for both Giza 171 and Sakha 102. One may notice from Table 9 that the cultivar Sakha 101 has the maximum percentage ratio of root mean square error and maximum negative percentage ratio of mean bias in both scenarios. In addition, the minimum percentage ratio of root

mean square error is reported for cultivar Giza 171, while the minimum negative percentage ratio of mean bias is registered for Giza 181. Therefore, the maximum decrease in grain yield will be for the cultivar Sakha 101 and the minimum increase will be for the cultivars Giza 171 and Sakha 102. However, the minimum decrease will be for the cultivar Giza 181 according to SRES B2, but it increased in SERES A2. In addition, most of the decrease in predicted grain yield using SRES B2 is greater than SRES A2.

It is obvious that the grain yield for all rice cultivars will be decreased compared to the measured one during the period 2010–2017 except for the cultivars Giza 171, Sakha 102, and Giza 181.

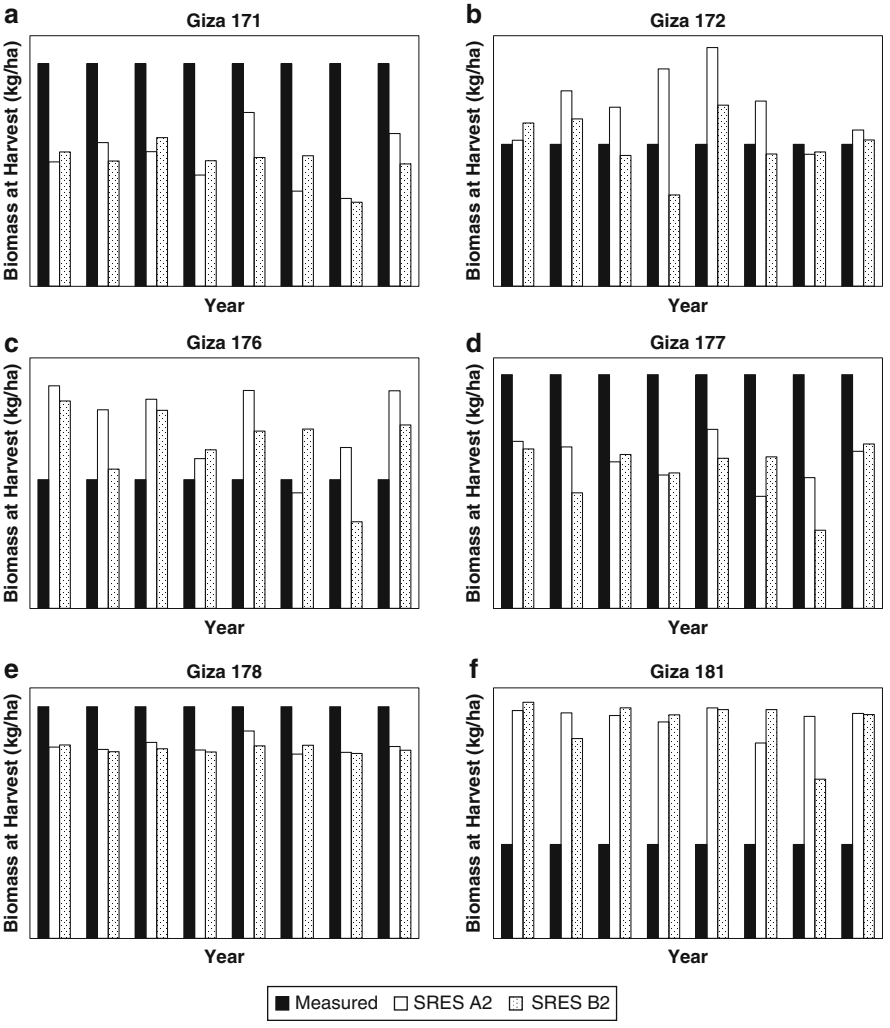

Fig. 3 (continued)

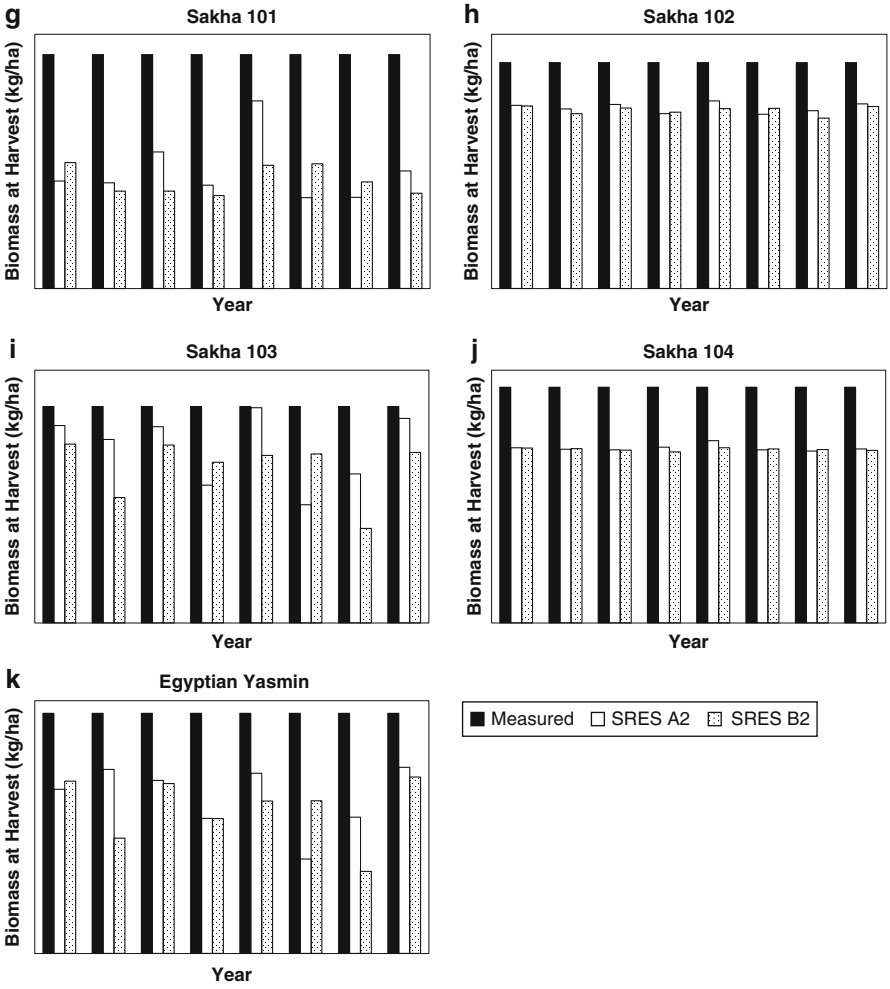

Fig. 3 (**a**–**k**) Comparison between measured and predicted biomass at harvest by using SRES A2 and SRES B2 emission scenarios for rice cultivars at Sakha

Future Directions

- The validation of the model has proved its high accuracy in prediction of rice parameters compared to measurements.
- The CERES-RICE model has high-performance percentage to predict both flowering and physiological maturity dates. However, this performance slightly decreases in the prediction of grain yield and biomass at harvest.

Table 8 Comparison between measured and predicted biomass at harvest and percentages of root mean square error, mean bias by using SRES A2 and SRES B2 emission scenarios for rice cultivars at Sakha

Cultivar	Measured	SRES A2	SRES B2
Giza 171	15,000	14,319	14,298
Giza 172	14,280	14,469	14,287
Giza 176	12,800	13,607	13,323
Giza 177	12,800	11,779	11,659
Giza 178	14,800	12,255	12,099
Giza 181	12,000	14,026	13,955
Sakha 101	14,220	12,619	12,487
Sakha 102	14,220	11,380	11,226
Sakha 103	12,000	11,427	11,154
Sakha 104	16,800	12,460	12,358
Egyptian Yasmin	15,300	13,981	13,786

	RMSE %		MB %	
Cultivar	SRES A2	SRES B2	SRES A2	SRES B2
Giza 171	4.72	4.76	−4.54	−4.68
Giza 172	1.74	0.88	1.32	0.05
Giza 176	7.49	5.67	6.31	4.09
Giza 177	8.21	9.26	−7.98	−8.91
Giza 178	17.44	18.30	−17.20	−18.25
Giza 181	16.94	16.60	16.89	16.29
Sakha 101	11.62	12.26	−11.26	−12.19
Sakha 102	20.07	21.13	−19.97	−21.06
Sakha 103	6.12	7.75	−4.77	−7.05
Sakha 104	25.86	26.44	−25.83	−26.44
Egyptian Yasmin	9.17	10.38	−8.62	−9.89

- The predicted flowering date, physiological maturity, and grain yield using SRES A2 scenario are greater than the predicted using SRES B2 except for a few years. However, in some rice cultivars, predicted biomass at harvest by SRES A2 is greater than the predicted by SRES B2 except for a few years.
- The predicted flowering date, physiological maturity, biomass at harvest, and grain yield for all rice cultivars decrease comparable to the measured ones during the period 2010–2017. However, the biomass at harvest and grain yield decrease greatly compared to both flowering date and physiological maturity.
- The results of this study indicate that the CERES-RICE model performance was very good under the Egyptian conditions. Therefore, the model could accurately be used in climate change impacts on rice.
- One may conclude that CERES-RICE model will be a very vital tool for farmers to avoid rice loss due to climate change.

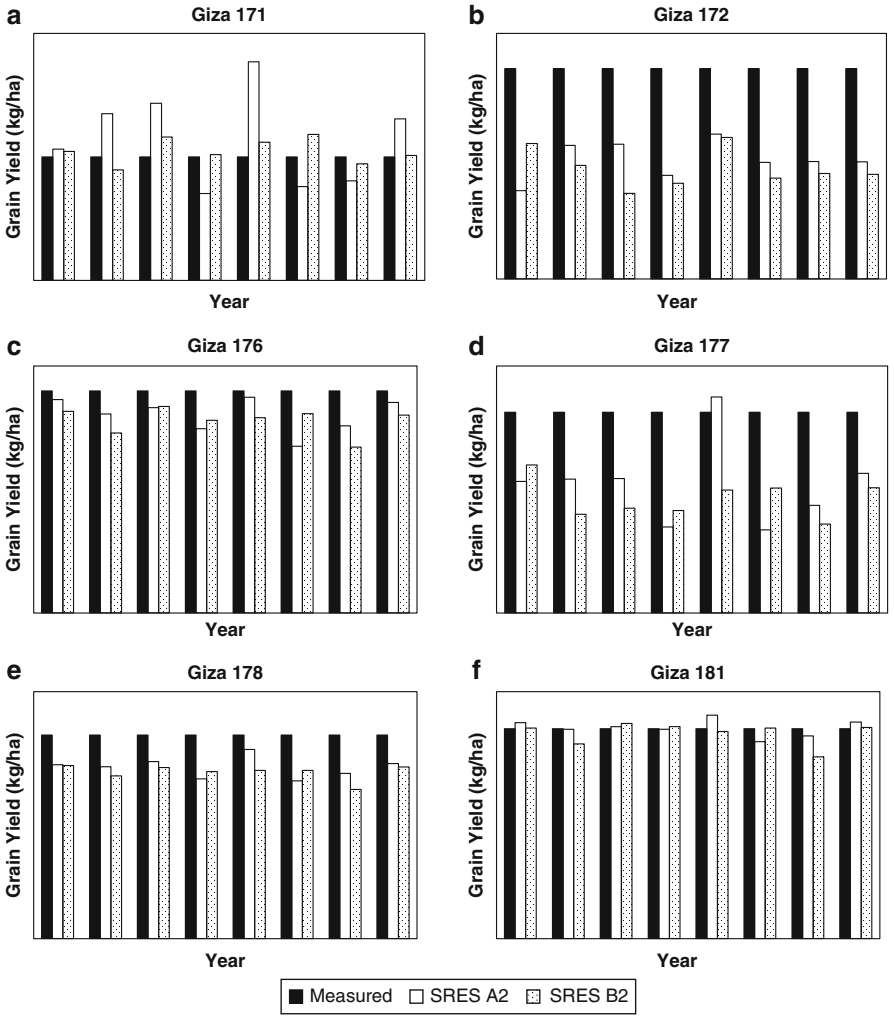

Fig. 4 (continued)

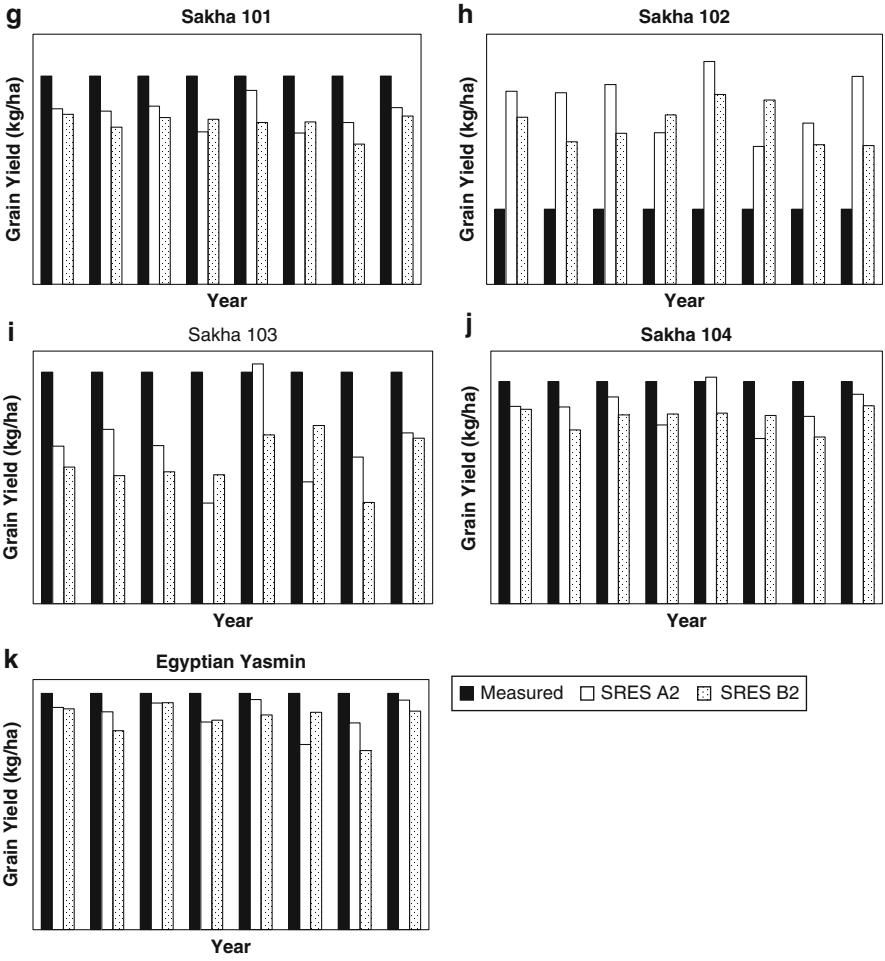

Fig. 4 (**a**–**k**) Comparison between measured and predicted grain yield by using SRES A2 and SRES B2 emission scenarios for rice cultivars at Sakha

Table 9 Comparison between measured and predicted grain yield and percentages of root mean square error and mean bias by using SRES A2 and SRES B2 emission scenarios for rice cultivars at Sakha

Cultivar	Measured	SRES A2	SRES B2
Giza 171	7500	7575	7524
Giza 172	8000	7482	7429
Giza 176	9000	8012	7793
Giza 177	7600	7236	7141
Giza 178	9900	8324	8085
Giza 181	8500	8540	8317
Sakha 101	10,000	8179	7750
Sakha 102	7600	8033	7941
Sakha 103	8100	7754	7677
Sakha 104	8800	7763	7378
Egyptian Yasmin	8500	7770	7586

	RMSE %		MB %	
Cultivar	SRES A2	SRES B2	SRES A2	SRES B2
Giza 171	2.57	0.71	1.00	0.31
Giza 172	6.59	7.26	−6.48	−7.14
Giza 176	13.12	14.52	−10.98	−13.41
Giza 177	6.86	7.41	−6.02	−7.25
Giza 178	16.59	18.67	−15.92	−18.34
Giza 181	3.74	5.51	0.46	−2.16
Sakha 101	19.32	22.90	−18.21	−22.5
Sakha 102	5.88	4.60	5.69	4.49
Sakha 103	4.83	5.42	−4.27	−5.23
Sakha 104	14.26	16.77	−11.78	−16.16
Egyptian Yasmin	10.52	12.34	−8.59	−10.76

References

Alexander L, Zhang X, Peterson TC (2006) Global observed changes in daily climate extremes of temperature and precipitation. J Geophys Res 111:D05109

Baker JT (2004) Yield responses of southern US rice cultivars to CO_2 and temperature. Agric For Meteorol 122:129–137

Baker JT, Allen LH Jr (1993) Effects of CO_2 and temperature on rice: a summary of five growing seasons. J Agric Meteorol 48:575–582

Boote KJ, Pickering NB, Baker JT, Allen LH Jr (1994) Modeling leaf and canopy photosynthesis of rice in response to carbon dioxide and temperature. Int Rice Res Notes 19:47–48

Church JA, White NJ (2006) A 20th century acceleration in global sea-level rise. Geophys Res Lett 33:L01602

Conroy JP, Seneweera S, Basra AS, Rogers G, Nissen-Wooller B (1994) Influence of rising atmospheric CO_2 concentrations and temperature on growth, yield and grain quality of cereal crops. Aust J Plant Physiol 21:741–758

EWUP (1983) Irrigation and production of rice in Abu Raya, Kafr El Sheikh Governorate. Technical report no. 9, NWRC, Delta Barrages, Cairo

FAO (2004) www.fao.org/rice2004/en/p4.htm. FAO, Egypt

Gordon C, Cooper C, Senior CA, Banks H, Gregory JM, Johns TC et al (2000) The simulation of sea surface temperature, sea ice extents and ocean heat transports in a version of the Hadley Centre coupled model without flux adjustments. Clim Dyn 16:147–168

Hansen JW, Indeje M (2004) Linking dynamic seasonal climate forecasts with crop simulation for maize yield prediction in semi-arid Kenya. Agric For Meteorol 125:143–157

Horie T, Matsui T, Nakagawa H, Omasa K (1996) Effect of elevated CO_2 and global climate change on rice yield in Japan. In: Omasa K, Kai K, Toda H, Uchijima Z, Yoshino M (eds) Climate change and plants in East Asia. Springer, Tokyo, pp 39–56

Horie T, Centeno HGS, Nakagawa H, Matsui T (1997) Effect of elevated carbon dioxide and climate change on rice production in East and Southeast Asia. In: Oshima Y (ed) Proceedings of the international scientific symposium on Asian Paddy Fields. College of Agriculture, University of Saskatchewan, Canada, pp 49–58

Hughes TP, Baird AH, Bellwood DR, Card M, Connolly SR, Folke C, Grosberg R, Hoegh-Guldberg O, Jackson JBC, Kleypas J, Lough JM, Marshall P, Nystrom M, Palumbi SR, Pandolfi JM, Rosen B, Roughgarden J (2003) Climate change, human pacts, and the resilience of coral reefs. Science 301:929–933

Hulme M, Jenkins GJ (1998) Climate change scenarios for the UK: scientific report. UKCIP technical report no 1. Climate Research Unit, Norwich

Hunt LA, Boote KJ (1994) Data for model operation, calibration, and validation. In: Tsuji GY, Hoogenboom G, Thornton PK (eds) IBSNAT: a system approach to research and decision-making. University of Hawaii, Honolulu

IPCC (2001) Summary for policymakers. In: Houghton JT, Ding Y, Griggs DJ, Noguer M, Van Der Linden PJ, Xioaosu D (eds) Climate change 2001: the scientific basis. Contribution of working group I to the 3rd assessment report of the Intergovernmental Panel on Climate Change. Cambridge University Press, Cambridge, 944 pp

IPCC-TGCIA (1999) Guidelines on the use of scenario data for climate impact and adaptation assessment. Version 1. 69 p. Prepared by Carter TR, Hulme M, and Lal M. Intergovernmental Panel on Climate Change (IPCC), task Group on Scenarios for Climate Impact Assessment. Available at http://ipcc-ddc.cru.uea.ac.uk/guidelines/guidance.pdf. Accessed June 2009

Jones PD, Moberg A (2003) Hemispheric and large-scale surface air temperature variations: an extensive revision and an update to 2001. J Clim 16:206–223

Jones PG, Thorntonb PK (2003) The potential impacts of climate change on maize production in Africa and Latin America in 2055. Global Environ Chang 13:51–59

Jones P, Allen LH Jr, Jones JW (1985) Responses of soybean canopy photosynthesis and transpiration to whole-day temperature changes in different CO_2 environments. Agron J 77:242–249

Kim HY, Lieffering M, Kobayashi K, Okada M, Miura S (2003) Seasonal changes in the effects of elevated CO_2 on rice at three levels of nitrogen supply: a free air CO_2 enrichment (FACE) experiment. Glob Chang Biol 9:826–837

Kimball BA, Kobayashi K, Bindi M (2002) Responses of agricultural crops to free-air CO_2 enrichment. Adv Agron 77:293–368

Kittel TGF, Rosenbloom NA, Royle JA, Daly C, Gibson WP, Fisher HH, Thornton P, Yates DN, Aulenbach S, Kaufman C, McKeown R, Bachelet D, Schimel DS (2004) VEMAP phase 2 bioclimatic database. I: Gridded historical (20th century) climate for modeling ecosystem dynamics across the conterminous USA. Clim Res 27:151–170

Leemans R, Solomon AM (1993) Modeling the potential yield and distribution of earth's crops under a warmed climate. Clim Res 3:79–96

Matthews RB, Kropff MJ, Bachelet D, van Laar HH (1995) Modeling the impact of climate change on rice production in Asia. CAB International, Wallingford, 289 p

Nakagawa H, Horie T (2000) Rice responses to elevated CO_2 and temperature. Glob Environ Res 3:101–113

Nakicenovic N, Alcamo J, Davis G, de Vries B, Fenhann J, Gaffin S et al (2000) Intergovernmental Panel on Climate Change (IPCC) special report on emission scenarios. Cambridge University Press, Cambridge, UK, 599 p

Pope VD, Gallani ML, Rowntree PR, Stratton RA (2000) The impact of new physical parameterization in the Hadley Centre Climate Model-HadCM3. Clim Dyn 16:123–146

Rosenzweig C, Parry ML (1994) Potential impact of climate change on world food supply. Nature 367:133–138

Sabaa MF, Sharaf MF (2000) Egyptian policies for rice development. Cah Options Mediterraneennes 40:25–36

Sedeek SM (2001) Studies of morphological and agronomical characteristics of some early varieties and lines of rice. MSc thesis, Faculty of Agriculture, Tanta University, Tanta

Torriani DS, Calanca P, Schmid S, Beniston M, Fuhrer J (2007) Potential effects of changes in mean climate and climate variability on the yield of winter and spring crops in Switzerland. Clim Res 34:59–69

Vinnikov KY, Grody NC, Robock A, Stouffer RJ, Jones PD, Goldberg MD (2006) Temperature trends at the surface and in the troposphere. J Geophys Res 111:D03106

Yamakawa Y, Saigusa M, Okada M, Kobayashi K (2004) Nutrient uptake by rice and soil solution composition under atmospheric CO_2 enrichment. Plant Soil 259:367–372

Climate Change Impacts, Vulnerability, and Adaptation in East Africa (EA) and South America (SA)

Anne Nyatichi Omambia, Ceven Shemsanga, and Ivonne Andrea Sanchez Hernandez

Contents

A.N. Omambia (✉)
National Environment Management Authority, Nairobi, Kenya
e-mail: tichiomambia@gmail.com

C. Shemsanga
Department of Water and Environmental Sciences and Engineering, Nelson Mandela Institution of Science and Technology-Tengeru, Tengeru, Arusha, Tanzania

Department of Environmental Engineering and Management, University Dodoma, Dodoma, Tanzania
e-mail: 7ceven@gmail.com

I.A. Sanchez Hernandez
Sustainability Development, AB Origen Fundación, Armenia, Quindio, Colombia
e-mail: colpacifico@hotmail.com

W.-Y. Chen et al. (eds.), *Handbook of Climate Change Mitigation and Adaptation*,
DOI 10.1007/978-3-319-14409-2_17

Abstract

In recent decades, global climate change has continued to cause devastating impacts to various places on Earth. Geographic and socioeconomic characteristics in East Africa (EA) and South America (SA) make the regions among the most vulnerable to the current temperature variations attracting several studies with wider implications. Presently, in these two regions, remarkable evidence of climate change includes repeated droughts and increase in drylands affecting water and food availability for humans, livestock, and wildlife (EA); intensification of climate-sensitive diseases; sea level rise; fast retreat of glaciers on Mount Kilimanjaro in Tanzania, Mount Kenya in Kenya, and Andean Mountains of South America; change in the rainfall patterns in the Amazon forests and in the whole of EA; and increasing of the frequency and intensity of the El Niño and La Niña phenomenon in the South Pacific that affect both EA and SA, among others. Although these two regions are not major contributors of greenhouse gases (GHGs), the poor conservation of strategic ecosystems through deforestation of the Amazon forests in SA and various forests in EA coupled with intensification of agriculture, land degradation, rapid rates of urbanization, and industrialization all driven by rapid population increase are putting a strain on valuable natural resources whose conservation would be critical in mitigating climate change. Adaptation measures have been constrained by climate change impacts. In both regions, poverty is widespread and climate change impacts have jeopardized most poverty alleviation initiatives including realization of some of the Millennium Development Goals (MDGs). Moreover, both regions have a strong dependency on rain-fed agriculture for economic development with hydroelectricity and biomass as main sources of energy. Consequently, adaptation measures are required for all the sectors but especially in agriculture, health, and energy where the loss of soil productivity, increasing spread of climate-sensitive diseases, and reduction of water and energy source supply are already threatening the social and economic security of both regions. Both regions have a wealth of indigenous knowledge and coping mechanisms of various local communities that should be incorporated into conventional adaptation measures of climate change. This chapter describes the main climate change impacts in EA and SA, vulnerabilities thereon, and adaptation measures that offer an opportunity to the two regions to develop in a sustainable way.

Introduction

Increasingly, many people across the world agree that climate change is the latest challenge facing humanity today and that nations must unite in addressing it. The reality of global climate change has been more evident in the recent past as significant scientific evidence clearly shows a warming trend in changing Earth climatic systems. Human development, especially industrialization, is largely blamed for significant release of greenhouse gases (GHGs) into the atmosphere in recent decades that have led to catastrophic changes in sea level rise, increase in natural disasters, and increase in global temperatures, among others.

Climate statistics and models indicate that over the course of the past century, the global surface temperature has warmed by about 0.8 °C, where 0.6 °C is likely to be from the last three decades alone (Hansen et al. 2006).

Traditionally, the bulk of the global GHGs contribution was credited to industrialized countries. Presently, major growing economies (Brazil, China, and India) and the transport and manufacturing sectors from other big cities in the developing world have observed a more significant contribution. For other developing countries, including those in South America and the East African region, their contribution toward climate change is largely blamed on land use change, land degradation, deforestation, and increased household energy needs, especially fuel wood consumption.

Although a few conflicting stands still exist across the globe regarding climate change issues, the heated debates that were not uncommon in the past few years have become less important. Consequently, global efforts toward addressing climate change have thus been seen through the establishment of the United Nations Framework Convention on Climate Change (UNFCCC) which came into force on March 21, 1994, with an overall framework to address climate change through intergovernmental efforts. In addition, the Kyoto Protocol was established alongside the UNFCCC which commits Annex I countries to undertake measures aimed at stabilizing GHG concentration in the atmosphere. All countries of the East African Community (EAC) and South America have ratified both the UNFCCC and the Kyoto Protocol and have actively participated and put mechanisms in place to implement the various agreements accruing from the annual UNFCCC Conference of Parties serving as the meeting of parties under the Kyoto Protocol (COPs/CMPs).

This chapter has focused on two unrelated regions, EA and SA, that are very vulnerable to climate change impacts but at the same time offering interesting adaptation and mitigation mechanisms humanity can learn from. Major climate change impacts, vulnerability, and adaptation options have been discussed. Some climate change impacts still considered of potential effects elsewhere are already happening within these two regions and hence give a wake-up call to the rest of the world for immediate combating actions. For example, the presence of climate-sensitive equatorial glaciers in the region offers a good opportunity to follow climate change trends and vulnerability. Thus, because of the diverse regional environmental

settings and socioeconomic characteristics, the regions offer the best opportunity to understand climate change details and how the developing countries live with climate change impacts, adaptation, and mitigation options thereby. For instance, it is now known that in EA, the ability to adapt to new conditions, exposure, and sensitivity changes to climate are determinant factors to the extent to which individual places are vulnerable to climate change impacts (Kelly and Adger 2000). In addition, the regions host some of the least developed countries and one of the emerging economies and thus are a good platform for socioeconomic comparisons.

The East African (EA) Picture

Brief Introduction of the EA Region

In its widest sense, the EA region includes Kenya, Tanzania, Uganda, Burundi, Rwanda, Sudan, and Ethiopia. Traditionally, the region was known to include only the three countries, Kenya, Uganda, and Tanzania, while politically, the current East African Community (EAC) block hosts the first five countries. The latter block has a rapid growing population currently standing at about 120 million people, most of whom are directly or indirectly employed in the agricultural sector. The inhabitants of the region have more or less comparable lifestyles and some forms of cooperation, long existed even before and during colonialism. During colonialism, for example, the former three countries had a well-developed cooperation in energy, monetary, transport, and communications sectors. To date, such important links continue to exist where they offer important contribution to regional economic growth and livelihood support during needy times like natural disasters which are not uncommon in the region (Maingu et al. 2003).

Biologically, the diverse environmental setting of the region has resulted in a number of endemism and very rich biological diversities. A number of rare species of aquatic and terrestrial ecosystems flourish in the region, both of which have a very big contribution in the economic development of the region. Its major wildlife ecosystems are internationally appreciated for their uniqueness and flourish in the region, including, among others, the Masai Mara Game Reserve in Kenya, Ngorongoro, Kilimanjaro, and Serengeti Wildlife Parks in Tanzania. One of the five internationally recognized centers in terms of high species richness and endemism, otherwise known as biological hot spots, is found in the Eastern Arc Mountain forests of EA (United Republic of Tanzania, URT 2007). The region also hosts a large portion of the Savannah, the richest known grassland in the world. The Eastern Arc Mountain forests and other regional forests make an important contribution in the energy sector in the region in which up to 90 % of the total energy usage is biomass dependent (Maingu et al. 2003). Moreover, the forests and the vast ocean area are very crucial in the control of carbon via the carbon cycle, while the diverse water bodies like large rivers and lakes are crucial for the socioeconomic sustainability of the region. These water bodies offer important services like irrigation,

hydropower, and domestic water to its fast-growing population, especially because the region has frequently been affected by severe water shortages (Hulme et al. 2001).

In addition, EA hosts Africa's tallest mountains (Mt. Kenya and Kilimanjaro) that still harbor rare tropical glaciers. The mountains have attracted several climate change studies that have added regional and extra-regional understanding of climate change trends. Geologically, the region is marked by the presence of the Rift Valley, semiarid to arid regions, and some of the most spectacular waterfalls that have been harnessed for hydropower projects. Furthermore, the region is rich in natural gas, coal, and different precious minerals including diamond, gold, and tanzanite, among others (Maingu et al. 2003). The neutral gas of coal is a notable contribution to the regional energy balance, while tanzanite is globally found in Tanzania only (United Republic of Tanzania, URT 2007).

Demographically, the region is home to thousands of pastoralists who remarkably herd their livestock mostly in the semiarid to arid areas of the region. The pastoralists provide a major portion of the livestock to the markets both within and beyond the region (Ensminger 1992; Kerven 1992) and as such are an important part to the regional gross domestic product (GDP) besides providing employment and important nutritional balance in the region. However, the livestock industry in the region is threatened by periodic droughts, the use of low breeds, and livestock diseases, inter alia. On the other hand, agriculture is the most important sector in the region considering the number of people it directly employs and its contribution to GDP and foreign exchange. Unfortunately, agriculture is mostly rain fed and severely impacted by uncertainty in rainfall patterns and intensity. Characteristically, agriculture in EA is largely subsistent, has low input, and is rain fed with only isolated cases of large-scale agriculture. This in turn leaves the region vulnerable to repeated crop failures, food insecurity, and increases in food prices (Hulme et al. 2001). Irrespective of the presence of the most productive soils and numerous water bodies, sadly the region is among the places where malnutrition is very high and periodic food aid has had to be provided. The situation has been made worse by the present climate change where rainfall has continued to be unpredictable, increasingly unreliable, and insufficient.

Meteorologically, EA is located in a complex climatic region in which the diverse topographical and hydrological interactions play an important role. The climate is mostly controlled by interactions between sea surface temperature (SST) forcing, large-scale atmospheric patterns, synoptic-scale weather disturbances (namely, trade winds and monsoons), tropical cyclones, subtropical anticyclones, easterly/westerly wave perturbations, and extratropical weather systems that are superimposed with regional factors like large lakes, topography, and maritime influence (Nicholson 1996; Ellis 1994). The above complexity renders climatic patterns within the region to change rapidly within a short distance and time. Consequently, the diurnal temperature range varies between 10 °C and 20 °C, while the annual temperature range is only 2 °C. On the other hand, mean annual bright sunshine is between <7 to 8 and 8 to >9 h/day in highlands and lowlands, respectively, while the regional mean annual net radiation varies between 450 and 550 cals/cm^2/day. The most important regional wind and pressure patterns include the Congo airstream with westerly and

southwesterly airflow, together with the northeast and southeast monsoons. Unlike the Asian southwestern monsoon, both East African monsoons are relatively dry, while the Congo airstream is humid and associated with rainfall (Nicholson 1996). Generally, East African rainfall is bimodal that is characterized by uncertainty both spatially and temporally. Predominantly, the rainfall occurs during boreal spring and comprises of long rains (March–May), while short rains come in autumn (September/October–December) season. The two rainy seasons occur when the Intertropical Convergence Zone (ITCZ) migrates from south to north through the equator. However, the above pattern varies significantly across the region, the uncertainty of which increases toward the dryer zones. In other words, rainfall is more patchily scattered in arid than in mesic systems (Ellis 1994). Within the region, the fluctuations in rainfall intensity are largely associated with east–west adjustments in the zonal Walker circulations that are linked to El Niño Southern Oscillation (ENSO). Studies have shown that humid areas in EA will become wetter while dry parts will turn out to be drier. The former will increase runoff, while the latter will significantly reduce it. In Tanzania, for example, two river basins are already said to have their runoff reduced (Nicholson 1996).

In this chapter, the discussions will be limited to the EA political block, the socio-environmental settings of which are considered useful in understanding local, regional, and extra-regional vulnerability and adaptations to global climate change.

Brief Introduction of Climate Change in EA

Although vulnerability to climate change impacts is increasingly becoming of ubiquitous nature, the best way of understanding climate change in EA is to ask "why is the region particularly vulnerable?"

EA is vulnerable because of various reasons, namely, the overdependency on natural resources and primary production; overreliance on rain-fed agriculture for livelihood support; low level of development; and inadequate institutional and economic capacities, all of which leave many persons vulnerable (Hulme et al. 2001; O'Brien et al. 2000). Climate change effects like changes in precipitation patterns and rising global temperatures are clearly affecting the region where they already disrupt people's livelihood, biodiversity, and ecosystems (Christensen and Hewitson 2007). Recent studies have shown that the region's economy largely depends on agriculture, livestock, tourism, wildlife, forestry, mining, industries, and marine and coastal resources, all of which are climate dependent and directly affected by the ongoing climate variability. Any impact on agriculture, which is the dominant contributor in terms of employment opportunity, income generation, and support to the population, leaves many livelihoods disrupted. In addition to the overdependence on natural resources, the vulnerability also roots from low level of development and generally of per capita income. The majority of the population in the region lives below respective national poverty lines and most of them with less than a dollar per day, especially in rural areas.

Furthermore, socioeconomic inequality within the population increases vulnerability and limits adaptation options to some individuals. The most obvious of such

inequality could be seen between the urban and rural populations, in which the latter suffers more from low development, low income, and poor access to public services compared to their urban counterparts (United Republic of Tanzania, URT 2007). In some places like Tanzania, vulnerability to climate change has even taken a gender dimension in which women are categorized more vulnerable on account of the deep-rooted socioeconomic barriers in the country.

Working with regional climate change projections, the region is set to observe both decreases and increases in rainfall of between 5 % and 10 % (June–August) and 5 % and 20 % (December–February), respectively. Sadly, the projections show that the increase in rainfall may come as a few large storms in early traditional wet season and hence complicate water management, soil erosion, and health services. Several development activities/projects in the region are either directly or indirectly impacted by climate change. This occurs when the variability impairs climate-dependent projects such as forest management, infrastructural developments, and agriculture, while indirect impacts happen when socioeconomic projects like health and education are impacted. Regrettably, for a good number of years, most governments in the region did not strategically link climate change and socio-development projects. Climate change factor was not clearly reflected in individual national development plans and policies. Only recently, and after significant climate change impacts, some governments in the region have practically linked the two.

Arguably, the negative impacts of climate change in the region are also complicated by other factors such as rapid population growth, widespread poverty of the inhabitants, and human and livestock diseases, among others. Even worse, under the current population growth rate, some studies already estimate a doubling in demand for water, food, and rangeland within 30 years (Ministry of Lands, Water and Environment (MLWE) 2002). Such statistics put EA in a very desperate situation, and effective measures must be taken sooner rather than later to counter the effects of climate change in the region. EA already has some social stressors which make the region even more vulnerable to climate change and thus limit adaptation ability. Such stressors include the following: governance problems, high population growth, land scarcity in some places, conflicts, and diseases such as malaria and HIV/AIDS.

Given the socioeconomic and technological capacity of the region, dealing with climate change will continue to be problematic because of numerous reasons. Most official strategies to livelihoods impacted by climate change are expensive and technical which renders poor implementation. This is where indigenous coping options which are plenty in the region, as will be seen later, could be integrated into the national strategies.

Regional Climate Change Vulnerability

The global climate change impacts like intensification of extreme weather events, sea level rise, alteration in temperatures, and distribution of precipitation are all evident in EA. Within the region, however, distribution of the effects of climate change is known to be nonuniform and arguably more noticeable from variations in

precipitation than temperature. For example, most studies indicate that the region will warm by between 2 °C and 4 °C by 2100 which is notably less compared to inner South Africa and Mediterranean Northwest Africa. Further projections show that regional warming in the twentieth century has been of the order of about 0.05 °C per decade. However, within the region itself, the projected warming is unlikely to be uniform where inner parts of the region are likely to warm more than coastal regions. On the other hand, a number of climate change-related droughts have been recorded in recent years with severe consequences to livelihood support systems and even deaths of both human and livestock (O'Brien et al. 2000; Christensen and Hewitson 2007). For example, studies have indicated that warm sea surface temperature may be to blame for the recent droughts between the 1980s and 2000s in equatorial and subtropical EA. Interestingly, however, historical records in the region show that over the course of the last century, there has been a net increase in the amount of rainfall (Hulme et al. 2001). Further studies show that the increasing rainfall and decreasing temperature in presently humid areas may increase river flow by up to 10–20 %, for example, in Uganda (Hulme et al. 2001). However, more recent studies suggest that whereas parts of equatorial EA are likely to have a 5–20 % increase in rainfall from December to February, the region will also observe a 5–10 % decrease in rainfall from June to August by as early as 2050. Certain parts of the region are known to be more vulnerable to climate variation than others. For instance, both increase in regional temperature and decrease in rainfall would leave most parts of Northern Uganda and many places in Tanzania with serious water scarcity (Ministry of Lands, Water and Environment (MLWE) 2002). Generally, presently, wet and dry places within the region will become wetter and drier, respectively. In Tanzania, for example, two rivers have their flow reduced directly because of the dwindling regional rainfall. Even more worrying, the observations show that the decrease in regional precipitation will most likely occur in the rational dry spell in the region and hence worsen frequency and severity of drought, hence desertification. Such relatively drastic changes in precipitation already have many socioeconomic and ecological negative impacts, among them reduced agricultural harvests, increased insects and fungal infestations, decreased biological diversity, and complicated hydropower availability, inter alia (Hulme et al. 2001).

Although climate change affects many biophysical and social aspects in the regions, the following categories considered as major issues will be used as a guideline for the discussion. Worth noting, some of these impacts have far-reaching influences and tend to trigger other vulnerability.

Natural Disasters: Droughts, Flooding, and Wildfires

Probably the claim that climate change is projected to aggravate frequency and intensity of extreme weather events (El Niño events, storms, droughts, and flooding) and wildfires can superlatively be understood from the EA region. The increased frequency and severity of the named natural disasters have in recent years caused injuries, deaths, famine, disease outbreaks, and even population displacement.

For example, the region has in recent years observed severe floods both in urban and rural areas (Conway 2002; Hellmuth et al. 2008; Action Aid International 2007). Although considered natural hazards, floods increasingly happen in cities where human activities are to be blamed. Urbanization, for example, has been observed to cover large areas in cities with roofs, roads, and pavements and thus restrict natural flow of water and percolation. Moderate storms in typical East African cities thus end up collecting enough water to cause floods, and thus their intensity has been growing as cities expand. Major towns including Nairobi, Kampala, and Dar es Salaam have witnessed periodic flooding which have repeatedly left widespread infrastructural and humanitarian costs (Action Aid International 2007). Flooding has also impacted the agricultural sector in which crop fields were swept away, nutrients leached, and top soils eroded. Even more worrying, both frequency and intensity of floods are worsened by the warm ENSO events. For example, the El Niño event in 1997 resulted in heavy rainfall and widespread flooding that was responsible for up to 1.7 m rise in the water level in Lake Victoria and severe damage to the agricultural sector (see Box 1). The flooding left many famers and pastoralists stranded with massive losses. Arguably as a sign of worsening situation, regional statistics show that between 1992 and 2008 up to 3,137,675 USD worth of humanitarian aids was spent on flooding-related disasters. Apart from flooding, drought is another climate disaster that has been very common in the region and is documented to be in close agreement with the regional climate change statistics. Between 1992 and 2008, droughts have claimed about USD 28,383,288 in humanitarian contributions to rescue lives within the region. Based on regional meteorological data, however, drought events may decrease in a few places while at the same time increase in other areas with major potential agroecological implications. Some of the most common implications in the region include desertification and deforestation that have been recorded to increase in many places. Based on the above statistics, it is clear that droughts bring more hardships to the people and have wider economical implication in the region than flooding (Action Aid International 2007).

Box 1: Showing Effects of El Niño in EA

Much of EA observed severe droughts in 1997 that was followed by devastating El Niño rains from October 1997 to March 1998 (Government of Kenya Meteorological Service 1998). The El Niño season was responsible for up to a fivefold increase in rainfall (Hulme et al. 2001) with severe consequences in infrastructure, agriculture, and health problems to both livestock and humans. The available statistics shows that up to 4,000 people died of flooding and many more died due to increased cases of malaria and cholera in the region. In addition, thousands of livestock died as a result of the flooding. The El Niño was economically costly as two major cash crops in many areas within the region, tea and coffee, were severely reduced. In addition there were widespread rotting of cereals notably wheat and maize in the region and

(continued)

Box 1: (continued)
consequently increased prices of the cereals (Nicholson 1996; Horn of Africa Review 1997). Furthermore, the much dependent source of foreign income, from tourisms, was as well hampered due to infrastructural problems. Furthermore, movements of farm inputs to farming areas, agricultural produces, and livestock to marketplaces were all impacted with significant increases in production costs.

Apart from that, other recent studies already show a clear linkage between climate change and incidents of wildfire within the region. Cases of bushfire due to periodic droughts and high temperatures are presently not uncommon within the region. One of such studies was done on Mt. Kilimanjaro where apart from the receding glaciers that everybody is worried about, there is a silent danger, periodic fires that are feared to have more ecological consequences than the diminishing glaciers. Because of the periodic fires on the mountain, it is argued that one-third of the forest cover has already been lost within the past seven decades alone. The fires on the mountain have been very serious to the extent that it is feared that the water sources in the fog interception zone will completely disappear within the next few years. It is thus argued that fires on the mountain may have far-reaching impacts on the eco-hydrological balance of the receding glaciers (Hemp 2005; Thompson et al. 2001). Apart from Mount Kilimanjaro, fire events directly connected to climate change have also been observed on other forest resources including on one of the world's biodiversity hot spots, namely, West Usambara and Uluguru Mountains (Mwandosya et al. 1998). Incidents of wildfires have also been reported in other regional ecosystems and projected to have more detrimental impacts in countries like Kenya where already large parts of the country lie in the arid and semiarid areas (MOENR 2002).

Sea Level Rise and the Salt Water Intrusion into Freshwater Sources

The EA region hosts a long strip of coastal area along the Indian Ocean that is shared by both Tanzania and Kenya. The ocean resource supports millions of livelihood and important cities for regional growth are found along the coast. Hitherto, studies from many parts of the world have shown only a small increase in sea levels, and/or reports still treat it among the potential effects of climate change. The sea level rise due to climate change can clearly be studied in EA where small islands such as Maziwe Island in Tanzania that was once attractive for tourists, fishermen, and researchers are now most of the time submerged and only habitable for a few hours during the day. Located about 15 nautical miles from a coastal town of Pangani in Tanzania, *Maziwe* Island is a clear wake-up call that the region is already suffering from sea level rise and demands further studies to establish consequential hydrogeological and ecological impacts. Note: Because of its importance and richness, the island was named among the national marine reserves in 1975 and is home

to 35 species of corals and more than 200 species of fish and is a wealthy source of algae, sponges, and sea grasses (United Republic of Tanzania and URT 2007).

Although Maziwe Island is the clearest threat of sea level rise in the region, many coastal towns and cities in Kenya and Tanzania remain at risk from the rising sea level (Magadza 2000). As seen earlier, most of these coastal towns in the region are of historical importance and attract many tourists every year. Indeed the submerging of the island would have significant socioeconomic and ecological implications like disruption of livelihoods and most importantly the regional GDP. Even more worrying, the sea level rise is already threatening freshwater availability through seawater intrusion affecting millions of coastal inhabitants who mostly depend on groundwater for domestic water supply. One such place where sea level rise is threatening such an important source of freshwater is Tanzania in which her aquifers and deltas are known to be at high risk. Other potential risks of sea level rise in the region include coastal erosion and losses of coral reef and mangroves in both Kenya and Tanzania (Magadza 2000).

Impacts on Water Availability, Agriculture, and Food Security

As seen earlier, it is worth mentioning that, even without climate change, agriculture in the region has many serious challenges, among them the overdependence on rainfall and soil degradation. Climate change is of a special concern in the agricultural sector since increasing temperature, changes in precipitation patterns, flooding, and generally water scarcity have all been linked to recent food insecurity in the region. About 80 % of EA livelihood depends on agriculture which regionally contributes around 40 % of the GDP (International Food Policy Research Institute (IFPRI) 2004). Agriculture in EA is highly vulnerable to climate vulnerability which often results to repeated crop failures, lower export earnings, and low domestic revenues, inter alia. Most EA countries are among the world leaders in terms of food insecurity, and climate variability will worsen diminishing harvests (Devereux and Edward 2004). Presently, over 40 % of mortality rates among Uganda's children are due to chronic droughts in the country. Many more children across EA are either stunted or underweight because of climate change-related malnutrition (The Global Humanitarian Forum 2009).

Research has shown that the overdependence in rain-fed agriculture has been leaving many rural livelihoods vulnerable to food insecurity partly due to the recent shift in growing season within the region. Although climate variability has been blamed for the worsening food insecurity, the vulnerability in the agricultural sector is also complicated by heavy reliance on the subsistence farming by the majority of farmers (Hulme et al. 2001). Note: African agriculture is the slowest in terms of productivity increase. Thus, global warming will only add tension to the already overstretched region and hence likely to affect even a greater number of individuals.

The recorded slight increase in temperature and decrease in rainfall within the region have already claimed many victims in terms of food insecurity. For example, the recorded decrease in rainfall of between 50 and 150 mm between March and May

from 1996 to 2003 was observed to have a corresponding decline in long-cycle crops in the region. As a result, many households abandoned maize (one of the long-cycle crop), the harvest of which directly depends on the availability of enough rainfall during the mentioned season above (see Box 2). In recent years, generally, drought has been observed to decrease water supplies with consequences in reduced crop productivity and the associated widespread famine in Northern Kenya and the Southern and central parts of Tanzania (see section "Natural Disasters: Droughts, Flooding, and Wildfires"). Another drought-related disaster could be traced in Rwanda where in 2005, the country observed massive crop failures in the Eastern province. In addition to the decrease in the amount of rainfall, agricultural systems in certain parts of EA have also been affected by too much rainfall. Equatorial EA has particularly been receiving increased amount of rainfall during El Niño season which resulted in periodic flooding often associated with sweeping away of crops (Hulme et al. 2001).

Box 2: Showing Potential Impacts of Climate Change on Agriculture

Tanzania is likely to lose up to 10 % of its grain harvest per year by 2080 (Mwandosya et al. 1998), among them, corn, which is a staple food and traditionally the most important source of carbohydrate in Tanzania. Already farmers are witnessing a significant decline in corn harvests and have attempted to grow other crops in its place. Should [CO_2] double and temperature increase by between 2 °C and 4 °C, an average of 33 % of maize harvests is likely to be lost by as early as 2075 (United Republic of Tanzania, URT 2007). In some places in central Tanzania, up to 80 % decreases in the maize harvest have been linked to climate change (United Republic of Tanzania, URT 2007; Mwandosya et al. 1998). In Tanzania, the flood- and/or drought-related famines have increasingly been common since the mid-1990s.

Climate change impacts on the agricultural sector will also have significant economic implications via interference with cash crops (Box 3). In Kenya, for example, agricultural losses from three cash crops in coastal areas, namely, coconuts, mangoes, and cashew nuts, could amount to about USD 500 million under a 1 m increase in sea level. The three crops also make a significant livelihood to many coastal dwellers in Tanzania and are under more or less similar threats (Easterling et al. 2007).

Box 3: Showing Potential Impacts of Climate Change on Cash Crops and the Associated Economic Implications in Kenya

Apart from food crops, climate change is also projected to affect major cash crops in the region with wider socioeconomic implications. Studies have shown that should the temperatures increase by 1.2 °C and if the changes in

(continued)

Box 3: (continued)
precipitation patterns continue, large areas of the world's second producer of tea (Kenya) will be made unfavorable for the crop. The latter would mean interference with over 25 % of Kenya's foreign exchange and up to 10 % loss of employment opportunity (Easterling et al. 2007).

Impacts on Human, Livestock, and Wildlife Health

Climate variability is ubiquitously known to be central in the reproduction and geographical distribution of a number of disease vectors. For example, recent projections show that a global rise of between 13 °C and 3 °C would enable mosquitoes to expand their natural range while survival chances of other disease vectors are likely to be increased with increasing rainfall. Within the region, the unprecedented extreme weather events, namely, high temperatures and severe rainfall, are blamed for the initiation of malaria epidemic in highland Rwanda, Uganda, Western Kenya, and Tanzania. It is well known that mosquito vectors thrive better under warmer temperatures; hence, global warming will most likely worsen cases of malaria. Within the region, generally, intensity and severity of climate-sensitive diseases, namely, dengue fever, Rift Valley fever (RVF), typhoid, cholera, malaria, dysentery, and a number of respiratory diseases, are all projected to worsen with ongoing climate alteration (The Global Humanitarian Forum 2009).

Malaria

Worsening of malaria cases has been recorded in many places within EA, and the epidemic is directly a result of changes in rainfall patterns, higher temperatures, deforestation, and generally environmental degradation (Hulme et al. 2001; Conway 2002; Mwandosya et al. 1998; Zhou et al. 2004). In close agreement to increasing numbers of malaria victims, regional studies already indicate an upward creeping of malaria cases directly because of recent modifications of vector habitats due to climate change (Müller 2010). For example, between 1960 and 1980, there were no recorded cases of highland malaria in highland EA, the case of which is no longer true in many highland areas like Lushoto and Kilimanjaro in Tanzania. The creeping of malaria into the highlands of EA is of particular concern since the local inhabitants of such places do not have a well-developed immunity against the disease and thus have a relatively increased mortality rate (Mwandosya et al. 1998; Müller 2010). Worrying predictions exist that more highlanders are likely to be further affected if the current trends will continue. The above trend is already witnessed in many places within the region where on top of climate change which is known to modify vector/microbial adaptations, the situation is also aggravated by regional socioeconomic changes, worsening of food production, and crippling health-care systems, inter alia (Conway 2002; Hellmuth et al. 2008; Mwandosya et al. 1998; World Health Organisation (WHO) Regional Office for Europe 2003).

Rift Valley Fever (RVF)

Hitherto, it is ubiquitously known that outbreaks of RVF are usually associated with heavy rainfall and warm temperatures. Within the last decade, several outbreaks of RVF in EA were directly attributed to worsening climate change impacts. Thus, the effects of climate change on human health within the region can further be appreciated by the close correlation between regional El Niño events and Rift Valley fever (RVF) epidemics in recent years. The observed regional trend has been that during warm ENSO events, the EA highland tends to receive unusual high rainfall which has a positive relationship with the number of recorded RVF outbreaks. Going deeper into historical records would reveal that about 75 % of all recorded cases of RVF occurred during the warm ENSO events between 1950 and 1998 (Patz et al. 2005). Such statistics give a worrying sign of what is likely to happen if full-scale impacts of projected negative effects of climate change on health sector would occur.

Cholera

The relationship between regional climate change and health sector can further be understood from cholera epidemics. Studies have shown that prolonged droughts often associated with scarce water resources, poor sanitation, and changes in rainfall and temperatures are periodical reasons behind regular outbreaks of cholera and other waterborne and diarrheal diseases in EA. Cholera cases are known to be worsened by wet seasons; thus any increase in the amount of rainfall as already is the case in some parts of EA (section "Natural Disasters: Droughts, Flooding, and Wildfires") would further elevate cases of cholera. As seen earlier, regional rainfall is projected to increase in coastal areas and Lake Victoria Basin, and the named localities above have already witnessed a relative increase in cases of cholera outbreaks (Mwandosya et al. 1998). The acute intestinal infection diseases that are caused by *Vibrio cholerae* can often become fatal and are now declared endemic in Lake Victoria Basin and have been of repeated occurrence in the region since 1978 (Mwandosya et al. 1998; World Health Organisation (WHO) Regional Office for Europe 2003). Available statistics show that the disease first caught the attention of EA coastal dwellers in 1836 where it left over 20,000 deaths in Zanzibar (Tanzania) alone and killed many more people in Kilwa (Tanzania), Malindi, and Lamu (the latter two in Kenya). A direct sign of the climate variability factors in cases of cholera outbreak in EA is seen from the fact that, cumulatively, more cases of the disease have been recorded over the past three decades, the same duration in which there has been worsening of climate change impacts.

Recently, the outbreak of poorly known diseases such as Chikungunya fever has also been linked to climate change in EA. It is known that warm and dry climatic conditions precede a typical outbreak of the disease. Following the prolonged drought for many seasons in EA, about 500,000 people mostly in the coastal areas were reported to be afflicted by the mosquito-spread viral disease (Shongwe 2009).

Apart from human health, livestock health has also been impacted by climate change in which there could be further infestation of tsetse flies, ticks, snails, and other disease vectors to previously safe zones. The former are already observed to

spread to Northeast Tanzania with the potential of reducing safe grazing range in the areas (Mwandosya et al. 1998). Furthermore, the impacts of climate change on healthy systems in EA have even affected wildlife ecosystems. In 1989, for example, large numbers of wild animals died of rinderpest which was directly attributed to regional climate change impacts (Mwandosya et al. 1998). Such big losses of wildlife coupled with declining biodiversity due to repeated drought in the region are likely to cripple the tourism sector, the major sources of foreign currency in the region.

Impacts on Environment: Deforestation, Fisheries, Biodiversity, Wildlife, Ecosystems, and Seawater Intrusion into Freshwater

Although major impacts on biodiversity in the region is presently believed to come from humans via overexploitation of natural resources and land use change, recent climate change scenarios have equally been threatening the biodiversity. Already studies show that there are changes in the migratory roots of wild animals in several precious ecosystems of EA. Even more worrying, studies have shown an upward shift in vegetation composition in major mountains in the region particularly on Mount Kilimanjaro. Generally, the climate variability already has its detrimental effects in dynamics of regional biomes and biodiversity integrity and richness.

Although most of the tropical fishes have adapted to warm waters, most of them might not survive temperatures beyond their critical thermal maxima due to recent climate change trends. The population of important fish species (*Tilapia mariae*) that occur in EA and are used as an important source of protein is likely to be affected if their preferred temperature (between 25 °C and 33 °C) will be exceeded. This particular species of fish has a thermal maximum of 37 °C beyond which they will not survive (Vuorinen et al. 1999; Siemien and Stauffer 1989). Ecologically, however, global warming might have even more effects as any such ecological imbalances will disturb the ecosystem and might result to losses of many more species. Other studies show that due to recent climate variability impacts in Lake Tanganyika there has been a 20 % decrease in primary production estimated to correspond to about 30 % of fish yields (Vuorinen et al. 1999).

In addition, researchers are already worried of the effects of climate change on the hydro-geochemistry of water bodies in EA that have a potential of significantly decreasing fish populations. Regional studies show that any slight increase in temperature is likely to affect the amount of dissolved (O_2) and the limnology of major lakes in the region (Fick et al. 2005). Already worrying studies show that significant effects might occur in Lakes Tanganyika and Victoria. The latter lake has in the 1980s observed massive deaths of fisheries due to low levels of dissolved oxygen as a result of decreased turnover in the lake (United Republic of Tanzania, URT 2007). It is widely believed that the trend is likely to be the same in other lakes in the region and calls for ecological studies to be carried so as to establish the situation. Any escalation in the effects of climate change on great lakes fisheries will have major socioeconomic implications as the lakes offer an important source of

employment, food to millions of people within the region, and even foreign exchange (United Republic of Tanzania, URT 2007).

Even more worrying, among the negative impacts of climate change that are already witnessed in EA include the problem of species invasiveness. It is already known that invasive species have better adaptive ability to climate change which puts them in a better competitive situation compared to other species. The latter is very worrisome as EA region has already witnessed a number of exotic species becoming uncontainable with detrimental ecological implications. Very delicate forest ecosystems in the Eastern Arc Mountain forests, like the East Usambara forest reserves, are already struggling with ecological impacts of several invasive species including *Lantana camara* and *Maesopsis eminii.* The problems of species invasion are not limited to terrestrial ecosystems; marine ecosystems have also witnessed a number of invasions including the water hyacinth and Nile perch in Lake Victoria. Studies show that the region may further be victimized by more colonization of invasive and other exotic specifies directly because of the ongoing global climate change (United Republic of Tanzania, URT 2007).

Although climate change is not the only problem affecting regional ecosystems, combined with other factors like overexploitation of resources and particularly land use changes (destruction of habitats), it may result to severe effects to regional biodiversity. The latter has directly affected forest resources, and availability of important products like fuel wood has been significantly affected. In addition, regional desertification has also been observed to expand.

Climate Change and Energy Crisis in EA

In order to be able to get a better picture of how the global climate change is complicating availability of energy in EA, the following basic is information is considered vital.

EA is blessed with a rich mixture of energy varieties that can be generalized into natural gas and coal in Tanzania, geothermal energy in Kenya and Tanzania, numerous hydropower sources, significant biomass in nearly all member countries, and recent discovery of oil reserves in Uganda and potentially in other countries. There is also rich potential for wind energy, biogas, and solar power in many places within the region (Maingu et al. 2003). Within EA, however, low level of regional development is clearly reflected in the energy characteristics and can statistically be studied from the percentage (%) energy consumption characteristics (Table 1).

In EA, the effects of climate change on regional energy stability can be observed from diverse angles. These include reduced availability of biomass, diminishing/dwindling water flow for hydropower generation, and most importantly destruction of infrastructures (roads, railways, electric poles) needed to transport and distribute various forms of energy.

From the table above, it is clear that the energy balance in all countries is largely dominated by biomass (mostly fuel wood, charcoal, and agricultural wastes). Since the effects of climate change include desertification, this is where it possesses its

Table 1 Showing levels of energy consumption in East Africa (EA)

Country	Petroleum (%)	Electricity (%) (major source of electricity)	Biomass (%)	Others (natural gas, solar power, wind power, etc.) (%)
Kenya	21.0	3.0 (mainly from hydropower, petroleum, and geothermal energy)	75.0	1
Uganda	6.1	1.1 (mainly from hydropower and petroleum)	92.8	–
Tanzania	8.0	1.2 (mainly from hydropower, natural gas, coal, and petroleum)	90.6	0.3

effects on the major source of energy. Wood is increasingly becoming rare in many places due to both human pressure and climate change (desertification); see section "Impacts on Environment: Deforestation, Fisheries, Biodiversity, Wildlife, Ecosystems, and Seawater Intrusion into Freshwater" above.

One potential mitigation option in the region's energy supply would be to embark on renewables which are not limited. However, the inclusion of the renewable into the energy mix has not been of any significant contribution in comparison to the massive potentials available among other reasons due to high initial costs involved and poor availability of necessary technologies (Maingu et al. 2003). A few promising attempts however exist in Kenya and much less in other countries where more than 150,000 solar PV units are installed contributing to over 5 MW to the country's power needs. Kenya is again leading in terms of wind energy harvesting where some 450 kW wind power system is already installed. Other countries including Tanzania have already identified several potential locations where wind is abundant round the year and some implementation attempts are ongoing (Maingu et al. 2003). On the other hand, biogas would be another potential source of energy in the region on account of the presence of many livestock. However, biogas technology has been around in the region for over 20 years, but its implementation has faced similar problems like solar energy. Isolated hope exists in Uganda and in other countries where a few plants have been installed and running. Interestingly, Uganda has also been a leading player in terms of power generation from industrial biomass residues. Promising units of power are currently being produced in three different sugar mills in the country. Kakira Sugar Works, for example, is currently producing 2.5 MW and plans to produce 15 MW when the unit is fully running. Tanzania has comparable installations in Kilombero Sugar Company with a few other potentials in other sugar industries like Mtibwa (Maingu et al. 2003). Efforts can still be made by individual governments within the region to invest in renewable energy as the current installation is mostly from private sector. Strengthening of such renewable energy sources into regional energy balance would help in dealing with periodic shortage of power due to repeated droughts in hydropower basins within the region which have hampered many development projects (Maingu et al. 2003).

Although EA is desperate in meeting its energy demands, if not carefully planned, some adaptations to climate change impacts on the energy sector are likely to leave the region to follow the destructive way as currently the situation is in Asia, particularly China. The recent incorporation of coal energy as a source of energy in Tanzania is seen to be as one adaptation option. Poor technology of harnessing energy from coal may add regional contribution to GHGs. The country has about $1{,}200 \times 10^6$ metric ton of proved coal reserves which could meet most of the energy needs in the country and potentially of the neighboring countries. Already the country is contributing about 6 MW to the national grid from coal, and the plan is to increase production to about 600 MW as an adaptation to the drought-prone hydropower. Given the low level of technology in the country, however, the capitalization of coal into the energy mixture is likely to contribute further to the problems of global climate change (Maingu et al. 2003).

Concomitant with the effects of climate change on availability as seen on biomass, hydropower is also periodically affected by drought, the frequency of which has been very high in the recent years. Like the rest of EA countries, Rwanda is also facing power shortage because of the impacts of climate change in its hydropower plants. For example, in 2006, the country spent 65,000 USD per day to generate emergence electricity because the Rugezi wetland had its water reduced to very low levels. Although the 1997 El Niño triggered heavy rain and subsequent flooding in many places in EA, it left certain parts of Kenya with severe drought that badly disrupted hydroelectricity power generation (Siemien and Stauffer 1989). In nearly all countries in EA, hydropower generation has suffered from climate change-related problems, namely, low water levels and siltation (Maingu et al. 2003). Worth noting, the proportion of electrification in the region is very low among other reasons due to financial constraints to expand the network, high prices of electricity, and generally low level of development (Maingu et al. 2003).

Livestock Sector

EA region is home to thousands of pastoralists. Interestingly, most livestock are mainly found in drier part of the EA like arid to semiarid regions. Worth noting, the drylands comprise of about two-thirds of Africa's land in which about 50 million people depend on livestock and/or dryland agriculture. Although climate variability is a common phenomenon of most drylands, in Africa and particularly EA, it has particularly influenced ecosystem structures and functions and consequently land use and lifestyles. It is worrying that in arid and semiarid regions, climate change may lead to loss of palatable forage to livestock and more drought-tolerant vegetations that are not suitable to livestock (MOENR 2002). The major climate change vulnerability to livestock sector in the region comes via repeated droughts that leave the areas with severe shortage of pasture and water (Box 4). As a result, there has been an increase in the number of conflicts between pastoralists, farmers, and

wildlife. The recent droughts have been severe to the extent of triggering communal fighting and even interwar between neighboring countries. Other vulnerabilities to the livestock sector include flooding. In recent years, flooding has been reported to sweep a large number of animals and made pastureland unavailable for livestock. In addition to drought and periodic flooding, livestock industry in EA is also affected by other factors like diseases epidemic, intertribal raiding, and declining pastureland due to rapidly increasing human populations among others.

Box 4: Showing Effects of Drought on Livestock Husbandry in EA
In 1997 the whole of EA observed one of the worst droughts which led to huge economic impacts to the pastoralists (World Food Program (WFP) 2000). In Uganda, frequency of environmental insecurity, livestock rustling, and intertribal fighting has increased, largely blamed on increased frequency of droughts; thus, pastoralists are forced to move beyond their land areas (Davidson et al. 2003; World Food Program (WFP) 2000). It is projected that as a direct consequence of climate change, Uganda may have a significant reduction in suitable areas for dairy farming and the entire livelihood of some pastoralists would be disrupted (Davidson et al. 2003).

Other Sectors

Tourism is a very important regional sector in terms of foreign exchange earnings. Surprisingly, a very few regional literatures exist patterning impacts of climate change on tourism sector. The effects of climate change on regional tourism mainly come through demolition of infrastructures that support tourism or disruption of the natural beauty of the tourism attractions. Major tourism attraction in the region, namely, Mount Kilimanjaro and Mount Kenya, and spectacular ecosystems such as wildlife and natural forests are all threatened by climate change (see section "Impacts on Environment: Deforestation, Fisheries, Biodiversity, Wildlife, Ecosystems, and Seawater Intrusion into Freshwater"). Furthermore, major tourism cities like Malindi, Mombasa, Lamu (in Kenya) Zanzibar, Dar es Salaam, Bagamoyo, Mtwara, and Tanga (in Tanzania) all lie in the coast where the projected sea level rise will have major socioeconomic implications (Mwandosya et al. 1998). The livelihood of many people in the coastal areas directly depends on the sector for living. Major infrastructures like hotels and other recreation structures are also threatened by the projected sea level rise (Maingu et al. 2003; Mwandosya et al. 1998). Like in other developmental activities, infrastructures such as roads and railways are very important for the sector but have periodically been swept away by flooding. The recent flooding in Tanzania which was associated with El Niño event swept a large part of the railway, and it is estimated that the country would require at least 6 months to fix it.

Socioeconomic Implications of Climate Change on EA Mountains

Diverse verticality of mountain ecosystem offers numerous microenvironments which in turn creates rich biodiversity. However, mountains are known to be very sensitive ecosystems that are often faced with conflicts between environmental conservation and human activities. Yet scientific evidence shows that most mountains are among vulnerable ecosystems to global warming. Rare mountain glaciers are close to the equator in a phenomenon that is only present in the three regions of the Earth: the Ecuadorian Andes, New Guinea, and EA. The latter hosts the two tallest mountains in Africa, Mt. Kilimanjaro (5,895 m) in Tanzania and Mt. Kenya (5,199 m) in Kenya, both of which are socio-ecologically very important to millions of people within the region. Many similarities exist regarding these tropical mountains, both of which are important tourism attractions, serve as an important source of water, are very rich in biodiversity, and are probably the most important for now; both are badly threatened by climate change and human pressure (Shongwe 2009). EA mountain slopes are under constant pressure from both commercial and subsistence farming. The most important climate-related threats on regional mountains include the unprecedented glacier recessions and periodic fires. The disappearance of the glaciers is not limited to the two mountains named above; another mountain in the region, Mount Rwenzori, has observed more or less the same trend (Shongwe 2009). Apart from interference with regional hydrological balance, the thinning of the glaciers has reduced the scenic values of the mountains with potential negative ramification to the tourism sector. Historical records show that these three mountains in EA began thinning in 1,880 proportional to the drop of water levels in regional great lakes. In this chapter, the impacts of climate change on Mt. Kenya and Kilimanjaro are discussed in the Box 5 (Fig. 1).

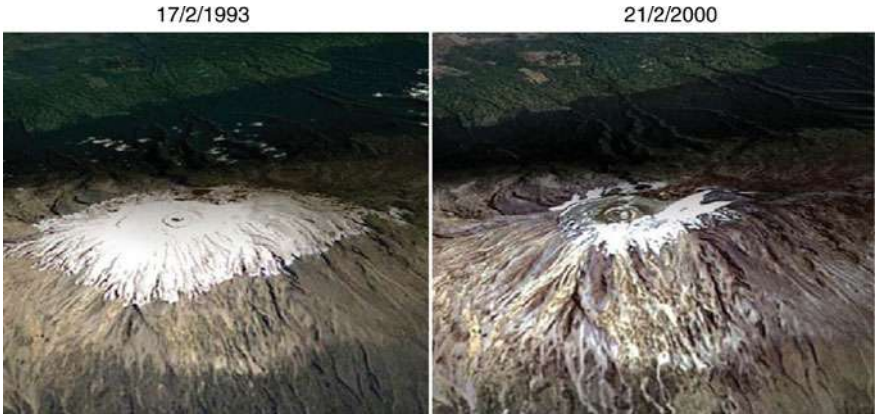

Fig. 1 Showing loss of Kilimanjaro glaciers and vegetation cover in a period of less than a decade (United Republic of Tanzania and URT 2007)

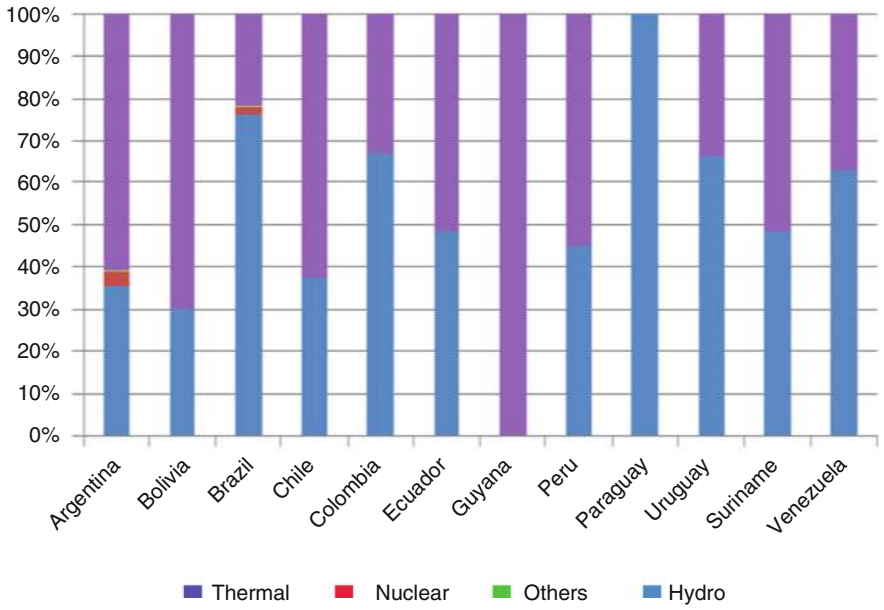

Fig. 2 Electricity production structure by country in 2008. Based on the information from the Latin American Energy Organization, OLADE, 2009. Energy Statistics Report 2009. Base year 2008

Box 5: Showing Retreat of Glaciers on Mount Kenya and Mount Kilimanjaro and the Associated Socioeconomic Impacts to the Society

Mount Kenya

On account of its uniqueness, Mt. Kenya is included among the list of world heritage sites and nicknamed a water tower in a semiarid region. The mountain contains several remnants of glaciers, all of which have been receding rapidly in the recent past (Fig. 2). For example, the Gregory and Lewis Glaciers have been showing unprecedented recession since the late nineteenth century. In 1990, there were 18 glaciers compared to only seven left by 2007. Studies show that the deteriorating water resources in the mountain and generally all other resources are attributed first and foremost to socioeconomic changes on the mountain but also on climate change consequences and seasonal aridity within the mountain's microclimates. The fast-thinning glaciers have badly affected the water supply to the already water-stressed areas of the region. In addition, nearly all the major rivers in Kenya begin from the mountain, with majority of the water coming from the middle and the summit of the mountain. The water levels in Tana and Athi Rivers among several rivers that originate from the mountain are currently among the worst affected. The flowing Tana

(continued)

Box 5: (continued)
and Athi Rivers are the main sources of water for the Seven Folks Dams, Kenya's key hydroelectric power generation plant. In addition to domestic use, the water is also used for agricultural activities that are important for the livelihood of the people. Hence, climate change consequences on the mountain could as well have impacts on the energy balance of the country. In addition, the mountain provides an important source of water to more than seven million people in the surrounding communities. Other studies in the region have indicated that reduction in water volume of these two rivers due to glacier disappearance on Mount Kenya will threaten the lives of over half of the Kenyan population (MOENR 2002).

Mount Kilimanjaro: The Roof of Africa

Like Mount Kenya, Mount Kilimanjaro which is found in Tanzania near the border with Kenya (3°04′S, 37°21′E) offers an excellent opportunity to study and understand regional climate change trends and vulnerability. Because of its importance, the mountain has received a worldwide attention that has attracted a series of studies, most of which giving worrying conclusions about its sustainability as a result of both climate change and human pressure. Arguably, the best way of studying the climate change vulnerability on Mt. Kilimanjaro is offered by its fast-thinning glaciers and its implications to the hydrology of the surrounding areas (Fig. 2). While the historical records show that the glaciers have been retreating since 1850, the current thinning is arguably the most alarming and fastest. Whereas the early retreat was likely due to natural climatic shifts, both the ongoing global warming and human pressure are blamed for the worse retreat ever recorded. Statistics show that there was about 4.2 km^2 of glaciers in 1976 compared to only 2.6 km^2 in 2000. The most recent studies on the mountain suggest that there will be no glaciers left on the mountain as early as 2020. The disappearance of the glaciers on the roof of Africa will have many negative consequences. The water from Mount Kilimanjaro is feeding the Pangani Basin where about 3.7 million Tanzanians live and many socioeconomic activities are carried out. The waters from the mountain are used for domestic, agricultural, and even hydropower production on the Nyumba ya Mungu dam. In addition, there are already changes in population dynamics and migration behaviors of species in the fragile ecosystems. Any further deterioration in the ecosystem would mean significant consequences as the Kilimanjaro National Park is the number one tourist attraction in the country. Unfortunately, because of climate variability and human pressure, there has been an increase in the number of fire events burning on the mountain that are likely to further degrade the eco-hydrological balance of the mountain (Christian 2006). Recent studies show that the fire is responsible for the ecological shift in species zones within

(continued)

Box 5: (continued)
the mountain (United Republic of Tanzania, URT 2007; Thompson et al. 2001; Mwandosya et al. 1998; Shongwe 2009; Sarmett and Faraji 1991).

Note: Because of its richness and shortage of land in Kilimanjaro region, Mt. Kilimanjaro area is among the most densely populated land in the country, the population of which is comparable to that of a typical city in Tanzania.

Coping with Extreme Climate Events

Indigenous Mechanisms

East Africans have a long history of living with consequences of extreme events like famine, drought, and invasion of locusts, among others. Historical records in Burundi, for example, show that during famine, affected population was forced to relocate to less affected places.

In addition to relocation, at times of extreme events, Burundians are documented to have worked as casual laborers in exchange for food. EA region is rich in such strategies albeit most of them need extra-local-level enforcement and might only help in a short term and/or for non-severe impacts (United Republic of Tanzania, URT 2007; Hulme et al. 2001; Davidson et al. 2003; Mwandosya et al. 1998). Although most of the local initiatives are unlikely to help people in the long term, they however do provide important help during disasters. Generally, important lessons can be learned from such initiatives and may be included in regional efforts to combat climate change.

An array of such coping mechanisms is analyzed and their strengths and weaknesses are discussed. The adaptive ability at the local level however differs from regions, households, and/or communities based on their respective environmental settings, socioeconomic backgrounds, and resource availability (Hulme et al. 2001).

Generally, most traditions in EA had strict customs and norms that ensured sustainable utilization of their natural conservation. One of such interesting forest ecosystem management could be traced to Burundi where certain biodiversity elements (plants and animals) were protected under traditional and religious beliefs. Apart from forest resources, such traditional conservation methods were presented for different plant types that were believed to have sacred values. Locally, referred to as *Intatemwa* and *Ikidasha* and translating, respectively, to what should not be cut and burned, such ecosystems were strictly prohibited from cutting and burning on account of their spiritual benefits. In the same society, felling down of live trees in Kibira forest was also firmly prohibited. Kinira forest, located at high altitude, was believed to be a conjunctiva between the Earth and the sky, and people generally respected both its virtual and physical services.

In addition, only a few people including the King and members of his kingdom were allowed to hunt in the forest. Generally, the combination of the traditional and religious beliefs above ensured sustainability of many of the sensitive ecosystems.

Such initiatives include the *shamba system* in Kenya and the *Ngitili* of the *Sukuma* agropastoralists of Tanzania. The former system works by allowing surrounding communities in the protected government forests to grow short seasonal food crops in the forest patches in which they are also expected to plant and manage trees. Farmers are not expected to establish permanent residence within the patches, and after a short time (3–5 years), they usually move and establish the same procedure to other forest patches. No payment is made to the farmers as both parties are beneficiaries in one way or another. The farmers are allowed to use the land the government assisted in reforestation. If this system is well managed and reinforced, it can save the twofold smoothly and help in improving the livelihood of the people and the carbon capture and storage (MOENR 2002). The latter system on the other hand is a common practice among the *Sukuma* agropastoralists of Shinyanga, Tanzania. It works by retaining areas of standing vegetation from the beginning to the end of the rainy period. Such areas, locally referred to as *Ngitili*, are usually closed to livestock grazing at the beginning of the rainy season and only made available to livestock during the dry period. The *Ngitili* thus serves to protect livestock from severe drought spells which are not uncommon in this region and at the same time serves to protect the ecology of the areas.

Apart from the strategies above, other communities of the region have other means of making a living during climate-related disasters. Such local-level coping mechanisms may include any of the following or their combination: switching to nonfarming activities, collection of wild fruits/vegetables/honey, remittances from migrant relatives and friends, and rarely selling one's assets (Conway 2002; Hellmuth et al. 2008). Nonfarming activities may include things like charcoal burning, handcrafting, casual laboring, and brick making. Although the contribution/income from such activities might be seen insignificant, it provides cushioning household to go through calamitous times like droughts and flooding. Regional lessons show that families that regularly receive remittances adapt better to climate change impacts than their counterparts who received nothing. Likewise the gathering of fruits, vegetables, and honey enables the household members to survive such times.

In the light of repeated droughts and their local experience, some societies in the region have turned into the use of local seed varieties and seed selection as a direct response to drought.

Studies have shown that some local grain varieties, for example, in Tanzania have better tolerance to drought than improved/high yield seed, and consequently farmers in drought-prone areas periodically grow local varieties. Such studies also indicate that the local varieties have longer shelf life than improved seeds.

Apart from that, some famers have replaced common crops like maize and beans with millet, sorghum, and cassava which are known to have better tolerance to drought. In addition, farmers cope with drought by including some livestock in their livelihood and establish some economic ties with pastoralists and markets and

practice other off-farm activities so as to diversify survival options (Galvin et al. 2002). Some farmers use their local skills and change planting seasons when drought is anticipated. When drought is expected, farmers have often changed the combinations in their intercropping to determine when to grow certain crops and switch between crops.

Apart from the survival strategies employed by indigenous farmers, EA pastoralists have also developed several coping mechanisms dealing with periodic droughts (Box 6). Such strategies include but not limited to economic diversification, migration to areas with better pastures, having diverse species of livestock, and intentional subjecting of herds to nutritional/drought-like stress so as to adapt them to stress period and hence increase their survival chance during disasters (Galvin et al. 2002).

Box 6: Showing Impacts of Climate Change on Sociocultural Aspects of Pastoralist Society in Tanzania and Their Subsequent Adjustments

Among the traditionally strict pastoralist societies in Tanzania include the Maasai who are entirely dependent on blood, milk, and meat from their herds for nutrition. Interestingly, the Maasai have started to practice crop farming in their means of livelihood (Grandin 1988), and non-pastoral foods like tea, corn, and sugar are increasingly becoming common. One of the reasons why the Maasai alongside other pastoralists in Tanzania have shifted to crop farming is the fact that their means of coping with climate variability to their livestock have been constrained by the current climate change pressure (Talle 1987).

Adapting Major Regional Sectors to Climate Change

Over the recent decades, the region has faced a number of climate-related calamities, namely, floods and droughts, which have crippled livelihood support systems. These have necessitated an array of adaptation strategies at various kinds of sectors including governments, private sectors, and individuals. For a long time, however, regional governments had failed to link climate change impacts on development projects. Major adaptation in this chapter will be discussed below, guided by vulnerability categories discussed above. Other specific adaptation strategies are also addressed. In recent years also, there has been recognition of the climate change challenges in regional policy issues.

Livestock Sector

Many methods have been suggested in dealing with climate change challenges on livestock sector. The most important adaptation method in practice includes reducing the number of livestock by keeping fewer healthier, more productive breeds. The latter has the potential of reducing pressure on pasture and water resources thus survive through calamitous periods like droughts (Ellis 1994). Other widely used

adaptation strategies include zero grazing and other improved methods of grazing that reduce environmental destruction (United Republic of Tanzania, URT 2007). The creation of livestock watering centers has a potential of reducing the number of livestock deaths due to shortage of water. The challenge with the latter option is on how to balance the water needs for the animals and avoid concentrating large numbers of livestock on the centers which might end up with further environmental degradation. Moreover, natural resource laws and policies especially on water and land need to be reviewed to allow pastoralists access to the resources without triggering tensions with farmers (Little and Brokensha 1987). It is under such circumstances where traditional land laws like the ones in Tanzania may be capitalized and integrated into regional strategies (United Republic of Tanzania, URT 2007). Finally, improvement of livestock extension services is vital where disaster preparedness information would easily and effectively be made to pastoralists before they occur (Hulme et al. 2001).

Health Sector

The most important means of adaptation in the health sector has been breaking breeding cycle of the disease vectors. The ongoing procedures for the control of malaria, for example, include improving drainage systems, removing stagnating water points, and bush clearance in residential areas, all of which aim at reducing mosquito multiplication (Mwandosya et al. 1998).

On the other hand, proper development and implementation of the early warning system for climate-sensitive diseases is another strategy that works better in reducing/controlling disease outbreaks. In addition, inclusion of the local skills on vulnerability, risks, and local coping options that have been used by the respective society is very important. For example, some local people within the region have well-developed skills on how to deal with both livestock and human health challenges (United Republic of Tanzania, URT 2003). Careful integration of local skills into the wider health sector may serve many lives. Tanzania's government has recognized potentials of traditional medicine and has included it in her medical research. Currently, a relatively well-advanced traditional medical center is fully operational at the Muhimbili National Hospital (Mwandosya et al. 1998).

Agriculture

Adaptation in agricultural sector probably requires the most attention as inhabitants in the region are among the global leaders in terms of food insecurity. Even more important, climate change is already estimated to have resulted in tripling food crises per year from 1980 to 2000.

Intensification of pests and diseases, changes in cropping timing, and shift in agricultural zones are consequences of climate variability that require immediate actions. Among the frequently suggested adaptation options within the region include, inter alia, the use of fast-maturing and drought-resistant crop varieties, inclusion of cover crops in the field, conservation tillage practices, and the use of green manure. However, the former strategy would require full involvement of the local people as certain farmers in the region objected certain varieties of

drought-resistant crops on grounds of their low markets and relatively high labor in their production (Mwandosya et al. 1998; Red Crescent Climate Centre, RCRCCC 2003). As climate-related failures in agriculture system intensified, agricultural sectors took the necessary steps like research in diseases and drought-resistant crops and early-maturing crop varieties. Kenya and Tanzania are leading the efforts in such researches and already promising results have been noted. In the former country, for example, 14 varieties of maize adapted to low available water are already in the field (MOENR 2002). Similar efforts are ongoing to other crops, namely, millet, sorghum, beans, and peas. In addition, different regional food security initiatives like national food reserves were created in nearly all countries in EA to help the population during times of disasters. Arguably, as a result of worsening situation, governments, nongovernmental organizations (NGOs), private sectors, and in some cases United Nations agencies are usually involved in such initiatives. Such initiatives often go down to district level so as to quickly deal with disasters when they occur. However, most of the initiatives have been hampered by lack of enough funding, high food prices, and mismanagement (Mwandosya et al. 1998).

Clean Energy and Energy-Serving Technology

In the EA region, most of the energy balance is met from biomass (Table 1). Any activity that would reduce the current rate of fuel wood consumption would thus help reduce deforestation and hence sequester more carbon. The use of fuel wood-saving stoves (efficient cookstoves) is regionally adapted as a promising strategy in dealing with energy crises. The latter is very important since land degradation, deforestation, and increase in desertification especially in arid and semiarid areas within this region have made availability of charcoal and fire wood very difficult and expensive (MOENR 2002). Interestingly, the declining biomass has necessitated regional studies on ways of consuming less biomass and higher efficiencies. Several types of fuel wood-saving stoves are in use and are proved to be very efficient. Most of these energy-saving stoves whose technology is simple and generally cheap use between 60 % and 70 % less fuel wood compared to traditional stoves (Maingu et al. 2003; United Republic of Tanzania, URT 2007; MOENR 2002). The potential of the stoves as a workable solution to reduce regional deforestation has caught the attention of nearly all regional governments, NGOs, CBOs, and other stakeholders and has been introduced to many parts of the region. As a result, the fuel wood-efficient stoves are now widely used in public institutions, hotel industry, and households. For example, a recent survey in Kenya has shown that there has been an increase in the number of households using the stoves from 4 % to 15 %. In Kenya alone, it is estimated that the increase in the use of the stoves would save about 7.7 million tons of fuel wood annually (MOENR 2002). Other countries in the region are also investing in these stoves and promising outcomes are already reported. In Tanzania, for example, efforts are being led by a nongovernmental organization called Tanzania Traditional Energy Development and Environmental Organization (TADEDO) where many stoves have been distributed countrywide (United Republic of Tanzania, URT 2007). Replication of similar efforts across the region would greatly contribute toward reduction in land degradation and deforestation since

biomass contributes over 70 % of domestic energy source in the East African region. Apart from fuel wood, other materials, namely, saw dusts, plant residuals, animal droppings, and some commercial wastes, have also been used in some of these energy-saving stoves.

In addition to the fuel wood efficiency that has a wide regional advocacy, efforts are also being made to reduce energy use and maximize efficiency in industries. Specific standards are currently operational in nearby countries regarding air quality control and generally environmental protection. Less fuel and high efficiency would all add to reduced GHGs emissions. In addition, there has been limitation in the importation of used vehicles and other machines beyond a certain age limit that have started to be implemented in most of the EA countries which in turn will contribute toward reduction in carbon emission (Maingu et al. 2003).

Other regional adaptation strategies in the energy sector include cogeneration and bioethanol production. The former mostly involves generation of electricity and heat from bagasse, a sugarcane waste product, by sugar industries. Kenya has currently one registered Clean Development Mechanism (CDM) project in this field, namely, the "35 MW Bagasse Based Cogeneration Project by Mumias Sugar Company Limited (MSCL)." On the other hand, ethyl-ethanol, a by-product of sugar processing, is relatively a clean form of energy that has multiple uses and is currently being explored by various sugar industries in Kenya. Regionally, such relatively clean energy projects are already running in Kenya and Tanzania with the potential of even further improvement to other parts (Maingu et al. 2003).

With climate change, regional cooperation in the energy sector is very important so as to compensate for potential shortfall in energy supplies. There exists a legal cooperation in the energy sector within the East African Community (EAC) member states stipulated under Article 101 of the Treaty for the establishment of the EAC. The treaty stipulates most legal issues that would ensure a smooth sharing of energy resources where member states are already sharing their energy resources (Maingu et al. 2003).

Generally, coping with climate change-related energy scarcity would require a combination of actions. The most reliable alternative to oil and biomass would be to strengthen the use of renewable energies like wind, geothermal, and solar energy. For example, geothermal energy generation in Kenya has proved to be a reliable and clean form of energy and has made a significant contribution to the national grid (Maingu et al. 2003). Further exploration of the geothermal energy into Tanzanian side would reduce the overdependence in natural forests and petroleum. Furthermore, investment into the relatively abundant supply of natural gas in Tanzania should be made central as natural gas has proved to be a relatively clean energy compared to oil and coal. Both of these attempts would additionally reduce the little regional contribution of CO_2 emission (Maingu et al. 2003).

Fight Against Disease

Because climate change has been observed to accelerate distribution and intensification of several diseases in EA, several adaptation strategies have been proposed in fighting diseases. Most regional efforts have been concentrated on malaria, the

number one global killer that has been responsible for over a million people annually. Because of the high motility rate it inflicts to people, several campaigns have been launched to eliminate the disease. Such regional campaigns range from the use of treated mosquito nets, rising awareness to the general public to the use of insecticides both indoors and in the environment. The latter strategy however needs to be taken with care so as to avoid potential environmental effects. Special attention has recently been addressed in highlands where the local inhabitants do not have the natural immunity against the disease and are thus vulnerable (Mwandosya et al. 1998). Other efforts are also addressed to other diseases such as cholera and typhoid fever. Vis-à-vis the latter case, water regional sanitation programs are threatened especially during wet seasons (World Health Organisation (WHO) Regional Office for Europe 2003). Apart from human diseases, isolated efforts are also directed toward the control of animal diseases. The latter efforts include the control of disease vectors by the use of insecticides and provision of sound breeding and extension services However, a few biological control agents of mosquitoes introduced in some areas, for example, rice-growing village of Mwea in Kenya, should be taken with care and closely monitored and controlled as cases of species invasion are not uncommon in EA (MOENR 2002) (see section "Impacts on Environment: Deforestation, Fisheries, Biodiversity, Wildlife, Ecosystems, and Sea-water Intrusion into Freshwater").

Flooding Control

With climate change, flooding calamities have been of repeated occurrence, and the latter has necessitated several adaptation strategies across the region. Among such measures include the construction of dams and dikes to prevent flooding. In Kenya, for example, such dikes are constructed on rivers Nzoia and Nyando. So as to reduce vulnerability to people, other efforts include coastal area conservation and conservation agriculture (Action Aid International 2007; MOENR 2002).

Water Harvesting, Irrigation Scheme Development, and Water-Serving Technology

Although the region is known for periodic droughts, there are periods of the year where surface runoff and flooding are common and could potentially be trapped for usage during water scarcity. The water which is most of the times wasted can potentially be trapped and used for domestic and industrial usage during drought episodes. Already efforts are being carried within the region where small- to large-scale water harvesting schemes are being done. For example, because of the increasing water scarcity in arid and semiarid regions in Kenya, rooftop rainwater collection and construction of water pans and dams are being facilitated by both the government and private sector (MOENR 2002).

In addition, East Africans have adapted to frequent droughts via irrigation development. As in the case with water harvesting, irrigation projects are well established in Kenya where recently some pastoralist societies have embarked on irrigated agriculture. The Narosura irrigation scheme run by the Maasai from the Narok district stands out to be the best example where horticultural crops are being

produced. Similar irrigation schemes are also run in Rwanda, Tanzania, and Burundi. Apart from the efforts above as climate change continued to cause water shortage in the region, water-serving technology has also became a mandatory in many of the agricultural and industrial sectors (MOENR 2002).

Environmental Conservation

As already discussed above, climate change is one of the factors for the recent environmental degradation in EA. In dealing with impacts of climate change on the environment such as soil erosion and water stress from flooding and rising global temperatures, respectively, regional governments, private sector, and other stakeholders have taken several environmental conservation steps and management of degraded ecosystems. In some parts of Kenya and Uganda, famers have adapted to farming methods that addresses both soil erosion and water loss. Increasingly, agroforestry, contour farming, and green manure are increasingly becoming common farming methods in many places in the region. On the other hand, special sectors/programs are put in place to address coastal resources in both Kenya and Tanzania (Magadza 2000). These include the Coastal Development Authority in Kenya and the integrated environmental program in Tanzania (Red Crescent Climate Centre, RCRCCC 2003). Issues of afforestation and reforestation have also been given significant emphasis in the region. For example, there is a region-wide tree planting campaign that has generally done very well. In Kenya, for example, the Green Belt Movement (GBM) led by the Nobel Prize Laureate Professor Wangari Maathai has received worldwide recognition for planting over 2,000 ha of trees. In collaborating with women groups in other parts of EA, the movement has successfully restored trees in farmlands, community lands, and even on school lands. Such local initiatives need to be assisted so as to deal with the increasing problem of regional desertification. The movement is now in the process of registering some of its afforestation/reforestation initiatives as Clean Development Mechanism projects and is already receiving financial assistance from the World Bank, among others (Patz et al. 2005).

Challenges and Opportunities for Combating Climate Change in EA

Before concluding this chapter, it would be worth to discuss something regarding regional challenges and opportunities in combating climate change.

The many opportunities available include the potential to develop reliable renewable energies within the region. As mentioned earlier, solar radiation and wind energy are not of short supply round the year (International Food Policy Research Institute (IFPRI) 2004). Potentials for geothermal energy are also very promising in Kenya and Tanzania. The former country is already producing a significant amount of electricity from geothermal energy and plans to increase its capacity even further. Albeit the region has observed a series of droughts and desertification has been reported in a number of places, it has many forests that can serve as important sink of carbon if long-term strategies regarding their sustainability would be ensured.

Because of the presence of large land cover in some countries like Tanzania, the potential of afforestation and reforestation exists with the added advantage of the geographical position which favors rapid growth of trees and hence sequesters carbon from the atmosphere (The Global Humanitarian Forum 2009; Little and Brokensha 1987). Generally, the region has the potential of being among the best beneficiaries of the UNFCCC's Reducing Emissions from Deforestation and Forest Degradation (REDD) mechanism.

On the other hand, apart from the challenges discussed so far, high above the list, poverty food insecurity and natural disasters, namely, droughts and floods, remain to be exigent. Within the region, poverty is strongly connected with deforestation and generally degradation and could thus limit the successful implementation of mitigation programs such as REDD. The challenge thus is to have effective disaster preparedness, reduce the proportion of populace that depend on rain-fed often unreliable agricultures, and have a working health-care system especially in rural areas and the provision of alternative livelihood support mechanisms (Government of Kenya Meteorological Service 1998; Patz et al. 2005; Red Crescent Climate Centre and RCRCCC 2003).

The South American Picture

A Brief of South America

South America occupies the landmass of the American continent located in the southern hemisphere, composed of 12 countries and covering 17 million square kilometers. It is bounded by Panama to the north, the Pacific Ocean to the west, and the Atlantic Ocean to the east. This region presented a population of 383 million and a gross domestic product (GDP) of 2.3 billion US dollars by 2007. The total exportations represented US$453 billion while the importations represented U$337 billion. The countries with the highest GDP per capita are Chile, Venezuela, Brazil, and Argentina (Andean Community (CAN) 2008). In this region 27,602,792 of inhabitants are indigenous (about 7.2 % of the region's population), with Peru showing the 46 %, Bolivia 21 %, and Ecuador 20 %. Additionally, for these countries indigenous population represents the 47 %, 71 %, and 43 % of the total respective national population (Roque 2005).

South America accounts for 27 % of freshwater of the world and 8 million square kilometers of forest. The region is the main global food producer and exporter and represents a hydrocarbon (oil and natural gas) offer estimated for 100 years (Comunidad 2010). The main representative organs in the political and economic agreements are the Union of South American Nations (UNASUR) which consists of all the 12 countries of South America, the Community of the Andean Countries (CAN) with the participation of the main four countries with a territory in the Andean Mountains (Bolivia, Colombia, Ecuador, and Peru), and the Common Market of the South (MERCOSUR) which consists of Argentina, Uruguay, Paraguay, Brazil, and Venezuela. Also, in the region the Amazon Cooperation Treaty

Organization was created by the countries with territory in the Amazon Forest (Bolivia, Brazil, Colombia, Ecuador, Guyana, Peru, Surinam, and Venezuela).

Climate Change Evidence in South America

The climate variability reported in the region is mainly indicated by the precipitation change, which presents an increase in Southern Brazil, Paraguay, Uruguay, Northeast Argentina, Northwest Peru, and Ecuador, while some decline is reported for Southern Chile, Southwest Argentina, and Southern Peru. The percentage of the variation in the precipitation presented a range variation between −5 and +6 in Colombia from 1961 to 1990, while in Uruguay, this tendency showed a positive variation of +20 between 1961 and 2002, which is also completely opposite to the one registered in Chile of −50 for the last 50 years (Magrin et al. 2007).

The temperature variability and its effects on climate events are not only different by region but also vary according to the season. Bolivia has showed major temperature variations in the humid months, a relationship which is also presented with the precipitation (General Secretariat of the Andean Community et al. 2007a). In the Central Andean region, the temperature variations registered between 1974 and 1998 are about 0.34 °C, which is 70 % more than the global average (General Secretariat of the Andean Community 2008), and maximum temperature variations (°C/10 years) of +0.2 and +0.2 are during the months of December, January, and February in Argentina-Patagonia for the last 50 years, with Argentina central presenting negative variations for the same periods that are presented by −0.2 to −0.8 (Tian et al. 2000).

The main climate events that have been identified in different ecosystems are strongly related to the Austral Oscillation and El Niño phenomena (General Secretariat of the Andean Community et al. 2007b; Wu et al. 2001; Jones et al. 2001). The interannual oscillation between cold and warm sea surface temperatures is known as El Niño and the Southern Oscillation phenomenon (ENSO). This phenomenon presented unusually strong warm events in 1982, 1983, 1997, and 1998, which is believed to have a relationship with global warming (Tsonis et al. 2003). This relationship has also been covered by other studies (WWF 2006) that studied data of atmospheric CO_2 concentration and the ENSO cycle to analyze the coupled climate–carbon cycle concluding that the terrestrial biosphere and the ocean carbon cycle behave in opposite senses, in which the land acts as a source while the sea acts as a net sink.

This is opposite to the dynamic described during La Niña, when sea performs as a source and land as a sink of carbon dioxide. Moreover, including decadal trend analysis, studies are showing that ENSO could be higher with warmer phases which are increasing with the global warming (Tsonis et al. 2003). On the other hand, studies have suggested that El Niño is activated to reverse positive global warming while La Niña reverses negative trends, concluding as well that ENSO could be sensitive to variation of global temperature but not at the actual value of global warming (WWF 2006).

The temperature of the surface in the Pacific is linked to the variability of the precipitations, which causes negative trends during warming events, especially in the wet seasons in the Andean region of the North of Bolivia and to the South of Peru, while in the North of the Andean, a systematic reduction is recorded in the Northeast of Ecuador and in Colombia (General Secretariat of the Andean Community et al. 2007b). Global warming can also cause a permanent El Niño state with major impacts in the Amazonia (Garcia 1999). Because of the relationship between global warming and ENSO and the influence of these events with land–climate dynamics, it is important to understand how sea sink dynamics can interact with land sources and the carbon cycle for creating mechanisms due to the protection and regulation of these cycles.

Climate Change Vulnerability in South America

The vulnerability of the region is not a linear process but a complex one related to feedbacks that increase the different risks and the vulnerability in both the natural and the human systems. In this way, the vulnerable factors described can be direct or feedback reactions resulting of the dynamic in social, natural, and/or linked human–natural systems, in which all are, associated to the climate events.

The main threats related to global warming are mainly associated with the climate variations of ENSO. This relationship causes/will cause stronger precipitation and droughts in the South American region affecting the natural hydrological cycles. The responses to the different events derived in South America are demonstrating a high vulnerability in the ecological and human systems. Because of the natural, social, cultural, political, and economical heterogeneity of the region, this vulnerability also varies through all the geography. As a result several risks are recognized for the water resources protection and supply, agriculture, health, energy security, and ecosystem protection especially in the Amazon Basin.

Ecosystem Vulnerability

The coastal area in South America is strongly exposed because the sea elevation, records show, ranges in variations over 1 mm per year for Colombia, Argentina, and Guyana and up to 4 mm/year for Brazil. In Argentina, the coastal area is already affected by the increased precipitations and landward winds (Magrin et al. 2007). Mangroves are already exposed, and risks associated with hurricanes and the sea level elevation have been recorded. Soil degradation is also worsened with climate change, estimating that more than the 20 % of the national territory could be degraded by the year 2050 in some countries like Chile, Ecuador, Paraguay, and Peru (ECLAC 2009). On the other hand, some studies estimated that the resilience of the Amazon Basin climate variations is zero, which in turn means that the conversion of this biome to a drier state threatens the key functionality of this ecosystem (representing the production of the 20 % of the global oxygen) (Thompson et al. 2009).

Some researches recognized that climate events, such as hurricanes, can expose the soil to erosion increasing the loss of nutrients. Vulnerability of these ecosystems is related to the Pacific temperature changes, to global warming, and also to local climate effects resulting from land clearing or land use change (Thompson et al. 2009). In Brazil, almost the 50 % of the country's rainforest may disappear by 2050 (Hall 2008). The effect of the long-term climatic variability has also been recognized in the northern part of the Amazonia where drier conditions have been noted since 1977 (WWF 2006). Moreover, the hydrological regime in the Amazon Basin presents more vigorous water cycles as a consequence of the increase in the evaporation and transpiration.

These specific ecosystems sustain water regimes depending on the relationships established between the sunlight, soil moisture, humidity, and cloud formation. As temperatures rise, the mountain cloud forests (also known as nebelwald which are forests with persistent wind-driven cloud) can present warming, affecting the hydrological cycles and exposing the local species to water stresses. As a result of extended dry seasons and lower water supply, vegetation is more vulnerable to fires and droughts (Foster 2001; World 2010).

With the 90 % of the Andean glaciers located in areas exposed to droughts and the 10 % in tropical humid areas, the retreating of glaciers can represent not only a loss of species but also impacts on the society and economy as energy, agriculture, and water supply, which are severally impacted for the present reduction in the ice covering (InWent 2008). Studies on glacier dynamics have included different variables to understand the impact of the climate variation and the retreat presented during the last decades. Cloud cover convection, precipitation, temperature, and humidity are related variables that have helped to monitor and estimate the past and future trends of glacier retreat. The temperature variation has increased by 0.11 °C every 10 years from 1950 (Kerven 1992), presenting a warming on the Pacific side and moderate variations in the eastern slopes (Conway 2002). Furthermore, increasing cloud cover is recognized over the north parallel 10°S in wetter seasons (December to February), while to the south of this parallel, the cover cloud is decreasing (General Secretariat of the Andean Community et al. 2007b). The cloud cover and convection have showed a decrease in the east of the Andes over the Amazon, while information analyzed for the humidity cannot be reconciled with this tendency (Vuille et al. 2003). The suppression of rainfall in the Amazon is additionally estimated as a result of changes in El Niño and weak Atlantic anticyclone (World Bank 2010).

Socioeconomic Vulnerability

The relationships of the damage ratio with the GDP show that countries like Peru, Bolivia, Ecuador, and Colombia (10 %) are more vulnerable than other countries demonstrating a direct link between GDP and vulnerability (General Secretariat of the Andean Community et al. 2007a). This social and agro-economic vulnerability is as well noted in Colombia, Ecuador, Peru, Brazil, and Bolivia by the World Bank (World Bank 2008). In addition to limited access to insurance, disparities in human development, and lack of climate-defense infrastructure, the poverty and low human

development are components that increase human vulnerability and reduce the capacity of society to adapt or respond to the climate impacts (UNDP 2007).

Driven by poverty and lack of proper planning, more population is localized on vulnerable zones. In Bolivia, the population growth rate in 1992 was 2.44 % increasing 3.47 % in the valley region by the year 2000. In the plains, the rates are higher with a growing rate of 3.89 % by 1992 and 3.26 % by 2000, with the 70 % located in the urban area (Calvo 2000). Additionally, by 1991 the homes under poverty were 78 % for the valleys and 70 % for the plains (Garcia 1999). This is a regional tendency where human settlements locate frequently on vulnerable areas, which added to extreme climate events is increasing the risk to natural threats.

Moreover, the vulnerability grows for indigenous population in the region. The major dependency of indigenous and traditional communities is on the natural resources, and because these resources could be more difficult to access or are reduced as a consequence of climate variation, these communities are exposed to negative effects (UICN 2008). Also, the location and economical activities of these communities are strongly associated to the services provided by the more affected ecosystems. Not only mountain or dry regions are occupied by different indigenous communities, but also tropical forests and some protected areas are the main zones of indigenous settlements.

It is estimated that large part of Latin Americans living in poverty are indigenous (Derruyttere 1997). The traditional and cultural backgrounds of these communities bring them to depend specially on the natural resources, creating dynamics of conservation and local development that can be threatened by the current effects of climate change. Poverty is a common factor in indigenous communities, and because of the loss and degradation of ecosystem services, the access to health systems, education, or information is more difficult for these populations.

The agricultural frontier is expanded as a result of the desertification of the ecosystems and the increasing of urban areas, causing the clearing of forests and the increase of the vulnerability by firing, soil erosion, and local climate variations as well. Although fossil fuels have been recognized as the main source of CO_2, the changes of the use of land and deforestation are the main causes of these emissions in Bolivia (83 %), Ecuador (70 %), and Peru (42 %) (General Secretariat of the Andean Community et al. 2007a). This tendency is representing a social threat because as much as 20 % of Brazilian Amazonia population depends on the region's natural resources and more than four million of rural inhabitants depend economically on these resources (ECLAC 2009).

Resulting from the glacier retreating and changes in hydrological cycles, the water resources are increasingly stressed exposing the population in South America to reduced availability of freshwater resources. Capital cities depend on high vulnerable ecosystems; 70 % of the population in Bogota is supplied with water from the Chingaza Natural Park, consisted of cloud forests and paramos, while Quito and Lima depend on water sources from important glaciers as the Antisana and Cotopaxi in Ecuador and the Chacaltaya in Peru (General Secretariat of the Andean Community 2008).

Agricultural Vulnerability

Agriculture is as well one of the main impacted components in South America. This sector is one of the most important in the regional economic development, accounting for 8.6 % of the gross domestic product (GDP) (Seo and Mendelsohn 2008). The most extensive droughts and reduction of precipitation in some areas reduce the productivity of crops. In Paraguay, decrease in cotton, wheat (by 2030), and soy (by 2050) is expected with sugarcane, cassava, and corn presenting an increase in crop yields as a result of the A2 climate scenario (climate scenarios were developed by the Emission Scenarios of the IPCC Special Report on Emission Scenarios; the A2 scenario includes a storyline and scenario family that describes a very heterogeneous world). For subsistence farms in Ecuador, 1 °C of temperature rising can increase crop yields but with retreating after temperatures reach 2 °C, and also banana, plantain, and cacao can be negatively affected with just a rise of 1 °C for intermediate farms (ECLAC 2009). In this way, it is also projected that small farmers (farms less than 30 ha) will get positive impacts for those situated in cold areas, but those located in warmer regions (Venezuela, Colombia, and the North of SA) may suffer negative consequences (Rodríguez 2007).

Some projections estimated different scenarios of temperature and rainfall variations to 2100; the first included an increase of 1.9 °C in the temperature and a 10 % increase of rainfall, and the other two estimated temperature rising of 3.3 °C and 5 °C with rainfall dropping by 5 % and 10 %, respectively. Following these projections a loss of land value of about 20 % (by 2060) and 53 % (by 2100) was calculated in the worst warming scenario and with smaller magnitudes in the other two. The study underlines the representativeness of the precipitation changes in the final values, with small household farms showing more vulnerability with higher temperature, while large commercial farms responded negatively to increasing precipitation (as these kinds of farms owned commercial livestock, what can be more affected by precipitation increase?) (Rodríguez 2007).

Impacts and Potential Risks Caused by Climate Change

ENSO has been related with malaria outbreaks in South America and childhood diarrheal disease in Peru (Siemien and Stauffer 1989). The IPCC predicts that the dry seasons can promote malaria, especially in the coast areas of Colombia, Venezuela, and Guyana, while with floods these epidemics are recurrent in the north coast of Peru. Also, prolonged droughts in Argentina, Chile, Paraguay, and Brazil increase the outbreaks of pulmonary hantavirus, while leishmaniasis, leptospirosis, and hyperthermia are outbreaks associated with the climate phenomenon (Magrin et al. 2007).

Power energy stations are presenting decreasing and suspension of the services because of the precipitation changes, increasing temperatures, and longer dry seasons corresponding to more frequent steady El Niño phenomena (see Box 7).

Box 7: News Summary

February, 2010

Paraguay faces energy shutdowns every day as result of the heat wave presented in February with high temperatures that also raise the energy consumption overcharging the capacity of the hydroelectrical system (BBC Mundo 2010).

October 21, 2009

The drought caused by El Niño has forced the energy interruptions in Venezuela. The reduction in the water levels of the rivers that supply the hydropower of different damns results in frequent electricity cutoffs in the country (IPS, Venezuela, 2009).

November, 2009

Ecuador faces the worst drought in the last 40 years that has reduced the reservoirs of the hydropower centrals and required the emergency declaration by the national government in the electricity sector. This situation has also required the increase in the energy imported from Peru and Colombia. The emergency was clear when the Paute hydroelectric plant reduced the production to 35 % of the total demand while the normal condition was of 60 % (La Hora, Ecuador, 2009).

Source: Arce, E. (2010) Paraguay also has energy crisis (in Spanish). BBC Mundo. Available on: http://www.bbc.co.uk/mundo/america_latina/2010/02/100208_1718_paraguay_energia_gz.shtml; Marquez, H. (2009), El Niño takes the water, the electricity and the water (in Spanish). Ambiente Venezuela; La Hora (2009) El Niño, El Niño is merciless with the countries of Latin America (in Spanish). Available on: http://www.lahora.com.gt/notas.php?key=58448&fch=2009-11-14

This tendency is representing a risk for the energy system in SA as electricity production is mainly based on hydroelectricity (see Fig. 2).

The present clearing rates and the agricultural frontier expansion are threatening the Amazon forest, a key global ecosystem. The increasing of evapotranspiration caused by higher temperatures will impact water cycles in the Amazon Basin. On the other hand, with the loss of vegetation and increased temperatures, a combination of lower evapotranspiration and precipitation causes a drying effect. Loss of species and ecosystem-type shifts are resulting from the global warming and increasing the vulnerability of human communities as well (WWF 2006). Furthermore, some features of the human communities settled in the Amazon region result in an increased risk for the conservation of this ecosystem and the sustainability of the human communities.

The high dependence on manual labor of small farmers in the Amazon and the information incompatibility between global and local dynamics increase the difficulty of these actors to develop adaptation and conservation measures

(continued)

Box 7: (continued)
(Brondizio and Moran 2008). As this ecosystem is one of the main regulators of the carbon dioxide and local climate and one of the main biodiversity regions in the planet, the current human and natural dynamics are generating a high risk in the loss of these functions and increasing the effects of climate variation in the region.

Adopting Climate Change Adaptation and Mitigation Measures in South America

The adaptation measures vary in different scales. In Peru, subregional strategies can be developed for the Clean Development Mechanism (CDM) or Adaptation under the National Strategy on Climate Change implemented since 2003. As a result, different actions on water management, food security, risk prevention, or hydroelectricity can be found (Patz et al. 2005). Moreover, Colombia is implementing the Integrated National Adaptation Plan (INAP): High Mountain Ecosystems, Caribbean Islands and Human Health (World Bank 2006) supported by a bilateral cooperation between the Netherlands and Japan. Additionally, many studies are still focused on the development of diagnostics, and in pilot phases, some transversal programs are found in Bolivia, where a national mechanism for climate change adaptation covering water resources, food security, health, human settlement and risk management, and ecosystems creates transversal programs in scientific research, capacity building and education, and anthropologic aspects and traditional knowledge (Commission on Climate Change and Development 2009).

Adapting to Climate Change

Information management is also part of the adaptation measures. More investments and technological development will take place as much as information is reliable and open markets as result of the people's perception on the necessity to adaptation (Commission on Climate Change and Development 2009). Counting on reliable, precise, and continuous information allows the governments to establish corrective measures for different sectors. Projects like the Community-Based Risk Screening Tool – Adaptation and Livelihoods (CRiSTAL) (to assess the systemic vulnerability) or Opportunities and Risks from Climate Change and Disasters (ORCHID) (to manage the risk, integrate adaptation, and identify opportunities to reduce vulnerability) are important developments with international support (Levine and Encinas 2008). Also, the Tropical Ocean Atmosphere Program provides observations of the upper tropical pacific from the middle of 1990 allowing the implementation of adaptive measures in agriculture planning, fire prevention, streamflow prediction for hydropower, and new applications in the health system (Magrin et al. 2007).

The Regional Role in Global Climate Change Mitigation

Mitigation actions in this region are mainly directed for the conservation and protection of forests as clue elements for sinking CO_2. In Colombia the first pilot project on adaptation by the Global Environment Facility (GEF) is being carried out, while Peru, Bolivia, and Ecuador are developing the proposal for the Andean Regional Project for Adaptation aimed at supporting pilot projects on glaciers and watersheds. Additionally, Ecuador is implementing a project through the water governance to reduce the vulnerability on climate change by an effective management of the water sources and better access to information on climate (General Secretariat of the Andean Community et al. 2007a).

On the other hand, some projects showed results on the ecosystem services demonstrating the complexity using these mechanisms. In Brazil, after 4 years, implementation of a project to pay for conservation services to small-scale farmers located in the Brazilian Amazon has presented combined results. This program developed by Proambiente has gathered about 4,200 participating families, from which the 42 % have reached payments over the R $650 (US$325) per household (Hall 2008). Also, the Juma Reserve REDD project has been established to prevent deforestation by the valuation of the services provided for the forests located in the southeastern region of the Brazilian state of Amazonas (do Planeta et al. 2008). The PES (payment for environmental services) presents a varied implementation; countries like Colombia and Ecuador count on important projects (e.g., the Face Reforestation Program for Ecuador, PROFAFOR (Spanish abbreviation), Carbon Sequestration Program, and the Pimampiro municipal watershed scheme) demonstrating advanced applications; however, Colombia presents some disadvantages in the payment to service providers, while countries like Bolivia and Venezuela show a higher skepticism and political barriers (Wunder 2007).

Otherwise, some challenges are recognized for the legal hurdles, and this aspect is observed on the Brazilian legislation for the concept of environmental services and their economic value which can be related to the water-use charges that do not place economical value on the water-conservation role of landowners (Hall 2008). Also, the complexity on the information related to the scientist and economical integration can affect the real operability of adaptation and mitigation measures. For this case, some studies have estimated that emission from both deforestation and fossil fuel combustion represents the 12 % which is 8 % less than the one estimated by the Intergovernmental Panel on Climate Change (IPCC) (Van der Werf et al. 2009).

Table 2 shows the ecological footprint for some countries in South America included in the estimations made by the Global Footprint Network (Footprint for Nations 2010) demonstrating the large biocapacity contained in the region and represented by their forests. South America counts on several advantages to develop adaptation and mitigation measures. Peru holds more than 40 projects equivalent to the reduction of about five million tons of CO_2 (General Secretariat of the Andean Community et al. 2007a). The Andean region including Venezuela and Chile has 570 million hectares of bio-productive area from which 200 million of supply goods

Table 2 Ecological footprint, ecological deficit, and main contributor of biocapacity, by country, 2006 (Elaborated based on information from Global Footprint Network (Footprint for Nations (2010) data tables http://www.footprintnetwork.org/en/index.php/GFN/page/footprint_for_nations/. Accessed September 29, 2010)

	Ecological footprint	Ecological (deficit) or reserve	Main type of biocapacity
Country name	2006	2006	2006
Argentina	3.0	4.1	Cropland (33 %)
Bolivia	2.4	16.9	Forest (82 %)
Chile	3.1	1.0	Forest (53 %)
Colombia	1.9	2.0	Forest (57 %)
Ecuador	1.9	0.4	Forest (57 %)
Paraguay	3.4	7.4	Forest (62 %)
Peru	1.8	2.3	Forest (67 %)
Venezuela (Bolivarian Republic of)	2.3	0.3	Forest (72 %)

and services absorb their own wastes, representing 370 million of global hectares valuated as 115,000 million dollars (General Secretariat of the Andean Community 2008).

The PES offers a great opportunity for countries to develop mitigation programs for the conservation of ecosystems and reforestation. For example, in Pimampiro, Ecuador, a farmer receives 12 $/ha/year for the conservation of primary forest; however, payments can vary for the same land use (a farmer in Heredia, Costa Rica, receives 57 $/ha/year for the same land use), and the implementation of PES has turned on an opportunity for farmers to develop conservation and productive activities (Kiersch et al. 2005).

The Climate Change Challenge for South America

South America's CO_2 emissions are relatively low; however, Brazil predominates the emissions of the region, while all the countries (excluding Paraguay) are presenting increase in the emissions, with Bolivia and Ecuador showing an increase of 69 % and 79 % between 1999 and 2008 relatively (see Fig. 3).

About 50 % of the $ktCO_2$ registered by 2012 belongs to energy-associated projects (see Fig. 4). This tendency is demonstrating the important participation in the Carbon Market reached by the implementation of energy projects.

Some projects in South America are demonstrating the potential of the region for implementing alternative energy and reduce CO_2 emissions (Table 3).

Despite the low participation of SA in the CDM, energy projects represent more than the 80 % of the $ktCO_2e$ registered by 2012 in all countries in the region (excluding Paraguay and Uruguay) (see Fig. 5). SA requires technological transfer to take advantage of the alternative energy potential, but better policies should be applied by participating in Global Carbon Market to achieve technology and

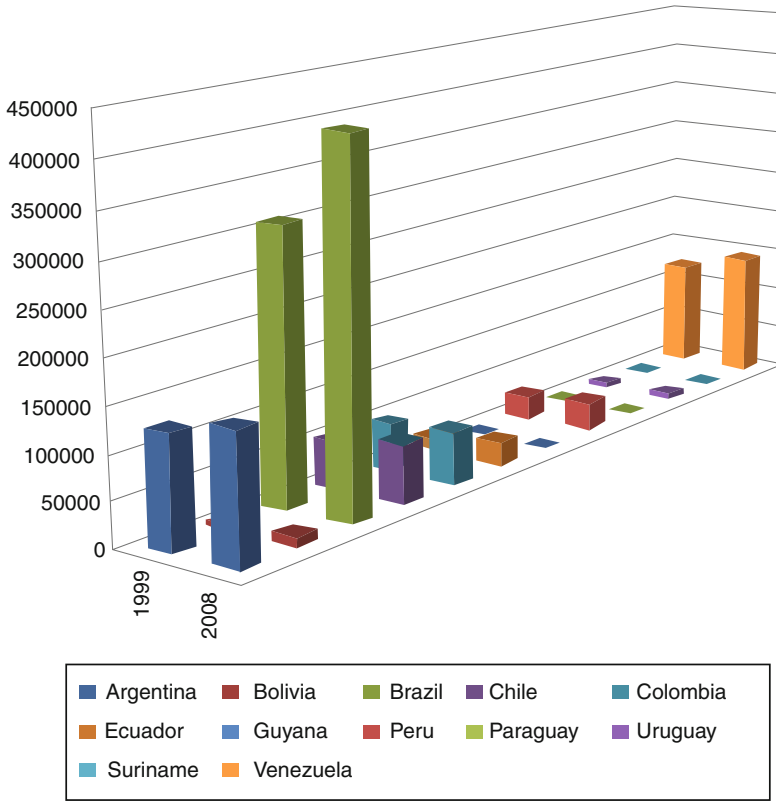

Fig. 3 CO_2 emissions (Gg) by country, 1999 and 2008. Elaborated based on the data from the Latin American Energy Organization, OLADE, 2009. Energy Statistics Report 2009. Base year 2008

resources transfer while protecting natural resources. A good example was given by Ecuador when it decided to pledge in a pioneering agreement with the United Nations to refrain from oil drilling in a pristine Amazon preserve in return for some US$3.6 billion ($4.9 billion) in payments from rich nations (Yasuni-ITT 2010).

Because of its ecological sensibility, in the sociocultural and economic context, South America is one of the main vulnerable regions in the planet facing climate change. This situation requires more accelerated and practical adaptation programs in the real scenario. Because the main natural and social characteristics bring different levels of risk, also the application of these programs should vary and be approached to different scales.

The main challenge for this region is to understand how global, regional, and local dynamics can impact the different local scenarios. At present, the main aim for combating climate change is to design more effective mitigation and adaptation measures for the specific and unique conditions, not only for the different countries, but also for the different communities and ecosystems contained within them. Policy

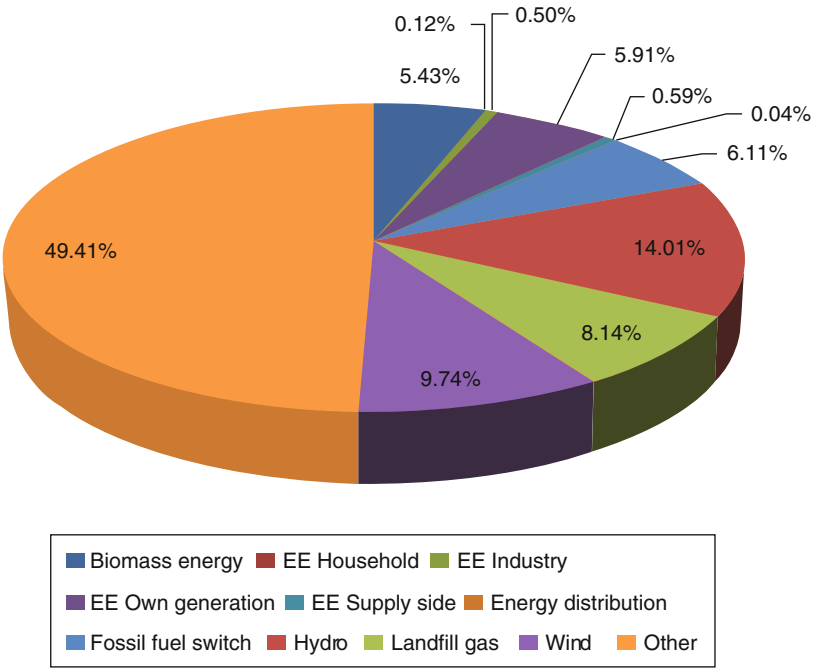

Fig. 4 Global sharing of $ktCO_2$ registered by project type by 2012. Elaborated based on the information from the data available at Carbon Market Data World ETS Database http://www.carbonmarketdata.com/. Accessed February 17, 2011

Table 3 CO_2 reduction potential by energy projects in South America (Elaborated based on the information from the *General Secretariat of the Andean Community, the United Nations Environment Programme (Regional Office for Latin America and the Caribbean), and the Spanish International Cooperation Agency (2007) and **Gerardo Siva Dias PR, Ribeiro WC, Sant Anna Neto JL, Zullo Jr. J (2009))

Country	CO_2 reduction potential (ton equivalent)	Kind of project
Ecuador*	307,000	Not specified
Bolivia*	17.7 million	Not specified
Colombia*	800,000	Jepirachi eolic project
Brazil**	84,165	Alta Mogiana Bagasse for electricity produced from fossil fuel energy stations by energy produced from sugarcane bagasse

integration of the countries to transform the natural resources and energy potential into operative projects is required. Regional scales, beyond national boundaries, should be integrated for designing regional actions toward the technological transfer for alternative energy development and conservation programs for vulnerable ecosystems like the Amazon, Glaciers, and forest cloud mountains.

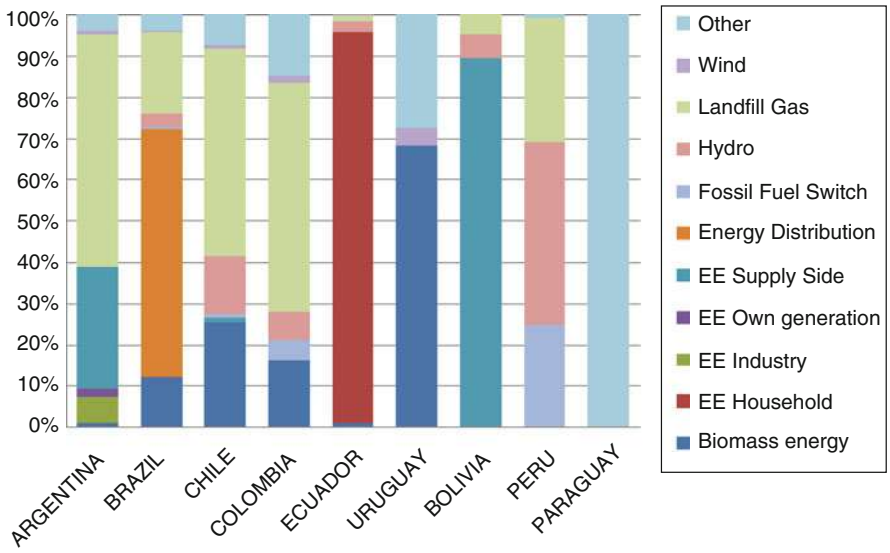

Fig. 5 National Sharing of $ktCO_2e$. Registered by project type by 2012 (Elaborated based on the information from the data available at Carbon Market Data World ETS Database http://www.carbonmarketdata.com/. Accessed February 17, 2011)

Future Direction to Combating Climate Change in SA and EA

Vis-à-vis the present climate change impacts, it is very unlikely that the negative effects on the environment and people's livelihood will improve any time soon. The latter necessitates helping vulnerable individuals/groups cope with the adverse effects and reestablish their means of livelihood after climate disasters. Worth noting, combating climate change in the regions would require both local and extra-local efforts in a number of ways. For instance, future adaptations and mitigations to climate change vulnerability will have to be reflected in all regional polices (MOENR 2002).

Coping with climate change challenges will have to go hand in hand with major adjustments in various policies and legislations. For instance, the potential for utilization of renewable energies, namely, biomass, solar power, geothermal, wind energy, biogas, and natural gas, would require significant regional governments' commitments in terms of policy adjustments and economic sacrifices. Successful harnessing of geothermal energy in Kenya, natural gas in Tanzania, and most of the renewable in Brazil could imply that proper policy adjustments could reduce power shortages in the regions. In recent years, however, significant efforts in structuring climate change policies have been taken by nearly all regional governments. Although the efforts may be considered insufficient compared to the impacts, they do provide a fundamental framework to dealing with regional climate change challenges. These include the establishment of national bodies with full mandates

on climate change issues and environment management at large and creation of several laws and legislations on environmental issues (The Global Humanitarian Forum 2009; Red Crescent Climate Centre, RCRCCC 2003). Arguably, as a sign of worsening situation, most recent government policy documents in the regions do recognize climate change as an important impediment to their sustainable development. For instance, most climate change issues are notably defined in the regional National Adaptation Program of Action (NAPA) reports (Red Crescent Climate Centre, RCRCCC 2003). In summary, the regional bodies dealing with climate change requires an inclusion of how such projects and/or policies with potential negative impacts to the environment will be addressed before being accepted for implementation. The latter makes it mandatory for extensive environmental impact assessment (EIA) to be carried out to such projects before they would be approved for implementation (The Global Humanitarian Forum 2009; Red Crescent Climate Centre, RCRCCC 2003). However, care must be taken as some of the suggestions in the NAPA reports provide suggestion that might not work in the region. For example, some suggestions in the reports are considered too expensive in the region and require unavailable technology. Failure to fully involve local people has been experienced in the region (particularly in Tanzania) where local people objected some drought-resistant crops on grounds that they were tasteless and lacked market value (Müller 2010). The latter have resulted in poor adaptation to climate change impacts and left on agriculture a significant number of the individuals vulnerable. While some of the suggestion might work in the long run, real solutions to the challenges of climate change vulnerability would come from an inclusion of a wealth of local skills dealing with climate change and disaster management at large.

In appreciating the importance of forests in carbon sinking, forests have regionally been advocated as one of the most important gears to combat climate change. In accordance with the global move, regional efforts put a lot of emphasis on both reforestation and afforestation programs (MOENR 2002). However, renewed efforts on forest management are needed as desertification has been increasing. In addition, special consideration needs to be taken on energy sector since a significant portion of regional energy balance is met from biomass energy (International Food Policy Research Institute (IFPRI) 2004). Capitalization on the abundant potentials of renewable energy would reduce pressure on the natural forests and the amount of carbon emitted.

Alongside the suggestions above, it is worth noting that the regions lack necessary expertise and economic ability to deal with climate change and associated issues. Emphasis must thus be concentrated on training local scientists, planners, and policy makers to prepare them to deal with the worsening situation in the regions. In addition, future direction of climate change in EA and SA will have to be concentrated on land use change since major regional contribution to the GHGs comes via land use change and deforestation.

Furthermore, the EA region has an abundant supply of carbon dioxide which requires purification only to be ready for industrial use. EA countries could capitalize on the natural supply of the gas and stop importation of the gas from other places. At present, most industries in Uganda, Tanzania, and Kenya still import carbon dioxide

which is seen as a wasted regional opportunity both to control carbon and investment. As a potential investment, the Carbacid Company in Kenya has started mining the gas for commercial purposes. Thus, both regional and even neighboring countries could meet all their carbon needs from the region without requiring importation of the gas. Similar efforts need to be strengthened in other regional countries and potentially stop importation of the gas all together.

Other areas where strengthening can be done to reduce vulnerability to climate change include accurate information gathering and dissemination. The latter is important since most times when climate disasters strike many people have been caught unaware/unprepared and thus increased vulnerability. In addition to that, renewed emphasis on local capacity building and decision-making should be made central in helping vulnerable groups to adapt better to climate change impacts. Because of the poor resource base in the regions, it is very important for funds whether in the form of credit or otherwise to be available to vulnerable groups after climate change disasters. Such funds can help affected individuals or groups to restock lost animals, buy farm inputs, and/or reestablish lost business or other means of livelihoods. The best way to ensure availability of funds to such groups/individual could be via rural credit mechanisms. Governments and other stakeholders should as well help rural credit mechanisms like pastoralists and/or cooperative unions get funds from financial institutions. This is important as regional studies have shown that individuals who have financial access like remittances from relatives generally recover faster and better from disasters.

Another potential area for future strengthening includes effective early warning systems on climate change disasters and effective information gathering and dissemination. Recent regional experiences have shown that climate change vulnerability is often worsened by failures to forecast potential climate disasters and poor communication between responsible authorities and the general population (Red Crescent Climate Centre, RCRCCC 2003). In the future, it would be very helpful to have a mechanism that would ensure such information is well forecasted and the general population is well prepared for the potential effects. Vis-a-vis to the above, it will be very helpful for regional bodies like meteorological departments and disaster management units to be equipped with advanced early warning systems for potential climate disasters and effective mechanisms to spread the necessary information. Albeit governments in both regions have taken certain steps in improving their disaster management units, further effort is still needed to improve them further by purchasing more accurate meteorological equipments and proper training of staff.

Finally, careful enforcement of environmental education in school curriculums may also prove to be a reliable means of reducing causes of climate change but most importantly help in regional adaptation and mitigation strategies. Because climate change and generally environmental degradation are presently appreciated to be developmental factors, it is crucial for regional education system to effectively prepare younger generations on environmental issues. Significant efforts have been made in recent years regarding inclusion of environmental aspects in school system, and several environmental-related degree and nondegree programs are being offered in colleges (The Global Humanitarian Forum 2009). Efforts can still be done to

improve such curriculums to enable real solutions to local climate change-related challenges. Inclusions of environmental course in non-environmental programs in schools would as well help a larger part of the society become environment sensitive.

Conclusion

In SA and EA, the negative climate change impacts are no longer potential threats but rather ongoing problems that have long been underestimated. Climate variability is already affecting many development projects and even threatens to undo some of the achievements made, including some of the Millennium Development Goals (MDGs). Generally, the regional climate change vulnerability requires immediate actions as several sensitive ecosystems like the coastal resources, Eastern Arc Mountain forests, the Amazon forests, Mount Kenya, Mount Kilimanjaro, and the Andean Mountains are already affected. The negative impacts on agricultural systems, water resources, biodiversity, energy availability, infrastructures, and health issues are unmistakably clear and worsened by the fast-growing population and widespread poverty, among others. Today, ordinary people in the villages know their ways of making a living and are threatened and are left with no option but to return to their indigenous survival skills. The status quo leaves the regions with potentials of being significant contributors of GHGs in the next decades via land degradation and especially deforestation of its fast-shrinking forest resources so as to meet basic needs such as fuel wood. The use of poor often polluting technologies in the struggle for economic development and the desires to meet the needs of the fast-growing population will also add to GHG contribution in the future. As these regions near their peaks in terms of economic and industrial development, this would mean that a more net contribution in GHGs is likely because the regions will be consuming more energy, a trend that is already evident.

Most adaptations and mitigation options suggested by international bodies and which are largely reflected in the regional climate change strategies have local implementation difficulties. Since the economic base of the regions is among the world's least, implementations of such technical, expensive, and often unavailable options might prove to be difficult and could leave many people vulnerable to climate change impacts. Fortunately, the regions have rich indigenous skills and adaptation measures that require strengthening and inclusion into the regional vision for combating and/or living with climate variability. Thus, meaningful relief from climate change vulnerability will have to include existing livelihood strategies and especially recognition of the traditional resource management including on land that are well developed in the regions. However, local survival skills to the harsh conditions like droughts have in recent years been overstretched and feared not to work in the long term.

Unfortunately, governments and development planners within the regions were late to recognize that climate change was an issue of development and needed to be incorporated into all development projects. Climate change issues were for the long time not clearly reflected into the regional development plans and mistakenly treated

as a separate entity resulting to bitter lessons. Because of the severity of the challenges of climate change to the delicate livelihood system in the regions, governments, private sector, and other stakeholders were forced to take decisive steps and recognize climate change to be an integral part of regional sustainable development.

Since major contributions to climate change causes come via land use change and natural resources exploitation, land and natural resources like forests need to be central in dealing with climate change in the regions. Land and forest policies necessitate reexamining and better enforcing so as to control/reduce desertification, a trend of which has in recent years been significant in the regions.

Moreover, because both the courses and impacts recognize no regional boundaries, regions must move with the rest of the world in combating climate change. Regional governments, private sectors, individuals, and other stakeholders need to play their expected roles in both adaptation and mitigation measures to combat climate change. On the other hand, where as the international efforts do provide important generalizations regarding climate variability, they should try as much as possible to recognize special vulnerability in SA and EA where many of their frameworks dealing with the variability might not work as expected and should locally be assisted to deal with their problems in specific ways. While generalization simplifies things, specific issues in the regions, like over 70 % of the population is dependent on biomass on EA, need to be noted and treated in a special way.

References

Action Aid International (2007) Unjust waters: climate change, flooding and the protection of poor Urban communities: experiences from six African cities. Africa's urban poor are struggling to cope with climate-induced flooding. Action Aid International, London

Andean Community (CAN) (2008) Main indicators in the South American countries 1998–2007 (in Spanish). Statistics Paper. Secretary General Andean Community. Lima. http://www.comunidadandina.org/estadisticas/SGde215.pdf. Accessed 12 Feb 2010

Brondizio ES, Moran EF (2008) Human dimensions of climate change: the vulnerability of small farmers in the Amazon. Phil Trans R Soc B 363:1803–1809

Calvo AF (2000) Demographic situation analysis of the country (in Spanish). Serie Documentos Tecnicos OPS, 2

Christensen H, Hewitson B (2007) Regional climate projections, Chapter 11. In: Solomon S et al (eds) Climate change 2007, the physical science base, contribution of working group 1 to the Fourth assessment report of the intergovernmental panel on climate change. Cambridge University Press, Cambridge, pp 848–940

Christian Aid (2006) The climate of poverty: facts, fears and hope. Christian Aid Report

Commission on Climate Change and Development (2009) Closing the gaps, Sweden www.ccdcommission.org. Accessed Dec 2010

Comunidad Andina (2010) Web page http://www.comunidadandina.org/sudamerica.htm. Accessed 24 Feb 2010

Conway D (2002) Extreme rainfall events and lake level changes in East Africa: recent events and historical precedents. In: Odada EO, Olago DO (eds) The East African great lakes: limnology, palaeolimnology and biodiversity, advances in global change research, vol 12. Kluwer, Dordrecht, pp 63–92

Davidson O, Halsnaes K, Huq S, Kok M, Metz B, Sokona Y, Verhagen J (2003) The development and climate nexus: the case of sub-Saharan Africa. Climate Policy 3S1:S97–S113

Derruyttere A (1997) Indigenous and sustainable development: the role of the Interamerican development bank (in Spanish). Banco Interamericano de Desarrollo. Departamento de Desarrollo Sostenible. Unidad de Pueblos Indígenas y Desarrollo Comunitario, Washington, DC

Devereux S, Edward J (2004) Climate change and food security. IDS Bull 35:22–30

do Planeta B, Sustentavel FA, do Estado AG (2008) The Juma sustainable development reserve project: reducing greenhouse gas emissions from deforestation in the state of Amazonas, Brazil project design document (pdd) for validation at "climate, community & biodiversity alliance (CCBA)" version 5.0 http://www.fas-amazonas.org/en/section/publications. Accessed Dec 2010

Easterling WE, Aggarwal PK, Batima P, Brander KM, Erda L, Howden SM, Kirilenko A, Morton J, Soussana JF, Schmidhuber J, Tubiello FN (2007) Food, fibre and forest products. In: Parry ML, Canziani OF, Palutikof JP, Van der Linden PJ, Hanson CE (eds) Climate change 2007: impacts, adaptation and vulnerability. Contribution of working group II to the fourth assessment report of the intergovernmental panel on climate change. Cambridge University Press, Cambridge, p 273313

ECLAC (2009) Economics of climate change in Latin America and the Caribbean Summary 2009, United Nations Santiago. http://www.eclac.org/publicaciones/xml/3/38133/2009-851-Summary-Economics_climate_change-WEB.pdf. Accessed 23 Mar 2010

Ellis J (1994) Climate variability and complex ecosystem dynamics: implications for pastoral development. In: Scoones I (ed) Living with uncertainty: new directions in pastoral development in Africa. Intermediate Technology, London, pp 37–57

Ensminger J (1992) Making a market: the institutional transformation of an African society. Cambridge University Press, New York

Fick AA, Myrick CA, Hansen LJ (2005) Potential impacts of global climate change on freshwater fisheries. A report for WWF, Gland

Footprint for Nations (2010) Data tables http://www.footprintnetwork.org/en/index.php/GFN/page/footprint_for_nations/. Accessed 29 Sep 2010

Foster P (2001) The potential impacts of global climate change on tropical montane cloud forests. Earth Sci Rev 55:73–106

Galvin KA, Ellis J, Boone RB, Magennis AL, Smith NM, Lynn SJ, Thornton P (2002) Compatibility of pastoralism and conservation? A test case using integrated assessment in the Ngorongoro Conservation Area, Tanzania. In: Chatty D, Colester M (eds) Displacement. Forced Settlement and Conservation, Berghahn/Oxford, pp 36–60

Garcia CL (1999) Urbanization, poverty and redistribution space of the Bolivian people (in Spanish). Revista electronic de Geografia y Ciencias Sociales 45(32)

General Secretariat of the Andean Community (2008) Climate change knows no borders climate change impact in the Andean Community (in Spanish). Secretary General Andean Community, Lima. http://revistavirtual.redesma.org/vol5/pdf/publicaciones/CAN-libro_cambioclimatico-0508.pdf. Accessed Feb 2011

General Secretariat of the Andean Community, the United Nations Environmental Program (Regional Office for Latin America and the Caribbean), and the Spanish International Cooperation Agency (2007) This climate is serious business an overview of climate change in the Andean Community (in Spanish). Secretary General Andean Community, Lima. http://revistavirtual.redesma.org/vol5/pdf/publicaciones/CAN-cambio_climatico_Cosa_seria_clima.pdf. Accessed Feb 2011

General Secretariat of the Andean Community, the United Nations Environmental Program (Regional Office for Latin America and the Caribbean), and the Spanish International Cooperation Agency (2007) The end of snowy heights? Glaciers and climate change in the Andean Community. Secretary General Andean Community, Lima. http://revistavirtual.redesma.org/vol5/pdf/publicaciones/cambio_climatico_fin_cumbres_nevadas.pdf. Accessed Feb 2011

Government of Kenya Meteorological Service (1998) The El-Niño Rains of Oct 1997–Jan 1998 in Kenya. Kenya meteorological department, Nairobi. www.meteo.go.ke/pws/elnino.html. Accessed Mar 2011

Grandin B (1988) Wealth and pastoral dairy production: a case study from Maasai land. Human Ecol 16(1):1–21

Hall A (2008) Better RED than dead: paying the people for environmental services in Amazonia. Phil Trans R Soc B 363:1925–1932

Hansen J, Ruedy R, Sato M, Lo K (2006) NASA Goddard Institute for space studies and Columbia University Earth Institute, New York. http://data.giss.nasa.gov/gistemp/2005/

Hellmuth ME, Moorhead A, Thomson MC, Williams J (eds) (2008) Climate risk management in Africa: learning from practice. International Research Institute for Climate and Society (IRI), Columbia University, New York

Hemp A (2005) Climate change driven forest fires marginalize the impact of ice cap wasting on Kilimanjaro. Global Change Biol 11:1013–1023

Horn of Africa Review (1997) Horn of Africa review compiled by the UNDP-EUE, 6/1-7/31. University of Pennsylvania, Philadelphia. www.sas.upenn.edu/Africa_Studies/Newsletters/har_797.html. Accessed Mar 2011

Hulme M, Doherty R, Ngara T, New M, Lister D (2001) African climate change: 1900–2100. Climate Res 17:145–168

International Food Policy Research Institute (IFPRI) (2004) Ending hunger in Africa: prospects for the small farmer. International Food Policy Research Institute (IFPRI), Washington, DC

InWent (2008) Climate change and retreat of glaciers in the Andean region: implications for water resources management. Rev Virtual REDESMA 2(3):19–23

Jones C, Collins M, Cox P, Spall S (2001) The carbon cycle response to ENSO: a coupled climate-carbon cycle l study. J Climate 14:4113–4129

Kelly PM, Adger WN (2000) Theory and practice in assessing vulnerability to climate change and facilitating adaptation. Clim Change 47:325–352

Kerven C (1992) Customary commerce: a historical reassessment of pastoral livestock marketing in Africa. ODI Agr Occas Pap 15. Overseas Development Institute, London

Kiersch B, Hermans L, Van H (2005) Payment schemes for water-related environmental services: a financial mechanism for natural resources management experiences from Latin America and the Caribbean. Paper presented on Seminar on environmental services and financing for the protection and sustainable use of ecosystems, Geneva, 10–11 Oct 2005

Levine T, Encinas C (2008) Adaptation to the climate change: experiences in Latin America (in Spanish). Rev Virtual REDESMA 2(3):25–32

Little PD, Brokensha DW (1987) Local institutions, tenure and resource management in East Africa. In: Anderson P, Grove R (eds) Conservation in Africa: people, policies and practice. Cambridge University Press, Cambridge, pp 193–209

Magadza CHD (2000) Climate change impacts and human settlements in Africa: prospects for adaptation. Environ Monitor Assess 61:193–205

Magrin G, Gay García C, Cruz Choque D, Giménez JC, Moreno AR, Nagy GJ, Nobre C, Villamizar A (2007) Latin America. In: Parry ML, Canziani OF, Palutikof JP, van der Linden PJ, Hanson CE (eds) Climate change 2007: impacts, adaptation and vulnerability. Contribution of working group II to the fourth assessment report of the intergovernmental panel on climate change. Cambridge University Press, Cambridge, pp 581–615

Maingu EM, Msyani C, Massawa E, Njihia J, Agatsiva JL, Apuuli B, Kahuma T, Mubiru P, Magezi SA (2003) Options for greenhouse gas mitigation in an integrated East African power development. In: Meena HE (ed) The centre for energy, environment, science and technology. Dar es Salaam, Tanzania, pp 6–32

Ministry of Lands, Water and Environment (MLWE) (2002) Initial national communication on climate change. Uganda

MOENR (2002) First national communication to the conference of the parties to the United Nations Framework Convention on Climate Change (UNFCCC). Ministry of Environment and Natural Resources. National Environment Secretariat, Nairobi

Müller B (2010) Copenhagen 2009, failure or final wake-up call for our leaders? Oxford Institute for Energy Studies, Oxford, p EV 49. ISBN 978-1-90755-04-6

Mwandosya MJ, Nyenzi BS, Luhanga ML (1998) The assessment of vulnerability and adaptation to climate change impacts in Tanzania. Centre for Energy Environment, Science and Technology (CEEST), Dar-es-Salaam. ISBN 9987612113

Nicholson SE (1996) A review of climate dynamics and climate variability in Eastern Africa. In: Johnson TC, Odada EO (eds) The limnology, climatology and paleoclimatology of the East African lakes. The international decade for the East African lakes (IDEAL). Gordon and Breach, Newark, pp 25–56

O'Brien K, Sygna L, Naess LO, Kingamkono R, Hochobeb B (2000) Is information enough?: user responses to seasonal climate forecasts in southern Africa. Centre for international climate and environmental research (CICERO), University of Oslo, Report No. 3, Oslo

Patz JA, Campbell-Lendrum D, Holloway T, Foley JA (2005) Impact of regional climate change on human health. Nature 438:310–317

Red Cross and Red Crescent Climate Centre, RCRCCC (2003) Preparedness for climate change. A study to assess the future impact of climate changes upon frequency and severity of disasters and the implications for humanitarian response and preparedness. IPCC Fourth Assessment Report, RCRCCC

Rodríguez VA (2007) Climate change, water and agriculture (in Spanish). Dirección de Desarrollo Rural Sustentable IICA. Comunica, edición N°1, II Etapa

Roque R (2005) Importance of collective lands of indigenous and African rural development (in Spanish). Futuros 11(3):135–161

Sarmett JD, Faraji SA (1991) The hydrology of Mount Kilimanjaro: an examination of dry season runoff and possible factors leading to its decrease. In: Newmark WD (ed) The conservation of Mount Kilimanjaro. IUCN, Gland, pp 53–70

Seo SN, Mendelsohn YR (2008) A Ricardian analysis of the impact of climate change on South American farms. Chilean J Agric Res 68(1):69–79

Shongwe SV (2009) The impact of climate change on health in the East, Central and Southern African (ECSA) region. ECSA Health Community, Arusha

Siemien MJ, Stauffer JRJ (1989) Temperature preference and tolerance of the spotted tilapia and Rio Grande cichlid. Archiv fur Hydrobiologie 115:287–303

Talle A (1987) Women as heads of houses: the organization of production and the role of women among pastoral Maasai of Kenya. Ethnos 52(1–2):50–80

The Global Humanitarian Forum (2009) Human impact report: climate change-the anatomy of a silent crisis. The Global Humanitarian Forum, Geneva. ISBN 978-2-8399-0553-4

Thompson J, Porras IT, Tumwine JK, Mujwahuzi MR, Katui-Katua M, Johnstone N, Wood L (2001) Drawers of water II: 30 years of changing domestic water use and environmental health in East Africa. IIED, London

Thompson I, Mackey B, McNulty S, Mosseler A (2009) Forest resilience, biodiversity, and climate change. A synthesis of the biodiversity/resilience/stability relationship in forest ecosystems. Secrétariat de la Convention sur la diversité biologique, Montréal. Technical series no. 43, 67 pp

Tian H, Melillo JM, Kicklighter DW, McGuire AD, Helfrich JV III, Moore BI, Vorosmarty CJ (2000) Climatic and biotic controls on annual carbon storage in Amazonian ecosystems. Glob Ecol Biogeogr 9:315–335

Tsonis AA, Hunt AG, Elsner JB (2003) On the relation between ENSO and global climate change. Meteor Atmos Phys 84:229–242

UICN (2008) Indigenous and traditional peoples and climate change Summary (in Spanish) http://cmsdata.iucn.org/downloads/uicn_pueblos_indigenas_y_cambio_climatico___version_resumida.doc. Accessed 23 Mar 2010

UNDP (2007) Human development report 2007/2008 fighting climate change: humanity solidarity in a divided world. http://hdr.undp.org/en/media/HDR_20072008_EN_Overview.pdf. Accessed 21 Mar 2010

United Republic of Tanzania, URT (2003) Initial national communication under the United Nations framework convention on climate change (UNFCCC). Office of the Vice President, Tanzania

United republic of Tanzania, URT (2007) National adaptation programme of action (NAPA). Vice president's office, division of environment. Government printers, Dar es Salaam

Van der Werf GR, Morton DC, DeFries RS, Olivier JGJ, Kasibhatla PS et al (2009) CO_2 emissions from forest loss. Nat Geosci 2:737–738

Vuille M, Bradley R, Werner M et al (2003) 20th century climate change in the tropical Andes: observations and model results. Clim Change 59:75–99

Vuorinen I, Kurki H, Bosma E, Kalangali A, Mölsä H, Lindqvist OV (1999) Vertical distribution and migration of pelagic Copepoda in Lake Tanganyika. Hydrobiologia 407:115–121

World Bank (2006) Project document on a proposed grant from the global environment facility trust fund in the amount of used 5.4 million for the benefit of the republic of Colombia through conservation international Colombia for the Colombia: integrated national adaptation program project, Bogota

World Bank (2008) Social dimensions of climate change report 2008. The World Bank, Washington, DC. http://www.crid.or.cr/digitalizacion/pdf/eng/doc17656/doc17656.htm. Accessed 28 Feb 2010

World Bank (2010) Climate change and clean energy initiative assessment of the risk of Amazon dieback main report. http://www.bicusa.org/en/Article.11756.aspx. Accessed 3 Mar 2010

World Food Program (WFP) (2000) Kenya's drought: no sign of any let up. WFP, Rome. www.wfp.org/newsroom/In_depth/Kenya.html. Accessed Mar 2011

World Health Organisation (WHO) Regional Office for Europe (2003) Methods for assessing human health vulnerability and public health adaptation to climate change. Health and global environmental change, vol 1. WHO Regional Office for Europe, Copenhagen

Wu Z, Schneider EK, Hu ZZ, Cao L (2001) The impact of global warming on ENSO variability in climate records. COLA Technical Report CTR 110

Wunder S (2007) Between purity and reality: taking stock of PES schemes in the Andes, Ecosystem Marketplace. http://www.ecosystemmarketplace.com/pages/dynamic/article.page.php?page_id=4585&section=home&eod=1. Accessed Dec 2010

WWF (2006) Climate change impacts in the Amazon: review of scientific literature. http://assets.panda.org/downloads/amazon_cc_impacts_lit_review_final.pdf. Accessed 9 Feb 2010

Yasuni-ITT (2010) To keep the oil reserves under earth (in Spanish). http://yasuni-itt.gob.ec/. Accessed Dec 2010

Zhou G, Minakawa N, Githeko AK, Yan G (2004) Association between climate variability and malaria epidemics in the East African highlands. In: Proceedings of the national academy of sciences of the United States of America, vol 101, Washington, DC, pp 2375–2380

Statistics in Climate Variability, Dry Spells, and Implications for Local Livelihoods in Semiarid Regions of Tanzania: The Way Forward

Ceven Shemsanga, A. N. N. Muzuka, L. Martz, H. Komakech, and Anne Nyatichi Omambia

Contents

C. Shemsanga (✉)
Department of Water and Environmental Sciences and Engineering, Nelson Mandela Institution of Science and Technology-Tengeru, Tengeru, Arusha, Tanzania

Department of Environmental Engineering and Management, University of Dodoma, Dodoma, Tanzania
e-mail: 7ceven@gmail.com

A.N.N. Muzuka • H. Komakech
Department of Water and Environmental Sciences and Engineering, Nelson Mandela Institution of Science and Technology-Tengeru, Tengeru, Arusha, Tanzania

L. Martz
Department of Geography, University of Saskatchewan, Saskatoon, SK, Canada

A.N. Omambia
National Environment Management Authority, Nairobi, Kenya

W.-Y. Chen et al. (eds.), *Handbook of Climate Change Mitigation and Adaptation*,
DOI 10.1007/978-3-319-14409-2_66

Abstract

The Dodoma municipality, a semiarid region of Tanzania, is characterized by limited rains, lack of surface water sources, and a high frequency of extreme climate events, particularly droughts and floods. These disadvantaged settings make it vital to study long-term climate trends for signals and patterns of shifting climate regimes for integrity of local livelihood support systems, especially agriculture, recharge, and pasture developments. The area has fairly long climate records, some of which extend to about 100 years. This chapter presents detailed analysis of six climate parameters, namely, rainfall (R), atmospheric relative humidity (ARH), temperature (T), sunshine (S), radiation (RD), wind speed (WS), and evaporation (ET) records from three meteorological stations, namely, Hombolo Agrovet (HMS), Dodoma (DMS), and Makutupora (MMS). The parameters above were statistically and graphically analyzed in four time scales, namely, monthly, seasonal, annual, and time series. The results showed the area is characterized by slight spatial variability in R intensity and T magnitudes with HMS having higher T and rains than DMS and MMS. Further there are clear decreasing trends in ARH and R, while T, S, WS, ET, and RD parameters showed characteristic increasing trends. Thus, except for extreme rain events, particularly El Niño-Southern Oscillations (ENSO), which are characterized by abnormally increased R magnitudes, R intensity has generally decreased in which over the past 91 years, there has been a net R decrease of 54 mm out of annual rains of only about 550 mm/year. Compared to annual time step, however, monthly step reveals more silent features like shortening of the growing seasons. Similarly, the frequency and severity of drought episodes are increasing, all of which adversely impact agriculture, pasture development, and recharge. Similarly, disappearance of R in some months, shifting seasonality, and general declining R intensities and magnitudes are clearly observed. May rains have largely disappeared, while in January, February, March, and April rains have decreased and hence shortening the length of growing season. On the other hand, clear warming trends and declining ARH were also observed. Yet the area is marked by cyclic wetting and drying events where in recent years, drying cycles have been prolonged. However, there is more variability in the mean minimum temperature (MMT) than in mean maximum temperatures (MMMT) in all stations. Between 1961 and 2012, there has been a net 1.13 and 0.778 °C increases in annual MMT and MMMT in DMS, respectively. Like for R trends, silent features are more evident under monthly T data than annual time steps where it is clear that June had the highest increase in MMT (1.54 °C), while April had the least (only 0.662 °C). However, both trends have the potential of affecting major livelihood support systems particularly agriculture and pasture development, but also local groundwater recharge that is vital for the local economy. The study area therefore offers a rare opportunity to understand and manage changing climate regimes including on extent of dry spells and longevity of growing seasons. The changing climate trends consequently call for significant adaptation and mitigation strategies so that local activities adjust to the current climate regimes particularly on onset and end of rainfall seasons and recharge fluxes.

Introduction

In recent years, the augments against climate change have lost path as its negative impacts become more severe and widespread, numerous times with major socioeconomic implications (Ebi 2014; Knox et al. 2012; Omambia et al. 2012). Globally, increasing evidence have been documented showing widespread changes in climate regimes with major implications in the life support systems like food security, shifting ecological range of disease vectors (Altizer et al. 2013; Harvell et al. 2002, 2009; Lafferty 2009; Thomson et al. 2012), submergence of islands and coastal resources (Barnett and Campbell 2010; Hearty and Neumann 2001; Nicholls 1995), and exuberated vulnerability to natural catastrophes (Omambia et al. 2012), to name but a few. In addition, climate change impacts are blamed for displacement of people and livestock which have often resulted to increased conflicts in Africa (Hendrix and Salehyan 2012; Maurel and Kubik 2014; Shemsanga et al. 2010; Burke et al. 2009).

Currently, many people in rural Africa witness major changes in growing seasons, rainfall intensity and distribution (Mary and Majule 2009; Sanga et al. 2013, 2014), temperature regimes, and disappearing and/or shrinkage of the surface water bodies like rivers and lakes (Boelee et al. 2013; Conway and Schipper 2011; Faramarzi et al. 2013; Hendrix and Salehyan 2012; Mutua and Koike 2013). Further, surface water bodies in Africa are declining leading to increasing conflicts between different water uses/users, namely, pastoralists, agriculturalists, hydropower plants, and water managers (Valimba 2004). On the other hand, drought and flood episodes are becoming more frequent and severe in many places in Africa (Cooper et al. 2013; Knox et al. 2012; Paavola 2008; Simon 2010). However, irrespective of the fact that many of these impacts have been recorded in Africa (Belloumi 2014; Mutua and Koike 2013), and whereas the continent is projected to be affected more by climate variability (Solomon 2007), little has been done on the ground in the manner of observed long-term climate trends, mitigation, and adaptation options (Belloumi 2014; Cooper et al. 2013; Ford et al. 2012; Rugai and Kassenga 2014; Sanga et al. 2013). Indeed the continent has limited ability/options to adapt to climate change impacts and functional mitigation measures due to high rates of poverty, limited infrastructure, and enabling resources to cope with the changes (Cooper et al. 2013; Rugai and Kassenga 2014; Sanga et al. 2013; Simon 2010). It is plausible therefore to carefully study how long climate variability impacts affect the content and hence be better prepared for the workable mitigations and adaptation measures on various sectors.

While the entire African continent is considered more vulnerable to negative climate change impacts, semiarid regions of Africa are already more affected (Fuller and Prince 1996; Majule 2008; Mary and Majule 2009; Mongi et al. 2010; Nelson and Stathers 2009; Paavola 2006; Rowhani et al. 2011). Irrespective of this dire situation, not much is known in the Dodoma municipality, a fast growing city in semiarid Tanzania, regarding long-term climate variability in terms of relative atmospheric humidity (RH), evaporation (ET), sunshine hours (S), radiation (RD),

temperature (T), wind speed (WS), and rainfall (R) patterns. The central issue of when did the key climate parameters locally started to change and at what magnitude compared to the local and global trends also remains unknown. In addition, although many strongly agree that the world climate systems are changing, the inter-seasonal and monthly variations of these core climate parameters in semiarid regions of the developing world are not well documented. Furthermore, past climate studies did not focus on frequency of droughts and monthly and seasonal climate variations, yet these are arguably more important for the local livelihood support system than the annual or higher time scales. While simple tools can make the general climate trends more available to local players, previous regional studies used complicated science and tools that are often out of reach to locals, experts, and decision-makers, hence making it difficult to appreciate the results and most importantly their usefulness.

The geographic, climate vulnerability, and meteorological characteristics of semiarid regions of Tanzania and East Africa in general, require close monitoring of trends in key climate parameters. This is partly so because these parameters directly affect key livelihood support systems of the populace especially agriculture which is predominantly rainfed, the main source of livelihood and employment (Shemsanga et al. 2010; Omambia et al. 2012; Craparo et al. 2015). Correct understanding of these climate parameters particularly when involving smaller and varied scales (monthly, seasonal, and annual) is important in such a region often faced with chronic shortages of water needed for its rapid socioeconomic development, rainfed agriculture, pasture development, and groundwater recharge. Small variations in these climate parameters at lower monthly time step have the potential of affecting local groundwater recharge, agriculture, and pastoralism activities among others. In spite of this importance, few studies have been done locally to ascertain long-term trends, evidence of shifting climate seasonality, yet such studies were all biased toward T and R leaving other pertinent parameters in understanding local climate dynamics unstudied. For instance, limited studies have indicated that the area has observed prolonged droughts and increased crop failure as a direct consequence of decreasing R regimes. Past studies in similar locality found that agriculture and livestock-keeping sectors were severely affected by decreasing R (Majule 2008; Mary and Majule 2009; Craparo et al. 2015). Irrespective of the robust local evidence that the local climate dynamics are changing fast, past studies did not sufficiently study changes in ET, T, S, D, WS, and ARH, all of which are key in understanding of climate patterns, moisture distribution, and local water balancing.

This study intends to statistically ascertain changes and patterns in key climate parameters, namely, R, T, ARH, WS, RD, and ET in relation to livelihood support systems vis-à-vis groundwater recharge, pasture development, and agriculture among others. It is hoped that such a broad and comprehensive understanding of the local climate regimes and their impacts on local livelihood support systems in comparison with the global climate trends would enable better decision-making on adaptation and mitigation from adverse climate variability impacts.

Case Study Description

The current work focuses on the Dodoma urban district. The area is bound by latitude 5°36′59″ and 6°14′50″ S and longitude 35°36′36″ and 36°01′54″ E (Fig. 1). The faulted and tectonically active crystalline basement area of Dodoma craton underlies the area. The metasedimentary rocks are mainly quartzites, iron-stones, micaceous quartzites, quartzo-feldspathic schists, and ferruginous quartzites (Shindo 1991; Nkotagu 1996a, b). Meteorologically, the area is in a semiarid region with low (550 mm/year) unimodal rains between October and May. Temperatures are lowest in July (about 13.0 °C) and highest in November (about 30.6 °C). The semiarid nature of the area can be appreciated from very high evapotranspiration (PET) rates averaging at 2000 mm/year; this rate is roughly fourfold annual rainfall (Shindo 1991). Hydrologically, the area is notable for its lack of permanent surface water bodies and a runoff/river network that is largely seasonal, flowing only during rainy seasons and a few weeks thereafter. Hence the area is heavily reliant of groundwater. The area has a moderate population growth rate (3.3 %), and it is projected that by 2025 total population will be 689,072 compared to 410,956 in 2012. Projections show that by 2025, 94,218 m^3/day of water will be needed in the municipality compared to about 38,006 m^3/day in 2002 (URT 2003).

Materials and Methods

The methods deployed included statistical and variability analyses of climate data, namely, RH, WS, E, S, RD, T, and R. Meteorological and groundwater level data were collected from Makutupora Met station (MMS) (1921–2013), Dodoma Met station (DMS) (1961–2013), and Hombolo Agrovet Met station (HMS) (1980–2013). These were statistically and graphically analyzed under four time steps, namely, monthly, annual, seasonal, and entire time series. However, studies show that extreme events in changing climate variability are more important than averages (Katz and Brown 1992) and, accordingly, those were especially plotted and analyzed.

Data analyses were done using Instat, v. 3.37®, SigmaPlot v11®, and MS-excel, 2007. Thornthwaite monthly water balance (TWMWB®) was used to further model and understand local climate parameters based on observed data. Further, these were used to analyze long-term climate variability, droughts severity, and long-term wetting and drying events/cycles. Local drought index (DI) was developed to assess drought trends by using the following equation (Rathore 2004):

$$DI = \frac{P - x}{SD} \tag{1}$$

where P = annual precipitation, X = long-term mean, and SD = standard deviation. The DI intensity values were then categorized accordingly DI = < −0.1 light drought (LD), DI = < −0.2 moderate drought (MD), DI = < −0.5 severe drought (SD), DI = < −0.8 very severe drought (VSD) (Rathore 2004). Khronostart1.1®

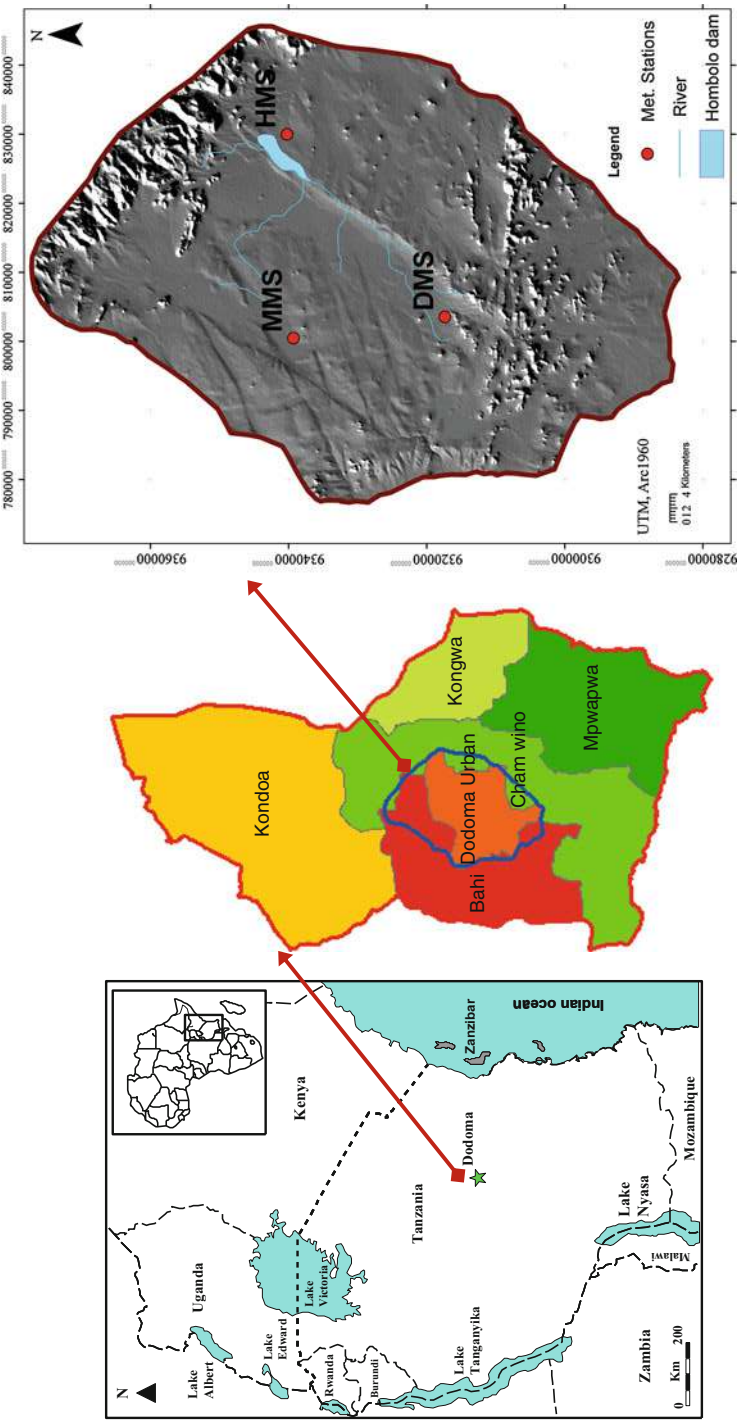

Fig. 1 Study area

software was used to determine when exactly the changes in rainfall occurred and how they varied across the entire time series, that is, when do they became significantly different from the trend. These were then compared and discussed along with the global patterns and shifts for any similarities and divergences.

In addition, extensive literature review on the current climate trend projections was performed. However, emphasis was put on simple techniques that are freely available to local experts and community with the aim that they would understand their local climatic regimes and consequently put working adaptations and mitigation measures in place. Thus, as much as possible, complicated science and expensive technologies were not employed in the current study as these are mostly unavailable to the local decision-makers and hence of little use.

Results and Discussions

Variability in Local Temperature Data

Analysis of T is important as it is a key driver for nearly all other climate parameters (Charman et al. 2009; Williams et al. 2013). Locally, T offers important climate variability signal trends with clear warming trends throughout the available time series. Figures 10 and 11 show that mean minimum temperature (MMT) and mean maximum temperatures (MMMT) have all increased over the available time series. However, these figures clearly show that there has been more significant temperature increases with the MMT than MMMT. Notice the shaper increases in MMT than in the MMMT (respectively, Figs. 10 and 11). Close observation of the T trend line and slope shows that between 1961 and 2012, there has been a net 1.13 and 0.778 °C increases in annual MMT and MMMT in DMS, respectively. Interesting to note, silent features are more evident under monthly than annual time steps where while both annual MMT and MMMT show increasing T, close observations of the monthly time step data reveal that some months had more increases in T than others (Figs. 10 and 11). The available time series suggest that June had the highest increase in MMT (1.54 °C), while April had the least of about 0.662 °C.

Similarly, the MMMT which until early 2000s had shown slow increases have recently shown much shaper increases (Fig. 11f, g, h, i, j, and l). Like for MMT, hidden and silent features are more obvious from monthly variations than annual time step in which microscale monthly variations are common with February recording the sharpest T increase (Fig. 11).

Therefore the increases in T will have important social economic consequences including on local water resources management, agriculture, and pasture developments. However, from monthly and annual average MMT and MMMT variations, it is clear that T has increased at all time scales. For instance, the MMT in 1982 and 2012 were, respectively, 18.1 °C and 19.7 °C a corresponding increase of 1.6 °C between these two points (Fig. 13b). These results correspond well with similar findings in comparable settings in Tanzania (Mary and Majule 2009; Swai et al. 2012a, b, c; Craparo et al. 2015) and recent climate downscaling and

projections. Worth noting, even minor increases in T have huge implications in the area as T is a key driver to other climate parameters like ET and the corresponding ARH (Fig. 22a, b), respectively. Thus, increases in T would in turn hamper potential groundwater recharge as more water would be involved in PET than infiltration and percolation (Calow et al. 1997, 2010; MacDonald et al. 2009, 2012; Ngongondo 2006).

Analysis of monthly average T for HMS and DMS reveals that the former has slightly higher T than the latter (Fig. 16b). Keeping other factors constant, these results mean that HMS is likely going to have slightly more PET than DMS as T is a vital driver for PET (Charman et al. 2009; Williams et al. 2013) and reiterates the role of micro-spatial T variability for local livelihood activities (Personal communication with Mr. Ntuza, Hombolo irrigation officer).

One reason why HMS has slightly higher T is to account for the fact that there are higher mountains (Chenene Mountains) in the NE which block advective winds from the depressions where HMS is located. In close connection with these findings, a recent study in the area concluded that, apart from the geology-related salinity in Hombolo Dam, high salinity in the dam was also due to excessive PET losses that is year-round higher than the R (Shemsanga et al. forthcoming). The increasing local T trend will only further exuberate the situation. Although for both HMS and DMS T are higher during the wettest month, January, hence more water losses, T is even higher for HMS during wet months; hence more water is likely to be lost via PET in Hombolo sub-catchment than in Dodoma urban sub-catchment (Fig. 16b). One can therefore plan to grow more of T-tolerant plants in HMS sub-catchment than in the DMS sub-catchment (personal communication with Mr. Ntuza, Hombolo irrigation officer).

Apart from the general warming trend in all data sets, notice that the annual MMT and MMMT have increased for up to 1.54 °C and 0.778 °C, respectively (Figs. 15 and 16). Notice also that similar warming trends are observed in the wettest month (January), driest month (September), warmest month (November), and coldest month (July) of the data set (Figs. 10, 11, and 16b). These findings are similar with current climate models that generally agree that the region is warming up fast (Cooper et al. 2013). These findings also agree with modeling and prediction results that show generalized warming trends across the continent (Mariotti et al. 2011). Further, these findings are also similar to studies from other localities in Eastern Africa with similar climatological settings (Kinh'Uyu et al. 2000). Previous studies and climate models have indicated that over the past 3 decades, there has been up to 0.6 °C in T (Omambia et al. 2012).

A study conducted at Makindu, a semiarid region of Kenya, had shown that if T is to rise by 3 °C, there would be a corresponding decrease in about 8 % in the length of growing periods (Cooper et al. 2009). By using HadCM3 model, the same study found that by 2050 the area will lose up to 5–20 % of the length of the growing season as a direct consequence of climate change. Yet increase in T has globally been associated with decreasing crop yield (Deryng et al. 2014; Liu et al. 2013; Liu et al. 2012; Deryng et al. 2014; Tao et al. 2015), and there are no reasons to think the

local increase in T will not affect the domestic agricultural sector, the largest employer in the county. For instance, it is argued that if in Tanzania T is to increase by between 2 °C and 4 °C, maize production will go down by about 33 % (Paavola 2008). Yet a recent study in northern Tanzanian highlands found that an increase in T had profound impacts in coffee yields (Craparo et al. 2015).

It is already known that T and moisture are key factors in the spread of disease vectors (Mary and Majule 2009). A recent study also modeled and linked malaria epidemic in Tanzania with increasing temperatures including in the highland where malaria was not endemic (Jones et al. 2007). This picture therefore shows that the area is very much threatened by climate variability, and adaptation measures must be considered for the local livelihoods.

Elsewhere in Africa, within the last few decades, the continent has observed widespread warming in many regions (Stocker 2014; Sabine 2014). By the end of the century, the continent's climate is further projected to have an increase of up to 2 °C in temperatures. Other projections put the continent at even higher risk (Burke et al. 2009; Hendrix and Glaser 2007; Faramarzi et al. 2013). These global projections are well translated in the current study area and would require major adaptation strategies. Such huge changes in climate dynamics are likely to impact on the local rainfed agriculture, recharge, and natural catastrophes like flooding and droughts where there has been an increase in the number of floods and drought episodes in the continent including in Tanzania and specifically in the study location as seen and discussed in the next subsection (Omambia et al. 2012; Shemsanga et al. 2010).

Rainfall Characteristics and Variability Data

Irrespective of the differences in longevity of the study, rainfall data shows similar declining trends in all three stations and at all time scales (time series, annual, seasonal, and monthly). However, the current findings show that there is high spatial and temporal rainfall variability (Fig. 3) where it is revealed that Hombolo sub-catchment receives more R (608 mm/year) than the Makutupora (548 mm/year) and Dodoma urban sub-catchments (581 mm/year) (Figs. 2 and 18b). These results also show that the annual average R is, respectively, 60 and 27 mm less in MMS and DMS than in HMS (Figs. 2 and 18b). Thus, the mountainous areas of Hombolo receive more R than the lowland areas of Makutupora and Dodoma urban (Fig. 1). These findings are similar with other local findings (Nkotagu 1996a, b, c; Rwebugisa 2008; Shindo 1994). The information on micro-scale spatial rainfall variability is important for planning types of crops to be grown and for management of groundwater in the area. For instance, from this information, it is most obvious that the shallow wells in Makutupora sub-catchment will have less recharge than Hombolo, for example, since shallow wells are mostly dependent on local rainfall (Al-manmi 2002; Cook and Herczeg 2000). Similarly, more of drought-resistant crops should be sought for Makutupora sub-catchment than for Hombolo.

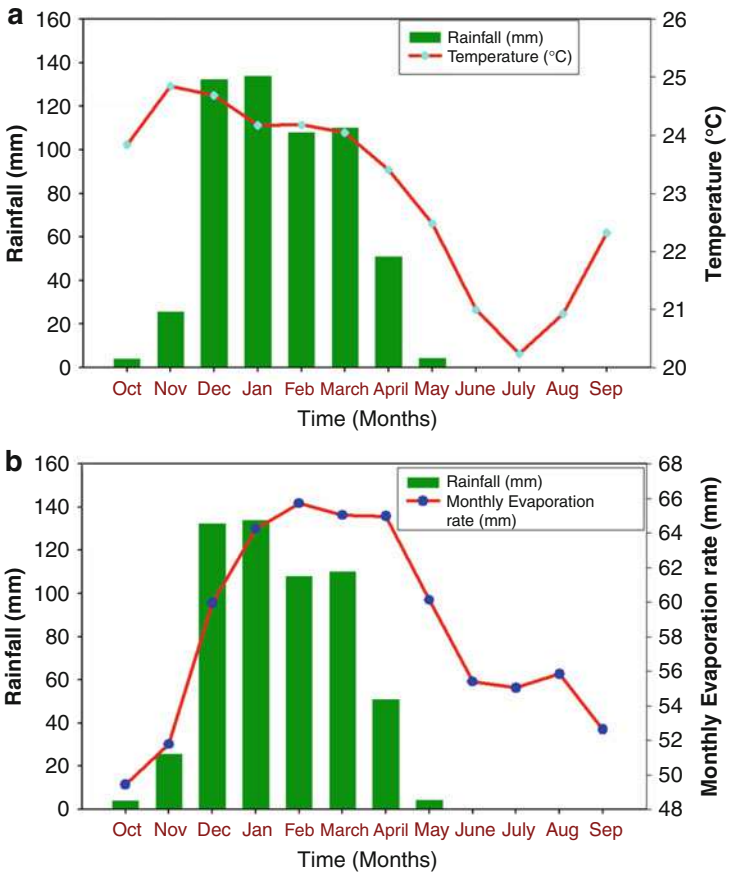

Fig. 2 (**a**) Climatograph of rainfall and temperature. (**b**) Rainfall and evaporation in the Dodoma municipality

From Fig. 3a, it is revealed that the regression of annual and May R at MMS has a slope of −0.592 and −0.556, respectively. Considering these values into account and taking the 91 years time series, this shows that there has been a net decrease in R of about 53.9 and 50.6 mm at an annual and May time step, respectively. This is a significant shift in the effective R for the area characterized by low rains (550 mm/year) that mostly come when T is highest (Fig. 16b).

Notice in the data set that all but one year that were completely with no April rains are clustered in the last 30 years. Notice also that there are significant declines in the amount of March rains from 2003 onward (Fig. 7). This may hint that April as is the case for May is no longer reliable for local livelihood support systems like agriculture and pasture development. This requires major adjustments in cropping seasonality and the choice of crops to be grown with more drought-resistant crops being the preferred choice. Similar patterns are observed for May rains for both DMS and

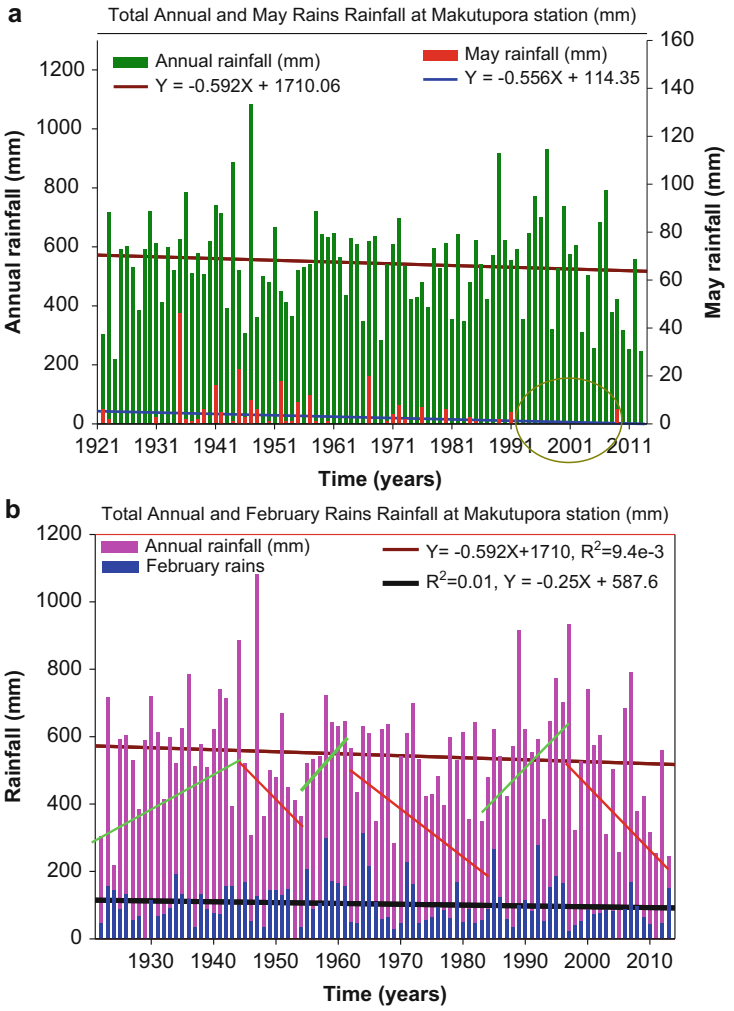

Fig. 3 (**a**) Total annual and May rains at MMS. (**b**) Total annual and February rains at MMS (mm)

HMS data sets (Figs. 4e and 5e). Further, such drops in the amount of R and the disappearance of April and May rains at Makutupora sub-catchment could adversely affect local recharge at Makutupora aquifer (well field) that supplies freshwater used in Dodoma city (the capital of Tanzania). This will further worsen the local hydrogeological balancing when already a recent study reported a decreasing dug wells yield and early drying of the well all of which were linked with decreasing R and increasing T & ET (Shemsanga et al. forthcoming).

It is interesting to note that while several years over the last 3 decades received no April rains at MMS (Fig. 7), DMS and HMS have continued to receive April rains although at a much reduced magnitude (Figs. 4d and 5d). Similarly, HMS has

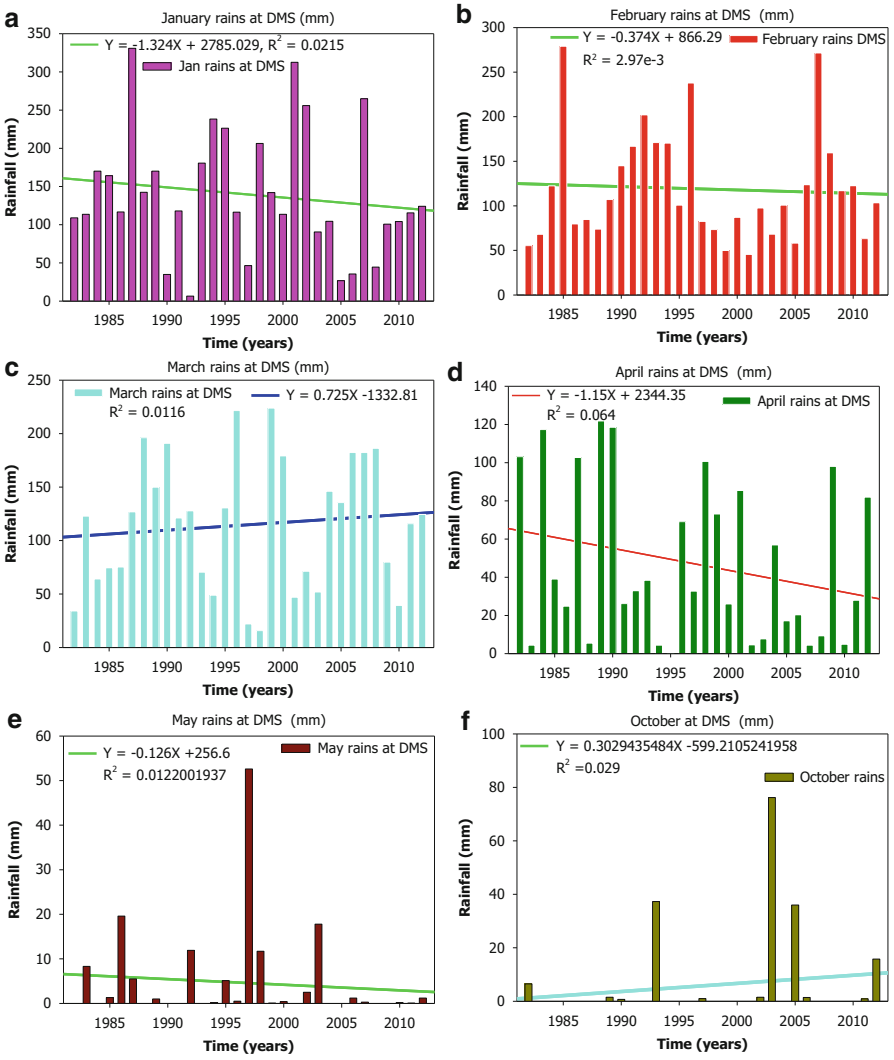

Fig. 4 Time series monthly rainfall trends at DMS

continued to receive more rains in May than DMS and MMS in that order. Such hidden and silent features are not vividly seen in annual and/or time series time step and may bring about a breakthrough in the timing of growing seasonality.

While some other local factors may play some roles, climate studies associate the widespread regional declines in R with increases in the Indian Ocean sea surface temperatures (SST) (Williams and Funk 2011). Similarly, a westward extension of the warm pole is blamed for some westward extension of the Walker circulations that dried most of EA (Williams and Funk 2011). The Indo-Pacific sea surface

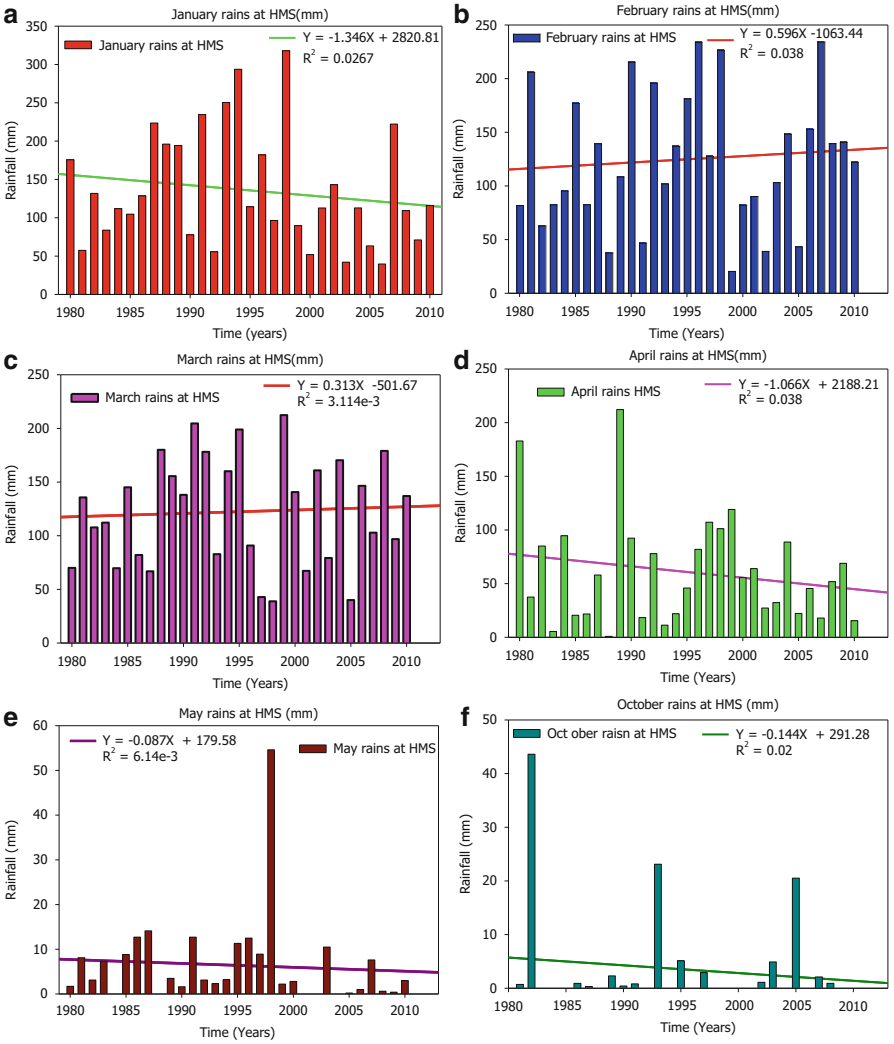

Fig. 5 Time series monthly rainfall trends at HMS

temperature plays pivotal roles in the failure of consecutive rainfall seasons in much of EA (Hoell and Funk 2014; Funk et al. 2014).

Despite the differences in longevity of the R data series from the three stations, notice that there are more or less clear and similar cyclic wetting and drying seasons. For instance, it is clear that from the early 1980s to late 1990s there were widespread wetting event seasonality (Figs. 3b, 6a, and b). The latter was followed by a drying event that is again uniformly observed in all three stations (Figs. 3b, 6a, and b). Furthermore, close observation of the pattern shows that in recent years, there have been longer drier seasons than wet seasons. This pattern however is of wide East

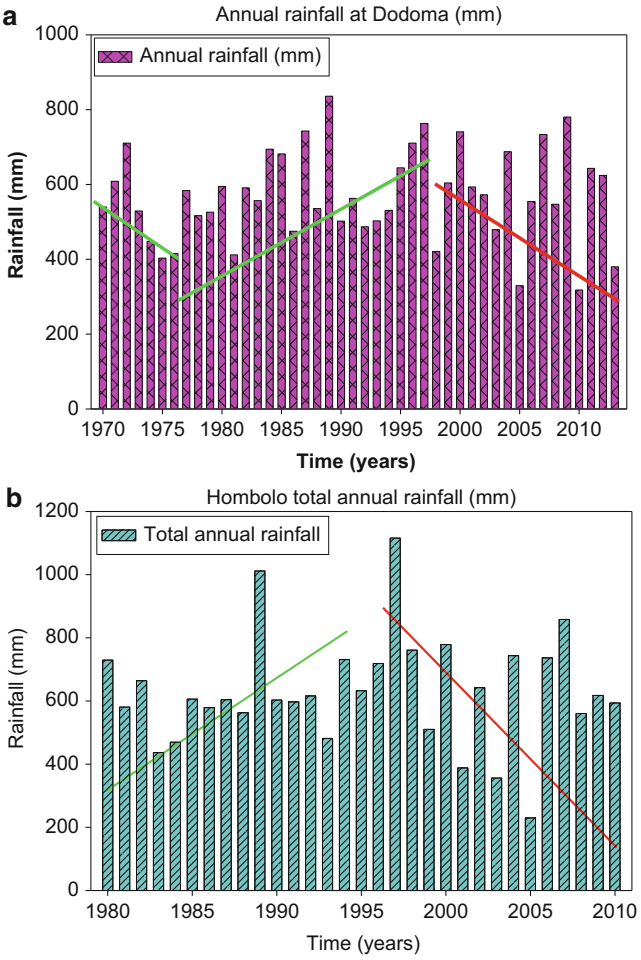

Fig. 6 Drying and wetting cycles at (**a**) DMS and (**b**) HMS

African implication and could be attributed to internal climate control parameters like thermohaline circulation, El Niño-Southern Oscillation, and changes in the ocean heat content (Cooper et al. 2008). For instance, closer similarity in the extended drier cycles can be seen in rainfall data from Kenya where in recent years there has been an extension of drier seasons in the rainfall data (Cooper et al. 2009, 2013).

Similar wetting and drying cycling was also reported in Zimbabwe between 1901 and 2007 rainfall data (Cooper et al. 2013; Hirji et al. 2002). Like already discussed, the extended drying events would therefore affect water budgeting in the area which would in turn affect groundwater recharge and availability of water for various socioeconomic activities like agriculture and pasture development.

Extreme Climate Events (Droughts and Floods)

In East Africa (EA), extreme climate events are particularly associated with floods and prolonged droughts that over the years have repeatedly cost human lives and widespread economic losses in terms of infrastructures, agricultural productivity, and domesticated and wild animal deaths, among others (Hendrix and Salehyan 2012; Maurel and Kubik 2014; Omambia et al. 2012; Shemsanga et al. 2010). According to Mr. Waziri (Tanzania Meteorological Agency TMA, central zone), recent years have witnessed more aggressive R events characterized by heavy downpours in a short time. "The rains are less evenly distributed and it is common to have a lot of R in a space of just hours leaving the rest of the season with little rains that are not productive in terms of cropping usefulness. Thus, the rains may be observed and the annual and monthly magnitude may even be the same but the bulk of the rains fall within a short time with very high force which ends up as runoff and triggering flash floods that destroy crops and infrastructure along the flow direction." Similar conclusions were reached by Valimba (2004).

In EA, the situation worsened in El Niño-Southern Oscillation events in which flash floods are very common (Valimba 2004). These years have characteristic heavy R associated with some floods. For instance, the severe ENSO-related floods of 1997/1998, the most severe in about 50 years, were specifically linked to the Indo-Pacific El Niño/Southern Oscillation (ENSO) and to sustained high sea surface temperatures (SST) in the Southwest Indian Ocean Valimba 2004). The extended 1976–1978 warm ENSO led to high R in the 1977–1979 (Fig. 18a). Generally, 2–8 years periodicity of East African Region is linked to the ENSO that is also the most rational inter-annual signal in the global climate patterns.

Evidence of Sifting Rainfall Seasonality

Close observation of time series for February, March, April, and May rains clearly shows generalized decreasing trends (Fig. 7). May being the end of rain season in Dodoma offers the best opportunity to understanding declining R variability (Figs. 3a, 4b, and 7). Notice that there have been virtually no May rains at MMS from 1992 to present except in 1999 when 6 mm of R was recorded. Thus, May rains have almost completely disappeared over the last 20 years. Specifically, no May rains were recorded from 2006 onward as opposed to previous years when up to 120 mm of R was recorded (Figs. 3a, 4b, and 7). Out of 9 years that HMS received no May rains, six were recorded in the last 15 years. Generally, in all three stations, May rains are significantly reduced and/or disappearing, a strong signal of worsening climate dynamics. Regression analysis shows that time series May rains have a slope of −0.556. Considering this value into account, it is clear that there has been a 50.6 mm of R from 1921 to 2012. This is a significant shift in the effective R for the area characterized by low rains that come mostly when T is highest (Fig. 16b).

The implications gathered here are that the useful R season is diminishing as onset of rains in October is also virtually disappearing (Figs. 5f and 7). This will affect cropping, pasture, and water resources, particularly recharge. January rains show that the rains have more or less stayed the same with no clear increase or decrease (Fig. 8). These require locals to grow drought-resistant and/or early-maturing

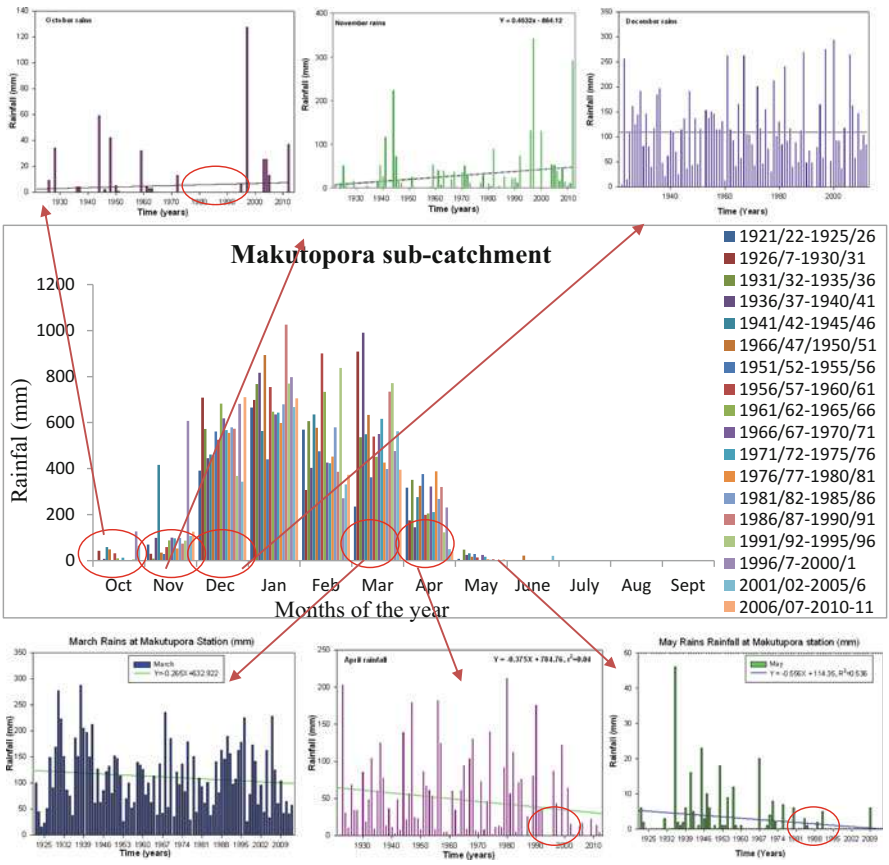

Fig. 7 Monthly temporal rainfall variability at MMS

crop varieties. Similar suggestions were given by other regional studies (Mary and Majule 2009; Swai et al. 2012a, b, c). Similarly, plans to harvest and store enough water for domestic, livestock, and irrigation should be planned as the main sources of water; dug wells have been drying early in recent years (Personal communication with Mr. Jackson in Mtumba suburb).

The area has a very high temporal variability in the amount of R received between the hydrological years (Fig. 8). For instance, going by March between 1936/1937 and 1940/1941, the area received over a thousand millimeters of R compared to only 200 mm between 1951/1952 and 1955/1956. Furthermore, considering March rains again at MMS, there has been a decrease of up to 800 mm between 1936/1937–1940/1941 and 2006/2007–2010/2011 (Fig. 8). Similarly, a close examination of the R patterns in April would reveal that between 1950/1952–1955/1956 and 2006/2007–2010/2011, there has been a decrease of up to 300 mm (Fig. 12). Similar R variability is recorded in other three stations (Fig. 9). However, high spatial and temporal R variability is typical for many semiarid regions of the country/world

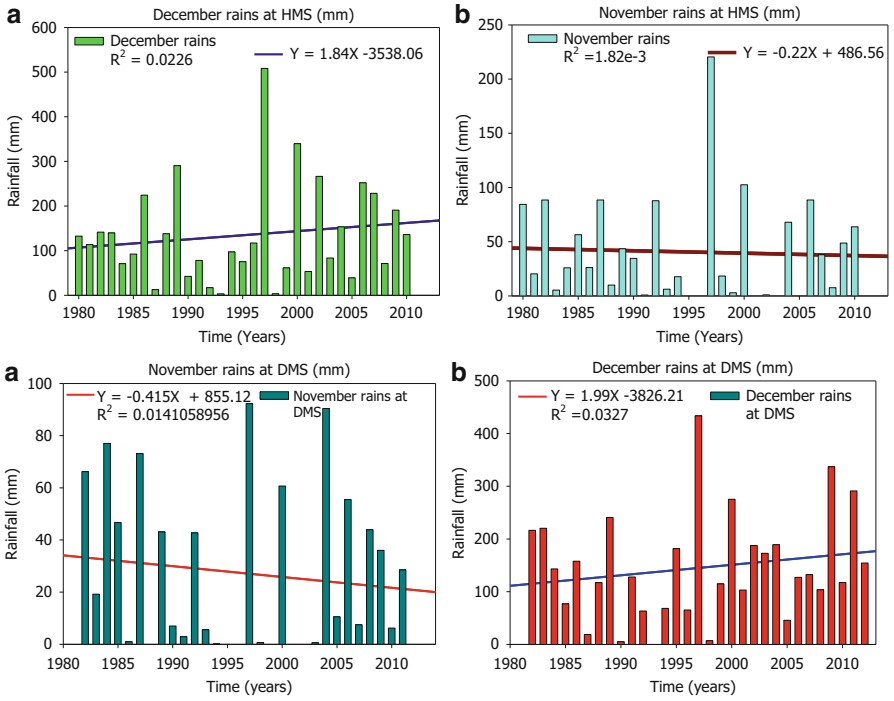

Fig. 8 Times series November and December monthly rainfall trends at DMS and HMS

(Graef and Haigis 2001; Mary and Majule 2009; Valimba 2004; Majule 2008; Rao et al. 2011). High temporal variability is also evident from the annual R data. From Fig. 7, it is evident that some years received very high rains (1947, 1989, and 1997), while others had very little R (1924, 1946, 1969, 2004, 2010, 2013). Notice that the occurrence of years with low rains has increased in recent years, whereas heavy rains are only associated with El Niño-Southern Oscillation (Figs. 3 and 7). These findings are similar to other local findings (Rwebugisa 2008; Taylor et al. 2013). Worth noting however, the high R recorded in 2004/2005 hydrological year is explained by the fact that the latter was an El Niño-Southern Oscillation. El Niño year in East Africa is known to exuberate high downpours (Cooper et al. 2013). Similar trends are also seen in other stations (Fig. 3a). The increased El Niño-Southern Oscillation events in Tanzania seem to favor surplus in which the maximum potential surplus was recorded in 1999 (Fig. 3a).

Drought Index (DI), Drying and Wetting Cycles

Close observation of the data series reveals that 47 out of 94 years from 1921 to 2014 were drought years. This means that there is a 47/94 change (50 %) of drought occurrences in the area. These show how vulnerable the area is to R stress and how R-dependent activities might be impacted. This roughly means that every second

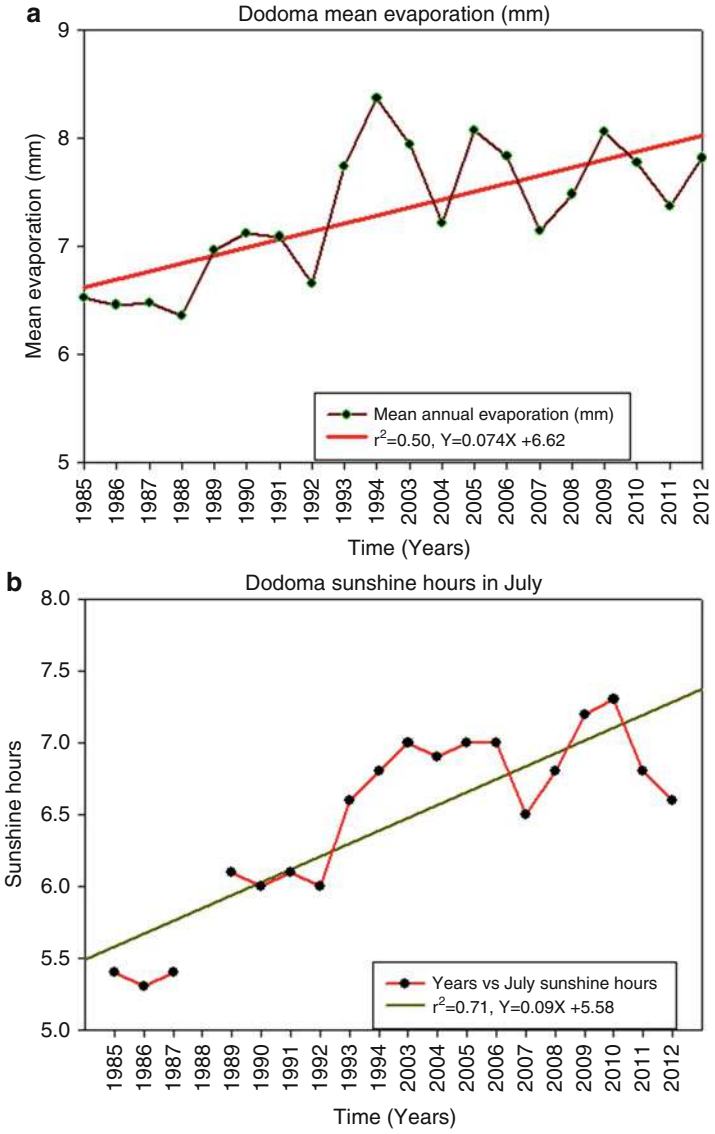

Fig. 9 Time series. (**a**) Annual mean evaporation (mm). (**b**) Dodoma sunshine hours in July

year, there has been some interference to rainfed agriculture, recharge, or pasture development. Out of 94 years, between 1921 and 2014, there were 47 years (50 %) that experienced some form of meteorological drought. Out of 20 years that experienced VSD, 10 occurred from 1977 to 2014 (a space of 37 years), while the other 11 occurred from 1921 to 1977 (a space of 56 years). In a similar way, out of 93 years of available R record, 4 and 2 and 3 and 2 years that experienced, respectively, SD

and MD were, respectively, recorded after and before 1977. Finally, out of 8 years that experienced LD, five occurred before 1997, while three followed after 1977. The bigger picture here is that lighter droughts were common in initial years of the data series, while severe droughts are more frequent in recent years; therefore, drought severity is gradually increasing, and R-dependent activities like agriculture and pasture development will continue to be adversely impacted. The increasing severity of drought is proportional with the general declining R and increasing T trends (Figs. 10, 11, 12, 13, 14, 15, 16, 17, 18, and 19). These findings support other regional studies that generally show drought is increasing (Mary and Majule 2009; Swai et al. 2012a, b, c). Studies already show that post-1970s drought characteristics in Southern Africa have been more extreme and widespread (Valimba 2004).

Although severity of drought could clearly be noticed to increase, some questions still remained, key among them being: When did the variability happen? Has it been uniform and continuous? Did we notice increasing, lengthening, and shortening wetting or drying cycles?

Thus, apart from visual assessment of R trend (Fig. 20b), the following two models were run to explain the situation more closely. Both Buishand and Pettitt models clearly show that local R is characterized by cyclic wetting and drying scenarios/cycles. Notice a prolonged drying events from 1972 to 1988 that were followed by a brief wetting event and then drying event again (Fig. 21a and b). Generally, the drying events are longer in latest time series data than in early time epoch. This drying event coincides well with the DI (Fig. 21a) suggesting worsening drought from 1977 onward. Notice also that the most recent wetting events (1957–1962 and 1987–2002) are brief compared to the earlier event in the data series (1927–1943) (Figs. 20b, 21a, and b). These results are also supported by other regional studies which concludes that the prolonged droughts from 1973 to 1976 (Fig. 20a and b) are attributed to extended 1973–1976 La Nina events (Valimba 2004; Nyenzi et al. 1999).

Relationship Between Rainfall and Groundwater Level (Recharge)

Record of groundwater head fluctuations (GHF) closely followed annual R trends with high annual R corresponding to high groundwater heads except for a few cases where high/low levels were preceded low/high R values (Fig. 5). This suggests that local R is the main source of recharge and any decreases in the R magnitudes and longevity will adversely impact groundwater resources (Shemsanga et al. forthcoming), the main sources of local fresh water for Dodoma city (Rwebugisa 2008; Kashaigili 2010). These findings are similar to previous studies in the area (Rwebugisa 2008; Taylor et al. 2013).

However, apart from the extreme R event, like 1997/1998 El Niño events in much of East African region (Valimba 2004), close analysis of the GHF trend suggests that groundwater has generally been declining as much as R trends (Fig. 22a). Figure 22a shows that, except for brief interruptions in groundwater level anomalies, there has been a prolonged groundwater level decline between 1969–1988, 1989–1994,

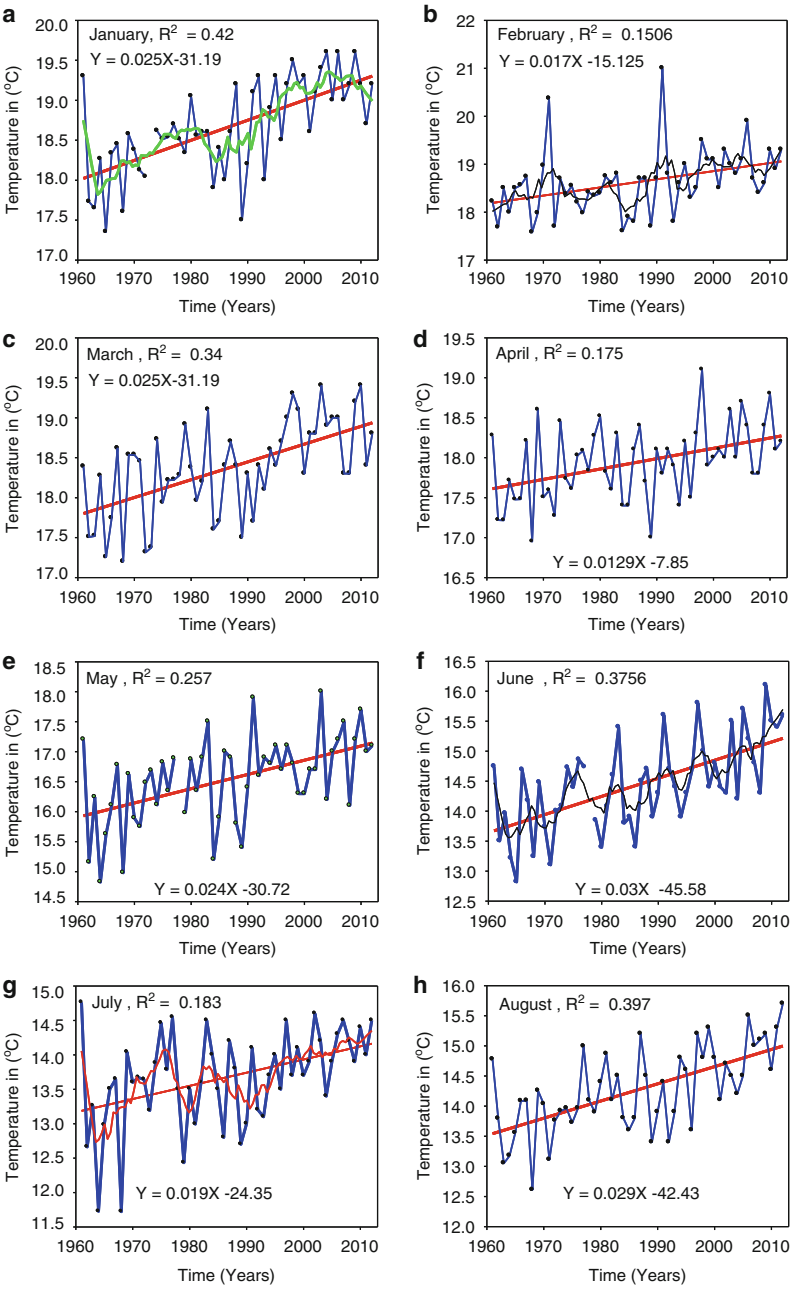

Fig. 10 (continued)

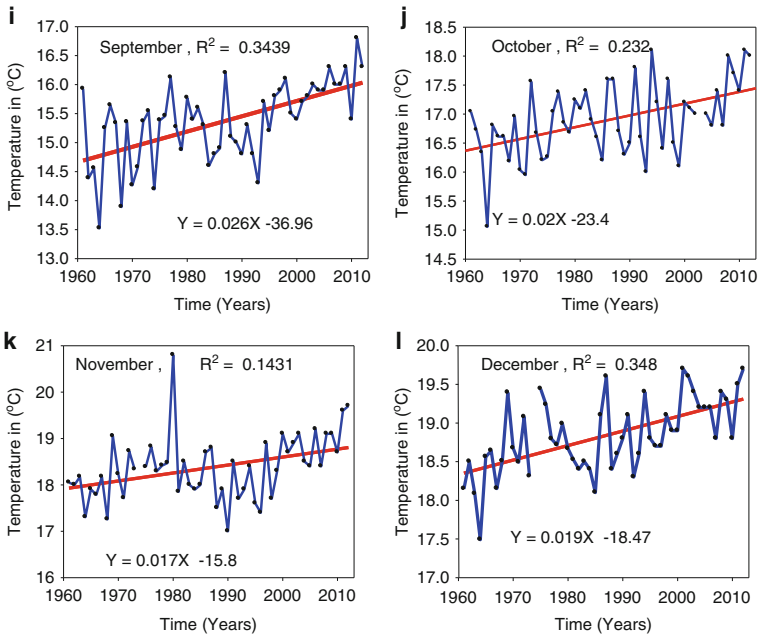

Fig. 10 Time series. Mean minimum monthly temperature at DMS

2001–2006, and 2007–present. These declines largely support epochs of the data series when R generally decreased except for a few cases. Further, this is in line with the local R trends that have been declining in much of East Africa (Omambia et al. 2012; Valimba 2004; Taylor et al. 2013). In an ongoing study, the general declining R trends have been associated with early drying up of dug wells and decreasing well yields in both shallow wells and deep wells (Shemsanga et al. forthcoming). Other regional studies also link ongoing climate variability with adverse impacts to groundwater availability and local livelihood support systems like agriculture and pasture development, especially to rural communities in semiarid regions (Calow et al. 1997, 2010; MacDonald et al. 2009; Ngongondo 2006).

Atmospheric Relative Humidity (ARH)

ARH is a useful parameter in showing potential changes in the sources of moisture for the atmosphere or changes in the dynamics of atmospheric circulations from both local and global forces (Kousari et al. 2011). The local annual mean ARH shows that there has been a steady decline in the percentage of ARH (Fig. 23a and b).

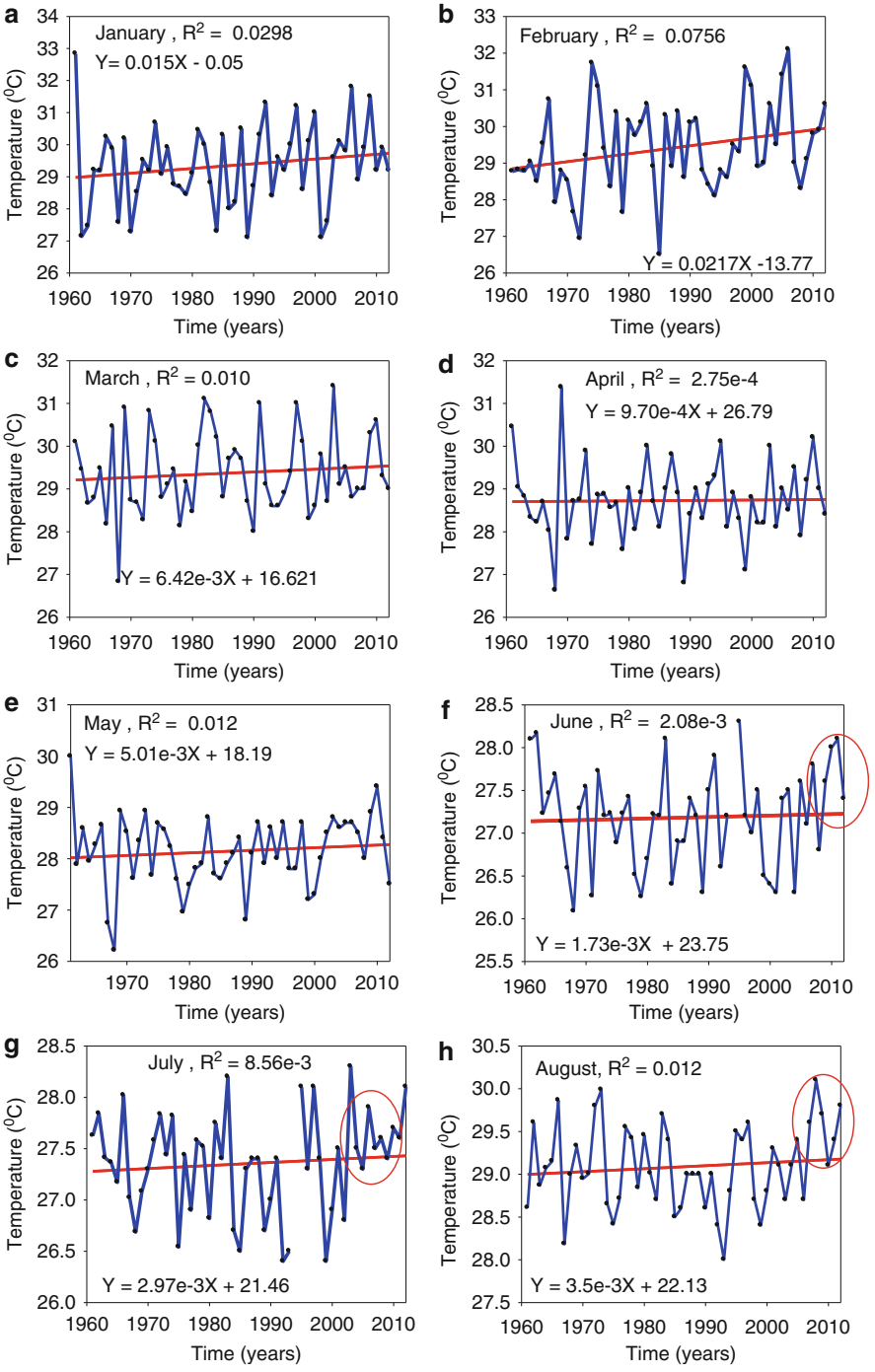

Fig. 11 (continued)

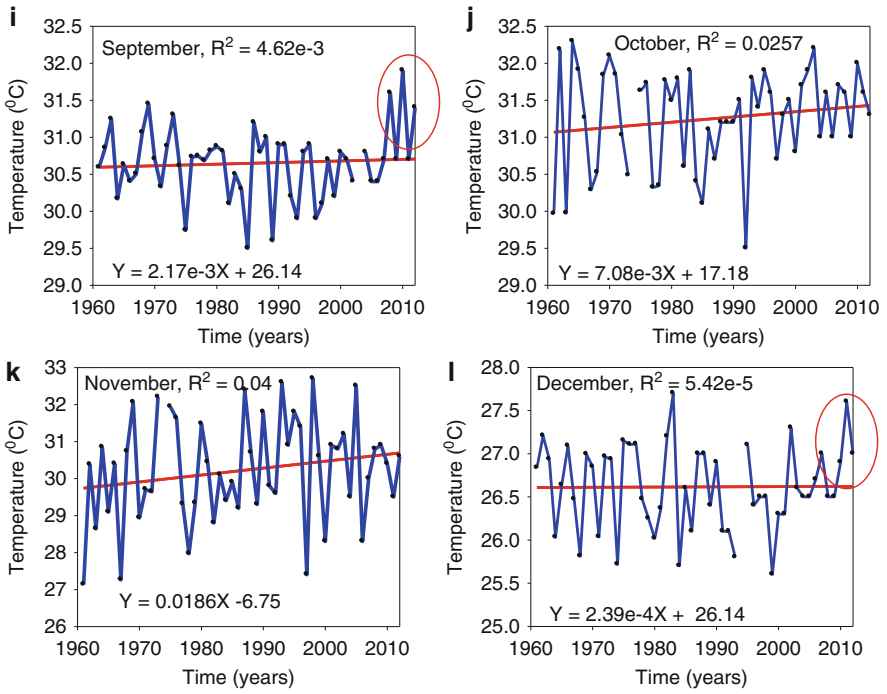

Fig. 11 Time series. Mean maximum monthly temperature at DMS

Analysis of seasonal variation in ARH shows significant decreases in wet and dry months (Fig. 23a) in which both dry and wet months (September and May, respectively) there records significant declining trends of about 7.37 % and 6.08 %, respectively, between 1982 and 2012. Considering regression for annual ARH, it is noted that the regression has a slope of −0.167. By working with the entire time series of this station (1981–2014), it is clear that there has been a 5.34 % decrease in ARH. This supports global patterns showing progressive climate-related declines in ARH magnitudes (Jung et al. 2010). Sharply declining amount of local ARH is a significant signal of changing climatic balances and/or decreases in the regional sources of moisture. These findings are similar to a study carried out in Iran where several stations had shown a decreasing ARH (Kousari et al. 2011).

The changes in sources of moisture locally could be attributed to several factors, key among them being decreasing R (Fig. 3a and b), decreasing vegetation cover and compositions (Allen 1985; Angelsen et al. 1999; Cline-Cole et al. 1990), decreasing soil moisture and shrinking water bodies (and other wet areas such as wetlands and rivers), and increasing WS (Al-manmi 2002). In line with the above, previous studies in Dodoma have recorded massive losses in vegetation cover which mostly came from high pressure on poles for construction, expansion of agricultural land, and fuelwood pressures (Allen 1985; Angelsen et al. 1999; Cline-Cole et al. 1990).

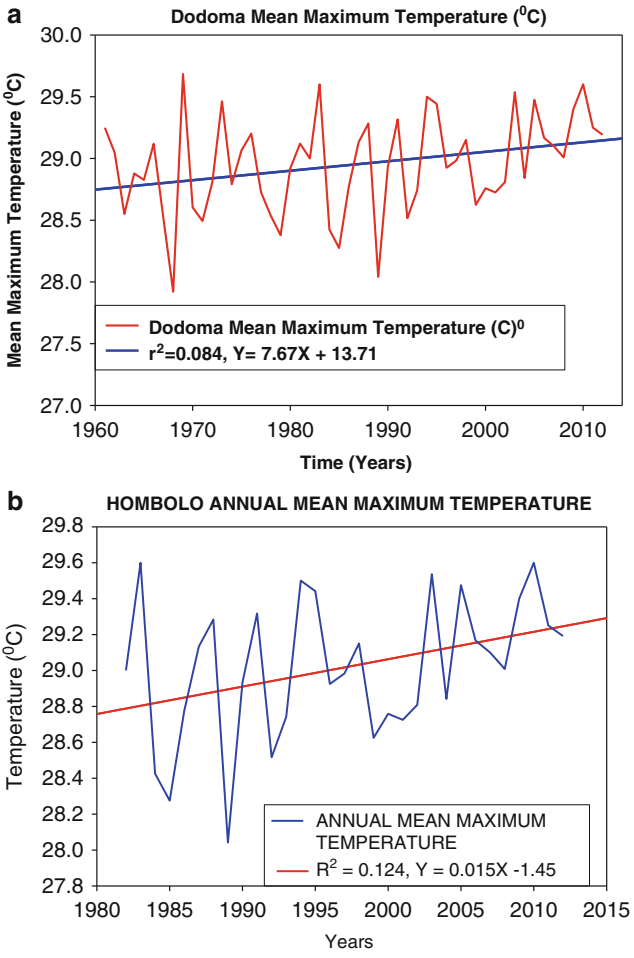

Fig. 12 Time series. Dodoma and Hombolo MMMT (°C)

In addition, increasing temperatures (Fig. 12 through 17), WS (Figs. 25 and 26), ET (Fig. 23a), radiation (Fig. 28a and b), and S (Figs. 23b to 24) could mean more water is lost immediately after rains via the process of PET leaving the rest of the year with minimum ARH. Locally, WS is at its maximum during the dry season which further blows away the available moisture and hence less detectable moisture in the atmosphere (Fig. 26a). Thus, changes in WS could also result in decreasing ARH as stronger winds blow the moisture away (Figs. 25 and 26). Notice that the mean monthly ARH at each month is higher at 9 am in the morning and relatively less at 3 pm in the evening. This relationship can explain why there has been a

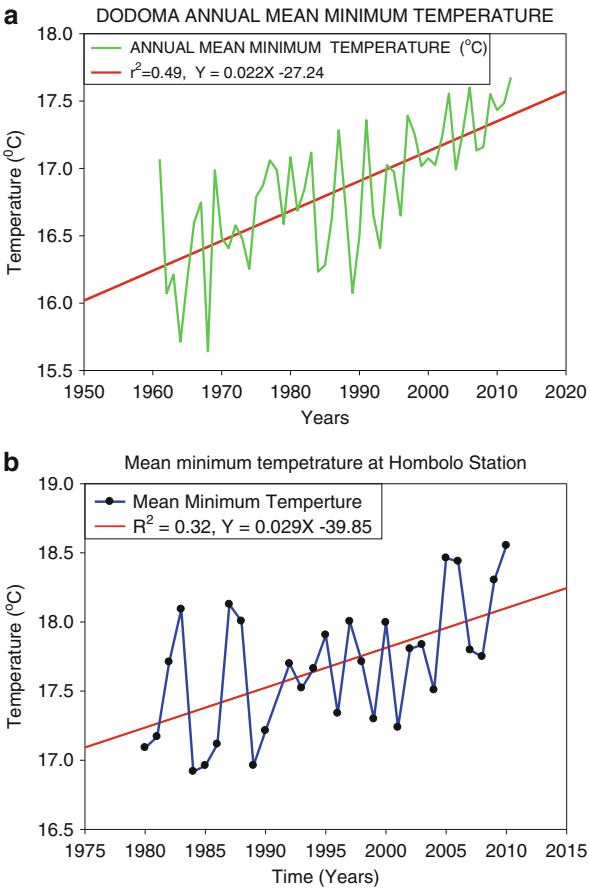

Fig. 13 (**a**) Time series MMT and (**b**) Mean MMT at DMS and HMS (°C)

general decline in percentage of ARH locally as T has been observed to increase with years (Figs. 2 and 10). Worth noting also, the minimum mean ARH is at its lowest in the peak of dry season when there is less water to be involved in PET and quickly increases as R begins in October. Thus, the declining ARH is most likely to be due to increasing T in dry, wet, coldest, and warmest seasons. This will in turn affect key livelihood support systems like local groundwater recharge and length of growing seasons.

Notice from Fig. 22 the close similarity between ARH and occurrence of R and T trends in which dry months have the lowest ARH, whereas the wettest months January and December have the highest. Indeed, T is a very important local climate driver and therefore should closely be monitored for meaningful mitigation and adaptation strategies against adverse climate impacts on water resources, agriculture and pasture development among others.

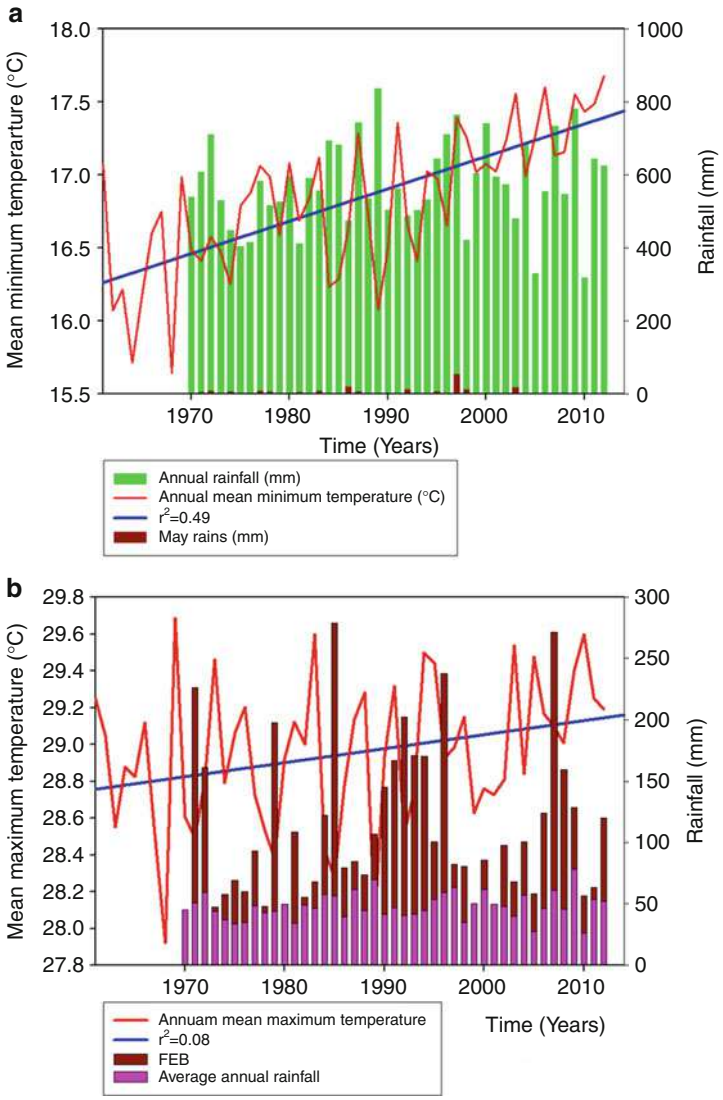

Fig. 14 Time series. (**a**) Annual and May rains and (**b**) average, annual, and February rains and MMT at DMS

Evaporation (ET) and Sunshine Hours (S)

Analysis of both S and ET data shows consistent increases in both parameters (Fig. 23a and b). The gradual increase in these two parameters suggests more water molecules are lost from the area. Thus, from the general increase in S, it is

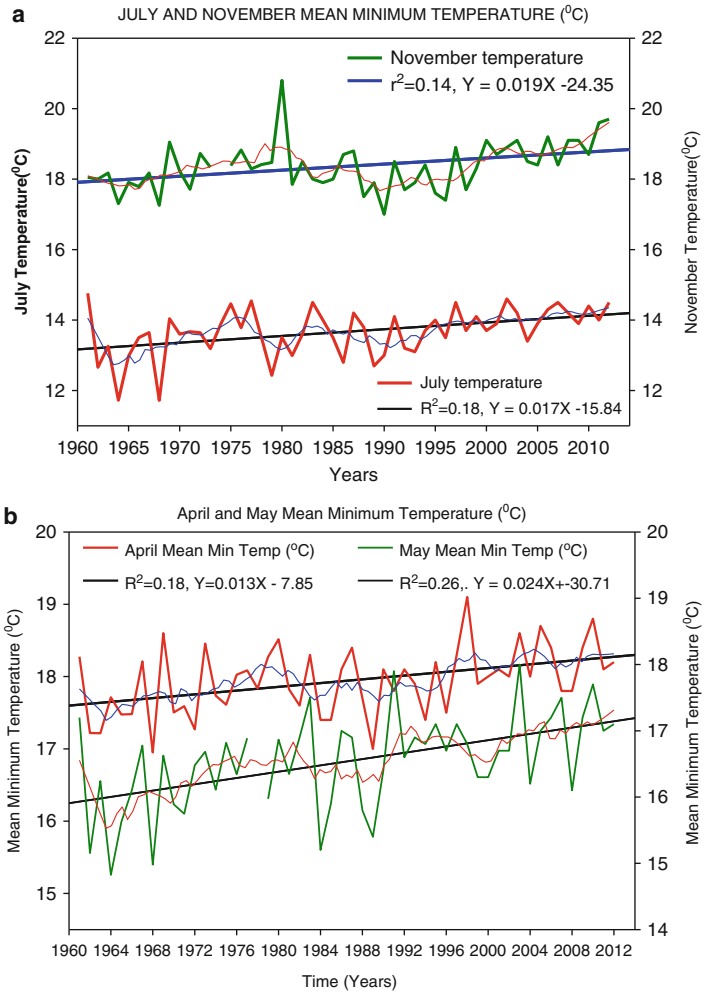

Fig. 15 (**a**) July and November MMT at DMS. (**b**) April and May MMT at DMS

not surprising to see that there has been a corresponding increase in ET rate (Fig. 23a and b). The increases in these two parameters can be explained by the proportional increases in T (Figs. 10, 11, 12, 13, 14, and 15) and (Fig. 29). The steady increases in S and ET, coupled with the decreasing amount of precipitation and ARH, could have major implications in the local water balancing. For instance, this could reduce the amount of water recharging the aquifers as the rate of recharge is inversely related to ET rate (Al-manmi 2002; Rwebugisa 2008; Shindo 1991). Past studies in the area indicated that annual PET is almost four times the amount of R leaving only a small proportion of water recharging the aquifer (Rwebugisa 2008; Shindo 1994);

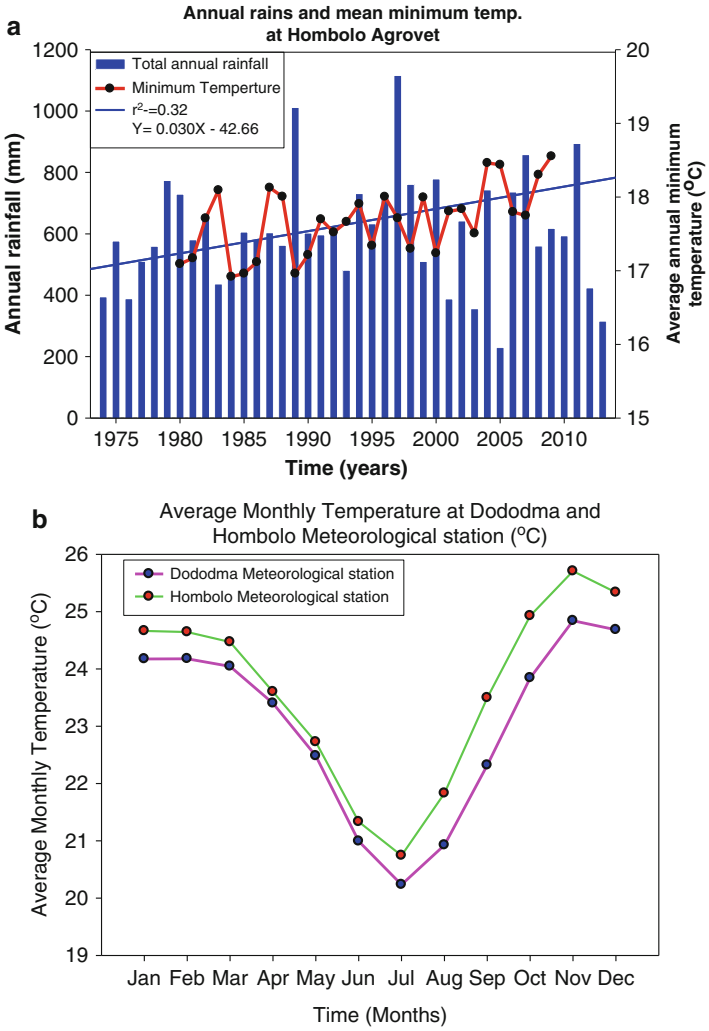

Fig. 16 (**a**) Annual average temperature and rainfall. (**b**) Mean monthly temperature in HMS (1980–2014)

therefore, the increases in these two parameters will lead to even lower proportions of water available for recharging. In addition, the increases in S and ET will both affect available water for plant growth and pasture development (Allen et al. 1998a; Stanhill and Cohen 2001; Nonhebel 1996; Wang et al. 2015; Deryng et al. 2014).

The relative higher ET in the area is also supported by modeling of the major climate data using TWMWB. The result of this model clearly shows that PET has

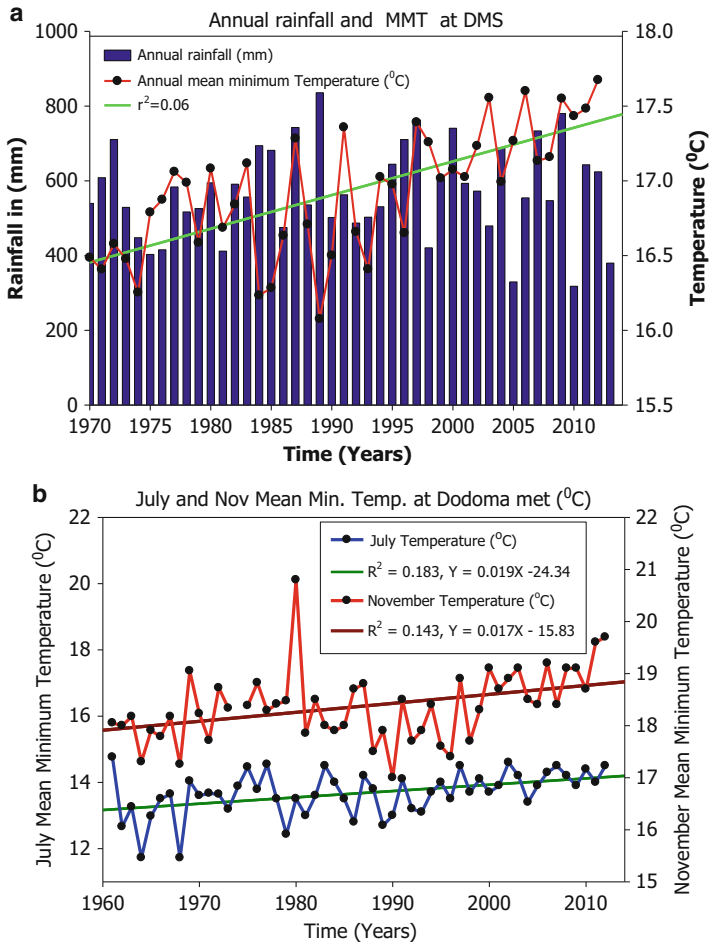

Fig. 17 Time series. (**a**) Annual rainfall and MMT at DMS. (**b**) July and November MMT at DMS

consistently been higher than that of R (Figure 26a and b). This could explain the absence of surface water bodies in the area (Shindo 1991; Rwebugisa 2008; Taylor et al. 2013). The river/runoff channels in the area only flow for a few weeks following rain events to account for characteristic high PET. Notice from Fig. 26a and b that TWMWB results support T time series data that HMS has higher T than DMS (Fig. 16b) and which leads to HMS to have higher PET than DMS (Fig. 26a and b). Past studies in the area reached similar conclusion and proposed artificial recharge schemes to be implemented to store the runoff water that often ends up to ET and flowing to the Indian Ocean and leaving the rest of the year with less water for the populace (Salama 1979).

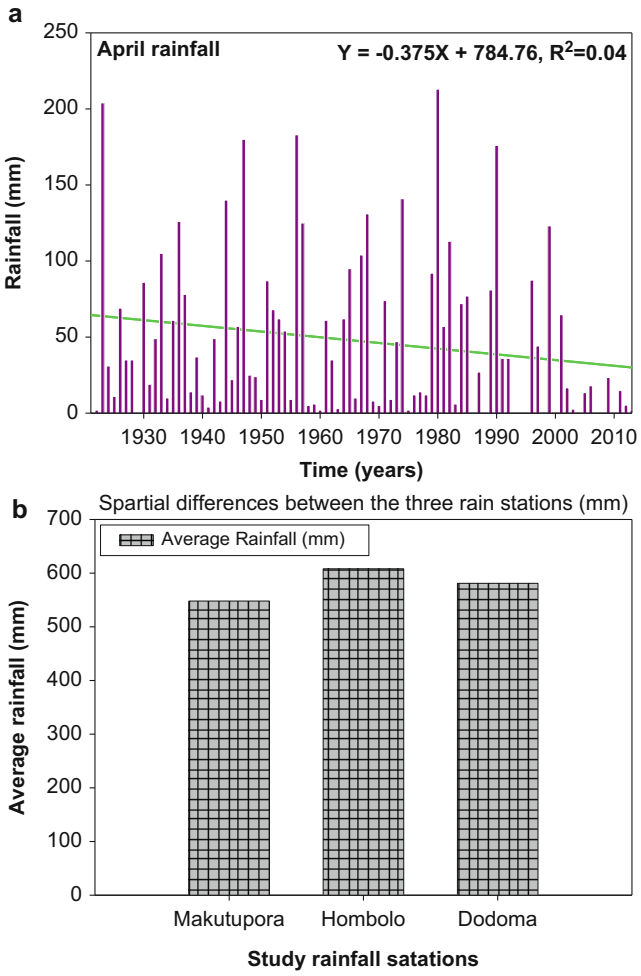

Fig. 18 (**a**) Times series April rains at MMS. (**b**) Variation of rainfall at MMS, HMS, and DMS

Wind Speed (WS)

Local wind speed parameter is marked by an increasing trend from the early 1980s that is followed by notable decreases from the early 1990s onward. Generally, the decreasing WS above was also recorded in various places of the world including in China (Jiang et al. 2010; Li et al. 2011). While changes in WS in China is partly attributed to urbanization especially uplifting of story buildings (Guo et al. 2011; Jiang et al. 2010; Li et al. 2011), locally the area around has largely remained the same, and therefore some other external forces like changes in the ocean surfaces are

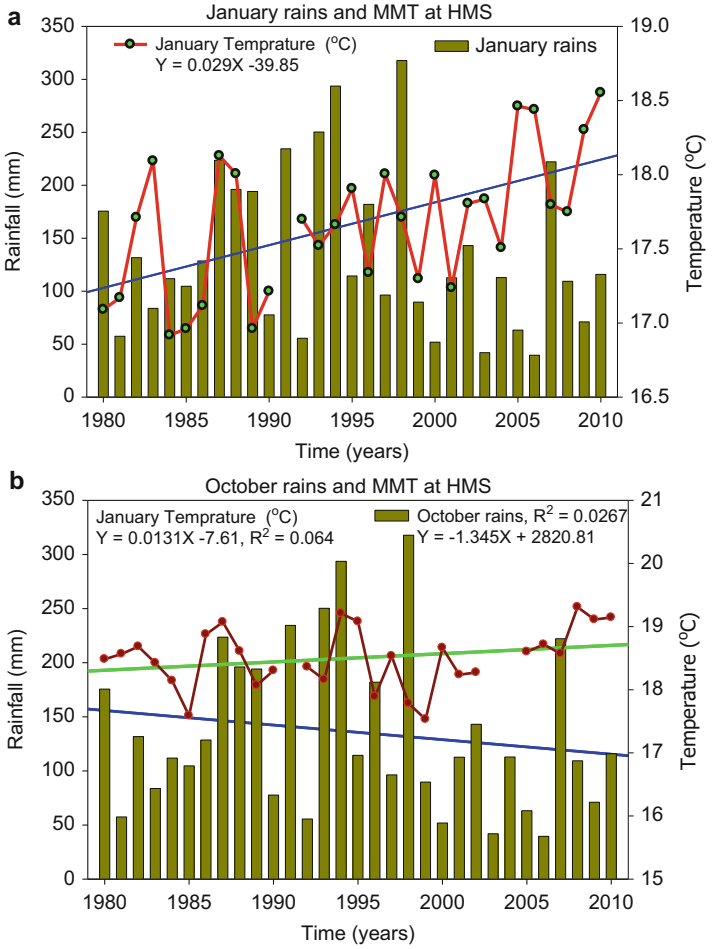

Fig. 19 January and October rains and MMT at HMS

thought to be the major cause or climate change related to lower-tropospheric pressure-gradient force (Guo et al. 2011). In Spain analysis of 67 land-based observation stations had also indicated that the WS had declined from 1961 to 2011. In these study stations, it became obvious that there were slight decreases in WS of between -0.016 m s^{-1} and -0.010 m s^{-1} per decade (Azorin-Molina et al. 2014).

Close observation of the entire data series however reveals that there has been some increases in WS (Fig. 27a and b). These dynamics will have major local implications as WS of an area is a very important parameter in many aspects including on local water budgeting between different water components

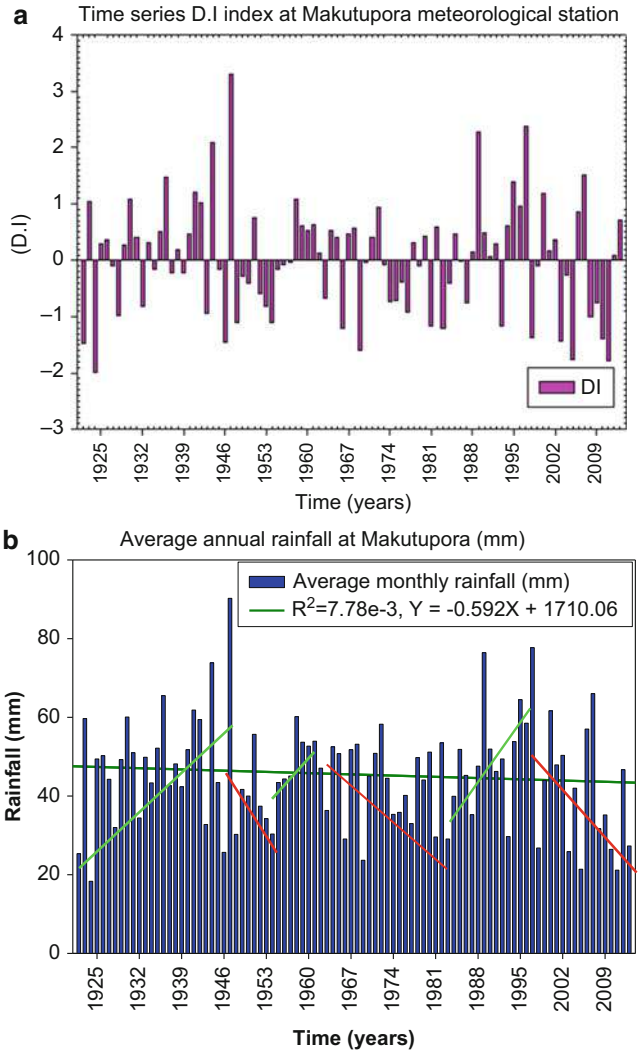

Fig. 20 (**a**) DI at MMS. (**b**) Time series average rainfall at MMS

(Allen et al. 1998b; Rayner 2007; Raz-Yaseef et al. 2012; Shenbin et al. 2006). The increasing WS has important reputations to distribution of moisture/ARH via enhanced PET (McVicar et al. 2012). Notice that the maximum WS occurs in September and October, while the average minimum WS comes in February (Fig. 29a). Similarly, there is stronger wind in the evening at 3 pm than in the morning at 9 am (Fig. 29a). This trend could explain why the area has observed an overall increase in PET following corresponding local T increases (Figs. 10 and 11).

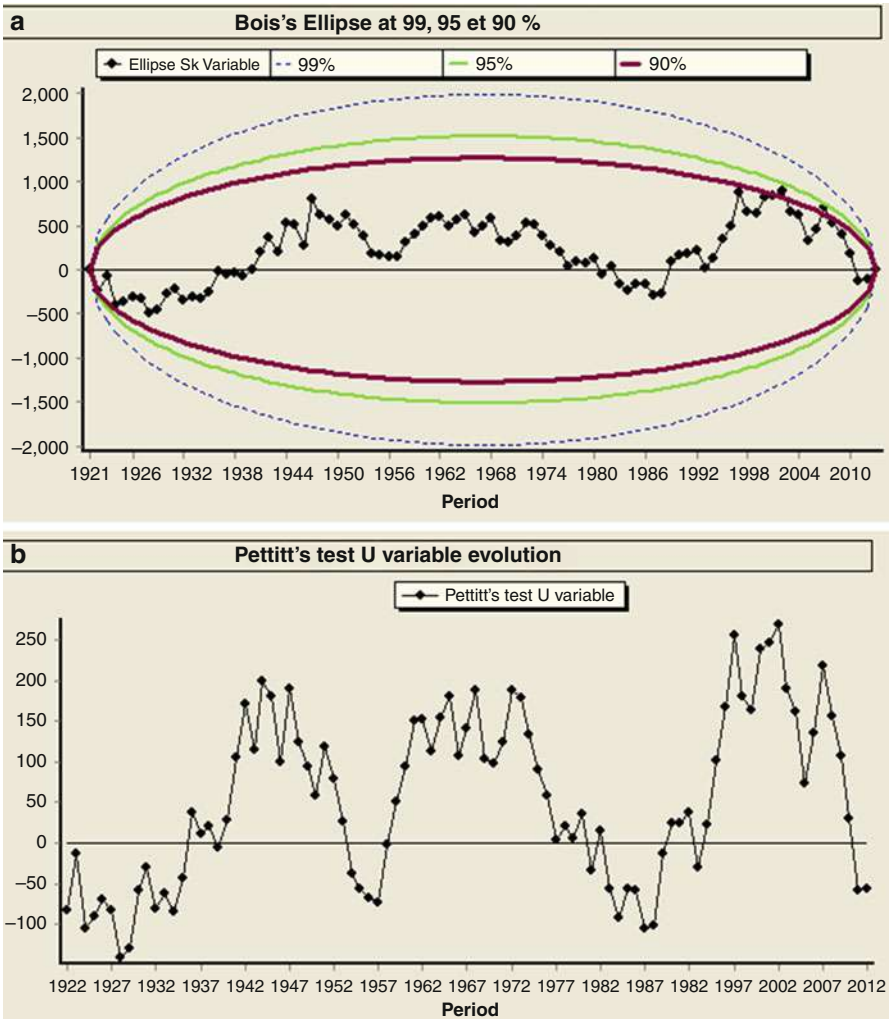

Fig. 21 Time series annual rainfall changes/fluctuation as modeled by Khronostart1.1

Thus, the maximum WS and ET occur at the hottest months of the year (November and October) which are wet months (Fig. 29a). Scholars link WS magnitudes with water resources dynamics where the windier the area is, the more the ET rate (McVicar et al. 2012); therefore these parameters must be properly monitored in the overall water resource management. Equally important, the maximum wind speed, RD, and ET all occur in October that is also the beginning of the rainy season. This relationship means that the bulk of the early rains will end up evaporating as these parameters directly favor more PET losses.

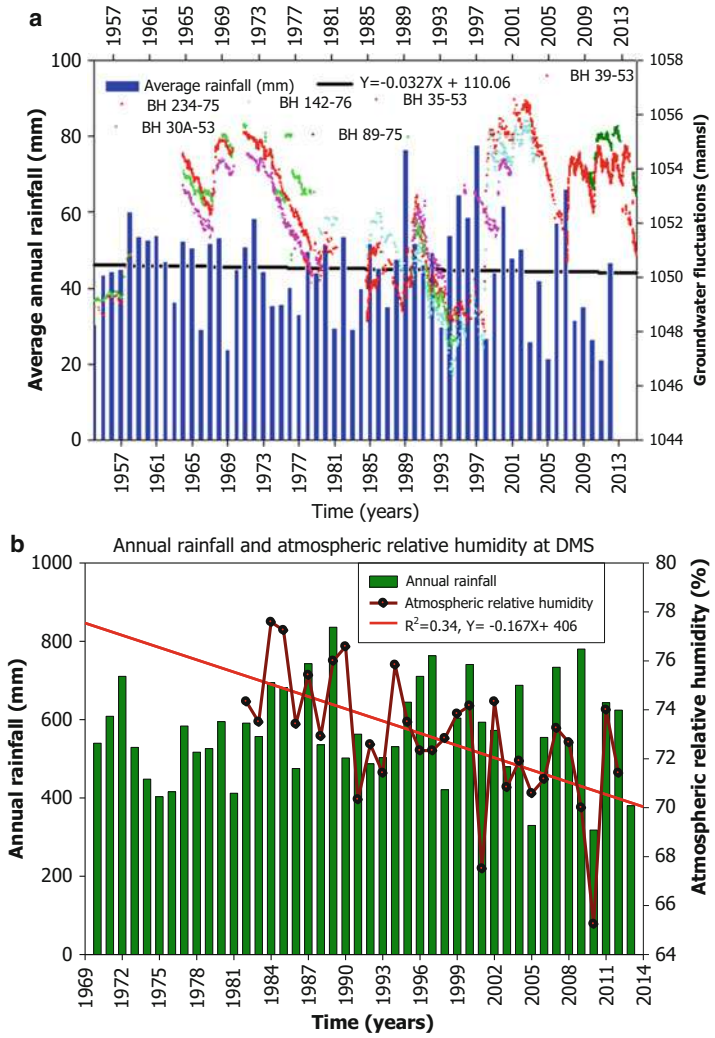

Fig. 22 Times series. (**a**) Rainfall magnitudes and hydrographs of the main observation boreholes at MMS. (**b**) Annual rainfall and ARH at DMS

Radiation (RD)

Solar radiation is one of the key parameters affecting climate and environment management strategies (Tang et al. 2011). Close observation of local SR data series suggests that like for the case of WS, the area is marked by increasing trends from the early 1980s followed by gradual decreases from 2002 onward. However, close observation of the data series suggests that over the entire time series, SR has slightly increased (Fig. 28a). Like for ET and WS magnitudes, SR has a huge effect

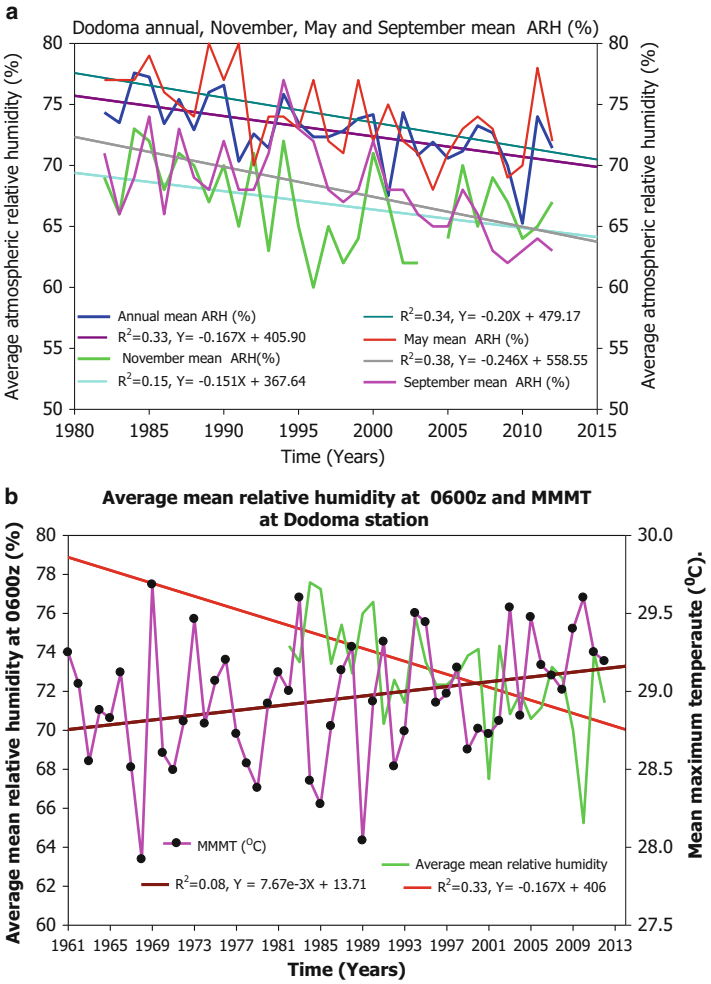

Fig. 23 Time series. (**a**) Annual, November, May, and September mean ARH. (**b**) Average ARH and MMT at DMS

on the climate dynamics including water balancing and distribution (Rathore 2004). Notice that the maximum RD occurs in October, while the minimum is in May, thus any increases in RD during wet months will adversely affect local water balancing since S trend has also increased (Fig. 29b). Thus, the highest radiation during wet months locally suggests that more water molecules would be in the vapor form and hence involved in PET losses (Fig. 28b). While analyzing radiation potentials in other Dodoma regions using 2002–2012 data series, similar findings were reached (Mking'imle 2013).

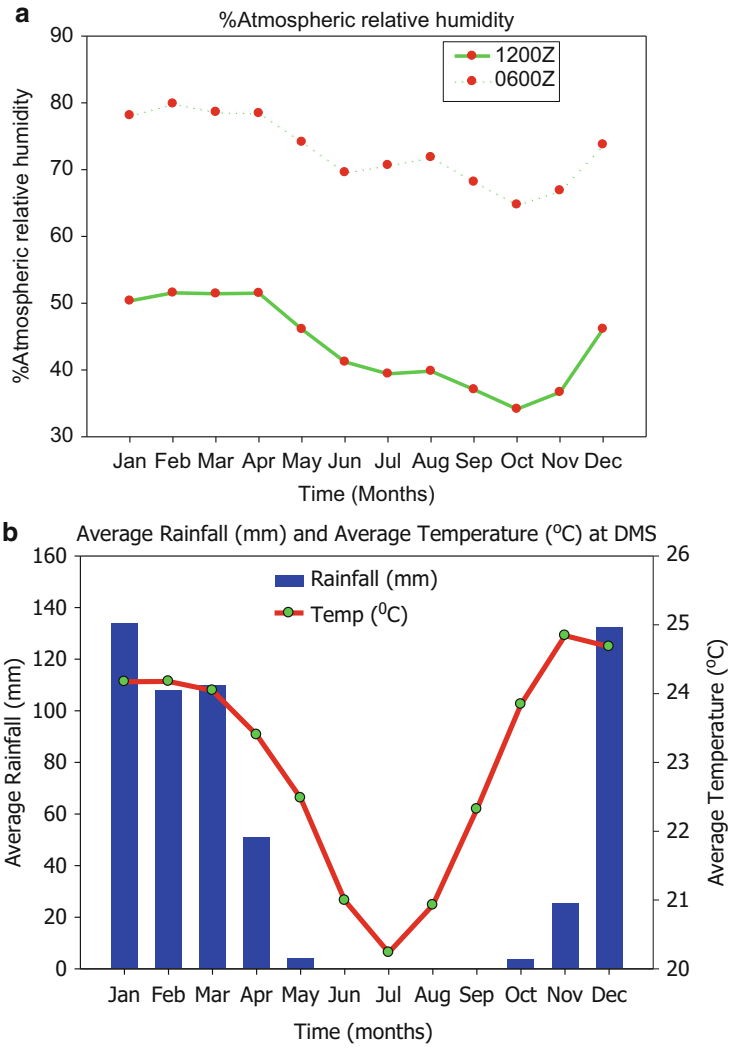

Fig. 24 Time series. (**a**) Average sunshine hours and radiation. (**b**) Sunshine hours in September at DMS (hours)

Studies across the world had indicated similar trends in SR where by using satellite observation, the decreasing trends were also observed in other parts of the world (Rathore 2004). Thus, studies show that global reduction in the amount of SR had a more global picture over the past 50 years (Stanhill and Cohen 2001). For instance, the amount of SR has observed an average decline of up to 2.7 % per decade (Stanhill and Cohen 2001). Studies in China had shown that there was widespread decline in the amount of SR in almost similar time series as recorded

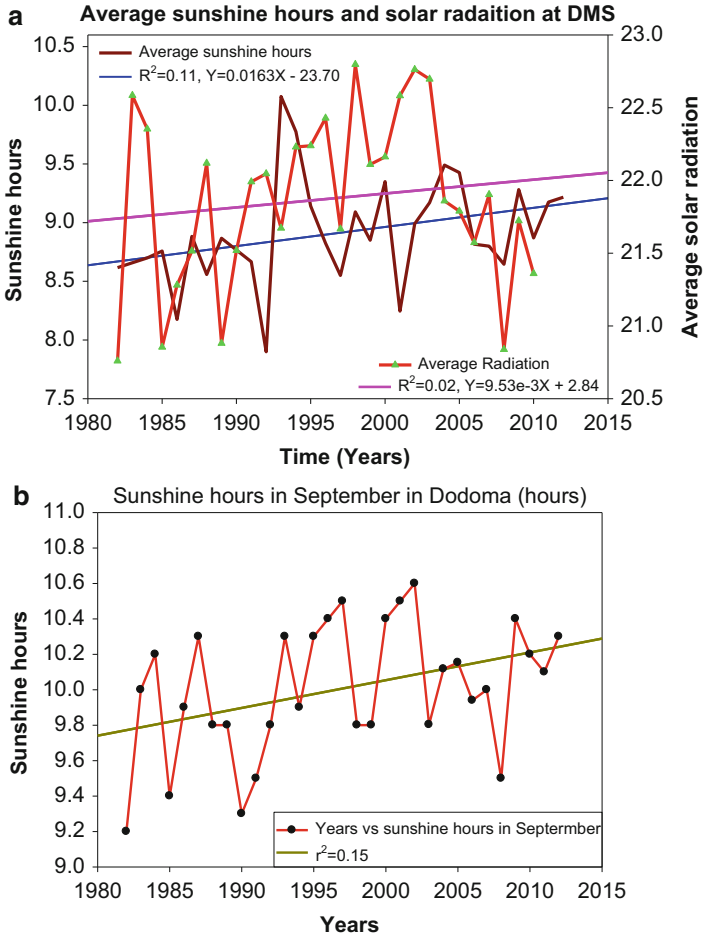

Fig. 25 Annual R and PET based on TWMWB modeling from (**a**) HMS and (**b**) DMS

in the current studies (Pavelic et al. 2012). In China the decreasing SR was further accompanied by the decreasing R which was also proportional to the amount of cloud cover. Locally, rainfall has also been declining (Fig. 3a) suggesting stronger similarities with the situation in China. The significant release of aerosol into the atmosphere from human activities and changes in land use could be one of the direct reasons to the decrease in SR (Pavelic et al. 2012). Variation in amount of SR with cloud cover is well-established science (Svensmark and Friis-Christensen 1997). Thus, the trends observed in Dodoma therefore are in agreement to similar global studies, and hence the wider causes could as well be the same. Currently, the widely accepted causes are human-related releases of aerosols; the sources and route of which do not recognize the political boundaries. These radiation dynamics will

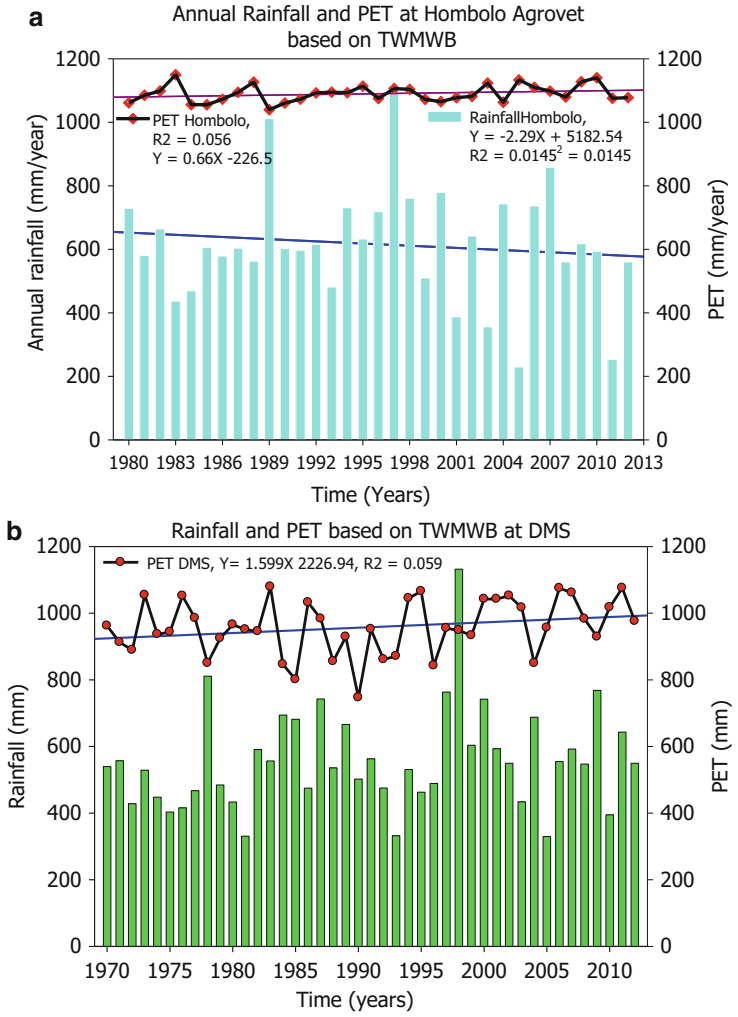

Fig. 26 (**a**) Monthly rainfall and mean ET at Hombolo Agrovet station. (**b**) Monthly rainfall and PET at DMS

inevitably adjust water, ecosystems, vegetation compositions, and primary productivity including on agricultural activities (Zhao and Running 2010). These relationships will need to be well studied in such an economy that is largely dependent on agriculture and livestock husbandry (Coulson 2011; Hella et al. 2011; Mgeni and Bangi 2014; Pedersen 2010). In Tanzania the releases of aerosols could directly be associated with the recent widespread adverse human activities, namely, deforestation activities and burning of fossil fuels (Mazvimavi 2002; Mking'imle 2013).

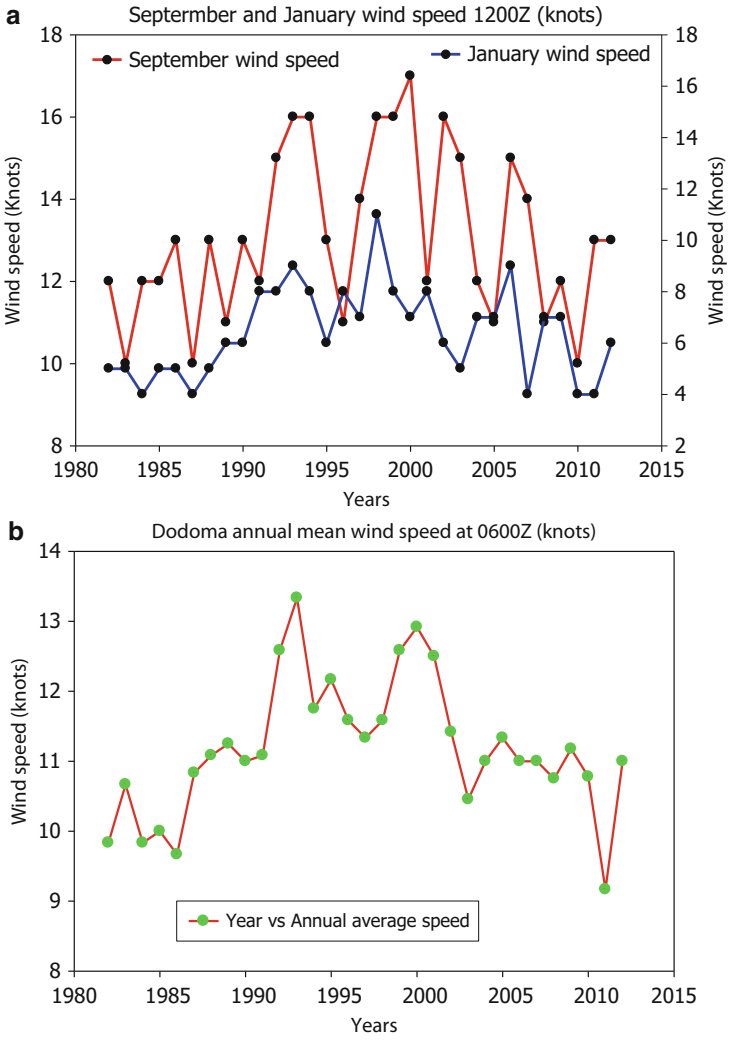

Fig. 27 Dodoma monthly mean atmospheric relative humidity (%)

Despite the fact that SR has locally decreased in recent years, the area still has a huge SR potential (Fig. 28a) that could be used for different uses including electrify generation (Mking'imle 2013) and therefore protect environment degradation (Mking'imle 2013). Worth noting, the country is still lagging behind in terms of electricity sufficiency production and supply. This remains the case when huge SR potential in Dodoma could be used to supply enough energy in Dodoma and beyond (Mking'imle 2013; Fig. 30).

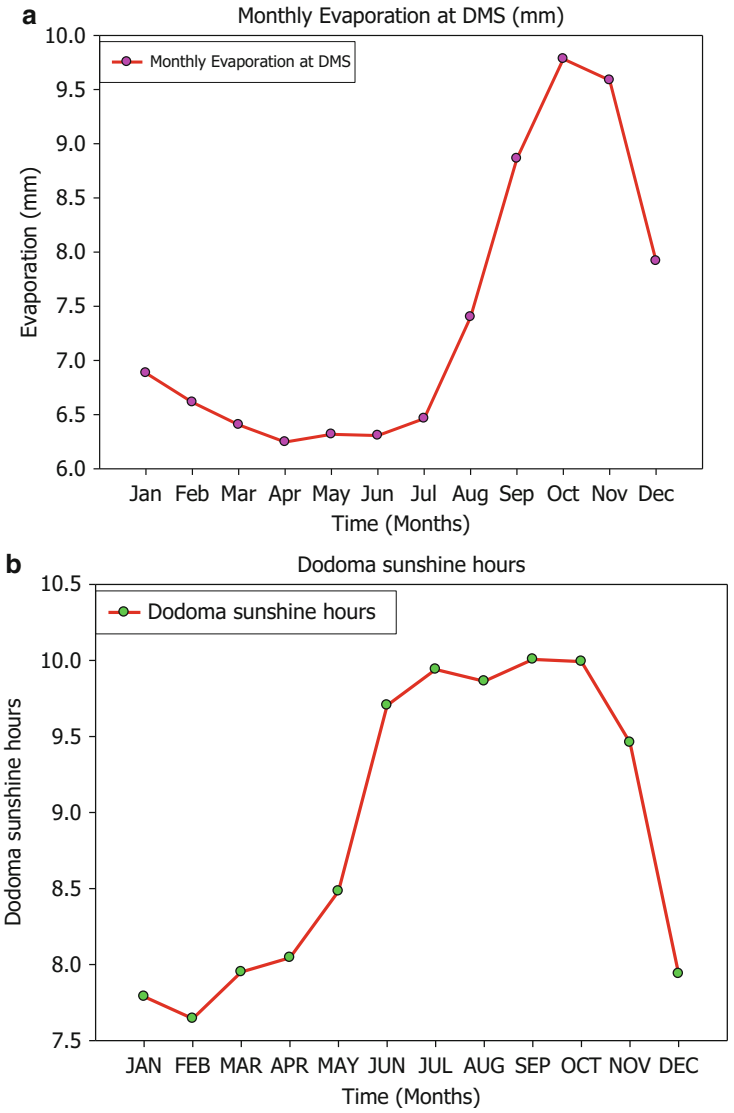

Fig. 28 (**a**) Dodoma September and January mean wind speed at 3 pm. (**b**) January and September mean wind speed at 3 pm

Conclusions and Recommendations

Analysis of major climate parameters (R, T, ARH, WS, RD, and ET) from MMS, HMS, and DMS, all located in the Dodoma municipality, a semiarid region of East Africa, was performed. The methods deployed include statistical, graphical

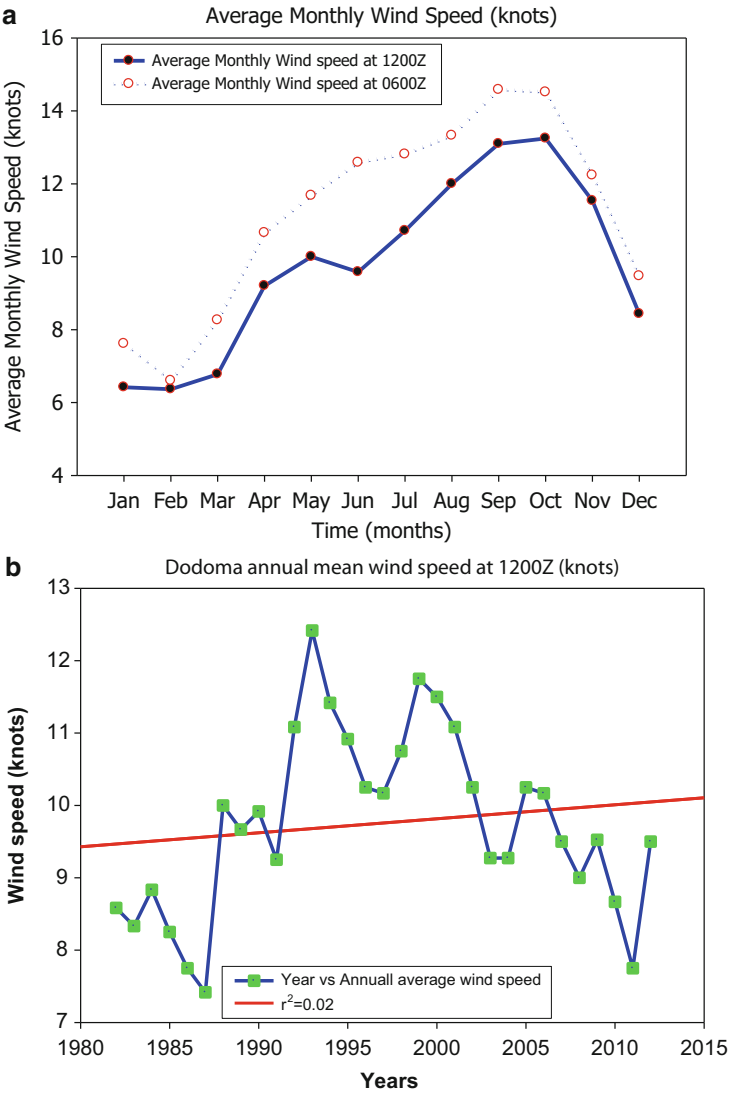

Fig. 29 (**a**) Dodoma monthly wind speed at 9 am and 3 pm. (**b**) Time series Dodoma mean monthly wind speed

modeling and extensive literature reviewing. The results show the area is not excluded from the global climate variability trends with nearly all climate parameters from the three stations showing similar trends and alterations, irrespective of the differences in their longevity. Thus, the global climate variability trends are well registered locally, offering lessons for more direct implications in terms of local

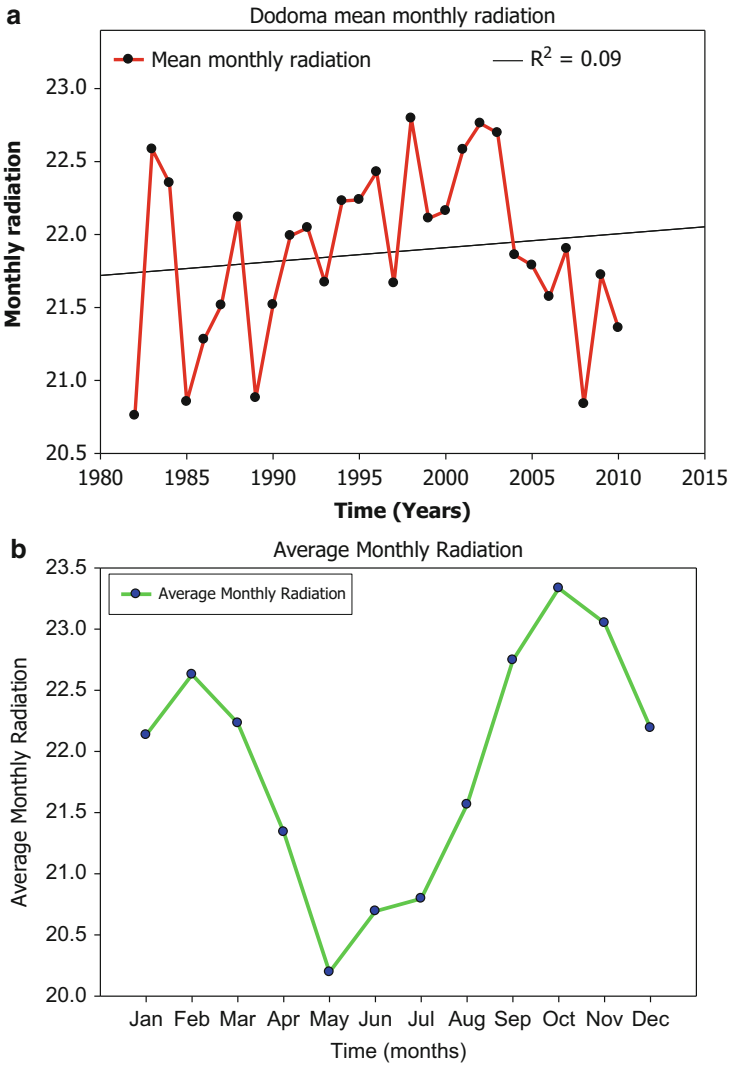

Fig. 30 (**a**) Time series Dodoma mean monthly radiation. (**b**) Dodoma average monthly radiation

livelihood support systems, namely, agriculture, pasture development, and groundwater recharge.

Locally, however, major variability is associated with T and R than with other parameters. The observed statistics clearly show that the number of rain days is diminishing and so are their magnitudes. On the other hand, it is clear that the area is getting warmer in both wet and dry seasons. Similarly, the declining ARH is likely to be linked to widespread decreases in vegetation cover and declining soil moisture and further strongly support observed R trend (the principal moisture sources), while

S and ET have slightly increased. Over the past 91 years, there has been a net R decrease of 54 mm in annual rains of only about 550 mm/year. Closer look at monthly time series reveals more hidden and silent details including strong signals of shifting R seasonality differences in the extent of decreasing and increasing climatic parameters. For instance, both May and April rains are ironically disappearing and/or significantly reduced suggesting a net reduction in the growing season and recharge cycles. Such silent features are generally not observed in annual time series.

On the other hand, like for R trends, hidden and silent features are more evident under monthly than annual T time steps where apart from the generalized warming trends, it is clear that June had the highest increase in MMT (1.54 °C), while April had the least (0.662 °C). Clearly changes in T and R (often key to the local livelihood support system like agriculture, pasture development, and groundwater recharge) will have major socioeconomic implications for the principally agrarian society. Declining R and increasing T further explain the repeated agricultural failures and livestock and wildlife deaths from shortage of pasture and water.

Furthermore, T and R are considered the most vital factors in the distributions of moisture and occurrence of disease vectors like mosquitoes. This could explain why in recent years in Tanzania malaria cases have worsened in areas where it was uncommon, like in the study area.

These findings should be reflected in adaptation and mitigation measures against the adverse impacts of climate change. These measures should include planting in accordance to the current R dates, planting early-maturing varieties, and planting drought- and high-temperature-resistant crops, among others. Measures to utilize less water should also be advocated among all water users in the area. Thus, there is a need to re-look at water allocation systems, and artificial groundwater recharge should be sought as an option as water would be protected from PET.

It is further recommended that future studies should include data from neighboring meteorological stations, satellite information and climate modeling and downscaling for a better understanding of the local climate trends in relation to a global picture. Similarly, it will be interesting to find out how the relatively well-established climate data trends and changes in land cover/use would be reflected in the surface water like river levels, sediment generation and characteristics, soil productivity, pasture development, soil moisture, etc.

References

Allen JC (1985) Wood energy and preservation of woodlands in semi-arid developing countries: the case of Dodoma region, Tanzania. J Dev Econ 19(1):59–84

Allen RG, Pereira LS, Raes D, Smith M (1998a) Crop evapotranspiration-guidelines for computing crop water requirements-FAO irrigation and drainage paper 56. FAO, Rome 300(9):D05109

Allen RG, Pereira LS, Raes D, Smith M (1998b) Crop evapotranspiration-guidelines for computing crop water requirements-FAO irrigation and drainage paper 56. FAO, Rome 300:6541

Al-manmi DA MA (2002) Water resources management in Rania area Sulaimaniyah NE-Iraq. University of Baghdad, PhD thesis

Altizer S, Ostfeld RS, Johnson PT, Kutz S, Harvell CD (2013) Climate change and infectious diseases: from evidence to a predictive framework. Science 341(6145):514–519

Angelsen A, Shitindi EFK, Aarrestad J (1999) Why do farmers expand their land into forests? Theories and evidence from Tanzania. Environ Dev Econ 4(3):313–331

Azorin-Molina C, Vicente-Serrano SM, McVicar TR, Jerez S, Sanchez-Lorenzo A, López-Moreno J-I, Revuelto J, Trigo RM, Lopez-Bustins JA, Espírito-Santo F (2014) Homogenization and assessment of observed near-surface wind speed trends over Spain and Portugal, 1961–2011. J Climate 27(10):3692–3712

Barnett J, Campbell J (2010) Climate change and small island states: power, knowledge, and the South Pacific. Earthscan

Belloumi M (2014) Investigating the impact of climate change on agricultural production in eastern and southern African countries (Vol. 3). Intl Food Policy Res Inst

Boelee E, Yohannes M, Poda JN, McCartney M, Cecchi P, Kibret S, Hagos F, Laamrani H (2013) Options for water storage and rainwater harvesting to improve health and resilience against climate change in Africa. Reg Environl Chang 13(3):509–519

Burke MB, Miguel E, Satyanath S, Dykema JA, Lobell DB (2009) Warming increases the risk of civil war in Africa. Proc Natl Acad Sci 106(49):20670–20674

Calow RC, Robins NS, MacDonald AM, Macdonald DMJ, Gibbs BR, Orpen WRG, Appiah SO (1997) Groundwater management in drought-prone areas of Africa. Int J Water Resour Dev 13(2):241–262

Calow RC, MacDonald AM, Nicol AL, Robins NS (2010) Ground water security and drought in Africa: linking availability, access, and demand. Groundwater 48(2):246–256

Charman DJ, Barber KE, Blaauw M, Langdon PG, Mauquoy D, Daley TJ, Karofeld E (2009) Climate drivers for peatland paleoclimate records. Quat Sci Rev 28(19):1811–1819

Cline-Cole RA, Main H, Nichol JE (1990) On fuelwood consumption, population dynamics and deforestation in Africa. World Dev 18(4):513–527

Conway D, Schipper ELF (2011) Adaptation to climate change in Africa: challenges and opportunities identified from Ethiopia. Glob Environ Chang 21(1):227–237

Cook PG, Herczeg AL eds (2012) Environmental tracers in subsurface hydrology. Springer Science & Business Media

Cooper P, Dimes J, Rao K, Shapiro B, Shiferaw B, Twomlow S (2008) Coping better with current climatic variability in the rain-fed farming systems of sub-Saharan Africa: an essential first step in adapting to future climate change? Agric Ecosyst Environ 126(1):24–35

Cooper P, Rao K, Singh P, Dimes J, Traore P, Rao K, Dixit P, Twomlow S (2009) Farming with current and future climate risk: advancing a 'Hypothesis of Hope' for rainfed agriculture in the semi-arid tropics. J SAT Agric Res 7:1–19

Cooper PJM, Stern RD, Noguer M, Gathenya JM (2013) Climate change adaptation strategies in Sub-Saharan Africa: foundations for the future. InTech Open, pp 327–356

Coulson A (2011) Kilimo Kwanza: a new start for agriculture in Tanzania. Working paper

Craparo ACW, Van Asten PJA, Läderach P, Jassogne LTP, Grab SW (2015) Coffea arabica yields decline in Tanzania due to climate change: Global implications. Agr Forest Meteorol 207:1–10

Deryng D, Conway D, Ramankutty N, Price J, Warren R (2014) Global crop yield response to extreme heat stress under multiple climate change futures. Environ Res Lett 9(3):034011

Ebi K, (2014) Assessing the health risks of climate change. In Global Climate Change and Public Health. Springer, New York, pp 307–317

Faramarzi M, Abbaspour KC, Vaghefi SA, Farzaneh MR, Zehnder AJ, Srinivasan R, Yang H (2013) Modeling impacts of climate change on freshwater availability in Africa. J Hydrol 480:85–101

Ford JD, Vanderbilt W, Berrang-Ford L (2012) Authorship in IPCC AR5 and its implications for content: climate change and Indigenous populations in WGII. Clim Change 113(2):201–213

Fuller DO, Prince SD (1996) Rainfall and foliar dynamics in tropical southern Africa: potential impacts of global climatic change on savanna vegetation. Clim Change 33(1):69–96

Funk C, Hoell A, Shukla S, Bladé I, Liebmann B, Roberts JB, Husak G (2014) Predicting East African spring droughts using Pacific and Indian Ocean sea surface temperature indices. Hydrol Earth Syst Sci 18(12):4965–4978

Graef F, Haigis J (2001) Spatial and temporal rainfall variability in the Sahel and its effects on farmers' management strategies. J Arid Environ 48(2):221–231

Guo H, Xu M, Hu Q (2011) Changes in near-surface wind speed in China: 1969–2005. Int J Climatol 31(3):349–358

Harvell CD, Mitchell CE, Ward JR, Altizer S, Dobson AP, Ostfeld RS, Samuel MD (2002) Climate warming and disease risks for terrestrial and marine biota. Science 296(5576):2158–2162

Harvell D, Altizer S, Cattadori IM, Harrington L, Weil E (2009) Climate change and wildlife diseases: when does the host matter the most? Ecology 90(4):912–920

Hearty PJ, Neumann AC (2001) Rapid sea level and climate change at the close of the Last Interglaciation (MIS 5e): evidence from the Bahama Islands. Quat Sci Rev 20(18):1881–1895

Hella JP, Haug R, Kamile IM (2011) High global food prices-crisis or opportunity for smallholder farmers in Tanzania? Dev Pract 21(4–5):652–665

Hendrix CS, Glaser SM (2007) Trends and triggers: climate, climate change and civil conflict in Sub-Saharan Africa. Political Geogr 26(6):695–715

Hendrix CS, Salehyan I (2012) Climate change, rainfall, and social conflict in Africa. J Peace Res 49(1):35–50

Hirji R, Malapo J (2002). Environmental sustainability in water resources management: A conceptual framework. In Hirji R, Johnson P, Maro P, Chiuta TM (Eds), Defining and mainstreaming environmental sustainability in water resources management in southern Africa. A SADC, IUCN, SARDC, World Bank Technical Report. pp1–20

Hoell A, Funk C (2014) Indo-Pacific sea surface temperature influences on failed consecutive rainy seasons over eastern Africa. Climate Dynam 43(5–6):1645–1660

Jiang Y, Luo Y, Zhao Z, Tao S (2010) Changes in wind speed over China during 1956–2004. Theor Appl Climatol 99(3–4):421–430

Jones AE, Wort UU, Morse AP, Hastings IM, Gagnon AS (2007) Climate prediction of El Niño malaria epidemics in north-west Tanzania. Malar J 6:162

Jung M, Reichstein M, Ciais P, Seneviratne SI, Sheffield J, Goulden ML, Zhang K (2010) Recent decline in the global land evapotranspiration trend due to limited moisture supply. Nature 467(7318):951–954

Kashaigili JJ (2010) Assessment of groundwater availability and its current and potential use and impacts in Tanzania. Report prepared for the International Water Management Institute (IWMI). Sokoine University of Agriculture, Morogoro

Katz RW, Brown BG (1992) Extreme events in a changing climate: variability is more important than averages. Clim Change 21(3):289–302

King' Uyu SM, Ogallo LA, Anyamba EK (2000) Recent trends of minimum and maximum surface temperatures over Eastern Africa. Journal of Climate 13(16):2876–2886

Knox J, Hess T, Daccache A, Wheeler T (2012) Climate change impacts on crop productivity in Africa and South Asia. Environ Res Lett 7(3):034032

Kousari MR, Ekhtesasi MR, Tazeh M, Naeini MAS, Zarch MAA (2011) An investigation of the Iranian climatic changes by considering the precipitation, temperature, and relative humidity parameters. Theor Appl Climatol 103(3–4):321–335

Lafferty KD (2009) The ecology of climate change and infectious diseases. Ecology 90(4):888–900

Li Z, Yan Z, Tu K, Liu W, Wang Y (2011) Changes in wind speed and extremes in Beijing during 1960–2008 based on homogenized observations. Adv Atmos Sci 28:408–420

Liu L, Wang E, Zhu Y, Tang L (2012) Contrasting effects of warming and autonomous breeding on single-rice productivity in China. Agric Ecosyst Environ 149:20–29

Liu L, Wang E, Zhu Y, Tang L, Cao W (2013) Effects of warming and autonomous reeding on the phenological development and grain yield of double-rice systems in China. Agric Ecosyst Environ 165:28–38

MacDonald AM, Calow RC, MacDonald DM, Darling WG, Dochartaigh BE (2009) What impact will climate change have on rural groundwater supplies in Africa? Hydrol Sci J 54 (4):690–703

MacDonald A, Bonsor H, Dochartaigh BÉÓ, Taylor R (2012) Quantitative maps of groundwater resources in Africa. Environ Res Lett 7:2–49

Majule A (2008) Climate change and variability: impacts on agriculture and water resource and implications for livelihoods in selected Basins. In: Towards climate change adaptation. In WEnt-Internationale Weiterbildung und Entwicklung gGmbH Publishing. ISBN: 978-3

Mariotti L, Coppola E, Sylla MB, Giorgi F, Piani C (2011) Regional climate model simulation of projected 21st century climate change over an all-Africa domain: comparison analysis of nested and driving model results. Journal of Geophysical Research 116(D15111): 12

Mary A, Majule A (2009) Impacts of climate change, variability and adaptation strategies on agriculture in semi-arid Tanzania: the case of Manyoni District in Singida Region, Tanzania. Afr J Environ Sci Technol 3(8):206–218

Maurel M, Kubik Z (2014) Climate variability and migration: evidence from Tanzania. Working Paper 104. Foundation pour les études et recherches sure developpement international, Paris

Mazvimavi D (2002) Watershed degradation and management. Defining and Mainstreaming Environmental Sustainability in Water Resource Management in Southern Africa. SADC, IUCN, SARDC, World Bank, Maseru/Harare/Washington, DC

McVicar TR, Roderick ML, Donohue RJ, Li LT, Van Niel TG, Thomas A, Grieser J, Jhajharia D, Himri Y, Mahowald NM (2012) Global review and synthesis of trends in observed terrestrial near-surface wind speeds: implications for evaporation. J Hydrol 416:182–205

Mgeni T, Bangi YI (2014) Is Kilimo kwanza a reliable answer to the paradox of hunger in the midst of plenty in Tanzania? Challenges and prospects of Kilimo kwanza (agriculture first) strategy in Tanzania. J Econ Sustain Dev 5(9):94–106

Mking'imle V (2013) Assessing the potential of solar energy utilization in central Tanzania, University of Nairobi

Mongi H, Majule AE, Lyimo JG (2010) Vulnerability and adaptation of rain fed agriculture to climate change and variability in semi-arid Tanzania. African Journal of Environmental Science and Technology 4(6)

Mutua F, Koike T (2013) Holistic view to integrated climate change assessment and extreme weather adaptation in the Lake Victoria Basin East Africa, AGU fall meeting abstracts, pp 1087

Nelson V, Stathers T (2009) Resilience, power, culture, and climate: a case study from semi-arid Tanzania, and new research directions. Gend Dev 17(1):81–94

Ngongondo CS (2006) An analysis of long-term rainfall variability, trends and groundwater availability in the Mulunguzi River catchment area, Zomba Mountain, Southern Malawi. Quat Int 148(1):45–50

Nicholls RJ (1995) Coastal megacities and climate change. GeoJournal 37(3):369–379

Nkotagu H (1996a) Application of environmental isotopes to groundwater recharge studies in a semi-arid fractured crystalline basement area of Dodoma, Tanzania. Afr Earth Sci 22:443–457

Nkotagu H (1996b) The groundwater geochemistry in a semi-arid, fractured crystalline basement area of Dodoma, Tanzania. J Afr Earth Sci 23(4):593–605

Nkotagu H (1996c) Origins of high nitrate in groundwater in Tanzania. J Afr Earth Sci 22(4):471–478

Nonhebel S (1996) Effects of temperature rise and increase in CO2 concentration on simulated wheat yields in Europe. Clim Change 34(1):73–90

Nyenzi BS, Kavishe MM, Nassib IR, Tilya FF (1999) Analysis of meteorological droughts in Tanzania. In: Proceedings of an interdisciplinary international conference on integrated drought management, Pretoria, 1999

Omambia AN, Ceven Shemsanga, and Ivonne Andrea Sanchez Hernandez (2012) Climate change impacts, vulnerability, and adaptation in East Africa (EA) and South America (SA). In: Handbook of climate change mitigation. Springer US, pp 571–620

Paavola J (2006) Justice in adaptation to climate change in Tanzania. MIT Press, Cambridge, MA

Paavola J (2008) Livelihoods, vulnerability and adaptation to climate change in Morogoro, Tanzania. Environ Sci Policy 11(7):642–654

Pavelic P, Giordano M, Keraita B, Ramesh V, Rao T (2012) Groundwater availability and use in Sub-Saharan Africa: a review of 15 countries (No. H046186). International Water Management Institute

Pedersen RH (2010) Tanzania's land law reform: the implementation challenge. Working paper

Rao K, Ndegwa W, Kizito K, Oyoo A (2011) Climate variability and change: farmer perceptions and understanding of intra-seasonal variability in rainfall and associated risk in semi-arid Kenya. Exp Agric 47(02):267–291

Rathore MS (2004/2005) State level analysis of drought policies and impacts in Rajasthan, India. Working paper 93: Drought Series Paper No. 6. IWMI, Colombo, 40 p

Rayner D (2007) Wind run changes: the dominant factor affecting pan evaporation trends in Australia. J Climate 20(14):3379–3394

Raz-Yaseef N, Yakir D, Schiller G, Cohen S (2012) Dynamics of evapotranspiration partitioning in a semi-arid forest as affected by temporal rainfall patterns. Agr Forest Meteorol 157:77–85

Rowhani P, Lobell DB, Linderman M, Ramankutty N (2011) Climate variability and crop production in Tanzania. Agr Forest Meteorol 151(4):449–460

Rugai D, Kassenga GR, (2014) Climate change impacts and institutional response capacity in Dar es Salaam, Tanzania. In:Climate Change Vulnerability in Southern African Cities. Springer International Publishing, pp 39–55

Rwebugisa RA (2008) Groundwater re-charge assessment in the Makutupora Basin, Dodoma, Tanzania, MSc thesis. International Institute for Geo-Information Science and Earth Observation, Enschede

Sabine C (2014) The IPCC fifth assessment report. Carbon 5(1):17–25

Salama RB (1979) Dodoma capital city water resources study. Government Printers, Dodoma

Sanga G, Moshi A, Hella J (2013) Small scale farmers' adaptation to climate change effects in Pangani basin and Pemba: challenges and opportunities. Int J Mod Soc Sci 2(3):169–194

Sanga G, Hella J, Mzirai N, Senga H (2014) Change on maize and beans production and compatibility of adaptation strategies in Pangani River Basin, Tanzania

Shemsanga C, Omambia AN, Gu Y (2010) The cost of climate change in Tanzania: impacts and adaptations. Journal of American Science 6(3):182–196

Shemsanga C, Muzuka ANN, Martz L, Komakechi H, Mihale L (forthcoming) Groundwater exploitation, the concept of sustainable yield and integrated water balance in aquifers of Dodoma, Tanzania. Submitted for publication

Shenbin C, Yunfeng L, Thomas A (2006) Climatic change on the Tibetan Plateau: potential evapotranspiration trends from 1961–2000. Clim Change 76(3–4):291–319

Shindo S (1991) Study on the recharge mechanism and development of groundwater in the inland area of Tanzania. Report of the Japanese-Tanzanian Research Mission (2). Chiba University

Shindo S (1994) Study on the recharge mechanism and development of groundwater in the inland area of Tanzania. Progress report of Japan-Tanzania joint research (3), Chiba University, Japan

Simon D ed., (2010) August. The challenges of global environmental change for urban Africa, Urban Forum. Springer, Netherlands 21(3): pp 235–248

Solomon S (2007) Climate change 2007-the physical science basis: Working group I contribution to the fourth assessment report of the IPCC (Vol. 4). Cambridge University Press

Stanhill G, Cohen S (2001) Global dimming: a review of the evidence for a widespread and significant reduction in global radiation with discussion of its causes and possible agricultural consequences. Agr Forest Meteorol 107(4):255–278

Stocker TF (ed) (2014) Climate change 2013: the physical science basis: Working Group I contribution to the Fifth assessment report of the Intergovernmental Panel on Climate Change. Cambridge University Press

Svensmark H, Friis-Christensen E (1997) Variation of cosmic ray flux and global cloud coverage-a missing link in solar-climate relationships. J Atmos Sol Terrl Phys 59(11):1225–1232

Swai O, Mbwambo J, Magayane F (2012a) Gender and perception on climate change in Bahi and Kondoa districts, Dodoma region, Tanzania. J Afr Stud Dev 4(9):218–231

Swai OW, Mbwambo JS, Magayane FT (2012b) Gender and adaptation practices to the effects of climate change in Bahi and Kondoa Districts Dodoma Region, Tanzania. J Sustain Dev 5(12)

Swai OW, Mbwambo JS, Magayane FT (2012c) Perceived effects of climate change on agricultural production: a gendered analysis done in Bahi and Kondoa districts, Dodoma region, Tanzania. Res Hum Soc Sci 2(9):59–68

Tang W-J, Yang K, Qin J, Cheng C, He J (2011) Solar radiation trend across China in recent decades: a revisit with quality-controlled data. Atmos Chem Phys 11(1):393–406

Tao F, Zhang Z, Zhang S, Rötter RP (2015) Heat stress impacts on wheat growth and yield were reduced in the Huang-Huai-Hai Plain of China in the past three decades. Eur J Agron 71:44–52

Taylor RG, Scanlon B, Döll P, Rodell M, Van Beek R, Wada Y, Treidel H (2013) Ground water and climate change. Nat Clim Change 3(4):322–329

Thomson M, Mantilla G, Platzer B, Willingham AL, World Health Organization and UNICEF, 2012. Assessment of research needs for public health adaptation to social, environmental and climate change impacts on vector-borne diseases in Africa: an informal expert consultation convened by the Special Programme for Research and Training in Tropical Diseases (TDR), Addis Ababa, Ethiopia, February 27–29, 2012

URT (2003) Socio-economic profile of Dodoma. National Bureau of Statistics, Dar-es-Salaam

Valimba P (2004) Rainfall variability in southern Africa, its influences on streamflow variations and its relationships with climatic variations, Rhodes University

Wang J, Wang E, Yin H, Feng L, Zhao Y (2015) Differences between observed and calculated solar radiations and their impact on simulated crop yields. Field Crop Res 176:1–10

Williams AP, Funk C (2011) A westward extension of the warm pool leads to a westward extension of the Walker circulation, drying eastern Africa. Climate Dynam 37(11–12):2417–2435

Williams AP, Allen CD, Macalady AK, Griffin D, Woodhouse CA, Meko DM, McDowell NG (2013) Temperature as a potent driver of regional forest drought stress and tree mortality. Nat Clim Change 3(3):292–297

Zhao M, Running SW (2010) Drought-induced reduction in global terrestrial net primary production from 2000 through 2009. Science 329(5994):940–943

Climate Change Adaptation, Mitigation, and the Attainment of Food Security in the Sudano-Sahelian Belt of Nigeria

Aishetu Abdulkadir

Contents

Abstract

Climate change and rainfall variability are evident in rainfall amount and the hydrologic growing season across the zone located between longitudes 3° and 15° east of the Greenwich meridian and latitudes 10° and 14° north of the Equator. These changes have continued to escalate the vulnerability of people's livelihood, as extreme weather conditions lead to reduction in agricultural yields which subsequently aggravate food insecurity. There is a general understanding of climate change and variability across the belt as indicated by the varying adaptation practices by individuals and communities to enable them to cope with the challenges of changing climate. Generally, in Nigeria, there are numerous crucial policies and programs aimed at addressing issues related to climate change adaptation and agricultural sustainability. However, the major concern is the level of implementation and its role in promoting, developing, and instituting effective adaptation strategies and practices that will enhance resilience of the

A. Abdulkadir (✉)
Centre for Disaster Risk Reduction and Development Studies (CDRM & DS), Federal University of Technology, Minna, Nigeria
e-mail: abuzaishatu@futminna.edu.ng

W.-Y. Chen et al. (eds.), *Handbook of Climate Change Mitigation and Adaptation*,
DOI 10.1007/978-3-319-14409-2_98

vulnerable communities. Consequently, bottom-up approaches should be developed and promoted to identify and document existing adaptation practices, alongside with assessing these adaptation practices for scaling up potential cost-effective practices for enhanced climate change adaptation, attainment of food security, and resilience.

The Sudano-Sahelian Belt of Nigeria

The Sudano-Sahelian belt of Nigeria is located between longitudes 3° and 15° east of the Greenwich meridian and latitudes 10° and 14° north of the Equator. However, in reality, this extends to about latitude 9° in recent times. The extreme northern part of the belt approaches the desert fringes, particularly sharing boundaries with the semiarid and arid zones of the Niger Republic. The states located in this zone are Sokoto, Kebbi, Zamfara, Katsina, Kano, Jigawa, Yobe, Borno, Gombe, Adamawa, Bauchi, and northern Kwara, Plateau, Niger, Nasarawa, and Taraba. Typical feature of this belt is land degradation in response to increase in both climate change and human activities: overcultivation and overgrazing.

The climate is characterized by alternate wet and dry seasons in response to the changes in pressure patterns. There is high variability in dates of onset and cessation of rains across the region which results in variability in length of the rainy season; this can also be attributed to the migratory patterns of the Intertropical Discontinuity (ITD). The rainy season in this belt is associated with late onset and early cessation which is associated with strong storms which destroy life and property. The rainy season in this zone has high rainfall intensity concentrated within a short period of time, thus increasing the rate and intensity of runoff. Hence, the Sudano-Sahelian zone is a moisture stress zone seen to be tending toward increased degradation. The latitudinal location of the belt also results in high temperature throughout the year, at about 27 °C. Generally, the highest temperature in the country is recorded in this zone. In addition, temperature range is highest in the northwest and northeast above 10 °C and reduces southward. The belt is dominated by savanna vegetation types: Guinea, Sudan, and Sahel savannas. The density of trees and grasses decreases northward, hence responding to climatic conditions.

Agriculture is the dominant economic activity in Northern Nigeria; crops such as groundnuts, cotton, millets, beans, Guinea corn, cassava, yam, and maize are cultivated in the region which also has the highest concentration of cattle in the country. In this belt the livelihood of rural farmers is highly tied to the availability of natural resource (land, water, and vegetation), thereby aggregating the impact and intensity of climate change on the community. A large proportion of the inhabitants depend on rain-fed agriculture. Also, irrigation scheme is employed mostly for cultivation of vegetable during the dry seasons but is characterized by low input and output.

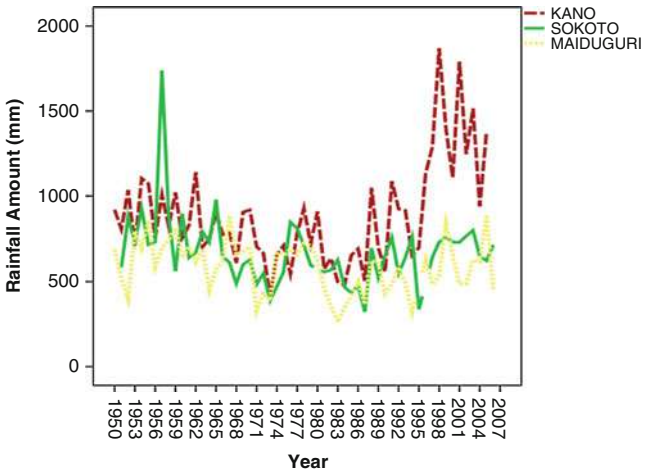

Fig. 1 Annual rainfall amount (1950–2007)

An Overview of Climate Change Impact in the Sudano-Sahelian Belt of Nigeria

The impact of climate change is already apparent across the Sudano-Sahelian zone of West Africa where a large proportion of the population engages in subsistent agriculture which is highly vulnerable to erratic weather conditions typical of the region. In Nigeria, climate changes coupled with increased human population and overexploitation of natural resources have aggravated environmental degradation which the teeming population rely on for their livelihoods. The recurring drought, desertification in the extreme Northern Nigeria, devastating flood across the riverine communities, soil erosion, and attendant loss of soil nutrients have continued to increase southward migration since the last century. Figures 1 and 2 depict the variability and gradual changes typical of the annual total rainfall amount and the hydrologic growing season in the three states across the belt. The vulnerability of developing countries and their populations to increased climate variability and change is of great concern and has attracted considerable research interest over the past decades with calls for increased funding for adaptation (Patt et al. 2010). These in addition to rainfall break, dry spell, drought, and flood during the growing season have continued to escalate the vulnerability of people's livelihood as extreme weather conditions lead to reduction in agricultural yields which subsequently aggravate individual/community poverty levels, susceptibility to climate change pressures, and food insecurity.

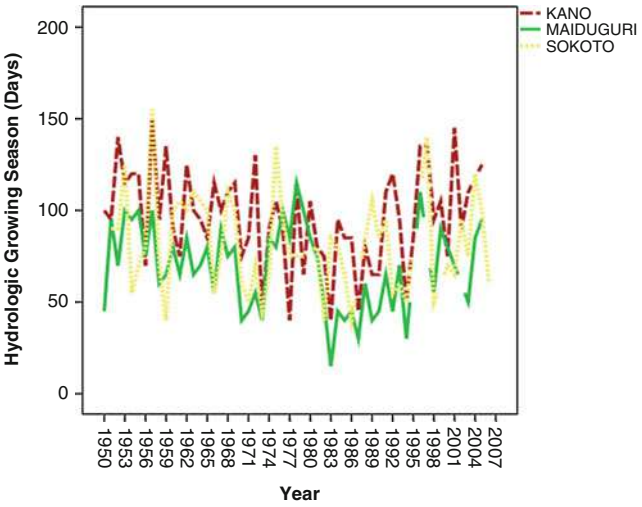

Fig. 2 Hydrologic growing season (1950–2007)

Climate Change Adaptation Practices and the Attainment of Food Security

There is a general understanding of climate change and variability across the belt as varying practices are being adapted by individuals and communities to enable them cope with the challenges of changing climate for the attainment of food security. The adaptation practices adopted are mixed farming, adoption of improved seeds that require less water and short maturing period, water conservation strategy, irrigation, and imbedding soil conservation culture through crop rotation. As such, agricultural adaptation that has always taken, and continues to take, place in Africa is responding more to perceived climate variability than climate change (Gina et al. 2008). These adaptation practices are taken to lessen the effects of climate change/variability and to increase socioeconomic well-being as well as enhance human livelihood. Adaptation to climate change is linked to sustainable socioeconomic development in the belt because large proportions of the inhabitants rely on natural resources (land and water) for their livelihood. They continue to identify measures for sustainable agriculture which is their main economic activity. Adaptation is adjusting the natural system or human system in response to actual or expected climatic stimuli or their effects (IPCC 2007). Basically, the emphasis has been on adjusting farming systems to expected climatic condition. How successful or otherwise these have been is yet to be determined. There is considerable knowledge gap with respect to climate change impact, vulnerability, and adaptation to increased climate variability and change (Molly and Brent 2011).

In recent times, the effect of climate change has forced farmers to diversify their economic activities, as most farming communities now combine crop cultivation and livestock farming or fishery. This to some extent is supported by the National Economic Empowerment and Development Strategy (NEEDS 2004) whose developmental plan is inspired by current challenges for vigorous growth. NEEDS emphasis is on job creation, strengthening the skill base, protecting the vulnerable, and promoting peace and security. This generally consists of robust plan to identify the major problems facing the various communities across the country with a view to proffering solutions using integrated economic development processes and programs across the tiers of the government (federal, state, and local government levels). However, the major concern is to what extent has the implementation of these robust plans reduced the vulnerability of the communities to climate change.

In a belt with the highest concentration of animal husbandry in the country, there is no realistic climate change adaptation practice as the existing adaptation practices are mainly reactive whereby the nomads move their animals southward for greener pastures, coupled with the fact that most of the local breed adapts to climatic stress. Livestock production in Africa and Southern Africa, especially its developing component, is vulnerable and at high risk of being severely affected by climate change (Rust and Rust 2013). This mobility will not only aggravate land, vegetation, and water degradation but also climate change as the dominance of grazing in the Guinea savanna in recent times is a potential for increased carbon dioxide emission into the atmosphere. The resultant problem of the practice is apparent in the widespread crisis between the traditional farmers and the encroaching nomads across the country. Consequently, there is an imperative need to maintain the existing grazing reserves and establish more grazing reserves to meet the growing demands of animal husbandry across the country. Furthermore, there should be capacity building for herders to enable them develop and adopt effective and affordable improved livestock management practices that will boost their adaptation to climate change.

The general approach to climate change adaptation in Nigeria has been top-down approach; usually, general policies and decisions are taken without the involvement of the communities or working together with the community groups to develop community-based climate change adaptation practices. The ministries and agencies should develop bottom-up approaches that will identify, document, quantify, and assess the existing adaptation practices for scaling up potential cost-effective practices that will enhance climate change adaptation and resilience. Integrating indigenous knowledge can add value to the development of sustainable climate change mitigation and adaptation strategies that are rich in local content and planned in conjunction with the people (Nyong et al. 2007). The community-based practices should be developed with the community by identifying their agricultural potentials and climate change challenges as well as promoting improved land and water management practices at community levels such that it will lead to the attainment of community food security in the country in general.

The Federal Government of Nigeria mandated the Nigerian Meteorological Agency (NIMET) to monitor weather and climate in Nigeria and provide meteorological information for sustainable development and safety of life and properties in the country. Hence, the agency annually gives detailed seasonal rainfall prediction (SRP) before the onset of rain so as to provide essential weather advisories and early warning to planners, decision makers, and the various operations in rainfall-sensitive socioeconomic sectors, e.g., transport, water resources, health, and agriculture. Onset and cessation dates, length of the rainy season, annual rainfall amount, expected changes in the prediction of the parameters, and socioeconomic implications are annually predicted to guide the farmers and stakeholders on the types of crops to be planted and what to expect of the growing season, dry spell, drought, and flood. Furthermore, the agency publishes agrometeorological products and services to advise the Federal Ministry of Agricultureand Rural Development and associated agencies as well as farmers to take advantage of the information contained in the two to enhance their adaptation to adverse weather conditions. NIMET – SRP (2015) predicted 3–13 days delay of onset of rains: late onset of growing season in Makurdi, Lokoja, and Enugu; early cessation of growing season in Zaria, Nguru, Kano, and Jos; shorter length of the growing season in Niger, Gusau, and Kaduna; below-normal rainfall amount in parts of the extreme southwest; and above-normal rainfall in Warri, Calabar, Bauchi, Gombe, and Nguru.

The seasonal rainfall prediction and agrometeorological products are beneficial to agriculture and other economic sectors as they contribute toward effective adaptation to the effect of climate change annually. However, considering the fact that large proportions of the vulnerable communities are uneducated, it is crucial to organize community-based sensitization programs that will enhance their understanding of these valuable information. These will reduce their vulnerability to climate-related hazards as it will enhance safe sowing and boost crop and food production. Developing countries are more exposed to experience the negative impacts of climate change owing to their fragile economic sectors and the reliance of many livelihoods on climate-sensitive sectors such as rain-fed agriculture (IPCC 2013; Stockmann et al. 2013; World Bank 2012). The relevant institutions, stakeholders, extension workers, and traditional leaders should strengthen community's capacity for climate change adaptation. Authorities, individuals, and communities' awareness will provide them with adequate capacity to act by adapting strategies for effective adaptation to the changing climate as well as facilitate the attainment of food security.

This general prediction needs to be developed into effective community- based early warning schemes that will be easily adapted by the immediate community and relevant stakeholders as cost-effective tools for climate change adaptation and attainment of food security. In the Sudano-Sahelian belt where about two-thirds of the population lives in rural areas, the starting point for the adaptation should be by promoting the culture of resilience based on existing community knowledge. In addition, the community should be well informed through dissemination of accurate and adequate information in local languages to enhance people's adaptation and resilience. Consequently, collection, compilation, and dissemination of relevant information and knowledge of climate change, vulnerabilities, and capacity at

Table 1 Agricultural research institutes in Northern Nigeria

Name of research institute	Mandate
Lake Chad Research Institute, P.M.B 1293, Gamboru Road Maiduguri, Borno State	Genetic improvement and development of production technologies for wheat, millet, and barley; the improvement of the productivity of the entire farming system in the northeastern zone
Institute for Agricultural Research, P.M.B 1044, Ahmadu Bello University, Samaru, Zaria	Genetic improvement and development of production and utilization technologies for sorghum, maize, cowpea, groundnut, cotton, and sunflower and the improvement of the productivity of the entire crop-based farming system in the northwest zone of Nigeria
National Cereals Research Institute, P.M.B 8, Badeggi, Bida, Niger State	Genetic improvement and production of rice, soybean, benniseed, and sugarcane and improvement of productivity of entire farming system of the central zone
Nigeria Stored Products Research Institute, P.M.B 1489, Km 3 Asa Dam Road, Ilorin, Kwara State	Research into improvement of major food and industrial crops and studies on stored product, pest and diseases, pesticide formulation, and residue analysis
National Animal Production Research Institute, P.M.B 1096, Shika, Zaria	Research on food, animal species, and forages
National Veterinary Research Institute, P.M.B 01, Vom	Research into all aspects of animal diseases and their treatment and control, as well as development and production of animal vaccines and sera
National Institute for Freshwater Fisheries Research, P.M.B 6006, New Bussa	Research into all freshwater fisheries and long-term effects of man-made lakes on ecology and environment throughout the country
National Agricultural Extension and Research Liaison Services, Ahmadu Bello University, Zaria	Research into technology transfer and adoption studies; overall planning and development of extension liaison activities nationally; collation and evaluation of agricultural information

community level will enhance climate change adaptation, mitigation, and resilience. The low adaptive capacity of crop farmers in Nigeria can be attributed to a variety of factors, including poverty, lack of access to resources, and poor infrastructure (Chinedum et al. 2011). Investigating the strategies for coping with current climate change will provide pointer for addressing adaption needs in Nigeria particularly in the area of food security and socioeconomic well-being.

Similarly, several agricultural research institutes are established across the zone (Table 1). Most of these institutes are mandated to conduct researches that will lead to sustainable agriculture in the zone through development of improved seed species that are today widely accepted by farmers across the zone. Ministries of agriculture have also continued to promote adoption of improved cultivation and higher-yield varieties through Agricultural Development Projects (ADP) that are widely spread across the country. The adoption of these improved species enhances community

capacity in adapting to climate change; practical adaptation initiatives tend to focus on risks that are already problematic (Barry and Johanna 2006). There are also centers like the Centre for Climate Change and Freshwater Resources (CCCFR) established in 1995 (as a linkage center of the Federal Ministry of Environment) to create awareness, educate, and train Nigeria's teeming population while conducting credible research to guide policy making. Centers like these should be empowered adequately and promoted to climate change institutes with the mandate to take leadership role in climate change monitoring, modeling, impact assessment, and development of adaptation and mitigation strategies that will enhance resilience to climate change. Generally, it is crucial to initiate polices, guidelines, programs, strategies, and projects to reduce vulnerability across the zone and help farmers adapt to the changing climate for the attainment of food security.

The National Emergency Management Agency (NEMA) in collaboration with the Federal Ministry of Education, in their contribution, has started the mainstreaming of climate change and disaster risk reduction (DRR) into basic and postbasic school curriculum. If accomplished and implemented, it will increase climate change awareness and subsequently enhance adaptation to climate change. However, it is also important to mainstream climate change into development interventions at the federal, state, and local government levels to enhance community climate change awareness and promote community-based adaptation policy such that it will lead to its incorporation into relevant socioeconomic activities at grass roots such as agriculture.

Climate Change Mitigation Strategies in the Sudano-Sahelian Belt of Nigeria

Since 1972, the United Nations General Assembly designated 5th of June as World Environment Day (WED), to stimulate awareness and understanding of the environment and the problems that besiege its sustainability; the Federal and States Ministries of Environment mark this day annually across the country with poorly planned and executed tree planting campaigns across the country. The practicality of these in climate change mitigation is still at very low level because in most cases these trees are hardly nurtured to maturity. The tree seedling should have been distributed to the endangered rural farmers that will be determined to plant and nurture them not only for climate change mitigation and resilience but also for enhanced community access to fruits, medicine, poverty reduction, enhanced livelihood, and attainment of food security.

Furthermore, the WED is generally used to encourage every Nigerian to plant trees in order to reduce emissions from deforestation and forest degradation (REDD) that is typical across the Sudano-Sahelian belt. To accomplish this, agroforestry is highly encouraged as economic tree seedlings are distributed to large-scale farmers by the ministry which not only help to mitigate climate change but also enhance community access to fruit and modify community microclimate (Plate 1). Nigeria's farmers reported that temperature and rainfall are increasing (Sofoluwe et al. 2011).

Plate 1 Large-scale agroforestry

Plate 2 Community's adaptation to climate change

This noble program should be well planned and implemented such that the rural farmers are incorporated or grassroots participation encouraged because it is a common method for rural community's adaptation to climate change (Plate 2). Through this, policy makers and environmentalists should have immensely contributed to climate change mitigation and improved standard of living as well as safeguarding biodiversity and preserving the natural environment. Furthermore, the Federal Ministry of Environment in collaboration with United Nations Development Programme (UNDP) and other partners is promoting the adoption of renewable energy across the country to promote the Nigerian Alliance for Clean Cookstoves (NACC) and is developing more efficient woodstoves to reduce consumption of biomass-based energy sources and to enhance climate change mitigation.

The agricultural management system is aggravating climate change impact as huge proportions of agricultural residue that cannot be consumed by animals are

burnt annually leading to the increased emission into the atmosphere. Crop residue burning is considered as a chief contributor of greenhouse gas (GHG) emissions in the atmosphere (Jordan et al. 2010). Thus, there is need to find appropriate methods which can enable farmers to incorporate these residues to land use practices as well as mitigate climate change and strengthen Africa's agricultural sectors to enable them to respond to growth in demand (John and Irene 2009). Improved management practice (IMP) techniques that will enhance soil organic matter storage with minimum soil disturbance through incorporation of crop residual into farming system should be promoted as its adoption will enhance climate change adaptation. Also, it will not only enhance soil fertility and crop performance but will also help in removing excess carbon dioxide from the atmosphere, thereby crucial for climate change mitigation and adaptation. In Nigeria rice straw and other crop residues are abundant; these can be incorporated into the soil as biological fertilizer in order to enhance soil sustainability and climate change adaptation and mitigation. Increasing atmosphere carbon dioxide is a dual consequence of poor management of crop residues and agricultural land practices (IPCC 2013). Thus, improved carbon sequestration necessitates adoption of improved land use management practices across the zone such that high-breed economic trees will be integrated into cultivated land for improved soil conservation, attainment of food security, and resilience to climate change.

Despite the fact that countries have ecological funds, it is not easy to determine what percentage of this goes to the climate change mitigation/adaptation. Climate change adaptation should be national priority such that it will be given its rightful place in planning for national development and supported with funds to implement adaptation strategies and enforce sustainable adaptation practices at large scale for the attainment of food security. Government at all levels, collaborative partners, and NGOs should specify certain percentage of fund for climate adaptation which should be invested in schemes and projects that will promote climate change adaption, mitigation, and resilience.

In Nigeria, available records in the Federal Department of Forestry show that Nigeria has a total of 1,160 constituted forest reserves covering over 10,752 ha of land, and this represents about 10 % of the total land area. Also, game reserves and national parks are excluded from this. However, most of these reserves only exist on paper and the Federal Department of Forestry argues that deforestation in Nigeria is now progressing at the rate of 3.5 % per annum. In Africa, for example, deforestation accounts for nearly 70 % of total emissions (FAO 2005). Furthermore, Anselm and Taofeeq (2010) stated that climate change is perhaps the most serious environmental threat to the fight against hunger, malnutrition, disease, and poverty in Africa, mainly through its impact on agricultural productivity. Hence, there is need to check the way in which people interact with these crucial resources such that it will reduce the rate of deforestation and increase biodiversity, conservation, and reforestation using introduced or indigenous species that will promote sustainability of the forest. These will not only enhance climate change adaptation and mitigation but contribute greatly toward the attainment of food security.

Future Direction

Generally, in Nigeria, there are numerous crucial policies and programs aimed at addressing issues related to climate change adaptation and agricultural sustainability. However, the major concern is the level of implementation and its role in promoting and developing institutions of effective adaptation strategies and practices that will enhance resilience of the vulnerable communities across the country. There should be an agency/organization empowered to collate, synthesize, implement, and promote climate change policies and programs at all levels of the government such that it will be widely adopted across the country particularly the vulnerable community. Bottom-up approaches should be developed and promoted to identify, document, and quantify existing adaptation practices, along with assessing these existing adaptation practices for scaling up potential cost-effective practices for enhanced climate change adaptation and resilience.

Institution and organization plans should be realistically implemented to enhance vulnerable community climate change adaptation and mitigation through such programs that will integrate environmental and natural resource development into socioeconomic development process for the attainment of food security and improved rural livelihood. Similarly, government interventions such as NEEDS should be channeled toward identifying the major problems facing the various communities across the country with a view to building their capacity in proffering solutions using integrated economic development processes and programs at community levels in job creation, strengthening the skill base, reducing vulnerability, and promoting peace and security that are today threatened across the country.

The federal, state, and local government initiatives should be proactive; the Nigerian Meteorological Agency (NIMET), NEMA, State Emergency Management Agency (SEMA), and ADP should collaborate in the development and communication of effective community-based early warning schemes as a cost-effective tool for climate change adaptation and attainment of food security. In addition to the agricultural research institutes well spread across the zone, climate change institutes should be established to take leadership role in climate change monitoring, modeling, and impact assessment, to collaborate with all the relevant agencies in the development of adaptation and mitigation strategies, and to initiate policy guidelines, programs, and projects that will enhance resilience to climate change. The institutes should identify ways of mainstreaming climate change into all developmental interventions at the federal, state, and local government levels as pathways for promoting community-based adaption policies at the grass roots. Bottom-up approaches should be enforced by identifying the varying community's agricultural potentials and the strategies of land and water management practices that will boost their adaptation to climate change.

WED should be marked by distributing tree seedlings to communities that will be determined to plant and nurture them not only for climate change mitigation and resilience but for enhanced community access to fruits, medicine, poverty reduction, improved livelihood, and attainment of food security instead of political tree planting

campaigns. Thus, agroforestry should be integrated into crop cultivation and animal husbandry by making economic tree seedlings available to small- and large-scale farmers. Renewable energy and clean cooking stoves should be promoted across the country, and more efficient stoves should be developed to reduce the use of fuel wood as source of energy as well as enhance climate change mitigation.

Furthermore, there is need to design and implement local adaptation strategies that will bridge the gap between scientific and local knowledge in order to create projects capable of increasing community adaptation and resilience. In addition to the high-breed crop varieties, relevant stakeholders should promote breeding of high-breed economic trees and make them available to farmers at subsidized rates. This will not only promote effective climate change adaptation but enhance mitigation and resilience. Diversification of the economy through provision of credit, cooperative, and micro-finance at lower interest rates should be promoted. Also, community-based organizations (CBOs), improved land and water management practices, irrigation strategies, building crop storages, developing marketing facilities, subsidizing agricultural inputs, and establishment of safe nets will enhance diversification of the economy. Generally, these are cost-effective tools for climate change adaptation, mitigation, and attainment of food security.

References

Anselm AE, Taofeeq AA (2010) Challenges of agricultural adaptation to climate change in Nigeria: a synthesis from the literature. Field Actions Sci Rep [Online] 4, online since 15 Feb 2010, connection on 25 Mar 2015. http://factsreports.revues.org/678

Barry S, Johanna W (2006) Adaptation, adaptive capacity and vulnerability. Glob Environ Chang 16(2006):282–292

Chinedum U, Robert UO, Abdullahi AY (2011) Climate change adaptation strategy technical report, agriculture sector; a compendium of studies commissioned and published by Building Nigeria's Response to Climate Change (BNRCC) Project, pp 49–68

FAO (2005) Global forest resources assessment. Food and Agriculture Organization, Rome, Italy.: http://wwwfao.org/forestry/fra2005 (accessed 24th June 214)

Gina Z, Anton C, Adriaan T, James A, Fernanda Z, Moliehi S, Ben S (2008) Climate change and adaptation in African agriculture. Report prepared for Rockefeller Foundation, by Stockholm Environment Institute

IPCC (2007) Climate change 2007: mitigation of climate change of working groups III to the fourth assessment report of the intergovernmental panel on climate change. Cambridge University Press, Cambridge, UK

IPCC (2013) Summary for policy makers, in climate change 2013; the physical science basis. Contribution of working group to the fifth Assessment report of the inter governmental panel on climate change. Cambridge University Press, Cambridge, UK

John DK, Irene S (2009) Climate change and food security in Africa. Centre for International Governance Innovation (CIGI). Special report on climate change in africa: adaptation, mitigation and governance challenges, pp 21–25

Jordan A, Zavala LM, Gil J (2010) Effects of mulching on soil physical properties and runoff under semi arid conditions in southern Spain. Elsevier 81:77–85

Molly EB, Brent M (2011) Climate change and agriculture in Africa: impact assessment and adaptation strategies. Eos Trans Am Geophys Union 89(47):474

NEEDS (2004) Meeting everyones NEEDS. National Planning Commission, Abuja. ISBN 0-9741708

NIMET – SRP (2015) Seasonal rainfall Prediction. Nigerian Meteorological Agency, ISO 9001 2008

Nyong A, Adesina F, Osman E (2007) The value of indigenous knowledge in climate change mitigation and adaptation strategies in the African Sahel. Mitig Adapt Strateg Glob Chang 12 (5):787–797

Patt AG, Tadross M, Nussbaumer P, Asante K, Metzger M, Rafael J, Goujon A, Brundrit G (2010) Estimating least-developed countries' vulnerability to climate-related extreme events over the next 50 years. Proc Natl Acad Sci 107:1333–1337

Rust JM, Rust T (2013) Climate change and livestock production: a review with emphasis on Africa. S Afr J Anim Sci 43(3):255–267

Sofoluwe NA, Tijani AA, Baruwa OI (2011) Farmers' perception and adaptation to climate change in Osun State. Niger Afr J Agric Res 6(20):4789–4794

Stockmann U, Adams MA, Crawford JW, Field DJ, Henakaarchchi N, Jenkens M (2013) The knowns, known unknowns and unknowns of sequestration of soil organic carbon. Agric Ecosyst Event 164:80–99

World Bank (2012) Carbon foot-printing of ARD projects; testing the ex-ante carbon balance appraisal tool. World Bank, Washington, DC

Understanding Climate Change Adaptation Needs and Practices of Households in Southeast Asia: Lessons from Five Years of Research

Herminia A. Francisco and Noor Aini Zakaria

Contents

Abstract

This chapter reports the main findings of research projects supported by the Economy and Environment Program for Southeast Asia (EEPSEA) over the last 5 years (2009–2013). The research projects reported focus on adaptation needs, climate change impacts, and the economics of adaptation projects as well as on efforts to link researchers with local government planners to enhance science-based adaptation planning. The lessons derived from these micro-level EEPSEA

H.A. Francisco (✉) • N.A. Zakaria
Economy and Environment Program for Southeast Asia (EEPSEA), Los Baños, Laguna, Philippines
e-mail: h.francisco@cgiar.org; aini@eepsea.net

W.-Y. Chen et al. (eds.), *Handbook of Climate Change Mitigation and Adaptation*,
DOI 10.1007/978-3-319-14409-2_67

studies are important because the impacts and adaptation solutions reported are often local, as they are carried out by households, communities, and local governments. Hence, these studies help in understanding how various groups are affected by climate change and what limits their adaptation choices, which are important in designing ways to increase their resilience to climate change.

Field-level assessment of impacts showed that extreme climate events (i.e., super typhoons and associated flooding) cost households more than a third of their annual household income per event. As future extreme climate events are expected to be more frequent and intense, future damage may be even bigger and will most likely drive vulnerable households toward extreme poverty. Household adaptation actions in the various study sites are generally very crude and mostly reactive (e.g., strengthening housing units, using sandbags during flooding, storing of food, evacuation) rather than preventive (e.g., relocation, building multistorey and stronger housing units). This is largely explained by the limited resources available to most vulnerable households for investment in stronger adaptation measures.

The studies also show that strengthening community ties can increase household and community resilience. It also increases the efficacy of using communities as vital conduits of climate information dissemination. Moreover, results indicate that climate communication policies and interventions should go beyond informing people of climate hazard risks; they should also provide information that would allow people to assess their capabilities as well as permit technical assessments of various adaptation options.

Local governments need support in adaptation planning. The two action research projects carried out with funding support from EEPSEA and collaborating organizations showed that local government officials are receptive to such research collaborations and are very much willing to learn from science-based adaptation planning. Research to identify efficient or cost-effective adaptation options was highly appreciated by local government units. They need support to seek climate financing for these adaptation programs however.

Introduction

The intensity and frequency of typhoons and flooding events, such as those experienced by the Philippines, Thailand, Vietnam, and Indonesia in the recent past, attest to the changed and changing climates that we all face. Southeast Asia's vulnerability to climate change is also confirmed in an Asian Development Bank report (ADB 2009) that cites the region's long coastlines, high population density and economic activity, and high dependence on agriculture and natural resources as a big reason for this vulnerability. The latest Intergovernmental Panel on Climate Change Report (IPCC 2014) affirmed these observations stating that the "risks of impacts that are severe, pervasive and irreversible is much greater if we stay on a path of continued high emissions." The areas under greatest threat are those around Manila Bay in the Philippines; in the low-lying coastal fringes of Sumatra,

Kalimantan, and Java in Indonesia; and in the Mekong (Vietnam), Chao Phraya (Thailand), and Irrawaddy (Myanmar) deltas (Handley 1992; Morgan 1993; Yusuf and Francisco 2009).

Asia as a whole is highly vulnerable to climate change. Anthoff et al. (2006) estimated that 105 million people in Asia would be at risk of having their homes inundated by a one-meter rise in sea level. In Bangladesh alone, a report by the United Nations Environment Program (UNEP 2008) mentioned that a one-meter rise in sea level would inundate 17,000 km^2 of the country's land, which is over 10 % of its total land mass.

Other parts of the world are not exempted. Countries in North America experience frequent hurricanes, often accompanied by storm surges and flooding, while others are suffering from extreme temperatures like heat waves or cold snaps. Extreme weather events like heat waves, floods, and droughts have also caused rising damage costs across Europe in recent years (Pittock 2003; Jones and Preston 2006). An increase in global temperature of 3.5 °C will result in damages worth at least €190 billion, representing a net welfare loss of 1.8 % of Europe's current gross domestic product (GDP) (European Commission 2014). Low-lying atoll countries in the Pacific such as the Kiribati, the Marshall Islands, Tokelau, and Tuvalu also face high risk from sea level rise (Garnaut 2010). The occurrence of climate change-related disasters is very likely to continue into the future (IPCC 2007).

The cost of climate change is very high. For instance, *Typhoon Haiyan* in the Philippines left more than 6,000 deaths with several thousands more missing. According to UN estimates, about 670,000 people were made homeless and 11 million people needed assistance for a long period given the extent of devastation that they suffered (Cumming-Bruce and Gladstone 2013). An article in *The Economist* placed the economic cost of Haiyan in the Philippines at USD 15 billion ("Typhoon Haiyan" 2013), which is 6 % of the country's 2013 GDP. The same article noted that the Vietnamese government averted damages by its quick and organized evacuation of 800,000 people from coastal communities (Ziervogel et al. 2013). Indeed, there are ways to prepare for catastrophes like this, but it must also be said that *Typhoon Haiyan*'s rage in the Philippines was of an unprecedented scale and intensity, which could have caught any government by surprise.

Our recent experiences with natural climate-related disasters are clearly showing us that the climate change debate is no longer about whether or not we should adapt; it is now an issue of *how* we can adapt more effectively and efficiently. Related to this is the question of how we can assist local government units (LGUs), communities, and households in improving their adaptive capacity. This chapter reports on the research findings of four (4) multi-country research projects supported by the Economy and Environment Program for Southeast Asia (EEPSEA) over the last 5 years (2009–2013). The research projects are focused on adaptation needs, climate change impacts, and the economics of adaptation projects as well as on efforts to link researchers with local government planners on adaptation planning.

The chapter is divided into five sections. The first part (section "Vulnerability to Climate Change and Impacts of Extreme Climate Events") presents an overview of the climate change vulnerability situation in Southeast Asia (SEA) based on the

work by Yusuf and Francisco (2009) and the household costs resulting from these extreme climate events based on studies in selected sites in the region. Section "Adaptation Practices and Factors Influencing Adaptation Choices" highlights the adaptation practices employed in the region and the determinants of adaptation choices. Section "Coastal Communities' Vulnerability and Adaptation Practices" expounds on adaptation by focusing on the experiences of three coastal villages in the Philippines, Vietnam, and Indonesia. Section "Working with Local Governments in Adaptation Planning" presents insights from experiences in pilot testing the EEPSEA vulnerability mapping approach as a prelude to identifying adaptation options based on a three-country grant in 2011 to the poverty-environment project, also supported by the International Development Research Centre. This section also provides insights from a 3-year grant to three research institutions in the region (the Philippines, Vietnam, and Cambodia) tasked with developing the adaptation planning capacity of LGUs and communities through participatory research. The final section (section "Lessons from EEPSEA-Funded Climate Change Adaptation Research in Southeast Asia: Future Directions") summarizes the key lessons learned from the 5-year multi-country research project carried out in countries identified as most vulnerable to climate change: the Philippines, Vietnam, Indonesia, Thailand, and Cambodia. Suggestions on how to move forward in the field of adaptation planning and economics research are advanced.

Vulnerability to Climate Change and Impacts of Extreme Climate Events

A Snapshot of Climate Change Vulnerability in Southeast Asia

In 2009, EEPSEA released the climate change vulnerability map for Southeast Asia (Yusuf and Francisco 2009). The program launched the report in the Philippines, Indonesia, and Vietnam with relevant policymakers and nongovernment organizations (NGOs) in attendance. The map (Fig. 1), which shows vulnerability to climate change at the subnational level, was well received as there was still very limited information on this at the time. While the map presents only a snapshot or a static picture of the situation using 2005–2008 information, it generated a lot of interest due to several reasons.

First, it shows how provinces or districts within a country compare with each other in terms of overall vulnerability, using the same set of indicators, namely, *hazards* (i.e., exposure to floods, drought, landslides, typhoons, and sea level rise), *adaptive capacity* (e.g., economic indicators like per capita income and poverty level, access to social services like education and health, infrastructure support like road and communication networks), and *sensitivity* (i.e., population at risk, represented by population density; ecological sensitivity, using hectares of protected areas).

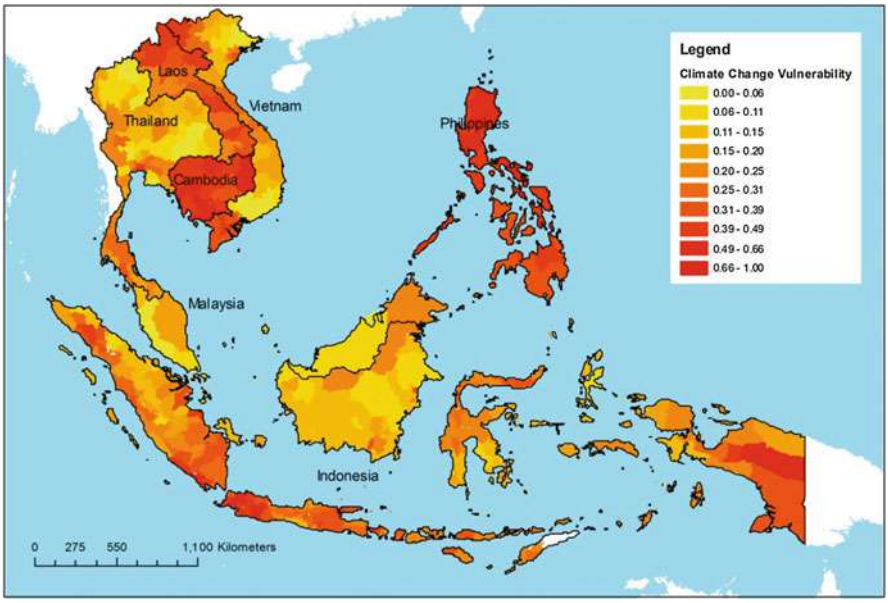

Fig. 1 Vulnerability to climate change in Southeast Asia (Source: Yusuf and Francisco 2009)

Second, the map is accompanied by a table that shows the contribution of the three elements (i.e., hazard exposure, lack of adaptive capacity, and sensitivity) to climate change vulnerability. It therefore shows areas where improvement in adaptive capacity is critical and areas where protection is a must, if exposure to hazard is the main driver of vulnerability. Likewise, it shows where vulnerability is caused by population and ecological sensitivity.

This is illustrated in Fig. 2. As shown, the main driver of vulnerability in Vietnam is exposure to hazards. Vietnam's long coastline, geographic location, and diverse topography and climates contribute to its being one of the most hazard-prone (storms and floods) countries in the Asia-Pacific region (World Bank 2011). In Indonesia, population density drives vulnerability in areas like Jakarta. Almost 230 million people inhabit Indonesia, with the majority (about 54 %) living on the island of Java (World Bank 2011). In poorer countries like Cambodia, low adaptive capacity is the dominant driver of vulnerability. The poor are the most vulnerable to the impacts of drought, floods, and landslides as they are highly dependent on climate-sensitive sectors like fisheries and forestry.

Finally, the map facilitated the active engagement of stakeholders in several countries and generated interest on how to downscale such a presentation at an even lower level of administration, such as towns and villages. Subsequently, EEPSEA provided modest funding support to pilot test the downscaling of this framework at the LGU level in several countries in the region as part of its research grants support (see section "Working with Local Governments in Adaptation Planning"

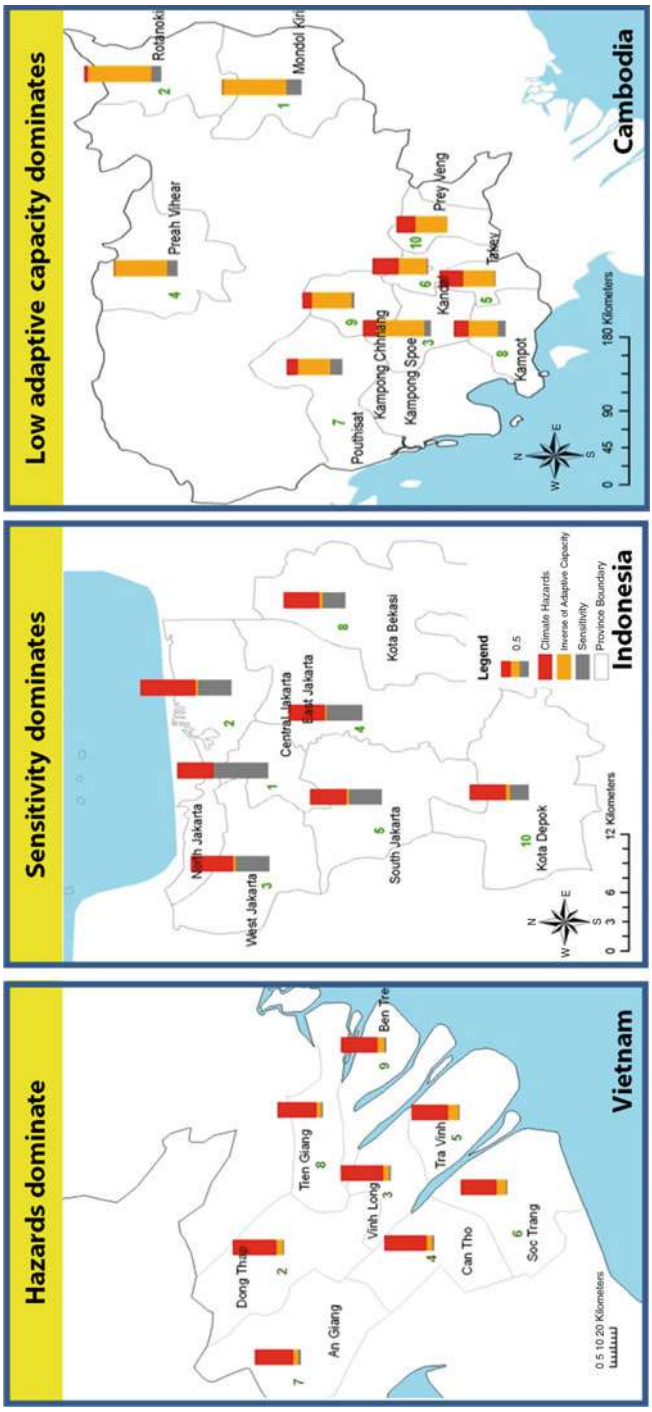

Fig. 2 Comparison of sources of vulnerability, three countries (Source: Yusuf and Francisco 2009)

discussion). The top 15 most vulnerable provinces/districts in each of the SEA countries where mapping was carried out are shown in Table 1.

Across SEA, the most vulnerable provinces and districts are found in the Philippines and Vietnam (largely from typhoons and flooding and low adaptive capacity) and Indonesia and Thailand (mostly from flooding and high sensitivity). A high degree of vulnerability can be noted for urban cities like Manila, Jakarta, and Bangkok, and this has been proven time and time again with yearly occurrences of multiple climate-related disasters like typhoons and flooding at these places. High population density, poor urban planning, and deforestation are factors that exacerbate these cities' sensitivity to climate change.

Jakarta's recent flood (Elyda and Dewi 2014) illustrates the vulnerability of urban cities to climate change. The flood affected 20,000 people (with seven reported dead) in 48 subdistricts where inundation of up to 6 m was experienced. While losses from this event were already big, the flood that took place in Jakarta in February 2007 remains unsurpassed. In the 2007 flood, nearly 60 % of the city was inundated, displacing 320,000 people and causing the death of 50.

The 2011 Thailand flooding is another example of the massive economic loss associated with climate change-related disasters. That was, by far, the worst flooding in 50 years that affected not only Bangkok but neighboring provinces as well. From July to December 2011, the Geo-Informatics and Space Technology Development Agency (GISTDA 2011) reported the inundation of 69 provinces covering 41,381 km^2. There were 815 reported deaths and damage to about 13 million rai (2.08 million hectares) of agricultural lands. This had a profound impact on food security in SEA as Thailand is a leading exporter of rice, a region staple (Loo et al. 2014).

Clearly, urban centers' high population density and high hazard exposure partly explain the high cost of damages from climate change, but other causes such as poor urban planning, clogging of waterways, and forest denudation are also partly to be blamed.

How Much Does a Household Suffer from Extreme Climate-Related Disasters?

The figures on losses and damages from any disaster could appear like mere statistics to most people, but to those on the ground, these numbers translate to economic loss and other forms of social loss or discomfort. We take a closer look at flooding damages and at how these had influenced those living in the affected areas of two studies most recently supported by EEPSEA (i.e., Wijayanti et al. 2014; Nabangchang et al. 2013) as well as of the five cross-country adaptation projects carried out in 2011.

Flooding Damages

Wijayanti et al. (2014) looked into the damages from the January 2013 Jakarta flooding that inundated houses and merchandise shops for about 3 days. It analyzed what factors influenced the level of damages using a flood damage model. In addition, it looked closely into the role of women in dealing with the flooding

Table 1 Top 15 vulnerable provinces/districts per country based on EEPSEA 2009 vulnerability mapping

Country	Top 15 vulnerable provinces/districts (2008 data)
Cambodia	Mondulkiri, Ratanakiri, Kampong Speu, Preah Vihear, Takev, Kandal, Pursat, Kampot, Kampong Chhnang, Prey Veng, Koh Kong, Svay Rieng, Stung Treng, Kampong Thom, and Battambang
Philippines	Manila, Benguet, Batanes, Ilocos Sur, Rizal, Bataan, Batangas, Bulacan, Abra, Albay, Quezon, Nueva Ecija, La Union, Aurora, and Mountain Province
Thailand	Krungthep, Samut Prakan, Nonthaburi, Samut Sakhon, Trang, Chachoengsao, Nakhon Si Thammarat, Surat Thani, Satun, Pattani, Ranong, Nakhon Nayok, Nakhon Pathom, Phatthalung, and Yala
Vietnam	Lai Chau, Dong Thap, Vinh Long, Can Tho, Tra Vinh, Soc Trang, An giang, Tien Giang, Ben Tre, Thai Binh, Minh Hai, Long An, Kien Giang, Thua Thien Hue and Son La
Lao PDR	Phongsali, Houaphan, Luang Namtha, Oudomxay, Saravan, Bokeo, Hammouan, Luang Prabang, Attapeu, Xekong, Borikhanxai, Xiangkhoang, Savannakhet, Viangchan, and Xaignabouri
Indonesia	Central, North, West, East, and South Jakarta, Kota Bandung, Kota Surabaya, Kota Bekasi, Kota Bogor, Kota Depok, Kota Palembang, Tangerang, Kota Tangerang, Kota Malang, and Jayawijaya
Malaysia	Sabah, Pulau Pinang, Kelantan, Terengganu, Perlis, Pahang, Kedah, Kuala Lumpur, Johor, Sarawak, Perak, Selangor, Melaka, Negeri Sembilan

Source: Yusuf and Francisco (2009)

situation. Specifically, a survey was conducted in two districts of South Jakarta (i.e., Pesanggrahan and Kebayoran Lama) covering three villages (i.e., Ulujami, Kebayoran Lama Utara, and Cipulir) and in two districts in West Jakarta (i.e., Kebon Jeruk and Cengkareng) covering three villages (i.e., Kedoya Selatan, Sukabumi Selatan, and Rawa Buaya).

As shown in Table 2, the nature and cost of the damages to households over a 3-day flooding event included damage to house structure and its content, cleanup cost, evacuation costs, loss of income (foregone income), and cost of illnesses.

The study found that the average loss to a household from the 3-day flooding is about USD 309.00. With a minimum daily wage of USD 5.00, this damage cost is huge. Inundation depth and duration, household income, and house area are positive and significant predictors of the level of flood damage based on the regression analysis carried out in the study.

For households engaged in small-scale trading or commercial enterprise, losses were three times higher than that of nonbusiness households. For this group, the losses took the form of damage to goods or merchandise, structural damage, and cleanup costs (Table 3).

The average flood damage to the business shops in the affected area over the 3-day flooding event was valued at USD 858. Consistent with the findings from nonbusiness household data, the main predictors of damages to the business group are inundation depth and duration, total floor area occupied by the business, and income, measured by turnover or sale per day.

Table 2 Average flood damage per house resulting from the January 17–19, 2013, flood event

Damage		Value (IDR)	Value (USD)	Percentage (%)
Direct	Structural damage	423,395	42	14
	Content damage (inside and outside)	1,881,703	188	60
Indirect	Cleanup cost	241,186	24	8
	Loss of income	290,345	29	9
	Evacuation and temporary house	117,383	12	4
	Cost of illnesses	142,252	14	5
Total		**3,096,264**	**309**	**100**

Cf: Wijayanti et al. (2014), Table 3 in the original report

Table 3 Average flood damage per unit business resulting from the January 17–19, 2013, flood event

Damage		Value (IDR)	Value (USD)	Percentage
Direct	Structural damage	564,800	56	7
	Content damage	1,543,060	154	18
Indirect	Turnover loss	5,252,704	525	61
	Temporary quarters	56,000	6	1
	Labor cost	383,667	38	4
	Cleanup cost	786,633	79	9
Total		**8,586,864**	**858**	**100**

Cf: Wijayanti et al. (2014), Table 7 in the original report

The second study was carried out in Bangkok, Thailand, by Nabangchang et al. (2013). In 2011, Thailand was hit by the worst flood experienced in 50 years. From July to December 2011, 69 provinces were affected, with a total inundation area of 41,381.8 km^2 (GISTDA 2011). The death toll reached 815, with three persons missing. Nearly 2.08 million hectares of agricultural land were damaged and the transportation of goods and services, particularly food supplies, was crippled because major roads were flooded and impassable.

The study looked at the damages incurred by households as a result of this long period of flooding. It surveyed some 500 households from the following districts: Bang Bua Thong district (in Nonthaburi province located west of Bangkok), Klong Luang district (in Pathum Thani province located north of Bangkok), and Don Muang district (northern Bangkok). The flooding in these districts was about 2 m at its highest level, with a flooding duration of 2–3 months. The households were interviewed twice with the first done immediately once the flooding begun to subside and the second done a year later. The intent of the second survey was to capture a more accurate estimate of flooding damages since most repairs and cleanup activities would have been completed by then. At the same time, some questions on the preferences for flooding insurance were asked.

Table 4 Mean household damages (in THB) by nature of damages and comparison of study results to World Bank 2012 estimates

	Bangkok		Nonthaburi		Pathum Thani	
Type of losses	WB	EEPSEA	WB	EEPSEA	WB	EEPSEA
Housing damage	2,565	136,387	3,240	99,704	4,701	41,342
Goods damages	19,486		19,686		19,448	
Cost of temporary shelter	17,276	3,770	19,455	3,780	22,023	731
Health-care cost	–	199	–	584	–	250
Household contributions to community efforts	–	1,832	–	1,383	–	3,568
Preventive costs	–	11,441	–	5,861	–	7,707
Others	–	35,089	–	45,766	–	41,574
Total	**40,336 (USD 1,310)**	**203,222 (USD 6,598)**	**43,399 (USD 1,409)**	**182,864 (USD 5,937)**	**47,179 (USD 1,532)**	**108,753 (USD 3,531)**

Source: Nabangchang et al. (2013)

Table 4 shows the damage estimates based on field interviews carried out in the three study areas. For comparison, it also shows the World Bank damage estimates provided immediately after the event. Nabangchang et al. (2013) estimated Bangkok residents' household losses at USD 6,598; USD 5,937 for Nonthaburi residents; and USD 3,531 for Pathum Thani residents. These numbers are three to five times higher than the estimates provided by the World Bank, showing that quick estimates can understate the extent of climate change impacts.

The big source of underestimation comes from the estimate of losses to the housing unit itself and damage to furniture and household appliances soaked underwater for a long time. This number is huge (38–67 % of total losses), most particularly for those residing in Bangkok and Nonthaburi. Nabangchang et al. (2013) also captured other losses that were not included in the World Bank estimates. These include, among others, expenditures to prevent water from coming into the house (e.g., use of sandbags and motor pump to get water out) and household contributions to community efforts to protect the village.

The cost to the households took the form of repair or replacement costs for damaged properties, cleanup costs, relocation costs, and foregone income during the disaster period. In terms of proportion to annual household income, the flood damages accounted for 44 % of annual household income in Nonthaburi, 30 % in Bangkok, and 29 % in Pathum Thani.

Typhoon Damages

Damages can take other forms, depending on the climate hazard. In the case of strong typhoons, production losses (crops, livestock, and fisheries destroyed by the typhoon) constitute a huge part of the overall damage cost.

The Philippines, Vietnam, and China are highly prone to natural disasters (i.e., earthquakes, volcanic eruptions, tropical cyclones, and floods) making them among the most disaster-prone countries in the world (Nhu et al. 2011; European Commission 2007). The Philippines is hit by an average of 20 typhoons per year as a result of its location along the Western Pacific Basin, the world's busiest typhoon belt (Heijmans and Victoria 2001). Vietnam is also highly vulnerable to climate change, especially its coastal areas (European Commission 2007) as well as Central Vietnam, which is likely to be hit by at least two typhoons per year (Tuan et al. 2012). An average of six typhoons hit China annually (Horiguchi 2014).

A team of researchers from the Philippines, Vietnam, and China looked into the damages caused by super typhoons that hit their respective countries from 2006 to 2007 (Table 5). *Typhoon Xangsane* hit Quang Nam province with intensity level 13 (134–149 kph) and was accompanied by heavy rains that led to flooding in Dai

Table 5 Average damage cost from extreme typhoons for the Philippines, Vietnam, and China, 2006–2007

	Damage costs (USD)					
	Philippines (2006)			Vietnam	China	
Items	Lowland	Coastal	All	(2006)	(2007)	Average
Damage/loss to household property	**601**	**792**	**687**	**204**	**695**	**529**
House	172	343	264	181	245	230
Household appliances	84	221	177	20	94	97
Vehicles/boats	326	196	222	2	353	192
Amenities (water supply, electricity, communication)	19	33	24	2	3	10
Damage/loss to household production	**662**	**244**	**524**	**174**	**300**	**336**
Crop/agriculture	575	158	380	123	142	215
Livestock and poultry	22	44	36	38	91	55
Fishing/aquaculture farm	–	43	43	3	51	33
Fishing (not included in aquaculture)	–	–		8	14	11
Household business	65	–	65	3	1	23
Foregone income	**185**	**72**	**130**	**13**	**681**	**275**
Loss of income/wages	79	43	61	1	34	32
Loss of business	106	29	70	12	647	243
Total	**1,448**	**1,108**	**1,341**	**391**	**1,676**	**1,140**
Average household income[a]	**–**	**–**	**3,955**	**3,145**	**5,068**	

Source: Phong et al. (2011)

[a]Philippine income data from the Philippine Statistics Authority (http://www.nscb.gov.ph/secstad/d_income.asp)

Vietnam income data from the General Statistics Office of Vietnam (http://www.gso.gov.vn)

China income data from the National Bureau of Statistics China (http://www.stats.gov.cn/english/statisicaldata)

Loc (Dai Loc People's Committee 2007 cited in Phong et al. 2010). The total damage was estimated at VND 578 billion (USD 27.5 million) (Phong et al. 2010). The same typhoon (locally named *Milenyo*) hit the Philippines on September 25–29, 2006. It was a category 4 super typhoon with a maximum speed of 230 kph. It affected 277 municipalities with the Southern Luzon provinces of Laguna, Cavite, and Batangas hit badly. Total damage was placed at PhP 6.6 billion (USD 137.5 million) (Peñalba and Elazegui 2011). *Typhoon Saomai* hit China in 2007 and was considered as the country's worst typhoon since 1951 (Yueqin et al. 2011). It caused substantial damages to property and livelihood and caused people to lose income for a short time due to flooding.

The losses that farming villages hit by super typhoons took the forms of: damage to houses and other properties; crop, fishery, and livestock production losses; and foregone income during and a few days after the event. The higher damage inflicted by *Typhoon Xangsane* in the Philippines compared to those from Vietnam reflects the fact that, historically, typhoons hit the former with greater intensity before it enters the latter. Vietnam's higher level of preparedness also helped lower the damage cost. The average damage from *Xangsane* in the Philippines was placed at USD 1, 341/household whereas this number is only USD 391/household in Vietnam. In the case of China study sites where a large number of small-scale household factories are found, the bigger percentage of household losses came from foregone income (Yueqin et al. 2011).

As a share to household income, the typhoon damages from one extreme typhoon could wipe out 34 % of the annual household income in the Philippines, 12 % in Vietnam, and 33 % in China. The average damage cost of USD 1,140/typhoon event across all sites amounted to about a third of the yearly household income, a significant amount particularly for communities with very low income to start with.

With the increasing frequency of super typhoons hitting the region in the last 5 years, those dependent on agriculture are facing serious threats that could drive people to extreme poverty. They would need to diversify their income sources, build stronger houses, or move to areas that are less vulnerable to climate change. They would need support from government and nongovernment development workers to enhance their adaptation capacity. The next section will discuss the results of several EEPSEA studies that aimed to understand the adaptation needs of communities in selected villages in the region.

Adaptation Practices and Factors Influencing Adaptation Choices

Adaptation to climate change is a complex, multidimensional, and multi-scale process (Bryant et al. 2000 cited in Tiwari et al. 2014). According to Tiwari et al. (2014), household adaptation choices are not only influenced by environmental variables but also by household socioeconomic characteristics. Supporting this notion, several studies found that farming experience, socioeconomic position, and access to resources and credit increase the probability of uptake of adaptation measures to climate change (Maddison 2007; Nhemachena and Hassan 2007).

A question that we want to answer in this section is "how have people been adapting to extreme climate events?" The five-country research that EEPSEA supported in 2007 looked specifically into this question. It identified adaptation practices of households, communities, and LGUs in selected study sites in Indonesia, Vietnam, Thailand, the Philippines, and China. The study sites in China, the Philippines, and Vietnam (Hue) were affected by typhoons and flooding while those in Thailand, Indonesia, and Vietnam (Hanoi) had to contend with riverine flooding. The study also analyzed what factors influenced their adaptation choices. A total of 2,005 households from nine villages in these five countries were interviewed (Table 6).

What Climate Change Adaptation Practices Were Being Practiced?

The cross-country researchers found that, for most countries, the proportion of households who were doing either behavioral or "structural" adaptation measures is less than half of the respondents. The behavioral adaptation practices included moving properties to safer places, evacuating when the warning is received, and storing 3–5 days worth of food and drinking water before the disaster hits. It is worth noting that majority of the Thai respondents (88 and 96 % of urban and rural respondents, respectively) knew the drill of moving their properties to safer places during flooding season (Table 7).

Those who engaged in soft structural adaptation measures were even fewer. These measures included reinforcing farmhouses with heavy objects or tying them to trees and using more durable housing materials where available and use of sandbags to protect the houses from flooding. Relatively well-off households have managed to build mezzanine or second floor areas to keep them protected during flooding, but these practices were carried out by less than 10 % of the household respondents. In Thailand, it was a common practice to use sandbags to protect the houses from the inflow of floodwater (Table 7).

In general, the survey on climate change adaptation (CCA) practices in the five countries demonstrated that in 2007–2009, CCA at the household level was still

Table 6 Type of ecozone and number of sample households

Study area	Type of ecozone covered by the survey	No. of sample households
China	Coastal	414
Indonesia	Coastal	190
Philippines	Lowland	200
	Coastal	200
Thailand	Urban	200
Central Vietnam (Hue)	Coastal	392
Northern Vietnam (Hanoi)	Inland	150
	Coastal	151

Source: Phong et al. (2011)

Table 7 Household behavioral and structural adaptation practices, 2007–2009

Adaptation strategies	Percentage of respondents adopting each strategy								
	China	Indonesia	Philippines		Thailand		Hanoi		Hue
			Lowland	Coastal	Urban	Rural	Inland	Coastal	
Behavioral adaptation									
Evacuate to safer place	49	26	30	28	15	2	48	23	25
Move properties to safer places	30	22	47	39	88	96	41	23	25
Store foods, drinking water, and other necessities	59	5	61	65	1	–	36	69	74
Trim trees near house	–	1	6	9	–	–	9	31	28
Structural adaptation									
Reinforce/repair house using more durable materials/resilient structures	69	46	44	59	–	–	30	33	91
Build mezzanine/second floor	1	8	–		4	1	9	10	9
Build scaffold	–	–	–	–	7	42	56	41	–
Use of sandbag/concrete-block dike	–	4	–	–	70	9	13	5	–
Reinforce pig and fish ponds	2	2	–	2	–		27	33	15
Plant trees along river	–	2	–	1	–	–	5	5	3

Source: Phong et al. (2011)

relatively low and, if done at all, was of the form that was considered "soft" and thus could hardly help mitigate impacts from climate change-related disasters.

Clearly, these adaptation measures, while needed, are not sufficient to protect the affected households from extreme events. Three options that were considered by experts as potentially having a bigger impact in reducing damages are (1) relocating households currently in flood-prone areas to safer places, (2) building a community safe shelter where people can evacuate to during disasters, and (3) buying disaster insurance for property or crop losses. The study teams asked the respondents if they will support these adaptation options and results are given in Table 8.

As shown in Table 8, building a community safe shelter is favored by majority of the respondents in all countries. This was not given as an option in the Philippine study sites as most villages considered the town's public schools as evacuation shelters. A good number of the respondents pointed out though that building a dedicated community safe shelter is constrained by limited financial resources available to the community.

Getting disaster insurance, if it becomes available, is favored by a third of the respondents. Those who did not support it said that the main constraint for getting insurance is the lack of knowledge on how it works and where it can be secured. This is something that a better information and outreach campaign could easily solve.

Relocation is, of course, not that popular for almost all study sites, except those from Indonesia where about 65 % expressed openness to this option. Those who refused this option considered the financial difficulty of doing this and the loss of social and economic ties as the main constraints.

What Determines Adaptation Practices?

An analysis of the factors affecting households' adaptation choices in this cross-country project was carried out and reported in Francisco et al. (2011). The authors used the data from four countries: the Philippines, Vietnam, Thailand, and China with a total sample size of 1,711 households. The households' adaptation practices were classified as either reactive or proactive. Those that were carried out when the disaster is about to happen or has begun to happen are reactive measures. This would include evacuation and practices like reinforcing housing structures. Proactive measures are those carried out long before the event happens, usually, in anticipation of the rainy season or typhoon months. These measures include monitoring information sent through the early warning system, constructing elevated housing units, and building concrete walls or dikes to prevent flooding. Sixty-four percent (64 %) of the households did some form of reactive measures and about 31 % undertook proactive measures. About 6 % did not do anything (Table 9).

Using a multinomial linear (MNL) regression analysis, the authors found that households where members had received training on disaster preparation are less likely to just perform reactive adaptation measures and are more likely to opt for

Table 8 Recommended adaptation action by experts and why some households do not take them

Adaptation strategies	Percentage of households willing to adapt each strategy and main reason of those not willing to adapt (in parenthesis)								
			Philippines		Thailand		Hanoi		
	China	Indonesia	Lowland	Coastal	Urban	Rural	Inland	Coastal	Hue
Behavioral adaptation									
Relocate to safer places	41 (*Financial constraint*)	63 (*Far from current job*)	42 (*Felt safer to stay in the current location*)	44	28 (*Don't know where to go*)	4	15 (*Not acceptable*)	2	12 (*Won't leave to protect property*)
Structural adaptation									
Build the community safe shelter	58 (*No gov't funds to do this*)	57 (*Costly and may not be effective*)	–	–	–	–	62 (*Lack of finances and land*)	59	72 (*Financial gap*)
Financial adaptation									
Buy disaster house/ crop insurance	47 (*Don't know where to get it*)	–	30 (*Financial constraint; Insurance company not credible*)	38	29 (*Not worth buying*)	40	39 (*Don't know insurance details; Not worth buying since event isn't frequent*)	44	20 (*Don't know how it works*)

Source: Phong et al. (2011)

Table 9 Classification of household adaptation practices in selected SEA countries

Adaptation choice	Frequency	Percentage
No adaptation (Y = 0)	99	5.8
Reactive measures (Y = 1)	1,090	63.7
Proactive measures (Y = 2)	522	30.5
Total	**1,711**	**100.0**

Source: Francisco et al. (2011)

proactive ones. Those with permanent types of houses and have more than a one-storey house are also likely to adopt proactive adaptation measures as well (Table 10). These variables are reflective of the higher economic status of the households, indicating that wealthier households would be more likely to take proactive adaptation measures.

Social capital (inferred from households seeking outside help) was also found to significantly influence household adaptation decisions. Those who sought help from outsiders (positive sign) would more likely use reactive measures. In contrast, those who found no need to seek help from others (negative sign), which is probably an indicator of economic independence, were more likely to opt for proactive measures (Table 10).

The adaptation choice analysis also reveals that increasing the number of information channels that provide news about extreme climate events will decrease the probability of undertaking reactive measures. This potential for rural climate information to support adaptation and climate risk management points to the need to make climate information more accurate, accessible, and useful for households (Roncoli et al. 2002; Ziervogel et al. 2005; Hansen et al. 2007 cited in Asfaw and Lipper 2011).

In terms of socioeconomic characteristics, a bigger household size is found to positively and significantly affect the probability of a household undertaking reactive adaptation measures. This indicates that with strength in number, people tend to be complacent about taking a more proactive stance to climate change. Moreover, the more educated households were more likely to implement proactive adaptation strategies than reactive ones. This is supported by Tiwari et al. (2014) who stated that households with more knowledge and information can be proactive in their response toward climate change. Other studies (Maddison 2006; Nhemachena and Hassan 2008) found that the age of the household head, which represents experience, positively correlated with the uptake of adaptation measures.

Finally, the analysis revealed that households were more likely to undertake reactive rather than proactive measures if they perceived the risk of future extreme climate events to be more severe than what they had previously experienced. This is unexpected and should be further investigated as this seems to imply the existence of an attitude of resignation to fate to climate change disasters.

This attitude of resignation was indeed expressed by some of the respondents. Their thinking is that since nature wills it, it cannot be controlled and is something we just have to live with. Surely, there are ways to reduce damages and this is the essence of undertaking effective adaptation measures to protect lives, property, and

Table 10 Marginal effects of the determinants of household adaptation decisions

Independent variables by variable group	No adaptation measure	Reactive measures	Proactive measures
Constant	**−0.1768*****	**0.9650*****	**−0.7882*****
Experience			
Frequency of extreme climate events experienced in the past	0.0035	−0.0405	0.0369
Received training on disaster preparedness in the last five years[a]	0.0073	**−0.1049****	**0.0976****
Traditional knowledge[a]	0.0050	−0.0264	0.0214
Exposure/sensitivity			
Permanence of house[a]	0.0090	**−0.1586*****	**0.1496*****
Number of storeys in house	−0.0011	**−0.0981*****	**0.0992*****
Wealth			
House ownership[a]	−0.0082	−0.0187	0.0269
Vehicle/boat ownership[a]	−0.0093	−0.0185	0.0279
Asked help from outside the household[a]	−0.0102	**0.1139*****	**−0.1037*****
Household characteristics and belief system			
Household size	**−0.0035****	**0.0120***	−0.0085
Educational level	0.0012	**−0.0168*****	**0.0157*****
Age of household head	**0.0009*****	−0.0020	0.0010
Believes that extreme event is a fate which the household has little control over[a]	0.0061	0.0452	−0.0513
Perceives future risk of extreme climate events[b]	0.0037	**0.0600****	**−0.0638****
Social capital			
Number of information channels	**0.0074*****	**−0.0597*****	**0.0523*****
Membership in organization[a]	**−0.0141***	0.0392	−0.0252
Participation in collective action[a]	−0.0014	0.0031	−0.0017
Length of stay in the area	**0.0005****	−0.0014	0.0009
China	−0.0216	**−0.2183*****	**0.2400*****
Philippines	**0.0736*****	**−0.3696*****	**0.2960*****
Thailand	**0.0634*****	**−0.5946*****	**0.5312*****
Pseudo-R^2	0.2488		
Log likelihood function	−1046.644		
Restricted log likelihood	−1393.303		
Chi-squared	693.319		
Prob(ChiSqd>X^2-value)	**0.00000*****		
% Correct prediction	74.46		
No. of observations	1,711		
Base category: no adaptation			

Cf: Francisco et al. (2011)
Note: ***, **, * = significant at 1 %, 5 % and 10 % level, respectively
[a]1 = yes, 0 = otherwise
[b]1 = more severe than what was experienced, 0 = otherwise

livelihood from extreme climate change disasters. In fact, everyone should also be thinking of mitigation because while it is true that our generation is already committed to climate change, there are efforts that can be done to slow down climate change for future generations.

Coastal Communities' Vulnerability and Adaptation Practices

Coastal areas in Asia face "an increasing range of stresses and shocks," which are intensified by climate change (Cruz et al. 2007). This is supported by a 170-country assessment by Harmeling (2011) on the impacts of extreme weather-related events such as storms, flood, and extreme temperatures. The assessment showed six Asian countries to be among the most vulnerable, namely, Bangladesh (rank 1), Myanmar (rank 2), Vietnam (rank 5), the Philippines (rank 7), Mongolia (rank 9), and Tajikistan (rank 10).

That coastal communities are highly vulnerable to climate change is widely recognized (IPCC 2007, 2014; ADB 2009, 2014). Their vulnerability comes from the rising sea level that accompanies the overall warming of temperature as well as the storm surges that accompanies the increased frequency and intensity of typhoons. Low physical and financial capacity for disaster preparedness also contributes, to some extent, to these areas' vulnerability to extreme climate events (Ward and Shively 2011; Adger 1999); wealthier countries typically suffer lower social losses than poorer countries (Kahn 2005).

The threat from sea level rise has been in the radar of climate discussions during the last few years, but the threat from storm surges became real only with the Philippines' experience during super *Typhoon Haiyan* in November 2013. In just less than an hour, the 13 ft storm surges with strong current experienced during *Haiyan* left a death toll of 6,300 with 1,785 left unaccounted for. A few months after the super typhoon, more than 52,000 families are still living in tents in the danger zone in Tacloban City as the local government struggled to find a 100-hectare relocation site for these people (Lowe 2014; Stevens 2014).

Given the critical situation that coastal communities face as a result of the changing climate, EEPSEA also supported several research projects on CCA in coastal areas. This effort was done in collaboration with the WorldFish Philippine Country Office (WF-PCO) and came in two sets of projects. The first project focused on understanding the adaptation practices and assessing the vulnerability of selected coastal communities in the Philippines, Vietnam, and Indonesia. The various studies part of this first project looked into the impacts and adaptation practices used in dealing with typhoons/flooding, coastal erosion, and saltwater intrusion at the household, community, and local government levels. Several planned adaptation options were then evaluated using cost-effectiveness analysis (CEA).

The second project, which is still ongoing, looks into intra-household impacts of climate change, how the various members are affected, and how they can be engaged to generate a stronger household adaptation plan. Table 11 shows the

Table 11 Summary of climate change hazards, impacts, and compounding issues in the study sites

Batangas, Philippines	Palawan, Philippines	Jakarta, Indonesia	Ben Tre, Vietnam
Hazards	***Hazards***	***Hazards***	***Hazards***
Sea level rise	More frequent and intense typhoons	Coastal erosion and seawater intrusion	More frequent and intense typhoons
Confounding environmental issues	Floods	Coastal or tidal flooding	Destructive flood and tidal surges from 1996 to 2008
Coastal erosion	***Confounding environmental issues***	Sea level rise	***Confounding environmental issues***
Sand quarrying	Mangrove cutting for charcoal, housing, and fencing materials	***Confounding environmental issues***	Sand mining
Illegal charcoal making from mangroves	Weak enforcement of coastal management laws	Loss of most of mangrove and coastal ecosystems	Salinity intrusion
Illegal fishing using blasting and cyanide	Illegal fishing	Large population	Heavy traffic of sea vessels
Fishing with fine mesh net and superlight	Burning of some upland areas for rice farming (*kaingin*)	Pollution that affects water quality, soil erosion	***Impacts***
Impacts	Expansion of private beachfront property	Absence of strong fisheries policy and overlapping jurisdictions	Loss of shelter and livelihood from typhoons
Damage to property (hotels, resort, houses, and boat) during typhoon	Inadequate protection of the fish sanctuary	***Impacts***	Land encroachment
Coral bleaching and increasing number of crown of thorns	***Impacts***	Land subsidence, coastal inundation, and coastal abrasion	Saltwater intrusion during the dry season leads to a shortage of freshwater for domestic and production uses
Impacts to livelihood and tourism in vulnerable coastal areas	Change in the fish species caught	Seawater intrusion has reached the National Monument	
House relocation due to coastal erosion	More houses and boats destroyed by typhoons	Increased turbidity of water affecting photosynthesis	
Mangrove areas, coral reefs, marine protected areas, and beaches now at risk	Coral bleaching	Decreasing water quality	
	Decreased land area due to coastal erosion	Change in the pattern of flow, bathymetry, and coastline	
	Loss of traditionally gleaned shells along the coastline	Sediment accumulation in the entrance of harbor lanes increases dredging costs	
	Seawater is hotter during the 3–4 pm gleaning activity		
	Bangus fry collected for the past 5–6 years declined significantly		

Cf: Perez et al. (2013), shown as Table 3 in the original study

climate change impacts considered in the different study sites and the compounding environmental stresses that those communities face in addition to climate change.

In particular, most communities had to deal with coastal erosion, sand quarrying, deforestation of forests and mangroves, and rampant illegal fishing, all of which could compound the impacts of climate change. What Table 11 further tells us is that efforts to address the development needs of these coastal communities need to be holistic since theirs is a complex environment that is not necessarily affected only by their coastal location. Instead, it is important to note that coastal communities live in an environment that traverses several ecosystems, some of which are linked to one another. They are also affected by an economic and governance system that influences their livelihood and hazard vulnerability, be it climate change or other hazards. Moreover, they are also assisted by the government and other development agencies in how they cope with climate change impacts. These coping measures are further discussed in the next section.

Adaptation Practices in Selected Coastal Villages

In the Philippines, it is noticeable that all local governments have formed a municipal disaster risk management council (MDRMC) that is funded using 5 % of the 20 % Development Fund (Table 12). This fund is used to provide disaster victims with food, particularly those who stay in evacuation centers during disaster events. The fund is also used to undertake information, education, and communication (IEC) campaigns on disaster risk reduction (DRR). In addition, local governments conduct dredging and river widening activities to reduce the flooding threat as well as to rehabilitate mangroves, which are now widely believed to provide protection from coastal erosion and flooding.

The same efforts are reported in the Indonesia and Vietnam study sites. In addition, Vietnam reports of technological support to farmers in the form of drought/flood-tolerant varieties and modified farming systems to suit the new climate (Table 12). Vietnam is also doing more structural measures, in the form of dike and pond system, to support livelihood. Indeed, as noted by Francisco (2008), there are a lot that countries in the region could learn from Vietnam on how they have been living with flooding.

Adaptation practices at the community and household levels were also obtained during the study. It is worth noting that most local government initiatives involved the community. Community folk participated in mangrove replanting, dike repairs and construction, and in other activities to improve their environment and help prepare for disasters. At the household level, adaptation practices included relocating and strengthening of houses, putting up defense structures like cement dikes, engaging in alternative livelihood activities to enhance financial security, and shifting fishing/farming practices to suit new and changed environments, particularly in Vietnam.

Table 12 CCA and disaster mitigation strategies in the study sites, 2012

Government-led initiatives	Community-based initiatives	Autonomous household adaptation practices
San Juan, Batangas, Philippines		
Organized MDRMC, which is financed by 5 % of the 20 % Development Fund Gave out cash support (e.g., PhP 1,000–2,000 to affected fisher folk) River dredging and widening to prevent flooding Regular IEC campaigns Maintenance of Marine Protected Areas, mangrove replanting, and engagement in "Billions of Trees Project" in 400 ha of upland, lowland, and beach side areas	Aquaculture and fish processing projects Mangrove replanting Crown-of-thorns starfish removal, as spearheaded by resort owners Typhoon warning system improvement and preparation for emergency evacuation Cleanup of drainage and flood control structures	Relocate or strengthen house structures Plant and sell mangrove seedlings Temporarily remove light structures in beach areas Join savings/credit cooperative Modify planting schedules
Honda Bay, Palawan, Philippines		
Passed an ordinance to conserve, protect, and restore (CPR) the Puerto Princesa City's sources of life Flood control project implementation and construction of breakwaters Mangrove reforestation Established a barangay disaster risk management council (BDRMC) with fund allocation	Establishment/ maintenance of fish sanctuary Participation in riverbank bioengineering projects (e.g., sea dike construction, mangrove reforestation) to reduce erosion and siltation Establishment of community-based early warning system and provision of temporary evacuation center	Use of indigenous materials to strengthen housing structures Use of cement and rocks to build dikes
Jakarta Bay, Indonesia		
Implemented measures related to watershed management and coastal and marine resources protection Conducted capacity building and community empowerment activities to implement watershed and marine and coastal resources management Promoted policies that integrate environmental concerns in economic development Encouraged institutional strengthening for river basin management and coastal and marine bay management	Community involvement in various initiatives to protect watershed and coastal and marine resources Construction of permanent embankments Drainage improvement and river dredging Mangrove planting	Clean the beach fronting their houses

(*continued*)

Table 12 (continued)

Government-led initiatives	Community-based initiatives	Autonomous household adaptation practices
Ben Tre Province, Vietnam		
Coastal zone management: road construction, dike upgrading, and mangrove protection *Freshwater resources management*"Acknowledgements" section has been deleted as it is not a part of the contribution structure. investment on irrigation systems for water storage, construction of dikes to prevent saltwater intrusion, and watershed management to protect water sources *Supported agricultural adaptation*: switch to salt-tolerant crops, investment on drought-tolerant crops, improvement of early warning system *Supported CCA for aquaculture and capture fisheries*: technological innovation in pond construction for improved water storage, introduction of fish-rice model in saline areas, and research to identify rich fishing grounds Information and awareness campaign on how to prepare for climate change	Mangrove forest protection Ensuring supply of freshwater for agriculture, aquaculture, and domestic needs (e.g., storage structure construction and provision of containers to harvest rainwater) Relocation of at-risk houses Participation in sea dike construction	Harvest rainwater Switch from black tiger shrimp to whiteleg shrimp to adapt to saline water Change cultivation schedules to avoid saltwater intrusion Use of sandbags to build dikes around the farm to prevent saltwater intrusion and seawater inflow

Source: Perez et al. (2013)

Cost-Effectiveness Analysis of Selected Adaptation Options

The results of a CEA of selected adaptation options, which were identified by LGUs as priority projects, are presented in Tables 13, 14, and 15. For the analysis, the researchers selected a common denominator, such as cost per unit of area protected or per household saved or protected. However, this is a very crude comparison as multiple types of benefits may be delivered by each of the adaptation options. For instance, a mangrove protection project will produce other types of benefits than what can be "produced" by installing a dike to protect a given area. As such, the comparison should be interpreted with caution. The last column in each of the next three tables provides some additional information regarding the interpretation of results.

For San Juan, Batangas, in the Philippines, sea wall construction and mangrove reforestation were compared, and results showed that it is a lot cheaper to prevent a kilometer of shoreline erosion using mangrove reforestation (Table 13). In addition,

Table 13 Cost-effectiveness analysis results for San Juan, Batangas, Philippines

Objective	Planned adaptation strategies	CE ratio	Notes
Protect the coastline from erosion	Sea wall construction	USD 0.16 M/ linear km of erosion prevented	Mangrove reforestation is not only more cost-effective but also offers other co-benefits like additional sources of income and marine biodiversity preservation
	Mangrove reforestation	USD 0.01 M/ linear km of erosion prevented	
Increase the number of households safe from typhoon/flooding	Zoning provisions and relocation	USD 0.07 M/ HH saved	The changing zoning provisions need to be accompanied by the removal of communities from areas they currently occupy, a very costly and socially unattractive option

Source:

this option produces other forms of benefits from the mangrove resources, both in terms of provisioning and regulating functions; if valued, these benefits will make this measure even more attractive.

The use of early warning system and the provision of evacuation shelter were also compared with improvement of zoning regulation and relocation. As expected, the latter was a lot more costly to implement as a way of protecting households from the negative impacts of flooding and/or typhoons. The early warning system is being put in place in many parts of the country.

A similar analysis was carried out for the Palawan, Philippines, study site (Babuyan in Honda Bay). Several options were evaluated: to protect households from storm surges (i.e., breakwater construction, dike construction, and mangrove reforestation), to protect them from inland flooding (i.e., upland reforestation, IEC with provision of temporary evacuation shelter, and household relocation), and to protect production areas (i.e., dike construction, riverbank rehabilitation, and river dredging). The results show the superiority of mangrove reforestation over structural measures, the cost-effectiveness of river dredging and riverbank rehabilitation, and support for an effective early warning system supplemented by IEC as part of DRR strategies (Table 14).

For the study sites in Jakarta Bay, Indonesia, several options with varying objectives were compared as shown in Table 15. River dredging[1] was found to be more cost-effective than the construction of new canals or embankment and even

[1]Note: The study did not indicate how often this has to be done.

Table 14 Cost-effectiveness analysis for Honda Bay, Palawan, Philippines

Objectives	Planned adaptation strategies	CE ratio	Notes
Protect households from storm surges and loss of property and minimize sand erosion	Breakwater construction	USD 0.276 M/HH	Mangrove reforestation is cost-effective in protecting households and properties and in minimizing sand erosion where mangroves are seen to thrive well
	Dike/levee construction	USD 0.032 M/HH	
	Mangrove reforestation	USD 0.019 M/HH	
Prevent river overflow and minimize siltation, which damage coconut plantations and fishponds	Riverbank rehabilitation using vetiver grass	USD 0.004 M/ha	The discussion on the planned options and cost-effectiveness (CE) ratios focused on prioritizing riverbed dredging together with riverbank rehabilitation using vetiver grass alone
	Riverbank rehabilitation using vetiver grass combined with mechanical method	USD 0.034 M/ha	
	Dike construction	USD 0.032 M/ha	
	River dredging	USD 0.002 M/ha	
Protect households from inland flooding	Upland reforestation	USD 926/HH	IEC is cost-effective but success depends on the maturity of the residents to react accordingly
	IEC/early warning system establishment and provision of temporary evacuation area	USD 120/HH	
	Household relocation	USD 2,234/HH	

Source:

mangrove rehabilitation. The high cost of mangrove rehabilitation is attributed to the need to purchase land from private landowners who already have rights over the areas previously occupied by mangroves. However, mangrove restoration is likely to make an even bigger contribution to the local economy in the face of climate change and the resulting increase in typhoon frequency and intensity (Tuan and Duc 2013). Mclvor et al. (2012) suggested that mangroves can potentially play a significant role in coastal defense and DRR.

Overall, one can see that the CEA results tend to favor mangrove reforestation over structural measures and river dredging in order to increase flood control function. The scientific basis for this claim was found in the study by Mazda

Table 15 Cost-effectiveness analysis for Jakarta, Indonesia

Site	Objectives	Planned adaptation strategies	CE ratio	Notes
Rorotan	Reduce the no. of HH affected by flooding	Construction of East flood canal	USD 307 M/ HH	The cost-effective option suitable in this area is the dredging of Sunter river
		Dredging of Sunter river	USD 0.695 M/ HH	
Marunda	Reduce the no. of HH affected by flooding and coastal flooding	Construction of permanent embankment	USD 2.5 M/ HH	The cost-effective option is planting mangroves
		Mangrove rehabilitation	USD 13.37/ HH	
Kalibaru	Reduce the no. of HH affected by flooding, coastal flooding, and saltwater intrusion	Road elevation	USD 2.64 M/ HH	The more cost-effective solution is to dredge Cakung river
		Dredging of Cakung river	USD 2.09 M/ HH	
Kamal Muara	Reduce the no. of HH affected by flooding and coastal flooding	Dredging of Pesanggrahan river	USD 2.09 M/ HH	The more cost-effective solution is to dredge Pesanggrahan river. A large portion of the cost of planting mangroves is the value of coastal land owned by private individuals or groups
		Mangrove rehabilitation	USD 2.43 M/ HH	
Muara Angke	Reduce the no. of HH affected by flooding and coastal flooding	Road elevation	USD 0.311 M/ HH	The more cost-effective solution is to elevate roads. Like in Kamal Muara, a large portion of the cost of planting mangroves is the value of privately-owned coastal land
		Mangrove rehabilitation	USD 2.07 M/ HH	

Source: Agus et al. (2013)

et al. (2006) and cited in Andrade et al. (2010). Moreover, the early warning system supplemented by evacuation shelter provision was found to be quite cost-effective compared with the other options evaluated. This finding is consistent with other studies' findings which validate the use of an early warning system as one of the most cost-effective measures to reduce damage cost (Hallegatte 2012; Linham and Nicholls 2010).

The next section describes efforts to link research with local government adaptation planning based on the experience from two cross-country projects implemented from 2011 to 2013.

Working with Local Governments in Adaptation Planning

Climate change will affect everyone. Differences on the impacts felt will depend on the locality's hazard exposure, the people's adaptive capacity, and the LGU's level of preparedness. This means that adaptation planning has to be locale specific to suit the conditions and capability of different local governments.

In order to bring research to the level where it can have impact, EEPSEA supported two multi-country projects to engage local government planners in adaptation planning in 2011–2013.

CBMS-EEPSEA Project

The main funding source of EEPSEA, the International Development Research Centre (IDRC), also supports a Community-Based Monitoring System (CBMS), a global project with presence in the Philippines, Vietnam, and Indonesia. The CBMS-EEPSEA partnership was carried out to pilot test the application of the EEPSEA framework on climate change vulnerability assessment and mapping at the local level using CBMS data and supplemented by data from other government sources. There are two outcomes that were expected from this initiative: (1) LGU level capacity building on understanding how to assess climate change vulnerability and (2) identification of adaptation strategies based on research done on this topic.

The study sites included (1) Vietnam, Kim Son district of Ninh Binh province in the North, Nghia Lo municipal of Yen Bai province in the North Mountainous Region, and Tam Ky town of Quang Nam province in the Central Region; (2) Indonesia, two villages in the province of Kota Pekalongan (Pasirsari village, Kecamatan Pekalongan Barat, and Panjang Wetan village, Kecamatan Pekalongan Utara); and (3) the Philippines, municipality of Carmona in Cavite province and Marinduque province.

Experience in pilot testing the climate change vulnerability framework shows that its main advantage is its simplicity, which allows local government decisionmakers to understand what factors they should consider when doing such an assessment. The ability to map information that allows government officials to immediately see how they fare relative to their neighbors was also found attractive.

Experience in using vulnerability mapping to aid in identifying suitable adaptation strategies varies across the participating country teams. The Philippine teams managed to bring the discussion to the point that they were able to identify the adaptation practices that need to be strengthened and those that need to be implemented as listed in Table 16 (Reyes 2012). The Vietnamese team shares that the process helped them understand the location and the sources of vulnerability but that these were not sufficient to assess what the community needs in order to adapt to the changing climate.

In a way, identifying the adaptation practices that the community or the local government could undertake is indeed only the first step. Given limited resources

Table 16 Adaptation strategies identified in the Philippine CBMS-EEPSEA project

Study site	Adaptation strategies identified
Carmona, Cavite	Strengthen current efforts in: river cleanup, solid waste management, and de-clogging of canals and waterways Conduct more orientations on DRR management, enhance DRR communication capability and early warning system with new equipment and strengthen flood forecasting, and upgrade evacuation and health facilities Install diversion canals, dams, and reservoirs to protect industrial and agricultural lands
Marinduque province	Review/update and enhance the provincial DRR management plan Strengthen the rehabilitation of watershed areas and reforestation projects through the National Greening Project (NGP), Bamboo Greenbelt Project, and other forest rehabilitation projects Build LGU and community capability and capacity on the various facets of DRR (i.e., warning, search and rescue, emergency relief, logistics and supply, communication and information management, emergency operation management, evacuation planning and management, health emergency education, and post disaster management) Establish/construct evacuation centers in safe areas and improve and construct roads and feeder roads, drainage facilities, footbridges, spillways, and floodways in priority areas Produce and disseminate natural hazard and geographic info system susceptibility maps and IEC materials and install Integrated Warning/ Communication and Response System Install automatic weather station in major critical areas such as Boac and Sta. Cruz

Source: Reyes (2012)

and varying capacity, an assessment of the economics of these measures and their technical and social acceptability must be carried out as well; these are not within the scope of the CBMS-EEPSEA project.

In the case of the Indonesian team, the adaptation policies and programs of the national and local governments were discussed and analyzed as a separate activity from the vulnerability mapping. The analysis revealed that current adaptation planning is largely addressing the hazard component of vulnerability, which they pointed out is a major limitation on account of the findings of the project. In particular, the CBMS-EEPSEA project showed clearly that adaptive capacity and sensitivity are equally important sources of vulnerability and should therefore be addressed as well.

All the project country teams recommended that similar efforts be done to assist other LGUs to better understand their vulnerability situation and to help them identify adaptation practices. To help evaluate the economic viability and acceptability of these identified strategies would require a longer time and a different set of skills, as demonstrated in EEPSEA's project with IDRC's Climate Change and Water program, which is discussed in the next section.

CCW-EEPSEA Project

In February 2011, EEPSEA and the IDRC program on climate change and water (CCW) awarded three 3-year research grants to institutions based in the Philippines, Vietnam, and Cambodia. The project, entitled "Building Capacity to Adapt to Climate Change in Southeast Asia," aimed to enhance the capacity of university researchers, provincial officials, LGU representatives, and other mass organizations in selected SEA countries by equipping them with knowledge on how to assess climate change causes and impacts and how to undertake an economic analysis of selected adaptation options.

Specifically, the collaborating partners were expected to undertake vulnerability analysis, prioritize adaptation options, and develop sound and feasible project proposals for funding. Based on the highly vulnerable sites identified in Yusuf and Francisco (2009), the project selected the following study sites: Kampong Speu in Cambodia (highly vulnerable to drought), Laguna in the Philippines (highly vulnerable to flooding), and Thua Thien Hue in Vietnam (exposed to flooding and typhoons).

The project adopts a multidisciplinary and participatory approach. Each country research team is composed of researchers with backgrounds in natural science, sociology, and economics. Their mandate was to work with their study site's local government officials in undertaking vulnerability assessment, in identifying and evaluating adaptation projects, and in developing the CCA proposal/plan for submission to donor agencies.

During project implementation, the research team implemented a series of training courses, joint field visits, and dialogues with community members. The key skills that the training courses addressed are vulnerability assessment and mapping following the framework used in Yusuf and Francisco (2009), evaluation of climate change impacts, economic analysis of adaptation options, and proposal development for adaptation funding support. Interestingly, many of the team members are now being involved in providing consultancy services on these areas in their own countries – a sure offshoot of their engagement in this project.

The engagement of the local government people in the project had brought about several benefits, namely, (1) greater awareness on climate change risks; (2) generation of risk maps, which were used to develop agricultural production plans for three subregions in Thua Thien Hue; (3) integration of climate risks in the socioeconomic development plan; and (4) improved knowledge on how to conduct vulnerability assessment and economic analysis of adaptation options as well as proposal development. They were also able to network with government people from other countries as the project hosted sharing and training meetings as part of the capacity building activities designed for the collaborators.

A post project survey was implemented to assess changes in knowledge and skills of the people involved in the project. All team members across the three countries demonstrated improved understanding of the climate change problem and a higher level of knowledge on the various tools that were used by the team. The

biggest improvement was noted among the research team members from Cambodia.

In terms of concrete actions taken up, local government partners in Thua Thien Hue have developed agricultural production plans based on the results of the climate change vulnerability map that was prepared through the project. The Thua Thien Hue LGU staff developed proposals to raise funds for the construction of local CCA measures, particularly better use of water in rice production.

The LGU partners in Laguna, Philippines, now have better appreciation and knowledge on how to implement vulnerability assessment and mapping and how to package proposals, but they acknowledged that they may not be able to carry these out on their own. Their reservation regarding their independent implementation/conduct of such activities is not due to perceived capacity constraint but more as a result of their busy schedules as they are responsible for multiple projects at the provincial office.

The project research findings also affirmed the findings of previous studies. First, that vulnerability to climate change is quite high and that it varies across areas. In Thua Thien Hue, Vietnam, households living in delta communes had higher adaptive capacity compared with households living in coastal and upland communes. The social capital was found to be generally high but limited infrastructure support, access to technology, and lower financial resources contributed to lower adaptive capacity for many households.

In Laguna, Philippines, higher vulnerability was noted among coastal communities compared with agriculture-based households. Interestingly, it was found that a big proportion of the vulnerable households are not knowledgeable about the threats posed by climate change. The most vulnerable households are often the most poor as well and so it probably makes no difference where their poverty stresses are coming from. In terms of experience with climate-related hazards, majority identified typhoons and flooding as the hazards posing the greatest threat based on experienced damages over the years, most intensely in the last few years. The biggest losses/damages come in the form of damages to houses and furniture. About 16 % of the households regularly experience evacuation, and a tenth of those interviewed had experienced permanent relocation as supported by the local government of Sta. Cruz, Laguna. The important role played by social capital, particularly those involving women's organizations, in accessing DRR programs was also highlighted in the Philippine study site.

The study site in Kampong Speu, Cambodia, is predominantly a farming community and is threatened mostly by drought, with flash floods occurring in certain areas only. Vulnerability was found highest in the eastern and central western regions of the province on account of the highest concentration of vulnerable communes in these areas. Farming households in lowland areas have been coping with drought conditions by shifting to short-duration crop varieties. Those in mountainous areas were found less willing to shift to new varieties, but they generally have more resources to cope with the impacts of a changing climate. For both sites, other adaptation strategies included: constructing and renovating canals, selling household assets, and migrating to

work outside the village (e.g., work in a garment factory, as household help, and in construction).

The teams also packaged adaptation proposals, which the LGUs can then submit for funding support: (1) a technology-based flood early warning system for the Sta. Cruz River Watershed in Laguna, Philippines; (2) improved irrigation system for Kampong Speu, Cambodia; and (3) upgrading of the An Xuan tributary banks and river dredging in Thua Thien Hue, Vietnam. These projects were found to be the most economically efficient option for the three sites based on the economic analysis of several alternative projects.

Lessons in Action Research: Working with Local Government Units

The researchers of the two projects considered working with the local governments both rewarding and productive. They are able to immediately share and discuss with local government planners their research results as the study progresses. The local government collaborators were involved more deeply in data analysis and presentation as they were engaged all throughout the project. Hence, there is joint ownership of the research reports, which was linked to adaptation planning more directly, unlike in the traditional research process. More importantly, there is improvement in the knowledge and skills of not only the researchers but also of their collaborating local government partners. All these are expected to result in a better understanding of the problem and a higher capacity to assess, evaluate, and decide on how it can be addressed.

Nonetheless, it must be mentioned that the heavy workload of the local government partners prevented them from being more engaged in the research process. They are only engaged in the project part time with DRR/climate change being only one of their many other responsibilities in their capacity as local government staff. The same can be said of the university researchers who are only working part time with the research. They meet and work with their collaborators only during meetings or major activities.

Perhaps, the project duration for the CCW-EEPSEA project is too long (i.e., 3 years), and that of the CBMS-EEPSEA project (i.e., 1 year) is too short. The CCW-EEPSEA project differs from the CBMS-EEPSEA project in that it is longer and thus has more resources. Its idea is to fully understand the various aspects of vulnerability by forming three teams (i.e., economic, social, and mapping teams) and to analyze and characterize who are the most vulnerable sectors in the locality. The team is comprised of university researchers, LGU representatives, and representatives from NGOs working in the community. On the second year, the potential and existing adaptation practices were identified and evaluated. An economic analysis of those options was carried out. In the last year, the team assisted the LGU in developing a proposal to seek support from donor organizations to fund their adaptation plans. This 3-year project completely contrasts with the 1-year duration of the CBMS-EEPSEA project, both in terms of depth of analysis and resources.

From a program point of view, it will appear that having 2 years for both projects will be a Pareto improvement. The CBMS-EEPSEA project would have more time to expand its adaptation analysis. On the other hand, 3 years may have been too long for the CCW-EEPSEA team as the members managed to do multiple assignments that took them away from a more concerted, focused analysis of the problem on hand. Somewhere in between these two project durations could result in a more intensive interaction between researchers and their local government partners as well as richer data collection and analysis.

Lessons from EEPSEA-Funded Climate Change Adaptation Research in Southeast Asia: Future Directions

Climate change is here to stay and is likely to get worse given that serious commitment to reduce greenhouse gas (GHG) emission will only happen starting 2020 *if*, *and only if*, the 2015 International Agreement with significant GHG reduction commitment will be signed by all countries in Paris. The prospect of having such a stronger agreement in place does not look good given how previous talks have failed on this front. We can only hope that our global leaders will come to their senses and put in place serious efforts to reduce GHG emission to slow down climate change.

On the positive side, it is good to hear about various countries' efforts to move toward a green economy by using more efficient technologies, building high energy savings, and investing on ecosystem reforestation or protection. However, these efforts cannot be done at a microscale – we need government commitment to pass stronger measures to reduce carbon emission. Surely, a carbon tax supplemented by programs to reduce impacts on the poor is a step in the right direction but is opposed in many countries because of strong lobbying pressure by those sectors who will be hit by this measure.

With the exception of climate deniers, everyone agrees that climate change poses a real threat to people, with some countries facing (and in fact, already experiencing) more serious challenges than others and the poor being more vulnerable to it. The various research supported by EEPSEA on CCA in SEA proved that the impact of extreme climate events on those affected is huge with an extreme event costing households up to 44 % of their annual household income. Depending on the number of extreme climate events (which unfortunately is expected to be more frequent and intense in the future), future damage can be even bigger and will most likely drive vulnerable households to extreme poverty.

Despite the severity of the situation, adaptation actions by SEA households are generally very crude and mostly in the form of reactive measures (e.g., strengthening housing units, using sandbags during flooding, storing of food, evacuation) rather than preventive ones (e.g., relocation, building multistorey and stronger housing units). Largely, this is explained by the limited resources available to most vulnerable households for investment in stronger measures. Moreover, in

many cases, there is still the hope that extreme events will not occur that often in the future or that they are used to this condition already and will be able to manage.

This complacency is now being addressed by enhanced IEC campaigns that most governments are launching toward DRR/climate change. A lot of this effort needs to be done more widely and intensely, but stronger adaptation investments need to be made if adaptation capacity or resilience is to be enhanced in areas most vulnerable to climate change. The financial resources available to these communities are undoubtedly small in relation to needs and efforts must be done to provide more resources and/or use more wisely the limited resources available. Hopefully, developing countries in the region will be able to access some of the adaptation funds available, and the economic analysis done on some of these measures was found to be economically viable.

Local governments need support in adaptation planning. The two action research projects carried out with funding support from EEPSEA and the collaborating organizations (IDRC's CBMS and CCW) showed that local government officials are receptive to such research collaborations and are very much willing to learn science-based planning. With more resources provided to free up some of their time during the conduct of such action research projects, a higher-level and more fruitful engagement can perhaps be expected from them. In addition, our experience shows that there are existing programs (e.g., CBMS, WorldFish, etc.) in most communities that researchers can tie up with so that synergy can be achieved in getting more resources and technical expertise in the action research.

Finally, given the urgency of the situation and the relatively higher level of research information now available from different organizations working in SEA, it is high time to move toward research that feeds directly into concrete actions, to not simply come up with plans and proposals but with adaptation projects/measures that can be readily implemented on the ground. This calls for action research with some funding available to pilot test adaptation projects that will be evaluated as part of the research. This is not going to be easy as there seems to be a dichotomy between research and development. In most cases, research organizations just do research while development organizations focus on development projects. This is so unfortunate in this instance since concrete actions supported by science are what we need to help prepare local governments, communities, and households to better adapt to climate change. Research alone oftentimes translates to *just pure talk*; action research is *walking the talk*.

References

ADB (Asian Development Bank) (2009) The economics of climate change in Southeast Asia: a regional review. Asian Development Bank, Manila

ADB (Asian Development Bank) (2014) Climate change and rural communities in the greater Mekong Subregion: a framework for assessing vulnerability and adaptation options. Asian Development Bank, Bangkok

Adger WN (1999) Social vulnerability to climate change and extremes in coastal Vietnam. World Dev 27(2):249–269

Agus HP, Siti Hajar S, Ivonne MR, Klaudia OS (2013) Climate Change Impact, Vulnerability Assessment, Economic and Policy Analysis of Adaptation Strategies in Jakarta Bay, Indonesia. Unpublished Research Report. Economy and Environment Program for Southeast Asia (EEPSEA), Philippines

Andrade AP, Fernandez BH, Gatti RC (2010) Building resilience to climate change: ecosystem-based adaptation and lessons from the field. International Union for Conservation of Nature (IUCN), Gland

Anthoff D, Nicholls RJ, Tol RSJ, Vafeidis AT (2006) Global and regional exposure to large rises in sea level: a sensitivity analysis. Working paper 96, Tyndall Centre for Climate Change Research, University of East Anglia

Asfaw S, Lipper L (2011) Economics of PGRFA management for adaptation to climate change: a review of selected literature. Commission on Genetic Resources for Food and Agriculture. Agricultural Economic Development Division (ESA), Food and Agriculture Organization (FAO), Rome

Cruz RV, Harasawa H, Lal M, Wu S, Anokhin Y, Punsalmaa B, Honda Y, Jafari M, Li C, Huu Ninh N (2007) Asia climate change 2007: Impacts, adaptations and vulnerability. In: Parry ML, Canziani OF, Palutikof JP, van der Linden PJ, Hanson CE (eds) Contribution of working group II to the fourth assessment report of the intergovernmental panel on climate change. Cambridge University Press, Cambridge, MA, pp 469–506

Cumming-Bruce N, Gladstone R (2013) U.N. Appeals for $301 million towards typhoon relief. The New York Times, 12 Nov 2013. http://www.nytimes.com/2013/11/13/world/asia/philippines-typhoon-haiyanresponse.html. Retrieved 13 Aug 2014

Elyda C, Dewi SW (2014) Jakarta braces for major flood. The Jakarta Post, 19 Jan 2014. http://www.thejakartapost.com/news/2014/01/19/jakarta-braces-major-flood.html. Retrieved 13 Aug 2014

European Commission (2007) Disaster preparedness in Vietnam. European commission article. http://ec.europa.eu/echo/files/policies/dipecho/presentations/vietnam.pdf

European Commission (2014) New study quantifies the effects of climate change in Europe. JRC News Release. Copenhagen 25 June 2014. https://ec.europa.eu/jrc/sites/default/files/jrc_20140625_newsrelease_climate-change_en.pdf

Francisco HA (2008) Adaptation to climate change needs and opportunities in Southeast Asia. ASEAN Econ Bull 25(1):7

Francisco HA, Predo CD, Manasboonphempool A, Tran P, Jarungrattanapong R, The BD, Peñalba LM, Tuyen NP, Tuan TH, Elazegui DD, Shen Y, Zhu Z (2011) Determinants of household decisions on adaptation to extreme climate events in Southeast Asia. Economy and Environment Program for Southeast Asia (EEPSEA), Singapore

Garnaut R (2010) The Garnaut climate change review in Australia. http://www.garnautreview.org.au/. Retrieved 12 Aug 2014

GISTDA (Geo-Informatics and Space Technology Development Agency) (2011) Radar satellite images and flood maps of the 2011 flood, May–Dec 2011

Hallegatte S (2012) A cost effective solution to reduce disaster losses in developing countries, hydro meteorological services, early warning, and evacuation. Policy research working paper 6058, World Bank

Handley P (1992) Before the flood. Climate Change May Seriously Affect Southeast. Far East Econ Rev 65(155):65–66

Harmeling S (2011) Global climate risk index 2011: who suffers most from extreme weather events? Weather-related loss events in 2009 and 1990 to 2009. A Briefing Paper. Germanwatch e.V. 24 pp

Heijmans A, Victoria L (2001) Citizenry-based & development-oriented disaster response. Centre for Disaster Preparedness and Citizens' Disaster Response Centre, Quezon City

Horiguchi C (2014) Rammasun is one of the strongest typhoons to hit Southeast China in recent years. http://www.rms.com/blog/2014/07/25/rammasun-is-one-of-the-strongest-typhoons-to-hit-southeast-china-inrecent-years/

IPCC (Intergovernmental Panel on Climate Change) (2007) Climate change 2007: impacts, adaptation and vulnerability. Contribution of working group II to the fourth assessment report of the intergovernmental panel on climate change. Cambridge University Press, Cambridge, MA

Jones RN, Preston BL (2006) Climate change impacts, risk and the benefits of mitigation. Commonwealth Scientific and Industrial Research Organisation, Canberra

Kahn M (2005) The death toll from natural disasters: the role of income, geography, and institutions. Rev Econ Stat 87(2):271–284

Linham MM, Nicholls RJ (2010) Technologies for climate change adaptation: coastal erosion and flooding, TNA guidebook series. United Nation for Economics Program, Roskilde

Loo YY, Billa L, Singh A (2014) Effect of climate change on seasonal monsoon in Asia and its impact on the variability of monsoon rainfall in Southeast Asia. Geosci Front. doi:10.1016/j.gsf.2014.02.009

Lowe A (2014) Typhoon Haiyan survivors in Tacloban face upheaval as city tries to rebuild. The Guardian. 8 May 2014. http://www.theguardian.com/world/2014/may/08/typhoon-haiyan-survivors-tacloban-philippines. Retrieved 13 Aug 2014

Maddison D (2006) The perception and adaptation to climate change in Africa. Discussion paper no. 10. Centre for Environmental Economics and Policy in Africa (CEEPA), University of Pretoria, Pretoria

Maddison D (2007) The perception of and adaptation to climate change in Africa. World bank policy research working paper, 4308.The World Bank, Washington, DC

Mazda Y, Magi M, Ikeda Y, Kurokawa T, Asano T (2006) Wave reduction in a mangrove forest dominated by *Sonneratia* sp. Wetl Ecol Manag 14:365–378

Mclvor A, Moller I, Spenser T, Spalding M (2012) Reduction of winds and swell waves by mangrove, Natural coastal protection series. Cambridge Coastal Research Unit working paper 40

Morgan J (1993) Natural and human hazards. In: Brookfield H, Byron Y (eds) Southeast Asia's environmental future: the search for sustainability. Oxford University Press, Kuala Lumpur

Nabangchang O, Leangcharoean P, Jarungrattanapong R, Allair M, Whittington D (2013) Economic costs incurred by households in the 2011 Bangkok flood. Economy and Environment Program for Southeast Asia (EEPSEA), Los Baños

Nhemachena C, Hassan R (2007) Micro-level analysis of farmers' adaptation to climate change in Southern Africa. IFPRI discussion paper 00714. International food policy research institute (IFPRI), Washington, DC

Nhemachena C, Hassan R (2008) Determinants of African farmers' strategies for adapting to climate change: multinomial choice analysis. Afr J Agric Resour Econ 2(1):83–104

Nhu OL, Thuy NT, Wilderspin I, Coulier M (2011) A preliminary analysis of flood and storm disaster data in Viet Nam, Global assessment report on disaster risk reduction. United Nations Development Program (UNDP), Hanoi

Peñalba LM, Elazegui DD (2011) Adaptive capacity of households, community organizations and institutions for extreme climate events in the Philippines. Economy and Environment Program for Southeast Asia (EEPSEA), Singapore

Perez ML, Sajise AJU, Ramirez PJB, Purnomo AH, Dipasupil SR, Regoniel PA, Nguyen KAT, Zamora GJ (2013) Economic analysis of climate change adaptation strategies in selected coastal areas in Indonesia, Philippines and Vietnam. Economy and Environment Program for Southeast Asia and Worldfish, Penang

Phong T, Tuan TH, The BD, Tinh BD, Penalba LM, Elazegui DD, Jarungrattanapong R, Manasboonphempool A, Yueqin S, Zhu Z, Li L, Lv Q, Wang X, Wang Y, Nghiem PT, Le TVH, Vu TDH, Pamela DM, Armi S, Safwan H, Dwi RP, Mamad TMMF, Taora V, Titania S, Saskya S, Alliza A, Wulan S, Francisco HA (2011) Cross-country analysis of household adaptive capacity. Unpublished Research Report. Economy and Environment Program for Southeast Asia (EEPSEA), Singapore

Pittock B (ed) (2003) Climate change: an Australian guide to the science and potential impacts. Australian Greenhouse Office, Canberra

Roncoli C, Ingram K, Kirshen P (2002) Reading the rains: local knowledge and rainfall forecasting among farmers of Burkina Faso. Soc Nat Resour 15:411–430

Reyes CM (2012) CBMS-EEPSEA PEP-Asia CBMS Network Climate Change Vulnerability Mapping in the Philippines: A Pilot Study. Unpublished Research Report. Economy and Environment Program for Southeast Asia (EEPSEA), Singapore.

Stevens A (2014) CNN's Andrew Stevens returns to Tacloban more than six months after Typhoon Haiyan, 19 June 2014. http://cnnpressroom.blogs.cnn.com/2014/06/19/cnns-andrew-stevens-returns-to-tacloban-more-than-six-months-after-typhoon-haiyan/. Retrieved 13 Aug 2014

Tiwari KR, Rayamajhi S, Pokharel RK, Balla MK (2014) Determinants of the climate change adaptation in rural farming in Nepal Himalaya. Institute of Forestry, Tribhuvan University, Pokhara

Tuan TH, Duc TB (2013) Cost- benefit analysis of mangrove restoration in Thi Nai Lagoon, Quy Nhon City, Vietnam. Asian cities climate resilience working paper series 4, 2013

Tuan AT, Phong T, Tran HT (2012) Review of housing vulnerability implications for climate resilient houses. Discussion paper series, Institute for Social and Environmental Transition-International

UNEP (United Nations Environment Program) (2008) An overview of the state of the world's fresh and marine waters, 2nd edn. http://www.unep.org/dewa/vitalwater/index.html

Ward P, Shively G (2011) Vulnerability, income growth and climate change. World Dev 40 (5):916–927

Wijayanti P, Tono H, Pramudita D (2014) Estimation of flood river damage in jakarta: the case of Pesanggrahan river. Economy and Environment Program of Southeast Asia (EEPSEA), Los Baños

World Bank (2011) Vulnerability, risk reduction and adaptation to climate change: Indonesia. http://sdwebx.worldbank.org/climateportalb/doc/GFDRRCountryProfiles/wb_gfdrr_climate_change_country_pofile_for_IDN.pdf

Yueqin S, Zhu Z, Li L, Lv Q, Wang X, Wang Y (2011) Analysis of household vulnerability and adaptation behaviors to Typhoon saomai, Zhejiang Province, China. Economy and Environment Program for Southeast Asia (EEPSEA), Singapore

Yusuf AA, Francisco HA (2009) Hotspots! Mapping climate change vulnerability in Southeast Asia. Economy and Environment Program for Southeast Asia (EEPSEA), Singapore

Ziervogel G, Bithell M, Washington R, Downing T (2005) Agent-based social simulation: a method for assessing the impact of seasonal climate forecasts among smallholder farmers. Agr Syst 83(1):1–26

Ziervogel G, Bithell M, Washington R, Downing T (2013) Typhoon Haiyan: worse than hell. The Economist, 16 Nov 2013. http://www.economist.com/news/asia/21589916-one-strongest-storms-ever-recorded-hasdevastated-parts-philippines-and-relief. Retrieved 13 Aug 2014

Impact of Climate Change, Adaptation, and Potential Mitigation to Vietnam Agriculture

Trinh Van Mai and Jenny Lovell

Contents

Abstract

The Institute for Agricultural Environment of Vietnam conducted a research to study climate change impacts on agriculture, develop climate change adaptation measures, and identify mitigation options. Climate change impacts were

M. Van Trinh (✉)
Institute for Agricultural Environment, Vietnam Academy of Agricultural Sciences, Phu do, South Tu Liem, Hanoi, Vietnam
e-mail: maivantrinh@gmail.com

J. Lovell
Environmental Studies Department, University of California Santa Cruz, Santa Cruz, CA, USA
e-mail: jmlovell@ucsc.edu

W.-Y. Chen et al. (eds.), *Handbook of Climate Change Mitigation and Adaptation*,
DOI 10.1007/978-3-319-14409-2_87

assessed through past, current, and future conditions. Past information showed damages due to extreme weather events. Current production and climate conditions showed potential vulnerability. Future climate change scenarios and crop growth modeling predicted long-term impacts on crop production. The impacts of many adaptation measures and mitigation options were evaluated to reduce risks and losses from climate change and to reduce greenhouse gas emissions. Results showed that climate change has caused strong impacts on agriculture in Vietnam. It has caused severe damages in the past, and it is likely to cause high vulnerability and heavy crop production losses in the future. Flat lands experience stronger impacts than highlands, with the Mekong River Delta suffering the strongest impacts, followed by the Coastal Central area and Red River Delta. As a country strongly impacted by climate change, it has suffered many extreme events and disasters. The agricultural sector has developed suitable adaptation measures to cope with the extreme events. Vietnam maintains a high agricultural productivity not only to feed more than 70 million people but also to export a high amount of food and foodstuffs. Vietnam is the leading cashew nut exporter, second highest rice exporter, and third highest coffee exporter in the world. However, with extensive areas of rice paddy production and high animal populations, Vietnam's agriculture contributes substantial greenhouse gas (GHG) emissions. As a result, the Vietnamese agricultural sector is developing and implementing many mitigation options, such as alternative wetting and drying irrigation, biogas digestion, composting, and converting rice land to non-rice land. These policies target a 20 % GHG emission reduction by 2020 in comparison to the "business-as-usual" scenario.

Introduction

Climate Change in Vietnam

Climate change is projected to impact human and ecosystems health at global, regional, country, and local scales. Due to human-induced greenhouse gas (GHG) emissions to the atmosphere, climate change will cause a cascade of environmental changes. These effects will particularly impact agricultural production.

The main causes of climate change are the accelerated increase of GHG-emitting activities, combined with the exploitation of carbon sinks, such as forests, and the destabilization of natural carbon sequestration mechanisms, such as oceans. The Kyoto Protocol aims to prevent and stabilize the emission of six main GHGs including carbon dioxide (CO_2), methane (CH_4), nitrous oxide (N_2O), hydrochlorofluorocarbons (HFCs), perfluorocarbons (PFCs), and sulfur hexafluoride (SF6). Of these GHGs, the most abundant and concerning is CO_2, which originates primarily from anthropogenic fossil fuel combustion of coal, oil, and gas. The second most important GHG is CH_4, which is emitted from landfills, enteric fermentation, air-cooling systems, coalmines, and natural gas.

These emissions increase GHG concentrations in the atmosphere, causing global warming and higher temperatures; glacial melting leading to the loss of lowlands and islands; shifting borders between ecological and agroecological zones that have existed for thousands of years; altering atmospheric, hydrologic, and biogeochemical cycles; and altering the functional components and quality of the hydrosphere, biosphere, and geosphere. These impacts ultimately result in profound changes in natural and human system productivity.

Because Vietnam is considered one of the countries most strongly impacted by climate change Dasgypta et al. (2007), the Government of Vietnam has paid a lot of attention to this issue. Climate change and sea level rise scenarios were developed for Vietnam as a foundation for assessment of impacts on sectors and regions in order to take proper responsive actions.

Extreme Events in Vietnam

Temperature

Changes in annual temperature over the past 50 years in Vietnam have been inconsistent in different regions. Overall, the average annual temperature increased by approximately 0.5 degrees Celsius (°C). The maximum temperature change ranged between −3.0 °C and 3.0 °C, and the minimum temperature change varied between −5.0 °C and 5.0 °C compared with the historical average (MONRE 2012), similar to the global temperature trends.

Rainfall

During the past 50 years, rainfall tended to decrease in northern regions but increased in southern regions. In the northern climate zones, rainfall has changed insignificantly in the dry season (from November to April) but decreased between 5 % and 10 % in the rainy season (from May to October). In the southern climate zones, rainfall decreased dramatically in the dry season but increased from 5 % to 20 % in the rainy season (MONRE 2012). However, the overall trend of average annual rainfall is to decrease in north and to increase in the south. In particular, rainfall increased by about 20 % in the southern central region compared to other regions (Table 1).

Typhoon

Annually there is an average of 12 typhoons or tropical depressions that affect Vietnam. Of these storm systems, 45 % originate from the Eastern Sea and 55 % originate from the Pacific Ocean (MONRE 2012). The Central Coastal areas of Vietnam, lying between 16°N and 18°N, and the Northern regions above 20°N, have the highest frequency of typhoons and tropical depressions.

Drought

Drought, including monthly water scarcity and seasonal scarcity, has increased overall but inconsistently. Drought impacts shift depending on the region and weather station within the same climate zone. Overall, the number of hot days

Table 1 Increase of temperature and changing of rainfall during 50 years in agro-climate zones of Vietnam

Agro-climate zone	Temperature (°C)			Rainfall (%)		
	January	July	Year	Period November–April	Period May–October	Year
Northern West	1.4	0.5	0.5	6	−6	−2
Northern East	1.5	0.3	0.6	0	−9	−7
Red River Delta	1.4	0.5	0.6	0	−13	−11
North Central	1.3	0.5	0.5	4	−5	−3
South Central	0.6	0.5	0.3	20	20	20
Central Highlands	0.9	0.4	0.6	19	9	11
Mekong River Delta	0.8	0.4	0.6	27	6	9

Source: IMHEN (2010a)

increased significantly across the country, especially in the Central and Southern regions.

Sea Level Rise

Satellite data from 1993 to 2010 indicated that the sea level in the Eastern Sea is rising at a rate of 4.7 mm per year. This translates to an average sea level rise along Vietnam's coastline of 2.9 mm per year. However, the coastal areas in the Central regions and the Southwestern region have higher sea level rise than other coastal areas.

Climate Change and Sea Level Rise Scenarios in Vietnam

In 2009, the Ministry of Natural Resources and Environment (MONRE 2009) published the first edition of Climate Change and Sea Level Rise Scenarios. The report included low-resolution forecasting for the seven climatic zones of Vietnam. MONRE designated the Vietnam Institute of Meteorology, Hydrology and Environment (IMHEN) as the leading agency on detailing and updating climate change and sea level rise scenarios for Vietnam. In collaboration with other research institutes, government agencies, and departments, the team prepared updates in 2010 and developed climate models and selective statistical tools specialized for Vietnam. Through this collaborative work, MONRE published the second edition of higher-resolution climate change and sea level rise scenarios for Vietnam in 2012 (MONRE 2012). The report included details at regional scales and an additional climatic extreme section.

Vietnam Agricultural Production

Although the agricultural sector only accounts for 20 % of Vietnam's gross domestic product (GDP), the industry plays a crucial role in Vietnam's economy. The sector is

responsible for feeding more than 70 million people. While Vietnam has seen a substantial increase in industrial production, the agricultural production has continued to increase at a slower rate over the past 10 years. The average annual growth rate of agriculture remained at about 3.5 % but has decreased in recent years due to the severe effects of climate and soil conditions. For example, in 2005 it accounted for 19.3 % of the GDP, and in 2012 it had only increased to 19.67 % of the GDP.

The makeup of Vietnam's agricultural outputs shows no significant change in recent years. Food crops are the biggest proportion of Vietnam's agricultural sector, accounting for 74.6 % of the total production. Crops are followed by livestock production, which accounts for 23.8 %, and agricultural services makes up the remaining 1.58 %. Crop production still plays the biggest role by far. There was a very slight decrease of the proportion of crop production between 2005 and 2012, from 76.39 % to 73.81 %. During this time livestock production filled that gap with an increase from 21.95 % to 24.65 %.

Crop production is dominated by annual crops, which account for 83.4 % of the area under production, and perennial crops, which account for 16.6 %. Most of the annual crops are cereals such as rice, maize, and soybeans, which make up 78.5 % of the annual crop production area. The remainders are commodity and annual industrial crops, covering about 9.4 % of the annual crop area. Because Vietnam's agricultural sector is dominated by annual crops, it is a highly important resource for food and economic security. Annual crop systems are highly vulnerable to weather and will be strongly impacted with a more variable and changing climate (Table 2).

Impact of Climate Change on Agriculture

Agriculture Vulnerability

According to Patnaik and Narayanan (2005) and Iyengar and Sudarshan (1982), agricultural vulnerability can be calculated using an index based on three factors: exposure to a hazard, sensitivity, and adaptability. This index approach is shown in Table 3.

Damages in Agriculture Production Associated with Climate Change

Damages Due to Natural Disaster, Drought, and Flood

Vietnam is located on the eastern seaboard of Southeast Asia, an area frequented by natural disasters. Climate change adds complexity to this system, increasing the frequency of typhoons and extreme hot and cold weather, droughts, landslides, and flooding. According to historical meteorological data, an average of 6.96 typhoons hit Vietnam annually between 1950 and 2008. The number of typhoons increased over the years, and, more importantly, these typhoons occurred later in the rainy season between 1990 and 2008. Between 1950 and 1990, typhoons would normally

Table 2 Area dynamics of some key crops in Vietnam

Year				2000	2005	2010	2011	2012
Agriculture land				12,644.3	13,287.0	14,061.1	14,363.5	14,579.2
In Which	Annual crops			10,540.3	10,818.8	11,214.3	11,420.5	11,481.5
	In which	Cereals crops		8399.1	8383.4	8615.9	8777.6	8872.3
		Rice		7666.3	7329.2	7489.4	7655.4	7753.2
			Spring rice	3012.3	2942.1	3085.9	3096.8	3124.3
			Autumn summer rice	2292.8	2349.3	2436.0	2589.5	2659.1
			Summer rice	2360.3	2037.8	1967.5	1969.1	1977.8
		Maize		730.2	1052.6	1125.7	1121.3	1118.3
		Soybean		2000	2005	2010	2011	2012
		Peanut		244.9	269.6	231.4	223.8	220.5
		Sugarcane		302.3	266.3	269.1	282.2	297.9
		Annual industrial crop		778.1	861.5	797.6	788.2	727.2
	Perennial cops			2104.0	2468.2	2846.8	2943.0	3097.7
	In which	Industrial		1451.3	1633.6	2010.5	2079.6	2215.0
		Fruit tree		565.0	767.4	779.7	772.5	765.9

Source: GSO (2013)

Table 3 Agriculture and aquaculture production from seven different agroecological zones in 2010

Group of factor	Parameter	Unit	Year	Relationship	RRD	NM	NCC	SCC	HL	SE	MRD
Exposure condition	Average max temp	°C	2010	+	26.4	25.7	29.1	30.8	30.5	32.1	31.9
	Average min temp	°C	2010	+	22.0	21.6	23.9	24.1	22.3	24.3	25.2
	Trend or temp increase within 50 years (1958–2007)	°C	2010	+	0.60	0.55	0.50	0.30	0.60	0.55	0.60
	Annual rainfall	mm	2010	+	1614.2	1450.6	2785.3	2526.5	1287.3	1162.7	2244.4
Sensitivity condition	Percentage of agricultural land	%	2010	+	38.268	14.913	15.842	17.769	29.775	46.036	63.066
	Water surface area	1000 ha	2010	+	124.900	69.860	54.500	25.100	11.100	61.700	727.400
	Population	head/km^2	2010	+	939	117	189	289	95	502	426
	Poor household	%	2010	+	8.3	29.4	20.4	20.5	22.2	2.3	12.6
	Coastal length	km	2010	+	267	250	639	1010	0	447	684
	Jobless %	%	2010	+	2.61	1.21	2.94	2.94	2.15	3.91	3.59
	Woman %	%	2010	+	50.72	50.11	50.46	50.79	49.33	51.25	51.28

(*continued*)

Table 3 (continued)

Group of factor	Parameter	Unit	Year	Relationship	RRD	NM	NCC	SCC	HL	SE	MRD
Adaptability condition	Agricultural value	Bil. VND	2010	–	4235	510	2771	7060	157	3071	34,991
	Rice yield	Tons/ha	2010	–	5.92	4.64	5.07	4.82	5.07	4.49	5.43
	Maize yield	Tons/ha	2010	–	4.52	3.32	3.99	3.99	4.92	5.2	5.29
	Peanut yield	Tons/ha	2010	–	5.28	8.85	2.04	2.04	2.93	5.16	3.1
	Fishing production	Tons	2009	–	10,744	175,051	219,583	452,213	3412	412,116	863,289
	Raising aquaculture production	Tons	2010	–	50,162	322,146	89,728	58,198	1502	91,727	1,838,638
	Raised fish production	Tons	2010	–	4859	243,818	62,437	12,325	14,702	62,433	1,419,010
	Raised shrimp production	Tons	2010	–	294	14,511	13,713	33,073	61	19,664	307,070
	Aquaculture export value	Bil. VND	2010	–	463.6	3843	2538.5	5080	146.3	4119.5	33,891.1

occur in August. However, between 1990 and 2008, they appeared regularly in October and November, much later in the season. There are also more extreme typhoons with higher intensity affecting the whole country. Historically, the highest typhoon speed was between 118 and 133 km per hour (km/h), which is an intensity of 12 on the typhoon Beaufort scale. In recent years typhoons have reached speeds of between 134 and 183 km/h, an intensity of 13–15. As a consequence of these more extreme events, there have been stronger impacts on agriculture production.

Data in Table 4 indicates that the average annual damage to agriculture during the period between 1995 and 2007 was 781.74 billion VND (equivalent to 54.9 million USD). This accounts for 0.67 % of agriculture's GDP (comparing to the 1.24 % GDP loss of all sectors caused by natural disasters). While agricultural production is a small portion of the country's income, the industry feeds more than 71.41 % of the population. Any damages to agriculture caused by natural disasters resulted in severe impacts on poor people, for whom it is very difficult to recover from a shock (Table 5).

Damages Due to Sea Level Rise

Without major action such as dyke reinforcements and improved drainage systems, a 1 m rise in mean sea levels along the coastline of Vietnam would cause an estimated threat of inundation to 17,423 km^2 (km^2) or 5.3 % of Vietnam's total land area (IMHEN 2010a). Specifically, it would threaten 39 % of the Mekong Delta, 10 % of the Red River Delta, and over 2.5 % of the Central Coast provinces. Moreover, 33 out of 63 provinces and municipalities, or 5 out of 8 economic regions, are threatened by severe inundation (IMHEN 2010a). The effects of sea level rise on saline water intrusion are significant, especially for the Mekong River Delta. In the period between 1980 and 1999, the 4 % salinity level reached 22.0 kilometers

Table 4 Damages in agriculture caused by natural disasters in Vietnam (1995–2007)

	Agriculture		All sectors		
Year	VND (million)	USD (million)	VND (million)	USD (million)	(%)[a]
1995	58,369	4.2	1,129,434	82.1	5.2
1996	2,463,861	178.5	7,798,410	565.1	31.6
1997	1,729,283	124.4	7,730,047	556.1	22.4
1998	285,216	20.4	1,797,249	128.4	15.9
1999	564,119	40.3	5,427,139	387.7	10.4
2000	468,239	32.2	5,098,371	350.2	9.2
2001	79,485	5.5	3,370,222	231.5	2.4
2006	954,690	61.2	18,565,661	1190.1	5.1
2007	432,615	27.7	11,513,916	738.1	3.8
Average damage/ year	781,764.11	54.9	6,936,716.6	469.9	11.6
Loss in GDP (%)	0.67	–	1.24		

Source: MARD (1995–2007)

[a]Percentage rate of agricultural GDP loss and total GDP loss

Table 5 Impact of extreme events on agriculture

Item	Unit	2001	2002	2003	2004	2005	2006	2007	2008
Total flooded rice area	Ha	132755.15	51025.4	210514.2	433790.7	537133.3	139230.8	173830.2	146945.5
+ Strong damaged	Ha	6678	2846	22987	9035.3	0	5370	4709.7	29932.35
+ Lost	Ha	15847.8	2669.2	41076	105336.5	30372.1	21348.1	33063.8	44627.54
Total flooded non-rice area	Ha	85528	43761.94	52617.9	44093.6	161455.3	122459.8	215059.2	325614
+ Strong damaged	Ha	4600	0	0	195	11	749.2	951.24	0
+ Lost	Ha	3027	10434	5924.9	3071.9	1709.5	23488.07	37767.8	189395.1
Flooded rice bed	Ha	3158.5	5.1	4.2	5327	0	0.5	2115	0
+ Lost	Ha	302	2.5	1.7	75	0	0.5	0	601.75
Cereal wetted and lost	Ton	17237	46065	43650.1	1029.5	6915.2	13345.5	79118.1	73392.9
Seed wetted and lost	Ton	287.7	726.025	311	442.01	1128.038	2565	8569	902.2
Lost industrial crop area	Ha	4796	33	831.1	0	306	1825.8	0	0
Damaged industrial crop	Ha	48824	1655	6939.4	505	26171.2	68842	16293.78	63753.33
Damaged sugarcane	Ha	17296	1368	11638.5	990.2	1829	3064	33769.1	6302.2
Damaged planted forest	Ha	5328	7	738.2	302	23524	34028.4	5403.88	3525.3
Falling tree	Tree	786995	13984	467063	13975	4014390	27549424	3100042	735191
Damaged fruit tree	Ha	51221	33637.3	7910.8	3881.5	66	86433	30647.16	5395.8
+ Died	Ha	7	201	500	0	0	3000	1761	0
Channel slide	M	282542	731124	73263	702904	166448	106720	994853	628230.8
Brocken bridge and water inlet	Piece	1335	638	3	7	70	140	132	450
Brocken water resources works	Piece	240	23	26	39	113	61	42	376
Damaged small water resource works	Piece	620	451	326	148	750	117	1926	1438
Lost water plank	Piece	974	509	669	981	36	377	1276	943
Flooded irrigation station	Piece	180	29	92	19	47	20	89	184
Sunk and lost board	Board	2033	26	184	97	382	1151	266	226
Damaged board	Board	344	0	1	122	89	1095	163	52

Sources: Department of Natural Disaster Management, MARD 2001–2008

(km) inland on the Red River. With 1 m mean sea level rise, by the end of the twenty-first century, the 4 % contour line will penetrate 4.5 km further inland into the Red River (IMHEN 2010b; Table 6).

Based on projected impacts due to sea level rise scenarios developed in 2009 and updated in 2012 by MONRE (2009, 2012), potential loss in rice production (rice equivalent) of the Mekong Delta will be about 7.6 million tons per year, equivalent to 40.52 % of the total rice yield toward 2100. If climate change and sea level rise happen as predicted in the scenarios and if the average annual yield of rice production remained unchanged, Vietnam would face serious problems of food shortages in 2100 with a 21.39 % rice yield lost.

Damages Caused by Changes in Climate Factors on Crop Production

For this damage, the impact of climate change on crop production was determined using crop growth models performed by the Institute for Agricultural Environment (Mai Van Trinh and Nguyen Hong Son 2011). The model used long-term climate factors such as maximum temperature, minimum temperature, rainfall, sunshine hour, humidity, and evaporation as the data inputs for the model. Potential rice, maize, and soybean yield in the spring and summer seasons, as well as yield changes due to altered climatic parameters, were determined in seven different ecological regions. Two provinces were selected for each region (Table 7).

Table 6 Forecast of rice yield loss according to 1 m sea level rise scenarios in MDR

Province	Total area (1000 ha)	Flooded area (1000 ha)	Flooded agricultural land (1000 ha)	Average rice yield (ton/ha/season)	Rice season (season)	Rice yield loss (1000 t)
Ben Tre	231.5	113.1	81.7	4.06	2.0	663.7
Long An	449.2	216.9	160.0	4.08	2.0	1305.3
Tra Vinh	222.6	102.1	83.5	4.43	2.0	739.9
Soc Trang	322.3	142.5	116.6	4.93	2.0	1150.1
Ho Chi Minh	209.5	86.2	39.2	3.17	2.0	248.6
Vinh Long	147.5	60.6	49.2	4.77	2.0	468.9
Bac Lieu	252.1	96.2	80.4	4.66	2.0	749.0
Tien Giang	236.7	78.3	60.1	4.90	2.0	588.5
Kien Giang	626.9	175.7	112.8	4.61	2.0	1040.5
Can Tho	298.6	75.8	64.6	5.18	2.0	669.6
Total	**2996.8**	**1147.4**	**848.1**	**44.79**	**2.0**	**7597.4**

Source: Tran Van The et al. 2010
MDR Mekong Delta River

Table 7 Damages of climate change on major crops of Vietnam

Parameter	2030 forecast		2050 forecast	
	Production (1000 t)	Percentage (%)*	Production (1000 t)	Percentage (%)*
1. Rice	**−1.966,4**	**−8.18**	**−3.634.7**	**−15,06**
Yield loss	−1.966,6	−8.10	−3.634,7	−14.97
Spring rice	−1.222,8	−7,93	−2.159,3	−14,01
Summer rice	−743,8	−8,40	−1.475,4	−16,66
2. Maize	**−500,4**	**−18,71**	**−880,4**	**−32,91**
3. Soybean	**−14,38**	**−3,51**	**−37,01**	**−9,03**

*Compare to 2008 production

IAE simulated crop yield for the years 2030 and 2050 under climate change conditions compared with normal climatic conditions. The simulation showed that rice yield will be reduced by 8.18 % and 15.06 % in 2030 and 2050; maize yield will be reduced by 18.71 % and 32.91 %; and soybean yield will be reduced 3.51 % and 9.03 %, respectively (Mai Van Trinh and Nguyen Hong Son 2011).

Quantify the Impacts Through Calculating Indexes

Vulnerability Index

Vulnerability indices of the agricultural sector for seven ecological zones were calculated following Patnaik and Narain (2005) and Iyengar and Sudarshan (1982). Results (Fig. 1) show that agricultural production in the Mekong River Delta and the South Central region are the most impacted by climate change with the highest vulnerability score. Their vulnerability is due to high annual rainfall, high average annual temperatures, high unemployment rate, long coastal exposure, and a large proportion of agricultural land.

Damage Index

Table 5 shows impacts of extreme events on agriculture, and Fig. 1 shows a damage index from 2001 to 2008. From these estimates, IAE concluded that South Central, North Central, and the Mekong River Delta were the most damaged by climate change. The Central Highlands, Northern Midlands, and Mountainous Areas are less affected. Particularly, in 2010 and 2011, there were 10 and 6 typhoons, respectively. These typhoons hit the North and South Central regions, causing extreme property damage, human injuries, and deaths.

Impact on Crop Production

Based on climatic changes such as temperature and rainfall under the scenarios from 2020 to 2025 and crop yields under regular cultivation conditions, a crop production impact index for seven ecological zones in Vietnam was calculated and presented in Fig. 1. The Red River Delta, Mekong River Delta, and North Central areas are the top three regions that scored the highest on the impact index.

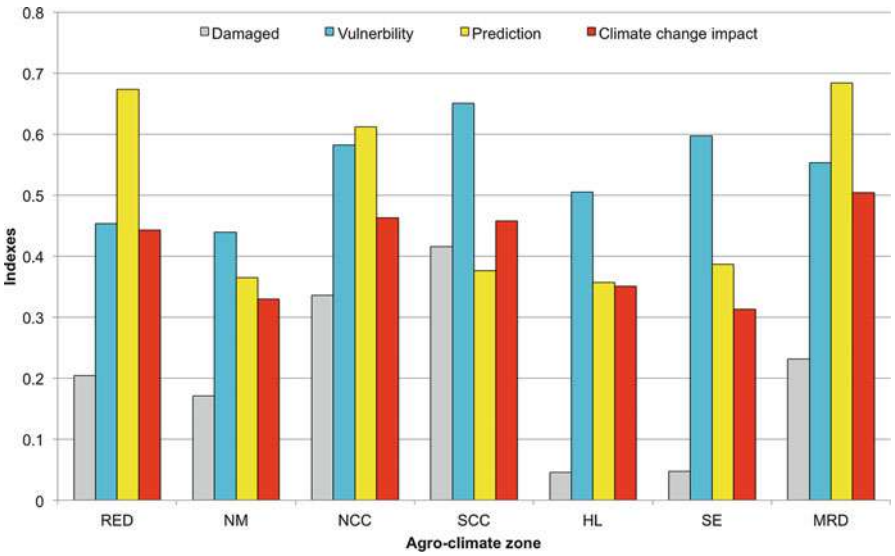

Fig. 1 Vulnerability indices, damages, crop yield prediction, and climate change impact

Indicators for Climate Change's Impact Assessment on Agricultural Sectors

An average of three indices were used as indicators to calculate impacts of climate change on different agricultural zones: a damage index, potential impact index (vulnerability), and forecasted impact index (impact of crop production). According to these indices, climate change will impact the Mekong River Delta the most, followed by the North and South Central Coast regions, and the Red River Delta. This result is also in line with the historical documentation of climate change in the regions. It can be used as a validated model to fully understand the impact of climate change and to develop adaptation measures and mitigation options for that region.

Climate Change Adaptation for Crop Production

Experiences in Climate Change Adaptation in Vietnam

In Vietnam, agricultural production is widely distributed in all ecological zones with climatic, geographic, soil, and crop characteristics. Because of this diversity, it is necessary and important to develop climate change adaptation measures for sustainable agricultural production in each region.

– *Northern Midlands and mountainous areas*: Rainfed crops that demand less water (such as sugarcane, cassava, and edible canna) are recommended to replace paddy rice. Additionally, upland rice and other crops that demand less water are

recommended for sloping land with the purpose of reducing dependence on the irrigation system and preventing soil erosion and degradation. In specific microecological zones in the high mountain areas with temperate climatic condition, Mai Van Trinh et al. (2014) recommend that farmers plant high-value medicine and herbal plants, such as black cardamom. This approach allows growers to gain the economic benefits of agricultural production while reducing impacts of extreme weathers, such as freezes and droughts, on perennial industrial crops. Farmers can also apply soil conservation methods on sloping land such as terrace farming, contour farming, windbreak, shading plants, and agro-forestry (Ha Dinh Tuan 2005). These valuable experiences can be transferred to other regions with the same conditions, facing the same climate change impacts.

- *Red River Delta*: The key crops of this region are paddy rice and annual industrial crops. Regarding climate change adaptation, changing the crop rotation, crop type, cropping calendar, and water supply are among the most popular methods to reduce risks from extreme events such as, drought, flood, and salinization. Specifically, for paddy rice production in the Red River Delta, the crop calendar can be changed with late transplanting of spring rice to avoid cold weather and increase rice yield. More importantly, changing of the crop calendar for an earlier summer season allows winter crops after the double rice crop. The farmers can achieve a better harvest with this modified crop calendar.
- *Central Coastal areas*: Adaptation measures in the Central Coast areas mainly focus on drought and desertification prevention for high water demand crops. Drought-tolerant crops are introduced to suitably grow in limited water supply conditions. New water sources, new farming methods, and modified cultivation techniques have also been introduced and implemented successfully in the region. For example, there is a new crop rotation including an annual rice, sweet potato, and cassava crop (Binh Dinh PPC 2010).
- *Southeast region:* As a semiarid ecological zone, adaptation measures in the Southeastern region mainly focus on changing the crop pattern and preventing drought for key crops such as cashew, peanut, sesame, sugarcane, and other annual industrial crops. IAE-ICRISAT (2010) showed that farmers in this region also want to reduce the rice production area and introduce other upland crops with lower water demand and higher profit values. These new crops, such as grapes and apples, improve grower's incomes and are more sustainable in drought conditions.
- *Central Highlands*: The main crops of the Central Highlands region are coffee, pepper, rubber, tea, and fruit tree. Most of adaptation measures aim to reduce water stress for these crops. In the same time, legume cover crops, fruit trees, and intercropping between annual crops and perennial crops should be implemented. These techniques increase income while maintaining soil moisture, protecting soil from erosion, and saving irrigation water.
- *Mekong River Delta:* As the most agriculturally productive region of the country, many adaptation measures, tools, and techniques are transferred to farmers in the Mekong River Delta. For example, extension workers promote suitable crop

selection, changing crop patterns or rotations, and integrating crop management to optimize crop production and reduce investment cost (Pham Quang Ha 2013).

Climate Change Adaptation Technologies

Prioritized Climate Change Adaptation Technologies in Agriculture

Plant Breeding

Using annual data on key crops between 1995 and 2008, IAE notes that rice, cassava, soybean, and sugarcane yields increased significantly (Table 8).

Yield increase under climate impact is a sign of strong adaptability in terms of food security. With the exception of a reduction in sweet potato production, yields from rice, maize, soybean, and peanut increased greatly between 1995 and 2008. Specifically, annual yields of rice, maize, and cassava production increased by 13.8, 3.3, and 5.0 million tons, respectively. The side benefits from yield improvements include increased photosynthetic biomass production, and therefore increased carbon sequestration in belowground biomass.

Climate change also causes changes in the frequency and severity of precipitation surplus and deficits. For example, Vietnam is experiencing a high number of rainfall events during the rainy season, which can lead to flooding and flash flooding. Conversely, less rainfall is associated with drought and salinization and works to increase the effects of sea level rise and saltwater intrusion. Observed data shows that saltwater intrusion moved inland from approximately 20 to 30 km from the shoreline in the Northern coastal line and between 50 and 70 km in the Southern coastal line (Mai Van et al. 2014). For this reason, the government encourages farmers to introduce and implement flood-, drought-, and salt-tolerant varieties. Many of rice varieties were introduced and successfully implemented in practice,

Table 8 Increase of crops' yield during 1995–2008

Unit, 1000 t							
Crop	RRD	NMR	CCR	CH	SE	MRD	Whole country
1. Rice	1568.4	1228.6	2238.0	508.3	372.8	7857.5	13,773.6
2. Maize	172.7	1.150.6	674.9	981.5	229.0	142.6	3351.3
3. Sweet potato	−275.0	25.8	−288.6	55.8	0.9	119.2	−361.9
4. Peanut	51.0	55.1	100.3	7.9	−31.1	16.1	199.3
5. Soybean	66.8	41.0	4.4	33.3	−7.8	−7.4	143.1
5. Cassava	23.1	721.7	2206.2	2072.4	2133.7	27.2	7184.3
6. Sugarcane	−77.5	858.5	3605.8	1172.3	169.2	−311.4	5416.9
7. Coffee	0.0	4.4	10.2	821.9	1.3	0.0	837.8

RRD Red River Delta, *MRD* Mekong River Delta, *CH* Central Highland, *SE* South East

such as rice varieties of OM5464 (Tran Thi Cuc Hoa 2011), OM5629, OM5981, and OM7368 (Lang et al. 2011).

Water-Saving Irrigation (WSI)

One of the impacts of climate change on agriculture is reducing available irrigation water. Many reservoirs in the upland areas tend to run out of water before the rainy season comes, causing drought late in the dry season. Hence, water-saving irrigation helps to save water, better contribute water resources for the whole season, and secure crop harvesting in the dry season.

System of Rice Intensification (SRI)

SRI was first introduced in Vietnam in 2003 in three provinces (Hanoi, Hoa Binh, Quang Nam). SRI uses the following practices: (i) using young seedlings (2.5 leaves or 8–15 days old); (ii) transplanting one plant per hill (instead of three or four); (iii) irrigating with a minimum of water (a thin water layer of 1–2 cm deep); (iv) applying more organic fertilizers and reducing nitrogen fertilizer; and (v) hand weeding (Uphoff 2002). These practices could be modified to suite local conditions. SRI practices were highly recognized and accepted by farmers and local authorities in the Northern region. The Ministry of Agriculture and Rural Development (MARD) officially adopted SRI as a good farming package by issuing Decision Number 3062/QĐ-BNN-KHCN on October 15, 2007. In 2011, 21 of 33 provinces in the Northern region applied and implemented SRI with total area of 185,065 ha and 1,070,384 participant farmers (PPD 2011).

Produce Compost from Crop Residues

Previously, crop residues or by-products were mostly used as fuel for cooking, roofing material, animal fodder, or tilled back into the fields. Recently, because rural areas are urbanizing, the traditional rice straw roof is being replaced by brick and concrete; wood cooking stoves are being replaced by gas, electricity, and coal; and crop residues are becoming obsolete. Burning these residues after harvesting is becoming popular practice but causes a serious air pollution and GHG emission problem. One of the suitable solutions is to produce compost using effective microbials.

Rice straw is shown to have many positive effects when used as a crop residue. Pham Thi Nhung (2006) carried out field experiments during the winter maize seasons of 2004 and 2005 with fertilizer application of 8 t manure per hectare (ha); 150 kilograms (kg) of nitrogen (N), 90 kg of phosphorus pentoxide (P_2O_5), and 90 kg of potassium oxide (K_2O) per ha; and 5 t of dried rice straw per ha. Results indicated that rice straw increased rice yield by 6–8 % compared to the control of no rice straw application. Rice straw supplementation with 10 % N, 10 % P2O5, and 10–20 % K_2O increased maize yield by 7–8 % above the control treatment. Increasing the supplement to 30–40 % K_2O does not change the maize's yield, and at 50 % the maize's yield's reduced 4 %. This illustrates that rice straw is a nice complement to input supplementation, increasing the efficiency and reducing the amount of nitrogen, potassium, and phosphorus needed.

Reduced Tillage

On sloping land: Tillage is one important field activity for cultivating maize, cassava, pachyrhizus, and edible canna in the central and mountainous provinces. Adoption of reduced tillage has significantly expanded with labor-saving benefits and introduction of better fertilizer and herbicide use (CYMMIT 1991). For example, in Son La Province (Northwest region), over 23 % of the area under production applied reduced tillage. This includes more than 30,000 ha out of total 130,000 ha of maize production. Farmers were interested with this farming technique, and they learned to practice it. The technique has also been widely implemented in five other mountainous provinces.

On flatland: No till is mainly applied in the winter crops after a double rice crop. For example, no till is used in soybean, potato, and maize by directly sowing the seeds on soil surface after harvesting of the summer rice and then covering the seed with rice straw. This farming technique has gradually expanded and is implemented in between 25 % and 60 % of the total winter soybean and potato crops in the Red River Delta (MARD 2009).

Biochar Application

Biochar, or charcoal, is produced by pyrolysis of biomass under the absence of oxygen or oxygen-limited conditions. Many scientists *consider* biochar "black gold" in agricultural production. Biochar contains carbon in stable pools with slowed decomposition that transforms to active forms (CO_2, CH_4, and other GHGs) recommend to use (Feng et al. 2012; Liu et al. 2011). Therefore, biochar has high potentials in improving soil properties by increasing the soil's water- and nutrient-holding capacity and protecting soil microorganisms and in improving yields. More importantly, biochar is considered an effective approach to carbon sequestration by storing carbon permanently in the soil. The agricultural sector of Vietnam produces huge amounts of crop residues which can be pyrolyzed to become biochar. With an annual production of 61 million tons of rice straw and other annual crop residues (IAE 2012), there is a large source of inputs for biochar production in Vietnam.

Soil Surface Cover

Farmers cover soil surface in well-drained land (on terraces); high-evaporative, arid land; and sandy land with low water-holding capacity. The materials for covering include rice straw, tree leaves and trunks, and nylon. The technique is widely applied in the Central region of Vietnam. The area is characterized by large areas of sandy soil with low soil organic matter, nutrient content, high vulnerability to drought, and low crop yield. Surface cover helps seeds to germinate more fully and faster, prevents weeds from emerging, maintains soil moisture, and reduces nitrogen volatilization. Soil cover is most often used on peanut, soybean, and sugarcane fields (Le Duy Thanh 2004).

Change Land Use from Rice to Fruit Tree

In many areas, rice is not the most suitable crop for the conditions. For example, in areas where land is elevated and unfavorable for irrigation infrastructure, soil fertility

is low, or soil is waterlogged due to a depression or sea level rise, usually rice yields are very low. One of the effective measures is converting rice to fruit tree orchards, especially in Mekong River Delta. Large areas of lowland paddy rice were shifted into fruit-fish systems, sculpting the land into alternating bunches of fruit trees and ditches for fish ponds.

Change Intensive Rice to Rice and Aquaculture

(i) *Paddy rice and fish/shrimp system*
Fish/shrimp systems are a growing trend in Mekong River Delta as an option for breaking away from solely rice farming. The old systems include an annual triple rice crop (three rice seasons per year) or double rice crop (two rice seasons per year). Because of changing climate and hydrological conditions, the low-elevation areas were deeply flooded and could not support the triple crop. Rice crops that are flooded at harvest time maintain low and unstable yields, usually in the rainy season in mid-September. In the fish/shrimp systems, the flooded land is used for raising fish or shrimp instead of growing rice in the late rainy season (third or second rice season). This land use is growing quickly in Mekong River Delta. As of 2008, there were 120,000 ha under fish/shrimp production. This trend is in line with the MARD policy to expand this land use type in Mekong River Delta to adapt to climate change and diversify production.

(ii) *Rice/duck system*
The rice/duck system has been implemented for a long time in the Mekong River Delta. The duck populations in the region as of 2010 reached 20 million (GSO 2011–2014), 70 % of which was released into the rice fields to seek food left after harvesting. However, in recent years, as the severe impacts of bird flu, field-free duck breeding is not recommended. It is recommended that ducks be raised in planned areas to reduce disease outbreaks (Table 9).

Climate Change Mitigation

GHGs Emission in Crop Production

Because agriculture is a leading sector for GHG emission reduction, MARD issued a plan for reducing GHG emissions by the year 2020 (Decision No. 3119, 2011). The plan focuses on the following solutions:

(i) *Applying advanced farming techniques.* This set of practices is aimed at rice production and includes water-saving irrigation such as SRI. Another part of the advanced farming techniques program is the “three reductions and three gains” program, which includes a reduction of seed, nitrogen fertilizer, and other chemical inputs and gains of crop yield, product quality, and economic

Table 9 Potential prioritized mitigation practices in agriculture

#	Practice	Properties	Prospect
1	Genetics	Increase carbon sequestration, increase biomass and yield Increase flood tolerance, salt tolerance, and drought tolerance	High
2	WSI (water-saving irrigation)	Water saving and reduction in irrigation Increase fertilizer use efficiency Reduce CH_4 emission	High
3	SRI	Reducing costs on seeds, fertilizers, pesticides, and irrigation Reduce CH_4 emission	High
4	Production of organic fertilizers from agricultural residues/by-products	Replacement of inorganic fertilizers Reduce emission of N_2O (from dry land) and CH_4 (from flooded land) Reduce environmental pollution from burning agricultural residues or agricultural waste	Medium
5	Biogas	Prevent environmental pollution from livestock production Reduce N_2O emission Collect biogas to replace other fuels (wood, coal, gas, etc.)	High
6	Minimum cultivation	Reduce soil erosion, soil run-off, and carbon loss Reduce costs on tillage and plowing	Medium
7	Biochar	Recovery of 50 % carbon in crop biomass Stabilized carbon in soil for long time and reduce emission Significantly improve soil properties including fertility Increase fertilizer efficiency, reduce N_2O emission Use as alternative fuel	Medium
8	Soil cover	Reduce soil erosion and carbon loss Reduce N_2O emission Save irrigation, fertilizers, and weeding labor Reduce using pesticides	Low
9	Conversion from rice production to fruit tree plantation	Reduce CH_4 emission	Medium
10	Conversion from three rice season system to two combined rice/fish/shrimp system	Increase efficiency and bring more benefit of lowlands	Medium

benefit. This strategy is nicknamed the "3R3G." Another campaign is called the "1M5R" and focuses on reducing adoption of one standard seed variety and reductions of overall seed inputs, nitrogen fertilizer, chemicals, water, and postharvest loses. Alternate wetting and drying irrigation (AWD) is also encouraged to save water and reduce GHG emissions.

AWD application has been shown to reduce the global warming potential (GWP) of rice production. Pandey et al. (2014) reported that AWD irrigation reduced methane emissions by approximately 67–71 %. While there is a slight increase in nitrogen oxide, overall, there is a 62–67 % reduction in CO_2 emissions.

(ii) *Change land use type from rice to short-duration industrial crops*

The total area of rice cultivation in Vietnam was 7.89 million ha (about 4.1 million ha rice land) in 2013 (GSO 2011–2014). However, according to development planning for the agricultural sector Mard (2010), rice cultivation will see a reduction to 3.8 million ha (about 7.0 million ha of cultivated rice land). Firstly, 0.266 million ha of rice cultivation will be converted to higher value annual industrial crops to reduce GHG emissions. This transition is expected to decrease emissions by 1.29 million tons of CO_2e (2.27 %).

(iii) *Change low yield/benefit rice land to high-value aquaculture (shrimp, fish)*

The main advantages of rice and fish/shrimp farming systems include obtaining higher economic benefits, reducing pesticide costs by 48–56 %, and increasing income by approximately $1375 per ha. According to MARD, in the Mekong River Delta, more than 600,000 ha of rice cultivation area could be converted to rice and fish/shrimp systems in order to reduce GHGs emission by 5.37 %, equivalent to a reduction of 3.06 million tons of CO_2.

(iv) *Effectively use rice straw*

Rice straw is increasingly going unused after the harvest, which poses a problem for disposal. However, the unused straw could represent a potential source for efficient reuse of waste materials and a reduction in GWP for crop production. It is reported that straw compost has also shown potential for maintaining N_2O emissions at a low level (Yao et al. 2010).

Pandey et al. (2014) carried field experiment in Red River Delta of Vietnam and found that the reuse of composted rice straw can reduce methane emissions by about 25–29 %, reduce nitrogen oxide by 5–20 %, and reduce CO_2 emissions by 24–28 %. In addition to compost, biochar that is pyrolyzed from rice straw Yanai et al. (2007) can improve soil fertility and crop yield (Table 10).

Identify and Analyze Technologies to Reduce GHG Emission in Agriculture

GHG reduction technologies are primarily applied in rice cultivation, in livestock breeding, and in altered fertilizer application on arable land.

Table 10 Potential GHG emission reduction from some crop production (Gg of CO_2e)

			Crop			
Measure	Rice	Maize	Soybean	Peanut	Cassava	Sugarcane
Business as usual (BAU)		1.020	0.177	0.239	0.089	1.270
Compost	9078.29	0.589	0.029	0.113	0.014	0.625
Biochar	3755.06	0.255	0.006	0.020	−0.001	0.897
Short-duration variety	9633.38		0.060	0.243	0.090	1.300
ICM			0.074	0.239	0.086	1.205
3R3G	7230.52					
NH_4SO_4	7858.27					
SRI	1304.26					

Source: Mai Van Trinh et al. 2012

Rice Production

Rice production is the most important agricultural subsector in Vietnam. According to Mai Van et al. (2014), GHG reduction technologies in rice cultivation should meet the following requirements: (1) increase rice yield, (2) increase economic benefits for farmers, (3) decrease investment costs, and (4) be sustainable.

Currently, two promising GHG reduction technologies in rice cultivation are being studied: irrigation management and nutrient management.

Irrigation management includes irrigating less, draining the soil, and keeping the soil humid during rice growth stages. The key stage to keep the soil humid is after top tillering until just before flowering and after ripening. By using this combination of irrigation management, experiments have shown a decrease in CH_4 emissions from rice as well as increased soil aeration and, hence, increase plant available nutrient. This option could be easily applied in lowlands with sufficient irrigation.

There are several options for mitigating GHG emissions using nutrient management techniques. Results of studies on emissions from rice fields indicate that both organic manure and nitrogen fertilizers increase CH_4 and N_2O emissions. Thus, increasing manure application needs to be paired with draining the soil to reduce CH_4 emission and increase N fertilizer use efficiency. By applying the correct N fertilizer amount to meet plant requirement in each growing stage, studies show reductions in N_2O emissions. Other mitigation options include changing the land use type from rice to upland crops; introducing drought-, flood-, and salt-tolerant crops; shifting the crop calendar; and implementing SRI. Farmers can also combine N fertilizer management and crop management to practice integrated crop management (ICM). Based on the program of integrated pesticide management (IPM), ICM aims to optimize water, soil, and solar conditions to optimize potential yield, reduce yield gaps, and lower GHG emissions.

Irrigation management is considered the most important approach for reducing CH_4 emissions from rice fields. Approaches can be implemented by mid-season drainage, AWD irrigation, and field expose-shallow irrigation (Table 11). All these

Table 11 Prioritized climate change mitigation technologies in agriculture

No.	Technology	Description	Prospect
1	Suitable nitrogen fertilization rate	Establish nitrogen formula suitable for soil property and crop characteristics; deep fertilizing, plant winter crops for better use of nitrogen residues from previous season	
2	Field water drainage during rice growth stages	Drain field water out during two stages: tillering and ripening in order to reduce CH4 emission and increase rice yield	
3	Surface expose drying and irrigation	Application cycle of shallow irrigation and water drain out (20–25 day/cycle) after transplanting in order to reduce CH4 emission and increase rice yield	
4	Application of short duration varieties	Application of short-term rice varieties (approximate 100 days of growth duration) with high yield and high disease and pest resistance to replace long duration varieties (more than 140 days of growth duration)	
5	Nutrient improvement by oriented additions of animal's feed	Oriented addition of nutrients in animal's feed (BMU cakes, urea, etc.)	
6	Application of stimulants in livestock production	Applying stimulants such as bovine somatotropin (BST) and anabolic steroid to improve and increase meat and milk quality and yield as well as reduce CH4 emission	
7	Biogas	Store livestocks' wastes under anaerobic condition to generate CH4 (biogas) for fuels. By-products from biogas are used as fertilizers or animal's feed	
8	Crop rotation to reduce soil organic carbon (SOC) loss	Applying conservation farming to maintain soil's water content. Planting legumes to increase soil's nitrogen fixation. Applying crop rotation suitable for soil properties and climate conditions	
9	Plant cover crops on sloping land to reduce soil erosion and maintain soil moisture	Planting different cover crops following contour line on sloping land. Digging holes to prevent soil erosion and recover soil from water run-offs	
10	Nutrient improvement by mechanical and chemical processes	Processing animal's feed through mechanical methods (grinding and blending) and chemical methods (fermentation, compost, micro-nutrient increase, etc.) in order to increased iggestiverate and meat yield	
11	Gene modification for livestocks	Apply gene engineering to create new livestock varieties with ability of rapid growth, high disease resistance	

mitigation options are suitable with local conditions but prioritized following the technology needs assessment (TNA) procedure (Quach Tat Quang et al. 2012).

Fertilization

The emission of N_2O is related to nitrogen in the soil and N fertilizer. Nitrogen is the key element in creating and increasing crop yield, making it both essential and potentially harmful in agricultural management. Fertilizer management can include many techniques. Farmers can perform a soil quality assessment in order to identify soil potential supply. Yield modeling can be used to identify the rate and amount of fertilizers to apply, based on soil properties and crop characteristic. Simple nutrient budgets and N testing can be used to identify the rate and time of fertilizer application. Farmers can also calculate their N balance from crop uptake, absorption, run-off, and emissions. Efficient use of manure and organic wastes used as fertilizers can reduce N emissions. Growers can also use winter crops to sequestrator remaining nitrogen from previous seasons or apply deep fertilization. Finally, growers can implement proper irrigation techniques and management to avoid fertilizer loss and check the soil's pH and acidity.

Cropland, Noncultivated Land, and Bare Land

Cropland

On actively cultivated croplands, farmers can conserve the soil by using alley cropping, contouring, terracing, crop residues to cover soil surface, reduced tillage, or no tillage. Mulching is practiced widely in sloping land areas to protect the soil from rain and wind erosion, limit evaporation, maintain water content in the soil, and prevent organic matter degradation. It also returns organic carbon and nutrients into the soil and reduces the costs of chemical fertilizer.

Fallow Land and Bare Land

Fallow and bare lands usually occur where there are unstable rainfall conditions, poor irrigation regimes, unfavorable transportation conditions, and poor humus. These lands occupy about 23 % of the nation. In these unfavorable soil conditions, many pedological processes lead to continued soil degradation and GHG emissions. Improvement and rehabilitation of these lands will improve ecological conditions, control soil erosion, reduce leaching, and reduce GHG emissions.

It is recommended to apply the following techniques to reduce GHG emission for noncultivated and bare lands:

- Plant green manure or grasses along the contour lines to prevent surface flows and retain sediment during high rainfall. Simultaneously, these buffers make terraces and soil traps along the contour lines to trap soil and prevent sedimentation from gently sloping surfaces.
- Apply intercropping, agro-forestry, and mix planting of annual crops and perennial crops. These practices have been implemented widely in hilly and mountainous areas. They were especially promoted as a key activity of the National Project

(Project 327) of regreening noncultivated and bare lands to protect against natural disasters, flash floods, and droughts in highlands
– Application of Sloping Agricultural Land Technology or SALT. SALT has certain advantages over both the traditional techniques of slash-and-burn (swidden agriculture) and conventional terrace farming. SALT enables farmers to stabilize and enrich the soil and to grow food crops economically. There is also a reduced need for expensive inputs like chemical fertilizers. In addition, SALT also conserves soil moisture and reduces pests and diseases. But most importantly, to a financially harried farmer, the technology can increase his or her annual income to almost threefold after only a period of 5 years.

Conclusion

Climate change strongly impacts Vietnam's agricultural sector. Damages have been documented in the past, the existing environment is highly vulnerable, and projections show high crop losses in the future. Flatlands are more strongly affected than highlands, in which the Mekong River Delta shows the most impacts. The Coastal Central area and Red River Delta follow the Mekong Delta. Vietnam experiences many extreme events and disasters each year. Climate change is projected to increase the frequency and severity of these weather events, damaging agricultural outputs. The agricultural sector has developed suitable adaptation measures to cope with climate change and keep production ongoing, not only feeding over 76 million people but also exporting a high amount of food and foodstuffs. Vietnam is the leading cashew nut exporter, second rice exporter, and third coffee exporter in the world. With a large area of paddy rice land and a large livestock sector, production processes in Vietnam have high GHG emissions. Thus, the agricultural sector is striving to implement many mitigation options such as AWD irrigation, composting, and converting rice land to non-rice land. With these mitigation measures, the sector plans to reach the target of reducing GHG emission by 20 % by 2020.

References

Binh Dinh PPC (2010) Binh Dinh province people committee report in 2010

CIMMYT (1991) Annual report: improving the productivity of maize and wheat in developing countries – an assessment of impact

Dasgypta S, Laplante B, Meisner C, Wheeler D, Yan J (2007) The impact of sea level rise on developing countries: a comparative analysis. World Bank policy research working paper 4136

Decision No. 3062 (2007) Decision No. 3062/QĐ-BNN-KHCN. In 15/10/2007 MARD issues a decision to acknowledge innovative/advance techniques and methods in rice cultivation

Decision No. 3119 (2011) Decision No. 3119/QĐ-BNN-KHCN. On approving programme of Green House Gas (GHG) emission reduction in the agriculture and rural development sector upto 2020

Decision no. 899/QĐ-TTg (2013) Approving the project "Agricultural restructuring towards raising added value and sustainable development"

Dobermann A, Walters DT, Adviento-Borbe MAA (2007) Global warming potential of high-yielding continuous corn and corn-soybean systems. Better Crops 91(3):16–19
Feng Y, Xu Y, Yu Y, Xie Z, Lin X (2012) Mechanism of biochar decreasing methane emission from Chinese paddy soils. Soil Biol Biochem 46:80–88
GSO (2013) General statistical office of Vietnam 2013
GSO (2011–2014) General Statistical Office of Vietnam from 2011–2014
Ha Dinh Tuan (2005) Farming techniques on sloping land. Selected proceeding from scientific conference of Vietnam Agriculture Science Institute (VASI)
IAE (2012) Potential of crop residue in "Viet Nam" agriculture, workshop proceeding on efficiency use g crop residue in Viet Nam agriculture, Hanoi 12/2013.
IAE-ICRISAT (2010) To the report of ICRISAT/ADB-RETA6349
IMHEN (2010a) Sea level rise scenarios and possible disaster risk reduction in Viet Nam, Institute of Meteorology, Hydrology and Environment, pp 24–25
IMHEN (2010b) Impacts of climate change on water resources and adaptation measures, Institute of Meteorology, Hydrology and Environment, pp 70–71
Iyengar NS, Sudarshan P (1982) A method of classifying regions from multivariate data. Econ Pol Wkly 2048–2052. Special Article
Le Duy Thanh (2004) Study technique of nylon covering crop to increase peanut yield on degraded soil in Viet Yen district, Bac Giang province, Hanoi University 124 pp
Liu Y, Yang M, Wu Y, Wang H, Chen Y, Wu W (2011) Reducing CH4 and CO2 emissions from waterlogged paddy soil with biochar. J Soils Sediments 11:930–939
Mai Van Trinh, Nguyen Hong Son (2011) Study the impact of climate change on cereal crop production in Vietnam, Science and Technology Journal of Agriculture and Rural Development. Minist Agric Rural Dev 12:3–9
Mai Van Trinh, Tran Viet Cuong (2012) Pyrolysis of rice straw and rice husk to produce biochar, material for improving soil fertility, crop yield and reducing Green House Gas (GHG) emission. In: Nguyen Van Tuat, Bui Chi Buu, Nguyen Van Viet, Nguyen The Yen (eds) Trends in rice research to overcome stresses in a changing climate. Agricultural Publishing House, Ha Noi, pp 366–372
Mai Van Trinh, Tran Van The, Dinh Vu Thanh (2014) Climate change and crop production. Agricultural Publishing House Ha Noi, pp 153 (Vietnamese)
MARD (2009) Ministry of agriculture and rural development's Agriculture production and plan to 2020
Mariam Trinh, Tran van The, Bui Thi Phuong (2012) An estimation of GHG reduction for the agriculture sector in Viet Nam, project's report for United Nations development (UNDP).
MONRE (2009) Climate change, sea level rise scenarios for Vietnam. Ha Noi, Vietnam
MONRE (2012) Climate change, sea level rise scenarios for Vietnam. Ha Noi, Vietnam
Lang NT, Van Tao N, Buu BC (2011) Marker-assisted backcrossing (mab) for rice submergence tolerance in Mekong delta. Omonrice 18:11–21
Patnaik U, Narayanan K (2005) Vulnerability and climate change: an analysis of the eastern coastal districts of India, Human security and climate change: an international workshop, Asker
Pham Quang Ha (2013) Survey and assessment impacts of climate change on agriculture and develop adaptation and mitigation measures for crop production and aquaculture in Vietnam. Research project report. Ministry for Agriculture and Rural Development
Pham Thi Nhung (2006) Study influence of burying agriculture residues to potassium pools in soil and crop yield on Eutric Fluvisols soil, Dan Phuong, Ha Tay province. MSc thesis, Hanoi Agriculture University
PPD (2009) Statistical data about implementation of SRI, Plant Protection Department
Quach Tat Quang, Nguyen Van Anh, Nguyen Thanh Hai (2012) Vietnam technology needs assessment for climate change mitigation and adaptation, summary report of technology needs assessment for climate change adaptation and mitigation of Vietnam, The Global Technology Needs Assessment, Ha Noi

Tran Thi Cuc Hoa (2011) Development of transgenic rice lines resistant to insect pests using Agrobacterium tumefaciens- mediated transformation and mannose selection system. Omonrice 18:1–10

Tran van The, Pham Quang Ha, Mariam (2010) Impact of climate change on Mekong delta river, scientific workshop proceeding, institute for agricultural environment.

Uphoff N (2002) Supporting food security in the 21st century through resource-conserving increases in agricultural production. Agric Food Secur 1:1–18

Yanai Y, Toyota K, Okazaki M (2007) Effects of charcoal addition on N_2O emissions from soil resulting from rewetting air-dried soil in short-term laboratory experiments. Soil Sci Plant Nutr 53:181–188

Yao Z, Zhou Z, Zheng X, Xie B, Mei B, Wang R, Bal Butterbach K, Zhu KJ (2010) Effects of organic matter incorporation on nitrous oxide emissions from rice-wheat rotation ecosystems in China. Plant Soil 327:315–330

Potential Impacts of the Growth of a Mega City in Southeast Asia: A Case Study on the City of Dhaka, Bangladesh

A. K. M. Azad Hossain and Greg Easson

Contents

Abstract

Megacities with populations of more than ten million people in compact urban areas are the most vulnerable environments on the earth. The impacts of climate change on these megacities will be multi-faceted and severe, especially in developing countries, due to fast growth rate and inefficient adaptation. It is very important therefore to understand the contributions of the growth of megacities to climate change, especially in the developing countries. Dhaka, the capital of Bangladesh, is one of the fastest-growing megacities in the world; its population

A.K.M.A. Hossain (✉)
National Center for Computational Hydroscience and Engineering (NCCHE), The University of Mississippi, Oxford, MS, USA
e-mail: ahossain@ncche.olemiss.edu

G. Easson
Mississippi Mineral Resources Institute, The University of Mississippi, Oxford, MS, USA
e-mail: geasson@olemiss.edu

W.-Y. Chen et al. (eds.), *Handbook of Climate Change Mitigation and Adaptation*,
DOI 10.1007/978-3-319-14409-2_68

increased from 6.621 million (in 1990) to 16.982 million (in 2014). Today, Dhaka is the 11th largest megacity in the world and is projected to be the 6th largest megacity in the world with a population of 27.374 million by the year 2030.

Remote sensing technology has been successfully used for mapping, modeling, and assessing urban growth and associated environmental studies for many years. This research investigates how the intensity of the urban heat island (UHI) effects correlates with continuous decrease in the greenness of the city of Dhaka, as measured from satellite observations. The results of this study indicate that Landsat imagery-derived normalized difference vegetation index (NDVI) can be used to investigate the changes in greenness in the city of Dhaka from 1980 to 2014. The changes in greenness can be correlated with the increase in the intensity of UHI effects in the city of Dhaka as determined using Landsat thermal data from 1989 to 2014.

Introduction

Urban populations grew rapidly throughout the nineteenth century, more by migration from the rural areas to the cities and manufacturing centers than by absolute population growth. Throughout the twentieth century, the number and sizes of cities grew, along with the percentage of the total population living in the cities (Schubel and Levi 2000). Since 1950, the worldwide urban population has grown from 746 million to 3.9 billion in 2014, 54 % of the total global population (United Nations 2014). Continued population growth and urbanization are predicted and it is projected to add 2.5 billion more people to the world's urban population by 2050 (United Nations 2014).

A large percentage of the urban growth is concentrated in the developing world, where the average urban growth rate for developing countries is 3.5 % per year, compared with a rate of less than 1 % per year for the developed countries (United Nations 1997; WRI 1998). Asia, despite its lower level of urbanization, is home to 53 % of the world's urban population. By 2050 it is projected that 90 % of the world's urban population will be in Asia and Africa (United Nations 2014).

The past several decades have seen the emergence of megacities, a metropolitan area with a total population in excess of ten million people (New Scientist Magazine 2006). A megacity can be a single metropolitan area or two or more metropolitan areas that have converged. The concept of megacities was initiated in 1987 to combine both theory and practice in the search for successful approaches to improve urban management and the conditions of daily life in the world's largest cities. The megacities concept was based on a collaborative effort among government, business, and community leaders of these megacities, in an attempt to shorten the time between the introduction of innovative ideas and their implementation and diffusion. The idea was coined not simply to identify, distill, and disseminate positive approaches but to strengthen the leaders and groups who are evolving the approaches and find sources of

support to multiply their efforts. The idea promotes a dual strategy that functions simultaneously at the practical and theoretical levels: (1) sharing "best practices" among the cities and putting the lessons of experience in the hands of decision makers and the public and (2) gaining a deeper understanding of the process of innovation and the consequences of deliberate social changes in the cities.

In 1950, New York and London were the world's only megacities (Schubel and Levi 2000). In 1990, the number of megacities had increased to 10, with a population of 153 million people, representing less than 7 % of the global urban population. By 2014, the number of megacities had nearly tripled to 28. The urban population in these megacities has grown to 453 million, and these areas now account for 12 % of the world's urban residents. The number of megacities is projected to increase to 41 by 2030 (United Nations 2014). Since most of the recent urban growth is concentrated in the developing world, the majority of the megacities are expected to be located in the developing world (Schubel and Levi 2000). Currently, 15 out of the 28 megacities are located in Asia, with the number projected to increase to 23 in Asia by 2030 (United Nations 2014). Table 1 shows the list of the current and projected megacities in the world.

The most vulnerable environments on the earth are the urban areas, especially the megacities. It is increasingly recognized that airborne emissions from major urban and industrial areas influence both air quality and climate change on scales ranging from regional to continental and global. The viability of important natural and agricultural ecosystems in regions surrounding highly urbanized areas is severely affected by the deteriorating urban air quality. Megacities also influence regional atmospheric chemistry. This situation is particularly acute in the developing world where the rapid growth of megacities is producing atmospheric pollution at unprecedented severity and extent (Gurjar et al. 2014).

The impacts of climate change due to urbanization are multi-faceted and severe. The impacts differ dramatically among the megacities in the developed and in the developing countries. The impacts in the developed countries are already adapted or being adapted with efficient technologies/policies/regulations, whereas in the developing countries, due to fast growth rate and inefficient adaptation, the impact is imminent and severe. There are also no signs that the governments in the developing countries will prove to be more capable in the future. These swarming, massive urban areas will continue to grow and should concern the world (Liotta and Miskel 2012).

It is very important therefore to understand the impacts of the growth of megacities on climate change. Studies on megacities at different spatial and temporal scales using various models will be required to understand their local-to-global impacts and implications (Gurjar et al. 2014). Lawrence et al. (2007) employed a global model to examine the outflow characteristics of pollutants from megacities. That model demonstrated the trade-offs between pollutant buildup in the region surrounding each megacity versus export to downwind regions or to the upper troposphere. Unfortunately, the coarse resolution of global atmospheric models and source inventories still presents difficulties to capturing the details of the impact of megacity emissions temporally and spatially (Gurjar et al. 2014).

Table 1 List of megacities (United Nations 2014)

Megacity	Country	Population (thousands)		Rank		Last 5 years' average growth (2010–2015)
		2014	2030	2014	2030	
Tokyo	Japan	37,833	37,190	1	1	0.6
Delhi	India	24,953	36,060	2	2	3.2
Shanghai	China	22,991	30,751	3	3	3.4
Mexico City	Mexico	20,843	23,865	4	10	0.8
Sao Paolo	Brazil	20,831	23,444	5	11	1.4
Mumbai	India	20,741	27,797	6	4	1.6
Osaka	Japan	20,123	19,976	7	13	0.8
Beijing	China	19,520	27,706	8	5	4.6
New York***	USA	18,591	19,885	9	14	0.2
Cairo	Egypt	18,419	24,502	10	8	2.1
Dhaka	Bangladesh	16,982	27,374	11	6	3.6
Karachi	Pakistan	16,126	24,838	12	7	3.3
Buenos Aires	Argentina	15,024	16,956	13	18	1.3
Kolkata	India	14,766	19,092	14	15	0.8
Istanbul	Turkey	13,954	16,694	15	20	2.2
Chongqing	China	12,916	17,380	16	17	3.4
Rio de Janeiro	Brazil	12,825	14,174	17	23	0.8
Manila	Philippines	12,764	16,756	18	19	1.7
Lagos	Nigeria	12,614	24,239	19	9	3.9
Los Angeles*	USA	12,308	13,257	20	26	0.2
Moscow	Russian Federation	12,063	12,200	21	31	1.2
Guangzhou	China	11,843	17,574	22	16	5.2
Kinshasa	Congo**	11,116	19,996	23	12	4.2
Tianjin	China	10,860	14,655	24	22	3.4
Paris	France	10,764	11,803	25	33	0.7
Shenzhen	China	10,680	12,673	26	29	1
London	UK	10,189	11,467	27	36	1.2
Jakarta	Indonesia	10,176	13,812	28	25	1.4

*Los Angeles-Long Beach-Santa Ana
**Democratic Republic of the Congo
***New York-Newark

Dhaka, the capital of Bangladesh, is one of the fastest-growing megacities in the world; its population increased from 6.621 million (in 1990) to 16.982 million (in 2014) (Table 1). Today, Dhaka is the 11th largest megacity in the world and is projected to be the 6th largest megacity in the world with a population of 27.374 million by the year 2030 (United Nations 2014).

The urban heat island (UHI) effect is an important impact of urbanization. Urban and suburban areas experience elevated temperatures compared to their surrounding rural areas (EPA 2015). The annual mean air temperature of a city with one million people or more can be 1.8–5.4 °F (1–3 °C) warmer than the surrounding area (OKe 1997). On a clear, calm night, this temperature difference can be as much as 22 °F (12 °C) (OKe 1987). The UHI effect for the city of Dhaka has already been recorded by several reports and articles (Ahmed et al. 2013). It is not yet however completely understood how the intensity of the UHI effect changes with the continuous growth of the city.

Remote sensing technology has been successfully used for urban growth and associated environmental studies for many years. This research investigates how the intensity of the UHI correlates with continuous decrease in the greenness of the city, as measured from satellite observations and using digital image processing techniques. The specific objectives include: (1) evaluating the changes in greenness from 1973 to 2014 using Landsat imagery-derived normalized difference vegetation index (NDVI), (2) estimating land surface temperatures (LST) using Landsat thermal imagery, and (3) investigating the potential of the Landsat-derived LST to evaluate the changes in the UHI effect.

Research Data

A time series of ten Landsat images covering Dhaka, Bangladesh, acquired from 1973 to 2014 were used in this research. The time series of imagery includes data acquired by Landsat 1 and Landsat 3 Multispectral Scanner (MSS), Landsat 4 and Landsat 5 Thematic Mapper (TM), Landsat 7 Enhanced Thematic Mapper Plus (ETM+), and Landsat 8 Operational Land Imager (OLI) and Thermal Infrared Sensor (TIRS). Table 2 lists the imagery acquisition dates and corresponding sensors and their characteristics. All ten data sets were used for visual analysis, but only selected imagery were used for vegetation and land surface temperature (LST) analysis. Table 3 shows the data usage matrix.

The spatial distribution of vegetation in Dhaka was mapped to evaluate the changes in greenness over time. A normalized difference vegetation index (NDVI) was used to detect the changes in greenness. NDVI was calculated for the imagery acquired in 1973, 1980, 1989, 2000, 2010, and 2014. The thermal sensor of the Landsat series became available with the launch of Landsat 4. The earliest thermal data available for this region was acquired in 1989, started the time series of LST data for 1989, 2000, 2010, and 2014 (Table 3).

The gradual changes in land use and land cover in and around the city of Dhaka from 1973 to 2014 are shown in Fig. 2. Figure 3 shows the net change in land cover and land use between 1973 and 2014.

Table 2 Satellite data acquired

Date	Sensor	VNIR bands	Spatial resolution (m)	Thermal bands	Spatial resolution (m)
Dec. 05, 1973	Landsat 1 MSS	4,5,6, and 7	60[a]	NA	NA
Feb. 20, 1980	Landsat 3 MSS	4,5,6, and 7	60[a]	NA	NA
Jan. 28, 1989	Landsat 4 TM	1,2,3, and 4	30	6	30[b]
Feb. 28, 2000	Landsat 7 ETM+	1,2,3, and 4	30	6	30[c]
Mar. 24, 2003	Landsat 7 ETM+	1,2,3, and 4	30	6	30[c]
Jan. 16, 2005	Landsat 5 TM	1,2,3, and 4	30	6	30[b]
Nov. 03, 2006	Landsat 5 TM	1,2,3, and 4	30	6	30[b]
Jan. 11, 2009	Landsat 5 TM	1,2,3, and 4	30	6	30[b]
Feb. 15, 2010	Landsat 5 TM	1,2,3, and 4	30	6	30[b]
Jan. 25, 2014	Landsat 8 OLI	2,3,4, and 5	30	10, 11	30[d]

[a]Original MSS pixel size was 79 × 57 m; production systems now resample the data to 60 m
[b]TM Band 6 was acquired at 120-m resolution but is resampled to 30-m pixels (after February 25, 2010)
[c]ETM+ Band 6 is acquired at 60-m resolution but is resampled to 30-m pixels (after February 25, 2010)
[d]TIRS bands are acquired at 100 m resolution but are resampled to 30 m in delivered data product

Table 3 Satellite data used

Date	Sensor	Visual inspection	NDVI	Thermal analysis
Dec. 05, 1973	Landsat 1 MSS	X	X	
Feb. 20, 1980	Landsat 3 MSS	X	X	
Jan. 28, 1989	Landsat 4 TM	X	X	X
Feb. 28, 2000	Landsat 7 ETM+	X	X	X
Mar. 24, 2003	Landsat 7 ETM+	X		
Jan. 16, 2005	Landsat 5 TM	X		
Nov. 03, 2006	Landsat 5 TM	X		
Jan. 11, 2009	Landsat 5 TM	X		
Feb. 15, 2010	Landsat 5 TM	X	X	X
Jan. 25, 2014	Landsat 8 OLI	X	X	X

Methods

This research is based on the hypothesis that satellite observation-based normalized difference vegetation index (NDVI) and land surface temperature (LST) can monitor changes in urban greenness in a megacity and the changes in the intensity of urban heat island (UHI) effect. Data acquired by Landsat satellites would be the best available option to achieve these results due to the extensive archive of imagery and consistency of the sensors.

Fig. 1 Location of the study site (not scaled)

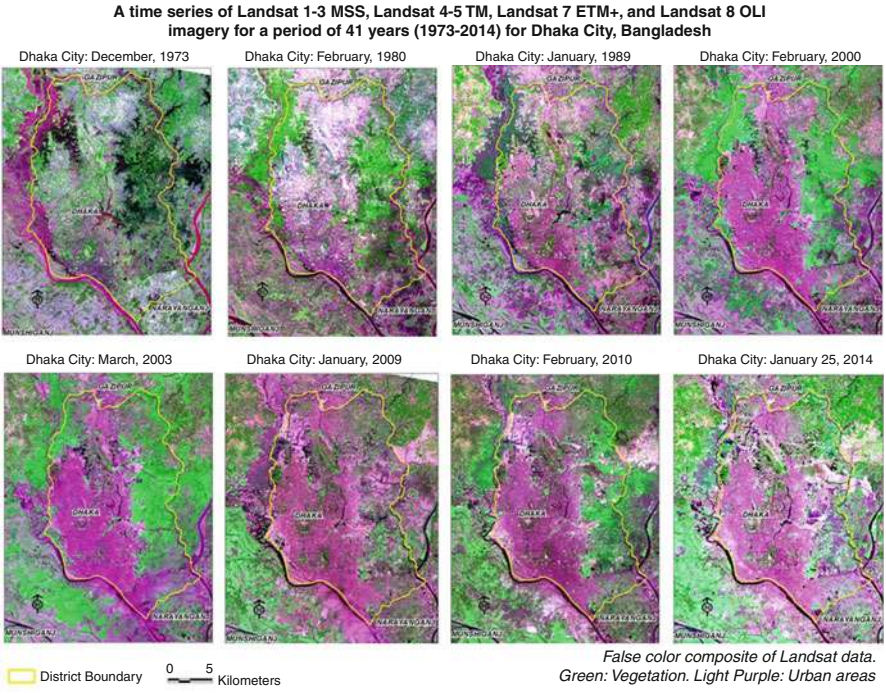

Fig. 2 Changes in land cover in Dhaka City

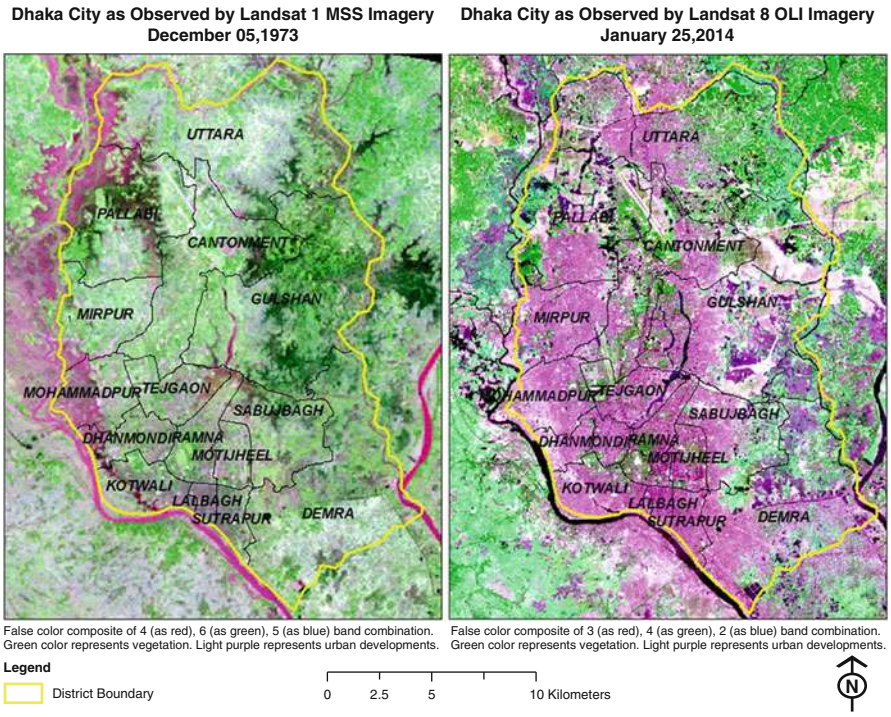

Fig. 3 Land use and land cover changes as observed by Landsat data

Normalized Difference Vegetation Index (NDVI)

The normalized difference vegetation index (NDVI) is an image enhancement technique, which can be used to describe the greenness or relative density and health of vegetation in an image. It is one of the most widely accepted and widely used vegetation indices. NDVI was first attributed by Rouse et al. (1973), but the concept was discussed by Kriegler et al. (1969). NDVI is commonly used as an indicator of relative biomass and greenness (Boone et al. 2000). The calculation of NDVI is based on the nature of the variation of reflectance values obtained from vegetated surfaces in the near-infrared (NIR) and red regions of the electromagnetic spectrum (EMS). The reflectance values of vegetation in the near-infrared (NIR) region are higher than that in the red region. NDVI provides a ratio of the NIR and the red bands (Eq. 1), eliminating any discrepancies that may occur in the imagery due to sensor differences or image quality issues, such as brightness and other interference (Hossain and Easson 2011). The NDVI can be computed for a wide variety of sensors depending on the availability of measurements in the NIR and red bands.

$$\mathrm{NDVI} = \frac{(\mathrm{NIR} - \mathrm{R})}{(\mathrm{NIR} + \mathrm{R})} \tag{1}$$

where NIR and R are pixel values of NIR and R bands, respectively.

Landsat data has been used for vegetation studies for many years. Since all the sensors used in Landsat data acquisitions consist of both visible and near-infrared (VNIR) channels (Table 2), it is possible to calculate NDVI using image data from all Landsat sensors. In this study, NDVI was calculated using imagery acquired by Landsat 1 MSS, Landsat 3 MSS, Landsat 4 TM, Landsat 5 TM, Landsat 7 ETM+, and Landsat 8 OLI satellites (Table 3). The NDVI calculation equations are as follows:

$$\mathrm{NDVI}_{\mathrm{Landsat1\_MSS}} = \frac{(\mathrm{Band7} - \mathrm{Band4})}{(\mathrm{Band7} + \mathrm{Band4})} \tag{2}$$

$$\mathrm{NDVI}_{\mathrm{Landsat3\_MSS}} = \frac{(\mathrm{Band7} - \mathrm{Band4})}{(\mathrm{Band7} + \mathrm{Band4})} \tag{3}$$

$$\mathrm{NDVI}_{\mathrm{Landsat4\_TM}} = \frac{(\mathrm{Band4} - \mathrm{Band3})}{(\mathrm{Band4} + \mathrm{Band3})} \tag{4}$$

$$\mathrm{NDVI}_{\mathrm{Landsat5\_TM}} = \frac{(\mathrm{Band4} - \mathrm{Band3})}{(\mathrm{Band4} + \mathrm{Band3})} \tag{5}$$

$$\mathrm{NDVI}_{\mathrm{Landsat7\_ETM+}} = \frac{(\mathrm{Band4} - \mathrm{Band3})}{(\mathrm{Band4} + \mathrm{Band3})} \tag{6}$$

$$\mathrm{NDVI}_{\mathrm{Landsat8\_OLI}} = \frac{(\mathrm{Band5} - \mathrm{Band4})}{(\mathrm{Band5} + \mathrm{Band4})} \tag{7}$$

Land Surface Temperature (LST)

Land surface temperatures (LSTs) in and around the city of Dhaka were estimated using the Level 1 thermal data acquired by Landsat 4–5 TM, Landsat 7 ETM+, and Landsat 8 TIRS sensors. The unitless digital number (DN) values of the thermal bands were digitally processed to corresponding radiance values. The processed radiance values were then used to calculate LST.

Conversion of DN to Radiance

Landsat 4–5 TM and Landsat 7 ETM+

During the generation of Level 1 data, pixel values from raw unprocessed imagery (Level 0 data) were converted to units of absolute radiance using 32-bit floating-point calculations. These absolute radiance values were then scaled to 8-bit values representing calibrated digital numbers (Q_{cal}) before output to the distribution media. Conversion of these calibrated digital numbers (Q_{cal}) in L1 products back

to the "at-sensor spectral radiance" (L_λ) requires knowledge of the original rescaling factors. The following equation (Eq. 8) was used to perform a radiance conversion for the Level 1 Landsat 4–5 TM and Landsat 7 ETM+ imagery (Chander and Markham 2003; Chander et al. 2009).

$$L_\lambda = \left(\frac{LMAX_\lambda - LMIN_\lambda}{Q_{calmax} - Q_{calmin}}\right)(Q_{cal} - Q_{calmin}) + LMIN_\lambda \tag{8}$$

where

L_λ = spectral radiance at the sensor's aperture in W/(m^2.sr.μm)
Q_{cal} = quantized calibrated pixel value in DNs
Q_{calmin} = minimum quantized calibrated pixel value corresponding to $LMIN_l$ (DN = 0)
Q_{calmax} = maximum quantized calibrated pixel value corresponding to $LMAX_l$ (DN = 255)
$LMIN_\lambda$ = spectral radiance that is scaled to Q_{calmin} in W/(m^2.sr.μm)
$LMAX_\lambda$ = spectral radiance that is scaled to Q_{calmax} in W/(m^2.sr.μm)

The required parameters were obtained from the Level 1 product metadata to process the acquired thermal data using Eq. 8. Equation 8 was modified to Eqs. 9, 10, and 11 and was used to obtain the at-sensor radiance values for the imagery acquired in 1989, 2000, and 2010, respectively.

$$L_{\lambda(L4\ TM\_1989)} = \left(\frac{15.303 - 1.238}{255 - 1}\right)(DN_{Band6} - 1) + 1.2378 \tag{9}$$

$$L_{\lambda(L7\ ETM\_2000)} = \left(\frac{12.650 - 3.20}{255 - 1}\right)(DN_{Band62} - 1) + 3.20 \tag{10}$$

$$L_{\lambda(L5\ TM\_2010)} = \left(\frac{15.303 - 1.238}{255 - 1}\right)(DN_{Band6}) + 1.238 \tag{11}$$

Landsat 8 TIRS

Landsat 8 TIRS data has two different thermal bands (Band 10 and Band 11), unlike Landsat 4–5 TM and Landsat 7 ETM+. The center wavelength and bandwidth of Band 10 are 10.9 and 0.6 μm respectively, whereas the center wavelength and bandwidth of Band 11 are 12.0 and 1.0 μm, respectively. In this study, Band 11 was used to estimate LST to be more comparable with Landsat TM and ETM+ thermal data. As proposed by USGS (2014), the conversion of DN values (Q_{cal}) to the "at-sensor spectral radiance" (L_l) was done using different approaches (comparing to Landsat TM and ETM+). Equation 12 was used in this case. This approach was also used in several recent research projects (e.g., Sameen and Kubaisy 2014).

$$L_\lambda = M.Q_{cal} + B \tag{12}$$

where

M is the radiance multiplier
B is the radiance add

The values of "radiance multiplier" and "radiance add" were obtained from Landsat 8 TIRS metadata (Table 4) for Band 11. These values were used in Eq. 12 to obtain Eq. 13, which was used to estimate LST for 2014 imagery acquisition date.

$$L_{\lambda(L8\ TIR_{2014})} = M * DN_{Band11} + B \tag{13}$$

Conversion of Radiance to LST

The obtained radiance values for all Landsat thermal data were converted to land surface temperature (LST) using Eq. 14. Since the obtained radiance values are of top of the atmosphere (at-sensor radiance), Eq. 14 was modified by adding an emissivity factor ($\mathcal{E}$) to minimize the influence of atmospheric distortion in the calculation (Eq. 15). Table 4 provides the values of K1 and K2 for Landsat 8 TIRS (Maher and Kubaisy 2014). Table 5 provides the values of K1 and K2 for Landsat 4–5 TM and Landsat 7 ETM + (Coll et al. 2010).

$$T_k = \frac{K_2}{\ln\left(\frac{K_1}{L_\lambda}\right) + 1} \tag{14}$$

$$T_k = \frac{K_2}{\ln\left(\frac{K_1.\varepsilon}{L_\lambda}\right) + 1} \tag{15}$$

where

T_k = effective at-satellite temperature in Kelvin
K_2 = calibrated constant 2 in Kelvin

Table 4 Landsat 8 TIR parameters

	TIR parameters			
			Thermal constants	
			K_1	K_2
TIR bands	Radiance multiplier (M)	Radiance add (B)	W/(m^2.sr.μm)	Kelvin
Band 10	0.0003342	0.1	774.89	1,321.08
Band 11	0.0003342	0.1	480.89	1,201.14

Table 5 Landsat TM and ETM+ thermal band calibration constants

	Constants	
	K_1	K_2
	Units	
Sensor type	$W/(m^2.sr.\mu m)$	Kelvin
Landsat 4 TM	671.62	1,284.30
Landsat 5 TM	607.76	1,260.56
Landsat 7 ETM+	666.09	1,282.71

K_1 = calibrated constant 1 in $W/(m^2.sr.\mu m)$
L_λ = spectral radiance at the sensor's aperture
e = emissivity (typically 0.95)

Equation 15 was then modified to form Eqs. 16–19 to calculate LST, in degrees Kelvin, for each different Landsat sensor by using corresponding values of L_λ, K_1, and K_2. After calculating LST in absolute temperature, the values were converted to degrees Celsius, using Eq. 20.

$$T_{k(L4\ TM_{1989})} = \frac{1260.56}{\ln\left(\frac{607.76 * 0.95}{L_{\lambda(L4\,TM\_1989)}}\right) + 1} \tag{16}$$

$$T_{k(L7\,ETM_{2000})} = \frac{1282.71}{\ln\left(\frac{666.09 * 0.95}{L_{\lambda(L7\,ETM\_2000)}}\right) + 1} \tag{17}$$

$$T_{k(L5\,TM_{2010})} = \frac{1260.56}{\ln\left(\frac{607.76 * 0.95}{L_{\lambda(L5\,TM\_2010)}}\right) + 1} \tag{18}$$

$$T_{k(L8\,TIR_{2014})} = \frac{1201.14}{\ln\left(\frac{480.89}{L_{\lambda(L8\,TIR\_2014)}}\right) + 1} \tag{19}$$

$$T_c = T_k - 273.15 \tag{20}$$

Results and Analysis

The processed NDVI and LST data were subset for Dhaka metropolitan area for analysis of changes in greenness and land surface temperature. The time series of Dhaka NDVI data was used to study the changes in greenness since 1980. The time series of Dhaka LST data was used to evaluate the changes in the intensity of urban heat island (UHI) impact since 1989.

Changes in Greenness

On the basis of the minimum and maximum values of NDVI, the lookup table of the entire time series data was scaled from −0.5 to 0.65 to visualize the changes in greenness over time. Figure 4 shows the NDVI time series for Dhaka city from 1980 to 2014. In Fig. 4, it is clearly seen that the average NDVI values decreased continuously from 1980 to 2014. The most dramatical change occurred between 1989 and 2000. The net change in greenness from 1980 to 2014 is also substantial as seen in Fig. 5.

Changes in the Urban Heat Island (UHI) Effects

The variation in the intensity of urban heat island (UHI) effects due to the changes in greenness in the city of Dhaka was evaluated by determining the changes in the nature of spatiotemporal distribution of land surface temperature (LST) over time. The Landsat satellite observed LST time series data were used in different ways to study the changes in the nature of spatiotemporal distribution of LST over time.

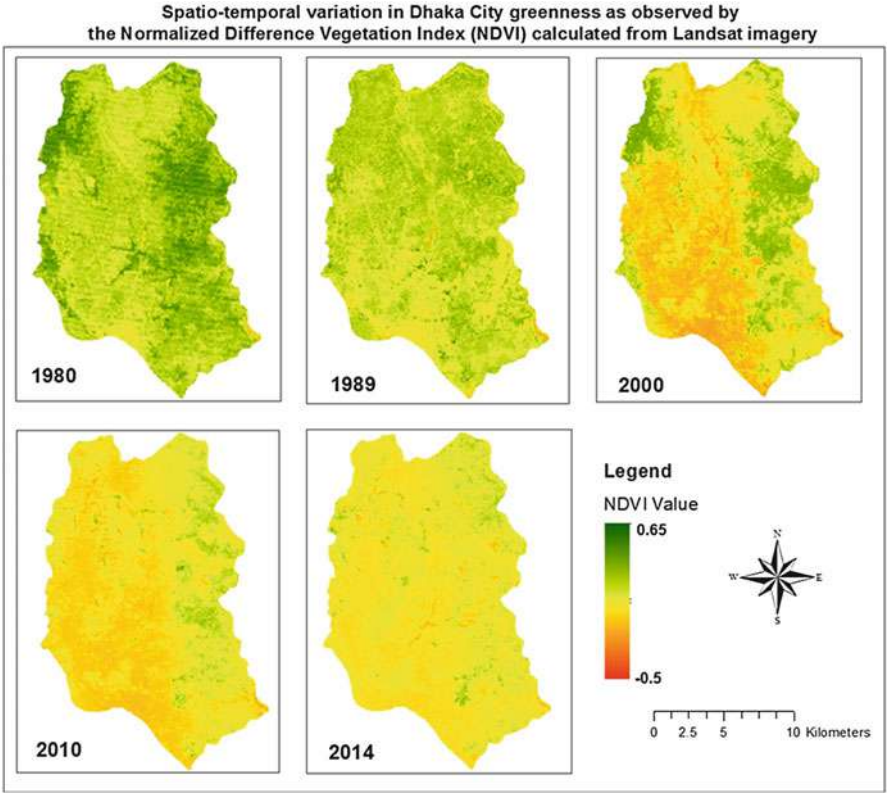

Fig. 4 Changes in greenness from 1980 to 2014 as observed by the Landsat data

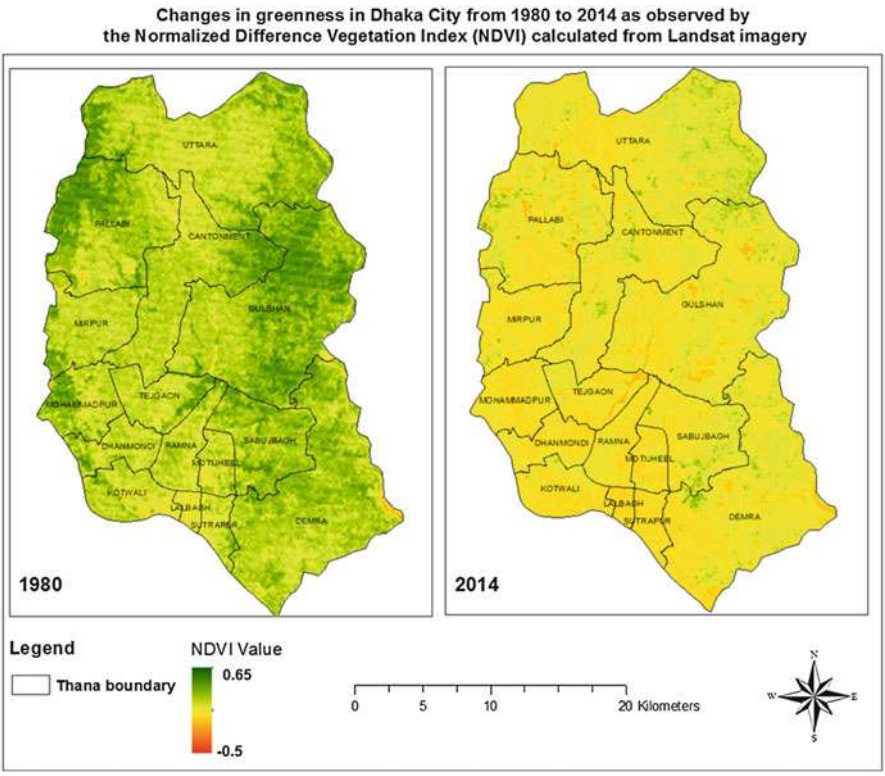

Fig. 5 Detailed changes in greenness from 1980 to 2014 as observed by the Landsat data (Thana is a kind of local administrative boundary like county)

At first, the LST distribution was visually analyzed by stretching the data lookup table from red to green. The red and green ends represent the maximum and minimum temperatures for each date. The areas covered by yellow represents approximately mean temperature for each date. Figure 6 shows the spatiotemporal distribution of Landsat observed LST in the city of Dhaka from 1989 to 2014. The LST imagery time series in Fig. 6 clearly shows that the areas characterized by high temperature extended substantially from 1989 to 2014, with significant increase from 1989 to 2000. Since the satellite imagery used in this study were acquired in different seasons of different years, it was not found reasonable to determine the absolute changes in LST variation by detecting the net changes in LST values.

The second approach focused on the variation in LST along specific cross-section profile. A cross-section line A-B was selected in the east-west direction on each LST data set to extract the temperature values along the line (Fig. 6). The extracted LST values along line A-B were plotted and compared with the mean LST value for the corresponding data acquisition dates. Figures 7, 8, 9, and 10 show the variation in LST along A-B in 1989, 2000, 2010, and 2014, respectively. This analysis supports

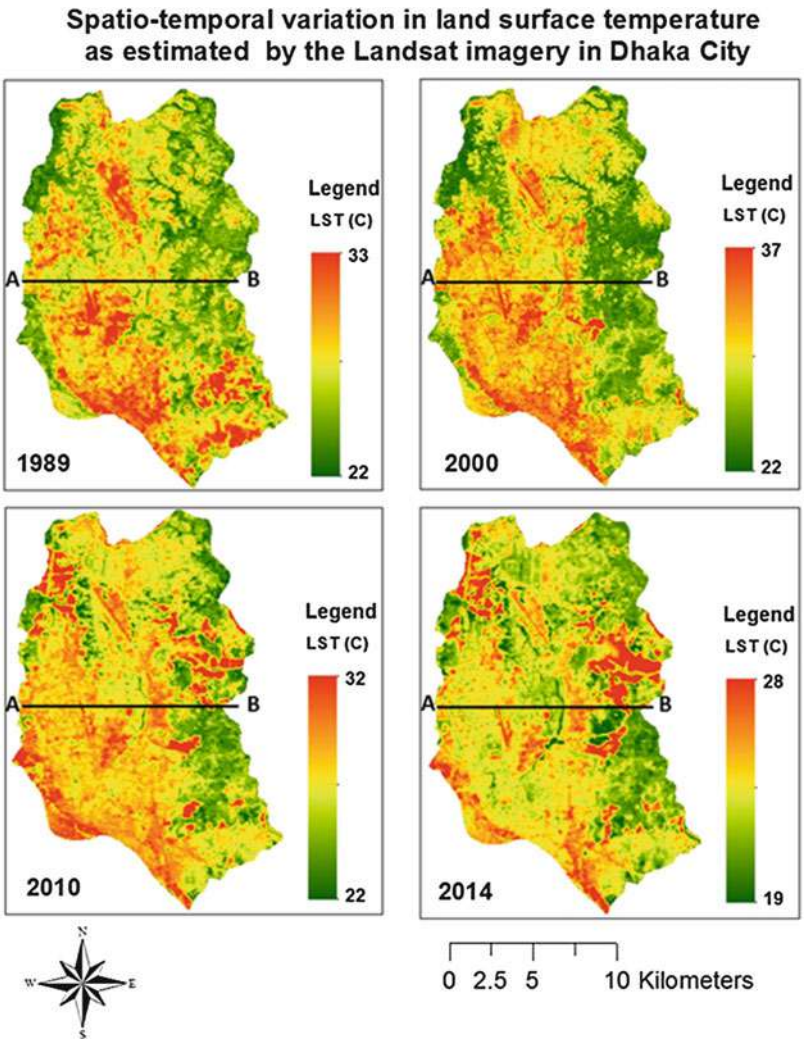

Fig. 6 Land surface temperature (LST) from 1989 to 2014 as observed by the Landsat data

the visual analysis performed earlier and also provided a more quantitative understanding of how the LST values changed over time in reference to the mean values.

The changes in the LST distribution pattern observed along line A-B provide a good quantitative evaluation of the changes in the intensity of UHI effects over time. However, the observation is limited in a particular direction and areas. The potential of image classification techniques was therefore evaluated to extend the quantitative analysis. The classification was performed based on the statistics of the satellite-observed LST imagery (Fig. 6) as shown in Table 6 and Figs. 11 and 12.

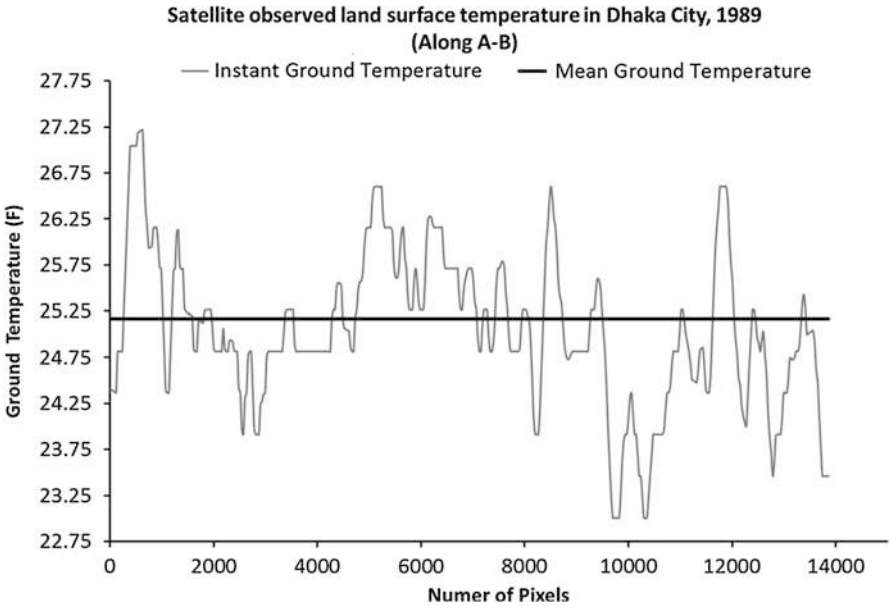

Fig. 7 Variation in LST along A-B in 1989

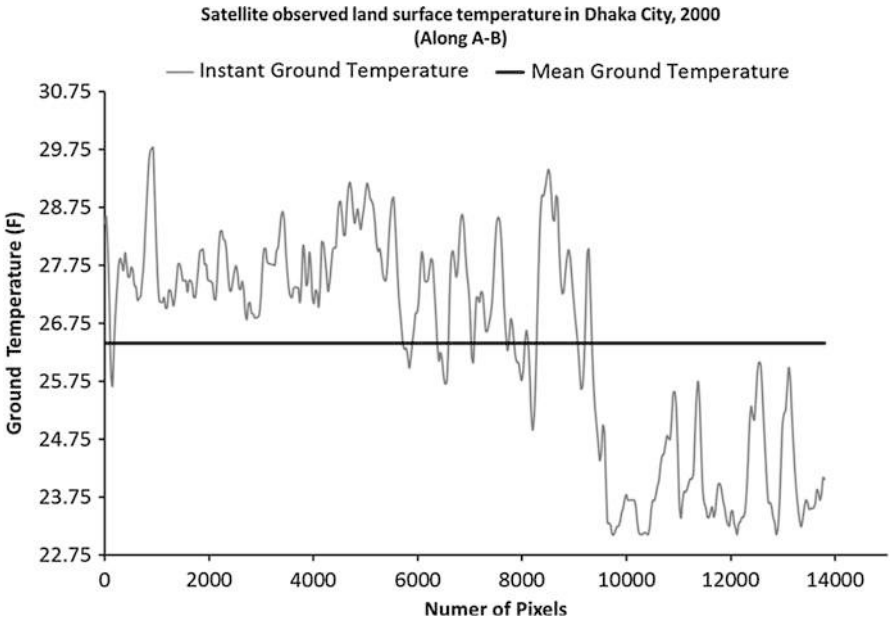

Fig. 8 Variation in LST along A-B in 2000

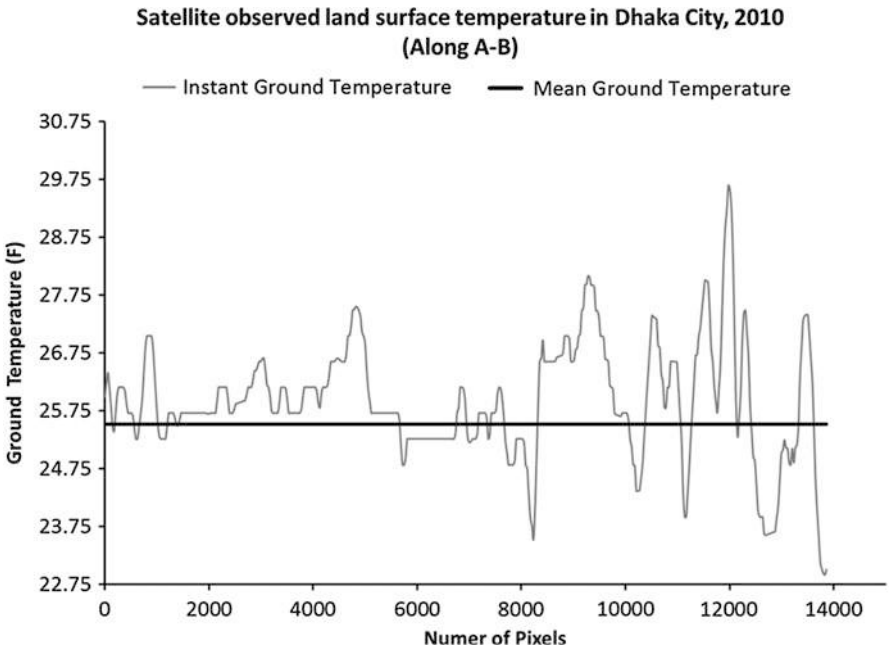

Fig. 9 Variation in LST along A-B in 2010

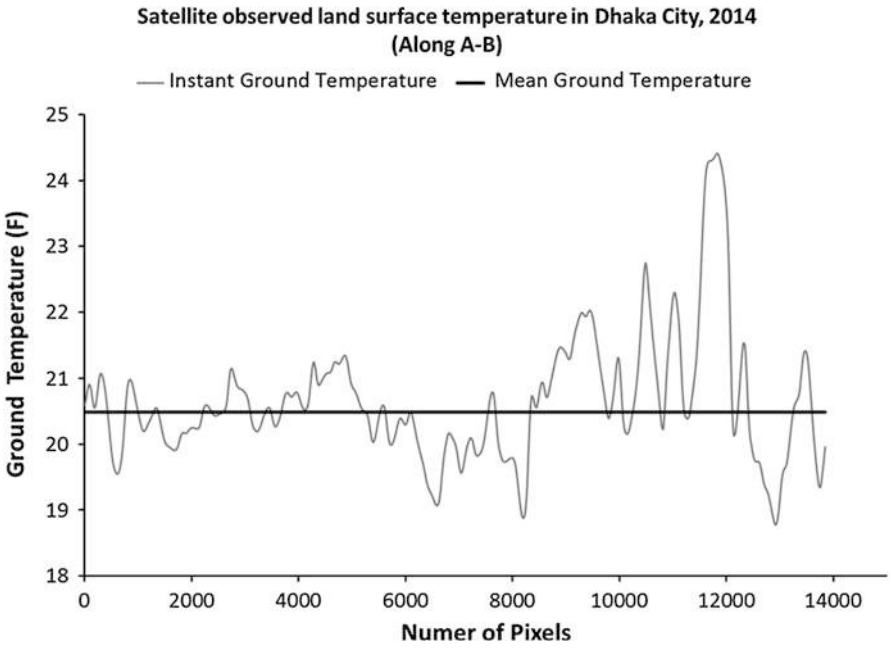

Fig. 10 Variation in LST along A-B in 2014

Table 6 Temperature statistics

Date	Sensor	Temperature statistics (°C)		
		Min	Max	Mean
1989	Landsat 4 TM	22.09	32.66	25.17
2000	Landsat 7 ETM+	21.61	36.63	26.41
2010	Landsat 5 TM	21.63	31.81	25.52
2014	Landsat 8 TIR	17.47	25.38	20.49

Each LST imagery was classified into five classes around the mean temperature to map the spatiotemporal distribution of the areas characterized by different levels of above mean temperature. The classes are as follows:

- Class 1: Areas with temperature equal or less than mean
- Class 2: Areas with temperature 1° higher than mean
- Class 3: Areas with temperature 2° higher than mean
- Class 4: Areas with temperature 3° higher than mean
- Class 5: Areas with temperature >3° higher than mean

Figures 13, 14, 15, and 16 show the distribution of LST pixels above mean LST in the city of Dhaka as observed in 1989, 2000, 2010, and 2014, respectively. The classified raster LST data were converted to vector data and polygons were simplified. The vector data with simplified polygons were used to calculate the areas covered by each LST regime (class).

The area calculations were plotted for different classes to compare them graphically. The area comparison plots improve the understanding of the changes in the intensity of UHI effect over time.

Figure 17 shows the comparison of the size of the areas characterized by total above mean temperature in the city of Dhaka from 1989 to 2014. The total size of the areas where LST remained above the mean increased continuously from 1989 to 2010 but decreased in 2014. Figure 18 shows the comparison of the size of the areas characterized by 1° above mean temperature in the city of Dhaka from 1989 to 2014. The total size of the areas where LST remained 1° above the mean decreased from 1989 to 2000, but increased since then continuously. Figure 19 shows the comparison of the size of the areas characterized by 2° above mean temperature in the city of Dhaka from 1989 to 2014. The total size of the areas where LST remained 2° above the mean increased from 1989 to 2000, but decreased since then. Figure 20 shows the comparison of the size of the areas characterized by 3° above mean temperature in the city of Dhaka from 1989 to 2014. The total size of the areas where LST remained 3° above the mean increased significantly from 1989 to 2000 and remained above 1989 since then.

Discussion and Conclusions

The number and size of megacities are increasing with the majority of the growth occurring in developing countries, especially in Asia and Africa. Understanding the potential impacts of the growth of megacities on the climate in Southeast Asia will

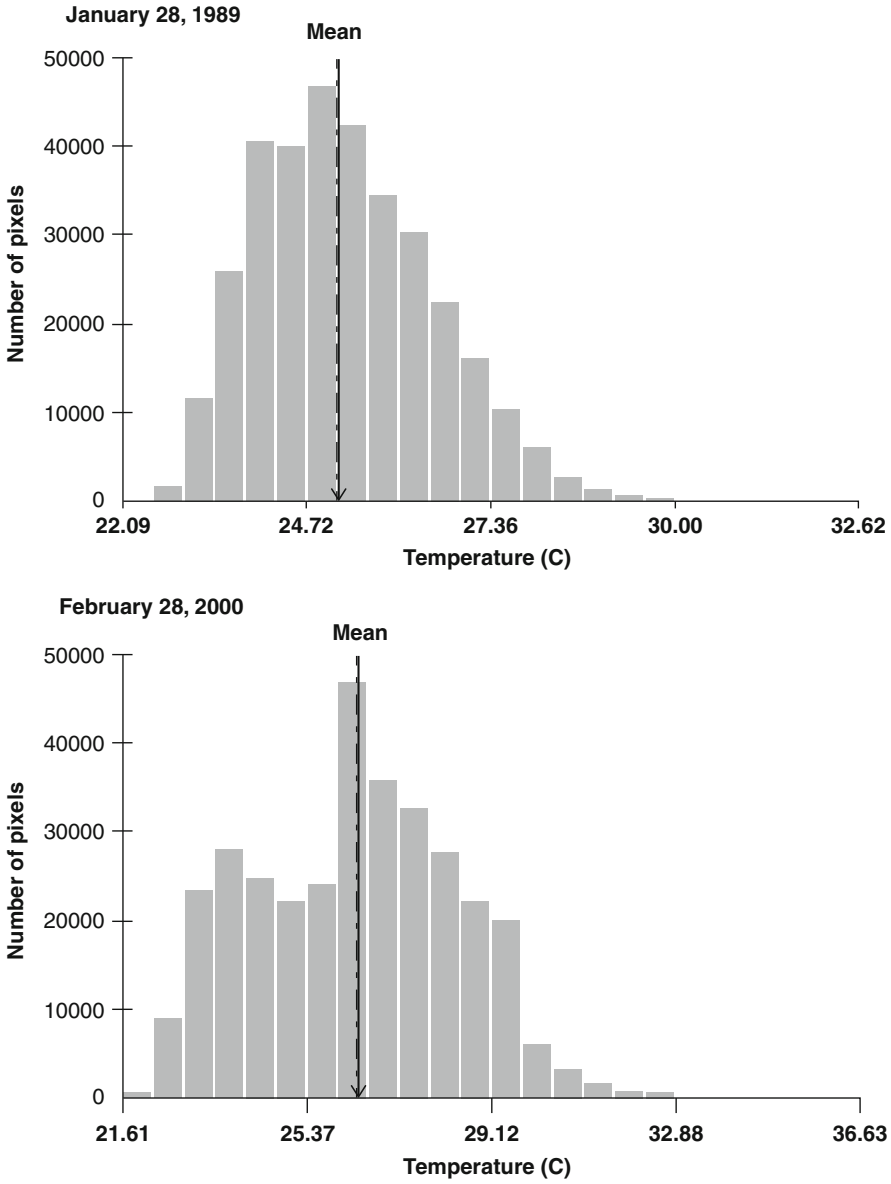

Fig. 11 LST mean for 1989 and 2000

provide insight for understanding the relationship between climate change and urban growth in the developing world. The analysis of the results obtained in this research for Dhaka, Bangladesh, shows that:

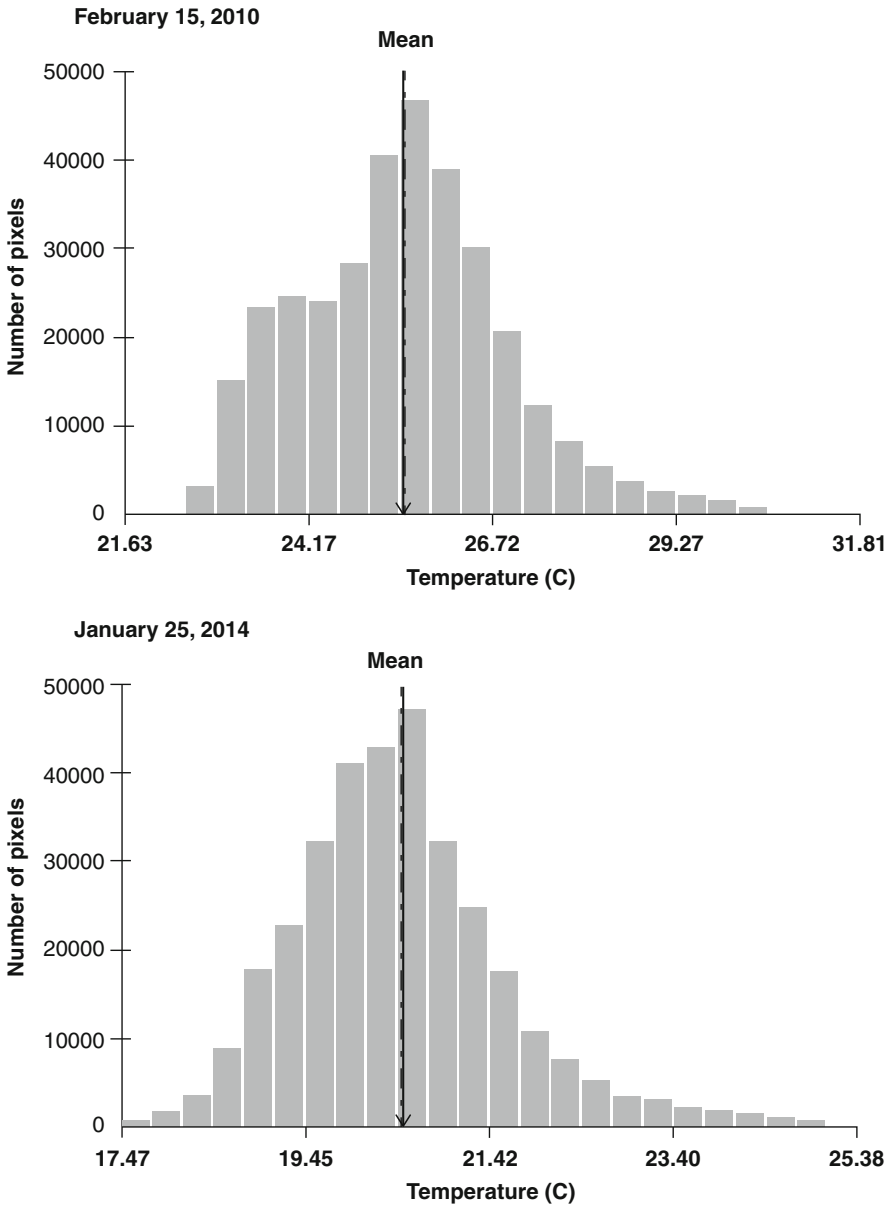

Fig. 12 LST mean for 2010 and 2014

- The land use and land cover change due to urban growth and development can be mapped and quantified using time series data acquired by the Landsat satellite programs from 1973 to date (Landsat 1–3 MSS, Landsat 4–5 TM, Landsat 7 ETM+, and Landsat 8 OLI and TIRS).

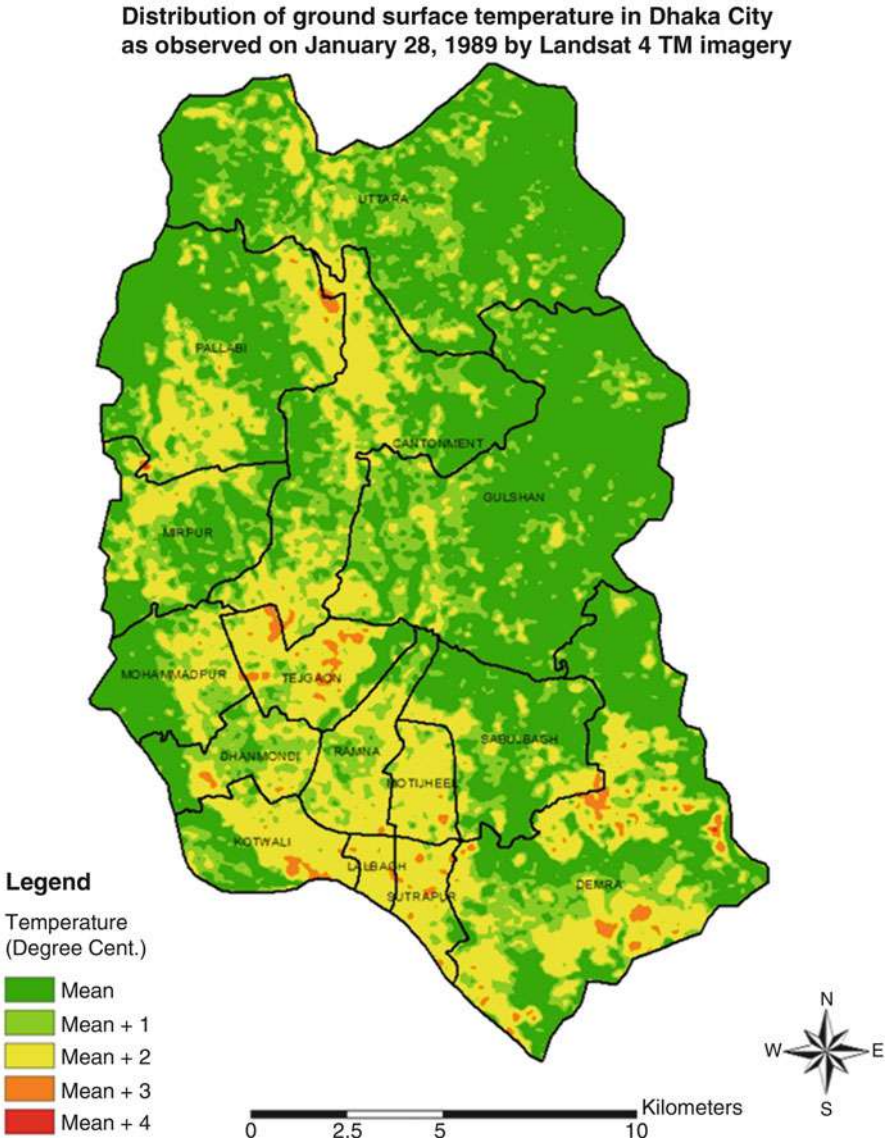

Fig. 13 Distribution of above mean temperature on January 28, 1989

- Landsat imagery-derived NDVI can be used to map and monitor the changes in greenness in growing megacities. It was observed that the average NDVI values in Dhaka decreased continuously from 1980 to 2014 with a significant change between 1989 and 2000.
- The changes in the land surface temperature (LST) can be used to determine the changes in the intensity of urban heat island (UHI) effect as a result of the growth

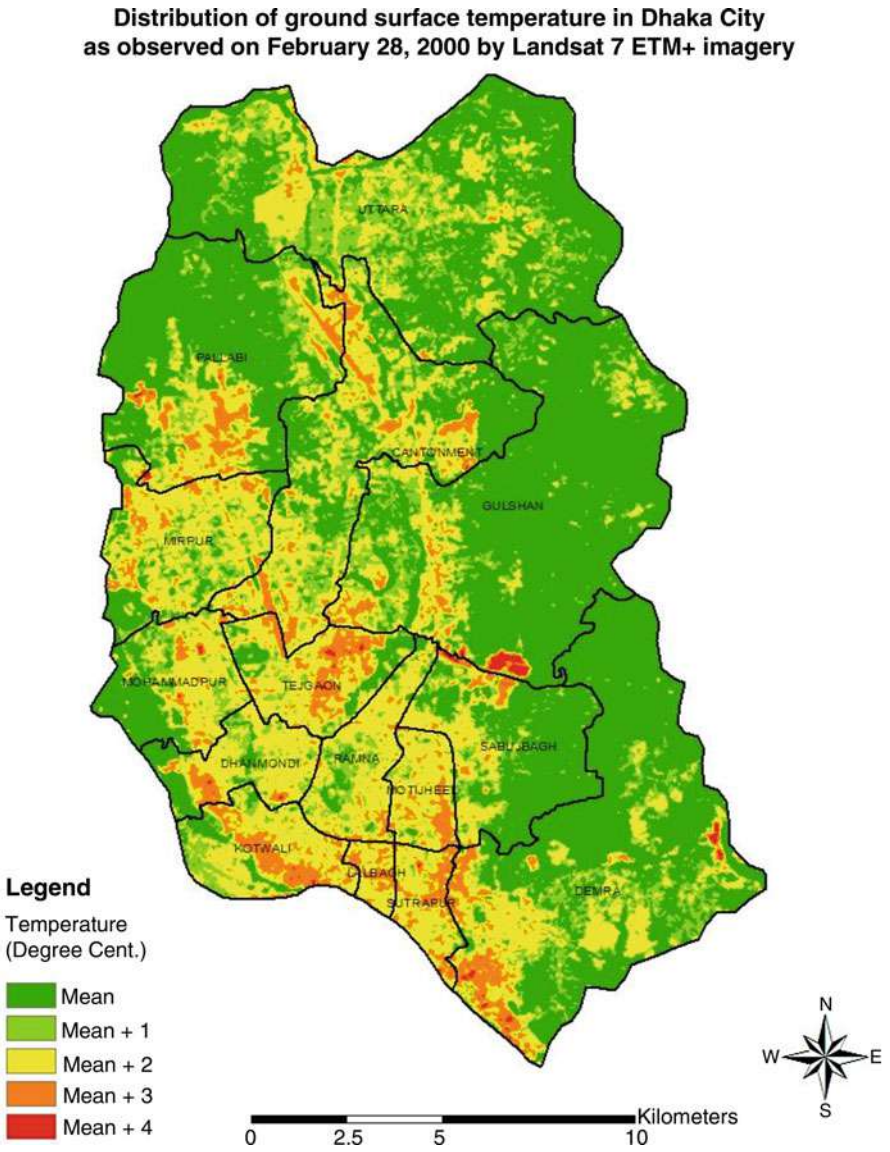

Fig. 14 Distribution of above mean temperature on February 28, 2000

and development in a megacity. The Landsat satellite-observed thermal data can be used to estimate continuous LST at 80–30 m spatial resolution from 1980 to date.

- It is possible to study the changes in the intensity of UHI effects in megacities, such as Dhaka, using the thermal data acquired by Landsat 4–5 TM, Landsat 7 ETM+, and Landsat 8 TIRS from 1989 to 2014. Visual inspection of the

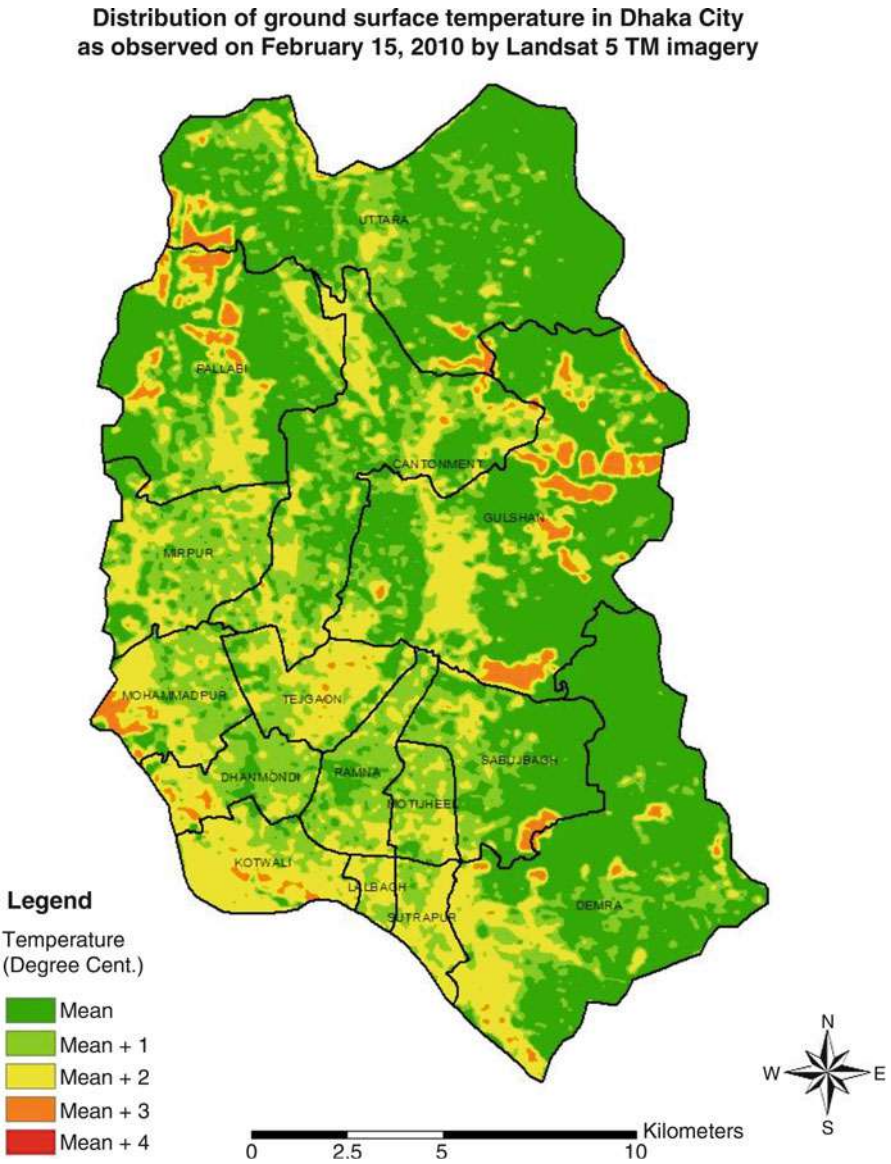

Fig. 15 Distribution of above mean temperature on February 15, 2000

Landsat-derived LST estimation can be used to interpret the changes in the intensity of UHI effects. However, a quantitative assessment of the changes in the spatiotemporal distribution of the LST over time is necessary to quantify the changes in the intensity of UHI effects. Image classification technique of the LST distribution can provide a reasonable solution in this regard. A five-class image classification scheme based on mean LST and 1, 2, 3, >3° above mean LST

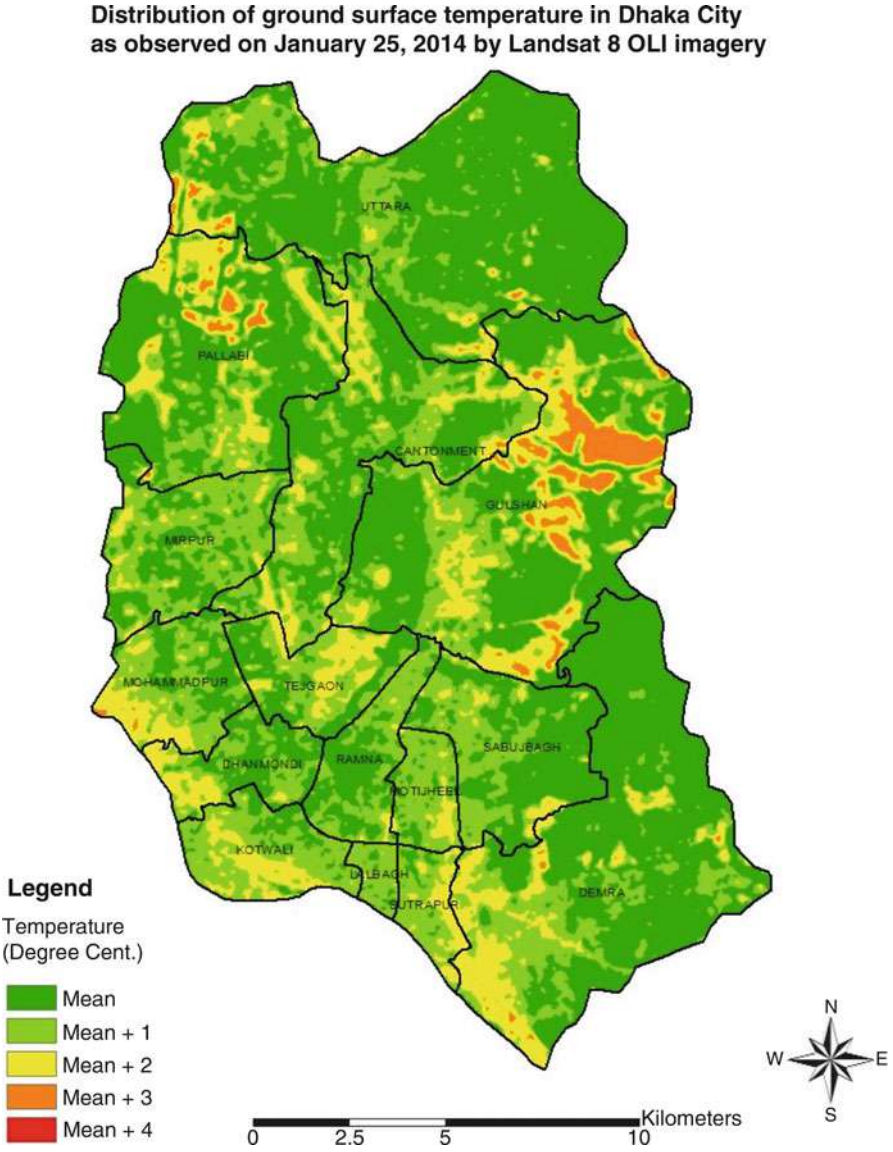

Fig. 16 Distribution of above mean temperature on January 25, 2014

provided a good understanding of the spatiotemporal variation of the above mean LST in Dhaka from 1980 to 2014.

- The imaging technology of LST (thermal data) by the Landsat 8 TIRS is different from that of the other Landsat sensors. The Landsat 8 TIRS data calibration approach used by NASA is also different. More research is needed to make the

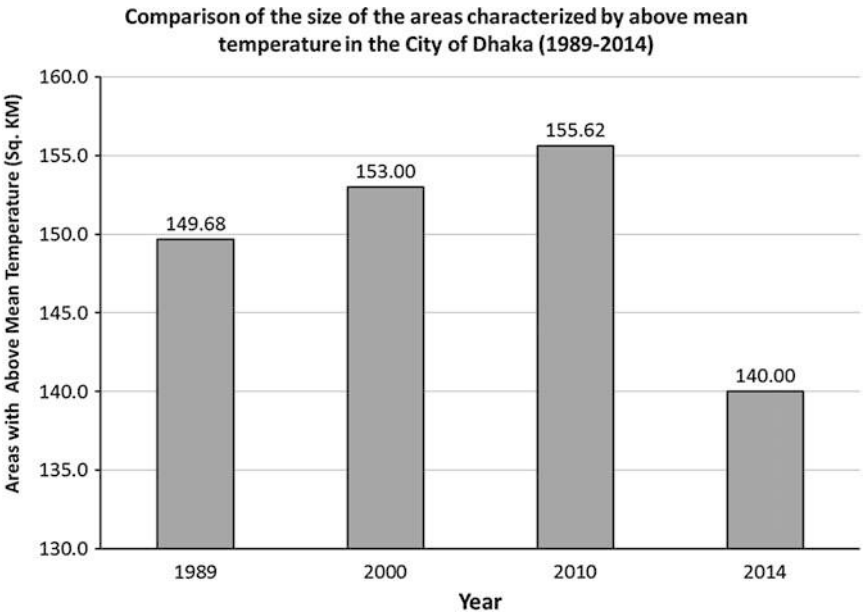

Fig. 17 Comparison of the size of the areas characterized by above mean temperature in the city of Dhaka (1989–2014)

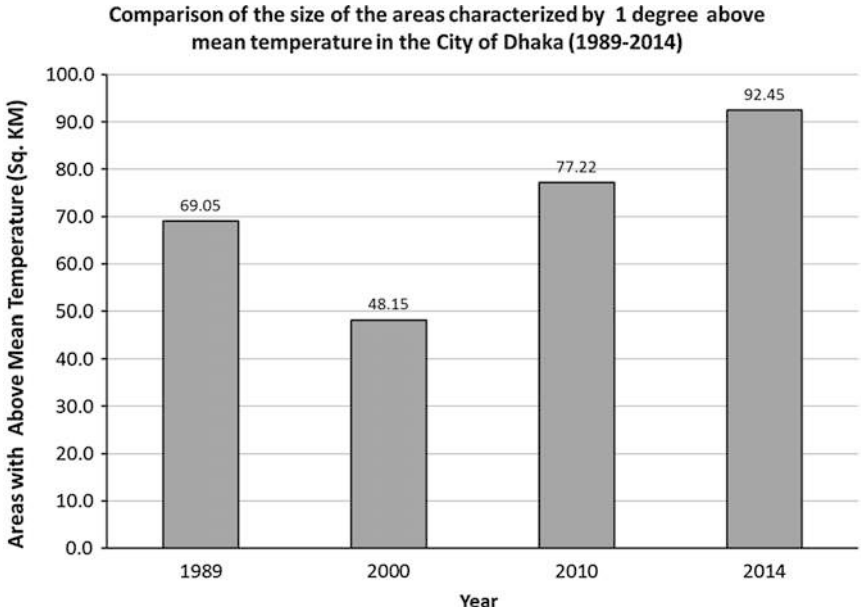

Fig. 18 Comparison of the size of the areas characterized by 1° above mean temperature in the city of Dhaka (1989–2014)

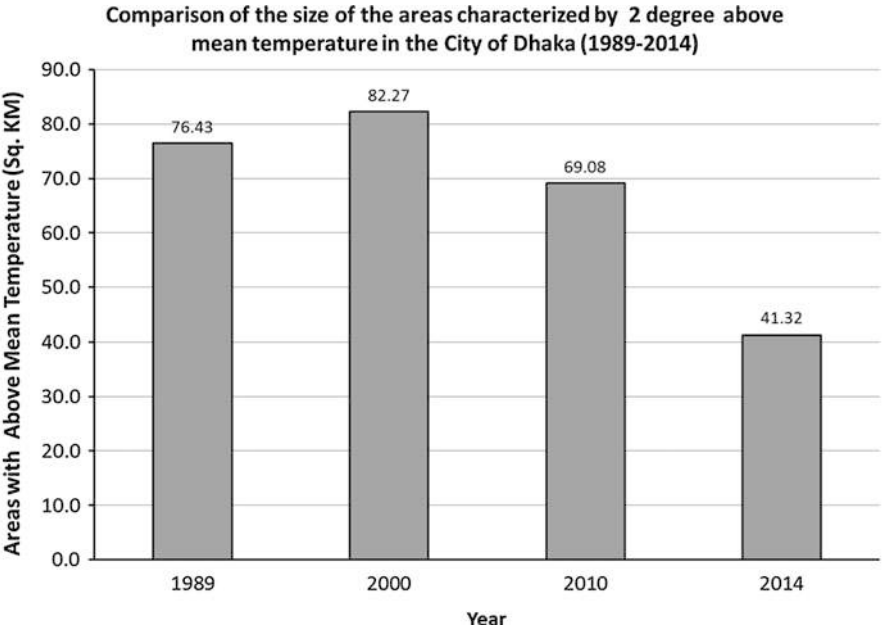

Fig. 19 Comparison of the size of the areas characterized by 2° above mean temperature in the city of Dhaka (1989–2014)

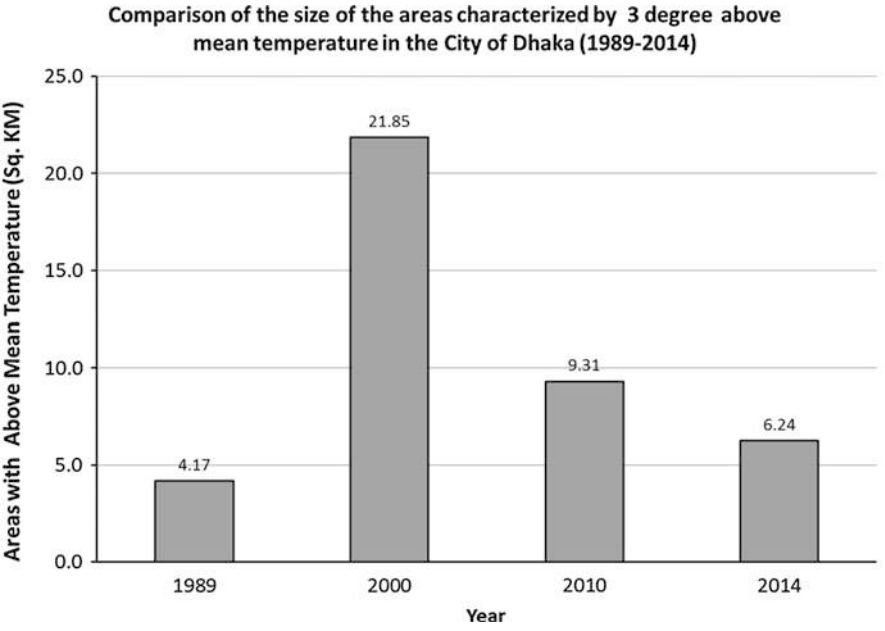

Fig. 20 Comparison of the size of the areas characterized by 3° above mean temperature in the city of Dhaka (1989–2014)

thermal data acquired by Landsat 8 TIRS and other Landsat sensors (TM and ETM+) comparable and reduce uncertainty.
- The interpretation of the changes in the greenness in the city of Dhaka was qualitative in nature in this study. It is recommended to use the surface reflectance-based NDVI calculation for the quantitative change detection studies.

Future Research Directions

The research presented in this chapter shows the potential of remote sensing data and image processing techniques to improve our current understanding about the impact of the growth of megacities in Southeast Asia on climate change. This study provides a good platform for future research to contribute in climate change studies following the emerging "bottom-up approach" (Hossain 2013). As part of this approach, initiatives are underway to extend the current research in the following directions.

- Categorize the NDVI and LST data for specific seasons and months so that the seasonal and monthly variations in land use and land cover and LST are minimized.
- Develop more statistically based methods to determine the changes in the intensity of UHI effects over time by normalizing the seasonal and monthly variations of LST.
- Extend this study to selected other megacities in both developing and developed countries to investigate if the developed methods/techniques work globally to determine the changes in the intensity of UHI effects due to urban growth.

Acknowledgments Thanks are due to NASA and USGS for providing all the Landsat data used in this research at free of charge. Thanks are also due to the National Center for Computational Hydroscience and Engineering (NCCHE) and Mississippi Mineral Resources Institute (MMRI) at the University of Mississippi for providing all the logistics and computing facilities for conducting this research.

References

Boone RB, Galvin KA, Lynn SJ (2000) Generalizing El Nino effects upon Maasai livestock using hierarchical clusters of vegetation patterns. Photogramm Eng Remote Sens 66:737–744

Chander G, Markham BL (2003) Revised Landsat-5 TM radiometric calibration procedures, and post-calibration dynamic ranges. IEEE Trans Geosci Remote Sens 41(11):2674–2677

Chander G, Markham BL, Helder DL (2009) Summary of current radiometric calibration coefficients for Landsat MSS, TM, ETM+, and EO-1 ALI sensors. Remote Sens Environ 113:893–903

Coll C, Galve JM, Sánchez JM et al (2010) Validation of Landsat-7/ETM+ thermal-band calibration and atmospheric correction with ground-based measurements. IEEE Trans Geosci Remote Sens 48(1):547–555

EPA (2015) Heat island effect. http://www.epa.gov/heatisland/. Accessed 20 Apr 2015

Gurjar BR, Nagpure AS, Singh TP et al (2014) Air quality in Megacities. The encyclopedia of earth. http://www.eoearth.org/view/article/149934/. Accessed 26 Jan 2015

Hossain A (2013) Flood inundation and crop damage mapping: a method for modeling the impact on rural income and migration in humid deltas. In: Roger P Sr (ed) Climate vulnerability: understanding and addressing threats to essential resources, vol. 5. Elsevier, Academic Pres, p 357–374. http://store.elsevier.com/product.jsp?locale=en_US&isbn=9780123847034

Hossain A, Easson G (2011) Predicting shallow surficial failures in the Mississippi river levee system using airborne hyperspectral imagery. Geomatics Nat Hazards Risk 3(1):55–78

Kriegler FJ, Malila WA, Nalepka RF et al (1969) Preprocessing, transformations and their effects on multispectral recognition. In: Proceedings of the sixth international symposium on remote sensing of environment. University of Michigan, Ann Arbor, pp 97–131

Lawrence MG, Butler TM, Steinkamp J et al (2007) Regional pollution potentials of megacities and other major population centers. Atmos Chem Phys 7:3969–3987

Maher IS, Kubaisy MHA (2014) Automatic surface temperature mapping in ArcGIS using Landsat-8 TIRS and ENVI tools, case study: Al Habbaniyah lake. J Environ Earth Sci 4(12):12–17

New Scientist Magazine (2006) How big can cities get? 17 June 2006, p 41

Oke TR (1987) Boundary layer climates. Routledge, New York

Oke TR (1997) Urban climates and global environmental change. In: Thompson RD, Perry A (eds) Applied climatology: principles & practices. Routledge, New York, pp 273–287

Rouse JW, Haas RH, Schell JA et al (1973) Monitoring vegetation systems in the Great Plains with ERTS. In: Third ERTS Symposium, NASA SP-351 I, pp 309–317

Schubel JR, Levi C (2000) The emergence of megacities. Med Glob Surviv 6(2):107–110

United Nation (2014) World urbanization prospects, the 2014 revision. Department of Economic and Social Affairs, United Nations, New York

United Nations (1997) The state of world population 1996: changing places: population, development and the urban future. United Nations, New York

USGS (2014) Using the USGS Landsat 8 product. http://landsat.usgs.gov/Landsat8_Using_Product.php. Accessed 20 Apr 2015

World Resources Institute (1998) World resources 1996–97: a guide to the global environment: the urban environment. Oxford University Press, Oxford

Potential of Solid Waste and Agricultural Biomass as Energy Source and Effect on Environment in Pakistan

S. R. Samo, K. C. Mukwana, and A. A. Sohu

Contents

S.R. Samo (✉)
Quaid-E-Awam University of Engineering, Science and Technology (QUEST), Nawabshah, Sindh, Pakistan
e-mail: sfaizsamo@yahoo.com

K.C. Mukwana
Energy and Environment Engineering Department, Quaid-E-Awam University of Engineering, Science and Technology (QUEST), Nawabshah, Sindh, Pakistan
e-mail: kcmukwana@quest.edu.pk; mukwana_99@yahoo.com

A.A. Sohu
Mechanical Engineering Department, QUCEST, Larkano, Sindh, Pakistan
e-mail: sabamydaughter@gmail.com

W.-Y. Chen et al. (eds.), *Handbook of Climate Change Mitigation and Adaptation*,
DOI 10.1007/978-3-319-14409-2_92

Abstract

The issue of waste management is now a global problem because it is not only damaging soils but also deteriorating the natural state of air and water. This chapter focuses on two important aspects of solid waste in Pakistan, i.e., domestic solid waste and agricultural solid waste. The industrial and commercial activities are contributing heavily in large quantity of solid waste. Solid waste comprises of heterogeneous substances. The most common substances may belong to paper, aluminum, plastic, glass, ferrous materials, nonferrous waste, yard waste, construction and demolition wastes, etc. The issue of management of solid waste in Pakistan is a major environmental problem. Various research findings indicate that solid waste generation in Pakistan varies from 0.283 to 0.612 Kg/capita/day, while various studies indicate that the waste generation growth rate is 2.4 % per year. As a general practice, solid waste is commonly dumped on low-lying land or open vacant land area. Then, it is burned by sanitary staff to reduce its volume so that the life span of the dumpsite can be enhanced. However, the dumped solid waste does not burn completely but rather produces clouds of smoke that can be seen from miles away. This causes obnoxious smell and creates a breeding ground for flies and rats.

Various findings indicate that currently, about 60,000 t/day of solid waste is generated in Pakistan. No weighing or segregation facilities are located at any disposal sites. The wastes generated from hospitals and industrial activities are simply treated as ordinary wastes. They are jointly collected and shifted to the dump sites. The research findings indicate that common composition of solid waste in Pakistan contains plastic, rubber, metal, paper, cardboard, textile waste, glass, food, animal waste, leaves, grass, straws and fodder, bones, wood, stones, and fines to certain extent. Out of this the food wastes are 8.4–21 % of the total solid waste; paper waste 15–25 %; leaves, grass, straw, and fodder 10.2–15.6 %; fines 29.7–47.5 %; and recyclables 13.6–23.55 %. Keeping in view this proportion of solid waste, a sustainable and viable management of solid waste may be adopted by recycling, composting, and waste to energy.

In the other part of the chapter, focus is on agricultural waste which is actually agricultural biomass. Being an agricultural country, huge quantity of biomass is generated and remains unutilized or burned in the agricultural fields causing air pollution. It can be observed from Tables 6, 7, 8, and 9 the biomass residue of

various crops such as wheat straw, rice husk, rice straw, cane trash, bagasse, and cotton stalk is in different ratios. These ratios are wheat and wheat straw ratio 1:1, 20 % rice husk found as waste in paddy, paddy and rice straw ratio 1:1, 23 % cane trash found as waste in sugarcane harvest, 30 % wet bagasse found as waste in sugarcane industry, and cotton and cotton sticks ratio 1:3.

Keeping in view the availability factor, the different agricultural residue biomass is used as animal feed and also as a raw source of energy at local level; hence, we theoretically consider 40 % availability of total average amount of agricultural residue biomass, i.e., 5354.73 × 103 t/year. Theoretically considering average calorific value of agricultural residue biomass 3500 KCal/Kg, then the theoretical energy content = 3500 k Cal/Kg × 5354.73 × 10^6 Kg = 1.91 × 10^{13}KCal (heating value) if this amount of heat energy is multiplied by 4.81 for converting K Cal into KJ = 7.97 × 10^{13} KJ or KW-S. Hence, the power plants of about 10,000 MW are possible to be installed in the province of Sindh with the use of only 40 % of single source by agricultural residue biomass of only major crops.

This step will help in reducing air pollution in the region as a whole, and on larger scale it will help in restoring the climatic changes occurring around the world.

Part A: Solid Waste and Its Management in Pakistan

Solid Waste

Solid waste can be explained as the waste that is discarded by the society as unwanted material with the understanding that it is of no any productive use and has passed through its ultimate use. Mostly it is in solid, semisolid, or liquid state and is thrown out from residential, commercial, or industrial premises. The Basel Convention defines wastes as, "substances or objects which are disposed of or are intended to be disposed of or are required to be disposed of by the provisions of the law" (Basel Convention 1989).

With the advancements, solid waste generation has increased enormously and consequently has started to cause environmental problems. In the past whatever the small quantity of solid waste used to be produced by the society, it was thrown in the open environment and the nature was capable to absorb it slowly and gradually without causing any significant harm or effect to the natural environment and the valuable environmental components of it. But the situation changed over time with the generation of large quantities of solid waste, and nature turned unable to replenish the damaging environment as the quantities of waste started to be disposed of in larger quantities. The issue of waste management is now a global problem because it is not only damaging soils but also deteriorating the natural state of air and water.

The large quantity of generation of solid waste is taking place due to changing lifestyles; increasing use of disposable items and excessive packaging are all adding to an increase in the quantity of solid waste being generated. The industrial and commercial activities are contributing heavily in large quantity of solid waste. Solid waste comprises of heterogeneous substances (APO 2004). The most common substances may belong to paper, aluminum, plastic, glass, ferrous materials, non-ferrous waste, yard waste, construction and demolition wastes, etc. (UNEP 2005).

The issues associated with solid waste management are complicated because of the quantity and diversity of the nature of waste as well as financial limitations in large cities. It is due to this reason that nowadays the authorities of municipal organizations, planners, and managers are concentrating on proper management of the solid waste so that it does not cause any adverse problem to the environment in general and human society in particular. The municipal solid waste management (MSWM) is generation, segregation, collection, transferring, transportation, and final dumping to the designated place. By this way it succeeds in addressing public health concerns, economics, conservation, aesthetics, and the environment.

For proper management it is essential to understand sources and types of solid waste (Hoornweg and Thomas 1999). These are given in Table 1.

Composition of Solid Wastes

Waste composition is used to describe the individual ingredients present in solid waste stream and their relative distribution. Knowledge of composition of solid wastes is important in evaluating and assessing the equipment needed, system and management programs, and plans needed for solid waste management. The municipal and commercial portion adds up about 50–75 % of total municipal solid waste generated in a society. The actual percentage distribution depends on the extent of the municipal services provided, location, season, economic conditions, population, social behavior, climate, market for waste materials, and other factors.

Solid Waste Issue in Pakistan

Like the rest of the world's urban areas, the issue of management of solid waste in Pakistan is a major environmental problem. Various research findings indicate that solid waste generation in Pakistan varies from 0.283 to 0.612 Kg/capita/day, while various studies indicate that the waste generation growth rate is 2.4 % per year. As a general practice solid waste is commonly dumped on low-lying land or open vacant land area. Then, it is burned by sanitary staff to reduce its volume so that the life span of the dumpsite can be enhanced. However, the dumped solid waste does not burn completely but rather produces clouds of smoke that can be seen from miles away. This causes obnoxious smell and creates a breeding ground for flies and rats.

Table 1 Sources and types of solid waste

S. no.	Sources	Locations from where solid waste is generated	Types of solid waste
1	Domestic	Single or multifamily housing units	Food waste, paper, cardboard, plastic, textiles, leather, yard waste, wood, glass, metals, ashes, special waste bulky items, consumer electronics, goods, batteries, oil
2	Factories	All locations where light and heavy manufacturing takes place, construction sites, power and commercial plants	Manufacturing process waste, scrap materials, construction and demolition wastes, rubbish, ashes, and special wastes
3	Commercial	Departmental stores, hotels, restaurants, markets, office buildings, etc.	Paper, cardboard, plastics, wood, food wastes, glass, metals, special wastes, hazardous wastes
4	Institutional	Schools, hospitals, prisons, government and private offices	Paper, cardboard, plastic, wood, food wastes, glass, metals, special waste
5	Construction or demolition	New construction sites, road repair, renovation sites, demolition of buildings, broken pavements	Wood, steel, concrete, dirt, etc.
6	Municipal services	Street cleaning, landscaping, parks, beaches, recreational areas, water and wastewater treatment plants	Street sweepings, landscape and tree/plant trimmings, general waste from parks, beaches, and other recreational areas, sludge
7	Agricultural	Crops, orchards, feedlots, agricultural farms, etc.	Spoiled food wastes, agricultural waste, rubbish, hazardous wastes

Source: Solid Waste Management in Asia Urban Development Sector Unit

This soil may have been used for more useful purposes and most important is that the possible recyclable materials are lost (ESMF 2009).

There is no proper waste collection system in any urban area at all. The solid waste is dumped on the streets. Different types of waste are not collected separately. There are no controlled sanitary landfill sites. Citizens are not aware of the relationship between ways of disposing of waste. As a result the overall natural environmental and public health problems emerged frequently. Figures 1, 2, 3, 4, 5, 6, 7, 8, 9, 10, 11, 12, 13, 14, 15, 16, and 17 given below reflect the solid waste dumped in an improper way in an open area (Pakistan's garbage disposal 2001).

Current Status of Solid Waste Generation in Pakistan

Various findings indicate that currently, about 60,000 t/day of solid waste is generated in Pakistan. No weighing or segregation facilities are located at any

Fig. 1 Improper dumping of solid waste in the vicinity of vacant residential area

disposal sites. The wastes generated from hospitals and industrial activities are simply treated as ordinary wastes. They are jointly collected and shifted to the dump sites (Wastes in Pakistan 2006). The estimated waste generations in different cities of Pakistan are given in Table 2.

Dumping of solid waste at abandoned open places and then its burning are the common practice. This thrown away waste has got lot of potential for recycling and is lost away easily. The total collection varies from 51 % to 70 %, while the rest of the solid waste stays behind on the streets. No relevant disposal facilities exist anywhere. It is unfortunate that no any city in Pakistan has acceptable solid waste management system right from generation of solid waste up to its final disposal. All such uncollected waste poses certain risk to the human health as well as results in clogging of drains and formation of stagnant pools of dirty water. This situation provides breeding ground for mosquitoes and flies that result in spreading malaria and cholera.

Common Composition of Solid Wastes in Pakistan

The research findings indicate that the common composition of solid waste in Pakistan contains plastic, rubber, metal, paper, cardboard, textile waste, glass, food, animal waste, leaves, grass, straws and fodder, bones, wood, stones, and fines to certain extent. Out of this the food wastes are 8.4–21 % of the total solid

Fig. 2 Improper dumping of solid waste in the low-lying area

waste; paper waste 15–25 %; leaves, grass, straw, and fodder 10.2–15.6 %; fines 29.7–47.5 %; and recyclables 13.6–23.55 % (UNEP 2005).

Environmental Problems Due to Solid Waste

Ground Pollution

As water whether surface or rain infiltrates deep down through solid waste, it causes leachate that comprises organic matter and may contain metallic substances like iron, mercury, lead, and zinc from discarded batteries and appliances. The leachate may also contain paints, chemical substances, pesticides, detergents, printing inks, etc. Such polluted water may cause serious impact on all living beings, including humans, and on an ecosystem.

Air Pollution

When solid waste is burned away in such an open place, heavy metals like iron and lead and harmful gases spread over the populated areas and result in air pollution. The blowing of wind also transfers finer solid waste substances, dust particles, and gases to the far-flung areas. The disintegration of solid waste in sunlight results in obnoxious smells and reduced visibility.

Fig. 3 Scavengers searching and collecting valuable items from improperly dumped solid waste

Health Hazards

The open dumping of solid waste initiates skin and eye infections and turns common in the prevailing area. Finer dust particles in the ambient air at or in the vicinity of dumpsites can cause respiratory problems in children and elders. The insects like flies breed on openly dumped waste and spread diseases like diarrhea, typhoid, all types of hepatitis, and cholera. Mosquitoes' bites transfer many viruses and parasites that cause diseases like malaria and yellow fever. Stray animals like dogs, cats, and rats staying and wondering around the dump site turn carriers of a variety of diseases including plague and fever. Even the sanitary staff engaged in handling and transferring of solid waste suffers from intestinal and skin diseases.

Major Constraints in Solid Waste Management in Pakistan

The proper management is missing in Pakistan because of numerous problems and issues. They include lack of infrastructure, inadequate budgetary allocations, lack of clear roles and responsibilities, uncontrolled disposal of solid waste (dumped in suburb and city boundaries), threat to public health and sanitation, and environmental pollution. In all such circumstances, solid waste solutions are not only with the engineers but can equally be distributed in between 50 % engineering and 50 % social – policy and institutional lack of participation and involvement (UNEP 2005).

Fig. 4 Scavengers intentionally burning the dumped solid waste and collecting exposed metallic items

Integrated Solid Waste Management Practices

Integrated solid waste management (ISWM) can be explained as a comprehensive waste prevention, recycling, composting, and disposal program through which the generated solid waste is managed in an environment-friendly way. A successful ISWM system focuses on prevention, recycling, and managing solid waste in such a way that it effectively protects human health and the natural environment. ISWM concentrates on sustainable solid waste management and involves in examining local needs and conditions. After this it selects the most suitable solid waste management methodologies for their strategies. Each and every activity needs careful collection and transportation of the waste to the final disposal point (Landfill design, U.S 1993).

Waste Prevention

Waste prevention is a term used for "source reduction" under which efforts are launched to prevent waste from being produced. The methodologies for waste prevention are the use of less packaging material, designing and manufacturing such items that can stay longer, and reusing repeatedly the products and materials which are once produced. Waste prevention supports in reduced handling, reduced treatment, and minimized disposal costs and in the end reduces the generation of methane.

Waste Recycling

Waste recycling may be defined as a process of collecting, reprocessing, and recovering certain waste substances, e.g., metals, glass, plastics, and paper, to

Fig. 5 Improperly dumped solid waste and its burning cause smoke and air pollution

Fig. 6 Improper dumping of solid waste causes damage to water and soil resources

produce new items. After collection, substances are segregated and forwarded to facilities that process them to manufacture new products and items and are made available as new products for their use. Recycling is the excellent option to resolve solid waste management issues. This technique of recycling exists in most cities. However, the recycling system differs from developing countries and developed countries. The advanced countries have established well-organized at-source segregation and recycling system, while in the developing countries, the system of recycling is not effective.

Fig. 7 Solid waste skip fully filled with waste and dropping down on the ground

Recycling converts materials into valuable raw materials that otherwise would have become useless waste and initiates a host of environmental, financial, and social benefits (Environment Protection 2011). There are at least five benefits for recycling of solid waste and they are as under:

(a) **Economic**
Possible economic benefit of waste prevention includes reduced waste disposal fees as the waste is not usually disposed free of cost; rather, substantial charges are to be paid by the producer. On the other hand, revenues can be earned from recycling commodities by selling the recyclable substances.

(b) **Environmental**
The environmental advantage lies in reduced energy consumption, reduced pollution, conservation of natural resources, and extension of valuable landfill capacity, which stimulate the development of greener technologies and prevent emissions of many greenhouse gases and water pollutants.

(c) **Employee Morale**
Employees' morale improves when they see the company taking steps to reduce waste through recycling. This enhanced morale certainly increases employee interest, productivity, and more waste prevention measures. Some companies use recycling revenues for employee recreation (i.e., picnics, holiday parties, etc.).

(d) **Corporate Image**
When customers and the surrounding neighborhoods see that the company is environmentally conscious, it creates a favorable image of the company. An enhanced corporate image might attract customers. It is noted from various surveys that more consumers now give preferences to a firm's environmental record when making purchasing decisions.

Fig. 8 Improperly dumped waste material alongside a wall of a residential house

(e) **Compliance**
Reducing solid waste through recycling means compliance with local or state solid waste regulations. Some stakeholders and organizations restrict the quantities or types of waste accepted at solid waste management facilities. By implementing an extensive and sustainable recycling program, the business can help ensure compliance with these requirements.

Waste Composting

Composting is the term used for degradation of organic materials under controlled conditions. This practice results in a marketable soil amendment or mulch. It is in fact a natural process that can be carried out with very simple human efforts. It can be systematically executed by reducing the composting time and space required and by minimizing the objectionable smells. The stabilized end products obtained after composting are rich in organic matter. These end products can act as a fine soil conditioner. But the concentrations of key nutrients such as nitrogen, phosphorus, and potassium are typically low in comparison to commercially manufactured fertilizers.

In the simplest composting systems, yard wastes are stacked in long, outdoor piles called windrows. A typical windrow might be 2 m high, 3 or 4 m wide, and tens of meters long. Their length is determined by the rate of input of new materials, the length of time that materials need for decomposition, and the cross-sectional area of the pile. The composting process is affected by temperature, moisture, pH, nutrient supply, availability of oxygen, bacteria, and fungi. These are principal players in the decomposition process. But microorganisms such as nematodes,

Fig. 9 Animals like dogs contract pathogens from the dumped solid waste material which spreads within the human settlements

mites, bugs, earthworms, and beetles also play a key role by physically breaking down the materials into smaller bits that are easier for microorganisms to attack (Integrated Agricultural Systems 2002).

A number of nutrients must be available to the microorganisms that are attacking and degrading the compost pile. The most important nutrients needed are carbon for energy, nitrogen for protein synthesis, and phosphorus and potassium for cell reproduction and metabolism. In addition, a number of nutrients are needed in trace amounts, including calcium, cobalt, copper, magnesium, and manganese.

Disposal (Landfilling and Combustion)

The landfilling and combustion activities are adopted to manage that solid waste which cannot be prevented or recycled. Under the method of landfilling, the solid waste is placed in properly designed, constructed, and managed landfills. In the landfills the dumped solid waste is safely contained permanently. The other method to handle this waste is through combustion. Combustion is the controlled burning of waste, which helps reduce its volume, and the burning process is called as incineration.

The Three Rs (Reduce, Reuse, and Recycle)

In today's world, reduce, reuse, and recycle, commonly referred as the three Rs for waste management, are effective measures that serve as alternatives to disposing

Fig. 10 Open dumping practice of solid waste in huge quantity on a large area

waste in landfills. Nowadays, various methods are available for properly managing the solid waste that is produced. The relevant municipal authority introduces an integrated approach to manage the generated solid waste along with combination of substitute options. The strategies of three Rs assist in reducing down the quantities of waste disposed away. The strategies of three Rs presently are helping out in conserving natural resources, landfill capacities, and energy. In addition to this, the three Rs save land and money. Choosing a new landfill has become complicated and more costly due to environmental bindings and opposition from the public living in the vicinity (Margaret Cunningham 2010).

(a) **Reduce**

The concept behind the option of reduce is not to produce the solid waste. This option can be practiced by purchasing carefully and being familiar with few guidelines like purchasing products in bulk quantity. Larger, economy-size items or those products that are confined in less packaging may be opted, avoiding overpackaged products, especially those which are packed with several materials such as foil, paper, or wooden boxes. Avoid disposable goods, such as paper plates, cups, napkins, razors, and lighters as their disposal contributes to the problem. Additionally, they are expensive because they are replaced again and again. Purchase long-lasting products that are durable or that carry good warranties. They will be long-lasting, save money in the long run, and save landfill capacities. At the office environments, make two-sided copies whenever possible. Maintain one master file instead of using several files.

Fig. 11 Scavenger is busy in openly burning the solid waste

Adopt the practice of using electronic mails or maintain a bulletin board for correspondence and communication. Also, adopt the practice of usage of cloth napkins instead of paper napkins.

(b) **Reuse**

The concept behind reuse is using again and again the products that are capable to do that. By adopting this practice, the paper material and plastic bags can be saved in larger quantities. More importantly, the broken appliances like furniture and toys can be repaired and made ready for reuse. Similarly, use a coffee can to act as a lunch box. Reuse successfully plastic microwave dinner trays as picnic dishes. Sell old clothes, appliances, toys, and furniture in garage sales or donate them to charities. Use resealable containers rather than plastic wrap. Use a ceramic coffee mug instead of paper cups. Reuse grocery bags or bring your own cloth bags to the store. Avoid taking any a bag from the shops until and unless they are really needed.

(c) **Recycling**

Recycling practice may be explained as a series of steps in which the used materials are processed and converted into raw material again and new products are remanufactured. These remanufactured items are sold as it is as a new product. The concerned organizations advise to purchase products made from recycled material. The remanufactured products are identified by a symbol called a recycling symbol. The recycling symbol indicates out one of the two things –

Fig. 12 Smoldering smoke coming out from dumped solid waste

either the product is made of recycled material or the item can be recycled. For instance, many plastic containers have a recycling symbol with a numbered code that indicates out the type of plastic resin it is made from. The users of the relevant plastic product can check out collection centers and curbside pickup facilities to see what they accept and start collecting those materials. Most commonly, the recyclable materials may include metal cans, newspapers, paper products, glass, and plastics. Preferences must be given to buying recycled materials at work when materials for office supply, office equipment, or manufacturing are needed. Speak to store management and ask for products and packaging that help in reducing down the solid waste. Prefer purchasing those items made from substances that are collected for recycling in the local area. Adopt practices for recycled paper for letterhead, copier paper, and newsletters.

Solid Waste Collection

Solid waste collection is the first operation of the solid waste management stream. More significantly, three parties play an important role in this operation, i.e., the producers of the waste, the municipal authority, and the sanitary staff. In order to execute this system, all the three parties have to work in close coordination; else, it will be difficult to yield the success. The producers must be familiar with their roles

Fig. 13 Improper dumping of solid waste and emerging smoke in the vicinity of vacant residential area

and responsibilities, and then there come the responsibilities of the municipal authorities and then the sanitary staff. For better performance the collection system can be classified in residential refuse collection systems, commercial waste collection, and recyclable material collection.

In executing waste collection system, there may be some influence of prevailing climate, topography, available transportation systems, traffic, roads, types of wastes, and population density. However, they can be managed by adopting best waste collection practices.

Waste Management Through Source Reduction

The solid waste that is not produced does not have to be collected is a simple concept. That is not the case in many other advanced countries in the world – especially those with modest domestic resources and limited land space for disposal, such as Germany and Japan. In such circumstances, strategies like good green design practices can be considered successful in reducing solid waste.

Green Product Design Strategies

The design that reduces the environmental impacts associated with the manufacture, use, and disposal of products is an important part of any pollution prevention

Fig. 14 Improper dumping of solid waste in the vicinity of vacant residential area

strategy. Companies that engage in such green product design are finding products that combine environmental advantages with good performance and price. The Office of Technology Assessment, USA, identifies two complementary goals of green design:

(a) Waste prevention
(b) Better material management

Waste prevention can be achieved by reducing the weight, toxicity, and energy use of products along with increasing the useful life of products. Better material management facilitates remanufacturing, recycling, and composting along with enhanced energy recovery opportunities.

Product System Life Extension

Products that do not wear out as quickly do not have to be replaced as often, which usually means that resources are saved and less waste is generated. Sometimes, products are discarded for reasons that have nothing to do with their potential lifetime. For example, computers become obsolete and clothing fashions change, but many products can continue to remain in service for extended periods of time if they are designed to be durable, reliable, reusable, remanufacturable, and repairable. Extending product life means consumers replace their products less often, which translates into decreased sales volume for manufacturers. Market share in the future may be driven to some extent by

Fig. 15 Improper dumping of solid waste and exposure of pollutants to the passersby

consumer demand for greener products. Consumers, of course, must make that happen.

Material Life Extension

Once a product has reached the end of its useful life, the materials from which it was made may still have economic value, and additional savings can result from avoiding disposal. The key design parameter for extending the life of materials is the ease with which they can be recycled. Products that have been designed to be recycled easily are becoming especially common in Germany. For example, Germany's requirement that automakers take back and recycle old automobiles has stimulated green design in companies such as BMW and Volkswagen. BMW already sells cars with plastic body panels that have been designed for disassembly and that are labeled as to resin type so they may more easily be recycled.

Material Selection

A critical stage in product development is selection of appropriate materials to be used. In green design, attempts are made to evaluate the environmental impacts associated with the acquisition, processing, use, and retirement of the materials under consideration. In some cases substituting one material for another can have a modest impact on the quality and price of the resulting product but can have a considerable impact on the environmental consequences.

Fig. 16 Large number of scavengers busy in searching valuable items from solid waste

Process Management

Manufacturing products requires raw materials and energy inputs. Both of which often can be managed more efficiently. The energy required to manufacture a product is an important component of a life cycle assessment. Process improvements that take advantage of waste-heat recovery, more efficient motors and motor controls, and high-efficiency lighting are almost always very cost effective.

Efficient Distribution

Methods of packaging and transporting products greatly affect the overall energy and environmental impacts associated with those products. Transportation costs are affected by the quantity and type of material shipped, which is in turn affected by packaging, trip distance, and type of carrier. The type of carrier is constrained by the terrain to be covered as well as the speed required for timely arrival. In general, shipping by boat is the least energy-intensive option, followed by rail, truck, and then air, which is fastest but requires the most energy per ton-mile transported.

Policy Options

Germany has shifted the burden of packaging disposal from the consumer back to manufacturers and distributors. Germany's Packaging Waste Law requires manufacturers and distributors to recover and recycle their own packaging wastes. The concept may even be extended to large durable goods, such as household appliances and automobiles. Germany's take-back policy is one of many examples of approaches that governments can take to encourage reduction in the environmental costs of products.

Fig. 17 Open transportation of collected solid waste and the sanitary staff involved in loading activity without relevant safety measures

Table 2 Estimated waste generation in different cities of Pakistan

S. no.	Name of city	Population	Waste generation rate Kg/capita/day	Daily waste generation (tons/day)	Annual waste generation (tons/year)
1	Karachi	1,66,31,255	0.613	10,195	37,21,160
2	Hyderabad	14,96,163	0.563	842	3,07,454
3	Peshawar	13,44,967	0.489	658	2,40,056
4	Faisalabad	28,08,982	0.391	1098	4,00,883
5	Quetta	6,57,788	0.378	248	90,755

Source: Sustainable Development Policy Institute Islamabad Pakistan

Labeling

Surveys have consistently shown that American consumers purchase products that are environmentally superior to competing products, even if they cost a bit more. Attempts by manufacturers to capture that environmental advantage have led to an overuse of poorly defined terms such as recyclable, recycled, eco-safe, ozone friendly, and biodegradable on product labels. Unfortunately, without a uniform and consistent standard for such terms, these labels are all too often meaningless or even misleading. For example, all soaps and detergents have been "biodegradable" since the 1960s. Aerosols "CFC-free, ozone friendly" have been the norm in the USA since the banning of CFCs for such applications in 1978.

Landfill Operations for Municipal Solid Waste

The properly designed landfills for disposal of municipal solid waste have brought a revolution in the place of traditional dumping of waste in the outskirts of residential settlements. The traditional waste dumping used to develop a variety of environmental pollution problems, viz., emergence of large number of flies, rats, airborne diseases, obnoxious smells/odors, and a black cloud of smoke.

The term landfill refers to physical facilities adopted for the final placement of solid wastes in the ground. There are few more terms which are used in this exercise of solid waste dumping. For example, **sanitary landfill** refers to engineered mechanism for the dumping of domestic solid wastes into the ground to reduce the public health and environmental impact, while the term **secure landfill** refers to the engineered facility for the dumping of hazardous wastes.

When the waste is placed in the landfills, biotransformation of organics takes place, and landfill gases and liquids are generated. The aerobic process starts to take place; then, it is followed by anaerobic processes. The aerobic processes produce and release carbon dioxide (CO_2) and liquid (H_2O), while the anaerobic process produces carbon dioxide (C_2O), methane (CH_4), and trace amounts of ammonia and hydrogen sulfide (Landfill manuals 1993).

Nowadays, the proper dumping of municipal solid waste in the properly designed and constructed land areas is referred as municipal solid waste landfills.

The term landfill refers to physical facilities adopted for the final placement of solid wastes in the ground. There are few more terms which are used in this exercise of solid waste dumping. For example "**Sanitary landfill**" refers to engineered mechanism for the dumping of domestic solid wastes into the ground to reduce the public health and environmental impact. While the term "**Secure landfill**" refers to the engineered facility for the dumping of hazardous wastes.

When the waste is placed in the landfills biotransformation of organics take place and landfill gases and liquids are generated. The starting take place aerobic process, then it is followed by anaerobic processes. The aerobic processes produce and release carbon dioxide (CO_2) and liquid (H_2O). While the anaerobic process produces carbon dioxide (C_2O), methane (CH_4) and trace amounts of ammonia and hydrogen sulfide (Environment Protection 2011).

Solid Waste Management Landfill Methods

There are various landfill methods which are discussed as under:

(a) **The trench method**
The trench method of landfills is used in level terrain. The trenches are dug by excavation in the ground. Solid waste is filled in the trenches and dirt is replaced on top of the buried material. After completion the trench is compacted.

(b) **The area method**
The area method is the most popular landfill method. In this method a side of a hill or a sloped area is found out. Then, refuse is dumped on the side of the slope and then covered with dirt. It continues until the entire slope is leveled.

(c) **The valley or ravine method**
The valley or ravine method is commonly used where large quantities of waste are generated by large cities. This method is used in an area with large depression or slope such as a valley or ravine. Usually, an area naturally developed is considered most suitable. Refuse is dumped in the depression and filled with dirt. The area is then compacted and built up.

Landfill Operation Classification

There are three classifications of landfills:

(a) **Class I landfills or secure landfills**
These landfills are designed for dumping of hazardous waste.
(b) **Class II landfills or monofills**
These landfills are designed for dumping of designated wastes, which are particular types of wastes such as incinerator ash or sewage sludge that are relatively uniform in characteristics.
(c) **Class III landfills or sanitary landfills**
These landfills are designed for dumping of municipal solid waste.

Though landfills remain the primary means of municipal solid waste disposal, three Rs of reduce, reuse, and recycling are beginning to have greater attraction in the waste management system.

Landfill Site Construction Requirements

The construction of a landfill site requires a step-by-step approach. The landfill activity planners and designers are basically concerned with the viability of a suitable site (Pak EPA 2011). In order to construct commercially and environmentally feasible landfill site, specific requirements must be kept in consideration. The specific requirements are discussed below:

(a) **Location**
The landfill site should be in easy access to transport the solid waste by road. The transfer stations may be established if the haul distance is far away or rail network is used for solid waste transportation. In addition to this, land value (cost of land), cost of meeting government requirements, and prospects of overall community served through the operation may also be considered before making any final decision. Types of construction, i.e., more than one landfill, may be used at a single site in order to enhance the life of the planned site for a very long time.
(b) **Stability**
It is the complete study of underlying geology at the planned landfill site, by studying the nearby area for earthquake faults or any such weak strata, underground water table, and location of nearby rivers, streams, and flood plains so that the landfill site stays intact.
(c) **Capacity**
Capacity refers to the quantity of solid waste that is to be dumped in the landfill area. The calculation of solid waste capacity is based on quantity of the wastes,

amount of intermediate and daily cover applied to it, and amount of settlement that the waste will undergo following tipping. The thickness of capping the landfill operation is considered along with construction of lining and drainage layers when it is completely filled at its end.

(d) **Protection of soil and water**
The solid waste is permanently dumped in the landfills. This permanent placement of solid waste needs installation of liner and collection systems. In addition to this arrangement for storm water control, leachate management and landfill gas migration may be seriously considered.

(e) **Nuisance and hazard management**
The overall operation of solid waste landfills is of critical nature. The solid waste is transported from one place to its final disposal. It is ensured that it does not cause any nuisance as there is a chance of it falling down from the loaded vehicle on its hauling path. The waste may possibly emit odor that is again a nuisance for the residents living on the haul-way path or near the landfill site. In some cases the solid waste may be infectious or hazardous in nature, and in that case special attention must be given while collection is performed.

Basic Features of Landfills

Moisture or water content in a landfill is important if the wastes are to decompose properly. The initial moisture contained in the wastes themselves is quickly dissipated, so it is water that percolates through the surface, sides, and bottom that eventually dominates the water balance in the landfill. Water percolating through the wastes is called leachate. Its collection and treatment is essential to the protection of the local groundwater.

Municipal solid waste landfills require composite liners and leachate collection system to prevent groundwater contamination. The composite liner consists of a flexible membrane liner (FML) above a compacted clay soil. Leachate is collected with perforated pipes that are situated above the FML. A final cover over the completed landfill is designed to minimize infiltration of water (BC Ministry of Environment 2013).

During waste decomposition, methane gas is formed so completed landfills need collection and venting system.

Sources of Methane: Landfill

On a global scale the methane gas emissions from landfill activities are estimated to be in between 30 and 70 million tons each year. It is believed that major releases of this landfill methane presently come from developed countries, where the levels of waste tend to be highest and no comprehensive methane recovery mechanism is adopted.

Landfills provide most suitable conditions for methanogenesis, with huge quantity dumping of organic material and prevailing anaerobic conditions. The larger quantities of waste which are dumped in landfills can produce methane for years to come after the closure of the landfills, as the waste passes through slow decay under the ground.

The municipal solid waste landfill activities are the largest human-related methane emissions. This landfill gas is easily captured and redirected if relevant

arrangement is made. Firstly, the commercial landfill gas energy (LFGE) recovery project was started in 1975 in Los Angeles. Gases are released during decomposition in landfills. When captured and converted to an alternative energy source, LFG is called biogas. The municipal solid waste decomposition releases methane ~50 %, $CO_2 \sim 45$ %, and $N_2 \sim 5$ % (Ahmed et al. 2013).

Methane release takes place from landfills either directly to the air or by diffusion through the soil cover and causes impacts on the natural environment.

Infectious Waste

Infectious waste is a waste that possesses potential risk of diseases or illness to human beings or a waste that is capable of causing infectious diseases. Segregation and labeling of infectious waste is carried out at its source of generation. When performing handling of infectious waste, it should be ensured that it must be carefully managed. The intactness of the packaging must be maintained and quicker bacterial growth and putrefaction is repressed. The containers in which sharps are placed must be impervious, rigid, puncture resistant, leak resistant, and sturdy so that they can sustain the risk.

Infectious waste may include human blood, body fluids, separated or removed away body organs through surgical operation, syringes, sharps, glassware, or all items used during the treatment activity on an infected patient.

Training for Handling Infectious Waste

Persons working with blood may be trained about blood-borne pathogens. The engaged staff working with animal contact may be trained with relevant training. The staff working with any waste that carries a potential risk of transmitting illness or disease to humans may be trained with infectious waste management. The staff engaged with infectious organisms having risk to cause illness or disease in healthy people, animals, or plants may be trained in biosafety.

Personal Protective Equipment for Handling Infectious Waste

The people who are engaged in handling infectious waste must be advised to wear relevant personal protective equipment (PPE), for example, wearing impermeable gloves for handling infectious waste. For splashing risk, wearing of eye protection or wearing shoe covers for walk-through hazards is advised.

Infectious Waste Storage

The noninfectious waste must be kept separate from infectious waste. If infectious waste is mixed by mistake with noninfectious waste, then it must be considered as infectious waste. Efforts should be made to minimize storage time duration. The area where infectious waste is placed must only be accessible by authorized personnel. The infectious waste storage area must be ventilated to outdoors. The area must be labeled with a warning sign in a clear and visible manner. The area must thwart exposure to common people, animals, and insects and disclosure to

weather. Red- or orange-colored bags are generally used for putting the infectious waste and are also called biohazard bags. The colored bags must be correctly sealed when filled. For leakage or seep hazards, leak-proof bins or bags should be used.

Labels for Infectious Waste

The universal biohazard symbol must be displayed at the place where infectious waste is placed. The biohazard symbol should be understandable from at least seven meters away from the placed bags containing infectious waste. A written message like "biohazard" or "biohazardous," "infectious waste," or "biomedical waste" must also be displayed.

Hazardous Waste

Wastes containing harmful components that are too dangerous to be handled in ordinary manner and sent to the landfill, dumped into the sewer system, or released into the atmosphere are hazardous substances. These can be in a form of a solid, liquid, contained gas, or sludge. Improper release of hazardous waste may seriously threaten the environment and human health. Hazardous waste is regulated from the moment it is created through the time of final disposal. Identification of listed hazardous wastes:

F-Listed Wastes
- Wastes from nonspecific sources
- Solvents from cleaning and degreasing operations
- Wastewater treatment

K-Listed Wastes
- Created from specific sources
- Chemical or pesticide manufacturing

P-Listed Wastes
- Acutely hazardous discarded commercial chemical products
- Arsenic trioxide

U-Listed Wastes
- Less hazardous discarded commercial chemical products

Future Changes in Solid Waste Composition

In terms of solid waste management planning, knowledge of future trends in the composition of solid waste and quantities is of great importance. As the time is passing, we are experiencing new lifestyles and for that we too adopt many practices; some of them are pointed as under:

(a) **Food waste**
The quantity of kitchen food waste collections has been changed significantly with the passage of time as a result of technological advancements and change in public health. Food processing and packaging industry and the use of kitchen food waste have affected the quantity of food waste. The proportion of food waste, by weight, has decreased as it is preserved or refrigerated for some time and used later on.

(b) **Paper and cardboard**
The proportion of paper and cardboard found in municipal solid waste stream has increased greatly over the past 50 years. All this happened due to excessive use of paper in offices and newspaper publications. This is expected to increase further in coming times.

(c) **Yard wastes**
The proportion of yard waste has also increased significantly, primarily due to passage of the relevant legislations that prohibit burning of yard wastes. By weight, yard waste currently accounts for about 16–24% of the waste stream.

(d) **Plastics**
The proportion of plastics in solid waste has increased significantly during the past 50 years. It is anticipated the use of plastic will continue to increase, but at a slower rate than during the past 25 years.

Future Directions

The way in which currently the solid waste is being managed is not an environment friendly. The incomplete collection of generated waste, lack of awareness from the common person to the chain of municipal authority, and ignorance toward segregation and open burning of waste are few issues out of many which need engineering and administrative approaches. The improper disposal has started causing numerous problems. The air is being polluted by addition of air pollutants in the atmosphere due to this open burning. The sewerage system is clogged and starts malfunctioning due to fallen down solid waste material. The freshwater bodies including canals and lakes as well as ocean water are heavily polluted, and its aquatic life and ecosystem are damaged. The receiving soils lose their fertility and deteriorate the landscaping. The scattered waste causes nuisance and foul smells in the prevailing area.

The solution lies in systematic approach of integrated solid waste management (ISWM). The individuals, the authorities of health-providing facilities, commercial areas, institutions, manufacturing facilities, etc. all need awareness and have to play participatory roles in order to perform their due responsibilities. The most important responsibility no doubt is on the part of municipal authorities. The municipal authorities should introduce separate waste collection system for recyclable waste for recycling, organic waste for composting, combustible waste for incineration, and the left out waste for properly maintained landfills. This will certainly help in properly managing the solid waste problem in Pakistan to a greater extent, and resultantly, the overall environment will be saved.

Fig. 18 *Mohenjo-daro*: Renowned place of archeological importance (Source: http://www.mohenjodaro.net)

Part B: Agricultural Biomass of Major Crops Produced in the Province of Sindh, Pakistan

Introduction

The province of Sindh, Pakistan, is historically important due to one of the oldest civilizations of the world, the Indus Valley Civilization, and the archeological site of Mohenjo-daro (Fig. 18). Since histories back the Indus Valley Civilization grew agriculture with Indus River as the source, agriculture is the backbone of our economy. In Sindh the major crops of wheat, rice, sugarcane, and cotton are on average annually grown on **2,41,22,600** ha, which produce an average of **1,87,98,930** t of major crops; as a result there is **1,36,34,340** t of average agriculture residue biomass annually. If only 40 % of this biomass residue is utilized for power generation, there will be more than **10,000 MW** of power plant generation capacity which is almost **81 %** replacement of fossil fuel power generation and **52 %** of overall generation capacity of Pakistan with Sindh province as the only source, while, if **35 %** of agricultural biomass residue of only major crops of Pakistan is utilized, there would be almost **double** of the installed capacity of Pakistan up to 2013 (Installed Capacity of Pakistan 19,360 MW).

Though there is a huge potential available in this region, if it is properly utilized, there could be double of our crop yields resulting double amount of agricultural

biomass residue, hence more poverty reduction and more environment-friendly energy generation for the future needs and development of the country at large.

Historical Background

History is evident about the emergence of the world's oldest civilizations, most of these civilizations born and flourished on the banks of the rivers – they needed freshwater to drink, to grow grains to feed, and to sail as a way of transportation. The first ancient civilizations arose in the Middle East, the Mesopotamia (land between two rivers Tigris and Euphrates); Egypt (Nile River); modern-day Pakistan, the Indus Valley Civilization (Indus River); and China, the Huang He (Yellow River) Valley.

The common factors of flourishing of these civilizations among all these were water and agriculture. The Indus Valley remained the host of ancient civilization of the world's human history; it is learned that the cloth used for the mummification in Egypt was exported from Mohenjo-daro. After the extermination of the Indus Valley Civilization, the new settlements grew slowly in the region (especially in the "doabs," the region lying between and reaching to the confluence of two rivers). Most of today's irrigation systems we have were an effort of the British authorities in the middle of the nineteenth century who managed the already existing system of low irrigation occurrences which evolved much earlier before the British rule; such systems were the small dams and inundation canals (*Ghar Wah*, the famous inundation canal constructed by the then Kalhora rulers of Sindh before the British in the region now known as Larkano District of Sindh). The British authorities expanded and modernized the whole irrigation water supply system of the Indus Basin known as Indus Basin Irrigation System (IBIS).

On the part of the British, they constructed in 1932 AC one the most famous barrages on the Indus River near Sukkur city of Sindh (known as Lord Lloyd or Sukkur barrage with seven canals taking from it) in the Sindh irrigation system (Sindh irrigation system is a part of IBIS). The Sindh irrigation system with three barrages, one pre-independence and two post-independence, and 14 main canals is one of the world's largest irrigation systems; the agricultural area of the province is irrigated by these 14 main canals.

The size of the area irrigated by the irrigation system in Sindh province is more than the area irrigated in Egypt, and it is one-and-a-half times the area irrigated in Mexico (van Steen Bergen 2014). The economy of the province is of dual nature; on the one side it has the country's biggest metropolitan city with Bin Qasim seaport and capital of Sindh province Karachi, which accounts for about 40 % of the population of the province and is the economic hub of the country as a whole. The rural population and area on the other side is mostly agricultural.

The rural Sindh is the most poverty stricken with huge manpower still with 35 % of the population below poverty line in 1999; one of the causes of this

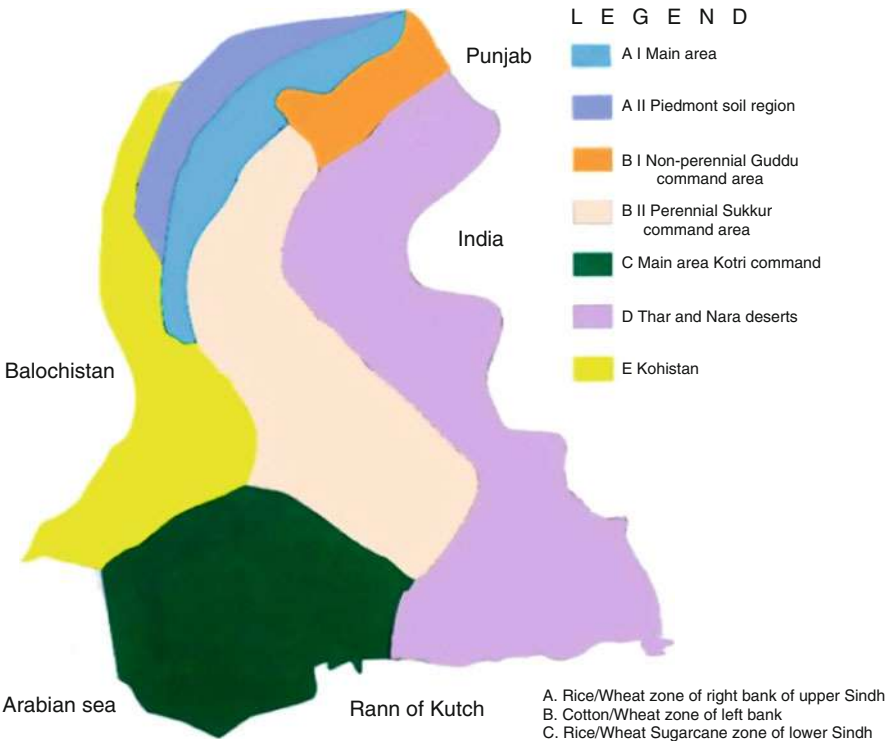

Fig. 19 Agricultural and ecological zones of Sindh province. Source: PARC

poverty is the great extent of inequity in land distribution. Big landlords with large farm cultivate their land through the tenants and land laborers and with mechanized equipments; mostly these equipments are tractors. Officially classified small farms are only 33 % the area of the size less 8 hectares (ha) (van Steen Bergen 2014).

Almost the entire agricultural area of the Sindh province is irrigated with 14 canals except limited areas in the west with spate irrigation, and agriculture in Tharparkar desert is rain fed. Rice, wheat, cotton, and sugarcane are the major crops mostly grown in the province; Fig. 19 gives the detail of command area and crops grown and includes desert area (van Steen Bergen 2014). The yield compared to the rest of the world which is much below is graphically shown in letter pages of this write-up. Mango and banana orchards are in districts of Hyderabad and Sanghar, guava is grown in Larkano District, and date palms are grown in Khairpur District. All are limited but high-valued horticulture, while mango and date palms are exported too.

The agricultural production of the province has increased more or less at the pace of population increase at a rate of 2–3 % a year, over the last 15 years (van Steen Bergen 2014).

Table 3 Barrages on Indus River in Sindh province

1. Guddu barrage	
(i) Left bank canals: one canal	01. The Ghotki Feeder (non-perennial)
(ii) Right bank canals: two canals	01. Desert Pat Feeder and 02.The Begari Sindh Feeder, (both are non-perennial canals)
2. Sukkur/Lord Lloyd barrage	
(i) Left bank canals: four canals	01. Khairpur West Canal, 02. Rohri Canal, 03. Khairpur East Canal, and 04. Eastern Nara Canal
(ii) Right bank canals: three canals	01. North West Canal, 02. Rice Canal, and 03. Dadu Canal
3. Kotri barrage	
(i) Left bank canals: three canals	01. The Akram Wah (Lined Canal), 02. The Fuleli Canal, and 03. The Pinyari Canal
(ii) Right bank canals: one canal	01. Kalri Baghar Feeder

Courtesy: Sindh Irrigation Department

The Irrigation System

The three gigantic barrages (namely, Guddu, Sukkur, and Kotri) on the Indus River in Sindh province (Table 3) supply irrigation water; the Sukkur barrage construction was completed in year 1932 pre-independence, while the other two barrages Kotri barrage construction completed in 1955 and Guddu barrage construction completed in 1962 both are post-independence barrages. Figures 20, 21, and 22 show the view of these three barrages.

The 14 main canals are fed by the above three gigantic barrages; further, the larger canals are subdivided into branches. Through the branches, distributaries, and minors, irrigation water is supplied to the agricultural lands through water courses. In the province of Sindh, there are 109 branch canals, 509 distributaries, and 902 minors (**Courtesy**: Sindh Irrigation Department).

Rohri Canal, and Eastern Nara Canal these off take from Indus river at Sukkur barrage on the left bank, both these serve command near about 1 million ha such is the huge size of Sindh irrigation system, these are one of the largest single Canal in the world (van Steen Bergen 2014). Out of these 14 main canals, some are non-perennial larger canals which flow seasonally (in summer season only when the river is in its high flows), and others are perennial which flow year-round (only closed in month of January for maintenance purpose).

The IBIS network for agriculture of our country Pakistan (Fig. 23) provides 90 % of fiber and food needs, while 10 % is provided through rain-fed (locally called barani) area. The IBIS has three dams, of which Tarbela Dam is a mega dam of Pakistan; the system also contains 19 barrages on river, 12 inter-river link canals, 45 big canal commands, and more than 1 million tube wells, including disposal network of agricultural effluent about 18,000 km length, with one drain carrying much part of agricultural saline effluent direct into the Arabian Sea known as Left Bank Outfall Drain (LBOD). The drainage network is still not connected as the

Fig. 20 Guddu barrage (Courtesy: Sindh Irrigation Department)

Fig. 21 Sukkur/Lord Lloyd barrage (Courtesy: Sindh Irrigation Department)

irrigation network is, resulting in such a large irrigated agricultural system that has not achieved the objective of poverty reduction. Further to the effect, the system even more deteriorated as time passes; the causes are detached management of different sectors (irrigation system, agriculture, environment, and social), as there is

Fig. 22 Kotri barrage (Courtesy: Sindh Irrigation Department)

deficiency in coordination among various water-related stakeholders and dearth of linkage of systemic process between economic, social, and environment; deficiency in execution of modern water management technologies; deprived water polices, especially in groundwater management; and poor maintenance and operation of the system as a whole (Lashari and Mahesar 2012).

As about 60 % population of the Sindh province of Pakistan is rural and their source of income is almost agriculture, so the economy of Sindh is agriculture dependent. The major crops are rice, wheat, cotton, and sugarcane; these crops make use of 68 % of area under crop, though in Sindh some horticulture crops are grown too, such as dates, bananas, and mangoes, including vegetables almost of all kinds seasonally. Total gross command area (GCA) of Sindh is 5.76 million hectare (Mha), and it is estimated that production of major crops in Sindh is reduced by 40–60 % as about 37.6 % of the total GCA is under waterlogging and salinity problems (Lashari and Mahesar 2012).

On the other hand, Table 4 shows the detail of 14-year data, where the net production of major cops and net cropped area vary from year to year depending upon availability of surface water and other factors such as to some extent introduction of modern techniques of hybrid seeds.

The contribution of Sindh province in overall national production of major agricultural crops from the 14-year data (i.e., from financial years 1997–1998 to

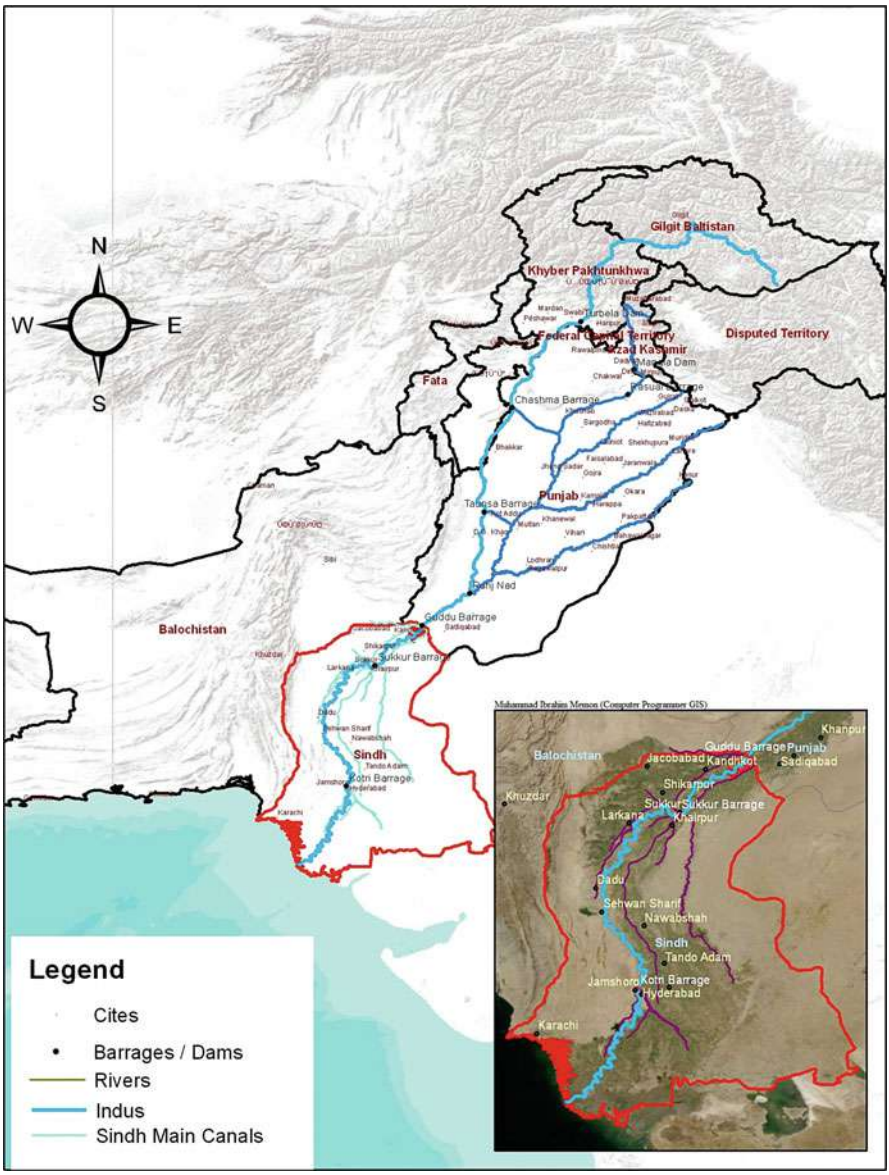

Fig. 23 Map of Pakistan and Sindh province showing IBIS (Source: SIDA.org.pk)

2010–2011) shows an average of 14 % to maximum 17 % in 2010–2011 in wheat, average of 34 % to maximum 36 % in 2008–2009 in rice, average of 27 % to maximum 29 % in 2007–2008 in sugarcane, and average of 23 % to maximum 33 % in 2009–2010 in cotton (*Pakistan Statistical Year Book of 2008 and 2011*).

Table 4 The production of major agricultural crops in Sindh province 14-year data

	Wheat		Rice (paddy)		Sugarcane		Cotton	
Cropping year	Area ha. (000)	Production (000) ton	Area ha. (000)	Production (000) ton	Area ha. (000)	Production (000) ton	Area ha. (000)	Production (000) bales (375 lbs each)
1997–1998	1120.2	2659.4	689.3	1840.9	261.6	15,999.6	600.3	2335.5
1998–1999	1123.7	2675.1	704.1	1930.3	270.8	17,050.7	630.2	2134.1
1999–2000	1144.2	3001.3	690.4	2123	230.6	14,290.8	633.5	2377.4
2000–2001	810.7	2226.5	540.1	1682.3	238.8	12,049.7	523.6	2141.1
2001–2002	875.2	2101	461.1	1159.1	240.7	11,416.3	547.4	2443.2
2002–2003	863.7	2109.2	488.3	1299.7	258.6	13,797.6	542.6	2411.8
2003–2004	878.2	2172.2	551.2	1432.8	259.9	14,611.8	561.4	2242.8
2004–2005	887.4	2508.6	543.9	1499.6	214.9	9357.4	635.1	3016.7
2005–2006	933.2	2750.4	593.2	1721	183.2	11,243.4	637.1	2648
2006–2007	982.2	3409.1	598.1	1761.8	214.7	12,529.2	570.1	2398.2
2007–2008	989.9	3411.4	594	1817.7	308.8	18,793.9	607.4	2536.2
2008–2009	1031.4	3540.2	733.5	2537.1	263.9	13,304.3	651.5	2978.3
2009–2010	1092.3	3703.1	707.7	2422.3	233.9	13,505.4	634.7	4270.7
2010–2011	1144.4	4287.9	361.2	1230.3	226.5	13,766.4	457	3536.8
Total	13,876.7	40,555.4	8256.1	24,457.9	3406.9	1,91,716.5	8231.9	37,470.8
Average of 14 years	991.19	2896.81	589.72	1746.99	243.35	13,694.04	587.99	2676.49

Courtesy (Pakistan Statistical Year Book 2008 and 2011)

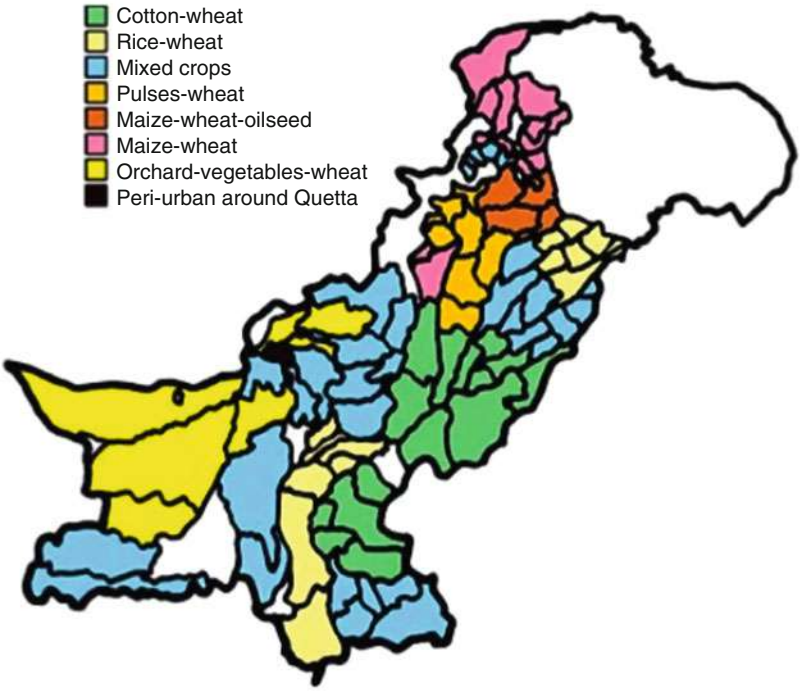

Fig. 24 Crop production regions (Source: FAO of UN)

The province of Sindh is the second largest province of Pakistan in terms of population and economy and is also known as the "Valley of Mehran." Mehran and Sindhu are the two well-known names of the Indus River. The name of province Sindh is also derived from word Sindhu – the Indus River – and it is the third largest province in terms of area which is 54,407 sq-miles (1,40,914 sq-km).

The total gross command area (GCA) of the province is 5.76 million hectares (Mha), and its culturable command area (CCA) is 2027Mha. The major crops grown are wheat, rice, sugarcane, and cotton; these major crops are cultivated on 68 % of total cropping area, and the rest is the horticulture crops. The irrigation network provides 48.76 million acre foot (MAF) of surface water to irrigate the command area, though the availability is generally 10–12% less than the above quantity of surface irrigation water. 5 MAF is the groundwater availability that is too unregulated, while the rainwater has good potential, but it is also not properly explored (Lashari and Mahesar 2012).

In horticulture, Sindh produces 88 % of chilies, 34 % of mangoes, and 73 % of banana grown in Pakistan. Others are the fodder crops, pulses, oil seeds, condiments, fruits, and vegetables (Kiani 2008).

Fig. 25 (**a**, **b**) Image of paddy crop sowing (Source: SARSO Sindh, Pakistan)

Figure 24 gives the detail of the entire Pakistan including the Sindh province region-wise major crops grown. In addition to this, in different regions various vegetables and other horticulture crops are also grown (Figs. 25, 26, 27, 28, 29, 30, 31, 32, 33, and 34).

Fig. 26 Image of grown paddy crop (Source: SARSO Sindh, Pakistan)

Fig. 27 Image of cotton crop sowing (Source: SARSO Sindh, Pak)

Pattern of Cropping and the Yield of Major Crops

Figure 35 gives the detail of cropping pattern of the entire country and Sindh province district and region wise; Table 4 shows the yield of major crops and area of each cultivated crop per year (wheat, rice, sugarcane, and cotton), while Fig. 36 and Table 5 show yield in kg/ha of different major crops for each year of Sindh province.

From Table 4, Table 5, and Fig. 36, it is very clear that all major crops from last 14-year data are in increasing trend in terms of cropping area, yield, and especially the average yield per hectare; the increase of average yield per hectare predicts the

Fig. 28 Image of grown cotton crop

future of agricultural production of the province on the positive side. For example, the cropping pattern and yield of major crops for the last 6 years (i.e., from 2004–2005 to 2010–2011) have remained worth noting as under:

Wheat in 2004–2005 area under crop was 887,400 ha and yield was 2827 Kg/ha, and in year 2010–2011 area under crop was 11,44,400 ha and yield was 3747 Kg/ha; cropping area increased by 22 % and yield per ha increased by 25 %.

Rice in 2004–2005 area under crop was 5,43,900 ha and yield 2757 Kg/ha, and in year 2010–2011 area under crop was 3,61,200 ha and yield 3406 kg/ha; cropping area decreased by 51 % (*the reason is Sindh province was the most affected region due to floods of cropping year 2010–2011*) even though yield per ha increased by 19 %, and if we compare cropping year 2008–2009 with that of 2004–2005, then the area under crop was 7,33,500 ha and yield 3459 Kg/ha; here cropping area increased by 26 % and yield per ha increased by 25 %.

Cotton in 2004–2005 area under crop was 6,35,100 ha and yield 808 Kg/ha, and in year 2010–2011 area under crop was 4,57,000 ha and yield 1316 Kg/ha; cropping area decreased by 39 % (*the reason is Sindh province was the most affected region due to super floods of cropping year 2010–2011*) even though yield per ha increased by 39 %, and if we match cropping year 2008–2009 with 2004–2005, then the area under crop was 651,500 ha and yield 902 Kg/ha; here cropping area increased by 2.5 % and yield per ha increased by 10 %.

Fig. 29 Image of ready cotton crop (Source: SARSO Sindh, Pakistan)

Sugarcane in 2004–2005 area under crop was 2,14,900 ha and yield was 43,543 Kg/ha, and in year 2010–2011 area under crop was 2,26,500 ha and yield 60,779 Kg/ha; cropping area increased by 5 % and yield per ha increased by 28 %.

From Table 5 it is clear from colored data and from Fig. 36 that the yield of major crops has gone under speedy increase in the last 6 years. The yield of wheat was 3747 Kg/ha and the yield of rice was more than 3400 Kg/ha.

However, it is also observed through data that some of the districts of Sindh Nawabshah and Khairpur were receiving the yield wheat around 4000 Kg/ha, while from field visits and meeting with progressive *zamindars* (land growers), the maximum was around 6000 Kg/ha. It is also observed through data and field visits that some of the paddy-growing districts of Sindh, Larkano, Shikarpur, Jacobabad, and Kandhkot, Kashmore, were getting paddy (using hybrid seed) yield around 5930 Kg/ha on average and some of the progressive *zamindars* (land growers) of the same area get yield maximum around 7907 Kg/ha.

From Figs. 37 and 38, evaluating the yield of wheat and rice in Sindh with the rest of the world's most advanced in yield of wheat and rice, the province of Sindh is 3747 Kg/ha, France 7280 Kg/ha, Germany 7750 Kg/ha, and the USA 8250 Kg/ha of wheat. Likewise, the yield of rice crop in Sindh is 3406 Kg/ha, the USA is more than 8000 Kg/ha, and Egypt is even more than 10,000 Kg/ha. But it is worth mentioning here that Sindh province has the capability to yield wheat of

Fig. 30 Image of grown wheat crop (Source: SARSO Sindh, Pakistan)

4000 Kg/ha to 6000 Kg/ha and rice about 6000 Kg/ha to 8000 Kg/ha as mentioned in the above paragraph regarding progressive land growers.

The province of Sindh has the capability of improving its yields as the trend shows in Fig. 36; the only requirement is the proper management of irrigation system and utilization of modern technologies and machinery while educating the farmers, tenants, and land growers.

The Rain-Fed (Nonirrigated) Area of Sindh

There are three prospective areas in Sindh where rain feed can be achieved; these are Thar desert, Khirhar hills, and Ubhan Shah hills; as shown green areas are canal-irrigated lands, while white areas are the rain-fed areas in Fig. 39 (Lashari and Mahesar 2012).

From Fig. 36, it is clear that the yield of major crops is on increasing trend but it is still low at national levels as of some progressive land growers are getting even more than the yields shown in Fig. 20, it means there is a potential gap that should be filled to increase the yield. Another point of focus is the rain-fed areas which are almost ignored and less considered which require more consideration that will result in significant growth in the production and yield. The sustainable irrigated agriculture is under threat from a number of issues which include increasing need of

Fig. 31 Image of wheat crop harvesting (Source: SARSO Sindh, Pak)

Fig. 32 Image of wheat grain (Source: SARSO Sindh, Pakistan)

water to meet raising population demand; poor maintenance of canal system causing inefficient service; waterlogging and salinity problems; excess use of groundwater resources resulting in exhausted groundwater aquifers, thus leaving large areas not viable for the poor farmers; insufficient field drainage system (even the existing field drainage effluent network not properly connected) which could dispose of agricultural effluent in due time; improper pricing or valuation of water; and scarce participation of consumers. Therefore, for the optimum production and crop yield, these areas need to be focused: competent and resourceful management including conservation of present water resources, equitable distribution of water in different areas and canal commands (from head to tail users), efficient drainage effluent interventions with well-connected networks for the maximization of crop

Fig. 33 Image of grown sugarcane crop

production, and reforms to be introduced within institutions to make the managing organizations more responsive, efficient, and dynamic (Lashari and Mahesar 2012).

The distribution and supply of irrigation water from head to tail has not remained reliable; people at the head get more water than the water users at the tail. As a result the set targets and objectives of irrigated agriculture are not being achieved, so the productivity is much lesser in quantity than it should have been. If reforms in irrigation sector are executed wholeheartedly, then farmers can play their important role to improve the productivity. Poor working of irrigation system since the 1960s is mainly due to water shortage which resulted into defective and unreliable supply, distribution, and finally inefficient use of irrigation water (Lashari and Mahesar 2012).

Biomass Residue of Agricultural Crops in the Province of Sindh

It can be observed from Tables 6, 7, 8, and 9 in columns from a to f that the biomass residue of various crops such as wheat straw, rice husk, rice straw, cane trash, bagasse, and cotton stalk is in different ratios, which is given below. These ratios are verified on-site and from research studies (Cerqueira et al. 2010; Figs. 40, 41, 42, and 43).

(a) Wheat and wheat straw ratio 1:1
(b) 20 % rice husk found as waste in paddy
(c) Paddy and rice straw ratio 1:1

Fig. 34 Image of harvested sugarcane crop (Source: SARSO Sindh, Pakistan)

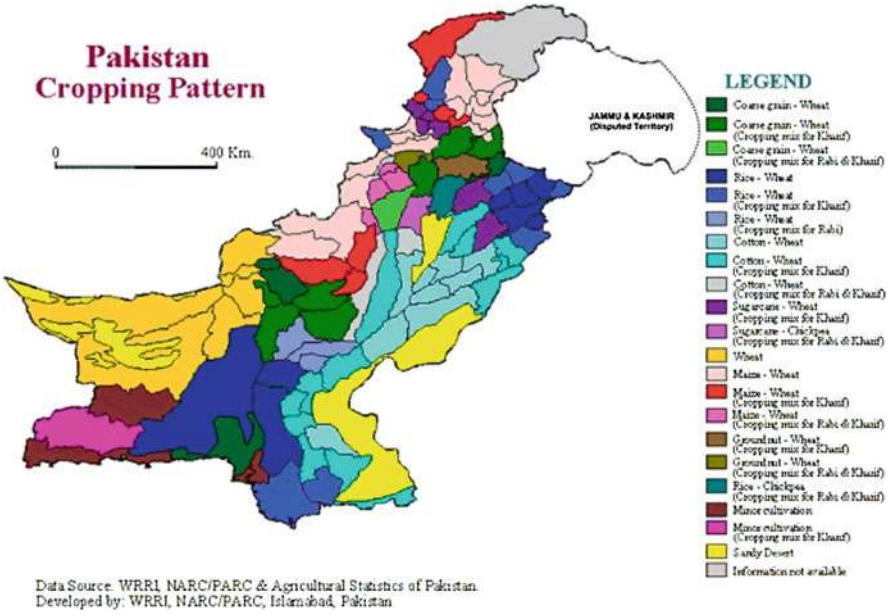

Fig. 35 Cropping pattern (Source: PARC)

(d) 23 % cane trash found as waste in sugarcane harvest
(e) 30 % wet bagasse found as waste in sugarcane industry
(f) Cotton and cotton sticks ratio 1:3

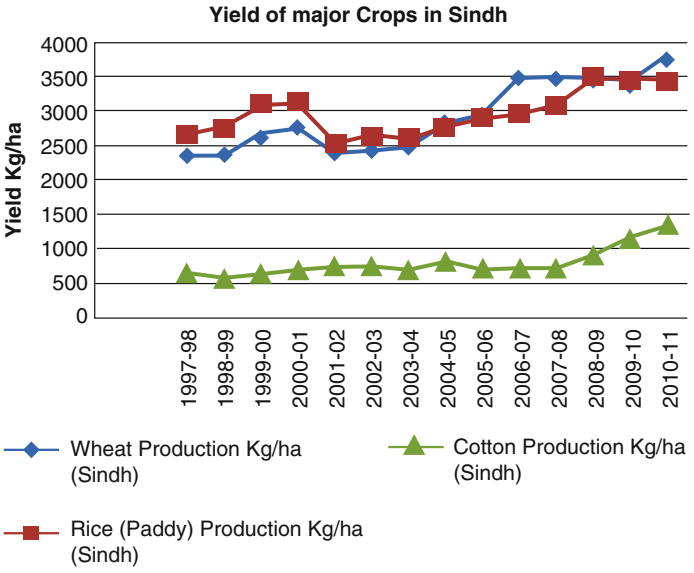

Fig. 36 Yield of major crops in Sindh

Table 5 Yield of major crops in Kg/ha of Sindh province

Cropping year	Wheat production Kg/ha	Rice (paddy) production Kg/ha	Cotton production Kg/ha	Sugarcane production Kg/ha
1997–1998	2374	2671	662	61,161
1998–1999	2381	2742	576	62,964
1999–2000	2623	3075	638	61,972
2000–2001	2746	3115	696	50,459
2001–2002	2401	2514	759	47,430
2002–2003	2442	2662	756	53,355
2003–2004	2473	2599	680	56,221
2004–2005	2827	2757	808	43,543
2005–2006	2947	2901	707	61,372
2006–2007	3471	2946	716	58,357
2007–2008	3446	3060	710	60,861
2008–2009	3432	3459	902	50,414
2009–2010	3390	3423	1145	57,740
2010–2011	3747	3406	1316	60,779

It may be observed from Tables 6, 7, 8, and 9 that annual average production of various agricultural major crops based on 14 years of data is a huge quantity which is given as under in Table 10.

From Tables 6, 7, 8, and 9, the total biomass residue of various agricultural major crops of 14 years and its average production are given as under in Table 11.

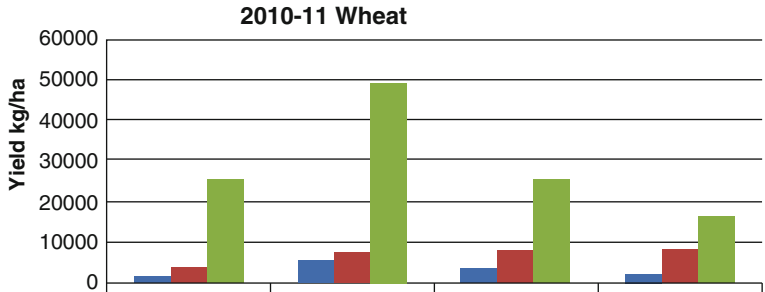

	Pak	France	Germany	U.K
Area (1000)ha	1144.4	5400	3320	1940
Yield kg/ha	3747	7280	7750	8250
Total Yield (1000)ton	25213.8	49300	25120	16000

Fig. 37 Wheat crop production and yield in the world

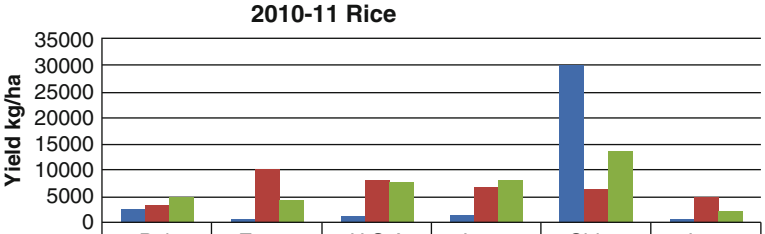

	Pak	Egypt	U.S.A	Japan	China	Iran
Area(1000)ha	2365.3	640	1370	1620	29800	630
Yield kg/ha	3406	10100	8070	6660	6590	4930
Total Yield (1000)ton	4823.3	4200	7620	7850	13500	2050

Fig. 38 Rice crop production and yield in the world

Total average amount of agricultural residue biomass of Sindh = **13,634.34** × **10^3t/year.**

Energy Content of Biomass Residue of Agricultural Crop in the Province of Sindh and Pakistan

Keeping in view the availability factor, the different agricultural residue biomass is used as animal feed and also as a raw source of energy at local level; hence, we theoretically consider 40 % availability of above total average amount of agricultural residue biomass, i.e., 5354.73 × 103 **t/year.**

Theoretically considering average calorific value of agricultural residue biomass **3500 KCal/Kg,** then the theoretical energy content = 3500 KCal/Kg×5354.73 × 10^6

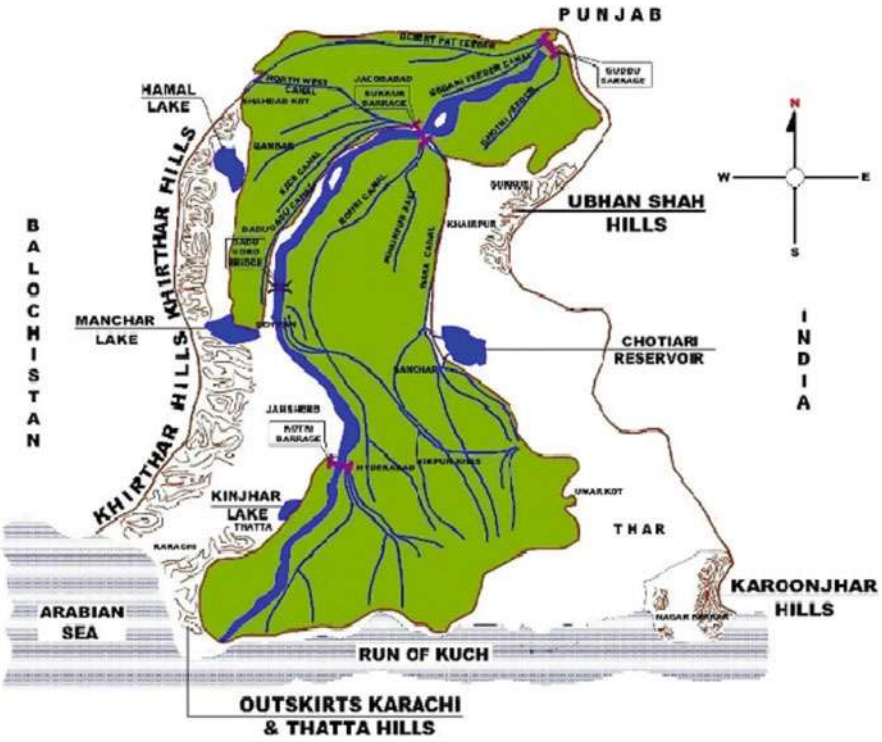

Fig. 39 Rain-fed and canal-irrigated lands (Source: Lashari and Mahesar (2012))

Kg = 1.91 × 10^{13}KCal (heating value) if this amount of heat energy is multiplied by 4.81 for converting K Cal into KJ = **7.97 × 10^{13} KJ or KW-S**.

With this theoretical heat content if converted into electrical energy with **40 %** overall power plant efficiency, then we have **3.2 × 10^{13} KW-S (el energy)**. Converting this for power plant to be installed, we'll have **8.9 × 10^{10} KWh = 10,120 MWYear.**

Hence, the power plants of about **10,000 MW** are possible to be installed in the province of Sindh with the use of only 40 % of single source by agricultural residue biomass of only major crops. By the end of the year 2013, the installed capacity of Pakistan is given in Table 12.

Then, the **10,000 MW** through agricultural residue biomass of major crops of Sindh province only will be 52 % of total installed capacity and 81 % of total fossil fuel installed capacity of Pakistan.

As already mentioned, that the *province of Sindh contributes significantly toward* overall national production of major agricultural crops from the 14-year data (i.e., from financial years 1997–1998 to 2010–2011) shows an average of 14 % to maximum 17 % in 2010–2011 in wheat, average of 34 % to maximum 36 % in 2008–2009 in rice, average of 27 % to maximum 29 % in 2007–2008 in sugarcane,

Table 6 Production of agricultural crop wheat and biomass residue in province of Sindh

	Wheat		
			a
Cropping year	Area (000) ha.	Production (000) ton	Wheat straw (000) ton
1997–1998	1120.2	2659.4	2659.4
1998–1999	1123.7	2675.1	2675.1
1999–2000	1144.2	3001.3	3001.3
2000–2001	810.7	2226.5	2226.5
2001–2002	875.2	2101	2101
2002–2003	863.7	2109.2	2109.2
2003–2004	878.2	2172.2	2172.2
2004–2005	887.4	2508.6	2508.6
2005–2006	933.2	2750.4	2750.4
2006–2007	982.2	3409.1	3409.1
2007–2008	989.9	3411.4	3411.4
2008–2009	1031.4	3540.2	3540.2
2009–2010	1092.3	3703.1	3703.1
2010–2011	1144.4	4287.9	4287.9
Total	13,876.7	40,555.4	40,555.4
Average of 14 years	991.19	2896.81	2896.81

Table 7 Production of agricultural crop rice (paddy) and biomass residue in province of Sindh

	Rice (paddy)			
			b	c
Cropping year	Area (000) ha.	Production (000) ton	20 % rice husk (000) ton	Rice straw ratio 1:1 (000) ton
1997–1998	689.3	1840.9	368.18	1840.9
1998–1999	704.1	1930.3	386.06	1930.3
1999–2000	690.4	2123	424.6	2123
2000–2001	540.1	1682.3	336.46	1682.3
2001–2002	461.1	1159.1	231.82	1159.1
2002–2003	488.3	1299.7	259.94	1299.7
2003–2004	551.2	1432.8	286.56	1432.8
2004–2005	543.9	1499.6	299.92	1499.6
2005–2006	593.2	1721	344.2	1721
2006–2007	598.1	1761.8	352.36	1761.8
2007–2008	594	1817.7	363.54	1817.7
2008–2009	733.5	2537.1	507.42	2537.1
2009–2010	707.7	2422.3	484.46	2422.3
2010–2011	361.2	1230.3	246.06	1230.3
Total	8256.1	24,457.9	4891.58	24,457.9
Average of 14 years	589.72	1746.993	349.40	1746.99

Table 8 Production of agricultural crop sugarcane and biomass residue in province of Sindh

	Sugarcane			
			d	e
Cropping year	Area (000) ha.	Production (000) tons	Cane trash 23 % (000) ton	Bagasse 30 % (000) ton
1997–1998	261.6	15,999.6	3679.908	4799.88
1998–1999	270.8	17,050.7	3921.661	5115.21
1999–2000	230.6	14,290.8	3286.884	4287.24
2000–2001	238.8	12,049.7	2771.431	3614.91
2001–2002	240.7	11,416.3	2625.749	3424.89
2002–2003	258.6	13,797.6	3173.448	4139.28
2003–2004	259.9	14,611.8	3360.714	4383.54
2004–2005	214.9	9357.4	2152.202	2807.22
2005–2006	183.2	11,243.4	2585.982	3373.02
2006–2007	214.7	12,529.2	2881.716	3758.76
2007–2008	308.8	18,793.9	4322.597	5638.17
2008–2009	263.9	13,304.3	3059.989	3991.29
2009–2010	233.9	13,505.4	3106.242	4051.62
2010–2011	226.5	13,766.4	3166.272	4129.92
Total	3406.9	1,91,716.5	44,094.795	57,514.95
Average of 14 years	243.4	13,694.0	3149.6	4108.2

Table 9 Production of agricultural crop cotton and biomass residue in province of Sindh

	Cotton		
			f
Cropping year	Area ha. (000)	Production (000) bales (375 lbs each)	Cotton stalk ratio 1:3 (000) ton
1997–1998	600.3	2335.5	1192.2
1998–1999	630.2	2134.1	1089.0
1999–2000	633.5	2377.4	1212.5
2000–2001	523.6	2141.1	1093.3
2001–2002	547.4	2443.2	1246.4
2002–2003	542.6	2411.8	1230.6
2003–2004	561.4	2242.8	1145.3
2004–2005	635.1	3016.7	1539.5
2005–2006	637.1	2648	1351.3
2006–2007	570.1	2398.2	1224.6
2007–2008	607.4	2536.2	1293.8
2008–2009	651.5	2978.3	1763.0
2009–2010	634.7	4270.7	2180.2
2010–2011	457	3536.8	1804.2
Total	8231.9	37,470.8	19,365.78
Average of 14 years	587.99	2676.49	1383.3

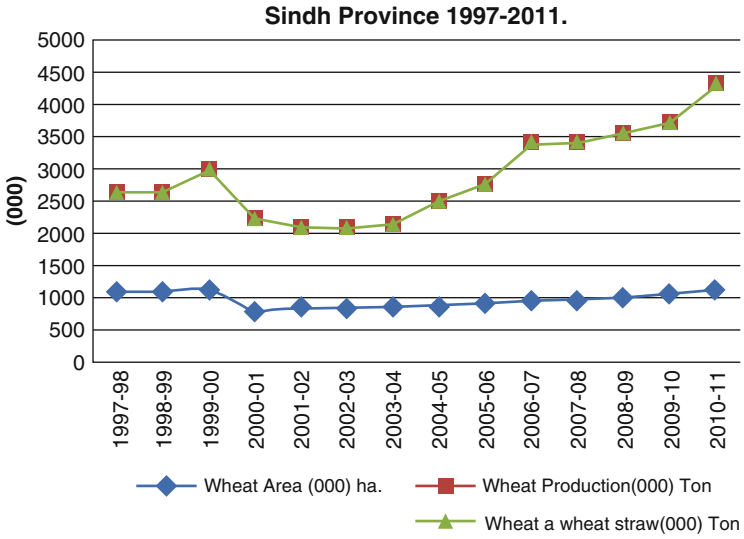

Fig. 40 Wheat crop and biomass residue wheat straw

and average of 23 % to maximum 33 % in 2009–2010 in cotton (*Pakistan Statistical Year Book of 2008 and 2011*).

Production of agricultural residue biomass in Pakistan is shown in Table 13 (by the production of major crops data of major crops *Pakistan Statistical Year Book of 2008 and 2011*) *on same considerations as* Table 11 for Sindh agricultural residue biomass.

Total average amount of agricultural residue biomass of Pakistan = **60,088.05**$\times$**10^3 t/year** as shown in Table 13. If the 35 % above total biomass agricultural residue produced in Pakistan could be utilized, about **39,026 MW** can be produced, which is very near to about 200 % of total installed capacity of all power plants in Pakistan.

This shows that there is huge potential of biomass that is available in Pakistan which could be utilized to meet the energy requirement and can overcome the energy crisis problem. At present, Alternative Energy Development Board Ministry of Water and Power Government of Pakistan has planned two power plants based on biomass waste in the province of Sindh; the details are given as under:

1. 12 MW biomass to energy power plant at Mirwah Gorchani Town, Mirpur Khas, Sindh
2. 9 MW biogas power plant at Pak Ethanol, Matli, Sindh. Letter of interest (LoI) issued to Pak Ethanol (Pvt) Ltd. for setting up power plant

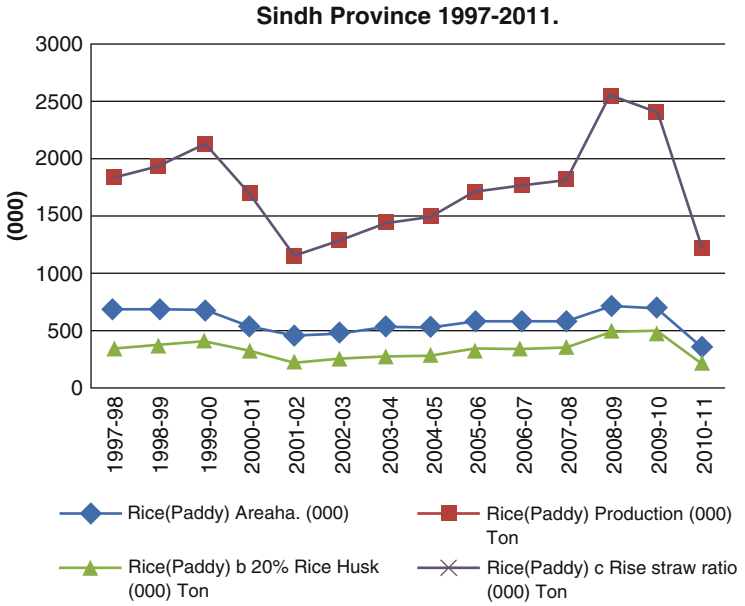

Fig. 41 Paddy/rice crop and biomass residue rice husk and rice straw

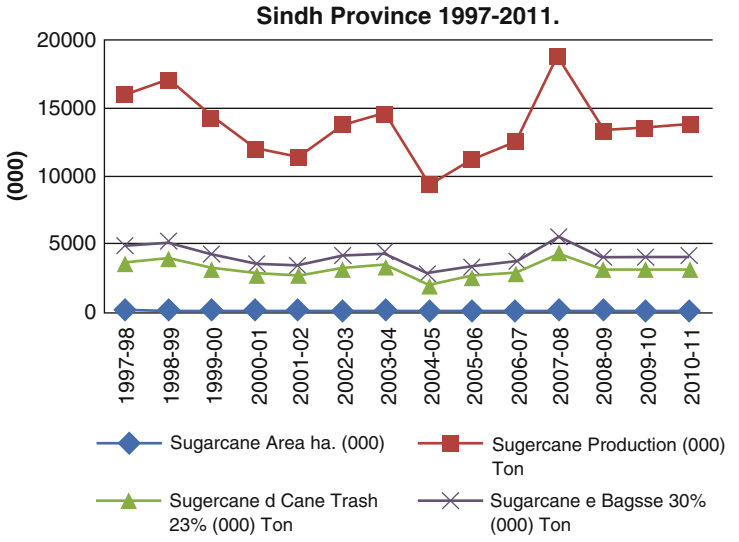

Fig. 42 Sugarcane crop and biomass cane trash and bagasse

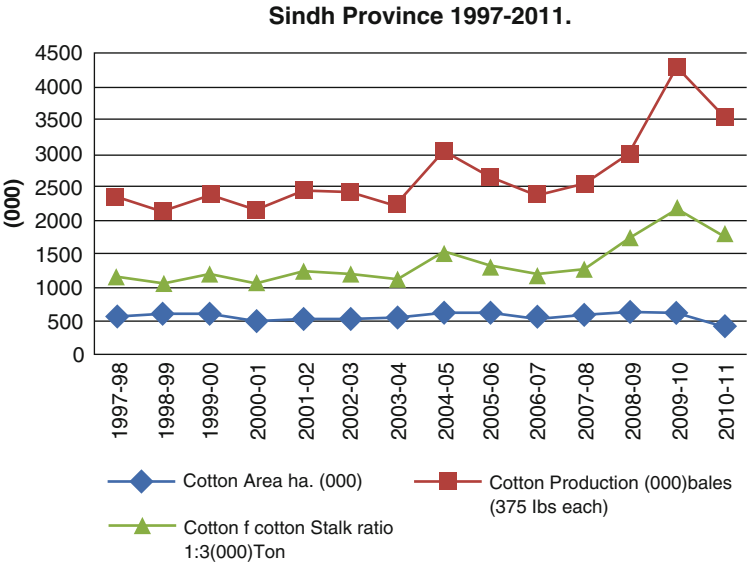

Fig. 43 Cotton crop and biomass residue cotton stalk

Table 10 Annual average productions based on 14 years of data of various agricultural major crops of Sindh

Crop	Production (000) ton
Wheat	2896.81
Rice (paddy)	1746.99
Sugarcane	13,694
Cotton	2676.5(000 bales, 375 lbs each)

Future Directions

Pakistan is bestowed by God with such great potentials which need to be exploited properly; it has such a climate with temperatures ranging from −50 °C to +50 °C; though we are facing difficulties with modernizing our agricultural and irrigation systems with the world today, still it has sufficient food to feed its population and to export, but there remains huge gap to be filled.

Our irrigation system is one of the largest systems of the world, and our agricultural command area is so expanded and large that it can also be compared to the huge agricultural commands of Egypt and Mexico.

Our agricultural lands have capability to produce yields to the world's best producing countries; to get such yields we have to improve all our systems related to agriculture as it is the backbone of our economy. To achieve such targets of which our agricultural lands and irrigation system are capable of, we must interlink various sectors which are helpful and beneficial to our agroeconomy. For this task, the irrigation department, agriculture department including farm water

Table 11 Production of agricultural residue biomass for Sindh province

Category	Agribiomass residue	Biomass total production in 14 years (million tons)	Average production per year (000) tons
a	Wheat straw (000) ton	40.56	2896.81
b	Rice husk (000) ton	4.90	349.40
c	Rice straw ratio (000) ton	24.50	1746.99
d	Cane trash (000) ton	44.10	3149.63
e	Bagasse (000) ton	57.52	4108.21
f	Cotton stalk ratio (000) ton	19.40	1383.30
Total average amount of agricultural residue biomass of Sindh (000) ton/year			13,634.34

Table 12 Total power installed capacity of Pakistan by 2013

Oil and gas	12,340	MW
Coal	160	MW
Total fossil fuel installed	12,500	MW
Others	6860	MW
Total installed as a whole	19,360	MW

Table 13 Production of agricultural residue biomass for Pakistan

Category	Agribiomass residue	Average production per year (000) tons
a	Wheat straw (000) ton	20,947.40
b	Rice husk (000) ton	1034.35
c	Rice straw ratio (000) ton	5171.77
d	Cane trash (000) ton	11,780.10
e	Bagasse (000) ton	15,365.33
f	Cotton stalk ratio (000) ton	5789.10
Total average amount of agricultural residue biomass of Pakistan (000) ton/year =		60,088.05

management, revenue department, and finance department should be interlinked starting from union council level by a focal person from each department to resolve related issues and to report to the higher authorities; every complaint must be recorded online and weekly progress-based reporting should be submitted, and to tackle the issue related to water with proper and well-connected agricultural drainage effluent networks, modernizing agriculture with farm water management and farm power machinery while at the same time educating the farmers, tenants, and land growers and revenue collection should be made accordingly while financing the growers and the tenants for better yields and proper pricing of the crops. As our economy is agrobased, hence research and development must be carried out in

every sector to improve our irrigation system, effluent drainage system, and agriculture at large.

Better yields will result in more production of agricultural residue biomass; consequently, we will have better economy at grassroots levels and poverty reduction, and we will be able to cater our energy requirements by utilizing some portion of agricultural residue biomass which is our own resource; this will further improve our economy.

References

(1999) Solid waste management in Asia. Hoornweg, Daniel with Laura Thomas. Working paper series no. 1. Urban Development Sector Unit. East Asia and Pacific Region

(2001) A comprehensive research on Pakistan's issues concerning garbage disposal and Government & Social efforts to improve them

(2002) The art and science of composting, A resource for farmers and compost producers. Center for Integrated Agricultural Systems

(2006) Techno-economic disposal of hospital wastes in Pakistan. J Med Res 45(02)

(2009) Environmental and Social Management Framework (ESMF), 4th edn

(2010) The 3 Rs of reducing solid waste: reuse, reduce & recycle, Margaret Cunningham

(2011) Characteristics of emissions from municipal waste landfills. Environ Prot Eng 37(4)

(2013) Revisiting Solid Waste Management (SWM): a case study of Pakistan. Sustainable Development Policy Institute Islamabad Pakistan. Int J Sci Footprints

Ahmed SI, Johari A, Hashim H, Mat R, Alkali H (2013) Landfill gas and its renewable energy potentials in Johor. Malaysia Int J Emerging Trends Eng Dev Issue 3:1

Asian Productivity Organization (2004–2005) Solid waste management: "issues and challenges in Asia". Report of the APO, Survey on solid waste management, Asian Productivity Organization, Japan, 2004–2005

BC Ministry of Environment (2013) Landfill criteria for municipal solid waste, 2nd edn. BC Ministry of Environment, Victoria

Cerqueira L, Edye LA, Wegener MK, Scarpare F, Renouf MA (2010) Report on "optimising sugarcane trash management for bio fuels production in Australia and Brazil" 2010

Director General Pak EPA, Environment, economic analysis of resources efficiency policies, Final report, August 2011

Draft guidelines for Solid Waste management, Pakistan Environmental Protection Agency, June 2005

http://en.wikipedia.org/wiki/Bagasse

International Environmental Technology Centre (UNEP) (2005) Solid waste management. International Environmental Technology Centre (UNEP)

Kiani A (2008) TFP and MIRR in the agricultural crop sub- sector of Sindh. Eur J Soc Sci 7

Landfill manuals, landfill design, U.S, Environmental Protection Agency, 26 July 1993

Lashari BK, Mahesar MA (2012) Potentials for improving water and agriculture productivity in Sindh, Pakistan. Sixteenth international water technology conference, IWTC 16 2012, Istanbul

Rice Knowledge Bank http://www.knowledgebank.irri.org/

The Basel convention on the control of hazardous wastes and their disposal adopted on 22 March 1989 by the conference of Plenipotentiaries in Basel, Switzerland

United Nations, Environment Program (2009) Developing Integrated Solid Waste Management plan, training manual

van Steen Bergen F (2014) Water charging in Sindh, Pakistan – financing large canal systems. Meta Meta Research

The Advanced Recycling Technology for Realizing Urban Mines Contributing to Climate Change Mitigation

Tatsuya Oki and Toshio Suzuki

Contents

Abstract

Coping with sustainable civilization and utilization of renewable energy, climate change mitigation is one of the big challenges. Obtaining metal resources from urban mines (waste) for supporting the civilization of human races will contribute not only to support sustainable development of civilization society to the future but also to mitigate climate change. Urban mines are one of the promising resources especially for poor natural metal resource countries such as Japan. Fortunately, Japan is one of the major rare metal consumers and also is capable of smelting rare metal by its own. Japan's urban mine will be more practical with top class recycling technology. In addition to these technological developments, it

T. Oki (✉)
National Institute of Advanced Industrial Science and Technology (AIST), Onogawa Tsukuba, Ibaragi, Japan
e-mail: t-oki@aist.go.jp

T. Suzuki
National Institute of Advanced Industrial Science and Technology (AIST), Nagoya, Japan
e-mail: toshio.suzuki@aist.go.jp

W.-Y. Chen et al. (eds.), *Handbook of Climate Change Mitigation and Adaptation*,
DOI 10.1007/978-3-319-14409-2_69

is necessary to reform the society system in order to realize productive and economical urban mines which overcome the natural mine. Furthermore, in order to continue a steady development of rare metal recycling, it is necessary to conduct well-planned technology development based on the prediction of the future material usage. In this chapter, the authors show the technical subjects for realizing total circulating usage of metal resources including rare metals and an attempt currently tackled in Japan.

Introduction

Huge metal resources are needed to support the civilization of mankind. Not only developed countries but also the remarkably developing Asian region has been consuming metal resources. In the past time, a lot of metal resources have been acquired from natural mines. Although a true depletion of the resources may be in the far future, the metal content of mines continues to decline gradually, and the amount of associated heavy metals and radioactive substances tend to increase. Total material requirement (TMR) which indicates the total amount of material usage to produce 1 ton of metal is usually utilized to compare the material consumption for production (Yamasue et al. 2009). For example, copper ore grade is decreasing year by year worldwide; as a result, the TMR of copper is increasing. This means that total energy consumption involved in the copper production increases. TMR increases especially for minor metals, which nowadays are very important for supporting advanced industries. Japan is being the world's largest minor metal-consuming country (in Japan, 47 species of minor metal are called "rare metals," as shown in Fig. 1), while the production of rare metals tends to be monopolized by certain countries and the world production volume of each rare metal is small. Therefore, the access to these metals can be easily restricted by the control of the production. In addition, environmental destruction is becoming a serious problem because the regulation for metal production is not well effective in such areas.

Figure 2 shows the estimated UO (urban ore)-TMR compared with NO (natural ore)-TMR (Yamasue et al. 2009). As can be seen, utilization of urban ore is already effective for minimizing the total energy consumption for almost all metal elements, and thus utilization of UO is considered to lead to mitigate the climate change in the future. In addition, considerably not far in the future, some of the metals are suspected to fall into critical shortage, and as a result, it is considered that maintenance of the substance society could be threatened. Deterioration of metal production efficiency and increase in the metal consumption mean an increase of the energy consumption for maintaining civilized society, which easily impacts on the climate change, too. Thus, an improvement of rare metal production technology for suppressing energy consumption for the metal production will be a significant step for climate change mitigation as well.

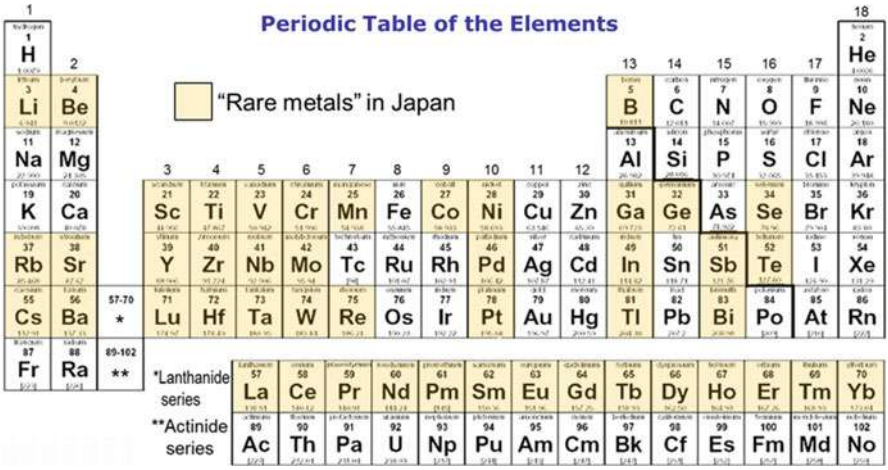

Fig. 1 Definition of the rare metals in Japan

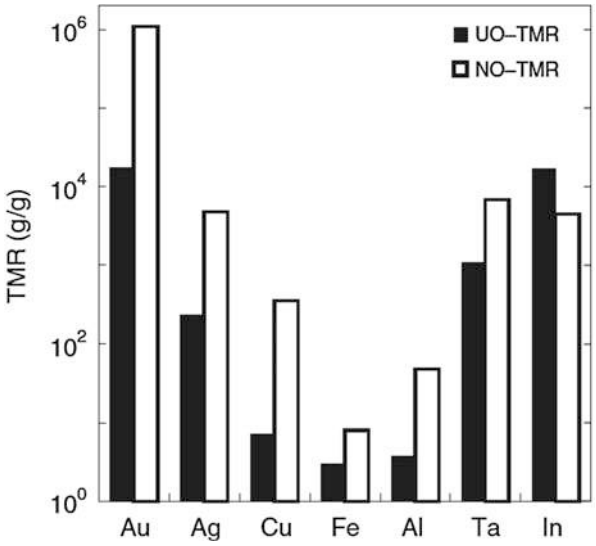

Fig. 2 The estimated UO-TMR compared with NO-TMR (From Ref. Yamasue et al. 2009)

On the other hand, almost all metal products remain somewhere on earth after usage. Some of them are soluble in water, but basically they exist in the solid state. According to the law of conservation of mass, most metals yielded ever from natural mines stay somewhere on earth, accumulated in the close area of human activities. Even in the narrow land of Japan, it is said that the total amount of accumulated metals in Japan is to surpass the annual metal consumption in the world. Thus, used products that are accumulated in the land have become to be called "urban mines." Most urban mines include products that have been routinely used without harmful substances and radioactive materials and are considered to be relatively safe

resources. Even when the metal quality of urban mines is not as high as that of natural mines where metals are concentrated by taking an enormous amount of time, for urban mine, it is possible to control of the distribution and concentration of the waste products for easy recycling. In the future, it will be possible to deliberately control the formation of urban mines, which will contribute not only to the sustainable development of civilized society but also to suppression of energy consumption due to the metal production, by extension, to contribute to climate change mitigation.

Although Japan is poor in natural resources, Japan has been supplying high-tech products to the world by importing the raw materials produced from natural mines overseas over the years. In recent years, however, due to the rise of resource nationalism, one experienced the soaring of metal prices and the imminence of supply itself. From such a background, a strategy is considered to attempt to collect resources, including rare metals from urban mines, and the strategic program has been carried out in Japan for the first time in the world. The purpose is not for recycling to reduce diffusion and waste of harmful substances but for thorough resource recovery. In this chapter, the recent efforts of the strategy in Japan will be shown, and a discussion will be presented on the development of urban mines that realize sustainable civilized society and the relaxation of climate change.

Recent Development of Urban Mines in Japan

From "Quantity Recycling" to "Quality Recycling"

Japan relies for most of the natural metal resources to support its manufacturing industry on imports from abroad, and in recent years Japan encountered a situation that stable supply of the resources, especially "rare metals," has been imminent by sudden export restriction and steep rises in metal prices. Since the characteristic of each rare metal is different from each element, it is difficult to be replaced by other rare metals, unlike energy resources. Therefore, even when weight-wise the usage of rare metals is negligible in the products, the shortage of the supply can lead to the stop of the production.

True depletion of metal resources is considerably ahead of the future, and a sufficient amount of metals should exist somewhere on earth; however, the stable supply is not a guaranteed issue. In addition, production efficiency of natural metal resources in the process will gradually decrease toward the depletion, which will require enormous energy and cost. This will become a significant impact on the manufacturing industry and the world economy.

By keeping the current situation that the society strongly depends on the natural metal resources, the world will become unsustainable at some point. On the other hand, the metals from natural mines, always, exist somewhere on earth. Most of them are already buried as wastes; some are used in the social infrastructure. Fossil energy disappears once it is used. Organic resources such as resin and paper are not possible to use repeatedly for a long period of time. However, the metals can be recycled forever in theory. Even if they lose product value, they still have industrial

value in the element itself; the smelting process can completely restore the original raw material.

The amount of recyclable metal is dependent on the degree of living standards and population in the area. Used products that are accumulated in a certain area (city) are called "urban mine" in contrast to the natural mine. In urban mine, resources can be acquired by recycling technology, not mine technology for a natural mine. Currently still good natural mines exist, and developing urban mines is not economical since recycling technologies are still costly. However, as the extraction of natural mines progresses to reduce the amount of reserves, the amount of reserves for urban mines increases. As described above, with the decline of natural mine production efficiency, one day, development of urban mines would become economically realistic. The pseudo-phenomenon actually occurred in Japan around 2010 due to import restrictions from soaring overseas metal prices. Therefore, in Japan, the development of urban mines was seriously considered in order to adapt the critical situation.

In Japan, recycling has been actively carried out since 1990. At the time, recycling was encouraged due to the shortage of waste disposal sites, and the aim of recycling was to reduce the amount of wastes, the so-called quantitative recycling. Target materials are abundant materials such as resin, glass, iron, and aluminum, and a major goal is to reduce the volume of wastes, not to recover the resource to reuse.

Until now, mass metals such as iron, aluminum, and precious metals have been recycled. But this time, "rare metal," which is not used in large quantities and not expensive as precious metals, attracted attention the most. Rare metals are also called "vitamins for industry" in Japan. Even if the usage is negligible, without it, it is no longer possible to manufacture a number of high-tech products. That temporal collapse of the balance of supply and demand, the situation that would be anticipated in the future, would be completely upsetting Japan.

Currently, there are few metal mines running in Japan, and raw materials have been imported and consumed by 120 million of Japanese people over the decades, and the several decades worth of materials has been accumulated in the national territory. This situation cannot still be called "urban mines" until the resource can be retrieved within a certain economy. While natural mines are formed by concentrating resources over incredibly long time, urban mines are not naturally formed by gathering a large amount of waste products. In other words, "urban mines" are not something to look for but to be intentionally developed (urban mining). Actually, urban mine development technology that realizes the reduction of the entropy of metal spread in land should be efficient and economical. When the urban mine development for retrieving rare metals was started in Japan, landfilled and reused wastes were not targeted, but the products owned by each person, "hoarding goods." The hoarded goods refer to digital home appliances that were not in use, sleeping in a desk drawer without being discarded.

In the early stage of urban mine development in Japan, where recycling infrastructure associated with the legislation in the 1990s is well established, it is thought that the rare metal can be easily recovered once the hoarded goods from the public are collected. The recovery operations of rare metal from small household appliances

in the designated area were conducted in 2008 in Japan. However, in reality, it was not possible to recycle the rare metals utilizing the existing recycling facilities.

Currently, among metals contained in the waste products, only noble metals (gold, silver, platinum, palladium, etc.) and some of base metals (iron, aluminum, copper, etc.) are recycled. Rare metals except for platinum and palladium are rarely recycled from waste products once available in the market. To realize the recovery system of rare metals from waste products, at least two problems must be overcome. First, used products widely spread to the consumers need to be stably collected when they are discarded. This requires the construction of rules and social systems. Second, it is required to develop the technology that realizes a high purity metal extraction from the collected waste products, high enough to be directly used by rare metal smelting and raw material manufacturers.

Although rare metal density is relatively high in small appliance wastes, the system for collecting these product wastes systematically did not exist until recently. Therefore, Small Appliances Recycling Act was made effective in Japan in 2013. It made it possible to collect small appliance wastes widely across the administrative area, being one breakthrough for the first problem. No obligation, however, exists on rare metal recovery. Without overcoming the latter technical problem, recycling of metals will only stay on recovering precious metals and part of the base metal even for small appliances wastes. Unlike recycling a conventional iron and aluminum used in construction materials, various rare metal concentrations in the waste products are about several hundreds to several thousands ppm. Thus, there exists a technical leap for recycling rare metals from small appliances in traditional recycling infrastructure, like trying surgery by using the pickaxe. At this time, "quality recycling" was started to be more paid attention to than "quantitative recycling," and the need for technological transformation had been widely recognized around 2010 in Japan.

Technical Challenges of Quality Recycling: Liberation

Physical Sorting Techniques and the Composition of the Waste Products

Because the amount of rare metals in waste products is very low compared to construction materials such as iron and aluminum, economical recovery of rare metals is difficult, and it is not practical to use hydrometallurgy processes with chemicals. Pyrometallurgy processes with high temperature, which are effective methods for recovering low concentrated copper and precious metals, are not ideal either because most of rare metals thermally dissolve and disperse into glass slug. Thus, it is of importance to separate copper and precious metals from the waste products by physical sorting before using smelting processes for rare metals. Development of low-cost physical sorting technology will be a key for realizing low concentrating rare metal recycling systems. Each waste product is thought to be consisting of various metal particles (hybrid particles) including rare metal particles. High purity sorting of rare metal strongly relies on the concentration and dispersion of the rare metal particles in the products.

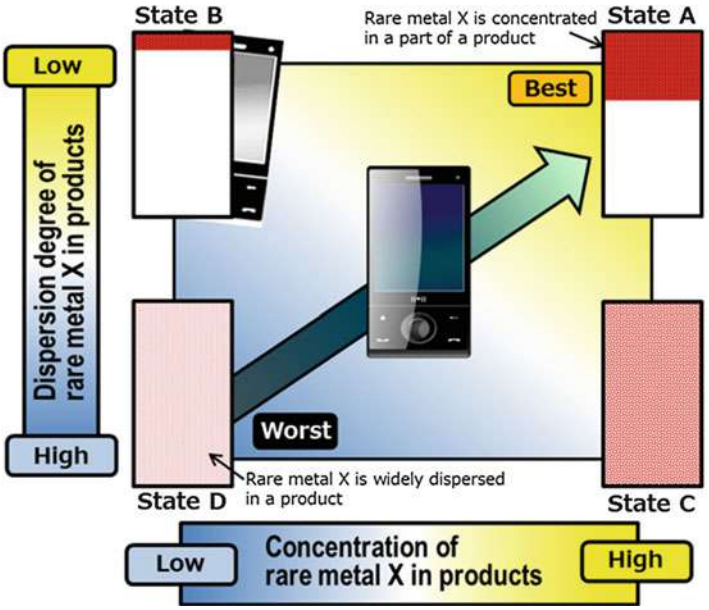

Fig. 3 Schematic image showing the existence status of rare metal in the waste product

Figure 3 is a schematic image showing the existence status of rare metal in the waste product. As can be seen, rare metal X is one of more than ten rare metals used in a smartphone and is considered to be concentrated by physical sorting. It is a great possibility of recovery if the concentration of the rare metal X is high enough after sorting. On the other hand, the possibility also depends on the dispersion of the rare metal X in the product. Here, dispersion is defined as the domain size (or distribution) of the rare metal X in the product. If the domain size is larger or the rare metal is concentrated in a particular area in the product, the dispersion of the rare metal X is considered to be small. Rectangular boxes in Fig. 3 show the rare metal X distribution in the product (smartphone). Status A is the best for physical sorting processes. The rare metal X exists in high concentration, locally in the product. In this case, it is quite easy to separate the particles with highly concentrated rare metal X from the rest of the particles by crushing or dismantling processes. This process is called "liberation – single separation." This is a very important operation in the physical sorting process and will be discussed later. Status A is not only easy for single separation but also for the rest of sorting operation due to the fact that the concentration of the rare metal X is high in the particles. The next best status for physical sorting is Status B at the upper left in Fig. 3. Even though the total amount of the rare metal X is low, it is expected to have liberation as good as Status A. Only this will cause difficulty at the latter operations in the process due to small amount of the rare metal X. Status C, even though the concentration of the rare metal X is high, is more difficult for liberation due to high distribution of X in the product. Status D is the worst scenario for physical sorting processes. In the case of a smartphone, they

typically have maldistribution of elements in the product, and thus it is not possible to apply physical sorting for single separation – liberation. Rather, they require very fine crushing processes to extract rare metal X. The required particle size after crushing totally depends upon the dispersion of the rare metal X. Usually, ordinal sorting processes can be applied down to several micron particle size, and it is not possible to apply physical sorting if liberation cannot be achieved still in this particle size.

Even when the liberation is possible for such small particles, it requires large amounts of energy for fine grinding. In addition, as discussed later, it also requires separation processes in the wet condition for less than 0.5 mm particles, while the millimeter size of particles can be applied to dry separation processes. The wet processes require another electric power for pumping water, water treatment process unit, which adds more energy consumption and cost. The product obtained by wet process is still not as good as that by dry sorting processes in the millimeter range. There is a trade-off between the purity and the recovery of X. Thus, the combination of fine grinding and wet separation processes is the last to be chosen in the physical sorting processes. These processes, however, are cost-effective compared to chemical processes and are effective for collecting the rate metals that are considered to be difficult to recycle. In the case of electrode and fluorescent materials that are used as fine powder, no crushing process is required and can be applied to wet sorting process in the ordinary recycling facility.

Importance of Liberation

Physical sorting processes for collecting metals from waste products require the decomposition of "hybrid" components into small "individual element" pieces in the first step. Large products may be decomposed by hand, and then, the pieces are sent to crushing processes. In many industrial processes, the purpose of crushing is to obtain uniform fine particles from complex particles, and the processes improve physical properties of the particles such as mobility, processability, and reactivity (Owada 2007). On the other hand, the goal of the physical sorting is to complete liberation. The ideal status is that a single element is a single particle. The element that is the target material for recycling can be atom, alloy metal or parts, etc. In the case of the particle including more than two elements, it is called "locked." It would be no problem when the locked material includes highly concentrated target material, and crushing processes would be effective for such locked constituents. If it is not the case, it is not possible to improve the purity of the element by utilizing physical sorting only. In the course of physical sorting processes, the crushing process is considered to be a pre-sorting process to realize the status of liberation, single separation of the target particle.

Figure 4 shows the 2D matrix model of liberation process, proposed by A. M. Gaudin (1939). It is a classical model, yet not enough for modeling the actual situation, but it helps in the understanding of the concept of liberation. Figure 4a shows the status before the crushing process, including target material in the matrix. "a" in the matrix is the size of locked and assuming that the product is cut into pieces

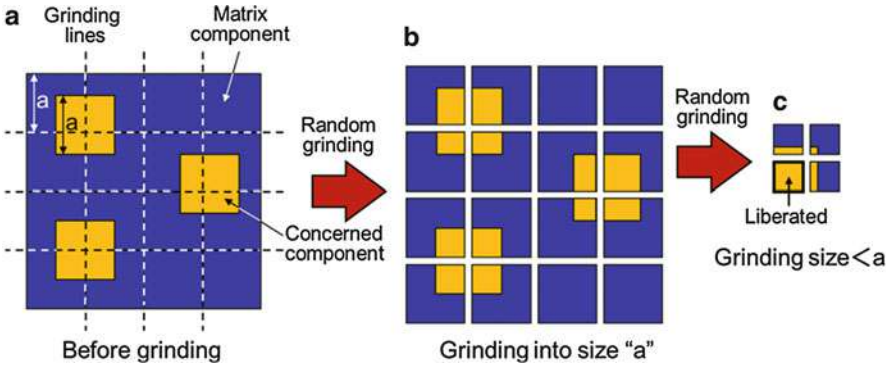

Fig. 4 2D matrix model of liberation process

uniformly with the size of "a," as shown in Fig. 4b, not influenced by the interface between the target material and the matrix. Some particles can be the status of liberation, but in the most of the pieces, the target material is still the status of locked. Another crushing process, the size less than "a," may lead to liberation status for the target material. In the actual process, such random crushing does not likely occur and the status of liberation can be easily obtained. Only the efficiency can be different for each crushing method; thus, wise choice of the method is crucial in order to realize high-quality liberation.

Figure 5 shows the schematic image of the relationship between progress of liberation and nonuniformity of crushed pieces. Let us consider Status A in Fig. 3 and apply crushing process in order to liberate the rare metal X. As crushing time proceeds, the particles become finer, and, eventually, particles of rare metal X are liberated. If this happens in a short period of time, which is the best scenario, the Status A shown in Fig. 5 will be realized, which leads to best pretreatment for physical sorting process. On the other hand, if longer crushing process time is required for liberating rare metal X, finer particles tend to be obtained, being Status B in Fig. 5 that is relatively difficult for physical sorting. Typically, Status B includes a wide range of particle size distribution, and it is almost impossible to collect particles under several microns by physical sorting process. Therefore, even when the nonuniformity of individual particle is realized, toward the right-hand side in Fig. 5, the status of well-mixed finer particles makes it difficult to separate the target particle. Also the same is applied to Status C in Fig. 5 where all particles are locked. To summarize, the process of liberation refers to achieving nonuniformity of individual particle by sacrificing the nonuniformity of the target material in the crushed product. The ideal situation is that nonuniformity of both individual particles and the target material is realized. Solid and broken lines in Fig. 5 show when the selective, optimized crushing process and random crushing process, respectively, are selected, which shows the idea of actual crushing process. Selective crushing is a very important technique to realize liberation at the coarse particle size. In order to realize efficient selective crushing, it is important to proceed to the breakup at the boundary

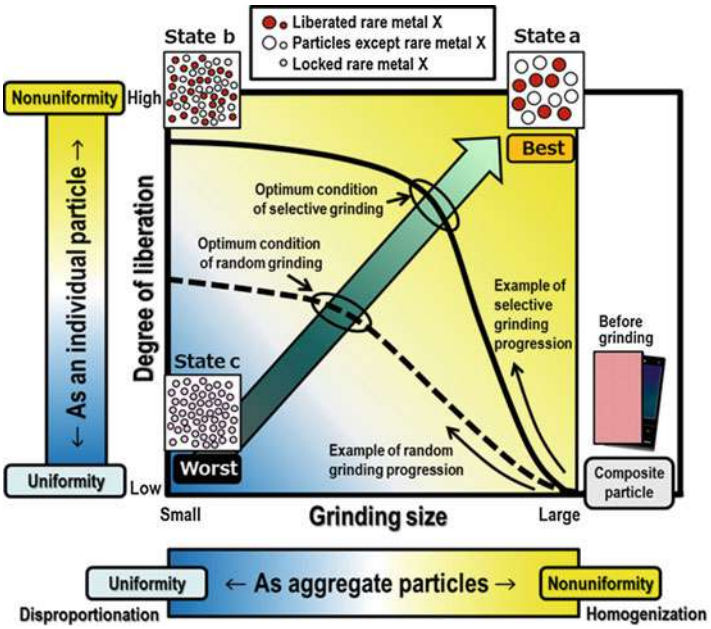

Fig. 5 Schematic image of the relationship between progress of liberation and nonuniformity of crushed pieces

of the rare metal X domain and the matrix. Since the waste products' properties are different, even considering culler phone, each one has different structure; strength, depending upon the model; manufacturer; and year of product; there is no all-fitted selective crushing machine. Currently, the selective crushing property of particular products is investigated by utilizing an existing crushing machine. Study of theoretical and systematic approaches is expected for realizing ideal selective crushing process.

Grinding Method Aiming at the Promotion of Liberation

Mechanical Crushing

Mechanical crushing is one of most realistic choices for early introduction to actual recycling plants. Mechanical crushing tends to break up products uniformly, and it is not easy to break up only at the interface as shown in Fig. 6a. It may, on the other hand, be possible to expect selective crushing as shown in Fig. 6b or c if there is a difference between mechanical properties of the target and the matrix. Figure 6b can be realized by combining thermal treatment and crushing processes, which were actually applied to the process for separating bone steel from concrete wastes (Mitsubishi Material Co, Ltd 2003; Matsumura 2003). Figure 6c can be realized by combining stirring and surface friction destruction processes.

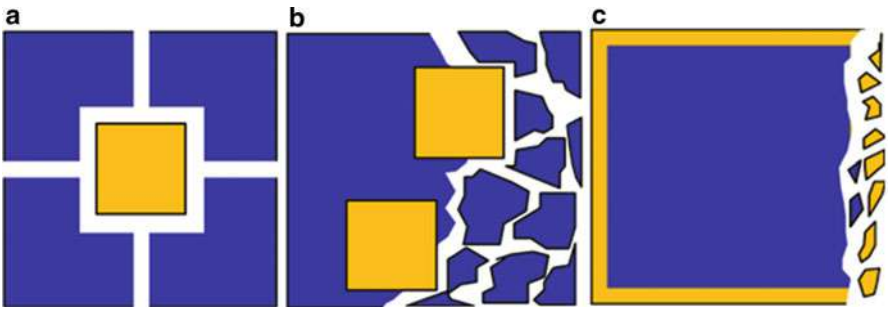

Fig. 6 Example of selective crushing for liberation

Not many cases are reported for metal recycling using mechanical crushing, but there is one good example, printed circuit boards. Actually, for the recycling of metal (copper) from the printed circuit board, the swing-type hammer mill process machine was applied, and it was found that the copper could be recycled as sphere particles due to its ductility (Furuyanaka et al. 1999). The selectivity of metal and nonmetal parts in the printed circuit board can be further improved by controlling the operating condition of the machine.

Other new processes are also under development (Koyanaka et al. 2006; Furuyanaka 2006; Koyanaka et al. 2006). One of them is the so-called active crushing method. It controls multiple operating conditions of impact crushing simultaneously during the actual operation. Single separation of target material, control of particle size, and ejection of crushed materials are optimized timely and continuously during the crushing operation.

Figure 7a shows the schematic image of the active crushing system (Furuyanaka 2006; Koyanaka et al. 2006). The system is based on the fast swing-type hammer mill, and the inverters for controlling hammer and feeder, electric air valve, and servo amplifier are connected to a PC, in which a certain operating pattern is programmed for automatic operation. In addition, the shape of the lining plate is also specially designed. Figure 7b and c shows examples of operating patterns for the speed of impact and the period of opening screen, which were actually applied to crushing circuit boards for TV after crushed using the cutter mill. As can be seen, the speed of hammer increases to 60 m/s with (b) 14 s and (c) 3 s, respectively. Using the pattern (c), one could obtain the metal separation efficiency of 50.6 %, with average particle sizes of 421 μm and 188 μm for metal and nonmetal, respectively. It was also shown that 59.6 % efficiency could be obtained by further optimization (Fig. 7b). As can be seen, accurate operation of mechanical crushing can provide realistic liberation of target materials. Not much verification so far is reported, but it is expected to increase the application of such techniques on recycling for portable devices.

Electrical Crushing

In order to realize the liberation of target materials without excess crushing, it is ideal to have selective separation at the boundary of target materials and the matrix.

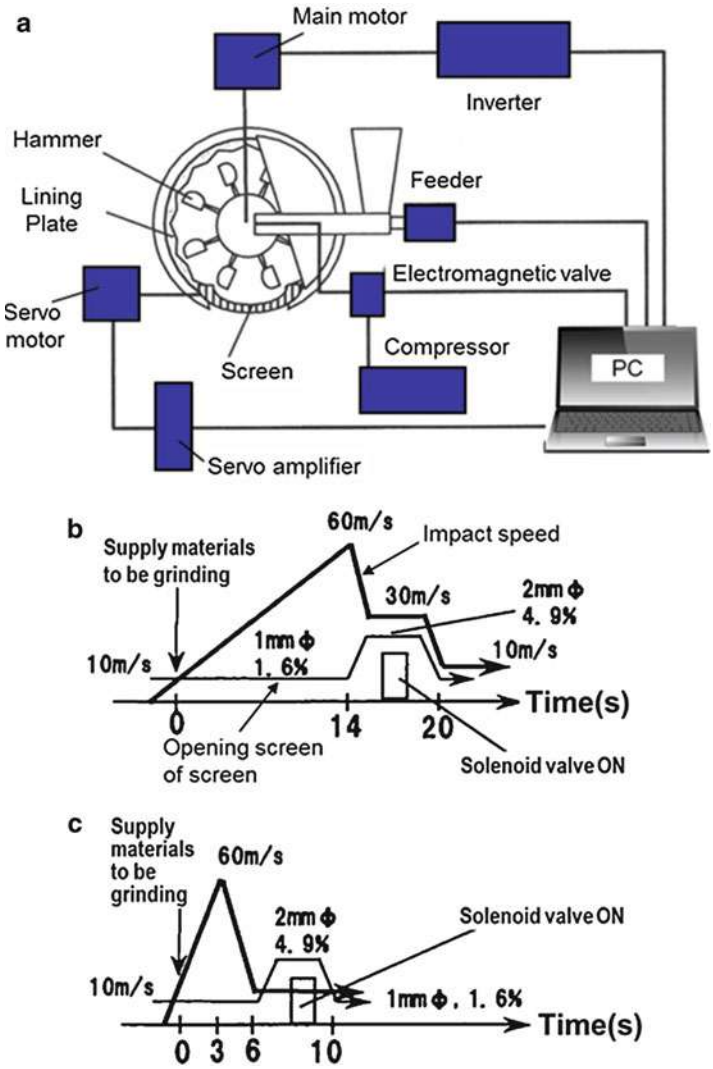

Fig. 7 (**a**) Schematic image of the active crushing system and (**b**, **c**) examples of operating patterns

Ordinal mechanical crushing methods, on the other hand, tend to result in uniform breakage, and it is difficult to crush designated area only. Therefore, electrical crushing is being considered, which allows crushing selectively along the boundary of the target material and the matrix. Mainly, there are two electrical crushing methods: electrical disintegration (ED) and electrohydraulic disintegration (EHD) methods. The ED method utilizes high voltage and large current in the liquid where particles (consisting of target material and matrix) are dispersed in a container. The particles are close to or touched at one electrode, and the other electrode is placed at

the other side of the container. The high-voltage pulse of several 10 kV in several 10 μs is applied, so the large current only flows at the boundary in the particles that leads to crush the particles along the boundary (Fujita et al. 2002). Many studies are reported especially for rocks, coals, and concretes and, in recent years, for liberation from used products on recycling purposes. For example, the method was applied to liquid crystal panels used for cellular phones and laptop computers, and it was confirmed that the panel was separated into two glass substrates, and indium (ITO) could be collected after different treatments (Shibayama et al. 2002).

The EHD method, on the other hand, utilized a shock wave generated by the large current flow in the liquid (Fujita et al. 2002). Explosives can be utilized instead of using the current flow. In either case, the shock wave generates tensile stress at the boundary and promotes selective crushes along the boundary. In the case of the cellular phone, it was reported that the shock wave propagated along the boundary between metal and resin and confirmed that metal parts were removed from the matrix (Kejun et al. 2001). As explained above, the electric crushing for liberation of used products is under development, and in the near future, it has a potential to be an innovative recycling method; however, it may also be difficult to introduce in the existing facilities due to the use of large current or explosives.

Alternative Technologies for Hand Dismantling and Picking: Easy Sensing

The most certain way to break up a complex product into pieces is dismantling. Dismantling is usually done by hand, while crushing is done by machines, and industrial robots may take human's place for dismantling processes in near future. From the technical point of view, dismantling is defined as liberating operation for individual product, while crushing as liberating operation for massed products. Thus, crushing is much more efficient and also cost-effective compared to dismantling. Nevertheless, hand dismantling is still the major method for recycling because it is an easier process for liberation. Actually, even in Japan (where the labor cost is considered to be higher), hand dismantling is applied for recycling motors, which are relatively large pieces, from used appliances. Since there is no almighty method for liberation, hand dismantling is still applied in many cases, even in some that are not cost-effective. Another advantage of hand dismantling is that breaking up and separation of pieces proceed in the same time. Although this method is very useful for applying for the variety of products, there is a limitation of this method from economical point of view, especially in Japan. Thus, the development of automated dismantling machines has been carried out, and some processes are successfully automated, for example, sorting process utilizing advanced sensing technology. This technology is very useful for getting rid of impurities from the uniform particle, but it cannot be applied to widely scattered pieces from dismantled products.

Under circumstances, the authors have been developing a cost-effective sorting machine utilizing "easy sensing" technology, alternative technologies for hand dismantling and picking. Instead of using expensive, high-performance sensors, this machine utilized a combination of cost-effective sensors, which were close to human sensibility, and highly controlled operation procedure based on the nature of target products.

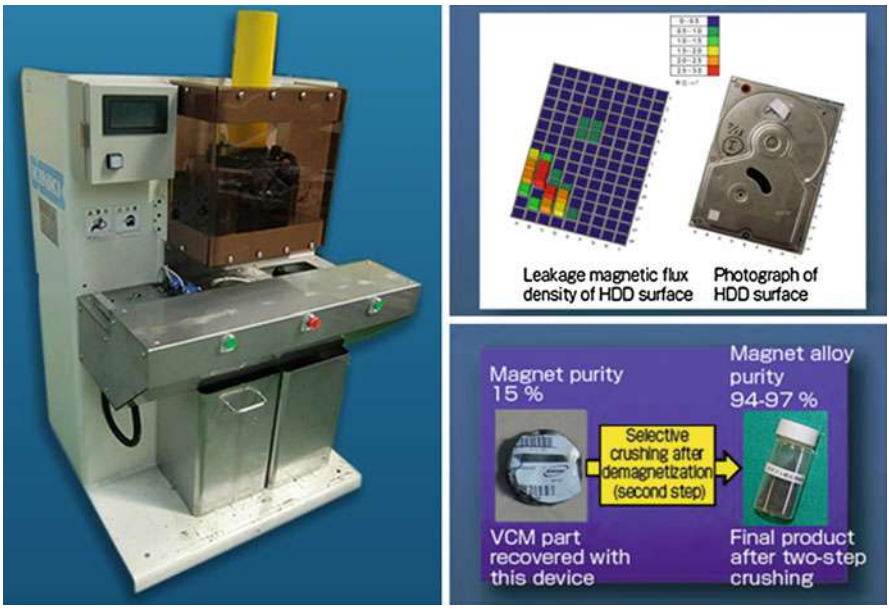

Fig. 8 Automatic collection of Nd magnet from HDD by HDD cutting separator (*HDD* hard disk drive)

For example, the authors have proposed a two-step crushing separation method for collecting neodymium magnets including rare-earth metal from hard disk drives (HDDs), "HDD cutting separator (HDD-CS)" as shown in Fig. 8. When HDD is normally crushed, the very strong neodymium magnets can be attached inside the crushing machine and cause many problems such as blockade at the screen. Even though they are luckily extracted out of the machine, they are agglomerated with metal pieces and not possible to be liberated. Thus, demagnetization process is typically applied in such case. Neodymium magnets have relatively low Curie temperature and can be demagnetized at around 350 °C. However, it is not cost-effective to use thermal energy only for extracting the magnet, 2 wt% of HDD, meaning that it requires 50 times more thermal energy for demagnetization. The HDD-CS solves such a problem by utilizing four magnetic sensors and location sensors that identify the leakage magnetic flux density and the position of magnets in the HDD without destruction. Then, the magnet is punched out with a nonmagnetic cutter. The accuracy of sensing is kept improving by optimizing the machine using the database of the leakage magnetic flux density for each HDD. This, small and cost-effective, machine realizes an automatic separation process of 400,000–1,000,000 HDD per year and can concentrate the magnet component ten times. After demagnetization, impact crushing, and screening processes, 94–97 % of magnetic alloy particles are successfully collected (Oki et al. 2011).

Another "easy sensing" technology, called "Arena Sorter," a sensor-based sorting technology, is also developed as an alternative hand selecting sensing technology. It

utilizes laser 3D measurement unit and weight detector that obtain the parameters (size, weight, and so on) of waste products, and they are recorded on the database. The system is operated using discrimination algorithm that utilizes neural network and the database (Koyanaka and Kobayashi 2011). For example of recycling cellular phones, the system successfully realized 90 % accuracy of automatic separation for tantalum capacitors from the cellular phones (Koyanaka et al. 2006).

Technical Challenges of Quality Recycling: High-Quality Separation

Challenges for the Optimization of Physical Sorting Processes

Even when ideal liberation is realized, particles still remain in a mixed status, and thus separation is required. For example, let us consider liberated metal particles including 100 ppm of target metal. This separation means that we need to pick up a target particle from a bucket filled with 10,000 particles. In the case of particles with centimeter order, separation by hand can be applied with high accuracy; however, it is not economical at the end.

As described above, one of the practical systems is sensor-based sorting system that utilizes materials' information obtained from the sensor. This can be cost-effective for such separation and is also called individual separation. Pressured air can be applied to the particle separation in the range of several mm–300 mm (Furuyanaka 2010). In addition, a variety of sensing technologies, such as color, images, transmission X-ray, and fluorescence X-ray, can be applied, and they are effective for the separation of specific particles (Owada et al. 2010). In the case of mixed particles consisting of many kinds of materials, on the other hand, accurate sensing cannot be expected. As the particle size decreases, it becomes more difficult to separate the particles. In this case, it may be more efficient to handle the particles as an aggregate. This is called "bulk separation" or "mass separation," which usually utilizes the difference in the properties of particles, such as density, magnetism, and wettability. In addition, the process can be categorized as dry separation and wet separation (usually in water). A dry separation process allows for high throughput and easy collection after separation, and a dry process unit is easy to install and cost-effective. On the other hand, a wet separation process utilizing bulk properties is expected to improve the separation efficiency compared to a dry separation process; however, it also has disadvantages that it consumes more energy for water circulation, dehydration, and drying processes. In addition, in many cases a surfactant is utilized in a wet separation process, which enlarges load for effluent treatment. After all, these two process types have an optimum range of particle sizes for separation as shown in Fig. 9. We conveniently define low-limit particle sizes shown in Fig. 9, and under certain reliability, low-limit particle sizes for dry and wet separation using bulk properties are 1 mm and 50 μm, respectively. As described above, if the liberation is achieved at the stage of coarse particles, dry separation can be applicable, and it realizes economical and highly efficient separation.

Once the crushing process is applied, it always generates fine particles less than 1 mm. Some rare metals in certain products have a tendency to be concentrated in the

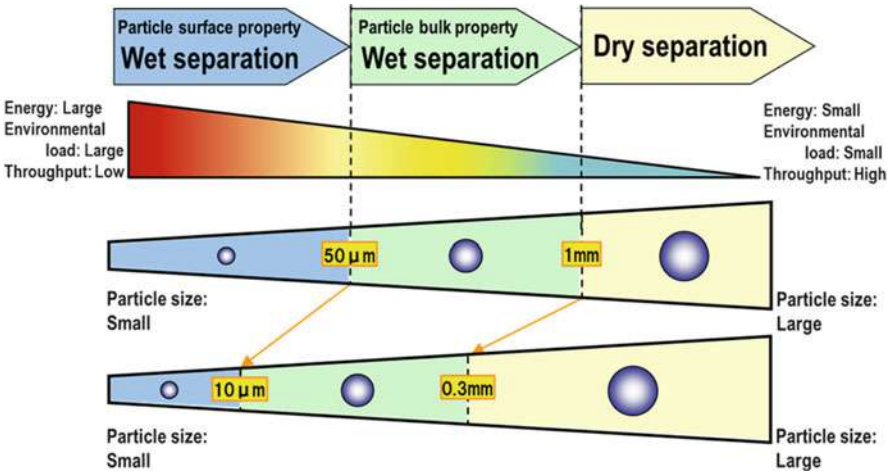

Fig. 9 Category of separation technology and concept of low limit of applicable particle size

particles, and thus, such fine particles will also need to be separated and collected (Oki 2008a; Oki et al. 2008). So far, the particles below 50 μm required wet separation processes utilizing surface property, such as flotation process. A recent study, on the contrary, showed the possibility of a dry process that realizes gravity concentration up to 10 μm particles using strong centrifugal force (Oki 2009).

On the contrary, one cannot achieve complete metal recycling no matter how individual elemental technology for recycling was developed. A great variety of products are manufactured and abolished in every year. Thus, construction of a flexible sorting process is necessary to cope with a change of such variations or the chronological changes. However, at the moment, the techniques to build these processes are not yet established, and one has to keep working on the development of these techniques to realize the most suitable sorting process and to derive the most suitable sorting condition.

Figure 10 shows the model of the simplest separation process, combining a grinder and a sorter. The targets fed to the sorting process have a variety of constituents such as various kinds of printed circuit boards and electric parts. The grinder itself also has a variety of models operable in the different treatment conditions. In addition, there are so many options for separation of crushed particles. Thus, although the model shown in Fig. 10 has only seven items, it gives ten million ways of separation processes, supposing that each item provides ten conditions. If 20 conditions were given for each item, 1.28 billion ways will exist. Since the efficiency of the liberation is determined as multiplication of grinding efficiency and separation efficiency, both processes need to be well optimized. Even if the simple model shown in Fig. 10 has one grinding and one separation process, the combination of possible patterns will be more than 100 million. In the actual case, a couple of grinding processes and three to ten of separation processes will be applied, which is an astronomical figure. Only a small portion of

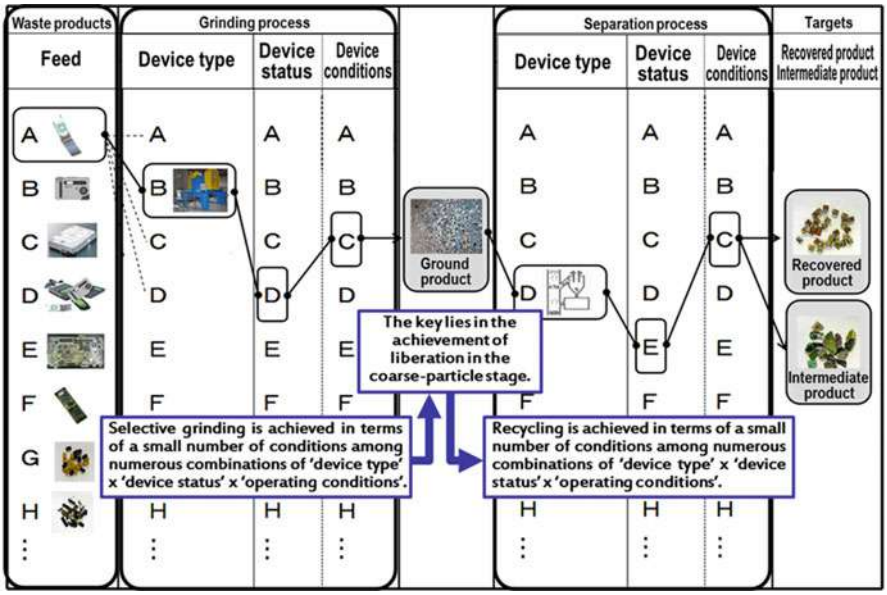

Fig. 10 The model of the simplest separation process

these patterns can actually be ideal physical separations for urban mine resources, and what makes it more difficult is that the cycle of product release is short and the amount and kind of rare metal are different from each product. Thus, one optimum separation pattern will no longer be effective in a short period. Because of this, it is very difficult to optimize the separation pattern, and in reality, they are operated under inefficient conditions.

Although the improvement of liberation processes by selecting optimum grinding and separation processes is important, it is very difficult to recognize the importance of the processes. Figure 11 shows the schematic image of a physical separation process that extracts and purifies rare metal X from waste product. For example, let us think about cellular phones as a feed. As described in Fig. 3, rare metal X can be located anywhere at the variety of status points in the cellular phone, and this affects the difficulty of liberation using a crushing process. In the crushing process, as shown in Fig. 5, the type of grinding machine and its operating conditions determine the size of particles and the degree of liberation. Even if the ideal liberation is realized such as Status A (or Status B) in Fig. 11, the results can be different depending upon the efficiency of the latter separation process. However, efficient separation after Status D does not often achieve higher purity of rare metal X than that of Status B with inefficient separation. Here, the information that can be obtained from typical recycle plants through the series of processes is threefold: (1) purity of rare metal X in the feed, (2) particle size after grinding, and (3) purity and yield of rare metal X after separation. Actually, important parameters that determine the quality of the entire process, such as the dispersion of rare metal X

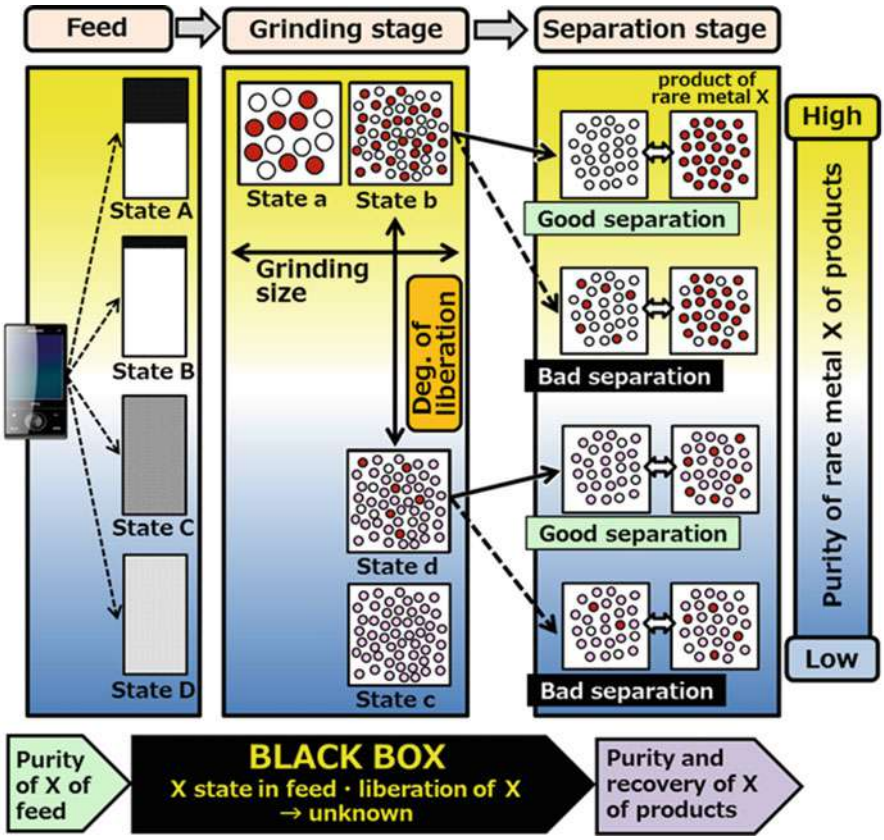

Fig. 11 The relationship between the selection of separation method and the degree of liberation

in the waste product and handy analysis method for the degree of liberation, do not exist. Important parameters in the processes from product feed to collection of separated particle are in the black box, and it is not possible to find out the source of problems such as poor purity of rare metal X after recycling. It could be due to the quality of liberation or separation. In this current situation, the concept of liberation and importance of selective grinding are not well recognized, and in not a few cases, only latter separation process is discussed without considering the degree of liberation.

In addition, component analysis of separated products does not provide sufficient feedback to the process for improvement, and this makes it difficult to optimize the process of physical separation. Development of simple and easy liberation measuring equipment, and the optimization of the selective grinding and sorting systems which depends on the liberation data, are indispensable issues for success of the rare metal recycling.

Selection of Sorting Technologies and Challenges

During the crushing process, particles with various sizes are generated. The ideal particle size range for better sorting results differs depending upon each sorting technology. Typically, the particles are separated into two or three particle size groups by a screening process, and an optimum sorting process is applied. The particles in the range below several hundred microns are usually not collected; however, collection of such particle range is becoming important especially for recycling precious metals and rare metals, as well as the sorting technology for such particle range.

In order to realize highly efficient, low-cost, and low-environmental impact sorting technologies, it is necessary to broaden the applicable particle range of each sorting technology, possibly of the technology in the right-hand side of the image shown in Fig. 8. For the example of improvement for the columnar pneumatic sorter, one of dry sorters, separation of 0.1 mm copper and aluminum particles is realized using model particles (Oki et al. 2007). A wet process can be utilized for finer particle separation where a dry process is no longer efficient. On the other hand, wet gravity concentration, based on particle bulk properties, still has the problem that the separation accuracy decreases as the particle size decreases due to low inertia. Typical particle size range for accurate separation is about 50 μm for conventional wet gravity concentrators such as shaking tables and spiral gravity concentrators. For the particle size below that, wet separation processes such as flotation using the surface properties of the particles can be effective. For the example of removal of ink from waste paper, flotation works very effectively. On the contrary, this process is not ideal for waste products with surface contamination that lower the separation efficiency significantly. Currently, application of wet separation techniques utilizing bulk property of particles is expected even for the particles below 50 μm.

Another gravity concentration technology utilizing strong centrifugal fields has been developed since the 1980s and has shown the possibility of gravity concentration up to 10 μ particles. Figure 12 shows a modified image of applicable particle sizes for each separation technology based on the literature by F. F. Aplan (2003). Among them, detailed information for conventional sorting technologies that can be used for mineral processing and metal recycling is available in the literature (Wills 2006). In this chapter, the authors focus on the gravity concentration technology that realizes wet separation of fine particles utilizing bulk properties. As the particle size decreases to below 50 μm, it becomes difficult to separate particles using wet gravity concentration. One of the reasons is that the mobility of particles in the water decreases and separation takes a lot of time. Another reason can be that it is difficult to separate the particles using the specific gravity difference as the inertia of the particles decreases. Gravity concentration using strong centrifugal fields, on the other hand, improves not only the mobility of particles but also the efficiency of separation.

Figure 13 shows the category of wet gravity concentration devices and the acceleration of gravity or centrifugal field affecting the separation (OKi 2008b).

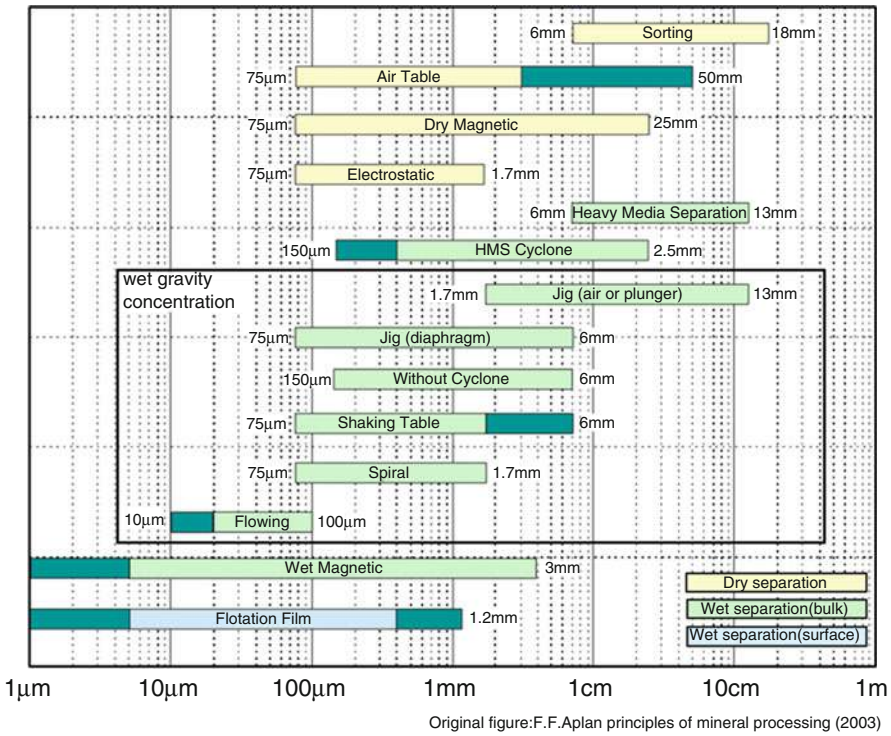

Fig. 12 Applicable particle sizes for each separation technology

Here, it shows the acceleration of rather small, lab-scale devices. Wet gravity concentration devices can be categorized into three types:

1. Water flow separation, method to separate utilizing particle sedimentation rate and velocity of the water stream
2. Film flow separation, method to separate utilizing the resistance between particles and water film on the slope and the friction between particles and the slope
3. Pulsatile flow separation, method to separate utilizing the upward and downward motion of water to differentiate the time reaching the bottom

Among these methods, separation by gravity settling, especially shaking table and jig, has been widely used for a long time as typical wet separation method. Hydro-cyclone using rotational flow and spiral separation devices are conventional installations for fine particles utilizing wet gravity concentration. In addition, the compulsive rotational wet gravity concentration method realized 10 μ particle separation utilizing strong centrifugal forces given by a mechanical rotating force. For the device shown in Fig. 13, maximum acceleration is in the range of 30–300 G (1 G = 9.80665 m s^{-2}). Although it is not possible to define the low-limit particle

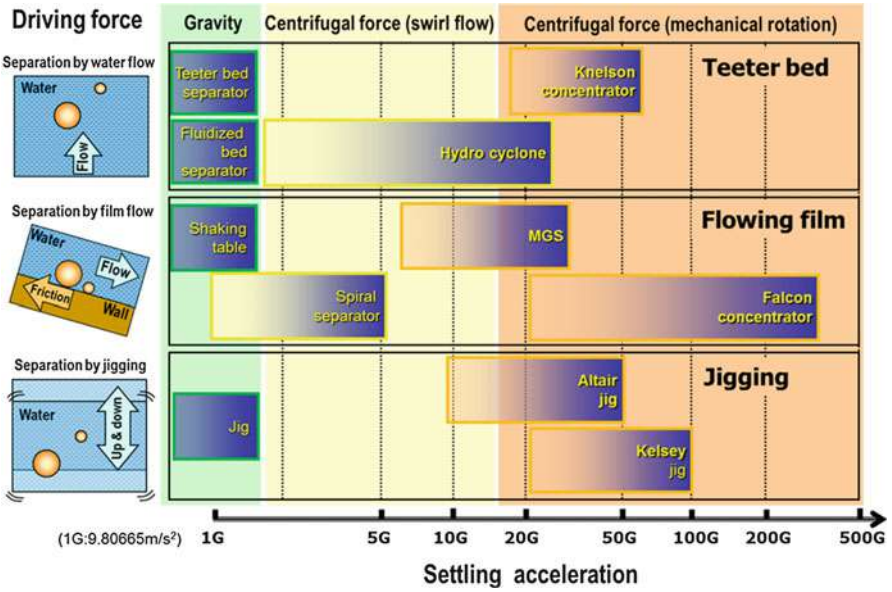

Fig. 13 Category of wet gravity concentration devices and settling acceleration

size or separation accuracy by the acceleration due to the difference in the particle motion or the method of particle collection, it is clear that the velocity and inertia of particles are increased by the acceleration. So far, compulsive rotational devices were utilized mainly overseas; however, the mechanism of particle separation and operability is still not clarified, and only few cases were applied to rare metal recycling. Since the wet process is promising, more application is expected in the future.

New Sorting Technology for Urban Mine Development: Smart Operation

A physical sorting process is usually combined from three to ten separation stages, and the combination of separation stages yields astronomical figures. Thus, most cases are abandoned before finding out the true performance of each device. To solve this situation, the authors have examined a system that promptly derives the optimum condition using a database and computer simulation. Without relying on experienced workers, the "smart operation" system realized automated operation at optimum condition. The system has been applied to recycling of printed circuit boards, and the author succeeded in the development of a sorting process that could collect tantalum capacitors at high purity for the first time in the world and achieved practical use upon introduction to a Japanese recycling plant in 2012.

Since tantalum is one of the most expensive rare metals and most of it is not recycled, the Japanese Government chose tantalum as one of five important metals (tungsten, tantalum, cobalt, neodymium, and dysprosium) that are preferentially recycled in 2012. Tantalum is mostly used in a tantalum capacitor on printed circuit

boards. At first, the recycling process of the printed circuit board for tantalum is developed based on the conventional liberation method (see Fig. 5). Considering the tantalum atom as the species of liberation, the authors aimed at the improvement of the liberation by fine grinding of the printed circuit board. After fine grinding, the authors conducted separation process based on the physical property of tantalum oxide, resulting in the concentration of tantalum to several times. Tantalum was, however, collected with a precious metal and other heavy metals due to low weight ratio of tantalum in printed circuit boards, around 1,000 ppm. As described before, rare metals such as tantalum need to be separated from copper or precious metals before pyrometallurgical treatment, and the recycling of tantalum could not be accomplished by the method mentioned above.

At first, it was considered that it was almost impossible to collect a certain electric element from a printed circuit board where various electronic elements were mixed. A phenomenon, however, was found that an electronic element was exfoliated from a printed circuit board as the original form by using a certain crushing device. Thus, we made an attempt to find out the most optimum separation pattern, considering the tantalum capacitor as the species of liberation and each electronic element has peculiar sorting properties. The authors classified over 400,000 electric elements in 320 categories according to the size and the function and built the database for their physical and sorting properties. Then, three kinds of separation methods, viz., size, specific gravity, and magnetic properties, are considered, and by numerical computation, the authors predicted the sorting result of approximately 2,055 trillion ways of patterns that include repetition use and performed narrowing of the optimum that a tantalum capacitor could concentrate afterward. As a result, the authors found the sorting process that realizes over 80 % of recovery of tantalum capacitors and purity of tantalum capacitors, from the mixture of exfoliated electric elements (Fig. 14, Oki et al. 2010).

Although the optimum sorting process pattern was clarified, there was no device that could realize the process pattern. Thus, the development of such device "inclined and low-intensity magnetic-shape separator" was conducted as the next step. This small device, rather used as an auxiliary unit, was a hybrid device that collected aluminum electrolytic capacitors at the inclined conveyor and collects quartz resonators at the low-magnetic field sorter. The device could collect iron and aluminum separately, and the rest that includes tantalum capacitor is sent to a special pneumatic sorter. This "double-tube pneumatic separator" is the main device of the sorting process and can control the airflow rates in the columns precisely using single blower. In the first column, elements heavier than the tantalum capacitor are collected by gravity, and in the second column, only tantalum capacitor is collected by gravity. The flow rate of the first column is slightly faster than that of the second one based on the numeric calculation. In order to realize highly accurate gravity concentration, this device introduces new operating parameters for both software and hardware. Especially, it is possible to operate automatically from the calibration of the device to the collection of elements by selecting the target elements (not only tantalum capacitor but also other elements) on the display, by operation control using electric element database (Oki et al. 2010).

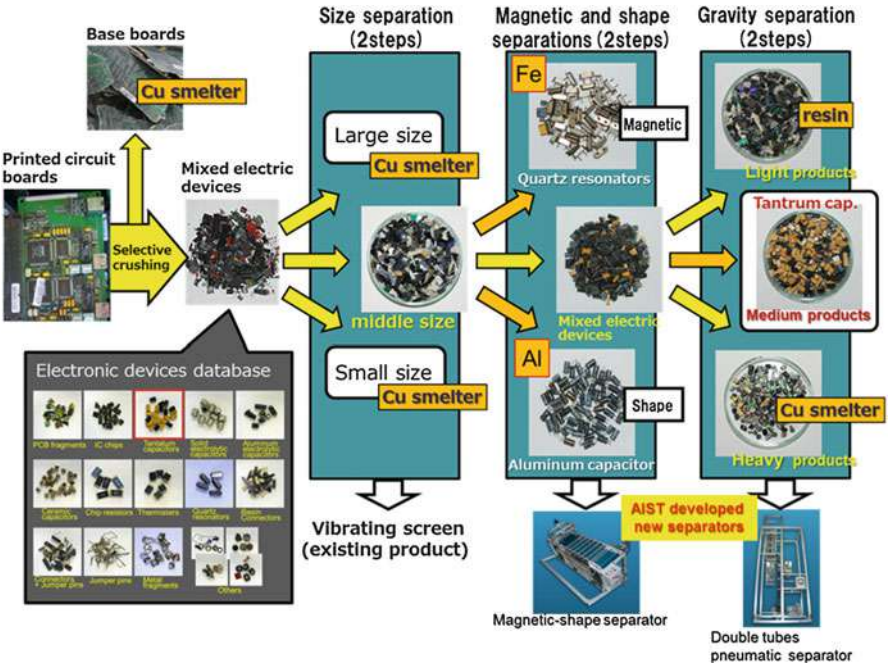

Fig. 14 Tantalum capacitor collecting process optimized by the simulation based on the database

It used to be assumed that the maximum separation efficiency of the tantalum capacitor was around 10–30 %; however, after such device development described above, the separation efficiency of 97 % was achieved by the trial run with a recycling plant where the device was installed (Oki et al. 2010, 2011). In this way, by using product information appropriately, it is possible to derive the most suitable sorting condition quickly and to recalculate the most suitable sorting condition by substitution of the information in the case of altering product specification, without going through again from the beginning. Use of the easy sensing technology and the smart operation technology just began, and it is expected that the development of recycling technology for other resources will progress further by the innovation of such physical sorting technology.

"Strategic Urban Mining" that Japan Aims for

Missing Link of Resource Circulation and Resource Circulation Interface Function

In recent years, the development of sensor-based sorting technology for recycling has been active around Europe, and in most of the cases, the mineral processing technology that was applied to the natural mine is converted into the physical

separation in the recycling. The mineral processing technology at the natural mine does not only utilize magnets for iron and gravity concentration for heavy metal but also make the most of the property of "minerals" based on the knowledge of geology and mineralogy, and minute sorting was conducted.

In addition, natural mines are usually developed for several decades, and there is enough time to optimize the mineral processing technology for a specific mineral. As a result, it is possible to obtain a variety of metals including rare metals economically.

On the other hand, when the technology is applied to urban mines, only the separating technology based on the element characteristic can be utilized due to less information of the waste products. As a result, except for precious metals, metals used for structural materials such as iron, aluminum, and copper became targets of the recycling.

In recent years in Japan, urban mines are expected to develop for supplying rare metals enough to manufacturing products; however, the technology still requires improvement from the conventional "quantity recycling" technology. The collection of rare metals was difficult in the old urban mine concept, but it can be said that a technical breakthrough will be achieved by compiling the characteristics of the waste products into a database and utilizing it for the separation process, as shown in the example of the tantalum capacitor.

On the other hand, however, the urban mining without considering infrastructure and system surrounding it does not realize efficient resource recovery as much as a natural mine can supply, even when new technology is introduced into a part of the resource circulation loop. Even if the recycling is promoted by both production and consumption sides, the resources do not circulate without considering an interface between both sides. In order to realize sustained circulation use of the strategic metals, it is important to construct a series of systems from the supply of reproduced raw materials to a product design, not only to develop resource recycling technology such as physical sorting. The authors thought that the introduction of innovative sorting technology and the eco-design functioned as a mediation technology, and the technology was named "resource circulation interface" (Fig. 15).

As discussed above, even if advancement of the physical sorting technology is accomplished, it will be difficult to apply it to all product forms with that alone due to the variety of the product designs released up to now. Thus, an easy recycling design (eco-design) can be considered to compensate for the technology gap. The effective and minimum easy recycling design can be achieved by the suggestion to the products as well as the design guidance of the parts and products that realized easy to sort without spoiling products' original function and charm. In this way, the improvement of the physical sorting technology is a key for the development of the urban mine including the interfacial function of global resource circulation of materials.

Aiming for Establishing Strategic Urban Mines

In order to succeed with efficient and deliberate urban mining, it is of importance to build a society system that introduces product eco-design and physical sorting

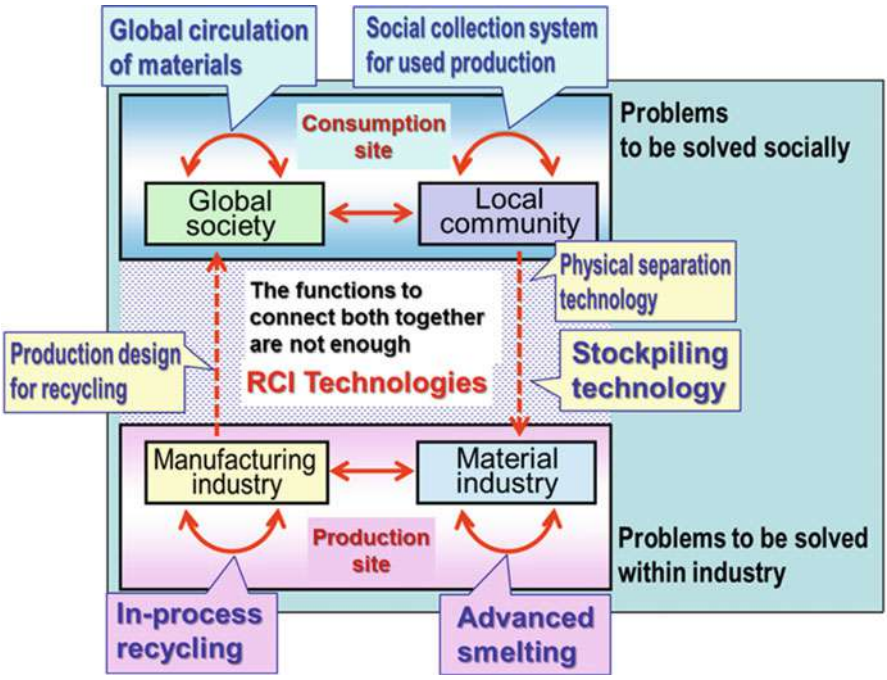

Fig. 15 Missing link and interfacial function of resource circulation

technology utilizing artifact databases. For this purpose, the authors have conducted a project called "Strategic Metal Resource Circulation Technology (Urban Mining)" between 2012 and 2014, aiming for the total development of urban mining in Japan. In this project, the authors specified important metals as "strategic metals" that are necessary to continue industrial activity and potentially have supply risk and evaluated the potential of urban mining and efficient collecting technologies. Venous industry (recycling industry), as shown in the upper part of Fig. 15, mainly focuses on the short-midterm technological subjects aiming for the development of urban mines that are scattered and disorderedly accumulated. Arterial industry (manufacturing industry) of the lower part of Fig. 16, on the other hand, focuses on the mid-long-term technological subjects for realizing a practical urban mining plan utilizing eco-design from manufacturer aspects.

As described above, by considering the demand and supply risk of metal resources, as well as the system that realizes deliberately and efficiently collecting strategic metals, the authors named their initiative "Strategic Urban Mine" in contrast to conventional disordered urban mines.

In addition, in November 2013, a new research base "Strategic Urban Mining Research Base (SURE)" was established in the National Institute of Advanced Industrial Science and Technology (AIST) for continuous research activity based

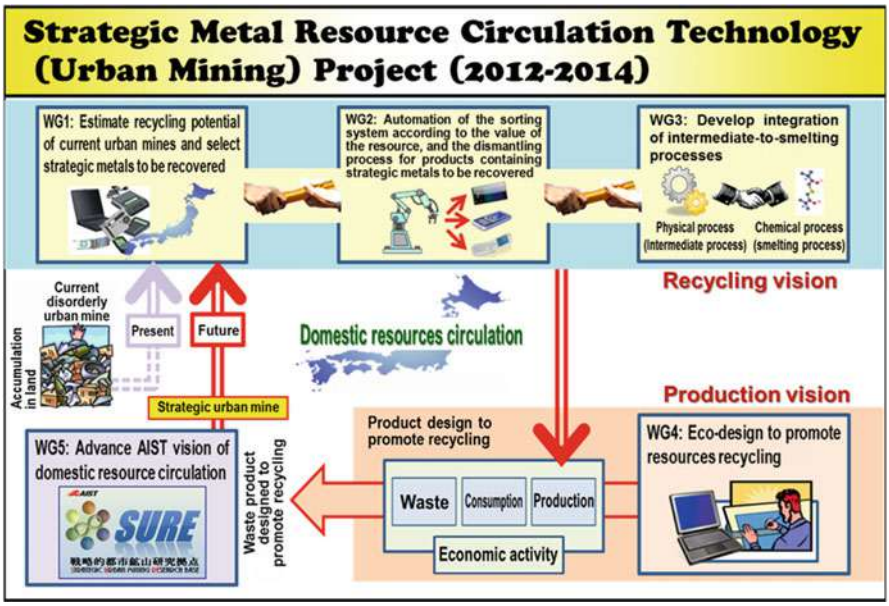

Fig. 16 Summary of Strategic Metal Resource Circulation Technology (Urban Mining) Project

on the project's concept. SURE holds 37 researchers from AIST (Fig. 17). And SURE maintains a laboratory for evaluation of sorting technology (SURE LATEST) at the AIST Tsukuba West site, aiming at the improvement of physical sorting technology. The laboratory has large space room and four separate rooms that hold about 60 physical sorting devices for grinding, crushing, and separation processes. Twenty of them were originally developed at the AIST (Oki 2012, 2013a, b, c, 2014a, b, c). Such open laboratory, the core of physical sorting technology, is the first attempt in Japan and expected to contribute accelerating development of urban mining development.

In order to introduce the strategic urban mine into the society, the support from industry side is necessary. For this purpose, the SURE consortium was organized in October 2014, together with companies related to metal resource circulation, aiming at an early realization of strategic urban mines by extracting needs from industry and society. Currently, the members of the consortium are 45 companies and 20 industry groups and public organizations and institutes.

Members of the SURE consortium discuss common subjects in the industry group or individual company's subjects such as eco-design and utilization technologies of recycled materials, in order to promote the strategic urban mining concept from the manufacturers' point of view. In addition, they can utilize the facility in SURE LATEST aiming at the extraction of potential problems at recycling plants for

Fig. 17 Structure of Strategic Urban Mining Research Base

better improvement of the technology. The SURE consortium is expected to propose a variety of new ideas related to urban mine development.

Future Prospects of Strategic Urban Mines

Obtaining enormous amount of metal resources from urban mines for supporting the civilization of human races will contribute not only to support sustainable development of civilization society to the future but also to mitigate climate change. While several incidents had happened in Japan, which accelerated the development of urban mining, up to now, there are still many issues that need to be solved from both technical and society system points of view. In this chapter, the authors showed the technical subjects for realizing total circulating usage of metal resources including rare metals and an attempt currently tackled in Japan.

Japan has already selected five important metals that need to be recycled and conducted related research on the nation level. It is, however, not possible to realize practical resource circulation with high international competitiveness if the technologies are developed individually.

Furthermore, even when one recycling technology has been established, the period of validity is not very long due to fast product cycle. The concentration of rare metal in the product also changes year by year, as well as characteristics of separation and crushing. In addition, the more a particular rare metal becomes important, the less material will be used in the product by promoting the use of alternative materials. It takes a lot of time to determine an ideal sorting pattern for a product from the enormous combination of crushing-sorting technologies, and when the process is ready, it is not a few cases that the target rare metal is no longer used anymore. Because of this, in the recycling process in many cases, a hand dismantling and picking process is used under inefficient conditions, and thus, the technology development does not always catch up with it.

In order to continue a steady development of rare metal recycling, it is necessary to conduct well-planned technology development based on the prediction of the future. From this point of view, there are two important forecasts: One is that which rare metals will be more important in the next 5 years and 10 years, in other words, which rare metals will be necessary to be recycled from urban mines. The other one is that we have to choose products from which rare metals are recycled. Currently in Japan, for the first one, five kinds of rare metals are selected as strategic rare metals; however, it is difficult to predict their true demand and price trend. At least, for the second one, those rare metals are already used in the products, and one can easily select appropriate products.

In order to proceed strategic urban mine development, the authors organized the Strategic Urban Mining Research Base (SURE) in the National Institute of Advanced Industrial Science and Technology (AIST). In this research base, the metals considered to be important in the next generation, not only rare metals, are designated to be “strategic metals,” and they are evaluated for their recycling potential. In addition, the database of physical properties for waste products is being constructed, and based on the database, automatic sorting technology for products including “strategic metal” and pre-smelting treatment technology are under development for preparing raw materials by recycling. These efforts will contribute to economical collection of strategic metal from the current “disordered urban mine” accumulated in the land.

Urban mines are one of the promising resources for Japan as a poor natural metal resource country. Fortunately, Japan is one of the major rare metal consumers and also is capable of smelting rare metal by its own. Japan’s urban mine will be more practical with the world top class recycling technology. In addition to these technological developments, it is necessary to reform the society system in order to realize productive and economical urban mine which overcomes the natural mines. The number of researchers and scientists will also be expected to increase for speeding up the development of technological aspect. Coping with sustainable civilization, utilization of renewable energy, and climate change mitigation is one of big challenges. All of them are interconnected, and from developing urban mine point of view, the activity of SURE including collaboration with private companies, and cultivation of human resources, is expected to contribute the climate change mitigation in the future.

References

Aplan FF (2003) Gravity concentration principles of mineral processing. SME, Colorado, pp 185–219

Fujita T et al (2002) Liberation as pre-treatment of recycling process by electrical crushing and water explosion. Resour Treat Technol 49:187–196

Furuyanaka S (2006) Active crushing of waste products – selective crushing technology for composite waste materials. Funtai Kogyou 38:57–64

Furuyanaka S (2010) Crushing technology and eco-recycle. NGT, Tokyo, pp 110–115

Furuyanaka S et al (1999) Evaluation of liberation property for impact crushing and gravity concentration of waste printed electric circuit board. Funtai Kogyou 36:479–483

Gaudin AM (1939) Principles of mineral dressing. McGraw-Hill, New York, pp 70–91

Kejun L et al (2001) Extraction of metals from disposed fragmented portable telephones by various leaching solution. Mater Trans 42:2519–2522

Koyanaka S, Ohya H, Endoh S (2006) New grinding technique to simplify the recycling process of scrap electronic devices. Rev Automot Eng 27:353–355

Koyanaka S et al. AIST web page. https://staff.aist.go.jp/s-koyanaka/ARENNA.pdf

Koyanaka S, Kobayashi K (2011) Res Conserv Recycl 55:515–523

Koyanaka S, Endoh S, Ohya H (2006) Effect of impact velocity control on selective grinding of waste printed circuit boards. Adv Powder Technol 17:113–126

Matsumura (2003) Concrete recycle technology. Consult Hokkaido 106:13–19

Mitsubishi Material Co, Ltd. (2003) Development of low environmental load type concrete from waste concrete. MITI Report of FY2003, Ministry of Economy, Trade and Industry

Oki T (2008) Proceeding of 16th environmental resource engineering symposium. pp 24–30

OKi T (2008) Screening, separation and gravity concentration. Min Mater Process Inst Jpn Tech Semin Book: 31–44

Oki T (2009) Funtai Gijutu 1(5):39–48

Oki T (2011) Proceedings of the conference of metallurgists (COM2011). pp 69–77

Oki T (2012) Physical sorting technology for rare earth recycle. Automob Technol 66(11):74–79

Oki T (2013a) Physical sorting technology for strategic development of urban mine – unused, refractory resources and Japan's resource vision. Systhesiology 6(4):238–245

Oki T (2013b) Physical sorting technology for strategic development of urban mine and future prospective. Kankyo Kanri 49(3):62–65

Oki T (2013c) Collection of electric element from waste printed circuit board based on the concept of strategic urban mining. Ceram Jpn 49(1):30–34

Oki T (2014) Urban mine development. Denki Hihyou 2014(2): 27–28

Oki T (2014b) Technical problems of rare metal recycle from waste portable appliances. Energy Resour 35(4):234–238

Oki T (2014c) Development of gas flow sorting device for the realization of strategic urban mine. Funtai Kogaku Gakkai-shi 51(7):527–531

Oki T et al (2007) Establishment of environmental friendly metal recycle system. AIST Environ Energy Symp Ser 1:20–24

Oki T et al (2008) Proc Spring Symp Min Mater Process Inst Jpn 2:91–92

Oki T et al (2010) IMPC2010. pp 3839–3844

Oki T et al (2011) Development of crushing and sorting device for collecting rare earth magnet from HDD. Kido-rui 58:34–35

Owada S (2007) Crushing/sorting technology. J Min Mater Process Inst Jpn 123:575–581

Owada S et al (2010) J Min Mater Process Inst Jpn: 153–156

Shibayama A et al (2002) Collection of materials from crushed liquid crystal panel using electrical crushing. J Min Mater Process Inst Jpn 118:490–496

Wills BA (2006) Will's mineral processing technology, 7th edn. Butterworth-Heinemann, Oxford

Yamasue E et al (2009) Novel evaluation method of elemental recyclability from urban mine – concept of urban ore TMR. Mater Trans 50(6):1536–1540

An Introductory Course on Climate Change

Wei-Yin Chen

Contents

W.-Y. Chen (✉)
Department of Chemical Engineering, The University of Mississippi, Oxford, MS, USA
e-mail: cmchengs@olemiss.edu

W.-Y. Chen et al. (eds.), *Handbook of Climate Change Mitigation and Adaptation*,
DOI 10.1007/978-3-319-14409-2_54

Abstract

The University of Mississippi offered a seminar course entitled Climate Change – Causes, Impacts and Solutions twice in the last 4 years. The immediate goal of this course is to raise the public awareness of the climate change issue. The second objective is to consolidate a knowledge base for the various outreach, education, and research activities on mitigating the climate change. Junior, senior, and graduate students of science and engineering majors were encouraged to take this course. About 25 speakers from Mississippi, Alabama, and Louisiana gave lectures that covered their expertise in a wide spectrum of areas that include causes, impacts, and solutions of climate change. The slides used in these lectures are posted on the course web site for public dissemination: http://home.olemiss.edu/~cmchengs/Global%20Warming/. Students chose a specific research topic for approval in the early stage of the class. They submitted their research papers and made presentations at the end of the semester. Their overall performance is based on their classroom enthusiasm, final report, and presentation. When the course was offered for the first time, they also made recommendations to the Chancellor's Ole Miss Green Initiative of the University of Mississippi on the reduction of carbon emissions in the community. This chapter discusses the motivation, content, and outcomes of this course in detail.

Introduction

Climate change is arguably the most serious environmental issue. As discussed in the previous chapters of this handbook, from the greenhouse gas emissions to the affected areas of climate change, it is an environmental problem unprecedentedly large in quantity and space. The causes of climate change are complex. Its impacts on weather, ecology, and economy are potentially severe. Technologies for mitigating climate change are costly, and the infrastructure of green technology has just started to emerge. The decline in the supply of high-quality crude oil has further increased the urgency to identify alternative energy resources and develop energy conversion technologies that are both environmentally sound and economically acceptable. Although the concept of sustainability is not new, it has become a household phrase as people become increasingly aware of the severity and scope of future climate change. Climate change has thus become the central issue of sustainability literacy. At the same time, there has been a shortage of workforce

in the organizations that require some, if not much, knowledge about climate change.

Scientists and engineers play a pivotal role in developing green technologies leading to climate change mitigation. Therefore, there is an urgent need to equip the graduates with adequate knowledge about climate change so that they can function effectively in their careers. Under such demand, a campaign on climate change mitigation was planned in fall 2007. Personally, it was another twist in my life. I came to the USA in 1973 as a graduate student in applied mathematics, but the "energy crisis" in 1974 changed my plan. I switched back to chemical engineering in 1975 and started my research in coal hydropyrolysis. I have been maintaining activities in areas of hydrocarbon fuel conversions and pollution control since then. Coal was called "black gold" and "king coal" in the 1970s. Coal remains a major and indispensible energy source, particularly for developing countries such as China and India. However, coal suffered a severe image problem in the last decade because of the concern of its greenhouse gas emissions. As a fossil fuel researcher, offering solutions to the climate change concern becomes not only an obligation but also a serious challenge.

About 30 faculty members of the University of Mississippi (UM) and scholars in the region enthusiastically joined the "climate change study group" in fall 2007. The activities of this group include offering courses, editing a handbook, collaborating on clean energy production and conservation research, sponsoring workshops, and developing outreach and public awareness activities. The climate change class is discussed herein, and this handbook has outgrown from this exercise.

The engineering school at the University of Mississippi has a relatively small faculty and student population. Faculty has a fairly tight teaching arrangement. Fortunately, the administrators shared the same views and enthusiasm about the course.

Students also have tight curricula with 128 credit hours requirement for engineering majors that have been imposed by the Institute of Higher Learning of the State of Mississippi. Most students of the engineering school have to take two elected courses in science and engineering before they graduate. Sixteen students enrolled the climate change class before the course application was approved by the administrator. Some of them were from Chemistry Department and School of Pharmacy. They were seniors and graduate students. This size is about the average for the engineering classes at the university. The course was offered for the first time in spring 2008 and subsequently in spring 2009.

Course Scope, Format, and Title

Students signed up for the class with curiosities, more or less, in different aspects: the course content, the instruction format, as well as the instructors' change in teaching style. The reports about global warming and climate change they heard in the news media just about every day had profoundly promoted their curiosity and interests in the issue. They were notably happy to see an introductory course on climate change. Students in sciences and engineering were used to analytical courses in rigid setting

that include formal lectures covering relatively narrow scope of subjects with well-developed techniques for the analyses. At the outset of the preparation for this course, it was decided to deliver the materials in seminar style for several reasons. Naturally, the broadness of the course subject requires multiple lecturers from many different fields. The question-and-answer session at the end of each lecture allows students to express their thoughts and imaginations. Different lecture topics for different sessions inspire their thoughts about the relations among these subjects. Students are indeed eager to learn a serious subject through in much relaxed atmosphere. Most of the students had taken my engineering mathematics and chemical engineering thermodynamics courses (the second semester course in thermodynamics) prior to my offer of the climate change class. They were pleasantly surprised to know that a course of quite different delivery and learning styles was offered.

The Intergovernmental Panel on Climate Change (IPCC) and Al Gore were awarded the Nobel Peace Prize when the course request was approved by the university. The gigantic three-volume IPCC's Fourth Assessment Report (AR4) provides a comprehensive assessment of many aspects of climate change analytically written and edited by a selected group of 559 scholars. At the outset of the course planning, it was decided to cover the same three areas as those covered by AR4, and the course was entitled Climate Change: Causes, Impacts and Solutions. The detailed structure of the course is discussed later in this chapter.

Speakers of the lectures were invited mainly from the UM as well as the universities in the region to cover the topics in the fields of causes, impacts, and solutions of climate change. Most of them accepted the invitations without hesitation since the invited lectures were their expertise. There were 25 formal lectures when the course was offered for the second time in 2009. About 60 % of these lectures focused on mitigation technologies. Each lecture lasts about 60 min followed by a 15-min question-and-answer session. Two sessions at the end of the semester were reserved for student presentations. Formal lecturers were asked to assign homework, which they will be asked to grade in the following week.

Textbooks and References

Vanek and Albright's *Energy Systems Engineering: Evaluation and Implementation* was chosen as the textbook (Vanek and Albright 2008). The authors introduce the system concept in the analysis of energy conversion technologies at its outset. It is an interesting and beneficial approach, although the "system" concept has been introduced in several engineering courses such as process control, dynamics, reaction engineering, engineering economy, etc.; this textbook applies the concept to several different aspects of the energy systems including material and energy balances, economics analysis, carbon cycle, etc. They are uniquely demonstrated in energy systems in one place. The authors introduce the science and engineering fundamentals, technological costs, and impact on natural environment of each of the selected energy systems. Major working equations associated with the technology are identified; the functions of these equations are consciously illustrated by short

representative examples. These equations effectively link the current issues of energy systems and climate change with materials introduced in other courses, such as economics, heat transfer, thermodynamics, etc. They also provide the readers with an overview of the context within which these systems are being implemented and updated today and into the future. Their presentation centers around the utilizations of alternative energy resources and their roles in climate change mitigation. An extensive online ancillary package for instructors provides an instructor's manual, solution files, course syllabus, MATLAB scripts, and teaching PowerPoint files. Vanek and Albright indeed made it a friendly book to both the students and the instructors. The book was published in late 2008, i.e., after the price surge of oil; therefore, the economic analysis is based on fairly reasonable data. Moreover, this textbook contains representative homework exercises that serve the pedagogical needs and broad in nature. The cost of this book is moderate. These features render it suitable for a one-semester, introductory textbook for engineering students who would like to know the alternative energy options. Specifically, it covers energy supply and demands, issues surrounding CO_2 emissions, factors affecting and models of energy systems, economic tools for energy systems, climate change and climate modeling, fossil fuel resources, stationary combustion systems, carbon sequestration, nuclear energy systems, solar resource, solar photovoltaic technologies, solar thermal applications, wind energy systems, transportation energy technologies, systems prospective on transportation energy, and a conclusion chapter on creating the twenty-first-century energy system. The book, however, lacks coverage on a number of important areas including biomass conversion systems, energy efficiency for buildings, geothermal energy, and advanced combustion systems including oxy-fuel combustion and chemical looping systems. The seminar class did not cover all the topics in this handbook; however, several scholars in the regions were invited to cover most of these topics.

IPCC's AR4 (Intergovernmental Panel on Climate Change 2007a, b, c) was introduced to the class early mainly because it provides the most comprehensive and up-to-date scientific, technical, and socioeconomic information about climate change. It is available online at no cost; the paper copies are available from Cambridge University Press at moderate costs. The students were asked to read the "Summary for Policy Makers and Technical Summary" for each volume (with a total size less than 300 pages) in the first 3 weeks of the course so that they can have a general understanding of the subject. Some of the slides for the introductory sessions were extracted from the online version of these reports. While AR4 presents the most detailed advanced analysis presented by the IPCC and others, it does not contain textbook-level explanations about most of the scientific and technological terminologies. The major portions of the AR4 (other than the "Summary for Policy Makers and Technical Summary") serve as an indispensable reference to the complex subject, which deserve frequent visits during their study.

The ambitious book written by Tester et al. (2005) was adopted as a reference. This decadelong effort of five MIT professors is the first single source of the sustainable energy utilizations when it was published in 2005. It assesses technologies of converting fossil fuels (oil, gas, and coal), nuclear energy, and renewable

energies (solar, biomass, wind, hydro-, and geothermal) and discusses energy storage, transmission, end use, and efficiency/conservation issues. These technologies are assessed in a political, social, economic, and environmental context with life cycle assessment and systems integration methods. This textbook has been used in a graduate course on sustainable energy many times at MIT. The book was recommended as an advanced reference.

Dessler and Parson (2010) provide an integrated treatment of the science, technology, economics, policy, and politics of climate change. Aimed at the educated nonspecialist, and at courses in environmental policy or climate change, the book clearly lays out the scientific foundations of climate change, the issues in current policy debates, and the interactions between science and politics that make the climate change debate so contentious and confusing. This new edition is brought completely up to date to reflect the rapid movement of events related to climate change. In addition, all sections have been improved; in particular, a more thorough primer on the basic science of climate change is included. The book also now integrates the discussion of contrarian claims with the discussion of current scientific knowledge, extends the discussion of cost and benefit estimates, and provides an improved glossary.

Web sites of major international and US organizations were introduced to the students:

- Intergovernmental Panel on Climate Change, http://www.ipcc.ch/
- United Nations Framework Convention on Climate Change, http://unfccc.int/2860.php
- United Nations Environment Programme, http://maps.grida.no/theme/climatechange
- World Meteorological Organization, http://www.wmo.int/pages/themes/climate/index_en.php#
- International Energy Agency, http://www.ieagreen.org.uk/
- United States Global Change Research Program, http://www.globalchange.gov/
- United States Climate Change Science Program, http://www.climatescience.gov/default.php
- United States Climate Change Technology Program, http://www.climatetechnology.gov/
- US Department of Energy, http://www.eia.gov/, http://www.energy.gov/environment/climatechange.htm, http://www.netl.doe.gov/technologies/carbon_seq/
- National Oceanic and Atmospheric Administration, http://www.noaa.gov/climate.html
- US Environmental Protection Agency, http://www.epa.gov/climatechange/
- US National Aeronautics and Space Administration, http://climate.nasa.gov/
- US National Science Foundation, http://www.nsf.gov/news/special_reports/climate/
- US Department of State, http://www.state.gov/g/oes/climate/
- National Academy of Science, http://www.koshland-science-museum.org/exhibitgcc/index.jsp
- Earth Policy Institute, http://www.earth-policy.org/

Table 1 2009 lectures

Session	Speakers	Title of lecture
1	Wei-Yin Chen	Overview of the causes of climate change – causes
2	Wei-Yin Chen	Overview of the impacts of climate change – impacts
3	Neil Manson	Reasoning economically about potential environmental catastrophes
4	Nathan Hammer	Atmospheric physics and chemistry
5	Charles Wax	Climate change – evidences and contrarian viewpoints
6	David Case	Climate change and US laws
7	David Case	International protocols and climate change
8	Yan Ding	Assessment of impact of sea level rise on coastal and estuarine infrastructure using numerical simulation model: CCHE2D-coast
9	Cris Surbeck	Effects of climate change on water resources
10	David Reed	Global climate change – impacts on biodiversity
11	Deb Gochfeld, Kristie Willett	Ecological and health impacts of climate change
12	Scott Gold	Surface chemistry and nanotechnologies: an approach for green energy
13	Jeff Roux	Energy conservation – use of foil radiant barriers to reduce residential/commercial energy usage in summer/winter for cooling/heating
14	Clint Williford	Biological conversion of biomass
15	Walter Cleland	Chemistry of CO_2
16	Waheed Uddin	Mobile and aerial sources of CO_2 and abatement strategies
17	Elizabeth Ervin	Nuclear energy: statistics
18	John Seiner	Fuel efficiency in transportation systems
19	Nathan Hammer	Photocatalytic reduction of CO_2 and water splitting
20	Robert Holt	Carbon sequestration
21	Wei-Yin Chen	Overview of the impacts of climate change – solutions
22	Robert Dahlin	Integrated gasification combined cycle (IGCC)
23	Tom Gale	Combustion on the horizon – oxy-fuel combustion and chemical looping
24	Amala Dass	Fuel cells
25	Steve Davis	Computational chemistry
26		Student presentations
27		Student presentations

Lectures Presented by Faculty and Scholars

Table 1 lists the lectures and speakers of the course in spring 2009. Among the 25 lectures, sessions 1, 3, 4, 5, 6, and 7 cover subjects in the "causes" category of climate change, sessions 2, 8, 9, 10, and 11 the "impacts," and the remaining 14 sessions the "solutions." Two sessions at the end of the semester are reserved

for students' project presentations. The contents of these 25 lectures are summarized below. More information about these lectures can be found in the slides used in these lectures, which have been uploaded for public dissemination: http://home.olemiss.edu/~cmchengs/Global%20Warming/.

Introduction to Climate Change: Causes, by Wei-Yin Chen

This is the first of three overview lectures given in this class that bore the same title of the course, one each on the causes, impacts, and solutions of climate change. The first two lectures covered the first two topics using one set of slides. The first introductory lecture on the causes covered the following topics:

- The rationale of offering a climate change class
- Impacts of increasing energy demand and lack of energy infrastructure on climate change challenges
- United Nation's efforts on climate change mitigation
- UNFCCC and Kyoto Protocol
- Total CO_2 emissions by country and CO_2 emission per capita
- Developed and developing nations' different views on CO_2 emission limits
- Paleoclimate archives and the scientific observations of greenhouse effects caused by human activities
- Greenhouse gases and their geographic and sectoral sources
- Radiative forcing of different greenhouse gases and their implication of human activities
- Nature climate change (i.e., the Milankovitch cycles) and its causes
- Thermohaline circulation and ice age
- Anthropogenic causes of climate change
- Natural carbon emission, carbon sinks, and carbon cycle and their relation with temperature rise and mitigation technologies

Finally, IPCC's comparison of economic development, population growth, and energy usage was used to illustrate the societal causes of global warming. The recent increase in CO_2 emissions was fueled more by economic growth than growing populations. It is not the poor masses, but the new and old rich that fuel global warming. And while energy and emission intensities have steadily decreased since the oil crisis in the 1970s, carbon intensity (carbon emission to energy consumption) has not. One conclusion could be drawn is that fixing prices for greenhouse gas emissions can help achieve emissions reduction, just like rising oil prices helped reduce energy and emissions intensity in the last decades.

Some of these slides were extracted from the IPCC's AR4 reports. Reading materials were assigned. Students were asked to start searching a term research topic.

Introduction to Climate Change: Impacts, by Wei-Yin Chen

The second lecture was on the impacts of climate change. History has shown that civilizations rise and fall to the pulse beats of climate. Erik Thorvaldsson's (known as Erik the Red) discovery of Greenland in 982 A.D. and the subsequent collapse of the Norse settlement less than 500 years later due to severe weather was one example. Flooding is generally believed to have caused the collapse of the Harappan civilization of India, 2500–1600 B.C. The outset of the lecture discussed how the analysis of climate predictability had actually promoted the evolution of modern chaos theory in the 1960s and 1970s.

Water's specific volume increases when the temperature rises. Sea level rise causes the most direct impact of temperature rises. Ice cap melting contributes a lesser degree of impact on sea level rise. Temperature rise also causes decline in biodiversity and natural disasters including droughts, heat waves, flooding, and cyclones. Sea level rise can contribute to disease spread and loss of traditional lifestyle. The natural disasters, in turn, can generate loss of traditional lifestyle, losses of water and food resources, biodiversity losses, economic losses, famines, casualties, and disease spread.

The abovementioned impacts were then discussed in more detail. IPCC's statistics and projections of these impacts are presented. The projected impacts on water resources, ecosystems, food productivity, coasts, and human health were presented as a function of warming from 1990 to 2100. As of 2007, there are concerns in all of these five areas. The projected sea level rise and its effects on land area, population, and GDP showed that Asia will have the most severe consequences. Records show an increasing trend of natural disasters, especially flooding and cyclones. The natural fluctuation of climate, El Nino and La Nina, was introduced. El Nino and La Nina originate in the Pacific Ocean but affect climate globally. The increase in El Nino frequency as the climate changes since 1970 has only recently been appreciated. The potential impact of sea level rise on the Nile Delta is presented. Its impacts on freshwater resources (ground- and surface water) of small islands and low-lying coastal area were explained. Freshwater, in turn, has profound influences on agriculture, ecosystems, and human health. Food production is affected by water, temperature, CO_2 level and ultraviolet radiation, and pest and diseases. Developing countries are expected to be affected more than the developed countries. Effects on tea and coffee productions in Kenya and Uganda were illustrated. Finally, the projected biodiversity loss between 2000 and 2050 and spread of several diseases, including malaria, were presented.

Reasoning Economically About Potential Environmental Catastrophes, by Neil Mason

At the outset of his lecture, Neil Mason, a philosophy professor, explained why environmental scientists should care about economics. It is known that economic evaluation mediates science and policy. The results of science never get translated

into action without some form of economic evaluation, either by private industry or by governmental regulators. Less obvious about the importance of economics is its role in moving forward a debate such as climate change. Skepticism about or outright denial of the results of scientific investigation can seem baffling, if not downright evil. Oftentimes, however, what is *really* going on is that skeptics or deniers (e.g., "intelligent design" proponents) wish to avoid the perceived evaluative implications (ethical, philosophical, religious, or economic) of the results of scientific investigation. Sometimes, the best way to move the debate forward is not to reiterate the science, but to address directly the evaluative presuppositions of the skeptics or deniers (e.g., "Why even think evolution is incompatible with belief in God?").

The major portion of the lecture covered the two competing approaches in making environmental policy decisions: the cost-benefit analysis (CBA) that has been the ascendancy in the USA (Sunstein 2005) and the precautionary principle (PP) that has been commonly adopted by the European Union and many of its member nations, as well as by the United Nations (Manson 2002; Sunstein 2005). The basic idea of CBA (Sunstein 2005) is to identify all potential costs and all potential benefits of a given course of action, assign to each cost and benefit both a probability of occurrence and a dollar value (positive or negative) of occurrence, crunch the numbers, and see whether the result is overall positive or negative. Using CBA, courses of action can be compared to see which course of action has the highest overall positive rating (or least bad negative rating). Then, policymakers should approve the course of action that maximizes net benefits or at least give some presumption in favor of that course of action (Sunstein 2005). Posner's CBA calculations (Posner 2003) regarding the building of the Brookhaven particle accelerator are illustrative (Sunstein 2005). With CBA, in order for a potential cost to factor into the decision, there is some estimate both of its dollar value and of its probability of occurrence that must be available; otherwise, that potential cost is a nonfactor.

The PP is considerably more vague than CBA, with a host of competing formulations (Manson 2002), but the basic idea is "better safe than sorry." Given that the results of our industrial/technological innovations cannot be foreseen, regulators are justified in restraining such innovations unless and until enough evidence comes in that the activity in question will *not* produce harmful results. The approach is "risk averse."

Standard objections to these approaches and responses are presented. Many examples are given. It is one of the lectures of this class that promotes critical thing about the basis in policymaking. As a homework exercise, the instructor asked the students to write an essay on what approach they would choose in determining the policies toward climate change.

Atmospheric Physics and Chemistry, by Nathan Hammer

Chemistry professor Nathan Hammer presented a lecture on atmospheric physics and chemistry. At its outset, the dynamical evolution of the Earth's atmospheric gas

since the primordial solar nebula 4.6 billion years ago was presented: from a composition similar to the emissions of today's volcanoes (rich in CO_2, H_2O, and H_2) to oxidizing gas that is rich in N_2 and O_2. O_2 has been stable in the atmosphere for 400 million years, as a result of photosynthesis and decay of organics on Earth. Trace gases are introduced. Among them, CO_2, CH_4, and N_2O are considered greenhouse gases due to their capabilities of absorbing vibration bands of the reflected sunlight from Earth's surface. Dr. Hammer presented the infrared absorption bands of these compounds and that result in trapping a fraction of reflected energy in the atmosphere. These trace greenhouse gases increase over time as the result of increasing use of fossil fuel combustion and activities of chemical industries. Human behaviors have caused increases in trace gas emissions that lead to the formation of photochemical smog from automobile tail gas and ozone depletion from chlorofluorocarbons (CFCs).

Geostrophic flow is driven by uneven distribution of pressure and temperature of Earth and the rotation of Earth (i.e., the Coriolis Effect); it, in turn, transports energy pole wards and reduces equator-to-pole temperature contrast. Prolonged temperature rise in this atmospheric circulation across the Pacific Ocean is called El Nino, or Southern Oscillation; similarly, prolonged temperature decrease is called La Nina. El Nino and La Nina usually happen 2–7 years with 9-month to 2-year durations. They cause global weather effects including droughts, hurricanes, moisture, and temperature patterns. Their causes, including global warming, are under active investigation.

The four layers of atmosphere were introduced: troposphere, stratosphere, mesosphere, and thermosphere. The chemical characteristics of their gas components and the temperature and pressure variations in these layers were discussed. In the troposphere, the main concerns are acidic gases, photochemical smog, and greenhouse gases. In the stratosphere, O_2 photochemically dissociates; the main issues are ozone depletion by nitrogen oxide (NO) and CFCs. The mesosphere is characterized by photochemical reactions of small diatomic molecules and reactions of atoms and ions. The thermosphere is characterized by ultraviolet radiation and ionic reactions. Dr. Hammer then discussed the mechanisms of the following chemical reactions or processes:

- Formation of photochemical smog starts with photochemical decomposition of NO_2 followed by ozone formation and a series of reaction involving volatile hydrocarbons.
- Ozone destruction by NO.
- Ozone destruction by hydroxyl radicals.
- Ozone destruction by CFCs.
- Aerosol formation dynamics.
- Ionic reactions.

The students were asked to write an essay about their understandings of the climate change as homework. The textbook by Wayne (1985), Seinfeld and Pandis (1998), and Jacob (1999) was recommended for additional information.

Global Climate Change: Scale and Complexities, by Charles Wax

The State climatologist and Mississippi State University Geosciences professor Charles Wax gave this lecture. At its outset, it covered the nature of climate change including the causes of Milankovitch cycles, sunspot activity, and emission of volcanic debris, which results in glaciations every 100,000 years and interglacials every 10,000 years. The correlations between the observed historical data between these nature phenomena were then discussed. The temperature decline after the medieval maximum, or the "little ice age," that took place between 1400 and 1900 AD, was at least partially due to the maunder minimum, or the prolonged sunspot minimum. It was suggested that the observed El Nino may be correlated with the Atlantic multidecadal oscillation documented in history. Coupled with changes in instrumental measurements and data interpretation methods, he mentioned the possibility that what have been observed may be part of a long story of ups and downs.

Climate Change and US Laws, by David Case

Law professor David Case gave two time-sensitive lectures, one on climate change and US laws and the other on climate change and international protocols. These lectures were given only weeks after President Obama was inaugurated. The proposals for climate change legislation at that time were discussed in detail: to include cap and trade, carbon tax, and Clean Air Act Amendment for regulating greenhouse gas emissions by EPA. The lecture covered the details of the process and subsequent developments, including Dr. Case's expectations on Obama administration's policy, of the 2007 *Massachusetts v. U.S. Environmental Protection Agency (EPA)*, 549 U.S. 497 (http://www.supremecourt.gov/opinions/06pdf/05-1120.pdf, 2007). *Massachusetts v. EPA* is a US Supreme Court case decided 5-4 in which 12 states and several cities of the USA brought suit against the EPA to force the agency to regulate carbon dioxide and other greenhouse gases as pollutants. Finally, the lecture covered the status of the National Environmental Policy Act (NEPA), Endangered Species Act (ESA), and common law litigation, such as *Connecticut v. American Electric Power* (S.D. N.Y. 2005) and *California v. General Motors* (N.D. Cal. 2007).

Climate Change and International Protocols, by David Case

Dr. Case's second lecture on *international protocols* focuses on the contributions of the multinational scientific body Intergovernmental Panel on Climate Change (IPCC). It covered IPCC's publications of the periodic Assessment Reports (AR), establishment of United Nations Framework Convention on Climate Change (UNFCCC), the functions of the Conference of Parties (COP), the journey of Kyoto Protocol, negotiations on post-Kyoto commitments, and skepticism about post-Kyoto regime. In addition to the *Massachusetts v. EPA* link mentioned above,

Dr. Case assigned three other reading assignments extracted from the book by Gerrard (2007).

Assessment of Impact of Sea Level Rise on Costal and Estuarine Infrastructure Using Numerical Simulation Model, by Yang Ding

Prof. Yan Ding of the National Center for Computational Hydroscience and Engineering gave a lecture on the impacts of sea level rise on costal and estuarine infrastructure using numerical simulation model. The lecture started with an overview on costal hazards due to hurricane, storm, and tides, current instrumental records for climate change, impacts of sea level rise, coastal zone structure, and coastal flood hazard zones. Most of this lecture was devoted to detailed numerical analysis of coastal and estuarine hydrodynamic and morphodynamic processes. Special cases were presented with comparison with recorded data. A list of references (including the slides on the web) was given, and the following homework assignments were assigned:

1. Find tidal datums in the Bench Mark Sheets of Gulfport Harbor, MS on the web site of NOAA Observational Data Interactive Navigation at http://tidesandcurrents.noaa.gov/gmap3/. Draw a figure to display the MSL, NGVD, and NAVD. Then, retrieve tidal datums in the Bench Mark Sheets of the USCG New Canal Station, Lake Pontchartrain, LA. Find the differences of the tidal datums between the two locations. Explain why they are different.
2. What are the impacts of sea level rise on coasts and coastal communities?
3. What are coastal zones? How are coastal flood hazard zones defined by Federal Emergency Management Agency?
4. What is the CCHE2D-Coast model? What are the model's capabilities to simulate coastal processes related to assessment of impacts of sea level rise?

Effects of Climate Changes on Water Resources, by Cristiane Queiroz Surbeck

Civil engineering professor Cristiane Queiroz Surbeck gave a lecture about the effects of climate changes on water resources. At its outset, the lecture covered the global ocean conveyor belt (thermohaline circulation), the effects of climate change on the circulation and therefore the distribution of Earth's water resource and quality and the hydrologic cycle. Then, the effects of climate change on water resources in the different regions of the North America were discussed. Through this case study, a few concepts and methods were discussed: the method for the estimation of hydrologic water budget through rainfall analysis, intensity-duration-frequency curves, and return period. A numerical example was given, and a specific water budget problem was given as homework.

Impacts of Global Climate Change on Biodiversity, by David Reed

Biology professor David Reed gave a lecture on the impacts of global climate change on biodiversity. At its outset, the definition, importance, and measure of biodiversity were covered. Origination and extinction through time have been observed in fossil record. The huge end-Permian mass extinction about 30,000 year ago marked the beginning of the diversity decline. The present extinction rate is shown to be at least 50 times higher than that of the post-Permian period. Cases of human-caused extinction were discussed. These cases led to the systematic and focal presentation of this lecture on the functions and importance of ecosystem services to the environment on Earth. These environmental services include food production, raw materials, recreation and water supply, atmospheric gases, water recycling, erosion control, soil formation, nutrient cycling, and purification of wastes. Plants are not only the sources of food, they are valuable sources of genetic materials, natural pesticides, and medicines. Climate change has shifted the range of 1,700 species toward the poles at an average rate of 6.1 km per decade, spread of diseases to higher elevations and more northerly latitudes, and population declines of polar bears and penguins. Since species habitats are more fragmented than in the past and are smaller than in the past, the impact of future climate change is expected to cause a higher rate of extinctions. About 10–20 % of all species on Earth are expected to go extinct by 2050.

Ocean and Human Health Consequences, by Deborah Gochfeld and Kristie Willett

Prof. Deborah Gochfeld of the National Center for Natural Products Research and Prof. Kristie Willett of Pharmacology made two related presentations in a joint seminar on ecological impacts of climate change. Dr. Gochfeld discussed the ocean health and Dr. Willett the human health consequences. These two lectures extend David Reed's biodiversity lecture into a more detailed analysis.

Dr. Gochfeld first introduced the ocean stressors imposed by humans: overfishing, pollution/sedimentation/eutrophication, and habitat modification, which reduce the resilience of species, communities, and ecosystems to climate change efforts. It was explained how local economies near major coral reefs benefit from an abundance of fish and other marine creatures as a food source and how drugs are produced from corals. The major portion of the lecture was devoted to the discussions about how climate change affects the seawater temperature, ocean chemistry (especially the decrease of carbonate ion, CO_3^{2-}, with increasing atmospheric CO_2 concentration), sea level rise, ocean circulation, solar and UV irradiance, and pathogen distribution and virulence. The results of these immediate effects were discussed in detail. For instance, changes in natural ocean circulation induce extreme weather, terrestrial climate, and disappearance of shallow water and intertidal habitats. Extreme weather, in turn, causes increased coastal erosion, especially beaches, increased river volume, flooding, drought, runoff (freshwater, sediment,

pollutants, nutrients), destruction of salt marshes, seagrass beds, mangroves, and coral reefs. Moreover, harmful algal blooms result from runoff of sediment, and nutrients are enhanced by elevated temperatures and solar radiation. Decrease in carbonate ion reduces the abilities of corals and other calcifying organisms (clams, oysters, mussels, and other important fish species) to produce skeletons or shells. Seawater rise causes flooded coastlines, wetlands, estuaries, disappearance of shallow water and intertidal habitats, and loss of nursery grounds, nesting, and feeding habitats of many organisms.

Dr. Willett's lecture covered stress-related problems, increased infectious disease, extreme events, increased number of poor, and increased agricultural yields. World Health Organization's (WHO) climate change site at http://www.who.int/globalchange/en/index.html was introduced at its outset. The primary, secondary, and tertiary impacts of climate change on human health at the outset were discussed. Temperature rise causes ozone and photochemical smog concentrations that induce several respiratory diseases and alleges. Statistics also illustrate that temperature correlates the populations of mosquitoes, ticks, snails, and parasites in contaminated water, which, in turn, transmit dengue fever, malaria, Lyme disease, schistosomiasis, and cholera. Extreme weather leads to flooding and drought that cause food shortage and malnutrition. The correlations between the temperature rise and the health issues observed in different parts of the world between 1990 and 1999 (Intergovernmental Panel on Climate Change 2007b) were also discussed. In addition to the IPCC report, WHO report (World Health Organization 2003) and EPA's climate change site, http://www.epa.gov/climatechange/ were assigned as the reading materials.

Surface Chemistry and Nanotechnology: An Approach to Green Energy, by Scott Gold

Prof. Scott Gold of the Louisiana Tech University gave a lecture on the surface chemistry and nanotechnology: an approach to green energy. This lecture covered two major portions: the sciences and technologies of template wetting nanofabrication and their technological applications in fuel cells and electrochemical supercapacitors. At the outset, it introduced the template materials, methods of wetting porous materials, reactive ion etching, sputtering processes, and posttreatment reactions that convert nanotube precursor to desired materials. He then discussed the applications of nanostructures from template wetting that include:

- Ceramics such as sulfated zirconia (superacid) for proton exchange membrane for fuel cells and acid catalysis
- Nanotubes of metals such as platinum, palladium, and gold as catalysts in fuel cells, and Raman spectroscopy
- Piezoelectric microelectromechanical systems (MEMS)
- Conductive and semiconducting polymers as electrical supercapacitors, photovoltaics, LEDs, photodiodes, sensor, and hydrogen storage

The second half of Dr. Gold's lecture focuses on fuel cells. Different types of fuel cells were introduced: alkaline, proton exchange membrane, direct methanol and other liquid fuels, phosphoric acid, molten carbonate, solid oxide, and enzymatic biofuel. Their applications and operating conditions were discussed. Research in fuel cells has been growing rapidly due to its low emissions, high-energy efficiency, and higher energy density than batteries. Reaction efficiency, design (current collection, fuel transport to catalyst, proton transport to membrane, and waste removal), material issues, and cost remain as technological barriers and research areas. Dr. Gold then presented the works of his group on nanofabrication: gold and platinum nanotubes on grapheme oxide (GO) and semiconducting polymer such as poly (3-hexylthiophene) (P3HT) nanotubes. Nanotube preparation and their enhancement in electron transfer rate coefficients for biofuel cell and supercapacitors were discussed in detail.

Energy Conservation: Use of Foil Radiant Barriers to Reduce Residential/Commercial Energy Usage in Summer/Winter for Cooling/Heating, by Jeff Roux

Prof. Jeff Roux of mechanical engineering gave this lecture on building design for energy conservation. At the outset, he presented the important role of energy conservation in climate change mitigation. IPCC AR4 concluded that the buildings sector will have the highest economical potential for global mitigation as a function of carbon price in 2030. Major currently available commercial technologies and practices for this sector include efficient lighting and daylighting, more efficient electrical appliances, heating and cooling devices, improved cook stoves, improved insulation, passive and active solar design for heating and cooling, alternative refrigeration fluids, and recovery and recycle of fluorinated gases. Key mitigation technologies and practices projected to be commercialized before 2030 include integrated design of commercial buildings including technologies such as intelligent meters that provide feedback and control and solar photovoltaic integrated in buildings. The research at the University of Mississippi on improved insulation for residential dwellings was then discussed. The lecture presented the characteristics and properties of various fibrous materials (fiberglass, rock wool, cellulose, and polystyrene and polyurethane foams) and their principles of operation. The large surface area of fibers inhibits the air within the insulation from moving. Air has a low thermal conductivity and is an excellent insulator if it can be made to remain stationary. The lecture also presented experimentally measured data (including summer and winter) at an occupied north Mississippi residence, which were transformed to various profiles such as time histories of temperature, heat flux, and water vapor concentrations. A mathematical model that incorporated conduction and radiation heat transfer and moisture transport was developed to predict the changes in total heat flux. Model predictions showed good correlations with the experimentally measured heat flux.

Biological Conversion of Biofuels, by Clint Williford

Dr. Clint Williford, professor of chemical engineering, gave a lecture entitled biological conversion of biofuels. The lecture started with an introduction on the historical correlations among oil price, supply, and demand. It then covered the greenhouse gas emissions from different sectors and fuel sources. Looking ahead, biomass conversion to fuels has been considered one of the seven wedges to maintain a constant CO_2 emission level between 2005 and 2055. This reduction corresponds to one billion tons of CO_2 per year, or an increase of bioethanol usage by 50 times. Nevertheless, the investment on biomass conversion grew rapidly in the last decade due to higher energy cost, concern for energy security, climate change, political supports, and technological maturity. The major portion of this lecture was on the current biofuel technologies: biodiesel, grain corn ethanol, cellulosic ethanol (cell EtOH), and biobutanol. In addition to the details of their conversion technologies, he explained the heat content of the products, pollutant emissions (unburned hydrocarbons, CO, particulate matter, and NO_x), fossil fuel replacement ratio, economics, and other issues during their usages. He then discussed his research on alternative biomass pretreatments for improved lignocellulosic ethanol production. Celluloses are abundant and widely spread. Conversion of cellulose to ethanol can relieve food demand from corn and cane; it is virtually eternal. Moreover, its positive impacts on CO_2 emission and nonrenewable replacement are both high (over 90 %) and have been spurring biofuel mandate. The technological difficulties of the conversion and its cost remain bottlenecks in its development. The separation of cellulose from lignin, however, requires innovations in the areas of the selections of enzymes, pretreatment process, and improved lignin utilizations. Dr. Williford also discussed the controversies of biofuels including the impact of deforestation, nitrous oxide emission from fertilizer, food price, and food export.

Chemistry of CO_2, by Walter Cleland

Professor of chemistry Walter E. Cleland gave a lecture on the chemistry of CO_2. This lecture was selected to promote critical thinking for developing innovative technologies for CO_2 capture and utilization. It started with an introduction of the various stable oxides of carbon, physical properties of CO_2, phase diagram, and Walsh diagram. Industrial processes involving CO_2 production and utilizations were then presented. CO_2 utilizations based on the physical properties of CO_2 include refrigeration fluid, cleaning solvent, solvent as a reaction media and extraction, and food and agrochemical applications such as beverage additives and fumigant. CO_2 utilizations based on the chemical properties of CO_2 include the production of urea, salicylic acid, inorganic carbonates and pigments, propylene carbonate, naturalization of caustic waste water, and CO_2 capture by various liquid and solid sorbents.

The majority of this lecture covered more detailed discussions of the CO_2 reactions for its production and utilizations. Productions of CO_2 mainly come from combustion and gasification of fossil fuels and their derivatives in stationary and

mobile sources. Fermentation, lime-kiln operations sodium phosphate manufacture, and natural gas wells also produce fairly sizable quantities of CO_2. CO_2 in these gas streams can be captured by amines (Girbotol process) and sodium or potassium carbonate process. CO_2, along with $KMnO_4$ (permanganate process) or $K_2Cr_2O_7$ (dichromate process), has been used to chemically reduce H_2S in gaseous streams to elemental sulfur.

The lecture then covered the reactions that involve CO_2 either as a reactant or as a product in the following categories: CO_2 reaction with H_2O; reaction with O_2, CO, and O_2; CO_2 with H_2 (reversed water-shift reaction); CO_2 with NH_3 (urea formation); CO_2 reactions with organics that have been used in carbon capture; coordination chemistry of CO_2 and metals; reaction of M-CO_2; reactions in biological systems; use of CO_2 as a C1 feedstock; carboxylation; polymerization; CO_2 reductions; and photochemical reduction of CO_2. The reactions of CO_2 with organics are of three major types: organic reaction with RO^- to form $ROCOO^-$, with RNH_2 to form $RNHCOO^-$ or RNHCONHR, and with RMgX or RLi to form $RCOO^-$. CO_2 is a poor ligand, but it does form a number of complexes and bonding modes with metals, which are important for activation of CO_2 in catalytic reduction reactions. For instance, M-CO_2 reacts proton or electrophile, such as R^+, and converts to M-CO or M-C(O)OR, respectively. CO_2 reacts with hydride, M-H, and forms M-O_2CH. Organophosphines, PR_3, react with M-CO_2 and O = PR_3. Isocyanide, M(CNR)-(CO_2), decomposes and forms RNCO and M-CO. Reactions of CO_2 in biological systems include animal metabolism, photosynthesis, enzyme-catalyzed carbonic acid decomposition, carboxylation of ribose, and catalytic reduction of CO_2 to CO. Using CO_2 as a C1 feedstock leads to the formation of carboxylates, lactones (RCOOR′), carbonates (RR′NCOOR″, ROC(O)OR′), ureas (RR′NCONRR′), and isocyanates (RNCO). Moreover, as a C1 feedstock, CO_2 reduces to formats ($HCOO^-$), oxalates ($^-O_2C\text{-}CO_2{}^-$), formaldehyde (H_2CO), CO, methanol, and methane. Carboxylation results in the formation of COO^- group on carbon, nitrogen, or oxygen atom in an organic compound such as direct carboxylation in ionic liquid from imidazolium carbonate. With metal-salen catalyst, polycarbonates form from epoxides and CO_2. Through metal and enzymatic catalytic mechanisms, CO_2 has been hydrogenated to formic acid and methanol. Finally, the fundamentals of photoelectrochemical reduction of CO_2 to formic acid and methanol were briefly discussed. A recent review by Beckman (2004) would be a valuable reading beyond this class.

Mobile and Area Source of Greenhouse Gas (GHG) and Abatement Strategies, by Waheed Uddin

Civil engineering professor Waheed Uddin gave a lecture on mobile and area source of greenhouse gas (GHG) and abatement strategies. This lecture introduced five topics:

- Quantifying traffic and built environment impacts on mobility and traffic congestion

- Evaluation of traffic and built environment impacts on GHG emissions and global warming
- Assessment of traffic and built environment impacts on air quality and public health
- Application of remote sensing and geospatial technologies and air pollution models for traffic visualization
- Environmental assessment and evaluation of abatement strategies

The transportation sector accounts for 28 % of total GHG emissions in the USA and 33 % of the nation's energy-related CO_2 emissions (EIA 2007). The USA in turn is responsible for 22 % of CO_2 emissions worldwide and for close to a quarter of worldwide GHG emissions (Energy Information Agency (EIA) 2007). Report has shown that GNP has been linearly proportional to the density of paved road, and GHG emissions have increased with increasing use of fossil fuels for the economic growth. Although average mileage per gallon of gasoline has increased 40.60 % from 1970 to 2000, average total fuel consumption per vehicle has decreased only 13.25 % from 1970 to 2000. Percent increase in vehicle mile traveled showed a strong correlation with increase in GDP. In addition to passenger cars, long haul tracks, light-duty trucks, aviation, marines, locomotives, motorcycles, and space missions are major portions of carbon emissions from mobile sources. Public transportation is one of the most significant means to reduce household carbon footprint. Moreover, traffic congestion and gridlock have steadily grown, and commuters spend 46 h annually stuck in traffic and waste five billion gallons of gas annually.

The lecture then covered carbon emission from buildings, whose carbon footprint can be extracted from high-resolution satellite imagery more cost effectively than traditional aerial photography. Large urban built-up areas (heat islands) demand more energy causing more carbon emissions and consequently more air quality degradation. As temperature rises, so does the likelihood that smog will exceed national standards of air quality; more power generation will produce more carbon emissions. As a result, sustainable transportation development must consider the following factors: land use, urbanization and social integration, built-up area effects on environment (air, water), built environment impacts on physical inactivity, traffic fatalities and injuries, traffic-related emissions and air pollution, traffic-related pavement noise impacts, construction process and material resources, energy demand, and diminishing natural resources.

To improve the spatial management and urban transport, it will be necessary to structure urban development with adequate transport policies and systems, manage efficiently the urban/rural/regional interfaces, and develop and implement enhanced GIS-based transport infrastructure asset management systems. Using the policy recommended by California's Climate Action Team (2007), Dr. Uddin stated the importance of "smart land use and intelligent transportation system (ITS)" to make the second-largest contribution toward meeting the state's ambitious GHG reduction goals. These policies include conservation and compact urban growth – by all government levels and by public, efficiency in vehicles by

vehicle manufacturer and consumers, efficiency in traffic flow by transport agency, better commercial truck fleet management by transporters, public mass transit, high-occupancy vehicle lanes, carpooling, flexible work hours, nonmotorized transport by government levels and by public, equity in road user charges for pollution and vehicle-mile traveled (VMT), and development in clean fuel and energy sources.

Nuclear Energy: Statistics, by Elizabeth Ervin

Civil engineering professor Elizabeth Ervin gave a lecture on nuclear energy with emphasis on statistical data. It was postulated at the outset that there are three motivations for developing nuclear energy today: it produces no controlled pollutants such as sulfur dioxides, nitrogen oxides, particulates, and GHG; it creates jobs and capital; and its image has changed in peoples' mind – 73 % of people approved its development in 2006. As a result, 36 new plants were under construction in 14 countries, and 223 had been proposed in 2006. A major human error at Chernobyl caused 56 deaths. However, the US civilian nuclear reactor program had resulted in zero fatality, compared to 33,134 coal miner and coal transporter deaths from 1938 to 1995 and 54,000 aviation deaths. Moreover, coal-fired power plant releases 100 times more radiations than equivalent nuclear reactor. At the presentation in 2008, there were 439 nuclear reactors operating in 31 countries; they provided 15.2 % of the world's electricity production in 2006 (34 % of EU and 20 % of USA). There were 104 commercial nuclear power reactor plants in the 64 sites and in 31 states in the USA. For seven states in 2006, nuclear energy made up the largest percentage of their electricity generated. Major unit operations of a nuclear power plant were introduced. Nuclear power generates economically competitive electricity, 1.82 cents per kWh, as compared to coal at 2.13 cents per kWh and natural gas 3.69 cents per kWh. Their power plants require much smaller spaces than those for biomass conversion plants, coal-fired power plants, and solar power plants. Disposal methods of nuclear fuel waste and low-level radioactive waste (LLRW) that consist of items that have come in contact with radioactive materials such as personal protective clothes have been developed. Fund, with an average of about 3.76 metric tons of dried used fuel per million dollars in the USA, has been committed to the management of nuclear waste. As of 2004, more than 690 containers have been loaded at 30 nuclear sites. This number is expected to grow to about 712 by 2015. Water discharged from a nuclear power plant contains no harmful pollutants and even meets regulatory standards for temperature. Prof. Ervin gave some facts about fission energy that are not commonly known. Nuclear energy has been widely adopted in medical procedures and cosmic. Many fruits and vegetables possess natural radioactivities. Uranium is a relatively abundant element (about as abundant as tin) that occurs naturally in Earth's crust. To resolve the shortage in nuclear workforce, the US Nuclear Regulatory Commission has created a curriculum education grant program as a multidisciplinary technical elective.

Fuel Efficiency in Transportation Systems, by Jack Seiner

The late Prof. Jack M. Seiner of mechanical engineering and National Center for Physical Acoustics gave a lecture entitled fuel efficiency in transportation systems. The lecture covered six topics: the motivation for transportation efficiency, carbon emissions by light-duty vehicles, alternative engine concepts, alternate fuels, alternate power sources, and roles of aerodynamic efficiency. The brief opening segment of his talk reiterated the major causes of climate change and the importance of improved energy conservation and enhanced fuel efficiency in transportation systems in climate change mitigation.

The discussion of carbon emissions by light-duty vehicles (the second part of the lecture) covered the concept of passenger miles per gallon (PMPG) for various transportation vehicles, estimation of auto sector CO_2 emissions, and global CO_2 emissions by economic sectors. It then reviewed the thermodynamics and thermal efficiencies of the two conventional piston-based engine cycles: the gasoline engine cycles and diesel engine cycles. These fundamentals led to major conclusions about the features and recent emphasis on diesel engines: diesel fuel has higher heat content than gasoline, and diesel engine has a 30–35 % higher thermal efficiency than conventional engine. For instance, a diesel engine in a light-duty vehicle such as a 2,000 lb Volkswagen Jetta gets 50 miles per gallon on the highway.

The discussion of alternate engines (the third part of the lecture) covered automotive gas turbines, rotary Wankel engine, Di Pietro rotary air engine, and other types of compressed-air cars. The history, design features, advantages, and technical issues of these technologies were discussed. The comparison of these engines considered the factors including pollutant emissions, efficiency, engine weight, fuel type, maintenance effort, life expectancy, number of parts, warm-up period, fuel flexibility, noise, and throttle lag.

In the discussion of alternate fuels (the fourth part of the lecture), the characteristics of gasoline with various alternate energy sources were compared: diesel, liquefied natural gas (LNG), compressed natural gas (CNG), ethanol and blended ethanol, liquid hydrogen, hydrogen at 150 bar, lithium, nickel metal hydride, lead acid battery, and compressed air. The number of vehicles that use these alternate fuels is increasing. Hydrogen and diesel have energy density higher than that of gasoline. Hydrogen does not have emission problems, but its storage in an efficient, safe, and cost-effective system has emerged as a major research area. Energies required for compression of H_2 to a gaseous state at high pressure and for liquefying H_2 are cost concerns. Energy loss in delivery in pipeline is another factor. Independently, means to store hydrogen by other materials have been investigated. Most of these works focus on hydrides, i.e., chemically bond hydrogen in a solid metal or carbon materials. In addition to hydrogen-packing density, performance indices include reversibility of hydrogen uptake and release, weight of hydride, kinetics of uptake and release, and the temperature and pressure dependence of H_2-hydride equilibrium. H_2 generation from hydrolysis of complex hydrides was discussed. Due to the complexity of these requirements, the US Department of Energy has announced a set of specific technical targets for hydrogen storage. The second half

of the discussion of alternate fuels was placed on biofuels. The historic development of "flexible fuel vehicles" was discussed first. He then discussed the feedstock, conversion technologies, emissions, policies, and challenges of various biofuels, with the emphases on the bioethanol and biodiesel. The serious challenges in the production of bioethanol include energy consumptions in the conversion of grain to ethanol (hydrolysis, distillation, drying, and emission control), water consumption, fertilizer use, and decrease in food supply. Biodiesel has a higher thermal efficiency than gasoline; the various sources of biodiesels, emissions prospective, and costs were then covered.

The alternate power sources for vehicles include hydrogen fuel cells, battery, and hybrids. This portion of the lecture covered the basic principles, comparison of various hydrogen storage systems, hybrid features and their prospective and their efficiencies in each of the energy conversion steps.

The last segment of this lecture covers the aerodynamic efficiency. It included the discussions of the factors influencing airplane ticket price per the nautical mile and nautical mile per gallon of gas. Recent development of blended wing body (BWB) for airplane design has shown advantages in weight of aircraft, fuel efficiency, and, therefore, the direct operating cost. The propulsion/airframe integration, aerostructure integration aerodynamics, and controls remain as major design challenges.

Photochemical Reduction of CO_2 and Water Splitting, by Nathan I. Hammer

Chemistry professor Nathan Hammer, a spectroscopist, gave a lecture on photochemical reduction of CO_2 and splitting of water. Solar energy is not only renewable, but also abundant. Indeed, more energy from sunlight strikes the Earth in 1 h (4.3×10^{20} J) than all the energy consumed on the planet in a year (4.1×10^{20} J). There is a high incentive to efficiently convert and store solar energy to reduce our reliance on fossil fuel. Photo- and electrochemical conversion of CO_2 and H_2O have been identified as one of the top five research areas in catalysis that require urgent attentions by the DOE's Basic Energy Science (Bell et al. 2007). Photocatalytic conversion of CO_2 to formic acid, formaldehyde, methanol, Co, and methane on catalyst surface has been demonstrated, and it is one of these potentially attractive approaches that brings CO_2 to a higher energy state by using solar energy. While CO_2 and H_2O react with photochemically excited electrons, water splitting takes place at electron holes. Water splitting can also be achieved by photolysis of water alone where O_2 forms on the photoanode and H_2 forms on cathode. The lecture covered the importance of these technologies, their fundamental reaction mechanisms, the role of band gap, and the characteristics and selection of catalysts in these photochemical reactions. It also includes several prominent works that demonstrate photochemical fixation of CO_2 on organic compounds, including the catalysts, reaction mechanisms, products, and secondary reactions.

Carbon Sequestration, by Robert Holt

Geology and geological engineering professor Robert Holt gave a lecture about his experiences in geologic carbon sequestration. He first explained the six known geologic sequestration options:

- Depleted oil and gas reservoirs
- Use of CO_2 in enhanced oil recovery
- Deep unused saline water-saturated reservoir rocks
- Deep unmineable coal seams
- Use of CO_2 in enhanced coal bed methane recovery
- Other suggested options including basalts, oil shales, and cavities

There are four CO_2 trapping mechanisms: structure and stratigraphic trapping, residual saturation trapping in large pores, solubility trapping by in situ water, and mineral trapping through chemical reactions. Mineral trapping is the most attractive process since it could immobilize CO_2 for a long time. However, it is comparatively slow because it depends on dissolution of silicate minerals. Security of trapped CO_2 (immobility) increases with time since the solubility and mineral trapping are slow.

The annual CO_2 consumption by the global chemical industries is only about 115 million metric tons, or less than 1 % of its production. At the same time, both natural and industrial analogues have provided evidences that geologic sequestration could be successful before other massive CO_2 utilization and storage technologies are developed. Distribution of natural analogues in the world, such as oil and gas reservoirs and CO_2 accumulation sites, is presented. Similarly, the distribution of industrial analogues in the world including natural gas storage, liquid waste disposal, and CO_2 injection for enhanced oil and gas recovery were presented. The lecture covered the CO_2 injection technology for enhanced recovery of hydrocarbons, the worldwide geologic storage potential, potential release pathways after injection, storage cost estimates, and monitoring technologies. Deep saline formation and sequestration in oil and gas fields have the highest capacities.

The last segment of his lecture covered the development of monitoring technologies at the University of Mississippi. The technology is based on a conceptual model for CO_2 transport in a saturated zone that involves buoyancy-driven CO_2 fingering with pulsation through coarse layers. It is visualized that pools of CO_2 are trapped beneath aquifer-confining layers; fingering and breakthrough of the trapped CO_2 occur when CO_2 pressure exceeds the non-wetting phase entry pressure. For phreatic aquifers, CO_2 moves into the unsaturated zone and pooling above the capillary fringe. Holt's research team has set up bench-scale apparatus and has been conducting field tests to answer the following basic scientific questions:

1. What controls CO_2 partitioning and dissolution into the aqueous phase?
2. What chemical reactions will occur and what are their rates?
3. What are the sizes of zones of detectable CO_2 and by-products?
4. What type of monitoring design will be required to insure detection?

Introduction to Climate Change: Solutions, by Wei-Yin Chen

This lecture was intended to give an overview on the solutions to climate change. It was originally arranged as session #12, the opening session on climate change mitigation, but scheduling issues left us few options except for this arrangement. The lecture included four major segments: energy conservation and efficiency, alternative energy sources, advanced combustion and gasification for efficient carbon utilization and enabling carbon capture and sequestration, and other advanced technologies.

The first segment on energy conservation and efficiency started with the IPCC's comparison (Intergovernmental Panel on Climate Change 2007c) of sectoral economical potential for global mitigation as a function of carbon price in 2030. The residential and commercial buildings sector leads the six other sectors in sectoral economical potential for global mitigation, which reflects the important role of energy conservation. Both building design and personal behaviors, such as the replacement of standard incandescent bulbs by compact fluorescent light bulb and shutting off lights and personal computers after work, could make notable contributions to carbon reduction. Energy supply sector ranks second in sectoral economical potential for global mitigation. Thus, the impact factors of various emerging technologies for power generation were discussed. According to IPCC's AR4, nuclear power, natural gas combined cycle, wind power, integrated coal gasification combined cycle (IGCC), pulverized coal combustion with oxygen (oxy-combustion) and carbon capture and sequestration (CCS), and pulverized coal combustion CCS are leading technologies that have the highest impact factors.

The segment on alternative energy sources covered the technical principles of nuclear energy, biofuels, wind and tide, geothermal energy, and solar energy. The rationale, scientific principles, and technologies are discussed. For the biofuel production and power generation, it covered biodiesel from vegetable oil and fat, ethanol from sugar cane and corn, ethanol from lignocellulosics, and thermal conversion of biomass.

The segment on advanced combustion and gasification for efficient carbon utilization and enabling carbon capture and sequestration covered the need for carbon capture and sequestration, the present sequestration technologies, and the post- and precombustion carbon capture technologies. Topics also included in the sequent discussion are basic design principles of oxy-fuel combustion, IGCC, chemical looping combustion, and integrated oxygen transport membrane for combustion.

The segment on other advanced technologies covered the fundamental principles of photocatalytic reduction of CO_2, electrochemical splitting of H_2O, and geoengineering approaches. The four geoengineering approaches include the use of stratospheric aerosols, cloud albedo enhancement, ocean iron fertilization, and sunshade geoengineering.

Integrated Gasification Combined Cycle (IGCC), by Robert Dahlin

Dr. Robert Dahlin, director of the Power Systems and Environmental Research of the Southern Research Institute, gave a lecture on IGCC. The lecture started with the presentation of the rationales behind the widespread use of coal in the USA: coal's abundance, wide availability, and more than 250 years' reserve (comparing to limited natural gas supply). IGCC flow sheets were used to discuss its major unit operations and the process features. These features include:

- Higher thermal efficiency than pulverized coal combustion
- Lower emissions
- Higher feedstock flexibility (coal, oil, natural gas, biomass, petroleum coke, and waste)
- Higher product versatility (chemicals, liquid fuels, power, and gas fuel)
- More economic means for CO_2 capture than pulverized-coal combustion (due to the higher CO_2 concentration from a gasifier)

Coal gasification was first used for streetlight in 1792. The USA had 1,200 gas plants in 1920s, but the discovery of natural gas led to demise of these plants. Increased energy demand, high natural gas prices, and stringent environmental regulations focused interests on IGCC. There are 117 operating plants and 385 gasifiers worldwide.

The lecture then covered the scientific reasons of the IGCC advantages over pulverized coal combustion mentioned above. IGCC removes the pollutants from synthesis gas before they are burned. High pressure and low gas volume provide favorable economics of pollutant removal; these operating characteristics also allow flexibility in pollutant concentration in feedstock. IGCC also produces less waste and consumes less water. IGCC uses two power cycles in series: gas turbine where power is generated from burning the syngas and steam turbine where power is generated from steam expansion. Syngas can also be used to produce chemicals and liquid fuels. Hydrogen can be used as a transportation fuel and fuel cell for generating electricity. These unit operations reveal not only the versatility of the IGCC process, but also a higher IGCC efficiency higher than that of pulverized coal combustion.

Some features of the 513 MW IGCC demonstration plant in Kemper County, Mississippi, were then discussed. Lignite will be its primary fuel and natural gas its backup. It has an air-blown rather than an O_2-blown gasifier. This modification eliminates the need of an air separation unit and reduces the capital and operating costs and cost of electricity. Moreover, it significantly reduces the emissions of SO_2, NO_2, CO, volatile organic compounds, and particulates. It is anticipated that about 50 % of the CO_2 will be captured.

The last segment of his lecture covered some of the research activities of Southern Company's IGCC Power Systems Development Facility (PSDF) at Wilsonville,

Alabama. These activities include the particulate removal by hot-gas filtration, high-temperature high-pressure particulate sampling system, development of drag correlations for the feeding system, tar cracking, gas clean up, and CO_2 capture. CO_2 capture for the high-pressure syngas in an IGCC plant will be less costly than a conventional pulverized coal combustion process. Southern Research is testing a wide spectrum of solvents and additives for capturing CO_2; representative data were presented.

Oxy-firing and Chemical Looping, by Thomas K. Gale

Dr. Thomas Gale, Power Systems Research Manager of the Southern Research Institute, presented his efforts on oxy-firing and chemical looping. Both are emerging carbon-capture-enabling technologies. The objective of Southern Research's oxygen-fired CO_2 recycle combustion project is to investigate, develop, optimize, and model O_2-fired utility boilers by:

- Retrofitting the existing Southern Company/Southern Research's 1 MW pilot-scale test facility
- Utilizing an advanced oxy-fired coal burner
- Measuring the operating and output responses to adjustable parameters
- Comparing these responses with CFD modeling results

The project has multiple participants. Coal is burnt by O_2 and recycled CO_2 in an oxy-fired boiler so that the flue gas contains mainly CO_2, not N_2 as the conventional pulverized coal combustion process. About 75 % of the CO_2 is recycled to avoid excessive flame temperature and maintain flow and heat transfer requirements. Thus, advanced burner for oxy-firing will be carefully signed to allow flame shape and heat release to be controlled and to provide a stable attached flame without natural gas assist. Since N_2 is not in the flue gas, the flue gas from an oxy-fired boiler has a 25 % volume of that from a conventional air-fired boiler, purification and compression are much less expensive for carbon sequestration. Air separation prior to combustion, however, creates sizable (about 25 %) energy penalty and notable electricity cost. Additional energy penalty comes from purification of CO_2 and compression and sequestration. These concepts were introduced in this lecture. Moreover, Southern Research's unique efforts were discussed that include Maxon oxy-fired burner, oxygen skid and piping system, distributed control system, gas flow control system, recycle system, safety system, conversion of facilities, axial temperature distribution and NO emissions from tests of two coals, computational fluid dynamics modeling conducted by Reaction Engineering International, and plans for the future tests. Parameter study for the future will be devoted to coal type, amounts of O_2 in primary flow, burner quarl tip, staging through the recycle-gas tip on the sides of the burner, and staging through the over-fired ports, and percentage of recycle. Flue gas composition, carbon burnout, inleakage, temperature profile, heat transfer, stability

of the test, acid-gas buildup, and apparent corrosion will be monitored during the tests.

In the second segment of the lecture, the basic concepts of the emerging chemical looping technology and Southern Research's research activities were introduced. An oxygen carrier, usually an oxidized metal, shuttles between two vessels in a cyclic chemical looping process. The oxide oxidizes (or gasifies) the fuel, such as coal and natural gas, in one reactor, while the reduced oxygen carrier is oxidized by air in a second reactor. Since the oxidant for burning fuel does not have N_2, the CO_2 concentration is high in the flue gas. Separation of CO_2 from the fuel oxidation reactor of chemical looping process is much less expensive than separating CO_2 from the flue gas of a pulverized coal combustor. Chemical looping is versatile, as it can be applied to both combustion and gasification.

Finally, Dr. Gale predicts the overall future of coal-fired power generation in the face of CO_2 emission regulation. Existing plants will have three choices as a result of immediate regulations: adding CO_2 scrubbers, retrofitting the boiler by installing oxy-firing with flue-gas recycle, or closing the plant. New plants may include oxy-fired furnace without much if any recycle and advanced thermodynamic cycles to offset the energy penalty or other advanced power systems such as oxy-fired IGCC. In the long term, chemical looping and IGCC look promising.

Fuel Cells, by Amala Dass

The lecture of chemistry professor Amala Dass included five arguments: fuel cell basics, fuel cell stacks and bipolar plates, types of fuel cells, proton exchange membrane fuel cells, and current status. A schematic is used to illustrate the major components and their functions in a hydrogen fuel cell (proton exchange membrane or PEM cell) at the outset. Slow reaction rate and hydrogen availability remain as challenges.

To gain high power output, multiple fuel cells are arranged in series, and bipolar plates are developed. PEM fuel cell uses relatively low temperature and can start quickly. It has been adopted in cars and buses. Five other major types of fuel cells have been developed: phosphoric acid, direct methanol (DMFC), alkaline (AFC), molten carbonate (MCFC), and solid oxide (SOFC). Hydrogen is the fuel for all of these fuel cells. The operating temperature ranges, electrolytes, catalysts, and operating characteristics of these fuel cells were discussed. Schematics were presented to illustrate the chemical structure and characteristics of the most popular PEM, Nafion. The strong C-F bond resists chemical attacks. Nafion's unique ionic properties are a result of incorporating perfluorovinyl ether groups terminated with sulfonate groups onto a tetrafluoroethylene (i.e., Teflon) backbone. The polymer is hydrophobic; the sulfonate side chains, SO_3^-, however, are hydrophilic. This leads to the desirable hydrophilic/hydrophobic micro-phase separated morphology. Advancement in nanotechnology has significantly enhanced efficiency of carbon-supported platinum catalysts.

Hydrogen is the common fuel for several types of the fuel cells mentioned above. The issues facing the infrastructure of hydrogen economy include H_2 production, delivery, storage, safety, and end-use materials. For fuel cell, the emerging technology faces challenges in the development of PEM stock, ancillary devices, fuel processors, fuel storage, fuel supply, and electric components. The industry for H_2-powered fuel cell (H_2FC) vehicles will have to overcome several critical technological barriers that include the hydrogen cost, H_2 storage capacity at reduced cost, and fuel cell cost with higher durability. It also has to overcome the economic and institutional barriers that include safety, codes and standard development, H_2 delivery infrastructure, domestic manufacturing and supply base, and public awareness and acceptance.

Computational Chemistry, by Steven Davis

Professor Steven Davis of the chemistry department gave an overview of computational chemistry techniques and their applications to reaction energetics and dynamics. The Hartree-Fock method was discussed along with its failure to include an accurate description of dynamic electron correlation. Characterization of chemical structures along potential energy surfaces was presented using the harmonic oscillator approximation to calculate vibrational frequencies to determine minima (stable structures) and maxima (transition states). Accurate potential energy surfaces were presented as determined using both single and multiconfigurational wave functions. Examples of highly strained structures with potential for solar energy storage were presented and their thermal isomerizations discussed. One such example, tricyclo[3.1.0.$0^{2,6}$]hexane (Davis et al. 2003), illustrated the necessity of using a multiconfigurational wave function plus Moller-Plesset perturbation theory to achieve accurate energies and correct electronic descriptions of transition states.

The use of trans double bonds in small hydrocarbon rings as a way to store potential energy was discussed and the advantages of using computational chemistry to determine relevant reaction pathways and energetics presented. The activation barriers were shown to be somewhat tunable by the substitution of heteroatoms for carbon atoms in the ring moiety (Davis et al. 2009). Multireferenced second-order Moller-Plesset perturbation theory (MRMP2) and coupled-cluster singles, doubles, non-iterative triplets [CCSD(T)] accuracies were compared for systems in which a single determinant was valid to provide a basis for accepting the MRMP2 energies for wave functions with strong multiconfigurational character.

A brief overview of how to choose the correct theoretical model to accurately determine chemical properties using computational chemistry was discussed. It was hoped that the students would gain an appreciation for the powerful tool computational chemistry has become as a companion to the experimentalist.

Table 2 Student presentations in 2008 and 2009

	Student	Research title
1	Damon Webster	Nuclear energy
2	Crystal Warren	Implementation of solar panels on commercial properties and the cost-based incentives
3	Joey Parkerson	Atmospheric carbon dioxide capture technologies
4	Michael McClure	Solar energy
5	Eddie Smith	Home energy efficiency
6	Archer Davis	Ice cores
7	Josh Sage	Hydroelectric energy
8	Leanna Smith	Green roofs
9	Brett Vescovo	US vs. global policy changes
10	Grady Cutrer	Green community
11	Sarah Mixon	Algae-based biofuels
12	Alison Kinnaman	Microremediation
13	Eric Williams	Biomass utilization
14	Shaolong Wan	Oxy-coal combustion
15	Benson Gathitu	Integrated gasification combined cycle
16	Guang Shi	Chemical looping combustion
17	Michael Brandes	Renewable wind energy
18	Whitney Hauslein	Ocean power
19	Katherine Osborne	Heat island infrastructure effects on climate change
20	Jonathan Jones	The hydrogen economy, hydrogen fuel cells, and implementation in Oxford, Mississippi
21	Ifejesu Eni-olorunda	The hydrogen economy – harnessing wind energy
22	Elizabeth Spence	How to go green
23	Ray Nalty	Weather control

Activities of the Students

Students were asked to choose a research topic at the beginning of the semester. They were asked to give a short oral report about their research status, questions, and difficulties in the middle of the semester. They were asked to give a term paper and an oral presentation at the end of the semester. A list of the students' presentations is given in Table 2. The topics range from offering tips in everyday life to modern technologies. Their presentations and papers were evaluated by a panel formed by a

group of faculties. Two outstanding works selected for the two awards were "Implementation of Solar Panels on Commercial Properties and the Cost-Based Incentives" by Crystal Warren and "Atmospheric Carbon Dioxide Capture Technologies" by Joey Keith Parkerson. They were given the title Ole Miss Idols of Climate Change Mitigation. In addition, each one of them received a $250 cash award. Their slides have been uploaded to the course Web site at http://home.olemiss.edu/~cmchengs/Global%20Warming/ along with the formal lectures.

Joey introduced the technology of capturing atmospheric CO_2 by using NaOH in a process that includes two chemical looping cycles: one involves NaOH/Na_2CO_3 and the other $Ca(OH)_2$/$CaCO_3$/CaO. In the sodium loop, NaOH is converted to Na_2CO_3 in an air/CO_2 contactor, and Na_2CO_3 is converted back to NaOH by $Ca(OH)_2$ in a causticizer. In addition to the causticizer, the calcium loop includes calciner and a slacker. $CaCO_3$ decomposes to CaO in the calciner, and CaO is hydrolyzed to $Ca(OH)_2$ in the slacker. Joey presented the capture technology as well as the cost evaluation, about $240 per ton of carbon. He argued that it would be competitive if compared to the cost for capturing carbon emitted from vehicles since no mobile device has to be carried.

Crystal proposed the widespread use of solar panels for commercial properties, legislative incentives for such installation, and mandatory installation by law. She presented the principles of solar panels, the rationales, cost estimate, and recommendations. Success stories of Wal-Mart, FedEx, and Google were discussed. She interviewed local business owners, including her mother and Wal-Mart, during her course of research. German government pays solar panel users 20 cents per kWh received from grid and receives 50 cents per kWh for energy sent back to grid. Crystal, on the other hand, proposed that federal, state, and local government each pays one third of the installation cost. She also proposed fixed energy prices for 15 years at 25 cents per kWh purchased from the grid and 50 cents per kWh for energy sent back to grid.

The Chancellor of the University of Mississippi launched the campus Green Initiative in the spring of 2008 when the course was offered for the first time. The students were excited about the initiatives; they felt that they can share their enthusiasms by transforming what they learned in the semester into actions. The Green Initiative, however, was in its infancy, and the administrators in charge had just started to organize a committee, which will eventually layout the tasks. The students decided to examine the current policies and facilities of the University and explore if there were rooms for improvement. They spent a few evenings together and deliberated their thoughts. The product of their discussions is a list of recommendations, which can be found at: http://home.olemiss.edu/~cmchengs/Global%20Warming/. An oral presentation was also made to the University administrators. The newly inaugurated provost, the retiring provost, and the university architect were among the participants for the presentation and its subsequent discussions. The two parts of the recommendations, policy and facility, were presented by the two students who were selected to be the idols of the climate change mitigation only a

couple of days earlier. In the last years, knowledge about climate change, sustainable energy, and environment has indeed been gradually incorporated into the curriculum. Research collaborations and outreach activities in these areas have increased. The University and City of Oxford, Mississippi, have established a public transportation. This course has notably induced public awareness.

Future Directions

Climate change affects the life of every living species on Earth. Only contributions from all concerned citizens could generate a monumental impact. Thus, climate change literacy must reach grassroot level that has several unprecedentedly large-scale characteristics. Disseminating climate change knowledge secures the immediate need of a strong workforce in the battle against climate change, which is gravely lacking. It raises public awareness and promotes actions of world citizens. More importantly, it is expected to catalyze innovations. In his State of the Union address of 2011 (Obama 2011), President Obama stated the philosophy of his science and technology: "This is our generation's Sputnik moment." The Russian Sputnik space satellite program in 1958 has stimulated the space race that, in turn, promoted innovations in many areas of science and technology. President Obama also characterized the nature of the new race in the same address: "We'll invest in biomedical research, information technology, and especially clean energy technology - an investment that will strengthen our security, protect our planet, and create countless new jobs for our people."

The clean energy activities are expected to grow rapidly in the near future. Mitigating GHG concentrations is closely related to the growths in energy demand, economy, and population. The adaption, impacts, and mitigation of GHG require knowledge in many different (if not all) fields and actions related to different sectors (if not all) of the civilization. Most notably, as this *Handbook* is organized, collaborations of political, legislative, educational, scientific, technological, and news media sectors will be necessary. For completeness, climate change literacy must cover all of these areas.

Science and technology will be in the core of these efforts. In the next few decades, there will be a wide range of research and development investments on the establishment of an alternative energy infrastructure, especially in the areas of biomass conversion, solar panel and concentrator, nuclear energy, wind turbine, hydropower, fuel cell, and geothermal energy. Fossil fuels, particularly coal, are abundant and widespread, and fossil fuel-based power generation is expected to remain a major driving force of the economy in the near future. CO_2 production, however, is much higher than its current utilization. Therefore, carbon capture and sequestration and large-scale utilization of CO_2 will be of great interests. Moreover, much attention will also be placed on technologies that enable carbon capture including chemical looping combustion, oxy-fuel combustion, and integrated

oxygen-transport membrane. Integrated coal gasification combined cycle (IGCC) is versatile and efficient. A hydrogen economy will depend on the development of technologies in several industrial sectors. Energy conservation and energy efficiency will be two major approaches to optimize the limited sources for power generation, transportation, buildings, and industrial sectors.

High-risk and high-impact innovations are not only required for clean energy research, but also desirable for science, technology, engineering, and mathematics (STEM) educations with emphasis on climate change literacy. Government investments on these topics are expected to increase worldwide. Efforts of the National Science Foundation (2011) and NASA (2011) are just two major sources for literacy funding in the USA. Synergistic collaborative alliances are welcome for generating projects with unique objectives and broad impacts. Creative use of information technologies, such as global seminars, could facilitate communication network. At the time of writing this chapter, the author has jointly offered a video, online global seminar class on sustainability with a colleague at the National Pingtung University of Science and Technology in Taiwan. The objectives of this course are to introduce modern issues to graduate students around the globe and to induce healthy and constructive debates representing the students in different regions of the world and different sectors of the society. In addition to the speed of the Internet, there is plenty of information available on the World Wide Web; therefore, Web-based teaching is expected to be more versatile and creative in the future.

Conclusions

Climate literacy can be offered with a group of faculties from different fields in various fashions. The broad nature of the subject renders it possible to cover only selected topics for the organized lectures and other topics for students' research. This course has generated a set of useful slides public dissemination. However, the Web sites mentioned in section "Lectures Presented by Faculty and Scholars" are also available.

Alternatively, some of the organized lectures can be replaced by students' deliberations on subjects such as "Should we promote the production of bioethanol as an alternative fuel?" or "Should we promote the growth of genetically altered plants for increased photosynthesis?" These discussions can certainly promote critical thinking about important issues and absorbing knowledge in related fields.

Activities of climate change literacy are expected to increase in the next decade. There will be more formal and short courses, workshops, summer camps, and outreach projects in other formats. Sustainability will be a central theme of these activities. With the adoption of modern information technology, climate change literacy is likely to accelerate President Obama's prediction that "This is our generation's Sputnik moment" (Obama 2011).

References

Beckman EJ (2004) Supercritical and near-critical CO_2 in green chemical synthesis and processing. J Supercrit Fluids 28:121–191

Bell AT, Gates BC, Ray D (2007) Basic research needs: catalysis for energy. Office of Basic Energy Science, US Department of Energy, Washington, DC

California's Climate Action Team (2007) Climate action team proposed early actions to mitigate climate change in California, California Protection Agency. http://www.climatechange.ca.gov/climate_action_team/reports/2007-04-20_CAT_REPORT.PDF

Davis SR, Nguyen KA, Lammertsma K, Mattern DL, Walker JE (2003) Ab initio study of the thermal isomerization of tricyclo[3.1.0.02,6]hexane to (Z, Z)-1,3-cyclohexadiene through the (E, Z)-1,3-cyclohexadiene intermediate. J Phys Chem A 107:198–203

Davis SR, Veals JD, Scardino DJ, Zhao Z (2009) Isomerization barriers and strain energies of selected dihydropyridines and pyrans with trans double bonds. J Phys Chem A 113:8724–8730

Dessler AE, Parson EA (2010) The science and politics of climate change: a guide to the debate, 2nd edn. Cambridge University Press, Cambridge

Energy Information Administration (EIA) (2008) Emissions of greenhouse gases in the United States 2007. Office of Integrated Analysis and Forecasting, U.S. Department of Energy, Washington, DC. http://www.eia.doe.gov/oiaf/1605/archive/gg08rpt/pdf/0573(2007).pdf

Energy Information Agency (EIA) (2007) Annual energy outlook, with projections to 2030. US Department of Energy, Washington, DC. http://ftp.eia.doe.gov/forecasting/0383(2007).pdf. Accessed 16 Sept 2011

Gerrard MB (2007) Global climate change and U.S. law. American Bar Association, Chicago, pp 17–25, 32–58, 61–85

Intergovernmental Panel on Climate Change (2007a) Climate change 2007 – the physical science basis: working group I contribution to the fourth assessment of the IPCC. Cambridge University Press, Cambridge. www.ipcc.ch

Intergovernmental Panel on Climate Change (2007b) Climate change 2007 – impact, adaptation and vulnerability: working group II contribution to the fourth assessment of the IPCC. Cambridge University Press, Cambridge. www.ipcc.ch

Intergovernmental Panel on Climate Change (2007c) Climate change 2007 – mitigation of climate change: working group III contribution to the fourth assessment of the IPCC. Cambridge University Press, Cambridge. www.ipcc.ch

Jacob DJ (1999) Atmospheric chemistry. Princeton University Press, Princeton

Manson N (2002) Formulating the precautionary principle. Environ Ethics 4(3):263–274

National Aeronautics and Space Administration (2011) Global climate change education project. Langley Research Center, Hampton. http://www.nasa.gov/offices/education/programs/descriptions/Global_Climate_Change_Education_Project.html

National Science Foundation (2011) FY 2012 budget request to congress, Washington, DC. http://www.nsf.gov/about/budget/fy2012/pdf/fy2012_rollup.pdf

Obama B (2011) State of unions address. US Capital, Washington, DC. http://www.whitehouse.gov/the-press-office/2011/01/25/remarks-president-state-union-address

Posner R (2003) Economic analysis of law. Aspen, New York

Seinfeld JH, Pandis SN (1998) Atmospheric chemistry and physics: from air pollution to climate change. Wiley, New York

Sunstein CR (2005) Cost-benefit analysis and the environment. Ethics 115:351–385

Tester JW, Drake EM, Driscoll MJ, Golay MW, Peters WA (2005) Sustainable energy choosing among options. MIT Press, Cambridge, MA

Vanek FM, Albright LD (2008) Energy systems engineering: evaluation and implementation. McGraw-Hill, New York

Wayne RP (1985) Chemistry of atmospheres. Clarendon, Oxford

World Health Organization (2003) Climate change and human health – risks and responses. Summary. World Health Organization, Geneva. ISBN 9241590815

Reducing Personal Mobility for Climate Change Mitigation

Patrick Moriarty and Damon Honnery

Contents

Abstract

In the high-mobility countries of the Organisation for Economic Cooperation and Development (OECD), many governments are seeking to reduce personal mobility, particularly car travel, for a variety of reasons. Reductions can be justified in general by concerns about global climate change, oil depletion and supply security, and traffic casualties. In urban areas, additional concerns are air pollution, traffic congestion, take-up of land by transport infrastructure, and quality of

P. Moriarty (✉)
Department of Design, Monash University, Melbourne, VIC, Australia
e-mail: patrick.moriarty@monash.edu

D. Honnery
Department of Mechanical and Aerospace Engineering, Monash University, Melbourne, VIC, Australia
e-mail: damon.honnery@monash.edu

W.-Y. Chen et al. (eds.), *Handbook of Climate Change Mitigation and Adaptation*,
DOI 10.1007/978-3-319-14409-2_51

urban life. Similarly, a variety of technological approaches are possible for addressing these problems in the context of global warming mitigation. This chapter examines policies for mobility reduction, as these can have a significant impact on climate change mitigation. It mainly restricts itself to the high-mobility countries of the OECD and uses four such countries (Australia, Japan, the UK, and the US) as case studies.

The approaches considered here include:

- Using modern Information Technology (IT) advances to promote travel substitution
- Car pooling, especially in urban areas
- Land use planning, particularly increased urban densities
- Encouraging the use of more environmentally friendly travel modes
- Raising the overall level (and perhaps also changing the structure) of motoring costs
- Reducing the convenience of car travel.

It is found that the use of IT, car pooling, and land use planning, whether voluntary or legislated, cannot be expected to produce much reduction in either car passenger-km or vehicle-km. Nor will reliance on voluntary approaches for car travel reduction by encouraging more use of environmentally friendly travel modes. Only the last two approaches can produce large and sustained reductions in travel greenhouse gas emissions, but heavy reliance on market forces such as very large increases in motoring costs is inequitable in OECD countries. The only equitable approach is to reduce the convenience of car travel, for example, by large travel speed reductions and by a reversal of the usual present ranking of travel modes: car, public transport, and active modes.

Abbreviations

ABS	Australian Bureau of Statistics
BITRE	Bureau of Infrastructure, Transport, and Regional Economics (Australia)
bp-k	billion passenger-km
BTS	Bureau of Transportation Statistics (US)
DfT	Department for Transport (UK)
EFMs	Environmentally friendly modes
EIA	Energy Information Administration (US)
GDP	Gross Domestic Product
GHG	Greenhouse gas
HOV	High occupancy vehicle
IEA	International Energy Agency
IPCC	Intergovernmental Panel on Climate Change
IT	Information Technology
OECD	Organisation for Economic Cooperation and Development
OPEC	Organization of the Petroleum Exporting Countries

PEB	Pro-environmental behavior
SBJ	Statistics Bureau Japan
TDM	Travel demand management
UN	United Nations
WBCSD	World Business Council for Sustainable Development

Introduction: Travel Reductions for Climate Mitigation

In the high-mobility countries of the Organisation for Economic Cooperation and Development (OECD), many governments are seeking to reduce personal mobility, particularly car travel, for a variety of reasons. Reductions can be justified in general by concerns about global climate change, oil depletion and supply security, traffic casualties, and even personal fitness (Moriarty and Kennedy 2004; Sallis et al. 2004). In urban areas, additional concerns are air pollution, traffic congestion, take-up of land by transport infrastructure, and quality of urban life.

A variety of technological approaches are possible for addressing the problems listed, including improving vehicular fuel efficiency and developing alternative fuels and power systems. This chapter examines policies for mobility reduction, as these can have a significant impact on climate change mitigation. Nevertheless, the other arguments given above for the desirability of travel reductions can help acceptance of such policies. Although this study is mainly restricted to examining travel in only four OECD countries (Australia, Japan, the UK, and the US), the conclusions should have more general application, at least to other high-mobility OECD countries.

The approaches considered here include:

- Using modern Information Technology (IT) advances to promote travel substitution
- Car pooling, especially in urban areas
- Land use planning, particularly increased urban densities
- Encouraging the use of more environmentally friendly travel modes
- Raising the overall level (and perhaps also changing the structure) of motoring costs
- Reducing the convenience of car travel.

What level of greenhouse gas (GHG) reduction in passenger transport might be needed to avoid serious anthropogenic climate change? It is here assumed that reductions in the transport sector, including surface passenger transport, will need to match those in the world economy overall. The 2013 Intergovernmental Panel on Climate Change (IPCC) Representative Concentration Pathway 2.6 (RCP2.6) has used models showing that CO_2 emissions from fossil fuels may have to be cut by the year 2050 to as little as 30.5 % of the year 2013 values, and fall to zero by 2070, if global temperature rises are to be limited to 2 °C (Stocker et al. 2013).

(The European Union regards a rise of 2 °C since the industrial revolution as representing a prudent limit for avoiding dangerous climatic change.) Others believe that CO_2 atmospheric concentration levels are already too high, and emissions thus need to be cut to zero before 2050 (Moriarty and Honnery 2011). In 2010, travel by all modes accounted for seven billion tonnes of CO_2-equivalent emissions, with about 72 % coming from road transport (Sims et al. 2014). For overall CO_2 reductions, transport cannot be ignored.

Assume that global energy-related CO_2 emissions have to follow the RCP2.6 limits and that by 2050 need to be cut to 2.9 billion tonnes of carbon (2.9 GtC) annual levels (Stocker et al. 2013). By 2050, passenger transport emission levels would also have to fall proportionally, if emission reductions are shared equally across sectors. But emission levels in the OECD countries are far higher than the world average. For example in 2013, the US emissions of CO_2 from fossil fuel combustion was 3.8 times the world average (BP 2014). If equal per capita emissions for the entire world's population are assumed by 2050, then (provided US share of world population remains at its present level) US surface passenger transport emissions would need to fall to around 8 % of their 2013 value. What this simple calculation shows is that reduction of a few percent in transport emissions will not suffice: a drastic reduction is needed.

Overall, this study finds that the use of IT, car pooling, and land use planning, whether voluntary or legislated, cannot be expected to produce much reduction in either car passenger-km or vehicle-km. Nor will reliance on voluntary approaches for car travel reduction by encouraging more use of environmentally friendly modes (EFMs) of travel. Only the last two approaches can produce large and sustained reductions in travel greenhouse gas emissions, but heavy reliance on market forces, such as very large increases in motoring costs, is inequitable, at least in highly motorized countries. The only equitable approach is to reduce the *convenience* of car travel, perhaps by large travel speed reductions and by a reversal of the usual present ranking of travel modes: car, public transport, and active modes.

Surface Transport Patterns in Four OECD Countries

Before attempting to discuss any specific policies for personal mobility reductions in any country, it is necessary to look at both the present transport situation and the path surface transport took in that country to reach the present position. Four OECD countries (Australia, Japan, UK, US), representing all four continents from which the OECD has members, were chosen as case studies. Together these countries span the range of transport-relevant parameters (for example, public transport share, gasoline costs, urban densities, car occupancy rates) found in OECD countries overall (The one exception is for non-motorized transport, so the experience of other OECD countries will be briefly considered for these modes.). These four countries also have good travel statistics available in English.

It is also important to look at possible *future* patterns of surface travel. Accordingly, both the forecasts of global and regional travel from the latest IPCC Report

(Sims et al. 2014) and official travel energy forecasts for the US have been included. In addition, the findings of researchers who have used the existence of travel time and money budgets to project travel in each of the various regions of the globe have been discussed. Levels of surface travel both much higher and much lower than at present have been predicted by various authorities.

Studying past, present, and projected future travel patterns are important for several reasons. Comparison of present travel in the four countries can reveal insights into where policy levers should be applied for climate mitigation. Understanding is needed, for instance, as to why surface travel per capita in Japan is so much lower than in the other countries studied. Discussion of projected travel by official organizations in, say, the year 2040 is also important. If travel reductions are going to occur anyhow because of over-riding changes in technology, the economy, or lifestyles, the remaining task would then be to merely guide these changes.

Present Transport Patterns

Vehicular Travel

Table 1 shows the composition of vehicular surface travel in passenger-km per capita in the four countries considered. It is evident from the table that in 1960, car travel was well-established as the dominant mode in the US, but was still negligible in Japan. Australia and the UK were in an intermediate position, with Australia closer to the US in car ownership and use. Both personal travel by motorcycles and light trucks have been included with car travel. Motorcycle travel is negligible today in each country (less than 1 %), except in Japan. Even in Japan, the share of motor cycle travel appears to have peaked in the 1980s and today is only a few percent of total passenger travel (Statistics Bureau Japan (SBJ) 2014).

Table 1 also shows that combined public transport patronage is today lower in the UK and the US than it was in 1960, but has grown slightly in Australia, and strongly in Japan, with most of the growth on rail. In fact, bus transport per capita peaked in Japan in the early 1970s at around 1,000 passenger-km/capita and has steadily fallen since. In contrast, train travel is resuming the strong growth that temporarily reversed in the mid-1990s.

Figure 1 demonstrates that per capita private car travel over the past 10–20 years appears to have leveled out in Australia, Japan, and the UK. Even in the US, car travel per capita has since 2004 flattened out as well, before the recent global financial crisis actually reduced per capita travel levels. In Great Britain, even *total* car, van and taxi travel, fell from 674 billion passenger-km (bp-k) in 2007 to 643 bp-k in 2012 (DfT 2013). It is evident that the very high levels attained in the US are unlikely to be reached by the other three countries – or by any other country, in or out of the OECD. And perhaps not even again in the US: the total number of vehicles registered per 1,000 population may have peaked in 2007 (Davis et al. 2013). Another feature of the graph is that the later the country began its push to mass car ownership, the lower the peak level of travel per capita.

Table 1 Per capita surface passenger-km of travel by mode and country, 1960 and 2011

Country	Year	Bus/tram[b]	Train	Car[c]	Total	Car %
Australia	1960	390	875	6,500	7,765	83.7
Australia	2011	870	670	13,620	15,155	89.9
Japan	1960	495	1,955	130	2,580	5.0
Japan	2011	705[d]	3,090	6,350[d]	10,145	62.6
UK[a]	1960	1,550	785	2,950	5,285	55.8
UK[a]	2011	685	1,110	10,530	12,325	85.4
US	1960	650	200	11,100	11,950	92.9
US	2011	1,510	195	20,310	22,015	92.3

[a]Averages are for Great Britain only, i.e., excluding Northern Ireland
[b]Includes a small amount of coastal sea transport
[c]Includes all private road vehicle travel
[d]2009 values
Sources: US Department of Transportation (DoT) (2011), Department for Transport (DfT) (2012), Bureau of Infrastructure, Transport, and Regional Economics (BITRE) (2013), Davis et al. (2013), DfT (2013), Bureau of Transportation Statistics (BTS) (2014), SBJ (2014)

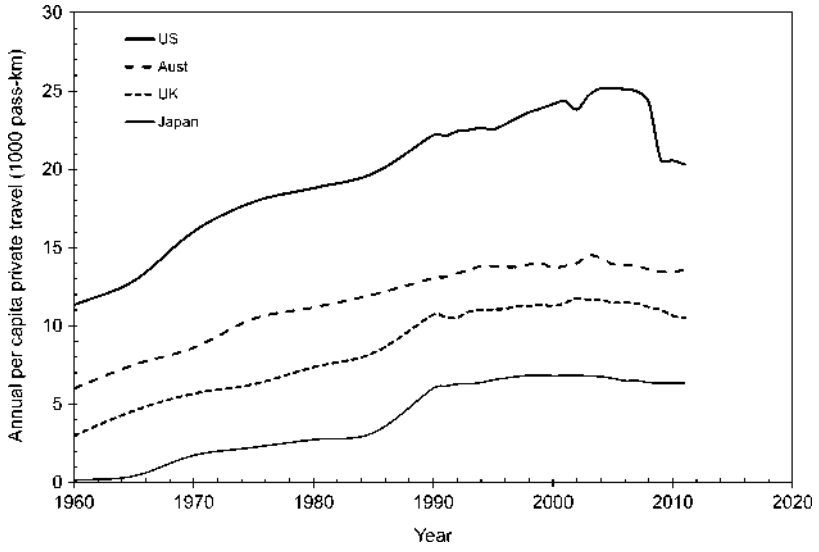

Fig. 1 Surface travel per capita versus year for Australia, Japan, the UK, and the US, 1960–2011 (Sources: As for Table 1)

In Australia, at least, males have been over-represented in car travel and under-represented in public transport travel compared with females. Further, females have been traditionally over-represented as car passengers, not drivers. This situation is changing, and today, the differences, although persisting, are small (Moriarty and Mees 2006). In all four countries, young female car driver licence-holding rates are approaching those for males. In a number of US states, there are now more female than male licence holders.

Non-Motorized Travel

So far, only vehicular surface travel has been considered. But non-motorized travel – walking and cycling – will, it is argued, be an important component of vehicular travel reductions for mitigating climate change. Non-motorized travel is better recorded for the journey to work trip, so most of the data presented here is for this trip type. For Melbourne, Australia, the available data span more than 50 years from 1951 to 2006, the date of the last national census. In Melbourne in 1951, about 11 % of work trips were by walking, with another 10 % on bicycle. By 2011, their share had fallen to 3.6 % and 1.3 %, respectively. Most of the drop in cycling had occurred by the late 1960s, although the fall in the share for walking was more uniform over time (Moriarty and Mees 2006). For Australia overall in 2011, the share of these modes was similar, with 4.5 % walking and 1.3 % cycling for the journey to work (BITRE 2013). As with motorized travel, females in the past had higher rates of non-motorized travel overall than males, but much greater rates of walking and lower rates of cycling for the work trip. Today their rate is similar to that for males.

For Great Britain overall, journey to work mode of travel data go back to 1890. In the 1890s decade, 59.4 % walked and 2.0 % cycled to work. Cycling peaked in the 1940s decade at 19.6 %, with a further 17.2 % walking (Pooley and Turnbull 2000). By 2008, the figures had fallen to 3 % for cycle and and 11 % on foot. In terms of travel distance, for all trip types cycling fell from 23 bp-k to about 4 bp-k between 1952 and 2007, although bicycle travel has been almost constant at between 4 and 5 bp-k for the past two decades (DfT 2012, 2013).

It is difficult to get data on the early use of non-motorized travel in Japan, but given the negligible vehicle ownership until the 1970s (ownership was only 5 per 1,000 population in 1960 (SBJ 2014)), the use of non-motorized modes was presumably high. In Tokyo, non-motorized trips were 25.8 % of the total in 1970 and still 21.7 % in 1990 for the journey to work (Newman and Kenworthy 1989, 1999).

In the US, these modes were even less used than in Australia, with 2.8 % walking for the work trip in the US overall in 2009 (BTS 2014). In 1983, the figure for walking was a little higher at 4.3 %. The highest level of walking to work was found in small cities and towns, with both large metropolitan areas and rural areas having somewhat lower levels (US Census Bureau 2012). Ausubel et al. (1998) presented a graph showing that daily walking per capita by Americans was around 4 km in 1880 and did not fall below 3 km until 1960, after which it fell rapidly to well below 1 km today.

These low values for non-motorized travel in the four countries today can be contrasted with several other OECD countries in Europe. Pucher and Dijkstra (2003) examined bicycle and walking trip-making in the urban areas in a number of OECD countries. Table 2 shows the results for selected countries for the year 1995.

The authors caution that the definition of a trip varies from country to country, but even so, the results are startling, and shows what is possible even today, given the right conditions. Climate seems to have a very little effect on the level of non-motorized trip-making. Sweden, part of which lies above the Arctic Circle, has far higher levels than several countries with more benign climates, such as

Table 2 Proportion of all urban trips by walking and cycling, various OECD countries, 1995

Country	All nonmotorized trips (%)	Walking (%)	Cycling (%)
US	7	6	1
Canada	12	10	2
England and Wales	16	12	4
France	28	24	4
Italy	28	24	4
Germany	34	22	12
Sweden	39	29	10
Denmark	41	21	20
Netherlands	46	18	28

Source: Pucher and Dijkstra (2003)

France and Italy. And as shown for 46 world cities by Newman and Kenworthy (1999) for 1990, the average for walking and cycling combined for the work trip was 5.1 % for six Australian cities, 4.6 % for 13 US cities, but 18.4 % for 11 European cities.

Predicted Future Transport Patterns

Vehicular Travel

Schafer and Victor (2000), following earlier work, argued that in all countries, both rich and poor, people have a fixed travel time budget per day. They therefore concluded that a shift from slower modes (public transport and non-motorized modes) to car travel is needed for people to travel further for a given daily time outlay. It is certainly the case that the observed decline in the share of these slower modes has been accompanied by a rise in car – and air – travel. They also postulated that in high-income countries, households spend a fixed share of their income on travel.

Personal travel levels themselves (including air travel, both domestic and international) were not anticipated to decline – indeed they saw large increases even in the high-mobility OECD countries. But to keep within their postulated daily travel time budget, they projected absolute declines in the level of car travel for present car-oriented countries, particularly the US, and large increases in high-speed travel (air and very fast train travel). Continued economic growth was seen as the method by which households could pay for this increased travel, while continuing to spend a constant share of household personal disposal income on travel. A variant of this approach has seen magnetically levitated (maglev) trains traveling at very high speeds in evacuated tunnels (to lower air friction) displacing car travel, presumably mainly for longer-distance trips (Ausubel et al. 1998; Moriarty and Honnery 2005).

Clearly, air travel within urban areas is not an option. But medium length trips are also unlikely to be made by high speed modes, even by high speed rail. Trips can only be at high speed if stops are very far apart, as there are definite limits to the rates

of acceleration and deceleration that humans can comfortably tolerate, which reduces average travel speed. Waiting at stops further reduces overall speeds. Although the surface travel reductions of Schafer and Victor do not translate into overall travel reductions (because of rising high speed travel) they do imply a reduction in future *surface* travel levels, including travel by car, in OECD countries.

But it is doubtful that people do in fact have constant travel time budgets, even when aggregated at the city-wide or even national level. And the empirical evidence also suggests that the share of disposable household income spent on travel has risen over time in the four countries studied here (Moriarty 2002b). Further, different sub-groups of the general population have very different average travel time outlays, as shown by the more than twofold travel time difference between female pensioners and full-time working males found in a 1986 Australian travel survey (Moriarty and Honnery 2005). Further, as U.K. researchers Lyons and Urry (2005) have stressed the increasing ability to use travel time for other activities, such as using a laptop on public transport trips, argues against individuals having fixed travel time budgets.

Other researchers, impressed by advances in the new IT, have also seen future reductions in surface travel. They have argued that not only surface travel, but all travel, urban and non-urban, surface and air travel, will decline because of substitution by IT. This view has been argued in some detail by MIT planner William Mitchell (2003). He used the term "demobilization" as a general term for the substitution of work, shopping, and other trips by networked computers. Others who have similarly envisaged a controlling role for IT as a means of travel substitution are Frances Cairncross (2001) and Joseph Pelton (2004).

As Tal (2008) has documented, the argument that IT will radically reduce travel has now been made for almost three decades. Actual results in the form of travel reductions that can be ascribed to teleworking or teleshopping so far have been disappointing (Moriarty and Kennedy 2000). There are two separate points that need to be examined when evaluating the "telework will reduce travel" argument:

- What is the present extent of teleworking and what is its likely growth in future?
- What impact does a given level of telework have on overall travel?

The numbers who telework for some or all of the time have not risen to anywhere near the levels forecast. Although Raiborn and Butler (2009) reported that in 2008, 11 % of the US workforce teleworked at least 1 day per month, up from 8 % in 2006, the percentage of "full-time equivalent" teleworkers will evidently be low. Even more important, teleworking households may not even reduce their travel overall. First, most households in OECD countries have more vehicle licence-holders than available personal vehicles. So even if a household car is not used for work travel on any given day, it may be used for other purposes by other household members – or by the teleworker for non-work trips.

Second, teleworking could affect the location decisions of households. If the commute trip by one or more household members is reduced through telework, the household may locate further away from the city center, where land prices are lower. At least for Australian cities, outer suburban (and non-urban) households travel

much further per capita than inner urban households (Moriarty 2002a). And for travel overall, including air travel, Smith (2008) has remarked that it is now so easy to plan travel by sitting at one's desk that IT could well have increased travel.

Similarly, teleshopping, or e-commerce, has also not fulfilled its early predictions; after more than a decade, e-commerce still only accounts for a 4 % share of all retail sales (US Census Bureau 2012), although for the category of computer hardware and software the share is much higher. With such a low overall share (and even at a much higher share, say 20 %), the effect on shopping trip frequency will probably be negligible, since a large variety of purchases are usually made on each shopping trip, even if only one shop (for example a super-market) is visited. It may also be true that much on-line shopping is additional to traditional shopping, and not a substitute.

None of these proposals for travel substitution is really new – all have low-tech precedents. A small proportion of the workforce has always worked from home. Mail order catalogues enabled remote shopping more than a century ago. Today, a telephone and a mailbox are still all that is needed for teleshopping. But whether a letter, telephone, or networked computer is used for ordering merchandise, it still needs to be physically delivered to the householder – with the exception of software. Any saving in private travel will thus be partly offset by a rise in freight vehicle travel. "Cyber universities" are less discussed today than they were a decade ago, but they are really just a new version of the old correspondence courses. In all, greater change probably came from the introduction of instantaneous communication with the telephone and the radio, than from the later introduction of modern IT.

Even if reductions in surface travel will not naturally occur by either the operation of travel time budgets or IT substituting for travel, there are other, more recent, arguments for future travel reductions. William Rees (2009) is a researcher who has a very pesimistic view on the likelihood of anything approaching "business-as–usual" in future cities. But his doubts are based on the need for very large reductions in both greenhouse gas emissions and oil consumption, and the limited ability of technical solutions like alternative fuels or efficiency gains to deliver in the limited time frame available.

All these views are in sharp contrast to the travel forecasts for OECD countries offered by various international and national authorities. The US Energy Information Administration (EIA) (2014), in its Annual Energy Outlook 2014, saw a gradual fall in US transport energy use, from 2012 to 2040, with transport energy in 2040 being 4.3 % below that in 2012 in the base case scenario. Nevertheless, vehicle-km by light vehicles was forecast to grow steadily from 2012 out to 2040 in the base case, even though it fell in the aftermath of the Global Financial Crisis.

The IPCC (Sims et al. 2014) warns that "Without policy interventions, a continuation of current travel demand trends could lead to a more than doubling of transport-related CO_2 emissions by 2050 and more than a tripling by 2100 in the highest scenario projections." The Organization of the Petroleum Exporting Countries (OPEC) (2013) gave an estimate of 897 million private transport vehicles in the world in 2010 and projected that this figure would rise to 1875 million in 2035. Although about two-thirds of all cars are presently in the OECD, the future annual growth in private vehicles in the OECD was forecast to be under 1 %. For China,

OPEC forecast car ownership to grow from 58 million in 2010 to a massive 442 million in 2035. This optimistic forecast assumes, of course, that neither oil availability nor concerns about global climate change impose limits.

Non-Motorized Travel

Most official future travel projections simply ignore non-motorized travel. If discussed at all, it is in the context of future travel in low-income countries. Schafer and Victor (2000) assumed that non-motorized forms of travel would be too slow for their time-constrained, high mobility future. Both the reports of the World Business Council for Sustainable Development (WBCSD) (2004) and the earlier IPCC reports devoted little space to non-motorized travel, with the WBCSD report assuming that it will gradually disappear as low-mobility societies move up the "ladder of mobility improvement," by which is meant that motorized travel will supplant it. Non-motorized travel was thus regarded as an inferior travel mode, and technical solutions (alternative fuels, vehicle efficiency improvements, etc.) were seen as the most important means of tackling climate change.

The very few available projections are thus usually only from advocates of these travel modes. Geurs and van Wee (2000) used backcasting to examine what changes were needed for a reduction in Dutch transport GHG emissions of 80–90 %. They concluded that compared to their "business as usual" scenario for 2030 transport, bicycle use, already high in the Netherlands (as shown in section "Non-Motorized Travel"), would need to double in terms of passenger-km in their major emissions reduction scenario. Given that car travel and motorbike/moped travel would need to be reduced by 50 % and 75 %, respectively, it is clear that cycling would become a major travel mode.

The present role of walking and cycling in the Netherlands demonstrates what is politically possible, even today. Income levels in the Netherlands are higher than most countries in the OECD, so that, unlike the situation in low-income countries, the popularity of these modes is not based on economic necessity. And at 51–54°N, the climate is less benign for walking/cycling that most other OECD countries. Nevertheless, its flat terrain and high population density are advantageous. In all OECD countries, however, there is increased concern about obesity and personal fitness (Pucher and Dijkstra 2003; Sallis et al. 2004). Non-motorized travel modes are well-placed to benefit from this concern.

Creating Environmentally Sustainable Behavior

Changing behavior as a means of achieving environmentally sustainable ends such as household travel and energy reductions is attractive because in principle it can be introduced rapidly. In fact, during gasoline shortages, changes in travel behavior can happen overnight, as motorists car pool, walk or use public transport to get to work. (However, after the emergency is over, very little permanent change in travel patterns has been observed.) These measures can also be very cheap to implement, compared with most other alternatives, and if voluntary, carry few political costs. The

important questions to ask of psychology are the following: How much change can be expected? Which approaches work best? Do voluntary approaches work better than more coercive approaches? Which demographic groups are most likely to change? In this section an attempt will be made to answer these questions, first for general environmental change and then for transport change.

General Principles for Change

Linda Steg (2008) has discussed three factors she considered important in promoting more environmentally sustainable behavior at the individual or household level: knowledge, motivation, and ability to make the necessary changes. Below, these three points are discussed in turn, then the significance of the findings for promoting pro-environment behavior (PEB) in general is discussed.

Knowledge is a necessary condition for adopting PEB. People have to be aware of the consequences of their consumption, such as their household domestic electricity use or private car use, on the physical environment. But consequences are not always easy to determine. For instance, the public's knowledge of the facts on climate change, and the reasons why nearly all climate scientists regard climate change as a serious problem, is generally poor, even among the educated populations of the OECD countries. The immense complexity of the climate change problem, with its multiple feedbacks operating at varying time scales, is one cause. Others include the significant natural variability of climate, making unambiguous attribution of cause difficult, and the stress on this uncertainty by industry groups with a strong interest in continued inaction on climate change.

Second, not only is knowledge important, but the public must be *motivated* to change their behavior in a more environmentally appropriate direction. When surveyed, most people in OECD countries profess to be concerned about the environment in general, but such concern does not always translate into action, as is shown by the continued rise in household energy consumption in many OECD countries, for example. Further, in the case of climate change mitigation, the link between individual reductions in GHG emissions and environmental benefit, particularly local, is tenuous. Other factors important for success or otherwise in achieving behavioral change include any extra costs and effort incurred, or any reduction in personal convenience. Policies will thus be more effective if they simply involve purchase of more energy-efficient equipment and do not restrict perceived freedom of choice (Steg 2008). Recycling involves no monetary costs and has been made convenient by the provision of recycling bins at households and businesses, and so has been widely adopted. Unfortunately, much household recycling may be only of marginal benefit in achieving ecological sustainability (Wikipedia 2014).

De Groot and Steg (2009) have further argued that ethical arguments (altruistic and biospheric considerations) for change in household practices are more effective than other approaches, such as those that stress cost savings. As they put it, it is better to get people to "act green" than to "act mean." Cost saving arguments can come undone when, for example, energy costs fall or household circumstances change. An

illustration of the former is the steep decline in sales of more energy-efficient hybrid electric vehicles in the US, following the fall of gasoline prices after mid-2008. Nevertheless, countries with higher costs for gasoline and domestic electricity and natural gas, in general use less energy.

Third, people must also be in a position to make the necessary changes. Money is often a barrier. Many households may not have the financial means to buy the new, more energy-efficient equipment, or to pay for retro-fitting their house to cut heating energy. They may find it easier to continue paying higher monthly or quarterly bills than to find the money for an energy efficiency improvement. It is not only physical or financial impossibility that matters; even cultural norms may make an action perceived as impossible.

Given these conditions needed for change, some suggestions for general strategies to promote environmental changes follow.

Promoting the purchase of more energy-efficient appliances (such as compact fluorescent globes in place of incandescent ones) can be a succesful strategy, especially if, as in this case, not only are the purchase costs low, but households suffer little inconvenience from the change. In the case of compact fluorescent globes, both costs and inconvenience were so minor that several governments have been able to mandate the phasing out of the less-efficient incandescent globes (Brown 2009). Changing the costs of energy, for example through a carbon tax, can also help reduce energy consumption, as can increasing the costs of travel. The road pricing schemes in London, and particularly Singapore, have had some success in reducing travel levels and marked success in changing travel patterns.

Researchers have found that higher income groups respond best to interventions for improving PEB. Studies in the US has shown that such groups are more likely to participate in "green energy" programs. For Australian capital cities, high income and high education households were also found to be more likely to have a strong environment commitment (Moriarty and Kennedy 2004). Torgler and García-Valiñas (2007) also reported that both better-educated and higher income individuals usually had stronger pro-environmental attitudes. They reasoned that "Wealthier citizens may have a higher demand for a clean environment and less environmental damages." On the other hand, in the US, sports utility vehicle ownership is much higher among the more affluent, and air travel in all countries is similarly concentrated among the well-off. Clearly, the issue of environmental support is a complicated one, where actions may not coincide with attitudes (Kennedy et al. 2009).

Thus the relationship between PEB and socioeconomic status is much more complex than revealed by surveys. Lower income households in OECD countries can be regarded as "involuntary environmentalists," because their per capita use of public transport is greater, while their use of domestic energy or water, is usually lower than that for higher income households. Similarly the higher levels of environmental concern usually (but not always) found for females (Torgler and García-Valiñas 2007) could have a similar basis. In any case, as shown in section "Present Transport Patterns," female use of more environmentally friendly transport modes is today not much better that that for males. These comments on involuntary environmentalism apply with even greater force to low income households of the

industrializing world. Nevertheless, higher income households, despite their greater resource use, are more likely to respond to campaigns for increased PEB (Gifford and Nilsson 2014).

Changing Travel Behavior

It is widely agreed that changing travel behavior is far harder than changing behavior for recycling or even general domestic energy conservation (e.g., Garling and Schuitema 2007; Dietz et al. 2009; Gifford and Nilsson 2014). In general, external constraints, whether real or perceived, on changing travel mode are usually severe in the car-oriented countries of the OECD. An important constraint is that alternatives to the car for any given trip usually involve longer travel times. It follows that bringing about voluntary change can be expected to be much more difficult than promoting other forms of pro-environmental behavior such as recycling. In addition, there are strong psychological benefits of car travel which other modes cannot match.

Clearly, transport GHG emission reductions would be easy if a carbon-neutral fuel was readily available at about the same price as existing petroleum-based transport fuels and could be used in existing vehicles. Proenvironment behavior would then be as easy as shifting to another brand of gasoline. But such a convenient solution to transport's GHG emissions will not be available for decades, if ever. Other approaches, such as travel demand management (TDM), are needed.

Dietz et al. (2009) have examined ways in which US households can voluntarily cut their carbon emissions. From behavioral research, they estimated that, nationally, the "reasonably achievable emissions reduction" potential in the household sector overall is 20 %. This reduction can be achieved in a decade, they argued, if "the most effective nonregulatory interventions are used." Although about 45 % of the estimated savings came from reductions in private vehicle fuel use, only about 11 % of this transport total came from travel reduction measures, namely from car pooling and trip chaining. Overall then, only 1 % (20 % $\times$ 0.45 $\times$ 0.11) of all household sector emissions could be reduced by voluntary TDMs. The authors assumed that only 15 % of households that were not currently car pooling or trip chaining would in fact voluntarily do so, if the most effective interventions were employed. In contrast, 90 % of households were anticipated to weatherize their houses.

Another US study (Greene and Schafer 2003) surveyed a large number of potential TDMs, both voluntary and legislated, to reduce vehicle-km of travel, including car pooling, congestion pricing, use of telecommuting, and land use planning. They estimated that combining all these approaches might reduce vehicular travel by around 10 %. Even this low figure – relative to what section "Introduction: Travel Reductions for Climate Mitigation" showed might be needed – they saw as representing an enormous challenge.

Garling et al. (2000) investigated the potential for voluntary reduction in car use by interviewing a number of randomly selected households in Goteborg, Sweden.

Respondents had reported beforehand they could eliminate at most 10 % of their car trips over the 8 days of the survey, but their actual reduction achieved over these 8 days was even less, because of unforeseen car trips. Stated intentions to reduce car travel were thus very different from actual behavioral changes. The authors concluded that a 10 % reduction, the same value as found for the US, was the most that could be expected from noncoercive measures.

Also in Goteborg, Hagman (2003) interviewed motorists about what they perceived as the advantages and disadvantages of car use. Interviewees were found to present the advantages in terms of their *personal* experience, for example, time savings. But only some disadvantages were based on personal experience; most were based on abstract arguments about adverse environmental effects. These arguments were derived from the media. Hagman thus concluded that "knowledge about advantages becomes absolute while knowledge about safety and environmental risks becomes relative and negotiable." He speculated that this difference could explain why presenting motorists with information on car travel's environmental costs has been unsuccessful in reducing driving.

It was reported above in section "General Principles for Change" that knowledge of the effects of consumption are considered important for promoting PEB in general. Tertoolen et al. (1998) used a field experiment in 1992 in the Netherlands to explore motorists' resistance to travel mode change. They found that providing information to car drivers on the monetary and environmental costs of car travel produced no measured reduction in driving, in line with other research. But Tertoolen and colleagues went further and claimed that information campaigns to reduce car use could have undesirable side effects. Their explanation was in terms of cognitive dissonance. If motorists cannot reconcile their general proenvironmental attitudes with information that their car use is damaging the environment, the dilemma can be resolved in two ways. The societally preferred way is of course to change behavior, but another way is by revising or even discarding their original proenvironmental attitudes. The authors show that the latter approach was common among their respondents. Motorists seem to react negatively to being branded as polluters, so that such an approach may not be at all effective in persuading them to use their cars less (Moriarty and Kennedy 2004).

Not all researchers would agree with De Groot and Steg (2009) that it is better to get people to "act green" rather than "act mean," at least for changing transport behavior. Wardman et al. (2007) used both revealed preference and stated preference surveys and modeling to find the most effective policies for reversing the steep decline in cycling noted in section "Non-Motorized Travel" in Great Britain. They argued that the best policy was a financial incentive for cycling to work. Payment of UK £2 daily to cyclists was found to double the level of cycling to work, whereas complete provision of segregated cycleways, an expensive undertaking, would only raise cycling by 55 %. Whether such modeled increases would actually occur is of course uncertain, but in any case, even a doubling of cycling commuter share would do little to reduce overall GHG emissions.

In an another recent study on factors affecting the success of programs to increase the use of cycling, Pucher et al. (2010) wrote:

> The current level of bicycling in a community also affects bicycling safety and the potential to further increase bicycling. Several studies have demonstrated the principle of "safety in numbers." Using both time-series and cross-sectional data, the studies find that bicycling safety is greater in countries and cities with higher levels of bicycling, and that bicycling injury rates fall as levels of bicycling increase. As the number of cyclists grows, they become more visible to motorists, which is a crucial factor in bicycling safety.

They added that as cycling use increases, "a higher percentage of motorists are likely to be bicyclists themselves, and thus more sensitive to the needs and rights of bicyclists."

They also showed the complexity of responses to policy initiatives to encourage cycling. Noncyclists in bicycle-oriented cities may respond much more positively to a given set of programs or infrastructure provision than noncyclists in cities with few cyclists. Context is very important. (Their findings are supported by the experience of cycling in Melbourne, discussed in section "Non-Motorized Travel," where it was shown that cycling to work collapsed in the 1950s – at precisely the time that car travel was growing rapidly.) Similar conclusions probably apply to policies to encourage walking – and even public transport.

Thus the overall empirical findings of behavior change psychologists and other researchers suggest that the prospects for voluntary travel reductions, at least, as a means of cutting energy use or GHG emissions, are not promising. Even using the most effective campaigns, only modest changes can be expected from voluntary transport change programs and even less from general media campaigns. These projected changes in travel behavior are small and reflect only the likely reductions in a "business as usual" transport future. As will be shown later, the *context* in which the changes are to take place matter a great deal. Even noncoercive measures could be effective if it becomes clear to the general populace that continuation of present practices is no longer an option. Unfortunately, in the context of adverse climate change, it was shown in section "General Principles for Change" that this is presently not the case.

Table 3 provides a list of TDMs under four categories, along with the percent savings considered possible by Greene and Schafer (2003) for individual measures. Both voluntary measures and what were seen as politically possible coercive interventions are included. In the next sub-section, a major voluntary trave change program in Australia is examined, and it is concluded that the findings of the psychologists are largely vindicated.

Voluntary Travel Reductions: An Australian Case Study

To evaluate the effectiveness of voluntary schemes, a case study from Australia is provided. In Australia, voluntary approaches to car travel reduction have mainly taken the form of TravelSmart interventions to encourage more use of environmentally friendly modes (EFMs) of travel – public transport, walking, and cycling. In contrast to other major Australian cities, where interventions have been small or nonexistent, the intervention in Perth, a city of about 1.7 million, was both far more

Table 3 Summary of travel demand reduction methods

General TDM category	Travel reduction method	Greene and Schafer (2003) vehicle-km savings estimates (%)
Physical change measures	Area-wide ridesharing	0.1–2.0
	Bicycle/pedestrian travel improvements	Less than 0.1
	Land-use planning to reduce trip distances e.g., mixed land use, "smart growth"	0.0–5.2
	Park-and-ride lots	0.1–0.5
	Public transport improvements e.g., improved intermodal interchanges	0.0–2.6
	High-occupancy vehicle (HOV) lanes	0.2–1.4
Legal policies	Prohibiting traffic in city centers	NA
	Decreasing speed limits	NA
	Compressed work week	0.0–0.6
	Parking control	NA
	Telecommuting	0.0–3.4
Economic policies	Parking pricing: work	0.5–4.0
	Parking pricing: nonwork	3.1–4.2
	Congestion pricing	0.2–5.7
	Tax on emissions per vehicle-km	0.2–0.6
	Decreasing costs for public transport	NA
Information and education measures	Individualized marketing	NA
	Public information e.g., advertizing campaigns for public transport	NA
	Giving feedback about consequences of behavior	NA
	Social modeling e.g., role model endorsement of public transport	NA

Sources: Greene and Schafer (2003), Rajan (2006), Garling and Schuitema (2007)

extensive and also earlier than in other cities, enabling an evaluation of the program.

The main idea was to target the less-committed motorists in a selected municipality, in recognition of the fact that while some of their trips have to be made by car, for many other trips presently made by car, EFMs are a real option, and the change could be made with only marginal loss of convenience. By providing information on these EFMs, the TravelSmart programs tried to shift some car trips to these modes. The information was tailored to the needs of the individual household, with local timetables for buses provided.

Such programs in Perth have now been in operation for more than a decade, and most of the city's total population have been targeted, so that reductions should appear at the city-wide level. As will be discussed later in section "Reducing Travel: Changing Urban Land Use Patterns" (see Table 5), levels of car passenger-km per capita, or car ownership, are today no lower than the

Table 4 Central Metropolitan Perth, Victoria Park, and South Perth journey to work, 1996 and 2001

	Central Metropolitan region		Victoria Park municipality		South Perth municipality	
Year	1996	2001	1996	2001	1996	2001
Population	117,700	121,950	26,720	27,690	36,450	37,520
Light vehicle travel (%)	78.2	75.5	76.1	75.9	83.7	81.9
Car occupancy rate	1.09	1.08	1.12	1.10	1.10	1.09
Public transport (%)	11.9	13.2	15.8	16.8	10.7	11.2
Walk/cycle (%)	8.1	9.5	5.9	5.6	3.9	4.8
All EFMs	20.0	22.7	21.7	22.4	14.6	16.0
EFM % rise 1996–2001		13.5		3.2		9.6

Source: Moriarty and Kennedy (2004)

average for Brisbane and Adelaide, cities closest in size and urban density. The initial municipality for comprehensive TravelSmart intervention was South Perth, which had blanket intervention in 2000. It is therefore useful to compare South Perth with the adjacent areas of Victoria Park and the Central Metropolitan region as controls, both at the 1996 Australian census, before the South Perth intervention, and 1 year later at the year 2001 census. As evidenced by the journey to work data in Table 4, no shift to a higher share of EFMs, or to a higher occupancy rate for the work trip was found as a result of the intervention 1 year earlier.

Any gains that were initially made thus do not appear to have persisted, although a 2006 evaluative report on all the Australian TravelSmart programs (Australian Greenhouse Office 2006) suggested that there is some "evidence that changes appear to be sustained for at least 5 years without maintenance or further intervention." And from the government TravelSmart website, it is evident that activities have ceased in recent years (TravelSmart Australia 2008). In fact, the website has not been updated since October 2008. But governments are willing to try these programs because it puts the responsibility on individuals to make the changes rather than on politicians facing re-election.

European experience with voluntary schemes has been similar. Garling and Schuitema (2007), after surveying the use of voluntary measures for TDM, summarized their findings thus:

> The conclusion is that non-coercive TDM measures alone are unlikely to be effective in reducing car use. Therefore, coercive TDM measures such as increasing cost for or prohibiting car use may be necessary but are difficult to implement because of public opposition and political infeasibility.

In summary, whatever the importance of voluntary approaches for promoting general conservation practices, they have not worked for private travel. The remainder of this chapter thus mainly looks at non-voluntary measures for reducing travel demand.

Reducing Travel: Changing Vehicle Occupancy Rates

Increasing the occupancy rate for cars appears to be an attractive greenhouse reduction method, for several reasons. First, it can be implemented with the existing vehicle fleet. Second, the costs are low compared with other approaches. Third, the potential is large: occupancy rates in OECD countries today are typically about 1.5 persons per car, or 30 % occupancy for a five-seater car. What is more, they were historically much higher, at around two persons per car in Australia and the US in the 1960s (Moriarty and Honnery 2008b).

Policies for increasing occupancy rates for personal vehicles can be voluntary or mandated. Neither approach has enjoyed much success. An important reason is that in all OECD countries, average household sizes have fallen in step with completed family size. In Japan, persons per private household have fallen from 3.28 in 1975 to 2.42 in 2010 (SBJ 2014). Fewer family members are then available to fill the car for weekend social trips. Figure 2 shows how US car occupancy rate (sports utility vehicles not included) has fallen in step with average US household size. The occupancy rates for cars appear to be tied very closely to the occupancy rates for houses.

In addition, cars per 1,000 population have risen in all four countries. As an example, in Melbourne, Australia, the car occupancy rate for the journey to work correlates almost perfectly ($R^2 = 0.99$) with persons per light vehicle available (Moriarty and Mees 2006). This suggests that occupancy rates for cars will be hard put to even maintain their present level if either car ownership continues to rise or household sizes continue their fall in OECD countries.

But even if a law was passed (and adhered to by motorists) requiring that average occupancy rates be doubled, it is doubtful that the net GHG reductions would be very significant. In order that roads do not choke up, a car-based passenger transport system requires trip origins and destinations, and so traffic, to be dispersed in both space and time. Only for commuting, with its low occupancy rates (less than 1.1 persons per car for Australian cities today), and travel concentrated in morning and evening peaks, would (say) a doubling of occupancy rates be feasible.

But whether GHG reductions would follow is uncertain: in California, Greene and Schafer (2003) reported that a car-pooling scheme did raise commuter car occupancy rates while in operation, but only at the expense of public transport patronage. Overall, they saw "area-wide ridesharing" as having the potential to reduce total US vehicle-km by 0.1–2.0 % and HOV lanes by 0.2–1.4 % (see Table 3).

Car pooling can also conflict with attempts by motorists to combine different trip purposes, another method of reducing car travel (i.e., vehicle-km traveled). To the extent that a car-pooling scheme was successful, it would radically change the *meaning* of private travel, replacing the perceived tyranny of public transport timetables with the new tyranny of dependency on the punctuality of others, often nonfamily members. Further, the circuitry of such chauffered trips will increase the total vehicle-km traveled, partly offsetting any GHG reductions. Since much of the easily arranged car pooling is already being done, it can be expected that major rises in car pooling would greatly increase this circuitry factor.

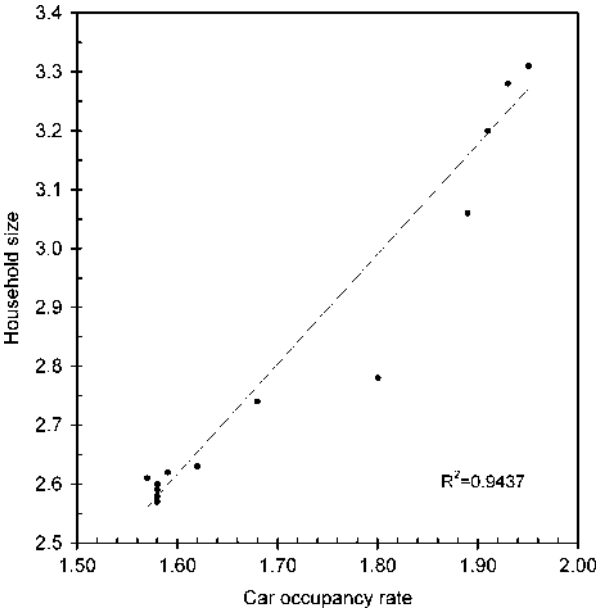

Fig. 2 Average household size versus car occupancy rate, US, 1960–2005 (Sources: US Census Bureau 2012; BTS 2014)

For public transport, the position is very different. As public transport loses patronage, the occupancy rates of public transport vehicles decrease. For the case of electric tramsin Melbourne, Australia, the occupancy rate fell from 24.6 in 1960, with overall patronage 783 million pass-km, to only 18.3 in 1980, 442 million pass-km (Newman and Kenworthy 1989). As patronage has grown strongly in recent years, occupancy is once again rising. Similar changes have been observed in Great Britain. Bus occupancy was 19 passengers per bus for 61.4 bp-k in 1974, fell to 8 passengers in 2000 at 46.2 bp-k, and has since risen to 10 passengers in 2007 at 50.8 bp-k (DfT 2013). Unlike car occupancy rates, public transport occupancies are independent of household size.

What this suggests is that public transport systems are often capable of much higher occupancy rates (but not often at peak hour, when many services are already at capacity loadings). Hence a shift to public transport from car can give a double boost to GHG reduction: one from the higher energy efficiency per seat-km that public transport enjoys over car travel, and second, from the higher occupancy rates possible from higher loadings (Moriarty and Honnery 2007, 2008b).

The reason for these occupancy rate changes is that when patronage falls, operators try to maintain service levels to prevent further passenger desertion. Conversely, as patronage rises, as is happening on many public transport systems in the OECD today, the rising patronage is initially accomodated on existing services, with additional services provided as required. In effect, if public transport patronage rises because of higher fuel prices, or rising congestion, seat occupancy increases naturally without any specific policy needed, either voluntary or nonvoluntary, for its increase.

In summary, public transport occupancy rates can be expected to rise, but the prospects for higher levels of car pooling are poor. Car pooling goes against several of the perceived advantages of the car, including privacy, direct travel between origin and destination, and no waiting (time of travel solely at the discretion of the driver). Instead, car pooling involves the need to negotiate with others, required levels of puntuality, choice of on-board music, and degree of driving caution. And even if car pooling could be politically mandated, the rise in occupacy rates would be partly illusory. In purely serve-passenger trips, the driver should not be counted as an occupant; public transport drivers are not counted. Increasing occupancy rates are not useful unless total transport GHG emissions are thereby reduced as well.

Reducing Travel: Changing Urban Land Use Patterns

Changing land use patterns is really only a mobility reduction option for urbanized areas, but in the OECD countries, 80 % or more of the total population live in urban areas. Many urban researchers have proposed such changes in existing cities as a means of both reducing vehicular travel overall, while increasing the share of public transport (e.g., Newman and Kenworthy 1999, 2006; Handy et al. 2006). The most discussed urban land use changes are policies to encourage (or mandate) increases in urban density. After allowing for differences in the definition of urban density for different cities – particularly if the cities are in different countries – urban densities can still vary by more than two orders of magnitude for different cities of the world (Newman and Kenworthy 1999). Figure 3 shows the exponential relationship for private travel versus urban density for 46 cities in Asia, Australia, Western Europe, and North America. Not only car travel, but all vehicular travel per capita, and transport energy consumption per capita, show similar curves.

While the density-private travel relationship is indeed strong, some caveats are in order. Australian and US cities, nearly all with densities of 1,000–2,000 persons/km^2, form a distinct group along the upper left-hand axis. For them, travel variations seem unrelated to density; all US cities had higher levels of car travel than any Australian city, even though the urban densities for the two countries fully overlapped. At the other extreme of the graph, in the bottom right-hand corner, lie six Asian cities, with very high urban densities and low levels of car travel. However, several also have much lower income levels than the other cities shown, and lower incomes will reduce both car ownership and travel.

The second problem relates to the definition of each city. The older cities of Europe often have boundaries that are much more restricted than those of Australian or North American cities, so that many of what would be called outer suburbs in the latter regions are excluded. Outer suburban residents typically travel much more than those living closer in and travel more by private transport (Moriarty 2002a). The result is lower recorded overall per capita urban travel levels in Europe's cities that would be the case if more extensive urban boundaries were used.

Travel per capita by residents in higher density areas of cities is usually lower than in areas of low density. A US example of this is found in the analysis by Fan and

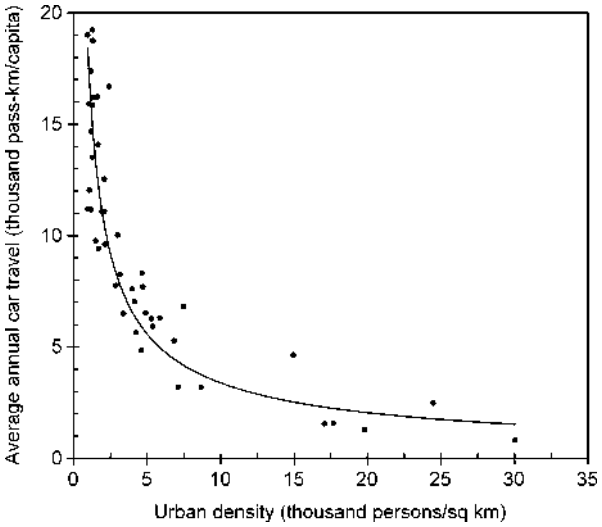

Fig. 3 Private vehicular travel per capita versus urban density, 46 world cities, 1990 (Source: Newman and Kenworthy 1999)

Khattak (2008) of the results of the 2006 Greater Triangle Region Travel Study in North Carolina. They concluded that travel overall in the region could be reduced by densification. But urban density tends to decrease with distance from the city center, and, as has just been shown, outer suburban residents travel more than inner city residents. An alternative explanation for their result might be that per capita travel rises with distance from the city center, as found for Melbourne, Australia (Moriarty 2002a).

The different areas of a city together form an interdependent urban system. If the inner city contains a surplus of workplaces over resident workers, as is true for many major cities, then workers from other areas must travel to fill these jobs. Similarly, the inner areas of major cities contain a variety of institutions and venues that are meant to serve the city as a whole, or even the entire region, many of them housed in or adjacent to the CBD. Examples include specialized shops and services, theatres, art galleries, and sports stadiums. Travel needs for inner area residents to these locations are minimized, but are of course higher for other urban residents.

Overall, of course, this arrangement of activities is efficient, minimizing total metropolitan-wide travel for (say) a major sporting event. Also helping reduce inner area car travel is the radial nature of many fixed rail urban networks, which results in denser and more frequent services there, and hence much greater public transport use per capita. Higher traffic congestion also discourages inner city residents from using cars for travel.

Looking at the four countries chosen, the urban densities of the three major Japanese cities – Tokyo, Osaka, and Nagoya – are far larger than those of the largest cities in Australia, the US, or even the UK. Indeed, the total annual number of motorized trips within a 50 km radius of central Tokyo was only slightly higher in 2009 than in 1995, and for street travel only (public and private), was lower in 2009

than in 1995. In a 50 km radius of central Osaka, vehicular trips also declined, with the total again lower in 2009 than in 1995 (SBJ 2014).

The very high job and population densities in these Japanese cities seem to have led to a saturation level for per capita vehicular travel at low levels compared with US or Australian cities. Further, only one-third of Tokyo trips, and about two-fifths of Osaka trips, are by private car. In Japan overall, the "car ownership intensity" (cars owned – which reflects car use – per unit of Prefectural Gross Income), correlates strongly ($R^2 = 0.8$) with the share of each prefecture living at high density (Moriarty 2007). A strong case can thus be made that very high urban densities, at least, lead to higher public transport patronage and far lower car travel levels.

Higher urban densities can potentially influence urban mobility levels (and mode choice) in two ways. First, for a given income level, a higher density city can support a higher density of shops and services of all kinds, simply because, for example, the total retail expenditure per km^2 will be higher. The distance to the nearest shopping center should therefore be lower in denser cities. The problem is that urban residents today don't necessarily use their nearest shopping center. A shopping survey from the 1990s in the city of Canberra, Australia's capital city with a population of around one-third of a million, illustrates this point (ABS 1998).

Canberra, unlike other major Australian cities, was consciously planned to have a defined hierarchy of shopping centers. In order of increasing size they are local centers, group centers, and town centers. In the survey, a local center was the nearest shopping center for 69 % of the city's population, a group center for 27 %, and for a town center, only 4 %. Yet only 19 % of households overall usually did their major food and grocery shopping at their nearest center. For the majority living nearest to a local center, nearly all of which have supermarkets, the figure fell to 5 %. (Nearest centers were, however, more popular for convenience items.) These findings can only be partly explained by the fact that the larger shopping centers were often closer to their workplaces, and sometimes presumably accessed from there.

These results can probably be extended to trip types of all kinds, as well as to other cities where, like Canberra, car travel is still perceived as both convenient and cheap. In support of this point, Moriarty and Beed (1988) compared the 1981 actual average trip length (airline) for the journey to work in Australia's major cities with the minimum average trip distance possible if all residences and workplaces were fixed, but workers could freely change workplaces. They found that such a change could halve work travel. Again, proximity to workplaces is not a sufficient condition for travel reduction.

By how much could urban density increases reduce vehicular travel and thus GHG emissions? Australia's five cities of one million-plus population provide a useful case study, particularly since the data are all collected using a common format. These cities – all state capitals – vary by over a factor of two in urban density from Brisbane to Sydney (see Table 5). Yet the two densest (Sydney and Melbourne) had a slightly higher level of vehicular passenger-km per capita than the three lower density cities (Brisbane, Perth, Adelaide). However, per capita public transport travel was much higher in these denser cities.

Table 5 Personal mobility, population, urban densities, five largest Australian cities, 2011

City	Population (millions)	Car (b-pk)	Public transport (b-pk)	Vehicular travel per capita (pass-km)	Density[a] (persons/ km^2)
Sydney	4.637	50.23	7.95	12,545	2,058
Melbourne	4.208	49.40	6.02	13,170	1,532
Brisbane	2.169	24.94	2.25	12,540	918
Perth	1.865	21.40	1.64	12,355	1,090
Adelaide	1.270	12.97	0.83	10,865	1,295

[a]2006 values
Sources: Moriarty and Mees (2006), BITRE (2013)

For low density cities, advances in traffic engineering techniques, together with the spread of traffic to off-peak times, may be able to accommodate some rise in urban density without making congestion much worse, which could explain the lack of response in Australian cities. For the US, Greene and Schafer (2003) reported that a doubling of local population and employment densities would only give a 5 % reduction in vehicle-km traveled (Table 3).

So, at best, even doubling the urban density of the smaller, lower density cities would achieve little in the way of travel reductions. It might be objected that for low-density Australian and US cities, all the above example shows that a mere doubling of urban density is not enough. But it is one thing to have the historically very high densities of many Asian cities – up to ten times Australian and US levels – but another to try to convert historically low density cities to very high density. It would also be enormously unpopular, and would in effect replace the political resistance to policies that directly reduce car travel (discussed below) with equally unpopular policies that might indirectly reduce travel.

Urban infrastructure has a lifetime of many decades – up to 70 years for houses, and even longer for transport right-of-ways. Even if the very large density changes were possible, it would take many decades to achieve. The world may not have that long for responding effectively to the challenge of global climate change.

A final argument against such large density increases concerns GHG emission reductions overall in the economy. Transport is an important, but not the only source of, emissions. All sections of the economy, not just the transport sector, will need to undergo drastic cuts in GHG emissions. An environmentally sustainable city might need somewhat lower density living to allow for households to supply much of their water needs from rainwater tanks, at least some food (mainly fruit and vegetables) from gardens, and part of their energy from rooftop photovoltaic cells and solar water heaters (Moriarty 2002a).

Neither the patterns found for Japan's largest three cities, nor those for the 13 US major cities analysed by Newman and Kenworthy (1999) fits this Australian pattern of vehicular travel per capita being independent of city size and density. In Japan, vehicular trips per capita in 2005 still showed a small *increase* with city size and population density (SBJ 2014), perhaps reflecting the continuing importance of public transport in these cities. This trend would fit in with the Australian experience,

where in 1947, when public transport dominated vehicular travel in Australian cities, vehicular travel per capita was *higher* in the higher density cities (which were also larger in size). In the US, there is a weak trend for cities with higher densities to have lower per capita vehicular travel – the opposite of Japan's experience, but more in line with the general world trend of per capita travel falling as urban density increases.

In summary, the very high historical urban densities achieved by the cities of Japan (and other Asian countries such as South Korea and China) do form an important constraint on the level of vehicular travel possible. At the low densities of many Australian and US cities, however, politically achievable density increases might not have much effect on total travel levels, although some shift to public transport should occur. But the short time frame the world has for climate change amelioration means that policy makers will have to work with cities largely as they presently exist. Further, as will be seen in section "Reducing Travel: Lowering the Convenience of Car Travel," for many cities the changes are unnecessary; the same result can be achieved by much more rapidly implemented changes to legislation.

Reducing Travel: Raising the Overall Level of Motoring Costs

Another possible approach is to increase significantly the costs of motoring, by adding further taxes on motoring fuels, and perhaps also increasing urban parking charges. Taxing motoring fuels has the advantage of reducing both urban and nonurban travel. Already, fuel taxes differ widely in the various OECD countries. Indicative gasoline and diesel prices for the year 2013 for various OECD countries, including those with the highest and lowest prices, are shown in Table 6. Since neither feedstock costs not refining costs vary much from country to country, most of the difference is due to different fuel taxes. Within the OECD countries, both gasoline and diesel prices vary by a factor of three. Combining this data with that for recent car travel from Fig. 1 suggests that the higher fuel prices found elsewhere in the OECD compared with the US is mainly responsible for the much higher levels of per capita travel in the US.

However, comparison of Japan and the UK shows the importance of factors other than fuel prices. Recent UK per capita car travel is 66 % higher than that in Japan, despite the higher gasoline prices in the UK. Less road space per vehicle in Japan, resulting in low travel speeds, is an important factor. Car travel in Australia is in turn higher than the UK, and petrol prices are lower. But when the higher urban densities of UK cities are also considered, and the lower national road space per vehicle, it seems that unacceptably high fuel price rises would be needed in Australia to ensure sufficient mobility reductions.

Nevertheless, by raising fuel taxes to a very high level, it would be possible to reduce car travel to any desired low level, both in urban and non-urban areas – assuming political feasibility – just as it was concluded that raising urban densities to very high levels would. It would also be very inequitable, particularly in Australia and the US, as suggested by the analysis above. In both these countries, households

Table 6 Indicative 2013 gasoline and diesel prices

Country	Gasoline (super) ($/l)	Diesel ($/l)
Australia	1.61	NA
Germany	2.11	1.60
Italy	2.34	1.85
Japan	1.66	1.30
Mexico	0.91	0.78
Norway	2.59	1.86
Turkey	2.68	2.40
UK	2.09	1.84
US	0.98	1.06

Source: IEA (2013)

having access to at least one car are fairly uniformly spread over all income groups, and only around 10 % of households are noncar owning. In Australia, at least, outer suburban households have, on average, a much lower income on a per capita basis compared with inner suburban households, but higher car ownership levels. They also have greater travel needs and have inferior public transport services (Moriarty 2002a). (In lower-income countries, on the other hand, where car ownership is often under 20 per 1,000 persons (OPEC 2013), raising fuel taxes would present much less of an equity problem.)

Surveys of motorists generally show that the respondents think that raising car travel costs will not be very effective in reducing travel (Steg 2008). But the actual responses to fuel cost rises tell a different story. (However, it may be that what the respondents really mean is that they do not *like* fuel costs rises and would prefer to see other measures adopted, such as cheaper, or more extensive, public transport provision.) Evidence for the efficacy of raised fuel prices comes from the effect of price rises on gasoline sales in the years before the global financial crisis. In Australia, per capita sales of fuel for light road vehicles peaked locally in 2004, and in 2012 were still below their 2004 level (ABS 2013). Similar effects seem to have occurred in a number of other OECD countries.

The fixed costs of car travel (including depreciation, registration, and insurance costs) presently dominate the annual costs of owning and running a car. For the US, Greene and Schafer (2003) found that for a 2001 model year car, gasoline costs were only 10.2 % of the total annual costs. However, this gives a misleading impression of their actual significance to motorists. Since fuel and parking costs are usually all that motorists perceive as the costs of car travel on a day-to-day basis, altering the *structure* of motoring costs could also reduce car travel.

At present, motorists can significantly reduce their unit costs by traveling more kilometers annually. Insurance and registration fees could be recovered by raising fuel taxes and could even be done so that the overall costs of motoring did not change for the average motorist. High annual travel motorists, however, would find themselves paying more per kilometer traveled, so that, once again, lower income outer suburban households might be disadvantaged.

Road pricing is an alternative market-based approach. Road space worldwide is still largely publicly provided, and freely available to all road users, regardless of the resulting congestion. Although toll roads, many of them privately owned, are centuries old, road pricing as a means of controlling traffic levels really began with the successful scheme in Singapore in 1975. The comprehensive and successful London scheme introduced in 2003 has led to renewed interest in road pricing in many other cities. Supporters can argue that since electronic road pricing is now technically feasible, rationing road space by electronic road pricing could be an important means for keeping urban congestion to tolerable limits. But road pricing, with its emphasis on road space scarcity, can only indirectly reduce vehicular travel and emissions. It can induce motorists to shift to public transport, but its main effect is probably to redirect traffic to other times and other untolled routes or destinations.

In summary, raising motoring costs can be an effective means of reducing car travel, but in OECD countries has adverse equity considerations. With less traffic on roads, average car speeds could (and probably would) be raised, resulting in a widening gulf between the high and low mobility sections of the population. Also, given that high-income households are more time-constrained than income-constrained, their car travel would rise, with an attendant rise in GHG emissions. In effect, the burden of reducing transport emissions would fall mainly on lower-income households. As discussed in section "General Principles for Change," they would become involuntary environmentalists. Major reductions in GHGs will not occur unless all sections of the population are engaged.

Nevertheless, it is likely that fuel cost rises – perhaps large ones – are unavoidable. Following record high costs for crude oil in the first half of 2008, prices slumped to under $40/barrel, but soon recovered and since 2011 annual prices have once again averaged over US$ 100/barrel (OPEC 2014). The age of cheap oil is over – unless the global economy collapses to such an extent that oil demand is greatly lowered. Higher motoring costs thus seem inevitable, and unlike measures such as reduced speed limits, will not be seen as the fault of governments of oil-importing countries.

Reducing Travel: Lowering the Convenience of Car Travel

Section "Reducing Travel: Changing Urban Land Use Patterns" has already discussed how high urban densities potentially allow trip distances to be shortened, although for low density cities, this potential is only very partially realized. But for very high densities of residents and workplaces, as in Japanese cities, another important effect occurs: because urban congestion is inevitably at high levels, the average speed of private car travel is much reduced, which tends to both lower car travel levels and raise the relative speed and economic viability of public transport, especially rail, with its own right-of-way. This is shown by Fig. 4, which plots for 1990, per capita car travel against the average car travel speed for the same sample of world cities as in Fig. 3, most of them (37) in OECD countries. The cities with low travel speeds and annual car travel are all in Asia. Although other factors are

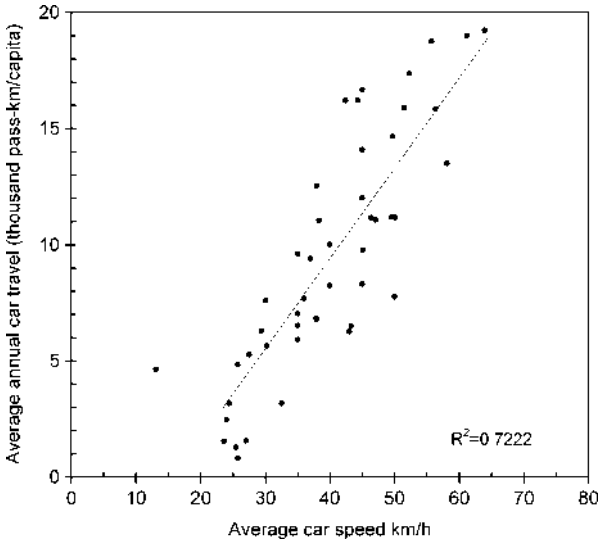

Fig. 4 Average per capita car travel versus average car speed for 46 world cities, 1990 (Source: Newman and Kenworthy 1999)

important, annual per capita car travel is clearly sensitive to average vehicle speed at least in cities.

As Table 1 showed, car travel is the overwhelming choice for surface travel not only for Australia and the US but also for the more densely populated UK. This perceived advantage of car travel over other modes arises from several causes. First, car travel, especially driving, produces psychological benefits such as mastery of the vehicle and the thrill of acceleration (Moriarty and Honnery 2005). Second, car travel allows much greater flexibility of travel: door-to-door travel at any time of the day or night, and so freedom from public transport timetables (even assuming public transport is an option). It also affords protection from the weather, greater perceived personal security, privacy from strangers, and the ability to transport much luggage. This last advantage is important for shopping and explains much of the popularity of drive-in shopping centers.

The third advantage concerns travel times. Because the extensive network of roads in most OECD cities is designed to provide vehicular access from origin to destination for almost every conceivable trip, distances by car are often shorter than by public transport (particularly fixed rail transport) for a given trip. Overall average trip travel times are also shorter by car because of higher average travel speeds; public transport has to make frequent stops to set down and pick up passengers. In general, car travel will always have an advantage over public transport modes on the first two factors discussed – it is inherent in the nature of private travel. But the third present advantage is not inherent in car travel: it results from the privileges granted to the car, such as speeding through residential areas, access to all areas of the city (usually including even the city center with its dense pedestrian traffic), and ability to park (even if a charge is made) at most locations (Moriarty and Honnery 2013).

As has been shown, in major Japanese cities where this third advantage is largely lacking, travel speeds by car are very low. The result is low vehicular travel levels overall, with rail replacing the car as the major travel mode. In Japan, such an effect has arisen "naturally"; its cities were largely formed before car travel was significant (Table 1). But given the political will, the privileges that have been given the car can be removed. Many cities in the OECD have taken tentative steps in this direction, with traffic-free central business districts, and priority for alternative travel modes, and "traffic calming" measures in residential districts.

But the city of Graz, Austria, with a population of 240,000 in the city proper, and 360,000 in the Greater Graz region, has gone furthest. In 1992, after a 2-year test period, the city imposed a 30/50 km/h speed limit on the entire road network. The 30 km/h limit was imposed on all side-roads and near centers such as schools and hospitals. These areas accounted for 80 % of the total city area. On all other roads, a 50 km/h limit was applied (European Local Transport Information Service 2008). The main purpose of the speed reductions was to improve road safety for all, but particularly pedestrians and cyclists, and to improve urban amenity. A modest reduction in the share of car travel has resulted and significant increase in cycling's share (Commission for Integrated Transport 2009).

The overall aim of policy would be to reverse the present transport priorities in OECD countries, so that non-motorized travel would be regarded as the default solution for urban trip-making, with public transport for back-up for necessary longer trips. Private vehicular travel would still be used in the transition to a low travel future, mainly in nonurban areas for longer trips difficult to service by public transport. The emphasis would be on "transport efficiency" (getting more access from each passenger-km) and less on mobility as an end in itself.

Future Directions

In this final section, the various arguments made in this chapter will be drawn together, in order to assess what policies for travel reductions would work in future in the various countries. Policies that work in cities will not always be effective in nonurban areas. Nor will policies that are successful in highly motorized countries necessarily be relevant in presently low-mobility countries. Further, the scope for vehicular travel reductions may be much smaller in congested cities like Tokyo, compared with many major cities in the US or Australia, with their far lower population and job densities.

First, an important concern when future mobility reduction policies are considered: Should the policies be voluntary, or mandated by governments? As discussed earlier, voluntary measures are easier to introduce and do not have the political costs to governments of more coercive measures. However, voluntary approaches to travel reduction have had little success. This conclusion should come as no surprise. After all, the decisive improvements in transport, from safety measures such as the installation of seat-belts and air bags, speed limits, and blood alcohol content limits, to technical environmental measures such as three-way catalytic converters, have all

been mandatory. So, of course, have been adherence to the highway code, proficiency tests and age limits for drivers, the requirement that vehicles have functioning brakes and turn indicator lights, tires with adequate tread, and so forth.

If measures are to be compulsory, what form should they take? They could involve very large changes to the monetary costs of motoring, as discussed in section "Reducing Travel: Raising the Overall Level of Motoring Costs." There, it was stressed that in highly motorized OECD countries it would prove inequitable, as reductions in motoring would mainly come from lower-income groups. Garling and Schuitema (2007) have also stressed that perceived fairness is important for public acceptability of TDM measures in general. In section "Reducing Travel: Lowering the Convenience of Car Travel," an alternative set of compulsory policies were explored. The main benefit of these approaches is that they target *all* travelers, because they change the relative travel speeds of the different modes. For many trips, EFMs would now become faster than car travel, particularly in areas closer to the city center. This loss of relative speed advantage for car travel could offset many of its inherent advantages, as already discussed.

An example from outside transport, from the authors' home city, Melbourne, illustrates these points well. Stream inflow volumes to Melbourne's water reservoirs have fallen over the past decade, while Melbourne's population has been growing rapidly (Melbourne Water 2014). Fortunately, when it became clear that reservoir levels were in sharp decline (together, they held less than 26 % of their design capacity in mid-2009), the problem was easily communicated to the public, and understood and accepted by all. So the state government was able to act fast and introduce policies to cut water use (although with recovery of reservoir levels since mid-2010, restrictions have been eased).

Of course, they were many exhortations for residents to do the "right thing" and conserve water. But ultimately the success of the program rested on the outright banning of certain categories of water use, such as car washing, for *all* residents – not by using market measures. Because the measures applied to all, their acceptance was much greater. One crucial reason why this policy could be successfully introduced can be seen by contrasting public perceptions of water shortages with that for global climate change. Unlike the disarray in opinions (at least by the public and the media) over the latter topic, which have still not abated, there were no media-promoted "Melbourne reservoir water level skeptics" to tell us that there really was plenty of water in the reservoirs or that alternatives to water would soon be available.

But what are the chances for success in introducing mandatory measures that could bring about very significant changes to travel behavior? World transport faces the twin problems of global climate change and depletion of conventional oil reserves. Climate change can be denied/avoided for a while longer – indeed, despite all the talk, international meetings, and the recently released IPCC report, this is the world's implicit response – but such a response is not an option for global oil depletion. The global annual available supply of *conventional* oil has likely peaked, and nonconventional supplies will be costly in both monetary and environmental terms and slow to develop. Oil use *per capita* peaked in 1978, and again in per capita terms has been constant from the early 1980s to the mid 2000s, but is now in slow

decline (BP 2014; UN 2014). If countries like China and India wish to increase their per capita use, it must fall in other countries if output is not raised. And given that most oil use is still in OECD countries, it is there that oil use must fall the most.

Climate scientists use the term external "external forcing" to refer to the way increased greenhouse gas concentrations are driving the planetary climate from thermal equilibrium. Given not only the strong attachment motorists presently have to their cars, but the lack of readily available and convenient alternatives to private travel, especially in the nonurban areas, it is likely that the "car culture" found in OECD countries will, in a similar manner, only change in a major way under "external forcing" of transport systems. Oil supply security issues and price rises will likely provide the initial external forcing in the future.

The Australian experience again provides a historical example of such external forcing. The only time when the fledgling car culture was seriously challenged was in 1929. Car ownership rose rapidly in the 1920s, but the Great Depression, followed by World War II and with it, gasoline rationing and the very low levels of car imports, stalled the rise of the car for two decades. Public transport patronage rose to record levels. Since then car travel has steadily increased its dominance of surface transport systems, both urban and nonurban. In recent years, however, driven by the crude oil price rises that began in the early 2000s (ABS 2013), Australia has seen not only sharp rises in public transport patronage but also a small reversal in market share (BITRE 2013). Similar gains have been recently reported for many other OECD countries, including the UK and Japan (DfT 2013; SBJ 2014).

Such rises in public transport patronage provide a benefit that can go far beyond that gained by substituting a given amount of passenger car travel by alternative (EFM) modes. In earlier papers (Moriarty and Honnery 2007, 2008a, b, 2013), the authors have advanced the idea that the dominant transport mode determines not only the modal share but also the total level of per capita vehicular travel and even the patterns of trip making. Australian historical experience suggests that the levels of vehicular travel are much lower when public transport dominates travel, as it did until the late 1940s. Consider the case of Melbourne. In 1947, public transport accounted for 80 % of vehicular travel and car travel 20 %. Yet within only 15 years, these percentages were reversed. Further, per capita travel levels today, with the car the dominant mode, are about four times those of 1947. What this demonstrates is that, under the right conditions, major transport changes can happen very fast.

Another important change was the shift in urban travel patterns. In 1947, vehicular travel in major Australian cities was strongly oriented toward the city center, since most workplaces, shopping expenditures and major centers for sports and entertainment were in the inner city area. Although many trips were local, such as visiting local shops and friends, most of these short trips were by nonmotorized means. Today, vehicular travel destinations are far more uniformly dispersed over the urban area (Moriarty and Honnery 2011). In each area of the city there is now a far better balance between workplaces and workers, shops and shoppers. Levels of personal travel *could* have been reduced, given this better balance. Instead, per capita levels rose several-fold in each of Australia's major cities. Most of this rise was for

discretionary trips such as shopping or social trips, rather than for nondiscretionary work or education trips. Overall, the suburbanization of many activities means that nonmotorized travel can now take over a large share of trips.

In urban areas of OECD countries, *localization* of activities will be increasingly needed. Residents will need to work, shop, recreate, and socialize more and more at the local level. This localization will in turn require both local areas to be more attractive, and residents to develop a "sense of place" and a sense of belonging. Urban planners will have to start thinking creatively about how to design areas for humans, rather than focusing mainly on traffic flow, the current preoccupation; urban planning is not reducible to traffic planning. The changes will also need to be implemented very quickly, as time is important if countries are to greatly cut not only transport's contribution to climate change but also oil consumption. As already mentioned, it is likely that impending oil shortages could act as a catalyst for necessary changes, forcing the public to realize that change is unavoidable and making their acceptance more likely.

Transport GHG reductions through personal travel reduction are different from other resource-using sectors in that synergistic effects come into play to a far greater extent than is possible elsewhere. Individuals can readily reduce their use of domestic energy or water use, even if their neighbours don't. Conversely, if the entire neighbourhood cuts its water use, it doesn't much help an individual household in the neighborhood reduce its own water use (except through peer pressure). But if, as advocated here, local shopping centers are used more intensively, the range of goods and services offered for sale will improve, most likely at the expense of the presently popular, drive-in centers. If public transport patronage rises greatly, service frequency will also rise and probably also service coverage. The latter could initially occur using buses, but in the longer term could be replaced by fixed-rail transport, if patronage justified it. For transport, government intervention will be crucial for success in changing to a new transport "logic."

How crises such as global climate change or oil depletion get interpreted is important for policy responses. However, while many people recognize as severe the challenges posed by oil depletion and global climate change, there are many others who don't see a problem, or if they do, think that one or more of a variety of tech fixes will solve these twin problems, without the need to resort to potentially unpopular measures such as mobility reductions. Policies promoting tech fixes are thus more likely to be tried first, and only when acknowledged to be inadequate, will the more fundamental changes advocated here be adopted.

This finally gives rise to another important question: whether incremental changes (such as the ongoing research and development of "green cars") will really help the move to an environmentally sustainable transport system. In section "Introduction: Travel Reductions for Climate Mitigation," it was shown how far reaching are the changes needed for OECD passenger transport. An analogy can help here: to get a couple of meters closer to the Moon, leaning a ladder against the back shed will suffice, but it is a dead-end approach for much closer approaches to the Moon. For that, a rocket must be built. However, other incremental approaches provide a very good fit to deeper change, including efforts to to make urban destinations more

accessible by active modes or to move people onto public transport. It is here that policy makers should focus their efforts in the interim period before more coercive policies must inevitably be introduced.

Acknowledgments Patrick Moriarty acknowledges the financial support of the Australasian Center for the Governance and Management of Urban Transport (GAMUT) for the research which underpins this book chapter. GAMUT is in turn funded by the Volvo Research and Education Foundations. He would also like to thank the Maintenance Technology Institute in the Department of Mechanical and Aerospace Engineering and the Department of Design, both at Monash University, for providing him with accomodation during the writing of this book chapter.

References

Australian Bureau of Statistics (ABS) (1998) Shopping preferences, ACT, October 1997. Canberra, Australia. ABS Cat No 8644 8

Australian Bureau of Statistics (ABS) (2013) Survey of motor vehicle use, Australia, 12 months ended 30 June 2012. Canberra, Australia. ABS Cat. No. 92080DO001_1230201206

Australian Greenhouse Office (2006) Evaluation of Australian TravelSmart projects in the ACT, South Australia, Queensland, Victoria and Western Australia: 2001–2005. Commonwealth of Australia, ACT. Available at http://www.travelsmart.gov.au/publications/evaluation-2005.html

Ausubel J, Marchetti C, Meyer P (1998) Toward green mobility: the evolution of transport. Eur Rev 6(2):137

BP (2014) BP statistical review of world energy 2014. BP, London

Brown LR (2009) Plan B 4.0: mobilizing to save civilization. Norton, New York/London

Bureau of Infrastructure, Transport and Regional Economics (BITRE) (2013) Yearbook 2013: Australian infrastructure statistics. Statistical report, Canberra

Bureau of Transportation Statistics (BTS) (2014) National transportation statistics. http://www.rita.dot.gov/bts/sites/rita.dot.gov.bts/files/publications/national_transportation_statistics/index.html

Cairncross F (2001) The death of distance, 2nd edn. Harvard Business School, Cambridge, MA

Commission for Integrated Transport (2009) Study of European best practice in the delivery of integrated transport: report on stage 2 – case studies. Available at http://www.cfit.gov.uk/docs/2001/ebp/ebp/stage2/05.htm

Davis SC, Diegel SW, Boundy RG (2013) Transportation energy data book: Edition 32. Oak Ridge National Laboratory, Oak Ridge, Tennessee, US. ORNL-6989

De Groot JIM, Steg L (2009) Mean or green: which values can promote stable pro-environmental behavior? Conserv Lett 2:61–66

Department for Transport (DfT) (2012) National travel survey: 2011. DfT, London. Available at https://www.gov.uk/government/uploads/system/uploads/attachment_data/file/35738/nts2011-01.pdf

Department for Transport (DfT) (2013) Transport statistics Great Britain 2013. DfT, London

Dietz T, Gardner GT, Gilligan J et al (2009) Household actions can provide a behavioral wedge to rapidly reduce U.S. carbon emissions. Proc Natl Acad Sci 106:18452–18456

Energy Information Administration (EIA) (2014) Annual energy outlook 2014. US Department of Energy, Washington, DC

European Local Transport Information Service (ELTIS) (2008) Citywide 30 km/h speed limit – City of Graz (Austria). Available at www.eltis.org/PDF/generate_pdf.php?study_id=1928&lan=en

Fan Y, Khattak AJ (2008) Urban form, individual spatial footprints, and travel: examination of space-use behavior. Transp Res Rec 2082:98–106

Garling T, Schuitema G (2007) Travel demand management targeting reduced private car use: effectiveness, public acceptability and political feasibility. J Soc Issues 63(1):139–153

Garling T, Garling A, Johansson A (2000) Household choices of car-use reduction measures. Transp Res A 34(3):309–320
Geurs K, van Wee B (2000) Backcasting to develop a sustainable transport scenario assuming emission reductions of 80–90 %. Innovation 13(1):47–62
Gifford R, Nilsson A (2014) Personal and social factors that influence pro-environmental concern and behaviour: a review. Int J Psych 49(3):141–157
Greene DL, Schafer A (2003) Reducing greenhouse gas emissions from US transportation. Pew Center on Global Climate Change. Available at http://www.pewclimate.org/docUploads/ustransp.pdf
Hagman O (2003) Mobilizing meanings of mobility: car users' constructions of the goods and bads of car use. Transp Res D 8(1):1–9
Handy S, Cao X, Mokhtarian P (2006) Correlation or causality between the built environment and travel behavior? Evidence from Northern California. Transport Res D 10:427–444
International Energy Agency (IEA) (2013) Key world energy statistics 2013. IEA/OECD, Paris
Kennedy EH, Beckley TM, McFarlane BL et al (2009) Why we don't "walk the talk": understanding the environmental values/behaviour gap in Canada. Human Ecol Rev 16(2):151–160
Lyons G, Urry J (2005) Travel time use in the information age. Transp Res A 39:257–276
Melbourne Water (2014) Available at http://www.melbournewater.com.au/waterdata/waterstorages/Pages/Storages-over-the-years.aspx
Mitchell WJ (2003) Me^{++}: the cyborg self and the networked city. MIT, Cambridge, MA
Moriarty P (2002a) Environmental sustainability of large Australian cities. Urban Policy Res 20 (3):233–244
Moriarty P (2002b) Household travel time and money expenditures. Road Transp Res 11(4):14–23
Moriarty P (2007) Environmental and resource constraints on Asian urban travel. Int J Environ Pollution 30(1):8–26
Moriarty P, Beed C (1988) Transport characteristics and policy implications for four Australian cities. Urban Policy Res 6(4):171–180
Moriarty P, Honnery D (2005) Determinants of urban travel in Australia. In: Proceedings of the 28th Australasian transport research forum, Sydney, 28–30 Sept 2005
Moriarty P, Honnery D (2007) Australian car travel: an uncertain future. In: Proceedings of the 30th Australasian transport research forum, Melbourne, 25–27 Sept 2007
Moriarty P, Honnery D (2008a) Low mobility: the future of transport. Futures 40(10):865–872
Moriarty P, Honnery D (2008b) The prospects for global green car mobility. J Clean Prod 16:1717–1726
Moriarty P, Honnery D (2011) Rise and fall of the carbon civilisation: resolving global environmental and resource problems. Springer, London
Moriarty P, Honnery D (2013) Greening passenger transport: a review. J Clean Prod 54:14–22
Moriarty P, Kennedy D (2000) Can telework reduce travel? In: IS 2000 conference, University of Woollongong, Dec 2000
Moriarty P, Kennedy D (2004) Voluntary travel change: an Australian case study. In: 3rd international conference on traffic and transport psychology, Nottingham, 5–9 Sept 2004
Moriarty P, Mees P (2006) The journey to work in Melbourne. In: Proceedings of the 29th Australasian transport research forum conference, Gold Coast, 27–29 Sept 2006
Newman P, Kenworthy J (1989) Cities and automobile dependence: an international sourcebook. Gower, London
Newman P, Kenworthy J (1999) Sustainability and cities: overcoming automobile dependence. Island, Washington, DC
Newman P, Kenworthy J (2006) Urban design to reduce automobile dependence. Opolis Int J Suburban Metropol Stud 2(1). Available at http://repositories.cdlib.org/cssd/opolis/vol2/iss1/art3. Article 3
Organization of the Petroleum Exporting Countries (OPEC) (2013) World oil outlook 2013. OPEC Secretariat, Vienna

Organization of the Petroleum Exporting Countries (OPEC) (2014) OPEC basket price. Available at http://www.opec.org/opec_web/en/
Pelton JN (2004) The rise of telecities: decentralizing the global society. The Futurist 38:28–33
Pooley CG, Turnbull J (2000) Modal choice and modal change: the journey to work in Britain since 1890. J Transp Geogr 8:11–24
Pucher J, Dijkstra L (2003) Promoting safe walking and cycling to improve public health: lessons from the Netherlands and Germany. Am J Public Health 3(9):1509–1516
Pucher J, Dill J, Handy S (2010) Infrastructure, programs, and policies to increase bicycling: an international review. Prev Med 50:S106–S125
Raiborn C, Butler JB (2009) A new look at telecommuting and teleworking. J Corp Account Financ 20(5):31–39
Rajan SC (2006) Climate change dilemma: technology, social change or both? An examination of long-term transport policy choices in the United States. Energy Policy 34:664–679
Rees WE (2009) The ecological crisis and self-delusion: implications for the building sector. Build Res Inf 37(3):300–311
Sallis JF, Frank LD, Saelens BE et al (2004) Active transportation and physical activity: opportunities for collaboration on transportation and public health research. Transp Res A 38:249–268
Schafer A, Victor D (2000) The future mobility of the world population. Transp Res A 34 (3):171–205
Sims R, Schaeffer R et al (2014) Transport. In: Edenhofer O, Pichs-Madruga R, Sokona Y et al (eds) Climate change 2014: mitigation of climate change. CUP, Cambridge, UK
Smith RA (2008) Enabling technologies for demand management: transport. Energy Policy 36:4444–4448
Statistics Bureau Japan (SBJ) (2014) Japan statistical yearbook 2014. Statistics Bureau, Tokyo. Also earlier editions. Available at http://www.stat.go.jp/english/data/nenkan/index.htm
Steg L (2008) Promoting household energy conservation. Energy Policy 36:4449–4453
Stocker TF, Qin D, Plattner G-K et al (eds) (2013) Climate change 2013: the physical science basis. Cambridge University Press, Cambridge/New York
Tal G (2008) Reduced overestimation in forecasting telecommuting as a travel demand management policy. Transp Res Rec 2082:8–16
Tertoolen G, van Kreveld D, Verstraten B (1998) Psychological resistance against attempts to reduce car use. Transp Res A 32(3):171–181
Torgler B, García-Valiñas MA (2007) The determinants of individuals' attitudes towards preventing environmental damage. Ecol Econ 63:536–552
TravelSmart Australia (2008) Available at http://www.travelsmart.gov.au/index.html
United Nations (UN) (2014) World population prospects: the 2012 revision. http://esa.un.org/unpd/wpp/index.htm. Accessed 15 July 2014
US Census Bureau (2012) The 2012 statistical abstract: PDF version. Also earlier editions. Available at http://www.census.gov/compendia/statab/2012edition.html
US Department of Transportation (DoT) (2011) Summary of travel trends: 2009 National Household Travel Survey. DoT, Washington, DC
Wardman M, Tight M, Page M (2007) Factors influencing the propensity to cycle to work. Transp Res A 41:339–350
Wikipedia (2014) Recycling. Available at http://en.wikipedia.org/wiki/Recycling
World Business Council for Sustainable Development (WBCSD) (2004) Mobility 2030: meeting the challenges to sustainability. WBCSD, Geneva

Nontechnical Aspects of Household Energy Reductions

Patrick Moriarty and Damon Honnery

Contents

Abstract

Domestic energy forms a significant part of total energy use in OECD countries, accounting for 22 % in the USA in 2011. Together with private travel, domestic energy reductions are one of the few ways that households can directly reduce their greenhouse gas emissions. Although domestic energy costs form a minor part of average household expenditure, the unit costs for domestic electricity and natural gas vary by a factor of 4 and 5, respectively, among OECD countries, and per capita use is strongly influenced by these costs. Other influences on domestic energy use are household income, household size, residence type (apartment/flat vs. detached house), and regional climate. Numerous campaigns have been carried out in various countries to reduce household energy use. A large literature

P. Moriarty (✉)
Department of Design, Monash University, Melbourne, VIC, Australia
e-mail: patrick.moriarty@monash.edu

D. Honnery
Department of Mechanical and Aerospace Engineering, Monash University, Melbourne, VIC, Australia
e-mail: damon.honnery@monash.edu

W.-Y. Chen et al. (eds.), *Handbook of Climate Change Mitigation and Adaptation*,
DOI 10.1007/978-3-319-14409-2_71

has analyzed both the results of these studies and the general psychology of pro-environmental behavior, yet the findings often seem to conflict with the national statistical data.

The authors argue that the rising frequency of extreme weather events (especially heat waves, storms, and floods), together with sea level rises, is likely to be a key factors in getting both the public and policy makers to treat global climate change as a matter of urgency. Costs of domestic energy are likely to rise in the future, possibly because of carbon taxes. But such taxes will need to be supplemented by other policies that not only encourage the use of more efficient energy-consuming appliances but also unambiguously support energy and emission reductions in all sectors.

Abbreviations

ABS	Australian Bureau of Statistics
EIA	Energy Information Administration (US)
EJ	Exajoule (10^{18} J)
EPR	Energy performance rating
EU	European Union
GHG	Greenhouse gas
GJ	Gigajoule (10^{9} J)
GNI	Gross national income
Gt	Gigatonne (10^{9} tonne)
IEA	International Energy Agency
IPCC	Intergovernmental Panel on Climate Change
IT	Information technology
MWh	Megawatt-hour (10^{6} W-hour)
NG	Natural gas
OECD	Organisation for Economic Co-operation and Development
ONS	Office for National Statistics (UK)
PCT	Personal carbon trading
PEB	Pro-environmental behavior
RCP	Representative Concentration Pathway
SBJ	Statistics Bureau Japan
SCC	Social cost of carbon
UHI	Urban heat island
UN	United Nations

Introduction

In 2011, world CO_2 emissions from energy and industry totalled 33.74 gigatonnes (Gt) (BP 2014). (A gigatonne = 10^{18} tonnes.) For the USA alone in 2011, total emissions were 5.5 Gt of CO_2, resulting from total energy use of 102.5 EJ (EJ = exajoule = 10^{18} J).

Of this total US energy, household energy use accounted for 22.6 EJ or 22.0 %, compared with 18.6 %, 31.4 %, and 28.0 % for the commercial, industry, and transportation sectors, respectively. The US Energy Information Administration (EIA) projects that domestic energy use in the USA will grow only slowly over the period 2012–2040, at an average of only 0.2 % per year (EIA 2014).

Along with private transport, cutting energy use at the household level is an important way for individuals to directly reduce their carbon footprint. (In this chapter, the terms "household energy use" and "domestic energy use" are used interchangeably.) Two possible approaches for reducing domestic energy consumption are, first, to encourage the purchase and use of domestic energy-using devices (see also chapter "► Energy Efficiency: Comparison of Different Systems and Technologies" in this handbook) and, second, by reducing the use of such devices. This could involve having fewer appliances (e.g., dispensing with second refrigerators in the household), running energy devices for fewer hours (e.g., turning off lights), or running at a lower setting (e.g., lowering thermostat settings in winter). This second approach to energy reductions is more important for household energy use than for either commercial buildings or industry, because for both of these sectors, energy costs are likely to be monitored more closely and policies for energy reduction, both technical and nontechnical, more readily implemented for purely economic reasons. Nevertheless, considerable scope still remains for both industry and commercial buildings to adopt these practices.

There is a further reason for a focus on domestic energy use. In many Organisation for Economic Co-operation and Development (OECD) countries in recent years, total primary energy use per capita, or even total primary energy use, has fallen (BP 2014). In the UK, for instance, total energy use has not risen for four decades, and total CO_2 emissions from fossil fuels peaked in 1970 and are now 26.5 % lower than the peak value. The problem is that recent decades have also seen the rise in imports to the OECD of energy- and CO_2-intensive manufactured products from Asia. As Davis and Caldeira (2010) show, such *embodied* CO_2 and energy can make a big difference to national emissions and energy statistics and render problematic the interpretation of energy time series data. Because domestic energy statistics only measure energy *used* by household equipment and not the embodied energy in the equipment, this problem is avoided.

This chapter is structured as follows. Section "Factors Affecting Domestic Energy Consumption" looks at patterns of domestic energy use in various selected OECD countries. Domestic energy prices, household income, household size, and climate were all found to be important for present domestic energy use. (In this chapter, the terms energy reductions and CO_2 reductions are used interchangeably, since, at the household level, energy reductions are – apart from rooftop solar devices and switching to gas from electricity for space and water heating – the only means available to reduce CO_2 emissions.) In section "Strategies for Household Energy Reductions," the numerous studies and field trials on reducing household energy use are reviewed. Researchers have looked at the effect of parameters such as income level, gender, age, and ethnicity on responsiveness to campaigns for energy reductions. The latest studies have concluded that significant energy reductions are

possible, but stressed that households face many barriers to reductions, including lack of relevant information. Building on the energy cost data in the previous section, the authors stress the importance of future carbon taxes for motivating energy reductions. In section "Future Directions," the possibility for conflicts between household energy savings and overall global climate change mitigation (or adaptation) is examined.

Factors Affecting Domestic Energy Consumption

Table 1 shows domestic energy consumption by end use for the USA for year 2011. Over half the energy use is for space heating and cooling (with the UK having a similar proportion (Steg 2008)), with almost one-fifth for water heating and refrigeration/freezers. Since 1993, the share for space heating has fallen, and the shares for both space cooling and appliances have risen (EIA 2013). Energy for space heating in the USA overall is expected to fall out to the year 2040, for space cooling to continue to increase (EIA 2014). Although space heating presently uses almost six times as much energy as space cooling in the USA overall, this ratio varies with regional climate. Households in colder climates spend a higher share of their total expenditure on fuel because of high winter fuel bills, which more than compensates for lower need for space cooling in the warmer months. In Australia, for example, in subtropical Brisbane (27° 30′ S), the figure is 2.1 %, compared with 3.5 % for temperate Hobart (43° S) (Australian Bureau of Statistics (ABS) 2012).

In OECD countries, nearly all of this domestic energy is supplied by reticulated electricity and natural gas. Table 2 shows the unit prices of these two domestic energy sources for 2012 for a number of OECD countries, including both the major economies and those with either very high or very low energy costs. The unit costs for domestic electricity and natural gas vary by a factor of 4 and 5, respectively, among OECD countries, with Mexico, one of the lowest-income OECD countries,

Table 1 Domestic energy use by function for the USA, 2011

Delivered energy consumption by end use	Share (%)
Space heating	43.03
Space cooling	7.54
Water heating	15.70
Refrigeration and freezers	4.07
Cooking	3.06
Clothes washers and dryers	2.48
Lighting	5.67
Dishwashers	0.88
Televisions and related equipment	2.97
Computers and related equipment	1.14
Other uses	13.47
Delivered energy	100.00

Source: EIA (2014)

having the lowest unit costs. The different costs have a large impact on domestic energy use. Comparing the USA and Japan, the much higher costs for domestic energy in Japan (2.3 times that of US electricity costs; see Table 2) coincide with a 3.5-fold reduction in domestic energy per capita (EIA 2014; Statistics Bureau Japan (SBJ) 2014). Only a small part of this difference can be explained by the 9.3 % higher gross national income (GNI)/capita reported for the USA (Table 2). Further, the slightly larger average household size in the USA compared with Japan (about 2.5 and 2.4 occupants, respectively) should, if anything, lower per capita domestic energy use. Similarly, the high-income, high-energy cost European countries (Denmark, Germany, and Sweden in Table 2) have much lower per capita domestic energy use than the USA. Further, the increase in domestic energy prices in the UK was seen as a partial explanation for the decrease in domestic energy use between 2005 and 2011 in England and Wales (Office for National Statistics (ONS) 2013).

The burden of domestic energy costs depends not only on unit prices but also on income level. As expected, the share of household expenditure spent on domestic energy declines for the higher-income quintiles (Table 3). However, higher-income

Table 2 Unit cost of domestic electricity and gas and per capita GNI for various OECD countries in 2012

Country	Electricity $/MWh	Gas $/MWh[a]	GNI/capita[b]
Denmark	383.43	123.09	59,870
Germany	338.75	90.32	45,170
Japan	276.76	NA	47,870
Mexico	90.20	30.36	9,640
Netherlands	238.24	98.7	48,110
Sweden	223.96	156.89	56,120
UK	220.74	73.65	38,500
USA	118.83	35.22	52,340

Sources: International Energy Agency (IEA) (2013b), World Bank (2014)
[a]Gross heating value
[b]Atlas method (US$ 2012)

Table 3 Domestic energy expenditure vs. household income quintile, Australia and Japan

Country	Lowest	Second	Third	Fourth	Highest	Average
Australia[a]	4.0 %	3.4 %	2.7 %	2.5 %	2.0 %	2.6 %
Australia[b]	1,147	1,460	1,616	1,929	2,294	1,721
Japan[c,d]	7.0 %	6.3 %	5.8 %	5.2 %	4.5 %	5.5 %
Japan[e]	162.6	178.7	187.8	197.8	224.7	190.5

Sources: ABS (2012), SBJ (2014)
[a]2009–2010 survey data
[b]$Aust (2009–2010) per year
[c]2012 survey data
[d]Only households with two or more persons are included
[e]In 1000 yen (2012) per year

households also have more persons per household (ABS 2012; ONS 2013; EIA 2014; SBJ 2014), so it may be that the greater energy efficiency possible with larger households explains some or all of the decrease. The UK statistics also measure domestic energy costs for quintiles ranked on an "equivalised disposable income," which adjusts for the number of persons per household (with, e.g., two adults counting as one unit, but two adults plus two children counting for 1.4 units) (ONS 2014). This 2012 UK data shows that, after such adjustment for size, the poorest fifth of households spent 10.9 % of their disposable income on domestic fuel, compared with only 2.8 % for the wealthiest quintile – nearly a fourfold difference. For both quintiles, the share of disposable household income spent on domestic fuel had risen since 2002 (from 8.0 % for lowest and from 1.7 % for highest), even though average domestic energy use in the UK had fallen by 17 % over the decade. Nevertheless, in absolute terms, the highest-income quintile spent more on domestic energy (and produced more CO_2 emissions) than the lowest-income quintile, and the same was true for gross expenditure on domestic energy in Japan and Australia (see Table 3).

Energy use in households also varies with housing type. A 2008 UK study (Druckman and Jackson 2008) found that those living mainly in flats ("city living") had a much lower share of weekly expenditure on energy than "countryside" residents, mainly living in detached houses. An earlier study in Australia (Moriarty 2002) found that inner-city residents of Melbourne and Sydney, with a high share of residents living in flats, spent a lower share of disposable income on household fuel than outer suburban residents or nonurban residents, both groups mainly living in detached houses. Along the same lines, a Canadian study (Larivière and Lafrance 1999) measured the residential electricity consumption of Québec's 45 most populous cities and towns and found that the per capita energy rose as the share of single dwellings increased. This result would be expected if electric power was an important form of heating in a cold climate.

The size of the residence (in square meters (m^2)) is also an important factor, particularly for domestic heating and cooling. It helps explain some of the large difference between US and Japanese energy use. In the USA in 2011, average residence size was 154.5 m^2, compared with only 94.1 m^2 for Japan overall and as low as 63.9 m^2 for Tokyo prefecture (2008 values, the latest available) (EIA 2014; SBJ 2014). The high population density of Japan and the resulting high land prices explain much of this difference. Other important differences are in both ownership and average size of appliances. For example, in Japan in 2009, only 27 % of households of two persons or more owned dishwashers; in the USA in 2009, the corresponding figure was 64 %. Also, both the number of refrigerators per 1,000 households and their average capacity were larger in the USA (EIA 2013; SBJ 2014).

The *behavior* of the occupants has also been found to be crucial. A British study (Pilkington et al. 2011) examined space heating demands in "a terrace of six similar, passive solar dwellings with sunspaces." Space heating demand per occupant was found to vary by a factor of 14. This finding clearly indicates both that behavioral factors are important for domestic energy use and also that considerable potential

exists for energy reductions. Further evidence comes from a study of 3,400 German homes: Sunikka-Blank and Galvin (2012) again found that dwellings with the same energy performance rating (EPR) varied widely in space heating energy use. (The EPR, measured in kWh/m^2 per year, assesses the overall energy efficiency of a building, either using actual or modeled energy use data (Corrado and Mechri 2009).) But they also found that (energy inefficient) dwellings with high EPR ratings consumed much *less* energy than calculated, while the reverse was true for low EPR (energy efficient) dwellings. Similar results appeared to hold for several other EU countries. They concluded that the potential energy savings from changes to occupant behavior may be far greater than assumed. Section "Strategies for Household Energy Reductions" looks further at this potential.

Strategies for Household Energy Reductions

Domestic energy reductions rely on far fewer policy options than are available for reducing household private travel energy. In addition to legislation on vehicular fuel efficiency (see also chapter "► Reducing Personal Mobility for Climate Change Mitigation"), authorities can also influence the *levels* of private travel (in vehicle-km) by measures such as street closures in the inner city, speed limit reductions, priority for public transport and nonmotorized modes, limits on availability of parking spaces, road pricing as in London and Singapore, reduced arterial road construction in urban areas, provision of improved public transport, as well as increased charges for parking and taxes on transport fuels. Authorities can implement these measures because most of the road systems, and often the public transport systems, are publicly owned. A further limit on the capacity of regulations to drive change is the much longer lifetimes of housing stock relative to road vehicles.

Apart from increasing fuel costs, these policy levers are not available for reducing domestic energy use. As with road vehicle efficiency, governments can legislate the use of energy-efficient light globes and establish energy ratings for domestic appliances and minimum insulation standards for new buildings. But too much intervention in the domestic sphere would meet strong popular resistance. Because of this, authorities must rely far more on voluntary behavior change (and domestic energy cost increases) for reducing domestic energy use than in other areas of energy use.

Nevertheless, domestic energy conservation has at least one important advantage over travel energy conservation. It is very difficult for individual households to reduce car travel if other households do not, particularly for countries like the USA, where car travel accounts for over 90 % of all surface vehicular travel. Even if car travel is reduced as a result of a campaign, households will usually soon relapse back to former practices, since car travel is usually faster than other modes. On the other hand, individual households can make domestic energy reductions even if others do not. This section first reviews the extensive social psychology literature (see section "Social Psychology and Pro-environmental Behavior") on pro-environmental behavior (PEB), particularly the importance of information provision (see section

"The Role of Information Provision") before examining the role of carbon taxes (see section "The Role of Monetary Approaches and Carbon Taxes") and, finally, the context for energy conservation (see section "The Context for Domestic Energy Conservation").

Social Psychology and Pro-environmental Behavior

A vast literature is now available on the application of social psychology to energy conservation, and pro-environmental behavior in general, together with policy recommendations. According to Dietz (2014), "modest policies" aimed at raising the efficiency of US household energy consumption (presently 22 % of total energy) could reduce overall CO_2 emissions in the USA by 7 %. Surveys in OECD countries have consistently found that the public regard protecting the environment and saving energy as important (Steg 2008; Booth 2009). Obviously, it is not how people respond to surveys about PEB (i.e., their stated attitudes toward the environment and energy conservation) that is important but whether or not households do in fact reduce their energy use and whether any such reductions continue in the long term. For as Dietz (2014) has also stressed, few studies with a social psychology approach are able to study actual environmental behavior, as distinct from *stated* intentions. A 2010 survey of energy use in Hungarian households has shown how stated intentions and actual behavior can differ. The survey of over 1,000 people found that those who "consciously act in a pro-environmental way" did not necessarily use less residential energy than respondents who did not exhibit PEB (Tabi 2013).

Much of the social psychology literature on PEB has concentrated on individual attributes. Jagers et al. (2014) found that 21 % of the respondents in a Swedish survey met the requirements for "ecological citizenship." Their conclusions found support for a strong relationship between ecological citizenship and PEB: "Our results suggest that *individuals who think along the lines of ecological citizenship are more likely than others to behave in an environmentally friendly way in their daily lives*." Yet PEB was measured by response to items such as "try to save household electricity" rather than comparing actual household electricity use with other householders; hence, pro-environmental attitudes rather than actual pro-environmental behavior were being measured.

Gifford and Nilsson (2014) have recently reviewed the various "personal and social factors that influence pro-environmental concern and behavior." We discuss here some of their findings relevant to methods for reducing household energy use. In general, survey respondents with more knowledge about environmental problems indicated greater overall environmental concern. (The role of information is discussed in more detail in section "The Role of Information Provision.) Interestingly, older people generally reported higher pro-environmental behavior than younger people and women more than men. Not only did the authors report that environmentalists "tend to be middle- or upper-middle-class individuals" but, at the national level, "environmental concern has a clear positive relation with gross domestic product (GDP) per capita."

Yet, as we have seen in section "Factors Affecting Domestic Energy Consumption," the higher-income quintiles in OECD countries have higher domestic energy use per household, and, globally, the OECD and other high-income countries have much higher primary energy use and CO_2 emissions per capita than low-income countries (IEA 2013b). Residents of low-income households and countries could thus be regarded as "involuntary environmentalists" (see Moriarty and Honnery 2012): their low incomes constrain their energy use and carbon emissions. Further, survey results are usually only given as percentage reductions, ignoring the fact that low-income households already use much less energy than the average. But in the USA, a recent study (Bohr 2014) found that income effects on belief about the reality of climate change were mediated by political beliefs. Briefly, lower-income Republicans regarded climate change as a more serious issue than higher-income Republicans, but the reverse was found true for Democrats. Clearly, one needs to be careful in evaluating the transfer of social psychology findings to the national energy policy domain.

A related point is the choice of *incentives* for promoting PEB. One fairly consistent result in the published literature is the apparent superiority of nonmonetary over monetary rewards. Steg (2008) has argued that domestic energy conservation is best served by appealing to normative and environmental values, because they provide a more enduring basis for change than ones which maximize personal interests, such as cost savings. If, for example, cost reductions disappear, then so will the conservation behavior, if formed on that basis. Overall, this view can be summed up by arguing that "green" reasons for change are superior to "mean" reasons (de Groot and Steg 2009). Dietz (2014) simply stated that "self-interest is only one of several values that underpin environmental decision making."

Turaga et al. (2010) reached similar conclusions and stated that the empirical evidence suggested that PEB was more likely for people whose "core values" could be described as "social altruistic" and/or "biospheric". Of course, this still leaves the problem of how to promote PEB in householders whose behavior is more in line with *homo economicus*. These researchers also warned that government policies might crowd out motivations for altruistic behavior. They thus stress the need to create "carefully structured institutions." The question of monetary incentives in the real world is, however, not so simple and is discussed in greater detail in section "The Role of Monetary Approaches and Carbon Taxes".

Steg (2008), looking specifically at domestic energy conservation, reported three *barriers* to conservation. The first barrier was that many households do not have sufficient knowledge of means to effectively reduce their energy consumption, as discussed in section "The Role of Information Provision." The second was the low-priority households attach to reducing energy use. As discussed in section "Factors Affecting Domestic Energy Consumption," domestic energy is typically only of the order of 5 % of household expenditure, although a higher proportion for low-income households. The third barrier was the high costs for some energy-saving strategies, particularly if it involved the purchase of more energy-efficient appliances. She reported that two general strategies can be used to reduce household energy use. First, use psychological insights to change householders' "knowledge,

perceptions, motivation, cognitions, and norms related to energy use and conservation." Second, alter the *context* in which energy use decisions are made; this important topic is treated in detail in section "The Context for Domestic Energy Conservation."

"Social marketing" has become popular as a means of changing people's attitudes and behavior on environmental issues. As defined by Corner and Randall (2011), social marketing "is the systematic application of marketing concepts and techniques to achieve specific behavioural goals relevant to the social good." Their study is a critique of the application of social marketing techniques in the UK to engage the public more fully on climate change. The study showed that the approach may in some circumstances be effective, particularly for encouraging PEB that needs only minor lifestyle changes, such as recycling household waste. However, given the scope of overall CO_2 reductions needed by the UK and other high-emitting countries, social marketing for carbon reductions appeared to be less effective, and some of the approaches tried were even counterproductive. One particular problem was that attempting to tailor messages to individual groups may lead to compromises that negatively impact PEB in the longer term and in other domains. In other words, it is risky to consider the various environmental problems (and even non-environmental problems) in isolation.

A complication of this type arises from what social psychologists term "moral licensing." According to Merritt et al. (2011), moral licensing "occurs when past moral behavior makes people more likely to do potentially immoral things without worrying about feeling or appearing immoral." Tiefenbeck et al. (2013) carried out a field experiment in 154 households of a 200-apartment complex in Greater Boston in the USA. The study examined the effect of a household water conservation program on electricity consumption. "The results show that residents who received weekly feedback on their water consumption lowered their water use (6.0 % on average), but at the same time increased their electricity consumption by 5.6 % compared with control subjects." They concluded that such moral licensing "can more than offset the benefits of focused energy efficiency campaigns, at least in the short-term." In some ways, this effect is similar to the well-known concept of "energy rebound," where improving energy efficiency makes the operation of energy-using devices cheaper, thus leading either to some increased use of such devices or using the money saved for other (energy-using) goods and services.

The Role of Information Provision

It seems intuitive that households need accurate information on both energy costs and energy use of specific household equipment. Studies have shown that there is indeed an information gap. Attari et al. (2010) conducted a nationwide US survey on estimated energy savings from such actions as turning off lights or replacing existing lights by more efficient ones. They concluded that "For a sample of 15 activities, participants underestimated energy use and savings by a factor of 2.8 on average, with small overestimates for low-energy activities and large underestimates for high-

energy activities." Householders may simply think that the unit energy consumption of an appliance is simply related to its size (Steg 2008). Correcting this bias would seem essential for domestic energy decision-making.

At least one government agency (the Office for National Statistics in the UK) saw better information as partly responsible for the observed declines in UK household energy use in recent years. The list of possible explanatory factors for household natural gas and electricity reductions included technical efficiency measures such as better cavity wall insulation and "improved efficiency of gas boilers and condensing boilers to supply properties with both hot water and central heating," as well as continuous rises in the price of domestic gas and electricity after the mid-2000s (ONS 2013). But they also saw the provision of better information to households as important, specifically the "introduction of energy rating scales for properties and household appliances, allowing consumers to make informed decisions about their purchases" and "generally increasing public awareness of energy consumption and environmental issues." But as the following discussion documents, simply providing more information can have unexpected effects on energy use.

The rise of the new information technology (IT) has greatly enlarged the scope for providing data on domestic energy use to households. There is now a growing literature on intelligent or smart cities and smart houses. Cook (2012) has described possible future houses equipped with a vast number of sensors ("ambient intelligence") to automatically adjust temperature and lighting levels, for example. A barrier to the realization of such smart houses is the privacy issue. But even if the privacy issue could be overcome, there are doubts about the extent of energy savings possible with such information provision alone. An Irish study (McCoy and Lyons 2014) reported the results of a controlled trial of 2,500 electricity consumers. Householders were supplied with smart meters which gave them detailed information on usage. They found that electricity use fell as expected, but compared to the control group, these householders invested less on energy-saving equipment. The authors speculated that householders might realize that conservation measures can be an alternative to energy efficiency investments. In other words, energy conservation and energy efficiency measures may not always be complementary measures, as is often assumed.

Delmas et al. (2013) performed a meta-analysis on 156 published "information-based energy conservation experiments" conducted over the period 1975–2012. The studies focused on household electricity savings. The type of information provided in the various experiments included items such as tips on how to save energy and the provision of detailed data on own energy use or that of peers. From these experiments, they found average measured savings in electricity use of 7.4 %. However, the savings found depended greatly on the type of information provided. The authors concluded that "strategies providing individualized audits and consulting are comparatively more effective for conservation behavior than strategies that provide historical, peer comparison energy feedback." They also reported potential problems with information campaigns, in that feedback on costs and monetary incentives led to relative *increases* in household electricity use.

Another recent study from the USA (Gromet et al. 2013) provided further evidence that simply giving more information will not necessarily encourage PEB in householders. In one study, they compared responses of self-identified political liberals with self-identified political conservatives. They showed that conservatives were *less* likely to buy more expensive but also more energy-efficient light bulbs if they were labeled as being good for the environment than if they were not so labeled. Responses were reversed for liberals. The researchers believed that "the political polarization surrounding environmental issues" in the USA was the explanation for their unexpected findings. This finding may not therefore be applicable to other OECD countries: in the EU, several conservative governments support deep cuts to CO_2 emissions.

The Role of Monetary Approaches and Carbon Taxes

One government policy often mentioned as both an important and necessary part of any carbon reduction strategy in all sectors of the economy is carbon taxes (Van Vuuren et al. 2011a). The European Union (EU) already has an emissions trading scheme (ETS), although the prices in 2013 were at historically low levels. Given that every tonne of CO_2 emitted, regardless of location, has the same climate effect, a global carbon market would be preferable. At present, though, apart from the multinational regional EU market, existing carbon markets are either national or even subnational (Newell et al. 2014). But reliance on market-based incentives can be criticized because it can (and has) led to abuses, particularly the "reducing emissions from deforestation and forest degradation" (REDD) scheme of the UN Framework Convention on Climate Change (Moriarty and Honnery 2011).

Nevertheless, such carbon taxes are sometimes regarded as providing motivation for domestic energy use reductions. Certainly, the cross-country evidence presented in section "Factors Affecting Domestic Energy Consumption" on domestic energy costs suggests that monetary considerations are important for energy use. The IPCC estimated that after 2050, carbon taxes required to meet Representative Concentration Pathway 2.6 (RCP2.6) target would need to be as high as $250 per tonne CO_2 (Van Vuuren et al. 2011b). Here, we provide a rough estimate of the effect such a tax would have on lower end OECD domestic electricity prices. In recent years, electricity generation in OECD countries overall has led to emissions of 0.434 tonne CO_2/MWh (IEA 2013a). At $250 per tonne CO_2, this works out as $108.5/MWh. From Table 2, this value would roughly double domestic electricity prices in Mexico and the USA.

An important question is whether such carbon taxes would be regressive. Dissou and Siddiqu (2014) have argued that they need not be, if seen in the context of a comprehensive analysis. They argued that "Most studies have assessed the distributional impact of carbon taxes through their effects on commodity prices alone, while ignoring their impact on individual welfare brought about by changes in factor prices." They found a U-shaped curve for income inequality (as measured by the Gini coefficient) when plotted against the level of carbon tax. Although maximum

income equity was found at a tax of about $50, a zero tax had about the same equity effect as one of over $100 per tonne CO_2. Nevertheless, a tax rate of $250 per tonne CO_2 would substantially increase inequality.

However, a carbon tax is not the only way of reducing emissions by monetary means. Starkey (2012) examined the equity effects of "personal carbon trading" (PCT). In this UK proposal, every adult would receive for free an equal carbon quota, with the sum of these quotas amounting to perhaps 40 % of total allowable national emissions. The author compared this proposal with other emission reduction schemes, including a carbon tax, and showed that these other schemes can be designed to be as equitable as any PCT one. Another possible approach is to alter the *structure* of domestic energy costs, with lower fixed costs on energy bills and higher unit costs for energy use. This change could be revenue neutral overall, but, again, its equity implications would need to be evaluated for each country. Future price rises for fossil fuels are likely inevitable; policies will have to be designed to ensure that lower-income households, who already pay a higher share of household income for domestic energy, are not be further disadvantaged.

The level of carbon tax necessary will depend on the costs of either replacing fossil fuels by nonfossil alternatives (renewable and nuclear energy) or the costs of various carbon sequestration methods. The latter include biological sequestration in plants (especially forests) and in soils and also mechanical sequestration techniques such as capturing CO_2 from the flue stacks of fossil fuel electricity plants, followed by compression, transport, and geological burial (Van Vuuren et al. 2011b; Moriarty and Honnery 2011). For details, see also chapter "▶ Reducing Greenhouse Gas Emissions with CO_2 Capture and Geological Storage" in this handbook. A recent study (Marshall 2013) found an extremely broad range of both the unit costs of various carbon sequestration methods – from $10 to $2,000/tonne CO_2 sequestered – and global potential (in Gt CO_2).

Of course, imposing such high carbon taxes would be unwarranted if it could be shown that the costs of climate *adaptation* (again, measured in $ per tonne of CO_2 or equivalent) were much smaller. Some economists have argued that the global economic costs of a 2 °C temperature rise will be small, and an official US estimate was that the "social cost of carbon" (SCC) was $37 per tonne of CO_2 emitted. However, these and similar results derived from economic models have been heavily criticized (Revesz et al. 2014). In any case, integrated climate models show that climate costs will rise in a nonlinear fashion as temperature rises beyond the nominal 2 °C "safe limit." Ackerman and Stanton (2012) have thus argued that the SCC could easily be an order of magnitude higher or, given certain assumptions, even infinite.

The Context for Domestic Energy Conservation

What will induce households, as well as policy makers, to take climate mitigation seriously? At present, despite the high profile of the climate change problem over the past two to three decades in both the press and scholarly publications, there has been

no real progress in mitigation: in 2013, emissions from fossil fuels were 2.1 % higher than in 2012 (BP 2014). Possible reasons for such climate inaction could include pressure from fossil fuel-based industries and energy-exporting countries, skepticism about the reality of global warming, and belief in the efficacy of future technical fixes such as aerosol geoengineering to painlessly solve the problem (see also chapter "▶ Geoengineering for Climate Stabilization" in this handbook). Interestingly, the Asian OECD countries (Japan and South Korea) both report very high levels of belief in the reality of global warming (Wikipedia 2014) and have insignificant fossil fuel reserves (BP 2014).

The Intergovernmental Panel on Climate Change (IPCC) (Stocker et al. 2013), in its latest report (Fifth Assessment Report (AR5)), warned that the world will increasingly face greater extremes in climate, particularly in the form of heat waves and high-intensity precipitation. Over the past century, global mean temperature has risen less than 1.0 °C, yet in temperate climates, daily variation can be 20 °C or more. Such variation makes it difficult for laypersons to feel the urgency that climate scientists feel. But already, recent heat waves in Europe and elsewhere have led to tens of thousands of excess deaths (Moriarty and Honnery 2014). Climate scientists speak of *climate forcing* (or radiative forcing, in watts per square meter) from GHGs. Analogously, it can be expected that the spread of extreme weather events, both in intensity and frequency, will provide the forcing for both the public and their policy makers in all countries to take decisive action on climate mitigation, although intense arguments will continue regarding the sharing of emission reductions between countries.

On the other hand, there is a disconnection between national costs for climate mitigation and benefits accruing to the same nation (Moriarty and Honnery 2014). Climate mitigation is an example of a global public good; these tend to be undersupplied by market economies. In contrast, most of the health benefits from reducing local air pollution in a city will accrue to that city. The problem would have been less serious when the OECD countries both had the highest per capita emissions of CO_2 *and* accounted for most of the global emissions. In 1965, the OECD produced 68.3 % of fossil fuel CO_2; in 2012, even a much enlarged OECD accounted for only 40.3 % (BP 2014). The urgent need for countries like China and India, still with relatively low emissions per capita, but large total emissions, to reduce their emission levels, will complicate popular acceptance of deep emission reductions in the OECD.

Another factor that must impact ordinary citizens' perception of both the need for reducing fossil fuel use and acceptance of high domestic fossil fuel energy prices is national fossil fuel reserve estimates. One set of reserve estimates, those of BP (2014), is shown in Table 4. Countries like Denmark, Japan, South Korea, and Sweden have negligible amounts of fossil fuels. German reserves are almost all low-quality lignite, which produces high CO_2 emissions per unit of delivered energy – an embarrassment for a country striving for "green" credibility. Even the UK, once the world leader in coal production, and, until recently, an important natural gas (NG) and oil producer, finds itself today with only a few years' reserves of all three fuels at their current production rates.

Table 4 Fossil fuel reserve estimates at the end of 2012 for various OECD countries, in EJ

Country	Oil	NG	Coal	All fossil fuels
Australia	22.3	143.2	1584.0	1749.4
Canada	993.2	75.4	141.0	1209.5
Denmark	4.0	1.5	2.6[a]	8.1
Germany	1.5	2.3	569.4	573.2
Japan	0.3	0.0	9.7	10.0
Mexico	65.1	15.1	28.9	109.1
South Korea	0.0	0.2	1.8	2.0
Sweden	0.0	0.0	0.0	0.0
UK	17.7	7.5	6.4	31.7
USA	199.9	320.3	4825.9	5346.0
World	9531.3	7058.0	17665.0	34254.3

Source: BP 2014
[a]In Greenland

Most fossil fuels used in these countries are thus imported, and so these importing countries are increasingly dependent on the continued goodwill of both oil- and NG-exporting countries. Restrictions on both oil and gas exports have been used for political purposes. In the USA, in contrast, the public is being led to believe that shale gas (and even shale oil) will lead once again to oil and gas independence for the USA. The *context* in which appeals to the public to conserve energy are made in OECD Europe or Asia, compared with fossil fuel-rich North America or Australia, is thus very different.

Future Directions

One important consideration for both future climate change mitigation and adaptation is to ensure that actions taken at the local level (such as an urban area) do not conflict with actions needed at the global level. Similarly, local actions for climate mitigation or adaptation must not conflict with policies needed for ecological sustainability in general.

One proposal for climate change mitigation is to paint urban building roofs (and even roads) with reflecting paint, in order to increase their albedo – the share of insolation that is reflected directly back into space (Royal Society 2009). Unlike most other geoengineering proposals, such roof whitening should meet with little international opposition, since the actions involved are clearly on national territory. It would also represent a means for households to directly mitigate climate change without reducing domestic energy use. And unlike most climate mitigation measures, most of the temperature reduction benefits would accrue to the urban area concerned (see also chapter "▶ Geoengineering for Climate Stabilization" in this handbook).

However, a recent study (Jacobsen and ten Hoeve 2012) modeled both local and global climate effects. The study found that although local temperature reductions

would indeed occur, the global effect would be a modest temperature increase. Even if different climate models were to give different results, the study illustrates the importance of such potential conflicts. A further problem is that "cool roofs" will reduce winter as well as summer temperatures, both inside and outside buildings. In temperate climates, domestic heating energy needs will therefore rise. Another study of reflective pavements (Yang et al. 2013) also found a similar unintended consequence: "reflected radiation from high-albedo pavements can increase the temperature of nearby walls and buildings, increasing the cooling load of the surrounding built environment and increasing the heat discomfort of pedestrians."

In section "Factors Affecting Domestic Energy Consumption," it was found that residents of apartment blocks, and higher urban density living in general, reduced household energy consumption. Increasing the residential density of cities might therefore appear as a way to lower energy use and carbon emissions. Further, increased urban density has also been promoted as a means of reducing urban car travel and their associated emissions (Moriarty and Honnery 2013). However, several possible conflicts arise. First, higher-density living might interfere with the ability to use passive solar energy for temperature control and natural lighting (Steemers 2003). Second, it might reduce the potential for individual households to use PV (photovoltaic) roof panels or solar hot water systems or, in low rainfall regions, tanks for rainwater storage. One also needs to consider the effect of urban density on the urban heat island (UHI) effect. Of course, reduction in household energy use will reduce urban waste heat, which is one component of the UHI effect. But according to Kleerekoper et al. (2012), a more important cause is the "urban canyon" effect, which prevents escape of radiant heat, and impervious surfaces, which prevent evaporative cooling. Both are likely to be more important in densely built-up urban areas.

This chapter has shown that deep reductions in household energy and thus CO_2 emissions will require a variety of compatible policies. The national statistical data presented in sections "Factors Affecting Domestic Energy Consumption" and "Strategies for Household Energy Reductions" showed that household domestic energy use is lowest in countries with low fossil fuel reserves; these countries also usually have higher prices for domestic energy use. Public support for decisive action on climate change varies from country to country and even in one country from month to month. However, the rise in frequency of extreme weather events – heat waves, storms, and floods – together with rising sea levels, is likely to increase support for action in all countries.

The review of domestic energy conservation campaigns discussed in section "Social Psychology and Pro-environmental Behavior" found only limited permanent measured energy reductions. But it could be that this disappointing result occurs because respondents presently do not really feel that energy security and fossil fuel depletion and climate change are serious problems that will necessarily involve major lifestyle changes. In future, it is likely that, for both fossil fuel depletion and climate change reasons, the context in which domestic energy decisions are made will change. Past research on domestic energy conservation may then be of little relevance. But new research will also have to take a more comprehensive view of

energy savings than in the past, to ensure that neither conflicts between energy efficiency and energy conservation do not occur nor conflicts between energy savings in different sectors.

References

Ackerman F, Stanton EA (2012) Climate risks and carbon prices: revising the social cost of carbon. Available at (http://dx.doi.org/10.5018/economics-ejournal.ja.2012-10)

Attari SZ, DeKay ML, Davidson CI et al (2010) Public perceptions of energy consumption and savings. Proc Natl Acad Sci 107(37):16054–16059

Australian Bureau of Statistics (ABS) (2012) 2009–10 household expenditure survey: summary of results. ABS, Canberra, Cat No 6530

Bohr J (2014) Public views on the dangers and importance of climate change: predicting climate change beliefs in the United States through income moderated by party identification. Clim Chang. doi:10.1007/s10584-014-1198-9

Booth C (2009) A motivational turn for environmental ethics. Ethics Environ 14(1):53–78

BP (2014) BP statistical review of world energy 2014. BP, London

Cook D (2012) How smart is your home? Science 335:1579–1581

Corner A, Randall A (2011) Selling climate change? The limitations of social marketing as a strategy for climate change public engagement. Glob Environ Chang 21:1005–1014

Corrado V, Mechri HE (2009) Uncertainty and sensitivity analysis for building energy rating. J Build Phys 33(2):125–156

Davis SJ, Caldeira K (2010) Consumption-based accounting of CO_2 emissions. Proc Natl Acad Sci 107:5687–5692

de Groot JIM, Steg L (2009) Mean or green: which values can promote stable pro-environmental behavior? Conserv Lett 2:61–66

Delmas MA, Fischlein M, Asensio OI (2013) Information strategies and energy conservation behavior: a meta-analysis of experimental studies from 1975 to 2012. Energy Policy 61:729–739

Dietz T (2014) Understanding environmentally significant consumption. Proc Natl Acad Sci 111 (14):5067–5068

Dissou Y, Siddiqu MS (2014) Can carbon taxes be progressive? Energy Econ 42:88–100

Druckman A, Jackson T (2008) Household energy consumption in the UK: a highly geographically and socio-economically disaggregated model. Energy Policy 36:3177–3192

Energy Information Administration (EIA) (2013) 2009 RECS survey data. Accessed on 18 Jun 2014 at (http://www.eia.gov/consumption/residential/data/2009/#sf?src=‹ Consumption Residential Energy Consumption Survey (RECS)-b1)

Energy Information Administration (EIA) (2014) Annual energy outlook 2014. US Department of Energy, Washington, DC

Gifford R, Nilsson A (2014) Personal and social factors that influence pro-environmental concern and behaviour: a review. Int J Psychol. doi:10.1002/ijop.12034

Gromet DM, Kunreuther H, Larrick RP (2013) Political ideology affects energy-efficiency attitudes and choices. Proc Natl Acad Sci 110:9314–9319

International Energy Agency (IEA) (2013a) CO_2 emissions from fuel combustion: highlights, 2013th edn. IEA/OECD, Paris

International Energy Agency (IEA) (2013b) Key world energy statistics 2013. IEA/OECD, Paris

Jacobson MZ, ten Hoeve JE (2012) Effects of urban surfaces and white roofs on global and regional climate. J Clim 25:1028–1044

Jagers SC, Martinsson J, Matti S (2014) Ecological citizenship: a driver of pro-environmental behaviour? Environ Polit 23(3):434–453

Kleerekoper L, van Esch M, Salcedo TB (2012) How to make a city climate-proof, addressing the urban heat island effect. Resour Conserv Recycl 64:30–38
Larivière I, Lafrance G (1999) Modelling the electricity consumption of cities: effect of urban density. Energy Econ 21:53–66
Marshall M (2013) Transforming earth. N Sci 220 (2938):10–11
McCoy D, Lyons S (2014) Better information on residential energy use may deter investment in efficiency: case study of a smart metering trial. MPRA paper no. 55402. http://mpra.ub.uni-muenchen.de/55402/
Merritt AC, Effron DA, Monin B (2010) Moral self-licensing: when being good frees us to be bad. Soc Personal Psychol Compass 4(5):344–357
Moriarty P (2002) Environmental sustainability of large Australian cities. Urban Policy Res 20 (3):233–244
Moriarty P, Honnery D (2011) Rise and fall of the carbon civilisation: resolving global environmental and resource problems. Springer, London
Moriarty P, Honnery D (2012) Chapter 51. Reducing personal mobility for climate change mitigation. In: Chen W-Y, Seiner JM, Suzuki T, Lackner M (eds) Handbook of climate change mitigation. Springer, New York
Moriarty P, Honnery D (2013) Greening passenger transport: a review. J Clean Prod 54:14–22
Moriarty P, Honnery D (2014) Future earth: declining energy use and economic output. Foresight 16(6):1–18
Newell RG, Pizer WA, Raimi D (2014) Carbon market lessons and global policy outlook. Science 343:1316–1317
Office for National Statistics (ONS) (UK) (2013) Household energy consumption in England and Wales, 2005–11. Accessed at http://www.ons.gov.uk/ons/dcp171766_321960.pdf
Office for National Statistics (ONS) (UK) (2014) Expenditure on household fuels 2002–2012. Accessed at http://www.ons.gov.uk/ons/rel/household-income/expenditure-on-household-fuels/2002—2012/sty-energy-expenditure.html
Pilkington B, Roach R, Perkins J (2011) Relative benefits of technology and occupant behaviour in moving towards a more energy efficient, sustainable housing paradigm. Energy Policy 39:4962–4970
Revesz RL, Howard PH, Arrow K et al (2014) Improve economic models of climate change. Nature 508:173–175
Royal Society (2009) Geoengineering the climate: science, governance and uncertainty. Royal Society, London
Starkey R (2012) Personal carbon trading: a critical survey. Part 1: equity. Ecol Econ 73:7–18
Statistics Bureau Japan (SBJ) (2014) Japan statistical yearbook 2014. Statistics Bureau, Tokyo, Available at http://www.stat.go.jp/english/data/nenkan/index.htm
Steemers K (2003) Energy and the city: density, buildings and transport. Energy Build 35:3–14
Steg L (2008) Promoting household energy conservation. Energy Policy 36:4449–4453
Stocker TF, Qin D, Plattner G-K et al (eds) (2013) Climate change 2013: the physical science basis. CUP, Cambridge, UK
Sunikka-Blank M, Galvin R (2012) Introducing the prebound effect: the gap between performance and actual energy consumption. Build Res Inf 40(3):260–273
Tabi A (2013) Does pro-environmental behaviour affect carbon emissions? Energy Policy 63:972–981
Tiefenbeck V, Staake T, Roth K et al (2013) For better or for worse? Empirical evidence of moral licensing in a behavioral energy conservation campaign. Energy Policy 57:160–171
Turaga RMR, Howarth RB, Borsuk ME (2010) Pro-environmental behavior: rational choice meets moral motivation. Ann N Y Acad Sci 1185:211–224
Van Vuuren DP, Edmonds J, Kainuma M et al (2011a) The representative concentration pathways: an overview. Clim Chang 109:5–31
Van Vuuren DP, Stehfest E, den Elzen MGJ et al (2011b) RCP2.6: exploring the possibility to keep global mean temperature increase below 2°C. Clim Chang 109:95–116

Wikipedia (2014) Climate change opinion by country. Accessed at http://en.wikipedia.org/wiki/Climate_change_opinion_by_country

World Bank (2014) GNI per capita, Atlas method (current US$). Available at http://data.worldbank.org/indicator/NY.GNP.PCAP.CD

Yang J, Wang Z, Kaloush KE (2013) Unintended consequences: a research synthesis examining the use of reflective pavements to mitigate the urban heat island effect. Arizona State University National Center of Excellence for SMART Innovations. Accessed at http://www.asphaltroads.org/assets/_control/content/files/unintended-consequences-1013.pdf

Bringing Global Climate Change Education to Middle School Classrooms: An Example from Alabama

Ming-Kuo Lee, Chandana Mitra, Amy Thomas, Tyaunnaka Lucy, Elizabeth Hickman, Jennifer Cox, and Chris Rodger

Contents

M.-K. Lee (✉) • C. Mitra
Department of Geology and Geography, Auburn University, Auburn, AL, USA
e-mail: leeming@auburn.edu; czm0033@auburn.edu

A. Thomas
Outreach Program, College of Sciences and Mathematics, Auburn University, Auburn, AL, USA
e-mail: alt0009@auburn.edu

T. Lucy • E. Hickman
Alabama Mathematics and Science Technology Initiative, Auburn University, Auburn, AL, USA
e-mail: tlk0006@auburn.edu; hickmep@auburn.edu

J. Cox
Alabama Science in Motion Program, Alabama State University, Montgomery, AL, USA
e-mail: jennifercox@alasu.edu

C. Rodger
Department of Mathematics and Statistics, Auburn University, Auburn, AL, USA
e-mail: rodgec1@auburn.edu

W.-Y. Chen et al. (eds.), *Handbook of Climate Change Mitigation and Adaptation*,
DOI 10.1007/978-3-319-14409-2_97

Abstract

A NASA-funded Innovations in Climate Education (NICE) Program has been launched in Alabama to improve high school and middle school education in climate change science. The overarching goal is to generate a better informed public that understands the consequences of climate change and can contribute to sound decision making on related issues. Inquiry-based NICE modules have been incorporated into the existing course of study for 9–12 grade biology, chemistry, and physics classes. New modules in three major content areas (earth and space science, environmental science, physical science) have been introduced to selected 6–8 grade science teachers in the summer of 2013 and 2014. The environmental science module allows students to explore the relationship between extreme climate events, water resources, and water pollution. In the earth science module, students investigate the effects of volcanic eruptions on Earth's atmospheric composition, global climate, and local landscape and water resources. The physical science module introduces students to the concept of urban climate and heating island effects. The NICE modules employ Roger Bybee's five E's of the learning cycle: engage, explore, explain, extend, and evaluate. Module learning activities include field data collection, laboratory measurements, and data visualization and interpretation. K-12 teachers are trained in the use of these modules for their classroom through unique partnership with Alabama Science in Motion (ASIM) and the Alabama Math Science Technology Initiative (AMSTI). Certified AMSTI teachers attend summer professional development workshops taught by ASIM and AMSTI specialists to learn to use NICE modules. Scientists are partnered with learning and teaching specialists and lead teachers to implement and test efficacy of instructional materials and models. This chapter serves as an example of how climate change education can be brought into K-12 schools.

Introduction

There is growing concern over the change that is occurring to Earth's climate and the impact it will have on the people, water resources, and ecosystems. Although the magnitude of climate change in the future is difficult to predict, there are likely to be effects on ecosystems and human systems such as agricultural, transportation, water supply, and health infrastructure – in ways people are only beginning to understand (International Panel on Climate Change 2007; National Academies 2008). These rapid changes make it less likely that human and natural systems will adapt. In order to deal with climate change impacts, greater efforts are needed toward educating the public about the science of climate change. The overarching goal is to improve the teaching and learning about global climate change through secondary education in a majority of high and middle schools in the state of Alabama, employing resources and data provided by NASA Innovations in Climate Education (NICE) Program.

In order to achieve this goal, new educational modules containing laboratory, field, and computer activities in targeted areas of global climate change education are developed. The main objective is to create modules that can be incorporated into the existing course of study for 6–12 grade science classes. Education modules used in high school classrooms were presented in the first edition of Handbook of Climate Change Mitigation (Lee et al. 2012). This paper presents the contents of new education modules developed for middle schools. High school and middle teachers are trained in the use of these modules for their classroom through partnership with Alabama Science in Motion (ASIM) and the Alabama Math Science Technology Initiative (AMSTI), respectively; both are administered by the Alabama State Department of Education. Specifically, the Alabama NICE program is designed to (1) improve understanding of climate change, enhance problem solving skills, generate greater interest in science, develop better informed persons capable of making decisions, and promote more interest in science, technology, engineering, and mathematics (STEM) careers among students; (2) enhance teachers' content knowledge of climate change and their ability to direct inquiry-based instruction and use of scientific data in the classroom; and (3) generate climate literacy, support for STEM education, climate conscious communities, and reduction in the carbon footprint among the diverse citizens of the state of Alabama.

Program Development and Implementation

Alabama Science in Motion Program

The NICE program is sustained through unique partnership with the Alabama Science in Motion (ASIM) and Alabama Math Science Technology Initiative (AMSTI) programs, which are funded by the Alabama State Department of Education. The program is free and allows all Alabama high and middle schools, no matter the size and location, to utilize the same high-tech, state-of-the-art laboratory and field equipment. In 1994 the governor of Alabama signed the Alabama Science in Motion program into legislation, and Alabama became the first state in the nation to institute a state-wide Science in Motion program. ASIM is administered by the Alabama Math Science Technology Initiative (AMSTI). In order for a school to be serviced by ASIM, they must be designated as an AMSTI school. This designation is given if all mathematics and science teachers and administrators come to 4 weeks of professional development training. At present over 40 % of the schools in the state are AMSTI schools. Of the current AMSTI schools, 80 % of the teachers attend a summer 2-week institute in biology, chemistry, or physics for years 1 and 2 of the program. The high school NICE modules are delivered in a separate four-day summer professional development workshop for teachers that have already received years 1 and 2 training. The NICE high school modules become the focal point for the professional development for all AMSTI teachers in grades 9–12 for ASIM year 3 and beyond training. The new NICE middle school modules were developed and delivered in the 2013 and 2014 professional development workshops for about

30 selected middle school teachers. The professional development workshops are delivered by ASIM and AMSTI specialists who are certified biology, chemistry, physics, and earth science teachers that serve their respective disciplines. This unique arrangement provides an equal opportunity for hands-on experimentation that many Alabama students would never experience. The program better prepares students for postsecondary education and recruitment into STEM disciplines.

Educational Modules

The NICE middle school education modules are developed by scientists in various content areas (e.g., earth and space science, environmental science, physical science) in conjunction with AMSTI specialists and lead teachers (Table 1). The modules employ Roger Bybee's (Bybee 1997) five E's of the learning cycle: engage, explore, explain, extend, and evaluate. The modules are aligned with the Alabama Course of Study, Alabama Graduation Examination, and National Learning Standards in Science, Geography, Technology, and Environmental Education (American Geographical Society 1994). Modules' learning activities include field data collection and laboratory measurements. Students employ remote sensing imagery and conduct

Table 1 Overview of NICE middle school educational modules

Science content areas	Main themes	Module activities
2.1. Earth and space science	Effects of volcanic activities on atmosphere and climate	2.1.1 Build a baking soda and vinegar volcano 2.1.2 Assess the reduction in light to Earth's surface using simple tools 2.1.3 Use graphic methods to explore impacts of volcanic eruption on climate
2.2 Hydrology–environmental science	Groundwater resource and climate change	2.2.1 Build an aquifer 2.2.2 Use the aquifer model to learn the basic vocabulary of groundwater and its hosting aquifers 2.2.3 Use the aquifer model to explore Earth's hydrologic cycle and impacts of climate change
2.3 Physical science	Urban heating island effects	2.3.1 Understand impacts of urbanization on local environment 2.3.2 Measure temperature and humidity to learn about pervious and impervious urban surfaces 2.3.3 Use remotely sensed images compare and contrast global cities 2.3.4 Watch a movie on renewable energy and analyze the pros and cons of adaptation and mitigation techniques for global climate change

hands-on laboratory experiments to investigate effects of global climate changes on physical environments and humans. NICE instructional materials include background content information (including an introductory Climate 101 Podcast), a detailed description of the specific exercise, pre-laboratory PowerPoint notes for teachers and students, pre- and post-laboratory test questions, and detailed procedures that utilizes the five E's of the learning cycle for each module. Climate 101 Podcast introduces teachers and students the basic key concepts and fundamental issues of global climate change. Students will leave the classroom with an understanding of the sources and impacts of climate change, the key national and international policies, and potential impact of climate change on human activity for many years to come. Currently, this climate change podcast is distributed as a DVD digital media file (including video and audio) via ASIM. The standards alignment (National Science Education Standards 1996) is articulated, and an equipment/materials list is generated, along with specific references. The modules enable students to gain hands-on experience in collecting and analyzing data, as well as to empower students and teachers to become more engaged in issues related to global climate change.

Earth and Space Science Module: Effects of Volcanic Activities on Atmosphere and Climate

Leading scientists: Ming-Kuo Lee

AMSTI specialist: Tyaunnaka Lucy, Jennifer Cox

Background. More than 50 volcanoes erupt each year worldwide and some of the catastrophic eruptions may change climate. For example, the 1991 eruption of Mt. Pinatubo in the Philippines blasted millions of tons of gases (e.g., sulfur dioxide) and solids (e.g., ash particles) into the atmosphere which circled the globe for weeks. These airborne-erupted materials (known as aerosols) may linger in the atmosphere for years before being flushed out by fluid motions (e.g., precipitation) in the atmosphere. These lingering aerosols can scatter the incoming solar radiation that reaches Earth's surface, resulting in lower temperature in the atmosphere. The sources of aerosols can be either natural (e.g., volcanic eruption) or anthropogenic (e.g., combustion of fossil fuels and biomass). A natural catastrophic volcanic eruption may cause a "measurable" change in Earth's climate on the timescale of several years (Russell et al. 1996). In addition to their effects on Earth's atmospheric composition and global climate, volcanic eruptions have effects in modifying the local landscape, weather, and water resources.

Learning goals and activities. Students learn (1) climate change can result from natural catastrophic events such as volcanic eruption and (2) understand the massive outpouring of gases and solids from volcanoes may increase the amount of aerosols in the atmosphere. In this activity students (1) build a baking soda and vinegar volcano, (2) assess the reduction in light to Earth's surface using simple tools, and (3) use simple graphing activities to illustrate climate impacts of volcanic eruption. This module is modified from a climate discovery educational module prepared by

the National Center for Atmospheric Research (NCAR) (http://eo.ucar.edu/educators/ClimateDiscovery/LIA_lesson8_9.28.05.pdf).

Engage. Students asked to read the following quote describing the conditions in Olongapo City, close to Mt. Pinatubo before and during its eruption in 1991.

> I was only 14 when it happened. But I remember that there was no sun for several days. The sky was either red or black. The ground was shaking all the time for days from the aftershocks. It was raining ashes and we had to wear a mask when we went outside. We also stayed inside the base for three days.

An image of the massive eruption of Mt. Pinatubo was provided (Fig. 1). Students brainstorm the changes in (1) the landscape near a volcano during and after an eruption and (2) in the atmosphere during and after an eruption. Students may be asked: What happens during a volcanic eruption and what materials are ejected from the volcano? What effects will the ejected materials have upon Earth's atmosphere? Students also make a list of potential changes for the landscape and water resources over time after a volcanic eruption. Teachers explain the eruption processes, materials ejected from volcanoes, and potential eruption impacts:

(a) The very hot magma (known as lava) leaves the magma chamber, forcing its way through the volcano and reaching Earth's surface. The lava flows down the sides of the volcano, cooling and solidifying over time, forming layers of ash and cinder along the cone. Some eruptions can be explosive, and ejected materials may include rock fragments (known as pyroclastic debris), ash (particles < 2 mm in diameter), and gas (H_2O, SO_2, and CO_2).

Fig. 1 An image of the massive eruption of Mt. Pinatubo on June 15, 1991 (From http://volcanoes.usgs.gov/hazards/gas/climate.php)

(b) The airborne-erupted materials (known as aerosols) may linger in the atmosphere for years before being flushed out by fluid motions like rain (e.g., precipitation) in the atmosphere. These lingering aerosols can scatter the incoming solar radiation that reaches Earth's surface, resulting in a lower temperature in the atmosphere. On the other hand, volcanic carbon dioxide, a known greenhouse gas, has the potential to promote global warming.
(c) Quick-moving lava (basaltic) with speeds up to 30 km/h can cover the land and create new rocks. The eruption of slow-moving lava (andesitic) forms a large mound (known as lava dome) above the vent. Explosive eruptions and accompanying earthquakes may trigger landslides. In cases where volcanoes are covered with snow and ice, water can mix with ash to form a mudflow called a lahar, which moves down the slope very quickly at speeds up to 50 km/h. The most common type of water contamination results from ash fall and causes a change in turbidity, acidity (pH), and toxic metals. Ash can clog streams and cause the turbidity (cloudiness of water caused by suspended solids) of water to rise and the pH of water to fall. Finer ash is able to carry more toxic metals and contaminate local water supply.

Explore

1. Students build a baking soda and vinegar volcano using the following steps:
   (a) First make the "cone" of volcano using model clay or dough. Make their own dough by mixing flour, cooking oil, and water. The dough should be smooth and firm. Mold the dough around the soda bottle into a volcano shape. Do not cover the hole or drop dough into it.
   (b) Mix vinegar (or warm water) with a pack of powdered drink mix.
   (c) Fill the bottle to about ¾ of its capacity with warm water.
   (d) Add 6–7 drops of detergent to the bottle contents. The detergent helps trap the bubbles produced by the reaction.
   (e) Add three tablespoons of baking soda to the liquid.
   (f) Slowly pour vinegar into the bottle until it starts to bubble and watch for the eruption (Fig. 2).
   (g) Recharge the volcano by adding more baking soda and vinegar.
2. Students assess the reduction of solar energy reaching Earth's surface following a volcanic eruption. Students use an infrared digital thermometer (i.e., an IR gun) to measure the temperature of a white surface exposed to direct sunlight. They then measure the temperature of a white surface in the shadow of Sun. Students compare and note the change in surface temperature. The white surface represents the surface of the Earth and sunlight obstruction represents the dust layer produced by a volcanic eruption that blocks incoming light.
3. Students explore the effects of a large eruption on the atmosphere and Earth's surface temperature. The illustrations of the Sun with different brightness (known as illumination) shown below reflect the amount of ashes and debris in the atmosphere. Students use a pocket light meter to measure how much illumination is spread over a given area in the illustration with maximum light (before

Fig. 2 AMSTI teachers built a baking soda and vinegar volcano

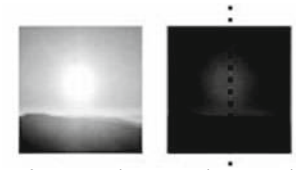

Before eruption During eruption

Measured illumination (in lux)		
Measured illumination (in fc)		

Fig. 3 Difference in the illustration with maximum light (before eruption) and minimum light (during eruption)

eruption) and minimum light (during eruption) (Fig. 3). The unit for illumination can be expressed either as lux (lumen per square meter) or foot-candle (fc, in lumen per square foot) (1 fc = 10.764 lx). Students draw two curves (amount of debris vs. time and temperature vs. time) in a diagram (Fig. 4) that demonstrates the impacts of volcanic eruption on atmosphere and Earth's surface temperature.

Explain. Students are asked to answer the following questions after the experiments:

(a) What type of gas is produced by mixing baking soda and vinegar? Will this gas be produced in real volcanoes? Is this gas considered a greenhouse gas?
(b) What are the temperatures of the white surface exposed to direct sunlight and those in the shadow of Sun? After a massive volcanic eruption, the airborne-erupted materials (known as aerosols) may linger in the atmosphere for years.

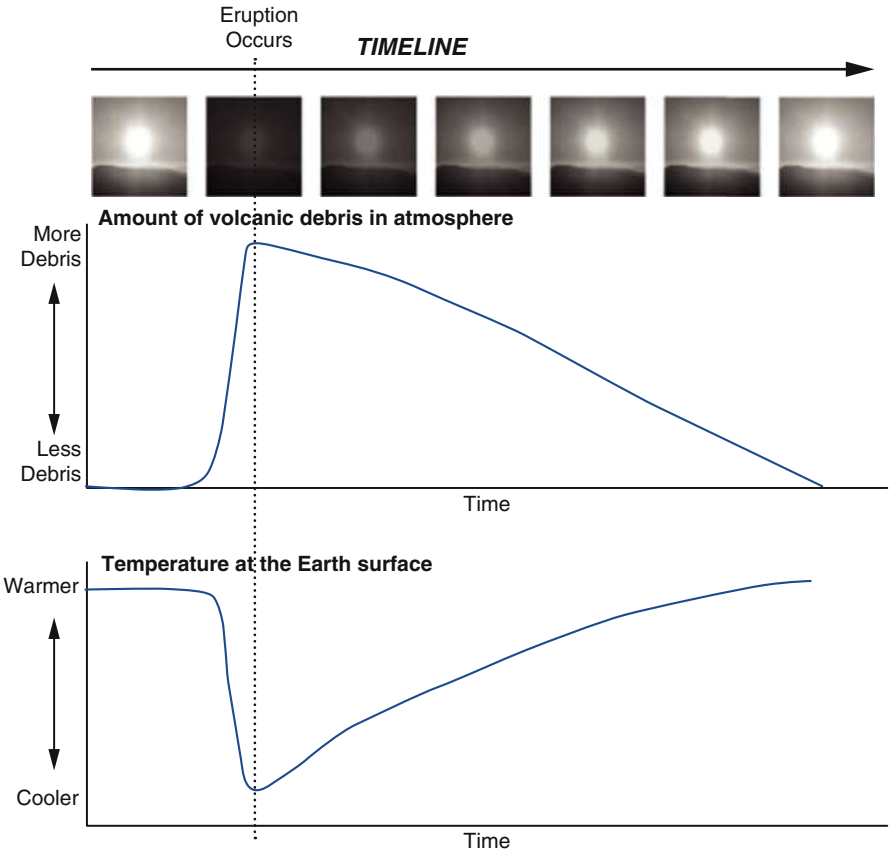

Fig. 4 The illustration of Sun before, during, and after a volcanic eruption

How do aerosols affect the incoming solar energy? How would Earth's surface temperature change (cooling or warming) in the years after a massive volcanic eruption?

(c) Use the illustrations of the Sun to answer the following questions:
- How does the relative amount of ash in the atmosphere change over time before, during, and after eruption?
- How will the amount of volcanic ash (and the change in ash through time) affect temperature on Earth's surface?
- Explain the correlation between the amount of ash and atmosphere temperature.

Extend. Students investigate what Earth's (geological) tectonic processes may cause volcanic eruption and where the active volcanoes are often located on Earth's surface. Students conduct research on selected supervolcanoes (e.g., Yellowstone) whose eruption in the past or modern time might dramatically affect Earth's atmosphere and climate.

Evaluation. Evaluations of student performance are based on (1) students' answers to pre-lab questions, (2) students' graphs (debris vs. time and temperature vs. time), (3) students' explanations on results, and (4) students' report on extension activities.

Equipment/materials needed. An infrared digital thermometer, an Extech light meter, man-made volcano ingredients (warm water, liquid dishwashing detergent, baking soda, vinegar, food coloring, or powdered drink mix).

Hydrology and Environmental Science Module: Groundwater Resource and Climate Change

Lead scientist: Ming-Kuo Lee

AMSTI specialists: Jennifer Cox, Tyaunnaka Lucy

Background. There is growing concern over the impacts of climate change on people and their water resources (Shat 2005; Foster 2006).Because of climate change, extremes in climate such as droughts and floods are likely to become more severe and more common (IPCC 2007, 2012; Karl et al. 2008). An increase in precipitation would lead to increases in surface runoff, sediment yields, nutrient loading, and release of human pollutants. An extended period of drought will lead to shortages of water and food supplies. Climate change can affect every component of our global freshwater budget, including precipitation, evaporation, groundwater, and surface stream flow and runoff (Chang and Jung 2010; Lee et al. 2013). Among various water resources, groundwater is the world's largest storage of clean freshwater. Groundwater is also the primary source of drinking water to nearly half of the world's population (Moench 2005) and the dominant source of water for irrigation and industrial activities. Future changes in climate and precipitation patterns will intensify pressure upon groundwater resources to meet the rapidly growing, global demand for freshwater.

Learning goals and activities. This module introduces students to the basic vocabulary used to describe groundwater and its hosting aquifers. Key terms (italicized) include *precipitation, surface runoff*, *water table*, *unsaturated zone, saturated zone, well casing,* and *well screen*. Students will build an aquifer to learn the fundamentals of Earth's hydrologic cycle, such as *recharge* and *discharge*, and the effects of rain, drought, and pumping on water table. After these activities students will better understand aquifers and the relationship between climate, water resources, and water pollution.

Engage. PowerPoint notes on basic groundwater and aquifer vocabulary, hydrologic cycles, and effects of climate change on water resources are presented to students by the teacher. Students then fill in the word boxes in the groundwater chart (Fig. 5), which show various components of the hydrologic cycle and a groundwater aquifer.

After learning the basic vocabulary and concepts, students build their own aquifer models (Fig. 6) using an aquifer kit provided by the NICE project team. Students follow the following steps: (1) Insert rubber stop into the drainage hole of the 1.5-gal

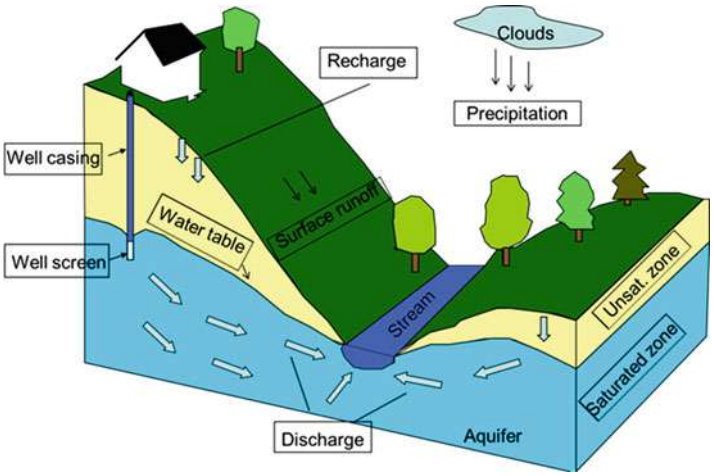

Fig. 5 A chart showing groundwater aquifer and hydrologic cycle

Fig. 6 ASMTI teachers built an aquifer tank model to demonstrate groundwater flow and contamination. Water can be added to simulate recharge or pumped out to simulate drought and overuse

tank; (2) slope a layer of gravel in the tank, with the lowest ground near the drainage hole; (3) insert a 1-in diameter well (a PVC pipe with holes drilled to serve as well screen) near the higher ground close to the side of the tank, with screen tapping the bottom gravel layer; (4) create a river by placing a clear plastic liner (with holes punched in the bottom) near the low ground; (5) lower a spray pump with plastic tubing to the screen interval in the PVC pipe; and (6) create a lake near high ground by patting down a thin layer of clay on a small circular depression.

Exploration

(a) Students simulate a precipitation event by slowly pouring water on ground surface using a cup with holes punched in the bottom. Some of the rain runs off on the surface into the river. Some of the rain moves down through the sediments and begins to fill up the aquifer (a process known as *recharge*). Students can see a river in the depression (discharge area) is fed directly by surface runoff and also by groundwater moving through the aquifer (a process known as *discharge*).
(b) Students mark the initial water table, saturated zone, and unsaturated zone (before the water table reaches the riverbed) using a water-soluble marker. They add more water and observe how the water table responds to rainfall. Students then use a spray pump (represents a municipal well) to withdraw groundwater from the aquifer. They observe how the water table declines in response to pumping. Groundwater cannot be withdrawn when the water table drops below the well screen interval.
(c) Students will slowly pour water into the lake underlain by clay, sand, and gravel. Students will compare the permeability of gravel, sand, and clay.
(d) Students simulate groundwater contamination by slowing pouring colored water (use food coloring or dye) on the ground near the water well, or students can spread colored powder (Kool-Aid) on the ground surface and then slowly pour water on the powder. Students observe how the contaminant reaches the groundwater and water well. Students will withdraw contaminated groundwater from the well using the pump.

Explain. Students are asked to answer the following questions after the experiments:

(a) Why some rainwater does not simply disappear on the surface while other rainwater quickly percolates through the ground? Are all the rock layers equally permeable?
(b) What happens to an aquifer when it rains? What happens to an aquifer when its groundwater is continuously withdrawn during a drought?
(c) Explain the concept of groundwater safety yield. What happens when the water table drops below the well screen?
(d) Explain why the safety and effectiveness of a water well depends upon its *siting*.
(e) Explain why a well needs to be properly sealed (known as well closure) when it is.
(f) List potential groundwater contaminants.

Extend. Students explore the concepts of the porosity of different geologic materials (i.e., clay, sand, and gravel) using the fluid saturation methods*. Students will find out which material is very porous (with pore spaces to store water) and permeable (allow fast water movement) and can make a productive aquifer for water supply. Contaminants must be removed from groundwater before it reaches

municipal water systems. Students will search and write a report on state-of-the-art groundwater remediation methods (i.e., remove contaminants by physical, chemical, and biological methods such as pump-and-treat, oxidation/reduction, and bioremediation). Information on specific groundwater cleanup technologies organized by type and contaminants can be found on the US Environmental Protection Agency (USEPA) website:

http://www.epa.gov/superfund/remedytech/remed.htm.

**Fluid saturation method can be used to measure the porosity. A clean and dried sample is weighted, saturated with a liquid of known density, and then reweighed. The weight change divided by the density of the fluid results is the pore volume. The volume of dried sample can be estimated using a beaker. Porosity is calculated as the ratio of fluid pore volume and volume of bulk sample.*

Example. The following procedure can be run to obtain pore and bulk volume of a sample and porosity using water with a density of 1 gm/cc. (1 cc = 1 mL):

1. *Weight of clean, dry sand:* $W_{dry} = 115$ *gms.*
2. *Bulk volume of clean, dry sand:* $V_b = 100$ cc (cc = cubic centimeters).
3. *Weight of sand saturated with liquid* $W_{\text{sat}} = 135$ gms ($\rho_w = 1$ gm/cc).
4. *Calculate the pore volume of fluid* $V_p = \frac{W_{\text{sat}} - W_{\text{dry}}}{\rho_w} = \frac{13\text{S} - 11\text{S}}{1} = 20$ cc.
5. *Porosity* $= \frac{V_p}{V_b} = \frac{20}{100} = 20\%$.

Evaluation. Evaluations of student performance are based on (1) students' aquifer model, (2) students' explanations of key terms and demonstration on aquifer model, and (3) students' report on extension activities.

Teachers use the following score sheet to evaluate students' work:

Aquifer Score Sheet

Students' Names: _____

Concept	Explain/ define	Demo/point out	Total
Groundwater recharge from precipitation	1	1. Recharge to groundwater	
Groundwater recharge from surface water	2	1. Existence of surface water 2. Recharge to groundwater	
Groundwater discharge to river	1	1. Water flow in river	
Water table	1	1. Point out the water table	
Saturated zone	1	1. Point out the saturated zone	
Unsaturated zone	1	1. Point out the unsaturated zone	
Permeability	1	1. Show permeability in 2 different materials	
Impact of a well has on groundwater	2	1. Water is withdrawn from well 2. Water level is lowered	
Groundwater contamination	1	1. Contamination is shown in groundwater	

(*continued*)

Concept	Explain/ define	Demo/point out	Total
Importance of well siting (location)	1	1. Location of wells to source of pollution	
Importance of well closure	1	1. Place cap on well	
Groundwater as part of hydrologic cycle	1	1. Connection among reservoirs	

Equipment/materials needed. 1.5-gal aquarium tank, gravels, sands, clays, one PVC pipe (1 in in diameter and 8 in long) with holes drilled to serve as the screen interval, PVC pipe cap, spray pump with plastic tubing, water-soluble marker, rain maker (plastic cup with holes in bottom), clear plastic liner (river), flashlight (to look down the well), food coloring, beakers, rubber stop, syringe (to drain water).

Physical Sciences Module: Urban Heating Island Effects

Lead Scientist: Chandana Mitra

AMSTI Specialist: Tyaunnaka Lucy

Background. Rapid urbanization has led to an increase in built-up area and impervious surfaces, increased greenhouse gas emissions, and more anthropogenic activities which are detrimental to the delicate yet complex environmental climate system of the Earth (IPCC 2007, 2012). Considered to be a cumulative effect of all these impacts is the urban heat island (UHI), defined as the difference of temperature between urban and surrounding rural areas. The urban heat island is a distinct "warm island" among the "cool sea" (Pérez and Peña 2010) which is graphically shown in Fig. 7. In countries like the USA, heat is the primary weather-related cause of death, and therefore, promotion of strategies for mitigating the UHI is a big concern for government agencies. There are two main UHI reduction strategies: first, to replace the black asphalt roofs with white-colored roofs and, second, to transform the concrete roofs to green roofs by planting grass and plants on them (Solecki et al. 2005). Overall the UHI can be mitigated by growing urban forests and parks and using more of renewable energy like solar and wind power instead of energy produced by fossil fuels. This would make the cities more sustainable and livable in future.

Learning goals and activities. This module introduces the basic knowledge about urbanization and what the impacts of rapid urbanization are on our environment. At the end of this activity, the students will understand how changing local environmental conditions like population increase, the materials you use on buildings, cars you drive, and the lifestyle you lead can affect city temperatures and create an urban heat bubble, also known as urban heat island. The students will be using infrared thermometers and hygrometers to measure the differences in temperature and moisture for different materials. They will also watch a movie that will give them an insight into the various renewable forms of energy which could be a solution to future climate change.

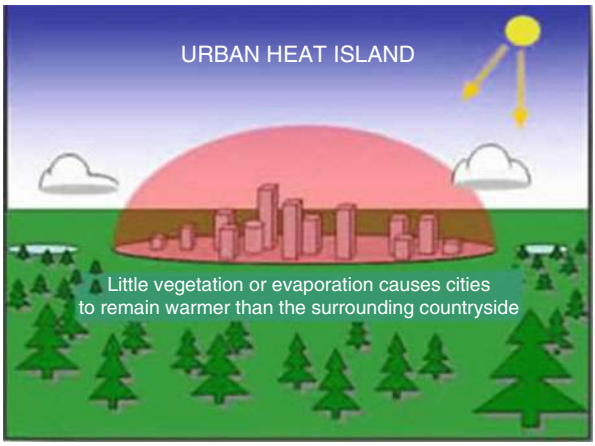

Fig. 7 Urban heat island source: http://www.nctcog.org/trans/sustdev/SDGreen/UrbHeatIsl.asp

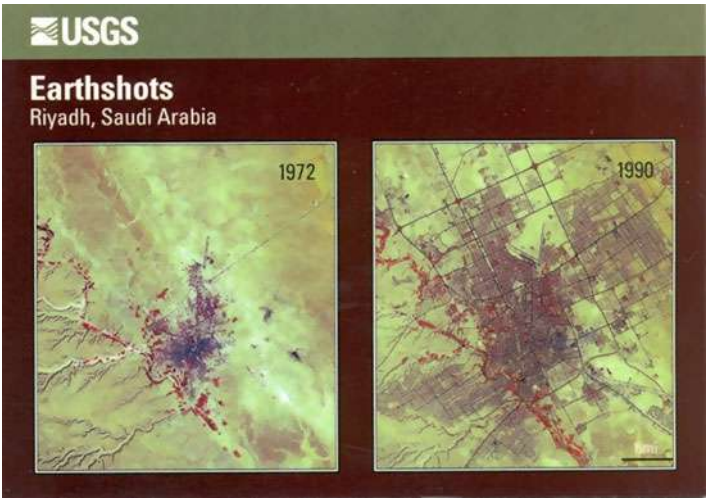

Fig. 8 Growth of Riyadh, Saudi Arabia (Source: USGS)

Engage. PowerPoint notes on urbanization, urbanization impact on climate change, permeable and impermeable surfaces, albedo, urban heat island, adaptation and mitigation techniques, and renewable energy will be provided.

To further engage the students, they will use tracing papers and the given Google and USGS images (http://earthshots.usgs.gov/earthshots/about#ad-image-0). With the help of the tracing papers, they will try to determine and see for themselves how cities are growing worldwide. A number of images downloaded from Earthshots–USGS will be provided, for example, Riyadh in Saudi Arabia (Fig. 8), Sydney in Australia (international), and Atlanta in the USA. This will give them an idea of the impact of uncontrollable city growth over short period of time and relate to the discussion earlier on impacts of population increase on environment.

The students will also be asked questions to engage them in a discussion involving their visit to Atlanta GA, did they see parks in Atlanta downtown, how much of Atlanta downtown is green, and what happens when a lot of people come and settle in a city. Besides these they will also be asked about the surface (green grass or concrete) they would like to walk on a hot afternoon, why people living in deserts wear white long robes, what happens when you burn coal, and whether they have heard about wind and Sun's energy usage. In this module Atlanta is the city of focus but the teacher can choose any big city which the students are familiar with. That will give the students a sense of involvement.

After learning the basic concepts and discussing the urbanization issues, students will use the instruments to measure temperature and humidity of various surfaces provided in the "urban heat island" kit by the NICE project team.

Exploration

(a) Option 1: Students will use infrared thermometers and hygrometers to measure the temperature of black and white surfaces and moisture level over a cemented concrete surface and a grass surface (Fig. 9). They will write their readings in the table provided below (can increase the rows if they feel like measuring more surfaces made of various materials). The students will calculate the differences and then discuss the reason why there is a difference in the temperatures. They will then relate the surface measurement differences to an urban environment. The teacher will help the students here by citing examples of heat absorption by black cars, white cars, desert people wearing long white robes, and black solar panels (example will be provided in the PowerPoint).

IR thermometer reading	Temperature (°C)	Temperature (°F)
White surface (roof if possible/white board) exposed to direct sunlight		
Dark black surface (roof if possible/black board) in direct sunlight		
Surface of black car		
Surface of white car		
Grass surface		
Concrete surface		
Hygrometer reading	Relative humidity (%)	
Concrete surface in direct sunlight		
Grass space in direct sunlight		
Concrete surface under shade of tree		
Green space under shade of tree		

Option 2: If the teacher wants, then he/she can make the students do a day-long study taking measurements every hour or every 2 h, documenting the temperature for different materials. They can prepare trend lines using graph papers (temperature and humidity variations vs. type of surface) to show how the

Fig. 9 AMSTI middle school teachers using IR thermometers to measure temperature of black cars and hygrometer to measure humidity of green grass

temperature varies depending on material in an urban environment. The teacher will help the students to relate the trend lines with urbanization and discuss the benefits of having white roof over black roofs and green space and urban parks over all impervious surfaces.

(b) The teacher will show in class the movie "Carbon Nation" (a movie on renewable energy) as a part of exploration. This movie is 84 min long which is one of the best climate change solution movies. The movie does not directly deal with the subject of climate change but focused mainly on using renewable energy which will help mitigate some of the effects of climate change and make our Earth a better place to live in.

Explain

(a) Why do you think dark roofs are hotter than white roofs? How does albedo help in reducing white roof temperatures?
(b) What are the problems of having dark roof?
(c) Do you think having green parks, green roofs, and green walls will help lessen the effect of UHI?
(d) The more concrete we have in our cities, the chances of having more urban flooding will increase – is this true? (The teacher will ask the students to relate this to the "Aquifer module" and make them relate urban flooding with impermeable surface and surface runoff.)
(e) Students will take notes while watching the movie "Carbon Nation" on the different types of renewable energy and what the benefits of each are. Is it possible to replace nonrenewable energy with renewable energy? Students will discuss the long-term and short-term benefits of using renewable energy.

Extend

(a) The students will use various methods (pictures and articles from magazines, journals, newspapers, Internet sources) to prepare charts and collages on the

things they learned during lab. They can work in groups. They will learn about each renewable energy, their limitations and examples from different parts of the world; try to find out if anywhere in their area solar power is harnessed; learn about electric cars and if they are better; and the gases that cause global warming and why they are increasing in the atmosphere.

(b) Students will investigate what would happen if there is an increase in heat in urban areas, discuss in class about ways in which population can be attracted away from cities to suburban areas, and conduct research on the growth of various cities in the USA and worldwide to see how cities are growing and at what rate.

(c) Another extension would be to talk to their neighbors and educate them on roof color and material and write a report on what feedback they received. The students can work in groups for this.

(d) Ask the students to find out if the city nearby or the city in which they live has a Climate Action Plan. They should search on the net cities which have implemented the maximum UHI mitigation techniques (Portland, Chicago, New York City, State of California).

Evaluation. Evaluations of student performance are based on (a) students' answers to questions based on PowerPoint notes, (b) their understanding of temperature and humidity differences and their effects on urban–rural climate patterns based on responses in class, (c) students' graphs (temperature and humidity variations vs. type of surface), (d) students' explanations of results and answer to the explain section, and (e) students' report on extension activities.

Equipment/materials needed. Overhead projector, an infrared digital thermometer, hygrometer, Google and USGS images showing growth of cities, tracing paper, reading material (urban heat island, city growth over time, adaptation and mitigation techniques to reduce urban heat island effect, renewable energy), two cardboard sheets (black and white) to represent different colored roofs.

Program Dissemination

Several methods of dissemination have been employed. Results of outreach activities and education materials were divulged through publications, conferences, and education symposium. Education modules used in high school classrooms and their evaluations were presented in the first edition of Handbook of Climate Change Mitigation (Lee et al. 2012). This paper presents the contents of new education modules developed for middle schools. Moreover, more than 10 papers have been presented at national conferences hosted by the American Geophysical Union, Geological Society of America, America View Fall technical meeting, and American Meteorological Society. Last, the College of Sciences and Mathematics hosted a climate change education symposium to educate faculty, graduate students, and undergraduate students on the interdisciplinary interface of sciences and mathematics. A forum "Frontiers in Global Climate Change" was held in the spring semester

of 2012. The leadership team served as the coordinating committee for the symposium. The keynote address was delivered in a fashion so that individuals not engaged in specifics of climate change research can become more informed. This forum enabled the leadership team to continue to meet and to refine background understanding regarding NICE education. In addition, it provided the leadership team with specific training in topics relevant to NICE. The symposium was advertised on-campus and to neighboring institutions in the region, which includes two historically Black colleges and universities: Alabama State and Tuskegee University. Media coverage was requested as well through Auburn University Office of Marketing and Communications.

Conclusions

Successful implementation of NICE education modules should enable significant advances in high school climate change science education. New resources including instruction materials for teachers and students have been developed in forms of laboratory handouts, database, laboratory kits, and multimedia products (podcast, movie, and PowerPoint files). The modules use new technology or innovative tools including computer software, web-based data search and visualization, and scientific data collections using sensors. The instruction materials are aligned with state and national academic standards, and teacher professional development program is implemented through partnership with ASIM and AMSTI programs. The overall teacher satisfaction from the teacher training was 4.88/5.00. The overall conclusion from the pre–post attitude assessment was the teachers came to the workshop interested in learning more about global climate change and were aware that it is an environmental concern that needs more public attention. While they also believe the government should be involved and NICE should be a national priority, they are not sure how at this point in time. After completing the module teacher training, the teachers reported a strong agreement that the content developed in the modules of this project for teaching global climate change concepts should be included in the Alabama secondary curriculum. At the culmination of the project, the team and AMSTI director will convene a final project meeting to disseminate the final evaluation results and plan for sustained delivery of NICE modules by AMSTI personnel.

A preliminary conclusion of this project is that high and middle schools can effectively partner with universities to offer students a meaningful and enriching science experience that increases their understanding of the concepts of Earth's system and climate change, and underscores the need to take action. Such a project can give these students access to expertise and equipment, thereby strengthening the connections between the universities, state education administrators, and the community. This project can serve as an example for improving K-12 school education in climate change science around the world to raise public awareness and perception.

Acknowledgments This project was supported by a grant from NASA NICE Program (NN09AL73G; Principal Investigator: Chris Rodger) and funding from the Alabama Science in Motion (ASIM) and Alabama Math Science Technology Initiative (AMSTI). We thank Mr. Matthew Williams (Office of Sustainability, Auburn University) for preparing a global climate change podcast as part of the instructional materials. We also thank America View, consortium of remote sensing scientists to expertise on satellite images.

References

American Geographical Society, Association of American Geographers, National Council for Geography Education, and National Geographic Society (1994) Geography for life national geography standards. National Geographic Research and Exploration, Washington, DC

Bybee RW (1997) Achieving scientific literacy: from purposes to practices. Heinemann Publisher, Portsmouth

Chang H, Jung I-W (2010) Spatial and temporal changes in runoff caused by climate change in a complex large river basin in Oregon. J Hydrol 388:186–207

Foster S (2006) Groundwater; sustainability issues and governance needs. Episodes 29:238–243

International Panel on Climate Change (2007) Climate change 2007: the physical science basis. Contribution of working group I to the fourth assessment report of the Intergovernmental Panel on Climate Change. Cambridge University Press, Cambridge, UK/New York

IPCC (2007) Climate change 2007: the physical science basis. In: Solomon SD, Qin M, Manning M, Marquis K, Averyt MMB, Tignor HL, Miller HL Jr, Chen Z (eds) Contribution of working group 1 to the fourth assessment report of the intergovernmental panel on climate change. Cambridge University Press, New York

IPCC (2012) In: Field CB, Barros V, Stocker TF, Qin D, Dokken DJ, Ebi KL, Mastrandrea MD, Mach KJ, Plattner GK, Allen SK, Tignor M, Midgley PM (eds) Managing the risks of extreme events and disasters to advance climate change adaptation. A special report of working groups I and II of the intergovernmental panel on climate change. Cambridge University Press, Cambridge, UK/New York, 582 pp

Karl RT, Meehl GA, Miller CD, Hassol SJ, Waple AM, Murray WL (eds) (2008) Weather and climate extremes in a changing climate. Regions of focus: North America, Hawaii, Caribbean, and U.S. Pacific Islands. U.S. Climate Change Science Program Synthesis and Assessment Product 3.3, 180 pp

Lee M-K, Marllin S, Fielman K, Marzen L, Lin Y, Birkhead R, Miller C, Norgaard P, Obley M, Cox J, Steltenpohl L, Wheeles E, Wooten M, Rodger C (2012) Bring global climate change education to Alabama Classroom. In: Handbook for climate change mitigation. Springer, New York, pp 1983–2028

Lee M-K, Natter M, Keevan J, Guerra K, Saunders JA, Uddin A, Humayun M, Wang Y, Keimowitz AR (2013) Assessing effects of climate change on biogeochemical cycling of trace metals in alluvial and coastal watersheds. Br J Environ Clim Change 3:44–66

Moench M (2005) Groundwater; the challenge of monitoring and management. In: World's Water, 2004–2005, P. Gleick, ed., Island Press, Washington DC, pp. 79–100

National Academies Report (2008) Understanding and responding to climate change. Highlights of the National Academies Reports. the National Academies, Washington, DC

National Science Education Standards (1996) National Research Council. National Academy Press, Washington, DC

Pérez AC, Peña MA (2010) The urban heat islands (UHI). http://www.urbanheatislands.com/. Last accessed on 16 Oct 2014

Russell PB, Livingston JM, Pueschel RF, Bauman JJ, Pollack JB, Brooks SL, Hamill P, Thomason LW, Stowe LL, Deshler T, Dutton EG, Bergstrom RW (1996) Global to microscale evolution of the Pinatubo volcanic aerosol derived from diverse measurements and analyses. J Geophys Res 101:18745–18763

Shat T (2005) Groundwater and human development; challenges and opportunities in livelihoods and environment. Water Sci Technol 51:27–37

Solecki WD, Rosenzweig C, Parshall L, Pope G, Clark M, Cox J, Wiencke M (2005) Mitigation of the heat island effect in urban New Jersey. Global Environ Change B Environ Hazards 6:39–49

Climate Change: Outreaching to School Students and Teachers

Dudley E. Shallcross, Timothy G. Harrison, Alison C. Rivett, and Jauyah Tuah

Contents

D.E. Shallcross (✉) • T.G. Harrison • A.C. Rivett
Bristol ChemLabS, School of Chemistry, University of Bristol, Bristol, UK
e-mail: d.e.shallcross@bris.ac.uk; t.g.harrison@bristol.ac.uk; ar9518@bristol.ac.uk

J. Tuah
Secretariat of Brunei Darussalam Technical and Vocational Education Council, Permanent Secretary Office (Higher Education), Ministry of Education, Bandar Seri Begawan, Brunei Darussalam
e-mail: jauyah.tuah@moe.edu.bn

W.-Y. Chen et al. (eds.), *Handbook of Climate Change Mitigation and Adaptation*,
DOI 10.1007/978-3-319-14409-2_53

Abstract

This chapter will describe some simple models that have been used to explain the basic principles of the Earth's climate to primary school students (aged 4–11), secondary school students (aged 11–16), post-16 students (16–19), and the general public (all ages) including those with disabilities. It will then describe a range of hands-on practical activities that demonstrate aspects of the climate system at the appropriate level. Assessment and impact of these activities on the learner's level of cognition are then presented showing that the hands-on approach is a most effective way of communicating such concepts irrespective of the age of the learner. Furthermore, the varied impacts of a "lecture demonstration," that is, a talk where points are illustrated by exemplar experiments that visually portray the science concept, are presented.

The many misconceptions that surround the understanding of the Earth's climate system and how teachers and other science communicators can deal with such issues in a classroom setting are discussed. The sourcing and use of the myriad datasets linked with the Earth's climate that are freely available for schools' projects are discussed with illustrations drawn from projects undertaken already.

Often the impact of such engagement activities on the provider themselves is ignored; here the tangible benefits to all providers involved are discussed with some case studies as illustrations.

Finally, the future prospect for the Earth's climate is nearly always portrayed as negative. In this chapter, the idea of stabilization wedges and ways that the worst-case scenarios for climate change can be averted is discussed. Using a variety of metrics, it is possible for a wide range of learners to appreciate the impact of any mitigation strategy, that is, literally "speaking in a language they can understand."

Introduction

The Need for Education in Climate Science

It is essential that teachers are armed with the correct (factual) information about the Earth's climate system, so that they can educate the next generation of students. It goes without saying that such education is essential so that these students can make informed decisions about their response to potential climate change. In the UK, climate chemistry is now included in many science courses that are taken by 16-year-old students, toward the end of compulsory education. Further work on climate change is part of advanced-level (A-level) chemistry and other courses that are taken by preuniversity students. Many of these courses have associated textbooks which do not go into sufficient depth to answer some of the questions that arise. More confusion results from incorrect information from a number of sources including the press, the Internet, and teachers that are not sufficiently knowledgeable about the topic (see section "Some Misconceptions Concerning Climate Change and Greenhouse Gases").

A fundamental problem is that a basic explanation of the Earth system and the need for naturally occurring greenhouse gases and their impact is often muddled.

The Research Councils UK (RCUK) (2002) was anxious that high-quality teacher training on the Earth's climate, and several other topics, was put in place by the creation of a daylong course to be hosted by the Science Learning Centres and run by experts in the field (Science Learning Centres 2004). The RCUK is split into seven sub-councils (arts and humanities, biosciences, engineering and physical science, economics and social science, medical, natural environment, and the science and technology facilities) and administers funding for research in the UK of around £2 billion a year in these areas. The Science Learning Centres were originally a network of nine regional centers and one national center, which provide continuing professional development for both primary and secondary teachers in the UK. These have recently contracted to five regional centers and the National Science Learning Centre in York. Therefore, in the UK, such a partnership was very potent in terms of its ability to bring expert researcher and teacher together. These courses are not compulsory for teachers to attend, and although feedback is very good, it will take a long time for the material to be disseminated from teacher to teacher. It is hoped

that one consequence of this chapter would be that it is of assistance to teachers and other educators looking to improve their understanding of climate science.

The Granny Model: Basic Concepts

Figure 1 introduces the Granny model; it consists of a heater and a very sensible Granny (grandmother). She wants to keep warm but knows that if she sits too far away from the heater, she will be cold and if she sits too close to the heater, she will be too warm. So she places her seat a sensible distance away from the heater so that she is neither too hot nor too cold, but just the right temperature (sometimes this is known as the Goldilocks hypothesis). The Granny represents the Earth and the heater is the Sun. It turns out that the Earth is just the right distance away from the Sun for the average surface temperature to be about 10 °C, based on simple heat flux arguments (see section "The Granny Model: The Underpinning Mathematics"), and this qualitative explanation works well at KS3 (Key Stage 3, 11–14-year-olds in the UK). There is a problem with this simple model, in terms of the Earth system, illustrated by Fig. 2. Clouds in the sky and ice at the Earth's surface act as mirrors and reflect back to space about 30 % of the energy arriving from the Sun. It turns out that about 6 % is reflected by ice at the surface and 24 % from the atmosphere (mostly by clouds), and this reflectivity (30 %) is known as the Earth's albedo, A (where $A = 0.3$). Other surfaces on the Earth are reflective but nowhere near as much as ice (see Table 1).

Figure 3 shows how this new feature can be incorporated into our Granny model. If it is imagined that Granny's pet dog has sat in front of the fire, it will block some of the heat from the heater reaching Granny. In the Earth system, the presence of clouds

Fig. 1 The Granny model, part 1. Mean temperature of the Earth is around 10 °C

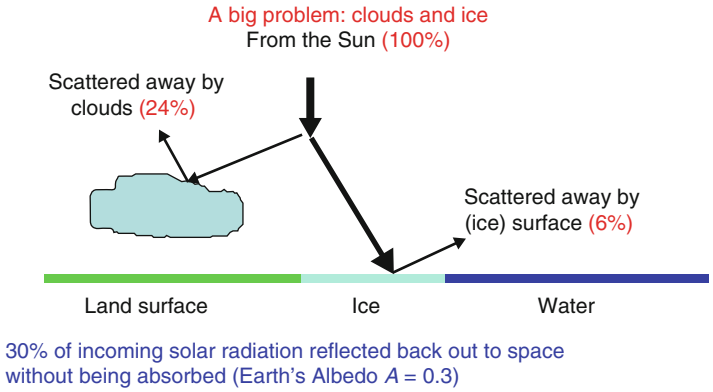

Fig. 2 A problem with the Granny model, part 1

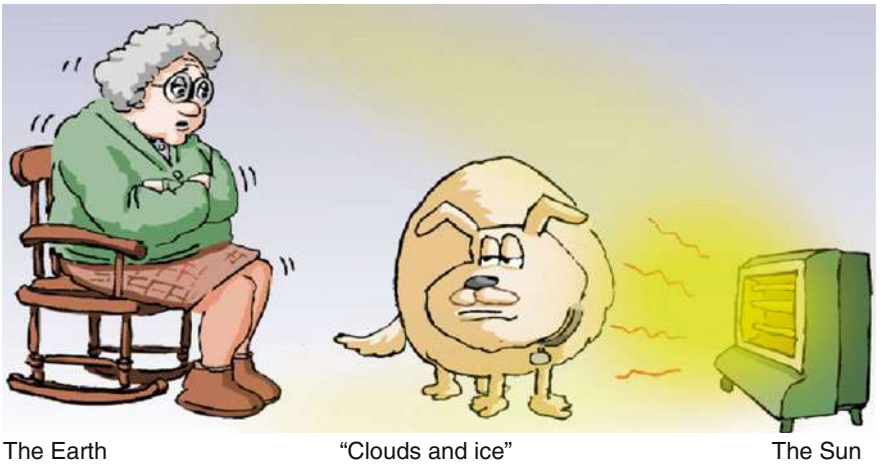

Fig. 3 The Granny model, part 2 (with clouds and ice). With clouds and ice mean temperature of the Earth ∼−18 °C

Table 1 Reflectivity of different types of surface with respect to incoming solar radiation

Surface type	Reflectivity (%)
Fresh snow	90–95
Dry sand	35–45
Grass-type vegetation	15–25
Needleleaf coniferous forest	10–20
Broadleaf deciduous forest	5–10

and ice would reduce the average surface temperature of the Earth to −18 °C, very cold indeed, making the Earth uninhabitable. The average surface temperature of the Earth is much hotter, so there must be a compensatory mechanism. What could the Granny do? She could move the pet out of the way (water is essential to the Earth, and one would not want to remove clouds and ice – even if they could be removed). She could move closer to the heater (although the Earth's orbit fluctuates, it cannot move close enough to the Sun to compensate; in any case, there are issues to do with evaporation of water and the formation of more cloud!). Finally, she could stay where she was and put on a blanket. The final option is what the Earth does; it puts on a blanket (greenhouse gases) to compensate for the loss of heat caused by clouds and ice.

For Fig. 4, the audience is asked to imagine that they are in space looking at the Earth and observing the heat being released from the surface of the Earth (in the infrared region). The figure clearly shows that not all of that heat escapes to space but that some is trapped by greenhouse gases in the atmosphere, such as carbon dioxide, ozone, and methane (CO_2, O_3, and CH_4), and that these act as a blanket around the Earth (or around the Granny).

Figure 5 now completes the Granny model where she has a blanket to offset the heat lost. The combination of these two effects (the Earth's albedo leading to cooling and the greenhouse gases leading to a warming) cancels out, ending up with an average surface temperature of about 16 °C. Hence, greenhouse gases are essential to

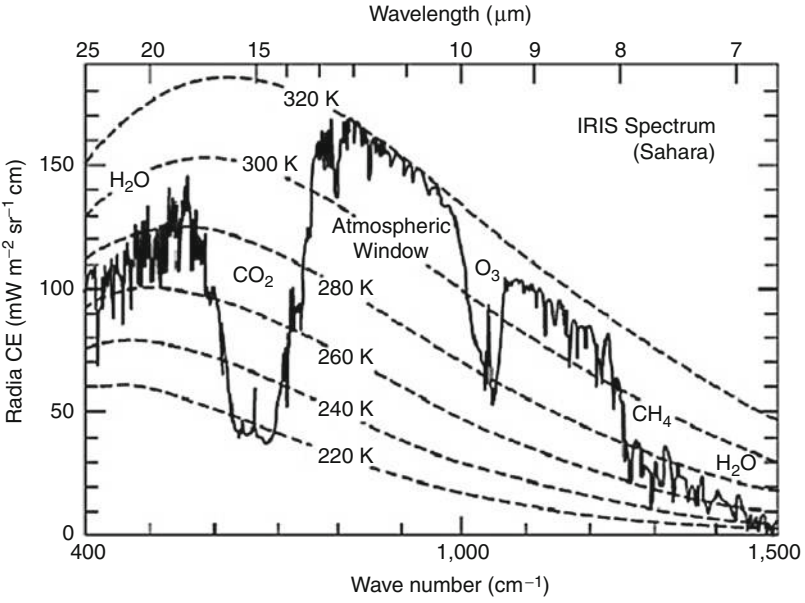

Fig. 4 Spectrum showing the outgoing infrared radiation from the Earth and the parts of the spectrum that are absorbed by greenhouse gases in the Earth's atmosphere

Fig. 5 Granny model, part 3 (clouds, ice, and greenhouse gases). With clouds and ice and greenhouse gases, the mean temperature of the Earth ~16 °C

the Earth system. A PowerPoint of this model is available for download from the Bristol ChemLabS outreach website at http://www.chemlabs.bristol.ac.uk/outreach/resources/Atmos.html.

The Granny Model: The Underpinning Mathematics

A First Attempt to Model the Climate

The simplest model of the climate is one where incoming solar energy and outgoing terrestrial energy emitted from the planet are equal, that is, an "energy in equals energy out" model or a balanced flux model. Throughout this section, it refers to energy; however, tacitly this means energy flux, that is, energy per second. It is known from measurements that the energy from the Sun reaching the top of the atmosphere, termed the solar constant S, is 1,370 W m^{-2}. If it is assumed that the radius of a perfectly spherical Earth is R_E, it can be seen that the Earth absorbs solar radiation over an area πR_E^2 (i.e., a flat disk of atmosphere) but emits energy from an area $4\pi R^2{}_E$ (i.e., from the entire surface), as illustrated in Fig. 6a, b. If an energy analysis is now carried out and it is assumed that energy in and energy out are the same, it is possible to arrive at the following:

$$\text{Energy in} = \text{Eneregy out} \tag{1}$$

$$\begin{aligned}&\text{Energy per unit area per unit time} \times \text{total area (disc)}\\ &= \text{Energy per unit area} \times \text{total surface area (sphere)}\end{aligned} \tag{2}$$

$$1370 \times \pi R_E^2 = \sigma T_E^4 \times 4\pi R_E^2 \tag{3}$$

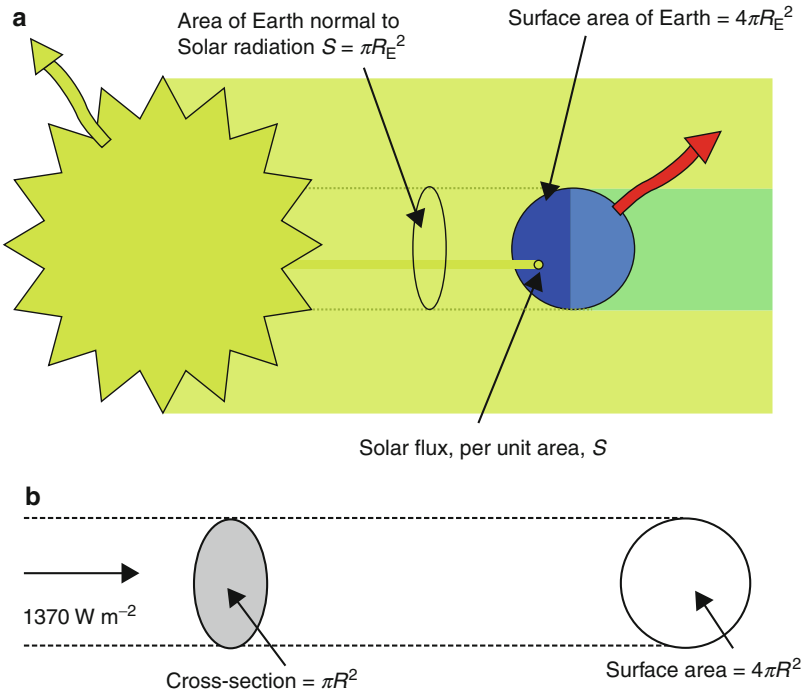

Fig. 6 (**a**) A schematic of a balanced flux model for the Earth. (**b**) A simplified version of the schematic of a balanced flux model for the Earth

Rearranging Eq. 3 yields an expression for the surface temperature of the Earth:

$$T_E^2 = \frac{1370}{4 \times 5.67 \times 10^{-8}} \tag{4}$$

$$T_E = 279 \text{ K} (6^\circ\text{C}) \tag{5}$$

First, it should be noted that the σT_E^4 comes from the Stefan-Boltzmann law. All bodies radiate energy as electromagnetic radiation. A blackbody absorbs all radiation falling on it and emits that radiation as a function of its surface temperature, where that flux of energy radiated is equal to σT^4; here σ is the Stefan-Boltzmann constant, 5.67×10^{-8} W m^{-2} K^{-4}, and T is the surface temperature of the body in Kelvin.

Second, a first glance at the result in Eq. 5 looks like a sensible figure for the average surface temperature of the Earth, maybe a little too cold. The problem with this very simple model is that some energy is reflected back out to space by clouds and ice without being absorbed. Approximately 24 % of the incoming energy is reflected by clouds, and another 6 % is reflected by the surface, for example, ice. This gives a total albedo (A) for the Earth of 30 % or 0.3. Therefore, the left-hand side of Eq. 4 must now be rewritten as $0.7 \times 1{,}370 \times \pi R_E^2$, and the calculation of T_E becomes

$$T_E^4 = \frac{1370 \times 0.7}{4 \times 5.67 \times 10^{-8}} \tag{6}$$

$$T_E = 255 \text{ K}(-18^\circ\text{C}) \tag{7}$$

This new value for the average surface temperature in Eq. 8 is obviously far too low and leads naturally to the question: "Why is the Earth so warm?" In order to answer this question, a slightly more complex model is needed.

A One-Layer Atmosphere Model

If it is assumed that the atmosphere is made up of a single layer of miscible gases, a more accurate model can be constructed that can be used by students using a spreadsheet. In this model, allowances are made for absorption by the atmosphere of the incoming visible light from the Sun and absorption of the outgoing infrared light emitted from the Earth.

Figure 7 summarizes the elements of the model. F_S is the solar constant divided by 4; hence, the incoming energy from the Sun is $F_S(1 - A)$, where A is the albedo, that is, removing that portion reflected back to space. This incoming energy is in the UV and visible region. τVIS is the fraction of this incoming energy that is transmitted through the atmosphere, that is, if the atmosphere absorbs it, all τVIS is zero, if the atmosphere absorbs none of it, τVIS is equal to 1. Hence, the energy reaching the surface of the planet is $F_S(1 - A) \times \tau$VIS. The Earth will act as a blackbody and will emit the energy denoted as F_g, from the surface of the Earth. This terrestrial radiation is centered in the infrared region of the spectrum. τIR is the fraction of infrared energy transmitted through the atmosphere, being zero if the atmosphere absorbs all of it and unity if the atmosphere absorbs none of it. Certain gases in the atmosphere do indeed absorb the infrared energy (greenhouse gases), and so outgoing energy is $F_g \times \tau$IR.

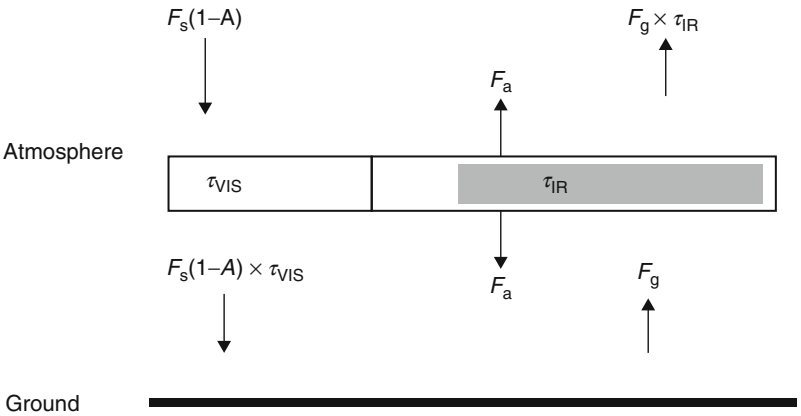

Fig. 7 Schematic of a one-layer atmosphere

Assuming that the energy from the atmosphere is denoted as F_a and that the energy in and out at the surface of the Earth and the top of the atmosphere are both balanced, then:

At the surface of the Earth,

$$F_S(1-A)\tau\text{VIS} + F_a = F_g \tag{8}$$

And at the top of the atmosphere,

$$F_g\tau\text{IR} + F_a = F_S(1-A) \tag{9}$$

Combining Eqs. 8 and 9,

$$F_g = \frac{F_S(1-A)(1+\tau\text{VIS})}{(1+\tau\text{IR})} \tag{10}$$

Finally, noting the Stefan-Boltzmann law once again, F_g can be expressed as

$$F_g = \sigma T_E^4 = \frac{F_S(1-A)(1+\tau\text{VIS})}{(1+\tau\text{IR})} \tag{11}$$

Equation 11 can be rearranged to make T_E the subject:

$$T_E = \left[\frac{F_S(1-A)(1+\tau\text{VIS})}{\sigma(1+\tau\text{IR})}\right]^{0.25} \tag{12}$$

Assuming that $F_S = 342.5$ W m^{-2} (solar constant divided by 4) and that τVIS $= 0.8$ and τIR $= 0.1$, then $T_E = 288.5$ K (15.5 °C). It is Eq. 12 that can be put into a package such as Microsoft Excel so that students may see the effects of changes in global temperature when parameters are changed.

A One-Layer Atmosphere Model Simulation

Further example output is shown in Table 2. In experiment 1, it is assumed that the atmosphere does not absorb any of the incoming or outgoing energy fluxes and the albedo is 0.3, giving a temperature of 254 K. If there are no clouds or ice ($A = 0.0$), the Earth then warms up in experiment 2–278 K, showing the importance of albedo. From experiment 2–3, the atmosphere now absorbs all the outgoing infrared radiation, and the Earth warms to 330 K. If clouds and ice are now introduced in experiment 4, the temperature drops to 302 K. These four factors, F_S, A, τVIS, and τIR, play a vital role in determining the surface temperature of the Earth, and students can investigate this for themselves. These models have been very popular with teachers and their students at secondary school in the UK and are beginning to be used in other countries.

Table 2 Output from the one-layer atmosphere model

Experiment				
Variables	1	2	3	4
FS/W m^{-2}	342.5	342.5	342.5	342.5
A	0.3	0.0	0.0	0.3
τVIS	1.0	1.0	1.0	1.0
τIR	1.0	1.0	0.0	0.0
T_E/K	254	278	330	302
T_E/°C	−19	5	57	29

Typical questions that could be asked that would require the students to use this model are:

1. Which of the variables has the greatest effect on average global temperature?

This is a somewhat open-ended question; one would first assume that the solar constant is the most important. However, if A approaches 1, that is, the Earth's surface becomes very reflective, covered in ice like the snowball Earth (see section "A One-Layer Atmosphere Model: Taking the Investigation Much Further"), then the temperature plummets.

2. What would happen to the surface temperature if the ice caps melted?

This question is asking the student to reduce A by approximately 6 %. It is quite surprising how much the temperature rises with modest reductions to the Earth's albedo.

3. If the average distance from the Earth to the Sun was increased by 1 % of the current value, what would the temperature be assuming albedo is 0.3, τIR = 0.3, and τVIS = 0.6?

This question opens up the importance of the solar constant and how small fluctuations in the Sun's energy (e.g., solar flares or sunspots) can affect surface temperature. Indeed, students can explore what would happen to the Earth's surface temperature if the Earth moved closer to the Sun or further away from it. As a simple approximation, one can assume that the Sun's energy is evenly spread over the surface of a sphere. Therefore, for simplicity it can be stated that the solar constant scales with $1/R^2$, so the solar constant $S = 1{,}370/R^2$, where $R = 1$ is defined as the distance from the Sun to the Earth at present. Therefore, if the distance from the Sun to the Earth is halved (just a bit further than Mercury is from the Sun), the solar constant increases by a factor of 4, and if the distance from the Sun to the Earth is quintupled (increased by a factor of 5 bringing the Earth slightly closer to the Sun than Jupiter), then S is reduced by a factor of 25 (see section "A One-Layer Atmosphere Model: Taking the Investigation Much Further").

Of course, far more challenging questions could be asked, for example:

1. The sand in the Sahara desert can be made into a glass mirror. If a perfectly reflecting mirror is put at the Earth's surface in the Sahara desert, it could reflect back incoming solar radiation and cool the planet.
2. How big would the mirror have to be in order to cool the planet by 1 °C?
3. What fraction of the Sahara desert would that be?

A One-Layer Atmosphere Model: Taking the Investigation Much Further

The one-layer atmosphere model opens us the possibility to investigate a myriad of interesting and more complex systems, and some of these are given here and tie in very well with current topics being presented at school level.

Surface Temperatures on Other Planets

The one-layer atmosphere model can be used to estimate the surface temperature on other planets. For simplicity, in the first instance, it can be assumed that the planet's atmosphere does not interact with energy entering or leaving the planet (τVIS and τIR are equal to 1) and that the planet's albedo is zero (nonreflecting). Using the approximation developed in question 3 from the previous section, $S(R) = 1{,}370/R^2$, it is then possible to work out the temperatures. Data for the relative distances are collected in Table 3, and from this an estimate of the surface temperature of each planet is then given and compared with actual measurements. It should be noted that these actual measurements are averages and should not be taken as the exact number.

Table 3 Estimates of the surface temperature of other planets in the solar system using the one-layer atmosphere model

Planet	D, Distance to Sun/millions of miles	D/D_{Earth}	S W m^{-2}	T K	T °C	T actual[a] °C
Mercury	36	0.4	8,562	441	168	167
Venus	67	0.7	2,796	333	60	457
Earth	93	1.0	1,370	278	5	10
Mars	142	1.5	609	228	−45	−46
Jupiter	484	5.2	51	122	−151	−153
Saturn	891	9.6	15	90	−183	−184
Uranus	1,790	19.2	4	65	−208	−197
Neptune	2,800	30.1	1.5	51	−222	−223

[a]Actual temperatures are taken fromhttp://wiki.answers.com/Q/What_is_the_surface_temperature_on_the_planets and http://theanswermachine.tripod.com/id2.html. Accessed 31 Aug 2010). Note that $S = 1{,}370/(D/D_{\text{Earth}})^2$ and $T = \{S/(4\sigma)\}^{0.25}$ (in Kelvin)

However, the first point is that the agreement is stunning apart from one planet, Venus. The surface temperature of Venus is much hotter than predicted. Why is this? It turns out that a runaway greenhouse effect has taken place and not even decreasing τIR to zero can reproduce the very hot temperature experienced (further modifications are required). The atmosphere of Venus is around 96 % CO_2, and the subsequent trapping of infrared radiation has caused the planet to experience much higher surface temperatures than predicted simply by its distance from the Sun.

Snowball Earth

Through geological evidence, it has been proposed that some 650 million years ago, the Earth was nearly completely covered in ice (see Hoffman et al. 1998). Such a snowball Earth is believed to have preceded the Cambrian explosion of life on Earth. Evidence for this comes from the fact that there are glacial deposits near the equator, and magnetic measurements also support this. In order for there to be glacial deposits in the tropics, there needs to be ice. Using the one-layer model, it is possible to investigate what would happen to surface temperature as the albedo (or amount of ice) increases. Taking τVIS and τIR to be equal to 1 for simplicity, it is then possible to calculate the effect on temperature as A is increased, that is, $A = 0$, $T = 278$ K, $A = 0.5$, $T = 234$ K, $A = 0.75$, $T = 197$ K, $A = 0.9$, and $T = 156$ K. It soon emerges that the model diverges from linearity and as A approaches zero the temperature plummets. To raise the temperature again, it is believed that greenhouse gases (CO_2 and CH_4) eventually rose to a level where the temperature started to rise again and ice melted causing a feedback on warming.

Global Dimming

It is a well-known phenomenon that one of the reasons that the Earth's surface temperature has not increased over the last 50 years as dramatically as originally predicted, even though greenhouse gas levels have increased significantly, is because of a process known as global dimming. In the process of burning fossil fuels, particulate matter is also released as well as water. It has been shown that the energy from the Sun reaching the Earth's surface has decreased since the 1950s by around 5 % (see Wild et al. 2005) and is believed to be caused by the addition of particles that increase the albedo of the Earth. The one-layer model can be used to investigate this impact by increasing the albedo (similar to snowball Earth in fact) of the Earth, where increasing A from 0.3 to 0.31, for example, cools the surface temperature by 1 °C, in keeping with the global dimming hypothesis. Indeed, the role of aerosols and volcanic eruptions (which inject sulfur-rich species into the atmosphere and lead to more cloud cover) can all be investigated using this model, all leading to a cooling.

Stratospheric Ozone Depletion and Climate Change

A topic that is often confused is the relationship between stratospheric ozone and climate. Ozone (O_3) is formed in the stratosphere, a region of the atmosphere between about 10 and 50 km in altitude. Its location arises because of the balance between the need for high-energy photons of light (UVC radiation) found in greater abundance the higher in altitude one goes and high pressures which decrease dramatically with increasing altitude. The reactions governing the formation of ozone are those derived by Chapman in the 1930s and are known as the Chapman mechanism and are summarized in reactions (Eqs. 13, 14, 15, and 16).

$$O_2 + h\nu \rightarrow O + O \sim 200 \text{ nm} \tag{13}$$

$$O + O_2 + M \rightarrow O_3 + M \tag{14}$$

$$O_3 + h\nu \rightarrow O + O_2 \sim 250 \text{ nm} \tag{15}$$

$$O + O_3 \rightarrow O_2 + O_2 \tag{16}$$

O_2 absorbs a photon of vacuum UV light (around 200 nm) and dissociates to form two O atoms in reaction (Eq. 13). The O atoms can add to O_2 in the atmosphere to form O_3, ozone, but need to have a relatively high pressure, denoted by M, so that the newly formed molecule can be stabilized. Since Eq. 13 is most efficient at the top of the atmosphere and Eq. 14 is most efficient at the bottom of the atmosphere, it is not surprising that somewhere in the middle the amount of ozone made is at a maximum, hence the location of the stratosphere. Ozone itself absorbs high-energy vacuum UV (around 250 nm), shown in reaction (Eq. 15). There are two important consequences of the ozone layer in the stratosphere. First, between O_2 and O_3, they filter out all the UVC radiation (200–280 nm) from the atmosphere which would cause life on the surface of the Earth to be severely compromised if it were not removed. Second, reaction (Eq. 15) gives out a lot of heat; hence, the stratosphere is a warm layer relative to the top of the troposphere (the layer of the atmosphere from 0 to 10 km approximately). This warm layer moderates the weather in the layer below and has other beneficial dynamical effects. The τVIS term relates directly to the absorption of the Sun's energy by O_3 and O_2. The one-layer model shows what would happen to the surface temperature if there was no ozone layer (e.g., $A = 0$, $\tau\text{VIS} = 1$, and $\tau\text{IR} = 1$) returning a value for $T = 278$ K, with an ozone layer ($A = 0$, $\tau\text{VIS} = 0.8$, and $\tau\text{IR} = 1$) $T = 271$ K, that is, a cooling of about 7 K or 7 °C.

Taking this further, it was discovered by Nobel Prize winner Paul Crutzen and others in the 1970s that the natural catalytic cycles reduce the amount of ozone in the stratosphere. These cycles arise from H_2O, CH_4, and N_2O being present in the atmosphere through natural cycles. If there was more ozone, that is, no natural removal processes, then $\tau\text{VIS} = 0.7$ may be a more reasonable number ($T = 267$ K), and the drop in surface temperature would be an additional 4 °C. Some may suggest that such a warming caused by gases released by biological processes occurring at the Earth's surface proposes a Gaia-type link, yet another interesting avenue for class discussion.

The destruction of stratospheric ozone will, of course, increase τVIS from 0.8 toward 1.0 and will lead to a warming of the surface. However, ozone is itself a greenhouse gas, and so by removing it, the amount of τIR transmitted would increase, that is, a cooling. So there is now an interesting balance to investigate, but this is not the end of the story. The species that have been responsible for polar stratospheric ozone depletion, the chlorofluorocarbons (CFCs) such as $CFCl_3$ and CF_2Cl_2, are also greenhouse gases (reducing τIR). So ozone is removed, which both cools and warms the planet, and in addition, the CFCs also warm the planet. These CFCs are in fact very potent greenhouse gases and absorb IR in the region known as the atmospheric window (see Fig. 4), a region of the spectrum where IR largely escapes to space.

Milankovitch Cycles and Ice Ages

Over the last 450,000 years, the Earth's climate has undergone four ice ages (glacial periods) where temperatures have been about 10 °C colder than they are today. During the ice age, large parts of the Earth were covered in ice. At the end of every ice age, there is a sudden rise in temperature (scientists are still trying to understand exactly why), and the Earth goes into a period known as an interglacial. This cycle of glacial and interglacial occurs on a timescale of about 100,000 years. Figure 8 shows this variation in temperature and comes from ice core data taken from Antarctica. What causes ice ages?

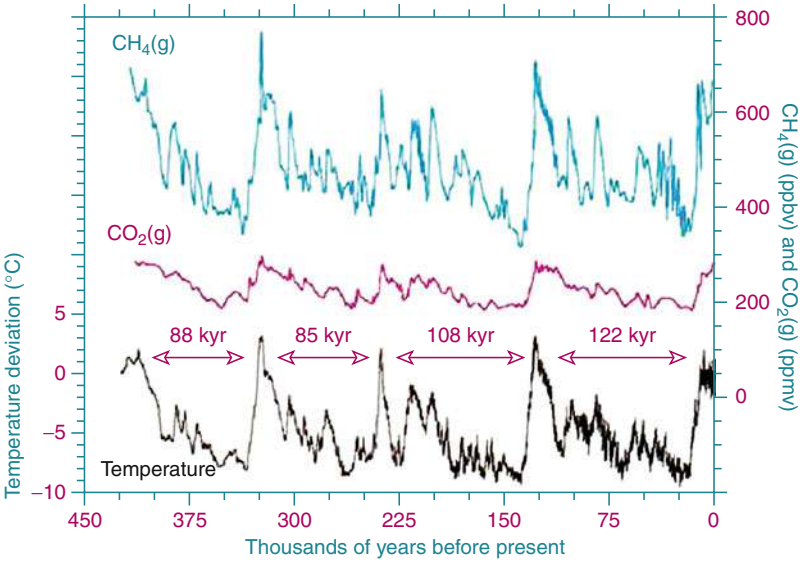

Fig. 8 Data taken from the Vostok ice core showing the changes in surface temperature and levels of CO_2 and CH_4 over the last 450,000 years

Milankovitch Cycles

Climate shifts correspond to three cycles related to Earth's orbit around the Sun that affect the intensity of solar heating (heat from the Sun). The discovery of these cycles is attributed to Milutin Milankovitch. These shifts are caused by gravitational attraction between the planets (mainly Jupiter) and Earth.

Eccentricity of Earth's orbit (see Fig. 9a) varies from nearly circular to elliptical. At low-eccentricity orbits, the average Earth-Sun distance is less, but when the Earth is in a more elliptical phase, the Earth-Sun distance is greater, and the heat from the Sun per unit area is less and leads to the onset of an ice age. This can be modeled by reducing S as the Earth-Sun distance increases. The timescale of this is about 100,000 years.

Axial tilt or obliquity of the Earth's axis of rotation (see Fig. 9b) changes from about 22° (currently 23.5°) to 24.5° and has a timescale of about 41,000 years. As the tilt increases, it changes the heat that reaches various parts of the Earth's surface.

Precession (wobble) changes the quantity of incident radiation (heating) arriving at each latitude during a season and has a timescale of about 22,000 years. These orbital cycles explain qualitatively why the Earth experiences ice ages (glacials) and interglacials. In Fig. 8, it can also be seen that two important greenhouse gases in the atmosphere, CO_2 and CH_4, also rise and fall with temperature. The reason for their fall as the Earth enters an ice age is because the surface of the Earth is being covered in more ice and this reduces the flux of CH_4 to the atmosphere from natural systems such as wetlands and animals and CO_2 from respiration. Using the one-layer model and increasing A (more ice) and increasing τIR (decreasing levels of greenhouse gases) from a base case will lead to a cooling, in agreement with observations. Therefore, past climates can also be investigated and explained by this model.

Present-Day Climate

There are many diagrams on the Internet and elsewhere that show how the surface temperature of the Earth has changed over the last 200 years. One thing is clear: Figure 8 shows that over the last 450,000 years, the level of CO_2 varied between about 170 and 280 ppm; today the level is around 400 ppm. Also during this period, CH_4 varied between about 350 and 700 ppb and is now around 1,750 ppb. Such a rise over the last 200 years has been conclusively shown to be due to the burning of fossil fuels. Evidence for this is interpreted from the carbon isotope ratio present in the sample. The one-layer model would suggest that such a rise in greenhouse gas levels should lead to a rise of about 1–3 °C in temperature. Part of the reason why the rise has not been on the high side is due to global dimming, mentioned earlier (see section "Stratospheric Ozone Depletion and Climate Change"). The point is that there should be no debate about warming due to increased levels of greenhouse gases; the debate should be how large the increase will be and how quickly it takes place. Data from present-day studies will be discussed in section "Impact and Assessment."

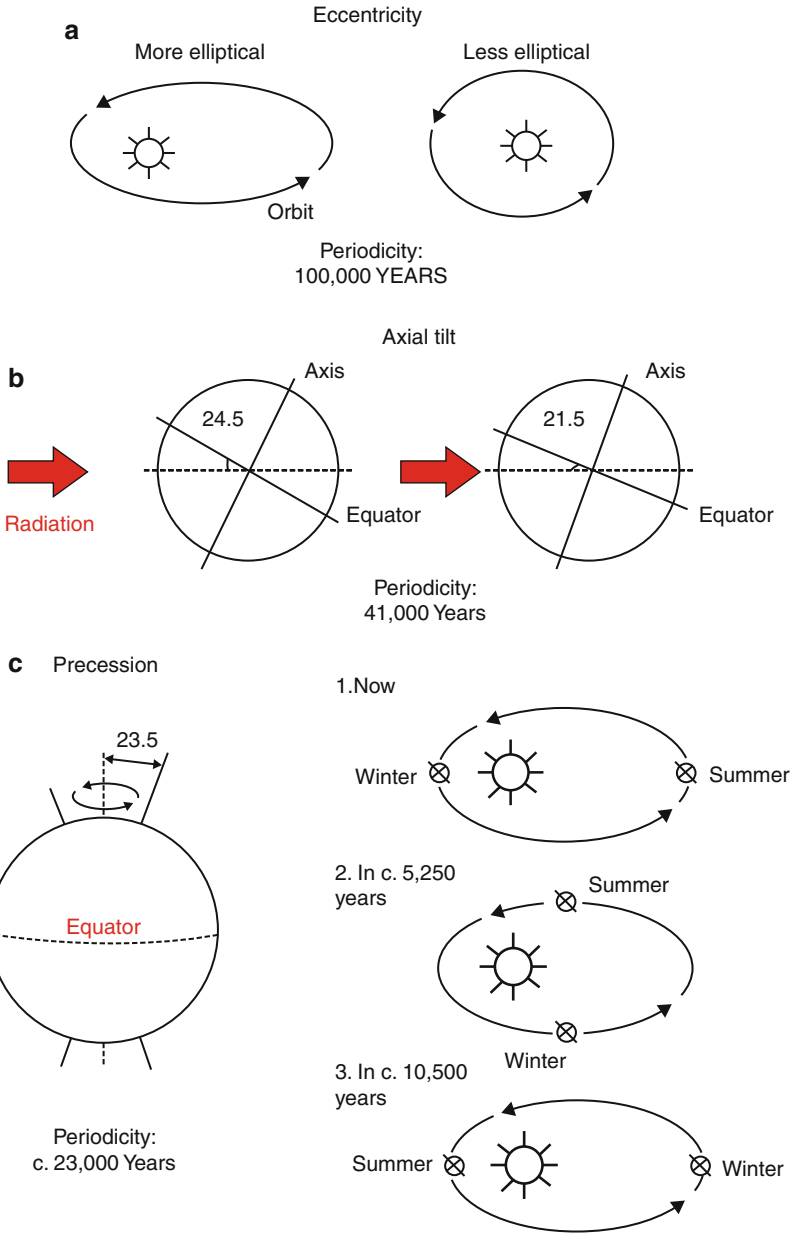

Fig. 9 (**a**) Eccentricity of the Earth's orbit around the Sun has a period of ca. 100,000 years. (**b**) Axial tilt of the Earth relative to the Sun has a period of ca. 41,000 years. (**c**) Precession of the Earth has a period of ca. 23,000 years

A Simple Mathematical Model That Can Be Used to Predict the Atmospheric Level of Greenhouse Chemicals Given Their Lifetime and Emission Rate

The following mathematical model should allow more able students and their teachers to make some more advanced predictions on the levels of greenhouse chemicals as a function of time given their emission rate and lifetime. Many scenarios can be explored to determine emission levels required to achieve a variety of equilibrium concentrations.

There is myriad of "greenhouse gases" in the Earth's atmosphere, i.e., many species can absorb infrared radiation over the wavelengths being emitted by the Earth. The most well known are CO_2, CH_4, and N_2O, but chlorofluorocarbons (CFCs), hydrochlorofluorocarbons (HCFCs), and in particular the hydrofluorocarbons (HFCs) also play a role. A fundamental concept in atmospheric science that is required is the *budget* of a compound. Put simply we consider the sources of the compound and the loss processes ("sinks") for the compound. If the *sources* and *sinks of a compound* balance, it will lead to a constant concentration being observed in the atmosphere. If sources are greater than sinks, then the concentration of that compound in the atmosphere will increase with time and vice versa. However, can we be more quantitative? If the budget is balanced, what will the constant concentration be and what controls this parameter? It turns out (see appendix for derivation) that the concentration of a compound A at time t, $[A]_t$, is

$$[A]_t = E/R\left(1 - \exp(-Rt)\right) \tag{17}$$

where E is the source or emission rate and R is the loss rate (units s^{-1}). We can use the concept of lifetime τ, which is simply the reciprocal of R (1/R), to rewrite Eq. 17:

$$[A]_t = \tau E(1 - \exp(-t/\tau)) \tag{18}$$

When sufficient time has elapsed, i.e., when an equilibrium has been established, a constant concentration of A, $[A]_{constant}$, is reached and is equal to E/R or τE. If the emission rate E increases, a new $[A]_{constant}$ is established which is bigger than before; if the emission rate decreases, the new $[A]_{constant}$ is now smaller. If R, the loss rate, increases, $[A]_{constant}$ decreases. If the loss rate decreases, $[A]_{constant}$ increases. Hence, the concentration of any compound, whether it is carbon dioxide, ozone, methane, nitrogen oxides, chlorofluorocarbons, etc., in the atmosphere is determined simply by E and R or E and τ. The overall impact will be a sum of the individual compound impacts.

Using the main greenhouse gas carbon dioxide (CO_2) as an example, we can imagine that there are natural processes, not involving human (anthropogenic) activity, releasing carbon dioxide (CO_2) into the atmosphere (respiration, aerobic decomposition of organic materials, natural forest fires, volcanic activity) and that

that CO_2 is taken up by plants via photosynthesis and in the oceans first as dissolution and then into the lengthier precipitation processes to form carbonate rock. This natural system leads to an equilibrium, and at that point the level of CO_2 is equal to a baseline concentration, $[CO_2]_{baseline}$. If there is now a constant emission of CO_2 arising from human activity (E_{human}), it will lead eventually to a new, higher-level $[CO_2]_{perturbed}$ which is larger than the baseline. This new-level $[CO_2]_{perturbed}$ is equal to

$$[CO_2]_{perturbed} = [CO_2]_{baseline} + E\tau \tag{19}$$

Current data, based on measurements in ice cores of trapped air deposited with preindustrial levels (before 1800) of CO_2, show that $[CO_2]_{baseline}$ ~280 ppm and that human activity is releasing about 8 ppm per year of CO_2 into the atmosphere (6.5 ppm due to fossil fuel combustion and cement production, etc., and 1.5 ppm through deforestation) and that about half of this stays in the atmosphere (the rest taken up by natural sinks within the lowest part of the troposphere by surface contact processes such as photosynthesis), so the annual emission of CO_2, E_{human}, is about 4 ppm per year. If we assume a lifetime of CO_2 in the whole of the atmosphere of ~100 years, the new CO_2 level will be

$$[CO_2]_{perturbed} = [CO_2]_{baseline} + E_{human}\tau = 280 + 4 * 100 = 680 \text{ ppm}$$

It should be noted that the natural sinks for carbon dioxide are within the boundary layer within the troposphere. If carbon dioxide were to be contained into the bottom 1–2 km of the troposphere, the lifetime of the CO_2 would be in the order of 4 years. Apart from a small reduction in carbon dioxide due to being dissolved out in rainfall at higher altitudes within the troposphere, there are no sinks for carbon dioxide above the boundary layer (approximately lowest 2 km). The carbon dioxide at high levels needs to be circulated through the boundary layer to be removed. This explains the difference in lifetime.

How long will it take to achieve the new equilibrium level?

$$[CO_2]_t = [CO_2]_{baseline} + \tau E_{human}\,(1 - \exp(-t/\tau)) \tag{20}$$

We can plot Eq. 20 as a function of time (Fig. 10) which shows that the time taken is between 200 and 300 years. However, the emission rate, E, of CO_2 is predicted to increase over the next 50 years if no action is taken, and hence the level of 680 ppm would be reached more quickly as a result. It should be noted that CO_2 is the dominant greenhouse gas (not including H_2O) at the time of writing; although gases such as methane (21 times more potent) and nitrous oxide (290 times more potent) are much better at absorbing infrared radiation than CO_2 on a molecule per molecule basis, their rise in concentration is 2.5×10^{-4} that of CO_2, and so their contribution is small but not insignificant to infrared radiation trapping.

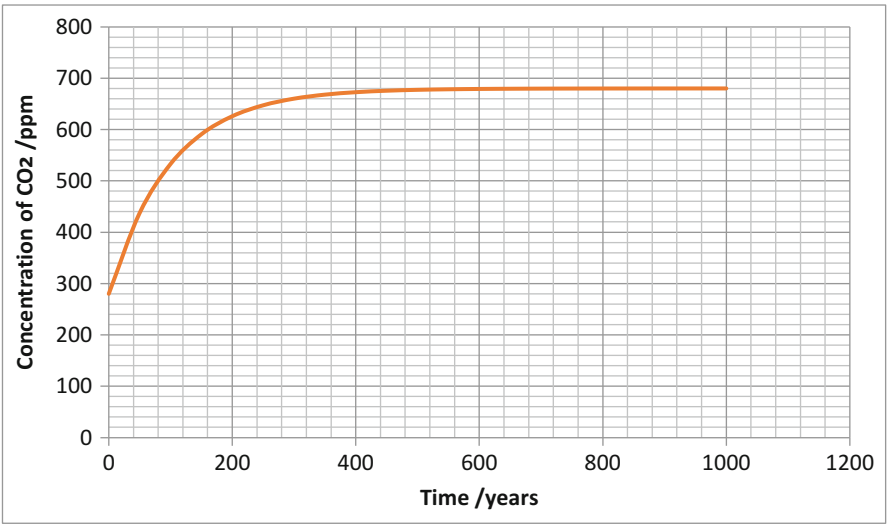

Fig. 10 Graph of concentration of carbon dioxide (ppm) against time (years)

What would emissions have to change by to reduce $[CO_2]_{perturbed}$ to 500 ppm?

$$[CO_2]_{perturbed} = 500 \text{ ppm} = [CO_2]_{baseline} + E_{human}\tau = 280 + E * 100$$
$$220 = 100E_{human}$$
$$2.2 = E_{human}$$

This amounts to a 45 % reduction in current emission rates.

Simple Mathematical Climate Model to Investigate the Role of the Oceans in *Slowing* Climate Change

The question of the impact of the oceans in taking up excess carbon dioxide from the atmosphere and the timescales involved is often queried. This simple model will allow exploration of these ideas.

$$\text{Mass of ocean} = 1.3 \times 10^{21}\text{kg}$$
$$\text{Heat capacity of water} \sim 4 \text{ Jg}^{-1}\text{K}^{-1}$$
$$\text{Heat capacity of the ocean} = 5.2 \times 10^{24}\text{JK}^{-1}$$

The heat capacity of the ocean is approximately 1,000 times that of the atmosphere, and so it can absorb excess thermal energy from the atmosphere.

If we imagine that since the year 1800 the increase in greenhouse gases has caused a rise in heating of ~1 Wm^{-2} (so-called radiative forcing) (http://www.ipcc.ch/), the total energy flux increase ΔE_f is

$$\Delta E_f = 1[Wm^{-2}] \times 4\pi R_E^2 (\text{surface area of the Earth where } R_E \text{ is the radius})$$
$$\Delta E_f = 4\pi\left(6.3781 \times 10^6\right)^2 W$$
$$\Delta E_f \sim 5 \times 10^{14} W$$

The time taken for this energy flux to cause a rise in temperature of 1 K in the atmosphere can now be calculated since energy (J) over power (watts) is time (seconds):

$$\text{Time}_{\text{atmosphere}} = 5 \times 10^{21}/5 \times 10^{14} = 1 \times 10^7 s \sim 116 \ \textit{days}$$

However, the time taken for this energy flux to cause a rise in temperature of 1 K in the ocean is

$$\text{Time}_{\text{ocean}} = 5.2 \times 10^{24}/5 \times 10^{14} = 1.04 \times 10^{10} s \sim 330 \ \text{years}$$

Hence, the timescales for climate change are driven by the ocean's thermal mass. It should be noted that this does not mean that temperature will not rise, but does mean that the timescale will be longer.

Climateprediction.net: Taking Part in Climate Simulations

Climateprediction.net is self-billed as "the world's largest climate forecasting experiment for the twenty-first century." It does this by recruiting help from people around the world who can offer time on their computers when their computers are switched on but are not being used to their full capacity. This is an example of citizen science that school students may wish to engage with.

The full climate model has many parameters that can be adjusted; to explore all of these parameters, an extremely large number of simulations must be performed. Even with the computer resources available to the climateprediction.net team, such an ensemble of simulations would take a very long time. The idea behind climateprediction.net is that anyone can download a version of the model that will explore one of these particular parameters from a group of preset scenarios. The model will take about 3 months to run in the background while one works, without compromising the speed of the computer.

Calculations are performed in three parts. The first part runs calculations using data from the years 1850 to 1900, checking the resulting predictions against temperature records: this is known as the calibration run. The second part runs a simulation from 1901 to 2000. The third stage then runs a simulation of the future climate (2000–2100) with one parameter changed, for example, the sensitivity of climate to uncertainties in the sulfur cycle. Once the calculations are complete, the data is automatically uploaded to the UK's Meteorological (Met) Office the next time the computer is online. The interface software which is provided free of charge with the simulation gives the computer user a graph of the changes to the climate, as they are calculated. Temperature variations by season with latitude, longitude, and

altitude are just some of the variables that can be visualized. Such features can enable a cross-curricular school project linking geography and the physical sciences. The climateprediction.net web site also offers information and resources specifically for schools (http://www.climateprediction.net/education/).

By August 2010, the project has run 74,842,477 model years and has 43,691 active hosts running the different simulations. In 2014, alone volunteers donated nearly 7,500 years of computing time completing half a million successful simulations. A set of current experiments may be found at the project web site as will details of how to get involved.

How does the simple model compare with more sophisticated models such as the Hadley Centre climate model used by the UK's Met Office? In fact, the two models are very similar, except that the Hadley Centre model does not consider the atmosphere as one layer but splits it into a number of boxes based on altitude, latitude, and longitude. For each box, the model directly calculates the amount of incoming UV/visible radiation transmitted and scattered within that box and the amount of outgoing infrared radiation transmitted by that box, based on the concentrations of key greenhouse gases and the surface area of cloud and ice. The most sophisticated versions of the Hadley Centre model also consider the heat flux into and out of the ocean and the uptake of CO_2 by vegetation. If the principles of the one-layer model are understood, comprehending the more complicated climate models is possible.

Writing Articles for School Students and Their Teachers

There are many publications, specialists, or otherwise that report new science to the general public, for example, *New Scientist*. There are also many publications that are aimed specifically at school students and their teachers. In Europe, examples include *Science in School* (http://www.scienceinschool.org/ last accessed February 21, 2015), *Physics Education* run by the Institute of Physics (http://iopscience.iop.org/0031-9120/ last accessed February 21, 2015), and *Chemistry Review* (http://www.york.ac.uk/chemistry/schools/chemrev/ last accessed February 21, 2015). In Brazil, the Ciência para Todos/ Science for All blogsite (http://www.ccell11.com/ last accessed February 21, 2015) aims to do this in Portuguese, Spanish, and English. Ideally, one would want cutting-edge research reported in a way that can be understood by the school community and indeed the general public. To do this effectively, articles should take into consideration the language and terminology that students are familiar with (Tuah et al. 2009); ideally then, the articles should be written by an expert in the field with the help of a practicing school teacher (Harrison et al. 2006; Shallcross and Harrison 2009). In 2005, at the School of Chemistry at the University of Bristol, the first ever full-time School Teacher Fellow (Shallcross and Harrison 2007a, b) position was established. Here an experienced secondary school science teacher was permanently seconded to work with the School of Chemistry, and one of the many things that took place was a rapid increase in the production of articles for a school audience. In concert with the School Teacher Fellow, researchers in the department have been encouraged to write such articles, and a number of

articles on aspects of climate change have also been written (Shallcross and Harrison 2007c, 2008a, b; Shallcross et al. 2009a, b). Elements of these articles focusing on practical and hands-on tools for education in climate science are given in the next section.

Practical and Hands-on Activities

A Climate Change Lecture Demonstration: A Pollutant's Tale

One method of effectively engaging with large numbers of the public on aspects of atmospheric chemistry and climate change is through a lecture demonstration. A lecture demonstration is different to a "chemistry magic show" because the experimental demonstrations chosen are used to illustrate the chemistry being discussed and are not just there for the "wow" factor. The "wow factor" is there in that some of the demonstrations are spectacular, but their use in telling the climate story is their primary value. The secondary aims are tied up with the promotion of chemistry and the "edutainment" value of the talk. One such portfolio of talks was created by the authors entitled "A Pollutant's Tale" together with its version aimed at primary school students "Gases in the Air." These have been performed in excess of 1,400 times in an 8-year period to a total audience of over 225,000 in twenty countries from China to New Zealand to South Africa to the USA and Europe (2006–2014). The several versions of the talk aimed at secondary school students and the wider public all contain the same experiments but the depth to which the explanations are given are age/prior knowledge appropriate. Some of the demonstrations used double-up to reinforce areas of knowledge required by the school curriculum. The talk is best given by two people but can be given by a suitably dexterous and informed individual. It needs 30 min setting up time and 20 min clear-up and can last from 50 to 80 min depending on the audience. The basic lecture demonstration is also now being given by other groups.

The lecture demonstration begins with a comparison of the Earth's atmosphere with the atmospheres of other planets in our solar system (Table 4). The gas giants being predominantly composed of hydrogen and helium give the excuse to set fire to balloons of these gases to reinforce knowledge of the chemistry of these gases and to start the lecture off with a bang. The chemistry of the gases in the Earth's atmosphere is next with experiments looking at liquid nitrogen and the production of oxygen via

Table 4 Three most abundant gases in each planetary atmosphere

Neptune	H_2 (80 %)	He (19 %)	CH_4 (1–2 %)
Uranus	H_2 (82 %)	He (15 %)	CH_4 (2.3 %)
Saturn	H_2 (96 %)	He (3 %)	CH_4 (0.45 %)
Jupiter	H_2 (93 %)	He (7 %)	CH_4 (0.3 %)
Mars	CO_2 (95 %)	N_2 (2.7 %)	Ar (1.6 %)
Venus	CO_2 (96 %)	N_2 (3.5 %)	SO_2 (0.015 %)
Earth	N_2 (78 %)	O_2 (21 %)	Ar (0.93 %)

the elephant's toothpaste experiment (catalytic decomposition of hydrogen peroxide using potassium iodide). From here the audience is introduced to volatile organic compounds (VOCs), a term for which most audiences have no knowledge. The audience is invited to analyze several examples of VOCs, that is, samples of plant origin VOCs such as lime, coconut, vanillin, and lavender are given to the audience to smell, by dipping thick blotting paper strips into a solution of these fragrances. These "smell sticks" are color-coded with food dye so that several samples may be given out at the same time. Synthetic versions of historically animal-derived fragrances of "whale vomit" (ambergris) and civet (originally extracted from the anal gland of the civet cat and still smelling like it) are also used. The question is raised "Where do all these smells go?" This question leads onto the subject of combustion, incomplete combustion being demonstrated by the production and ignition of acetylene and complete combustion of methanol vapor in the "whoosh bottle experiment" (see section "Methanol Whoosh Bottle"). The true demise of the VOCs via free radical mechanisms is then given to appropriately experienced audiences. From here the talk goes onto other pollutants starting with nitrogen dioxide (see section "Nitrogen Dioxide Preparation"). The audience is taken through some research data on the nitrogen dioxide concentration in a city across a day, and its connectivity with photochemical smog is developed with audiences whose background knowledge is suitable.

A major section of the talk then targets carbon dioxide with inspection of Bristol CO_2 levels over a year's data capture and then to the "Keeling CO_2 curve" from Mauna Loa. A moment is taken to look at why Hawaii and also to get the audience to consider that studying science could get them to some very pleasant places to work! Two very basic demonstrations with dry ice (solid CO_2) are performed, the inflation of rubber gloves showing that dry ice sublimes and also that carbon dioxide is soluble in water and will neutralize an alkaline solution becoming weakly acidic (see section "Solubility of CO_2 in Water/Precipitation of Calcium Carbonate"). Three to five minutes are then taken to explain climate using the Granny model (see sections "The Granny Model: Basic Concepts" and "The Granny Model: The Underpinning Mathematics"). A graph of temperature data for the past 150 years is shown which then leads onto the computer modeling of the climate. This is done showing both natural forcings and human contributions and finally the sum of the two. The use of computer modeling to first be able to match the past events before it can be used to make predictions is discussed. The predictions on temperature and rainfall for the area of the world that the lecture demonstration is being delivered are then highlighted. The question "What can be done about it?" is then posed. A graph showing the carbon emissions by year from 1955 to 2055 is put up. The wedge of carbon needed to be removed to avoid the "business as usual" situation is highlighted, and the Pacala and Socolow (2004) stabilization wedge idea is explained. The take-home message then becomes that no one has to wait around for someone to invent ways of removing carbon. In fact, there are already 11 technologies that currently exist. If the social and political willpower were present employing these technologies, it would not only remove the projected carbon load but even reduce it below the current levels. It is very important to leave younger students with a positive message rather than one of

"gloom and doom." The final demonstrations, to end on a bang, are a reminder of the chemistry of helium and hydrogen (a fossil fuel replacement). One version of the PowerPoint of "A Pollutant's Tale" may be downloaded from http://www.chemlabs.bristol.ac.uk/outreach/A-Pollutant-Tale.html, and Spanish and German translations are available from the same webpage.

Demonstrations and Experiments That Can Be Done in School to Augment Climate Change Education

There are a number of chemicals that are important to consider for climate change, either as contributors to climate (soot and carbon dioxide formation), as alternative fuels (methanol and hydrogen), or as alternative energy sources. In this section, several classroom demonstrations and experiments to introduce these materials and describe how they can be used to enliven climate change lessons or lectures are presented. *Safety note*: Local rules and regulations on health and safety should be applied before trying these out. Always practice the experiments before presenting them in front of students, and the environment that the experiments are to be performed in should be taken into account.

Soot/Particulate Carbon

Soot fits into the category of airborne particulate matter. Particles are considered hazardous when they are less than 5 μm in diameter, as they are not filtered out by the upper respiratory tract before entering the lungs.

Black carbon will enhance global warming, but not all particles in the atmosphere do. It all depends on their optical properties: if the particles are very reflective, like a mirror (e.g., sea-salt particles), they can reflect incoming solar radiation back to space and decrease the radiation that reaches the Earth, causing a reduction in surface temperature. If they are dark, such as soot, they will absorb incoming and even outgoing radiation and enhance warming.

Soot is a product of incomplete combustion of carbonaceous fuels, for example, in car motors, central heating, or power stations. There are a number of reactions that can produce soot. The simplest teacher demonstration is to burn small pieces of expanded polystyrene packaging, holding them with tongs over a heatproof mat. The yellow flame produced is very smoky, and the smoke contains black specks of carbon. However, this is not a suitable reaction for students to perform, as the polystyrene drips molten droplets of burning material; instead, the teacher should demonstrate this. Another teacher demonstration, that is a little more spectacular, is the combustion of glucose with an oxidizer. If 5 g of glucose powder is mixed with 5 g of potassium chlorate on a heatproof surface, it can be ignited by a few drops of concentrated sulfuric acid. The eruption of flame also produces a lot of gray smoke which can be discussed in terms of incomplete combustion (safety note: this experiment must not be made by students, as it is dangerous).

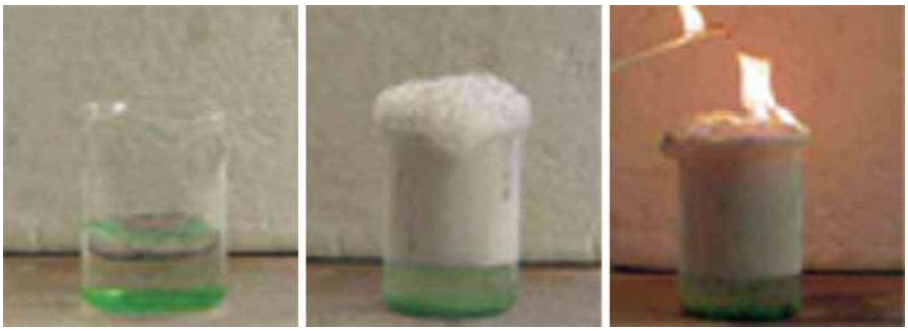

Fig. 11 Addition of calcium carbide to water (with some washing-up liquid added) and then ignition of the resulting foam

If a class experiment to produce soot is needed, the combustion of freshly prepared acetylene (ethyne, C_2H_2) gas is an entertaining reaction (see Fig. 11). Take a 250 ml glass beaker, place it on a heatproof mat, and half fill the beaker with water. Add a good squirt of washing-up liquid (to trap the acetylene gas produced as a foam) to the water and also a few pieces of calcium carbide (CaC_2). The reaction is immediate, liberating bubbles of acetylene. The teacher or student can then use a lit splint, taper, or match to ignite the foam. This burns dramatically with a yellow flame with smuts of carbon.

$$CaC_2 + 2H_2O \rightarrow Ca(OH)_2 + C_2H_2 \tag{21}$$

Solubility of CO_2 in Water/Precipitation of Calcium Carbonate

If dry ice is available, an interesting experiment can be performed to demonstrate the solubility of carbon dioxide in water. This can be used to introduce a discussion about the uptake of carbon dioxide (CO_2) by the oceans as a possible mechanism for removing carbon dioxide from the atmosphere. For this very visually impressive reaction (see Fig. 12), add a handful of dry ice (take care to avoid cold temperature burns) to a large (1 l) beaker of water that has been made alkaline (pH = ~12) with sodium hydroxide solution and to which a small volume of universal (pH) indicator has been added.

Apart from the impressive condensation of water vapor, forming a cloud above the beaker, the formation of carbonic acid (a weak acid) causes a series of color changes to the indicator from purple through to orange (see Fig. 12). For a more impressive cloud, use hot water, as there is more water vapor to condense. The condensation is caused by very cold carbon dioxide gas produced when the dry ice

Fig. 12 Tim Harrison and Dudley Shallcross with dry ice reacting in alkaline water

sublimes, using energy from the much hotter water. Some of the carbon dioxide dissolves in the water.

A small piece of dry ice placed in limewater (calcium hydroxide solution, $Ca(OH)_{2\,(aq)}$) can also be used to show the precipitation of carbon dioxide as calcium carbonate. The oceans of the world dissolve carbon dioxide gas and can precipitate calcium carbonate, which is used in shell construction by numerous creatures. The rate of dissolution is too slow to compensate for the increase in atmospheric carbon dioxide:

If no dry ice is available, then a 2 l drink bottle could be filled with carbon dioxide gas, and about 30 cm^3 of 2 mol dm^{-3} sodium hydroxide can be added. Place the cap on the bottle and shake. The bottle should start to collapse as the carbon dioxide gas reacts with the sodium hydroxide, thus reducing the pressure inside the bottle. The solution forms exothermically so that it gets warm. This shows that carbon dioxide gas is acidic. This has implications for the change in the ocean's pH as the high concentrations dissolve over time.

Methanol Whoosh Bottle

Methanol is a biofuel, an alternative to fossil or nuclear fuels, and this experiment can be used to demonstrate its combustion. In addition to being a renewable fuel, methanol has the advantage over fossil fuels of not releasing "stored" carbon dioxide into the atmosphere; instead, it recycles carbon dioxide that is in the environment anyway.

Fig. 13 Igniting the methanol "whoosh" bottle experiment

Methanol vapor (which is toxic) can be ignited inside an 18–20 l plastic water bottle of the type used in water dispensers. Note that after the experiment, the container will no longer be fit for its original purpose! Be warned some polymers used to make these containers may melt! Also the water bottle must be dry, as the tops of wet bottles tend to melt during the combustion!

Pour around 20 ml of methanol (methyl alcohol, CH_3OH) into a dry 20 l water bottle and shake to vaporize. The pressure of the vapor can be sensed by the hand held over the bottle's mouth if the room is warm. Pour out the surplus liquid methanol. Put the bottle behind a transparent safety screen on the floor and away from any overhead heat, flame, flash sensors, or curtains. Put a lighted taper or long match to the mouth of the water bottle, holding it at arm's length with fingers outstretched. A blue flame will erupt with a loud roar as the methanol vapor completely combusts (see Fig. 13). The experiment should not be repeated with the same container until it is dry again otherwise the methanol burns more slowly and the top of the container begins to melt! Using ethanol or methylated spirits is not recommended as more heat is generated and the container gets very hot. Some demonstrators use propan-2-ol as the fuel. Ethanol burns too hot to do this safely.

Another dramatic demonstration of combustion uses 5 g of glucose mixed with 5 g of potassium chlorate on a heatproof mat. A few drops of concentrated sulfuric acid initiate the reaction between the powders which produces flame and smoke, as also mentioned above. This is a variant on the more well-known "screaming jelly baby" demonstration where a soft jelly sweet is quickly inserted into a clean boiling

tube a quarter full of potassium chlorate which has been heated strongly until molten. In both cases, the potassium chlorate being an oxidizer can be thought of as releasing oxygen to allow the sugar to burn releasing energy as heat and light from the fuel/air mixture.

Hydrogen-Filled Balloons

This teacher demonstration could be used to introduce hydrogen as an alternative fuel to replace fossil fuels and especially to raise the question of whether the combustion product is a greenhouse gas.

One way to demonstrate that hydrogen is a fuel is to fill a balloon with hydrogen (from a cylinder) and tether it to a chair placed away from sensors and flammable materials (such as posters, blinds, or curtains) using a piece of thin string. Ignite the balloon using a lit taper or match, fastened to the end of a meter ruler or a long pole at arm's length. Students should remain several meters away, as during the resultant explosion bits of the rubber balloon tend to fly in all directions. Those with sensitive hearing should place their hands over their ears. The flame and heat energy liberated are spectacular (see Fig. 14) and should lead to discussion of hydrogen's suitability as a fuel.

Fig. 14 Igniting a hydrogen-filled balloon

The Reduction of Iron Oxide on a Match Head

The use of blast furnaces in the iron and steel industries contributes to the atmospheric concentration of carbon dioxide. The crucial reaction, which reduces iron oxide to pure iron by means of carbon monoxide, is

$$Fe_2O_{3(s)} + 3CO_{(g)} \rightarrow 2\ Fe_{(s)} + 3CO_2(g) \tag{22}$$

Students can mimic this reaction on the head of a match! Moisten an unlit match with water and roll into sodium carbonate (Na_2CO_3) powder, and then in iron oxide powder (Fe_2O_3), so that both stick to the match head. Use a second match to ignite the first and let it burn for a moment or two. Crunch the first match head onto a watch glass or Petri dish. Drag a magnet against the underside of the watch glass; the small particles of iron formed will be visible as they follow the magnet's pull. Try this with the starting materials to show that no magnetic materials were initially present. The match provides both the energy for the reaction and the carbon monoxide as a reducing agent. The sodium carbonate acts as a flux material.

Alcohol Burners

Unburned hydrocarbons enter the atmosphere and are oxidized by the hydroxyl radical (•OH) to form predominantly alcohols and carbonyls. Therefore, starting with an alcohol reduces the number of oxidation steps that must take place. Computer model simulations show that the concentration of •OH in the atmosphere is increased when hydrocarbons are swapped for alcohols and carbonyls. Increasing the concentration of •OH will increase the removal rate of greenhouse gases containing a C–H bond. It is also well known that the oxidation of alcohols leads to smaller production of secondary pollutants such as tropospheric ozone. Therefore, using alcohols has a positive effect on both air quality and the removal of greenhouse gases. Moreover, the smaller alcohols can be removed, to a small extent, by physical processes such as dry (taken up by a surface) and wet (rain, fogs, and aerosols) deposition, whereas their hydrocarbon counterparts cannot.

Alcohol burners are the small burners made of glass (see Fig. 15), complete with a wick, which traditionally come with children's chemistry sets and are readily available from school equipment companies. They can be used to determine the energy released in the combustion of shorter primary alcohols such as methanol, ethanol, propan-1-ol, butan-1-ol, and pentan-1-ol. The production of such fuels is a topic in its own right. Note it is too dangerous to use petrol or diesel in these burners.

Fuel Cells

Fuel cells produce electricity from a reaction between a fuel such as an alcohol or hydrogen at the anode and an oxidizing agent such as oxygen or chlorine at the

Fig. 15 Alcohol burner setup under a beaker to which a known volume of water is to be added

cathode. The fuel and the oxidizing agent react in the presence of an electrolyte. A fuel cell is different from a chemical battery because in fuel cells reactants can be replenished, whereas the chemicals being consumed in batteries are not, as they are sealed. A fuel cell will continue to work as long as its reactants are replaced.

There are several demonstration fuel cells available for purchase to show the principle to students. In an alcohol/air fuel cell (see Fig. 16), the cell consists of two parts: an adapted plastic beaker with a conductive pad connected to a terminal (the anode) and an insert containing the catalyst. A defined volume of a source of alcohol (such as antifreeze) or of an alcohol itself (such as propan-1-ol) is mixed with 55 ml of alkali (such as sodium hydroxide) and put into the plastic beaker. The insert (colored red in the image) is put into the beaker to complete the cell. Air can pass through the insert into the alkaline alcohol mixture.

The voltage produced by the fuel cell can easily be measured using a cheap multimeter/voltmeter.

Grätzel Cells

Grätzel cells, also called "nanocrystalline dye solar cells" or "organic solar cells," convert sunlight into electricity directly. Named after their inventor, Michael Grätzel, a Swiss engineer, the function of Grätzel cells is based on artificial photosynthesis using natural dyes found in cherries, blackberries, raspberries, and blackcurrants, among others. These purple-red dyes, known as anthocyanins, are very easy for school students to extract from fruits and leaves by simply boiling them up in a small volume of water and filtering.

Fig. 16 Fuel cell using gin to generate electricity

These cells are very promising because they are made of low-cost materials and do not need elaborate apparatuses to manufacture. Although their conversion efficiency is less than that of the best thin-film cells, their price/performance ratio (kWh m^{-2} $annum^{-1}$) is high enough to allow them to compete with fossil fuel electrical generation. Commercial applications, which were held up due to chemical stability problems, are now forecast in the European Union Photovoltaic Roadmap to be a potentially significant contributor to renewable electricity generation by 2020.

Grätzel cells separate the two functions provided by silicon in a traditional cell design: normally, the silicon both acts as the source of photoelectrons and provides the electric field to separate the charges and create a current. In the Grätzel cell, the bulk of the semiconductor is used solely for charge transport, while the photoelectrons are provided from a separate photosensitive dye (the anthocyanin). Charge separation occurs at the surfaces between the dye, semiconductor, and electrolyte.

The dye molecules are quite small (nanometer sized), so in order to capture a reasonable amount of the incoming light, the layer of dye molecules needs to be made fairly thick, much thicker than the molecules themselves. To address this problem, a nanomaterial is used as a scaffold to hold large numbers of the dye molecules in a 3D matrix, increasing the number of molecules for any given surface area of cell. In existing designs, this scaffolding is provided by the semiconductor material (titanium oxide), which serves double duty.

Production of Biofuels from Vegetable Oils

There are a number of ways of making biofuels from a range of vegetable oils, but the reaction is essentially the same. A biofuel is made by alkaline hydrolysis of the triglycerides in a vegetable oil and the following reesterification of the triglycerides to the methyl ester (a transesterification is done to obtain a less viscous fuel, which is termed biodiesel). In practice, both steps can take place in the same preparation, provided a mixture of methanol in alkali is used. This mixture contains the methoxide ion. During hydrolysis, a fatty acid is liberated from the triglyceride. Together with the methoxide ion, the methyl ester of the fatty acid is then formed. Glycerol (propan-1,2,3-triol) is a waste product of this last reaction. The disposal or use of the glycerol is one of the challenges for this growing industry.

One can either use a large tube or a reflux method involving Quickfit^{TM} laboratory glassware. If using a reflux for the reaction, the biofuel can be separated from the glycerol by solvent extraction. If the experiment is being performed by students in a well-equipped laboratory, the products formed from several different starting vegetable oils can be compared using GCMS (gas chromatography-mass spectrometry).

In the simpler preparation, 12–13 ml of a vegetable oil of choice is put into a boiling tube with 2 ml of potassium hydroxide in methanol (5 % w/w). The liquids are mixed without shaking to prevent trapping air and foaming. The mixture is left to stand in a water bath at 60 °C. The reaction rate can be followed by measuring the viscosity: one can time how long it takes for a small ball bearing to drop through a defined depth of the mixture in the tube every 5 min at regular intervals for up to 2 h. Furthermore, you can leave a sample for a whole day in these conditions to observe the extent of hydrolysis. *Note*, if previously used vegetable oil is utilized, please remember to strain out any food residues first!

Nitrogen Dioxide Preparation

Few students make or even see the gas nitrogen dioxide (NO_2) as it is poisonous, and science teachers are put off by the necessary risk assessment. Nitrogen dioxide can be made in small volumes very simply using a source of copper and concentrated nitric acid. In the UK, it is permissible to use copper coinage as a source of copper and as such adds to the interest of the demonstration. If coinage use is not possible, then a spatula of copper turnings – not bulk copper metal or copper powder – should be used. The copper is placed in a wide-necked conical flask or 400 ml beaker placed on a white tile against a white background to make the color change more easily seen.

After a short while, orange-brown fumes of nitrogen dioxide can be seen. The reaction increases speed after a few moments. Provided there are no drafts, the density of the gas may be seen by pouring out the gas from the reaction vessel. The acidity of the gas may be demonstrated using damp universal indicator paper or blue litmus. Some closer members of the audience may get to smell the chlorine-like odor,

and it may remind them of the smell that is sometimes detected near busy roads or outside of central heating boiler ducts. The reaction may be stopped by diluting the acid in the reaction vessel with water. The blue color of hydrated copper (II) can be seen.

The color of the gas is important, indicating that it absorbs light at around 400 nm. The NO_2 is easily broken down to NO and O atoms by this photolysis process. The O atom produced can add to O_2 as shown in reaction (Eq. 14) and gives rise to the production of ozone near the surface. Such production of ozone near the surface is bad for animal and plant health and is associated with photochemical smog. As the oxidizing properties of nitric acid are concentration dependent, this reaction has a number of other teaching uses.

Detection of Atmospheric Carbon Dioxide Levels Using IR Sensors

Carbon dioxide (CO_2) is the most commonly known greenhouse gas. One might well ask how levels of CO_2 are measured in air samples, particularly as their concentrations are so low. A lot of people will remember from their own school science lessons that carbon dioxide can be detected through the use of limewater (saturated calcium hydroxide solution) where the clear and colorless solution turns chalky, misty, and milky or forms a white precipitate depending on interpretation. All these descriptions refer to the formation of a suspension of calcium carbonate ($CaCO_3$). Few have any understanding of how the concentration of carbon dioxide in the atmosphere can be known. Few will have any understanding of infrared spectroscopy and its link with molecular bonding.

How Do Infrared (IR) Sensors Work?

Two types of carbon dioxide sensors have been used with school students and teachers (Harrison et al. 2006): one which allows gas to diffuse into the sensor and one which is pumped. They both work in similar ways.

Carbon dioxide molecules absorb energy at specific frequencies of infrared radiation and use the corresponding energies to stretch or bend the covalent bonds between the carbon and oxygen atoms accordingly. Low energies cause a bond-bending motion, and high energies cause bond stretching. The frequencies at which this occurs are within the infrared part of the electromagnetic spectrum (between 4,000 and 650 wavenumbers, corresponding to 2.5–15 μm). A wavenumber is the unit commonly used in spectroscopy to relate wavelength to energy. A wavenumber ($1/\lambda$) is the reciprocal of wavelength (λ) and is directly proportional to energy. This absorbance at this wavelength can be used to determine the CO_2 concentration in the air.

There are two main types of carbon dioxide sensors (Harrison et al. 2006). The more expensive research sensors pump air through the sensor, while the cheaper devices rely on diffusion. For either type of detector, air passes into the absorption cell. This is effectively a small darkened cylinder within the sensor. At one end of the

absorption cell, there is an infrared light source coupled to a fixed wavelength filter, which provides a narrow band source of infrared light, for CO_2 at around 2,350 cm^{-1} (wavenumbers, i.e., 4.3 μm). At the other end of the tube, there is an infrared detector or photon counter that measures the infrared light intensity. The more CO_2 molecules are in the air sample, the more infrared radiation is absorbed in the cell, and the less infrared radiation reaches the detector. For small absorptions, the Beer-Lambert law shows that

$$\text{Concentration} = \frac{(1 - (I/I_0))}{\sigma l} \tag{23}$$

where

l is the path length (length of the cell).

σ is the absorption cross section for CO_2 at the wavelength being used and is known to a high accuracy.

(I/I_0) is the ratio of infrared radiation arriving at the detector when the cell is empty (I_0) to when it has an air sample in it (I).

I_0 is not measured for each reading, but will be measured frequently to check that there are no appreciable fluctuations in the instrument infrared light intensity.

Students who have used such sensors (see Fig. 17a, b), on loan from the University of Bristol, have been surprised that the carbon dioxide reading inside an empty classroom is much greater than that outside, the latter being well above 0.037 % (370 ppm) as reported for the CO_2 atmospheric concentration in some textbooks. New school buildings in the UK appear to have windows that are not designed to be opened! Simple experiments in a lecture theater with ~200 students show that the CO_2 concentration will reach ~1,400 ppm after 50 min.

The CO_2 sensors that have been used with students are tuned to the CO_2 ν_3 asymmetric bond stretch at 2,349 wavenumbers (Harrison et al. 2006). An asymmetric stretch is where the carbon-oxygen double bonds (C=O) absorb energy and one of the two bonds lengthens, while the other one contracts. For CO_2, there can only be one asymmetric stretch. This particular bond stretch is important because carbon dioxide is the only molecule present in high quantities in the atmosphere to absorb at 2,439 wavenumbers. Therefore, only absorption by CO_2 can cause a change in infrared light intensity at this wavelength. It is common for an optical sensor to be tuned to a specific frequency where the molecule absorbs. Usually it is the most intense absorption that is chosen to be detected because there will be the greatest sensitivity. Using the method with other gases, this is not always possible as there may be others that also absorb in that region. In that case, a different absorption is chosen free from interferences.

Examples of simple investigations that can be made with such sensors without logging include measuring the levels inside a classroom before and after it is in use, measuring roadside levels of carbon dioxide and the differences that are there in moving away from the road (wind direction, season, time of day also play a part),

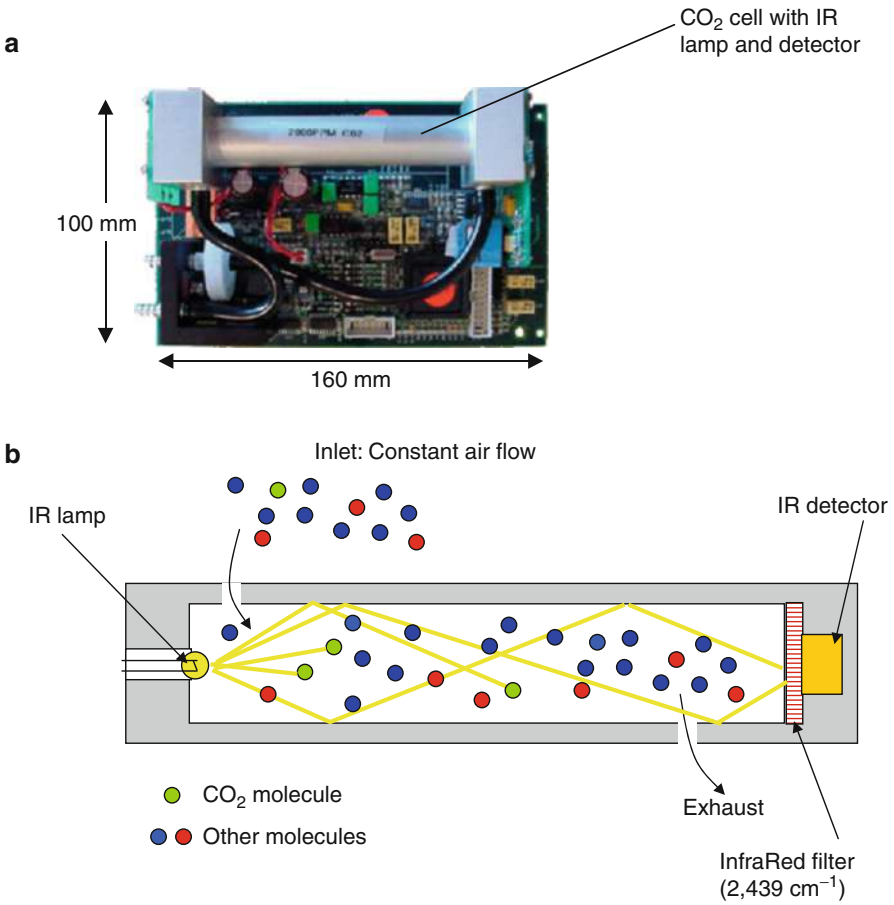

Fig. 17 (**a**) Internal circuitry of the CO_2 detector. (**b**) A schematic of the CO_2 cell within the sensor 2,439 cm^{-1} = 4.1 μm

and measuring levels above and below trees and other vegetation. With a logging device, simple investigations of the change in concentration in a classroom during the lesson, with and without windows and doors open, are easy to do. Roadside data measurements over a period of time provide a rich source of information not only about emissions from cars but also about the dynamics of the atmosphere. Fourier transform analysis (Harrison et al. 2006) of these data has revealed cycles of minutes (corresponding to traffic light signal cycles), 8 h (rush hour peaks), 12, and 24 h revealing the rising and falling of the Earth's boundary layer. Very-long-term measurements, of course, provide seasonal cycles that a student can investigate and reveal, even in urban measurements, a winter peak and summer trough caused by photosynthesis.

Impact and Assessment

"How does one know that what one does in terms of climate change outreach is doing any good?" is often a question asked of work with primary and secondary school students or indeed with the wider public. It is often a question asked of prospective funders either directly or by implication on grant applications when the use of evaluators is required. In this section, some feedback methods are discussed that may be useful for employment in outreach activities.

A major current issue in the field of science communication is evaluating the impact of activities designed to engage people with science and technology. Evaluation is widely seen as the primary tool to identify best practice and provide empirical evidence of the positive impact of such activities. However, there is no standard method for doing this or for comparing the results.

The majority of published evaluations involve the use of quantitative data generated through written questionnaires. Using such methods to evaluate the impact of short-duration activities is often inappropriate or impractical. Are there alternatives to the traditional questionnaire for obtaining feedback about the impact of some types of science communication activity? What are the effects, if any, of the activities on participants?

Generic Learning Outcomes

In a recent research exercise, Rivett (2009) investigated a number of physical science outreach events, including the use of lecture demonstrations at primary and secondary level on atmospheric chemistry and climate change. These activities were evaluated using a variety of unconventional techniques. The events were evaluated using *postcard writing, children's drawings, comments boards and walls, observation*, and *unsolicited and teacher feedback*. An *interactive voting* system and some *written questionnaires* developed and administered by third parties were also utilized. These largely focused on identifying the immediate to short-term impact of the activities. They generated largely qualitative data but included a quantitative component.

These data were analyzed using the *Generic Learning Outcome* [GLO] (Generic Learning and Archives Council 2008) framework, which is becoming a common evaluative tool across the Museum and Science Centre sector. GLOs are a way to look at different types and levels of impact using one tool. The model stems from a view of learning as a personal and individual experience, which is context dependent. Five categories are used to code participants' responses: *knowledge and understanding*; *skills*; *attitudes and values*; *enjoyment, inspiration, and creativity*; and *activity, behavior, and progression*.

The alternative evaluation techniques tested resulted in the production of a large amount of useful data and a greater range and depth of information on impact than might be expected. The qualitative nature of the tools is more appropriate for small

sample sizes (which might lack statistical significance). They were generally uncomplicated to use and simple to analyze using the GLO framework.

- *Write a postcard* feedback revealing the greatest range and depth of learning outcomes, comparable with an externally designed *written questionnaire*.
- *Observations* were a rich source of data, but did not necessarily capture the impact on all participants. *Teacher feedback* provided information about a range of learning outcomes, but not from the pupils' own perspective. *Children's drawings* gave some useful information about a limited range of learning outcomes.
- *Comments boards* provided a deeper insight into participants' experiences than initially expected, but generally only about a subset of learning outcomes. To generate meaningful data about impact, questions must be carefully worded to guide responses.
- *Unsolicited feedback* does not give reliable evidence of learning outcomes, but can be analyzed to provide limited information about impacts.
- *Interactive voting* provided the least information about impact in this study, because the questions asked generally did not focus on learning outcomes.
- The major category of learning outcome reported by participants is *enjoyment*, but evidence for *knowledge* gained, changes in *attitudes*, and *behavior* is also strong. It is the questions asked which hold the key to elucidating different learning outcomes.

Suggested Questions to Discern Different Learning Outcomes

The evaluation techniques differed in their level of convenience. Data collection tools such as the *postcard feedback* and *Post-it note comments* were cheapest and simplest to administer and could be analyzed rapidly using the GLO method.

The majority of these techniques can only evaluate the immediate impact of the activity. This is due to when they are administered, which could be instantly after the event or at the most up to 1 or 2 weeks afterward. Asking participants to complete these styles of evaluation, a significant amount of time afterward is impractical and becomes more a test of memory than anything else. Teacher feedback was shown to provide an indication of longer-term impact, although this may be rather subjective.

The GLO framework is a useful coding device which allows wider comparisons with other studies. It enables outcomes beyond immediate "reaction" level to be investigated in a meaningful way. The GLO approach reveals that impact is not a neat, linear process but occurs at many levels and over a multiplicity of timescales.

The learning outcomes themselves are extremely varied. There may be no or even a negative impact, a transient effect, or something deep and long lasting. The level of impact is impossible to predict and is not the same for all participants. Discovering the medium- to long-term impact of any of these activities is beyond the scope of the techniques tested.

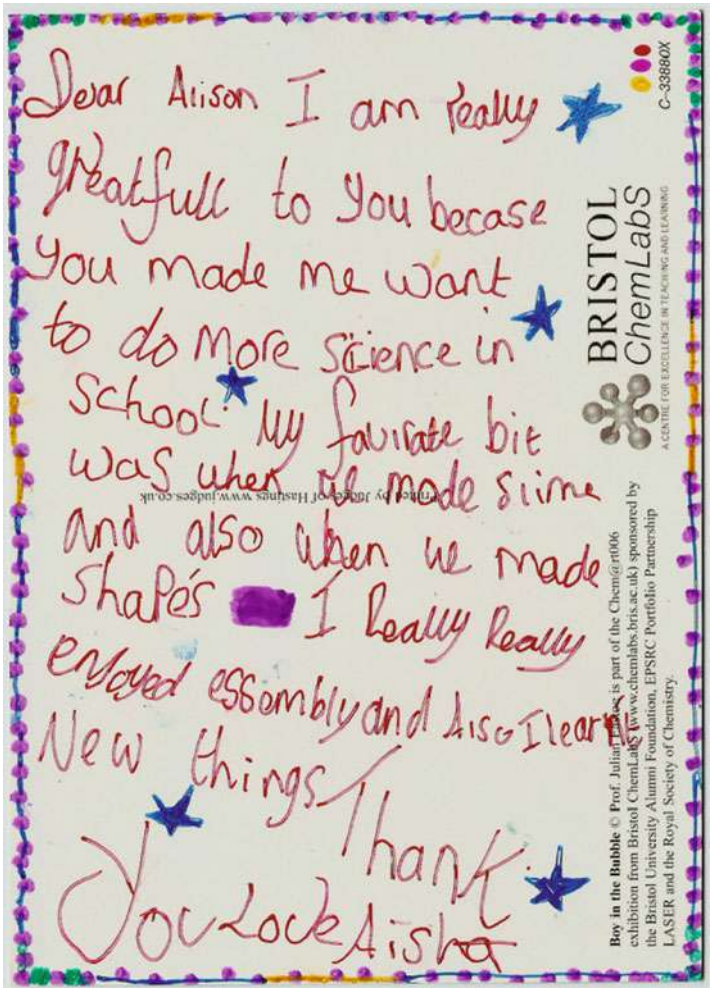

Fig. 18 A postcard from a primary school student, providing feedback on an activity

However, a learner's enthusiasm for a subject is usually retained much longer than memory of facts or content. There is evidence that memorable activities which provide positive experiences of science can affect future behavior. Given the right support, situational interest may become sustained and so increase motivation and satisfaction with a subject.

Science communication activities like those investigated are just one part of the many and varied experiences in people's lives. A single event cannot be expected to have a significant impact on the life choices of the majority of participants. What can make a difference is ensuring, through thorough and reliable evaluation, that there are a range of high-quality opportunities for people of all ages to experience different aspects of science, meet role models, and develop their interest and abilities.

Table 5 Suggested questions that can be used for evaluation of activities

What was your favorite part of the day	*Formative/process/ enjoyment*
Was there anything you did not like	*Formative/process/attitudes*
Please tell me anything you learned today	*Knowledge/skills*
How did today make you feel about science	*Attitude/enjoyment*
Did you find out how to do anything new or do anything better	*Skills/knowledge*
Do you think you will do any science activities following this event	*Behavior/attitudes*

The study identified a number of techniques which provide a range and depth of information about the learning outcomes experienced by respondents. They can easily be embedded into science communication activities and do not require time-consuming analysis.

The impact of the physics and chemistry activities studied was found to be very positive for the majority of participants and was similar to those found in other studies. A myriad of effects are seen at a variety of levels and over a range of timescales.

This postcard (Fig. 18) sums up how a simple evaluation method can pay dividends in terms of the level of information gathered and show true evidence of the potential impact of science communication activities. A list of suggested questions for a GLO analysis is provided in Table 5.

Some Misconceptions Concerning Climate Change and Greenhouse Gases

The following are the main misconceptions that workshops with students or with teachers have unearthed. It is important for all educators working in climate change to realize that ideas and models that are commonly used with peers are not general knowledge and the "obvious" needs to be spelled out. One such example with a group of experienced teachers was the term "aerosol," which was only considered to be a spray can!

All greenhouse gases are synthetic/man made.

No, several natural processes release gases which can absorb outgoing infrared radiation (i.e., they are greenhouse gases), for example, CO_2 is produced during respiration and natural combustion, N_2O is produced by denitrifying bacteria in soil, and CH_4 is generated by termites and cows.

Global warming means that the entire planet will warm up evenly everywhere.

No, warming will be quickest at the North Pole and slowest in the southern ocean.

All pollution in the atmosphere causes global warming.

No, for example, air pollution that leads to aerosol formation can cool the planet down (global dimming), e.g., SO_2 emissions.

All greenhouse gases are bad for the planet.

No, a natural background level is essential for the average surface temperature to be habitable (see sections "The Granny Model: Basic Concepts" and "The Granny Model: The Underpinning Mathematics").

If more carbon dioxide means a warmer temperature, surely faster photosynthesis at the higher temperatures will remove the excess CO_2.

Photosynthesis is controlled by enzymes, so at some temperature this process will stop. Also, at higher CO_2 levels, stomatal conductance drops (the plant does not have to work so hard to obtain CO_2), and there is evidence that its physiology changes significantly.

If burning waste materials produces CO_2, then why not simply not burn organic waste instead of letting it rot.

This is a contentious issue; during rotting, a myriad of gases are released into the atmosphere, and many will be greenhouse gases that will eventually be converted to CO_2 in the atmosphere. So there is a strong argument to burn the waste, harness the energy, and capture the CO_2 produced.

CO_2 is worse than methane.

Figure 4 shows us that CO_2 already absorbs a significant fraction of outgoing infrared radiation around 660 cm^{-1} (25.2 μm), and therefore to absorb more would require a bigger jump in concentration than that for CH_4. It turns out that CH_4 is 21 times more potent than CO_2 over long timescales.

Carbon dioxide is always heavier than air.

Below 100 km, gases are all well mixed in the Earth's atmosphere, and even though CO_2 is heavier than air, it is well mixed.

It is only burning fossil fuels that causes emissions of CO_2.

Respiration also produces CO_2 as do a number of key industrial processes such as iron and steel, aluminum, and cement production.

Datasets That Can Be Used in a Class Setting

There are many datasets that are freely available, such as the UK National Air Quality Archive (NETCEN) (1996), that are a fantastic resource for students and teachers who want to have more hands-on activities concerned with air quality and climate change. However, the main problem is finding out about these archives, being able to access them and, of course, being able to comprehend what these data are and how to use them. A very profitable way forward is to provide background material for teachers and to run master classes in how to use these data. Through these classes, it has been possible to refine the notes provided and extend the scope of the class. There are also datasets that are well documented such as the Advanced Global Atmospheric Gases Experiment (AGAGE) dataset.

One such use of a dataset was research into how fireworks affected air quality during the UK's Bonfire Night. Students from several year groups from three schools were instructed on how to handle data from the UK-AIR website (http://uk-air.defra.gov.uk), and their research was published (Harrison and Shallcross 2011).

AGAGE

AGAGE (1978) is a project that has run since 1978 (then called the Atmospheric Lifetime Experiment, ALE) and consisted originally of five surface stations that were spread across the Northern and Southern Hemisphere, away from major pollution sources. These sites were in Ireland, the USA, Barbados, American Samoa, and Australia (see Fig. 19) and use gas chromatography coupled with a variety of detectors to measure CFCs (chlorofluorocarbons), compounds that were responsible for depleting stratospheric ozone and their replacements the HCFCs and HFCs (hydrochlorofluorocarbons and hydrofluorocarbons). In addition to these gases, measurements of key species such as CO_2, CH_4, and N_2O are made. Extensive information is available, and clear notes on data are provided. Using data such as that from AGAGE can transform classroom teaching and cognition on the subject of climate.

Global Warming Potentials

It is useful to define a concept called the global warming potential or GWP. In the "Introduction" section, it was explained why greenhouse gases are so important to the Earth's climate system and that to be a greenhouse gas, it needs to absorb infrared radiation corresponding to the wavelengths shown in Fig. 4. The most important of these greenhouse gases is CO_2, and the GWP is defined relative to CO_2. The GWP is calculated using a computer model and allows greenhouse gases to be "ranked" in

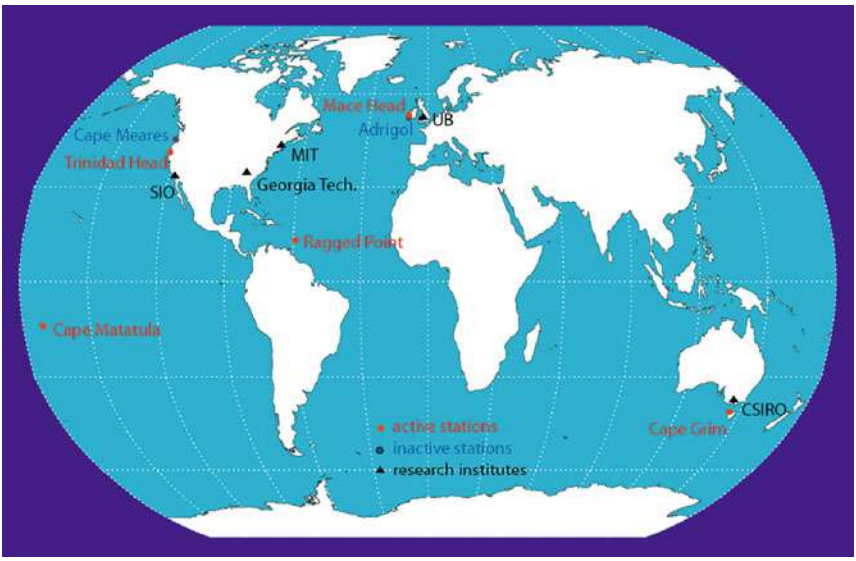

Fig. 19 Original surface sites for the AGAGE project

Table 6 Some global warming potentials for a range of trace gases over a 20-year and 100-year time horizon

Trace gas	Lifetime (years)	GWP time horizon 20 years	GWP time horizon 100 years
CO_2	~120	1	1
CH_4	10	63	21
N_2O	150	270	290
$CFCl_3$	60	4,500	3,500
CF_2HCl	15	4,100	1,500
CF_2Cl_2	130	7,100	7,300

terms of their potency. It is not too difficult to see that the two factors that determine a GWP are how strongly does the gas absorb infrared radiation emitted by the Earth (effectively the size of the absorption cross section of the gas) and how much of the gas (determined by its source strength and lifetime) is present. In a GWP computer model, one would typically release a unit mass of CO_2 and a unit mass of the gas whose GWP is to be determined. After 20 model years, the radiative forcing or heat trapped by CO_2 is calculated and scaled so that it equals 1. Using this scaling factor, the radiative forcing of the gas under inspection is also calculated. The model is run for 100 model years, and the radiative forcing is calculated again and scaled to CO_2. Some data from key greenhouse gases are collected in Table 6. The table reports the GWP on a 20-year and 100-year time horizon and, because of the definition, CO_2 in unity always. Interestingly, for all other gases, the GWP either increases from a 20-year time horizon to a 100-year one or decreases. Further inspection shows that those gases that have a shorter lifetime than CO_2, that is, CH_4, $CFCl_3$, and CF_2HCl, all decrease, while the remaining two, N_2O and CF_2Cl_2, whose lifetimes are longer than CO_2 increase. This change in GWP with time (hence the need to stipulate the time horizon) arises because if the gas is removed more quickly than CO_2, relative to the year 20, the ratio of X/CO_2 in the year 100 will have decreased, that is, far more of X will have been removed than CO_2. Hence, with time the effectiveness of the gas will decrease, that is why the GWP of CH_4 drops from 63 to 21, for example. In a similar vein, N_2O is longer lived than CO_2, and so with time the CO_2 will decay more rapidly, and the N_2O becomes even more effective with time. Regardless of lifetime, it is clear that species containing C–F and C–Cl bonds have very high GWPs. This was explained in section "Stratospheric Ozone Depletion and Climate Change," that is, that these gases absorb in the region known as the atmospheric window and have high absorption cross sections, coupled with their lifetime, leading to the high GWP. Compounds of particular concern are the PFCs (perfluorocarbons), fully fluorinated saturated hydrocarbons (e.g., CF_4 and C_2F_6). These molecules have incredibly long lifetimes (sometimes known as immortal molecules) and very large absorption cross sections and can therefore have a GWP of many thousands. It has been speculated that if man colonizes another planet such as Mars, PFCs would be needed in the terraforming process to flood the atmosphere with high GWP gases and raise the surface temperature.

Methods Used to Monitor Greenhouse Gases

It is instructive to know how the levels of greenhouse gases in the atmosphere are determined. First, the site of the monitoring station is important; it needs to be away from major pollution sources, so that changes to the background concentration can be determined. This criterion dictated where the AGAGE stations would be located (see Fig. 19), and it also then requires that the stations are in remote locations. Hence, the monitoring systems need to be robust, reliable, and low maintenance. For the majority of gases, gas chromatography (Fig. 20) with either an ECD (electron capture detector) or an FID (flame ionization detector) or a mass spectrometer is used. Since many of these gases are present in trace quantities, the air mass must first be pre-concentrated, and to achieve this, a cooled microtrap (−50 °C) containing some solid adsorbent is used to trap the gases of interest (ADS in the figure). Many liters of air can be trapped in this way, and once collected this slug of air can be driven off the trap in 1–2 s by ballistic heating. This slug of concentrated air is then separated into its components by passing it through a GC (gas chromatography) column. As the gases pass over a solid or liquid phase (an adsorbent), some bond to the surface more efficiently than others, and so separation takes place. For gases such as CFCs, HCFCs, and N_2O, which have electronegative elements such as F, O, and Cl, an ECD is a good detector. An ECD consists of a beta (electrons) emitter that provides a baseline current. As the molecule passes through the beam, it absorbs electrons and a dip in current is observed. This invention of Lovelock is incredibly sensitive. For other species, they can either be burned in a flame, where ions are produced and detected, or "weighed" using a mass spectrometer.

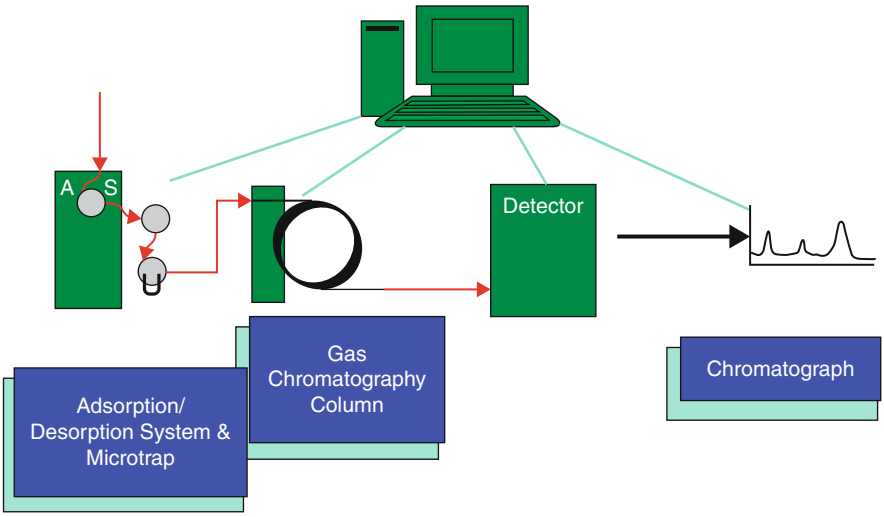

Fig. 20 Schematic of a gas chromatography system used in the AGAGE project

Outreach: Impact on Providers and Others

What Is the Impact on Postgraduates and Researchers Who Engage with Schools, Teachers, and the General Public?

There are several reasons why researchers such as postgraduates should get involved with outreach in topics such as climate change excluding the most important one, which is that taking part in well-organized and well-thought-through activities is great fun!

Communication Skills

Working with school students causes researchers to evaluate the language that they use to communicate their work. Researchers who only used to communicating their science to peers do not always realize that their language is very specific and has acceptance of mutually understood models. They forget that this language and use of models are not widely understood by others. Working with school students directly, or writing articles for them, brings this home. The advantage for the researcher is being able to communicate their work to wider audiences including to those less expert. There are many instances when it may be vital to be able to explain to someone what research you are doing, for example, a potential funder. To younger researchers, the opportunity to give presentations to groups of school students increases their confidence and makes the delivery of talks at seminars and conferences of their peers a less daunting task than it would otherwise be. For younger researchers, it also forces them to really understand the background to their material, as they will almost certainly be asked that obvious but not trivial question about their subject, by an enthusiastic teacher or student.

Role Models

School students still see stereotypes of scientists as being male, middle-aged with long white hair. Putting young researchers, perhaps with colored hair and studs through their noses, in front of school students makes a big difference. Bristol ChemLabS outreach often has requests for outreach teams to be composed of specific gender and racial types to act as role models in particular places. For example, in areas in certain countries of social deprivation with a high proportion of immigrant descendents, to have teachers that are from that group can have an amazing impact on the student's enthusiasm. In another instance, a totally female team was requested to work with primary aged girls who had become disillusioned with science and mathematics. The feedback from both implied that these targeted role models had the desired effect.

Supervisors

Many supervisors may be reluctant to let their postgraduates engage in outreach activities as this removes them from the research laboratory environment. Students report that they really value short periods spent away from their labs engaged in outreach. Students give as examples, coming back into the labs afresh, the ability to

look at their work with renewed enthusiasm as they treat outreach engagements as "periods of tranquility" in an otherwise chaotic work program. Indeed, some students have only managed to complete their PhDs because of this outlet. In other cases, the climate change science being presented to school students has suddenly clarified the point of a piece of PhD research and then has led to it moving on in a new direction.

Increased Employment Prospects

Students can access many more potential careers such as those directly involved in science communication and teaching. Working for an outreach team also gives them additional referees that can comment on their skills for these and other positions. Increasingly, employers value the soft skills, such as communication and team work skills, over technical expertise of graduate chemists. Outreach work can develop these.

Impact on Recipients

Well-focused activities with supporting resources can have a lasting (Harrison and Shallcross 2010; Tuah et al. 2009) impact on teachers and their students, in terms of cognition in this subject area. Through schools one can also interact with whole families, for example, parents. A combination of lecture demonstrations, model workshops, and hands-on practical sessions has been found to be a powerful portfolio for a wide range of learner types and ages. Such approaches have also worked well for those with disabilities, for example, visually impaired.

Is Climate Change All Gloom and Doom? Introducing Stabilization Wedges

When learning about climate change, the students can become despondent easily. They can feel that warming of the Earth and the resultant consequences are inevitable. Both to give some hope to the students and to demonstrate to them the potential of scientific research, ideas presented in a recent paper by two leading climate scientists (Pacala and Socolow 2004) can be introduced into lessons. Their paper discusses how CO_2 levels can be stabilized and other carbon-based greenhouse gas emissions into the atmosphere using technologies that already exist.

Stephen Pacala and Robert Socolow devised the concept of stabilization wedges as a way to reduce carbon emissions over the next 50 years. Figure 21 shows how carbon emissions have increased over the last 50 years and how they are predicted to change in the next 50 years largely based on changes in population. By 2055, it is predicted that there will be 14 gigatons (billion tons) of carbon (GtC) emitted per year if nothing is done now. This will lead to a level of CO_2 in the atmosphere that is around three times the CO_2 level before the industrial revolution started and is predicted to cause a rise in the Earth's average surface temperature of 1–5 °C.

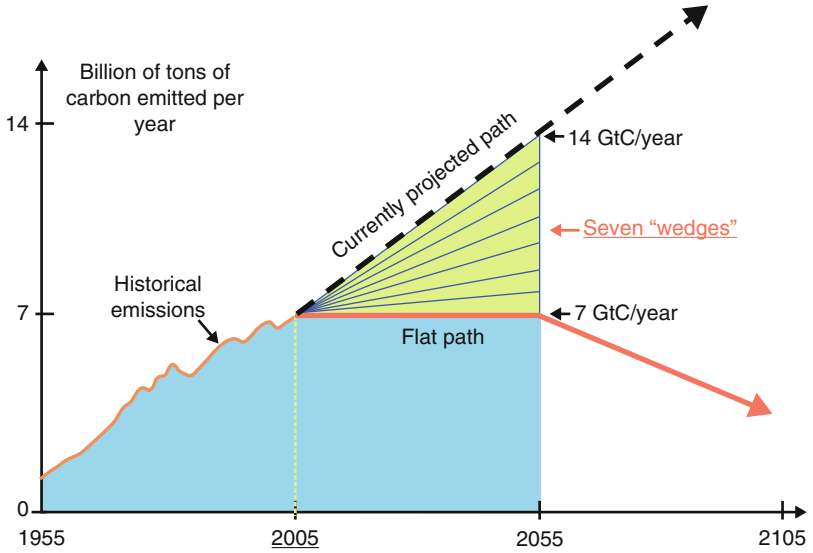

Fig. 21 Carbon emissions, past, present, and future, and the concept of stabilization wedges

Pacala and Socolow suggest that the objective is to maintain carbon emissions at their present levels of 7 GtC per year. As there is no one method to remove this carbon burden, they devised the idea of stabilization wedges. A wedge represents an activity that reduces emissions to the atmosphere that starts at zero today and increases linearly until it accounts for 1 GtC per year of reduced carbon emissions in 50 years. The cumulative total is therefore 25 GtC of reduced emissions over 50 years.

What Activities May Achieve This Effect?

Improved Fuel Economy

A typical car emits a ton of carbon into the air each year. There are one billion cars in use today, and the figure will grow to two billion. Two wedges could be saved if their fuel economy were improved from 30 miles per gallon (mpg) of fuel to 60 mpg.

Reduced Use of Cars

Assuming an increase by 2055 to two billion cars and assuming that no improvement in fuel economy was achieved, a wedge could be saved if the number of miles traveled was reduced from 10,000 miles per year to 5,000 miles per year. Both of these options could save more than one wedge if there is an overprediction regarding the increase in the number of cars in use by 2055. More use of telecommunication and mass transit will reduce the use of cars further.

More Efficient Buildings

Many savings can be made in terms of energy efficiency in buildings, for example, replacing all the world's incandescent light bulbs with compact fluorescent lights would provide a saving of one fourth of one wedge. However, to save one wedge of carbon requires a cut in carbon emissions from buildings of 25 % by 2055. This can be achieved using known and established approaches to energy efficiency. The largest savings are in space heating and cooling, water heating, lighting, and electric appliances.

Improved Power Plant Efficiency

Currently, coal-powered plants operate at about 32 % efficiency and are responsible for about 25 % of all carbon emissions. Improving plant efficiency to 60 % through use of better turbines, fuel cells, etc., would save half a wedge if the quantity of coal-based electricity is unchanged. Emissions from power plants can be reduced both by changing the fuel and by converting the fuel to electricity more efficiently at the power plant.

Decarbonization of Electricity and Fuels

For example, per unit of electricity, carbon emissions are half as large from natural gas power plants as from coal-based power plants. A wedge would be achieved by displacing 1,400 GW of baseload coal with baseload gas by 2055. However, a wedge would require an amount of natural gas equal to that used for all purposes today. A wedge worth of gas would require 50 LNG (liquefied natural gas) tanker deliveries every day or the equivalent of 50 Alaska gas pipelines. This scenario also assumes that no losses of CH_4 (which has a higher GWP than CO_2, see above) would occur during exploration and distribution.

Carbon Capture and Storage

One wedge of carbon can be saved by providing carbon capture and storage at 800 GW of baseload coal plants of 1,600 GW of natural gas plants. A wedge will require injecting a volume of CO_2 equal to the amount of oil extracted every year back into subsurface locations. There are currently less than ten CO_2 storage (pilot) projects that each injects one million tons of CO_2 per year. By 2055, 3,500 will be needed.

Decarbonization of Electricity and Fuels: Nuclear Fission

The rate of installation of nuclear power plants required to save one wedge of carbon from electricity is equal to the global rate of nuclear expansion from 1975 to 1990. Phasing out of nuclear electric power would create the need for another half wedge of emission cuts. There are of course continuing issues concerning removal and storage of nuclear waste, natural catastrophes (compare Fukushima), and the threat of terrorism.

Increased Use of Renewable, Nonfossil, Energy Sources, Including Wind, Electricity, Photovoltaic Electricity, and Biofuels

Installed wind capacity has been growing at about 30 % per year for more than 10 years. It is around 50 GW peak at present, and therefore a wedge of carbon would require 40 times the current deployment. The wind turbines would occupy about 30 million hectares (about 3 % of the area of the USA), some on land and some out to

sea. However, since the windmills would be widely spaced, it is possible to use the land for other purposes as well. A wind electricity wedge would require a combined land area the size of Germany.

The current global deployment of photovoltaics is about 3 GW peak, with a growth factor of about 30 % per year. Therefore, to save 1 GtC per year would require an increase in the deployment by a factor of 700 by 2055 giving 2,000 GW peak. This would be equivalent to an area of about 2 million hectares, assuming an output of 1,000 W peak per m^2 or 2–3 m^2 per person. A photovoltaic electricity wedge would require an array of photovoltaic panels with a combined area about 12 times that of metropolitan London.

Biofuels such as ethanol can replace fossil fuels, but a wedge of first-generation biofuels (e.g., ethanol from sugar cane or biodiesel from rapeseed or soy bean) could be achieved by the production of 34 million barrels per day of ethanol to replace gasoline by 2055. This assumes that the ethanol is from fossil-free carbon and is 50 times larger than the current production rate. This would require 250 million hectares of high-yield plantations equivalent to one sixth of the world's cropland. One wedge from biofuels (first generation) would require planting an area the size of India with biofuel crops. For details, see the respective chapter on biofuels in this handbook.

The pros and cons of implementing each of these technologies would make both interesting projects and the subjects for class debates whether in science or in social studies. The approaches – as well as the problems they are designed to reduce – will impinge more on the lives of the young rather than on their teachers or the authors of this chapter. All options are based on current technologies, and therefore some of these options may well provide more savings as technology improves. The consequences of these do generate comment particularly from younger audiences.

Deforestation

If the current rate of clear-cutting of primary tropical forest were reduced to zero, over the next 50 years that would save half a wedge. A further half wedge would be saved if reforestation of 250 million hectares of tropical land (currently 1,500 million hectares) or 400 million hectares of temperate forest (currently 700 million hectares) took place over the next 50 years. One wedge of saving would require new forests over an area the size of the continental USA.

Soil Management

Conversion of forest or natural grassland to cropland leads to aeration of the soil through annual tilling. This practice accelerates the decomposition of stored carbon and releases it back into the atmosphere. It is believed that 55 GtC has been lost from soils (two wedges worth) historically. Currently, 110 million hectares out of a total of 1,600 million hectares of cropland worldwide undergo conservation tilling. Conservation tilling will involve nondisruption to the soil, for example, drilling of seeds without plowing, soil erosion control, and planting of cover crops. It is feasible that a half to one wedge can be saved through conservation tilling of all croplands. Currently, conservation tillage is practiced on less than 10 % of global cropland.

Conclusions and Summary

The need to make the public more aware of climate change and the potential consequences of it, not only on planet Earth as a whole but also on the individual, is going to increase. Frequently aired radio and television programs, whether for an educated public or school-aged students, need to be made. Articles in popular magazines and not just science-specific journals need to be written for a range of audiences. If possible, access to scientists well versed in public communication at venues that do not intimidate such as bars and social centers, rather than university lecture theaters, for *café scientifique* experiences is going to be needed. Naturally, all these will be pointless if the level of communication is not appropriate to the audience.

In schools in the UK, there has been a major move to promote "science literacy" so that students can make educated decisions about information they receive on a great number of issues from nuclear power to alternative fuels and to evaluate adverts and newspaper articles. These students also look at "how science works," so they are also taught about how research is funded and now can have opinions as to whether research in some areas should be funded. These are of course not just future major consumers and tax payers but are also the voters of tomorrow. Whether this education trend will develop more widely or not, scientists need to communicate their findings as widely and in an accessible way as possible.

The models developed in this chapter and associated practical experiments have enhanced the cognition of teachers and students with respect to the Earth's climate system. It provides these learners with tools to carry out their own investigations and projects and does not require expensive equipment or facilities. The Earth's climate system can be distilled to something that can be understood by the vast majority of people, and it is a great shame that at present there is still considerable misunderstanding that persists. The notion of stabilization wedges is a very powerful one and provides learners with some light at the end of the tunnel. Using the models developed, it is possible to carry out simple calculations and arrive at the estimates provided in terms of land area required, for example. The ability to make such "back of the envelope" calculations not only is a very useful life skill but allows the learner to critically assess the viability of each option presented. There is clearly much still to do in terms of providing the tools to allow new learners to understand the underpinning science of this important topic. However, the material described in this chapter makes a start at least on this road.

Even More Contemporary Atmospheric Chemistry: Criegee Biradicals

Many school science curricula may expect examples of contemporary science. One recent case in atmospheric chemistry concerns the Criegee biradical. It involves elements of preuniversity chemistry such as free radicals, alkenes, and ozonolysis. In 1949, Criegee and Wenner first proposed that ozonolysis of alkenes such as ethene proceeds through carbonyl oxide intermediates, such as the $\bullet CH_2OO\bullet$ biradical.

First, an adduct is formed, and this cyclic structure decomposes rapidly to form a carbonyl and a Criegee intermediate (the details can be found elsewhere in this reference work). Such biradicals had not been detected until recently when a group of British and American researchers succeeded using the Advanced Light Source at the University of California (Berkeley, USA) and photoionization mass spectrometry (PIMS). The importance: free radicals regulate ozone levels in the stratosphere and oxidation rates throughout the lower atmosphere, and some of the accepted atmospheric chemistry is now being rethought through. An outline of the fundamental science for teachers has been published (Shallcross and Harrison 2013).

Future Directions

The Bristol ChemLabS outreach project, the range of activities being described here, is a sustainable program. While the activities such as lecture demonstrations; writing of articles suitable for teachers, school students, and members of the public; and teacher training will continue, their scope will expand. Already, requests for inclusion of climate change sessions for the Prince's Teaching Trust which supports newly qualified (chemistry) teachers and teacher training sessions in Perth, Australia, are being planned. The Royal Society of Chemistry has recently awarded a grant to the ChemLabS team to deliver lecture demonstration training to postgraduate chemists in other universities, several of whom it is hoped will adopt "A Pollutant's Tale" for their own delivery, as has been done in South Africa. Last, an interactive climate change book, suitable for navigation by members of the public of all ages and prior knowledge, is being considered. The climate change challenges are not going away in the short term, and so the outreach needs to educate will not either.

References

AGAGE (1978) http://agage.eas.gatech.edu/. Accessed 29 Oct 2014

Generic Learning Outcomes, Museums Libraries and Archives Council (2008) www.inspiringlearningforall.gov.uk/toolstemplates/genericlearning. Accessed 27 Oct 2014

Harrison TG, Shallcross DE (2010) What should be expected of successful engagement between schools, colleges and universities? Sch Sci Rev 91(335):97–102

Harrison T, Shallcross D (2011) Smoke is in the air: how fireworks affect air quality. Science in School 21:47–5

Harrison T, Shallcross D, Henshaw S (2006) Detecting CO_2 – the hunt for greenhouse-gas emissions. Chem Rev 15(3):27–30

Hoffman PF, Kaufman AJ, Halverson GP, Schrag DP (1998) A Neoproterozoic snowball earth. Science 281(5381):1342–1346. doi:10.1126/science.281.5381.1342

NETCEN (1996) UK National Airquality Archive. http://www.airquality.co.uk/. Accessed 27 Oct 2014

Pacala S, Socolow R (2004) Stabilization wedges: solving the climate problem for the next 50 years with current technologies. Science 305:968–972

RCUK (2002) www.rcuk.ac.uk. Accessed 29 Oct 2014

Rivett AC (2009) A study into the feasibility and validity of using alternatives to questionnaires to evaluate the impact of a selection of physics & chemistry science communication activities. Thesis (M.Sc.), University of Bristol

Science Learning Centres (2004) https://www.sciencelearningcentres.org.uk/. Accessed 21 Feb 2015

Shallcross DE, Harrison TG (2007a) A secondary school teacher fellow within a University chemistry department: the answer to problems of recruitment and transition from secondary school to University and subsequent retention? Chem Educ Res Pract 8:101–104

Shallcross DE, Harrison TG (2007b) The impact of School Teacher Fellows on teaching and assessment at tertiary level. New Dir 3:77–78

Shallcross DE, Harrison TG (2007c) Climate change made simple. Phys Educ 42:592–597

Shallcross DE, Harrison TG (2008a) Climate change modelling in the classroom. Sci Sch 9:28–33. www.scienceinschool.org/2008/issue9/climate. Accessed 21 Feb 2015

Shallcross DE, Harrison TG (2008b) Practical demonstrations to augment climate change lessons. Sci Sch 10:46–50. www.scienceinschool.org/2008/issue10/climate. Accessed 21 Feb 2015

Shallcross DE, Harrison TG (2009) Hydrogen in the earth's atmosphere. Chem Rev 19(2):2–6

Shallcross D, Harrison T (2013) Radical changes in our atmosphere. Education in Chemistry, Royal Society of Chemistry, 22–25 Sept

Shallcross DE, Harrison TG, Henshaw SJ, Sellou L (2009a) Fuelling interest: climate change experiments. Sci Sch 11:38–43. www.scienceinschool.org/2009/issue11/climate. Accessed 27 Oct 2014

Shallcross DE, Harrison TG, Henshaw SJ, Sellou L (2009b) Looking to the heavens: climate change experiments. Sci Sch 12:38–43. www.scienceinschool.org/2009/issue12/climate. Accessed 27 Oct 2014

Tuah J, Harrison TG, Shallcross DE (2009) The advantages perceived by schoolteachers in engaging their students in university-based chemistry outreach activities. Acta Didactica Napocensia 2(3):31–44

Wild M, Gilgen H, Roesch A, Ohmura A, Long CN, Dutton EG, Forgan B, Kallis A, Russak V, Tsvetkov A (2005) From dimming to brightening: decadal changes in solar radiation at Earth's surface. Science 308(5723):847–850. doi:10.1126/science.1103215

Geoengineering for Climate Stabilization

Maximilian Lackner

Contents

Abstract

Engineering the climate by means of carbon dioxide removal (CDR), Earth radiation management (ERM), and/or solar radiation management (SRM) approaches has recaptured the attention of scientists, policy makers, and the

M. Lackner (✉)
Institute of Advanced Engineering Technologies, University of Applied Sciences FH Technikum Wien, Vienna, Austria
e-mail: maximilian.lackner@tuwien.ac.at

W.-Y. Chen et al. (eds.), *Handbook of Climate Change Mitigation and Adaptation*,
DOI 10.1007/978-3-319-14409-2_72

public. Climate engineering is being assessed as a set of tools to deliberately, and on a large scale, moderate or retard global warming. There are several concepts available, like injecting aerosol-forming SO_2 into the stratosphere or placing huge objects in orbit to partly shade Earth from incoming radiation or fertilizing the ocean with iron for increased algae growth and creation of carbon sinks. Such concepts are highly speculative, and irrespective of whether they would work, they bear huge risks, from adversely affecting the complex climate system on a regional or global scale to potentially triggering droughts, famine, or wars. More research is needed to better understand promising concepts and to work them out in depth, so that options are made available in case they should become necessary in the future, when climate change mitigation and adaptation measures do not suffice and fast action becomes imperative. Apart from the technological hurdles, which are anyhow mostly far beyond today's engineering capabilities, huge social, moral, and political issues would have to be overcome. The purpose of this chapter is to highlight a few common concepts of CDR, ERM, and SRM for climate engineering to mitigate climate change.

Introduction

Climate engineering (also dubbed geo-engineering, geoengineering) is defined as "the deliberate large-scale intervention in the Earth's climate system, in order to moderate global warming" (Shepherd 2009). Another, more positive term found in the literature is "climate remediation" or "climate intervention."

It can be considered a variant of macroengineering (the implementation of extremely large-scale design projects such as the Panama Canal) and similar in type to terraforming (planetary engineering, i.e., altering the environment of an extraterrestrial world). The expression is not to be confused with **geological engineering** (likewise termed geoengineering or geotechnical engineering, which is concerned with the design and construction of earthworks, including excavations, hydraulic fracturing (fracking), drilling, and underground infrastructure).

Climate engineering can be seen as the most desperate, bizarre climate change mitigation measure. Yet, due to slow progress with conventional and incremental measures, it has recaptured widespread attention among scientists, politicians, and the public. Climate engineering or "hacking the planet" (Kintisch 2010) is hyped as "quick fix" and "only solution" on the one hand and bedeviled and rejected as wacky idea, simply gambling, being impossible, and very dangerous on the other hand. Some see it as a metaphoric "Faustian bargain" or man's attempt to "play God." Finally, one needs to acknowledge that climate engineering concepts mostly "treat the symptoms rather than cure the illness" of climate change.

It is not so easy to find one's position toward climate engineering, and according to Heyward and Rayner (2013), some "scientists involved in geoengineering discourse convey mixed messages about the need for technocratic management of the

anthropocene at the same time as expressing strong commitments to the importance of public participation in decision making about geoengineering." The Intergovernmental Panel on Climate Change (IPCC) states that every option has to be considered, yet it expresses a critical attitude toward climate engineering due to the inherent, unknown risks and assesses it in its 2007 report as "largely speculative and unproven and with the risk of unknown side-effects." It was around the year 2008 (Ming et al. 2014) to 2009 that a critical discourse of geoengineering started to emerge, mainly in American magazines (Biello 2009; Kunzig 2008) and German newspapers (Anshelm and Hansson 2014). Kennedy et al. (2013) write that "No study of coping with climate change is complete without considering geoengineering."

Social science teaches that transformation dynamics evolve from hope-inspired alternative choices rather than fear-driven technical constraints (Stirling 2014). With a lot of disappointment from commitment and implementation of climate change mitigation measures over the last years, and continued GHG emissions, many scientists feel certain despair, giving an inclination toward options provided by climate engineering.

Climate engineering can be considered a complementary approach to conventional measures: Preserving the climate (quick fix) while CO_2 is gradually brought under control by natural and/or artificial processes. In this scenario, climate engineering would "buy time" for mankind and the globe.

The major issue, even with reversible actions of climate engineering, is that the climate system is very complex. Identifying unintended consequences is not a trivial – if at all possible – task. Such consequences could be most severe and irreversible, like droughts or wars. In this context, it is worthwhile to think about the theory of chaos, which is rooted in the pioneering work of MIT meteorologist and mathematician Edward N. Lorenz (1963). Moreover, a slight drifting of the continents or a minor shifting of ocean currents may bring ice to one land and desert sands to another; see Lorenz (1972).

Safe Limits

The concept of Earth as a self-regulatory system was developed in the late 1960s by J. E. Lovelock and became popular under the name "Gaia hypothesis" and "Daisyworld" model (it is a parable on the biological homeostasis of the global environment. "Daisyworld" contains white and black flowers. When temperatures rise, more white daisies grow, increasing reflection. Sinking temperatures are counteracted by a growth of black daisies: They absorb more sunlight. Hence the balance of white to black daisies controls the temperature and stabilizes it. The simplistic Daisyworld model intuitively describes the coupling between climate and the biosphere). Lovelock's concept is being discussed controversially (Weaver and Dyke 2012; Boston 2008). For sure nature can buffer anthropogenic impact to some extent, but not endlessly, and climate change is testimony for this finite buffering capacity.

In their seminal paper "A safe operating space for humanity" (compare *The Limits to Growth* work by the Club of Rome in 1972), Rockström et al. write that "Although Earth has undergone many periods of significant environmental change, the planet's environment has been unusually stable for the past 10,000 years. This period of stability — known to geologists as the Holocene — has seen human civilizations arise, develop and thrive" (Rockström et al. 2009). They define nine interlinked planetary boundaries, three of which have already been overstepped. For instance, the estimated safe threshold identified for atmospheric CO_2 is 350 ppm or a total increased warming of 1 W/m^2 (current warming is approx. 1.9 W/m^2 radiative forcing from 400 ppm of CO_2 (Butler and Montzka 2013), not considering the additional radiative forcing by other greenhouse gases such as CH_4).

Climate Engineering Approaches

Climate engineering is still in its infancy, at a theoretical stage, where ideas are being generated, discussed, and elaborated. The Secretariat of the Convention on Biological Diversity concluded that "There is no single geoengineering approach that currently meets all three basic criteria for effectiveness, safety and affordability. Different techniques are at different stages of development, mostly theoretical, and many are of doubtful effectiveness" (Secretariat of the Convention on Biological Diversity 2012).

Global climate engineering is untested and mostly untestable (MacMynowski et al. 2011). Its roots go back to 1965, when advisors to US President Lyndon B. Johnson suggested spreading reflective particles over 13 million km^2 of ocean in order to reflect an extra 1 % of sunlight away from Earth (Kintisch 2010). This was one of the first high-level acknowledgements of climate change. Interestingly, no suggestions to cut down CO_2 emissions were reported to have been made. The president did not follow these early geoengineering suggestions.

Even prior to that, in 1955, John von Neumann foresaw "forms of climatic warfare as yet unimagined" in *Fortune* magazine (von Neumann 1955). In 1974, the Russian researcher Mikhail Budyko suggested that cooling down the planet could be achieved by burning sulfur in the stratosphere, which would create a haze from the resulting aerosols (higher albedo) (Teller et al. 1997). This and other concepts will be touched upon below. Space-based geoengineering concepts build upon Tsiolkovsky's and Tsander's 1920s idea of utilizing mirrors for space propulsion (Kennedy et al. 2013). As these examples show, ideas to engineer the climate came up quite early.

Small-scale weather modification can already be achieved today, e.g., by cloud seeding to induce rainfall. The historical Project "Stormfury" (1962–1983) attempted to weaken tropical cyclones with silver iodide (Willoughby et al. 1985). For a brief review on "rainmaking attempts" and "weather warfare," which is outside the scope of this chapter, see Chossudovsky (2007) and *Climate Modification Schemes*, American Institute of Physics (AIP) (2011). Weather modification action has been limited by the international community, e.g., during war by the 1977 UN

Environmental Modification Convention. Another regulation in this respect is the London Convention (1972) and its 1996 Protocol, which are global agreements regulating dumping of wastes at sea. Article 6 prohibits exports of wastes for dumping in the marine environment, which includes, e.g., CO_2 in CCS (carbon capture and storage) schemes (Dixon et al. 2014).

Examples where man has modified local climate (impacts) include artificial snow in skiing resorts or irrigation for crop yield amelioration. Previous environmental interventions by man have sometimes brought about unwanted – and unexpected – effects, also in the near past, e.g., streamlining riverbeds leading to local floods or the creation of urban heat islands.

Joe Romm, founding editor of the blog Climate Progress, has linked "geoengineering to a dangerous course of chemotherapy and radiation to treat a condition curable through diet and exercise — or, in this case, emissions reduction" (McGrath 2014). Al Gore, former vice president of the USA, was quoted on climate engineering to be "utterly mad and delusional in the extreme." He said that searches for an instant solution were born out of desperation, were misguided, and could lead to an even bigger catastrophe (Goldenberg 2014). "The idea that we can put a different form of pollution into the atmosphere to cancel out the effects of global warming pollution is utterly insane" (Goldenberg 2014).

In fact, the idea of "engineering" the Earth's climate is a shocking one. There is yet little information available, and "technically feasible" concepts are totally vague on costs, effectiveness, reversibility, risks, and side effects.

However, serious scientists have started to investigate options for climate engineering more deeply, since swift remedial action might be needed once the Earth's climate system reaches a "tipping point" (positive feedback, thermal runaway, e.g., thawing of permafrost releases CH_4, which further increases temperatures). It seems necessary to study climate engineering, to be prepared. There is also the threat of unilateral action by another country (Dean 2011), should a local benefit from such action be expected. Tipping point rhetoric is challenged in Heyward and Rayner (2013).

Climate engineering ideas and concepts fall into two broad groups: **carbon dioxide removal (CDR)** and **solar radiation management (SRM)**. Several researchers discern **Earth radiation management (ERM)** from SRM, where ERM techniques focus on atmospheric convection enhancement (building of thermal bridges) and increasing outgoing IR heat radiation (i.e., long wavelength). The focus of SRM is on (short wavelength) incoming radiation. The term ERM was introduced by David L. Mitchell et al. (2011). He includes CRD and cirrus cloud reduction into SRM (Mitchell and Finnegan 2009). CRD techniques are remediation, whereas SRM are intervention.

CDR techniques are generally not considered that controversial, and they do not seem to introduce global risks, as they work on the local scale. Costs and technical feasibility have been limiting CDR deployment, e.g., reforestation or CCS. CRD attacks the root cause of climate change. However, the effects work slowly to bring down temperatures again.

SRM targets an increase in the amount of solar energy radiated back into space, effectively dimming the Sun. The necessary albedo enhancement is envisioned for

deserts, oceans, mountains, clouds, and also manmade objects like roofs or roads. Prominent concept examples include deployment of giant orbiting sunshields in space, emission of huge amounts of SO_2 (Crutzen 2006) and particles into the stratosphere to mimic the action of volcanoes, increase of the Earth's albedo by "painting" deserts white, spraying sea water into the atmosphere to produce and whiten clouds, redirecting ocean streams and changing their salinity (Could a massive dam 2010), or pumping seawater into pole regions and creating ice. Such techniques bear the risk of upsetting the Earth's natural rhythms. SRM approaches act quickly. However, they do not remove the root cause of climate change, mainly CO_2 levels in the atmosphere, so other aspects like ocean acidification are not tackled.

Raymond Pierrehumbert, professor in Geophysical Sciences at University of Chicago, said "The term 'solar radiation management' is positively Orwellian. It's a way to increase comfort levels with this crazy idea" (Rotman 2013).

According to Shepherd (2009), CDR methods should be regarded as preferable to SRM methods. SRM methods are expected to be cheaper, though.

The Royal Society wrote in a 2009 report (Shepherd 2009): "Solar Radiation Management methods could be used to augment conventional mitigation. However, the large-scale adoption of Solar Radiation Management methods would create an artificial, approximate, and potentially delicate balance between increased greenhouse gas concentrations and reduced solar radiation, which would have to be maintained, potentially for many centuries. It is doubtful that such a balance would really be sustainable for such long periods of time, particularly if emissions of greenhouse gases were allowed to continue or even increase."

Although technological hurdles exist, it is expected that devising working technologies (i.e., installations that cool the atmosphere) are easier than understanding their effects or how governance (Shepherd 2009) should be applied.

The focus of this chapter lies on SRM, which directly modify the Earth's radiation balance; compare Fig. 1. It also covers CDR, which influences the global carbon cycle (see Fig. 2), and ERM, as well as touching upon governance and other related aspects of climate engineering.

Radiation Balance

Energy on Earth mainly comes from the Sun. The solar constant is approx. 1,361 W/m^2, which translates into a power of 1.730×10^{17} W for the entire Earth. The average incoming solar radiation is approx. ¼ of the solar constant (342 W/m^2). The radiation balance of the Earth is shown in Fig. 1 in a simplified version.

Climate engineering aims at modifying this radiation balance to achieve a lower net heating effect. In climate science, **radiative forcing** or climate forcing is defined as the difference of insolation (sunlight) absorbed by the Earth and energy radiated back to space. Currently, it is 2.916 W/m^2, which corresponds to 479 $CO_{2\text{-eq}}$. 1.88 W/m^2 thereof is due to CO_2 and 0.51 W/m^2 due to CH_4 (Butler and Montzka 2013).

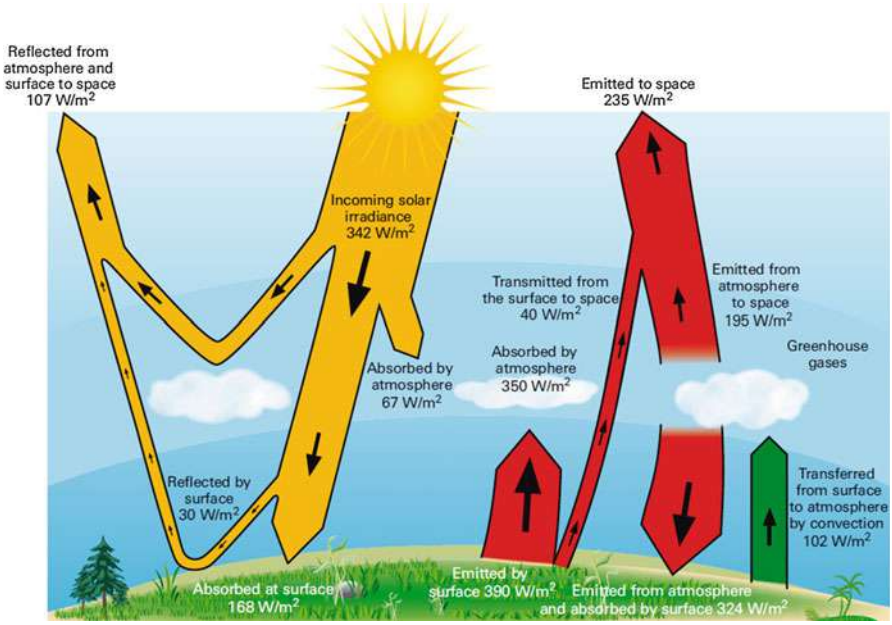

Fig. 1 Schematic showing the global average energy budget of the Earth's atmosphere. *Yellow* indicates solar radiation; *red* indicates heat radiation; and *green* indicates transfer of heat by evaporation/condensation of water vapor and other surface processes. The width of the *arrow* indicates the magnitude of the flux of radiation and the numbers indicate annual average values. At the top of the atmosphere, the net absorbed solar radiation is balanced by the heat emitted to space (Source: Shepherd 2009)

Global Carbon Cycle

Figure 2 shows the simplified global carbon cycle in Gt of carbon per year (1 Gt = 1 Pg = 10^{15} g). One can see that the ocean is the largest sink.

The various carbon sinks present opportunities for geoengineering. Subsets of special techniques are **biogeoengineering** and **Arctic geoengineering**. In biogeoengineering, plants or other living organisms are used or modified to beneficially influence the climate on Earth, e.g., by creating carbon sinks. An example is iron fertilization of the oceans. Iron is a growth-limiting factor, so fertilization would be expected to produce more algae, taking up CO_2, like land-based biomass.

"Global dimming" is an aspect that could be exploited for climate engineering. Monoterpenes from boreal forests (Rinnan et al. 2011; Aaltonen et al. 2011) were found to contribute to global dimming (cooling), apart from being a CO_2 sink, so tree planting would be a working biogeoengineering approach. **Global dimming**, generally, is caused by an increase in particulates such as sulfate aerosols in the atmosphere due to human action. The effect of anthropogenic global dimming has interfered with the **hydrological cycle** by reducing evaporation and so may have reduced rainfall in some areas. Global dimming also creates a cooling effect that may

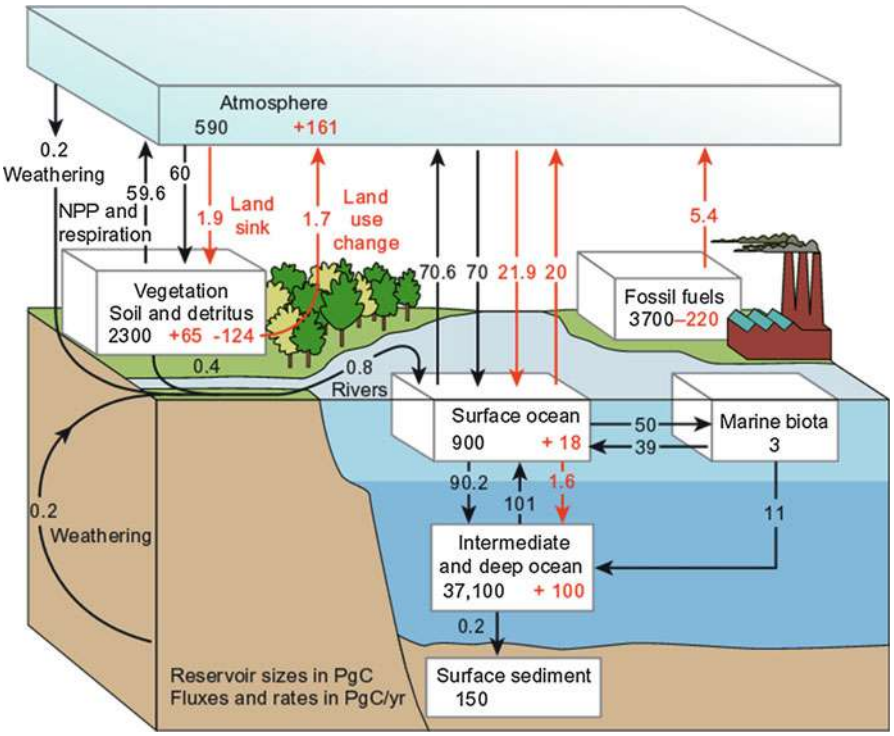

Fig. 2 Simplified representation of the global carbon cycle. The values inside the boxes are standing stocks (in Pg C); the *arrows* represent annual fluxes (Pg C/y). The *black arrows* and *numbers* show the preindustrial values of standing stocks and fluxes; the *red arrows* and *numbers* indicate the changes due to anthropogenic activity (Source: Cole 2013)

have partially counteracted the effect of greenhouse gases on global warming. With sulfur levels in fuels being further reduced, e.g., for ships, the global warming contribution of combustion emissions will increase in the future.

Arctic geoengineering focuses geographically on the Arctic, which plays a key role in maintaining current climate due to its albedo and stored methane. The Arctic ice is disappearing quickly, though, and concepts have been envisioned to support ice buildup.

Impacts of Climate Engineering

The targeted impact of climate engineering is to bring down global air and surface temperatures. Undesired side effects might also occur, though, particularly in SRM schemes. Several researchers have run computer models to investigate the effect of blocking part of the solar radiation. Shading the Sun would, according to the models,

reduce the global temperatures, but also lead to profound changes to precipitation patterns including disrupting the Indian Monsoon (Shepherd 2009). Anthropogenic SO_2 in the stratosphere at a level necessary to counteract the radiative forcing of human CO_2 and CH_4 could cut rainfall in the tropics by 30 % (Ferraro et al. 2014). Also, it would lead to acid rain. There is further concern that SO_2 in the troposphere can harm the ozone layer; see also section "Stratospheric Sulfate Aerosols."

Evidence that such action would in fact result in a net cooling was provided by the eruption of the volcano Mt. Pinatubo in the Philippines in June 1991. It resulted in a −0.5 °C variation in the Earth surface temperature, due to the effect of sulfate aerosol-induced albedo enhancement. However, already by the year 1995, the effect had vanished, and the temperature returned to the former value (Gomes and de Araújo 2011). Note: Another volcanic event with transient, global impact on the climate was the 1815 eruption of Mount Tambora in Indonesia, which led to a "year without summer" and famine due to reduced crop yields (Stilgoe et al. 2013a).

Sticking with this geoengineering example, potential side effects of SO_2 injected into the stratosphere by, e.g., balloons, artillery, or jet planes, are:

- CO_2 emissions from the missions
- Litter, e.g., from returning balloon shells
- Noise, e.g., from the artillery
- Depletion of ozone
- Regional droughts, e.g., in Africa and Asia from weaker monsoon activity
- Impact on cloud formation, particularly cirrus clouds, with unpredicted effects
- Acidic rain, leading to further ocean acidification, and other effects on the ecosystem
- Whitening of the sky due to aerosols, more diffuse radiation
- Less yield from solar energy collectors, impacting renewable energy production
- Temperature changes in the stratosphere, influencing atmospheric circulations in the troposphere with unknown effects

The Geoengineering Model Intercomparison Project (GeoMIP) around Ben Kravitz assesses the projected impacts of geoengineering by different climate models, focusing on SRM (http://climate.envsci.rutgers.edu/GeoMIP/publications.html). In 2013, 12 climate models simulating quadrupled atmospheric carbon dioxide levels and a corresponding reduction in solar radiation were compared (Kravitz 2013). In Fig. 3, an overview by the Convention on Biological Diversity (http://www.cbd.int/convention/) shows which intended and unintended effects might result from geoengineering.

It is expected that both SRM and SDR would affect biodiversity and ecosystems, which finally have a significant impact on human well-being. As stated above, quantification of intended and also identification of unintended consequences of SRM and to a lesser extent ERM and CDR techniques are difficult to achieve.

On the benefits, risks, and costs of stratospheric geoengineering, see e.g., Robock et al. (2009).

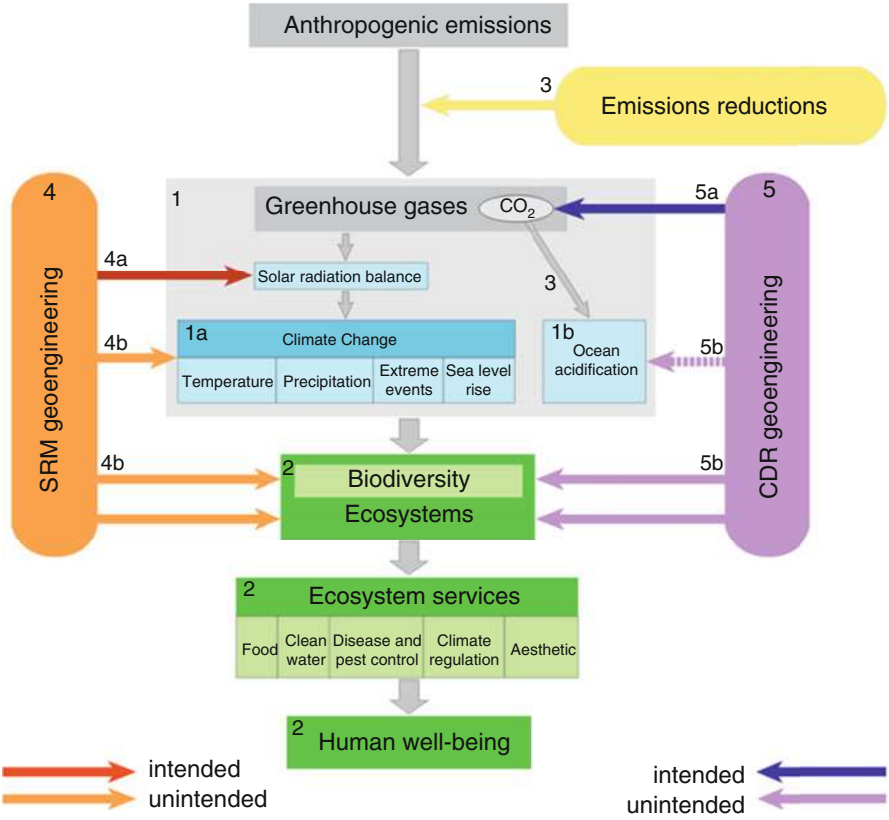

Fig. 3 Conceptual overview of how greenhouse gas emission reductions and the two main groups of geoengineering techniques may affect the climate system, ocean acidification, biodiversity, ecosystem services, and human well-being (Numbers refer to the chapters in the cited source, from which reproduction with permission was made (Secretariat of the Convention on Biological Diversity 2012))

Legal, Moral, and Social Issues

"Whose hand will be on the planetary thermostat?"(Robock 2014). Action by one nation would impact climate globally, but who is entitled to enact and control climate engineering? Would the target of climate engineering be to reduce future global warming, i.e., to maintain current temperatures; to limit global warming to, e.g., 2 K; or to bring back temperatures to preindustrial levels? Who would set the target? These questions cannot be answered at this point in time, as outlined in this section of this chapter.

Legal Issues

Signed by 150 government leaders at the 1992 Rio Earth Summit, the Convention on Biological Diversity is dedicated to promoting sustainable development. Conceived as a practical tool for translating the principles of Agenda 21 (a voluntarily implemented action plan of the United Nations with regard to sustainable development), it states "that no climate-related geo-engineering activities that may affect biodiversity take place, until there is an adequate scientific basis on which to justify such activities and appropriate consideration of the associated risks for the environment and biodiversity and associated social, economic and cultural impacts, with the exception of small-scale scientific research studies" (http://www.cbd.int/convention/). Thereby, private or public experimentation and adventurism are avoided, yet research is possible. R&D in climate engineering is justified so that man understands his options once a said environmental tipping point has been surpassed (contingency planning to have "something on the shelves" when needed). Research priorities in this respect are worked out in Shepherd (2009).

Moral and Social Issues

While anthropogenic greenhouse gas emissions are an unwanted side effect, climate engineering constitutes a large-scale, intentional effort to alter the climate.

Responsibilities and global political governance are not clear. It is conceivable that different governments have different targets for global temperatures. Some areas of the world show higher crop yield in an elevated temperature scenario, for instance. So actions by one country to alter the climate, motivated by expected local benefits, might result in war. Multilateral commitments and agreements over time periods of several 100 years would be necessary, as this is the time that, e.g., SO_2 from climate engineering would have to remain in the stratosphere in a delicate balance with anthropogenic CO_2 emissions it is offsetting, so there would also have to be imperative controls over CO_2 levels at the same time.

The governance of emerging science and innovation is discussed in Stilgoe et al. (2013b), citing canceling the geoengineering project "SPICE" (see below) as an example. For public perception of geoengineering, see Corner et al. (2013) and Sikka (2012). Governance principles concerning climate engineering were also elaborated in the 2010 Asilomar International Conference on Climate Intervention Technologies (http://climate.org/resources/climate-archives/conferences/asilomar/report.html).

Preliminary Climate Engineering Field Experiments

Climate engineering has a global scale, and documented field trials to date are very limited. Some concepts can hardly be tested at all.

Fig. 4 Whitening the mountain Chalon Sombrero in Peru in a geoengineering pilot project (Source: Collyns 2010)

One of the largest experiments, known as **LOHAFEX**, was an Indo-German fertilization experiment in 2009, in which six tonnes of iron as iron sulfate solution was spread over an area of 300 km^2 (Ebersbach et al. 2014) in the South Atlantic. It was expected to trigger an algal bloom, resulting in CO_2 update and some of the algae ending up in the ocean bed as carbon sink.

A much disputed, similar experiment was carried out in July 2012 by entrepreneur Russ George, who put approx. 100 t of iron sulfate into the Pacific Ocean several hundred miles west of the islands of **Haida Gwaii**/Canada. The intention was to increase the production rate of phytoplankton for salmon fishing (Sweeney 2014).

In 2005, a pilot project in Switzerland to **cover a glacier** with a reflective foil was carried out. On the Gurschen glacier, it was found that the blanket reduced the melding by 80 % (Pacella 2007). More trials on an area of more than 28,000 m^2 were done on the Vorab glacier (Pacella 2007).

Painting the Andes: In 2009, the World Bank has awarded a seed grant to 26 innovative climate adaptation projects, selected from 1,700 proposals (World Bank). Among them was one idea from Peruvian inventor Eduardo Gold to whiten the Chalon Sombrero peak in the Andes (Collyns 2010). This pilot project (see Fig. 4) has received positive media attention.

In the UK **SPICE** project (Stratospheric Particle Injection for Climate Engineering, 2015), a trial balloon flight was planned; see Fig. 5.

The idea was to send a balloon 1 km into the sky and to eject water droplets. These droplets should create clouds, increasing the albedo. The experiment had to be canceled due to opposition from environmental groups (Shukman 2014; Zhang et al. 2015).

Tree planting (reforestation, afforestation) (Zomer et al. 2008; Schirmer and Bull 2014; Trabucco et al. 2008) and peatland restoration (Bonn et al. 2014) activities are

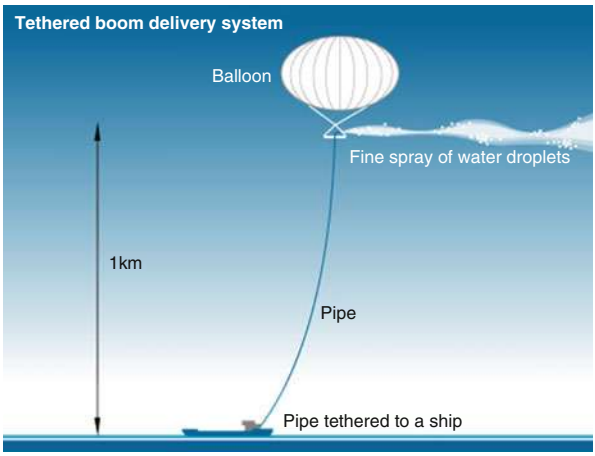

Fig. 5 Concept of the SPICE experiment (Source: Vidal 2011)

being considered in several parts of the world. According to the IPCC, reforestation refers to establishment of forest on land that had recent tree cover, whereas afforestation refers to land that has been without forest for longer time periods (IPCC 2015).

Cool roof experiments: In cities, the temperature is typically 1–3 °C higher than in the surrounding countryside, due to, e.g., heat-absorbing infrastructure such as dark asphalt parking lots and dark roofs (Oke 1997). By increasing the reflectivity, more radiation is sent back into space, and energy costs (air conditioning) can be reduced. Pilot projects are, e.g., the "White Roof Project" (http://www.whiteroofproject.org/) and New York's "NYC °CoolRoofs" (http://www.nyc.gov/html/coolroofs/html/home/home.shtml).

Keeping groundwater level and salinity low. In Australia, rising levels of salty groundwater pose a problem for farmers. By pumping that groundwater into shallow evaporation ponds, crops are protected, with a positive side benefit of increased albedo (Edmonds and Smith 2011); see Fig. 6 (note that "geoengineering" is a side effect here).

Edmonds and Smith (2011) also describe reflective covers on water bodies to prevent evaporation losses. According to Ming et al. (2014), 40–50 % of the water stored in small farm dams of "hot" countries may be lost due to evaporation. Such covers, as a side effect, increase the albedo and thereby contribute to climate change mitigation; compare Fig. 7.

Proposed Strategies for Climate Engineering

Potential approaches are surface based (e.g., albedo modification of land or ocean), troposphere based (e.g., cloud whitening), stratosphere based (e.g., injection of SO_2 or Al_2O_3), and space based (e.g., gigantic space-based mirrors, lenses, or sunshades). Below, several selected concepts are briefly introduced.

Fig. 6 Image of a 700 × 900 m^2 wheat field in Western Australia in which a 66 m diameter evaporation pond was created (Source: Edmonds and Smith 2011)

Fig. 7 Reflective evaporation covers on a mine reservoir at Parkes in Australia (Edmonds and Smith 2011)

Carbon Dioxide Removal (CDR)

As mentioned above, the first set of concepts can be summarized as CO_2 removal schemes (CDR) as visually summarized in Fig. 8.

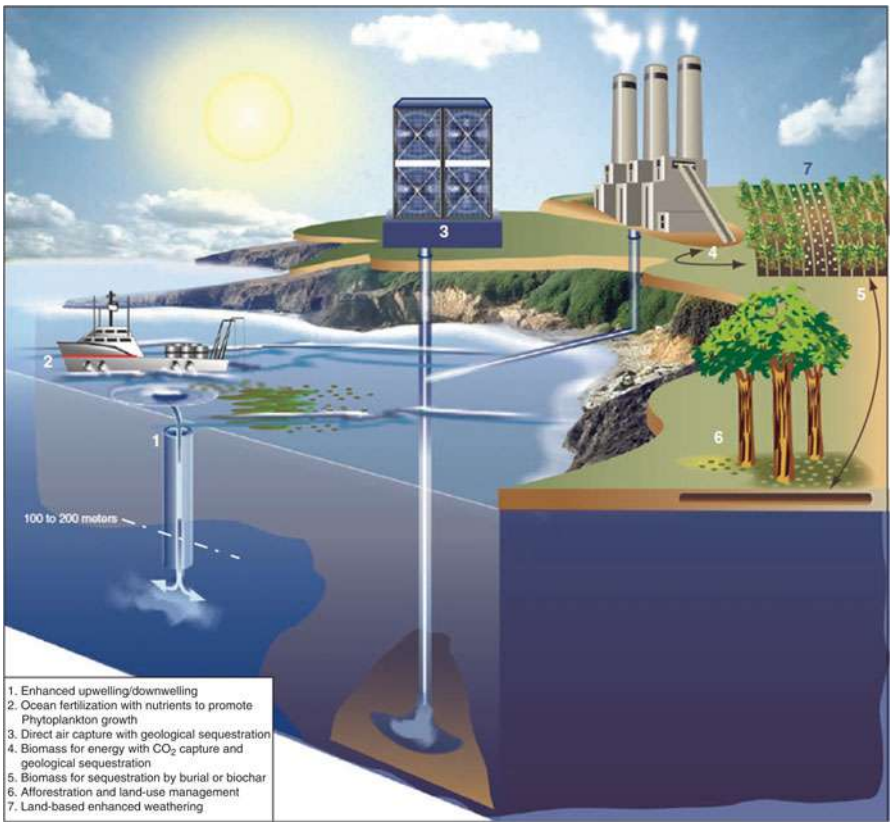

Fig. 8 Depiction of some popular CDR concepts. See text for details (Source: Climate 2010)

Carbon capture and storage (CSS) and carbon sequestration projects are out of the scope of this chapter; see elsewhere in this handbook and in the DOE/NETL CO_2 capture and storage roadmap (2010). Other CDR concepts include (Shepherd 2009):

- Use of biomass as carbon sink.
- Protection of and (re)creation of terrestrial carbon sinks such as grasslands.
- Enhanced weathering to remove CO_2 from the atmosphere.
- Direct capturing of CO_2 from the ambient air (concepts to wash CO_2 out of the atmosphere include "artificial trees" and scrubbing towers), known as industrial air scrubbing (IAS) or direct air capture (DAC) (de_Richter et al. 2013). Costs are expected to be prohibitively high (House et al. 2011).
- Enhancement of oceanic uptake of CO_2, for example, by fertilization of the oceans with naturally scarce nutrients such as iron or by changing ocean currents.
- Biochar (when biomass is pyrolyzed, char (biochar) remains. It can be mixed with soil to create terra preta, a carbon sink (Hyland and Sarmah 2014)).

There are numerous other concepts, such as removing (dark) vegetation from the mountain tops or changing the composition of ship and aircraft exhaust. The interested reader will find a collection of ideas in various internet sources such as Wikipedia. Out of the concepts presented from (Shepherd 2009) above, two are described briefly as an example.

Enhanced Weathering

In enhanced weathering, inorganic matter is used to take up CO_2, a process that occurs in nature, but slowly. For instance, if carbonates are formed, CO_2 is stored long term. This chemical approach to geoengineering involves land- or ocean-based techniques. Examples of land-based enhanced weathering techniques are in situ carbonation of silicates such as ultramafic rocks (ultrabasic rocks, which are igneous and metaigneous rocks with a very low silica content and a high magnesium and iron content). Ocean-based techniques involve alkalinity enhancement of the sea, e.g., by grinding, dispersing, and dissolving olivine, limestone, silicates, or calcium hydroxide against ocean acidification and for CO_2 sequestration. Enhanced weathering is considered as one of the most cost-effective options. CarbFix (2015) is a feasibility project of enhanced weathering in Iceland. For details on mineral carbonation/mineral sequestration, see, e.g., Herzog (2002) and Goldberg et al. (1998).

Bioenergy with Carbon Sequestration (BECS), Biochar, and Wood Burning

BECS is a hybrid approach in which bioenergy crops are grown and used as fuel, and the CO_2 emissions are captured and stored (see CCS elsewhere in this handbook). Biochar and BECS could together contribute a carbon sink of 14 GtC/year by 2100 (Edenhofer et al. 2012). The concept of burying wood in anoxic environments (e.g., deep in the soil) is that decomposition would be much slower, providing a long-term carbon sink; compare Fig. 9. According to Zeng (2008), the long-term carbon sequestration potential for wood burial is 10 ± 5 GtC per year, and currently about 65 GtC is available on the world's forest floors in the form of coarse woody debris suitable for burial. The cost for wood burial is estimated to be lower than the typical cost for power plant CCS. Approx. 100 tC are bound as coarse wood carbon from a typical mid-latitude forest area of 1 km^2 in 1 year (Zeng 2008). However, there is the potential for counterproductive emissions of methane from anaerobic decomposition of the buried wood.

It is estimated that, by storing carbon in deep sediments, deep ocean sequestration can capture up to 15 % of the current global CO_2 annual increase. It was hence suggested to dump crop residues in the deep ocean (Strand and Benford 2009).

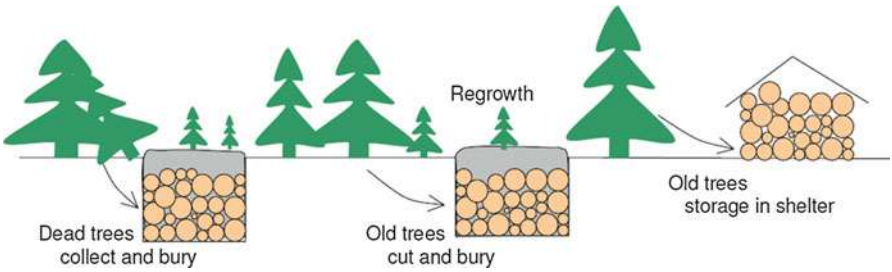

Fig. 9 Schematic diagram of forest wood burial and storage (Source: Zeng 2008)

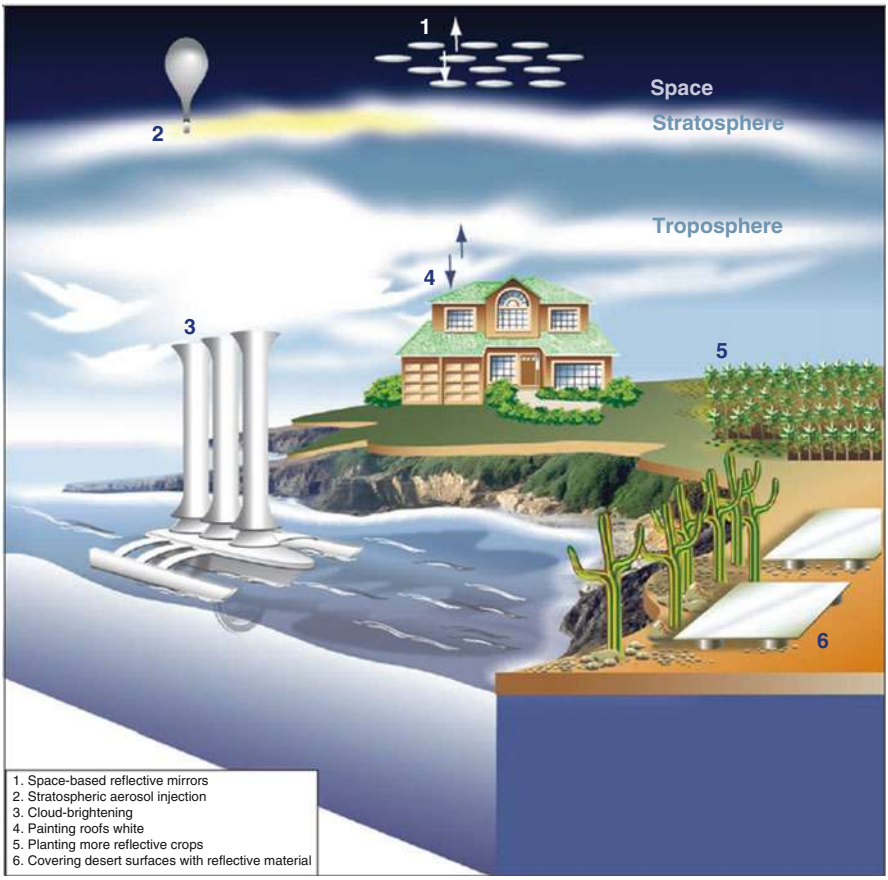

Fig. 10 Depiction of solar radiation management (Source: Climate 2010)

Solar Radiation Management (SRM)

The second set of techniques for climate engineering is the SRM category. SRM stands for "solar radiation management" or "sunlight reflection methods;" compare Fig. 10.

Four of such SRM concepts are explained below.

Cloud Reflectivity Modification

This approach considers altering the reflectivity of clouds in two ways: thinning of cirrus clouds and brightening (low) marine clouds. High, cold cirrus clouds let sunlight penetrate but capture infrared radiation. Hence, thinning or removing cirrus would have a net cooling effect on Earth. By contrast, low, warm clouds (stratocumulus, which cover approx. 1/3 of the ocean's surface) reflect sunlight efficiently. This "cloud whitening" or "marine cloud brightening" could be achieved with cloud condensation nuclei (CCN) such as fine seawater droplets. The effect is considered to be more pronounced on the sea than on the land, as clouds over the landmass have more (natural and anthropogenic) CCN available. Proposed schemes include seawater sprays produced by unmanned ship, ocean foams (Evans et al. 2010) from air bubble bursting, ultrasonic excitation (Barreras et al. 2002), and electrostatic atomization.

Stratospheric Sulfate Aerosols

SO_2 is known to cause global dimming, as it leads to aerosol formation, and the aerosols reflect sunlight. The mechanism is that SO_2 is oxidized to sulfuric acid, which is hygroscopic, has a low vapor pressure, and hence forms aerosols (Robock 2014). It was suggested to inject sulfur into the stratosphere as SO_2, sulfuric acid, or hydrogen sulfide by artillery, aircraft, and balloons (Rasch et al. 2008). According to estimates by the Council on Foreign Relations, "one kilogram of well placed sulfur in the stratosphere would roughly offset the warming effect of several hundred thousand kilograms of carbon dioxide" (Victor et al. 2009).

This approach was estimated to be over 100 times cheaper than producing the same temperature change by reducing CO_2 emissions (Keith et al. 2010). The SO_2 injection would have to be maintained, as tropospheric sulfur aerosols have a comparatively short atmospheric lifetime. Also, other particles have been considered, e.g., Al_2O_3.

Space Lenses, Space Mirrors, and "Dyson Dots"

Space-based concepts aim at transforming the solar constant into a controlled solar variable (Kennedy et al. 2013). They envision large space-based objects, which might be manufactured on the moon, mining local materials, or using material from asteroids. Concepts of giant lenses (Early 1989), dust rings (Bewick et al. 2013), and sunshades (Kosugi 2010) to block part of the Sun's incoming radiation using the effects of reflection, absorption, and diffraction were worked out. A convex lens with 1,000 km in diameter is considered sufficient, and in a Fresnel embodiment, it would only be a few millimeters thick (Early 1989). Shading the Sun by approx. 55,000 orbiting mirrors with 100 km^2 size, made from wire mesh, or by trillions of smaller mirrors (comparable to a DVD), was suggested (Ming et al. 2014); however, such

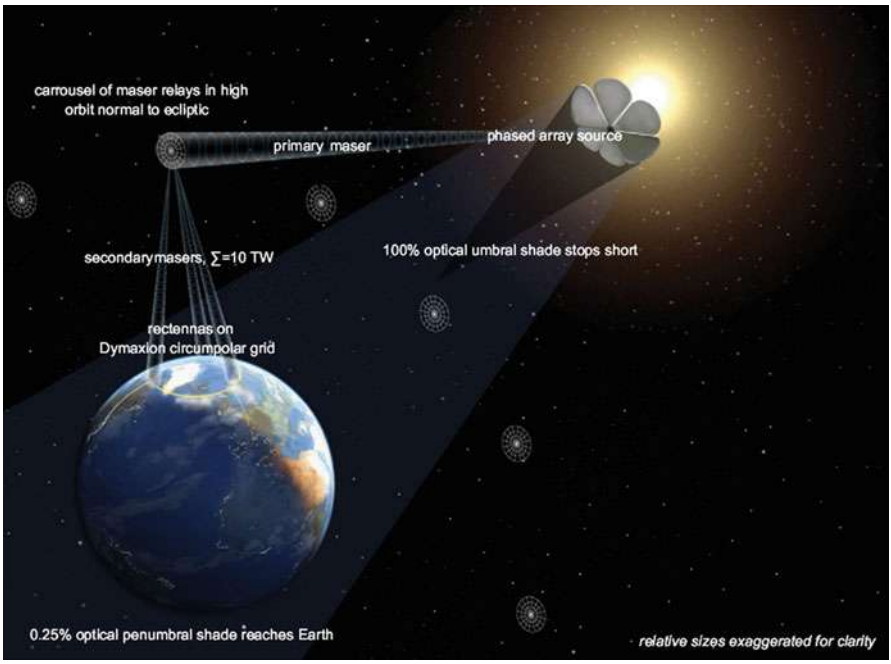

Fig. 11 Dyson dot concept with "self-funding" master energy delivery to the Earth (Reproduced with permission from Kennedy et al. 2013)

concepts are widely viewed as unrealistic. Current engineering capabilities are far from being able to realize such science-fiction-like concepts, not speaking about the costs, which are estimated at a century worth of global domestic product of all nations combined (Ming et al. 2014).

The "mirrors and smoke in space" concept was refined and coined "Dyson dots" (Kennedy et al. 2013). The concept is to place one or more large lightsail(s) in a radiation-levitated position sunward of the Lagrange point 1 (L1, SEL1). In this point, the gravitational forces on an object exerted by Earth and the Sun are equal. L1 is approx. 1.5 million km from Earth.

A 700,000 km^2 parasol in L1 would reduce insolation on Earth by at least 0.25 %. A photovoltaic power station on the sunny side of the parasol could "beam" energy to Earth via a maser (microwave laser) on the order of global demand, hence essentially funding the entire project. The "Dyson dot" concept is shown in Fig. 11.

The expression "Dyson dot" is based on the concept of a "Dyson sphere," a hypothetical megastructure imagined by Freeman Dyson in 1960, who speculated in a science article entitled "Search for Artificial Stellar Sources of Infrared Radiation" that advanced extraterrestrial civilizations could have housed in their star with a megastructure, maximizing energy capturing.

A 0.25 % reduction in the Sun's energy output was observed in the period of mid-sixteenth to mid-seventeenth century dubbed "sunspot cycle shutdown time,"

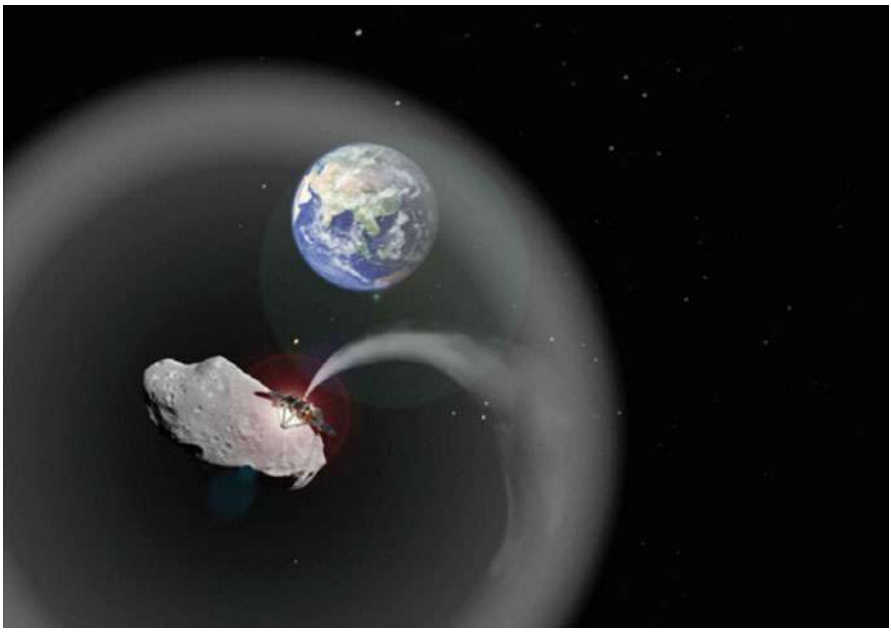

Fig. 12 Impression of an L1 positioned dust cloud for space-based geoengineering (Source: Bewick et al. 2012)

"Maunder Minimum," or "Little Ice Age," so this order of magnitude is what space geoengineers are aiming at.

Dust Clouds

Clouds of extraterrestrial dust placed in the vicinity of the L1 point are an alternative concept to thin-film reflectors, aiming at significantly reducing the manufacturing efforts. The material should be mined from captured asteroids, being moved by solar collectors or mass drivers (Bewick et al. 2012); see Fig. 12.

For details on such a dust concept, see, e.g., Bewick et al. (2012). Dust for sunlight blocking might also be mined on the moon.

Other Greenhouse Gas Remediation Ideas

There are many other geoengineering concepts than those introduced above, some of which are mentioned here:

CFC Destruction by Lasers

Chlorofluorocarbons (CFC) are persistent in the atmosphere, having huge GWP, yet they are accessible via their photochemistry (Stix 1993). Extremely powerful lasers might be used to break up tropospheric CFC.

Ocean Heat Transport

Ocean heat transport (downwelling of ocean currents) is outlined in Zhou and Flynn (2005). This concept aims at changing oceanic currents to shovel heat energy to deeper regions of the ocean. Also, solar-driven heat pumps might be used to this end.

Methane Remediation

Since methane is also a GHG of big concern, other geoengineering concepts target reducing CH_4 emission, e.g., by soil oxidation into CO_2 (Tate 2015).

ERM and Energy Production

Earth radiation management (ERM) aims at increasing the long wavelength radiation sent into space, which today is being trapped by GHG. ERM can be combined with energy production in so-called meteorological reactors (Ming et al. 2014). The term "meteorological reactor" stands for a climate engineering installation that fulfills two purposes: reduction of radiative forcing and energy production. Possible embodiments are:

- Solar updraft tower
- Solar downdraft energy tower
- Atmospheric vortex engine
- Heat pipes
- Radiative cooling, emissive energy harvesters (EEH)

Figure 13 shows an overview of such ERM schemes.

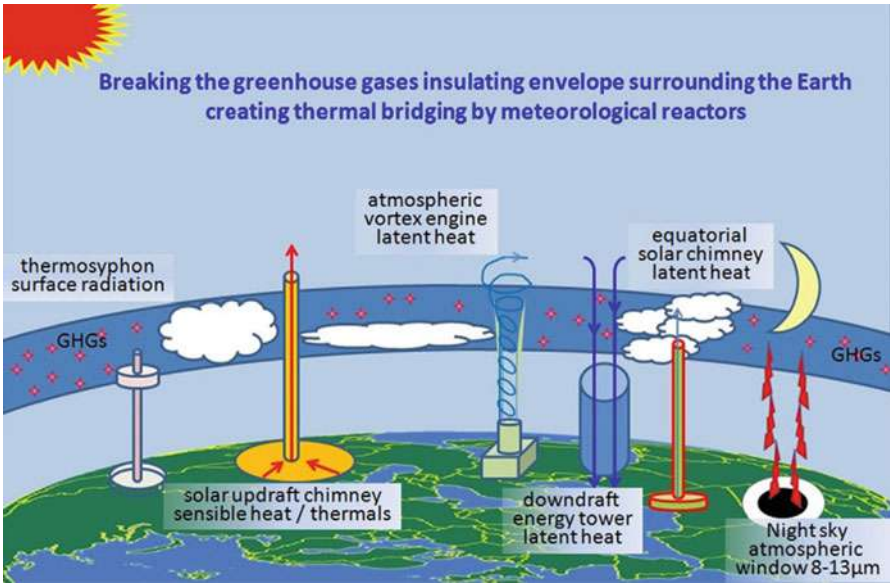

Fig. 13 Principal longwave radiation targets of meteorological reactors (Source: Ming et al. 2014)

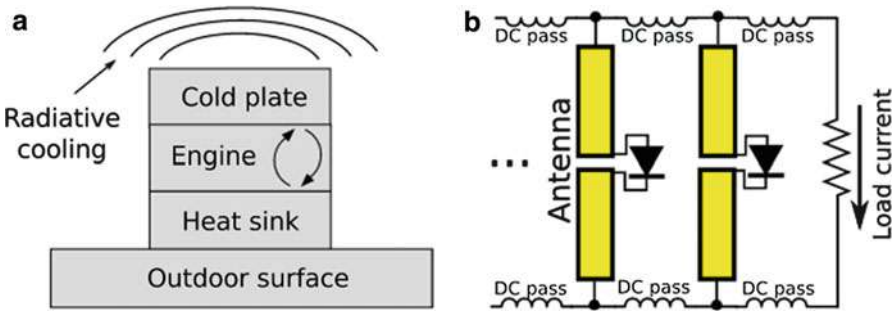

Fig. 14 Two possible EEH designs. (**a**) In a thermal EEH, a heat engine operates between the ambient temperature and a radiatively cooled plate. (**b**) In an infrared rectenna EEH, the whole panel is at ambient temperature, but the circuit's electrical noise is coupled to the cold radiation field via antennas (Source: Byrnes et al. 2014)

The "chimney effect" is used to create air motion, which can drive a generator. The hot air is moved into higher layers of the atmosphere, where it can radiate off heat energy. In Fig. 14, emissive energy harvesters (EEH) designs are depicted.

For details on "meteorological reactors" in ERM mode, see Ming et al. (2014) and http://www.solar-tower.org.uk/meteorological-reactors.php.

Climate Engineering in the Context of Climate Change Mitigation and Adaptation

Figure 15 is an illustration of the conceptual relationship between SRM and CDR with climate change adaptation and mitigation, in the context of the interdependent human and climatic systems.

The Kaya identity (O'Mahony 2013) mentioned in the caption of Fig. 15 is based on Japanese scientist Kaya and can mathematically be expressed as F = pop * (GDP/pop) * (E/GDP) * (F/E), with F being global anthropogenic CO_2 emissions, pop being global population growth, G the world GDP, and E the global energy consumption. Carbon emissions F can be estimated as the product of growth (pop), economic expansion (GDP/pop), energy intensity (E/GDP), and carbon efficiency (F/E).

Is It Geoengineering or Not?

The term geoengineering expresses, as stated initially, deliberate *large-scale* intervention in the Earth's climate system. CDR methods with a local to regional and/or low global impact are hence not real geoengineering approaches. The delineation is not exactly clear-cut. An attempt was made by the 2011 IPCC Expert Meeting on Geoengineering; see Fig. 16.

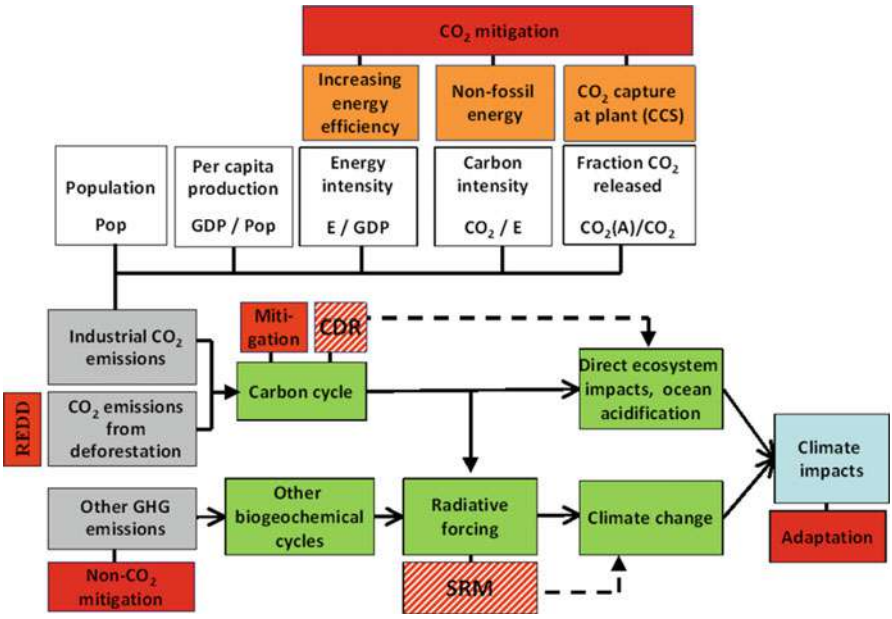

Fig. 15 Illustration of mitigation, adaptation, solar radiation management (*SRM*), and carbon dioxide removal (*CDR*) methods in relation to the interconnected human, socioeconomic, and climatic systems and with respect to mitigation and adaptation. The *top* part of the figure represents the Kaya identity. REDD stands for Reducing Emissions from Deforestation and Forest Degradation (Source: Edenhofer et al. 2012)

As Fig. 16 shows, ocean fertilization and ocean alkalinization are seen as geoengineering-type projects, as can be large afforestation/reforestation.

Discussion

Having presented some geoengineering concepts, a discussion about their targeted effectiveness and commercial viability has to be carried out. Geoengineering appraisals in their context frames were studied in Bellamy et al. (2012), where "climate emergency," "insufficient mitigation," and "climate change impacts" were cited most often. The appraisals were found to be mostly expert analytic, involving calculations/computer modeling, expert reviews and opinions, economic assessments, and MCA (multi-criteria analysis) (Bellamy et al. 2012). This study also investigated the frequency of different geoengineering proposals; see Fig. 17.

Stratospheric aerosols and space reflectors were investigated most often. There was a balance between solar- and carbon-based concepts.

A qualitative ranking of storage potentials and local vs. global impact is shown in Fig. 18.

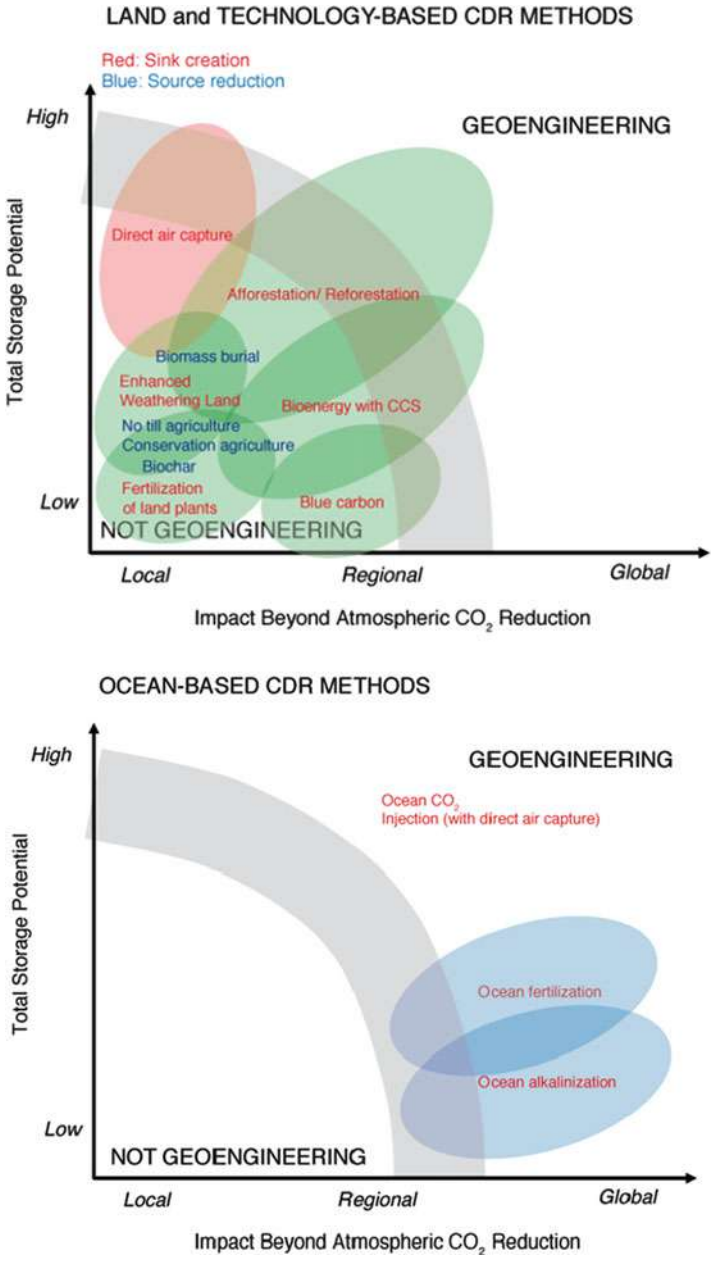

Fig. 16 Scale and impact are important determinants of whether a particular CDR method and specific application should be considered as geoengineering or not. Note that the specific positioning of the different methods is only illustrative and does not constitute a consensus view of the experts participating in the 2011 IPCC Expert Meeting on Geoengineering that produced this chart (Source: Edenhofer et al. 2012)

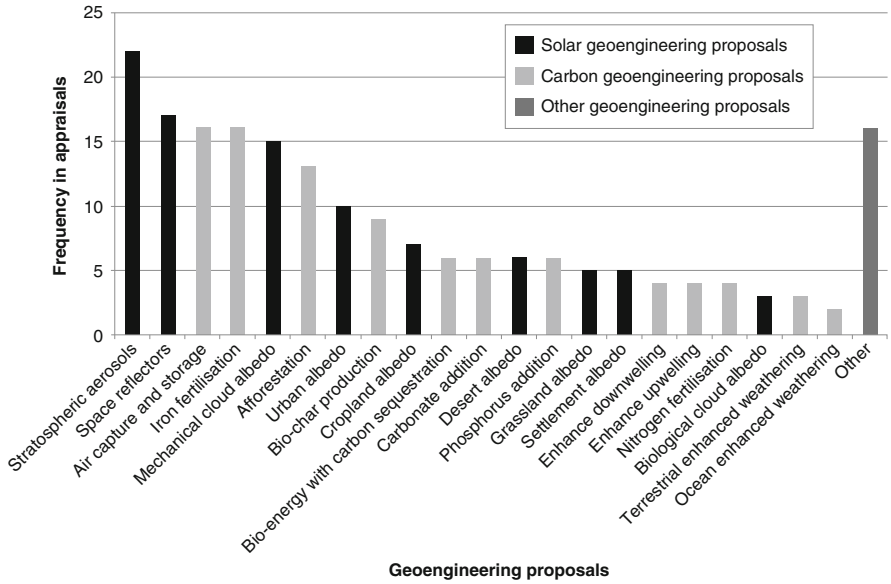

Fig. 17 Relative abundance of geoengineering concepts in the scientific literature. "Others" were cited no more than once (Source: Bellamy et al. 2012)

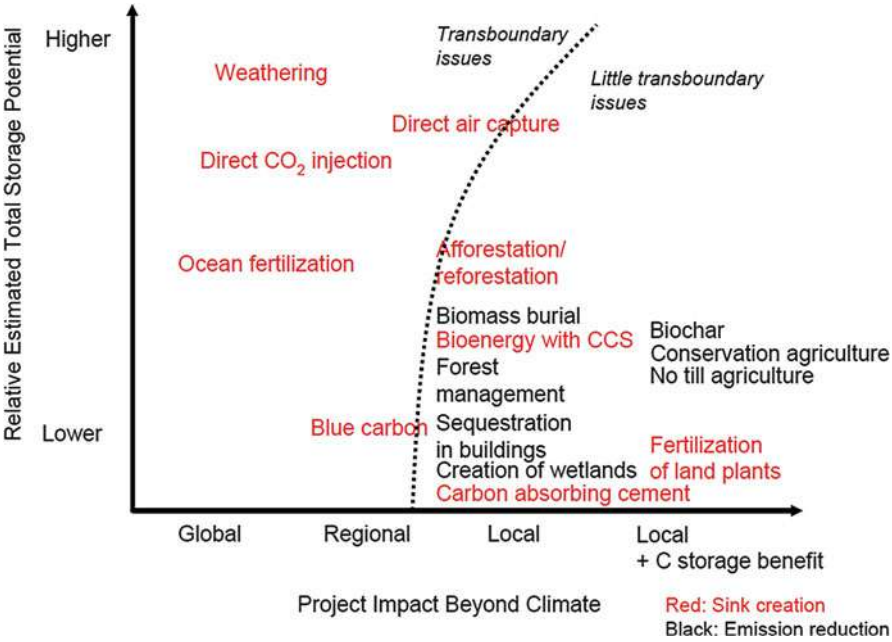

Fig. 18 The relative estimated total storage potential for emission reduction and sink creation projects at different scales (Source: Edenhofer et al. 2012)

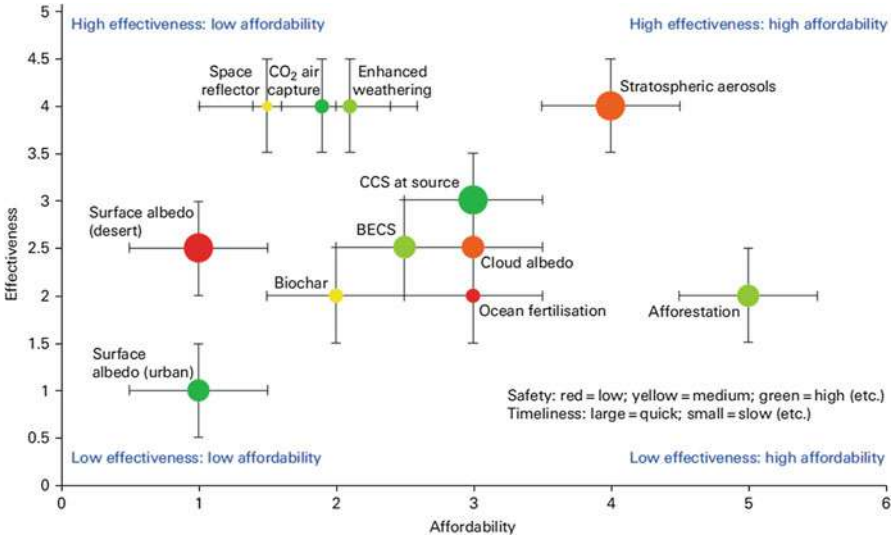

Fig. 19 Preliminary overall evaluation of the geoengineering technique (Shepherd 2009)

As Fig. 18 shows, concepts with a large estimated global potential are carbon sinks, with the ocean being particularly important. For these, transboundary issues arise.

Blue carbon is the carbon captured by the world's oceans and coastal ecosystems (Blue Carbon Initiative 2015).

An overall evaluation in terms of affordability and effectiveness, reproduced from Shepherd (2009), is shown in Fig. 19.

The color of the bullets in Fig. 19 indicates the level of system safety (red = low; yellow = medium; green = high), whereas the size of the bullets relates to the timeliness of the techniques (large = quick; small = slow). One can see from Fig. 19 that urban surface albedo enhancements like "white roofs" are safe, but lack effectiveness technically and financially. Afforestation, also a safe technique, is affordable, but has a lower effectiveness potential than stratospheric aerosols, which are more risky, are more costly, and take more time. Such comparison charts can help define research priorities.

Results from another, similar study are depicted in Figs. 20 and 21.

Lenton and Vaughan (2009) concludes "only stratospheric aerosol injections, albedo enhancement of marine stratocumulus clouds, or sunshades in space have the potential to cool the climate back toward its pre-industrial state. Strong mitigation, combined with global-scale air capture and storage, afforestation, and bio-char production, i.e., enhanced CO_2 sinks, might be able to bring CO_2 back to its pre-industrial level by 2100, thus removing the need for other geoengineering."

A third study (Goes et al. 2010) which is being presented here has compared four scenarios: BAU (business as usual), CO_2 abatement, intermediate geoengineering (next 50 years), and continuous geoengineering from the present until 2150; see

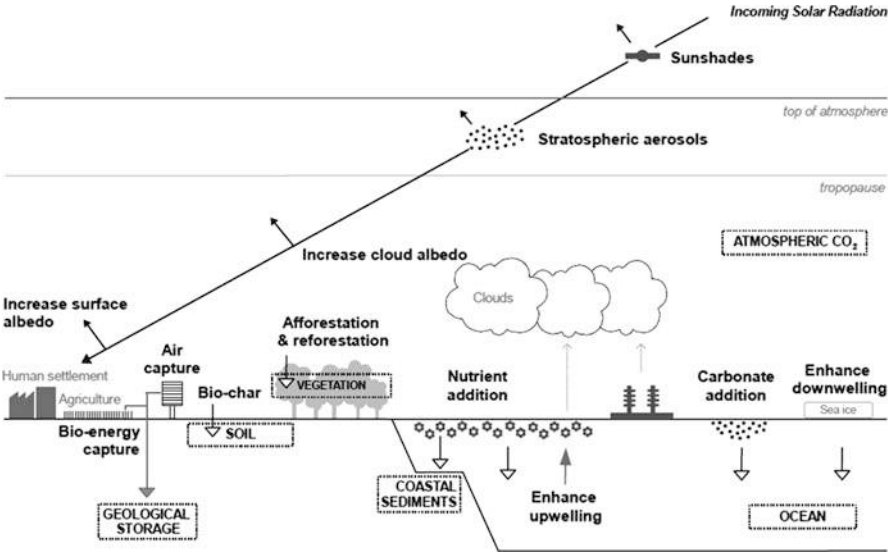

Fig. 20 Schematic overview of the climate geoengineering proposals considered. *Black arrowheads* indicate shortwave radiation; *white arrowheads* indicate enhancement of natural flows of carbon; *gray downward arrow* indicates engineered flow of carbon; *gray upward arrow* indicates engineered flow of water; *dotted vertical arrows* illustrate sources of cloud condensation nuclei; and *dashed boxes* indicate carbon stores (Source: Lenton and Vaughan 2009)

Figs. 22 and 23. The two geoengineering scenarios deploy stratospheric aerosol injection.

CO_2 emissions are assumed to be equally increasing in all scenarios except the abatement one. Two key observations from this study (Goes et al. 2010) are:

- Radiative forcing in the "intermediate geoengineering" scenario would reach the same levels as that in the BAU scenario soon after the geoengineering was stopped.
- Compared to the BAU scenario, a temperature rise of up to 1.5 K per decade, as opposed to less than 0.5 K per decade, would result. Such a strong change might finally be even worse for flora and fauna – and humans than a steady increase.

Figure 23 gives projections on the costs of the four scenarios.

As one can deduct from Fig. 23, damage and total costs of the BAU and intermediate geoengineering scenarios are highest, whereas the continuous geoengineering scenario presents itself as the economically most favorable one. As the authors conclude, aerosol geoengineering for CO_2 abatement can be an economically ineffective strategy. Failure to sustain the aerosol forcing can lead to huge and abrupt changes to the climate: "Substituting aerosol geoengineering for greenhouse gas emissions abatements constitutes a conscious risk transfer to future generations, in violation of principles of intergenerational justice which demands that present

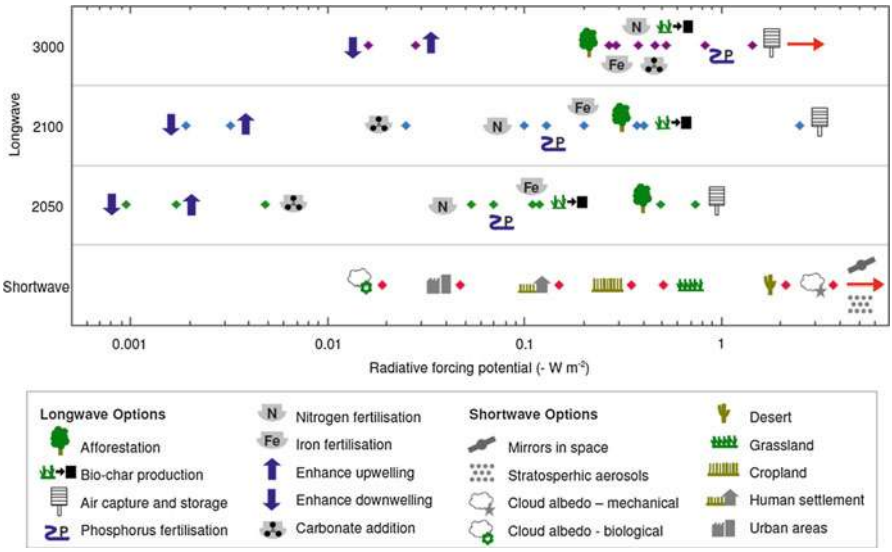

Fig. 21 Summary of estimates of the radiative forcing potential of different climate geoengineering options from Lenton and Vaughan (2009). The potential of longwave (CO_2 removal) options is given on three different time horizons, assuming a baseline strong mitigation scenario. The *rightward pointing arrows*, which refer to mirrors in space, stratospheric aerosols, and air capture and storage on the year 3,000 timescale, indicate that their potential could be greater than suggested by the diamonds (which in these cases represent a target radiative forcing to be counteracted: 3.71 W/m^2 due to 2 × CO_2 = 556 ppm for the shortwave options and 1.43 W/m^2 due to 363 ppm CO_2 in the year 3000 under a strong mitigation scenario) (Source: Lenton and Vaughan 2009)

generations should not create benefits for themselves in exchange for burdens on future generations" (Goes et al. 2010).

Conclusions

As this brief, introductory chapter to geoengineering has shown, several concepts that at first sight look tempting to "quickly fix global warming" have been developed. Ideas range from more tree planting to huge constructions in space, they include techniques to substantially alter the albedo of manmade objects, deserts, or mountains, and they consider injecting vast amounts of chemicals into the ocean and/or the stratosphere. At the present time, the consequences of such measures, and even the magnitude of their very effect, are hard if not impossible to predict, possibly generating huge risks from irreversibly messing up the complex climate system of our Earth for centuries, altering rainfall patterns, and provoking severe military activities, to name but a few possible side effects. Yet, climate engineering poses an option to deal with the impending aggravation of climate change, and once scientists know more about the various options, one or the other of them might in fact become a viable support in global climate change mitigation and adaptation

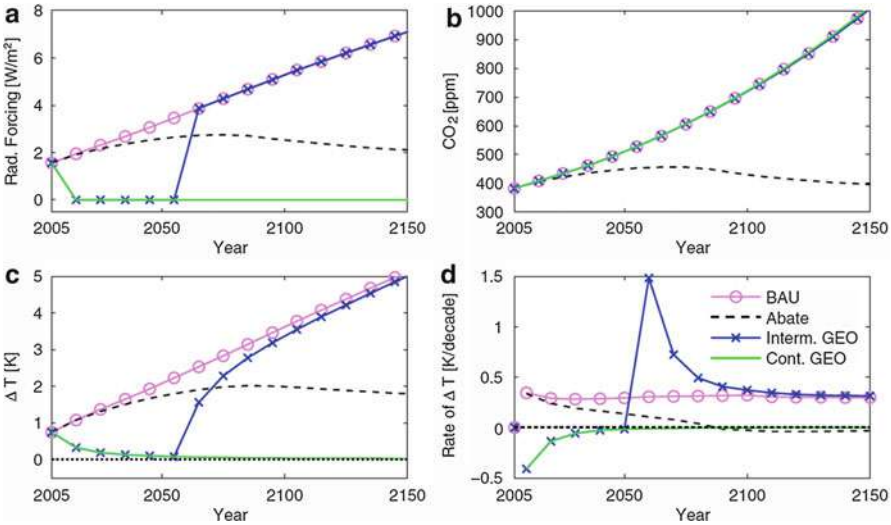

Fig. 22 Radiative forcing (panel **a**), global mean atmospheric CO_2 (panel **b**), global mean surface temperature change (panel **c**), and the rate of global mean surface temperature change (panel **d**) for BAU (*circles*), abatement (*dashed line*), intermittent geoengineering (*crosses*), and continuous geoengineering (*solid line*). Note that these results neglect potential economic damages due to aerosol geoengineering forcing. *BAU* business as usual, *GWP* gross world product (Source: Goes et al. 2010)

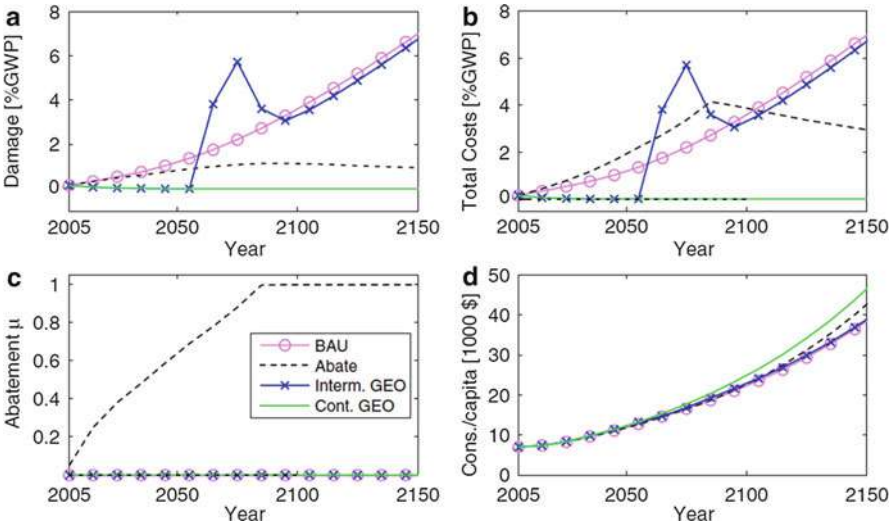

Fig. 23 Economic damage of climate change (panel **a**), total costs (i.e., CO_2 abatement costs and climate change damages cost), abatement, (panel **b**), fraction of CO_2 abatement (panel **c**), and per capita consumption (panel **d**) for BAU (*circles*), optimal abatement (*black dashed line*), intermittent geoengineering (*crosses*), and continuous geoengineering (*solid line*). Note that these results neglect potential economic damages due to aerosol geoengineering forcing. *BAU* business as usual, *GWP* gross world product (Source: Goes et al. 2010)

measures to bring the anthropogenic impacts back under control. On the question of geoengineering ethics, Alan Robock concludes that "in light of continuing global warming and dangerous impacts on humanity, indoor geoengineering research is ethical and is needed to provide information to policymakers and society so that we can make informed decisions in the future to deal with climate change. This research needs to be not just on the technical aspects, such as climate change and impacts on agriculture and water resources, but also on historical precedents, governance, and equity issues. Outdoor geoengineering research, however, is not ethical unless subject to governance that protects society from potential environmental dangers. . .Perhaps, in the future the benefits of geoengineering will outweigh the risks, considering the risks of doing nothing. Only with geoengineering research will we be able to make those judgments" (Robock 2012).

So to conclude, one can say that climate engineering is an interesting topic of research, and CDR techniques that are less risky than SRM techniques might complement conventional climate change mitigation actions. For approaches with global impact, clear governance rules need to be established and enforced.

Outlook

Research of geoengineering should be enhanced, as recommended, e.g., by the UK Royal Society, the American Meteorological Society, the American Geophysical Union, the US Government Accountability Office, and prominent scientists (Robock 2014). Unrealistic and potentially dangerous concepts will be abandoned, and new, innovative ones emerge, possibly providing new options for climate change mitigation and adaptation.

References

Aaltonen H, Pumpanen J, Pihlatie M, Hakola H, Hellén H, Kulmala L, Vesala T, Bäck J (2011) Boreal pine forest floor biogenic volatile organic compound emissions peak in early summer and autumn. Agr Forest Meteorol 151(6):682–691

Anshelm J, Hansson A (2014) Battling Promethean dreams and Trojan horses: revealing the critical discourses of geoengineering. Energy Res Soc Sci 2:135–144

Barreras F, Amaveda H, Lozano A (2002) Transient high frequency ultrasonic water atomization. Exp Fluids 33:405–413

Bellamy R, Chilvers J, Vaughan NE, Lenton TM (2012) Appraising geoengineering. Tyndall Centre for Climate Change Research, working paper 153, June 2012

Bewick R, Sanchez JP, McInnes CR (2012) The feasibility of using an L1 positioned dust cloud as a method of space-based geoengineering. Adv Space Res 49(7):1212–1228

Bewick R, Lücking C, Colombo C, Sanchez JP, McInnes CR (2013) Heliotropic dust rings for Earth climate engineering. Adv Space Res 51(7):1132–1144

Biello D (2009) World's craziest geoengineering scheme. http://www.scientificamerican.com/podcast/episode/worlds-craziest-geoengineering-sche-09-09-03/

Blue Carbon Initiative (2015) http://thebluecarboninitiative.org/

Bonn A, Reed MS, Evans CD, Joosten H, Bain C, Farmer J, Emmer I, Couwenberg J, Moxey A, Artz R, Tanneberger F, von Unger M, Smyth M-A, Birnie D (2014) Investing in nature: developing ecosystem service markets for peatland restoration. Ecosyst Serv 9:54–65

Boston PJ (2008) Gaia hypothesis. In: Reference module in earth systems and environmental sciences, from encyclopedia of ecology. Elsevier Science Ltd, Amsterdam, pp 1727–1731

Butler JH, Montzka SA (2013) The NOAA annual greenhouse gas index (AGGI). NOAA/ESRL Global Monitoring Division. http://www.esrl.noaa.gov/gmd/aggi/aggi.html (2015)

Burke J (2010) Could a massive dam between Alaska and Russia save the Arctic? Huffington Post. 27 Nov 2010. Retrieved 10 Mar 2011

Byrnes SJ, Blanchard R, Capasso F (2014) Harvesting renewable energy from Earth's mid-infrared emissions. Proc Natl Acad Sci U S A 111(11):3927–3932

CarbFix (2015) https://www.or.is/en/projects/carbfix

Chossudovsky M (2007, Dec 7) Weather warfare: beware the US Military's experiments with climatic warfare. The Ecologist, Global Research. http://www.globalresearch.ca/weather-warfare-beware-the-us-military-s-experiments-with-climatic-warfare/7561

Climate Modification Schemes, American Institute of Physics (AIP) (2011) http://www.aip.org/history/climate/RainMake.htm

Cole JJ (2013) Chapter 6 – The carbon cycle: with a brief introduction to global biogeochemistry. In: Fundamentals of ecosystem science. pp 109–135

Collyns D (2010) Can painting a mountain restore a glacier? BBC. http://www.bbc.co.uk/news/10333304

Corner A, Parkhill K, Pidgeon N, Vaughan NE (2013) Messing with nature? Exploring public perceptions of geoengineering in the UK. Glob Environ Change 23(5):938–947

Crutzen PJ (2006) Albedo enhancement by stratospheric sulfur injections: a contribution to resolve a policy dilemma? Clim Change 77:211–220

de_Richter RK, Ming T, Caillol S (2013) Fighting global warming by photocatalytic reduction of CO_2 using giant photocatalytic reactors. Renew Sustain Energy Rev 19:82–106

Dean C (2011) Group urges research into aggressive efforts to fight climate change. http://www.nytimes.com/2011/10/04/science/earth/04climate.html?_r=0

Dixon T, Garrett J, Kleverlaan E (2014) GHGT-12, update on the London protocol – developments on transboundary CCS and on geoengineering. Energy Procedia 63:6623–6628

DOE/NETL carbon dioxide capture and storage RD&D roadmap, Dec 2010. http://www.netl.doe.gov/File%20Library/Research/Carbon%20Seq/Reference%20Shelf/CCSRoadmap.pdf

Early JT (1989) Space-based solar shield to offset greenhouse effect. J Br Interplanet Soc 42:567–569. http://www.see.ed.ac.uk/~shs/Climate%20change/Data%20sources/Early%20earth%20shield1989.pdf

Ebersbach F, Assmy P, Martin P, Schulz I, Wolzenburg S, Nöthig E-M (2014) Particle flux characterisation and sedimentation patterns of protist plankton during the iron fertilisation experiment LOHAFEX in the Southern Ocean. Deep Sea Res I Oceanogr Res Pap 89:94–103

Edenhofer O, Pichs-Madruga R, Sokona Y, Field C, Barros V, Stocker TF, Dahe Q, Minx J, Mach K, Plattner G-K, Schlömer S, Hansen G, Mastrandrea M (2012) IPCC expert meeting on geoengineering, meeting report, Lima, 20–22 June 2011, ISBN 978-92-9169-136-4

Edmonds I, Smith G (2011) Surface reflectance and conversion efficiency dependence of technologies for mitigating global warming. Renew Energy 36:1343–1351

Evans J, Stride E, Edirisinghe M, Andrews D, Simons R (2010) Can oceanic foams limit global warming? Climate Res 42(2):155–160. doi:10.3354/cr00885. edit

Ferraro AJ, Highwood EJ, Charlton-Perez AJ (2014) Weakened tropical circulation and reduced precipitation in response to geoengineering. Environ Res Lett 9:014001 (7 pp)

Goes M, Tuana N, Keller K (2010) The economics (or lack thereof) of aerosol geoengineering. In: Climatic change. Springer. doi:10.1007/s10584-010-9961-z, http://www.aoml.noaa.gov/phod/docs/Goes_etal_2011.pdf

Goldberg P, Chen Z-Y, O'Connor W, Walters R, Ziock H (1998) CO_2 mineral sequestration studies in US. http://www.netl.doe.gov/publications/proceedings/01/carbon_seq/6c1.pdf

Goldenberg S (2014) Al Gore says use of geo-engineering to head off climate disaster is insane, theguardian.com, Wednesday 15 Jan 2014. http://www.theguardian.com/world/climate-consensus-97-per-cent/2014/jan/15/geo-al-gore-engineering-climate-disaster-instant-solutio
Gomes MS de P, de Araújo MSM (2011) Artificial cooling of the atmosphere – a discussion on the environmental effects. Renew Sustain Energy Rev 15(1):780–786
Herzog H (2002) Carbon sequestration via mineral carbonation: overview and assessment (PDF). Massachusetts Institute of Technology. Retrieved 5 Mar 2009
Heyward C, Rayner S (2013) A curious asymmetry: social science expertise and geoengineering. Climate geoengineering governance working paper series: 007. http://geoengineering-governance-research.org/perch/resources/workingpaper7heywardrayneracuriousasymmetry.pdf
House KZ et al (2011) An economic and energetic analysis of capturing CO_2 from ambient air. Proc Natl Acad Sci U S A 108:20428–20433
Hyland C, Sarmah AK (2014) Chapter 25 – Advances and innovations in biochar production and utilization for improving environmental quality. In: Bioenergy research: advances and applications. Elsevier Ltd, Amsterdam, pp 435–446
IPCC (2015) 2.2.3. Afforestation, reforestation, and deforestation. http://www.ipcc.ch/ipccreports/sres/land_use/index.php?idp=47
Keith DW, Parson E, Morgan MG (2010) Research on global sun block needed now. Nature (Nat Publ Group) 463(7280):426–427
Kennedy RG III, Roy KI, Fields DE (2013) Dyson dots: changing the solar constant to a variable with photovoltaic lightsails. Acta Astronaut 82(2):225–237
Kintisch E (2010) Hack the planet: science's best hope – or worst nightmare – for averting climate catastrophe. Wiley, Hoboken. ISBN 0-470-52426-X
Kosugi T (2010) Role of sunshades in space as a climate control option. Acta Astronaut 67 (1–2):241–253
Kravitz B (2013) Geoengineering has its limits. Nature 501:9. doi:10.1038/501009a
Kunzig R (2008) Geoengineering: how to cool earth – at a price. Scientific American. http://www.scientificamerican.com/article/geoengineering-how-to-cool-earth/
Lenton TM, Vaughan NE (2009) The radiative forcing potential of different climate, geoengineering options. Atmos Chem Phys 9:5539–5561. www.atmos-chem-phys.net/9/5539/2009/
Lorenz EN (1963) Deterministic non-periodic flow. J Atoms Sci 20:130–141
Lorenz EN (1972) Predictability: does the flap of a butterfly's wings in Brazil set off a tornado in Texas? American Association for the Advancement of Science, 139th meeting, 29 Dec 1972. http://eaps4.mit.edu/research/Lorenz/Butterfly_1972.pdf
MacMynowski DG, Keith DW, Caldeira K, Shin HJ (2011) Can we test geoengineering? Energy Environ Sci 4:5044–5052
McGrath M (2014) Geoengineering plan could have 'unintended' side effect. http://www.bbc.com/news/science-environment-25639343
Ming T, de_Richter R, Liu W, Caillol S (2014) Fighting global warming by climate engineering: is the Earth radiation management and the solar radiation management any option for fighting climate change? Renew Sustain Energy Rev 31:792–834
Mitchell DL, Finnegan W (2009) Modification of cirrus clouds to reduce global warming. Environ Res Lett 4:1–8
Mitchell DL, Mishra S, Lawson RP (2011) Cirrus clouds and climate engineering: new findings on ice nucleation and theoretical basis. In: Planet earth. Intech, Rijeka, pp 257–288
O'Mahony T (2013) Decomposition of Ireland's carbon emissions from 1990 to 2010: an extended Kaya identity. Energy Policy 59:573–581
Oke TR (1997) Urban climates and global environmental change. In: Thompson RD, Perry A (eds) Applied climatology: principles & practices. Routledge, New York, pp 273–287
Pacella RM (2007) Duct tape methods to save the earth: insulate the glaciers. Pop Sci. http://www.popsci.com/node/3245

Rasch PJ, Tilmes S, Turco RP, Robock A, Oman L, Chen C, Stenchikov GL, Garcia RR (2008) An overview of geoengineering of climate using stratospheric sulphate aerosols. Philos Transact A Math Phys Eng Sci 366(1882):4007–4037

Rinnan R, Rinnan Å, Faubert P, Tiiva P, Holopainen JK, Michelsen A (2011) Few long-term effects of simulated climate change on volatile organic compound emissions and leaf chemistry of three subarctic dwarf shrubs. Environ Exp Bot 72(3):377–386

Robock A (2012) Is geoengineering research ethical? Peace Secur 4:226–229

Robock A (2014) Stratospheric aerosol geoengineering. Issues Environ Sci Techol (special issue "Geoeng Clim Syst") 38:162–185

Robock A, Marquardt A, Kravitz B, Stenchikov G (2009) Benefits, risks, and costs of stratospheric geoengineering. Geophys Res Lett 36, L19703. doi:10.1029/2009GL039209

Rockström J, Steffen W, Noone K, Persson Å, Chapin FS III, Lambin EF, Lenton TM, Scheffer M, Folke C, Schellnhuber HJ, Nykvist B, de Wit CA, Hughes T, van der Leeuw S, Rodhe H, Sörlin S, Snyder PK, Costanza R, Svedin U, Falkenmark M, Karlberg L, Corell RW, Fabry VJ, Hansen J, Walker B, Liverman D, Richardson K, Crutzen P, Foley JA (2009) A safe operating space for humanity. Nature 461:472–475. doi:10.1038/461472a

Rotman D (2013) A cheap and easy plan to stop global warming. http://www.technologyreview.com/featuredstory/511016/a-cheap-and-easy-plan-to-stop-global-warming/

Rusco F, Stephenson J (2010) Climate change, a coordinated strategy could focus federal geoengineering research and inform governance efforts, report to the Chairman, Committee on Science and Technology, House of Representatives, GAO-10-903. United States Government Accountability Office (GAO). http://www.gao.gov/assets/320/310105.pdf

Schirmer J, Bull L (2014) Assessing the likelihood of widespread landholder adoption of afforestation and reforestation projects. Glob Environ Chang 24:306–320

Secretariat of the Convention on Biological Diversity (2012) Geoengineering in relation to the convention to biological diversity: technical and regulatory matters. CBD technical series no 66. Montreal, ISBN 92-9225-429-4. http://www.cbd.int/doc/publications/cbd-ts-66-en.pdf

Shepherd J (2009) Geoengineering the climate: science governance and uncertainty. The Royal Society, London. https://royalsociety.org/policy/publications/2009/geoengineering-climate/

Shukman D (2014) Geo-engineering: climate fixes 'could harm billions'. http://www.bbc.com/news/science-environment-30197085. Accessed 5 Jan 2015

Sikka T (2012) A critical theory of technology applied to the public discussion of geoengineering. Technol Soc 34(2):109–117

SPICE Stratospheric Particle Injection for Climate Engineering (2015) http://www.spice.ac.uk/

Stilgoe J, Watson M, Kuo K (2013a) Public engagement with biotechnologies offers lessons for the governance of geoengineering research and beyond. PLoS Biol 11(11). doi:10.1371/journal.pbio.1001707

Stilgoe J, Owen R, Macnaghten P (2013b) Developing a framework for responsible innovation. Res Policy 42:1568–1580

Stirling A (2014) Transforming power: social science and the politics of energy choices. Energy Res Soc Sci 1:83–95

Stix TH (1993) Removal of chlorofluorocarbons from the troposphere, Plasma Science. IEEE conference record – abstracts, 1993 I.E. international conference on, ISBN 0-7803-1360-7

Strand SE, Benford G (2009) Ocean sequestration of crop residue carbon: recycling fossil fuel carbon back to deep sediments. Environ Sci Technol 43(4):1000–1007. doi:10.1021/es8015556

Sweeney JA (2014) Command-and-control: alternative futures of geoengineering in an age of global weirding. Futures 57:1–13

Tate KR (2015) Soil methane oxidation and land-use change – from process to mitigation. Soil Biol Biochem 80:260–272

Teller E, Hyde R, Wood L (1997) Global warming and ice ages: prospects for physics-based modulation of global change (PDF). Lawrence Livermore National Laboratory. Retrieved 30 Oct 2018. See pages 10–14 in particular

Trabucco A, Zomer RJ, Bossio DA, van Straaten O, Verchot LV (2008) Climate change mitigation through afforestation/reforestation: a global analysis of hydrologic impacts with four case studies. Agr Ecosyst Environ 126(1–2):81–97

Victor DG, Granger Morgan M, Apt J, Steinbruner J, Ricke K (2009) The geoengineering option: a last resort against global warming?. Geoengineering. Council on Foreign Affairs. Retrieved 19 Aug 2009

Vidal J (2011) Giant pipe and balloon to pump water into the sky in climate experiment. The Guardian. http://www.theguardian.com/environment/2011/aug/31/pipe-balloon-water-sky-climate-experiment

von Neumann J (1955) Can we survive technology? Fortune, June, pp 106–108, 151–152. Reprinted in Sarnoff D (ed) (1956) The fabulous future: America in 1980. Dutton, New York, pp 33–48

Weaver IS, Dyke JG (2012) The importance of timescales for the emergence of environmental self-regulation. J Theor Biol 313:172–180

Willoughby HE, Jorgensen DP, Black RA, Rosenthal SL (1985) Project STORMFURY, a scientific chronicle, 1962–1983. Bull Am Meteorol Soc 66:505–514

World Bank and Partners Award $4.8 Million to 26 Innovative Ideas to Save the Planet, http://web.worldbank.org/WBSITE/EXTERNAL/COUNTRIES/AFRICAEXT/EXTAFRSUMESSD/EXTFORINAFR/0,,contentMDK:22389504~menuPK:2493506~pagePK:64020865~piPK:149114~theSitePK:2493451,00.html. Accessed 16 Jan 2015

Zeng N (2008) Carbon sequestration via wood burial. Carbon Balance Manage 3:1. doi:10.1186/1750-0680-3-1, http://www.cbmjournal.com/content/3/1/1

Zhang Z, Moore JC, Huisingh D, Zhao Y (2015) Review of geoengineering approaches to mitigating climate change. J Clean Prod 15:898–907

Zhou S, Flynn PC (2005) Geoengineering downwelling ocean currents: a cost assessment. Clim Change 71(1–2):203–220. doi:10.1007/s10584-005-5933-0

Zomer RJ, Trabucco A, Bossio DA, Verchot LV (2008) Climate change mitigation: a spatial analysis of global land suitability for clean development mechanism afforestation and reforestation. Agr Ecosyst Environ 126(1–2):67–80

Social Efficiency in Energy Conservation

Patrick Moriarty and Damon Honnery

Contents

Abstract

Global energy use, fossil fuel carbon dioxide (CO_2) emissions, and atmospheric CO_2 levels continue to rise, despite some progress in mitigation efforts. Improving energy efficiency is seen as an important means of reducing emissions, but absolute reductions in global energy use remain elusive because of continued growth in the numbers of important energy-using devices such as transport vehicles, and energy rebound. Limiting the rise in average surface temperature above preindustrial to 2 °C is widely regarded as the limit for avoiding dangerous anthropogenic climate change. Given the magnitude of CO_2 emission reductions necessary for this limit to be met, other approaches are needed for reducing energy use and its resultant emissions. This chapter discusses social efficiency (nontechnical means for reducing energy use) and stresses the social

P. Moriarty (✉)
Department of Design, Monash University, Melbourne, VIC, Australia
e-mail: patrick.moriarty@monash.edu

D. Honnery
Department of Mechanical and Aerospace Engineering, Monash University, Melbourne, VIC, Australia
e-mail: damon.honnery@monash.edu

W.-Y. Chen et al. (eds.), *Handbook of Climate Change Mitigation and Adaptation*,
DOI 10.1007/978-3-319-14409-2_73

and environmental context in which energy consumption occurs in various sectors. Three important sectors for energy use, transport, buildings, and agriculture, are used to illustrate the potential for social efficiency in energy reductions. We argue that by focusing more clearly on the human needs energy use is meant to satisfy, it is possible to find new, less energy-intensive ways of meeting these needs.

Abbreviations

ABS	Australian Bureau of Statistics
CO_2-eq	Carbon dioxide equivalent
EIA	Energy Information Administration (US)
EJ	Exajoule (10^{18} joule)
GHG	Greenhouse gas
GJ	Gigajoule (10^9 joule)
Gt	Gigatonne (10^9 tonne)
IEA	International Energy Agency
IPCC	Intergovernmental Panel on Climate Change
IT	Information technology
MJ	Megajoule
OECD	Organisation for Economic Co-operation and Development
p-km	Passenger-km
SBJ	Statistics Bureau Japan
t-km	Tonne-km
UK	United Kingdom
v-km	Vehicle-km

Introduction

Most studies on energy efficiency focus on technical efficiency measures such as megawatt-hour output of electricity per megajoule (MJ) of primary energy input for a power station, or vehicle-km per MJ of fuel input for a car. While the potential for technical efficiency improvements in energy-consuming devices is large (Cullen et al. 2011) and efficiency gains are expected to be a major factor in future carbon mitigation scenarios (Van Vuuren et al. 2011a, b), the results to date have been disappointing. Many barriers, both technical and socioeconomic, hinder the implementation of energy efficiency policies. Global energy use and fossil fuel CO_2 emissions continue to grow (BP 2015), resulting in a steady climb in atmospheric CO_2 levels.

Further, energy efficiency is subject to the well-known *rebound effect*. Rebound occurs because efficiency improvements (e.g., in light bulbs or passenger cars) lower the cost of operation, either encouraging more use of the energy-using device or allowing the money so saved to be spent on other energy-using goods or services (Druckman et al. 2011; Moriarty and Honnery 2015). A related concept is the demonstration effect of present lifestyles in high-income countries on the

expectations of residents of industrializing countries. If their ownership of energy-intensive goods such as private vehicles or air conditioners rises to levels near those prevailing in high-income countries, any efficiency gains will be swamped by rising global use. Technical energy efficiency is important for carbon mitigation, but needs to be supplemented by nontechnical measures for deep carbon reductions. Energy efficiency measures are discussed in detail in the chapter "▶ Energy Efficiency: Comparison of Different Systems and Technologies".

It is not enough that the energy (or carbon) intensity of economies – primary energy (or carbon) consumed per unit of gross national income – be reduced; absolute levels of fossil fuel energy must also be greatly cut.

As used here in the context of energy conservation, the term *social efficiency* refers to a system-based approach that stresses the social and environmental context in which energy consumption occurs in various sectors. As Haas et al. (2008) have stressed, households and organizations do not use energy for its own sake; they use it to enjoy the *energy services* it provides. Put simply, social efficiency will refer to nontechnical means for reducing energy use. As discussed, technical efficiency improvements are made by getting more output from a given energy input, such as electric output per unit of fossil fuel input energy; social efficiency improvements, on the other hand, are made by getting more social "value" from each unit of the output of an energy-using device (Moriarty and Honnery 1996, 2014).

It is instructive to compare approaches in climate change modeling and energy efficiency studies. Climate scientists have utilized general circulation models for decades and, more recently, coupled carbon-climate models. Such modes have been used to show, for example, that afforestation could exacerbate climate change (Keller et al. 2014). The newly grown forests would decrease the albedo (the fraction of the insolation reflected directly back into space), offsetting the carbon sequestration in the trees. With the exception of the rebound literature, energy efficiency research, in contrast, mostly does not look at effects on other energy sectors.

To illustrate both the approaches used and the potential for social energy efficiency, this chapter focuses on three important energy-using sectors as case studies: transport, both passenger and freight; energy use in buildings, both household dwellings and commercial buildings; and agriculture, particularly for food production. These case studies were chosen not only for their importance for global energy use and greenhouse gas (GHG) emissions but also because they illustrate different aspects of social efficiency.

By examining social efficiency in these three sectors, we hope to point to new ways at looking at energy and GHG emissions reductions. In particular, we stress the need to examine more closely *what energy is used for* (Shove and Walker 2014). As energy researcher Benjamin Sovacool (2014) put it: "Academic researchers frequently obsess over technical fixes rather than ways to alter lifestyles and social norms." The usual, technical approach is to find ways of performing existing tasks more efficiently; instead we ask whether the tasks should be done in the first place and whether the human needs underpinning energy use can be met in a different, less energy-intensive way.

Social Efficiency: Transport

In 2012, the fuel for all modes of vehicular transport, including both passenger and freight, accounted for 27.9 % of global final demand for energy, up from 23.1 % in 1973 (International Energy Agency (IEA) 2014). Transport is heavily reliant on fossil fuels (96.6 % in 2012) and global road vehicle numbers are still rising rapidly. GHG emissions from this sector are thus rising, and it will be very difficult for technical solutions alone to stop further rises, let alone greatly reduce them.

Passenger Transport

The conventional measure of the passenger transport task is passenger-km (p-km). For example, 10 p-km is generated if one passenger travels 10 km or ten passengers each travel for 1 km. Transport efficiency in turn is measured as p-km per MJ of primary fuel. Measures such as miles per gallon and liters per 100 km are still widely used for vehicle efficiency, but suffer from two drawbacks. First, the useful output of passenger travel is p-km rather than vehicle-km (v-km); in other words, the occupancy rate is important. With this measure of output, buses can now be compared with car travel. Second, although liters per 100 km is useful for comparing the efficiency of various petrol or diesel-fueled vehicles, it is not useful for comparing electric-powered vehicles, whether for private or public transport, with vehicles that run on liquid fuels. But p-km/MJ of primary enables fair comparison of all passenger transport modes, regardless of energy source or vehicle carrying capacity (Moriarty and Honnery 2012).

However, even though p-km is a more useful measure than v-km, transport is still mainly a *derived demand*. Although some travel, especially by car, is undertaken for its own sake, in most cases travelers undergo the monetary and time costs required in order to access out-of-home activities such as working, education, or shopping. Access to activities, not mobility, is the real purpose of transport; hence one measure of the social efficiency of passenger transport would be *access* per primary MJ of transport fuel. Obviously, all else being equal, doubling the occupancy rate of all vehicular transport should double the access achieved per primary MJ. Occupancy rates are covered in more detail in the chapter "▶ Reducing Personal Mobility for Climate Change Mitigation".

Of course, it is much easier to measure p-km than it is to measure access, which has a subjective component. As Halden (2011) has stated: "accessibility is an attribute of people and goods rather than transport modes or service provision." Mobility may be easy to measure, but given that travel is mainly a derived demand, he further argued that it is difficult to say whether more travel is better than less.

How can access be improved? The journey to work trip will be used to illustrate the possibilities. First, we need to define two terms, *minimum average work trip length* and *actual average work trip length*. For convenience, we will use the example of cities and assume that all workplaces within the city boundaries are filled by resident workers. The minimum average work trip length for any city will

then be the average distance traveled to work if workplaces are fixed, but workers can change residences such that total travel to work for all city residents is minimized. The actual average work trip length is that calculated from origin-destination studies of citywide work trip patterns. Clearly, total work travel will be less if the actual average distance is close to the minimum.

Studies have shown that, in real cities, there is a large amount of "excess" work travel. For a range of US and Australian cities, actual work travel was found to be roughly twice the minimum. On the other hand, for a sample of Japanese and South Korean cities, actual work travel was much closer to the minimum (Moriarty and Honnery 2013). The much higher densities of the latter cities compared with US and Australian cities, and the accompanying traffic congestion, are important explanatory factors. However, even if excess work travel is very low, overall work travel could still be reduced in some cities. This happens if there is a mismatch between residences and workplaces – if, for example, workplaces are largely located in one area of a city and residents (and thus workers) in other areas. With the rise of the service sector (and the decline in manufacturing jobs) in Organisation for Economic Co-operation and Development (OECD) cities, this potential mismatch is disappearing. Jobs such as those in the education, health, retail shopping, and other service sectors serve a local area and so are found intermingled with residential areas. With manufacturing, in contrast, the intended market for the products is far wider, often national or even international in scope, and so did not need to be close to residential areas. The result of the rising share of service jobs is improvement in the balance of workplaces and resident workers at the local level (Australian Bureau of Statistics (ABS) 2013; Cervero 1996).

For other trip types, access is more difficult to define. For shopping, access is not only a function of distance to the nearest shopping center but also the range of shops available. Authorities can and do improve resident access to services by strategic location of schools, parks, local government offices, and health centers, for example. As discussed in the chapter "► Reducing Personal Mobility for Climate Change Mitigation" (Section 7), if we lower the *convenience* of car travel in an attempt to reduce its external costs (e.g., air and noise pollution, GHG emissions, community disruption, traffic casualties), the balance between private travel and other modes will be fundamentally altered. In particular, nonmotorized modes will now be relatively more convenient, as well as faster and safer. Vehicular trips for different purposes will be combined more often, and preferred destinations for discretionary trips will change. In brief, if we remove the *priority* accorded to vehicular travel, especially by car, overall vehicular travel will fall. But access levels need not decline with reduced (vehicular) travel, since travel patterns and the intensity of use of various local services can be expected to change over time to maintain access levels.

As Gabrielli and von Karman (1950) showed many decades ago, there is a trade-off between speed and energy efficiency. Slower modes of transport are usually more energy efficient. So an important way of lowering the convenience of car travel is by speed reductions. This will not only reduce transport energy use but also traffic-related air and noise pollution. It will also reduce the frequency and severity

of traffic accidents, both for vehicle occupants and for nonmotorized travelers. For the latter group, research has found that at "impact speeds of 32 km/h, only about 5 % of pedestrians are killed and injuries are minor. At 48 km/h, 50 % are killed and many are seriously injured, while at 80 km/h most do not survive the impact" (Moriarty and Honnery 1999, 2008). Similarly, vehicle impacts with other vehicles or roadside objects are reduced in both number and severity. These benefits can be used to justify lower speed levels.

Even before the global financial crisis, land passenger travel per capita had started decreasing in a number of OECD countries (Millard-Ball and Schipper 2011). However, air travel continues its strong growth, except for Japan, where it has been falling since the year 2000 (Statistics Bureau Japan (SBJ) 2014). Globally, Airbus projects air travel to grow at an average rate of 4.7 % over the years 2014–2033, with international tourism a key driver (Airbus 2014). Hence, an important approach to reducing fuel use and GHG emissions in air transport is the substitution of more local for international tourist destinations. Why do so many people feel the need for international holidays and distant travel in general? One reason is the large and rising number of people, often from lower-income countries, working in wealthier countries (OECD 2014), who visit their families or friends in their home country. Another possible reason is the stress of modern industrial life and work, which impels people to take their vacations in distant locations to get away from this situation (Chen and Petrick 2013). What these examples do show is that global social and economic conditions form part of the explanation of the present high levels of travel.

Finally, we need to explore the ways in which the new information technology (IT) affects travel behavior. Although this question has been explored for nearly four decades, no definitive answer has emerged. Dal Fiore et al. (2014) concluded, as others have, that the new IT, especially mobile technology, has the potential to both increase and decrease levels of passenger travel. Given that per capita vehicular travel levels are falling in many OECD nations, it is possible that either IT is now actively decreasing travel levels or that it is at least enabling people to cope with less travel.

Freight Transport

In a similar manner to passenger transport, technical freight transport efficiency can be measured by tonne-km (t-km) of payload freight per MJ of primary fuel. Even more so than for passenger travel, the efficiency of the various freight modes varies by two to three orders of magnitude (Edenhofer et al. 2014), with air transport being by far the least energy efficient (but the fastest) form of freight transport.

Although freight trucks in all weight classes have shown technical efficiency gains in recent years (in terms of t-km/primary MJ), there has also been a trend toward increased use of smaller freight vehicles for delivery. In Australia overall, but especially in urban areas, light commercial vehicles are carrying a rising share of total t-km (ABS 2013). In London, the same trend has been found and is expected

to continue out to the year 2050 (Zanni and Bristow 2010). Such trends undo some of the efficiency gains in truck freight transport. "Just-in-time" logistics is intended to keep parts inventory in manufacturing to a minimum. One consequence is that delivery frequencies have risen, and average loads have decreased. In effect, the private costs of inventory have fallen, but at the expense of increased external costs for highway freight. The list of external costs for road freight vehicles is similar to those already discussed for road passenger travel.

The "occupancy rate," or payload to tare weight ratio, for freight vehicles is just as important as for passenger travel. For specialized transport vehicles, such as oil or liquefied natural gas tankers, return loads are not feasible. For general goods carriers, two-way loadings can often be improved by better logistics planning, resulting in overall energy reductions (Edenhofer et al. 2014). But a prior question should be: is this particular freight transport needed at all? Most tonne-km of freight globally is moved by international ocean vessels. In most OECD countries, large volumes of products are either imported from other countries or from a different region of the same country. Yet similar products are often also made in the importing country or region. Consumer choice may be important; the point that is often overlooked is that the external costs of the necessary freight transport are unpaid, leading to underpricing of the imported goods.

However, social changes already underway could move freight in a more sustainable direction. Recently much attention has been given to "food miles" and a general preference for locally produced goods, such as that sold at farmers' markets. Food miles represent the distance between the point of food production and the point of consumption. Van Passel (2013) has shown that the concept needs to be modified to meet the charge of oversimplification. He argued for its extension to include freight transport externalities and even added that "all relevant economic, social, and ecological aspects should be taken into account." Many existing food products are endorsed as variously being "fair trade," "organically grown," or "dolphin safe" and often have detailed nutritional information on their packets. In the future we could well see information such as the energy costs, kilometers of transport, and transport mode added to labels. Just as many countries worry about energy security, food security could also become more important for consumer preferences. This point is discussed further in the section "Social Efficiency: Agriculture."

As an example of the kind of systems thinking needed about freight, Schewel and Schipper (2012) have examined in detail "retail goods movement" in the USA, which in 2009 accounted for 6.6 % of US energy demand. They start with the point of import or of manufacture, followed by transport of these goods to a central warehouse, then distribution to individual shops, and finally transport, usually by car, of the purchased goods to the consumer's final destination. They point out the conflict that can arise between freight transport energy costs and the final consumer's energy costs. The trend toward fewer, larger stores has improved freight energy efficiency by allowing use of higher capacity trucks, but on the other hand, shoppers have had to drive further to the more widely spaced retail outlets. This retail case study shows that it is not always possible to separate passenger travel energy from freight transport energy.

Social Efficiency: Buildings

According to the Intergovernmental Panel on Climate Change (IPCC), in 2010 "buildings accounted for 32 % of total global final energy use" (Edenhofer et al. 2014). They were also responsible for 19 % of energy-related GHG emissions, or 9.18 Gt CO_2-eq., when electricity-related emissions were included. Further, according to the IPCC, this "energy use and related emissions may double or potentially even triple by mid-century." Although building energy is growing strongly in industrializing countries, in the core OECD countries, and the economies in transition, total building energy, both direct and indirect, has peaked (Edenhofer et al. 2014). But, as pointed out in the chapter "► Nontechnical Aspects of Household Energy Reductions" (Section 2)", research has shown that occupant behavior can make a huge difference in domestic energy use and presumably for commercial buildings as well. Thus, it is becoming increasingly acknowledged that the social context in which building energy use occurs is crucial.

Energy use in buildings is different from energy use in passenger transport in that it can and does occur without a human presence. In many cases, this raises few problems: refrigerators, freezers, and electric clocks are best left running continuously. But lighting and space heating/cooling in buildings, as well as computers, televisions, radios, and other appliances, are often left running, whether or not humans are there to enjoy the energy services provided. Even when not running, their standby energy use can be collectively important. Rather than measuring the power consumption of, for example, a television set, a possible measure of social efficiency might be the number of person-hours of actual viewing per hour the set is operating or per MJ of energy the device consumes.

In OECD countries, by far the most important energy use in buildings is for space heating and cooling. Yet temperature controls for both heating and cooling could be set much closer to ambient levels, if clothing more appropriate to outside temperatures were worn indoors. For offices, it would mean that dress codes would need to change to allow more appropriate clothing for the season. One problem with fixed temperature settings is that it weakens the possibility of *acclimatization* to seasonal temperatures. For example, in hot regions of the world, Auliciems (2009) has reported that inhabitants preferred temperatures of "34 °C or even higher." This seasonal or regional acclimatization can be lost where air-conditioning of buildings is common.

Passive solar energy is in some ways a misnomer, since its use requires a far more active participation by building occupants for space heating or cooling, for example, than does mechanical air-conditioning, which merely requires a thermostat setting. Passive solar can be used for lighting as well as thermal conditioning of buildings. For residences, use of passive solar involves the judicious opening and shutting of windows and blinds for temperature control and lighting and even varying the timing and use of cooking stoves and ovens, depending on whether the heat will add or subtract from thermal comfort. In some situations, it may be worthwhile investigating a change to hours of employment as a means of improving occupant comfort. Passive solar (in the form of wind energy) can also be used for

clothes drying, but in many communities the use of outdoor clothes drying is still banned (Lee 2009), because of the claim that clothes lines are unsightly.

The case study by Pilkington et al. (2011) in the UK showed the importance of occupant behavior for making the most of energy savings from passive solar design. The six terrace houses studied were of identical design, with superefficient insulation and "sunspaces." They found that space heating use per occupant varied by a factor of 14. The main reason for the variation was that the higher energy users kept the internal doors open on winter days. Overall, the approach we advocate here can be contrasted with the "smart buildings" approach. Instead of predetermined settings, even if set by the occupants, we advocate that the building occupants actively respond to changing ambient conditions and adjust openings and shading accordingly.

Just as for passenger transport, the occupancy rate of buildings is important in determining energy use. For residences, the occupancy rate has generally fallen in recent decades in most OECD countries, a consequence of both declining family size and rising incomes (e.g., ABS 2012; SBJ 2014; US Census Bureau 2012). The result is that dwelling space (in m^2) per occupant has also risen, which tends to raise the energy for heating or cooling and lighting energy per occupant. If the trend toward declining household size could be reversed, not only would domestic energy efficiency rise but the occupancy rate for cars, and thus their energy efficiency, would also rise. Possibilities for increase include young adults staying at home longer and multi-family and group households. Both the latter groups are already common in many OECD countries, forming an increasing share of total households (e.g., ABS 2012). However, they have not been able to stem the overall fall in household sizes.

Social Efficiency: Agriculture

Modern industrial agriculture is not only heavily reliant on energy, especially petroleum-based fuels, but is also a major producer of the GHGs methane and nitrous oxide, as well as CO_2. Over the years 2000–2100, the IPCC estimated that average annual emissions of all GHGs from agriculture were in the range 5.0–5.8 Gt CO_2-eq., compared with all-sector global 2010 emissions of 49 Gt CO_2-eq. (Edenhofer et al. 2014). For these reasons alone, a change is needed in the way the world produces its food and fiber. But present agricultural methods also produce a host of other serious environmental problems and costs, including air and water pollution, loss of biodiversity, soil erosion, and soil salinity.

The emphasis in industrial agriculture is on cost minimization per unit of output, given that its products must compete in the marketplace. However, these costs are usually viewed in a narrow accounting sense; the *external costs* (including GHG emissions and the other costs listed above) can often be ignored (Weis 2010), just as they often are for transport. These environmental costs, such as surface water pollution, will incur energy costs for their remediation (Moriarty and Honnery 2011).

Ho and Ulanowicz (2005) investigated the energy return (in terms of food kilojoules) to energy input ratio for three types of agricultural systems: preindustrial, semi-industrial, and full-industrial. They found that the range of energy return ratios for the first two systems was 6.9–11.5 and 2.1–9.7, respectively. For the full-industrial agricultural systems, the ratio was little better than unity. It appears that trying to coax more output per hectare in industrial agriculture is subject to diminishing returns on the largely fossil fuel energy invested (Bos et al. 2013). While it may save land (and for industrial agriculture, land rent, real or imputed, is an important part of production costs), such systems carry higher energy costs, as well as higher general environmental costs.

A narrow technical approach to GHG emissions from agriculture can also lead to conflicts for overall climate mitigation. Emphasis on CO_2 emissions reduction may lead to nitrous oxide emissions from fertilizer being overlooked. And the projected use of corn stover for conversion to liquid fuels runs the risk of increased soil erosion and loss of soil carbon. Using corn stover (and other agricultural wastes) for bioenergy will enable some fossil fuel carbon to be left in the ground, but soil carbon losses could partly or wholly offset this benefit.

Nevertheless, for agriculture, we have to look wider than these biophysical environmental impacts. McMichael (2011), in his article on multi-functionalism in agriculture and the "food sovereignty" movement, stressed that farming is not simply about food production, vital though this is. It is valued also for "its contribution to ecosystem management, landscape protection, rural employment, fostering farming knowledge, rural life, cuisine maintenance, and regional heritage." The recognition of the importance of multi-functionalism means that agriculture has diverse impacts on overall energy use; agriculture's energy use implications go far beyond that involved in food and fiber production, even after the energy costs of environmental damages are taken into account. Whether or not these energy costs incurred in other sectors are greater or less for alternative than for industrial agricultural practices is presently unknown; the important point is that they should be considered in the analysis of the total energy costs of agriculture. Farming is a *social* activity.

When discussing passenger transport in section "Passenger Transport," we emphasized the importance of the question: What is the purpose of transport? Similarly, we need to ask: What is the purpose of agricultural production? What are the products used for? The answer might seem obvious, since food is a basic human necessity, with no substitutes. However, according to the Food and Agriculture Organization (OECD/FAO 2014), in 2014, 34.4 % of the global grain harvest (estimated at 2.461 Gt) was fed to livestock, with a further 6.8 % used for liquid fuel production. The FAO expects the share of these nonfood uses to rise modestly in the future, together reaching 42.3 % of the grain harvest by 2023. Grain provides the bulk of the human diet. Other important agricultural foodstuffs used for feedstock for animals or for fuels include soybeans, oilseeds, and sugarcane. It is true that feedstocks are used to produce meat and dairy produce. However, in many OECD countries, including the USA and Australia, meat and dairy produce consumption is well in excess of the level regarded as producing a healthy diet. Further,

one billion people still suffer dietary deficiencies of various kinds (Conway 2012). If the world shifted to a more vegetarian diet, this deficiency could be remedied.

A related issue is food waste: much of the food that is produced and intended for direct human consumption is not eaten but wasted. For industrializing countries, food losses are greatest in the immediate post-harvest part of the food supply chain. In contrast, for OECD countries, the greatest overall food losses resulted at the food retailer, food services industry, and household levels (Parfitt et al. 2010). Atkinson (2014) has even claimed that half the food supplied in high-income countries is thrown away uneaten. As a solution, Parfitt et al. have called for "[C]ultural shifts in the ways consumers value food" and educating the public on the environmental costs of such food waste.

Urban agriculture could also be an important means for reducing food production energy use. Teng et al. (2011) have estimated that, worldwide, around 800 million nominally urban residents are involved in food production, many of them full time, especially in low-income cities. But food production is also growing in popularity in OECD cities. Growing food in cities for the household's own use reduces the relevant "food miles" discussed in section "Freight Transport" to zero, thus cutting freight energy use. According to Ackerman et al. (2014), urban farms can also potentially produce a range of social and economic similar to rural farms: "Urban agriculture not only provides a source of healthful sustenance that might otherwise be lacking, it can also contribute to a household's income, offset food expenditures, and create jobs." It also helps the environmental sustainability of the city, and larger urban farms can provide job training for underserved populations. Varying diets to match the growing seasons of locally produced fruit and vegetables can also reduce agricultural transport costs.

Future Directions

If efforts at mitigating climate change in the coming decades are no better than those in recent decades, the world could be heading to a 4 °C rise in average surface temperature above preindustrial values by the century's end. Although some adaptative measures will be clearly needed, since further climate change is unavoidable given climate (and social) inertia, adaptation cannot be expected to cope with such a temperature rise. At a 4 °C rise, the broadly linear response so far observed in various climate subsystems may break down (New et al. 2011), resulting in changes difficult to predict. Adaptation efforts would then be continuously aiming at a moving target.

Hence, mitigation is the only long-term solution to climate change, and the later it is postponed, the more drastic will be the changes needed. There are encouraging signs that the world's leaders are starting to appreciate how serious the climate change problem is. The European Union now binds its member states to reduce their GHG emissions by at least 40 % from 1990 levels by 2030, mainly through improved energy efficiency and more renewable energy. The world's largest carbon emitter, China, has recently pledged to stabilize its GHG emissions by 2030, and the

second largest, the USA, has promised that by 2025, its emissions will be 14–16 % less than those in 1990 (Anon 2014; Malakoff 2014). Although technical solutions will doubtless be the preferred approach to meet these targets, the latest IPCC report on mitigation (Edenhofer et al. 2014) has placed far more emphasis on nontechnical approaches than did the earlier IPCC reports.

A key advantage of technical energy efficiency improvements is that they are a much better fit to the existing growth-oriented market economies than the social efficiency approaches discussed here. At present, most of these social efficiency measures are not politically feasible. But, in addition to the GHG reduction targets just discussed, changes are under way which will ensure that, in future, social efficiency is less "unthinkable" than it is today. Rockström et al. (2009) have discussed nine "planetary limits" which Earth is approaching, including climate change, ocean acidification, and the rate of biodiversity loss. To this list must be added the global depletion of fossil fuels, particularly oil, and of key minerals essential for industrial economies.

The official position is still that reserves of fossil fuels are more than enough to sustain rising production for decades to come (BP 2015; Energy Information Administration (EIA) 2014). The IPCC (Stocker et al. 2013) projects that natural gas will be an important component of future energy use, being seen as especially valuable as a transition fuel to a low carbon future, because of its low CO_2 emissions per unit of energy compared with coal or oil.

In contrast to this optimistic position, recent research (Inman 2014) has cast doubt on the long-term future for shale gas, which was thought to have large reserves, particularly in the USA. A fine-grained analysis of US shale formations has found that the "sweet spots" where production is presently occurring are not typical of the formations as a whole. Overall, US natural gas production could peak within a decade and then fall sharply. If the US example serves as a model for shale gas production globally, the decarbonization of the energy supply could even be reversed. More generally, Schindler (2014) and others (e.g., Höök and Tang 2013) have stressed that oil, both conventional and unconventional, will peak soon, and natural gas and even coal will peak within a very few decades as well. If the potential for renewable energy to reduce GHG emissions is also less than anticipated, energy reductions will have to be the main approach for GHG reductions.

In the future, then, we can expect to see greatly increased attention to system approaches to energy use, as well as more research that combines both technical and social approaches to energy, for the following reasons:

- Rising energy costs for producing energy partly offset any gains in device energy efficiency.
- Energy rebound significantly offsets any gains in energy efficiency.
- As evidenced by the continued rise in atmospheric concentrations of CO_2 and GHGs overall, the current emphasis on technical solutions is not working.
- Many of the easily made technical energy efficiency measures have already been implemented; those remaining will be progressively more difficult to implement. In contrast, social efficiency potential has barely been tapped.

This chapter has shown that it is usually very difficult to neatly compartmentalize the various energy sectors. Improving freight energy efficiency may negatively impact on passenger transport efficiency, for example. A large range of social practices impact on energy uses, as shown in this chapter. The efficiency of providing thermal comfort in buildings can be greatly improved by changes to the lifestyles of the occupants, including their clothing choices, and by the active use of passive solar energy. Agricultural practices can affect both transport energy costs and the energy costs of ecosystem maintenance. Choosing a diet with less meat and dairy products can greatly improve the overall energy efficiency of national and global food systems. If the world is to produce the carbon mitigation effort needed to avoid disruptive climate change, the question that will increasingly need to be asked is: What is the energy for? What we have termed social efficiency is an attempt to address this vital question.

References

Ackerman K, Conard M, Culligan P et al (2014) Sustainable food systems for future cities: the potential of urban agriculture. Econ Soc Rev 45(2):189–206

Airbus (2014) Global market forecast: flying on demand 2014–2033. Accessed on 8 Dec 2014 at http://www.airbus.com/company/market/forecast/

Anon (2014) On the road to a climate fix. New Sci 13 Dec: 8–9

Atkinson A (2014) Urbanisation: a brief episode in history. City 18(6):609–632

Auliciems A (2009) Human adaptation within a paradigm of climatic determinism and change. Chapter 11. In: Ebi KL, Burton I, McGregor G (eds) Biometeorology for adaptation to climate variability and change. Springer Science + Business Media B.V, Dordrecht

Australian Bureau of Statistics (ABS) (2012) 2009–10 Household expenditure survey: Summary of results. Cat No 6530 ABS, Canberra. (Also earlier surveys)

Australian Bureau of Statistics (ABS) (2013) Survey of motor vehicle use, Australia, 12 months ended 30 June 2012. ABS Cat. No. 92080DO001_1230201206

Bos JFFP, Smit AL, Schröder JJ (2013) Is agricultural intensification in The Netherlands running up to its limits? Wagening J Life Sci 66:65–73

BP (2015) BP statistical review of world energy 2015. BP, London

Cervero R (1996) Jobs-housing balance revisited: trends and impacts in the San Francisco Bay area. J Am Plan Assoc 62(4):492–511

Chen C-C, Petrick JF (2013) Health and wellness benefits of travel experiences: a literature review. J Travel Res 52(6):709–719

Conway G (2012) One billion hungry: can we feed the world? Cornell University Press, Ithaca

Cullen JM, Allwood JM, Borgstein EH (2011) Reducing energy demand: what are the practical limits? Environ Sci Technol 45:1711–1718

Dal Fiore F, Mokhtarian PL, Salomon I et al (2014) "Nomads at last"? A set of perspectives on how mobile technology may affect travel. J Transp Geogr 41:97–106

Druckman A, Chitnis M, Sorrell S et al (2011) Missing carbon reductions? Exploring rebound and backfire effects in UK households. Energy Policy 39:3572–3581

Edenhofer O, Pichs-Madruga R, Sokona Y et al (eds) (2014) Climate change 2014: mitigation of climate change. CUP, Cambridge, UK

Energy Information Administration (EIA) (2014) Annual energy outlook 2014. US Department of Energy, Washington, DC

Gabrielli G, von Karman T (1950) What price speed? Specific power required for propulsion of vehicles. Mech Eng 72(10):775–781

Haas R, Nakicenovic N, Ajanovic A et al (2008) Towards sustainability of energy systems: a primer on how to apply the concept of energy services to identify necessary trends and policies. Energy Policy 36:4012–4021
Halden D (2011) The use and abuse of accessibility measures in UK passenger transport planning. Res Transp Bus Manag 2:12–19
Ho M-W, Ulanowicz R (2005) Sustainable systems as organisms. Biosystems 82:39–51
Höök M, Tang X (2013) Depletion of fossil fuels and anthropogenic climate change – a review. Energy Policy 52:797–809
Inman M (2014) The fracking fallacy. Nature 516:28–30
International Energy Agency (IEA) (2014) Key world energy statistics 2014. IEA/OECD, Paris
Keller DP, Feng EY, Oschlies A (2014) Potential climate engineering effectiveness and side effects during a high carbon dioxide-emission scenario. Nat Commun 5:3304. doi:10.1038/ncomms4304
Lee A (2009) The right to dry. New Sci 2732:26–27
Malakoff D (2014) China's peak carbon pledge raises pointed questions. Science 346:903
McMichael P (2011) Food system sustainability: questions of environmental governance in the new world (dis)order. Glob Environ Change 21:804–812
Millard-Ball A, Schipper L (2011) Are we reaching peak travel? Trends in passenger transport in eight industrialized countries. Transp Rev 31(3):357–378
Moriarty P, Honnery D (1996) Social factors in household energy conservation. In: Proceeding of 13th Clean and Environ Conference, 22–25 Sept, Adelaide, 186–191
Moriarty P, Honnery D (1999) Slower, smaller and lighter urban cars. Proc Inst Mech Engr 213 (D):19–26
Moriarty P, Honnery D (2008) Low mobility: the future for transport. Futures 40(10):865–872
Moriarty P, Honnery D (2011) Is there an optimum level for renewable energy? Energy Policy 39:2748–2753
Moriarty P, Honnery D (2012) Energy efficiency: lessons from transport. Energy Policy 46:1–3
Moriarty P, Honnery D (2013) Greening passenger transport: a review. J Clean Prod 54:14–22
Moriarty P, Honnery D (2014) Reconnecting technological development with human welfare. Futures 55:32–40
Moriarty P, Honnery D (2015) Reliance on technical solutions to environmental problems: caution is needed. Environ Sci Tech 49:5255–5256
New M, Liverman D, Schroeder H et al (2011) Four degrees and beyond: the potential for a global temperature increase of four degrees and its implications. Phil Trans R Soc A 369:6–19
OECD (2014) OECD factbook 2014: economic, environmental and social statistics. OECD, Paris, Available at: http://dx.doi.org/10.1787/factbook-2014-en
OECD/Food and Agriculture Organization (FAO) (2014) OECD-FAO agricultural outlook 2014 OECD, Paris. Available at: http://dx.doi.org/10.1787/agr_outlook-2014-en
Parfitt J, Barthel M, Macnaughton S (2010) Food waste within food supply chains: quantification and potential for change to 2050. Phil Trans R Soc B 365:3065–3081
Pilkington B, Roach R, Perkins J (2011) Relative benefits of technology and occupant behaviour in moving towards a more energy efficient, sustainable housing paradigm. Energy Policy 39:4962–4970
Rockström J, Steffen W, Noone K et al (2009) A safe operating space for humanity. Nature 461:472–475
Schewel LB, Schipper LJ (2012) Shop 'till we drop: a historical and policy analysis of retail goods movement in the United States. Environ Sci Technol 46:9813–9821
Schindler J (2014) Chapter 2: The availability of fossil energy resources. In: Angrick M et al (eds) Factor X: policy, strategies and instruments for a sustainable resource use, vol 29, Eco-Efficiency in Industry and Science. Springer, Dordrecht
Shove E, Walker G (2014) What is energy for? Social practice and energy demand. Theory Cult Soc 31(5):41–58
Sovacool BK (2014) Energy studies need social science. Nature 511:529–530

Statistics Bureau Japan (SBJ) (2014) Japan statistical yearbook 2014. Statistics Bureau, Tokyo, Available at http://www.stat.go.jp/english/data/nenkan/index.htm. (Also earlier editions)
Stocker TF, Qin D, Plattner G-K et al (eds) (2013) Climate change 2013: the physical science basis. CUP, Cambridge, UK
Teng, P, Escaler M, Caballero-Anthony M (2011) Urban food security: feeding tomorrow's cities. Significance June, pp 57–60
US Census Bureau (2012) The 2012 statistical abstract: historical statistics. Available at http://www.census.gov/compendia/statab/hist_stats.html
Van Passel S (2013) Food miles to assess sustainability: a revision. Sust Dev 21:1–17
Van Vuuren DP, Edmonds J, Kainuma M et al (2011a) The representative concentration pathways: an overview. Clim Change 109:5–31
Van Vuuren DP, Stehfest E, den Elzen MGJ et al (2011b) RCP2.6: exploring the possibility to keep global mean temperature increase below 2°C. Clim Chang 109:95–116
Weis T (2010) The accelerating biophysical contradictions of industrial capitalist agriculture. J Agrar Chang 10(3):315–341
Zanni AM, Bristow AL (2010) Emissions of CO_2 from road freight transport in London: trends and policies for long run reductions. Energy Policy 38:1774–1786

Measuring Household Vulnerability to Climate Change

Sofie Waage Skjeflo

Contents

Abstract

This chapter summarizes research on the potential impacts of climate change on households, with a particular focus on contributions from different methodological approaches to understanding impacts for households in developing countries. Agriculture has been a central focus of this literature, both because of the sensitivity of the agricultural sector to a changing climate and also because of the importance of agriculture for the livelihoods of the poor. The literature review shows that developing countries are largely expected to be disproportionally hurt by projected changes in temperature, precipitation, and extreme events. On the other hand, the actual household level response to these changes is not well understood, and there are still gaps in the methodological approaches to understanding these issues. The recent literature reveals promising approaches that may complement and improve existing methods as more data becomes available.

S.W. Skjeflo (✉)
UMB School of Economics and Business, Norwegian University of Life Sciences, Ås, Norway
e-mail: sofie.skjeflo@vista-analyse.no; sofieskjeflo@gmail.com

W.-Y. Chen et al. (eds.), *Handbook of Climate Change Mitigation and Adaptation*,
DOI 10.1007/978-3-319-14409-2_74

Introduction

Despite remarkable achievements in improving standards of living and reducing the proportion of the world's population living in poverty over the past century (Easterlin 2000; Chen and Ravallion 2010), securing basic needs remains a challenge for a large share of the global population. In 2010, the estimated share of the world's population living in extreme poverty, defined as less than $1.25 per day measured in purchasing power parity terms, was about 20 % (World Bank 2014). In sub-Saharan Africa, the estimated share is almost 50 % (World Bank 2014). The majority of the world's poor live in rural areas and rely on agriculture as their main livelihood (World Bank 2014). In the face of a changing climate, the challenge of improving the livelihoods of the poor may be even greater (IPCC 2014). The physical characteristics of agriculture create a strong link between the climate, agriculture, and poverty (Porter et al. 2014). Understanding the potential impacts of climate change therefore requires knowledge of how the rural poor might be affected, through which channels and how policies to improve livelihoods interact with these impacts.

This chapter aims to give an overview of the literature on climate change impacts in developing countries, with a particular emphasis on agriculture in sub-Saharan Africa. The focus is on the contributions of different methodological approaches to understanding climate change in rural developing countries, as well as empirical findings. After discussing the direct impacts of changing temperature and precipitation trends, the household level response to these impacts is discussed. This requires an understanding of household characteristics and the context in which rural households interact, which is discussed in section Household Heterogeneity and Market Characteristics. The final section concludes with some challenges for future research.

Climate Change Impacts on Agriculture

The most recent report from the Intergovernmental Panel on Climate Change (IPCC) concludes that the climate system is warming and that it is very likely that weather extremes have become more frequent and severe due to climate change (IPCC 2013). Projections show that continued greenhouse gas emissions will cause average temperatures to increase further, and there is high confidence that the near-term increase will be larger in tropical and subtropical regions than midlatitude regions. Projections for average precipitation are less clear. It is likely that precipitation variability will increase, but the projections are uncertain and vary considerably across regions in sub-Saharan Africa (IPCC 2013). Figure 1 shows the trends and projected trends in temperature and precipitation for Africa. The top left panel of the figure shows the trend in temperature from 1901 to 2012, where white areas are areas where there is insufficient data to conclude on any trend. The top right panel shows the projected difference in annual mean temperature between mid- and late twenty-first century and 1986–2005. The projections for the RCP8.5, or the

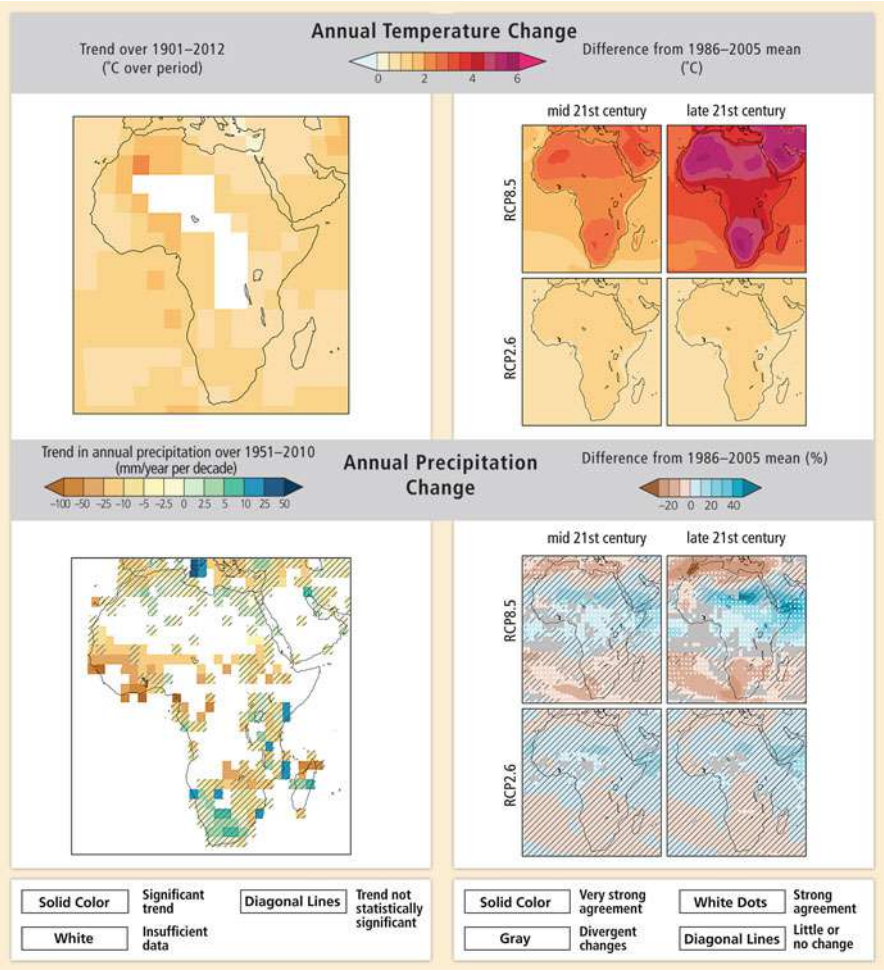

Fig. 1 Observed and projected changes in annual average temperature and precipitation (*top panel*, *left*). Map of observed annual average temperature change from 1901 to 2012, derived from a linear trend [WGI AR5 Figures SPM.1 and 2.21] (*bottom panel*, *left*). Map of observed annual precipitation change from 1951 to 2010, derived from a linear trend [WGI AR5 Figures SPM.2 and 2.29]. For observed temperature and precipitation, trends have been calculated where sufficient data permit a robust estimate (i.e., only for grid boxes with greater than 70 % complete records and more than 20 % data availability in the first and last 10 % of the time period). Other areas are white. *Solid colors* indicate areas where trends are significant at the 10 % level. *Diagonal lines* indicate areas where trends are not significant (*top and bottom panel*, *right*). CMIP5 multi-model mean projections of annual average temperature changes and average percent changes in annual mean precipitation for 2046–2065 and 2081–2100 under RCP2.6 and 8.5, relative to 1986–2005. *Solid colors* indicate areas with very strong agreement, where the multi-model mean change is greater than twice the baseline variability (natural internal variability in 20-year means) and >90 % of models agree on sign of change. *Colors* with *white dots* indicate areas with strong agreement, where >66 % of models show change greater than the baseline variability and >66 % of models agree on sign of change. *Gray* indicates areas with divergent changes, where >66 % of models show change

"business-as-usual" scenario, show up to 6° warming by the end of the twenty-first century in some areas of Africa. The RCP2.6 scenario, which is a scenario with aggressive mitigation efforts where emissions are near zero by the end of the century, also shows warming in Africa, highlighting that adaptation efforts may be needed even if emissions are cut dramatically. The bottom two figures show that observed trends and projected changes in precipitation are much less clear, with missing data preventing clear insights on past trends.

Studies of impacts of climate change in developing countries have to a large extent focused on impacts through agriculture, both because of the importance of the agricultural sector in terms of production and employment and because of the sensitivity of this sector to climate change (Arndt et al. 2012).

Early studies of quantitative impacts of climate change on agriculture relied on crop simulation models to simulate the impact of changing temperature, precipitation, and concentration of CO_2 in the atmosphere on crop growth (Kurukulasuriya and Rosenthal 2003). These models capture the effect of genetic factors; climate variables such as solar radiation, maximum and minimum temperatures, and precipitation; as well as soil characteristics and farm management practices on yields (Parry et al. 1999). The models can also take into account the fertilization effect of increased CO_2 concentration in the atmosphere, as explained by Darwin and Kennedy (2000), and different adaptation options can be simulated by exogenously changing planting dates, fertilization, irrigation, and so forth.

Since these models require detailed input and are constructed for separate crops, the applications of crop models for country- or region-level studies of Africa are scarce (Hertel and Rosch 2010; Thurlow et al. 2012). Thurlow et al. (2012) therefore use a less detailed hydro-crop model in their study of impacts of climate variability on Zambian agriculture. Based on climatic and agronomic statistics from the past three decades, their hydro-crop model predicts 14–77 % maize yield losses in the most drought-prone agroecological zone during a severe drought event and up to 48 % yield losses during more moderate drought events.

An application at a more aggregated scale is provided by Jones and Thornton (2003) who use global circulation model (GCM) output to generate weather scenarios for surfaces in Africa and Latin America up to 2055. The authors do not state which emission scenarios the simulations are based on. The GCM output is used to produce daily weather data that is used in the CERES-Maize crop model. The model simulations are run under the assumption of current varieties and farm practices, i.e., without adaptation. The results show that three quarters of the countries in Africa and

Fig. 1 (continued) greater than the baseline variability, but <66 % agree on sign of change. Colors with *diagonal lines* indicate areas with little or no change, where <66 % of models show change greater than the baseline variability, although there may be significant change at shorter timescales such as seasons, months, or days. Analysis uses model data and methods building from WGI AR5 Figure SPM.8 (See also Annex I of WGI AR5. [Boxes 21-2 and CC-RC] Source: page 1207 in Niang et al. (2014))

Latin America can expect declining maize yields. An exception is the Ethiopian highlands which are expected to experience up to 100 % increases in yields.

Nelson et al. (2009) use the DSSAT biophysical crop modeling system to predict impacts of climate change on crop yields under the A2 SRES scenario (Nakicenovic and Swart 2000) simulated with two different climate models. The direct biophysical impact on crop yields is calculated without any adaptation and both with and without the fertilization effect from CO_2 and is reported to be negative for rain-fed wheat, but with mixed results (some increases and some decreases) for rain-fed maize. For sub-Saharan Africa, the direct impact of climate change on maize yields is negative for both climate models, although a precise estimate is not provided. The numerical results reported are highly aggregated for rain-fed and irrigated maize, which makes it difficult to compare these results with the country-level study above. When taking into account farmers' adaptation to price changes due to climate change, for instance, through adapting crop mix and input use, a 10 % decrease in maize production for sub-Saharan Africa is predicted. This estimate is based on the partial equilibrium IMPACT model.

Taking into Account Adaptation

As emphasized by several authors, the direct impacts of climate change on crop yields may not be good predictors of the economic impacts of climate change (Mendelsohn et al. 1994; Mendelsohn and Dinar 1999; Skoufias et al. 2011). First of all, if the estimated impacts have not taken into account farmers' response to changing conditions, they could overestimate the negative impacts, as farmers may adapt to climate change by switching crops and agricultural techniques, diversifying income sources, or migrating (Kurukulasuriya and Rosenthal 2003). To avoid what they called the "dumb farmer bias," Mendelsohn et al. (1994) therefore introduced a "Ricardian approach" – examining the importance of climate for land values – to take into account adaptation by farmers. The Ricardian approach uses cross-sectional data and bases the analysis on returns to land under different climatic conditions, thus capturing that farmers will adapt to climate change by switching to technologies and crops that yield the highest return to their land. This method estimates long-run impacts of climate change, incorporating all available adaptations. Mendelsohn (2008) summarizes recent studies of impacts of climate change for agriculture in developing countries, using the Ricardian approach. Based on cross-sectional farm-level data from eleven African countries, the marginal effect of increased temperature on net revenues is found to be a 6 % decrease, on average. However, the studies reported show large variations of impacts depending on whether it is the impact of mean climate changes or climate variability that is assessed, whether farms are irrigated, geographic locations, and in which season climate variability occurs. Average estimates can therefore hide large variations. For instance, the effect on net revenues on dryland farms is estimated to be −8 %, while it is estimated that irrigated farms can expect a 3 % increase in net revenue from

marginal warming. The impact of decreased precipitation also shows large variations, although both irrigated and rain-fed farming are expected to lose.

Early criticism of the Ricardian approach was raised by Cline (1996) and Darwin (1999), where Cline (1996) argues, among other things, that ignoring relative price changes due to climate change is likely to underestimate welfare losses, considering the price inelastic demand for food. In addition, Hanemann (2000) argues that the Ricardian approach will overestimate the adaptation choices available to the individual farmer. Burke and Lobell (2010) add that this critique is particularly relevant for poor farmers in developing countries, where access to suitable alternative crops for crop switching may be limited and the cost of switching may be high due to risk aversion or strong consumer preferences for a particular crop.

A number of studies investigate the determinants of adapting to climate change in developing countries using cross-sectional data. For instance, Deressa et al. (2009) and Bryan et al. (2009) find that important constraints to adaptation include lack of information, financial constraints, and lack of access to land for households in South Africa and Ethiopia.

Di Falco and Veronesi (2013) investigate the determinants of adaptation and the impact of different adaptation strategies on net crop revenues in Ethiopia. They use cross-sectional data on 941 farm households and spatially interpolated climate data. Survey respondents were asked about what, if any, adjustments they made in their farming practices in response to long-run shifts in temperature and precipitation. Of the farmers that adapted, more than 95 % reported changing crop varieties, soil conservation, and water conservation or water-harvesting strategies. To correct for selection bias when estimating the impact of adapting on farm net revenues, the authors use a multinomial endogenous switching regression, where the choice to adapt is estimated in a first step. As instrumental variables (see, for instance, Wooldridge 2010) for adaptation in the second step, past experience with climate extremes and access to information about farm techniques are used in the regression that estimates the impact of adaptation, along with climate variables, on farm net revenues. The second step corresponds to the Ricardian approach discussed above. From the first stage, the authors find that temperature, rainfall, soil conditions (where those with very fertile soils are less likely to adapt), household size, and past experience with climate extremes are significantly correlated with the decision to adapt using various strategies. The results from the second step are used to estimate counterfactual net revenues, which are used to calculate the treatment effect of various adaptation strategies for farm net revenues. They find no significant effect of adopting adaptation strategies in isolation, but a portfolio of adaptation strategies significantly increases net farm revenues. In line with the previous literature on this subject, they find that switching crops is one of the most rewarding strategies to adapt to climate change, but only when carried out in combination with soil or water conservation. Adopting all three strategies simultaneously does not increase net revenues more than only one of the conservation strategies in combination with crop switching.

An important weakness of the abovementioned studies is the reliance on cross-sectional data. Despite attempts to control for factors that may bias the results, the

decision to adopt is likely to be dependent on unobservable household characteristics that are also correlated with, for instance, farm revenues. Similarly, household unobservables may influence the variables that are correlated with the decision of whether or not to adopt adaptation strategies, as well as the adoption decision itself, thus biasing the estimated coefficient on the determinants of adoption. Using panel data makes it possible to control for time-invariant unobservables by exploiting the variation within households over time, and this approach is increasingly used in recent studies of impacts of climate change and climate variability. Recent studies exploit observed variation in temperature and precipitation to investigate impacts of climate change on economic outcomes, while controlling for time-invariant unobservables by using fixed effects panel data analysis, i.e., exploiting the variation *within* a spatial unit over time, rather than cross-sectional variation. An example from African agriculture is the study by Schlenker and Lobell (2010), who exploit panel data on crop yields for five staple crops in sub-Saharan Africa, coupled with weather data, while controlling for country fixed effects. They use their estimated impacts to predict the effects of various scenarios for future temperature and precipitation and find consistently negative impacts on yields. This holds for all crops except cassava, which the authors argue does not have a well-defined growing season, resulting in a poor model fit (Schlenker and Lobell 2010).

A review of papers using this approach is provided by Dell et al. (2013), who argue that the strength of the literature is to provide causal evidence on the impact of contemporary weather (rainfall, precipitation, and extreme events) on economic outcomes such as agriculture, health, and conflict. They also argue that there are challenges in extrapolating from the impacts of weather to impacts of long-run climate change, which may be larger (due to intensification) or smaller (due to adaptation).

To the author's best knowledge, there are very few studies explicitly looking at farm-level adaptation to climate change in developing countries using panel data. One exception is a working paper by Taraz (2013), who uses panel data on more than 8,000 Indian farm households from three crop seasons between 1970 and 1999, as well as district level agricultural panel data, both coupled with gridded monthly climate data from the University of Delaware. She exploits variation in monsoon regimes, periods of more common droughts or floods, typically lasting three to four decades, to investigate farmer's adaptation to a marginal change in climate. The results show that farmers adapt their crop portfolio as well as investment in irrigation following particularly dry or wet decades, controlling for wealth and time-invariant household characteristics. However, she also finds that this adaptation is only able to mitigate 15 % of the losses farmers are exposed to due to the adverse shift in climate.

In a developed country setting, Burke and Emerick (2013) use variation in longer-term temperature and precipitation in the USA to study whether farmers can adapt to gradual climate change. As argued by the authors, relying on short-run weather variability to say something about adapting to long-run climate change may overestimate adaptation (if short-run strategies are not "sustainable" in the longer run) or understate adaptation (if there is more flexibility in the longer run). They therefore model changes in agricultural outcomes over time as a function of changes

in temperature and precipitation while controlling for country-level time-invariant unobservables and state-level time-variant unobservables, by using fixed effects analysis as discussed above. Their findings indicate very limited adaptation taking place and little or no mitigation compared to impacts of short-run climate variability. Their results imply potentially large negative impacts of projected climate change by mid-century.

Household Heterogeneity and Market Characteristics

A second objection to relying on crop model simulations alone to assess impacts of climate change in rural developing countries is that the distribution of impacts across the population will depend on heterogeneity in terms of productive assets and whether the households are net producers or net consumers of food (Skoufias et al. 2011).

The second aspect is best captured in a model that incorporates price changes due to climate change. In an early study, Rosenzweig and Parry (1994) use results from crop simulation models in a global trade model and find that despite adaptation, cereal prices are expected to increase due to climate change. Their finding is confirmed by more recent studies, for instance, those reviewed by Schmidhuber and Tubiello (2007). Taking into account the likely change in relative prices due to climate change also responds to the critique of the Ricardian approach for being a partial equilibrium.

A computable general equilibrium (CGE) model takes into account autonomous adaptation to climate change, in the sense that changing market prices for goods and factors of production create incentives to reallocate resources (for instance, to increase food production if food prices increase) and substituting between different food crops in consumption. CGE models are, briefly stated, multisector equilibrium models where prices and production are determined simultaneously. As discussed by Arndt et al. (2012), this approach makes it possible to trace the causal links and mechanisms through which biophysical changes (e.g., decreased crop yields) impact the economy.

Several studies have explored impacts of climate change by using CGE models of developing countries. Using the crop yield impacts from the hydro-crop model described above, Thurlow et al. (2012) analyze impacts of climate variability and climate change on growth and poverty in Zambia. They use a dynamic CGE model which is also linked to a microsimulation component to calculate impacts on poverty. The model disaggregates agricultural production into five agroecological zones to take into account the differential impacts of climate variability and change on these subregions. Two sets of simulations are run; impacts of climate variability over a ten-year period are investigated by simulating 32 different rainfall patterns/sequences based on observations from 1976 to 2007. Impacts of climate change are investigated by simulating three different climate scenarios up to 2025, the SRES B1 scenario and two alternative scenarios with 2° warming by 2025 and 15 % decrease in rainfall in one scenario and 15 % increase in rainfall in the other. The

authors find that the impacts of climate variability dominate the impacts of climate change, but in combination, they both have serious impacts on growth and poverty. The mean climate variability impact is a 0.4 % reduction in GDP each year, reduced maize production by 30 kg/capita, and an average change in the poverty rate by 2.25 % over the ten-year period, with a larger increase in urban than rural poverty. The impacts of climate change are sensitive to the assumptions made concerning rainfall changes, but even under the most pessimistic climate change scenario, the impacts are less than half of those resulting from climate variability.

Another CGE study that focuses on climate variability is the study by Pauw et al. (2011), which looks at economy-wide impacts of droughts and floods on Malawi as well as adaptation through adoption of drought-resistant maize varieties. Production losses in agriculture estimated in a stochastic drought and flood model are simulated in a CGE model of Malawi, and the authors find that Malawi on average looses 1.7 % of GDP annually due to droughts and floods. The CGE model disaggregates farm households according to landholding size and region, as well as urban and rural nonfarm households. Farmland is disaggregated according to land size, and labor is disaggregated according to skill level. This allows detailed modeling of the economy with links between production, factor markets, and household incomes and thus a detailed analysis of impacts on household welfare. The changes in expenditures for each household group are combined with household survey data to calculate changes in the poverty rate. The largest increase in poverty is for rural nonfarm households, while the largest impact on earnings is for small-scale farmers. These farmers rely to a large extent on maize, which is vulnerable to droughts, and the increase in crop prices in response to the drought is not sufficient to compensate the production loss. If farmers adapt to climate variability by adopting drought-resistant maize, the overall poverty rate decreases and GDP increases; however, the authors do not discuss how these benefits are distributed across household categories.

Hertel et al. (2010) assess implications of three climate change impact scenarios (resulting in low, medium, and high productivity) for agriculture on a set of 15 developing countries. For instance, the low-, medium-, and high-productivity scenarios for coarse grains for Malawi imply −22, −10, and 2 % changes in yields by 2030. These impact estimates are based on recent studies and are direct yield impacts, i.e., without adaptation. The authors use the Global Trade Analysis Project (GTAP) model with a microsimulation component for poverty analysis to study impacts of the productivity change on world market prices and poverty of household groups in the different countries. The simulations show that average crop prices do not change much under the medium-impact scenario and that average poverty impacts are also small. For coarse grains, world market prices are still expected to increase as much as 15 % in the medium scenario and 62 % in the low-productivity scenario. The results also show that poverty impacts can be disaggregated into effects on costs of living and effects on earnings, where the earnings effect varies considerably depending on which activity households engage in. For some households, the positive earnings effect from increased crop prices may outweigh the effect of increased costs of living. Adding together these effects, the authors find that the median poverty impact

on self-employed agricultural households is positively correlated with the productivity shock, while the opposite is true for the self-employed nonagricultural households. Urban wage earners experience a poverty increase in all cases, but normally constitute a small share of the poor. For African countries, the large negative impact on yields does not permit poverty reduction for the self-employed agricultural households, even in the low-productivity, high-price scenario. The authors conclude that in order to assess impacts on livelihoods and poverty in developing countries, detailed information on earnings and poverty in household groups is needed, and it is necessary to look beyond the most likely impact scenarios.

The results imply that taking into account the likely increase in food prices due to climate change implies a positive "earnings effect" on farm households that sell some of their produce, and accounting for this effect may reverse the negative impact of climate change for some households. Using a static CGE model of Malawi, Skjeflo (2013) shows that negative productivity shocks to maize cause increased domestic maize prices, which are beneficial for large landholders. On the other hand, urban poor and small-scale farmers are hurt by higher food prices because they are net buyers of food and spend a large share of their income on food. This is shown in Fig. 2, where the welfare impact of the negative productivity shock to maize for eight household groups is measured by the equivalent variation as percent of baseline expenditures. The figure shows that small-scale farm households, who constitute the majority of the rural households in Malawi, experience a small welfare decrease

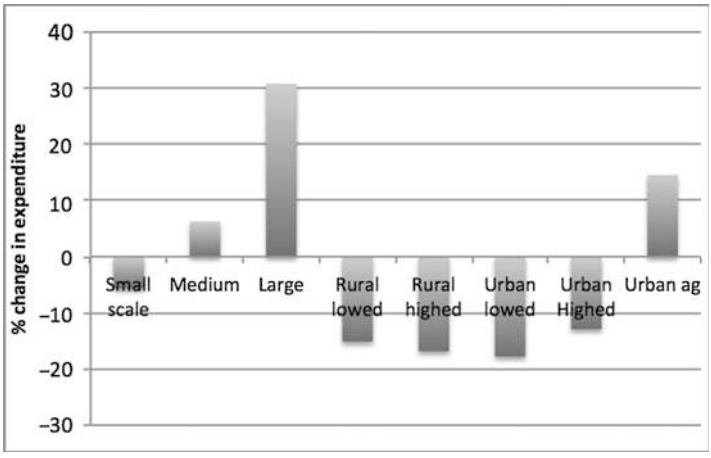

Fig. 2 Welfare impacts of negative productivity shocks to maize due to climate change by 2030 in Malawi. Welfare change measured by the equivalent variation, as percent of baseline household expenditures. Household groups: small scale = small-scale farm households, medium = medium-scale farm households, large = large-scale farm households, rural lowed = rural nonfarm households with low education, rural highed = rural nonfarm households with high education, urban lowed and highed defined similarly, urban ag = urban farm households (Source: page 1698 in Skjeflo (2013))

despite higher maize prices. Farm households with larger landholdings benefit from the productivity shock because of increased crop prices. Urban households, and especially urban households with little or no education, are particularly vulnerable because of the large share of their income that is spent on food.

The CGE studies discussed above are based on aggregate models that assume perfect factor and product markets, while econometric studies have shown numerous constraints to adaptation at the household level, many of them related to market imperfections. As previously mentioned, studies from South Africa and Ethiopia find that access to credit is a main constraint to adapting to climate change among farm households, as well as access to land (in Ethiopia) and information about adaptation options and climate projections (Deressa et al. 2009; Bryan et al. 2009; Di Falco et al. 2012).

The fundamental dependence of agriculture on weather and natural resources creates a strong link between the environment and the rural economy in developing countries. In a seminal paper, Binswanger and Rosenzweig (1986) show how the immobility of land causes spatial dispersion, high transport costs, and synchronic timing of production activities in agriculture, while heterogeneity in input factors contributes to asymmetric information. Weather variability is linked to yield risk, market price risk, and uncertain optimal timing of production activities. Binswanger and Rosenzweig (1986) show how a combination of these factors may explain credit market imperfections, labor and land market imperfections, as well as output market imperfections. The dual role of farm households as producers and consumers of food is therefore also likely to be important when assessing household vulnerability to climate change. This is in line with the basic farm household model by Singh et al. (1986). They also showed that when markets for goods that the farm household both consumes and supplies (such as food or labor) fail, production decisions are no longer independent from consumption decisions. A number of studies have shown the implications of non-separability for farm household behavior, for instance, in terms of low supply response to price incentives (de Janvry et al. 1991) and nonlinear supply (Löfgren and Robinson 1999).

Morton (2007) discusses potential impacts of climate change on smallholder agriculture and mentions lack of market access for smallholders as a non-climatic stressor that increases smallholders' vulnerability to climate change. As previously discussed, market imperfections may also act as constraints to adaptation for farm households, and they are also likely to affect how households respond to planned adaptation policies. Market characteristics will also shape the response of households to increased climate risk due to climate change. To the extent that climate shocks are common shocks that simultaneously affect households in an area, the scope for informal risk-sharing strategies is limited (Dercon 2002). Formal credit and insurance markets are often missing or imperfect in developing countries (Besley 1995), and the effect of increased climate variability on households will depend on their ability to smooth income and consumption through risk management strategies. These strategies may in themselves have important impacts on poverty, by locking poor households in low-risk, low-return agriculture (Dercon 2002). Weather risk may thus contribute to increased inequality.

Future Directions

The studies summarized above show that climate change is expected to harm less developed countries disproportionally. However, as has been extensively discussed in the literature, it is not sufficient to rely on the direct impacts of changing temperatures and precipitation, or more severe and frequent climate extremes, without taking into account households' responses to these changes. An early suggestion to incorporate this important aspect into studies of climate change impacts is the Ricardian approach. This approach has been criticized for failing to take into account the likely impact of climate change on food prices and for overestimating the range of adaptation options available to the individual farmer. Another problem is the reliance on cross-sectional data, causing concerns for omitted variable bias. This is also a concern for the existing studies of farm-level adaptation to observed variation in temperature, precipitation, and climate extremes in less developed countries. As a way of bypassing this problem as well as dealing with the importance of changing prices, a number of studies use CGE models to investigate the impacts of climate change for household groups in developing countries. A valid criticism against this approach is the assumption of well-functioning markets in poor, rural economies. The recent empirical literature that exploits variation in observed weather across time within spatial units seems like a promising approach to improved understanding of climate change impacts. These studies are rare for developing countries, perhaps because of data quality and availability issues, for instance, if one wishes to investigate actual adaptation to gradual changes in climate and not weather variation. However, as more and better data becomes available, this seems like a promising approach. Existing and new approaches should be used to complement each other in order to gain new and robust insights to the potential impacts of climate change for households.

References

Arndt C, Chinowsky P, Robinson S, Strzepek K, Tarp F, Thurlow J (2012) Economic development under climate change. Rev Develop Econom 16(3):369–377

Besley T (1995) Chapter 36 Savings, credit and insurance. In: Behrman J, Srinivasan TN (eds) Handbook of development economics, vol 3. Elsevier, Amsterdam, pp 2123–2207

Binswanger HP, Rosenzweig MR (1986) Behavioural and material determinants of production relations in agriculture. J Develop Stud 22(3):503–539

Bryan E, Deressa TT, Gbetibouo GA, Ringler C (2009) Adaptation to climate change in Ethiopia and South Africa: options and constraints. Environ Sci Policy 12(4):413–426

Burke M, Emerick K (2013) Adaptation to climate change: evidence from US agriculture. Unpublished, University of California, Berkeley

Burke M, Lobell D (2010) Food security and adaptation to climate change: what do we know? In: Climate change and food security. Springer, Dordrecht, pp 133–153

Chen S, Ravallion M (2010) The developing world is poorer than we thought, but no less successful in the fight against poverty. Quartr J Econom 125(4):1577–1625

Cline WR (1996) The impact of global warming of agriculture: comment. Am Econom Rev 86:1309–1311
Darwin R (1999) The impact of global warming on agriculture: a Ricardian analysis: comment. Am Econom Rev 89:1049–1052
Darwin R, Kennedy D (2000) Economic effects of CO_2 fertilization of crops: transforming changes in yield into changes in supply. Environ Model Assessment 5(3):157–168
de Janvry A, Fafchamps M, Sadoulet E (1991) Peasant household behaviour with missing markets: some paradoxes explained. Econom J 101(409):1400–1417
Dell M, Jones BF, Olken BA (2013) What do we learn from the weather? The New Climate-Economy Literature. J Econom Literature 52(3):740–98
Dercon S (2002) Income risk, coping strategies, and safety nets. World Bank Res Observ 17(2):141–166
Deressa TT, Hassan RM, Ringler C, Alemu T, Yesuf M (2009) Determinants of farmers' choice of adaptation methods to climate change in the Nile Basin of Ethiopia. Glob Environ Chang 19(2):248–255
Di Falco S, Veronesi M (2013) How can African agriculture adapt to climate change? A counterfactual analysis from Ethiopia. Land Econ 89(4):743–766
Di Falco S, Yesuf M, Kohlin G, Ringler C (2012) Estimating the impact of climate change on agriculture in low-income countries: household level evidence from the Nile Basin, Ethiopia. Environ Res Econom 52(4):457–478
Easterlin RA (2000) The worldwide standard of living since 1800. J Econom Perspect 14(1):7–26
Hanemann WM (2000) Adaptation and its measurement. Clim Change 45(3):571–581
Hertel TW, Rosch SD (2010) Climate change, agriculture, and poverty. Appl Econ Perspect Pol (Autumn 2010) 32(3):355–385
Hertel TW, Burke MB, Lobell DB (2010) The poverty implications of climate-induced crop yield changes by 2030. Glob Environ Chang 20(4):577–585
IPCC (2013) Summary for policymakers. In: Stocker T, Qin D, Plattner G-K, Tignor M, Allen S, Boschung J, Nauels A, Xia Y, Bex V, Midgley P (eds) Climate change 2013: the physical science basis. Contribution of working group I to the fifth assessment report of the intergovernmental panel on climate change. Cambridge University Press, Cambridge, UK/New York
IPCC (2014) Summary for policymakers. In: Field C, Barros V, Dokken D, Mach K, Mastrandrea M, Bilir T, Chatterjee M, Ebi K, Estrada Y, Genova R, Girma B, Kissel E, Levy A, MacCracken S, Mastrandrea P, White LL (eds) Climate change 2014: impacts, adaptation, and vulnerability. Part A: global and sectoral aspects. Contribution of working group II to the fifth assessment report of the intergovernmental panel on climate change. Cambridge University Press, Cambridge, UK/New York
Jones PG, Thornton PK (2003) The potential impacts of climate change on maize production in Africa and Latin America in 2055. Glob Environ Chang 13(1):51–59
Kurukulasuriya P, Rosenthal S (2003) Climate change and agriculture: a review of impacts and adaptations. World Bank, Washington, DC
Löfgren H, Robinson S (1999) Nonseparable farm household decisions in a computable general equilibrium model. Am J Agric Econom 81(3):663–670
Mendelsohn R (2008) The impact of climate change on agriculture in developing countries. J Nat Res Policy Res 1(1):5–19
Mendelsohn R, Dinar A (1999) Climate change, agriculture, and developing countries: does adaptation matter? World Bank Res Observ 14(2):277–293
Mendelsohn R, Nordhaus WD, Shaw D (1994) The impact of global warming on agriculture: a Ricardian analysis. Am Econom Rev 84(4):753–771
Morton JF (2007) The impact of climate change on smallholder and subsistence agriculture. Proc Natl Acad Sci 104(50):19680–19685
Nakicenovic N, Swart R (2000) Special report on emissions scenarios. Edited by Nebojsa Nakicenovic and Robert Swart, pp 612. ISBN 0521804930. Cambridge University Press, Cambridge, UK, July 2000, p 1

Nelson GC, Rosegrant MW, Koo J, Robertson R, Sulser T, Zhu T, Ringler C, Msangi S, Palazzo A, Batka M et al (2009) Climate change: Impact on agriculture and costs of adaptation. International Food Policy Research Institute, Washington, DC

Niang I, Ruppel O, Abdrabo M, Essel A, Lennard C, Padgham J, Urquhart P (2014) Africa. In: Field C, Barros V, Dokken D, Mach K, Mastrandrea M, Bilir T, Chatterjee M, Ebi K, Estrada Y, Genova R, Girma B, Kissel E, Levy A, MacCracken S, Mastrandrea P, White LL (eds) Climate change 2014: impacts, adaptation, and vulnerability. Part B: regional aspects. Contribution of working group II to the fifth assessment report of the intergovernmental panel on climate change. Cambridge University Press, Cambridge, UK/New York

Parry M, Rosenzweig C, Iglesias A, Fischer G, Livermore M (1999) Climate change and world food security: a new assessment. Glob Environ Chang 9:S51–S67

Pauw K, Thurlow J, Bachu M, Van Seventer DE (2011) The economic costs of extreme weather events: a hydrometeorological CGE analysis for Malawi. Environ Develop Econom 16 (02):177–198

Porter J, Xie L, Challinor A, Cochrane K, Howden S, Iqbal M, Lobell D, Travasso M (2014) Food security and food production systems. In: Field C, Barros V, Dokken D, Mach K, Mastrandrea M, Bilir T, Chatterjee M, Ebi K, Estrada Y, Genova R, Girma B, Kissel E, Levy A, MacCracken S, Mastrandrea P, White LL (eds) Climate change 2014: impacts, adaptation, and vulnerability. Part A: global and sectoral aspects. Contribution of working group II to the fifth assessment report of the intergovernmental panel on climate change. Cambridge University Press, Cambridge, UK/New York

Rosenzweig C, Parry ML (1994) Potential impact of climate change on world food supply. Nature 367(6459):133–138

Schlenker W, Lobell DB (2010) Robust negative impacts of climate change on African agriculture. Environ Res Lett 5(1):014010

Schmidhuber J, Tubiello FN (2007) Global food security under climate change. Proc Natl Acad Sci 104(50):19703–19708

Singh I, Squire L, Strauss J (1986) Agricultural household models: extensions, applications, and policy. Johns Hopkins University Press, Baltimore

Skjeflo S (2013) Measuring household vulnerability to climate change – why markets matter. Glob Environ Chang 23(6):1694–1701

Skoufias E, Rabassa M, Olivieri S, Brahmbhatt M (2011) The poverty impacts of climate change – a review of the evidence. World Bank Policy Research Paper. World Bank, Washington, DC

Taraz V (2013) Adaptation to climate change: historical evidence from the Indian monsoon. Department of Economics, Yale University, New Haven

Thurlow J, Zhu T, Diao X (2012) Current climate variability and future climate change: estimated growth and poverty impacts for Zambia. Rev Develop Econom 16(3):394–411

Wooldridge JM (2010) Econometric analysis of cross section and panel data. MIT Press, Cambridge, MA

World Bank (2014) World development indicators 2014. http://www.scribd.com/doc/222646575/World-Development-Indicators-2014. Accessed 26 Aug 2014

Fracking

Qingmin Meng

Contents

Abstract

Natural gas has gained a dominant role in current world clean energy development due to the significant advances in horizontal drilling and hydraulic fracturing. Hydraulic fracturing, also known as fracking that is now increasing exponentially across the world, is the process of extracting natural gas from shale rock layers or other tight rock formations within the earth. Specifically, horizontal drilling combined with traditional vertical drilling allows injection of highly pressurized fracking fluids into the shale layers to create new channels within the rock, from which natural gas is released at much higher rates than traditional drilling. For example, the USA holds the largest known shale gas reserves in the world. Fracking in the USA has boosted economy and local community growth. However, studies have found that hydraulic fracking threatens water resources, harms air quality, changes landscapes, and damages ecosystems. Furthermore, methane emissions from drilling, fracking processes, and the related natural gas storage and transportation have become a critical issue, which raises the question whether hydraulic fracking can mitigate world climate

Q. Meng (✉)
Department of Geosciences, Mississippi State University, Starkville, MS, USA
e-mail: qmeng@geosci.msstate.edu

W.-Y. Chen et al. (eds.), *Handbook of Climate Change Mitigation and Adaptation*,
DOI 10.1007/978-3-319-14409-2_62

change. Some studies have obtained significantly different conclusions of climate mitigation impacts of fracking. More studies and further measuring and observational surveys are needed in order to have a comprehensive understanding of hydraulic fracturing's impacts on climate mitigation.

Introduction

In the media, hydraulic fracturing (fracking) often refers to the two steps applied for extracting natural gas trapped in shale formations. The first step is to drill down to the sedimentary rocks and then drill sideways for a mile or more. This horizontal drilling has been widely practiced since the 1980s to extract conventional oil and gas. In the second step, the producers must deploy hydraulic fracturing; using high pressure, fracking pumps into open fractures in the rocks with millions of gallons of water, sand, and chemicals that allow oil and gas to flow. Fracking was introduced into gas mining as early as in 1940s and then was efficiently combined with horizontal drilling in 1990s.

Fracking has resulted in significant economic hopes and opportunities such as employment, income, and tax revenue growth in shale play regions but with increasing public awareness and concerns about the environmental impacts of hydraulic fracturing. Many studies have talked about the processes of hydraulic fracturing and its environmental impacts including surface and groundwater resources (e.g., Osborn et al. 2011), air pollution (e.g., Howarth et al. 2011a), seismic activities (e.g., seismosoc.org 2015), environmental and the population at risks of fracking (Meng 2015a), and landscape and ecosystem disturbance (Meng 2014). In this chapter, the author summarizes a comprehensive understanding of the conception and technological process of fracking, its development, and its worldwide extent and then focuses on methane emissions and a concise summary of current understanding of its climate impacts.

Hydraulic Fracturing (Fracking)

Instead as a "drilling process" as a lot of media state, hydraulic fracturing in fact is a specific process used after the drilled hole is completed. Hydraulic fracturing or "fracking" is the propagating of fractures in a rock layer caused by a highly pressurized compound fluid creating small cracks, or fractures, in underground geological formations to free unconventional resources of natural gas, oil, and other hydrocarbons captured inside tight sandstones, shales, and other low-permeability geological formations. These geological formations, known to contain hydrocarbons, have served as sources for conventional oil or gas. However, the gas and oil in them were generally be deemed as unrecoverable due to their low porosity and permeability. The advancements of technology in hydraulic fracturing and horizontal drilling have resulted in significant progresses recently (Kuuskraa

et al. 2011), and drilling now can be done kilometers underground and to horizontal distances of 3 km and even more exploring shale, sandstone, and other formations as thick as only 30 m.

A well is hydraulically fractured after horizontal drilling is completed and then the drilling rig is moved off site. Water tanks and water-hauling trucks come to the well site. The fracking operation is to start when the sand haulers, pump truck, blender, and control van arrive. After all pieces of equipment are joined together, they will be connected to the wellhead with high-pressure hoses. Then, the equipment is tested before the actual fracture stimulation will start. This fracking operation may need several hours to even several days, which depends on the geological characteristics and the number of fracture zones. There is then typically a very high-level noise and truck traffic becomes the most noticeable signal in the operation process. Generally, 8000–80,000 m^3 (2–20 million gallons) of water and proppants including sand and chemicals are pumped underground into the horizontal or directional wells at high pressures (69,000–138,000 kPa), which are sufficient to fracture impermeable rock formations. Rock fractures induced by high-pressure, high-volume hydraulic fracturing allow natural gas and oil to flow from the formation to the well and up through the well to the ground surface. In this process, chemical- and sand-laden watery fluid will be pumped down into the well and the watery gas or oil will eventually be collected. Therefore, in order to prevent the fluid from entering the water supply, steel surface or intermediate casing needs to be inserted into the well. Additionally, cement needs to be filled into the annulus and the space between the casing strings and the drilled hole. Once the cement has set, the drilling continues from the bottom of the surface or intermediate cemented steel casing to the next depth. Using smaller steel casing each time, this process is repeated until the gas and oil-bearing reservoir is reached often between 1900 and 4000 m in depth.

Fracturing fluids, typically including water, sand, and proprietary chemical mixes, are injected down the well bore into the impermeable rock formations. The fluids that create the initial fractures are then mixed with thicker fluids that include sand and gelatin. When the fluids flow back up, sand remains in the fractures and props the rock open, which maintains open pathways to the well. This allows the gas or oil to seep from the rock into pathways, up and through the well and till the ground surface for collection. According to volume of fracturing fluids used, one can classify fracking into low-volume and high-volume hydraulic fracturing. Up to 20 million liters of water for an individual well can be needed for high-volume hydraulic fracturing applied to the completion of tight gas and shale gas fracking. Low-volume fracking used to stimulate high-permeability reservoirs typically needs 75,000–300,000 l of fluid per well. One also needs to understand that 15–80 % of the fluid returns to the ground surface and is often called wastewater, when the fracking procedure is completed. The wastewater often contaminates fracturing chemicals and subsurface constituents, which include toxic organic compounds, heavy metals, and naturally occurring radioactive materials. Remaining untreated or not adequately secured, this wastewater can result in harmful environmental and health effects.

A larger fracking field is needed to take into account the space for equipment and material storage for fracture stimulation. A typical fracking site is about 4–5 acres,

which is used to hold the numerous truck-mounted pumps, temporary storage tanks, and fracture-treat large tractor trailer trucks, and the original landscape is totally changed (Meng 2014). Once a vertical hole is drilled, a downhole drilling motor is inserted into the hole to begin horizontal drilling. For instance, it takes over 350 pieces of pipe for a 3000 m horizontal well. Production casing is inserted into the full length of the wellbore when the target distance is completed. Casing wells is a critical process because it permanently secures the wellbore and it prevents hydrocarbons form seeping out, and at this point, a temporary wellhead is installed. A perforating gun is lowered by wire line into the casing and an electrical current is sent down and sets off a charge that shoots small holes through the casing and cement. Then, the well will be fracked and a permanent wellhead is installed once fracking is completed with a built pipeline to transport the gas to the pipeline network.

Biocides are widely used in fracking since bacterial colonies can clog or obstruct fracking wells and make it hard to extract gas after fracturing. However, people do not have a complete list of the biocides currently used in fracking. While biocides are a small portion of fracking fluid, we need to understand that up to $>$ 500 mg/L and, given total fluid volumes surpassing 10 million L per horizontal well, a total amount of biocides per fracking event can exceed 1000 gal (McCrudy 2011; Nicot and Scanlon 2012; Aminto and Olson 2012). Many of the biocides are degradable through abiotic and biotic especially aerobic processes, but some can potentially transform into severe or persistent compounds, while the understanding of biocides' degradation and sorption in high pressure and salt and organic matter concentrations is very limited (Kahrilas et al. 2015). Some of the fluids stay underground, and some return to the surface as wastewater and are collected for disposal, which are often injected into deep ground that are called wastewater wells.

Gas yield per well can be much different across shale plays, but currently there is limited available statistics about production of fracking wells. In Marcellus Shale region, USA, an average yield of a gas well is between 5700 to 290,000 m^3 per day. In the first and second year, the yield can be 57,000–114,000 m^3 per day; in the third and fourth year, the yield can be 28,000–56,000 m^3 per day (Marcellususa.com).

Fracking Across the World

Many countries, including but not limited to Algeria, Argentina, Australia, Brazil, Canada, China, France, Libya, Mexico, Poland, Russia, South Africa, the USA, and Venezuela, are estimated to possess at least $\sim 3 \times 10^{12}$ m^3 [$\sim$100 trillion ft^3 (Tcf), or 1×10^{14} ft^3] of recoverable shale gas (Kuuskraa et al. 2011; Schulz et al. 2010). In Fig. 1, the US Energy Information Administration (EIA) has summarized and compared the technically recoverable shale gas and oil resources of the whole world between the USA and the regions outside the USA. Global estimates for recoverable shale gas are $\sim 206 \times 10^{12}$ m^3, which is for at least 60 years of current global usage in 2013, and global estimated shale oil resources are now 345 billion barrels (Bbbl; one barrel = 42 US gallons) (US Energy Information Administration

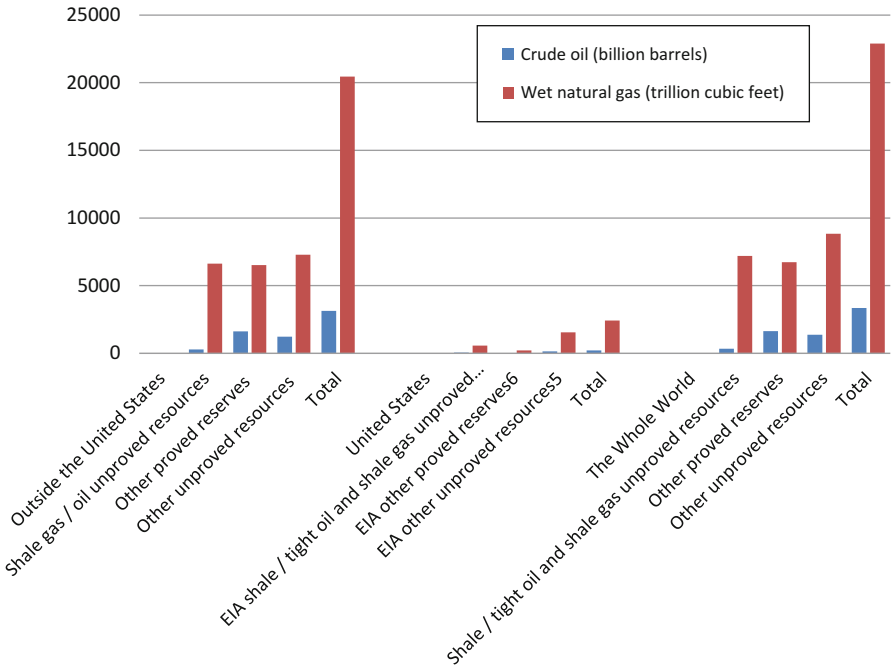

Fig. 1 Technologically recoverable shale gas and shale oil resources across the world. They are plotted using the data estimated by the US Energy Information Administration (2013)

2013). In the USA, average estimates of the technically recoverable shale gas resource doubled to 600–1000 Tcf (17–28 $\times$ 10^{12} m^3) in 2013, and the technically recoverable shale oil resource rose by 40 % to 58 Bbbl (US Energy Information Administration 2013). However, these are only substantial resource estimates, which are a type of guesses because large-scale production of shale and other unconventional gas and oil resources is currently in its introduction phase (Meng 2015b).

Fracking has been applied in the whole world for about 60 years, but in the various countries, the fracking processes can be different. In the USA, one early type of fracking called slickwater fracking was used to extract natural gas in the Barnett Shale in Texas in 1998. This fracking technique was made possible by integrating microseismic three-dimensional imaging supported by federal agencies such as the Department of Energy and recent advances in directional drilling (Shellenberger and Nordhaus 2011). Drilling into shale now accounts for about 30 % of the US gas production (Dopp 2012). Today, fracking often means the combination of advanced high-pressure, high-volume hydraulic fracturing and horizontal drilling, which in fact employs cutting-edge technologies and now is mostly responsible for surging natural gas or petroleum production. In the USA, fracking has been involved in safe applications to shale, but other tight rock formations have also been explored by drilling about 2 km or more below the surface before gradually turning horizontal (Fig. 2). Compared to shale gas, tight gas is produced from reservoir rocks with

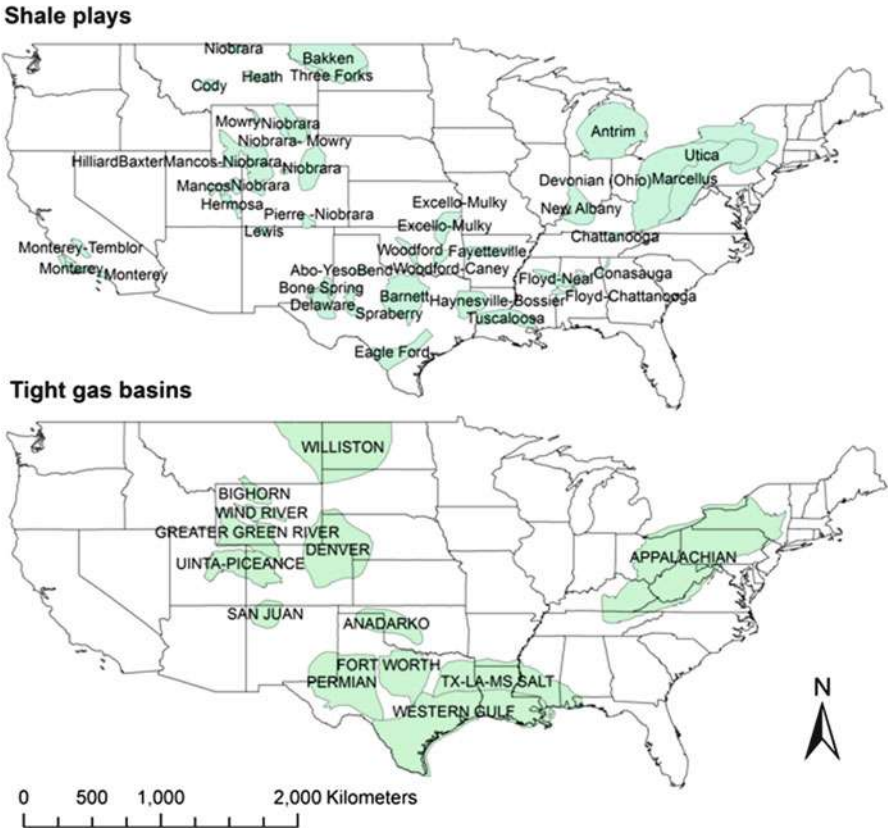

Fig. 2 Shale plays and tight gas basins in the USA

much lower permeability so that massive hydraulic fracturing is needed to create fractures in the reservoirs less than 0.1 millidarcy matrix permeability and less than 10 % matrix porosities (Law and Spencer 1993; Sharif 2007). When a well is drilled, cased, and cemented, small perforations are made in the horizontal portion of the well pipe, and in reality, a single surface site/fracking pad often accommodates a number of wells. A typical mixture of water (90 %), sand (9.5 %), and chemical additives (0.5 %) is pumped at high pressure through the well into tight rock formations in order to create microfractures, which are held open by the grains of sand. Chemical additives play a number of roles, such as to reduce friction and prevent pipe corrosion.

From at least the mid-1960s, fracking has been widely used by the petroleum industry in Canada (Milne and Howie 1966). Massive fracking has been used across Alberta from the late 1970s to regain natural gas from the Spirit River Formation, which is a typical low-permeability sandstone formation (Cant and Ethier 1984). Fracking currently is applied to the development of the fields Cardium, Duvernay,

Montney, and Viking in Alberta, Bakken in Saskatchewan, Montney, and Horn River in British Columbia.

Germany began to apply fracking to gas wells in tight sandstone in 1975, and it quickly became a common technology in the period 1978–1985, when more wells used fracking than in any other European country. Most fracking used water- or oil-based gels in Germany (Mader 1989), and the Rotliegend Sandstone is the most popular target formation for fracking, which has been the source of most of German natural gas production (Koehler 2005).

In the UK, fracking has been used commonly in North Sea gas and oil fields from the late 1970s (Mader 1989) and has been used in about 200 British onshore gas and oil wells since the early 1980s. However, fracking did not attract public attention until it was proposed for onshore shale gas wells in 2007 (British Geological Survey 2012).

Fracking also has been recently used in developing countries. The South African government strongly campaigns for fracking in order to extract enough natural gas across the country, which is treated as a "bridge-fuel" between coal and alternative fuels in this country. However, people recognized that the significant amount of loss of methane to the environment in the process of fracking through leakage from fracking sites is considerable. A temporary moratorium on hydraulic fracturing for shale gas in South Africa's Karoo region was imposed in 2011 due to the public pressure, examining concerns about environmental degradation and particularly groundwater safety (Hweshe 2012). China completed its first horizontal shale gas well in 2011. A global shale gas study has indicated that China's technically recoverable shale gas reserves could be almost 50 % higher than those of the USA (Watts 2011).

Methane Emission from Fracking Process

According to estimations by the US Environmental Protection Agency (EPA), methane (CH_4) is the second most prevalent greenhouse gas (GHG). CH_4 is mainly emitted in the USA from human activities. CH_4 accounted for about 9 % (equivalent to CO_2) of all US greenhouse gas emissions from human activities (EPA 2010). Methane is emitted from sources such as wetlands and human activities such as leakages from natural gas systems and the raising of livestock. Although methane's lifetime in the atmosphere is much shorter than that of carbon dioxide (CO_2), CH_4 is more efficient at trapping radiation than CO_2. The impact on climate change for CH_4 is over 20 times greater than CO_2 over a 100-year period. Globally, over 60 % of total CH_4 emissions come from human activities (EPA 2010).

Methane is emitted from industry, agriculture, and waste management activities. According to EPA's overall green gas emissions' estimation, the largest source of CH_4 emission is natural gas and petroleum systems in the USA (Fig. 3). Methane is the primary component of natural gas. Most often CH_4 is emitted to the atmosphere in the processes of production, processing, storage, transmission, and distribution of

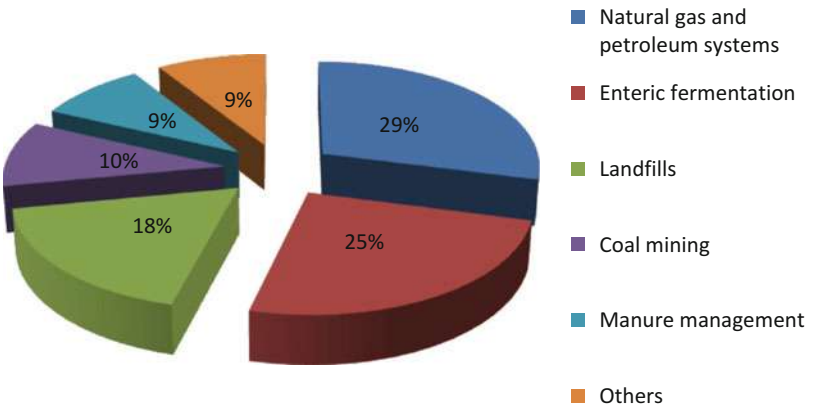

Fig. 3 Methane emission sources in the USA

natural gas. Methane emission from hydraulic fracking is more complex than that from conventional gas mining.

During fracking well completion, natural gas starts flowing up the well, accompanied by some of the water and chemicals used to crack the rock. In fracking processes, completion practices and regulations differ from region to region and by companies. The flowback water, also called wastewater, is most often pumped into an open wastewater pit dug on site, where methane and volatile organic compounds (VOCs) directly flow into the air. Flowback mixtures sometimes are also contained in tanks, either open or closed and thus with vapors vented or flared too. When a fracking well has been completed, production operations become similar to conventional natural gas extraction.

There are also potential methane emissions during production and fracking processes. Potential emissions include incomplete combustion during flaring, fugitive emissions of natural gas from equipment leaks, and intentional venting from oil and wastewater storage tanks or ponds. Natural gas produced with fracking liquids and oil will be richer in VOCs than a well producing mostly natural gas. Natural gas-powered compressor engines, flaring units, and centralized processing and compression facilities at fracking pad sites also contribute CO_2, CO, NOx, and VOCs such as formaldehyde, PM (soot), and polycyclic aromatic hydrocarbons. Fugitive emissions encompass the GHG methane and varying amounts of VOCs including aromatics such as the carcinogen benzene and the hazardous air pollutant toluene.

Actual gas emissions are different from region to region. This depends on natural gas and oil composition, separation requirements, and different state regulations (Moore and Bar-Ilan 2013). Some estimates of the fraction of natural gas production vented or flared on federal lands in the Western USA ranged from 0.34 % to 5 % of the total production volume (US Government Accountability Office 2010). However, 29 % to 36 % of the natural gas extracted from the Bakken Shale in North Dakota was vented or flared between May 2011 and December 2012, which is mainly due to a

lack of infrastructure such as access to pipelines and other processing infrastructure (US Energy Information Administration 2014). As the official Colorado inventory for the Denver basin indicated, more than 70 % of total VOC emissions from all sources in the region resulted from 6000 more oil and condensate storage tanks, even with stringent controls in place (Wells 2012). However, the state estimate of total VOC emissions from gas and oil operations was only half the estimate obtained from actual field measurements in the Denver Basin (Pétron et al. 2014).

Regional and national estimations of total methane emissions associated with hydraulic fracking remain uncertain and are an important topic of considerable research (Howarth et al. 2011b). Official EPA estimates of annual methane emissions from natural gas production operations have varied greatly in the last decade, which ranged between about 0.2 % (US Environmental Protection Agency 2010) and 1.5 % (US Environmental Protection Agency 2011, 2012) of the national gross natural gas production. Similarly, a study indicated that national emissions from natural gas production operations in 2011 were 0.42 % of gross production (Allen et al. 2013), which is very close to the estimate of 0.49 % according to the 2013 EPA inventory and EIA (Energy Information Administration, USA) production statistics.

Research is also needed to examine methane leakage during natural gas transmission and distribution. In the USA, there are about 2.2 million miles of natural gas distribution mains and hundreds of thousands of miles of higher-pressure transmission pipelines. According to the US EPA inventories, losses during transmission and distribution are about 0.7 % of total production, which is the largest loss of any step in the natural gas supply chain (US Environmental Protection Agency 2013). Other estimates of the amount of gas lost in the process of natural gas transport are 1.4 % for Russia (Lelieveld et al. 2005) and 5.3 % for the UK (Mitchell et al. 1990). Although new methane mapping technologies have allowed to check and map pipeline leakage of natural gas across cities (Jackson et al. 2014; Phillips et al. 2013), it is still a grand challenge to regionally and nationally assess natural gas leakage during transport.

Unlike these bottom-up emission measurements and inventory estimates, substantially larger regional-scale leakage rates have been found by recent atmospheric studies using airborne and tall-tower measurements in the western USA. Karion et al. (2013) estimated that 55,000 $\pm$ 15,000 kg CH_4 per hour leaked into the atmosphere in the Uintah Basin, which amounts to a rate of 6.2–11.7 % of total natural gas production in the region. Pétron et al. (2014) measured 4 % leakage in the oil- and gas-producing Denver Basin, Colorado. In these two basins, aggregated methane emissions seem significantly larger than the US EPA 2013 estimated 1.4 % total leak rate. A recent synthesis suggests that total methane emissions from anthropogenic activities in the USA, including oil and gas production, were 50 % higher than EPA estimates (Brandt et al. 2014; US Environmental Protection Agency 2013). The emissions from gas and oil can be underestimated by as much as a factor of five in the South Central USA according to a recent study (Miller et al. 2013). It is apparent that more research work is needed, and a common understanding that methane losses are larger than current EPA estimates is acceptable.

Climate Mitigation?

Unfortunately, whether methane emissions are large enough to offset the advantage in methane's combustion efficiency compared to coal in electricity generation is still unclear (3.2 % lost gas in total) (Alvarez et al. 2012). If it is so, people believe that better information on the sources of leaks and advanced gas transport technology can significantly reduce future leakage and fugitive greenhouse gas emissions, and therefore improve local and regional air quality in the future. How much hydraulic fracturing and unconventional resource extraction reduce total GHG emissions in the future is unknown. Current lower energy prices from increased supply would probably increase energy consumption and encourage users to natural gas from other energy sources including coal, nuclear, and renewables.

Using the data of the National Energy Modeling System projections from the US Energy Information Administration (EIA), Newell and Raimi (2014) showed that in the USA, gas and oil price would fall significantly under a "high natural gas and oil resource" scenario compared with a reference scenario. While total energy use would be about 3 % higher as a result, total GHG emissions could remain about 0.5 % lower than in the reference scenario, which could be mainly because of the natural gas displacement of coal for electricity generation. Likewise, other researchers concluded that increased natural gas supply such as hydraulic fracturing might decrease GHG emissions slightly in the USA and globally, but it seems impossible to change global GHG concentrations substantially (Newell and Raimi 2014; Energy Modeling Forum 2013; Edmonds and McJeon 2013).

On the other hand, an increase of the total GHG emissions is still possible, which partially depends on the extent to which cheaper natural gas and oil reduce the market penetration of other green energy sources, such as renewables and nuclear power. Large emissions with an average of 34 g CH_4/s (2.937 t/day) per well from seven hydraulic fracking pads were checked and quantified in the drilling phase (Caulton et al. 2014). Howarth et al. (2011a) also concluded that 3.6–7.9 % of lifetime shale gas production migrates to the atmosphere through venting or leaking over the lifetime of a well and that 1.9 % of the total gas production is emitted as methane through well completion.

Furthermore, Schneising et al. (2014) used the SCIAMACHY (Scanning Imaging Absorption spectroMeter for Atmospheric CHartographY) satellite remote sensing to quantify methane emissions from the Bakken and Eagle Ford formations that are the fastest growing oil production regions in the USA. They found that methane emissions in the Bakken and Eagle Ford formations have increased by 990 $\pm$ 650 kt CH_4 $years^{-1}$ and 530 $\pm$ 330 kt CH_4 $years^{-1}$ between the periods 2006–2008 and 2009–2011. These emission estimates correspond to leakages of 10.1 % $\pm$ 7.3 % and 9.1 % $\pm$ 6.2 % in terms of energy content, which directly puts fracking's immediate climate benefit in question and therefore indicates that current inventories very likely underestimate the fugitive emissions from Bakken and Eagle Ford. This remote sensing-based top-down estimate is calculated using long-term satellite data, which complements previous measurement-based results of other regions. For example, these estimates are similar to the earlier results of an average of 4.0 %

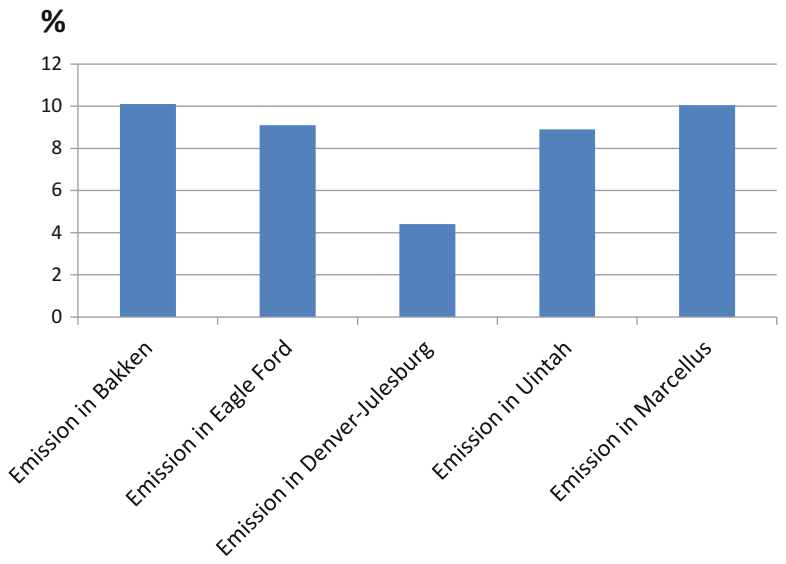

Fig. 4 High methane emission rates (%) in different hydraulic fracturing regions in the USA

(2.3–7.7 %) for the Denver-Julesburg (Pétron et al. 2012), 8.9 % (6.2–11.7 %) for the Uintah Basin (Karion et al. 2013), and a possible range of 2.8–17.3 % for the Marcellus shale formation (Caulton et al. 2014), which are described in Fig. 4. We also need to understand that it is possible to reduce methane emissions by adopting green completion technology, which could considerably lower leak rates to the EPA inventory estimates at selected fracking sites in the Appalachian, Gulf Coast, Midcontinent, and Rocky Mountain regions in the USA (Allen et al. 2013).

Future Directions

Currently, public concerns and scientific research mainly focus on risks to surface water and groundwater resources, the air impacts, and the induced seismicity. Minimal research has been carried out exploring fracking's impacts on ecosystem and landscape disturbance and local and global climate changes. The author believes that some challenging research questions and topics in climate mitigation can include:

1. To establish reliable and standard ways to accurately measure fracking-caused methane emissions. Independent state and federal efforts are needed to evaluate and improve current emission inventories in order to increase accuracy.
2. To develop long-term emission inventory and monitoring systems. Short period intensive studies are also needed to supply independent measurements and to support long-term monitoring adjustments.

3. To locally, regionally, and globally estimate methane emissions and to estimate and model the local, regional, and global climate impacts of fracking. To understand and model the relationship between methane emissions and climate changes is another challenging topic in fracking and climate mitigation.
4. To create national and worldwide spatial and temporal databases for fracking and its methane emissions and make them publically available.

References

Allen DT, Torres VM, Thomas J, Sullivan DW, Harrison M et al (2013) Measurements of methane emissions at natural gas production sites in the United States. Proc Natl Acad Sci U S A 343:733–735

Alvarez RA, Pacala SW, Winebrake JJ, Chameides WL, Hamburg SP (2012) Greater focus needed on methane leakage from natural gas infrastructure. Proc Natl Acad Sci U S A 109:6435–6440

Aminto A, Olson MS (2012) Four compartment partition model of hazardous components in hydraulic fracturing fluid additives. J Natl Gas Sci Eng 7:16–21

Brandt AR, Heath GA, Kort EA, O'Sullivan F, Pétron G et al (2014) Methane leaks from North American natural gas systems. Science 343:733–735

British Geological Survey (2012) The unconventional hydrocarbon resources of Britain's Onshore Basins – Shale Gas "Interview with Dan Steward, Former Mitchell Energy Vice President". Breakthrough blog. The Breakthrough Institute. 20 Dec 2011. Accessed 1 Apr 2015

Cant DJ, Ethier VG (1984) Lithology-dependent diagenetic control of reservoir properties of conglomerates, Falher member, Elmworth Field, Alberta. Bull Am Assoc Pet Geol 68(8):1044

Caulton DR, Shepson PB, Santoro RL, Sparks JP, Howarth RW, Ingraffea AR, Cambaliza MOL, Sweeney C, Karion A, Davis KJ, Stirm BH, Montzka SA, Miller BR (2014) Toward a better understanding and quantification of methane emissions form shale gas development. Proc Natl Acad Sci 111(17):6237–6242

Dopp T (13 Feb 2012) New Jersey Senate Committee Again Passes Gas-Fracking Ban. Businessweek. Accessed 1 Apr 2015

Edmonds J, McJeon H (2013) Implications of abundant natural gas. Presented at Abundant Gas Workshop, 29 Apr, Global Technology Strategy Project, Cambridge, MD. http://www.globalchange.umd.edu/data/gtsp/topical_workshops/2013/spring/presentations/Edmonds_ImplicationsOfAbundantGas_2013-04-29.pdf

EPA (2010) Methane and nitrous oxide emissions from natural sources. U.S. Environmental Protection Agency, Washington, DC

Howarth RW, Santoro R, Ingraffea A (2011a) Methane and the greenhouse-gas footprint of natural gas from shale formations. Clim Change 106:679–690

Howarth RW, Ingraffea A, Engelder T (2011b) Natural gas: should fracking stop? Nature 477:271–275

Hweshe F (17 Sept 2012) South Africa: international groups rally against Fracking, TKAG claims. West Cape News. Accessed 13 Apr 2015

Jackson RB, Down A, Phillips NG, Ackley RC, Cook CW et al (2014) Natural gas pipeline leaks across Washington, DC. Environ Sci Technol 48:2051–2058

Kahrilas GA, Blotevogel J, Stewart PS, Borch T (2015) Biocides in hydraulic fracturing fluids: a critical review of their usage, mobility, degradation, and toxicity. Environ Sci Tech 49:16–32

Karion A, Sweeney C, Pétron G, Frost G, Hardesty RM et al (2013) Methane emissions estimate from airborne measurements over a western United States natural gas field. Geophys Res Lett 40:4393–4397

Koehler M (2005) Productivity of frac stimulations in the German Rotliegend: theoretical considerations and practical results. Society of Petroleum Engineers, Paper 94250-MS, June 2005
Kuuskraa V, Stevens S, Van Leeuwen T, Moodhe K (2011) World shale gas resources: an initial assessment of 14 regions outside the USA. Adv. Resour. Int. Rep., prepared for US Energy Information Administration, Department of Energy, Washington, DC
Law BE, Spencer CW (1993) Gas in tight reservoirs – an emerging major source of energy. In: Howell DG (ed) The future of energy gasses. US Geological Survey Professional Paper 1570. pp 233–252. Washington, USA: United States Government Printing Office
Lelieveld J, Lechtenboehmer S, Assonov SS, Brenninkmeijer CAM, Dienst C et al (2005) Greenhouse gases: low methane leakage from gas pipelines. Nature 434:841–842
Mader D (1989) Hydraulic proppant fracturing and gravel packing. New York, USA: Elsevier, pp 176, 178
Marcellususa.com. Natural Gas Lessor's Royalty Calculator. www.marcellususa.com/RoyaltyCalculator2.aspx. Accessed 19 May 2015
McCrudy R (2011) Hight rate hydraulic fracturing additives in non-Marcellus unconventional shales. In: Proceedings of the technical workshops for the hydraulic fracturing study: chemical & analytical methods, EPA 600/R-11/066; US Environmental Protection Agency, Washington, DC
Meng Q (2014) Modeling and prediction of natural gas fracking pad landscapes in the Marcellus Shale region, USA. Landsc Urban Plan 121:109–116
Meng Q (2015a) Spatial analysis of environment and population at risk of natural gas fracking in the state of Pennsylvania, USA. Sci Total Environ 515–516:198–206
Meng Q (2015b) Modeling and prediction of natural gas fracking pad landscapes in the Marcellus Shale region, USA. A rejoinder to Klein and Manda's commentary. Landsc Urban Plan 136:52–53
Miller SM, Wofsy SC, Michalak AM, Kort EA, Andrews AE et al (2013) Anthropogenic emissions of methane in the United States. Proc Natl Acad Sci U S A 110:20018–20022
Milne JES, Howie RD (1966) Developments in eastern Canada in 1965. Bull Am Assoc Pet Geol 50 (6):1298
Mitchell C, Sweet J, Jackson T (1990) A study of leakage from the UK natural gas distribution system. Energy Policy 18:809–818
Moore T, Bar-Ilan A (2013) Upstream oil and gas emission inventories: regulatory and technical considerations. Presented at "Air Quality and Oil & Gas Development in the Rocky Mountain Region Workshop," 21 Oct, Boulder. http://www.wrapair2.org/pdf/Moore_Barilan_OandG_Inventories. Accessed 15 Mar 2015
Newell RG, Raimi S (2014) Implications of shale gas development for climate change. Environ Sci Technol. doi:10.1021/es4046154
Nicot JP, Scanlon BR (2012) Water use for shale-gas production in Texas, US. Environ Sci Technol 46(6):3580–3586
Osborn SG, Vengosh A, Warner NR, Jackson RB (2011) Methane contamination of drinking water accompanying gas-well drilling and hydraulic fracturing. Proc Natl Acad Sci U S A 108:8172
Pétron G et al (2012) Hydrocarbon emissions characterization in the Colorado Front Range: a pilot study. J Geophys Res 117(D4):D04304. doi:10.1029/2011JD016360
Pétron G, Karion A, Sweeney C, Miller BR, Montzka SA et al (2014) A new look at methane and nonmethane hydrocarbon emissions from oil and natural gas operations in the Colorado Denver-Julesburg Basin. J Geophys Res 119(11):6836–6852
Phillips NG, Ackley R, Crosson ER, Down A, Hutyra LR et al (2013) Mapping urban pipeline leaks: methane leaks across Boston. Environ Pollut 173:1–4
Schulz HM, Horsfield B, Sachsenhofer RF (2010) Shale gas in Europe: a regional overview and current research activities. Pet Geol Conf Ser 7:1079–1085
Seismosoc.org (2015) Fracking confirmed as cause of rare "felt" earthquake in Ohio. http://www.seismosoc.org/society/press_releases/BSSA_105-_Skoumal_et_al_Press_Release.pdf. Accessed 13 Apr 2015

Sharif A (2007) Tight gas resources in Western Australia. PWA, Sept 2007
Shellenberger M, Nordhaus, T (16 Dec 2011) A boom in shale gas? Credit the feds. The Washington Post
US Energy Information Administration (2013) Technically recoverable shale oil and shale gas resources: an assessment of 137 shale formations in 41 countries outside the United States. http://www.eia.gov/analysis/studies/worldshalegas/pdf/overview.pdf. Accessed 13 Apr 2015
US Energy Information Administration (2014) Natural gas gross withdrawals and production. US Energy Information Administration, Independent Statistics and Analysis, US Department of Energy, Washington, DC. Last modified 30 June. http://www.eia.gov/dnav/ng/ng_prod_sum_a_EPG0_FGW_mmcf_a.htm
US Environmental Protection Agency (2010) US greenhouse gas sources and sinks inventory: 1990–2008. Rep. EPA 430-R-10-006, 15 Apr, US Environmental Protection Agency, Washington, DC. http://www.epa.gov/climatechange/Downloads/ghgemissions/508_Complete_GHG_1990_2008.pdf. Accessed 15 Mar 2015
US Environmental Protection Agency (2011) US greenhouse gas sources and sinks inventory: 1990–2009. Rep. EPA 430- R-11-005, 15 Apr, US Environmental Protection Agency, Washington, DC. http://www.epa.gov/climatechange/Downloads/ghgemissions/US-GHG-Inventory-2011-Complete_Report.pdf. Accessed 15 Mar 2015
US Environmental Protection Agency (2012) Oil and natural gas sector: new source performance standards and national emission standards for hazardous air pollutants reviews. Final rule. EPA-HQ-OAR-2010-0505, FRL-9665-1. Fed Regist 77(159):49490–49598
US Environmental Protection Agency (2013) US greenhouse gas sources and sinks inventory: 1990–2011. Rep. EPA 430- R-13-001, 22 Apr, US Environmental Protection Agency, Washington, DC. http://www.epa.gov/climatechange/Downloads/ghgemissions/US-GHG-Inventory-2013-Main-Text.pdf
US Government Accountability Office (2010) Federal oil and gas leases: opportunities exist to capture vented and flared natural gas, which would increase royalty payments and reduce greenhouse gases. Report to congressional requesters, GAO-11-34, Oct, Washington, DC. http://www.gao.gov/products/GAO-11-34. Accessed 15 Mar 2015
Watts J (21 Apr 2011) China takes step towards tapping shale gas potential with first well. London: guardian.co.uk. Accessed 15 Mar 2015
Wells D (2012) Condensate tank emissions. Presented at Int. Emiss. Invent. Conf. Sess. 6, Oil Gas Explor. Prod., 13–15 Aug, Tampa. http://www.epa.gov/ttnchie1/conference/ei20/session6/dwells.pdf. Accessed 15 Mar 2015

Transport Through Porous Media: Case Studies of CO_2 Sequestration, CO_2-Oxygen Reaction in Oxy-Combustion, and Oxygen Transport in Membrane at High Temperatures

Aishuang Xiang

Contents

Abstract

Global warming and climate change have been linked to man-induced carbon dioxide (CO_2) emissions due to the correlation between raised global surface

A. Xiang (✉)
Chemical Engineering Department, Massachusetts Institute of Technology, Cambridge, MA, USA
e-mail: xaishuang@gmail.com

W.-Y. Chen et al. (eds.), *Handbook of Climate Change Mitigation and Adaptation*,
DOI 10.1007/978-3-319-14409-2_76

temperatures and increased ambient CO_2 concentrations during the last century. The man-made CO_2 emissions are primarily from burning of fossil fuels for energy production and transportation. To limit the emissions, CO_2 sequestration has been applied to inject CO_2 into various deep surface formations after capturing CO_2 from the flue gases. The topic of transport through porous media in this chapter is to summarize investigations of migration of CO_2 after sequestration, gas transport through coal particles during oxy-combustion, and oxygen transport in membranes during air separation. A general mechanism has been provided first in the introduction to briefly explain transport through porous media. The following sections, respectively, include a general review of recent literatures on the subjects of CO_2 migration after sequestration, CO_2-oxygen transport in oxy-combustion, and oxygen transport in membrane at high temperatures. Understanding the fundamental mechanisms and processes of the transport through porous media allows mathematical models to be used to evaluate and optimize the performance and design of these systems.

Introduction

Gas transport in porous media occurs in a number of important applications including environmental remediation of contaminated sites (Xiang et al. 2013), drying of industrial and food products (Sam Saguy et al. 2005), coal-based oxy-combustion (Edge et al. 2011), and carbon sequestration (Ho and Webb 2006). Understanding the fundamental mechanisms and processes of the transport through porous media allows mathematical models to be used to evaluate and optimize the performance and design of these systems.

Readers can understand the topic from three aspects: the processes and models, measurements and monitoring, and some applications. The focus of this chapter is on climate change-related gas transport in porous media, and a few important examples include CO_2 migration after sequestration, CO_2-oxygen transport in oxy-combustion, and oxygen transport in membranes at high temperatures.

Processes and models present fundamentals associated with gas transport in porous media like mass, momentum, and heat transport mechanisms. Interactions between gas and the media surface or between species in the continuum phase may occur and affect the transport of the gas. Figure 1 illustrates the porous medium containing a two-phase system: γ-phase, the liquid or gas phase, and the κ-phase, the impermeable solid phase (Ho and Webb 2006). Two types of averages in terms of the average volume, V (illustrated in Fig. 1), should be defined in order to develop the local volume-averaged equations.

The first of these is the *superficial average* of some function ψ_γ which is defined according to

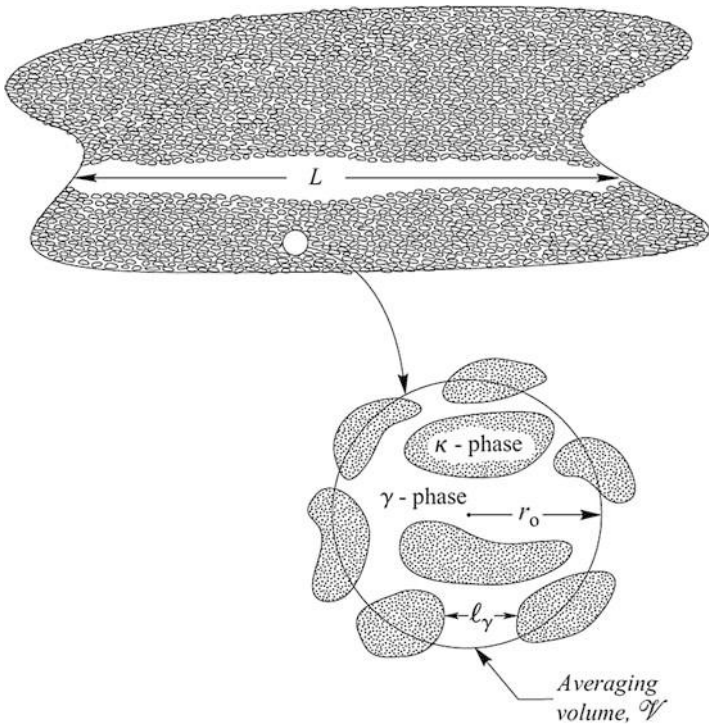

Fig. 1 The porous medium containing a two-phase system: γ-phase, the liquid or gas phase, and the κ-phase, the solid phase (Reproduced by permission)

$$\langle \psi_\gamma \rangle = \frac{1}{\mathscr{V}} \int_{V_\gamma} \psi_\gamma \mathrm{d}V \tag{1}$$

while the second is the *intrinsic average* which is defined by

$$\langle \psi_\gamma \rangle^\gamma = \frac{1}{V_\gamma} \int_{V_\gamma} \psi_\gamma \, \mathrm{d}V \tag{2}$$

These two averages are related according to

$$\langle \psi_\gamma \rangle = \varepsilon_\gamma \langle \psi_\gamma \rangle^\gamma \tag{3}$$

in which ε_γ is the volume fraction of the γ-phase defined explicitly as

$$\varepsilon_\gamma = \frac{V_\gamma}{\mathscr{V}} \tag{4}$$

The application of the two types of averages was demonstrated in section "General Transport Mechanism" to develop the local volume-averaged equations.

Various methods have been used to measure gas transport processes and parameters at the laboratory and field scales. Measurements of the diffusion coefficient, permeability, flow rate, constituent concentration, and mass flux of gas were described in this chapter with the three applications of CO_2 migration after sequestration, CO_2-oxygen transport in oxy-combustion, and oxygen transport in membrane at high temperatures.

Literature review has been given separately for the three applications as well as a summary of transport fundamental studies in the porous media. This chapter provides a general review of the different processes, models, and experimental methods associated with the three applications of gas transport in the porous media. The author hopes that readers can develop an understanding of the topics and an appreciation for the three applications covered in this chapter.

General Transport Mechanism

Momentum Transfer

The momentum transfer in the porous media also includes the continuity equation and the linear momentum equation. The former has been given by Ho and Webb (2006) as

$$\frac{\partial \rho_\gamma}{\partial t} + \nabla \cdot \left(\rho_\gamma \mathbf{v}_\gamma\right) = 0 \tag{5}$$

When the density can be treated as a constant, this reduces to

$$\nabla \cdot \mathbf{v}_\gamma = 0, \tag{6}$$

and the local volume-averaged form is given by

$$\nabla \cdot \left\langle \mathbf{v}_\gamma \right\rangle = 0 \tag{7}$$

This form of the continuity equation is an attractive approximation for the case of dilute solution mass transfer. For non-dilute solutions, the approximation given by Eq. 7 may not be acceptable.

Ho and Webb (2006) also demonstrated the development of the linear momentum equation in the form of the superficial velocity, and the final form was given by

$$\left\langle \mathbf{v}_\gamma \right\rangle = -\frac{\mathbf{K}}{\mu_\gamma}\left[\nabla\left\langle p_\gamma \right\rangle^\gamma - \rho_\gamma \mathbf{g} - \underbrace{\left(\mu_\gamma/\varepsilon_\gamma\right)\nabla^2\left\langle \mathbf{v}_\gamma \right\rangle}_{\text{Brinkman correction}}\right] - \underbrace{\mathbf{F}\cdot\left\langle \mathbf{v}_\gamma \right\rangle}_{\text{Forchheimer correction}} \tag{8}$$

in which **K** and **F** have been deliberately chosen to produce a momentum equation containing the *superficial average* velocity rather than the *intrinsic average* velocity and $\mu_\gamma/\varepsilon_\gamma$ is sometimes referred to as the *Brinkman viscosity*. When values of the Brinkman viscosity are different from $\mu_\gamma/\varepsilon_\gamma$, it means that this term is being used as an empirical correlating factor.

The deduction of Eq. 8 began with the governing equation for $\boldsymbol{v}_\gamma$ given by

$$\frac{\partial}{\partial t}\left(\rho_\gamma \mathbf{v}_\gamma\right) + \nabla \cdot \left(\rho_\gamma \mathbf{v}_\gamma \mathbf{v}_\gamma\right) = \rho_\gamma \mathbf{g} - \nabla p_\gamma + \mu \nabla^2 \mathbf{v}_\gamma \tag{9}$$

in which variations in the density and viscosity in the viscous term have been ignored.

Mass Transfer

Ho and Webb (2006) have developed a convenient form of the general mass transfer equation in the porous media:

$$\underbrace{\varepsilon_\gamma \frac{\partial \langle c_{A\gamma}\rangle^\gamma}{\partial t}}_{\text{accumulation}} + \underbrace{\nabla \cdot \langle c_{A\gamma}\, \mathbf{v}_{A\gamma}\rangle}_{\text{transport}} = \underbrace{\langle R_{A\gamma}\rangle^\gamma}_{\text{homogeneous reaction}} \underbrace{- a_v \frac{\partial \langle c_{As}\rangle_{\gamma\kappa}}{\partial t}}_{\text{adsorption}} + \underbrace{a_v \langle R_{As}\rangle_{\gamma\kappa}}_{\text{heterogeneous reaction}} \tag{10}$$

where C_{As} represents the surface concentration of species A (moles per unit area) and R_{As} represents the molar rate of production of species A owing to heterogeneous reaction (moles per unit area per unit time). A connection between the surface concentration, C_{As}, and the bulk concentration, $C_{A\gamma}$, is required in order to obtain a solution for $C_{A\gamma}$ and therefore the intrinsic concentration, $\langle C_{A\gamma}\rangle^\gamma$. The two classic connections are the linear interfacial flux relation given by

$$\left(c_{A\gamma}\, \mathbf{v}_{A\gamma}\right) \cdot \mathbf{n}_{\gamma\kappa} = k_{A1}\, c_{A\gamma} - k_{-A1} c_{As}, \text{ at the } \gamma - \kappa \text{ interface}, \mathrm{A} = 1, 2, \ldots, \mathrm{N} \tag{11}$$

and the approximation of local adsorption equilibrium (Whitaker 1986; 1999). For a linear adsorption isotherm, this latter connection is given by

$$c_{As} = K_{\mathrm{eq}}\, c_{A\gamma}, \text{ at the } \gamma - \kappa \text{ interface}, \quad \mathrm{A} = 1, 2, \ldots, \mathrm{N} \tag{12}$$

A more convenient form of Eq. 10 has been given by Ho and Webb (2006):

$$\varepsilon_\gamma \frac{\partial \langle c_{A\gamma}\rangle^\gamma}{\partial t} + \nabla \cdot \left(\langle \mathbf{v}_\gamma\rangle \langle c_{A\gamma}\rangle^\gamma\right) = \langle \nabla \cdot \mathbf{J}_{A\gamma}\rangle + \underbrace{\nabla \cdot \langle \widetilde{\mathbf{v}}_\gamma \widetilde{c}_{A\gamma}\rangle}_{\text{dispersive transport}} + \langle R_{A\gamma}\rangle^\gamma - a_v \frac{\partial \langle c_{As}\rangle_{\gamma\kappa}}{\partial t} + a_v \langle R_{As}\rangle_{\gamma\kappa} \tag{13}$$

in which the volume average velocity has been expressed in terms of the superficial average, $\langle \boldsymbol{V}_\gamma \rangle$, rather than the intrinsic average, $\langle \boldsymbol{V}_\gamma \rangle^\gamma$.

In the following sections, we will provide a general review of the different processes, models, and experimental methods of the gas transport in the porous media associated with the three applications of CO_2 migration after sequestration, CO_2-oxygen transport in oxy-combustion, and oxygen transport in membrane at high temperatures.

CO_2 Migration After Sequestration

Introduction

Global warming and climate change have been linked to man-induced carbon dioxide (CO_2) emissions due to the correlation between raised global surface temperatures and increased ambient CO_2 concentrations during the last century (Oelkers and Cole 2008; Lackner 2003). The man-made CO_2 emissions were on the order of 3.45×10^{10} tonnes/year in 2012 (Olivier et al. 2013) and are primarily from burning of fossil fuels for energy production and transportation. To put the number in comparison, the total anthropogenic CO_2 emissions are on the order of 2.7×10^{10} tonnes/year in 1999 (Reichle et al. 1999). To limit the emissions, CO_2 sequestration has been applied to capture CO_2 from the flue gases and to inject CO_2 into various deep surface formations through underground geological storage, ocean storage, and mineral carbonation of carbon dioxide (Lackner 2003; Metz et al. 2005). In addition, the captured CO_2 can be stored as biomass in forests and soils (Oelkers and Cole 2008). If sequestration is to achieve this goal, it must operate on a multiterawatt scale while sequestering almost all produced CO_2, and it must also be safe, environmentally acceptable, and stable (Lackner 2003).

Called geologic carbon sequestration, this process aims to prevent CO_2 from entering the atmosphere by storing it permanently in three main target formations, specifically, depleted oil and gas reservoirs, brine formations, and deep unmineable coal seams (Kaszuba et al. 2003; Lackner 2003; Metz et al. 2005). An impermeable cap rock is essential because CO_2 density is generally less than that of water, so buoyancy tends to drive CO_2 upwards, back to the surface (Oelkers and Cole 2008). CO_2 sequestration through ocean storage means the injection of captured CO_2 into the ocean, usually at depths greater than 1000 m, where it would be isolated from the atmosphere (Adams and Caldeira 2008). Mineral carbonation aims to create stable carbonate minerals such as magnesite ($MgCO_3$) and calcite ($CaCO_3$) by reacting CO_2 with silicate minerals containing magnesium and calcium (Oelkers and Cole 2008). Such minerals are stable over geologic timescales, so sequestration by this method would minimize risk of later leakage back to the atmosphere. Storing CO_2 in forests and soils is a potential alternative to the above industrial sequestration methods. The use of forests for CO_2 storage will require (1) that forests be managed to grow continuously and

(2) that the carbon harvested from forests not be returned to the atmosphere (Johnson 1992). The potential for forests to sequester CO_2, however, is limited (Nilsson and Schopfhauser 1995) due to the limited hectares of trees available worldwide for afforestation.

Of the potential target formations for geologic carbon sequestration, depleted natural gas (CH_4) reservoirs appear to be obvious targets for initial utilization for several reasons. First, depleted gas reservoirs have a proven record of long-term gas containment and capacity as evidenced by their exploitation for CH_4 production. Second, there is an infrastructure of wells and pipelines, knowledge of the local subsurface conditions, and history of industrial activity at gas fields that favor implementation of CO_2 injection. Third, natural gas reservoirs are typically depleted and uneconomic even though 10–40 % of the original gas in place is still in the reservoir. Thus, the possibility exists to inject CO_2 into depleted gas reservoirs to increase reservoir pressure and produce additional CH_4 for economic benefit. Oldenburg (2006) has provided a detailed review on the CO_2 transport through porous depleted natural gas (CH_4) reservoirs.

Among several alternatives for CO_2 removal through geologic carbon sequestration, sequestration of CO_2 in coal seams has also been proposed as a promising strategy because of high gas storage capacity of coal. This technique also has a scientific and technological advantage compared to other proposed techniques for CO_2 sequestration due to the knowledge and experience gained in the area of gas production from coal seams over the years (Karacan and Mitchell 2003). White et al. (2005) reviewed the storage of captured CO_2 in coal seams with a methane recovery process. The review topics include an evaluation of the coal seam properties relevant to CO_2 sequestration, such as density, surface area, porosity, diffusion, permeability, transport, rank, adsorption/desorption, shrinkage/swelling, and thermochemical reactions; a leak detection using direct measurements, chemical tracers, and seismic monitoring; a discussion of gaps in our knowledge base that will require further research and development; etc.

Once injected, CO_2 will be in a supercritical fluid state at depths greater than approximately 800 m (2600 ft) and will be in either a liquid or gaseous state at lesser depths (Schnaar and Digiulio 2009). In all cases, CO_2 will be less dense than native groundwater and will migrate vertically due to density and pressure differentials and laterally due to pressure differentials. This section of the book chapter focused on gas transportation through porous media after sequestration in the coal seams, and review of the literature was limited to the mathematical modeling and simulation of gas transport and to the techniques measuring the chemical and physical properties of gas and subsurface.

Modeling and Simulation

Schnaar and Digiulio (2009) have provided a detailed review of the computational modeling of the geologic sequestration of carbon dioxide. Existing studies demonstrate the use of modeling in project design, site characterization, assessments

of leakage, and site monitoring. Particularly informative components of existing modeling studies include parameter sensitivity analyses, evaluation of numerical artifacts, code comparison, and demonstrations of model calibration to site monitoring data. Modeling the injection and sequestration of CO_2 bears unique challenges, such as the need to properly characterize CO_2 transport properties across a large range of temperatures and pressures and the need to couple multiphase flow, reactive transport, and geomechanical processes. In addition, the volumes of CO_2 that may be injected are largely unprecedented, and an appropriate amount of site characterization across the potentially impacted area will be difficult.

A coal bed (known as coal seams in Europe) contains a natural system of orthogonal fractures known as the cleat, which imparts some permeability to it (Holloway 2001). Although the solid coal does not contain a significant amount of conventional porosity, it does contain micropores of 20°A in diameter and mesopores of 20–500°A in diameter. The mesopores account for most of the pore volume and the micropores for most of the internal surface area (Jones et al. 1992). These commonly contain a natural gas known as coalbed methane (CBM). CO_2 has a greater affinity to be adsorbed onto coal than methane. Thus, if CO_2 is pumped into a coal seam, not only will it be stored by becoming adsorbed onto the coal, it may displace any methane at the adsorption sites (Gunter et al. 1996).

Several subsurface processes, collectively referred to as trapping mechanisms, may promote long-term sequestration of CO_2 (Metz et al. 2005). These include physical containment beneath low-permeability, high-entry-pressure strata (i.e., caprock), trapping as a residual, nonmobile fluid phase in formation pore space (i.e., capillary trapping), dissolution into resident groundwater, precipitation of C-bearing minerals, and sorption of CO_2 onto mineral surfaces. Modeling the transportation of CO_2 through porous media after sequestration in the coal seams includes some of these subsurface processes.

A wide variety of modeling exercises have been reported in the peer-reviewed literature for geologic sequestration of CO_2 (Schnaar and Digiulio 2009). Here listed some reports related to fate of CO_2 after sequestration in coal seams. Simulations have been conducted considering enhanced coalbed CH_4 production with CO_2 sequestration and consideration of CO_2 sorption to coalbed seams (Bromhal et al. 2005). Simulations including mineral precipitation and dissolution reactions have been conducted for injection into fractured caprock (Gherardi et al. 2007). The impact of relative permeability hysteresis and residual fluid trapping by capillary forces in three-dimensionally heterogeneous media has also been considered (Juanes et al. 2006; Flett et al. 2007; Doughty 2007). Subsurface flow of CO_2 has been coupled to a simplified atmospheric flow model to examine the fate of CO_2 that reaches the ground surface (Oldenburg and Unger 2004). To summarize, subsurface fluid flow models used for CO_2 sequestration activities vary in complexity and may include routines for multiphase flow, heat transport, reactive transport, and geomechanical processes. Traditionally, models have been developed as separate entities to simulate these processes. At best, present-day simulators address and couple a subset of these processes.

Use of Modeling to Design Geologic Sequestration Systems

Schnaar and Digiulio (2009) have summarized the use of modeling to design geologic sequestration systems. Computational models can be used to aid in the siting and design of geologic sequestration operations. For example, models can be used to optimize the number, depth, orientation (i.e., vertical, horizontal, or angled), flow rate, and maximum injection pressure of injection wells to maximize CO_2 trapping processes. Keith and others (Keith et al. 2004; Leonenko and Keith 2008) demonstrated that CO_2 dissolution can be accelerated by optimizing the geometry of injection wells and the pump age of brine to maximize the CO_2-brine interface. Several studies have demonstrated the use of modeling to assess design strategies for geologic sequestration during enhanced hydrocarbon recovery (e.g., Jessen et al. 2005; Kovscek and Cakici 2005).

Models can be used to demonstrate how formation heterogeneity can be taken advantage of to increase capillary trapping and dissolution. Simulations reported by Doughty et al. (2001) and Doughty and Pruess (2004) demonstrated that the interplay between geologic heterogeneity and buoyancy-driven flow is crucial in determining where and how effective structural and stratigraphic traps are and how CO_2 is distributed in space. They reported that the presence of discontinuous low-permeability lenses resulted in sinuous, vertically extensive plumes that increased the interfacial contact area and contact time between CO_2 and groundwater compared with a homogenous case. Therefore, there was an increased potential for CO_2 trapping via dissolution, capillary trapping, and mineral precipitation for the heterogeneous case.

Use of Modeling to Inform Site Monitoring

Schnaar and Digiulio (2009) summarized an example of how numerical modeling can be used to compare the spatial resolution and sensitivity of various geophysical monitoring techniques. The study used three-dimensional, multiphase-flow, numerical modeling and rock-property relations developed from log data at the Schrader Bluff field on the North Slope of Alaska (Hoversten and Gasperikova 2004). The analysis considered the application of electromagnetic and seismic geophysical techniques, as well as other techniques, for monitoring injection at a site on the North Slope. Results showed that there would be a clear change in seismic amplitudes and the amplitude vs. offset signature associated with changes in water and CO_2 saturation, both of which could be used to make quantitative estimates of saturation changes. An electromagnetic surface technique was evaluated as a method to quantitatively measure changes in brine saturation in the reservoir. Simulation results suggested that the injected CO_2 would result in changes in the electrical field of an order of magnitude above the background electrical noise.

Modeling Leakage of Carbon Dioxide to the Vadose Zone and Atmosphere

In the event of CO_2 leakage, the vadose zone is the last subsurface domain that CO_2 would traverse as it moves toward the root zone, the atmosphere, and the indoor air of buildings, where it could pose a threat to ecosystems and human health at

relatively low concentrations (e.g., Lewicki et al. 2006). Schnaar and Digiulio (2009) have summarized the modeling leakage of carbon dioxide to the vadose zone and atmosphere. In the vadose zone, leaking CO_2 would be in a gaseous form and CO_2-air mixtures would be denser than the surrounding air. Simulations reported by Oldenburg and Unger (2003), however, suggested that pressure differentials caused by leakage of CO_2 at the water table could result in upward vertical movement of CO_2 and release to the atmosphere. The magnitude of this pressure differential was shown to increase with leakage rate and decrease with the radius of the source zone (i.e., larger source zones are associated with diffusing leakage relative to direct leakage from wells). Simulations also suggested that attenuation due to CO_2 dissolution into infiltrating water was minimal in cases where CO_2 leakage was ongoing and that barometric fluctuations had little impact on time-averaged CO_2 atmospheric release rates. Sensitivity analyses demonstrated several scenarios wherein CO_2 concentrations at the soil surface were large enough (i.e., mole fraction >0.3) to cause adverse ecological impacts.

Oldenburg and Unger (2004) coupled subsurface and surface-layer transport models to further evaluate subsurface-atmospheric interactions. The above-ground surface layers were established in a numerical code by setting a porosity equal to unity and permeability values to mimic a logarithmic wind velocity profile. Simulation results were consistent with earlier simulations in that relatively large CO_2 concentrations were observed in vadose-zone air (i.e., a CO_2 mole fraction approaching unity); however, CO_2 concentrations in the surface layers were orders of magnitude smaller than in the subsurface due to dilution in wind. Lower CO_2 concentrations in the surface air were observed in simulations with greater wind speeds.

Simulations also suggested that some CO_2 would reenter the subsurface in the direction downwind of surface release due to dissolution in infiltrating water. In the event that significant leakage occurs from the injection zone, remediation may be required in groundwater and the vadose zone. Vadose-zone remediation strategies for gaseous CO_2 would probably be similar to those currently used for volatile organic compound contaminated sites, which are primarily based on soil vapor extraction (SVE) systems. Zhang et al. (2004) evaluated several design strategies for SVE-based remediation of CO_2. Two-dimensional radial simulations demonstrated that the use of a vertical well SVE system provided modest improvements to remediation efficiency when compared with natural attenuation or passive strategies. The use of an impermeable cover did not improve remediation removal rates. Three-dimensional simulations suggested that the use of complementary vertical and horizontal wells in the SVE system may improve remediation efficiency compared with strictly vertical or horizontal well cases.

Existing Codes

Several codes have been developed for multiphase flow and transport problems (Schnaar and Digiulio 2009). Codes reported in the literature used for the modeling of CO_2 sequestration can also be applied or modified to simulate CO_2 migration after sequestrating in the coal seams. The codes include those developed primarily

for petroleum reservoir engineering (STARS, Law and Bachu 1996; ECLIPSE, Zhou et al. 2004; Juanes et al. 2006; CHEARS, Flett et al. 2007; and CMG-GEM and CMG-IMEX) and codes developed at the US Dep. of Energy national labs for a range of multiphase flow and transport problems (CRUNCH, Knauss et al. 2005; TOUGH series, Finsterle 2004; Xu et al. 2006; Doughty and Pruess 2004; Doughty 2007). These codes vary not only in the physical processes and governing equations but also in numerical techniques such as the spatial discretization methods, iteration approaches, and gridding routines.

Measurements

Measurements of chemical and physical properties include collecting site information and monitoring the migration of CO_2 after sequestration. X-ray CT and SEM were used to observe the gas storage and transport in a coal sample from Zonguldak Basin (Turkey) (Karacan and Okandan 2001; Karacan and Mitchell 2003). In these studies, a coal sample was placed in an X-ray transparent core holder that enables applying confining pressure and gas pressure separately. Images were processed and quantified to calculate the porosity and gas adsorption rate at different local positions. These data, together with SEM pictures at the same local points, revealed that different lithotypes show different rate behaviors in consolidated sample. These data were also used to study the equilibrium isotherm parameters and to investigate the kinetics of the adsorption process for calculating the diffusivity of CO_2 in different microlithotypes.

Monitoring of geologically sequestered CO_2 is required to protect the environment as well as the health and safety of the public. White et al. (2005) reviewed the monitoring and verification of geologically sequestered CO_2. Migration of CO_2 can be monitored using a variety of techniques. The simplest monitoring method is to measure the pressure (White et al. 2005). To monitor the possible leakage of CO_2 and CH_4 to the surface, it is necessary to determine the flux of these gases emanating from the earth above the coalbed on a seasonal basis before CO_2 is sequestered (Klusman 2003). A monitoring technique that allows determination of a slow and/or intermittent leak of CO_2 to the surface is required. This can be done using a tracer. A tracer is an extraneous substance that is added to the CO_2. White et al. (2005) summarized the use of tracer to determinate such kind of leakages.

Geophysical methods represent another major category of monitoring tools that will be applied to monitor the fate and integrity of geologically sequestered CO_2. Interested readers can refer to the literature review by White et al. (2005).

Summary

Gas transport through porous media is a very important topic in CO_2 sequestration and migration. Storage of CO_2 in the coalbed has been proposed as a promising strategy because of high gas storage capacity of coal. However, mathematical

modeling studies in this subject are very limited though much more experimental work was reported in the literature. Since modeling and simulation can be used to evaluate and optimize the performance and design of these systems, researchers could put more effort in modeling CO_2 injection and migration for the sequestration process in the coal seams.

CO_2-Oxygen Transport in Oxy-Combustion

Introduction

Oxy-fuel combustion is currently considered to be one of the major technologies for carbon dioxide capture. A book (Zheng 2011) has focused on the development of oxy-fuel combustion technologies using coal as fuel. Coal plays a very important role in our day-to-day lives. In a comprehensive report published in 2008, the International Energy Agency (IEA) predicted that the demand for coal will surpass oil in absolute terms between 2030 and 2050 and will become the predominant fuel for the world (IEA, 2008–1). Coal as an energy source has a number of negative environmental impacts, including (but not limited to) the release of particle matter, oxides of sulfur and nitrogen, carbon monoxide (CO), and trace metals such as mercury. Therefore, it is necessary to develop clean coal technology.

Currently, there are three major CO_2 capture technologies that have reached the level of industrial-scale demonstration: post-combustion capture, precombustion capture, and oxy-fuel combustion (Shaddix 2012). Oxy-fuel combustion is a very elegant approach for CO_2 capture that uses oxygen instead of air for combustion. By eliminating nitrogen from the oxidant gas stream, it is possible to produce a CO_2-enriched flue gas ready for sequestration after water has been condensed and other impurities have been separated out. Oxy-fuel combustion for CO_2 capture incorporates three main components: the air separation unit that provides oxygen for combustion, the furnace and heat exchangers where combustion and heat exchange take place, and the CO_2 capture and compression unit. The heat transfer characteristics and its impacts on boiler design were studied for furnaces of various sizes under oxy-fuel operation, and it is concluded that an oxy-fuel-fired furnace can have the same heat transfer rate as an air-fired one with lower furnace exit temperature and higher gas emissivity. Therefore, current boiler design principles and operational practice can be easily adopted for oxy-fuel combustion (Tan et al. 2006; Wall et al. 2005).

Research into oxy-fuel combustion of coal has involved a diverse set of experiments and modeling studies, from the most fundamental aspects to pilot-scale experimental testing and full-scale boiler CFD modeling (Shaddix 2012). Pulverized coal combustion represents the vast majority of the installed power plant capacity, and most of the oxy-fuel combustion research to date has focused on applications of diluting the oxygen to produce similar radiant and convective heat transfer profiles as existing in conventional air-fired coal boilers. Since CO_2 has higher volumetric heat capacity than N_2, the average mixture of oxygen and

recycled flue gas (predominately CO_2, with high concentrations of moisture, in some cases) must be composed of approximately 28 % O_2. Consequently, coal particles in the oxy-fuel boilers are igniting and burning in vastly different chemical and thermal environments than in conventional air-fed boilers. This has motivated a revisit of fundamental studies of coal particle ignition and char combustion phenomena in a CO_2 bath gas, which provide key information for CFD modeling and oxy-fuel burner design. This section of the chapter focuses on the transport phenomena through the porous coal particles in the oxygen-fed boilers during the oxy-combustion.

Modeling and Simulation

For oxy-combustion with flue gas recirculation, elevated levels of CO_2 and steam affect the heat capacity of the gas, radiant transport, and other gas transport properties. A topic of widespread speculation has concerned the effect of gasification reactions of coal char on the char burning rate. To assess the impact of these reactions on the oxy-fuel combustion of pulverized coal char, Hecht et al. (2012) computed the char consumption characteristics for a range of CO_2 and H_2O reaction rate coefficients for a 100 μm coal char particle reacting in environments of varying O_2, H_2O, and CO_2 concentrations using the kinetics code SKIPPY (Surface Kinetics in Porous Particles). Their results indicate that gasification reactions reduce the char particle temperature significantly (because of the reaction endothermicity) and thereby reduce the rate of char oxidation and the radiant emission from burning char particles. However, the overall effect of the combined steam and CO_2 gasification reactions is to increase the carbon consumption rate by approximately 10 % in typical oxy-fuel combustion environments. In addition, the gasification reactions have increasing influence as the gas temperature increases (for a given O_2 concentration) and as the particle size increases. Gasification reactions account for roughly 20 % of the carbon consumption in low-oxygen conditions and for about 30 % under oxygen-enriched conditions.

Chen et al. (2012) reviewed the oxy-fuel combustion of pulverized coal in the aspects of characterization, fundamentals, stabilization, and CFD modeling. The technical review of oxy-coal combustion covered the most recent experimental and simulation studies. Numerical models for subprocesses were used to examine the differences between combustion in an oxidizing stream diluted by nitrogen and carbon dioxide. The review introduced the evolution of this technology from its original inception for high temperature processes to its current form for carbon capture, followed by a discussion of various oxy-fuel systems proposed for carbon capture. The review also discussed the characteristics of oxy-fuel combustion in the context of heat and mass transfer, fuel delivery and injection, coal particle heating and moisture evaporation, devolatilization and ignition, char oxidation and gasification, as well as pollutants formation. Further, the review included advances in sub-models for turbulent flow, heat transfer and reactions in oxy-coal combustion

simulations, and the results obtained using the CFD modeling. It was summarized that distinct characteristics in oxy-coal combustion necessitate modifications of CFD sub-models because the approximations and assumptions for air-fuel combustion may no longer be valid. Based on the review, research needs in this combustion technology were suggested.

Geier et al. (2012) reported on the development and application of an extended single-film reaction model that includes both oxidation and gasification reactions. The traditional single-film nth-order Arrhenius char oxidation model was extended by including additional heterogeneous reactions of char with CO_2 and H_2O, as is required to accurately predict char particle temperatures and char consumption rates in both conventional and oxy-combustion environments. The performance of the model has been systematically interrogated in comparison to experimental data for two US coals (a Powder River Basin subbituminous coal and a low-sulfur, high-volatile bituminous coal) for a variety of model assumptions. The analysis with the extended single-film model showed that incorporation of both steam and CO_2 gasification reactions is required to maintained reasonable values for activation energy of the reactions. The modification of the traditional single-film char burnout model achieved the goal of improving CFD predictions of oxy-fuel combustion of pulverized coal char particles by focusing on the model performance in predicting experimentally observable data (particle temperature) of char particles burning in N_2 and CO_2 baths with different contents of O_2.

Kim et al. (2014) used burnout simulations of coal char particles with apparent char reactivity and a single-film model that includes the Stefan flow effect on mass and energy transfer, to study the impact of CO_2 gasification on the oxy-combustion of pulverized coal chars. The simulations revealed that gasification reaction by CO_2 improves the char burnout time and carbon consumption and decreases the char particle temperature. Also, the simulations indicate the gasification reaction has a greater influence on the char burnout time and the relative contribution to carbon consumption in an oxygen-deficient environment and a greater influence on the particle temperature in an oxygen-enriched environment. However, this tendency according to oxygen level is also influenced by the gas temperature. In addition, the influence of the gasification reaction on char combustion increases as the gas temperature increases and as the particle size increases. Although more reliable rate parameters and insight of the influence of boundary layer heat release are needed, the simulation study shows that it is important to include gasification reaction by CO_2 when simulating char combustion in the oxy-fuel combustion environments.

Measurements

In order to fully understand the results of pilot-scale tests and to accurately predict scale-up performance through CFD modeling, Murphy and Shaddix (2006) have measured the combustion rates of two pulverized coal chars in both conventional

and oxygen-enriched atmospheres. The study used a combustion-driven entrained flow reactor equipped with an optical particle-sizing pyrometry diagnostic and a rapid-quench sampling probe. Oxygen-enriched combustion was found to significantly increase the char combustion temperature and to reduce the char burnout time, as expected. The optical kinetic data, interpreted with a single-film oxidation model, demonstrate increasing kinetic control in enriched-oxygen combustion, despite the faster particle combustion rates. Char burnout rates and char particle temperatures are predicted reasonably well when applying a char burnout model with the derived kinetics.

Gonzalo-Tirado et al. (2013) determined the kinetics of CO_2 gasification for coals of different ranks under oxy-combustion conditions. Combustion reactions were performed in a flow reactor consisting of a cylindrical, externally heated tube (1.6 m long, 78 mm inner diameter), in which the fuel particles are pneumatically injected by means of an insulated gun. Samples of partially burnt particles were collected at increasing distances from the injection point with an isokinetic probe. Higher activation energies and lower char reaction rates (in the conditions explored) were found for char gasification than for oxidation, and the coal rank influenced both sets of kinetics.

Kim et al. (2014) applied a new experimental approach to directly measure the CO_2 gasification rate of a subbituminous coal char at high temperatures and atmospheric pressure. Sandia National Laboratories' laminar entrained flow reactor facility was employed for this study, and char particle size-temperature statistics were measured using a particle-sizing pyrometer, i.e., the velocity, diameter, and temperature of individual burning char particles. A water-cooled sampling probe with helium-quench gas dilution was used to collect char samples at selected heights for determination of char burnout.

Summary

Computational fluid dynamic (CFD) simulations traditionally rely on the computational efficiency of single-film global kinetic oxidation models to predict char particle temperatures and char conversion rates in pulverized coal boilers. In oxy-fuel combustion with flue gas recirculation, char combustion occurs in the presence of elevated CO_2 levels and, frequently, elevated water vapor levels (when employing wet flue gas recirculation). Also, local oxygen concentrations can be quite high in the vicinity of oxygen injection lances. The suitability of existing approaches to modeling char combustion under these conditions has been unclear. In particular, previous work has shown that both boundary layer conversion of CO and gasification reactions of steam and CO_2 need to be included to give reasonable agreement with the experimental measurements, for particles over 60 μm in size. Large physical domain sizes and high computational complexity dictate the use of fairly coarse meshes for the spatial domain and application of simplified coal combustion models, which inevitably reduces the range of process conditions for which the simulation software produces reliable results.

Oxygen Transport in Membrane at High Temperatures

Introduction

It was introduced in section "CO_2-Oxygen Transport in Oxy-Combustion" that oxy-fuel combustion for CO_2 capture incorporates three main components: the air separation unit that provides oxygen for combustion, the furnace and heat exchangers where combustion and heat exchange take place, and the CO_2 capture and compression unit. This section of the book chapter focused on the technology of oxygen separation using membrane at high temperatures. The use of selective membranes to separate certain components from a gas stream, for example, separating oxygen from nitrogen in the oxy-fuel combustion system is a relatively novel capture concept (Mondal et al. 2012). Membranes are semipermeable barriers able to separate substances by various mechanisms (solution/diffusion, adsorption/diffusion, molecular sieve, and ionic transport). These are available in different material types, which can be either organic (polymeric) or inorganic (carbon, zeolite, ceramic, or metallic) and can be either porous or nonporous.

Oxygen separation technologies currently include polymer membranes, pressure swing adsorption (PSA), vacuum swing adsorption (VSA), cryogenics, chemical looping combustion (CLC), and ceramic autothermal recovery (CAR) (den Exter et al. 2009). Polymeric membranes are used for oxygen enrichment or depletion of air, and the polymers are commonly based on among others polyphenyloxide (Parker Gas Separation) and polyimides (air products). The separation is based on preferred dissolution and diffusion of oxygen over nitrogen in these materials, but the operating temperature is limited by the thermal stability of the polymers used. The PSA and VSA technologies are based on the preferred absorption of nitrogen in, for example, zeolite beds. Cryogenics is currently the most developed mature large-scale oxygen production technology, and this technology can also be used to produce nitrogen and argon. In CLC, a metal or metal oxide is oxidized by air in one reactor and transferred to a reduction reactor that is fed with, for example, syngas. The CAR concept uses a set of two or more batch reactors alternating between oxidation and reduction cycles, containing a perovskite material that is cycled between two oxygen contents.

High-temperature oxygen transport membranes (OTMs) have been proposed for plants using high purity O_2 for fuel conversion. These include both plants that partially oxidize feedstocks to produce syngas and power plants with CO_2 capture based on oxy-fuel combustion (Chiesa et al. 2013). The optimal OTM operating temperature is between 800 °C and 900 °C when integrating as a permeator in a gas turbine of an integrated gasification combined cycle (IGCC) plant and is between 700 °C and 900 °C for heavy fuel oxy-combustion. All these applications require high operation temperatures of the OTMs.

den Exter et al. (2009) clearly identified that the high-temperature ceramic membranes that selectively transport oxygen are the high-temperature oxygen transport membranes (OTMs). They are referred to with several acronyms of

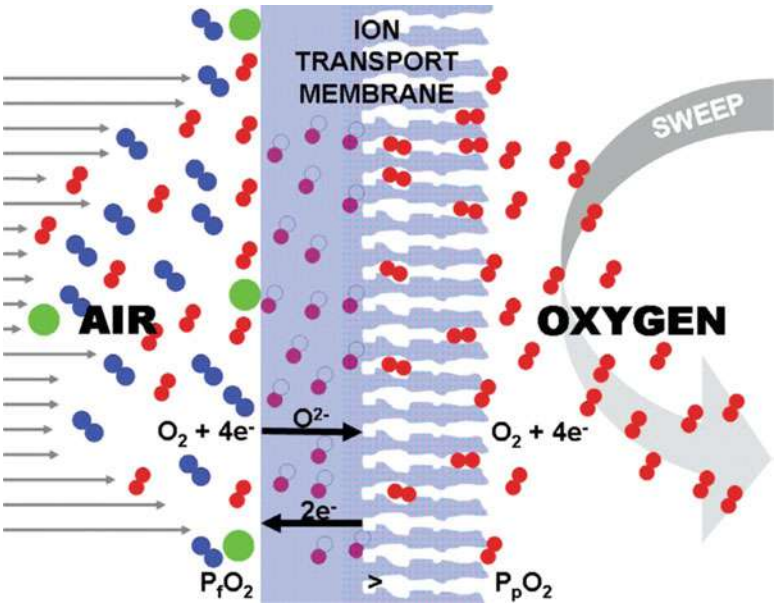

Fig. 2 Schematic representation of the transport of oxygen through an ion transport membrane consisting of a dense (*left*) and porous (*right*) part. The sweep can be either "inert," for example, CO_2 or H_2O, or "fuel," for example, CH_4 (den Exter et al. 2009)

which OTM (oxygen transport membranes), ITM (ion transport membranes), and MIEC (mixed ionic electronic conducting) membranes prevail. They also pointed out the two main applications of high-temperature membrane technology are the production of high purity oxygen as a valuable chemical and as a reactant for various (partial) oxidation processes such as methane conversion. Most OTM materials are only permeable to oxygen at temperatures above 700 °C (975 K) (Foy and McGovern 2005). OTM technology integrates O_2 separation and combustion in one unit. A schematic representation of the air separation process using OTM as a whole is presented in Fig. 2 (den Exter et al. 2009). The driving force for the transport of oxygen is a difference in partial oxygen pressure (p_{O2}) between the feed and permeate side of the membrane. Figure 2 also demonstrates that the OTM consists of an inert porous support (*right*) coated with a dense gas separation layer (*left*).

There are three main types of ceramics with ion transport capabilities: perovskite, fluorite, and mixed (Foy and McGovern 2005). OTM reactors supply pure oxygen through the membrane to the sweep side where a fuel is introduced and oxidized. Examining the fundamentals of catalytic fuel conversion and how they couple with oxygen permeation and gas-phase reactions requires detailed and complex models (Hong et al. 2013a, b). Due to the coupling between catalytic fuel conversion and oxygen permeation, and the high operation temperature,

a detailed analysis is needed to account for the coupling of oxygen permeation, gas-phase flow and transport, and homogeneous and heterogeneous chemistry in terms of the local thermodynamic state on both sides of the membrane surface.

The modeling of the flow process considers a numerical solution of the conservation equations of mass, momentum, energy, and species in the axisymmetric flow domain (Ben-Mansour et al. 2012). The oxygen permeation across the membrane depends upon the prevailing temperatures and the oxygen partial pressure at both sides of the membrane. In the following section, modeling and simulation studies of the flow process were summarized.

Modeling and Simulation

Understanding the theory of the OTM is very important for the modeling and simulation studies. Foy and McGovern (2005) provided a summary of the theory. There are a number of factors that affect the passing of oxygen through the membrane. Firstly the oxygen must reach the membrane. It is possible that due to transport in the flow of gas on the feed side of the membrane, the flux could be limited. After the oxygen reaches the membrane, it is adsorbed onto the surface. Surface exchange effects can be identified by a difference in the normalized values for different thicknesses of the same material. Once the oxygen has reached the surface and been adsorbed onto it, it is transported through the ceramic by bulk transport through the ceramic lattice, which contains oxygen ion vacancies. The oxygen flux across the membrane is given by the Nernst-Einstein equation above 700 °C (975 K) where the flux is directly proportional to the absolute temperature and inversely proportional to the thickness of the membrane. The flux is also proportional to the natural log of the ratio of oxygen partial pressures across the membrane. This explains why the flux can be much higher when an oxygen-consuming reaction occurs on one side of the membrane.

Modeling studies conducted so far have rarely related the heterogeneous chemistry for perovskite oxygen transport membranes to the local thermodynamic state and have not resolved its coupling with the oxygen permeation and gas-phase transport and reactions in detail (Hong et al. 2013a, b). Akin and Lin (2004) assumed different permeation mechanisms and two limiting oxidation kinetics: either extremely fast reaction or no conversion. Using a simple reactor model such as a continuously stirred tank reactor (CSTR), they examined how the oxidation reaction rates, the reducing gas flow rate, and the feed-side oxygen partial pressure influence the oxygen permeation rate. Based on the same CSTR model, Rui et al. (2009) investigated the effect of the finite chemical kinetic rates on the oxygen permeation rate. Results from these studies have shown that chemical reactions and their kinetic rates have substantial influence on the oxygen permeation. These models considered a CSTR and assumed arbitrary reaction rates. Wang and Lin (1995) estimated catalytic kinetic parameters assuming that perovskite membranes behave catalytically in a way similar to Li/MgO membranes and

applied them to the CSTR model, while Tan et al. (2008) used the kinetic parameters of perovskite membranes with a plug flow reactor (PFR) model.

Hong et al. (2013a, b) developed a physical model that resolves spatially the gas-phase flow, incorporates detailed homogeneous chemistry, and accounts for oxygen permeation. Hong et al. (2013a, b) further revised this model to incorporate heterogeneous chemistry on the membrane surface. The surface and bulk species and their reactions are coupled with the local thermodynamic state near the membrane in the gas phase. Using spatially averaged, i.e., reactor level, measurements available in the literature, numerical simulations have been used to develop the heterogeneous chemistry that resolves both oxygen surface exchange and catalytic fuel conversion.

Computational fluid dynamics was also applied to model the oxygen transport in a lab-scale experimental setup for permeation testing of oxygen transport membranes using finite element analysis (Gozálvez-Zafrilla et al. 2011). The modeling considered gas hydrodynamics and oxygen diffusion in the gas phase and vacancy diffusion of oxygen in a perovskite disk-shaped membrane at 1273 K. In a first step, the model was set to obtain the diffusion coefficient of oxygen. The parametric study showed that the setup geometry and flow rate in the air compartment did not have major influence in the oxygen transport. However, very important polarization effects in the sweep-gas (argon) compartment were identified. The highest oxygen permeation flux and the lowest oxygen concentration on the membrane surface were obtained for the following conditions (in increasing order of importance): (1) a large gas inlet radius, (2) a short gas inlet distance, and (3) a high gas flow rate. The computational fluid dynamics method has also been applied by Habib et al. (2013a, b), and the solver of the Fluent software was used with a series of user-defined functions (UDFs) in a Cartesian coordinate system.

To summarize, the modeling of the flow process considers a numerical solution of the conservation equations of mass, momentum, energy, and species in the axisymmetric flow domain. A representative OTM flow schematic for modeling study has been given by Hong et al. (2013a, b) and was reproduced in Fig. 3. The flow process couples the gas-phase flow, transport and chemical reactions, and oxygen permeation flux and heat flux across the membrane.

Conservation of Mass

According to the configuration in Fig. 3, Hong et al. (2012) used the following as the continuity equation:

$$\frac{\partial \rho}{\partial t} + \frac{\partial V}{\partial y} + \rho U = -\frac{\rho}{T}\frac{\partial T}{\partial t} - \sum_{k=1}^{N} \frac{\rho \overline{W}}{W_k}\frac{\partial Y_k}{\partial t} + \frac{\partial V}{\partial y} + \rho U = 0 \tag{14}$$

where ρ is the density, V is the normal velocity, U is the transverse velocity, W is the mixture molecular weight, W_k is the molecular weight of species k, and N is the number of gas-phase species.

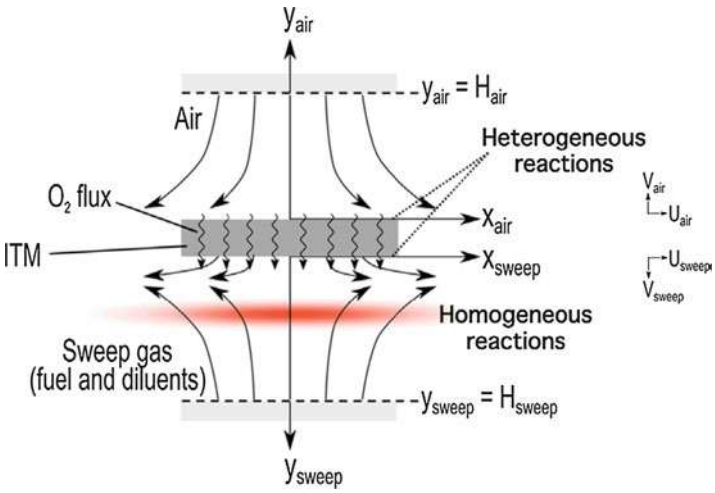

Fig. 3 Planar, finite-gap stagnation flow configuration of the OTM flow schematic for modeling study (Hong et al. 2013)

Conservation of Momentum

According to the configuration in Fig. 3, Hong et al. (2012) proposed the conservation of momentum in the x-direction and used the following equation:

$$\rho\frac{\partial U}{\partial t}+V\frac{\partial U}{\partial y}+\rho U^2+\Lambda_x-\frac{\partial}{\partial y}\left(\mu\frac{\partial U}{\partial y}\right)=0 \tag{15}$$

where ρ is the density, V is the normal velocity, U is the transverse velocity, $\Lambda_x=\frac{1}{x}\frac{dp}{dx}$ and is the scaled transverse pressure gradient (kg/m^3/s^2), and μ is the dynamic viscosity.

Conservation of Energy

Hong et al. (2013) coupled the thermal energy balance of the membrane in their mathematical models and considered the conductive, convective, and diffusive heat transfer with the gaseous domain and the heat release from the surface reactions as well as the thermal radiation between the membrane and the reactor walls. According to the configuration in Fig. 3, Hong et al. (2012) used the following as the conservation of energy equation:

$$\rho\frac{\partial T}{\partial t}+V\frac{\partial T}{\partial y}+\frac{1}{c_p}\left[\sum_{k=1}^{N}\hat{h}_k\dot{\omega}_k+\sum_{k=1}^{N}j_k c_{p,k}\frac{\partial T}{\partial y}-\frac{\partial}{\partial y}\left(\lambda\frac{\partial T}{\partial y}\right)\right]=0 \tag{16}$$

where ρ is the density, V is the normal velocity, $\dot{\omega}_k$ is the molar production rate of species k, c_p is the mixture specific heat, $c_{p,k}$ is the specific heat of species k, $\hat{h}_k$ is the molar enthalpy of species k, λ is the mixture thermal conductivity, N is the number of gas-phase species, and j_k is the flux of species k in the y direction.

Conservation of Species

Hong et al. (2013) distinguished three domains for the conservation of species with heterogeneous chemistry. The three domains were illustrated in Fig. 4 as gaseous, surface, and bulk domains. The gaseous and bulk domains are volumetric domains, whereas the surface domain is an interface domain between these two volumetric domains. The transport-chemistry interaction in each domain is modeled using the appropriate form of the differential equations, and the surface reactions are used to connect them. The bulk species concentration in the direction of the membrane thickness is governed by bulk diffusion, and the control volume approach is used to relate the volumetric bulk domain with the interface domain. The species conservation within the surface domain is accounted for by surface reaction without species transport or mass fluxes. When coupling the heterogeneous kinetic mechanism, the species concentration at and immediately below the surface domain is used.

Ben-Mansour et al. (2012) specified the binary mass diffusion coefficient of the component i in the component j to determine the diffusion coefficient. The corresponding diffusion coefficient in the mixture is computed by

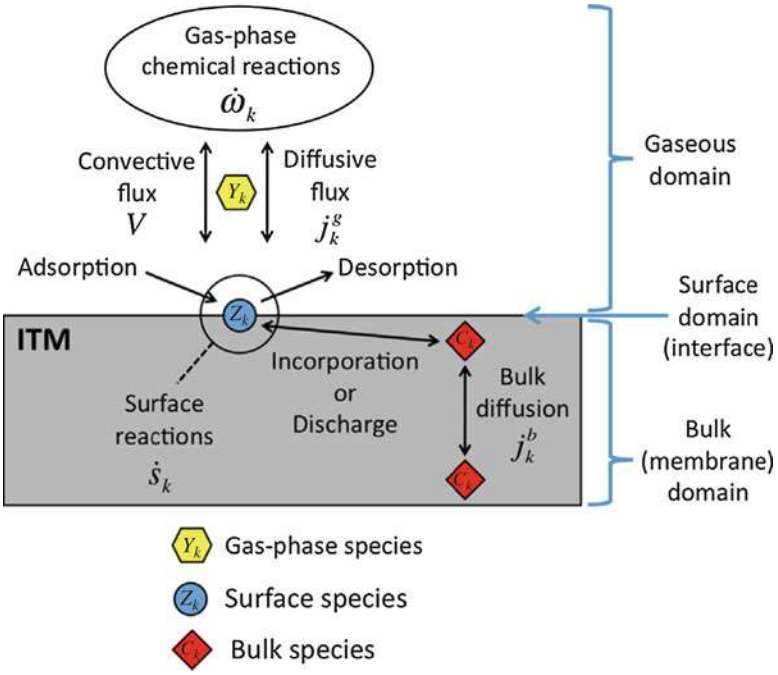

Fig. 4 Three domains (i.e., gaseous, surface, and bulk domains) and the species belonging to each domain (i.e., Y_k = gas-phase species in the gaseous domain, Z_k = surface species in the surface domain, and C_k = bulk species in the bulk domain). The gaseous and bulk domains are volumetric domains, whereas the surface domain is an interface domain between these two volumetric domains (Hong et al. 2013)

$$D_{i,\mathrm{m}} = \frac{1 - X_i}{\sum_{j,j\neq i}\left(\frac{X_i}{\mathrm{D}_{i,j}}\right)} \tag{17}$$

Gozálvez-Zafrilla et al. (2011) modeled the transport of oxygen in the membrane by a Fickian diffusion mechanism of oxygen vacancies in the structure. The transport depends on the concentration gradient of oxygen vacancies and a diffusion coefficient which is a material property.

Measurements

Chemical and Physical Properties

Zeng et al. (2009) applied the Archimedes method using mercury to obtain the relative density of the ceramic membrane. They also analyzed the phase composition of the membrane intermediate material by X-ray diffraction (XRD), measured the O1s XPS spectra of the powders with VG ESCALAB MKII, and analyzed with the Gaussian peak software.

Park et al. (2008) applied SEM to measure the morphologies of the calcined powder and membrane. They painted the rectangular specimens with silver paste to measure the electrical conductivity with a *dc* four-probe method as a function of temperature (100–900 °C) in 80 % N_2-20 % O_2 and in 1 % O_2/N_2 atmosphere at a flow rate 100 mL · min^{-1}.

Transport Properties

Oxygen permeation tests were performed by numerous researchers (Zeng et al. 2009; Park et al. 2008; Tan et al. 2012; Sunarso et al. 2009; Wang et al. 2014). Gas phase chemistry detection was involved in all these studies. In this section of the book chapter, we only representatively listed two studies.

Zeng et al. (2009) measured the oxygen permeation through the membranes using the experimental setup: one side of a disk-shaped membrane was exposed to atmospheric air and the other side was swept with flowing helium or pure CO_2 to carry away the permeated oxygen. The total flow rate on the feed side of the membranes was set to be 100 mL · min^{-1} and the flow rate on the permeate side to 50 mL · min^{-1}. To verify the O_2/CO_2 production concept, a one-end closed membrane tube was sealed in an alumina tube by silver to form a permeation cell. The shell side of the tube was exposed to a pressurized air (3 bar), and the core side was swept with a flowing CO_2 injected through an alumina tube. The effluent from the permeated (lower p_{O2}) side of the membrane was analyzed with online gas chromatography.

Park et al. (2008) measured the oxygen permeation using the setup shown in Fig. 5. The membrane permeation cell was assembled with the membrane, alumina tube, and sealant. Prior to oxygen permeation test, the cell part was purged with He gas to remove the air in permeation cell tube and to confirm

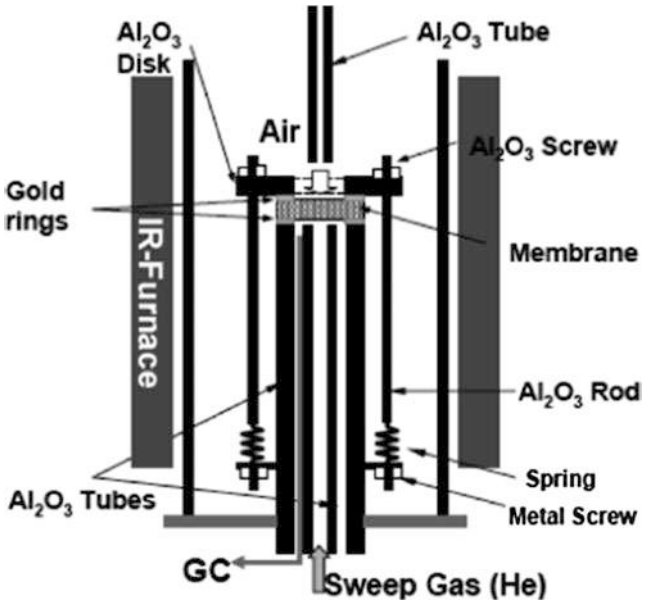

Fig. 5 The schematic diagram of a permeation test cell (Park et al. 2008)

sealing of the assembly consisted of alumina tubes, membrane, and sealant for 20 h. The leakage through membrane during oxygen permeation test was also measured for all runs at each temperature, and the oxygen permeation fluxes were corrected on the basis of the measured leakage. Permeation study was performed within the temperature range of 750–950 °C. The oxygen content in the permeate stream was measured with a gas chromatograph, and the oxygen flux was determined by:

$$J_{O_2}[\mathrm{mL/min\,cm^2(STP)}] = \frac{F_{\mathrm{total}}[\mathrm{mL/min}]\, y_{O_2}[v\%] - \text{leakage correction}}{A\,[\mathrm{cm^2}]} \tag{18}$$

where F_{total} is corresponding with the total flow rate of the permeation stream in which the oxygen concentration is y_{O2}, A is the effective membrane surface area, and *leakage correction* means the calculating oxygen flux from leakage.

Thermal Properties

Thermogravimetric analysis (TA) was carried out for the OTM materials. Tan et al. (2012) reported to use TA with 500 mg of the crashed hollow fiber sample in a sample holder. The sample was heated 25–950 °C at a rate of 10 °C · min^{-1} in CO_2 or nitrogen (flow rate = 50 mL · min^{-1}).

Summary

Numerous reports have been on the study of the oxygen transport membrane, and the OTM technology has been proved a popular topic. However, due to the complexity of the flow process through the membrane system, much further effort is still required to understand the fundamentals and to improve the performance of the OTM at high temperatures.

Future Directions

In this book chapter, the author first listed the general mechanism to briefly explain transport through porous media. Then, a general review was given of the different processes, models, and experimental methods of the gas transport in the porous media associated with the three applications of CO_2 migration after sequestration, CO_2-oxygen transport in oxy-combustion, and oxygen transport in membrane at high temperatures. Due to the broadness of the topic, the author suggested readers to further refer to the listed references of each topic if interested.

The topic of oxygen transport at high temperatures is popular recently. Many efforts have been put in exploring new materials for OTM, while less efforts have been made in understanding the transport mechanism. Due to the high working temperature, the OTM requires materials having strict properties so that it is very popular for researchers to study materials with high performance. It is very important to understand the transport mechanism in order to develop the new materials.

References

Adams EE, Caldeira K (2008) Ocean storage of CO_2. Elements 4:319–324

Akin FT, Lin JYS (2004) Oxygen permeation through oxygen ionic or mixed-conducting ceramic membranes with chemical reactions. J Membr Sci 231(1–2):133–146

Ben-Mansour R, Habib MA, Badr HM, Nemitallah M (2012) Characteristics of oxy-fuel combustion in an oxygen transport reactor. Energy Fuel 26(7):4599–4606

Bromhal GS, Sams WN, Jikich S, Ertekin T, Smith DH (2005) Simulation of CO_2 sequestration in coal beds: the effects of sorption isotherms. Chem Geol 217:201–211

Chen L, Yong SZ, Ghoniem AF (2012) Oxy-fuel combustion of pulverized coal: characterization, fundamentals, stabilization and CFD modeling. Prog Energy Combust Sci 38(2):156–214

Chiesa P, Romano MC, Kreutz TG (2013) 10 – use of membranes in systems for electric energy and hydrogen production from fossil fuels (Handbook of membrane reactors). In: Basile A (ed) Handbook of membrane reactors. Woodhead publishing series in energy, vol 2. Woodhead Publishing, Cambridge, pp 416–455

den Exter MJ, Haije WG, Vente JF (2009) Viability of ITM technology for oxygen production and oxidation processes: material, system, and process aspects. In: Inorganic membranes for energy and environmental applications. Springer, New York, pp 27–51

Doughty C (2007) Modeling geologic storage of carbon dioxide: comparison of hysteretic and non-hysteretic curves. Energy Convers Manag 48:1768–1781

Doughty C, Pruess K (2004) Modeling supercritical carbon dioxide injection in heterogeneous porous media. Vadose Zone J 3:837–847

Doughty C, Pruess K, Benson SM, Hovorka SD, Knox PR, Green CT (2001) Capacity investigation of brine-bearing sands of the Frio Formation for geologic sequestration of CO2. Pap. P. 32. In: Proceedings of the national conference on carbon sequestration, 1st, Washington, DC, 14–17 May 2001 [CD-ROM]. USDOE/NETL-2001/1144. U.S. Department of Energy, National Energy Technology Laboratory, Pittsburgh, PA

Edge P, Gharebaghi M, Irons R, Porter R, Porter RTJ, Pourkashanian M, ... Williams A (2011) Combustion modelling opportunities and challenges for oxy-coal carbon capture technology. Chem Eng Res Des 89(9):1470–1493

Finsterle S (2004) Multiphase inverse modeling: review and iTOUGH2 applications. Vadose Zone J 3:747–762

Flett M, Gurton R, Weir G (2007) Heterogeneous saline formations for carbon dioxide disposal: impact of varying heterogeneity on containment and trapping. J Pet Sci Eng 57:106–118

Foy K, McGovern J (2005) Comparison of ion transport membranes. In: Proceedings of 4th annual conference on carbon capture and sequestration, Alexandria, Virginia, pp 2–5

Geier M, Shaddix CR, Davis KA, Shim HS (2012) On the use of single-film models to describe the oxy-fuel combustion of pulverized coal char. Appl Energy 93:675–679

Gherardi F, Xu T, Pruess K (2007) Numerical modeling of self-limiting and self-enhancing caprock alteration induced by CO2 storage in a depleted gas reservoir. Chem Geol 244:103–129

Gonzalo-Tirado C, Jimenez S, Ballester J (2013) Kinetics of CO_2 gasification for coals of different ranks under oxy-combustion conditions. Combust Flame 160(2):411–416

Gozálvez-Zafrilla JM, Santafé-Moros A, Escolástico S, Serra JM (2011) Fluid dynamic modeling of oxygen permeation through mixed ionic–electronic conducting membranes. J Membr Sci 378(1):290–300

Gunter WD, Gentzis T, Rottenfusser BA, Richardson RJH (1996) Deep coalbed methane in Alberta, Canada: a fuel resource with the potential of zero greenhouse gas emissions. In: Proceeding of 3rd international conference carbon dioxide remov, Cambridge, MA, pp 217–22

Habib MA, Ben Mansour R, Nemit-allah MA (2013a) Modeling of oxygen permeation through a LSCF ion transport membrane. Comput Fluids 76:1–10

Habib MA, Ahmed P, Ben-Mansour R, Badr HM, Kirchen P, Ghoniem AF (2013b) Modeling of a combined ion transport and porous membrane reactor for oxy-combustion. J Membr Sci 446:230–243

Hecht ES, Shaddix CR, Geier M, Molina A, Haynes BS (2012) Effect of CO_2 and steam gasification reactions on the oxy-combustion of pulverized coal char. Combust Flame 159 (11):3437–3447

Ho CK, Webb SW (eds) (2006) Gas transport in porous media, vol 20. Springer, Dordrecht

Holloway S (2001) Storage of fossil fuel-derived carbon dioxide beneath the surface of the earth. Annu Rev Energy Environ 26(1):145–166

Hong J, Kirchen P, Ghoniem AF (2012) Numerical simulation of ion transport membrane reactors: oxygen permeation and transport and fuel conversion. J Membr Sci 407–408:71–85

Hong J, Kirchen P, Ghoniem AF (2013a) Laminar oxy-fuel diffusion flame supported by an oxygen-permeable-ion-transportmembrane. Combust Flame 160(3):704–717

Hong J, Kirchen P, Ghoniem AF (2013b) Analysis of heterogeneous oxygen exchange and fuel oxidation on the catalytic surface of perovskite membranes. J Membr Sci 445:96–106

Hoversten GM, Gasperikova E (2004) Non-seismic geophysical approaches to monitoring. p 1071–1112. In Thomas DC, Benson SM (eds) Carbon dioxide capture for storage in deep geologic formations: results from the CO_2 capture project, vol 2. Geologic storage of carbon dioxide with monitoring and verification, Elsevier, Amsterdam. IEA (International Energy Agency) (2008–1), Energy technology perspectives: scenarios & strategies to 2050, Paris, 2008

Jessen K, Kovscek AR, Orr FM Jr (2005) Increasing CO_2 storage in oil recovery. Energy Convers Manag 46:293–311

Johnson DW (1992) Effects of forest management on soil carbon storage. Water Air Soil Pollut 64:83–120

Jones AH, Bell GJ, Schraufnagel RA (1992) A review of the physical and mechanical properties of coal with implications for coal-bed methane well completion and production. Coalbed Methane, SPE Repr. Ser. no. 35, Richardson, Soc. Pet. Eng, pp 14–26

Juanes R, Spiteri EJ, Orr FM Jr, Blunt MJ (2006) Impact of relative permeability hysteresis on geological CO_2 storage. Water Resour Res 42:W12418

Karacan CÖ, Mitchell GD (2003) Behavior and effect of different coal microlithotypes during gas transport for carbon dioxide sequestration into coal seams. Int J Coal Geol 53(4):201–217

Karacan CO, Okandan E (2001) Adsorption and gas transport in coal microstructure: investigation and evaluation by quantitative X-ray CT imaging. Fuel 80:509–520

Kaszuba JP, Janecky DR, Snow MG (2003) Carbon dioxide reaction processes in a model brine aquifer at 200 C and 200 bars: implications for geologic sequestration of carbon. Appl Geochem 18(7):1065–1080

Keith DW, Hassanzadeh J, Pooladi-Darvish M (2004) Reservoir engineering to accelerate dissolution of stored CO_2 in brines. In Wilson M et al (ed) Proceedings of international conference on greenhouse gas control technologies, 7th, Vancouver, BC, Canada, vol 2. Elsevier Science, Amsterdam, pp 2163–2167, 5–9 Sept 2004

Kim D, Choi S, Shaddix CR, Geier M (2014) Effect of CO_2 gasification reaction on char particle combustion in oxy-fuel conditions. Fuel 120:130–140

Klusman RW (2003) Evaluation of leakage potential from a carbon dioxide EOR/sequestration project. Energy Convers Manag 44(12):1921–1940

Knauss KG, Johnson JW, Steefel CI (2005) Evaluation of the impact of CO_2, co-contaminant gas, aqueous fluid and reservoir rock interactions on the geologic sequestration of CO_2. Chem Geol 217:339–350

Kovscek AR, Cakici MD (2005) Geologic storage of carbon dioxide and enhanced oil recovery: II. Co-optimization of storage and recovery. Energy Convers Manag 46:1941–1956

Lackner KS (2003) A guide to CO_2 sequestration. Science 300:1677–1678

Law DH-S, Bachu S (1996) Hydrogeological and numerical analysis of CO_2 disposal in deep aquifers in the Alberta sedimentary basin. Energy Convers Manag 37:1167–1174

Leonenko Y, Keith DW (2008) Reservoir engineering to accelerate the dissolution of CO_2 stored in aquifers. Environ Sci Technol 42:2742–2747

Lewicki JL, Birkholzer JT, Tsang CF (2006) Natural and industrial analogues for leakage of CO_2 from storage reservoirs: identification of features, events, and processes and lessons learned. J Environ Geol 52:457–467

Metz B, Davidson O, de Coninck H, Loos M, Meyer L (2005) IPCC special report on carbon dioxide capture and storage. Intergovernmental panel on climate change, Geneva (Switzerland). Working group III

Mondal MK, Balsora HK, Varshney P (2012) Progress and trends in CO_2 capture/separation technologies: a review. Energy 46(1):431–441

Murphy JJ, Shaddix CR (2006) Combustion kinetics of coal chars in oxygen-enriched environments. Combust Flame 144(4):710–729

Nilsson S, Schopfhauser W (1995) The carbon-sequestration potential of a global afforestation program. Clim Change 30:267–293

Oelkers EH, Cole DR (2008) Carbon dioxide sequestration a solution to a global problem. Elements 4(5):305–310

Oldenburg CM (2006) Gas transport in porous media, vol 20. Springer, Dordrecht, pp 419–425

Oldenburg CM, Unger AJA (2003) On leakage and seepage from geologic sequestration sites: unsaturated zone attenuation. Vadose Zone J 2:287–296

Oldenburg CM, Unger AJA (2004) Coupled vadose zone and atmospheric surface-layer transport of carbon dioxide from geologic carbon sequestration sites. Vadose Zone J 3:848–857

Olivier J, PBL JGO, Janssens-Maenhout G, PBL JAP, PBL MA, Middelburg M (2013) Trends in global CO_2 emissions. 2013 report PBL publication number: 1148. www.pbl.nl/en or edgar.jrc.ec.europa.eu

Park JH, Kim JP, Kwon HT, Kim J (2008) Oxygen permeability, electrical property and stability of $La_{0.8}Sr_{0.2}Co_{0.2}Fe_{0.8}O_3$-delta membrane. Desalination 233(1–3):73–81

Reichle D, Houghton J, Kane B, Ekmann J, Benson S, Clarke J, Dahlman R, Hendrey G, Herzog H, Hunter-Cevera J, Jacobs G, Judkins R, Ogden J, Palmisano A, Socolow R, Stringer J, Surles T, Wolsky A, Woodward N, and York M (1999) Carbon sequestration research and development. U.S. Department of Energy, Washington, DC, DOE/SC/FE-1

Rui Z, Li Y, Lin YS (2009) Analysis of oxygen permeation through dense ceramic membranes with chemical reactions of finite rate. Chem Eng Sci 64(1):172–179

Sam Saguy I, Marabi A, Wallach R (2005) New approach to model rehydration of dry food particulates utilizing principles of liquid transport in porous media. Trends Food Sci Technol 16(11):495–506

Schnaar G, Digiulio DC (2009) Computational modeling of the geologic sequestration of carbon dioxide. Vadose Zone J 8(2):389–403

Shaddix CR (2012) Coal combustion, gasification, and beyond: developing new technologies for a changing world. Combust Flame 159(10):3003–3006

Sunarso J, Liu S, Lin YS, da Costa JD (2009) Oxygen permeation performance of $BaBiO_{3-1}$ ceramic membranes. J Membr Sci 344:281–287

Tan Y, Croiset E, Douglas M, Thambimuthu K (2006) Combustion characteristics of coal in a mixture of oxygen and recycled flue gas. Fuel 85:507–512

Tan X, Li K, Thursfield A, Metcalfe IS (2008) Oxyfuel combustion using a catalytic ceramic membrane reactor. Catal Today 131(1–4):292–304

Tan X, Liu N, Meng B, Sunarso J, Zhang K, Liu S (2012) Oxygen permeation behavior of La0. 6Sr0. 4Co0. 8Fe0. 2O3 hollow fibre membranes with highly concentrated CO_2 exposure. J Membr Sci 389:216

Wall T, Gupta R, Buhre B, Khare S (2005) Oxy-fuel (O_2/CO_2, O_2/RFG) technology for sequestration-ready CO_2 and emission compliance. In: Proceedings of the 30th international technical conference on coal utilization and fuel systems, Clearwater, 17–21 Apr 2005

Wang W, Lin YS (1995) Analysis of oxidative coupling of methane in dense oxide membrane reactors. J Membr Sci 103(3):219–233

Wang Z, Kathiraser Y, Soh T, Kawi S (2014) Ultra-high oxygen permeable BaBiCoNb hollow fiber membranes and their stability under pure CH_4 atmosphere. J Membr Sci 465:151–158

Whitaker S (1986) Transient diffusion, adsorption and reaction in porous catalysts: the reaction controlled, quasi-steady catalytic surface. Chem Eng Sci 41:3015–3022

Whitaker S (1999) The method of volume averaging. Kluwer, Dordrecht

White CM, Smith DH, Jones KL, Goodman AL, Jikich SA, LaCount RB, Schroeder KT (2005) Sequestration of carbon dioxide in coal with enhanced coalbed methane recovery a review. Energy Fuel 19(3):659–724

Xiang A, Yan W, Koel BE, Jaffé PR (2013) Poly (acrylic acid) coating induced 2-line ferrihydrite nanoparticle transport in saturated porous media. J Nanoparticle Res 15(7):1–9

Xu T, Sonnenthal E, Spycher N, Pruess K (2006) TOUGHREACT: a simulation program for non-isothermal multiphase reactive geochemical transport in variably saturated geologic media: applications to geothermal injectivity and CO_2 geological sequestration. Comput Geosci 32:145–165

Zeng Q, Zu YB, Fan CG, Chen CS (2009) CO2-tolerant oxygen separation membranes targeting CO_2 capture application. J Membr Sci 335(1–2):140–144

Zhang Y, Oldenburg CM, Benson SM (2004) Vadose zone remediation of carbon dioxide leakage from geologic carbon dioxide sequestration sites. Vadose Zone J 3:858–866

Zheng L (ed) (2011) Oxy-fuel combustion for power generation and carbon dioxide (CO_2) capture. Woodhead Publishing, Cambridge

Zhou W, Stenhouse MJ, Arthur R, Whittaker S, Law DH-S, Chalaturnyk R, Jazrawi W (2004) The IEA weyburn CO_2 monitoring and storage project: modeling of the long-term migration of CO_2 from weyburn. In: Wilson M et al (ed) Proceedings of international conference on greenhouse gas control technologies, 7th, Vancouver, BC, Canada. vol 1. Elsevier Science, Amsterdam, pp. 721–729, 5–9 Sept 2004

Part III

Climate Change Mitigation: Energy Conversation, Efficiency, and Sustainable Energies

Energy Efficiency: Comparison of Different Systems and Technologies

Maximilian Lackner

Contents

M. Lackner (✉)
Institute of Advanced Engineering Technologies, University of Applied Sciences FH Technikum Wien, Vienna, Austria
e-mail: maximilian.lackner@tuwien.ac.at

W.-Y. Chen et al. (eds.), *Handbook of Climate Change Mitigation and Adaptation*,
DOI 10.1007/978-3-319-14409-2_24

Abstract

The efficient use of energy, or energy efficiency, has been widely recognized as an ample and cost-efficient means to save energy and to reduce greenhouse gas emissions. Up to 1/3 of the worldwide energy demand in 2050 can be saved by energy efficiency measures. In this chapter, several important aspects of energy efficiency are addressed. After an introduction and definition of energy efficiency, historic development and state-of-the-art and future trends of energy efficiency are presented in the light of life cycle assessment and total cost of ownership considerations. Energy efficiency in the sectors energy production, energy transmission and storage, transportation, industry, buildings, and appliances is reviewed. Concurrent measures such as recycling or novel materials are also discussed and touched upon. Energy conservation is covered in the final section of this chapter. References for deeper study are provided with an emphasis on guidelines on how to improve energy efficiency. Given the breadth of the subject, only exemplary coverage can be aimed for. The purpose of this chapter is to highlight the significance of energy efficiency and to provide cross-learnings from achievements in different sectors so that energy efficiency in the readers' own facilities and installations can be assessed and improved with cost-effective means as a contribution to climate change mitigation, cost savings, and improved economic competitiveness.

Introduction

Energy in the everyday world is a range of commodities, for instance, thermal or electrical. It is a scalar physical quantity that is defined by the amount of work that can be done by a force. Energy comes in different forms: Classical mechanics distinguishes between kinetic and potential energy. In the everyday world, one can see chemical, thermal, gravitational, light, and electrical energy, to name but a few. These forms of energy can be transformed into each other. The SI unit of energy is joule [J], with other common units being kilowatt hour [kWh], tonne of oil equivalent [toe], and British thermal unit [btu, BTU]:

$1\ J = 1\ kg\ m^2\ s^{-2} = 1Ws$
$1\ kWh = 3.6*10^6\ J$
1 toe = 41.868 GJ = 11,630 kWh
1 btu = 1.060 kJ; 1 quad = 10^{15} (1 quadrillion) btu = 1.06×10^{18} J

The worldwide energy consumption is on the order of 500 exajoules (5×10^{20} J) per year, which corresponds to an average consumption rate of 15 terawatts (1.5×10^{13} W).

Energy efficiency, i.e., the efficient use of energy, describes the use of less energy to achieve the same level of energy service. Energy efficiency is a universally applicable concept relevant for consumers and industry alike. It can be achieved by a more efficient technology, an improved process, or a change of individual behavior. Energy efficiency can, according to the IEA's World Energy Outlook 2014, "close the competitiveness gap caused by differences in regional energy prices" (IEA 2014a).

The International Energy Agency (IEA) promotes energy security amongst its 29 member countries through collective response to physical disruptions in oil supply and provides research and analysis on energy. The annual World Energy Outlook is the IEA's "flagship" publication, which is widely recognized as an authoritative source for global energy projections and analyses. It provides medium- to long-term energy market projections, ample statistics, and recommendations for governments and the energy business.

Obstacles toward the introduction of energy efficiency are often not imposed by technical or economic reasons but rather by the habits, norms, and mindset of our social institutions, often termed "market barriers." Therefore, apart from increasing research and development (R&D) to create and improve energy-efficient technologies and appliances, one has to address the issue from other angles such as policy-making (Blok et al. 2004), too. The proliferation of energy-efficient technologies requires stimuli outside the scope of technical, and economic, logic arguments.

Also, it has to be noted that the proliferation of technically and economically superior technology is a gradual one (Jaffe and Stavins 1994). Subsidies can have an important effect on the penetration rate of new energy technologies (Lund 2006), as can industry agreements (Grossman and Krueger 1991).

In its most current World Energy Outlook (IEA 2014a), released in November 2014, the International Energy Association (IEA) has compared the "central scenario," a kind of baseline or BAU (business as usual or reference) scenario, to its suggested course of action to control climate change, which is termed "for 2 °C target" scenario. In the WEO 2009, it was called "450 scenario", as a limit of 450 ppm of $CO_{2\text{-eq}}$ in the atmosphere would limit temperature increase to 2 °C. In the reference scenario, worked out for the period to 2040, the world is set for a rise in temperature of up to 6 °C, leading to severe global challenges in terms of irreversible environmental damage and energy security. The notion that energy security can be an issue has existed since the OPEC oil embargo of 1973 (otherwise known as the oil crisis), followed by the second energy crisis 6 years later. It was recently revived in

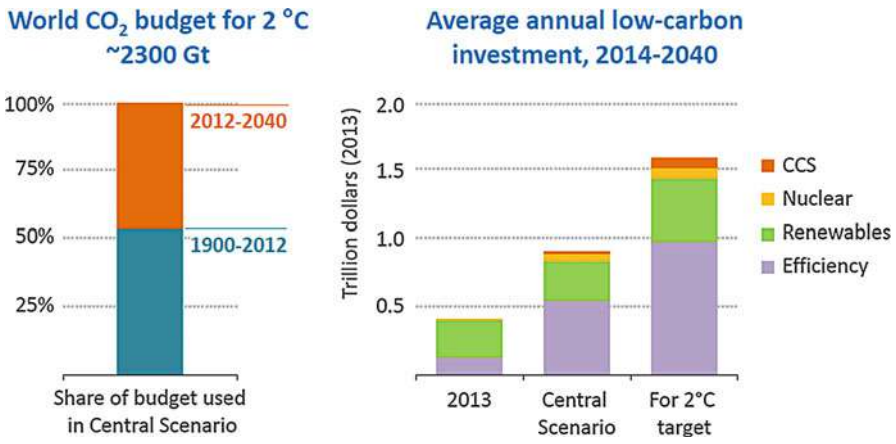

Fig. 1 In the central scenario of WEO's Energy Outlook 2014, the entire global budget of $CO_{2\text{-eq}}$ to 2100 is used up by 2040 (*left*). Investments to achieve the 2 °C target are ~2/3 in the energy efficiency domain (*right*) (Source: IEA 2014b)

Central Europe in the winters of 2006 and 2009 (Gow 2009; Hollinger 2014) due to natural gas supply cuts.

Globally, crude oil prices exceeding for the first time 100 USD per barrel in the same year have also led to concerns about energy security in terms of affordability and sustainability. There is no straightforward definition for energy security. In Kruyt et al. (2009), indicators based on availability, accessibility, affordability, and acceptability were created. With depleting fossil fuel sources and concentration of these in fewer regions, not all of which are considered politically stable, it can be anticipated that fossil fuel prices will go up and will fluctuate more strongly, partly driven by speculation. Today, the world relies to approx. 80 % on fossil fuels for primary energy production.

The IEA "450 scenario" demands for fossil fuel consumption to peak by 2020 and for energy-related CO_2 emissions to be cut from 28.8 Gt in 2007 to 26.4 Gt in 2030 (IEA 2009). In the "for 2 °C target," the world's CO_2 budget is given as 2,300 Gt, of which more than 50 % was emitted from 1900 to 2012; see Fig. 1.

As it can be seen in Fig. 1, the largest contribution to CO_2 abatement – approx. 2/3 – can be made by energy efficiency measures. Another strong contribution comes from changes in the mix of power generation technologies.

Table 1, based on IEA (2009), shows the worldwide energy-related CO_2 emissions.

Similar results, focused on the USA, were found in Granade et al. (2009). As a conclusion, one can say that energy efficiency has a huge potential. In this chapter, several aspects of energy efficiency for climate change mitigation are highlighted. Complete coverage of the topic cannot be provided within the scope of this chapter, so a selection has been made to present some of the most relevant areas related to energy efficiency.

Table 1 Global CO_2 emissions in the "reference scenario" and the "450 scenario" in the 2009 World Energy Outlook of the IEA, compare Fig. 1 (Source: IEA 2009)

CO_2 emissions	1990	2007	2030, reference scenario	2030, 450 scenario
Total	20.9 Gt	28.8 Gt	40.2 Gt	26.4 Gt
Per capita	4.0 t	4.4 t	4.9 t	3.2 t
Power generation	36 %	41 %	44 %	32 %
Transport	22 %	23 %	23 %	29 %
Industry	19 %	17 %	15 %	17 %
Buildings	14 %	10 %	8 %	10 %
Others	10 %	10 %	9 %	11 %

What Is Energy Efficiency

Energy efficiency is, as the term implies, the efficient use of energy, i.e., using a lower amount of energy to achieve the same level of energy service (Patterson 1996). It can be achieved by improved behavior or by more efficient technology.

Thermodynamics teach that energy can only be transformed. According to the first law, energy can neither be created nor destroyed. A change in the internal energy of a system, U, can be achieved by adding heat Q or work W:

$$\mathrm{d}U = \mathrm{d}Q - \mathrm{d}W \tag{1}$$

where $\mathrm{d}Q$ and $\mathrm{d}W$ are incremental changes in heat and work, respectively (the minus denotes that positive work is being done by the system).

Equation 1 can be rewritten as

$$\mathrm{d}U = T\mathrm{d}S - p\mathrm{d}V \tag{2}$$

where the work done by the system during expansion is $p\mathrm{d}V$. The amount of heat added to the system can be described by $\mathrm{d}Q = T\mathrm{d}S$ with T being the temperature and S the entropy. In a heat engine, thermal energy is converted to mechanical energy by exploiting a temperature gradient between a hot and a cold reservoir for an energy transfer. The efficiency of such a heat engine is given by the ratio of useful power to heat energy input. It can be derived as follows:

$$\mathrm{d}W = \mathrm{d}Q_\mathrm{c} - (-\mathrm{d}Q_\mathrm{h}) \tag{3}$$

$\mathrm{d}W = -p\mathrm{d}V$, i.e., the work done by the engine.
$\mathrm{d}Q_\mathrm{h} = T_\mathrm{h}\mathrm{d}S_\mathrm{h}$, i.e., the heat energy taken from the high-temperature reservoir.
$\mathrm{d}Q_\mathrm{c} = T_\mathrm{c}\mathrm{d}S_\mathrm{c}$, i.e., the heat energy delivered to the cold-temperature reservoir.

In the reversible Carnot heat engine cycle ($\mathrm{d}S_\mathrm{c} = \mathrm{d}S_\mathrm{h}$, i.e., no net change in the entropy), the maximum efficiency is

Table 2 Efficiencies of power plants (Source: Curzon and Ahlborn (1975), Callen (1985))

Power plant	Technology	T_c (°C)	T_h (°C)	η (Carnot)	η (endoreversible)	η (observed)
A	Coal fired	25	565	0.64	0.40	0.36
B	Nuclear power	25	300	0.48	0.28	0.30
C	Geothermal power	80	250	0.33	0.178	0.16

$$\eta_{\max} = 1 - \frac{\mathrm{d}Q_c}{\mathrm{d}Q_h} = 1 - \frac{(T_c \mathrm{d}S_h)}{(-T_h \mathrm{d}S_h)} = 1 - \frac{T_c}{T_h} \tag{4}$$

The Carnot efficiency is a theoretical one, because it considers an infinitesimally small temperature change. As for "real" heat engines such as internal combustion engines or power plants, one is typically after a sizeable power output, which is an irreversible process. Therefore, the ideal, reversible Carnot process does not well describe the efficiency of a technical system. Taking the concept of endoreversible thermodynamics (Hoffmann et al. 1997) into consideration, the efficiency of a heat engine operating in irreversible mode can be obtained as

$$\eta = 1 - \sqrt{\frac{T_c}{T_h}} \tag{5}$$

This expression is known as the endoreversible efficiency or Chambadal-Novikov efficiency (Chambadal 1957; Novikov 1958). It allows a more realistic estimation of the efficiency of a heat engine, which can be termed semi-ideal. The endoreversible efficiency takes the destruction of **exergy** in an irreversible process into consideration. Exergy is the highest possible useful work during a process that brings the system into equilibrium with a heat reservoir (Perrot 1998; Dewulf et al. 2008; Demirbas et al. 2000; Wall et al. 1994; Prins et al. 2004). It was introduced by Gibbs as a special form of the Gibbs available energy. Exergy is the **work potential** of a system. It can be potential (gravitational or magnetic force field), kinetic (velocity), physical (pressure, temperature), or chemical (composition) (Dewulf et al. 2008). Exergy analysis can be used to determine inefficiencies.

Table 2, compiled from Curzon and Ahlborn (1975) and Callen (1985), shows the comparison of the Carnot and Chambadal-Novikov efficiencies of three power plants to their actual ones.

From the above table, it can be seen that the endoreversible efficiency predicts the observed one well. In Cullen and Allwood (2010), theoretical efficiency limits for energy conversion devices are reviewed.

The combination of energy efficiency and renewable energy is often referred to as **sustainable energy**. Sustainability was defined in 1983 by the UN World Commission on Environment and Development as follows: "Sustainable development is development that meets the needs of the present without compromising the ability of future generations to meet their own needs."

Energy productivity, similar to energy efficiency, has a narrower scope. It is defined as ratio of output divided by energy consumption, e.g., GDP/energy consumption in terms of liter oil equivalent of that economy from its energy balance table (GDP = gross domestic product).

Another aspect related to energy efficiency in the context of climate change mitigation is the concept of **greenhouse gas emission factors**. Apart from CO_2, other greenhouse-active gases can be emitted, such as CH_4, N_2O, or halocarbons. Office of Energy Efficiency, Natural Resources Canada (2002), provides an overview.

There is a huge potential for energy efficiency improvements. Three recent studies on this topic are Electric Power Research Institute (EPRI) (2015) and Granade et al. (2009), making projections until 2020, and IEA (2009), which extends its forecasts to 2030. It needs to be stressed that such impressive potentials can only be turned into reality if significant initiatives are launched. Program costs have to be catered for, too. Different approaches to measure energy efficiency in industry are shown in Phylipsen et al. (1997). Indicators of energy efficiency are discussed in Bor (2008) and Ang (2006). Another important consideration in energy efficiency is the entire life cycle of a product. **Life cycle energy efficiency** (Malça and Freire 2006) not only considers actual use of a piece of equipment but also its production and disposal (see section "Life Cycle Assessment (LCA)" later). **Energy efficiency trading** can only be mentioned here. It is discussed in Mundaca (2009). A detailed overview on energy efficiency is provided in McLean-Conner (2009).

Significance of Energy Efficiency

There is – unfortunately – no such thing as a perpetuum mobile. As a consequence, energy can only be transformed from one form into another one, which happens under certain losses (see also above). Users of mobile phones, notebooks, and any other mobile device will naturally and subconsciously appreciate energy efficiency – because energy is obviously a scarce resource in these applications. Service life and hence usefulness will depend on the efficiency and energy density of the gadget (Mitsos et al. 2007). However, energy efficiency is a much broader topic.

Energy is the leading source of anthropogenic greenhouse gas emissions, approx. 65 % (IEA 2009), and hence needs to be at the core of climate change mitigation actions. In the IEA's reference scenario, the global energy demand is set to increase by 40 % from 2007 to 2030, reaching 16.8 billion toe (IEA 2009). 90 % of this increase is predicted to happen in non-OECD countries, with India and China accounting for half (IEA 2009). Global electricity demand is projected to grow by even 76 % from 2007 to 2030, requiring 4,800 GW of additional capacity. This is five times the existing US capacity (IEA 2009).

In the proposed course of action, the "450 scenario," more than 50 % of all (necessary) energy savings are realized by energy efficiency measures. The target is an energy-efficient and low-carbon economy. By 2050, energy efficiency measures could cut the total worldwide energy consumption by as much as 1/3 (IEA 2009).

Energy efficiency has a large-scale effect. Apart from addressing global warming, energy security and fossil fuel depletion are tackled, alongside solid savings for individuals, enterprises, and nations at large.

Air quality, particularly in urban areas and in developing countries, can also be improved by energy efficiency measures. There are other environmental co-benefits, too, from implementing energy efficiency measures.

By focusing on energy efficiency rather than on increasing energy production, a cost-effective, "soft" energy path is followed. The term "negawatt" was coined two decades ago to describe electricity that "*wasn't created due to energy efficiency*" (Joskow and Marron 1993).

Energy efficiency has been widely recognized as a vast, low-cost energy source (Granade et al. 2009). The reason why this unused potential is so large stems from the multitude of barriers that impede energy efficiency today (Granade et al. 2009; Schleich 2009; Jaffe and Stavins 1994). Unlike the production factors of labor and capital, which have been seen impressive optimization since the industrial revolution, energy is far from being at the lowest possible level.

Energy efficiency has become part of the political agenda in many countries (Al-Mansour et al. 2003). Monitoring energy intensity is common practice since the 1973 oil crisis. How policies can increase energy efficiency is shown in Geller et al. (2006) for the OECD countries (OECD = Organization for Economic Co-operation and Development; 34 member countries, which are considered highly developed) and in Vine (2002) for the state of California, a leading region for energy efficiency as will be referred to in this chapter of the handbook.

For corporations, energy efficiency is an important pillar for the "triple bottom line," i.e., their performance in economic, social, and environmental aspects. Businesses and consumers alike start taking energy considerations into account for decision making. It is estimated that energy is a strategic factor for 40 % of all global revenue (McKinsey & Company, Inc. 2009). Unpredictable volatility in fuel prices, driven by depletion of crude oil and speculation, places a burden on companies and economies as a whole, which they feel needs to be controlled. Stern (2007) provides an overview on the economic aspects of climate change. With energy efficiency being the easiest way to save energy, it is highly relevant to mitigate climate change effects and their detrimental consequences.

Benefits of Energy Efficiency

Energy efficiency offers several direct and indirect benefits, some of which are obvious. The reduction of pollution and greenhouse gas emissions aids the environment. For businesses, reduced energy bills will translate into competitive advantages. Also, energy efficiency measures can lead to higher worker productivity and reduced sick leave rate (Granade et al. 2009) as concurrent benefits. Consumers can enjoy increased comfort levels (Jaffe and Stavins 1994), particularly those living in low-income households. Indirect benefits, as an example, also related to health (less drafty and damp rooms after the implementation of energy efficiency measures in

private homes such as insulation upgrading). As a nation, a key benefit is an improvement in energy security, another one that reduced exposure to volatility in energy prices. There has also been a wide discussion on job creation by the quest for energy efficiency. While it is true that energy-intensive production processes are shifted toward developing countries, leading to job losses in countries of the European Union and the USA, for instance, there should be a net positive effect from the job market stimuli provided by energy efficiency. For instance, the market for building insulation is estimated at 10–12 billion USD for the USA alone (Granade et al. 2009).

An overview on the market size for energy efficiency in the USA is provided by Ehrhardt-Martinez and Laitner (2008).

Some considerations on actual and potential job creation by energy efficiency improvement programs are provided by Granade et al. (2009), where the potential for the USA is estimated to lie between 600,000 and 900,000 jobs over the next decade in direct, indirect, and induced jobs.

Energy efficiency will not be the sole solution. There will still be a need for new, additional power plants, partly to meet increased demand, partly to replace old ones. Also, there might be additional demand that is now unaccounted for, e.g., to power electric vehicles (Granade et al. 2009) that are likely to replace traditional cars to some extent. A national commitment to green buildings has the potential to generate 2.5 million and to support 8 million American jobs (US Green Building Council 2015), with similar prospects being offered in other countries. The job market potential of clean energy is reviewed in Wei et al. (2010).

Downside of Energy Efficiency

While energy efficiency as such is indisputably a good thing, there are several aspects that have to be considered to avoid detrimental overdoing. First, the **economics** have to be considered. In a competitive landscape, corporations will only implement energy efficiency measures that "pay for themselves" (see also later). High upfront investments are one of the barriers toward better energy efficiency. Apart from costs, **complexity** is another aspect to consider. In order to improve the efficiency of a plant or an engine, advanced control systems are required, which need to be maintained. Capable technicians and additional resources have to be provided to that end. The most economic process might not be the most reliable one. As **operability** of technical equipment, particularly in the capital-intensive process industry, is of utmost importance, some concessions to energy efficiency are sometimes well accepted from a process point of view. For many production plants, 1 day of additional, unplanned shutdown per year will mean the difference between profit and loss. Also, plant personnel might focus on other aspects than energy efficiency when operating a unit or equipment (Moore 2005) to safeguard "trouble-free" operation or simply be too busy to concentrate on continuously optimizing energy usage. Another extreme, hypothetic example of an inefficient energy saving attempt

would be a person having an accident at home because of not turning on the light when fetching something from the cellar or during the night.

For these reasons, it might happen and even be advisable not to squeeze out the last bit of energy efficiency from a given system, but rather to act with commonsense.

Energy Efficiency Versus Energy Demand: The Rebound Effect

The effect that energy efficiency improvements on the microlevel (i.e., machines and individual plants in industry) do not fully translate into the expected energy savings on the aggregate level (such as the economy) is termed **rebound effect** or **Jevons paradox**. It is also called the **Khazzoom-Brookes postulate**. The rebound effect can be direct or indirect. If it is >100 %, it is called "backfire" (Sorrell 2009). Simply put, energy efficiency makes energy services cheaper, so demand tends to increase. This concept is called "elasticity of demand." A more economic car might tempt its owner to drive faster and further, thus partially offsetting potential energy savings. A car producer can decide to install more electronic devices for increased driver comfort in a car that has been made more fuel efficient, thanks to the use of lightweight construction materials and a better engine.

The extent of the rebound effect depends on the elasticity of demand, which tends to be stronger with consumers than with industrial plants (Sorrell 2009).

William Stanley Jevons studied the rebound effect during the industrial revolution (Sorrell 2009). In his 1865 book *The Coal Question* (Jevons 2008), he was pondering over the question whether efficiency measures would really lower actual coal consumption, based on empirical evidence that after efficiency improvements with steam engines and in steel production, the actual energy consumption had soared. For more information, see Saunders (1992) and Herring and Sorrell (2009).

Energy Intensity

Intensity is an ambiguous term. In physics, it is power per unit area [W/m^2], a time-averaged energy flux. In heat transfer, intensity commonly denotes the radiant heat flux per unit area per unit solid angle [$W \cdot m^{-2} \cdot sr^{-1}$].

Here, energy intensity is an economic concept as a measure of the energy efficiency of a nation's economy. It is calculated as units of primary energy consumption per unit of GDP or value added, measured in [MJ/$] or [toe/$]. The energy intensity of a country is influenced by many factors, for instance, the climate. Economic productivity and standards of living contribute as well as the energy efficiency of buildings and appliances, traffic patterns (public transportation vs. individual cars), and the way energy is being produced (EIA 2015).

Energy intensity can hence be used as a surrogate for aggregate energy efficiency. Countries differ strongly by energy intensity, and within countries, there are marked differences amongst regions. In the USA, a state with superior energy efficiency

performance is California, which has established leadership in, e.g., per capita energy consumption (Rosenfeld 2008; Vine et al. 2006). The energy efficiency of different countries is assessed in Utlu and Hepbasli (2007). The term "energy intensity" can also be applied to a production process as a synonymous expression for specific energy consumption, based on quantity [kg] or value added [$] or [€]; see also section "Energy-Intensive Industries."

Emission Intensity (Carbon Intensity)

Another concept is the emission intensity. It is the average emission rate of a given pollutant from a given source related to the intensity of a specific activity, e.g., grams of CO_2 per MJ of energy produced [g/MJ]. The term emission intensity is often used interchangeably with "**carbon intensity**" and "**emission factor**" in the climate change discussion. Other greenhouse gases and pollutants can be considered, too, by calculating CO_2 equivalents (CO_2-eq). Table 3 provides an overview on emission intensities, compiled from Bilek et al. (2008).

The subscripts in Table 3 stand for "thermal" and "electric." In combined heat and power (CHP, cogeneration), both heat and power are produced from a combustion process, boosting overall efficiency (see later).

Historical Development of Energy Efficiency

A proverb says "Things that cost nothing have little value." In this sense, as long as easy access to energy is available, there are few incentives to use it wisely. History tells several lessons here. Visitors to Greek islands will witness testimony of one such unsustainable practice exercised centuries ago, i.e., chopping down trees to build ships without reforestation. There are countless other examples of unsustainable acts related to resource and energy efficiency in the past, some of which have even led to the extinction of a local human population (Bologna and Flores 2008). The global oil crises in the 1970s were an event that has triggered several measures for energy efficiency on a large scale, e.g., the creation of the DoE (Department of Energy) in the USA. In the following decade, when crude oil prices

Table 3 Emission intensities (Source: Bilek et al. 2008). The ratio of H/C is 4 in natural gas, which is higher than in oil and especially coal, leading to lower CO_2 emissions per kWh

Fuel/resource	Electric g(CO_2-eq)/kWh_e
Coal	863–1,175
Oil	893
Natural gas	587–751
Nuclear power (U)	60–65
Hydroelectricity	15
Photovoltaics	106
Wind power	21

went down again, there was reduced motivation to focus attention on energy efficiency in many areas. The industrial sector has improved its energy efficiency continuously over the last 30 years, partly in order to reduce variable production costs and to improve competitive advantage (one also has to take into account that a significant part of energy-intensive production facilities was transferred to low-labor-cost countries in, e.g., Asia). Economic growth, a trend toward increased personal mobility and toward larger homes and the use of more and more appliances, amongst others, has led to a steady increase of absolute energy demand in most industrialized countries.

As a result, the overall energy intensities in the USA have declined as follows between 1980 and 2005 (Granade et al. 2009):

Residential sector	−11 %
Commercial sector	−21 %
Industrial sector	−42 %

While the national per capita energy consumption in the USA has grown by 1.3 % per year from 1977 to 2007, which means a doubling, it remained almost constant in California.

In the EU, the average efficiency of gas-fired power plants has increased from 34 % in 1990 to 50 % in 2005 and is expected to increase to 54 % by 2015 (Graus and Worrell 2009). For coal-fired power plants, the efficiency, also based on the lower heating value, went up from 34 % in 1990 to 38 % in 2005 and is expected to increase to 40 % by 2015. These trends are visualized in Fig. 2.

As the developed world has built its industry, specific energy consumption was constantly improved. Yet the largest share of historic and current global emissions comes from developed countries. Many people now fear that while other countries race through their development, they might expel "their share," i.e., high amounts of pollutants, into the atmosphere. China, for instance, has been able to maintain economic growth of greater than 9 % from 1980 to 2000, while the energy demand only increased by 3.9 % per year (Lin 2007). This shows that energy demand does not necessarily have to outpace economic growth during the early stages of industrialization and development (Lin 2007).

A word of caution: Many scientific publications, as well as the public opinion, believe in decreasing energy intensity over time. This hypothesis is often only an assumption, which needs to be proven. In Le Pen and Sévi (2010), the authors conclude that many energy efficiency trends on a national level follow a stochastic nature; see Fig. 3.

In Schipper et al. (2005), historic developments and future trends of energy efficiency are discussed. Megatrends (Naisbitt 1985) will also have an impact on energy efficiency. How they are perceived can differ strongly (Atilla Oner et al. 2007).

In general, there have been strong improvements in certain areas with respect to energy efficiency, some of which were countered, though, by rebound effects.

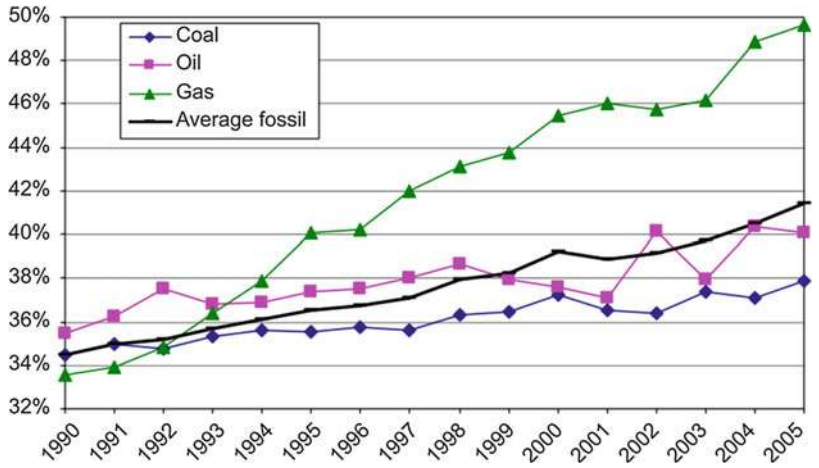

Fig. 2 Energy efficiency trends of fossil fuel combustion in the EU27 (Reprinted with permission from Elsevier from Graus and Worrell (2009))

Assessing Energy Efficiency Improvements

Energy efficiency improvements can be achieved by technological progress or by changes in behavior. They can be measured.

However, for a correct assessment, the following factors have to be taken into account:

- Erosion of part of the improvements by the rebound effect (see above)
- Comparability of data (same year, same boundary conditions)
- Selection of a proper baseline

The baseline for measuring energy efficiency is of utmost importance to avoid wrong conclusions. This is elaborated with an example from the transportation industries below, viz., the fuel consumption of aircraft over time. Figure 4 shows a data compilation of how fuel efficiency of commercial aircraft was improved over the last decades.

Taking the Comet 4 as a baseline, fuel consumption was reduced by 70 % in modern aircraft. Approx. 40 % of the improvements are attributed to engine efficiency improvements, and 30 % to airframe efficiency improvements (IPCC 2000).

The **de Havilland Comet** was the world's first commercial jet airliner (Davies and Birtles 1999).

Figure 4 was taken from an IPPC report. The IPCC (**Intergovernmental Panel on Climate Change**) is a renowned, scientific intergovernmental body established to evaluate the risk of climate change caused by human activity (Intergovernmental

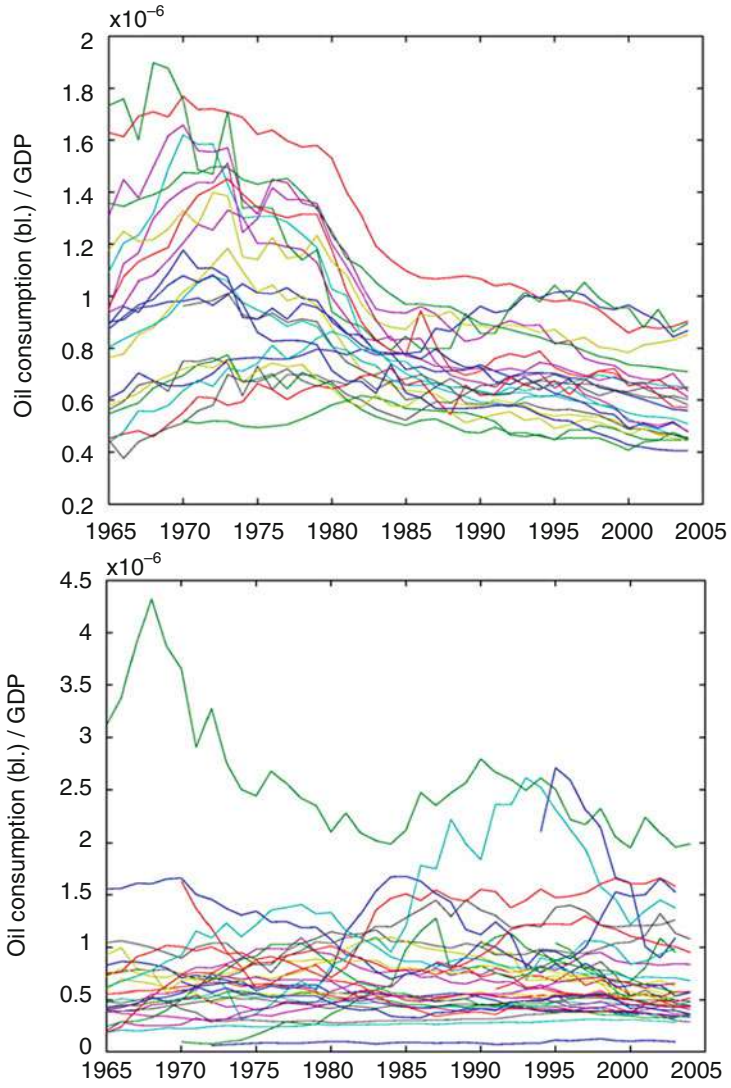

Fig. 3 Stochastic movement of energy consumption. *Left*: oil consumption per unit of GDP for OECD countries from 1965 to 2005. *Right*: same data for non-OECD countries (Reprinted with permission from Elsevier from Le Pen and Sévi (2010))

Panel on Climate Change (IPCC) 2015). It was awarded the 2007 Nobel Peace prize together with Al Gore. In Peeters et al. (2005), the authors argue that the pre-jet era was ignored in the above IPCC discussion and that the Comet 4 is an unsuitable baseline. From the conclusions of that report (Peeters et al. 2005):

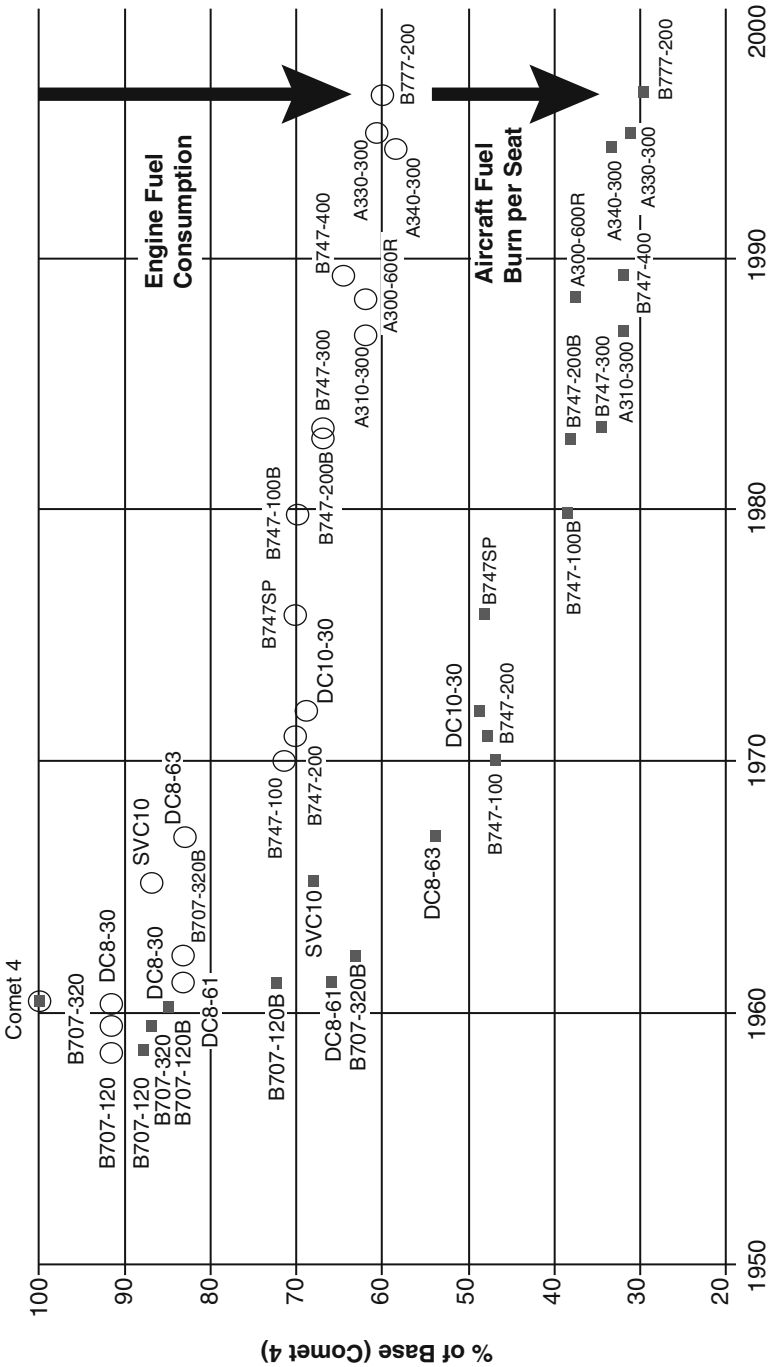

Fig. 4 Fuel efficiency of commercial aircraft over the last 50 years. See text for details. Reprinted with permission (Source: IPCC 2000)

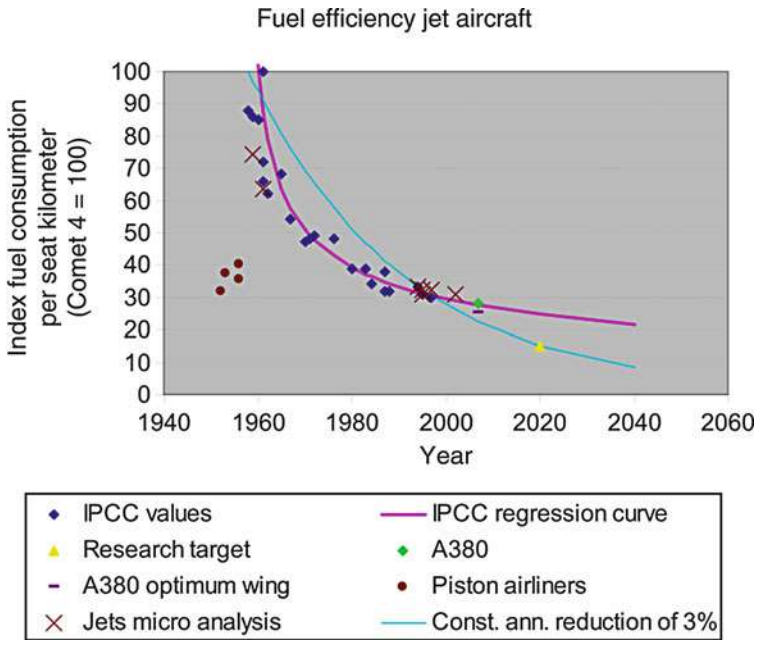

Fig. 5 IPCC graph with additional data (Reprinted with permission from Peeters et al. (2005))

> The later piston-powered airliners were at least twice as fuel-efficient as the first jet-powered airliners; If, for example, the last piston-engine aircraft of the mid-fifties are compared with a typical turbojet aircraft of today, the conclusion is that the fuel efficiency per available seat-kilometre has not improved. . .. The last piston-powered aircraft appear to have had the same energy efficiency per available seat-kilometre as average modern jet aircraft. The most modern jet aircraft (such as the B777-200 or B737-800) are slightly more efficient per available seat-kilometre.

The findings from this study are depicted in Fig. 5.

As it can be seen in Fig. 5, slight changes in the assumptions will lead to strong deviations in the results. This has to be borne in mind when assessing and comparing energy efficiency studies presented by various interest groups.

Innovation and New Technologies for Energy Efficiency

In order to increase energy efficiency, innovation (Christensen et al. 2001) is needed. By innovation, either of the following energy efficiency improvements can be achieved:

- Carrying out the same task or process with less energy
- Utilizing the same amount of energy to produce more output or higher value
- Redefining the task or process so that the new way consumes less energy

Innovation can take place in incremental steps or in a disruptive way, when a new technology is developed, for instance. The electric light bulb, being condemned as energy inefficient today, was one such disruptive innovation, which has been around for more than a century. So in order to innovate, engineers and researchers might be tempted to search and build more knowledge in their own area of expertise and to innovate as much as possible in their very own fields. This strategy has proven successful – take the famous Bell Labs (Gehani 2003) as an example. Fifty years ago, the Bell Labs were generating every new technology that the telephone business needed, and the telephone business, in turn, was using all of Bell Labs' innovations. Bell Labs were virtually unbeatable. However, the rules of innovation have changed somehow over time. The Bell Labs invented the transistor, which clearly is one of their greatest discoveries. However, Bell Labs did not recognize the value of the transistor, and they gave it away for little money. The transistor, hence after, was extremely successful, but with the main use not being in the telecommunications industry. On the other hand, the very innovation that revolutionized the telecommunications industry – the fiberglass cable – was developed outside that industry. This phenomenon has been observed in many industries over the last 50 years (Drucker 2003) – the major innovations with the biggest impact for an industry are not likely to come out of the industry itself but will rather be "born" in a different area.

The significance of this development for the realm of energy efficiency is as follows: Energy efficiency can be improved in many ways. In a passenger car, for instance, an advanced engine, lightweight plastics components instead of steel or tires causing less rolling friction will all serve the same final purpose of energy efficiency.

Innovation takes time until its full potential is being realized, though. In Lund (2006) the market penetration rates of new energy technologies were studied. It is concluded there that the time for a takeover of market share from 1 % to 50 % varies from less than 10 years to 70 years, with takeover times below 25 years being associated with end-use technologies. Long investment cycles render the energy production industry inert to change.

Typical Energy Efficiencies

The energy of photosynthesis is on the order of 1 %, with a fraction of approx. 0.2 % being stored as biomass. Sugarcane exhibits peak storage efficiencies of up to 8 % (Hall and Rao 1999). The first steam engines, designed as external combustion engines, had efficiencies on the same order of magnitude.

To visualize the energy balance, i.e., the energy efficiency, of a process or machine, a Sankey diagram can be used. For exergy, Grassmann diagrams (Hinderink et al. 1999) are deployed (though both terms are sometimes used interchangeably in the literature).

An example for a Grassmann diagram for nitric acid production is shown in Fig. 6 (Hinderink et al. 1999).

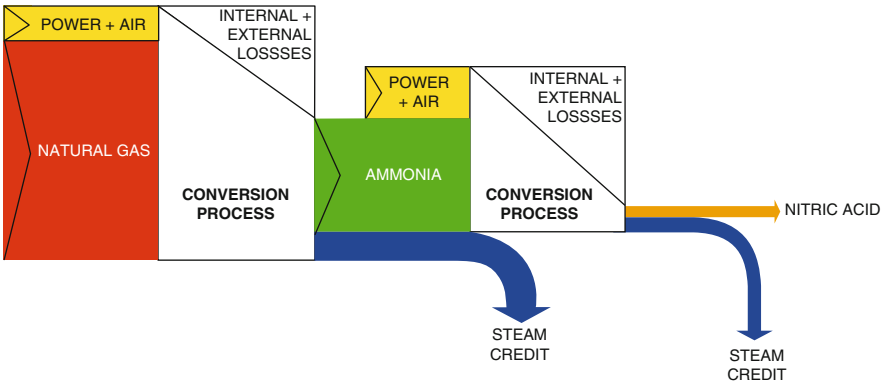

Fig. 6 Simplified Grassmann diagram for the production of nitric acid (Hinderink et al. 1999) (Reproduced by permission of the Royal Chemical Society (*RCS*))

The Grassmann diagram can be seen as an energy flow diagram, visually explaining which fraction of the total, initial energy ends up in the final product.

In order to obtain typical energy efficiencies, or reference energy efficiencies, a benchmark is deployed. The benchmark in energy efficiency is given by the state-of-the-art and so-called BAT (best available technology) values. However, BAT values are often difficult to obtain, as corporations tend to keep them secret and patents do not always provide full disclosure.

The energy efficiency and carbon intensity of a given process depend on the system boundaries that are considered and on the energy path. For instance, whether electricity for a hybrid car has been produced in a coal-fired power plant or by solar cells will heavily impact the overall efficiency (see also section "Life Cycle Assessment (LCA)").

Actual efficiencies will depend on a large number of factors such as the condition of a given system or appliance. Examples are the load of an engine, maintenance on motors, and usage patterns. This is obvious for every car owner who wants to reach the "official" fuel consumption of his/her car.

When energy efficiency potentials are presented in the literature, one has to be careful not to overestimate or mix up the various potentials, which are:

- Technical potential
- Economic potential
- Maximum achievable potential (considering factors such as demographics, market conditions, and regulatory factors)
- Realistic achievable potential (taking historic data into account)

People adapt to change at different rates. Take popular technologies as an example. Even for microwave ovens and mobile phones, it took 10–15 years for market penetration. Therefore, the realistically achievable potential is never equal to

the full technical potential. Also, the effort to obtain a large part of any potential saving will increase along the way.

For energy efficiencies of various technologies, processes, and appliances, the reader is referred to the respective chapters of this handbook and to the specialized, referenced literature.

Benchmarking of Energy Efficiency

There are no useful reference data for absolute energy efficiency from a thermodynamic or theoretical point of view. Rather, one can only compare a given process or technology route, device, or method to other solutions in the lab or in the field, so that the best available technology (BAT) or state of the art can be determined empirically. Such a benchmarking exercise focused on energy efficiency will yield interesting results. In Phylipsen et al. (2002), for instance, it was found that the energy consumption of the steelmaking plants in several countries was 25–70 % above the best plant. In the cement industry, the average consumption was 2–50 % higher than the very best plant energy efficiency.

Benchmarking can be used by operators of industrial plants to compare their energy efficiency, and ultimately their competitiveness, to that of their contenders.

Consumers can use relative indications of energy efficiency, such as the Energy Star® label, to easily spot energy-efficient appliances as a guide for purchase decisions.

It needs to be mentioned that comparing like with like is crucial. If, for instance, steelmaking plants in two countries are to be compared, sectoral differences must be taken into account (Phylipsen et al. 2002) (if, e.g., there is plenty of secondary steel available, energy efficiency will "automatically" be higher). Also, regional differences in feedstock quality (Worrell et al. 2000a) or climatic conditions will affect the energy efficiency of a given plant. More information of reliable reference data for energy efficiency comparisons on a national level can be found in Doukas et al. (2008).

In mature industries, energy efficiency differences from plant to plant are not expected to be very large, because improvements tend to be incremental.

Generally, there is a lack of energy efficiency benchmark standards for industry at large and factories in various sectors (Yang 2010), secrecy and antitrust legislation being important impeding factors. There exist corporate benchmarks in some companies that operate multiple plants or sites. Several consultants carry out benchmarking studies in various industries, e.g., Solomon Associates for steam crackers, Phillip Townsend Associates for polymerization plants, Plant Services International for ammonia and urea plants, and PDC (Process Design Center) for more than 50 petrochemical processing plants (The International Energy Association in Collaboration with CEFIC 2007), to cite a few examples. These benchmarks present generalized and anonymized data with which the energy efficiency and the competiveness of one's own plant can be compared to the industry average.

Energy Efficiency World Records

A world record in energy efficiency of a car was set in 2005 as 5,134 km per liter of gasoline equivalent, operating on a hydrogen-powered PEMFC (polymer electrolyte membrane fuel cell) (Santin 2005) during the Shell Eco-Marathon. It challenges students around the world to design, build, and drive the most energy-efficient car and has three annual events in Asia, America, and Europe. On the website of the competition (Shell Eco Marathon 2015), additional records on energy efficiency are highlighted, e.g., an equivalent of 3,771 km with 1 l of fuel with a combustion engine-powered car in 2009 (5 years earlier, the record was 3,410 km). These figures, equally impressive and irrelevant for current practical road transportation, show that there is plenty of potential left to increase energy efficiency, even beyond current imagination.

Some Not-So-Energy-Efficient Inventions and Practices

Here are some examples of low-energy-efficient appliances and habits, most of which might soon astonish people that they even existed in our times:

- Incandescent light bulbs
- Huge private cars such as SUV with single occupancy
- Standby function on electrical appliances in households
- Patio heaters to warm open areas outside the house
- Melting snow in cities such as New York City to dispose of it
- Flaring of hydrocarbons in petroleum refineries
- Room temperature regulation by opening and closing a window, while keeping the heater switched on
- Water ring pumps to produce an industrial vacuum

In a typical household, appliances on standby use up 10 % of the total amount of electricity consumed. This is equivalent to 400–500 kWh annually, virtually wasted with no energy service rendered.

Barriers to Energy Efficiency

There is no doubt about the fact that energy efficiency offers cost-effective energy savings. However, the full potential has barely been tapped into. There are several barriers, associated with financial limitations, uncertainty, or others. They can also be classified as structural and behavioral and related to availability (Granade et al. 2009).

Though businesses and households are responsible for implementing most energy efficiency investments, it is their governments to provide the right bordering conditions to catalyze investments in energy efficiency by offering tax incentives,

Table 4 Estimated persistence of energy efficiency measures (Source: Climate Action 2015)

Years following implementation (installation)	Remaining energy efficiency impact	
	Electricity-related measures (%)	Fuel-related measures (%)
1	99.69	100
2	95.97	99.46
3	89.59	98.51
4	85.14	97.84
5	84.02	97.11
6	78.32	89.75
7	78.22	89.75
8	78.22	89.75
9	74.58	89.70
10	66.73	87.45

education, or other facilitation. One reason why the potential for energy efficiency has not yet been realized to its full extent is the fact that high upfront investments are often necessary, whereas the savings accrue incrementally over the subsequent years (Granade et al. 2009). Also, the energy efficiency improvement potentials are highly fragmented (Granade et al. 2009). Apart from low awareness, the difficulty to measure energy efficiency improvements in several areas contributes to slow progress. Barriers to energy efficiency are discussed in Granade et al. (2009), alongside the following potential actions to break down these barriers:

- Information and education
- Incentives and financing
- Codes and standards

Experience shows that consumers are particularly hostile toward funding of energy efficiency measures, compared to businesses, even if the economics are reasonable. They apply hyperbolic discounting, meaning that immediate value is regarded significantly higher than future one.

Barriers toward energy efficiency improvements in industrial settings are reviewed in Schleich (2009).

Another interesting question is the durability of energy efficiency measures, which was studied in Climate Action Team (2015), the results of which are given in Table 4.

The percentages in Table 4 reflect the portion of the first year energy savings that remain throughout the full lifetime of the studied energy efficiency measures. A distinction was made between measures focused on saving electrical energy and measures to save fuel. It can be seen that already after a few years, considerable losses from the initial gains are encountered, which can be explained by various factors depending on the efficiency measure. "Hard-wired" energy efficiency initiatives will generally be lasting longer than those based on behavioral changes (see also below).

An example on how energy efficiency can stagnate if the economic and organizational conditions are not in favor of it, such as prevailing low electricity prices, is shown for the Swedish building industry in Nässén and Holmberg (2005) and Nässén et al. (2008).

Aspects of financing energy efficiency, another prominent barrier, are outlined in Taylor et al. (2008), Lee et al. (2003), Jechoutek and Lamech (1995), and Clark (2001). Barriers to energy efficiency in general are reviewed in Sorrell et al. (2004).

Levels of Energy Efficiency: From Process to Behavior

Energy efficiency can be achieved by various means.

A product can be manufactured in a way that energy is used efficiently, either during its production or during its use. A process can be energy efficient by itself, or it can produce energy-efficient outcomes. The same applies for services. Here are some examples of more and less efficient products and processes:

- Office lighting by compact fluorescent lights/LED versus traditional incandescent light bulbs
- Modern compact passenger car versus older, mid-sized model
- Cement production by the dry process versus the wet process
- Air separation by pressure swing adsorption versus air separation by cryogenic air cooling and fractionated distillation
- Steel manufacture from scrap metal versus ore

It is desirable to have efficient equipment and processes in place. However, these can be operated in very inefficient ways. The magnitude of loss in energy efficiency by "bad" operation can be as large as the difference between competing processes and equipment items (Moore 2005). Some examples of these "bad" operation aspects are:

- Excessive speeding with a car, which strongly increases fuel consumption/km
- Neglected maintenance on insulation of window frames in a private home
- Keeping office lights on overnight when they are not needed
- Operating plant utilities at full capacity during idle production times
- Not repairing leakages on compressed air pipelines

In contrast to the installation of new, more energy-efficient equipment, or the design of a more energy-efficient process, operation thereof requires constant attention (compare also the table above, showing the stunning erosion of energy efficiency gains over a few years' time). By continuously working on a mindset toward energy efficiency, for instance, by having employees turn off idle equipment and by fostering continuous improvement, also small, individual savings can add up.

In Moore (2005), some aspects of why operators in control rooms do not always give utmost importance to energy efficiency are listed:

- Lack of urgency, little incentives to value long-term performance versus the short term
- Preference of steady-state operation versus short-term optimization efforts
- Comfort, trading economy against less effort
- Individual work history and anecdotes making risk perception highly personal
- Different levels of skills and knowledge
- Instinct to preserve assets rather than maximize their utilization
- Little effect of administrative control measures alone
- Focus drift due to distraction

The most economic mode of operation of a plant in the process industries, for instance, is not always the most convenient one (Moore 2005). This will lead operators to at least partly refrain from energy efficiency optimization.

Such "human factors" can be improved by considering the **usability** of processes and equipment. Whereas the usefulness of a man-made tool or installation is related to user satisfaction, the term us(e)ability denotes the ease with which it can be deployed. In general, usability can be defined as a measure of the ease with which a system can be learned or used; its safety, effectiveness, and efficiency; and attitude of its users toward it (Jordan et al. 1996). In Nachreiner et al. (2006) and Nishitani et al. (2000), two examples of the successful application of usability and **usability engineering** in process control systems and industrial plants are given.

Energy Efficiency Investments

As energy-efficient technologies often have higher initial investment costs than older, less advanced ones, economic considerations will determine the extent to which energy efficiency is considered for new investments and for retrofits alike. The TCO (total cost of ownership) approach will clearly recommend energy efficient, but typically more expensive installations, in many cases. Investing in "the right technology," if it is not supported by a sound business case of yearly energy bill savings, will be easier during the construction of a new building or factory than when one wants to apply for funds, corporate and federal alike, later on. In industry, one can distinguish between:

- Pure capacity investments
- Pure energy efficiency investments
- Hybrid capacity and energy efficiency investments

Common appraisal methods for investment projects in industry are:

- Payback period
- Net present value (NPV)

- Internal rate of return (IRR): discount rate where NPV = 0
- Strategic fit

Approval can be based on an evaluation of several of these parameters, by a ranking or by fulfilling a certain cutoff criterion. To test the validity of the profitability calculation of such a project, a sensitivity analysis can be carried out by varying the most important parameters. Monte Carlo simulation enhances the quality of such simulations (Lackner 2007). Real options (Rugman and Li 2005) can also be used. While debottlenecking investments, which increase production capacities, usually have short payback periods and high IRRs, often exceeding 50 %, energy efficiency investments sometimes cannot make it over the 10 % hurdle. If the funds for investment projects are limited, naturally those with higher IRR will be preferred. Energy efficiency investments can be carried out at a lower IRR than a corporation's normal hurdle rate (IRR), because the associated risk is generally lower than for a capacity investment (energy savings can be predicted more reliably).

Often, when "selling" an energy efficiency project in a corporation, one had to better avoid the term "energy" and describe potential projects as "efficiency" or "productivity" improvement projects when presenting them to decision makers.

Energy has a different importance for various sectors. Those industries which are energy intensive will suffer more from high and volatile energy prices than the ones incurring only a small percentage of their costs from energy bills. It is estimated that out of the total global economic activity (according to the International Monetary Fund (IMF) US$77.609 trillion (GDP) or US$106.998 trillion (purchasing power parity, PPP) for 2014), 40 % comes from companies where energy plays a strategic role (McKinsey & Company, Inc. 2009). The sectors concerned are transportation, building and construction, energy-intensive industries, engineering, IT (information technology), and the energy industry. For companies in these sectors, energy can have a direct or indirect effect, i.e., on their own production costs or on the acceptance of their products.

On the other side, there are industries, such as education, retail, insurance, and healthcare, which do not depend as much on energy competitiveness.

Introducing Energy Efficiency Programs

It is estimated that most organizations have a potential for 10–20 % energy efficiency improvement, which will materialize in the bottom line. In order to improve energy efficiency in a company or another larger institution, an **energy survey** or an **energy audit** can be a first step to map out the saving potential. More information on such energy audits can be found in Sustainable Energy Ireland (SEI) (2015) and Carbon Trust (2015). They consist of data collection ("hard facts" such as electricity consumption and interviews on common practices) and internal and external benchmarking. There is currently a lack of qualified energy auditing staff (Yang 2010). Checklists can help to uncover inefficiencies in processes and equipment.

In the EU, Directive 2012/27/EU of 25 October 2012 on energy efficiency has introduced compulsory energy audits for large corporations in an attempt to foster energy consumption reduction.

Using off-peak hour electricity is an option to shrink the electricity bill. How to manage energy efficiency in a corporation is described in Russell (2009). To which extent agreements foster energy efficiency is analyzed in Rietbergen et al. (2002).

Combustion

Combustion plays a critical role in energy efficiency considerations, as approx. 80 % of global primary energy is produced by combustion processes. Combustion processes have the single largest human influence on climate with 80 % of anthropogenic greenhouse gas emissions (Quadrelli and Peterson 2007). Fuels can be fossil or renewable (biomass). They are gaseous, liquid, and solid.

Combustion is used in power plants for electricity and heat production, transportation, and other areas (see sections below for details). Figure 7 shows the global trend in CO_2 emissions over the last 140 years (source: Quadrelli and Peterson 2007).

As it can be inferred in Fig. 7, the increase in anthropogenic, combustion-derived CO_2 emissions has almost been an exponential one. For the impact on climate change, not only the efficiency of a combustion process itself but also emissions generated during fuel production and transportation have to be considered. For instance, for every kg of mined coal, 1.2–16.5 g of the greenhouse gas methane (GWP = 21) are emitted (Office of Energy Efficiency, Natural Resources Canada 2002).

Combustion can be carried out in furnaces (see section "Power Plants and Electricity Production" below) and boilers, in internal and external combustion engines, and in gas turbines (Pilavachi 2000; Boyce 2006; Farzaneh-Gord and Deymi-Dashtebayaz 2009).

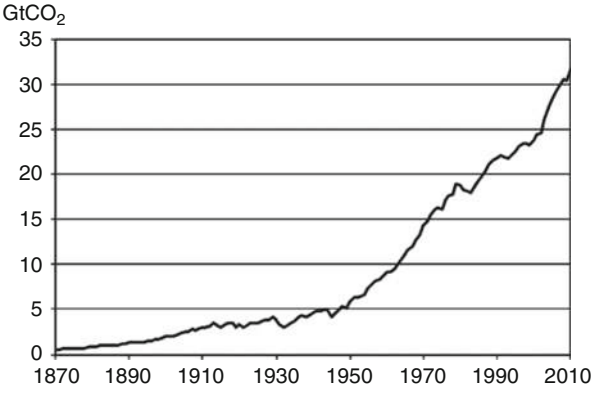

Fig. 7 Trend in CO_2 emissions from fossil fuel combustion (Source: Carbon Dioxide Information Analysis Center, Oak Ridge National Laboratory, US Department of Energy, Oak Ridge, TN, USA). Units: Gigatons of CO_2 (Reprinted with permission from International Energy Agency (2014))

Pyrolysis and gasification are special cases of combustion. These processes can be used to obtain gaseous or liquid fuels from biomass or coal in conjunction with a Fischer-Tropsch (van Vliet et al. 2009; Prins et al. 2004) or other synthesis processes. Due to the removal of moisture and ash and the effect of deoxygenation, liquid hydrocarbons derived from biomass have a threefold energy density and are hence more advantageous for transportation and storage (Demirbas et al. 2000). See also chapter "► Gasification Technology" in this handbook.

Heat recovery from flue gases is a particularly energy-efficient measure. For steam systems, for instance, 1 % of fuel can be saved for every 25 °C reduction in exhaust gas temperature (Galitsky 2008).

In Quadrelli and Peterson (2007), recent trends on CO_2 emissions from fuel combustion are reviewed. For combustion in general, see Lackner et al. (2010) and Lackner et al. (2013).

Power Plants and Electricity Production

12 % of man's total energy is made up by electricity, a fraction that is expected to rise to 34 % until 2025 (Ibrahim et al. 2008).

Energy efficiency in electricity production can be defined as the energy content of the produced electricity divided by the primary energy input, with reference to the lower heating value (Graus and Worrell 2009).

The lower heating value (LHV, or net calorific value) assumes that the water formed in combustion remains as vapor.

In **cogeneration**, the overall efficiency can be increased, because the (by-product and formerly waste) heat is used. Cogeneration is also dubbed **CHP** (combined heat and power).

Power production is carried out by (large) public power and CHP plants and by so-called **autoproducers**. These are users such as chemical factories which produce their own power and heat. In the EU, autoproducers account for 8 % of the total power generation (Graus and Worrell 2009). Electricity production plants have an efficiency of around 30–40 %, whereas combined heat and power (CHP, cogeneration) yields up to 90 % (Office of Energy Efficiency, Natural Resources Canada 2002). For the installed base of CHP, see CHP Installation Database (2015).

In the EU, the energy efficiencies for coal-fired power production range from 28 % (Slovak Republic) to 43 % (Denmark). On a global scale, the spread for oil-fired power plants is an efficiency of 23 % for the Czech Republic and 46 % for Japan (Graus and Worrell 2009).

The efficiency of a given power plant is dependent on its age. The younger a plant, the higher its energy efficiency was (intuitively) found to be (Graus and Worrell 2009). These findings are in line with another study (Phylipsen et al. 2002), which revealed that the least energy-efficient plants are not always located in developing countries. Apart from the age of a plant, its fuel mix, size, and load account for the big differences in efficiencies mentioned above (see also section "Cross-Cutting Technologies" below).

State-of-the-art power plants based on coal and gas have energy efficiencies of 46 % and 60 %, respectively (Graus and Worrell 2009).

It is estimated that the replacement of inefficient coal-fired power plants by more efficient coal- or gas-fired ones, particularly in China and in the USA, can reduce global CO_2 emissions by 5 % (IEA 2009). In Canada in 1988, according to the Canadian Industry Program for Energy Conservation (CIPEC), the average CO_2 emissions in electricity production were 0.22 t/MWh, with a spread of 0.01 in Quebec to 0.91 in Alberta (Office of Energy Efficiency, Natural Resources Canada 2002).

Demand side management (DMS) can help to level peak electricity demand (Loughran and Kulick 2004). This will be even more important as more renewable energy plants (wind, solar) are installed, where electricity production and consumption hardly coincide.

Energy is increasingly being produced **from waste**. Methane can be extracted from landfills for power production in gas engines. Waste incineration uses the energy content of waste and converts it to a low-volume, inert residue. While previously the focus of waste incineration plants was on low-emission combustion to get rid of the waste, today the energy efficiency of these plants has become important, too. In Bujak (2009), an incineration plant for medical waste is presented. It is equipped with a heat recovery system and can extract 660–800 kW of usable energy from 100 kg/h of medical waste with an energy efficiency between 47 % and 62 %. New and innovative pyrolysis and gasification technologies for energy-efficient waste incineration are presented in Malkov (2004). In Dijkgraaf and Vollebergh (2004), waste incineration is compared to landfilling, and in Cherubini et al. (2009), a life cycle assessment (LCA) (Guineé 2002) of waste management strategies is performed.

Energy Transmission and Distribution

Today, electricity production is centralized, with large power plants being coupled to a complex distribution network.

Energy transmission and distribution cannot be performed in a totally loss-free way (leaving apart superconductivity, where electrical resistance is exactly zero). In Europe, they typically amount to 4–10 % and hence reduce the overall efficiency of power supply by several percent points (Graus and Worrell 2009).

For the USA, EIA estimates that national electricity transmission and distribution losses are approx. 6 % (FAQ and US Energy Information Administration). In India, losses are estimated at 32 %, which is significantly above the global average of 15 % (Joshi and Pathak 2014).

Transporting the fuel to end users is more cost effective yet also consumes substantial amounts of energy (see sections below). Natural gas, for instance, is being pumped across long distances, because placing a gas power station next to the gas field and transmitting the electricity and heat would result in a considerably lower overall efficiency than compressing and moving the gas through pipelines.

Globally, Russia is the largest producer and transporter of natural gas. Methane emissions from the Russian natural gas long distance network are estimated at approximately 0.6 % of the natural gas delivered (Lechtenböhmer et al. 2007).

Energy Storage

The need for more and cleaner energy leads to an increase in distributed generation (DG) and renewable energy sources (RES) (Hadjipaschalis et al. 2009). Since such sources like wind power are not as reliable and as simple to adjust to demand fluctuations as conventional power plants, they could be coupled with energy storage systems.

Power demand by (end) users fluctuates strongly. Typically the lowest consumption during a 24-h period is nearly half the peak demand (compare Fig. 8).

Today, with a mainly centralized electricity production scheme, there is only a small storage capacity available, amounting to approx. 90 GW or 2.6 % of the total production of 3,400 GW (Ibrahim et al. 2008). With DG and RES on the increase, it is expected that energy storage, more specifically electrical energy storage, will gain significance on a local (small) and regional (large) level.

Energy can be stored in various ways, for instance, as:

Potential energy	Pumped hydro storage (PHS, i.e., pumping water up into a reservoir, so that it can later drive a turbine) or compressed air energy storage systems (CAES, i.e., compressing gas in a cylinder)
Kinetic energy	Accelerating a flywheel
Chemical energy	Batteries (Rydh and Sandén 2005), fuel cells (H_2)
Thermal energy	Use of sensible or latent heat (Ibrahim et al. 2008), e.g., of NaOH

Lead batteries are well known for the storage of energy; however, they are heavy and inapt for high cycling rates. Rydh and Sandén (2005) discuss the energy efficiency of batteries.

In Ibrahim et al. (2008) and Hadjipaschalis et al. (2009), an overview on current and future energy storage technologies is given. They differ in their maturity, target use (e.g., portable or fixed, long- or short-term storage), specific power (power density) [W/kg] and specific energy (energy density) [Wh/kg], the lifetime (number of cycles), the self-discharge rate, and the costs per installed kWh. Hydrogen storage options are reviewed in Hirscher and Hirose (2010).

In Ibrahim et al. (2008), the energy efficiencies of various energy storage technologies are compared.

An interesting option for electrical energy storage is power to gas (P2G, PtG) (Gahleitner 2013).

Energy storage (and conversion) is always associated with losses.

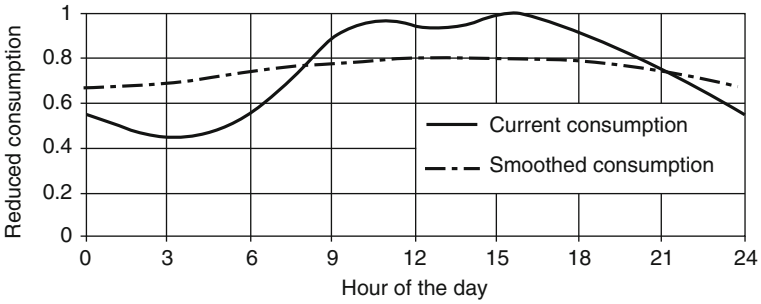

Fig. 8 Average daily power consumption in France (Reprinted with permission from Elsevier from Ibrahim et al. (2008)). Peak demand happens in the morning and afternoon, with the lowest demand being met in the early morning hours

Life Cycle Assessment (LCA)

Life cycle assessment (LCA) (Guineé 2002), also called life cycle analysis, is a holistic view on a product or service. As the name implies, all steps from its raw material production, manufacturing, transportation, distribution, use, and disposal are considered to determine the overall effect that a given product has on the environment. LCA is rooted in the ISO14001 environmental management system standard, more specifically in ISO 14040, 14041, 14042, and 14043 (ISO 2015). The ISO standard for energy management is ISO 50001.

Variants of life cycle analysis are:

Cradle-to-grave analysis	(Full life span)
Cradle-to-cradle analysis	(Including recycling)
Cradle-to-gate analysis	(Partial process)
Gate-to-gate analysis	(One step)
Well-to-wheel analysis	(Used in the automotive industry; see below)
Wire-to-water efficiency	(Used for pumps; see later)

Eco-balance is a synonymous expression for LCA.

An illustrative example for the value of LCA is the use of plastic materials for insulation purposes. Within 4 months of use, the energy savings can equal the energy needed for production, with a service life of up to over 50 years (The International Energy Association in Collaboration with CEFIC 2007).

In transportation, LCA is typically done as well-to-wheel (WtW) analysis, which is an overall fuel efficiency calculation (there are also the standard LCA studies for cars, ranging from production to use and disposal). **WtW efficiency**, detailed in Braungart et al. (2007), van Vliet et al. (2009), Svensson et al. (2007), and Hekkert et al. (2005), is a similar concept as **life cycle energy efficiency** (Malça and Freire 2006). Both concepts can be understood as overall efficiencies of a process chain, calculated as the product of the individual efficiencies.

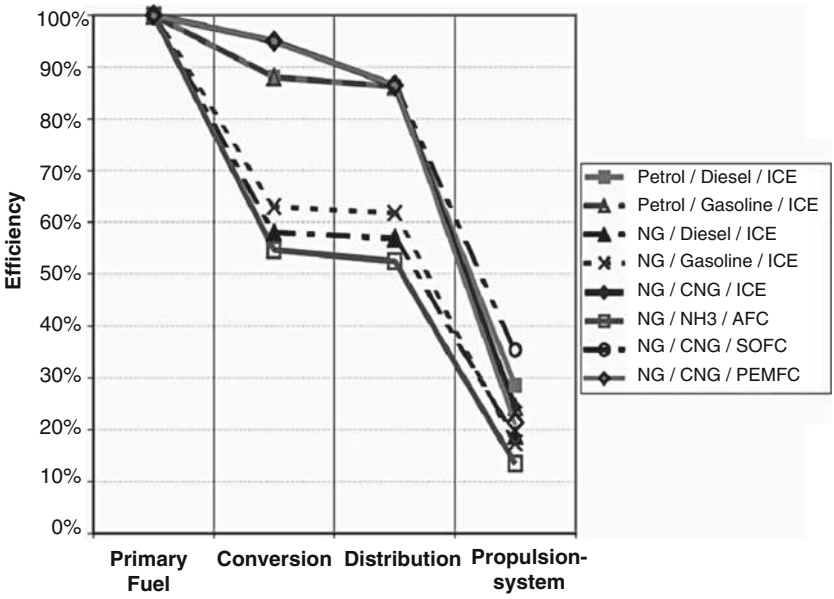

Fig. 9 Well-to-wheel efficiencies under hot starting conditions (Reprinted with permission from the Society of Automotive Engineers (*SAE*) from Ellinger et al. (2001)); *ICE* internal combustion engine, *NG* natural gas, *CNG* compressed natural gas, *AFC* alkaline fuel cell, *SOFC* solid oxide fuel cell, *PEMFC* polymer electrolyte membrane fuel cell

WtW efficiencies allow meaningful comparisons between different technologies, for instance, internal combustion engines (ICEs) versus fuel cell (FC) vehicle technologies. They provide for a fair comparison. Figure 9, taken with permission from Ellinger et al. (2001), shows the efficiency chain for different automotive propulsion systems under hot start conditions.

In Fig. 9, the WtW efficiency is calculated as the product of conversion efficiency η_c, distribution efficiency η_t, and propulsion system efficiency η_p as shown in equation 6:

$$\eta = \eta_c \eta_t \eta_p \tag{6}$$

The conversion efficiency η_c for gasoline and diesel production in a refinery is quoted as 88 % in Heitland et al. (1990) and as 63 % for their production from methanol according to the Lurgi process (20 years ago), and the distribution efficiency η_t as 97–98 % in The International Energy Association in Collaboration with CEFIC (2007).

In Fig. 9, it can be seen that the CNG-SOFC (compressed natural gas-solid oxide fuel cell) combination achieved the best overall efficiency of around 35 %, with the best internal combustion engine performance being 29 % for diesel from crude oil (the International Energy Association in Collaboration with CEFIC 2007).

The **eco-balance** of biodiesel, for instance, has to consider the consumption of fossil fuels and materials for its production, e.g., the use of lubrication oil. Another important term is that of the **energy path**. The production process will strongly impact energy consumption. Methanol, for instance, can be produced via a path starting from sugarcane (1st-generation biofuel), from lignocellulosis (2nd-generation biofuel), or from natural gas (traditional), which will yield different eco-balances.

An interesting website on LCA is run by the US Environmental Protection Agency (EPA) (http://www.epa.gov/nrmrl/std/lca/lca.html 2015).

A related concept to LCA is the **embodied energy** (Venkatarama Reddy and Jagadish 2003). It is often used for buildings (see later). Also in other industries, significant amounts of energy are "stored" in the final product. In the case of the petrochemical and chemical industries, which consume 30 % of global industrial energy, more than half of the energy is locked up in the final products (the International Energy Association in Collaboration with CEFIC 2007) and can be recaptured at the end of their lifetime.

The total life cycle of a product can not only be assessed with regard to energy use and environmental aspects but also from an economic point of view – in terms of costs. In this case, one speaks about **life cycle costs** (**LCC**) or total cost of ownership (TCO).

Recycling is an important aspect of life cycle assessment. The primary energy demand for "new" materials is often considerably higher than that needed to recycle them from waste. For instance, if aluminum cans are recycled, the energy consumption will only be 5 % of the energy needed to make them from virgin bauxite ore. Scrap metal, glass, paper, and plastics should be recycled to make best use of their "energy content," as primary production tends to consume more energy than secondary one. In the case of plastics, "thermal recycling" is an advantageous, final use if other types of recycling are not feasible. The 3Rs (**reduction, reuse, recycling)** are approaches to limit the quantity of primary raw material demand, hence contributing to sustainability.

Total Cost of Ownership (TCO)

The total cost of ownership (TCO) concept acknowledges the fact that the use of any equipment has two types of costs associated with it:

- Initial investment costs
- Running costs over the entire useful lifetime (energy, maintenance, disposal, etc.)

For industrial pumps, for instance, which are typically in service for 15–20 years, the initial investment cost is often less than 5 % of total incurred costs (Tutterow et al. 2002). For a majority of industrial assets and facilities, the lifetime energy will dominate the life cycle costs, which is also the case for many equipment items in private homes. More information on TCO can be found in Braun and Leiber (2007),

US Department of Energy (2005), and Sorrell et al. (2004), with the latter two providing ample coverage of economic evaluation of energy efficiency.

Energy Efficiency in Various Sectors

In the following sections, energy efficiency in various areas is discussed. As is shown in Fig. 1 and Table 1, major consumers of energy are end users, power plants, transportation, industry, buildings, and others, each of which showing potential for cost-effective energy efficiency improvements.

Agriculture and Food

Agricultural activities make a strong contribution to anthropogenic climate change.

Greenhouse gas emissions from this sector account for 22 % of global total emissions, which is similar to the contribution level of industry and greater than that of transportation. Livestock production (including transport of livestock and its feeding) accounts for nearly 80 % of the sector's emissions (McMichael et al. 2007). The two strong greenhouse gases (GHG), methane and nitrous oxide (which are closely linked with livestock production), contribute much more to this sector's warming effect than does carbon dioxide (McMichael et al. 2007). Emission factors of CO_2 and CH_4 for livestock are estimated at 36–3,960 and 0.01–120 kg per head and year, respectively (Office of Energy Efficiency, Natural Resources Canada 2002). Agricultural operations not only put strain on global climate by CH_4 emissions from cattle but also by energy consumption, which is concentrated in the areas of irrigation, process heat applications, and refrigeration. Irrigation pumps, refrigerated warehouses, greenhouses, and postharvest processing offer various potentials for energy efficiency improvements. A nice example is provided by some Dutch greenhouses, which are heated by gas engines, the CO_2 from which is fed into the greenhouses to fertilize the plants and to boost their growth (Lugt et al. 1996). In Oude Lansink and Bezlepkin (2003), different heating methods for greenhouses are compared. In Ramírez et al. (2006a), the energy efficiency of the Dutch food industry is reviewed, and in Ramírez et al. (2006b) that of the European dairy industry. Additional case studies of recent improvements in energy efficiency in the agricultural industry are discussed in Swanton et al. (1996).

The energy use for the production of various agrichemicals, such as herbicides, growth regulators, and fungicides, ranges from 120 to 550 MJ/kg of active ingredient (Saunders et al. 2006), taking production, packaging, and transportation into account (Saunders et al. 2006). The application rate of these chemicals further determines the total energy consumption per kg of agricultural product.

Food miles are a very simplistic concept relating to the distance food travels as a measure of its impact on the environment (Saunders et al. 2006). While a lower number of "food miles" will generally render a product more energy efficient, because transportation ways are shorter, a food commodity that is produced with

high energy efficiency, e.g., by low use of fertilizers, and that has a long mileage to the consumer can still have a lower environmental impact that foodstuff manufactured close to the end customer in an otherwise inefficient way. This simple example shows that energy efficiency aspects are closely interwoven and often difficult to compare, not only in the agricultural industry. Globalization affects the food industry as much as it does high-tech goods.

Ecuador is the world's largest banana exporter. The carbon footprint of Ecuadorian export bananas was found to range from 0.45 to 1.04 kg CO_2-equivalent/kg banana (Iriarte et al. 2014).

In Wang (2008), energy efficiency in the food industry is treated in detail.

Transportation and Logistics

Our world has become global, so that people and goods are being transported between countries and continents on a large scale. The IEA predicts significant improvements in energy efficiency in transportation; however, these will be more than offset by increased travel (IEA 2009) and further globalization.

Fuel efficiency in transportation ranges from a few megajoules per kilometer and passenger for a bicycle to several 100 MJ for a helicopter. Approx. 1/3 of the energy consumption in transportation is used for freight movement (Sorrell et al. 2009), which accounts for 8 % of total anthropogenic CO_2 emissions. Most of these emissions stem from trucks (heavy goods vehicles, HGV), which account for most freight activities in most countries, e.g., 68 % of all tonne kilometers in the UK (Sorrell et al. 2009). Ample road networks make cargo distribution by HGV convenient and efficient in terms of time and costs.

Externalities are the costs or benefits that affect parties who did not choose to incur that cost or benefit (Buchanan and Stubblebine 1962). An example for such a negative externality is air pollution or climate change by transportation: The costs are born neither by car producers nor by motorists. For a discussion of freight and transportation externalities, see Ranaiefar and Amelia (2011).

For details on transportation and climate change, see the subsections below and also chapter "▶ Fuel Efficiency in Transportation Systems" in this handbook.

Road Transportation and Internal Combustion Engines

Although rail and ship transportations are more efficient and environmentally benign than road transportation, trucking is still heavily used for reasons of flexibility, costs, and timeliness, not only in weakly developed areas, to move goods and people.

Most vehicles on the road today are powered by internal combustion engines (ICE).

Engine and propulsion system selection for cars is based on various criteria such as driving performance, range, and safety. ICE burn gasoline and diesel, the latter being primarily for trucks. In some countries, cars and trucks with natural gas-, ethanol-, and hydrogen-propelled engines constitute a fleet fraction next to those

with alternative systems such as electrical batteries or air buffer tanks. In Brazil, ethanol fuel has become popular. It is mostly produced from sugarcane, whereas the USA use corn as feedstock. For biodiesel, the Americas use soybean, whereas Europe mainly deploys rapeseed (1st generation biofuels). Hydrogen is chiefly obtained by water electrolysis.

Internal combustion engines have become more efficient over the last decades. The largest losses in gasoline engines are encountered by throttling the engine (Ellinger et al. 2001).

Taylor (2008) estimates that over the next decade, an efficiency improvement of another 6–15 % is feasible. Various optimizations such as direct fuel injection, variable valve timing, supercharging, downsizing, exhaust gas recirculation, onboard fuel reforming, and powertrain improvements, e.g., on the gearbox, are being tested and implemented (Ellinger et al. 2001). The reuse of losses also offers significant potentials, for instance, recuperative braking or the extraction of heat from exhaust gases, as it is a state of the art in power plants (economizers).

Stationary engines, such as large gas engines for power backup or landfill gas use, can be operated in steady mode at optimum efficiency. Combustion engines in mobile machines have to perform well over a wide range of load, which yields poorer overall efficiency.

A novel, promising combustion technology for engines is HCCI (homogeneous charge compression ignition) (Zhao 2007). HCCI is a hybrid between an auto-ignited diesel engine and a spark-ignited Otto engine in that it deploys auto-ignition of a homogeneous fuel-air mixture. Alternative ignition systems (Lackner 2009) such as laser ignition are also expected to improve fuel economy. For a discussion on internal combustion engines for future cars, see Lackner et al. (2005).

Passenger Cars

It is estimated that by 2030, 60 % of all new cars sold will be **hybrids**, plug-in hybrids, and **electric vehicles**, as opposed to 1 % today (IEA 2009). Hybrid cars combine an electric engine and an internal combustion engine. Dual fuel concepts (natural gas and diesel, for instance) are also feasible. The CO_2 intensity of the passenger car fleet in 2030 is estimated to be 90 g of CO_2/km, compared to 205 g/km in 2007, as a worldwide average. In OECD countries, it should reach 80 g, in the EU 70 g, and in India and China 110 and 90 g, respectively, in 2030, the latter ones down from 225 and 235 g, respectively, in 2007 (IEA 2009). On the other hand, a large increase in the global number of cars is anticipated, particularly in developing nations such as China and India.

Hybrids use regenerative breaking to recapture energy that would otherwise dissipate. The effect on fuel economy of such cars is particularly pronounced in stop-and-go city traffic.

Fuel economy of private cars is governed by the following aspects:

- Technology advances of the car, e.g., weight reduction or better engine
- Driving habits (use of air-condition, cruising speed, payload in the car, etc.)

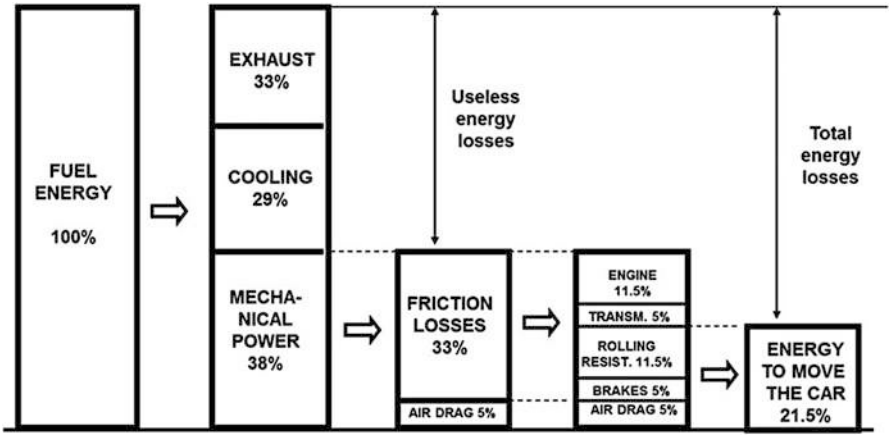

Fig. 10 Energy losses in passenger cars (Reproduced with permission from Elsevier from Holmberg et al. (2012))

- Maintenance (no clogged air filters, correct tire pressure, etc.)
- Weight (lightweight construction materials can save fuel over the entire lifetime)

Figure 10 shows the breakdown of passenger car energy consumption (Holmberg et al. 2012).

In passenger cars, one-third of the fuel energy is used to overcome friction in the engine, transmission, tires, and brakes. The direct frictional losses, without braking friction, are 28 % of the fuel energy. In total, only 21.5 % of the fuel energy is used to move the car.

Potential solutions to reduce friction in passenger cars include the use of advanced coatings and surface texturing technology on engine and transmission components, new low-viscosity and low-shear lubricants and additives, and tire designs with reduced rolling friction (Holmberg et al. 2012).

There is plenty of information available for consumers who want to pick an energy-efficient car, e.g., one website run by the US EPA (http://www.fueleconomy.gov/ 2015).

In California, **partial zero emission vehicles (PZEVs)** were introduced to satisfy part of the state's **zero emission vehicle** (ZEV) program (Collantes and Sperling 2008).

In Johansson and Åhman (2002), options for carbon-neutral passenger transport are reviewed.

Thomas (2009) compares fuel cell and battery electric vehicles. The primary energy efficiencies of alternative powertrains in vehicles are discussed in Åhman (2001)). In Ellinger et al. (2001), the energy efficiency of internal combustion engines and fuel cells for automotive use with different fuels is assessed. It is concluded there that fuel cells have an advantage during hot start conditions, but suffer from efficiency losses during cold starts (Ellinger et al. 2001).

Although the energy efficiency of a fuel cell-powered car is not the best, the environmental performance of a vehicle burning hydrogen from solar generation in a low-noise, virtually emission-free fuel cell is outstanding. It is expected that the fraction of fuel cell cars will increase over the next decade, with an accompanying growth of the necessary infrastructure.

Ships

Nifty percent of the world's trade is carried by the international shipping industry, supported by 50,000 merchant ships (http://www.ics-shipping.org/publications/ 2015). Over the last four decades, total seaborne trade is estimated to have quadrupled, from just over 8,000 billion tonnes-miles in 1968 to over 32,000 billion tonnes-miles in 2008 (http://www.ics-shipping.org/publications/ 2015). In 2011, figures were 42.8 billion tonnes-miles or 8.7 billion tonnes according to UNCTAD (United Nations Conference on Trade and Development) and the ITF (International Transport Forum 2013).

Seaborne shipping is one of the most energy-efficient means of transportation, especially for large, bulky goods.

Here is a comparison of energy efficiency of different transportation modes, taken from a study by the Swedish Network for Transport and the Environment (Table 5) (http://www.ics-shipping.org/publications/ 2015).

It has to be noted that the table above is slightly biased in favor of sea transportation, as the aircraft mentioned is an outdated one used on a short-haul flight.

Ships can be driven by different technologies (Schneekluth and Bertram 1998) with diesel engines being most common. The resistance of the ship's hull, the design or the propeller, and the tonnage are important factors for its energy efficiency as well. The impact of shipping on the atmosphere and on the climate is discussed in Eyring et al. (2010). The auxiliary powering of ships by kitelike devices is discussed in Burgin and Wilson (1985) and Kim and Park (2010). Spinning vertical rotors installed on a ship to convert wind power into thrust based on the Magnus effect, so-called Flettner rotors, are another option to increase energy efficiency. Microbubbles as a means of reducing skin friction on ships are studied in Kodama et al. (2000). Different propulsion systems for LNG carriers are discussed in Chang et al. (2008). LNG (liquefied natural gas) is expected to gain an increasing importance.

Table 5 Energy consumption in different transportation modes (dwt is the deadweight tonnage (also known as deadweight, DW or dwt), a measure of how much weight a ship can safely carry. It is the sum of the weights of cargo, fuel, ballast water, crew, etc.) (Source: http://www.ics-shipping.org/publications/ 2015)

Mode	Air	Road	Sea	Sea
Comment	B727-200 (1,200 km flight)	Medium-sized truck	Cargo ship, 2,000–8,000 dwt	Cargo ship, >8,000 dwt
Energy consumption	4.07 kWh/(ton*km)	0.49 kWh/(ton*km)	0.08 kWh/(ton*km)	0.06 kWh/(ton*km)

Rail Transportation

Intuitively, rail transportation of people and cargo is amongst the most environmentally friendly modes of movement. Technological progress has increased energy efficiency in rail transportation, too. According to Kemp (1997), aerodynamic drag per seat at 150 km/h was cut by half over 30 years. Train speed determines energy efficiency. The energy consumption for a high-speed train from London to Edinburgh increases from 30 to almost 60 kWh/seat as the speed goes up from 225 to 350 km/h (Kemp 1994). The American railway corporation Amtrak reported an energy use of 2,935 BTU per passenger-mile (1.9 MJ/passenger-km) in 2005 (Amtrak 2015).

A critical factor in energy efficiency of trains is the occupancy. If a train is only 25 % loaded, the fuel consumption per passenger and seat can be worse than with economic cars and modern aircraft as shown in Kemp (2004).

For a discussion on the potential role of high-speed trains in future sustainable transportation, see Kamga and Yazici (2014).

Air Transportation

Aviation has helped shape our current business dealings and lifestyles significantly. Virtually any point on the globe has got into easy reach within 24 h. Air transportation is used for cargo and people. It has contributed approx. 3.5 % to global greenhouse gas emissions in 1990 with a projection of 15 % or more in the future (Penner et al. 1999). The impact of aviation on climate change is not only driven by CO_2 emissions but also by H_2O emissions at high altitude (Williams et al. 2002). Due to the long residence time of water vapor at aircraft cruising altitude, it can disproportionally contribute to global warming by reflecting and retaining infrared radiation (compare the effect of natural clouds). Biofuels for aviation (Marsh 2008) were already tested in a proof-of-concept study (BBC 2008), provoking mixed feelings amongst critics. Winglets (Marks 2009) and lightweight materials (Marsh 2007) are two commonly known concepts to increase fuel efficiency of aircraft, hence increasing energy efficiency. See also Figs. 4 and 5.

The impact of service network topology on air transportation efficiency is discussed in Kotegawa et al. (2014).

In a recent study on the impact of airline mergers and hub reorganization on aviation fuel consumption, it was found that a typical airline merger in the USA has a fuel saving potential of 25–28 % (Ryerson and Kim 2014). Renewable fuels in aviation are discussed in Winchester et al. (2013).

Pipeline Transportation

Pipelines (Ellenberger 2010), i.e., conduits of pipe, can be used to transport liquids, gases, and slurries. The Romans built aqueducts for water transportation some 2,000 years ago. An early industrial pipeline was installed in Austria in 1595 to transport brine from Hallstatt to Ebensee for salt production (Bedford and Pitcher 2005). Today, pipelines are commonly used to transport petroleum, natural gas, and other commodities over large distances. A comparison of natural gas transportation by

LNG tankers and pipelines is made in Elvers (2007). LNG compression and regasification consume 7–13 % of the original amount of natural gas, as well as roughly 0.15 % per day of marine transport, which adds about another 1 % to overall energy losses. Pipeline transportation of natural gas results in energy losses of approx. 1 % per 1,000 km. Therefore, an intercontinental 8,000 km pipeline would involve energy losses of roughly 10 %, which is approx. half the amount of transportation by LNG tankers over the same distance (Elvers 2007). The transportation of liquids in pipelines versus onboard of trucks is compared in Pootakham and Kumar (2010) and (Ghafoori et al. (2007). The conveying of coal as slurry in pipelines is assessed in Kania (1984). In industrial plants, pneumatic conveying (dense phase or dilute phase conveying of a solid in air) and hydraulic conveying (solids in liquid carrier media) are used to transport materials between various processing sections. Variable speed drives (VSD) for pneumatic conveying blowers are a means of enhancing energy efficiency versus blowing off excess air at low conveying capacities for the transportation of solids in the gas phase. Kumar et al. (2007) review the transportation of biomass in pipelines. It is concluded that long distances and high throughput rates make such systems economic, as is generally the case with pipeline transportation.

Industry

Industry accounts for a high fraction of the global energy consumption; see Table 1. The energy intensity varies strongly from 52.3 end-use BTUs per USD of value added in cement production to 0.4 end-use BTUs per USD in computer assembly (Granade et al. 2009). Ten end-use BTUs per USD can be set as limit for energy-intensive industries as done in Granade et al. (2009).

There is a huge potential for energy savings in industry, yet the biggest opportunities for optimization are not easily known to the people involved (Yang 2010).

Approximately 2/3 of the energy saving potential can be found in specific process steps of energy-intensive industries, whereas 1/3 resides in various areas of nonenergy-intensive ones. Savings can be realized by more efficient processes or by more efficient equipment.

Crosscutting Technologies

Equipment which is used in different sectors of industry, such as lighting, motors, boilers, and pumps, is subsumed as crosscutting technologies. For these, best practices (see, e.g., US Department of Energy 2010) and general recommendations can be formulated that are valid for several branches and sectors of industry. Generally, there exist untapped-into saving potentials in:

- Waste heat recovery
- Steam systems
- Motor systems
- Pumps (Tutterow et al. 2002)

- Lighting
- Buildings
- Utilities

For quantifying energy efficiency potentials, there are various methods (Phylipsen et al. 1997).

Here are some aspects of energy efficiency that are relevant for many industries:

Process design: The largest contribution to energy efficiency is made during the design of a process. If a product, for instance, has to be heated up and cooled down several times, chances are high that the process is not energy efficient. Also, an implemented production process is difficult to change.

Overcapacity: Design capacity should meet the needs for a process in terms of vessel size, engine power, etc. Overdesign always costs money – not only in the investment phase but most likely also later on, when energy consumption is higher than necessary. Overcapacities of process equipment should normally not exceed 10 % of the overall design capacity.

Debottlenecking: If a plant can be deblottlenecked, i.e., the output can be increased by making some small modifications, one typically has a highly profitable project. Also from an energy efficiency perspective, debottleneckings frequently lower the specific energy consumption of a product, thus making it more energy efficient.

Measuring, monitoring: In order to be able to track energy efficiency measures, it is necessary to measure accurately and regularly actual consumption values of electricity and other utilities such as compressed air or cooling water. Only by monitoring them actively will deviations be spotted.

Automatic controls: Automatic process control is generally faster and more accurate than a manual one and also less prone to errors. Therefore, a production process can be carried out in the most energy-efficient way if it is automatically controlled (Szentennai and Lackner 2014). Automation will be more economic for large processing plants where the investment costs can be diluted over the volume.

Compressed air: Leaks of air from pipes can easily lead to 20–50 % efficiency loss of a compressed air system. Preventive maintenance and the timely repair of leaks will help to minimize running costs. A pressure reduction of the entire system can often be considered, as instrument air (plant air) typically only needs to have ~6 bar pressure, which is less than the design pressure of many compressor systems. If the operating pressure is reduced by just 1 bar, energy savings of over 5 % can result.

Maintenance: If industrial assets are not properly being taken care of, their energy consumption tends to increase. Advanced maintenance techniques such as risk-based maintenance, preventive maintenance, thermography, and others will help to keep energy efficiency up. Cutting costs on maintenance can bring short-term gains at the expense of increased risk and deferred costs. A typical yearly maintenance budget for industrial plants would be 2 % of the investment value, depending of course on the process.

Cogeneration: Production sites that produce their own electricity should seriously consider combined heat and power (CHP). If there is no need for heat in the installation itself, there might be an opportunity to sell the heat, e.g., for district heating purposes. Cogeneration will use the heat which would otherwise be wasted, thereby increasing the energy efficiency. For details, see Raj et al. (2011) and Çakir et al. (2012).

Motors and drives: It is estimated that 2/3 of all electricity consumption in industry is used to drive various motors (US Department of Energy 2010), so there is a huge optimization potential. The "motor challenge" is a recent program to improve motor efficiency (Energy Efficient Motor Driven 2010). Typical energy efficiencies of motors are 80–90 %, with advanced models reaching 97 % (Office of Energy Efficiency, Natural Resources Canada 2002).

Variable speed drives: An engine's energy consumption can be matched to the load by using a variable speed drive (VSD). VSDs can be realized with a frequency converter coupled to an engine. Up to 50 % of energy can be saved. Today, only an estimated 10 % of all engines in industry are equipped with VSD. A large number of motors are still controlled by throttling valves in pump systems or vanes in fan applications. By throttling, a part of the produced output immediately goes to waste. Speed control with intermediate transmission such as belt drives, gearboxes, and hydraulic couplings adds to the inefficiency of the system and requires the motor to run at full speed. Another drawback is that such systems typically require more maintenance. They can be noisy, too.

Pumps: It is estimated that pumps consume 25 % of the electricity in US manufacturing facilities (Galitsky 2008). Industrial pumps have a lifetime of 20 years and longer. Pump efficiency is defined as the pump's fluid power divided by the input shaft power and is influenced by hydraulic effects, mechanical losses, and internal leakages. Pump manufacturers have devised many ways to improve pump efficiencies. For example, the pump surface finish can be made smoother by polishing to reduce hydraulic losses. A "good" efficiency for a pump will vary depending on the type of the pump. A more useful efficiency term is the **wire-to-water efficiency**, which is the product of the pump and motor efficiency. An even better measure of efficiency for analysis purposes is the **system efficiency**, which is defined as the combined efficiency of the pump, motor, and distribution system. See also Tutterow et al. (2002) and "Life Cycle Assessment (LCA)" above.

Blowers and fans: Fans move air as pumps move liquids. They can often be optimized for energy efficiency, e.g., by adding a VSD. For details, see, e.g., Gunner et al. (2014).

Energy management system: An energy management system (EMS) is the energy equivalent of an environmental management system. Generally, industrial sites or units that consume more than 1,000 toe/day should have a dedicated **energy manager**, who will "pay himself/herself" by economizing on energy bills. A guideline for energy management is provided by Office of Energy Efficiency, Natural Resources Canada (2002). The standard ISO 50001 can serve as guidance.

Several smaller units instead of large one: Instead of one large pump which is controlled with a bypass, several smaller pumps might be more energy efficient, matching power consumption to the process needs. The same consideration might work for air compressors, etc.

Energy audit and energy survey: These tools were mentioned already earlier in this chapter in the context of the EU Directive 2012/27/EU of 25 October 2012 on energy efficiency. Energy audits and energy surveys can be administered by internal or external staff. Generally speaking, it is vital for the success of an energy efficiency program in a corporation to have the support of a senior, recognized executive and to make the effort lasting by introducing energy performance indicators, which can be linked to employee's targets and performance management.

Load shifting (using off-peak electricity) (Favre and Peuportier 2014): If energy-intensive production processes can be concentrated in off-peak hours, the energy bill will be lower. This will also have positive effects on the environment, as peak electricity demand often needs to be produced in a not-so-efficient way.
For details, see, e.g., demand side management in smart grid operation in López et al. (2015).

Load shedding (Kanimozhi et al. 2014): By reducing peak electricity consumption, energy costs can also be reduced.

Insulation: Process insulation can be optimized for energy efficiency. A waterlogged insulation transfers heat 15–20 times faster than a dry one, and one filled with ice even 50 times faster (Office of Energy Efficiency, Natural Resources Canada 2002)!

Using waste heat: Heat losses are a major sink for energy. Process heat in general can be upgraded using **absorption heat pumps (AHP)** (Wei et al. 2014). Heat losses in flue gases are a particularly large term: If flue gases exist and the chimney too hot, significant amounts of heat are wasted (up to 1 % of fuel savings for 25 °C colder flue gas temperature (Galitsky 2008)); see also cogeneration. As for **heat exchangers**, cleaning and optimization can bring additional energy efficiency gains (Wang et al. 2009).

An overview on energy efficiency improvement potentials in industry is given in Rajan (2002) and Bannister (2010), the latter focusing on mechanical systems. Industrial energy efficiency in Asia, where a large part of global energy-intensive industry has settled, is treated in United Nations (2006).

Steam and Boilers

Steam engines are gone; however, still 37 % of the fossil fuel burned in the US industry is used to produce steam (Einstein et al. 2001). Steam is the working fluid in steam turbines for electricity production. It is used in various industries to transfer and to store heat, as it is a capacious reservoir for thermal energy because of the high heat of vaporization of water.

The chemical industry uses significant amounts of steam as process heat, one reason being that steam is generated as a by-product in some processes in integrated

chemical production sites. Steam in general can be produced efficiently in cogeneration plants. In contrast to district heating networks to heat private homes, cogeneration plants in industry can be operated at full capacity all year round. Steam is produced in **boilers**. Energy efficiency measures for boilers include:

- Improved process control
- Reduced excess air
- Improved insulation
- Maintenance
- Recovery of heat from flue gas
- Recovery of steam from blowdown
- Optimization of fuel mix

For steam distribution systems, the following measures are effective:

- Improved insulation
- Improved steam traps
- Steam trap monitoring
- Leak repairs
- Condensate return

In Einstein et al. (2001), information on steam systems in industry and their energy use and energy efficiency improvement potentials are outlined. Detailed information on boilers is given in Heselton (2004).

Energy-Intensive Industries

There are certain "heavy industries" that consume a large fraction of total energy output. In China, for instance, the top 1,000 energy-intensive enterprises consumed 30 % of China's total energy and 50 % of the total industrial energy in 2007 (NDRC 2007). Energy intensity is a specific quantity, expressed as kWh/kg of product or as kWh/monetary unit (value added, often in USD). Above an arbitrary threshold of ten end-use BTUs per USD, one can speak about energy-intensive industries (Granade et al. 2009). This classification is valid for the production of:

Cement	(Calcination process, clinker production)
Steel	(Coke consumption)
Aluminum	(Primary metal production by electrolysis)
Ores	(Mining operations)
Pulp and paper	(Mechanical pulping)

These industries have a strong effect on global energy consumption, because they are not only energy intensive as such but because they produce high amounts of materials per year. The global steel production, for instance, is in excess of one million tonnes (Lackner 2010). The IEA predicts big improvements in energy efficiency in industry, which are expected to be more than offset by higher output

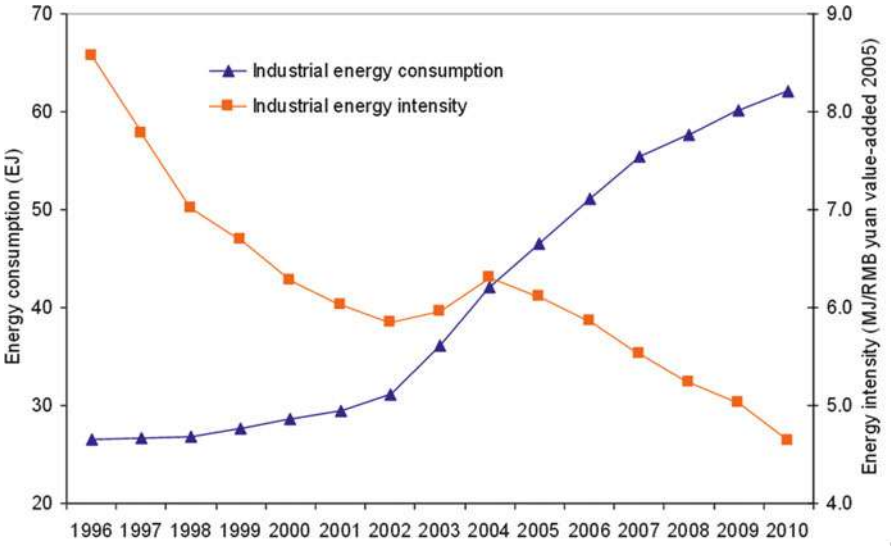

Fig. 11 China's industrial energy consumption and intensity from 1996 to 2010 (Reproduced with permission from Ke et al. (2012))

of steel and cement (IEA 2009), especially in the developing world, to which countries like Brazil, Russia, India, China (BRIC), Mexico, and South Korea belong. Figure 11 shows the trend in China's industrial energy consumption and intensity from 1996 to 2010 (Ke et al. 2012).

The industrial energy consumption of China increased significantly from 1996 to 2010, especially after 2002.

By 2010, China's industrial energy intensity had decreased 46 % below the 1996 level (Ke et al. 2012).

Energy production in China is largely based on coal combustion, with efficiencies being approx. 10 % lower than in Europe or the USA (Nuo and Gaoshang 2008). The CO_2 emissions from coal combustion are naturally higher than those from other fuels with a lower C/H ratio. Several technology options to reduce energy consumption and CO_2 emissions in energy-intensive industries are reported in Yudken and Bassi (2009); see also below.

Iron and Steel

In the iron and steel industry, as the name implies, iron production and steel production are the main processes (Berns et al. 2008). Iron can be produced along different routes. The classic path is the production of pig iron from ore and coke in the blast furnace, which is then further processed into steel in the basic oxygen furnace (BOF) or the open hearth furnace (OHF), the first one being more energy efficient. Smelt reduction and direct reduction (DR) are two other, advanced routes to iron. The electric arc furnace (EAF) is used to produce secondary steel from scrap.

Table 6 Potential technologies to make energy-intensive production processes more efficient (Source: Yudken and Bassi (2009) from IEA, DOE, AISI, Aluminum Association, Korean Energy Institute)

Technology option	Description	Time frame
Pulverized coal and plastic waste injection	Pulverized coal is already used by more than 50 % of all US BOFs	ST-MT
New reactor designs	Uses coal and ore fines (COREX™, FINEX™)	MT
Paired straight hearth furnace	Substitutes coal for coke in blast furnaces, lower costs, uses 2/3 energy	MT-LT
Molten oxide electrolysis	Produces iron and oxygen, no CO_2	LT
Hydrogen flash melting	Uses hydrogen in shaft furnaces, no CO_2	MT
Geological sequestration and steelmaking		MT-LT

ST short term (2010–2015), *MT* medium term (2015–2030), *LT* long term (2030–2050)

In China, the energy consumption per tonne of steel has declined from 1.43 to 0.52 toe between 1980 and 2005 (Wei et al. 2007). Integrated steel plants have a specific primary energy consumption ranging from 19 to 40 GJ/t of steel (Gale and Freund 2014), with minimills that use scrap steel being more efficient. Technology options for reducing energy use and CO_2 emissions in the iron and steel industry are tabulated in Table 6, reproduced from Yudken and Bassi (2009).

Aluminum

Worldwide primary aluminum production is projected to increase from 23 to 38 million tonnes by 2020 (Gale and Freund 2014). The primary aluminum (Moors 2006) production, starting from bauxite via electrolysis (Hall-Héroult process), is a very energy-intensive process, contributing 1 % of total anthropogenic greenhouse gas emissions in 1995 with about 364 million tonnes/year CO_2-equivalent (Gale and Freund 2014).

Secondary aluminum production (Li et al. 2006) consumes approx. 5 % of the energy needed for primary production. Existing and potential future processes for bauxite processing are reviewed in Smith (2009). Technology options for reducing energy use and CO_2 emissions in primary aluminum are summarized in Table 7, reproduced from Yudken and Bassi (2009).

Other Primary Metals

Generally, one can distinguish between pyrometallurgical and hydrometallurgical processes. The ore content of a deposit influences energy efficiency as the chosen process does. The energy demand for comminution is described in Tromans (2008). Energy efficiency of a lead smelter is discussed in Morris et al. (1983), and energy efficiency of copper and magnesium production in Alvarado et al. (2002) and Cherubini et al. (2008), respectively. Processes for the production of steel, aluminum, copper, lead, and zinc are reviewed from an energy perspective in Stepanov

Table 7 Potential technologies to make energy-intensive production processes more efficient (Source: Yudken and Bassi (2009) from IEA, DOE, AISI, Aluminum Association, Korean Energy Institute)

Technology option	Description	Time frame
Wetted, drained cathode technology		MT-LT
Alternative cell concepts	Combines inert anode, drained cathodes	LT
Carbothermic and kaolinite reduction process on commercial scale	Alternatives to the Hall-Héroult process	LT

ST short term (2010–2015), *MT* medium term (2015–2030), *LT* long term (2030–2050)

and Stepanov (1998). Sintering processes and their energy efficiencies are discussed in Musa et al. (2009) for one system, and scale-up in metallurgy in general in Lackner (2010).

Pulp and Paper

The pulp and paper (P&P) industry is a very energy-intensive one.

Pulp is being produced from wood by the kraft process, with electricity as additional input and output, plus steam as an output. An efficient kraft pulp mill can be a net exporter of heat and electricity (Jönsson and Algehed 2010).

Industry practice shows that in the past, most energy-efficient measures were limited to low-investment, high-return projects, with typically 5 % energy savings with a 1-year payback time (Costa et al. 2007), with a lot of potential still untapped into.

In current paper mills, steam savings of up to 30 % are deemed feasible (Kilponen et al. 2001; Costa et al. 2009; Axelsson et al. 2008; Nordman and Berntsson 2009; Lutz 2008).

Energy efficiency savings can be obtained from the use of different fuels, which are typically wood, bunker oil, and black liquor (Costa et al. 2007), the latter being a by-product of the transformation of wood chips into pulp. Typical energy efficiencies in the industry for bark combustion are 67 % (based on the higher heating value) and 80 % for bunker oil combustion, respectively (Costa et al. 2007).

In Jönsson and Algehed (2010), the utilization options for excess steam and heat at kraft pulp mills are studied. Traditional ways are increased electricity production and district heating, whereas increased sales of biomass as bark and/or extracted lignin and carbon capture and storage (CCS) are new pathways.

There is a trend toward additional products, complementing the traditional pulp and paper output, by biofuels, pellets, lignin, carbon fibers, and other specialty chemicals (Jönsson and Algehed 2010) from pulp and paper plants.

In Costa et al. (2007), the economics of **trigeneration** in a kraft pulp mill are discussed. In trigeneration, pulp production, waste heat upgrading, and power production are simultaneously carried out (compare **polygeneration**). Absorption heat pumps (AHP) can be used to cool waste heat streams and to extract energy from them.

Table 8 Potential technologies to make energy-intensive production processes more efficient (Source: Yudken and Bassi (2009) from IEA, DOE, AISI, Aluminum Association, Korean Energy Institute)

Technology option	Description	Time frame
Black liquor gasification	In demonstration, R&D; commercially available 2030; 15–23 % gain	MT-LT
Efficient drying technology	R&D now; commercial demo, 2015–2030; commercial, 2030 onward	MT-LT

ST short term (2010–2015), *MT* medium term (2015–2030), *LT* long term (2030–2050)

Technology options for reducing energy use and CO_2 emissions in the paper and paperboard industry, reprinted from Yudken and Bassi (2009), are summarized here in Table 8.

Recycling is another option to increase energy efficiency of paper products. For details on energy efficiency options in the pulp and paper industry, see Worrell et al. (2001).

Cement

The cement industry, already 15 years ago, exceeded 1.5 billion tonnes of annual output, making it a huge consumer of energy. For cement production, first clinker has to be made, which is then blended with approx. 5–70 % additives such as gypsum and fly ash to yield cement. This first step is the most energy-intensive one. Limestone ($CaCO_3$) is burnt with silicon oxides, aluminum oxides, and iron oxides. There is a wet process and a dry process, the latter one being more energy efficient. As cement plants (Deolalkar 2009) consume significant amounts of energy, approx. 4 GJ/t of cement produced (Khurana et al. 2002), energy efficiency programs have been extensively applied to various plants (da Graça Carvalho and Nogueira 1997; Utlu et al. 2006; Mandal and Madheswaran 2010; Worrell et al. 2000a; Doheim et al. 1987). For each t of cement, approx. 0.5 t of CO_2 are generated (Office of Energy Efficiency, Natural Resources Canada 2002).

In Worrell et al. (2000a), potentials for energy efficiency improvements in the US cement industry are discussed, and in Liu et al. (1995) those for China.

CO_2 and energy intensity reductions in cement production can be achieved by:

- Modification of the product composition (less clinker)
- Use of alternative cements (e.g., mineral polymers)
- Improving the energy efficiency of the process and process equipment
- Introduction of a different process (e.g., change from wet to dry process)
- Replacement of high-carbon fossil fuels by low-carbon fossil fuels

A trend in the cement industry is the use of waste fuels such as tires. Recommendations on energy efficiency and cost saving opportunities for the cement industry can be found in Worrell and Galitsky (2008).

Glass Production

Glass is a ubiquitous material that comes as sheet glass (produced in the float glass process), hollow glass (for glass containers), automotive glass, optical glass, and other glasses such as glass fiber and glass wool. Its production is an energy-intensive process. According to Sheredeka et al. (2001), 74 % of production costs are typically raw materials, fuels, and electricity. Recycling of glass offers a good way of increasing energy efficiency. One recycled bottle can save approx. 0.1 kWh (Glass Manufacturing Industry Council (GMIC) 2015). In http://www.osti.gov/glass/bestpractices.html (2015), best practices for energy efficiency improvements in the glass industry are provided. A detailed treatise of energy efficiency potentials in the American glass industry can be found in Worrell et al. (2008).

Petroleum Refining

In a petroleum refinery (oil refinery) (Fahim et al. 2009), crude oil is processed into various petroleum products such as naphtha, gasoline, diesel, and liquefied petroleum gas (LPG). Refineries are complex, chemical plants that are usually highly integrated. Crackers, for instance, can produce lightweight hydrocarbons as basic feedstock for the petrochemical industry (see also below).

Energy efficiency in a petroleum refinery can be tackled from various angles. Like in industry in general, there is usually optimization potential in cogeneration, steam systems, heat transfer systems, and motors; see also Coletti and Macchietto (2009a, b), Bevilacqua and Braglia (2002), Wenkai et al. (2003), Fath and Hashem (1988), Najjar and Habeebullah (1991), and McKay and Holland (1981) for details reported in the literature. Worrell et al. (1994a) estimated the energy saving potential for refineries to be around 15 %.

The determination of the energy efficiency of a certain process is a somewhat tricky task, as it depends on boundary limits to be drawn. Alireza Tehrani Nejad (2007) attempts to allocate CO_2 emissions in petroleum refineries to various petroleum products. One aspect of the petrochemical and chemical industry in general that has to be noted here with respect to energy efficiency is that the energy contained in the feedstock is partly converted to heat and power but also remains in the final products to some extent, providing potentials for recycling at the end of the various materials' lifetimes (feedstock recycling or thermal recycling).

Recommendations on energy efficiency and cost saving opportunities in refineries can be found in Worrell and Galitsky (2005).

Petrochemicals

Petrochemicals are products derived from petroleum (Meyers 2004) other than fuels for combustion. The petrochemical industry consumes approx. 8 % of total oil production for the manufacture of various products (The International Energy Association in Collaboration with CEFIC 2007) ranging from plastics, rubbers, and solvents to various fine chemicals. Two important upstream processes are **cracking** (fluid catalytic cracking, steam cracking) for the production of olefins such as ethylene and propylene and **reforming** (catalytic reforming) for the production of aromatics.

Table 9 Potential technologies to make energy-intensive production processes more efficient (Source: Yudken and Bassi (2009) from IEA, DOE, AISI, Aluminum Association, Korean Energy Institute)

Technology option	Description	Time frame
High-temperature furnaces	Able to withstand more than 1,100 °C	MT-LT
Gas turbine integration	Higher-temperature CHP for cracking furnace	MT-LT
Advanced distillation columns		MT-LT
Combined refrigeration plants		MT-LT
Biomass-based system options	Feedstock substitution	LT

ST short term (2010–2015), *MT* medium term (2015–2030), *LT* long term (2030–2050)

Worldwide, more than 10^7 t of propylene, $6.5*10^6$ t of ethylene, and $7*10^6$ t of aromatics are produced per year. From these primary petrochemicals, to which also synthesis gas can be counted, a wide range of chemical products is made. Energy efficiencies of a steam cracker are reported in Tuomaala et al. (2010) and Ren et al. (2008). Naphtha crackers are estimated to consume 31.5 GJ/t of energy (Worrell et al. 2000b).

The gross energy requirement (GER) for major petrochemical products such as ethylene, propylene, butadiene, and benzene is reviewed in Worrell et al. (1994a).

Technology options for reducing energy use and CO_2 emissions for petrochemicals are shown here in Table 9, from Yudken and Bassi (2009).

Below, details on some petrochemical products with respect to energy efficiency are reviewed.

Polymers

The polymer industry has ramped up plastic production between 1950 and 2007 from 1.5 to 260 million tonnes (Johansson 2015) worldwide, which corresponds to an annual growth rate of more than 9 %, making plastics ubiquitous and versatile construction materials. Today, plastic production has reached 300 million tonnes per year (http://www.essentialchemicalindustry.org/processes/recycling-in-the-chemical-industry.html 2015). Polyolefins are the most common plastics, with polyethylene (PE) and polypropylene (PP) accounting for the largest fraction, followed by polyvinylchloride (PVC), polystyrene (PS) and expanded polystyrene (EPS), polyethylene terephthalate (PET), polyurethane (PUR), and others, e.g., engineering plastics such as polycarbonate (PC).

Polymers can be produced with different technologies, ranging from radical reactions (high-temperature and high-pressure processes such as for high-density polyethylene (HDPE)) to catalytic processes (at more moderate conditions), which show varying energy efficiencies.

The gross energy requirements for the production of low-density polyethylene (LDPE), PP, PS, and PVC are 69.8, 61.6, 81.5, and 55.7 GJ/t, respectively (Worrell et al. 1994a). Plastic production uses 8 % of the world's oil production, 4 % as feedstock and 4 % during manufacture (University of York 2010).

Cogeneration and heat recovery in polymerization processes are discussed in Budin et al. (2006).

In Europe, the recycling rate of plastics has reached 51.3 % (21.3 % recycling and 30.0 % energy recovery, i.e., combustion) (Johansson 2015).

Worrell et al. (1994a) investigated potential energy savings in the production of plastics. That study found that the technical potential for energy efficiency savings varies from 12 % for PE to 25 % for PVC. Further information on energy use in plastic production can be found in Patel and Mutha (2004).

Alternative feedstocks, biopolymers, and feedstock recycling (Scheirs 2006) are emerging trends in the industry with impact on energy efficiency.

Chemical Industry

The chemical industry uses crude oil, natural gas, and coal, apart from electricity, both as raw materials and as fuels to produce more than 50,000 different products. More than half of the energy used by the chemical industry is processed as feedstock, which means that it is transformed into various products such as chemicals or polymers. Most energy is consumed by the production of a few small, intermediate compounds. In the chemical industry, energy costs account for 10–15 % of total manufacturing costs (Bieling 2007). For some processes such as electrolysis, energy costs can exceed 50 % of production costs. The DOE estimates potential energy savings within the chemical industry to be approximately 20 %.

Strategies to improve energy efficiency in the chemical industry are process improvements, cogeneration, integration, and the introduction of energy management systems (EMS).

Integration means that rather than producing a single chemical, a production location should strive to use its feedstock to make the desired final product, while utilizing by-products as well. If several production steps, such as crude oil distillation, cracking, and polymerization, can be done in one location, costly and wasteful transportation and storage steps can be avoided (compare the German concept of an integrated chemical complex, the "Verbund." At the largest chemical Verbund site, BASFs, Ludwigshafen, synergies amount to 500 million € per year, 150 million € out of which are attributed to energy savings (The International Energy Association in Collaboration with CEFIC 2007)).

Process design is also an important consideration for energy efficiency, as different unit operations (McCabe et al. 2004) have varying energy demands.

In Worrell et al. (2000b), energy use and energy intensity of the US chemical industry are analyzed. A general review on sustainability and energy efficiency in the chemical industry is provided by de Swaan Arons (2010).

Below, some details on various products of the chemical and process industries with respect to energy efficiency are compiled.

Actual energy consumption values for the production of chemicals are significantly higher than the theoretical demand stipulated by thermodynamics.

A "clean-sheet redesign," not considering cost-effectiveness, would offer a potential for energy savings in chemical production of up to 95 % (Granade et al. 2009; Hinderink et al. 1999).

Catalysts, as they lower the activation energy, can generally increase energy efficiency, particularly enzymatic catalysts for several particular reactions.

Process intensification and **polygeneration** are two emerging technologies that could reduce energy demand in the chemical industry.

By process intensification (Etchells 2005), more compact and efficient plants can be designed. Polygeneration using natural resources is detailed in Serra et al. (2009).

An overview on energy efficiency in the chemical industry is provided in Worrell and Blok (1994) and Worrell et al. (1994a, b, 2000c). **Green chemistry** is discussed in Poliakoff et al. (2002) and Anastas and Warner (2000).

Ammonia

Ammonia is one of the inorganic chemicals with the highest yearly production volume. Its global consumption is in excess of 10^7 t. NH_3 is the precursor to most industrially produced nitrogen-containing compounds. More than 80 % of ammonia is processed to fertilizers. Ammonia production consumes more than 1 % of all man-made power (Max Appl 2006). CO_2 emissions in ammonia production are estimated to be 1.58 t for each t of the product (Office of Energy Efficiency, Natural Resources Canada 2002). Energy consumption is quoted as 39.3 GJ/t for feedstock (natural gas) plus 140 kWh/t electricity, totaling to 40.9 GJ/t (based on higher heating value, corresponding to 37.1 GJ/t based on lower heating value) (Worrell et al. 2000b). Without considering the natural gas, the primary energy consumption for ammonia production is 16.7 GJ/t (Worrell et al. 2000b).

For energy efficiency studies and improvement potentials in ammonia production, see Panjeshahi et al. (2008) and Rafiqul et al. (2005). The use of ammonia as a fuel is described in Zamfirescu and Dincer (2009).

The specific energy consumption for the production of urea is estimated at 2.8 GJ/t (1994) (Worrell et al. 2000b).

Fertilizers

Nitrogen-bearing fertilizer production is a very energy-intensive industry. Ammonia is the most important intermediate chemical compound here (see also above). Table 10 shows the energy use and emission intensity for the production of various fertilizer components, reprinted from Wells (2001):

An early review on energy efficiency in fertilizer production is provided by Mudahar and Hignett (1985). Energy efficiency in the fertilizer industry is reviewed in Ladha et al. (2005), Abdul Quader (2003), Kumar (2002), Mudahar and Hignett (1985), and Fadare et al. (2010).

Nitrogen fertilizer production has an additional impact on climate change, mainly via N_2O emissions (Stuart et al. 2014).

Table 10 Energy requirements to manufacture fertilizer components plus associated CO_2 emissions (Source: Wells 2001)

Component	Energy use [MJ/kg]	Emissions [kg CO_2/MJ]
N	65	0.05
P	15	0.06
K	10	0.06
S	5	0.06
Lime	0.6	0.72

Methanol

Methanol can be produced by steam reforming from methane (Rosen and Scott 1988). It can also be obtained from coal (Li et al. 2010) and various biomass products (Hamelinck and Faaij 2002) such as sugarcane. Methanol has seen increased interest for its use in:

- Direct methanol fuel cells (Jiang et al. 2004)
- Fuel for combustion engines (Agarwal 2007)
- Feedstock for chemical industry (Olah et al. 2009)

In 1994, the specific energy consumption for the production of methanol was 38.4 GJ/t (based on higher heating value) (Worrell et al. 2000b). Best practice in 2013 was 9.0–10.0 GJ/t.

Figure 12 shows today's energy losses in the chemical industry for the major chemicals, amongst them methanol. Catalysis bears a great potential for further energy reduction (DECHEMA 2013).

Industrial Gases

A wide variety of gases is industrially produced and sold in compressed or liquid state. Apart from air, oxygen and nitrogen are amongst the most commonly used industrial gases (Häring et al. 2007), others being argon (welding), carbon dioxide, and methane. Oxygen and nitrogen have traditionally been produced through cryogenic air separation where air is cooled and pressurized until it becomes a liquid with

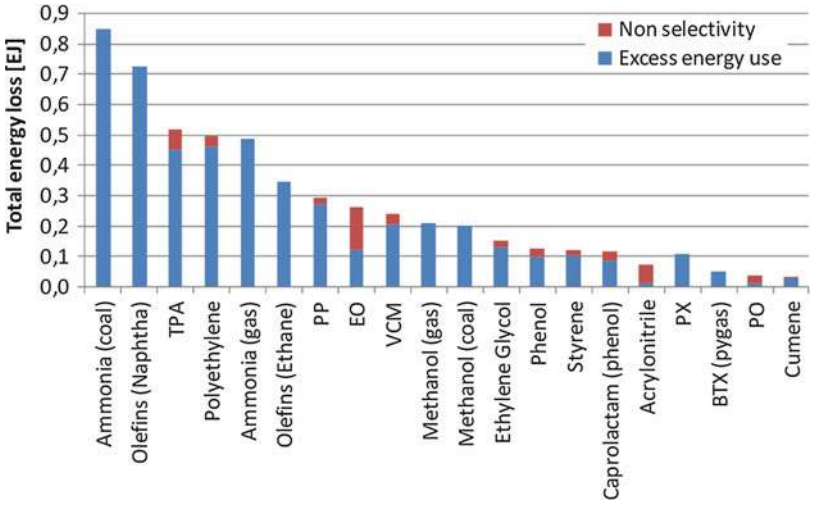

Fig. 12 Cumulated theoretical total energy loss for major chemical processes based on 2010 production volumes (Source: DECHEMA 2013). *TPA* terephthalic acid, *PP* polypropylene, *EO* ethylene oxide, *VCM* vinyl chloride monomer, *PX* paraxylene, *BTX* benzene, toluene, xylene, *pygas* pyrolysis gasoline, *PO* propylene oxide

the various gases being extracted through fractionated distillation. The associated energy consumption is estimated to be 1.8–2.0 GJ/t of oxygen or nitrogen (Worrell et al. 2000b).

Other energy-efficient technologies such as pressure swing adsorption (PSA) (Sharma 2009) and membrane separation (Koros and Fleming 1993) are increasingly used.

For a comparison of cryogeny versus membranes for oxygen-enriched air (OEA) production, see Belaissaoui et al. (2014).

Methane can be produced through anaerobic fermentation (biogas) and methanogenesis (through bacteria). Also, hydrogen can be produced by bacteria (Xia et al. 2014); see also below.

An article on energy efficiency gains in gas production (thermal gasification) is given by Kumar et al. (2010).

Chlorine

Chlorine is produced through electrolysis of a salt solution (brine), which is an energy-intensive process requiring between 3,065 and 3,960 kWh/t (Worrell et al. 2000b). The coproducts caustic soda (sodium hydroxide, NaOH) and hydrogen gas (H_2) are obtained, with the major markets for chlorine being PVC (polyvinylchloride) manufacturing, inorganic chemicals, propylene oxide, water treatment, and organic chemicals.

The chlorine industry is reviewed in Johnston and Stringer (2001).

Technology options for reducing energy use and CO_2 emissions in chlor-alkali manufacturing are summarized from Yudken and Bassi (2009) in Table 11.

Hydrogen

Hydrogen is regarded as an interesting option, as transportation fuel, and as storage medium for electricity, being produced from renewable resources. The "hydrogen economy" (Ball and Wietschel 2009) is often seen as a straightforward solution to many issues around pollution and global warming. Despite all the potential that lies in the technical exploitation of hydrogen, it needs to be borne in mind that the hydrogen – as clean as it is as such – has to be produced. Hydrogen from nuclear power is treated in Hori (2008) and Yildiz and Kazimi (2006).

It is the overall energy efficiency (system efficiency) that will determine whether hydrogen will be used on a large scale as energy carrier. For details, see Page and Krumdieck (2009).

Table 11 Potential technologies to make energy-intensive production processes more efficient (Source: Yudken and Bassi (2009) from IEA, DOE, AISI, Aluminum Association, Korean Energy Institute)

Technology option	Description	Time frame
Convert mercury process and diaphragm process plants to membrane technology	Combined electrolytic cell with a fuel cell, using hydrogen by-product	MT-LT

ST short term (2010–2015), *MT* medium term (2015–2030), *LT* long term (2030–2050)

A comparison of thermochemical, electrolytic, photoelectrolytic, and photochemical solar-to-hydrogen production technologies is made in Wang et al. (2012).

Pharmaceutical Industry

The US pharmaceutical industry has energy expenses of approx. one billion USD per year (Galitsky 2008), which, being only a small fraction of total production costs, is still significant, given the fact that energy savings will translate into direct and predictable earnings. In the pharmaceutical industry, there are three overall stages:

- R&D
- Production of bulk pharmaceutical substances
- Formulation of the final products

Table 12 shows the distribution of energy use (Galitsky 2008) in this sector.

Twenty-five percent of the total energy is used for plug loads and processes, 10 % for lighting, and 65 % for HVAC (heating, ventilation, and air-conditioning). The biggest potential can hence be found in R&D and bulk manufacturing.

Public Sector and Community Infrastructure

The public sector is another area where energy efficiency potential exists.

Awareness of energy efficiency and conservation is a major topic. In a typical office, nearly 40 % of the electricity consumption occurs after closing hours (Danish Ministry of Transport und Energy 2005). In China, the energy consumption in the building sector is 25 % of total energy consumption. The energy use in urban buildings in megacities like Beijing and Shanghai are about 90 % of the whole energy consumption in buildings (Jiang 2011). It was found that amongst these urban buildings, the energy use in **public buildings** is higher than in other building sectors (Jiang 2011). China's Ministry of Construction has issued six energy efficiency design standards to the building sector since 1995, where the latest one is the design standard for energy efficiency in public buildings, aiming at a 50 % reduction of energy consumption in new and refurbished public buildings. Beijing and

Table 12 Pharmaceutical industry and energy use (Source: Galitsky 2008)

Area	Distribution of energy use (%)
R&D	30
Offices	10
Production of bulk pharmaceutical substances	35
Formulation, packaging, and filling	15
Warehouse	5
Miscellaneous	5
Total	100

Shanghai governments have also issued their local energy saving standards for public buildings with 65 % and 50 % of energy saving, respectively (Jiang 2011).

Government institutions can apply energy-efficient procurement and create awareness for energy savings. Public buildings (see also next section) offer energy efficiency increase potential, as does, for instance, the lighting infrastructure of public roads.

For enhancing energy efficiency in public buildings, local energy audit programs were found to be successful (Annunziata et al. 2014).

Energy efficiency in **public lighting** is discussed in Radulovic et al. (2011).

Desalination plants are important in several parts of the world. Their energy efficiencies for different technologies are assessed in Mesa et al. (1997), Tay et al. (1996), Al-Kharabsheh (2006), Gomri (2009), and Charcosset (2009).

Another important infrastructure is **data centers**. Their energy efficiency is discussed, e.g., in Todorovic and Kim (2014).

Buildings

Buildings have a strong and long-lasting impact on global energy consumption, because they are constructed for typically 50–100 years. In 2005, 39 % of the total energy consumption in the USA stemmed from commercial and residential buildings (US Green Building Council 2015). They accounted for as much as 70 % of total electricity consumption (US Green Building Council 2015). There is hence a huge potential for what is known as **green buildings**.

The residential sector in the USA is expected to account for 29 % of the US energy consumption in 2020 (Granade et al. 2009), driven by population growth, larger homes, and more electric and electronic gadgets in private households. The specific energy use for heating of buildings, a major parameter for their energy efficiency, is given in kWh/(m^2*year).

Key determinants for energy efficiency of buildings are:

- Location and surroundings
- Insulation
- Heating technology

Sealing of ducts, basement insulation, and improved heating equipment are seen as major efficiency opportunities in private homes in the USA (Granade et al. 2009).

Heat pumps are particularly energy efficient. There are three types of heat pumps: air to air, water source, and ground source. Ground source heat pumps typically use four times less electrical energy than direct electrical heaters.

Deviations in energy efficiency from the design requirements to actual performance may come from:

- Errors in the design
- Errors in the construction

- Incorrect operation
- Lack of maintenance
- Changed use of the building

Various tools, such as an **energy survey** or an **energy audit**, can help uncover efficiency potentials.

On average, heating and cooling account for almost half of a typical utility bill. Drafty rooms can be improved by checking windows and doors. The HVAC (heating, ventilation, air-conditioning) system often offers potential for improvement and so does the lighting. Compact fluorescent lights (CFL) are more efficient than electric bulbs.

Passive buildings (Miller et al. 2009) and **zero net energy (ZNE) buildings** (Hernandez and Kenny 2010; Elkinton et al. 2009) are more energy efficient than traditional ones. For ZNE buildings, **embodied energy** (Venkatarama Reddy and Jagadish 2003) can be considered. This is the quantity of energy required to manufacture and transport the materials utilized for their construction.

According to Venkatarama Reddy and Jagadish (2003), the total embodied energy of load-bearing masonry buildings can be reduced by 50 % when energy-efficient/alternative building materials are used.

Landscaping around private homes can also bring measurable energy savings. Carefully positioned trees can save up to 25 % of a household's energy consumption for heating and cooling. They can, apart from giving a nice appearance, provide shade and shelter from wind. Payback times for such planting measures can be as low as several years (DOE 1995).

Microgeneration for individual houses is another interesting technology option for the energy savvy.

A small combined heat and power (CHP) system to produce electricity and heat for a community or a single household is known as microgeneration (Entchev et al. 2004). The most promising technologies are Stirling engines and fuel cells in a size range of approx. 1–10 kW_e. Total efficiencies can be typically 80–88 % (Entchev et al. 2004).

It is estimated that in US buildings, 1/3 of the total energy consumption can be saved at a cost of 2.7 $c/kWh (Brown 2008); see also for natural gas savings there. Figure 13 shows the electricity saving potential for the residential area, and Fig. 14 the same scenario for the commercial sector.

It can be seen in Fig. 13 that in the residential area, a huge potential exists for TV sets, lighting, and space cooling, with freezers already being rather optimized. Figure 14 takes a look at the commercial sector.

In the commercial sector, space cooling and lighting offer large potential, with the most cost-effective opportunities residing in space heating and ventilation. Energy efficiency in the residential area is covered in International Energy Agency (2008). A guide on energy efficiency for home owners can be found in Krigger and Dorsi (2008).

Smart metering has been suggested for enhancing residential energy efficiency (Anda and Temmen 2014).

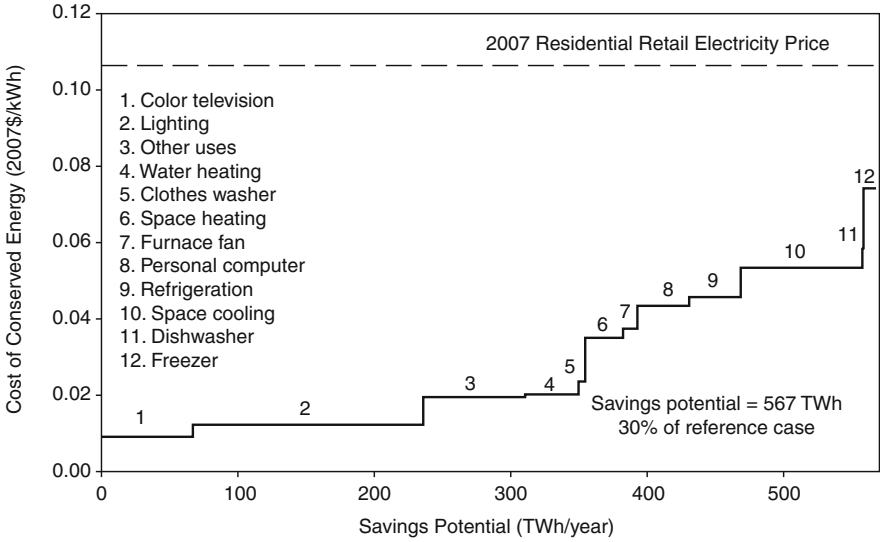

Fig. 13 Residential electricity saving potential in the year 2030 (Reprinted with permission from Brown (2008))

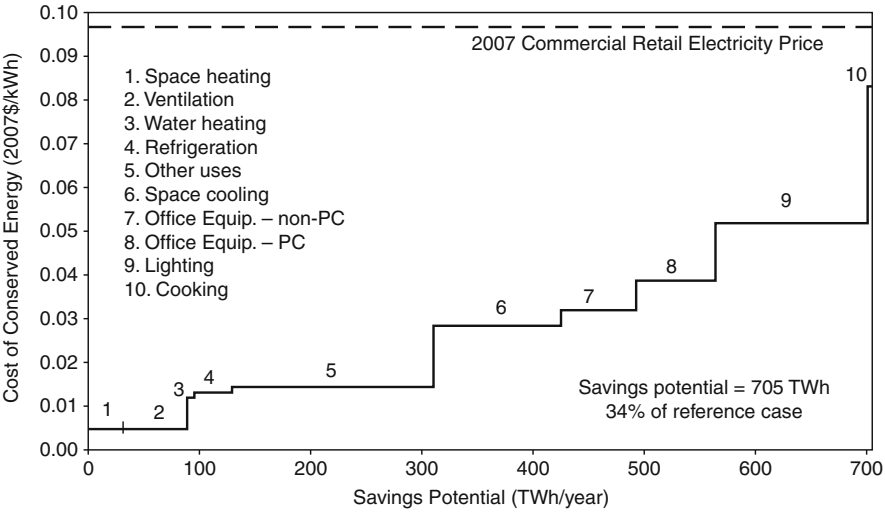

Fig. 14 Commercial electricity saving potential in the year 2030 (Reprinted with permission from Brown (2008))

Appliances

Appliances are a collection of electrically powered devices, which can be found in nearly every household. They account for approx. 20 % of a typical household's energy consumption, with refrigerators, washing machines, and dryers at the top of the consumption list. A "cheap" device can become very costly over its entire lifetime of up to 10 or 20 years (see TCO concept above).

In 1978, California took a leading national role in the USA by establishing the first building and appliance standards in the country. Nearly 85 % of all dishwashers in California are Energy Star™ compliant (see later), and 50 % of refrigerators and washing machines conform to these standards, too. What is even more impressive, however, is that this increase in market share occurred within no more than 7 years; see Fig. 15, reprinted with permission from Next 10's California Green Innovation Index (2010).

Typical renewal cycles of appliances in industrialized countries, here the USA, are shown in Fig. 16, reprinted from Okura et al. (2006).

Modern appliances consume significantly less energy than older ones.

Lighting

Lighting has played a large part in the public discussion on energy efficiency. As traditional incandescent bulbs, which have an efficiency on the order of 1 % to produce light, are being phased out in many countries, mild panic-buying could be observed in 2009 (Jamieson 2009). Some consumers oppose the compact fluorescent lights (CFL), which typically cost four times as much as traditional bulbs. The fact that their energy consumption is one-fifth and that payback times are typically short has not convinced all consumers (yet). There are reservations against the hue of the

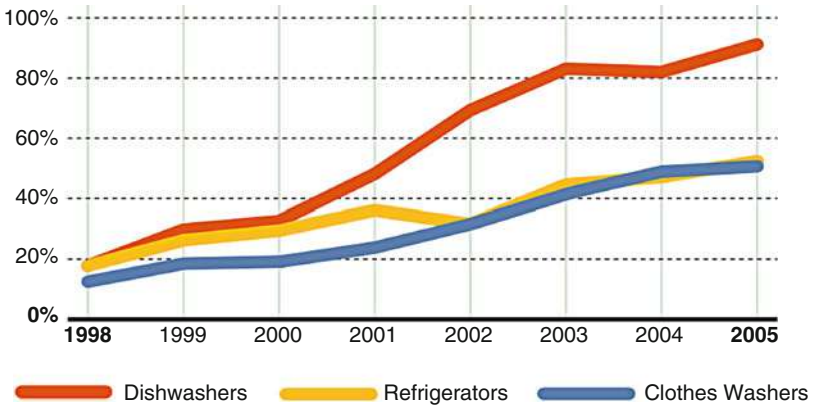

Fig. 15 Market share of Energy Star™ appliances in California (Reprinted with permission from Next 10's California Green Innovation Index (2010))

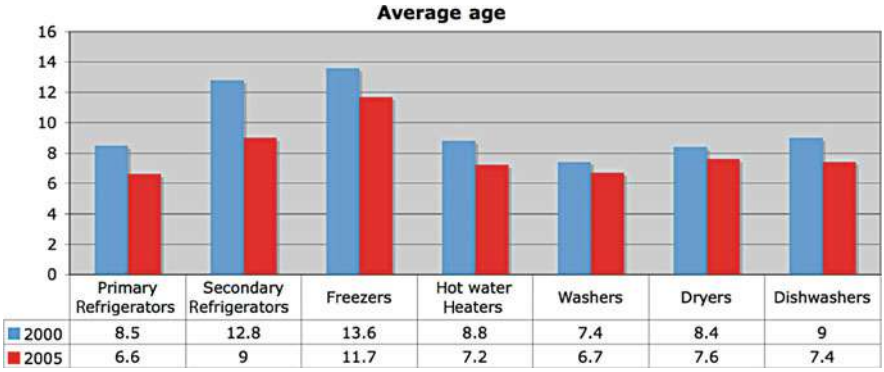

Fig. 16 Appliance renewal cycles (Reprinted with permission from Okura et al. (2006))

Table 13 Number luminous flux emitted by common light sources (Reproduced with permission from Gan et al. (2013)). Lumen is the SI unit of luminous flux, a measure of the total quantity of visible light emitted by a source

Lamp	Lamp wattage	Lumens
Incandescent lamp	75 W	950
Compact fluorescent lamp	15 W	810
Fluorescent lamp	36 W	2,400
LED	18 W	1,600

CFL's light. CFL that work in dimmers tend to cost more than standard CFL. In Techato et al. (2009), a life cycle analysis of CFL is made. An alternative to CFL is light-emitting diodes (LED) (Principi and Fioretti 2014; Gan et al. 2013). For a comparison of typical light sources, see Table 13.

Consumers

Up to 2/3 of household energy use is for space heating, water heating, and refrigeration (Granade et al. 2009) with lighting playing a lesser role. Another significant share is held by the "**plug load**". "Plug load" is a collective term for electrical devices and small appliances. These are virtually hundreds of small devices in private homes, consuming electricity. The biggest shares are held by TV sets (22 %), DVD players (5 %), PCs (5 %), and microwave ovens (3 %) (Granade et al. 2009). **Standby power consumption** is a huge energy waster. In Japan, the annual per household standby electricity consumption could be reduced from 437 to 308 kWh from 2002 to 2005 (Granade et al. 2009). Figure 17 shows typical energy expenditures for Swedish households, reproduced from Nässén et al. (2008).

It is assumed that with a tripling of energy prices, energy use of private households would decrease by 30 % (Nässén et al. 2008). Energy consciousness of consumers has increased over the last years, partly induced by various initiatives such as Energy Star™; see also below.

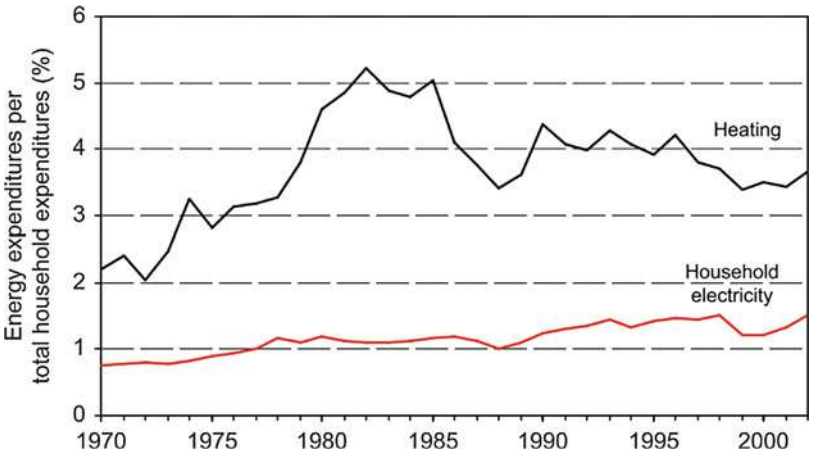

Fig. 17 Annual average of expenditures of households on energy for heating and electricity (Reprinted with permission from Elsevier from Nässén et al. (2008))

Tips and Tricks for Consumers

There are plenty of tips and tricks in various organizations' and authorities' brochures and Internet pages for consumers on how to lower their utility bills. Most of them are commonsense, but it is worthwhile to take a look at them to capture some fast savings. Here are a few examples of often unused potential in private homes:

- The temperature of the refrigerator is too low.
- The refrigerator is positioned in a confined space.
- The washing machine is operated half empty with too warm water temperature.
- Open food is stored in refrigerators (liquids need to be covered, and food should be wrapped to avoid moisture release).
- Untight windows.
- Time is not considered (peak electricity is most costly).

Ample advice on how to save energy (energy conservation and energy efficiency) in the household can be found in the internet, e.g., from governmental sites such as (http://energy.gov/energysaver/articles/energy-saver-guide-tips-saving-money-and-energy-home 2015) or organizations like the OECD (http://www.oecd.org/greengrowth/40317373.pdf 2015).

Initiatives for Energy Efficiency

Energy efficiency improvements do not come "naturally", at least not at the desired speed. In order to overcome the known barriers toward energy efficiency, which were outlined above in this chapter, government action can help. Numerous programs and initiatives to educate people about and to promote energy efficiency have

been started by governments, NGOs (nongovernmental organizations), NPOs (non-profit organizations), for-profit entities, and visionary individuals such as business owners and public celebrities. One such initiative is **Energy Star™**.

The Energy Star® label is used to identify energy-efficient appliances. It was initiated by the DOE (US Department of Energy) and the EPA (US Environmental Protection Agency). Products with the Energy Star™ label usually exceed minimum efficiency standards by a substantial amount.

More information on Energy Star® can be found at (http://www.energystar.gov/ 2015) and (http://www.eu-energystar.org/ 2015). The impact of agreements on energy efficiency is reviewed in Grossman and Krueger (1991).

Other Aspects

There are countless areas for hidden or for indirect energy efficiency improvements, some of which are being touched upon here.

Advanced **packaging**, for instance, can save substantial amounts of materials to achieve the same level of good protection. Lightweight packaging will make transportation over long distances more energy efficient. One example is the replacement of bulky glass bottles by composite containers of (recycled) cardboard and plastics.

In **information technology** (IT), there is often an untapped potential for energy savings and efficiency improvements. Anyone who has witnessed the large air-conditioning systems for server rooms will immediately see the potential offered by what has become known as **green computing**. More details can be found in Minas and Ellison (2009) and Namboodiri (2009).

The **service sector** can also contribute to more energy efficiency. **Electronic banking, video telephony,** and **teleconferencing** (Liang et al. 2007), **telecommuting** (Nelson et al. 2007; Rhee 2008), and **fleet management** (D'Agosto and Ribeiro 2004) are just a few examples where energy for traveling can be economized.

In general, shifting employment and economic activity from manufacturing to the service sector saves energy and cuts greenhouse gas emissions, because the service sector is much lower in energy intensity.

Energy efficiency potentials in hospitals are discussed in Sloan et al. (2009).

Energy efficiency under extreme conditions is reviewed in Tin et al. (2010).

Energy Conservation

Being a broader term than energy efficiency, energy conservation is about using less energy, with a lower energy service being delivered. Sometimes, it is used synonymously with energy efficiency. Energy saving is without doubt the quickest, most effective, and most cost-efficient way for reducing greenhouse gas emissions, as well as improving air quality, especially in developing countries and in densely populated areas. An example of energy conservation on a private level is, for instance, driving

less with one's car. An organization can study its office lighting setup to remove costly over-illumination, for example.

For more information on energy conservation, see Thumann and Dunning (2008), Patrick et al. (2007), Chirarattananon and Taweekun (2003), Jin et al. (2009), Markis and Paravantis (2007), Lin (2007), and Al-Mofleh et al. (2009).

Further Study and Reading

In this section, a few terms that are related to energy efficiency were compiled as a starting point for further exploration by the interested reader.

Dematerialization: By this expression, one can understand the decline of weight and "embedded energy" (cf. embodied energy) of materials in industrial end products over time or, more broadly speaking, the absolute or relative reduction in the quantity of materials required to serve economic functions (Wernick et al. 1996; Tapio et al. 2007). On the one hand, one can observe a decline in weight of certain good such as PCs; on the other hand, people tend to use more materials as their comfort level increases (e.g., larger homes, larger cars). Trends of dematerialization are reviewed in Wernick et al. (1996). A similar term is **ephemeralization**, which was coined by R. Buckminster Fuller. It is the ability of technological advancement to do "*more and more with less and less until eventually you can do everything with nothing*" (Buckminster Fuller 1973).

Industrial Ecology: Being defined as a "systems-based, multidisciplinary discourse that seeks to understand emergent behaviour of complex integrated human/natural systems" (Allenby 2006), industrial ecology strives at sustainability and eco-efficiency. More information on the topic can be found in Frosch and Gallopoulos (1989).

Eco-efficiency: According to the World Business Council for Sustainable Development (WBCSD), it is expressed as:

- Reduction in the material intensity of goods or services
- Reduction in the energy intensity of goods or services
- Reduced dispersion of toxic materials
- Improved recyclability
- Maximum use of renewable resources
- Greater durability of products
- Increased service intensity of goods and services

More information can be found in World Business Council for Sustainable Development (WBCSD) (2000).

Water efficiency: Water efficiency is closely linked to water conservation. It can be defined as the accomplishment of a function, task, process, or result with the minimal amount of water feasible. Effluent reuse is one important means of achieving water efficiency (White and Howe 1998). It is estimated that each m^3 of water utilized in the industrial and service sectors generates at least 200 times more wealth

than it does in the agricultural sector (Beaumont 2000). This suggests that water-intensive production will be shifted from arid regions to those with more water (compare the shift of CO_2-intensive production to certain areas). Here, the concept of **virtual water** (Allan 2005; Chapagain 2006) steps into place. Virtual water, also called **embedded water, embodied water**, or **hidden water**, refers to the water needed to manufacture a good or service.

Yearly individual water consumption is on the order of 1 m^3 for drinking, 100 m^3 for domestic use, and 1,000 m^3 embedded in food. This shows that the concept of virtual water is closely linked to water efficiency and ultimately to energy efficiency.

Other burning topics related to energy are the **affordability** of energy and **access** to **energy**, which are both not secured for a high number of people.

Conclusions

This chapter has taken a look at energy efficiency in industry, transportation, the private sector, and other areas, exploring a topic of high relevance for climate change mitigation. Energy use efficiency is the cheapest and easiest source of energy, with a huge unused potential. It is estimated that up to 1/3 of the worldwide energy demand in 2050 can be saved by energy efficiency measures.

In its "International Energy Outlook 2014," the EIA (US Energy Information Administration) mentions a growing energy efficiency in the transportation sector, which, in OECD Europe, already induced a decline in consumption of liquid fuels (EIA (US Energy Information Administration) 2014). Energy efficiency has started to proliferate, and there is still a lot of potential.

In this chapter, aspects of energy efficiency from various sectors were presented, spanning historic data, current levels, and future trends. An emphasis is placed on providing brief information and references on how energy efficiency improvements can be realized.

References

Abdul Quader AKM (2003) Natural gas and the fertilizer industry. Energy Sustain Dev 7(2):40–48

Agarwal AK (2007) Biofuels (alcohols and biodiesel) applications as fuels for internal combustion engines. Prog Energy Combust Sci 33(3):233–271

Åhman M (2001) Primary energy efficiency of alternative powertrains in vehicles. Energy 26(11):973–989

Al-Kharabsheh S (2006) An innovative reverse osmosis desalination system using hydrostatic pressure. Desalination 196(1–3):210–214

Allan JA (2005) Virtual water: a strategic resource global solutions to regional deficits. Ground Water 36(4):545–546

Allenby B (2006) The ontologies of industrial ecology. Prog Ind Ecol 3(1/2):28–40

Al-Mansour F, Merse S, Tomsic M (2003) Comparison of energy efficiency strategies in the industrial sector of Slovenia. Energy 28(5):421–440

Al-Mofleh A, Taib S, Mujeebu MA, Salah W (2009) Analysis of sectoral energy conservation in Malaysia. Energy 34(6):733–739
Alvarado S, Maldonado P, Barrios A, Jaques I (2002) Long term energy-related environmental issues of copper production. Energy 27(2):183–196
Amtrak (2015) http://www.amtrak.com/. Accessed 1 Jan 2015
Anastas P, Warner JC (2000) Green chemistry: theory and practice. Oxford University Press, Oxford. ISBN 978-0198506980
Anda M, Temmen J (2014) Smart metering for residential energy efficiency: the use of community based social marketing for behavioural change and smart grid introduction. Renew Energy 67:119–127
Ang BW (2006) Monitoring changes in economy-wide energy efficiency: from energy–GDP ratio to composite efficiency index. Energy Policy 34(5):574–582
Annunziata E, Rizzi F, Frey M (2014) Enhancing energy efficiency in public buildings: the role of local energy audit programmes. Energy Policy 69:364–373
Atilla Oner M, Nuri Basoglu A, Sýtký Kok M (2007) Megatrends as perceived in Turkey in comparison to Austria and Germany. Technol Forecast Soc Chang 74(4):538–557
Axelsson E, Olsson MR, Berntsson T (2008) Opportunities for process-integrated evaporation in a hardwood pulp mill and comparison with a softwood model mill study. Appl Therm Eng 28 (16):2100–2107
Ball M, Wietschel M (2009) The hydrogen economy: opportunities and challenges. Cambridge University Press, Cambridge. ISBN 978-0521882163
Bannister K (2010) Industrial energy efficiency handbook: eliminating energy waste from mechanical systems. Mcgraw-Hill Book. ISBN: 978-0071490665, New York, USA
BBC (2008) Airline in first biofuel flight, BBC News UK, Sunday, 24 Feb 2008. http://news.bbc.co.uk/2/hi/7261214.stm. Accessed 1 Jan 2015
Beaumont P (2000) The quest for water efficiency – restructuring of water use in the Middle East. Water Air Soil Pollut 123(1–4):551–564
Bedford N, Pitcher G (2005) Austria, Lonely planet Austria. Lonely Planet Publications, Torino, page 56. ISBN 978-1740594844
Belaissaoui B, Le Moullec Y, Hagi H, Favre E (2014) Energy efficiency of oxygen enriched air production technologies: cryogeny vs membranes. Sep Purif Technol 125:142–150
Berns H, Theisen W, Scheibelein G (2008) Ferrous materials: steel and cast iron. Springer, Berlin. ISBN 978-3540718475
Bevilacqua M, Braglia M (2002) Environmental efficiency analysis for ENI oil refineries. J Clean Prod 10(1):85–92
Bieling H-H (2007) Chemical reaction – an energy-intensive industry finds the solution in CHP. Cogeneration & On-Site Power. http://www.cospp.com/articles/article_display.cfm?ARTICLE_ID=288130&p=122. Accessed 1 Jan 2015
Bilek M, Hardy C, Lenzen M, Dey C (2008) Life-cycle energy balance and greenhouse gas emissions of nuclear energy: a review. Energy Convers Manag 49(8):2178–2199
Blok K, Luiten EEM, De Groot HLF (2004) The effectiveness of policy instruments for energy-efficiency improvement in firms: the dutch experience. Springer, Dordrecht. ISBN 978-1402019654
Bologna M, Flores JC (2008) A simple mathematical model of society collapse applied to Easter Island. EPL 81:48006
Bor YJ (2008) Consistent multi-level energy efficiency indicators and their policy implications. Energy Econ 30(5):2401–2419
Boyce MP (2006) The gas turbine engineering handbook, 3rd edn. Elsevier, Oxford. ISBN 978-0750678469
Braun E, Leiber W (2007) The right pump lowers total cost of ownership. World Pumps 2007 (491):30–33

Braungart M, McDonough W, Bollinger A (2007) Cradle-to-cradle design: creating healthy emissions – a strategy for eco-effective product and system design. J Clean Prod 15 (13–14):1337–1348
Brown R (2008) U.S. building-sector energy efficiency potential. Lawrence Berkeley National Laboratory, LBNL paper LBNL-1096E. Retrieved from http://www.escholarship.org/uc/item/8vs9k2q8. Accessed 1 Jan 2015
Buchanan JM, Stubblebine WC (1962) Externality. Econ New Ser 29(116):371–384
Buckminster Fuller R (1973) Nine chains to the moon. Jonathan Cape, London. ISBN 978-0224008006
Budin R, Mihelić-Bogdanić A, Sutlović I, Filipan V (2006) Advanced polymerization process with cogeneration and heat recovery. Appl Therm Eng 26(16):1998–2004
Bujak J (2009) Experimental study of the energy efficiency of an incinerator for medical waste. Appl Energy 86(11):2386–2393
Burgin N, Wilson PA (1985) The influence of cable forces on the efficiency of kite devices as a means of alternative propulsion. J Wind Eng Ind Aerodyn 20(1–3):349–367
Çakir U, Çomakli K, Yüksel F (2012) The role of cogeneration systems in sustainability of energy. Energy Convers Manag 63:196–202
Callen HB (1985) Thermodynamics and an introduction to thermostatistics, 2nd edn. Wiley, New York. ISBN 978 0471862567
Chambadal P (1957) Les centrales nucléaires, vol 4. Armand Colin, Paris, pp 1–58
Chang D, Rhee T, Nam K, Chang K, Lee D, Jeong S (2008) A study on availability and safety of new propulsion systems for LNG carriers. Reliab Eng Syst Saf 93(12):1877–1885
Chapagain AK (2006) Globalisation of water: opportunities and threats of virtual water trade. Taylor & Francis, London. ISBN 978-0415409162
Charcosset C (2009) A review of membrane processes and renewable energies for desalination. Desalination 245(1–3):214–231
Cherubini F, Raugei M, Ulgiati S (2008) LCA of magnesium production: technological overview and worldwide estimation of environmental burdens. Resour Conserv Recycl 52 (8–9):1093–1100
Cherubini F, Bargigli S, Ulgiati S (2009) Life cycle assessment (LCA) of waste management strategies: landfilling, sorting plant and incineration. Energy 34(12):2116–2123
Chirarattananon S, Taweekun J (2003) A technical review of energy conservation programs for commercial and government buildings in Thailand. Energy Convers Manag 44(5):743–762
CHP Installation Database (2015) ICF International/EEA. http://www.eea-inc.com/chpdata/index.html. Accessed 1 Jan 2015
Christensen CM, Overdorf M, Thomke S (2001) Harvard business review on innovation. Mcgraw-Hill Professional. ISBN: 978-1578516148, New York, USA
Clark A (2001) Making provision for energy-efficiency investment in changing markets: an international review. Energy Sustain Dev 5(2):26–38
Climate Action Team (2015) http://www.climatechange.ca.gov/climate_action_team/index.html. Accessed 1 Jan 2015
Coletti F, Macchietto S (2009a) A heat exchanger model to increase energy efficiency in refinery pre heat trains. Comput Aided Chem Eng 26:1245–1250
Coletti F, Macchietto S (2009b) Predicting refinery energy losses due to fouling in heat exchangers. Comput Aided Chem Eng 27:219–224
Collantes G, Sperling D (2008) The origin of California's zero emission vehicle mandate. Transp Res A Policy Pract 42(10):1302–1313
Costa A, Paris J, Towers M, Browne T (2007) Economics of trigeneration in a kraft pulp mill for enhanced energy efficiency and reduced GHG emissions. Energy 32(4):474–481
Costa A, Bakhtiari B, Schuster S, Paris J (2009) Integration of absorption heat pumps in a Kraft pulp process for enhanced energy efficiency. Energy 34(3):254–260
Cullen JM, Allwood JM (2010) Theoretical efficiency limits for energy conversion devices. Energy 35(5):2059–2069

Curzon FL, Ahlborn B (1975) Efficiency of a carnot engine at maximum power output. Am J Phys 43:22–24

D'Agosto M, Ribeiro SK (2004) Eco-efficiency management program (EEMP) – a model for road fleet operation. Transp Res Part D: Transp Environ 9(6):497–511

da Graça Carvalho M, Nogueira M (1997) Improvement of energy efficiency in glass-melting furnaces, cement kilns and baking ovens. Appl Therm Eng 17(8–10):921–933

Danish Ministry of Transport and Energy (2005) Action plan for renewed energy-conservation. ISBN: 87-7844-564-7, Copenhagen, Denmark. http://188.64.159.37/graphics/Publikationer/Energipolitik_UK/Action_plan_for_renewed_energy_conservation/index.htm

Davies REG, Birtles PJ (1999) Comet: the world's first jet airliner. Paladwr Press, McLean. ISBN 1-888962-14-3

de Swaan Arons J (2010) Efficiency and sustainability in the energy and chemical industries: scientific principles and case studies, 2nd edn. CRC Press, Boca Raton. ISBN 978-1439814710

DECHEMA (2013) Energy and GHG reductions in the chemical industry via catalytic processes: ANNEXES. http://www.dechema.de/dechema_media/Chemical_Roadmap_2013_Annexes-p-4582-view_image-1-called_by-dechema2013-original_site-dechema_eV-original_page-124930.pdf. Accessed 1 Jan 2015

Demirbas A, Caglar A, Akdeniz F, Gullu D (2000) Conversion of olive husk to liquid fuel by pyrolysis and catalytic liquefaction. Energy Sources Part A Recov Util Environ Eff 22 (7):631–639

Deolalkar SP (2009) Handbook for designing cement plants. CRC Press. ISBN: 978-8178001456, Boca Raton, USA

Dewulf J, van Langenhove H, Muys B, Stijn B, Bakshi BR, Grubb GF, Paulus DM, Sciubba E (2008) Exergy: its potential and limitations in environmental, science and technology. Environ Sci Technol 42(7):2221–2232

Dijkgraaf E, Vollebergh HRJ (2004) Burn or bury? A social cost comparison of final waste disposal methods. Ecol Econ 50(3–4):233–247

DOE (1995) Landscaping for energy efficiency. DOE/GO-10095-046 FS 220, The Energy Efficiency and Renewable Energy Clearinghouse (EREC), Merrifield, USA. http://www1.eere.energy.gov/library/pdfs/16632.pdf

Doheim MA, Sayed SA, Hamed OA (1987) Analysis of waste heat and its recovery in a cement factory. Heat Recovery Syst CHP 7(5):441–444

Doukas H, Papadopoulou AG, Psarras J, Ragwitz M, Schlomann B (2008) Sustainable reference methodology for energy end-use efficiency data in the EU. Renew Sustain Energy Rev 12 (8):2159–2176

Drucker PF (2003) The essential Drucker: the best of sixty years of Peter Drucker's essential writings on management. HarperCollins, New York. ISBN 978-0060935740

Ehrhardt-Martinez K, Laitner JA (2008) The size of the U.S. energy efficiency market: generating a more complete picture. ACEEE, Washington, DC

EIA (2015) US Energy Information Administration. http://www.eia.doe.gov/emeu/international/energyconsumption.html. Accessed 1 Jan 2015

EIA (U.S. Energy Information Administration) (2014) International energy outlook 2014. http://www.eia.gov/forecasts/ieo/pdf/0484%282014%29.pdf. Accessed 1 Jan 2015

Einstein D, Worrell E, Khrushch M (2001) Steam systems in industry: energy use and energy efficiency improvement potentials. Lawrence Berkeley National Laboratory, LBNL paper LBNL-49081. Retrieved from http://www.escholarship.org/uc/item/3m1781f1. Accessed 1 Jan 2015

Electric Power Research Institute (EPRI) (2015) http://www.epri.com/. Accessed 1 Jan 2015

Elkinton MR, McGowan JG, Manwell JF (2009) Wind power systems for zero net energy housing in the United States. Renew Energy 34(5):1270–1278

Ellenberger P (2010) Piping and pipeline calculations manual: construction, design fabrication and examination. Butterworth Heinemann, Amsterdam. ISBN 978-1856176934

Ellinger R, Meitz K, Prenninger P, Salchenegger S, Brandstätter W (2001) Comparison of CO_2 emission levels for internal combustion engine and fuel cell automotive propulsion systems. SAE paper 2001-01-3751, Warrendale, USA. http://papers.sae.org/2001-01-3751/
Elvers B (2007) Handbook of fuels: energy sources for transportation. Wiley-VCH, Weinheim. ISBN 978-3527307401
Energy Efficient Motor Driven Systems (2010) The Motor Challenge Programme. http://www.motor-challenge.eu/. Accessed 1 Jan 2015
Entchev E, Gusdorf J, Swinton M, Bell M, Szadkowski F, Kalbfleisch W, Marchand R (2004) Micro-generation technology assessment for housing technology. Energy Build 36(9):925–931
Etchells JC (2005) Process intensification: safety pros and cons. Process Saf Environ Prot 83 (2):85–89
Eyring V, Isaksen ISA, Berntsen T, Collins WJ, Corbett JJ, Endresen O, Grainger RG, Moldanova J, Schlager H, Stevenson DS (2010) Transport impacts on atmosphere and climate: shipping. Atmos Environ 44(37):4735–4771
Fadare DA, Bamiro OA, Oni AO (2010) Energy and cost analysis of organic fertilizer production in Nigeria. Energy 35(1):332–340
Fahim MA, Al-Sahhaf TA, Lababidi HMS (2009) Fundamentals of petroleum refining. Elsevier Science & Technology, Amsterdam. ISBN 978-0444527851
FAQ, US Energy Information Administration (2014) How much electricity is lost in transmission and distribution in the United States? http://www.eia.gov/tools/faqs/faq.cfm?id=105%26t=3. Accessed 1 Jan 2015
Farzaneh-Gord M, Deymi-Dashtebayaz M (2009) A new approach for enhancing performance of a gas turbine (case study: Khangiran refinery). Appl Energy 86(12):2750–2759
Fath HES, Hashem HH (1988) Waste heat recovery of dura (Iraq) oil refinery and alternative cogeneration energy plant. Heat Recovery Syst CHP 8(3):265–270
Favre B, Peuportier B (2014) Application of dynamic programming to study load shifting in buildings. Energy Build 82:57–64
Frosch RA, Gallopoulos NE (1989) Strategies for manufacturing. Sci Am 261(3):144–152
Gahleitner G (2013) Hydrogen from renewable electricity: an international review of power-to-gas pilot plants for stationary applications. Int J Hydrog Energy 38(5):2039–2061
Gale J, Freund P (2014) Greenhouse gas abatement in energy intensive industries. IEA Greenhouse Gas R&D Programme. http://ccs101.ca/assets/Documents/ghgt5.pdf. Accessed 1 Jan 2015
Galitsky C (2008) Energy efficiency improvement and cost saving opportunities for the pharmaceutical industry, an ENERGY STAR guide for energy and plant managers. Lawrence Berkeley National Laboratory, LBNL paper, LBNL-57260. Retrieved from http://www.escholarship.org/uc/item/9zw158vm. Accessed 1 Jan 2015
Gan CK, Sapar AF, Mun YC, Chong KE (2013) Techno-economic analysis of LED lighting: a case study in UTeM's faculty building. Procedia Eng 53:208–216
Gehani N (2003) Bell Labs: life in the crown jewel. Silicon Press, Summit. ISBN 978-0929306278
Geller H, Harrington P, Rosenfeld AH, Tanishima S, Unander F (2006) Polices for increasing energy efficiency: thirty years of experience in OECD countries. Energy Policy 34(5):556–573
Ghafoori E, Flynn PC, Feddes JJ (2007) Pipeline vs. truck transport of beef cattle manure. Biomass Bioenergy 31(2–3):168–175
Glass Manufacturing Industry Council (GMIC) (2015) http://www.gmic.org/. Accessed 1 Jan 2015
Gomri R (2009) Energy and exergy analyses of seawater desalination system integrated in a solar heat transformer. Desalination 249(1):188–196
Gow D (2009) Russia-Ukraine gas crisis intensifies as all European supplies are cut off. The Guardian, 7 Jan 2009. http://www.theguardian.com/business/2009/jan/07/gas-ukraine. Accessed 1 Jan 2015
Granade HC, Creyts J, Derkach A, Farese P, Nyquist S, Ostrowski K (2009) Unlocking energy efficiency in the U.S. economy, McKinsey Global Energy and Materials. McKinsey & Company, Washington DC. http://www.mckinsey.com/client_service/electric_power_and_natural_gas/latest_thinking/unlocking_energy_efficiency_in_the_us_economy

Graus W, Worrell E (2009) Trend in efficiency and capacity of fossil power generation in the EU. Energy Policy 37:2147–2160
Grossman G, Krueger A (1991) Environmental impacts of a North American free trade agreement, National Bureau of Economic Research, Working paper, 3914. NBER, Cambridge, MA
Guineé JB (2002) Handbook on life cycle assessment: operational guide to the ISO standards, 2nd edn, Eco-efficiency in industry and science. Springer, Dordrecht. ISBN 978-1402005572
Gunner A, Hultmark G, Vorre A, Afshari A, Bergsøe NC (2014) Energy-saving potential of a novel ventilation system with decentralised fans in an office building. Energy Build 84:360–366
Hadjipaschalis I, Poullikkas A, Efthimiou V (2009) Overview of current and future energy storage technologies for electric power applications. Renew Sustain Energy Rev 13(6–7):1513–1522
Hall DO, Rao K (1999) Photosynthesis, 6th edn. Cambridge University Press, Cambridge. ISBN 978-0521644976
Hamelinck CN, Faaij APC (2002) Future prospects for production of methanol and hydrogen from biomass. J Power Sources 111(1):1–22
Häring H-W, Belloni A, Ahner C (2007) Industrial gases processing. Wiley-VCH, Weinheim. ISBN 978-3527316854
Heitland H, Hiller H, Hoffmann HJ (1990) Factors influencing CO_2 emission of future passenger car traffic. MTZ 51:2
Hekkert MP, Hendriks FHJF, Faaij APC, Neelis ML (2005) Natural gas as an alternative to crude oil in automotive fuel chains well-to-wheel analysis and transition strategy development. Energy Policy 33(5):579–594
Hernandez P, Kenny P (2010) From net energy to zero energy buildings: defining life cycle zero energy buildings (LC-ZEB). Energy Build 42(6):815–821
Herring H, Sorrell S (2009) Energy efficiency and sustainable consumption: the rebound effect, Energy, climate and the environment. Palgrave, New York. ISBN 978-0230525344
Heselton KE (2004) Boiler operator's handbook. Marcel Dekker, New York. ISBN 978-0824742904
Hinderink P, van der Kooi HJ, De Swaan Arons J (1999) On the efficiency and sustainability of the process industry. Green Chem 176–180. http://www.rsc.org/delivery/_ArticleLinking/DisplayArticleForFree.cfm?doi=a909915h%26JournalCode=GC. Accessed 1 Jan 2015
Hirscher M, Hirose K (2010) Handbook of hydrogen storage: new materials for future energy storage. Wiley-VCH, Weinheim. ISBN 978-3527322732
Hoffmann KH, Burzler JM, Schubert S (1997) Endoreversible thermodynamics. J Non-Equilib Thermodyn 22(4):311–355
Hollinger P (2014) Europe risks 'significant' gas shortages this winter. Financial Times, 11 July 2014. http://www.ft.com/cms/s/0/a119b2e4-082e-11e4-acd8-00144feab7de.html#axzz3NCxSbl9h. Accessed 1 Jan 2015
Holmberg K, Andersson P, Erdemir A (2012) Global energy consumption due to friction in passenger cars. Tribol Int 47:221–234
Hori M (2008) Nuclear energy for transportation: paths through electricity, hydrogen and liquid fuels. Prog Nucl Energy 50(2–6):411–416
http://www.energystar.gov/ (2015). Accessed 1 Jan 2015
http://www.epa.gov/nrmrl/std/lca/lca.html (2015). Accessed 1 Jan 2015
http://www.essentialchemicalindustry.org/processes/recycling-in-the-chemical-industry.html (2015). Accessed 1 Jan 2015
http://www.eu-energystar.org/ (2015). Accessed 1 Jan 2015
http://www.fueleconomy.gov/ (2015). Accessed 1 Jan 2015
http://www.ics-shipping.org/publications/ (2015). Accessed 1 Jan 2015
http://www.osti.gov/glass/bestpractices.html (2015). Accessed 1 Jan 2015
Ibrahim H, Ilinca A, Perron J (2008) Energy storage systems – characteristics and comparisons. Renew Sustain Energy Rev 12(5):1221–1250
IEA (2009) World energy outlook 2009. International Energy Association (IEA), Paris. ISBN 9789264061309

IEA (2014a) World energy outlook 2014. ISBN 978-92-64-20804-9. http://www.iea.org/W/bookshop/477-World_Energy_Outlook_2014. Accessed 1 Jan 2015
IEA (2014b) World energy outlook 2014. Presentation to the Press. http://www.worldenergyoutlook.org/media/weowebsite/2014/WEO2014_LondonNovember.pdf. Accessed 1 Jan 2015
Intergovernmental Panel on Climate Change (IPCC) (2015) http://www.ipcc.ch/. Accessed 1 Jan 2015
International Energy Agency (2008) Promoting energy efficiency investments: case studies in the residential sector. Organization for Economic Cooperation & Development, Paris. ISBN 978-9264042148
International Energy Agency (2014) CO_2 emissions from fuel combustion, IEA statistics. http://www.iea.org/publications/freepublications/publication/CO2EmissionsFromFuelCombustionHighlights2014.pdf. Accessed 1 Jan 2015
International Transport Forum (2013) Statistics brief, Dec 2013, Global transport trends in perspective. http://www.internationaltransportforum.org/statistics/StatBrief/2013-12-Trends-Perspective.pdf. Accessed 1 Jan 2015
IPCC (2000) Aviation and the global atmosphere. IPCC special reports on climate change. http://www.grida.no/publications/other/ipcc_sr/?src=/climate/ipcc/aviation/avf9-3.htm. Accessed 1 Jan 2015
Iriarte A, Almeida MG, Villalobos P (2014) Carbon footprint of premium quality export bananas: case study in Ecuador, the world's largest exporter. Sci Total Environ 472:1082–1088
ISO (2015) http://www.iso-14001.org.uk/index.htm. Accessed 1 Jan 2015
Jaffe AB, Stavins RN (1994) The energy-efficiency gap, what does it mean? Energy Policy 22 (10):804–810
Jamieson A (2009) Customers buy up traditional light bulbs before switch to low energy alternatives. The Telegraph, 18 Apr 2009. http://www.telegraph.co.uk/technology/news/5179266/Customers-buy-up-traditional-light-bulbs-before-switch-to-low-energy-alternatives.html. Accessed 1 Jan 2015
Jechoutek KG, Lamech R (1995) New directions in electric power financing. Energy Policy 23 (11):941–953
Jevons WS (2008) The coal question. Lulu Press, Gloucester. ISBN 978-1409952312
Jiang P (2011) Analysis of national and local energy-efficiency design standards in the public building sector in China. Energy Sustain Dev 15(4):443–450
Jiang R, Rong C, Chu D (2004) Determination of energy efficiency for a direct methanol fuel cell stack by a fuel circulation method. J Power Sources 126(1–2):119–124
Jin JC, Choi J-Y, Yu ESH (2009) Energy prices, energy conservation, and economic growth: evidence from the postwar United States. Int Rev Econ Financ 18(4):691–699
Johansson J-E (2015) Compelling facts about plastics, plastics Europe. http://www.plasticseurope.org/. Accessed 1 Jan 2015
Johansson B, Åhman M (2002) A comparison of technologies for carbon-neutral passenger transport. Transp Res Part D: Transp Environ 7(3):175–196
Johnston P, Stringer R (2001) Chlorine and the environment: an overview of the chlorine industry. Springer, Dordrecht. ISBN 978-0792367970
Jönsson J, Algehed J (2010) Pathways to a sustainable European kraft pulp industry: trade-offs between economy and CO_2 emissions for different technologies and system solutions. Appl Therm Eng 30(16):2315–2325
Jordan P, Jordan JW, McClelland IL (1996) Usability evaluation in industry. Taylor & Francis, London. ISBN 978-0748404605
Joshi R, Pathak M (2014) Decentralized grid-connected power generation potential in India: from perspective of energy efficient buildings. Energy Procedia 57:716–724
Joskow PL, Marron DB (1993) What does a negawatt really cost? Further thoughts and evidence. Electr J 6(6):14–26

Kamga C, Yazici MA (2014) Achieving environmental sustainability beyond technological improvements: potential role of high-speed rail in the United States of America. Transp Res Part D: Transp Environ 31:148–164
Kania JJ (1984) Economics of coal transport by slurry pipeline versus unit train: a case study. Energy Econ 6(2):131–138
Kanimozhi R, Selvi K, Balaji KM (2014) Multi-objective approach for load shedding based on voltage stability index consideration. Alex Eng J 53(4):817–825
Ke J, Price L, Ohshita S, Fridley D, Khanna NZ, Zhou N, Levine M (2012) China's industrial energy consumption trends and impacts of the Top-1000 Enterprises Energy-Saving Program and the Ten Key Energy-Saving Projects. Energy Policy 50:562–569
Kemp RJ (1994) The European high speed network. In: Feilden GBR, Wickens AH, Yates I (eds) Passenger transport after 2000 AD. Spon Press, London. ISBN 0419194703
Kemp RJ (1997) Rail transport in the next Millennium, Visions of Tomorrow. IMechE 150 year symposium, London. ISBN: 186058098X
Kemp R (2004) Take the car and save the planet. Power Eng 18(5):12–17
Khurana S, Banerjee R, Gaitonde U (2002) Energy balance and cogeneration for a cement plant. Appl Therm Eng 22(5):485–494
Kilponen L, Ahtila P, Parpala J, Pihko M (2001) Improvement of pulp mill energy efficiency in an integrated pulp and paper mill. In: Proceedings ACEEE summer study on energy efficiency in industry, Washington DC, pp 363–374. http://aceee.org/files/proceedings/2001/data/papers/SS01_Panel1_Paper32.pdf
Kim J, Park C (2010) Wind power generation with a parawing on ships, a proposal. Energy 35 (3):1425–1432
Kodama Y, Kakugawa A, Takahashi T, Kawashima H (2000) Experimental study on microbubbles and their applicability to ships for skin friction reduction. Int J Heat Fluid Flow 21(5):582–588
Koros WJ, Fleming GK (1993) Membrane-based gas separation. J Membr Sci 83(1):1–80
Kotegawa T, Fry D, DeLaurentis D, Puchaty E (2014) Impact of service network topology on air transportation efficiency. Transp Res Part C Emerg Technol 40:231–250
Krigger J, Dorsi C (2008) The homeowner's handbook to energy efficiency: a guide to big and small improvements. Saturn Resource Management, Helena. ISBN 978-1880120187
Kruyt B, van Vuuren DP, de Vries HJM, Groenenberg H (2009) Indicators for energy security. Energy Policy 37(6):2166–2181
Kumar S (2002) Cleaner production technology and bankable energy efficiency drives in fertilizer industry in India to minimise greenhouse gas emissions – case study. In: Greenhouse gas control technologies – 6th international conference, Pergamon Press, Oxford. pp 1031–1036
Kumar A, Cameron JB, Flynn PC (2007) Pipeline transport of biomass. Appl Biochem Biotechnol 113(1–3):27–39
Kumar A, Demirel Y, Jones DD, Hanna MA (2010) Optimization and economic evaluation of industrial gas production and combined heat and power generation from gasification of corn stover and distillers grains. Bioresour Technol 101(10):3696–3701
Lackner M (2007) Innovation in business unit pipe: shaping a strategy for the future. Master thesis, LIMAK Johannes Kepler University Business School, Linz
Lackner M (ed) (2009) Alternative ignition systems. ProcessEng Engineering GmbH, Vienna. ISBN 978-3902655059
Lackner M (ed) (2010) Scale-up in metallurgy. ProcessEng Engineering GmbH, Vienna. ISBN 978-3-902655-10-3
Lackner M, Winter F, Geringer B (2005) Chemie im Motor. Chemie in unserer Zeit 4:228–229
Lackner M, Winter F, Agarwal AK (2010) Handbook of combustion. Wiley-VCH, Weinheim. ISBN 978-3527324491
Lackner M, Palotás AB, Winter F (2013) Combustion: from basics to applications. Wiley-VCH, Weinheim. ISBN 978-3527333516

Ladha JK, Pathak H, Krupnik TJ, Six J, van Kessel C (2005) Efficiency of fertilizer nitrogen in cereal production: retrospects and prospects. Adv Agron 87:85–156
Le Pen Y, Sévi B (2010) What trends in energy efficiencies? Evidence from a robust test. Energy Econ 32(3):702–708
Lechtenböhmer S, Dienst C, Fischedick M, Hanke T, Fernandez R, Robinson D, Kantamaneni R, Gillis B (2007) Tapping the leakages: methane losses, mitigation options and policy issues for Russian long distance gas transmission pipelines. Int J Greenhouse Gas Control 1(4):387–395
Lee M-K, Park H, Noh J, Painuly JP (2003) Promoting energy efficiency financing and ESCOs in developing countries: experiences from Korean ESCO business. J Clean Prod 11(6):651–657
Li T, Hassan M, Kuwana K, Saito K, King P (2006) Performance of secondary aluminum melting: thermodynamic analysis and plant-site experiments. Energy 31(12):1769–1779
Li Z, Gao D, Chang L, Liu P, Pistikopoulos EN (2010) Coal-derived methanol for hydrogen vehicles in China: energy, environment, and economic analysis for distributed reforming. Chem Eng Res Des 88(1):73–80
Liang Y, Lee Y-C, Teng A (2007) Real-time communication: internet protocol voice and video telephony and teleconferencing. In: Multimedia over IP and wireless networks. Academic Press, New York, pp 503–525
Lin J (2007) Energy conservation investments: a comparison between China and the US. Energy Policy 35(2):916–924
Liu F, Ross M, Wang S (1995) Energy efficiency of China's cement industry. Energy 20(7):669–681
López MA, de la Torre S, Martín S, Aguado JA (2015) Demand-side management in smart grid operation considering electric vehicles load shifting and vehicle-to-grid support. Int J Electr Power Energy Syst 64:689–698
Loughran DS, Kulick J (2004) Demand-side management and energy efficiency in the United States. Energy J 25(1):19–44
Lugt PM, de Niet A, Bouwman WH, Bosma JCN, van den Bleek CM (1996) Catalytic removal of NO_x from total energy installation flue-gases for carbon dioxide fertilization in greenhouses. Catal Today 29(1–4):127–131
Lund P (2006) Market penetration rates of new energy technologies. Energy Policy 34 (17):3317–3326
Lutz E (2008) Identification and analysis of energy saving projects in a Kraft mill. Pulp Paper Can 109(5):13–17
Malça J, Freire F (2006) Renewability and life-cycle energy efficiency of bioethanol and bio-ethyl tertiary butyl ether (bioETBE): assessing the implications of allocation. Energy 31 (15):3362–3380
Malkov T (2004) Novel and innovative pyrolysis and gasification technologies for energy efficient and environmentally sound MSW disposal. Waste Manag 24(1):53–79
Mandal SK, Madheswaran S (2010) Environmental efficiency of the Indian cement industry: an interstate analysis. Energy Policy 38(2):1108–1118
Markis T, Paravantis JA (2007) Energy conservation in small enterprises. Energy Build 39 (4):404–415
Marks P (2009) 'Morphing' winglets to boost aircraft efficiency. New Sci 201(2692):22–23
Marsh G (2007) Airbus takes on Boeing with reinforced plastic A350 XWB. Reinf Plast 51 (11):26–27, 29
Marsh G (2008) Biofuels: aviation alternative? Renew Energy Focus 9(4):48–51
Max Appl (2006) Ammonia. In: Ullmann's encyclopedia of industrial chemistry. Wiley-VCH, Weinheim
McCabe WL, Smith J, Harriott P (2004) Unit operations of chemical engineering, 7th edn. Mcgraw-Hill, New York. ISBN 978-0072848236
McKay G, Holland CR (1981) Energy savings from steam losses on an oil refinery. Eng Cost Prod Econ 5(3–4):193–203
McKinsey & Company, Inc. (2009) Energy: a key to competitive advantage, new sources of growth and productivity. Anja Hartmann, Wolfgang Huhn, Christian Malorny, Martin Stuchtey, Thomas

Vahlenkamp, Detlef Kayser, Detlev Mohr, Claudia Funke Frankfurt/Germany http://www.mckinsey.com/~/media/mckinsey/dotcom/client_service/sustainability/pdfs/energy_competitive_advantage_in_germany.ashx
McLean-Conner P (2009) Energy efficiency: principles and practices. Pennwell, Tulsa. ISBN 978-1593701789
McMichael AJ, Powles JW, Butler CD, Uauy R (2007) Food, livestock production, energy, climate change, and health. Lancet 370:1253–1263
Mesa AA, Gómez CM, Azpitarte RU (1997) Design of the maximum energy efficiency desalination plant (PAME). Desalination 108(1–3):111–116
Meyers RA (2004) Handbook of petrochemicals production processes. Mcgraw-Hill Professional, New York. ISBN 978-0071410427
Miller FP, Vandome AF, McBrewster J (2009) Zero-energy building. Energy efficiency in British housing, energy conservation, passive house. Alphascript Publishing. ISBN: 978-6130023331, Beau Bassin, Mauritius
Minas L, Ellison B (2009) Energy efficiency for information technology: how to reduce power consumption in servers and data centers. Intel Press, Santa Clara. ISBN 978-1934053201
Mitsos A, Chachuat B, Barton PI (2007) What is the design objective for portable power generation: efficiency or energy density? J Power Sources 164(2):678–687
Moore DA (2005) Sustaining performance improvements in energy intensive industries. In: Proceedings of the twenty-seventh industrial energy technology conference, New Orleans, ESL-IE-05-05-31, 10–13 May 2005
Moors EHM (2006) Technology strategies for sustainable metals production systems: a case study of primary aluminium production in The Netherlands and Norway. J Clean Prod 14 (12–13):1121–1138
Morris DR, Steward FR, Evans P (1983) Energy efficiency of a lead smelter. Energy 8(5):337–349
Mudahar MS, Hignett TP (1985) Energy efficiency in nitrogen fertilizer production. Energy Agric 4:159–177
Mundaca L (2009) Energy Efficiency Trading: concepts, practice and evaluation of tradable certificates for energy efficiency improvements. VDM Verlag, Saarbrücken. ISBN 978-3639139730
Musa C, Licheri R, Locci AM, Orrù R, Cao G, Rodriguez MA, Jaworska L (2009) Energy efficiency during conventional and novel sintering processes: the case of Ti–Al_2O_3–TiC composites. J Clean Prod 17(9):877–882
Nachreiner F, Nickel P, Meyer I (2006) Human factors in process control systems: the design of human–machine interfaces. Saf Sci 44(1):5–26
Naisbitt J (1985) Megatrends: ten new directions transforming our lives. Grand Central Publishing, New York. ISBN: 978-0446512510,
Najjar YSH, Habeebullah MB (1991) Energy conservation in the refinery by utilizing reformed fuel gas and furnace flue gases. Heat Recovery Syst CHP 11(6):517–521
Namboodiri V (2009) Algorithms & protocols towards energy-efficiency in wireless networks. VDM Verlag, Saarbrücken. ISBN 978-3639157024
Nässén J, Holmberg J (2005) Energy efficiency – a forgotten goal in the Swedish building sector? Energy Policy 33(8):1037–1051
Nässén J, Sprei F, Holmberg J (2008) Stagnating energy efficiency in the Swedish building sector – economic and organisational explanations. Energy Policy 36(10):3814–3822
NDRC (2007) Bulletin of energy consumption in the top 1000 Chinese enterprises. Beijing, Sept 2007 (Chinese)
Nelson P, Safirova E, Walls M (2007) Telecommuting and environmental policy: lessons from the ecommute program. Transp Res Part D: Transp Environ 12(3):195–207
Next 10's California Green Innovation Index (2010) http://www.nextten.org/environment/greenInnovation.html. Accessed 1 Jan 2015
Nishitani H, Kawamura T, Suzuki G (2000) University – industry cooperative study on plant operations. Comput Chem Eng 24(2–7):557–567

Nordman R, Berntsson T (2009) Use of advanced composite curves for assessing cost-effective HEN retrofit II. Case studies. Appl Therm Eng 29(2–3):282–289
Novikov II (1958) The efficiency of atomic power stations. J Nucl Energy II 7:125–128 (translated from Atomnaya Energiya 3:409 (1957))
Nuo G, Gaoshang W (2008) Analysis on China's energy efficiency. Energy China 7:32–36
Office of Energy Efficiency, Natural Resources Canada (2002) Energy efficiency planning and management guide. Canadian Industry Program for Energy Conservation, Ottawa. ISBN 0-662-31457-3
Okura S, Rubin R, Brost M (2006) What types of appliances and lighting are being used in California residences? http://mail.mtprog.com/CD_Layout/Day_2_22.06.06/1615-1815/ID147_Okura_final.pdf, http://escholarship.org/uc/item/7qz3b977. Accessed 1 Jan 2015
Olah GA, Goeppert A, Surya Prakash GK (2009) Beyond oil and gas: the methanol economy, 2nd edn. Wiley-VCH, Weinheim. ISBN 978-3527324224
Oude Lansink A, Bezlepkin I (2003) The effect of heating technologies on CO_2 and energy efficiency of Dutch greenhouse firms. J Environ Manage 68(1):73–82
Page S, Krumdieck S (2009) System-level energy efficiency is the greatest barrier to development of the hydrogen economy. Energy Policy 37(9):3325–3335
Panjeshahi MH, Ghasemian Langeroudi E, Tahouni N (2008) Retrofit of ammonia plant for improving energy efficiency. Energy 33(1):46–64
Patel M, Mutha N (2004) Plastics production and energy. Encycl Energy 3:81–91
Patrick DR, Fardo S, Richardson RE (2007) Energy conservation guidebook, 2nd edn. CRC Press, Boca Raton. ISBN 978-0849391781
Patterson MG (1996) What is energy efficiency? Concepts, indicators and methodological issues. Energy Policy 24(5):377–390
Peeters PM, Middel J, Hoolhorst A (2005) Fuel efficiency of commercial aircraft, an overview of historical and future trends, NLR-CR-2005-669. Nationaal Lucht- en Ruimtevaartlaboratorium, National Aerospace Laboratory NLR. http://www.transportenvironment.org/Publications/prep_hand_out/lid/398. Accessed 1 Jan 2015
Penner JE, Lister DH, Griggs DJ, Dokken DJ, McFarland M (1999) Aviation and the global atmosphere; a special report to IPCC working groups I and III. Cambridge University Press, Cambridge
Perrot P (1998) A to Z of thermodynamics. Oxford University Press, Oxford. ISBN 978-0198565529
Phylipsen GJM (Dian), Blok K, Bode J-W (2002) Industrial energy efficiency in the climate change debate: comparing the US and major developing countries. Energy Sustain Dev 6(4):30–44
Phylipsen GJM, Blok K, Worrell E (1997) International comparisons of energy efficiency-methodologies for the manufacturing industry. Energy Policy 25(7–9):715–725
Pilavachi PA (2000) Power generation with gas turbine systems and combined heat and power. Appl Therm Eng 20(15–16):1421–1429
Poliakoff M, Fitzpatrick JM, Farren TR, Anastas PT (2002) Green chemistry: science and politics of change. Science 297:807–810
Pootakham T, Kumar A (2010) A comparison of pipeline versus truck transport of bio-oil. Bioresour Technol 101(1):414–421
Principi P, Fioretti R (2014) A comparative life cycle assessment of luminaires for general lighting for the office – compact fluorescent (CFL) vs Light Emitting Diode (LED) – a case study. J Clean Prod 83(15):96–107
Prins MJ, Ptasinski KJ, Janssen FJJG (2004) Exergetic optimisation of a production process of Fischer–Tropsch fuels from biomass. Fuel Process Technol 86:375–389
Quadrelli R, Peterson S (2007) The energy–climate challenge: recent trends in CO_2 emissions from fuel combustion. Energy Policy 35(11):5938–5952
Radulovic D, Skok S, Kirincic V (2011) Energy efficiency public lighting management in the cities. Energy 36(4):1908–1915

Rafiqul I, Weber C, Lehmann B, Voss A (2005) Energy efficiency improvements in ammonia production – perspectives and uncertainties. Energy 30(13):2487–2504
Raj NT, Iniyan S, Goic R (2011) A review of renewable energy based cogeneration technologies. Renew Sustain Energy Rev 15(8):3640–3648
Rajan GG (2002) Optimizing energy efficiencies in industry. McGraw-Hill Professional, London. ISBN 978-0071396929
Ramírez CA, Blok K, Neelis M, Patel M (2006a) Adding apples and oranges: the monitoring of energy efficiency in the Dutch food industry. Energy Policy 34(14):1720–1735
Ramírez CA, Patel M, Blok K (2006b) From fluid milk to milk powder: energy use and energy efficiency in the European dairy industry. Energy 31(12):1984–2004
Ranaiefar F, Amelia R (2011) Freight-Transportation Externalities, Logistics Operations and Management, pp 333–358
Ren T, Patel MK, Blok K (2008) Steam cracking and methane to olefins: energy use, CO_2 emissions and production costs. Energy 33(5):817–833
Rhee H-J (2008) Home-based telecommuting and commuting behavior. J Urban Econ 63 (1):198–216
Rietbergen MG, Farla JCM, Blok K (2002) Do agreements enhance energy efficiency improvement?: analysing the actual outcome of long-term agreements on industrial energy efficiency improvement in The Netherlands. J Clean Prod 10(20):153–163
Rosen MA, Scott DS (1988) Energy and exergy analyses of a production process for methanol from natural gas. Int J Hydrog Energy 13(10):617–623
Rosenfeld A (2008) Energy efficiency: the first and most profitable way to delay climate change. EPA Region IX, California Energy Commission, Sacramento
Rugman AM, Li J (2005) Real options and international investment. Edward Elgar, Northampton. ISBN 10: 1840649011
Russell C (2009) Managing energy from the top down: connecting industrial energy efficiency to business performance. CRC Press. ISBN: 978-1439829967, Boca Raton, USA
Rydh CJ, Sandén BA (2005) Energy analysis of batteries in photovoltaic systems. Part II: energy return factors and overall battery efficiencies. Energy Convers Manag 46(11–12):1980–2000
Ryerson MS, Kim H (2014) The impact of airline mergers and hub reorganization on aviation fuel consumption. J Clean Prod 85:395–407
Saunders H (1992) The Khazzoom-Brookes postulate and neoclassical economic growth. Energy J 13(14):131–148
Saunders C, Barber A, Taylor G (2006) Food miles – comparative energy/emissions; performance of New Zealand's agriculture industry, vol 285, Research report. Agribusiness & Economics Research Unit, Lincoln University, Christchurch. ISBN 0-909042-71-3
Scheirs J (2006) Recycling of waste plastics. In: Pyrolysis and related feedstock recycling technologies: converting waste plastics into diesel and other fuels. Wiley, ISBN: 978-0470021521, Weinheim, Germany
Schipper L, Meyers S, Howarth RB, Steiner R (2005) Energy efficiency and human activity: past trends, future prospects. Cambridge University Press, Cambridge. ISBN 978-0521479851
Schleich J (2009) Barriers to energy efficiency: a comparison across the German commercial and services sector. Ecol Econ 68(7):2150–2159
Schneekluth H, Bertram V (1998) Ship propulsion. In: Ship design for efficiency and economy, 2nd edn. Butterworth Heinemann, Oxford, pp 180–205
Serra LM, Lozano M-A, Ramos J, Ensinas AV, Nebra SA (2009) Polygeneration and efficient use of natural resources. Energy 34(5):575–586
Sharma SD (2009) Fuels – hydrogen production|gas cleaning: pressure swing adsorption. In: Encyclopedia of electrochemical power sources. Elsevier Science & Technology, Amsterdam/ Netherlands, pp 335–349
Shell Eco Marathon (2015) http://www.shell.com/home/content/ecomarathon/about/current_records/. Accessed 1 Jan 2015

Sheredeka VV, Krivoruchko PA, Polokhlivets EK, Kiyan VI, Atkarskaya AB (2001) Energy-saving technologies in glass production. Glas Ceram 58(1–2):70–71
Sloan P, Legrand W, Chen JS (2009) Energy efficiency. In: Sustainability in the hospitality industry. Butterworth Heinemann, Oxford, pp 13–26
Smith P (2009) The processing of high silica bauxites – review of existing and potential processes. Hydrometallurgy 98(1–2):162–176
Sorrell S (2009) Jevons' Paradox revisited: the evidence for backfire from improved energy efficiency. Energy Policy 37(4):1456–1469
Sorrell S, O'Malley E, Schleich J (2004) The economics of energy efficiency: barriers to cost-effective investment. Edward Elgar, Cheltenham. ISBN 978-1840648898
Sorrell S, Lehtonen M, Stapleton L, Pujol J, Champion T (2009) Decomposing road freight energy use in the United Kingdom. Energy Policy 37(8):3115–3129
Stepanov V, Stepanov S (1998) Energy use efficiency of metallurgical processes. Energy Convers Manag 39(16–18):1803–1809
Stern N (2007) The economics of climate change: the stern review. Cambridge University Press, Cambridge. ISBN 978-0521700801
Stuart D, Schewe RL, McDermott M (2014) Reducing nitrogen fertilizer application as a climate change mitigation strategy: Understanding farmer decision-making and potential barriers to change in the US. Land Use Policy 36:210–218
Sustainable Energy Ireland (SEI) (2015) http://www.sei.ie. Accessed 1 Jan 2015
Svensson AM, Møller-Holst S, Glöckner R, Maurstad O (2007) Well-to-wheel study of passenger vehicles in the Norwegian energy system. Energy 32(4):437–445
Swanton CJ, Murphy SD, Hume DJ, Clements DR (1996) Recent improvements in the energy efficiency of agriculture: case studies from Ontario, Canada. Agric Syst 52(4):399–418
Santin J (2005) Swiss fuel cell car breaks fuel efficiency record. Fuel Cells Bull 2005(8):8–9
Szentennai P, Lackner M (2014) Advanced control methods for combustion. Chem Eng 2–6:08
Tapio P, Banister D, Luukkanen J, Vehmas J, Willamo R (2007) Energy and transport in comparison: immaterialisation, dematerialisation and decarbonisation in the EU15 between 1970 and 2000. Energy Policy 35(1):433–451
Tay JH, Low SC, Jeyaseelanb S (1996) Vacuum desalination for water purification using waste heat. Desalination 106(1–3):131–135
Taylor AMKP (2008) Science review of internal combustion engines. Energy Policy 36 (12):4657–4667
Taylor RP, Govindarajalu C, Levin J (2008) Financing energy efficiency: lessons from Brazil, China, India, and beyond. World Bank, Washington, DC. ISBN 978-0821373040
Techato K-a, Watts DJ, Chaiprapat S (2009) Life cycle analysis of retrofitting with high energy efficiency air-conditioner and fluorescent lamp in existing buildings. Energy Policy 37 (1):318–325
Tehrani Nejad M A (2007) Allocation of CO_2 emissions in petroleum refineries to petroleum joint products: a linear programming model for practical application. Energy Econ 29(4):974–997
The International Energy Association in Collaboration with CEFIC (2007) Feedstock substitutes, energy efficient technology and CO_2 reduction for petrochemical products, A workshop in the framework of the G8 dialogue on climate change, clean energy and sustainable development, Paris, France
Thomas CE (2009) Fuel cell and battery electric vehicles compared. Int J Hydrog Energy 34 (15):6005–6020
Thumann A, Dunning S (2008) Plant engineers and managers guide to energy conservation, 9th edn. CRC Press, Boca Raton. ISBN 978-1420052466
Tin T, Sovacool BK, Blake D, Magill P, El Naggar S, Lidstrom S, Ishizawa K, Berte J (2010) Energy efficiency and renewable energy under extreme conditions: case studies from Antarctica. Renew Energy 35(8):1715–1723
Todorovic MS, Kim JT (2014) Data centre's energy efficiency optimization and greening – case study methodology and R&D needs. Energy Build 85:564–578

Tromans D (2008) Mineral comminution: energy efficiency considerations. Miner Eng 21 (8):613–620
Tuomaala M, Hurme M, Leino A-M (2010) Evaluating the efficiency of integrated systems in the process industry–case: steam cracker. Appl Therm Eng 30(1):45–52
Tutterow V, Casada D, McKane A (2002) Pumping systems efficiency improvements flow straight to the bottom line. Lawrence Berkeley National Laboratory, LBNL paper LBNL-51043. Retrieved from http://www.escholarship.org/uc/item/8s4315r9. Accessed 1 Jan 2015
UK Carbon Trust (2015) http://www.carbontrust.co.uk. Accessed 1 Jan 2015
United Nations (2006) Energy efficiency guide for industry in Asia. United Nations, Nairobi. ISBN 978-9280726473
University of York (2010) Recycling in the chemical industry. http://www.wasteonline.org.uk/resources/InformationSheets/Plastics.htm. Accessed 1 Jan 2015
US Department of Energy (2005) A manual for the economic evaluation of energy efficiency and renewable energy technologies. International Law & Taxation, Washington, DC. ISBN 978-1410221056
US Department of Energy (2010) Energy efficiency & renewable energy, best practices, motors, pumps and fans. http://www1.eere.energy.gov/industry/bestpractices/motors.html. Accessed 1 Jan 2015
US Green Building Council (2015) http://www.usgbc.org. Accessed 1 Jan 2015
Utlu Z, Hepbasli A (2007) A review on analyzing and evaluating the energy utilization efficiency of countries. Renew Sustain Energy Rev 11(1):1–29
Utlu Z, Sogut Z, Hepbasli A, Oktay Z (2006) Energy and exergy analyses of a raw mill in a cement production. Appl Therm Eng 26(17–18):2479–2489
van Vliet OPR, Faaij APC, Turkenburg WC (2009) Fischer–Tropsch diesel production in a well-to-wheel perspective: a carbon, energy flow and cost analysis. Energy Convers Manag 50 (4):855–876
Venkatarama Reddy BV, Jagadish KS (2003) Embodied energy of common and alternative building materials and technologies. Energy Build 35(2):129–137
Vine E (2002) Promoting emerging energy-efficiency technologies and practices by utilities in a restructured energy industry: a report from California. Energy 27(4):317–328
Vine E, Rhee CH, Lee KD (2006) Measurement and evaluation of energy efficiency programs: California and South Korea. Energy 31(6–7):1100–1113
Wall G, Sciubba E, Naso V (1994) Exergy use in the Italian society. Energy 19(12):1267–1274
Wang L (2008) Energy efficiency and management in food processing facilities. CRC Press, Boca Raton. ISBN 978-1420063387
Wang Y, Feng X, Cai Y, Zhu M, Chu KH (2009) Improving a process's efficiency by exploiting heat pockets in its heat exchange network. Energy 34(11):1925–1932
Wang Z, Roberts RR, Naterer GF, Gabriel KS (2012) Comparison of thermochemical, electrolytic, photoelectrolytic and photochemical solar-to-hydrogen production technologies. Int J Hydrog Energy 37(21):16287–16301
Wei Y-M, Liao H, Fan Y (2007) An empirical analysis of energy efficiency in China's iron and steel sector. Energy 32(12):2262–2270
Wei M, Patadia S, Kammen DM (2010) Putting renewables and energy efficiency to work: how many jobs can the clean energy industry generate in the US? Energy Policy 38 (2):919–931
Wu W, Wang B, Shi W, Li X (2014) An overview of ammonia-based absorption chillers and heat pumps. Renew Sustain Energy Rev 31:681–707
Wells C (2001) Total energy indicators of agricultural sustainability: dairy farming case study. Ministry of Agriculture and Forestry, Wellington
Wenkai L, Hui C-W, Hua B, Tong Z (2003) Material and energy integration in a petroleum refinery complex. Comput Aided Chem Eng 15(Part 2):934–939
Wernick IK, Herman R, Govind S, Ausubel JH (1996) Materialization and dematerialization: measures and trends. Daedalus 125(3):171–198

White SB, Howe C (1998) Water efficiency and reuse: a least cost planning approach. In: Proceedings of the 6th NSW recycled water seminar, Sydney
Williams V, Noland RB, Toumi R (2002) Reducing the climate change impacts of aviation by restricting cruise altitudes. Transp Res Part D: Transp Environ 7(6):451–464
Winchester N, McConnachie D, Wollersheim C, Waitz IA (2013) Economic and emissions impacts of renewable fuel goals for aviation in the US. Transp Res A Policy Pract 58:116–128
World Business Council for Sustainable Development (WBCSD) (2000) Eco-efficiency: creating more value with less impact. World Business Council for Sustainable Development, Geneva. ISBN 2-94-024017-5
Worrell E, Blok K (1994) Energy savings in the nitrogen fertilizer industry in the Netherlands. Energy 19(2):195–209
Worrell E, Galitsky C (2005) Energy efficiency improvement and cost saving opportunities for petroleum refineries. Lawrence Berkeley National Laboratory, LBNL paper LBNL-56183. Retrieved from http://www.escholarship.org/uc/item/96m8d8gm. Accessed 1 Jan 2015
Worrell E, Galitsky C (2008) Energy efficiency improvement and cost saving opportunities for cement making, an ENERGY STAR® guide for energy and plant managers. Ernest Orlando Lawrence Berkeley National Laboratory, LBNL-54036-Revision
Worrell E, De Beer JG, Faaij APC, Blok K (1994a) Potential energy savings in the production route for plastics. Energy Convers Manag 35(12):1073–1085
Worrell E, Cuelenaere FA, Blok K, Turkenburg WC (1994b) Energy consumption of industrial processes in the European union. Energy 11(19):1113–1129
Worrell E, Martin N, Price L (2000a) Potentials for energy efficiency improvement in the US cement industry. Energy 25(12):1189–1214
Worrell E, Phylipsen D, Einstein D, Martin N (2000b) Energy use and energy intensity of the U.S. chemical industry. Lawrence Berkeley National Laboratory, LBNL paper LBNL-44314. Retrieved from http://www.escholarship.org/uc/item/2925w8g6. Accessed 1 Jan 2015
Worrell E, Phylipsen D, Einstein D, Martin N (2000c) Energy use and energy intensity of the U.S. chemical industry, LBNL-44314. Lawrence Berkeley National Laboratory, Berkeley
Worrell E, Martin N, Anglani N, Einstein D, Khrushch M, Price L (2001) Opportunities to improve energy efficiency in the U.S. pulp and paper industry. Lawrence Berkeley National Laboratory. LBNL paper LBNL-48354. Retrieved from http://www.escholarship.org/uc/item/7sv597fv. Accessed 1 Jan 2015
Worrell E, Galitsky C, Masanet E, Graus W (2008) Energy efficiency improvement and cost saving opportunities for the glass industry: an energy star guide for energy and plant managers. Lawrence Berkeley National Laboratory, Publication no LBNL-57335-Revision
Xia A, Cheng J, Ding L, Lin R, Song W, Zhou J, Cen K (2014) Enhancement of energy production efficiency from mixed biomass of *Chlorella* pyrenoidosa and cassava starch through combined hydrogen fermentation and methanogenesis. Appl Energy 120:23–30
Yang M (2010) Energy efficiency improving opportunities in a large Chinese shoe-making enterprise. Energy Policy 38:452–462
Yildiz B, Kazimi MS (2006) Efficiency of hydrogen production systems using alternative nuclear energy technologies. Int J Hydrog Energy 31(1):77–92
Yudken JS, Bassi AM (2009) Climate policy and energy-intensive manufacturing impacts and options. Millenium Institute, 2111 Wilson Boulevard, Suite 700, Arlington 22201. http://www.globalurban.org/Climate_Policy_and_Energy-Intensive_Manufacturing.pdf. Accessed 1 Jan 2015
Zamfirescu C, Dincer I (2009) Ammonia as a green fuel and hydrogen source for vehicular applications. Fuel Process Technol 90(5):729–737
Zhao H (2007) HCCI and CAI engines for the automotive industry. Woodhead Publishing, Cambridge. ISBN 978-1845691288

Fuel Efficiency in Transportation Systems

Maximilian Lackner, John M. Seiner, and Wei-Yin Chen

Contents

Abstract

Transportation of people and of goods plays an important role in modern life. It is a major source of anthropogenic CO_2. This chapter, after introducing some fundamentals of natural climate fluctuations as described by Milankovitch cycles,

John M. Seiner: deceased

M. Lackner (✉)
Institute of Advanced Engineering Technologies, University of Applied Sciences FH Technikum Wien, Vienna, Austria
e-mail: maximilian.lackner@tuwien.ac.at

J.M. Seiner

W.-Y. Chen
Department of Chemical Engineering, The University of Mississippi, Oxford, MS, USA
e-mail: cmchengs@olemiss.edu

W.-Y. Chen et al. (eds.), *Handbook of Climate Change Mitigation and Adaptation*,
DOI 10.1007/978-3-319-14409-2_18

describes the causes and consequences of man-made climate change and the motivation for increased fuel efficiency in transportation systems. To this end, contemporary and future ground-based and air-based transportation technologies are discussed. It is shown that concepts that were already given up, such as turbine-driven cars, might be worthwhile for further studies. Alternative fuels such as hydrogen, ethanol and biofuels, and alternative power sources, e.g., compressed air engines and fuel cells, are presented from various perspectives. The chapter also addresses the contribution of CO_2 emissions of the supply chain and over the entire life cycle for different transportation technologies.

Introduction

The purpose of this chapter is to introduce current concepts being examined to increase fuel efficiency in transportation systems in order to reduce their impact on unfavorable climate change. This is a daunting task that will take the cooperation and sacrifice of most of the entire human population to avoid a premature catastrophic event. Now, other chapters of this handbook reveal the salient scientific reasons for climate change, and the reader is encouraged to consult these chapters. However, here it is only necessary to establish that global warming or cooling has continually occurred by natural causes since Earth's formation. This can be deduced from examining the so-called Milankovitch cycles (Kukla and Gavin 2004).

Transportation of people (passengers) and goods (freight, cargo) can be done on the land, the sea, and the air. Approx. 50 % of all transportation emissions are from passenger transport (Lipscy and Schipper 2013). One can distinguish between individual transportation (e.g., cars, bikes) and mass transportation (e.g., trains, planes, buses). Land-based transportation is achieved on highways and on railroads. Travel intensity and choice of transportation mode depend on personal preference, income, and country (Lipscy and Schipper 2013). Trip distance, e.g., to work for commuters, is also an important driver (Muratori et al. 2013). Goods can also be moved in pipelines. With the globalization of the economy and shifts in lifestyle habits, transportation has become more and more important over the last 100 years, both in the industrial and the developing world. Figure 1 below, in an exemplary fashion, shows the increase in energy consumption for transportation in China.

According to Zhang et al. (2011a), highways have become the dominant mode of transportation in China. The energy consumption in this mode increased from 1980 to 2006 from 36.4 % to 61.5 %. Other economies have seen similar developments. As Fig. 1 shows, other transportation systems have seen more and more usage as well.

Transportation systems are mainly driven by fossil fuels, predominantly those made from crude oil. The reason is that liquid fuels such as gasoline and diesel have high energy content that are safe and convenient to handle at low costs.

Energy efficiency of transportation systems can be defined as the amount of energy needed for a certain task, e.g., the transportation of one passenger or one unit of cargo over a certain distance. Transportation and energy is reviewed in

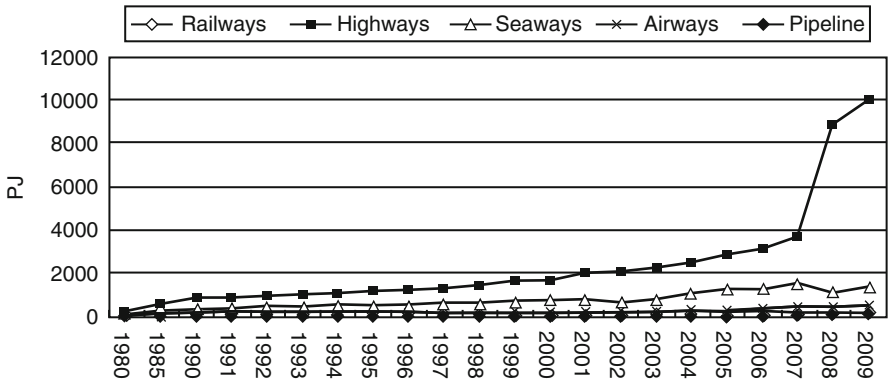

Fig. 1 Chinese transportation sectors and their energy consumption from 1980 to 2009 (Reproduced with permission from Zhang et al. 2011b)

Greene (2004). Energy efficiency is the most economic way for climate change mitigation (Kamal 1997). Therefore, efforts need to be taken to improve energy efficiency of transportation systems.

Since the year 2000, the world production of gasoline (petrol) has matched consumption of this product. This has led to sporadic shortfalls of gasoline at the pumps along with elevated costs. Beyond the uncertainty of future fuel costs, the predictions for effects of global warming on the planet are very severe, and it is important that mankind addresses the issue of how transportation systems contribute to this problem. Today there are over one billion vehicles in the world, and within 20 years, the number will double (Sperling et al. 2010), largely a consequence of China's and India's explosive growth. Figure 2 takes a look at the projected number of cars in China. An impressive increase is expected over the next years (Hao et al. 2011).

Figures 1 and 2 depict the situation in China, which was chosen as a showcase example here, as China is currently one of the world's major emitters of anthropogenic CO_2.

At the present time, as shown in this chapter, there are only partial solutions to reduce the impact of transportation systems on global warming. Energy conservation by avoiding travel is one option. Technical improvements to transportation systems are another approach.

Readers will note that the production of CO_2, a by-product from the combustion of carbonaceous fuels such as gasoline with air, has been linked to a global increase in temperature. With an increase in the Earth's temperature comes melting of the ice caps and a rise of sea level on coastal cities. Of most concern is an accompanying change in composition of the Earth's fragile atmosphere. Millions of years ago the Earth had a very different atmosphere than it does today, where ice caps were melted and instead had lush forests. The percentage of O_2 was over 30 %, a level that would support large mammals, as it did, but not the present human population. Therefore, it is imperative that economical methods be found to reduce the emission of CO_2 if mankind is to have a sustainable future. Tim Flannery (2006) (http://www.

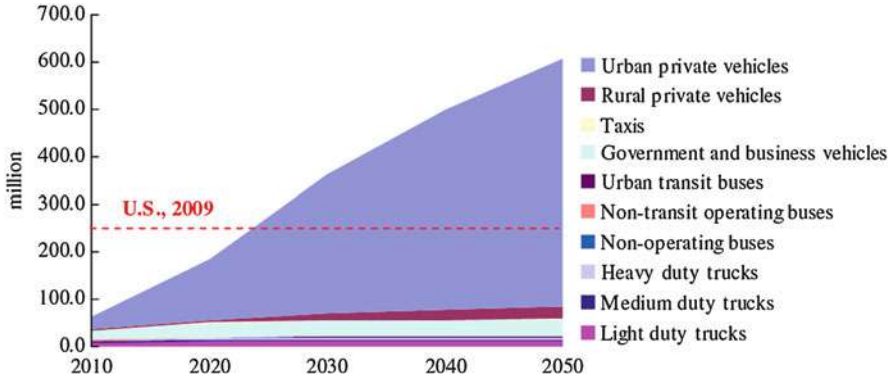

Fig. 2 Projection of China's vehicle population through 2050 (Reproduced with permission from Hao et al. 2011)

theweathermakers.org/) pointed out in his book that to stay below the threshold for melting of the ice sheets in Greenland and West Antarctica, it would be needed to reduce CO_2 emissions by 80 % from today's levels. This corresponds to no more than 30 lb of CO_2 per person per day. Further, Flannery predicts that if progress in reaching the above goal is not enough, only 20 % of the present world population will reach the year 2050. Professor Tim Flannery is an Australian mammalogist, paleontologist, environmentalist, and global warming activist.

In this chapter, the case for the reduction of CO_2 emissions from transportation systems is made. Solutions to efficient reductions are an evolutionary process where incremental change may represent mankind's only solution. With this viewpoint prior automotive designs that were introduced years ago and that failed to gain acceptance but may deserve another evaluation will be discussed. Present-day automotive engines utilize fuel injection systems instead of carburetors and represent the main reason for increased fuel mileage. Consequently, this chapter will also examine various engine cycles. Other measures such as lightweight construction materials, car pooling, and traffic management can also reduce fuel consumption. There is also a need to consider alternate fuels not only for emissions, but also reduction of the dependence on oil. Thus, the use of biofuels and hydrogen as substitutes for oil will be discussed. This is such a broad effort that this chapter will only be able to introduce a few concepts for automotive applications. Concepts for other landborne plus air- and seaborne transportation will be touched upon. The authors will also briefly discuss fuel cells, hybrid vehicles, and electric vehicles. Aircraft with respect to fuel efficiency will shortly be addressed. There is no question that aircraft play an important role in contemporary lifestyle, but they require significant energy to perform their mission. Thus it will be necessary to introduce radical designs that would substantially reduce the fuel burn rate.

The Issue

Since Earth's formation, the atmosphere's composition and temperature has changed dramatically due to the Earth's cooling. However, there is another factor that affects the temperature of the atmosphere that is related to gravitational attraction between the planets and the sun. This gravitational attraction produces an eccentricity of the Earth's orbit, obliquity of the Earth's axis, and precession of the Earth's axis of rotation. These effects have various periods as was first noted by Milankovitch who observed the following periods of the Earth's axis: Wobble cycles of 19,000 and 23,000 years, tilt cycle of 41,000 years, and cycles of 100,000 and 400,000 years to the Earth orbit around the sun (Kukla and Gavin 2004). The Earth's orbit transitions periodically between a circular and an elliptical orbit. When on an elliptical orbit, the Earth's distance to the Sun has periods where it is the greatest, and the Earth's atmosphere is cold (i.e., ice age). Currently, the Earth is in a more circular orbit, and the Earth's temperature is warmer. These Milankovitch cycles are of course natural events that mankind cannot interfere with. During previous periods the ice caps were melted, and in the USA, alligators extended as far north as Denver. Data gathered from the Antarctica ice shelf allow researchers to infer the air temperature of the Earth at that location going back 400,000 years from analysis of cores drilled into the ice. Further analysis of these cores also permits one to estimate the percentage of CO_2 in the atmosphere during this period of time. One can also deduce that during nearly circular orbits, the Earth's temperature is the warmest, and during elliptical orbits, the Earth's temperature is the coldest. The temperature spikes around 320,000, 210,000 and 130,000 years before today's time and now have elevated contents of CO_2 in the atmosphere. The warming periods that occurred beyond present day were controlled by natural events. However, during the present cycle that includes the Industrial Revolution, there appears to be a large increase in the percentage of CO_2 that is significantly higher than recorded for previous cycles: the CO_2 concentration in the atmosphere is elevated by 100 ppm due to human action. During the warm periods where the Earth's orbit is nearly circular, the peak concentration of CO_2 has been in the order of 275 ppm CO_2. Today (January 2015) it has spiked to just under 400 ppm (The Keeling Curve et al. 2015), about 40 % higher than in preindustrial times and higher than in any other period in at least 800,000 years. The level of atmospheric CO_2 is rising at a rate of approximately 2 ppm/year. This increase can be attributed to the presence of humans on Earth and their rapid consumption of energy, i.e., by the combustion of fossil fuels. A fair question to ask is what are the major contributors to CO_2 production and how the CO_2 concentration is related to Earth's average temperature. From Fig. 3, one can see that there are three main contributors to the production and emission of CO_2 in the atmosphere from burning fossil fuels, cement production, and land use change. The figure, reproduced from the 5th IPCC Assessment Report (2013), also shows the CO_2 sinks. These represent the areas where technology developments to reduce CO_2 are needed.

The question then is how this increase in concentration of CO_2 modifies the average temperature of the planet.

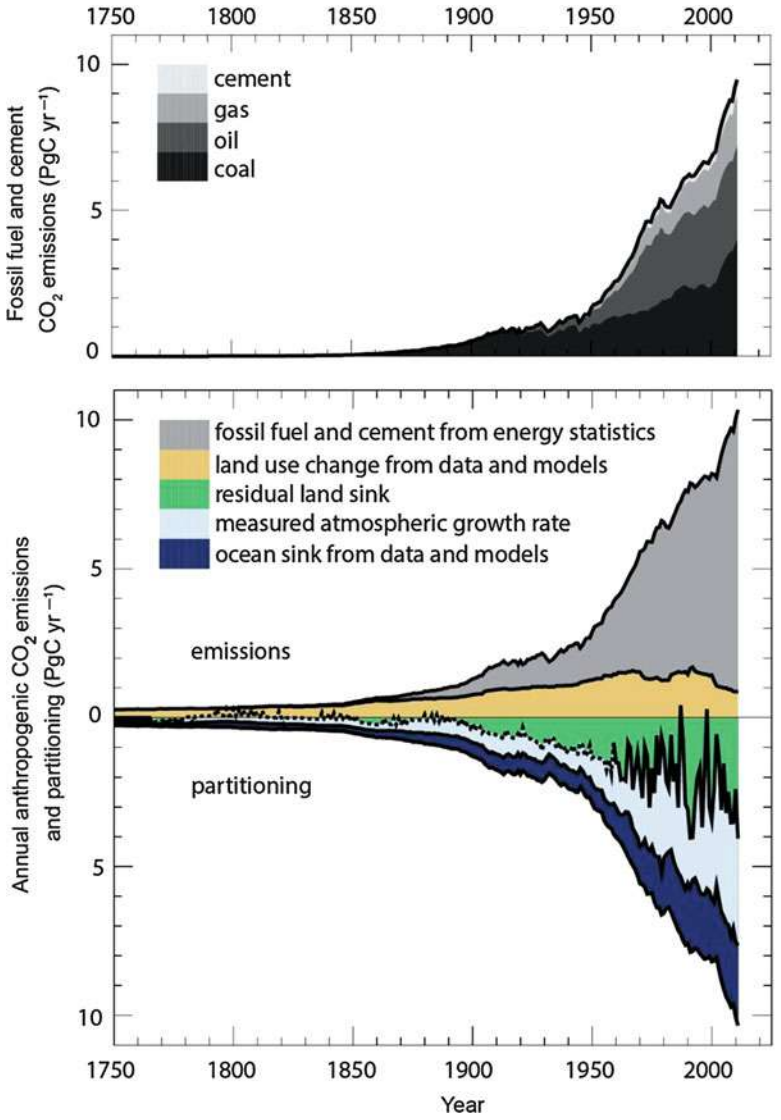

Fig. 3 Leading contributors to production of CO_2 and sinks (Reproduced from IPCC 2013)

Note that CO_2 is not the only anthropogenic greenhouse gas, but also the most important one. Most of the natural greenhouse effect is caused by water vapor.

Other important greenhouse gases are CH_4, N_2O, and SF_6. CH_4 emissions are also produced by the transportation sector, e.g., as losses from natural gas (and biogas) production and distribution and as unburnt hydrocarbon emission from the combustion process.

It is very surprising how small an increase in CO_2 concentration contributes to the average temperature around the globe. Now, the atmosphere has reached a level of said ~400 ppm. This means that the world has seen a nearly 2 °C increase in temperature over that of preindustrial times. Even with this small increase in average temperature, many today can recall changes that have occurred and are noteworthy (for more information on narrative research in climate change, see, e.g., (Paschen and Ison 2014). In the early 1900s, people would drive their cars across Lake Ontario to Toronto, Canada, on the frozen ice sheet. This lake has not frozen over for more than 50 years. In Southern Virginia, James River used to freeze over as late as the 1950s, but no longer. Predictions by Flannery are that if an atmospheric CO_2 concentration between 900 and 1,000 ppm is reached, in the future only one in five people would survive. Now, aside from observations that have occurred with an increase in global temperature, one can observe that the ice sheets have already begun to melt. Figure 4 shows the extent of the Arctic sea ice averaged over the period 1979 to 2007 for the months May to September. Following Fig. 5, one can see that the ice shelf does not restore itself until September. In a typical year the ice sheet would begin to grow again in August, but now in August it is still melting. With melted ice sheets, the Earth's thermal energy balance is changed since more heat from the Sun is absorbed by the Earth rather than being reflected back into space. Thus, the cycle is intensified.

Figure 5 below shows the thickness of the ice sheet north of Greenland in the 1950s and the prediction by NOAA (National Oceanic and Atmospheric Administration) for the year 2050, which shows the ice sheet is predicted to be reduced to half its previous size.

Therefore, there is a strong motivation to increase the fuel efficiency of transportation systems for people and freight to mitigate anthropogenic climate change. Several aspects will be discussed below.

Carbon Emissions by Light Duty Vehicles

It can be seen that since the beginning of the Industrial Revolution, the planet's atmosphere has increased in temperature by almost 2 °C. Not a large increase, but big enough to start significant melting of the ice caps. One can see that the temperature increase can be linked to a large increase in CO_2 in the atmosphere. Combustion of solid (coal), liquid (gasoline, diesel), or gaseous (natural gas) fuels, to a significant fraction for transportation purposes, is the major contributor to the production of anthropogenic CO_2. Natural gas has a higher H/C ratio than diesel or gasoline. Therefore, it is more climatically benign when being burnt in engines (note that the greenhouse warming potential [GWP] of CH_4 is ~20 times that of CO_2, so CH_4 emissions are to be avoided).

A natural question to ask at this point is what percentage of CO_2 production is due to transportation and which countries are the major contributors. DeCicco et al. provide a graphic illustration of each sector's contribution in Fig. 6. The estimates shown in this figure only include the use of fossil fuel. As can be seen,

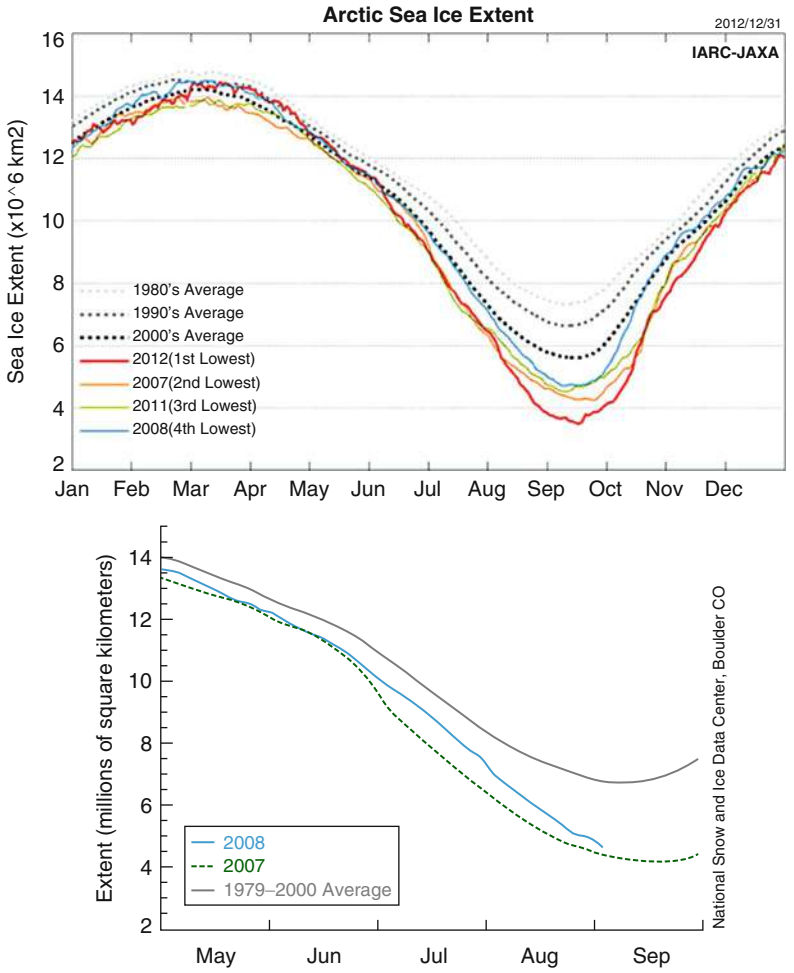

Fig. 4 Annual cycle of the Arctic sea ice extent for 2012 (*red*), 2007 (*orange*), 2011 (*green*), and 2008 (*blue*). *Dashed lines* show decadal means for the 2000s (*black dashes*), 1990s (*gray dashes*), and 1980s (*light-gray dashes*) (Source: IARC/JAXA Sea Ice Monitor, http://www.ijis.iarc.uaf.edu/en/home/seaice_extent.htm) (Walsh 2014)

over 40 % of the CO_2 emissions are from the production of home electricity and heat. Light-duty vehicles only account for 10 % of the production, and almost half of that is produced in the USA with a significant nearly a quarter from Europe. One observes that only a little over 2 % occurs in China and India. In the next 20 years, China and India are expected to grow and consume an amount equal to the USA (compare also Figs. 1 and 2).

A substantial growth in CO_2 production by light-duty vehicles would require additional refineries throughout the world, or extreme shortages at the pump would

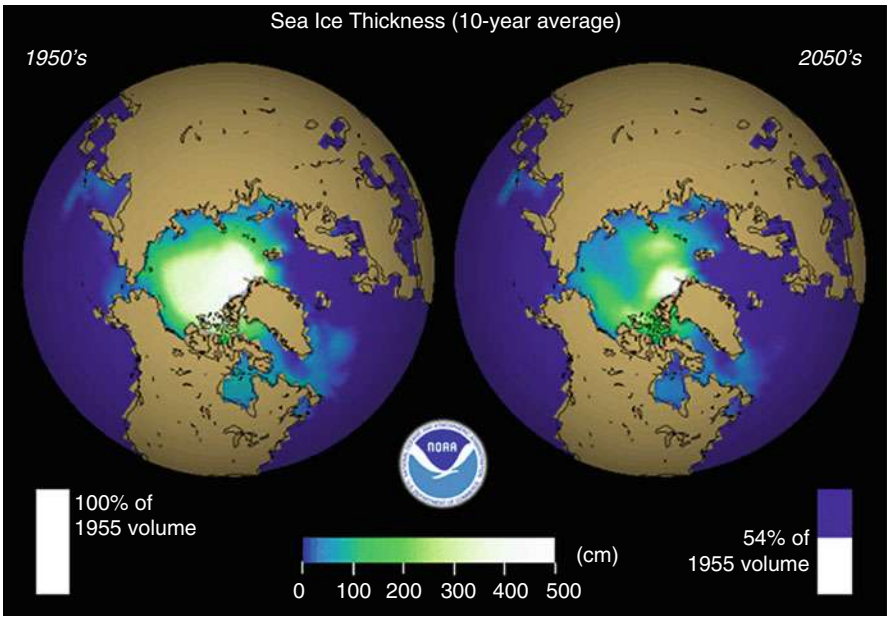

Fig. 5 Melting of the polar ice cap (Reprinted with permission from the National Snow and Ice Data Center 2015)

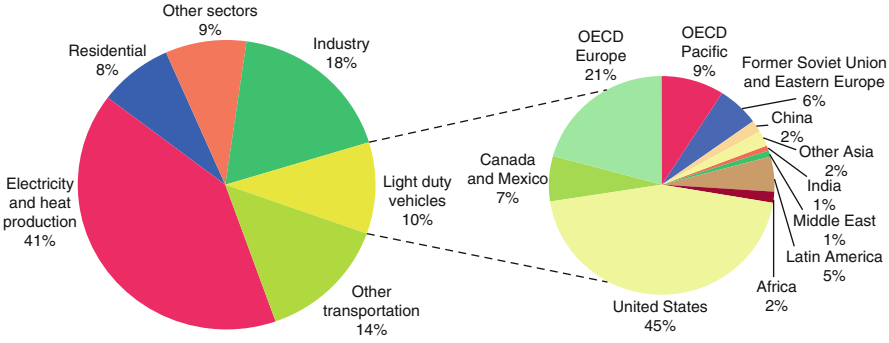

Fig. 6 Estimates for CO_2 production by sector and light-duty vehicles. *Left*: Global carbon emissions by sector (6,814 $*10^6$ t). *Right*: Light-duty vehicle carbon emissions by region ($680*10^6$ t). (Reprinted with permission from DeCicco et al. 2015)

occur. Energy conservation will play a more realistic role in the future to avoid the problem of fuel shortage, but this cannot be expected to take effect until existing vehicles are replaced with ones using new technology. DeCicco also addressed this issue, and in Fig. 7a, one can see that old SUVs dominate the carbon burden share

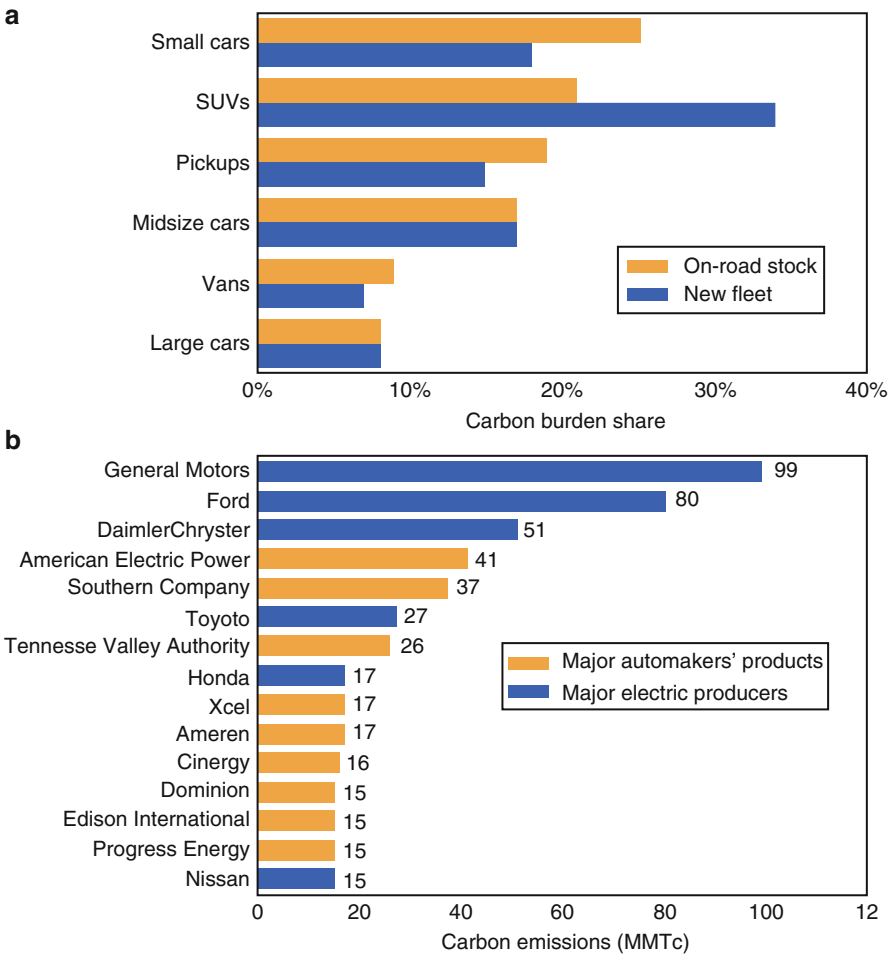

Fig. 7 Carbon emissions by new versus old vehicles and electric producers. (**a**) CO2 pollution as % of new & old vehicles. (**b**) Carbon emissions: auto & electric producers DeCicco et al., Global Warming on the Road (DeCicco et al. 2015)

and that both new and old midsize cars contribute equally. Carbon emissions by cars dominate those associated with electric producers, see Fig. 7b. These statistics indicate that there is a need to adopt a policy to retire existing vehicles as soon as possible and, in particular, SUVs.

DeCicco et al. point out that there are three factors that govern the production of carbon dioxide in the transportation sector. The first is related to travel demand, the second to automotive efficiency, and the third to carbon content per gallon of fuel. Aside from reducing the distance travelled per year by car or light-duty truck, it is of interest to know how alternate means for ground transportation compare to decide which mode to emphasize. Table 1 shows a compilation of results by the US

Table 1 Efficiency of various transportation systems 1 gal (~3.7854 l) of gasoline contains approximately 114,000 BTU (120 MJ) of energy. MPGe = miles per gallon gasoline equivalent. This measure of the average distance travelled per unit of energy consumed compares the energy consumption of alternative fuel vehicles. 1 MPGe ≈ 0.0182 km/kW · h ≈ 0.005 km/MJ

Transport mode	Average passengers per vehicle	Efficiency per passenger	
Vanpool	6.1	1,322 BTU/mi	2.7 l/100 km (87 MPGe)
Motorcycles	1.2	1,855 BTU/mi	3.8 l/100 km (62 MPGe)
Rail (Amtrak)	20.5	2,650 BTU/mi	5.4 l/100 km (43 MPGe)
Rail (transit light and heavy)	22.5	2,784 BTU/mi	5.7 l/100 km (41 MPGe)
Rail (commuter)	31.3	2,996 BTU/mi	6.1 l/100 km (38 MPGe)
Air	96.2	3,261 BTU/mi	6.7 l/100 km (35 MPGe)
Cars	1.57	3,512 BTU/mi	7.2 l/100 km (33 MPGe)
Personal trucks	1.72	3,944 BTU/mi	8.1 l/100 km (29 MPGe)
Buses (transit)	8.8	4,235 BTU/mi	8.7 l/100 km (27 MPGe)

Department of Energy (DOE) for the efficiency of various transportation systems in terms of energy expended per passenger with an estimate of an equivalent number of liters per 100 km. The efficiency in Table 1 is estimated in terms of BTU/mile and also in miles per gallon.

Table 1, from the US Department of Energy in 2008, clearly indicates the value of carpooling with a van that would carry six passengers. On a per passenger basis, the vanpool achieves 87 $MPGe_{US}$, an efficiency that would be hard to match by an automobile with a single passenger. Only motorcycles nearly match the vanpool. Personnel trucks are listed as one of the most inefficient modes of transportation with cars, only slightly better. Transit buses are the worst form primarily due to the constant stopping and starting needed to pick-up and let off passengers.

Carbon Generated by Combustion with Air

Each barrel contains 42 gal (159 l) of crude oil and consists of various petroleum products as shown in Fig. 8. As one can observe, only about half a barrel of crude can be refined into gasoline (after fractionated distillation, several processes in a refinery such as cracking can shift the product mix).

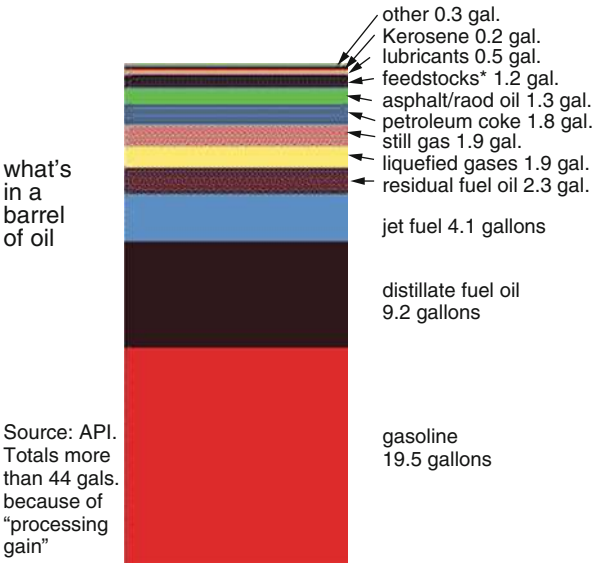

Fig. 8 Products obtained from refining a crude barrel of oil (Reproduced with permission from Gibson Consulting 2015). *API* American Petroleum Institute

The amount of CO_2 emitted per gallon is governed by the Code of Federal Regulations (40CFR600.113) (Title 40 2015). The carbon content of gasoline per gallon is 2,421 g, whereas the carbon content of diesel fuel per gallon is 2,778 g.

Recall the words of Tim Flannery who said that to prevent the ice sheets from melting, every human had to be on a diet of 30 lb or less of carbon a day. So each person could only use about a gallon and a half of gasoline each day. The ability to use only a gallon and a half each day strongly suggests an elusive goal. While one may not be able to meet this goal, earnest conservation steps can ease the way into the inevitable. One of the first conservation steps one can take is to consider engine thermodynamic cycles to see if there is any advantage. Toward this purpose, the bare essentials associated with the spark and compression ignition engines are discussed.

The four-stroke engine cycle was first patented by Eugenio Barsanti and Felice Matteucci in 1854. An illustration of the four-stroke cycle, reproduced from Obert (1973), is shown in Fig. 9. There, one sees the position of the cylinder head, intake valve, exhaust valve, and spark ignition for one entire cycle. Figure 10a, b show that the thermodynamic model for either SI (spark ignition) or CI (compression ignition) during intake and exhaust is considered to be an isentropic process (=constant entropy). During cycles of heat in or out, the thermodynamic model is far from isentropic. Note that for compression ignition engines, during combustion, the process takes place at constant pressure.

For the ideal combustion, the efficiencies associated with the stoichiometric combustion of these fuels with air are illustrated in Fig. 10. For gasoline, this is given by

$$C_8H_{18} + 12^{1/2}O_2 + 47N_2 \rightarrow 8CO_2 + 9H_2O + 47N_2$$

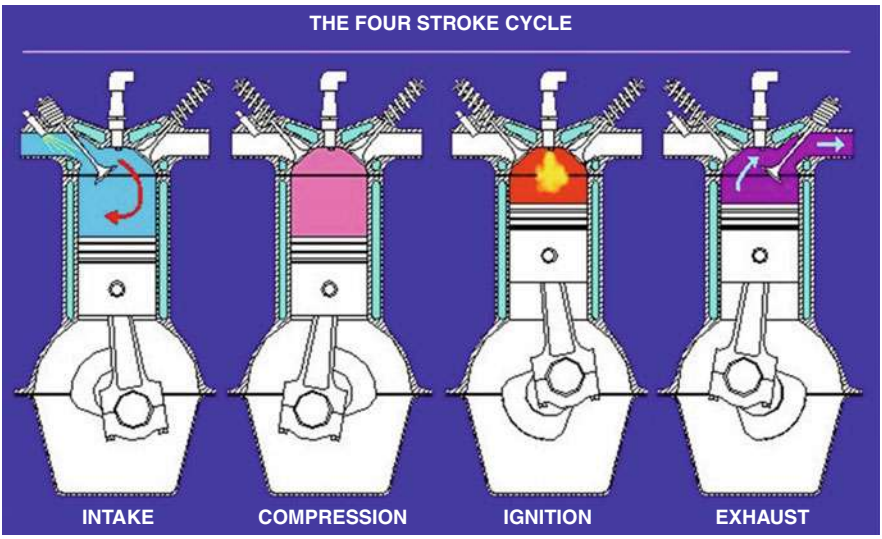

Fig. 9 Graphic illustration of four-stroke compression ignition engine (Reproduced from Obert 1973)

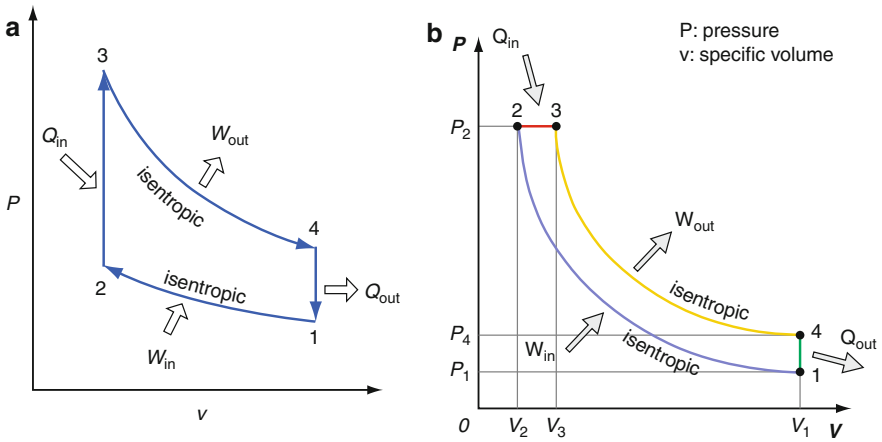

Fig. 10 Idealized four stroke for SI and CI combustion models. (**a**) Otto cycle Pv Diagram. (**b**) Diesel cycle Pv Diagram(Reproduced from Obert 1973). *P*, pressure; *v*, volume; *W*, work; *Q*, heat; *SI*, spark ignition; and *CI*, compression ignition

where following Fig. 10a one can note

$$Q_{Arev} = c_v(T_3 - T_2) \quad \eta_t = \frac{Q_A + Q_R}{Q_A} = 1 - \frac{T_1}{T_2} = 1 - \frac{1}{r_v^{\gamma-1}}$$
$$Q_{Rrev} = c_v(T_1 - T_4)$$

where r_v is the engine compression ratio. As an example, consider the following: engine compression ratio, $r_v = 8$; ambient temperature, $T_a = 540\ ^\circ R$ (300 K); ambient pressure, $P_a = 14.7$ psia (101.3 kPa = 1.014 bar); and then one has that

$$\eta_t = 1 - \frac{1}{r_v^{\gamma-1}} = 1 - \frac{1}{8^{0.4}} = 0.565 = 56.5\%$$

Factoring in transmission and drive train, the overall gasoline-powered automobile efficiency is approx. 17 % (Obert 1973). Quite remarkable, about 83 % of the available energy is wasted on the gasoline-powered internal combustion engine. Even the thermal efficiency of the four-stroke ideal diesel engine cycle appears more attractive. Consider the Pv diagram shown in Fig. 10b, which shows air coming into the system at constant pressure and air being discharged from the system at constant pressure. Based on this cycle one can derive that the reversible heat added and discharged is given by

$Q_{Arev} = c_v(T_3 - T_2)$
$Q_{Rrev} = c_v(T_1 - T_4)$, and since $\left(\frac{T_3}{T_2}\right)^\gamma = \left(\frac{T_4}{T_1}\right)$, the thermal efficiency is given by

$$\eta_t = \frac{Q_A + Q_R}{Q_A} = 1 - \left(\frac{1}{\gamma}\right)\left(\frac{T_4 - T_1}{T_3 - T_2}\right) = 1 - \frac{1}{r_v^{\gamma-1}}\left[\frac{r^\gamma - 1}{\gamma(r-1)}\right]$$

Typical values for the diesel cycle are compression ratios near 25 to ensure auto ignition. A diesel engine takes in just air, compresses it, and then injects fuel into the compressed air. The heat of the compressed air lights the fuel spontaneously. A typical thermal efficiency computed from the above equation using a compression ratio of 25 is a value $\eta_t = 0.264$. Note: Diesel engines are in general 30–35 % more efficient than gasoline-powered vehicles; however, efficiency strongly depends on the vehicle load.

The energy efficiency of alternative power trains in vehicles is discussed in Åhman (2001).

Otto and diesel engines are most commonly used in transportation. The Wankel engine is another concept with less proliferation. It operates without pistons. The Mazda RX-8 is one example of a car that deploys a Wankel engine. Table 2 shows some aspects of Wankel engines.

Experiments with turbine-powered cars were carried out in the USA around 1960. The following pros and cons were identified (Table 3).

Gas turbines are very efficient at high speeds and constant load. They need time to reach optimum operating conditions, and they produce thrust rather than torque. The problem with vehicles is that they are operated in several load conditions and often only for short distances.

Although the concept of turbine cars was abandoned soon after their appearance, they might still offer an interesting route to future efficient cars, so new research is carried out in this area, for instance, on micro-gas turbines (MGT) to recharge battery packs, in particular, for electric vehicles (EVs) (Sim et al. 2013).

Table 2 Assessment of the Wankel engine (Reproduced with permission from Hege 2006)

Pros	Cons
High power output/unit weight	Rotating seals reduce engine compression ratio
Good fuel/air mixing	Large fraction of unburned fuel lowers the efficiency
Even combustion	Excessive noise due to rotating seals

Table 3 Assessment of turbine-powered automobiles (Reproduced from Hege 2006)

Pros	Cons
Low maintenance Long engine life expectancy Reduction of number of parts by 80 % No warm-up period, easy low-temperature start No stall at sudden overload Hot but clean exhaust gases Low oil consumption Operation on wide fuel variety	High fuel consumption at idle due to high rpm throttle lag from idle as the engine spools up. High temperature of exhaust gases, low efficiency High noise emissions Expensive

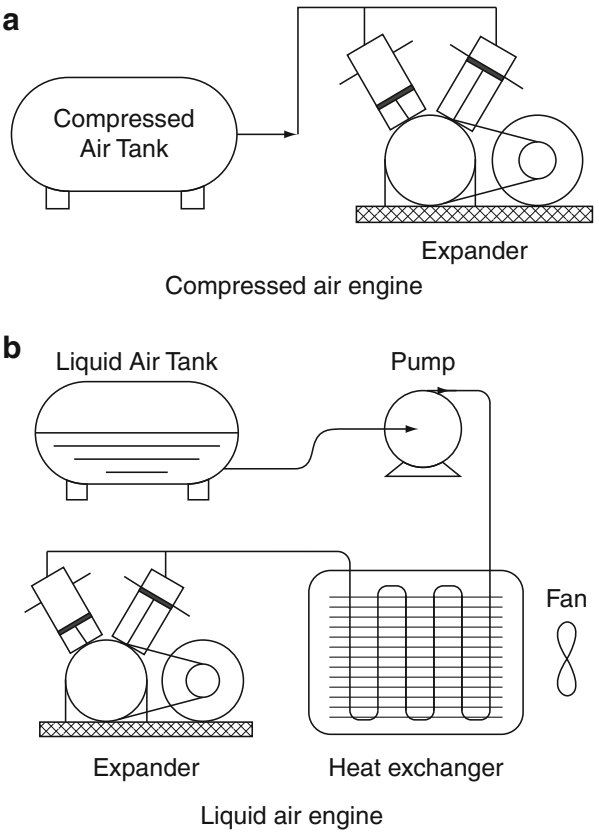

Fig. 11 Air-fuelled engines (Reproduced with permission from Chen et al. 2011)

Another technology is the "air fuelled engine." It can be operated by compressed air (Miller et al. 2010) or by liquid air, yielding zero tailpipe emissions (Chen et al. 2011), compare Fig. 11.

Due to the high energy consumption of air liquefaction plants, the compressed air-powered engines have a better energy efficiency than the liquid air ones (28.3 % to 36.0 % vs. 12.8 % to 17.0 % for the setups studied in Chen et al. 2011). Compared to liquid hydrocarbon fuels, compressed air has a lower energy density.

A novel concept for internal combustion engines is HCCI (homogeneous charge compression ignition) (Zhao 2007). It is a kind of hybrid between a compression ignition and a spark ignition engine, in that a homogeneous fuel/air mixture is brought to autoignition. This combustion mode resembles the typical "knocking" in gasoline engines. It is fast and hard to control. However, HCCI offers the potential of low-pollution and high-efficiency automotive engines.

Alternative Fuels

With depleting fossil fuel resources, costs go up and supply shortages might occur, apart from the emission of CO_2 into the atmosphere from the burning of these fuels. Alternative fuels can be unconventional fossil fuels (such as those derived from shale gas (Mallapragada et al. 2014), methane hydrate, fracking, etc.) and "renewable" fuels. This section focuses on renewable fuels, which are produced directly or indirectly from sunlight, without the need to turn to fossil fuels. The following energy carriers have been envisaged as fuels for combustion engines and/or fuel cells:

- Hydrogen
- Ethanol
- Ammonia (Zamfirescu and Dincer 2009)
- Methane
- Methanol

These fuels can be produced via various routes, both from fossil and renewable resources. Methane is also the main constituent of biogas. There are so-called flexible-fuel (flex fuel) vehicles that can run on several fuels, e.g., ethanol. A blend of gasoline and 85 % ethanol is called E85. Flex-fuel vehicles (FFV) have been produced since the 1980s. Ethanol (von Blottnitz and Ann Curran 2007) and biodiesel (Ticker 2003) are two common "biofuels." Fischer Tropsch synthesis and biomass gasification are important processes to obtain fuels from biomass, apart from anaerobic digestion and fermentation. Fuels from waste are also considered biofuels. Oil crops yield fuels from extraction and pressing of suitable plants (Tickell 2000). Also, aquatic biomass such as certain algae can be used, e.g., for biodiesel production.

There is also some controversy around biofuels. Two issues associated with biofuels are

- Potential competition over farmland with food crops
- Water consumption associated with their production (see concept of virtual water, Allan 2011)

One can distinguish between 1st, 2nd, and 3rd generation of biofuels.

First-generation biofuels are made from foodstuff (ethanol from corn, biodiesel from soybean, or rapeseed via transesterification). They are mature and available on the market.

Second-generation biofuels are produced from lignocellulose. There are thermal and enzymatic processes to break of the biopolymers into smaller units.

There are also "1.5 G" biofuels, which utilize the full plant of 1G fuels.

The first 1.5G and 2G biofuel commercial production plants are on stream. Their advantage is that no competition over arable land with food crops exists. Also, 2G biofuels can be grown on marginal land.

Third-generation biofuels target algae for "green" fuel production, as they are expected to yield more biomass per area than land-based fuels. They could use sewage as nutrient, and avoid land usage (land use change, e.g., through deforestation to produce cropland), which also contributes to climate change.

Energy produced from biomass was initially considered carbon neutral because biomass is renewable through photosynthesis. Controversies, however, have emerged about the various impacts of promoting the use of first-generation biofuels. Major concerns about using bioethanol as fuel include the following issues:

- Corn is a food source, and corn ethanol production will reduce food availability. Developing countries that depend on the corn donation from the west have already experienced food shortages.
- Fertilizer is required in corn production; both cost and energy consumption are incurred during fertilizer production. Moreover, unprecedentedly large scale use of fertilizer alters the natural nitrogen cycle and induces other ecological/environmental problems that have already been identified as threats.
- About 5 gal of water are needed in the production of each gallon of ethanol in a plant; this does not consider the amount of water it takes to grow the corn. So potable water shortages might result from excessive bioethanol production.
- Bioethanol production requires energy input. Ethanol purification by distillation is energy intensive and usually involves consumption of natural gas, which, in turn, produces CO_2 from fossil fuel. As a result, while bioethanol utilization reduces fossil fuel dependence, it is not a completely carbon neutral process.

Widespread adoption of bioethanol will cause redistribution of the world's natural resources and wealth. The actual environmental and societal costs of bioethanol are likely to be much higher. A good starting point for a healthy debate on this issue can be found at (Schulz 2007).

The transportation of energy carriers also consumes, naturally, energy. In Hamelinck et al. (2003), the energy consumption of biofuel transportation from production site to point of use is discussed, so that biofuels are not entirely carbon

Table 4 Energy density of various fuels

Fuel	Volumetric (Wh/l)	Gravimetric (Wh/kg)
Diesel	10,942	13,762
Gasoline	9,700	12,200
LPG (liquefied petroleum gas)	7,216	12,100
Propane	6,600	13,900
Ethanol	6,100	7,850
Methanol	4,600	6,400
Liquid hydrogen	2,600	39,000
Hydrogen (150 bar)	405	39,000
Nickel-metal hydride	100	60
Lead acid battery	40	25
Compressed air	17	34

neutral or even carbon negative. The carbon balance of several biofuels is even worse than that of gasoline or diesel. A detailed life cycle assessment is necessary.

When assessing biofuels, next to climate change, abiotic depletion, acidification, eutrophication, and human toxicity (Petersen et al. 2015) need to be considered.

Second- and third-generation biofuels hold promise for CO_2 emission savings.

The share of biofuels is expected to increase significantly over the next decade. An important aspect of alternative fuels, apart from their specific costs, is the energy density (see Table 4).

From the above Table 4, one can see that compressed air has a low energy density both in terms of volume and weight. The energy density is important for the range of a vehicle. Gases can be stored in compressed form, as hydrides or as a liquid in cryogenic conditions. Liquefaction can consume a considerable amount of energy. For hydrogen, one can define the gravimetric storage density. It is the weight of hydrogen being stored divided by the weight of the storage and delivery system. A typical value is 2–4 %. Storage has to be achieved in a safe, cost-effective, and efficient way. Alanates are a promising material class for hydrogen storage (Gross et al. 2002). Hydrides, this is chemically bond hydrogen in a solid material. This storage approach should have the highest hydrogen-packing density. However, storage media have to meet several requirements:

- Reversible hydrogen uptake/release
- Lightweight with high capacity for hydrogen
- Rapid kinetic properties
- Equilibrium properties (p, T) consistent with near-ambient conditions

There are two solid-state approaches:

- Hydrogen absorption (bulk hydrogen)
- Hydrogen adsorption (surface hydrogen)

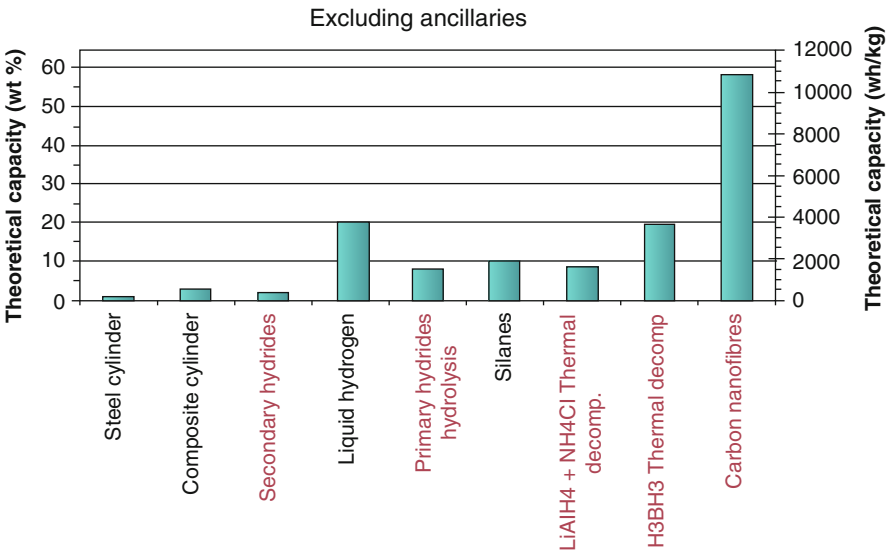

Fig. 12 Graphic illustration of hydrogen storage methods. *Red color* indicates that the technologies have not reached maturity yet (Reproduced from Obert 1973)

For details on hydride storage, see Agresti (2010).

Figure 12 compares several storage methods for hydrogen. Hydrogen can be produced, e.g., by electrolysis (solar power) or gasification.

Renewable energies for sustainable development are discussed in Lund (2007).

Alternative Power Sources

Electric cars come as battery-powered and fuel-cell-powered models. For a comparison on "well-to-wheel" energy pathways, see, e.g., (Eaves and Eaves 2004). So-called hybrid vehicles use a combination of an internal combustion engine (ICE) plus an electric motor (van Vliet et al. 2010).

Air Transportation

According to Chèze et al. (2011), world air traffic should increase by about 100 % between 2008 and 2025. The world jet fuel demand is expected to increase by about 38 % during the same period (Chèze et al. 2011). Aircraft manufacturers have reduced the specific fuel consumption of their equipment over the last decades, e.g., by using more efficient turbines, lightweight construction materials, and improved design. More radical concepts might help lower specific fuel consumptions further. Blended-wing-body (BWB) aircraft are promising constructions currently being studied. Their benefits are 10–15 % less weight and 20–25 % less fuel

consumption. Challenges today are the integration of the propulsion system into the airframe, aerodynamics, and control. An important aspect for the fuel efficiency of aircraft is the so-called aerodynamic efficiency. It determines its range with all other parameters kept constant. For details, see Qin et al. (2004).

CO_2 emissions and energy efficiency of aircraft are treated in Lee (2010), Babikian et al. (2002), Lee et al. (2004), and Morrell (2009).

Cargo

Freight transportation is a huge industry. Goods are moved by sea, air, and land, where seaborne transportation has the highest share with over 30,000 billion tonne-miles per year. Sea transportation aboard large container ships has a particularly advantageous energy efficiency compared to other modes. Because of concerns for the air quality in harbors and port cities, the emissions from ships have recently received more attention. For details on CO_2 emissions from shipping activities and their mitigation, see Fitzgerald et al. (2011), Villalba and Gemechu (2011), Cadarso et al. (2010), Geerlings and van Duin (2011), Heitmann and Khalilian (2011), Schrooten et al. (2009).

Means of Energy Efficiency

Energy efficiency improvements can be achieved in various ways.

By training staff, an "energy saving mindset" can be created. It can yield fuel savings directly, without the need for significant investment costs. However, the impact will not be as long lasting as technical improvements. Building upon the above idea of different means to achieve energy efficiency gains, the following Fig. 13 below highlights four energy conservation strategies for road transportation and their monetary impact, reproduced with permission from Litman (2005).

In Parry et al. (2014), an analytical framework for comparing the welfare effects of energy efficiency standards and pricing policies for reducing gasoline, electricity, and carbon emissions is discussed.

Comparison of Different Transportation Technologies

A key question related to energy efficiency in transportation is how various modes compare to each other. This is shown in an exemplary way for the greenhouse gas emissions (g CO_2 equivalents) per PKT (PKT = passenger kilometer travelled). In that paper (Chester and Horvath 2009), it is concluded that the total life cycle energy inputs and greenhouse gas emissions for road, rail, and aircraft transportation on top of the tailpipe emissions are 63 %, 155 %, and 31 %, respectively. This means that in the case of rail transportation, the major part of CO_2 emissions does not occur during the use of the vessel for a journey, but rather in related areas such as infrastructure

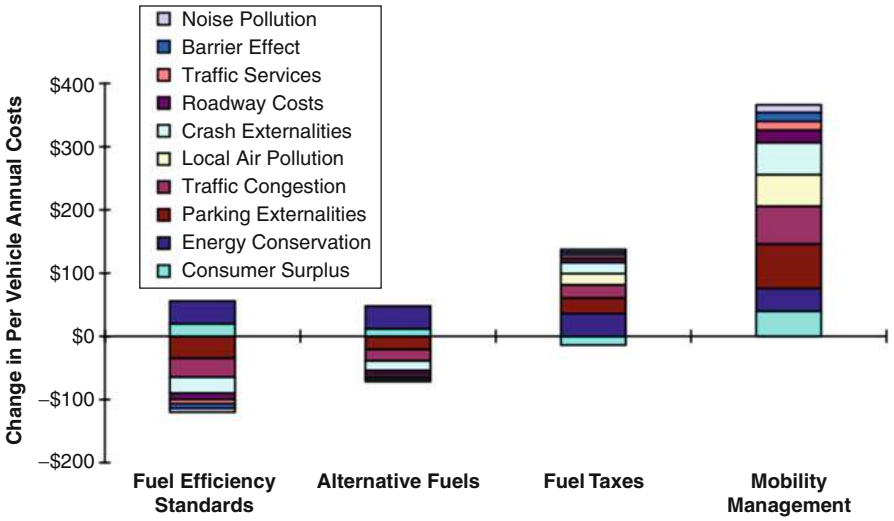

Fig. 13 Cost impact of four different strategies for energy conservation. Above the 0 line, benefits are shown, and below costs. The barrier effect refers to delays that motorized traffic causes to other modes of transportation. In Litman (2005), it is valued at 0.7 cent per vehicle kilometer. For more details, the reader is referred to Litman (2005)

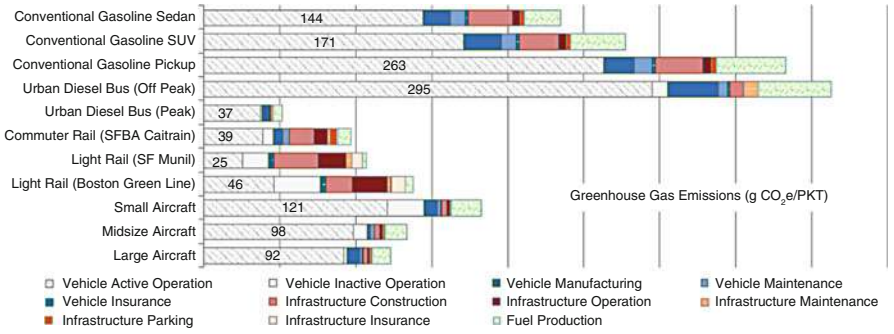

Fig. 14 Total GHG (greenhouse gas) emissions per PKT (passenger kilometer travelled). The components of vehicle operation are depicted in *grey*, while other vehicle components are shown in *blue shades*. Infrastructure components are shown in *red* and *orange*. Fuel production components carry *green* color. All components appear in the order of the legend (Reproduced with permission from Chester and Horvath 2009)

construction and infrastructure operation. The infrastructure for railways is more complex than that of large aircraft, for instance.

As can be seen from Fig. 14 above, it is important to consider infrastructure and supply chain aspects when comparing different transportation modes for their energy efficiency. The (assumed) passenger occupancy is one parameter that strongly affects the results of such studies.

Energy efficiency of rail transportation is detailed in Miller (2009); of buses in Ally and Pryor (2007); and of aircraft in Lee (2010), Babikian et al. (2002), Lee et al. (2004) and Morrell (2009).

Future Directions

Over the last years, a "green" development has emerged, and sustainability has become a buzzword also among consumers and in the transportation industries. In Utlu and Hepbasli (2007), the energy efficiencies of different sectors in several countries are compared (see Fig. 15 below). One can spot that they range from 35 % to 70 %. There is a big potential for savings in all sectors, and it is largest in the transportation area, followed by utilities, residential/commercial, and industrial sectors.

The efficiency of vehicles on US roads from 1923 to 2006 is discussed in Sivak and Tsimhoni (2009). In Romm (2006), Joseph Romm ponders on the car and fuel of the future, and in Azar et al. (2003), global energy scenarios in transportation until 2100 are developed. By looking at Fig. 15, one can assume that the transportation sector offers plenty of potential for energy efficiency improvements. An interesting study (Åkerman and Höjer 2006), which is partly reproduced below, has attempted to quantify these potentials, see Tables 5 and 6.

For cargo transportation, airships might be an energy-efficient means of transportation in future (Liao and Pasternak 2009).

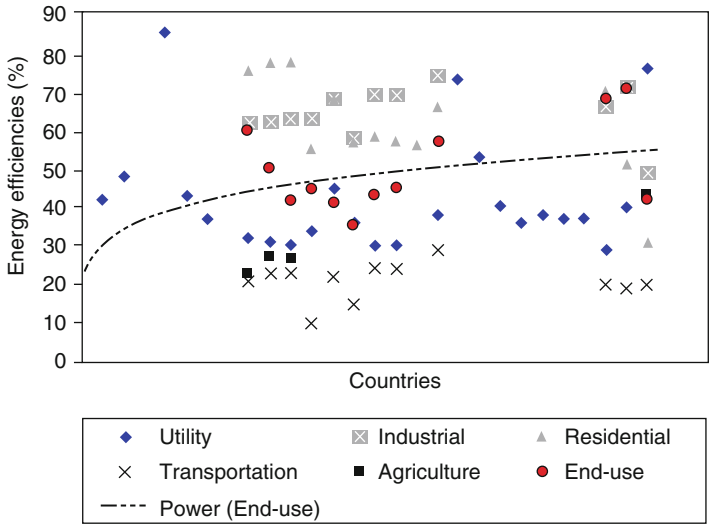

Fig. 15 Energy efficiencies of different countries by sector. In transportation, the potential for improvement seems biggest (Reproduced with permission from Utlu and Hepbasli (2007))

Table 5 Potential to reduce the energy use per passenger-km in Sweden from 2000 to 2050. The occupancy and speed are kept constant (Reproduced with permission from Åkerman and Höjer 2006) (see there for details)

	kWh/ passenger-km, 2000	Potential change by 2050 (%)	kWh/ passenger-km, 2050
Car, combustion mode, 1,2 pass/car (<100 km)	0.75	−75	0.20
Car, electric mode (<100 km)			0.10
Small electric city vehicle			0.07
Car, combustion mode, 2 pass/car (>100 km)	0.32	−65	0.12
Bus (<100 km)	0.22	−60	0.09
Bus (>100 km)	0.13	−40	0.07
Ferry (20 knots)	0.60	−30	0.42
High-speed ferry (40 knots)	1.80	−30	1.30
Rail (<100 km)	0.16	−50	0.08
Rail, 200 km/h (<100 km)	0.11	−50	0.05
Air	0.57	−44	0.32

Table 6 Potential to reduce the energy use per tonne-km in Sweden from 2000 to 2050. The load factor and speed are kept constant (Reproduced with permission from Åkerman and Höjer 2006) (see there for details)

	kWh/tonne-km, 2000	Potential change by 2050 (%)	kWh/tonne-km, 2050
Lorry (<100 km)	0.70	−40	0.42
Lorry (>100 km)	0.25	−30	0.17
Light lorry (<3.5 t)	–	−45	–
Rail	0.05	−30	0.20
Ferry (20 knots)	0.20	−30	0.14
Cargo ship	0.05	−30	0.04
Air	3.00	−44	1.68

Future energy-efficient transportation systems can be developed based on new radical approaches such as blended-wing-body aircraft or by revisiting “old” ideas such as turbine cars.

It is expected that energy efficiency in the transportation sector will increase in the coming years, also driven by cost-saving attempts, see Fig. 16 as an example (Iran).

One can see that there was a fluctuation in both the energy and exergy efficiencies in the period between 1998 and 2009, and the minimum value of energy and exergy efficiencies occurred in the previous year. Some socioeconomic and political reasons, such as the increase and decrease in the export of petroleum and import of petroleum products, the establishment of new refineries, national subsidies, international sanctions, and war are considered as the main reasons for changes in the

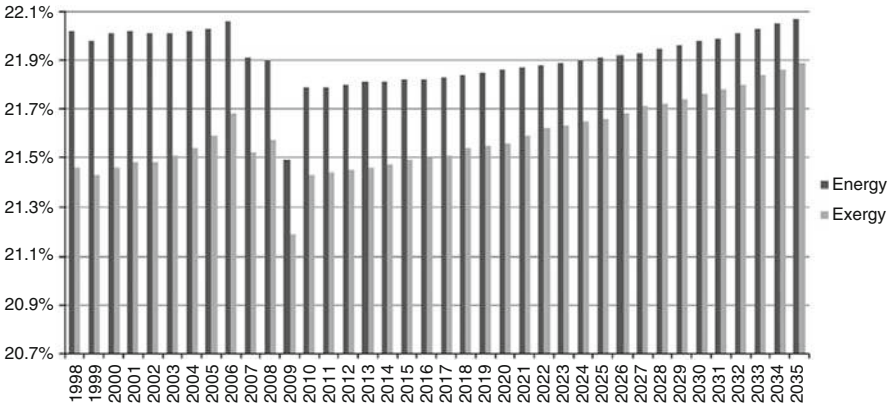

Fig. 16 Overall energy and exergy efficiencies in Iran between 1998 and 2035 (Source: Zarifi et al. 2013)

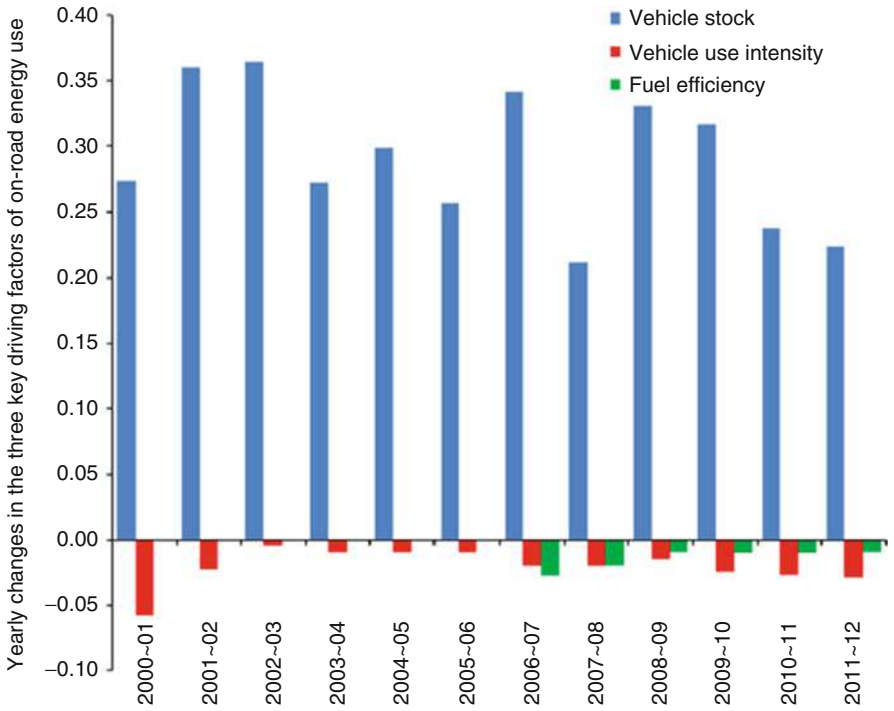

Fig. 17 Relative changes in the three driving factors behind energy use in the road transport sector in China (Source: Wu and Huo 2014)

contribution of each fuel and, consequently, change in the overall energy and exergy efficiencies during the previous years (Zarifi et al. 2013).

It has to be borne in mind that efficiency improvements in transportation can be offset by increased mobility, see Fig. 17 (example of China).

In this chapter, several aspects of energy and fuel efficiency on the transportation industries were touched upon. For comparisons, well-to-wheel (WTW) efficiencies need to be considered (Mallapragada et al. 2014). For further reading, see the cited references and also the chapter "Energy Efficiency" in this handbook. For an in-depth discussion of alternate fuels, see the following chapters in this handbook: Biochemical Conversion of Biomass to Fuels, Hydrogen Production, Conversion of Syngas to Fuels, and Integrated Gasification Combined Cycle (IGCC). Another interesting, promising approach is onboard reforming of fuels (Martin and Wörner 2011).

References

Agresti F (2010) Hydrogen storage in metal and complex hydrides: from possible niche applications towards promising high performance systems. VDM Verlag Dr. Müller, Saarbrücken. ISBN 9783639313444

Åhman M (2001) Primary energy efficiency of alternative powertrains in vehicles. Energy 26 (11):973–989 (Original Research Article)

Åkerman J, Höjer M (2006) How much transport can the climate stand? – Sweden on a sustainable path in 2050. Energy Policy 34(14):1944–1957

Allan T (2011) Virtual water: tackling the threat to our planet's most precious resource. IB Tauris, London. ISBN 978–184511984

Ally J, Pryor T (2007) Life-cycle assessment of diesel, natural gas and hydrogen fuel cell bus transportation systems. J Power Source 170(2):401–411

Azar C, Lindgren K, Andersson BA (2003) Global energy scenarios meeting stringent CO_2 constraints – cost-effective fuel choices in the transportation sector. Energy Policy 31 (10):961–976

Babikian R, Lukachko SP, Waitz IA (2002) The historical fuel efficiency characteristics of regional aircraft from technological, operational, and cost perspectives. J Air Transp Manag 8 (6):389–400

Cadarso M, López L-A, Gómez N, Tobarra M (2010) CO_2 emissions of international freight transport and offshoring: measurement and allocation. Ecol Econ 69(8):1682–1694

Chen H, Ding Y, Li Y, Zhang X, Tan C (2011) Air fuelled zero emission road transportation: a comparative study. Appl Energy 88(1):337–342

Chester MV, Horvath A (2009) Environmental assessment of passenger transportation should include infrastructure and supply chains. Environ Res Lett 4:024008

Chèze B, Gastineau P, Chevallier J (2011) Forecasting world and regional aviation jet fuel demands to the mid-term (2025). Energy Policy 39(9):5147–5158

DeCicco J, Fung F, An F (2015) Global warming on the road, environmental defense. http://www.edf.org/documents/5301_Globalwarmingontheroad.pdf

Eaves S, Eaves J (2004) A cost comparison of fuel-cell and battery electric vehicles. J Power Source 130(1–2):208–212

Fitzgerald WB, Howitt OJA, Smith IJ (2011) Greenhouse gas emissions from the international maritime transport of New Zealand's imports and exports. Energy Policy 39(3):1521–1531

Flannery T (2006) The weather makers. Grove Atlantic, New York. ISBN 9780802142924

Geerlings H, van Duin R (2011) A new method for assessing CO_2-emissions from container terminals: a promising approach applied in Rotterdam. J Cleaner Prod 19(6–7):657–666
Gibson consulting (2015) http://www.gibsonconsulting.com/
Greene DL (2004) Transportation and energy. In: Encyclopedia of energy. Academic, Amsterdam/Boston, pp 179–188
Gross KJ, Thomas GJ, Jensen CM (2002) Catalyzed alanates for hydrogen storage. J Alloy Compound 330–332:683–690
Hamelinck CN, Suurs RAA, Faaij APC (2003) International bioenergy transport costs and energy balance. Universiteit Utrecht, Copernicus Institute, Science Technology Society, Utrecht. ISBN 9039335087
Hao H, Wang H, Yi R (2011) Hybrid modeling of China's vehicle ownership and projection through 2050. Energy 36(2):1351–1361
Hege JB (2006) The Wankel rotary engine: a history. Mcfarland, Jefferson. ISBN 978–0786429059
Heitmann N, Khalilian S (2011) Accounting for carbon dioxide emissions from international shipping: burden sharing under different UNFCCC allocation options and regime scenarios. Marine Policy 35(5):682–691
http://www.theweathermakers.org/ (2015)
IPCC (2013) http://www.ipcc.ch/report/graphics/index.php?t=Assessment%20Reports&r=AR5%20-%20WG1&f=Chapter%2006
Kamal WA (1997) Improving energy efficiency – the cost-effective way to mitigate global warming. Energy Convers Manag 38(1):39–59
Kukla G, Gavin J (2004) Milankovitch climate reinforcements. Global Planet Change 40 (1–2):27–48
Lee JJ (2010) Can we accelerate the improvement of energy efficiency in aircraft systems? Energy Convers Manag 51(1):189–196
Lee JJ, Lukachko SP, Waitz IA (2004) Aircraft and energy use. In: Encyclopedia of energy. Academic, Amsterdam/Boston, pp 29–38
Liao L, Pasternak I (2009) A review of airship structural research and development. Prog Aerosp Sci 45(4–5):83–96
Lipscy PY, Schipper L (2013) Energy efficiency in the Japanese transport sector. Energy Policy 56:248–258
Litman T (2005) Efficient vehicles versus efficient transportation. Comparing transportation energy conservation strategies. Transp Policy 12(2):121–129
Lund H (2007) Renewable energy strategies for sustainable development. Energy 32(6):912–919
Mallapragada DS, Duan G, Agrawal R (2014) From shale gas to renewable energy based transportation solutions. Energy Policy 67:499–507
Martin S, Wörner A (2011) On-board reforming of biodiesel and bioethanol for high temperature PEM fuel cells: comparison of autothermal reforming and steam reforming. J Power Source 196 (6):3163–3171
Miller AR (2009) Applications – transportation, rail vehicles: fuel cells. In: Encyclopedia of electrochemical power sources. Academic, Amsterdam/Boston, pp 313–322
Miller FP, Vandome AF, McBrewster J (2010) Compressed-air energy storage: compressed-air vehicle. Compressed-air engine, compressed air car, air compressor, load profile, compressed air, … gas, fireless locomotive, vehicle-to- grid. Alphascript Publishing. ISBN: 978–6130271428, Saarbrücken/Germany
Morrell P (2009) The potential for European aviation CO_2 emissions reduction through the use of larger jet aircraft. J Air Transp Manag 15(4):151–157
Muratori M, Moran MJ, Serra E, Rizzoni G (2013) Highly-resolved modeling of personal transportation energy consumption in the United States. Energy 58(1):168–177
National Snow & Ice Data Center (2015) http://nsidc.org/
Obert EF (1973) Internal combustion engines and air pollution, vol 3. Addison Wesley, New York. ISBN 978–0700221837
Parry IWH, Evans D, Oates WE (2014) Are energy efficiency standards justified? J Environ Econ Manag 67(2):104–125

Paschen J-A, Ison R (2014) Narrative research in climate change adaptation – exploring a complementary paradigm for research and governance. Res Policy 43(6):1083–1092
Petersen AM, Melamu R, Knoetze JH, Görgens JF (2015) Comparison of second-generation processes for the conversion of sugarcane bagasse to liquid biofuels in terms of energy efficiency, pinch point analysis and Life Cycle Analysis. Energy Convers Manag 91:292–301
Qin N, Vavalle A, Le Moigne A, Laban M, Hackett K, Weinerfelt P (2004) Aerodynamic considerations of blended wing body aircraft. Prog Aerosp Sci 40(6):321–343
Romm J (2006) The car and fuel of the future. Energy Policy 34(17):2609–2614
Schrooten L, De Vlieger I, Panis L, Chiffi C, Pastori E (2009) Emissions of maritime transport: a European reference system. Sci Total Environ 408(2):318–323
Schulz W (2007) The costs of biofuels. Chem Eng News 85(51):12–16, http://pubs.acs.org/cen/coverstory/85/8551cover.html
Sim K, Koo B, Kim CH, Kim TH (2013) Development and performance measurement of micro-power pack using micro-gas turbine driven automotive alternators. Appl Energy 102:309–319
Sivak M, Tsimhoni O (2009) Fuel efficiency of vehicles on US roads: 1923–2006. Energy Policy 37 (8):3168–3170
Sperling D, Gordon D, Schwarzenegger A (2010) Two billion cars: driving toward sustainability. Oxford University Press, New York. ISBN 978–0199737239
The Keeling Curve, Scripps Institution of Oceanography, UC San Diego, USA, https://scripps.ucsd.edu/programs/keelingcurve/. Accessed 1 Jan 2015
Tickell J (2000) From the fryer to the fuel tank: how to make cheap, clean fuel from free vegetable oil: The complete guide to using vegetable oil as an alternative fuel. GreenTeach Publishing, Sarasota. ISBN 978–0966461602
Ticker J (2003) From the fryer to the fuel tank. GreenTeach Publishers, Sarasota. ISBN D-9707227-0
Title 40 (2015), Protection of environment, Sec. 600.113-93, Fuel economy calculations, http://edocket.access.gpo.gov/cfr_2010/julqtr/40cfr600.113-93.htm
Utlu Z, Hepbasli A (2007) A review on analyzing and evaluating the energy utilization efficiency of countries. Renew Sustain Energy Rev 11(1):1–29
van Vliet OPR, van Vliet OPR, Kruithof T, Turkenburg WC, Faaij APC (2010) Techno-economic comparison of series hybrid, plug-in hybrid, fuel cell and regular cars. J Power Source 195 (19):6570–6585
Villalba G, Gemechu ED (2011) Estimating GHG emissions of marine ports – the case of Barcelona. Energy Policy 39(3):1363–1368
von Blottnitz H, Ann Curran M (2007) A review of assessments conducted on bio-ethanol as a transportation fuel from a net energy, greenhouse gas, and environmental life cycle perspective. J Clean Prod 15(7):607–619 (Original Research Article)
Walsh JE (2014) Intensified warming of the arctic: causes and impacts on middle latitudes. Global Planet Change 117:52–63
Wu L, Huo H (2014) Energy efficiency achievements in China's industrial and transport sectors: how do they rate? Energy Policy 73:38–46
Zamfirescu C, Dincer I (2009) Ammonia as a green fuel and hydrogen source for vehicular applications. Fuel Process Technol 90(5):729–737 (Original Research Article)
Zarifi F, Mahlia TMI, Motasemi F, Shekarchian M, Moghavvemi M (2013) Current and future energy and exergy efficiencies in the Iran's transportation sector. Energy Convers Manag 74:24–34
Zhang M, Li H, Zhou M, Mu H (2011a) Decomposition analysis of energy consumption in Chinese transportation sector. Appl Energy 88(6):2279–2285
Zhang M, Li G, Mu HL, Ning YD (2011b) Energy and exergy efficiencies in the Chinese transportation sector, 1980–2009. Energy 36(2):770–776
Zhao H (2007) HCCI and CAI engines for the automotive industry. Woodhead Publishing, Cambridge, UK. ISBN 978–1845691288

Thermal Insulation for Energy Conservation

David W. Yarbrough

Contents

Abstract

The use of thermal insulations to reduce heat flow across the building envelope has been an accepted energy conservation strategy for many decades. Materials available for use as building insulation include naturally occurring fibers and particles, man-made fibers, reflective systems, cellular plastics, evacuated systems, aerogels, and hybrid insulations that combine two or more types of insulation. This chapter discusses the basic theory of insulation and the way they are evaluated. Performance limitations are identified, and discussion of the performance of building elements that represent combinations of insulation and other building material is contained in this chapter. The importance of air infiltration and moisture control is discussed. The language associated with thermal insulation technology and key thermal properties have been included to help the reader use the vast literature associated with building thermal insulation.

D.W. Yarbrough (✉)
R&D Services, Inc., Cookeville, TN, USA
e-mail: dave@rdservices.com

W.-Y. Chen et al. (eds.), *Handbook of Climate Change Mitigation and Adaptation*,
DOI 10.1007/978-3-319-14409-2_19

Introduction

The objectives of modern building design are to provide a comfortable living environment with minimum use of external energy for heating and cooling. In fact, the present target is the construction of "zero energy buildings" that provides conditioned living space, light, and utilities without net energy from exterior sources. This is accomplished by optimum use of wind energy, solar energy, and ground coupling combined with building envelope design that limits heat flow across walls, ceilings or roof cavities, and floors using thermal insulation, reduction of air infiltration, advanced window design, and reduction of thermal bridging. These objectives are major items of interest in the field of building science. This chapter will start with a discussion of thermal insulation: properties, evaluation, and use. This will be followed by observations related to thermal bridging, air infiltration, and new materials.

This chapter discusses the reduction in heat flow by low thermal conductivity materials (insulations). The control of air movement and moisture transport across the building envelope (wall, ceiling, and floor) are additional factors to be considered. Fibrous or particulate insulations seldom provide significant resistance to air infiltration caused by wind-induced pressure differences between the inside and outside of the structure. When these materials are used, additional steps such as caulking and sealing or housewraps are used to provide a barrier to air infiltration. Materials such as cellular plastic insulation (closed cell) can provide a barrier to airflow when installed without cracks or defects. Thermal insulation also plays a role in controlling moisture transport and accumulation. Condensation within the building envelope occurs when the temperature at a location is equal or less than the "dew-point" temperature. The dew-point temperature depends on the actual air temperature (dry-bulb temperature) and the relative humidity. The temperatures within the building envelope depend on the interior temperature, the exterior temperature, and the materials including insulation that are present in the building envelope. Condensation and accumulation of water depend, as a result, on bulk movement of air through the building envelope, diffusion of water vapor through the construction materials, and the temperature profile in the building envelope.

Thermal Insulation Use in Buildings

Heat moves across the building envelope by three mechanisms: convection, conduction, and radiation. Thermal insulations are designed to reduce heat flow by radiation and convection without significantly increasing conduction. There are also insulations that reduce conductive heat transfer by altering the gas phase. The various types of insulation change each type of heat flow by different amounts. Heat transfer of convection can occur within porous materials if buoyant forces resulting from density differences overcome the friction between the moving gas (air, in most cases) and bounding surfaces, fibers, or particles. This "free" convection is eliminated in most cases by insulations such as fiberglass, rock wool, or cellulose.

Air moving within a porous material or region will absorb energy from the warm side of a region and reject it to the cool side of the region. Air moving through a leaky insulated region due to a pressure difference caused by wind or fans, forced convection, means that exterior air is being exchanged for interior air. Airflow into the building is matched by air moving out of the building. In addition, air moving through a porous or fibrous insulation changes the temperature profile within the insulation, and the resulting heat flow by conduction and radiation is changed (Anderlind and Johansson 1983; Yarbrough and Graves 1997). Thermal insulations designed to reduce radiation by the use of reflective (low thermal emittance) surfaces often have a significant amount of internal convection, and as a result, the performance of enclosed reflective air spaces depends on the direction of heat flow (down, up, or horizontal). The convective contribution to the overall heat flow is taken into account when reflective insulation is evaluated and labeled.

A large number of building insulations rely on the low thermal conductivity of air for their performance. This type of insulation includes most of the fibrous materials like fiberglass, rock wool, cellulose, polyester, wool or cotton, and open-cell cellular plastic. A second large class includes closed-cell cellular plastics that contain a gas with a thermal conductivity lower than air with correspondingly high thermal resistance values. The performance of closed-cell insulations requires that the low-conductivity gas remains in the cells unchanged. In general, these insulations are evaluated for average long-term thermal resistance since there are inevitable changes in the cell-gas composition due to air entering the cells or outward loss of the low thermal conductivity gas. There is also a type of insulation that contains fibers or cells that are so small that they interfere with the collisions between gas-phase molecules and consequently reduce the thermal conductivity below that of the gas under normal conditions. The thermal conductivity of a gas depends on both temperature and pressure and is the result of gas molecule collisions. If the gas-phase molecules do not collide, then heat flow through the gaseous part of the insulation is reduced or eliminated. This occurs when the average distance between collisions is greater than the average dimensions of the space available. One type of super-insulation is based on the use of evacuated regions (elimination of the gas phase). All of these concepts are presently represented by commercial products. Table 1 contains a listing of some insulations that are available for use in buildings. Insulation manufactured as batts is usually dimensioned to fit standard construction, while loose-fill insulation is pneumatically installed using especially designed equipment or poured in place. Table 2 contains thermal resistance values for selected building materials and thermal insulations. These are example values not intended to represent any specific product.

There are a wide variety of natural materials mostly fibrous or particulate that are used around the world as insulations. References such as the *ASHRAE Handbook of Fundamentals* (ASHRAE 2009), AIRAH (2007), and Materials for Energy Conservation in Buildings (Hall 2010) contain tables of physical properties for insulating materials and detailed discussions about the use and evaluation. Table 3 contains qualitative information about the relative performance for commonly encountered conditions for the insulations in Table 1.

Table 1 Building insulations

Insulating material	Type	Examples
Air	Fibrous	Fiberglass – batts and loose fill
		Rock wool – batts and loose fill
		Cellulose – batts and loose fill
		Cotton – batts
		Polyester – batts
		Wool – batts
	Cellular plastic	Spray-applied polyurethane (open cell)
		Expanded polystyrene (board or slab)
		Polyisocyanurate (board stock or slab)
	Particulate	Perlite
		Vermiculite
	Reflective	Reflective insulations
		Radiant barriers
Gas other than	Cellular plastic	Spray-applied polyurethane (closed cell)
		Extruded polystyrene (board or slab)
		Polyisocyanurate (board or slab)
		Phenolic
		Gas-filled panels
Reduced pressure	Particulate	Evacuated panels containing silica
		Evacuated panels containing perlite
Nano-materials		Aerogels
		Nano-fibers

Table 2 Thermal resistivity values for selected building materials at 75 °F (24 °C)

Material	R for 1-in. thickness (ft^2 h °F/Btu)	RSI for 25-mm thickness (m^2 K/W)
Wood	0.8–1.4	0.14–0.25
Concrete		
High density	0.1	0.018
Low density	0.5–1	0.09–0.18
Fiberglass batt	3.1–4.2	0.55–0.74
Fiberglass loose fill	2.0–2.4	0.35–0.42
Cellulose loose fill	3.5–3.7	0.62–0.65
Cellular plastic		
Open cell	3.0–3.5	0.53–0.62
Closed cell	5.0–6.5	0.88–1.15

Several entries in Table 3 indicate an increase in conduction because solids such as glass, rock, paper, plastic, or wood have much greater thermal conductivity than air. If air is displaced by a solid particle or fiber, then the heat flow by conduction will increase.

Table 3 Relative performance of commonly used building insulations

Type of insulation	Free convection	Conduction	Radiation
Fiberglass, rock wool, and cellulose	Eliminates	Increases	Reduces
Cellular plastics – air	Eliminates	Increases	Reduces
Cellular plastics – gas	Eliminates	Decreases	Reduces
Reflectives	Reduces	Increases	Greatly reduces

Fibrous materials such as fiberglass, rock wool, cellulose, or open-cell plastics present some resistance to airflow resulting from a pressure difference but do not perform as "air barriers." Closed-cell plastic insulation can perform as an air barrier material in sufficiently thick and without cracks or holes due to shrinkage or weathering. Reflective insulations have an effect on convection when they divide the space they occupy into discrete regions with reduced temperature differences and increased surface area to resist the movement of the enclosed air.

Horizontally applied porous insulation can exhibit a loss in thermal resistance due to upward convection (Graves et al. 1994; ASTM C 1373 (2014)). This phenomena occurs in cold climates where there is a large temperature difference across the insulation that create significant air density differences in the air.

Thermal Performance Evaluation of Building Insulation

The thermal performance of building insulation is commonly characterized by its thermal resistance designed by "R (ft^2 h °F/Btu)" or "RSI (m^2 K/W)" depending on the system of units being used. The thermal resistance is defined by Eq. 1 where the denominator is referred to as "apparent thermal conductivity." This terminology is used since the equation used to describe heat flow by conduction (Fourier's law) is used to describe heat flow by all mechanisms:

$$R = t/k_a \tag{1}$$

- [t] is thickness in inches.
- [k_a] is apparent thermal conductivity in Btu in./ft^2 h °F.
- [R] is thermal resistance in ft^2 h °F/Btu.

$$RSI = t/\lambda$$

- [t] is thickness in meters.
- [λ] is apparent thermal conductivity in W/m K.
- [RSI] is thermal resistance in m^2 K/W.

Another property called thermal resistivity, R^* or RSI^*, is related to thermal resistance as shown by Eq. 2. Equation 1 indicates that R or RSI scales linearly

with thickness. This is valid as long as k_a or λ has been determined using test specimens thick enough to avoid surface effects (the thickness effect) (Fine et al. 1981):

$$R^* = R/t \quad \text{or} \quad 1/ka \tag{2}$$

[R^*] has units ft^2 h °F/Btu in.

$$RSI^* = RSI/t \quad \text{or} \quad 1/\lambda$$

[RSI^*] has units m K/W.

Building codes and requirements are usually discussed in terms of R-values or RSI-values, while manufacturers and marketers often quote resistivity values, R^* or RSI^*.

The total thermal resistance (R_T or RSI_T) of an assembly consisting of layers of materials perpendicular to the direction of heat flow is additive:

$$R_T = R_1 + R_2 + R_3 + \cdots \tag{3}$$

A given section of a building envelope (e.g., a wall) will likely consist of at least three materials: an inner sheathing, an insulation filled region, and an external sheathing or façade. The total thermal resistance from the interior surface to the exterior surface is the sum of the individual resistances. The design for energy conservation involves selection of materials with high thermal resistance in order to reduce heat flow across an area, A, as shown by Eq. 4. The greater the R_T or RSI_T the smaller the heat flow:

$$Q = A \cdot \Delta T/R_T \tag{4}$$

- [A] is area perpendicular to heat flow direction (ft^2 or m^2).
- [ΔT] is ($T_{hot} - T_{cold}$) in °F or K.
- [R_T or RSI_T] is total thermal resistance.
- [Q] is heat flow in Btu/h or watts.

Standardized test methods are used to determine the thermal resistance values for building materials for the purpose of labeling and design calculations. In the case of thermal insulation materials, the most commonly used apparatus is described in the test method ASTM C 518 (ASTM C 518 (2014)). Figure 1 is a photograph of two heat flow meters. The apparatus is designed to provide values for three of the four quantities in Eq. 4 (Q, A, and ΔT). A value for R can then be calculated. The apparent thermal conductivity, k_a, can be calculated from the thickness of the test material using Eq. 1. This test method provides steady-state physical property values for materials that have been conditioned to prevent water (moisture) movement in the test specimen during the test. Thermal testing of building elements is accomplished using a hotbox facility to be discussed later.

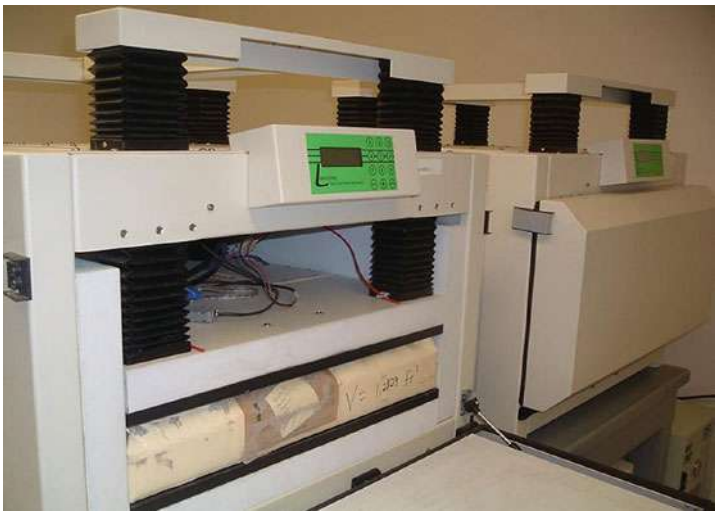

Fig. 1 Photograph of two heat flow meters (*open* and *closed*). The *brown* test specimen is between two *black* isothermal plates. The front is closed during a test

Factors That Affect Thermal Resistance

The thermal resistance of practically all materials depends on the temperature of the material. The temperature is usually characterized as the average of the warm side temperature and the cool side temperature. Thermal resistance measurements are generally made with a relatively small temperature difference such as 50°F or 28°C and an average temperature specified by labeling conventions. The average temperature is 75°F (23.9°C) in some parts of the world and as low as 50°F (10°C) in some locations. The laboratory test methods are generally capable of measuring the thermal resistance over the temperature range anticipated for buildings.

In most cases, the thermal resistance of building insulations decreases as the temperature increases (or increases as the temperature decreases) when other factors are held constant. This is easily understood for the insulations that are based on air. The thermal conductivity of air increases with temperature thus reducing the thermal resistance of the insulation in question. Equations 5a and 5b are relations between temperature and thermal conductivity of air for the limited temperature range likely to be encountered in buildings. Actual variation with temperature of the apparent thermal conductivity will differ from that of air because there are other heat flow mechanisms. Variations of the thermal resistance of insulation materials with temperature have been measured and reported (Abdou and Budaiui 2005):

$$k_{air} = 0.18 + 0.027^{*}(T(^{\circ}F) - 75)/100 \qquad (5a)$$

$$32 < T < 176^{\circ}F$$

k_a with units Btu in./ft^2 h °F

$$\lambda_{air} = 0.026 + 0.0070^{*}(T(^{\circ}C) - 24)/100 \quad (5b)$$

$$0 < T < 80^{\circ}C$$

λ_a with units W/m K.

An important observation about air-based insulations follows from approximate values given by Eq. 5. The maximum possible R-value at a given temperature that can be achieved by an air-based thermal insulation can be calculated from the thermal conductivity of air. The maximum occurs when there is no convection present, and all radiation has been eliminated. The heat transfer by conduction is all that is left. The solid components of the insulation will have thermal conductivities greater than air meaning that k_{air} is a lower bound on k_a. Equation 1 gives $R_{max} = 5.56$ for 1-in. thickness at 75°F and $RSI_{max} = 0.96$ for 25-mm thickness at 24°C. Practical air-based insulation invariable has R-values less than the maximum value because radiation is not completely blocked, and there is a conductive contribution from the solid material in the insulation.

The thermal resistances of cellular plastic insulations containing a gas other than air or a gas mixture with thermal conductivity less than that of air also decrease with increase in temperature as long as the composition of the gas trapped in the cells does not change. In some cases, it is possible to have temperatures low enough to condense the low thermal conductivity gas components in a closed-cell foam thus changing the cell-gas composition. Generally, this means that the fraction of gas that is low thermal conductivity decreases and the overall thermal conductivity increases. If this phenomena occurs, then the thermal resistance decreases as the temperature decreases. As a result of the aging phenomena, the performance of closed-cell cellular plastic insulation is evaluated in terms of an average value over a long period of time such as 15 years. This is called the long-term thermal resistance (LTTR). There are consensus laboratory methods for determining LTTR (ASTM C 1303 2014).

Air movement through porous or fibrous insulations like fiberglass, rock wool, or cellulose changes the heat flow rates in or out of a building. The heat content of air depends on its temperature. Cold air entering a building must be heated to the interior set point temperature. Conversely, warm air entering the building is cooled to the interior set point temperature. In both cases, there is an expenditure of energy to maintain the temperature in the conditioned space. In addition, the movement of air through the insulation changes the temperature profile in the insulation which in term changes the rate of heat flow through the insulation. The movement of air through insulated regions can also carry water vapor into the building thus adding another item of cost, for example, the removal of excess water by condensation and heating or cooling the water vapor transported by air. These factors provide motivation for construction that reduces air infiltration to as low a level as health considerations permit.

The thermal resistance of compressible insulations like fiberglass, rock wool, polyester, or cellulose depends on the density (mass per unit volume) of the material as installed in the building envelope. Insulation manufacturers specify the thickness and

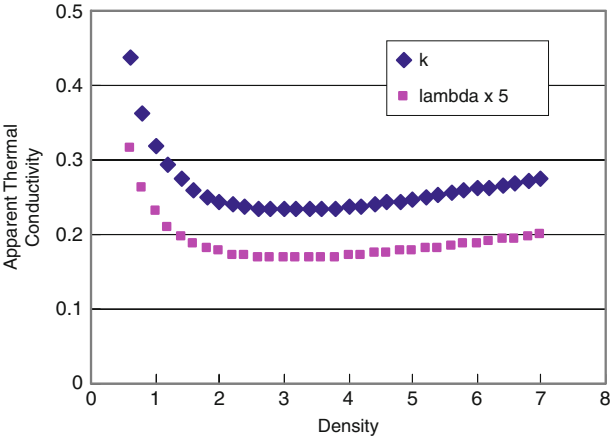

Fig. 2 Apparent thermal conductivity as a function of density (lb_m/ft^3). The curve labeled k has units Btu in/ft^2 h °F, while the curve labeled lambda × 5 has units W/m K. Multiply the density in the figure by 16.02 to obtain density with units kg/m^3

density (or weight per unit area) of their product that is required to achieve a specific R or RSI. If the specified thickness and weight of material are not achieved, then the R or RSI will likely be different from the target value. Each insulation type has a characteristic curve like that shown in Fig. 2. The curve in Fig. 2 shows data for an example material with constant composition and fiber diameter at a constant temperature (Siegel and Howell 1971). As the density of the insulation changes, the three heat transfer contributions (conduction, convection, and radiation) change, and the overall rate of heat transfer changes. When the density of the insulation is low, the curve indicates that the apparent thermal conductivity will decrease as density increases (thermal resistance will increase), while the high-density state shows increasing apparent thermal conductivity with increasing density (decreasing thermal resistance). Every thermal insulation product has its own characteristic curve. Thermal insulations are labeled and sold with a thickness at which the advertised R will be achieved. The thermal resistance will be different if compressed to thicknesses other than that on the label because as the thickness changes, the density changes (Robinson and Powell 1957).

Figures 3 and 4 show R-values for a 1-in. thickness of insulation and RSI-values for 25-mm thickness of insulation for the material illustrated in Fig. 2. The important point here is the significant change in the insulation performance per unit thickness as the density (amount of material per unit volume) is changed.

Reflective Insulations

Enclosed air spaces with low emittance surfaces provide resistance to heat flow by reducing or nearly eliminating radiative transfer across the air space. This is readily shown by the following equation for the net radiation, Q_{rad}, between large parallel planes with emittances ε_1 and ε_2 (Siegel and Howell 1971):

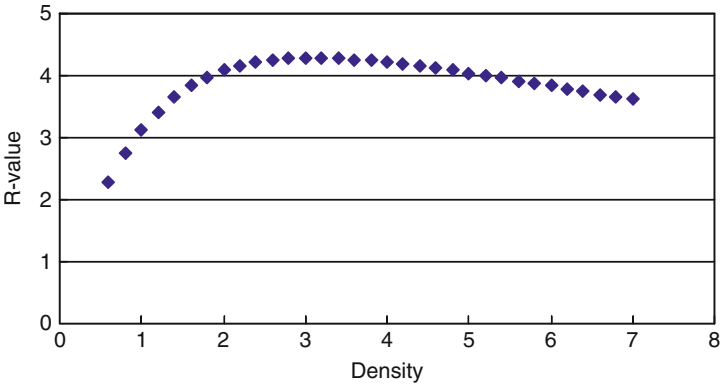

Fig. 3 R-value for a 1 in. of insulation at the indicated density units: R-value (ft^2 h °F/Btu) density (lb_m/ft^3)

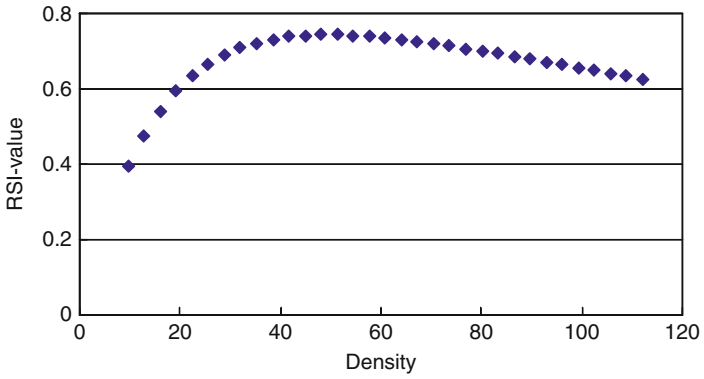

Fig. 4 R-value for 25 mm of insulation at the indicated density units: RSI-value (m^2 K/W) density (kg/m^3)

$$Q_{rad} = E\{A \cdot \sigma \cdot (T_{hot}^4 - T_{cold}^4)\} \tag{6}$$

- Q_{rad} is net radiation from the hot surface to the cold surface (Btu/h or watts).
- A is the area perpendicular to the heat flow (ft^2 or m^2).
- T_{hot} and T_{cold} are absolute temperatures (R or K).
- σ is the Stefan-Boltzmann constant 0.1712×10^{-8} (Btu/h ft^2 °R^4) or 5.669×10^{-8} (W/m^2 K^4).

$$E = (1/\epsilon_1 + 1/\epsilon_2 - 1)^{-1} \tag{7}$$

The heat transfer by radiation is directly proportional to the effective emittance (E), a quantity that varies from 0 (a perfect reflector) to 1 (a perfect absorber or block body). A large number of building materials (wood, masonry, and common

Table 4 Examples of effective emittance values

Surface	ϵ_1	E with ($\epsilon_2 = 0.9$)	E with ($\epsilon_2 = \varepsilon_1$)
Aluminum foil	0.03	0.030	0.015
Metallized film	0.05	0.050	0.026
Coating	0.25	0.243	0.143
Wood	0.90	0.818	0.818

Table 5 Maximum radiation exchange and reductions

T_{hot} °F (°C)	T_{cold} °F (°C)	Q with E = 0.9 (kW)	Q with E = 0.05 (kW)	Reduction (kW)
70 (21.1)	65 (18.3)	1.54	0.09	1.45
100 (37.8)	90 (32.2)	3.59	0.20	3.39
100 (37.8)	85 (29.4)	5.31	0.30	5.01

nonmetallic paints) have emittances near 0.9. A few emittance values (ε) are listed in Table 4 along with calculated values for E. The first column contains E with one surface having a low emittance, while the other surface is wood or a common building material. The second column contains E for low emittance surfaces on both sides of the reflective air space.

The bracketed term in Eq. 6 provides the maximum net radiation between the two surfaces for a given area and specific temperatures. Table 5 contains a few examples of the radiation term between two wood or two masonry surfaces and the reduction that can be achieved by changing one surface to emittance 0.05.

The results in Table 5 are for an area of 100 ft^2 (9.3 m^2) and the indicated temperatures.

The total heat flow across a reflective air space can be approximated by Eq. 8 where the term h_c represents heat transport by convention and conduction (Robinson and Powell 1957). The term h_c is determined from an experimental measurement of total heat flow with a subsequent subtraction of the radiative term. The term h_c can be determined from published equations and hotbox data (Robinson and Powell 1957; Desjarlais and Yarbrough 1991). Since h_c includes convection, the values depend on the heat flow direction. The standard ISO 6946 also provides a method for determining h_c (ISO 6946 (2005)):

$$\begin{aligned} Q_{total}/A &= (h_{rad} + h_c) \cdot \Delta T \\ h_{rad} &= 4 \cdot E \cdot \sigma \cdot T_m^3 \\ T_m &= (T_{hot} + T_{cold})/2 \\ \Delta T &= (T_{hot} - T_{cold}) \end{aligned} \tag{8}$$

Table 6 contains some examples of enclosed reflective air space thermal resistances for a single enclosed air space with E = 0.03. The *ASHRAE Handbook of Fundamentals* contains reflective air space thermal resistances for various conditions (ASHRAE (2009)).

Table 6 Single reflective air space thermal resistance values at $T_m = 77\ °F\ (25\ °C)$

Thickness in. (mm)	ΔT °F (°C)	Thermal resistance ft² h °F/Btu (m² K/W)		
		Down	Horizontal	Up
0.47 (12)	18 (10)	2.38 (0.42)	2.33 (0.41)	1.87 (0.33)
0.94 (24)	18 (10)	4.43 (0.78)	3.41 (0.60)	2.04 (0.36)
1.50 (38)	18 (10)	5.85 (1.03)	3.24 (0.57)	2.16 (0.38)
0.47 (12)	27 (15)	2.38 (0.42)	2.38 (0.42)	1.70 (0.30)

Envelope R-Values

Heat flow across a section of the building envelope depends on the temperatures of the regions on both sides on the element and the thermal resistances between the regions. The situation is best discussed for a wall section that does not include doors or windows. The resistance between the regions includes layers of different building materials and in many cases materials positioned in the direction of heat flow (thermal bridges). Heat flow calculations are commonly based on U-values (overall heat transfer coefficient) that take into account all of the materials between the bounding regions and surface film resistances:

$$Q = U \cdot A \cdot \Delta T \tag{9}$$

- U, Btu/ft² h °F or (W/m² K)
- A, ft², or (m²)
- ΔT, °F, or (K or °C)
- Q, Btu/h, or (W)

In order to avoid the complication of wind and the difference between the temperature of the outside air and the temperature of sunlit wall, the outside surface of the wall will be taken as region 1, and the inside air temperature will be taken as region 2. The U in this case will include an inside air film resistance (R_{film}), an interior sheathing material resistance (R_1), the resistance of the wall structure (R_s), the exterior sheathing (R_2), and final exterior wall material (R_3). For this case, U is given by Eq. 10:

$$U = 1/(R_{film} + R_1 + R_s + R_2 + R_3) \tag{10}$$

$$R_T = 1/U \tag{11}$$

R_s is the complication in the equation for U since in many cases, the region is not a homogeneous layer of material. If the wall is a layer of material like concrete, brick, or solid wood, then the denominator in Eq. 10 is a sum of resistances. If the wall is a wood frame or timber wall type of structure, then there are parallel paths (commonly two) for heat to move across this region. One path is through the insulated region, while the second path is through the frame or timber region. Equation 12 is often

used to calculate a value for R_{cav} where f_c is the fraction of the wall area that bounds cavity and f_w is the fraction that bounds the wood framing ($f_c + f_w = 1$). The f values depend on the design of the framing. For example, nominal 2 × 4-in. wood framing placed 16 in. on center with double top plates and a single bottom plate has $f_w = 0.14$ for a ceiling to floor distance of 8 ft. The corresponding value for f_c is 0.87. This means that only 86% of the wall area is insulated by installing material in the cavity formed by wood framing members:

$$f_w = (14.5 \cdot 91.5)/(16.0 \cdot 96) = 0.86$$

If R_w 4.2 ft^2 h °F/Btu is taken as the resistance for the wood in the direction of heat flow and R_c 15 ft^2 h °F/Btu is taken for the resistance of the insulation, then the value for R_s from Eq. 1 is 11.03. If R_c is 11, then R_s is 8.97:

$$R_s = 1/(f_w/R_w + f_c/R_c) \tag{12}$$

Specification of values such as $R_{film} = 0.68$, $R_1 = 0.5$, $R_2 = 0.45$, and $R_3 = 0.2$ permits an evaluation of U for R_c 15. The R_T describes the overall resistance of the structure between the inside air and the exterior surface. If an exterior air film is included, then it can be added to the result for R_T:

$$U = 1/(0.68 + 0.5 + 11.24 + 0.5 + 0.45 + 0.2) = 0.0737$$
$$R_T = 13.57$$

This example is intended to show several factors to consider. The total thermal resistance of the wall is not equal to the thermal resistance of the cavity insulation even though it includes several additional resistance factors. The total resistance of the wall depends on the design (e.g., spacing) of the structure and the materials used to build the structure. If metal is substituted for wood, then the resistance R_w drops to near zero, and thermal resistance in the path through the metal structure has to be added. A few examples of steel wall resistances taken from an American Iron and Steel Institute publication (American Iron and Steel Institute 1995) are shown in Table 7. The data for R 11, R 13, and R 15 cavity insulations are for 3.625-in. steel framing that is 24 in. on center, while R 19 is for 6.0-in. framing that is 24 in. on

Table 7 R_{tot} for steel stud walls

R cavity	R sheathing	R_{total}
ft^2 h °F/Btu (m^2 K/W)		
11 (1.937)	1.0 (0.176)	7.0 (1.23)
13 (2.289)	1.0 (0.176)	7.3 (1.29)
15 (2.642)	1.0 (0.176)	7.6 (1.34)
19 (3.346)	1.0 (0.176)	8.0 (1.41)
11 (1.937)	5.0 (0.881)	13.0 (2.29)
13 (2.289)	5.0 (0.881)	13.6 (2.40)
15 (2.642)	5.0 (0.881)	14.3 (2.52)
19 (3.346)	5.0 (0.881)	15.0 (2.64)

Fig. 5 An open hotbox (Photo courtesy of the BTRIC, Oak Ridge National Laboratory, USA)

center. R sheathing refers to continuous insulation placed perpendicular to the direction of heat flow. This is R_2 in Eq. 10.

The U-values for building assemblies can be measured using a hotbox facility that can be used to test relatively large test specimens, 9 by 16 f. (2.7 by 4.88 m), for example. The total heat flow at steady state from a warm region to a cold region is determined from a measurement of heat input to maintain the temperature of the warm region ASTM C 1363 (2014). A hotbox measurement includes heat transfer by all mechanisms. Figure 5 is a photograph of a rotatable hotbox used for building assemblies. The outline of a test specimen can be seen between the two sections of the hotbox. The two sections are closed to perform a test.

Concrete masonry walls and concrete block walls represent a somewhat different type of situation in that the R_s is representing a layer of material. Solid concrete walls built using "standard" weight concrete (density of 100–125 lb/ft^3) have thermal resistance values of approximately 0.1 ft^2 h °F/Btu per inch of thickness. An 8-in.-thick wall using this material has an R of about 0.8 ft^2 h °F/Btu. Masonry blocks with interval cells (air filled) have slightly high R-values (range 1.5–2.0) that depend on the density of the concrete used to produce the blocks. Insulation can be added to cells to make modest increase in the resistance of the blocks. Application of the parallel path idea introduced above shows that a concrete block with insulation core region has a maximum R of about 3 ft^2 h °F/Btu that is achieved as the resistance of the core material becomes very large. This situation is remedied in part by adding layers of insulation usually on the interior side of the wall. When this is done, the concrete or block wall resistance becomes R_2 in Eq. 10, and the interior insulation system becomes R_s.

In many cases, the performance of massive walls is improved by the dynamics of absorbing and discharging heat as the outside temperature changes. This is called "the mass effect." The mass effect is sometimes described by a factor called the "dynamic benefit for massive walls (DBMS)." The DBMS is a multiplier that describes the thermal performance in terms of a "dynamic R" (Kosny et al. 2001):

$$\text{Dynamic } R = \text{Conventional R} \cdot \text{DBMS} \tag{13}$$

DBMS values range from 1 to perhaps 4. The DBMS depends on the temperature variation in a given location and the mass, specific heat, density, and thermal conductivity of the construction material in question. The determination of a DBMS value generally requires computer simulations of the structure to determine the factor DBMS that will result in equal performances of the massive wall and a conventional wall with specified thermal resistance. For the present discussion, it is sufficient to note that massive walls can demonstrate thermal performance that is much better than anticipated from the relatively modest conventional R.

Attic or roof cavity insulation receives a lot of attention since the roof surface can become very hot due to solar radiation and very cold due to radiation to the night sky. Attic spaces or roof cavities are often ventilated to remove moisture from the occupied part of the building and remove some heat. The attic space insulation is commonly located on the attic floor directly above the conditioned space. In some applications, the insulation is placed directly below the roof deck. This latter application is sometimes combined with a non-ventilated attic strategy.

Attic floor insulation is commonly viewed as a continuous layer of material of uniform thickness. A small correction can be applied to account for the presence of structural members buried in the insulation (ceiling joists), but this is a minor factor in modern times with insulation thicknesses that are much greater than the height of the ceiling joist. The depth of attic floor insulation is dictated in part by economic factors since there is often sufficient space for large thicknesses of insulation. This is in contrast with walls with fixed amount of space for insulation. Attic thermal resistance recommendations and requirements vary around the world with current recommendations as high as R 60 ft^2 h °F/Btu (RSI 10.6 m^2 K/W) rated at 75°F or 24°C. A wide variety of insulations in the form of batts (or blankets) or loose-fill insulation that is pneumatically installed or poured is used. The important considerations in choosing attic insulation type and R-value include mechanical stability of the insulation, moisture absorption/desorption, and fire performance.

Mechanical stability is important since the thermal resistance depends on thickness as shown by Eq. 1. If the insulation loses thickness, then its thermal resistance will be reduced. In the case of loose-fill insulations, this phenomena is called "settling." As an insulation settles, its density increases, and the apparent thermal conductivity changes.

An analysis of data for most of the common types of insulation shows that settling or thickness reduction results in R-value reduction. Some insulation products, cellulose, for example, are labeled to account for settling after the material is installed. Some insulations contain binders or adhesives to reduce settling after the

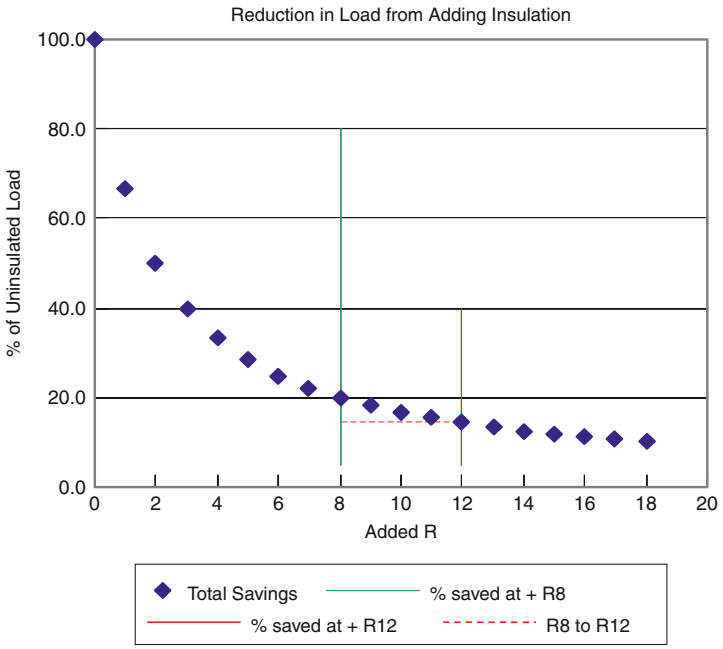

Fig. 6 Example of diminishing return

insulation is installed. Stabilized cellulose is an example of this type of insulation (ASTM C 1497 (2010)).

A builder or designer should be aware of the settling phenomena and examine the care with which the insulation manufacturer deals with this issue. The resistance of attic insulation to ignition or spread of fire is important because the attic region operates at elevated temperatures in the summer, often contains electrical wiring, and sometimes contains hot surfaces such as lights, flues, or chimneys.

Some types of insulation, for example, cellulose, cellular plastic, plastic fiber, wool, and wood fiber, can be ignited and will burn. These insulations are often treated with fire-retardant chemicals to reduce smoldering tendency and limit the spread of fire on the surface. Care must be taken to keep material that can ignite and burn away from potentially hot surfaces. The condition of electrical wiring can also be a safety issue especially if the wiring becomes buried in a material that will ignite and burn. An understanding of the fire-retardant chemicals being used, their long-term stability, and the manufacturer testing and quality control is important and difficult. At a minimum, the user of the insulation should verify that the product undergoes regular verification of its fire resistance and that permanence of the fire-retardant chemicals has been established.

A combination of Eqs. 6 and 11 introduces an interesting and overlooked concept about insulation: a diminishing return. Consider, for example, the heat flux (Q/A) through a region when the temperature difference (ΔT) is specified. The heat flux is inversely proportional to R as shown in Fig. 6.

Table 8 Anticipated savings from increased attic insulation

R total	R added	Heat flux reduction (%)	Base heat flux (%)
2	0	0.0	100.0
10	8	80.0	20.0
14	12	85.7	14.3
15	13	86.7	13.3
20	18	90.0	10.0
25	23	92.0	8.0
30	28	93.3	6.7
35	33	94.3	5.7
60	58	96.7	3.3

The diamonds in Fig. 6 represent the percent of heat flux calculated for a ceiling with added R-value to an uninsulated ceiling assigned the value R 2. Adding R 8 to the ceiling to provide a total R of 10 reduces the ceiling heat flux to 20 % of the uninsulated value. Adding R 12 reduces the ceiling heat flux to 15 % of the uninsulated value. Table 8 extends the added R-value to R 60 showing the rapidly declining savings to be expected. The same type of calculation would apply to other parts of the building envelope.

Below floor insulation is used when there is space below the floor or when the building is positioned on a slab. Slab insulation is often limited to the perimeter region with insulation installed either on the interior or exterior side of the foundation perpendicular to the heat flow direction. The amount of thermal resistance recommended for perimeter application is generally in the range R 5–R 10 (RSI 0.9–1.8).

There are several strategies for insulating floors above the ground (with crawl space). One technique involves installing fiberglass batt insulation between the floor joists. A water vapor retarder is usually installed below the insulation to keep water vapor from condensing on the bottom of the flooring. Reflective insulations are also used in below-floor applications either as single sheet materials attached to the bottom edge of the floor joists or between floor joists. Multilayer reflective insulation has also been used in the application.

Hybrid Systems

Different types of insulations are being combined to economically enhance overall performance. Combinations of spray polyurethane insulation and fiberglass or reflective insulation are examples of this type of system. When installed in a wall cavity, the spray foam can provide an airtight seal and a level of thermal resistance that depends on the thickness of the foam. The wall cavity is then filled with a mass insulation such as fiberglass or provided with a reflective insulation. In either case, the thermal resistance of the cavity is the sum of the thermal resistance of the foam and the thermal resistance of the insulation used to fill the cavity. The benefits of such a system are enhanced thermal resistance and a barrier to air infiltration.

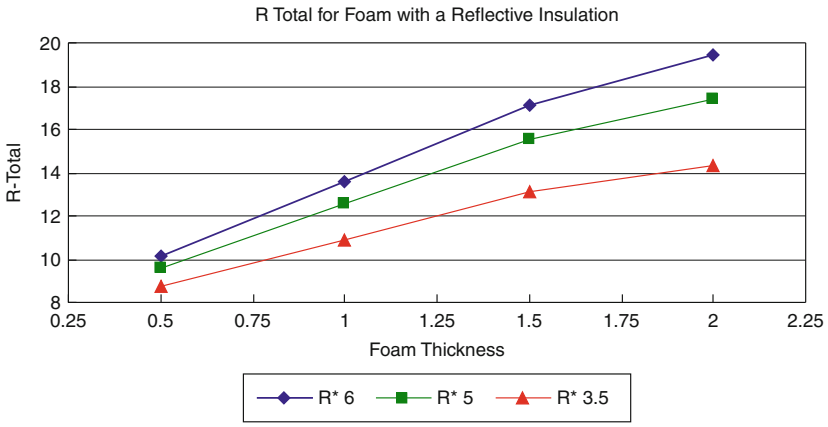

Fig. 7 Total R for a hybrid insulation system combining cellular foam and a reflective insulation

Figure 7 shows calculated values for a wall element containing a layer of spray polyurethane foam and a reflective insulation assembly with R = 6.8−7.8 (RSI = 1.2−1.4). The curves in Fig. 7 are for foams with thermal resistivities, R^*, from 3.5 ft^2 h °F/Btu (open cell) to 6 ft^2 h °F/Btu (closed cell). The total space for the hybrid system is 5.5 in. (140 mm).

Summary

This chapter has outlined some of the fundamental considerations related to building insulation. Important properties have been identified and factors that affect performance have been discussed. The selection of thermal protection for the building envelope must include consideration of moisture transport and a requirement that air infiltration be addressed. In many cases, this means that materials in addition to thermal insulation will be required. Air barrier materials and water vapor retarders are examples. In some cases, thermal insulation serves dual purposes such as being an air barrier and a thermal insulation.

Future Directions

Future developments in the area of building insulation will no doubt find increased use of super-insulations such as vacuum panels, aerogel insulation, and gas-filled panels.

Conventional insulations will be improved by adding components to block radiation (opacifiers). Phase-change material will be added to conventional insulation to provide for improved dynamic performance. The rate of advance in these areas is tied to cost of the materials, cost of energy, and availability of energy.

Advanced technologies that proved materials or systems that provide thermal resistance that changes with conditions will lead to new levels of energy conservation and contribute to construction of "zero energy buildings." Variable resistance insulations can be used to take maximum use of incoming solar energy.

References

Abdou AA, Budaiui IM (2005) Comparison of thermal conductivity measurements of building insulation materials under various operating temperatures. J Build Phys 29(2):171–184

AIRAH (2007) Technical handbook, 4th edn. The Australian Institute of Refrigeration, Air Conditioning and Heating, Melbourne

American Iron and Steel Institute (1995) Thermal design and guide for exterior walls, RG-9405

Anderlind G, Johansson B (1983) Dynamic insulation – a theoretical analysis of thermal insulation through which a gas or fluid flows. Swedish Council for Building Research, Document D8. Available from Svensk Byggtjanst, Box 7853, S-103 99 Stockholm, Sweden

ASHRAE (2009) Heat, air, and moisture control in building assemblies – material properties. In: Handbook of fundamental. American Society of Heating, Refrigerating and Air-Conditioning Engineers, Atlanta (Chap 26)

ASTM C 1303 (2014) Standard test method for predicting long-term thermal resistance of closed-cell foam insulation. In: 2014 Annual book of ASTM standards, vol 04.06, West Conshohocken, PA, pp 734–753

ASTM C 1363 (2014) Standard test method for thermal performance of building materials and envelope assemblies by means of a hot box apparatus In: 2014 Annual book of ASTM standards, vol 04.06, West Conshohocken, PA, pp 798–841

ASTM C 1373 (2014) Standard practice for determination of thermal resistance of attic insulation under simulated winter conditions. In: 2014 Annual book of ASTM standards, vol 04.06, West Conshohocken, PA, pp 850–857

ASTM C 1497 (2014) Standard specification of cellulose fiber stabilized thermal insulation. In: 2014 Annual book of ASTM standards, vol 04.06, West Conshohocken, PA, pp 921–925

ASTM C 518 (2014) Standard test method for steady-state thermal transmission properties by means of the heat flow meter apparatus. In: 2014 Annual book of ASTM standards, vol 04.06, West Conshohocken, PA, pp 156–171

Desjarlais AO, Yarbrough DW (1991) Prediction of the thermal performance of single and multi-airspace reflective insulation materials. ASTM STP 1116:24–43

Fine HA, Jury SH, Yarbrough DW, McElroy DL (1981) Heat transfer in building thermal insulation: the thickness effect. ASHRAE Trans 87(Pt 2):539–568

Graves RS, Wilkes K, McElroy DL (1994) Thermal resistance of attic loose-fill insulations decrease under simulated winter conditions. Therm Conduct 22:215–226

Hall MR (ed) (2010) Materials for energy efficiency and thermal comfort in buildings. Woodhead, Oxford

ISO 6946 (2005) Building components and building elements-thermal calculation method

Kosny J, Kossecka E, Desjarlais A, Christian J (2001) Dynamic thermal performance and energy benefits of using massive walls in residential buildings. Oak Ridge National Labs and Polish Academy of Sciences. http://www.ornl.gov

Robinson HE, Powell FJ (1957) The thermal insulation value of airspaces. Housing research paper 23. U.S. Department of Commerce, National Bureau of Standards (NIST), Washington, DC, USA

Siegel R, Howell JR (1971) Thermal radiation heat transfer. McGraw-Hill, New York

Yarbrough DW, Graves RS (1997) The effect of air flow on measured heat transfer through wall cavity insulation. J ASTM Int 4(5):94–100

Thermal Energy Storage and Transport

Satoshi Hirano

Contents

S. Hirano (✉)
Thermal and Fluids Systems Group, Energy Technology Research Institute, National Institute of Advanced Industrial Science and Technology (AIST), Tsukuba, Japan
e-mail: hirano@ni.aist.go.jp

W.-Y. Chen et al. (eds.), *Handbook of Climate Change Mitigation and Adaptation*,
DOI 10.1007/978-3-319-14409-2_20

Abstract

The efficient use of energy is important to restrain the emission of greenhouse effect gases. Thermal energy storage and heat transport technology enable to utilize the renewable energy and the waste heat which are generally unstable, maldistributed, and thin. They also enable to operate energy devices at a highly efficient condition. This chapter introduces some basic research and development activities of thermal energy storage and heat transport, especially latent heat utilization. First, the following fundamental knowledge of thermal energy storage is explained: (1) the functions of thermal energy storage, (2) the classification of storage methods, (3) the characteristics of thermal energy storage materials especially phase change materials (PCMs), and (4) the constitutions of thermal energy storage devices. Other characteristics and challenges of latent heat thermal energy storage (LHTES) which utilize supercooling phenomenon are also explained. Second, several examples of the practical use of LHTES including the utilization of snow and ice are discussed. In the same way, several characteristics and examples of the practical use of the heat transport using latent heat are also explained. Furthermore, recent developments on the following research subjects are introduced: (1) thermal energy storage for hot water supply using the supercooling phenomenon of sugar alcohol, (2) heat storage for space heating using the supercooling of hydrate, (3) the improvement of thermal characteristics of paraffin wax as a PCM, (4) a steam accumulator using sugar alcohol, (5) pipeless heat transport using sugar alcohol or hydrate, and (6) heat transport method using the microencapsulated PCM slurry.

Introduction

Global warming and depletion of fossil fuels are two major problems that are caused by large-scale energy consumption. To resolve these problems, the current practice of focusing on inexpensive energy use should be reconsidered, and the focus should be shifted to efficient energy use that does not adversely affect the environment. From the heat usage point of view, there are many heat demands within a temperature range of 0–200 °C. Although the heat demands can be basically provided by waste heat and renewable energy such as solar heat, most of them are directly provided by combustion of fossil fuels (Fig. 1). Such waste heat and solar heat are usually unstable and dispersing thinly.

By using thermal energy storage, such thin heat can be stored temporarily, so that the instability of heat supply can be smoothed. Thus thermal energy storage is the essential technology for utilizing such unstable or thin renewable heat. Thermal energy storage has another important feature which enables to generate and use energy efficiently because thermal energy storage can store energy during slack demand times (e.g., at night) and provide energy during high demand times (e.g., during the day). To meet a given peak demand, energy storage permits smaller power plants to be built, and it also permits them to be continually run at peak operating efficiency.

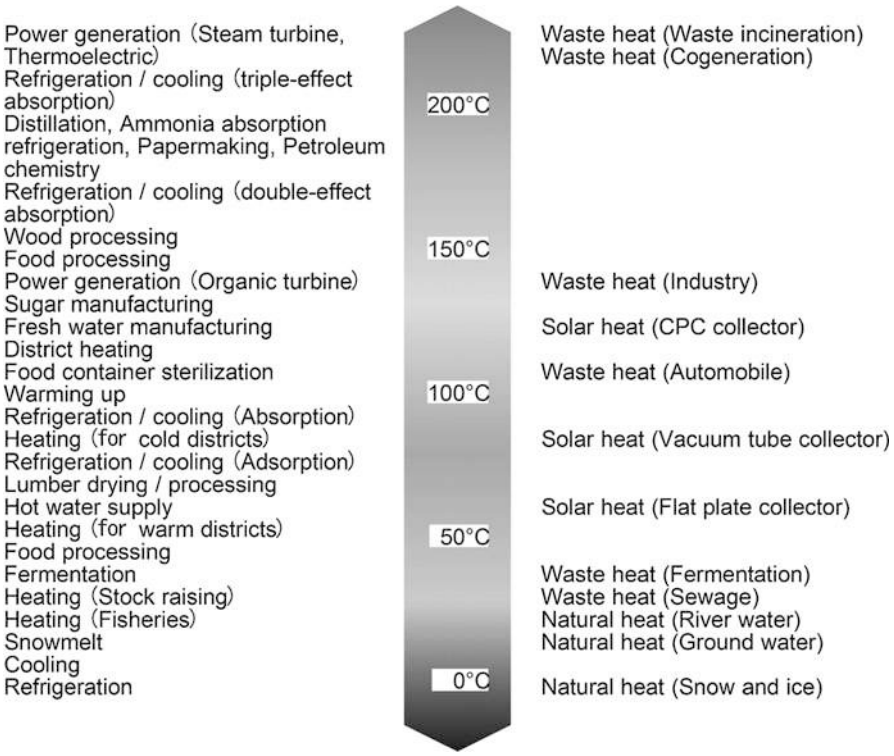

Fig. 1 Heat demands and heat sources by renewable energy and waste heat from 0 °C to 200 °C

By using heat transport, various heat sources can be connected and various heat demands which are located far from the heat sources can be fulfilled. The heat transport technology also enables to use a variety of heat sources such as a boiler, waste heat, and solar heat. Therefore, heat transport is the key technology to realize the thermal network among heat sources and heat demands, which can minimize the capacity of each heat source.

This chapter describes fundamental technology and the recent research trend of thermal energy storage and its application to heat transport.

Fundamentals of Thermal Energy Storage

Solar System and Thermal Energy Storage

The quantity and quality of heat supply from natural energy generally change with time. It is only during the daytime that solar energy can be acquired. Particularly, direct solar radiation is provided only at the time of fine weather. Heat demand in the commercial sector and residential sector, on the other hand, is apt to concentrate in

the morning and evening rather than in the daytime. Therefore, to improve the utility value of solar energy and magnify the application field of the energy, the technologies to collect and store solar heat in the daytime and to supply the stored heat during the high demand times become important.

Figures 2 and 3 show general components of solar systems with the thermal energy storage which can temporarily store the heat from solar collectors and can supply the stored heat on demand. Three thermal processes, (1) charging, (2) keeping, and (3) discharging, are necessary for thermal energy storage. The simplest constitution of a thermal energy storage method is that an object of heating is contacted to a thermal energy storage body or is included in the body as shown in Fig. 2a.

In Fig. 2, all the above thermal processes (1–3) are done passively. For example, there are houses and buildings which adopt this thermal energy storage method to use solar heat. The system using this method is called a passive solar system. If the system is designed such that the solar heat goes to the structure of a building through a transparent thermal insulation as shown in Fig. 2b and such that the time taken for thermal conduction from the structure to the indoor wall is about half a day, this storage method can automatically supply solar heat for space heating in the

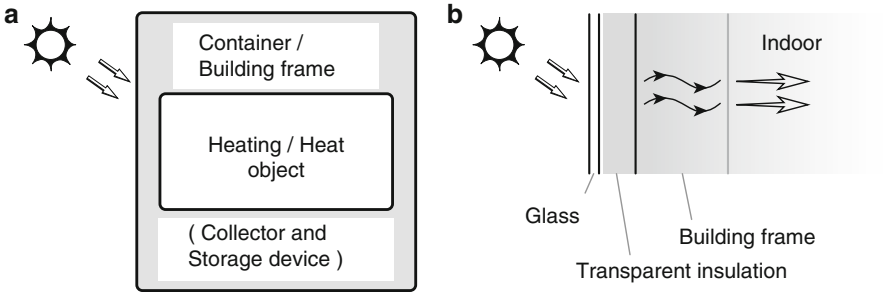

Fig. 2 (**a**) Component of passive thermal energy storage device and (**b**) application to heating by wall heat storage

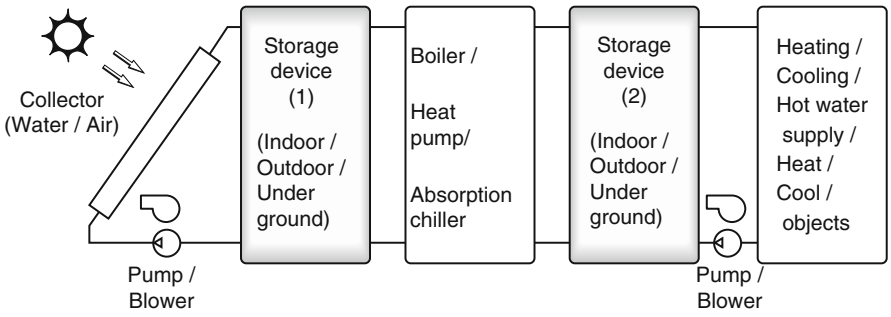

Fig. 3 Configuration of an active solar system

nighttime. Although the passive thermal energy storage is simple in constitution, it is difficult to control the above processes (1–3) depending on the condition. Therefore, the thermal optimization of the system is important in designing such passive systems.

Figure 3 shows the example of an active solar system which carries out the above three thermal processes actively. Each device shown in Fig. 3 is appropriately selected depending on the objective of the system. For example, a solar domestic hot water system corresponds to the simplest composition of the system shown in Fig. 3. The domestic hot water system consists of a solar collector and a water tank for thermal energy storage, both of which are installed on a roof. Cold water which flows into the collector is heated by solar heat in the daytime, which causes natural convection of the water and circulates the water between the collector and the tank. Thereby the water temperature in the tank gradually rises to a high temperature for hot water supply after sunset.

Water is the most convenient medium to transport heat among the components shown in Fig. 3. In the system which deals with the lower temperature than the freezing point of water, nonfreezing fluid is usually used as a heat transfer medium. On the other hand, in the system which deals with the higher temperature than a room temperature, an organic compound or chloride is often used for a heat transfer medium. In the system in which heat transfer medium is not water, a heat exchanger is often used in the storage device to heat the water. Air is sometimes used for the heat transfer medium in the solar collector because air can directly be used for space heating or for heating.

The thermal energy storage device (1) in Fig. 3 can regulate the fluctuation of heat supply. When the output from the thermal energy storage device (1) is short in temperature or quantity for heat demand, boilers, heat pumps, or absorption chillers are used as an auxiliary heat source. The thermal energy storage device (2) in Fig. 3 can regulate the fluctuation of heat demand. If the quantities of heat supply and heat demand can be patternized, either thermal energy storage device (1) or (2) is omitted by designing the system matching the fluctuation of the quantities. Optimization of operating temperature and equipment capacity based on the thermal performance of each component is necessary for designing the system with thermal energy storage.

Functions of Thermal Energy Storage

The effects of thermal energy storage are classified into three functions as shown in Fig. 4, that is to say, phase regulation between heat supply and heat demand (Fig. 4a), an amplification of heat supply (Fig. 4b), and smoothing of heat supply (Fig. 4c). For example, the function of phase regulation is utilized when solar heat gained in the daytime is used to supply hot water in the nighttime. The amplification function of heat supply is utilized when solar heat gradually gained through a year is used for heating in winter concentratedly. The smoothing function of heat supply is utilized when solar heat gained under an unstable weather condition is used for solar thermal power generation at constant output.

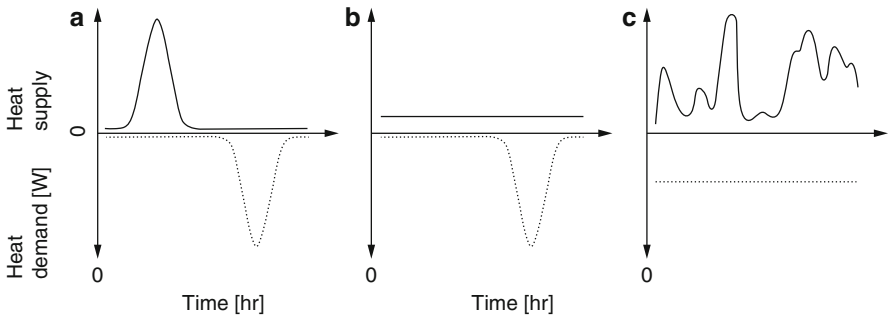

Fig. 4 Functions of thermal energy storage. (**a**) Phase regulation, (**b**) amplification, (**c**) smoothing

In many practical uses, these three functions should be properly selected and combined to fit applications. For example, the passive thermal energy storage device in Fig. 2 uses two functions: the phase regulation shown in Fig. 4a and the smoothing shown in Fig. 4c. The active thermal energy storage system in Fig. 3 uses all the three functions: the phase regulation, the amplification, and the smoothing shown in Fig. 4.

Classification of Thermal Energy Storage Methods

A material absorbs or discharges heat when the kinetic energy or the potential energy of the atoms or the molecules in the material changes by temperature change or phase transition. Besides, a material absorbs or discharges heat when the condition of the atomic bond or the molecular bond changes by chemical reaction. Thermal energy can be temporarily stored by using these phenomena as necessary. Table 1 shows the example of thermal energy storage methods classified by physical and chemical phenomena which are used to store heat.

Thermal energy storage methods using the physical change of a material are classified into the following three methods: (1) The thermal energy storage method which uses the absorption and discharge effects of heat caused by the temperature change of materials is called sensible heat thermal energy storage (SHTES). The SHTES is applied to hot water bags or electric water heaters with water tanks. (2) The thermal energy storage method which uses the absorption and discharge effects of heat caused by the phase transition of materials is called latent heat thermal energy storage (LHTES). The LHTES is applied to ice pillows or ice storage air conditioners. (3) The thermal energy storage method which uses the adsorption and desorption heats of material is called adsorption thermal energy storage. The adsorption storage is applied to air conditioners or chillers. The particular classification of SHTES and LHTES in Table 1 is mentioned later.

Thermal energy storage methods using the chemical change of a material are classified into the following three methods: (1) The thermal energy storage method which uses the endothermic and exothermic reactions of materials is called chemical

Table 1 Thermal energy storage methods

Use of physical change of materials	
Sensible heat thermal energy storage (SHTES)	Conventional SHTES (e.g., hot water storage)
	Soil thermal energy storage/underground thermal energy storage
	Aquifer thermal energy storage
	Solar pond
Latent heat thermal energy storage (LHTES)	Conventional LHTES (e.g., ice storage)
	Supercooled thermal energy storage
Adsorption thermal energy storage	
Use of chemical change of materials	
Chemical thermal energy storage (CTES)	Conventional CTES (e.g., reversible reaction between calcium hydroxide and calcium oxide)
	Metal hydride thermal energy storage
	Concentration difference thermal energy storage

thermal energy storage (CTES). Because repeatability becomes premise as for the functions of thermal energy storage, it is necessary for the reaction of CTES to be reversible. As subspecies of the CTES, there are (2) metal hydride thermal energy storage and (3) concentration difference thermal energy storage using heat of dilution.

Thermal Energy Storage Materials

Any substance can be used as thermal energy storage material in theory. The effectiveness as thermal energy storage materials depends on thermophysical properties like specific heat, transition point, and heat of transition. However, practicable materials are limited by chemical properties like deliquescence, efflorescence, corrosiveness, noxiousness, heat resistance, and economy.

Table 2 shows heat capacities per 1 L of several familiar materials used as heat storage materials (The Japan Society of Mechanical Engineers (JSME) 2009). In a room temperature, water is the best material for SHTES system in point of cost, safety, and thermal energy storage density. At a high temperature over several hundred degrees Celsius, rocks and bricks are effective as materials for SHTES system, too.

Table 3 shows melting points and heats of fusion per 1 L around the melting points of several familiar materials (Hirano 2002). Water is also the most suitable phase change material (PCM) for LHTES systems which is operated near 0 °C. Ice storage systems are good examples of LHTES systems and are widely spread today. Paraffin is one of usable PCMs. The heat of fusion per unit volume of paraffin is small because both density and heat of fusion per unit mass are small. Besides, inflammability of low-melting-point paraffin is high. However, paraffin has low noxiousness, and the influence of supercooling (mentioned later) before freezing is small. Therefore, paraffin is used as a comparatively cheap PCM.

Table 2 Heat capacities of ordinary materials per 1 L

Material	Heat capacity (J/K)
Water	4170[a]
Mild steel	3720[b]
Loam (water content 37 %)	3440[a]
Basalt	2670[c]
Sand and clay (water content 22 %)	2350[a]
Limestone concrete	2160[a]
Chamotte brick	2000[a]
Asphalt	1950[a]
Cedar (water content 48 %)	540[b]

[a]At 20 °C
[b]At 27 °C
[c]At 127 °C

Table 3 Heat of fusion of ordinary materials per 1 L

Material	Melting point (°C)	Heat of fusion (kJ/L)
Water	0	306
Polyethylene glycol #400	8	97
Sodium sulfate decahydrate	32	334
Disodium hydrogen phosphate dodecahydrate	36	384
Sodium acetate trihydrate	58	356
Paraffin wax	42 ∼ 70[a]	120 ∼ 190[a]
Polyethylene glycol # 6,000	57	201
D-Threitol	87	328
Erythritol	118	416
Mannitol	167	422
Tin	232	422
Aluminum	660	940

[a]Depending on the number of carbon atoms in a molecule

Hydrate is also one of the useful PCMs. Noxiousness of most hydrate is low. However, supercooling and segregation (mentioned later) become a problem when the hydrate is used as a PCM. Sugar alcohol is one of the safe and promising PCMs. However, the supercooling and cost of sugar alcohol may be problematic. Thus the further utilization of hydrate or sugar alcohol is expected in the future LHTES systems because the thermal energy storage densities of hydrate and sugar alcohol are larger than that of paraffin.

Thermal Energy Storage Devices

In the thermal energy storage device shown in Fig. 3, suitable mechanisms are necessary to control the three processes: (1) charging, (2) keeping, and (3) discharging. For the control of the processes, most thermal energy storage

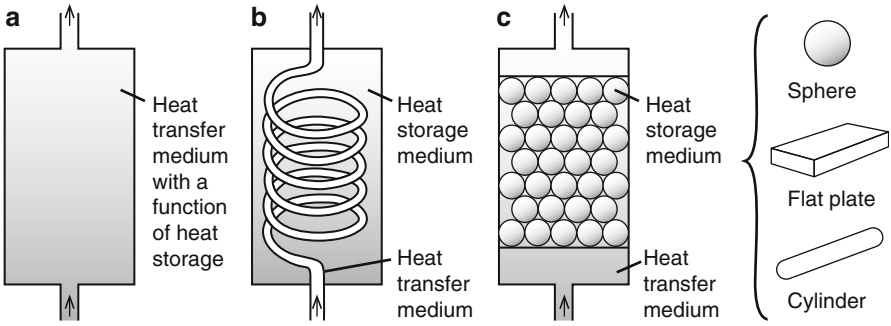

Fig. 5 Typical configuration of thermal energy storage device. (**a**) Combined use of heat transfer medium and heat storage material, (**b**) separation by pipe, (**c**) separation by capsule

devices take either constitution shown in Fig. 5. When the storage space for a heat transfer medium is installed in the middle of piping shown in Fig. 5a, the abovementioned thermal processes (1–3) can be carried out simply by injecting and extracting the heat transfer medium if necessary. For example, water as a heat transfer medium also functions as a heat storage medium in a solar domestic hot water system. The thermal energy storage is given only by sensible heat when the phase of the heat transfer medium does not change within the temperature range of operation. On the other hand, when hydrates, inclusion compounds, or clathrate compounds of hydrocarbon or fluorocarbon, or fluids like the ice slurry are used as the heat transfer media, latent heat is also available to use along with sensible heat.

In the thermal energy storage tank shown in Fig. 5a, the heat transfer medium is easily mixed if the agitating behavior by the inflow motion of the heat transfer medium is strong. In this case, the storage tank is called a mixed tank. The mixed-type heat storage tank provides a high performance in the smoothing function of Fig. 4c. However, the available energy easily decreases in the mixed tank because the temperature difference is easily lost by the agitating behavior. On the other hand, if the mixing behavior by the inflow motion of the heat transfer medium is small, the thermal stratification due to density variations is easily formed in the heat storage tank. In this case, the storage tank is called a stratified tank. The heat storage tank of thermally stratified type can easily maintain available energy in the tank. To promote the formation of plug flow in the stratified tank, a diffuser or a manifold is often used.

For example, the thermal energy storage device for a solar system is considered. The efficiency of a solar collector which is installed in the upstream side of the thermal energy storage device becomes higher as the temperature difference between the solar collector and the ambient air becomes smaller. The efficiency of the thermal appliances such as a heat pump installed in the downstream side of the thermal energy storage device becomes higher as the output temperature of the storage device becomes higher. Therefore, the thermal energy storage device of thermally stratified type is more profitable in efficiency of the solar system than the mixed-type device (Duffie and Beckman 1991).

One practicable idea for solar energy systems is the use of a pond as the thermal energy storage tank and a solar collector. The pond for this purpose is called a solar pond. The heat transfer medium flows into the solar pond and flows out from the pond with gained solar heat to supply heat. A wide pond is advantageous to collect solar heat. However, the gained solar heat is usually going to be dissipated and lost easily from the surface of the pond to the ambient air because of natural convection in the pond. On this account, an inverse thermal stratification is applied to reduce the heat dissipation. Sodium chloride, polymer compound, porous structure, or honeycomb structure is added to the pond to form the inverted temperature profile in the direction of depth such that the temperature in the lower layer is higher than that in the upper layer. Salt lakes are just available to use as the solar ponds.

In cold districts, it is necessary for antifreezing fluids to be used as the heat transfer medium to prevent freezing. When the antifreezing fluid can be just used for not only the heat transfer medium but also the heat storage medium, thermal energy storage devices shown in Fig. 5a can be applied. On the other hand, the thermal energy storage device shown in Fig. 5b, c is used when the heat storage medium is different from the heat transfer medium. The materials listed in Tables 2 and 3 can be used as the heat storage materials for the system shown in Fig. 5b, c. In the constitution shown in Fig. 5b, c, the heat exchange rate between the heat transfer medium and the heat storage medium is one of the most significant factors to determine the thermal time constant of the device. It is effective to broaden the contact area between both media for improving the heat exchange rate. It is also convenient to handle the heat storage medium when the medium is divided into small pieces. Therefore, the heat storage media are usually filled into the plural small capsules shown in Fig. 5c whose shape is spherical, cylindrical, or flat.

There are several methods which use the underground soil and rocks as the heat storage medium. The method which is called soil thermal energy storage or underground thermal energy storage uses the antifreezing fluid and the soil as the heat transfer medium and the heat storage medium shown in Fig. 5b, respectively. The method which is called aquifer thermal energy storage uses the underground water for the heat transfer medium and uses underground rocks and sands for the heat storage medium as in Fig. 5c. Above both methods using the earth are effective for a large quantity and long-term thermal energy storage. When the storage period is longer than a season, the method is particularly called seasonal thermal energy storage. For example, the surplus solar heat gained in the summer can be effectively utilized in the winter by the seasonal thermal energy storage.

Characterization of Thermal Energy Storage

In a thermal energy storage system, quantity of stored sensible heat, Q_s (J); quantity of stored latent heat, Q_l (J); and quantity of stored heat of reaction, Q_r (J), are given in the next equations, respectively:

$$Q_s = m\int c(T)dT \tag{1}$$

$$Q_s \approx mc\Delta T = \rho V c\Delta T \tag{2}$$

$$Q_l = m\Delta_f H M_f \tag{3}$$

$$Q_r = n\Delta_r H R_f \tag{4}$$

where $c(T)$ is the specific heat at temperature T(J/g/K); M_f, melting fraction (defined by [melted mass]/[total mass]); m, mass (g); n, number of moles (mol); R_f, reacting fraction (defined by [reacted mass]/[total mass]); T, temperature (K); V, volume (m^3); $\Delta_f H$, heat of fusion (J/g); $\Delta_r H$, heat of reaction (J/mol); ΔT, temperature change (K); and ρ, density (g/m^3).

If the temperature dependence of specific heat of the thermal energy storage material is small or if the temperature change of the material during the storage processes is small, Eq. 1 can be approximated by Eq. 2. The quantity of stored heat in the SHTES system is governed only by Eq. 1. Storage process with the LHTES system is usually accompanied by temperature change before and after the phase transition. Therefore, the quantity of stored heat in the LHTES system is usually governed by Eqs. 1 and 3. Storage process with the CTES system is usually accompanied by temperature change or by temperature change and phase transition before and after the reaction. Therefore, the quantity of stored heat in the CTES system is usually governed by Eqs. 1 and 4 or Eqs. 1, 3, and 4.

The efficiency of thermal storage, η, and the efficiency of a heat storage tank, η_t, defined by the following equations are used for typical indexes to characterize the performance of a thermal energy storage device:

$$\eta = Q_{out}/Q_{in} \tag{5}$$

$$\eta_t = Q_{out}/Q_{th} \tag{6}$$

where Q_{out} is the output thermal energy (J); Q_{in}, input thermal energy (J); and Q_{th}, theoretical storage capacity of thermal energy (J).

The efficiency of available energy, exergy, based on the environmental temperature is also important to evaluate the performance of the storage devices with which the charging and the discharging processes occur in a specific small temperature range such as the LHTES system.

Each thermal energy storage method is characterized in Table 4. The thermal energy storage density is defined by the quantity of heat which can be stored in a unit mass or in a unit volume of the storage material. The SHTES has a lot of embodiments and is technically mature. The LHTES has some technical issues in repeatability, stability, or profitability except an ice storage system, one of the LHTES systems. Thus, the technology of the LHTES is in the middle of development. Although the CTES has the highest functionality, there are many pending issues including the material compatibility.

Table 4 General merits and demerits of three methods of thermal energy storage

Rating item	SHTES	LHTES	CTES
Storage density	X	Δ	O
Stability of output temperature	X	O	O
Repetition stability	O	Δ	X
Responsibility	O	Δ	Δ
Safety	Δ	Δ	Δ
Initial cost	O	Δ	X

SHTES sensible heat thermal energy storage, *LHTES* latent heat thermal energy storage, *CTES* chemical thermal energy storage

The thermal energy storage density of the LHTES device is larger than that of the SHTES device. Therefore, LHTES is more advantageous than SHTES for the applications where the size of heat storage systems must be minimized, for example, in urban areas. The temperature of the heat storage medium during the charging and discharging processes of sensible heat varies with time. On the other hand, the temperature of the heat storage medium during the charging and discharging processes of latent heat is maintained at the transition point. This is the reason that LHTES is more advantageous than SHTES in point of the storage efficiency of available energy. In addition, the repeatability of the storage processes of LHTES is comparatively stable. Thus, further application of LHTES is expected. From the following section, thermal energy storage and heat transport which use latent heat of PCMs will be explained in detail.

Phase Change Thermal Energy Storage

General Feature of Phase Change Materials

It is well experienced routinely that ice absorbs large heat of fusion and cools surrounding substances during melting process. In this case, water functions as a PCM. Many candidates of PCMs were listed up in various kinds of literature especially in 1970s when we experienced two oil crises. Among those candidates, however, many of them were substances with toxicity, noxiousness, corrosiveness, irritation, oxidizability, combustibility, or inflammability. Thus the number of available materials for PCMs has been decreasing as regulations for the use of chemical substances have been strengthened.

As typical examples of PCMs, paraffin, hydrate, and sugar alcohol are recently attracting attention. Major physical properties of water (Hirano 2002), *n*-eicosane (Kosaka et al. 1980), disodium hydrogen phosphate dodecahydrate (DHD) (Hirano et al. 2001), and erythritol (Kakiuchi 2008) are given in Table 5. Compared with water in Table 5, the following points are given as the characteristics of the three materials: paraffin, hydrate, and sugar alcohol. Hydrate and sugar alcohol are profitable to densification of thermal energy storage because densities are larger

Table 5 Comparison of physical properties of water, *n*-eicosane, DHD, and erythritol

Property	(Phase)	Water	*n*-eicosane	DHD	Erythritol
Density (kg/m^3)	(Solid)	917[a]	830	1520[c]	1480[e]
	(Liquid)	999.84[a]	780	1447[d]	1300[f]
Specific heat (kJ/kg·K)	(Solid)	2.101[b]	1.9	2.00[c]	1.38[e]
	(Liquid)	4.2174[a]	2.3	3.45[d]	2.77[f]
Thermal conductivity (W/m·K)	(Solid)	2.09[a]	0.34	1.02[c]	0.73[e]
	(Liquid)	0.565[a]	0.15	0.61[d]	0.33[f]
Melting point (°C)		0	36.4	35.54	119
Heat of fusion	(kJ/kg)	333.6	247	265.6	330
	(kJ/L (liquid))	333.5	193	384.3	429

[a]0.0 °C
[b] −2.2 °C
[c]32 °C
[d]36 °C
[e]20 °C
[f]140 °C

than that of water. On the other hand, paraffin is disadvantageous for densification of thermal energy storage because the density is small. It is effective to use not only latent heat but also sensible heat of hydrate for thermal energy storage because the specific heat of hydrate is as large as that of water. The utilization effect of sensible heat of paraffin and sugar alcohol is not large compared with water due to the same reason. Hydrate and sugar alcohol are disadvantageous in the heat exchange during the phase change process because thermal conductivities of them are about a half of that of water. Paraffin is more disadvantageous in the heat exchange during the phase change process because the thermal conductivity of paraffin is only about a quarter of that of water.

The selection of the suitable material for PCMs depends on the place where the heat storage device is used as well. For a mobile heat storage system, not only the volume of the heat storage medium but also the weight becomes an important factor. For a stationary heat storage system, on the other hand, the volume of the heat storage medium is overwhelmingly more important than the weight of the medium. Figure 6 shows the relationships between the melting points and heats of fusion per unit volume for several candidates of PCMs whose melting points exist between 0 °C and 200 °C. The unit volume of each material except water is based on the volume in the liquid phase at around the melting point because the maximum quantity of the material filled in a capsule is limited by the volume in the liquid phase. The unit volume of water is based on the volume in the solid phase at around the melting point because the volume of water decreases after melting. In comparison with the heat of fusion of water which is used for an ice storage air-conditioning system, the heats of fusion of hydrate and sugar alcohol are large, and the heats of fusion of paraffin and other organic substances are small.

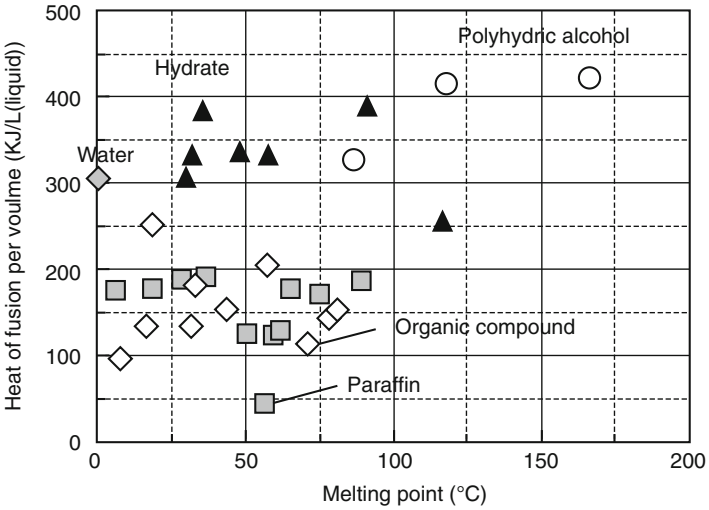

Fig. 6 Example of heats of fusion per unit volume of some promising PCMs in the liquid phase

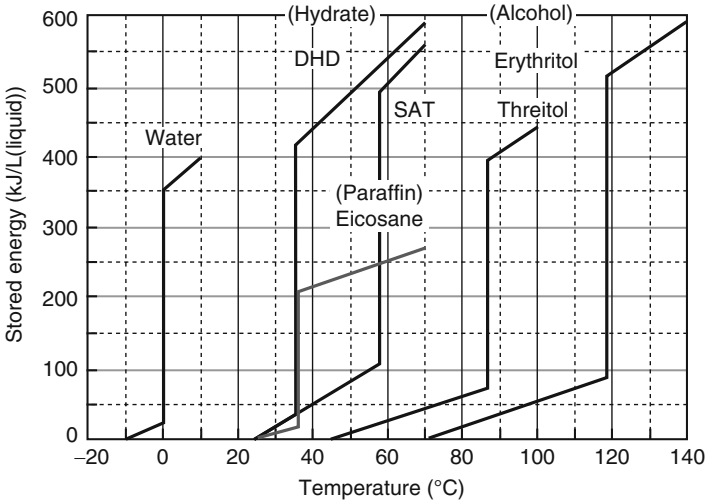

Fig. 7 Temperature dependence of the thermal energy which can be stored per unit volume

Thermal Energy Storage Density

It is extremely rare for practical LHTES systems to use only latent heat. The LHTES systems usually use not only latent heat but also sensible heat in the proper operating temperature range including the transition point of the heat storage medium. Figure 7 expresses the variations of the thermal energy which can be stored in each proper

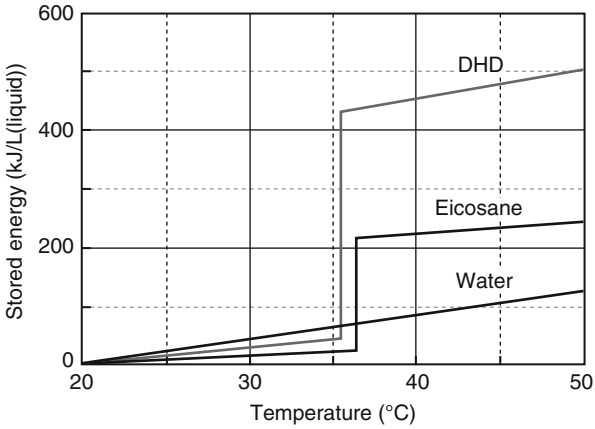

Fig. 8 Comparison of the thermal energy which can be stored per unit volume in the temperature range from 20 °C to 50 °C

temperature range about *n*-eicosane, disodium hydrogen phosphate dodecahydrate (DHD), sodium acetate trihydrate (SAT), threitol, and erythritol as typical examples of paraffin, hydrate, and sugar alcohol. Hydrate can store large energy because both specific heat and heat of fusion are large; thus it is effective to use hydrate with a wide temperature range. On the other hand, both specific heat and heat of fusion of paraffin are small. Thus the superiority of LHTES with paraffin over the SHTES with water becomes lower as the operating temperature range of paraffin becomes wider.

For example, Fig. 8 gives the variations of the thermal energy which can be stored per unit volume of water, *n*-eicosane, and DHD when the materials are heated from 20 °C to 50 °C. The thermal energy which can be stored with *n*-eicosane by the temperature rise of 30 °C is about twice as much as that with water. By the way, when the temperature rise from 35.9 °C to 36.9 °C is considered, the thermal energy which can be stored with water by this temperature rise is 4.2 kJ/L. On the other hand, the thermal energy which can be stored with *n*-eicosane by the same temperature rise, 1 °C, as that of water is evaluated at 195 kJ/L including heat of fusion. In this temperature change, 1 °C, the thermal energy which can be stored with *n*-eicosane is 46 times larger than that with water. That is to say, the superiority of the thermal energy storage density of LHTES against SHTES deteriorates when the range of the operating temperature of LHTES system becomes wide.

Variations of the thermal exergy (available energy) which can be stored per unit volume of the PCMs are shown in Fig. 9 when 20 °C is assumed to be the standard environmental temperature. Sugar alcohol can store larger exergy than hydrate and paraffin because the melting point is high. In other words, the quality of the thermal energy which can be stored with sugar alcohol is high. Thus, LHTES with sugar alcohol has high added value for space heating or hot water supply. To use PCMs shown in Fig. 6 effectively, it is important to make better use of the merits of each PCM and to make up for the demerits of it. Besides, the development of new materials located in the upper part of the graph in Fig. 6 is eagerly awaited in future.

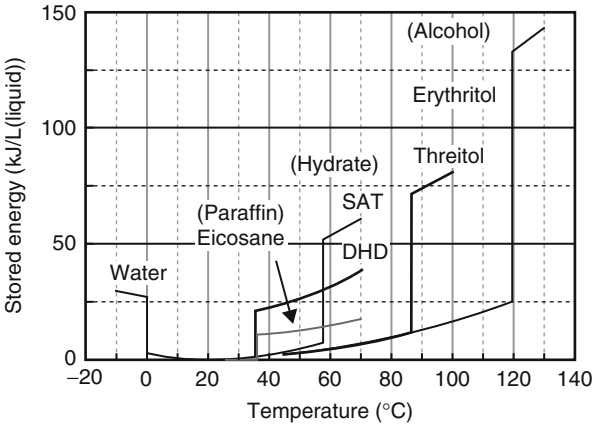

Fig. 9 Temperature dependence of the thermal energy which can be stored per unit volume

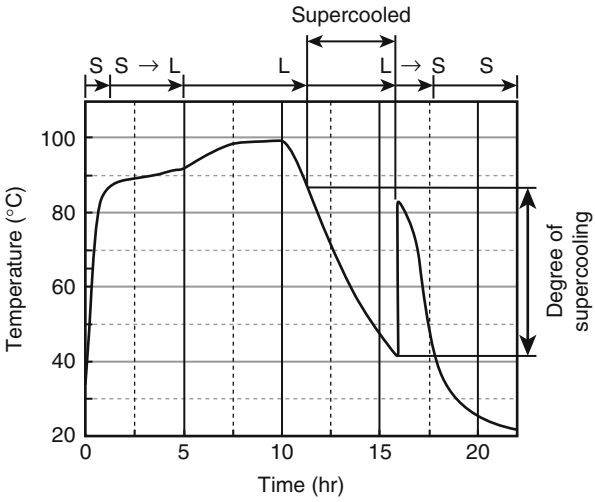

Fig. 10 Example of the temperature variation of D-threitol during melting and solidification processes. The letters "S" and "L" are mean solid phase and liquid phase, respectively

Supercooling and Segregation

A material changes its phase from solid to liquid (fusion) or vice versa (solidification) ideally at the melting point. Practically, however, the temperature gap between fusion and solidification processes occurs. For example, Fig. 10 shows the temperature variation of D-threitol during melting and solidification processes. In Fig. 10, a heating operation increases the temperature of the threitol in the solid phase. The threitol starts to melt at the melting point, 87 °C. After the threitol completely melted, the melt is cooled to the room temperature. By the cooling operation, the temperature of the threitol falls to the melting point. However, the solidification process does not start at the melting point. The melt is continuously cooled to the lower temperature than the melting point, in the liquid phase called a supercooled state.

Supercooling phenomenon is caused by not the delay of thermal conduction in the melt, but the difference in free energy between a liquid phase and a solid phase. To generate a crystal nucleus in the melt, it is necessary for the radius of the molecular cluster in the melt to exceed the critical size which is determined from the relationship between the volume-free energy and the surface-free energy. Therefore, the supercooled state is maintained in the metastable state unless the melt is cooled to the spontaneous nucleation temperature, about 41 °C in Fig. 10. The difference between the spontaneous nucleation temperature and the melting point is equivalent to the maximum degree of supercooling of the material. The maximum degree of supercooling depends not only on the intensive properties, such as the melting point, but also on extensive properties, such as the mass of the material filled into a container.

Once the solidification starts by the generation of a crystal nucleus, the temperature of the threitol recovers to the melting point as is shown in Fig. 10. After that, the threitol continues releasing heat of solidification till solidification is completed. The supercooling phenomenon is easily observed in hydrate and sugar alcohol.

There are two aspects to the supercooling phenomenon that the supercooling of a PCM is favorable for LHTES or unfavorable for it. When the heat of solidification of a PCM is kept in the supercooled state at the lower temperature than the melting point, the heat loss from the PCM to the ambient air can be reduced. In this case, the supercooling becomes a favorable phenomenon for LHTES. On the other hand, even when the heat of solidification of a PCM is demanded, the latent heat is not obtained due to the supercooling unless the temperature of the PCM falls to the spontaneous nucleation temperature below the melting point. In this case, the supercooling becomes an unfavorable phenomenon for LHTES. Most research on LHTES has been conducted from the latter viewpoint. Thus, great efforts of research and development of PCMs have been focused on the prevention technology against supercooling.

The research on the prevention technology against supercooling became in earnest from the research by Telkes in 1940s. Telkes discovered that the sodium tetraborate decahydrate was effective as a nucleating agent for sodium sulfate decahydrate (Telkes 1954). The nucleation cannot be promoted easily even if the additive for nucleation is kept in the solid phase. It is considered that the effect of the nucleating agent and the factor of the induction of nucleation are different among base materials, so that it is necessary to discover the agents by a trial-and-error method. Discovery of nucleating agent by Telkes attracted next research, and from 1950s to 1980s, several nucleating agents were discovered, and several physical nucleation methods were invented. However, there are many PCMs whose proper nucleating agents are not found yet.

Segregation in hydrate is another challenging phenomenon as well as the supercooling. In the melt of the hydrate, the hydrate of the lower order which crystallized in advance by peritectic reaction is going to precipitate in the melt due to density variations. The hydration reaction of the higher order does not completely proceed if the hydrate of the lower order precipitates before it takes in more water molecules and becomes the original hydrate of the higher order. Segregation causes

the substantial decrease in heat of fusion and the functional deterioration as a PCM. Therefore, proper inhibitors for segregation or stabilizers such as thickeners and polymers for liquid adsorption have been developed. However, the optimization of the proportion of the segregation inhibitors to a PCM is necessary because the inhibitors cause decrease in the storage density of thermal energy.

The maximum degrees of supercooling of paraffin and some other organic substances are smaller than those of hydrate and sugar alcohol. Besides, the segregation does not occur in paraffin and any other organic substances. Those advantages are two of the reasons why paraffin and other organic substances are often used as PCM at around a room temperature.

Research and Development Situation

Looking back upon the progress, the two oil crises in the 1970s accelerated research and development on thermal energy storage methods in the industrial world and the academic world. From the second half of the 1970s to the first half of the 1980s, various kinds of materials and their application methods were searched for throughout the world and put in order. Besides, most of theoretical or experimental analyses concerning melting or solidification processes of PCMs or performances of the thermal energy storage with PCMs were conducted in this epoch. After that, the number of the research and development on thermal energy storage temporarily decreased. Recently, however, the number is a little increasing by a cognitive surge to the global warming issue represented by the Kyoto Protocol. Many of the articles related to phase change thermal energy storage were reported from 1980 to 1990, and many books and literature summarizing the reports were published after that.

However, physical properties of PCMs including mixtures are not fully known even though the names of the materials are well known. Besides, it is not rare that physical properties of PCMs listed in handbooks and literature include gross errors or the transmitted errors by using references which made mistakes of numerical mentions when the properties are quoted from original references (Hirano et al. 2001). The LHTES systems are generally used in the broad temperature range from the lower temperature than the melting point of a PCM to the upper temperature. Therefore, the temperature and pressure dependences of the physical properties of PCMs are important to the effectual design of the system. However, such detailed data are available only for several PCMs.

The technology of LHTES at the lower temperature than the room temperature has advanced by the research for more than 10 years after the oil crises. For example, an ice storage air-conditioning system has been downsized, improved in efficiency, and widespread. The research on LHTES by natural snow and ice was advanced as snow-utilization and snow-persistence technologies, and demonstration tests came into operation. Food storage and transport are suitable for use of snow and ice because the added values of the food storage and transport are higher than that of space cooling. The food transport at a low temperature with ice has been used

Table 6 Features of commercial encapsulated PCMs

Melting point (°C)	Heat of fusion (kJ/kg)	Principal component
58	226	Sodium acetate trihydrate
47	212	Sodium acetate compound
29	188	Calcium chloride hexahydrate
25	150	(The same as above)
17	145	(The same as above)
14	145	(The same as above)
0	333	Sodium carbonate aqueous solution
−3	308	Ammonium carbonate aqueous solution
−4	286	Potassium chloride aqueous solution
−10	283	Ammonium chloride aqueous solution
−15	293	(The same as above)
−16	289	(The same as above)
−21	222	Sodium chloride aqueous solution

conventionally as methods to retain the freshness. As food culture became rich, the uses of natural snow and ice came to attract attention not only for simple freshness retainment but also for increase and retainment in flavor. The lower the storage temperature of food is, the longer the preservation term is. However, the storage at the optimal temperature around the freezing point of water is good for the point of increase and retainment in flavor. The proper storage temperature, humidity, and period are actually different among food. For example, from the room temperature to the ice point, the flavor of rice becomes much superior as the storage temperature becomes lower. However, it is reported that the additional improvement of flavor of rice is small even if the storage temperature is kept at the lower temperature than the ice point (Hirano 2006).

The PCMs are often filled in containers of proper size such as in Fig. 5c and the containers are tightly sealed. The subdivision of the PCMs to the containers accelerates the heat exchange rate between the PCMs and the heat transfer medium and stabilizes the characteristic of phase change. In addition, the subdivision to the containers improves handling ability and prevents the PCMs from contamination. The manufacturing technology of encapsulated PCMs of which the containers are mainly made of polyolefin resin was developed in the 1980s. The heat-resistant temperature of polyolefin resin for the containers is about 70–100 °C. As a result, the spread of ice storage systems and floor heating systems with LHTES advanced.

Examples of the physical properties of the commercial encapsulated PCMs are listed in Table 6 (Mitsubishi Chemical Engineering 1999; Phase Change Products 2009). In the heat storage systems which use heat transfer media, convective heat transfer is dominant over the heat exchange between the PCMs and the heat transfer media. Thus spherical or cylindrical containers are often used in encapsulating PCMs to increase the contact area between the PCMs and the media. For example, the shapes of most PCM capsules on the market for hot water supply systems and for

space cooling and heating systems are spherical or cylindrical. The melting points of the PCMs in the spherical or cylindrical capsules are set to various temperatures which are shown in Table 6, in response to the purposes of uses.

In the heat storage systems which do not use heat transfer media, thermal conduction is dominant over the heat exchange between the PCMs and the cooling or heating objects. Thus, tabular containers are often used in encapsulating PCMs to increase the contact area between the PCMs and the objects. For example, the shapes of most PCM capsules on the market for floor heating systems are tabular. The materials of the container are selected from a soft film or a hard resin depending on applications. Several types of encapsulated PCMs which use sodium sulfate decahydrate (melting point is 32 °C) or sodium acetate trihydrate (adjusted melting point is 43 °C) are put on the market for floor heating systems (Hirano 2009a). Besides on the market, there are tabular encapsulated PCMs which use sodium sulfate decahydrate (adjusted melting point is 23 °C) for the heat capacity of passive solar systems. For equipment of the blackout indemnification of communication repeating facilities, tabular encapsulated PCMs of which the melting points are 36 °C are put on the market. For leveling the temperature of battery, there are resin-packaged PCMs of which the melting points are 29 °C.

As unique examples of the use of PCMs, there are warm keeping trays which use PCMs for maintaining the temperature of food. The melting points of the PCMs in the trays are set to various temperatures in response to the purposes. For maintaining the temperature of the hot water of baths, warm keeping packs are put on the market. These warm keeping packs are also usable as hot water bottles. Furthermore, there are flexible warm keeping mats for pets. Both warm keeping packs and mats use the organic compounds such as polyethylene glycol whose melting point is between 40 °C and 60 °C.

Phase Change Heat Transport

Transport Methods

Steam discharges large heat of condensation when it changes to liquid water. Therefore, steam has been used for long as a heat transport medium using the phase change between gas and liquid. However, to use the phase change between gas and liquid at around the room temperature, the decompression of the heat transport system or the use of the medium with a low boiling point is necessary. Besides, in using the phase change between gas and liquid, there is a problem of the thermal energy transport density defined by the quantity of heat which can be transported in a unit mass or in a unit volume of the transport material.

For instance, Table 7 gives the physical properties of ice, liquid water, and steam, respectively (Hirano 2002; International association for the properties of water and steam (IAPWS) 1998). The transporting power for gas is smaller than that for liquid, and the heat of condensation per unit mass is larger than the heat of solidification. However, the heat of condensation per unit volume is smaller than the heat of

Table 7 Comparison of physical properties of ice, liquid water, and steam

Property	Ice	Liquid water		Steam
Density (kg/m^3)	917[a]	999.84[a]	958.4[c]	0.5981[c]
Specific heat (kJ/kg·K)	2.101[b]	4.2174[a]	4.217[c]	2.077[c]
Thermal conductivity (W/m·K)	2.09[a]	0.565[a]	0.679[c]	0.0250[c]
Phase transition point (°C)	0	–	–	100
Heat of phase transition (kJ/kg)	333.6	–	–	2256
Heat of phase transition (kJ/L(liquid))	333.5	–	–	1.349

[a]0.0 °C
[b] −2.2 °C
[c]100 °C

solidification because the density in the gas phase is small. Thus heat transport using the phase change between solid and liquid has been researched and developed as a promising method at around the room temperature.

The heat transport methods with fusion and solidification are as follows: (1) a method to freeze the heat transfer medium partially and flow the slurry in piping, (2) a method to suspend fine grains of PCMs in the heat transfer medium and flow the emulsion in piping, (3) a method to suspend encapsulated PCMs with micro-dimensions in the heat transfer medium and flow the suspension in piping, (4) a method to fill up storage tanks with PCMs and carry the tanks by freight trains, freighters, or automobiles between heat source equipment and heat demand equipment. As for the transport density of thermal energy, the same argument as LHTES basically stands up. That is to say, the transport density depends on the content of PCMs in the base fluids, heat of fusion of PCMs, and so on.

The spread of phase change heat transport has not been advanced because of the same economical efficiency as phase change thermal energy storage. The clogging in the piping by the solidification or the aggregation of the PCMs is one of the serious issues in phase change heat transport. Therefore, suitable mechanism for preventing the clogging is necessary. Besides, the durability of the microcapsule shell generally deteriorates in a hot water, so that the improvement of heat resistance of the shell is required in the future.

Research and Development Situation

Around the 1990s, research and development of heat transport technologies by a hydrate slurry and a microcapsule slurry were conducted as the applications of phase change thermal energy storage technology at a low temperature, and part of the technologies was put to practical use. For example, a transport technology of latent heat at a low temperature with a tetra-*n*-butylammonium bromide (TBAB) aqueous solution (heat of fusion is 193–206 kJ/kg) was put to practical use (New Air Conditioning System Division 2009). The crystal deposition temperature of a TBAB aqueous solution is adjustable in the range from 0 °C to 12 °C by the concentration of the aqueous solution. When the crystal deposition temperature of

the hydrate slurry is higher than 0 °C, the coefficient of performance of chillers for generating the hydrate slurry becomes larger than that for generating the ice slurry, which reduces the consumption of electric power for generating the hydrate slurry holding the same latent heat as the ice slurry.

The viscosity of the hydrate slurry is larger than that of water. On the other hand, the thermal energy transport density of the hydrate slurry is larger than that of water, which can reduce the flow rate of the heat transport medium for air-conditioning. Since the reduction of the flow rate reduces the pressure drop in piping, the consumption of electric power for transporting the slurry is less than that for water. Therefore, the reduction of the transportation power of a heat transport medium and the improvement of the operation efficiency of a refrigerating machine are concurrently achieved if high-density heat transport is taken at 7 °C where the efficiency of cooling operation of the air in rooms is high.

The application of subsumption compounds except TBAB to the heat transport is also examined. Besides, the research of freezing control technology by synthetic polymers is conducted as research to improve the latent heat transport (Inada 2006). The substitution effect of natural antifreezing protein (AFP) was found in cheap heavy chemicals like polyvinyl alcohol.

Examples of Recent Technical Development

Thermal Energy Storage System for Hot Water Supply

In the temperature range for a hot water supply, paraffin waxes, organic compounds, and sugar alcohol shown in Fig. 6 are considered to be comparatively safe PCMs. In respect to the storage density of thermal energy and thermal conductivity, however, paraffin waxes and organic compounds are inferior as PCMs. Besides, there are no proper hydrates which are safe, have reproducibility in repetition of phase change, and have the melting point in the temperature range for a hot water supply. Therefore, sugar alcohol attracts much attention in the 2000s, and the proper methods for using the material have been studied (Kakiuchi 2008). The attractive points of sugar alcohol are its safeness used as medicines and food and its proper melting point for hot water supply. On the other hand, it was difficult to use sugar alcohol effectively as a PCM because the maximum degree of supercooling of sugar alcohol is large.

For example, in Fig. 10, the solidification of D-threitol whose melting point is 87 °C cannot be triggered unless the threitol is once cooled to around 40 °C because the spontaneous nucleation temperature is about 40 °C. That is to say, the heat of solidification of the threitol cannot be immediately extracted at the melting point. If the heat for cooling the threitol to the spontaneous nucleation temperature cannot be used, about 40 % of the heat stored in the threitol will be lost for the nucleation process. On the other hand, the heat of solidification can be saved in the supercooled state at a low temperature for a long term if the release time of the supercooled state is controlled actively. Besides, if the heat for cooling the threitol to the spontaneous

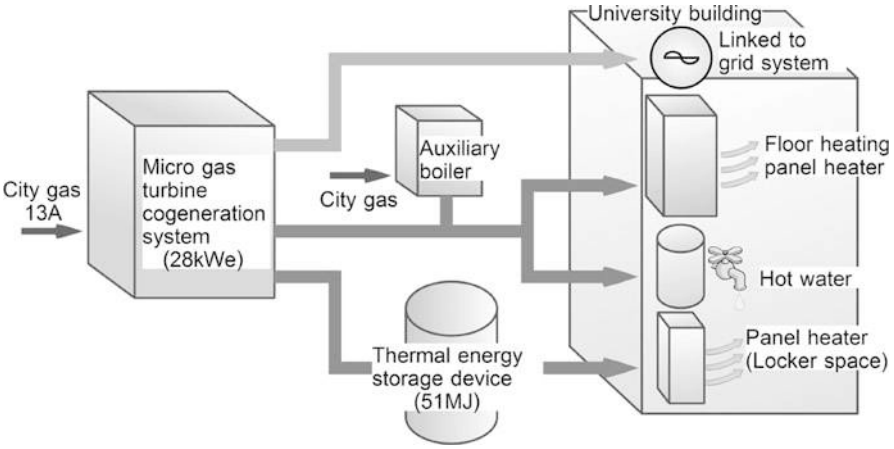

Fig. 11 Cogeneration system with hot water supply and space heating by thermal energy storage

nucleation temperature can be used effectively, the stored heat can be discharged twice in separate hours before and after the storage period in the supercooled state.

As an example of the applications of the LHTES using supercooling, a cogeneration system with the LHTES of D-threitol is shown in Fig. 11 (Hirano 2009b; Hirano and Takeuchi 2009). The system was installed in a building of the university located in Sapporo, Japan. The heat engine of the system is a micro gas turbine (MGT). The shaft power of the MGT drives a generator (27 kW). The exhaust gas of the MGT heats water for hot water supply with heat exchangers. Thus the cogeneration system can simultaneously supply both electricity and heat to the building. In the daytime, the hot water is partially supplied to the LHTES unit to store the surplus heat from the MGT. During the nighttime when the MGT is not operated, the LHTES unit can supply hot water in response to the demand of space heating.

In this system, the supercooled thermal energy storage unit with dual tanks illustrated in Fig. 12 enables the use of the threitol for thermal energy storage. The threitol is filled into thin and long cylindrical copper capsules. The capacity of each capsule is 912 mL. The storage tank is 166 L in capacity and is filled up with 96 capsules. The heat of fusion of the encapsulated threitol is 28 MJ in total. The storage tank is partitioned into two sections by thermal insulation. The PCM capsules exist in both sides of the partition. The upper large section, 152 L in capacity, is used for thermal energy storage. The lower small section, 1.6 L, is used for initiating nucleation in the supercooled threitol. The trigger for nucleation is the circulating water in the piping of the system at the room temperature. Circulation of the water through the nucleation section for only 5 min cools the bottom of each PCM capsule, which initiates nucleation in the supercooled threitol.

Figure 13 shows the variations of the thermal output and the outlet temperature of the circulating water from the storage unit during a daily storage cycle. As the charging process, the threitol is heated for 12 h by the exhaust heat from the MGT.

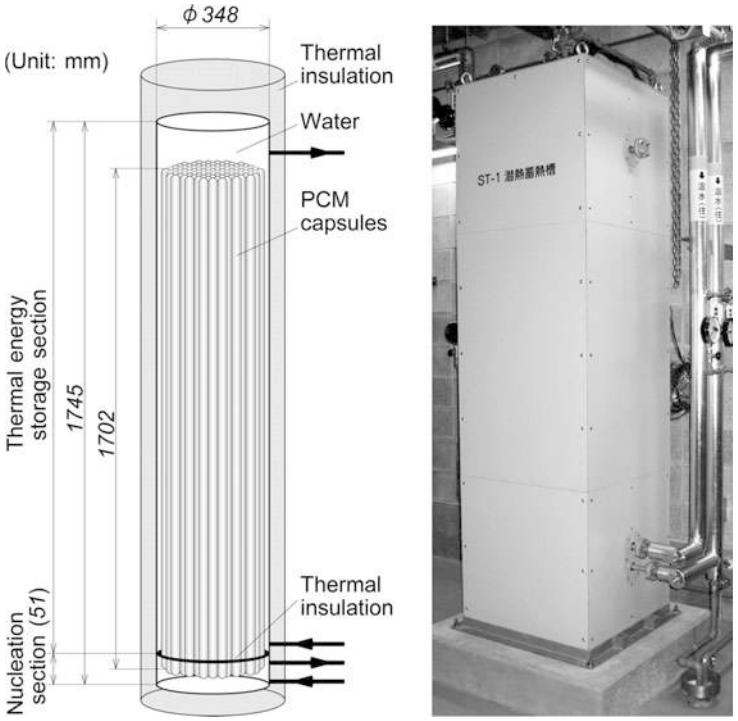

Fig. 12 Supercooled thermal energy storage unit

Fig. 13 Thermal output and the outlet temperature of the circulating water from the storage unit during a daily storage cycle

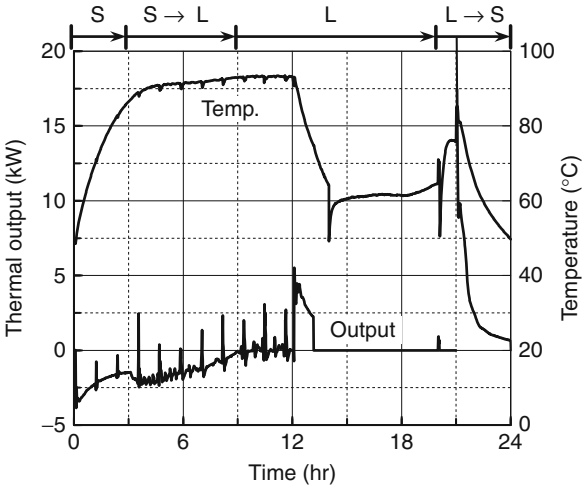

After the threitol completely melted, part of the sensible heat is discharged from the storage unit as the first thermal output, which makes the threitol supercooled. As the keeping process, the heat of solidification of the threitol is completely kept for about 8 h in the nighttime. After the supercooled storage, the threitol is intentionally nucleated to discharge the remained latent heat and sensible heat from the storage unit as the second thermal output. The two thermal outputs from the storage unit are used for space heating after and before the operation of the MGT. The heat for cooling the threitol in the nucleation section to the spontaneous nucleation temperature was equivalent to only the 1 % of the heat which is retained with the storage unit just after the charging process. Furthermore, the cooling heat for the nucleation operation can be used to preheat the circulating water in the piping effectively. By these processes, the 91 % of heat retained with the storage unit just after the charging process can be effectively used for space heating in the evening and early in the morning.

Heat Storage System for Heating

There are floor heating systems using solar heat gained in the daytime of fine weather day. The gained solar heat is partially stored in a thermal energy storage device or underfloor slab. The stored solar heat is emitted indoors gradually, and floor heating continues from night to the early morning of the following day. However, the additional heat is sometimes necessary for heating in the next morning because of the shortage of the available stored heat by the conventional thermal energy storage device. The reason for the shortage is that the stored heat by the conventional LHTES or SHTES is always dissipated into the ambient air regardless of a demand. The active use of the supercooling phenomenon in addition to the conventional systems enables the thermal energy storage device to store solar heat, midnight power, and so on effectively for half a day, or beyond cloudy days, a weekend, or a season. In the operating temperature range from 30 °C to 60 °C, the hydrate is superior as a PCM for space heating in point of the storage density of thermal energy as is shown in Fig. 6.

Thus the research on the floor heating system as illustrated in Fig. 14 has been conducted (Hirano et al. 2010). The PCM is disodium hydrogen phosphate dodecahydrate (cf. Table 5). The DHD is filled into thin and long cylindrical capsules made of polypropylene. The capacity of the capsule is 1,810 mL. Fifty-six capsules are horizontally embedded in the floor between subfloor joints. The heat of fusion of the encapsulated DHD is 25 MJ in total. By the supercooled storage of the hydrate, the system can effectively radiate the stored heat twice. For example, part of the sensible heat of the DHD in the liquid phase can be discharged in the evening, which makes the DHD supercooled. After the supercooled storage in the nighttime, the DHD is intentionally nucleated on the following morning and can discharge the remained latent heat and sensible heat.

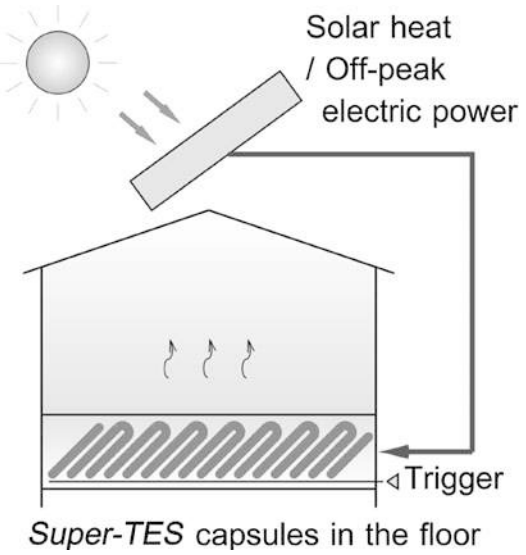

Fig. 14 Floor heating system with supercooled thermal energy storage

One of the most interesting applications of this storage method is the system which can store solar heat for cloudy or rainy days. If the storage system in the floor is divided into several sets and each set can be operated individually on demand, the stored solar heat can be partially discharged depending on more heat demands than twice. For example, after the supercooled storage in the nighttime, only a half of the sets is intentionally nucleated on the following morning, and the half of the stored latent heat is discharged and remained sensible heat as the second thermal output if it is cloudy or rainy. Then the remaining latent heat can be discharged from the remaining half of the sets as the third thermal output on the next morning of the cloudy or rainy day.

Furthermore, research on the seasonal LHTES using the supercooling phenomenon has been conducted. For example, the performance of a long-term LHTES unit using DHD as a PCM was experimentally investigated (Hirano and Saitoh 2007). The storage tank used in the experiment is partitioned into two sections by thermal insulation as is already shown in Fig. 12. The PCM capsules exist in both sides of the partition. The capacity of the storage tank is 53 L in total and the tank holds 31 capsules of DHD. The heat of fusion of the encapsulated DHD is 9.1 MJ in total. The result of the experiments shows that the storage unit can control the nucleation of the DHD after the supercooled storage for 203 days. From the result of the storage operation between 22 °C and 66 °C, the sensible heat of the unit was released to the room and lost. However, the latent heat is kept in the supercooled DHD, and the 49 % of the initial stored heat could be discharged by the nucleation operation after half a year.

Paraffin is chemically stable and is comparatively cheap. Therefore, the development of application of paraffin to PCMs at around room temperature is still continuing. The thermal conductivity of paraffin, especially in the solid phase, is small as

shown in Table 5, which deteriorates the heat exchange with the heat transfer medium. In addition, the separation of the solid phase of paraffin from the wall surface of the container easily occurs with thermal contraction during solidification. Therefore, the heat exchange of paraffin in the solid phase with the heat transfer medium often becomes rate-determining process of the storage device. On this account, research to promote heat transfer by mixing carbon fibers in paraffin or impregnating paraffin into a porous metal has been conducted. Besides, the application of paraffin to the warm keeping containers to transport corneas, joints, and skin for grafting has been studied as the application to high-value-added objects (Hirano 2009a).

Steam Accumulator

Steam accumulators are often used in the facilities that the consumption of thermal energy is large and the consumption of steam varies with time intensely. The steam accumulator is the device which stores the steam generated by a boiler as pressurized water and smooths the temporally variable steam supply to manufacturing processes. The heat dissipation from the conventional steam accumulator to the ambient air tends to be large because the surface area of the accumulator is large. Besides, depending on thermal load, a steep output variation is sometimes demanded to the steam accumulator every several minutes. The heat of solidification per unit volume is larger than the heat of condensation as is mentioned in section "Transport Methods." Therefore, the steam accumulator can be downsized if the phase change between solid and liquid is applied to. The downsizing by the solid–liquid phase change reduces the surface area of the accumulator, which reduces the heat dissipation from the accumulator to the ambient air by around 50 % at the maximum.

Thus, the steam accumulator which uses one type of sugar alcohol, mannitol (cf. Table 3), as a PCM is proposed (Hoshi and Saitoh 2001). The mannitol is filled into long and thin capsules made of copper. The storage tank is 190 L in capacity and is filled up with 190 capsules. Heat of fusion of the encapsulated mannitol is 23 MJ in total. To use mannitol as a PCM, there occurs a problem regarding supercooling in the discharging process because the maximum degree of supercooling of the pure mannitol amounts to about 50 °C. Therefore, the method to restrain the maximum degree of supercooling to about 15 °C by adding calcium sulfate as a nucleating agent has been adopted. The steam accumulator generated 200–250 kg/m^3 of steam at the flow rate of 30–40 kg/h. Besides, the combined system of the steam accumulator of mannitol with solar collectors and a disk turbine of the organic Rankine cycle is proposed (Saitoh 2008).

Pipeless Heat Transport

Many factories and incineration plants, which are potential heat sources, are usually located far from office areas and residential areas where the heat is consumed. It is

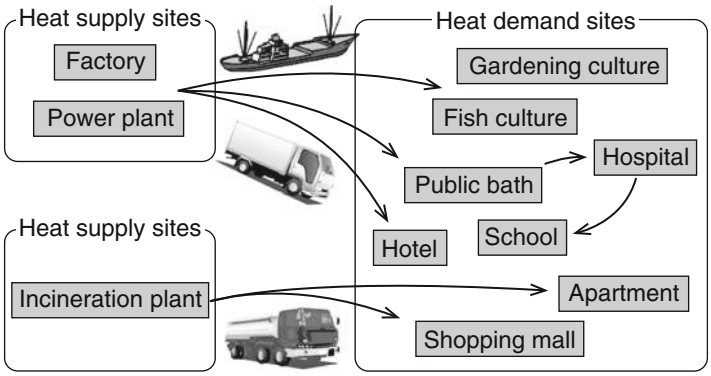

Fig. 15 Pipeless heat transport

important to transport heat efficiently for using the exhaust heat from the factories effectively. Thus the transport methods using PCMs from the heat supply site to the heat demand site by car, freight train, or ship as shown in Fig. 15 have been investigated.

For example, truck transportation systems using erythritol (cf. Table 3) or sodium acetate trihydrate (cf. Table 3) as PCMs were proposed and tested in several fields (Aoki 2007; Kawai et al. 2006). In the field tests, the PCMs filled into stainless steel tanks are melted and solidified by the heat exchange of direct contact with heat transfer oil. The proper capacity of the storage tank for the truck transport depends on the road condition and the traffic regulation. For example, the proper capacity of the storage tank for transportation in Japan is estimated to be 5–20 m^3.

The results of the field tests show that the charging process of thermal energy to the storage tank was completed in a heat supply site in about 2 h. The discharging process was completed in a heat demand site in about 4 h. The distance of conveyance that truck transportation is advantageous on energy is evaluated to be less than about 20 km. The most serious assignment at present is how to improve the investment effect. The promotion of the heat exchange rate between the PCMs and the heat transfer medium can improve the capacity utilization and cost-effectiveness.

Microcapsule Slurry Heat Transport

Building materials, fibers of clothes, and heat transfer media are just available for heat storage media for SHTES. However, the thermal energy storage densities of those materials are smaller than those of PCMs. Thus several methods to improve the thermal energy storage densities of those materials have been studied. One of the methods is mixing those base materials with the fine grains of PCMs which are insoluble to the base materials. Encapsulated paraffin or polyethylene glycol is often

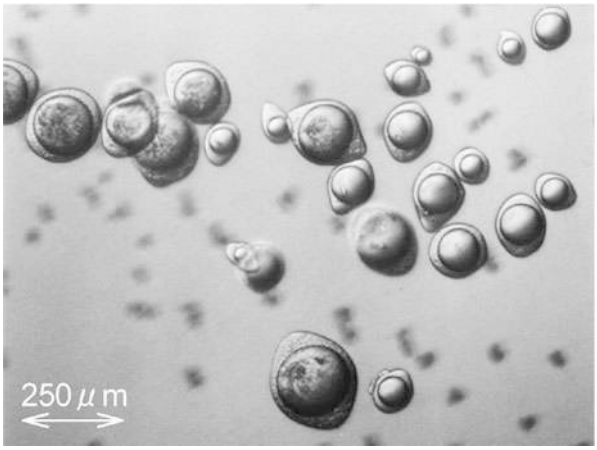

Fig. 16 Microencapsulated PCM particles produced by coacervation method (gelatin wall) (Photography by Takeuchi H et al.)

used as fine grains of PCMs. The diameters of the PCM capsules are usually on the order of micrometer. Gelatin, melamine resin, or urea resin is used for the shell of microcapsules. The PCMs can be mixed into various kinds of base materials by encapsulating the PCMs in a micro-size. Besides, the capsulation makes it easy to handle the PCMs and widens the surface area for heat transfer. The microencapsulated PCMs are applied to high-density heat transport by the slurry mixed with heat transfer media. Besides, the PCMs are applied to the passive thermal energy storage as thermal mass and to warm keeping sheets.

In the 1990s, several researches of slurry heat transport for space cooling were conducted. Figure 16 shows the microencapsulated PCMs that *n*-octadecane is coated with gelatin (Takeuchi et al. 1998). The addition of the particle dispersion agent prevents the aggregation among the PCM capsules, which is important to maintain the performance of the PCM slurry. It is necessary to raise the concentration of the microcapsules for increasing the thermal energy storage density of the slurry. When the concentration of the microcapsules in the slurry increases, the flow velocity range for laminar flow expands because the apparent viscosity of the slurry increases. Then there is the optimal flow velocity of the PCM slurry that the pressure loss for circulating the slurry becomes smaller than that for the pure heat transfer medium. When the PCM slurry is circulated at such optimal flow rate, the consumption of electric power by pumps can be reduced.

The results of the endurance test of the PCM capsules and the heat exchange test of the PCM slurry are shown in Figs. 17 and 18, respectively. If the capsule diameter is smaller than dozens of micrometers, the damage of the capsule by the transportation pumps is prevented (Fig. 17). Besides, if the particle concentration in the slurry increases, the overall coefficient of heat transfer of the slurry decreases (Fig. 18). Decrease in coefficient of heat transfer reduces the heat dissipation from piping to the ambient air. Therefore, the microencapsulated PCM slurry becomes effective for long-distance heat transport.

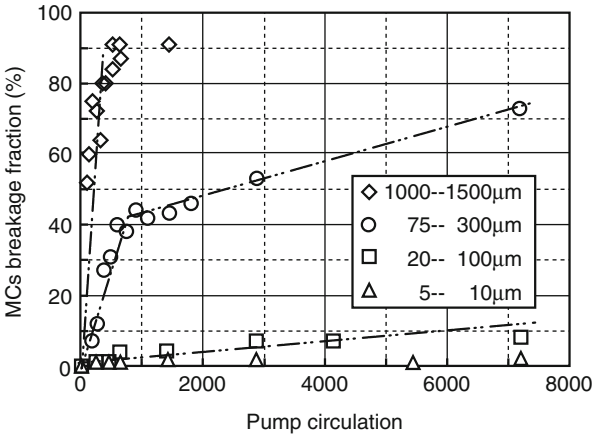

Fig. 17 Breakage fraction of the microcapsules by thermal cycles

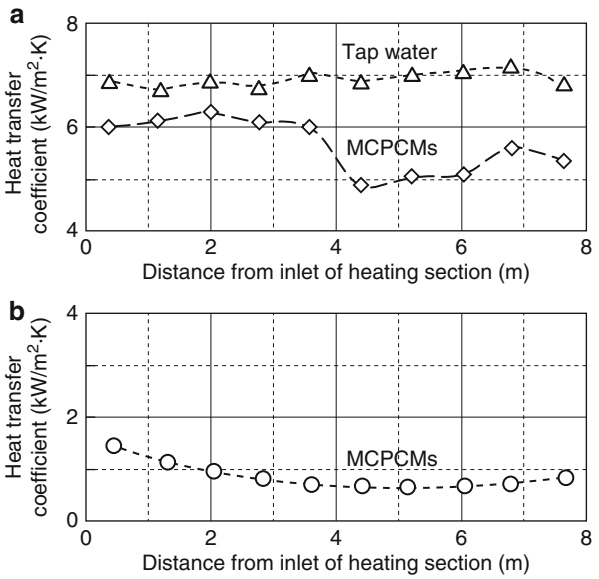

Fig. 18 Heat transfer coefficients of the microcapsule PCM slurry for the cases of (**a**) turbulent flow (particle size, 5 μm; particles concentration, 15 vol.%; Reynolds number = 12,000; flow velocity = 1.33 m/s) and (**b**) laminar flow (particle size, 5 μm; particle concentration, 25 vol.%; Reynolds number = 1,900; flow velocity = 1.22 m/s)

Future Directions

Thermal energy storage and heat transport enable to promote the utilization of waste heat and renewable energy which are unstable, maldistributed, and thin in general. In addition, high densities of thermal energy storage and heat transport enable to reduce heat loss during heat storage and transportation. However, except water or rock, the introduction of high-density thermal energy storage and heat transport is not advanced in point of cost-effectiveness.

The issue of the material cost can be improved by modification of manufacturing methods and mass productions. For example, although threitol has been produced by a synthetic process conventionally, a fermentation method to produce D body was recently discovered (Ueda and Yasuda 2004), which leads the manufacturing cost of D-threitol to the same level as erythritol. The issue of the overall cost of the system can be improved by using technology like the supercooled thermal energy storage which raises added value.

The 1970s and 1980s, when characteristics of various kinds of materials and applications for thermal energy storage were investigated, can be considered as the first golden age of research and development of thermal energy storage and heat transport. In the near future, the creation and application of novel PCMs which are designed by computational chemistry and synthetic process will be required as well as the revolution of the manufacturing methods which use microorganisms, and developments of high-value-added utilization technology.

References

Aoki I (2007) Thermal energy storage transport system by erythritol (Waste heat transport system by direct contact latent heat thermal energy storage technology). In: Development of thermal energy transport system. Japan Society of Refrigerating and Air Conditioning Engineers, Tokyo

Duffie JA, Beckman WA (1991) 8 energy storage. In: Duffie JA, Beckman WA (eds) Solar engineering of thermal processes, 2nd edn. Wiley, New York

Hirano S (2002) Phase change thermal energy storage. J Jpn Inst Energy 81(8):691–699

Hirano S (2006) 4°4 Technology for utilizing thermal energy at low temperature. In: Japan Solar Energy Society (ed) Solar energy utilization technology. Ohmsha, Tokyo

Hirano S (2009a) Research and development trends on latent heat thermal energy storage. J Jpn Solar Energy Soc 35(4):11–17

Hirano S (2009b) Field test study of cogeneration using supercooled thermal energy storage. In: New energy technology for society, http://www.aist.go.jp/Portals/0/resource_images/aist_e/research_results/publications/pamphlet/today/new_energy_technology_for_society.pdf. 17 June 2015. National Institute of Advanced Industrial Science and Technology (AIST), Tokyo

Hirano S, Saitoh TS (2007) Long-term performance of latent heat thermal energy storage using supercooling. In: Proceedings of ISES solar world congress 2007 V, Beijing, pp 2741–2745

Hirano S, Takeuchi H (2009) Performance of thermal energy storage unit using supercooling of D-threitol. Papers & Programme of the 8th international conference on sustainable energy technologies, Aachen, Paper 214

Hirano S, Saitoh TS, Oya M, Yamazaki M (2001) Temperature dependence of thermophysical properties of disodium hydrogenphosphate dodecahydrate. J Thermophys Heat Transf 15 (3):340–346

Hirano S, Shibasaki N, Kudo T (2010) Characteristics of thermal storage and radiation in floor heating system using supercooled thermal energy storage. In: Proceedings of renewable energy 2010, Yokohama, Paper O-Th-3-2

Hoshi A, Saitoh TS (2001) A study of solar steam accumulator with high temperature latent heat thermal energy storage (2nd report; fundamental characteristics of steam accumulator). J Jpn Solar Energy Soc 27(5):41–48

Inada T (2006) Growth control of ice crystals by poly (vinyl alcohol) and antifreeze protein in ice slurries. Chem Eng Sci 61(10):3149–3158

International association for the properties of water and steam (IAPWS) (1998) Revised release on the IAPS formulation 1985 for the thermal conductivity of ordinary water substance. IAPWS, London

Kakiuchi H (2008) Development trend of latent heat or chemical thermal energy storage material. In: NTS (ed) Energy storage and transport, electricity/heat/chemistry. NTS, Tokyo

Kawai A, Kamano H, Okuyama S, Shikata I (2006) Experimental report (I) by latent heat storage transportation system "TransHeat Container." Kurimoto technical report 54, pp 12–17

Kosaka M, Asahina T, Taoda H (1980) Recent research on thermal energy storage (7) about latent heat type thermal energy storage materials for space heating/hot water supply. Reports of the Government Industrial Research Institute, Nagoya, vol 29-2, pp 53–62

Mitsubishi Chemical Engineering (1999) Main ingredients of thermal energy storage materials in STL thermal energy storage system. Mitsubishi Chemical Engineering, Tokyo

New Air Conditioning System Division (2009) Hydrate slurry thermal energy storage air-conditioning system. JFE Engineering, Yokohama

Phase Change Products (2009) Product range of phase change materials. Phase Change Products, Western Australia

Saitoh TS (2008) Final version of solar SHINLA turbine generation system. In: Proceedings of JSES/JWEA joint conference, Tottori, pp 381–382

Takeuchi H, Pyatenko AT, Yamagishi Y, Sugeno T, Ishige T (1998) Characteristics of microencapsulated phase change material slurry as energy transportation refrigerant. Thermal Sci Eng 6(1):162–167

Telkes M (1954) Composition of matter for the storage of heat. US Patent No. 2677664

Ueda M, Yasuda M (2004) Microbial production of rare sugars by biotransformation and fermentation: L-Ribose and D-Threitol. Monthly Fine Chem 33(9):52–60

The Japan Society of Mechanical Engineers (JSME) (2009) V-3 properties of solid, V-4·1·1 properties of ordinary water. In: The Japan Society of Mechanical Engineers (JSME) (ed) JSME data book: heat transfer, 5th edn. JSME, Tokyo

Smart Grid

Dawood Al Abri, Arif S. Malik, Mohammed Albadi, Yassine Charabi, and Nasser Hosseinzadeh

Contents

D. Al Abri (✉) • M. Albadi • N. Hosseinzadeh
Department of Electrical and Computer Engineering, Sultan Qaboos University, Muscat, Oman
e-mail: alabrid@squ.edu.om; mbadi@squ.edu.om; hosseinz@squ.edu.om

A.S. Malik
Department of Electrical and Computer Engineering, College of Engineering, Sultan Qaboos University, Muscat, Oman
e-mail: asmalik@squ.edu.om

Y. Charabi
Department of Geography, Sultan Qaboos University, Muscat, Oman
e-mail: yassine@squ.edu.om

W.-Y. Chen et al. (eds.), *Handbook of Climate Change Mitigation and Adaptation*,
DOI 10.1007/978-3-319-14409-2_78

Abstract

Smart grid holds a great promise for a cleaner, more efficient power; healthier air; and lower greenhouse gas emissions. A smart grid vastly improves energy efficiency and is already revolutionizing our energy future. A smart power grid delivers electricity from suppliers to consumers using digital technology with two-way communication to control appliances at consumers' homes to save energy, reduce cost, and increase reliability and transparency. A smart grid includes an intelligent monitoring system that keeps track of all electricity flowing in the system. It also incorporates the capability of integrating renewable electricity, such as solar and wind, at the consumer end. For houses equipped with solar panels and/or wind turbines, the goal is for them to consume no more energy than they produce and to produce net zero carbon emissions. The future with smart grid may look like a lot of distributed "green" generation at the consumer end replacing the conventional generation and thus easing its way to more sustainable future energy needs.

This chapter will start with an introduction that provides an overview of conventional power grid and its evolution to smart grid. It will then discuss the worldwide applications of the smart grid and its technologies in sections "Worldwide Applications of Smart Grids" and "Smart Grid Technologies," respectively. Renewable energy (RE) is considered as a universal remedy for solving current climate change or global warming threats. Section "Renewable Energy Resources in the Grid: Challenges and Opportunities" will discuss a number of potential challenges and opportunities in integrating RE with the existing grid.

One way to decrease the electrical load is a concept called demand response (DR). DR programs give consumers the ability to voluntarily reduce electricity usage at specific times of the day (such as peak hours) during high electricity prices or during emergencies (such as preventing a blackout). The benefit of DR is not only in the economic cost savings but also in the environmental costs. The DR programs and their benefits derived from the smart grid will be discussed in section "Demand Response for Smart Grid."

With the smart grid's promises of a more reliable, robust electric delivery system comes the virtual representation of that system used to make operational decisions. The source of the basic data for this virtual representation is the geographical information system (GIS). The importance of GIS interface with the smart grid will be highlighted in section "Geographical Information System Interface with Smart Grid."

Communication networks play a crucial role in facilitating smart grid functionality as being able to adapt to load and demand changes, intelligently manage bidirectional

data flow, and crucially enhance system reliability, robustness, security, and sustainability. In section "Smart Grid Networking and Communication Technologies," the role of the communications network in smart grid operation will be described together with its main functionalities. The increase of data transfer through the grid communications network raises many concerns regarding the network security and privacy. These aspects will be tackled in more detail in section "Security and Privacy."

Given the environment of the smart grid, the amount of data handling will increase tremendously. Conventional data storage and management will encounter great difficulties. Section "Cloud Computing for the Smart Grid" will explore the use of cloud computing to tackle this problem.

Control systems are required across broad geographical and industry scales in real time – from devices to power system wide, from fuel sources to consumers, from utility pricing to demand response, etc. Section "Advances and Challenges in the Development of Smart Grids" will deal with the advances and challenges in the development of the smart grid. Of course, the transition from conventional to smart grid should weigh the costs and benefits related to implementation. These are discussed in section "Smart Grid Economics."

Many countries are greatly interested to shift from conventional grid to smart grid. In the last section "Future Directions: Road Map to "Mature" Smart Grids," a model is discussed that can provide guidance and a road map to establish a fully functioning "mature" smart grid.

Introduction

Producing electricity from fossil fuels is one of the major factors of atmosphere pollution, which results in global warming. For example, approximately 40 % of total US GHG emissions are produced from electric utilities (Jung and Yeung 2011). Oil- and coal-fired power plants are the most widespread means for bulk generation and are responsible for GHG emissions.

To reduce this effect, the world has started shifting toward producing electricity from renewable sources of energy, such as solar, wind, and geothermal energy systems. After more than a decade of various campaigns, the world leaders are now close to an agreement on actions to save the environment and to reduce causes of climate change. "World leaders agreed that climate change is a defining issue of our time and that bold action is needed today to reduce emissions and build resilience and that they would lead this effort" (United Nations 2014). Therefore, renewable energy sources are growing fast. However, without the appropriate enabling technologies linking them to the grid, their potential will not be fully realized (Department of Energy 2008). Smart grid provides such enabling technologies.

The power networks around the globe are evolving from conventional grids to smart grids. In the conventional model, the power is generated in power stations and flows in an interconnected transmission network to a distribution system. The power flow in the distribution system has a one-way direction from power substations toward loads.

In contrast to the conventional grid, the distribution system in a smart grid provides a two-way power flow between customers and utilities. Customers have the option of generating electricity using renewable energy systems and exporting energy to the grid at times that they select. Meters become smart by having the capability of measuring quantities of interest in both directions of power flow and by having the feature of a two-way communication between the customers and the power utilities. Storage devices will be available to store the excess of produced energy and release to the network when needed. As a whole, then, the system becomes more efficient and reliable and provides a better configuration to absorb high penetration of renewable energy sources compared with the conventional grids.

Smart grid is a result of utilizing the communication and control technology in the power grid to give customers flexibility in controlling the way that they consume electricity and to give utilities more control on the power flow. The development of smart grid is not directly caused by the expansion of renewable energy sources, but connecting these sources to the grid is one of the driving forces in the development of smart grids.

A smart grid may have different meanings in different applications. One definition is given as follows (SRA 2035 2012):

> A smart grid is an electricity network that can intelligently integrate the actions of all users connected to it—generators, consumers and those that do both—in order to efficiently deliver sustainable, economic and secure electricity supplies.

Smart grid deployment must include information and communications technology, regulatory framework, standardization usage, commercial considerations, environmental impact, societal requirements, and governmental laws.

> Smart grids incorporate information and communications technology into every aspect of electricity generation, delivery and consumption in order to minimize environmental impact, enhance markets, improve reliability and service, and reduce costs and improve efficiency (International Renewable Energy Agency (IRENA) 2013).

By reducing system energy losses and controlling loads on the power network, a smart grid reduces the need for electricity generation and, therefore, reduces greenhouse emissions that otherwise would be produced.

Smart grid can facilitate economical downstream GHG reduction opportunities by boosting energy efficiency (in both grid efficiency and end-use conservation), as well as enabling greater integration of renewables (in both utility-scale projects and distributed generation). Furthermore, smart grid infrastructure can help to enable widespread transport electrification that not only can dramatically reduce GHG and other emissions but can also serve to enhance energy security by making less dependence on fossil fuels.

The smart grid is an encouraging advancement for developed and developing countries because it inaugurates a new era of power system management and will help the governments to attain their targets in the energy sector. In the framework of climate change, the transition to smart grid is an imperative to reduce greenhouse gas emissions and requires a clear diagnosis of the abovementioned considerations.

Worldwide Applications of Smart Grids

Each nation has slightly different goals in pursuing smart grid technologies and programs and a slightly different definition of what constitutes a smart grid (Schneider Electric 2012). For the USA, smart grid is the national economic stimulus and grid modernization. For Europe, however, the focus is on greenhouse gas reduction and energy system improvement. Meanwhile, South Korea and Japan focus on green growth through the use of information technology and the introduction of renewable energies and related technologies, respectively.

Smart grid infrastructure, including grid automation upgrades as well as smart metering, is expected to represent a huge market opportunity and will attract $200 billion in worldwide investment between 2008 and 2015 (Bouvier and Strubel 2010). In fact, for 2010, the US and the Chinese governments have decided to invest more than $7.1 billion and $7.3 billion, respectively, in the development of smart grid technologies (BuddeComm 2010). Meanwhile, the annual investment in Europe is estimated to be approximately five billion euros. The EU's blueprint for financing its Strategic Energy Technology Plan estimates that the cost of upgrading interconnections and building new super grid connections to supply Europe securely would cost over 200 billion euros by 2050 (BuddeComm 2010). Similarly, Australia has allocated approximately AU$100 million for a National Energy Efficiency Initiative to develop an innovative smart grid energy network. The project combines broadband with intelligent grid technology and smart meters in homes and will enable greater energy efficiency and better integration of renewable energy sources, such as solar and wind power. For Africa, smart grid technology is expected to help address its chronic power shortage in a market growing at around 10 % per annum (Power 2010).

Smart Grid Technologies

It is believed that the transmission network is already considerably smart even in the conventional grids. However, distribution networks of the conventional grids are far from being smart! Smart grid technologies can add intelligence to these networks. However, "at the residential level, smart grid must be simple, 'set-it-and-forget-it' technology, enabling consumers to easily adjust their own energy use" (Department of Energy 2008).

Many types of technologies can be utilized in a smart grid. While some of them are more specific to smart grid, other technologies may be commonly used in both conventional and smart grids. Smart grid technologies should generally facilitate communication, information management, and control of the grid.

Smart grid technologies can be put into four functional categories (Department of Energy 2008):

- ***Information collectors:*** To make a grid smart, data should be collected from many system locations using various types of sensors. These sensors generally measure performance-related characteristics of electricity system components.

An example is a meter, called smart meter, which continually measures the power imported or exported by any customer. These meters are connected to the network by an advanced metering infrastructure (AMI), which refers to two-way electricity meters and the communications and data processing equipment required to collect smart meter data and deliver it to the grid operator (King 2005).

- Another example is a set of sensors that track temperature, vibration, and other characteristics of a transformer. Other sensors may also be used to collect information, such as meters that measure electricity characteristics (voltage, current, etc.) of a distribution line.
- ***Information assemblers, displayers, and assessors***: This category includes devices that accept information and display and/or analyze it.
- ***Information-based controllers***: These devices control the behavior of other devices to achieve some goals based on the information received. Examples of these goals are reduction of energy consumption at peak-demand times, demand-side management, voltage regulation, improvement of power quality, increase of reliability and efficiency, etc.
- ***Energy/power resources***: Included in this category are technologies that can contribute to the generation of electricity, storage of electrical energy, or reduction of demand.

Renewable Energy Resources in the Grid: Challenges and Opportunities

Renewable Energy Challenges

The increased penetration level of renewable energy-based generation facilities in the electricity grid brings up many issues and uncertainties, which are related mainly to economic efficiency, energy security, and owner financial issues. A brief description of each of these issues is given below.

Economic Efficiency

Economic efficiency means maximizing the net value of the benefits gained from the available resources (Au and Au 1983). In the renewable energy-based generation facility context, it means efficient and optimum deployment of these units. Market structure, operation, and pricing determine whether these units are integrated efficiently or not (IEA 2002). Market structure has a major influence on the efficient penetration of renewable energy-based generation units to the system. The liberalization of the wholesale market is not enough when the distribution level is still a monopoly. This monopoly could hinder the penetration of renewable energy units by imposing standby tariffs and high prices for ancillary services. To overcome this problem, the regulator should ensure nondiscriminatory access of these units to the grid once technical issues are resolved. For efficient market operation, liberalization of the retail market would provide customers the option to locally generate their own electricity when electricity prices are high.

The participation of renewable energy-based generation facilities in electricity markets involves difficulties because the wholesale markets were originally designed for large central generation plants. Policy intervention is necessary to enable small renewable energy units to actively participate in the market. For example, facility owners must use the expensive spot market to cover for any discrepancy between expected needs and actual demand/generation, if the owner decides to participate in the market.

The liberalization of electricity markets evolved in price fluctuation. Higher prices of electricity during peak periods and lower prices during off-peak periods favor new generation units' deployment during peak hours. In many places, electricity prices are not sensitive to location, and electricity markets have a uniform market price. In such a case, the true value of renewable energy-based generation facilities is underestimated. Units' location plays an important role in reducing transmission and distribution (T&D) losses, relieving distribution network congestion, deferring or avoiding T&D infrastructure upgrades and reinforcement, and providing ancillary services. The restructuring of electricity prices is crucial for the true value of these units to be realized. Using locational marginal prices, as in standard market design, will enable efficient investment decisions (Bhattacharya et al. 2001).

Energy Security

The large penetration of renewable energy-based generation facilities in the system can affect energy security. This effect can appear in two forms: primary fuel diversification and power system reliability. Renewable energy technologies help in diversifying the primary fuel of electrical energy from depending on fossil fuels as a primary source of energy. The main reliability concern for renewable energy technologies in this context is the fact that these units are nondispatchable because of natural or operational intermittency. In such cases, these units might not be able to respond to demand variations, and this condition in turn reduces the system's ability to provide reserve power when necessary (IEA 2002).

Owner Financial Issues

Renewable energy-based generation facilities have higher capital cost per kW of installed capacity than conventional central power plants. In many cases, governmental incentives and subsidies are necessary to facilitate the integration of some renewable-based technologies.

Utilities may require the owner of renewable energy-based generation facilities to pay for studies and sometimes system upgrades to ensure the reliability, safety, and power quality of the system. When not regulated, distribution companies might impose high standby charges. According to the theory of economic efficiency, the power producer should pay for all the costs for upgrading the distribution system. Therefore, owners of renewable generation facilities should pay for the cost incurred by the distribution system operator. These costs could be very high if the system needs to be reinforced. By contrast, large central plants do not pay for transmission system upgrades and reinforcements. Thus, a fair solution is for owners of renewable

generation facilities to pay a connection fee and for the rest of the cost to be covered by customers as part of the operating cost (IEA 2002).

Renewable Energy Potential Benefits

Utilities can benefit from using renewable generation facilities in their planning process. Owners and customers can use renewable generation facilities to reduce their cost of energy. Additionally, the integration of renewable generation facilities can benefit all other members of society.

Utility Applications

Deferred or Avoided T&D Expansion

Renewable generation facilities are becoming a viable choice in power delivery system planning (El-Khattam 2004). Utilities can avoid expensive network expansion and other network reinforcements by encouraging the installation of renewable generation facilities at selected locations. These facilities have the potential to relieve transmission congestion and reduce power losses in both T&D networks. Since T&D system costs represent a considerable share of the total price of electricity, these facilities could save up to 30 % of electricity costs on average (IEA 2002). Moreover, extending the network to remote areas is economically not practical. Utilities could gain substantial savings by using locally generated power. The costs of network capacity expansion projects would otherwise be reflected in the price of electricity paid by consumers. Utility planning tools could be used to assess potential utility value to be gained by using renewable generation facilities instead of relying completely on conventional capacity expansion (El-Khattam 2004).

Reduced System Losses

Power losses (I^2R) are proportional to the resistance, "R," of the power path and the loading, "I," of the line. Unlike central plants, small renewable generation facilities are located near consumers; therefore, the resistance in the current path is much lower than that between central plants and electricity consumers. Moreover, renewable generation facilities will reduce the loading of transmission lines and relieve heavily loaded lines, leading to more reduction in power loss. Numerous studies demonstrated that loss reduction depends on renewable generation facility penetration, technology, dispersion, location, and reactive power control (Albadi et al. 2013; Quezada et al. 2006). The value of this benefit can be substantial in some cases where system losses are high. Although loss reduction calculations can be done using power flow calculations, a lot of data are required, and the results are valid only for certain loading profiles. Nevertheless, with certain loading levels, especially with light loads, the renewable generation facilities might result in increasing the energy losses compared with situations for which these facilities are not used.

Voltage Support to Electricity Grid

Similar to other types of distributed generation (DG) units, renewable generation facilities can be used to support the distribution system voltage profile through the injection of reactive power. This in turn improves power quality for nearby customers and reduces losses in distribution systems. Losses are reduced when reactive power is locally provided; consequently, this minimizes the reactive component of the current flowing in the system. The benefit of this application is not substantial because other cheaper means for voltage support could be available, such as switched capacitors. Moreover, voltage support is characterized as a localized problem (Ackermann et al. 2001).

Customer Applications

Lower Cost of Electricity

The T&D cost of electricity represents 30 % of the total price on average. Customers with on-site generation might find that the cost of installing and operating on-site generation is less than the cost of buying electricity from the grid. The difference between the two costs represents the value of this benefit to the customer. This value is case sensitive and depends on electricity price, load profile, renewable generation facility capital cost, and operation and maintenance costs. Studies have reported that the benefits of this application mainly drive most customers in considering deployment of DG units in general (Ackermann et al. 2001). They are obviously the main drivers for most customers in market environments where the cost of electricity from the public grid is higher than the cost of energy from locally available renewable generation facilities.

Consumer Electricity Price Protection

Renewable generation facilities can minimize the risks associated with electricity price volatility when price spikes appear because of congestion, generation shortage, and market power (Albadi and El-Saadany 2008). Moreover, the owner will have the flexibility of switching between renewable generation facilities and utility generation if real-time pricing (RTP) is used. The size of this benefit depends on price volatility and customer risk preferences (Ackermann et al. 2001).

Enhanced Demand Response and Elasticity

Without on-site generation, most customers do not have the means to react to changes in electricity price and its volatile fluctuations. Yet on-site generation appeals to customers with its desirable flexibility. Customers with installed on-site generation units will certainly consider generating their own electricity instead of buying from the grid when electricity prices are higher than that for their own generation. This situation will appear as a demand response and elasticity in electricity markets, ultimately reducing electricity prices and price volatility for the benefit of all consumers (Albadi and El-Saadany 2008). Given the intermittency nature of most renewable energy resources, having storage is essential to realize this benefit. The value of this benefit will increase as on-site generation penetration levels

increase, up to a certain level – beyond which the value starts decreasing. Although this benefit is very difficult to quantify, it can be estimated using market simulation tools (Albadi and El-Saadany 2008).

Improved Reliability and Power Quality

For customers concerned with both the reliability and quality of main grid power, using on-site renewable generation facilities is an attractive solution. Reliability in this context can be expressed as the expected duration of an outage over a period, while the power quality is expressed by the frequency of occurrence and duration of voltage sags. The value of this application depends on the frequency, duration, and timing of interruptions and voltage sags. Obviously, this condition differs from one class of customers to another and sometimes even within the same class (C. E. Commission 2004). The value of higher reliability and power quality is the main motivation for installing on-site generation facilities in places, such as hospitals, high-rise buildings, and process industries, with sensitive loads. The value of this application is characterized by avoiding the costs incurred in case of interruption (Gumerman et al. 2003). This value is customer dependent, and it can reach very high levels in some industries. Given the intermittency nature of most renewable energy resources, having storage is essential to improve reliability and power quality.

Consumer Control

Renewable generation facilities offer a useful alternative to customers seeking independence from utility power, generally individualistic consumers who want to be in charge of everything in their daily life, including supplying electricity requirements. Another group of candidates are consumers who want to obtain their electricity needs from a certain source, such as from environmentally friendly units (Gumerman et al. 2003).

Other Benefits

Improving Grid Security

Using local renewable generation facilities to supply part of the electricity demand will reduce grid dependence on large central plants and the transmission system, which could be forced out of the system or become inoperative because of vandalism or natural events. This use will in turn reduce the impact of critical system component failures. Although this benefit is spread to the whole of society and could be substantial, it is very difficult to quantify. As an example of this benefit, the International Energy Agency (IEA) reported that the availability of standby generation helped in reducing blackout risks during California's electricity crisis of 2001 (IEA 2002). Furthermore, diversifying the fuel source is advantageous to system security.

Effects on Land Use

Some renewable generation facilities have smaller footprints, that is, they require less space compared with central plants. For example, with rooftop photovoltaic

systems and wind turbines installed in farming areas, the utilization of the roof and the land is minimal. Moreover, the installation of renewable generation facilities does not need, or at least reduces, T&D infrastructure space requirements compared with central plants. A property located in an urban area is obviously worth more than one that is remotely located away from the grid. With the deployment of renewable generation facilities in rural areas, the price difference is decreased, and customers have more flexibility in deciding about the location of their projects. However, estimating the value of DG land use effects is very difficult (Gumerman et al. 2003).

Reducing Opposition to Central Power Plants and Transmission Lines

Many individuals and groups oppose building new power plants and transmission line projects for a variety of reasons, including environmental and property value concerns, among others. They can exert a tremendous force to stop new central plants and transmission lines. It is expected that renewable generation facilities will not be faced with such strong opposition. The value of this benefit is complex and difficult to estimate. One method of estimating this value is by comparing property value before and after the project (Gumerman et al. 2003).

Reducing Emissions

Emissions, such as NO_x and CO_2, are by-products of electricity generation. Renewable generation technologies do not produce emissions when converting renewable energy to electricity. This benefit affects all of society but is difficult to evaluate. Owners of renewable generation facilities receive incentives for reducing the health risks associated with emissions (Gumerman et al. 2003).

Supporting Renewable Portfolio Standards Goals

Renewable portfolio standards (RPSs) are legislations that mandate utilities to generate a minimum percentage of the electricity through use of renewable energy sources. Having renewable generation facilities in the system makes RPS achievable. The value of allowing a utility to meet RPS is presented by renewable energy credits and incentives to renewable facilities owners.

Demand Response for Smart Grid

Demand response (DR) can be defined as the changes in electricity usage by end-use customers from their normal consumption patterns in response to changes in the price of electricity over time. DR may include incentive payments designed to induce lower electricity use at times of high wholesale market prices or when system reliability is jeopardized. DR actions include all intentional electricity consumption pattern modifications by end-use customers that are intended to alter the timing, level of instantaneous demand, or total electricity consumption (Albadi and El-Saadany 2008).

Table 1 Customer response actions

Target	Action examples	Cost
Reducing demand during peak periods	Changing thermostat settings temporarily	Temporary loss of comfort
Shifting demand from peak to off-peak periods	Shifting some household activities, rescheduling industrial activities	Residential customer: no cost Industrial customer: rescheduling cost
Reducing demand during peak and/or off-peak demand	Using on-site generation, using more energy-efficient appliances	Installation cost and/or fuel cost

Table 2 Classification DR of programs

Program types	1. Price based (market led or economic based)	2. Incentive based (system led, emergency based, stability based)	
		A. Classical DSM	B. Market based
Program examples	Time-of-use (TOU) rate Critical peak pricing (CPP) Extreme day pricing (EDP) Extreme day CPP (ED-CPP) Real-time pricing (RTP)	Direct load control Interruptible/ curtailable load	Emergency DR Demand bidding Capacity market Ancillary service market

A customer response can be achieved by three general actions (Valero et al. 2007). Each of these actions involves cost and measures taken by the customer, as described in Table 1.

DR Programs

DR can be achieved through different programs: price based and incentive based. Incentive-based programs are classified into two types (Albadi and El-Saadany 2008): classical demand-side management (DSM) and market-based programs, as shown in Table 2.

In classical incentive-based programs, participating customers receive participation payments, usually as a bill credit or discount rate, for their participation in the programs. In market-based programs, participants are rewarded with money for their performance, depending on the amount of load reduction during critical conditions. The price-based programs are based on dynamic pricing rates in which electricity tariffs are not flat; the rates fluctuate following the real-time cost of electricity. Many economists claim that RTP programs are the most direct and efficient DR programs suitable for competitive electricity markets and should be the focus of policy makers (Albadi and El-Saadany 2008; Bloustein 2005).

DR Benefits and Cost

DR benefits fall under four main categories: participant, market wide, reliability, and market performance benefits (Albadi and El-Saadany 2008), as shown in Table 3.

Table 3 DR benefits

Category	Participant	Market wide	System reliability	Market performance	Environmental benefits
Benefit examples	Incentive payments Bill savings	Reduce electricity prices Avoid/ defer capacity costs	Reduce outages Diversify system operator resources	Reduce market power Reduce price volatility Offer more options to customers	Better land utilization Air and water quality improvement Reduction of natural resources depletion

Table 4 DR benefits

Burden owner	Participant		Program owner/operator	
Cost category	Initial	Operation	Initial	Operation
Cost examples	Enabling technology Response plan/ strategy On-site generation Capital expenditure (CAPEX)	Inconvenience Lost business Rescheduling On-site generation Operation expenditure (OPEX)	Advanced metering infrastructure (AMI) Customer education campaign	Marketing campaign Incentive payments Administration Program evaluation

Participants in classical DSM incentive-based programs are entitled to receive incentive payments for their participation, whereas market-based customers will receive payments based on their performance. The DR benefits extend to other nonparticipating customers through an overall electricity price reduction because of more efficient utilization of the available infrastructure and avoided or deferred infrastructure enforcements and upgrades. DR programs allow customers to participate in reducing forced outages and their consequences. Customer participation provides the system operator more resources to maintain system reliability (US Department of Energy 2006; International Energy Agency 2003).

Another benefit of DR programs is the improvement of electricity market performance. Participants have more choices in the market even when retail competition is not available. With the market-based programs and dynamic pricing programs, consumers can manage their consumption, and therefore, they have an impact on the market through reducing market power and price volatility. The indirect benefits of DR programs to the environment include better land utilization as a result of avoided/deferred new electricity infrastructure, better air and water quality as a result of efficient use of resources, and extended lifetime of natural resources.

A classification of DR program costs is shown in Table 4. Both DR program operator/owner and participants incur initial costs before the implementation of

the program and operational costs during the program (Albadi and El-Saadany 2008).

The program participant's initial costs include the installation of enabling technologies, such as smart thermostats, peak load controls, energy management systems, and on-site generation units. In addition, a response plan/strategy that will be implemented in case of an event should be established before the enrolment. Depending on the response plan, operation cost varies (US Department of Energy 2006). Some cost components are more difficult to quantify than others. For example, it is difficult to quantify the reduction of comfort that may result if a customer decides to reset the thermostat (International Energy Agency 2003). Other event-relevant costs are easier to quantify, for instance, lost business or rescheduling of industrial processes or activities. Fuel and maintenance costs need to be considered if a participant decides to use a backup on-site generation unit.

The program owner/operator initial costs include building an AMI that covers both metering and communication sides depending on the type of DR program (s) under consideration. For example, advanced metering systems to measure, store, and transmit energy usage at required intervals is a prerequisite to the implementation of RTP programs. Another important element before commissioning DR programs is customer education. Operation costs that might be incurred by the DR program owner/operator are administration and management costs in addition to incentive payments in the case of incentive-based programs. The continuous marketing for commissioned program and the continuous evaluation of the program are important components of the program operation costs and are essential for the success of the program.

Geographical Information System Interface with Smart Grid

The implementation of the smart grid passes through multiple phases that require strategy of deployment and include numerous challenges. A challenge associated with the technology is finding a way to make efficient use of the large amounts of data collected by the meters. In this regard, geographical information system (GIS) technology will play a key role in the automation strategy in that it will provide the initial infrastructure data that will fuel the automated analytics. In addition, the results of analytics on the intelligent grid are best presented in a geographic dimension. The smart grid is also a heavy investment that necessitates a financial risk analysis. Much like electronic banking, the smart grid is not the sum total of its components but how those components work together.

Role of GIS in the Smart Grid

A smart grid requires real-time analytic engines able to analyze the network, determine the current state and condition of the system, predict what may happen, and develop a plan. These engines receive data from the electric power operators and

outside parties, such as weather services, through an AMI. AMI is a combination of smart meters, data management, communications network, and applications specific to metering and plays a key role in smart grid technology, and many electric power operators began smart grid implementation with AMI (Schneider Electric 2012).

Although AMI was considered for a long time as the masterpiece technology of the smart grid, electric power operators now see the distribution management system (DMS) as one of the most key components of an effective smart grid strategy. The DMS is driven by a network model, which must reflect precisely the following forms of data:

- Network asset information
- Real-time data
- Time series data
- Transactional data

An enterprise GIS database is the key in managing the network model in terms of data integrity and quality. Enterprise GIS is also the most dynamic system feeding the DMS, through managing and securing the workflow for update of asset information. GIS can provide an accurate and up-to-date network model that can be easily served to all smart grid information systems, including supervisory control and data acquisition (SCADA), outage management system, and DMS (Schneider Electric 2012).

Challenges of GIS Data Quality

The quality of GIS database is a serious challenge for the performances expected from DMS functionality. A network model handled with inaccurate or stale GIS data leads to ineffective results. The frequent causes of data errors are mainly related to import and conversion of data from CAD systems, with a lack of network integrity rules to GIS. Errors such as transformer/customer connectivity and voltage mismatches are recurrent and can be linked to poor data management workflow when graphic work design (GWD) is accomplished with a non-GIS platform. This kind of data error requires an incessant data correction and leads to a long backlog and a network model that is certainly not quite accurate (Schneider Electric 2012).

Nowadays, the distribution network is dynamic and in perpetual changing, with demand from customers for more electric power, seasonal variability of load and power demand, and occurrences of outages. For this reason, the GWD process by which the electric power operators sustain and upgrade their infrastructure is involved in daily work, and their network model must be built in a manner that can be quickly and accurately updated (Flynn 2007).

The design of the GWD is highly complex and contains multidimensional workflows. It requires simultaneous design and collaboration. Thus, the enterprise of the complex GWD workflows is very critical because multiple designs might implicate a shared asset like pole or fuse. The GWD process is also characterized by

its long transaction and partial posting because some designs might take years to achieve and other portions take a week.

GIS-based GWD is the optimal solution to avoid a long backlog and errors in the core data of the network model. Most significantly, the GIS-based GWD process is built with central asset and network repository, for fast and accurate design and timely network model update. In other words, workflow designers do not need to develop their own designs or to redigitize existent designs in GIS and to import designs from CAD systems. GIS-based GWD is much more productive than any other systems in terms of design optimization and is also a confirmed solution for preserving network model date accuracy (Bouvier and Strubel 2010).

Smart Grid Networking and Communication Technologies

The expected amount of data generated by different subsystems within the smart grid is quite huge. These data include smart meter readings, diagnostic sensor measurements, control information, real-time pricing (RTP), etc. As a result, networking is an essential ingredient in the smart grid vision to transfer this huge amount of data between various devices, applications, and subsystems. Although there is no networking standard that emerged as the de facto standard for smart grid, there are few essential requirements for any such standard, including supporting quality of service (QoS), reliability, high availability, and wide coverage and ensuring security and privacy (Fang et al. 2012). It is unlikely that there will be a single networking technology used in the smart grid. It is more realistic to expect several networking technologies used in various parts of the grid that should be integrated in a broader communication framework. At this point, one may wonder why not use the existing supervisory control and data acquisition (SCADA) system for data transfer. Unfortunately, the current SCADA cannot support the new requirements for smart grid. In particular, existing SCADA systems do not sufficiently support the real-time requirement (Galli et al. 2011), which is essential for dynamic control and optimization of the power system. For example, in the current SCADA systems, sensors report measurements asynchronously (Galli et al. 2011). Designing an efficient communication infrastructure for smart grid will require taking into consideration many new challenges, including the following (Yu et al. 2011):

- Huge amount of data that will be generated by the various smart devices in the smart grid.
- High variability of traffic during the day because of the changes in the volume of data generated based on the dynamics of the grid (e.g., switching order of equipment based on RTP).
- Interoperability between the various technologies that will be used in the different parts of the smart grid (generation, transmission, distribution, control, etc.).
- Different QoS requirements are needed for different data flow. For example, control commands will have stringent time-delay requirements compared with the monthly utility bill data.

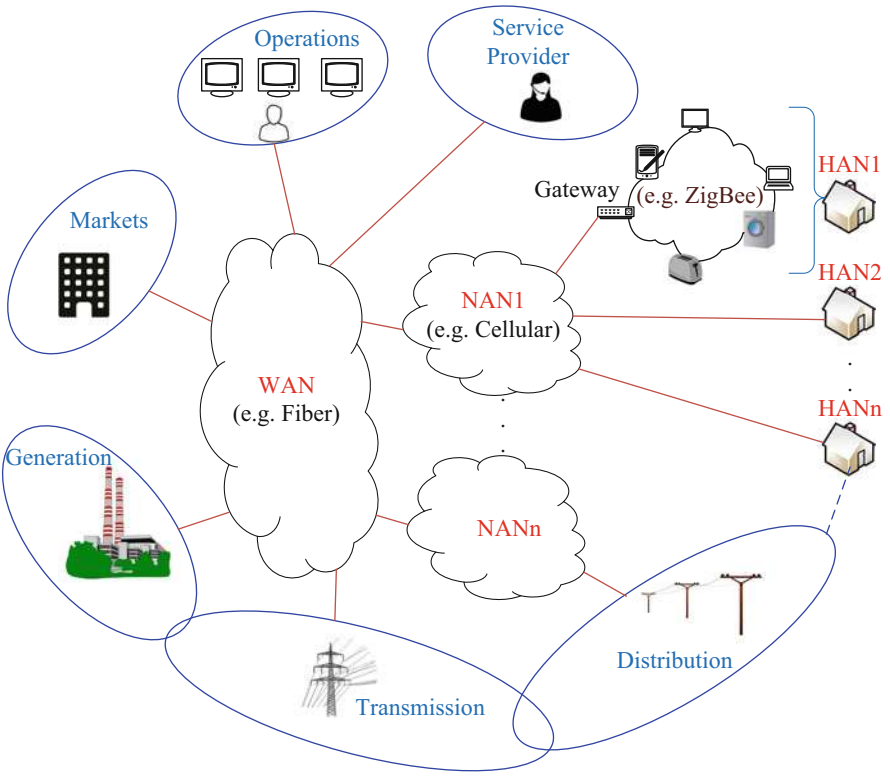

Fig. 1 Smart grid network architecture

- The need to secure the data transmitted to protect the critical grid infrastructure from attacks that could disrupt the normal operation of the grid.

Network Architecture

The large number of devices and subsystems that need to communicate with each other in the smart grid will require hierarchical networking architecture to facilitate the manageability and scalability of the overall communications infrastructure. One level of networking will be done at the home level where various smart appliances are connected together to form a home area network (HAN), as shown in Fig. 1. Through the HAN, a controller can orchestrate the operation of other appliances (e.g., turn on/off) in accordance with the dynamics of the smart grid (e.g., prices). Communication outside the home (e.g., from meter to power provider) will be done through a gateway that is connected to a neighborhood area network (NAN). NANs will be connecting multiple HANs and subsystems that exist within a neighborhood. A NAN may be used to aggregate data from various sources to reduce the load on the network core. These NANs will be connected to the rest of the smart grid domain

(generation, transmission, etc.) through a wide-area network (WAN). Given the huge volume of traffic that the WAN needs to handle, it is vital that high-speed networking technologies should be utilized in constructing the WANs.

Networking Technologies

This section briefly reviews the networking technologies that can be utilized in the smart grid. These technologies can be classified into two: wired and wireless.

Wired Networking Technologies

Power-Line Communication

In power-line communication (PLC), the same lines used to transfer power are utilized to carry the data. This is very attractive because the infrastructure is already widely available, which means that the investment required to utilize it for communication purposes is minimal. On the downside, the PLC environment is very harsh because of time- and frequency-varying signal attenuation, various types of noises injected by loads, and dependence on location, network topology, and loads connected (Biglieri 2003). Characterizing these various impairments is essential to create a reliable communication system. However, such a task is very challenging because of the dynamic nature of loads connection/disconnection to the grid (Sutterlin and Downey 1999). Moreover, although PLC had been used for Internet access and home networking, the many incompatible standards hinder its wide deployment (Galli et al. 2011). Some of the main PLC issues that need to be resolved are the type of communication modulation scheme, scheme that nodes should use to access the power line to send their data (i.e., medium access control [MAC]), and routing the data to the final destination. Galli et al. (2011) advocated that PLC is one suitable networking technology for future smart grid that can support various applications over all voltage levels (LV, MV, HV), such as remote fault detection, remote control, and vehicle-to-grid communication.

Digital Subscriber Line

Digital subscriber line (DSL) is a high-speed access technology that utilizes the same wires as the conventional phone system to provide network access. The basic idea is to use the spectrum above the range used by the phone system. DSL is an umbrella term that is used to represent a family of standards (the most popular being the asymmetric DSL). The achievable data rate depends on the variant of DSL and the cable length and condition. It can range from 256 kbps up to 1 Gbps in the new G. fast standard (Timmers et al. 2013). Considering its widespread use, it may be used by utility companies to collect smart grid data (e.g., meter reading). In fact, some companies have already utilized this option in their smart grid projects (see, e.g., Gungor et al. 2011).

Optical Networking

Optical fiber has an extremely large bandwidth that makes it an attractive choice in providing high data communication rates compared with copper-based media. The capacity of fiber exceeds 100 Tbit/s (Essiambre et al. 2013). Another advantage of optical fiber is that it has a good immunity characteristic to interference caused by electrometric signals. Thus, it is a good candidate for a communication media for a high-voltage environment (Gungor and Lambert 2006). Optical networking solution is also attractive for the core of the network to carry the huge amount of data between the various subsystems (e.g., SONET/SDH). The biggest hurdle in using optical fiber is the high initial deployment cost. To overcome this, existing public optical fiber infrastructure may be utilized at the beginning, and then private optical fiber should be gradually deployed to serve the needs of the smart grid network. As in the DSL case, optical fibers may be utilized to transmit data from customers to utility companies in areas where fibers are used as a broadband access technology (e.g., passive optical network (Banerjee et al. 2005)).

Wireless Networking Technologies

WiFi

WiFi is a wireless technology based on the IEEE802.11 standard, which specifies the lower two layers of OSI model (MAC and physical) for implementing wireless network. The IEEE802.11 has various specifications that utilize different frequency ranges (2.4 GHz, 5 GHz, 60 GHz) and provide data rates that vary from 1 Mbps in the legacy IEEE802.11 to approximately 7 Gbps in the IEEE802.11ad (Cordeiro et al. 2010), which is promoted under the name Wireless Gigabit Alliance. The range varies and can reach up to 70 m indoor and 250 m outdoor although it may be extended by various techniques (e.g., increase antenna power). Compared with other short-range wireless technology, WiFi consumes more power, which is a concern for power-limited mobile devices. Using WiFi is a viable in-home network because of its wide use to create WLAN in homes.

ZigBee

ZigBee is a standard developed by the ZigBee Alliance (http://zigbee.org) that is based on the IEEE802.15.4 standard. The focus of the IEEE802.15.4 is on the physical and MAC layers for low-rate, low-power personal area networks, whereas ZigBee focuses on the higher layer of the networking stack (Ergen 2004). The goal of ZigBee is to provide standards that address the needs for automation and control for low-power and low-rate application. The smart energy profile of ZigBee is an application profile that is developed for communicating energy-related information, such as pricing and consumption (Bilgin and Gungor 2012). The ZigBee is one of the technologies that the US National Institute for Standards and Technology (NIST) has identified for customer-premise smart grid technology. Research suggests that ZigBee is suitable for low-rate and low-voltage environments that do not require high reliability and tight deadlines (Bilgin and Gungor 2012). The main disadvantages of using ZigBee are low bit rate and interference that may occur with other

networking technologies that share the same license-free spectrum, particularly WiFi within the 2.4 GHz industrial, scientific, and medical (ISM) band (Yi et al. 2011).

Z-Wave

Z-Wave is an automation, control, and status monitoring technology. This technology is based on ITU-T G.9959 for its MAC and physical layer specification. Its main focus is on interoperability between devices utilizing this technology (http://www.z-wavealliance.org/). Like ZigBee, it targets low-rate and low-power applications, and it operates in the sub-1 GHz band, which makes it immune to interference from WiFi and other wireless technologies that operate in the 2.4 GHz band. A large number of products support this technology. Thus, it is a strong contender for the home networking arena.

DASH7

DASH7 is a low-power and low-rate wireless technology based on the ISO 18000-7 standard for radio frequency identification for devices operating in the 433 MHz bands. The nominal coverage range of this technology is 250 m (Norair 2009). This wide range makes it a good alternative to ZigBee, and hence, this reduces the number of devices and delay (Usman and Shami 2013). For example, one master DASH7 device may be sufficient to coordinate with all other devices in a home environment. The main method of communication used in this technology is a command-response model that sends small chunks of data abruptly (Norair 2009).

Cellular Communication

One of the main advantages of cellular communication technologies is that the infrastructure already exists in most places. This situation enables rapid deployment of smart grid solutions that are based on cellular networks. The option is viable for linking different smart grid entities that are located over a wide geographic area. Many companies from around the globe are utilizing the existing cellular network infrastructure for collecting the data from the smart meters (Gungor et al. 2011). The only concern regarding this communication option is the possible degradation in performance during peak usage hours by ordinary cellular service users, which may affect mission-critical smart grid applications.

Satellite Communication

Given its extensive coverage, satellite communication may be an attractive solution for remote areas where no other communications infrastructure exists. From an economical point of view, the installation cost of other technologies may cost more than using satellite communication. For example, satellite communication had been used for monitoring and controlling remote substations (Gungor and Lambert 2006). On the downside, satellite communication suffers from long round-trip delays compared with other terrestrial networking technologies. Moreover, weather conditions have a pronounced effect on the performance of satellite links.

Networking Research Challenges

- Integration between the smart grid system and Internet of Things (IoT) objects to achieve the goals of the smart grid. In IoT, objects are envisioned to communicate and cooperate with each other to create some smart service. For example, the IoT objects can cooperate between themselves in future smart homes to reduce the power consumption when needed by the smart grid and without dependence on a central controller to coordinate the process. Another example is to use the IoT sensors to monitor a power transmission line to prevent or recover from disasters (e.g., Liu et al. 2011).
- Reliable simulation of the smart grid. Simulation is one of the important tools used to analyze the performance of the systems. Given that the smart grid involves interaction between cyber and physical systems, a reliable approach to simulate such cyber-physical systems is essential to advance the field. Although some researchers had tackled this problem by combining well-known simulators for the different domains (e.g., ns2 for simulating networks) encompassed by the smart grid (e.g., Lin et al. 2011), it is unclear if this is the best and most optimum approach to handle the smart grid simulation. This issue needs further investigations to assess the reliability of the simulation results obtained by such an approach. Emphasis should also be given to optimization of the simulation environment to handle the large number of devices, the huge amount of data these devices generate, and the dynamic interactions between the various physical and cyber systems.
- Optimization/coexistence of different wireless technologies that operate over the same frequency band. With the expected huge growth of number of devices that will be connected to the Internet wirelessly, considerable interference is expected to happen between these devices that may impair the network connectivity and hence may have undesirable effects on the overall operation of the smart grid. Analyzing these effects and proposing optimal coexisting schemes will be crucial.

Security and Privacy

Security

The use of networking technologies will inevitably require security to ensure the continuous operation of the smart grid. Given that the smart grid is a large and complex system that encompasses many networking technologies, new unforeseeable security risks are likely to emerge that are not part of the current network security solutions. Hence, a new and fresh approach is necessary to handle them. For example, an attacker that successfully compromises a control center may be able to interrupt service or cause blackout in severe cases. Ideally, the smart grid should be able to withstand all sorts of attacks targeting it. However, in practice, guarding against all attacks is not feasible. Hence, the system should be designed to achieve important security goals that provide assurance that the system can deal

safely with the attack targeting these specific security goals. Desirable security goals include the following (Dzung et al. 2005):

Confidentiality: This goal refers to ensuring that the data are not disclosed except to authorized personnel. For example, meter readings and management messages should be kept confidential to protect the private data of consumers from being viewed by unauthorized entities (Yan et al. 2011).

Integrity: This objective refers to protecting the data from modification by unauthorized entities.

Availability: The aim here is to ensure that only authorized entities have a timely and reliable access to the services or resources. This is one of the most essential requirements to ensure that power is delivered to the consumers without interruption.

Authentication: This goal deals with verifying entity claim about its identity. This is a crucial security goal since most of the other services depend on knowing the entity involved. For example, proper authentication is essential to determine if a person is authorized to issue control commands that may affect the overall operation of the grid.

Authorization (access control): This security objective deals with granting access to services to authorized entities only. As mentioned previously, there is a strong dependence on identifying the entity correctly (i.e., authentication) to determine whether to permit or deny access to the requested resource.

Auditability: This refers to the ability to reconstruct the events and behavior of the system over a previous period. Achieving this goal helps in analyzing attacks and learning the causes and weaknesses that led to compromising the system.

Nonrepudiability: This goal refers to the ability to provide an evidence, which withstands the scrutinizing of a trusted third party, of which entity initiated a certain action even if that entity is not cooperating. This is very useful to resolve accountability and liability disputes.

Third-party protection: This goal prevents any damage that may happen to a third party because of any compromise to the IT system. Since the grid consists of many systems interconnected to one another, compromising one system may cause damage to another, which may have undesirable consequences, from loss of reputation to legal liability for the caused damage.

Attacks

Once the attacker manages to compromise a system by exploiting some weakness, he may execute many forms of attacks, including the following (Mo et al. 2012):

Denial of service (DoS): This form of attack targets the availability of the system and aims to deny the authorized personnel from accessing the system services in a timely fashion. Such attack, if successful, could easily disrupt the overall operation of the smart grid by denying the authorized personnel the timely access to critical information or control equipment to react to contingency.

Data modification/injection: In this attack, the malicious intruder attempts to modify data exchange between different entities or falsely inject fake data. For example, the attacker can alter smart meter data to cheat the utility companies by modifying the consumption readings to low values. It is even possible that an attacker can modify the readings of several power meters so that such modification is not detectable by state-estimation mechanisms employed by utility companies to detect bad data (Giani et al. 2011). Another example that may cause DoS attack is to inject lower (or negative) prices that will lead to a spike in consumption and possible blackout.

Eavesdropping: This form of attack aims to capture the network traffic to obtain sensitive information, such as power usage, pricing, and commands to subsystems, thus violating the confidentiality requirement.

Malware spreading: The attacker can spread a malware through the smart grid network, which enables him to retrieve sensitive information and/or control devices.

Countermeasures

Cryptography and key management: Cryptography will be an essential ingredient to accomplish many of the goals for the smart grids. Many cryptographic protocols require a shared secret (known as key) for bootstrapping the scheme. The keys could be the same in both communicating devices (i.e., symmetric key cryptography), or the keys could be different although they are related (i.e., public key cryptography). However, although the keys are related in public key cryptography, obtaining one key from the other is computationally infeasible. Symmetric key schemes are usually faster than the public key cryptography systems, but their disadvantage is the key distribution problem. For proper security, the symmetric key cryptography requires each pair of devices to have a shared key. Consequently, developing an efficient scheme to distribute the shared key between the different communicating pairs is a challenging task considering the huge number of devices that exist in the smart grid. Therefore, applying the current scheme may not be feasible in all parts of the grid, and hence, new lightweight cryptographic protection schemes will be necessary (e.g., Fouda et al. 2011). Moreover, managing the huge number of keys and related tasks, such as updating and revoking the key, is not a trivial task (see Smith 2012).

Secure architecture: The overall design of the smart grid network should be resilient to attacks. The design considerations include (Mo et al. 2012) choosing a resilient network topology, securing routing protocols, and securing forwarding.

System and device security: This area deals with preventing an attacker from exploiting vulnerabilities that exist in software that enable the attacker to commit malicious attacks, such as privilege escalation, bypassing authentication, and installing malicious code. One promising approach to verify the authenticity of the code and detect the presence of malware is a technique called code attestation. This technique enables an external entity to obtain the signature of the software running in the system and hence detect the presence of malware if the signature is altered (Mo et al. 2012).

Intrusion detection: The goal here is to detect attacks and possibly attempt to handle them safely. Usually, intrusion detection works by detecting anomaly in the network operation. However, a traditional scheme may need modification to accommodate attacks that are unique to the smart grid. For example, a selfish renewable power source may stop providing power to the grid, which may sabotage the overall operation of the grid. Detecting such selfish sources is unique to the smart grid (Li et al. 2012).

Privacy

Privacy may be defined broadly as keeping one's own information to oneself. According to the US cyber security working group (The Smart Grid Interoperability Panel and Cyber Security Working Group 2010), four dimensions of privacy should be considered in the context of the smart grid. These dimensions are as follows:

- Privacyof personal information: This includes any information related to the individual (e.g., civil identification number, occupation, etc.).
- Privacy of the person: This is related to the person's own body (e.g., medical devices used by the person).
- Privacy of personal behavior: This is related to the person's activities (e.g., sleeping, watching TV, etc.).
- Privacy of personal communication: This is related to protecting the individual's communication from unwarranted surveillance.

Obviously, the privacy concerns exist even in the old grid although at a lower scale. For example, the monthly consumption can be used to infer the occupancy status of the house during the month. In the future smart grid, the larger amount of data collected at shorter time intervals, the larger the concern on infringement on the personal privacy. The following examples illustrate the sort of personal information that may be gleaned from data pertaining to the smart grid (The Smart Grid Interoperability Panel and Cyber Security Working Group 2010):

- The activities within the person's dwelling can be constructed by comparing the electrical profile of various appliances with the observed consumption pattern reported by the smart meter of the individual. In addition, the pattern of use and the number of individuals present in the dwelling may be deduced.
- The data about plug-in electric vehicle (PEV), such as charging time and location, can be used to construct travel pattern and location of the owner.
- The use of live energy data can be used to conduct real-time surveillance to determine things, such as the presence inside the dwelling, sleeping/waking hours of owner, or where they are inside the dwelling.
- The health pattern and risk can be determined by monitoring, through appliance profiling, the frequency of meals, the cooking method (e.g., microwave or oven), time in front of TV, time using treadmills, etc.

The personal information that can be learned from data collected by the smart grid is attractive to many parties, including the following:

- Law enforcement to perform surveillance on suspected criminals
- Criminals and other unauthorized users to determine house appliances and the best time for burglary
- Appliance manufacturers to determine usage pattern and efficiency
- Marketing companies to perform targeted marketing

Hence, safeguarding and protecting this information is an essential requirement for privacy. The issue of privacy cannot be tackled by pure technical solution; privacy laws are necessary in this regard.

Research Challenges

- **Modeling the impact of attacks on smart grid:** Given the cyber-physical nature of the smart grid, an attack that is not considered a serious threat in the purely cyber system may be devastating in the smart grid. Real-time control may be disrupted by introducing a small amount of delay that may not be an issue in other less time-sensitive applications. Therefore, modeling and characterizing the impact of different attacks on the smart grid are essential to develop a robust and secure future smart grid.
- **Cryptographic algorithms and key management:** Although a vast number of cryptographic schemes have been proposed to meet the security goal requirements in traditional network security arena, many of them may be computationally intensive to be used in the smart grid environment, and they could introduce unacceptable delays for real-time applications. Hence, adopting existing solutions for a smart grid environment or developing new lightweight cryptographic protocols will be necessary to meet the security requirements of the grid without affecting its performance. Moreover, the efficient management of the cryptographic keys (e.g., distributing, updating, revoking, etc.) required for many of the schemes is also essential considering the huge number of devices/subsystems that exist in the grid. The cryptography and key management is one of the top priority research areas identified by the US cyber security working group (The Smart Grid Interoperability Panel and Cyber Security Working Group 2010).

Cloud Computing for the Smart Grid

Cloud computing may be defined as delivering a computing solution over the Internet as opposed to building this solution in-house. For example, an application (e.g., energy-usage visualization) may be run on the infrastructure provided by the cloud computing service provider instead of running it on a dedicated server. The cloud computing paradigm provides many advantages compared with the traditional

computing paradigm where each organization runs its own data center. These advantages include the following:

- Rapid deployment of services: Organization needs to ink a contract with a cloud service provider to start deploying a new service.
- Scalability: Customer may request additional (or less) resources from the service provider if the demand for service warrants such request.
- Pay per use: Customer pays according to his or her use of computing resource as specified in the agreement with the service provider.
- Economy of scale: Many customers share the same computing resources.
- Ease of maintenance: All maintenance issues, such as troubleshooting and upgrading, are handled by the service provider.

Three main service models exist in the cloud computing arena:

- Software as a service (SaaS): The client is provided with access to software running in the cloud infrastructure of the provider.
- Platform as a service (PaaS): The client is provided with a platform for application development (typically, it includes operating system, programming language development platform, database, and web server).
- Infrastructure as a service (IaaS): The client is given access to hardware (typically virtual).

The cloud computing paradigm can contribute to the advancement of the future smart grid by providing services essential to the operation of the grid, such as the following (Markovic et al. 2013):

- Processing and storing the large amount of data generated by the grid (e.g., meter and sensor readings)
- Running smart grid applications, such as AMI
- Functioning as a virtual power plant by acting as a flexible consumer that can adjust its consumption based on the computing power

Advances and Challenges in the Development of Smart Grids

The smart grid development and implementation in many countries is underway and growing rapidly. The theoretical and technological advancements move this development forward.

> Advances in distributed sensing, modeling, and control may contribute toward the development of an effective, intelligent, distributed control of power system networks. Assets optimization, novel control algorithms, control/coordination of energy storage, advanced power electronics, cyber security, policies, and technologies play important roles in the smart grid of the future (Massoud Amin 2011).

Nevertheless, challenges exist in the technological field. A power grid, particularly in its smart grid configuration, is a complex dynamic system. One of the challenges for developing a smart grid is using systems science, controls, and applied mathematics to perform the following (Massoud Amin 2011):

- Modeling
- Robust control
- Further expansion of the theory underpinnings of complex interactive systems
- Dynamic interaction in interdependent layered networks
- Disturbance propagation in networks
- Forecasting and handling uncertainty and risk

Some obstacles hinder smart grid implementation. Key barriers appear to be policy related, social, or regulatory, rather than technical. These obstacles are summarized by Giordano et al. (2013) as follows:

- Lack of interoperability and standards
- Regulatory barriers: uncertainty over roles and responsibilities in new smart grid applications and uncertainty over sharing of costs and benefits and consequently over new business models
- Consumer resistance to participating in trials

The range of regulatory arrangements might present significant barriers to the replicability of project results in different countries.

Smart Grid Economics

Smart grid is generally characterized by high investment costs and low operating costs. However, the benefits are many, and some are hard to monetize. Some of the challenges that are recognized in the cost-benefit evaluation of smart grid projects are as follows (Jackson 2011):

- The streams of smart grid costs and benefits are characterized by uncertainty caused by a variety of technologies, software, programs, and operational practices that influence over a sufficiently long planning horizon.
- Smart grid benefits are systemic in nature and are only realized once the entire system is in place and market players have taken up their roles.
- The uncertainty of consumer participation and response is another challenge the utility companies face in deciding the economics of the smart grid. The active participation of customers in hourly load contribution is an essential factor in determining the benefits of many smart grid solutions.

The GridWise Alliance (a consortium of public and private stakeholders that include utilities, IT companies, equipment vendors, new technology providers, and

academic institutions) recommended (Nibler and Masiello 2009) that smart grid project costs should consist of the following:

- Retrofits to transmission apparatus with smart grid capabilities, such as flexible AC transmission technologies, high-efficiency technologies (e.g., low-loss or superconducting technologies), high-speed switchgear, new voltage transient suppression technologies, etc.
- Transmission monitoring, control, and optimization, including sensors, communications, and computer systems and software
- Distribution monitoring, control, and optimization, including sensors, communications, and computer systems and software
- Smart grid technologies focused on renewable facilitation, such as inverters capable of providing voltage var support, governor response, and power system stabilization to protection/automation systems, feeder and station protection and automation systems developed for high local renewable penetration, etc.
- Advanced metering including advanced meters, communications infrastructure, and computer systems and software capable of providing a variety of functionalities, including RTP, remote connect/disconnect, integration of electric vehicles and HANs at some level, power quality sensing and communications, etc.
- Communications infrastructure to support the smart grid, including distribution automation and advanced metering
- Microgrids capable of high reliability/resiliency and islanded operation
- Integration of distribution automation, feeder automation, AMI, and microgrid technologies
- Technologies to assist in the efficient integration of plug-in hybrid vehicles
- Consumer integration into energy markets and grid operations
- IT, communications, and field automation projects concentrated on achieving compliance with cyber security standards

The most elaborate work performed for the estimation and calculation of the benefits of the smart grid is by the Electric Power Research Institute (EPRI) of the USA. The EPRI methodology (EPRI Report 2010, 2012, 2013) provides a framework for evaluating the economic, environmental, reliability, safety, and security benefits from the perspective of the different stakeholder groups (utilities, customers, and society). The methodology developed a systematic way of defining and estimating the benefits of the smart grid. The first EPRI report (2010) outlined an initial approach to quantify and monetize the 22 benefits of the smart grid. These benefits included optimized generation operation; deferred generation, transmission, and distribution capacity; reduced ancillary service cost; reduced congestion cost; reduced equipment failure; reduced maintenance cost; reduced meter reading cost; reduced electricity theft; reduced emissions; and reduced wide-scale blackouts, among others. A list of benefits with a small description of each is presented below. A complete guide to the calculation of benefits can be found in EPRI Report (2010, 2012, 2013) and European Commission JRC Report (2012):

1. *Optimized generation operation*: Better forecasting and monitoring of load and grid performance coupled with ancillary services that may come from stationary electricity storage and/or PEV would enable grid operators to dispatch a more efficient mix of generation to reduce cost. The optimized generation operation benefit is likely to be estimated rather than calculated.
2. *Deferred generation capacity investments*: Reduction in system peak demand by end-use customers in response to changes in electricity prices could lead to reduction/deferral of generation capacity. The benefit could be monetized as follows:

$$\begin{aligned}\text{Value}\,(\$) = \quad & \text{Annual capital carrying charge of new generation}\,(\$/\text{year}) \\ & \times \text{Time deferred}\,(\text{years})\end{aligned}$$

3. *Reduced ancillary service cost*: Ancillary services are services required to ensure that electricity can be transmitted reliably, efficiently, and securely. These services include regulation and operating reserves, maintenance of power frequency, and the cost-based services of scheduling, system control and dispatch, voltage control, and black start. Ancillary services could be reduced if generators follow load more closely. The benefit of these services is hard to assess as their requirements vary significantly from year to year and are market based.
4. *Reduced congestion cost*: Transmission congestion occurs when scheduled market transactions (generator and load) result in power flow over a transmission line that exceeds the power-carrying capability of the line. When congestion occurs in a competitive market, there is a risk of price hike from utilities that control transmission services. The reduced congestion cost benefit can be realized through DR and making use of DG.
5. *Deferred transmission capacity investment*: Reducing the overloads on transmission lines results in better asset management and reduction in the potential needs for upgrades. This can be achieved by the use of DR and customer energy resources, such as DG, energy storage, and PEV. The benefit could be monetized as follows:

$$\begin{aligned}\text{Value}\,(\$) = \quad & \text{Annual capital carrying charge of upgrade}\,(\$/\text{year}) \\ & \times \text{Time deferred}\,(\text{years})\end{aligned}$$

6. *Deferred distribution capacity investment*: Similar to transmission lines, closer monitoring and load management on distribution feeders could potentially postpone the need for upgrades or defer the capacity additions.
7. *Reduced equipment failure*: Reducing mechanical stresses on central generating equipment and T&D apparatus increases service life and reduces the probability of premature failure. The reduced equipment failure can be realized through four functions: fault current limiting, dynamic capability rating, diagnosis and notification of equipment condition, and enhanced fault protection.

8. *Reduced distribution equipment maintenance cost*: Online diagnosis and notification of equipment condition could eliminate or reduce the need to send the maintenance staff in the field to check the equipment condition.
9. *Reduced distribution operation costs*: Automatic feeder switching and automatic voltage and reactive power control through capacitors' switching eliminate the need for field crew required to carry out switching. The avoided cost benefit can be calculated by the difference of distribution operations cost before and after the implementation of the smart grid.
10. *Reduced meter reading costs*: Real-time load measurement and management would eliminate the need of meter readers and hence the cost related to sending them to read the meter manually.
11. *Reduced electricity theft*: Smart meters can detect any meter tampering. Moreover, any event of electricity theft can be detected by the real-time load measurement and management system.
12. *Reduced electricity losses*: Automatic voltage regulation and reactive power control, real-time load measurement and management, and real-time transfer functions of the smart grid help manage peak feeder loads, locate electricity production closer to load, and ensure that the voltage remains within the standard limits while minimizing the reactive power provided. These measures reduce the peak load and improve the power factor, thus reducing the T&D line losses for a given load served.
13. *Reduced electricity cost*: Customer electricity use optimization function could help alter customer usage patterns (DR with price signals or direct load control) or help reduce the cost of electricity during peak times by using DG or customer storage (plug-in vehicles or stationary electricity storage).
14. *Reduced sustained outages*: A sustained outage is one that lasts more than 5 min excluding major outages and blackouts (European Commission JRC Report 2012). Adaptive protection, automated feeder switching, automated islanding and reconnection, enhanced fault protection, and other functions of the smart grid together with DG and storage could reduce the likelihood of outage and allow the system to be reconfigured in time to help restore the service to as many customers as possible. The benefit to consumers is based on the value of service provided by the utility.
15. *Reduced major outages*: The following functions help in the reduction of major outages: wide-area monitoring, visualization, and control; automated islanding and reconnection; real-time load measurement and management; and real-time load transfer. These functions can isolate portions of the system that include DG that could help in serving the isolated customers until the service is fully restored.
16. *Reduced restoration cost*: The cost of restoring the service may include the cost related to line crew labor, material equipment, and support services, such as logistics, call centers, media relations, and other professional staff time. The reduced restoration cost benefit could be realized through the following functions: adaptive protection, automated feeder switching, diagnosis and notification of equipment condition, and enhanced fault protection.

17. *Reduced momentary outages*: A momentary outage is classified that lasts less than 5 min (European Commission JRC Report 2012). The reduced momentary outage benefit could be realized through enhanced fault protection and stationary electricity storage. The value of this benefit is based on the value of service metrics that are typically determined by customer class (residential, commercial, industrial) and may vary geographically.
18. *Reduced sags and swells*: A voltage sag is a short-duration reduction in voltage that can occur because of short circuit, overload, or starting of electrical motor, whereas voltage swell, which is a momentary increase in voltage, happens when a heavy load turns off in a power system. The frequency and severity of voltage fluctuations can be reduced by locating high-impedance faults more quickly and precisely. The reduced sags and swells benefit could be realized through enhanced fault protection and stationary electricity storage.
19. *Reduced CO_2 emissions*: This benefit is achieved through several functions and enabled energy resources in the smart grid, such as power flow control, automated feeder switching, automated voltage and reactive power control, real-time load measurement and management, customer electricity, customer electricity use optimization, DG, stationary electricity storage, and plug-in vehicles. An example of its benefit could come from reduced vehicle rolls for operation and maintenance and meter reading; fewer T&D line losses; reduction in peak demand and use of central generation, which is mainly fossil fuel based; and use of DG, which is mainly renewable energy based.
20. *Reduced SO_x, NO_x, PM-10, and other emissions*: The reduction of SO_x, NO_x, PM-10, and other pollutants is achieved with the same functions and enabled energy resources as discussed above for CO_2 emissions. The benefit could also come from reduced truck rolls, less use of central generation, etc.
21. *Reduced oil usage*: The benefit could be realized through automated feeder switching, diagnosis and notification of equipment condition, real-time load measurement and management, and PEVs. The functions that provide this benefit eliminate or minimize the need of sending line workers or crew to the switch location to operate it. Similarly, the typical number of trips to perform maintenance per feeder would be reduced. Meanwhile, the electrical energy used by PEVs displaces the equivalent amount of gasoline. Making use of DG, which is mainly renewable energy based, would reduce the usage of fossil fuel energy.
22. *Reduced wide-scale blackouts*: The reduced wide-scale blackouts benefit is achieved through wide-area monitoring and visualization, dynamic capability rating, and enhanced fault detection functions. These functions allow the grid operator to view and monitor a better picture of the bulk power system and then allow for better coordination of resources and operations between regions, which would lower the probability of wide-area blackouts. The value of this benefit is estimated by calculating the "expected" number of blackouts that could be avoided and the cost of each event.

After identifying the types of costs and benefits involved in smart grids, it would be worthwhile to see whether these smart grids lead to financial savings over the

existing grids or not. Therefore, two case studies of developed countries, USA and Great Britain, and one case study of a developing country, Oman, are discussed (Babic 2014).

The Case of USA: In 2011 (EPRI Report 2011), the EPRI made a forecast that the cost to upgrade the US grid to "smart" status would be between $338 billion and $476 billion and would generate benefits of between $1,294 billion and $2,028 billion, for a projected benefit-to-cost ratio of between 2.8 and 6.0 to 1. However, US utility smart grid business cases typically forecast benefit-to-cost ratios of between 1.1 and 3.0 to 1. These studies are mainly based on macroeconomic analysis. In 2013 (Smart Grid Consumer Collaborative 2013), the Smart Grid Consumer Collaborative (SGCC) completed a review of available research quantifying the actual – rather than forecast – benefits and costs to help stakeholders analyze and maximize the value of various capabilities. SGCC is a consumer-focused nonprofit organization formed to promote an understanding of the benefits of modernized electrical systems among all stakeholders in the USA. The stakeholders are consumer advocates; environmental advocates; regulators; consumers; legislators; utilities; and hardware, software, and service suppliers to the utility industry, among others. This report summarizes available research in terms consumers can understand and synthesizes findings in a "per-customer" context whenever possible. SGCC presents the results of two cases: the "reference case" and the "ideal case." The reference case is made with a set of conservative assumptions and the ideal case with aggressive assumptions that one can hope to achieve. The analysis is performed assuming 13-year project life, incorporating 3 years of implementation and 10 years of operation. Based on available research and incorporating the reference and ideal case assumptions detailed in the report, the ratio of benefits to costs ranges from 1.5 to 2.6 to 1 in the reference and ideal cases, respectively. The net benefit of the estimated net present value (NPV) is approximately $247 per customer in the reference case and $713 per customer in the ideal case.

The Case of Great Britain: The study is carried out by Ernst & Young (EY) in 2012 (Ernst & Young 2012) to determine the economic benefits of smart grid deployment in British economy. This report draws on existing British and international studies and interviews conducted with relevant stakeholders and EY economic analysis, as well as some assumptions introduced, where access to more detailed information has been limited, in order to conduct the analysis. The report has two broad, major conclusions. The first is that the benefits of moving toward smart grid development in a timely fashion far outweigh the risks and appear robust across a number of different scenarios. The second is that the timely creation of a smart grid can prompt noteworthy benefits in other industries, providing an appreciable boost to growth, jobs, and exports. The analysis in this report indicates that an incremental £23 billion NPV is required between 2012 and 2050 on smart investments to upgrade the distribution network, whereas a total of £27 billion NPV is required for a complete smart grid deployment. However, this is significantly cheaper than pursuing a conventional investment strategy in grids that

cost £46 billion NPV. Therefore, the study concludes that smart grid investment strategy could deliver cost savings of as much as £19 billion NPV over conventional technology investment strategy.

The Case of Oman: This study (Malik and Bouzguenda 2013) evaluated the long-term load management benefits of the smart grid in terms of avoided cost of generation, transmission, and distribution in the Sultanate of Oman. The avoided generation cost is calculated by taking the difference between the costs of two optimal generation expansion plans of 26 years. The first plan is with the base load forecast, and the second plan is with the modified load forecast caused by load management. The T&D capacity cost is calculated indirectly using the concept of asset distribution in a power system. The savings in T&D losses and environmental benefits are also estimated. The projected benefits from the smart grid range from $2.3 to $4.2 billion, which covers the assumed cost of upgrading the grid that may be somewhere between 1.4 and 2.0 billion dollars for 560,000 households. However, both the cost and the benefit estimates are based on certain assumptions and have limitations. For example, the cost of doing load management is not included. By contrast, the benefits of the smart grid are only partially estimated; benefits such as reduced ancillary service cost, reduced congestion cost, reduced equipment failure, reduced maintenance cost, reduced meter reading cost, reduced electricity theft, self-healing, avoiding blackouts, the use of renewable energy sources, etc., are not considered.

Future Directions: Road Map to "Mature" Smart Grids

There is no doubt that there are numerous economic and environmental benefits of the smart grid, and for that reason, so many developed and developing countries are already progressing toward smart grid deployment (see, e.g., Smart Grid Consumer Collaborative 2013; Ernst & Young 2012; Malik and Bouzguenda 2013; Ontario Smart Grid Forum 2013; Fadaeenejada et al. 2014). Tracking the progress of smart grid development is a topic of intense interest around the world (Fadaeenejada et al. 2014). It is also an overwhelming task, given the effects of smart grid beyond the electricity sector into other areas of society. Recent IEA report says that smart grid deployment in EU countries is steadily growing, but available deployment data do not give a full picture (IEA 2014). The report also warns that the current rate of deployment is insufficient and recommends promoting the development metrics, national data collection, and international data coordination. To measure and monitor the progress of smart grid development, a management tool called the smart grid maturity model (SGMM) has been developed by utilities for utilities (Carnegie Mellon University 2014a).

The SGMM model provides a framework for understanding the current state of smart grid deployment and capability within an electric utility and provides a context for establishing future strategies and work plans as they pertain to smart grid implementations. It is composed of eight model domains, and each contains six defined levels of maturity, ranging from level 0 (lowest) to level 5. Domains are

Table 5 Maturity levels and their characteristics

Maturity levels	Name	Maturity characteristics
5	Pioneering	Breaking new ground, industry-leading innovation
4	Optimizing	Optimizing smart grid to benefit entire organization, may reach beyond organization, increased automation
3	Integrating	Integrating smart grid deployments across the organization, realizing measurably improved performance
2	Enabling	Investing based on clear strategy, implementing first projects to enable the smart grid (may be compartmentalized)
1	Initiating	Taking the first steps, exploring options, conducting experiments, developing smart grid vision
0	Default	Default level (status quo)

logical groupings of smart grid-related capabilities and characteristics. The eight domains of the model are as follows:

1. Strategy, Management, and Regulatory (SMR)
2. Organization and Structure (OS)
3. Grid Operations (GO)
4. Work and Asset Management (WAM)
5. Technology (TECH)
6. Customer (CUST)
7. Value Chain Integration (VCI)
8. Societal and Environmental (SE)

The six levels of maturity (see Table 5) represent defined stages of an organization's progress toward achieving its smart grid vision in terms of automation, efficiency, reliability, energy and cost savings, integration of alternative energy sources, improved customer interaction, and access to new business opportunities and markets. By assessing its current maturity level in each domain and taking steps to increase its levels as appropriate, an organization moves closer to obtaining the desired benefits of adopting and implementing smart grid technology.

As of year 2014, 142 major investor-owned utilities and small public power utilities in the USA and in 29 countries are using SGMM (Carnegie Mellon University 2014b). The model has proven to be a valuable tool for utilities to help in:

- Identifying the smart grid landscape
- Developing a shared smart grid vision and road map
- Communicating with internal and external stakeholders using a common language
- Prioritizing options and supporting decision-making
- Comparing progress over time and to the rest of the community
- Measuring progress
- Preparing for and facilitating change

References

Ackermann T, Andersson G, Söder L (2001) Distributed generation: a definition. Electr Power Syst Res 57:195–204

Albadi MH, El-Saadany EF (2008) A summary of demand response in electricity markets. Electr Power Syst Res 78:1989–1996

Albadi MH et al (2013) Optimal allocation of solar PV systems in rural areas using genetic algorithms – case study. Int J Sustain Eng 6(4):301–306

Au T, Au T (1983) Engineering economics for capital investment analysis. Allyn and Bacon, Boston

Babic J (2014) Agent-based modeling of electricity markets in a smart grid environment 2014 [Online]. http://www.fer.unizg.hr/_download/repository/KDI_Jurica_Babic.pdf. Accessed 14 Nov 2014

Banerjee A et al (2005) Wavelength-division-multiplexed passive optical network (WDM-PON) technologies for broadband access: a review [DInvited]. J Opt Netw 4(11):737–758

Bhattacharya K, Bollen MHJ, Daalder JE (2001) Operation of restructured power systems. Kluwer, Boston

Biglieri E (2003) Coding and modulation for a horrible channel. IEEE Commun Mag 41(5):92–98

Bilgin BE, Gungor VC (2012) Performance evaluations of ZigBee in different smart grid environments. Comput Netw 56(8):2196–2205

Bloustein E (2005) School of planning and public policy, assessment of customer response to real time pricing, Rutgers. The State University of New Jersey [Online]. http://www.policy.rutgers.edu

Bouvier S, Strubel P (2010) Deploying a smarter grid through cable solutions and services. White paper Nexans

BuddeComm (2010) 2009 global smart grids – intelligent energy technology [Online]. http://www.budde.com.au/Research/Global-Smart-Grids-Intelligent-Energy-Technology.html. Accessed 10 Apr 2010

C. E. Commission (2004) DG definition and cost-benefit analysis – policy inventory, Sacramento, CA 95814-5512, California

Carnegie Mellon University (2014a) Smart grid maturity model: matrix. Version 1.2

Carnegie Mellon University (2014b) SGMM around the world [Online]. http://resources.sei.cmu.edu/asset_files/Webinar/2014_018_101_303535.pdf. Accessed 19 Nov 2014

Cordeiro C, Akhmetov D, Park M (2010) Ieee 802.11Ad: introduction and performance evaluation of the first multi-gbps wifi technology.In: Proceedings of the 2010 ACM international workshop on mmWave communications: from circuits to networks, New York, pp 3–8

Department of Energy, USA (2008) The smart grid: an introduction [Online]. http://energy.gov/sites/prod/files/oeprod/DocumentsandMedia/DOE_SG_Book_Single_Pages.pdf. Accessed 7 May 2015

Dzung D et al (2005) Security for industrial communication systems. Proc IEEE 93(6):1152–1177

El-Khattam W (2004) Power delivery system planning implementing distributed generation. University of Waterloo, Waterloo

EPRI Report (2010) Methodological approach for estimating the benefits and costs of smart grid demonstration projects. EPRI, Palo Alto, 94303-0813

EPRI Report (2011) Estimating the costs and benefits of the smart grid: a preliminary estimate of the investment requirements and the resultant benefits of a fully functioning smart grid. EPRI, Palo Alto, 1022519

EPRI Report (2012) Guidebook for cost/benefit analysis of smart grid demonstration projects: revision 1, measuring impacts and monetizing benefits. EPRI, Palo Alto, 1025734

EPRI Report (2013) Guidebook for cost/benefit analysis of smart grid demonstration projects: revision 2. EPRI, Palo Alto, 3002002266

Ergen SC (2004) ZigBee/IEEE 802.15. 4 summary, vol 10. UC Berkeley, California, USA

Ernst & Young (2012) Smart grid: a race worth winning? A report on the economic benefits of smart grid. London

Essiambre R-J, Ryf R, Fontaine NK, Randel S (2013) Breakthroughs in photonics 2012: space-division multiplexing in multimode and multicore fibers for high-capacity optical communication. IEEE Photonics J 5(2):0701307

European Commission JRC Report (2012) Guidelines for conducting a cost-benefit analysis of smart grid projects. Joint Research Centre, Petten

Fadaeenejada M et al (2014) The present and future of smart power grid in developing countries. Renew Sustain Energy Rev 29:828–834

Fang X et al (2012) Smart grid – the new and improved power grid: a survey. IEEE Commun Surv Tutor 14(4):944–980

Flynn B (2007) What is the real potential of the smart grid? In: The AMRA international symposium, Reno, 30 Sept–3 Oct 2007

Fouda MM et al (2011) A lightweight message authentication scheme for smart grid communications. IEEE Trans Smart Grid 2(4):675–685

Galli S, Scaglione A, Wang Z (2011) For the grid and through the grid: the role of power line communications in the smart grid. Proc IEEE 99(6):998–1027

Giani A et al (2011) Smart grid data integrity attacks: characterizations and countermeasures. In: Smart grid communications (SmartGridComm), 2011 I.E. international conference on, Brussels, Belgium, pp 232–237

Giordano V et al (2013) Smart grid projects in Europe: lessons learned and current developments. European Commission, Joint Research Centre, Institute for Energy and Transport, Luxembourg: Publications Office of the European Union. © European Union, 2011

Gumerman EZ et al (2003) Evaluation framework and tools for distributed energy resources. Lawrence Berkeley National Laboratory, Berkeley

Gungor VC, Lambert FC (2006) A survey on communication networks for electric system automation. Comput Netw 50(7):877–897

Gungor VC et al (2011) Smart grid technologies: communication technologies and standards. IEEE Trans Ind Inf 7(4):529–539

IEA (2002) Distributed generation in liberalised electricity markets. Paris. Organization for Economic Co-operation and Development (OECD)/International Energy Agency (IEA)

IEA (2014) Tracking clean energy progress 2014: energy technology perspectives 2014 excerpt IEA input to the clean energy ministerial [Online]. http://www.iea.org/publications/freepublications/publication/Tracking_clean_energy_progress_2014.pdf. Accessed 18 Nov 2014

International Energy Agency (2003) The power to choose – demand response in liberalized electricity markets. OECD, Paris

International Renewable Energy Agency (IRENA) (2013) Smart grids and renewable – a guide for effective deployment [Online]. http://www.irena.org/DocumentDownloads/Publications/smart_grids.pdf. Accessed 7 May 2015

Jackson J (2011) The utility smart grid business case: problems, pitfalls and ten real-world recommendations. In: 2nd annual evaluating the business case for smart grid investments, Orlando, 20–21 Oct 2011

Jung M, Yeung P (2011) Connecting smart grid & climate change. Silver Spring Networks. http://www.silverspringnet.com/pdfs/SSN_WP_ConnectingSmartGrid-1109.pdf. Accessed 3 Dec 2014

King C (2005) Advanced metering infrastructure (AMI). DRAM Coalition [Online]. www.oregon.gov/PUC/electric_gas/010605/king.pdf?ga=t. Accessed Nov 2012

Li X et al (2012) Securing smart grid: cyber attacks, countermeasures, and challenges. IEEE Commun Mag 50(8):38–45

Lin H et al (2011) Power system and communication network co-simulation for smart grid applications. In: Innovative smart grid technologies (ISGT), 2011 I.E. PES, California, USA, pp 1–6

Liu J et al (2011) Applications of internet of things on smart grid in China. In: Advanced communication technology (ICACT), 2011 13th international conference on, South Korea, pp 13–17

Malik A, Bouzguenda M (2013) Effects of smart grid technologies on capacity and energy savings – a case study of Oman. Energy 54:365–371
Markovic DS et al (2013) Smart power grid and cloud computing. Renew Sustain Energy Rev 24:566–577
Massoud Amin S (2011) Smart grid: overview, issues and opportunities – advances and challenges in sensing, modeling, simulation, optimization and control. Eur J Control 5(6):547–567
Mo Y et al (2012) Cyber–physical security of a smart grid infrastructure. Proc IEEE 100 (1):195–209
Nibler V, Masiello R (2009) Handbook for assessing smart grid projects. Prepared by KEMA Inc. for GridWise Alliance [Online]. http://www.gridwise.org. Accessed 10 Nov 2014
Norair JP (2009) Introduction to DASH7 technologies. Dash7 Alliance Low Power RF Tech Overv
Ontario Smart Grid Forum (2013) Ontario smart grid progress assessment: a vignette, Toronto [Online]. http://www.ieso.ca/documents/smart_grid/Smart_Grid_Progress_Assessment_Vignette.pdf. Accessed 18 Nov 2014
Power (2010) Which country's grid is the smartest? [Online]. http://www.powermag.com/issues/cover_stories/Which-Countrys-Grid-Is-the-Smartest_2345.html. Accessed 9 Apr 2010
Quezada V et al (2006) Assessment of energy distribution losses for increasing penetration of distributed generation. IEEE Trans Power Syst 21:533–540
Schneider Electric (2012) GIS-based design for effective smart grid strategies [Online]. http://tvt.schneider-electric.com/forms/smart_grid/upload/GIS-Based-Design-for-Effective-Smart-Grid-Strategies.pdf. Accessed 7 May 2015
Smart Grid Consumer Collaborative (2013) Smart grid economic and environmental benefits: a review and synthesis of research on smart grid benefits and costs, Atlanta, GA
Smith SW (2012) Cryptographic scalability challenges in the smart grid. In: ISGT, Washington DC, USA, pp 1–3
SRA 2035 (2012) [Online]. http://www.futured.es/wp-content/uploads/downloads/2012/04/sra2035.pdf. Accessed 7 May 2015
Sutterlin P, Downey W (1999) A power line communication tutorial-challenges and technologies. In: International symposium on power-line communications and its applications, Lancaster, UK, pp 15–29
The Smart Grid Interoperability Panel and Cyber Security Working Group (2010) NISTIR 7628 guidelines for smart grid cyber security
Timmers M et al (2013) G.fast: evolving the copper access network. IEEE Commun Mag 51 (8):74–79
U.S. Department of Energy (2006) Benefits of demand response in electricity markets and recommendations for achieving them. Report to the United States Congress [Online]. http://eetd.lbl.gov
United Nations (2014) Climate summit 2014 – catalyzing action. The Chair's Summary, UN Headquarters, New York [Online]. http://www.un.org/climatechange/summit/2014/09/2014-climate-change-summary-chairs-summary/. Accessed Nov 2014
Usman A, Shami SH (2013) Evolution of communication technologies for smart grid applications. Renew Sustain Energy Rev 19:191–199
Valero S et al (2007) Methods for customer and demand response policies selection in new electricity markets. IET Gener Transm Distrib 1:104–110
Yan Y, Qian Y, Sharif H (2011) A secure and reliable in-network collaborative communication scheme for advanced metering infrastructure in smart grid. In: Wireless communications and networking conference (WCNC), 2011 IEEE, Mexico, pp 909–914
Yi P, Iwayemi A, Zhou C (2011) Developing ZigBee deployment guideline under WiFi interference for smart grid applications. IEEE Trans Smart Grid 2(1):110–120
Yu R et al (2011) Cognitive radio based hierarchical communications infrastructure for smart grid. IEEE Netw 25(5):6–14

Concentrated Solar Thermal Power

Anjaneyulu Krothapalli and Brenton Greska

Contents

Abstract

In spite of several successful alternative energy production installations in recent years, it is difficult to point to more than one or two examples of a modern industrial nation obtaining the bulk of its energy from sources other than oil, coal, and natural gas. Thus, a meaningful energy transition from conventional to renewable sources of energy is yet to be realized. It is also reasonable to assume that a full replacement of the energy currently derived from fossil fuels with energy from alternative sources is probably impossible over the short term. For example, the prospects for large-scale production of cost-effective renewable

A. Krothapalli (✉)
Department of Mechanical Engineering, Florida State University, Tallahassee, FL, USA
e-mail: kroth@eng.fsu.edu

B. Greska
Cameron International, Houston, TX, USA
e-mail: bgreska@sustaintech.com; bgreska@sustaintech.com

W.-Y. Chen et al. (eds.), *Handbook of Climate Change Mitigation and Adaptation*,
DOI 10.1007/978-3-319-14409-2_33

electricity remain to be generated utilizing either the wind energy or certain forms of solar energy. These renewable energies face important limitations due to intermittency, remoteness of good resource regions, and scale potential. One of the promising approaches to overcome most of the limitations is to implement many recent advances in solar thermal electricity technology. In this section, various advanced solar thermal technologies are reviewed with an emphasis on new technologies and new approaches for rapid market implementation.

The first topic is the conventional parabolic trough collector, which is the most established technology and is under continuing development with the main focus being on the installed cost reductions with modern materials, along with heat storage. This is followed by the recently developed linear Fresnel reflector technologies. In two-axis tracking technologies, the advances in dish-Stirling systems are presented. More recently, the solar thermal electricity applications in two-axis tracking using tower technology are gaining ground, especially with multi-tower solar array technology. A novel solar chimney technology is also discussed for large-scale power generation. Non-tracking concentrating solar technologies, when used in a cogeneration system, offer low-cost electricity, albeit at lower efficiencies – an approach that seems to be most suitable in rural communities.

Introduction

Solar thermally generated electricity is a low-cost solar energy source that utilizes complex collectors to gather solar radiation in order to produce temperatures high enough to drive steam turbines to produce electric power. For example, a turbine fed from parabolic trough collectors might require steam at 750 K and reject heat into the atmosphere at 300 K, thus having an ideal thermal (Carnot) efficiency of about 60 %. Realistic overall conversion (system) efficiency of about 35 % is feasible with intelligent management of waste heat. The solar radiation can be collected by different concentrating solar power (CSP) technologies to provide high temperature heat. The solar heat is then used to operate a conventional power cycle, such as Rankine (steam engine), Brayton (gas turbine engine), or Stirling (Stirling engine) (Decher 1994). While generating power during the daytime, additional solar heat can be collected and stored, generally in a phase-change medium such as molten salt (Pilkington Solar International GmbH 2000). The stored heat can then be used during the nighttime for power generation. A simple schematic, shown in Fig. 1, describes the main elements of such a system.

The markets and applications for CSP dictate the category of the system and its components. Typically, the general categories considered by size are small ($<$100 kW), medium ($<$10 MW), and large ($>$10 MW). The CSP systems can be made of combinations of different collectors, power cycles, and, if required, thermal storage technologies. The CSP system processes heat like any conventional power plant, and, as such, the plant efficiency depends primarily upon the operating temperature. Therefore, the useful energy produced will depend on the solar-field collection and

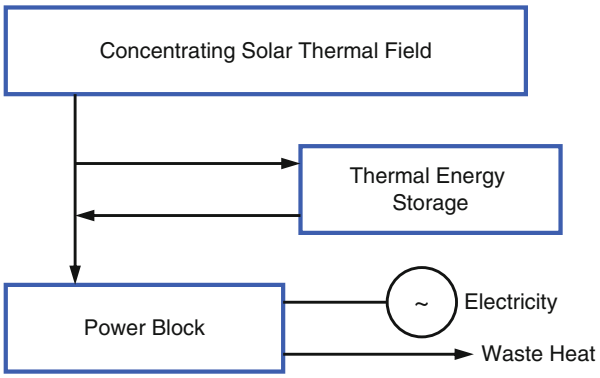

Fig. 1 Main components of a concentrating solar power (CSP) system

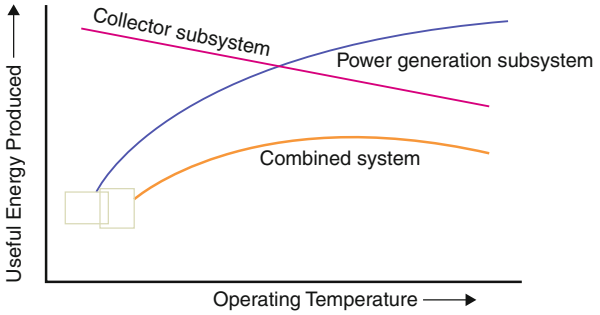

Fig. 2 CSP system efficiency variation with operating temperature

the power cycle efficiencies, as illustrated in Fig. 2. The efficiency of a solar collector field is defined as the quotient of usable thermal energy versus received solar energy. The power generation subsystem efficiency is the ratio of net power out to the heat input.

The different CSP technologies that will be explored in the following sections are parabolic trough, central tower receiver, dish-Stirling, linear Fresnel, and solar chimney. CSP technologies require sufficiently large (>5.2 kWh/m^2/day) direct normal irradiance (DNI), as opposed to PV technologies that can use diffuse, or scattered, irradiance as well (Duffie and Beckman 2006). The history of the Solar Electricity Generating Systems (SEGS) in the southwest desert of California (Jensen et al. 1989), where DNI is quite favorable for CSP, shows impressive cost reductions as shown in Fig. 3. These parabolic trough plants have been operating successfully for over three decades, thus providing valuable data. As indicated in the figure, the advanced concepts, with large-scale implementation and improved plant operation and maintenance, provide a great opportunity for further reductions in the levelized electricity cost (LEC), a topic that will be discussed later. Life cycle assessment of emissions and land surface impacts of the CSP systems suggest that they are best suited for greenhouse gas and other pollutant reductions. CSP systems are also best suited, because of the effortless capture of the waste heat, for multi-generation applications, such as the simultaneous production of electricity and water

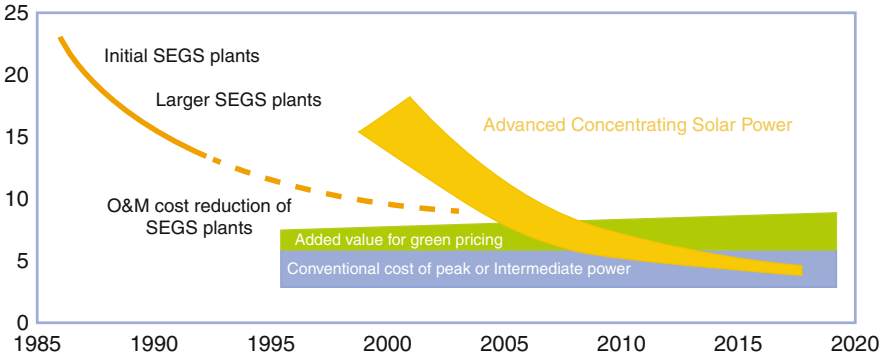

Fig. 3 Levelized electricity cost (cents/kWh) projections of CSP (Source: Solar Paces)

purification. Because of rapid developments occurring both in technology and electricity market strategies, CSP has the greatest potential of any single renewable energy area. It also has significant potential for further development and achieving low cost because of its guaranteed fuel supply (the sun).

In this chapter, a succinct review of the current technologies is given together with an assessment of their market potential. While describing some of the recent approaches in some detail, the activity around the world will also be included.

Solar Radiation

The potential for CSP implementation in any given geographic location is largely determined by the solar radiation characteristics (Duffie and Beckman 2006). The total specific radiant power per unit area, or radiant flux, that reaches a receiver surface is called irradiance and it is measured in W/m^2. When integrating the irradiance over a certain time period, it becomes solar irradiation and is measured in Wh/m^2. When this irradiation is considered over the course of a given day, it is referred to as solar insolation, which has units of $kWh/m^2/day$ ($= 3.6\ MJ/m^2/day$). However, by assigning a number of useful solar hours in a given day, then the units simplify to W/m^2. As such, the terms irradiance and insolation are typically used interchangeably. Solar radiation consists primarily of direct beam and diffuse, or scattered, components. The term "global" solar radiation simply refers to the sum of these two components. The daily variation of the different components depends upon meteorological and environmental factors (e.g., cloud cover, air pollution, and humidity) and the relative earth-sun geometry. The direct normal irradiance (DNI) is synonymous with the direct beam radiation, and it is measured by tracking the sun throughout the sky. Figure 4 shows an example of the global solar radiation that is measured on a stationary two flat plates and a plate that is tracking the sun. The measured DNI is also included, and its lower value can be attributed to the fact that it does not account for the diffuse radiation component (Molenbroek et al. 2008).

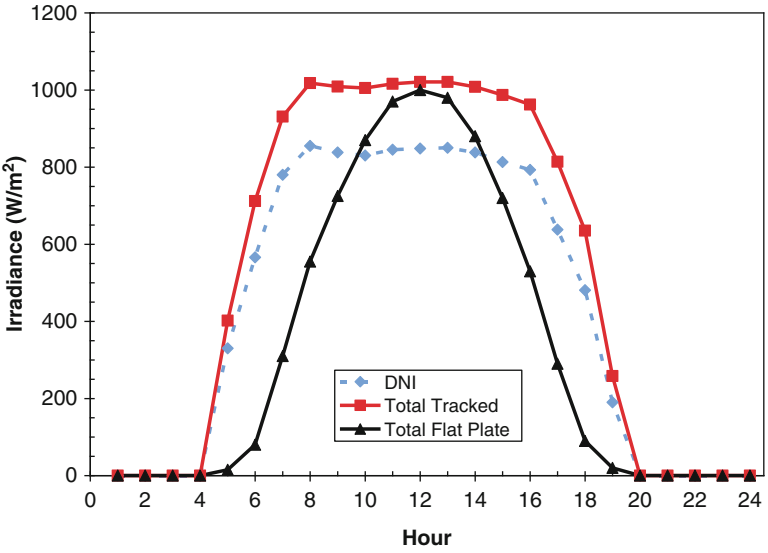

Fig. 4 Solar irradiance variation within a day measured on a flat plate positioned horizontal and tracking the sun and direct normal irradiance (DNI) (Source: Molenbroek 2008)

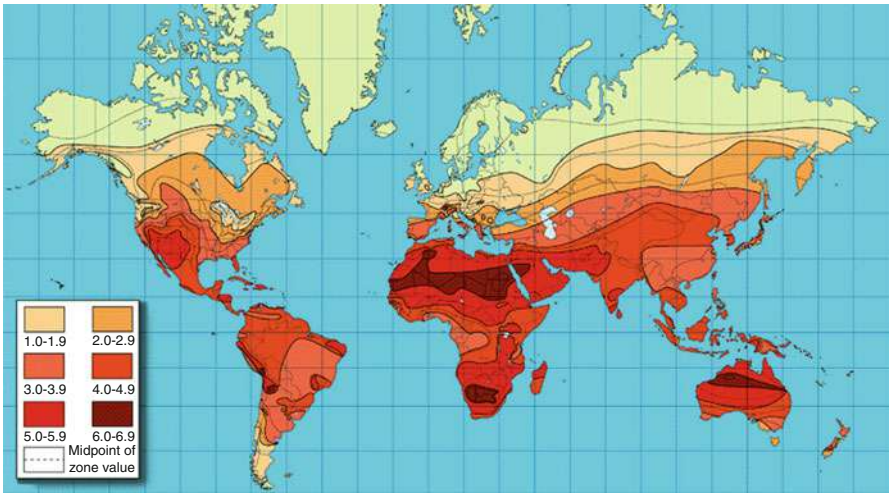

Fig. 5 The solar insolation (kWh/m^2/day) on an optimally tilted surface during the worst month of the year (Source: http://www.meteostest.ch)

In CSP applications, the DNI is important in determining the available solar energy. It is also for this reason that the collectors are designed to track the sun throughout the day. Figure 5 shows the daily solar insolation on an optimally tilted surface during the worst month of the year around the world (www.meteotest.ch;

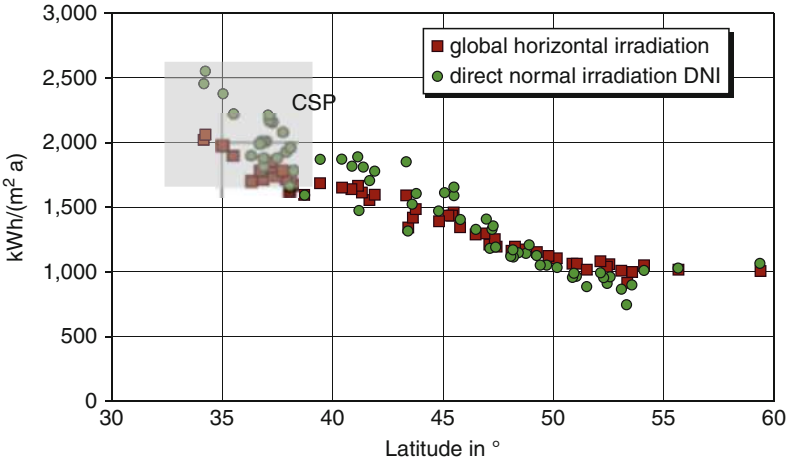

Fig. 6 Annual global irradiation in Europe and the USA (Source: Volker Quaschning, DLR & Manuel Blanco Muriel, CIEMAT, Spain)

Table 1 Annual DNI at selected locations

Location	Site latitude	Annual DNI (kWh/m^2)
United States		
Barstow, California	35°N	2,725
Las Vegas, Nevada	36°N	2,573
Tucson, Arizona	32°N	2,562
Alamosa, Colorado	37°N	2,491
Albuquerque, New Mexico	35°N	2,443
El Paso, Texas	32°N	2,443
International		
Northern Mexico	26–30°N	2,835
Wadi Rum, Jordan	30°N	2,500
Ouarzazate, Morocco	31°N	2,364
Crete, Greece	35°N	2,293
Jodhpur, India	26°N	2,200

www.wrdc-mgo.nrel.gov). Regions represented by light and dark red colors are most suitable for CSP implementation. The annual DNI value will also greatly influence the levelized electricity cost (LEC), which will be discussed later. Typical values of DNI at different latitudes and selected locations around the world are given in Fig. 6 and Table 1. Based on the information presented here, it can be seen that desert and equatorial regions appear to provide the best resources for CSP implementation.

CSP Technologies

Parabolic Trough Technology

This technology is comprised of relatively long and narrow parabolic reflectors with a single-axis tracker to keep the sun's image in focus on a linear absorber or receiver. This technology uses reflectors curved around the rotation axis (which is typically oriented east-west) using a linear parabolic shape, which has the property of collecting nearly parallel rays from the direct solar beam in a line image. A long pipe receiver can be placed at the focus for heating of heat transfer fluid (Fig. 7). The receiver is normally a tube, which contains a heat transfer fluid or water for direct steam generation.

The two major components of the collector subsystem are the parabolic trough reflector, including its support structure, and the receiver, also referred to as the heat collector element. Important factors for the most efficient parabolic trough reflector include the stability and accuracy of the parabolic profile, optical error tolerance, method of fabrication, material availability, and strength constraints. The geometry, length of the trough, the aperture, and rim angle will dictate the amount of heat collection. Since there are a large number of collector modules in a typical plant, the cost optimization requires minimizing the material weight (steel or aluminum), the operations needed to manufacture the structure, and the assembly of the elements that compose the collector (Gee and Hale 2006). A typical modern structure using

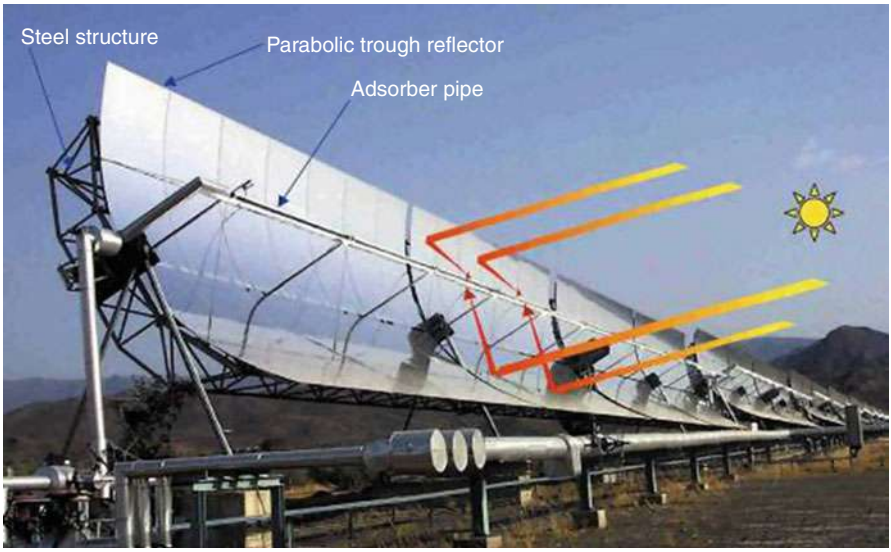

Fig. 7 A typical parabolic trough system (Source: http://www.abengoasolar.com)

Fig. 8 *Left*: parabolic trough space frame structure (Source: NREL). *Right*: lightweight trough with reflective thin film mirror (Farr and Gee 2009)

aluminum space frame technology to support the reflector is shown in Fig. 8. These are considerably lighter per unit of aperture area compared to standard steel structures.

All utility-scale parabolic trough installations to date have utilized silvered glass mirrors as reflectors (Fig. 7). These reflectors are limited in size and are typically driven by manufacturing limitations, strength, handling, shipping, and installation issues. These parabolic trough modules will have between 20 and 40 mirrors mounted to a single space frame module. The mirrors are typically 4–5 mm thick and are mounted to the structural frame with bolted connections. Alternatively, a UV-stabilized mirror film (i.e., ReflecTech™) laminated onto an aluminum substrate (Fig. 8b) provides a reflectance of about 94 % (Farr et al. 2009). The weight of the modern reflective surface is about 3.5 kg/m^2 versus 10 kg/m^2 (2.1 lbf/ft^2) for glass mirrors and allows for a lower initial cost.

The receiver must achieve high efficiency with high solar absorptance, low thermal losses, and minimum shading. The receiver typically consists of a pipe with a solar-selective coating encased in a glass tube throughout which there is a vacuum. The most commonly used thermal receiver is the SCHOTT PTR™

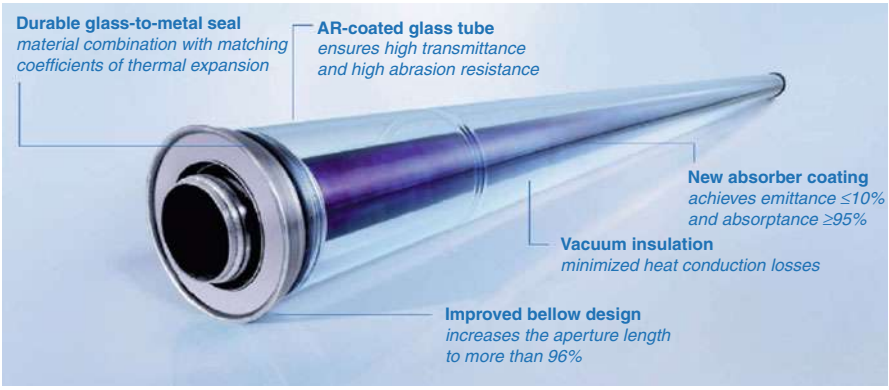

Fig. 9 Schott PTR™ 70 receiver

70 (http://www.schottsolar.com/global/products/concentrated-solar-power/schott-ptr-70-receiver/), shown in Fig. 9, which has a highly selective absorber coating on a stainless steel tube that has an outside diameter of 70 mm. The tube is enclosed in a glass cylinder with vacuum insulation to minimize the long-wave IR radiation and convection losses. The receiver tube supports are designed to minimize any receiver deflection and sunlight blockage. This particular configuration is in widespread use, but it has a number of drawbacks, which include the fact that it is difficult to maintain the vacuum seals, especially after welding, and, as has been observed, the heat transfer fluid and solar-selective coating off-gas hydrogen into the vacuum tube, thus negating the convection reducing effects of the tube.

The typical thermal conversion efficiency (net heat collected/incident solar radiation over the trough aperture area) for a parabolic trough is shown in Fig. 10 for the PT-1 concentrator (Dudley et al. 1995). The efficiency is largely affected by the collector thermal and optical losses. Since the radiation losses are proportional to the fourth power of the temperature, the efficiency decreases rapidly with increasing working fluid temperature. The nominal operating temperature of many plants (e.g., SEGS) is about 400 °C (~350 °C above ambient) operating at a thermal conversion efficiency of about 50 % at best. The trend over the last 25 years has been to make larger collectors with higher concentration ratios in order to improve the collector thermal efficiency. However, due to increased material manufacturing and installation costs of the large aperture (>6 m) troughs, the LEC still remains high for widespread implementation.

The concentrating parabolic trough systems typically produce power based on the Rankine cycle, which is the most fundamental and widely used steam-power cycle. The cycle starts with superheated steam generated by the heat collected from the parabolic trough field. The superheated vapor expands to lower pressure in a steam turbine that drives a generator to convert the work into electricity. The turbine exhaust steam is then condensed and recycled as the feed water for the superheated steam generation to begin the cycle again. The simple steam cycle thermodynamic efficiency can be as high as 35 %. Considering that the generator sets are better than

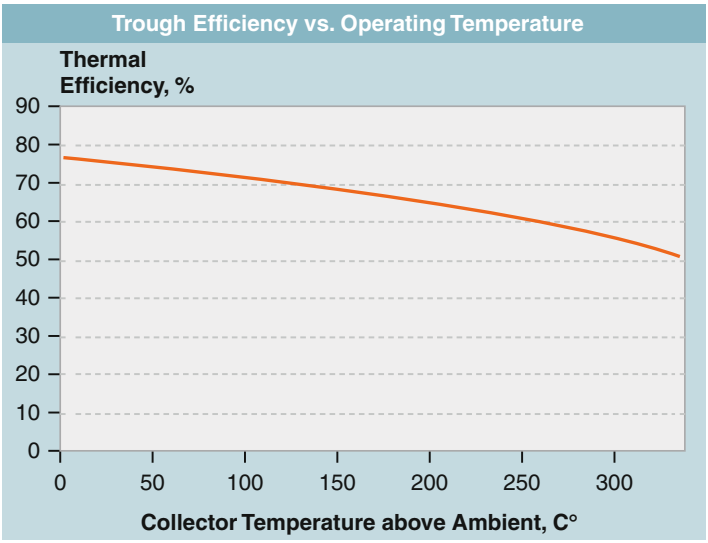

Fig. 10 The variation of the thermal efficiency of a parabolic collector with operating temperature (Dudley et al. 1995)

90 % efficient in converting the shaft power into electricity, it is expected that the cycle can produce electricity at an efficiency in excess of 30 %. As such, the total combined plant efficiency (solar to electricity) is best estimated to be about 15 %. The SEGS system experience shows that the annual solar to electric efficiency varies from 10.7 % to 14.6 %, with the higher number corresponding to the case where thermal storage is included in the plant. Although the plant efficiency appears low when compared to conventional fossil fuel-based plants, the operation and maintenance (O&M) costs are negligible due to the absence of any fuel costs, thus making the LEC largely depend on the capital costs. It is useful to think in terms of the cost/efficiency ratio to determine the viability of the CSP plant. Although much of the recent effort is on increasing the efficiency of the plant, it is more useful to find ways to reduce capital costs, thereby reducing the LEC. Hence, the following is a discussion assessing the component costs for a parabolic trough plant.

Figure 11 gives a breakdown of the investment costs associated with a typical parabolic trough plant utilizing the Rankine steam cycle (Brakmann et al. 2002). As the pie chart indicates, the majority of the initial investment cost is associated with the solar field. Much progress has been made recently with the introduction of lightweight space frame structure designs and the development of efficient highly reflective film (www.reflectechsolar.com), such as ReflecTech™ and 3M's new solar mirror film (http://solutions.3m.com). The heat transfer fluid (HTF) system moves the heat from the solar field to the power block, and it requires an HTF with the following properties: high-temperature operation with high thermal stability, good heat transfer properties, low energy transportation losses, low vapor pressure, low

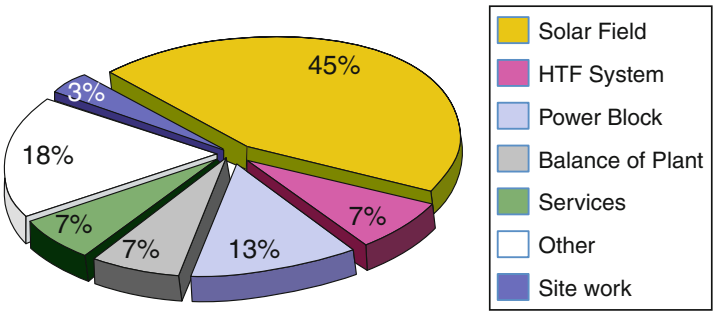

Fig. 11 Typical cost breakdown of a parabolic trough SEGS plant

freeze point, low hazard properties, good material compatibility, low hydrogen permeability of the steel pipe, and economical product and maintenance costs. As a result, synthetic organic HTFs are most suitable for the parabolic trough plants. For example, SYLTHERM™ 800, a high-temperature HTF by Dow Chemical Company, can be used in liquid form up to 400 °C and meets many of the requirements delineated above (http://www.dow.com/webapps/lit/litorder.asp?filepath=heattrans/pdfs/noreg/176-01469.pdf&pdf=true). The last of the major components is the power block, which consists of a conventional steam turbine-based system, the costs of which are well established and a number of new players from China and India have made the prices quite competitive. Any significant reduction in the cost of any of these three major components will result in a lower LEC for CSP systems.

The most recent 64 MW (nominal) installation in Nevada (Nevada Solar One), shown in Fig. 12, uses 5.77 m aperture parabolic troughs with PTR-70 receivers, resulting in a geometric concentration ratio of 26. The total solar field is 357,200 m^2 and the plant site area is 1.62 km^2. Field inlet and outlet temperatures are 300 °C and 390 °C, respectively. The solar steam turbine inlet temperature is about 371 °C at 86.1 bar. The plant uses a supplementary gas heater to provide 2 % of the total heat requirement. The plant produces about 134×10^6 kWh of electricity annually, which yields a plant capacity factor of about 0.24. Coal power plants have a capacity factor on the order of 0.74, and as such they can produce the equivalent electricity output from a 21 MW plant. The solar to electricity efficiency of the plant (Fig. 13 shows the plant schematic) is estimated, based on the annual DNI of 2,573 kWh/m^2, to be 14.6 %. The CO_2 emission reduction (as compared to a equivalent coal plant) is estimated to be about 100,000 MT/year. A typical electricity production in a day is depicted in Fig. 14, where the hourly DNI variation is also displayed. The total installed cost of the project was $266 million resulting in a nominal price of about $4.15/W. With medium temperature (250–300 °C) parabolic troughs and advanced receiver designs, it is anticipated that the installed costs may reach as low as $2.50/W, thus making the parabolic trough systems competitive with many other renewable energy solutions.

The ability to provide near-firm power through the use of thermal energy storage is gaining prominence. This characteristic differentiates CSP from PV technology, as

Fig. 12 *Left*: parabolic trough field. *Right*: power block at Nevada Solar One power plant (Source: www.acciona-na.com)

the utilities can tailor the use of CSP electricity as needed. The thermal storage can also provide more uniform output over the day and increase annual electricity generation, thereby increasing the plant capacity factor. For example, while solar energy availability peaks at noon, demand peaks in the late afternoon when the

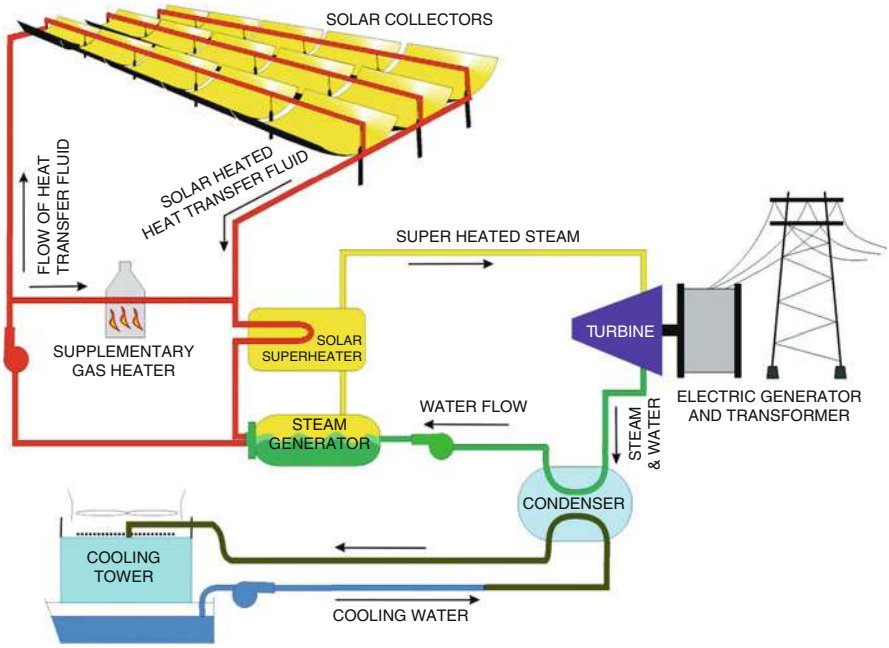

Fig. 13 Nevada Solar One plant schematic (Source: www.acciona-na.com)

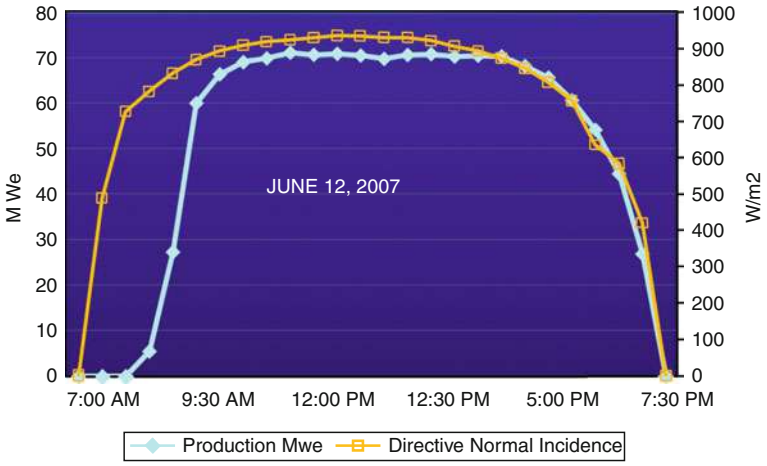

Fig. 14 Nevada Solar One electricity output and DNI for a typical summer day (Source: www.acciona-na.com)

energy from the sun is already going down. Figure 15 shows a parabolic trough plant schematic with molten salt thermal storage incorporated (Kearney and Morse 2010). A high-temperature thermal energy storage option has been developed for parabolic troughs that use molten nitrate salt as the storage medium in a two-tank system; it has

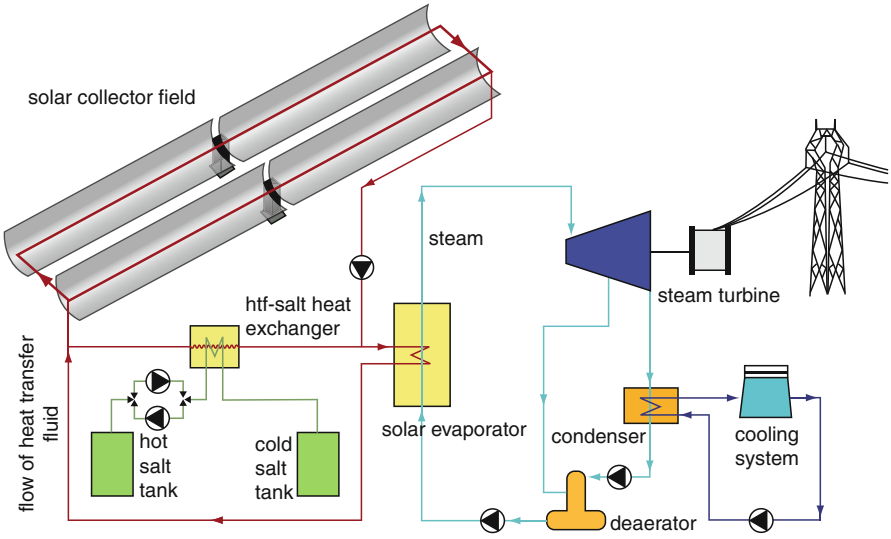

Fig. 15 A schematic of a parabolic trough plant with added thermal storage (Kearney and Morse 2010)

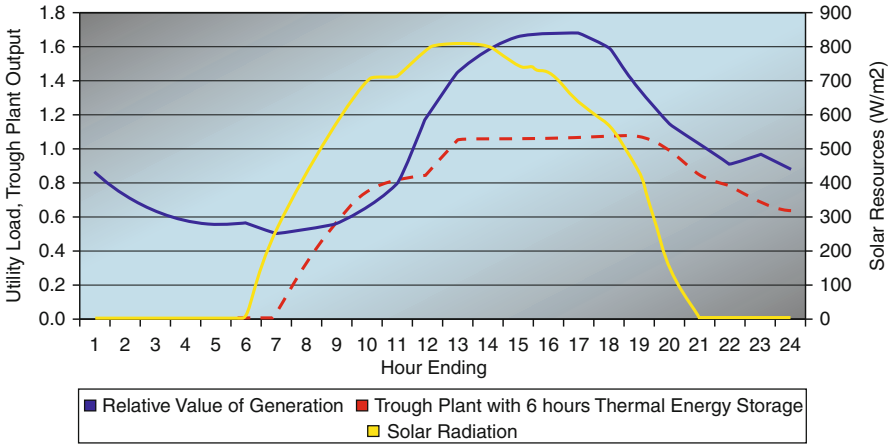

Fig. 16 The effect of storage on utility load during a typical day (Kearney and Morse 2010)

an oil-to-salt heat exchanger to transfer thermal energy from the solar field to the storage system (Laing et al. 2009). A more desirable option under development is an advanced heat transfer fluid (HTF) that is thermally stable at high temperatures, has a high thermal capacity and a low vapor pressure, and remains a liquid at ambient temperatures. The effect of storage to follow the utility system demand is clearly depicted in Fig. 16. When compared to the data shown in Fig. 14, where the

electricity supply follows closely with the sun's energy, the storage extends the availability of electricity through evening hours.

The performance of SEGS plants, the successful development of Nevada Solar One, and the progress made by industry innovations have greatly increased interest in utility-scale CSP projects in the USA and Europe. Abengoa Solar's proposed 250 MW Solana parabolic trough plant provides an example of the potential of this technology (http://www.abengoasolar.com/corp/web/en/our_projects/solana/).

Linear Fresnel Reflector Technology

Fresnel lenses are used as solar concentrators where the reflector is composed of many long row segments of flat mirrors, which concentrate beam radiation onto a fixed receiver, located at few meters height, running parallel to the mirrors axis of rotation (Fig. 17). Linear Fresnel follows the principles of parabolic trough technology but replaces the curved mirrors with long parallel lines of flat, or slightly curved, mirrors. Unlike parabolic troughs where the aperture is limited to few meters, a large aperture can be achieved by the linear Fresnel reflector at low cost. Although the original idea is quite old (Francia 1961, 1968), only recently has this concept been brought to fruition by two teams in Australia and Belgium. The concentration ratios used in this system are quite similar to those achieved using parabolic troughs (10–80). Hence, the operating temperatures are also in the same range of the parabolic trough systems, 250–400 °C. A picture of the Solarmundo prototype system (Häberle et al. 2002) erected in Liege, Belgium, is shown in Fig. 18. The collector area is 2,500 m^2 (25 m wide and 100 m long) and the absorber tube has an outer diameter of 18 cm. The prototype used a black (nonselective) absorber. However, in order to achieve satisfactory thermal performance, a highly selective absorber coating that is stable at high operation temperatures must be applied. A pilot plant, a 1 MW (peak) thermal, system similar to the prototype was built at PSA

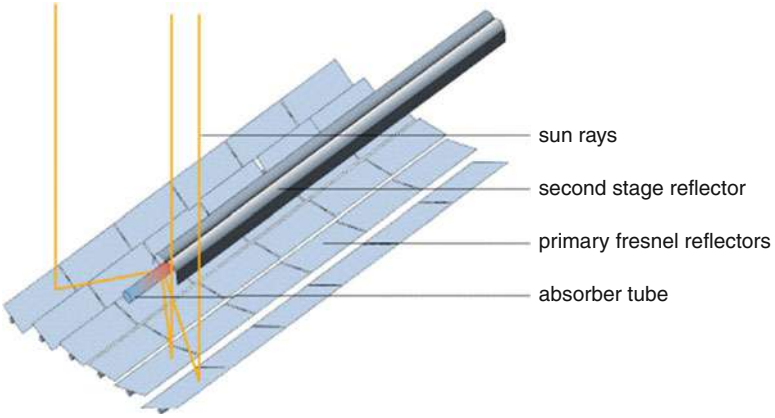

Fig. 17 The principle of a typical Fresnel collector (Haberle et al. 2002)

Fig. 18 2,500 m^2 reflected area Fresnel concentrator prototype in Belgium (Haberle et al. 2002)

in Almeria, Spain. Water flows through this absorber pipe, which is heated to temperatures of up to 450 °C. This produces steam (as in a conventional power plant), which is converted into electrical energy through the use of a steam turbine.

A 5 MW_e compact linear Fresnel reflector (CLFR) power plant was built by Ausra in California as a demonstration plant (www.ausra.com) (Fig. 19). The solar-field aperture area was 26,000 m^2, with three lines, each 385 m length with a mirror width of 2 m. The plant produces 354 °C superheated steam at 70 bar. The CLFR utilizes multiple absorbers, which is an alternate solution to the linear Fresnel reflector (LFR) where only one linear absorber on a single linear tower is used. This prohibits any option of the direction of orientation of a given reflector. Therefore, if the linear absorbers are close enough, individual reflectors will have the option of directing reflected solar radiation to at least two absorbers. This additional factor gives potential for more densely packed arrays, since patterns of alternative reflector inclination can be set up such that closely packed reflectors can be positioned without shading and blocking.

The main advantages of linear Fresnel are its lower investment and operational costs. Firstly, the flat mirrors are cheaper and easier to produce than parabolic curved reflectors and so are readily available from manufacturers worldwide. The structure also has a low profile, with mirrors just 1 or 2 m aboveground. This means the plant

Fig. 19 The Ausra 5 MW Kimberlina solar thermal demonstration plant (Source: http://www.ausra.com)

can operate in strong winds and it can use a lightweight, simple collector structure. Although the technology offers a simpler and more cost-effective solution, it has not been tested long enough to determine its viability as an alternative to parabolic trough technologies.

Dish-Stirling Technology

Dish-Stirling systems are relatively small units that track the sun and focus solar energy onto a cavity receiver at the focal point of the reflector, where it is absorbed and transferred to a heat engine/generator. The ideal concentrator shape is a paraboloid of revolution (Fig. 20, left). Some concentrators approximate this shape with multiple spherically shaped mirrors supported with a truss structure (Fig. 20, right). An engine based on the Stirling cycle is most commonly used in this application due to its use of an external heat supply that is indifferent to how the heat is generated (Saad 1997). Hence, it is an ideal candidate to convert solar heat into mechanical energy. The high-efficiency conversion process involves a closed cycle engine using an internal working fluid (usually hydrogen or helium) that is recycled through the engine. The working fluid is heated and pressurized by the solar receiver, which in turn powers the Stirling engine. Stirling engines have decades of recorded operating history. For over 20 years, the Stirling Energy System (www.stirlingenergy.com) dish-Stirling system has held the world's efficiency record for converting solar energy into electricity with a record of 31.25 % efficiency. Their size typically ranges from 1 to 25 kW with a dish that is 5–15 m in diameter. Because of their

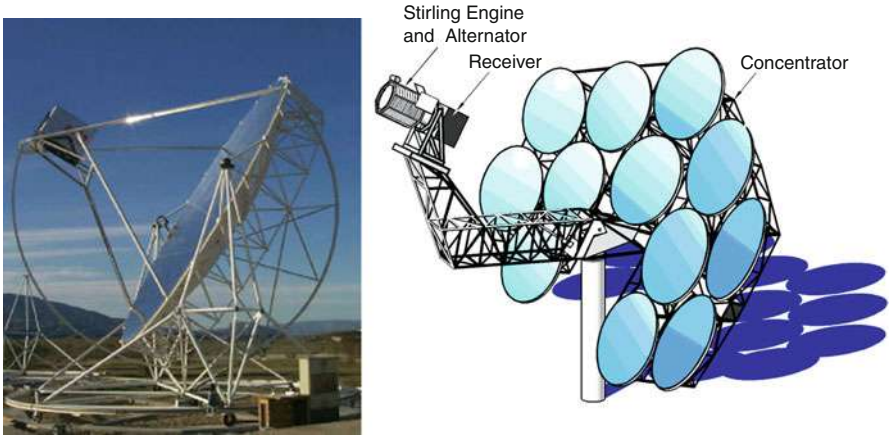

Fig. 20 *Left*: Euro Dish (Source: http://www.sbp.de). *Right*: SAIC-Sandia dish (Source: http://www.energylan.sandia.gov/)

size, they are particularly well suited for decentralized applications, such as remote stand-alone power systems.

One of the most advanced dual-axis tracking parabolic dish-Stirling systems is manufactured by Stirling Energy Systems (SES), and it produces 25 kW_e peak power (at 1,000 W/m^2 DNI) (www.stirlingenergy.com). This unique design uses a radial solar concentrator dish structure that supports an array of curved glass mirror facets as shown in Fig. 21. The dish has a diameter of about 11.6 m (glass surface area ≈90 m^2), which results in a concentration ratio of about 7,500. The heat input from the sun is focused onto solar receiver tubes (at a focal length of 7.45 m) that contain hydrogen gas. The solar receiver is an external heat exchanger that absorbs the incoming solar thermal energy. This heats and pressurizes the gas in the heat exchanger tubing, which in turn powers the Stirling engine at a typical operating temperature of about 800 °C. A generator that is connected to the engine then provides the electrical output. Waste heat from the engine is transferred to the ambient air via a radiator system similar to those used in automobiles. The gas is cooled by a radiator system and is continually recycled within the engine during the power cycle. The solar energy to electricity peak conversion efficiency is reported as 31.25 %. A much smaller 3 kW_e advanced parabolic dish-Stirling system is manufactured by Infinia (Fig. 21). The single free-piston Stirling engine uses helium in a hermetically sealed system, thereby avoiding maintenance issues generally associated with moving parts. The solar to electric peak efficiency is reported to be around 24 %.

Dish-Stirling systems are quite flexible in terms of size and scale of deployment. Owing to their modular design, they are capable of both small-scale distributed power output and large-scale, utility-scale projects. Although dish-Stirling systems have been tested and proven for over two decades with no appreciable loss in the key performance criteria, there were no utility-scale plants in operation until very recently. Within the past year, 60 SES SunCatcher™ systems were installed as part

Fig. 21 *Left*: SES Sun Catcher™ (Source: http://www.stirlingenergy.com/). *Right*: Power Dish™ by Infinia (Source: http://www.infiniacorp.com)

of the Maricopa Solar demonstration plant in Arizona (Fig. 22). The plant is currently operational and it is capable of producing 1.5 MW_e. Two other plants in California, totaling over 1.4 GW are slated to begin construction soon using thousands of the SES systems. A similar 1 MW system is under construction in Villarrobledo, Spain, using the Infinia 3 kW units (www.infiniacorp.com). The successful installation and operation of these dish-Stirling systems in a scale beyond a handful of units will demonstrate their technical viability for the large-, utility-scale plants. Unlike steam cycles, this technology uses no water in the power conversion process, a key benefit compared to other CSP plants.

Current installed cost for the dish-Stirling systems at demonstration scale, with few units (mostly built in semiautomated manufacturing facilities), is about $6,000/kW. This cost is approximately distributed with 40 % in the concentrator and controls, 33 % in the power conversion unit, and the remaining 27 % of the costs in the balance of plant and installation of the system. Mass production techniques, such as those employed at the automotive scale, will provide great cost benefits to these systems. With the economies of scale in their favor and because of higher solar to electricity efficiency (25–30 %), the dish-Stirling systems will become competitive with the photovoltaic and parabolic trough systems. However, unlike the parabolic trough systems, the 20-year life cycle costs of these systems are yet to be determined.

Power Tower Technology

The solar central receiver power tower is a concept that has been under study both in the USA and Spain over the last three decades. This technique utilizes a central

Fig. 22 *Left*: 1.5 MW Maricopa Solar installation (Source: http://www.srpnet.com/maricopasolar). *Right*: 1 MW solar installation in Villarrobledo, Spain (Source: http://www.infiniacorp.com)

power tower that is surrounded by a large array of two-axis tracking mirrors – termed heliostats – that reflect direct solar radiation onto a fixed receiver located on the top of the tower. The typical concentration ratio for this approach is in excess of 400. Within the receiver, a fluid transfers the absorbed solar heat to the power block where it is used to generate steam for a Rankine cycle steam engine/generator. Until recently, the largest demonstration plant employing this technology was the 11.7 MW_e "Solar One" plant in Barstow, California (Fig. 23), that was constructed and operated in the 1980s. Solar One operated at a nominal temperature of 510 °C and it had a peak solar to electric efficiency of about 8.7 %. In the 1990s, Solar One was converted to "Solar Two" through the addition of additional heliostats and a two-tank molten salt storage system to improve the capacity factor of the system (www1.eere.energy.gov/library/pdfs/28751.pdf).

Two important components of the power tower technology are the heliostats and the receiver. Heliostats are the most important cost element of the power tower plant, and they typically contribute to about 50 % of the total plant cost. Consequently, much attention has been paid to reduce the cost of heliostats to improve the economic viability of the plant. The most commonly used design is the two-axis sun-tracking pedestal-mounted system as shown in Fig. 24. A heliostat consists of a

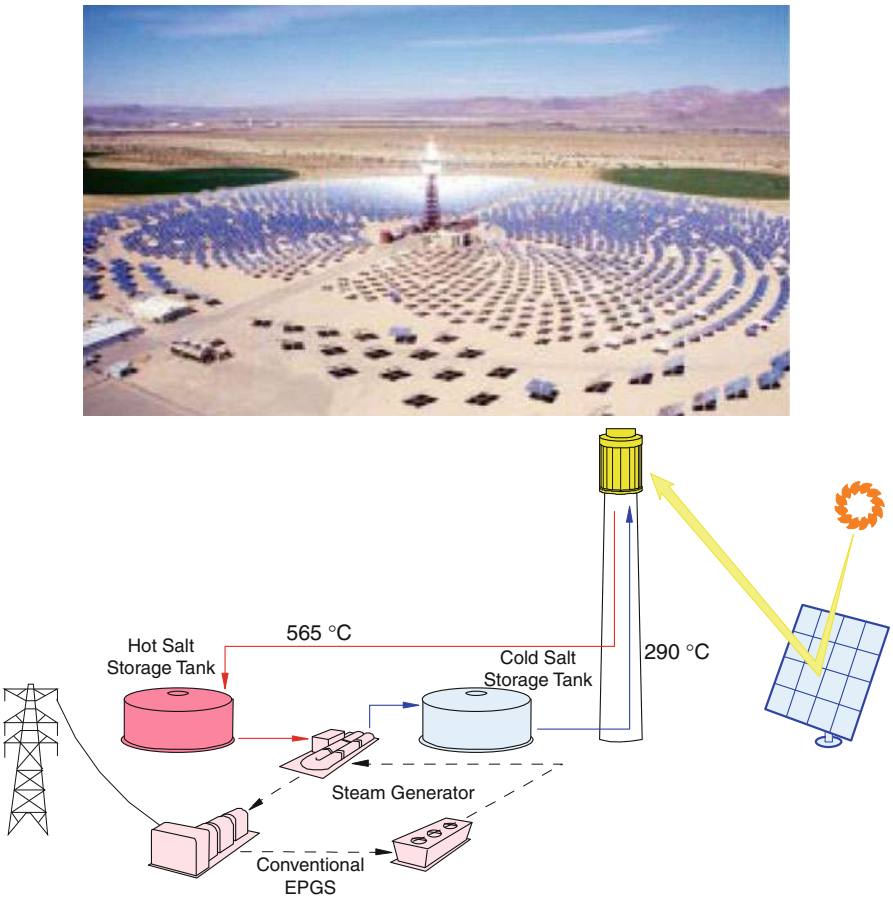

Fig. 23 *Left*: Solar One/Two central solar tower receiver plant. *Right*: schematic of the plant's major components (Source: USDOE)

large mirror with the motorized mechanisms to actuate it, such that it reflects sunlight onto a given target throughout the day. A heliostat array is a collection of heliostats that focus sunlight continuously on a central receiver. A 148 m^2 ATS glass/metal heliostat has successfully operated for over 20 years at the National Solar Thermal Test Facility in Albuquerque, USA, without much degradation of the beam quality. It has also survived high winds in excess of 40 m/s. Depending upon the production rates, the installed price of the ATS heliostat was estimated to be between $126 and 164 per square meter (Kolb et al. 2007). With increasing installations, the estimated installation price will be around $90/$m^2$. The Sandia study also suggests that large heliostats are more cost efficient than small ones on a cost per square meter basis (Kolb et al. 2007).

A relatively new facility that began operation in 2006 is the PS10 solar power tower in Spain (10 MW Solar Thermal Power Plant for Southern Spain 2006). The

Fig. 24 Typical advanced heliostat field (Source: Plataforma Solar de Almeria – PSA, Spain)

main goal of the PS10 project was to design, construct, and operate a power tower on a commercial basis and produce electricity in a grid-connected mode. This 11 MW_e facility generates about 23,000 MWh of grid-connected electricity annually at an estimated solar to electricity efficiency of about 15 %. However, it should be noted that the plant also uses natural gas for 12–15 % of its electricity production. The solar radiation is concentrated through the use of 624 reflective heliostats, each of which has a 121 m^2 curved reflective surface, arranged in 35 circular rows, as shown in Fig. 25. As a result, the total reflective surface is 75,216 m^2. The heliostats concentrate the solar radiation to a cavity receiver that is located at the top of a 115 m high tower. The cavity receiver is basically a forced circulation radiant boiler designed to use the thermal energy supplied by the concentrated solar radiation flux to produce more than 100,000 kg/h of saturated steam at 40 bar and 250 °C. The saturated steam is then sent to the turbine where it expands to produce mechanical work and electricity. For cloudy transient periods, the plant has a saturated water thermal storage system with a thermal capacity of 20 MWh, which is equivalent to an effective operational capacity of 50 min at 50 % turbine workload. This is a relatively short storage time, partially because the tower uses water rather than molten salt for heat storage. The water is held in thermally clad tanks and reaches temperatures of 250–255 °C (instead of around 600 °C for systems using salt).

The investment cost of the PS10 plant was about 35 million euros, thus resulting in an installed cost of about 3,000 euros per kW_e. Of this cost, the heliostat cost was reported to be about 140 euros/m^2. From this experience, it appears that about 30 % of the total installed cost of a solar power tower goes toward the heliostat expense.

A second-generation plant, referred to as PS20, has twice the PS10 output (20 MW), with 1,255 two-axis sun-tracking heliostats. The receiver is located on top of a 165 m tower, and it utilizes the same technology as that of PS10 for electricity generation. The new plant features include control and operational systems enhancements, an improved thermal energy storage system, and a higher efficiency receiver.

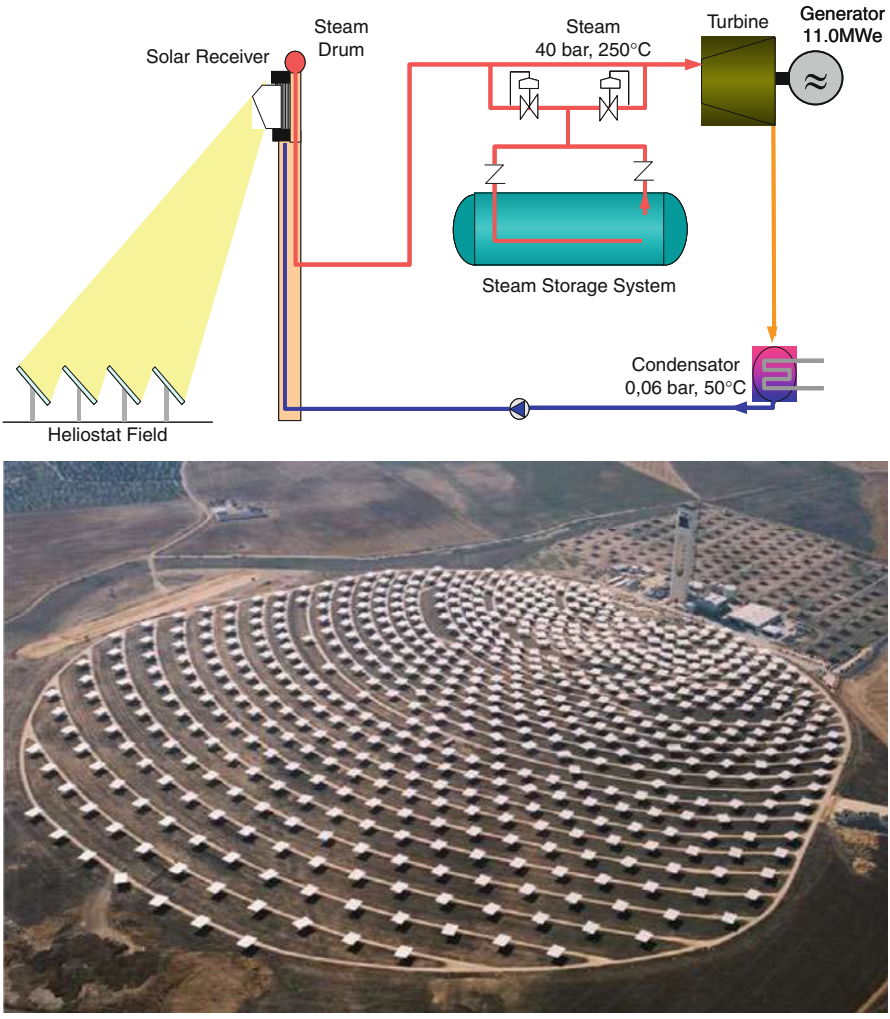

Fig. 25 PS10 11 MW central receiver tower project in southern Spain. *Left*: plant schematic. *Right*: the PS10 plant aerial picture (Source: Abengoa Solar)

A utility-scale 400 MW solar tower power project, referred to as the "Ivanpah Solar Power Complex," is being built in California by a consortium led by Bright Source Energy, and it is operational in 2013 (www.brightsourceenergy.com). The heliostats in this project will consist of smaller flat mirrors, termed the LPT 550, each having a reflecting area of 14.4 m^2. Fifty thousand of these LPT 550 heliostats will be required for every 100 MW of installed capacity. The receiver is a traditional high-efficiency boiler positioned on top of the tower. The boiler tubes in the receiver are coated with a solar-selective material that maximizes energy absorbance, and there are sections within the receiver for steam generation, superheating, and reheating.

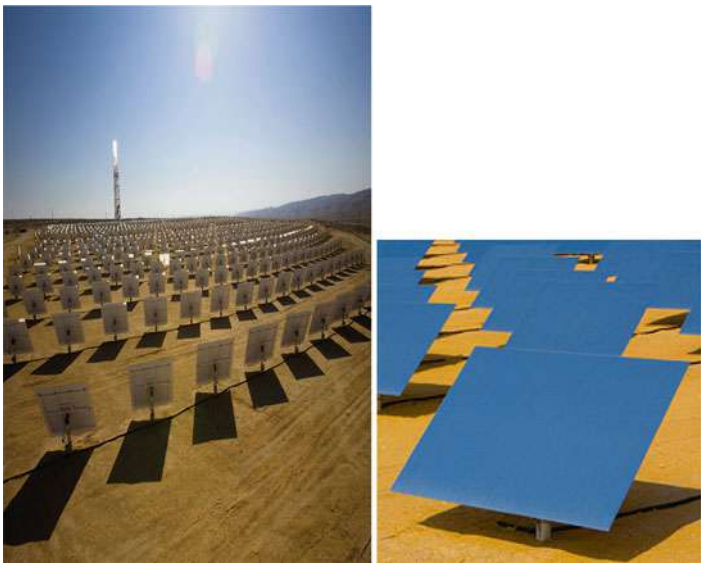

Fig. 26 The LPT 550 central receiver tower demonstration plant in Israel's Negev desert. *Left*: heliostat field with central tower. *Right*: 7.22 m^2 heliostat (Source: Brightsource Energy)

This results in the generation of superheated steam at 550 °C and 160 bars (unlike the saturated steam that is produced in the PS10 and PS20). The power block consists of a conventional Siemens steam turbine generator with a reheat cycle and auxiliary functions of heat rejection, water treatment, water disposal, and grid interconnection capabilities. The technology demonstration plant, as shown in Fig. 26, has 1,641 heliostats (reflecting area ~12,000 m^2) with each measuring 2.25 × 3.21 m (7.22 m^2). The tower height was 75 m (60 m tower plus 15 m receiver), and the thermal energy collected by the receiver was between 4.5 and 6 MW_{th}. Because of the higher operating temperature, the solar to electrical efficiency of these plants is expected to be about 20 %. Although there is not yet any experience with utility-scale plant installations, it appears that the installation cost of these plants may be in the range of \$3,000/kW_e.

In an attempt to bring down the installed cost of the solar power plant technology, eSolar, a California company introduced a modular/distributed tower design with a 1 m^2 reflected area heliostat (www.esolar.com). These much smaller heliostats, with fully automated two-axis sun tacking system, are easy to assemble and install in large numbers. Each central tower unit is capable of producing 2.5 MW_e through the use of 12,000 mirrors that reflect the radiation onto a 47 m high tower. The thermal receiver in the tower has external evaporator panels for producing superheated steam at 440 °C and 60 bar. Figure 27 shows a technology demonstration plant with two-tower system that nominally produces 5 MW_e of electricity. Since the performance details of the plant are not disclosed in any public domain, it is difficult to assess the solar to electric efficiency and the installed plant cost. In principle, the

Fig. 27 5 MW twin central receiver tower facility with 1 m^2 heliostats in California (Source: eSolar)

smaller heliostats are easy to manufacture, install, and maintain. However, the solar energy collection may involve significant losses due to spillage reaching the thermal receiver. Hence, it is important to study the pilot plant performance characteristics before a utility-scale plant design is considered.

Solar Chimney Power Plant Technology

A solar chimney power plant has a high chimney (tower) that is surrounded by a large collector roof made of either glass or resistive plastic supported on a framework (Fig. 28) (von Backstrom et al. 2008). Toward its center, the roof curves upward to join the chimney, thus creating a funnel. Solar radiation (direct and diffuse) strikes the collector and transmits part of its energy that heats up the ground and the air underneath the collector roof. At the ground surface, part of the transmitted energy is absorbed and the rest is reflected back to the roof, where it is subsequently reflected to the ground. The multiple reflections result in a higher fraction of energy absorbed by the ground. The warm ground surface heats the adjacent air through natural convection. The buoyant air follows the upward incline of the roof until it reaches the chimney, thereby drawing in more air at the collector perimeter. The natural and forced convection set up between the ground and the collector flows at high speed through the chimney and drives wind generators at its bottom. As the air flows from the collector perimeter toward the chimney, its temperature increases, while the velocity remains constant due to the increasing collector height at the center as shown in the schematic (Fig. 28). The pressure difference between the outside cold air and the hot air inside the chimney causes the air to flow through the turbine. The ground under the collector roof behaves as a storage medium and can even heat up

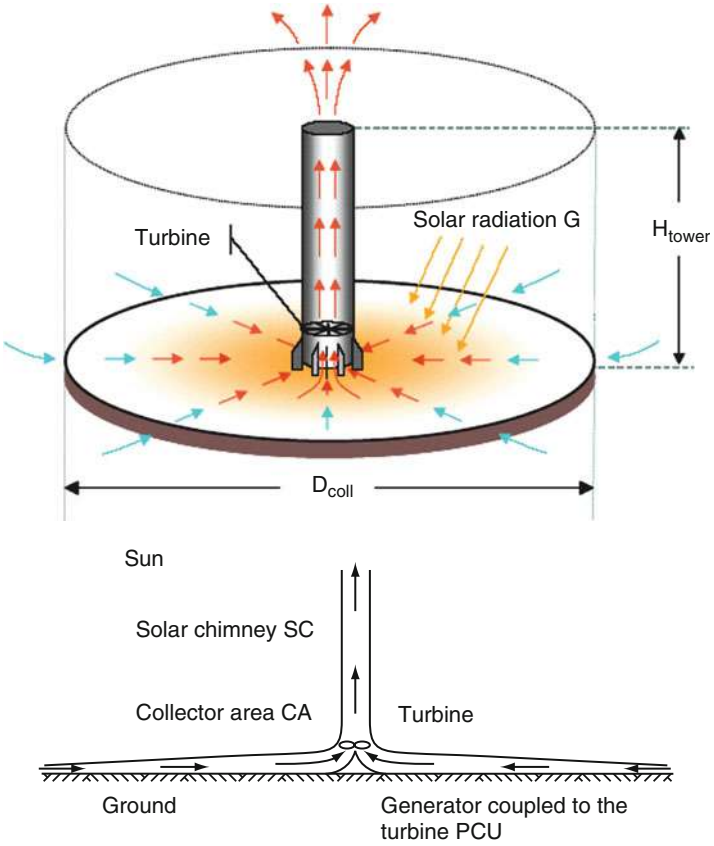

Fig. 28 *Left*: an artist rendering of a 5 MW solar chimney plant (Source: http://www.sbp.de). *Right*: a schematic indicating the main components of the plant (von Backstrom et al. 2008)

the air for a significant time after sunset. The efficiency of the solar chimney power plant is below 2 % and depends mainly on the height of the tower. As a result, these power plants can only be constructed on land that is very cheap or free. Such areas are usually situated in desert regions. However, this approach is not without other uses, as the outer area under the collector roof can also be utilized as a greenhouse for agricultural purposes.

A 200 m high solar chimney demonstration plant based was constructed in Manzanares, Spain (http://www.youtube.com/watch?v=XCGVTYtJEFk). The peak power output of this demonstration plant was 50 kW, and it operated for over 8 years without any significant degradation in performance. However, as with other CSP plants, the minimum economical size of the solar chimney power plant is in the several MW range. Although no pilot plant has been built to demonstrate the viability of this technology in the MW range, computer simulations suggest its promise as a low-cost solar thermal technology. Figure 29 shows the results from

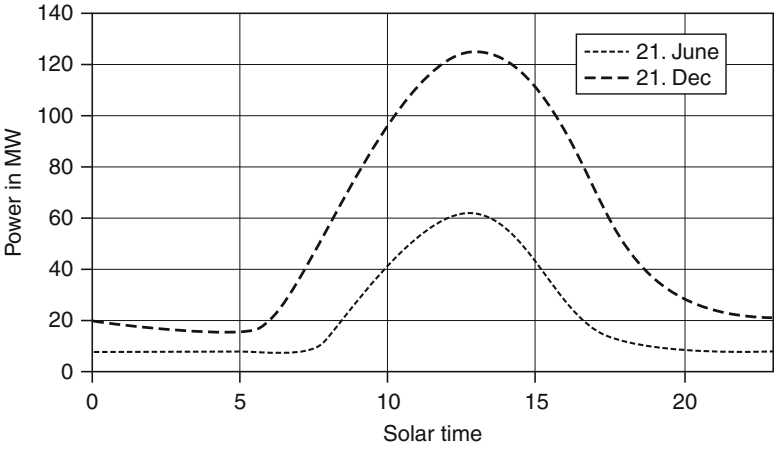

Fig. 29 Simulated results of electrical power output of solar chimney power plant during summer and winter (von Backstrom et al. 2008)

a simulation of a large-scale solar chimney power plant with a 5,000 m collector diameter (~20 km^2 area) and a chimney height of 1,000 m and inside diameter 210 m (von Backstrom et al. 2008). With the vast expanse of unpopulated land in Australia, it may be possible to economically erect a solar chimney plant of this size.

Nonimaging Concentrator Technology

All of the concentrating technologies discussed thus far require some type of active solar tracking in order to account for the change in the elevation of the sun on any given day and throughout the year. Nonimaging concentrators, such as the compound parabolic concentrator (CPC), allow for the use of a non-tracking stationary concentrator that can account for the daily and annual excursion in solar elevation (Meinel and Meinel 1976). Figure 30 illustrates how the light rays in a commercial CPC collector are concentrated when the source is directly overhead (left), such as solar noon on the equinox, and when it is at the acceptance angle of the CPC design (right), such as would be observed during the solstice.

The stationary benefit of the CPC comes at the expense of a concentration ratio of 2 for the design. This is an order of magnitude lower than what can be achieved through the use of a parabolic trough, but it is twice that of a typical flat-plate collector. As such, the CPC design is capable of producing sensible heat at temperatures well in excess of 120 °C, thus making it a good candidate for use with an absorption refrigeration system. It can also be paired with a low-temperature power cycle, such as an organic Rankine cycle, to generate electricity. The resulting system would be fairly inefficient when compared to a dish-Stirling system, but it would have a cost-to-efficiency ratio that would make it attractive for use in rural areas.

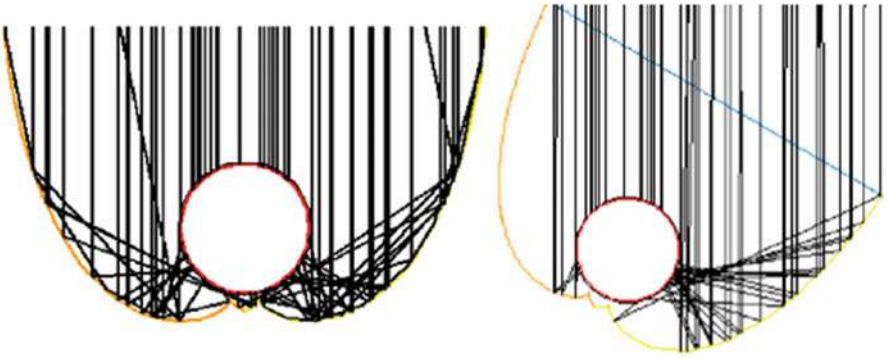

Fig. 30 Ray tracing diagrams for the Winston Series CPC. *Left* – incoming light rays directly overhead. *Right* – incoming light rays at the acceptance angle of the design (Source: www.soalrgenix.com)

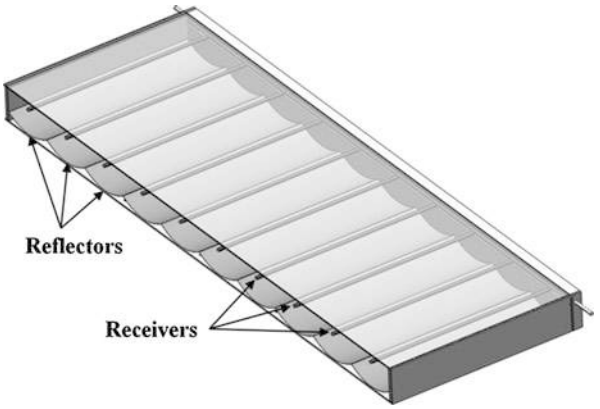

Fig. 31 Cutaway of multiple parabolic trough flat-plate collector

Industrial process heat from solar energy is becoming important in many industries such as pharmaceutical and textile, etc. In this context, the goal is to create a solar collector that can produce thermal energy in the medium temperature range (100–150 °C). To achieve this goal, a collector is designed to emulate features of existing flat-plate and CPC collectors while utilizing parabolic trough collector (PTC) geometry (Pandolfini et al. 2013).

The Multiple Parabolic Reflector Flat Panel Collector (MPFC) applies aspects of a stationary panel with the reflector geometry of a PTC. Multiple parabolic reflectors are arranged in an array within the envelope of the panel (Fig. 31). A tubular receiver is associated with each reflector, collecting the reflected light. The receivers are able to transverse within the panel independently from the reflectors. This allows for collection of concentrated light while the entire panel remains stationary.

The main feature of the MPFC is its moving receiver (which differs from conventional stationary reflector designs). Movement of the receiver is along a

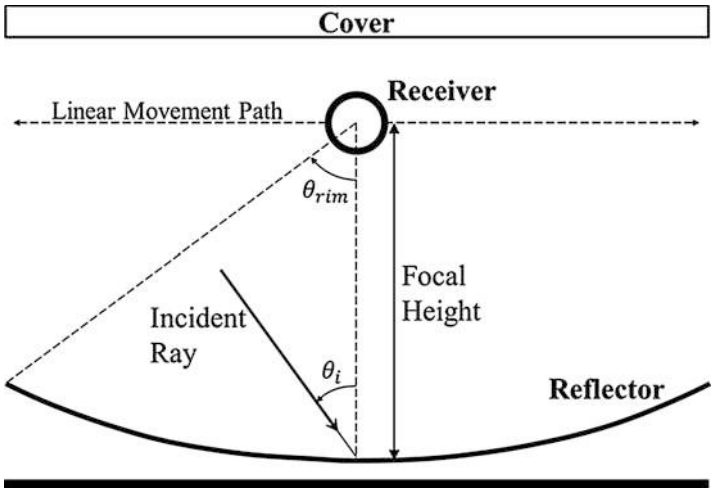

Fig. 32 A schematic of a single section of the MPFC

constant height, located through the focal point of the reflector. A motor controls the movement of the receiver assembly. The motor moves a rack-and-pinion system that in turn moves the receiver array. Position of the receiver must be accurate because it determines the optical gain of the receiver. The placement of the receiver causes some loss of solar energy that is determined by the incident angle of the sun on the reflector, θ_i. However, the reflector and the receiver designs are both optimized to collect solar energy over the course of a year.

Analysis of this new design is based on two parameters that affect the amount of light collected: concentration ratio, C, and rim angle, θ_{rim} (Fig. 32). The concentration ratio is defined as the ratio of the collector aperture area to the receiver's surface area. The rim angle defines the angle swept around the focal point, from the surface normal to the edge of the parabolic reflector.

Ray tracing is used to determine an optimal rim angle. The amount of light accepted by the receiver at concentration ratio of 6 is found greatest for $50 < \theta_{rim} < 60°$. Figure 33 shows the receiver placed at the focal height f. The receiver is allowed to be positioned at any horizontal position at this height. The ideal placement for the receiver is where the edge of the receiver is tangent to the caustic surface with the center of the receiver within the caustic envelope. The relative position of the receiver will change as θ_i changes, seen in Fig. 33.

The MPFC being stationary as the sun moves across the sky enables the receiver to accept varying amounts of radiation with minimal tracking except the receiver tubes move with respect to a parabolic reflector. The simplicity of the MPFC design makes it a cost-viable alternative to other collector types for producing heat at medium temperatures. For example, the levelized cost of energy (LCOE) is estimated at $\$0.006/kWh_{th}$ at a collection temperature of about 125 °C over its lifetime of about 20 years.

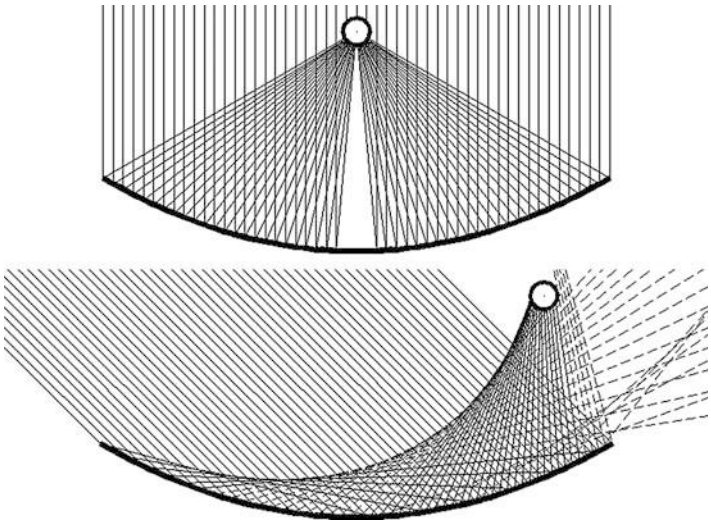

Fig. 33 Reflected rays at $\theta_i = 0^\circ$ (*top*), $\theta_i = 45^\circ$ (*bottom*)

Concentrating Solar Power (Thermal) Systems Economics

The concentrating solar power (CSP) for electricity generation technologies examined in the previous sections is the most dominant and has the greatest potential for commercialization. Current projects are targeted so that they meet specific needs at an economic benefit. Once success is achieved, the price points will come down, and good economics will drive the CSP projects. The following discussion is included here to indicate that CSP is becoming more economically attractive. Component manufacturers, utilities, and regulators are making decisions now that will determine the scale, structure, and performance of the CSP industry. Since each country's approaches to the renewable electricity industry are different, only the observations that are more common globally are included here. When considering the economic viability of CSP, often the levelized electricity cost (LEC) is calculated and compared among different technologies. Therefore, in the following, a general method is given for determining LEC.

The LEC is dependent on many variables related to the site, technology chosen, and the plant financing. The LEC is defined as (Pitz-Paal et al. 2005)

$$\text{LEC} = \frac{CRF \times K_I + K_{OM} + K_F}{E}$$

where

$$\text{CRF} = \frac{k_d(1+k_d)^n}{(1+k_d)^n - 1} + k_i$$

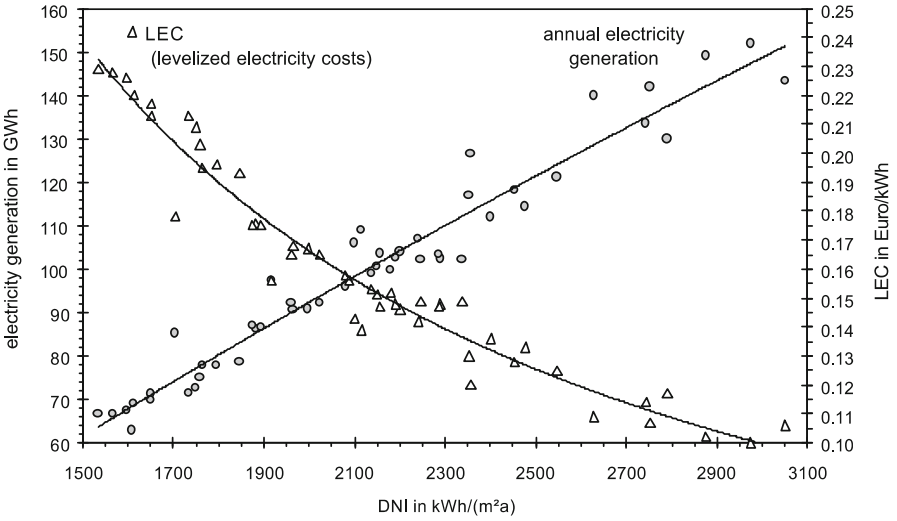

Fig. 34 The variation of annual electricity generation and LEC for a 50 MW_e parabolic trough plant with a 375,000 m^2 solar field for fifty chosen sites (Quaschning et al. 2001)

CRF is capital recovery factor, K_I total investment of the plant, K_{OM} annual operation and maintenance costs, K_F annual fuel costs (any fossil fuel, such as natural gas), E annual net electricity revenue, k_d debt interest rate, n depreciation period in years (~30), and k_i annual insurance rate (~1 %).

The many factors that determine the LEC vary greatly due to government subsidies, tax incentives, and annual net electricity production. One of the key parameters in the above formula is the determination of the annual electricity generation, which depends largely on the available DNI at the plant location. For example, Fig. 34 shows the impact of the annual DNI on the annual power generation and the LEC of a 50 MW_e parabolic trough SEGS type power plant with a 375,000 m^2 solar field. The economic parameters (e.g., discount rate of 6.5 %, solar-field costs of 200 euro/m^2, power block costs of 1,000 euro/kW, and O&M costs of 3.7 million euro per annum) have been kept constant (Quaschning et al. 2001). Although some of the financial data may be outdated, the intent here is simply to show that the annual electricity generation is approximately proportional to the DNI. This suggests that a careful analysis needs to be carried out for the determination of an economically optimized project site that not only depends on the solar irradiance (DNI) but on many other influencing parameters.

The present evaluation estimates (Fig. 35) from a number of sources that the LEC for CSP systems, shown here as cost of electricity (COE), will be around \$0.15–0.20/kWh, assuming a load demand between 9:00 am and 11:00 pm. However, the absolute cost data on many of the CSP systems considered here, and those planned for commercial deployment around the world, is largely unavailable so these numbers must be considered with some caution. Cost reductions

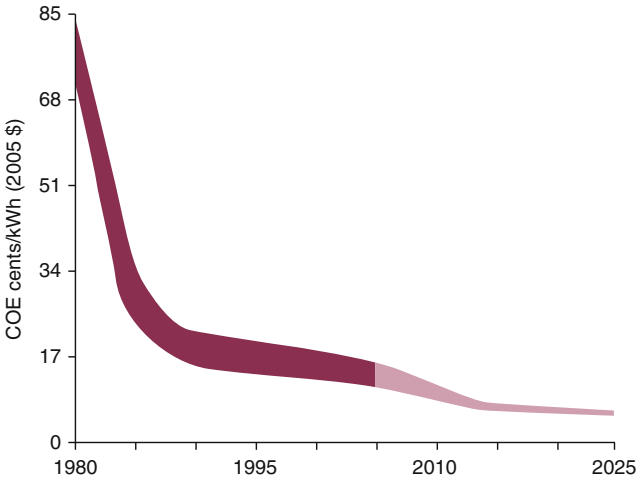

Fig. 35 The variation of the LEC for concentrating solar thermal power (Source: National Renewable Energy Laboratory, USA)

due to technological improvements, such as the implementation of thermal storage, and large-scale deployment are estimated to be around 10–30 % for parabolic trough systems, 20–35 % for central receiver systems, and 20–40 % for dish-Stirling systems (Quaschning et al. 2001). Given the rapid deployment of CSP systems, it is suggested that within the next 5 years, the LEC will be $0.10–0.15/kWh. With the additional benefit of carbon credits, CSP technology is poised to become the dominant solar electricity generating plant development in places where there is good DNI.

Summary and Conclusions

Concentrating solar thermal power (CSP) is a proven technology, which has significant potential for further development and achieving low cost. The history of the Solar Electricity Generating Systems (SEGS) in California demonstrates impressive cost reductions achieved up to now, with electricity costs ranging today between $0.10 and $0.15/kWh. Advanced technologies, mass production, economies of scale, and improved operation will allow for a reduction in the cost of solar-produced electricity to a competitive level within the next 5–10 years. Hybrid solar-and-fuel plants, at favorable sites, making use of special schemes of finance, can already deliver competitively priced electricity today. With over two decades of experience, parabolic trough technology is mature enough that its investment cost estimates can be made with confidence. Given the rapid growth contemplated within the immediate future (mostly in the southwest USA) and medium temperature CSP systems (250–300 °C), it is very likely that the LEC price target of $0.10/kWh may well be met within the next 3 years using the parabolic trough technology. When the

parabolic trough technology is combined with biomass gasification in a hybrid system, the overall plant efficiency will be substantially increased, thus resulting in a relatively low LEC. This is an approach that is ideally suited for regions of moderate DNI (5.2–5.5 kWh/m^2/day) and for distributed power applications (1–5 MW power plants). A greater opportunity lies in the thousands of niche markets that are primed for smaller-scale (1–10 MW) parabolic trough projects at a lower cost.

The central receiver tower (CRT) systems are being pursued aggressively by a number of companies with approaches that mostly differ in the heliostat size. The distributed approach with multiple towers appears to gain prominence because of their lower installation costs. Both parabolic trough and central tower systems benefit from heat storage, especially when the power demand is during off-peak solar hours. The CRT systems are best suited in areas of good annual solar insolation (>2,000 kWh/m^2/year) and utility-scale plant sizes (>50 MW). Because of the steam cycle used in the power block, the water availability can be an issue, especially in desert regions. The problem can be overcome by the use of an air-cooling system, which will have the adverse effect of reducing the overall plant efficiency.

The recent advances made in dish-Stirling systems in improving their solar to electric efficiency in the range of 30 % make them attractive for utility-scale power plant implementation. Because of their small unit electricity output (<25 kW), they are most attractive for distributed applications, especially when hermetically sealed Stirling engines are used as this may result in much lower operation and maintenance costs.

In summary, CSP is poised to become a significant player in the renewable electricity generation in countries where a significant solar energy resource is available, such as those near desert and equatorial regions.

References

10 MW Solar Thermal Power Plant for Southern Spain (2006) Final technical progress report, MNE5-1999-356, European Commission. http://www.ec.europa.eu/energy

Brakmann G, Kearney D (2002) The status and prospects of CSP technologies. In: International executive conference on expanding the market for concentrating solar power (CSP) – moving opportunities into projects, Berlin, June 2002

Decher R (1994) Energy conversion – systems, flow physics and engineering. Oxford University Press, New York

Dudley VE, Evans LR (1995) Test results: industrial solar technology parabolic trough solar collector, SAND94-1117. Sandia National Laboratories, Nov 1995

Duffie JA, Beckman WA (2006) Solar engineering of thermal processes, 3rd edn. Wiley, Cape Canaveral

Farr A, Gee R (2009) The SkyTrough™ parabolic trough solar collector. ES2009-90090. In: ASME 3rd international conference on energy sustainability, San Francisco

Francia G (1961) Un nouveau collecteur de l'energie rayonnante solaire: theorie et verifications experimentales. In: United Nations conference on new sources of energy, Rome, pp 554–588

Francia G (1968) Pilot plants of solar steam generation systems. Solar Energy 12:51–64

Gee RC, Hale MJ (2006) Solargenix energy advanced parabolic trough development. NREL/CP-550-39206, Nov 2006

Häberle A, Zahler C, Lerchenmüller H, Martins M, Wittwer C, Trieb F, Dersch J (2002) The Solarmundo line focussing fresnel collector. Optical and thermal performance and cost calculations. In: Steinfeld A (ed) Proceedings of 11th SolarPaces international symposium on concentrated solar power and chemical energy technologies. Paul Scherrer Institute, Zurich
http://solutions.3m.com
http://www.abengoasolar.com/corp/web/en/our_projects/solana/
http://www.dow.com/webapps/lit/litorder.asp?filepath=heattrans/pdfs/noreg/176-01469.pdf&pdf=true
http://www.schottsolar.com/global/products/concentrated-solar-power/schott-ptr-70-receiver/
http://www.youtube.com/watch?v=XCGVTYtJEFk
Jensen C, Price H, Kearney D (1989) The SEGS power plants: 1988 performance. In: 1989 ASME international solar energy conference, San Diego, April 1989
Kearney D, Morse F (2010) Bold, decisive times for concentrating solar power. Solar Today 24 (4):32–35
Kolb GJ, Davenport R, Gorman D, Lumia R, Thomas R, Donnelly M (2007) Heliostat cost reduction. ES2007-36217. In: Proceedings of the ASME energy & sustainability conference, Long Beach, June
Laing D, Bauer T, Lehmann D, Bahl C (2009) Development of a thermal energy storage system for parabolic trough power plants with direct steam generation. ES 2009-90038. In: Proceedings of the ASME 2009 energy and sustainability conference, San Francisco, July 2009
Meinel AB, Meinel MP (1976) Applied solar energy – an introduction. Addison Wesley, Reading
Molenbroek E (2008) Concentrating solar power status and potential. ECOFYS Report, September
Pandolfini J (2013) Design and development of the multiple parabolic reflector flat panel collector (MPFC) to generate medium temperature heat, Ph.D. Dissertation, Florida State University
Pilkington Solar International GmbH (2000) Survey of thermal storage for parabolic trough power plants. NREL/SR-550-27925. NREL, Golden
Pitz-Paal R, Dersch D, Milow B (2005) European concentrated solar thermal road-mapping (ECOSTAR), SES6-CT-2003-502578, Deutsches Zentrum fur Luft-und Raumfahrt e.V (DLR), Germany
Quaschning V, Kistner R, Ortmanna W (2001) Simulation of parabolic trough power plants. In: Proceedings of the 5Th Cologne solar symposium, Cologne, pp 46–50
Saad MA (1997) Thermodynamics – principles and practice. Prentice Hall, New Jersey, pp 403–407
von Backstrom TW, Harte R, Hoffer R, Kratzig WB, Kroger DG, Niemann H-J, van Zijl GPAG (2008) State and recent advances in research and design of solar chimney power plant technology. VGB Power Tech 7:64–71
www.ausra.com
www.brightsourceenergy.com
www.esolar.com
www.infiniacorp.com
www.meteotest.ch
www.reflectechsolar.com
www.stirlingenergy.com
www.wrdc-mgo.nrel.gov. NREL: National Renewable Energy Laboratory, Bolder
www1.eere.energy.gov/library/pdfs/28751.pdf

Harvesting Solar Energy Using Inexpensive and Benign Materials

Susannah Lee, Melissa Vandiver, Balasubramanian Viswanathan, and Vaidyanathan (Ravi) Subramanian

Contents

S. Lee • M. Vandiver • V.R. Subramanian (✉)
Department of Chemical and Metallurgical Engineering, Chemical and Materials Engineering Department, LME 310, MS 388, University of Nevada, Reno, NV, USA
e-mail: ravisv@unr.edu

B. Viswanathan
National Center for Catalysis Research, Indian Institute of Technology Madras, Chennai, Tamil Nadu, India
e-mail: bvnathan@iitm.ac.in

W.-Y. Chen et al. (eds.), *Handbook of Climate Change Mitigation and Adaptation*,
DOI 10.1007/978-3-319-14409-2_32

Abstract

Historically, the growth and prosperity of human civilization have mainly been propelled by fossil energy (coal and petroleum) usage. Decades of tested and proven technologies have led to a continuous increase in demand for fossil-based fuels. As a result, we are now finding ourselves at the threshold of a critical tipping point where environmental consequences and global climate can be irreversibly affected and hence cannot be ignored. More than ever before, our unending and rapidly growing need for energy has necessitated urgent action on efforts to examine alternative forms of energy sources that are eco-friendly, sustainable, and economical.

There are several alternatives to fossil-based fuels. These include biomass, solar, wind, geothermal, and nuclear options as prominent and possible sources. All these options can assist us with reducing our dependence on fossil fuels. Solar energy, being one of them, has the unique potential to meet a broad gamut of current global energy demand. These include domestic applications such as solar-assisted cooking, space, heating, as well as industrial processes such as drying. Solar energy utilization in several key areas such as electricity generation (photovoltaics), clean fuel production (hydrogen), environmental remediation (photocatalytic degradation of pollutants), and reduction of greenhouse gases (CO_2 conversion to value-added chemicals) is also of great interest. A key challenge that must be addressed to boost commercialization of solar energy technologies, and common to these applications, is material properties and solar energy utilization efficiency. To realize large-scale and efficient solar energy utilization, application-based materials with a unique combination of properties have to be developed. The material has to absorb visible light and be cost competitive, composed of earth-abundant elements, and nontoxic, all at the same time.

This chapter consists of ten sections. The first introduction section consists of a detailed discussion on the importance of energy in human activity, the effects of fossil fuels on climate and human lifestyle, and materials that meet many of the above criteria. The second section provides a short and critical comparison of solar energy with other alternatives. The third section provides a quick review of the basic concepts of solar energy. The commonly employed toolkits used in the characterization of materials for solar energy conversion are discussed in section "Toolkit for Characterization of Photoactive Materials (PMs).". Some of these tools can be used to evaluate specific optical, electronic, and catalytic properties of materials. Section five discusses the main categories of materials that are either commercialized or under development. The challenges to developing new materials for solar energy conversion are addressed in section "Materials for Solar Energy Utilization". Section "Integrating Tested Concepts of Solar Energy Utilization to Produce Fuels in an Effective Way" outlines some of the main strategies to test the promising materials before a large-scale commercialization attempt is initiated. Section "Commercial Ventures" profiles companies and institutions that are engaged in efforts to evaluate, improve, and commercialize solar energy technologies. This segment provides information about the product from a few representative companies around the world and their niche in the commercial market. Section "Future Work" provides a general outlook into the trend in solar energy utilization, commercialization, and its future. Finally, section "Conclusion" provides the authors' concluding perspective about the solar energy as a pathway for reducing our dependence on fossil fuels. At the conclusion of this chapter, we have also provided over 100 references that are highly recommended for further in-depth study into various aspects of solar energy.

Introduction

Importance of Energy in Human History

Energy has been one of the basic requirements for human activity and has played a pivotal role in human history. Research has been undertaken that correlates the increased availability of energy within a society to its citizens to an increase in the standard of living conditions. The nineteenth century saw the ushering of a technology revolution, a period in time that contributed to a significant improvement in the quality of human life while witnessing an increasing demand for energy in order to maintain these improved standard living conditions. Fossil fuels were critical to the industrial revolution that accompanied technological development during this era. The latter twentieth century saw a rapid increase in the demand for various other forms of energy in different parts of the world. Moreover, it is anticipated that this voracious demand for energy will only increase in the foreseeable future as many more countries of the world strive to improve quality of life for their citizenry (Hultman 2007; Weiss et al. 2009; Rotmans and Swart 1990).

Table 1 2003 US energy consumption

Source	Amount	QBtu	Percent
Coal	1.08×10^9 t	22.6	23.0
Natural gas	21.8×10^{12} ft^3	22.5	22.9
Petroleum	6.72×10^9 bbl	39.1	39.8
Nuclear	757×10^9 kWh	7.97	8.1
Renewable	578×10^9 kWh	6.15	6.3
Total		98.3	100

Present Sources of Large-Scale Energy

The US Department of Energy's 2003 Annual Energy Report divides US energy usage into four main categories with a percentage of the total US 98.3 QBtu/year usage: residential usage (21.23 %), commercial (17.55 %), industrial (32.52 %), and transportation (26.86 %). This same report then proceeds to break down the 2003 US energy consumption which is shown in Table 1.

As is evident from Table 1, fossil fuels (coal, petroleum, and natural gas) make up 85.7 % of the US energy consumption, making them the first and by far the predominantly used sources (Danielsen 1978). The reason for a predominantly fossil-fuel-based economy is that (1) the technologies and infrastructure using fossil-based fuels have been well developed over several decades and (2) the comparatively lower cost of fossil fuels in relation to other types of energy sources.

The next highest US energy consumption after the fossil fuel is nuclear energy. Nuclear energy has been extensively exploited as an energy source in several developed countries as an alternate to fossil fuels and is a promising eco-friendly energy source for large-scale applications (Lenzen 2008; Germogenova 2002). However, nuclear energy has a high capital cost, vulnerability to man-made disruption, and the potential to be used for destructive purposes. Furthermore, a tremendous challenge lies in changing negative public perception about nuclear technology, stemming from perceived danger due to prior unfortunate nuclear-related incidents in Chernobyl, USSR, and Three Mile Island, USA. It is to be noted that the trend in the United States' energy consumption has been reflected in several developed countries as well.

Issues with Large-Scale Usage of Fossil Fuels

In spite of the availability of several energy sources for large-scale usage, fossil fuels have been one of the most cost competitive, easily accessible, widely available, and therefore a more attractive option. It continues to be the primary form of cheap energy source in many countries with wide-ranging economic portfolios. However, with the continued use of fossil fuels coupled with a demand, their detrimental impact on climate and environment has forced us to reexamine the viability of relying further on this form of energy as mankind's primary resource for the future. Speculated major concerns are climate change, health hazards, and potential for

Table 2 Issues with continued reliance on fossil fuels as a primary resource for mankind's energy needs

Problem areas for fossil fuels	Specifics	Description
Climate change issues	Global warming	Emission of greenhouse gases such as CO_2 traps solar heat which raises atmospheric temperature
	Sea level rise	Rise in sea levels due to global warming can lead to flooding of low-lying areas
	Alternation of weather pattern resulting from temperature change	Draughts, floods, hurricanes, and tornados can critically impair local/regional economic activities such as agriculture and even lead to displacement of the population
Health hazard	Tailpipe/stack emissions	SO_x, NO_x, and particulates in emissions can reduce air quality by promoting smog formation which may lead to health hazards such as lung cancer
Economic risks	Unsteady supply of increasingly finite resources	Increasing demand for finite resources can lead to spiraling prices (price fluctuations) that can hurt or even stunt economic growth
Others	Geopolitical instability	Extreme reliance on very few sources where political situation can become unfavorable
	Man-made disruption	Disruption of stable supply of energy due to activities such as terrorism
	Land destruction	Environmental impact on local animal and plant life

economic chaos. The details of some leading concerns regarding continued dependence on fossil fuel as a primary resource are listed in Table 2.

Need for an Alternate Energy Focus

A closer look at other alternatives to meet mankind's demand for energy is urgently needed. The reasons cited in Table 2 highlight the need for a serious reexamination of mankind's approach to identifying, researching, and implementing possible options of energy resources. The key criteria for choosing an alternative energy form are: (a) sustainability, (b) eco-friendliness, (c) availability, (d) cost (capital and operating), (e) political will to change status quo by modifying governmental public policies, (f) population support, (g) technological reliability, and (h) safety aspects. It has to be first understood that no single form of energy can offset fossil-fuel usage completely and continue to meet the rising demands globally. It is also perhaps a smart decision to avoid focusing on just one form of alternate energy, but explore a diversified energy portfolio. It is generally agreed that an energy portfolio containing a mix of various forms of non-fossil-based alternative ranked using the above criteria should be tailored based on region- or country-specific needs.

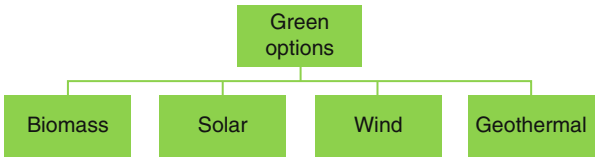

Scheme 1 Green energy options that have potential to meet global energy needs

Options Available to Us

There are several non-fossil-fuel-based alternatives that have been examined as possible energy sources (Tester et al. 2005). The United States and Europe are leading the effort in examining the induction of non-fossil alternatives into mainstream energy sector. However, there is still a long way to go in this direction. For example, current US consumption of renewable energy forms – wind, biomass, geothermal, and solar – is 6.3 %, a very small fraction of the total 98.3 QBtu of energy used by the United States. Some of the pros and cons of these green alternatives are discussed next.

Wind Energy

Wind power is broadly defined as the conversion of wind energy into a useful form of energy-utilizing machinery such as sailing vessels, windmills, and wind turbines (Scheme 1). Wind energy shows promise as a replacement for fossil fuels as an energy source; theoretical estimates indicate that global output from wind can be the equivalent of ~5,800 quads of energy per year (AWEA 2010) (1 quad = 172 million barrels of oil =425 million tons of coal). Moreover, wind power has certain advantages over other renewable forms of energy such as solar energy, for the wind can blow day and night, sunny or cloudy, and often is strongest during dark, overcast winter storms when energy is needed for heating and getting solar energy is not possible.

However, wind power also has its limitations. Many devices that convert wind energy need specific wind velocities to work efficiently, and as a result, these specific wind velocities are often location specific, limiting the areas in which wind energy conversion devices can be used. Furthermore, contentious issues such as potential harm to endangered birds due to the rotating blades, noise concerns, health concerns, and the effects on aesthetics of the landscape due to the presence of several hundred windmills in a farm need to be resolved. Countries such as the United States (Knoll and Klink 2009) and England (Price et al. 1996) are seriously considering or have projects underway to harvest wind energy. The data from such case study locations should be carefully examined and appropriate changes have to be made to address the aforementioned concerns to exploit wind energy on a larger scale.

Biomass Energy

Biomass is a renewable energy source because the energy it contains comes from the sun. Plants capture the sun's energy via the process of photosynthesis. Photosynthesis converts carbon dioxide from the air and water from the ground into

carbohydrates, complex compounds composed of carbon, hydrogen, and oxygen. Later when these carbohydrates are combusted, fermented, or gasified for energy utilization, they turn back into carbon dioxide and water and release the sun's energy that they contain. Through this cyclic process, biomass functions as a sort of natural and potentially infinite battery for storing solar energy. Depending on the biomass source and method used for releasing the captured energy, biomass energy can have the potential to supply 79 QBtu of energy (this is 80 % of the US energy consumption). However, in order to reach this output, the current 350×10^6 acres of land being harvested in the United States would have to be used solely for biomass production. This leads to the main disadvantage of biomass – the land needed to produce the biomass often leads to competition with land for food, destruction of forests, and with some biomass technologies, such as ethanol, food crops are used directly (Sanderson 2007). However, biomass from solid maniple waste and new research investigating biomass produced from nontraditional sources such as coffee waste or algae-based biofuel production possibly positively influence technological and commercial advances within this field (Oliveira et al. 2008; Kondamudi et al. 2008).

Geothermal Power

Geothermal power utilizes the continuous flow of heat energy from the hot interior of the earth to its surface, by means of space heating and the generation of electricity. Unlike fossil fuels, biomass, wind, and solar, geothermal has the capacity to sustain itself in a continuous closed-loop system using heat from the earth's crust.

Moreover, the world's geothermal energy reserve is recorded at 10^8 QBtu, a million times the total yearly US energy consumption. Unfortunately, current geothermal energy is limited by locations where natural reserves occur and the heat energy can be tapped in a commercially viable manner; however, there are new technologies being researched, such as the Normal Geothermal Gradient and Hot Dry Rock technologies, which would expand geothermal usage tremendously.

Solar Power

It is to be noted that solar energy can be considered as the indirect source for wind (solar-driven temperature changes cause wind movement) and biomass (chlorophyll pigments absorbing sunlight to grow plants/biomass). However, we do not focus on that aspect often when we talk about solar power. Solar power harnesses the radiant light and heat given off by the sun and is unquestionably the most universally available and least utilized form of renewable energy resource. It is estimated that the earth receives 162,000 TW of energy from the sun (Ginley et al. 2008). If one assumes that earth has a land mass of approximately 20 %, the fraction of energy reaching land is ~32,400 TW, a fraction of the world's yearly energy consumption! If it is possible to build systems that can harness this solar energy, it could solve mankind's energy problems. However, the biggest challenge is the development of materials that can economically and efficiently convert solar energy into useful forms at a commercially viable efficiency. This chapter focuses on solar energy

and some of the factors that are pivotal to using solar energy as a resource for meeting global energy needs.

For further details on these topical areas, the readers are referred to four chapters on biomass and one chapter on wind energy in this text.

Solar Energy

The following sections assume that the reader already has a fundamental knowledge of solar energy. For a review of these concepts, there are numerous publications in circulation that cover these fundamentals in greater detail.

What Is Solar Energy?

Solar radiation consists of light of different wavelengths (energy). The energy associated with each wavelength can be estimated using the equation $E = h\frac{c}{\lambda}$, where E = energy (eV), h = Planck's constant (6.6×10^{-34} J s), λ = wavelength of light (nm), and c = velocity of light (3×10^{8} m/s). As the wavelength of light increases, the energy associated with that wavelength decreases. Solar energy received at the surface of the earth also depends on the location (zenith angle) and effects of atmospheric interference (pollution or turbidity). In general, the irradiance at the surface reduces toward the poles and increases with atmospheric pollution. The solar spectrum can be divided into several regions. These include far-UV (<200 nm), UV (200–400 nm), visible (400–700 nm), infrared (700–1,400 nm), and far-infrared (>1,400 nm). The distribution of energy associated with sunlight can be identified to different regions and may be approximated as UV <5 %, visible ~40–50 %, and the rest being infrared. The heat associated with the solar energy can be attributed to the infrared part of the solar spectrum. Photoactive materials involved in solar energy conversion respond to the irradiation by absorbing solar energy and undergoing electronic and/or chemical transformations. The primary step is a process of generating oppositely charged species called excitons or electrons and holes (Bahnemann 2004; Mills et al. 1993). A secondary process may involve production of electricity (flow of electrons) or initiation of chemical reactions that result in product(s) that have energy applications.

Advantages/Disadvantages of Solar Energy

Just as the other forms of energy resources have advantages and limitations, solar energy has its own set of benefits as well as drawbacks. These points are compared in Table 3.

Table 3 Advantages and disadvantages of solar energy

Advantages	Disadvantages
1. Universally available, infinite energy source, and free. Complementary technologies ensure continuous availability	Large area required to produce sizeable power (may not be possible to harvest solar energy in densely populated areas)
2. Clean eco-friendly, very low maintenance, supports local economy "*green jobs*," and does not contribute to global warming	Some materials used currently in solar energy conversion can be expensive and toxic and may require carefully planned disposal protocols
3. Sustainable and free of geopolitical instabilities. No security issues	Weather patterns can be a source of unpredictable interference
4. Political support and incentives to switch to solar energy systems are favored in many countries	Public awareness about incentives (rebates) and education is still low and needs a significant boost
5. Solar energy usages range from food processing (solar cookers) to large-scale electricity generation	Solar conversion efficiencies in most applications are low. Efficiency improvement via materials development is a key challenge

Applications of Solar Energy

Traditionally, the most common forms of solar energy usage have been harvesting the heat associated with the solar radiation, which is later utilized in applications such as cooking, space heating, and drying. Many of these applications have undergone technical refinement over time leading to cost competitive, efficient, and wide-scale usage. A brief discussion on some of these applications is presented in section "Principles of Solar Energy Utilization." Figure 1 shows the breadth of applications that employ various aspects of solar power. Since the 1900s, efforts to use solar energy for energy generation involved focusing on the direct production of electricity, liquid, and gaseous fuels utilizing solar energy. Of particular interest, and also a great challenge, is using solar energy to sequester CO_2 for producing value-added products such as fuels and control its emissions into the environment at the same time. The objective is to address two of mankind's fundamental challenges: provide sustainable energy and reduce impact on climate. Due to the criticality of these challenges, CO_2 control using solar energy is an emerging area of research.

From an environmental perspective, the applications of solar energy in waste treatment cannot be ignored. Photocatalytic degradation of a wide variety of gas-phase and liquid-phase pollutants assists in keeping the atmosphere and water bodies clean. This process involves the destruction of potentially toxic materials through a series of steps into relatively benign intermediates and later into CO_2 and water. Depending on the nature of the pollutant(s), the application of solar energy for environmental protection can therefore be a simple and cost-effective method to treat recalcitrant materials. A limited discussion of this aspect of solar energy utilization is provided later (sections "CO_2 Conversion," "Example 1: Integrated Organic Waste Treatment and Fuel Cell System," and "Example 3: Bioprocesses to Convert Waste to Energy Using Algae").

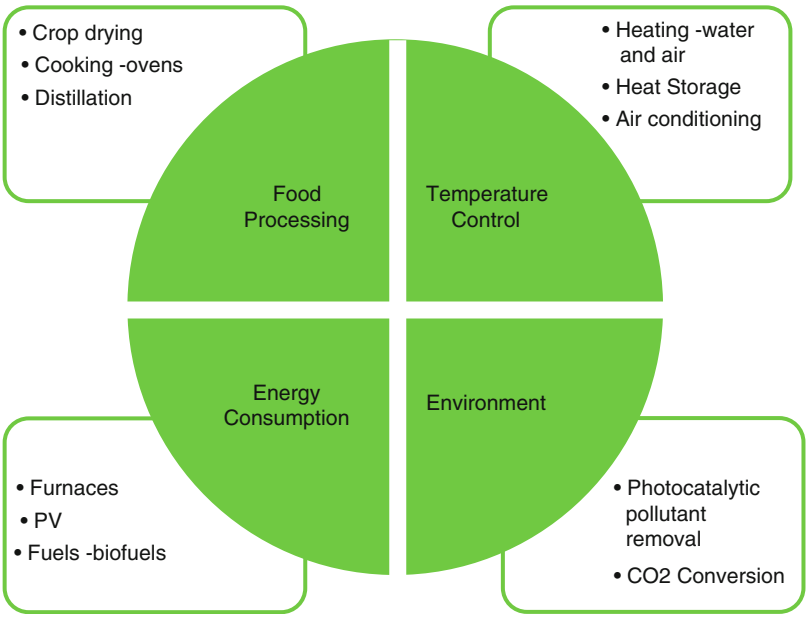

Fig. 1 Solar energy can be utilized in a wide range of applications from processing of agricultural precuts to energy generation to environmental remediation

Principles of Solar Energy Utilization

This section discusses the principles of solar energy utilization in commonly used applications such as water purification, residential heating, food processing, biofuel production, photovoltaics, water splitting, and CO_2 conversion to hydrocarbons.

Space and Water Heating

Space heating is often used in residential and commercial areas (Bezdek et al. 1979; Sakai et al. 1976; Kulkarni et al. 2007; Kalogirou 2009; García-Valladares et al. 2008; Han et al. 2010). The process involves utilizing heat from the sun in order to provide comfortable living conditions in an eco-friendly manner. Space heating involves careful planning of the design of structures based on the orientation of the sun. The differences in the densities of warm and cold air are exploited to cause an artificially induced circulation in a confined space. The roof can be slanting or flat and made of partially transparent glass, permitting natural illumination. The principle design of one form of a well-designed space heating system, including the general steps involved, is schematically illustrated in Fig. 2a. A slight variation of this concept can also be used in heating water. A typical setup may include off-the-

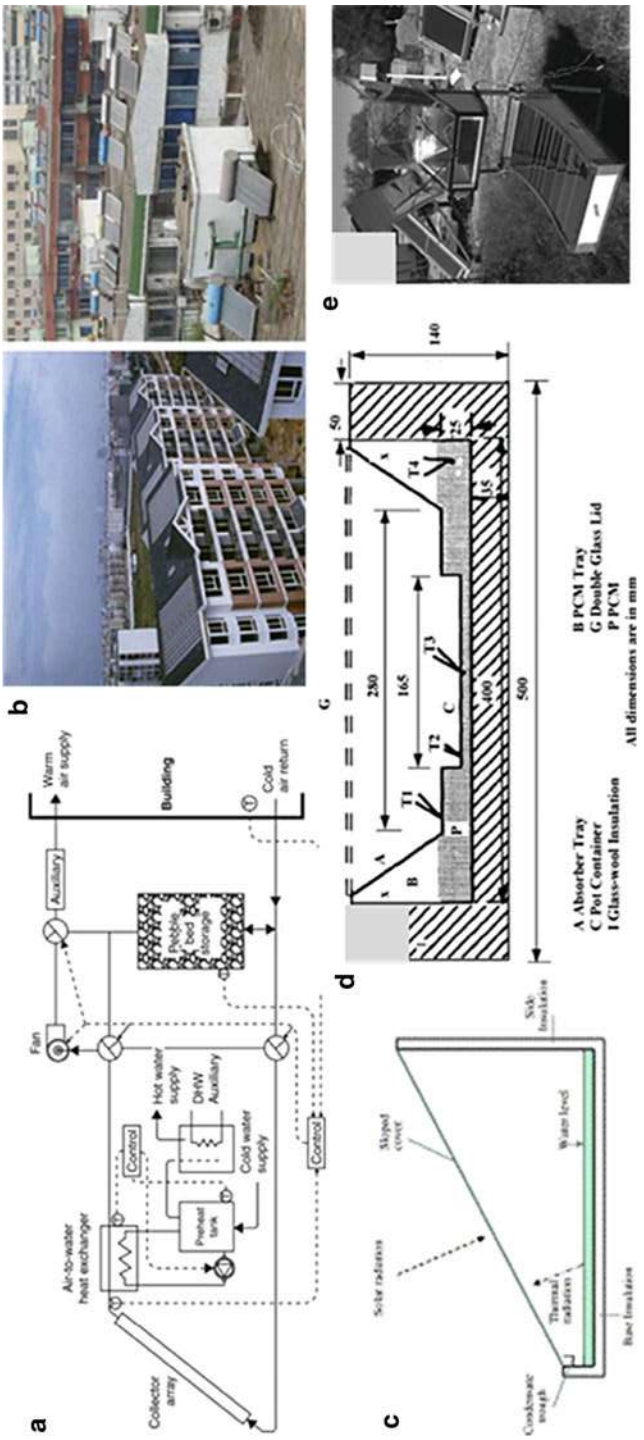

Fig. 2 The use of solar energy in several applications has been studied extensively. Here are some examples where solar energy is utilized in (**a**) large-scale and (**b**) small-scale portable water heater, (**c**) solar still, and (**d**, **e**) solar cooker. Refer to section "Principles of Solar Energy Utilization" for details (Reprinted with permission from Elsevier)

shelf metallic heat-conducting tubes that carry water through a blackened enclosure exposed on one side to solar radiation. This produces water fit for domestic use. Figure 2b shows the pictures of solar water heating apparatus on the roofs of buildings in China. Benefits of employing such eco-friendly approaches may include significant cost savings in utility bills, reduced illumination costs, reduced dependence on fossil-based fuels, and protected earth's climate by minimization of carbon footprint.

Water Purification Using Solar Stills

Solar stills (or solar distillation) are used for producing portable water from impure and/or scarce water resources (Kaushal and Varun 2010; Tiwari et al. 1996, 2003; Khalifa and Hamood 2009). A solar still can be used in places with little or no infrastructure such as deserts, regions with mines that have potential ground water contamination, in areas that have frequent disruptions in utilities (power and water supply), and as an emergency survival kit. The principle of operation of a solar still is shown in Fig. 2c. Heat energy from the sun facilitates evaporation followed by condensation of water. The still consists of a lower darkened region with a transparent cover (glass or polymer) placed at an inclination that allows solar radiation to pass through. The bottom of the still often houses the impure water and can be maintained dark if needed to maximize absorption of heat from the sun. The source of this water can be groundwater, industrial effluents, agricultural runoffs, wastes from poultry/diary, or other sources. The absorbed heat is transferred to the water which evaporates and then condenses on the inner side of the cover. The condensate trickles down along the slope of the cover and collects in a separate reservoir, providing water fit for consumption. Since water has to be boiled to kill microorganisms such as bacteria, a solar still may not be able to do this effectively as boiling is not always achieved at the still operating temperatures. One can fabricate a crude still using materials such as transparent plastic, a water-resistant darkened polystyrene sheet, and stones.

Food Processing

Solar energy can be used in cooking, drying of organic matter, and in the elimination of pests that threaten crops (Sharma et al. 2009a, b; Tiwari et al. 1994; Harmim et al. 2008). Solar cookers are the simplest form of food processing equipment. The concept is similar to a solar still or solar water heater. Incident as well as reflected sunlight is absorbed by a dark vessel that contains the food material that has to be cooked. A simple solar cooker can be made of a wooden box, with a glass wool liner and aluminum reflector sheets. A schematic representation of a solar cooker is shown in Fig. 2d. Figure 2e shows a photograph of a household solar cooker. Solar cookers can be especially effective in countries along the equator since they receive significant amounts of solar radiation for a better part of the day peaking right around the

midday periods. Therefore, solar radiation can be easily used to cook a midday lunch in a reasonable time. Larger area solar dryers consist of wooden boxes with ventilation holes in the sides. These holes assist in air circulation. Dry air carries the moisture generated from the organic matter outside. The top of the box is covered with glass or flexible polymeric materials at a latitude-based angle to allow maximum sunlight. These boxes can be used to dry organic matter: fruits, vegetables, or fish.

Solar-Assisted Biofuel Production

Fuels obtained from a biological source such as an organic matter (plants and waste matter) are called biofuels: (Hou and Zheng 2009; Vorayos et al. 2006; De Falco et al. 2009) vegetable oil (biodiesel), bioalcohols (ethanol), and biogas (methane) are common examples (Hou and Zheng 2009; Vorayos et al. 2006; De Falco et al. 2009; Peterson and Hustrulid 1998). The principles involved in the production of these biofuels vary vastly depending on the type of approach used for the biofuel production. However, common to all these processes is the (1) cyclic nature of CO_2 from the sunlight being utilized by a plant to the utilization of this stored energy and (2) the requirement that a catalyst drives this reaction. Figure 3 illustrates the different types of catalyst-driven reactions. Among the four pathways shown in Fig. 3, pathways I and II are benefited due to solar energy usage in the left side. Solar energy is absorbed by catalysts such as chlorophyll to form chemical energy in vegetables and plants. This in turn can be converted using appropriate catalysts to biodiesel and/or ethanol. The carbon cycle for an energy crop produced from the rape plant is shown in Fig. 4a. Solar energy is utilized in pathways III and IV to drive products in the right side. Path III utilizes microorganisms such as algae which drive the photoconversion of CO_2 to value-added fuels. In pathway IV, redox chemistry at the photocatalyst surface is central to the conversion of CO_2 to value-added chemicals. The development of biofuels using solar energy is very promising, and this approach to solar energy conversion can be a major player in the energy mix for the future.

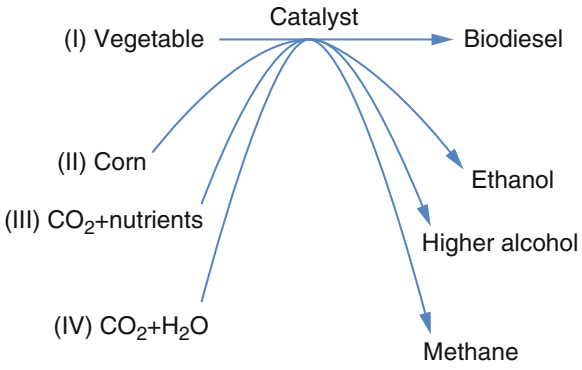

Fig. 3 The production of biofuels can be carried out using different raw materials in the presence of a catalyst

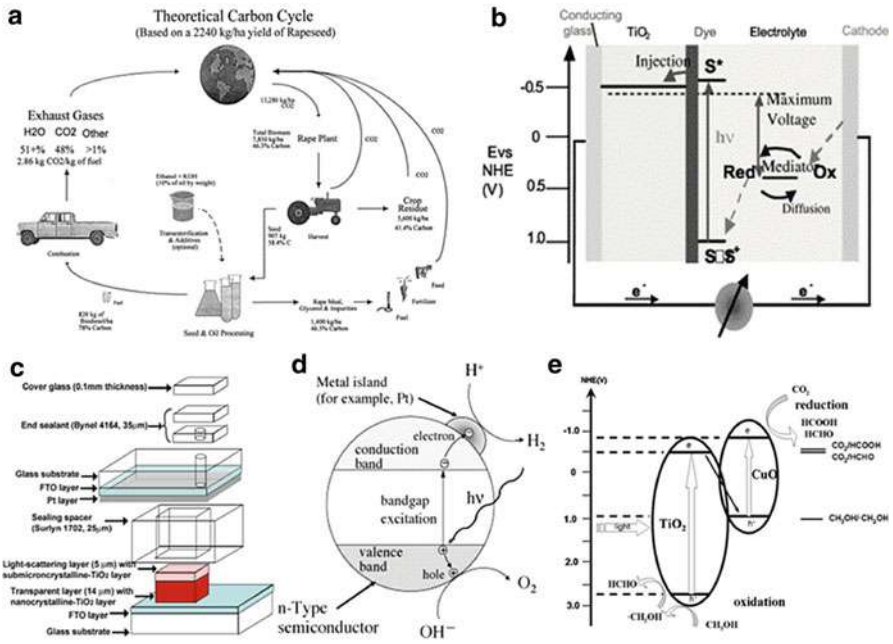

Fig. 4 (**a**) Schematic of the steps involved in biofuel cycle, (**b**) the process of solar energy conversion to electricity using a PV device, (**c**) the exploded view of a dye-sensitized solar cell, (**d**) mechanism of redox processes in a photocatalyst, and (**e**) CO_2 photocatalytic reduction using solar energy over a semiconductor oxide photocatalyst (Reprinted with permission from Elsevier)

Solar Photovoltaics (PV)

A photovoltaic device converts solar energy to electricity through two main steps: the energy from the solar radiation is absorbed by the photoactive material(s) to produce excited electrons, and these electrons then tunnel through the material to the external circuit to generate a photocurrent (Bube 1990; Server 2010; Takeda et al. 2009; Landi et al. 2005; Ito et al. 2008). Figure 4b shows the operating principle of a solar cell based on a combination of an inorganic material called titanium dioxide (TiO_2) and a visible light-absorbing dye. Figure 4c shows the parts of a dye-sensitized solar cell. In this system, electron–hole pairs are generated due to the light absorbed by the dye, and it tunnels though an underlying TiO_2 layer to a collecting conducting glass substrate. An electrolyte is present between the anode (conducting glass) and the cathode of a PV device. The role of the electrolyte is to function as a redox couple and facilitate replenishing of the charges at the photoanode. Composite systems are often used to (1) improve light absorbance, (2) promote charge separation, and (3) increase the overall performance efficiency of the solar cell. Tandem cells, inorganic composite-based solar cells, and dye-sensitized solar cells are some examples of popular photovoltaic devices. An ideal solar cell is one which is able to absorb most of the solar radiation (usable parts

of the solar radiation are ultraviolet, visible, and infrared) and generate electricity with a high level of solar-to-electric power conversion efficiency (η). Investments in the area of solar photovoltaics have been growing at an incredible rate in the last decade (REN21-Secretariat 2010). Improvement in technology, low material and processing costs, and political incentives have been identified as the major factors contributing to solar PV growth in developed as well as developing countries.

Photocatalytic Oxidative (Water Splitting) and Reductive (CO_2 → Fuel) Reactions

Solar energy can be used to drive different types of chemical reactions yielding many value-added products (Kudo and Miseki 2009; Aroutiounian et al. 2005; Matsuoka et al. 2007; Teramura et al. 2010; Anpo et al. 1995; Qin et al. 2011). Water splitting, CO_2 control, and environmental remediation are popular examples of such solar-driven reactions. The principle behind these different reactions is essentially the same. In a photocatalyst surface, both oxidative (electron liberating) and reductive (electron gaining) reactions can occur simultaneously as shown in Fig. 4d. In either type, the photocatalyst driving the reaction has to straddle the reaction of interest if it were to be performed without the application of an external electric field or bias. In photooxidative reactions such as water splitting and environmental remediation using oxidation, hole or hydroxyl radicals generated at the valence band of the semiconductor are often the main participating agents. Photocatalytic water splitting involves the hydrogen formation at the cathode and oxygen formation at the anode. Reduction reactions are performed by the electrons at the conduction band. Examples of reductive reactions include CO_2 reduction to hydrocarbons such as methane, methanol, or methyl formate (Fig. 4e) and reductive precipitation of toxic heavy metals such as mercury and cadmium from waste streams. For a detailed discussion on the mechanistic aspects of the redox reactions on a photocatalyst surface, readers are referred to a few representative reviews in the literature (Bahnemann 2004; Mills et al. 1993; Hoffmann et al. 1995; Linsebigler et al. 1995; Fujishima et al. 2000; Gogate and Pandit 2004; Mor et al. 2006; Rajeshwar et al. 2001).

Toolkit for Characterization of Photoactive Materials (PMs)

Photoactive materials or PMs for solar-to-energy conversion can be simple (consisting of one element or compound) or complex (consisting of several materials in the form of a composite). Often, synthesis procedures for complex PMs employ preformed materials as building blocks. To improve the performance of the PMs, one has to examine surface, optical, electronic, and catalytic properties of the material (s) as they start to take the desired shape or form. There are several tools that can be employed to evaluate material properties at various stages of synthesis. Some of these stages include formation, phase transformation, growth, photoactivity before and after integration with other materials, and performance after the entire device has

Table 4 Optical, surface, and electrochemical measurements that can be performed to determine the properties of photoactive materials

Category	Instrument	Purpose
Optical	Spectrometer	UV–vis absorption
	FT IR	Interaction with other materials (composite formation), synthesis progress
Surface	SEM, TEM, HRTEM	Surface morphology (shape, size, aspect ratio), crystallinity, size distribution
	BET	Surface area
	TGA-DSC	Thermal stability, phase transition properties
	XRD	Crystallinity, compound formation
	AFM	Surface properties (morphology, roughness) of films
Electronic	V_{OC}, I/t, V/t, I/V	Photoelectrochemical properties (of interest in, e.g., PV, photoelectrocatalytic water splitting), Mott–Schottky, band edges
	Incident photon to current efficiency	Effectiveness of materials to convert solar to electric energy

been fabricated. Table 4 is a list of some common tools used to evaluate material performance. A detailed description of some of these tools is also provided below. (Note: For brevity, only commonly used tools representing each of the three categories below are discussed.)

FT IR Fourier transform infrared spectrometer, *SEM* scanning electron microscope, *HR(TEM)* high-resolution (transmission electron microscope), *TGA-DSC* thermogravimetric analyzer-differential scanning calorimeter, *XRD* X-ray diffraction, *AFM* atomic force microscope, V_{oc} open circuit potential, *I/t* current–time, *V/t* voltage–time, *I/V* current–voltage

Photoelectrochemical Measurements

PMs produce charge carriers such as electrons and holes on photoillumination. These charge carriers are the basis of any activity involving the PMs. A knowledge of electron–hole transport in photoelectrochemical systems is critical to designing nanostructured materials (especially composites) with high efficiency. Factors that may contribute to altering this efficiency of charge generation are the composition of the nanostructure, film thickness (if it is a film), light intensity, electrolyte, and its concentration. An essential requirement in a photoactive system is the need to maximize the separation between the photogenerated charges. Careful consideration of other aspects such as mode of illumination (front and back faces for films), which depends on the film thickness, decides the extent of light conversion. Photoelectrochemical techniques provide the necessary means for the evaluation of a nanostructured photoactive composite to maximize light energy conversion and its application in energy production. In the case of films, the commonly used setup

for the electrochemical measurements involves a light source (solar simulator), appropriate filters to control light intensity and wavelength, and a cell consisting of three electrodes. The PM to be analyzed is deposited as a film on a conducting medium and is called the working electrode. It is flanked with a reference and counter-electrode. The activity of the PM can be determined in the presence of white light and/or light of different wavelengths. Electrochemical measurements typically involve the estimation of the open circuit potential (V_{oc}), current–voltage characteristics (cyclic voltammetry), and the estimation of efficiency. These measurements can provide information on the effectiveness of the photoelectrode to perform solar-to-electric power conversion, water splitting, or fuel production (CO_2 to value-added chemical). Efficiency is calculated in the form of incident photon to current conversion efficiency (IPCE). IPCE and other optical tools can provide information about what material is contributing to photoactivity and which region of the solar spectrum is effectively utilized. Further details of these types of analysis and the features of the plots obtained in these measurements are discussed in an earlier work (Subramanian 2007).

Spectroscopy

Spectroscopy chiefly involves absorption and fluorescence measurements (Lakowicz 2006; Workman 1998). Most of the materials participating in solar-assisted energy production can include metals, semiconductors, insulators, polymers, organic dyes, and composites of materials from these groups. These materials can exhibit absorption to varying degrees and in different regions of the light spectrum. Absorption spectroscopy is therefore an invaluable tool to probe the optical properties of the photoactive material. In the nanometer size, materials demonstrate interesting optical properties. For example, noble metals exhibit unique properties due to the development of plasmon band. Semiconductors exhibit size-dependent optoelectronic properties called quantization effect. While most of the materials exhibit absorbance, a few materials demonstrate fluorescence. Fluorescence involves energy liberated by a photoactive system when charge/energy exchange between a material and surroundings leads to the material transitioning to a steady base (unexcited state). If a material is fluorescent, conventionally both fluorescence and absorption spectroscopy is used. The layout of a fluorescence measurement system is shown in Scheme 2. Typically, the material absorbs light of a higher energy, and the emission from the material, usually of lower energy, is probed at an angle of 90° to the incident beam. Complementary usage of fluorescence and absorption for probing interactions in composites (such as TiO_2–Au) is generally applied for photoactive materials and enables a deeper understanding of the interactions in the composite. Charge transfer processes, ground and excited state interactions' bonding, and complexations between interacting molecules are some of the aspects studied using these optical techniques.

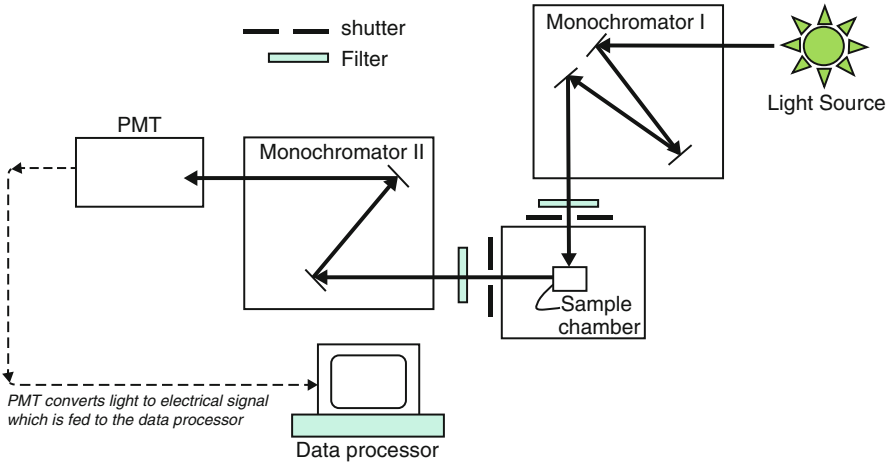

Scheme 2 Simplified layout of a general spectrofluorometer

Transient Studies

Several composites can display interactions in the sub-second time domain. These interactions usually take place by charge and energy transfer and could be in the order of micro-, nano-, pico-, and femtosecond time domains. A flash photolysis study which is primarily carried out to elucidate this mechanism involves an elaborate setup consisting of an array of optics (lens, filters, photomultipliers, and monochromators) and a light source. While the source is a laser beam of known wavelength which initiates the materials in the composite to excited state, a probe beam (usually from a xenon lamp) is used to investigate the changes due to the incident monochromatic light. Scheme 3 shows a typical laser flash photolysis setup. Transient study plots are designated as difference absorption spectra (Kamat et al. 2002; Bahnemann et al. 1997) and help one to shed light on the dynamics occurring in the sub-second timescales. Pulse radiolysis (for steady state one can use γ-radiolysis) is employed to observe the effect of highly reactive species such as hydroxyl radicals and aqueous electrons on a composite system. Bombardment of water with high-energy ionizing radiation produces reductive and oxidizing species as shown below.

$$H_2O \rightarrow e_{aq}^{-} H^{\bullet}, H^{\bullet}, H_2, H_2O_2, H_3O^{+}, OH^{-}$$

Reactivity of a certain radical with the semiconductor–metal composite can be observed by selectively scavenging out other radicals from the system using different agents.

The above section provides an overview of different techniques that can be used to determine the photoelectrochemical properties of materials. Several of these techniques can be performed by a reasonably well-trained student. These techniques can be used as a screening step to determine the use of a material for a certain application.

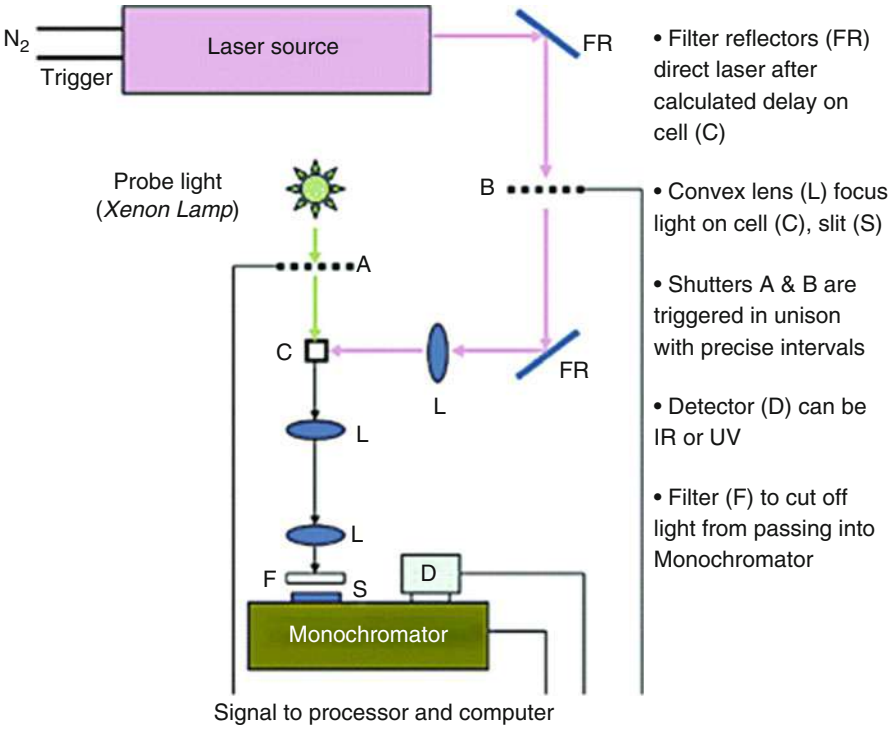

Scheme 3 Schematic of the laser flash photolysis setup for probing charge transport dynamics in the sub-second timescale using a nitrogen excitation laser (337 nm)

Materials for Solar Energy Utilization

Photoactive compounds or composites have to pass a set of very stringent criteria to qualify as a material for solar energy utilization. This section discusses some of these criteria. A brief overview of the methods that can be used for the synthesis of photoactive materials and device fabrication is discussed. This is followed by a summary of the state of various popular photoactive materials and their limitations. The materials used in PV, water splitting, and CO_2 conversion applications are discussed in detail toward the end of this section.

What Is the Holy Grail in Photocatalysis?

The properties that one has to look for in materials for photocatalytic applications include: solar response, availability, toxicity, processability, compatibility, stability, cost, and recyclability. Specific details of these aspects are listed below:

- Response to wide range of wavelengths in solar radiation (ability to effectively utilize maximum parts of the solar spectrum).
- Availability (large supply of materials).
- Process ability (amenable to large processing techniques and preferably cost-effective).
- Absence of any toxic effects (preference is minimally environmental and/or health hazard).
- Compatibility (flexibility to couple with other materials with the intent to improve optical, electronic, and/or catalytic properties).
- Stability (providing consistent performance without significant deterioration over time).
- Cost competitive (this is directly related to availability).

These are the major criteria that a material must fulfill to be considered as a promising candidate in photocatalysis.

It is not possible to rank all known materials based on all these aspects. In this work, the authors have therefore focused on a select few materials based on applications and which meet several of the aforementioned selection criteria.

Review of Synthesis Procedures for Photocatalysts

There are several methods that can be used for the synthesis of materials for solar energy conversion. These include wet chemical methods (such as sol–gel and reverse micelle techniques) and chamber-based methods (such as chemical vapor deposition and atomic layer deposition). Wet chemical methods usually involve using precursors of the materials that form the photoactive material, agents that participate in the transformation of the precursor to the desired final product (this may include complexing agents, stabilizers, and initiators). Detailed description of the merits of different wet chemical methods can be found in reviews by several authors (Best and Dunstan 2009; Wang et al. 2009; Cui et al. 2008; Strobel et al. 2006) including one from the authors' group (Kar et al. 2008). Chamber-based methods can be expensive initially due to higher capital cost and the need for possible sophisticated materials handling. In contrast to the wet chain methods, they do not require several agents and can oftentimes lead to a product that is much purer. Anodization and layer-by-layer self-assembly (or successive ionic layer adsorption and reaction – SILAR) process are often used to prepare composite particles using preformed materials as building blocks. They are rather simple, generic protocols customizable to the synthesis of different materials. Oftentimes these methods are used to prepare the anode and/or the cathode of a solar energy harvesting device separately, and then a different method has to be used to integrate these elements to form the device (PV or photoelectrochemical (PEC) cell).

System Integration

The fabricated materials have to be integrated to form a device prior to its application in solar energy conversion. A film-based PEC device is often used in water splitting reactions. A PEC system consists of an anode, cathode, and an electrolyte. The electrolyte is often the source of the fuel (e.g., aqueous solution of an alcohol produces hydrogen by splitting water in the electrolyte). A slurry-based PEC system does not have a clear separation of the anode and cathode since the catalyst acts as a center where both redox activities occur simultaneously, whereas a dye-sensitized solar cell device consists of an anode, cathode, and electrolyte that are clearly separate from one another. On the other hand, a slurry system has no distinct anode–cathode; the particles itself act as PEC, as referred to in Bard's concept (Bard 1979).

Previous Attempts in Materials Development

A list of different materials that can be used as a photocatalyst is provided in section "Materials for Photovoltaics, Water Splitting, and CO_2 Reduction." Titanium dioxide (TiO_2) has been the most popular and extensively studied photocatalyst for its ability to harvest solar energy, and hence it is first discussed here (Zach et al. 2006). It demonstrates good stability over a wide pH range, compatibility with other materials, environmental friendliness, and low cost. Its applications include solar energy conversion (photovoltaics) (Gratzel 1991, 2001) and hydrogen production (by photocatalytic water splitting) (Aroutiounian et al. 2005). However, TiO_2 has some significant limitations. For example, TiO_2, by itself, has high charge recombination rates compared to its combination with other materials such as dyes or semiconductors. TiO_2 alone has very limited light-harvesting ability (it only absorbs UV light) (Ni et al. 2007). Several reviews have discussed the photoactivity of TiO_2 and its composites for different applications (Rajeshwar et al. 2001; Kalyanasundaram and Gratzel 1997; Cheng et al. 2005; Cozzoli et al. 2004; Robel et al. 2006; Frank et al. 2004). The photoactivity of TiO_2 can be significantly improved by dye sensitization (Kalyanasundaram and Gratzel 1997), altering its composition (such as doping) (Cheng et al. 2005; Choi et al. 1994) and/or combining TiO_2 with other materials (Rajeshwar et al. 2001; Cozzoli et al. 2004; Robel et al. 2006). These efforts have been reasonably successful in improving the performance of TiO_2 composites. With respect to photovoltaic applications, the efficiency of light absorbance and improvement in charge separation of TiO_2-based nanocomposites still remain low ($\sim$10–12 %). The limitations of TiO_2-based materials can be attributed to the absence of flexibility for altering the inherent photoactivity of TiO_2 itself (because there is just one cation site (Ti) available for manipulation of electronic properties). In this context, a photoactive material, whose inherent electronic properties can be altered with greater flexibility, is needed.

Silicon-based solar cells are probably the most reliable, with proven high efficiencies ($\eta = 10$–20 %) based on the nature of crystallite size and manufacturing methods (Perezalbuerne and Tyan 1980; Kurtz et al. 2007; Schropp 2004; Kazmerski 2006). However, silicon for high-efficiency applications is becoming increasingly expensive. Complex processing routines also drive manufacturing costs high. Chalcogenide films made of various combinations of Cu, In, Ga, As, Cd, Se, and Te can be tuned to absorb significant visible light and show near optimal photovoltaic performance ($\eta \sim 20$ %) (Goetzberger et al. 2003) but pose toxicity concerns to environment and can require expensive reagents, and processing cost is high (Bube 1990; Dhere et al. 2005). Multijunction devices can produce very high efficiencies (>35 %) (Baur et al. 2007), but one of the issues is the transparency required to activate underlying layers. Photoactive polymers with fullerenes as the electron transport agent are significantly simple to process compared to Si-based devices but are limited in their stability during long-term operations (Cravino 2007; Liang et al. 2008).

Materials for Photovoltaics, Water Splitting, and CO_2 Reduction

The following section provides a list of materials for photovoltaic, water splitting, and CO_2 reduction applications. The selection of materials is based on meeting one or more of the following criteria: cost effectiveness, eco-friendly, and ease of synthesis.

Photovoltaics

Solar cells can be distinguished on the basis of their overall *solar-to-electric* conversion efficiency into several categories. Several reviews have discussed different aspects of PV (Bube 1990; Gratzel 2005; Thomas et al. 1999; Green 2007; Guenes and Sariciftci 2008; Catchpole et al. 2001). Table 5 provides a comparison of the different technologies available today and how these technologies rank with respect to each other. Many of the materials identified here either have been commercialized or offer promise for commercialization due to aspects such as cost competitiveness or eco-friendliness or ease of process ability. In general, all solar cell technologies known today are designed for niche applications and come with advantages and disadvantages. Therefore, the choice of a solar cell technology is usually made based on the type of application and the length of time the cell is expected to be in service. A summary of the advantages and disadvantages of the different types of cells is provided in the following sections. *(Chemical formulas are shown in the table for brevity. Readers are referred to citations for details.)*

Water Splitting

Water splitting can be performed in the presence or absence of sacrificial agents. Based on the approach employed, several reviews have discussed the materials (Kudo and Miseki 2009; Aroutiounian et al. 2005; Best and Dunstan 2009;

Table 5 Materials for photovoltaic applications

Material	Reason	Refs.
CdTe	Low-cost preparation technique, high conductivity, appropriate band gap, recycling methods developed	Oktik (1988), Bosio et al. (2006), Miles et al. (2005)
$CuInSe_2$	Low-cost, non-vacuum preparation technique	Oktik (1988), Kaelin et al. (2004), Eberspacher et al. (2001)
TiO_2	Continuous non-vacuum process by simple printing techniques	Kay and Gratzel (1996)
	Combination rapid thermal process and layer-by-layer spin coating preparation	Tao et al. (2010)
	TiO_2 nanotube array in ionic liquid electrolyte cell	Kuang et al. (2008)
	TiO_2 nanorod assembly	Wei et al. (2006)
a-Si	Low-cost encapsulation method	Kondo et al. (1997)
$CuInS_2$	Low-cost vapor deposition preparation	Hou and Choy (2005)
	Low-cost, non-vacuum preparation technique with solution coating and reduction-sulfurication technique	Todorov et al. (2006)
	Synthesized hollow nanospheres from common inorganic metal salts using surfactant-assisted chemical route	Zhang et al. (2008)
Thin crystalline silicon	Thin-film reduced cost	Catchpole et al. (2001), Shah et al. (2006)
ZnO/Al_2O_3	Cheaper hybrid PV cells	Damonte et al. (2010)
$CuGaInSe_2$	High-efficiency, low-cost thin film	Miles et al. (2005)
Nafion	Charge transport material to be used with ZnO or CdTe	Feng et al. (2009)
$ZnPc/C_{60}$	Organic PV cell, low-cost, experiment with rubrene doping	Taima et al. (2009)
PbSe	Lower-cost, high-efficiency semiconductor material	Hanrath et al. (2009)
Carbon nanotube (w/TiO_2)	Alternative to platinum as a counter-electrode in DSSCs	Muduli et al. (2009), Lee et al. (2009)
P3HT/PCBM	BJH cell that is lightweight, flexible, low-cost production	Honda et al. (2009)
	Preparation by low-cost quick-drying technique, improved efficiency over other techniques	Ouyang and Xia (2009)
FeS_2	P3HT nanowires and $PC_{61}BM$ or $PC_{71}CM$	Xin et al. (2010)
	Lower cost due to abundance and production than silicon and $>$ or $=$ efficiency	Wadia et al. (2009)
FeS and FeS_2	Nanosheet films from reaction of iron foil and sulfur powder, for photocathodes in tandem solar cell with TiO_2 as photoanode	Hu et al. (2008)

Wang et al. 2009; Rajeshwar 2007; Woodhouse and Parkinson 2009). The following segments list some of the popular materials that have been used successfully for water splitting. Properties of the materials are listed in column 2. Oxides, oxide composites, and non-oxides are common materials for driving water splitting reactions. Other materials such as perovskites, sillenites, and pyrochlores are also promising families of compounds that demonstrate water splitting. However, these materials may be difficult to synthesize, and more research has to be performed to determine the applicability of such materials for water splitting reactions (Table 6).

CO_2 Conversion

Due to global environmental concern, the research in utilization of solar energy for CO_2 conversion and/or control is gaining momentum. Several articles (Hinogami et al. 1998; Koci et al. 2009; Li et al. 2008; Wang et al. 2010; Tseng et al. 2004; Wu et al. 2005) have addressed this topic, and readers are directed to these articles for further information. Table 7 lists some of the articles that demonstrate the application of a few leading and representative materials for CO_2 conversion.

Challenges and Limitations to Materials

Mathematical models that consider thermodynamic limits and the near impossibility to convert solar energy to other forms of energy without generating entropy pins the maximum attainable theoretical efficiency of conversion of solar energy at 85 % (Wurfel 2002). Specific to photovoltaics, silicon (Si) solar cells (both single and polycrystalline) have been by far the most studied devices with the greatest market penetration and demonstrate the highest efficiencies (10–25 % for wafers, 4–20 % for modules) (Green 2007; Miles et al. 2007). However, increasing demand for Si, material processing, and device manufacturing costs have led to the opportunity for other non-Si-based technologies to enter the commercial market (Green 2007; Guenes and Sariciftci 2008). Thin-film processing technologies that use amorphous silicon (a-Si) is less expensive if single junction solar cells are of interest. However, single junction a-Si solar cells have low efficiencies (3–4 %), and employing amorphous thin films in a multijunction type cell (e.g., using a-Si and a-Si_xGe_{1-x}) can improve efficiencies up to 6–8 % (Green 2007) and make them commercially viable (Guha and Yang 2006) but again increases cost. Comparative efficiencies of silicon-based and non-silicon-based solar cells are discussed at length in literature (Goetzberger et al. 2003).

Alternate to Si cells are compound semiconductor solar cells; GaAs, InGaP, and copper indium gallium selenides (CIGS) are popular examples that have tremendous commercial potential but are presently limited by processing cost and hence used only in niche areas such as space applications (Bosi and Pelosi 2007). Using these in a multijunction format to boost efficiencies to the order of 6–8 % and possibly reducing processing cost could bring the technology for terrestrial use (application in on-demand and on-site power generation) (Bosi and Pelosi 2007). Alternate concepts on how to overcome efficiency limitations using tandem cells, intermediate band gap

Table 6 Materials for photocatalytic water splitting to produce hydrogen

Material	Properties	Refs.
a-Si	Relatively high conversion efficiency, no catalyst degradation, low-cost hydrogen production	Rocheleau et al. (1998)
	Inexpensive, efficient, and renewable hydrogen source	Kelly and Gibson (2006)
TiO_2	Surface engineering to increase active sites for reaction	Nowotny et al. (2006)
	Carbon-doped TiO_2 increases efficiency of water splitting	Park et al. (2006)
	Nano-size photocatalyst, low-cost, environmentally friendly	Ni et al. (2007)
	Nanostructured photocatalyst to reduce material cost	Hu et al. (2010)
	Nanotube and nanowire arrays for improved efficiency	Shankar et al. (2009)
	Carbon modified n-type TiO_2 photoelectrodes to increase conversion efficiency	(Shaban and Khan 2008)
	Efficient photocatalyst prepared by environmentally friendly microwave-assisted hydrothermal process	Somasundaram et al. (2007)
Si/TiO_2	Si doping improves efficiency, low-cost solar-to-chemical conversion	Takabayashi et al. (2004)
Fe_2O_3	Require smaller overpotential to oxidize water, single solar cell power, lower production costs	Nowotny et al. (2006)
	Ag-Fe_2O_3 nanocomposite photocatalyst as efficient, low-cost PEC	Jang et al. (2009a)
	Doping to improve efficiency	Jang et al. (2009b)
	Thin layer of Fe_2O_3 using nanostructured host scaffold of WO_3	Sivula et al. (2009)
ZnO	Low-cost oxide semiconductor	Aroutiounian et al. (2005)
$SrTiO_3$	Low-cost oxide semiconductor	Aroutiounian et al. (2005)
WO_3	Fe^{3+}/Fe^{2+} redox over WO_3, efficient photocatalyst, low-cost option	Miseki et al. (2010)
	Nanoporous WO_3 for improved efficiency	Guo et al. (2007)
$CuInS_2$	High H_2 evolution in presence Na_2S/Na_2SO_3 as sacrificial electron donors under visible light radiation	Zheng et al. (2009)
Cu_2O	Cheaper synthesis than similar photocatalyst	Ma et al. (2008)
	Cu_2O powders in coupled with WO_3 in suspension had good H_2 evolution	Kawai et al. (1992)
	High absorption efficiency, nontoxic, elements abundant	Somasundaram et al. (2007)

(*continued*)

Table 6 (continued)

Material	Properties	Refs.
In_2O_3	Nitrogen doping shows better photoelectrochemical activity for water splitting than N-doped TiO_2	Reyes-Gil et al. (2007)
SnO_2/α-Fe_2O_3	High purity, low-cost, environmentally friendly production	Niu et al. (2010)
CdS	CdS glass composite to reduce photocorrosion of powder form	Liu et al. (2010)
(CdS/TiO_2)	CdS/TiO_2 nanotubes showed greater efficiency than either material alone	Li et al. (2010)

solar cells, and quantum dot (QD) solar cells as discussed in this review have to be explored (Solanki and Beaucarne 2007). Dye-sensitized solar cells (DSSC) may be a cost-effective option, a significant limitation being dye cost and stability and corrosion of metal components of the cell due to the usage of the popular iodine–iodide-based, charge shuttling electrolyte (Toivola et al. 2009). Recombination of photogenerated charges, mainly due to irregularity in the periodicity of the materials, has to be addressed or the performance of a solar cell improved (Frank et al. 2004).

To improve the application of low-cost, high-efficiency solar cells, low-cost ink technologies need to be developed to make it possible to develop a sort of spray paint methodologies to prepare bulk high-efficiency solar cells (Hillhouse and Beard 2009). International standardization of cost for solar cell fabrication is being developed and tested (Chamberlain 1980). Organic material-based solar cells are relatively new and far from becoming *state-of-the-art* devices. However, they are gaining popularity and there is some market activity with devices offering efficiencies of 4–6 % (Hoppe and Sariciftci 2004). Due to the fact that solar systems are open to the elements and the moving nature of the sun, issues such as tracking to maintain efficiency of the system and protection against dust and minimizing the impact of cloud interference have to be considered for reliable operation of the system. One has to explore the development of new materials and applications for solar energy utilization and minimize the use of environmentally toxic materials such as Cd (Bauer 1993). Other emerging areas such as band gap engineering and multilayered systems (high-efficiency tandem cells) for solar energy utilization have to be examined as well (Khaselev and Turner 1998; Goswami et al. 2004).

Integrating Tested Concepts of Solar Energy Utilization to Produce Fuels in an Effective Way

One method to improve solar energy utilization is to develop "smart and integrated systems" that can perform several solar-driven processes that are complementary in nature. The benefits of such an approach are as follows:

Table 7 Materials for photocatalytic reduction of CO_2

Material	Reason	Refs.
TiO_2	TiO_2 anchored on glass act as active photocatalyst for reduction of CO_2 with H_2O	Anpo (1995)
	Highly dispersed anchored TiO_2 to reduce CO_2 to CH_4, Cu loading increased CH_3OH	Anpo et al. (1995)
	TiO_2 nanoparticles, found 14 nm to be optimum photocatalyst	Koci et al. (2009)
	Simple synthesis methods to form highly active nanocomposite photocatalyst	Li et al. (2008)
	TiO_2 pellets reduced CO_2 in the presence of water vapor under UV irradiation	Tan et al. (2006)
	Cu-loaded TiO_2 increases photoreduction CO_2, shown Cu(I) as primary active site	Tseng et al. (2004)
	Cu–TiO_2 optical fibers transform CO_2 to hydrocarbons at higher efficiencies	Wu et al. (2005)
	Highly dispersed TiO_2 within zeolite cavities for efficient CO_2 reduction	Yamashita et al. (1998)
	TiO_2 on a SnO_2 glass substrate to form bilayer catalyst, high photocatalytic activity	Tada et al. (2000)
	Effect of metal depositing on TiO_2, improved efficiency	Xie et al. (2001)
CdSe	CdSe/Pt/TiO_2 photocatalyst producing high yield of CH_4 with CH_3OH, H_2, and CO as minor products	Wang et al. (2010)
CdS	Effective photocatalytic reduction, increased efficiency with excess Cd^{2+}	Fujiwara et al. (1997)
Ti-Si	Ti-containing silicon thin films higher reduction than powdered photocatalyst	Ikeue et al. (2002)
Titanium silicalite	UV irradiation reduction of CO_2 with H_2 to CH_4, Ti believed to provide active site	Yamagata et al. (1995)
Poly (3-alkylthiophene)	Photocatalyst in the presence of phenol to produce salicylic acid	Kawai et al. (1992)
$BiVO_4$	Photocatalytic ethanol production under visible light	Liu et al. (2009)
$CaFe_2O_4$	Nonpoisonous, cheap, p-type semiconductor with small band gap	Matsumoto et al. (1994)
Ga_2O_3	Photoreduction of CO_2 with H_2 at room temperature and ambient pressure	Teramura et al. (2008)
$InTaO_4$	Common water splitting semiconductor, now tested CO_2 reduction. Reduction potential increased by adding NiO cocatalyst	Pan and Chen (2007)
(K, Na, Li)TaO_3	Photocatalytic reduction of CO_2 to CO in presence of H_2	Teramura et al. (2010)

1. Maximizing solar energy utilization
2. A one-stop system for multiple applications
3. Improved utilization of land (this benefit can be a significant advantage in places with costly real estate and where limited land may be available for solar energy)
4. Potential for improved energy efficiency, reduced ecological impact, and greater benefits for human activity

Three examples are presented below that illustrate these aspects.

Example 1: Integrated Organic Waste Treatment and Fuel Cell System

An interesting concept that combines two traditional applications of photocatalysis, environmental remediation and energy generation, to form a photo-fuel cell device is discussed below (Antoniadou et al. 2010). Photocatalytic degradation of organic environmental waste results in the formation of hydrogen ions which can be tapped to produce hydrogen molecules in order to use them as a clean fuel. The organic "fuel" wastes can be a part of a photoelectrochemical device that is comprised of two electrodes, (1) a photoanode that essentially consists of the photocatalyst where holes oxidize the organics to liberate H^+ ions, (2) a cathode where the ions are reduced to form hydrogen, and (3) an electrolyte consisting of water, organics, and some salt (essential for ionic conductivity). A schematic of the setup and a prototype of the device are shown in Fig. 5; TiO_2 coated on a fluorine-doped tin oxide (FTO) substrate is used as a photoanode for oxidation of organics. One can expand on this concept a step further by (1) matching the pollutants in a manner that maximizes photooxidation on the basis of redox properties of the materials involved, (2) mechanism of degradation, or (3) potential for H^+ ion generation to improve the yield of hydrogen.

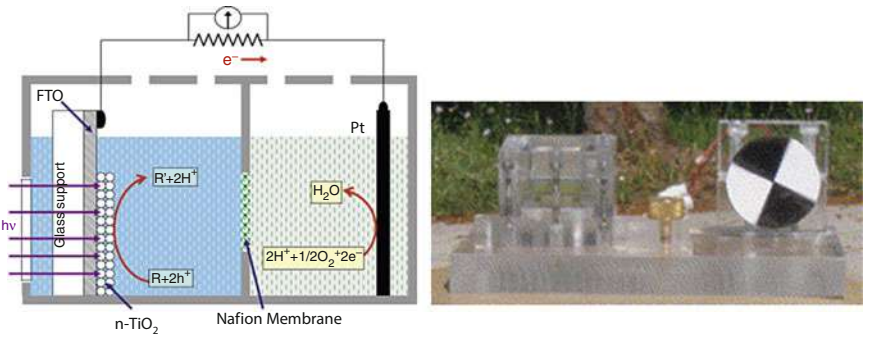

Fig. 5 Schematic representation of a two-compartment PEC cell. The openings at the *upper part* represent gas inlets and outlets. The chemical reactions shown are only indicative examples. The system can be used with other combination of pollutants to produce energy (Reprinted with permission from Elsevier)

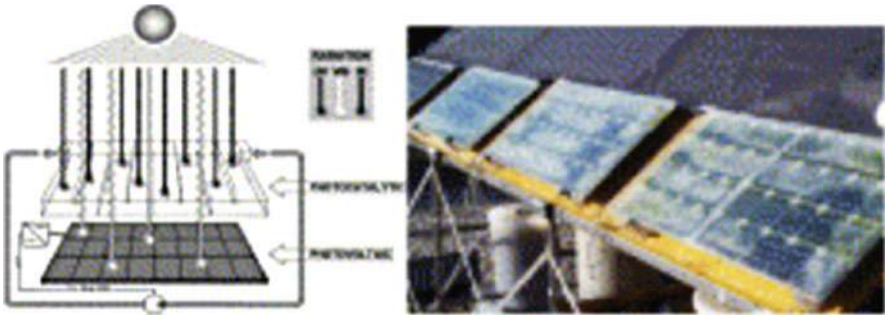

Fig. 6 Schematic representation of a hybrid photocatalytic-photovoltaic system powered using internally generated energy (Reprinted with permission from Elsevier)

Example 2: A Hybrid Photocatalytic-Photovoltaic System (HPPS)

A research group from Switzerland has pioneered the development of an autonomous eco-friendly HPPS system which utilizes solar energy to perform photodegradation of pollutants and a PV system to generate power for operating the system simultaneously (Sarria et al. 2005). This three-tiered system consists of (1) a sun-facing top layer where UV-assisted photodegradation of pollutants is performed, (2) an intermediate water layer which functions as an IR filter to regulate temperature, and (3) a visible light-absorbing PV device that produces electricity at the bottom to power a recirculation pump associated with the system. A schematic of the system is shown in Fig. 6. The system thus does not draw any external power for performing the waste treatment. The system consists of four PV modules and has an overall volume of 25 L. This is an example of a smart integrated system that utilizes UV, visible, and IR parts of the solar spectrum to combining photodegradation of pollutants and producing electricity. A possible direction to further improve the efficiency of such systems may be to focus on trying to harvesting IR photons to produce electricity using new photocatalysts.

Example 3: Bioprocesses to Convert Waste to Energy Using Algae

Man-made emissions such as CO_2 from industries have adverse effects on the environment; the realization of the negative effects of such emissions has led to international protocol and policy changes such as cap-and-trade agreements to control environmental impact (Kunjapur and Eldridge 2010; Pittman et al. 2011; Walke 2009). On the other hand, the shortage of transportation fuels has necessitated the need to develop alternate sources of energy. These two challenges can potentially be addressed simultaneously using algae.

Algae-based systems can assist in green house gas control by consuming CO_2 to produce a variety of useful products. Algae in the presence of sunlight, water, and

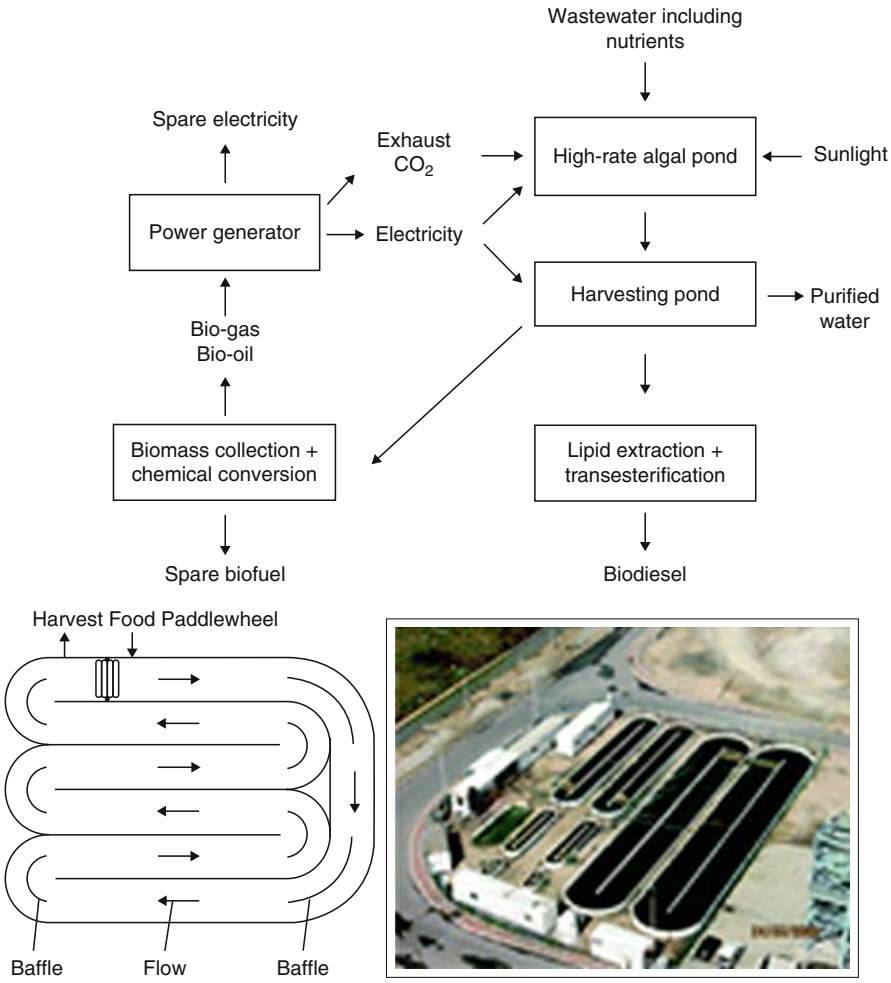

Fig. 7 The steps involved in biodiesel production using waste water, solar energy, and CO_2, and the picture of an actual raceway facility implementing about process (Top) (Reprinted with permission from Elsevier and ACS)

CO_2 nutrients produce biofuels (for transportation), solid biomass (burned to produce heat or electricity), hydrogen, or oxygen. A schematic of the pathway for some of these products is shown in Fig. 7. This approach is considered a promising solution to global environmental and energy needs. Photobioreactors or raceway ponds are two common methods to contact algae with light, CO_2, and nutrients. An example of a raceway pond is shown in Fig. 7.

In a generic parlance, these examples help reinforce the old adage – *One man's junk is another man's treasure*.

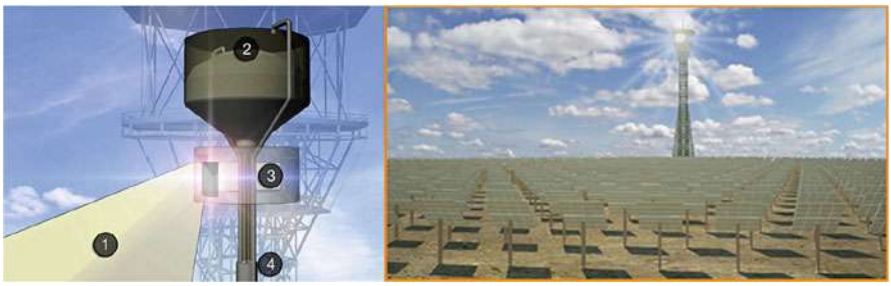

Fig. 8 Schematic of Sundrop Fuels® system to concentrate solar energy onto the thermochemical reactor for gasification and the ground view of heliostat mirrors used to concentrate solar energy

Example 4: Solar-Powered Biomass Gasification

Biomass gasification is the process of converting organic material to syngas, primarily carbon monoxide and hydrogen, which can be used to produce various forms of energy and fuels (Sundrop Fuels Inc 2010; In Biomassmaganzine.com 2010). Organic biomass is reacted at high temperatures with a specific amount of oxygen and water to produce syngas. The syngas is then purified and can be used for electricity generation, production of liquid fuels, or production of hydrogen gas. The problem with traditional gasification processes is that a large amount of energy is required to generate the high temperatures necessary for gasification. This energy is typically supplied by coal-fired power plants or by burning part of the biomass feedstock. Researchers at several Colorado universities in collaboration with the National Renewable Energy Laboratory have developed a rapid solar-thermal reactor that can be used for biomass gasification. In this process, a number of mirrors are used to concentrate solar energy to a single point producing extremely high reactor temperatures, in excess of 2,000 °C. Sundrop Fuels has applied this technology at their solar-driven biomass gasification facility in Louisville, Colorado. Sundrop Fuels uses thousands of solar heliostat mirrors on the ground to direct concentrated solar energy to a thermochemical reactor atop a high tower. Feedstock entering the reactor is converted to syngas at 1,300 °C. Figure 8 shows a schematic representation of the solar-driven gasification process. The syngas is then cleaned and processed to create "green" gasoline, diesel, and aviation fuels. Biomass gasification is a promising technology for producing a number of fuels, and the use of concentrated solar energy eliminates traditional energy losses during thermal energy generation.

Commercial Ventures

The progress in the development of materials for solar energy utilization in the last few decades has permitted a wide variety of solar cell-based commercial ventures to fulfill contemporary specific niches and markets. Furthermore, solar companies are constantly researching and refining their manufacturing processes to discover more

Table 8 Commercial companies involved in the design of solar energy conversion systems

Company	Headquarter's location	Solar cell technology	Website
Konarka Technologies	Lowell, MA	Power plastics	http://www.konaraka.com
Dyesol	Queanbeyan, NSW, Australia	High purity dye solar cell	http://www.dyesol.com
Inventux Technologies	Berlin, Germany	Solar micromorph thin-film modules	http://www.inventux.com

economical and eco-friendly solar cells that will satisfy emerging markets and cliental needs. Within this section, we will profile three solar companies: Konarka Technologies, Dyesol, and Inventux Technologies. Table 8 briefly introduces these companies.

Konarka® Technologies

Konarka Technologies is an international solar company receiving recognition worldwide for developing a third-generation organic photovoltaic technology-based solar cell (Konarka 2009). An organic photovoltaic cell utilizes conductive polymers or small carbon-based molecules for light absorption and charge transport, respectively, while traditional electronics use inorganic conductors such as copper. Konarka's chief technology, Power Plastic, was invented by the company's cofounder and Nobel Prize laureate, Dr. Alan Heeger. Power Plastic is a photoreactive polymer material and can be printed or coated inexpensively onto flexible substrates using roll-to-roll manufacturing; it is comprised of several thin layers: a photoreactive printed layer, a transparent electrode layer, a plastic substrate, and a protective packaging layer, as illustrated in Fig. 9.

Unique Features

Konarka's Power Plastic has several advantages over other organic photovoltaic technologies. These include:

- Tunable cell chemistry to absorb specific wavelengths of light as well as broad spectrum
- To capture both indoor and outdoor light and convert it into direct energy in the form of electric current
- To perform its function using all recyclable materials
- Being thin, lightweight, and flexible

Applications

Konarka's Power Plastic has four major end-product applications. These include:

- Microelectronics: powering sensors, smart cards, and low-power applications
- Portable power: solar-powered sensors, backpacks, and cell phone chargers

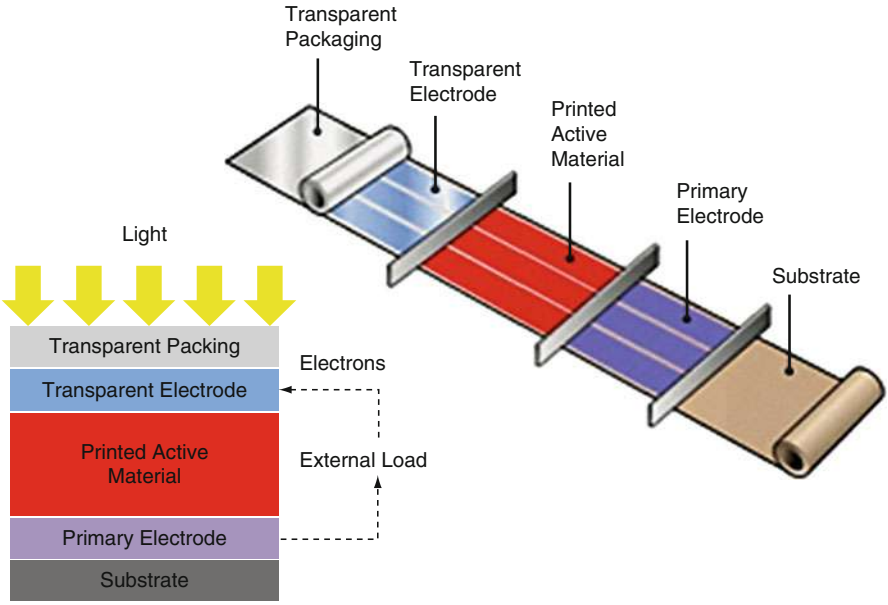

Fig. 9 Illustration of power plastic layers (modified from the Konarka® website)

- Remote power: accessing renewable power at stadiums, carports, and airports
- Building integrated applications (BIPV): custom-manufactured applications roof, windows, and walls

Cost per Watt

Konarka's Power Plastic technology has already reduced the cost of manufacturing solar cell so that it is less than $1 per watt; moreover, Konarka states that through mass production, this cost will be further reduced to approximately $0.10/W.

Future Plans

Konarka is currently developing two future applications for Power Plastic which are under development by Konarka and Arch Aluminum %26 Glass:

- Manufacturing transparent and opaque solar cells for integrated curtain walls and windows components
- The ability for this technology to work off-angle permitting the technology to expand to other niches

Konarka's ongoing research involves conducting advanced research in power fibers, bifacial cells, and tandem architecture. The resulting products of this ongoing research would permit Konarka to expand solar power technology to woven textiles

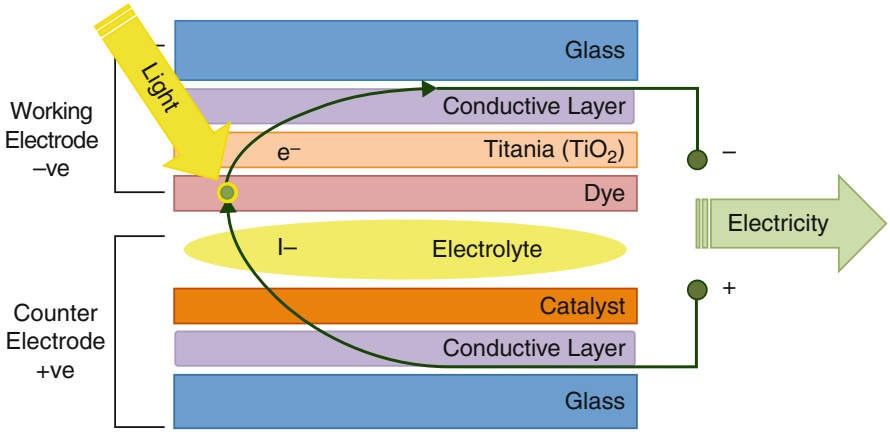

Fig. 10 The fundamental DSC structure design consideration (taken from the Dyesol® website)

via power fibers. Bifacial cells being transparent in nature would permit the solar cells to generate electricity from inside and outside light while allowing the technology to double as a see-through window. Tandem architecture would increase the efficiency of organic photovoltaic devices to 15 % through the process of stacking series-connected subcells.

Dyesol®

Dyesol manufactures and sells high purity dye solar cell (DCS) materials, titania pastes, sensitizing dyes, electrolytes, and electrode catalysts (Dyesol 2010). As seen in Fig. 10, the DSC structure consists of a layer of nanoparticulate titania (titanium dioxide) which is formed on a transparent electrically conducting substrate and photosensitized via a single ruthenium (Ru)-based dye layer. An iodide-tri-iodide-based electrolyte redox system is placed between a layer of photosensitized titania and a second electrically conducting catalytic substrate.

Unique Features

Some advantages of using DSC technology versus other contemporary silicon-based photovoltaic technology are that they:

- Are much less sensitive to angle of incidence of radiation – it is a "light sponge" soaked with dye.
- Perform over a wide range of light conditions.
- Have low sensitivity to ambient temperature changes.
- Are much less sensitive to shadowing and can be diode-free.
- Are an option for transparent modules, thus enabling wider applications.

- Are truly bifacial: They absorb light from both faces and can be inverted.
- Are versatile: DSC power can be amplified by tandem and optical techniques without the use of concentrators.

The resulting DSC panels are more versatile because they are less sensitive to the angle of the solar radiation, allowing them to be installed on vertical walls and in low-light areas; moreover, they can be transparent and can be designed in various color schemes permitting more attractive architectural integration options than those available for silicon.

Applications

Dyesol's patented products and their applications are listed below:

- Interconnected Glass Module: This design is for applications where longest lifetime is needed for exposed mounting and to be isostructural to and replacing the existing structure. Electrical interface can be typically via a short DC bus to a local area network for distribution or inversion to AC.
- SureVolt Solar Range: Maintain voltage at all light levels, having high resistance to damage through impact, bending, tension, torsion, and compression. The range is ideally suited for use in portable consumer electronics, military, and indoor applications, as well as developed landscape infrastructure.

Dyesol's dye solar cells (DSC) are marketed to low light, dappled light, and indoor light markets, a market that only DSC can address.

Cost per Watt

The *Photovoltaic World* May/June 2009 magazine stated at the anticipated 7 % Dyesol efficiency the resulting cost of DSC technology was $1.00/W.

Future Plans

Dyesol appears to have two major future goals:

1. To outsource to working in collaboration with wireless technology and tandem products
2. To enhance power out devices to direct chemical production and complete building solutions

Inventux Technologies

Inventux is a solar energy company that specializes in the development, production, and marketing of environmentally friendly, silicon-based thin-film solar (micromorph thin-film) modules (Inventux 2010). The combination of an amorphous with a microcrystalline cell is termed a micromorph cell. Micromorph cells

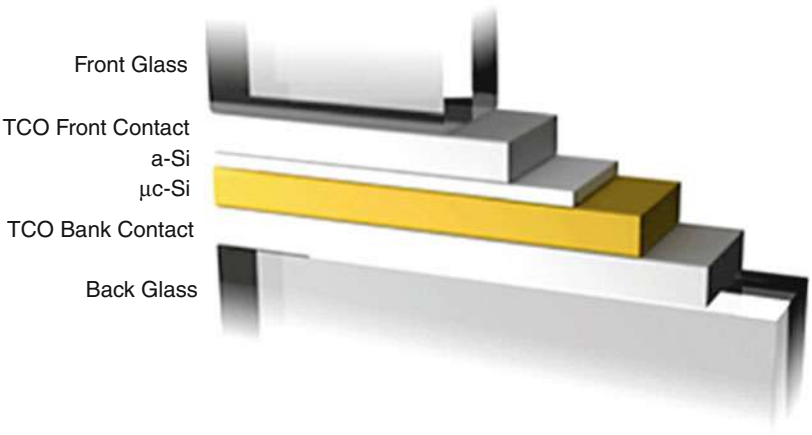

Fig. 11 Thin-film photovoltaic modules layer composition (taken from the Inventux® website)

thus represent the most consistent advancement of amorphous silicon-based tandem cell technology. Figure 11 illustrates the thin-film photovoltaic modules layer composition. The glass serves both as a substrate for the thin-film PV cell and a component of the later encapsulation of the element. The various layers are successively deposited on the front glass. To produce the absorber layers, the plasma-enhanced chemical vapor deposition (PECVD) using gaseous silicon hydrogen compounds became generally accepted. The production of the front and back contact layers (transparent conductive oxide – TCO) takes place by applying low-pressure chemical vapor deposition (LPCVD).

Unique Features

Inventux' solar modules contain absorbers made of amorphous and microcrystalline silicon. Amorphous and microcrystalline silicon are suitable to be combined in a tandem solar cell, since the different band gaps facilitate an enhanced utilization of solar radiation and manufacturing can be done using the same technology. Several of the advantages and benefits of using Inventux Solar Technologies PV modules are:

- The extremely thin 0.002-mm absorber layer requires only a minimum amount of raw material (silicon); the layer thickness is just one-hundredth of that of conventional photovoltaic technology.
- Exploitation of a broader light spectrum as well as fewer shading losses as with crystalline modules, up to 30 % higher yield during inhomogeneous light conditions compared to crystalline modules and a wider range of applications possible.
- By far better temperature behavior at good solar radiation conditions as with crystalline technology, higher yields at full load conditions.
- Monolithic module configuration, as opposed to crystalline cell configuration – with its electrically required spacing, only very little inactive module surface exists.

- Monolithic wiring during the process makes subsequent manual production steps superfluous.
- Series connection of solar cells leads to a relatively high open circuit voltage of the modules, minimized conduction losses, and reduced cabling work.
- Due to the very high spectral acceptance, they have the highest efficiency potential in the area of silicon-based thin-film photovoltaics.

Applications

Inventux thin-film photovoltaic modules are particularly suitable for large, grid-connect photovoltaic systems; moreover due to the micromorph tandem structure wide light spectrum absorption capabilities, Inventux technologies can be used during inhomogeneous light conditions and climate conditions.

Cost per Watt

Inventux Solar Technologies implements Oerlikon Solar's micromorph technology in the company's manufacturing processes. Oerlikon claims that through the incorporation of advanced fabrication designs, the company's turnkey tandem junction technology would be capable of producing modules for $0.70/W by the end of 2010.

Commercial Venture that Employs Tested Concepts of Solar Energy Utilization to Produce Fuels in an Effective Way

Algenol® (2010) is a US-based firm that proposes sequestering CO_2 from power plant exhausts and producing transportation fuel from it. The company plans to use water and sunlight to produce value ethanol (an additive to gasoline). A schematic of their proposed flow sheet is shown in Fig. 12. The firm focuses on the production of

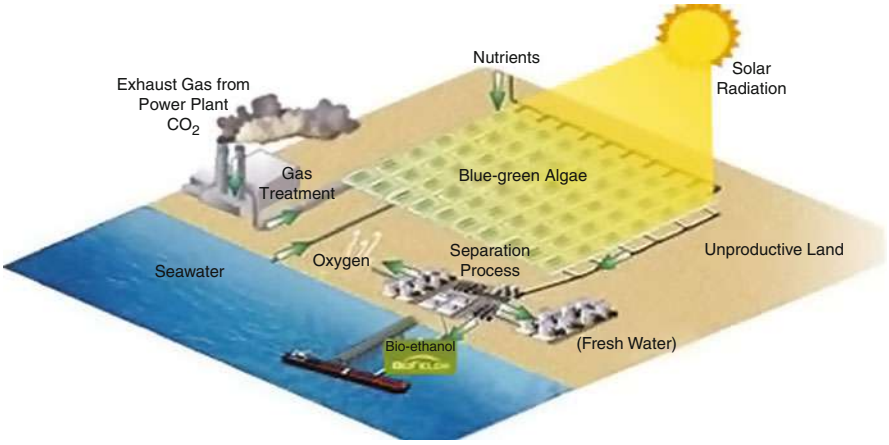

Fig. 12 An artistic rendition of a plant showing CO_2 capture from exhaust of a power plant and its utilization in a biofuel production facility. http://www.treehugger.com/files/2008/06/algenol-algae-biofuel-race-process-economics-advantage.php

ethanol from algae without destroying the algae. A unique highlight of their system is the possibility of growing the algae in land areas that may be deemed unfit for agricultural activities, for example, a desert-like environment. They are planning to build commercial facilities in the United States and Mexico in the near term for large-scale ethanol production. The company plans to sell ethanol at a price of $3.00/gal and is expected to be a major player in the value ethanol market in the near future.

Other Types of Solar Companies

A list of other solar companies from different regions around the world is provided next. These companies are involved in manufacturing products that utilize solar energy in different processes. The reader is referred to the links provided for further information.

Company	Headquarter's location	Solar cell technology	Website
Auria Solar	Taiwan	Amorphous silicon thin film	http://www.auriasolar.com/
First Solar	Phoenix, AZ	Cadmium telluride	http://www.firstsolar.com
Evergreen Solar Inc	Marlboro, MA	String ribbon crystalline silicon	http://evergreensolar.com/en/
OriginOil	Los Angeles, CA	Biofuel with solar	http://www.originoil.com/
Schüco	US location	Solar cooling	http://www.schueco.com/web/com
	Union City, CA	Solar hot water	
Solar Biofuels	Queensland, Australia	Solar biofuels (biomass)	http://www.solarbiofuels.org/
Northern Lights Solar Solutions	Winnipeg, MB Canada	Solar heating	http://www.solartubs.com/
Silicon Solar	Ithaca, NY	Portable solar power solutions	http://www.siliconsolar.com/index.html
DesignLine	Christchurch, New Zealand	Solar-powered bus (Tindo in Adelaide, Australia)	http://www.designlinecorporation.com/

Future Work

Solar research is no longer considered as a small blimp in the energy field. The last three decades of work has in fact brought it to a position where it has been accepted as a serious competitor to many traditional/nontraditional sources of energy. This is evident from the skyrocketing growth rate for solar-based technologies in the world.

However, much needs to be done. Several critical areas require further development to cement the status of solar as a reliable, large-scale, and everlasting source of energy for mankind. To make solar commercial, economical, and lasting, development has to be simultaneously realized along three fronts: scientific, pilot-scale testing and processing, and rapid evaluation and commercialization of promising technologies. A brief insight into future directions along these lines is provided. The scientific step is the most important aspect of all the three stages. Material properties, or rather constraints, are an area that clearly is the limiting factor and greatest challenge to solar energy commercialization. Since solar energy harvesting requires a close interaction of materials with elements and in some instances requires operation under extreme conditions, materials stability is of paramount importance. Solar-to-electric conversion technologies have the potential to transform mankind's energy needs. However, materials that demonstrate stable performance without undergoing chemical transformations and consisting of earth-abundant elements are urgently needed. Researchers have to focus on developing low-cost, wide-spectrum solar energy harvesters. The improvement of solar conversion or utilization efficiency is critical. To achieve efficiency improvements, fundamental understating of material properties such as charge transport, recombination dynamics, and thermal management is needed. One approach to accelerate materials identification and its testing is to employ a combinatorial analysis method. There have been some efforts in this direction, but more is needed. Past research has abundantly shown that multi-element/multi-compound systems as light harvesters are the correct way to move toward realizing efficient solar harvesters. Stacking different materials built on-site or assembling prefabricated compound(s) is required to improve light absorbance as well as efficient transformation of absorbed energy. Combinatorial techniques have to be developed to analyze libraries of possible compounds and to expedite the identification of formulations for maximizing light absorbance and its testing. In stage II, one really needs to focus on the techniques to synthesize solar energy harvesters and convertors on a large scale. Issues such as reliable scale-up material properties (identical and reproducible product) and cost competitiveness have to be addressed at the pilot scale. Approaches such as screen or ink-jet printing have been considered to be very promising techniques to reproduce lab-scale results on a commercial scale. These techniques have to be tested and perfected before further large-scale ventures. Performance data of extended use of solar energy convertors is still limited. Therefore, such data along with weather patterns and its influence on solar energy transformation has to be obtained. Realistic modeling predictions and long-term solar energy outputs have to be generated before using solar as the alternative source of energy for human activity. Stage III will require a large-scale effort on the part of governments (policy makers), green technology companies (research entities and venture capitalists), and public at large to come together to make solar energy a lasting and impacting form of alternate energy source. There are several evidences of governments getting sensitized to such needs, and short-term incentives are provided to test the people's acceptance of the technologies and market reactions. However, there is still no leading technology within the solar energy conversion technologies that can be considered as the one solution for mankind's energy needs. Therefore, the search has to go on.

Conclusion

Solar energy utilization has immense potential due to the range of applications in which it can be utilized. The core issue with solar energy is materials development. There has been significant progress in this area thanks to cutting-edge research in different parts of the world. Market penetration-driven favorable incentives now have to drive the commercialization of promising technologies. The authors are of the opinion that it is no longer necessary to follow *a wait and watch approach* for solar energy systems as many of these systems have passed that stage. One has to take concerted efforts to (1) customize systems based on geographical needs, (2) cost considerations, (3) long-term goals, and (4) institutional support. Solar energy systems are going to play a significant role in future energy portfolios regardless of the applications.

Acknowledgments The authors thank Prof. Wei-Yin Chen for the opportunity to make this contribution. Vaidyanathan Subramanian would like to thank the representatives of Konarka®, Dyesol®, and Inventux Technologies® for their time and contributions. He would also like to thank Prof. Misra and York Smith for their insights as well as the Department of Energy (Grant # DE-EE0000272) for the financial support.

References

Algenol (2010) vol 2010. http://www.algenolbiofuels.com/
Anpo M (1995) Solar Energy Mater Solar Cells 38:221
Anpo M, Yamashita H, Ichihashi Y, Ehara SJ (1995) J Electroanal Chem 396:21
Antoniadou M, Kondarides DI, Labou D, Neophytides S, Lianos P (2010) Solar Energy Mater Solar Cells 94:592
Aroutiounian VM, Arakelyan VM, Shahnazaryan GE (2005) Solar Energy 78:581
AWEA (2010) vol 2010. American Wind Energy Association, Washington, DC
Bahnemann D (2004) Solar Energy 77:445
Bahnemann DW, Hilgendorff M, Memming R (1997) J Phys Chem B 101:4265
Bard AJ (1979) J Photochem 10:59
Bauer GH (1993) Appl Surf Sci 70–71:650
Baur C, Bett AW, Dimroth F, Siefer G, Meuw M, Bensch W, Kostler W, Strobl G (2007) J Solar Energy Eng Trans ASME 129:258
Best JP, Dunstan DE (2009) Int J Hydrogen Energy 34:7562
Bezdek RH, Hirshberg AS, Babcock WH (1979) Science 203:1214
Bosi M, Pelosi C (2007) Prog Photovolt 15:51
Bosio A, Romeo N, Mazzamuto S, Canevari V (2006) Prog Cryst Growth Char Mater 52:247
Bube RH (1990) Annu Rev Mater Sci 20:19
Catchpole KR, McCann MJ, Weber KJ, Blakers AW (2001) Solar Energy Mater Solar Cells 68:173
Chamberlain RG (1980) Eur J Oper Res 5:405
Cheng P, Gu MY, Jin YP (2005) Prog Chem 17:8
Choi WY, Termin A, Hoffmann MR (1994) J Phys Chem 98:13669
Cozzoli PD, Fanizza E, Comparelli R, Curri ML, Agostiano A, Laub D (2004) J Phys Chem B 108:9623
Cravino A (2007) Polym Int 56:943
Cui Y, Du H, Wen LS (2008) J Mater Sci Technol 24:675

Damonte LC, Donderis V, Ferrari S, Meyer M, Orozco J, Hernandez-Fenollosa MA (2010) Int J Hydrogen Energy 35:5834
Danielsen AL (1978) Rev Bus Econ Res 13:1
De Falco M, Giaconia A, Marrelli L, Tarquini P, Grena R, Caputo G (2009) Int J Hydrogen Energy 34:98
Dhere NG, Kulkarni SS, Jahagirdar AH, Kadam AA (2005) J Phys Chem Solids 66:1876
Dyesol (2010) Solar cell technology. Dyesol, Queenbeyan
Eberspacher C, Fredric C, Pauls K, Serra J (2001) Thin Solid Films 387:18
Feng ZF, Zhou JZ, Xi YY, Lan BB, Guo HH, Chen HX, Zhang QB, Lin ZHJ (2009) J Power Sources 194:1142
Frank AJ, Kopidakis N, van de Lagemaat J (2004) Coord Chem Rev 248:1165
Fujishima A, Rao TN, Tryk DA (2000) J Photochem Photobiol C 1:1
Fujiwara H, Hosokawa H, Murakoshi K, Wada Y, Yanagida S, Okada T, Kobayashi H (1997) J Phys Chem B 101:8270
García-Valladares O, Pilatowsky I, Ruíz V (2008) Solar Energy 82:613
Germogenova TA (2002) Prog Nucl Energy 40:1
Ginley D, Green MA, Collins R (2008) MRS Bull 33:355
Goetzberger A, Hebling C, Schock HW (2003) Mater Sci Eng R Rep 40:1
Gogate PR, Pandit AB (2004) Adv Environ Res 8:501
Goswami DY, Vijayaraghavan S, Lu S, Tamm G (2004) Solar Energy 76:33
Gratzel M (1991) Coord Chem Rev 111:167
Gratzel M (2001) Nature 414:338
Gratzel M (2005) MRS Bull 30:23
Green MA (2007) J Mater Sci Mater Electron 18:S15
Guenes S, Sariciftci NS (2008) Inorganica Chim Acta 361:581
Guha S, Yang J (2006) J Non Cryst Solids 352:1917
Guo YF, Quan X, Lu N, Zhao HM, Chen S (2007) Environ Sci Technol 41:4422
Han J, Mol APJ, Lu Y (2010) Energy Policy 38:383
Hanrath T, Veldman D, Choi JJ, Christova CG, Wienk MM, Janssen RAJ (2009) ACS Appl Mater Interfaces 1:244
Harmim A, Boukar M, Amar M (2008) Solar Energy 82:287
Hillhouse HW, Beard MC (2009) Curr Opin Colloid Interface Sci 14:245
Hinogami R, Nakamura Y, Yae S, Nakato Y (1998) J Phys Chem B 102:974
Hoffmann MR, Martin ST, Choi WY, Bahnemann DW (1995) Chem Rev 95:69
Honda S, Nogami T, Ohkita H, Benten H, Ito S (2009) ACS Appl Mater Interfaces 1:804
Hoppe H, Sariciftci NSJ (2004) Mater Res 19:1924
Hou XH, Choy KL (2005) Thin Solid Films 480:13
Hou Z, Zheng DX (2009) Appl Therm Eng 29:3169
Hu Y, Zheng Z, Jia HM, Tang YW, Zhang LZ (2008) J Phys Chem C 112:13037
Hu XL, Li GS, Yu JC (2010) Langmuir 26:3031
Hultman NE (2007) Curr Hist 106:376
Ikeue K, Nozaki S, Ogawa M, Anpo M (2002) Catal Lett 80:111
In Biomassmaganzine.com (2010) http://www.biomassmagazine.com/article.jsp?article_id=1674%26q=%26page=all
Inventux Technology (2010) vol 2010, Berlin
Ito S, Murakami TN, Comte P, Liska P, Grätzel C, Nazeeruddin MK, Grätzel M (2008) Thin Solid Films 516:4613
Jang JS, Yoon KY, Xiao XY, Fan FRF, Bard AJ (2009a) Chem Mater 21:4803
Jang JS, Lee J, Ye H, Fan FRF, Bard AJ (2009b) J Phys Chem C 113:6719
Kaelin M, Rudmann D, Tiwari AN (2004) Solar Energy 77:749
Kalogirou SA (2009) Solar space heating and cooling: processes and systems. Elsevier, Amsterdam
Kalyanasundaram K, Gratzel M (1997) Proc Indian Acad Sci Chem Sci 109:447
Kamat PV, Flumiani M, Dawson A (2002) Colloids Surf A Physicochem Eng Asp 202:269

Kar A, Sohn Y, Subramanian V (2008) Chapter 10. Synthesis of oxide semiconductors, metal nanoparticles and semiconductor–metal nanocomposites. Research Signpost, Trivandrum (Invited)
Kaushal A, Varun (2010) Renew Sustain Energy Rev 14:446
Kawai T, Kuwabara T, Yoshino K (1992) J Chem Soc Faraday Trans 88:2041
Kay A, Gratzel M (1996) Solar Energy Mater Solar Cells 44:99
Kazmerski LL (2006) J Electron Spectros Relat Phenomena 150:105
Kelly NA, Gibson TL (2006) Int J Hydrogen Energy 31:1658
Khalifa AJN, Hamood AM (2009) Solar Energy 83:1312
Khaselev O, Turner JA (1998) Science 280:425
Knoll A, Klink K (2009) Renew Energy 34:2493
Koci K, Obalova L, Matejova L, Placha D, Lacny Z, Jirkovsky J, Solcova O (2009) Appl Catal B Environ 89:494
Konarka Technology (2009) Lowell, vol 2010
Kondamudi N, Mohapatra SK, Misra M (2008) J Agric Food Chem 56:11757
Kondo M, Takenaka A, Ishikawa A, Kurata S, Hayashi K, Nishio H, Nishimura K, Yamagishi H, Tawada T (1997) Solar Energy Mater Solar Cells 49:127
Kuang D, Brillet J, Chen P, Takata M, Uchida S, Miura H, Sumioka K, Zakeeruddin SM, Grtzel M (2008) ACS Nano 2:1113
Kudo A, Miseki Y (2009) Chem Soc Rev 38:253
Kulkarni GN, Kedare SB, Bandyopadhyay S (2007) Solar Energy 81:958
Kunjapur AM, Eldridge RB (2010) Ind Eng Chem Res 49:3516
Kurtz S, Friedman D, Geisz J, McMahon W (2007) J Cryst Growth 298:748
Lakowicz JR (2006) Principles of fluorescence spectroscopy, 3rd edn. Springer, Boston
Landi BJ, Castro SL, Ruf HJ, Evans CM, Bailey SG, Raffaelle RP (2005) Solar Energy Mater Solar Cells 87:733
Lee WJ, Ramasamy E, Lee DY, Song JS (2009) ACS Appl Mater Interfaces 1:1145
Lenzen M (2008) Energy Convers Manag 49:2178
Li GH, Ciston S, Saponjic ZV, Chen L, Dimitrijevic NM, Rajh T, Gray KA (2008) J Catal 253:105
Li C, Yuan J, Han B, Jiang L, Shangguan WF (2010) Int J Hydrogen Energy 34:3621–3630
Liang YY, Xiao SQ, Feng DQ, Yu LP (2008) J Phys Chem C 112:7866
Linsebigler AL, Lu GQ, Yates JT (1995) Chem Rev 95:735
Liu YY, Huang BB, Dai Y, Zhang XY, Qin XY, Jiang MH, Whangbo MH (2009) Catal Commun 11:210
Liu M, Jing D, Zhao L, Guo L (2010) Int J Hydrogen Energy 35:7127–7133
Ma LL, Lin YL, Wang Y, Li JL, Wang E, Qiu MQ, Yu Y (2008) J Phys Chem C 112:18916
Matsumoto Y, Obata M, Hombo J (1994) J Phys Chem 98:2950
Matsuoka M, Kitano M, Takeuchi M, Tsujimaru K, Anpo M, Thomas JM (2007) Catal Today 122:51
Miles RW, Hynes KM, Forbes I (2005) Prog Cryst Growth Char Mater 51:1
Miles RW, Zoppi G, Forbes I (2007) Mater Today 10:20
Mills A, Davies RH, Worsley D (1993) Chem Soc Rev 22:417
Miseki Y, Kusama H, Sugihara H, Sayama K (2010) J Phys Chem Lett 1:1196
Mor GK, Varghese OK, Paulose M, Shankar K, Grimes CA (2006) Solar Energy Mater Solar Cells 90:2011
Muduli S, Lee W, Dhas V, Mujawar S, Dubey M, Vijayamohanan K, Han SH, Ogale S (2009) ACS Appl Mater Interfaces 1:2030
Ni M, Leung MKH, Leung DYC, Sumathy K (2007) Renew Sustain Energ Rev 11:401
Niu MT, Huang F, Cui LF, Huang P, Yu YL, Wang YS (2010) ACS Nano 4:681
Nowotny J, Bak T, Nowotny MK, Sheppard LR (2006) J Phys Chem B 110:18492
Oktik S (1988) Prog Cryst Growth Char Mater 17:171
Oliveira LS, Franca AS, Camargos RRS, Ferraz VP (2008) Bioresour Technol 99:3244
Ouyang JY, Xia YJ (2009) Solar Energy Mater Solar Cells 93:1592

Pan PW, Chen YW (2007) Catal Commun 8:1546
Park JH, Kim S, Bard AJ (2006) Nano Lett 6:24
Perezalbuerne EA, Tyan YS (1980) Science 208:902
Peterson CL, Hustrulid T (1998) Biomass Bioenergy 14:91
Pittman JK, Dean AP, Osundeko O (2011) Bioresour Technol 102:17–25
Price T, Bunn J, Probert D, Hales R (1996) Appl Energy 54:103
Qin S, Xin F, Liu Y, Yin X, Ma W (2011) J Colloid Interface Sci 356:257
Rajeshwar K (2007) J Appl Electrochem 37:765
Rajeshwar K, de Tacconi NR, Chenthamarakshan CR (2001) Chem Mater 13:2765
REN21-Secretariat (2010) Renewable energy 2010 global status report
Reyes-Gil KR, Reyes-Garcia EA, Raftery D (2007) J Phys Chem C 111:14579
Robel I, Subramanian V, Kuno MK, Kamat PV (2006) J Am Chem Soc 128:2385
Rocheleau RE, Miller EL, Misra A (1998) Energy Fuels 12:3
Rotmans J, Swart R (1990) Environ Manag 14:291
Sakai I, Takagi M, Terakawa K, Ohue J (1976) Solar Energy 18:525
Sanderson KW (2007) Cereal Foods World 52:5
Sarria V, Kenfack S, Malato S, Blanco J, Pulgarin C (2005) Solar Energy 79:353
Schropp REI (2004) Thin Solid Films 451–452:455
Server H (2010) Photovoltaics: solar electricity and solar cells in theory and practice. Germany
Shaban YA, Khan SUM (2008) Int J Hydrogen Energy 33:1118
Shah A, Meier J, Buechel A, Kroll U, Steinhauser J, Meillaud F, Schade H, Domine D (2006) Thin Solid Films 502:292
Shankar K, Basham JI, Allam NK, Varghese OK, Mor GK, Feng XJ, Paulose M, Seabold JA, Choi KS, Grimes CA (2009) J Phys Chem C 113:6327
Sharma A, Chen CR, Lan NV (2009a) Renew Sustain Energy Rev 13:1185
Sharma A, Chen CR, Murty VVS, Shukla A (2009b) Renew Sustain Energy Rev 13:1599
Sivula K, Le Formal F, Gratzel M (2009) Chem Mater 21:2862
Solanki CS, Beaucarne G (2007) Energy Sustain Dev 11:17
Somasundaram S, Chenthamarakshan CRN, de Tacconi NR, Rajeshwar K (2007) Int J Hydrogen Energy 32:4661
Strobel R, Baiker A, Pratsinis SE (2006) Adv Powder Technol 17:457
Subramanian V (2007) Interface 16:32
Sundrop Fuels Inc. (2010) Louisville, vol 2010. http://www.sundropfuels.com/index.html
Tada H, Hattori A, Tokihisa Y, Imai K, Tohge N, Ito S (2000) J Phys Chem B 104:4585
Taima T, Sakai J, Yamanari T, Saito K (2009) Solar Energy Mater Solar Cells 93:742
Takabayashi S, Nakamura R, Nakato Y (2004) J Photochem Photobiol A Chem 166:107
Takeda Y, Kato N, Higuchi K, Takeichi A, Motohiro T, Fukumoto S, Sano T, Toyoda T (2009) Solar Energy Mater Solar Cells 93:808
Tan SS, Zou L, Hu E (2006) Catal Today 115:269
Tao J, Sun Y, Ge MY, Chen X, Dai N (2010) ACS Appl Mater Interfaces 2:265
Teramura K, Tsuneoka H, Shishido T, Tanaka T (2008) Chem Phys Lett 467:191
Teramura K, Okuoka S, Tsuneoka H, Shishido T, Tanaka T (2010) Appl Catal B Environ 96:565–568
Tester JW, Drake EM, Driscoll MJ, Golay MW, Peters WA (2005) Sustainable energy-choosing among options. MIT Press, Cambridge, MA
Thomas MG, Post HN, DeBlasio R (1999) Prog Photovoltaics 7:1
Tiwari GN, Bhatia PS, Singh AK, Sutar RF (1994) Energy Convers Manag 35:535
Tiwari GN, Kumar S, Sharma PB, Khan ME (1996) Appl Therm Eng 16:189
Tiwari GN, Singh HN, Tripathi R (2003) Solar Energy 75:367
Todorov T, Cordoncillo E, Sanchez-Royo JF, Carda J, Escribano P (2006) Chem Mater 18:3145
Toivola M, Halme J, Miettunen K, Aitola K, Lund PD (2009) Int J Energy Res 33:1145
Tseng IH, Wu JCS, Chou HY (2004) J Catal 221:432
Vorayos N, Kiatsiriroat T, Vorayos N (2006) Renew Energy 31:2543

Wadia C, Alivisatos AP, Kammen DM (2009) Environ Sci Technol 43:2072
Walke C (2009) Cap and trade, EPA, vol 2010
Wang M, Na Y, Gorlov M, Sun LC (2009) Dalton Trans 6458
Wang CJ, Thompson RL, Baltrus J, Matranga C (2010) J Phys Chem Lett 1:48
Wei QS, Hirota K, Tajima K, Hashimoto K (2006) Chem Mater 18:5080
Weiss M, Neelis M, Blok K, Patel M (2009) Clim Change 95:369
Woodhouse M, Parkinson BA (2009) Chem Soc Rev 38:197
Workman JJ (1998) Chapter 2. Ultraviolet, visible, and near infrared spectroscopy. Academic, Chestnut Hill
Wu JCS, Lin HM, Lai CL (2005) Appl Catal A Gen 296:194
Wurfel P (2002) Physica E Low Dimens Syst Nanostruct 14:18
Xie TF, Wang DJ, Zhu LJ, Li TJ, Xu YJ (2001) Mater Chem Phys 70:103
Xin H, Reid OG, Ren GQ, Kim FS, Ginger DS, Jenekhe SA (2010) ACS Nano 4:1861
Yamagata S, Nishijo M, Murao N, Ohta S, Mizoguchi I (1995) Zeolites 15:490
Yamashita H, Fujii Y, Ichihashi Y, Zhang SG, Ikeue K, Park DR, Koyano K, Tatsumi T, Anpo M (1998) Catal Today 45:221
Zach M, Hagglund C, Chakarov D, Kasemo B (2006) Curr Opin Solid State Mater Sci 10:132
Zhang A, Ma Q, Lu MK, Yu GW, Zhou YY, Qiu ZF (2008) Cryst Growth Des 8:2402
Zheng L, Xu Y, Song Y, Wu CZ, Zhang M, Xie Y (2009) Inorg Chem 48:4003

Greenhouse Gas Emission Reduction Using Advanced Heat Integration Techniques

Kailiang Zheng, Helen H. Lou, and Yinlun Huang

Contents

Abstract

Consuming about 20 % of total energy annually in the USA (according to DOE in 1994), the chemical industry is a major source of greenhouse gas (GHG) emissions. It has been widely recognized that a significant reduction of energy

K. Zheng (✉) • H.H. Lou
Dan F. Smith Department of Chemical Engineering, Lamar University, Beaumont, TX, USA
e-mail: kevinnzheng@gmail.com; kevin.zheng@bayer.com; Helen.lou@lamar.edu

Y. Huang
Lab for Multiscale Complex Systems Science and Engineering, Department of Chemical Engineering and Materials Science, Wayne State University, Detroit, MI, USA
e-mail: yhuang@wayne.edu

W.-Y. Chen et al. (eds.), *Handbook of Climate Change Mitigation and Adaptation*,
DOI 10.1007/978-3-319-14409-2_21

consumption and GHG emissions in chemical processes must implement advanced heat integration technologies in a holistic way.

Heat integration is a family of technologies for improving energy efficiency. The technologies can be applied to the design of heat exchanger networks, heat-integrated reaction-separation systems, etc. Pinch analysis is the foundation of heat integration. In this chapter, the applicability of pinch technology in GHG emission reduction is reviewed first. Furthermore, the concept of "total site," which is valuable for energy targeting and integration at regional level, is described. A "total site" includes not only traditional industrial processes but also commercial and residential energy users into the scope.

Then, more advanced concepts in heat integration are introduced. The concepts are developed based on the observation of problems arising in heat integration applications – stability of heat-integrated systems in operation. The known modeling work addressing these issues will be reviewed thoroughly. The basic principles on how the disturbance-propagation-rejection models for these major chemical processing systems can be adopted in process synthesis and analysis stages will be discussed.

The concept of "total site" has been further extended to greenhouse gas emission targeting and reduction. Carbon dioxide (CO_2) emission-focused pinch analysis methodology is reviewed, which is valuable for obtaining the optimal energy resource mix of fossil fuel and renewable energy for the regional or national energy sector.

Introduction

The chemical industry is one of the largest energy-consuming sectors in the USA. According to the US DOE's analysis, this industry consumes approximately 20 % of the total industrial energy consumption (1994) and contributes in a similar proportion to the nation's greenhouse gas (GHG) emissions. There are great potentials to reduce the energy demand and GHG emissions in chemical process systems using advanced heat integration technologies. The basic heat integration methodology was developed in the past decades under the label "Pinch Analysis." Some key points have been published at the end of 1970, but it was Linnhoff and his coworkers (1994) who developed the basis of pinch technology, which is now considered as the foundation of heat integration.

Pinch analysis was originally developed based on thermodynamic principles to identify the optimal energy recovery strategies between the matches of hot and cold streams. It provides tools that allow the users to investigate energy flows within a process and identify the most economical ways of maximizing heat recovery and of minimizing the demand for external utilities purchased elsewhere (e.g., steam and cooling water), thus contributing to GHG emission reduction. The core concept is to match the available internal heat sources (hot streams) with the appropriate heat sinks (cold streams) to maximize the energy recovery and minimize the cost of external heat sources. Some specialized software packages for implementing the

pinch point analysis are available, such as Super Target™ (KBC Energy Services), Aspen Pinch™, Hextran™ (Simsci), and Honeywell Exchangernet™. Taking the Super Target™ suite, for example, it allows the user to carry out an in-depth pinch analysis for the heat integration within processes, columns, and a large site, respectively, using the PROCESS, COLUMN, and SITE modules.

Over the past decades, pinch analysis has been successfully used to reduce energy consumption site wide (Matsuda et al. 2009) and in individual processes. The applications of pinch analysis in industrial sectors such as oil refining, chemicals, pulp and paper, etc., can typically identify opportunities for 10–35 % energy consumption savings (Natural Resources Canada 2003). Due to its powerful function, the application of pinch analysis is extended to many fields, such as wastewater treatment (Rossiter 1995; Wang and Smith 1994), hydrogen integration (El-Halwagi et al. 2003; Towler et al. 1996), emission targeting (Dhole and Linnhoff 1993a), and even financial management (Zhelev 2005).

In this chapter, the fundamentals of pinch analysis are briefly introduced first. It will cover all of the following aspects: setting energy targets by the construction of composite curves, grid diagram for developing the heat exchanger network (HEN), plus/minus principles for process modifications, appropriate placement of units, principles of data extraction, mathematical programming approach, total site concept, etc. Then, more advanced concepts about the controllability and operability issues of heat integration system are addressed. A disturbance propagation and control (DP&C) model is introduced to the HEN design approach to handle the disturbance issue. This will lead to the optimal design solution both in the criteria of economic cost and controllability. At last, a novel carbon emission pinch analysis (CEPA) methodology, which is developed from traditional pinch analysis, is introduced for emission reduction targeting and planning from industrial sites to regional or national energy sectors. It can identify the minimal usage of low carbon emission yet high-cost energy resources and obtain the optional energy resources allocation scheme.

The Basics of Pinch Analysis

Pinch analysis is a rigorous, structured approach for identifying the bottlenecks in industrial process energy use. The minimum theoretical utility requirement in a process (target) can be calculated for overall energy use, as well as for specific utilities (LP, HP steam, cooling water, etc.) ahead of any detailed heat integration system design activities. Pinch technology can be used to extend the analysis to the site-wide integration of a number of processes by means of utility systems. When considering any pinch-type problem, the same principles apply:

- A process can be defined in terms of supplies and demands (or sources and sinks) of energy.
- The optimal solution can be achieved by appropriately matching sources and sinks by following thermodynamic laws.

- The defining parameter in determining the suitability of matches is the temperature of streams.
- Inefficient transfer of resource can block identification of an optimal solution.

Energy Targets

Constructing the composite curves. The most fundamental concept in pinch analysis is the so-called composite curve. Composite curves are used to determine the minimum energy consumption target for a given process system. The curves are profiles of heat availability (demonstrated by the hot composite curve) and heat demands (shown by the cold composite curve). The degree to which the curves overlap is a measure of the potential for heat recovery, as illustrated in Fig. 1. The gray zone in Fig. 1, where two composite curves overlap (heat duty wise), is the amount of heat that can be recovered through heat integration.

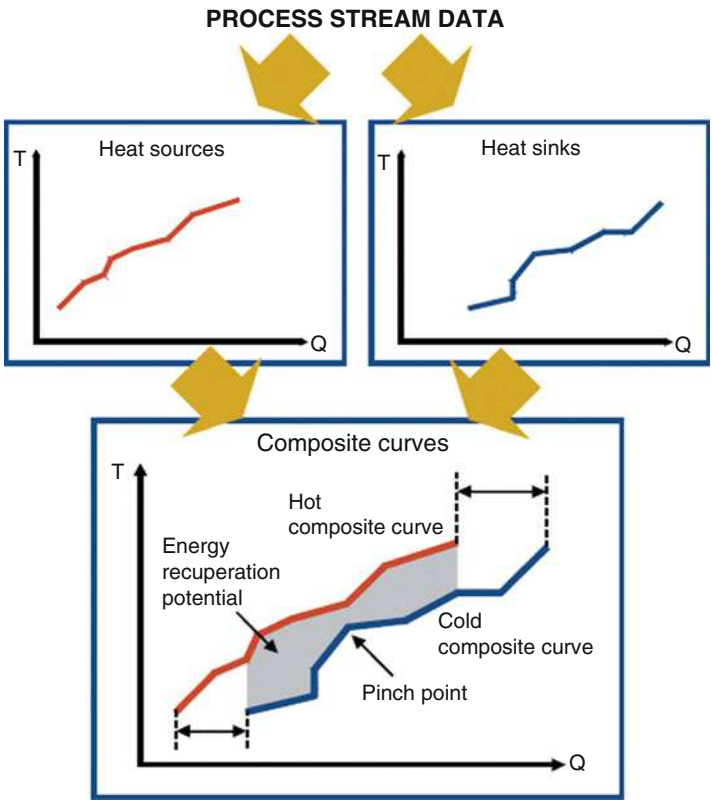

Fig. 1 The composite curves (Natural Resources Canada 2003)

Table 1 Example data for building composite curves (Natural Resources Canada 2003)

Stream	Stream type	Supply temperature (°C)	Target temperature (°C)	Heat duty (kW)	CP (kW/°C)
1	Hot	200	100	2,000	20
2	Hot	150	60	3,600	40
3	Cold	80	120	3,200	80
4	Cold	50	220	2,550	15

To construct the curves, it requires only a complete and consistent energy balance of the process. The data are used to define the process streams in terms of their temperatures, mass flow rates, as well as heat capacities and heating or cooling requirements. These data can be obtained from one or all of the following ways: plant measurements, design data, and simulation. Once identified, these process streams are then divided into sources and sinks.

A source is the stream that has a certain amount of heat to be removed, out of which a fraction or whole can be recovered. Such process streams are called hot streams. A sink corresponds to a stream that must be heated, which is called a cold stream. In pinch analysis, process streams should be identified and then divided into source and sink streams. This step is called data extraction, which is crucial for any pinch analysis. The following example explains how to do the data extraction:

Table 1 presents the stream data chosen to illustrate the construction of the composite curves. The following elements are necessary:

- Stream or segment temperatures: the supply temperature T_s and the target temperature T_t
- Heat capacity flow rate of each stream or segment, defined as $CP = \frac{\Delta H}{\Delta T}$ where ΔH is the enthalpy variation over the temperature interval ΔT and CP is defined as mass flow rate (kg/s) × heat capacity (KJ/(°C · kg)) and has a unit of kW/°C. For example, stream 2 is cooled from 150 °C to 60 °C, releasing 3,600 kW of heat. Its CP value is 40 kW/°C.

Figure 2a shows the hot streams plotted individually on a temperature-duty (or temperature-enthalpy) diagram. The slope of composite curve is the inverse of the CP value. By adding the enthalpy changes of the individual streams within each temperature interval, the hot composite cure is constructed as shown in Fig. 2b. Note that in Fig. 2b, from 150 °C to 100 °C, the slope of the composite curve in this section is reduced. In a similar way, the cold composite curve can be constructed, as illustrated in Fig. 2c and d.

Determining the energy targets. An important part of pinch analysis is the minimum energy requirement (MER) for a given process or plant. This information is used to identify the maximal potential for improvement before starting the detailed process design. To determine the minimum energy target of a process, the cold composite curve is moved left horizontally toward the hot composite curve, as shown in Fig. 3a. Please note that the enthalpy axis measures relative quantities,

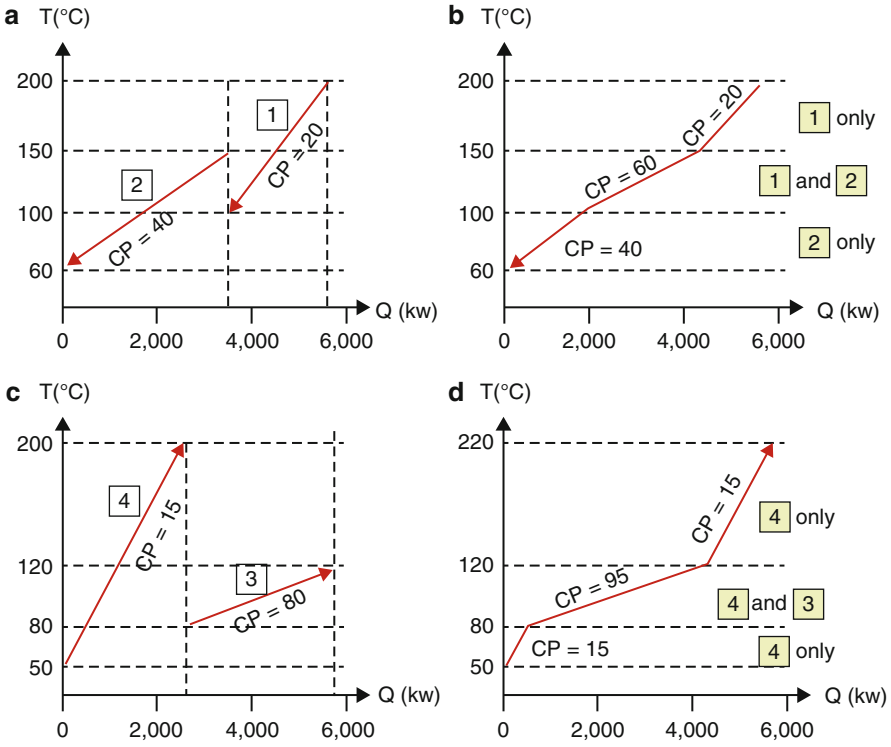

Fig. 2 Constructions of composite curves (Natural Resources Canada 2003)

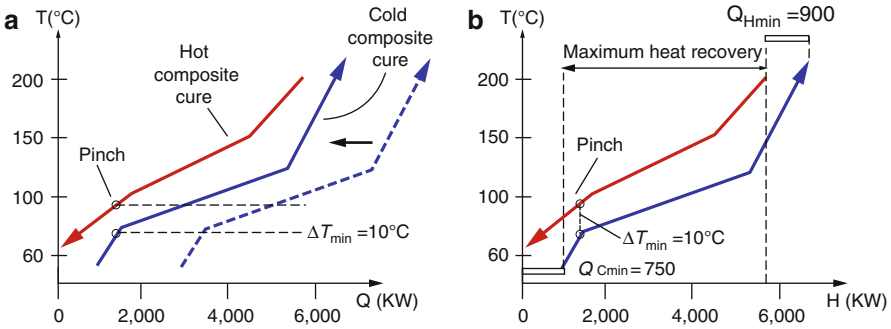

Fig. 3 Determine the energy targets by using the composite curves (Natural Resources Canada 2003)

and it only represents the enthalpy change of process streams. Moving a composite curve horizontally does not, in any way, change the stream data. The relative position of the composite curves depends on the minimum allowable temperature difference, $\Delta T_{\min}$, which is the minimum temperature difference that is allowed in a heat

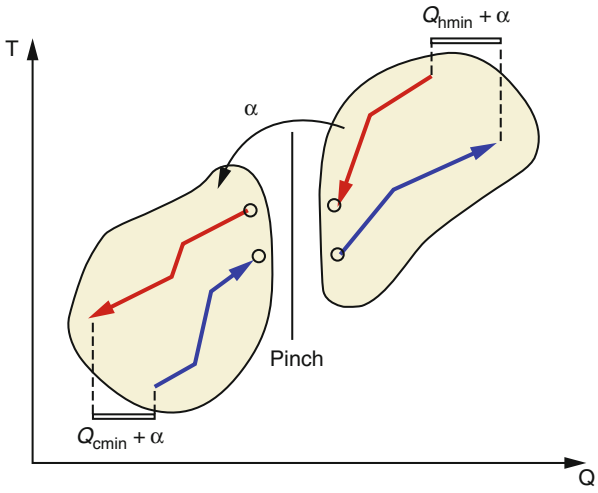

Fig. 4 Heat transfer across the pinch point (Natural Resources Canada 2003)

exchanger (note that the value of ΔT_{min} is usually given before design based on engineering experience; optimal determination of its value is a complicated problem). This also determines the pinch position where the heat transfer between the hot and cold streams is the most constrained. A value of 10 °C is used in this example.

In Fig. 3b, the overlap between the composite curves is the maximum heat recoverable between the hot and cold streams in the process; the remaining heating and cooling needs are the minimum hot utility requirement ($Q_{H\ min}$) and the minimum cold utility requirement ($Q_{C\ min}$) of the process, respectively, for the chosen ΔT_{min}. In this example, the minimum hot utility requirement ($Q_{H\ min}$) is 900 kW and the minimum cold utility requirement ($Q_{C\ min}$) is 750 kW, respectively, as indicated in Fig. 3b.

As demonstrated in the above example, pinch analysis enables the setting of targets for minimum energy consumption prior to any detailed heat exchanger network (HEN) design and allows to quickly indentify the scope of energy savings at an early stage of synthesis.

The point of the closest approach between the two composite curves, where ΔT_{min} is reached, is known as the pinch point. The pinch point is determined by the minimum temperature difference that will be accepted in any heat transfer unit. The pinch principle states that any design where heat is transferred across the pinch will require more energy than the minimum requirement. Consequently, the pinch point divides the problem into two independent subsystems, that is, the hot-end subsystem and the cold-end subsystem.

In principle, the region above the pinch only requires hot utility, while the region below the pinch only requires cooling utility (see Fig. 4). According to pinch design rules, no heat should be transferred from the hot-end subsystem to the cold-end subsystem. For example, if α amount of cross-pinch heat is transferred from the subsystem above the pinch to that below the pinch, then this cross-pinch heat needs

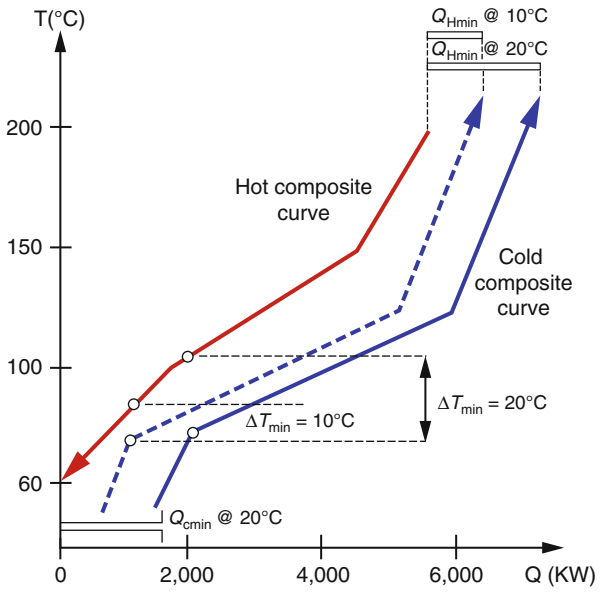

Fig. 5 Effect of ΔT_{min} (Natural Resources Canada 2003)

to be supplied by an equivalent amount of hot utility above the pinch plus the same amount of cold utility below the pinch. Needless to say, this situation should be avoided in any case.

Selection of ΔT_{min}. Generally, saving energy may increase the capital cost, and thus, often, there is a need of a trade-off between capital and energy costs. This can be demonstrated by examining the composite curves. As the separation between hot and cold composite curves (ΔT_{min}) increases, the overlap between the hot and cold streams becomes reduced, thereby decreasing opportunities for heat recovery and in turn increasing the utility cost (Fig. 5). Meanwhile, if ΔT_{min} is increased, which means the permissible minimum temperature driving force between the hot and cold streams is increased, this will allow a greater temperature difference in any heat exchanger. Then, heat exchangers would be smaller in size, thereby making the capital cost for individual heat exchanger lower. Thus, the higher energy cost may be offset by the reduced capital cost of heat exchangers.

Figure 6 shows a generalized trend of energy cost and capital cost when ΔT_{min} changes. It is very obvious that for any given plant, there exists an optimum value of ΔT_{min} which can minimize the total cost of energy and capital. If the cost of energy and the cost of heat exchangers are known for a given plant, it is possible to predict the optimum value of ΔT_{min} ahead of detailed design. In practice, ΔT_{min} for a particular process is often selected by the two factors: the shape of composite curves and the engineer's experience. For chemical processes, and where utilities are used for heat transfer, ΔT_{min} values are typically in the range of 10–20 °C. For low temperature process using refrigeration, a lower ΔT_{min} value, for example, 3–5 °C, could be used to minimize expensive power demands in a refrigeration system.

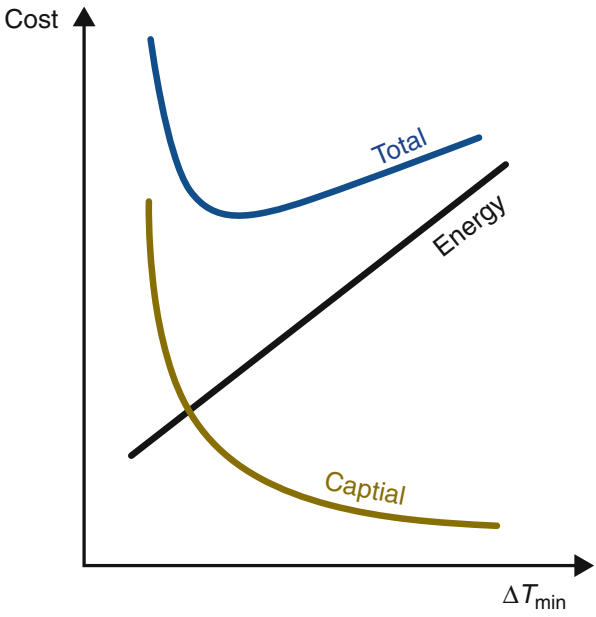

Fig. 6 Energy/capital trade-off (Natural Resources Canada 2003)

Targeting for multiple utilities: *the grand composite curve.* Most processes are heated and cooled using several different utility levels (e.g., different steam pressure levels, furnace flue gas, cold water, refrigeration levels, etc.). It is desirable to increase the use of cheap utility levels and decrease the use of expensive utility levels. For example, using low-pressure (LP) steam instead of high-pressure (HP) steam and cooling water instead of refrigeration can reduce the energy cost.

Composite curves can provide the overall energy targets. However, they do not clearly indicate the exact amount of energy needed to supply by various utility levels. The grand composite curve, which plots process energy deficit (above the pinch) and energy surplus (below the pinch) as a function of temperature, can handle this problem and determine the multiple utility targets.

To construct the grand composite curve, a small mathematical adjustment must be made to the composite curves. The hot composite curve is shifted down and the cold composite curve is shifted up separately by 1/2 ΔT_{min} each, until they touch at the pinch point. The resulting composite curves are referred as the shifted curves and have no real physical meaning. They are merely a step in the construction procedure, which ensures that the resulting grand composite curve shows the required zero-heat flow at the pinch point.

The grand composite curve is generated by plotting the heat load difference between the hot and cold composite curves as a function of temperature (Fig. 7). It provides a graphical representation of the heat flow through the process, from the hot utility to those parts of process above the pinch point, and from the process below the pinch point to the cold utility. The pinch point is where the curve intercepts the temperature axis (Fig. 7).

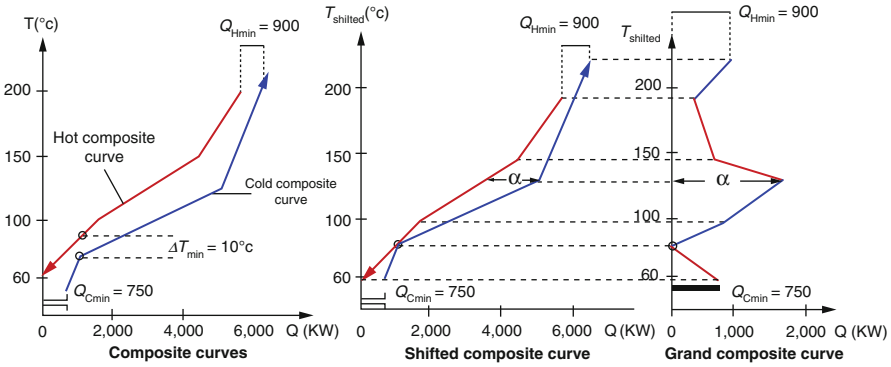

Fig. 7 Construction of the grand composite curve (Natural Resources Canada 2003)

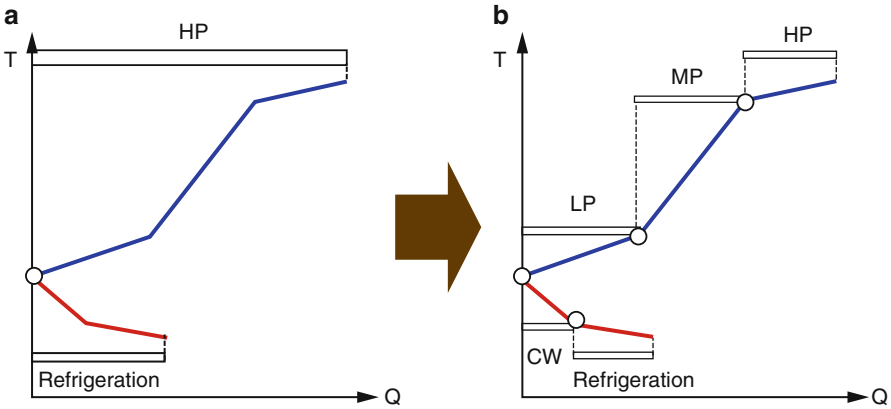

Fig. 8 The grand composite curve for multiple utilities targeting: (**a**) before targeting; and (**b**) after targeting (Natural Resources Canada 2003)

Figure 8a shows a grand composite curve where high-pressure (HP) stream is used for heating and refrigeration is used for the cooling process. In order to reduce the utility costs, some intermediate utilities, such as medium-pressure (MP) steam, low-pressure (LP) steam, and cooling water (CW), can be used as an alternative. Figure 8b shows targets for these alternative utilities.

The target for an LP steam is determined by plotting a horizontal line at the LP steam temperature from the T-axis until it intercepts the grand composite curve. The MP steam target can be obtained in a similar way. The remaining heating duty is satisfied by the HP steam. A similar procedure can be done below the pinch to determine the use of cooling water instead of refrigeration. In summary, the grand composite curve is one of the basic tools used in pinch analysis for the selection of

appropriate utility levels and for targeting optimal heat loads of various utility levels to minimize the total utility cost.

Heat Exchanger Network Design

The targeting step in a pinch analysis includes targeting for minimal energy usage, targeting for process modifications, targeting for multiple utilities, and appropriate placement of heat engines and heat pumps. The aim of targeting step is to explore various process improvement options, such as energy recovery, process modification, and utility system integration, quickly and easily without going into the detail of heat integration design. The key improvement options identified in the targeting stage need to be realized in the detailed design. The heat exchanger network (HEN) design procedure which is based on pinch principle can translate the idea of improvement option into specific detailed design. This design procedure uses the so-called grid diagram to represent the heat exchanger networks. This method will systematically lead the designer to good network design schemes that achieve the energy targets within practical limits.

Grid diagram. Figure 9 illustrates a grid diagram, which is a working frame for synthesizing a heat exchanger network (HEN). The hot streams run from left to right at the top, while the cold streams run in the opposite direction at the bottom, as illustrated in Fig. 9. The vertical line with two arrows connecting the hot stream with cold stream represents the heat exchanger between process streams. Heaters on cold steams and coolers on hot streams are shown with circles. The process pinch location is represented by a dashed line dividing the grid diagram into two parts. The pinch hot and cold temperatures obtained from composite curves by the determined $\Delta T_{\min}$ are

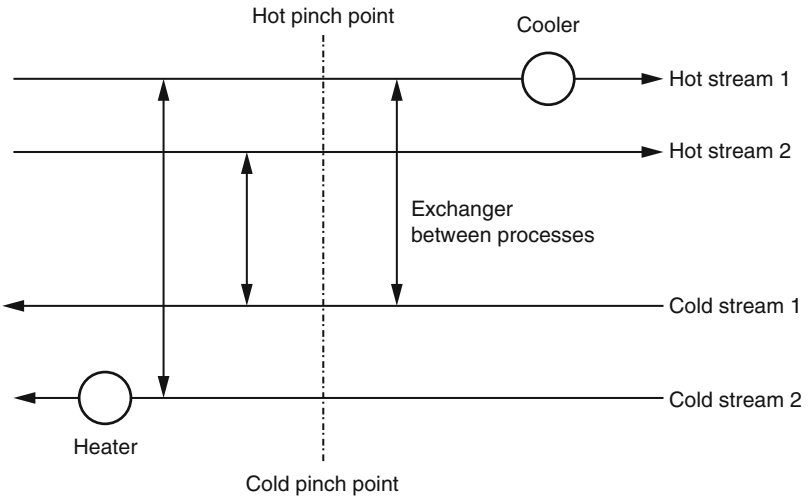

Fig. 9 Grid diagram for developing the heat exchanger network

shown at the top and bottom of the dashed line. The process above the pinch (heat sink) is on the left side of the dashed pinch line, and the process below the pinch (heat source) is on the right side. Overall, in the grid diagram, the temperatures of streams decrease from the left side (above the pinch) to the right side (below the pinch).

According to the pinch principles discussed before, the process is divided into two independent subsystems at the pinch point and any heat transfer across the pinch will require more energy than the minimum requirement. Thus, the HEN design should be conducted in two steps, above the pinch and below the pinch, respectively. The design starts at the pinch, where the heat transfer is most constrained. To determine the match of steams sequentially, heuristic feasibility rules could be used. Note that stream matching can be also determined by rigorous mathematical programming methods (Papoulias and Grossmann 1983; Yee et al. 1990; Floudas 1995; Floudas and Grossmann 1986; Ciric and Floudas 1990).

For a pinch match above the pinch (at the left side), the following heuristic rule can be followed, that is, $CP_{\text{hot}} \leq CP_{\text{cold}}$. In this context, *CP* means mass flow rate × specific heat capacity. This rule can be easily understood by the fact that only hot utility is needed above the pinch, so the *CP* value of the cold streams must be greater than the *CP* value of the hot streams.

Similarly, below the pinch (at the right side), for each pinch match, the following heuristic rule holds: $CP_{\text{hot}} \geq CP_{\text{cold}}$. The two rules above can be summarized as $CP_{\text{in}} \leq CP_{\text{out}}$. It means for a match at the pinch, the *CP* value of the stream going out of the pinch must be greater than the *CP* value of the stream coming into the pinch. For example, when considering the process above the pinch, the *CP* of hot stream, which is coming into the pinch, is smaller than the *CP* of cold stream, which is going out of the pinch.

Number of matches, paths, and loops. Linnhoff and coworkers (1994) pointed out that the minimum number of units (matches) N_E needed to recover the energy between N_s process streams using N_u utilities can be expressed by the following equation, if the synthesis problem cannot be feasibly divided into two or more energy-independent problems:

$$N_E = N_s + N_u - 1$$

If there are N_{loop} loops present in the network, this equation can be modified as:

$$N_E = N_s + N_u - 1 + N_{\text{loop}}$$

The concept of path means a physical connection through streams and heat exchangers for the transfer of energy between utilities. A path allows the modification of the temperature difference between hot and cold streams. A loop is a closed trajectory connecting several heat exchangers. These two concepts are very useful in the optimization of heat exchanger network design.

Reducing the HEN. The HEN design for minimum energy requirements based on the pinch principle ensures the maximal energy recovery, thus minimizing the energy cost. However, this design may increase the number of units needed, and thus

demanding a high equipment cost. In this case, merging some units and reducing the number of equipments may contribute more significantly to the total cost saving through trade-off between the capital and operating costs. The final optimization of the design will depend on the cost of energy and equipment in the particular case analysis. As a rule of thumb, breaking the loop including the heat exchanger with the smallest load and removing this unit in a loop can greatly reduce the total cost of the design. The loss of energy recovery capacity due to the reduction of small units can be partly compensated by increasing the heat transfer area of large units. This can be explained by the fact that for small heat exchangers, the fixed capital cost of equipment, which includes installation, instrumentation, control, supervising, and maintenance costs, is usually larger than the cost of incremental heat transfer area.

Appropriate Placement and Process Modifications

Appropriate placement of units. The appropriate placement principle determines the optimal location of individual units against the pinch. It applies to heat engines, heat pumps, distillation columns, evaporators, furnaces, and any other operating units which can be represented in terms of heat sources and sinks.

In the process industry, the use of combined heat and power systems has been increased significantly. In such cogeneration units, the heat rejected by a heat engine, such as steam turbine, gas turbine, or diesel engine, is used as hot utility and integrated into the process. If a heat engine is integrated across the pinch, as

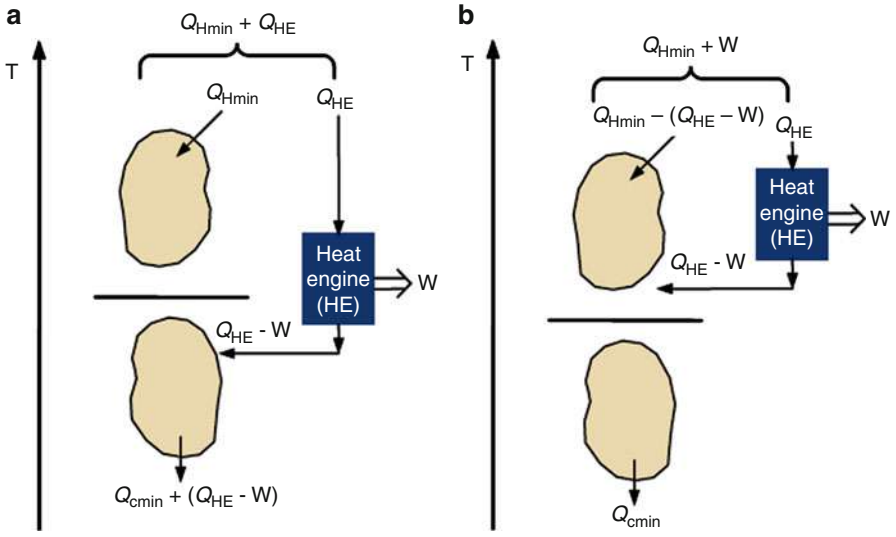

Fig. 10 Integration of heat engine exhaust: (**a**) across the pinch; and (**b**) above the pinch (Natural Resources Canada 2003)

shown in Fig. 10a, the process will still require the same amount of utilities ($Q_{H\ \mathrm{min}}$). When the heat engine is completely integrated above the pinch as shown in Fig. 10b, the heat is rejected to the heat sink region of the process, thus exploiting temperature differences between the utility and process and producing work at a very high efficiency. After integration, the import of W amount of extra energy from heat sources can produce W amount of shaft work, and the efficiency of heat to work conversion appears close to 100 %. A similar situation will arise when heat engine is completely integrated below the pinch.

Heat pumps, such as vapor compression and refrigeration, are systems that absorb heat at a low temperature in an evaporator, consume shaft work to compress the working fluid, and reject heat at a higher temperature in a condenser. If the pump is located completely above the pinch, it simply transforms power into heat, which is

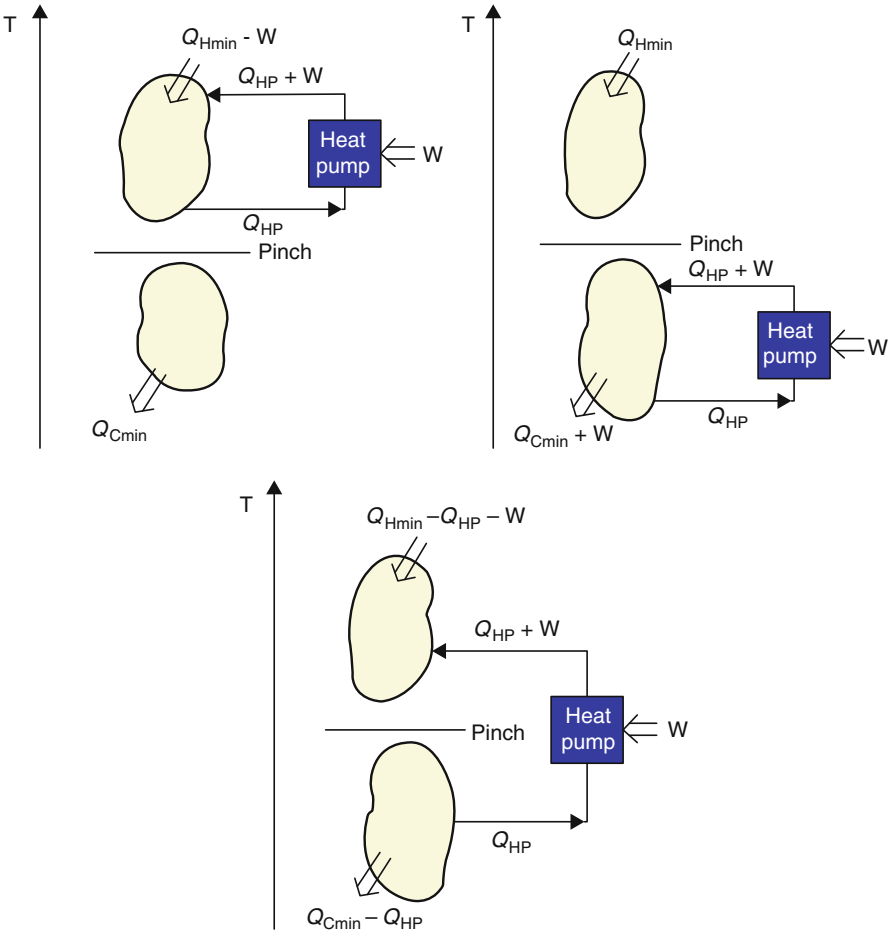

Fig. 11 Integration of a heat pump above, below, and across the process pinch (Natural Resources Canada 2003)

not economical. If it is placed completely below the pinch, the situation is even worse because work is transformed into waste heat. The only appropriate way to place a heat pump is across the pinch, where heat is absorbed below the pinch and rejected above the pinch, as shown in Fig. 11.

In fact, the principles introduced above can be concluded as the Townsend and Linnhoff heuristics (Seider et al. 2003):

1. When positioning heat engines to reduce the total utilities, place them entirely above or below the pinch.
2. When positioning heat pumps to reduce the total utilities, place them across the pinch.

Plus/minus principle in process modifications. For a process, the heat and material balance determines the shape of the composite curves and then the minimum energy requirements set by the curves. By changing the heat and material balance, the composite curves would change accordingly. Thus, it is possible to further reduce the energy requirement of the process. There are several parameters that could be changed, such as distillation column operating pressures and reflux ratios, feed vaporization pressures, etc. There are so many choices that a guide is needed to confidently predict the parameters that could be changed to reduce the energy consumption. By applying the thermodynamic rules based on pinch analysis, which is called the "plus/minus principle," it is possible to identify the appropriate process modifications that will improve the energy recovery significantly. In general, the hot utility can be reduced by (1) increasing hot stream (heat source) duty above the pinch and (2) decreasing cold stream (heat sink) duty above the pinch. Similarly, the cold utility target can be reduced by (1) decreasing hot stream duty below the pinch and (2) increasing cold stream duty below the pinch. This is termed as the plus/minus principle for process modifications. This simple principle provides a reference for any adjustment in process heat duties, such as vaporization of a recycle, etc., and indicates which modifications would be beneficial and which would be detrimental.

Often, it is possible to change temperatures rather than heat duties. It is clear from the composite curves that temperature changes confined to one side of the pinch will not have any effect on the energy targets. However, temperature changes across the pinch can change the energy targets for the process. For example, reducing the feed vaporization pressure (cold stream) may move the feed vaporization duty from above the pinch (minus) to below the pinch (plus). Hence, a reduction of vaporization duty is achieved in both hot and cold utilities. This can be considered as an application of plus/minus principle twice.

When a cold stream is removed from the region above the pinch and placed below the pinch, certainly, the shape of cold stream composite curve will change accordingly. The hot utility needed will diminish by the exact amount of cold utility moved. Similarly, moving a hot stream from the region below the pinch to above the pinch will reduce the hot utility consumption. In general, the above observations for beneficially shifting process temperatures can be summarized as follows: (1) shift hot streams from below the pinch to above and (2) shift cold streams from above the pinch to below.

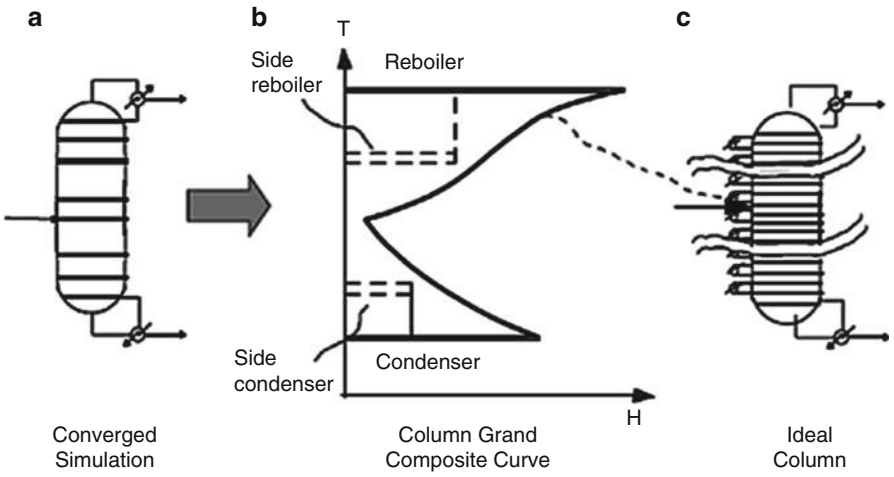

Fig. 12 Column grand composite curve (Linnhoff March 1998)

Modifications of distillation column. Distillation column unit is the basic processing step in many chemical plants. Although distillation is highly energy-intensive, consuming energy in the magnitude of several MJ/s, it has a low thermodynamic efficiency (less than 10 % for a difficult separation). Thus, it is one of the important areas for heat integration. During the retrofit or new column design, pinch analysis can be exploited to identify the targets for appropriate column modifications in order to reduce utility cost and to improve energy efficiency. Some software packages, such as Super Target™ (KBC Energy Services), Aspen Pinch™, provide advanced software tools for the implementation of column targeting and modifications.

Figure 12 shows an example of the column grand composite curve (CGCC) (Dhole and Linnhoff 1993b), a tool that is used for column pinch analysis. CGCC is based on the concept of minimum thermodynamic condition for a distillation column, which pertains to thermodynamically reversible column operation. In this ideal condition, a distillation column would operate at minimum reflux, with an infinite number of stages, and with side reboilers and side condensers placed at each stage with appropriate heat loads for the operating and equilibrium lines to coincide, as shown in Fig. 12c. In other words, the reboiling and condensing loads are distributed over the whole column. The stage-enthalpy (stage-H) or temperature-enthalpy (T-H) profiles for such an ideal column therefore can represent the theoretical minimum heating and cooling requirements of the column operation. These profiles are termed as the column grand composite curves (CGCC).

Most industrial columns have certain inevitable losses or inefficiencies. In order to set realistic targets for the column modifications, these losses must be allowed. To handle this problem, Dhole and Linnhoff (1993b) developed a practical near-minimum thermodynamic condition (PNMTC) approach, which is adopted by many software. This approach takes into account the losses or inefficiencies

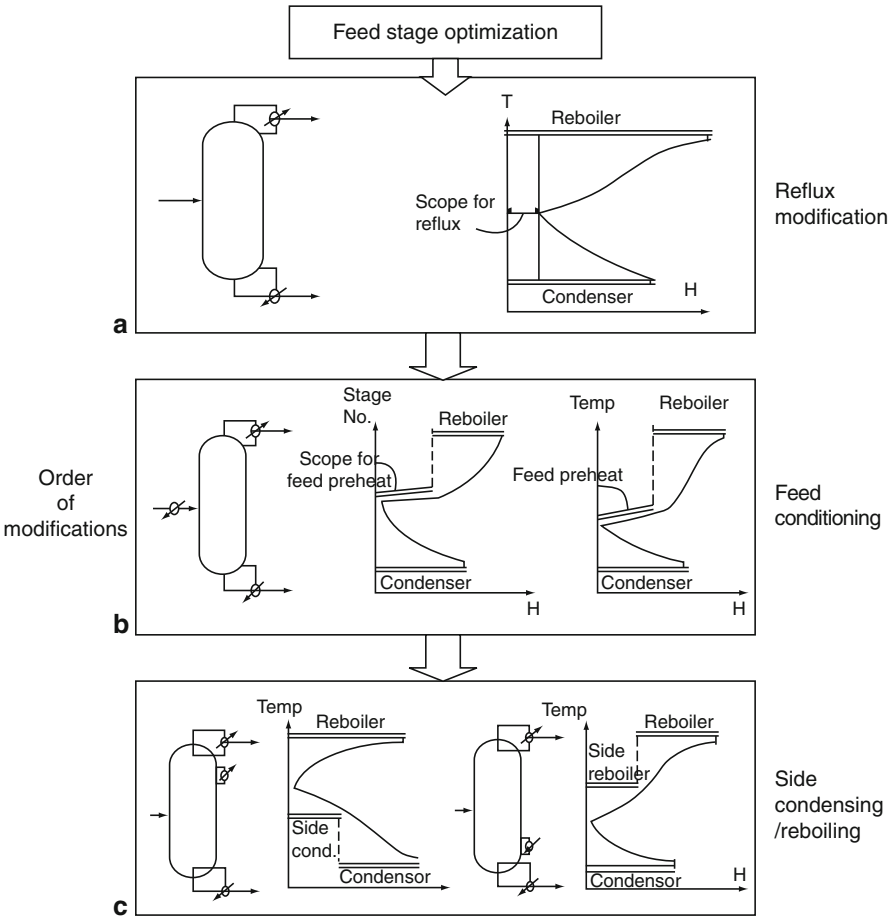

Fig. 13 Using column grand composite curve to identify column modifications (Linnhoff March 1998)

introduced through practicalities of column design, such as pressure drop, multiple side products, side strippers, sharp separations, etc. The procedure for constructing the CGCC starts from a converged column simulation. From the simulation, the necessary column information is extracted on a stage-wise basis. Then, the equations for equilibrium and operating lines are solved simultaneously at each stage for designated light-key and heavy-key components. The enthalpy deficits used in plotting the CGCC are calculated at each stage. At last, these enthalpy deficits are cascaded to construct the CGCC either in stage-H or T-H dimensions.

Like the grand composite curve for a process, the CGCC provides a thermal profile for the column and can be used for identifying the targets for potential column modifications, such as feed location, reflux ratio, feed conditioning (preheating or precooling), and side condensing or reboiling. Based on the

inspection of the CGCCs, the following order of implementation of different column modifications is recommended as shown in Fig. 13: feed location (appropriate placement), reflux ratio modification (reflux ratio vs. no. of stages), feed conditioning (preheating or precooling), and side condensing or boiling.

Feed location needs to be carried out first since it may strongly interact with other column modifications. The feed enthalpy strongly influences the shape of CGCC near the feed stage. And the CGCC usually shows a pinch point near the feed stage. Inspection of the CGCC can identify any distortions due to inappropriate feed location. Normally, this kind of distortions will be apparent since the stage-H CGCC will have significant projections at the feed location (pinch point). This is due to a need for extra local reflux to compensate for the inappropriate feed location. The optimal feed stage can be obtained by trying alternate feed locations and observing its influence on the reflux ratio. When the feed is introduced too high up in the column, there will be a sharp enthalpy change on the condenser side of the stage-H CGCC, and the feed should be moved down. Similarly, when the feed is introduced too low, there will be a sharp change on the reboiler side of the stage-H, and the feed should be moved up. The optimal feed location not only removes the distortion in the stage-H CGCC but also reduces the condenser and reboiler duties.

Out of many other column modification options, the scope of reflux improvement must be considered first since it results in direct heat load savings at both reboiler and condenser. In Fig. 13a, the horizontal gap between vertical axis and T-H CGCC pinch point indicates the scope for reduction in heat duties through reduction of reflux ratio. When the reflux ratio is reduced (while increasing the number of stages to maintain the separation), the gap will decrease, and the CGCC will move closer to the vertical axis, thus reducing the condenser and reboiler duties. It must be noted that when the reflux ratio is reduced, the number of stages will increase to maintain the desired separation. Thus, to obtain an optimal reflux ratio, the increase in the capital cost due to the increase of stages should be traded off against the savings in the operating cost due to reduced condenser and reboiler loads.

Inappropriate feed condition usually results in a sharp enthalpy change in the CGCCs near the feed location and increases the heat load of condenser or reboiler. The scope of feed conditioning can be identified from the sharp enthalpy changes on the stage-H or T-H CGCCs. Figure 13b shows an example that the feed needs to be preheated. The extent of the sharp enthalpy change on the CGCCs determines the appropriate preheating duty needed. Feed preheating not only reduces the reboiler duty but also reduces the temperature levels at which the hot utility (for the reboiler and the feed preheater) needs to be supplied. For feed precooling, the situation is similar. Changes in the heat duty of feed preheaters or precoolers will lead to similar duty changes in the reboiler or condenser loads.

After the modification of feed conditioning, side condensing/reboiling should be analyzed. An appropriate side reboiler, like the feed preheaters, not only reduces the heat loads of column reboiler but also reduces the temperature levels at which the hot utility (for the main reboiler and the side reboiler) needs to be supplied. In Fig. 13c, the two CGCCs show the potential for side condensing and reboiling, respectively.

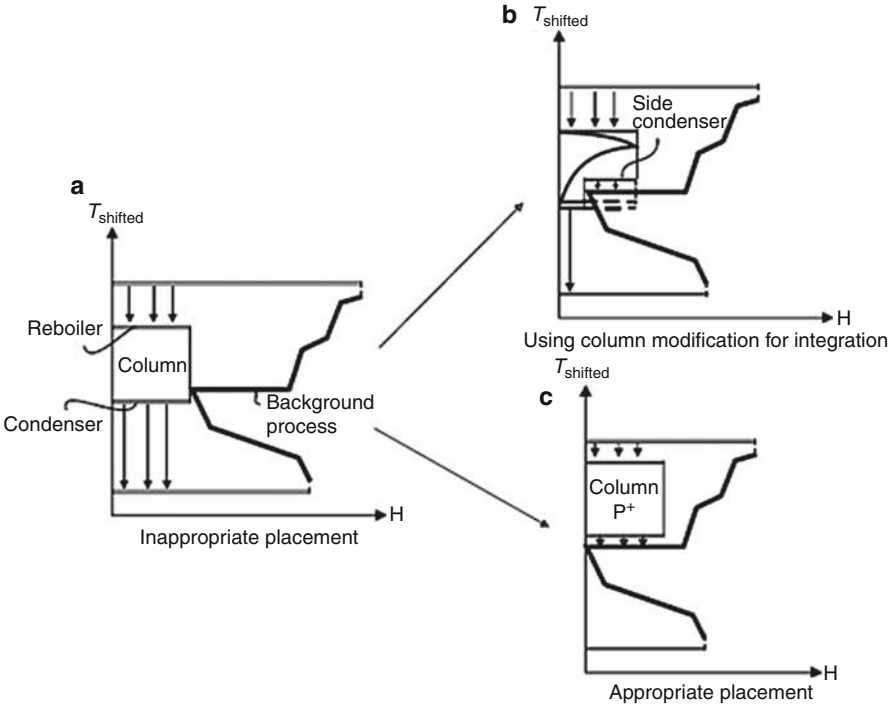

Fig. 14 Appropriate integration of a distillation column with the background process (Linnhoff March 1998)

In general, feed conditioning is preferred to side reboiling or side condensing as it offers a more moderate and convenient temperature level. Meanwhile, feed conditioning is external to the column and therefore easier to be implemented than side condensing/reboiling.

Till here, several ways of improving column thermal efficiency by stand-alone column modifications and their sequence are presented. In many cases, it is possible to further improve the overall energy efficiency of the process by appropriately integrating the column with the background process.

Figure 14 illustrates three examples of integrating the distillation column with the background process. The background process is represented by its grand composite curve. Figure 14a shows an example of an inappropriately placed column with its temperature range across the pinch temperature of the background process and without any potential for integration with the background process. Figure 14b illustrates a case that although the column temperature range still crosses the pinch temperature of the background process, a side condenser can be added to further improve the overall thermal efficiency as identified by the CGCC.

Figure 14c presents a different alternative integration scheme, which allows a complete integration between the column and the background process. In this scheme, the column pressure is increased to move the CGCC to one side of the

process pinch point instead of crossing the pinch. Thus, the overall energy consumption of this scheme is just the energy consumption of the background process.

Although appropriate column integration can provide significant energy benefits, these benefits must be considered together with the relevant issues, like the associated capital investment and difficulties in operation.

Data Extraction

Before the pinch analysis can be done, various process information is needed. Note that the amount of information available from plant measurement, data acquisition systems, and simulation models of a process can be very large, and most of the data may be of no relevance to the analysis. It is thus necessary to identify and extract only the information that truly captures the relevant sources and sinks and their interactions with the overall process. The required data involves process stream heating and cooling information, utility stream information, cost information, and some background information regarding the processes. In summary, the following data need to be collected for each process stream: mass flow rate (kg/s), specific heat capacity (kJ/kg·°C), supply and target temperature (°C), and heat related to a phase change (kJ/kg). Additionally, for the utilities and the existing heat exchangers, the following information needs to be acquired: existing heat exchanger area (m^2), heat transfer coefficient of heat exchangers ($kW/(m^2 \cdot °C)$), and utilities available in the process (water temperature, steam pressure levels, etc.).

Data extraction could be time-consuming and must be performed carefully as the results of pinch analysis strongly depend on this step. Poor data extraction can easily lead to missed opportunities for the process improvement. In extreme cases, poor data extraction can falsely show that the existing process design is already the optimal one in energy efficiency. Data extraction needs to be conducted in an appropriate way, which only accepts the critical parts of the existing design that cannot be changed. A key objective of data extraction is to recognize the parts of process that can be further modified during the analysis (e.g., adding new heat exchangers, changing the process temperatures, etc.). If during the data extraction, all the features of existing design are considered as fixed, then there will clearly be no scope for improvement. If the extraction does not consider any features of the existing design, then the pinch analysis conducted later may overestimate the potential benefits.

At the beginning of a data extraction, it is recommended that all process streams be included. The constraints, such as distance between processes, operability, and control and safety issues, can be considered later on. The experienced specialists may include some constraints at the beginning of data extraction. This can speed up the overall analysis; however, lots of experience is required to ensure that potential heat integration opportunities are not excluded by adding these constraints earlier. Hence, data extraction requires lots of experience, and there are many sector specifics for data extraction. Not all of them can be covered here; however, some important heuristic rules have been developed as guidelines over the past years.

Do not mix streams at different temperatures. In a process flow sheet, the streams at different temperatures cannot be directly mixed together, as such direct non-isothermal mixing acts as a direct contact heat exchanger. Such mixing may involve cross-pinch heat transfer and therefore increase the overall external utility requirement. It should not become a fixed feature of the data extraction. For example, if the pinch is located at 70 °C, then mixing a stream at 90 °C with a stream at 50 °C will create a cross-pinch heat transfer and increase the energy targets. To avoid this, if mixing must take place due to process reasons, then the isothermal mixing must be considered. The streams involved in mixing should be considered independently and extracted separately as being mixed at the same target temperature.

Do not carry over features of the existing solution. This rule is illustrated with the example whose process flow sheet is shown in Fig. 15. Based on the original data extraction generated from the process flow sheet in Fig. 15, a HEN design is conducted using pinch analysis. The original data extraction and corresponding HEN design are illustrated in Fig. 16. Because the HEN design from pinch analysis, consisting of one heater, one cooler, and two exchangers, is identical to the existing process flow sheet design in Fig. 15, it seems that the existing flow sheet design is already optimized and there is no opportunity for further improvement. The pinch analysis results in no benefit.

However, the original flow sheet is not an optimal design and the original data extraction is not appropriate. Figure 17 shows an appropriate method of data extraction from the existing process flow sheet and the corresponding HEN design. All the three cold streams previously extracted can be denoted as just one cold stream, and likewise, only one hot stream needs to be extracted. The improved design is much simpler and easier to control. It shows significant additional potential

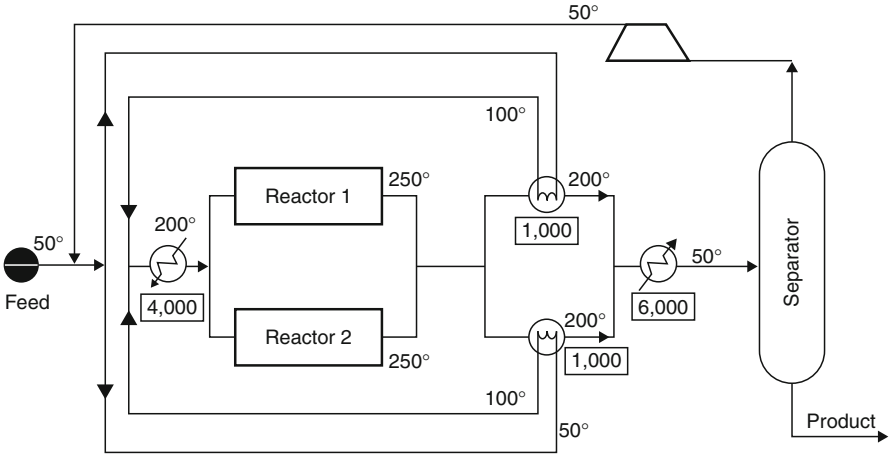

Fig. 15 Example process flow sheet for data extraction (Linnhoff March 1998)

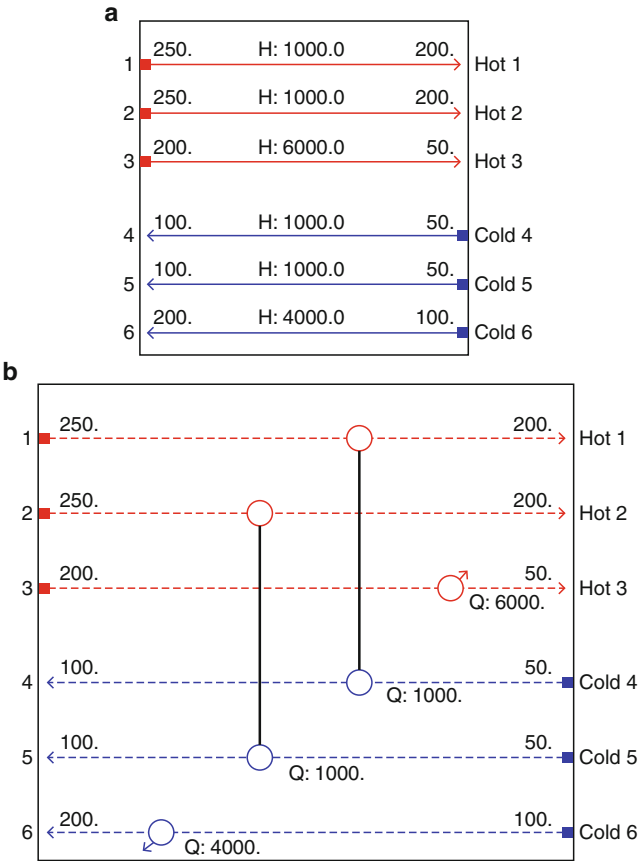

Fig. 16 Original data extraction and HEN design (Linnhoff March 1998)

for improved energy recovery and reduces both the equipment cost and energy cost. The "appropriate" data extraction does not exclude any potential energy-saving opportunities. As this example illustrates, the practitioner should be careful in separating the relevant stream data from the original process flow sheet design and should not take over features from it.

Do not consider true utility streams. A true utility stream is a utility stream (steam, flue gas, cooling water, refrigerant, cooling water, etc.) that can be replaced in principle by any other stream (process or utility) for heat recovery. One of the goals of using pinch analysis is to reduce the usage of utilities. Therefore, if utility streams are extracted in a similar way to process streams, they will be considered as fixed features and thus no opportunities of reduction in utility use will be identified. However, in some cases, it is not practical to replace the utility streams by any other form of heat recovery. The utility streams are not true utility streams and need to be extracted as process streams. This is often the case for steam dryers, ejectors, and turbine drives. For example, when steam is required in a shift reactor to enhance the

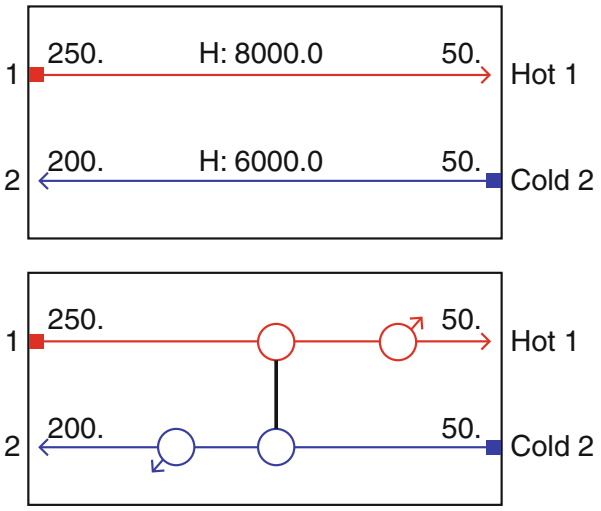

Fig. 17 Improved data extraction and HEN design (Linnhoff March 1998)

shift process, the steam is not a true utility. The steam is not just used for heating but is necessary for the reaction and cannot be replaced. In this situation, the steam must be extracted as a cold stream, to be heated and vaporized from the original feed condition to the appropriate steam temperature and pressure for the reaction.

Identify hard and soft constraints. A hard constraint would be a constraint that cannot be changed in any way, like the inlet temperature of a reactor, while a soft constraint is often open to change within certain range. An example of a soft constraint is the discharged temperature of a product stream going to storage, which is often flexible within a range. It is sometimes possible to achieve more heat recovery by changing the soft constraints, such as temperature, pressure, and enthalpy conditions of streams, at the data extraction stage. So the soft constraints should be ideally extracted and the plus/minus principle for process modifications should be applied.

Total Site Concept

In the previous part, heat and power integration for a single process has been studied. Typically, industrial processes, such as refinery and petrochemical processes, operate as parts of large sites or factories. A total site is originally defined as an industrial system consisting of several processes, whose material and energy needs are supplied by a central utility system. For example, in a large site where direct heat integration between processes (e.g., heat exchange between two streams from different processes) is difficult due to a long distance between them, indirect heat integration may be achieved through a utility system. By integrating a number of processes via the steam system, additional inter-process heat recovery can be achieved. Figure 18 shows a schematic of a typical process industry site involving several processes, A, B, and C. These individually operated processes, some with

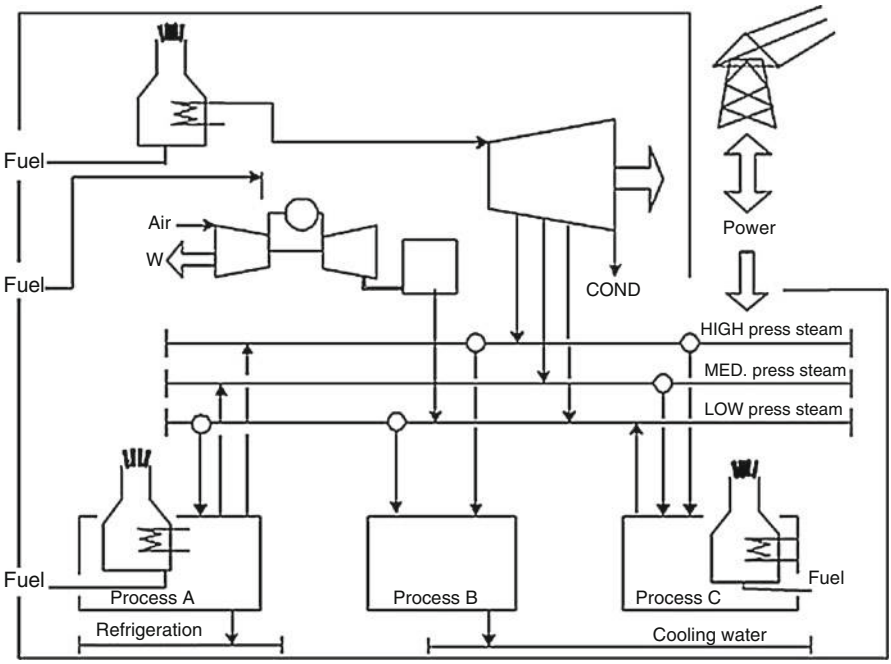

Fig. 18 Schematic of a site whose separately operated processes are linked indirectly through the utility system (Natural Resources Canada 2003)

their own utilities, are served by a central utility system. The utility system consumes fuel, generates power, and supplies the necessary steam through several steam mains. There are both consumption and recovery of process steam via the steam mains between the different processes. Usually the individual production processes and the central services are controlled by different departments and operated independently. The site infrastructure therefore usually suffers from an inadequate overview design and control. For example, in a site involving 50 production processes, the grand composite curve of each individual process will suggest different steam levels. To minimize the total energy and capital cost of the whole site, it requires an approach to consider the individual process issues along with the site-wide utility planning together to identify the correct compromise in steam levels and loads.

A graphical method, the so-called total site profiles, was first introduced by Dhole and Linnhoff in 1993 (1993a). Klemes et al. (1997) then extended this methodology to site-wide applications. This method allows a target to be set for the total site heat recovery. Site-wide analysis usually starts with a kickoff meeting to determine the detail levels each process should be studied and the scope of total site data extraction. In general, not all processes need to be analyzed at the same level. For example, some units may lack enough data for the analysis, and some processes do not need a detailed study due to their small size or low complexity.

Three models, black box, gray box, and white box, are used to represent the broad categories of detail level that may be applied to a process. Black-box processes are not to be studied in detail and only the overall utility consumption is considered. This may be because their energy consumption is very small, or heat recovery projects may be difficult to implement, or it is just not the right time for the company to invest in that area. So these processes are simply represented by their existing utility consumption profiles.

Gray-box processes only consider heat transfer that involves utilities. These processes usually have small scope of process-process heat exchange but have significant utility use. In these cases, the process streams that are heated or cooled by utility are considered; however, the process-process heat exchange matches are not considered. In this way, the process/utility interface can be optimized in a site-wide area instead of internal optimization within the process. Again, there is no need to conduct individual pinch analyses for the processes.

White-box processes need to perform a detailed pinch analysis. These are usually complex processes with significant energy consumption. For these processes, grand composite curves are constructed. The source and sink profiles of these white-box processes, together with those of black-box processes and gray-box processes, are further modified to construct the site source sink profile (SSSP) which consists of a site heat source profile and a site sink profile. The construction procedure involves selecting parts of the grand composite curves that are satisfied by the central utility system and shifting the temperature. It is not the same as simply combining all the process stream data together into a single site data set, which would allow some far from realistic scenarios. Those scenarios do not consider the realistic constraints, such as distances, controllability, flexibility, etc., which will reduce the number of integration possibilities. For the detailed construction procedure, please see reference (Linnhoff March 1998).

Figure 19 illustrates the construction site source sink profiles for a site consisting of four white-box processes (A, B, C, and D) and several other gray-box and black-box processes. In the total site profiles diagram, the site heat sources are shown on the left side and the site heat sinks are shown on the right side.

Total site analysis is used to determine the potential for maximizing indirect heat integration through central utilities. The analysis can identify the optimal balance of process steam generation via heat recovery and consumption, and also the optimum steam header pressures. After the site source profile and site heat sink profile are plotted, the composite curves of steam generation and consumption are also constructed. The heat should transfer from the heat source profile to the steam generation profile to generate steams. And also, the heat from the steam usage profile should transfer to the heat sink profile by the consumption of steam. By superimposing the current utility balance onto the site source and sink profiles, thermodynamic targets for heat and power cogeneration can be set graphically. Figure 20 shows the site source sink profiles and utility profiles for a site-wide analysis. On the left side of Fig. 20a, the gap between the process heat sources profile and the current steam generation profile shows that there is a potential to generate additional high-pressure steam through heat recovery from process heat sources.

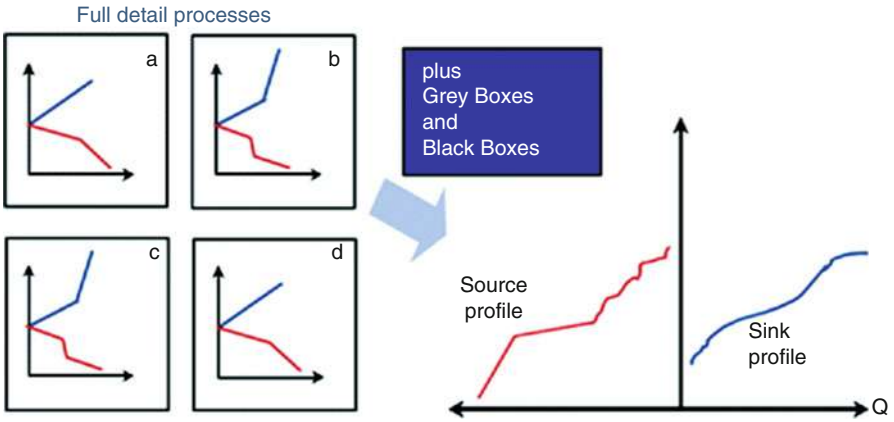

Fig. 19 Construction of the site-wide source sink profiles (Natural Resources Canada 2003)

Similarly, on the right side of Fig. 20a, the gap between the process heat sink curve and the current steam consumption curve shows that much of the medium-pressure steam usage can be substituted by low-pressure steam to reduce the steam energy consumption.

Figure 20b shows the target for optimal steam generation through heat recovery from process heat sources and the target for optimal steam consumption (heat load and pressure levels). On the left side of Fig. 20b, the optimal additional high-pressure steam generation can be identified through shifting the existing steam generation profile toward process heat sources profile. This will effectively increase the heat integration between processes indirectly through the utility system and reduce the need of external hot utility for steam generation. Similarly, on the right side of Fig. 20b, the optimal heat load and pressure levels of steam consumption can be targeted by shifting the existing steam consumption profile toward process heat sinks profile.

Typically, a site-wide pinch analysis can be carried out in two phases. The objective of the first phase is to get a reliable target for overall, site-wide savings and to identify the potential area that is likely to yield greatest benefits during the following second phase. In this way, engineering hours are minimized both in phase 1, through the judicious selection of black- and gray-box processes, and in phase 2, by not having to study every data in detail. In phase 2, further project packages need to be developed, and the strategic total site road map can be constructed. After the work of phase 1, it is possible to establish the relationship between investment and benefit of all the projects in the site. Such a representation is called the road map for the site development. The road map includes project details such as savings, investment, effect on emissions, and the compatibility of projects with each other. Each route in a road map consists of a series of mutually compatible projects. Each project package is explored for its technical and economic feasibility. The road map forms a rigorous basis for the designer or planner to plan a route or a strategy for long-term site development on all energy-related issues.

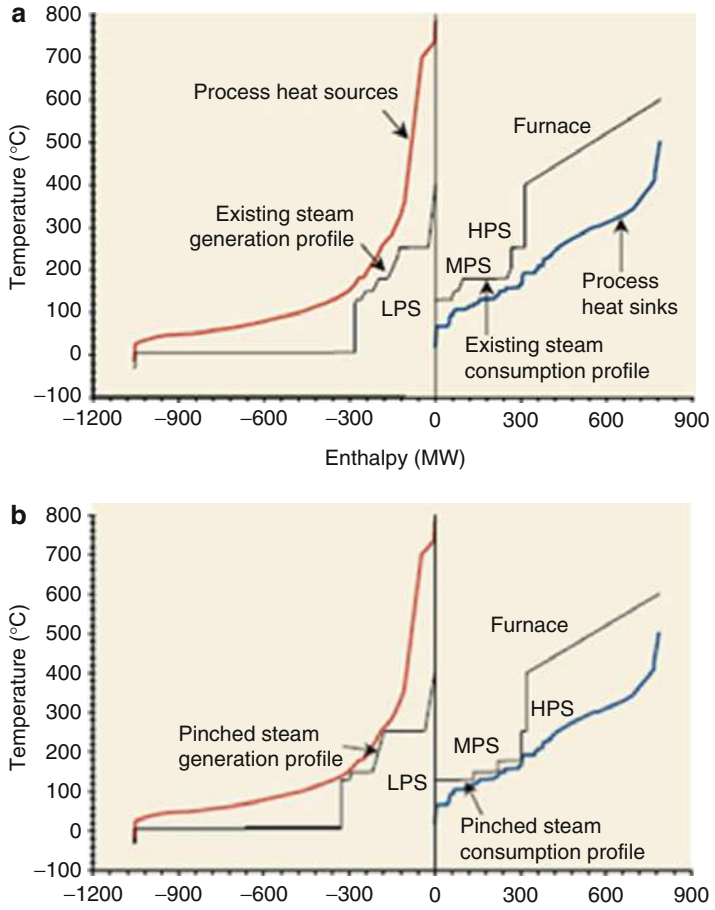

Fig. 20 (**a**) The existing total site profiles before targeting. (**b**) Total site profiles after targeting (Natural Resources Canada 2003)

As a summary, the key steps in total site pinch analysis can be listed as follows:

1. Individual process pinch analysis: Starting from heat and material balances of individual processes, pinch analysis establishes key options for process modifications, energy recovery (savings in noncentral utilities), and targets for multiple utilities. The grand composite curves are ready for use in total site analysis.
2. Total site pinch analysis: The site source sink profiles and the central utility generation and usage curves are constructed. They can help to set targets for the utility system improvements and process-wise improvements. The assumptions of steam system instep (1), such as the pressure of steam mains, need to be reset if they are changed in this step (2).

3. Identification of specific projects and construction of road map: The targets obtained through previous steps need to be further implemented in detail. Then the specific projects are put together in a coherent plan involving alternative routes of compatible projects.
4. Final selection of project alternatives from total site road map.

The site-wide analysis technique can be a very powerful approach for oil refining, petrochemical, and iron and steel plants, as well as regional energy sectors. Some software applications based on this approach are currently available. The SuperTarget software package (KBC Energy Services, UK), allows engineers to undertake total site pinch analysis using its site module. Kazuo Matsuda et al. (2009) applied the total site pinch analysis to one of the largest heavy chemical complexes in Japan which has 31 sites consisting of process industries including a petrochemical, refinery, and power company. Their study demonstrates that despite the very high efficiency of the individual process plants in the complex, the area-wide pinch technology can identify a huge amount of energy-saving potential. In their study, a large amount of energy saving, 0.9×10^6 GJ/year, was achieved by the implementation of area-wide integration projects.

An important innovation about the total site concept has been presented by Perry et al. (2008), who extended this concept. Traditionally, a total site includes only a set of industrial processes. Perry et al. made a further improvement by including commercial and residential energy users into the total site concept. The resultant process collections are termed as locally integrated energy sectors.

Mathematical Programming Approach for HEN Design

Over the past decades, heat-integrated system and HEN design have been extensively studied. Most of the contributions to this research can be classified as either a sequential or a simultaneous synthesis method (Furman and Sahinidis 2002). Generally speaking, mathematical programming represents a class of alternative techniques in spite of pinch analysis. Linear programming (LP) method and mixed integer linear programming (MILP) (Papoulias and Grossmann 1983) are both sequential methods.

The simultaneous synthesis methods are primarily mixed integer nonlinear programming (MINLP) (Yee and Grossmann 1990) formulations of HEN problems. The approach is based on a stage-wise superstructure representation that contains all possible network configurations and process stream matches. In each stage, potential heat exchange may take place between any pair of hot and cold streams. This MINLP model can simultaneously optimize and synthesize the capital and energy cost, and other structural features, as steam splitting and bypass design. While the MINLP can be formulated easily, unfortunately, it is frequently difficult to obtain converged solutions using the algorithms available today in systems like GAMS, especially when the number of streams is large and the models are complex. It is beyond the scope of this text to cover in detail the

approaches to formulating and solving MINLPs. However, in the next section of this chapter, a disturbance propagation and rejection (DPR) embedded MINLP model is introduced for HEN design.

Disturbance Propagation and Control Modeling for the Design of Highly Controllable Heat-Integrated Systems

Traditionally, in most process synthesis activities, only the cost is considered when targeting the optimal solution. This practice can give rise to the designs at the minimum total annualized investment. Process operational issues, especially structural controllability, are usually not a concern in the design procedure, while only steady-state condition is considered. As a consequence, the operational controllability of the "optimal" design solution generated by the aforementioned traditional method may be questionable. In the worst case, an (economically) optimally designed process may not be operable, as shown in Yang et al. (1996), where a real industrial example is described, where the originally designed HEN experiences various disturbances of temperatures and heat capacity flow rates in operation. Industrial practice has made it clear that process controllability should be part of the process synthesis work. This has led to the introduction of an active research area, called integration of process design and control (IPDC) (McAvoy 1987; Huang and Fan 1992; Elliott and Luyben 1995).

The analysis of disturbance propagation (DP) and disturbance rejection (DR) is conducted extensively in flexibility and controllability analysis. Flexibility is a system's capability of absorbing long-term variations appearing at the inlet of process (Papalexandri and Pistikopoulos 1994; Kotjabasakis and Linnhoff 1986). Controllability is referred to as the system's capability of withstanding short-term disturbances. Yang et al. (1996, 2000, 2005; Lou and Huang 2002) introduced a simplified, first-principle-based modeling approach to evaluate DP in HENs, MENs (Mass Exchanger Network), distillation networks, and heat-integrated reaction system design at the steady-state level. Integrating this quantitative analysis approach into traditional process synthesis can lead to the optimal design satisfying both economic and operational objectives.

Disturbance Propagation Modeling

The DP modeling approach introduced below is general, and it will be integrated into a super structure-based MINLP (mixed integer nonlinear programming) model, through a case study, to generate a cost-effective and highly controllable network.

In the process synthesis stage, the precise information of process disturbance is usually unavailable. Meanwhile, a worst-case design is usually sufficient, though may not be optimal. Thus, the estimated maximum magnitude of each disturbance can be used instead. For a HEN operated at a given normal operating condition, the known types of disturbances can be expressed as the maximum fluctuation of stream

source temperature (δT^s) and that of heat capacity flow rate (δMc_p). After propagating these disturbances of input source streams, the resulting DP model can predict the stability of the target temperature of each stream by the obtained δT^t, which stands for the largest deviation from the normal operating target points. Yang et al. (1996) developed a DP modeling methodology for a heat exchanger unit as well as a HEN that can contain any number of hot and cold streams. By neglecting the high-order differentiation terms and replacing the logarithmic mean temperature difference by an arithmetic mean term (Yan et al. 2001), the model can be simplified to a linear one and is summarized below.

Unit-based DP model. A DP model for a single heat transfer unit (HTU) can be written as follows:

$$\delta T^t = D_t \delta T^s + D_m \delta M c_p \tag{1}$$

or

$$\begin{pmatrix} \delta T_h^t \\ \delta T_c^t \end{pmatrix} = \begin{pmatrix} 1-\alpha & \alpha \\ \beta & 1-\beta \end{pmatrix} \begin{pmatrix} \delta T_h^s \\ \delta T_c^s \end{pmatrix} + \begin{pmatrix} (2-\alpha)\alpha_h & -\alpha_c \alpha \\ \beta \alpha_h & -\alpha_c (2-\beta) \end{pmatrix} \begin{pmatrix} \delta MC_{ph} \\ \delta MC_{pc} \end{pmatrix} \tag{2}$$

where

$$\alpha = \frac{T_h^s - T_h^t}{T_h^s - T_c^s}, \tag{3}$$

$$\beta = \frac{T_c^t - T_c^s}{T_h^s - T_c^s}, \tag{4}$$

$$\alpha_h = \frac{T_h^s - T_h^t}{2MC_{p_h}}, \tag{5}$$

$$\alpha_c = \frac{T_c^t - T_c^s}{2MC_{p_c}}, \tag{6}$$

where D_t and D_m are temperature and heat capacity flow rate-related disturbance propagation matrix, respectively; T and δT are the stream temperature and temperature fluctuation, respectively; Mc_p and δMc_p are the heat capacity flow rate and its fluctuation, respectively; superscripts s and t refer to source and target, respectively; and h and c refer to hot and cold streams, respectively. The above model can be used to provide a quick and accurate quantification of DP through the propagation in a heat exchanger.

System DP model. The unit-based DP model in Eq. 1 can be applied to any heat transfer unit (HTU) in a HEN. Thus, the DP model for the i-th HTU, named E_i, in a HEN can be expressed as:

$$\delta T_{E_i}^{\text{out}} = D_{t_{E_i}} \delta T_{E_i}^{\text{in}} + D_{m_{E_i}} \delta M c_{p_{E_i}} \tag{7}$$

If a HEN contains N_e heat exchangers, a system DP model can be established directly by lumping all the single unit-based models in the sequence of exchanger numbers. This procedure yields the following equation:

$$\delta T^{*\text{out}} = D_{t_E}^{*} \delta T^{*\text{in}} + D_{m_E}^{*} \delta M c_p^{*} \tag{8}$$

where

$$\delta T^{*\text{in}} = \left[\left(\delta T_{E_1}^{\text{in}} \right)^T \left(\delta T_{E_2}^{\text{in}} \right)^T - \left(\delta T_{E_{Ne}}^{\text{in}} \right)^T \right]^T, \tag{9}$$

$$\delta T^{*\text{out}} = \left[\left(\delta T_{E_1}^{\text{out}} \right)^T \left(\delta T_{E_2}^{\text{out}} \right)^T - \left(\delta T_{E_{Ne}}^{\text{out}} \right)^T \right]^T, \tag{10}$$

$$\delta M_{c_p}^{*} = \left[\left(\delta M c_{P_{E_1}} \right)^T \left(\delta M c_{P_{E_2}} \right)^T - \left(\delta M c_{P_{E_1^e}} \right)^T \right]^T, \tag{11}$$

$$D_{t_E}^{*} = \text{diag}\left\{ D_{t_{E_1}}, D_{t_{E_2}}, \cdots, D_{t_{E_{Ne}}} \right\}, \tag{12}$$

$$D_{m_E}^{*} = \text{diag}\left\{ D_{m_{E_1}}, D_{m_{E_2}}, \cdots, D_{m_{E_{Ne}}} \right\}, \tag{13}$$

The superscript Tin equations designate the transpose operation of corresponding matrix, which interchanges the rows and columns of matrix. The "diag" in Eqs. 12 and 13 means the matrix $D_{t_E}^{*}$ and $D_{m_E}^{*}$ are diagonal matrices, which is a square matrix whose elements outside the main diagonal are all zero. The dimensions of vectors $\delta T^{*\text{in}}$, $T^{*\text{out}}$, and $\delta M C_p^{*}$ are all $2\,N_e \times 1$, and the $D_{t_E}^{*}$ and $D_{m_E}^{*}$ are both $2\,N_e \times 2\,N_e$ matrices. It is needed to point out that $\delta T^{*\text{ in}}$ and $\delta T^{*\text{ out}}$ contain a number of N_m intermediate temperatures. An intermediate temperature is the temperature of a stream between two adjacent heat transfer units (HTUs). N_m can be calculated by the following Eq. 14:

$$N_m = 2N_e - N_s - N_{\text{split}}, \tag{14}$$

where N_e is the number of HTUs; N_s is the total number of hot streams and cold streams; and N_{split} is the total number of stream branches after splitting.

After several steps of mathematical processing, a general system DP model can be derived as bellow:

$$\delta T^{t} = \underline{D_t} \delta T^{s} + \underline{D_m} \delta M c_p \tag{15}$$

where

$$\underline{D_t} = D_{t11} + D_{t12}(I - D_{t22})^{-1} D_{t21}, \tag{16}$$

$$\underline{D_m} = D_{m1} + D_{t12}(I - D_{t22})^{-1} D_{m2}. \tag{17}$$

Those underbars in the equations do not have any mathematical meaning and are just symbols to differentiate from other matrix variables. For the detailed deduction of this model, please refer to the work of Yang et al. (2006).

DP-based network structure representation. To derive those matrices in the DP model, a structural matrix S, whose dimension is $(2\ N_e - N_{\text{split}}) \times 2\ N_e$, should be constructed. Matrix S can be decomposed into two sub-matrices, $S_1(N_s \times 2\ N_e)$ and $S_2(N_m \times 2\ N_e)$, whose definitions are given below.

In sub-matrix S_1, each row is designed for a hot or cold stream, and the columns are divided into N_e pairs. Each pair is assigned for a specific heat transfer unit (HTU). In each pair, the left column corresponds to the hot stream going through the HTU, and the right column corresponds to the cold stream through the unit. A stream may be split into a number of branches, going through different HTUs and mixing together. In this case, the splitting ratios are reflected by the matrix elements corresponding to the streams. Each element has a value between 0 and 1, where 0 represents streams not going through the units – a fraction represents the splitting portion going through the unit – and 1 means the stream going through units without splitting.

In sub-matrix S_2, each row represents the intermediate streams between two adjacent HTUs. The definition of columns is the same as sub-matrix S_1. Each element of matrix S_2 represents the connection modes of the intermediate stream with an HTU. [1], [1], or 0 is assigned to the element to represent an intermediate stream entering, leaving, or not going through an HTU, respectively.

DP model-embedded HEN synthesis approach. HEN synthesis can be fulfilled by mixed integer nonlinear programming (MINLP) method, following the procedures of network representation, mathematical optimization model formulation, and optimal solution identification. The DP model introduced above can be integrated in the optimization model to take account of controllability issues in HEN design.

Problem statement. In an HEN synthesis problem, there are a set I of hot process streams, a set J of cold process streams, and a set K of superstructure stages. Each hot or cold process stream has a specified heat capacity flow rate, and their inlet and outlet temperatures are also specified exactly or given as inequalities. A set of hot and cold utilities, along with their temperatures, are also known. Meanwhile, the predicted max-min source temperature disturbance and flow rate fluctuations are also given along with the permissible target temperature fluctuations. The objective of the synthesis is to determine a network structure with the minimum total annual cost (TAC) satisfying the permissible target temperature fluctuation requirement.

Stream-based superstructure. The first step of the synthesis is constructing a stream-based superstructure. An HEN superstructure can be developed by a graph-theoretical approach (Floudas 1995). Figure 21 shows a two-stage superstructure for a two hot and **two** cold stream synthesis problems, which will be studied in this case. All units and their inputs and outputs are represented as a set of nodes in the graph, where all possible connections are linked between pairs of units. The key elements of

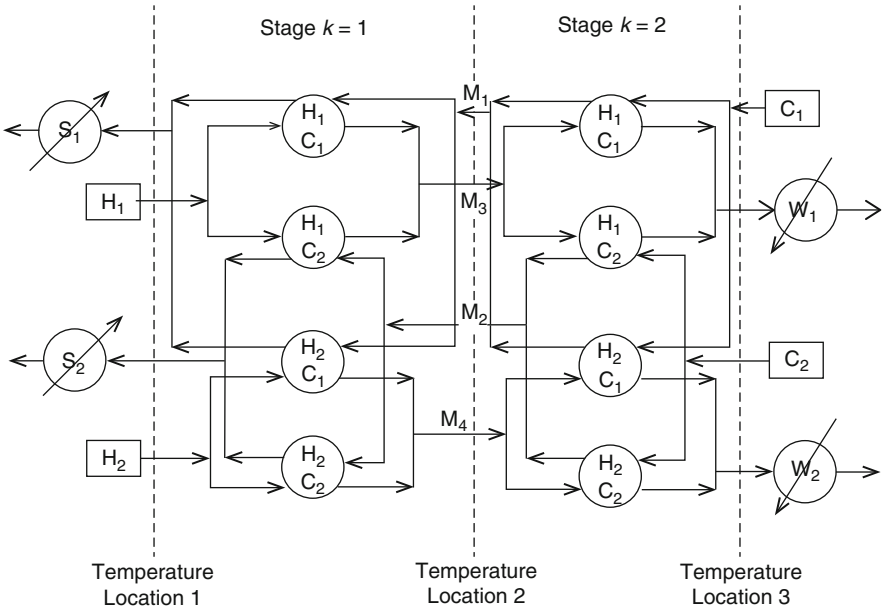

Fig. 21 Two-stage superstructure for two hot streams and two cold streams (Yan et al. 2006)

a superstructure are HTUs, mixers, and splitters. An HTU is denoted as a large circle, while a mixer or splitter is denoted as a small dot. Each HTU has a splitter at its inlet and a mixer at its outlet.

Problem formulation. After the construction of HEN superstructure, the next step is to formulate the synthesis problem with mathematical equations.

Objective function. The total annual cost (TAC) is the combination of the utility cost and heat exchangers' related cost, such as the cold utility cost, hot utility cost, fixed charges, and area cost for heat exchangers between streams. TAC should be minimized and can be formulated as (Yan et al. 2006):

$$\begin{aligned}
&\min \sum_{i\in I} C_{CU} Q_{cu,i} + \sum_{j\in J} C_{HU} Q_{hu,j} + \sum_{i\in I}\sum_{j\in J}\sum_{k\in K} CF_{i,j} y_{i,j,k} \\
&+ \sum_{i\in I} CF_{cu,i} y_{cu,i} + \sum_{j\in J} CF_{hu,j} y_{hu,j} \\
&+ \sum_{i\in I}\sum_{j\in J}\sum_{k\in K} C_{i,j}\left(\frac{Q_{i,j,k}}{U_{i,j}\left[\Delta T_{i,j,k}\Delta T_{i,j,k+1}\left(\Delta T_{i,j,k}+\Delta T_{i,j,k+1}\right)/2\right]^{1/3}}\right)^{0.6} \\
&\quad + \sum_{i\in I} C_{i,cu} + \left(\frac{Q_{cu,i}}{U_{cu,i}\left[\Delta T_{cu,i}\left(T_i^t - T_{cu}^s\right)\left(\Delta T_{cu,i} + T_i^t - T_{cu}^s\right)/2\right]^{1/3}}\right)^{0.6} \\
&\quad \sum_{j\in J} C_{j,cu} + \left(\frac{Q_{hu,j}}{U_{hu,j}\left[\Delta T_{hu,j}\left(T_{hu}^s - T_j^t\right)\left(\Delta T_{hu,j} + T_{hu}^s - T_j^t\right)/2\right]^{1/3}}\right)^{0.6},
\end{aligned} \tag{18}$$

where C_{CU} is the per-unit cost of cold utility; $Q_{cu,\ i}$ stands for the heat exchanged between hot stream i and the cold utility; C_{HU} is the per-unit cost of hot utility; $Q_{hu,\ j}$ stands for the heat exchanged between cold stream j and the hot utility; CF is the fixed charge for heat exchangers; C is the area cost coefficient; the exponent 0.6 in this equation is a constant used by many researchers to analyze the area cost of heat exchangers; T^s and T^t are inlet and outlet temperatures, respectively; U is the heat transfer coefficient; $Q_{i,\ j,\ k}$ is the heat exchanged between hot process stream i and cold process stream j in stage k; $\Delta T_{i,\ j,\ k}$, is the temperature approach for the match of hot stream i and cold process stream j in stage k; $\Delta T_{cu,\ i}$ is the temperature approach for the match of hot stream i and the cold utility; $\Delta T_{hu,j}$ is the temperature approach for the match of cold process stream j and hot utility; variable $y_{i,\ j,\ k}$ stands for the existence of a match between hot process stream i and cold process stream j in stage k; $y_{cu,\ i}$ stands for the existence of a match between hot stream process i and cold utility; and $y_{hu,\ j}$ stands for the existence of a match between cold stream process j and hot utility. The binary variables represent the existence of unit for a match and the values are either 1 or 0.

$$y_{i,j,k}, y_{cu,i}, y_{hu,j} \in \{0,1\}, \quad \forall i \in I, \forall j \in J, \forall k \in K \tag{19}$$

Constraints. This MINLP problem should be subject to the following constraints.

Energy balance constraints. The overall energy balance for each process streams should be observed. For example, the amount of energy each hot (cold) process stream releases (obtains) by the difference of source and target stream temperature should be equal to the sum of heat transferred between process streams and heat transferred to (from) cold utilities (hot utilities).

Also, the energy balance for each stream is each superstructure stage and the energy balance for the utility streams should be respected.

Temperature feasibility constraints. The temperature of each stream should decrease monotonically along with the temperature locations.

Logical constraints. The temperature approach between the streams that exchanged heat should not exceed the maximum temperature difference. Meanwhile, the exchanged heat of process streams and utilities cannot exceed an upper limit.

System controllability constraints. Besides the above constraints, the target temperature fluctuations of streams should be limited in permissible ranges, which are the controllability-related constraints.

$$\delta T_{\max}^{t(-)} \leq \delta \underline{T}^t \leq \delta T_{\max}^{t(+)} \tag{20}$$

where $\delta \underline{T}^t$ is the vector for target temperature fluctuations and $\delta T_{\max}^{t(-)}$ and $\delta T_{\max}^{t(+)}$ are vectors for the maximum negative and positive target temperature fluctuations, respectively.

The DP-based network structure matrix S can be constructed according to the approach introduced in the previous section. Then, based on this structure matrix S

and the binary variables, an HEN system DP model can be constructed as introduced before. Through the system DP model, the target temperature fluctuations $\delta \underline{T}^t$ can be obtained from the source temperature disturbances $\delta \underline{T}^s$ and source heat capacity flow rate disturbances Mc_p.

Optimal solution identification. After the formulation of objective function and various constraints, the last step in this synthesis approach is the optimization of the model. This DP-embedded MINLP model can be solved using the general algebraic modeling system (GAMS).

Case application of DP-embedded HEN synthesis approach. Yan et al. (2006) studied the case of Yee and Grossmann (1990) for the incorporation of DP into the HEN design procedure. This design problem has two hot streams and two cold streams. The design data including the disturbance information are listed in Table 2. The stage-wise superstructure is already shown in Fig. 21. There are 12 possible matches and therefore 12 binary variables. According to this superstructure, a structure matrix S is also generated and listed in Table 3. The "M" labeled stream in Table 3 stands for the intermediate stream between two adjacent heat transfer units. In this case, three scenarios are studied and each has a different control requirement. In each scenario, the control requirements, which are the maximum negative and positive target temperature fluctuations $\delta T^{t(-)}_{\max}$ and $\delta T^{t(+)}_{\max}$ act as one of the constraints. The optimal HEN of this scenario can be obtained by solving the DP-embedded MINLP problem using GAMS.

For further detailed calculations, please refer to the work of Yan et al. because only the results are provided here. Table 2 listed the control requirements, the actual temperature fluctuations, and the TAC of each scenario. Figures 22, 23, and 24 give the optimal HEN solution of each scenario under different control specifications. The symbol "E" in these figures represents the heat exchangers.

Comparing the three optimal solutions, it is obvious that solution A in scenario I has the simplest HEN structure (Fig. 22) and the minimum TAC ($ 450,072 in Table 2). This is because in scenario I, there are no constraints imposed on the maximum negative and positive target temperature fluctuations $\delta T^{t(-)}_{\max}$ and $\delta T^{t(+)}_{\max}$, and actually, this is the traditional synthesis case where no control issues are considered. However, when the strict control requirements are specified, this optimal solution

Table 2 Stream data for the synthesis problem (Yan et al. 2006)

Stream	T^s (°C)	T^t (°C)	Mc_p (kW/°C)	$\delta T^{s(+)}$ (°C)	$\delta T^{s(-)}$ (°C)
Hot 1	180	75	30	5	0
Hot 2	240	60	40	0	0
Cold 1	40	230	35	0	−5
Cold 2	120	300	20	0	−5
The heat transfer coefficients: $U_{i,j} = U_{cu,i} = 0.8$ kW/(m^2·°C); $U_{hu,j} = 1.2$ kW/(m^2·°C)					
The per-unit cost of utilities: $C_{CU} = 20$ $/(kW/year); $C_{HU} = 80$ $/(kW/year)					
The area cost coefficients: $C_{i,j} = C_{i,cu} = 1{,}000$; $C_{hu,j} = 1{,}200$					

Table 3 Structural matrix for the superstructure of case study (Yan et al. 2006)

	HTU_1		HTU_2		HTU_3		HTU_4		HTU_5		HTU_6		HTU_7		HTU_8	
Stream	H	C	H	C	H	C	H	C	H	C	H	C	H	C	H	C
H_1	$\frac{Q_{1,1,1}}{Q_{1,1,1}+Q_{1,2,1}}$	0	$\frac{Q_{1,2,1}}{Q_{1,1,1}+Q_{1,2,1}}$	0	0	0	0	0	$\frac{Q_{1,1,2}}{Q_{1,1,2}+Q_{1,2,2}}$	0	$\frac{Q_{1,2,2}}{Q_{1,1,2}+Q_{1,2,2}}$	0	0	0	0	0
H_2	0	0	0	0	$\frac{Q_{2,1,1}}{Q_{2,1,1}+Q_{2,2,1}}$	0	$\frac{Q_{2,2,1}}{Q_{2,1,1}+Q_{2,2,1}}$	0	0	0	0	0	$\frac{Q_{2,1,2}}{Q_{2,1,2}+Q_{2,2,2}}$	0	$\frac{Q_{2,2,2}}{Q_{2,1,2}+Q_{2,2,2}}$	0
C_1	0	$\frac{Q_{1,1,1}}{Q_{1,1,1}+Q_{2,1,1}}$	0	0	0	$\frac{Q_{2,1,1}}{Q_{1,1,1}+Q_{2,1,1}}$	0	0	0	$\frac{Q_{1,1,2}}{Q_{1,1,2}+Q_{2,1,2}}$	0	0	0	$\frac{Q_{2,1,2}}{Q_{1,1,2}+Q_{2,1,2}}$	0	0
C_2	0	0	0	$\frac{Q_{1,2,1}}{Q_{1,2,1}+Q_{2,2,1}}$	0	0	0	$\frac{Q_{2,2,1}}{Q_{1,2,1}+Q_{2,2,1}}$	0	0	0	$\frac{Q_{1,2,2}}{Q_{1,2,2}+Q_{2,2,2}}$	0	0	0	$\frac{Q_{2,2,2}}{Q_{1,2,2}+Q_{2,2,2}}$
M_1	{1}	0	{1}	0	0	0	0	0	[1]	0	[1]	0	0	0	0	0
M_2	0	0	0	0	{1}	0	{1}	0	0	0	0	0	[1]	0	[1]	0
M_3	0	[1]	0	0	0	[1]	0	0	0	{1}	0	0	0	{1}	0	0
M_4	0	0	0	[1]	0	0	0	[1]	0	0	0	{1}	0	0	0	{1}

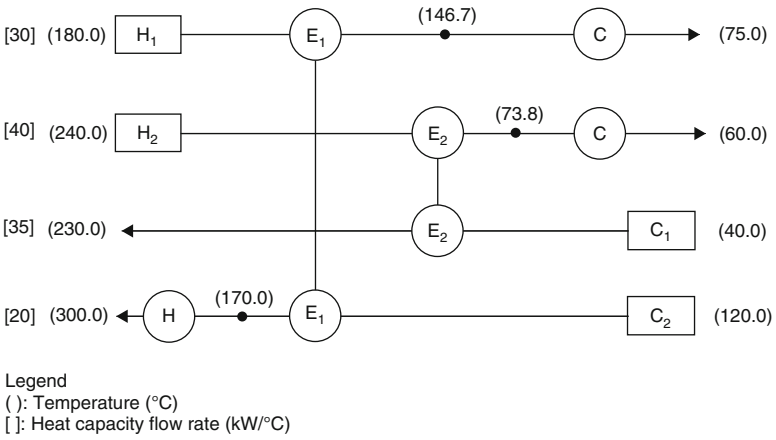

Fig. 22 Solution A for the HEN synthesis problem in scenario I (Yan et al. 2006)

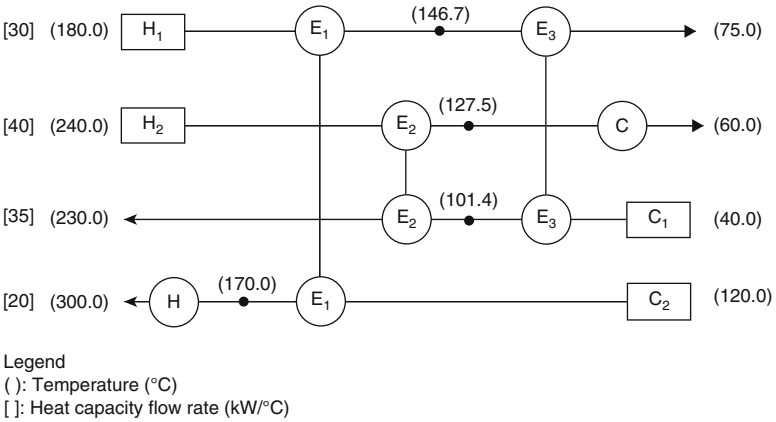

Fig. 23 Solution C for the HEN synthesis problem in scenario III (Yan et al. 2006)

may not qualify. For example, in scenario III, the control requirement $\delta T_{\max}^{t(-^{+})}$ of cold stream 2 is within the range of ± 1 °C, which is far beyond the actual temperature fluctuations of $(-3.3, 6.6)$°C in scenario I. This indicates solution A will not meet the control requirements of scenario III, and this indicates that integrating DP model into the HEN design procedure can generate the optimal result which meets the control requirements. Plus, different control specifications can be imposed on the synthesis problem according to the real process. Comparing scenarios II and III, stricter control requirements are imposed on cold stream 2 and hot stream 1, and a higher TAC is needed in scenario III. The higher TAC is kind of the trade-off for stricter control requirements (Table 4).

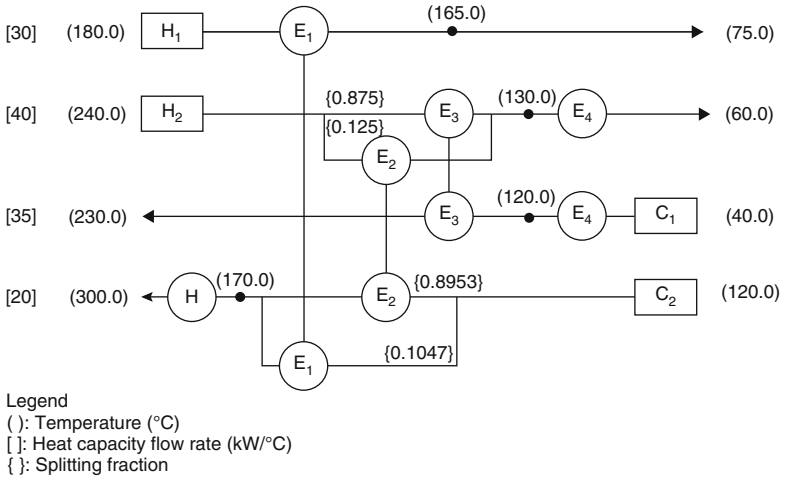

Fig. 24 Solution B for the HEN synthesis problem in scenario II (Yan et al. 2006)

Table 4 Comparison of the solutions under different control requirements (Yan et al. 2006)

	Case I(solution A)		Case II (solution B)		Case III (solution C)	
Streams	$\delta T^{t(\pm)}_{\max}$(°C)	δT^{t}(°C)	$\delta T^{t(\pm)}_{\max}$(°C)	δT^{t}(°C)	$\delta T^{t(\pm)}_{\max}$(°C)	δT^{t}(°C)
Hot 1	–	3.7/−4.2	±6	2.0/−5.5	±2	1.0/−1.3
Hot 2	–	0.0/−4.2	±4	2.0/−4.0	±4	0.6/−3.9
Cold 1	–	0.0/−0.3	±1	0.2/−0.4	±3	1.0/−2.8
Cold 2	–	6.6/−3.3	±10	6.6/−3.3	±1	0.9/−0.8
TAC ($/year)	450,072		450,759		468,013	

Disturbance Propagation and Control (DP&C) Model-Embedded Synthesis Approach

The DP model introduced above can be used to quickly estimate the maximum deviation of system outputs under various types of disturbances. However, the DP models do not consider any control actions for disturbance rejection (DR). This can lead to a conservative network design. In operation, a HEN is always controlled through regulating bypass flow rates associated with heat exchangers. Thus, Yan et al. (2001) further extend Yang's DP model to a disturbance propagation and control (DP&C) model where control actions are taken into account. This model can be embedded into a HEN design procedure to optimally select the locations and nominal fractions of bypasses with the minimum penalty on capital cost.

The system DP&C model is expressed below. For the detailed derivations, please refer to the work of Yan et al. (2001).

$$\delta \underline{T}^{t} = \underline{B}\underline{\delta f} + \underline{D_t}\underline{\delta T}^{s} + \underline{D_m}\underline{\delta M c_p} \tag{21}$$

where

$$\underline{B} = B_1 + D_{t_{12}}(\mathrm{I} - D_{t_{22}})^{-1}B_2 \tag{22}$$

$$\underline{D_t} = D_{t_{11}} + D_{t_{12}}(\mathrm{I} - D_{t_{22}})^{-1}D_{t_{21}} = \left(\underline{D_{t_h}}^T \underline{D_{t_c}}^T\right)^T; \tag{23}$$

$$\underline{D_m} = D_{m_1} + D_{t_{12}}(\mathrm{I} - D_{t_{22}})^{-1}D_{m_2} = \left(\underline{D_{m_h}}^T \underline{D_{m_c}}^T\right)^T; \tag{24}$$

$\delta\underline{T}^t$ and $\delta\underline{T}^s$ are vectors of maximum stream temperature deviation for the target and source temperature, respectively; $\underline{B}$ is the process-gain matrix; $\delta\underline{f}$ is the vector of maximum fluctuations of bypass nominal fractions; and $\underline{D_t}, \underline{D_m}, B_1, B_2$, etc. are relative matrices.

Disturbance rejection with minimum economic penalty. While a bypass of a heat exchanger can help to reject disturbances, its installation must cause an increment of heat transfer area and the capital cost. A trade-off between the DR and cost must be made in the bypass selection. Figure 25 illustrates how the stream target temperature fluctuation (δT^t) and the increment heat transfer area ($\Delta A_E/A_E$) are related to the nominal fraction of a bypass (f_E). The nominal fraction of a bypass (f_E), can be

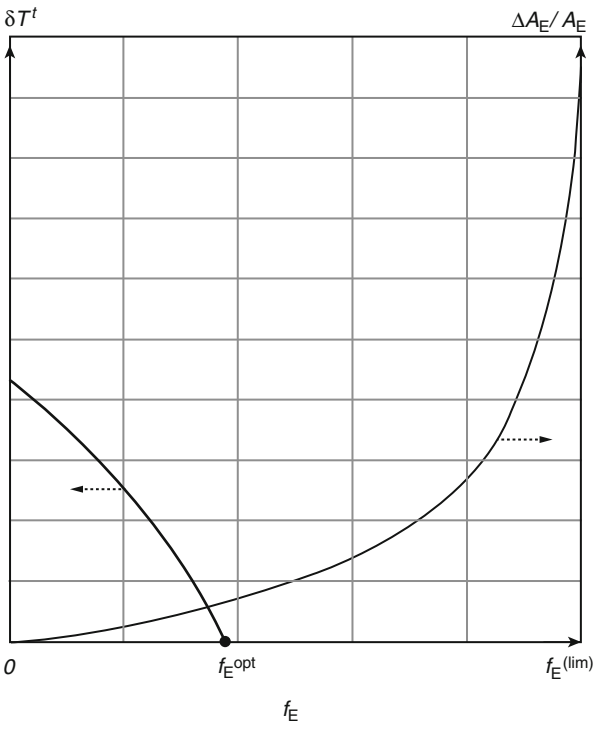

Fig. 25 Relationship of target temperature, heat transfer area, and bypass fraction (Yan et al. 2001)

selected from 0 (no bypass) to the upper limit $f_E^{(lim)}$. As shown in Fig. 25, when f_E increases, δT^t will decrease, while $\Delta A_E/A_E$ will increase. In this study, the optimal solution is defined as the one realizing complete disturbance rejection at the steady state and with minimum increment of heat transfer areas. Any nominal fraction value below the optimal value f_E^{opt} will not realize complete DR. Meanwhile, any value above f_E^{opt} will have more area increment with the same complete DR level, and this is certainly not desirable.

Case study: design of bypasses and control loops for a four-stream HEN. Yan et al. (2001) developed an iterative design procedure to determine the optimal locations and nominal fractions of bypasses in a HEN design and applied this method to a four-stream HEN design case previously studied by Yee and Grossmann (1990). For simplicity, only the problem statement and the solution are provided here to demonstrate the efficacy of this approach.

Table 5 and Fig. 26 show the steady-state design data as well as source disturbance information and control requirements of the selected case.

Table 5 Design data for the four-stream HEN synthesis problem (Yan et al. 2001)

Stream no.	T^s (K)	T^t (K)	Mc_P (kW/K)	$\delta T^{s(+)}$ (K)	$\delta T^{s(-)}$ (K)	$\delta T^{t(+)}_{max}$ (K)	$\delta T^{t(-)}_{max}$ (K)
H_1	620.0	385.0	10.0	5	0	0	0
H_2	720.0	400.0	15.0	0	0	5.5	−5.5
C_1	300.0	560.0	20.0	0	−5	0	0
C_2	280.0	340.0	30.0	0	−5	4.0	−4.0

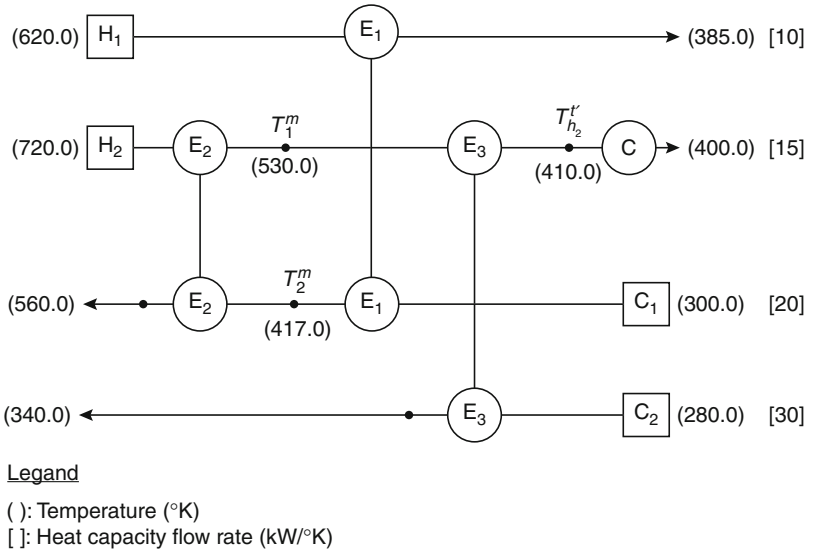

Fig. 26 Original four-stream HEN design (Uzturk and Akman 1997)

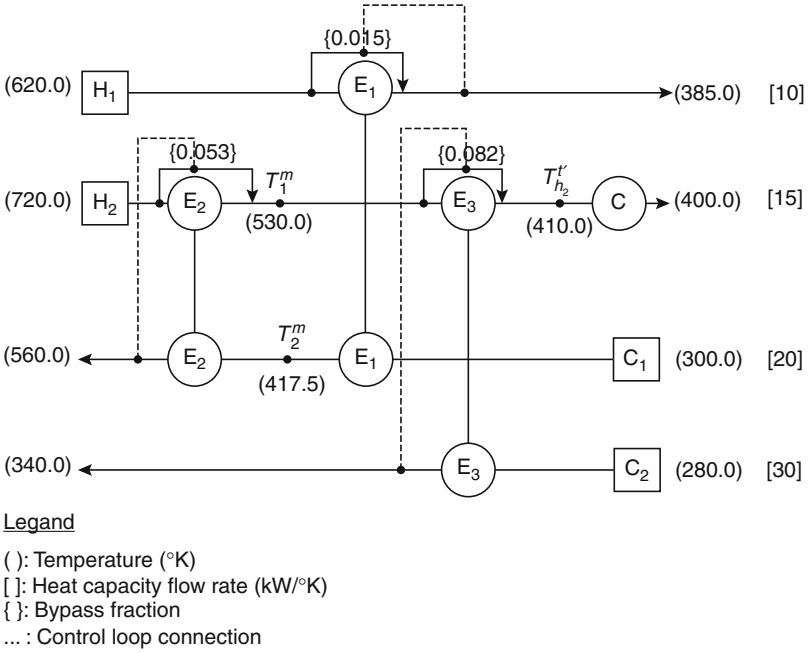

Fig. 27 Optimal bypass design for the HEN by the DP&C approach (Yan et al. 2001)

The resulting optimal bypass design with control loops by the DP&C approach is shown in Fig. 27. Uzturk and Akman (1997) also studied the same problem and their result is shown in Fig. 28. Table 6 compares the different design results in total costs. The design solution by DP&C model is 6 % cheaper than that by Uzturk and Akman. In addition, the RGA (relative gain array) analysis reveals that the solution by DP&C method has no system interaction among loops at steady state. By contrast, the design in Fig. 28 has considerable interactions among loops.

To sum up, the disturbance propagation and control (DP&C) method can quantify the disturbance propagation and disturbance rejection by using bypasses in the HEN design process. It can help to design the fewest bypasses with their nominal fractions for complete disturbance rejection with minimum economic penalty. The application strongly demonstrates the robustness and efficacy of this DP&C-based HEN design approach.

Emissions Targeting and Planning: CO_2 Emissions Pinch Analysis (CEPA)

Emission targeting by pinch analysis has been reported by Linnhoff and Dhole (1993a) using the total site analysis concept. Total site in their work refers to industrial systems incorporating several processes, which are serviced by a central

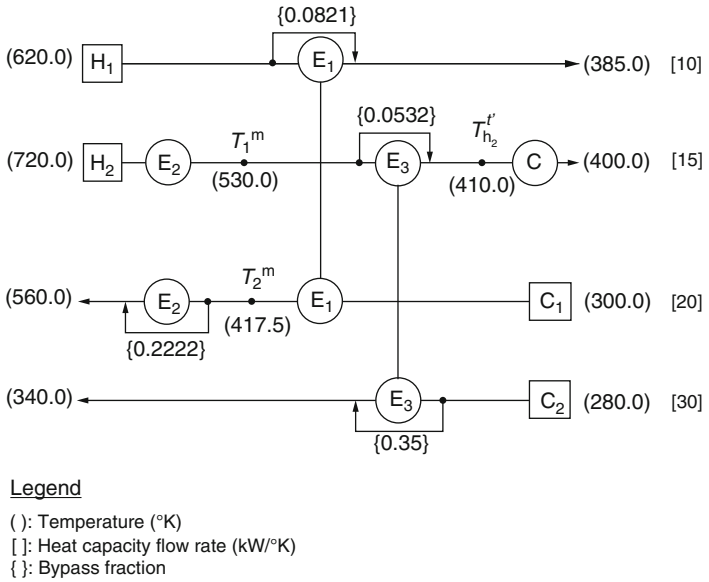

Fig. 28 Bypass design for the same HEN by Uzturk and Akman (1997)

Table 6 Comparison of different design results (Yan et al. 2001)

Heat exchanger	Original design (no bypass), area (m^2)	DP&C design (with bypass), area (m^2)	Uzturk and Akman design (with bypass), area (m^2)
E_1	34.7	35.4	39.1
E_2	42.3	44.3	49.2
E_3	22.8	23.7	25.8
ΣE_i	99.8	103.4	114.1
Cost	$24,386	$24,905	$26,408

energy-utility system. Although emission targeting by pinch analysis was introduced in those studies, the early applications were limited to within industrial facilities. Tan and Foo (2007) reformulated the traditional "total site" concept (Dhole and Linnhoff 1993a; Klemes et al. 1997; Linnhoff and Dhole 1993) and presented a novel application of pinch analysis for the preliminary planning of a country's energy sector. The carbon emissions pinch analysis (CEPA) was first developed by Tan and Foo and coworkers (2007; Foo et al. 2008; Lee et al. 2009) for emission targeting and reduction from industrial sites to macroscales (e.g., regional or national energy sectors).

Crilly and Zhelev utilized the CEPA method to analyze the Irish electricity sector (Crilly and Zhelev 2008). Detailed description of the procedure for implementing the CEPA methodology can be found in Crilly and Zhelev (2008). The following is a brief illustration of the novel method.

When planning energy sectors, it occurs very often that emission constraints will present. This is especially common in the industrialized countries such as Germany and Ireland where CO_2 emission limits are applied during the Kyoto/post-Kyoto setting. Thus, the problem arises when considering how to identify energy allocation schemes to meet the specified emission limits. If only environmental issues are considered, it is naturally desirable to maximize the use of low-carbon or zero-carbon energy sources, such as wind, hydroelectric, solar, biomass energy, etc. However, in real-world planning scenarios, economic issues need to be considered. Due to the high cost of renewable energy sources mentioned above, it is often desirable to determine the minimum amount of low-carbon or zero-carbon energy sources required to meet the national or regional emission limits and energy demand, which is known as the defined pinch point. The CEPA method can be used to determine the minimum quantity of low-carbon or zero-carbon energy sources needed and the energy allocation scheme among different energy resources in order to meet the specified emission limits and energy demand.

Ireland's electricity sector. In Ireland, GHG emissions come from various industrial sectors, including electricity generation, transportation, other manufacturing and service industries, as well as agricultural and waste-treatment sectors. The emissions in 2005 have an overall 25.48 % increase as compared with the 1990 level. This amount is far above Ireland's permissible 13 % increase in overall GHG emissions under the European Union (EU)'s Burden-Sharing Agreement on the Kyoto Protocol. For Ireland's electricity sector, it contributed a 23.33 % share of Ireland's overall GHG emissions in 2005 (21.40 % in 1990) and took a substantial 32.66 % of Ireland's total primary energy requirement (TPER), according to the publications from the government. In 2005, the TPER can be classified using the following actual energy resource (AER) mix (Crilly and Zhelev 2008):

1. Fossil fuel: natural gas (NG) ∼40.09 %, coal (C) ∼27.77 %, oil (O) ∼15.16 %, and peat (P) ∼10.02 %
2. Electricity: imported electricity (IE) from Scotland ∼3.45 %
3. Renewable energy sources (RESs): landfill gas, biomass, and other biogas ∼0.57 %, hydro ∼1.06 %, and wind ∼1.88 %

In the short-to-medium future of Ireland's electricity sector, a well-designed optimal energy resource (OER) mix is required to satisfy both the energy needs and emission limit. The renewable energy source-electricity (RES-E) has its disadvantages, such as high cost, limited public acceptability, inherent intermittency/variability, lack of predictability and poor reliability, etc. Thus, only the absolute minimum amount of RES-E should be employed in the optimal energy resource (OER) mix for the sector.

Application of CEPA. The basis of the approach is the construction of the composite curves of both the demand and the supply. These composite curves are then manipulated and shifted depending on the desired objectives. Crilly and Zhelev applied the CEPA to the electricity sector based on the data sources from the Sustainable Energy Authority of Ireland (SEAI), which is set up by the Ireland

Table 7 The past and forecasted AER mixes and OER mixes for the sector in 2005 and 2010, respectively (Crilly and Zhelev 2008)

	RESs	NG	Oil	Coal	Peat	IE	Total
EF$\left(\mathrm{t}\frac{\mathrm{CO_{2(e)}}}{\mathrm{TJ}}\right)$	0	56.8	75.6	94.6	116.7	120.0	–
Past AER $\mathrm{mix_{2005}}$							
% of total TJ/year	3.51	40.09	15.16	27.77	10.02	3.45	100.00
TJ/year	7,494	85,578	32,364	59,285	21,395	7,369	213,485
Mt CO_2(e)/year	0.00	4.86	2.45	5.61	2.50	0.88	16.30 > $\mathrm{KL_{2005}}$
Past OER $\mathrm{mix_{2005}}$ (by CEPA)							
% of total TJ/year	9.83	40.09	15.16	27.77	7.15	0.00	100.00
TJ/year	20,994	85,578	32,364	59,285	15,264	0.00	213,485
Mt CO_2(e)/year	0.00	4.86	2.45	5.61	1.78	0.00	14.70 = $\mathrm{KL_{2005}}$
Projected AER $\mathrm{mix_{2010}}$							
% of total TJ/year	7.20	56.52	0.14	30.74	2.38	3.02	100.00
TJ/year	17,585	137,997	335	75,069	5,820	7,369	244,175
Mt CO_2(e)/year	0.00	7.84	0.03	7.10	0.68	0.88	16.53 > $\mathrm{KL_{2010}}$
Projected OER $\mathrm{mix_{2010}}$ (by CEPA)							
% of total TJ/year	8.02	56.52	0.14	30.74	2.38	2.20	100.00
TJ/year	19,585	137,997	335	75,069	5,820	5,369	244,175
Mt CO_2(e)/year	0.00	7.84	0.03	7.10	0.68	0.64	16.29 = $\mathrm{KL_{2010}}$

government as its national energy authority. The data for the actual energy resource (AER) mix in 2005 is shown in Table 7. The energy demand (consumption) and resource (supply) composite curves (CC) before shifting are plotted in Fig. 29. More specifically, the figure depicts a correlation between the amount of CO_2 or $CO_{2\,(\mathrm{equivalent})}$ per unit time and the amount of energy per unit time. It shows a slope of the amount of CO_2 per unit energy for any line segments, which is also the emission factor. The resource composite curve is constructed by plotting cumulatively the quantity of electricity generated for the several fuel resources against total emissions from those resources. The emission factor (EF) (i.e., the amount of emissions produced per unit of electricity, $\left(\mathrm{t}\frac{\mathrm{CO_{2(e)}}}{\mathrm{TJ}}\right)$ for each energy resources is also provided in Table 7. The fuel source with the lowest emission factor is plotted first, followed by the next lowest and so on. In this resource composite curve, the renewable energy source is plotted first, followed by natural gas, oil, coal, peat, and imported electricity. The slope of each line segment is equal to the emission factor of corresponding energy resource. All emissions factors are expressed as carbon equivalent and include all relevant greenhouse gases.

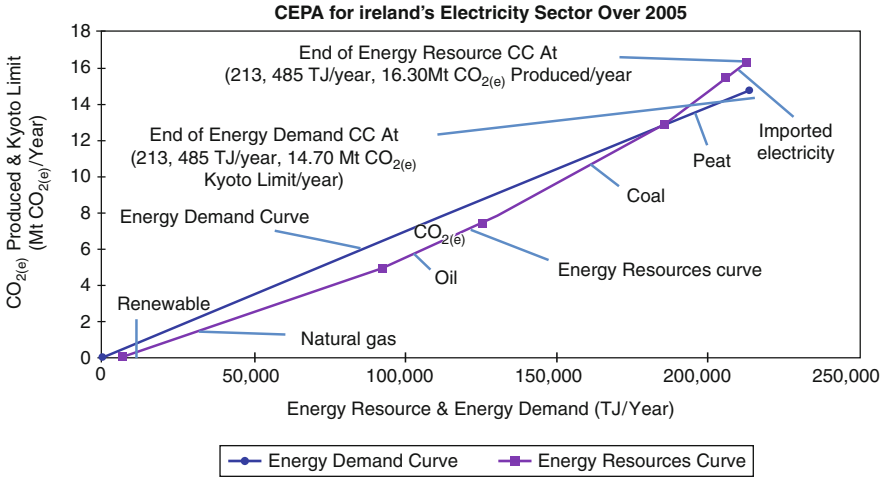

Fig. 29 CEPA applied to Ireland's electricity sector over 2005: before shifting of energy resource CC (Crilly and Zhelev 2008)

Ireland permitted an increase of its overall GHG emissions by no more than 13 % per year during 2008–2012, as compared to the baseline year of 1990, which is 55.75 Mt $CO_{2(e)}$. Thus, Ireland's environmental protection agency determined a leveled-out Kyoto limit (KL) of 62.99 Mt $CO_{2(e)}$ for each year between 2008 and 2012. The Kyoto limit KL_{2005} for 2005 is 61.78 Mt $CO_{2(e)}$ by the principle of interpolation. Because the electricity sector had a 23.79 % share of the actual overall GHG emissions of 69.63 Mt $CO_{2(e)}$ in 2005, this sector should be allocated the same percentage of the KL_{2005}, which equated to 14.70 Mt $CO_{2(e)}$. This value is the vertical ordinate for the top end of the energy demand curve as shown in Figs. 29 and 30.

The energy demand composite curve is also constructed using the same method as the energy resource composite curve. It is assumed that the emissions from various demand sectors are proportional to the electricity usage and therefore will produce a straight line from the origin to the end of the demand composite curve. The horizontal ordinate for the top end of both the energy demand curve and energy resource composite curve should share the same value because the demand (or consumption) should match the resource (or supply) in any given year. The slope of the demand line is known as the grid emission factor (GEF), which is simply the average emission factor for the entire system. In this case, the EF for the energy demand curve is 69.0 $\mathrm{t}\frac{CO_{2(e)}}{TJ}$.

In Fig. 29, it is easy to find that the top end of the resource curve is above the top end of the energy demand curve, which shows the AER mix led to more emissions than the permitted KL of the electricity sector. Thus, the energy resource composite curve needs to be shifted horizontally to the right to get rid of the excess emissions. Figure 30 shows a shifted energy resource composite curve that meets the Kyoto limit for the sector. The energy resource CC is shifted horizontally to the right until it intersects with the top end of energy demand CC, and this is the CO_2 emission pinch

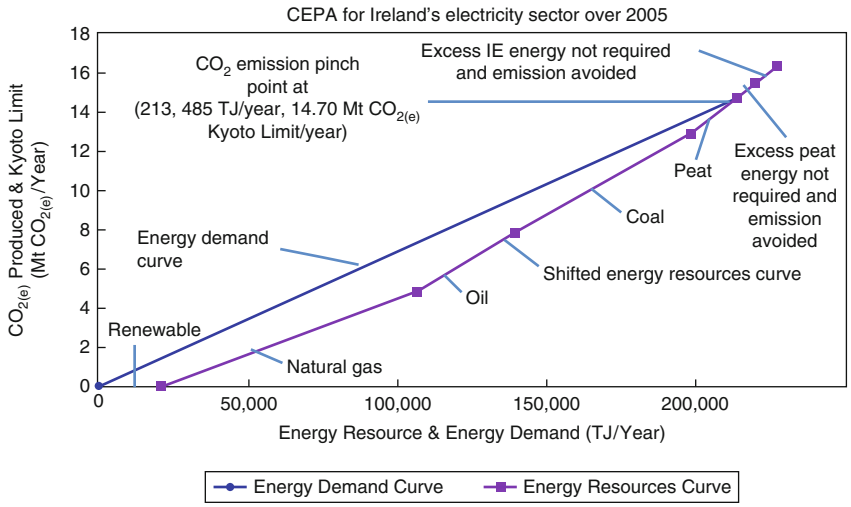

Fig. 30 CEPA applied to Ireland's electricity sector over 2005: after shifting of energy resource CC (Crilly and Zhelev 2008)

point. At this pinch point, the energy resources not only provide a total amount of 213,485 TJ energy per year (meeting the annual energy demand) but also release 14.70 Mt $CO_{2(e)}$ emissions (meeting the Kyoto limit of emission). In this way, the amount that the resource CC has been shifted then becomes the minimal amount of renewable energy that needs to be added in order to meet the emission target. The overhang of the resource CC to the right of the pinch point represents the amount and type of energy resources that need to be substituted by renewable energy. In this case, the renewable energy portion of the energy resource CC increases, the portion of imported electricity is totally substituted, and the portion of electricity from peat generation decreases as illustrated in Fig. 30. By increasing the energy resources with low-emission factors and decreasing energy resources with high-emission factors, the shifting procedure achieved the desired objective, that is, the emissions produced by the resources equal to the Kyoto limit of the demand. Meanwhile, the other objective of using the minimum amount of renewable energies due to their disadvantages is also achieved by this horizontal shift procedure. Each of the line segments of the shifted energy resource CC is measured off in order to get the optimal energy resource (OER) mix in 2005, which is also the optimal energy resource allocation scheme of the sector. The corresponding emissions produced by each of these optimal amounts are also measured. All of the measured data are listed in Table 7.

Further adaptations to CEPA. Crilly and Zhelev made a forecasting adaptation to the CEPA methodology, which is briefly introduced here. If the optimal energy resource (OER) mix in the future can be predicted, then the sector's policymakers can use this information to guide the future development plan of the sector. For example, in the near future, Ireland will close old and inefficient power plants and

create new power generation plants. The ahead-of-time knowledge of the future OER mix will be particularly useful for the policymakers to decide which form of power generation plant should be constructed. As long as the future actual energy resource (AER) mix is available, the future OER mix can be obtained using the same CEPA procedure described in the proceeding section. The future AER mix can be projected based on the energy model linked with macroeconomic model together with many key forecast parameters, such as GDP growth, population growth, fuel prices, etc. In 2006, the Sustainable Energy Authority of Ireland (SEAI), Ireland's national energy authority, published the projected AER mix for the electricity sector in 2010, which is shown in Table 7. Crilly and Zhelev used that information to forecast the OER mix that the energy sector in 2010 should have. Their forecast is also listed in Table 7. Analyzing those data, the OER mix in 2010 will need to have the input of RESs rising from 7.2 % of the AER mix to 8.2 %. This important and invaluable information will give the relevant policymakers and stakeholders 3 years time in advance to make up for this forecasted shortfall of renewable energies in 2010 for the analysis made in 2007.

Future Trends

Heat integration is one branch of process integration technologies. In the authors' view, there are several directions that can be considered as potentially promising for the future of process integration.

Process integration, especially the newer development, has not been used as widely as it could be. It is likely to see a wider range of application in process integration. Still, there is much work to be carried out in the research of integrating heat-integrated network with separation systems and reactor designs and the consideration of operational issues as well. Heat integration is closely related to mass integration by nature. Although extension of pinch analysis to mass integration field, such as water pinch and hydrogen pinch, has already been applied to industries successfully, systematic methods in this area are still in development. Utilizing advanced optimization techniques to solve process integration problems is very promising.

With the advancement of computer technology, a new generation of more powerful software tools for process integration may emerge. Comparing to the process simulation software, which is relatively mature, the process integration software is at its infancy. Process integration problems are generally complex tasks at considerable scales and involve comprehensive interactions. The development of powerful commercial software for process integration is instrumental for its wider application.

Climate change has recently become a major focus of industry and government. Pinch analysis has been extended to solve emissions and energy footprint problems to meet the environmental goals with technical and economic constraints simultaneously. Several methodological (graphical and numerical) approaches have been developed to handle problems such as energy allocation, segregated targeting, and retrofit planning. Meanwhile, similar approaches for considering energy, land, and

water footprint issues in energy and biofuel systems have been developed. Regarding the increasing concerns on climate change, more methodologies and applications are expected in this area.

Conclusion

Heat integration is a family of methodologies that can be used to improve energy efficiency, reduce energy consumption, and minimize GHG emissions. Pinch analysis can be considered as the foundation of heat integration. It can identify the maximal heat recovery and minimal external utility needs for the system before any detailed design. As a powerful tool, pinch analysis extends its application to many other fields, such as waste reduction, wastewater treatment, refinery hydrogen management, emission targeting, etc.

In spite of the total annualized cost, the HEN design must always consider the operability and controllability issues as well. During operations, various disturbances of temperatures and heat capacity flow rates always present. The disturbance propagation and control (DP&C) model-embedded HEN design approach can estimate the disturbance propagation and reject the severe disturbances through bypass design. This method can generate an optimal design solution satisfying both the economic and control objectives, thereby ensuring the achievement of high energy efficiency and low emissions.

The novel carbon emission pinch analysis (CEPA) methodology, developed based on traditional pinch analysis, can identify the minimal quantity of low-carbon-emission energy resources needed to meet both the emission limit and energy requirement and the optimal energy allocation scheme, for a regional or national energy sector. It can provide invaluable information for the decision-makers and stakeholders.

Acknowledgments This work is in part supported by the National Science Foundation under Grants Nos. 0737104, 0736739, and 0731066.

References

Ciric AR, Floudas CA (1990) A comprehensive optimization model of the heat exchanger network retrofit problem. Heat Recovery Syst CHP 10(4):407–422

Crilly D, Zhelev T (2008) Emissions targeting and planning: an application of CO_2 emissions pinch analysis (CEPA) to the Irish electricity generation sector. Energy 33(10):1498–1507

Dhole VR, Linnhoff B (1993a) Total site targets for fuel, co-generation, emissions and cooling. Comput Chem Eng 17:S101–S109

Dhole VR, Linnhoff B (1993b) Distillation column targets. Comput Chem Eng 17(5–6):549–560

El-Halwagi MM, Gabriel F, Harell D (2003) Rigorous graphical targeting for resource conservation via material recycle/reuse networks. Ind Eng Chem Res 42(19):4319–4328

Elliott TR, Luyben WL (1995) Capacity-based economic approach for the quantitative assessment of process controllability during the conceptual design stage. Ind Eng Chem Res 34(11):3907–3915

Floudas CA (1995) Nonlinear and mixed-integer optimization. Oxford University Press, Oxford
Floudas CA, Grossmann IE (1986) Synthesis of flexible heat exchanger networks for multi period operation. Comput Chem Eng 10(2):153–168
Foo DCY, Tan RR, Ng DKS (2008) Carbon and footprint-constrained energy planning using cascade analysis technique. Energy 33(10):1480–1488
Furman KC, Sahinidis NV (2002) A critical review and annotated bibliography for heat exchanger network synthesis in the 20th century. Ind Eng Chem Res 41:2335–2370
Huang YL, Fan LT (1992) Distributed strategy for integration of process design and control: a knowledge engineering approach to the incorporation of controllability into heat exchanger network synthesis. Int J Comput Chem Eng 16(5):496–522
Klemes J et al (1997) Targeting and design methodology for reduction of fuel, power and CO_2 on total sites. Appl Therm Eng 17(8–10):993–1003
Kotjabasakis E, Linnhoff B (1986) Sensitivity tables for the design of flexible process (I) – how much contingency in heat exchanger networks is cost-effective. Chem Eng Res Des 64:197–211
Lee SC et al (2009) Extended pinch targeting techniques for carbon-constrained energy sector planning. Appl Energy 86(1):60–67
Linnhoff March (1998) Introduction to pinch technology. Linnhoff March, Cheshire
Linnhoff B, Dhole VR (1993) Targeting for CO_2 emissions for total sites. Chem Eng Technol 16 (4):252–259
Linnhoff B et al (1994) A user guide on process integration for the efficient use of energy, 2nd edn. IChemE, Rugby
Lou HH, Huang YL (2002) Rapid prediction of disturbance propagation in a non-sharp ternary separation system. J Chin Inst Chem Eng 33(1):87–94
Matsuda K et al (2009) Applying heat integration total site based pinch technology to a large industrial area in Japan to further improve performance of highly efficient process plants. Energy 34(10):1687–1692
McAvoy TJ (1987) Integration of process design and process control. In: McGee HA, Liu YA Jr, Epperly WR (eds) Recent development in chemical process and plant design. Wiley, New York, p 186
Natural Resources Canada (2003) Pinch analysis: for the efficient use of energy, water and hydrogen. CANMET Energy Technology Center of Natural Resources, Canada
Papalexandri KP, Pistikopoulos EN (1994) Synthesis and retrofit design of operable heat exchanger networks: 1. Flexibility and structural controllability aspects. Ind Eng Chem Res 33:1718–1737
Papoulias SA, Grossmann IE (1983) A structural optimization approach in process synthesis-II. Heat recovery networks. Comput Chem Eng 7:707–721
Perry S, Klemeš J, Bulatov I (2008) Integrating waste and renewable energy to reduce the CFP of locally integrated energy sectors. Energy 33:1489–1497
Rossiter AP (1995) Waste minimization through process design. McGraw-Hill, New York
Seider WD, Seader JD, Lewin DR (2003) Product and process design principles synthesis, analysis, and evaluation, 2nd edn. Wiley, New York
Tan RR, Foo DCY (2007) Pinch analysis approach to carbon-constrained energy sector planning. Energy 32(8):1422–1429
Towler GP et al (1996) Refinery hydrogen management: cost analysis of chemically-integrated facilities. Ind Eng Chem Res 35:2378–2388
Uzturk D, Akman U (1997) Centralized and decentralized control of retrofit heat-exchanger networks. Comput Chem Eng 21:S373–S378
Wang YP, Smith R (1994) Wastewater minimisation. Chem Eng Sci 49:981–1006
Yan QZ, Yang YH, Huang YL (2001) Cost-effective bypass design of highly controllable heat exchanger networks. AlChE J47:2253–2276
Yan QZ, Xiao J, Huang YL (2006) Synthesis of highly controllable heat integration systems. J Chin Inst Chem Eng 37(5):457–465
Yang YH, Gong JP, Huang YL (1996) A simplified system model for rapid evaluation of disturbance propagation through a heat exchanger network. Ind Eng Chem Res 35:4550–4558

Yang YH, Lou HH, Huang YL (2000) Steady state disturbance propagation modelling of heat integrated distillation processes. Chem Eng Res Des 78(2):245–254

Yang YH, Huang YL, Lou HH (2005) A structural disturbance propagation model for the conceptual design of highly controllable heat-integrated reaction systems. Chem Eng Commun 192 (8):1096–1115

Yee TF, Grossmann IE (1990) Simultaneous optimization models for heat integration-II. Heat exchanger network synthesis. Comp Chem Eng 10:1165–1184

Yee TF, Grossmann IE, Kravania Z (1990) Simultaneous optimization models for heat integration-I. Area and energy targeting and modeling of multi-stream exchangers. Comput Chem Eng 14:1151–1164

Zhelev TK (2005) On the integrated management of industrial resources incorporating finances. J Cleaner Prod 13(5):469–474

Modern Power Plant Control for Energy Conservation, Efficiency Increase, and Financial Benefit

Pal Szentannai

Contents

Abstract

Process control takes place in all power plants. The main task of all automatic controllers is to assure the optimal values of their controlled variables under all circumstances. The quality of operation of these controllers has evidently a crucial effect on the way of operation of the entire power plant. Whether a power plant – based on either renewable resources or fossil fuels – is operated in a highly effective way, or is a rather resource-consuming one, is evidently of

P. Szentannai (✉)
Department of Energy Engineering, Budapest University of Technology and Economics, Budapest, Hungary
e-mail: szentannai@energia.bme.hu

W.-Y. Chen et al. (eds.), *Handbook of Climate Change Mitigation and Adaptation*,
DOI 10.1007/978-3-319-14409-2_22

very high importance regarding emissions and other ecological aspects. This fact is the reason for discussing in this chapter the possible ways for increasing the level of control quality in power plants.

An overview will be given at the beginning about the ways and tools the advanced control methods offer – in case of their more intensive applications in power plants – for protecting the environment and for mitigating the climate change. It will be followed by a concise but goal-oriented introduction of the most relevant control methods together with their evaluations regarding the aspects of their applicabilities in power plants. Because the way toward obtaining the environmental benefits offered by the advanced control methods is not a trivial one, some considerations, aspects, and hints will be given on this issue in the next part. A few successful power plant applications will be introduced afterward, and the actual main development directions will be outlined at the very end of this chapter.

Nomenclature

$A(q)$	Polynomial in the ARX model
$a_1 \ldots a_5$	Free parameters of the cost function
$B_1\ (q)$	Polynomial in the two-input ARX model
$B_2\ (q)$	Polynomial in the two-input ARX model
$b_1 \ldots b_5$	Free parameters of the cost function
C_{CO} mol/m^3	Molar concentration of CO in the flue gas
C_{NO} mol/m^3	Molar concentration of NO in the flue gas
e	Control error
$e(t)$	Equation error of the ARX model
K	Cost function
q	Time shift operator
r	Air distribution: ratio of primary air to total air
r	Reference signal (set point)
t s	Time
u	Control signal (process input)
$\dot{V}_A$ m^3/s	Total air flow
$\dot{V}_P$ m^3/s	Primary air flow
$\dot{V}_S$ m^3/s	Secondary air flow
y	Controlled variable
y_M	Controlled variable modeled
ϑ, T K	Bed temperature

Introduction

The practically exclusively used control method in power plants is currently the PID (proportional-integral-derivative (Evans 1954)) algorithm. The well-known, clear-sighted effects of its three parameters, the easy and uniform methods for setting

them, and the multiply proofed, stable operation assure its widespread success in many industrial branches, including the energy industry (Åström and Hägglund 1995; Datta et al. 2000; Visioli 2006; O'Dwyer 2009; Smith 2009; Yu 2006). Besides these clear advantages, the PID controller does have its limitations (which will be discussed later in this chapter), and parallel, modern control theory offers a wide range of advanced control methods. The basic ideas of the most important such methods will be briefly introduced in this chapter, together with the conclusions in the special aspect of their applicabilities in power plants. These introductions will be extended with practical hints regarding their realizations in new or existing power plants of any type, and some practical examples will be introduced too.

The problem discussed in this chapter is a rather unusual one! No compromise must, namely, be made between economical and ecological interests, because the benefits of applying advanced control methods in power plants serve both in the same time. It is evident, namely, that increasing the efficiency or decreasing the resource-consuming manner of operation (referring to any sorts of fuel, water, air, or even valuable components under decreased thermal stress) serves both of those goals in parallel. In spite of the limited number of advanced control applications in power plants, the published results show clear, numerically expressible benefits, an overview of which will also be given in this chapter.

The total number of industrial applications of advanced control techniques has increased rapidly worldwide, but the distribution of these applications among industry branches is considerably unequal. While chemical industry alone had more than 7,000 running applications of the most popular solution (Model Predictive Control, MPC) in 2005, the number of similar applications in power plants at that time was definitely below 100 (Dittmar and Pfeiffer 2006). Interesting is also the dynamic rate of increase of those applications in the chemical industry: their number has been doubled practically every 5 years since 1995.

The goal of this chapter is nothing else but to encourage operators and owners of power plants together with decision makers for applying advanced control methods also in power plants in order to contribute to both global climate change mitigation and local financial benefits.

For building a basis, some elementary ideas and notational practice of the control theory will be outlined here for those readers who are unfamiliar with this area.

The central element of a control system is always the *process* (or *plant*, P) to be controlled as shown in Fig. 1. The process can be affected by its input signal u (*plant input* or *control signal*), and its response is its output signal y (*controlled variable*). The process is often affected by *disturbances* (d) too, which may be either measurable or unmeasurable. In the classical control theory, all the above signals are considered as scalars, but throughout this chapter, they will be handled as vector variables – without any extra markings like boldfaced or underlined letters. It means that the current discussions may also refer to systems having multiple input and multiple output signals. In most cases of the following discussion, several signals (several real measuring points) can be handled jointly as components of one variable, which will be handled as a multidimensional vector variable (like in the algebra).

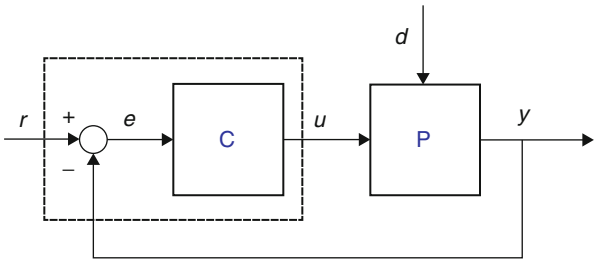

Fig. 1 Basic elements of a closed loop control system – introduction of the notation used throughout the discussion of advanced control methods. Each variable may represent several physical variables joined as a multidimensional vector variable

The *process* to be controlled is generally not an entire system (e.g., a whole power plant or a boiler), much rather only a subprocess of it. In some books, papers, and theoretical discussions, the borders and list of inputs and outputs of the *process* are considered as predefined characteristics of the system. A definitely differing approach will be followed throughout this chapter. The theoretical and practical considerations on defining the borders of the process P are, namely, a key toward successful control, and a high level of knowledge of both power engineering and control sciences is required in this essential step.

Another important element of a control system is the *controller* (C) itself. In the classical approach, its input is the *control error* (e), which is the deviation between *controlled variable* (y) and *reference signal* (or *set point*, r). In some advanced control methods, both *controlled variable* and *reference signal* will be considered, not only their actual difference. In the case of multi-output processes, also the reference signals must be multidimensional vector variables, of course.

The goal of controller design is to set the internal behavior of the controller C so that the process output y could keep or follow the value prescribed by the reference signal r. Throughout this design procedure, the instationary behavior of the process also must be considered. The goal of the science of control theory is to develop such design procedures for many different plant types. The modern control theory has reached a really high amount of very useful results throughout its theoretical work; however, these results are still rarely utilized in power plants. The possible utilizations of these results and their environmental (and also financial) benefits will be discussed throughout the rest of this chapter.

Environmental Benefits Offered by Advanced Control Methods in Power Plants

Energy conservation and efficiency increase of power plants are important goals to be considered throughout their basic design efforts. But how can these goals be supported by the real-time controllers? The next figure shows just one example. According to this example, a better control may keep the superheated steam

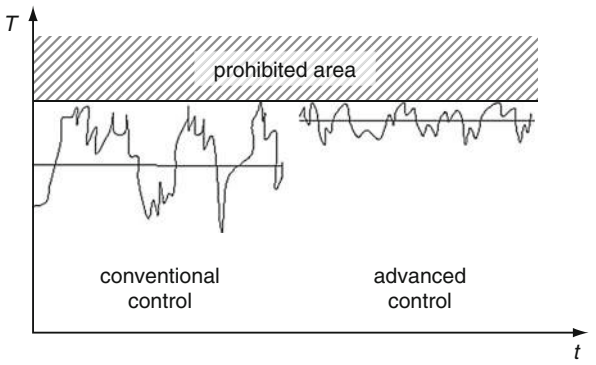

Fig. 2 Environmental benefit from applying advanced control. Narrower band of fluctuation allows higher average live steam temperature, which directly results in higher plant efficiency

temperature of a thermal power plant within a narrower band (Fig. 2). This decreased fluctuation in turn allows a higher set point of the same temperature, since the properties of the steel material used determine the maximum permissible steam temperature. And a higher average live steam temperature directly increases the efficiency of the plant, which means a direct decrease in fuel consumption. As a further consequence, the amount of emitted pollutants (including CO_2) will be significantly decreased while producing the unchanged amount of electricity and heat. It is important to mention here that this positive effect is valid not only for fossil-fueled power plants but in an identical fashion also for biomass fueled or other ones. Similarly, an increased efficiency of wind mills, photovoltaic power plants, or hydroelectric power stations will reduce the energy demand to be produced from fossil resources.

An obvious case of obtaining direct environmental benefit in the steady-state operation was discussed in this simple example only. It is important to mention already here that modern control techniques offer a much wider range of areas where direct environmental and economic benefits can be expected. The most important such benefits can be listed as follows:

- Reaching higher efficiency in steady states (which directly results in lower fuel consumption and emission – as introduced in the example above)
- Making load changes smoother and less resource consuming (by means of considering and limiting thermal stresses which in turn results in increased lifetimes)
- Making the start-up periods faster (which directly results in savings in fuel consumption)
- Increasing the level of supply by making the power plant a more flexible one in the energy market (which increases the potential of thermal power plants for compensating the uneven supply of wind farms)

Besides the steam temperature control discussed in the above example, a number of further control tasks exist in power plants. An excellent overall summary of their specific goals and classical solutions can be found in Klefenz (1986, 1991). The basic components of power plants are often extended nowadays with different subprocesses

in order to fulfill some specific or newly set requirements. These subprocesses require in most cases some own control tasks like the minimization of the ammonia slip in the flue gas in DENOX facilities. It is important to emphasize that advanced control techniques discussed in this chapter can be applied for all abovementioned groups of power plant control tasks, and in all cases, similar direct economic and environmental benefits are expected due to their higher level of intelligence.

What is the secret behind advanced control techniques that allows them to offer such benefits? Let us answer this question using the example of one of the most frequently used techniques, model predictive control (MPC). Its most important properties are as follows:

- Its control actions are *based on future values* calculated by an integrated process model.
- It can inherently *consider constraints* regarding, e.g., allowed operating areas and actuator positions, speed limits.
- *Multivariable* control is naturally handled allowing an integrated compensation of cross effects.

This chapter and its approach are definitely not against the traditional PID (proportional-integral-derivative) controller! There are the definite reasons for the worldwide and branchwide success and high proliferation of the PID controller technique. It is also certain that the PID controller technique has had a nearly exclusive role in all branches of the industry from the nineteenth century onward, and it will keep its role in the future as well. However, it is also obvious that the PID control technique does have its limitations. The most important cases – together with just a few power plant examples – for which the efficient application of the PID control technique is strongly limited, can be given as follows:

- For MIMO (multi-input, multi-output) systems with significant couplings (e.g., heat and power controls of turbogenerator groups)
- For strongly nonlinear processes (e.g., engines and turbines)
- For time-variant processes (e.g., waste incinerators)
- For cases where better control performance is required

The examples given in brackets behind the above bullets could be extended with a really high number of cases from the power generation industry. This makes it an evidence that power plants are typical applications where it is definitely advisable to apply advanced controllers.

Introduction of the Advanced Control Methods of Highest Potentials in Power Plants

Which are the most important advanced control methods? What are their basic ideas? In which cases are they advantageous and where are their limits? These questions will be discussed in this section – but from the special aspect of their possible

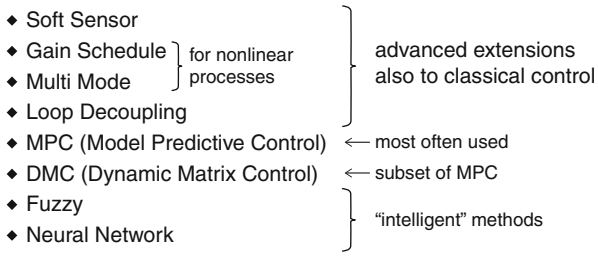

Fig. 3 The most important advanced control methods from the aspect of their applicabilities in power plants

applications in power plants. Figure 3 gives a schematic overview of those advanced control methods that seem to be of the highest potential regarding their applications in power plants or have proven already their successful applicabilities in the energy industry. This figure will be used as a road map throughout this section.

It will be seen – after studying the basic ideas of the above methods – that most of them use process models for reaching a better control quality. A wide variety of model structures, depths, and approaches is available, and their presences seem to be general characteristics of the advanced control methods. The reason for it can be understood easily, and it can be summarized as follows: *the better the process is known by its controller, the higher control quality can be expected*. According to this, the efforts in process modeling and simulation are of the highest importance. And further on this statement seems to be true also for the person who intends to design the control system of an entire energy technology system like a power plant. According to this, a deep knowledge of the power plant, its subprocesses, thermal, chemical, and practical engineering aspects, operation environment, etc., must be well known for realizing a successful, high-quality (advanced) control system. A mathematical description of the selected process may not be enough, since just the procedure of drawing the borders of the subprocesses requires all the above theoretical and practical knowledge and experiences, and this beginning step is crucial regarding the later success.

The basics of the most important advanced control methods will be discussed in the next subsections. However, their detailed theoretical analyses are no goals of the current chapter, since these aspects (e.g., stability issues) are discussed in detail for numerous particular cases in the original research articles and textbooks. In spite of this, a special care will be taken throughout the current discussions on the aspects of their possible roles, advantages, and limiting characteristics regarding their possible applications in power plants for reaching environmental benefits and financial results.

Soft Sensor

In some cases, a significant difficulty in building effective control loops is the lack of a measured variable characterizing well the actual state of the process. A wide variety of theoretical and simple practical reasons may cause this situation like a significant

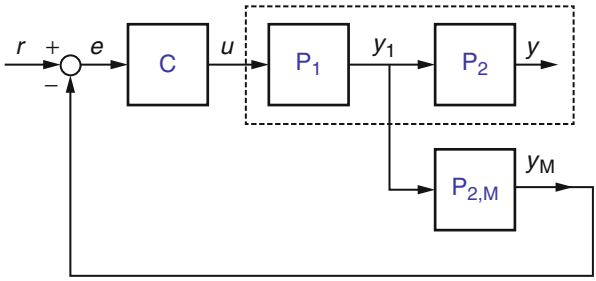

Fig. 4 Soft sensor is practically a model ($P_{2,M}$) of a subprocess (P_2). The calculated version (y_M) of an unmeasurable process variable (y) can be used for control on the basis of the measurement of another "primary" variable (y_1)

time delay between the core process and its measurable output signal, a signal being very difficult or expensive to measure accurately, a signal burdened with significant noise or other inaccuracies, and so on.

Soft sensor may be a good solution for these cases. Its basic idea (see Fig. 4) is to measure other, easily accessible process variables being in strong relationship with the required one, and the later one will be deduced from the measured one. For doing this deduction, a model will be used in all cases.

Some special cases of the approach of *soft sensor* are known in the literature under their own names. *Kalman filter* is a broad set of tools for the cases where the measured data contains significant noise and other inaccuracies, while the *Smith predictor* gives a very interesting theoretical solution for processes with pure time delays. A significant technical relevance has in this field the so-called state optimal control. This advanced technique was applied successfully in several power plants in classical control environments in the 1990s, and it was mostly used for controlling the superheated steam temperature. This process can be, namely, characterized by a significant time delay being dependent also upon the actual plant load; however, modeling this SISO (single-input, single-output) system is not too difficult. Determining the actual rate of combustion in a boiler can be mentioned as a further example, because an accurate measurement on the steam or hot water side indicates any changes significantly later than the primary processes that originated them.

Gain Schedule and Multimode Control

A practical extension of all linear controller design methods toward nonlinear processes are *gain schedule* and *multimode* control. The idea behind both of them is to choose always among a number of predefined control configurations depending upon the actual operating point.

The first step in designing such a control system is to identify an appropriate variable to be used as *scheduling variable*, which may be the plant load signal in most power plant applications. Thereafter, a set of operating points will be chosen within the whole range of the scheduling variable, and any (advanced or classical) simple control design methods will be applied to each. During the online operation of the system, always one control configuration will be activated according to the actual value of the scheduling variable. The only difference between the two

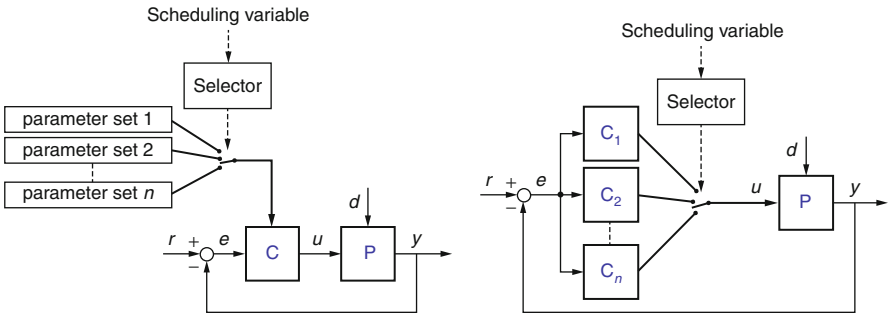

Fig. 5 Basic ideas of gain schedule (*left*) and multimode control (*right*)

subjected methods is that while in the case of *gain scheduling*, only the parameter settings of an unchanged controller will be updated according to the actual values of the scheduling variable, in the case of *multimode* control, the whole controller itself – as visible in Fig. 5.

As an evident advantage of these approaches, well-known linear control methods can be used also for nonlinear processes. However, only slight nonlinearities can be handled on this way, because otherwise the frequent switches between the actually used controllers or control parameters would result in unpredictable behaviors. This phenomenon indicates also a drawback of this method: the switches may result in unsmooth operation.

Regarding the applicabilities of these two similar control methods in power plants, it can be stated that they can be effectively applied, because the main nonlinearities in these applications can be easily characterized by the plant load signal as the scheduling variable. The nonlinearities caused by the varying actual load is in most cases exactly in the range where an unchanged linear controller cannot be used effectively anymore, but these nonlinearities still allow the applications of these simple methods. An advantage of the first subjected method is its simplicity, while the later one allows its application also in such cases where the use of different control algorithms at different operating points is necessary.

Loop Decoupling

In many practical cases, the control loops are not really independent from each other. This fact can easily be observed very often in power plants when a change in one control loop affects the other. The reason is, of course, that because of the presence of strong couplings (dashed lines in Fig. 6) inside the entire process, it cannot be considered as a set of independent one-dimensional (SISO) subsystems. It is in reality a coupled multidimensional process, which should be handled by the methods developed for multidimensional control problems, since the methods and tools developed for one-dimensional cases (e.g., the PID controller) cannot satisfactory solve the multidimensional problems. Control engineers often try to smooth out the

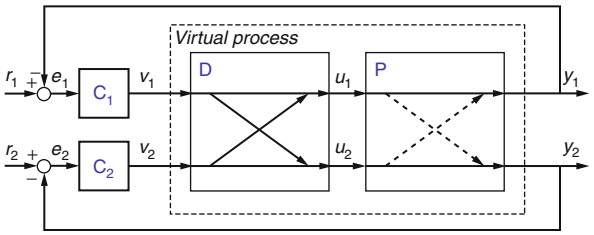

Fig. 6 Inserting a well-designed decoupler (D) between controllers (C_1, C_2) and process (P) results in a virtual process having no internal cross couplings. This virtual process can be controlled by means of independent, one-dimensional controllers designed according to any (e.g., classical) control design methods

most disturbing cross effects by means of several empirical tools. However, a relatively simple overall theoretical solution exists for tracing back the multidimensional problem to a set of one-dimensional problems, and these one-dimensional control tasks can already be solved by means of common (advanced or classical) controller design methods.

A so-called decoupler (D in Fig. 6) will be designed and applied according to well-known, relatively simple design procedures, the details of which will not be discussed here. The goal of such a *decoupler* is to build a virtual process, the inputs of which are the inputs of the decoupler and the outputs are the outputs of the real process. The control loops of this resultant virtual process are independent from each other already.

Loop decoupling can easily be realized also in the existing control system of an existing power plant; since most DCS (digital control system) software allows the insertion of extra multiplier blocks, the decoupler is built up in most cases. Their actual values shall be determined off-line by well-known standard procedures, which require also a process model. The controllers C_1 and C_2 will be designed afterward, also off-line, by considering the dynamic characteristics of the resultant virtual process *decoupler + process* (the inputs of which are v_1 *and* v_2, the outputs, y_1 *and* y_2 in Fig. 6).

Model Predictive Control

The control method having the highest potential regarding industrial applications (including power plant applications as well) and also the highest number of successfully running industrial realizations is *model predictive control* (*MPC*). This is already a complete control method, which cannot be considered as a simple extension to the classical ones. This is a model-based method, which entirely handles also multidimensional processes. A further practical advantage of MPC regarding its industrial realization is its entire capability for handling constraints like maximal and minimal possible flow rates, valve positions, and other technological prescriptions. Model predictive control has several variations and development directions; its

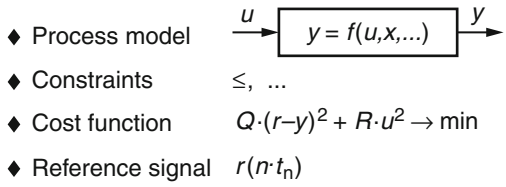

Fig. 7 A priory requirements of the MPC method

common basic idea will be summarized below – with special respect to its power plant applications for energy conservation and efficiency increase.

The initial requirements of this control method are a *process model*, a set of *constraints*, a *cost function*, and the future values of the *reference signal* up to a certain horizon as shown in Fig. 7.

A *process model* can be used theoretically in any programmed form. In practical applications, empirical models (black box models) are often used because they can be generated relatively easily by means of available identification procedures based on pure input, output measurements. Nevertheless, physical modeling (or at least using semiempirical models) is rather advisable, because a deep understanding of the controlled process (represented in such a model) gives definitely a great help in controlling it successfully. Processes, where identification-based empirical models are practically unusable, are the ones characterized by long-term conservation behaviors. It is important to emphasize here, because this is a frequent case in power plant processes! The long-term fuel and bed material accumulation in fluidized bed combustors (FBC) is a typical case, but grate firing and some other power plant processes are of very similar characteristics.

The mathematical procedure of MPC does inherently handle also constraints, which should be given as relational operators referred to any available variables of the model or the control structure. This characteristic of MPC makes it a very practice-oriented one in case of its application in power plants, as discussed above. An interesting utilization of this property of MPC is the inclusion of some technological constraints (e.g., thermal stresses) which cannot be considered directly in the case of most other control methods.

A very clear formulation of the goal of the control is the *cost function* (or *target function*), which gives the weighting between two opposite interests. A very low control error can, namely, be achieved at the expense of a very intensive actuator operation and vice versa. In Fig. 7, Q and R are the weightings, which are matrices in the general, multidimensional case. They represent the relative importances of these two aspects, where the matrix elements refer to the individual physical control errors (differences between set points and measured outputs) and actuator activities.

The reference signal can be either a constant set point or a function of time. Because the basic version of MPC is a timely discrete one, the future values of the reference signal should be available in the time steps $n \cdot t_n$.

The task the controller has to execute online at each time step is to solve the quadratic optimization problem with constraints. Because this problem is a well-

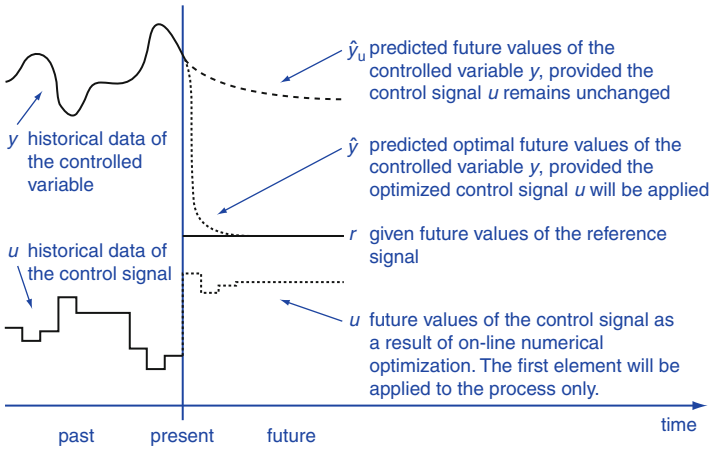

Fig. 8 Way of operation of the model predictive control. This method inherently handles also multidimensional processes and timely changing reference signals; however, for a better visibility, the much simpler single-input single-output case is indicated here. The inherent consideration of constraints is also not visible in this figure

known one for a longer while, numerous effective solver algorithms are available in the literature of mathematics. They will be adapted and used in the model predictive controllers, the operational procedure of which is the following.

In each time step, the optimization problem formulated above will be solved numerically, and its result is the optimal future time series of the control signal u (Fig. 8). Not the whole time series but only its first element will be applied to the system, because in the next time step, the same optimization procedure will deliver a newer, updated control signal. In this way, the actually applied control signal will consider also the latest measured process data, which behavior acts as an effective tool against model inaccuracies being present of necessity.

As a summary to MPC, it can be stated that this advanced control method offers excellent properties that can be utilized well also in power plants. That is why an increasing number of its applications in any types of power plants would be definitely a very effective tool for energy conservation, efficiency increase, and emission reduction. However, for realizing such applications, expert knowledge is required covering both power engineering and advanced control engineering.

Dynamic Matrix Control

A rather simple version of model predictive control (MPC) is dynamic matrix control (DMC). Simplicity means here a procedure of significantly less online computational demand, which is an advantage regarding its applications in power plants.

This early version of MPC can use the process model in a predefined simple form only, which is the so-called dynamic matrix. A drawback of this simplicity is, of

course, the higher inaccuracy of the model in most cases. As a further difference compared to the basic MPC approach, DMC does not handle constraints entirely, which fact may also be either an advantage or disadvantage depending upon the specific application.

Fuzzy Control

Both *fuzzy control* and *neural network control* came from the direction of artificial intelligence research, and that is why they are often called *intelligent* control methods (although this naming does not mean any rank differences compared to other advanced techniques).

Fuzzy logic is an alternative direction of the set theory. According to the approach of the classical set theory, a point may either belong to a set or definitely not. In the fuzzy set theory, a membership function will be used instead, which is ranged from 0 to 1. It is important to mention at this point that human thinking seems to be much closer to the later approach, since nobody could clearly define the borders of the set "youth." The unsharp borders of this set are indicated in Fig. 9, which shows them as an example on fuzzy membership functions.

All measured data in fuzzy control will be classified into fuzzy sets, and this initial step of fuzzy control is called *fuzzification*. A given actual value of a measurement may belong to more sets in the same time. According to the basic idea of fuzzy logic introduced above, several sets will be defined by their membership functions like "very low," "low," "medium," etc., and these membership functions are usually overlapped.

The next step does no more deal with exact measured data; it uses the fuzzified states only (like "pressure is low"). In this second step, decisions will be made according to some rules implemented during the design process of the fuzzy controller. These rules are rather simple ones like "IF pressure is *low* THEN set discharge valve position to *somewhat open.*"

The final step in fuzzy control is called *defuzzification.* Output values will be formed here from the resulted decisions by means of output membership functions in such a

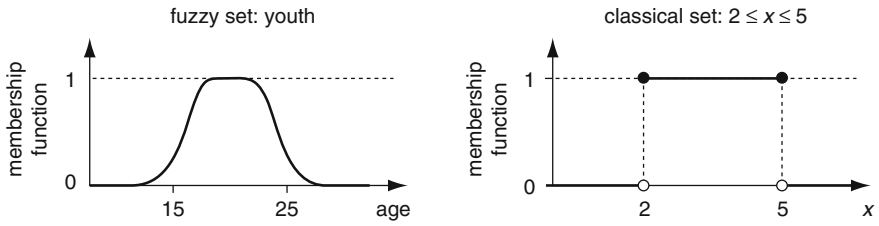

Fig. 9 A fuzzy membership function to the fuzzy set described by the human expression "youth" (*left*). Membership functions can be used also in the classical set theory, but their borders are "crisp" (*right*)

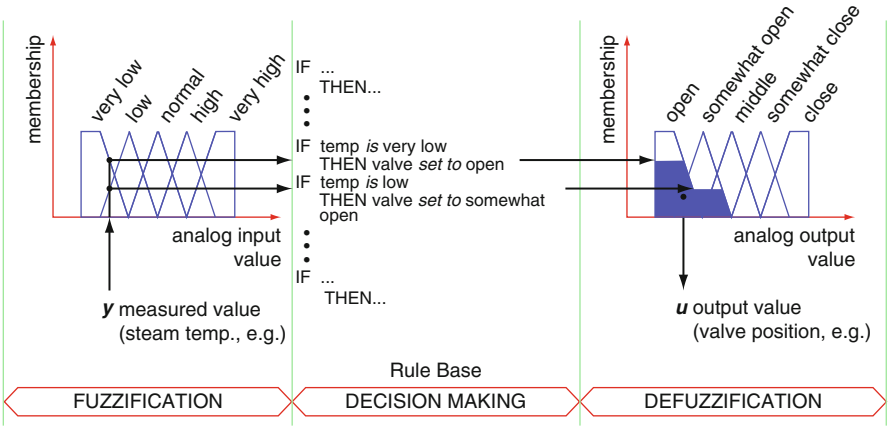

Fig. 10 Internal structure of the fuzzy controller. Extension toward multivariable and dynamic control is possible

way that the parallel decisions will be weighted by those membership values which resulted from them. The whole procedure is indicated in Fig. 10 in a simplified manner.

Regarding its usability in power plants, fuzzy control can be characterized by the next advantages (+) and disadvantages (−):

- + Easy realization of human/expert knowledge, because the way of representation of the operational requirements is very close to the human thinking.
- + Low-cost realization is possible, because fuzzification and defuzzification may be realized by means of low-cost sensors and actuators, respectively, and decision making is a procedure requiring relatively low computational capacities.
- − Unsmooth output signals may be resulted by the discretized way of operation of the decision-making procedure.
- − The overall stability of the control system can rarely be guaranteed because of the heuristic setup of the controller.

Neural Network

Neurons are the basic elements of the nervous system. Many of them work in parallel, and the interactions between them determine the way of operation of the entire system. The junctions where these interactions take place are called synapses, and the magnitude of transferring signals from one neuron to another one through a certain synapse can be changed throughout the normal biological learning process. One neuron may receive several input signals from others, but it generates only one output signal.

The above (general and simplified) description is the basis of the artificial neural networks (NN), which can be used also as controllers (Fig. 11).

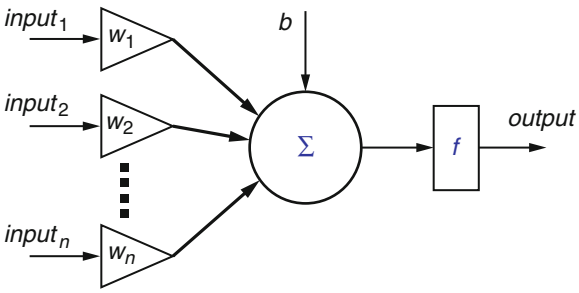

Fig. 11 One artificial neuron. In a layer of a neural network, several neurons act in parallel. In a neural network, some layers will be applied. w_i represents the weighting factors and b is an additive, the actual settings of which is the result of the learning process

A very important characteristic of neural networks is their abilities for learning. It practically means certain procedures for finding the optimal set of the weighting factors w_i and additive constants b so that in case of a set of inputs, the network would result in its desired set of outputs. Several search procedures are known, which depend also upon the actual form of the neuron output function f.

The application of this theoretical background for the purposes of controlling a process still has a number of different approaches.

If, for example, the neural network learns the inverse behavior of the process, applying the desired process output on the neural network input, its output will result the process input necessary for that desired process output. Beyond this theoretically simple application, many further successful ways of industrial applications are known. Also several combinations of fuzzy control and neural networks are applied, and both of these "intelligent" methods are often used as value-added extensions to other control solutions.

Proposed Ways of the Introduction of Advanced Control into Power Plants

The introduction of advanced control methods offers a number of ecological and economical benefits as discussed above; however, the way of their implementation is not an evident one (Szentannai 2010). One must be aware of the special requirements of modern control techniques compared to those of the traditional, PID-based ones. As a general and strongly simplified observation, it can be stated that modern techniques are based on more detailed calculations. This is the reason for their requiring significantly higher computational capacities. Computers capable of such performance became commercially available low-cost standard ones in recent years, and many people use equipment of that capacity in everyday life. However, the reliability of these computers is definitely below the level expected in power plants. Moreover, most industrial control systems were designed for lower computational capacities only. A further problem can result from the fact that only a few digital control systems (DCSs) are equipped with standard software tools required to program an advanced control application.

In this actual situation, one must distinguish between two different cases: application *in a new power plant* or application *in an existing power plant* equipped with traditional controllers.

The first case seems to be easier, since the new control system of a new power plant can be designed according to the special needs of the selected advanced control method. This first means the appropriate selection of the hardware and software structure of the DCS to be applied: a system capable of these control methods should be installed.

In spite of this theoretically simple and straightforward method, a more conservative approach will be proposed here to realize the benefits of advanced control strategies in new power plants. During the construction of a new power plant, it may be more advantageous and secure to program and use traditional control loops in the commissioning period of the whole power plant technology and to set up advanced controllers in a second phase only after reaching stable and secure operation. In most cases, commissioning in any case is followed by a longer period of fine-tuning the entire power generation technology, which should be used also for setting up, fine-tuning, and testing the final, modern control system as software changes in the unchanged DCS. This approach also allows a final comparison between traditional and advanced controls.

In the second case, an existing power plant is running with its complete, proved, and stable traditional control system. In this case, the purpose of the introduction of an advanced control technique is to achieve and utilize its benefits outlined above. While doing this, one should not forget that the existing stable operation is of much higher actual importance than any advantages the new controller may offer. In other words, the benefits of the introduction of the advanced controller must be achieved in such a way that stability of the existing control system will by no means be lost. A good practice for this is to retain the existing control system as a supervisor above the new one. The supervisor should stay idle as long as the difference between the outputs of new and advanced controllers remains below a given threshold. This limit may be increased stepwise by the control engineer after appropriate periods of reliable operation of the new control technique, allowing more and more effective utilization of its benefits.

Another question in this case is the choice of hardware on which to run the new control algorithm. Since the existing control system is generally not capable of doing this, an external platform is required. A rather general configuration is proposed in Fig. 12, which indicates both hardware and software structure, together with the necessary communication pathway.

This scheme should be considered as a typical arrangement only and must be modified according to the actual environment in each particular case. Positioners are, e.g., in many cases realized outside the DCS (digital control system), sometimes as distributed local ones. Some device border lines must be actualized in this case; however, even in such a case, no change is proposed to the general concept of keeping the positioners outside the advanced controller.

As visible on the above figure, the high-level parts (the traditional, one-dimensional PID controllers) of the existing control loops will be replaced by

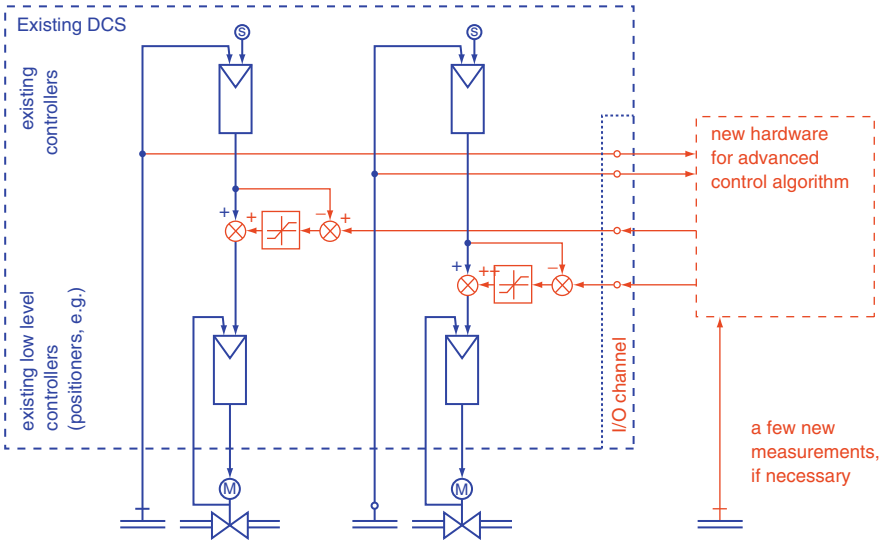

Fig. 12 Proposed typical hardware and software configuration for applying advanced control in a power plant originally equipped with a traditional control system. Benefits of the modern control will be utilized while the proven and secure operation of the original control system will be retained (*Thick lines*, existing system; *thin lines*, advanced control extension)

the advanced controller, but the replaced elements will become effective again if and when the new control outputs show an unlikely degree of variance from those of the original control system. This proposed method of implementation assures a secure way to realizing the benefits of advanced control techniques.

This scheme may also be applicable in the case of a new power plant, the only difference being that the communication channel between old and new hardware can be omitted since the capacity of the DCS can be chosen to satisfy the higher computation needs of an integrated implementation of the advanced algorithm also. This is possible nowadays without any remarkable surplus in the DCS price.

Successful Applications of Advanced Control in Power Plants

Applying the latest results of the control theory also in power plants is not only a theoretical possibility! A number of applications are known from the literature; some of them will be introduced in this section. A general, interesting characteristics of these applications is that they serve the ecological goals not only through increasing the plant efficiency (which directly results in energy conservation and reduced total flue gas emission including CO_2), but most of them also bring about further environmental benefits.

After the literature overview, a case study will be given where not only the basic idea and the results will be shown but also the complete solution in detail. For those

who want to go deeper or want to have a broader overview of advanced control applications in different types of power plants, a recently published book can be proposed (Szentannai 2010).

Some Published Applications

Ruusunen (2010) applied the *soft sensor* technique on two grate-fired combustors based on solid biomass (wood chips, wood pellets, and fuel peat) of 30 and 300 kW thermal capacities. His goal was to compensate the combustion power fluctuations being present in these small-scale biomass fired boilers due to inhomogeneous fuel quality and unequal feeding capacity. The stabilized and accurate combustion power is, namely, critical for maintaining low emissions and stable operating conditions.

Based on the model-based approach, fuel power changes could be compensated by the controller before they affected the heat output of the boiler, enabling continuous and delay-free monitoring of disturbances. As inputs of the soft sensor, some temperature measurements were used, the locations of which were found to be critical.

Operational experiences have shown that through the applied advanced control strategy, the standard deviations of the heat output and CO reduced by 40 %. Also 25 % reduction of CO concentration was measured during the test period, and the fluctuation of the oxygen concentration was reduced by 45 % in the same time. The increase in boiler efficiency is also very attractive: 1–2.4 % points!

Havlena and Pachner (2010) reported a successful application of multivariable Model Predictive Control (MPC). Their goal was to improve stability key process variables, effectiveness of limestone use, and boiler combustion efficiency under emission limits. Two circulating fluidized bed (CFB) boilers were originally operated with standard PID control strategy. As the fluidized bed combustion process shows strong interactions between process variables, standard PID control did not fully meet the operational requirements. The boilers are fueled by a mixture of coal and coke, and the nominal steam production is 310 t/h each.

A very simple, half-empirical (gray box) model was set up including also the long-term storage characteristics of this combustor type.

The bed temperatures were originally manually kept between 860 °C and 900 °C by the operators. After the introduction of the model-based advanced control technique, these temperatures are automatically maintained with standard deviation below 1 °C at a given reference value, which is optimal for in situ SO_2 removal. The SO_2 emissions, originally only monitored, are now controlled and held within a very narrow band (<25 mg/m^3). As further environmental benefits of this application of the MPC technique, reduction of the flue gas O_2 emission to 2.5 % resulted in boiler efficiency increase by 0.25–0.5 % point. Another important result was the improved boiler responsiveness to load demand changes, which is very important for compensating the unpredictable load balance changes of the electricity system, caused by changes in the wind power intensities, for example.

Franke and Doppelhamer (2006) applied the nonlinear MPC technique on a 700 MW coal-fired power plant, which has to perform full start-up and shutdown processes very often. A special characteristics of this application is that not only ordinary process variables are considered by the controller but also new measured data being important regarding lifetimes of valuable boiler components.

During start-up, fast temperature changes cause intensive spatial temperature differences in thick-walled parts, in particular, headers behind the superheaters and spherical fittings in the live steam pipe. These spatial temperature differences cause thermal stress, which cause fatigue up to destruction. This is why the thermal differences in the mostly exposed places will be measured and considered in the current application of MPC, which advanced control technique is able to handle such constraints inherently.

After taking into operation this new control method, the overall start-up time could be reduced by about 20 min and the start-up costs by about 10 % in the 700 MW power plant. It is of very high environmental importance also in case of its being a coal-fired power plant, because the CO_2 emission was reduced accordingly, and this increased flexibility increases in turn the possible share of wind power in the electricity network.

An Optimum Control Application Discussed in Detail

After the above literature overview, a selected advanced control solution will be introduced as a detailed example. A new combustion control strategy for fluidized bed combustors (FBCs) will be discussed in this section.

The basic goal of combustion control is always identical, regardless of the actual combustion technique or control strategy, namely, setting the air flow rate so that optimal combustion conditions can be assured under the actual fuel feed, fuel composition, and other circumstances. Despite this strong similarity, significant differences appear between the FBCs and other combustion technologies, since in case of fluidized bed combustion,

- The combustion air must assure not only optimal combustion but also appropriate fluidization.
- The combustion air must be set with respect to the actual fuel inventory, not to the actual fuel feed rate.
- The air distribution between primary and secondary air is a supplementary task of high importance.

The proposed approach in setting up the control strategy follows the traditional way of formulating a *cost function* (also called *target function*) to be minimized, but the significant differences listed above will be considered as well. While the traditional combustion control has one control variable only (the air flow), the new one is two-dimensional, since the optimal flow rates of both primary and secondary air

must be controlled. While the traditional combustion control considers a few losses only (basically, incomplete combustion loss because of too low air flow and heat loss by exhaust gas because of too high air flow), the new one must consider also some others of significant influences. The list of aspects proposed to be built into the new cost function is as follows:

- Satisfactory fluidization must be assured in the lower section of the combustion chamber (below the secondary air inlet).
- Satisfactory fluidization must be assured in the upper section of the combustion chamber (above the secondary air inlet).
- The characteristic bed temperature must not be too high.
- Total CO emission must not be too high (or it must not exceed its threshold).
- Total NO emission must not be too high (or it must not exceed its threshold).

This list of terms was found to be sufficient in practical cases. Limiting the bed temperature also from below was found to be unnecessary, for example, because other terms of the list assure already that this deviation cannot happen. As a mathematical representation of this set of terms, exponential functions are proposed because of their easy-to-handle ability both numerically and analytically and also because of their abilities for being parameterized so that different limiting shapes can be realized from a nearly linear manner up to a practically sharp threshold. According to this, the proposed form of the cost function K (which is to be minimized by the combustion control) is the following:

$$\begin{aligned} K = &\exp\left(a_1 \cdot \dot{V}_\mathrm{P} + b_1\right) \\ &+\exp\left(a_2 \cdot \left(\dot{V}_\mathrm{P} + \dot{V}_\mathrm{S}\right) + b_2\right) \\ &+\exp\left(a_3 \cdot \vartheta + b_3\right) \\ &+\exp\left(a_4 \cdot C_\mathrm{CO} \cdot \left(\dot{V}_\mathrm{P} + \dot{V}_\mathrm{S}\right) + b_4\right) \\ &+\exp\left(a_5 \cdot C_\mathrm{NO} \cdot \left(\dot{V}_\mathrm{P} + \dot{V}_\mathrm{S}\right) + b_5\right) \end{aligned} \tag{1}$$

The proposed control concept allows other cost functions as well, of course. Its parameters should be set according to the actual local needs dictated by the technology (e.g., temperature, fluidization), environmental goals (e.g., emission limits), and any further economical circumstances (e.g., prices of losses). In the actual case, the next set of parameters was found to be the best, and this one was used throughout the further investigations:

$$\begin{aligned} &a_1 = -0.24\ \mathrm{s/m^3}; a_2 = -0.11\ \mathrm{s/m^3}; a_3 = \ 0.018\ \mathrm{1/K}; \\ &a_4 = \ 0.15\ \mathrm{s/(m^3 \cdot ppm)}; a_5 = \ 0.015\ \mathrm{s/(m^3 \cdot ppm)}; \\ &b_1 = \ 5.4; b_2 = \ 7.91; b_3 = -19.4; b_4 = -3; b_5 = -3. \end{aligned}$$

The task formulated previously (to minimize the cost function) should be realized by an appropriately designed controller. Furthermore, it is believed that better control performance can be reached on the basis of better knowledge of the process to be

controlled. While in case of the traditional PID controller the whole information about the process is represented by only three parameters, advanced control theories use more detailed models.

In the investigated case, a comprehensive mathematical model of the fluidized bed combustion will be used for setting up and testing the advanced control scheme. This model was developed and validated by means of measurements on a 300 MW_{th} industrial FBC unit by the author, and it was published elsewhere (Szentannai 1998).

The actual control task is not the most general one: the minimum place of a calculated variable should be found in this case, and not a given set point of the controlled variable should be followed as generally. Different approaches are known for a controller configuration to solve the model-based optimum control problem outlined above; some of them are listed here:

- Off-line optimum seeking algorithms can be run on the programmed model and cost function while simulating a high variety of operating conditions. The found optimal settings can then be stored in a real-time (online) controller.
- An online optimum seeking algorithm can be realized in the real-time controller.
- The above closed loop optimum seeking controller can be supported by initial guesses coming from either the off-line optimum search (first bullet above) or learned previous results of the online search (second bullet).
- Further model-based online optimum seeking procedures can be developed based on the results of the advanced control theory.

The second approach will be discussed here in detail, since this one can be considered as a basis for further enhancements either upstairs or downstairs.

The idea of the proposed control structure is simple; it traces back the optimum control task to an ordinary control task. According to this, the gradient of the actual value of the cost function should be controlled to zero (Fig. 13) according to the principle of the extremum-seeking control philosophy (Blackman 1962; Zhanga and Ordóñez 2009).

All process variables of the fluidized bed combustor involved in the cost function will be continuously measured, of course. Their actual values will be forwarded to the block that calculates the actual scalar value of the cost function, the minimum of which should be found and set by the remaining elements of the control structure. Its gradient should be estimated in the next block. The space of search is two-dimensional spanned by the manipulated variables $\dot{V}_P$ and $\dot{V}_S$, but in practice it often seems to be better to handle to use another space defined by the coordinate transformation $\dot{V}_A = \dot{V}_P + \dot{V}_S$, $r = \dot{V}_P/\dot{V}_A$ where $\dot{V}_A$ is *total air* and r is *air distribution*.

In the gradient estimator, a known identification method will be used first. A two-dimensional, discrete-time ARX model will be identified online, which standard method delivers the model in the following form:

$$A(q) \cdot \Delta y(t) = B_1(q) \cdot \Delta u_1(t) + B_2(q) \cdot \Delta u_2(t) + e(t), \tag{2}$$

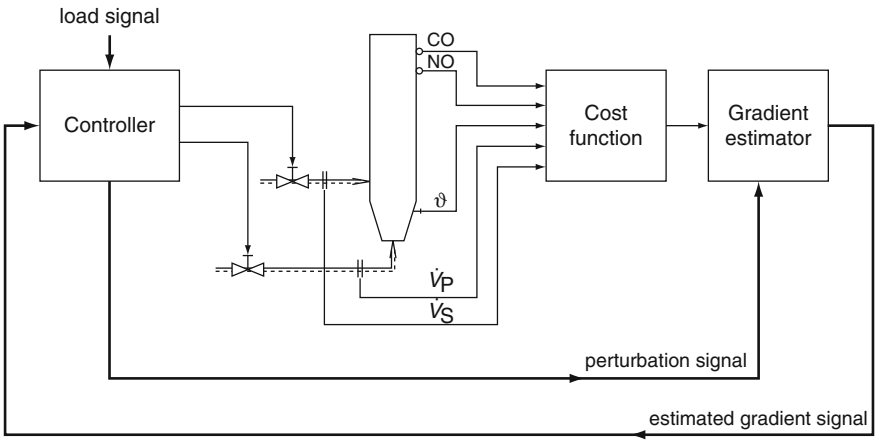

Fig. 13 The proposed structure of combustion control using extremum seeking control developed for fluidized bed combustors

where q is the time shift operator, $y(t)$ is the process output (which is the K value in the actual case), and Δu_1 and Δu_2 are the process inputs ($\dot{V}_P$ and $\dot{V}_S$ in the actual case). This procedure needs to know also the perturbation signal, which will be defined and added to the inputs by the controller block. The results of the identification procedure are in this case the coefficients of the polynomials $A(q)$, $B_1(q)$, and $B_2(q)$. The final output of this block (the gradient estimates) can be calculated according to

$$\frac{\partial K}{\partial \dot{V}_A} = \left.\frac{B_1(q)}{A(q)}\right|_{q=1} \tag{3}$$

$$\frac{\partial K}{\partial r} = \left.\frac{B_2(q)}{A(q)}\right|_{q=1}. \tag{4}$$

The controller block in the proposed control structure (Fig. 13) can be any traditional controller. The set point is zero, and the process variable to be controlled is the estimated gradient delivered by the block described above. In the actual, first implementation of the scheme, a rather simple, conservative control law was built in: the (two-dimensional) controller step will be set always proportional to the negative gradient received. A flat sawtooth signal of very low amplitude compared to the effective outputs added to a random binary signal (of low amplitude as well) was chosen as perturbation signal needed for the ARX identification. It is generated within the control block, it is added to the calculated control output, and it is forwarded extra to the ARX identifier located in the *gradient estimator* block. The load signal of the block is introduced to the controller block for further developments only, as an additional information for learning the optimum values once found.

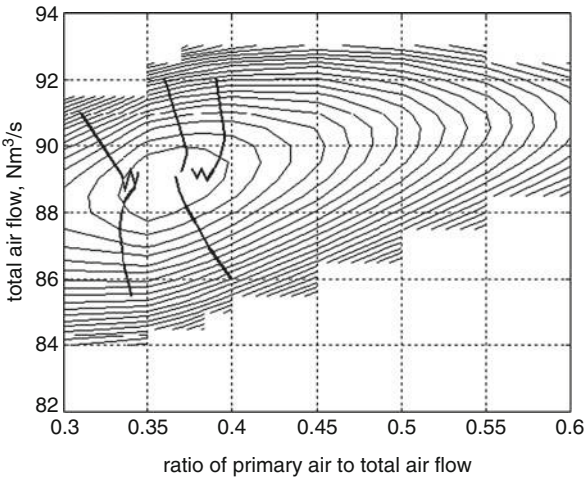

Fig. 14 Trajectories of the extremum seeking control from different starting points

The control strategy was realized in the simulation environment Matlab-Simulink©. The model described above was used throughout the simulation tests and also for plotting the surface of the cost function over the $\dot{V}_A - r$ space. (The surface of this function is not visible for the online controller, of course.) Figure 14 shows the paths of some simulated searches that started from different initial guesses far from the optimum. The results are satisfactory, and the controller succeeded in shifting the fluidized bed combustion system close to its optimum in all cases.

Based on the current results, further tests of the new control strategy are planned after implementing it on an industrial-sized fluidized bed combustor. The model-based control development allows also a number of further investigations. The optimal primary and secondary air flows as functions of the actual boiler load were calculated, for example, and the resulted functions were rather similar to those found by others experimentally to be the best (Bunzemeier 1992; Edelmann 1992). Further research will focus on the application of the programmed mathematical model in other model-based control procedures offered by the advanced control theory according to the bulleted list at the beginning of this section.

Future Directions

Actual trends and successful examples of numerous applications of advanced control techniques in power plants indicate their significant benefits both ecologically and economically. This double positive effect predicts their dissemination in the

upcoming years, in spite of their current time lag compared to similar applications in other industry branches.

Besides the somewhat higher computational capacities required by these methods, the most significant bottleneck in their dissemination seems to be the lack of technicians familiar with both power engineering and modern control theory. This aspect should be considered in the education already, where besides the theoretical background, the application-oriented issues together with the available controller realizations and software packages should also be introduced to the future engineers.

All advanced control methods have really good outlooks for successful applications in power plants; however, the model-based ones seem to be more advantageous and prosperous in this area. The explanation is simple: if a controller has more information about the process (e.g., in form of a model), it has better chances for a successful control. This statement explains also the handicap of the traditional PID controller, its whole knowledge about the process is, namely, only three digits, its three parameters. Model predictive control (MPC) is that model-based control technique which has really good inherent properties for its power plant applications and which seems to be the mostly used one. Very good commercial packages are available for its linear version, and theoretical and practical extensions toward strongly nonlinear cases can also be built up. The realization of these methods requires nowadays generally a computational platform outside of the standard digital control system (DCS) of the plant, but in the near future the commercial DCSs will be hopefully equipped with all the hardware and software components required for their integrated realizations. Some steps toward this direction can be observed already at the most significant DCS suppliers worldwide, and this further development will be warmly welcome by those who are interested in the environmental and financial optimization of the energy industry.

Regarding the model types to be built into the model-based controllers, gray box models and mathematical models seem to be more advantageous and successful contrary to black box models, because the later types generally do not consider long-term storage effects, which are typical in some combustion processes. But not only because of this significant advantage can be predicted a more intensive dissemination of gray box models and mathematical models in the near future. The needed amount of work of power engineers for setting up such models is, namely, not so high in the control enhancement project, and their presence is needed by all means because drawing the borders of the multivariable process is a key, and it cannot be done without their technological knowledges.

Acknowledgments The author is grateful to ProcessEng Engineering GmbH, Vienna, Austria, and to Periodica Polytechnika Civil Engineering, Budapest, Hungary, for permitting to use some materials published by the author earlier in Szentannai (2010, 2011).

References

Åström KJ, Hägglund T (1995) PID controllers: theory, design, and tuning. International Society for Measurement and Control, Research Triangle Park, p 343. ISBN 1556175167

Blackman PF (1962) Extremum-seeking regulators. In: Westcott JH (ed) An exposition of adaptive control. Pergamon, Oxford

Bunzemeier A (1992) Mathematisches Modell zur regeldynamischen Analyse eines Dampferzeugers mit zirkulierender Wirbelschichtfeuerung. Fortschritt-Bericht VDI, Reihe 6, Nr 273

Datta A, Ho M-T, Bhattacharyya SP (2000) Structure and synthesis of PID controllers. Springer, London, p 233. ISBN 1852336145

Dittmar R, Pfeiffer B-M (2006) Modellbasierte Prädiktive Regelung in der industriellen Praxis. Automatisierungstechnik 54(12):590–601

Edelmann H (1992) Modellierung der Dynamik und des Regelverhaltens für einen Dampferzeuger mit zirkulierender Wirbelschichtfeuerung. Dissertation Universität GH Siegen. Fortschrittsbericht VDI, Reihe 6, Nr 275

Evans W (1954) Control-system dynamics, Electrical and electronic engineering series. McGraw-Hill, New York, p 282. ASIN B00005XDYG

Franke R, Doppelhamer J (2006) Online application of Modelica models in the industrial IT extended automation system 800xA, Modelica 2006, 4–5 Sep 2006. The Modelica Association, pp 293–302 https://modelica.org/events/modelica2006/Proceedings/proceedings/Proceedings2006_Vol1.pdf

Havlena V, Pachner D (2010) Model-based predictive control of a circulating fluidized bed combustor. In: Szentannai P (ed) Power plant applications of advanced control techniques. ProcessEng, Vienna, pp 43–67. ISBN 978-3-902655-11-0

Klefenz G (1986) Automatic control of steam power plants. Bibliographisches Institut, Zürich, p 248. ISBN 9783411016990

Klefenz G (1991) Die Regelung von Dampfkraftwerken. BI-Wiss.-Verl, Mannheim, p 240. ISBN 9783411152841

O'Dwyer A (2009) Handbook of PI and PID controller tuning rules. Imperial College Press, London, p 608. ISBN 1848162421

Ruusunen M (2010) Advanced combustion power stabilization method for a grate-fired biomass boiler. In: Szentannai P (ed) Power plant applications of advanced control techniques. ProcessEng, Vienna, pp 113–134. ISBN 978-3-902655-11-0

Smith CL (2009) Practical process control: tuning and troubleshooting. Wiley-Interscience, Hoboken, p 431. ISBN 0470381930

Szentannai P (1998) Energetics for the environment: modelling of fluidized bed combustion. In: Gépészet '98, proceedings of first conference on mechanical engineering, Technical University of Budapest, 28–29 May 1998. Springer Hungarica, Budapest, pp 750–754. ISBN 963 699 078 6 https://www.antikvarium.hu/konyv/aradi-p-csaszi-f-gepeszet-98-1-2-394258?ID=394258

Szentannai P (ed) (2010) Power plant applications of advanced control techniques. ProcessEng, Vienna, p 500. ISBN 978-3-902655-11-0

Szentannai P (2011) Mathematical modeling and model-based optimum control of circulating fluidized bed combustors. Period Polytech Civ Eng:20–1029 http://www.pp.bme.hu/ci/article/view/467

Visioli A (2006) Practical PID control. Springer, London, p 10. ISBN 1846285852

Yu C-C (2006) Autotuning of PID controllers. Springer, London, p 261. ISBN 978-1-84628-036-8

Zhanga C, Ordóñez R (2009) Robust and adaptive design of numerical optimization-based extremum seeking control. Automatica 45:634–646

Mobile and Area Sources of Greenhouse Gases and Abatement Strategies

Waheed Uddin

Contents

W. Uddin (✉)
Department of Civil Engineering, The University of Mississippi, Oxford, MS, USA
e-mail: cvuddin@gmail.com; cvuddin@olemiss.edu

W.-Y. Chen et al. (eds.), *Handbook of Climate Change Mitigation and Adaptation*,
DOI 10.1007/978-3-319-14409-2_23

Abstract

This chapter discusses mobile and area sources of carbon dioxide (CO_2) and other greenhouse gas (GHG) emissions. The CO_2 emissions from mobile sources are accounted globally for 23 % of world energy-related GHG emissions in 2004. In the United States, the CO_2 emissions in 2004 from mobile sources included 28 % of all anthropogenic GHG emissions, and the missions from mobile sources grew 29 % between 1990 and 2004. The CO_2 emissions for several megacities, the carbon footprint expressed in CO_2, and the CO_2 per capita used as a sustainability scale are also reviewed. Traffic congestion and gridlock in most urban areas and cities have grown substantially worse over the years, causing commuters to waste millions of hours in traffic jams. The resulting vehicle emissions have adverse impacts on the environment, both in air quality degradation and increases in GHG. Examples are presented on contributions of built environment and transportation-related air pollution and GHG emissions from mobile sources, cities, and other populated areas.

The heat island effect causes an increase in surface temperature and air temperature in the built-up areas of a city. Urban sprawl and associated transportation-related emissions also tend to increase area temperature. An increase in air temperature results in a higher rate of photochemical reactions that form ground-level ozone and smog during hot summer days. Additionally, it requires extra electricity to cool down buildings in summer days, resulting in increased energy demands, larger air-conditioning bills, and elevated emissions of GHG and ozone precursors.

Sustainable multimodal transportation network and urban infrastructure facilities are warranted to support urban communities in view of the demand of energy, reduce public health hazards resulting from air pollution and urban smog, and mitigate adverse impacts of GHG emissions on the environment. Innovative geospatial applications of high-resolution satellite imageries are presented to estimate built-up area and traffic volume. Real-time intelligent transportation system technologies can also improve traffic flow, reduce congestion and air pollution, and decrease GHG emissions. Government agencies and cities worldwide can use CO_2 emission per capita sustainability scale for evaluating effectiveness of sustainable transportation and development policies. Country laws and regulations to reduce transport-related emissions and international accords on global responsibility for CO_2 reductions are reviewed.

Introduction

Overview

A well-maintained network of transportation infrastructure and an adequate supply of energy are two indispensable pillars of any economy as they support the transport and mobility needs of the public, industries, agriculture and other businesses, and quality of life. The highway network of a country forms the backbone of its transportation infrastructure by providing connectivity needs that allow for the safe and efficient mobility of people and goods. It also represents investments of billions of dollars in every country. Figure 1 illustrates world ranking in road length, and Fig. 2 shows vehicle stocks of selected countries (ORNL 2003). The United States (USA) leads the world in automobile ownership with approximately 137 million registered cars as of 2008 that is 0.74 % up from 136 million cars in 2007 (DOT 2007, 2008). The proportion of cars in the vehicle fleet is much higher in the United States compared to most industrialized and developing countries. Approximately 25 % of all world petroleum produced, which is a primary source of carbon emissions, is consumed in the United States (ORNL 2004). About 66.5 % of this is used by the transportation sector in the United States to provide safe and efficient mobility.

As of 2007, the transportation sector includes over 254 million road transport vehicles which comprise of 93.3 % cars and other automobiles, 2.8 % motorcycles, 0.3 % buses, and 3.6 % trucks (DOT 2007). However, trucks travel almost twice as

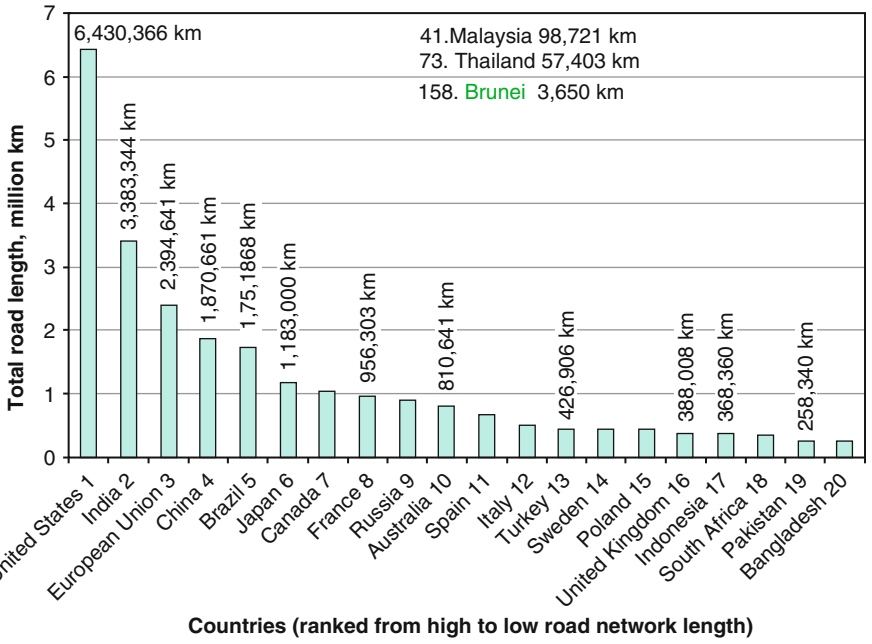

Fig. 1 World ranking in road length

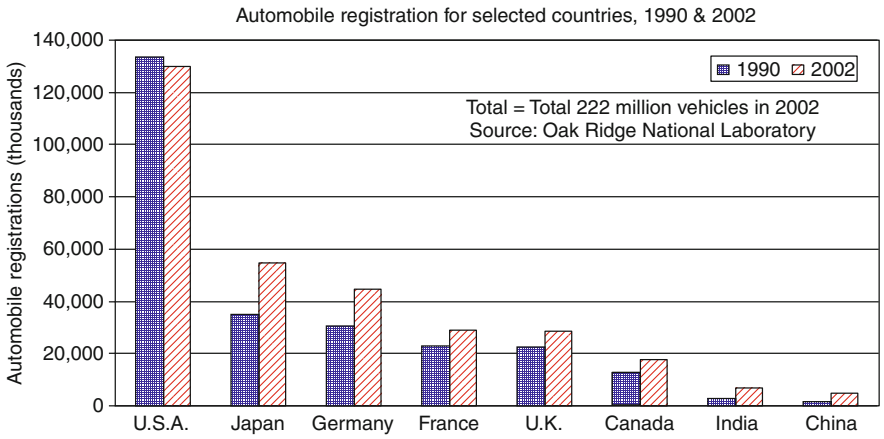

Fig. 2 Car ownership trends in selected countries

much as cars per vehicle per year and consume 3.5 times more fuel than cars per vehicle. Travel demand has been increasing consistently in the United States since the construction of the interstate highway system causing congestion, gridlock, air pollution, GHG emissions, and physical deterioration of pavements from the higher proportion of truck traffic on the national highway system (GAO 2002a, b; EPA 2005a). Additionally, aircraft, trains, and ships provide vital links in the transportation infrastructure network of the United States. In 2009, 704 million passengers were enplaned on US airlines domestically and internationally, which is expected to reach one billion passengers a year by 2023 (FAA 2010). Worldwide, 2.4 billion passengers are expected to depart on scheduled airline flights in 2010, compared to 2.1 billion passengers reported in 2006 (IATA 2007, 2010). Growth in urban areas and cities (Auch et al. 2004) contributes to area and mobile GHG emissions resulting from consumption by buildings, industries, and roads (EPA 2005a; EIA 2000).

According to the IPCC report, 33 billion tons of anthropogenic CO_2 is emitted annually, 7.3 billion tons is absorbed by the ocean, 7.3 billions of tons is absorbed by the forests, and 18.3 billon tons accumulated in the atmosphere (IPCC 2007). The industrialized countries contain 20 % of the population and produce 46 % of the greenhouse gases. Anthropogenic carbon emissions from transportation and populated areas are estimated to be 77 % globally (IPCC 2007), in addition to the industrial emission from coal- and fossil fuel-based power-generating plants and industries. The CO_2 emissions from mobile transportation sources are accounted globally for 23 % of the world energy-related GHG emissions in 2004 and 28 % in the United States. Between 1990 and 2007, the US inventory of anthropogenic GHG emission includes electricity, transportation, industrial, agriculture, and residential and commercial sectors (Fig. 3). The transportation sector accounts for 28 % of all anthropogenic GHG emissions in the United States, trailing the electricity sector at 34 % (EPA 2005a). Over 600 coal fire-powered plants contribute to electricity generation and GHG emissions in the United States, and coal remains the source

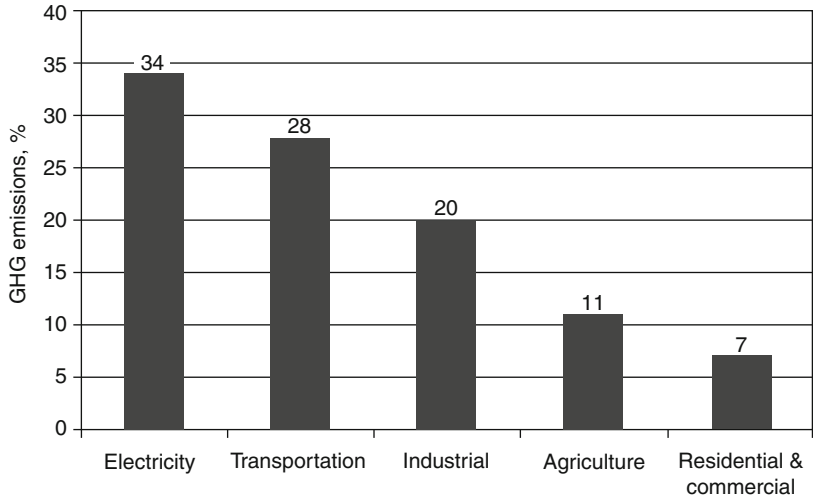

Fig. 3 Inventory of US greenhouse gas emissions

of 50–70 % of electricity in the United Kingdom, India, and China. Worldwide, the number of vehicles has grown tenfold since 1950, and the present number is estimated to be about 630 million vehicles. Worldwide, vehicle inventory will continue increasing sharply as the world population migrates to urban areas, energy demand grows, and air quality degrades in cities (United Nations 1999; WHO/UNEP 1992, 2009; WBCSD 2004; EEA 2008; WHO 2009a).

Travel demands over the past two decades already surpassed capacity limits of the road infrastructure, not only in the United States but also in most urban areas worldwide. This growth in travel demand and congestion directly contributes to increases in air pollution and greenhouse gases, mobility costs, user operation costs, public health costs, and other societal costs. The resulting vehicle emissions and demand on energy (due to the increased built areas and population migration from rural areas) have had adverse impacts on the environment, both in air quality degradation and increases in GHG (WHO/UNEP 1992; WHO 2009a; Uddin and Boriboonsomsin 2005, 2006; Uddin et al. 2005; 2009a, b; Osborne 2009; Headrick 2010; Uddin 2006; 2007, 2009, 2010a, b; Uddin and Uddin 2010). The GHG emissions are well-known contributors to global warming, rising sea levels and temperatures, and climate change mechanisms. This chapter focuses on traditional uses of petroleum-based gasoline and diesel which fuel the transportation sectors.

Objectives

The objectives are to:

1. Review the current and future trends of emission contributions from transportation and area sources, including built-up urbanized areas and their adverse

impacts on global warming and climate change indicators, ground-level air quality, and public health.
2. Discuss abatement strategies for greenhouse gas emissions by implementing sustainable transport and traffic management, smart growth and mixed use urban planning, mass transit multimodal solutions, alternative fuel, and vehicle fuel efficiency technologies.
3. Present best practices and use of geospatial analysis, life cycle costs and benefits, and value engineering to evaluate effectiveness of abatement strategies for sustainable transportation infrastructure and urban growth to reduce their contributions of air pollution and greenhouse gases.

Environmental Sustainability Challenges

Sustainability Definition

Sustainability has been defined in different variations. The following definition is used in this chapter: "to meet the current needs without depleting natural resources and compromising the ability of future generations to meet their own needs for sustaining a comfortable quality of life."

A "sustainability scale" is defined as carbon footprint in terms of carbon dioxide per capita. Sustainable transportation and development policies strive to minimize adverse impacts on the environment while conserving natural resources.

Environment, Energy, and GHG Emissions

Environment and energy are greatly impacted by transportation system planning and operation, urban growth and land-use practices, and travel modes available to and used by the population. After the Clean Air Act of 1970, the EPA's federal environmental regulations and vehicle technology innovations (such as catalytic converter) in the United States have resulted in the removal of lead from the fuel and vehicle emissions (Uddin and Boriboonsomsin 2005). Other vehicle emissions affect the ground-level air quality and greenhouse gases. This creates significant changes in the ecocycle involving water, oxygen, and carbon dioxide, all essential in sustaining human, animal, and plant life. The following six criteria pollutants have been recognized as the most damaging to the public health and the environment for which the US EPA established the National Ambient Air Quality Standards (NAAQS) (Uddin and Boriboonsomsin 2005; Bernow and Marron 1990): ground-level ozone (O_3), carbon monoxide (CO), oxides of nitrogen (NOx), sulfur dioxide (SO_2), particulate matter (PM_{10} and $PM_{2.5}$), and lead (Pb). The notation PM_{10} is used to describe particles of aerodynamic diameter 10 μm or less, and $PM_{2.5}$ represents particles of aerodynamic diameter 2.5 μm or less. Ground-level O_3 is formed through the photochemical reaction of nitrogen dioxide (NO_2) and volatile organic compounds (VOC) in the presence of sunlight, which are produced by petroleum-fueled vehicles. Methane (CH_4) is a species among VOC.

Carbon dioxide (CO_2) emissions are directly proportional to fuel consumption. Nitrous oxide (N_2O) and VOC emissions are affected by vehicle emission

control technologies for motorized vehicles on roads. The three pollutants (CO_2, CH_4, N_2O), not specifically regulated in the United States, are the principal "greenhouse gases" which, through increased concentrations in the atmosphere, can contribute to global warming and associated climate change on global and regional scales. NO_x and CO (predominantly vehicle emissions) also contribute to greenhouse warming (Bernow and Marron 1990). In principle, all molecules having two or more atoms can contribute to greenhouse warming due to their absorption of light in the infrared region. CO is a short-lived species in the atmosphere and therefore cannot contribute much. NO_x's role is not all bad. NO induces OH radical in the stratosphere, which, in turn, breaks down CH_4 – a GHG with a stronger warming force.

The overall uncertainty in CH_4 and N_2O emission estimates for the US inventory of mobile sources of GHG emissions is relatively minor due to the fact that these emissions are a small part of total highway vehicle GHG emissions. The significance of uncertainty in non-road vehicle modes (such as snowmobiles, off-road tractors and desert vehicles, lawn mowers, etc.) is low given the relatively small quantity of GHG released by these sources (Bernow and Marron 1990).

Urgent Need for Environmentally Sustainable Transportation Policies

The travel demand on the road infrastructure network in the United States has increased more than its capacity. Consequently, emissions from mobile sources grew 29 % between 1990 and 2004 (Davis and Hale 2007). Commuters waste millions of hours and gallons of fuel in traffic congestion. Each year, about 20 million barrels of diesel fuel are consumed by idling long-haul trucks in the United States, which produce about ten million tons of carbon emissions (Gaines et al. 2006). Additionally, residential emissions have increased 13 % in the last two decades. Both ground transportation and aviation emissions are adversely affecting the global atmosphere more than coal burning plants. They will have greater impacts in the coming years due to the expected exponential growth of vehicle and aviation transport worldwide and especially in the emerging economies. The emerging economies of China, India, and Brazil are all following the path of the United States and other industrialized nations in developing transportation infrastructure assets, increasing their transportation fleet, and accelerating carbon emissions. As reviewed in later sections, the rapid urban growth in developing countries and increase in the number of cities with five million inhabitants or more are expected to grow from 40 in 2001 to 58 in 2015. This growth in transport vehicles and urbanized areas will result in a higher energy demand and greater GHG emissions. A 50 % rise in energy use and carbon emissions is expected worldwide by the year 2030 (EIA 2007a). Therefore, mobile sources of CO_2 emissions will remain significant contributors to the release of greenhouse gases and its transport into the upper atmosphere. There is an urgent need to improve assessment of the contributing factors and find practical and cost-effective solutions. This will help to evaluate the benefits and economic costs of alternative abatement strategies before making major decisions on regional and global levels for an effective mitigation approach.

Related Research Sources

This chapter summarizes an up-to-date literature review of the Internet sources, published papers and reports, news articles, as well as research studies undertaken by the author. The resources referenced and used include:

- Federal agencies in the United States, European agencies, and other international organizations (ORNL 2003, 2004; DOT 2007, 2008; GAO 2002a, b; EPA 2005a, 2008a; FAA 2010; IATA 2007, 2010; Auch et al. 2004; EIA 2000; IPCC 2007; United Nations 1999; WHO/UNEP 1992, 2009; WBCSD 2004; EEA 2008; WHO 2009a; EIA 2007a), including:
  - US Department of Transportation (USDOT), Federal Highway Administration (FHWA), Federal Aviation Administration (FAA), Oak Ridge National Laboratory (ORNL), Environmental Protection Agency (EPA), US Energy Information Administration (EIA) of Department of Energy (DOE), US Geological Survey (USGS), General Accounting Office (GAO), and Transportation Research Board (TRB) reports of the National Academies
  - International Airlines Transport Association (IATA), International Energy Agency (IEA), Intergovernmental Panel on Climate Change (IPCC), Organization of Economic Cooperation and Development (OECD), United Nations Environment Programme (UNEP), United Nations Population Fund (UNPF), World Business Council for Sustainable Development (WBCSD), and World Health Organization (WHO)
- Funded and graduate research studies conducted by the author at the Center for Advanced Infrastructure Technology (CAIT), University of Mississippi, since 1999, for air quality modeling and GHG analysis, terrestrial and spaceborne remote sensing, geospatial analysis, and built-up area and traffic attribute extraction from imagery (WHO 2009a; Uddin and Boriboonsomsin 2005, 2006; Uddin 2006; Uddin et al. 2005, 2009a, b; Osborne 2009; Headrick 2010; Uddin 2007, 2009, 2010a, b; Uddin and Uddin 2010)
- Published books, papers, reports, news stories, and web documents, as referenced in the following sections

Mobile Sources of GHG Emissions

Mobility Needs and Transportation-Related CO_2 Emissions

Transportation and Economic Prosperity

Having "efficient public mobility" and "safe and secure transportation infrastructure assets" is imperative for mobility needs, distribution of resources and goods through intermodal facilities, assistance to communities during disasters and emergencies, and other services to society. The economic prosperity of a country is strongly associated with the relative size and physical condition of its road network, which is the most important component of its transportation infrastructure according to the

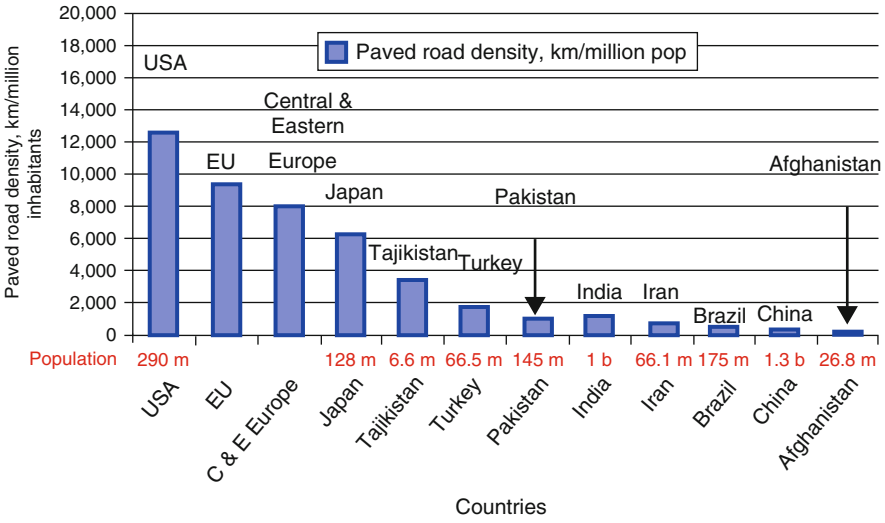

Fig. 4 Comparison of paved-road density of industrialized and developing countries, 2001

World Bank's study (Hudson et al. 1997). The study reports that the road infrastructure asset inventory shows high positive correlation with the gross national product (GNP) per capita of a country. The GNP per capita reflects a country's total market value of the goods and services produced annually divided by the population. High paved-road density values in km per million inhabitants (Uddin et al. 2005; Queiroz and Gautam 1992) are reported for industrialized countries (Fig. 4). Comparatively, low values of this important economic development indicator are observed in developing countries. However, China's expressways and highways will exceed most other developed countries within the next decade due to accelerated construction programs. India, Brazil, and several other countries are also expanding their road and highway networks to provide connectivity to a larger number of their populated areas and serve the mobility needs of the public, agriculture, and industries. The World Bank's use of only paved-road density for correlation with economic prosperity indicator is misleading because it ignores other transport infrastructure assets of a country such as rail and water transport. Rail infrastructure represents a significant modal share in Europe and most developing countries for serving passenger and freight travel demands.

Regardless of a region's characteristics such as culture, income, or geography, people on average spend a significant amount of time traveling on the road and/or wasting fuel on congested roadways. People in less developed regions spend a great deal of their time traveling to and from destinations due to lack of transportation facilities and/or urbanization, while people in more developed countries such as Japan, Western Europe, and the United States spend half of their time leisurely traveling and the other half in route (Schäfer et al. 2009). The US automobile ownership in terms of persons per motor vehicle is estimated at 1.27 persons per

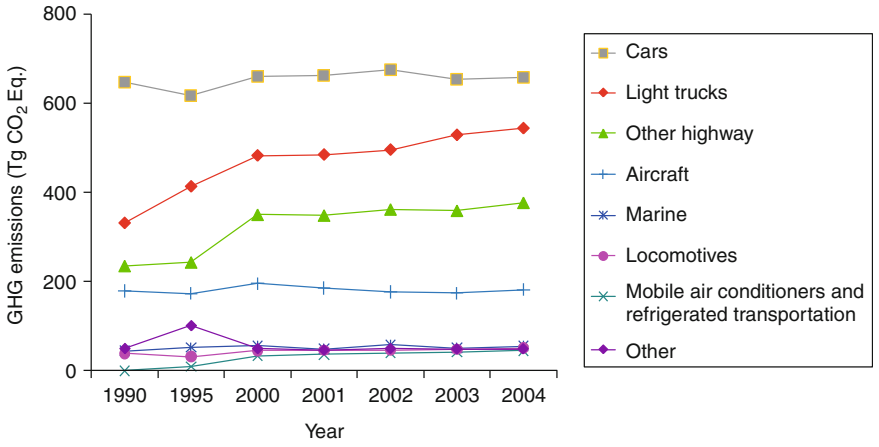

Fig. 5 US greenhouse gas emissions from all mobile sources, by travel mode and vehicle

car considering 235.9 million registered automobiles in 2007 which include cars, vans, pickup truck, and sport-utility vehicle (SUV). Brazil has 48 million vehicles as of 2006 and a population of 175 million that translates to 3.6 persons per vehicle. The 2008 automobile ownership rate (total number of motor vehicles per 1,000 population) of 842 in the United States is higher compared to other countries, such as Brazil's rate of 156 motor vehicles per 1,000 population as of 2009. Vehicle mix indicates the utilization of different modes on roads. Traffic demand can also largely impact air quality, public health, and public safety on society as well. Accurate and timely collections of traffic attributes are necessary for traffic management, performance evaluation of transportation systems, and measuring emission inventory.

Mobile Sources of GHG

Figure 5 shows the US greenhouse gas emissions from all mobile sources, by travel mode and vehicle type between 1990 and 2004 (EPA 2005a). Figure 6 shows the US transportation emissions by transport mode. Aviation produced about 9 % of transportation GHG emissions in 2003, the largest source of non-road transportation GHG emissions. In total, aircraft GHG emissions decreased about 3 % from 1990 to 2003. Following a substantial decline in travel after the terrorist attacks on September 11, 2001, in the United States, passenger travel rose more rapidly than the GHG emissions due to a higher number of seats occupied. Aircraft emissions have risen due to increased passenger travel and freight activities, but this has been offset by the improved fuel efficiency of aircraft and their operations. Between 1990 and 2003, passenger miles traveled on domestic services increased by 48 %, from 345.9 to 505.2 billion passenger miles. This is higher the than 31 % increase in light-duty vehicle passenger miles over the same period (EPA 2008a). The United States accounts for approximately 40 % of all commercial aviation and 50 % of all general aviation activity in the world (Uddin 2010c). The US airlines carried 20.4 % more

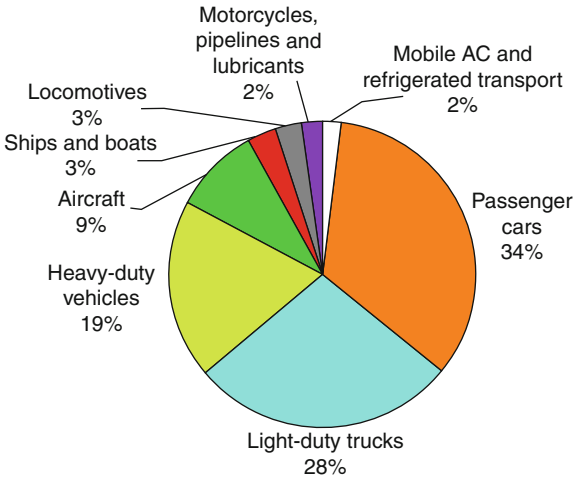

Fig. 6 US transportation-related GHG emissions, 2004

passengers and cargo traffic in 2007 compared to that in 2000, but they used 3 % less fuel in doing so. This resulted in a reduction of 5.1 million tons of CO_2 emissions in 2007 compared to that in 2000, and the FAA's satellite-based Next Generation Air Transportation System (NextGen) is expected to increase efficiency and further reduce the aviation GHG emission (McCarthy 2010). Therefore, the main concern of mobile GHG emission is from on-road vehicles which make up 81 % of the transportation-related emissions.

In the last three decades, the total number of vehicle miles driven rose to 2.9 trillion miles per year, four times faster than the rate of population growth of the United States. Per capita vehicle mile traveled (VMT) in 2003 was 9,941. This indicates that vehicle fuel efficiency and improvements in emission control may be offset by increased VMT in the United States (McCarthy 2010). The VMT distribution by vehicle on roads is plotted in Fig. 7 (ORNL 2004). The vehicle mile travel proportions of 58.1 % by automobiles and 36.5 % by trucks show a significant amount of freight by roads at 3.46 times less fuel efficiency.

Older model vehicles and absence of effective vehicle emission regulations and testing will yield higher amounts of emissions. Not all states in the United States have emission testing programs (such as Mississippi), but the manufacturers strictly follow federal emission and fuel efficiency regulations in all states. In many countries where there are no stringent emission regulations and/or no effective enforcement control, older model and relatively aged vehicles are used to make more trips and pollute roads more with both GHG and other pollutants. This was the case in China where, in the 1990s, most automobiles, including cars and trucks, were still using 10–20-year-old technologies and polluting urban areas with more than ten times emissions compared to the United States and Japan. In view of rapidly growing economy and vehicle fleet, China has already embarked upon a national program to implement lead-free fuel, fuel economy requirements, and emission standards to

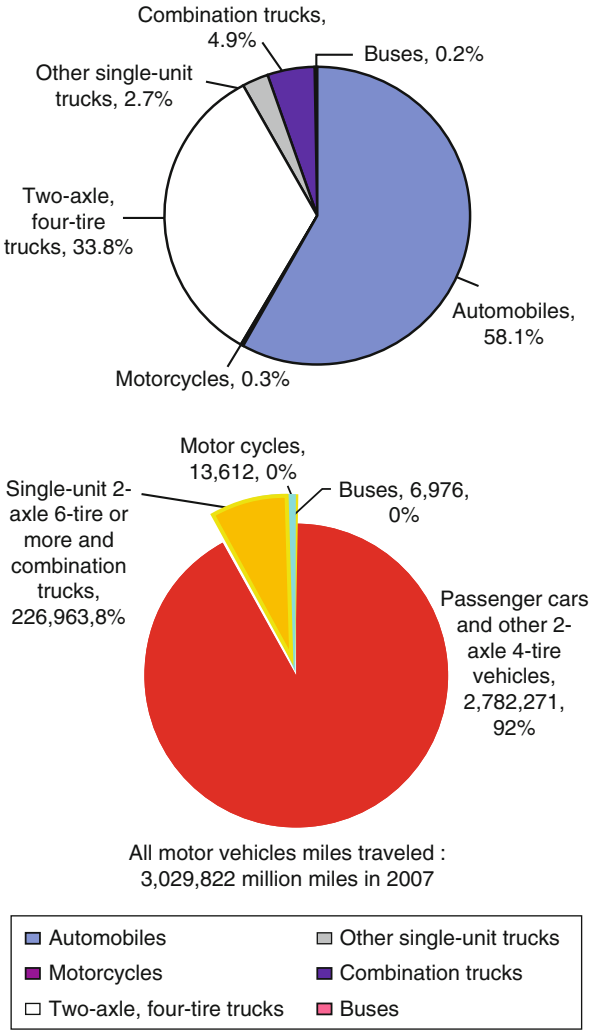

Fig. 7 Vehicle fleet mix distribution (*left*) and VMT distribution (*right*) in the United States

reduce vehicular emission. Old vehicle technology is still common in many other cities of developing countries. Reportedly, some 70 % of the 18 million people in Kolkata (formerly known as Calcutta) in India suffer from respiratory disorders caused by air pollution (BBC 2007).

Science Models of CO_2 Emissions from Traffic Volume Demand

Methodology for CO_2 Emissions from Vehicle Mile Traveled

The CO_2 emission problem inherent to the mobile transportation originates from the burning of petroleum-derived fuel (gasoline and diesel) for power. The burning of

petroleum and natural gas fuel primarily emits CO_2 which represents 82 % of the total US anthropogenic GHG emissions (EIA 2007a).

The GHG emission inventory data are reported in units of tons of carbon dioxide equivalent (CO_2e), which allows emissions of greenhouse gases of different heat trapping potential to be combined for a direct comparison of different GHG emission inventory. In the United States, 28 % of all GHG emissions are from the transportation sector as shown in Fig. 3 (EPA 2005a). Other criteria emissions contribute greatly to pollute ground-level air and cause smog, ozone, cancer, lung disease, and respiratory disease. The following methodology is used by the US EPA to estimate CO_2 emission from vehicle mile traveled data (EPA 2005b).

Assumptions:

- CO_2 emissions from a gallon of gasoline = 19.4 lbs (assuming 99 % of carbon is eventually oxidized)
- CO_2 emissions from a gallon of diesel fuel = 22.2 lbs (assuming 99 % of carbon is eventually oxidized)
- Average fuel efficiency for gasoline passenger car = 20.3 miles per gallon (mpg)
- Average fuel efficiency for diesel truck = 5.9 mpg
- Typical vehicle travel (cars, vans, light trucks combined) = 12,000 miles per year

CO_2 emissions:

$$\{(\text{number of miles driven per year})/\text{average vehicle fuel effiiciency}\} * \text{pounds of } CO_2 \text{ emitted pergallon} \quad (1)$$

Example:

$$\begin{aligned} CO_2 \text{ Emissions for passenger vehicle} &= \{12,000/20.3\} * 19.4 \\ &= 11,468 \text{ lbs} \\ &= 5.7 \text{ tons per year per passenger vehicle} \end{aligned}$$

$$\begin{aligned} CO_2 \text{ Emissions for diesel truck} &= \{12,000/5.9\} * 22.2 \\ &= 45,153 \text{ lbs} \\ &= 22.6 \text{ tons per year per truck} \end{aligned}$$

This example shows that due to very low fuel efficiency, diesel trucks produce four times more CO_2 in comparison to typical cars.

Natural gas is accounted for 28.5 % of fossil energy use in 2008, but only 21.4 % of the total energy-related CO_2 emissions in the United States (EIA 2009). Carbon intensity of natural gas is 55 % of the carbon intensity of coal and 75 % of the carbon intensity for petroleum. Therefore, a hybrid vehicle operating on mostly compressed natural gas (CNG) and liquid natural gas (LNG) may be assumed to emit 75 % of the CO_2 emission calculated for petroleum fuel using Eq. 1. These types of hybrid vehicles are common in several countries, including Brazil and Pakistan (Uddin 2007), but the CNG and LNG consumption is accounted for only 6.9 % transportation share of energy consumption in the United States in 2003 (ORNL 2004).

Energy- and Transportation-Related Global CO_2 Emissions

Recent Department of Energy (DOE) data of the 2008 US inventory of anthropogenic GHG emission shows seven billion metric tons of CO_2e. This includes 5.814 million metric tons of energy-related emissions of which 40.6 % is for electric power generation, 33.1 % transportation-related emission, and 26.3 % produced by residential buildings, commercial sources, and industries (EIA 2009). About 25 % of all world petroleum produced was consumed in the United States. About 66.5 % of this was used by the transportation sector in the United States, as shown in Fig. 8 (EIA 2007b). Consumption of fossil fuel produces CO_2 that is distributed by source in the United States as 42 % from petroleum, 37 % from coal, and 21 % from natural gas. The 1990 data from OECD countries shows that highways account for 94 % air pollution from all transportation modes. About 81 % of GHG emission comes from on-road vehicles, as shown in Fig. 6 for the 2004 emission inventory in the United States (EIA 2007b). The United States, in turn, was responsible for 20 % of energy-related CO_2 emissions worldwide in 2006, though the country accounts for only 5 % of the world's population. In comparison, China's share of global energy-related CO_2 emissions was 21 %, which is projected to grow to 29 % in 2030, and China accounts for 51 % of the projected increase worldwide during this period, followed by India with 7 % projected increase (EIA 2009).

Multimodal Transportation and Travel Demand Management

CO_2 Footprint Indicators of Multimodal Travel

It is useful to compare CO_2 emissions for vehicle distance traveled per person and freight distance traveled per ton to assess their impacts on the sustainability scale. Transportation accounts for 23 % of all global CO_2 emissions, and Fig. 9 shows the CO_2 footprint (grams per passenger per km) contributed by each travel mode for one

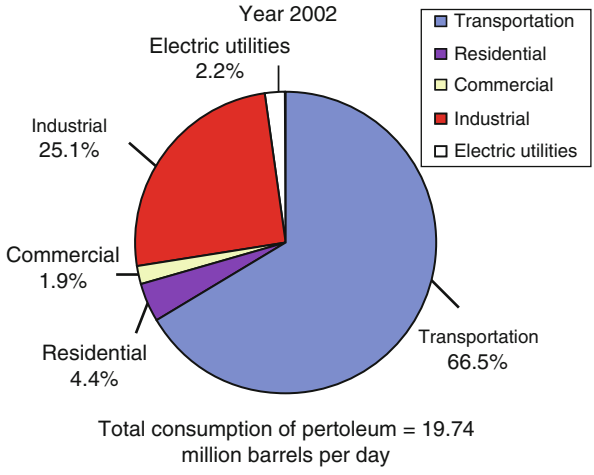

Fig. 8 Distribution of annual consumption of petroleum fuel by sectors

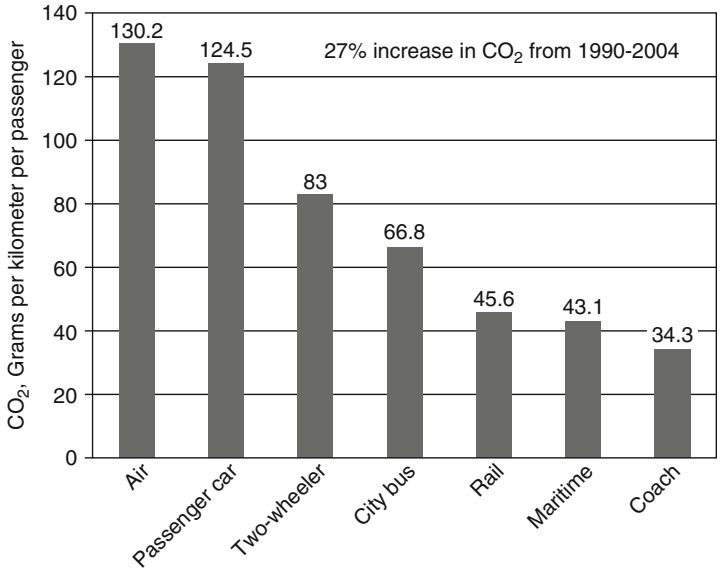

Fig. 9 Production of CO_2 emission by transport mode

person to travel 1 km (EEA 2008; Allianz 2010). Clearly, aviation and passenger car travelers are the most polluting modes of transportation, and rail/train is one of the lowest polluting at one-third CO_2 footprint emission. This shows that public bus and other mass transit modes will reduce emissions significantly in urban areas and cities. In 2005, public transportation (transit buses, mass transit rail) reduced carbon emission by 6.9 million metric tons and avoided 400,000 t of other GHG emissions in the United States (Davis and Hale 2007). The CO_2 footprint emission of freight truck travel per ton km will be several times larger than that by freight train considering that:

- A diesel truck's fuel efficiency is poor at 9.4 km (5.9 miles) per gallon, and on the average a truck travels approximately 40,000 km (25,000 miles) annually, about twice that of an average car travel.
- Truck CO_2 footprint emission is estimated at 25 g per ton km of freight travel by road assuming an average 20 metric tons of freight per truck per km at above fuel efficiency.
- Rail CO_2 footprint emission is estimated at 5–10 g per ton km of freight travel by rail/train. However, the actual emission by rail/train will be even less because trains are able to carry several times more freight than a truck and it would be more economic than a freight truck.

Traffic gridlock and delays on roads and highways further deteriorate air quality by producing excess vehicle emissions. Additionally, road user time is wasted at slower speeds in congested hours of travel. Unlike road vehicles, a dual-track rail

infrastructure keeps trains moving at designated speeds safely, efficiently, and free of "gridlock" eliminating unnecessary emissions. Figure 10 shows the growth trends in passenger and freight travel demands during 1970–2000 in the United States. An indication of the deficit between travel demand and capacity is the congestion, which is measured in terms of traffic density or travel time. The GAO stated that the US interstate highways have become more congested than other similar roads (GAO

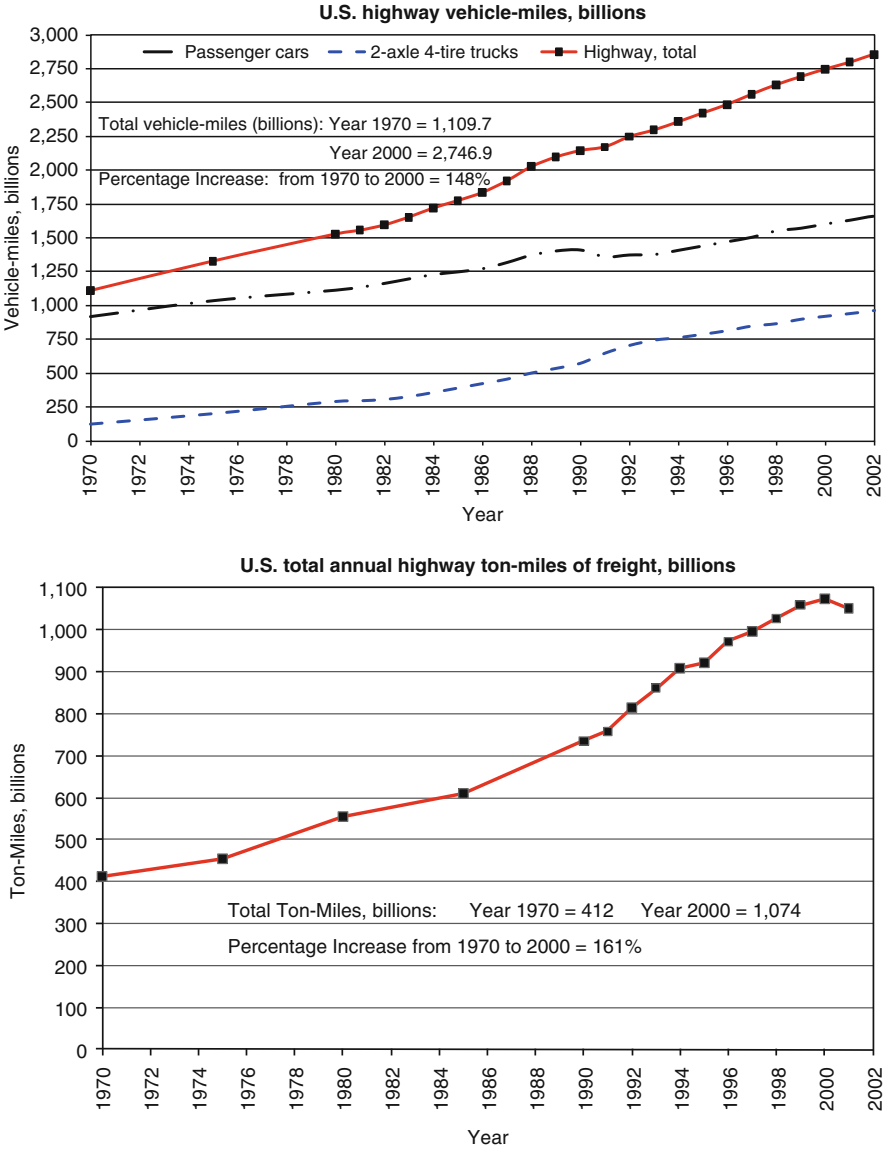

Fig. 10 US travel demand trends; (*left*) VMT, (*right*) freight ton miles

2002a) and that metropolitan areas are reportedly having problems with congestion and degraded air quality (GAO 2002b). The overall density of traffic on the interstate highway system has increased 31.7 % over the past decade. More recent US studies on changes in mobility patterns, driving in the built environment, federal guidelines, and states' efforts (Pisarski 2006; TRB 2009; NCHRP 2010a; Keck et al. 2010) indicate that CO_2 footprints and GHG emissions are being used as one of the key performance indicators of urban and regional traffic management and transportation infrastructure asset management.

Repercussions of Traffic Congestion on Air Pollution and Commuters' Woes

Urban Growth and Travel Demand, and Congestion

As of 2008, for the first time in history, more than half of the world's population lives in towns and cities, as reported by the United Nations (United Nations 1999). Urbanization is very high in industrialized and developed countries, where as of 2000, 75 % of the population lives in urban areas. The urban growth during the last five decades has increased travel demand more than the infrastructure supply, resulting in frequent traffic jams and long peak hours. As reported in TIMES, the term gridlock apparently originated in New York City during a transit workers' strike in 1980, when a surge of commuter autos paralyzed Manhattan's street grid (Koepp 1988). American workers are frequently caught in traffic because commuting patterns have changed drastically in recent decades. Figure 11 shows that road bottlenecks and traffic incidents contribute 65 % to congestion (Uddin and Uddin 2010).

It is estimated that commuters spend millions of hours annually stuck in traffic congestion and waste billion gallons of gas. In 2003, the US commuters suffered 43.8 million total person-hours delay in urbanized areas at an average 25-h delay per person and resulting in 15 gal of fuel wasted per person (ORNL 2004; Uddin and Uddin 2010; Schrank and Lomax 2008). This increment in congestion directly affects the increase in air pollution and greenhouse gases, mobility costs, user operating costs, public health costs, discomfort and stress, and other societal costs.

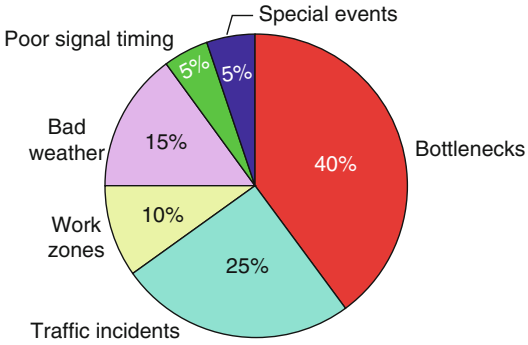

Fig. 11 Causes of traffic congestion (From US data)

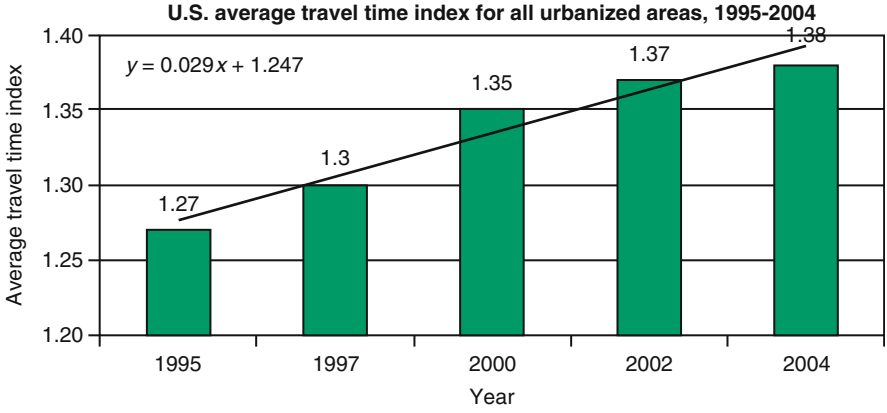

Fig. 12 Increased congestion trend in urban areas of the United States, indicated by average TTI

Travel Time Delay Comparisons

The Travel Time Index (TTI) is another indication of traffic congestion used in the United States to compare travel time delays in several urbanized areas (Schrank and Lomax 2008). It is the ratio of peak-period travel time during congested condition to free-flow travel time for a given road section. A TTI of 1.3, for example, indicates that a 20-min free-flow trip will take 26 min during the peak travel time periods, a 6-min (30 %) travel time penalty. Figure 12 illustrates the trend of average TTI for urbanized areas in the United States for the time period 1995–2004. While it depicts that the TTI is on a rise, for the period of data shown, it was below 1.40. The TTI has increased 12 % in the last decade in urbanized areas in the United States. This number is higher approaching 2.0 or more, for some cities such as Los Angeles and New York. The TTI value estimated in 2007 for Karachi, Pakistan, was of the order of 3.5–4.0 during several hours of peak travel. This high ratio indicated undesirable congestion and provided basis to study traffic congestion in Karachi. Strategies were recommended using geographical information system (GIS) and intelligent transportation system (ITS) technologies to enhance traffic management as discussed later in the section "Geospatial Analysis of Built Environment and Traffic Demand Impacts" (Uddin and Ali 2007).

Health Risks Associated with Transport Patterns, Travel Behavior, and Built Environment

Besides other environmental hazards, built environment and transport-related emissions pose serious health risks to cities in developed countries and the majority of cities in developing countries. In the United States (TRB 2005, 2009; Keck et al. 2010; NCHRP 2010b) and Europe (WHO 2004, 2009b), transport-related health and environment risks have been a major focus of research and transport policy formulation. However, in many developing countries, transport-related health

risks have not received attention and priority for investment and policy actions (ORNL 2004; WHO 2009b). Important health risks and public health hazards due to transport and travel patterns include the following (Uddin et al. 2005; Uddin 2006, 2007; Uddin and Uddin 2010; TRB 2005; WHO 2004, 2009b):

- *Public health hazards from urban air pollution*: Increased exposure to air pollution is associated with higher rates of cardiovascular and respiratory diseases, asthma, and other diseases, which are estimated to kill nearly one million people each year worldwide.
- *Traffic fatalities and injuries*: Road transport is responsible for another estimated 1.2 million deaths and 50 million injuries; pedestrians and cyclists are among the groups most at risk. A significant proportion of injuries in developing countries is related to the lack of safe space for bike/motorcycle and nonmotorized transport.
- *Health risks due to physical inactivity*: Motorization and built environment are the driving force in lifestyles which lack physical activity, especially in the United States and other car-culture countries where urban sprawl requires many more trips. Physical inactivity is a risk factor for cardiovascular diseases; cancers of the breast, colon, and rectum; and diabetes mellitus. Globally, the lack of or insufficient routine physical activity is reported to cause an estimated 3.2 million deaths annually.

Additionally, the urban sprawl type land use favors car owners and promotes poverty and social inequalities (Uddin et al. 2005; Uddin and Uddin 2010). Over the past two decades, even as many developed cities have been rediscovering the health and environmental benefits of walking and cycling, nonmotorized travel is in decline in many cities of developing countries (WHO 2009b).

Commuters' Woes

Commuters stuck in long traffic jams lose patience and drive under stress. The 2010 report on IBM Global Commuter Pain Study surveyed 8,192 motorists in 20 cities on six continents to better understand consumer thinking toward traffic congestion crisis and environmental concerns related to higher levels of auto emissions (IBM 2010). The study Index gauges physical, emotional, and economic toll that everyday traffic has on commuters based on the following ten issues: (1) commuting time, (2) time stuck in traffic, (3) price of gas already too high, (4) traffic gotten worse, (5) start–stop traffic problem, (6) driving causing stress, (7) driving causing anger, (8) traffic affecting work, (9) driving stopped due to bad traffic, and (10) decision not to make trip due to traffic. The study's Pain Index ranks each city on a scale of 1–100, with 100 being the most onerous, as shown in Fig. 13.

The following highlights of the study provide useful insight into traveler's perception and evaluation of the transport and traffic management in their respective cities:

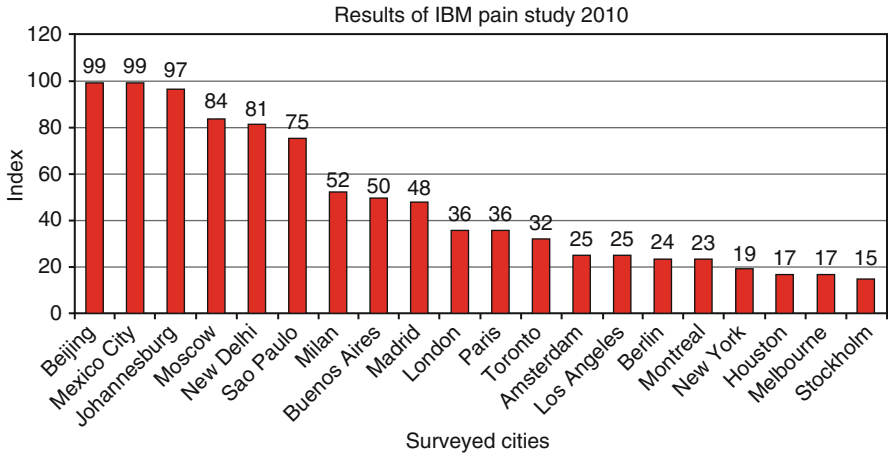

Fig. 13 Result of Pain Index summarized from 2010 IBM Global Commuter Pain study

- Overall traffic has gotten worse in the past 3 years according to the 67 % majority.
- Eight cities scoring 50 or more ranked as having horrible (worse) traffic, with Beijing and Mexico City topping the list of worst traffic and only Milan from Europe included in the list.
- Twelve other cities with bearable (better) traffic are in North America, Europe, and Australia with scores of less than 50, and the best two cities being Melbourne and Stockholm.
- While over 90 % of the respondents in New York and Los Angeles reported driving to work, only 32 % reported so in Paris, 34 % in Amsterdam and Buenos Aires, and 37 % in Milan.
- After driving, the most popular form of transportation was bus – at 12 %. The two cities with the most painful commutes, Beijing and Mexico City, have 44 % and 32 % commuters using bus, respectively. (Traffic in these cities would be more horrible if so many people did not travel by bus.)
- The perception of worsening traffic stemmed in large part from being stuck in traffic for significant lengths of time. This was indicated by 87 % of the respondents who were stuck in roadway traffic during the last 3 years.
- The average delay due to traffic congestion was 1 h for the surveyed cities worldwide – very similar to the figure for the United States alone in the previous two Commuter Pain surveys conducted by IBM. (Note: This number is not directly comparable to the delay hours stated in section "Repercussions of Traffic Congestion on Air Pollution and Commuters' Woes" for US urbanized areas.)
- Responding to the harmful effects of traffic on the health of commuters in any way, 57 % said yes. Among those respondents, increased stress (30 %) and anger (27 %) were the primary manifestations. Increased stress was most prominent in Mexico City (56 %), São Paulo (55 %), New Delhi (45 %), Buenos Aires (44 %), and Beijing (40 %), while anger prevailed in Beijing (53 %), Moscow (51 %),

New Delhi (48 %), and Mexico City (43 %). All of these cities were among those identified in the survey as having especially "painful" commutes.

The above insights from the commuter's survey in large cities are useful considering that cities are driving engines of a country and predicted to grow further and contribute more GHG emissions (Koch-Kraft 2008), as noted below:

- Seventy-eight percent of all CO_2 emissions originate in cities (including mobile sources and built-up areas).
- Eighty percent of economic growth is predicted in cities in emerging industrialized and developing countries.
- Sixty-six percent of the population will be in cities by 2030 with 350 million more urban dwellers in China and India.

Area- and Built Environment-Related GHG Sources

Open Area Sources and Built Environment Effects

GHG from Open Areas

Open area sources of GHG emissions include (predominantly CO_2 except where noted different):

- Petroleum fuel-related emissions during extraction, shipment, refining, storage, and distribution
- Industrial emissions (manufacturing, factories producing steel and other metals)
- Construction material production (cement, asphalt mix, plastics)
- Fires from industrial and commercial incidents (e.g., the oil well fire of 2010 in the Gulf of Mexico)
- Forest fires due to heat and dry spells which are increasingly caused by climatic changes but also blamed on clearing forest land for agriculture and development purposes
- Open burning of solid waste (commonly seen around most cities in developing countries whereas some industrialized countries use for energy production such as incinerators used in Denmark for heating homes in winter)
- Portable electric generators running on gasoline (again a common scene in many developing countries)
- Wastewater treatment areas and solid waste landfill (primarily emitting methane)
- Livestock (methane emissions) and manure management practices (methane and N_2O emissions)
- Agriculture land sources (N_2O emissions from agricultural soils and methane emissions from rice cultivation)
- Deforestation (carbon stock loss) and land-use management (soil carbon pool changes)

The IPCC report (IPCC 1996) provides further information on GHG inventory associated with wastewater and solid waste, manure management, agriculture, forest (including deforestation), and land-use changes. No further discussion is undertaken on the contribution of these open sources since the focus here is on mobile and built area sources of GHG emissions.

Heat Island Effects in the Built Environment

For the first time in history, more than half of the world's population live in towns, cities, and megacities. Towns are generally located in rural areas and smaller than a city in population. Cities are human settlements with a typical population of as small as a few thousands to several millions. On the other hand, a city is called a megacity if it is inhabited by ten million people or more. A major detrimental effect of urbanization is runoff from rapid urban growth and constructed impervious surfaces that continue to degrade coastal and inland waters. Buildings use 36 % of total energy, consume 65 % of electricity, and produce 30 % of greenhouse gas emissions in the United States (EIA 2000). These concerns must be addressed in the design and management of urban growth and cities. In most rural environments, people live amidst moderately abundant vegetation, but in most urban environments, trees are removed, and vegetation is relatively sparse. Vegetation cover has a profound influence on solar energy flux because vegetation absorbs radiation in the most energetic infrared part of the solar spectrum to use in photosynthesis (Landsberg 1981). The unused fraction of the incoming solar energy is either transpired with water or reflected at near-infrared wavelengths. Most materials used in the built-up areas absorb a significant fraction of this incoming solar energy and reradiate it as sensible heat (Landsberg 1981; Oke 1982). Man-made dark constructed surfaces, such as buildings, concrete, and asphalt, absorb more heat from sunlight in comparison to other natural surfaces (soils, grass, trees, and water bodies). This is due to the low solar reflectivity of dark surfaces or albedo (the ratio of the amount of light reflected from a material to the amount of light incident on the material). These low albedo surfaces can raise the local ambient air temperature in an area by as much as 8 °F (4 °C) over the surrounding areas (Pomerantz et al. 2003; Rosenfeld et al. 1998). This phenomenon is known as the "heat island" effect.

A growing percentage of the population lives in urban areas where this heat island effect is more pronounced and induces physical stress, loss of productivity, and even death during heat waves. The heat island effect has been observed even in smaller towns, and on hot summer days, the surface temperature of the constructed surfaces (asphalt, concrete, buildings) during the hottest hours can be significantly higher than the daily maximum air temperature depending on solar radiation, clouds, and wind speed. Using 1-m satellite imagery to classify surfaces and conducting thermal analysis (Uddin and Tang 1999), a surface temperature map of Oxford, Mississippi, in the United States was developed. Figure 14 shows the surface temperature plotted for a strip along the east–west cross section of the city layout plan (Uddin and Boriboonsomsin 2006). The surface temperature difference between the inner city and outskirts can be much higher for larger metropolitan urban areas. A similar analysis for Memphis, Tennessee, showed built-up area about 67.3 % of the total

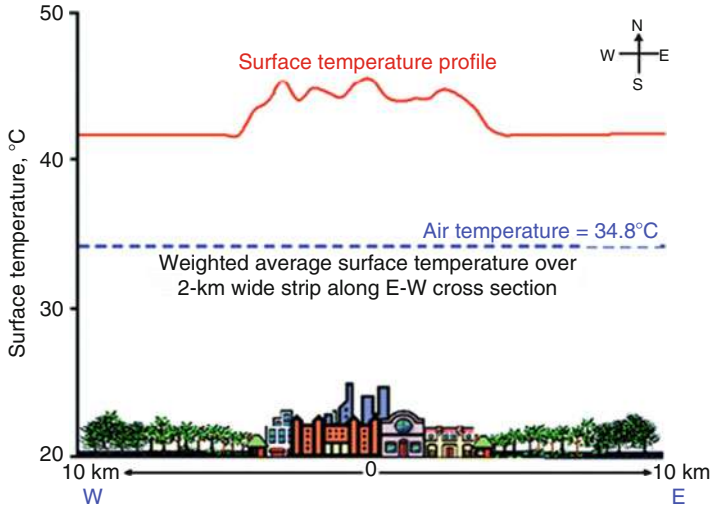

Fig. 14 Heat island effect in Oxford, Mississippi, United States

area of 1,211 km^2. Other non-built natural surfaces include 16.9 % trees, 12.5 % grass, 2.8 % water, and 0.5 % soil. The average surface temperature on the hottest hour of summer is 55.9 °C, which is 21.1 °C higher than the maximum air temperature of 34.8 °C that day due to about three times more built-up surfaces in Memphis than in Oxford, Mississippi. The heat island effect is compounded in most urbanized and populated areas by higher energy use in summer, vehicle traffic density, and emissions from congested conditions.

In many areas of the United States, a warming of 2.2 °C (4 °F) could increase ground-level O_3 concentrations by about 5 % (Akbari 2005). Air quality is also degraded due to the increase in O_3 and PM levels. Additionally, it requires extra electricity to cool down buildings in summer days, which results in increased energy demands, larger air-conditioning bills, and greater demand on power consumption. In the United States, about one-sixth of all electricity generated (about $40 billion per year) is used to air-condition buildings (Rosenfeld et al. 1998). This in turn increases air pollution.

Impacts of Urbanization and Megacities

Historical Overview of Urbanization and Current Trends in Growth of Megacities

The following discussions about historical development of cities, urbanization, and growth of megacities in modern times are based upon historical facts and extensive published research reviewed for this chapter (Wikipedia 2009; Abhat et al. 2005; DB Research 2008; Molina and Molina 2004; WRI 2007; MEGAPOLI 2009; City

Mayors Development 2007). A chronological account of birth of cities to modern era's megacities follows:

- *Pre-Christian era before Roman Empire*: Probably the birth of the world's first city took place on the plains of Mesopotamia near the banks of the Tigris and Euphrates Rivers in what is now Iraq in the Middle East. The development of the metropolis of *Athens* in ancient Greece was a milestone for all future mankind, where a disciplined civil society evolved with planned buildings, iconic architectural structures, institutions of learning, and sports stadium facilities.
- *Rome*: The first major populous city in the world became *Rome* when the Roman Empire spread to most parts of Europe and the Middle East. Rome was populated by more than one million people in 5 AD when the world's population was only 170 million. Romans were the first civil engineers and urban planners building roads and bridges for transportation, aqueducts for water supply, massive temples and sports structures, urban housing, and suburbs. It was the largest, wealthiest, and most politically important city in Europe for over a thousand years. Its population declined to about 20,000 during the Early Middle Ages, and it became a city of ruins. However, Roman roads and bridges served Europe until the times of Late Middle Ages and Industrial Revolution since the modern roads were not built until the 1800s.
- *Constantinople and Chang'an*: The city of *Istanbul* in modern-day Turkey was the Eastern Roman Byzantine Empire's seat and known as *Constantinople.* With its well-planned city streets, port, and commerce infrastructure, it remained a large prosperous metropolitan city for hundreds of years as well as during the Ottoman's Islamic Empire until the late 1800s. Istanbul has grown rapidly in the twentieth century, and with ten million population, it is now ranked 21 in the list of the top 25 megacities in the year 2006. The Chinese Imperial capital city of Chang'an was located northwest of today's Xi'an during the Han Dynasty. Around AD 750, Chang'an had an estimated one million people within city walls as recorded in Chinese history.
- *Cities in the modern era of 1800 to the mid-twentieth century*: In 1800, *Beijing* and *London* were the only major cities with populations of over one million. During the 1800s, only 3 % of the world's population lived in cities, which rose to 47 % by the end of the twentieth century. The invention of steam power and railways facilitated intercity traffic and commerce. But the discovery of petroleum and invention of the gasoline-powered car in the early 1900s revolutionized transportation, provided freedom of mobility, promoted manufacturing and businesses, and accelerated growth of cities and urban population through migration from countryside and abroad. In 1900, North America and Europe possessed nine out of the ten largest cities in the world.
- *Post-World War II era and emergence of megacities*: A city with a population of ten million or more has been generally described as a megacity. In 1950, New York, London, Tokyo, Paris, Chicago, and Moscow were inhabited by the world's largest metropolitan populations. New York City was the only megacity urban area with a population of over ten million. Since then, many megacities

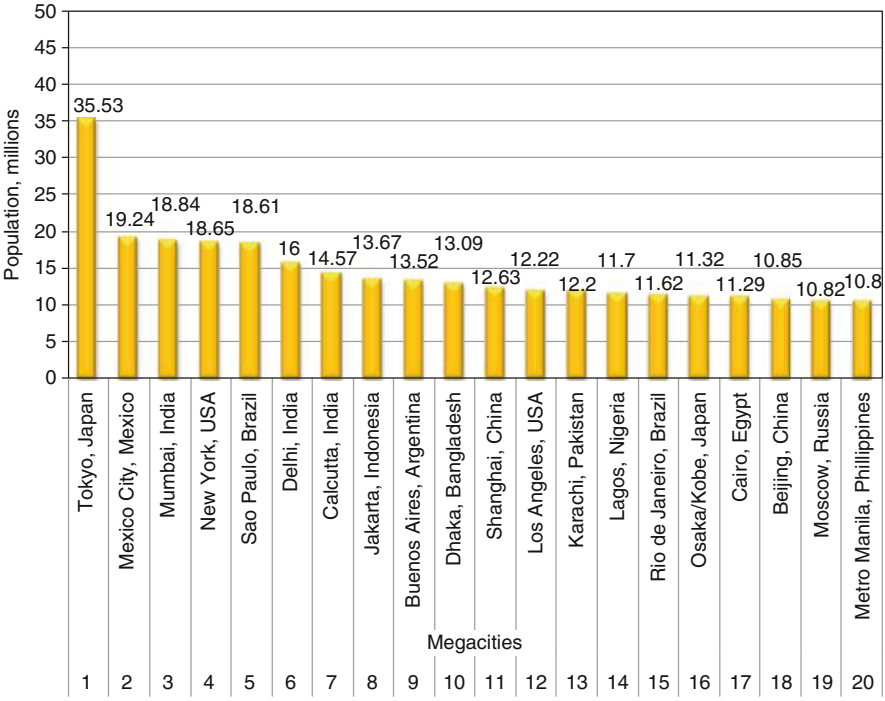

Fig. 15 Top 20 megacities in the world ranked by descending population, 2006

have evolved, and the majority of these are outside North America and Europe. This increase has happened as the rest of the world's population moves toward the high urbanization levels of North America and Western Europe, 75–85 %.

The largest megacity in the twenty-first century is the Greater Tokyo Area. Figure 15 shows the top 20 megacities in the world as of 2006, where New York is ranked number 4 and Los Angeles at 12 (DB Research 2008; City Mayors Development 2007). There is no other city from North America or Western Europe in the list. The increase in urban population is expected to be most dramatic in the developing countries of Asia and Africa. One study predicts that Asia alone will have at least ten megacities by 2025 (Wikipedia 2009). Additionally, the number of cities with five million inhabitants or more is expected to increase worldwide from 40 (year 2001) to 58 (year 2015).

Urban Population Density Impacts

The ratio of central city to metro population in the US urbanized areas decreased 30 % in 50 years from 0.57 in 1950 to 0.38 in 2000 (TRB 2009). Suburbs and outskirts of cities have typically low density, resulting in longer driving distances to work, more cars on roads, increased congestion, and higher GHG emissions. Dense population and demand on energy and mobility make the environment of a large city

and urbanized area different from the environment of smaller towns in rural and other uninhabited areas. Cities and urban areas are now major contributors of GHG emission, air pollution, and associated health risks (United Nations 1999; WHO/UNEP 1992, 2009; WBCSD 2004; EEA 2008; WHO 2009a; Uddin 2006, 2009; Uddin and Uddin 2010; Molina and Molina 2004; WRI 2007; MEGAPOLI 2009). Cities are sources of most of the anthropogenic GHG, other air pollutants, and aerosols that are known to alter the state of the global atmosphere and climate. Megacities produce 12 % of the anthropogenic CO_2 emissions and lesser fractions of the methane and nitrous oxide emissions. Even emission levels are maintained at that of the year 2005, simulation results show that megacities will be responsible for a 225-mK warming over the next 100 years with just under 90 % of this warming due to the CO_2 (MEGAPOLI 2009). Cities drive economic and societal development in all countries and offer better economic prosperity than rural areas, which is the primary cause of urban migration. At the same time, they are the largest consumers of natural resources and the biggest sources of pollution and greenhouse gas emissions. City inhabitants own more automobiles due to higher income levels and greater needs for mobility. This highlights the important role cities should play in mitigating climate change mechanisms.

Urbanization and Motorization Links

Uddin et al. (Uddin et al. 2005) discuss linkage between road transport and urbanization which affects physical inactivity, safety and traffic fatalities, air pollution and environmental degradation, public health, societal costs, quality of life, and social integration problems. Additionally, diminishing energy resources are equally important issues for environmentally sustainable transportation policy and decision-making.

Urban Growth and Travel Demand

Travel demand (number of vehicles and vehicle km traveled) is at its highest level both for automobile and truck traffic. Particularly, high traffic density and associated congestion is a constant reminder of the adverse impacts of urbanization as indicated by road users' woes in large cities (Fig. 13). As reported by City Mayors organization (City Mayors Development 2007) based on the key findings of a survey of 522 decision-makers from 25 megacities, "solving transportation issues has the highest priority in the cities surveyed, and air pollution is seen as the main environmental issue."

The link between urbanization and motorization has been strong in the United States and other industrialized countries due to greater mobility needs (Auch et al. 2004; Uddin and Uddin 2010; Pisarski 2006; Koepp 1988; Kozel 2007). This link is also displaying in emerging economies and developing countries. The change in travel pattern has significantly impacted travel demand on roads, which is typically indicated by Average Annual Daily Traffic (AADT) volume and vehicle mile traveled. These statistics have steadily increased over the years in the United

States (Uddin and Uddin 2010; Pisarski 2006), as shown by changes during 1970–2000: 58 % increase in vehicles registered, 148 % increase in total vehicle miles, and 161 % increase in total freight ton miles. Significant travel demand indicators (in 2007 except where noted otherwise) in the United States were (DOT 2007, 2008; Uddin and Uddin 2010):

- *Number of vehicles registered*: 254.4 million, 93.3 % (cars, 2-axle 4-tire vehicles) and 3.5 % (2-axle 6-tire or more trucks, combination)
- *Total vehicle miles*: 3.08 billion, 92 % (cars, 2-axle 4-tire vehicles) and 8 % trucks and less than 0.5 % (bus and motorcycles)
- *Total freight ton miles*: 1,293 billion (year 2005)
- *Average miles traveled per vehicle*: 11,720 miles (cars) and 25,141 miles (trucks)
- *Fuel economy (average miles traveled per gallon of fuel)*: 20.4 miles (cars), 5.9 miles (trucks), 6.1 miles (buses), and 56.2 miles per gallon (motorcycles)

Figure 16 shows the 2008 vehicle miles traveled and GHG emissions (DOT 2008), which indicate that though all trucks combined accounted for only 7.6 % VMT, they emitted 60 % CO_2 of all on-road vehicles. In comparison, cars contributed 54.3 % VMT but only emitted 39 % CO_2, implying that mobile GHG emissions are undesirably high even outside cities where most trucks operate. The results of a comparative study of national transportation policies over the last 25 years in the United States and France by Gires (Gires 2005) show that in the early 2000s:

- The US consumption of fuel and emission levels has not changed much due to the increase in car ownership, more travel mileage, and larger market share of fuel gulping SUVs and pickup trucks that has risen to 50 %.
- The average gasoline consumption has remarkably decreased by more than 20 % in France, but diesel market share rose by 70 %.

Figure 17 shows that car ownership per 1,000 population in large cities of industrialized countries was 2–30 times that of the major cities of developing countries based on the data from the 1990s (Imran 2010). This implies that the cities in developed and industrialized countries will have significantly higher GHG emissions due to higher AADT, larger number of car trips, and low fuel economy of on-road vehicles.

A reasonably quantifiable sustainability scale is CO_2 emission per capita that can be used by government agencies and cities for evaluating the performance of sustainable transportation policies. Using the 2007 daily vehicle demand volume (DOT 2007; Uddin 2010a; Molina and Molina 2004; WRI 2007; Imran 2010), vehicle fleet composition, typical vehicle miles driven per day, and CO_2 calculations (Eq. 1), transportation-related on-road vehicle emissions were estimated for many US cities including two megacities (New York and Los Angeles) and compared with three megacities in developing countries (São Paulo, Brazil; Mexico City, Mexico; and Karachi, Pakistan) as a part of research by Headrick (Headrick 2010; Uddin and Uddin 2010). The CO_2 calculations assumed that bus and trucks are operated on

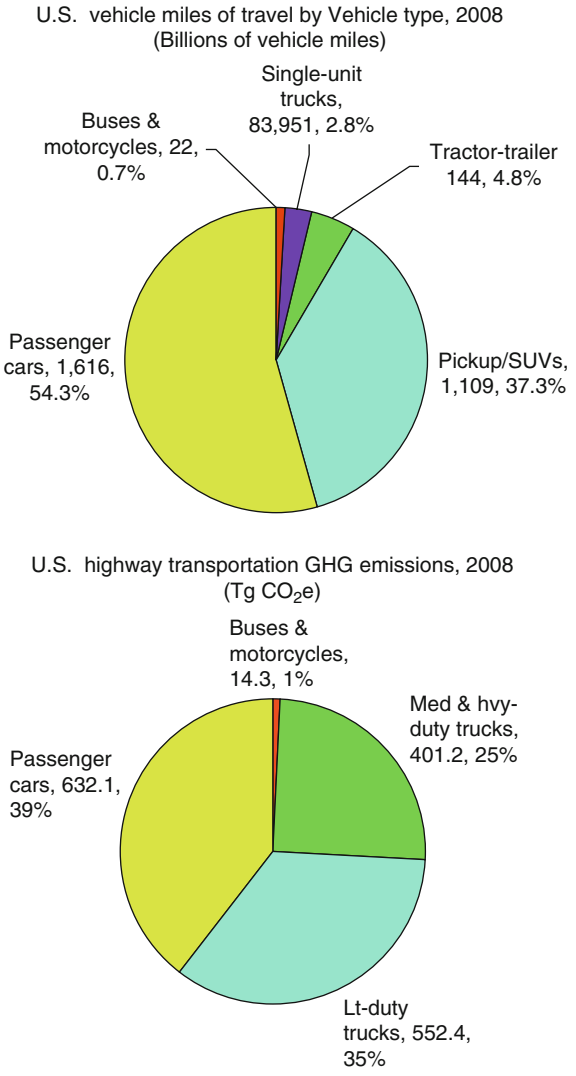

Fig. 16 Vehicle miles traveled and GHG emissions in the United States, 2008

diesel and cars and other passenger vehicles run on gasoline. The results of annual CO_2 emission per capita sustainability index, plotted in Fig. 18 (Headrick 2010; Uddin and Uddin 2010), and population data show that:

- In comparison to US cities, the CO_2 per capita for the three megacities of the developing world is substantially less (1.4 for São Paulo, 0.4 for Mexico City, and 0.4 for Karachi).
- The CO_2 per capita is the highest for Montgomery, Alabama (8.9 t), which is one of the eight US cities at 5.6 t or higher CO_2 per capita, followed by five more

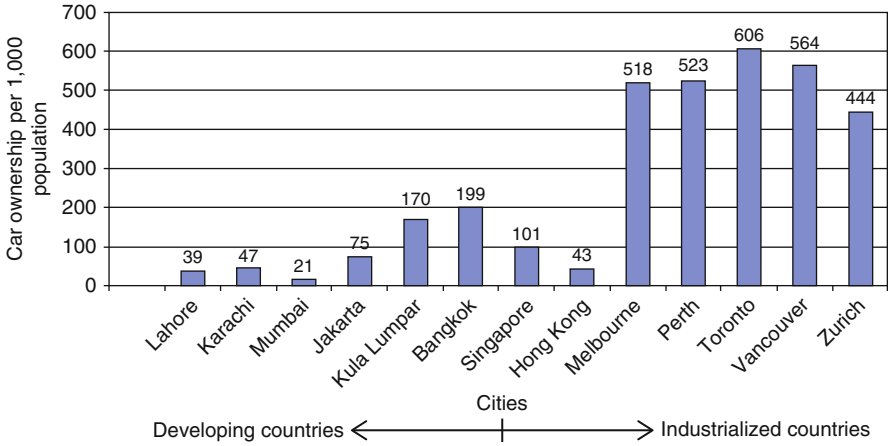

Fig. 17 Comparison of car ownership per 1,000 people in selected cities, 1990s

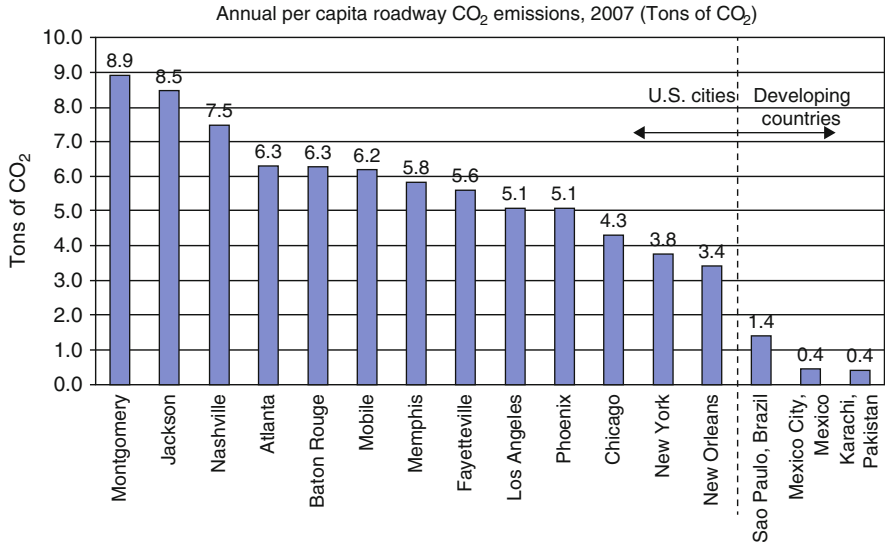

Fig. 18 Comparison of selected US cities and three megacities abroad on sustainability scale

populous cities at 5.1–3.4 t (Los Angeles, Phoenix, Chicago, New York, and New Orleans).

- New York and Los Angeles top the list at 68.4 and 62.7 million tons of CO_2 emissions annually for the two highest CO_2 emissions, followed by Chicago (38.7), Atlanta (28.3), São Paulo (25.0), Phoenix (17.6), Mexico City (7.6), Nashville (7.4), and lesser emissions for all other cities.

- Except for New York (18.2 million), Los Angeles (12.3 million), and Chicago (nine million), populations of other US cities range from 0.2 to 4.5 million in 2007. Populations of megacities abroad range high, from 17.7 million (São Paulo), 17.4 (Mexico City), and 14.0 (Karachi).
- However, population density (1,000 persons per sq. mile) of the three megacities abroad is 3.5–5 times higher than Los Angeles, the highest population density city in the United States (6.3 for Los Angeles and 4.1 for New York).

The above CO_2 per capita analysis assumes all vehicular traffic is operated by gasoline for cars and other automobiles and diesel for trucks. The CO_2 per capita will be less for São Paulo, where up to 25 % of cars operate on ethanol and biofuel, and Karachi, where up to 70 % of cars and an increasing number of auto-rickshaws operate as hybrid vehicles mainly on CNG. Furthermore, this analysis shows that the three megacities of developing countries have less car traffic volume on roads and more people traveling by mass transit and other modes of public transportation in comparison to most US cities.

The impact of utilizing efficient multimodal mass transit systems on reducing CO_2 emitted by on-road vehicles is evident in large cities and urbanized areas both in the United States (such as New York City) and developing countries (e.g., São Paulo and Singapore). New York City Mayor's office of planning and sustainability compiled 2005 GHG emission inventory results considering all mobile, buildings, and other area sources (New York City 2007). The results showed that (1) contributions of 20 % were from on-road vehicles and 3 % from transit and (2) on the sustainability scale New York City, at 7.1 metric tons CO_2e emission per capita, ranked next higher to London, while the average US emission per capita was 3.5 times that of New York City (Fig. 19). The above comparison of citywide GHG emission per capita and preceding analysis of on-road GHG emission per capita for several US cities and megacities in emerging economies and developing countries

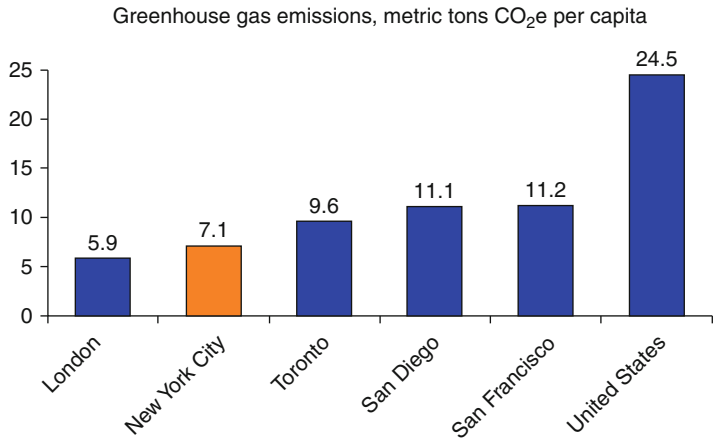

Fig. 19 New York City on sustainability scale based on 2005 GHG emission inventory

clearly demonstrate the strong link between urbanization and motorization in producing GHG emissions.

Geospatial Analysis of Built Environment and Traffic Demand Impacts

Modern geospatial analysis and GIS software tools and availability of aerial and spaceborne remote sensing data provide new opportunities for mapping and spatial analysis of the built environment including land use, urban growth, transportation network, and traffic demand volume and temporal characteristics.

GIS Maps of Urbanized Areas, Urban Growth, and Built-Up Areas in the United States

The USGS has used Landsat satellite imagery data for mapping of the continental United States into the National Land Cover Dataset (NLCD) of 1992. This dataset has been updated by the NLCD 2001 project which uses both Landsat5 and Landsat7 data from 1999 to 2003. The purpose of using both satellites was to prevent clouds from adversely affecting data availability. The spatial resolution of both NLCDs is 30 m. During the period from 1973 to 1992, the urban area of Las Vegas, Nevada, grew dramatically throughout the level basin (Auch et al. 2004).

Built-up areas from imagery and geospatial analysis of NLCD 2001 land cover class maps were estimated for the city of Memphis, Tennessee, and used to create a surface temperature map (Fig. 20) for a hot summer day. The weighted surface temperature for the study area of Memphis in Tennessee was 55.9 °C as discussed in detail by Uddin et al. (2009a). This was 21.1 °C higher than the maximum air temperature of 34.8 °C that day. The availability of high-resolution commercial satellite imageries provides new opportunities to develop computationally efficient geospatial analysis tools for estimating built-up and natural surface areas. For example, the NLCD 2001 map of Oxford, Mississippi, overestimated the built-up area by 43 % in comparison to geospatial analysis of 1-m multispectral satellite imagery.

Imagery-Based Geospatial Analysis for Karachi Metropolitan Road Network GIS and Traffic Demand Volume

A recent traffic management study for the megacity of Karachi, Pakistan, was sponsored by the United States Agency for International Development (USAID) under its "US-Pakistan Science and Technology Cooperative Program" and implemented by the National Academy of Sciences (NAS) during 2007–2010 (Uddin 2009). The project is primarily focused on improving urban traffic flow management and air quality using GIS and spaceborne remote sensing technologies. Karachi is inhabited by more than 14 million people in 2007, and its population is growing at an annual 5 % due to migration from the countryside. Karachi's existing roadways are over-congested and inadequate considering its rapidly growing daily traffic volume demand. More than 40 % road fatalities involve pedestrians. No

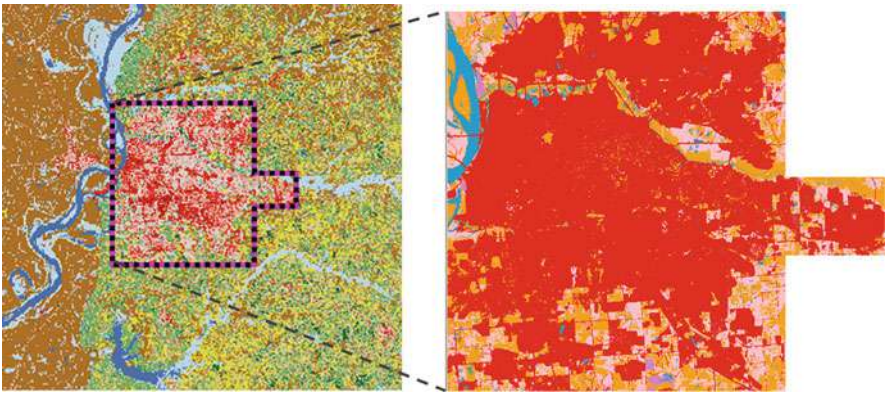

CAIT surface classes	Percentage area from NLCD2001	Predicted surface temperature, °C
1. Built-up area	67.4	61.1
2. Grass	12.5	46.8
3. Tree	16.9	45.3
4. Soil	0.5	54.1
5. Water	2.8	34.4
Weighted average surface temperature		55.9

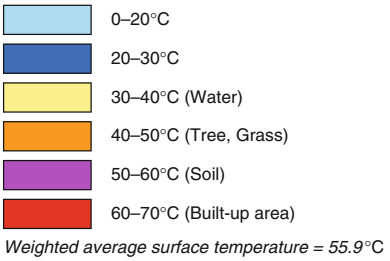

Fig. 20 (*Top left*) Memphis boundary shown on NLCD map, (*top right*) surface temperature map of Memphis, (*bottom left*) summary of built and non-built areas for Memphis, (*bottom right*) legend used for surface temperature scale

improvement in public transport, transit fleet, and operation is evident by overcrowded transit buses and vans (Uddin and Ali 2007). However, the City's Command and Control Centre (CCC), essentially an ITS-based traffic video surveillance system implemented during 2008–2010, is a significant addition to its infrastructure for incident management and crime prevention. The ITS video surveillance system is further helping to reduce emergency response time and promote timely utilization of traffic police for traffic flow management during peak hours and crash incidents. There is no comprehensive road network and land-use GIS, infrastructure database, and traffic volume demand data. The 0.6-m multispectral satellite imagery (Karachi-1) was used to extract vector maps of transportation network, buildings, and other land-use footprint planimetrics (Uddin et al. 2009b; Uddin 2010a).

An innovative geospatial methodology for extracting traffic count data from high-resolution imagery was developed and validated using selected road sections of Gulfport and Oxford, Mississippi, USA (Osborne 2009; Uddin 2010a). This methodology extracts traffic counts from the imagery to calculate average measured density per lane. Posted traffic speed, jamming density, and measured density and flow relationships are used to calculate expected speed. Speed multiplied by density gives volume per hour for the hour of the imagery. Furthermore, daily traffic volume can be estimated if the fraction of traffic volume in that hour based on hourly volume distribution for the entire day is known. The geospatial methodology for traffic data

extraction was then implemented for the Karachi road network. The hourly volume factor was estimated from on-road video data analysis of an arterial in Karachi. Average daily traffic volumes were calculated for 40 road sample sections selected from a factorial design, and a traffic volume map was created using GeoMedia Pro and 0.6-m Karachi-1 imagery as well as Google Earth Imagery for areas outside Karachi-1 imagery scene. The results for all sampled road sections of Karachi yielded an average AADT of 49,564 vehicles per day (Osborne 2009). Most major and multilane roads experienced high hourly traffic volume and poor level of service (Headrick 2010; Uddin 2010a). The results indicated that the average daily traffic volume was affected significantly by road classification and area of the city (71 % inner city vs. 29 % outskirts). These data were used to calculate CO_2 emissions as discussed later.

GHG Abatement Strategies

The worldwide reduction of greenhouse gases and the efficient use of energy in urban, transportation, and industrial applications are important issues for all countries. Recognizing the continuing global increase in mobile travel, the application of traffic congestion-reducing strategies must be implemented in order to meet the target GHG levels and infrastructure needs. In the United States, several traffic management strategies have been widely implemented in recent years in order to improve traffic flow and reduce traffic congestion. These strategies include Travel/Transportation Demand Management (TDM) in urban areas, mass transit deployment, use of ITS technologies, and signal-free corridors and road junction design alternatives. In 2005, public mass transportation in the United States reduced carbon emission by 6.9 million metric tons and avoided 400,000 t of other GHG emissions (Davis and Hale 2007). Simulation studies have shown the promise of reduction in CO_2 and improved air quality as a result of increased vegetation in urban areas.

Sustainable Transport and Traffic Management Solutions

Transport Demand Management and Sustainable Strategies to Reduce CO_2 Emissions

The transportation sector's CO_2 emissions are a function of vehicle fuel efficiency, fuel carbon content, and VMT. Energy and climate policy initiatives at the federal and state levels have focused almost exclusively on technological advances in vehicles and fuels. The evolving gridlock problems and their societal and environmental impacts require innovative solutions to manage urban growth, VMT, and vehicle use. Therefore, any "solution" to the global warming and climate change crisis must involve slowing the growth of CO_2 emissions from mobile sources in the United States. The same is applicable to all other industrialized and rapidly developing countries where car ownership and single-occupancy vehicle (SOV) use are increasing at alarming rates, such as China, Brazil, and India. The worldwide per

capita passenger kilometer traveled per year is expected to increase 48 % between 2000 and 2050 with the highest increase (279 %) projected for China (WBCSD 2004; EEA 2008). An important factor in energy consumption increase is population and urban growth rate, which is high in almost all emerging cities in developing countries. It is imperative to consider the following abatement strategies to reduce mobile GHG sources (Uddin 2009; Molina and Molina 2004; Foletta and Heyen-Perschon 2009):

- *Motorized travel demand reduction*: Reduce the amount of passenger kilometers traveled and freight ton kilometers traveled, discourage SOV trips to ease congestion, and decrease motorcycle traffic to improve road user safety.
- *Idling long-haul trucks on highway rest stops and truck parks*: Eliminate the practice of idling long-haul trucks for long hours (a common scene on US highways). States should use highway patrol to enforce, encourage trucker employers to pay for motel/hotel accommodation for the night, and consider penalty charges for "polluting" trucks who follow this practice.
- *Sustainable multimodal transport implementation*: Implement less polluting mass transit transport strategies for urban mobility with less or fewer emissions per km travel, and increase freight modal share of efficient freight rail.
- *Nonmotorized travel promotion*: Make policy and facilities to promote nonmotorized trips in congested inner city areas.
- *Vehicle inspection and emission testing program*: Develop and enforce regulations for annual vehicle inspection and emission testing programs by developing testing and maintenance facilities and workforce.
- *Transport technology improvements*: Improve performance of transport mode engines and vehicles (lightweight vehicles, smart/intelligent cars) for more safe and efficient use of petroleum fuel and design hybrids to use alternative energy sources with reduced or zero carbon emissions.
- *Regulatory measures based on technology*: Enforce regulations on fuel efficiency, emission levels, and market share of hybrid and battery-driven vehicles.
- *Market-based economic instruments (congestion pricing and emission trading)*: Consider densely trafficked downtown areas, urban roads, and other surrounding corridors as good candidates for congestion pricing to reduce congestion and emissions. Emission trading has been most widely applied in the United States to reduce power plant emissions and is a candidate for global CO_2 trading.
- *Public awareness campaigns*: Develop and conduct public education and awareness campaigns (to implement any of the above strategies successfully) in cooperation with civil society groups.

Technology improvement programs initiated in California have resulted in a slow but consistent reduction in air pollution over the last four decades (Molina and Molina 2004). This is a testimony of regulatory enforcements and public awareness considering there has been consistent urban growth and increase in vehicle kilometers traveled. Congestion pricing schemes need public awareness and support (as implemented successfully in London and Singapore).

Metropolitan Transportation Demand Management

Examples of travel demand and transportation system management actions and TDM marketing to improve traffic operations in large cities and urban areas include (Uddin and Uddin 2010; NCHRP 2010a):

- *Improved traffic flow*: Replacement of stop-controlled intersections by modern roundabout, reversible lanes, transit-stop relocation, removal of encroachments, and ITS traveler's information and congestion warning system.
- *Priority treatment of high-occupancy vehicles*: Dedicated high-occupancy vehicle (HOV) lanes, bus preemption of traffic signals, ITS surveillance and traveler's information technologies, toll policies, and all electronic toll charge system.
- *High-occupancy automobile use*: Car pooling, van pooling, ridesharing, and discouraging use of single-occupancy vehicles.
- *Non-automobile, biking, or pedestrian trips*: Nonmotorized travel modes and auto-restricted zones.
- *Reduced peak-period travel and delays*: Flexible hours, congestion pricing, and peak-period truck restrictions. These strategies are also applicable for nonrecurring events such as adverse weather conditions (hurricane, snow, ice, or rain), work zones, special events, and major incidents and emergencies.
- *Parking management*: Enforcement of parking regulations, video surveillance, park-and-ride facilities, and parking disincentives (e.g., very high parking fee and charges for parking tickets).
- *Transit and paratransit service improvements*: Transit incentives and marketing, transit shelters, terminals, transit-fare-collection techniques, connectivity with other transportation services, and ITS technologies for improved deployment and scheduling.
- *Transit management of efficiency measures*: Routing and surveillance, on time and reliable service, vehicle communications, and maintenance policies to provide state of good repair.
- *Large capacity change alternative on existing roadways*: Travel time reduction for a large capacity alternative is 30 % for one-way operation, 30 % for reversible flow, and 50 % for left-turn prohibition. Additionally, crashes and incidents tend to reduce, while capacity is increased for a large capacity change alternative.
- *Innovative shared transport infrastructure alternative*: Transportation and urban planning approach should be changed toward the green and cool approach by reducing the number of autos on the road and increasing innovative shared transportation and transit alternatives.

Clearly, there is a need to design innovative transport infrastructure to operate at low speeds for shared use of commuters for many congested cities with thriving downtowns and existing ground-level mass transit systems and underground subway/metro tracks. Mass transit systems include bus transit, bus rapid transit (BRT), and light rail transit (LRT). Examples of such metropolitan cities are Chicago, New York, Los Angeles, and many European cities where simply there is no space to increase capacity by building more traditional transport facilities. Costs are also

very high for adding more bus lanes to expand BRT operations. The answers to the urban commuter problem in such developed and congested cities are dedicated elevated transportation pathways maximizing the use of existing right-of-ways of public roads. The key to the success of this innovative approach is in selecting the "right" vehicle technology that can be lightweight and energy efficient. Powered by electricity or magnetic levitation (Maglev) technology and operated at city speed range, a personal rapid transit system is a sustainable pollution free solution for urban areas and cities (Uddin and Uddin 2010). This innovative "green" transport alternative can be economically justifiable based on life cycle costs and benefits.

Smart Growth, Space Planning, and Sustainable Infrastructure

Mixed Land Use and Compact Development to Reduce Cars on Roads in Cities

Encouraging mixed land use and compact development will mitigate and avoid the many flaws of traditional urban development. Urban sprawl and suburban development are characterized by low densities, automobile intensive strip development, poorly connected streets, automobile-oriented transportation planning and traffic management, and detached single family homes and similar land use. Dense or compact development typically involves medium to high densities, more vibrant-centered development, interconnected streets, pedestrian-friendly and transit-friendly road design, and mixed uses of land and roads. Cities should increase the deployment and use of public transport and cool commuting alternatives. Urban growth is inevitable worldwide as metropolitan cities offer more job opportunities, excellent community facilities, and a better quality of life to people migrating from rural areas or smaller cities. Realizing that a single solution is not the answer, a combination of the following abatement strategies should be evaluated to explore practical solutions for reducing transportation-related emissions:

- *Promote smart growth*: Examples include high urban density, less travel distance for commuting to work and shopping, green spaces, and energy conservation.
- *Implement space planning applications*: Space planning approach will be helpful to achieve sustainable growth on ground, below ground, and elevated structures.
- *Establish green and cool cityscapes and communities in and around cities*: Some examples include light-colored, eco-friendly block pavements for sidewalks and parking lots. Residents and homeowners should be given tax-break incentives for the use of white- and light-colored roofs to reduce heat island effects. Similarly, use of solar panel and green roof should be supported to promote energy conservation and renewable energy.
- *Develop sustainable multimodal infrastructure*: Sustainable multimodal transport facilities and operations are possible by providing less polluting mass transit, discouraging SOV use, and introducing safe pathways for walking trips and dedicated bike lanes for nonmotorized travelers.

- *Reduce congestion in cities and metropolitan areas*: Congestion can be reduced by deploying efficient public transportation, ITS technologies to improve operational efficiency, and reducing number of vehicles on roads to ease congestion.
- *Use GIS- and ITS-based speed data to visualize congestion and air pollution trends*: Introduction of geospatial analysis and online GIS visualization products to show public near real-time status of congestion reduction, improvement in air quality from reduced pollution, and reduction in GHG emissions. This education and media campaign will promote wider voluntary use of fuel-efficient cars, public transport, and energy conservation.
- *Consider sustainability related to natural resources and energy demand*: Life cycle analysis of sustainable transport infrastructure assets and mitigation strategies should look into all opportunities related to conservation of materials and energy sources, space-use and land-use planning, and multimodal transportation policies (Uddin 2010b). Two major areas for sustainable road infrastructure assets are (1) pavement construction and maintenance and (2) non-pavement assets (such as bridges, sidewalks, drainage).

Multimodal Alternatives for Travel in Cities, Intercity Connectivity, and Regional Transport

A multimodal transport system makes efficient use of the space and existing transport infrastructure in cities and urban areas having limited funding resources. Historically, an underground mass transit rail subway system provided good use of the space, but its construction and expansion are very expensive. Such rail subway systems may not be the best cost-effective solution in megacities of emerging economies and developing countries. In comparison, the construction of a designated bus lane costs only a fraction of a comparable subway rail line. The bus transit and BRT systems can be implemented in any megacity, adapted quickly, and provide good connectivity to rail network.

Regional and intercity rail network should play an important role in a multimodal approach to reduce GHG emissions. Rail engines are becoming less polluting in compliance with the EPA's clean air non-road diesel rules of 2004 and 2008 (EPA 2008b) with reductions of 99 % in sulfur, up to 90 % in PM, and 80 % in NO_x emissions. Rail locomotives are four times more fuel efficient than trucking, and a train can carry the freight of 280 or more trucks reducing highway congestion and significant reduction in GHG and other emissions (AAR 2010a, b). Electric-powered high-speed rail technology for efficient intercity and regional passenger transport can alleviate plaguing problems of urban and highway traffic congestion, wastage of gasoline fuel, vehicle emissions of criteria air pollutants, and GHG emissions. In the recent years, the US government has committed billions of dollars to several states for constructing high-speed rail corridors (Uddin and Uddin 2010).

Consumption and Hidden Cost of Petroleum

The hunger for petroleum fuel by transportation is enormous in every country. Most countries and especially developing countries spend a sizable amount of their national budgets on crude oil. In 2002, about 11 million barrels of crude oil

equivalent per day was burnt by highway vehicles in the United States (ORNL 2004). The share of light automobiles was 8.5 million barrels, and medium/heavy freight trucks consumed about 2.4 million barrels. In comparison, total rail traffic consumed only 260,000 barrels per day with a major portion (245,000 barrels) by freight train and only 15,200 barrels by passenger rail. The US share of petroleum consumption was 25.3 % of the total world consumption of 79.08 million barrels of petroleum per day in 2003 (ORNL 2004). The accelerated industrialization and economic prosperity of China has made it the second largest petroleum consumer after the United States. The known worldwide petroleum reserves are being diminished every year. The protection of this commodity and its supply has been a major reason of US military expenditures in the Middle East. One such estimate of 1996 is 20–40 billion dollar annual cost to defend all US interests in the Persian Gulf (Delucchi and Murphy 1996). The 2000s Iraq war cost is even substantially higher. (The gasoline cost at fill station may exceed $7 per gallon if the "petroleum protection war cost" is accounted for.) This hidden cost of petroleum is generally ignored in economic evaluation.

Alternative Energy and Fuel, Vehicle Innovations, and Nonmotorized Transport

Cities face challenges of inadequate parking space and polluting transport services. Recent transportation policies and strategies, such as congestion pricing and the use of BRT and LRT systems, have shown some benefits by reducing the number of cars on roads. The key to success for achieving sustainability in the transportation system is to reduce the number of vehicles and number of trips on roads. Increased shares of nonmotorized trips by mixed land use and pedestrian-friendly road design are complimentary strategies to reduce vehicle volume on roads. Sustainable solutions to mobility require a combination of multimodal strategies with reduction of cars on congested roads, reduction in gasoline vehicles, increased share of biofuel vehicles, and zero carbon battery-powered vehicles. Sustainable mass transit strategies include vehicles running on natural gas (CNG and LNG), liquid petroleum gas (LPG), biodiesel, and hybrid and other energy-efficient technologies.

Vehicle efficiency policies and government regulations can be effective if supported by the public. For example, California required that 2 % of vehicle sales had to be zero-emission vehicles by 1998, considering that battery-powered vehicles would meet this need. Initially this was not achieved, but research in hybrid gasoline-electric vehicles is paid off by creating small batteries that could be continuously recharged by a small gasoline-powered generator (Molina and Molina 2004). These near zero-emission hybrid vehicles are now popular and fuel efficient by almost doubling the mileage of a traditional small car.

Some countries with CNG vehicles in use as of 2007 (Uddin 2007) rank in the following order (total number of CNG vehicles in parenthesis): Argentina (1.454 million), Brazil (1.303 million), Pakistan (1.300 million), Italy (0.410 million), India (334,000), the United States (142,000), and China (125,000). The number of

CNG vehicles in the United States is approximately 10 % of the three highest ranking users of CNG vehicles (Argentina, Brazil, and Pakistan). The US consumption of CNG was only 6.4 % followed by 0.4 % LNG consumption in 2004. The United States should consider taking advantage of its large domestic reserves of natural gas for consumption in hybrid cars and other light vehicles. Federal government can take the lead by converting all government-owned cars to gasoline/natural gas hybrid vehicles. Federal and state government agencies can require car manufacturers to produce certain percentage of new cars each year with CNG/gasoline hybrid technology. It will not take a new infrastructure to supply gas because a comprehensive gas pipeline network already exists throughout the United States.

GIS-Based Decision Support System and Value Engineering

Geospatial Mapping and GIS Decision Support System Examples

Spaceborne and airborne remote sensing technologies, GIS and geospatial visualization tools, and air pollution models can be used to prevent and mitigate the adverse effects of transportation systems. GIS-based decision support systems should be developed for identifying the problem areas, vulnerability assessment of transportation infrastructure, and life cycle benefit–cost analysis. A geospatial analysis of CO_2 inventory by states for 1990 and 2003 in the United States, reported by EPA (2008a), indicates:

- Carbon dioxide emissions in 2003 are 15 % above 1990 levels.
- The five states that produce the least amount of transportation emissions are Vermont, Rhode Island, Delaware, South Dakota, and the District of Columbia. These are smaller and less populated areas.
- California, Texas, Florida, New York, and Pennsylvania remain the five states with the highest emissions in 2003 as in 1990.
- This shows that these five states, containing large populated urban metropolitan cities, produce more emissions than other smaller and rural states.

The GIS maps are not shown here for brevity, but this analysis shows an example of GIS-based decision support system on the regional and national level. These results can be used by federal and state agencies to make a decision related to the allocation of funds among states and cities for planning and implementing GHG abatement strategies. Another example of GIS-based decision support system is quantification of built and non-built surface areas in a city. An increase in the percentage area of these built-up surfaces will definitely increase the weighted average surface temperature (by surface area). The increased urban area temperature and increased traffic emission result in air quality degradation which adversely impacts lung disease sufferers. The associated public health cost is about 19 % of the total societal costs, as shown in a previous study in Oxford, Mississippi (Uddin and Boriboonsomsin 2006).

Value Engineering and Life Cycle Analysis

Value engineering (VE) enables to evaluate a cost-effective solution by selecting alternative technologies and methods to achieve reduction in overall life cycle costs without compromise to safety and efficiency. The traditional life cycle analysis (LCA) considers agency costs and user costs associated with pavement life cycle (Uddin et al. 2005). Agency costs for building and maintaining roads require lots of natural resources, such as asphalt, aggregate, cement, concrete, and steel. User costs include vehicle operating cost (voc). For example, the pavement roughness condition deteriorates with time and traffic repetitions that can influence fuel and oil consumption, tire deterioration, and vehicle maintenance. These voc components have been well established in the World Bank's and the US FHWA studies (Uddin et al. 2005). The present worth of life cycle vehicle operating cost is in the range of 18–29 cents per vehicle mile for two-lane rural roads in good to poor condition. The PSI scale (0 for the worst and 5 for the best) is used to define surface condition of pavements. Figure 21 shows the relative weights of these voc components and the influence of Pavement Serviceability Index (PSI) on voc (Uddin et al. 2005).

As pavement surface deteriorates, PSI reduces and voc increases. Reduction in voc due to improved pavement condition and travel time saved due to increased capacity and reduced congestion has been traditionally used to calculate life cycle benefits. However, vehicle emission-related and air pollution-related environmental and societal costs have been lacking from the traditional LCA practice of highway project evaluation. The effects of transportation-related emissions and air pollution on public health and associated medical costs are reviewed and summarized by Uddin (2006). These cost models, congestion pricing, and carbon emission taxes can be used for a comprehensive life cycle analysis to evaluate sustainable alternative transportation and development strategies as a part of value engineering analysis. The life cycle analysis strategies for sustainable transportation system and development should consider:

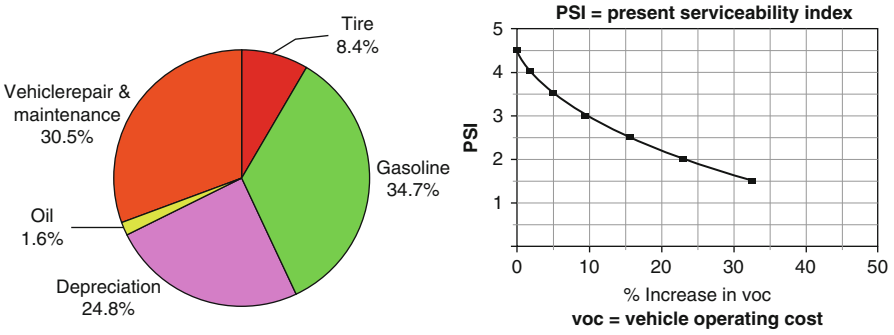

Fig. 21 Road vehicle operating cost components (*left*) and voc increase due to pavement deterioration indicated by lower present serviceability index of road pavements (*right*)

- Providing sufficient and safe mobility to commuters to be productive in the workplace.
- Supporting commercial businesses to flourish without losing potential customers.
- Improving mobility using multimodal approach as a part of the space planning concept.
- Increasing mass transit mode share by increasing car parking prices and using transit modes operating on alternative less polluting energy.
- Improving traffic flow management through video surveillance and other ITS technologies to reduce congestion and gridlocks, user delays, wastage of fuel in queues, and emissions.
- Evaluating and implementing less polluting and more efficient rail and pipeline solutions for freight transport in place of current dependence on highway trucks. The diesel-gulping trucks are highly polluting and emit several times more GHG emissions than alternative freight rail mode. This strategy will also require the construction and management of intermodal facilities.
- Creating new financing opportunities by collecting transportation-related carbon emission tax from trip makers and giving incentives of no such tax for commuters who predominantly use transit.
- Constructing more green spaces and promoting nonmotorized cycling and walking.
- Monitoring air quality and striving for less air pollution and clear skies.
- Reducing backlog of infrastructure and preserving state of good repair using increased revenues by collecting higher fuel taxes on gasoline and diesel.
- Serving more people and creating/preserving jobs.

Life Cycle Analysis of Sustainable Transport Solutions and Value Engineering Case Study

Agency costs for building and maintaining roads require lots of natural resources, such as asphalt, aggregate, cement, concrete, and steel. The process of constructing, pavement material processing, and compacting operations consumes significant amount of fuel and energy. The service life of a typical asphalt highway pavement is 10–15 years, whereas the life of a typical concrete highway pavement is 15–30 years. Functional life of road vehicles is also limited to 10–15 years. In comparison, alternative mass transit of a regional/national high-speed rail (HSR) network and personal rapid transit (PRT) in urbanized areas can last several times longer with less maintenance cost. These alternatives are also safer due to operation on dedicated pathways with no vehicle conflict or congestion. Life cycle analysis of costs and benefits should be evaluated for a longer analysis period of 60–70 years as a part of value engineering evaluation. Over this analysis period, the track-based mass transport system lasts without major rehabilitation or reconstruction, operated typically on electricity. During this period, road infrastructure and vehicle fleets need to be replaced one to three times. Road vehicle operating cost (Fig. 21) is a large component of road user cost (Uddin et al. 2005), which is substantially reduced by the proportion of the road users who switch to the new transit technology. Other benefits include reduction in fuel and low pollution cost. The benefits from each

alternative should include user benefits as well as societal benefits per passenger km or freight ton kilometer which include savings from reduced fuel consumption, time saved due to less delay, public health benefits from reduced air pollution, fewer crash-/accident-related costs, and lesser societal costs due to reduction in CO_2 emissions.

In metropolitan cities and urban areas, dedicated elevated PRT pathways provide a sustainable solution to the urban commute and congestion by maximizing the use of existing right-of-ways of public roads. This will require the selection of the "right" PRT vehicle technology that can be lightweight and energy efficient. The PRT infrastructure requires the use of elevated structures and efficient cleaner energy sources of electricity and Maglev for PRT operations designed to reduce congestion and impacts on the environment. Examples are Swedish SkyCab (electricity driven) and Brazilian Cobra Maglev vehicle/track systems (Uddin and Uddin 2010). The approach to determine economic cost is derived from a study of the traffic volume data, where there are new lines built, users' time savings, number of users willing to pay for such a transport, release of capacity in congested roads, and broader economic benefits including development of less developed regions and creation of jobs. The life cycle economic evaluation includes several financial considerations such as present worth analysis of benefits and costs over a reasonable analysis period considering an appropriate discount rate and calculating the net present value (NPV) of minimum two alternatives. The base alternative is "do nothing," and the reduction in user delay hours and emissions is considered an indirect benefit from the new alternative transit strategy.

To illustrate life cycle benefit and cost analysis of a PRT system, it is assumed that the agency cost for building a 30–40 miles/h speed PRT system on elevated alignment may cost around four million US$ per km, much lower than an HSR system. The PRT's annual operating cost will also be significantly lower than an HSR alternative due to energy-efficient and lightweight vehicle technology. The PRT construction cost of a 10-km stretch is about 40 million dollars with annual 0.5 million dollar operating cost. Assume that each person using the PRT system saves annually 25 h of delay at $16 per hour and avoids wastage of 15 gal of fuel and oil at $3 per gallon. Therefore, for 20,000 commuters (or 20 % car owners in the daily traffic volume) using PRT instead of driving single-occupancy cars, the total user saving is about nine million dollars annually. This example implies that the PRT's initial construction cost is covered within 5 years (at 0 % discount rate) just by considering annual user saving. This analysis simply ignores the passenger fare revenue that will be an agency benefit. Additionally, the societal benefit will be enormous in terms of reduction in CO_2 at 2,765 t daily or about one million tons annually (Uddin and Uddin 2010). Other indirect benefits include less air pollution, reduction in associated public health cost, less risk of on-road crashes, and increased productivity. Showing this type of evidence to the traveling public and other stakeholders, they can be persuaded to approve the PRT system implementation. Building and operating these innovative energy-efficient and cleaner mass transit solutions in metropolitan areas and other large cities can be successful if disincentives are in place to discourage commuters from driving their cars.

Monitoring, Targets, and Applicable Laws

The US EPA uses standard models for measuring and preparing inventory of GHG from all possible sources (EPA 2008a). It is also important to make real-time measurements to assess impacts of mobile and area sources of air pollution and greenhouse gases on air quality and global warming. The methods reviewed will benefit practitioners and decision-makers involved in federal, statewide, tribal, metropolitan, or small community transportation planning agencies.

Terrestrial Remote Sensing and Space-Based Monitoring

The annual emission inventories from transportation and industrial sources need to be verified by measuring CO_2 and other air pollutants. Monitoring of air quality involves analysis of air samples for criteria air pollutants (short lived, requiring frequent measurements) and CO_2 (long lived) emissions (Molina and Molina 2004). Monitoring methods range from simple passive sampling and measuring techniques to continuous gas analyzers and remote sensors. The measurement quantifies the amount of CO_2 higher than the background level in which traffic or other anthropogenic emissions are absent.

Remote Sensing Monitoring of CO_2 and Other Air Pollutants

Remote sensing LIght Detection and Ranging (LIDAR) active sensor in infrared band is used for CO_2, measurements. Tunable differential absorption LIDAR was used for real-time in situ measurements of air pollutants in a previous study for air quality modeling (Uddin 2002). The remote sensing instrument can be set up near any highway or industrial area and measure CO_2 and other emissions in different spectral bands using a target 1 km away (Velasco and Roth 2009). An eddy covariance (EC) flux remote sensing equipment has been used in several studies for measuring CO_2 levels, usually mounted at the top of towers or masts at least twice the mean height of the surrounding buildings. The EC system consists of an ultrasonic anemometer to measure wind fluctuations coupled with an infrared gas analyzer to measure water vapor and CO_2 measuring from 2 to 20 times per second. The results of CO_2 measurements from several cities in the United States, Europe, South America, and Asia showed that built-up areas provide a constant source of CO_2 (Velasco and Roth 2009; Andrade 2007; CO_2 Science 2006). The level of emissions is higher for densely populated larger cities with high traffic volume such as that shown for São Paulo, Brazil, by measuring CO_2 and other pollutants inside and outside road tunnels (Andrade 2007); Mexico City and Singapore (Velasco and Roth 2009); Paris, France; and Phoenix, United States (CO_2 Science 2006). The Paris study results revealed that atmospheric CO_2 concentrations near surface throughout the country outside Paris averaged 415 ppm, which was significantly lower than 950 ppm observed in the city. Furthermore, considering other air pollutants and aerosols in addition to GHG, cities are the source of most of the pollutants

that are known to alter the state of the global atmosphere and the climate. Therefore, cities play an important role in mitigating the GHG emissions (Velasco and Roth 2009).

Spaceborne Remote Sensing for Pollution Monitoring

Recent National Aeronautics and Space Administration (NASA) satellites and European Organisation for the Exploitation of Meteorological Satellites (EUMETSAT) use both active and passive remote sensing instruments to probe throughout the troposphere (McMillan et al. 2009). These instruments measure atmospheric aerosols, clouds, and trace gases across the spectrum from the ultraviolet to the microwave bands. The Atmospheric InfraRed Sounder (AIRS) and Advanced Microwave Sounding Unit (AMSU) are deployed onboard the NASA's Aqua satellite. These spaceborne sensors see 70 % of the Earth both day and night and provide detailed vertical retrievals of temperature and water vapor and weighted free tropospheric concentrations of CO, CH_4, CO_2, and O_3 (McMillan et al. 2009).

In addition to spaceborne remote sensing measurements of emissions, geospatial analysis of spaceborne satellite imagery provides a remote sensing alternative to estimate built-up area estimates and traffic volume for any city or urban area in the world, as discussed previously for Karachi (Osborne 2009; Headrick 2010; Uddin 2009, 2010a). This approach is especially useful where these citywide data are not measured on routine basis. Karachi port area extracted from 0.6-m satellite imagery showed 58.7 % built-up area and 41.3 % non-built area (ocean, river, soil, grass, trees). Accurate and timely collections of traffic attributes are necessary for traffic management and calculation of mobile GHG emissions for sustainability performance evaluation of transportation systems. Furthermore, the imagery-based traffic volume method can be used to fill up missing daily traffic volume and identify candidate locations for ITS traffic video surveillance installation. The 2007 estimated daily traffic volume for the entire megacity was 9.3 million vehicles. Daily traffic volume per sq km in the inner city buffer is about ten times more than the traffic volume in the outskirt area. This also implies that vehicle emission of air pollutants is also higher in the inner city area, which is adversely affecting the public health of residents and commuters alike. The traffic congestion on most major roads and vehicle emissions are adversely affecting travel time productivity and air quality. Based on the US EPA procedures (Eq. 1), citywide CO_2 emission from the imagery-based road traffic volume is estimated 5.5 million tons as of 2007 for Karachi (Headrick 2010; Uddin 2010a).

The United States and European Initiatives

Sustainable Transport Policies

Although CO_2 emissions from road transport and road passenger kilometers continue to grow, fuel efficiency per passenger kilometer is improving. Road ton kilometers are increasing but truck fuel efficiency is not. It is important to recognize that improvements in energy efficiency of vehicles, less polluting fuel like CNG, and

nonfossil fuels are still not enough to counteract the growth in transport demand. Therefore, measures focused on reducing transport demand or shifting demand to more sustainable modes of transportation are extremely important to provide significant emission reduction results. A sustainable solution requires a shift to multimodal transportation systems with emphasis on reducing travel time to commute and better facilities for bikes and nonmotorized modes. It has been argued that improvements in energy efficiency of vehicles and nonfossil fuels are not enough to counteract the increasing road travel demand and transportation-related GHG emission (McCarthy 2010). Therefore, measures focused on reducing transport demand or shifting demand to more sustainable modes of transportation are extremely important to provide significant emission reductions. A sustainable transportation and development policy should encourage building parks, preserving wooded areas, and providing additional water bodies as an integral part of the built environment and residential neighborhood "green" communities. Reduction of energy consumption and emissions requires ecological-friendly pavement materials and related technologies with minimum use of traditional hot mix asphalt (Uddin 2010b).

Recent Transport- and GHG-Related Regulations, Policies, and Initiatives in the United States

The EPA and USDOT federal agencies are drawing on current laws to mandate fuel efficiency standards and reduced GHG emissions per mile traveled by passenger vehicles. Several legislative and regulatory actions, being undertaken in the United States to reduce transportation-related GHG emissions as reviewed in EIA (2009) and based upon the recent news, include:

- The EPA as required by public law 110–161 (December 26, 2007) developed a mandatory reporting rule for GHG on September 22, 2009. The rule requires emitters of GHGs from 31 different source categories to report their emissions to the EPA. Approximately 80–85 % of total US GHG emissions from 10,000 facilities are expected to be covered by the rule. Reporters must begin to monitor their emissions on January 1, 2010; the first annual emission reports will be due in 2011.
- On April 2, 2007, the US Supreme Court authorized the EPA under Section 202 (a)(1) of the Clean Air Act (CAA) to announce that the six key GHGs pose a threat to public health and welfare for current and future generations and that GHG emissions from new motor vehicles and motor vehicle engines contribute to climate change.
- The draft rule of EPA, published in the Federal Register on October 27, 2009, limits the applicability of CO_2 emission standards under the CAA to new and modified stationary sources that emit more than 25,000 million tons CO_2e annually. The EPA expects that 14,000 large industrial sources, which are responsible for nearly 70 % of US GHG emissions, will be required to obtain Title V operating permits. This threshold rule would cover power plants, refineries, and other large industrial operations but except small farms, restaurants, schools, and other small facilities.

- EPA recently released the RFS2 volumetric requirements for 2010, calling for approximately 8 % of the total gasoline and diesel pool to consist of renewable content, mostly from corn-based ethanol.
- According to the EPA requirements, a larger percentage of renewable fuels will consist of these second- and third-generation biofuels, such as algal diesel and cellulosic ethanol. By 2022, advanced biofuels will comprise almost 60 % of the renewable fuel mandate. In this way, the move to renewable fuels will contribute a greater share of the drop in transportation's GHG emissions.
- The American Recovery and Reinvestment Act of 2009 ("The Stimulus Bill") was signed into law by President Obama on February 17, 2009. Under the Act, the DOE received $36.7 billion to fund renewable energy, carbon capture and storage, energy efficiency, and smart grid projects, among others. The projects are expected to provide reductions in both energy use and GHG emissions.
- The Energy Independence and Security Act of 2007 (EISA) mandated national GHG emission standards for mobile sources, authorized by the CAA, and updated Corporate Average Fuel Economy (CAFE) standards, required by EISA.
- On September 15, 2009, EPA and USDOT formalized an agreement announced in May 2009 between the Administration and automobile industry stakeholders to accelerate the existing CAFE mandate and impose nationwide the tailpipe GHG standards sought by California.
- On September 25, 2009, the State of California imposed a fee on carbon emissions, the second government body in the United States (after Boulder, Colorado). The fee will be used to fund implementation of the State's GHG cap-and-trade program. The fee is expected to raise $63 million per year from approximately 350 large emitting entities in the State. The state law will go into effect in fiscal year 2010–2011 and will be apportioned among entities on the basis of their annual GHG emissions, at a cost of approximately 15.5 cents per million ton CO_2e.
- In March 2010, EPA and DOT released emissions and CAFE standard that will go into effect by 2012 and increase the fuel economy of passenger vehicles by 2016. By model year 2016, the combined car and truck standard will be 250 g of CO_2 emissions per mile. Additional GHG standards to improve air-conditioning systems in vehicles will achieve the fuel economy equivalent of 35.5 miles per gallon.
- In May 2010, President Obama's memorandum directed EPA and US DOT to begin the rule-making process for further reductions for model year 2017 through 2025. The memorandum also directed both EPA and National Highway Traffic Safety Administration (NHTSA) to establish fuel efficiency and GHG standards for commercial medium and heavy-duty trucks, starting with model year 2014, in accordance with the CAA and EISA.
- On September 15, 2009, the United States, Canada, and Mexico expressed their support for a proposal to include chlorofluorocarbons (HFCs) under the Montreal Protocol. These gases are used primarily in refrigeration and air-conditioning applications. The proposal calls for reductions in the consumption and production of HFCs around the world, with developed nations taking the lead.

Global Accords and Developing World Efforts

International Climate Change Mitigation Accords

The United Nations Framework Convention on Climate Change (UNFCC) has been the primary organization for international accords (http://unfccc.int/essential_background/items/2877.php). *The Kyoto Protocol* was initially adopted on December 11, 1997, in Kyoto, Japan. Under the Protocol, 37 countries committed themselves to a reduction of greenhouse gases, and all member countries gave general commitments. The benchmark 1990 emission levels were accepted by the Conference of the Parties of the Convention, which were the values of "global warming potential" calculated for the IPCC Second Assessment Report. These figures are used for converting the various greenhouse gas emissions into comparable CO_2e when computing overall sources and sinks.

In December 2008, the fourteenth *Conference of the Parties to the United Nations Framework Convention on Climate Change* and the fourth *Meeting of the Parties to the Kyoto Protocol* were held in Poznan, Poland. Key areas of discussion included the following:

- Governments shifted into "full negotiating mode" in hopes of delivering a comprehensive new climate change agreement in December 2009 in Copenhagen, Denmark.
- The European Union called on developed countries as a group to reduce their emissions to 30 % below 1990 levels by 2020 and on developing countries to reduce their emissions by 15–30 % below business-as-usual levels.
- Ministers encouraged the parties to view the global economic crisis as an opportunity to address climate change and, simultaneously, contribute to economic recovery, rather than as a hindrance to progress on climate change.

On March 28, 2009, US President Obama launched the *Major Economies Forum on Energy and Climate*. The Forum facilitated dialog among the major economies, leading up to an agreement at the fifteenth *Conference of the Parties to the UNFCC* in Copenhagen. Further, the Forum seeks to advance joint ventures to develop clean energy resources. Discussions have centered on adaptation, mitigation, measuring, reporting and verification, and technological cooperation. At least 29 countries indicated that they will join the accord representing more than 70 % of global greenhouse gas emissions. Major countries committed to cut emissions below 1990 levels by 2020 are as follows: the United States by 17 %, China by 40 %, India at least 20 %, Brazil at least 36 %, South Africa by 34 % in emissions from coal, and the European Union by at least 20 % in its overall emissions.

The United Nations Conference on Climate Change in Cancun, Mexico, concluded on December 10, 2010. Over 190 countries of the UNFCC agreed on a new international deal "The Cancun Agreement" to mitigate global warming impacts. This is the latest climate change agreement after the Kyoto Protocol. The Cancun Agreement adopted 33 pages of text outlining a framework for further progress of

negotiating emission reductions, monitoring and verifying emissions, funding adaptation, and forest protection. The key points of the agreement included:

- Carbon dioxide capture and storage in geological formations will be included as an eligible project activity.
- The 37 countries are allowed to fulfill their greenhouse gas emission obligations by investing in projects that reduce emissions in developing countries.
- Action is included to protect the world's forests because deforestation accounts for nearly one-fifth of all global carbon dioxide emissions.
- Technology transfer will be facilitated to reduce GHG emissions through innovation in transport infrastructures.
- A Green Climate Fund of US$30 billion of new contributions for the period 2010–2012 is established to help the most vulnerable developing countries adapt to the unavoidable impacts of climate change and reduce their carbon footprints.
- In the longer term, developed countries committed to a goal of mobilizing jointly US$100 billion per year by 2020 to address the needs of poorer countries. A "significant share" of new multilateral funding for adaptation should flow through the Green Climate Fund, which will be managed by the World Bank for the first 3 years, delegates agreed.

The United Nations Collaborative Programme on Reducing Emissions from Deforestation and Forest Degradation in Developing Countries (REDD) has lead REDD efforts in some countries in 2010, such as Bolivia, Congo, Indonesia, Panama, Tanzania, Vietnam, and Zambia. More info is available from http://www.un-redd.org. Inventory and monitoring of forest is an essential step for such efforts, including the use of airborne and spaceborne remote sensing technologies. After the Cancun agreement, many developing countries are initiating REDD plans to preserve national forests, such as announced by the Environment Minister of Pakistan during the international biodiversity conference on December 31, 2010 (International conference on biodiversity is our life).

Lack of Multimodal Transport Strategy Consideration by International Lending Institutions

As a part of the infrastructure loan evaluation, the World Bank and other international lending institutions historically did not encourage multimodal strategy evaluation for transportation infrastructure loan projects in urban areas or at regional levels, as evidenced by the following discussion. Since the World Bank's first loans during the late 1940s to finance the reconstruction of the postwar economies of Western Europe, the World Bank has loaned more than $330 billion to developing countries (Driscoll 1996). The latest data shows that the World Bank's worldwide lending accounts for 20 % in the transport sector (World 2010). Total loan amount of about $33 billion in the last decade was dispersed to transport infrastructure and services. Of that, a significant 73 % was spent on roads, with the remaining only 27 % on rail, ports, aviation, and transport services (Martin 2007). Highway project analysis traditionally lacked considerations for congestion, vehicle emissions, and

public health impacts in comparison of life cycle costs and benefits of roads versus rail transportation strategies. Additionally, the World Bank financing of the transport vehicle fleet has been decreasing, and effort has been made to transition from public to private enterprises, especially for freight haul trucks. This in turn became impetus for building more roads with higher emitting vehicular traffic and increasing the decay of (lower emission per passenger) rail infrastructure in many countries.

The World Bank increased its efforts in recent years to provide developing countries greater access to finance and technology for climate change mitigation efforts. However, climate change mitigation was considered in less than 20 % of the World Bank's energy sector lending in 2005 (Sohn et al. 2005). Additional funding sources in recent years include the Clean Technology Fund (CTF) in 2008 (Weiss and Logan 2008), Climate Investment Funds (CIF) fund, and Global Environment Facility (GEF) funds, established in 1991 (Rooke et al. 2009). However, some groups of civil society (Martin 2007; Sohn et al. 2005; Rooke et al. 2009) are skeptical of the World Bank's CTF and other environment-related financing programs because of the evidence of unsustainable growth outcomes of loan projects, including more spending on oil, coal, and gas (94 % in 2007–2008 alone), privatization and export-driven production which do not emphasize on environmental sustainability, lack of gender justice by ignoring women from loan negotiations, and priority for highway funding, resulting in decay of rail infrastructure. These concerns and future use of Green Climate Fund created by the UNFCC's 2010 Cancun Agreement warrant that the World Bank and other international lending institutions should change their outlook of transport and energy loan evaluation policies, considering the adverse impacts of GHG emission, air pollution, and social and economic deterioration of the poor and women.

Best Practices

Annually 33 billion tons of anthropogenic CO_2 emission is produced worldwide (Andrade 2007; The Realignment 2009). A significant part of the anthropogenic CO_2 emission is produced by on-road vehicles, especially in cities. These emissions can be reduced by implementing more efficient and low fuel mass transit systems and other sustainable multimodal transport strategies. A successful sustainable transportation policy requires all stakeholders (car manufacturers and dealers, general public, and government agencies) and policy makers to set goals to reduce emissions on national levels. Examples of the best practices of abatement strategies for transport alternative and their effectiveness evaluation methods are discussed in this section. These best practices will be viable options for adaptation and implementation by other urbanized areas and megacities in the rest of the world.

United States Examples

Reductions in transport-related emissions and subsequent improvements in air quality have been made through government enforcements of regulations and voluntary participation by the industry and the public in the United States. The

current economic recession has shown an inherent vulnerability in the automotive industry due to the slump in demand of new cars. The "Cash For Clunkers" program, initiated by Obama Administration in the United States, was extremely successful to remove older fuel drinking cars from the roads. Additionally, according to the US Treasury (The Realignment 2009), the $3 billion spent on the program produced 42,000 jobs, sold 700,000 cars, and created 0.3–4 % worth of gross domestic product (GDP).

Statewide efforts (California and Maryland): With 36 million inhabitants, California is the most populated state. California Department of Transportation (Caltrans) operates and maintains 15,269 highway miles which is less than 9 % of total 170,000 miles of public roads. California's highway network supports the sixth largest economy in the world due to its rich agriculture and timber production, diverse industries, computer technology firms, and movie industry (NCHRP 2010a). Caltrans evaluates transportation project delivery using several key indicators of performance measures/outcomes: travel time and delay (mobility), travel modal choice (accessibility), person- and vehicle-traveled distance (productivity), condition index (system preservation), crashes/fatalities (traveler safety and security), and indictors of air quality, noise, and energy consumption (environmental quality). California's Climate Action Team expects "smart land use and intelligent transportation" to make the second largest contribution toward meeting the state's ambitious GHG reduction goals (EIA 2009).

Maryland is relatively a small state, ranked 42nd in area, but it is the fifth densest state in the United States with an estimated population of 5.6 million. Per capita VMT is nearly the same as the US average, with nearly 75 % VMT occurring in urbanized areas (Keck et al. 2010). Maryland State Highway Administration (SHA) operates and maintains 5,263 highway/road centerline miles, which represents less than 20 % of the total 29,265 roadway centerline miles in the state. However, the highway network carries 70 % of the total VMT in the state. Mass transit infrastructure consists of subway, light rail, and bus service. Currently, 82 % of freight moves by roads with half of the freight simply passing through the state. Maryland publishes the annual attainment report on transportation system performance in five categories against target values (NCHRP 2010a). These performance measures include driver satisfaction, percent of highway network in preferred condition, acres of wetland or wildlife habitats restored, fuel usage of light vehicle fleet, user cost saving due to incident management, transport-related emission by region, transport-related GHG emissions, vehicle emission reduction, travel demand management performance, reduction in VMT through park and ride, bicycle and pedestrian fatalities and injuries, percentage of highway centerline miles with a bicycle level of comfort target and miles of highways with marked bicycle lanes, and percentage of SHA road centerline miles in urban areas with sidewalks and percentage of sidewalks compliant with the Americans with Disabilities Act (ADA). A success story for a multimodal highway project was the Intercounty Connector (ICC) designed to relieve congestion between two major corridors (Interstate Highway I-270 and I-95) in Montgomery and Prince George's counties (NCHRP 2010a).

Sustainable energy and transport strategies in major cities (Atlanta, Georgia, and Austin, Texas): Atlanta, Georgia, has been a nonattainment urban area for many years due to higher level of air pollution. One of the factors for its program success is TDM marketing by the Georgia Department of Transportation (GDOT) to reduce congestion and GHG emissions, using reliable performance metrics to pitch its messages to the public (Keck et al. 2010). For example, the Clean Air Campaign (CAC), a not-for-profit corporation, was formed in 1996 by collaboration between government, business, and civic organizations (Keck et al. 2010). Originally funded by the GDOT as a public awareness campaign for air quality degradation associated with vehicle emissions, the CAC began to conduct employer outreach in 2000. For the most part, this role focuses on changing travel behaviors through informed decision-making and public education campaign. The most effective TDM marketing programs involve a variety of partners within a community, including public officials, community organizations, and individual support transportation alternatives. These partner organizations include Transportation Management Association (TMA), Employer Service Organizations (ESOs), Rideshare matching and guaranteed ride home (GRH) service, and Vanpool services. Through these TDM efforts commuting alternatives in the Atlanta metro area boasts an annual reduction in pollution and the following benefits each year (Keck et al. 2010):

- Sixteen million car trips eliminated from metro Atlanta roadways
- More than 200,000 t of pollution not released into the air
- More than $156 million estimated in reduced commute costs
- Thirty million dollars estimated in health-related cost savings due to improved air quality

Austin, Texas: The city of Austin, Texas, initiated its energy conservation and GHG reduction program in 2007. By winning the 2010 national climate protection award on September 29, 2010, Austin has been recognized nationally for reaching the 5th milestone of monitoring and verifying results of the city's carbon reduction plans (City of Austin 2010). This was announced by the Local Governments for Sustainability, USA, which is associated with the International Council for Local Environmental Initiatives (ICLEI). The city of Austin has implemented an innovative transportation user fee (TUF) which averages $30–40 annually for a typical household in their utility bills. This charge is based on the average number of daily motor vehicle trips made per property, reflecting its size and use. This regulation rewards households that reduce their vehicle ownership. The city provides exemptions to residential properties with occupants that do not own or regularly use a private motor vehicle for transportation or if they are 65 years of age or older. The Austin Climate Protection Plan, developed by the city to reduce GHG emissions, includes many elements (City of Austin 2010) such as:

- Making all city facilities and operations carbon neutral by 2020
- Reducing Austin Energy's carbon footprint and making any new electricity generation carbon neutral

- Enhancing Austin Energy's Green Building program for achieving energy efficiency in buildings
- Engaging businesses and citizens to reduce their carbon footprints

London, United Kingdom

London implemented a congestion pricing program effective February 2003 that charges drivers £5 each time they enter the central city (22 km^2 area, 1.2 % of greater London), similar to the toll charged at major bridge crossings (Molina and Molina 2004; Limanond 2010). This congestion-designated zone is surrounded by perimeter roads that serve as its boundaries. The charge is enforced by fixed and mobile surveillance cameras that are linked to automatic licensed plate number recognition technology. Heavy penalty of £80 is assessed against the vehicle owner if the charge is not paid by midnight. There is also a 90 % discount for residents of the congestion zone. There is a concern about negative financial impact on the local retail sector and on wider economy (Molina and Molina 2004). The program showed the following benefits to Central London: a 30 % reduction of car travel, average travel speed increased from 13 to 17 km/h, and congestion delay reduced by 30 % (Limanond 2010). The reduction in vehicular traffic volume also improved air quality. The levels of NO_x, PM_{10}, and CO_2 concentrations in London decreased by 16–19 % after the congestion pricing program was implemented (Limanond 2010).

Mexico City

Metropolitan Mexico City ranks second in the 2006 list of megacities at 19.24 million population (Fig. 15). The city expanded in the late 1930s when a combination of rapid economic growth, population growth, and a considerable rural migration filled the city with people. Mexico City houses 80 % of all the firms in the country, and 2.6 million cars and buses bring people to work and shop in them. Street vendors make up an enormous part of Mexico's job force (Abhat et al. 2005). The extensive industrial and commercial activities within the city are primarily responsible for its prosperity as well as many of the environmental problems. High levels of emissions are responsible for permanent respiratory problems suffered by more than one million people. Air quality degradation worsens by the fact that Mexico City is situated in a basin (Abhat et al. 2005). The geography prevents winds from blowing away the pollution, trapping it above the city. More than 30 % of the city's vehicles are more than 20 years old. The city has been striving to implement solutions which include (Abhat et al. 2005; DB Research 2008):

- Bicycles and motorcycles are popular. Numbers of cars are reduced on roads by enforcing the law of banning cars on roads on certain weekdays.
- A thriving LRT system is in operation for years, with nine lines and 75 miles of tracks and more under construction.
- The metrobus public transport system has significantly contributed in improving both air quality and easing transport problems. Bus journey times have been halved, and CO_2 emissions have been reduced by 80,000 t a year.

São Paulo, Brazil

The megacity of São Paulo has a population of 18.61 million and ranks 5th in the 2006 list of top megacities (Fig. 15). Although it is home to only 15 % of the country's inhabitants, this megacity consumes 60 % of Brazil's energy. The city emitted 83 million tons of CO_2 in 2003. In metropolitan São Paulo, there were 2,000 major industrial facilities and 7.2 million passenger and commercial vehicles as of 2006, which include 93.5 % light-duty and 6.5 % heavy-duty diesel vehicles (Andrade 2007). Approximately 76.3 % of the light-duty vehicles burn a mixture of 78–80 % gasoline, 22 % consume ethanol (referred to as gasohol), and 17.2 % use hydrated ethanol (95 % ethanol + 5 % water). In comparison, up to 10 % ethanol is used in gasoline in the United States for cars and light vehicles. On a daily basis, public transportation plays a key role in meeting the transportation needs of people living in and commuting from 39 municipalities in São Paulo. São Paulo's complex but successful public bus transit system operates over 26,000 buses on nearly 2,000 routes carrying up to 11 million people daily. The bus system uses especially constructed bus lanes, which enable bus commuters to avoid traffic jams on the streets and buses to travel faster than cars (Molina and Molina 2004; Andrade 2007). There are also several rail transit systems and connecting train lines. A noncontact smart card allows riders discounted prices for multiple rides and makes for easier transitions between bus, train, and subway transit systems.

Bangkok, Thailand

Bangkok has long been considered a city plagued by congestion and poor air quality. The country and metropolitan city governments adapted several environmental strategies in the 1990s and included the formation of environmental law enforcement bodies. The key steps for automobile emission reductions were phasing out lead from fuel by the mid-1990s by making unleaded gas cheaper, introducing vehicle inspection and maintenance programs, and reducing the number of cars on roads by providing better public mass transport options. Bangkok Mass Transit Authority operates air-conditioned and ordinary buses. Articulated buses used in the BRT system are for 90, and other buses are for 40–50 passengers. However, the ordinary buses are being phased out (DB Research 2008; MEGAPOLI 2009). Most of the buses run on diesel, but they are being converted to a cleaner and cheaper natural gas vehicle (NGV) engine. Recently, it operates new routes of NGV-powered air-conditioned vans, shuttling people between the city center and suburban communities.

Future Directions

There is a strong link between mobile sources of GHG, air quality, and the transportation sector. First, transportation emissions are the main cause of air quality problems in many megacities and large urban centers. This seems to be the trend in the megacities of the developing world, where these emissions will soon become the

dominant source of air pollutants. Second, economic growth is closely linked to personal and freight transportation and efficient mobility; thus, restrictions of transportation activities for improving air quality could hinder economic growth. The challenge is thus to improve air quality and reduce GHG emissions while ensuring personal and freight mobility.

Livable Cities and Eco-friendly Lifestyles

A 2004 report by the US National Academies examined the influence of the built environment on physical inactivity in the United States and recommends that opportunities be provided to increase physical activity and study social marketing when changes are made to the built environment – whether retrofitting the existing facilities or constructing new developments and communities (TRB 2005). The lack of physical mobility and walking as a means of traveling about has attributed to obesity and related health problems in US cities. Similar concerns about transport equity are discussed in a 2009 WHO report (WHO 2009b). Modern cities have typically been designed for cars and vehicular traffic. Unlike residents in urban areas, residents in rural places are less likely to walk to work or commercial establishments. This is the case in Mississippi, a rural state which has been ranked one of the top three states for obesity problems for the past several years.

Transport infrastructure and traffic operation management also influence livability of a city and eco-friendliness of its people. Zurich, Switzerland, topped the 2007 list of the most livable cities in Western Europe. Zurich' shares of commuter trips include 24 % walking trips, 40 % public transport, and 36 % private automobiles (Gires 2005). The proportion of private automobiles is almost less than half of the automodal share in other major cities of the western world and Australia. Additionally, bikeways, well-managed intercity rail services, and about 2,000 trains traveling daily to different destinations reflect the eco-friendly lifestyles of Zurich's inhabitants. The long-term sustainability vision adopted by New York City also includes better transit mobility, less congestion, and nonmotorized transport facilities (New York City 2007). Many cities in Western countries have been recognizing the health and environmental benefits of walking and cycling and are trying to provide safe eco-friendly facilities for these activities. However, during the same period, nonmotorized trips in many cities of the developing world have been declining due to a focus on improving motorized vehicle flow on roads and ignoring the needs of pedestrians and other people who depend on mass transit vehicles to commute.

Sustainable Accessibility, Mobility, Commuting, and Economic Prosperity

Mobility and access to affordable and clean transportation to all people in a city is the key to economic growth, social welfare, and quality of life. In emerging economies

and developing countries, economic growth drives development and prosperity. Inadequate mobility places limitations on the poor and other disadvantaged groups to job access, educational institutions, medical care and hospitals, safe recreational facilities, as well as making them more susceptible to fire, rain, and other natural hazards. However, in many large cities of the developing world, adequate mass transit and public transportation modes are not sufficiently provided and managed. Millions of other inhabitants without cars waste long hours in congestion and unsafe travel. Traffic safety data from Karachi shows that in 2007 more than 40 % road fatalities involved pedestrians (Jumma 2008). People in many megacities suffer from stress, air pollution-related health problems, and deterioration of quality of life.

Sustainable mobility is defined as the ability to meet people's mobility needs without adversely impacting societal or ecological values for present and future generations. Due to the important role of nonmotorized modes of travel in promoting better livable cities, a more suitable term is *sustainable accessibility*. Transport strategies for sustainable accessibility and mobility should be environmentally sustainable, socially sustainable to ensure equity among all sectors of the society, and economically and financially sustainable (WRI 2007). Sustainable accessibility is imperative when planning and implementing nonmotorized and multimodal transportation strategies to support sustainable growth of cities while responding to mobility and accessibility needs of all sectors of the society.

Equity and Shared Responsibility

Emissions from fuel combustion are growing faster for the transport sector than for other sectors; this growth is more pronounced in the developing world than in the industrialized and developed countries. Increases in CO_2 emissions have been seen in all transport modes, but particularly in road transport.

Passenger and Freight Rail Modal Share

Emissions from mobile sources in the United States grew 29 % between 1990 and 2004 (Davis and Hale 2007). Residential emissions have increased 13 % in the last two decades. Commuters waste millions of hours and gallons of fuel in traffic congestion in and around cities. Lots of emphasis for reducing congestion and GHG emissions have been on increasing the modal share of mass transit, increasing car fuel efficiency and reducing volume of cars and other two-axle automobiles by travel demand management strategies (car pooling, HOV lanes, and increasing parking prices downtown). The executive branch of the US government and Congress has put forth little known effort to reduce truck travel and associated GHG emissions. Publicly, no pressure has been put on truck travel which produces three to four times more GHG emissions for every gallon of fuel in comparison to cars. Fuel efficiency drive has not been geared to trucks. Considering freight truck business employs millions of heavy truck drivers, both technologically and politically, and there is little pressure on the trucking industry to reduce GHG emissions.

The EPA data (EPA 2005a) also shows that in the United States (a) medium and heavy trucks used for freight travel produced 410.8 million tons of CO_2e emissions in 2007, amounting to 79.5 % increase from 1990, and (b) the truck share of total transportation-related GHG emission was 20.5 % in 2007. But what is the real cost of truck-related GHG emissions and physical damage to road and highways? Here are some underlying facts:

- Trucks occupy more lane space on publicly owned and financed urban roads, intercity roads, and all types of public highways.
- Trucks worsen congestion on urban and suburban highways and cause safety problems and crashes.
- Trucks pay a small share of their use of roads and highways and none for construction or maintenance costs.
- Trucks cause most of the physical damage to pavement structures and bridges, which are structurally designed for truck weight and cumulative applications over the highway design life. Car traffic has virtually no deterioration effect on pavements.
- The road and highway infrastructure is totally built and maintained by taxpayer's money, and trucking companies do not have to factor these costs in their business decisions.
- In other words, freight trucks are being subsidized heavily by taxpayer money for providing and maintaining the road and bridge infrastructure.

A national transport policy decision is needed to apply additional charge or fee on trucks for (1) road-use charge on lump-sum annual basis or truck-travel distance basis, (2) pavement damage cost attributed by annual distance driven, and (3) carbon emission charges per ton mile or ton km because of their significant carbon footprint. The revenue should be used to improve road infrastructure condition, build more intermodal facilities at primary distribution centers throughout the United States, and encourage businesses to use rail mode more often and for longer regional destinations. For example, Norway and Germany have implemented road-use pricing and road tolls on freight trucks; however, several civil society groups argue that this toll revenue should not be simply used on road maintenance and reducing congestion on roads, but to invest in other alternatives, for example, fuel-efficient and mass transit transport.

Compliance with EPA rules for emission reductions of locomotives (EPA 2008b) and more use of fuel-efficient rail transportation of freight throughout the United States and passenger travel on heavily trafficked road corridors will reduce the mobile GHG emissions significantly and improve air quality. Moreover, freight rail mode is privately owned in the United States, and, unlike freight trucks, no taxpayer money is used to subsidize freight rail and bridge infrastructure costs. Here are some numbers reported by the US rail industry (AAR 2010a, b):

- Rail locomotives are four times more fuel efficient than trucking; therefore, moving freight by train instead of truck reduces GHG emissions by 75 %.

- Replacing just 10 % long-haul freight trucks by rail can reduce GHG emissions annually by 12 million tons. This reduction is equivalent to taking off two million cars from roads or planting 280 million trees.
- A train can carry the freight of 280 or more trucks reducing highway congestion and creating space for 1,100 or more cars.
- Rail track costs about 2–4 million dollars per mile in relatively short time in comparison to about 10–15 million dollars per mile for highway construction and 5–10 years to build and for higher life cycle costs due to pavement maintenance needs.

Unlike road vehicles, a dual-track rail infrastructure keeps trains moving at designated speeds safely and efficiently with no "congestion" and no extra emission. The purpose of this discussion is that equal opportunity should be provided by the authorities to rail/train operators on selected long-distance corridors to compete with freight truck operators and expressways for regional commuters. This approach should be considered as a national policy and priority matter. The freight trucks in the United States are subsidized by operating on public highways, whereas the rail/train operators do not have similar assistance of public funds for constructing and maintaining rail infrastructure. Unfortunately, similar disparity is happening in most developing countries where rail generally is operated by public agencies like highways, but rail gets little or no funding to modernize its train stocks and rail infrastructure. National transportation policies have been derived from the lack of understanding of the mobile sources of GHG emissions and effects of other road transportation-related pollutants on public health and quality of life. This led to a gradual decline in rail service quality over the last three decades because passenger rail transport has been predominantly used by the poor people.

Traditionally European countries have been building and using a passenger rail infrastructure. Lately, China has been striving to build rail infrastructure and promoting passenger rail service. Passenger rail mode has been popular in these countries for providing connectivity to airports, as well as for serving commuters in urban areas and intercity corridors. The megacity of São Paulo has been a leader in Brazil in multimodal passenger transport of electric powered commuter rail that serves millions of commuters every day in harmony with BRT and several transit bus routes. By intermodal integration through one electronic ticket accepted by all these services, congestion and travel time were reduced significantly, which led to lower CO_2 emissions (InfrastructureGlobal 2012). Brazil invested in elevated monorail lines in São Paulo and other cities that opened for service just before the 2014 Soccer World Cup.

Recently, an economic viability study was conducted that recommended a commuter rail combined with intercity rail service in the rural area of the Mississippi Gulf Coast (CAIT 2014). Major highways on the Gulf Coast suffer from severe traffic congestion with an average travel speed on I-10 near Gulfport reducing by over 20 % to or below 55 mph (88 kmph). The study revealed that trams and street rail cars, BRT, and high-cost tram or light rail transit are not feasible for the rural area due to degradation of highway traffic capacity from lane occupancy and rail track

intrusion. These also add safety risks of mixed multimodal traffic. Consequently, these modes are not technically feasible from value engineering perspectives of functional and safety requirements. The monorail line is not recommended due to very high initial capita cost. The final recommended strategies include commuter rail passenger service on existing freight rail tracks: (1) "Casino Train" in E-W corridor and (2) commuter rail line "Beach Train" in N-S corridor. Considering direct revenues only (fare, advertising on train and stations, annual fee charges to concessions on stations and shuttle service operators), the breakeven period is 6–7 years until the rail service will become financially self-sustaining (CAIT 2014). Other benefits include an increase in income from casino patrons and tourists/visitors, additional gaming and sales tax revenues, reduction in emissions, and fuel cost savings as a result of moving a significant number of auto commuters to rail lines. Economic development impacts will create a total of 500 jobs and boost regional economy.

Involving Stakeholders and Public for Sustainable Transport and Mitigation Strategies

Successful implementation of socially equitable and environmentally sustainable development requires area monitoring of air pollutants including CO_2, life cycle cost analysis, marketing plans, involvement of all stakeholders (oil and motor vehicle industries, retail businesses, and transport services), and public awareness campaigns for shared responsibility within a region and globally. It is estimated that 30 % of fuel is wasted in congested cities in finding parking places. Many car manufacturers are working on future concept cars for megacity markets to serve the city center area without traditional carbon footprint (Moves 2010). These small lightweight lithium battery-powered green cars are designed for lower speeds and very small or zero CO_2 emission per mile. By reducing vehicular emissions, air quality will be protected, greenhouse gases will be reduced, and the effect on global warming will diminish. In order to develop and implement green transport technologies to reduce GHG emissions, it is recommended for governments at national, state/provincial, and local levels to institute policies and provide initiatives for green technology growth. At the same time, a push for public support is crucial for the future success of green technology implementation so that it may be firmly established in the long term.

Stakeholders' cooperation and involvement are required for the following: (1) sustainable development of the built environment, (2) identification of less polluting transportation technologies, and (3) implementation of abatement strategies to mitigate congestion and its adverse impacts on traffic safety, global warming, and air quality. Stakeholders should be identified at community, regional, and national levels. An integrated approach involving all stakeholders can help manage and reverse many blighted parts of our cities, urban and suburban communities, and rural and industrial areas to livable conditions. Governments must take initiatives to increase public awareness of mobile GHG problems, mitigate adverse transportation impacts and sprawl, and improve air quality and quality of life of millions of people each year. The use of nongovernmental organizations (NGOs) (WRI 2007; Foletta

and Heyen-Perschon 2009; Jumma 2008) and public–private partnerships should be promoted to create environmentally and financially sustainable transport management strategies.

During the last few years, social media has been extensively used by interested people, news media, and the general public to convey news and campaign messages. Blogging and Twitter have empowered all people in a region or globally to interact and communicate with others (InfrastructureGlobal 2011; Twitter 2014). Environmental awareness, energy, CO_2 emissions, and climate change impacts are popular topics on social media, which have been powerful to educate, disseminate information, and raise global concerns to reduce carbon emissions.

Global Responsibility for CO_2 Reductions

During 2013 and 2014 major initiatives have emerged on international levels to reduce CO_2 and other harmful emissions from energy and transport sectors. Climate change impacts are triggering major natural disasters in some Asian countries who are not major contributors to global GHG emissions, displacing millions of people and destructing their economies (Twitter 2014). The White House launched its Climate Action Plan (CAP) in 2013 to prepare US citizens and communities for climate change adaptation in response to an increase in frequency of weather-related floods and coastal hurricane disasters (White 2014). The most recently concluded climate change talks in Peru's capital Lima in December 2014 reached agreement on carbon targets for all countries (The Guardian 2014). And with 2014 on course to be the hottest year on record, activists and campaigners warned that the plan was far too weak. Countries are expected to declare their proposed emission reduction targets by March 2015. China, with 8,548 million tons of CO_2 emissions from energy in 2012 overtaking the United States by 38 %, will formally pledge to cut its greenhouse gas emissions, joined by similar pledges from India, Brazil, and other developing countries.

Concluding Remarks

The vehicle emission and demand on energy (due to the increased built areas and population migration from rural areas) have adverse impacts on the environment, both in air quality degradation and increases in greenhouse gas emission. Governments throughout the world must consider reduction in greenhouse gas emissions and other air pollution a national priority. Further, they should involve all stakeholders in finding multimodal solutions including nonmotorized trips for the mobility and accessibility in growing cities and long-haul transport needs to support development and economy. A reasonably quantifiable sustainability scale is CO_2e emission per capita that can be used worldwide for evaluating performance of sustainable transportation and development policies by government agencies and cities.

The worldwide reduction of greenhouse gases from transportation sources and the efficient use of energy in urban and industrial applications should be important for

sustaining the quality of life of current and future generations. Although awareness has increased in the public related to the global damaging effect of greenhouse gas emission and public health hazards from other air pollution, when it is directly tied to economic prosperity, survival, and individual freedom to travel by car, vehicle emissions and air pollution becomes secondary. By providing knowledge to decision-making authorities in both industrialized and developing countries, it is expected that they will be able to adapt and implement many available high payoff research products in response to sustainable national transportation planning priorities.

Acknowledgments The author's research was primarily conducted at the Center for Advanced Infrastructure Technology (CAIT) of the University of Mississippi. Thanks are due to the author's former graduate students Katherine Osborne, Jessica Headrick, Bikila Wodajo, Carla Brown, and Kanok Boriboonsoms for their contributions. Thanks are also due to CAIT research assistants Eric Shackelford for the CO_2 calculations associated with road vehicle emissions in selected cities, Seth Cobb for assistance in the Gulf Coast passenger rail study and Cherrelle Williams for editorial assistance.

References

AAR (2010a) Freight railroads help reduce greenhouse gas emissions. American Association of Railroads (AAR), Washington, DC. http://www.aar.org/Environment.aspx. Accessed 12 Sept 2010

AAR (2010b) Freight railroads: reducing highway gridlock. American Association of Railroads, Washington, DC. http://www.aar.org/Environment.aspx. Accessed 12 Sept 2010

Abhat D, Dineen S, Jones T, Motavalli J, Sanborn R, Slomkowski K (2005) Cities of the future. Environ Mag XVI(5):1–2. http://www.emagazine.com/view/?2849. Accessed 28 Aug 2010

Akbari H (2005) Energy saving potentials and air quality benefits of urban heat island mitigation. Lawrence Berkeley National Laboratory, California. http://HeatIsland.LBL.gov/, http://www.epa.gov/heatislands/impacts/index.htm. Accessed 9 Feb 2009

Allianz (2010) Energy – InfoGraphic: transportation emission compared. 03 Sept 2009. www.knowlegde.allianz.com/en/media/graphics. Accessed 20 Aug 2010. http://knowledge.allianz.com/nopi_downloads/images/co2_emissions_96dpi.jpg

Andrade MF (2007) Air quality impairment associated to local sources in the megacity of São Paulo, Brazil. InterfacEHS J Integr Manage Occup Health Environ 2(5):1–17. http://www.interfacehs.sp.senac.br/images/artigos/104_pdf.pdf. Accessed 20 July 2010

Auch R, Taylor J, Acevedo W (2004) Urban growth in American cities: glimpses of U.S. urbanization. Circular 1252, U.S. Geological Survey, U.S. Department of the Interior. http://pubs.usgs.gov/circ/2004/circ1252/#Purpose. Accessed 28 Aug 2010

BBC (2007) BBC world news. http://www.BBC.com. Accessed 3 May 2007

Bernow SS, Marron DB (1990) Valuation of environmental externalities for energy planning and operations. Tellus Institute, Boston

CAIT (2014) Economic Viability of Mississippi Gulf Coast Rail Service Revival. NCITEC white paper, Center for Advanced Infrastructure Technology (CAIT), University of Mississippi, 2014. http://www.olemiss.edu/projects/cait/ncitec/NCITEC-WhitePaper-GC.pdf. Accessed 20 Nov 2014

City Mayors Development (2007) Solving transport issues has highest priority for megacities: Siemens AG. http://www.citymayors.com/development/megacities.html. Accessed 28 Aug 2010

City of Austin (2010) City of Austin wins national climate protection award. http://www.ci.austin.tx.us/acpp/default.htm. Accessed 10 Oct 2010

CO_2 Science (2006) Carbon dioxide (urban CO_2 dome – cities outside U.S.) – summary. Center for the Study of Carbon Dioxide and Global Change, Tempe. http://www.co2science.org/subject/u/summaries/urbanco2dome.php

Davis T, Hale M (2007) Public transportation's contribution to U.S. greenhouse gas reduction. SAIC, McLean

Delucchi MA, Murphy J (1996) U.S. military expenditures to protect the use of Persian-gulf oil for motor vehicles. UCD-ITS-RR-96-3 (15), University of California, Davis

DOT (2007) Highway statistics 2007. Federal Highway Administration, U.S. Department of Transportation, Washington, DC. http://www.fhwa.dot.gov/policyinformation/statistics/2007/vm1.cfm. Accessed 9 Mar 2010

DOT (2008) Highway statistics 2008. Federal Highway Administration, U.S. Department of Transportation, Washington, DC. http://www.fhwa.dot.gov/policyinformation/statistics/2008/vm1.cfm. Accessed 10 June 2010

Driscoll DD (1996) The IMF and the World Bank how do they differ? http://www.imf.org/external/pubs/ft/exrp/differ/differ.htm. Accessed 20 Sept 2010

EEA (2008) Greenhouse gas emission trends and projections in Europe 2008, tracking progress towards Kyoto targets. European Environment Agency (EEA), Copenhagen

EIA (2000) Trends in building-related energy and carbon emissions: actual and alternate scenarios. Presentation at summer study on energy efficiency in buildings, sponsored by the American council for an energy-efficient economy, 21 Aug 2000 by Stephanie J. Battles and Eugene M. Burns. Energy Information Administration (EIA), U.S. Department of Energy, Washington, DC. http://www.eia.doe.gov/emeu/efficiency/aceee2000.html. Accessed 12 Mar 2009

EIA (2007a) International energy annual outlook. Energy Information Administration, U.S. Department of Energy, Washington, DC

EIA (2007b) Annual energy outlook 2007. DOE/EIA-0383(2007). Energy Information Agency, U.S.Department of Energy, Washington, DC. http://www.eia.doe.gov/oiaf/aeo/index.html. Accessed 15 Dec 2009

EIA (2009) Emissions of greenhouse gases report. DOE/EIA-0573(2008). Energy Information Agency, U.S. Department of Energy, Washington, DC. http://www.eia.doe.gov/oiaf/1605/ggrpt/. Accessed 15 Dec 2009

EPA (2005a) Emission facts: average carbon dioxide emissions resulting from gasoline and diesel fuel. EPA420-F-05-001. U.S. Environmental Protection Agency (EPA), Washington, DC. http://www.epa.gov/otaq/climate/420f05001.htm. Accessed 7 Mar 2010

EPA (2005b) Emission facts: average carbon dioxide emissions resulting from gasoline and diesel fuel. EPA420-F-05-001. U.S. Environmental Protection Agency, Washington, DC. http://www.epa.gov/oms/climate/420f05001.pdf. Accessed 7 Mar 2010

EPA (2008a) Inventory of U.S. greenhouse gas emissions and sinks: 1990–2006. U.S. Environmental Protection Agency, Washington, DC

EPA (2008b) Locomotives. http://www.epa.gov/otaq/locomotives.htm. Accessed 30 Aug 2010

FAA (2010) FAA aerospace forecast fiscal years 2010–2030. Federal Aviation Administration (FAA), U.S. Department of Transportation, Washington, DC. http://www.faa.gov/data_research/aviation/aerospace_forecasts/2010-2030/. Accessed 10 Aug 2010

Foletta N, Heyen-Perschon J (2009) Global transport development. Institute for Transportation and Development Policy (ITDP), Hamburg. http://www.itdp-europe.org/assets/documents/Global_Transport_Development_2009.pdf

Gaines L, Vyas A, Anderson JL (2006) Estimation of fuel use by idling commercial trucks. Paper No. 06–2567. In: CD proceedings, 85th annual meeting. Transportation Research Board, Washington, DC, 22–26 Jan 2006

GAO (2002a) Physical conditions of the interstate highway system have improved, but congestion and other pressures continue. Highway Infrastructure, Report Number GAO-02-1128 T. General Accounting Office (GAO), Washington, DC

GAO (2002b) Environmental protection: federal government could help communities better plan for transportation that protects air quality. Testimony Report Number GAO-02-988 T. General Accounting Office, Washington, DC

Gires J-M (2005) Hydrocarbons challenges for long term sustainable transportation. In: Presentation, environment 2005 – international conference on sustainable transportation in developing countries, Abu Dhabi, 30 Jan–2 Feb 2005

Headrick J (2010) Geospatial analysis of roadway traffic volume, flow simulation, and air pollution impacts in the built environment. M.S. thesis, University of Mississippi, Mississippi

Hudson WR, Haas R, Uddin W (1997) Infrastructure management. McGraw Hill, New York. (Japanese edition 2001, Chinese edition 2005)

IATA (2007) IATA 2007 annual report. International Air Transport Association (IATA), Washington, DC. http://www.iata.org/NR/rdonlyres/9CE110BA-B989-448F-9991-67DF69397A6D/0/ar2007.pdf. Accessed 30 Dec 2007

IATA (2010) Air transport market analysis, April 2010. International Air Transport Association, Washington, DC. www.iata.org/economics. Accessed Aug 2010

IBM (2010) The globalization of traffic congestion: IBM 2010 commuter pain survey. IBM. http://www-03.ibm.com/press/us/en/pressrelease/32017.wss. Accessed 10 Sept 2010

Imran M (2010) Sustainable urban transport in Pakistan: an institutional analysis. Int Plann Stud 15 (2):119–141, Taylor and Francis. http://www.informaworld.com/smpp/title~content=t713426761. Accessed 8 July 2010

InfrastructureGlobal (2011) Eastern United States Devastated By Hurricane Irene – No Break from Onslaught of Natural Disasters, 2011. http://infrastructureglobal.com/?p=485. Accessed 14 July 2014

InfrastructureGlobal (2012) Sustainable Mass Transit in Cities: Reducing Congestion and Car Emissions in the World by Deploying Metros and Clean Buses, 2012. http://infrastructureglobal.com/?p=2882. Accessed 10 Dec 2014

Bhatti, G Raza, Soomro Shireen (2010) Proceedings, International Conference on "biodiversity is our life." Center for Biodiversity and Conservation, Shah Abdul Latif University, Khairpur (Mir's), Sindh, Pakistan, 29–31 Dec 2010, e-tALK Newsletter, vol 3(12). http://bgarden.salu.edu.pk

IPCC (1996) Revised 1996 IPCC guidelines for national greenhouse gas inventories: reporting instructions. http://www.ipcc-nggip.iges.or.jp/public/gl/guidelin/annex3ri.pdf. Accessed 20 Feb 2011

IPCC (2007) Climate Change 2007: Mitigation. The Intergovernmental Panel on Climate Change. http://www.ipcc.ch/. Accessed 20 Dec 2009

Jumma R (2008) Road traffic injury research and prevention centre (Presentation). Urban Resource Centre, Karachi, 8 Feb 2008. http://www.urckarachi.org/Forums.HTM. Accessed 15 Sept 2010

Keck D, Patel H, Scolaro AJ, Bloch A, Ryan C (2010) Accelerating transportation project and program delivery: conception to completion. NCHRP Report 662, National Cooperative Highway Research Program, TRB, Washington, DC

Koch-Kraft A (2008) Future megacities combating climate change. Fifth BMBF Forum for Sustainability, Berlin. www.future-megaciries.org. Accessed 20 Aug 2010

Koepp S (1988) Gridlock! TIME Magazine, 12 Sept 1988, pp 52–60

Kozel SM (2007) Roads to the future, capital beltway. Updated 30 Sept 2007. http://www.roadstothefuture.com/Capital_Beltway.html. Accessed 28 Aug 2010

Landsberg HE (1981) The urban climate. Academic, New York

Limanond T (2010) Travel demand management policies. Sustainable Urban Transport Project (SUTP). http://www.sutp.org/index.php?option=com_content&task=view&id=136&lang=uk. Accessed 15 Sept 2010

Martin B (2007) At the crossroads: which way the World Bank's transport strategy? Bretton Woods Project, London, Update 11 July 2007. http://www.brettonwoodsproject.org/art-554319. Accessed 15 Sept 2010

McCarthy JE (2010) Aviation and climate change. Report 7–5700 for U.S. Congress, Congressional Research Service

McMillan W, Yurganov L, Krueger A, Hoff R, Barnet CD, Gleason J, Celarier E, Krotkov N, Liu X, Kurosu T, Osterman G, Torres O (2009) Satellite observations of megacity air pollution, biomass burning emissions, and their long-range transport. In: Presentation, 11th conference on atmospheric chemistry, 15 Jan 2009. http://ams.confex.com/ams/89annual/techprogram/paper_149714.htm. Accessed 12 Sept 2010

Megacity Moves (2010) Motor Trend Magazine, July 2010, pp 20–22

MEGAPOLI (2009) Megacities: emissions, urban, regional and global atmospheric pollution and climate effects, and integrated tools for assessment and mitigation. MEGAPOLI-NL05-09-12, (5). http://megapoli.dmi.dk/nlet/MEGAPOLI_NewsLet05.pdf. Accessed 28 Aug 2010

Molina M, Molina L (2004) Megacities and atmospheric pollution. J Air Waste Manage Assoc 54 (6):644–680

NCHRP (2010a) State department of transportation role in the implementation of transportation demand management programs. Research Results Digest 348, National Cooperative Highway Research Program (NCHRP), TRB, Washington, DC

NCHRP (2010b) NCHRP web-only document 152: assessing mechanisms for integrating transportation-related greenhouse gas reduction objectives into transportation decision making. National Cooperative Highway Research Program, TRB, Washington, DC

New York City (2007) Inventory of New York city greenhouse gas emissions. Mayor's office of long-term planning and sustainability. http://www.nyc.gov/html/planyc2030/downloads/pdf/emissions_inventory.pdf. Accessed 10 Sept 2010

Oke TR (1982) The energetic basis of the urban heat island. Q J Roy Meteorol Soc 108(1):24

ORNL (2003) Transportation energy data book, 23rd edn. Report ORNL-6793. Oak Ridge National Laboratory, Oak Ridge, Prepared for U.S. Department of Energy

ORNL (2004) Transportation energy data book, 24th edn. Report ORNL-6970. Oak Ridge National Laboratory, Oak Ridge, Prepared for U.S. Department of Energy

Osborne K (2009) GIS-based urban transportation infrastructure management using spaceborne remote sensing data. M.S. thesis, University of Mississippi, Mississippi

Pisarski AE (2006) Commuting in America. NCHRP Report 550, National Cooperative Highway Research Program, TRB, Washington, DC. www.trb.org

Pomerantz M, Pon B, Akbari H, Chang SC (2003) The effect of pavements' temperatures on air temperatures in large cities. Report LBNL-43442, Lawrence Berkeley National Laboratory, California, April 2000. Heat Island Group. http://eande.lbl.gov/HeatIsland/. Accessed 2 Apr 2003

Queiroz C, Gautam S (1992) Road infrastructure and economic development: some diagnostic indicators, Policy research working paper series. The World Bank, Washington, DC

DB Research (2008) Megacities: boundless growth. Deutsche Bank Research. http://www.dbresearch.com/PROD/DBR_INTERNET_EN-ROD/PROD0000000000222116.pdf. Accessed 10 Sept 2010

Rooke A, Zuckerman E, Schalatek L (2009) Doubling the damage: World Bank climate investment funds undermine climate and gender justice. Gender Action, Washington, DC. www.genderaction.org

Rosenfeld AH, Akbari H, Romm JJ, Pomerantz M (1998) Cool communities: strategies for heat island mitigation and smog reduction. Energy Build 28(1):51–62

Schäfer A, Jacoby HD, Heywood JB, Waitz IA (2009) The other climate threat: transportation. Am Sci 97(6):476–483

Schrank D, Lomax T (2008) Six congestion reduction strategies and their effects on mobility. Texas Transportation Institute, College Station, Texas. http://mobility.tamu.edu/resources/. Accessed 12 Dec 2009

Sohn J, Nakhooda S, Baumert K (2005) Mainstreaming climate change at the multilateral development banks. World Resources Institute, Washington, DC

The Guardian (2014) Lima Climate Change Talks Reach Global Warming Agreement. *The Guardian*, December 14, 2014. http://www.theguardian.com/environment/2014/dec/14/lima-climate-change-talks-reach-agreement. Accessed 14 Dec 2014

The Realignment (2009) Gas-free cars and high speed rail. http://realignmentproject.wordpress.com/2009/09/16/gas-free-cars-and-high-speed-rail/. Accessed 15 Sept 2010

TRB (2005) Does the built environment influence physical activity? Examining the evidence. TRB Special Report 282. TRB, The National Academies Press, Washington, DC

TRB (2009) Driving and the built environment: the effects of compact development on motorized travel, energy use and CO2 emissions. TRB Special Report 298, Transportation Research Board (TRB), Washington, DC. www.trb.org

Twitter (2014) Worldwide over 28 million displaced due to natural #disasters in 2013: Asia 91 %; Top 9 countries in South & East Asia. @drwaheeduddin 12:12 am 20 Dec 2014 from Twitter

Uddin W (2002) Transportation, air quality, and remote sensing laser measurements of air pollutants related to highway traffic in Mississippi – Oxford and Tupelo. Achievements of the DOT-NASA Joint Program on Remote Sensing and Spatial Information Technologies Application to Multimodal Transportation 2000–2002, U.S. DOT, pp 9–10

Uddin W (2006) Air quality management using modern remote sensing and spatial technologies and associated societal costs. Int J Environ Res Public Health MDPI 3(3):235–243

Uddin W (2007) Assessment of transportation related safety and public health impacts using remote sensing and geospatial analysis technologies. In: Proceedings, seventh Malaysian road conference, Kuala Lumpur, 17–19 July 2007, pp 1–16

Uddin W (2009) Development of an ITS-based traffic management model for metropolitan areas of Pakistan with Karachi as a pilot study – annual report, year 3. Pakistan-US Science and Technology Cooperative Program, National Academy of Sciences (NAS)/U.S. Agency for International Development. http://sites.nationalacademies.org/PGA/dsc/pakistan/PGA_052872. Accessed 21 Sept 2010

Uddin W (2010a) Spaceborne remote sensing data for inventory and visualization of transportation infrastructure and traffic attributes. In: CD proceedings, first international conference on sustainability transportation and traffic management, Karachi, 1–3 July 2010, pp 3–12

Uddin W (2010b) Environmental, energy, and sustainability considerations for life-cycle analysis of pavement systems. In: International workshop on energy and environment in the development of sustainable asphalt pavements. U.S. National Science Foundation (NSF) and China NSF, Xian, 7–9 June 2010

Uddin W (2010c) Remote sensing and geospatial technologies for inventory and condition monitoring of transport infrastructure assets. In: Proceedings, second international conference on transport infrastructure, ICTI, São Paulo, 4–6 Aug 2010

Uddin W, Ali M (2007) Karachi metropolitan intelligent transportation system (MITS) stakeholders group workshop executive summary report. Pakistan-US Science and Technology Cooperative Program, National Academy of Sciences (NAS)/U.S. Agency for International Development. http://sites.nationalacademies.org/PGA/dsc/pakistan/PGA_052872. Accessed 10 Aug 2010

Uddin W, Boriboonsomsin K (2005) Air quality management using vehicle emission modeling and spatial technologies. In: Proceeding, environment 2005 – international conference on sustainable transportation in developing countries, Abu Dhabi, 30th Jan–2nd Feb 2005, pp 841–861

Uddin W, Boriboonsomsin K (2006) A consideration of heat-island effect in ground-level ozone forecasting model and its application in rural areas of northern Mississippi. Paper 06–1954. In: CD proceedings, 85th annual meeting. Transportation Research Board, Washington, DC, 22–26 Jan 2006

Uddin W, Tang L (1999) Effects of thermal gradient on asphalt pavement performance. In: Proceeding of the third international congress on thermal stresses, Cracow, 13–17 June 1999, pp 383–386

Uddin W, Uddin U (2010) Sustainable personal rapid transit strategies for congested cities and urban communities. In: Proceedings, second international conference on transport infrastructure, ICTI, São Paulo, 4–6 Aug 2010

Uddin W, Borinoonsomsin K, Garza S (2005) Transportation related environmental impacts and societal costs for life-cycle analysis of costs and benefits. Int J Pavement 4(1–2):92–104

Uddin W, Brown C, Dooley E Scott, Wodajo BT (2009a) Geospatial analysis of remote sensing data to assess built environment impacts on heat-island effects, air quality and global warming. Paper 09–3416. In: CD proceedings, 88th annual meeting. Transportation Research Board, Washington, DC, 11–15 Jan 2009

Uddin W, Wodajo BT, Osborne K, White M (2009b) Expediting infrastructure condition assessment for disaster response and emergency management using remote sensing data. In: Proceedings, MAIREPAV6 – sixth international conference on maintenance and rehabilitation of pavements and technological control, Torino, 8–10 July 2009

United Nations (1999) Prospects for urbanization – 1999 revision. United Nations Department of Economic and Social Affairs, Population Division, New York

Velasco E, Roth M (2009) Measuring emissions of greenhouse gases and air pollutants in cities. Innovation 9(1):15–17. http://www.innovationmagazine.com/volumes/v9n1/preserved-docs/15_17.pdf

WBCSD (2004) Mobility 2030: meeting the challenges to sustainability. World Business Council for Sustainable Development (WBCSD), Conches

Weiss MA, Logan J (2008) The World Bank's clean technology fund. RS 22989, Congress Research Service Report to U.S. Congress

White House (2014) Fact Sheet: The President's Climate Data Initiative: Empowering America's Communities to Prepare for the Effects of Climate Change, 2014. http://www.whitehouse.gov/the-press-office/2014/03/19/fact-sheet-president-s-climate-data-initiative-empowering-america-s-comm. Accessed 28 Mar 2014

WHO (2004) World report on road traffic injury prevention. World Health Organization, Geneva. http://www.who.int/worldhealthday/2004/infomaterials/world_report/en/summary_en_rev.pdf. Accessed 10 Aug 2010

WHO (2009a) Megacities and urban health. World Health Organization (WHO), Centre for Health Development, Kobe City. http://www.who.or.jp/2009/reports/Megacities_Report_DEC09.pdf. Accessed 28 Aug 2010

WHO (2009b) Healthy transport in developing cities. Health and Environment Linkages Initiative (HELI). United Nations Environment Programme (UNEP), World Health Organization (WHO), Geneva

WHO/UNEP (1992) Urban air pollution in megacities of the world. World Health Organization, United Nations Environment Programme, Blackwell, Oxford

WHO/UNEP (2009) Healthy transport in developing cities. Health and Environment Linkages Initiative (HELI), United Nations Environment Programme (UNEP), World Health Organization (WHO), Geneva

Wikipedia (2009) Megacity. http://en.wikipedia.org/wiki/Megacity. Accessed 21 July 2010

World Bank (2010) www.worldbank.org. Accessed 20 Sept 2010

WRI (2007) EMBARQ background paper on global transportation and motor vehicle growth in the developing world – implications for the environment. World Resources Institute (WRI). http://earthtrends.wri.org/features/view_feature.php?fid=54&theme=4. Accessed 10 Aug 2010

Biomass as Feedstock

Debalina Sengupta and Ralph W. Pike

Contents

D. Sengupta (✉)
Texas A&M University, College Station, TX, USA
e-mail: sengupta.debalina@epa.gov

R.W. Pike
Minerals Processing Research Institute, Louisiana State University, Baton Rouge, LA, USA
e-mail: pike@lsu.edu

W.-Y. Chen et al. (eds.), *Handbook of Climate Change Mitigation and Adaptation*,
DOI 10.1007/978-3-319-14409-2_25

Abstract

The world has a wide variety of biofeedstocks. Biomass is a term used to describe any material of recent biological origin, including plant materials such as trees, grasses, agricultural crops, or animal manure. In this chapter, the formation of biomass by photosynthesis and the different mechanisms of photosynthesis giving rise to biomass classification are discussed. Then, these classifications and composition of biomass are explained. The various methods used to make biomass amenable for energy, fuel, and chemical production are discussed next. These methods include pretreatment of biomass, biochemical routes of conversion like fermentation, anaerobic digestion, transesterification, and thermochemical routes like gasification and pyrolysis. An overview of current and future biomass feedstock materials, for example, algae, perennial grass, and other forms of genetically modified plants, is described including the current feedstock availability in the United States.

Introduction

The world is dependent heavily on coal, petroleum, and natural gas for energy and fuel and as feedstock for chemicals. These sources are commonly termed as fossil or nonrenewable resources. Geological processes formed fossil resources over a period of millions of years by the loss of volatile constituents from plant or animal matter. The human civilization has seen a major change in obtaining its material needs through abiotic environment only recently. Plant-based resources were the predominant source of energy, organic chemicals, and fibers in the western world as recently as 200 years ago, and the biotic environment continues to play a role in many developing countries. The discovery of coal and its usage has been traced back to fourth century B.C. Comparatively, petroleum was a newer discovery in the nineteenth century, and its main use was to obtain kerosene for burning oil lamps. Natural gas, a mixture containing primarily methane, is found associated with the other fossil resources, for example, in coal beds. The historical, current, and projected use of fossil resources for energy consumption is given in Fig. 1. Petroleum, coal, and natural gas constitute about 86 % of resource consumption in the United States. The remaining 8 % comes from nuclear, and 6 % comes from renewable energy. Approximately 3 % of total crude petroleum is currently used for the production of chemicals, the rest being used for energy and fuels.

The fossil resources are extracted from the earth's crust, processed, and burnt or converted to chemicals. The proven reserves, in North America, for coal were 276,285 million tons (equivalent to 5,382 EJ [exajoule $= 10^{18}$ J]) in 1990, for oil were 81 billion barrels (equivalent to 476 EJ) in 1993, and for natural gas were 329×10^3 billon ft^3 (equivalent to 347 EJ) in 1993 (Klass 1998). The United States has considerable reserves of crude oil, but the country is also dependent on oil imports from other countries for meeting the energy requirements. The crude oil price has fluctuated over the past 40 years, the most recent price increase over $130

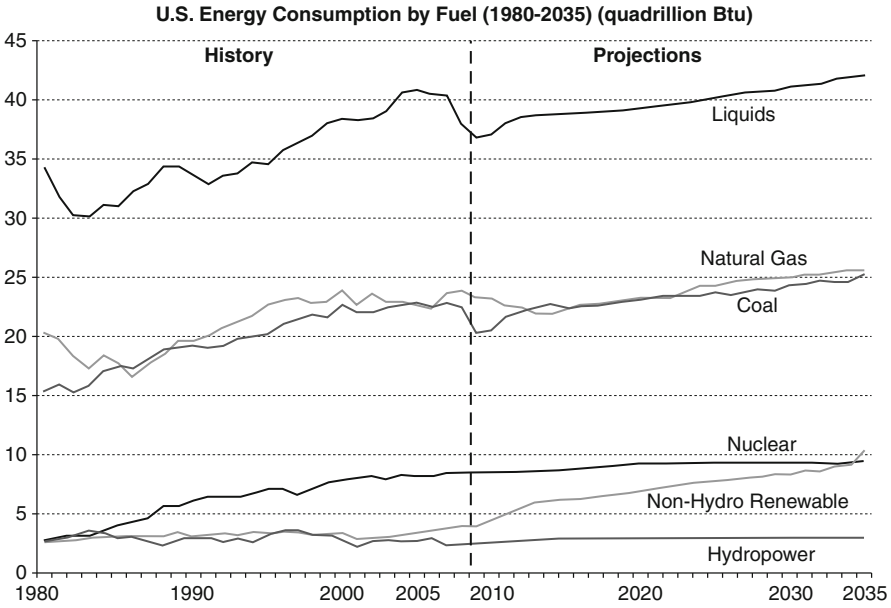

Fig. 1 Energy consumption in the United States, 1980–2035 (EIA 2010)

per barrel being in 2008. The EIA published a projection of the price of crude oil over the next 25 years, where high and a low projections were given in addition to the usual projection of crude oil price, as shown in Fig. 2 (EIA 2010). The projection shows a steady increase in price of crude to above $140 per barrel in 2035. With a high price trend, the crude can cost over $200 per barrel.

The fossil resources are burnt or utilized for energy, fuels, and chemicals. The process for combustion of fossil resources involves the oxidation of carbon and hydrogen atoms to produce carbon dioxide and water vapor and releasing heat from the reactions. Impurities in the resource, such as sulfur, produce sulfur oxides, and incomplete combustion of the resource produces methane. The Intergovernmental Panel on Climate Change identified that changes in atmospheric concentration of greenhouse gases (GHG), aerosols, land cover, and solar radiation alter the energy balance of the climate system (IPCC 2007). These changes are also termed as climate change. The green house gases include carbon dioxide, methane, nitrous oxide, and fluorinated gases. Atmospheric concentrations of carbon dioxide (379 ppm) and methane (1,774 ppb) in 2005 were the highest amounts recorded on the earth (historical values computed from ice cores spanning many thousands of years) till date. The IPCC report states that global increases in CO_2 concentrations are attributed primarily to fossil resource use. In the United States, there was approximately 5,814 million metric tons of carbon dioxide released into the atmosphere in 2008, and this amount is projected to increase to 6,320 million metric tons in 2035 (EIA 2010) as shown in Fig. 3.

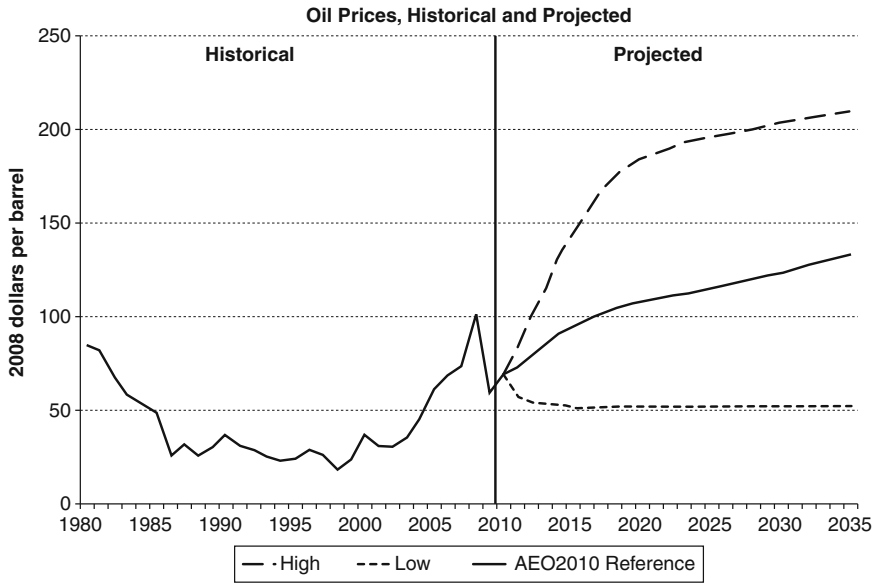

Fig. 2 Oil prices (in 2008 dollars per barrel), historical data, and projected data (Adapted from EIA (2010))

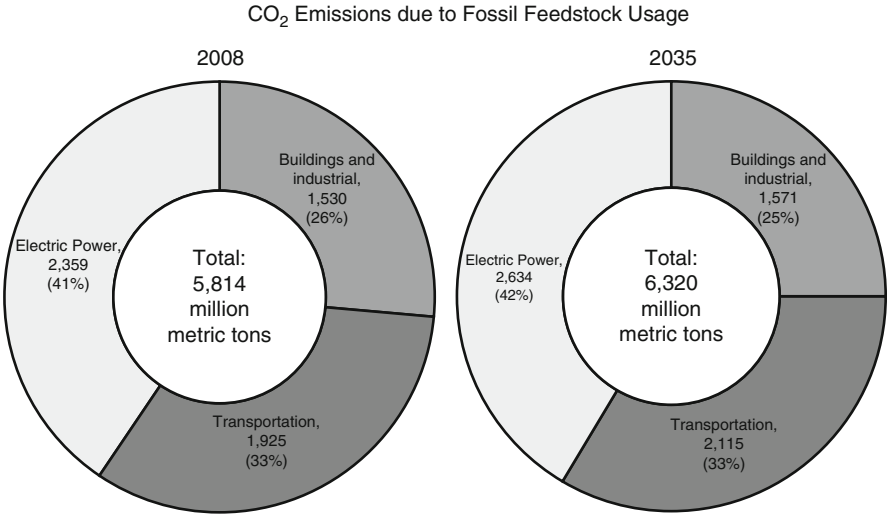

Fig. 3 Carbon dioxide emissions in 2008 (current) and 2035 (projected) due to fossil feedstock usage (Adapted from EIA (2010))

The increasing trends in resource consumption, resource material cost, and consequent increase carbon dioxide emissions from anthropogenic sources indicate that a reduction of fossil feedstock usage is necessary to address climate change.

This has prompted world leaders, organizations, and companies to look for alternative ways to obtain energy, fuels, and chemicals.

Thus, carbon fixed naturally in fossil and nonrenewable resources over millions of years is released to the atmosphere by anthropogenic sources. A relatively faster way to convert the atmospheric carbon dioxide into useful resources is by photosynthetic fixation into biomass. The life cycle of the fossil resources showed that the coal, petroleum, and natural gas all are derivatives of decomposed biomass on the earth's surface trapped in geological formations. Thus, biomass, being a precursor to the conventional nonrenewable resources, can be used as fuel, generate energy, and produce chemicals with some modifications to existing processes.

Biomass can be classified broadly as all the matter on earth's surface of recent biological origin. Biomass includes plant materials such as trees, grasses, agricultural crops, and animal manure. Aquatic plants, such as algae, also undergo photosynthesis and provide good sources for carbohydrates and lipids. Just as petroleum and coal require processing before the use as feedstock for the production of fuels, chemicals, and energy, biomass also requires processing such that the resource potential can be utilized fully. As explained earlier, biomass is a precursor to fossil feedstock, and a comparison between the biomass energy content and fossil feedstock energy content is required. The heating value of fuel is the measure of heat released during the complete combustion of fuel at a given reference temperature and pressure. The higher or gross heating value is the amount of heat released per unit weight of fuel at the reference temperature and pressure, taking into account the latent heat of vaporization of water. The lower or net heating value is the heat released by fuel excluding the latent heat of vaporization of water. The higher heating values of some bioenergy feedstocks, liquid biofuels, and conventional fossil fuels are given in Table 1. It can be seen from the table that the energy content of the raw biomass species is less than bioethanol, and biodiesel compares almost equally to the traditional fossil fuels.

This chapter gives an outline for the use of biomass as feedstock. The following sections will discuss various methods for biomass formation, biomass composition, conversion technologies, and feedstock availability.

Biomass Formation

Biomass is the photosynthetic sink by which atmospheric carbon dioxide and solar energy are fixed into plants (Klass 1998). These plants can be used to convert the stored energy in the form of fuels and chemicals. The primary equation of photosynthesis is given by Eq. 1:

$$6CO_2 + 6H_2O + \text{Light} \rightarrow C_6H_{12}O_6 + 6O_2 \quad (1)$$

The photosynthesis process utilizes inorganic material (carbon dioxide and water) to form organic compounds (hexose) and releases oxygen. The Gibbs free energy change for the process is +470 KJ per mole of CO_2 assimilated, and the

Table 1 Heating value of biomass components (Klass 1998; McGowan 2009)

Component	Heating value (gross) (GJ/MT unless otherwise mentioned)
Bioenergy feedstocks	
Corn stover	17.6
Sweet sorghum	15.4
Sugarcane bagasse	18.1
Sugarcane leaves	17.4
Hardwood	20.5
Softwood	19.6
Hybrid poplar	19.0
Bamboo	18.5–19.4
Switchgrass	18.3
Miscanthus	17.1–19.4
Arundo donax	17.1
Giant brown kelp	10.0 MJ/dry kg
Cattle feedlot manure	13.4 MJ/dry kg
Water hyacinth	16.0 MJ/dry kg
Pure cellulose	17.5 MJ/dry kg
Primary biosolids	19.9 MJ/dry kg
Liquid biofuels	
Bioethanol	28
Biodiesel	40
Fossil fuels	
Coal (low rank; lignite/sub-bituminous)	15–19
Coal (high rank; bituminous/anthracite)	27–30
Oil (typical distillate)	42–45

corresponding enthalpy change is +470 KJ. The positive sign on the energy denotes that energy is absorbed in the process. The initial product for biochemical reactions for photosynthetic assimilation is sugars. Secondary products are derived from key intermediates of the biochemical reactions and include polysaccharides, lipids, and proteins. A wide range of other organic compounds may also be produced in certain biomass species, such as simple low molecular weight organic chemicals (e.g., acids, alcohols, aldehydes, and ethers), complex alkaloids, nucleic acids, pyrroles, steroids, terpenes, waxes, and high molecular weight polymers such as polyisoprenes. A detailed description of how these components are formed from the intermediates is beyond the scope of this chapter. The basic reactions for photosynthesis will be discussed in this section, and the key products will be explained.

Photosynthesis is a two-phase process comprising of the "light reactions" (in the presence of light) and "dark reactions" (in the absence of light). The light reactions capture light energy and convert it to chemical energy and reducing power. In the

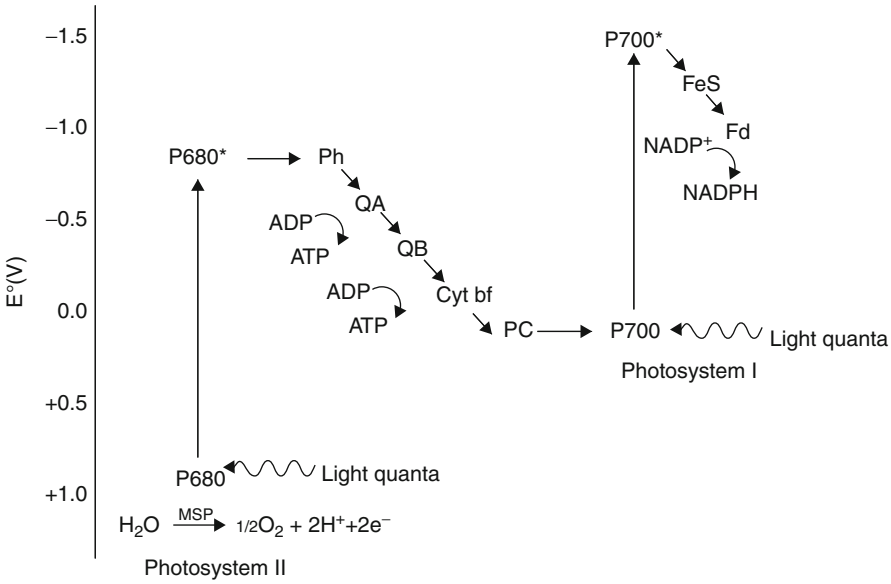

Fig. 4 Z-scheme of biomass photosynthesis P680 and P700 is the chlorophylls of the photosystem II and I, respectively. (*MSP* manganese stabilizing protein, *Ph* pheophytin, *Q* quinone, *Cyt* cytochrome, *PC* plastocyanin, *FeS* nonheme iron-sulfur protein, *Fd* ferredoxin) (Adapted from Drapcho et al. (2008))

dark reactions, chemical energy and the reducing power from light reactions are used to fix atmospheric carbon dioxide.

The light reaction in photosynthesis is explained using the "Z-scheme" diagram as shown in Fig. 4 (Drapcho et al. 2008). Solar energy in the wavelength range of 400–700 nm is captured by chlorophylls within the cells of plants and microorganisms like green algae or cyanobacteria. The flow of electrons is shown in Fig. 4. Two photosystems, photosystem I and photosystem II, are used in the light reactions. All the terms in Fig. 4 are not explained in this text, but the most important intermediates are listed below the figure. In photosystem II (PSII), light energy at 680 nm wavelength is used to split water molecules as shown in Eq. 2:

$$2H_2O \overset{\text{light energy}}{\rightarrow} O_2 + 4H^+4e^- \tag{2}$$

The electrons are accepted by the chlorophyll in PSII and reduce it from a reduction potential of +1 V to approximately −0.8 V. The electrons are then transferred to photosystem I (PSI) through a series of membrane-bound electron carrier molecules. ATP (adenosine triphosphate) is produced as the electrons are transferred due to a proton-motive force that develops as protons are pumped across the thylakoid membrane. Acceptance of the electron reduces the potential of PSI to approximately −1.4 V. The reduction potential of PSI is then sufficient to reduce ferrodoxin, which

in turn reduces NADP+ to NADPH. This NADPH is used to reduce inorganic carbon for new cell synthesis.

Thus, the light reactions are common to all plant types, where eight photons per molecule of carbon dioxide excite chlorophyll to generate ATP (adenosine triphosphate) and NADPH (reduced nicotinamide adenosine dinucleotide phosphate) along with oxygen (Klass 1998). The "Z-scheme" transfers electrons from a low chemical potential in water to a higher chemical potential in NADPH, which is necessary to reduce CO_2.

The ATP and NADPH produced in the light reactions react in the dark to reduce CO_2 and form the organic components in biomass via the dark reactions and regenerate ADP (adenosine diphosphate) and $NADP^+$ (nicotinamide adenosine dinucleotide phosphate) for the light reactions. The biochemical pathways and organic intermediates involved in the reduction of CO_2 to sugars determine the molecular events of biomass growth and differentiate between various kinds of biomass.

In photosynthesis, CO_2 enters the leaves or stems of biomass through stoma, the small intercellular openings in the epidermis. These openings provide main route for photosynthetic gas exchange and water vapor loss in transpiration. The dark reactions can proceed in accordance with at least three different pathways, the Calvin-Benson cycle, the C4 cycle, and the CAM cycle, as discussed in the following sections.

The Calvin-Benson Cycle

The Calvin-Benson cycle is shown in Fig. 5. The overall reaction for the Calvin cycle is given in Eq. 3. Plant biomass species, which use the Calvin-Benson cycle to form products, are called the C3 plants (Klass 1998).

$$6CO_2 + 12\ \ NADPH + 18\ \ ATP \rightarrow C_6H_{12}O_6 + 12NADP^+ + 18\ \ ADP \quad (3)$$

This cycle produces the 3-carbon intermediate 3-phosphoglyceric acid (3-phosphoglycerate) and is common to fruits, legumes, grains, and vegetables. C3 plants usually exhibit low rates of photosynthesis at light saturation, low light saturation points, sensitivity to oxygen concentration, rapid photorespiration, and high CO_2 compensation points. The light saturation point is the light intensity beyond which it is not a limiting factor for photosynthesis. The CO_2 compensation point is the CO_2 concentration in the surrounding environment below which more CO_2 is respired by the plant than is photosynthetically fixed. Typical C3 biomass species are alfalfa, barley, chlorella, cotton, *Eucalyptus*, *Euphorbia lathyris*, oats, peas, potato, rice, soybean, spinach, sugar beet, sunflower, tall fescue, tobacco, and wheat. These plants grow favorably in cooler climates.

The C4 Cycle

The C4 cycle is shown in Fig. 6. In this cycle, CO_2 is initially converted to 4-carbon dicarboxylic acids (malic or aspartic acids) (Klass 1998). Phosphoenolpyruvic acid

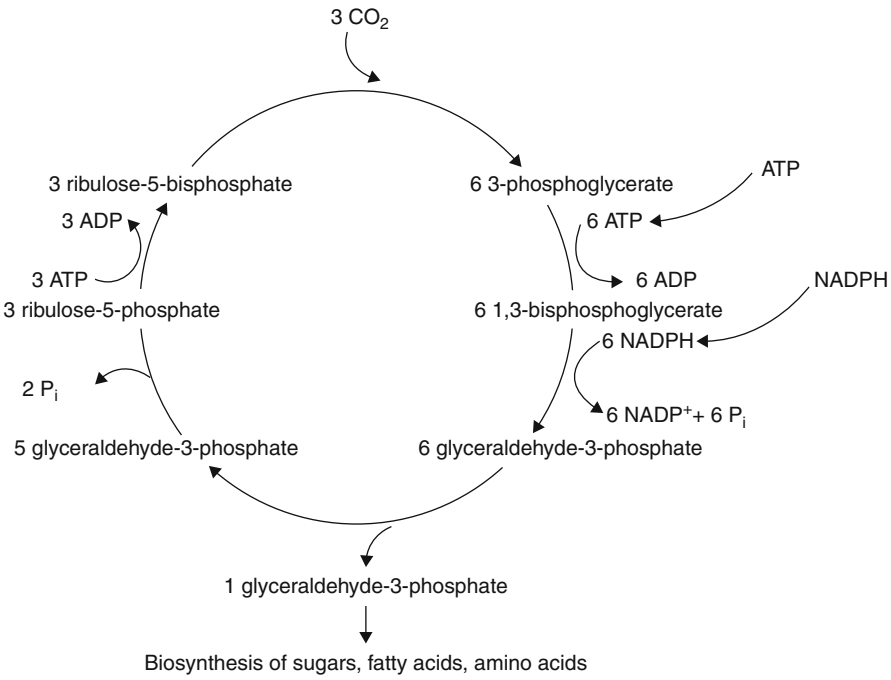

Fig. 5 Calvin-Benson cycle for photosynthesis (Adapted from Drapcho et al. (2008))

reacts with carbon dioxide to form oxaloacetic acid. Malic or aspartic acid is formed from the oxaloacetic acid. The C4 acid is transported to bundle sheath cells where decarboxylation occurs to regenerate pyruvic acid, which is returned to the mesophyll cells to initiate another cycle. The CO_2 liberated in the bundle sheath cells enter the C3 cycle described above, and it is in this C3 cycle where the CO_2 fixation occurs. The subtle difference between the C3 and C4 cycles is believed to be responsible for the wide variations in biomass properties. Compared to C3 biomass, C4 biomass is produced in higher yields with higher rates of photosynthesis, high light saturation points, and low levels of respiration, low carbon dioxide compensation points, and greater efficiency of water usage. Typical C4 biomass includes crops such as sugarcane, corn, and sorghum and tropical grasses like Bermuda grass.

The CAM Cycle

The CAM cycle is the crassulacean acid metabolism cycle, which refers to the capacity of chloroplast containing biomass tissues to fix CO_2 in dark reactions leading to synthesis of free malic acid (Klass 1998). The mechanism involves β-carboxylation of phosphoenolpyruvic acid by phosphoenolpyruvate carboxylase enzyme and the subsequent reduction of oxaloacetic acid by maleate dehydrogenase.

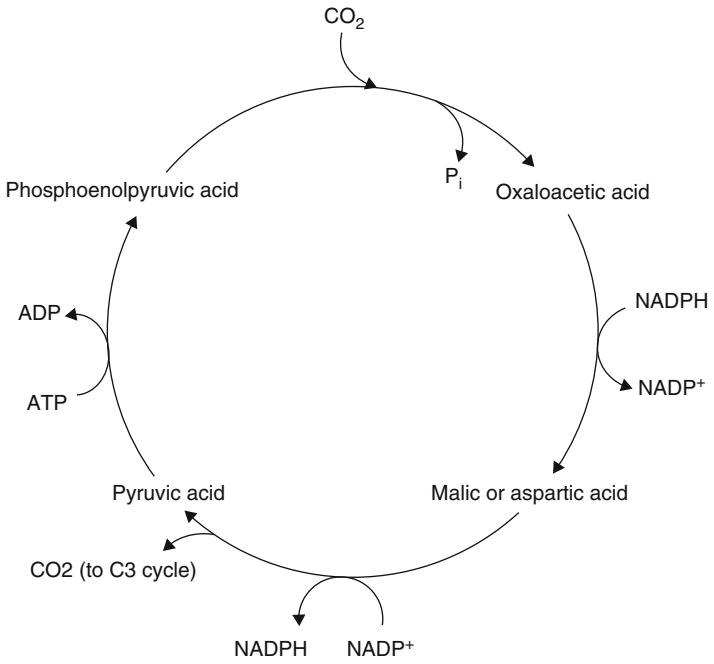

Fig. 6 Biochemical pathway from carbon dioxide to glucose for C4 biomass (Adapted from Klass (1998))

Biomass species in the CAM category are typically adapted to arid environments and have low photosynthesis rates and higher water usage efficiencies. Plants in this category include cactus and succulents like pineapple. The CAM has evolved so that the initial CO_2 fixation can take place in the dark with much less water loss than C3 or C4 pathways. CAM biomass also conserves carbon by recycling endogenously formed CO_2. CAM biomass species have not been exploited commercially for use as biomass feedstock.

Thus, different photosynthetic pathways produce different intermediates leading to different kinds of biomass. The following section discusses the different components in biomass.

Biomass Classification and Composition

The previous section gave the mechanisms for the formation of biomass by photosynthesis. The classification and composition of biomass will be discussed in this section. Biomass can be classified into two major subdivisions, crop biomass and wood (forest) biomass. There are other sources of biomass, like waste from municipal areas and animal wastes, but these can be traced back to the two major sources. Crop biomass primarily includes corn, sugarcane, sorghum, soybeans, wheat, barley,

rice, etc. These contain carbohydrates, glucose, starch, or oils as its primary constituents. Wood biomass is composed of cellulose, hemicellulose, and lignin. Examples of woody biomass include grasses, stalks, stover, etc. Starch and cellulose are both polymeric forms of glucose, a 6-carbon sugar. Hemicellulose is a polymer of xylose. Lignin is composed of phenolic polymers. Oils are composed of triglycerides. Other biomass components, which are generally present in minor amounts, include proteins, sterols, alkaloids, resins, terpenes, terpenoids, and waxes.

Apart from crop and woody biomass, a class of microorganisms exist which are capable of producing biomass. These are single-celled organisms like algae or cyanobacteria and have the capability of photosynthesis to produce oils, carbohydrates, proteins, etc. These are discussed in details in a later section.

The components of biomass are discussed in details below.

Saccharides and Polysaccharides

Saccharides and polysaccharides are hydrocarbons with the basic chemical structure of CH_2O. The hydrocarbons occur in nature as 5-carbon or 6-carbon ring structure. The ring structures may contain only one or two connected rings, which are known as monosaccharides, disaccharides, or simply as sugars, or they may be very long polymer chains of the sugar building blocks.

The simplest six-sided saccharide (hexose) is glucose. Long-chained polymers of glucose or other hexoses are categorized either as starch or cellulose. The characterization is discussed in the following sections. The simplest five-sided sugar (pentose) is xylose. Pentoses form long-chain polymers categorized as hemicellulose. Some of the common 6-carbon and 5-carbon monosaccharides are listed in Table 2.

Starch is a polymer of glucose as the monomeric unit (Paster et al. 2003). It is a mixture of α- amylose and amylopectin as shown in Fig. 7. α-Amylose is a straight chain of glucose molecules joined by α-1,4-glucosidic linkages as shown in Fig. 7a. Amylopectin and amylase are similar except that short chains of glucose molecules branch off from the main chain (backbone) as shown in Fig. 7b. Starches found in nature contain 10–30 % α-amylose and 70–90 % amylopectin. The α-1,4-glycosidic linkages are bent and prevent the formation of sheets and subsequent layering of polymer chains. As a result, starch is soluble in water and relatively easy to break down into utilizable sugar units.

Lignocellulosic Biomass

The non-grain portion of biomass (e.g., cobs, stalks), often referred to as agricultural stover or residues, and energy crops such as switchgrass are known as lignocellulosic biomass resources (also called cellulosic). These are comprised of cellulose, hemicellulose, and lignin (Paster et al. 2003). Generally, lignocellulosic material contains 30–50 % cellulose, 20–30 % hemicellulose, and 20–30 % lignin. Figure 8a illustrates

Table 2 Common 6-carbon and 5-carbon monosaccharides

6-Carbon sugars	Structure	5-Carbon sugars	Structure
D-Fructose	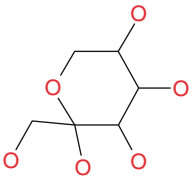	D-Xylose	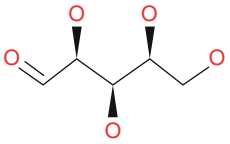
D-Glucose	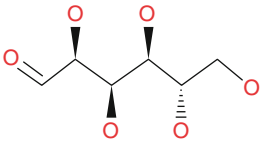	D-Ribulose	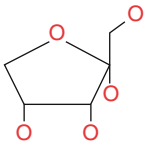
D-Gulose	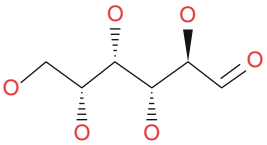	D-Ribose	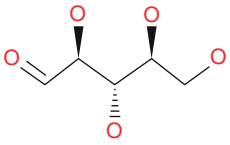
D-Mannose	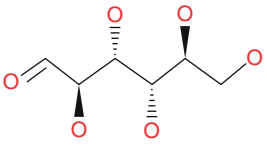	D-Arabinose	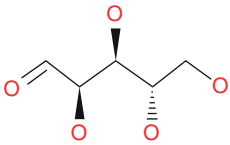
D-Galactose	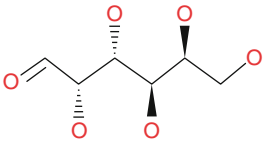		

how cellulose, hemicellulose, and lignin are physically mixed in lignocellulosic biomass. Figure 8b illustrates how pretreatment is necessary to break the polymeric chains before cellulose and hemicellulose can be used for chemical conversions. Some exceptions to this are cotton (98 % cellulose) and flax (80 % cellulose). Lignocellulosic biomass is considered to be an abundant resource for the future bio-industry. Recovering the components in a cost-effective way requires pretreatment processes discussed in a later section.

Cellulose

Cellulosic biomass comprises 35–50 % of most plant material. Cellulose is a polymer of glucose with degree of polymerization of 1,000–10,000 (Paster et al. 2003). Cellulose is a linear unbranched polymer of glucose joined together by $\beta - 1,4$-glycosidic linkages as shown in Fig. 9. Cellulose can either be crystalline or amorphous. Hydrogen bonding between chains leads to chemical stability and insolubility and serves as a structural component in plant walls. The high degree of crystallinity of cellulose makes lignocellulosic materials much more resistant than

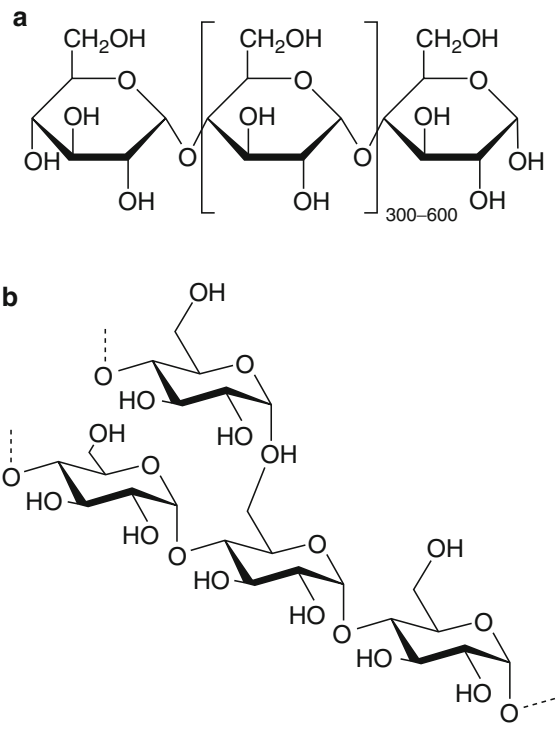

Fig. 7 Structure of starch; (**a**) α-amylose; (**b**) amylopectin

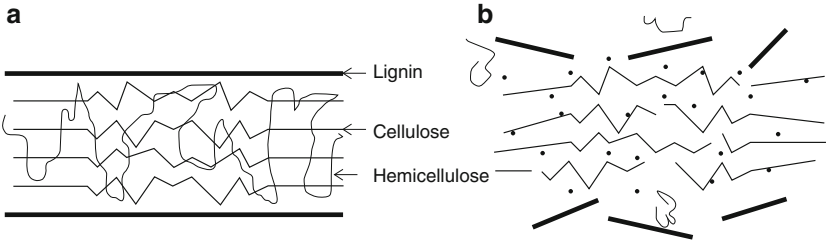

Fig. 8 (**a**) Physical arrangement of lignocellulosic biomass; (**b**) lignocellulosic biomass after pretreatment

starch to acid and enzymatic hydrolysis. As the core structural component of biomass, cellulose is also protected from environmental exposure by a sheath of lignin and hemicellulose. Extracting the sugars of lignocellulosics therefore involves a pretreatment stage to reduce the recalcitrance (resistance) of the biomass to cellulose hydrolysis.

Hemicellulose

Hemicellulose is a polymer containing primarily 5-carbon sugars such as xylose and arabinose with some glucose and mannose dispersed throughout (Paster et al. 2003).

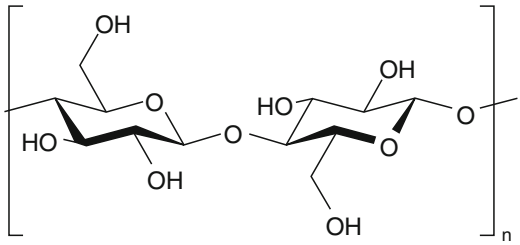

Fig. 9 Structure of cellulose

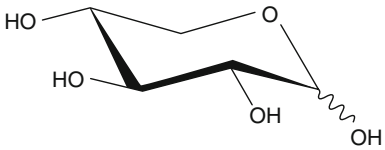

Fig. 10 Structure of xylose, building block of hemicellulose

The structure of xylose is shown in Fig. 10. It forms a short-chain polymer that interacts with cellulose and lignin to form a matrix in the plant wall, thereby strengthening it. Hemicellulose is more easily hydrolyzed than cellulose. Much of the hemicellulose in lignocellulosic materials is solubilized and hydrolyzed to pentose and hexose sugars during the pretreatment stage. Some of the hemicellulose is too intertwined with the lignin to be recoverable.

Lignin

Lignin helps to bind the cellulose/hemicelluloses matrix while adding flexibility to the mixture. The molecular structure of lignin polymers is very random and disorganized and consists primarily of carbon ring structures (benzene rings with methoxyl, hydroxyl, and propyl groups) interconnected by polysaccharides (sugar polymers) as shown in Fig. 11. The ring structures of lignin have great potential as valuable chemical intermediates, mainly aromatic compounds. However, separation and recovery of the lignin is difficult. It is possible to break the lignin-cellulose-hemicellulose matrix and recover the lignin through treatment of the lignocellulosic material with strong sulfuric acid. Lignin is insoluble in sulfuric acid, while cellulose and hemicellulose are solubilized and hydrolyzed by the acid. However, the high acid concentration promotes the formation of degradation products that hinder the downstream utilization of the sugars. Pyrolysis can be used to convert the lignin polymers to valuable products, but separation techniques to recover the individual chemicals are lacking. Instead, the pyrolyzed lignin is fractionated into a bio-oil for fuels and high phenolic content oil which is used as a partial replacement for phenol in phenol-formaldehyde resins.

Lipids, Fats, and Oils

Oils can be obtained from oilseeds like soybean, canola, etc. Vegetable oils are composed primarily of triglycerides, also referred to as triacylglycerols.

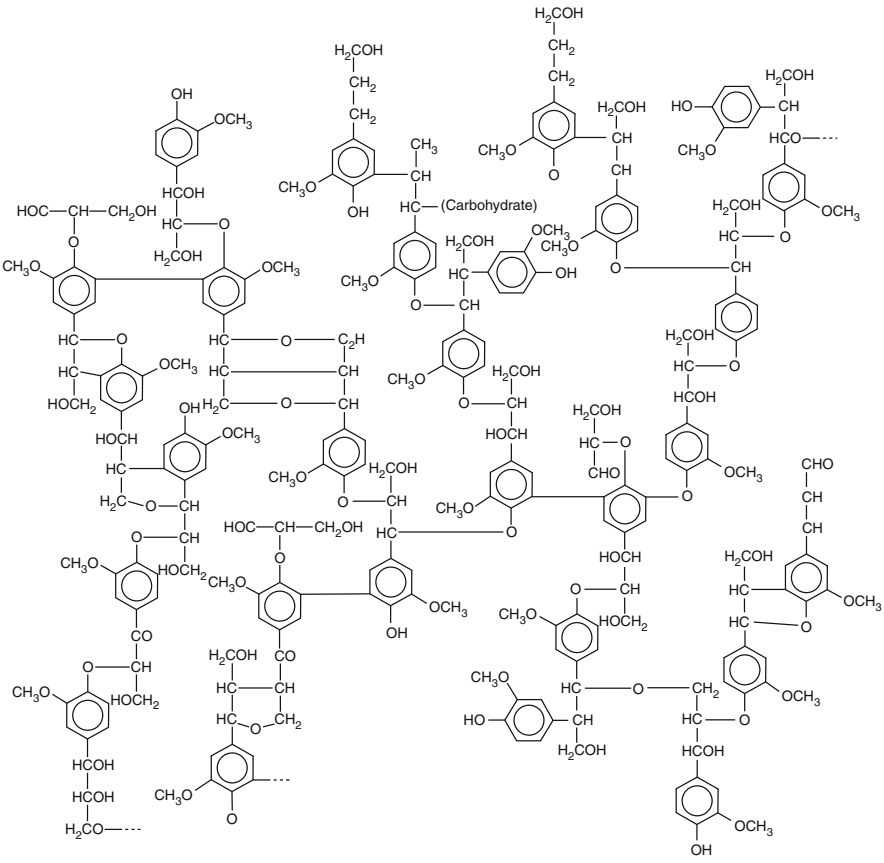

Fig. 11 Structure of lignin (Glazer and Nikaido 1995)

Triglycerides contain a glycerol molecule as the backbone with three fatty acids attached to glycerol's hydroxyl groups. The structure of a triglyceride is shown in Fig. 12 with linoleic acid as the fatty acid chain. In this example, the three fatty acids are all linoleic acid, but triglycerides could be a mixture of two or more fatty acids. Fatty acids differ in chain length and degree of condensation. The fatty acid profile and the double bonds present determine the property of the oil. These can be manipulated to obtain certain performance characteristics. In general, the greater the number of double bonds, the lower the melting point of the oil.

Proteins

Proteins are polymers composed of natural amino acids, bonded together through peptide linkages (Klass 1998). They are formed via condensation of the acids through the amino and carboxyl groups by removal of water to form polyamides.

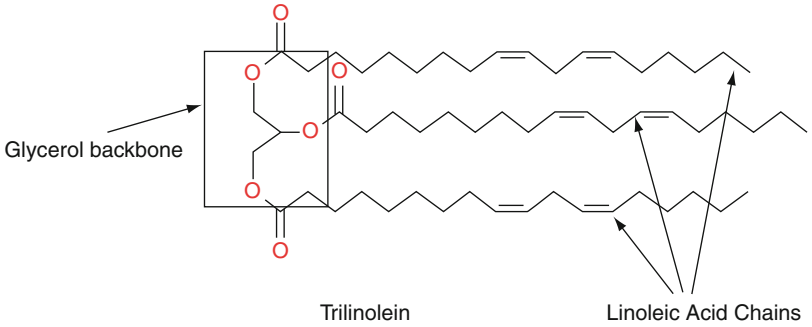

Fig. 12 Formation of triglycerides (linoleic acid as representative fatty acid chain)

Table 3 Amino acid groups present in proteins

Family	Amino acids
Glutamate	Glutamine, arginine, proline
Aspartate	Asparagine, methionine, threonine, isoleucine, lysine
Aromatic	Tryptophan, phenylalanine, tyrosine
Serine	Glycine, cysteine
Pyruvate	Alanine, valine, leucine

Proteins are present in various kinds of biomass as well as animals. The concentration of proteins may approach zero in different biomass systems, but the importance of proteins arises while considering enzyme catalysis that promotes the various biochemical reactions. The apparent precursors of the proteins are amino acids in which an amino group, or imino group in a few cases, is bonded to the carbon atom adjacent to the carboxyl group. Many amino acids have been isolated from natural sources, but only about 20 of them are used for protein biosynthesis. These amino acids are divided into five families: glutamate, aspartate, aromatic, serine, and pyruvate. The various amino acids under these groups are shown in Table 3.

Table 4 gives the composition of some biomass species based on the above components. The biomass types are marine, fresh water, herbaceous, woody, and waste biomass, and a representative composition is given in the table. Other components not included in the composition are ash and crude protein.

Biomass Conversion Technologies

The conversion of biomass involves the treatment of biomass so that the solar energy stored in the form of chemical energy in the biomass molecules can be utilized. Common biomass conversion routes begin with pretreatment in case of cellulosic and grain biomass and extraction of oil in case of oilseeds. Then the cellulosic or starch containing biomass undergoes fermentation (anaerobic or aerobic),

Table 4 Component composition of biomass feedstocks (Klass 1998; McGowan 2009)

Name	Celluloses (dry wt %)	Hemicelluloses (dry wt %)	Lignins (dry wt %)
Corn stover	35	28	16–21
Sweet sorghum	27	25	11
Sugarcane bagasse	32–48	19–24	23–32
Hardwood	45	30	20
Softwood	42	21	26
Hybrid poplar	42–56	18–25	21–23
Bamboo	41–49	24–28	24–26
Switchgrass	44–51	42–50	13–20
Miscanthus	44	24	17
Arundo donax	31	30	21
RDF (refuse-derived fuel)	65.6	11.2	3.1
Water hyacinth	16.2	55.5	6.1
Bermuda grass	31.7	40.2	25.6
Pine	40.4	24.9	34.5

gasification, or pyrolysis. The oil in oilseeds is transesterified to get desired product. There are other process technologies including hydroformylation, metathesis, and epoxidation, related with direct conversion of oils to fuels and chemicals, the details of which are not included in this chapter.

Biomass Pretreatment

Biomass is composed of components such as starch, sugars, cellulose, hemicellulose, lignin, fats, oils, etc., as described in the previous section. Often two or more of these components are physically mixed with each other, and a pretreatment is necessary before the chemical energy in biomass molecules can be utilized in a useful way. For example, lignocellulosic biomass is composed of cellulose, hemicelluloses, and lignin. The cellulose and hemicelluloses are polysaccharides of hexose and pentose. Any process that uses biomass needs to be pretreated so that the cellulose and hemicellulose in the biomass are broken down to their monomeric form. Pretreatment processes produce a solid pretreated biomass residue that is more amenable to enzymatic hydrolysis by cellulases and related enzymes than native biomass. Biocatalysts like yeasts and bacteria can act only on the monomers and ferment them to alcohols, lactic acid, etc. The pretreatment process also removes the lignin in biomass which is not acted upon by enzymes or fermented further.

Pretreatment usually begins with a physical reduction in the size of plant material by milling, crushing, and chopping (Teter et al. 2006). Some of the equipment used in the industry for size reduction include rotary breaker, roll crusher, hammer mill,

impactor, tumbling mill, and roller mill. The size of biomass particles needs to be reduced to nominal size of 1–6 mm (Womac et al. 2007). For example, in the processing of sugarcane, the cane is first cut into segments and then fed into consecutive rollers to extract cane juice rich in sucrose and physically crush the cane, producing a fibrous bagasse having the consistency of sawdust. In the case of corn stover processing, the stover is chopped with knives or ball milled to increase the exposed surface area and improve wettability. Corn is hammer milled to flour before it is transferred to cook tanks.

The physical reduction in size enables a wider surface area to come in contact for further chemical conversions. However, physical size reduction is an energy-intensive process, and an optimum size reduction is required to balance energy consumption and conversion efficiency. For example, recent research in corn fermentation using finer ground corn enables the liquefaction to be conducted at lower temperatures, and this process is known as cold starch hydrolysis.

After the physical disruption process, the biomass may be chemically treated to remove lignin. This is shown in Fig. 8b. Lignin forms a coating on the cellulose microfibrils in untreated biomass, thus making the cellulose unavailable for enzyme or acid hydrolysis. Lignin also absorbs some of the expensive cellulose-active enzymes.

The following chemical pretreatment processes are employed for biomass conversion.

Hot wash pretreatment: This pretreatment concept was developed at the National Renewable Energy Laboratory and uses hot water or hot dilute acids at temperatures above 135 °C to wash out the solubilized lignin and hemicellulosic sugars (Tucker et al. 2011). The hot wash pretreatment process involves the passage of hot water through heated stationary biomass and is responsible for solubilization of the hemicellulose fraction (Teter et al. 2006). The hemicellulose is converted to pentose oligomers by this process which needs to be further converted to respective monosaccharides before fermentation. The performance of this pretreatment process depends on temperature and flow rate, requiring about 8–16 min. About 46 % of lignin is removed at high rates and temperatures. The hydrothermal process does not require acid resistant material for the reactors, but water use and recovery costs are disadvantages to the process.

Acid hydrolysis: Hydrolysis is a chemical reaction or process where a chemical compound reacts with water. The process is used to break complex polymer structures into its component monomers. The process can be used for the hydrolysis of polysaccharides like cellulose and hemicelluloses (Katzen and Schell 2006). When hydrolysis is catalyzed by the presence of acids like sulfuric, hydrochloric, nitric, or hydrofluoric acids, the process is called acid hydrolysis. The reactions for hydrolysis can be expressed as in reaction given by Eqs. 4 and 5:

$$\text{Cellulose (Glucan)} \rightarrow \text{Glucose} \rightarrow 5-\text{Hydroxymethylfurfural} \rightarrow \text{Tars} \quad (4)$$

$$\text{Hemicellulose (Xylan)} \rightarrow \text{Xylose} \rightarrow \text{Furfural} \rightarrow \text{Tars} \quad (5)$$

The desired products of hydrolysis are the glucose and xylose. Under severe conditions of high temperature and acid concentrations, the product tends to form hydroxymethylfurfural, furfural, and the tars.

Dilute sulfuric acid is inexpensive in comparison to the other acids. It has also been studied and the chemistry well known for acid conversion processes (Katzen and Schell 2006). Biomass is mixed with a dilute sulfuric acid solution and treated with steam at temperatures ranging from 140 °C to 260 °C. Xylan is rapidly hydrolyzed in the process to xylose at low temperatures of 140–180 °C. At higher temperatures, cellulose is depolymerized to glucose, but the xylan is converted to furfural and tars. The pretreatment conditions used in lignocellulosic biomass (corn stover) feedstock-based ethanol process by (Aden et al. 2002) were acid concentration of 1.1 %, residence time of 2 min, temperature maintained at 190 °C, and a pressure of 12.1 atm.

Concentrated acids at low temperatures (100–120 °C) are used to hydrolyze cellulose and hemicelluloses to sugars (Katzen and Schell 2006). Higher yields of sugars are obtained in this case with lower conversion to tars. The viability of this process depends on low-cost recovery of expensive acid catalysts.

Enzymatic hydrolysis: Acid hydrolysis explained in the previous section has a major disadvantage where the sugars are converted to degradation products like tars. This degradation can be prevented by using enzymes favoring 100 % selective conversion of cellulose to glucose. When hydrolysis is catalyzed by such enzymes, the process is known as enzymatic hydrolysis (Katzen and Schell 2006). The temperature and pressure for enzymatic hydrolysis depend on the particular enzyme and its tolerance to a particular temperature. A detailed discussion of the particular temperatures for enzymes is beyond the scope of this chapter.

Enzymatic hydrolysis is carried out by microorganisms like bacteria, fungi, protozoa, insects, etc. (Teter et al. 2006). Advancement of gene sequencing in microorganisms has made it possible to identify the enzymes present in them which are responsible for the biomass degradation. Bacteria like *Clostridium thermocellum*, *Cytophaga hutchinsonii*, *Rubrobacter xylanophilus*, etc., and fungi like *Trichoderma reesei* and *Phanerochaete chrysosporium* have revealed enzymes responsible for carbohydrate degradation.

Based on their target material, enzymes are grouped into the following classifications (Teter et al. 2006). Glucanases or cellulases are the enzymes that participate in the hydrolysis of cellulose to glucose. Hemicellulases are responsible for the degradation of hemicelluloses. Some cellulases have significant xylanase or xyloglucanase side activity which makes it possible for use in degrading both cellulose and hemicelluloses.

Ammonia fiber explosion: This process uses ammonia mixed with biomass in a 1:1 ratio under high pressure (21 atm) at temperatures of 60–110 °C for 5–15 min, and then there is explosive pressure release. This process, also referred to as the AFEX process, improves saccharification rates of various herbaceous crops and grasses. The pretreatment does not significantly solubilize hemicellulose compared to acid pretreatment. The conversions achieved depend on the composition of

feedstock, e.g., over 90 % hydrolysis of cellulose and hemicellulose was obtained after AFEX pretreatment of Bermuda grass (Sun and Cheng 2002). The volatility of ammonia makes it easy to recycle the gas (Teter et al. 2006).

Fermentation

The pretreatment of biomass is followed by the fermentation process where pretreated biomass containing 5-carbon and 6-carbon sugars is catalyzed with biocatalysts to produce desired products. Fermentation refers to enzyme catalyzed, energy yielding chemical reactions that occur during the breakdown of complex organic substrates in presence of microorganisms (Klass 1998). The microorganisms used for fermentation can be yeast or bacteria. The microorganisms feed on the sucrose or glucose released after pretreatment and converts them to alcohol and carbon dioxide. The simplest reaction for the conversion of glucose by fermentation is given in Eq. 6:

$$C_6H_{12}O_6 \rightarrow 2C_2H_5OH + 2CO_2 \tag{6}$$

An enzyme catalyst is highly specific, catalyzes only one or a small number of reactions, and a small amount of enzyme is required. Enzymes are usually proteins of high molecular weight (15,000 < MW < several million Daltons) produced by living cells. The catalytic ability is due to the particular protein structure, and a specific chemical reaction is catalyzed at a small portion of the surface of an enzyme, called an active site (Klass 1998). Enzymes have been used since early human history without knowing how they worked. Enzymes have been used commercially since the 1890s when fungal cell extracts were used to convert starch to sugar in brewing vats.

Microbial enzymes include cellulase, hemicellulase, catalase, streptokinase, amylase, protease, clipase, pectinase, glucose isomerase, lactase, etc. The type of enzyme selection determines the end product of fermentation.

The growth of the microbes requires a carbon source (glucose, xylose, glycerol, starch, lactose, hydrocarbons, etc.) and a nitrogen source (protein, ammonia, corn steep liquor, diammonium phosphate, etc.). Many organic chemicals like ethanol, succinic acid, itaconic acid, lactic acid, etc., can be manufactured using live organisms which have the required enzymes for converting the biomass. Ethanol is produced by the bacteria *Zymomonas mobilis* or yeast *Saccharomyces cerevisiae*. Succinic acid is produced in high concentrations by *Actinobacillus succinogenes* obtained from rumen ecosystem (Lucia et al. 2007). Other microorganisms capable of producing succinic acid include propionate producing bacteria of the *Propionibacterium* genus, gastrointestinal bacteria such as *Escherichia coli*, and rumen bacteria such as *Ruminococcus flavefaciens*. Lactic acid is produced by a class of bacteria known as lactic acid bacteria (LAB) including the genera *Lactobacillus*, *Lactococcus*, *Leuconostoc*, *Enterococcus*, etc. (Axelsson 2004).

Commercial processes for corn wet milling and dry milling operations and the fermentation process for lignocellulosic biomass through acid hydrolysis and enzymatic hydrolysis are discussed in details in chapter "► Chemicals from Biomass."

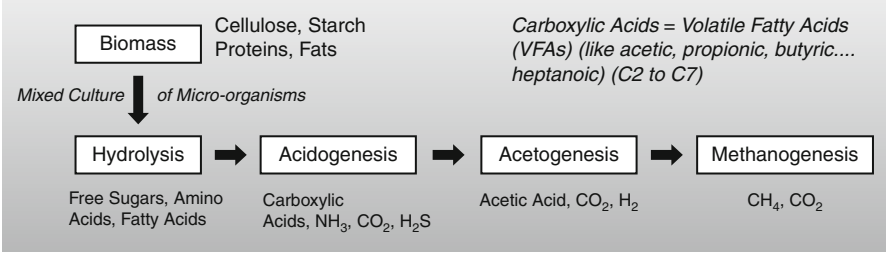

Fig. 13 Anaerobic digestion process

Anaerobic Digestion

Anaerobic digestion of biomass is the treatment of biomass with a mixed culture of bacteria to produce methane (biogas) as a primary product. The four stages of anaerobic digestion are hydrolysis, acidogenesis, acetogenesis, and methanogenesis as shown in Fig. 13.

In the first stage, hydrolysis, complex organic molecules are broken down into simple sugars, amino acids, and fatty acids with the addition of hydroxyl groups. In the second stage, acidogenesis, volatile fatty acids (e.g., acetic, propionic, butyric, valeric) are formed along with ammonia, carbon dioxide, and hydrogen sulfide. In the third stage, acetogenesis, simple molecules from acidogenesis are further digested to produce carbon dioxide, hydrogen, and organic acids, mainly acetic acid. Then in the fourth stage, methanogenesis, the organic acids are converted to methane, carbon dioxide, and water.

Anaerobic digestion can be conducted either wet or dry where dry digestion has a solid content of 30 % or greater, and wet digestion has a solid content of 15 % or less. Either batch or continuous digester operations can be used. In continuous operations, there is a constant production of biogas; while batch operations can be considered simpler, the production of biogas varies.

The standard process for anaerobic digestion of cellulose waste to biogas (65 % methane-35 % carbon dioxide) uses a mixed culture of mesophilic or thermophilic bacteria (Kebanli 1981). Mixed cultures of mesophilic bacteria function best at 37–41 °C, and thermophilic cultures function best at 50–52 °C for the production of biogas. Biogas also contains small amount hydrogen and a trace of hydrogen sulfide, and it is usually used to produce electricity. There are two by-products of anaerobic digestion: acidogenic digestate and methanogenic digestate. Acidogenic digestate is a stable organic material comprised largely of lignin and chitin resembling domestic compost, and it can be used as compost or to make low-grade building products such as fiberboard. Methanogenic digestate is a nutrient-rich liquid, and it can be used as a fertilizer but may include low levels of toxic heavy metals or synthetic organic materials such as pesticides or PCBs depending on the source of the biofeedstock undergoing anaerobic digestion.

Kebanli et al. (1981) give a detailed process design along with pilot unit data for converting animal waste to fuel gas which is used for power generation. A first-order

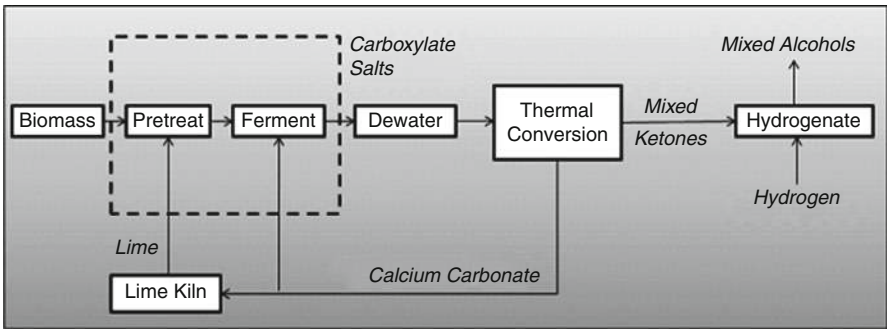

Fig. 14 Flow diagram for the MixAlco process using anaerobic digestion (Granda 2007)

rate constant, 0.011 ± 0.003 per day, was measured for the conversion of volatile solids to biogas from dairy farm waste. In a biofeedstock, the total solids are the sum of the suspended and dissolved solids, and the total solids are composed of volatile and fixed solids. In general, the residence time for an anaerobic digester varies with the amount of feed material, type of material, and the temperature. Resident time of 15–30 days is typical for mesophilic digestion, and residence time for thermophilic digestion is about one-half of that for mesophilic digestion. The digestion of the organic material involves mixed culture of naturally occurring bacteria, each performs a different function. Maintaining anaerobic conditions and a constant temperature is essential for the viability of the bacterial culture.

Holtzapple et al. (1999) describe a modification of the anaerobic digestion process, the MixAlco process, where a wide array of biodegradable material is converted to mixed alcohols. Thanakoses et al. (2003) describe the process of converting corn stover and pig manure to the third stage of carboxylic acid formation. In the MixAlco process, the fourth stage in anaerobic digestion of the conversion of the organic acids to methane, carbon dioxide, and water is inhibited using iodoform (CHI_3) and bromoform ($CHBr_3$). Biofeedstocks to this process can include urban wastes, such as municipal solid waste and sewage sludge, and agricultural residues, such as corn stover and bagasse. Products include carboxylic acids (e.g., acetic, propionic, butyric acid), ketones (e.g., acetone, methyl ethyl ketone, diethyl ketone), and biofuels (e.g., ethanol, propanol, butanol). The process uses a mixed culture of naturally occurring microorganisms found in natural habitats such as the rumen of cattle to anaerobically digest biomass into a mixture of carboxylic acids produced during the acidogenic and acetogenic stages of anaerobic digestion. The fermentation conditions of the MixAlco Process make it a viable process, since the fermentation involves mixed culture of bacteria obtained from animal rumen, which is available at lower cost compared to genetically modified organisms and sterile conditions required by other fermentation processes.

The MixAlco process is outlined in Fig. 14 where biomass is pretreated with lime to remove lignin. Calcium carbonate is also added to the pretreatment process. The resultant mixture containing hemicellulose and cellulose is fermented using a mixed

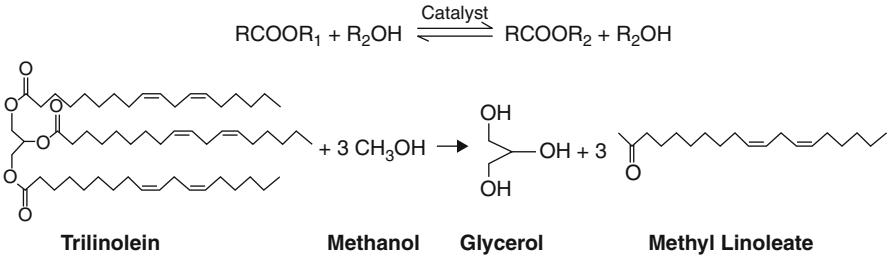

Fig. 15 General transesterification reaction with an example for $RCOOR_1$ as trilinolein and R_2OH as methanol

Table 5 Carboxylic acid products at different culture temperatures (Granda 2007)

Acid	40 °C	55 °C
C2 – Acetic	41 wt%	80 wt%
C3 – Propionic	15 wt%	4 wt%
C4 – Butyric	21 wt%	15 wt%
C5 – Valeric	8 wt%	<1 wt%
C6 – Caproic	12 wt%	<1 wt%
C7 – Heptanoic	3 wt%	<1 wt%
	100 wt%	100 wt%

culture of bacteria obtained from cattle rumen. This process produces a mixture of carboxylate salts which is then fermented. Carboxylic acids are naturally formed in the following places: animal rumen, anaerobic sewage digesters, swamps, termite guts, etc. The same microorganisms are used for the anaerobic digestion process, and the acid products at different culture temperatures are given in Table 5.

The MixAlco process proceeds to form carboxylate salts with the calcium carbonate. Dewatering process removes water. Then the carboxylate salts are thermally decomposed to mixed ketones like acetone, diethyl ketone, and dipropyl ketones. The mixed ketones can then be converted to ethanol by hydrogenation using Raney nickel catalyst at a temperature of 130 °C and pressure of 12 atm in a stirred tank reactor for 35 min.

Transesterification

In biomass conversion processes, transesterification refers to the reaction of an alcohol with natural oil containing triglycerides to produce monoalkyl esters and glycerol (Meher et al. 2006). The glycerol layer settles down at the bottom of the reaction vessel. Diglycerides and monoglycerides are the intermediates in this process. Figure 15 shows the general reaction for transesterification with an example for trilinolein as the representative triglyceride and methanol as the representative alcohol.

A wide variety of vegetable oils and natural oils can be used for transesterification. Table 6 gives a list of oils that can be used with their respective constituent fatty acid content. Linoleic acid and oleic acid are the main constituents for soybean oil. Algae oil composition varies according to the species of algae chosen and is discussed in a later section on algae. The alcohols that can be used for transesterification depend on the type of esters desired. Methanol (CH_3OH) gives methyl esters, and ethanol (C_2H_5OH) produces ethyl esters.

The catalyst used for transesterification may be an acid, a base, or a lipase. The commonly used catalysts are given in Table 7 along with their advantages and disadvantages (Meher et al. 2006; Fukuda et al. 2001; Ma and Hanna 1999).

The mechanism of alkali-catalyzed transesterification is described in Fig. 16. The first step involves the attack of the alkoxide ion to the carbonyl carbon of the triglyceride molecule, which results in the formation of a tetrahedral intermediate. The reaction of this intermediate with an alcohol produces the alkoxide ion in the second step. In the last step the rearrangement of the tetrahedral intermediate gives rise to an ester and a diglyceride.

The mechanism of acid-catalyzed transesterification of vegetable oil (for a monoglyceride) is shown in Fig. 17. It can be extended to di- and triglycerides. The protonation of carbonyl group of the ester leads to the carbocation, which after a nucleophilic attack of the alcohol produces a tetrahedral intermediate. This intermediate eliminates glycerol to form a new ester and to regenerate the catalyst.

Both the triglycerides in vegetable oil and methyl esters from the transesterification of vegetable oils can be used as monomers to form resins, foams, thermoplastics, and oleic methyl ester (Wool and Sun 2005). A thermosetting polymer is formed by the polymerization of triglycerides with styrene using a free radical initiator, and curing for 4 h at 100 °C that has very good tensile strength, rigidity, and toughness properties. Lignin can enhance toughness, and it can be molded to a material with an excellent ballistic impact resistance. Triglycerides can be functionalized to acrylated, epoxidized soybean oil that can be used for structural foam that has biocompatibility properties. Methyl esters can be functionalized to epoxidized oleic methyl ester and acrylated oleic methyl ester which can be polymerized with comonomers methyl methacrylate and butyl acrylate to form oleic methyl ester. A monolithic hurricane-resistant roof has been designed using these materials.

The methyl esters formed from transesterification from vegetable oil can be used as diesel in diesel engines, and this is referred to as biodiesel. Haas et al. (2006) describe an industrial-scale transesterification process for the production of biodiesel from the transesterification of soybean oil. Figure 18 gives a schematic overview of the process model. A two-reactor model was designed with crude degummed soybean oil as feedstock with phospholipid content of less than 50 ppm and negligible fatty acids, sodium methoxide catalyst, and methanol as the alcohol. The design contained three sections, a transesterification section, a purification section, and a glycerol recovery section. The transesterification section consisted of two sequential reactors. The purification section had a centrifugation column which separated esters from the aqueous phase. The glycerol recovery and purification section also consisted of a centrifugal reactor and subsequent distillation and

Table 6 Fatty acid compositions of common oils (percentages)

Fatty acid	Soybean (Meher et al. 2006)	Cottonseed (Meher et al. 2006)	Palm (Meher et al. 2006)	Lard (Meher et al. 2006)	Tallow (Meher et al. 2006)	Coconut (Meher et al. 2006)	Sunflower (Zamora 2005)
Lauric	0.1	0.1	0.1	0.1	0.1	46.5	–
Myristic	0.1	0.7	1	1.4	2.8	19.2	–
Palmitic	10.2	20.1	42.8	23.6	23.3	9.8	7
Stearic	3.7	2.6	4.5	14.2	19.4	3	5
Oleic	22.8	19.2	40.5	44.2	42.4	6.9	19
Linoleic	53.7	55.2	10.1	10.7	2.9	2.2	68
Linolenic	8.6	0.6	0.2	0.4	0.9	0	1

Table 7 Commonly used catalysts in transesterification and their advantages and disadvantages (Meher et al. 2006; Fukuda et al. 2001; Ma and Hanna 1999)

Type	Commonly used compounds/ enzymes	Advantages	Disadvantages
Alkali catalysts	NaOH, KOH, $NaOCH_3$,$KOCH_3$ (other alkoxides are also used)	1. Faster than acid-catalyzed transesterification	1. Ineffective for high free fatty acid content and for high water content (problems of saponification) 2. Energy intensive 3. Recovery of glycerol difficult 4. Alkaline wastewater requires treatment
Acid catalysts	HCl, H_2SO_4, H_3PO_4, sulfonic acid	1. Good for processes with high water content and free fatty acids	1. Slow process compared to alkali (alkoxides) 2. Required after treatment of triglycerides with alkoxides formed for purification purposes
Enzyme/ lipase/ heterogeneous catalysts	*M. miehi*, *C. antarctica*, *P. cepacia*, *C. rugosa*, *P. fluorescens*	1. Possibility of regeneration and reuse of the immobilized residue 2. Free fatty acids can be completely converted to alkyl esters 3. Higher thermal stability of the enzyme due to the native state 4. Immobilization of lipase allows dispersed catalyst, reducing catalyst agglomeration 5. Separation of product and glycerol is easier using this catalyst	1. Some initial activity can be lost due to volume of the oil molecules 2. Number of support enzyme is not uniform 3. Biocatalyst is more expensive that the natural enzyme

evaporation columns for 80 % (w/w) glycerol as a by-product. The cost analysis of the overall process was done with a depreciable life of 10 years and an escalation rate of 1 %. Annual production capacity for the methyl ester plant was set at 10×10^6 gal. With a feedstock cost of $0.236/lb of soybean oil, a production cost of $2.00/gal of methyl ester was achieved.

Gasification/Pyrolysis

Thermal conversion processes such as gasification can be used to convert biomass to synthesis gas, a mixture of carbon monoxide and hydrogen. The products and yields

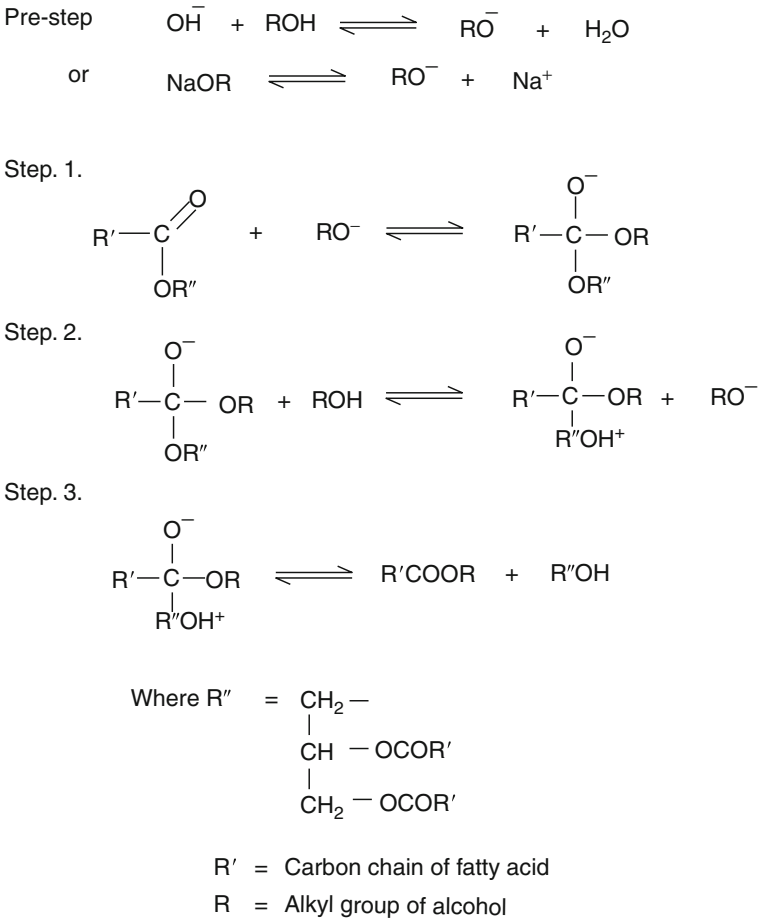

Fig. 16 Mechanism of alkali-catalyzed transesterification (Adapted from Meher et al. (2006))

depend on feed composition, dimension of feed particles, heating rate, temperature, and reaction time (Klass 1998). A detailed discussion for gasification is included in a later chapter.

In biomass gasification, steam and oxygen are used to produce synthesis gas where the amount of steam and oxygen are controlled to produce carbon monoxide and hydrogen with a minimum amount of carbon dioxide and other products. Synthesis gas is a 1:1 mixture of carbon monoxide and hydrogen. In the 1800s coal gasification was used to provide syngas used for lighting and heating. At the beginning of the twentieth century, syngas was used to produce fuels and chemicals. Many of the syngas conversion processes were developed in Germany during the First and Second World Wars at a time when natural resources were becoming scarce for the country and alternative routes for hydrogen production, ammonia synthesis,

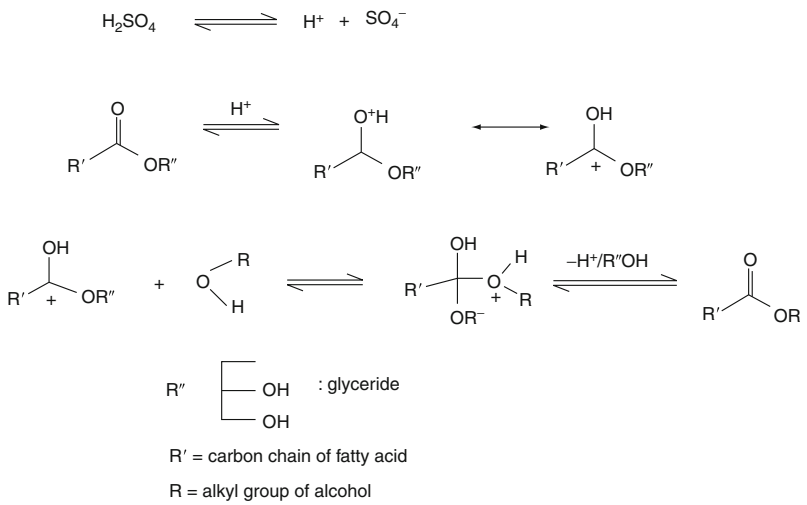

Fig. 17 Mechanism of acid-catalyzed transesterification (Adapted from Meher et al. (2006))

and transportation fuels were a necessity. With the development of the petroleum industry in the 1940s and beyond, the economics of many of these syngas routes became unfavorable and was replaced by petroleum-based processes. The Fischer-Tropsch synthesis reactions for the catalytic conversion of a mixture of carbon monoxide and hydrogen into liquid alcohol fuels was one such process developed in Germany.

The United States has the highest proven reserves of coal among all its natural resources. Coal co-fired with biomass and complete biomass gasification processes are alternatives that are being considered for the production of syngas for fuels and chemicals. The US DOE multiyear program plan for 2010 outlines the fuels, energy, and chemicals that can be produced from the thermochemical routes for biomass processing (DOE 2010b; Spath and Dayton 2003). Biomass gasification technologies are similar to coal gasification and both produce similar product gases. However, biomass contains more volatile matter, gasification occurs at lower temperatures and pressures than coal, and pyrolytic chars are more reactive than coal products. The increase in pressure lowers equilibrium concentrations for hydrogen and carbon monoxide and increases the carbon dioxide and methane concentrations. Biomass contains oxygen in cellulose and hemicellulose which makes them more reactive than oxygen deficient coal. Volatile matter in biomass is about 70–90 % in wood as compared to 30–45 % in coal.

There are three types of biomass gasification processes – pyrolysis, partial oxidation, and reforming. Pyrolysis, as explained before, is the combustion of biomass in absence of oxygen. Partial oxidation is the process where less than stoichiometric quantity required for complete combustion is used, and partially oxidized products are formed. Steam reforming process involves the reaction of biomass with steam.

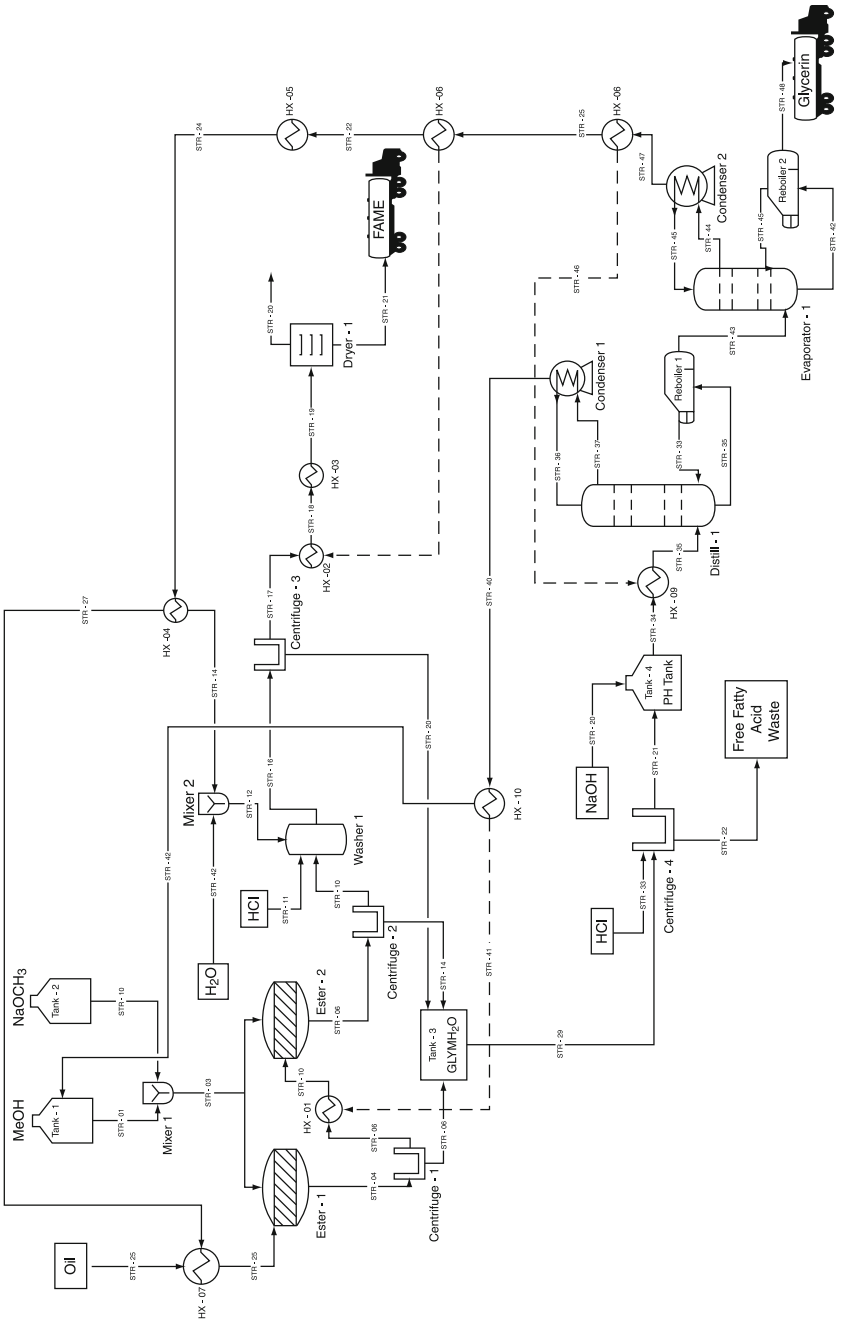

Fig. 18 A process model for the production of biodiesel and glycerol (Adapted from Haas et al. (2006))

The energy content of product gases from biomass gasification can be varied. Low-energy content gases (100–300 BTU/scf) are formed when there is direct contact of biomass feedstock with air (Klass 1998). Dilution of product gases with nitrogen occurs during the gasification process. Medium-energy gases (300–700 BTU/scf) are obtained from directly heated biomass gasifiers when oxygen is used and from indirectly heated biomass gasifiers when air is used, and heat transfer occurs via inert solid medium. High-energy product gases (700–1,000 BTU/scf) are obtained when gasification conditions promote the formation of methane and other light hydrocarbons.

Commercial biomass gasification facilities started worldwide in the 1970s and 1980s. Typically, gasification reactors comprise of a vertical reactor that has drying, pyrolysis, and combustion zones. Synthesis gas leaves the top of the reactor, and molten slag leaves the bottom of the reactor. The reactions that take place in the reactor are given in Eqs. 7, 8, and 9 using cellulose as representative of biomass (Klass 1998).

Pyrolysis:

$$C_6H_{10}O_5 \rightarrow 5CO + 5H_2 + C \tag{7}$$

Partial oxidation:

$$C_6H_{10}O_5 + O_2 \rightarrow 5CO + 5H_2 + CO_2 \tag{8}$$

Steam reforming:

$$C_6H_{10}O_5 + H_2O \rightarrow 6CO + 6H_2 \tag{9}$$

Synthesis gas is used in the chemical production complex of the lower Mississippi river corridor to produce ammonia and methanol. Currently, ammonia and methanol are produced using synthesis gas from natural gas, naphtha, or refinery light gas. Nearly 12.2 billion pounds of methanol are produced annually in the USA, and most of the methanol is converted to higher-value chemicals such as formaldehyde (37 %), methyl tertiary butyl ether (28 %), and acetic acid (8 %) (Paster et al. 2003). Ethanol can be produced from the synthesis gas, and Fischer-Tropsch chemistry is another approach to convert synthesis gas to chemicals and fuels. The chemicals that can be produced include paraffins, monoolefins, aromatics, aldehydes, ketones, and fatty acids.

Pyrolysis is the direct thermal decomposition of the organic components in biomass in the absence of oxygen to yield an array of useful products like liquid and solid derivatives and fuel gases (Klass 1998). Conventional pyrolysis is the slow, irreversible, thermal degradation of the organic components in biomass in absence of oxygen and includes processes like carbonization, destructive distillation, dry distillation, and retorting. The products of pyrolysis under high pressure and

temperature include mainly liquids with some gases and solids (water, carbon oxides, hydrogen, charcoal, organic compounds, tars, and polymers). The pyroligneous oil is the liquid product formed and mainly composed of water, settled tar, soluble tar, volatile acids, alcohols, aldehydes, esters, and ketones. The solid derivative from pyrolysis is referred to as biochar. Biochar can be used as a soil amendment and as a carbon sequestration medium. Depending on pyrolysis conditions and feedstock, the liquid product contains valuable chemicals and intermediates. The separation of these intermediates in a cost-effective manner is required. Pyrolysis can be slow, or fast, depending on the residence time and temperature. Slow pyrolysis occurs between 500 °C and 900 °C and produces low-energy gas, pyrolytic oil, and charcoal. Fast pyrolysis is operated in the range of 400 − 650 °C and residence times of a few seconds to a fraction of a second.

ConocoPhillips has funded a $22.5 million and 8-year research program at Iowa State University to develop new technologies for processing lignocellulosic biomass to biofuels (C & E News 2007). The company wants to investigate routes using fast pyrolysis to decompose biomass to liquid fuels.

Faustina Hydrogen Products LLC announced a $1.6 billion gasification plant in Donaldsonville, Louisiana. The plant will use petroleum coke and high sulfur coal as feedstocks instead of natural gas to produce anhydrous ammonia for agriculture, methanol, sulfur, and industrial-grade carbon dioxide. The hydrogen is produced for ammonia production from the water gas shift reaction of synthesis gas. Synthesis gas will be produced from gasification of coal and petroleum coke instead of natural gas. Capacities of the plant include 4,000 t per day of ammonia, 1,600 t per day of methanol, 450 t per day sulfur, and 16,000 t per day of carbon dioxide. Mosaic Fertilizer and Agrium Inc. have agreements to purchase the anhydrous ammonia from the plant. The carbon dioxide will be sold to Denbury Resources Inc. for the use in enhanced oil recovery of oil left after conventional rig drilling processes in old oil fields in Southern Louisiana and the Gulf Coast. The rest of the carbon dioxide would be sequestered and sold as an industrial feedstock. The facility claims to have the technology to capture all the carbon dioxide during manufacturing process.

Eastman Chemical Company, a Fortune 500 company, will provide the Faustina gasification plant with necessary maintenance and services and plans to have a 25 % equity position along with a purchase contract to buy the methanol produced in the plant. Eastman Chemicals will use methanol to make raw materials like propylene and ethylene oxide. Faustina is also backed by D. E. Shaw Group and Goldman Sachs.

Eastman Chemicals also plans to have 50 % stake in a $1.6 billion plant to be built in Beaumont, Texas, in 2011 (Tullo 2007). The plant will use gasification to produce syngas. Eastman will use the syngas to produce 225 million gallons of methanol and 225,000 metric tons of ammonia per year at Terra Industries in Beaumont. Air Products & Chemicals will supply 2.6 million metric tons per year of oxygen to the gasifiers and market the hydrogen produced in the complex.

Biomass Feedstock Availability

The challenge with biomass feedstock usage is the availability of biomass on an uninterrupted basis. Biomass, as a feedstock, has a wide variation due to a number of causes. These include climate and environmental factors like insolation, precipitation, temperature, ambient carbon dioxide concentration, nutrients, etc.

The availability of land and water areas for biomass production is important for the sustainable growth of biomass. The land capability in the United States is classified according to eight classes by the USDA and is given in Table 8. There have been numerous studies on the availability of biomass as feedstock in the United States, the most recent survey and estimation being undertaken by Perlack et al. (2005). Their findings are summarized in this section for land biomass resources.

The land base of the United States is approximately 2,263 million acres, including the 369 million acres of land in Alaska and Hawaii (Perlack et al. 2005). The land area is classified according to forest land, grassland pasture and range, cropland, special uses like public facilities, and other miscellaneous uses like urban areas, swamps, and deserts. The distribution of the total land areas according to these categories is given in Fig. 19. About 60 % of the total land base in the lower 48 states having some potential for growth of biomass.

The two major categories of biomass resources availability are forest resources obtained from forest land and agricultural resources obtained from crop land (or agricultural land). The detailed classification of the biomass resources is given in Fig. 20. The primary resources are often referred to as virgin biomass, and the secondary and tertiary are referred to as waste biomass. Currently, slightly more than 75 % of biomass consumption in the United States (about 142 million dry tons) comes from forestlands. The remainder (about 48 million dry tons), which includes biobased products, biofuels, and some residue biomass, comes from cropland.

Table 8 Land capability classification (Source: USDA)

Class	Description
Class I	Contains soils having few limitations for cultivation
Class II	Contains soils having some limitations for cultivation
Class III	Contains soils having severe limitations for cultivation
Class IV	Contains soils having very severe limitations for cultivation
Class V	Contains soils unsuited to cultivation, although pastures can be improved and benefits from proper management can be expected
Class VI	Contains soils unsuited to cultivation, although some may be used provided unusually intensive management is applied
Class VII	Contains soils unsuited to cultivation and having one or more limitations which cannot be corrected
Class VIII	Contains soils and landforms restricted to use as recreation, wildlife, water supply, or aesthetic purposes

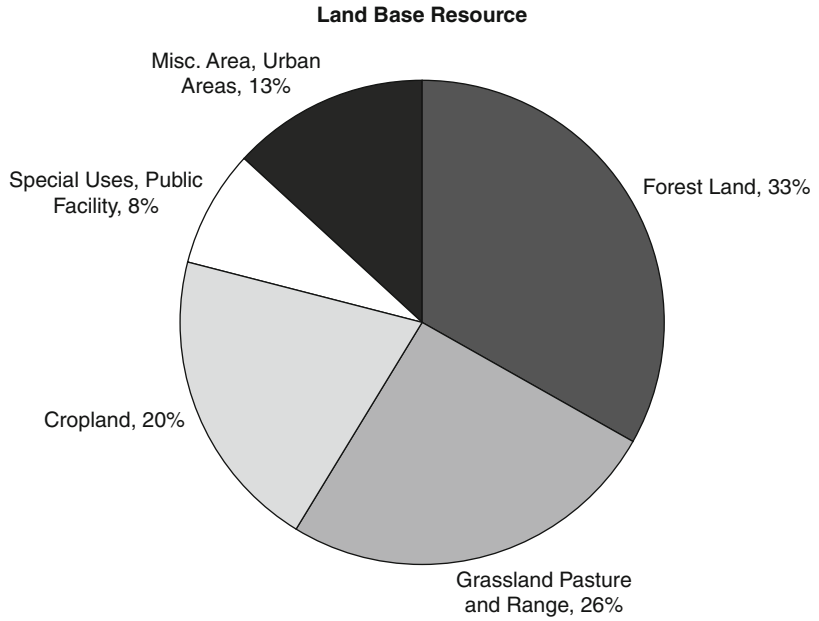

Fig. 19 United States land-based resource (Perlack et al. 2005)

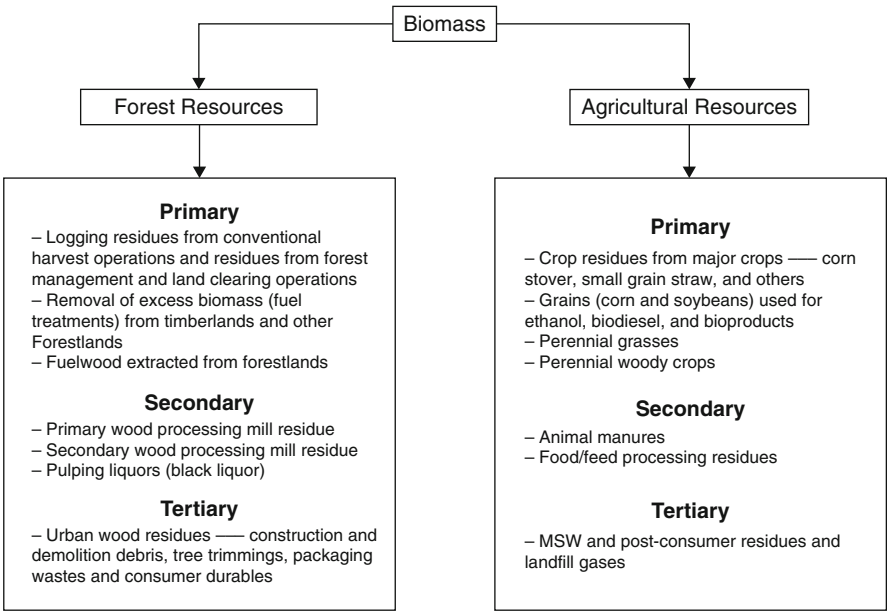

Fig. 20 Biomass resource base (primary, secondary, and tertiary biomass) (Adapted from Perlack et al. (2005))

Forest Resources

Forest Land Base

The total forest land resource base in the United States is approximately 749 million acres (one-third of the total land resource). The forest land is grouped into unreserved "timberland," "reserved land," and "others." The 749 million acres is divided into 504 million acres of timberland capable of growing 20 ft^3 per acre of wood annually, 166 million acres of forestland classified as "other" (incapable of growing 20 ft^3 per acre of wood annually and hence used for of livestock grazing and extraction of some nonindustrial wood products) and 78 million acres of reserved forestland used for parks and wilderness. "Timberland" and the "other" land are considered as the resource base that can be utilized for forest biomass resources.

Types of Forest Resource

The primary forest resources include logging residues and excess biomass (not harvested for fuel treatments and fuelwood) from timberlands. Logging residues are the unused portions of growing-stock and non-growing-stock trees cut or killed by logging and left in the woods. Fuelwood is the wood used for conversion to some form of energy, primarily for residential use.

The processing of sawlogs and pulpwood harvested for forest products generates significant amounts of mill residues and pulping liquors. These are secondary forest resources and constitute the majority of biomass in use today. The secondary residues are used by the forest products industry to manage residue streams, produce energy, and recover chemicals. About 50 % of current biomass energy consumption comes from the secondary residues.

The various categories in which primary and secondary forest resources can be grouped are given below (Fig. 21):

- *Logging residue*: The recovered residues generated by traditional logging activities and residues generated from forest cultural operations or clearing of timberlands. These constitute about 67 million dry tons of residues, of which 41 million is currently available for bioenergy and biobased products.
- *Fuel treatments* (*forest land*): The recovered residues generated from fuel treatment operations on timberland and other forestland. Fuel treatments are the procedures by which forests are treated so as to reduce the fuel value in the wood. The amount of biomass potentially available as feedstock for bioenergy and biobased products is 60 million dry tons per year.
- *Fuelwood*: The direct conversion of roundwood to energy (fuelwood) in the residential, commercial, and electric utility sectors currently includes 35 million dry tons per year and used for space and process heating applications.
- *Forest products industry residues and urban wood residues*: These include the utilization of unused residues generated by the forest products industry, urban residues including those discarded from construction and demolition operations,

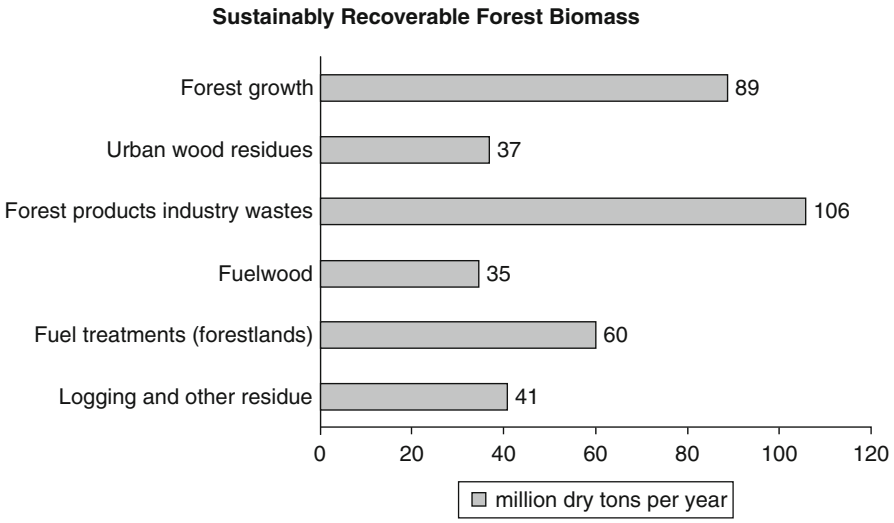

Fig. 21 Estimate of sustainably recoverable forest biomass (Adapted from Perlack et al. (2005))

and residues from tree trimmings, packaging residues, and wood-based consumer durables giving a total of 143 million dry tons per year.

- *Forest growth*: Forest growth and increase in the demand for forest products will increase the contribution of forest biomass by an additional 89 million dry tons annually.

The estimate of currently recoverable forest biomass is given in Fig. 21. The approximate total quantity is 368 million dry tons annually. This includes about 142 million dry tons of biomass currently being used primarily by the forest products industry and an estimated 89 million dry tons that could come from a continuation of demand and supply trends in the forest products industry.

Limiting Factors for Forest Resource Utilization

The 368 million tons of potential forest biomass feedstock base is constrained by some restrictions for exploitation. For forest resources inventory, development in forest utilization relationships and land ownership is expected to play a major role in utilizing the resource. There are three major limiting factors for forest residues from fuel treatment thinning resource, namely, accessibility (having roads to transport the material and operate logging/collection systems, avoiding adverse impacts on soil and water), economic feasibility (value of the biomass compared against the cost of removing the material), and recoverability (function of tree form, technology, and timing of the removal of the biomass from the forests).

Forest products industry processing residues include primary wood processing mills, secondary wood processing mills, and pulp and paper mills. Residues from these sources include bark, sawmill slabs and edgings, sawdust, and peeler log cores,

residues from facilities which use primary products and black liquor. A significant portion of this residue is burnt or combusted to produce energy for the respective industries. Excess amount of residue remain unutilized after the burning and combustion and can be used in biomass processes. Urban wood residues include municipal solid wastes and construction and demolition debris. A part of it is recovered, and a significant part is unexploited. Finally, future forest growth and increased demands in forest products are likely to affect the availability of forest resources for biomass feedstock base. In summary, all of these forest resources are sustainably available on an annual basis, but not currently used to its full potential due to the above constraints. For estimating the residue tonnage from logging and site clearing operations and fuel treatment thinning, a number of assumptions were made by Perlack et al. (2005):

- All forestland areas not currently accessible by roads were excluded.
- All environmentally sensitive areas were excluded.
- Equipment recovery limitations were considered.
- Recoverable biomass was allocated into two utilization groups – conventional forest products and biomass for bioenergy and biobased products.

Summary for Forest Resources

Thus, biomass derived from forestlands currently contributes about 142 million dry tons to the total annual consumption in the United Sates of 190 million dry tons. With the increased use of potential and currently unexploited biomass, this amount of forestland-derived biomass can increase to approximately 368 million dry tons annually. The distribution of the forest resource potential is summarized in Fig. 22. This estimate includes the current annual consumption of 35 million dry tons of fuelwood extracted from forestland for residential, commercial, and electric utility purposes; 96 million dry tons of residues generated and used by the forest products industry; and 11 million dry tons of urban wood residues. There are relatively large amounts of forest residue produced by logging and land clearing operations that are currently not collected (41 million dry tons per year) and significant quantities of forest residues that can be collected from fuel treatments to reduce fire hazards (60 million dry tons per year). Additionally, there are unutilized residues from wood processing mills and unutilized urban wood. These sources total about 36 million dry tons annually. About 48 % of these resources are derived directly from forestlands (primary resources). About 39 % are secondary sources of biomass from the forest products industry. The remaining amount of forest biomass would come from tertiary or collectively from a variety of urban sources.

Agricultural Resources

Agricultural Land Base

The agricultural land resource base for the United States is approximately 455 million acres, approximately 20 % of the total land base in the country. Out of this, 349 million acres is actively used for crop growth, 39 million acres constitutes idle

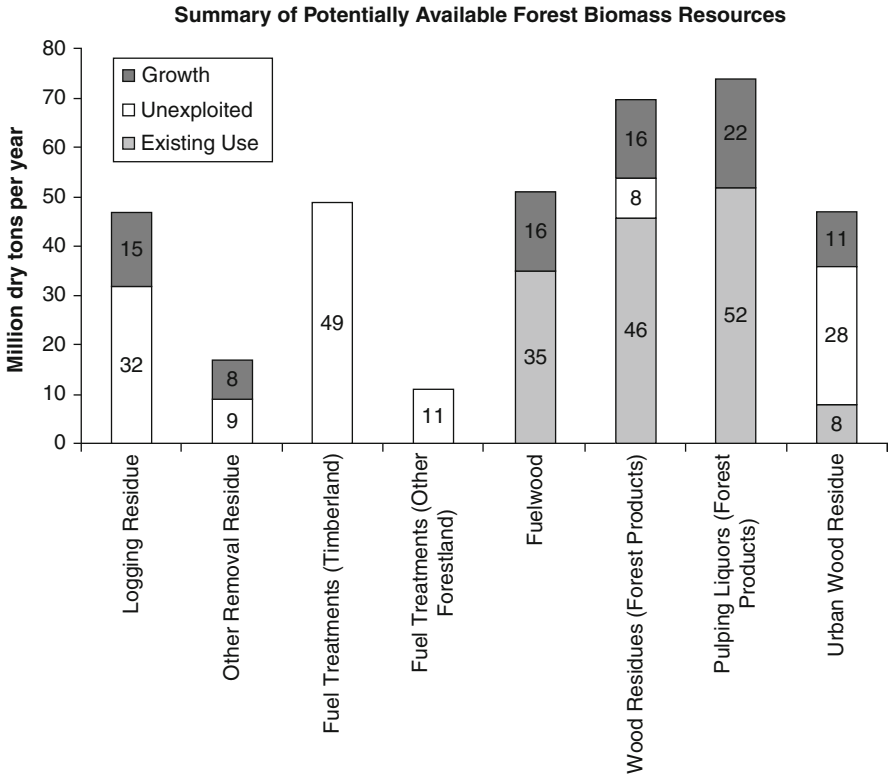

Fig. 22 Summary of potentially available forest biomass resources (Adapted from Perlack et al. (2005))

cropland, and 67 million acres is used for pasture. Cropland utilization is affected by soil and weather conditions, expected crop prices, and government incentives. Crop land is also lost due to conversion of the land for other uses like urban development, etc. The major food crops planted acreage constitutes wheat, soybeans, and rice. The feed crops include corn, sorghum, and hay. The fallow and failed land is a part of cropland. Apart from cropland, there is idle land which includes acreage diverted from crops under the Acreage Reduction Program (ARP), the Conservation Reserve Program (CRP), and other federal acreage reduction programs. The cropland used only for pasture is also separately accounted for. The distribution of agricultural land base and planted crop acreages in the United States is shown in Fig. 23.

Types of Agricultural Resource

The agricultural resource base is primarily comprised of grains and oilseeds in the United States. Currently, grains are primarily used for cattle feed. Grains, primarily corn, can be used for producing ethanol, and oilseeds, primarily soybeans, can be used to produce biodiesel. Approximately 93 % of the total US ethanol is produced from corn. Apart from these, agricultural residues, like corn stover, can also be used

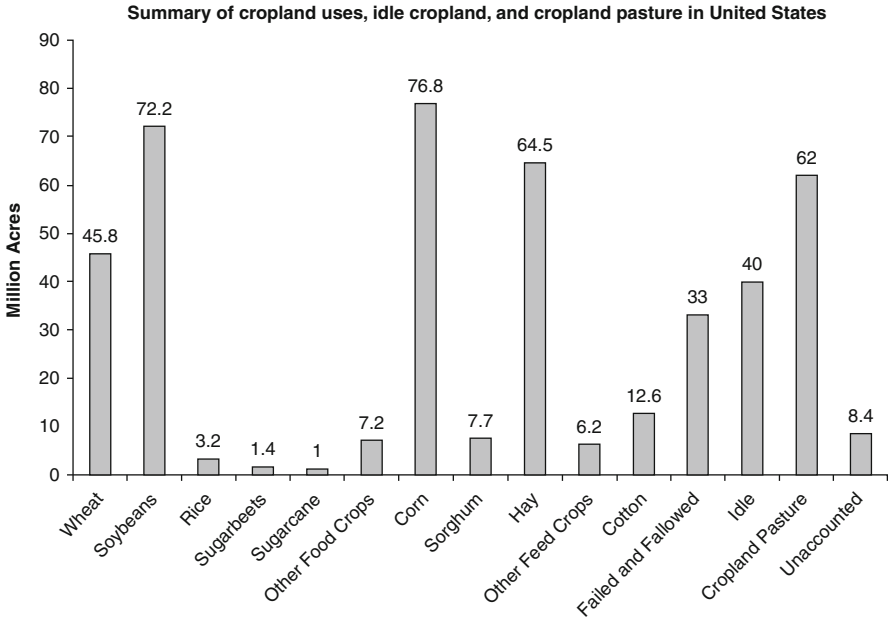

Fig. 23 Summary of agricultural land usage by major crops in United States (Adapted from Perlack et al. (2005))

for producing ethanol. In the United States, approximately 428 million dry tons of annual crop residues, 377 million dry tons of perennial crops, 87 million dry tons of grains, and 106 million dry tons of animal manures, process residues, and other miscellaneous feedstocks can be produced on a sustainable basis (Perlack et al. 2005). This resource potential was evaluated based on changes in the yields of crops grown on active cropland, crop residue-to-grain or crop residue-to-seed ratios, annual crop residue collection technology and equipment, crop tillage practices, land use change to accommodate perennial crops (i.e., grasses and woody crops), biofuels (i.e., ethanol and biodiesel), and secondary processing and other residues. Three scenarios were evaluated for availability of crop biomass, and they are given below.

Current Availability of Biomass Feedstocks from Agricultural Land

The current availability scenario studies biomass resources current crop yields, tillage practices (20–40 % no-till for major crops), residue collection technology (~40 % recovery potential), grain to ethanol and vegetable oil for biodiesel production, and the use of secondary and tertiary residues on a sustainable basis. The amount of biomass currently available for bioenergy and bioproducts is about 194 million dry tons annually as shown in Fig. 24. The largest source of this current potential is 75 million dry tons of corn residues or corn stover, followed by 35 million dry tons of animal manure and other residues.

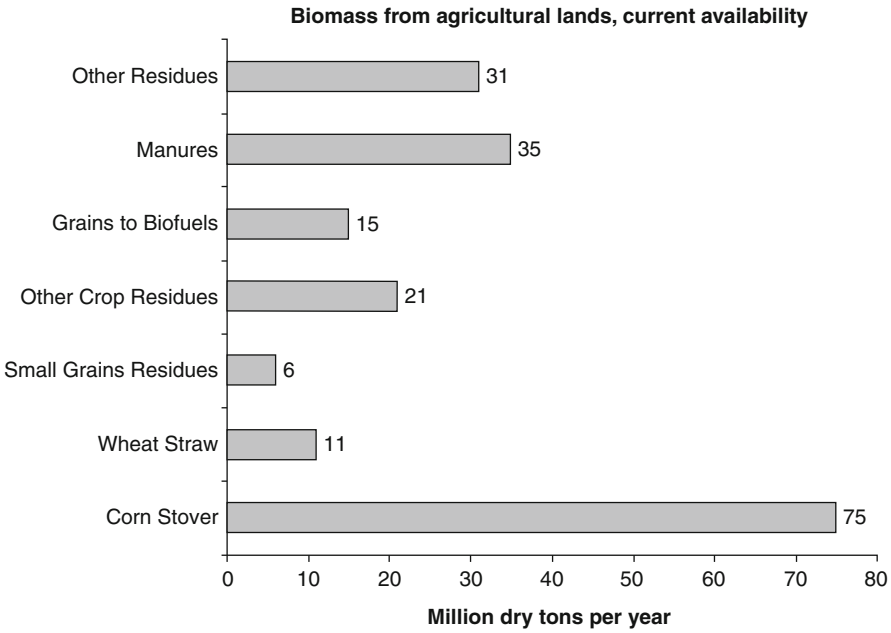

Fig. 24 Current availability of biomass from agricultural lands (Perlack et al. 2005)

Biomass Availability Through Technology Changes in Conventional Crops with No Land Use Change

This scenario analyzed the biomass availability of conventional crops achieved through technology changes. The land utilization for conventional crops projected for 2014 was used for this analysis. Technology changes to increase crop yields and improve collection equipment, and sustainable agricultural practices were considered in this scenario. Corn yields were assumed to increase by 25–50 % from 2001 values, while yields of wheat and other small grains, sorghum, soybeans, rice, and cotton are assumed to increase at rates lower than for corn. The increased production of corn contributed to increase in corn stover as residue. Soybeans contributed no crop residue under a moderate yield increase of about 13 % but made a small contribution with a high yield increase of about 23 %. The collection of these residues from crops was increased through better collection equipment capable of recovering as much as 60 % of residue under the moderate yield increases and 75 % under the high yield increases, but the actual removal amounts depend on the sustainability requirements. No-till cultivation method was assumed to be practiced on approximately 200 million acres under moderate yield increases and all of active cropland under high yields. The amount of corn and soybeans available for ethanol, biodiesel production, or other bioproducts was calculated by subtracting amounts needed to meet food requirements plus feed and export requirements from total quantities. All remaining grain was assumed to be available for bioproducts. Further, about 75 million dry tons of manure and other secondary and tertiary residues and wastes and 50 % of the biomass

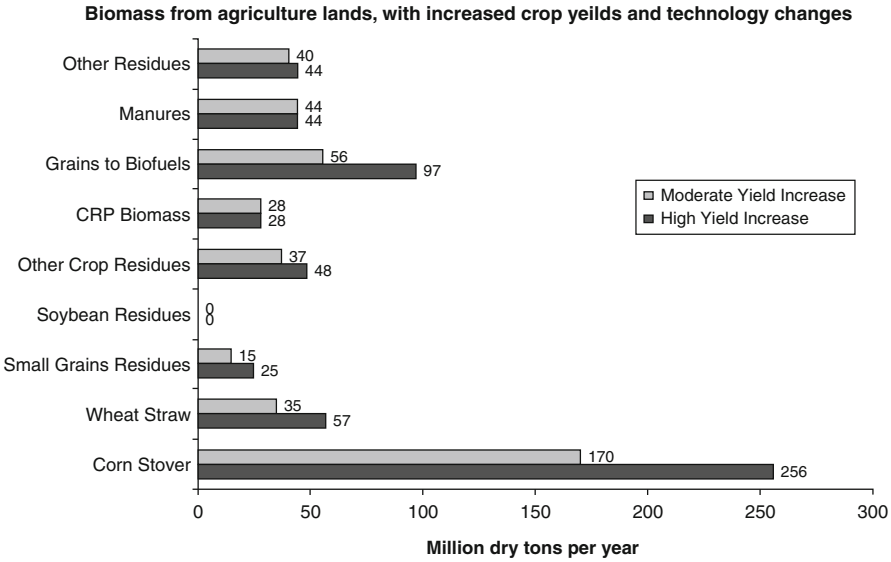

Fig. 25 Availability of biomass for increased crop yields and technology changes (Perlack et al. 2005)

produced on CRP lands (17–28 million dry tons) were assumed to be available for bioenergy production. Thus, this scenario for the use of crop residue results in the annual production of 423 million dry tons per year under moderate yields and 597 million dry tons under high yields. In this scenario, about two-thirds to three-fourths of total biomass are from crop residues, as can be seen in Fig. 25.

Biomass Availability Through Technology Changes in Conventional Crops and New Perennial Crops with Significant Land Use Change

This scenario assumes the addition of perennial crops, land use changes, and changes in soybean varieties, as well as the technology changes assumed under the previous scenario. Technology changes are likely to increase the average residue-to-grain ratio of soybean varieties from 1.5 to a ratio of 2.0. The land use changes considered in this scenario included the conversion of land for growth of perennial crop on 40 million acres for moderate yield increase or 60 million acres for high yield increase. Woody crops produced for fiber were expanded from 0.1 million acres to 5 million acres, where they can produce an average annual yield of 8 dry tons per acre. Twenty-five percent of the wood fiber crops are assumed to be used for bioenergy and the remainder for other, higher-value conventional forest products. Perennial crops (trees or grasses) grown primarily for bioenergy expand to either 35 million acres at 5 dry tons per acre per year or to 55 million acres with average yields of 8 dry tons per acre per year. Ninety-three percent of the perennial crops are assumed available for bioenergy and the remainder for other products. A small fraction of the available biomass (10 %) was assumed as lost during the harvesting

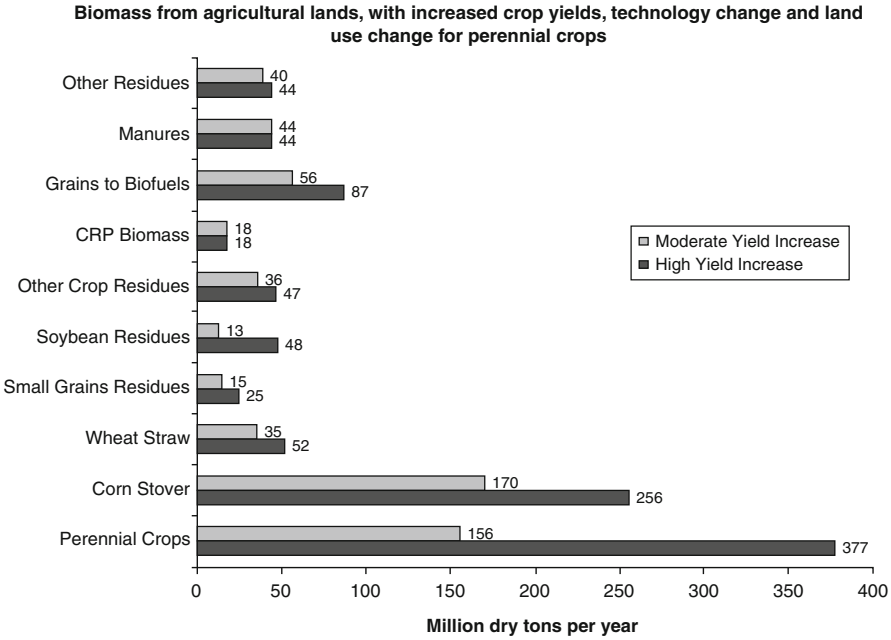

Fig. 26 Availability of biomass for increased crop yields and technology changes and inclusion of perennial crops (Perlack et al. 2005)

operations. This scenario resulted in the production of 581 (moderate yield) to 998 million (high yield) dry tons as shown in Fig. 26. The crop residues increased even though conventional cropland was less because of the addition of more soybean residue together with increased yields. The single largest source of biomass is the crop residue, accounting for nearly 50 % of the total produced. Perennial crops account for about 30–40 % depending on the extent of crop yield increase (i.e., moderate or high).

Limiting Factors for Agricultural Resource Utilization

The annual crop residues, perennial crops, and processing residues can produce 998 million tons of potential agricultural biomass feedstock. The limiting factors for the utilization of crop residues and growth of perennial crops for the purpose of feedstock generation will require significant changes in current crop yields, tillage practices, harvesting and collection technologies, and transportation. Agricultural residues serve as a land cover and prevent soil erosion after harvesting of crops. The removal of large quantities of the residue can affect the soil quality by removal of soil carbon and nutrients and may need to be replenished with fertilizers. The fertilizers, in turn, require energy for production, and hence the optimum removal of the residues needs to be evaluated. Perennial crops require less nutrient supplements and are better choices for preventing soil erosion compared to annual crops, and they are considered for planting.

Important assumptions made for this evaluation of agricultural biomass availability by Perlack et al. (2005) included the following:

- Yields of corn, wheat, and other small grains were increased by 50 %.
- The residue-to-grain ratio for soybeans was increased to 2:1.
- Harvest technology was capable of recovering 75 % of annual crop residues (when removal is sustainable).
- All cropland was managed with no-till methods.
- Fifty five million acres of cropland, idle cropland, and cropland pasture were dedicated to the production of perennial bioenergy crops.
- All manure in excess of that which can applied on-farm for soil improvement under anticipated EPA restrictions was used for biofuel.
- All other available residues were utilized.

Summary for Agricultural Resources

Thus, biomass derived from agricultural lands currently available for removal on a sustainable basis is about 194 million dry tons. This amount can be increased to nearly one billion tons annual production through a combination of technology changes, adoption of no-till cultivation, and land use change to grow perennial crops. The amount of biomass available without the addition of perennial crops but high crop yield increase would be 600 million dry tons. Approximately the same amount of biomass would be produced on agricultural lands with moderate crop yield increase and addition of perennial crops. The distribution of the agricultural resource potential is summarized in Fig. 27.

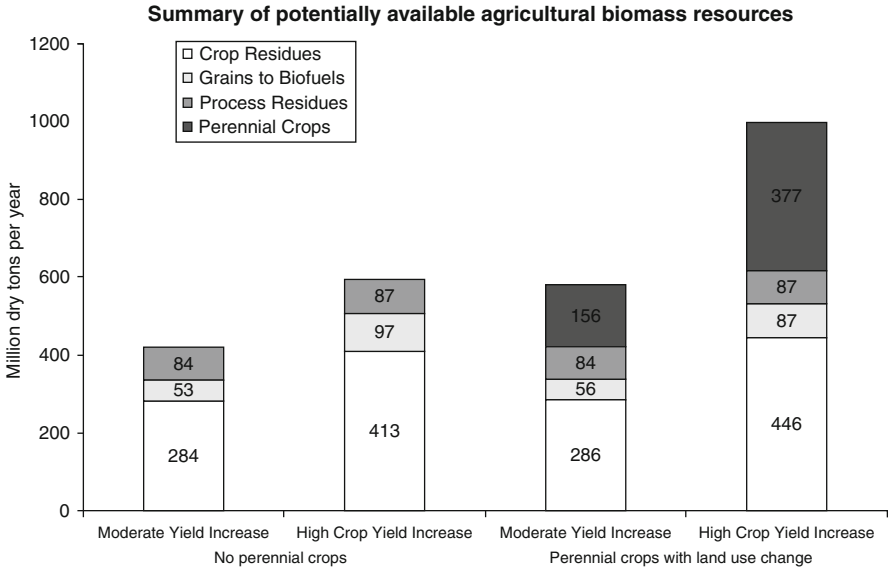

Fig. 27 Summary of potentially available agricultural biomass resources (Perlack et al. 2005)

Aquatic Resources

The previous sections discussed conventional biomass feedstock options grown on land. Apart from the crop and forest biomass resources, other organisms that undergo photosynthesis are cyanobacteria and algae. There are several ongoing attempts to find the ideal growth conditions for cultivating algae on a sustainable basis. Key areas of research interests in algae include high per-acre productivity compared to typical terrestrial oilseed crops, non-food-based feedstock resources, the use of otherwise nonproductive, non-arable land for algae cultivation, utilization of a wide variety of water sources (fresh, brackish, saline, and wastewater), and production of both biofuels and valuable coproducts. The Energy Efficiency and Renewable Energy Laboratory at the Department of Energy commissioned a working group assess the current state of algae technology and to determine the next steps toward commercialization (DOE 2010a). The workshop addressed the following topics and technical barriers in algal biology, feedstock cultivation, harvest and dewatering, extraction and fractionation of microalgae, algal biofuel conversion technologies, coproducts production, distribution and utilization of algal-based fuels, resources and siting, corresponding standards, regulation and policy, systems and techno-economic analysis of algal biofuel deployment, and public-private partnerships. This section aims to capture some of those efforts. A model algal lipid production system with algae growth, harvesting, extraction, separation, and uses is shown in Fig. 28. Methods to convert whole algae into biofuels exist through anaerobic digestion to biogas, supercritical fluid extraction and pyrolysis to liquid or vapor fuels, and gasification process for production of syngas-based fuels and chemicals. Algae oil can supplement refinery diesel in hydrotreating units or be used as feedstock for the biodiesel process. The research on algae as a biomass feedstock is a very dynamic field currently, and the potential of algae seems promising as new results are presented continuously.

Methods to cultivate algae have been developed over the years. Recent developments in algae growth technology include vertical reactors (Hitchings 2007) and bag reactors (Bourne 2007) made of polythene mounted on metal frames, eliminating the need for land use for cultivation. The NREL Aquatic Species Program (Sheehan et al. 1998) mentions "raceway" ponds design for growth of algae. This method required shallow ponds built on land area and connected to a carbon dioxide source

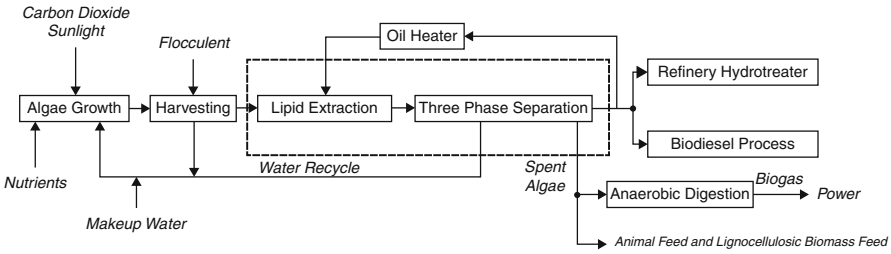

Fig. 28 Model algae lipid production system (Adapted from Pienkos and Daezins (2009))

Table 9 Comparison of productivity between algae and soybean (Pienkos and Daezins 2009)

Productivity	Soybeans	Algae		
		Low productivity (10 g/m^2/day) 15 % TAG	Med. productivity (25 g/m^2/day) 25 % TAG	High productivity (50 g/m^2/day) 50 % TAG
Gallons/acre	48	633	2,637	10,549
Total acres	63.6 million	63.6 million	25 million	6.26 million
Gallons/year	3 billion	40 billion	66 billion	66 billion
Petrodiesel (%)	4.5	61	100	100

such as a power plant. Productivity in these pond designs was few grams/m^2/day. Other designs include tubular cultivation facilities, and the semi-continuous batch cultures gave improved production rates of algae. For example, the 3D Matrix System of Green Fuel Technologies Corporation have an average areal productivity of 98 g/m^2/day (ash free, dry weight basis), with highs of over 170 g/m^2/day achieved during a run time of 19 days (Pulz 2007).

Algae have the potential for being an important source of oil and carbohydrates for production of fuels, chemicals, and energy. Carbon dioxide and sunlight can be used to cultivate algae and produce algae with 60 % triglycerides and 40 % carbohydrates and protein (Pienkos and Daezins 2009). A comparison in productivity between algae and soybean is given in Table 9. The table shows that even at low productivity of algae, yields are more than 10 times in gallons per acre when all the United States soybean acreage is utilized for algae. Higher yields are obtained at medium and high productivity levels of algae (higher triacylglycerols) with reduced acreage requirements. The algae oil resulting from low productivity can replace approximately 61 % of the total United States diesel requirements, as compared to only 4.5 % for soybean oil-based diesel. The other advantage, at these yields, algae can capture up to 2 billion tons of carbon dioxide while photosynthesis.

However, the growth of algae on a large scale for production of oil and chemicals seems to be the most important barrier at this stage. The following technologies developed seem promising ways to cultivate algae, apart from traditional open pond systems. These are discussed on a per case basis, with the companies that have developed these technologies. Some of the current research trends in algae bioreactor systems are presented in the following sections.

Raceway Pond Systems

"Raceway" design for algae growth included shallow ponds in which the algae, water, and nutrients circulate around a "racetrack" as shown in Fig. 29 (inset) (Sheehan et al. 1998). Motorized paddles help to provide the flow and keep algae suspended in water and circulated back up to the surface on a regular frequency. The ponds are shallow to ensure maximum exposure of sunlight (sunlight cannot penetrate beyond certain depths). The ponds are operated as continuous reactors with

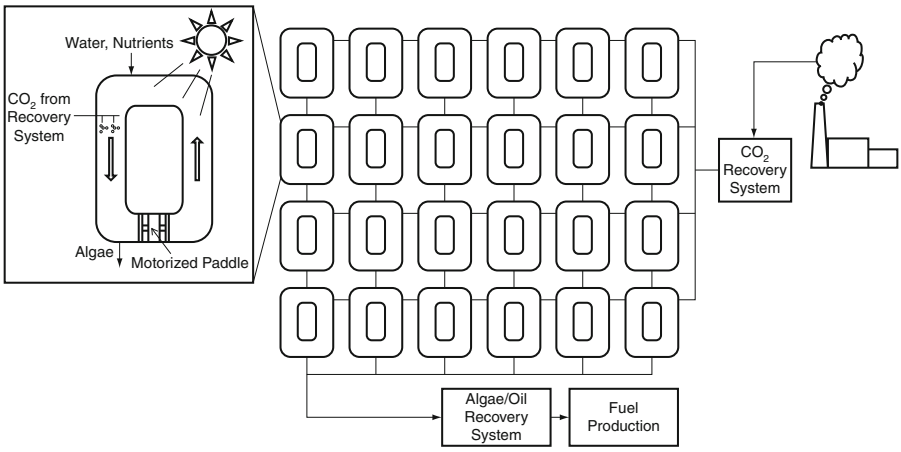

Fig. 29 Algae raceway design (inset) and algae farm system for algae growth (Adapted from Sheehan et al. (1998))

water and nutrients fed to the pond and carbon dioxide bubbled through the system. The algae containing water is removed at the other end of the pond. The algae is then harvested and processed for oil extraction.

The concept of the raceway design for algae growth can be extended to an algae farm as shown in Fig. 29. This consists of numerous ponds similar to the raceway in which algae is grown and harvested. The size of these ponds is measured in terms of surface area (as opposed to volume) as the surface area is critical to capturing sunlight. The productivity is measured in terms of biomass produced per day per unit of available surface area. These designs required large acres of land and thus obtained the scale of farms. The open bioreactor system for a 50 square meters and width 1.2 m algae cultivation facility at the microalgal culture facility of UH Marine Center is shown in Fig. 30.

Algenol Biofuels: Direct to Ethanol^{TM} Process

Algenol biofuels have developed metabolically engineered algae species to produce ethanol in closed bioreactor systems. The proprietary Capture Technology^{TM} bioreactors hold single-cell cyanobacteria in closed and sealed plastic bag units preventing contamination, maximize ethanol recovery, and allow fresh water recovery. The advantage of the process lies in the fact that it is a one-step process where the cyanobacteria utilize the carbon dioxide to convert it to ethanol and secrete the ethanol from the cell (Voith 2009). There is a requirement for strict maintenance of growth parameters such as CO_2, nutrients, water, pH, temperature, salinity, and other environmental conditions for the engineered species of microorganism. The process to make ethanol from algae utilizes 1.5 million tons of carbon dioxide per 100 million gallons of ethanol produced. Algenol, The Dow Chemical Company, and the Department of Energy have teamed to produce ethanol using this technology at

Fig. 30 Microalgal culture facility at the UH Marine Center (Photo: Dr. Edward Laws, LSU School of the Coast and Environment)

Dow's Freeport, Texas, site. Dow would contribute with 25 acres of their site, carbon dioxide source, and technical expertise for the $25 million project. Dow plans to utilize their expertise in film technology to device ideal bioreactor for the system with optimum sunlight penetration.

ExxonMobil Algae Research

ExxonMobil is funding $600 million for algae research partnered with Synthetic Genomics, Inc. to identify and develop algae strains to produce bio-oils at low costs (Kho 2009). The research will also determine the best production systems for growing algal strains, for example, open ponds or closed photobioreactor systems. The company also plans for scale-up to large amounts of CO_2 utilization and developing integrated commercial systems.

Shell Algae Research

Shell and HR Biopetroleum formed a joint venture company in 2007, called Cellana, to develop an algae project for a demonstration facility on the Kona Coast of Hawaii

Island. The site was leased from the Natural Energy Laboratory of Hawaii Authority (NELHA) and is near existing commercial algae enterprises, primarily serving the pharmaceutical and nutrition industries.

The facility will grow only nonmodified, marine microalgae species in open-air ponds using proprietary technology. Algae strains used for the process are indigenous to Hawaii or approved by the Hawaii Department of Agriculture.

Green Fuels Technology

GreenFuel Technologies developed a process that grows algae in plastic bags using CO_2 from smokestacks of power plants via naturally occurring species of algae. The CO_2 source can also come from fermentation or geothermal gases. Algae can be converted to transportation fuels and feed ingredients or recycled back to a combustion source as biomass for power generation. Industrial facilities do not need any internal modifications to host a GreenFuel algae farm. In addition, the system does not require fertile land or potable water. Water used can be recycled, and wastewater can be used as compared to oilseed crops' high water demand. With high growth rates, algae can be harvested daily.

Valcent Products

32A vertical reactor system is being developed by Valcent Products, Inc. of El Paso, Texas, using the 340 annual days of sunshine and carbon dioxide available from power plant exhaust.

Enhanced Biofuel Technology and A2BE Carbon Capture, LLC, are some of the firms that use the concept of raceway pond design and algae farm for production of algae for biofuels. Research is underway to determine the species of algae for oil production and the best method of extracting the oil. Extraction methods being evaluated include expeller/press, hexane solvent extraction, and supercritical fluid extraction and are the more costly step in the process. Approximately 70–75 % of algae oil can be extracted using expeller press, while 95 % oil can be extracted by hexane solvent oil extraction and 100 % oil extracted using supercritical fluid extraction.

Algae Species

Algae are plant-like microorganisms that preceded plants in developing photosynthesis, the ability to turn sunlight into energy. Algae range from small, single-celled organisms to multicellular organisms, some with fairly complex differentiated form. Algae are usually found in damp places or bodies of water and thus are common in terrestrial as well as aquatic environments. Like plants, algae require primarily three components to grow: sunlight, carbon dioxide, and water. Microalgae are the most efficient in photosynthesis, with 60–70 % of each cell's volume capable of photosynthesis (Arnaud 2008). The algae also do not have roots, stems, or leaves, which diverts resources to produce hydrocarbons. Algae cells contain light-absorbing chloroplasts and produce oxygen through photosynthesis. Biologists have categorized microalgae in a variety of classes, mainly distinguished by their pigmentation,

life cycle, and basic cellular structure. The four most important (in terms of abundance) are (Sheehan et al. 1998):

- The diatoms (Bacillariophyceae): These algae dominate the phytoplankton of the oceans, but are also found in fresh and brackish water. Approximately 100,000 species are known to exist. Diatoms contain polymerized silica (Si) in their cell walls. All cells store carbon in a variety of forms. Diatoms store carbon in the form of natural oils or as a polymer of carbohydrates known as chrysolaminarin.
- The green algae (Chlorophyceae): This type of algae is abundant in freshwater, for example, in a swimming pool. They can occur as single cells or as colonies. Green algae are the evolutionary progenitors of modern plants. The main storage compound for green algae is starch, though oils can be produced under certain conditions.
- The blue-green algae (Cyanophyceae): This type of algae is closer to bacteria in structure and organization. These algae play an important role in fixing nitrogen from the atmosphere. There are approximately 2,000 known species found in a variety of habitats.
- The golden algae (Chrysophyceae): This group of algae is similar to the diatoms. They have more complex pigment systems and can appear yellow, brown, or orange in color. Approximately 1,000 species are known to exist, primarily in freshwater systems. They are similar to diatoms in pigmentation and biochemical composition. The golden algae produce natural oils and carbohydrates as storage compounds.

The program initially looked into over 3,000 strains of organisms, which was then narrowed down to about 300 species of microorganisms. The program concentrated not only on algae that produced a lot of oil, but also with algae that grow under severe conditions – extremes of temperature, pH, and salinity.

Algal biomass contains three main components: carbohydrates, proteins, and natural oils. Algae contains 2–40 % of lipids/oils by weight. The composition of various algal species is given in Table 10. These components in algae can be used for fuel or chemicals production in three ways, mainly production of methane via biological or thermal gasification, ethanol via fermentation, or conversion to esters by transesterification (Sheehan et al. 1998). *Botryococcus braunii* species of algae has been engineered to produce the terpenoid C30 botryococcene, a hydrocarbon similar to squalene in structure (Arnaud 2008). The species has been engineered to secrete the oil, and the algae can be reused in the bioreactor. A further modification to the algae is smaller light collecting antennae, allowing more light to penetrate the algae in a polythene container reactor system. A gene, tla1, is responsible for the number of chlorophyll antennae and can be modified to reduce the chlorophyll molecules from 600 to 130. Botryococcene is a triterpene and, unlike triglycerides, cannot undergo transesterification. It can be used as feedstock for hydrocracking in an oil refinery to produce octane, kerosene, and diesel.

Dry algae factor is the percentage of algae cells in relation with the media where is cultured, e.g., if the dry algae factor is 50 %, one would need 2 kg of wet algae

Table 10 Percentage composition of protein, carbohydrate, lipids, and nucleic acid composition of various strains of algae (Sheehan et al. 1998)

Strain	Protein	Carbohydrates	Lipids	Nucleic acid
Scenedesmus obliquus	50–56	10–17	12–14	3–6
Scenedesmus quadricauda	47	–	1.9	–
Scenedesmus dimorphus	8–18	21–52	16–40	–
Chlamydomonas reinhardtii	48	17	21	–
Chlorella vulgaris	51–58	12–17	14–22	4–5
Chlorella pyrenoidosa	57	26	2	–
Spirogyra sp.	6–20	33–64	11–21	–
Dunaliella bioculata	49	4	8	–
Dunaliella salina	57	32	6	–
Euglena gracilis	39–61	14–18	14–20	–
Prymnesium parvum	28–45	25–33	22–38	1–2
Tetraselmis maculata	52	15	3	–
Porphyridium cruentum	28–39	40–57	9–14	–
Spirulina platensis	46–63	8–14	4–9	2–5
Spirulina maxima	60–71	13–16	6–7	3–4.5
Synechococcus sp.	63	15	11	5
Anabaena cylindrica	43–56	25–30	4–7	–

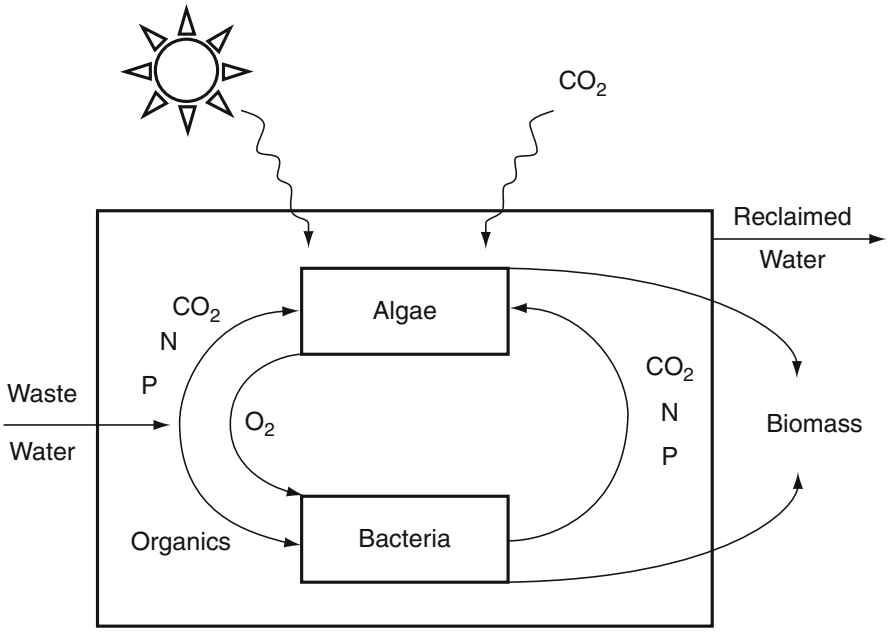

Fig. 31 Schematic diagram for wastewater treatment with algae and production of biomass (Lundquist 2011)

(algae in the media) to get 1 kg of algae cells. Lipid factor is the percentage of vegoil in relation with the algae cells needed to get it, i.e., if the algae lipid factor is 40 %, one would need 2.5 kg of algae cells to get 1 kg of oil.

Carbon dioxide sources for algae growth can be from pipelines for CO_2, flue gases from power plants, or any other sources rich in carbon dioxide. The flue gases from power plants were previously not considered as suitable algae cultivation land was not found near power plants. However, with newer designs of algae reactors linked with power plants, the flue gases can be suitable sources for algae cultivation. Water usage for algae growth is also a concern for design. In an open pond system, the loss of water is greater than in closed tubular cultivation or bag cultivation methods. The water can be local industrial water and recycled after harvesting algae.

Algae can be used in wastewater treatment, as wastewater contains nutrients for algae growth. The advantages for wastewater treatment using algae include the production of oxygen with low-energy input, removal of soluble nitrogen and phosphorus, fixation of atmospheric carbon dioxide, and the production of biomass (Lundquist 2011). The simple schematic in Fig. 31 shows how algae and bacteria can be used to produce biomass.

Conclusion

The chapter aimed to give an overview of the use of biomass as the next-generation feedstock for energy, fuels, and chemicals. The formation of biomass gave the methods in which atmospheric carbon dioxide is fixed naturally to different types of biomass. The classification of biomass into starch, cellulose, hemicellulose, lignin, lipids and oils, and proteins helped to understand the chemical composition of biomass. Biomass species are available in nature as a combination of the components, and it is important to separate the components for the use as energy, fuels, and chemicals. Various conversion technologies are employed for the separation of the components of biomass to make it more amenable, and these include pretreatment, fermentation, anaerobic digestion, transesterification, gasification, and pyrolysis.

The availability of biomass on a sustainable basis is required for the uninterrupted production of energy, fuels, and chemicals. The current forest biomass feedstock used per year is 142 million metric tons. This can be potentially increased to 368 million metric tons which include currently unexploited and future growth of forest biomass. The agricultural biomass currently available per year on a sustainable basis is 194 million dry tons. This amount can be potentially increased to 423–527 million metric tons per year with technology changes in conventional crops and 581–998 million metric tons with technology and land use changes in conventional and perennial crops.

Apart from crop and forest biomass, research in algae and cyanobacteria is ongoing for the production of carbohydrate-based and oil-based feedstock. These processes are currently constrained primarily by the successful scale-up to meet the biomass needs. However, recent advances in photo-bioreactors and algae ponds show considerable potential for large-scale growth of algae as biomass feedstock.

Future Directions

The biomass resource base is capable of producing feedstock for a sustainable supply of fuels, energy, and chemicals. However, technological challenges, market drivers, fossil feedstock cost fluctuations, and government policies and mandates play a significant role in utilizing the full potential of the biomass resources. Ideally, the biomass is regenerated over a short period of time when compared to fossil resources. This period can be few years for forest resources, seasonal for agricultural crops, and days for algae and cyanobacteria. Biomass is the source for natural atmospheric carbon dioxide fixation. Thus, with the use of biomass as feedstock for energy, fuels, and chemicals, the dependence on fossil resources can be reduced, and climate change issues related to resource utilization can be addressed.

References

Aden A, Ruth M, Ibsen K, Jechura J, Neeves K, Sheehan J, Wallace B (2002) Lignocellulosic biomass to ethanol process design and economics utilizing co-current dilute acid prehydrolysis and enzymatic hydrolysis for corn stover, NREL/TP-510-32438. National Renewable Energy Laboratory, Golden

Arnaud C (2008) Algae pump out hydrocarbon biofuels. Chem Eng News 86(35):45–48

Axelsson L (2004) Lactic acid bacteria: classification and physiology. In: Salmien S, Wright AV, Ouwehand A (eds) Lactic acid bacteria: microbiological and functional aspects. Marcel Dekker, New York

Bourne Jr JK (2007) Green dreams. National Geographic Magazine. http://ngm.nationalgeographic.com/print/2007/10/biofuels/biofuels-text. Accessed 8 May 2010

C & E News (2007) ConocoPhillips funds biofuel research. Chem Eng News 85(18):24

DOE (2010a) Biomass multi-year program plan March 2010. Energy efficiency and renewable energy (US DOE). http://www1.eere.energy.gov/biomass/pdfs/mypp.pdf. Accessed 8 May 2010

DOE (2010b) National algal biofuels technology roadmap. Energy efficiency and renewable energy (US DOE). Draft document: https://e-center.doe.gov/iips/faopor.nsf/UNID/79E3ABCACC9AC14A852575CA00799D99/$file/AlgalBiofuels_Roadmap_7.pdf. Accessed 8 May 2010

Drapcho CM, Nhuan NP, Walker TH (2008) Biofuels engineering process technology. McGrawHill, New York. ISBN 978-0071487498

EIA (2010) Annual energy outlook 2010. Report No. DOE/EIA-0383(2010). Energy Information Administration, Washington, DC

Fukuda H, Kondo A, Noda H (2001) Biodiesel production by the transesterification of oils. J Biosci Bioeng 92(5):405–416

Glazer AW, Nikaido H (1995) Microbial biotechnology: fundamentals of applied microbiology. W.H. Freeman, San Francisco. ISBN 0-71672608-4

Granda C (2007) The MixAlco process: mixed alcohols and other chemicals from biomass in: seizing opportunity in an expanding energy marketplace, alternative energy conference. LSU Center for Energy Studies. http://www.enrg.lsu.edu/Conferences/altenergy2007/granda.pdf

Haas MJ, McAloon AJ, Yee WC, Foglia TA (2006) A process model to estimate biodiesel production costs. Bioresour Technol 97(4):671–678

Hitchings MA (2007) Algae: the next generation of biofuels, Fuel Fourth Quarter 2007. Hart Energy, Houston

Holtzapple MT, Davison RR, Ross MK, Aldrett-Lee S, Nagwani M, Lee CM, Lee C, Adelson S, Kaar W, Gaskin D, Shirage H, Chang NS, Chang VS, Loescher ME (1999) Biomass conversion to mixed alcohol fuels using the MixAlco process. Appl Biochem Biotechnol 79(1–3):609–631

IPCC (2007) Climate change 2007: synthesis report. http://www.ipcc.ch/pdf/assessment-report/ar4/syr/ar4_syr.pdf. Accessed 8 May 2010

Katzen R, Schell DJ (2006) Lignocellulosic feedstock biorefinery: history and plant development for biomass hydrolysis. In: Kamm B, Gruber PR, Kamm M (eds) Biorefineries – industrial processes and products, vol 1. Wiley-VCH, Weinheim. ISBN 3-527-31027-4

Kebanli ES, Pike RW, Culley DD, Frye JB (1981) Fuel gas from dairy farm waste, Agricultural energy, vol II Biomass energy crop production, ASAE publication 4-81, 3 vols. American Society of Agricultural Engineers, St. Joseph

Kho J (2009) Big oil bets on biofuels. Renewable Energy World. http://www.renewableenergyworld.com/rea/news/article/2009/07/bio-oil-bets-on-biofuels. Accessed 8 May 2010

Klass DL (1998) Biomass for renewable energy, fuels and chemicals. Academic, San Diego. ISBN 0124109500

Lucia LA, Argyropolous DS, Adamopoulos L, Gaspar AR (2007) Chemicals, materials and energy from biomass: a review. In: Argyropoulos DS (ed) Materials, chemicals and energy from forest biomass. American Chemical Society, Washington, DC. ISBN 978-0-8412-3981-4

Lundquist TJ (2011) Production of algae in conjunction with wastewater treatment. http://www.nrel.gov/biomass/pdfs/lundquist.pdf. Accessed 8 Mar 2011

Ma F, Hanna MA (1999) Biodiesel production: a review. Bioresour Technol 70(1):1–15

McGowan TF (2009) Biomass and alternate fuel systems. American Institute of Chemical Engineers/Wiley, Hoboken. ISBN 978-0-470-41028-8

Meher LC, Vidya Sagar D, Naik SN (2006) Technical aspects of biodiesel production by transesterification – a review. Renew Sustain Energy Rev 10(3):248–268

Paster M, Pellegrino JL, Carole TM (2003) Industrial bioproducts: today and tomorrow. Department of Energy report prepared by Energetics Inc. http://www.energetics.com/resourcecenter/products/studies/Documents/bioproducts-pportunities.pdf. Accessed 8 May 2010

Perlack RD, Wright LL, Turhollow AF, Graham RL (2005) Biomass as feedstock for a bioenergy and bioproducts industry: the technical feasibility of a billion-ton annual supply. USDA document prepared by Oak Ridge National Laboratory, ORNL/TM-2005/66, Oak Ridge

Pienkos PT, Daezins A (2009) The promise and challenges of microalgal-derived biofuels. Biofuels Bioprod Biorefin 3(4):431–440

Pulz O (2007) Evaluation of GreenFuel's 3D matrix algae growth engineering scale unit. APS Red Hawk Power Plant. http://moritz.botany.ut.ee/~olli/b/Performance_Summary_Report.pdf. Accessed 8 May 2010

Sheehan J, Dunahay T, Benemann J, Roessler P (1998) A look back at the U. S. Department of Energy's aquatic species program – biodiesel from algae, NREL/TP-580-24190. National Renewable Energy Laboratory, Golden

Spath PL, Dayton DC (2003) Preliminary screening – technical and economic feasibility of synthesis gas to fuels and chemicals with the emphasis on the potential for biomass-derived syngas, NREL/TP-510-34929. National Renewable Energy Laboratory, Golden. http://www.nrel.gov/docs/fy04osti/34929.pdf. Accessed 8 May 2010

Sun Y, Cheng J (2002) Hydrolysis lignocellulosic materials ethanol production review. Bioresour Technol 83:1–11

Teter SA, Xu F, Nedwin GE, Cherry JR (2006) Enzymes for biorefineries. In: Kamm B, Gruber PR, Kamm M (eds) Biorefineries – industrial processes and products, vol 1. Wiley-VCH, Weinheim. ISBN 3-527-31027-4

Thanakoses P, Black AS, Holtzapple MT (2003) Fermentation of corn stover to carboxylic acids. Biotechnol Bioeng 83(2):191–200

Tucker MP, Nagle NJ, Jennings E, Lyons R, Elander R (2011) Hot-washing of pretreated corn stover using integrated sunds horizontal screw and jaygo pretreatment reactors with

pneumapress automatic pressure filter. http://www1.eere.energy.gov/biomass/pdfs/34331.pdf. Accessed 8 Feb 2011
Tullo AH (2007) Eastman pushes gasification. Chem Eng News 85(32):10
Voith M (2009) Dow plans algae biofuels pilot. Chem Eng News 87(27):10
Womac AR, Igathinathane C, Bitra P, Miu P, Yang T, Sokhansanj S, Narayan S (2007) Biomass pre-processing size reduction with instrumented mills. http://www.biomassprocessing.org/Publications/2-Papers_presented/ASAE%20Paper%20No%20056047%20biomass_instrumentedmills_Womac%20et%20al.pdf. Accessed 8 Feb 2011
Wool RP, Sun XS (2005) Bio-based polymers and composites. Elsevier/Academic, Burlington
Zamora A (2005) Fats, oils, fatty acids, triglycerides. http://www.scientificpsychic.com/fitness/fattyacids1.html. Accessed 8 May 2010

Biochemical Conversion of Biomass to Fuels

Swetha Mahalaxmi and Clint Williford

Contents

Abstract

Biomass can provide both hydrocarbon fuels and chemical compounds such as alcohols, gums, sugars, lipid-based products, etc. Biomass-derived fuels have acquired a lot of attention during recent years because of the abundance of supply of resources and lower green house gas emissions. Grasses, agricultural residues, animal residues and waste, used oils, etc., can be used as starting materials in the production of biofuels. Ethanol and biodiesel have found greatest application and contribute significantly to fuels. However, there is growing interest in other alternatives: hydrogen, methane, butanol, renewable diesel, and petroleum compatible fuels from advanced catalytic biotech processes. Characteristics of various feedstocks and fuels, processes for conversion of biomass to biofuels,

S. Mahalaxmi (✉) • C. Williford
Department of Chemical Engineering, The University of Mississippi, Oxford, MS, USA
e-mail: swetha.mahalaxmi@gmail.com; drwill@olemiss.edu

W.-Y. Chen et al. (eds.), *Handbook of Climate Change Mitigation and Adaptation*,
DOI 10.1007/978-3-319-14409-2_26

the physical, chemical factors, and limitations affecting the conversion of biomass to fuels are discussed in this chapter. Process parameters include pH, temperature, and residence time. Additionally, chemical parameters include carbon source, nutrients, acid and alkaline hydrolysis agents, and phenolic inhibitors and sugars generated within the process. Several limitations to bioconversion of biomass are described such as size reduction, crystallinity, byproduct inhibition to fermentation, deactivation of cellulases, ethanol tolerance by yeast, and cofermentation of various sugars. Recent innovations and future developments in recombinant DNA technology and protein engineering are aimed at overcoming limitations to bioconversion. Understanding the limitations and applying suitable biotechnological applications will support future developments for producing biofuels.

Introduction

With increasing demands for transportation fuel, renewable sources of energy content, have gained importance in the recent years. Important fuel parameters are energy content, combustion quality such as octane or cetane number, volatility, freezing point, toxicity, and its adaptability to current combustion engines (Lee et al. 2008c). Biofuels such as hydrogen, methane, ethanol, butanol, and biodiesel are of current interest in replacing (in partial or complete) gasoline to mitigate greenhouse gas emissions.

Table 1 presents comparative data for various fuels against gasoline and can be produced from biochemical conversion of biomass. Current working status of these fuels is also mentioned in the Table 1. Among the fuels mentioned in the table, butanol and biodiesel (biodiesel from pure vegetable oils) can be used in existing gasoline and diesel engines respectively with a little modification. For others, engine modification is required. For ethanol, lower blends in gasoline do not require engine modification. Use in higher blends requires engine modification. Engine modification is required for some nongasoline fuels due to difference in their air-fuel ratio, latent heat of evaporation, and corrosiveness. Air-fuel ratio of gasoline is 14.6 kg air for 1 kg of fuel. However, 10 % v/v ethanol blend of gasoline has 3.5 % w/w oxygen in the fuel which influences the air-fuel ratio at which the engine performs. Engine management systems in modern vehicles adjust the air-fuel ratio to maintain the stoichiometric oxygen in the fuel. Absence of engine management system or use of higher blend gasolines/biodiesel alters the air-fuel ratio, therefore requiring engine modification. Ethanol and biodiesel have higher latent heat of evaporation compared to gasoline, which may present difficulties with starting in cold conditions. To avoid cold start difficulties, vehicles require a small tank fitted to accommodate gasoline to initiate combustion. Moreover, viscosity of biodiesel increases during cold conditions requiring alternative starting methods for vehicles using higher blends of biodiesel. Higher blends of ethanol are known to be corrosive on fuel lines and tanks; therefore, vehicles using 20 % v/v ethanol blend gasoline require to have nickel-plated steel fuel lines and tank.

Table 1 Properties of various biofuels (Adapted from sources Lee et al. (2008c) and http://en.wikipedia.org/wiki/Energy_density)

	Hydrogen	Methane	Ethanol	Butanol	Biodiesel	Gasoline
Heat of vaporization (KJ/Kg)	451.9	760	920	430	2,639.9	360
Energy density (MJ/L)	10.1 (liq)	0.0378	19.6	29.2	37.3	32.0
Research octane number	>130	135	129	96	>25	97–98
Air to fuel ratio	34	17.2	9.0	11.2	13.5	14.6
Freezing point (°F)	−435	−296.5	−173.2	−128.7	26–66	−40
Flash point, closed cup (°F)	−423	−306.4	55	84	212–338	−45
Solubility in water, volume%	–	–	100	9	Negligible	Negligible
Technology	Microbial	Microbial	Microbial	Microbial	Chemical	Chemical
				Chemical	Enzymatic	Physical
Status	Laboratory	Industrial	Industrial	Laboratory	Industrial	Industrial
					Laboratory	
Engine application	Blend	Blend	Blend	Blend	Blend	N/A
	Pure	Pure	Pure	Pure	Pure	
Current engine modification	Required	Required	Required for higher blends	Not required	Not required[a]	N/A

[a]Not required for lower blending

Various sources such as agricultural residues, municipal waste, animal waste, perennial grasses, etc., are used for conversion to biofuels. In this chapter, processes of production of biofuels, hydrogen, methane, ethanol, butanol, and biodiesel are described with recent progress. Applications of recombinant DNA technology and bioengineering to overcome production bottlenecks and enhance fuel production are discussed.

Sources

Biomass represents all materials derived from plant, animal, and microbial origins. Classification of biomass used in conversion to biofuels may be based on the origin (plant/animal), carbon source (woody/herbaceous), and physical and chemical characteristics. However, biomass from plant origin is considered highly desirable for its abundance and potential to mitigate emission of greenhouse gases. Carbohydrate monomers in plants are formed through photosynthesis, in which the atmospheric carbon dioxide is converted by sunlight to chemical energy. Moreover, the same amount of carbon dioxide is released, when biomass-derived fuels for energy are used, as taken up during the plant growth using sustainable means, therefore, production of more biomass, consequently mitigates and not add up to the atmospheric carbon dioxide (McKendry 2002).

Biomass can be majorly divided into woody plants, herbaceous plants or grasses, aquatic plants, and manures. Among these, some herbaceous plants, aquatic plants, and manures contain high moisture content and are suitable for wet processing or biochemical processing. Aqueous processing or wet processing is generally initiated through enzyme action. This method is suitable for high moisture content biomass because of challenged efficiency of overall energy retrieval, compared to the energy required for drying involved in dry processing. Moisture content, carbon source, and cellulose to lignin ratio are the most important factors affecting the wet process. Biomass with low moisture content is subjected to dry process or thermal treatment such as gasification, pyrolysis, and combustion. Factors that influence the dry processes are ash content, alkali, and trace components as they adversely affect the thermal conversion processes (McKendry 2002).

The products of wet processes are ethanol, butanol, and biogas. Ethanol and butanol products majorly depend on the plant composition – cellulose, hemicellulose, and lignin. Cellulose, hemicellulose, and lignin are the three main components of any plant material. Cellulose is a polymer of glucose with linear chains of (1,4)-D-glucopyranose units in β-configuration with an average molecular weight of around 100,000. Another polymer of glucose with linear chains of (1,4)-D-glucopyranose units in α-configuration, called amylose constitute about 20 % of starch. Starch also includes amylopectin, a branched polymer chain of D-glucose molecules called α-1,6 glycosidic linkage (Shuler and Kargi 2008). Starch can be more easily digested to sugars compared to cellulose due to the beta configuration and high crystallinity offered by cellulose linear structure. Starch can be obtained

from any of the food storage units of plants, while cellulose constitutes all the other parts of the plant.

Hemicellulose is a heterogeneous polymer of pentoses (xylose and arabinose) primarily xylose, hexoses (mannose, glucose, and galactose), and sugar acids. Although it is not covalently bonded, it is tightly bonded to the surface of each cellulose microfibril. Cellulose digestibility to sugars partially depends on the hemicellulose content.

After cellulose and hemicellulose, lignin is the third most abundant biopolymer, consisting primarily of phenylpropane units most commonly linked by ether bonds. It provides structural support , through its hydrophobic nature impermeability, and resistance to microbial and oxidative attack (Feldman 1985; Chang and Holtzapple 2000). Additionally, woody plants have higher lignin than herbaceous plants, thus imparting lesser strength in the latter due to loosely bound fibers (Saha 2004). Lignin also inhibits the conversion of carbohydrates to ethanol making it imperative to maximize the elimination of lignin in biomass. However, woody plants having higher lignin proportions resist moderately severe treatments, unlike herbaceous biomass. Some herbaceous plants like switch grass and miscanthus (*Miscanthus*) require less severe treatments for lignin removal. Since lignin alone causes inhibition to conversion of sugars and to ethanol, cellulose to lignin ratio is an important factor effecting conversion. Removed lignin can be used for combustion in boilers for energy generation.

For dedicated energy crops, cultivation of herbaceous plants is greatly encouraged for biochemical conversion to fuels compared to the woody biomass for several reasons such as, lesser harvest time, ease of harvesting, usage of surplus land, less intensive agricultural practices, less lignin content, and less severe treatment for conversion. Selection of plants for energy production depends on the climatic conditions, geographical location, and availability and type of treatment employed (either thermal or biochemical).

In the UK, a perennial crop, *miscanthus*, has attained a lot of attention for energy production through biochemical conversion due to the ease in growing, harvesting, and good annual yield. This thin-stemmed crop has been considered a good energy crop due to its annual harvest and low mineral content and is grown in ten countries in Europe. In the USA, another thin-stemmed crop, switch grass, is a model crop for the Oak Ridge National Laboratory, as it yields high ethanol from fermentation with the existing technologies. Its low ash and alkali content allow it to be used for combustion. Brazil, one of the pioneers for the production of ethanol, for fuel uses sugarcane as the source (McKendry 2002). Sources of biomass other than herbaceous plants include agricultural residues such as wheat straw, rice straw, corn fiber, corn stover, baggase, etc. Animal residues such as pig slurry (Murphy and McCarthy 2005), cattle dung, horse dung (Kalia and Singh 1998), etc., are used for biogas production, which upon upgrading to >97 % methane, can be used as transport fuel. Marine algae have gained importance as potential sources for biofuel production, both as substrates for fermentation to hydrogen, ethanol, and butanol, and as oil-rich sources for biodiesel production. Due to their less energy and water requirement, higher carbon dioxide capture and negligible lignin, they are considered as superior

to terrestrial biomass (Tran et al. 2010; Jung et al. 2011). However, several factors including availability, moisture content, and cellulose/lignin ratio impact the biochemical production of biofuels.

Process Overview

Major processes involved in the biochemical production of biofuels are biomass handling, biomass pretreatment, hydrolysis, and fermentation. However, depending on the source of biomass, the route of conversion to biofuel and the type of biofuel, the series of processes can alter. Figure 1 shows a schematic representation of some common unit operations and processes for the biofuels mentioned in section "Biofuels."

Handling

Biomass, either grown or obtained from various sources, needs to be transported to the production sites for biochemical conversion to fuels. Postharvest it is prepared as bales, pellets, and briquettes for which the biomass has to be size reduced. Size reduction is an important mechanical preprocessing step to increase the bulk density and flowability of particles for transportation. Biomass is generally ground to 3–8 mm particles to compact it into pellets or briquettes of higher density. Important parameters in evaluating the efficiency of size reduction are particle size, particle size distribution, shape, surface area, density, and energy efficiency of mill used (Miao et al. 2011). Due to the unavailability of a continuous supply of biomass feedstocks, storage of biomass becomes important to ensure uninterrupted supply for continuous production of biofuels. Although outdoor storing of wood chunks is a commonly practiced method, studies show that terpenes are emitted from wood due to the exposure of direct heat from sunlight (Rupar and Sanati 2005). Large silos and specially constructed facilities are used for biomass storage

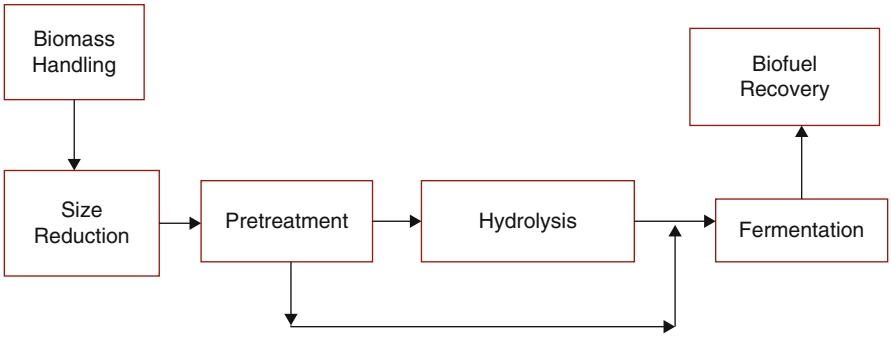

Fig. 1 Schematic representation of processes in biochemical conversion of biomass to fuels

to protect feedstock from the effects of weather, rodents, and microbial growth. Microbial growth during storage causes loss of substrate and also has the potential to result in self-ignition due to exothermic reactions. Therefore, it is required to maintain dry conditions to allow little microbial activity in the biomass during storage. Field drying postharvest is a common method for drying in sunny regions. However, thermal or mechanical drying techniques using drum driers are available for drying biomass after harvest and before storage in colder regions (Venturi et al. 1999).

Pretreatment

Pretreatment plays an important role in the biochemical conversion yields of biofuels. Complex structures in biomass are broken down into oligomeric subunits through pretreatment. These oligomers are further broken down into monomeric units during hydrolysis and fermentation. Pretreatment enhances the product yields by disrupting and solubilizing the hemicelluloses and lignin structures in biomass. Key properties affecting the conversion of lignocellulose are the crystallinity of cellulose, degree of polymerization, moisture content, available surface area, and lignin content (Chang and Holtzapple 2000). The aim of pretreatment is to disrupt the lignocellulosic structure by (1) removing hemicellulose, increasing mean pore size, and facilitating the entrance of enzymes and hydrolysis; (2) removing or redistributing lignin to reduce its "shielding" effect (Alvira et al. 2010).

Pretreatment processes will ideally achieve the following (Yang and Wyman 2008):

- High yields for multiple crops, sites ages, and harvesting times
- Highly digestible pretreated solid
- Minimum amount of toxic compounds
- Biomass size reduction not required
- Operation in reasonable size and moderate cost reactors
- Nonproduction of solid-waste residues
- Effective at low moisture content
- Obtains high sugar concentration (from hydrolysis)
- Fermentation compatibility (minimal production of inhibitors)
- Lignin recovery
- Minimum heat and power requirements

Main Classes of Pretreatment

The main classes of pretreatment covered in this chapter are mechanical, chemical, physiochemical, and biological. Mechanical pretreatment is discussed at this point as it applies to most process trains for biomass conversion. Chemical, physiochemical, and biological pretreatments are described in section "Pretreatment," as they pertain most closely to bioethanol production. At that point, characteristics making acid and alkali pretreatments suitable for methane production are also discussed.

Mechanical

Milling uses grinding to reduce particle size and crystallinity. Specific surface area is increased and degree of polymerization gets decreased. Numerous milling systems can be employed: ball, hammer, roller, colloid, and vibro energy milling (Alvira et al. 2010; Taherzadeh and Karimi 2008). Coupled with other pretreatment, milling can increase hydrolysis yield for lignocellulose by 5–25 % and reduces digestion time by 23–59 % (Delgenes et al. 2003; Hartmann and Ahring 2000). There are limits to effectiveness. Size reduction below #40 mesh does not improve hydrolysis yield or rate (Chang and Holtzapple 2000). Power requirements are large, which will limit economic feasibility (Hendriks and Zeeman 2009).

- Chemical (section "Pretreatment")
  - Acid pretreatment – concentrated and dilute
  - Alkali pretreatment – NaOH, $Ca(OH)_2$, or ammonia
- Physiochemical (section "Pretreatment")
  - Thermal processes include liquid hot water (LHW) and steam pretreatment
  - Steam explosion
  - Ammonia explosion (and CO_2 explosion)
  - Other physiochemical methods include organosolv and wet oxidation
- Biological pretreatment – brown and white soft-rot fungi (section "Pretreatment")

Alvira et al. conclude that chemical and thermochemical methods are the most effective and promising technologies for industrial applications (Alvira et al. 2010). They suggest combination of different pretreatments should be considered for optimal fractionation of components and high yields. They also stress the need for additional fundamental research plant cells to better understand the reactions induced by pretreatment.

Taherzadeh and Karimi (2008) concluded that concentrated acids, wet oxidation, solvents, and metal complexes are effective, but too expensive (Fan et al. 1987; Mosier et al. 2005a). They concluded that steam pretreatment, lime pretreatment, LHW systems, and ammonia-based pretreatments have a high potential. Eggeman and Elander (2005) presented an economic evaluation showing only small differences in cost for five different pretreatment technologies (dilute acid, hot water, ammonia fiber explosion (AFEX), ammonia recycle percolation (ARP), and lime). This analysis appears in the special issue "Coordinated development of leading biomass pretreatment technologies" (Wyman et al. 2005). Optimizing enzyme blends and hydrolysate conditioning may better differentiate process economics.

Hydrolysis and Fermentation

During hydrolysis, breaking down of polymeric and oligomeric cellulosic structure, to simpler molecules such as glucose, cellobiose, xylose, galactose, arabinose, and mannose, takes place. It is done by the action of either chemical or enzymatic agents. Enzymatic hydrolysis is a complex process that takes place at the solid/liquid

interphase. Several processes such as chemical and physical changes in the solid biomass, primary hydrolysis of soluble intermediates from the surface, and secondary hydrolysis to ultimately simpler molecules such as glucose take place simultaneously (Balat 2007). More discussion about enzymes used in hydrolysis is provided in section "Hydrolysis."

Conversion of simpler carbohydrates to alcohol through action of microbes is called as fermentation. Fermentation is both substrate and microbe specific, more details about fermentation are mentioned in section "Biofuels" for each biofuel, hydrogen, methane, ethanol, butanol, and biodiesel.

A combination of hydrolysis and fermentation is another process where simultaneous breaking down of complex carbohydrates to simpler ones and converting to alcohol takes place. This process is commonly called as simultaneous saccharification and fermentation (SSF). Product yields from SSF are higher than separate hydrolysis and fermentation (SHF), as the end product inhibition during hydrolysis of higher carbohydrates to glucose and cellobiose, is relieved by simultaneous fermentation of glucose to ethanol (Balat 2007).

Hydrolysis and fermentation are carried out in both batch and continuous modes. Batch reactors require higher reactor volume compared to the continuous reactors to achieve similar product yields. Two basic types of continuous reactors used in biochemical reactions are continuously stirred tank reactor (CSTR) and plug flow reactor (PFR). Most commonly, CSTR is used for hydrolysis and fermentation during the biochemical production of biofuels. Studies show usage of a packed bed reactor (PBR) in comparison with upflow anaerobic sludge bed (UASB) for the production of hydrogen from organic fraction of municipal solid waste, where the PBR was packed with municipal solid waste. The retention times of 50 and 24 h gave maximum hydrogen yields of 23 % v/v and 30 % v/v (based on volume of waste) for PBR and UASB, respectively (Alzate-Gaviria et al. 2007). Another study investigated combined or sequential two-stage processes involving coproduction of hydrogen and methane since hydrogen is an intermediate byproduct of methane production (Park et al. 2010; Zhu et al. 2008; Koutrouli et al. 2009). Dissolved oxygen and heat transfer are known to be limited by reactor volume. Fermentation for hydrogen, methane, ethanol, and butanol production is anaerobic, and the reactor volume is not limited by the dissolved oxygen and heat transfer when run in continuous mode. Therefore, CSTR fermentation systems with recycling of cell mass are sufficient to overcome solvent toxicity and limited cell growth (García et al. 2011).

Biofuels

Hydrogen

Biohydrogen is considered as a potential biofuel for the future, it is produced from biomass through different routes and their combinations. Gasification of biomass is one of the routes; refer to the chapters on thermal conversion of biomass, integrated

gasification for combined cycle (IGCC), and conversion of syngas to fuels in this handbook for more details about the gasification process. Hydrogen is a natural byproduct of many microbial processes under anaerobic conditions. Certain microbes release hydrogen from water in the presence of sunlight and/or carbon dioxide. Microbes that derive carbon from carbohydrates and need sunlight as a source of energy to release hydrogen are called phototrophic or photosynthetic organism (e.g., *Rhodobacter*) and those that derive their carbon from carbon dioxide and energy from sunlight are called photoautotrophic organisms (e.g., green microalgae and cyanobacteria) (Wukovits et al. 2009). Different fermentative processes, based on different sources of energy and their combinations, are anaerobic fermentation, dark fermentation, photo fermentation, direct photolysis, indirect biophotolysis, and fermentative water-gas shift reaction. The majority of these processes combine microbiological routes led by several microbes.

Anaerobic fermentation is a four-stage process carried out by a consortium of microbes. In the first stage, the complex organic components are converted to simpler components (e.g., sugars) by hydrolysis. In the second stage, the products of hydrolysis are further broken down to short-chain fatty acids by acidogenic bacteria. During the third stage, acidogenesis, the products of second stage are converted to acetic acid, hydrogen, and carbon dioxide. In the final stage, methanogenesis, the products from the third stage are used by the methanogenic bacteria to produce methane. Thus, hydrogen in this process is an intermediate product and its production can be increased by increasing the substrate content in the raw material used.

Figure 2 represents three different two-stage routes that are under active investigation. In the first stage, optimized technologies of above-mentioned conventional methods are used to convert biomass to organic acids and hydrogen. In the second stage, additional energy such as light, electricity, and methane and hydrogen from the first stage are used for achieving stoichiometric conversions. Although this combination of two stages produces a mixture of methane and hydrogen, the process can be developed to achieve hydrogen stream. Dark fermentation is carried out by the anaerobes that convert biomass substrate to hydrogen under the absence of light and is shown in Fig. 2. This process is similar to the first three stages of anaerobic fermentation where the initial raw substrate is simpler carbohydrate. For a complex substrate, hydrolysis such as a chemical/physical pretreatment of biomass is required to break down the complex polymeric biomass substrate to simpler monomeric and oligomeric carbohydrates, which can be later converted to organic acid, carbon dioxide, and hydrogen by anaerobes during dark fermentation. Reaction (1) represents a general formula for hydrogen metabolism from glucose. It is evident that in the presence of hydrogenase enzyme, 4 moles of hydrogen are released for every 1 mole of glucose. Thermophilic bacteria, that grow at high temperatures (above 60 °C) ferment biomass, produce hydrogen at higher rates than the mesophilic bacteria that grow at moderate temperatures (below 50 °C), due to aseptic conditions maintained at high temperatures. Additionally, hydrogen production depends on the other byproduct organic acids present in the effluent. Acetic acid and other organic acids have an inhibitory effect on the growth of microbes, consequently influencing

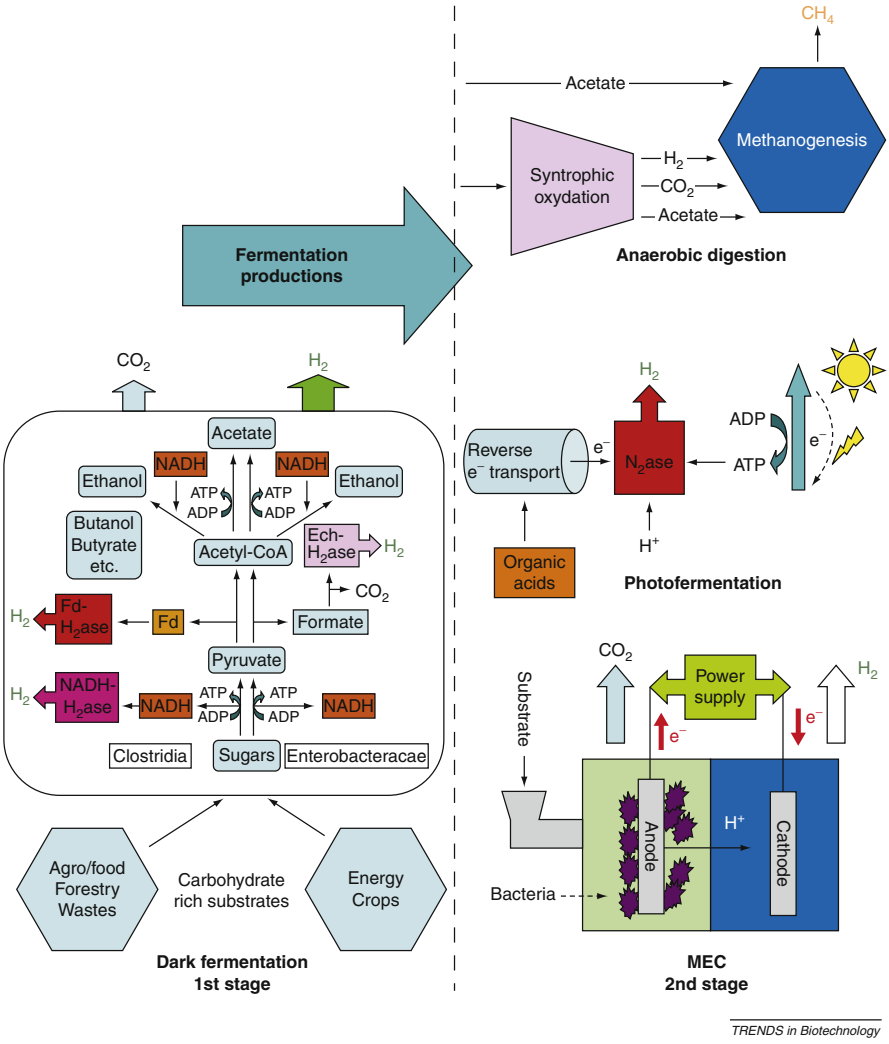

Fig. 2 Different two-stage routes for conversion to hydrogen and methane (Hallenbeck and Ghosh 2009)

hydrogen yield. Besides its inhibitory effect, acetic acid influences the pH of the system, thus affecting the activity of hydrogenase enzyme responsible for the production of hydrogen.

$$C_6H_{12}O_6 + 2H_2O \rightarrow 2CH_3COOH + 2CO_2 + 4H_2 \quad (1)$$

Photo fermentation involves a series of biochemical reactions such as anaerobic digestion. However, unlike dark fermentation, it requires light for energy during the process of hydrogen production. Simple, short-chain fatty acids are converted to

carbon dioxide and hydrogen catalyzed by nitrogenase enzyme in the absence of nitrogen by purple nonsulfur bacteria or green micro algae. Reaction (2) describes the conversion process. Theoretically, 4 moles of hydrogen are produced for every mole of acetic acid but, in practice, part of the acetic acid is used for the production of cells. Moreover, large surface area is required to capture the necessary light energy, making it practically challenging in terms of bioreactor design. Transparent tubular reactors and flat panel reactors consisting of transparent rectangular boxes are under investigation (Wukovits et al. 2009).

$$CH_3COOH + 2H_2O + \text{light energy} \rightarrow 4H_2 + 2CO_2 \quad (2)$$

Combination of the above-mentioned fermentations enhances the yield of hydrogen production. One such combination is dark fermentation and anaerobic digestion in which the monomeric components of the polymeric biomass are converted to biohydrogen. Dark fermentation and photo fermentation is another combination process that theoretically yields 12 moles of hydrogen for every mole of hexose sugar. This approach, called "Hyvolution," would allow complete digestion of biomass, enhancing small-scale, cost-effective production of hydrogen, which otherwise is limited by thermodynamic considerations (Wukovits et al. 2009).

Another approach mentioned in the second stage (lower right of Fig. 2) employs microbial electrohydrogenesis cells (MECs). In this method, electricity is applied to a microbial fuel cell that provides the necessary energy to convert the byproducts (typically organic acids) of the first stage into hydrogen (Hallenbeck and Ghosh 2009).

Several raw materials such as kitchen waste, animal waste, agricultural residues, etc., are used as substrates for biohydrogen production. Fermentation of kitchen waste devoid of plastic and bones was used to produce hydrogen with a maximum efficiency of 4.77 LH_2/(L reactor day) in a continuous stirred tank reactor (Shi et al. 2009). Use of second-generation feedstocks that are of cellulose origin such as corn stalks, wheat straw, switch grass, and *miscanthus* further enhance economical production of hydrogen. Pretreated lipid extracted microalgal biomass residue (LMBR) showed threefold hydrogen yields compared to the untreated LMBR (Yang et al. 2010). However, noncellulosic components such as xylose require conversion by a fermentative organism. High-thermophilic mixed culture was developed for xylose fermenting to biohydrogen at 1.36 ± 0.03 mol H_2/mol xylose consumed (Kongjan et al. 2009).

Organisms belonging to genus *Clostridium* such as *Clostridium butyricum*, *C. acetobutylicum*, *C. saccharoperbutylacetonicum*, and *C. pasteurianum* are often used in the anaerobic production of hydrogen. Anaerobic thermophilic bacterial fermentation to hydrogen is the most suitable option due to increasing chemical and enzymatic reaction rates at high temperatures. Additionally, thermophilic processes yield lesser undesirable products as compared to mesophilic processes (Koskinen et al. 2008). An optimized fermentation of hydrolysate obtained from treating sugarcane bagasse with 0.5 % H_2SO_4 under 121 °C and 1.5 kg/cm^2 in autoclave for 60 min was obtained at initial pH 5.5 and initial total sugar

concentration of 20 g/L at 37 °C (Pattra et al. 2008). Thus, initial pH and total sugar concentration are important factors for an optimal hydrogen yield. However, an increase in hydrolysate (sugar) concentrations from 25 % (v/v) to 30 % (v/v) led to no hydrogen production. Further, an increase in lag time was observed from 11 to 38 h for an increase in hydrolysate concentrations from 20 % (v/v) to 25 % (v/v) for a mixed thermophilic dark fermentation process (Kongjan et al. 2010). Supplemental glucose and xylose with a ratio of 2:3 along with suitable pH control and inoculum concentration are realized to be the key factors for enhanced hydrogen production (Prakasham et al. 2009).

Finally, biophotolysis is a low productivity method for hydrogen gas production. It involves dissociation of water by solar energy using green micro algae. The process takes place in two ways, direct biophotolysis and indirect biophotolysis. In direct biophotolysis, the microbes split the water into oxygen and hydrogen using sunlight by releasing two photons, which can either reduce carbon dioxide or form hydrogen in the presence of hydrogenase enzyme. However the released oxygen has an inhibitory effect on the hydrogenase enzyme which can be overcome by indirect biophotolysis. Indirect biophotolysis is carried out by cyanobacteria, in which water and carbon dioxide form carbohydrates and oxygen via photosynthesis. The second stage involves either dark fermentation or a combination of dark and photo fermentation to produce hydrogen. Fermentative water-gas shift reaction is another biological route in which carbon monoxide in the presence of water is converted to carbon dioxide and hydrogen (Wukovits et al. 2009).

Methane

Methane is the main component of natural gas which is used as an energy carrier and raw material all over the world (Seiffert et al. 2009). Biogas produced from anaerobic digestion of biomass contains methane which can be used for energy purposes. The biochemical conversion of manure and other biomass to methane involves three stages.

In the first stage, hydrolysis, enzymes produced by strict anaerobes such as *Clostridia*, *Bactericides*, and *Streptococci*, break up the complex molecules such as lipids, polysaccharides, proteins, fats, nucleic acids, etc., to simpler molecules such as monosaccharides, amino acids, fatty acids, etc. In the second stage, acidogenesis, a group of bacteria ferment the byproducts of hydrolysis to acetic acid, propionic acid, and butyric acid. In the third stage, methanogenesis, methanogens convert the acetic acid, hydrogen, and carbon dioxide into methane and carbon dioxide.

Figure 3 shows a block diagram of biogas production from manure. Biogas production is greatly affected by temperature. Anaerobic fermentation is effective mostly at mesophilic (15–40°C) and thermophilic (50–60°C) temperature ranges. Therefore, the reactors are coated with biomass residues such as charcoal and even constructed in a sun-facing direction to avoid cold winds and make maximum use of heat available from nature (Anand and Singh 1993). Reactors have been designed to have a polythene sheet covering the top of it to utilize the energy from sun to heat up the reactor contents even during winter (Bansal 1988).

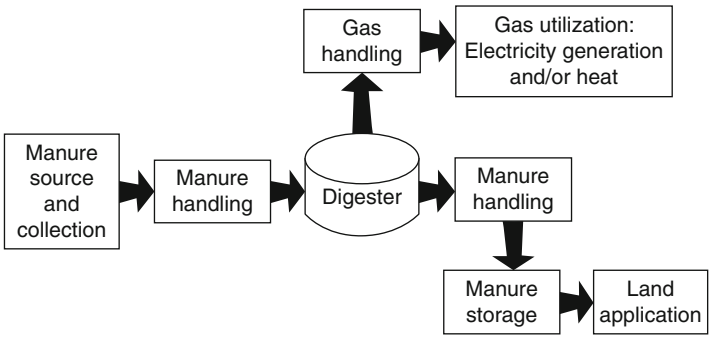

Fig. 3 Block diagram of biogas production from manure (Source: http://pubs.ext.vt.edu/442/442-881/442-881.html)

As acetic acid and hydrogen produced during the process decrease the pH of the system, pH maintenance is another important parameter affecting the methane production, the desired pH being 6.8–7.2. Several techniques are involved in enhancing the production of biogas, such as addition of organic and inorganic additives, microbial strains, recycling of digested slurry, and maintaining C:N ratio. Additives, such as powdered green leaves, allow adsorption of substrate to increase localized concentration and enhance microbial growth. Addition of Ca and Mg salts act as microbial energy supplements and avoid foaming. Recycling of slurry avoids loss of active culture which otherwise occurs through the effluent stream. As the microbes tend to utilize carbon 25–30 times faster than nitrogen for the production of methane, maintaining C:N ratio is another critical factor in efficient production of biogas (Yadvika et al. 2004).

Biomethane can be distributed into the natural gas grid. In the case of existing pipelines in UK, Italy, and Germany, this concept is called the "green gas concept" (Åhman 2010). However, to employ biogas as a transportation fuel, concentration of biogas to 97 $\pm$ 1 % of methane by removing the carbon dioxide is required (Power and Murphy 2009). About 30–60% of the wet biomass can be converted to methane by anaerobic digestion, while the remaining residue can be used as biofertilizer (Åhman 2010). Coproduction of methane and hydrogen using a two-stage anaerobic digestion process is another way to optimize simultaneous production of methane and hydrogen (Zhu et al. 2008).

An energy input approximating 22 % of the fuel value is utilized in the production of biomethane, compared to approximately 57 % in the production of bioethanol (Power and Murphy 2009). The majority of the difference arises from the thermal energy consumption involved in the distillation of ethanol and drying of the residue obtained from fermentation. Thus methane's gaseous nature has an added advantage over liquid biofuels. However, biomethane losses during digestion and upgrading constitute about 7.41 % of total biogas produced. Minimizing these losses and improving infrastructure efficiency for biomethane is needed to enhance the utility of methane relative to ethanol (Power and Murphy 2009).

Ethanol

Ethanol is the most extensively studied biofuel to date and has gained great attention as sustainable biofuel. Bioethanol production and utilization is estimated to reduce green house gas emissions, improve agricultural economy, enhance rural employment, and increase national security (Mabee and Saddler 2009). Bioethanol has higher octane number, broader flammability limits, higher flame speeds, and higher heats of vaporization than gasoline, which allow for higher compression ratio, shorter burn time, and leaner burn engine. A major problem with ethanol is its water solubility and azeotropic mixture formation with water, limiting separation during distillation, consequently intensifying the cost of the separation process. Other major disadvantages include lower energy density than gasoline, low vapor pressure (making cold starts difficult), and toxicity to ecosystems (Balat 2007). However, ethanol is a 35 % oxygenated fuel and reduces particulate and NO_x emissions. It increases combustion efficiency as it provides a reasonable antiknocking value. It can be blended with gasoline in various amounts, ranging from 5 % to 85–100 %, for use in the existing internal combustion engines, where 85 % (E85, meaning 85 % ethanol in gasoline) blends are used in flexible fuel vehicles (FFVs). Table 2 shows various blends of ethanol in gasoline used in different countries worldwide. In pure ethanol cars, sulfur emissions have totally disappeared; gasoline-driven cars with ethanol replacing lead have negligible carbon monoxide emissions (Goldemberg et al. 2008).

Substrates used for the production of bioethanol vary with the availability of feedstock and geographical location. The USA and Brazil are the two major bioethanol producers in the world. Sugarcane and cane molasses are the substrates for the ethanol production in Brazil as is cornstarch in the USA (Almeida et al. 2007). Other substrates used are cassava, sugar beet, wheat, etc. However, use of food products like corn and cassava for ethanol production has an inflating effect on the prices of these staple crops and an effect on their supply. Additionally, storage of high concentration sugar substrates is liable to microbial contamination

Table 2 Common gasoline ethanol blends available in various countries (Balat 2007)

	Common vehicles	Flexible fuel vehicles (FFVs)
USA	E10	E85
Canada	E10	E85
Sweden	E5	E85
India	E5	–
Australia	E10	–
Thailand	E10	–
China	E10	–
Columbia	E10	–
Peru	E10	–
Paraguay	E7	–
Brazil	E20, E25	Any blend available

and requires sophisticated storage methods, such as refrigeration, which in turn requires energy use over long periods (Dodic et al. 2009). Work by Dodic et al. suggests the use of intermediate products such as thick juice in sugar beet production as substrates for ethanol production, in order to reduce storage volume and microbial contamination. Use of lignocellulosic materials such as switch grass, *miscanthus*, sorghum, and corn stover is highly encouraged due to high substrate availability, economic feasibility of production, and storage, and due to other reasons mentioned in section "Sources" of this chapter. Waste mushroom logs have been studied for their potential as substrates for ethanol production where 12 g/L ethanol concentration was obtained as against 8 g/L concentration for normal logs (Lee et al. 2008b). Mahua flowers were investigated for their potential as substrates for ethanol fermentation, with ethanol productivity of 3.13 g/kg flower/h at 77.1 % efficiency (Mohanty et al. 2009).

Lignocellulosic biomass consists of majorly cellulose, hemicelluloses, and lignin of which cellulose is the most desired component for ethanol production. Ethanol is produced from the sugars that are present in the cellulose in polymeric form. Biomass is initially preprocessed, such as size reduced and washed for ease of handling and removal of soil. As shown in Fig. 4, the first major stage requires release of sugars from the cellulose-hemicellulose-lignin matrix; the second major stage involves the hydrolysis of higher sugars and fermentation of the monomeric sugars to ethanol; and the third stage involves the separation of ethanol from the fermentation broth.

Pretreatment

Pretreatments for bioethanol production may be performed using chemicals such as sulfuric acid, sodium hydroxide, ammonium hydroxide, supercritical ammonia, and supercritical carbon dioxide at both high and low temperature and pressure conditions to separate undesirable components such as lignin from biomass. Pretreatment disrupts the biomass structure and increases the surface area to enhance enzyme

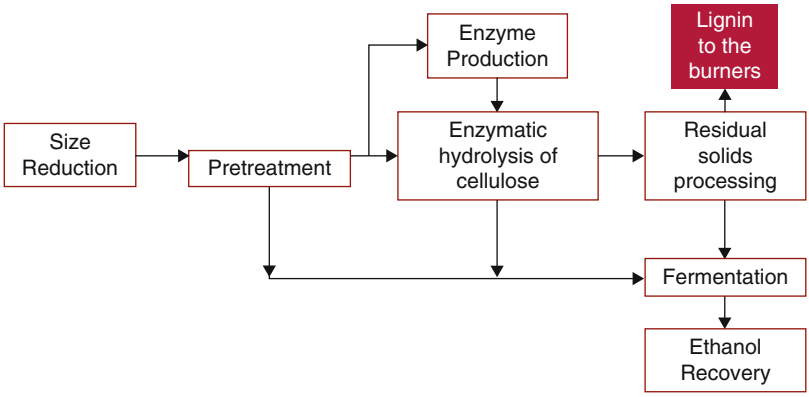

Fig. 4 Cellulosic ethanol "sugar platform"

access during the hydrolysis stage. Several pretreatment methods such as hot water treatment, steam explosion, dilute sulfuric acid treatment, and ammonia fiber expansion can be employed to remove lignin and/or depolymerize lignocelluloses structure in biomass.

Thermal processes include liquid hot water (LHW) and steam pretreatment. At temperatures above 150–180°C, hemicellulose and then lignin begin to dissolve (Bobleter 1994a; Garrote et al. 1999). Hot water pretreatment primarily dissolves hemicellulose to increase access for enzyme hydrolysis and to limit formation of inhibitors (Mosier et al. 2005a). Liquid hot water has removed up to 80 % of the hemicellulose to improve enzymatic hydrolysis by increasing the accessible surface area of the cellulose (Mosier et al. 2005a; Laser et al. 2002). pH should be kept between 4 and 7 to maintain hemicellulosic sugars in oligomeric, reducing formation of degradation products and thus inhibitors (Mosier et al. 2005a). Hemicellulose can be hydrolyzed to form acids which further hydrolyze the hemicelluloses (Gregg and Saddler 1996). The main advantages for LHW are recovery of pentoses, minimization of inhibitors, compared to steam explosions and minimal need for chemical and neutralization as compared to dilute acid pretreatment (Taherzadeh and Karimi 2008). Hot water pretreatment of lignocellulosic biomass has three types of reactor configurations, cocurrent, counter current, and flow through. In cocurrent pretreatment, biomass and water are heated to a desired temperature and held in the reactor for a controlled residence time before cooling. In counter current flow system, biomass slurry and water are allowed to flow in opposite directions into the reactor. In flow through configuration, hot water is allowed to flow through a stationary bed of biomass (Mosier et al. 2005b). Therefore, pretreatment technologies have been developed to be carried out in both batch and continuous flow reactor configurations.

Steam explosion has been widely tested in lab and pilot-scale systems. Biomass is pressurized with steam at 160–260°C for several seconds to minutes and pressure is rapidly released. Mechanical forces separate fibers and the high temperature promotes conversion of acetyl groups to acetic acid (Alvira et al. 2010; Taherzadeh and Karimi 2008). The main action of the acetic acid is probably to catalyze the hydrolysis of soluble hemicellulose oligomers (Bobleter 1994b). Lignin is redistributed and some removed (Pan et al. 2005). Removing hemicellulose increases accessibility of enzymes to the cellulose (Alvira et al. 2010). The advantages of steam explosion include use of larger chip size, reduced need for acid catalyst, high sugar recovery, and feasibility for industrial-scale use (Alvira et al. 2010). The primary disadvantages include partial hemicellulose degradation and generation of inhibitory compounds (Oliva et al. 2003). Steam explosion can be combined with addition of sulfur dioxide and sulfuric acid to enhance recovery of cellulose and hemicellulose. It improves the solubilization of hemicelluloses, lowers optimal treatment temperatures, and partially hydrolyzes cellulose (Brownell et al. 1986; Tengborg et al. 1998). Acid addition is particularly effective with softwoods, which have a low content of acetyl groups (Sun and Cheng 2002).

Acid pretreatment removes hemicellulose to make cellulose more accessible. It can also hydrolyze fermentable sugars. Acid pretreatment can be practiced using

high concentrations of acid (generally sulfuric) at low temperatures or low concentrations at high temperatures (Taherzadeh and Karimi 2008). Use of concentrated acid requires corrosion resistant process equipment. Recovery of the acid is energy intensive and produces degradation products inhibitory to fermentation (Alvira et al. 2010; Taherzadeh and Karimi 2008; Chisti 1996). Use of dilute acid is more promising, for example at 0.1–1 % sulfuric acid at 140–190°C. This achieves almost total hemicellulose removal and high cellulose conversion (Taherzadeh and Karimi 2008). Production of inhibitory compounds is lessened (Hendriks and Zeeman 2009). Addition of nitric acid greatly improves solubilization of lignin in newspaper (Xiao and Clarkson 1997). The use of acid pretreatment for methane production is more forgiving because methanogens can tolerate the inhibitory compounds (Xiao and Clarkson 1997; Benjamin et al. 1984).

Alkali pretreatment uses NaOH, $Ca(OH)_2$, or ammonia. Lime is very effective (Hendriks and Zeeman 2009). It removes acetyl groups and has lower cost and less safety concerns. Solvation and saponification reactions (Hendriks and Zeeman 2009) lead to swelling. The swelling increases internal surface area of cellulose, decreases polymerization and crystallinity, and disrupts lignin structure and removes some lignin and hemicellulose (Taherzadeh and Karimi 2008), increasing accessibility to enzymes enhancing saccharification (Kassim and El-Shahed 1986). Processing can be done at low (ambient) temperature (Xu et al. 2007) for long time periods (24 h) or at elevated (120–130°C) levels for minutes to hours (Silverstein et al. 2007). Production of inhibitory compounds is significantly less (Taherzadeh and Karimi 2008). But, solubilization and redistribution of lignin and modifications in crystalline state of lignin can counteract the benefits of the method (Gregg and Saddler 1996). Addition of hydrogen peroxide to alkaline pretreatment enhances lignin removal and improves enzymatic hydrolysis (Carvalheiro et al. 2008). Alkaline pretreatment, as with acid, is more forgiving for production of methane versus ethanol (Pavlostathis and Gossett 1985).

Ammonia fiber explosion or "expansion" (AFEX) is analogous to the steam expansion method. Anhydrous ammonia is added to biomass at approximately 1 kg NH_3: 1 kg dry and held at temperatures of approximately 100–120°C for several minutes. Pressure is rapidly released, swelling and disrupting the lignocellulose structure (Alvira et al. 2010; Taherzadeh and Karimi 2008). Only a solid residue is produced and a little hemicellulose and lignin are removed (Wyman et al. 2005). Enzyme hydrolysis yields and ethanol production are increased (Alizadeh et al. 2005). AFEX does not produce inhibitors, although some lignin may remain on the biomass surface (Alvira et al. 2010). It is more effective on lower-lignin crop residues and herbaceous crops than woody material (Wyman et al. 2005).

CO_2 explosion uses CO_2 at high pressure to penetrate the pores of lignocellulose. Explosive depressurization disrupts the cellulose and hemicellulose structure and improves enzymatic hydrolysis. Supercritical conditions at 35 °C and 73 bar remove lignin and increase digestibility more effectively (Alvira et al. 2010). However, pretreatment with appropriate conditions is a highly desirable step for lignocellulosic biomass to improve its digestibility.

Other physiochemical methods include organosolv and wet oxidation. Organosolv uses organic solvents to dissolve lignin. Solvent recovery is essential, and inexpensive, low molecular weight alcohols are favored. The recovery of low molecular weight lignin as a coproduct is potentially a significant advantage (Pan et al. 2005). Wet oxidation uses water and oxygen under elevated pressure and temperature (Taherzadeh and Karimi 2008). Hydrogen peroxide can be used at ambient temperature can also be used to enhance enzymatic hydrolysis (Azzam 1989). Batch treatment of corn stover using $FeCl_3$ in tubular reactors resulted in the hydrolysis yield of 98 % compared to 22.8 % yield for the untreated corn stover (Liu et al. 2009).

Biological pretreatment primarily uses brown and white soft rot fungi that degrade lignin and hemicelluloses (Taherzadeh and Karimi 2008). White rot fungi in particular have been evaluated and several shown to have high delignification efficiency (Kumar et al. 2009). Increase in total sugar yields during hydrolysis has been reported for switch grass preprocessed with *Phanerochaete chrysosporium* for 7 days (Mahalaxmi et al. 2010). Advantages include low energy and chemical requirements and ambient conditions. However, hydrolysis rates after biological pretreatment are low, and more research is needed (Alvira et al. 2010).

Hydrolysis

Hydrolysis of the pretreated biomass can be performed both chemically and biochemically. Chemical hydrolysis uses a continuous two-step dilute sulfuric acid process. The first step involves low temperature treatment and the second step, a high temperature treatment, as hemicellulose depolymerizes at lower temperature than the cellulose polymer. In the first step, the hemicellulosic fraction is removed, followed by the second step in which hexose release occurs. A batch process, using concentrated sulfuric acid, is also used for biomass hydrolysis; however, the use of concentrated acid requires high capital investment due to the requirement of corrosive resistant process equipment. Additionally, it requires acid recycling and recovery for economic viability of the process (Balat 2007).

Biochemical hydrolysis is the most sought out process in recent years and is commonly called as saccharification. It is initiated by enzymes that cleave the cellulose-lignin matrix into various monomeric, dimeric, and oligomeric sugars. Most common enzymes that act synergistically for cellulose hydrolysis, called cellulases, are endoglucanases or endo-1,4-β-glucanases (EG), exoglucanases or cellobiohydrolases (CBH), and β-glucosidases (BGL). While endoglucanases cleave the intramolecular bonds of the cellulose polymer, CBH and BGL catalyze the release of cellobiose and glucose from oligomeric ends and glucose from cellobiose respectively as shown in the Fig. 5. A synergistic effect of an enzyme component system consisting of at least endo-β-glucanases, exo-β-glucanases, and β-glucosidases results in hydrolytic efficiency (Sun and Cheng 2002; Maeda et al. 2011).

Enzymes related to hemicellulose hydrolysis, hemicellulases, are majorly endo-1,4- β-xylanase, β-xylosidase, α-glucuronidase, α-L-arabinofuranosidase, and acetylylan esterase as shown in Fig. 6. Therefore, the hydrolysate contains both

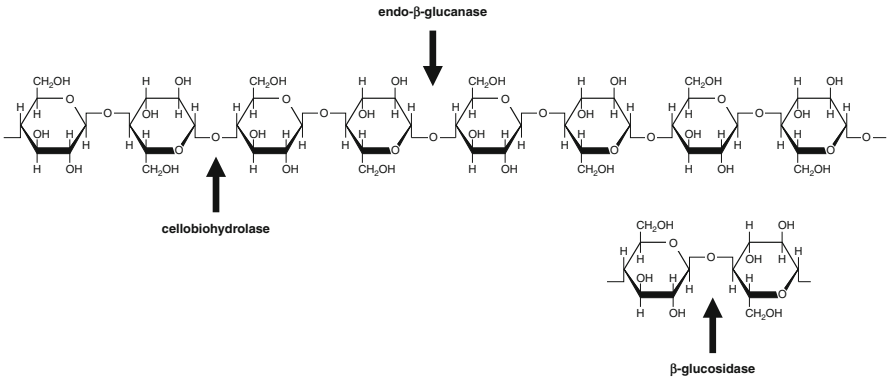

Fig. 5 Molecular structure of cellulose and site of action of endoglucanase, cellobiohydrolase, and β-glucosidase (Kumar et al. 2008)

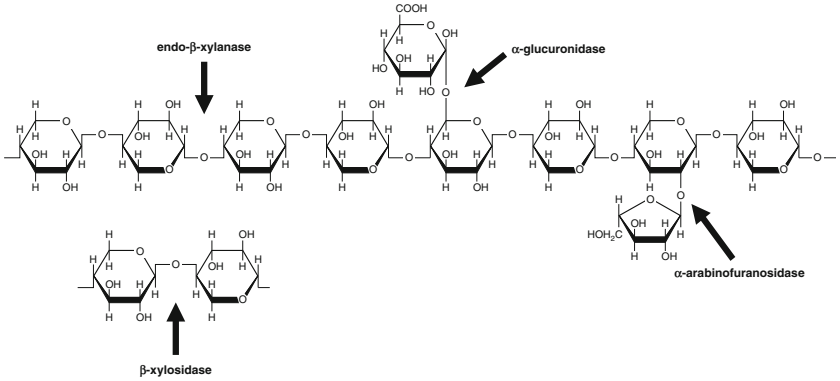

Fig. 6 Polymeric chemical structure of hemicellulose and targets of hydrolytic enzymes involved in hemicellulosic polymer degradation (Kumar et al. 2008)

hexoses and pentoses and their oligomeric forms depending on the treatment (Kumar et al. 2008).

Various bacteria such as *Clostridium*, *Cellulomonas*, *Bacillus*, *Thermomonospora*, *Ruminococcus*, *Bacteriodes*, *Erwinia*, *Acetovibrio*, *Microbispora*, and *Streptomyces* produce these enzymes to hydrolyze lignocelluloses. Fungi such as *Trichoderma*, *Ceriporiopsis*, *Aspergillus*, and *Sporotrichum* also possess the cellulolytic abilities to hydrolyze lignocellulosic biomass. Therefore, enzyme extracts from these cultures are used for hydrolyzing biomass and recent developments in enzyme technology have reduced their price of production significantly.

The factors that influence the enzymatic hydrolysis are mainly temperature, pH, and substrate concentration. At low substrate concentration, increase in substrate concentration increases the yield and the reaction rate of hydrolysis. However, at

high substrate concentration, yield and reaction rate decrease due to substrate inhibition of enzymes (Sun and Cheng 2002; Chisti 1996). Temperature and pH for enzyme activity varies by the microbe source from which it is derived. However, most commonly used industrial cellulases are derived from wild and modified strains of *Trichoderma reesei* and have an optimum temperature between 45 °C and 50 °C. Hydrolysis yields are also increased by addition of surfactants such as Tween-20. It is reported that the addition of Tween-20 resulted in 8 % increase in ethanol and 50 % reduction in cellulases dosage, increase in enzyme activity and the hydrolysis rate (Sánchez and Cardona 2008).

Consolidated microbial treatment of biomass is another method of saccharification of biomass. Loss of sugars during the process is inevitable, due to the consumption by microbes, which makes the use of enzyme extracts advantageous for hydrolysis. Enzyme hydrolysis is limited byproduct inhibition, which requires continuous removal of hydrolysis products apart from the use of BGL for subsequent conversion of the generated cellobiose to glucose. Therefore, simultaneous saccharification and fermentation (SSF) is a potential solution for product inhibition, where release of glucose using enzyme hydrolysis and its subsequent fermentation to ethanol by yeast take place in the same system (Balat 2007).

Fermentation

Fermentation of biomass to ethanol is commonly carried out using yeast such as *Saccharomyces* and *Pichia*, bacteria such as *Zymomonas* and *Escherichia*, and fungi such as *Aspergillus.* Products of hydrolysis and sugars are converted to ethanol producing carbon dioxide as byproduct and energy for cell growth. The most commonly used microbe *Saccharomyces cerevisiae* ferments sugars to ethanol at almost anaerobic conditions, although it requires a certain amount of oxygen for essential polyunsaturated fats and lipids. Figure 7 depicts the ethanol fermentation pathway of *Saccharomyces* from glucose. It briefly describes the conversion of glucose to ethanol through intermediate biochemical reactions involving NAD^+ and NADH (Nicotinamide adenine dinucleotide – oxidized and reduced forms, respectively). Since lignocellulosic biomass consists of several components such as pentoses, hexoses, and acids (acetic acid), degradation products derived from the pretreatment stage could inhibit the fermentation process. Chemical, physical, and biological methods have been developed to overcome the inhibition effect of these compounds by detoxification. *Trichoderma reesei* has been reported to degrade the inhibitors present in willow hydrolysate after steam pretreatment. Overnight extraction of spruce hydrolysate with diethyl ether at pH 2 showed detoxification effects with ethanol yields comparable to the reference fermentation. Detoxification by alkali treatment at pH 9 using $Ca(OH)_2$ and readjustment of pH to 5.5 allowed better fermentability due to precipitation of toxic compounds (Palmqvist and Hahn-Hägerdal 2000).

Usually, the temperature of operation is in the mesophilic range (15–40°C) for most of the species mentioned above. Increases in temperature beyond the optimum condition result in a decrease in ethanol yield and eventually in cell death. Another important factor in maintaining good cell growth is pH, generally a pH range of 6.5–7.5 (Aminifarshidmehr 1996) is suitable for ethanol fermentation for most of the

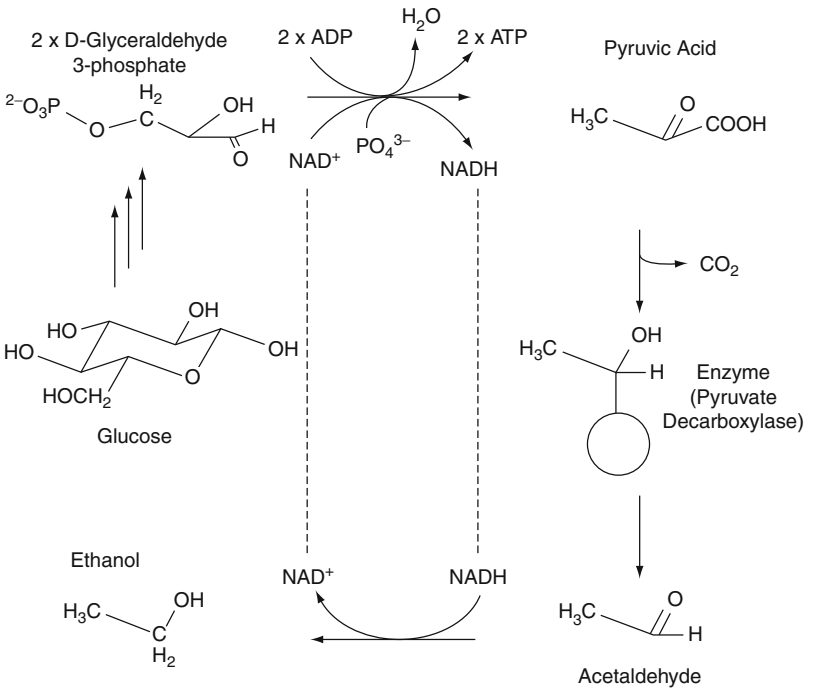

Fig. 7 Ethanol fermentation pathway of *Saccharomyces*

strains, although, yeast and fungal strains can tolerate up to 3.5–5.0. pH below 4.0 reduces the potential of bacterial contamination thus alleviating the requirement of severe aseptic techniques (Balat 2007).

Fermentation of biomass is affected by several other factors such as ethanol tolerance, substrate concentration, and byproduct inhibition. Ethanol tolerance is one of the factors which determine the maximum ethanol concentration that can be reached during fermentation, as most of the microbes responsible for fermentation cannot tolerate high concentrations of ethanol, eventually leading to cell death. *Zymomonas* has higher ethanol tolerance and achieves 5 % higher ethanol yields, as compared to the other yeast strains (Mohagheghi et al. 2002). Increase in substrate concentration decreased the ethanol yield. However, batchwise charging of substrate reduces this kind of inhibition. Therefore, fed-batch reactors are more suitable for industrial applications. Byproduct inhibition is overcome by chemical, mechanical, or biological detoxification as mentioned above (Balat 2007).

Butanol

Butanol is a colorless liquid which causes a narcotic effect at high concentrations. It is used as a solvent in biopharmaceutical, chemical, and cosmetic applications because of its high solubility in organic solvents and low water miscibility. Its physical properties very closely resemble those of gasoline, making it a potential

additive in partial or complete to transportation fuel (Lee et al. 2008c). Butanol can also be used as a replacement fuel to gasoline-driven engines with minimum or no changes; it can also be blended with gasoline at much higher composition than ethanol as butanol has similar energy content as that of gasoline. It can be added to gasoline at the refinery and distributed through existing gasoline pipeline unlike ethanol, as butanol is less corrosive and does not absorb water (Dürre 2008).

Butanol, a four carbon primary alcohol, can be synthesized both chemically and biochemically; chemical synthesis of butanol is conducted majorly by three methods, namely, Oxo synthesis, Reppe synthesis, and crotonaldehyde hydrogenation. However, the discussion of this chapter is limited to biochemical conversion of biomass to butanol.

In biochemical route, butanol is a fermentation product of anaerobic bacteria *Clostridium acetobutyliticum*, *Clostridium butyricum*, etc. Industrial production of butanol dates back to 1914 during World War I, as a byproduct in the production of acetone (which was used in war ammunition) by fermentation using *C. acetobutyliticum*. Although there was no immediate application of butanol during that time, later in 1920s in the USA, it was used to replace amyl acetate, a product from amyl alcohol, a solvent for lacquers in the automobile industry. By the 1950s, 66 % of the butanol used in the world was produced biochemically. However, due to increased biomass cost and low crude oil prices, crude oil replaced butanol as a transportation fuel (Dürre 2007). Substrates used for butanol production can be of both starch and cellulose origin such as molasses, corn fiber, wheat straw, etc. However, the conflict of using food substrates for fuel production regulates the usage of starch-based substrates. Figure 4, which depicts the flow of processes for ethanol, can also be applied for butanol. However, fermentation of biomass is carried out by butanol producing bacteria.

The biochemical routes involved in butanol formation are given in Fig. 8 (Lee et al. 2008c). Butanol formation takes place through the glucose-pyruvate-butyraldehyde route. Butanol fermentation is a biphasic transformation consisting of an acidogenic phase which occurs during exponential growth phase and solventogenic phase. During the acidogenic phase, acid-forming pathways are activated, and acetate, butyrate, hydrogen, and carbon dioxide are produced as major products. Acetone, butanol, and ethanol/propanol are the products of solventogenic phase which occurs after the exponential growth phase (Lee et al. 2008c). Both acidogenic and solventogenic phases can be seen in the Fig. 8 based on the final products produced in the two phases. The solventogenic phase is a response to the increased acid production after acidogenic phase, which if not initiated, would lead to a decrease in the extracellular pH, and finally to cell death due to increasing proton gradient between inner and outer cellular environments (Dürre 2008). Therefore, pH control has a very crucial effect on butanol production, and it requires being in the acidic range for the solventogenic phase.

Solvent toxicity is another major concern that causes cell death, due to cell wall weakening in the presence of acetone, ethanol, and butanol (the most toxic compound), leading to low product concentrations and productivity (Lee et al. 2008c). Solvent toxicity can be overcome by continuous removal of the solvents through

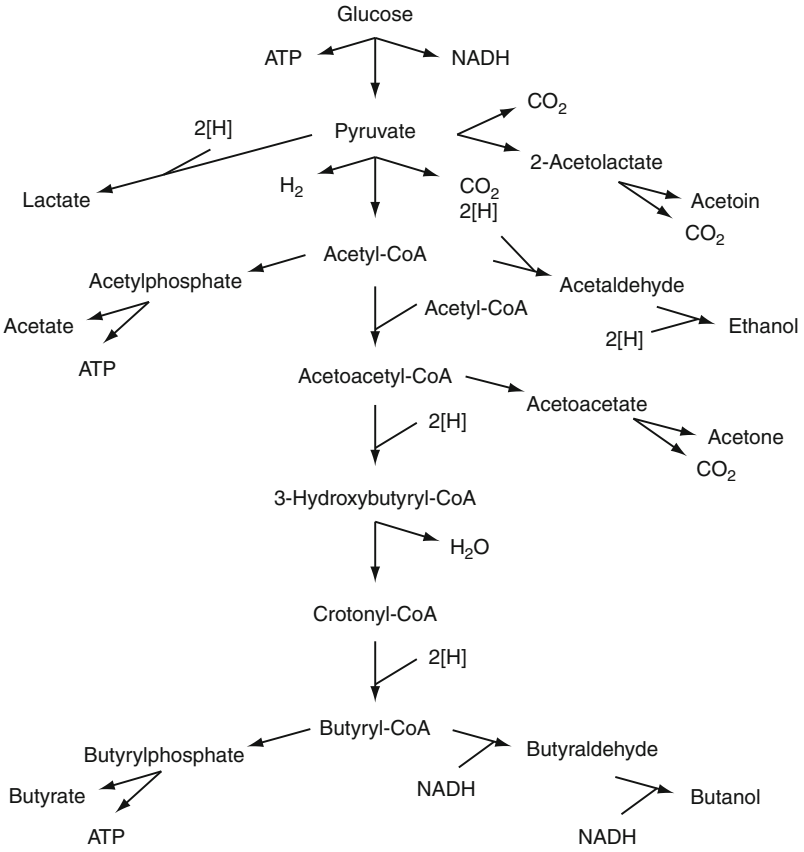

Fig. 8 Butanol fermentation pathway of *Clostridium acetobutylicum* (Dürre 2008)

various unit operations. Traditionally, butanol formed is separated by distillation which is a cost-intensive operation due to its high boiling point. Alternative methods for butanol separation are adsorption, gas stripping, liquid-liquid extraction, perstraption, pervaporation, and reverse osmosis (Dürre 2007). Each of these processes has certain limitations, among which, gas stripping is simple and successful in spite of low selectivity, as it can be used in a continuous operation for removing butanol. Liquid-liquid extraction requires use of a solvent that is noninhibitory to the microbes. In pervaporation, butanol is selectively diffused through a membrane and evaporated without removing the medium components necessary for the microbial growth (Qureshi et al. 1999). However, it is limited by fouling of membranes by the particles present in the fermentation broth.

Biodiesel

Biodiesel is a biofuel derived from transesterification of fats and oils with properties similar to the petroleum diesel. It can be blended with diesel or used directly in the

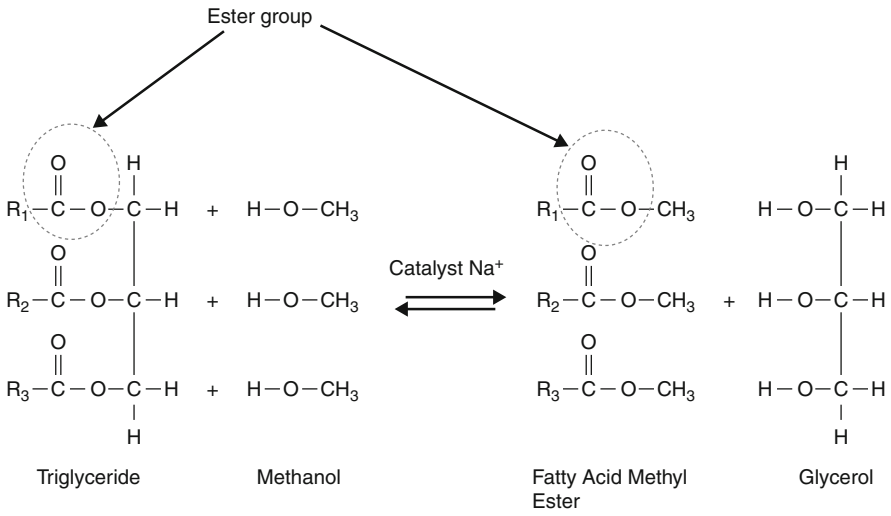

Fig. 9 Formation of biodiesel (Fatty acid methyl ester)

existing diesel engines without significant modifications. The main advantage of biodiesel is that, as a biomass-derived fuel, it produces 78 % less (net) carbon dioxide emissions, compared with that for petroleum-derived diesel fuel. Because its structure is nonaromatic, it combusts more efficiently, producing 46.7 % less carbon monoxide emissions, 66.7 % less particulate emissions, and 45.2 % less unburned hydrocarbons compared to conventional diesel. Therefore, it can be used in highly sensitive environments such as marine and mining environments (Helwani et al. 2009). Additionally, its high boiling point (about 150 °C) and presence of fatty acids impart lesser volatility and higher lubricating effect respectively, on engines, eventually reducing wear and tear and enhancing longer service life (Al-Zuhair 2007).

Biodiesel is conventionally produced from transesterification of oil (triglycerides) with alcohol (methanol) in the presence of an acid, base, or enzyme catalyst with glycerin as byproduct as shown in Fig. 9.

The sources of oil include oil seed plants such as palm, rapeseed, soybean, castor, and jatropha, used oils, lard, animal fat residue, etc. Palm oil having the highest yield of around 4,000 kg of oil per hectare is considered to be the best source of oil for biodiesel production (Al-Zuhair 2007). However, the majority of the cost involved in biodiesel production arises from the cost of the feedstock oil. Further, with the increasing edible oil consumption, it is more economical and environmentally sustainable to employ used oils and nonedible oils for biodiesel production. The major differences between the fresh and used oils are the moisture and free fatty acid (FFA) content, with used oils having high moisture and FFA content, which affect the acid- and alkaline-catalyzed transesterification, respectively. Alternatively, animal fats from waste residues are a useful source of oils. However, the heat at their high melting points denatures the enzymes used during enzyme-catalyzed

transesterification. Other sources of oil are oleaginous yeasts and filamentous fungi which on their outer surface secrete oil (Miao and Wu 2006).

As mentioned earlier, biodiesel production process can be alkali, acid, or enzyme catalyzed depending on the amount of FFAs and moisture present in the oil feedstock. The stoichiometry from Fig. 9 suggests oil to methanol ratio to be 1:3. However, for equilibrium to proceed toward the formation of biodiesel, use of excess alcohol is suggested.

During an alkali-catalyzed reaction, the oils in the presence of excess methanol are converted to fatty acid methyl esters and glycerin (Fig. 10). Alternately, during an acid-catalyzed reaction the triglycerides are esterified followed by a transesterification process (Fig. 11) (Schuchardt et al. 1998). Low FFA-containing feedstock is more suitable for alkali-catalyzed transesterification and high FFA-containing ones for acid-catalyzed reaction. FFAs present in oils during base-catalyzed reaction react with the oils to form soap and emulsions that hinder the purification processes of biodiesel apart from base consumption (Basu and Norris 1996). Alkaline methoxides are high biodiesel yielding base catalysts with short reaction times, even at very low (0.5 mol%) concentrations. However, they are more expensive than metal hydroxides (KOH and NaOH) (Helwani et al. 2009). On the other hand, acid-catalyzed reactions are 400 times slower than the alkali-catalyzed transesterification (Al-Zuhair 2007) and less sensitive to FFA content. The presence of water greatly inhibits the conversion due to catalyst deactivation.

The major reaction parameters affecting the biodiesel conversion are temperature, oil/methanol ratio, FFA, and moisture contents. An increase in temperature will increase the conversion the most appropriate range being 60–70°C, the alcohol boiling range at atmospheric pressure.

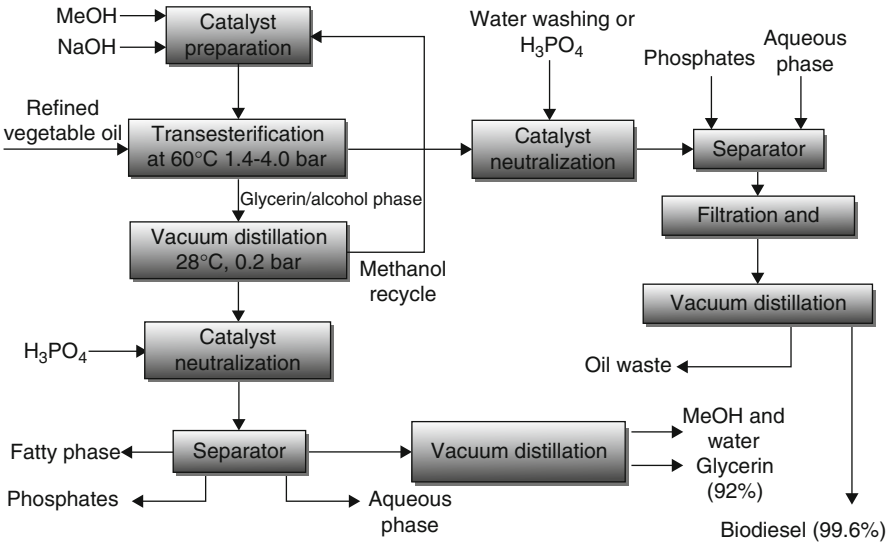

Fig. 10 Block diagram for base-catalyzed production of biodiesel (Helwani et al. 2009)

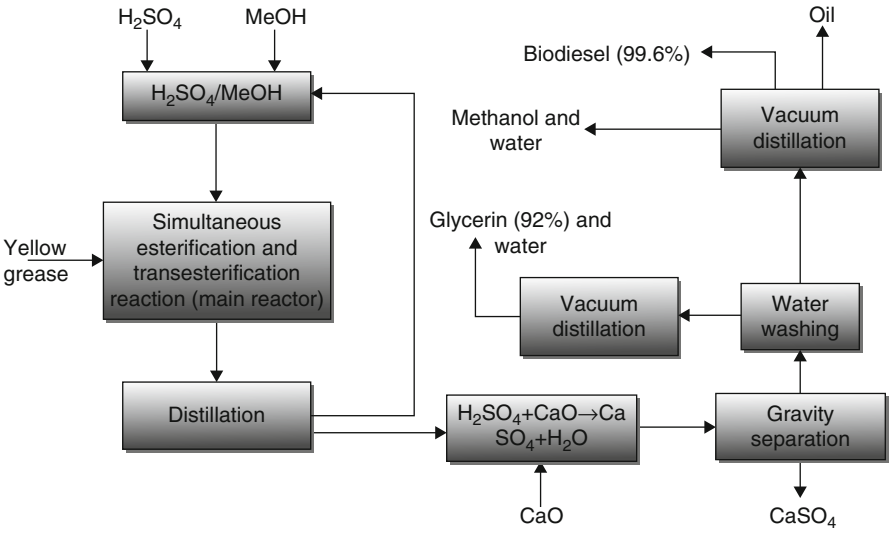

Fig. 11 Block diagram for acid-catalyzed production of biodiesel (Helwani et al. 2009)

Enzyme-catalyzed transesterification is achieved using lipases obtained from organisms such as *Candida rugosa*, *Pseudomonas fluorescens*, *Rhizopus oryzae*, *Burkholderia cepacia*, *Aspergillus niger*, *Thermomyces lanuginosa*, and *Rhizomucor miehei* (Al-Zuhair 2007). Enzymes are more compatible in terms of usage of a wide range of feedstocks, fewer processing steps, and fewer separation steps. Enzymes do not form soaps with the FFAs present in the feedstock, which allows the use of spent oils and animal fats for biodiesel production. They can convert both FFAs and triglycerides (TAG) simultaneously without another pretreatment step for converting FFAs to TAG (Fjerbaek et al. 2009). An increase in temperature increases the enzymatic conversion of biodiesel due to increased rate constants and lesser mass transfer limitations (Al-Zuhair et al. 2003). Additionally, optimal water content increases the biodiesel conversion as lipase acts as an interface between the aqueous and organic phases which allow its activation by rendering suitable conformation for transesterification (Panalotov and Verger 2000). However, they are currently facing challenges related to lower reaction rate, high cost, and loss of activity.

Methanol is the most widely used alcohol for biodiesel production due to its availability from syngas. However, it is required to use an alcohol produced from a renewable source, such as ethanol, to make biodiesel production a completely green process. Additionally, methanol is toxic and renders lipases inactive at high concentrations. Therefore, methyl acetate can be used as a methyl acceptor in place of methanol, as it still has no negative effects on Novozyme 435, the only commercial lipase known, used for biodiesel production from soybean oil (Du et al. 2004). Immobilization of lipases is considered an economical process to overcome the

limitations of using a batch process and employing a continuous process to enable glycerol separation for higher conversion rates (Watanabe et al. 2002).

Genetic Engineering Approaches

With the above background of conversion of biomass to fuels, it is evident that several factors such as biomass composition, pH, temperature, by-products, etc., have a potential impact on the biofuel production. Process factors such as pH and temperature can be maintained using appropriate reactor and process conditions. Intrinsic factors such as biomass composition, product tolerance such as ethanol and butanol tolerance, specific binding of enzymes, and byproduct inhibition will remain potential challenges without recombinant DNA technology.

Recombinant DNA technology is comprised of five general procedures (Nelson and Cox 2008):

1. A desired segment of the microbe DNA of interest is cut using sequence-specific endonucleases which are nucleotide cleaving enzymes, otherwise called restriction endonucleases. These endonucleases act as molecular scissors to obtain the required nucleotide sequence.
2. A small molecule of DNA capable of self-replication is selected. These molecules, called cloning vectors, are generally plasmids or viral DNA which can be coupled with the nucleotide sequence obtained from the previous step.
3. The two segments are incubated in the presence of DNA ligase to obtain a recombinant DNA.
4. Recombinant DNA is introduced into the host cell for replication. The most common host cell used is *E. coli* for its well-understood DNA metabolism and its well-characterized bacteriophages (viruses that live on bacteria) and plasmids.
5. After cell replication, the host cells with recombinant DNA are identified and used for expression.

The most commonly used host cells for metabolic engineering are *Escherichia coli*, *Zymomonas mobilis*, and *Saccharomyces cerevisiae* as their genetic maps are the most well studied (Banerjee et al. 2010). They are facultative anaerobes with fast growth rates and viability (Lee et al. 2008a). Incorporation and expression of pyruvate decarboxylase and alcohol dehydrogenase II genes from *Z. mobilis* into *E. coli* has resulted in high yields of ethanol from the utilization of both pentoses and hexoses, as against only hexoses (Banerjee et al. 2010). Although the recombinant strains are helpful in exploring the solutions for pathway-related problems, their industrial sustenance is limited due to the lack of robustness. Recombinant *E. coli* can produce isopropanol, n-butanol, and fatty acid ethyl esters through various engineered pathways (Atsumi and Liao 2008).

Modification of enzymes used in hydrolysis of biomass to produce sugars is generating immense interest. However, it is noticed that the enzymes belonging to the same class have different amino acid sequences conferring low level of

homogeneity, for example CBH1 (*T. reesei*) has <65 % amino acid identity in the nonredundant database. Additionally, cellulases from fungal origin have different optimized conditions than those from the prokaryotic origin and to predict a better choice between them is a challenge. Prediction of biochemical activity of an enzyme from its amino acid sequence is unreliable, and the only better way to evaluate it is to employ the extracted cellulase for hydrolysis and test it on various substrates (Banerjee et al. 2010). Alternatively, manipulation of plant species is directed toward altering its components such as lignin. Rastogi and Dwivedi discussed altering the lignin of woody species by introducing *omt* or *f5h* gene to introduce syringyl units in lignin to increase the paper pulping capability (Rastogi and Dwivedi 2008). Modification of lignin can be a potential area of research to increase the enzymatic digestibility and hydrolysis for enriching animal feed and enhancing biofuel production respectively.

Another area where genetic engineering principles can be applied is biomass cultivation. It is understood that by increasing the light interception efficiency and solar energy conversion to biomass, the productivity and yield of cultivation can be increased. Genetic engineering techniques can be applied to identify and manipulate the genes related to light reception and energy conversion to biomass in plants for dual interest, mitigation of elevated levels of atmospheric carbon dioxide, and increasing crop yield (Jansson et al. 2010).

Recombinant DNA technology is also used as a means to identify various enzymatic activities present in an organism. Two β-glucosidases were identified from *Pichia etchellsii* by cloning and expression of the corresponding genes in *E. coli* (Wallecha and Mishra 2003).

Advanced Fuels from Biochemical Conversion

Algal biofuels are of growing interest, where microalgae are grown in either closed or open photobioreactors to produce fatty acids. Although, algae use the sunlight with the same photosynthetic efficiency as that of land plants, the productivity of algal systems is much higher than plant biomass, as they do not produce roots, stems, and other structures. However, the extraction and processing costs during oil extraction from algae are challenging and require being minimized (Kaparaju et al. 2009). In an alternative use of algae, macro algae cells are used to tap the sunlight, and the tapped energy is converted to electricity. The excited electrons in the chloroplasts of the algae are intercepted through gold electrodes to create a tiny electrical current (Alternative energy).

The University of California, Los Angeles, is conducting research on microbes producing fuels from proteins rather than utilizing them for their growth. The microbes are induced to produce certain kind of proteins, which can be converted to fuels (Alternative energy).

Modified cyanobacteria utilize atmospheric carbon dioxide and sunlight to produce isobutanol which can be used as biofuel. Bacteria-powered battery is a very recent development, contrary to the belief that bacteria cannot produce electricity.

The byproducts of bacterial metabolism produce ions which pass through an ion filtering membrane, and then through an external circuit, converting the chemical energy provided by the bacteria to electrical energy (Alternative energy).

Isobutene, a fuel additive is produced through natural enzyme, rather than from the traditional petroleum-based route, by Prof. Thomas Bobik and his doctoral student David Gogerty. They have identified a new natural enzyme which can convert glucose found in plants to isobutene and is called as Bobik's enzyme. A limitation with the enzyme is the time taken to convert glucose to isobutene. However, efforts are in progress to reduce the conversion time for industrial feasibility (Alternative energy).

Qteros and Applied Clean Tech are working together to produce ethanol from wastewater and have developed technologies to handle the sludge remaining from the wastewater plant. Tobacco oil is another promising biofuel that is being studied by the researchers in Biotechnology Foundation Labs at Thomas Jefferson University. Current research is being conducted on improving the oil production from the tobacco leaves. Tobacco is a very attractive source for biofuel as it is not used in food production. Two genes in the plant have been modified to result in 6.8 % of oil per dry weight in leaves (Alternative energy).

Future Directions

It is evident from the above discussion that biofuels have high potential for meeting the needs of the transportation sector and supporting fuel independence and greener living. Choice of biomass and its properties are critical for optimum production of biofuel. Biomass selection depends on its availability, type of pretreatment employed, and the biofuel desired for production and their economics. Exploring various sources of biomass and improving the system of biomass collection and handling can improve the availability of biomass. Chemical, physical, or microbial techniques that can enrich the biomass composition are very desirable. Improvements in reactor design, process conditions, and other engineering aspects help optimize the biofuel production process. Adaptation and modifications of engine systems to biofuel use and innovation of newer ones is another important area of interest. Application of biotechnological tools such as recombinant DNA technology and genetic engineering can be used to overcome the bottlenecks of biochemical conversion and microbial robustness.

References

Åhman M (2010) Biomethane in the transport sector-an appraisal of the forgotten option. Energy Policy 1:208–217

Alizadeh H, Teymouri F, Gilbert T et al (2005) Pretreatment of switchgrass by ammonia fiber explosion (AFEX). Appl Biochem Biotechnol 1:1133–1141

Almeida JRM, Modig T, Petersson A et al (2007) Increased tolerance and conversion of inhibitors in lignocellulosic hydrolysates by *Saccharomyces cerevisiae*. J Chem Technol Biotechnol 4:340–349
Alternative energy. http://www.alternative-energy-news.info/technology/biofuels/. Accessed 8 Aug 2011
Alvira P, Tomás-Pejó E, Ballesteros M et al (2010) Pretreatment technologies for an efficient bioethanol production process based on enzymatic hydrolysis: a review. Bioresour Technol 13:4851–4861
Alzate-Gaviria LM, Sebastian PJ, Pérez-Hernández A et al (2007) Comparison of two anaerobic systems for hydrogen production from the organic fraction of municipal solid waste and synthetic wastewater. Int J Hydrog Energy 15:3141–3146
Al-Zuhair S (2007) Production of biodiesel: possibilities and challenges. Biofuels Bioprod Biorefin 1:57–66
Al-Zuhair S, Hasan M, Ramachandran KB (2003) Kinetics of the enzymatic hydrolysis of palm oil by lipase. Process Biochem 8:1155–1163
Aminifarshidmehr N (1996) The management of chronic suppurative otitis media with acid media solution. Otol Neurotol 1:24–25
Anand RC, Singh R (1993) A simple technique, charcoal coating around the digester, improves biogas production in winter. Bioresour Technol 2:151–152
Atsumi S, Liao JC (2008) Metabolic engineering for advanced biofuels production from *Escherichia coli*. Curr Opin Biotechnol 5:414–419
Azzam AM (1989) Pretreatment of cane bagasse with alkaline hydrogen peroxide for enzymatic hydrolysis of cellulose and ethanol fermentation. J Environ Sci Health B 4:421–433
Balat M (2007) Global bio-fuel processing and production trends. Energy Explor Exploit 3:195–218
Banerjee S, Mudliar S, Sen R et al (2010) Commercializing lignocellulosic bioethanol: technology bottlenecks and possible remedies. Biofuels Bioprod Biorefin 1:77–93
Bansal NK (1988) A techno-economic assessment of solar assisted biogas systems. Energy Sources 4:213–229
Basu HN, Norris ME (1996) Process for production of esters for use as a diesel fuel substitute using a non-alkaline catalyst. US Patent 5,525,126
Benjamin MM, Woods SL, Ferguson JF (1984) Anaerobic toxicity and biodegradability of pulp mill waste constituents. Water Res 5:601–607
Bobleter O (1994a) Hydrothermal degradation of polymers derived from plants. Prog Polym Sci 5:797–841
Bobleter O (1994b) Hydrothermal degradation of polymers derived from plants. Elsevier, Kidlington
Brownell HH, Yu EKC, Saddler JN (1986) Steam-explosion pretreatment of wood: effect of chip size, acid, moisture content and pressure drop. Biotechnol Bioeng 6:792–801
Carvalheiro F, Duarte LC et al (2008) Hemicellulose biorefineries: a review on biomass pretreatments. National Institute of Science Communication and Information Resources, New Delhi
Chang V, Holtzapple M (2000) Fundamental factors affecting biomass enzymatic reactivity. Appl Biochem Biotechnol 1:5–37
Chisti Y (1996) Biotechnology advances. In: Wyman CE (ed) Handbook on bioethanol: production and utilization. Taylor & Francis, Washington, DC
Delgenes JP, Penaud V, Moletta R (2003) Pretreatments for the enhancement of anaerobic digestion of solid wastes. ChemInform 34(13). doi:10.1002/chin.200313271
Dodic S, Popov S, Dodic J et al (2009) Bioethanol production from thick juice as intermediate of sugar beet processing. Biomass Bioenergy 5:822–827
Du W, Xu Y, Liu D et al (2004) Comparative study on lipase-catalyzed transformation of soybean oil for biodiesel production with different acyl acceptors. J Mol Catal B Enzym 3–4:125–129
Dürre P (2007) Biobutanol: an attractive biofuel. Biotechnol J 12:1525–1534
Dürre P (2008) Fermentative butanol production. Ann N Y Acad Sci 1:353–362

Eggeman T, Elander RT (2005) Process and economic analysis of pretreatment technologies. Bioresour Technol 18:2019–2025
Fan LT, Gharpuray MM, Lee YH (1987) Cellulose hydrolysis. Springer, Berlin
Feldman D (1985) Wood-chemistry, ultrastructure, reactions, by D. Fengel and G. Wegener, Walter de Gruyter, Berlin and New York, 1984, 613 pp. Price: 245 DM. J Polym Sci 11:601–602
Fjerbaek L, Christensen KV, Norddahl B (2009) A review of the current state of biodiesel production using enzymatic transesterification. Biotechnol Bioeng 5:1298–1315
García V, Päkkilä J, Ojamo H et al (2011) Challenges in biobutanol production: how to improve the efficiency? Renew Sust Energy Rev 2:964–980
Garrote G, Domínguez H, Parajó JC (1999) Hydrothermal processing of lignocellulosic materials. Eur J Wood Wood Prod 3:191–202
Gogerty DS, Bobik TA (2010) Formation of isobutene from 3-hydroxy-3-methylbutyrate by diphosphomevalonate decarboxylase. Appl Environ Microbiol 76(24):8004–8010
Goldemberg J, Coelho ST, Guardabassi P (2008) The sustainability of ethanol production from sugarcane. Energy Policy 6:2086–2097
Gregg D, Saddler J (1996) A techno-economic assessment of the pretreatment and fractionation steps of a biomass-to-ethanol process. Appl Biochem Biotechnol 1:711–727
Hallenbeck PC, Ghosh D (2009) Advances in fermentative biohydrogen production: the way forward? Trends Biotechnol 5:287–297
Hartmann H, Ahring BK (2000) Increase of anaerobic degradation of particulate organic matter in full-scale biogas plants by mechanical maceration. Water Sci Technol 3:145–153
Helwani Z, Othman MR, Aziz N et al (2009) Technologies for production of biodiesel focusing on green catalytic techniques: a review. Fuel Process Technol 12:1502–1514
Hendriks ATWM, Zeeman G (2009) Pretreatments to enhance the digestibility of lignocellulosic biomass. Bioresour Technol 1:10–18
Huo Y-X, Cho KM, Lafontaine Rivera JG, Monte E, Shen CR, Yan Y, Liao JC (2011) Conversion of proteins into biofuels by engineering nitrogen flux. Nat Biotechnol 29:346–351
Jansson C, Wullschleger SD, Kalluri UC et al (2010) Phytosequestration: carbon biosequestration by plants and the prospects of genetic engineering. Bioscience 9:685–696
Jung K-W, Kim D-H, Shin H-S (2011) Fermentative hydrogen production from *Laminaria japonica* and optimization of thermal pretreatment conditions. Bioresour Technol 3:2745–2750
Kalia AK, Singh SP (1998) Horse dung as a partial substitute for cattle dung for operating family-size biogas plants in a hilly region. Bioresour Technol 1:63–66
Kaparaju P, Serrano M, Thomsen AB et al (2009) Bioethanol, biohydrogen and biogas production from wheat straw in a biorefinery concept. Bioresour Technol 9:2562–2568
Kassim EA, El-Shahed AS (1986) Enzymatic and chemical hydrolysis of certain cellulosic materials. Agric Waste 3:229–233
Kongjan P, Min B, Angelidaki I (2009) Biohydrogen production from xylose at extreme thermophilic temperatures (70°C) by mixed culture fermentation. Water Res 5:1414–1424
Kongjan P, O-Thong S, Kotay M et al (2010) Biohydrogen production from wheat straw hydrolysate by dark fermentation using extreme thermophilic mixed culture. Biotechnol Bioeng 5:899–908
Koskinen PEP, Lay C-H, Puhakka JA et al (2008) High-efficiency hydrogen production by an anaerobic, thermophilic enrichment culture from an Icelandic hot spring. Biotechnol Bioeng 4:665–678
Koutrouli EC, Kalfas H, Gavala HN et al (2009) Hydrogen and methane production through two-stage mesophilic anaerobic digestion of olive pulp. Bioresour Technol 15:3718–3723
Kumar R, Singh S, Singh O (2008) Bioconversion of lignocellulosic biomass: biochemical and molecular perspectives. J Ind Microbiol Biotechnol 5:377–391
Kumar P, Barrett DM, Delwiche MJ et al (2009) Methods for pretreatment of lignocellulosic biomass for efficient hydrolysis and biofuel production. Ind Eng Chem Res 8:3713–3729
Laser M, Schulman D, Allen SG et al (2002) A comparison of liquid hot water and steam pretreatments of sugar cane bagasse for bioconversion to ethanol. Bioresour Technol 1:33–44

Lee SK, Chou H, Ham TS et al (2008a) Metabolic engineering of microorganisms for biofuels production: from bugs to synthetic biology to fuels. Curr Opin Biotechnol 6:556–563
Lee J-W, Koo B-W, Choi J-W et al (2008b) Evaluation of waste mushroom logs as a potential biomass resource for the production of bioethanol. Bioresour Technol 8:2736–2741
Lee SY, Park JH, Jang SH et al (2008c) Fermentative butanol production by *Clostridia*. Biotechnol Bioeng 2:209–228
Lee H, Choi S (2015) An origami paper-based bacteria-powered battery. Nano Energy 15:549–557
Liu L, Sun J, Li M et al (2009) Enhanced enzymatic hydrolysis and structural features of corn stover by FeCl3 pretreatment. Bioresour Technol 23:5853–5858
Mabee WE, Saddler JN (2009) Bioethanol from lignocellulosics: status and perspectives in Canada. Bioresour Technol 13:4806–4813
Maeda RN, Serpa VI, Rocha VAL et al (2011) Enzymatic hydrolysis of pretreated sugar cane bagasse using *Penicillium funiculosum* and *Trichoderma harzianum* cellulases. Process Biochem 5:1196–1201
Mahalaxmi S, Jackson C, Williford C et al (2010) Estimation of treatment time for microbial preprocessing of biomass. Appl Biochem Biotechnol 5:1414–1422
McKendry P (2002) Energy production from biomass (part 1): overview of biomass. Bioresour Technol 1:37–46
Miao X, Wu Q (2006) Biodiesel production from heterotrophic microalgal oil. Bioresour Technol 6:841–846
Miao Z, Grift TE, Hansen AC et al (2011) Energy requirement for comminution of biomass in relation to particle physical properties. Ind Crop Prod 2:504–513
Mohagheghi A, Evans K, Chou Y-C et al (2002) Cofermentation of glucose, xylose, and arabinose by genomic DNA-integrated xylose/arabinose fermenting strain of *Zymomonas mobilis* AX101. Appl Biochem Biotechnol 1:885–898
Mohanty SK, Behera S, Swain MR et al (2009) Bioethanol production from mahula (*Madhuca latifolia L.*) flowers by solid-state fermentation. Appl Energy 5:640–644
Mosier N, Hendrickson R, Ho N et al (2005a) Optimization of pH controlled liquid hot water pretreatment of corn stover. Bioresour Technol 18:1986–1993
Mosier N, Wyman C, Dale B et al (2005b) Features of promising technologies for pretreatment of lignocellulosic biomass. Bioresour Technol 6:673–686
Murphy JD, McCarthy K (2005) The optimal production of biogas for use as a transport fuel in Ireland. Renew Energy 14:2111–2127
Nelson DL, Cox MM (2008) Lehninger principles of biochemistry. W. H Freeman, New York
Oliva J, Sáez F, Ballesteros I et al (2003) Effect of lignocellulosic degradation compounds from steam explosion pretreatment on ethanol fermentation by thermotolerant yeast *Kluyveromyces marxianus*. Appl Biochem Biotechnol 1:141–153
Palmqvist E, Hahn-Hägerdal B (2000) Fermentation of lignocellulosic hydrolysates. I: inhibition and detoxification. Bioresour Technol 1:17–24
Pan X, Xie D, Gilkes N et al (2005) Strategies to enhance the enzymatic hydrolysis of pretreated softwood with high residual lignin content. Appl Biochem Biotechnol 1:1069–1079
Panalotov I, Verger R (2000) Enzymatic reactions at interfaces: interfacial and temporal organization of enzymatic hydrolysis. In: Baszkin A, Norde W (eds) Physical chemistry of biological interfaces. Marcel Dekker, New York
Park MJ, Jo JH, Park D et al (2010) Comprehensive study on a two-stage anaerobic digestion process for the sequential production of hydrogen and methane from cost-effective molasses. Int J Hydrog Energy 12:6194–6202
Pattra S, Sangyoka S, Boonmee M et al (2008) Bio-hydrogen production from the fermentation of sugarcane bagasse hydrolysate by *Clostridium butyricum*. Int J Hydrog Energy 19:5256–5265
Pavlostathis SG, Gossett JM (1985) Alkaline treatment of wheat straw for increasing anaerobic biodegradability. Biotechnol Bioeng 3:334–344
Power NM, Murphy JD (2009) Which is the preferable transport fuel on a greenhouse gas basis; biomethane or ethanol? Biomass Bioenergy 10:1403–1412

Prakasham RS, Brahmaiah P, Sathish T et al (2009) Fermentative biohydrogen production by mixed anaerobic consortia: impact of glucose to xylose ratio. Int J Hydrog Energy 23:9354–9361
Qureshi N, Meagher MM, Hutkins RW (1999) Recovery of butanol from model solutions and fermentation broth using a silicalite/silicone membrane. J Membr Sci 1–2:115–125
Rastogi S, Dwivedi UN (2008) Manipulation of lignin in plants with special reference to *O*-methyltransferase. Plant Sci 3:264–277
Rupar K, Sanati M (2005) The release of terpenes during storage of biomass. Biomass Bioenergy 1:29–34
Ryu WH, Bai S-J, Park JS, Huang Z, Moseley J, Fabian T, Fasching RJ, Grossman AR, Prinz FB (2010) Direct extraction of photosynthetic electrons from single algal cells by nanoprobing system. Nano Lett 10(4):1137–1143
Saha BC (2004) Lignocellulose biodegradation and applications in biotechnology. In: Saha BC, Hayashi K (eds) Lignocellulose biodegradation. American Chemical Society, Washington, DC
Sánchez ÓJ, Cardona CA (2008) Trends in biotechnological production of fuel ethanol from different feedstocks. Bioresour Technol 13:5270–5295
Schuchardt U, Sercheli R, Vargas RM (1998) Transesterification of vegetable oils: a review. J Braz Chem Soc 9(1):199–210
Seiffert M, Kaltschmitt M, Miranda JA (2009) The biomethane potential in Chile. Biomass Bioenergy 4:564–572
Shi Y, Zhao X-T, Cao P et al (2009) Hydrogen bio-production through anaerobic microorganism fermentation using kitchen wastes as substrate. Biotechnol Lett 9:1327–1333
Shuler ML, Kargi F (2008) Bioprocess engineering basic concepts. Prentice Hall International Series, New York
Silverstein RA, Chen Y, Sharma-Shivappa RR et al (2007) A comparison of chemical pretreatment methods for improving saccharification of cotton stalks. Bioresour Technol 16:3000–3011
Sun Y, Cheng J (2002) Hydrolysis of lignocellulosic materials for ethanol production: a review. Bioresour Technol 1:1–11
Taherzadeh M, Karimi K (2008) Pretreatment of lignocellulosic wastes to improve ethanol and biogas production: a review. Int J Mol Sci 9:1621–1651
Tengborg C, Stenberg K, Galbe M et al (1998) Comparison of $SO_2$and H_2SO_4 impregnation of softwood prior to steam pretreatment on ethanol production. Appl Biochem Biotechnol 1:3–15
Tran NH, Bartlett JR, Kannangara GSK et al (2010) Catalytic upgrading of biorefinery oil from micro-algae. Fuel 2:265–274
Venturi P, Gigler JK, Huisman W (1999) Economical and technical comparison between herbaceous (*Miscanthus* × *giganteus*) and woody energy crops (*Salix viminalis*). Renew Energy 1–4:1023–1026
Wallecha A, Mishra S (2003) Purification and characterization of two [beta]-glucosidases from a thermo-tolerant yeast *Pichia etchellsii*. Biochim Biophys Acta 1649(1):74–84
Watanabe Y, Shimada Y, Sugihara A et al (2002) Conversion of degummed soybean oil to biodiesel fuel with immobilized Candida antarctica lipase. J Mol Catal B Enzym 3–5:151–155
Wukovits W, Schnitzhofer W et al (2009) Fuels – hydrogen production, biomass: fermentation. In: Dyer CK, Moseley PT, Ogumi Z, Rand DAJ, Scrosati B, Garche J (eds) Encyclopedia of electrochemical power sources. Elsevier, Amsterdam
Wyman CE, Dale BE, Elander RT et al (2005) Coordinated development of leading biomass pretreatment technologies. Bioresour Technol 18:1959–1966
Xiao W, Clarkson WW (1997) Acid solubilization of lignin and bioconversion of treated newsprint to methane. Biodegradation 1:61–66
Xu Z, Wang Q, Jiang Z et al (2007) Enzymatic hydrolysis of pretreated soybean straw. Biomass Bioenergy 2–3:162–167
Yadvika S, Sreekrishnan TR et al (2004) Enhancement of biogas production from solid substrates using different techniques-a review. Bioresour Technol 1:1–10

Yang B, Wyman CE (2008) Pretreatment: the key to unlocking low-cost cellulosic ethanol. Biofuels Bioprod Biorefin 1:26–40

Yang Z, Guo R, Xu X et al (2010) Enhanced hydrogen production from lipid-extracted microalgal biomass residues through pretreatment. Int J Hydrog Energy 18:9618–9623

Zhu H, Stadnyk A, Béland M et al (2008) Co-production of hydrogen and methane from potato waste using a two-stage anaerobic digestion process. Bioresour Technol 11:5078–5084

Thermal Conversion of Biomass

Zhongyang Luo and Jingsong Zhou

Contents

Abstract

Bioenergy is presently the largest global contributor of renewable energy. Biomass thermal conversion has significant potential to expand in the production of heat, electricity, and fuels for transport. In addition, energy from biomass can contribute significantly toward the objectives of reducing greenhouse gas emissions and alleviating problems related to climate change. There are three main thermal processes – combustion, gasification, and pyrolysis – to convert the biomass into various energy products.

Combustion is well established and widely practiced with many examples of dedicated plant and co-firing applications. At present, biomass co-firing in modern coal power plants is the most cost-effective biomass use for power generation. Due to feedstock availability issues, dedicated biomass plants for combined heat and power (CHP) are typically of smaller size.

Z. Luo (✉) • J. Zhou
State Key Laboratory of Clean Energy Utilization, College of Energy Engineering, Zhejiang University, Hangzhou, Zhejiang, People's Republic of China
e-mail: zyluo@zju.edu.cn; zhoujs@zju.edu.cn

W.-Y. Chen et al. (eds.), *Handbook of Climate Change Mitigation and Adaptation*,
DOI 10.1007/978-3-319-14409-2_27

Gasification provides a competitive way to convert diverse, highly distributed, and low-value lignocellulosic biomass to syngas for combined heat and power generation, synthesis of liquid fuels, and production of hydrogen (H_2). A number of gasifier configurations have been developed. Biomass integrated gasification combined cycles (BIGCC) using black liquor are already in use. Gasification can also coproduce liquid fuels, and such advanced technologies are currently being investigated in research and pilot plants.

Pyrolysis is thermal destruction of biomass in the absence of air/oxygen to produce liquid bio-oil, syngas, and charcoal. Fast pyrolysis for liquid fuel production is currently of particular interest because liquid fuel can be stored and transported more easily and at lower cost than solid biomass. Pyrolysis technology is currently at the demonstration stage, and technologies for upgrading the bio-oil to transport fuels are applied at the R&D and pilot stage.

This chapter provides an overview of the state-of-the-art knowledge on biomass thermal conversion: the recent breakthrough in the technology, the current research and development activities, and the challenges associated with its increased deployment.

Introduction

Due to the rapid outgrowth of population and urbanization, renewable energy is of growing importance in responding to concerns over the environment and the security of energy supplies. Among the renewable energies, one of the most important energy sources in near future is biomass. In general, any organic non-fossil fuel can be considered a biomass fuel. These are the substances in which solar energy can be stored. Plants produce biomass continuously by the process of photosynthesis. Currently biomass is gaining more and more attention worldwide. Because of its potential in neutral in relation to global warming, biomass fuels are considered environmentally friendly. There is no net increase in CO_2 for the utilization of biomass if it is replanted. And biomass is the fourth largest source of energy in the world, accounting for about 15 % of the world's primary energy consumption (Chen et al. 2003). The potential of biomass to help to meet the world energy demand has also been widely recognized. Today biomass contributes about 10–15 % (or 45 $\pm$ 10 EJ) of the energy demand. On average, in the industrialized countries biomass contributes about 9–14 % to the total energy supplies, but in developing countries this is as high as one-fifth to one-third (Khan et al. 2009).

Usual composition of biomass comprises cellulose, hemicellulose, lignin, extractives, and inert ash. Biomass resources can be divided into two categories, i.e., natural and derived materials. These categories can further be subdivided as agriculture waste, forest products, and energy crops. Biomass fuels and residues can be converted to energy via thermochemical, biological, and mechanical or physical processes. Thermochemical conversion processes, a significant way used for the recovery of energy from biomass, draw the most attention of the world. The three basic approaches of different thermochemical processing are combustion,

gasification, and pyrolysis. Combustion burns biomass directly with excess oxygen in the temperature of 800–1,000 °C to obtain a range of outputs like heat, mechanical power, or electricity. It is already a worldwide and well-established commercial technology with applications in most industrialized and developing countries. And combustion systems are widely available at domestic, small industrial, and utility scales. Gasification converts biomass to a combustible gas mixture through partial oxidation of biomass at high temperatures of 800–900 °C. It has traditionally received the most R&D support as it offers potentially higher efficiencies compared with combustion. Generally, comparing to coal gasification systems, most of the available biomass gasifiers are still in the development or early demonstration process. Pyrolysis is thermal destruction of biomass in the absence of air/oxygen. Pyrolysis of biomass starts at 350–500 °C and goes to 700 °C with the liquid oil, gases, and solid products. Different condition leads to the formation of products in different proportions. Fast pyrolysis is still at a relatively early stage of development but offers the benefits of a liquid fuel with concomitant advantages of easy storage and transport as well as comparable higher power generation efficiencies at the smaller scales of operation that are likely to be achieved from bioenergy systems compared to fossil-fueled systems.

Biomass Thermal Conversion

Combustion

Of all thermochemical conversion technologies available for biomass, combustion is the most developed and most frequently applied because of its low costs and high reliability. Its commercial availability is high, and there is a multitude of options for integration with the existing infrastructure on both large- and small-scale levels (van Loo 2004).

Combustion Process of Biomass

During combustion, the biomass first loses its moisture at temperatures up to 100 °C, using heat from other particles that release their heat values. As the dried particle heats up, volatile gases containing hydrocarbons, CO, CH_4, and other gaseous components are released. In a combustion process, these gases contribute about 70 % of the heating value of the biomass. Finally, char oxidizes and ash remains.

Combustion characteristics for different types of biomass vary slightly depending upon the particular chemical composition, physical properties, and ash characteristics of the given fuel. One of the most important properties of biomass fuel that must be considered during the combustion process is the fuel moisture content. In most cases, the moisture contents of the residues are determined by the process of separating the residues from the crop product. High moisture content can lead to poor ignition and reduction of the combustion temperature, which in turn hinders the combustion of the reaction products and consequently affects the quality of combustion (Demirbas 2004; Werther et al. 2000; Jenkins et al. 1998).

Compared to solid fossil fuels, the properties of biomass are of great difference, which may result in different combustion behaviors. The differences may be summarized as follows:

1. Biomass fuels generally have higher volatile contents, less carbon and more oxygen, and lower specific heating value than coal.
2. Pyrolysis starts at a lower temperature for biomass fuels.
3. The fractional heat contribution by volatiles in biomass is of the order of ~70 % compared to ~36 % for coal.
4. Biomass fuels, for example, straw, have more free alkali in ash, which may aggravate the slagging and fouling problems.
5. Compared to coal chars, biomass chars have higher oxidation reactivity, probably as a result of the presence of alkalis (catalytically active) in the char matrix.

All these have significant influence on the thermal utilization of biomass fuels and the choice of the appropriate combustion technology.

Status of Biomass Combustion Technology

Biomass combustion power plants differ mainly in the areas of boiler designs, fuel composition, and environmental regulations. Pretreatment facilities are designed according to the difference between characteristics of the biomass and the demands by the boiler system, while flue gas cleaning is designed according to the difference between the environmental demands and the emissions of the boiler flue gases. Steam turbines and generators that are used in the different plants do not show many differences in basic design, except for differences between condensing and combined heat and power technology (CHP) applications.

Different biomass combustion systems are available for industrial purposes. Broadly, they can be defined as fixed-bed combustion, fluidized-bed combustion, and dust combustion. Boiler capacity of each combustion technology is different, with the corresponding value shown in Table 1.

The two most common types of boilers for biomass combustion are fixed-bed systems and fluidized-bed combustors, both of which have good fuel flexibility and

Table 1 The corresponding capacity range of biomass combustion boilers

Biomass combustion boilers		Capacity
Fixed bed	Stoves	2–12 KW
	Boilers	5–35 KW
	Pellets	5–100 KW
	Understoker	5 KW–2 MW
	Moving grate	200 KW–50 MW
Fluidized bed	Bubbling fluidized bed	5–100 MW
	Circulating fluidized bed	5–100 MW
Dust	Dust	5–14 MW
	Co-firing with pulverized coal	10–250 MW

can be fueled entirely by biomass or co-fired with coal. Suspension burners are often used to co-fire milled biomass pellets or raw biomass with pulverized coal or natural gas, in which the air-dried biomass fuels (with relatively low moisture content, e.g., <25 wt%) must be finely pulverized (e.g., particle feed size <6 mm) and have a relatively low share (e.g., less than 25 % on energy basis). The following description is in accordance with the combustion form (van den Broek et al. 1995).

Fixed-Bed

Fixed-bed combustion systems include grate furnaces and underfeed stokers. Primary air passes through a fixed bed, where drying, gasification, and charcoal combustion take place in consecutive stages. The combustible gases are burned in a separate combustion zone using secondary air.

Grate Furnace

Grate furnaces are appropriate for burning biomass fuels with high moisture content, different particle sizes, and high ash content. Usually, the capacity goes up to around 20 MWth. Mixtures of wood fuels can be used but straw, cereals, and grasses may cause problems due to their different combustion behavior, low moisture content, and low ash melting point. The fuel burns in a fixed or mobile grate, and in a relatively static state, the air required during combustion comes from the bottom through the grate. The combustion time of fuel after entering the furnace can be controlled by the movement or vibration of the grate, and finally, the ash left falls below the grate into the pit at the tail. The grate and walls can be air-cooled or water-cooled to avoid slagging problems. The design and control of the grate are aimed at guaranteeing smooth transportation and even distribution of the fuel and a homogeneous primary air supply over the whole grate surface. Irregular air supply may cause slagging and higher amounts of fly ash and may increase the oxygen needed for complete combustion.

Grate combustion is divided into chain grate, reciprocating grate, vibrating grate, and so on. The chain grate boilers are now less used because the fuel is hard to burn out, resulting from the uneven fuel layer and air distribution. Among the different types of grates, vibrating grates may have the longest life and highest availability. It is made of panel walls with drilled holes in the fins for the primary air. The grate is part of the boiler pressure system and connected to furnace walls by flexible connection pipes, designed for the vibrations. Instead of a continuous ash discharge in a traveling grate, a vibrating grate utilizes an intermittent ash removal system where the grate surface vibrates at high frequency and low amplitudes for about 2 % of the time to move the solids forward and discharge the ash at the end of the grate. This type of grate uses very few moving parts, and the drive mechanism is outside the heat and flame, which increases grate life, reduces maintenance costs, and results in high equipment availability (Yin et al. 2008).

After many years of exploration and development, Denmark has had mature experience with the grate combustion technology, and pure straw power generation and combined heat and power have been spread across the country. The most famous technology is water-cooled vibrating grate combustion boiler, which has been

applied in many other countries such as Sweden, Spain, Finland, England, and China. In Denmark, crops are packed according to uniform standards to bales when harvesting and trucked to warehouse of power plants and then the crop bales transported by belt to the furnace.

Crop bales have two main combustion ways when feeding into the furnace: one is "cigar burning," where big bales are pushed continuously into the combustion chamber where they burn from the end, and the other, bales are broken up and chopped before feeding into furnace.

Underfeed Stoker

Underfeed stokers represent a cheap safe technology for small- and medium-scale systems up to about 6 MWth. The fuel is fed into the combustion chamber by screw conveyors from below and is transported upward on a grate. Underfeed stokers are suitable for biomass fuels with low ash content (wood chips, sawdust, pellets) and small particle sizes (up to 50 mm). Underfeed stokers have a good partial load characteristics and simple load control. Load changes can be achieved more easily and quickly than in grate furnaces because of its better control of the fuel supply.

Fluidized Bed

Among the available technologies, fluidized beds are proving to be one of the best because of their flexibility, stability, and efficiency. They are used worldwide to combust both coal and biomass. Depending on the fluidization velocity, bubbling and circulating fluidized-bed combustion can be distinguished. Circulating fluidized-bed combustion technology has been widely used in small-scale thermal power-generating unit and develops quickly toward large-scale and high parameter (Khan et al. 2009).

Biomass generally has high water content and low calorific value. The inherent advantages of fluidized beds make them an attractive option for the combustion of biomass. In a fluidized bed, biomass fuel is burned in a self-mixing suspension of gas and solid bed material (usually silica sand and dolomite) in which air for combustion enters from below. The intense heat transfer and mixing provide good conditions for complete combustion with low excess air demand. Using internal heat exchanger surfaces, flue gas recirculation, or water injection, a relatively low combustion temperature is maintained in order to prevent ash sintering in the bed. Due to the good mixing achieved, fuel flexibility is high, although attention must be paid to particle size and impurities contained in the fuel. Fluidized-bed combustion plants usually operate at full load.

At present, utilization of biomass by fluidized-bed combustion technology has a considerate scale worldwide. The fuel is mainly forestry waste and other low-alkali biomass. There are lots of companies working at the development and application of this technology (Jana 2004), typical ones are AE & E, Foster Wheeler, B & W, and Kvaerner, with its main applications in Europe and the USA. The fluidized boilers developed by B & W have been in operation since late 1980s. In Sweden, with branches, leaves, and other forest wastes as fuels of large fluidized-bed boilers, the thermal efficiency can reach 80 %. Applying the circulating fluidized bed of Foster

Wheeler, the moist content of biomass residues burned can reach as high as 60 % in Finland. In China, there are abundant biomass resources of high potassium content such as rice and wheat straw. In addition to the water-cooled vibrating grate technology introduced from Denmark, Zhejiang University developed a new fluidized combustion technology based on particular boiler design and combustion organization. Through a series of different-scale thermal experiments and industrial practices, it proved to be a successful combustion technology using crop residues (Yu et al. 2010).

Suspension Combustion

Dust combustion is suitable for fuels available as small, dry particles such as wood dust. A mixture of fuel and primary combustion air is injected into the combustion chamber. Combustion takes place while the fuel is in suspension; the transportation air is used as primary air. Gas burnout is achieved after secondary air addition. An auxiliary burner is used to start the furnace. When the combustion temperature reaches a certain value, biomass injection starts and the auxiliary burner is shut down. Due to the explosion-like gasification process of the biomass particles, careful fuel feeding is essential. Since the fuel and air are well mixed, only a small amount of excess air is required. This results in high combustion efficiency.

However, there is irreconcilable conflict between the high temperature needed by suspension combustion and the high-alkali characteristic of some special biomass such as straw. Few practical projects directly carried out the suspension burning of biomass, most co-fired it with coal in a small blending ratio in the existing coal-fired plants.

Problems Related to Biomass Combustion

The most problems during biomass combustion are ash related. Biomass usually has high contents of alkali oxides and salts, the low melting points of which may lead to various problems during combustion (Werther et al. 2000; Demirbas 2005).

Agglomeration

During the combustion of agricultural residues in fluidized beds, a major problem is bed agglomeration. Agglomeration begins when part of the fuel ash melts and causes adhesion of bed particles. In addition to the adhesion effect of the sintered ash, the alkali oxides or salts can react with Si compounds of the bed material to form eutectic mixtures with low melting points. Beginning of agglomeration in the fluidized bed is often indicated by the occurrence of temperature gradients in the bed and the presence of large fluctuation of the bed pressure. When the feeding of the fuel continues, the extent of agglomeration will increase and may eventually lead to defluidization of the whole bed (Demirbas 2005; Bartels et al. 2008; Chirone et al. 2006; Elisabet et al. 2005).

Fouling and Slagging

The constituents of the ash formed as a result of the combustion process reacting with flue gases or with other components, in a complex mechanism, forming a

variety of compounds that may be in gaseous, liquid, or solid state. Gaseous or liquid-phase constituents form deposits on the cooled surfaces or furnace walls leading to slagging and fouling, respectively. The term "slagging" characterizes deposits on furnace walls or other surfaces exposed to predominantly radiant heat. Fouling refers to deposits on surfaces in the heat recovery section. Fouling is generally associated with reduction in heat-transfer rates and corrosion (Werther et al. 2000; Baxter 1993).

Corrosion

Ash deposition from biomass fuels that contain certain chemicals can also create corrosion and erosion of metals. The two most abundant inorganic elements in wheat straw are Si and K, which form silicates with a low melting point. The combustion of the straw leads to the condensation of molten silicates, which are likely to cause fouling and corrosion in combustion systems. Metals in combustion systems are exposed to chemical attack when silicates are present because protective layers of oxides can be relatively soluble and/or reactive in silicate slags (Werther et al. 2000; Nielsen et al. 2000).

Some Measures

In the process of biomass combustion and utilization, there have been some efficient ways to solve fouling, slagging, and corrosion problems such as reducing fuel alkali metal content (co-firing with coal or appropriate pretreatment); raising the melting point of fuel ash by additives such as kaolinite, bauxite, and emalthite; and applying new type of bed material (non-SiO_2 bed material: feldspar, dolomite, and magnesite as well as ferric oxide and alumina). Meanwhile, to reduce the combustion temperature appropriately without influencing normal operation of fluidized bed is also a good option (Khan et al. 2009; Elisabet et al. 2005).

Co-firing Coal and Biomass

Biomass can be directly fired in dedicated boilers. However, co-firing biomass and coal has technical, economical, and environmental advantages over the other options. By co-firing biomass with coal, a continuous supply of biomass would not be an issue, since the boiler plant would always have the primary fuel, coal, for 100 % utilization (Baxter 2005).

Technology Options for Co-firing

Co-firing is a family of technologies. These include blending biomass with coal on the fuel pile, separately injecting biomass into a boiler, and gasifying biomass for subsequent firing in an electricity-generating system (Tillman 2000; Sami et al. 2001).

Blending Biomass with Coal on the Fuel Pile

This simple approach to blending biomass with coal for subsequent introduction into the boiler is the least-cost approach to co-firing. It provides good mixing, high combustion efficiencies, and low emissions. When this approach to co-firing is

employed in pulverized combustion boilers, it will have significant impact on the pulverizer. And the percentage of biomass that can be added to the total fuel blend is at very low levels. Also it is important to note that the type of biomass blended with coal is limited. For example, bark can cause significant problems because it can be very stringy. Usually, wood chips, sawdust, and straw are used for this kind of co-firing. And wood chip was found to be the most favorable co-firing fuel in terms of ease of combustion and reduced emissions of NO_x and SO_2.

Co-firing with Separate Injection

This approach involves separately preparing the biomass and then firing it in the boiler. The biomass is introduced simply at another injection point. This approach, which involves more equipment than blending on the coal pile, can accomplish higher percentage co-firing in pulverized combustion boilers. It has the advantage of better control over fuel flow rates. Thermal output similar to coal-only firing requires higher biomass feed rates. Thus, separate feeders facilitate controlling the biomass feed rate independent of the coal feed rate. Using a single feed line for a blend fuel has the risk of agglomeration occurring in the supply line, which may lead to a disconnection or blockage in the fuel supply. On the other hand, separate feed lines and separate burners increase capital and maintenance costs.

Gasification-Based Co-firing

The gasification approach to co-firing has significant potential, for it permits the use of biomass in other solid fuel combustion systems without significant influence on it. In gasification-based co-firing, biomass is first fed to a gasifier in order to generate a producer gas. The gas is then fired in a boiler or in a duct burner between a combustion turbine and a heat recovery steam generator. Gasification-based co-firing addresses several issues commonly associated with co-firing including accomplishing complete combustion in a furnace with a very short gas residence time, separating biomass ash from coal ash, and providing a means for co-firing in natural gas-fired electricity-generating systems. While it is the most capital-intensive approach to co-firing, it is also the most flexible in terms of the base fuel considered (coal, oil, natural gas) and the electricity-generating system appropriate to its application.

Major Technical Considerations When Co-firing Biomass with Coal

Co-firing biomass with coal, in comparison with single coal firing, helps reduce the total emissions per unit energy produced. Coal and biomass fuels are quite different in composition. Co-firing biomass with coal has the capability to reduce both NO_x and SO_x levels from the existing pulverized coal-fired power plants. In addition, biomass ash with notable carbon content has been used as effective reburning fuel for NO reduction, and it was reported that about 85 % of NO reduction efficiency appears achievable at a stoichiometric ratio 0.945 (Chen and Gathitu 2006). This can be considered a special co-firing process. Biomass offers important advantages as a combustion feedstock due to the high volatility of the fuel and the high reactivity of both the fuel and the resulting char. However, it should be noticed that in comparison

with solid fossil fuels, biomass contains much less carbon and more oxygen and has a low heating value (Baxter 2005; Tillman 2000; Demirbas 2003). There are still many important issues that are yet unanswered regarding coal-biomass blend combustion.

Fuel Preparation and Handling

Because biomass fuels are hygroscopic, have low densities, and have irregular shapes, they should generally be prepared and transported using equipment designed specifically for that purpose. In some cases, however, they can be directly metered on the coal belt conveyor. Care must be taken to prevent skidding, bridging, and plugging in pulverizers, hoppers, and pipe bends.

Ash Deposition

Rates of ash deposition from biomass fuels can greatly exceed or be considerably less than those from firing coal alone. This is attributable only partially to the total ash content of the fuels. Deposition rates from blends of coal and biomass are generally lower than indicated by a direct interpolation between the two rates. Experimental evidence supports the hypothesis that this reduction occurs primarily because of interactions between alkali (mainly potassium) from the biomass and sulfur from the coal.

Fly Ash Utilization

The majority of the fly ash generated from coal combustion worldwide is used either as a concrete additive or for other purposes. However, current standards preclude the use of fly ash as a concrete additive from any source other than coal. The technical case for precluding the use of fly ash from co-firing wood with coal appears to be unjustified. However, the less comprehensive data available for herbaceous biomass fuels suggest that alkali, chorine, and other properties may compromise several important concrete properties. Strict interpretation of many standards that are the basis for regulations and policy for many institutions would preclude all fly ash from use in concrete if it contains any amount of non-coal-derived material, including co-fired fly ash. Though these standards are under active revision, this may take many years to complete (van Loo and Koppejan 2008).

Gasification

Biomass gasification is a thermal conversion technology that converts biomass into a combustible gas through high-temperature partial oxidation reaction. The product gas mainly consists of carbon monoxide (CO), carbon dioxide (CO_2), hydrogen (H_2), methane (CH_4), and water (H_2O) but also contains contaminants such as char particles, tars, and ash. The syngas can be used to produce a wider variety of outputs: electricity, heat and power, liquid fuels, and synthetic chemicals. Hence, different demands of the market can be met. The utilization of biomass gasification technology mainly depends on syngas purification technologies and syngas quality control technologies. At present, biomass gasification system is undergoing the transformation from demonstration to commercialization. The well-known manufacturers of

commercial biomass gasifiers are Bioneer, PRM Energy, Foster Wheeler, and Lurgi Umwelt.

Gasification Process of Biomass

The gasification process is a sequence of interconnected reactions: the first step is quick drying. The second step is fast pyrolysis at 300–500 °C. Char, condensable hydrocarbons, tars, and gases are produced. The following step is gasification, namely, partial oxidation reaction between pyrolysis production and oxygenant. During gasification, part of the biomass is converted to char and tar instead of syngas. Reduction and conversion of char and tar can also increase syngas yield and overall conversion efficiency. Hence, the product syngas quality depends on: raw material composition, water content, temperature, heating rate, type of gasifier, and oxidation of pyrolysis products. The reaction process is as follows:

Oxidation: $C + O_2 \rightarrow CO_2,\ 2C + O_2 \rightarrow 2CO$
Boudouard: $C + CO_2 \rightarrow 2CO$
Steam reforming: $CH_4 + H_2O(g) \rightarrow CO + 3H_2$, $CH_4 + 2H_2O(g) \rightarrow CO_2 + 4H_2$
Water-gas reaction: $C + H_2O(g) \rightarrow CO + H_2$, $C + 2H_2O(g) \rightarrow CO_2 + 3H_2$
Water-gas shift reaction: $CO + H_2O(g) \rightarrow CO_2 + H_2$

In the gasification process, the oxidant can be air, pure O_2, steam, CO_2, air/steam, O_2/steam, CO_2/steam. The advantages and technical challenges of different gasifying agents are listed in Table 2. In addition, CO_2 gasification is very promising. CO_2 from the gasification or combustion can be used as gasifying agent. But there are few operational examples.

Table 2 Advantages and technical challenges of different gasifying agents

Method	Gas composition	LHV	Advantages	Technical challenges
Air gasification	CO, CO_2, H_2, CH_4, N_2, tar	~3–6 MJ/m^3 (Gabra et al. 2001; Zainal et al. 2002)	Simple equipment, easy operation and maintenance, low cost	Syngas with high N_2 content (>50 %) and low heating value, combustion problems (especially gas turbine)
Oxygen gasification	CO, CO_2, H_2, CH_4, tar	~10–12 MJ/m^3	Good syngas quality	High cost of operation and air separation
Steam gasification	CO, CO_2, H_2, CH_4, tar	~10–15 MJ/m^3 (Rapagna et al. 2000; Gil et al. 1999)	High H_2 content (>50 %), high heating value	An indirect or external heat supply, corrosion, and high tar content
Pyrolytic gasification	CO, CO_2, H_2, CH_4, tar	~15–20 MJ/m^3	Syngas with medium heating value	Low system efficiency

Status of Biomass Gasification Technology

The gasifier is the core component of biomass gasification equipment. There are three main types of gasifiers: fixed bed, fluidized bed, and entrained-flow bed. According to a recent survey about the gasifier manufacturers, 75 % of gasifiers offered commercially were downdraft fixed bed, 20 % were fluidized bed (including circulating fluidized beds), 2.5 % were updraft fixed bed, and 2.5 % were other types (Knoef 2000).

Fixed-Bed Gasifier

Working characteristics: the chopped biomass materials are put into the reactor from the top. The gasification reactions occur slowly in the gasifier. Fixed-bed reactors have countercurrent (updraft), cocurrent (downdraft), and very seldom crosscurrent mass flow.

Due to its simple design, easy operation, and reliable performance, fixed-bed gasifier is widely applied. However, compared with other types of reactors, low and nonuniform heat and mass transfer in the fixed-bed reactors (Wang et al. 2008) lead to large quantities of tars and char in the syngas. That increases the system complexity and investment of subsequent processing. Therefore, small-scale gasifiers are more economical.

Updraft gasifiers are mainly used for heating (Kurkela 2000). Its upper size is around 2.5 MWe. The most well-known manufactures of updraft fixed-bed gasifiers are Bioneer and PRM Energy. About 10 Bioneer gasifiers are operational for district heating in Finland and Sweden. PRM Energy has 18 units in operation producing heat for industrial drying application or low-pressure steam (Knoef 2001–2003). Downdraft gasifiers are more attractive for small-scale application up to around 1.5 MWe. In principle, downdraft gasifier is suitable for electric power generation. But it has not achieved industrialization.

Fluidized-Bed Gasifier

Working characteristics: the pulverized raw material and inert sands are put into the reactor. The material particles, sands, and gasifying agents can be heated evenly by good contacting among each other under the blowing of gasifying agent. A certain state of "boiling" is presented in the reactor. Therefore, fluidized beds have fast heat up, high gasification rate, great production capacity, and high syngas yield. Tar content is low since its secondary cracking under the high temperature and uniform temperature field. But high dust content is in the gas phase. Due to the complicated structure and large equipment investment of fluidized-bed reactor, large-scale gasification system is more economical.

The types of fluidized-bed gasifiers can be divided into single fluidized-bed gasifier, double fluidized-bed gasifier, and circulating fluidized-bed gasifier.

Atmospheric bubbling fluidized-bed gasifiers at pilot scale and commercial application in small to medium scales ($\sim$25 MWth) can be in reliable operation. Circulating fluidized-bed gasifiers are more suitable for large scale ($-$100 MWe) with attractive market. Examples include the TPS (Termiska Processer AB)

atmospheric process (Waldheim et al. 2001) and the Varnamo pressurized system (Stahl et al. 2001). The world's most mature biomass gasification technology is "fast internal circulating fluidized-bed" (FICFB) technology. The most successful biomass gasifier for power generation is "Güssing" gasifier in Australia, which is based on the high-temperature pyrolysis to produce syngas with medium heating value. It has been successfully run >15,000 h to generate electricity 2 MWe.

According to the blowing pressure of gasification agent, gasifiers have atmospheric gasifiers (0.11 ~ 0.15 MPa) and pressurized gasifiers (1.8 ~ 2.25 MPa). The pressurized gasifier with high-temperature and high-pressure outgas is suitable for the large-scale system for power generation. A gas compression process in the downstream system for the gas turbine or liquefaction could be avoided in the pressurized gasification process, in the short term, either pressurized circulating fluidized-bed, bubbling bed, or pressurized bubbling bed gasifiers have the lack of market appeal mainly due to the complex system and high construction cost of large pressure shell. And the pressurized gasification process often uses pure O_2 as gasifying agent to improve the gas quality. Hence, special security measures are required to guarantee safe operation.

Entrained-Flow-Bed Gasifier

Work characteristics: fine biomass powder as raw material carried by the high-speed air flow is injected into the gasifier with gasifying agent. In the reactor, solid particles are dragged along with the gas stream. Their properties of dispersing and flowing in the airflow are similar to the flow of mass points of gas. This generally means short residence times (typically 1 s) and high temperatures (typically 1,300 ~ 1,500 °C). Hence, entrained-flow gasification is of high reaction rate, large capacity, high carbon conversion, and improved syngas without tar and phenol and little environmental pollution.

Now entrained-flow gasification technology is mainly used in coal gasification industry. The most mature technology of entrained-flow gasification is Koppers-Totzek (KT) technology, which is in the atmospheric pressure operation. And pressurized entrained-flow gasification technology is successfully developed: Shell and Prenflo technology can feed dry coal powder, and Texaco and Destec technology can feed water-coal slurry or oil.

Although there are many commercial coal-based entrained-flow gasifiers, the experience in the biomass-based gasifiers is still little. Experimental results show: biomass ash in the entrained-flow gasifiers is difficult to melt under the operating temperature (1,300 ~ 1,500 °C), due to ash containing high contents of CaO and alkali metal generally found in the gas phase, which can reduce the ash melting point. However, a slagging gasifier is preferred over a non-slagging gasifier: (1) little slagging can never be avoided and (2) a slagging gasifier is more fuel flexible, but it needs to add a fluxing material (silica or clay) to achieve melting properties at required temperature.

Currently, the research on biomass entrained-flow gasification is at the stage of experimental study and numerical simulation. The CARBO-V system of Colin (CHOREN) in the German city of Freiburg, Saxony, is the most advanced biomass

gasification system for bio-oil production in the industrial level. Energy Research Centre of the Netherlands (ECN) studied the feasibility of biomass entrained-flow gasification, ash melting properties, the feeding device, pressurization methods, and the selection of gasification routes (Drift et al. 2004). Biomass Technology Group of the Netherlands (BTG) investigated the bio-oil entrained-flow gasification (Venderbosch and Prins 1998). Zhejiang University of China designed the reactor, investigated biomass gasification characteristics, residual carbon properties, the volatile issue of alkali metal, and pretreatment of raw materials; and established a dynamic model about the gasification process (Zhao 2007).

In recent years, countries in the world usually pressurized entrained-flow gasifiers for the research on the biomass gasification using powder materials. As a potential gasification technology, pressurized gasification has become a hot research spot. How to effectively realize the pressurized entrained-flow gasification of biomass is the focus of future research.

Syngas Quality Control and Cleaning Technology

Any gasification process for synthesis gas will produce pollutants: particulate, condensable tars, alkali metal compounds, H_2S, HCl, NH_3, HCN, COS, etc. (Van et al. 1995). So deep purification is needed according to the requirements of the downstream gas appliances and the use restrictions of catalyst. In general, Fischer-Tropsch synthesis demands higher standards of gas cleaning than biomass integrated gasification combined cycle (BIGCC). At present, the common feedstock for Fischer-Tropsch synthesis is the relatively clean natural gas. Hence, actual cleaning specifications for some specific biomass contaminants are not known. Some specifications for biomass gasification are estimated based on the practical experience.

Ash Particles

Ash particles in the product gas can be mainly purified by mechanical clarification. The particle reduction of different methods can be seen in Table 3. Most of them are operated at low temperatures. Some are at high temperatures, such as the operation temperature of ceramic filters which is 600 °C. Ceramic filter according to its structure types can be divided into bag-type ceramic filters, webbing ceramic filters, tubular ceramic filters, cross flow ceramic filters, cellular-type ceramic filter, and so on. Low-temperature cleaning technology has been realized in industrialization and

Table 3 The particle reduction of different methods

Method	Particle reduction (%)	Particle size
Wash tower	95–98 %	>1 μm
Jet scrubber	95–99 %	>1 μm
Granular-bed filter	99 %	
Bag filter	99 %	>0.1 μm
Cyclone separator	90 %	>10 μm
Inertial dust separator	≤70 %	20–30 μm
Wet electrostatic precipitator	>99	

Table 4 The tar yield of different gasification processes

Gasification method	Tar content in syngas (g/Nm^3)
An air-blown circulating fluidized-bed (CFB) biomass gasifier	10
Updraft fixed-bed gasifier	100
Downdraft fixed-bed gasifier	1
Other gasifier	0.5 ~ 100

Table 5 The effect of different methods on removing tars

Method	Tar reduction (%)
Water scrubber	10–25
Venturi scrubber	50–90 (Hasler 1997)
Fabric filter	0–50
Rotating particle separator	30–70
Wet electrostatic precipitator	40–70 (Paasen and Rabou 2004)

more mature than high-temperature cleaning. But the pollution problems of low-temperature cleaning are more serious, such as secondary pollution caused by wastewater from washing and wet ESP. Compared with low-temperature cleaning, high-temperature cleaning can improve system energy efficiency, can reduce the operating cost from the utilization of high-temperature syngas, and also can be combined with the high-temperature fuel cells for heat and power generation (Ma et al. 2005).

Tar

Biomass tar is a light hydrocarbon and phenolic mixture. "Naphthalene" is the most difficult compound to reform.

Tar will cause many severe problems. It will condense into liquid below its dew point temperature to lead to clogged, blockage, or corrosion in the downstream pipeline, filters, or equipment. It is difficult to completely burn tar. Gas facilities such as internal combustion engines and gas turbines would be damaged. Table 4 shows the tar yield of different gasification processes.

Tar removal, conversion, or destruction has been one of the greatest technical challenges for the successful development of commercial gasification technologies (Dayton 2002). For this reason, most applications require the product gas with a low tar content, of the order 0.05 g/m^3 or less.

The methods to remove tar are mechanical cleaning, low-temperature cleaning, high-temperature cleaning, thermal cracking, and catalytic cracking. The operation and economical analysis shows that mechanical cleaning and catalytic cracking are suitable for small-scale plants and large-scale plants, respectively.

Mechanical Cleaning

The common mechanical methods are considerably efficient in removing tar accompanied with effective particles capture (Hasler and Nussbaumer 1999). Table 5

shows the effect of different methods on removing tars. However, the cost of mechanical cleaning system is usually high. And it only removes the tar from the product gas, while the energy in the tar is lost. Now a new tar removal system called OLGA (OLGA is the Dutch acronym for oil-based gas washer) is developed. In this system, heavy tars, 99 % phenol, and 97 % of the heterocyclic tars can be removed (Boerrigter 2005). The lab test results (Hasler 1997) show that active carbon has good removal efficiency for high-boiling hydrocarbons and phenols. Meanwhile, the "tar" and the active carbon itself can be recycled as a feedstock. But the tars' accumulation on the carbon is difficult to clean completely to cause the blockage of active carbon filters.

Thermal Cracking

In thermal cracking method, the raw gas derived from gasification or pyrolysis is heated to high temperatures. The tar molecules can be cracked into lighter gases.

Biomass-derived tar is very refractory and hard to crack by high temperature alone. Three ways are beneficial for tar's splitting decomposition reaction. The first method is to increase the residence time such as the utilization of fluidized-bed reactor. But the improving effect is not obvious. The second method is increasing the area of the heating surfaces, but it depends on the mixture grade of various compositions. The last method is adding oxygen or air to strengthen the partial oxidation of tar, which increases the CO content at the expense of conversion efficiency decrease and operation cost enhancement.

Catalyst Cracking

At present, the catalytic cracking is the most effective way to remove the tar. It is divided into low-temperature catalytic reforming (350 $\sim$ 600 °C) and high-temperature catalytic reforming (500 $\sim$ 800 °C). Catalysts are as follows: nickel-based catalyst, dolomite, alkali metals, and nano-catalyst.

Nickel-based catalyst supported on SiO_2 and Al_2O_3 can be used at low temperatures or at high temperatures for catalytic cracking. Although nickel-based catalyst has good effect on cracking tars, it is very expensive and easy to lose activation because of the carbon deposition, H_2S poisoning, and catalyst attrition.

Compared to nickel-based catalyst, the abundant naturally occurring catalysts such as dolomite $CaMg(CO_3)_2$ are cheaper. And it is the most common and effective catalyst for tar removal (Rapagna et al. 2000). However, the conversion of tars over dolomite cannot reach 90–95 % or more (Zhang 2003). And it is difficult for dolomite to crack the heavy tar components (Karlsson and Ekström 1994). In addition, due to its low melting point, dolomite is very easy to melt to cause deactivation.

Adding inexpensive alkali metal catalyst to biomass raw material can significantly reduce tar content through dry mixing or wet impregnation. Many studies (Brown et al. 2000; Kumar et al. 1997; Elliott and Baker 1986) suggest that potassium has a better catalytic effect on tar cracking compared to other alkali metals (such as Na, Li, Ca, etc.). But the alkali metal in the furnace would lead to

agglomeration, sintering, fluidization performance degradation, blockage in the pipes, and other metal catalyst deactivation.

Currently, some novel metals have been widely used as catalysts for tar cracking. It is found that $Rh/CeO_2/SiO_2$ has the best catalytic performance: little carbon deposition at low temperatures and high and stable activity even under the presence of high concentrations of H_2S (280 ppm) (Tomishige et al. 2005). In addition, nano-Ni catalyst ($NiO/\gamma\text{-}Al_2O_3$) also can improve the quality of synthesis gas and reduce the tar in the gasification process (Li et al. 2008).

Plasma Methods

Some studies demonstrated that corona discharge could also decompose the organic components, which can be used to reduce the tar content. Tests (Heesch and Paasen 2000) were carried out on a wood gasifier, which was designed to produce a 100 kW electrical output. The dust removal efficiency was about 72–95 %. Conversion efficiencies of heavy tar components and light tar components were 68 % and ~50 %, respectively. In addition to capturing dust and tar, plasma technology can operate at high temperatures.

Alkali Metal

In the biomass gasification process, the problems associated with alkali metals are mainly caused by the main nonmetallic components: Si and alkali metal potassium in the ash. Si reacts with K at temperature less than 900 °C. For this reason, Si-O-Si bond is broken to form silicate or to react with sulfur to form sulfate. The melting points of silicate and sulfate are lower than 700 °C. So they are easy to deposit on the walls of reactors or pipes to cause sintering, corrosion, anti-fluidization, or blockage. These problems can be mitigated by leaching and fractionation as the two main pretreatments (Arvelakis et al. 2002, 2005; Arvelakis and Koukios 2002). However, mechanical fractionation could reduce up to 50 % of the ash content in the biomass. The remaining ash would still produce such problems (Arvelakis et al. 2005). Eighty percent of the alkali metals in the syngas can be separated together with the coke through the cyclone.

Syngas Utilization

Gas Centralized Supply

In the developing countries, in addition to the heat and power supply, biomass gasification technology has been mainly applied for domestic cooking in the way of gas centralized supply.

The process of biomass gasification system project for central gas supply: straw is put into the gasifier and converted into combustible gas through pyrolysis and gasification reactions. The dust and tars in the combustible gas are removed by the downstream cleaner. Then the clean gas stored in the air storage can be delivered to the every user of this system.

The main types of gasifiers used in the biomass gasification system project for central gas supply are pyrolysis gasifiers, updraft fixed-bed gasifiers, pressurized

updraft fixed-bed gasifiers, downdraft fixed-bed gasifiers, and fluidized-bed gasifiers. Downdraft fixed-bed gasifier is the most often used reactor in all of them.

But the operation rate of village-level straw gasification system for centralized cooking gas supply is still very low. There are many reasons for this. Technically the syngas quality is low due to the low heating value and the high contents of CO and N_2. Contents of tars and dust in the combustible gas are high. The whole centralized gas supply system is not fully used. The syngas should be utilized in many ways to improve the utilization rate of system such as power generation, preheating, and drying grain and other agricultural products. From a policy and economic point of view: limited by the capital cost, the system needs to be as simple as possible. Therefore, the system cannot be perfectly designed, leaving some operation difficulties and environmental problems (Bridgwater et al. 1999a). Therefore, most of the domestic cooking fuel projects need government financial support now.

Combined Heat and Power Generation

Due to its properties of energy saving and environmental conservation, combined heat and power generation (CHP) technology has been the focal point of worldwide attention as an alternate energy source for traditional source.

The major conversion technologies of biomass-based CHP systems are combustion, gasification, pyrolysis, biochemical/biological processes, and chemical/mechanical processes. Combustion technology is widely used at large- and medium-scale systems. Although gasification technology is still developing, this technology has great potential for CHP. The main types of gasifiers for CHP systems are updraft/downdraft fixed-bed gasifiers, fluidized-bed gasifiers, circulating fluidized-bed gasifiers, and entrained-flow gasifiers. Internal combustion engines and turbine can use cleaned product gas to produce heat and power. Gasification-based CHP system potentially has higher electricity efficiency than a direct combustion-based CHP system. Moreover, syngas from biomass gasification can increase the bio-based fuel percentage used in the existing pulverized combustors without any concern about plugging of the coal-feeding system during co-firing of biomass coal. But gasification-based CHP systems have not been realized in commercialization till now. The unstable gasification process leads to the great changed quality of the synthetic gas and higher content of tars, which seriously damage engines. And to reduce system cost, the gasification-based system is short of automatic measurement and control measures to result in the varied system performance.

According to CHP capacity, it can be divided into large-scale, medium-sized, small-scale, and microscale CHP. Biomass is best suited for decentralized, small-scale, and microscale CHP systems due to its intrinsic properties. On one hand, small-scale and microscale biomass CHP systems can reduce transportation cost of biomass and provide heat and power where they are needed. On the other hand, it is more difficult to find an end user for the heat produced in larger CHP systems. Generally speaking, the concept “small-scale CHP” means combined heat and power generation systems with electrical power less than 100 kW. “Microscale CHP” is also often used to denote small-scale CHP systems with an electric capacity smaller

than 15 kWe. Biomass-based CHP systems are generally smaller than coal-based systems. And the power efficiency of biomass-based CHP is also lower, only about 85–90 %, as 30–34 % and 22 % of electricity will be used for biomass drying and solid-waste treatment, respectively. A typical CHP system at large scale is biomass integrated gasification combined cycles (BIGCC). The overall efficiency of the BIGCC system is about 86 % and the electrical efficiency is about 33 % (Miccio 1999). "VEGA" gasification system developed by Sydkraft AB Company of Sweden uses BIGCC technology for district heat and power supply. Buggenum IGCC system in the Netherlands uses the mixtures of biomass and coal to generate power (250 MW). Currently small- and medium-scale CHP systems have not been commercialized due to high investment, low return, and some technical barriers.

Synthesis Techniques

Syngas can be converted to a liquid fuel or chemicals through synthesis technology.

The major synthesis technologies are methanol synthesis, Fischer-Tropsch synthesis, methane synthesis, hydroformylation of olefins synthesis, and hydrogen in organic synthesis. The features of different technologies are in Table 6.

Fischer-Tropsch synthesis is one of the biomass indirect liquefaction technologies. Under the appropriate condition (20 $\sim$ 40 bar, 180 $\sim$ 250 °C), syngas as raw material is synthesized into the liquid fuels (hydrocarbons with different chain lengths). Fischer-Tropsch synthetic oil can be divided into three categories according to different raw materials (see Table 7). The synthesis process includes gasification, gas purification, transformation and reforming, synthesis, and upgradation. The optimal molar ratio of H_2 and CO for Fischer-Tropsch synthesis is 2 $\sim$ 2.5, preferably 2.1. Currently the cheap Fe-based catalyst is commonly used for industrial Fischer-Tropsch synthesis. However, it will strengthen the water-gas reaction to produce too much useless CO_2 at the expense of large CO consumption. Moreover, when it is used in slurry bed reactors at low temperatures, the small particles of Fe-based catalyst are hardly separated from the product wax. The Co-based catalyst precisely overcomes these deficiencies. Hence, the current developed catalysts are mostly cobalt-based catalysts with high activity, high factor of chain elongation, and long life. The main reactors are fixed bed and circulating fluidized bed. The F-T synthesis is used on a technical scale nowadays only at SASOL (coal based) in South Africa and at Shell (natural gas based) in Malaysia. However, biomass synthesis gas for the Fischer-Tropsch synthesis is still of less attention.

Obstacles to Commercialization

The application obstacles are divided into technical and nontechnical barriers to obstruct development of biomass gasification technology.

Technical barriers are shown as follows:

1. *Biomass resources*: As a resource with the properties of low density and dispersion, there are substantial logistical problems in collection and transport as well as high costs. Moreover, biomass has the characteristic of its seasonality. So it is difficult to achieve large-scale gasification plants for power generation.

Table 6 The features of different synthesis technologies (Wang et al. 2008; Reinhard 2002)

Synthesis	Product	Principle	Catalyst	Industrialization
Methanol synthesis	Methanol	$CO + 2H_2 \rightarrow CH_3OH + 90$ kJ/mol	High-pressure process: copper-containing catalysts	Yes
		$CO_2 + 3H_2 \rightarrow CH_3OH + H_2O + 49.6$ kJ/mol	Low-pressure process: CuO/ZnO/M (M = Al, CrO, mixed oxide of zinc and aluminum)	
F-T synthesis	F-T oil	$CO + 2H_2 \rightarrow [-CH_2-] + H_2O - 165$ kJ/mol	Cobalt or iron	Yes
Methane synthesis	Methane	$CO + 3H_2 \rightarrow CH_4 + H_2O + 206.4$ kJ/mol	Mg-promoted Ni catalysts with diatomaceous earthenware as carrier	Yes
Hydroformylation	Aldehyde	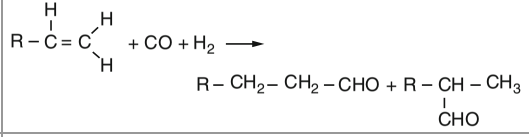	Cobalt carbonyl hydride, cobalt- or rhodium-phosphine complexes	Yes
Hydrogen in organic synthesis	Chemicals	$A + nH_2 \rightarrow BH_2n$	Raney nickel, copper, molybdenum, especially inert metals (Pt, Pd)	No

Table 7 The features of different Fischer-Tropsch synthetic oil

Fisher-Tropsch synthesis fuels	Advantages	Disadvantages	Commercialization
Coal-based oil (coal to liquid)	Oil quality is better than the products of direct liquefaction	High content of arene, a low cetane number for diesel oil product, no applications for CO_2 zero emission	Sasol in Malaysia
Natural gas-based oil (gas to liquid)	A high cetane number, does not contain aromatic compound and sulfur	No applications for CO_2 zero emission	Shell in South Africa
Biomass-based oil (biomass to liquid)	A neutral carbon fuel, does not contain the impurities that are always in mineral oil		No
	A high cetane number, can be used as additives or used as clean fuel for diesel engines		

2. *Feeding*: In the feeding process, the problems with bridging, blockage, and instability are often caused due to low-dense materials and mixed residues with varying characteristics.
3. *Gasification technology*: There is a need to improve the equipment reliability. The immature technology makes it difficult to open market and commercialize.
4. *Purification*: The difficulties of purifying tail gas are how to solve the fouling and corrosion of the heat exchanger and pipes, tar removal/cracking, and continuous operation.
5. *Prime mover*: Experience about biomass syngas utilized in operation of prime mover is little, such as allowable contamination, allowable emissions, engine, fuel cell, Stirling, and turbine (specifications to product gas).

Nontechnical barriers are shown as follows:

1. *Emission standard*: The standards of allowable emissions differ from country to country.
2. *Public perception*: At present, due to large investment, small return, and no significant effect of gasification technology on social benefits, the public are rather negative with no confidence.
3. *Infrastructure*: Many aspects affect economy of biomass gasification – investment channel, collection and transportation cost, and so on. To take the power generation for an example, some countries do not have regulations regarding the incorporation of electricity derived from biomass into the existing grid network.
4. *Capital cost*: Investment cost of gasification projects are high, particularly the cost of collection and transportation of raw materials. Sometimes in order to

reduce costs, the system has to be as simple as possible. Therefore, this results in some sectors such as tar treatment, and gas cleaning cannot be perfectly designed, leaving some operation difficulties and environmental problems.

5. *Environmental protection*: In recent years, countries in the world advocate environmental protection energetically, as well as energy saving and emission reduction. But the real fact is that not all the biomass gasification technology can meet environmental requirements. Although some techniques, such as centralized gas supply systems for domestic cooking in rural areas, can achieve obvious social benefits, in practice gasification stations are difficult to really make a profit from it due to the high cost of antipollution measures.

Pyrolysis

Pyrolysis is the initial chemical stage of combustion and has been used for charcoal production from wood since ancient Egyptian times. And biomass pyrolysis is a process in which biomass is heated in the absence of oxygen to decompose into char, gaseous products, and liquid product "bio-oil." The significant development of biomass pyrolysis happens in the 1980s, when many researchers began to observe an increasing liquid product yield obtained from fast pyrolysis with a rapid heating rate and a short cooling time (Graham et al. 1984). Crude bio-oils have a high water content of about 15–30 %, a high acidity (PH value of 2.8–3.8), a high density of about 1,200 kg/m^3, a low heating value of 14–18.5 MJ/kg, and a large range of viscosities depending on the feedstock and pyrolysis conditions (Zhang et al. 2007). And they are multicomponent mixtures of different chemical families, such as acids, ketones, alcohols, aldehydes, esters, sugars, and phenols (Garcia-Perez et al. 2007). The deleterious properties of corrosiveness, high viscosity, and thermal instability limit the high-quality applications of bio-oils, but corresponding upgrading technologies are developed to explore promising ways for substituted transport fuel production (Xu et al. 2008; Balat and Balat 2009). Moreover bio-oils from this conversion technology have a positive environmental effect compared to most coal- or petroleum-derived fuels due to the low levels of aromatics and sulfur.

Pyrolysis Process of Biomass

The physical conditions of biomass pyrolysis, such as temperature, heating rate, and residence time, have been identified to have a profound influence on the product yields and composition. As shown in Table 8, pyrolysis is classified as slow, conventional, fast, and flash pyrolysis mainly depending on the temperature and heating rate. The terms of "slow pyrolysis" and "fast pyrolysis" are somewhat arbitrary and have no precise definition of the times or heating rates involved in each. Conventional pyrolysis may be in the range of slow pyrolysis, and flash pyrolysis is also termed as fast pyrolysis. Slow pyrolysis is similar to carbonization and produces large amounts of charcoal. This charcoal as a solid fuel is cleaner than that from fossil fuels without the impurities of lead, sulfur, or mercury, which is the best option in the process of iron reduction and sugar refinement and as the absorbent

Table 8 Classification of biomass pyrolysis technologies (Huber et al. 2006; Mohan et al. 2006)

Pyrolysis type	Temperature (°C)	Heating rate	Residence time	Main products
Carbonization	400	Very low	Days	Charcoal
Slow pyrolysis	400–600	Low	Hours	Charcoal, liquids, gases
Conventional pyrolysis	600	Low	5–30 min	Charcoal, liquids, gases
Fast pyrolysis	400–650	High	0.1–2 s	Liquids
Flash pyrolysis	<650	Very high	<1 s	Liquids or chemicals and gases
Vacuum pyrolysis	400	Medium	2–30 s	Liquids

or soil amendment (Peláez-Samaniego et al. 2008). Fast pyrolysis produces 60–75 wt% of liquid bio-oil, 15–25 wt% of solid char, and 10–20 wt% of noncondensable gases varied with the feedstock used. The maximum bio-oil yield of up to 80 wt% dry feed is obtained from wood fast pyrolysis at 500–520 °C with residence times not more than 1 s (Bridgwater et al. 1999b). In order to obtain a high liquid bio-oil yield, fast pyrolysis is well in research and development in recent years among the whole world. The suitable conditions include (1) very high heating and heat-transfer rate and a finely ground biomass feedstocks, (2) carefully controlled pyrolysis temperature of about 420–550 °C, and (3) short vapors residence times in reactors and rapid vapors cooling times (Huber et al. 2006; Mohan et al. 2006). A number of fast pyrolysis technologies have been commercialized mainly by Ensyn Technologies (seven Rapid Thermal Processing plants used circulating fluidized bed have been built in the USA and Canada; the largest has the capacity to process 100 t of dry residual wood per day), Dynamotive (three fast pyrolysis plants which adopted fluidized bed are in operation and the largest is 200 t/day plant in Guelph), and BTG (the Empyro plant, the largest pyrolysis plant in Europe, can convert 5 t dry wood into oil, steam, and electricity per hour in the rotary cone reactor).

Status of Biomass Fast Pyrolysis Technology

Fast Pyrolysis for Bio-oil Production from Various Feedstocks

Various feedstocks have been used in fast pyrolysis process for bio-oil production, ranging from bark, wood, agricultural wastes/residues, nuts, seeds, algae, grasses, and forestry residues to energy crops such as *Miscanthus* and *Sorghum*. Wood materials are widely used for bio-oil production due to the high bio-oil yield and quality. Luo et al. (2004) conducted the fast pyrolysis of wood feedstock such as *Pterocarpus indicus*, *Cunninghamia lanceolata*, and *Fraxinus mandshurica* in a fluidized-bed reactor and obtained the optimum bio-oil yield of about 56 % at the temperature 500 °C. Park et al. (2008) obtained a bio-oil yield of about 50 wt% of the product from Radiata pine sawdust fast pyrolysis at 400–450 °C in a bubbling fluidized bed. In addition to wood residues, agricultural waste and algae are also rich in raw materials. The highest bio-oil yield of about 55 wt% was obtained from rice husk and cotton stalk fast pyrolysis in a fluidized bed at 465 °C and 510 °C, and

these products could be directly used as a fuel oil in a boiler or a furnace on the basis of heat value, stability, miscibility, and corrosion characteristics analysis (Zheng 2007; Zheng et al. 2008). Miao et al. (2004) investigated the fast pyrolysis of microalgae (*Chlorella protothecoides* and *Microcystis aeruginosa*) in a fluidized bed at 500 °C with a heating rate of 600 °C/s and a vapor residence time of 2–3 s. The yield of bio-oil was 18 % and 24 %, respectively, and the properties were considered more suitable for fuel oil usages than bio-oil from lignocelluloses materials, with a higher heating value of 29 MJ/kg, a density of 1.16 kg/L, and a viscosity of 0.10 Pa s.

Reactors for Fast Pyrolysis

Besides the influence of biomass feedstocks, the types of reactor are the dominant factor, which directly determine the yield and physicochemical properties of bio-oils. The breakthrough of fast pyrolysis technology is the development of reactors. During the last two decades, several kinds of reactors have been explored to meet the rapid heat-transfer requirements. The main highlights of the important reactors that are available for the commercialization of pyrolysis technology will be discussed below.

Bubbling Fluidized-Bed Reactors

Bubbling fluidized-bed reactors are usually used in biomass pyrolysis for bio-oil production. They are easy to construct, operate, and even be scaled up, providing good temperature control and efficient heat transfer to biomass particles due to high solid density all along. Heating can be achieved in a variety of ways such as hot wall, hot tubes, hot inert gases, hot fluidizing gas, hot sand, etc. However, heat transfer to bed at large scales of operation has to be considered carefully due to scale-up limitations of different methods of heat transfer. A key feature of fast pyrolysis is the need to separate the by-product char from the vapors as quickly and completely as possible because char is a vapor-cracking catalyst and can significantly reduce the bio-oil yields. The rapid and effective char separation is usually achieved by ejection and entrainment followed by separation in one or more cyclones, so careful design of sand and biomass/char hydrodynamics is important. Fluidized-bed reactors give good and consistent performance with high liquid yields of typically 70–75 wt% from wood on a dry-feed basis, when biomass particle sizes are as small as less than 2–3 mm. Therefore, fluidized-bed reactors are commonly used for bio-oil production, including the academic researches in the Waterloo laboratory, Aston University, Leeds University, and National Renewable Energy Laboratory (NREL) and all the demonstration projects of Dynamotive. However, relatively low bio-oil yields of about 50–55 wt% are obtained in the same type of reactors in recent years (Luo et al. 2004; Park et al. 2008; Miao et al. 2004; Bridgwater 2003). The detailed different configuration of reactors is one of the reasons, but the main reason may be caused by the different efficiencies of quench coolers. So the R&D of condensation devices is very important to further improvement of the reactors.

Circulating Fluidized-Bed/Transported-Bed Reactors

Circulating fluidized bed (CFB) has many similar features to bubbling fluidized bed except that the residence time for the char is almost the same to it for vapors and gas (Bridgwater 2003). The advantage of CFBs is that they are suitable for very large throughputs, even though the hydrodynamics are complex and heat-transfer modes are not identified. The disadvantages are related to the separation of attrited char particles from pyrolysis vapors and careful control of closely integrated char combustion reactor to ensure that the temperature and heat flux match the process and feed requirements. Heat supply is usually from recycled heated sand through 80 % conduction, 19 % gas-solid convective transfer, and 1 % radiation (Bridgwater 1999), so their heat-transfer rates are not as high as fluidized beds and obviously affected by the biomass/sand ratio. In addition, impurities imported from hot char or adhered in recycled sand are mainly composed of alkali metals, which decrease the liquid product yield, increase the char yield, and improve the thermal stability of bio-oils (Nowakowski et al. 2007; Wang et al. 2006).

Ablative Pyrolysis Reactor

Ablative pyrolysis is substantially different in concept compared to the other methods of fast pyrolysis, which must adopt small biomass particles to ensure the high heat-transfer rate. The mode of reaction in ablative pyrolysis is completed by the high relative motion between particles and reactor wall. So heat is transferred from the hot reactor wall surface to melt biomass in virtue of high pressures, achieved due to centrifugal force in NREL or mechanically in Aston University. The wall temperature has to be limited to a maximum of about 625 °C to ensure the production of a liquid film between the wall and the particles which then vaporizes and leaves the reactor and to avoid severe coke deposition at the wall (Bridgwater and Peacocke 2000). The reactions in ablative pyrolysis are limited by heat-supply rate to the reactor rather than heat-transfer rate to the particles, so large feed sizes can be used without the requirement for fluidizing gas. Usually, ablative reactors are small and intensive but hard to scale up economically. The original design capacity of the vortex reactor in NREL is 50 kg/h biomass but the factual maximum throughput is 36 kg/h. Development focuses of ablative reactors are on the improvements of the bio-oil quality rather than reactor throughput currently. One of few researches related to the reactor configuration is the comparison of contact ablative pyrolysis and radiant ablative pyrolysis, on the basis of the values of ablation thickness and velocity and of product fractions and compositions, to show their advantages and drawbacks (Lédé 2003).

Vacuum Pyrolysis Reactor

Vacuum pyrolysis reactor is actually not a true fast pyrolysis, as the heat-transfer rate both to and through the solid biomass is much slower than that observed in other reactors and the solid residence time is very high. Vacuum pyrolysis can produce larger particles of biomass than most fast pyrolysis, which decompose into primary fragments when heated in the reactor and then quickly vaporize under reduced pressure. The properties of rapid volatilization and no carrier gas of vacuum

pyrolysis directly cause a less content of char particles in liquid product due to lower gas velocities. A pilot vacuum reactor with continuous feed rate of 15 kg/h, operated at 500 °C under 15 kPa, was used to produce bio-oil and investigate the characterization of bio-oils from softwood and hardwood (Garcìa-Pérez et al. 2007). Liquid yields of 45 wt% and 53 wt% on dry feed were obtained from softwood and hardwood with higher char yields than fast pyrolysis systems. However, there are no successful large throughput demonstrations that adopted vacuum pyrolysis technologies due to the complicated mechanics and poor heat-mass transfer rates.

Auger Reactor

Auger pyrolysis is a novel pyrolysis technology compared with other pyrolysis technologies (Brown 2009). The main features are that it is compact and does not require carrier gas and can continuously decompose biomass at low temperature of about 400 °C. Augers are used to transport feedstocks through an oxygen-free cylindrical heated tube. Hot sand as a heat-transfer medium can increase the heat supply from auger reactor. When heated, particles begin to decompose and volatilize followed by the separation of char and vapors. This design consequently reduces energy costs; moreover, the vapor residence time can be modified by increasing the length of the heated zone.

Rotating Cone Pyrolyzer

The rotating cone reactor is developed by Twente University and demonstrated by Biomass Technology Group of the Netherlands (BTG) in the 1990s. Biomass particles are fed into an impeller that is mounted at the base of the heated rotating cone together with an excess flow of inert materials, which have less carrier gas and sand or some catalytic particles (Wagenaar et al. 1994). These are then flung on to the heated surface to be pyrolyzed while being transported spirally upward along the hot cone wall. Produced char and sand drop into a fluidized bed surrounding the cone, from where they are lifted to a separate fluid-bed combustor, where char is burned to heat the sand used as the recycled heat-transfer medium. The reactor is very compact but complex integrated of three subsystems, including rotating cone reactor, riser for sand recycling, and fluidized bed for char combustion. So they are hard to scale up.

Development Recommendations

According to the above-discussed contents, some details should be paid more attention to the improvement of biomass to bio-oil processes, which allow easier scale up and significantly improved energy efficiency.

1. For pyrolysis reactor, it is important to develop an independent heat-supply source, which allows more design flexibility and easier control. Moreover, if the operated temperature can be minimized to about 400–450 °C, energy consumption will be obviously decreased compared to that consumed in 500–550 °C.
2. For the char separation, more efficient cyclones are urgently needed to separate char from pyrolysis vapors or aerosols with the minimum attrition of char

Table 9 Typical properties of the bio-oils (Czernik and Bridgwater 2004; Bridgwater 2004)

Properties	Value		Notes
	Bio-oil	Heavy oil	
Moisture content (wt%)	15–30	0.1	Water comes from moisture in the feed and reaction water and cannot be separated
pH	2.5		The low pH value comes from organic acids, e.g., acetic acid
Density	1.2	0.94	Bio-oil has about 40 % of the energy content of fuel oil on a weight basis but 60 % on a volumetric basis
Elemental composition			Typical elemental composition is affected by both the feedstocks and the produced solid char
C	54–58	85	Typical data is 57
H	5.5–7	11	Typical data is 6
O	35–40	1.0	Typical data is 37
N	0–0.2	0.3	The N content is trace
Ash	0–0.2	0.1	All ash is associated with the char content and affected by char separation
HHV (MJ/kg)	16–19	40	With the consideration of high moisture content of about 25 %, bio-oil has a high heating value
Viscosity, at 500 °C (cP)	40–100	180	Viscosity depends on the feedstocks, water content, light, and aging
Solids (wt%)	0.2–1	1.0	0.1 wt% is a good level, and 1 wt% is often encountered
Distillation residue (wt%)	Up to 50	1.0	Water addition can be tolerated up to about 35 %. Bio-oil is miscible with polar solvents such as methanol but totally immiscible with petroleum-derived fuels

particles, which have significant influence on quenching and applications of bio-oils. And as the by-product, the more clean char is better.

3. For quenching system, a rapid quenching time and a small recycle ratio (i.e., a small gas/biomass feed ratio) are required. It is the weakest part in the biomass-to-bio-oil development.

Properties of Bio-oils

Bio-oil is also called pyrolysis oil, wood oil, liquid smoke, wood distillates, etc., in the related researches and reports. Bio-oils are dark brown, are smelly, have high acidity, and have free-flowing organic liquids, produced from the decomposition and fragment of the main biomass components, namely, cellulose, hemicelluloses, and lignin. The special and complex physicochemical properties of bio-oils require careful characterizations of bio-oils and comprehensive considerations before any applications, storage, upgrading, and utilization.

Physical Properties

The physical properties of bio-oils are well documented in the literatures (Mohan et al. 2006; Lu et al. 2009a; Czernik and Bridgwater 2004; Bridgwater 2004). The

typical properties are described in Table 9, which are significantly different from that of the heavy fuel oil. The moisture content in bio-oils varies over a wide range (15–30 wt%) depending on the feedstocks and process conditions. The presence of water has both negative and positive effects on the oil properties. It lowers the heating value of bio-oils, especially the LHV and flame temperature, and contributes to the increase in ignition delay and decrease of combustion heat release rate. But the existence of water in bio-oils improves flow characteristics during pumping and atomization and leads to lower NO_x emissions. The presence of oxygen in many oil components is the primary reason for differences in the properties and behavior observed between hydrocarbon fuels and biomass pyrolysis oils. The high oxygen content of 35–40 % results in a low energy density that is less than 50 % of that for conventional fuel oils and immiscibility with hydrocarbon fuels. An even more important consequence of the organic oxygen is the thermal instability of bio-oils. The viscosity decreases at higher temperatures much faster than for petroleum-derived oils and a significant reduction can also be observed by addition of polar solvents. The undesired effect is the viscosity increase with time during storage or handling processes due to the chemical reactions between compounds leading to the formation of large molecules. Moreover, the corrosiveness is severe at elevated temperature and with the increase in water content. These properties have a significant influence on the behavior of bio-oils during combustion and consequently applications for energy production in standard equipment. Bio-oils are combustible but not flammable due to the high content of nonvolatile components contained (Hristov et al. 2004).

Chemical Properties

From a chemical point of view, bio-oils are characterized by the presence of oxygenated compounds, such as furan derivatives, carboxylic acids, alcohols, dihydroxyphenols, and dimethoxyphenols, derived from the decomposition of biomass components. Typical components and their yields of commercial wood-derived bio-oils produced from Biomass Technology Group of the Netherlands (BTG), Dynamotive, Ensyn, and Pyrovac (adopted vacuum reactors located in Quebec, Canada) are summarized in Table 10. Major compounds exist in the four kinds of bio-oils except for some differences in yields, which are caused by types of wood material, reactors, liquid collection methods, etc. In addition, properties and compositions of bio-oils from other feedstocks (like agriculture residues and forest residues) are also concluded by many researches (Mohan et al. 2006; Zheng 2007; Branca et al. 2005, 2006; Uzun et al. 2007).

Bio-oils are composed of molecules with different sizes derived from the depolymerization and fragmentation of cellulose, hemicelluloses, and lignin. Moreover, the composition of bio-oils is influenced by various factors, such as reactor type, operating conditions, and feeding materials. For example, the results of conventional fast pyrolysis indicate that faster rates enhance the formation of levoglucosan and hydroxyacetaldehyde with a diminution of carboxylic acids (Branca et al. 2003). Detailed classification systems use categories such as acids, aldehydes, phenols, furans, alkenes, aromatics, ketones, and saccharides (Mohan et al. 2006), and

Table 10 Yields and boiling point temperature of bio-oil components (Branca et al. 2005)

Compound	T_b (K)	BTG (wt %)	Dynamotive (wt %)	Ensyn (wt%)	Pyrovac (wt %)
Formaldehyde	253.9	2.63	2.07	0.83	0.76
Acetaldehyde	294	0.92	1.01	0.68	0.55
Glycolic acid	323	0.57	0.50	0.31	1.07
Glyoxal	324	1.51	1.32	0.84	0.92
Methanol	337.8	0.91	1.03	0.39	0.07
(5H)-Furan-2-one	360	0.54	0.62	0.50	0.51
Group I	300–360	7.86	7.75	3.96	4.48
Water	373.2	30.4	21.1	20.3	15.7
Hydroxyacetaldehyde	383	6.65	5.65	3.69	2.54
5-Hydroxymethylfurfural	388	0.49	0.52	0.23	0.83
Acetic acid	391.2	3.17	2.46	4.73	2.25
Butanol	390.6	3.15	2.85	1.29	0.80
Group II	360–400	44.42	33.16	30.59	22.42
Propionic acid	414.2	0.28	0.33	0.66	0.30
Hydroxypropanone	418.7	2.82	3.91	1.63	1.10
2-Methyl-2-cyclopentenone	431.4	0.06	0.17	0.14	0.53
2-Furfural	434.7	0.35	0.53	0.53	0.30
N-butyric acid	436	1.08	0.98	0.93	1.43
Group III	400–450	6.51	8.37	5.39	5.39
Phenol	455	0.08	0.10	0.23	0.32
o-Cresol	464.3	0.02	0.04	0.08	0.13
Syringaldehyde	465.6	0.04	0	1.16	0.07
p-Cresol	475	0.02	0.04	0.05	0.12
Guaiacol	478.2	0.36	0.53	0.21	0.33
4-Methyl guaiacol	494.2	0.65	1.23	0.23	0.41
Group IV	450–500	1.57	2.86	2.54	2.57
1,2-Benzendiol	518	0	0.13	0.10	0.91
Eugenol	526.4	0.42	0.71	1.80	0.24
Syringol	536	0.16	0.14	0.61	0.21
Vanillin	538.7	0.82	0.29	0.08	0.25
Isoeugenol (cis + trans)	540.5	1.41	2.80	0.49	1.18
Group V	500–550	3.08	4.66	3.49	3.25
Levoglucosan	659	2.96	4.48	3.71	3.72
Cellobiosan	–	1.80	2.30	0	0.70
Group VI	>550	4.93	7.22	4.04	4.89

representative compounds include acetic acid, formic acid, levoglucosan, hydroxypropanone, 2-furaldehyde, and hydroxyacetaldehyde (Garcia-Perez et al. 2007). The chemical composition of bio-oil can be manipulated by changing the thermal conditions of pyrolysis, but complex bio-oils are recalcitrant to complete

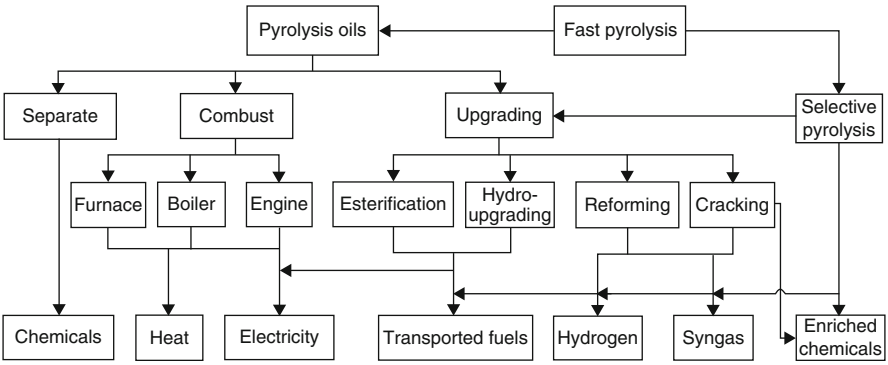

Fig. 1 Applications of bio-oils from fast pyrolysis process

chemical characterization, which is hindered by the limitations of modern analytical equipment.

Applications of Bio-oils

The most significant issues of bio-oils as fuels are poor volatility, high viscosity, coking, corrosiveness, and cold-flow problems. Though these problems limit the utilization of bio-oils, they also have many applications, mainly including direct combustion in boilers or furnaces to supply heat or to generate electricity and substitution for transported fuels after upgrading. Figure 1 summarizes some existing concepts of bio-oil applications, which can be divided into two classes: primary and high-grade applications.

Primary Applications of Bio-oils

Bio-oils are renewable liquid fuel, with a lower heating value of about 18 MJ/kg compared with 43 MJ/kg for diesels. They can be used as fuels in boilers, engines, or gas turbines for the production of heat, power, and combined heat and power (CHP). Compared to combustion and gasification of biomass, fast pyrolysis has the advantage that a liquid intermediate is produced, stored, and then transported to centralized locations economically. Thus, bio-oil production and heat or power generation can be carried out independently at different locations and times and at good efficient scales (Brammer et al. 2006).

Heat Generation

As discussed above, bio-oils have lower heating values compared with fossil fuels due to the high content of oxygenated compounds and water, but their combustion characteristics are similar to light fuel oils. So direct combustion of bio-oils can supply residential or industrial heating, which have been under operations in many regions. Currently, the consideration and improvement of this application are referred to three major issues. Bio-oils are too acidic to be used in the existing residential boilers, meaning that bio-oils should have to be processed or stainless

steel used; the modification of nozzles or burners is also necessary to ensure efficient ignition or combustion. Researches on the removal of oxygenated compounds and part of water are essential to improve the combustion behaviors.

Power Generation

One of the common applications for bio-oils is as a fuel for power generation. But attentions should be paid that boilers, especially engines and turbines, are specially designed to use bio-oils, rather than the conventional commercial engines. Organizations testing bio-oil in engines include Wartsila Diesel in Finland, Onnrod Diesel in Great Britain, and Orenda in Canada. One of the alterations to the turbine includes changing the fuel system and nozzle to handle a higher flow rate. Because of the high viscosity of bio-oils, the efficiency of fuel atomization is also an issue that must be addressed to achieve complete combustion. All these changes in the fuel pump, feed linings, and the injection system provide opportunities for applications for bio-oils to replace natural gas, diesel, and other fossil fuels in the industrial equipment.

As bio-oils are insoluble with petro-derived fuels, it is not possible to mix the fuels before combustion without emulsification. Emulsions of bio-oil and standard diesel or other fossil fuels have been produced and tested in diesel engines. Some researches investigate the emulsification effect on thermal stability of the fuel blends and observe that the emulsions are more stable than the crude bio-oils; the higher the bio-oil content, the higher the viscosity of the emulsion; and the optimal range of emulsifier to provide acceptable viscosity is between 0.5 % and 2 % (Chiaramonti et al. 2003a, b). Moreover, suitable emulsification can decrease the viscosity and corrosiveness of the fuel blends compared with original bio-oils (Ikura et al. 2003). Emulsification does not demand redundant chemical transformations, but the high cost and energy consumption input cannot be neglected. The accompanying corrosiveness to the engine and the subassemblies is inevitably serious.

Chemical Separation

More than 400 kinds of compounds have been identified in bio-oils. Some enriched compounds, such as acetic acid, hydroxyacetaldehyde, and phenols, can be separated by adding solvents into bio-oils. Phenols, consisting of relatively small amounts of phenol, eugenol, and cresols and much larger quantities of alkylated phenols, which are also called lignin-derived fractions, are present in high concentrations. The lignin-derived fraction is comprised of a total phenolic content of about 30–80 % and is considered more reactive in usage as an extender within resin formulations without requiring any further extraction or fractionation procedures. Many attractive results about pyrolyzed phenol substitution for resins have been reported (Wang et al. 2009a, b). However, resin producers want to market the reproducible, precisely tailored resin compositions that the end users demand. So the variability of chemical compositions has gained resin producers' attention in developing commercial resins from bio-oils.

Table 11 Properties of bio-oils after hydrodeoxygenation (Elliott 2007)

Properties	High-pressure liquefaction	Flash pyrolysis	Hydrodeoxygenation bio-oils
Elemental analysis			
C	72.6	43.5	85.3–89.2
H	8.0	7.3	10.5–14.1
O	16.3	49.2	0–0.7
S	<45	29.0	0.005
H/C ratio	1.12	1.23	1.40–1.97
Density (g/mL)	1.15	24.8	0.796–0.926
Moisture (wt%)	5.1	24.8	0.001–0.008
HHV (MJ/kg)	35.7	22.6	42.3–45.3
Viscosity (cP)	15,000 (61 °C)	59 (40 °C)	1.0–4.6 (23 °C)
Aromatic/aliphatic carbon	–	–	38/62–22/78
Octane number	–	–	77
Distillation range (wt%)			
IBP-225 °C	8	44	97–36
225–350 °C	32	Coked	0–41

Bio-oils Upgrading for High-Grade Applications

Hydrodeoxygenation (Hydro-upgrading)

Crude fossil fuel oil processing techniques typically focus on the removal of nitrogen and sulfur, as well as molecular weight reduction. In contrast, treatment of bio-oils will mainly be more focused on oxygen removal and molecular weight reduction. Hydrodeoxygenation of bio-oils involves treating bio-oils at moderate temperature of 250–400 °C with high-pressure H_2 (10–18 MPa) and continuous H_2 feed rate (volume ratio of H_2/bio-oil, 100–700) (Peterson et al. 2008). Processes refer to hydrotreating and hydrocracking, often in the presence of some catalysts. A number of different catalysts are employed, including nickel, cobalt, molybdenum, and platinum. Comprehensive reviews on hydrodeoxygenation have been written by Furimsky (2000) and Elliott (2007). As shown in Table 11, the energy content and the stability of bio-oils after upgrading are significantly increased. The high-pressure liquefaction is a method for bio-oil upgrading, which takes place in a water-rich phase, rather than an oil-rich phase, which eliminated the need for recycle but employed subsequent alkaline and acid treatments (Davis et al. 1982). The disadvantages are that it consumes H_2 and even requires high-pressure H_2. Moreover, hydrodeoxygenation process needs complicated equipments, advanced techniques, and excess cost and usually is forced to stop due to catalyst deactivation and reactor clogging. Future work in hydrodeoxygenation may be focused on developing decreased H_2 combustion system modified through mass and energy balance calculation and exploring and texting novel high-efficiency catalysts.

Catalytic Steam Reforming

The strategy of catalytic steam reforming is based on producing hydrogen from bio-oils in conjunction with other products that have greater value and can reduce the cost of hydrogen, which firstly start to develop in the 1990s by NREL. The original concept is that bio-oils are fractionated into two fractions based on water solubility. The water-soluble fraction is to be used for hydrogen production, and the water-insoluble fraction could be used in adhesive productions. Bio-oils are usually steam reformed using a nickel-based catalyst at 750–850 °C, followed by a shift reaction to convert CO to CO_2. The reactions in catalytic steam reforming of bio-oils are described as follows. The yield of hydrogen is limited with a maximum of only 8.6 g H_2/100 g bio-oil (Milne et al. 2001). Control of coke formation is a key aspect of this process. Loss of activity of the nickel catalysts after a few hours forces periodic regeneration. It is well known that CO_2 from a pressure swing absorption step can effectively remove the coke. There are currently no commercial deployment opportunities for hydrogen production, but this method remains viable. Several model compounds were successfully steam reformed, such as acetic acid, ethyl alcohol, acetone, phenol, cresol, and aqueous fraction of bio-oil.

$$\text{Biomass} + \text{Energy} \rightarrow \text{Bio} - \text{oil} + \text{Char} + \text{Gas impurities (pyrolysis)}$$
$$\text{Bio} - \text{oil} + \text{Water} \rightarrow \text{CO} + \text{H}_2\text{(reforming)}$$
$$\text{CO} + \text{Water} \rightarrow \text{CO}_2 + \text{H}_2\text{(shift reaction)}$$
$$\text{CH}_{1.9}\text{O}_{0.7} + 1.26\,\text{H}_2\text{O} \rightarrow \text{CO}_2 + 2.21\,\text{H}_2$$

Steam reforming of bio-oils can also produce syngas, composed of CO and H_2. Then syngas is converted into a range of fuels depending on the ratio of CO/H_2. The fuels include hydrogen by the water-gas shift reaction, methanol by methanol synthesis, alkanes by Fischer-Tropsch synthesis, ethanol by fermentation, etc.

Catalytic Cracking

Catalytic cracking is one of the routes for obtaining gasoline and other lighter products from fast pyrolysis oils. The initial catalysts were clays and amorphous silica alumina and were evolved with time to zeolites, specially the use of rare earth-Y (REY) and finally to the ultrastable-Y (USY), REUSY, and multi-zeolite catalysts used today (Tamunaidu and Bhatia 2007). Bio-oils can be upgraded using zeolite catalysts to reduce oxygen content and improve thermal stability. Zeolite upgrade is operated in the temperature range of 350–500 °C, atmospheric pressure, and gas hourly space velocities of around 2. The products are consisted of hydrocarbons, water-soluble organics, water, oil-soluble organics, gases, and coke. A number of chemical reactions occur including dehydration, cracking, polymerization, deoxygenation, and aromatization. By alternation cracking steps, bio-oils can be mainly decomposed into H_2, CO or CO_2, and coke. Then the coke is burnt by O_2 addition in the regeneration step. Catalytic cracking provides an interesting means of controlling the coke formed during bio-oil cracking. Moreover, the process may run autothermally. Different chemical compounds in bio-oils have a significant difference in reactivity and coke formation rates. Therefore, separation prior to reaction is

a positive prevention method for coke formation and catalyst attrition. It is necessary to incorporate the reactor and catalyst design as well as optimum process operation conditions in order to further improve the bio-gasoline production (Ong and Bhatia 2010).

Selective Pyrolysis of Biomass

In recent years, selective pyrolysis has aroused a great interest due to the advantages of operating at atmospheric pressure and in the absence of hydrogen. Selective pyrolysis is different from conventional fast pyrolysis, which is usually aimed at the maximum bio-oil yield and is to drive the pyrolysis of biomass toward the products of interest (Zhu and Lu 2010). The application of proper catalysts can effectively optimize the distribution of bio-oil composition and improve the quality of bio-oil as well as produce value-addition chemicals. Many studies have been focused on the catalysts of acids and alkali metal salt. The application of sulfated metal oxides (SO_4^{2-}/TiO_2, SO_4^{2-}/ZrO_2, SO_4^{2-}/SnO_2) significantly decreases or completely eliminates the formation of levoglucosan due to the enhancement of dehydration reactions (Lu et al. 2009b), while suitable concentration of phosphoric acid can govern levoglucosan/levoglucosenone ratio produced from cellulose pyrolysis (Dobele et al. 2005). Alkali metal salts such as K_2CO_3, NaCl, KCl, $MgCl_2$, and $CaCl_2$ have an obvious influence on gaseous products resulting in an increase in gas yield and a decrease in tar yield (Nishimura et al. 2009; Shimada et al. 2008). Currently catalytic upgrading of pyrolysis vapors using zeolites and noble metals is a potentially promising method for removing oxygen from organic compounds and converting them to hydrocarbons (French and Czernik 2009). Zeolites (Y and ZSM type) exhibit a strong influence on pyrolysis behavior of cellulose, reducing the overall yields of anhydrosugars to convert into hydrocarbons (Fabbri et al. 2007). Noble metals, for example, Pt and Ni, are widely applied in bio-oil catalytic reforming to improve the yields of gaseous products especially hydrogen (Zhao et al. 2009; Iojoiu et al. 2007).

Application of Biochar

Biochar as the by-product of biomass pyrolysis is of increasing interest because of concerns about climate change caused by emissions of carbon dioxide (CO_2) and other greenhouse gases (GHG).

Biochar is a stable charcoal of rich carbon produced by biomass pyrolysis under fully or partially anoxic conditions and at relatively low temperature (below 700 °C). The carbon content of biomass char varies as the pyrolysis temperature changes (Bruun et al. 2010). Biochar has a high surface area, high nutrient-retention capacity, and high water-retention capacity due to its porous structure (Zhang et al. 2009).

Biochar as a Potent Soil Amendment

Biochar has a large surface area because of its pore structure just as charcoal. Therefore, biochar has a high water-retention capacity. Application of biochar will increase the water-holding capacity of agricultural soil. In addition, the application of biochar is related to soil moisture and soil texture (Zhang et al. 2009). But further

studies are needed to clarify whether this may help balance fluctuations in water availability to plants (Karhu et al. 2011).

There are several ways for biochar to improve soil fertility. In the first place, biochar in the soil has a high nutrient-retention capacity because biochar can increase soil cation exchange capacity to enhance cation adsorption and improve pH of the soil. For example, rice hull char can increase pH in both soils to some extent, mainly by decreasing the contents of exchangeable acid and exchangeable Al, and increase the content of exchangeable bases and the base saturation (Yuan and Xu 2010). Furthermore, biochar addition benefits for the growth of fungus and nitrogen-fixing microbial groups, improving soil fertility and increasing crop yields (Song and Gong 2010; Diana et al. 2010). So, as a soil amendment, biochar makes soil more fertile, preserves cropland diversity, and reduces the need for some chemical and fertilizer inputs, which indirectly boosts food security and reduces water pollution.

Application of biochar could not only improve the physical and chemical properties of soil and increase soil fertility but also adsorb heavy metals (such as cadmium, arsenic, etc.), prevent the plant from uptaking of pollutants, and improve the effect of environmental remediation to a certain extent. The effects on the mobility, bioavailability, and toxicity of specific elements vary with the applying amendments to multielement contaminated soils (Luke et al. 2010; Luke and Marta 2011).

Biochar as a Powerful Tool to Combat Climate Change

The carbon in biochar resists degradation and can hold carbon in soils for hundreds to thousands of years. Biochar is produced through pyrolysis or gasification – processes that heat biomass in the absence (or under reduction) of oxygen.

In addition to creating a soil enhancer, sustainable biochar practices can produce oil and gas by-products that can be used as fuel, providing clean, renewable energy. When the biochar is buried in the ground as a soil enhancer, the system can become "carbon negative."

Biochar and bioenergy coproduction can help combat global climate change by displacing fossil fuel use and by sequestering carbon in stable soil carbon pools. It may also reduce emissions of nitrous oxide.

Future Directions

Combustion

At present, large-scale biomass combustion power generation projects were mainly concentrated in Europe and the USA and other developed countries. However, due to the variety of resources, most of the applied projects are using wood-based raw materials such as branches, wood chips, and waste wood as the main fuel, only a small part blending a small part of the crop stalks. In the area of crop stalk combustion power generation, Denmark has made outstanding achievement, represented by water-cooled vibrating grate technology of BWE. In 1988, the first crop stalk combustion power plant was constructed in Denmark. Since then, more

than 100 plants have been established in the past years, and it makes biomass become the very important energy resource in Denmark. In order to overcome the biomass fuel supply fluctuations, large-scale power plants generally co-fire it with coal. Meanwhile, in order to improve the economics of biomass power plants and thermal efficiency, now the combined heat and power technology (CHP) is widely used.

After many years of development, there have been no major technical obstacles of biomass combustion power generation. However, lots of work still need to be done. The biomass resources are of great varieties and scattered, which result in difficult collection and transportation. At present, the equipments and processing flow for collection, transportation, and pretreatment of biomass are not perfect, which is the key factor of scale-up biomass power generation.

In the future, the utilization of high-alkali biomass will become more and more important. In order to improve the share of electricity generation from biomass combustion, co-firing represents a cost-effective, short-term option at large scale.

Gasification

Among the different gasification technologies, the biomass gasification is the most promising biomass technology that has great potential to be further developed. Though there is a great achievement in the research and development of this technology, several developmental constraints exist including pollution issues, competitiveness with electricity generated by conventional fuel, and system scale. Environmental protection and energy conservation may be a driving force of further development of the biomass gasification technologies.

1. *Scale*: At present, due to financing problems, the development of small-scale gasification plants is restricted. But the development of large-scale plants is also restricted because of the problems with collection and transportation. To handle the relations of the two issues is the great impetus for gasification development.
2. *Feeding*: Because of the seasonality of biomass, it is necessary to improve the feasibility of the gasification equipment for different raw materials either separately or in mixed form. Compared to the direct gasification of raw biomass materials, the overall efficiency of oil/gas gasification is low. But it is easier to realize continuous oil and system compression using oil as raw material, which can effectively reduce costs and achieve economy. Hence, it is necessary to research and develop the pyrolysis oil/gas gasification technology.
3. *Combined heat and power (CHP) technology*: Although large- and medium-scale CHP plants have been commercialized, small- and microscale plants used for heat supply for buildings are easier to find an end user than larger CHP systems. So small- and microscale plants need more research.
4. *Contamination*: Some specifications for biomass gasification are estimated based on the practical experience. So it is necessary to investigate the rules of pollutant emission in the biomass gasification process.

5. *Purification*: A complete set of specific specification for pollutants in the product gas is needed. For example, the requirements for Fischer-Tropsch synthesis are very stringent. And the relatively clean natural gas is the common feedstock for Fischer-Tropsch synthesis. But the actual cleaning specifications are not known for some specific biomass contaminants.
6. *Policy*: Since the industrialization process of biomass gasification would take a long period to reflect the importance of biomass gasification in an environmental protection field, the government should offer sustainable assistance for development, such as increasing support funds, setting up of special project assessment institute, and setting up of special funds with an aim to drive society investment and cultivate mature market.

Pyrolysis

Bio-oils have the considerable advantages of being storable and transportable as well as the potential to supply the amount of valuable chemicals; there are many challenges facing fast pyrolysis that relate to technology, product characterization, and applications.

The challenges are as follows:

1. Design a well-integral fast pyrolysis system, making the reactor in perfect cooperation with char separation, liquid quenching, liquid collection, and fuel applications.
2. Decrease the cost of bio-oil production and increase the energy efficiency.
3. Set up standards for testing the physicochemical properties of bio-oil.
4. Develop widely the applications of bio-oils before and after upgrading.
5. Bio-oil is incompatible with conventional fuels and its users are unfamiliar with this material.
6. Dedicated fuel handing systems are needed.
7. Develop environmental health and safety issue evaluation in handing, transport, and usage.
8. Encourage developers to implement bio-oil and by-product applications.

References

Arvelakis S, Koukios EG (2002) Physicochemical upgrading of agroresidues as feedstocks for energy production via thermochemical conversion methods. Biomass Bioenergy 22:331–348

Arvelakis S, Gehrmann H, Beckman M et al (2002) Effect of leaching on the ash behaviour of olive residue during fluidized bed gasification. Biomass Bioenergy 22:55–69

Arvelakis S, Gehrmann H, Beckmann M et al (2005) Preliminary results on the ash behavior of peach stones during fluidized bed gasification: evaluation of fractionation and leaching as pre-treatments. Biomass Bioenergy 28:331–338

Balat M, Balat H (2009) Recent trends in global production and utilization of bio-ethanol fuel. Appl Energy 86(11):2273–2282

Bartels M, Lin WG, Nijenhuis J et al (2008) Agglomeration in fluidized beds at high temperatures – mechanisms, detection and prevention. Prog Energy Combust Sci 34(5):633–666
Baxter LL (1993) Ash deposition during biomass and coal combustion-a mechanistic approach. Biomass Bioenergy 4(2):85–102
Baxter L (2005) Biomass-coal co-combustion: opportunity for affordable renewable energy. Fuel 84:1295–1302
Boerrigter H (2005) "OLGA" tar removal technology. The Energy research Centre of the Netherlands, ECN-C-05-009
Brammer J, Lauer M, Bridgwater A (2006) Opportunities for biomass-derived "bio-oil" in European heat and power markets. Energy Policy 34(17):2871–2880
Branca C, Giudicianni P, Blasi C (2003) GC/MS characterization of liquids generated from low-temperature pyrolysis of wood. Ind Eng Chem Res 42:3190–3202
Branca C, Blasi C, Elefante R (2005) Devolatilization and heterogeneous combustion of wood fast pyrolysis oils. Ind Eng Chem Res 44(4):799–810
Branca C, DiBlasi C, Elefante R (2006) Devolatilization of conventional pyrolysis oils generated from biomass and cellulose. Energy Fuels 20(5):2253–2261
Bridgwater A (1999) Principles and practice of biomass fast pyrolysis processes for liquids. J Anal Appl Pyrol 51:3–22
Bridgwater A (2003) Renewable fuels and chemicals by thermal processing of biomass. Chem Eng J 91:87–102
Bridgwater A (2004) Biomass fast pyrolysis. Therm Sci 8:21–49
Bridgwater A, Peacocke G (2000) Fast pyrolysis processes for biomass. Renew Sust Energy Rev 4:1–73
Bridgwater AV, Beenackers AACM, Spila K et al (1999a) An assessment of the possibilities for transfer of European biomass gasification technology to China. European Community, Belgium
Bridgwater A, Meier D, Radlein D (1999b) An overview of fast pyrolysis of biomass. Org Geochem 30:1479–1493
Brown JN (2009) Development of a lab-scale auger reactor for biomass fast pyrolysis and process optimization using response surface methodology. MS thesis, Iowa State University, Ames
Brown RC, Liu Q, Norton G (2000) Catalytic effects observed during the co-gasification of coal and switchgrass. Biomass Bioenergy 18:499–506
Bruun EW, Hauqqaard-Nielsen H, Ibrahim N et al (2010) Influence of fast pyrolysis temperature on biochar labile fraction and short-term carbon loss in a loamy soil. Biomass Bioenergy 35 (3):1182–1189
Chen WY, Gathitu BB (2006) Design of mixed fuel for heterogeneous reburning. Fuel 85:1781–1793
Chen G, Andries J, Spliethoff H (2003) Catalytic pyrolysis of biomass for hydrogen rich fuel gas production. Energy Convers Manag 44:2289–2296
Chiaramonti D, Bonini M, Fratini E et al (2003a) Development of emulsions from biomass pyrolysis liquid and diesel and their use in engines-Part 1: emulsion production. Biomass Bioenergy 25(1):85–99
Chiaramonti D, Bonini M, Fratini E et al (2003b) Development of emulsions from biomass pyrolysis liquid and diesel and their use in engines-Part 2: tests in diesel engines. Biomass Bioenergy 25(1):101–111
Chirone R, Miccio F, Scala F (2006) Mechanism and prediction of bed agglomeration during fluidized bed combustion of a biomass fuel: effect of the reactor scale. J Chem Eng 123 (3):71–80
Czernik S, Bridgwater A (2004) Overview of applications of biomass fast pyrolysis Oil. Energy Fuels 18(2):590–598
Davis H, Figueroa C, Schaleger L (1982) Hydrogen or carbon monoxide in the liquefaction of biomass. In: World hydrogen energy conference IV, Pasadena
Dayton D (2002) A review of the literature on catalytic biomass tar destruction. Report No. NREL/TP-510-32815. National Renewable Energy Laboratory, Golden. http://www.osti.gov/bridge

Demirbas A (2003) Sustainable cofiring of biomass with coal. Energy Convers Manag 44:1465–1479
Demirbas A (2004) Combustion characteristics of different biomass fuels. Prog Energy Combust Sci 30:219–230
Demirbas A (2005) Potential applications of renewable energy sources, biomass combustion problems in boiler power systems and combustion related environmental issues. Prog Energy Combust Sci 31:171–192
Diana N, Marco R, Kam-Rigne L et al (2010) Contrasted effect of biochar and earthworms on rice growth and resource allocation in different soils. Soil Biol Biochem 42:1017–1027
Dobele G, Rossinskaja G, Dizhbite T et al (2005) Application of catalysts for obtaining 1, 6-anhydrosaccharides from cellulose and wood by fast pyrolysis. J Anal Appl Pyrol 74 (1–2):401–405
Drift A van der, Boerrigter H, Coda B et al. (2004) Entrained flow gasification of biomass: ash behaviour, feeding issues, and system analyses. ECN-C-04-039. ECN, Petten
Elisabet B, Marcus Ö, Anders N (2005) Mechanisms of bed agglomeration during fluidized-bed combustion of biomass fuels. Energy Fuel 19(3):825–832
Elliott DC (2007) Historical developments in hydroprocessing bio-oils. Energy Fuels 21 (3):1792–1815
Elliott DC, Baker EG (1986) The effect of catalysis on wood gasification tar composition. Biomass 9:195–203
Fabbri D, Torri C, Baravelli V (2007) Effect of zeolites and nanopowder metal oxides on the distribution of chiral anhydrosugars evolved from pyrolysis of cellulose: an analytical study. J Anal Appl Pyrol 80(1):24–29
French R, Czernik S (2009) Catalytic pyrolysis of biomass for biofuels production. Fuel Process Technol 91(1):25–32
Furimsky E (2000) Catalytic hydrodeoxygenation. Appl Catal A 199(2):147–190
Gabra M, Pettersson E, Backman R et al (2001) Evaluation of cyclone gasifier performance for gasification of sugar cane residue-Part 1: gasification of bagasse. Biomass Bioenergy 21:351–369
Garcia-Perez M, Chaala A, Pakdel H et al (2007) Characterization of bio-oils in chemical families. Biomass Bioenergy 31(4):222–242
Garcìa-Pérez M, Chaala A, Pakdel H et al (2007) Vacuum pyrolysis of softwood and hardwood biomass: comparison between product yields and bio-oil properties. J Anal Appl Pyrol 78(1):104–116
Gil J, Corella J, Aznar MP et al (1999) Biomass gasification in atmospheric and bubbling fluidized bed: effect of the type of gasifying agent on the product distribution. Biomass Bioenergy 17:389–403
Graham R, Bergougnou M, Overend R (1984) Fast pyrolysis of biomass. J Anal Appl Pyrol 6 (2):95–135
Hasler XX (1997) Evaluation of gas cleaning technologies for small scale biomass gasifiers. Swiss Federal Office of Energy and Swiss Federal Office for Education and Science, Zurich
Hasler P, Nussbaumer T (1999) Gas cleaning for IC engine applications from fixed bed biomass gasification. Biomass Bioenergy 16:385–395
Heesch BEJM, Paasen SV (2000) Pulsed corona tar cracker. IEEE Trans Plasma Sci 28:1571–1575
Hristov JY, Stamatov V, Honnery DR et al. (2004) Radiant heating of a bio-oil droplet: a quest for a suitable most and scaling of pre-explosion conditions. In: 15th Australasian fluid mechanics conference, Sydney
Huber GW, Iborra S, Corma A (2006) Synthesis of transportation fuels from biomass: chemistry, catalysts, and engineering. Chem Rev 106(9):4044–4098
Ikura M, Stanciulescu M, Hogan E (2003) Emulsification of pyrolysis derived bio-oil in diesel fuel. Biomass Bioenergy 24(3):221–232
Iojoiu E, Domine M, Davidian T et al (2007) Hydrogen production by sequential cracking of biomass-derived pyrolysis oil over noble metal catalysts supported on ceria-zirconia. Appl Catal A 323:147–161

Jana S (2004) Biomass technologies & experiences with biomass utilization. Final[R]
Jenkins BM, Baxter LL, Miles TR Jr et al (1998) Combustion properties of biomass. Fuel Process Technol 54:17–46
Karhu K et al (2011) Biochar addition to agricultural soil increased CH_4 uptake and water holding capacity – results from a short-term pilot field study. Agric Ecosyst Environ 140:309–313
Karlsson G, Ekström C (1994) The development of a biomass IGCC process for power and heat production. In: Proceedings of the eighth European conference on biomass for energy, environment, agriculture and industry, Vienna
Khan AA, de Jong W, Jansens PJ et al (2009) Biomass combustion in fluidized bed boilers: potential problems and remedies. Fuel Process Technol 90:21–50
Knoef HAM (2000) Inventory of biomass gasifier manufacturers and installations. Final Report to European Commission, Contract DIS/1734/98-NL. Biomass Technology Group B.V., University of Twente, Enschede. http://www.gasifiers.org/
Knoef H (2001–2003) Technology brief: fixed-bed gasification. Task 33: thermal gasification of biomass. IEA Bioenergy Agreement. http://media.godashboard.com/gti/IEA/FixedBedGasificationr.pdf
Kumar VA, Anil KV, Pant KK (1997) Potassium-containing calcium aluminate catalysts for pyrolysis of n-heptane. Appl Catal A Gen 162:193–200
Kurkela E (2000) PROGAS – gasification and pyrolysis R&D programme 1997–1999. In: Proceedings conference on power production from biomass III, gasification & pyrolysis R&D&D. VTT, Espoo
Lédé J (2003) Comparison of contact and radiant ablative pyrolysis of biomass. J Anal Appl Pyrol 70(2):601–618
Li J, Xiao B, Liang DT et al (2008) Development of Nano-NiO/Al_2O_3 catalyst to be used for tar removal in biomass gasification. Environ Sci Technol 42:6224–6229
Lu Q, Li W, Zhu X (2009a) Overview of fuel properties of biomass fast pyrolysis oils. Energy Convers Manag 50(5):1376–1383
Lu Q, Xiong W, Li W et al (2009b) Catalytic pyrolysis of cellulose with sulfated metal oxides: a promising method for obtaining high yield of light furan compounds. Bioresour Technol 100 (20):4871–4876
Luke B, Marta M (2011) The immobilisation and retention of soluble arsenic, cadmium and zinc by biochar. Environ Pollut 159:474–480
Luke B, Eduardo MJ, Jose LGE (2010) Effects of biochar and greenwaste compost amendments on mobility, bioavailability and toxicity of inorganic and organic contaminants in a multi-element polluted soil. Environ Pollut 158:2282–2287
Luo Z, Wang S, Liao Y et al (2004) Research on biomass fast pyrolysis for liquid fuel. Biomass Bioenergy 26(5):455–462
Ma L, Verelst H, Baron GV (2005) Integrated high temperature gas cleaning: tar removal in biomass gasification with a catalytic filter. Catal Today 105:729–734
Miao X, Wu Q, Yang C (2004) Fast pyrolysis of microalgae to produce renewable fuels. J Anal Appl Pyrol 71(2):855–863
Miccio F (1999) Gasification of two biomass fuels in bubbling fluidized bed. In: Proceedings of the 15th international conference on fluidized bed combustion, Savannah, pp 16–19
Milne T, Elam C, Evans R (2001) Hydrogen from biomass: state of the art and research challenges. NREL IEA/H2/TR-02/001
Mohan D, Pittman C, Steele P (2006) Pyrolysis of wood/biomass for bio-oil: a critical review. Energy Fuels 20(3):848–889
Nielsen HP, Frandsen FJ, Dam-Johansen K et al (2000) The implications of chlorine-associated corrosion on the operation of biomass-fired boilers. Prog Energy Combust Sci 26:283–293
Nishimura M, Iwasaki S, Horio M (2009) The role of potassium carbonate on cellulose pyrolysis. J Taiwan Inst Chem Eng 40(6):630–637
Nowakowski D, Jones J, Brydson R et al (2007) Potassium catalysis in the pyrolysis behaviour of short rotation willow coppice. Fuel 86:2389–2402

Ong Y, Bhatia S (2010) The current status and perspectives of biofuel production via catalytic cracking of edible and non-edible oils. Energy 35(1):111–119
Paasen SVB, Rabou L (2004) Tar removal with wet ESP: parametric study. In: The second world conference and technology exhibition on biomass for energy, industry and climate Protection, Rome, pp 205–210
Park H, Park Y, Kim J (2008) Influence of reaction conditions and the char separation system on the production of bio-oil from radiate pine sawdust by fast pyrolysis. Fuel Process Technol 89:797–802
Peláez-Samaniego M, Garcia-Perez M, Cortez L et al (2008) Improvements of Brazilian carbonization industry as part of the creation of a global biomass economy. Renew Sust Energy Rev 12 (4):1063–1086
Peterson A, Vogel F, Lachance R et al (2008) Thermochemical biofuel production in hydrothermal media: a review of sub- and supercritical water technologies. Energy Environ Sci 1:32–65
Rapagna S, Jand N, Kiennemann A et al (2000) Steam-gasification of biomass in a fluidised-bed of olivine particles. Biomass Bioenergy 19:187–197
Reinhard R (2002) Biomass gasification to produce synthesis gas for fuel cells, liquid fuels and chemicals. Task 33: thermal gasification of biomass (2001–2003). IEA Bioenergy Agreement. http://media.godashboard.com/gti/IEA/TechnologybriefSynthesisGas.pdf
Sami M, Annamalai K, Wooldridge M (2001) Co-firing of coal and biomass fuel blends. Prog Energy Combust Sci 27:171–214
Shimada N, Kawamoto H, Saka S (2008) Different action of alkali/alkaline earth metal chlorides on cellulose pyrolysis. J Anal Appl Pyrol 81(1):80–87
Song YJ, Gong J (2010) Effects of biochar application on soil ecosystem functions. Ludong Univ J Nat Sci Ed 26(4):361–365
Stahl K, Neergaard M, Nieminen J (2001) Final report: Varnamo demonstration programme. In: Bridgwater AV (ed) Progress in thermochemical biomass conversion. Blackwell Science, London, pp 549–563
Tamunaidu P, Bhatia S (2007) Catalytic cracking of palm oil for the production of biofuels: optimization studies. Bioresour Technol 98(18):3593–3601
Tillman DA (2000) Biomass cofiring: the technology, the experience, the combustion consequences. Biomass Bioenergy 19:365–384
Tomishige K, Asadullah M, Kunimori K (2005) Novel catalyst with high resistance to sulfur for hot gas cleaning at low temperature by partial oxidation of tar derived from biomass. Catal Commun 6:37–40
Uzun B, Pütün A, Pütün E (2007) Composition of products obtained via fast pyrolysis of olive-oil residue: effect of pyrolysis temperature. J Anal Appl Pyrol 79:147–153
van den Broek R, Faaij A, van Wijk A (1995) Biomass combustion power generation technologies [R]. Energy from biomass: an assessment of two promising systems for energy production. http://www.projects.science.uu.nl/nws/publica/95029.htm
van Loo S (2004) Biomass combustion and cofiring [R]. Task 32, IEA Bioenergy
van Loo S, Koppejan J (2008) Handbook of biomass combustion and co-firing [M]. Earthscan, London
Van RR, Oudhuis ABJ, Faaij A (1995) Modelling of a biomass-integrated-gasifier/combined-cycle (BIG-CC) system with the flowsheet simulation program Aspen-plus. Netherlands Energy Research Foundation ECN, Petten
Venderbosch RH, Prins W (1998) Entrained flow gasification of bio-oil for synthesis gas. BTG Biomass Technology Group b.v. University of Twente
Wagenaar BM, Prins W, van Swaaij WPM (1994) Pyrolysis of biomass in the rotating cone reactor: modeling and experimental justification. Chem Eng Sci 49(24):5109–5126
Waldheim L, Morris M, Leal M et al (2001) Biomass power generation: sugar cane bagasse and trash. In: Bridgwater AV (ed) Progress in thermochemical biomass conversion. Blackwell Science, London, pp 509–523

Wang J, Zhang M, Chen M et al (2006) Catalytic effects of six inorganic compounds on pyrolysis of three kinds of biomass. Thermochim Acta 444:110–114
Wang LJ, Weller CL, Jones DD et al (2008) Contemporary issues in thermal gasification of biomass and its application to electricity and fuel production. Biomass Bioenergy 32:573–581
Wang M, Leitch M, Xu C (2009a) Synthesis of phenolic resol resins using cornstalk-derived bio-oil produced by direct liquefaction in hot-compressed phenol-water. J Ind Eng Chem 15 (6):870–875
Wang M, Leitch M, Xu C (2009b) Synthesis of phenol-formaldehyde resol resins using organosolv pine lignins. Eur Polym J 45(12):3380–3388
Werther J, Saenger M, Hartge EU et al (2000) Combustion of agricultural residues. Prog Energy Combust Sci 26:1–27
Xu J, Jiang J, Sun Y et al (2008) Bio-oil upgrading by means of ethyl ester production in reactive distillation to remove water and to improve storage and fuel characteristics. Biomass Bioenergy 32(11):1056–1061
Yin CG, Lasse AR, Søren KK (2008) Grate-firing of biomass for heat and power production. Prog Energy Combust Sci 34:725–754
Yu CJ, Qin JG, Xu J et al (2010) Straw combustion in circulating fluidized bed at low temperature: transformation and distribution of potassium. Can J Chem Eng 88:875–880
Yuan JH, Xu RK (2010) Effects of rice-hull-based biochar regulating acidity of red sail and yellow brown soil. J Ecol Rural Environ 26(5):472–476
Zainal ZA, Rifau A, Quadir GA et al (2002) Experimental investigation of a downdraft biomass gasifier. Biomass Bioenergy 23:283–289
Zhang XD (2003) The mechanism of tar cracking by catalyst and the gasification of biomass. The dissertation of Zhejiang University
Zhang Q, Chang J, Wang T et al (2007) Review of biomass pyrolysis oil properties and upgrading research. Energy Convers Manag 48(1):87–92
Zhang WL, Li GH, Gao WD (2009) Effect of biomass charcoal on soil character and crop yield. Chin Agric Sci Bull 25(17):153–157
Zhao H (2007) PHD thesis in experimental and theoretical research on entrained flow gasification of biomass for syn-gas, Zhejiang University
Zhao M, Florin N, Harris A (2009) The influence of supported Ni catalysts on the product gas distribution and H2 yield during cellulose pyrolysis. Appl Catal B 92:185–193
Zheng J (2007) Bio-oil from fast pyrolysis of rice husk: yields and related properties and improvement of the pyrolysis system. J Anal Appl Pyrol 80(1):30–35
Zheng J, Yi W, Wang N (2008) Bio-oil production from cotton stalk. Energy Convers Manag 49 (6):1724–1730
Zhu XF, Lu Q (2010) In: Maggy Ndombo Benteke Momba (ed) Production of chemicals from selective fast pyrolysis of biomass, biomass. Sciyo. ISBN: 978-953-307-113-8

Chemicals from Biomass

Debalina Sengupta and Ralph W. Pike

Contents

Abstract

The different biomass conversion routes to chemicals will be described in this chapter. Chapter "► Biomass as Feedstock," gives an overview of the methods used to obtain chemicals from biomass. These processes along with some other chemical conversions can be used for the manufacture of chemicals from biomass. A list of chemicals compiled based on the carbon number in the chemicals will be discussed in this chapter. Some of these chemicals are presently made

D. Sengupta (✉)
Texas A&M University, College Station, TX, USA
e-mail: sengupta.debalina@epa.gov

R.W. Pike
Minerals Processing Research Institute, Louisiana State University, Baton Rouge, LA, USA
e-mail: pike@lsu.edu

W.-Y. Chen et al. (eds.), *Handbook of Climate Change Mitigation and Adaptation*,
DOI 10.1007/978-3-319-14409-2_28

from nonrenewable feedstock like natural gas and petroleum, while others are new chemicals that have potential to replace nonrenewable feedstock-based chemicals. Transesterification process is used to produce propylene chain of chemicals from glycerin. Fermentation is used to produce ethanol which is converted to ethylene and can be used for ethylene chain of chemicals. The chemicals discussed in this chapter include recent advances in chemistry, and processes discussed include new frontiers for research in biomass to chemical production.

Introduction

Crude oil is the single largest source of energy for the USA, followed by natural gas and coal. Approximately 3 % of the total crude oil is used as feedstock for the production of chemicals (Banholzer et al. 2008). Natural gas is used for the production of fertilizers and supplies energy to the production processes. Petroleum refineries extract and upgrade valuable components of crude oil using various physical and chemical methods into a large array of useful petroleum products. While the USA is one of the world's largest producers of crude oil, the country relies heavily on imports to meet the demand for petroleum products for consumers and industry. This reliance on international ties to petroleum trade has led to numerous upheavals in the industry over the last four decades, the most recent being when crude oil prices reached $134 per barrel in 2008 (Banholzer et al. 2008), as shown in Fig. 1. Natural disasters such as hurricanes in the Gulf Coast region (Katrina and Rita in 2005 and Gustav in 2008) caused major damages to offshore oil-drilling platforms and disruption of crude oil supply. The natural gas prices, shown in Fig. 2, have also varied from $4 per cubic feet in 2001 to $13 per cubic feet in 2008 (EIA 2010b).

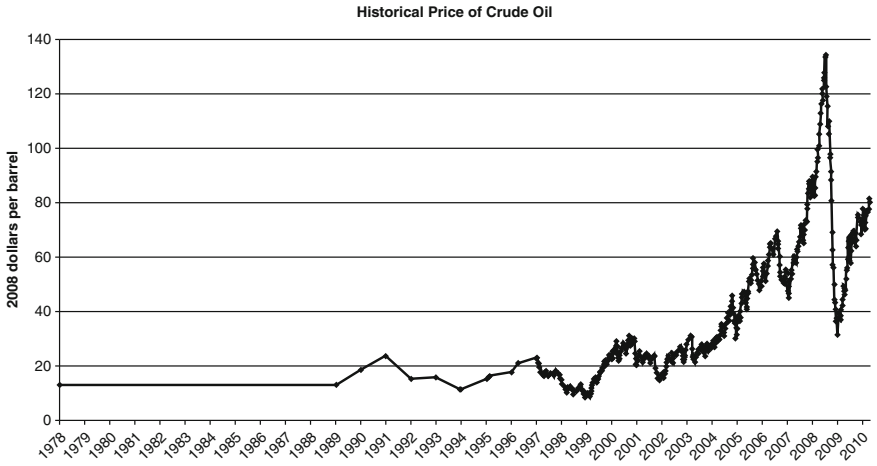

Fig. 1 Historical crude oil prices (EIA 2010a)

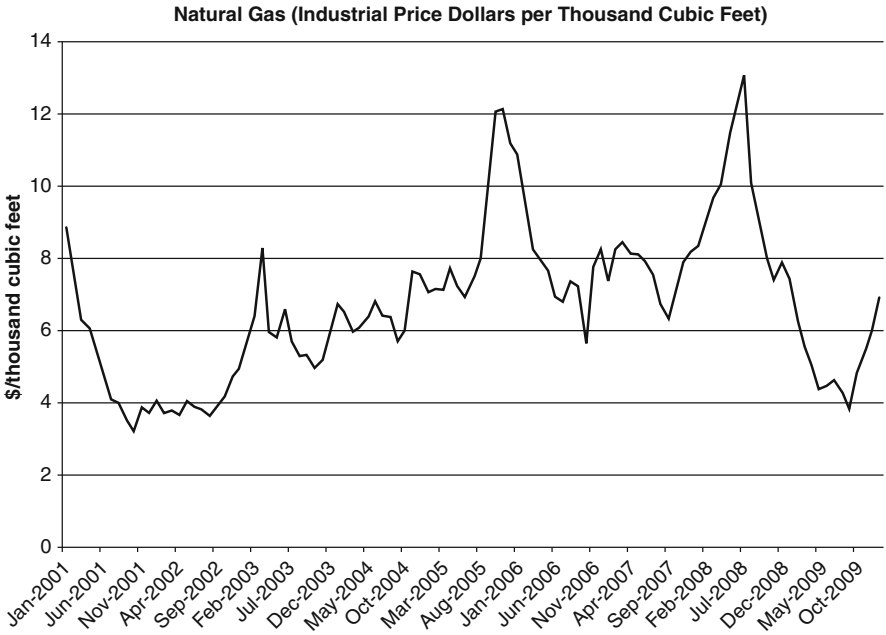

Fig. 2 Natural gas prices (EIA 2010b)

The consumption of energy resources in the world added 30.4 billion tons of carbon dioxide in 2008, an increase of approximately 12 billion tons higher than 1980 figures (EIA 2010c). The rate of carbon dioxide emissions is expected to go higher, unless alternate methods for obtaining energy, fuels, and chemicals are developed. Renewable resources are considered for supplementing and eventually substituting the dependence on oil and natural gas. These resources include biomass, wind, hydroelectric, and solar energy. These resources convert an alternate form of energy (different from fossil resource) into power, fuels, or chemicals. Some of these resources (wind, solar, hydroelectric) do not emit large quantities of carbon dioxide during resource utilization and thus are cleaner choices compared to fossil resources. This also reduces the dependence on foreign oil imports.

The processes for the production of chemicals involve the conversion of traditional or conventional forms of energy (petroleum and natural gas) to materials by rearranging the atoms from the components, mainly carbon, hydrogen, and oxygen. The shift to renewable resources for the production of chemicals offers biomass as the only choice of raw material because only biomass can provide the necessary carbon, hydrogen, and oxygen atoms. The rest of the renewable resources can be used as supplement for energy requirements for the conversion processes. Also, carbon dioxide utilized in photosynthetic processes to produce biomass is released when biomass is used. This allows the immediate use of atmospherically fixed carbon dioxide to be released to the environment, which in turn will be used for biomass formation. The transition from fossil feedstock to biomass feedstock

requires extensive process technology changes, market penetration of new chemicals from biomass replacing existing chemicals, and process energy requirements.

Chemicals from Nonrenewable Resources

The chemical industry in the USA is an integral part of the country's economy, producing more than 70,000 products each year. About 24 % of the chemicals produced become raw materials for other products within the industry. For example, ethylene is the fourth largest produced chemical in the USA, with 24 million short tons produced in 1997 (Energetics 2000). The Department of Energy gives an extensive list of chemicals and allied products manufactured in the USA, identified by SIC (Standard Industrial Classifications) codes. The major US chemical industry SIC codes and their corresponding products are given in Table 1.

Based on the classifications of industrial chemicals in Table 1, they can be divided into five chains of chemicals. These include the ethylene chain, the propylene chain,

Table 1 Major US chemical industry SIC codes and their products (Adapted from Energetics (2000))

SIC	Major products
281 Industrial inorganic chemicals	
2812 Alkalies and chlorine	Caustic soda (sodium hydroxide), chlorine, soda ash, potassium, and sodium carbonates
2813 Industrial gases	Inorganic and organic gases (acetylene, hydrogen, nitrogen, oxygen)
2819 Industrial inorganic chemicals (not otherwise classified)	Compounds of aluminum, ammonium, chromium, magnesium, potassium, sodium, sulfur, and numerous other minerals; inorganic acids
282 Plastics and rubbers	
2821 Plastic materials and resins	Synthetic resins, plastics, and elastomers (acrylic, polyamide, vinyl, polystyrene, polyester, nylon, polyethylene)
2822 Synthetic rubber	Vulcanizable rubbers (acrylic, butadiene, neoprene, silicone)
286 Industrial organic chemicals	
2865 Cyclic crudes and intermediates	Distilling coal tars; cyclic intermediates, i.e., hydrocarbons, aromatics (benzene, aniline, toluene, xylenes); and organic dyes and pigments
2869 Industrial organic chemicals (not otherwise classified)	Aliphatic/acyclic organics (ethylene, butylene, organic acids), solvents (alcohols, ethers, acetone, chlorinated solvents), perfumes and flavorings, rubber processors and plasticizers
287 Agricultural chemicals	
2873 Nitrogenous chemicals	Ammonia fertilizer compounds, anhydrous ammonia, nitric acid, urea, and natural organic fertilizers
2874 Phosphatic chemicals	Phosphatic materials, phosphatic fertilizers

the benzene–toluene–xylene (BTX) chain, the agricultural chemicals chain, and the chlor-alkali industry (Energetics 2000). Among these, the production of ethylene, the building block for the ethylene chain of chemicals, depends on the availability of petroleum feedstock. Propylene, a building block for the propylene chain of chemicals, is almost entirely produced as a coproduct with ethylene in the steam cracking of hydrocarbons. The BTX chain of chemicals is coproduced by the catalytic reforming of naphtha. The agricultural chemicals, like ammonia, urea, ammonium phosphate, etc., are primarily dependent on natural gas for the production of hydrogen. Thus, the present chemical industry is almost entirely dependent on fossil resources for the production of chemicals. A significant amount of carbon dioxide and other greenhouse gases is also released during the production of these chemicals.

Historically, there had been no governmental regulations on carbon dioxide emissions by chemical industries. However, the increased concerns due to global warming, climate change, and pollution reduction programs prompted the US Government House of Representatives to pass the American Clean Energy and Security Act of 2009 (ACES 2010). This bill, if passed, would introduce a cap and trade program aimed at reducing the greenhouse gases to address climate change. The Environmental Protection Agency issued the Mandatory Reporting of Greenhouse Gases Rule in December 2009 (EPA 2010). The rule requires reporting of greenhouse gas (GHG) emissions from large sources and suppliers in the USA and is intended to collect accurate and timely emission data to inform future policy decisions. Under the rule, suppliers of fossil fuels or industrial greenhouse gases, manufacturers of vehicles and engines, and facilities that emit 25,000 t or more per year of GHG emissions are required to submit annual reports to EPA.

With the government initiatives and increased global concerns for greenhouse gas emissions, alternate pathways for production of chemicals from biomass are required. This chapter focuses on the use of biomass as feedstock for chemicals. This is an ongoing research area, and the chemicals discussed in this chapter are not an exhaustive list; however, an attempt is made to include the most promising chemicals from biomass that have the potential for commercialization and can replace the existing chain of chemicals from fossil resources.

Chemicals from Biomass as Feedstock

The world has a wide variety of bio-feedstocks that can be used for the production of chemicals. Biomass includes plant materials such as trees, grasses, agricultural crops, and animal manure. The components of biomass are shown in Fig. 3, and it can be seen that all the biomass components are molecules of carbon, hydrogen, and oxygen atoms. Biomass can be divided into five major categories as shown in the figure: starch, cellulose, hemicellulose, lignin, and oils. Cellulose, hemicellulose, and lignin are components of woody biomass, grasses, stalks, stover, etc. Starch and cellulose are both polymeric forms of hexose, a 6 carbon sugar. Hemicellulose is a polymer of pentose. Lignin is composed of phenolic polymers, and oils are

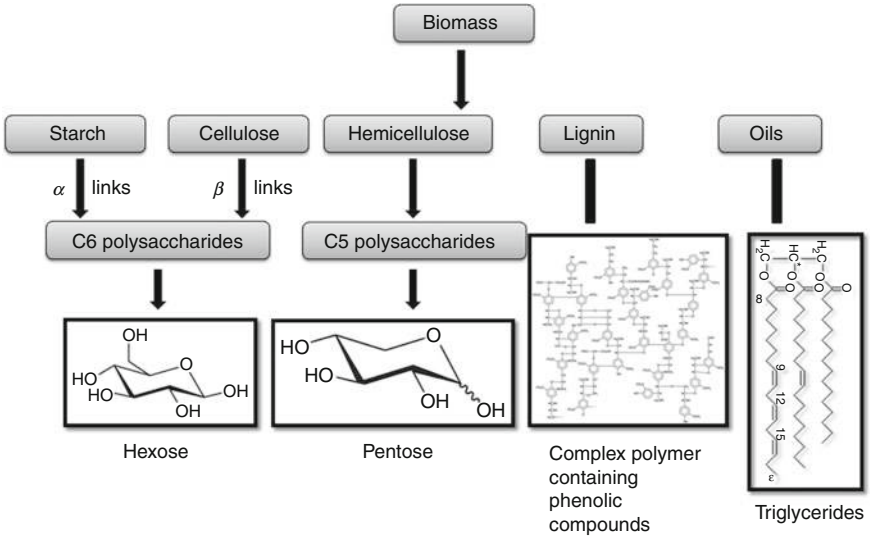

Fig. 3 Biomass classifications and components

triglycerides. Starch is primarily found in corn, sweet sorghum, and other crops. Sugarcane contains the sugar in monomeric form, but extraction of juice is required. Other biomass components, which are generally present in minor amounts, include sterols, alkaloids, resins, terpenes, terpenoids, and waxes.

The feedstock availability in the USA currently includes 142 million dry tons per year of forest biomass with a possibility of increasing it to 368 million dry tons per year (Perlack et al. 2005). The agricultural biomass currently available is 194 million dry tons per year with a possible increase to 998 million dry tons per year. Forest biomass is the biomass obtained from forestland (land having at least 10 % tree cover) and is naturally or artificially regenerated. Agricultural biomass is the biomass obtained from cropland designated for the harvested row crops and closely sown crops, hay and silage crops, tree fruits, small fruits, berries, tree nuts, vegetable and melons, and other minor crops. Apart from forest and agricultural biomass, algae can be produced from power plant exhaust carbon dioxide and used for chemical synthesis.

Figure 4 shows the different routes for the production of chemicals from biomass. The feedstock base includes natural oils, sugars, and starches as carbohydrates, cellulose, and hemicellulose. The main conversion technologies used are transesterification, fermentation, anaerobic digestion, acid dehydration, gasification, and pyrolysis. The primary products given in the figure are not an exhaustive list, but some representative chemicals.

There are primarily two different platforms of conversion technologies for converting biomass feedstock to chemicals, the biochemical platform and the thermochemical platform (DOE 2010a). The biochemical platform focuses on the

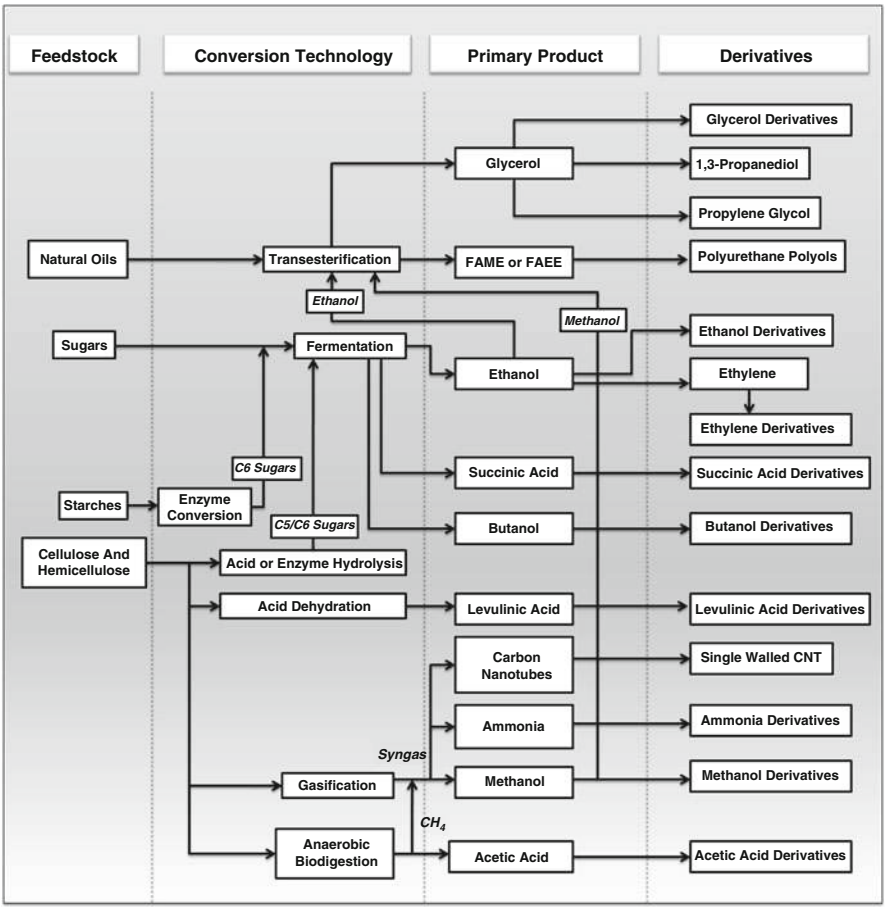

Fig. 4 Biomass feedstock conversion routes to chemicals

conversion of carbohydrates (starch, cellulose, hemicellulose) to sugars using biocatalysts like enzymes and microorganisms and chemical catalysts. These sugars are then suitable for fermentation into a wide array of chemicals. Apart from this, chemical catalysis used in transesterification reaction can produce fatty acid methyl and ethyl esters (FAME and FAEE) and glycerol. The fermentation products such as ethanol and butanol can be a starting material for numerous chemicals, for example, ethanol can be converted to ethylene and introduced to the propylene chain of chemicals. The glycerol produced as by-product in the transesterification process can be converted to produce the propylene chain of chemicals. The thermochemical platform uses technology to convert biomass to fuels, chemicals and power via thermal and chemical processes such as gasification and pyrolysis. Intermediate products in the thermochemical platform include clean synthesis gas or syngas (a mixture of primarily hydrogen and carbon monoxide) produced via gasification

and bio-oil and biochar produced via pyrolysis. Synthesis gas is conventionally manufactured from natural gas, so the gasification procedure to produce synthesis gas from biomass is a possible replacement for the fossil resource.

The various chemicals that can be manufactured from biomass are compiled based on carbon numbers and given in the following section. Some of these chemicals are presently made from nonrenewable feedstock like natural gas and petroleum, while others are new chemicals that have potential to replace nonrenewable feedstock-based chemicals. This description is not exhaustive but serves as a starting point for identifying the processes and feedstocks for conversion to chemicals.

Biomass Conversion Products (Chemicals)

Biomass can be converted to chemicals using the routes described in the previous section. The Biomass Research and Development Act of 2000 had set up a Biomass R&D Technical Advisory Committee which has fixed a goal of supplying the USA with 25 % of its chemicals from biomass by the year 2030 (Perlack et al. 2005). Bulk chemicals can be defined as those costing $1.00–$4.00 per kg and produced worldwide in volumes of more than 1 million metric tons per year (Short 2007). The production cost of these chemicals can be reduced by 30 % when petrochemical processes are replaced by biobased processes. Some of these chemicals are discussed in the following sections.

Single Carbon Compounds

Methane

Methane from natural gas is an important industrial raw material for the production of acetylene, synthesis gas, methanol, carbon black, etc. (Austin 1984). Natural gas is a nonrenewable source, and ways to produce methane from biomass are needed.

Methane can be produced from the anaerobic digestion of biomass, primarily waste biomass (e.g., corn stover, sewage sludge, municipal solid waste, etc.). Methanogenic bacteria are comprised of mesophilic and thermophilic species that convert biomass in the absence of oxygen. Anaerobic digestion of biomass is the treatment of biomass with a mixed culture of bacteria to produce methane (biogas) as a primary product. The four stages of anaerobic digestion are hydrolysis, acidogenesis, acetogenesis, and methanogenesis. In the first stage, hydrolysis, complex organic molecules are broken down into simple sugars, amino acids, and fatty acids with the addition of hydroxyl groups. In the second stage, acidogenesis, volatile fatty acids (e.g., acetic, propionic, butyric, valeric) are formed along with ammonia, carbon dioxide, and hydrogen sulfide. In the third stage, acetogenesis, simple molecules from acidogenesis are further digested to produce carbon dioxide, hydrogen, and organic acids, mainly acetic acid. Then in the fourth stage, methanogenesis, the organic acids are converted to methane, carbon dioxide, and water. The last stage produces 65–70 % methane and 35–30 % carbon dioxide

(Brown 2003). Anaerobic digestion can be conducted either wet or dry where dry digestion has a solid content of 30 % or greater and wet digestion has a solid content of 15 % or less. Either batch or continuous digester operations can be used. In continuous operations, there is a constant production of biogas, while batch operations can be considered simpler; the production of biogas varies. Advantages of anaerobic digestion for processing biomass include the ability to use non-sterile reaction vessels, automatic product separation by outgassing, and relatively simpler equipment and operations. The primary disadvantages for the process are slow reaction rates and low methane yields.

The methanation chemistry from carbon monoxide and carbon dioxide is given by the reactions in Eqs. 1 and 2 (NETL 2011). Synthetically, the methanation process takes place over nickel catalyst fixed-bed reactors, known as methanators. The reactions are highly exothermic, and a catalyst system that can maintain its activity after prolonged exposure to high temperatures is required. Three types of methanation reactor configurations include equilibrium-limited fixed-bed reactors in series, throughwall-cooled fixed-bed reactor, and slurry bubble reactor (NETL 2011):

$$CO + 3H_2 \rightarrow CH_4 + H_2O \quad (1)$$

$$CO_2 + 4H_2 \rightarrow CH_4 + 2H_2O \quad (2)$$

An innovative process using pyrolytic gasification for methane production from biomass is given by Klass (1998) and shown in Fig. 5. Biomass is fed to the pyrolysis reactor operating at 800 °C. The reactor temperature is maintained at this temperature by sand fed from the combustion reactor at 950 °C. The biomass decomposes into pyrolysis gas (~40 % CO, ~30 % H_2, and others) which exits from the top of the reactor. Char is deposited on the sand which is sent to the combustion reactor, and air is fed to this reactor to maintain the temperature at

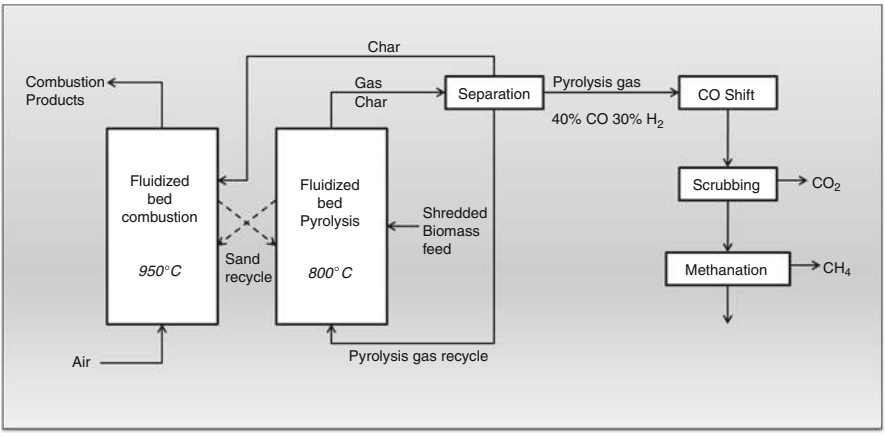

Fig. 5 Pyrolytic gasification process using two fluidized bed reactors (Adapted from Klass (1998))

950 °C from combustion of the char. The pyrolysis gas can then be sent to a methanation reactor as shown in Fig. 5.

Methanol

Methanol was historically produced by the destructive distillation of wood (Wells 1999). Currently, 97 % of methanol production is based on natural gas, naphtha, or refinery light gas. Large-scale methanol manufacture processes based on hydrogen–carbon oxide (carbon mono- and dioxides) mixtures were introduced in the 1920s. In the 1970s, low-pressure processes replaced high-pressure routes for the product formation. Currently, methanol is produced using adiabatic route of ICI and isothermal route of Lurgi. Capacities of methanol plants range from 60,000 to 2,250,000 t/year. Nearly 12.2 billion pounds of methanol are produced annually in the USA, and around 85 % of it is converted to higher-value chemicals such as formaldehyde (37 %), methyl tertiary butyl ether (28 %), and acetic acid (8 %) (Paster et al. 2003).

Synthesis gas, an intermediate in the conventional methanol process from natural gas, can be produced from gasification of biomass (Spath and Dayton 2003). The details of gasification process have been discussed in an earlier chapter. The conventional process for methanol synthesis and the process modification for utilizing biomass as feedstock are given in Fig. 6.

Two Carbon Compounds

Ethanol

Ethanol has been produced by fermentation of carbohydrates for many thousands of years (Wells 1999). Economic, industrial manufacture of ethanol began in the 1930s.

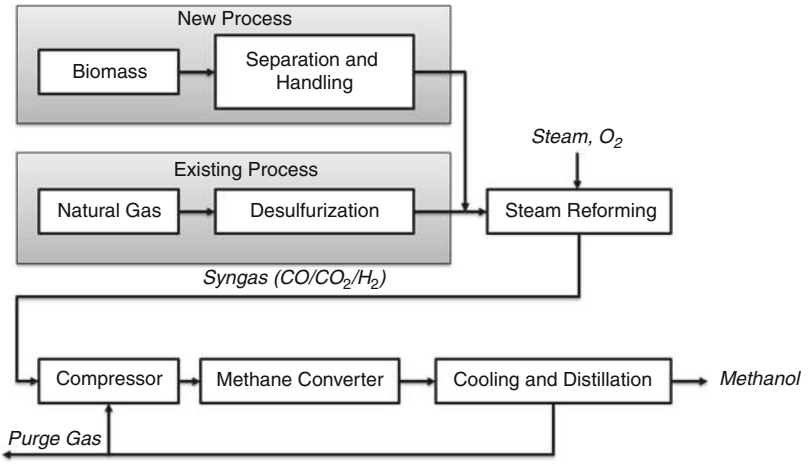

Fig. 6 Conventional methanol process with modification for biomass-derived syngas (Adapted from Spath and Dayton (2003))

Current processes to produce ethanol in the industry include direct and indirect hydration of ethylene and carbonylation of methyl alcohol and methyl acetate. Industrial uses of ethanol include use as solvents and in the synthesis of chemicals (Wells 1999). Forty-five percent of total industrial ethanol demand is for solvent applications. It is a chemical intermediate for the manufacture of esters, glycol ethers, acetic acid, acetaldehyde, and ethyl chloride, and this demand as intermediate accounts for 35 % of its production. Ethanol can also be converted to ethylene and that serves as a raw material for a wide range of chemicals that are presently produced from petroleum-based feedstock. Since ethylene is an important building block chemical and ethanol is its precursor, the processes for manufacture of ethanol are discussed in details in this section. There are four case studies presented for conversion of lignocellulosic biomass to ethanol.

Increasing prices of crude petroleum has prompted the research for manufacture of ethanol from biomass sources. Ethanol can be produced by the fermentation of starch (corn), sugar (sugarcane), or waste lignocellulosic biomass like corn stover or switchgrass. The processes for conversion depend on the feedstock used. The reaction for fermentation of glucose to ethanol is given by Eq. 3:

$$C_6H_{12}O_6 \rightarrow 2C_2H_5OH + 2CO_2 \tag{3}$$

Sugars can be directly converted to ethanol using *Saccharomyces cerevisiae* without any pretreatment (Klass 1998). For starch-containing grain feedstock, the cell walls must be disrupted to expose the starch polymers so that they can be hydrolyzed to free, fermentable sugars as yeast does not ferment polymers. The sugar polymers in grain starches contain about 10–20 % hot-water-soluble amylases and 80–90 % water-insoluble amylopectins. Both substances yield glucose or maltose on hydrolysis. Cellulosic or lignocellulosic biomass is mainly composed of crystalline and amorphous cellulose, amorphous hemicelluloses, and lignin as binder. The main problems associated with using this feedstock lie in the difficulty of hydrolyzing cellulosics to maximize glucose yields and the inability of yeasts to ferment the pentose sugars which are the building blocks of the hemicelluloses.

Capacities of biomass feedstock-based ethanol plants range from 1.5 to 420 million gallons per year in the USA (EPM 2010). Currently, 60 % of the world's biobased ethanol is obtained from sugarcane in Brazil. Sugar from sugarcane is used directly as a solution from the grinding of the cane, and it is sent directly to fermentor rather than proceeding with clarification, evaporation, and crystallization to produce raw sugar that is sent to a sugar refinery. The corn dry-grind process for the production of ethanol is described by (Klass 1998) and shown in Fig. 7. The production of ethanol in the USA increased from nearly 2 billion gallons in 1999 to over 13 billion gallons in 2010 (DOE 2010b; EPM 2010) as shown in Fig. 8.

Cellulosic biomass refers to a wide variety of plentiful materials obtained from plants, including certain forest-related resources (mill residues, precommercial thinning, slash, and brush), many types of solid wood waste materials, and certain agricultural wastes (including corn stover, sugarcane bagasse), as well as plants

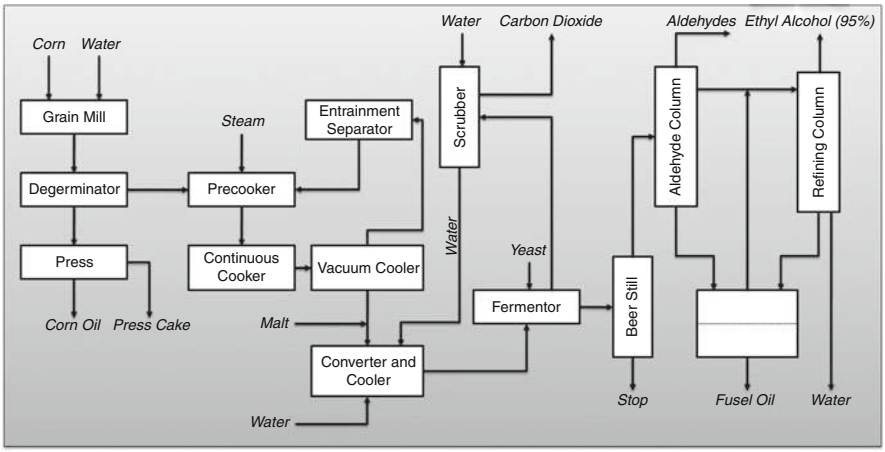

Fig. 7 Corn dry-grind operation to ethanol (Adapted from Klass (1998))

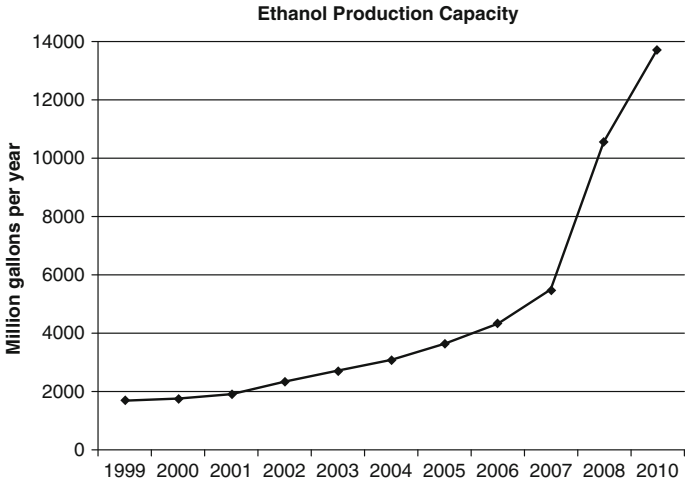

Fig. 8 Production of ethanol in the USA from 1999 to 2010 (EPM 2010; DOE 2010a)

that are specifically grown as fuel for generating electricity. These materials can be used to produce ethanol which is referred to as "cellulosic ethanol." The cellulosic biomass contains cellulose, hemicellulose, and lignin. The cellulose and hemicellulose are converted to sugars using enzymes, which are then fermented to ethanol. Figure 9 gives the BCI process for the conversion of cellulosic biomass (sugarcane bagasse) to ethanol.

Six plants were selected by DOE to receive federal funding for cellulosic ethanol production (DOE 2007). These plants received a sum of $385 million for biorefinery

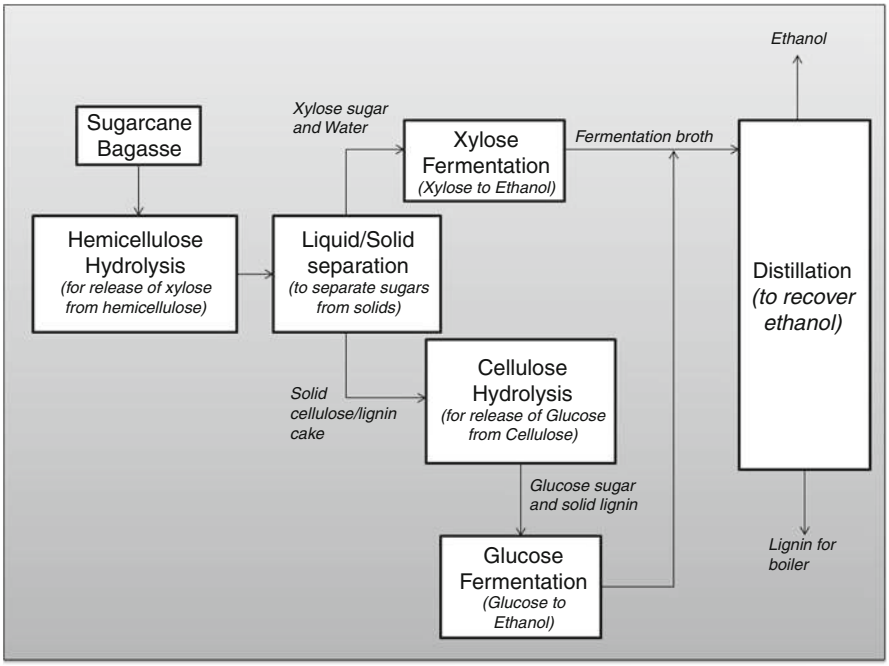

Fig. 9 BCI process for converting sugarcane bagasse to ethanol (Adapted from Smith (2005))

projects for producing more than 130 million gallons of cellulosic ethanol per year. Table 2 gives a list of these plants with their capacity of producing ethanol.

Four case studies are given in this section where biomass is converted to ethanol. The first two cases are production of ethanol from cellulosic biomass, the third case is a fermentation process of glycerol to produce ethanol, and the fourth case discusses fermentation of syngas to ethanol. There are several other methods to produce ethanol from biomass including corn, sugarcane, sugarcane bagasse, etc. The fermentation of corn to ethanol is a well-established process (Klass 1998), and detailed descriptions of corn wet milling and dry milling procedures have been given by Johnson (Johnson 2006). Approximately 93 % of the ethanol currently produced in the USA comes from corn, and 3 % comes from sorghum (DOE 2010b). Other feedstocks include molasses, cassava, rice, beets, and potatoes. However, these are primarily food and feed crops, and there is considerable debate on their usage, for example, the use of corn as feed versus feedstock. Cellulosic biomass to ethanol production is not yet fully developed for large-scale production, and some of these attempts are discussed in the following cases. The first two cases are discussed on the basis of selection on raw material and the optimum selection of plant size. These are currently the major concerns for a cellulosic feedstock-based ethanol industry, and research is ongoing to reduce the cost of ethanol for these factors.

Table 2 DOE-funded cellulosic ethanol plants (DOE 2007)

Plant name/ location/start-up year	Feedstock	Feedstock capacity (t/day)	Products	Notes
Abengoa Bioenergy Biomass of Kansas LLC Colwich, Kansas, 2011	Corn stover Wheat straw Sorghum Stubble Switchgrass	700	Ethanol: 11.4 million gal/year Syngas	Thermochemical and biochemical processing
ALICO, Inc. LaBelle, Florida 2010	Yard Wood Vegetative wastes (citrus peel)	770	Ethanol: 7 million gal/year (first unit) 13.9 million gal/year (second unit) Power: 6,255 KW Hydrogen Ammonia	Gasification fermentation of syngas to ethanol
BlueFire Ethanol, Inc. Southern California 2009 (plant in Fulton, MS)	Sorted green waste and wood waste from landfills	700	Ethanol: 19 million gal/year	Concentrated acid processing fermentation
Broin Companies Emmetsburg, Palo Alto County, Iowa 2010	Corn fiber Corn stover	842	Ethanol: 125 million gal/year Chemicals Animal feed	Fermentation of starch and lignocellulosic biomass (25 %)
Iogen Biorefinery Partners, LLC Shelley, Idaho 2010	Agricultural residues: wheat straw, barley straw, corn stover, switchgrass, and rice straw	700	Ethanol: 18 million gal/year (first plant) 250 million gal/year (future plants)	Enzymatic process converting cellulose to ethanol
Range Fuels, Inc. Near Soperton, Treutlen County, Georgia 2011	Unmerchantable timber and forest residues	1,200	Ethanol: 10 million gal/year (first unit) ~40 million gal/year (commercial unit) Methanol: 9 million gal/year (commercial unit)	Thermochemical Catalytic syngas conversion

Case Study 1: Iogen Process for Ethanol Production from Wheat Straw and Corn Stover

Tolan (2006) discussed Iogen's process for the production of ethanol from cellulosic biomass. Iogen was one of the six companies identified by DOE to receive federal funding to produce ethanol from lignocellulosic feedstock. Iogen's facility produces 2,000 gal/day of ethanol from wheat straw in a pilot plant, with proposal to scale up to 170,000 gal/day (60 million gal/year). The Iogen process uses steam explosion pretreatment for chopped, milled wheat straw mixed with corn stover. High-pressure steam and 0.5–2 % sulfuric acid are added to the feedstock at a temperature of 180–260 °C. The acid hydrolysis releases the hemicellulose and converts it to xylose. The residence time in the pretreatment reactor is 0.5–5 min. The pressure is released rapidly to enable the steam explosion process. Hemicellulose reacts first in the process according to the reaction given in Eq. 4. The dilute sulfuric acid produces xylose monomer, which dehydrates to furfural according to the reaction given in Eq. 5 under further pretreatment conditions. Similar reactions occur for arabinose. Small amounts of cellulose react to glucose according to the reaction given in Eq. 6 and further degrade to hydroxymethylfurfural according to the reaction given in Eq. 7. The lignin depolymerizes in this process but is insoluble in the acid or water:

$$(C_5H_8O_4)_n + H_2O \rightarrow (C_5H_8O_4)_{n-1} + C_5H_{10}O_5 \tag{4}$$

$$C_5H_{10}O_5 \rightarrow C_5H_4O_2 + 3H_2O \tag{5}$$

$$(C_6H_{10}O_5)_n + H_2O \rightarrow (C_6H_{10}O_5)_{n-1} + C_6H_{12}O_6 \tag{6}$$

$$C_6H_{12}O_6 \rightarrow C_6H_6O_3 + 3H_2O \tag{7}$$

The next step is the preparation of cellulase enzymes and cellulose hydrolysis. In the Iogen process, *Trichoderma*, a wood-rotting fungus, is used to produce cellulase enzymes. The cellulases are prepared in submerged liquid cultures in fermentation vessels of 50,000 gal. The liquid broth contains carbon source, salts, complex nutrients like corn steep liquor, and water. The carbon source is important and includes an inducing sugar (like cellobiose, lactose, sophorose, and other low molecular weight oligomers of glucose) promoting cellulase growth as opposed to glucose which promotes growth of the organism. The nutrient broth is sterilized by heating with steam. The fermenter is inoculated with the enzyme production strain once the liquid broth cools down. The operating conditions of the fermenter are 30 °C at a pH 4–5. The temperature is maintained using cooling coils of water, and pH is maintained using alkali. Constant stream of air or oxygen is passed to maintain aerobic conditions required for *Trichoderma*. The cellulase enzyme production process requires about one week and, at the end of the run, is filtered across a cloth to remove cells. The spent cell mass is disposed in landfills. Cellulase enzymes can be directly used at Iogen's ethanol manufacturing facility. The enzymes can also be stored provided that it is sterilized against microbial contamination by using sodium benzoate and protein denaturation by using glycerol. Iogen reduces the cost

of their ethanol manufacture by having an on-site cellulase manufacture facility, reducing costs due to storage and transportation of enzymes. The cellulase enzymes are conveyed to hydrolysis tanks to convert cellulose to glucose.

The slurry from pretreatment containing 5–15 % total solids is fed into hydrolysis tanks having a volume of 200,000 gal. Crude cellulase enzymes broth is added in dosages of 100 l/t of cellulose. The contents are agitated to keep material dispersed in the tank. The hydrolysis proceeds for 5–7 days. The viscosity of the slurry decreases, and lignin remains as insoluble particles. The cellulose hydrolysis process yields 90–98 % conversion of cellulose to glucose. Enzymatic hydrolysis of cellulose occurs according to Eqs. 8 and 9:

$$(C_6H_{10}O_5)_n + H_2O \rightarrow (C_6H_{10}O_5)_{n-2} + C_{12}H_{22}O_{11} \tag{8}$$

$$C_{12}H_{22}O_{11} + H_2O \rightarrow 2C_6H_{12}O_6 \tag{9}$$

The cellulose hydrolysis is followed by sugar separation and fermentation using recombinant yeast capable of fermenting both glucose and xylose. The hydrolysis slurry is separated from lignin and unreacted cellulose using a plate-and-frame filter. The filter plates are washed with water to ensure high sugar recovery. The sugar stream from pretreatment section is pumped into fermentation tanks. The lignin cakes can be used for power generation by combustion, and excess electricity can be sold to neighboring plants.

The sugar stream is fermented with genetically modified *Saccharomyces* yeast capable of fermenting both glucose and xylose. The yeast is well developed for plant operations with good ethanol tolerance. The rates and yields of xylose fermentation are not high in the current process leaving scope for further improvement. The fermentation broth obtained after fermentation is pumped into a distillation column. Ethanol is distilled out at the top and dehydrated. The yield of ethanol obtained in the process is 75 gal/t of wheat straw.

The feedstock selection for the Iogen process depended on the following considerations:

- *Low cost*: Desired feedstock should be available and delivered to plant at low cost. Primary and secondary tree growth, sawdust, and wastepaper have existing markets and were not considered for the process.
- *Availability*: Feedstock availability should be consistent and in the order of 800,000 t/year which is not generally available from sugarcane bagasse.
- *Uniformity*: Feedstock availability should be consistent, and hence municipal waste containing foreign matter was discarded.
- *Cleanliness*: High levels of silica can cause damage to equipment. Microbial contamination and toxic or inhibitory products should be prevented from the feedstock.
- *High potential ethanol yield*: Cellulose and hemicellulose should be present in high percentage in the feed to yield maximum ethanol by fermentation. Wood and forestry waste has high lignin content which inhibits fermentation.

- *High efficiency of conversion*: The efficiency of conversion in the Iogen process depended on arabinan and xylan content in feedstock. These are constituent hemicelluloses, and low content of these required high quantities of enzyme for conversion to cellulose, thereby increasing the process cost.

Case Study 2: NREL Process for Conversion of 2,000 t/day of Corn Stover

Aden et al. (2002) and Humbird and Aden (2009) discuss the use of lignocellulosic biomass for the production of ethanol from corn stover. The plant size was such that 2,000 t/day of corn stover was processed in the facility. The overall plant diagram is given in Fig. 10. The cost estimate is based on the assumption that the plant developed is an "nth" plant of several plants that are already built using the same technology and are operating. The target selling price of ethanol is $1.07 per gallon with a start-up date for plant in 2010. This cost was increased in an updated report (Humbird and Aden 2009) to $1.49 per gallon of ethanol. The conceptual design for this plant includes equipment design, corn stover handling, and purchase of enzymes from commercial facilities like Genencor International and Novozymes Biotech. The design did not take into account the sale of by-products which are important commodity and specialty chemicals, but the report mentions that reduction of price of ethanol is possible with the sale of these chemicals. The design of the facility is divided into eight sections: feedstock storage and handling; pretreatment and hydrolyzate conditioning; saccharification and co-fermentation; product, solids, and water recovery; wastewater treatment; product and feed chemical storage; combustor, boiler, and turbogenerator; and utilities. The process description for conversion of biomass is similar to the Iogen process for corn and wheat straw as raw material.

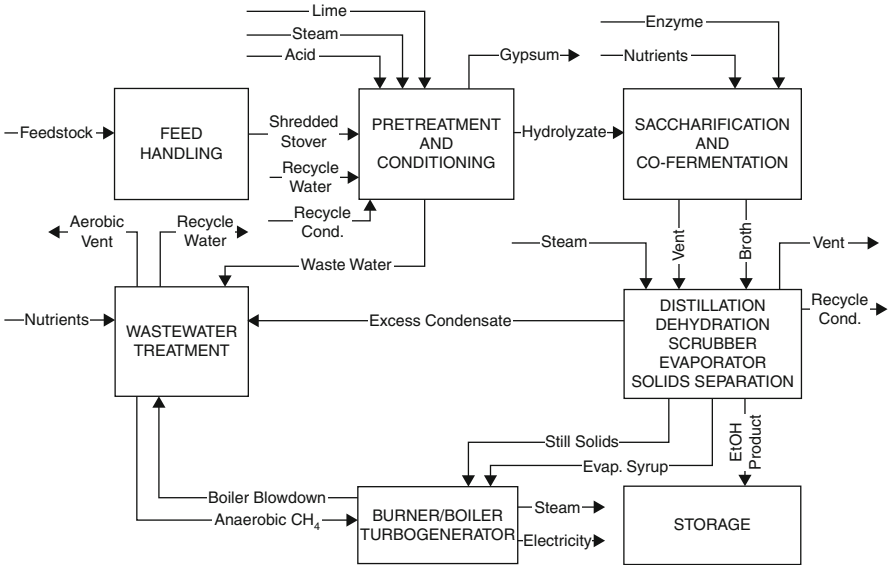

Fig. 10 Overall process diagram for corn stover conversion to ethanol (Aden et al. 2002)

The NREL report gave the following considerations for the selection of plant size between 2,000 and 4,000 t/day. These are listed below:

- *Economies of scale*: The capital cost for equipment varies with equipment size according to the Eq. 10. If exponential, "exp," equals 1, linear scaling of plant size occurs. However, if the exponential value is less than 1, then the capital cost per unit size decreases as the equipment becomes larger. The NREL uses a cost scaling exponent of 0.7:

$$\text{New cost} = \text{Original cost}\left(\frac{\text{New size}}{\text{Old size}}\right)^{\exp} \tag{10}$$

- *Plant size and collection distance*: The distance traveled to collect corn stover increases as the plant size increases because more stover is required for feed. This collection distance is estimated as the radius of a circle around the plant within which the stover is purchased. This area around the plant is calculated using the Eq. 11:

$$\text{Area}_{\text{collection}} = \left(\text{D}_{\text{strover}} / \left(\text{Y}_{\text{strover}} * \text{F}_{\text{available acres}} * \text{F}_{\text{land in crops}}\right)\right) \tag{11}$$

  where
  $\text{Area}_{\text{collection}}$ is the circle of collection around the plant
  D_{stover} is the annual demand for stover by an ethanol plant
  Y_{stover} is metric tons stover collected per acre per year
  $\text{F}_{\text{available acres}}$ is the fraction of total farmland from which stover can be collected
  $\text{F}_{\text{land in crops}}$ is the fraction of surrounding farmland containing crops.

  The fraction of available acres takes into account the land use due to roads and buildings within the farmland. For example, if the farm area has 25 % roads and other infrastructure, then the fraction of available land, $\text{F}_{\text{available acres}}$, is 0.75. The $\text{F}_{\text{land in crops}}$ is a variable parameter depending on the ability of farms around the ethanol plant to contribute to the corn stover demand. The parameter is used to vary the dependence of plant size on collection distance. The radius of collection is calculated from the $\text{Area}_{\text{collection}}$. The price of ethanol is also a function of plant size and percentage of available acres.
- *Corn stover cost*: The corn stover raw material cost depends on two direct costs: the cost of baling and staging stover at the edge of the field and the cost of transportation from the field to the plant gate. Apart from these, a farmer's premium and cost for fertilizers also add up to the direct costs for corn stover as a raw material. A life cycle analysis of the corn stover represents that 47 % of cost was in the staging and baling process, 23 % was for transport of stover to plant, 11 % was farmer premium for taking the risk of added work of collecting and selling the residue, and the rest 12 % for fertilizer supplement for the land. This method of analysis gave a value of $62 per dry metric ton of corn stover. The report suggests that this cost will be reduced considerably over time with new technology for collecting and transporting stover, and an assumption of $33 per

dry metric ton of corn stover was taken for further analysis. However, the update to the report in 2009 suggested that the cost for feedstock increased to $69.60 per dry ton of corn stover in 2007, which can be reduced to reach $50.90 per dry ton in 2012 (Humbird and Aden 2009).

- *Corn stover hauling cost*: The corn stover hauling cost (cost for farm to gate of plant) depended on distance from plant. The hauler cost is a function of radial distance from the plant. An increase in hauling cost shows the optimum plant size range to decrease. For 50 % increase in hauling costs per ton-mile, plant size range decreases from 2,000 to 8,000 t/day to 2,000–5,000 t/day. For a 100 % increase, the optimal plant size is at around 3,000 t/day, and the price of ethanol increases drastically above or below this price.
- *Total cost of ethanol as a function of plant size*: The total cost of ethanol as a function of plant size was determined with the total feedstock and non-feedstock costs. The analysis was done with two plant sizes of 2,000 and 10,000 t/day of stover. A net savings occurred for plant sizes between 6,000 and 8,000 t/day of stover. Below 2,000 t/day, the selling price per gallon of ethanol increased rapidly. A minimum optimal plant size between 2,000 and 4,000 t/day of corn stover was obtained for collection from 10 % corn acres around a conversion plant.

Case 3: Ethanol from Fermentation of Glycerol

Ito et al. (2005) described a process where ethanol is produced from glycerol-containing waste discharged after transesterification process. *Enterobacter aerogenes* HU-101 microorganism is used to ferment the glycerol-rich waste, and yields of 63 mmol/l/h of H_2 and 0.85 mol/mole glycerol of ethanol were reported using porous ceramics as support to fix cells in the reactor. There are no reports of scale-up of this process.

Case 4: Ethanol from Synthesis Gas Fermentation

Synthesis gas can be used as feed to a fermentor that uses anaerobic bacteria to produce ethanol. Although it uses some of the oldest biological mechanisms in existence, technical barriers to be overcome include organism development, gas–liquid mass transfer, and product yield (Spath and Dayton 2003; Phillips et al. 2007; Snyder 2007).

Spath and Dayton (2003) give a description of the process for conversion of synthesis gas to ethanol. The first step in the process is to convert biomass to synthesis gas, and the syngas is then converted to ethanol using fermentation. The feedstock for this process was wood chips derived from forests. Wood chips are primarily composed of cellulose, hemicellulose, and lignin. However, this process can use any biobased feedstock as feed, which can be gasified to syngas. The overall schematic diagram is given in Fig. 11.

The feed is received and placed in temporary storage on-site. It is then sent to the gasifier where it is converted into a raw syngas mixture rich in carbon monoxide and hydrogen. The indirect BCL/FERCO process gasifier was used for the production of syngas from biomass (Spath and Dayton 2003). The equipment include an indirectly heated gasifier with operating temperature at 700–850 °C and pressures slightly

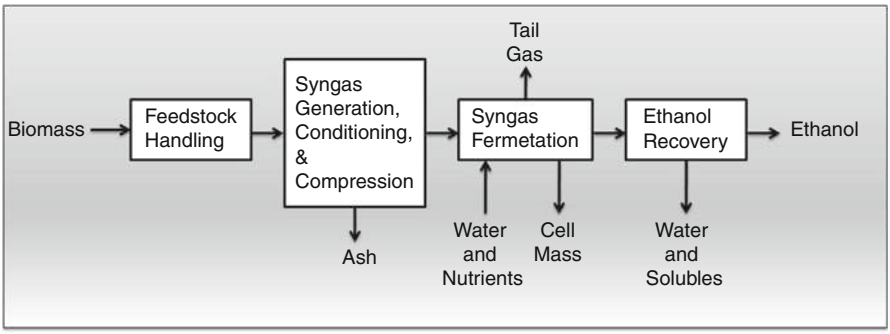

Fig. 11 Synthesis gas to ethanol process (Adapted from Spath et al. (2003))

greater than atmospheric. The biomass feed is dried and then fed to a fast fluidized bed where it is converted into a raw syngas. The resulting syngas contains significant amounts of methane, ethylene and other light hydrocarbons, and tars which can be removed in the gas-conditioning steps. The conditioned syngas is then fed to fermentation reactor where it is converted to ethanol using bacteria. The resulting fermentation broth is diluted, typically containing 2 % or less of ethanol. The ethanol can be recovered from the broth using recovery schemes (distillation, molecular sieves) used in the existing corn ethanol industry. The cell mass produced can be recycled as a portion of the feed to the gasifier. One advantage of the syngas fermentation route is that the chemical energy stored in all parts of the biomass, including the lignin fraction, contributes to the yield of ethanol. Equation 12 gives the method to calculate the capacity of ethanol produced by this process:

$$\mathrm{P} = \frac{F \times \mathrm{HHV}_F \times \eta_{\mathrm{Gas+Cond}} \times X_{\mathrm{CO+H_2/EtOH}}}{1.5 \times 10^5} \tag{12}$$

where

P, production of ethanol, million gal/year
F, feed rate, tons/day (dry basis)
HHVF, higher heating value of the feed in Btu/lb (dry)
$\eta_{\mathrm{Gas+Cond}}$, cold gas efficiency of gasifier + conditioning steps (a fraction less than 1)
$X_{\mathrm{CO + H2/EtOH}}$, average conversion of CO and H_2 to ethanol, as a fraction of theoretical

Spath and Dayton (2003) give the overall reactions for the process as given in Eqs. 13, 14, 15, and 16. The microorganisms used for ethanol production from syngas mixtures are anaerobes that use a heterofermentative version of the acetyl-CoA pathway for acetogenesis. Acetyl-CoA is produced from CO or H_2/CO_2 mixtures in this pathway. The acetyl-CoA intermediate is then converted into either acetic acid or ethanol as a primary metabolic product. Carbon monoxide is a better

substrate than carbon dioxide and hydrogen because the change in free energy is more favorable as shown in Eqs. 13, 14, 15, and 16:

$$6CO + 3H_2O \rightarrow CH_3CH_2OH + 4CO_2 \quad \Delta G = -48.7 \text{ kcal/mol} \tag{13}$$

$$2CO + 6H_2 \rightarrow CH_3CH_2OH + 3H_2O \quad \Delta G = -28.7 \text{ kcal/mol} \tag{14}$$

$$4CO + 2H_2O \rightarrow CH_3COOH + 2CO_2 \quad \Delta G = -39.2 \text{ kcal/mol} \tag{15}$$

$$2CO_2 + 4H_2 \rightarrow CH_3COOH + 2H_2O \quad \Delta G = -25.8 \text{ kcal/mol} \tag{16}$$

The ratio of ethanol to acetate produced depends upon the strain and fermentation conditions. The organisms are inhibited by low pH and acetate ion concentration. Typically, the pH is kept at 4.5 for the production of ethanol (Spath and Dayton 2003).

The organisms used are mesophilic or thermophilic bacteria, with temperature optimums ranging from room temperature to 90 °C. High operating temperatures, low carbohydrate levels, low pH, and high CO levels (inhibitory to methanogens) reduce the risk of contamination (Spath and Dayton 2003).

The fermentor can be a simple gas-sparged tank reactor, operating in batch or continuous mode. A two-stage fermentation system with cell recycle has been suggested as a better alternative. The syngas fermentation performance is not tied to a specific H_2/CO mixture, but organisms prefer CO more than H_2 (Spath and Dayton 2003).

Spath and Dayton (2003) also report the cost analysis for the gasification process and fermentation. A facility for gasification processing 2,000 t (dry) per day of wood would produce 48.5 million gal/year of ethanol based on an ethanol yield of 71 gal/t. Fixed capital was estimated at $153.6 million or $3.17 per annual gallon of capacity. Cash costs were $0.697 per gallon with feedstock cost at $25 per ton. The price required for a zero net present value for the project with 100 % financing and 10 % real after-tax discounting, known as rational cost, was $1.33 per gallon.

Phillips et al. (2007) described the feasibility of a forest resource-based thermochemical pathway conversion to ethanol and mixed alcohols. Hybrid poplar was used as feed for the indirect gasification process. The detailed design included seven sections, namely, feed handling and drying, gasification, gas cleanup and conditioning, alcohol synthesis, alcohol separation, steam cycle, and cooling water. The syngas was heated to 300 °C and 1,000 psi pressure and converted to the alcohol mixture across a fixed-bed catalyst. The minimum cost of ethanol based on the operating cost was $1.01 per gallon. A similar study with syngas from high-pressure oxygen blown direct gasifiers gave a minimum cost of ethanol based on the operating cost as $1.95 per gallon (Dutta and Philips 2009).

Acetic Acid

Acetic acid was first made by the fermentation of ethyl alcohol, and a very dilute solution of it is used as vinegar (Wells 1999). Small quantities of acetic acid are recovered from pyroligneous acid liquor obtained from the destructive distillation

of hardwood. The modern acetic acid industry began with the commercial availability of acetylene which was converted to acetaldehyde and then oxidized to acetic acid. The three commercial processes for the manufacture of acetic acid are oxidation of acetaldehyde, liquid phase oxidation of *n*-butane or naphtha, and carbonylation of methyl alcohol. The carbonylation of methyl alcohol is the dominant technology because of low material and energy costs and the absence of significant by-products. Capacities of acetic acid plants range from 30,000 to 840,000 t/year.

Synthesis gas is the raw material for the carbonylation process at low temperature and pressure using a proprietary catalyst, rhodium iodide, developed by BASF and Monsanto. The synthesis gas can be produced alternately from biobased feedstock using gasification and pyrolysis as described in previous chapter. The fermentation of syngas can also be used to produce acetic acid, as shown in Eqs. 15 and 16.

Acetic acid can be produced by the anaerobic digestion of biomass. The four stages of anaerobic fermentation are given in the section for methane. The fourth stage of methane formation can be inhibited by the use of iodoform or bromoform, thus producing carboxylic acids, hydrogen, and carbon dioxide. Biomass is converted to acetic acid (CH_3COOH) under non-sterile anaerobic conditions according to Eq. 17 (Holtzapple et al. 1999). Glucose ($C_6H_{12}O_6$) is used for illustration for this reaction:

$$C_6H_{12}O_6 + 2H_2O + 4NAD^+ \rightarrow 2H_3CCOOH + 2CO_2 + 4NADH + 4H^+ \quad (17)$$

The reducing power of nicotinamide adenine dinucleotide (NADH) may be released as hydrogen using endogenous hydrogen dehydrogenase as shown by the reaction in Eq. 18:

$$NADH + H^+ \rightarrow NAD^+ + H_2 \quad (18)$$

Methanogens are microorganisms that can produce methane by reacting carbon dioxide produced with hydrogen. The reaction is given in Eq. 19:

$$CO_2 + 4H_2 \rightarrow CH_4 + 2H_2O \quad (19)$$

Acetic acid can also be converted to methane in the presence of methanogens. So, the potential to convert all biomass to methane exists. The production of methane according to Eq. 19 can be inhibited by the addition of iodoform or bromoform. Thus, combining reactions in Eqs. 17 and 18, Eq. 20 is obtained where acetic acid is produced from glucose and the production of methane is inhibited:

$$C_6H_{12}O_6 + 2H_2O \rightarrow 2H_3CCOOH + 2CO_2 + 4H_2 \quad (20)$$

Conversion of biomass mixtures of sugarcane bagasse/chicken manure (Thanakoses et al. 2003a), municipal solid waste/sewage sludge (Aiello-Mazzarri et al. 2006), and corn stover/pig manure (Thanakoses et al. 2003b) to carboxylic acids has been reported.

Forty-four percent of acetic acid is converted to vinyl acetate which is used to form polyvinyl acetate and polyvinyl alcohols used for paints, adhesives, and plastics. Twelve percent of acetic acid is converted to acetic anhydride which is used to manufacture cellulose acetate, paper-sizing agents, a bleach activator, and aspirin. Thirteen percent of acetic acid is used to produce acetates and esters used in solvents for coatings, inks, resins, gums, flavorings, and perfumes. Twelve percent of acetic acid is used in the production of terephthalic acid (TPA) used for polyethylene terephthalate (PET) bottles and fibers.

Cellulose acetate is a cellulose derivative prepared by acetylating cellulose with acetic anhydride (Wells 1999). Fully acetylated cellulose is partially hydrolyzed to give an acetone-soluble product, which is usually between a di- and a tri-ester (Austin 1984). The esters are mixed with plasticizers, dyes, and pigments and processed in different ways depending on the form of plastic desired. The important properties of cellulose acetate include mechanical strength, impact resistance, transparency, colorability, fabricating versatility, moldability, and high dielectric strength (Austin 1984). Cellulose acetate is used to manufacture synthetic fibers like rayon, based on cotton or tree pulp cellulose.

Research has been reported using waste cellulose from corn fiber, rice hulls, and wheat straw to produce cellulose acetate (Ondrey 2007a). The raw materials are milled, slurried in dilute sulfuric acid, and pretreated in an autoclave at 121 °C. This is followed by the acetylation to cellulose triacetate under ambient conditions at 80 °C, using acetic acid, acetic anhydride, methylene chloride, and trace amounts of sulfuric acid. The cellulose acetate is soluble in methylene chloride and separated easily from the reaction medium. Conversions of cellulose to cellulose acetate have been 35–40 % in a laboratory study. The incentive to pursue this line of work was the price of cellulose acetate, approximately $2.00 per pound, a more valuable product than ethanol.

Ethylene

Ethylene ranks fourth among chemicals produced in large volumes in the USA with about 48 billion pounds produced in 1997 (Energetics 2000). It is a principal building block for the petrochemicals industry, with almost all of the ethylene produced being used as a feedstock in the manufacture of plastics and chemicals.

Ethylene is used as a raw material in the production of a wide variety of chemicals and polymers as shown in Fig. 12 (Energetics 2000). Polyethylene (PE) is used in the manufacture of plastic films, packaging materials, moldings (e.g., toys, chairs, automotive parts, and beverage containers), wire and cable insulation, pipes, and coatings. The production of polyethylene in USA in 1997 was about 27 billion pounds (Energetics 2000), which increased to 60 billion pounds in 2008 (ICIS 2009). Ethylene dichloride is used to manufacture polyvinyl chloride (PVC) which is used in drainage and sewer pipes, electrical conduits, industrial pipes, wire and cable coatings, wall panels, siding, doors, flooring, gutters, downspouts, and insulation. The US chemical production of ethylene dichloride was over 20 billion pounds in 1997. The US production of PVC was about 14 billion pounds in 1997. Ethylene oxide is used for the production of ethylene glycol which is a commonly

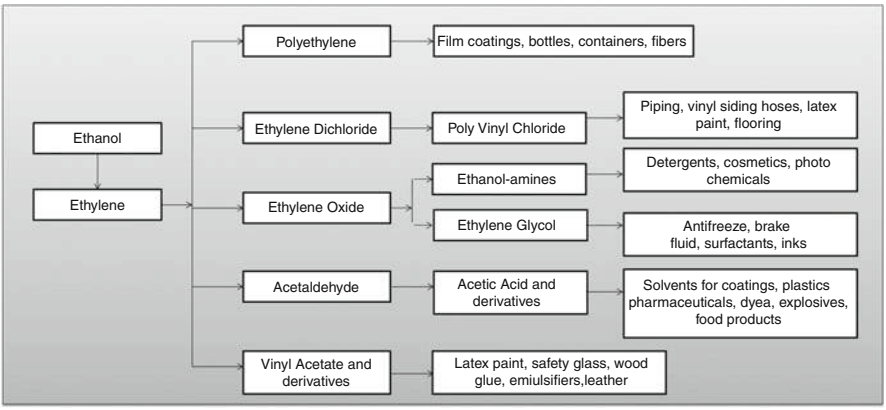

Fig. 12 Ethylene product chain (Adapted from Energetics (2000))

used antifreeze. Ethylene glycol also serves as a raw material in the production of polyester, used for manufacturing textiles. Ethylene oxide and ethylene glycol are both listed among the top 50 chemicals produced in the USA, with ethylene oxide ranking twenty-seventh (7.1 billion pounds in 1997) and ethylene glycol ranking twenty-ninth (5.6 billion pounds in 1997).

World demand for ethylene was about 180 billion pounds in 1998 and was predicted to reach 250 billion pounds by 2005 (Energetics 2000). The polyethylene industry was a 100 billion pound market with over 150 producers worldwide in 1998 (Energetics 2000). The global market for polyvinyl chloride was estimated at about 7.5 billion pounds capacity.

The petroleum refining industry is the major supplier of raw materials for ethylene production, and a large percentage of ethylene capacity is located at petroleum refineries that are in close proximity to petrochemical plants (Energetics 2000). Naphtha and gas oil are the primary sources from which ethylene is obtained. In Western Europe and some Asian countries (South Korea, Taiwan, Japan), naphtha and gas oil account for 80–100 % of the feed to ethylene crackers. Overall, more than 50 % of ethylene production capacity is currently located at refineries. However, the current resources of petroleum are being depleted for use as fuels, and the rising price of petroleum feedstock opens up new areas for research for the production of ethylene.

Ethanol can be used for the production of ethylene by dehydration. Ethanol, for the dehydration process to ethylene, can be produced from biomass feedstock as described in the earlier section. Ethanol is vaporized by preheating with high-pressure steam before passing over a fixed bed of activated alumina and phosphoric acid or alumina and zinc oxide contained in a reactor (Wells 1999). The reaction for dehydration of ethanol to ethylene is given in Eq. 21:

$$C_2H_5OH \rightarrow C_2H_4 + H_2O \tag{21}$$

The reactor can be isothermal or adiabatic, with temperature maintained at 296–315 °C. The reaction is endothermic, and the heat is supplied by condensing vapor latent heat. The temperature control in the reactor is important to prevent the formation of acetaldehyde or ethers as by-products. The gas is purified, dried, and compressed using conventional steps. A fluidized bed modification of this process has been developed with efficient temperature controls and conversions up to 99 %.

Takahara et al. (2005) have discussed the use of different catalysts for the dehydrogenation of ethanol into ethylene. The dehydration of ethanol into ethylene was investigated over various solid acid catalysts such as zeolites and silica–alumina at temperatures ranging from 453 K to 573 K under atmospheric pressure. Ethylene was produced via diethyl ether during the dehydration process. H-mordenites were the most active for the dehydration.

Philip and Datta (1997) reported the production of ethyl tert-butyl ether (ETBE) from biomass-derived hydrous ethanol dehydration over H-ZSM-5 catalyst. Temperatures between 413 K and 493 K were studied for the process, at partial pressures of ethanol less than 0.7 atm and water feed molar ratio less than 0.25.

Varisli et al. (2007) reported the production of ethylene and diethyl ether by dehydration of ethanol over heteropoly acid catalysts. The temperature range studied for this process was 413–523 K with three heteropoly acids, tungstophosphoric acid (TPA), silicotungstic acid (STA), and molybdophosphoric acid (MPA). Very high ethylene yields over 0.75 were obtained at 523 K with TPA. Among the three HPA catalysts, the activity trend was obtained as STA > TPA > MPA.

Tsao and Zasloff (1979) describe a detailed patented process for a fluidized bed dehydration with over 99 % yield of ethylene. Dow Chemical and Crystalsev, a Brazilian sugar and ethanol producer, announced the plans of 300,000 t/year ethylene plant in Brazil to manufacture 350,000 t/year of low-density polyethylene from sugarcane-derived ethanol. Braskem, a Brazilian petrochemical company, announced their plans to produce 650,000 t of ethylene from sugarcane-based ethanol which will be converted to 200,000 t/year of high-density polyethylene (C&E News 2007).

Three Carbon Compounds

Glycerol

Glycerol, also known as glycerine or glycerin, is a triol occurring in natural fats and oils. About 90 % of glycerol is produced from natural sources by the transesterification process. The rest 10 % is commercially manufactured synthetically from propylene (Wells 1999).

Glycerol is a major by-product in the transesterification process used to convert the vegetable oils and other natural oils to fatty acid methyl and ethyl esters. Approximately 10 % by weight of glycerol is produced from the transesterification of soybean oil with an alcohol. Transesterification process is used to manufacture fatty acid methyl and ethyl esters which can be blended in refinery diesel. As the production of fatty acid methyl and ethyl esters increases, the quantity of glycerol

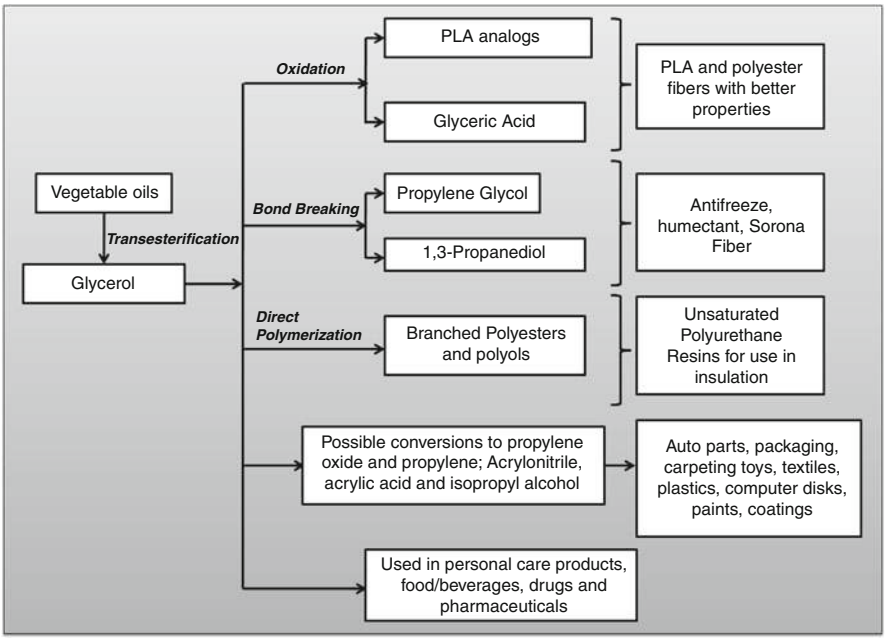

Fig. 13 Production and derivatives of glycerol (Adapted from Energetics (2000) and Werpy et al. (2004))

manufactured as a by-product also increases the need to explore cost-effective routes to convert glycerin to value-added products.

Glycerol currently has a global production of 500,000–750,000 t/year (Werpy et al. 2004). The USA is one of the world's largest suppliers and consumers of refined glycerol. Referring to Fig. 13, glycerin can potentially be used in a number of paths for chemicals that are currently produced from petroleum-based feedstock. The products from the glycerol are similar to the products currently obtained from the propylene chain. Uniqema, Procter & Gamble, and Stepan are some of the companies that currently produce derivatives of glycerol such as glycerol triacetate, glycerol stearate, and glycerol oleate. Glycerol prices are expected to drop if biodiesel production increases, enabling its availability as a cheap feedstock for conversion to chemicals. Small increases in fatty acid consumption for fuels and products can increase world glycerol production significantly. For example, if the USA displaced 2 % of the on-road diesel with biodiesel by 2012, almost 800 million pounds of new glycerol supplies would be produced.

Dasari et al. (2005) reported a low pressure and temperature (200 psi and 200 °C) catalytic process for the hydrogenolysis of glycerol to propylene glycol that is being commercialized and received the 2006 EPA Green Chemistry Award. Copper chromite catalyst was identified as the most effective catalyst for the hydrogenolysis of glycerol to propylene glycol among nickel, palladium, platinum, copper, and copper chromite catalysts. The low pressure and temperature are the advantages for

the process when compared to traditional process using severe conditions of temperature and pressure. The mechanism proposed forms an acetol intermediate in the production of propylene glycol. In a two-step reaction process, the first step of forming acetol can be performed at atmospheric pressure, while the second requires a hydrogen partial pressure. Propylene glycol yields >73 % were achieved at moderate reaction conditions.

Karinen and Krause (2006) studied the etherification of glycerol with isobutene in liquid phase with acidic ion exchange resin catalyst. Five product ethers and a side reaction yielding C_8-C_{16} hydrocarbons from isobutene were reported. The optimal selectivity toward the ethers was discovered near temperature of 80 °C and isobutene/glycerol ratio of 3. The reactants for this process were isobutene (99 % purity), glycerol (99 % purity), and pressurized with nitrogen (99.5 % purity). The five ether isomers formed in the reaction included two monosubstituted monoethers (3-*tert*-butoxy-1,2-propanediol and 2-*tert*-butoxy-1,3-propanediol), two disubstituted diethers (2,3-di-*tert*-butoxy-1-propanol and 1,3-di-*tert*-butoxy-2-propanol), and one trisubstituted triether (1,2,3-tri-*tert*-butoxy propane). *Tert*-butyl alcohol was added in some of the reactions to prevent oligomerization of isobutene and improve selectivity toward ethers.

Acrylic acid is a bulk chemical that can be produced from glycerol. Shima and Takahashi (2006) reported the production of acrylic acid involving steps of glycerol dehydration, in gas phase, followed by the application of a gas-phase oxidation reaction to a gaseous reaction product formed by the dehydration reaction. Dehydration of glycerol could lead to commercially viable production of acrolein, an important intermediate for acrylic acid esters, superabsorber polymers, or detergents (Koutinas et al. 2008). Glycerol can also be converted to chlorinated compounds such as dichloropropanol and epichlorohydrin. Dow and Solvay are developing a process to convert glycerol to epoxy resin raw material epichlorohydrin (Tullo 2007a).

Several other methods for conversion of glycerol exist; however, commercial viability of these methods is still in the development stage. Some of these include catalytic conversion of glycerol to hydrogen and alkanes and microbial conversion of glycerol to succinic acid, polyhydroxyalkanoates, butanol, and propionic acid (Koutinas et al. 2008).

Lactic Acid

Lactic acid is a commonly occurring organic acid, which is valuable due to its wide use in food and food-related industries and its potential for the production of biodegradable and biocompatible polylactate polymers. Lactic acid can be produced from biomass using various fungal species of the *Rhizopus* genus, which have advantages compared to the bacteria, including their amylolytic characteristics, low nutrient requirements, and valuable fermentation fungal biomass by-product (Zhang et al. 2007).

Lactic acid can be produced using bacteria also. Lactic acid-producing bacteria (LAB) have high growth rate and product yield. However, LAB have complex nutrient requirements because of their limited ability to synthesize B-vitamins and

amino acids. They need to be supplemented with sufficient nutrients such as yeast extracts to the media. This downstream process is expensive and increases the overall cost of production of lactic acid using bacteria.

An important derivative of lactic acid is polylactic acid. BASF uses 45 % corn-based polylactic acid for its product ecovio®.

Propylene Glycol

Propylene glycol is industrially produced from the reaction of propylene oxide and water (Wells 1999). Capacities of propylene glycol plants range from 15,000 to 250,000 t/year. It is mainly used (around 40 %) for the manufacture of polyester resins which are used in surface coatings and glass fiber-reinforced resins. A growing market for propylene glycol is in the manufacture of nonionic detergents (around 7 %) used in petroleum, sugar, and paper refining and also in the preparation of toiletries, antibiotics, etc. Five percent of propylene glycol manufactured is used in antifreeze.

Propylene glycol can be produced from glycerol, a by-product of transesterification process, by a low pressure and temperature (200 psi and 200 °C) catalytic process for the hydrogenolysis of glycerol to propylene glycol (Dasari et al. 2005) that is being commercialized and received the 2006 EPA Green Chemistry Award.

Ashland Inc. and Cargill have a joint venture underway to produce propylene glycol in a 65,000 t/year plant in Europe (Ondrey 2007b, c). Davy Process Technology Ltd. (DPT) has developed the glycerin to propylene glycol process for this plant. The plant is expected to start up in 2009. The process is outlined in Fig. 14. This is a two-step process where glycerin in the gas phase is first dehydrated into water and acetol over a heterogeneous catalyst bed, and, then, propylene glycol is formed in situ in the reactor by the hydrogenation of acetol. The per pass glycerin conversion is 99 %, and by-products include ethylene glycol, ethanol, and propanols.

Huntsman Corporation plans to commercialize a process for propylene glycol from glycerin at their process development facility in Conroe, Texas (Tullo 2007a).

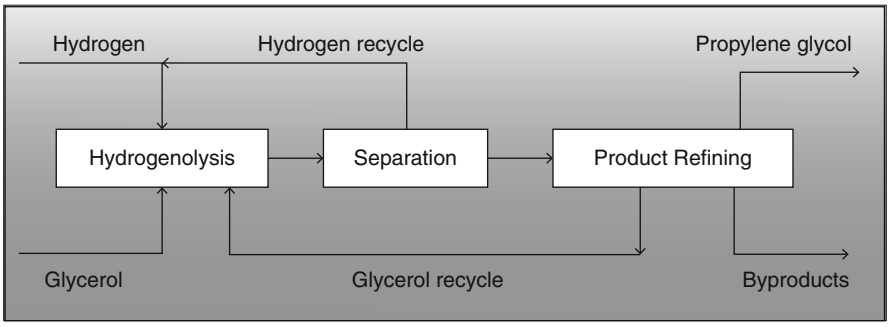

Fig. 14 DPT process for manufacture of propylene glycol from glycerol by hydrogenolysis (Ondrey 2007c)

Dow and Solvay are planning to manufacture epoxy resin raw material epichlorohydrin from a glycerin-based route to propylene glycol.

1,3-Propanediol

1,3-Propanediol is a derivative that can be used as a diol component in the plastic polytrimethylene terephthalate (PTT), a new polymer comparable to nylon (Wilke et al. 2006). Two methods to produce 1,3-propanediol exist, one from glycerol by bacterial treatment and another from glucose by mixed culture of genetically engineered microorganisms.

A detailed description of various pathways to microbial conversion of glycerol to 1,3-propanediol is given by Liu et al. (2010). Mu et al. (2006) give a process for conversion of crude glycerol to propanediol. They conclude that a microbial production of 1,3-propanediol by *Klebsiella pneumoniae* was feasible by fermentation using crude glycerol as the sole carbon source. Crude glycerol from the transesterification process could be used directly in fed-batch cultures of *K. pneumoniae* with results similar to those obtained with pure glycerol. The final 1,3-propanediol concentration on glycerol from lipase-catalyzed methanolysis of soybean oil was comparable to that on glycerol from alkali-catalyzed process. The high 1,3-propanediol concentration and volumetric productivity from crude glycerol suggested a low fermentation cost, an important factor for the bioconversion of such industrial by-products into valuable compounds. A microbial conversion process for propanediol from glycerol using *K. pneumoniae* ATCC 25955 was given by Cameron and Koutsky (Cameron and Koutsky 1994). With a $0.20/lb of crude glycerol raw material, a product selling price of $1.10/lb of pure propanediol, and a capital investment of $15 MM, a return on investment of 29 % was obtained. Production trends in biodiesel suggest that the price of raw material (glycerol) is expected to go down considerably, and a higher return on investment can be expected for future propanediol manufacturing processes.

DuPont Tate and Lyle Bio Products, LLC, opened a $100 million facility in Loudon, Tennessee, to make 1,3-propanediol from corn (CEP 2007). The company uses a proprietary fermentation process to convert the corn to Bio-PDO, the commercial name of 1,3-propanediol used by the company. This process uses 40 % less energy and reduces greenhouse gas emissions by 20 % compared with petroleum-based propanediol. Shell produces propanediol from ethylene oxide, and Degussa produces it from acrolein. It is used by Shell under the name Corterra to make carpets and DuPont under the name Sorona to make special textile fibers.

Acetone

Acetone is the simplest and most important ketone. It is colorless, flammable liquid miscible in water and a lot of other organic solvents such as ether, methanol, and ethanol. Acetone is a chemical intermediate for the manufacture of methacrylates, methyl isobutyl ketone, bisphenyl A, and methyl butynol, among others. It is also used as solvent for resins, paints, varnishes, lacquers, nitrocellulose, and cellulose acetate. Acetone can be produced from biomass by fermentation of starch or sugars

via the acetone–butanol–ethanol fermentation process (Moreira 1983). This is discussed in detail in the butanol section below.

Four Carbon Compounds

Butanol

Butanol or butyl alcohol can be produced by the fermentation of carbohydrates with bacteria yielding a mixture of acetone and butyl alcohol (Wells 1999). Synthetically, butyl alcohol can be produced by the hydroformylation of propylene, known as the oxo process, followed by the hydrogenation of the aldehydes formed yielding a mixture of *n*- and *iso*-butyl alcohol. The use of rhodium catalysts maximizes the yield of *n*-butyl alcohol. The principal use of *n*-butyl alcohol is as solvent. Butyl alcohol/butyl acetate mixtures are good solvents for nitrocellulose lacquers and coatings. Butyl glycol ethers formed by the reaction of butyl alcohol and ethylene oxide are used in vinyl and acrylic paints and lacquers and to solubilize organic surfactants in surface cleaners. Butyl acrylate and methacrylate are important commercial derivatives that can be used in emulsion polymers for latex paints, in textile manufacturing, and in impact modifiers for rigid polyvinyl chloride. Butyl esters of acids like phthalic, adipic, and stearic acid can be used as plasticizers and surface-coating additives.

The process for the fermentation of butanol is also known as Weizmann process or acetone–butanol–ethanol fermentation (ABE fermentation). Butyric acid-producing bacteria belong to the *Clostridium* genus. Two of the most common butyric acid-producing bacteria are *C. butylicum* and *C. acetobutylicum*. *C. butylicum* can produce acetic acid, butyric acid, 1-butanol, 2-propanol, and H_2 and CO_2 from glucose, and *C. acetobutylicum* can produce acetic acid, butyric acid, 1-butanol, acetone, H_2, CO_2, and small amounts of ethanol from glucose (Klass 1998). The acetone–butanol fermentation by *C. acetobutylicum* was the only commercial process of producing industrial chemicals by anaerobic bacteria that uses a monoculture. Acetone was produced from corn fermentation during World War I for the manufacture of cordite. This process for the fermentation of corn to butanol and acetone was discontinued in 1960s for unfavorable economics due to chemical synthesis of these products from petroleum feedstock.

The fermentation process involves conversion of glucose to pyruvate via the Embden–Meyerhof–Parnas (EMP) pathway; the pyruvate molecule is then broken to acetyl-CoA with the release of carbon dioxide and hydrogen (Moreira 1983). Acetyl-CoA is a key intermediate in the process serving as a precursor to acetic acid, ethanol. The formation of butyric acid and neutral solvents (acetone and butanol) occurs in two steps. Initially, two acetyl-CoA molecules combine to form acetoacetyl-CoA, thus initiating a cycle leading to the production of butyric acid. A reduction in the pH of the system occurs as a result of increased acidity. At this step in fermentation, a new enzyme system is activated, leading to the production of acetone and butanol. Acetoacetyl-CoA is diverted by a transferase system to the production of acetoacetate, which is then decarboxylated to acetone. Butanol is produced by reducing the butyric acid in three reactions. Detailed descriptions of

batch fermentation, continuous fermentation, and extractive fermentation systems are given by Moreira (1983).

DuPont and BP are working with British Sugar to produce 30,000 t/year or biobutanol using corn, sugarcane, or beet as feedstock (D'Aquino 2007). UK biotechnology firm Green Biologics has demonstrated the conversion of cellulosic biomass to butanol, known as Butafuel. Butanol can also be used as a fuel additive instead of ethanol. Butanol is less volatile, not sensitive to water, less hazardous to handle, less flammable, has a higher octane number, and can be mixed with gasoline in any proportion when compared to ethanol. The production cost of butanol from biobased feedstock is reported to be $3.75/gal (D'Aquino 2007).

Succinic Acid

Succinic acid was chosen by DOE as one of the top 30 chemicals which can be produced from biomass. It is an intermediate for the production of a wide variety of chemicals as shown in Fig. 15. Succinic acid is produced biochemically from glucose using an engineered form of the organism *Anaerobiospirillum succinici-producens* or an engineered *Escherichia coli* strain developed by DOE laboratories (Werpy et al. 2004).

Zelder (2006) discusses BASF's efforts to develop bacteria which convert biomass to succinate and succinic acid. The bacteria convert the glucose and carbon dioxide with an almost 100 % yield into the C4 compound succinate. BASF is also developing a chemistry that will convert the fermentation product into succinic acid derivatives, butanediol and tetrahydrofuran. Succinic acid can also be used as a monomeric component for polyesters.

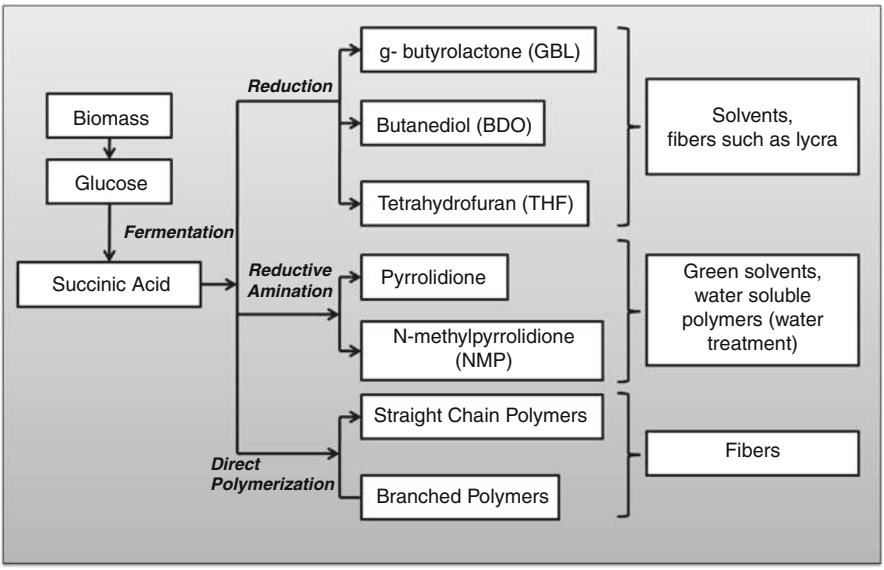

Fig. 15 Succinic acid production and derivatives (Werpy et al. 2004)

Snyder (2007) reports the successful operation of a 150,000 fermentation processes that use a licensed strain of *E. coli* at the Argonne National Laboratory. Opportunities for succinic acid derivatives include maleic anhydride, fumaric acid, dibasic esters, and others in addition to the ones shown in Fig. 15. The overall cost of fermentation is one of the major barriers to this process. Low-cost techniques are being developed to facilitate the economical production of succinic acid (Werpy et al. 2004).

BioAmber, a joint venture of Diversified Natural Products (DNP) and Agro Industries Recherche et Development, will construct a plant that will produce 5,000 t/year of succinic acid from biomass in Pomacle, France (Ondrey 2007d). The plant is scheduled for start-up in mid-2008. Succinic acid from BioAmber's industrial demonstration plant is made from sucrose or glucose fermentation using patented technology from the US Department of Energy in collaboration with Michigan State University. BioAmber will use patented technology developed by (Guettler et al. 1996), for the production of succinic acid using biomass and carbon dioxide.

Aspartic Acid

Aspartic acid is an α-amino acid manufactured either chemically by the amination of fumaric acid with ammonia or the biotransformation of oxaloacetate in the Krebs cycle with fermentative or enzymatic conversion (Werpy et al. 2004). It is one of the chemicals identified in DOE top 12 value-added chemicals from biomass list. Aspartic acid can be used as sweeteners and salts for chelating agents. The derivatives of aspartic acid include amine butanediol, amine tetrahydrofuran, aspartic anhydride, and polyaspartic with new potential uses as biodegradable plastics.

Five Carbon Compounds

Levulinic Acid

Levulinic acid was first synthesized from fructose with hydrochloric acid by the Dutch scientist G.J. Mulder in 1840 (Kamm et al. 2006). It is also known as 4-oxopentanoic acid or γ-ketovaleric acid. In 1940, the first commercial scale production of levulinic acid in an autoclave was started in the USA by A.E. Stanley, Decatur, Illinois. Levulinic acid has been used in food, fragrance, and specialty chemicals. The derivatives have a wide range of applications like polycarbonate resins, graft copolymers, and biodegradable herbicide.

Levulinic acid (LA) is formed by treatment of 6 carbon sugar carbohydrates from starch or lignocellulosics with acid. Five carbon sugars derived from hemicelluloses like xylose and arabinose can also be converted to levulinic acid by addition of a reduction step subsequent to acid treatment. The following steps are used for the production of levulinic acid from hemicellulose (Klass 1998). Xylose from hemicelluloses is dehydrated by acid treatment to yield 64 wt% of furan-substituted aldehyde (furfural). Furfural undergoes catalytic decarbonylation to form furan. Furfuryl alcohol is formed by catalytic hydrogenation of the aldehyde group in

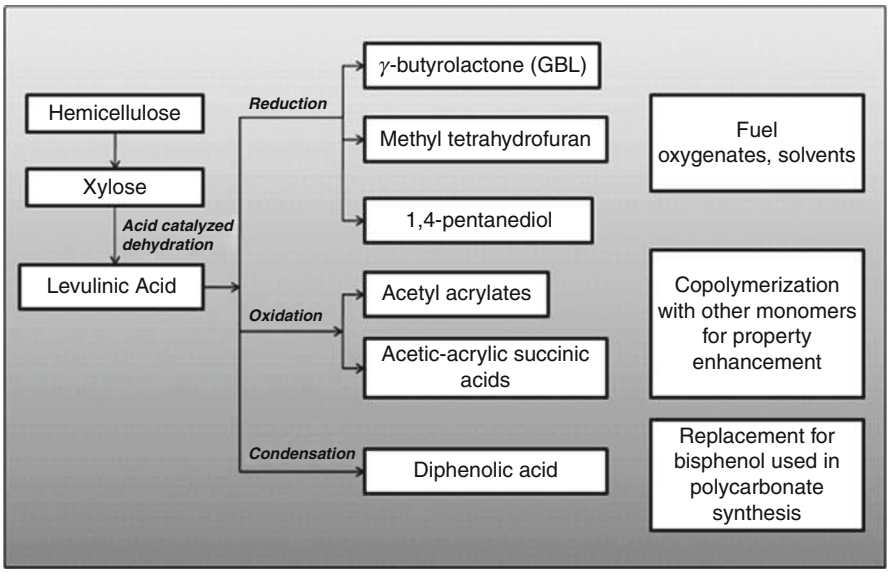

Fig. 16 Production and derivatives of levulinic acid (Adapted from Werpy et al. (2004))

furfural. Tetrahydrofurfuryl alcohol is formed after further catalytic hydrogenation of furfural. Levulinic acid is formed from tetrahydrofurfuryl alcohol on treatment with dilute acid. Werpy et al. (Werpy et al. 2004) report an overall yield of 70 % for the production of levulinic acid.

A number of large-volume chemical markets can be addressed from the derivatives of levulinic acid (Werpy et al. 2004). Figure 16 gives the production of levulinic acid from hemicellulose and the derivatives of levulinic acid. In addition to the chemicals in the figure, the following derivative chemicals of LA also have a considerable market. Methyltetrahydrofuran and various levulinate esters can be used as gasoline and biodiesel additives, respectively. δ-Aminolevulinic acid is a herbicide and targets a market of 200–300 million pounds per year at a projected cost of $2.00–3.00 per pound. An intermediate in the production of δ-aminolevulinic acid is β-acetylacrylic acid. This material could be used in the production of new acrylate polymers, addressing a market of 2.3 billion pounds per year with values of about $1.30 per pound. Diphenolic acid is of particular interest because it can serve as a replacement for bisphenol A in the production of polycarbonates. The polycarbonate resin market is almost 4 billion lb/year, with product values of about $2.40/lb. New technology also suggests that levulinic acid could be used for production of acrylic acid via oxidative processes. Levulinic acid is also a potential starting material for the production of succinic acid. The production of levulinic acid-derived lactones offers the opportunity to enter a large solvent market, as these materials could be converted into analogs of N-methylpyrrolidinone. Complete reduction of levulinic acid leads to 1,4-pentanediol, which could be used for production of new polyesters.

A levulinic acid production facility has been built in Caserta, Italy, by Le Calorie, a subsidiary of Italian construction Immobilgi (Ritter 2006). The plant is expected to produce 3,000 t/year of levulinic acid from local tobacco bagasse and paper mill sludge through a process developed by Biofine Renewables.

Hayes et al. (2006) give the details of the Biofine process for the production of levulinic acid. This process received the Presidential Green Chemistry Award in 1999. The Biofine process involves a two-step reaction in a two-reactor design scheme. The feedstock comprises of 0.5–1.0 cm biomass particles comprised of cellulose and hemicellulose conveyed to a mixing tank by high-pressure air injection system. The feed is mixed with 2.5–3 % recycled sulfuric acid in the mixing tank. The feed is then transferred to the reactors. The first reactor is a plug-flow reactor, where first-order acid hydrolysis of the carbohydrate polysaccharides occurs to soluble intermediates like hydroxymethylfurfural (HMF). The residence time in the reactor is 12 s at a temperature of 210–220 °C and pressure of 25 bar. The diameter of the reactor is small to enable the short residence time. The second reactor is a back-mix reactor operated at 190–200 °C and 14 bar and a residence time of 20 min. LA is formed in this reactor favored by the completely mixed conditions of the reactor. Furfural and other volatile products are removed, and the tarry mixture containing LA is passed to a gravity separator. The insoluble mixture from this unit goes to a dehydration unit where the water and volatiles are boiled off. The crude LA obtained is 75 % and can be purified to 98 % purity. The residue formed is a bone-dry powdery substance or char with calorific value comparable to bituminous coal and can be used in syngas production. Lignin is another by-product which can be converted to char and burned or gasified. The Biofine process uses polymerization inhibitors which convert around 50 % of both 5 and 6 carbon sugars to levulinic acid.

Xylitol/Arabinitol

Xylitol and arabinitol are hydrogenation products from the corresponding sugars xylose and arabinose (Werpy et al. 2004). Currently, there is a limited commercial production of xylitol and no commercial production of arabinitol. The technology required to convert the 5 carbon sugars, xylose and arabinose, to xylitol and arabinitol, can be modeled based on the conversion of glucose to sorbitol. The hydrogenation of the 5 carbon sugars to the sugar alcohols occurs with one of many active hydrogenation catalysts such as nickel, ruthenium, and rhodium. The production of xylitol for use as a building block for derivatives essentially requires no technical development. Derivatives of xylitol and arabinitol are described in Fig. 17.

Itaconic Acid

Itaconic acid is a C5 dicarboxylic acid, also known as methyl succinic acid, and has the potential to be a key building block for deriving both commodity and specialty chemicals. The basic chemistry of itaconic acid is similar to that of the petrochemical-derived maleic acid/anhydride. The chemistry of itaconic acid to the derivatives is shown in Fig. 18.

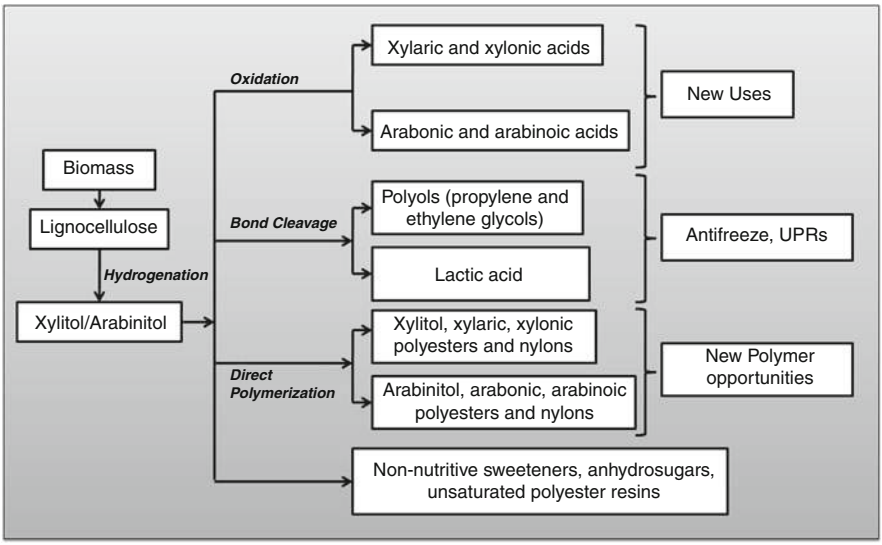

Fig. 17 Production and derivatives of xylitol and arabinitol (Adapted from Werpy et al. (2004))

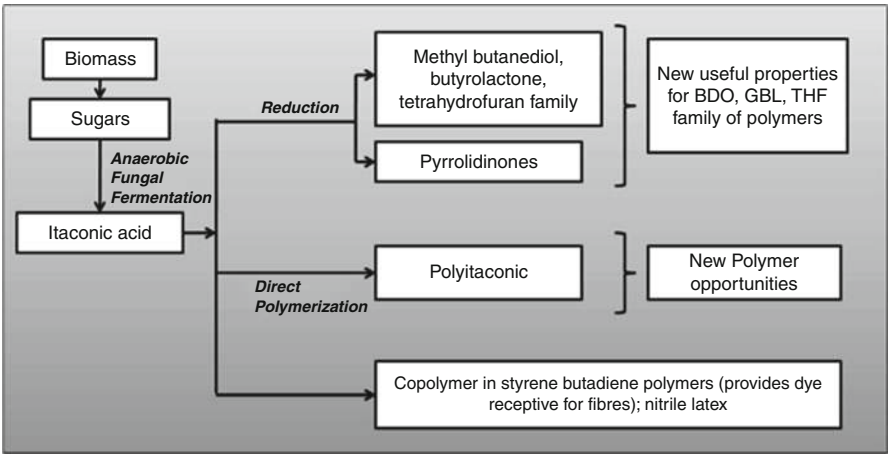

Fig. 18 Production and derivatives of itaconic acid (Adapted from Werpy et al. (2004))

Itaconic acid is currently produced via fungal fermentation and is used primarily as a specialty monomer. The major applications include the use as a copolymer with acrylic acid and in styrene–butadiene systems. The major technical hurdles for the development of itaconic acid as a building block for commodity chemicals include the development of very low-cost fermentation routes. The primary elements of improved fermentation include increasing the fermentation rate, improving the final

titer, and potentially increasing the yield from sugar. There could also be some cost advantages associated with an organism that could utilize both C5 and C6 sugars.

Six Carbon Compounds

Sorbitol

Sorbitol is produced by the hydrogenation of glucose (Werpy et al. 2004). The production of sorbitol is practiced commercially by several companies and has a current production volume on the order of 200 million pounds annually. The commercial processes for sorbitol production are based on batch technology, and Raney nickel is used as the catalyst. The batch production ensures complete conversion of glucose.

Technology development is possible for conversion of glucose to sorbitol in a continuous process instead of a batch process. Engelhard (now a BASF-owned concern) has demonstrated that the continuous production of sorbitol from glucose can be done continuously using a ruthenium on carbon catalyst (Werpy et al. 2004). The yields demonstrated were near 99 % with very high weight hourly space velocity.

Derivatives of sorbitol include isosorbide, propylene glycol, ethylene glycol, glycerol, lactic acid, anhydrosugars, and branched polysaccharides (Werpy et al. 2004). The derivatives and their uses are described in Fig. 19.

2,5-Furandicarboxylic Acid

FDCA is a member of the furan family and is formed by an oxidative dehydration of glucose (Werpy et al. 2004). The production process uses oxygen or electrochemistry. The conversion can also be carried out by oxidation of 5-hydroxymethylfurfural,

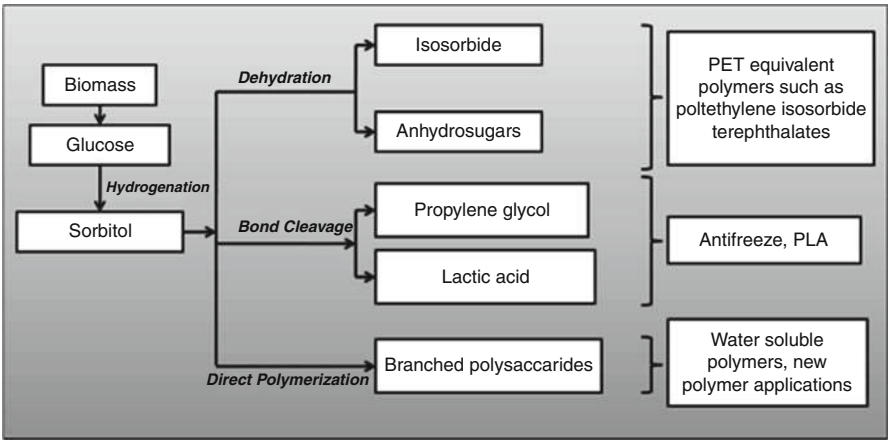

Fig. 19 Production and derivatives of sorbitol (Adapted from Werpy et al. (2004))

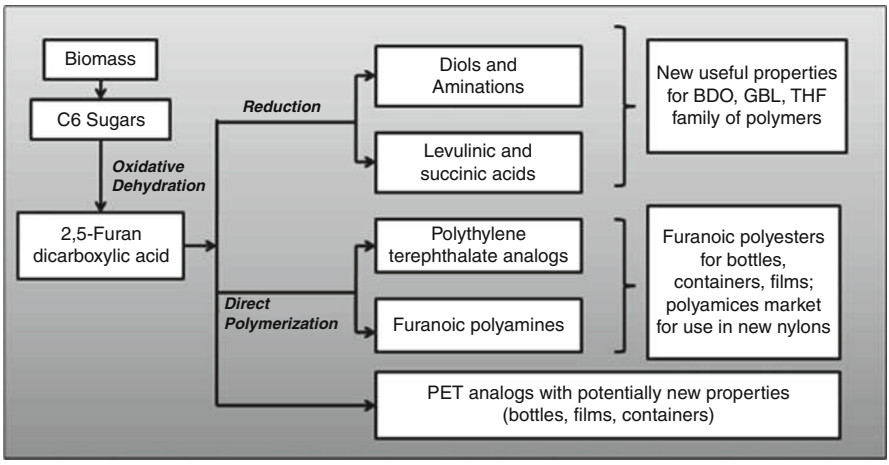

Fig. 20 Production and derivatives of 2,5-FDCA (Werpy et al. 2004)

which is an intermediate in the conversion of 6 carbon sugars into levulinic acid. Figure 20 describes some of the potential uses of FDCA.

FDCA resembles and can act as a replacement for terephthalic acid, a widely used component in various polyesters, such as polyethylene terephthalate (PET) and polybutylene terephthalate (PBT) (Werpy et al. 2004). PET has a market size approaching 4 billion pounds per year, and PBT is almost a billion pounds per year. The market value of PET polymers varies depending on the application, but is in the range of $1.00–3.00/lb for uses as films and thermoplastic engineering polymers. PET and PBT are manufactured industrially from terephthalic acid, which, in turn, is manufactured from toluene (Wells 1999). Toluene is obtained industrially from the catalytic reforming of petroleum or from coal. Thus, FDCA derived from biomass can replace the present market for petroleum-based PET and PBT.

FDCA derivatives can be used for the production of new polyester, and their combination with FDCA would lead to a new family of completely biomass-derived products. New nylons can be obtained from FDCA, either through reaction of FDCA with diamines or through the conversion of FDCA to 2,5-bis(aminomethyl)-tetrahydrofuran. The nylons have a market of almost 9 billion pounds per year, with product values between $0.85 and $2.20 per pound, depending on the application.

Biopolymers and Biomaterials

The previous section discussed the major industrial chemicals that can be produced from biomass. This section will be focused on various biomaterials that can be produced from biomass. Thirteen thousand million metric tons of polymers were made from biomass in 2007 as shown in Fig. 21 out of which 68 % are natural rubber. New polymers from biomass, which attribute to a total of 3 % of the present

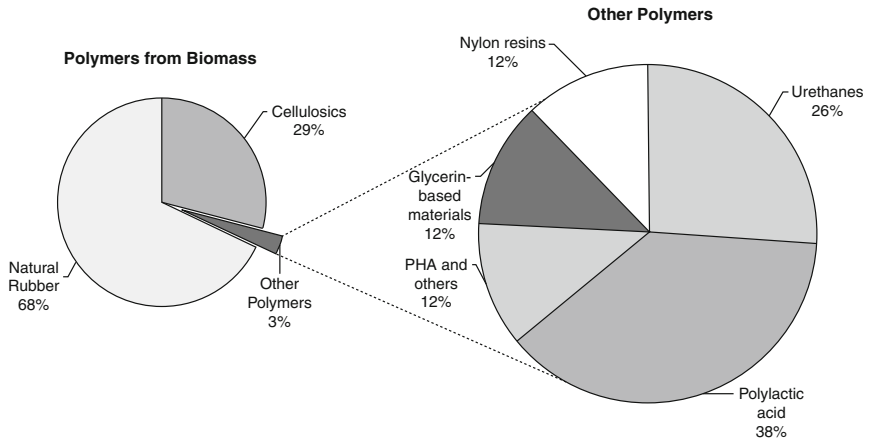

Fig. 21 Production of polymers from biomass in 2007 (13,000 million metric tons) and breakdown of "other polymers" (Tullo 2008)

market share of biobased polymers, consist of urethanes, glycerin-based materials, nylon resins, polyhydroxyalkanoates (PHA), and polylactic acid (PLA) (Tullo 2008). A new product from a new chemical plant is expected to have a slow penetration (less than 10 %) of the existing market for the chemical that it replaces. However, once the benefits of a new product are established, for example, replacing glass in soda bottles with petrochemical-based polyethylene terephthalate, the growth is rapid over a short period of time. Most renewable processes for making polymers have an inflection point at $70 per barrel of oil, above which the petroleum-based process costs more than the renewable process. For example, above $80 per barrel of oil, polylactic acid (PLA) is cheaper than polyethylene terephthalate (PET) (Tullo 2008). Table 3 gives a list of companies that have planned new chemical production based on biomass feedstock along with capacity and projected start-up date. Government subsidies and incentives tend to be of limited time and short-term value. Projected bulk chemicals from biobased feedstocks are ethanol, butanol, and glycerin.

Some of these biomaterials have been discussed in association with their precursor chemicals in the previous section. The important biomaterials that can be produced from biomass include wood and natural fibers, isolated and modified biopolymers, agromaterials, and biodegradable plastics (Vaca-Garcia 2008). These are outlined in Fig. 22. The production process for poly(3-hydroxybutyrate) is given by Rossell et al. (2006), and a detailed review for polyhydroxyalkanoates (PHA) as commercially viable replacement for petroleum-based plastics is given by Snell and Peoples (2009).

Lignin has a complex chemical structure, and various aromatic compounds can be produced from lignin. Current technology is underdeveloped for the industrial scale production of lignin-based chemicals, but there is considerable potential to supplement the benzene–toluene–xylene (BTX) chain of chemicals currently produced

Table 3 Companies producing biobased materials from biomass (Tullo 2008)

Company name	Location	Start-up date	Product	Capacity (t/year)	Notes
Telles	Clinton, Iowa	Q2, 2009	Polyhydroxyalkanoate (PHA) or Mirel	50,000	Joint venture between Metabolix and Archer Daniels Midland, fermented with K-12 strain of *Escherichia coli* genetically modified to produce PHA directly (about 3.5 % lower energy consumption compared to conventional plastics), biodegradable of PHA
Cereplast	Seymour, Indiana	Completed, 2008	Polylactic acid (PLA)-based compound	25,000	Cereplast working with PLA from NatureWorks to make it more heat resistant comparable to polypropylene or polystyrene
PSM North America	China	In production	Plastarch material (PSM)	100,000	80 % industrial starch and 8 % cellulose mixed with sodium stearate, oleic acid, and other ingredients. It can be processed like a petrochemical plastic, can withstand moisture, and is heat tolerant
Synbra	The Netherlands	2009	Polylactic acid (PLA)	5,000	PLA technology developed by Dutch lactic acid maker Purac and Swiss process engineering firm, Sulzer
Green Bioscience	Tianjin, China	–	Polyhydroxyalkanoate (PHA)	10,000	DSM has invested in this firm

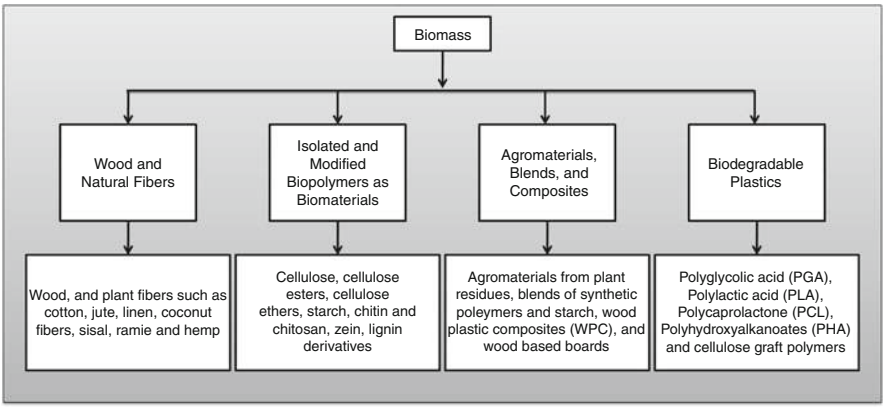

Fig. 22 Biomaterials from biomass (Vaca-Garcia 2008)

from fossil-based feedstock. Osipovs (2008) discusses the extraction of aromatic compounds such as benzene from biomass tar.

Natural Oil-Based Polymers and Chemicals

Natural oils are mainly processed for chemical production by hydrolysis and or transesterification. Oil hydrolysis is carried out in pressurized water at 220 °C, by which fatty acids and glycerol are produced. The main products that can be obtained from natural oils are shown in Fig. 23. Transesterification is the acid-catalyzed reaction in the presence of an alcohol to produce fatty acid alkyl esters and glycerol. Fatty acids can be used for the production of surfactants, resins, stabilizers, plasticizers, dicarboxylic acids, etc. Epoxidation, hydroformylation, and metathesis are some of the other methods to convert oils to useful chemicals and materials. Sources of natural oil include soybean oil, lard, canola oil, algae oil, waste grease, etc.

Soybean oil can be used to manufacture molecules with multiple hydroxyl groups, known as polyols (Tullo 2007b). Polyols can be reacted with isocyanates to make polyurethanes. Soybean oil can also be introduced in unsaturated polyester resins to make composite parts. Soybean oil-based polyols have the potential to replace petrochemical-based polyols derived from propylene oxide in polyurethane formulations (Tullo 2007b). The annual market for conventional polyols is 3 billion pounds in the USA and 9 billion pounds globally.

Dow Chemical, the world's largest manufacturer of petrochemical polyols, also started the manufacture of soy-based polyols (Tullo 2007b). Dow uses the following process for the manufacture of polyols. The transesterification of triglycerides gives methyl esters which are then hydroformylated to add aldehyde groups to unsaturated bonds. This is followed by a hydrogenation step which converts the aldehyde group to alcohols. The resultant molecule is used as a monomer with polyether polyols to build a new polyol. Urethane Soy Systems manufactures soy-based polyols at Volga,

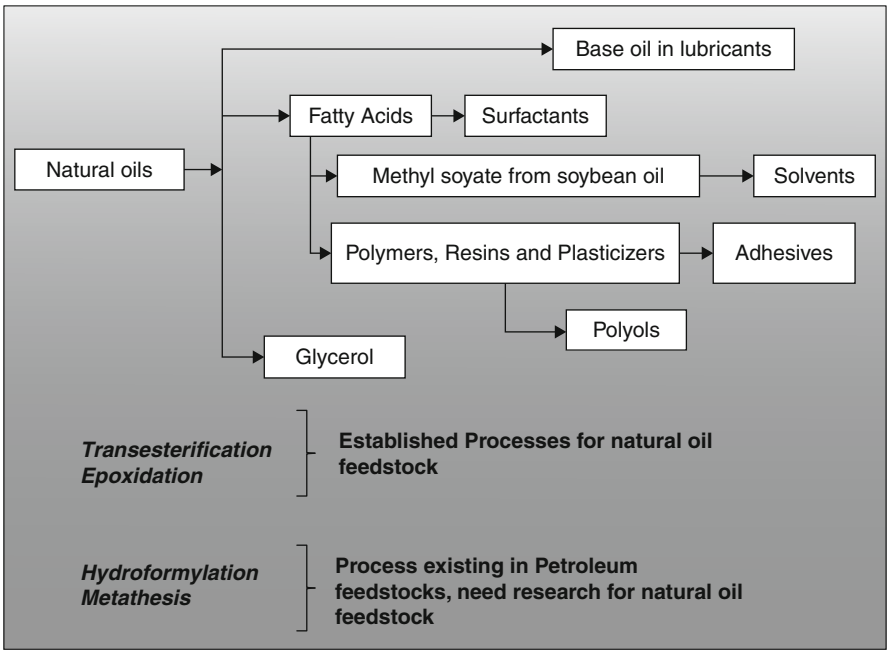

Fig. 23 Natural oil-based chemicals

South Dakota, with a capacity of 75 million pounds per year and supplies them to Lear Corp., manufacturer of car seats for Ford Motor Company. The company uses two processes for the manufacture of polyols: an autoxidation process replacing unsaturated bonds in the triglycerides with hydroxyl groups and a transesterification process where rearranged chains of triglycerides are reacted with alcohols. BioBased Technologies® supplies soy polyols to Universal Textile Technologies for the manufacture of carpet backing and artificial turf. Johnson Controls uses their polyols to make 5 % replaced foam automotive seats. The company has worked with BASF and Bayer MaterialScience for the conventional polyurethanes and now manufactures the polyols by oxidizing unsaturated bonds of triglycerides. The company has three families of products with 96 %, 70 %, and 60 % of biobased content.

Soybean oil can be epoxidized by a standard epoxidation reaction (Wool and Sun 2005). The epoxidized soybean oil can then be reacted with acrylic acid to form acrylated epoxidized soybean oil (AESO). The acrylated epoxidized triglycerides can be used as alternative plasticizers in polyvinyl chloride as a replacement for phthalates.

Aydogan et al. (2006) give a method for the potential of using dense (sub-/supercritical) CO_2 in the reaction medium for the addition of functional groups to soybean oil triglycerides for the synthesis of rigid polymers. The reaction of soybean oil triglycerides with $KMnO_4$ in the presence of water and dense CO_2 is presented in this paper. Dense CO_2 is utilized to bring the soybean oil and aqueous $KMnO_4$

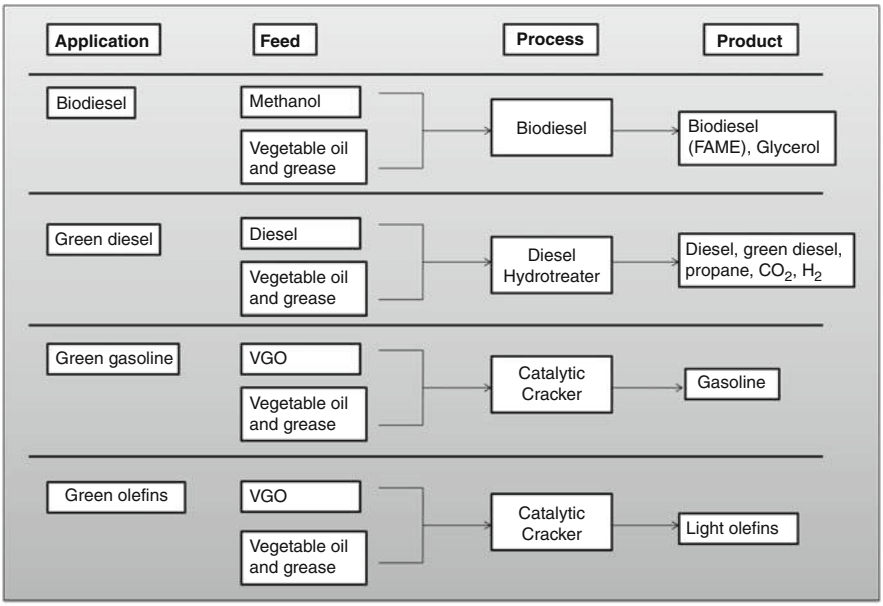

Fig. 24 Processing routes for vegetable oils and grease (Holmgren et al. 2007)

solution into contact. Experiments are conducted to study the effects of temperature, pressure, $NaHCO_3$ addition, and $KMnO_4$ amount on the conversion (depletion by bond opening) of soybean–triglyceride double bonds (STDB). The highest STDB conversions, about 40 %, are obtained at the near-critical conditions of CO_2. The addition of $NaHCO_3$ enhances the conversion; 1 mol of $NaHCO_3$ per mole of $KMnO_4$ gives the highest benefit. Increasing $KMnO_4$ up to 10 % increases the conversion of STDB.

Holmgren et al. (2007) discuss the uses of vegetable oils as feedstock for refineries. Four processes are outlined as shown in Fig. 24. The first process is the production of fatty acid methyl esters by transesterification process. The second process is the UOP/Eni Renewable Diesel Process that processes vegetable oils combined with the crude diesel through hydroprocessing unit. The third and fourth processes involve the catalytic cracking of pretreated vegetable oil mixed with virgin gas oil (VGO) to produce gasoline, olefins, light cycle oil, and clarified slurry oil. Petrobras has a comparable H-Bio process where vegetable oils can also be used directly with petroleum diesel fractions.

Conclusion

As in petroleum and natural gas, various fractions are used for the manufacture of various chemicals; biomass can be considered to have similar fractions. All types of biomass contain cellulose, hemicellulose, lignin, fats, and lipids and proteins as main

constituents in various ratios. Separate methods to convert these fractions into chemicals exist. Biomass containing mainly cellulose, hemicellulose, and lignin, referred to as lignocellulosics, can also undergo various pretreatment procedures to separate the components. Steam hydrolysis breaks some of the bonds in cellulose, hemicellulose, and lignin. Acid hydrolysis solubilizes the hemicellulose by depolymerizing hemicellulose to 5 carbon sugars such as pentose, xylose, and arabinose. This can be separated for extracting the chemicals from 5 carbon sugars. The cellulose and lignin stream is then subjected to enzymatic hydrolysis where cellulose is depolymerized to 6 carbon glucose and other 6 carbon polymers. This separates the cellulose stream from lignin. Thus, three separate streams can be obtained from biomass. The cellulose and hemicellulose monomers, glucose, and pentose can undergo fermentation to yield chemicals like ethanol, succinic acid, butanol, xylitol, arabinitol, itaconic acid, and sorbitol. The lignin stream is rich in phenolic compounds, which can be extracted, or the stream can be dried to form char and used for gasification to produce syngas.

Biomass containing oils, lipids, and fats can be transesterified to produce fatty acid methyl and ethyl esters and glycerol. Vegetable oils can be directly blended in petroleum diesel fractions, and catalytic cracking of these fractions produces biomass-derived fuels. Algae have shown great potential for use as source of biomass, and there have been algae strains which can secrete oil, reducing process costs for separation. Algae grow fast (compared to food crops), fix atmospheric and power plant flue gas carbon sources, and do not require freshwater sources. However, algae production technology on an industrial scale for the production of chemicals and fuel is still in the research and development stage. Growth of algae for biomass is a promising field of research.

The glycerol from transesterification can be converted to propylene glycol, 1,3-propanediol, and other compounds which can replace current natural gas-based chemicals. Vegetable oils, particularly soybean oil, have been considered for various polyols with a potential to replace propylene oxide-based chemicals.

Future Directions

These technologies outlined above can be further developed to produce a wide array of chemicals, and further research is needed for the commercialization of these chemicals.

Nearly 5.6 billion metric tons of carbon dioxide were emitted to the atmosphere in 2008 from utilization of fossil resources (EIA 2010b). The world production of polymers from biomass was 13 billion metric tons. There is opportunity to further convert biomass to chemicals and materials, and further research is required in that direction. The derivatives and market penetration of new chemicals from biomass are needed. The lignin stream from cellulosic biomass is an important source of aromatic chemicals such as benzene, toluene, xylene, etc. and can contribute to the BTX chain of chemicals.

This chapter outlined the various chemicals that are currently produced from petroleum-based feedstock that can be produced from biomass as feedstock. New polymers and composites from biomass are continually being developed which can replace the needs of current fossil feedstock-based chemicals.

References

ACES (2010) H.R.2454 – American clean energy and security act of 2009. http://www.opencongress.org/bill/111-h2454/show. Accessed 8 May 2010

Aden A, Ruth M, Ibsen K, Jechura J, Neeves K, Sheehan J, Wallace B (2002) Lignocellulosic biomass to ethanol process design and economics utilizing co-current dilute acid prehydrolysis and enzymatic hydrolysis for corn stover, NREL/TP-510-32438. National Renewable Energy Laboratory, Golden

Aiello-Mazzarri C, Agbogbo FK, Holtzapple MT (2006) Conversion of municipal solid waste to carboxylic acids using a mixed culture of mesophilic microorganisms. Bioresour Technol 97(1):47–56

Austin GT (1984) Shreve's chemical process industries, 5th edn. McGraw-Hill, New York. ISBN 0070571473

Aydogan S, Kusefoglu S, Akman U, Hortacsu O (2006) Double-bond depletion of soybean oil triglycerides with KMnO4/H2 in dense carbon dioxide. Korean J Chem Eng 23(5):704–713

Banholzer WF, Watson KJ, Jones ME (2008) How might biofuels impact the chemical industry? Chem Eng Prog 104(3):S7–S14

Brown RC (2003) Biorenewable resources: engineering new products from agriculture. Iowa State Press, Iowa. ISBN 0813822637

C&E News (2007) Dow to make polyethylene from sugar in Brazil. Chem Eng News 85(30):17

Cameron DC, Koutsky JA (1994) Conversion of glycerol from soy diesel production to 1,3-propanediol. Final report prepared for National Biodiesel Development Board. Department of Chemical Engineering, UW-Madison, Madison

CEP (2007) $100-million plant is first to produce propanediol from corn sugar. Chem Eng Prog 103(1):10

D'Aquino R (2007) Cellulosic ethanol – tomorrow's sustainable energy source. Chem Eng Prog 103(3):8–10

Dasari MA, Kiatsimkul PP, Sutterlin WR, Suppes GJ (2005) Low-pressure hydrogenolysis of glycerol to propylene glycol. Appl Catal Gen 281(1–2):225–231

DOE (2007) DOE selects six cellulosic ethanol plants for up to $385 million in federal funding. http://www.energy.gov/print/4827.htm. Accessed 2 Oct 2007

DOE (2010a) Biomass multi-year program plan March 2010. Energy efficiency and renewable energy (US DOE). http://www1.eere.energy.gov/biomass/pdfs/mypp.pdf. Accessed 8 May 2010

DOE (2010b) Biomass energy databook. United States Department of Energy. http://cta.ornl.gov/bedb/biofuels.shtml. Accessed 8 May 2010

Dutta A, Philips SD (2009) Thermochemical ethanol via direct gasification and mixed alcohol synthesis of lignocellulosic biomass, NREL/TP-510-45913. National Renewable Energy Laboratory, Golden

EIA (2010a) Weekly United States spot price FOB weighted by estimated import volume (dollars per barrel), Energy Information Administration. http://tonto.eia.doe.gov/dnav/pet/hist/LeafHandler.ashx?n=PET&s=WTOTUSA&f=W. Accessed 8 May 2010

EIA (2010b) Annual energy outlook 2010, Energy Information Administration. Report no. DOE/EIA-0383(2010)

EIA (2010c) Total carbon dioxide emissions from the consumption of energy (million metric tons), Energy Information Administration. http://tonto.eia.doe.gov/cfapps/ipdbproject/IEDIndex3.cfm?tid=90&pid=44&aid=8. Accessed 8 May 2010

Energetics (2000) Energy and environmental profile of the U.S. chemical industry, Energy efficiency and renewable energy (US DOE). http://www1.eere.energy.gov/industry/chemicals/pdfs/profile_chap1.pdf. Accessed 8 May 2010

EPA (2010) Mandatory reporting of greenhouse gases rule, United States Environmental Protection Agency. http://www.epa.gov/climatechange/emissions/ghgrulemaking.html. Accessed 8 May 2010

EPM (2010) Plants list. Ethanol producers magazine. http://www.ethanolproducer.com/plant-list.jsp. Accessed 8 May 2010

Guettler MV, Jain MK, Soni BK (1996) Process for making succinic acid, microorganisms for use in the process and methods of obtaining the microorganisms. US Patent no. 5,504,004

Hayes DJ, Fitzpatrick S, Hayes MHB, Ross JRH (2006) The biofine process – production of levulinic acid, furfural and formic acid from lignocellulosic feedstock. In: Kamm B, Gruber PR, Kamm M (eds) Biorefineries – industrial processes and products. Wiley-VCH, Weinheim. ISBN 3-527-31027-4

Holmgren J, Gosling C, Couch K, Kalnes T, Marker T, McCall M, Marinangeli R (2007) Refining biofeedstock innovations. Petrol Tech Q 12(4):119–124

Holtzapple MT, Davison RR, Ross MK, Aldrett-Lee S, Nagwani M, Lee CM, Lee C, Adelson S, Kaar W, Gaskin D, Shirage H, Chang NS, Chang VS, Loescher ME (1999) Biomass conversion to mixed alcohol fuels using the MixAlco process. Appl Biochem Biotech 79(1–3):609–631

Humbird D, Aden A (2009) Biochemical production of ethanol from corn stover, 2008: state of technology model, NREL/TP-510-46214. National Renewable Energy Laboratory, Golden

ICIS (2009) Ethylene. ICIS Chem Bus 276(15):40

Ito T, Nakashimada Y, Senba K, Matsui T, Nishio N (2005) Hydrogen and ethanol production from glycerol-containing wastes discharged after biodiesel manufacturing process. J Biosci Bioeng 100(3):260–265

Johnson DL (2006) The corn wet milling and corn dry milling industry - a base for biorefinery technology developments. In: Kamm B, Gruber PR, Kamm M (eds) Biorefineries – industrial processes and products. Wiley-VCH, Weinheim. ISBN 3-527-31027-4

Kamm B, Kamm M, Gruber PR, Kromus S (2006) Biorefinery systems – an overview. In: Kamm B, Gruber PR, Kamm M (eds) Biorefineries – industrial processes and products, vol 1. Wiley-VCH, Weinheim. ISBN 3-527-3102

Karinen RS, Krause AOI (2006) New biocomponents from glycerol. Appl Catal A 306:128–133

Klass DL (1998) Biomass for renewable energy, fuels and chemicals. Academic, California. ISBN 0124109500

Koutinas AA, Du C, Wang RH, Webb C (2008) Production of chemicals from biomass. In: Clark JH, Deswarte FEI (eds) Introduction to chemicals from biomass. Wiley, Chichester. ISBN 978-0-470-05805-3

Liu D, Liu H, Sun Y, Lin R, Hao J (2010) Method for producing 1,3-propanediol using crude glycerol, a by-product from biodiesel production. Publication No. 2010/0028965 A1. http://www.freepatentsonline.com/20100028965.pdf. Accessed 8 May 2010

Moreira AR (1983) Acetone-butanol fermentation. In: Wise DL (ed) Organic chemicals from biomass. The Benjamin Cummind Publishing, Menlo Park. ISBN 0-8053-9040-5

Mu Y, Teng H, Zhang D, Wang W, Xiu Z (2006) Microbial production of 1,3-propanediol by Klebsiella pneumoniae using crude glycerol from biodiesel preparations. Biotechnol Lett 28(21):1755–1759

NETL (2011) Gasifipedia, supporting technologies, Methanation. http://www.netl.doe.gov/technologies/coalpower/gasification/gasifipedia/5-support/5-12_methanation.html. Accessed 8 Mar 2011

Ondrey G (2007a) Coproduction of cellulose acetate promises to improve economics of ethanol production. Chem Eng 114(6):12

Ondrey G (2007b) Propylene glycol. Chem Eng 114(6):10

Ondrey G (2007c) A vapor-phase glycerin-to-PG process slated for its commercial debut. Chem Engr 114(8):12

Ondrey G (2007d) A sustainable route to succinic acid. Chem Eng 114(4):18
Osipovs S (2008) Sampling of benzene in tar matrices from biomass gasification using two different solid-phase sorbents. Anal Bioanal Chem 391(4):1409–1417
Paster M, Pellegrino JL, Carole TM (2003) Industrial bioproducts: today and tomorrow. Department of Energy Report prepared by Energetics, Inc, Columbia. http://www.energetics.com/resourcecenter/products/studies/Documents/bioproducts-pportunities.pdf
Perlack RD, Wright LL, Turhollow AF, Graham RL (2005) Biomass as feedstock for a bioenergy and bioproducts industry: the technical feasibility of a billion-ton annual supply. USDA document prepared by Oak Ridge National Laboratory, ORNL/TM-2005/66, Oak Ridge
Philip CB, Datta R (1997) Production of ethylene from hydrous ethanol on H-ZSM-5 under mild conditions. Ind Eng Chem Res 36(11):4466–4475
Phillips S, Aden A, Jechura J, Dayton D, Eggeman T (2007) Thermochemical ethanol via indirect gasification and mixed alcohol synthesis of lignocellulosic biomass, NREL/TP-510-41168. National Renewable Energy Laboratory, Golden
Ritter S (2006) Biorefineries get ready to deliver the goods. Chem Eng News 84(34):47
Rossell CEV, Mantelatto PE, Agnelli JAM, Nascimento J (2006) Sugar-based biorefinery – technology for integrated production of Poly(3-hydroxybutyrate), sugar, and ethanol. In: Kamm B, Gruber PR, Kamm M (eds) Biorefineries – industrial processes and products, vol 1. Wiley-VCH, Weinheim. ISBN 3-527-31027-4
Shima M, Takahashi T (2006) Method for producing acrylic acid. US Patent no 7,612,230
Short PL (2007) Small French firm's bold dream. Chem Eng News 85(35):26–27
Smith RA (2005) Analysis of a petrochemical and chemical industrial zone for the improvement of sustainability, M. S. thesis. Lamar University, Beaumont
Snell KD, Peoples OP (2009) PHA bioplastic: a value-added coproduct for biomass biorefineries. Biofuels Bioprod Biorefin 3(4):456–467
Snyder SW (2007) Overview of biobased feedstocks. Twelfth new industrial chemistry and engineering conference on biobased feedstocks, Council for Chemical Research, Argonne National Laboratory, Chicago, 11–13 June 2007
Spath PL, Dayton DC (2003) Preliminary screening – technical and economic feasibility of synthesis gas to fuels and chemicals with the emphasis on the potential for biomass-derived syngas, NREL/TP-510-34929, National Renewable Energy Laboratory, Golden. http://www.nrel.gov/docs/fy04osti/34929.pdf. Accessed 8 May 2010
Takahara I, Saito M, Inaba M, Murata K (2005) Dehydration of ethanol into ethylene over solid acid catalysts. Catal Lett 105(3–4):249–252
Thanakoses P, Alla Mostafa NA, Holtzapple MT (2003a) Conversion of sugarcane bagasse to carboxylic acids using a mixed culture of mesophilic microorganisms. Appl Biochem Biotechnol 107(1–3):523–546
Thanakoses P, Black AS, Holtzapple MT (2003b) Fermentation of corn stover to carboxylic acids. Biotechnol Bioeng 83(2):191–200
Tolan JS (2006) Iogen's demonstration process for producing ethanol from cellulosic biomass. In: Kamm B, Gruber PR, Kamm M (eds) Biorefineries – industrial processes and products, vol 1. Wiley-VCH, Weinheim. ISBN 3-527-31027-4
Tsao U, Zasloff HB (1979) Production of ethylene from ethanol. US Patent no 4,134,926
Tullo AH (2007a) Soy rebounds. Chem Eng News 85(34):36–39
Tullo AH (2007b) Firms advance chemicals from renewable resources. Chem Eng News 85(19):14
Tullo AH (2008) Growing plastics. Chem Eng News 86(39):21–25
Vaca-Garcia C (2008) Biomaterials. In: Clark JH, Deswarte FEI (eds) Introduction to chemicals from biomass. Wiley, Chichester. ISBN 978-0-470-05805-3
Varisli D, Dogu T, Dogu G (2007) Ethylene and diethyl-ether production by dehydration reaction of ethanol over different heteropolyacid catalysts. Chem Eng Sci 62(18–20):5349–5352
Wells GM (1999) Handbook of petrochemicals and processes, 2nd edn. Ashgate, Brookfield
Werpy T, Peterson G, Aden A, Bozell J, Holladay J, White J, Manheim A (2004) Top value added chemicals from biomass: vol 1 Results of screening for potential candidates from sugars and

synthesis gas. Energy Efficiency and Renewable Energy (US DOE). http://www1.eere.energy.gov/biomass/pdfs/35523.pdf. Accessed 8 May 2010

Wilke T, Pruze U, Vorlop KD (2006) Biocatalytic and catalytic routes for the production of bulk and fine chemicals from renewable resources. In: Kamm B, Gruber PR, Kamm M (eds) Biorefineries – industrial processes and products, vol 1. Wiley-VCH, Weinheim. ISBN 3-527-31027-4

Wool RP, Sun XS (2005) Bio-based polymers and composites. Elsevier Academic, Amsterdam. ISBN 0-12-763952-7

Zelder O (2006) Fermentation – a versatile technology utilizing renewable resources. In: Raw material change: coal, oil, gas, biomass – where does the future lie? Ludwigshafen, 21–22 Nov 2006. http://www.basf.com/group/corporate/en/function/conversions:/publish/content/innovations/events-presentations/raw-material-change/images/BASF_Expose_Dr_Zelder.pdf. Accessed 8 May 2010

Zhang ZY, Jin B, Kelly JM (2007) Production of lactic acid from renewable materials by Rhizopus fungi. Biochem Eng J 35(3):251–263

Hydrodeoxygenation (HDO) of Bio-Oil Model Compounds with Synthesis Gas Using a Water Gas Shift Catalyst with a Mo/Co/K Catalyst

Rangana Wijayapala, Akila G. Karunanayake, Damion Proctor, Fei Yu, Charles U. Pittman, and Todd E. Mlsna

Contents

Abstract

Bio-oil is a renewable and carbon-neutral energy source. It is made by the fast pyrolysis of biomass at elevated temperatures followed by condensation of vapors and aerosols that are removed rapidly from the pyrolysis chamber. Raw bio-oil contains significant amounts of oxygenated compounds which reduce its fuel quality. Upgrading raw bio-oil using hydrodeoxygenation (HDO) is one

R. Wijayapala • A.G. Karunanayake • D. Proctor • C.U. Pittman • T.E. Mlsna (✉)
Department of Chemistry, Mississippi State University, Starkville, MS, USA
e-mail: htw21@msstate.edu; uak1@msstate.edu; ddp110@msstate.edu; cpittman@chemistry.msstate.edu; tmlsna@chemistry.msstate.edu

F. Yu
Agricultural and Biological Engineering, Mississippi State University, Starkville, MS, USA
e-mail: fyu@abe.msstate.edu

W.-Y. Chen et al. (eds.), *Handbook of Climate Change Mitigation and Adaptation*,
DOI 10.1007/978-3-319-14409-2_79

solution to increase fuel quality. Guaiacol and furfural are important model oxygen-containing compounds present in raw bio-oil. HDO of guaiacol and furfural with a dual Cu-based water–gas shift and Mo/Co/K HDO catalyst system in a static catalyst basket was studied in the gas phase in a batch autoclave using H_2/CO at 4.0 MPa (total partial pressure of CO + H_2) and temperatures of 200 °C, 250 °C, and 300 °C. Syngas HDO using two syngas mixtures (H_2/CO/N_2 ratios of 47:47:6 (50/50 syngas) and 18:23:46 (bio-syngas)) was compared to hydrogen alone, which is traditionally used in bio-oil upgrading. Liquid and gas products were analyzed using GC/MS. Temperature and catalyst both exert significant effects on conversion and product selectivity. Guaiacol conversions of 79–86 % were observed in both 50/50 syngas and bio-syngas systems at 300 °C, with 24–29 % cyclohexane formed in 4 h. Furfural exhibited ~100 % conversion in 4 h at 300 °C with both syngas systems. Reaction products from upgrading with syngases had a higher total heat of combustion but lower energy density than the products from reactions with pure H_2. For example, 0.04 mol (4.96 g) of guaiacol has a total heat of combustion of 143.4 kJ with an energy density of 28.9 kJ/g (3.59 MJ/mol). Reaction products from upgrading the same amount of guaiacol with H_2 had a total energy content and energy density of 146.6 ± 0.4 kJ and 38.8 ± 0.2 kJ/g (3.66 MJ/mol), respectively, compared to 153.6 ± 0.4 kJ and 35.8 ± 0.1 kJ/g (3.84 MJ/mol) for the product upgraded with bio-syngas. This, and product selectivity, suggests incorporation of some C from CO in these syngas reactions.

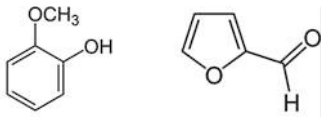

Guaiacol Furfural

Introduction

Worldwide energy consumption began increasing dramatically, beginning with the Industrial Revolution. This trend continues today and energy needs are expected to double in the next 50 years as more of the world becomes developed (Shafiee and Topal 2009). Fossil fuels are a major energy source and continued use of these finite reserves will lead to depletion with time. Greenhouse gas emissions of CO_2 are a harmful consequence of fossil fuel combustion and a major contributor to global warming. Development of alternative fuel sources is needed which will provide energy while reducing CO_2 emissions.

Conversion of biomass into biofuels has been studied to fulfill our clean energy needs (Alonso et al. 2010; Bridgwater 2006; Adjaye and Bakhshi 1995a). A portion of CO_2 emissions produced during formation and use of biofuels is consumed during photosynthesis for plant growth. Biofuel versus fossil fuel use would

lower greenhouse gas emissions. Many currently available "first-generation" (Stöcker 2008) biofuels (ethanol) come from the edible plant carbohydrates and fermentation. This competes with food demand from a rapidly growing population, raising food prices. The so-called "second-generation" technologies for the production of fuels allow the use of a wide range of nonfood "cellulosic" biomass feedstocks (Stöcker 2008). This includes agricultural residues (e.g., straw, bagasse, corn stover), wastes (e.g., paper, manures, cardboard, sawmill residues), and specially grown energy crops (e.g., *Miscanthus*, willow, switchgrass) (Huber and Corma 2007; Huber et al. 2006). Cellulosic-containing biomass consists of biopolymers such as cellulose (35–50 %), hemicelluloses (15–25 %), and lignin (15–30 %) (Mohan et al. 2006).

Thermochemical Conversion of Biomass

Biomass can be converted by gasification to synthesis gas or by fast pyrolysis to raw bio-oil. Catalytic upgrading of these raw materials can lead to transportation-grade fuels. Gasification converts biomass into synthesis gas, consisting of carbon monoxide and hydrogen. Pyrolysis of biomass produces raw bio-oil, which is an unstable complex mixture, consisting of various organic and inorganic compounds and water (Huber et al. 2006; Mohan et al. 2006). An advantage of both these thermochemical approaches is that all of the biomass (cellulose, hemicelluloses, and lignin) can be fed and consumed during conversion without isolating specific components first. A major disadvantage is significant loss of original calories present in the biomass during conversion.

Pyrolysis of Biomass

Biomass pyrolysis is the decomposition of biomass using elevated temperatures while limiting oxygen. During this process, gases, liquids, and solids (chars) are produced (Mohan et al. 2006). The compositions of the product depend on the feedstock, residence time, and pyrolysis temperature. Pyrolytic decomposition of hemicelluloses occurs between 250 °C and 400 °C; cellulose decomposes at a somewhat higher temperature of 310–430 °C, while lignin decomposes at 300–530 °C (Williams and Besler 1996). Dehydration of cellulose begins around 300 °C and produces unsaturated polymers and char. Depolymerization of cellulose to form smaller units begins at ~400 °C (Lange 2007). At higher temperatures, breaking of C–C and C–H bonds produces C_{2-4} oxygenates and gases (CO, CO_2, H_2, and CH_4) (Lange 2007).

Different pyrolysis modes result in different product compositions as reported by Bridgwater (Bridgwater 2006) (Table 1). Commercial value exists in liquid (Alonso et al. 2010), char (Bridgwater 2006), and gas products (Delgado et al. 1997), contributing to the importance of biomass pyrolysis. Biomass pyrolysis production

Table 1 Average product yields formed by different dry wood pyrolysis methods (Bridgwater 2006)

Method	Operation conditions		Liquid (%)	Gas (%)	Char (%)
	Temperature	Residence time			
Fast	Moderate temperature, around 500 °C	Short hot vapor residence time ~1 s	75	13	12
Intermediate	Moderate temperature, around 500 °C	Moderate hot vapor residence times ~10–20 s	50	30	20
Slow (carbonization)	Low temperature, around 400 °C	Very long residence time	30	35	35
Gasification	High temperature, around 800 °C	Long residence times	5	85	10

methods continue to be extensively studied and optimized to increase the value of each component.

Bio-oil yield under optimum fast pyrolysis conditions (typically between 425 °C and 500 °C with a vapor residence time of a 1 s) may reach 70–80 % of the biomass, with 20–25 % water (Delgado et al. 1997). Slow pyrolysis (400 °C with a residence time of ~8 min) (Ashworth et al. 2014) produces more biochar and considerably increases the yield of water (up to 35–40 %) (Bridgwater 2006). Longer residence times of ~1 h (Ashworth et al. 2014) and lower temperatures of around 400 °C reduce bio-oil yields while increasing the yields of char to about 30 wt%. Higher temperatures around 700 °C at very high heating rates produce more gases (up to 80 wt%) (Bridgwater 1994). Salts and acids which are formed during the pyrolysis can influence the quality of the bio-oil.

Oxygenated compounds found in bio-oil derive their oxygen content from the oxygen originally present in the cellulose, lignin, and hemicellulose components of the biomass. This is because the biomass is fed to the reactor either under nitrogen or through a valve which seals the reactor from air. The only oxygen gas that can be fed under those conditions is with the air that enters with the biomass particles or pellets. The biomass fed to the reactor is 2000 or more times as dense as the air occupying the volume between biomass particles. Thus, even if 80 % of this volume is air (~20 % of this is oxygen), the moles of oxygen in the feed are negligible versus what would be needed to measurably influence the product distributions.

Gasification of Biomass

Gasification of biomass is performed under controlled amounts of oxygen and steam at elevated temperature (500–800 °C) to produce bio-syngas (Delgado et al. 1997). Steam use can generate the water–gas shift reaction (Eq. 1) and steam reforming reaction (Eqs. 2 and 3). CO and hydrocarbons produced during gasification can react with water to produce H_2. Equation 1, the water–gas shift

reaction, converts carbon monoxide and water into carbon dioxide and hydrogen. Equations 2 and 3 convert hydrocarbons produced during the gasification process into CO and H_2. Small amounts of added oxygen can reduce coke formation by combustion of the carbonaceous material to CO_2 and other volatile chemicals (van Steen and Claeys 2008). Steam can increase the H_2/CO ratio in the resulting synthesis gas (van Steen and Claeys 2008). Syngas can be used directly for power generation as a methane substitute or converted into fuel-range hydrocarbons by Fischer–Tropsch (FT) synthesis with appropriate catalysts (van Steen and Claeys 2008).

$$CO + H_2O \rightleftharpoons CO_2 + H_2 \quad (1)$$

$$CH_4 + H_2O \rightleftharpoons CO + 3H_2 \quad (2)$$

$$C_xH_{2y} + xH_2O \rightleftharpoons xCO + (x + y)H_2 \quad (3)$$

Bio-oil Upgrading

Fast pyrolysis of biomass with a residence time of 1 s at moderate temperatures (425–500 °C) can be used to produce bio-oil in high yields (60–75 %). Regardless of the production method, raw pyrolysis bio-oil's high organic oxygen (20–40 %) and water (15–30 %) contents lead to low energy densities, thermal and chemical instabilities, acidity, undesirable odors, and corrosive properties (Bridgwater 1994). Microphases are frequently present in bio-oil and easily observable under magnification (Mohan et al. 2006). Tiny solid char particles are common which catalyzed reactions on their surfaces further enhancing instability (Mohan et al. 2006). Upgrading is required to convert raw fast pyrolysis oil into a useable form for transportation fuels (Mohan et al. 2006; Boateng et al. 2008; Bridgwater et al. 1999). Several approaches (cracking, decarbonylation, decarboxylation, hydrocracking, hydrodeoxygenation, and hydrogenation) were reported for bio-oil upgrading (Adjaye and Bakhshi 1995b; Wildschut et al. 2009). These reactions take place in the presence of catalysts at elevated pressure and temperature. Examples of each reaction type are given in Fig. 1.

Fast pyrolysis oils contain liquid organic components that include organic acids, ketones, aldehydes, furans, phenolic compounds, guaiacol, syringol, sugar-based compounds, and water (Mohan et al. 2006; Ingram et al. 2007). The large phenolic content in bio-oil results from lignin pyrolysis and may reach 30 % of the organic components (Zhang et al. 2007). Guaiacol, among the more abundant fragments from lignin (Mohan et al. 2006; Bridgwater et al. 1999; Ingram et al. 2007; Zhang et al. 2007; Mullen and Boateng 2008; Bridgwater 2003; Bridgwater et al. 2001; Bridgwater and Peacocke 1999; Huber et al. 2005; Bridgwater 1996; Czernik and Bridgwater 2004), is present at levels of approximately 0.94 wt% in pine wood and 0.18–0.51 wt% in switchgrass- and alfalfa-derived pyrolysis oils (Ingram et al. 2007; Mullen and Boateng 2008). Furfural is produced during thermal

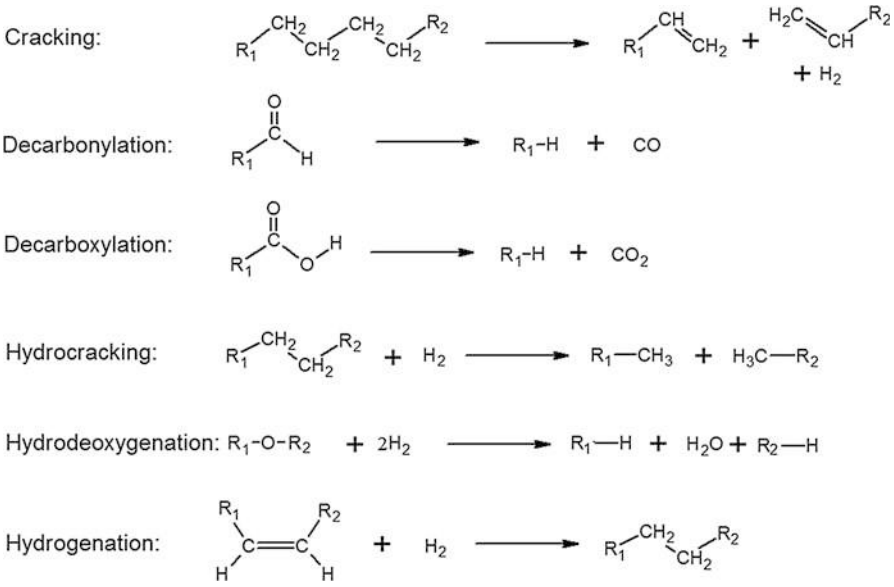

Fig. 1 Bio-oil upgrading reactions

decomposition of glucose, cellulose, and hemicelluloses (Mohan et al. 2006; Bridgwater et al. 1999; Ingram et al. 2007; Zhang et al. 2007; Mullen and Boateng 2008; Bridgwater 2003; Bridgwater et al. 2001; Bridgwater and Peacocke 1999; Huber et al. 2005; Bridgwater 1996; Czernik and Bridgwater 2004).

Hydrodeoxygenation (HDO) is similar to hydrodesulfurization (HDS) which is used extensively in the oil refineries to remove sulfur from organic molecules. During HDO, oxygen is removed from the organic compound as water. Separated organic and aqueous phases are often found after the reaction (Venderbosch et al. 2010).

Deoxygenation upgrading is generally conducted at elevated hydrogen pressure and temperatures (Grange et al. 1996). HDO is generally performed at pressures between 10 and 30 Mpa (Venderbosch and Prins 2010; de Miguel Mercader et al. 2010). Higher pressures increase hydrogen solubility in the bio-oil and H_2 absorption on the catalyst surfaces. This serves to increase rate and decrease coking (Kwon et al. 2011). Theoretically, about 25 mol H_2 per one kg of bio-oil is required to completely deoxygenate the bio-oil. However, excess hydrogen (35–420 mol/kg) typically is used for HDO reactions (Venderbosch et al. 2010; Elliott et al. 2009).

Industrial HDO reactions are typically done in a flow reactor with liquid hourly space velocities (LHSV) of 0.1–1.5 h^{-1} (McCall et al. 2012), while batch reactions, often used for research applications, are typically completed in 2–5 h (Wildschut et al. 2009). HDO is conducted at temperatures between 250 °C and 450 °C (Adjaye and Bakhshi 1995a). Recently, the effect of temperature on upgrading was studied using wood-based bio-oil in a fixed-bed flow reactor at 14 Mpa H_2 with a Pd/C

catalyst. The upgraded liquid product yield decreased from 75 % to 56 % when increasing the temperature from 310 °C to 360 °C. More gas products were produced at the higher temperature. At temperatures over 340 °C, hydrocracking becomes more favorable than HDO (Elliott et al. 2009).

Noble metal (Ru, Rh, Pd, and Pt) catalysts are reported to show good activity for HDO reactions; however, their higher prices make them unattractive (Yakovlev et al. 2009). Ni, Co, Mo, and Cu metals can be used as alternatives to the noble metal catalysts. However, these catalysts are reported to suffer from lost activity due to catalyst coking (Yakovlev et al. 2009).

Several dual metal catalyst systems (Zhao et al. 2009; Zhang et al. 2006), including Co/Mo combinations, have been used to promote bio-oil HDO reactions (Furimsky 2000). Previous HDO studies of the model compound guaiacol under hydrogen followed its conversion into phenol, catechol, and fully deoxygenated cyclohexane, cyclohexene, and substituted benzenes using hydrogen and Mo/Co catalysts (Laurent and Delmon 1994; Bredenberg et al. 1982; Lin et al. 2011). Guaiacol conversion to phenol has also been achieved by removal of methanol via hydrogenolysis of the aromatic C–O bond using Co/Mo, along with a competing formation of catechol by loss of the methyl group (Ferrari et al. 2001; Ferrari et al. 2002). Catalyst acidity promotes both coke formation (Centeno et al. 1995) and guaiacol conversion. Potassium modification of alumina-supported Mo/Co alters the catalyst's acidity and reduces coke formation during guaiacol conversion (Centeno et al. 1995; Wijayapala et al. 2014). Ni/Mo/S and Co/Mo/S catalysts have been widely used for HDO (Elliott 2007). Ni and Co act as promoters by donating electron density to the Mo, weakening the Mo–S bond. Loss of sulfur creates vacant sulfur sites for HDO (Massoth et al. 2006). However, during the electron donation process, Mo–S is converted into Mo–O which reduces catalyst activity (Romero et al. 2010).

Transition metal catalysts for HDO reactions should be bifunctional. Oxygen-containing compounds must be activated during the process and a hydrogen adsorption active site is also needed. A support is often used with transition metals to achieve this bifunctionality. The transition metal can act as the active site for dissociative hydrogen absorption and then it can donate a hydrogen atom to promote the HDO reaction. The supporting material can act as the active site for the oxy-compound complexation as described in Fig. 2 (Mallat and Baiker 2000; Vargas et al. 2004).

Hydrogen gas has been used for almost all bio-oil upgrading studies (Mallat and Baiker 2000; Vargas et al. 2004; Fisk et al. 2009). Upgrading reactions typically include HDO, which induces C–O bond cleavage and produces water (Bridgwater 1996). The water–gas shift (WGS) reaction (Eq. 1) can be used to generate H_2 from CO + H_2O and to vary H_2 and CO compositions (Patt et al. 2000; Sun et al. 2010). *Herein, we examined Mo/Co/K loaded on a ZSM-5 support to catalyze HDO reactions of guaiacol and furfural with 50/50 syngas and bio-syngas (a green and renewable source of hydrogen and carbon monoxide). Mo/Co/K on a ZSM-5 support was also simultaneously used with a Cu-based low-temperature WGS catalyst for HDO reactions of guaiacol and furfural using the same syngas sources.* The reactions were conducted at 200–300 °C and a 4 MPa initial CO + H_2 pressure in batch gas phase reactions.

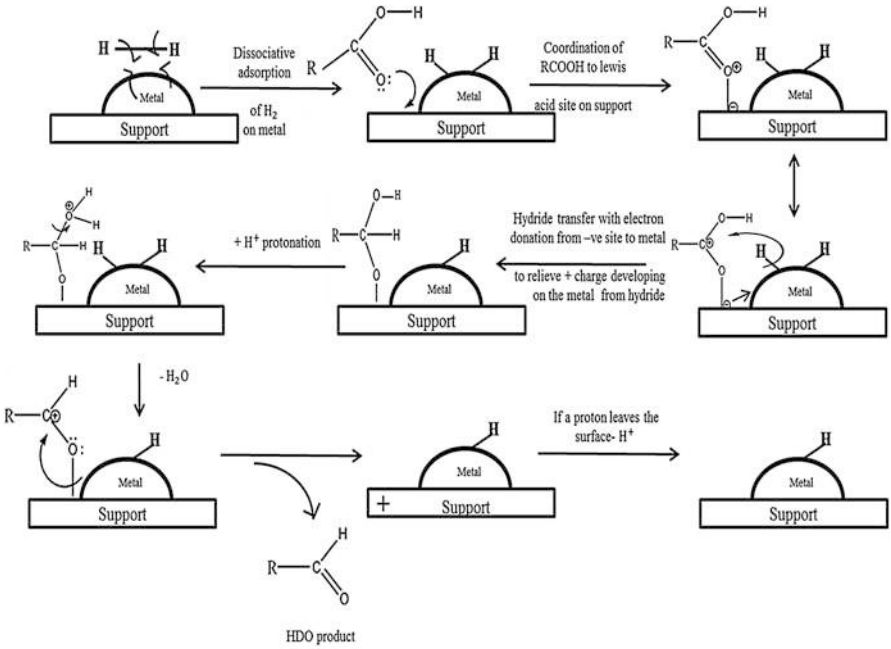

Fig. 2 Schematic diagram of one catalyst process showing the synergistic relationship of the transition metal and the support

The presence of CO and the WGS catalyst can increase H_2 partial pressure by reaction with both H_2O formed during HDO and also the water present in bio-oil. In model compound work, no water will be present at the start. However, the WGS reaction should lower the water content of the products produced by HDO. These upgrading reactions were compared to analogous HDO reactions using only H_2. *It is conceivable that CO may independently remove oxygen from organic compounds, forming CO_2*. Since Mo/Co/K on ZSM-5 is a known Fischer–Tropsch (FT) catalyst (van Steen and Claeys 2008), *it is also possible that syngas-induced HDO of guaiacol and furfural might occur concurrently with FT chemistry*. If so, hydrocarbons formed by FT reactions would enhance the upgraded product's heating value.

Experimental

Catalyst Preparation

Mo/Co/K/ZSM-5 was prepared using incipient wetness impregnation (Liu et al. 2009). The ammonium form of ZSM-5 ($SiO_2/Al_2O_3 = 50$) (50.0 g) obtained from Zeolyst International was impregnated with an aqueous solution of 4.60 g $(NH_4)_6Mo_7O_{24} \cdot 4H_2O$ (Sigma-Aldrich). This Mo/ZSM-5 was then impregnated

with an aqueous solution of 12.35 g $Co(NO_3)_2 \cdot 6H_2O$ (Sigma-Aldrich). Finally this Mo/Co/ZSM-5 was impregnated with an aqueous solution of 1.25 g K_2CO_3 (Sigma-Aldrich). The samples were then calcined in air at 500 °C for 3 h and pelletized into 0.45–0.8 mm particles for activity tests. The designated (after calcination) loading was 5 wt% for Co with 5 wt% Mo and 1.4 wt% K. The WGS catalyst was purchased from Alfa Aesar (copper-based low-temperature water–gas shift catalyst, HiFUEL W220 pellets 3.1 × 3.1 mm).

Catalyst Characterization

Catalyst surface areas were determined by N_2 physical adsorption using a BET surface area analyzer (Monosorb Quantachrome). First, the samples were degassed at 280 °C under flow of 30 % nitrogen in helium. Atomic absorption (AAS) analyses were conducted using Mo, Co, Cu, and K standards (Sigma-Aldrich AAS standard) to determine the metal wt% values. Acid digestion was used to extract the metal from the supporting surface prior to analysis. Carbon % of the used catalysts was determined using an elemental analyzer (CE 440; Exeter Analytical, Inc.). Catalyst characterization results are discussed in Results and Discussion.

Catalytic Upgrading Guaiacol and Furfural with Syngas

Guaiacol and furfural HDO reactions with syngas were performed in a 500 mL stainless steel static reactor controlled with a Parr 4843 reactor controller. The combinations of substrate, gases, catalyst, and temperature employed (54 total combinations) are listed in Table 2. The catalyst (2.0 g or 2.0 g of each when using dual catalysts) was used with two different syngas mixtures: syngas 50/50 H_2/CO/N_2 (47:47:6) and bio-syngas (mole% H_2, 17.83 %; CO, 22.66 %; N_2, 46.04 %; CH_4, 1.76 %; C_2H_4, 0.25 %; O_2, 0.88 %; CO_2, 10.60 %) and also with H_2 (99.99 %). Guaiacol (Sigma-Aldrich) or furfural (Sigma-Aldrich) (0.0400 mol) were used as the substrates. They were loaded into the reactor at room temperature. The catalyst was loaded into a static basket mesh holder placed well above the substrate (guaiacol or furfural) liquid level. After purging with the gas to be used, this reactant gas was introduced, pressurizing the reactor at ambient temperature. Then the reactor was heated to the designated reaction temperature (200 °C, 250 °C, or 300 °C) which raised the total pressure to 4.0 MPa in each case.

After the 4 h reaction, the reactor was allowed to cool to ambient temperature before effluent gas was collected into a 1 L Tedlar bag and analyzed using a gas chromatograph (SRI 8610C) equipped with both thermal conductivity (TCD) and flame ionization (FID) detectors. A ShinCarbon ST 100/120 (2 m 1 mm ID 1/16″ OD silicone) packed column and an MXT-1(60 m 0.53 mm ID 5.00 μm) capillary column were employed for separation of inorganic gases and light hydrocarbons. Liquid products were removed and the reactor was washed three times with 5.0 mL

Table 2 Reaction conditions used for each catalyst system

Substrate	Gas	Catalyst	Temperature (°C)[a]
Guaiacol	50/50 syngas	Mo/Co/K	200, 250, 300
		WGS	200, 250, 300
		WGS + Mo/Co/K	200, 250, 300
	Bio-syngas	Mo/Co/K	200, 250, 300
		WGS	200, 250, 300
		WGS + Mo/Co/K	200, 250, 300
	Hydrogen	Mo/Co/K	200, 250, 300
		WGS	200, 250, 300
		WGS + Mo/Co/K	200, 250, 300
Furfural	50/50 syngas	Mo/Co/K	200, 250, 300
		WGS	200, 250, 300
		WGS + Mo/Co/K	200, 250, 300
	Bio-syngas	Mo/Co/K	200, 250, 300
		WGS	200, 250, 300
		WGS + Mo/Co/K	200, 250, 300
	Hydrogen	Mo/Co/K	200, 250, 300
		WGS	200, 250, 300
		WGS + Mo/Co/K	200, 250, 300

[a]In all cases, the reactor was charged at ambient temperature with the reactant gas so that it reached a 4.0 MPa partial pressure (hydrogen + carbon monoxide) once the target temperatures of 200 °C, 250 °C, and 300 °C were achieved

of ethyl acetate (Sigma-Aldrich, LC–MS Grade). The washings were collected and added to the liquid products. An internal standard, chlorobenzene-d_5 (Sigma-Aldrich) (0.100 mL), was added and the mixture diluted to 25.0 ml in a volumetric flask. GC/MS analysis of the mixture was performed on a GC/MS (Agilent 7890A) equipped with DB-1 column (GC, DB-1-60 m 0.32 mm 1.0 μm). Peak area comparisons with the internal standard using product response factors allowed for quantification.

Results and Discussion

Catalyst Characterization

Catalyst surface areas and metal compositions are listed in Table 3. Impregnating ZSM-5 with Mo, Co, and K significantly reduced the surface area from 422 m^2/g to approximately 300 m^2/g, indicating that the added metals block some zeolite channels. A smaller drop in Mo/Co/K/ZSM-5 surface area was observed after the 50/50 syngas catalytic reactions at 300 °C with guaiacol than those with furfural, implying somewhat more catalyst coking occurred during furfural HDO under the same conditions. In contrast, Cu-based WGS catalyst's surface area dropped sharply and coke deposited during both guaiacol and furfural HDO. After HDO

Table 3 Catalyst elemental analysis, surface area, and percent carbon after HDO

	Surface area (m^2/g)			Elemental analysis[a] Wt(%)				Carbon (%)[b]	
Catalyst	Calcined	Used[c] (Guaiacol)	Used[c] (Furfural)	Mo	Co	K	Cu	C % (Gua.)	C % (Fur.)
ZSM-5	422	.....	.....	–	–	–	–		
ZSM-5/Mo/Co/K[d]	299	270	252	4.19	4.24	1.16	–	4.2	8.3
Cu-based WGS[e]	84.6	49.1	41.0	–	–	–	38.2	6.1	11.5

[a]Elemental analyses (atomic absorption) were performed on catalysts after calcination and before HDO reactions
[b]Using an elemental analyzer (CE 440; Exeter Analytical, Inc.)
[c]Catalysts were used in 4 h reactions with syngas 50/50 at 4.0 MPa partial pressure ($CO + H_2$) at 300 °C, prior to BET analysis
[d]No WGS catalyst was used
[e]No HDO catalyst was used

reactions, 4.2 and 8.3 %C were found on the WGS catalyst for these two substrates, respectively. Carbon depositions observed on the used catalysts at 200 °C, 250 °C, and 300 °C are shown for H_2, 50/50 syngas, and bio-syngas reactions in Fig. 3. AAS analysis confirmed the expected Mo/Co composition of the fresh catalyst after calcinations (Table 3).

HDO of Guaiacol and Furfural

HDO of guaiacol and furfural was studied individually with Mo/Co/K and Cu-based WGS catalysts and then with the dual system of both catalysts (Table 2). HDO reactions under hydrogen were used as reference results to compare with the catalyst activity in syngas reactions. Guaiacol and furfural conversions at 200–300 °C were determined (Tables 4 and 5) following their disappearance by GC/MS.

Temperature has a significant impact on the guaiacol conversion with all three reagent gases with the three different catalyst systems (Table 4). At the highest temperature (300 °C) employed, the maximum guaiacol conversions were observed for each gas and each catalyst. The conversions of guaiacol in the presence of the dual catalysts (Mo/Co/K + WGS) were almost the same as the conversions using the single Mo/Co/K catalyst under hydrogen at 200 °C, 250 °C, and 300 °C. However, a significant difference in guaiacol conversion was found with both syngas compositions using Mo/Co/K versus the dual (Mo/Co/K + WGS) catalyst. The dual catalyst system exhibited the higher conversions with both syngases at all three temperatures. However, using only Mo/Co/K resulted in considerably lower conversions with both syngases than with hydrogen only (where the initial hydrogen

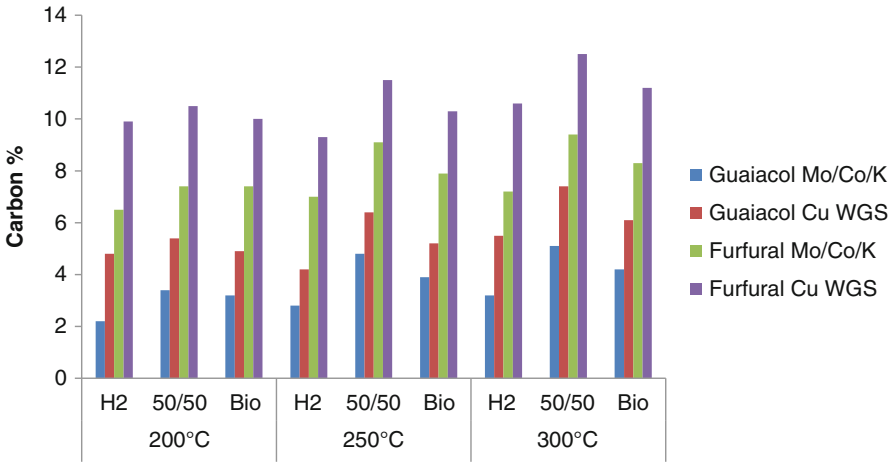

Fig. 3 Carbon percentage found on the used Mo/Co/K and Cu-based WGS catalyst and after HDO reaction of guaiacol and furfural in the due catalyst reactions

Table 4 Guaiacol conversions in HDO reactions with Mo/Co/K and WGS catalysts at 200 °C, 250 °C, and 300 °C under 50/50 syngas, bio-syngas, and H_2 after 4 h

	Syngas 50/50			Bio-syngas			Hydrogen		
Catalyst	200 °C	250 °C	300 °C	200 °C	250 °C	300 °C	200 °C	250 °C	300 °C
Mo/Co/K	16.7[a]	32.4	45.4	13.6	27.1	39.5	26.7	60.4	88.4
WGS	11.2	14.2	16.7	10.2	11.9	13.7	14.8	17.4	19.2
Mo/Co/K + WGS	24.6	55.2	86.1	20.2	44.5	79.2	28.4	62.4	91.4

[a]All conversions are expressed as percent guaiacol conversion

Table 5 Furfural conversions in HDO reactions with Mo/Co/K and WGS catalysts at 200 °C, 250 °C, and 300 °C under 50/50 syngas, bio-syngas, and hydrogen after 4 h[a]

	Syngas 50/50			Bio-syngas			Hydrogen		
Catalyst	200 °C	250 °C	300 °C	200 °C	250 °C	300 °C	200 °C	250 °C	300 °C
Mo/Co/K	88.1[a]	90.1	94.2	85.1	89.4	93.6	97.1	100	100
WGS	69.4	85.3	89.4	65.7	84.1	88.5	70.4	88.2	90.4
Mo/Co/K + WGS	95.6	100	100	94.1	100	100	98.4	100	100

[a]All conversions are expressed as percent conversion of furfural conversion

pressure was higher). This illustrates the significance that the WGS catalyst plays in the dual catalyst system for HDO of guaiacol with syngas.

Higher conversions were observed for furfural than guaiacol under these conditions. When the reaction temperature was maintained at or above 250 °C, complete furfural conversion was achieved in 4 h using the dual (Mo/Co/K + WGS) catalyst with each type of syngas (Table 5). HDO rates increased at higher temperatures for all the catalyst systems, with all reagent gases. The products from both guaiacol and furfural HDO treatments were analyzed by GC/MS using chlorobenzene-d_5 as an internal standard and response factors from standards. The product selectivity (S_i) is expressed in Eq. 4, where n_i is the number of moles of product i and c_i is the number of carbon atoms in product i. The selectivity, S_i, is the percentage of the total number of carbon atoms found in the specified product i ($n_i \times c_i$) versus the number of carbon atoms in the starting material ($n_a^0 \times c_a$). This tracks carbon from the amount in either the guaiacol or furfural changed to the reactors to the products. If the sum of all S_i values exceeds 100 %, that would indicate that carbon has entered into the products from the CO of the syngas reagent gas.

$$S_i = \frac{n_i \times c_i}{n_a^0 \times c_a} \times 100\% \tag{4}$$

n_i = Number of moles of product i
c_i = Number of carbon atoms in product i
n_a^0 = Initial number of moles of guaiacol or furfural
c_a = Number of carbon atoms in guaiacol or furfural

These selectivities are obtained from experimental measurements of the product selectivities (S_i) observed in HDO of guaiacol and furfural. These are shown in Table 6.

Guaiacol reactions produced significant amounts of cyclohexane and cyclohexene after 4 h at 300 °C using all three reactant gases. Both syngases converted guaiacol into deoxygenated products, although using only H_2 generated slightly higher cyclohexane and cyclohexene selectivities. Cyclohexane and cyclohexene selectivities decreased at 200 °C and 250 °C. 1,2-Dimethoxybenzene selectivity was significantly higher using either syngas compared to employing H_2 at 300 °C.

A major question of interest is: can carbon from CO be incorporated into the liquid HDO reaction products? Evidence of carbon incorporation into the liquid products from CO was obtained. Guaiacol HDO products from both 50/50 syngas and bio-syngas reactions at 300 °C exhibited product selectivity totals exceeding 100 % (Table 6a). This means more carbon was found in the liquid products than was present in the reagent guaiacol placed into the reaction vessel. Therefore, this carbon could only have come from CO. This was only observed at 300 °C and the amounts were small (see Table 6a). However, three repetitions of each experiment were performed and the amounts of extra carbon beyond the guaiacol charged exceeded the standard deviation in these experiments. Future reactions will be done

Table 6 HDO product selectivities at 200 °C, 250 °C, and 300 °C for all three reagent gases over the Mo/Co/K + WGS dual catalyst after 4 h for (a) guaiacol and (b) furfural

(a) Guaiacol HDO product selectivities (S_i)									
	300 °C[a]			250 °C			200 °C		
Products	H_2	50/50	Bio	H_2	50/50	Bio	H_2	50/50	Bio
Guaiacol	**8.6**	**13.9**	**20.8**	**37.6**	**44.8**	**55.5**	**71.6**	**75.4**	**79.8**
Cyclohexane	33	29.2	24.3	5.7	4.8	3.2	0.3	0	0
Cyclohexene	23	17.6	17.7	8.9	6.3	5.6	0.7	0.2	0.1
1,2-Dimethoxybenzene	8.3	20.2	17.9	12.6	24.1	23.2	18.7	7.8	5.4
1,2-Benzenediol	12	7.1	4.9	28.5	15.6	8.9	6.4	14.1	12.9
Benzene	9	4.2	3.2	2.6	1.2	0.8	0.5	0.5	0.3
3-Methylbenzene-1,2-diol[b]	_	1	1.7	_	_	_	_	_	_
Methylcyclohexane	1.4	2.2	1.3	_	_	_	_	_	_
Methoxybenzene	0.5	0.3	0.1	1.3	0.7	0.2	_	_	_
Phenol	1.3	0.6	0.9	1.5	0.7	0.8	0.5	0.3	0.1
Hydroxymethylcyclopentane	0.2	0.3	0.2	_	_	_	_	_	_
Cyclohexanol	0.7	0.3	0.5	0.1	0.1	0.1	_	_	_
1,2-Dimethoxycyclohexane	0.8	1.2	1.8	_	_	_	_	_	_
2-Methoxy-5-methylphenol	0.2	0.3	1	_	_	_	_	_	_
4-Methylphenol[b]	_	1.6	1.9	_	_	_	_	_	_
2-Methylphenol[b]	_	1.2	1.5	_	_	_	_	_	_
3-Ethylphenol[b]	_	0.6	0.7	_	_	_	_	_	_
2,4-Dimethylphenol[b]	_	0.3	0.2	_	_	_	_	_	_
Totals[c]	98.9[d]	102.2[d]	100.6[d]	98.8[d]	98.2[d]	98.2[d]	98.7[d]	98.4[d]	98.6[d]
Standard deviation[e]	±0.29	±0.31	±0.27						

(b) Furfural HDO product selectivities									
	300 °C			250 °C			200 °C		
Products	H_2	50/50	Bio	H_2	50/50	Bio	H_2	50/50	Bio
Furfural	_	_	_	_	_	_	1.6	4.4	4.6
2-Methylfuran	65.2	69.7	66.6	67.2	75.2	77.4	72.4	76.2	78.2
Furan	26.9	22.1	22.5	27.7	19.4	15.1	24.3	17.7	15.2
2-Hydroxymethylfuran	2.1	0.3	0.4	1.3	0.1	0.1	_	_	_
Pentane	1.7	_	_	_	_	_	_	_	_
Cyclohexene[f]	_	3.1	4.2	_	2.4	3.1	_	0.4	0.6
Cyclohexane[f]	_	0.9	1.5	_	0.5	1.3	_	_	_
Cyclopentene[f]	_	2.2	1.9	_	0.6	0.3	_	_	_
Totals[g]	95.9	98.3	97.1	96.2	98.2	97.3	98.3	98.7	98.6

[a]Average of three repeated runs
[b]Products found only when using syngas
[c]Relative mole% (moles of carbon in the sum of the product/moles of carbon in initial guaiacol)
[d]Totals over 100 % were achieved with syngases, indicating incorporation of carbon from CO into the products
[e]Standard deviation of the three repeated experiments
[f]Expected FT reaction product (found only when using syngas)
[g]Relative mole% (moles of carbon in the sum of the products/moles of carbon in initial furfural)

at 325 °C and 350 °C to determine if this additional carbon in the products increases.

Alkyl-substituted phenols appear in guaiacol HDO reaction products (at 300 °C) only when using syngas as shown in Table 6a. Methylation and ethylation of phenol probably occur via Friedel–Crafts alkylation by methanol and ethanol formed by Fischer–Tropsch reaction of syngas on Mo/Co/K, but these FT reactions cannot occur with H_2 (see Eq. 5). The formation of methanol and dimethyl ether was observed from syngas over this catalyst previously (Wijayapala et al. 2014). Char or coke formation or incomplete liquid product collection could explain the missing carbon (totals below 100 % for Table 6a and b). Used catalysts exhibited carbon weight percentages of 2–12 wt%. These are shown in Fig. 3.

$$\mathrm{CO} + \mathrm{H_2} \xrightarrow[\substack{\mathrm{FT} \\ 300\ ^\circ\mathrm{C}}]{\mathrm{Mo/Co/K}} \mathrm{CH_3OH}, \quad \mathrm{CH_3CH_2OH} \tag{5}$$

Furfural reactions exhibited high selectivity to furan and methylfuran. Totally deoxygenated products such as pentane, cyclohexane, and cyclopentene are also formed. Cyclic aliphatic hydrocarbons were found only in furfural/syngas reactions and not in furfural/H_2 reactions, suggesting CO was involved in product formation, perhaps via Fischer–Tropsch (FT) routes.

Two control reactions were performed to probe if FT chemistry was involved. Syngas-only reactions were carried out using the dual Mo/Co/K + WGS catalysts at 300 °C, where no guaiacol or furfural was present. No cyclic aliphatic or olefinic compounds were formed after 4 h (Table 7). This suggests that the cyclic hydrocarbons shown in Table 6 are probably produced from reactions involving guaiacol or furfural. A second experiment reacted guaiacol at 300 °C with only CO (no H_2) over the Mo/Co/K + WGS catalyst for 4 h (Table 8). Very little conversion occurred. This small amount of conversion seen could have resulted from thermal conversion generating small amounts of water, which, in turn, led to some H_2 formation by the WGS reaction.

Oxygen removal is one measure of bio-oil upgrading. Catalyst activity was defined by the degree of deoxygenation (HDO %). HDO % is defined here simply as the percentage of the initial oxygen in the substrate charged to the reactor that remains in the liquid product. This is expressed in Eq. 6 (Bykova et al. 2012), where a_i is the number of oxygen atoms contained in a given component of the product i and n_i is the number of moles of product i. The product of n_i and a_i is summed from all product components over the starting material where n_a^0 is the initial number of moles of guaiacol or furfural. The 2 factor is used because there are two oxygen atoms in each guaiacol and furfural molecule.

$$\mathrm{HDO}\% = \left[1 - \frac{\sum_i n_i a_i}{n_a^0 \times 2}\right] \times 100 \tag{6}$$

Table 7 Product distribution percentages found with 50/50 syngas and Mo/Co/K + WGS catalyst without guaiacol or furfural at 4 h

Products	200 °C	250 °C	300 °C
Carbon monoxide	74.3	65.2	58.5
Carbon dioxide	12.5	16.9	20.1
Methane	2.0	2.7	3.3
Ethene	0.8	1.0	1.3
Propane	0.5	0.7	0.8
2-Methylpropane	0.3	0.4	0.5
2-Methylbutane	3.0	4.1	4.9
Pentane	2.6	3.5	4.2
2-Methylpentane	1.0	1.4	1.6
Hexane	0.2	1.5	1.7

Table 8 Product distribution from the reaction of guaiacol with CO over the Mo/Co/K + WGS dual catalyst at 300 °C for 4 h. No H_2 was added

Products	Relative content %[a]
Guaiacol	93.28
Phenol	0.65
4-Methylphenol	0.47
Methoxymethylphenol[b]	0.35
4-Methylbenzene-1,2-diol	0.34
2-Methylphenol	0.24
Dimethylphenol[b]	0.22
Methoxymethylphenol[b]	0.21
1,2-Dimethoxybenzene	0.15
2-Methoxy-4-methylphenol	0.15
Dimethylphenol[b]	0.13
Methoxybenzene	0.12
Dimethylphenol[b]	0.11

[a]GC/MS spectrum relative area percentage
[b]Specific isomer not determined

HDO % (Table 9) reflects the oxygen removal capability of the catalyst when reactions are compared at identical conditions and reaction times. A higher HDO% indicates less oxygen in the products. The distribution of reaction products with 0, 1, or 2 oxygen atoms from guaiacol HDO over Mo/Co/K + WGS at 300 °C after 4 h can be found in Fig. 4.

The HDO % of guaiacol was higher using hydrogen than using either syngas. The largest difference in product selectivities for guaiacol upgrading at 300 °C (Table 6) was found for 1,2-dimethoxybenzene (8.3, 20.2, and 17.9 % for H_2, 50/50 syngas, and bio-syngas, respectively). The amount of this compound peaks at 4 h and then decreases in hydrogen reactions. 1,2-Dimethoxybenzene is thought to form from the addition of methanol to the guaiacol hydroxyl function (*O*-methylation) with loss of water. Methanol can be produced from syngas via FT processes over Mo/Co/K on ZSM-5 (Wijayapala et al. 2014). However, acid-catalyzed methylation of guaiacol by another guaiacol molecule could also occur.

Table 9 HDO % of guaiacol and furfural reactions catalyzed by Mo/Co/K + WGS at 300 °C for 4 h[a]

Substrate	Hydrogen	50/50 syngas	Bio-syngas
Guaiacol	68.8	53.7	48.9
Furfural	51.8	53.8	55.1

[a]HDO % is the percentage of oxygen that was initially present in the initial substrate removed by the HDO reaction and no longer found in the product

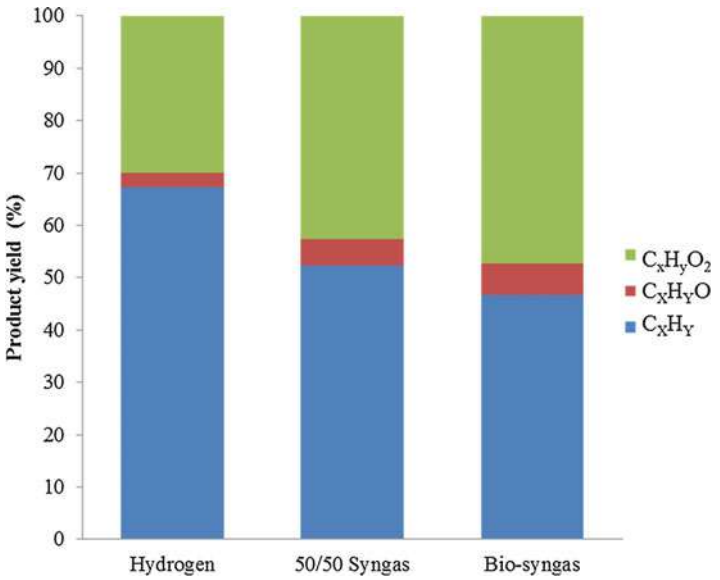

Fig. 4 Yields of compounds with different numbers of retained oxygen atoms for guaiacol HDO over Mo/Co/K + WGS at 300 °C after 4 h (C_xH_yO, single-oxygen-atom-containing oxygenates; $C_xH_yO_2$, dioxygen-atom-containing oxygenates; C_xH_y, products without oxygen)

Product distribution versus time curves was obtained by running identical reactions for different lengths of time before analyzing the products. H_2, 50/50 syngas, and bio-syngas were used individually to upgrade both guaiacol and furfural with the dual catalyst (Mo/Co/K + WGS). Guaiacol conversion (falling curves) and the product selectivities for cyclohexane and 1,2-dimethoxybenzene with the three different gases versus time are shown in Fig. 5.

Guaiacol consumption with H_2, 50/50 syngas, and bio-syngas at 300 °C was essentially complete after 8 h. Reaction with pure hydrogen occurred faster than those with either syngas. However, if the initial hydrogen partial pressure in syngas reactions were adjusted to be equal to these in the pure H_2 cases, this would no longer be true. The product distributions changed little after 8 h with all three gases. The initial partial H_2 pressures in the syngas reactions were lower than with pure H_2. This lower H_2 pressure slows hydrodeoxygenation and hydrogenation. At high initial H_2 pressures, hydrodeoxygenation/hydrogenation is favored and conversion

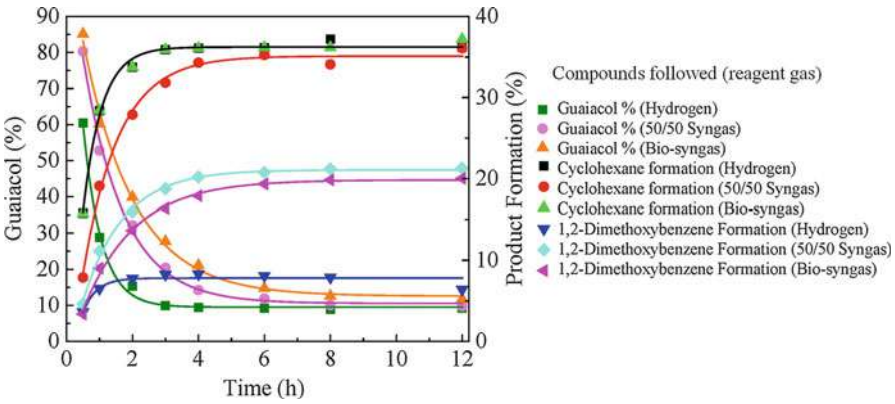

Fig. 5 Guaiacol consumption and cyclohexane and 1,2-dimethoxybenzene formation versus reaction time using the dual catalyst (Mo/Co/K + WGS) at 300 °C for all three reagent gases

is accelerated. The pressure falls with time in these constant volume reactions. The WGS catalyst produces in situ H_2 from water formed during HDO in the syngas reactions. This raises the hydrogen partial pressure and facilitates the HDO and hydrogenation of guaiacol. Cyclohexene formation versus time (not shown in Fig. 4) initially rises, reaches a maximum, and then decreases. Cyclohexane continues to increase as the hydrogenation of cyclohexene generates cyclohexane. The product distributions versus time over the Mo/Co/K + WGS catalyst at 300 °C are shown in Table 10. When 50/50 syngas was reacted alone over the Mo/Co/K + WGS dual catalyst, no cyclohexane or cyclohexene were formed. However, C-1 through C-6 linear and branched alkanes were produced (Table 7). Thus, cyclohexane and cyclohexene formed in guaiacol HDO must be derived from guaiacol.

Furfural was consumed more rapidly (~4 h, Fig. 6) than guaiacol (Fig. 5). The yield of the two main products (furan and 2-methylfuran) reached their maximum values after 3 h using all three reagent gases. Cyclohexane and cyclohexene were formed along with cyclopentene. The product distributions formed as a function of time over the dual catalyst system at 300 °C 50/50 syngas are summarized in Table 11. Since cyclohexene, cyclohexane, and cyclopentene were not formed in 50/50 syngas reaction alone over the dual catalyst from 200 °C to 300 °C, the cyclic hydrocarbons must have originated from furfural. Reaction schemes (Schemes 1 and 2) are proposed for the HDO of guaiacol and furfural based on the product analyses with time (all product formation percentages are shown in Tables 10 and 11).

In guaiacol HDO, the methoxy group is demethylated by hydrogenolysis of the O–CH_3 bond (Scheme 1). This forms catechol and methane. Demethoxylation of guaiacol leads to the formation of phenol and methanol (Nimmanwudipong et al. 2011). Hydrogenolysis of phenol's OH group cleaves the $C_{aromatic}$–OH bond forming benzene. Subsequent hydrogenation of the aromatic ring can result in cyclohexane (Nimmanwudipong et al. 2011). Guaiacol can be converted to phenol

Table 10 Guaiacol reaction product formation verses reaction time using the dual catalyst (Mo/Co/K + WGS) at 300 °C[a]

Products	Product formation %							
	0.5 h	1 h	2 h	3 h	4 h[b]	6 h	8 h	12 h
Guaiacol	80.1	51.4	28.3	17.9	13.9	12.9	12.7	12.4
Cyclohexane	6.2	15.1	22.0	25.1	29.2	30.1	30.0	30.1
Cyclohexene	3.3	10.8	18.4	18.9	17.6	17.1	17.3	18.2
1,2-Dimethoxybenzene	4.6	11.1	16.0	18.7	20.2	20.8	21.2	18.2
1,2-Benzenediol	2.1	4.3	7.8	7.4	7.1	6.9	6.7	4.5
Benzene	3.2	4.6	4.8	5.6	4.2	3.9	3.8	2.1
3-Methylbenzene-1,2-diol	–	–	–	0.4	1.0	1.2	1.3	1.1
Methylcyclohexane	–	–	–	1.2	2.2	2.2	2.3	2.9
Methoxybenzene	0.1	1.0	0.8	0.7	0.3	0.3	0.2	0.3
Phenol	0.2	0.6	1.1	1.4	0.6	0.5	0.4	0.6
Hydroxymethylcyclopentane	–	–	–	0.1	0.3	0.3	0.3	0.3
Cyclohexanol	–	0.2	0.4	0.5	0.3	0.2	0.1	0.3
1,2-Dimethoxycyclohexane	–	0.2	0.4	1.0	1.2	1.3	1.3	3.5
2-Methoxy-3-methylphenol	–	–	0.0	0.2	0.3	0.3	0.4	0.5
4-Methylphenol	–	–	0.1	0.7	1.6	1.6	1.6	3.1
2-Methylphenol	–	–	0.1	0.6	1.2	1.2	1.2	1.8
Ethylphenol	–	–	–	0.3	0.6	0.6	0.5	1.9
2,4-Dimethylphenol	–	–	–	0.2	0.3	0.3	0.4	2.6

[a]Tentative chemical identities were determined using internal standards, retention times, and NIST library software. Quantification was determined using standard calibration curves

[b]The 4 h data represents average from three experiments

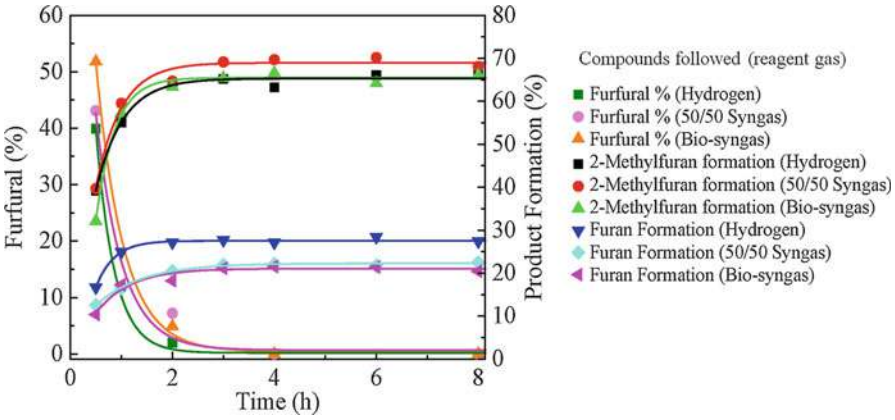

Fig. 6 Furfural consumption and 2-methylfuran and furan formation versus reaction time using the dual catalyst (Mo/Co/K + WGS) at 300 °C for all three reagent gas compositions

Table 11 Product formation verses reaction time for furfural HDO using the dual catalyst (Mo/Co/K + WGS) at 300 °C using 50/50 syngas

Products	Product formation % (based on furfural)						
	0.5 h	1 h	2 h	3 h	4 h	6 h	8 h
2-Methylfuran	39.7	59.5	64.7	69.1	69.7	70.2	68.1
Furan	12.6	16.5	20.5	21.9	22.1	21.8	22.5
2-Hydroxymethylfuran	3.2	5.2	2.0	0.7	0.3	0.1	0.1
Cyclohexene	–	1.6	3.4	3.5	3.1	3.2	3.3
Cyclohexane	–	0.3	0.5	0.6	0.9	0.9	0.8
Cyclopentene	–	–	0.4	2.0	2.2	2.5	2.5

via direct demethoxylation, and/or the observed product, methoxybenzene, can be demethylated to phenol by methanol. Methoxybenzene can also undergo demethoxylation by hydrogen to benzene, followed by hydrogenation to cyclohexene and cyclohexane. Ring hydrogenation of phenol produces cyclohexanol (see Table 10). Then, dehydration to cyclohexene can be followed by hydrogenation to cyclohexane. *O*-Methylation of guaiacol gives dimethoxybenzene.

O-Methylation of phenol or guaiacol readily occurs in the presence of methanol or dimethyl ether (Shen et al. 2005), both of which form from syngas over this catalyst system (Wijayapala et al. 2014). Phenol will readily be *C*-methylated at *ortho* and *para* positions over the Mo/Co/K catalyst which is supported on ZSM-5, a strong catalyst for electrophilic aromatic substitution.

Furfural (Scheme 2, Table 11) produced 2-methylfuran (~70 %) by hydrodeoxygenation of the aldehyde group. This likely occurred through aldehyde hydrogenation to 2-hydroxymethylfuran followed by facile loss of water from the reactive alpha CH_2OH group. The formation of 2-hydroxymethylfuran is seen to rise early

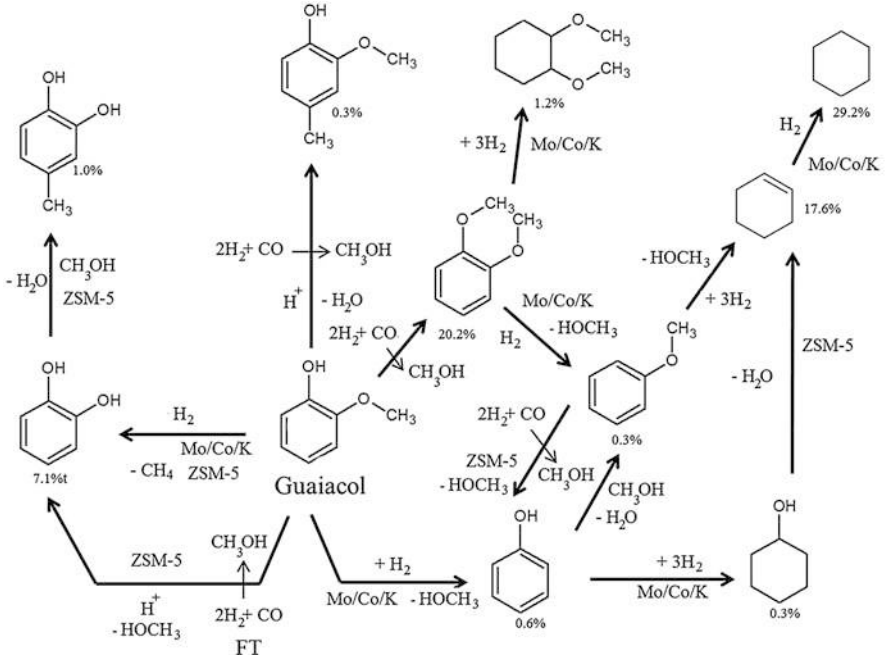

Scheme 1 Proposed scheme for guaiacol conversion to ten observed products with 50/50 syngas over Mo/Co/K + WGS at 300 °C. Product yields are given after 4 h

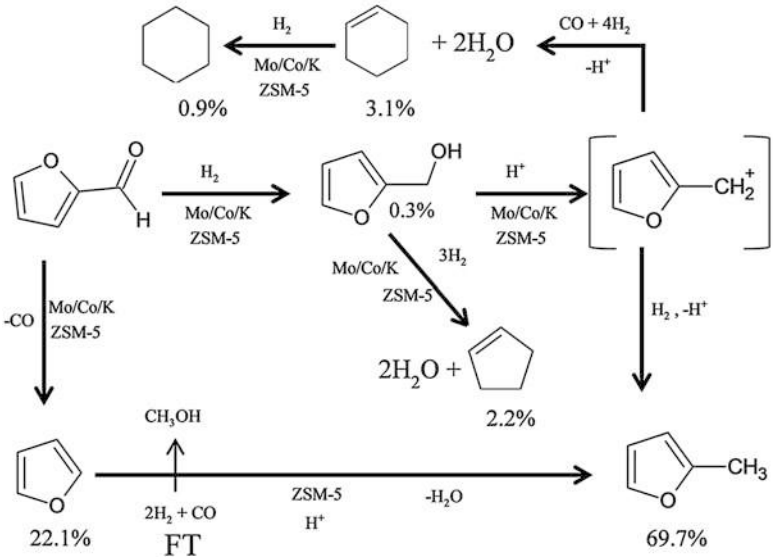

Scheme 2 Proposed scheme for furfural HDO with 50/50 syngas over Mo/Co/K + WGS at 300 °C after 4 h

and then fall (Table 11). Decarbonylation of the furfural aldehyde function produces furan (Modak et al. 2012). Furan is formed in ~22 % yield between 3 and 8 h. The formation of cyclohexene, cyclohexane, and cyclopentene, each with one carbon more than furfural, was observed with syngas, but not with hydrogen, in furfural HDO (Table 11). Since these three products were not formed from 50/50 syngas over Mo/Co/K + WGS without furfural present, these arose from furfural. The presence of methanol or dimethyl ether, formed in FT routes, could give 2-methylfuran by electrophilic aromatic substitution. Carbon addition to the furan ring, originating from CO, with concurrent removal of the oxygen must occur to convert the C-5 furfural or a product resulting from it to cyclohexene or cyclohexane. However, we have no evidence to support a specific pathway for this or for cyclopentene formation.

The heat of combustion defines the energy content in a fuel. The total heat of combustion of guaiacol and furfural liquid products in kJ is found in Tables 12 and 13, respectively. The energy density (kJ/g) was calculated using the number of moles of each product determined from GC/MS and the standard enthalpy of combustion (ΔH_c°) for each product. The mass of each product mixture was determined from the number of moles and molecular weight for each product. The results for both guaiacol and furfural HDO reactions after 4 and 12 h at 200 °C, 250 °C, and 300 °C can be found in Table 14. Product mixtures obtained by upgrading with all three gases exhibited higher total heats of combustion and energy densities kJ/g than the initial guaiacol and furfural feeds. The guaiacol products from H_2 (300 °C and both 4 and 12 h) upgrading had a lower total energy but higher energy density than upgrading with the bio-syngases. In contrast, the furfural H_2 upgrading product at these same conditions (300 °C, 4 and 12 h) exhibited both lower total energies and lower energy densities than the product upgraded with the bio-syngas.

The heat content (kJ) of the guaiacol product mixture versus reaction time for 300 °C upgrading reactions using the dual catalyst is shown in Fig. 7. A significant gap exists between the hydrogen and syngas upgrading. *Syngas upgrading leads to higher heats of combustion*. After 12 h, products from the 50/50 syngas guaiacol upgrade gave a 156.4 ± 0.5 kJ versus 146.6 ± 0.4 kJ for the product made under hydrogen (9 kJ difference for 0.0400 mol of starting material). *This is due to a product selectivity with syngas that favors higher heat of combustion products*. Reaction products with an increased total energy content are a potential benefit of upgrading with synthesis gas compared to hydrogen particularly when used in fuel applications.

Catalyst recycle was tested both with and without a catalyst washing step. Used catalyst was washed with ethyl acetate and dried for 24 h at 125 °C under air, before reuse. Product selectivities and CO conversions were examined to evaluate loss of activity and the reusability of the Mo/Co/K + WGS catalyst (Fig. 8). Catalysts lose activity more rapidly when reused without washing. About 50 % of the activity was lost after the catalyst had been used twice. However, 98 % activity is retained after three cycles, if the washed catalyst is recycled.

Table 12 Calculation of the heat of combustion of the liquid product obtained by upgrading guaiacol with Mo/Co/K + WGS at 200, 250, and 300 °C for 4 h (number of moles of each product was used with the heat of combustion of each compound found in references (Matos et al. 2003; Linstrom and Mallard))

		Heat of combustion (kJ) (kJ/mol × number of moles) guaiacol (143 kJ)								
Heat of combustion (kJ/mol)	Products	300 °C			250 °C			200 °C		
		H_2	50/50[a]	Bio[b]	H_2	50/50	Bio	H_2	50/50	Bio
3587	**Guaiacol**	12.2	19.7	29.5	53.3	63.1	78.2	101.4	106.4	112.9
3920	Cyclohexane	51.2	45.2	37.6	8.8	7.4	4.9	0.5	0.0	0.0
3752	Cyclohexene	34.1	26.1	26.2	13.2	9.3	8.3	1.0	0.3	0.1
4287	1,2-Dimethoxybenzene	14.1	34.2	30.3	21.3	40.6	39.1	31.6	13.2	9.1
2856	Catechol	13.6	8.0	5.5	32.2	17.5	10.0	7.2	15.9	14.5
3267	Benzene	11.6	5.4	4.1	3.4	1.5	1.0	0.6	0.6	0.4
2856	3-Methylbenzene-1,2-diol	0.0	1.1	1.9	0.0	0.0	0.0	0.0	0.0	0.0
4565	Methylcyclohexane	2.5	4.0	2.3	0.0	0.0	0.0	0.0	0.0	0.0
3783	Methoxybenzene	0.7	0.4	0.1	1.9	1.0	0.3	0.0	0.0	0.0
3058	Phenol	1.6	0.7	1.1	1.8	0.8	1.0	0.6	0.4	0.1
3938	Hydroxymethylcyclopentane	0.3	0.5	0.3	0.0	0.0	0.0	0.0	0.0	0.0
3730	Cyclohexanol	1.0	0.4	0.7	0.1	0.1	0.1	0.0	0.0	0.0
5183	1,2-Dimethoxycyclohexane	1.6	2.5	3.7	0.0	0.0	0.0	0.0	0.0	0.0
4215	2-Methoxy-5-methylphenol	0.3	0.5	1.7	0.0	0.0	0.0	0.0	0.0	0.0
3705	4-Methylphenol	0.0	2.3	2.8	0.0	0.0	0.0	0.0	0.0	0.0
3696	2-Methylphenol	0.0	1.8	2.2	0.0	0.0	0.0	0.0	0.0	0.0
4353	3-Ethylphenol	0.0	1.0	1.2	0.0	0.0	0.0	0.0	0.0	0.0
4348	2,4-Dimethylphenol	0.0	0.5	0.3	0.0	0.0	0.0	0.0	0.0	0.0
		144.9	154.4	151.7	136.1	141.4	142.9	143.0	136.8	137.2

[a]50/50 syngas
[b]Bio-syngas

Table 13 Calculation of the heat of combustion of the product from furfural upgrading with Mo/Co/K + WGS at 200, 250, and 300 °C for 4 h (product wt% was used with the heat of combustion of each compound found in reference (Linstrom and Mallard))

		Heat of combustion(kJ) (kJ/mol × number of moles) (furfural 93.5 kJ)								
Heat of combustion (kJ/mol)	Products	300 °C			250 °C			200 °C		
		H_2	50/50[a]	Bio[b]	H_2	50/50	Bio	H_2	50/50	Bio
2339	**Furfural**	0.0	0.0	0.0	0.0	0.0	0.0	1.5	4.1	4.3
2562	2-Methylfuran	66.8	71.4	68.2	68.9	77.1	79.3	74.2	78.1	80.1
2088	Furan	22.5	18.5	18.8	23.1	16.2	12.6	20.3	14.8	12.7
2548	2-Hydroxymethylfuran	2.1	0.3	0.4	1.3	0.1	0.1	0.0	0.0	0.0
3535	Pentane	2.4	0.0	0.0	0.0	0.0	0.0	0.0	0.0	0.0
3752	Cyclohexene	0.0	4.7	6.3	0.0	3.6	4.7	0.0	0.6	0.9
3920	Cyclohexane	0.0	1.4	2.4	0.0	0.8	2.0	0.0	0.0	0.0
3291	Cyclopentene	0.0	2.9	2.5	0.0	0.8	0.4	0.0	0.0	0.0
		93.8	99.1	98.6	93.3	98.5	99.1	96.0	97.6	98.0

[a]50/50 syngas
[b]Bio-syngas

Table 14 Energy density (kJ/g) and total energy (kJ) of product mixtures from guaiacol and furfural upgraded over Mo/Co/K + WGS using the two synthesis gas mixtures versus only hydrogen after 4 and 12 h (Tables 12 and 13)

			300 °C			250 °C			200 °C		
Quantity[a]	Units	Time (h)	H_2	50/50	Bio	H_2	50/50	Bio	H_2	50/50	Bio
Energy	kJ/g	4	38.8	36.7	35.8	30.6	30.6	30.4	29.3	28.8	28.7
Density		12	38.8	36.7	35.8	–	–	–	–	–	–
Total	kJ	4	144.9	154.4	151.7	136.1	141.4	142.9	143.0	136.8	137.2
Energy		12	146.6	156.4	153.6	–	–	–	–	–	–
			300 °C			250 °C			200 °C		
Quantity[b]	Units	Time (h)	H_2	50/50	Bio	H_2	50/50	Bio	H_2	50/50	Bio
Energy	kJ/g	4	31.2	32.0	32.2	31.0	31.6	31.9	31.0	30.8	30.8
Density		12	31.3	32.1	32.2	–	–	–	–	–	–
Total	kJ	4	93.8	99.1	98.6	93.3	98.5	99.1	96.0	97.6	98.0
Energy		12	89.3	94.8	96.6	–	–	–	–	–	–

[a]The heat of combustion of guaiacol charged to the reactor (28.9 kJ/g, 143.4 kJ for 4.96 g)
[b]The heat of combustion of furfural charged to the reactor (24.3 kJ/g, 93.5 kJ for 3.82 g)

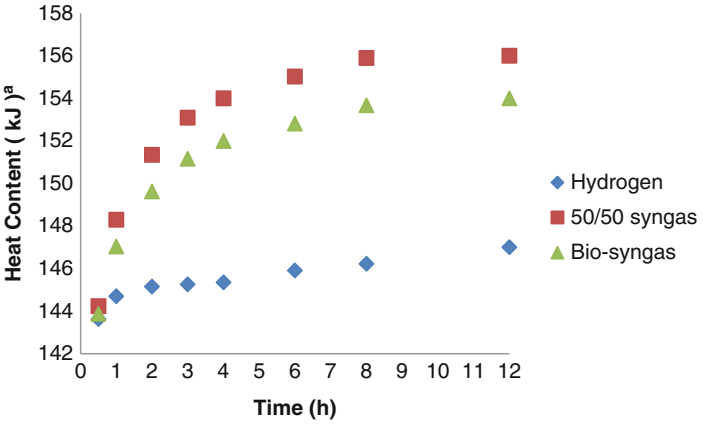

Fig. 7 Heat content (kJ) of the product mixtures obtained from guaiacol HDO reactions over the dual Mo/Co/K + WGS catalyst at 300 °C versus reaction time. [a]Product heat content from its calculated heat of combustion

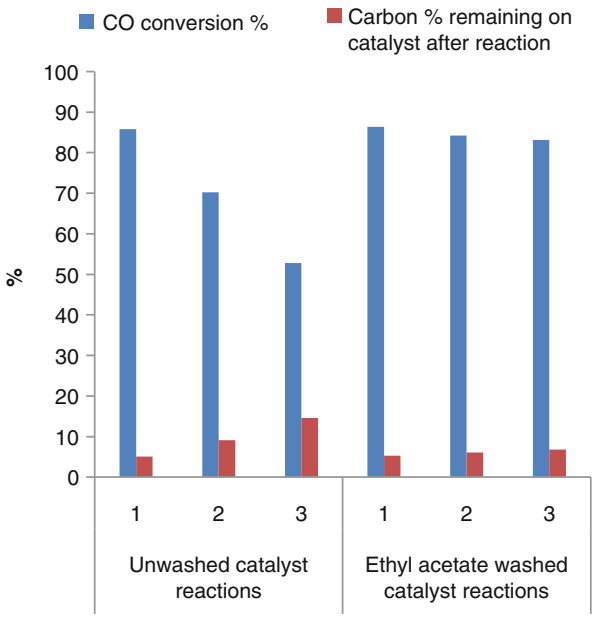

Fig. 8 CO % conversion and C wt% found on the used catalyst (Mo/Co/K + WGS shift catalyst using guaiacol and 50/50 syngas at 300 °C). CO conversion decreased and C wt% on the used catalyst increased in reactions employing recycled unwashed catalyst. Washing the used Mo/Co/K + WGS catalysts with ethyl acetate reduced progressive loss of CO conversion upon recycling the catalyst

Conclusions

The upgrading of bio-oil model compounds, guaiacol and furfural, using syngas or hydrogen and a dual catalyst system (Mo/Co/K + WGS) showed that syngas reactions (same total initial pressure but lower H_2 partial pressure) gave slower but competitive conversions compared to H_2. This occurs even though the H_2 partial pressure was much lower in the syngas reactions. All furfural upgrading reactions, at or above 300 °C, resulted in 100 % conversion of furfural's aldehyde functional group. In raw bio-oil, aldehydes are known to participate in oligomerization and oxidation reactions contributing to raw bio-oil instability. Upgrading reactions that remove this functional group lower oxygen content and increase bio-oil stability. Furfural conversion was complete (primarily producing 2-methylfuran ~70 % and furan ~22 %) after 4 h under hydrogen and both syngases at 250 °C and 300 °C. At 300 °C, furfural HDO% was slightly higher with syngas ~54 % compared to H_2 at 51.8 %. Guaiacol conversion increased with increasing temperature and was faster under hydrogen at 300 °C (~90 % at 3 h) than under the syngases (~90 % at 8 h).

Guaiacol HDO products from both 50/50 syngas and bio-syngas reactions at 300 °C exhibited products with more total carbon than that in the starting guaiacol (e.g., selectivity totals exceeding 100 %, Table 6a). This suggests incorporation of carbon into the liquid products from CO. This incorporation of carbon from syngas resulted in additional products, not found from H_2 upgrading, and a higher heat of combustion using syngas upgrading (156 and 154 kJ) versus hydrogen (147 kJ). Increased product energy content represents a compelling advantage of syngas upgrading, compared to H_2 upgrading, when developing new routes to biomass-derived transportation-quality liquid fuels.

This work identified a catalyst system, which effectively converted a model bio-oil aromatic phenol arising from lignin pyrolysis and a model furan aldehyde derived from cellulose pyrolysis, respectively, to more hydrophobic compounds with less oxygen. Products included alkanes and ethers using bio-syngas as the hydrogen source. The use of syngas, instead of pure hydrogen for HDO reactions, represents a new green bio-oil model upgrading route with considerable oxygen removal and increased energy density products. This represents an endorsement for more bio-oil upgrading research using syngas in place of hydrogen under a much wider range of conditions and substrate feeds.

Future Directions

Future work will focus on studying additional model compounds which are present in raw bio-oil (e.g., furfuryl alcohol, acetic acid, isoeugenol, hydroxyacetone, etc.) with a number of different functional groups including ethers, aldehydes, ketones, alcohols, esters, and carboxylic acids. Raw biomass pyrolysis liquids will also be studied. Once catalysts and conditions are optimized in a static reactor, efforts will shift to optimizing in a flow reactor. The H_2/CO ratio will be varied. Higher

pressures (5–10 MPa), various H_2/CO ratios and higher temperatures (300–400 °C), and gas hourly space velocities will also be investigated. We have demonstrated that model bio-oil compounds can be upgraded from treatment with bio-syngas. The ultimate goal of this work would be the commercial use of catalysts and reaction conditions to upgrade raw bio-oil in a flow system utilizing bio-syngas to produce a commercial-grade liquid fuel with the required heating value, acid value, water content, and density.

Acknowledgments This material is based upon work performed through the Sustainable Energy Research Center at Mississippi State University and is supported by the US Department of Energy under award DE-FG3606GO86025 and US Department of Agriculture under award AB567370MSU.

References

Adjaye JD, Bakhshi NN (1995a) Catalytic conversion of a biomass-derived oil to fuels and chemicals I: model compound studies and reaction pathways. Biomass Bioenergy 8(3):131–149

Adjaye JD, Bakhshi NN (1995b) Production of hydrocarbons by catalytic upgrading of a fast pyrolysis bio-oil. Part I: conversion over various catalysts. Fuel Process Technol 45(3):161–183

Alonso DM, Bond JQ, Dumesic JA (2010) Catalytic conversion of biomass to biofuels. Green Chem 12(9):1493–1513

Ashworth AJ, Sadaka SS, Allen FL, Sharara MA, Keyser PD (2014) Influence of pyrolysis temperature and production conditions on switchgrass biochar for use as a soil amendment. BioResources 9(4):7622–7635, 14 pp

Boateng AA, Mullen CA, Goldberg N, Hicks KB, Jung H-JG, Lamb JFS (2008) Production of bio-oil from alfalfa stems by fluidized-bed fast pyrolysis. Ind Eng Chem Res 47(12):4115–4122

Bredenberg JBS, Huuska M, Räty J, Korpio M (1982) Hydrogenolysis and hydrocracking of the carbon-oxygen bond: I. Hydrocracking of some simple aromatic O-compounds. J Catal 77(1):242–247

Bridgwater AV (1994) Catalysis in thermal biomass conversion. Appl Catal Gen 116(1–2):5–47

Bridgwater AV (1996) Production of high grade fuels and chemicals from catalytic pyrolysis of biomass. Catal Today 29(1–4):285–295

Bridgwater AV (2003) Renewable fuels and chemicals by thermal processing of biomass. Chem Eng J 91(2–3):87–102

Bridgwater T (2006) Biomass for energy. J Sci Food Agric 86(12):1755–1768

Bridgwater AV, Peacocke GVC (1999) Fast pyrolysis processes for biomass. Renew Sustain Energy Rev 4(1):1–73

Bridgwater AV, Meier D, Radlein D (1999) An overview of fast pyrolysis of biomass. Org Geochem 30(12):1479–1493

Bridgwater AV, Czernik S, Piskorz J (2001) An overview of fast pyrolysis. Blackwell, Oxford, pp 977–997

Bykova MV, Ermakov DY, Kaichev VV, Bulavchenko OA, Saraev AA, Lebedev MY, Yakovlev VA (2012) Ni-based sol–gel catalysts as promising systems for crude bio-oil upgrading: guaiacol hydrodeoxygenation study. Appl Catal Environ 113–114:296–307

Centeno A, Laurent E, Delmon B (1995) Influence of the support of CoMo sulfide catalysts and of the addition of potassium and platinum on the catalytic performances for the hydrodeoxygenation of carbonyl, carboxyl, and guaiacol-type molecules. J Catal 154(2):288–298

Czernik S, Bridgwater AV (2004) Overview of applications of biomass fast pyrolysis oil. Energy Fuel 18(2):590–598

de Miguel Mercader F, Groeneveld MJ, Kersten SRA, Way NWJ, Schaverien CJ, Hogendoorn JA (2010) Production of advanced biofuels: co-processing of upgraded pyrolysis oil in standard refinery units. Appl Catal Environ 96(1–2):57–66

Delgado J, Aznar MP, Corella J (1997) Biomass gasification with steam in fluidized bed: effectiveness of CaO, MgO, and CaO–MgO for hot raw gas cleaning. Ind Eng Chem Res 36(5):1535–1543

Elliott DC (2007) Historical developments in hydroprocessing bio-oils. Energy Fuel 21(3):1792–1815

Elliott DC, Hart TR, Neuenschwander GG, Rotness LJ, Zacher AH (2009) Catalytic hydroprocessing of biomass fast pyrolysis bio-oil to produce hydrocarbon products. Environ Prog Sustain Energy 28(3):441–449

Ferrari M, Maggi R, Delmon B, Grange P (2001) Influences of the hydrogen sulfide partial pressure and of a nitrogen compound on the hydrodeoxygenation activity of a CoMo/Carbon catalyst. J Catal 198(1):47–55

Ferrari M, Delmon B, Grange P (2002) Influence of the impregnation order of molybdenum and cobalt in carbon-supported catalysts for hydrodeoxygenation reactions. Carbon 40(4):497–511

Fisk CA, Morgan T, Ji Y, Crocker M, Crofcheck C, Lewis SA (2009) Bio-oil upgrading over platinum catalysts using in situ generated hydrogen. Appl Catal Gen 358(2):150–156

Furimsky E (2000) Catalytic hydrodeoxygenation. Appl Catal Gen 199(2):147–190

Grange P, Laurent E, Maggi R, Centeno A, Delmon B (1996) Hydrotreatment of pyrolysis oils from biomass: reactivity of the various categories of oxygenated compounds and preliminary techno-economical study. Catal Today 29(1–4):297–301

Huber GW, Corma A (2007) Synergies between bio- and oil refineries for the production of fuels from biomass. Angew Chem Int Ed 46(38):7184–7201

Huber GW, Chheda JN, Barrett CJ, Dumesic JA (2005) Production of liquid alkanes by aqueous-phase processing of biomass-derived carbohydrates. Science 308(5727):1446–1450

Huber GW, Iborra S, Corma A (2006) Synthesis of transportation fuels from biomass: chemistry, catalysts, and engineering. Chem Rev 106(9):4044–4098

Ingram L, Mohan D, Bricka M, Steele P, Strobel D, Crocker D, Mitchell B, Mohammad J, Cantrell K, Pittman CU Jr (2007) Pyrolysis of wood and bark in an auger reactor: physical properties and chemical analysis of the produced bio-oils. Energy Fuel 22(1):614–625

Kwon KC, Mayfield H, Marolla T, Nichols B, Mashburn M (2011) Catalytic deoxygenation of liquid biomass for hydrocarbon fuels. Renew Energy 36(3):907–915

Lange J-P (2007) Lignocellulose conversion: an introduction to chemistry, process and economics. Biofuels Bioprod Biorefin 1(1):39–48

Laurent E, Delmon B (1994) Study of the hydrodeoxygenation of carbonyl, carboxylic and guaiacyl groups over sulfided CoMo/γ-Al_2O_3 and NiMo/γ-Al_2O_3 catalysts: I. Catalytic reaction schemes. Appl Catal Gen 109(1):77–96

Lin Y-C, Li C-L, Wan H-P, Lee H-T, Liu C-F (2011) Catalytic hydrodeoxygenation of guaiacol on Rh-based and sulfided CoMo and NiMo catalysts. Energy Fuel 25(3):890–896

Linstrom PJ, Mallard WG. NIST Chemistry WebBook, NIST standard reference database number 69. National Institute of Standards and Technology, Gaithersburg

Liu S, Gujar AC, Thomas P, Toghiani H, White MG (2009) Synthesis of gasoline-range hydrocarbons over Mo/HZSM-5 catalysts. Appl Catal Gen 357(1):18–25

Mallat T, Baiker A (2000) Selectivity enhancement in heterogeneous catalysis induced by reaction modifiers. Appl Catal Gen 200(1–2):3–22

Massoth FE, Politzer P, Concha MC, Murray JS, Jakowski J, Simons J (2006) Catalytic hydro deoxygenation of methyl-substituted phenols: correlations of kinetic parameters with molecular properties. J Phys Chem B 110(29):14283–14291

Matos MAR, Miranda MS, Morais VMF (2003) Thermochemical study of the methoxy- and dimethoxyphenol isomers. J Chem Eng Data 48(3):669–679

McCall MJ, Brandvold TA, Elliott DC (2012) Fuel and fuel blending components from biomass derived pyrolysis oil. Google Patents

Modak A, Deb A, Patra T, Rana S, Maity S, Maiti D (2012) A general and efficient aldehyde decarbonylation reaction by using a palladium catalyst. Chem Commun 48 (35):4253–4255

Mohan D, Pittman CU Jr, Steele PH (2006) Pyrolysis of wood/biomass for bio-oil: a critical review. Energy Fuel 20(3):848–889

Mullen CA, Boateng AA (2008) Chemical composition of bio-oils produced by fast pyrolysis of two energy crops. Energy Fuel 22(3):2104–2109

Nimmanwudipong T, Runnebaum R, Block D, Gates B (2011) Catalytic reactions of guaiacol: reaction network and evidence of oxygen removal in reactions with hydrogen. Catal Lett 141 (6):779–783

Patt J, Moon D, Phillips C, Thompson L (2000) Molybdenum carbide catalysts for water–gas shift. Catal Lett 65(4):193–195

Romero Y, Richard F, Brunet S (2010) Hydrodeoxygenation of 2-ethylphenol as a model compound of bio-crude over sulfided Mo-based catalysts: promoting effect and reaction mechanism. Appl Catal Environ 98(3–4):213–223

Shafiee S, Topal E (2009) When will fossil fuel reserves be diminished? Energy Policy 37(1):181–189

Shen ZL, Jiang XZ, Mo WM, Hu BX, Sun N (2005) Catalytic *O*-methylation of phenols with dimethyl carbonate to aryl methyl ethers using [BMIm]Cl. Green Chem 7(2):97–99

Stöcker M (2008) Biofuels and biomass-to-liquid fuels in the biorefinery: catalytic conversion of lignocellulosic biomass using porous materials. Angew Chem Int Ed 47(48):9200–9211

Sun Y, Hla SS, Duffy GJ, Cousins AJ, French D, Morpeth LD, Edwards JH, Roberts DG (2010) High temperature water–gas shift Cu catalysts supported on Ce–Al containing materials for the production of hydrogen using simulated coal-derived syngas. Catal Commun 12 (4):304–309

van Steen E, Claeys M (2008) Fischer-tropsch catalysts for the biomass-to-liquid (BTL)-process. Chem Eng Technol 31(5):655–666

Vargas A, Bürgi T, Baiker A (2004) Adsorption of activated ketones on platinum and their reactivity to hydrogenation: a DFT study. J Catal 222(2):439–449

Venderbosch RH, Prins W (2010) Fast pyrolysis technology development. Biofuels Bioprod Biorefin 4(2):178–208

Venderbosch RH, Ardiyanti AR, Wildschut J, Oasmaa A, Heeres HJ (2010) Stabilization of biomass-derived pyrolysis oils. J Chem Technol Biotechnol 85(5):674–686

Wijayapala R, Yu F, Pittman CU Jr, Mlsna TE (2014) K-promoted Mo/Co- and Mo/Ni-catalyzed Fischer–Tropsch synthesis of aromatic hydrocarbons with and without a Cu water gas shift catalyst. Appl Catal Gen 480:93–99

Wildschut J, Mahfud FH, Venderbosch RH, Heeres HJ (2009) Hydrotreatment of fast pyrolysis oil using heterogeneous noble-metal catalysts. Ind Eng Chem Res 48(23):10324–10334

Williams PT, Besler S (1996) The influence of temperature and heating rate on the slow pyrolysis of biomass. Renew Energy 7(3):233–250

Yakovlev VA, Khromova SA, Sherstyuk OV, Dundich VO, Ermakov DY, Novopashina VM, Lebedev MY, Bulavchenko O, Parmon VN (2009) Development of new catalytic systems for upgraded bio-fuels production from bio-crude-oil and biodiesel. Catal Today 144(3–4):362–366

Zhang Q, Chang J, Wang TJ, Xu Y (2006) Upgrading bio-oil over different solid catalysts. Energy Fuel 20(6):2717–2720

Zhang J, Toghiani H, Mohan D, Pittman CU Jr, Toghiani RK (2007) Product analysis and thermodynamic simulations from the pyrolysis of several biomass feedstocks. Energy Fuel 21(4):2373–2385

Zhao C, Kou Y, Lemonidou AA, Li X, Lercher JA (2009) Highly selective catalytic conversion of phenolic bio-oil to alkanes. Angew Chem 121(22):4047–4050

Biochar from Biomass: A Strategy for Carbon Dioxide Sequestration, Soil Amendment, Power Generation, and CO_2 Utilization

Vanisree Mulabagal, David A. Baah, Nosa O. Egiebor, and Wei-Yin Chen

Contents

V. Mulabagal (✉) • D.A. Baah
Department of Chemical Engineering, Tuskegee University, Tuskegee, AL, USA
e-mail: vmulabagal@mytu.tuskegee.edu; dbaah@mytu.tuskegee.edu

N.O. Egiebor
Department of Chemical Engineering and Division of Global Engagement, The University of Mississippi, Oxford, MS, USA
e-mail: negiebor@olemiss.edu

W.-Y. Chen
Department of Chemical Engineering, The University of Mississippi, Oxford, MS, USA
e-mail: cmchengs@olemiss.edu

W.-Y. Chen et al. (eds.), *Handbook of Climate Change Mitigation and Adaptation*,
DOI 10.1007/978-3-319-14409-2_80

Abstract

Biochar is a stable form of carbon produced via the pyrolysis of biomass for use in sustainable environmental and agricultural practices. The concept of biochar was originally triggered from the ancient practice in which humans deliberately mixed carbonized biomass into soils to enrich the soil quality and fertility. According to the International Biochar Initiative (IBI), biochar can be defined as "A solid material obtained from the thermo-chemical conversion of biomass in an oxygen-limited environment." Biomass-derived biochar production has been demonstrated as a potentially viable strategy for developing negative carbon emission technologies for climate change mitigation and also as a material for effective amendment of relatively poor agricultural soils. Most interestingly, ongoing biochar research work has expanded broadly, stretching from its traditional core in the environmental and agricultural science to include studies in the use of biochar for energy generation and as adsorbents for pollution treatment applications. However, the use of biochar for carbon sequestration and soil amendment has attracted more interests by research scientists globally. The use of biochar as a material for soil amendment is closely linked with its potential for climate change mitigation by carbon sequestration. Specifically, the properties of biochar include resistance to microbial degradation and chemical transformations, high surface areas, high water retention capacity, cation-exchange capacity, and its effectiveness as support and substrate for soil microbes. These characteristics endow biochar with a greater potential to become a highly useful source of materials for improving agricultural productivity through soil quality enhancement while simultaneously sequestering CO_2 from the atmosphere to mitigate climate change. On a separate front, a recent study of acoustic and photochemical interactions of CO_2 with carbonaceous materials seems to warrant feasibility research in the future for exploring novel routes of CO_2 utilization and CO_2 capture. Moreover, biochar's ability to absorb electromagnetic radiation and emit far-infrared wavelength radiation has promoted research, development, and commercialization of biochar's applications in medical and health therapies.

Introduction

For decades, significant interest has been paid to research activities on biomass-derived biochar for environmental and agricultural purposes. The key properties such as resistance to microbial degradations, chemical transformations, and preservation for geological time periods have provided recognition for biochar application as a potential strategic material for carbon sequestration and soil improvement. The concept of biochar originated from the ancient practice in which humans were deliberately

mixing burned biomass into soils to enrich the soil quality (O'Neill et al. 2009). These enriched soil deposits, known as terra preta and found in the Amazonian Basin, appear to have substantially altered soil properties and led to long-term carbon storage and crop improvement (Lehmann 2003; Lehmann et al. 2009).

Biochar, being a thermochemically derived recalcitrant carbon, has multiple definitions based on its production conditions and intended applications. The International Biochar Initiative (IBI 2012) provided a standardized definition for biochar as "A solid material obtained from the thermo-chemical conversion of biomass in an oxygen-limited environment." Lehmann and Joseph (2009) described biochar as "A carbon-rich product obtained when biomass such as wood, manure or leaves is heated in a closed container with little or unavailable air" (Lehmann and Joseph 2009), whereas two more definitions given by Shackley et al. (2012) and Verheijen et al. (2010) were "The porous carbonaceous solid produced by the thermo-chemical conversion of organic materials in an oxygen depleted atmosphere that has physicochemical properties suitable for safe and long-term storage of carbon in the environment" (Shackley et al. 2012), and "Biomass that has been pyrolyzed in a zero or low oxygen environment applied to soil at a specific site that is expected to sustainably sequester carbon and concurrently improve soil functions under current and future management, while avoiding short- and long-term detrimental effects to the wider environment as well as human and animal health"(Verheijen et al. 2010).

Biomass-derived biochar has been increasingly discussed by experts as a potential strategy for developing negative carbon emission technologies, climate change mitigation, soil quality, and food security (Lal 2004; Lehmann et al. 2009; Lehmann and Joseph 2009; Manya 2012; Paustian et al. 2000; Xu et al. 2012; Zhao et al. 2013a). To mitigate global climate change and ensure food security for a growing global population, biochar-based techniques have been extensively used for many years to improve the environment by carbon sequestration, reduce greenhouse gas emissions, and enhance soil quality and crop productivity (Laird 2008; Lehmann 2007; Lehmann et al. 2006; Sohi et al. 2010). The multiple benefits associated with biochar are shown diagrammatically in Fig. 1.

Figure 1 shows how human activities impact global climate change and this is represented in two categories and designated carbon negative and carbon positive. Carbon negative is a phrase used to describe any activity that removes more carbon or CO_2 from the atmosphere. For example, the process of photosynthesis is a classic carbon neutral phenomenon. Ultimately, the world will need to become carbon negative if the increasing buildup of atmospheric CO_2 is to be reversed. Thus, a sustainable global environmental future requires strategies to facilitate the use of energy resources that enable the reduction of concentrations of CO_2 and other greenhouse gases in the atmosphere. Low-cost and sustainable ways to achieve net negative carbon emissions from human activities involve the use of technologies such as the hydrogen fuel cell, solar and wind power, and other renewable energy sources. They are critical to achieving the net negative emission goal. On the contrary, carbon positive processes are those which add carbon to the environment. Whereas the thermochemical transformation of biomass into biochar is carbon positive with respect to the atmosphere, the addition of biochar to soil is carbon

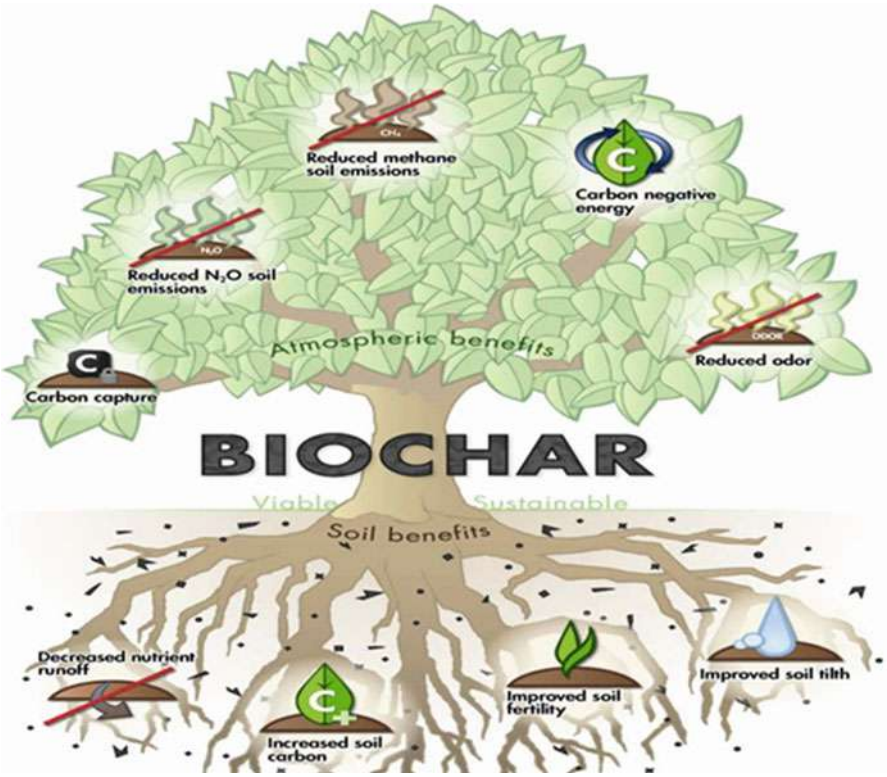

Fig. 1 Environmental and agricultural benefits associated with biochar (Source: International Biochar Initiative (IBI); http://www.biocharinternational.org/)

negative and desirable. Converting biomass carbon to biochar carbon is known to help in sequestering 50 % of the initial carbon compared to the low amounts retained after burning or normal biological decomposition. The stabilization of biomass carbon to carbonized biochar under sustainable procedures is an imperative component in a multi-phased strategy to reduce and offset GHG emissions globally. An added benefit to this solution is the potential for simultaneous enhancement in agricultural production through increased soil carbon content, improved soil fertility and soil tilth, water retention capacity, and reduced nutrient depletion. The physical properties of biochar contribute to its intrinsic multifunctional ability as a tool for environmental management. When biochar is present in the soil, its contribution to the physical nature of the system may involve significantly influencing texture, structure, porosity, and consistency through changing the bulk surface area, pore-size distribution, particle-size distribution, density, and packing. The effect of biochar on soil physical properties may then have a direct impact on plant growth because the penetration depth and availability of air and water within the root zone is determined largely by the physical makeup of soil horizon (Downie et al. 2009). In this chapter, the authors have summarized information related to biochar production

techniques, characterization methods, and its potential benefits for carbon sequestration and soil amendment purposes.

Biochar Production Pyrolysis

Pyrolysis is a thermochemical process involving conversion of organic material into a carbon rich solid (char/biochar/charcoal) and volatile materials such as gases (syngas) and liquids (bio-oil) by heating in the absence of oxygen (Demirbas and Arin 2002). The solid product obtained in pyrolysis process is known as char/biochar or charcoal and contains around half of the carbon of the original organic matter. A simple schematic representation of main products of pyrolysis is shown in Fig. 2. Pyrolysis process has been used for decades. Production of charcoal as an unintentional residue from cooking fires by Cro-Magnon man has been reported 38,000 years ago (Antal and Grønli 2003). Pyrolysis and gasification methods have been used for the production of synthetic crude oil from coal since Victorian times.

Based on the heating rate applied to the biomass in order to reach the intended pyrolysis temperature, pyrolysis is classified into slow pyrolysis and fast pyrolysis. Techniques such as intermediate pyrolysis, flash pyrolysis, and hydrothermal carbonization and gasification methods have also been employed but less frequently compared to slow and fast pyrolysis.

Slow Pyrolysis

Slow pyrolysis involves slower heating rates and longer solid and vapor residence times. The temperatures used in slow pyrolysis are typically 400 °C and the heating rate is about 5–7 °C/min. In slow pyrolysis, the yield of biochar is higher compared

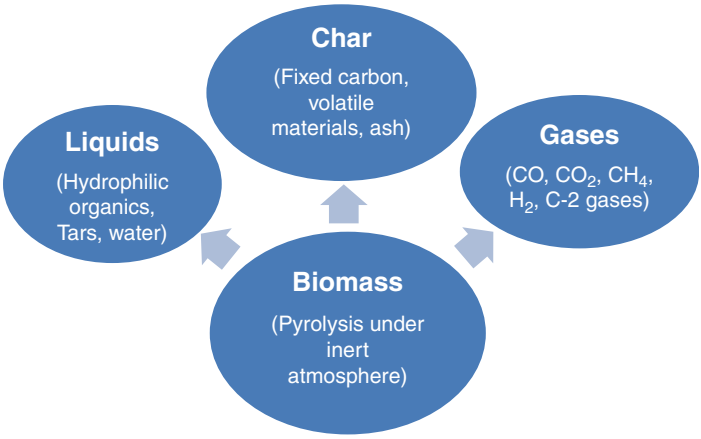

Fig. 2 Major products formed in biomass pyrolysis

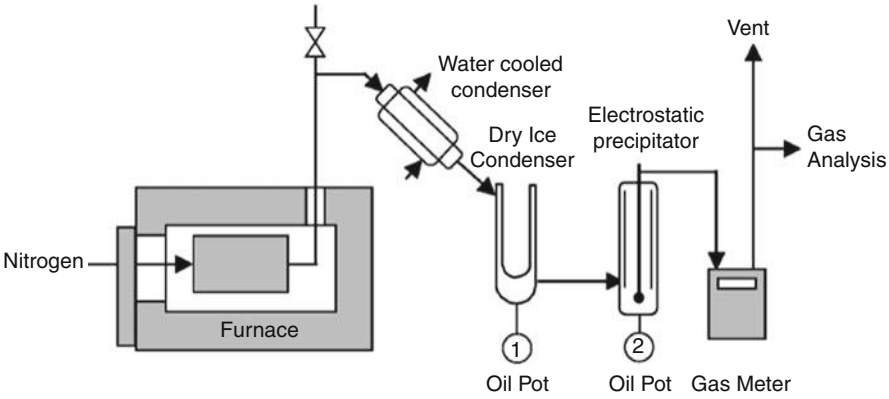

Fig. 3 Schematic representation of slow pyrolysis setup (Bridgwater et al. 2007) (Copyright © 2014 Interscience Enterprises Ltd)

to liquid and gas products formed. In the past, slow pyrolysis of biomass using pits and mounds or kilns was common practice. Bridgwater et al. (2007) demonstrated product yields and characteristics in slow pyrolysis of eucalyptus mallee, and the experimental setup reported in this study is shown in Fig. 3 (Bridgwater et al. 2007).

Fast Pyrolysis

Fast pyrolysis involves high heating rates and short vapor residence times. The pyrolysis reaction temperature applied in this process is usually around 500 °C. Fast pyrolysis requires feedstocks with smaller particle size (<2 mm) and a setup that is capable of removing vapors quickly from the presence of the hot solids. Fluid beds, stirred or moving beds, and vacuum pyrolysis system designs have been used for this application. Commercial processes using fast pyrolysis method have been reviewed and reported (Bridgwater et al. 1999; Bridgwater and Peacocke 2000). In fast pyrolysis the biomass heating rate is very rapid (>300 °C/min) and used specifically to obtain high yields of single-phase bio-oil. A fast pyrolysis experimental setup reported by Bridgwater et al. (2007) is shown in Fig. 4. Since the fast pyrolysis process yields higher concentrations of volatiles, its value for soil applications is limited. Fast pyrolysis produces 50–85 % of bio-oil, 5–25 % of solid char, and 10–20 % of gases, depending on the nature of feedstock and operating conditions.

Other Techniques

Methods such as intermediate pyrolysis, flash pyrolysis, hydrothermal carbonization, and gasification have also been reported. Intermediate pyrolysis was used in electronic waste disposal feedstock (Hornung 2013). The performance of this

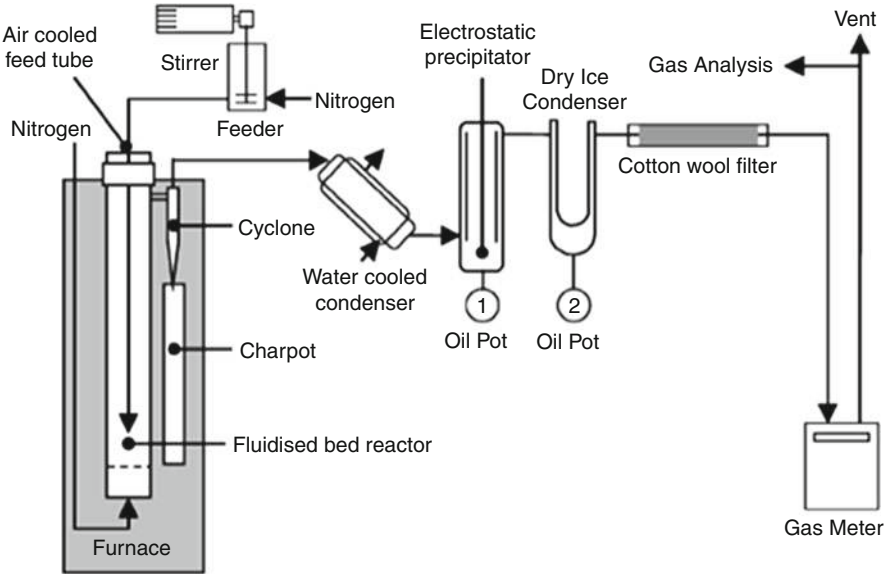

Fig. 4 Schematic representation of fast pyrolysis setup (Bridgwater et al. 2007) (Copyright © 2014 Interscience Enterprises Ltd)

method is very similar to slow pyrolysis and there is not much literature available. Flash pyrolysis methods are similar to fast pyrolysis but required higher temperatures and shorter residence times (Demirbas and Arin 2002). However, hydrothermal carbonization is used in the conversion of biomass into carbon-rich solids in water at high temperatures and pressure (Kruse et al. 2013). Since water is used in hydrothermal carbonization process, there is no need to dry feedstock prior to carbonization and it is a useful method for liquid biomass conversion. The gasification method involves partial combustion of biomass in a gas flow containing a controlled level of oxygen at high temperatures ranging from 500 °C to 800 °C. The main product in this process is syngas.

During pyrolysis, the heat transfer rate is one of the important parameters for determining the product yield and properties. According to IEA (2007), biochar product yields in slow and fast pyrolysis are 35 % and 12 %, respectively (IEA 2007). Depending on the pyrolytic conditions such as temperature, heating rate, vapor residence time, and biomass feedstock composition, the physiochemical properties and quality of biochar vary widely (Enders et al. 2012; Ronsse et al. 2013). Masiello (2004) explained that at low temperature, biochar chemical composition is closer to the original feedstock, while high temperature biochar is closer to graphite (Masiello 2004). Biochar produced at low temperature has high volatile matter and lower fixed carbon and ash contents than its high temperature counterpart (Bourke et al. 2007). Earlier studies have demonstrated that biochar with high volatile organic content contributed to nitrogen immobilization and microbial

activity reduction which negatively affected plant growth (Deenik et al. 2010; Spokas et al. 2012). Thus, it is clear that improving the yield of biochar for carbon sequestration and agricultural purposes has been associated with slow pyrolysis in which production gas and liquid co-products will be reduced (Angın 2013; Crombie et al. 2013; Demiral and Ayan 2011; Demirbas 2004; Hossain et al. 2011; Manya 2012; Mašek et al. 2013; Ronsse et al. 2013). Prior to use, a key step involves the evaluation of biochar characteristics that are responsible for its quality and efficacy for the intended application. The details of various biochar characterization methods have been summarized.

Biochar Characterization

The physicochemical properties and composition of the feed biomass are a function of the content of cellulose, hemicellulose, lignin, and extractives. Once the biochar is produced, determining key characteristics using relevant analytical techniques enable the understanding of the potential of the biochar product for proposed applications. Especially the temperature used in the pyrolysis process has shown an impact on both biochar production distribution and the nature of biochar (Kim et al. 2010; Méndez et al. 2013). When the pyrolysis temperature is higher, less biochar is generated and the microstructure develops more effectively. If the temperature is too high, the loss of carbon and other functional group elements on the surface is excessive. The chemical composition, pH, surface charge, and thermal stability of biochar, as well as the heavy metal fate in the biochar body, are also functions of pyrolysis temperature. The information obtained by physicochemical characterization of biochar may help understand the environmental and agronomic functions and facilitates production of desired biochar which offers specified benefits. Properties such as bulk density, elemental composition (ultimate analysis), pH, proximate analysis, and surface properties will help in assessing the biochar quality (Okimori et al. 2003). The details of analytical methods used to characterize biochar properties have been summarized.

Bulk Density

Since the solid density of biochar is directly related to its mechanical strength, it can be used to estimate the biochar's relative ability to withstand wear and tear during soil applications. Generally, the biochar has a higher density than the biomass feedstock from which it was derived. Bulk density is defined as weight per unit volume of material and expressed in kilograms per cubic meter (kg/m^3). Bulk density of biochar is measured by adding a known amount of mass into a container of known volume. Generally, biochar bulk density is around 0.2–0.5 g/cm^3 (Brewer et al. 2014; Özçimen and Karaosmanoğlu 2004).

Elemental Composition

Elemental analysis is generally performed by combusting biochar under excess oxygen using an Elemental Analyzer (EA). This analysis includes quantitative estimation of carbon, hydrogen, nitrogen, sulfur, and oxygen. Also, elemental ratios of C:O, O:H, and C:H are reported as reliable methods to measure the extent of pyrolysis of biochar (Cheng et al. 2008; Kuzyakov et al. 2009). Chan and Xu (2009) reported that during pyrolysis, biomass carbonizes to yield biochar which is highly recalcitrant in nature and has a potential impact on soil health and productivity (Chan and Xu 2009). Thus, quantification of elemental components and their ratios of biochar samples are very important to assess their quality as they may influence soil properties.

pH

Measuring pH is crucial to choose the right char for soil applications depending on the soil nature. The simplest way to measure pH is to make a char and water slurry and use a standard laboratory pH meter. Biochar pH is known to be neutral to basic.

Functional Group Analysis

Qualitatively, Fourier transform infrared spectroscopy (FTIR) is frequently used to detect functional groups in biochar samples. The information is helpful in comparing biochar samples produced under different conditions. Some of the selective stretching group frequencies of biochar samples in IR spectra include O-H (3,400 cm^{-1}), aliphatic C-H (3,000–2,860 cm^{-1}), aromatic C-H (3,060 cm^{-1}), and the carbonyl (C = O) (1,700 cm^{-1}) functionalities.

Proximate Analysis

Proximate analysis of biochar includes parameters like volatile organic compounds (VOCs), moisture content, ash content, and fixed carbon. Biochar VOCs are formed during pyrolysis by breakdown or rearrangement of chemical structures present in biomass feedstock. Biochar VOCs have greater impact on plant and microbial responses to biochar amendments because they are known to inhibit/stimulate microbial and plant processes (Baldwin et al. 2006; Klinke et al. 2004). Analyzing VOC content in biochar prior to soil amendment may avoid adverse agronomic effects. Analytical methods such as pyrolysis-gas chromatography/mass spectrometry (pyr-GC/MS) methods have been developed for VOC analysis in biochar samples (Clough et al. 2010; Galipo et al. 1998; Spokas et al. 2011). Thermogravimetric analysis (TGA) has been used routinely to determine the moisture content,

volatiles, percentage of fixed carbon, and ash content in biochar samples (Garcia et al. 2013; Kim et al. 2010; Kim and Agblevor 2007; Ottaway 1982; Slaghuis and Raijmakers 2004).

Surface Property Characterization

The surface area characteristic is expressed in the extent of porosity of the biochar which in turn depends on the cell structure of the starting materials. The best-known and most commonly used method for evaluating specific surface areas of biochar materials is the Brunauer-Emmett-Teller (BET) nitrogen physisorption method. For example, if feedstock has larger pore sizes, it can yield biochar with larger surface area resulting in greater nutrient retention properties. These larger pores can also enhance microbial activity (Warnock et al. 2007). In addition, scanning electron microscopy (SEM) has been used for studying the morphology of biochar materials. SEM analysis helps in obtaining details about pore structure and their distribution among the biochar produced under different pyrolysis conditions and from different biomass sources (Fang et al. 2013; Özçimen and Karaosmanoğlu 2004; Shaaban et al. 2013). Figure 5 shows SEM images of biochar produced from wood sources (Fig. 5a), sugarcane bagasse (Fig. 5b), and goat droppings (Fig. 5c) and pyrolyzed at 550 °C. Different physical microstructural property is represented in these images. The macroporous structures in wood derived biochar are arranged in an array of parallel domains, whereas that for the sugarcane bagasse is expressed in a radial distribution. Biochar from goat dropping may only be microporous.

Other analytical instruments used to determine biochar properties include X–ray photoelectron spectroscopy (XPS), energy dispersive X-ray spectroscopy (EDX), near-edge X-ray absorption fine structure (NEXAFS) spectroscopy, nuclear magnetic resonance (NMR) spectroscopy, gas chromatography/mass spectrometry (GC/MS), and total organic carbon (TOC) analyzer (Chintala et al. 2012; Fernandes and Brooks 2003; Keiluweit et al. 2010; Lee et al. 2010; Moon et al. 2013; Srinivasan and Sarmah 2014). Studies on characterization of biochar properties have been respired in the literature (Abdel-Fattah et al. 2014 ; Ahmad et al. 2014; Brewer et al. 2014; Chia et al. 2014; Hmid et al. 2014; Jindo et al. 2012; Liu et al. 2014; Mimmo et al. 2014; Novak et al. 2009; Pujol et al. 2013; Rajkovich et al. 2012; Shaaban et al. 2013; Stanger et al. 2013; Zhao et al. 2013b). Overall, detailed characterization of biochar samples provides valuable information useful in understanding the environmental and agronomic efficacy of biochar samples in depth.

Biochar Benefits: Carbon Sequestration

For the past few decades, CO_2 emissions in the atmosphere have been increasing significantly each year. It has been estimated that each year approximately 2 Gt of carbon is set free as CO_2 in response to deforestation and degradation of soils.

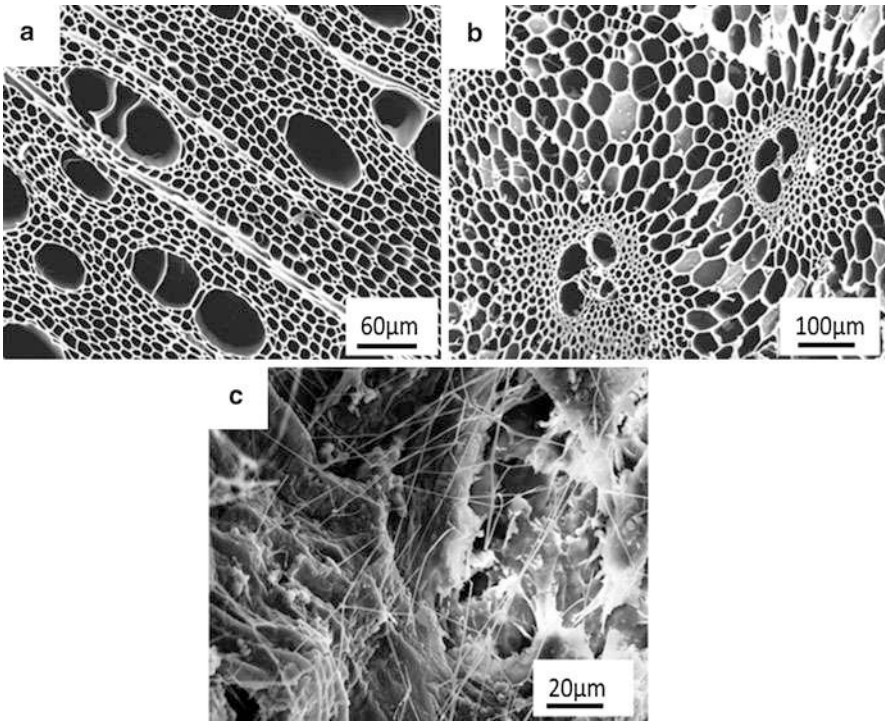

Fig. 5 Scanning electron microscope (SEM) images showing macroporosity of a wood-derived (**a**), sugarcane bagasse (**b**), and goat dropping (**c**) biochar produced by slow pyrolysis: The biochar samples were gold coated and imaged with beam energy of 20 kV on a Zeiss EVO 50VP SEM

The US Department of Energy (USDOE) has estimated that by 2020 the global, annual net production of CO_2 will be 33.8 billion metric tons (USDOE 2010). Energy sources, fires, deforestation, and soil degradation activities have been contributing to increasing the levels of CO_2 emissions into the atmosphere. Since CO_2 is the foremost greenhouse gas (GHG), its enrichment in the atmosphere triggers an increase in atmospheric temperature and ultimately results in global climate change. Researchers have been looking for potential strategies to mitigate climate change by either reducing greenhouse gas emissions or by carbon sequestration, e.g., in aboveground soils. In the past, the Intergovernmental Panel on Climate Change (IPCC) has listed several climate change mitigation options: (1) carbon capture and storage, (2) energy efficiency, (3) switch to low-carbon fuels, (4) nuclear power, (5) renewable energy, (6) enhancement of biological sinks, and (7) reduction of non-CO_2 greenhouse gas emissions (IPCC 2005). Among these options enhancing biological sinks and carbon capture and storage can balance CO_2 in the atmosphere. But again carbon capture and storage concept is associated with high energy consumption generating additional emissions associated with carbon capture. However, the other mitigation approaches are only

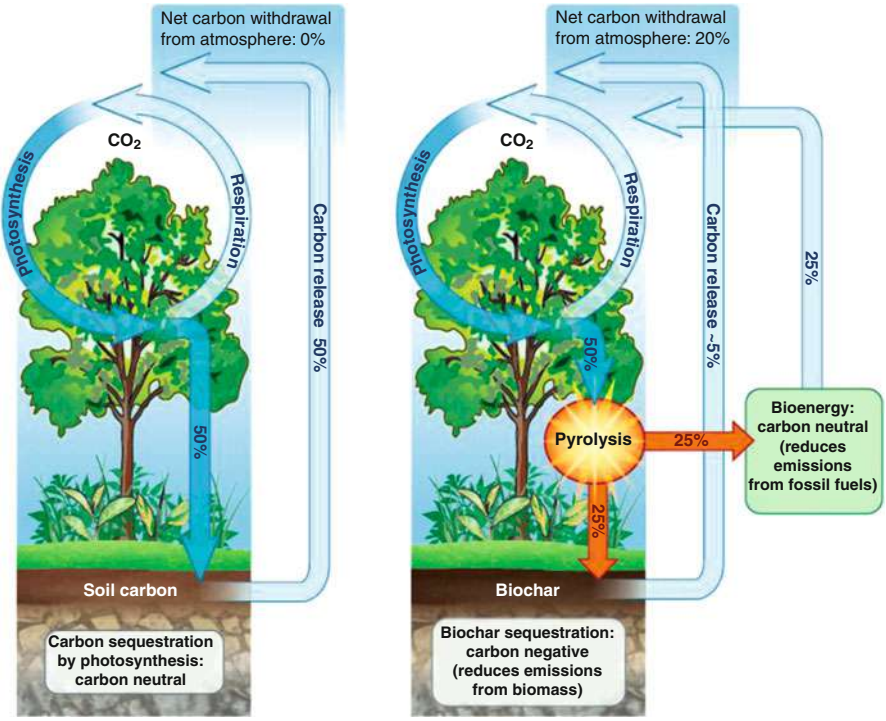

Fig. 6 Illustration of normal and biochar-based carbon cycles (Lehmann 2007) (Copyright © 2007 Nature Publishing Group)

preventive or controlling measures. The carbon cycle function in natural and biochar-based scenarios is shown in Fig. 6. In the case of normal cycle, plants absorb atmospheric carbon dioxide as part of the biological carbon cycle but they are inadequate to handle huge amounts of carbon dioxide released in the atmosphere. So the net carbon withdrawal by the natural carbon cycle from the atmosphere is zero. In addition, plants decay and this biomass releases captured carbon dioxide into the atmosphere. If this biomass is converted into biochar and used to amend soil, the net carbon withdrawal from the atmosphere is 20 % as shown in Fig. 6. Additionally, biochar-based carbon cycle can reduce emissions by 12–84 % and offers the opportunity to convert bio-energy into a carbon-negative strategy (Lehmann 2007).

During the biomass pyrolysis, bio-oil, biochar, and syngas are the three main products. These products can influence the global carbon cycle in the following ways. All the main products obtained during pyrolysis can be used as energy sources which can reduce fossil energy use. In general, biomass decomposition can release a significant amount of carbon dioxide into the atmosphere. By pyrolyzing the biomass, the biochar with enriched stable carbon is produced and will remove carbon

dioxide from the atmosphere that would otherwise be released into the atmosphere through bacterial decomposition in the soil. This biochar added into soil becomes a carbon sink and long-term carbon storage.

Biochar carbon sequestration is fundamentally different from other forms of carbon sequestration. It refers to the capture and subsequent storage of carbon to prevent it from being released into the atmosphere (Duku et al. 2011). The primary effect of biochar production on greenhouse gas fluxes is the avoidance of emissions that would have occurred had the biomass been left to decompose. For example, biochar from herbaceous and woody feedstock sources is found to have a carbon content of 60.5–66.7 % and 74.5–80 %, respectively. One can assume from these figures that for every ton of biochar applied to the soil, 0.61–0.80 t of carbon (equivalent to 2.2–2.93 t of CO_2) can be sequestered (Galinato et al. 2011). Using the highest carbon content of the wood-based biochar (i.e., 80 %) and the CO_2 offset price range of $1 to $31/MT CO_2 (West and McBride 2005), the approximate value of biochar carbon sequestration is $2.93–$90.83/MT biochar. Biochar carbon sequestration might avoid difficulties such as accurate monitoring of soil carbon due to spatial and temporal variation which are the main barriers to inclusion of agricultural soil management in emissions trading. Using the turnover rate and the quantity of carbon has been suggested as a method to be used in assessment of the carbon sequestration potential and that could be done independently from biochar use as soil amendment or other non-fuel purposes.

Biochar Benefits: Soil Amendment

Since biochar is produced from waste biomass such as crop residues, manures, timber and forestry residues, and green waste, its use as a soil amendment has been suggested as a sustainable approach in achieving soil fertility and enhanced crop productivity along with other environmental benefits (Chan et al. 2007). In the past, highly fertile carbon-rich terra preta soils in Central Amazonia are widely cited as evidence that charcoal addition to soils brings benefits to the soils (Lehmann 2003). Due to the increasing recognition for the potential of the terra preta as a model for modern agriculture, the use of biomass-derived biochar has raised a lot of research and development interests (Lehmann 2003; Lehmann et al. 2009). Biochar soil amendment becomes a practice to improve soil fertility and crop productivity while maintaining high levels of soil carbon (Ibrahim et al. 2013; Lehmann et al. 2011). Biomass-derived biochar has been proposed as a potential strategy to enhance soil fertility and crop productivity that can boost food security. Studies have shown that the application of biochar to soil enhances soil fertility by increasing the soil cation-exchange and water retention capacities as well as microbial activity, thereby improving agricultural productivity (Lehmann 2007; Lehmann and Rondon 2006).

Enhanced Soil Fertility and Crop Productivity

Effect of Biochar pH and Surface Properties on Nutrient Availability and Cation-Exchange Capacity (CEC)

Once biochar was amended into soil, it exists as soil aggregates rather than free organic matter, thus making up the overall structure of the soil (Liang et al. 2008). According to Sohi, the soil texture and chemistry can be modified based on biochar's pH and surface properties (Sohi 2012). Also, the chemically active biochar surface properties change soil nutrient dynamics and can act as a catalyst for soil functions. A statistical meta-analysis undertaken by Jeffery et al. (2011) to evaluate the relationship between the application of biochar and crop productivity showed an overall small, but statistically significant benefit of biochar application to soils on crop productivity. Even though the grand mean increase is 10 %, the mean results for each analysis performed within the meta-analysis covered a wide range (from −28 % to 39 %) with the greatest (positive) effects with regard to soil analyses being observed in acidic (14 %) and neutral pH soils (13 %) and in soils with a coarse (10 %) or medium texture (13 %). This observation suggests that two of the main mechanisms for yield increase may be a liming effect and an improved water holding capacity of the soil, along with improved crop nutrient availability (Jeffery et al. 2011). Generally, biochar pH values are neutral to basic ranging from pH 6.2 to 9.6 (Chan and Xu 2009). Effects of biochar on soil chemistry appear to arise from modification of soil pH. In the case of acidic soil, there is a reduction in cation-exchange capacity (CEC) and nutrient availability observed with lower pH values. In addition to the nature of the feedstock, a significant importance to biochar properties is the temperature of production. The production temperature influences properties such as the biochar surface chemical characteristics (pH), bulk surface area, and carbon content. Although it has been argued that other factors such as soil type, soil chemistry, organic matter content, and climate may be of greater importance to the agricultural impact of biochar incorporation, the importance of production temperature cannot be overlooked (Mukome et al. 2013). Typically, there is little or no cation-exchange capacity of soil organic matter at very low pH, but this increases with higher pH, and biochar is no exception. However, the point at which the CEC (cation-exchange capacity) of biochar is zero (point of zero charge, pzc) is dependent on the production temperature. It is seen from Fig. 7 that both pH and surface area of biochar appear to increase with production temperature, as carbon yield decreases and so the optimum temperature is probably within the range of 450–550 °C.

CEC is a measure of the surface charge in a soil or a biochar and refers to the ability of a soil/biochar to hold onto nutrients. The benefits for soil work both ways as it will absorb nutrients and prevent leaching yet release the nutrients when required by plants. The level of CEC of biochar gives an indication of the abundance of negatively charged sites on the biochar which can retain exchangeable cations that are essential plant macronutrients, e.g., NH_4^+ and Ca^{2+} (Carrier et al. 2012). For example, Lehmann (2003) demonstrated that biochar reduced leaching of NH_4^+, maintaining it in the surface soil where it is available for plant uptake. The production of a partially oxygenated biochar that possesses enhanced cation-exchanging

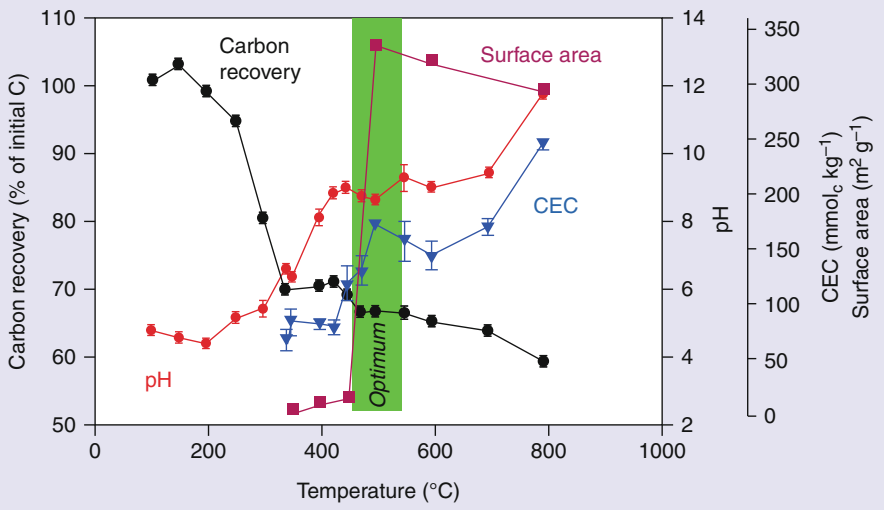

Fig. 7 The impact of temperature on biochar properties. Temperature effects on carbon recovery, cation-exchange capacity (measured at pH 7), pH, and surface area are shown here (Lehmann 2007) (Copyright © 2007 Ecological Society of America)

property by reaction of the biochar source with oxygenating compounds such that the biochar homogeneously acquires oxygen-containing cation-exchanging groups has been reported with oxygenated biochar possessing CEC of at least 140 mmol/kg (Lee et al. 2011, 2013). This concept is based on the experimental finding that the O:C atomic ratio in biochar material correlates with its cation-exchange capacity. Along with aging, the CEC capability increases as evidenced in the terra preta soils of the Amazon (Glaser et al. 2002). Charges on the high surface area can increase cation-exchange capacity (CEC), thereby increasing a soil's ability to retain and supply nutrients. It is well known that both organic and mineral fractions of soil contribute to cation-exchange capacity. The cation-exchange capacity controls the flush of ammonium ions after fertilizer application and mineralization of soil organic matter. This mineralization of organic matter helps in mitigating loss of nitrate leaching. Ash content, phosphorus, potassium and other trace elements present in biochar may impact on crop growth (Steiner et al. 2007).

It is important to note that even though the CEC of biochar is hampered at the pzc, the biochar surface is still available for sorption interactions with other chemical species through hydrogen bonding. For example, the hydrophobic surface of wood-derived biochar has been demonstrated to enhance perchlorate adsorption via H-bonding to oxygen containing groups on the biochar surface (Fang et al. 2013). The principle is illustrated in the schematic in Fig. 8. The totally hydrophilic aliphatic biomass surface (which is unreceptive to ClO_4^- anion) when subjected to pyrolysis and transformed into biochar acquires an aromatic hydrophobic nature. The newly created hydrophobic surface interacts through H-bonding with the ClO_4^- anion. Fang et al. (2013) suggested that it is possible to tune the sorption properties

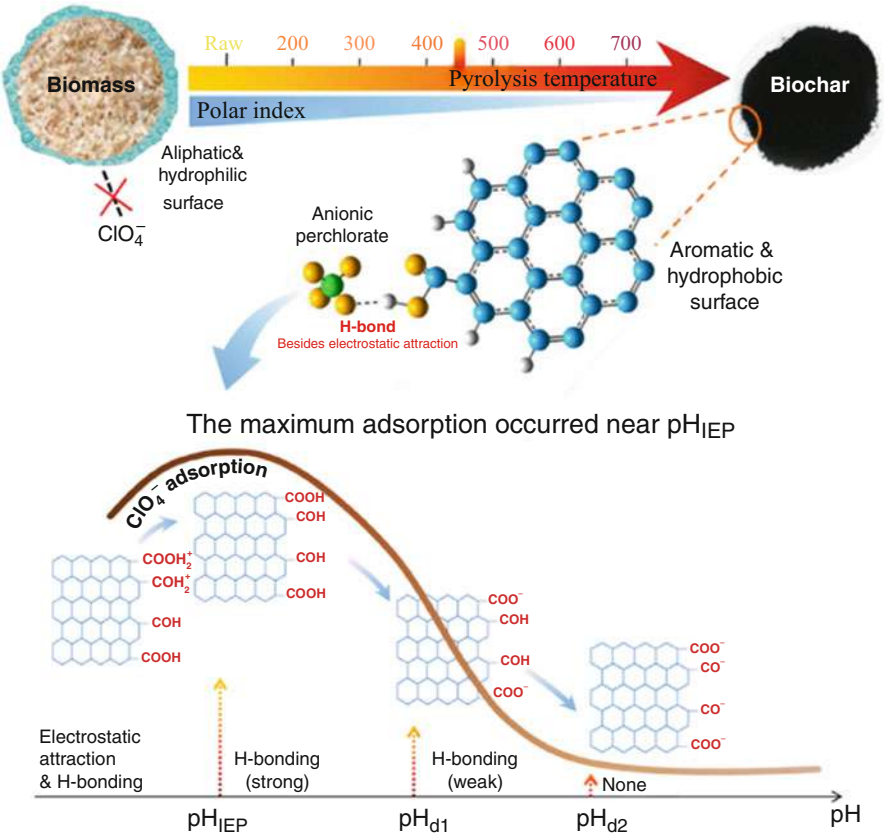

Fig. 8 The schematic of pH-dependent perchlorate (ClO_4^-) adsorption mechanisms onto high temperature biochar with different structural properties and surface functional groups. The maximum adsorption occurred at the point of zero surface charge (Fang et al. 2013) (Copyright © 2013 American Chemical Society. IEP = isoelectric point; d1 =; d2 =)

of biochar by changing the solution pH and concluded that the maximum adsorption interaction occurs at the point of zero charge. The surface area of biochar has a significant impact on the magnitude of interactions between biochar and the soil environment. The surface properties of biochar derived from biomass is crucial in understanding water retention, nutrient retention, sorption capability, and microbial activity of biochar (Day et al. 2005; Fernandes and Brooks 2003; Yu et al. 2006).

Habitat for Microbial Activity

Biochar addition to soil has been shown to increase microbial activity as well as microbial efficiency. In fact, enhanced microbial activity influences the nutrient availability, moisture retention, and cation-exchange capacity (CEC) and is associated with plant growth. Due to porous nature, biochar has been shown to improve soil microorganism abundance and cause effects on nutrient cycle and soil structure

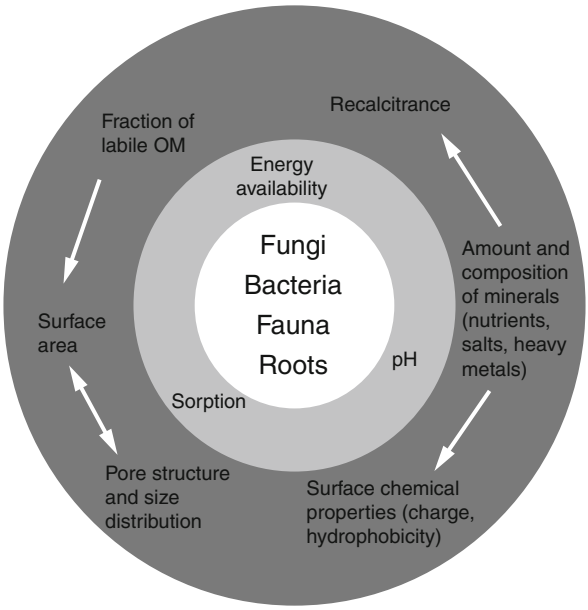

Fig. 9 A schematic overview of correlation between biochar properties and soil microbial community: outer circle represents biochar properties; intermediate circle denotes soil process which influences the microbial community, whereas inner circle shows a qualitative estimation of the strength of the connection. White arrows indicate influence between biochar properties (Lehmann et al. 2011) (Copyright © 2011 Elsevier Ltd. OM =)

that leads to soil growth (Grossman et al. 2010; O'Neill et al. 2009; Pietikäinen et al. 2000; Rutigliano et al. 2014). This scenario has been evidenced further in terra preta soils of the Amazonian Basin (Atkinson et al. 2010). Various biochar properties that influence the soil microbial community and relation between biochar properties and soil microbial community have been documented (Lehmann et al. 2011). The proposed correlation between biochar properties and soil microbial community reported by Lehmann et al. 2011 is illustrated in Fig. 9. Substantial research evidence documenting stimulation of indigenous arbuscular mycorrhizal fungi by biochar has positive impact on plant growth due to increase in nutrient availability, moisture retention, and cation-exchange capacity (Rondon et al. 2007; Warnock et al. 2007). Biochar has demonstrated its function as soil conditioner by making nutrients available to plants and improving soil structure. The surface area and pore structure properties of biochar can increase soil water holding capacity, and the micro-pore spaces with positively charged surfaces can improve soil water retention and in turn reduce nutrient loss through leaching (Lehmann and Joseph 2009; Verheijen et al. 2010). In addition to the chemical stabilization of nutrients, modification of the physical structure of the bulk soil may result in biochar not simply increasing the capacity of soil to retain water, but also nutrients in soil solution. CEC of biochar may be due to leaching of hydrophobic compounds from biochar or by increasing carboxylation of carbon through abiotic oxidation (Cheng et al. 2006).

Mobility and Bioavailability of Heavy Metals

Growing human activities and industrial revolution have resulted in the concentration of metal such as cadmium (Cd), copper (Cu), and lead (Pb) in contaminated

soils. These heavy metals may have negative consequences on agricultural productivity and human health. Thus, in contaminated soils, heavy metals such as Cd, Cu, and Pb and their mobility and bioavailability are of agricultural and environmental concern. Biochar soil amendment has been considered to be an alternative remediation method to not only promote plant growth but also reduce the mobility of metals in contaminated soil (Beesley et al. 2010, 2014; Houben et al. 2013; Uchimiya et al. 2011b). Several studies have demonstrated that biochar soil amendment was successful in retaining these heavy metals in contaminated soils (Clemente et al. 2010; Tang et al. 2013; Uchimiya et al. 2010, 2011a). The presence of various functional groups and the highly porous nature of biochar have demonstrated it to be very effective in the adsorption of heavy metals. The pH of biochar also plays an important role in controlling the mobility of heavy metals. Studies have explained that an increase in pH and CEC affects the metal immobilization process (Beesley et al. 2011; Uchimiya et al. 2011a). Therefore, biochar has been considered a potential amendment for promoting the establishment of a plant cover and phytostabilization strategies on contaminated soils (Beesley et al. 2011).

Pesticide Sorption

Biochar is considered as a universal sorbent. Compared to natural soil, biochar-amended soil has greater sorption ability due to its large surface area and charge density (Liang et al. 2006). Application of biochar as sorbent is a cost-effective approach and has shown strong affinity for organic contaminants (Yang and Sheng 2003; Yu et al. 2010). The usage of pesticides in agricultural practice poses a potential risk of groundwater pollution. These environmental contaminants have been monitored in groundwater. Based on solubility and dissipation behavior in soil, these contaminants may represent elevated risk of leaching. This leaching process is affected by sorption and desorption behaviors in soil. Biochar works as a super sorbent and decreases the leaching potential of these contaminants in soils which further helps to mitigate groundwater contamination (Ahmad et al. 2014; Guo et al. 2006; Loganathan et al. 2009). The mechanism for the sorption characteristic of biochar has been proposed by Ahmad et al. (2014) and the details have been illustrated in Fig. 10.

The large surface area (1,000 m^2/g), micro-, meso-, and macro-porosity, diverse surface and bulk properties of biochar has imparted to it different sorption properties of biochar (Downie et al. 2009). It is unsurprising that the presence of biochar in soil plays an influential role in the sorption properties of soil. The application of biochar to the sorption or removal of organic and inorganic pollutants has been tested using four theoretical isotherm models, namely, Langmuir, Freundlich, Dubinin-Radushkevich, and Temkin models (Zhang et al. 2011). The Langmuir model is described by the following equation:

$$\frac{C_e}{q_e} = \frac{1}{Q_0 K_L} + \left(\frac{1}{Q_0}\right) C_e \tag{1}$$

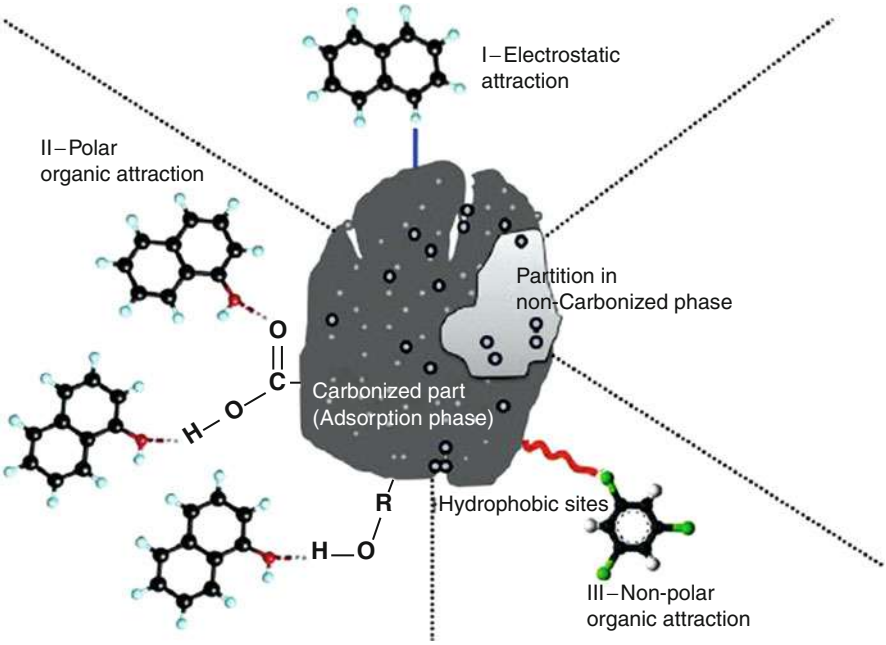

Fig. 10 Biochar interaction with organic contaminants: Electrostatic attraction between biochar and organic contaminant (I), polar organic contaminant (II), and non-polar organic contaminant (III). (Ahmad et al. 2014) (Copyright © 2014 Elsevier Ltd)

where q_e and C_e are, respectively, the amount adsorbed per gram of adsorbent (mg/g) and the solute concentration in solution (mg/l) at equilibrium and Q_0 and K_L are constants related to the maximum adsorption capacity (mg/g) and the intensity of adsorption(l/mg), respectively. An essential characteristic of the Langmuir isotherm is explained in terms of the dimensionless separation factor (R_L) defined by the equation

$$R_L = \frac{1}{1 + K_L C_i} \tag{2}$$

where C_i is the initial concentration.

The Freundlich's model is described by the equation

$$In\, q_e = In\, K_F + \left(\frac{1}{n}\right) In\, C_e \tag{3}$$

where K_F (mg/g) is the adsorption capacity of the adsorbent and n gives an indication of how favorable the adsorption process is.

The Dublin-Radushkevich equation has a linear representation of the form

$$In\ q_e = In\ Q_0 - K_{DR}\ \varepsilon^2 \tag{4}$$

where K_{DR} (mol^2/K^2) is a constant related to the mean adsorption energy and ε is the Polanyi potential which can be calculated from the equation

$$\varepsilon = RT\ In\left(1 + \frac{1}{C_e}\right) \tag{5}$$

A plot of In q_e versus ε^2 gives K_{DR} as the slope and Q_0 and the intercept.

The Temkin equation is also given in a linear form as

$$q_e = B_T\ InK_T + B_T\ InC_e \tag{6}$$

where $B_T = RT/b_T$, the constant b_T is related to the heat of adsorption, and K_T is the equilibrium binding constant corresponding to the maximum binding energy.

The Langmuir and Freundlich models have been most commonly used to describe adsorption isotherms. These adsorption isotherms describe the relation between the adsorbate loading on the adsorbent (Q_e) and the liquid-phase concentration of the adsorbate (C_e) at equilibrium conditions. The Langmuir model corresponds to the homogeneous monolayer adsorption, whereas the Freundlich model defines the adsorption onto adsorbents with heterogeneous surface (Yang et al. 2014). Additionally, the dynamics of an adsorption process in terms of the order and the rate constants has been evaluated using the pseudo-second-order kinetic equation given as

$$\frac{t}{Q_t} = \frac{1}{K_2 Q_{\max}^2} + \frac{1}{Q_{\max}} t \tag{7}$$

$$Q_t = K_w\ t^{1/2} + I\ (\text{Weber} - \text{Morris model}) \tag{8}$$

where $Q_{\max}$ and Q_t are the adsorption capacities (mg/g) at the equilibrium and at time t, respectively; K_2 and K_w are the constants of pseudo-second-order and the Weber-Morris model, respectively; and I is the intercept (Yang et al. 2013, 2014). The units of K_2 and K_w are g/(mg. min) and (mg/g).$min^{-1(½)}$, respectively.

Altering Nitrous Oxide (N_2O) Emissions

Global nitrous oxide (N_2O) emissions mainly originate from soil due to the extensive use of nitrogen (N) fertilizers in agriculture. N_2O is one of the potent greenhouse gases (GHG) released into the atmosphere from both natural (about 60 %) and anthropogenic sources (approximately 40 %), and its atmospheric concentration in 2013 was about 325.9 parts per billion. Its estimated impact on climate is 298 times greater than equal emissions of carbon dioxide, over a period of 100 years. Biochar

addition to soils reduces nitrous oxide (N_2O) emissions by slowing down the nitrogen cycle, possibly as results of an increase in the carbon/nitrogen ratio (Ussiri et al. 2009). Further, crop productivity enhancement is possible with biochar amendment with no or minimal fertilizers, which helps in mitigating other greenhouse gas emissions from soil and on indirect emissions. Irrigation costs can be reduced by biochar amendment.

Emerging Applications in Power Generation

Scientific Background

With the goals of developing novel CO_2 capture and utilization technologies, a recent study by Chen et al. (2014) used biochar as a substrate in their study of CO_2 reactions with carbonaceous materials at temperatures below 100 °C. Their study synthesized scientific observations and principles from disparate fields: chemically and photochemically induced CO_2 fixation on carbon, acoustic physics and chemistry, structural characteristics of biochar, and solvent-induced swelling of carbonaceous materials. Each of these strands will be described below. The relevant hypotheses, tests of these hypotheses, and technological implications are discussed in later sections.

Chemically and Photochemically Induced CO_2 Fixation on Carbon

At the outset of their efforts, Chen et al. (2014) sought new CO_2 fixation processes, such as the Kolbe-Schmitt reaction R1 below (Kolbe 1860; Schmitt 1885; Lindsey and Jeskey 1957) that could represent the initial steps for viable CO_2 utilization and capture.

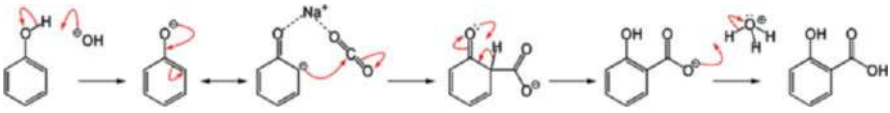

(*R*1)

The reverse reaction of R1, i.e., the desorption of CO_2, has a desorption energy of 24–29 kJ per mole of CO_2 (Dewar et al. 1988; Bonneau-Gubelmann et al. 1996) which is within the range for the CO_2 desorption by amines that has been considered the most viable means of CO_2 capture and desorption. The hydroxyl groups can also be functionalized by amine through a linker such as sulfonic acid. Since the synthesis procedure is designed mainly for CO_2 capture (Brunelli et al. 2012) but not directly for CO_2 utilization or reuse, no detailed discussion is given here.

While reaction R1 might be considered for CO_2 capture, the resultant product is expected to have a lower heating value than the reactant phenol, so the reaction cannot be considered as a major CO_2 recycle route for fuel production. On the other

hand, photochemical or photocatalytic CO_2 fixation, recently reviewed by Kumar et al. (2012) and by Izumi (2013), could add heating value through reductive photocarboxylation, in which the aromatic structures are also reduced by the addition of hydrogen. This was first accomplished by Tazuke et al. (1975, 1986) by Hg-lamp irradiation of a solution of an aromatic hydrocarbon and CO_2 in the presence of an electron donor (*N*,*N*-dimethylaniline, DMA) and a hydrogen atom donor (dimethylformamide, DMF). Instead of using a liquid solvent, Chateauneuf et al. (2002) used supercritical CO_2 in their reductive photocarboxylations. The reaction equilibrium favors carboxylated product under high CO_2 pressure. Nearly complete conversion of anthracene was observed at 35 °C and 2,000 psi, with DMA as the electron donor and 2-propanol as the hydrogen atom donor. About 57 % of the product was dihydrocarboxylic acid. This carboxylation reaction can be stated as

$$\begin{aligned} \mathrm{PAH} + \mathrm{h}\nu \rightarrow \mathrm{PAH}^{*} + \mathrm{DMA} \rightarrow \mathrm{PAH}^{\bullet -} + \mathrm{CO_2} \\ \rightarrow \mathrm{PAH}^{\bullet} - \mathrm{CO_2}^{-} + \mathrm{iPrOH} \rightarrow \mathrm{H-PAH-CO_2}^{-} \end{aligned} \qquad \text{(R2)}$$

The key to the remarkably high conversion of anthracene rests on the role of the electron donor in forming the reaction intermediate $PAH^{\bullet -}$, a charged free radical, by electron transfer to the photochemically excited PAH*.

The thermal carboxylation of phenolic PAHs R1 and reductive photochemical carboxylation R2 of PAHs promoted the authors' interests in fixing CO_2 on naturally available carbonaceous materials. These CO_2 fixation reactions could serve as a major step for CO_2 capture and CO_2 utilization. Due to the reductive nature of the photochemical R2, the resultant product should have higher heating value than the reactant PAH, and thus the CO_2 is recycled to an energy source in a cradle-to-cradle carbon cycle. The process would be most attractive if the carbonaceous material were a renewable biomass, as will be described below.

Sonochemical and Sonophysical Effects

Acoustic cavitation consists of at least three distinct, successive stages: nucleation, bubble growth, and implosive collapse (Ince et al. 2001). During the collapse stage, the energy released is so extreme that trapped gases undergo molecular fragmentation, which is the underlying phenomenon in homogeneous sonochemistry. This collapse is accompanied by the emission of light, or sonoluminescence (SL) (Suslick and Flannigan 2008). Spectroscopic analyses of SL reveal that the temperature and pressure can reach 20,000 K and several thousand bar, respectively (Suslick and Flannigan 2008). Water splits during the bubble-collapse stage, and the formation of oxygen, hydroxyl, and peroxyl radicals is attractive for oxidizing organic waste in water and for the oxidative desulfurization of fuels (Mason 1990). Strongly reducing protons also form during water splitting.

Sonication has been widely adopted to enhance mixing and reduce mass transfer limitations in liquid/solid interactions. Ultrasound is also capable of leaching fine minerals such as K, Na, S, Cl, P, Mg, Ca, Fe, and Al, from porous carbonaceous materials (Ahmed et al. 2004). As a result of mineral leaching, the internal surface

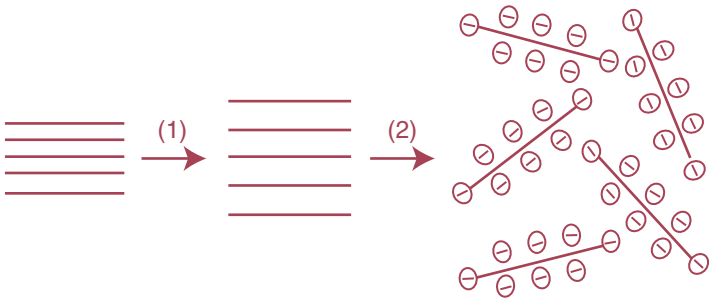

Fig. 11 Graphite can be oxidized to graphite oxide (Step 1), which can be exfoliated into single-layer platelets of graphene oxide (GO) by ultrasound (Step 2)

area of carbon increases, which, in turn, creates higher heating value and higher rates of fluid-surface reactions such as gasification, thus improving the efficiency of the carbon fuel.

Graphite can be oxidized to graphite oxide, producing intercalated hydroxyl and epoxide groups and a disrupted sp^2-bonded carbon network. Stankovich et al. (2006) demonstrated that graphite oxide in phenyl isocyanate is completely exfoliated by ultrasound (150 W) for 1 h, producing single-layer graphene oxide (GO); see Fig. 11. GO platelets are expected to be more reactive than graphitic oxide clusters due to the higher contact area in GO, a feature that will be discussed below. The interests in conducting ultrasound treatment on biochar (see below) were to induce positive benefits on the heating value of the biochar by inducing exfoliation of its graphite oxide, along with mineral removal and water splitting.

Structural Characteristics of Biochar

Chen et al. (2014) chose biochar (Fig. 12) for their ultrasonic and photocatalytic treatments for several structural reasons.

First, biomass-derived (Hammes and Schmidt 2009) and coal-derived (Franklin 1951) chars and petroleum coke (Yen et al. 1961) contain stacks of graphite oxide clusters with reactive carbon edges which could serve as binding sites for CO_2. Ultrasound-exfoliated GO will be even more reactive than the raw char. Second, biochar is more porous than coal-derived char and petroleum coke and is expected to have a higher rate of fluid/solid reactions. Third, the acidic ions of dissolved CO_2 in water can enhance the dissolution of metal ions in the biochar. Fourth, TiO_2 in char is a known semiconductor; it could serve as an electron donor in photocatalytic reductive fixation of aromatics and CO_2, while H_2O can serve as the desired hydrogen donor. Biochar is thus an attractive, renewable carbonaceous material to investigate the treatments proposed.

Solvent-Induced Swelling of Carbonaceous Materials

It has been demonstrated that coal, biomass, and coal-derived chars can be swelled by solvents, including CO_2 and H_2O, after breakage of the cross-links in their macromolecular structure (Gathitu et al. 2009; Mirzaeian and Hall 2006, 2007).

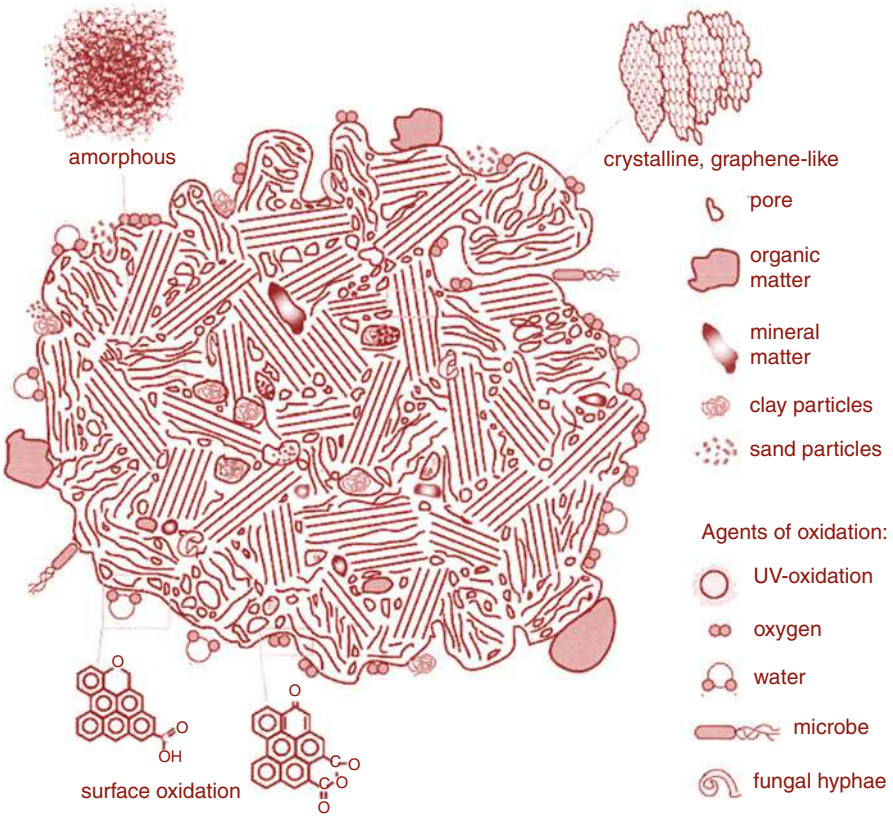

Fig. 12 Graphite oxide clusters form the backbone of the biochar structure (Hammes and Schmidt 2009)

Hydrogen bonds, especially those contributed by hydroxyl and carboxyl groups, have been considered by many as the major cross-links between aromatic clusters (Larsen and Gurevich 1996). The swelled carbonaceous materials have higher porosity and, therefore, higher gas/solid reactivity in processes such as gasification (Wall et al. 2002), which suggests the potential benefits of treating carbon with CO_2 and H_2O (see Fig. 13).

Tested Hypotheses and Technological Implications

Hypotheses

Consideration of the acoustic and photochemical interactions of CO_2 with PAHs as discussed above led Chen et al. (2014) to a set of hypotheses. To start with, they hypothesized that in a single reactor of biochar with CO_2 and H_2O, ultrasound would simultaneously induce the following synergistic chemical and physical processes:

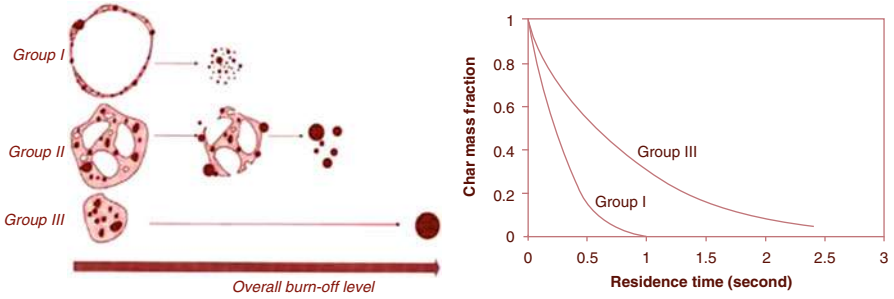

Fig. 13 Porous carbons (Group I particles) possess a higher gasification rate than non-porous carbons (Group III particles) (Wall et al. 2002) (Copyright © 2002 Elsevier Science Ltd)

graphite oxide exfoliation, water splitting, leaching of minerals, carboxylation, hydrogenation, and swelling. As a result, the treated biochar would have a higher heating value, higher reaction rates, and fewer operational and maintenance problems in the subsequent power-generation processes. Moreover, any CO_2 fixed reductively on biochar could be recycled in power/heat generation, thus creating a cradle-to-cradle carbon cycle.

Secondly, Chen et al. (2014) hypothesized that in a single contactor of biochar with CO_2 and H_2O and suitable donors, solar irradiation would induce the following synergistic chemical and physical processes simultaneously: carboxylation, hydrogenation, water splitting, and swelling. As a result, the treated biochar would have a higher heating value and higher reaction rates.

Results of Hypothesis Testing

Ultrasonic and photocatalytic treatments of a sorghum-derived biochar with CO_2 and H_2O at 60 °C resulted in the following observations (Chen et al. 2014):

- Remarkable increases in heating value (HV) for both treatments: 50 % increase for ultrasonic treatment and 20 % increase for photochemical treatment
- Large increases in internal surface area (up to 16-fold) for both types of treatment
- Significant leaching of minerals (60–98 % of Si, K, and Na) that are detrimental to power generation but beneficial to soil after they are captured in the leachate (water)
- Significant hydrogenation, calculated as 9 % additional hydrogen after ultrasonic treatment and 24 % additional hydrogen after photochemical treatment
- Carbon fixation, calculated as 13 % additional carbon after ultrasonic treatment and 16 % additional carbon after a simultaneous photochemical and ultrasonic treatment
- No significant change in oxygen content of the biochar

Further, Fourier transform infrared (FTIR) spectroscopy suggests that carboxylation occurs during photochemical treatments (Chen et al. 2014). The increase in internal surface area (by N_2-BET) during ultrasound treatment is lower than that

from photochemical treatment, suggesting the possibilities of surrendering mesopore volume by exfoliated GO platelets during ultrasound treatment. The increases in heating value result from the combined processes of carbon fixation, mineral removal, and, in the photochemical treatment, hydrogenation. The observed increases in carbon and hydrogen content are attributable, in part, to carboxylation, water splitting, and hydrogenation; H_2O and CO_2 are the only H and C sources in the treatments. These observations are consistent with their hypotheses, although much work remains to optimize the conditions and elucidate the responsible mechanisms.

Implications for Sustainable Technologies

The results discussed above suggest new paradigms for the following technologies:

- Ultrasonic pretreatment of biochar (or other selected carbon feedstock) prior to gasification for simultaneously increasing thermal efficiency, decreasing CO_2 emissions, and reducing operational issues
- Photochemical pretreatment of biochar (or other selected carbon feedstock) prior to gasification, for increasing hydrogen content
- CO_2 capture by functionalized nanographene oxide (GO), phenolic compounds, and char-derived polycyclic compounds that have not been the focus of a systematic CO_2 capture study

Figure 14 illustrates the major streams and variables in a pretreatment process, ultrasonic or photochemical, before the char is fed into a gasifier and combustor.

Power generation with a pretreatment unit offers several sustainable benefits since it is expected to:

- Have higher thermal efficiency due to the 20–50 % higher heating value of the char
- Have a higher power-generation rate due to the more porous nature (16×) of the char

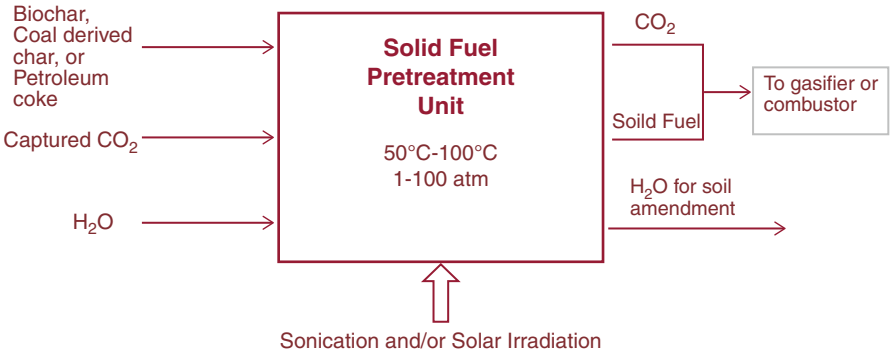

Fig. 14 Streams and variables of a pretreatment process

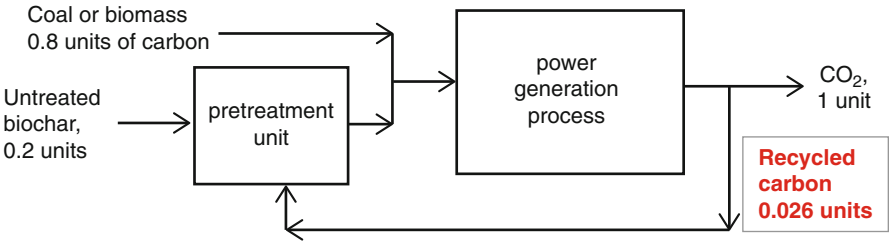

Fig. 15 The ultrasound-treatment unit recycles 2.6 % carbon in the feed, thus creating a cradle-to-cradle carbon cycle

- Exhibit fewer operational and maintenance issues such as fouling and slagging due to the removal of detrimental minerals K, Na, and Si (60–98 %)
- Offer a new CO_2 capture and utilization route since carbon in biochar picks up CO_2 in treatment
- Offer a waste (biochar) utilization route
- Return the soil nutrients, K and Na, in the leachate back into the soil

The benefits of such treatment on thermal efficiency and CO_2 recycling are not merely incremental. Assuming char's heating value increases by 50 % and 20 % of such increase is used by the pretreatment process, the energy output from char combustion will be 1.40 times that of the untreated char. For a co-generation power plant that uses char as only 20 % of its fuel source, with the rest from coal or biomass (see Fig. 15), the overall energy output will increase to 28 % (20 % × 1.40), resulting in a net gain of 8 % in the total output. This would be considered a significant improvement for power plants.

A carbon balance has been conducted for a co-gasification process where 20 % of carbon in the feed comes from biochar based on the 13 % increase in biochar's carbon content during treatment. Figure 15 illustrates the impact of introducing an ultrasonic biochar pretreatment unit on CO_2 emissions prior to biochar's injection into a gasifier. It suggests that the pretreatment unit renders it possible to recycle about 2.6 % of burned carbon fixed in the char. In a co-generation process shown in Fig. 15, the treatment results in 13 % carbon fixation on char and, therefore, 2.6 % carbon recycle – creating a cradle-to-cradle carbon cycle. The scale of this CO_2 uptake is noteworthy. The anthropogenic production of CO_2 is so high that the current total CO_2 utilization does not account for even 1 % of overall CO_2 emissions, and a single technology capable of using 1 % of its CO_2 emissions can be considered a major contribution (Styring et al. 2012).

The efficiency of ultrasound energy output was estimated by using a short treatment time of 3 min, which results in a 19 % increase in heating value (see Fig. 16). The energy consumed by the sonicator during the 3-min treatment was 0.65 kcal/g, which is less than the increase in heating value of the biochar, 0.91 kcal/g, during the 3-min treatment (from 4.83 to 5.74 kcal/g). Although the energy gain (the difference between these two quantities) seems to be limited, it is expected that a

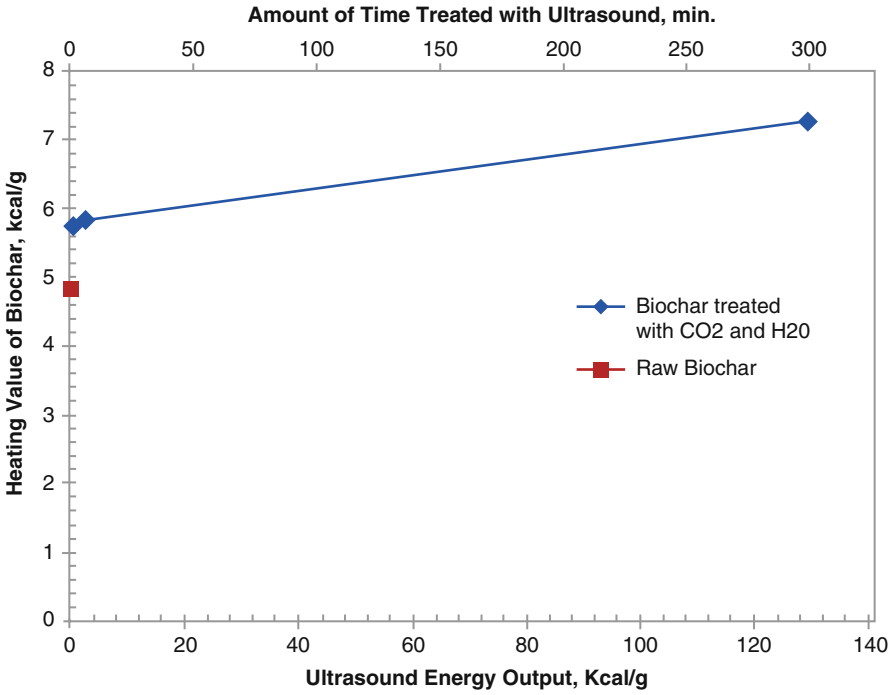

Fig. 16 Ultrasound power increases biochar's heating value. Biochar was treated with (CO_2 + H_2O) and 90-W ultrasound transducer (Chen et al. 2014) (© 2014 American Institute of Chemical Engineers)

majority of the ultrasound energy was dissipated in its surroundings through several modes in the initial apparatus, in which cavitation consumes only a small fraction of the energy. Ultrasound treatment induces energy gain mainly through the loss of mineral content and increases in hydrogen and carbon contents as a result of the treatment. These synergistic physical and chemical processes are believed to be the results of carboxylation, water splitting, hydrogenation, graphite oxide exfoliation, leaching, swelling, etc.

In practice, ultrasonic energy can be used much more efficiently by directly inserting a high-power ultrasonic horn into the solution in the treatment reactor. Thus, the test data indeed support the potential benefits in energy efficiency and the economics of installing a biochar pretreatment reactor prior to gasification or combustion. The pretreatment concept is technically viable. For instance, Mahamuni and Adewuyi (2010) reviewed the costs of various commercial advanced oxidation processes (AOPs) involving similar ultrasound devices for waste-water treatment, containing ideas for further reducing the costs for advanced ultrasound-treatment processes. Pretreatment is also viable because CO_2, H_2O, and residual heat are usually readily available in power plants.

Medical Applications

Biochar has many technological applications even though it is usually considered a by-product in biofuel production. As discussed above, biochar has been adopted in soil amendment and remediation of organic and inorganic contaminants in soil and water. Interests in biochar have intensified in the last decade mainly due to biochar's stability in sequestrating carbon in soil and its use for soil amendments. More recently, Nguyen and Pignatello (2013) evaluated biochar's ability in recovery and containment of marine oil spills. The study of ultrasonic and photochemical interactions of biochar with CO_2 and water (Chen et al. 2014) has provided foundations to explore novel technologies for CO_2 utilization and CO_2 capture.

On a separate front, biochar's medical applications have been scrutinized. We include only a short discussion for completeness since it is not directly related to mitigating climate change. Interestingly, most of these applications were developed with bamboo biochars in China, Japan, and Taiwan where bamboo is widespread. As stated by Zhong et al. (2010), bamboo can be harvested more than 20 times than trees on the same area. It can be harvested annually and regenerated without replanting. It sequestrates up to 12 t of CO_2 per hectare and generates 30 % more oxygen than trees during its growth.

Most of the medical applications of bamboo biochars are based on their abilities to generate far-infrared (FIR) radiations and negative ions (Lou et al. 2007). Bamboo biochar has 15.3–24.1 cmol/kg cation-exchange capacity. Bamboo biochar adsorbs nitrate-nitrogen more effectively than activated carbon (Mizuta et al. 2004). The negative ions generated by bamboo biochar remove the odors and refresh air.

Bamboo char has high electrical conductivity; chemically modified bamboo biochar has been used for developing lithium-sulfur batteries (Gu et al. 2015). Bamboo charcoal can generate a good amount of negatively charged ions that have the property of giving electrons to nearby matters, while charcoal adsorbs positive ions. Bamboo char dissipates electromagnetic (EM) waves emitted by devices such as television, personal computers, cell phones and microwave over, etc., by bouncing them, and the released EM waves can be absorbed by bamboo char due to its high electrical conductivity. The absorbed energy is then dissipated as far-infrared (FIR) emissions. Teraoka et al. (2004) reported that FIR emitted by bamboo biochar at wave lengths between 4 and 16 μm inhibits the growth of Henrietta Lacks (HeLa) cervical cancer cells in vitro at 37 °C. At ambient temperatures, ~25 °C, FIR inhibits tumor growth in mice (Nagasawa et al. 1999; Udagawa et al. 2000; Hamada et al. 2003). Ishibashi et al. (2008) found that the FIR-induced inhibitions of proliferations of cancer cells are controlled by basal expression level of heat shock protein 70A. Moreover, whole-body FIR irradiation at wave length between 7 and 12 μm is believed to improve human health and sleep by keeping the body warm, enhancing the blood circulation, and reducing blood pressure (Honda and Inoue 1988; Inoue and Kabaya 1989; Wang et al. 2006). A number of bamboo char-based food, beauty care, textile, sleepwear and health support products are commercially available.

Conclusions

Pyrolysis process converts biomass organic matter to biochar and increases the recalcitrance of carbon which becomes more resistant to chemical and/or biological decay. Due to its recalcitrant nature, biochar has long-term stability and its soil amendment utilization has been proposed as a way to store carbon in the soil for longer periods than if biomass was left to decay. The physical and chemical properties of biochar support soil health by altering the pH in acidic soils, increasing water retention capacity, and enhancing nutrient availability and microbial activity. Since biochar has high sorption capacity, its agricultural soil amendment will be helpful in reducing leaching of pesticides and pollutants in soil. Much more research is required to establish characterization methods and best management practices for biochar applications in various fields that can help to understand the mechanisms underlying biochar applications for soil amendment and environmental applications. In conclusion, based on the extensive research evidence, it is clear that biochar is indeed a viable soil amendment option for agricultural and environmental purposes worldwide.

References

Abdel-Fattah TM, Mahmoud ME, Ahmed SB, Huff MD, Lee JW, Kumar S (2014) Biochar from woody biomass for removing metal contaminants and carbon sequestration. J Ind Eng Chem doi:10.1016/j.jiec.2014.06.030

Ahmad M, Rajapaksha AU, Lim JE, Zhang M, Bolan N, Mohan D . . . Ok YS (2014) Biochar as a sorbent for contaminant management in soil and water: a review. Chemosphere 99:19–33. doi:10.1016/j.chemosphere.2013.10.071

Angın D (2013) Effect of pyrolysis temperature and heating rate on biochar obtained from pyrolysis of safflower seed press cake. Bioresour Technol 128:593–597. doi:10.1016/j.biortech.2012.10.150

Antal MJ, Grønli M (2003) The art, science, and technology of charcoal production†. Ind Eng Chem Res 42(8):1619–1640. doi:10.1021/ie0207919

Atkinson CJ, Fitzgerald JD, Hipps NA (2010) Potential mechanisms for achieving agricultural benefits from biochar application to temperate soils: a review. Plant and Soil 337(1–2):1–18

Baldwin IT, Halitschke R, Paschold A, von Dahl CC, Preston CA (2006) Volatile signaling in plant-plant interactions: "talking trees" in the genomics era. Science 311(5762):812–815. doi:10.1126/science.1118446

Beesley L, Moreno-Jiménez E, Gomez-Eyles JL (2010) Effects of biochar and greenwaste compost amendments on mobility, bioavailability and toxicity of inorganic and organic contaminants in a multi-element polluted soil. Environ Pollut 158(6):2282–2287. doi:10.1016/j.envpol.2010.02.003

Beesley L, Moreno-Jiménez E, Gomez-Eyles JL, Harris E, Robinson B, Sizmur T (2011) A review of biochars' potential role in the remediation, revegetation and restoration of contaminated soils. Environ Pollut 159(12):3269–3282. doi:10.1016/j.envpol.2011.07.023

Beesley L, Inneh OS, Norton GJ, Moreno-Jimenez E, Pardo T, Clemente R, Dawson JJC (2014) Assessing the influence of compost and biochar amendments on the mobility and toxicity of metals and arsenic in a naturally contaminated mine soil. Environ Pollut 186:195–202. doi:10.1016/j.envpol.2013.11.026

Bonneau-Gubelmann I, Michel M, Besson B, Ratton S, Desmurs J (1996) Carboxylation of hydroxylation of hydroxy aromatic compounds. Indus Chem Libr 8:116–128

Bourke J, Manley-Harris M, Fushimi C, Dowaki K, Nunoura T, Antal MJ (2007) Do All carbonized charcoals have the same chemical structure? 2. A model of the chemical structure of carbonized charcoal†. Ind Eng Chem Res 46(18):5954–5967. doi:10.1021/ie070415u

Brewer CE, Chuang VJ, Masiello CA, Gonnermann H, Gao X, Dugan B. . . Davies CA (2014) New approaches to measuring biochar density and porosity. Biomass Bioenergy 66:176–185. doi:10.1016/j.biombioe.2014.03.059

Bridgwater AV, Peacocke GVC (2000) Fast pyrolysis processes for biomass. Renew Sustain Energy Rev 4(1):1–73. doi:10.1016/S1364-0321(99)00007-6

Bridgwater AV, Meier D, Radlein D (1999) An overview of fast pyrolysis of biomass. Org Geochem 30(12):1479–1493. doi:10.1016/S0146-6380(99)00120-5

Bridgwater AV, Carson P, Coulson M (2007) A comparison of fast and slow pyrolysis liquids from mallee. Int J Glob Energy Issues 27(2):204–216

Brunelli NA, Didas SA, Venkatasubbaiah K, Jones CW (2012). Tuning cooperativity by controlling the linker length of silica-supported amines in catalysis and CO_2 capture. J Am Chem Soc 134:13950–13953

Carrier M, Hardie AG, Uras U, Gorgens J, Knoetze J (2012) Production of char from vacuum pyrolysis of South-African sugar cane bagasse and its characterization as activated carbon and biochar. J Anal Appl Pyrolysis 96:24–32

Chan KY, Xu Z (2009) Biochar: nutrient properties and their enhancement. Biochar Environ Manag Sci Technol 51:67–84

Chan KY, Van Zwieten L, Meszaros I, Downie A, Joseph S (2007) Agronomic values of greenwaste biochar as a soil amendment. Soil Res 45(8):629–634. doi:10.1071/SR07109

Chateauneuf JE, Zhang J, Foote J, Brink J, Perkovic MW (2002) Photochemical fixation of supercritical carbon dioxide: the production of a carboxylic acid from a polyaromatic hydrocarbon. Adv Environ Res 6:487–493

Chen WY, Mattern DL, Okinado E, Senter JC, Mattei AA, Redwine CW (2014) Photochemical and acoustic interactions of biochar with CO_2 and H_2O: applications in power generation and CO_2 capture. AIChE J 60:1054–1065

Cheng C-H, Lehmann J, Thies JE, Burton SD, Engelhard MH (2006) Oxidation of black carbon by biotic and abiotic processes. Org Geochem 37(11):1477–1488. doi:10.1016/j.orggeochem.2006.06.022

Cheng C-H, Lehmann J, Engelhard MH (2008) Natural oxidation of black carbon in soils: changes in molecular form and surface charge along a climosequence. Geochim Cosmochim Acta 72(6):1598–1610. doi:10.1016/j.gca.2008.01.010

Chia CH, Singh BP, Joseph S, Graber ER, Munroe P (2014) Characterization of an enriched biochar. J Anal Appl Pyrolysis 108:26–34. doi:10.1016/j.jaap.2014.05.021

Chintala R, Clay DE, Schumacher TE, Malo DD, Julson JL (2012) Optimization of oxygen parameters for determination of carbon and nitrogen in biochar materials. Anal Lett 46(3):532–538. doi:10.1080/00032719.2012.721103

Clemente R, Hartley W, Riby P, Dickinson NM, Lepp NW (2010) Trace element mobility in a contaminated soil two years after field-amendment with a greenwaste compost mulch. Environ Pollut 158(5):1644–1651. doi:10.1016/j.envpol.2009.12.006

Clough TJ, Bertram JE, Ray JL, Condron LM, O'Callaghan M, Sherlock R R, Wells N S (2010) Unweathered wood biochar impact on nitrous oxide emissions from a bovine-urine-amended pasture soil all rights reserved. No part of this periodical may be reproduced or transmitted in any form or by any means, electronic or mechanical, including photocopying, recording, or any information storage and retrieval system, without permission in writing from the publisher. Permission for printing and for reprinting the material contained herein has been obtained by the publisher. Soil Sci Soc Am J 74(3):852–860. doi: 10.2136/sssaj2009.0185

Crombie K, Mašek O, Sohi SP, Brownsort P, Cross A (2013) The effect of pyrolysis conditions on biochar stability as determined by three methods. GCB Bioenergy 5(2):122–131. doi:10.1111/gcbb.12030

Day D, Evans RJ, Lee JW, Reicosky D (2005) Economical CO_2, SOx, and NOx capture from fossil-fuel utilization with combined renewable hydrogen production and large-scale carbon sequestration. Energy 30(14):2558–2579. doi:10.1016/j.energy.2004.07.016

Deenik JL, McClellan T, Uehara G, Antal MJ, Campbell S (2010) Charcoal volatile matter content influences plant growth and soil nitrogen transformations all rights reserved. No part of this periodical may be reproduced or transmitted in any form or by any means, electronic or mechanical, including photocopying, recording, or any information storage and retrieval system, without permission in writing from the publisher. Permission for printing and for reprinting the material contained herein has been obtained by the publisher. Soil Sci Soc Am J 74(4): 1259–1270. doi: 10.2136/sssaj2009.0115

Demiral İ, Ayan EA (2011) Pyrolysis of grape bagasse: effect of pyrolysis conditions on the product yields and characterization of the liquid product. Bioresour Technol 102(4):3946–3951. doi:10.1016/j.biortech.2010.11.077

Demirbas A (2004) Effects of temperature and particle size on bio-char yield from pyrolysis of agricultural residues. J Anal Appl Pyrolysis 72(2):243–248. doi:10.1016/j.jaap.2004.07.003

Demirbas A, Arin G (2002) An overview of biomass pyrolysis. Energy Sources 24(5):471–482. doi:10.1080/00908310252889979

Dewar MJS, Dieter KM (1988) Mechanism of the chain extension step in the biosynthesis of fatty acids. Biochemistry 27:3302–3308

Downie A, Crosky A, Monroe P (2009) Biochar for environmental management: science and technology. Earthscan, London, pp 13–32

Duku MH, Gu S, Hagan EB (2011) Biochar production potential in Ghana – a review. Renew Sustain Energy Rev 15(8):3539–3551

Enders A, Hanley K, Whitman T, Joseph S, Lehmann J (2012) Characterization of biochars to evaluate recalcitrance and agronomic performance. Bioresour Technol 114:644–653. doi:10.1016/j.biortech.2012.03.022

Fang Q, Chen B, Lin Y, Guan Y (2013) Aromatic and hydrophobic surfaces of wood-derived biochar enhance perchlorate adsorption via hydrogen bonding to oxygen-containing organic groups. Environ Sci Technol 48(1):279–288

Fernandes MB, Brooks P (2003) Characterization of carbonaceous combustion residues: II. Nonpolar organic compounds. Chemosphere 53(5):447–458. doi:10.1016/s0045-6535(03)00452-1

Franklin R (1951) Crystallite growth in graphitizing and non-graphitizing carbons. Math Phys Sci 1097:196–218

Galinato SP, Yoder JK, Granatstein D (2011) The economic value of biochar in crop production and carbon sequestration. Energy Policy 39(10):6344–6350

Galipo RC, Egan WJ, Aust JF, Myrick ML, Morgan SL (1998) Pyrolysis gas chromatography/mass spectrometry investigation of a thermally cured polymer. J Anal Appl Pyrolysis 45(1):23–40. doi:10.1016/S0165-2370(98)00059-X

Garcia R, Pizarro C, Lavin AG, Bueno JL (2013) Biomass proximate analysis using thermogravimetry. Bioresour Technol 139:1–4. doi:10.1016/j.biortech.2013.03.197

Gathitu BB, Chen WY, McClure MC (2009) Effects of coal interaction with supercritical CO_2: physical structure. Ind Eng Chem Res 48:5024–5034

Glaser B, Lehmann J, Zech W (2002) Ameliorating physical and chemical properties of highly weathered soils in the tropics with charcoal – a review. Biol Fertil Soils 35(4):219–230. doi:10.1007/s00374-002-0466-4

Grossman J, O'Neill B, Tsai S, Liang B, Neves E, Lehmann J, Thies J (2010) Amazonian anthrosols support similar microbial communities that differ distinctly from those extant in adjacent, unmodified soils of the same mineralogy. Microb Ecol 60(1):192–205. doi:10.1007/s00248-010-9689-3

Gu X, Wang Y, Lai C, Qiu J, Li S, Hou Y, Martens W, Mahmood N, Zhang S (2015) Microporous bamboo biochar for lithium−sulfur batteries. Nano Res 8(1):129–139. Doi:10.1007/s12274-014-0601-1

Guo G, Zhou Q, Ma L (2006) Availability and assessment of fixing additives for the in situ remediation of heavy metal contaminated soils: a review. Environ Monit Assess 116 (1–3):513–528. doi:10.1007/s10661-006-7668-4

Hamada Y, Teraoka F, Matsumoto T, Madachi A, Toki F, Uda E, Hase R, Takahashi J, Matsuura N (2003) Effects of far infrared ray on Hela cells and WI-38 cells. Int Congr Ser 1255:339–341

Hammes K, Schmidt MWI (2009) Changes of biochar in soil. In: Lehmann J, Joseph S (eds) Biochar for environmental management: science and technology. Earthscan, London

Hmid A, Mondelli D, Fiore S, Fanizzi FP, Al Chami Z, Dumontet S (2014) Production and characterization of biochar from three-phase olive mill waste through slow pyrolysis. Biomass Bioenergy. doi:10.1016/j.biombioe.2014.09.024

Honda K, Inoue S (1988) Sleep-enhancing effects of far-infrared radiation in rats. Int J Biometeorol 32(2):92–94

Hornung A (2013) Intermediate pyrolysis of biomass, Chap 8. In: Rosendahl L (ed) Biomass combustion science. Technology and engineering. Woodhead, Cambridge, pp 172–186

Hossain MK, Strezov V, Chan KY, Ziolkowski A, Nelson PF (2011) Influence of pyrolysis temperature on production and nutrient properties of wastewater sludge biochar. J Environ Manage 92(1):223–228. doi:10.1016/j.jenvman.2010.09.008

Houben D, Evrard L, Sonnet P (2013) Mobility, bioavailability and pH-dependent leaching of cadmium, zinc and lead in a contaminated soil amended with biochar. Chemosphere 92(11):1450–1457. doi:10.1016/j.chemosphere.2013.03.055

Ibrahim HM, Al-Wabel MI, Usman ARA, Al-Omran A (2013) Effect of conocarpus biochar application on the hydraulic properties of a sandy loam soil. Soil Sci 178(4):165–173. doi: 10.1097/SS.0b013e3182979eac

Ince NH, Tezcanli G, Belen RK, Apikyan IG (2001) Ultrasound as a catalyzer of aqueous reaction systems: the state of the art and environmental applications. Appl Catal B Environ 29:167–176

Inoue S, Kabaya M (1989) Biological activities caused by far-infrared radiation. Int J Biometeorol 33(3):145–50

International Biochar Initiative (IBI) (2012) Standard product definition and product testing guidelines for biochar that is used in soil. http://www.biochar-international.org/newsletter

International Energy Agency (IEA) (2007) Bioenergy biomass pyrolysis. IEA Bioenergy. www.ieabioenergy.com

IPCC (2005) Special report on carbon dioxide capture and storage, prepared by working group III of the Intergovernmental Panel on Climate Change. In: Sohi et al (eds) Cambridge University Press, Cambridge

Ishibashi J, Yamashita K, Ishikawa T, Hosokawa H, Sumida K, Nagayama M, Kitamura S (2008) The effects inhibiting the proliferation of cancer cells by far-infrared radiation (FIR) are controlled by the basal expression level of heat shock protein (HSP) 70A. Med Oncol 25:229–237

Izumi Y (2013) Recent advances in the photocatalytic conversion of carbon dioxide to fuels with water and/or hydrogen using solar energy and beyond. Coordin Chem Rev 257:171–186

Jeffery S, Verheijen FGA, van der Velde M, Bastos AC (2011) A quantitative review of the effects of biochar application to soils on crop productivity using meta-analysis. Agr Ecosyst Environ 144(1):175–187

Jindo K, Suto K, Matsumoto K, García C, Sonoki T, Sanchez-Monedero MA (2012) Chemical and biochemical characterisation of biochar-blended composts prepared from poultry manure. Bioresour Technol 110:396–404. doi:10.1016/j.biortech.2012.01.120

Keiluweit M, Nico PS, Johnson MG, Kleber M (2010) Dynamic molecular structure of plant biomass-derived black carbon (biochar). Environ Sci Technol 44(4):1247–1253. doi:10.1021/es9031419

Kim SS, Agblevor FA (2007) Pyrolysis characteristics and kinetics of chicken litter. Waste Manag 27(1):135–140. doi:10.1016/j.wasman.2006.01.012

Kim S-J, Jung S-H, Kim J-S (2010) Fast pyrolysis of palm kernel shells: influence of operation parameters on the bio-oil yield and the yield of phenol and phenolic compounds. Bioresour Technol 101(23):9294–9300. doi:10.1016/j.biortech.2010.06.110

Klinke HB, Thomsen AB, Ahring BK (2004) Inhibition of ethanol-producing yeast and bacteria by degradation products produced during pre-treatment of biomass. Appl Microbiol Biotechnol 66(1):10–26. doi:10.1007/s00253-004-1642-2

Kolbe H (1860) Ueber Synthese der Salicylsäure. Annalen der Chemie and Pharmacie 113:125–127

Kruse A, Funke A, Titirici M-M (2013) Hydrothermal conversion of biomass to fuels and energetic materials. Curr Opin Chem Biol 17(3):515–521. doi:10.1016/j.cbpa.2013.05.004

Kumar B, Llorente M, Froehlich J, Dang T, Sathrum A (2012) Photochemical and photoelectrochemical reduction of CO_2. Annu Rev Phys Chem 63:541–69

Kuzyakov Y, Subbotina I, Chen H, Bogomolova I, Xu X (2009) Black carbon decomposition and incorporation into soil microbial biomass estimated by 14C labeling. Soil Biol Biochem 41(2):210–219. doi:10.1016/j.soilbio.2008.10.016

Laird DA (2008) The charcoal vision: a win–win–win scenario for simultaneously producing bioenergy, permanently sequestering carbon, while improving soil and water quality all rights reserved. No part of this periodical may be reproduced or transmitted in any form or by any means, electronic or mechanical, including photocopying, recording, or any information storage and retrieval system, without permission in writing from the publisher. Agron J 100(1):178–181. doi: 10.2134/agrojnl2007.0161

Lal R (2004) Soil carbon sequestration impacts on global climate change and food security. Science 304(5677):1623–1627. doi:10.1126/science.1097396

Larsen JW, Gurevich I (1996) A method for counting the hydrogen-bond cross-links in coal. Energy Fuels 10:1269–1272

Lee JW, Kidder M, Evans BR, Paik S, Buchanan AC 3rd, Garten CT, Brown RC (2010) Characterization of biochars produced from cornstovers for soil amendment. Environ Sci Technol 44(20):7970–7974. doi:10.1021/es101337x

Lee JW, Buchanan AC, Evans BR, Kidder MK (2011) PCT/US2011/020306

Lee JW, Lee J, Buchanan AC III, Evans B, Kidder M (2013) Oxygenation of biochar for enhanced cation exchange capacity. In: Lee JW (ed) Advanced biofuels and bioproducts. Springer, New York, pp 35–45

Lehmann J (2003) Amazonian dark earths: origin, properties, management. Kluwer, Dordrecht

Lehmann J (2007) Bio-energy in the black. Front Ecol Environ 5(7):381–387

Lehmann J, Joseph S (2009) Biochar for environmental management: science and technology. In: Lehmann J, Joseph S (eds), Earth Scan, London & Sterling, VA, 416 p

Lehmann J, Rondon M (2006) Bio-char soil management on highly weathered soils in the humid tropics. Biological approaches to sustainable soil systems. CRC Press, Boca Raton, pp 517–530

Lehmann J, Gaunt J, Rondon M (2006) Bio-char sequestration in terrestrial ecosystems–a review. Mitig Adapt Strat Glob Chang 11(2):395–419

Lehmann J, Czimczik C, Laird D, Sohi S (2009) Stability of biochar in soil. Biochar Environ Manag Sci Technol. In: Lehmann et al. (eds), Earth Scan, London & Sterling, VA, pp 183–205

Lehmann J, Rillig MC, Thies J, Masiello CA, Hockaday WC, Crowley D (2011) Biochar effects on soil biota–a review. Soil Biol Biochem 43(9):1812–1836

Liang B, Lehmann J, Solomon D, Kinyangi J, Grossman J, O'Neill B, Neves EG (2006) Black carbon increases cation exchange capacity in soils. Soil Sci Soc Am J 70(5):1719–1730. doi:10.2136/sssaj2005.0383

Liang B, Lehmann J, Solomon D, Sohi S, Thies JE, Skjemstad JO . . . Wirick S (2008) Stability of biomass-derived black carbon in soils. Geochimica et Cosmochimica Acta 72(24):6069–6078. doi:10.1016/j.gca.2008.09.028

Lindsey AS, Jeskey H (1957) The Kolbe-Schmitt reaction. Chemistry 57:583–620

Liu X, Li Z, Zhang Y, Feng R, Mahmood IB (2014) Characterization of human manure-derived biochar and energy-balance analysis of slow pyrolysis process. Waste Manag 34(9):1619–1626. doi:10.1016/j.wasman.2014.05.027

Loganathan VA, Feng Y, Sheng GD, Clement TP (2009) Crop-residue-derived char influences sorption, desorption and bioavailability of atrazine in soils all rights reserved. No part of this periodical may be reproduced or transmitted in any form or by any means, electronic or

mechanical, including photocopying, recording, or any information storage and retrieval system, without permission in writing from the publisher. Permission for printing and for reprinting the material contained herein has been obtained by the publisher. Soil Sci Soc Am J 73(3): 967–974. doi: 10.2136/sssaj2008.0208

Lou CW, Lin CW, Lei CH, Su KH, Hsu CH, Liu ZH, Lin JH (2007) PET/PP blend with bamboo activated charcoal to produce functional composites. J Mater Process Technol 192:428–433

Mahamuni NN, Adewuyi YG (2010) Advanced oxidation processes (AOPs) involving ultrasound for waste water treatment: a review with emphasis on cost estimation. Ultrason Sonochem 17:990–1003

Manya JJ (2012) Pyrolysis for biochar purposes: a review to establish current knowledge gaps and research needs. Environ Sci Technol 46(15):7939–7954. doi:10.1021/es301029g

Mašek O, Budarin V, Gronnow M, Crombie K, Brownsort P, Fitzpatrick E, Hurst P (2013) Microwave and slow pyrolysis biochar: comparison of physical and functional properties. J Anal Appl Pyrolysis 100:41–48. doi:10.1016/j.jaap.2012.11.015

Masiello CA (2004) New directions in black carbon organic geochemistry. Mar Chem 92 (1–4):201–213. doi:10.1016/j.marchem.2004.06.043

Mason TJ (1990) Chemistry with ultrasound. In: Mason TJ (ed) Critical reports on applied chemistry 28, Society for Chemical Industry. Elsevier, London

Méndez A, Tarquis AM, Saa-Requejo A, Guerrero F, Gascó G (2013) Influence of pyrolysis temperature on composted sewage sludge biochar priming effect in a loamy soil. Chemosphere 93(4):668–676. doi:10.1016/j.chemosphere.2013.06.004

Mimmo T, Panzacchi P, Baratieri M, Davies CA, Tonon G (2014) Effect of pyrolysis temperature on miscanthus (*Miscanthus* × *giganteus*) biochar physical, chemical and functional properties. Biomass Bioenergy 62:149–157. doi:10.1016/j.biombioe.2014.01.004

Mirzaeian M, Hall PJ (2006) The interactions of coal with CO_2 and its effects on coal structure. Energy Fuels 20:2022–2027

Mizuta K, Matsumoto T, Hatate Y, Nishihara K, Nakanishi T (2004) Removal of nitrate-nitrogen from drinking water using bamboo powder charcoal. Bioresour Technol 95:255–257

Moon DH, Park JW, Chang YY, Ok YS, Lee SS, Ahmad M, Baek K (2013) Immobilization of lead in contaminated firing range soil using biochar. Environ Sci Pollut Res Int 20(12):8464–8471. doi:10.1007/s11356-013-1964-7

Mukome FND, Zhang X, Silva LCR, Six J, Parikh SJ (2013) Use of chemical and physical characteristics to investigate trends in biochar feedstocks. J Agric Food Chem 61 (9):2196–2204

Nagasawa Y, Udagawa Y, Kiyokawa S (1999) Evidence that irradiation of far-infrared rays inhibits mammary tumour growth in SHN mice. Anticancer Res 19(3A):1797–800

Nguyen, HN, Pignatello JJ (2013) Laboratory tests of biochars as absorbents for use in recovery or containment of marine crude oil spills. Environ Eng Sci 30(7):374–380

Novak JM, Busscher WJ, Laird DL, Ahmedna M, Watts DW, Niandou MAS (2009) Impact of biochar amendment on fertility of a southeastern coastal plain soil. Soil Sci 174(2):105–112. doi:10.1097/SS.1090b1013e3181981d3181989a

Okimori Y, Ogawa M, Takahashi F (2003) Potential of Co_2 emission reductions by carbonizing biomass waste from industrial tree plantation in South Sumatra, Indonesia. Mitig Adapt Strat Glob Chang 8(3):261–280. doi:10.1023/B:MITI.0000005643.79908.5a

O'Neill B, Grossman J, Tsai MT, Gomes JE, Lehmann J, Peterson J, Thies JE (2009) Bacterial community composition in Brazilian Anthrosols and adjacent soils characterized using culturing and molecular identification. Microb Ecol 58(1):23–35. doi:10.1007/s00248-009-9515-y

Ottaway M (1982) Use of thermogravimetry for proximate analysis of coals and cokes. Fuel 61(8):713–716. doi:10.1016/0016-2361(82)90244-7

Özçimen D, Karaosmanoğlu F (2004) Production and characterization of bio-oil and biochar from rapeseed cake. Renew Energy 29(5):779–787. doi:10.1016/j.renene.2003.09.006

Paustian K, Six J, Elliott ET, Hunt HW (2000) Management options for reducing CO_2 emissions from agricultural soils. Biogeochemistry 48(1):147–163. doi:10.1023/A:1006271331703

Pietikäinen J, Kiikkilä O, Fritze H (2000) Charcoal as a habitat for microbes and its effect on the microbial community of the underlying humus. Oikos 89(2):231–242. doi:10.1034/j.1600-0706.2000.890203.x

Pujol D, Liu C, Gominho J, Olivella MÀ, Fiol N, Villaescusa I, Pereira H (2013) The chemical composition of exhausted coffee waste. Ind Crops Prod 50:423–429. doi:10.1016/j.indcrop.2013.07.056

Rajkovich S, Enders A, Hanley K, Hyland C, Zimmerman A, Lehmann J (2012) Corn growth and nitrogen nutrition after additions of biochars with varying properties to a temperate soil. Biol Fertil Soils 48(3):271–284. doi:10.1007/s00374-011-0624-7

Rondon M, Lehmann J, Ramírez J, Hurtado M (2007) Biological nitrogen fixation by common beans (*Phaseolus vulgaris L.*) increases with bio-char additions. Biol Fertil Soils 43(6):699–708. doi:10.1007/s00374-006-0152-z

Ronsse F, van Hecke S, Dickinson D, Prins W (2013) Production and characterization of slow pyrolysis biochar: influence of feedstock type and pyrolysis conditions. GCB Bioenergy 5(2):104–115. doi:10.1111/gcbb.12018

Rutigliano FA, Romano M, Marzaioli R, Baglivo I, Baronti S, Miglietta F, Castaldi S (2014) Effect of biochar addition on soil microbial community in a wheat crop. Eur J Soil Biol 60:9–15. doi:10.1016/j.ejsobi.2013.10.007

Schmitt R (1885) Beitrag zur Kenntniss der Kolbe'schen Salicylsäure Synthese. J für Praktische Chemie 31:397–411

Shaaban A, Se S-M, Mitan NMM, Dimin MF (2013) Characterization of biochar derived from rubber wood sawdust through slow pyrolysis on surface porosities and functional groups. Procedia Eng 68:365–371. doi:10.1016/j.proeng.2013.12.193

Shackley S, Carter S, Knowles T, Middelink E, Haefele S, Haszeldine S (2012) Sustainable gasification–biochar systems? A case-study of rice-husk gasification in Cambodia, part II: field trial results, carbon abatement, economic assessment and conclusions. Energy Policy 41:618–623. doi:10.1016/j.enpol.2011.11.023

Slaghuis JH, Raijmakers N (2004) The use of thermogravimetry in establishing the Fischer tar of a series of South African coal types. Fuel 83(4–5):533–536. doi:10.1016/j.fuel.2003.10.002

Sohi SP (2012) Agriculture. Carbon storage with benefits. Science 338(6110):1034–1035. doi:10.1126/science.1225987

Sohi S, Krull E, Lopez-Capel E, Bol R (2010) A review of biochar and its use and function in soil. Adv Agron 105:47–82

Spokas KA, Novak JM, Stewart CE, Cantrell KB, Uchimiya M, Dusaire MG, Ro KS (2011) Qualitative analysis of volatile organic compounds on biochar. Chemosphere 85(5):869–882. doi:10.1016/j.chemosphere.2011.06.108

Spokas K, Novak J, Venterea R (2012) Biochar's role as an alternative N-fertilizer: ammonia capture. Plant and Soil 350(1–2):35–42. doi:10.1007/s11104-011-0930-8

Srinivasan P, Sarmah AK (2014) Characterisation of agricultural waste-derived biochars and their sorption potential for sulfamethoxazole in pasture soil: a spectroscopic investigation. Sci Total Environ 502c:471–480. doi:10.1016/j.scitotenv.2014.09.048

Stanger R, Wall T, Lucas J, Mahoney M (2013) Dynamic Elemental Thermal Analysis (DETA) – a characterisation technique for the production of biochar and bio-oil from biomass resources. Fuel 108:656–667. doi:10.1016/j.fuel.2013.02.065

Stankovich S, Dikin DA, Dommett GHB, Kohlhaas KM, Zimney EJ, Stach EA, Piner RD, Nguyen ST, Ruoff RS (2006) Graphene-based composite materials. Nature 442:282–286

Steiner C, Teixeira W, Lehmann J, Nehls T, de Macêdo J, Blum WH, Zech W (2007) Long term effects of manure, charcoal and mineral fertilization on crop production and fertility on a highly weathered Central Amazonian upland soil. Plant and Soil 291(1–2):275–290. doi:10.1007/s11104-007-9193-9

Styring P, Jansen D, de Coninck H, Reith H, Armstrong K (2011) Carbon capture and utilisation in the green economy: using CO_2 to manufacture fuel, chemicals and materials. Report no. 501, The Centre for Low Carbon Futures 2011 and CO_2 Chem Publishing 2012, July 2011

Suslick K, Flannigan J (2008) Inside a collapsing bubble: sonoluminesence and the conditions during cavitation. Annu Rev Phys Chem 59:659–683

Tang J, Zhu W, Kookana R, Katayama A (2013) Characteristics of biochar and its application in remediation of contaminated soil. J Biosci Bioeng 116(6):653–659. doi:10.1016/j.jbiosc.2013.05.035

Tazuke S, Ozawa H (1975) Photofixation of carbon dioxide: formation of 9,10-dihydrophenanthrene-9,carboxylic acid from phenanthrene-amine-carbon dioxide systems. J Chem Soc Chem Commun 7:237–238

Tazuke S, Kazama S, Kitamura N (1986) Reductive photocarboxylation of aromatic hydrocarbons. J Org Chem 51:4548–4553

Teraoka F, Hamada Y, Takahashi J (2004) Bamboo charcoal inhibits growth of HeLa cells in vitro. Dent Mater J 23(4):633–637

Uchimiya M, Lima IM, Klasson KT, Wartelle LH (2010) Contaminant immobilization and nutrient release by biochar soil amendment: roles of natural organic matter. Chemosphere 80(8):935–940. doi:10.1016/j.chemosphere.2010.05.020

Uchimiya M, Klasson KT, Wartelle LH, Lima IM (2011a) Influence of soil properties on heavy metal sequestration by biochar amendment: 1. Copper sorption isotherms and the release of cations. Chemosphere 82(10):1431–1437. doi:10.1016/j.chemosphere.2010.11.050

Uchimiya M, Klasson KT, Wartelle LH, Lima IM (2011b) Influence of soil properties on heavy metal sequestration by biochar amendment: 2. Copper desorption isotherms. Chemosphere 82(10):1438–1447. doi:10.1016/j.chemosphere.2010.11.078

Udagawa Y, Nagasawa H (2000) Effects of far-infrared ray on reproduction, growth, behaviour and some physiological parameters in mice. In vivo 14(2):321–6

U.S. DOE (2010) Biomass multi-year program plan (MYPP). Office of the biomass program. Energy Efficiency and Renewable Energy, U.S. Department of Energy

Ussiri DAN, Lal R, Jarecki MK (2009) Nitrous oxide and methane emissions from long-term tillage under a continuous corn cropping system in Ohio. Soil Tillage Res 104(2):247–255. doi:10.1016/j.still.2009.03.001

Verheijen F, Jeffery S, Bastos A, Van der Velde M, Diafas I (2010) Biochar application to soils. Institute for Environment and Sustainability, Luxembourg

Wall TF, Liu GS, Wu HW, Roberts DG, Benfell KE, Gupta S, Lucas JA, Harris DJ (2002) The effects of pressure on coal reactions during pulverized coal combustion and gasification. Progr Energ Combus 28:405–433

Wang GW, Hu GZ, Kong Q, He HB, Xu L (2006) Research progress in properties of bamboo activated charcoal. J Bamboo Res 25(4):9–12

Warnock D, Lehmann J, Kuyper T, Rillig M (2007) Mycorrhizal responses to biochar in soil – concepts and mechanisms. Plant and Soil 300(1–2):9–20. doi:10.1007/s11104-007-9391-5

West TO, McBride AC (2005) The contribution of agricultural lime to carbon dioxide emissions in the United States: dissolution, transport, and net emissions. Agr Ecosyst Environ 108 (2):145–154. doi:10.1016/j.agee.2005.01.002

Xu T, Lou L, Luo L, Cao R, Duan D, Chen Y (2012) Effect of bamboo biochar on pentachlorophenol leachability and bioavailability in agricultural soil. Sci Total Environ 414:727–731. doi:10.1016/j.scitotenv.2011.11.005

Yang Y, Sheng G (2003) Enhanced pesticide sorption by soils containing particulate matter from crop residue burns. Environ Sci Technol 37(16):3635–3639. doi:10.1021/es034006a

Yang Z-H, Xiong S, Wang B, Li Q, Yang W-C (2013) Cr(III) adsorption by sugarcane pulp residue and biochar. J Cent South Univ 20(5):1319–1325

Yang Y, Lin X, Wei B, Zhao Y, Wang J (2014) Evaluation of adsorption potential of bamboo biochar for metal-complex dye: equilibrium, kinetics and artificial neural network modeling. Int J Environ Sci Technol 11(4):1093–1100

Yen TF, Erdman JG, Pollack SS (1961) Investigation of the structure of petroleum asphaltenes by X-ray diffraction. Anal Chem 33:1587–1594

Yu XY, Ying GG, Kookana RS (2006) Sorption and desorption behaviors of diuron in soils amended with charcoal. J Agric Food Chem 54(22):8545–8550. doi:10.1021/jf061354y

Yu X, Pan L, Ying G, Kookana RS (2010) Enhanced and irreversible sorption of pesticide pyrimethanil by soil amended with biochars. J Environ Sci 22(4):615–620. doi:10.1016/S1001-0742(09)60153-4

Zhang H, Tang Y, Liu X, Ke Z, Su X, Cai D, Yu Z (2011) Improved adsorptive capacity of pine wood decayed by fungi *Poria cocos* for removal of malachite green from aqueous solutions. Desalination 274(1–3):97–104

Zhao G, Mu X, Wen Z, Wang F, Gao P (2013a) Soil erosion, conservation, and eco-environment changes in the loess plateau Of China. Land Degrad Dev 24(5):499–510. doi:10.1002/ldr.2246

Zhao L, Cao X, Mašek O, Zimmerman A (2013b) Heterogeneity of biochar properties as a function of feedstock sources and production temperatures. J Hazard Mater 256–257:1–9. doi:10.1016/j.jhazmat.2013.04.015

Zhong Z, Flanagan R, Yang H (2010) Bamboo biochar as a potential source of soil humic substance in soil ecosystems. Slides presented at the international symposium on environmental behavior and effects of biomass-derived charcoal, Hangzhou, 9–11 Oct 2010. See http://www.biochar-international.org/sites/default/files/zheke_Zhong.pdf

Wind Energy

Manfred Lenzen and Olivier Baboulet

Contents

M. Lenzen (✉) • O. Baboulet
ISA, School of Physics-A28, The University of Sydney, Sydney, NSW, Australia
e-mail: m.lenzen@physics.usyd.edu.au; olivier.baboulet@centraliens-nantes.net

W.-Y. Chen et al. (eds.), *Handbook of Climate Change Mitigation and Adaptation*,
DOI 10.1007/978-3-319-14409-2_34

Abstract

Electricity is perhaps the most versatile energy carrier in modern economies, and it is therefore fundamentally linked to human and economic development. Electricity growth has outpaced that of any other fuel, leading to ever-increasing shares in the overall mix. This trend is expected to continue throughout the following decades, with large – especially rural – segments of the world population in developing countries climbing the "energy ladder" and becoming connected to power grids (UNDP, World energy assessment: 2004 update. United Nations Development Programme, New York, 2004). Electricity therefore deserves particular attention with regard to its contribution to global greenhouse gas emissions, which is reflected in the ongoing development of low-carbon technologies for power generation. The main purpose of this chapter is to provide a bridge between detailed technical reports and broad resource and economic assessments on wind power. The following aspects of wind energy are covered: the global potential of the wind resource, technical principles of wind energy converters, capacity and load characteristics, life-cycle characteristics, current scale of deployment, contribution to global electricity supply, cost of electricity output, and future technical challenges. Wind power is the second-strongest-growing of renewable electricity technologies, with recent annual growth rates of about 34 %. The technology is mature and simple, and decades of experience exist in a few countries. Due to strong economies of scale, wind turbines have grown to several megawatts per device, and wind farms have now been deployed offshore. The wind energy industry is still small but competitive: 120 GW of installed wind power contributes only about 1.5 % or 260 TWh to global electricity generation at average capacity factors of around 25 % and levelized costs between 3 and 7 US¢/kWh, including additional costs brought about by the variability of the wind resource. The technical potential of wind is larger than current global electricity consumption, but the main barrier to widespread wind power deployment is wind variability, which poses limits to grid integration at penetration rates above 20 %. Life-cycle emissions for wind power alone are among the lowest for all technologies; however, in order to compare wind energy in a systems view, one needs to consider its low capacity credit: adding emissions from fossil-fuel balancing and peaking reserves that are required to maintain overall systems reliability places wind power at about 65 g/kWh. Wind power's contribution to twenty-first-century emission abatement is potentially large at 450–500 Gt CO_2.

Introduction

Electricity[1] is perhaps the most versatile energy carrier in modern economies, and it is therefore fundamentally linked to human and economic development. Electricity growth has outpaced that of any other fuel, leading to ever-increasing shares in the

[1]Responsible for the section on technical principles of wind energy converters

overall mix. This trend is expected to continue throughout the following decades, with large – especially rural – segments of the population in developing countries climbing the "energy ladder" and becoming connected to power grids (UNDP 2004). Electricity therefore deserves particular attention with regard to its contribution to global greenhouse gas emissions, which is reflected in the ongoing development of low-carbon technologies for power generation.

Parts of this chapter are based on a report on the status of electricity-generating technologies (Lenzen and Badcock 2009; Lenzen 2010). That report was commissioned with the objective of providing an up-to-date snapshot of multiple criteria related to electricity generation, but not with the objective to provide a tool or a basis for multi-criteria decision analysis.

Why the need for a new assessment of the state of wind energy, or for that matter, electricity-generating technologies? This work does not aim to replace milestone reports such as the Energy Technology Perspectives (IEA 2008a) or the World Energy Assessment (UNDP 2004). Its main focus is twofold: (a) to provide more technical information than is usually found in global assessments on critical technical aspects, such as variability of wind power, and (b) to capture the most recent findings from the international literature.

The chapter unfolds by presenting an up-to-date summary reviews on the following aspects of wind energy:

1. Global potential of resource
2. Technical principles of wind energy converters
3. Capacity and load characteristics
4. Life-cycle characteristics
5. Current scale of deployment
6. Contribution to global electricity supply
7. Cost of electricity output
8. Future directions

The chapter concludes with a summary.

Global Potential of Resource

In 2008, the global capacity of wind energy converters was 121 GW, generating about 260 TWh of electricity or about 1.5 % of global electricity production (WWEA 2008). Most of the capacity (Fig. 1) is installed in the USA (25 GW) and in the EU (about 65 GW), followed by China (12 GW) and India (10 GW).

Wind energy deployment has been increasing rapidly throughout the past decade, recording growth rates of around 30 % since 1996 (Fig. 2). More than half of the 2008 additions occurred in the USA and in China (Fig. 3), with the USA overtaking Germany as the leader in installed wind capacity.

Measurements from numerous surface and balloon-launch monitoring stations suggest that the global technical potential from onshore wind energy exceeds current

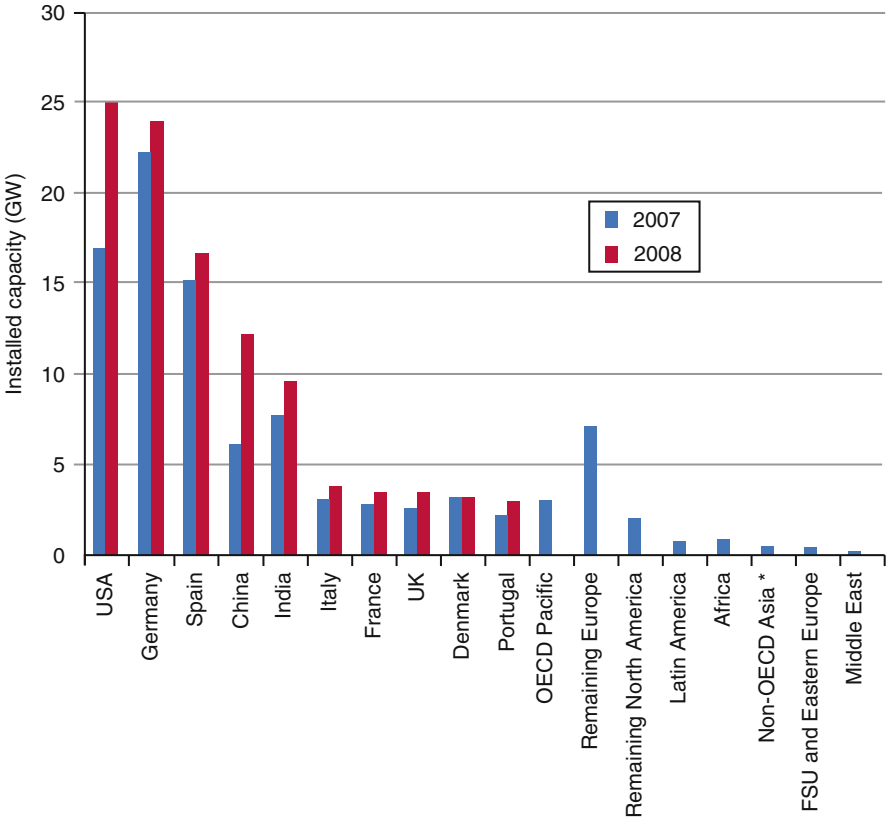

Fig. 1 Installed wind power capacity by region (Compiled from WWEA (2008), GWEC (2008)) (*Asia excludes China and India)

world electricity demand. Using global grid-cell data, Hoogwijk et al. (2004) undertake a detailed assessment of:

1. The theoretical potential (the energy content of global wind).
2. The geographical potential of onshore wind. Hoogwijk et al. assessment excludes land areas with wind speeds below 4 m/s (if the cutoff point had been 6 m/s, areas with current wind turbine installations would have been excluded). It also excludes areas unavailable for turbine installation, such as nature reserves and areas with other functions, and urban areas and high altitudes above 2,000 m with low air density. For further details, Table 1 in Hoogwijk et al. (2004) provides suitability factors, which shows the percentage of a land area available for wind turbine installation.
3. The technical potential (extrapolating wind data to hub height, considering wake effects and realistic power densities in MW/km^2, applying average capacity factors, subtracting downtime).

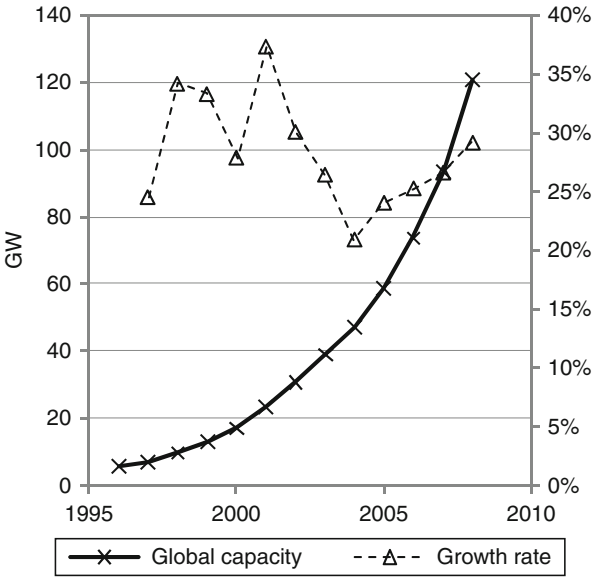

Fig. 2 Historical development of installed wind power capacity and annual growth rates (Compiled from WWEA (2008), GWEC (2008))

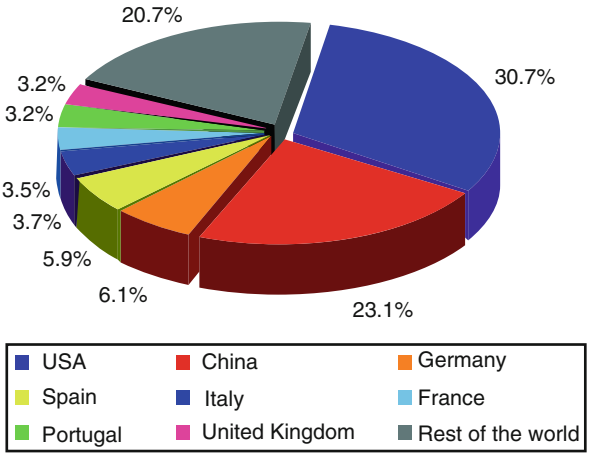

Fig. 3 Regional shares of added capacity in 2008 (After WWEA (2008))

4. The economic potential, given the cost of alternative sources (calculating rated turbine power optimized for grid-cell wind conditions, regressing capital cost and turbine output as a function of rated power and an economies-of-scale factor).

While the theoretical onshore potential exceeds humankind's energy consumption by a few 100-fold, Hoogwijk et al. (2004) estimate the technical potential to be about 100 PWh/year and the economic potential at cost below 7 US¢/kWh to be about 20 PWh/year, both of which still exceed current global electricity consumption. This is consistent with previous studies (Archer and Jacobson (2005) and

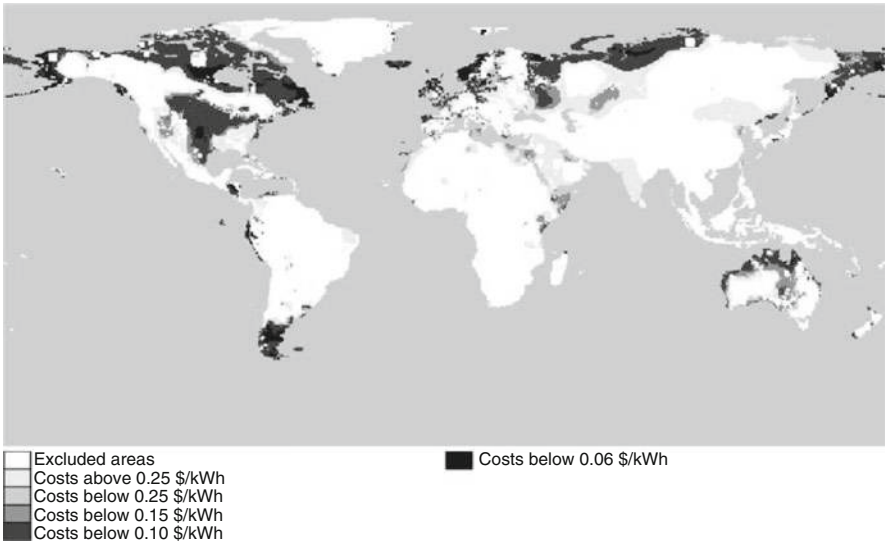

Fig. 4 The economic potential of onshore wind power (After Hoogwijk et al. (2004))

references listed by Hoogwijk et al. (2004) in their Sect. 7.2). However, most of the economic onshore potential – 15 PWh/year – is concentrated in a few remote regions (Fig. 4), namely, the north of Canada (8 PWh/year), Patagonia (4 PWh/year), Siberia (2 PWh/year), and the coastal regions of Australia (1 PWh/year). Only about 5 PWh/year overlaps with regions of significant electricity consumption, the Central USA (3 PWh/year), Western Europe (1 PWh/year), and Central America (1 PWh/year). Relatively small potential is found in Africa, South Asia, and Southeast Asia. The regional technical potentials given by Hoogwijk et al. (2004) are confirmed in studies on the USA (US Department of Energy et al. 2008), India (Carolin Mabel and Fernandez 2008), and China (Changliang and Zhanfeng 2009). Hoogwijk et al. (2004) do not include any grid integration, transmission, and distribution issues in their assessment, which is instead dealt within their later publication (Hoogwijk et al. 2007). The resolution of their global assessment is also such that it cannot account for specific circumstances at the small-region geographical level. In India, for example, the technical potential is further limited by transmission capacity of the grid (Carolin Mabel and Fernandez 2008).

Offshore potential is estimated to be even higher (see Kempton et al. (2007)), but reliable wind data are often lacking (Hoogwijk et al. 2004). Offshore wind power is currently seen as more expensive than onshore wind but at higher penetration rates in the longer term could offer more benefits than onshore because of its more level output and its proximity to large coastal cities (Snyder and Kaiser 2009).

The later assessment of wind by Hoogwijk et al. (2007) takes into account a whole range of effects occurring with increasing penetration, such as output smoothing and increasing interconnection, depletion of the wind resource, requirements of

reliability backup and short-term spinning reserves, and increasingly discarded excess wind energy.

The potential of wind power is hence not limited by the resource potential but instead by how much can be integrated into existing power supply systems without causing major supply and demand imbalances and at acceptable costs (Holttinen 2008). At a given penetration rate, wind power's mitigation potential would depend on future electricity demand. Assuming steady increases in turbine size (from 1.5 MW in 2007 to 2 MW in 2030) and capacity factor (from 25 % in 2007 to 30 % in 2030), the GWEC (2008) projects a moderate growth scenario to lead to 1,400 GW capacity in 2030 (generating 3,500 TWh) and 1,800 GW in 2050 (4,800 TWh). Assuming a 2030 demand of 30 PWh, this scenario is equivalent to an average penetration rate of just over 11 % (compare GWEC (2008, p. 40)). 2050 annual CO_2 mitigation would then amount to about 4.4 Gt CO_2/year. Extrapolating this trend linearly to 2,100 yields a crude estimate of 350 Gt CO_2 total mitigation potential. In addition, the GWEC (2008) reference scenario yields about 1.7 Gt CO_2/year in 2050, or 150 Gt CO_2 until 2100, and the advanced scenario yields about 8.2 Gt CO_2/year in 2050, or 650 Gt CO_2 until 2100. These scenarios are consistent with estimates by the GWEC (2008, pp. 38, 45–46). A long-term global penetration rate of around 20 % is perhaps realistic (compare estimates of 15–20 % in Resch et al. (2008)) given that (a) large economic potential is not available in all world regions and (b) current research indicates substantial difficulties of integrating wind at penetration rates higher than 20 % (Hoogwijk et al. 2007). This corresponds to a total mitigation potential of about 450–500 Gt CO_2. For comparison, Hoogwijk et al. (2007) arrive at potentially avoided CO_2 emissions of 1 Gt CO_2/year, just in OECD Europe and the USA, at carbon prices of around US $30–50/t CO_2. This figure is in the ballpark of the estimate given above.

Technical Principles of Wind Energy Converters

This section discusses modern wind energy conversion systems. However, before setting forth the different types of wind turbines along with their design principles and characteristics, a reminder of the origin of winds, followed by a brief overview of the historical development of wind-powered devices, will first unfold.

Wind power is actually a form of solar power as winds result from solar radiation. Sunbeams entering the atmosphere heat the Earth's surface but not evenly across the surface and over time. Indeed, the equator receives more energy from the sun than the poles and dry land surfaces absorb, retain, and release heat at different rates than the oceans. Consequently, air masses surrounding the Earth's surface warm and cool at different rates. Since hot air masses are lighter than cold ones, they rise and reduce the atmospheric pressure below them drawing in cooler air masses. This creates a global atmospheric convection system that gives birth to winds. Since these air masses are in motion, they have kinetic energy. Wind energy converters capture this kinetic energy and then convert it into a useful form of energy such as electricity or mechanical power.

Sailboats and sailing ships have been using the power of the wind for at least the last 3,000 years. However, the first recorded use of (vertical-axis) windmills to operate irrigational and agricultural projects was in the seventh century BC in the Afghan highlands. The most ancient historical documents pertaining to horizontal-axis windmill technology date from about 1,000 AD and were found in the regions of Persia, Tibet, and China. From there, the technology spread westward to Europe where it was later, at the beginning of the twelfth century, extensively used to grind flour (Ackermann and Söder 2002).

Another seven centuries or so will pass before the first windmill designed for electricity production is built in Scotland in 1887 by Professor James Blyth. Set up in his holiday cottage, his 10-m-high wind turbine charged accumulators engineered by the Frenchman Camille Alphonse Faure to power the lighting of the cottage, thus making it the first residential area in the world to have electricity supplied by wind power (Shackleton 2009). A precursor of modern horizontal-axis wind generators was developed in Yalta, USSR, in 1931. This 100 kW generator mounted atop a 30-m tower was reported to have a capacity factor of 32 %, quite close to current wind machines (Wyatt 1986).

On the eve of the twenty-first century, rising concerns over energy security of supply and global warming paved the way to an expansion of interest in all available forms of renewable energy in general and in wind power in particular. Like this, and boosted in addition by readily available wind resources and economies of scale, worldwide grid-connected wind capacity doubled approximately every 3 years during the 1990s. After the 2003 surge in oil prices due to the geopolitical situation in the Middle East, interest in commercial wind power further expanded.

Modern Wind Energy Conversion Systems

Wind power is the conversion of the kinetic energy of winds into another form of energy, either mechanical or electricity. If the useful form of energy is mechanical (to, for instance, pump water or grind stones), the converter is generally referred to as a windmill. In contrast, if the useful form of energy is electricity, the converter is called a wind turbine or a wind energy converter. In the following section, focus will be on the latter technology, that is, to harness the kinetic energy of wind to produce electricity.

Before examining modern wind energy conversion systems, it is important to bear in mind that only a given fraction of the (kinetic) energy of wind can effectively be harnessed. If all the energy was to be extracted by a wind turbine, the air mass would come to a stop in the intercepting rotor area jamming the cross-sectional area for the following air masses. The theoretical limit of the kinetic energy of the wind that can be harnessed by a hypothetical ideal wind energy extraction machine (referred to as Betz's law and derived by combining the fundamental laws of conservation of mass and energy) is 16/27 (59.3 %).

Wind energy conversion systems can either depend on aerodynamic drag (force acting in a direction opposite to the oncoming flow velocity) or on aerodynamic lift.

Most of modern wind turbines are based on the aerodynamic lift. The resulting force stemming from the blades intercepting the air flow has two components: a (drag force) component in the direction of the flow and a (lift force) component perpendicular to the drag. The lift force is a multiple of the drag force and consequently the main driving power of the rotor, by means of which it produces the necessary driving torque.

The orientation of the spin axis of wind turbines based on aerodynamic lift (lift-type wind turbine) can be either vertical or horizontal. However, horizontal-axis machines are more commonly used for large-scale industrial applications (AWEA 2009).

Horizontal-Axis Wind Turbines

Horizontal-axis wind turbines (HAWTs) consist of a tower atop of which a nacelle containing the rotor, the generator, and an optional gearbox is mounted.

There exist diverse mechanisms to position the nacelle into or out of the wind. Small turbines are pointed by a wind vane, while large ones most of the time use a wind sensor coupled with a servomotor to electrically yaw (align) the nacelle toward or away from the wind depending on the signal sent by the wind sensor.

Since the power in the wind is a cube of the wind speed, the converted mechanical power must always be controlled at high wind speed. This power output control can be achieved by stall control (the blade position remains unchanged but natural turbulences occurring behind the blades in high wind speed reduce the aerodynamic forces and thus the power output), pitch control (the blade angle of attack is reduced at higher wind speed and so are consequently the aerodynamic forces and the power output), or a combination of the two, active stall regulation (the blade angle of attack is fine-tuned to create stall along the blade).

If the wind speed rises above the cutout wind speed threshold (usually varying between 20 and 30 m/s), the turbine is shut off and the rotor is turned out of the wind to avoid potential damage to the primary turbine structure. In so doing, a substantial quantity of energy is wittingly lost. However, equipment capital costs required to strengthen the primary structure to resist wind speeds over the cutout wind speed threshold will likely be larger than the value of the lost energy that could have had otherwise been harvested over the lifetime of the wind turbine.

The number of blades of a horizontal-axis wind turbine depends on its purpose. Turbines designed with two or three blades are usually more suited for electricity generation, while turbines designed with 20 or more blades are generally more suited for mechanical operations (e.g., water pumping).

While most generators are designed to run in the range of 1,200–1,800 rpm (revolutions per minute), large wind turbine rotors most of the time operate at speeds between 10 and 60 rpm. To convert the slow rotational speed of the blades to the higher speeds necessary to drive the electrical generators, gearboxes are therefore used on a majority of large turbines. However, direct mechanical connection (direct drive) can also be achieved with generators designed to run at very low rpm. Such

generators usually consist of many poles (the required rpm of a generator depends on the number of pole pairs) and are very large (large diameter to accommodate the large number of poles) in comparison to generators attached to gearboxes (NREL 2001).

A fixed-speed turbine technology imposes the rotational rate of the turbine to that of the electric grid, whereas a variable-speed turbine technology allows the speed of the rotor to be proportional to the wind speed. In so doing, the former technology forgoes a substantial amount of wind potential, while the latter, in contrast, considerably improves the aerodynamic efficiency in high wind and allows to run at lower speeds so that, everything else being kept equal, a variable-speed technology collects more energy than its fixed-speed counterpart. However, this enhanced energy capture that comes at a high price because of the expensive embedded power electronics and control systems can be economically counterbalanced by fixed-speed wind turbines.

Drawbacks of HAWTs are that the tall towers and blades, up to 90 m long, are difficult to transport and to erect, necessitating tall and expensive cranes and skilled operators. In addition, their imposing structures make them pointedly visible across large areas, disrupting sceneries and landscapes, sometimes leading to local opposition.

In spite of turbulence issues, downwind HAWTs have also been engineered. First, because no additional mechanism for maintaining them aligned with the wind are necessary and second because in high winds, blades can bend, which decreases their swept area and subsequently their wind resistance. However, since turbulences ultimately lead to fatigue failures, horizontal-axis wind turbines are almost exclusively upwind machines.

Vertical-Axis Wind Turbines (VAWT)

The main advantage of this disposition, especially at sites where the wind direction is highly patchy, is that the turbine does not need to be pointed into the wind to be effective. In addition, the generating machinery and gearbox can be placed at ground level, easing maintenance and lowering material requirement.

However, drawbacks are that the driving torque of the rotor varies more noticeably within each turn, the static torque is rather low, and the rotor has to be started up by using the generator as a motor (Sesto and Casale 1998). In addition, it is difficult to erect vertical-axis turbines atop towers. Consequently they are most of the time erected close to the foundations upon which they rest (ground or building rooftop, for instance). It entails that, for a given installed capacity, less wind energy can be harnessed as wind blows slower at lower altitude. In addition, air masses flowing close to the ground are turbulent, potentially producing vibration, and subsequently noise and bearing wear, increasing the maintenance and/or shortening the equipment lifetime (Golding 1997). In contrast, the wind always strikes at a consistent angle the face of a horizontal-axis blade whatever the position in the rotation ensuring a consistent lateral wind loading during a revolution, reducing

vibration and audible noise. Moreover, as opposed to HAWTs, blades, which are fixed to the shaft, cannot be adjusted (pitched), so that power output can be controlled only by aerodynamic stall.

Characteristics of a Wind Turbine

A wind turbine installation is made up of subsystems to harness the energy from the wind (rotor), to point the turbine into the wind (yaw mechanism), and to convert the mechanical rotation into electrical power (generator), as well as subsystems to start, stop, and control the turbine. Horizontal-axis medium to large size grid-connected wind turbines (>100 kW) currently occupy the biggest market share and are expected to principally account for wind deployment in the near future (Ackermann and Söder 2002). This section therefore specifically focuses on their designs that can be divided into three parts (NREL 2006):

- A tower on top of which the nacelle is mounted
- The rotor that includes blades
- The generator that includes an electrical generator, control electronics, and most of the time a gearbox

The Tower

The tower is an important part of a wind turbine primarily because it supports the nacelle and the rotor. The tubular steel tower design is the most widespread technological choice, even though there exist other alternatives like lattice towers or concrete towers. Towers are conical, with their diameter decreasing toward the nacelle, to enhance their strength on the one hand and reduce their material intensity on the other.

In areas with a high surface drag, it is better to erect tall towers since the wind blows faster farther away from the ground. More specifically, wind speed follows in daytime the wind profile power law, which foresees that wind speed rises proportionally to the seventh root of altitude (Peterson and Hennessey 1978). Consequently, doubling the altitude of a turbine theoretically increases the expected wind speeds by 10 % and the expected power by 34 %. However, to avoid buckling, increasing the tower height generally entails enlarging the diameter of the tower as well.

Rotor: Blade Design and Count

Turbine blades, sometimes slightly tilted up, are positioned significantly ahead of the tower and made rigid to prevent them from being shoved into the tower by high winds. Most modern large-scale wind turbine rotor blades are therefore made of

glass fiber-reinforced plastics (e.g., epoxy), which, besides, allows for low rotational inertia and quick accelerations, should gusts of wind occur (variable-speed turbines). In contrast, previous generations of (fixed-speed) wind turbines whose rotational speed is imposed by the AC frequency of the power lines are manufactured with heavier steel blades and therefore higher inertia (Sahin 2004).

The determination of the number of blades depends on the purpose of the wind turbine as aforementioned. Wind turbines for electricity generation usually use either two or three blades even though two-bladed designs are more the exception than the norm for large-scale grid-connected horizontal-axis wind turbines.

The rotor moment of inertia of a three-bladed wind turbine is simpler to comprehend than that of a two-bladed one. In addition, three-bladed wind turbines are often better accepted for their visual aesthetics and are responsible for lower audible noise than their two-bladed counterparts (Thresher and Dodge 1998). Furthermore, during the yawing (alignment) of the nacelle in or out of the wind, a cyclic load is exercised on the root end of every blade and whose magnitude is function of the blade position. Three-bladed turbines see their cyclic load symmetrically balanced when combined at the turbine drivetrain shaft, contributing to smoother maneuvers during yawing.

On the flip side, two-bladed wind turbines, when equipped with a pivoting teetered hub, can also nearly filter out the cyclic loads into the turbine driveshaft and system during yawing. Moreover, the tower top weight is lighter and so consequently is the whole supporting structure, lowering associated costs. In addition, two-bladed turbines can have a higher rotational speed than their three-bladed counterparts. Indeed, the degree of rigidity necessary to avoid hindrance with the tower imposes a lower limit on the thinness of the blades and subsequently (a lower limit) on their mass. However, this is only true for upwind machines as bending of blades enhances tower clearance for downwind ones. Likewise, cheaper gearbox and generator costs can be achieved with two-bladed turbines as faster rotational speeds reduce peak torques in the turbine drivetrain. Lastly, the fewer the number of blades the higher the system reliability is, chiefly through the dynamic loading of the rotor into the tower and turbine drivetrain systems.

Electrical Generator

The energy captured by the blades is subsequently passed onto the generator via a transmission system consisting of a rotor shaft with bearings, brakes, an optional gearbox, as well as a generator.

Whereas the power generation industry resorts almost integrally to synchronous generators because of their variable reactive power production (voltage control), most wind turbines generate electricity through (six-pole induction) asynchronous generators that are directly connected with the electricity grid. However, some designs also use directly driven synchronous generators (Ackermann and Söder 2002).

Electrical generators produce AC (alternating current) power by definition. While the previous generations of (fixed-speed) wind turbines spin at a constant speed governed by the frequency of the grid they are connected onto, new (variable-speed)

ones most of the time rotate at the speed that produces electricity most efficiently being given the actual wind conditions. This can be achieved either using direct AC-to-AC frequency converters (cycloconverters) or using DC current link converters (AC to DC to AC). Although variable-speed turbines require costly power electronics that in addition generate supplementary power loss, a substantially larger fraction of the wind energy can be harnessed by the rotor (NREL 2001).

Control Electronics

Wind conditions being highly variable across sites and over time, a wind turbine is designed to operate over a large range of wind speeds (usually between 12 and 16 m/s). Therefore, to avoid any potential damage to the primary turbine structure during operation in strong winds while ensuring an optimal aerodynamic efficiency of the rotor in light ones, the rotational speed and torque of the rotor must permanently be monitored and controlled. There are several approaches to successfully achieve this (power output) control.

Stall Regulation

This technique requires the rotor to spin at a constant speed (independent of the wind speed). When a wind stream is intercepted in the rotor area, it creates natural turbulences right behind the blades. This is called the stall effect. As a result, aerodynamic forces (induced drag or drag associated with lift) are reduced and so subsequently is the power output of the rotor (Ackermann and Söder 2002).

If the stall effect is a complicated dynamic process to comprehend, stalling is an easy power output control to practically implement as the faster the wind blows, the larger the stall effect is (passive regulation). However, stalling increases the (ordinary) drag by increasing the cross section of the blade facing the wind.

Pitch Control

Pitching the angle of attack of the blades into (respectively out of) the wind increases (respectively reduces) the aerodynamic forces and subsequently the power output of the rotor. One of the main technical challenges associated with designing pitch-controlled wind turbines is getting the blades to furl (to swing out of the wind) swiftly enough in case of a gust of wind. Seemingly, these systems must be able to adjust the pitch of the blades by a fraction of a degree at a time, depending on the wind speed, to control the power output.

The pitching system in medium and large size grid-connected wind turbines is usually based on a hydraulic system, controlled by a computer system. To prevent an eventual hydraulic power failure to furl the blades, pitch regulation systems are also spring-loaded.

By permanently fine-tuning at an optimum angle the rotor blades (even in low-wind conditions), pitch-controlled turbines achieve a better yield at low-wind sites than stall-regulated turbines. In addition, the thrust exercised by the rotor on both the tower and the foundation being significantly lower for pitch-controlled turbines than their stall-regulated counterparts, the primary structure of the former is less material intensive and likely incur lower costs. Moreover, stall-regulated (fixed-pitch) turbines must be shut down when the cutout wind speed threshold is reached, whereas pitch-controlled ones can progressively evolve toward a spinning mode as the rotor operates in a no-load mode at the maximum pitch angle (fully furled turbine).

On the flip side, once the stall effect becomes effective (in high wind conditions), the power oscillations occurring on stall-regulated turbines and stemming from the wind oscillations are smaller than those occurring on pitch-controlled turbines in a corresponding regulated mode (Ackermann and Söder 2002).

Active Stall Regulation

This regulation system is a combination between and a culmination of pitch and stall approaches. It is a combination because, to optimize the aerodynamic efficiency of the rotor and to ensure a torque large enough to create a turning force in light winds, the rotor blades are pitched like in a pitch-controlled wind turbine, whereas after the rated capacity is reached, they are pitched in the opposite direction (than that of a pitch-controlled turbine) in order to increase their angle of attack and install them into a deeper stall.

It is a culmination because active stall regulation achieves a power output control smoother than the jerky one associated with pitch-controlled turbines while still preserving at the same time the advantage of pitch-controlled turbines over stall-regulated ones to turn the blades parallel to the airflow (the so-called low-load feathering position) and subsequently reducing the thrust on the turbine structure (Ackermann and Söder 2002).

Wind Farms

Groups of turbines are often combined into wind farms whose installed capacity can range from a few to several 100 MW. The largest wind farm for commercial production of electric power, situated in Texas, USA, combines 421 turbines into a 735 MW plant. Such turbines are usually three bladed and have high tip speeds (the ratio between the rotational speed of the tip of a blade and the actual velocity of the wind) of 300 km/h. Their supporting structures tower from 60 to 90 m above ground, while their associated blades range from 20 to 40 m in length. Wind plants have short construction lead times, even compared to those of transmission infrastructure.

Trends

Variable-speed turbines with pitch control using either direct driven synchronous ring generator or double-fed asynchronous generators are likely to become the norm, not the exception. However, cost of energy is and will remain the key driving force of wind energy growth. Therefore, if variable-speed turbines are to become a sound economic winner, additional costs incurred by power electronics required by most variable-speed designs must clearly be counterbalanced by the enhanced energy capture.

Capacity and Load Characteristics

Wind energy converters are dependent on the wind, and hence turbine output varies over time, across all timescales ranging from seconds to up to years. Measuring, modeling, and understanding this variability are crucial for site selection and also for integration of wind power into electricity grids.

In 2008, the global capacity of wind energy converters was 121 GW, generating about 260 TWh of electricity (WWEA 2008). This yields a capacity factor of about 24.5 % (Fig. 5).

Plant outages are not as problematic with wind power as they are with fossil, nuclear, or large hydro, because numerous wind plants are usually distributed over a wide geographical area (Archer and Jacobson 2007). Such decentralization in a power supply system reduces the requirements for contingency reserve, since this type of reserve is mostly tied to the largest potential source of failure, which is the largest single generator in the system (Holttinen et al. 2008). Output from wind farms can be expected to be smoother than that of a single turbine, but smoothing effects on larger scales may not be so significant and may also vary between regions. While smoothing effects are discernible when comparing single turbines with wind farms and regions (Fig. 6, and also a similar figure for the UK in Oswald et al. (2008)), combining regions as such may not necessarily lead to much additional smoothing because of strong correlations in the wind regime over large distances (Fig. 7). Østergaard (2008) artificially combines the wind output of West and East Denmark (which are not connected into a common grid) and obtains only small averaging effects. Oswald et al. (2008) uses weather maps to demonstrate the correlation and variability of wind regimes across a large area combining Ireland, the UK, and Germany (Fig. 7). His findings (confirmed for Germany in Weigt (2008, Sect. 3.1 and Fig. 4)) cast doubt on the effectiveness of a trans-channel "supergrid" in smoothing out variations in wind load. Holttinen et al. (2009) present a detailed account of variability across geographical and temporal scales. Archer and Jacobson (2003) present wind speed data for a single site, and three and eight sites in Kansas, USA, and show how the frequency of low-wind events decreases as the number of included sites increases.

However, wind generators cannot – without storage – react to changes in demand because unlike hydropower they cannot follow a fluctuating demand (Fig. 8). Therefore, in the absence of supply matched end uses, they require a flexible electricity grid

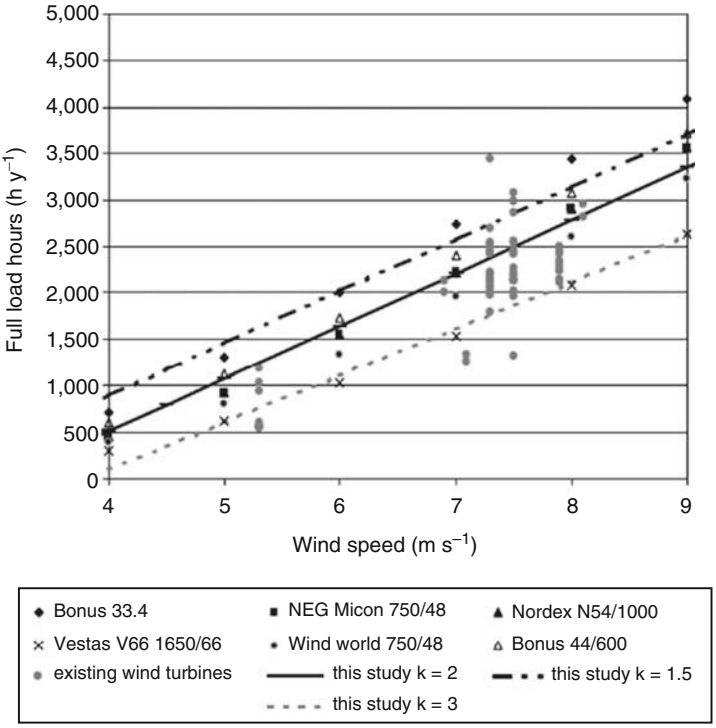

Fig. 5 Average capacity factor as a function of wind speed. Most turbines operate in a range between 2,000 and 3,000 full load hours, which is equivalent to capacity factors between 23 % and 34 % (After Hoogwijk et al. (2004); *k* is the Weibull wind speed distribution parameter). For wind farms at certain windy sites, average capacity factors of up to 45 % are reported (Archer and Jacobson 2007)

with a sufficient portion of technologies that can react quickly to demand changes, such as hydropower or natural-gas-fired plants (GWEC 2008; Söder 2004).

The *average capacity* factor of 24.5 % given above does not reflect the circumstance that electricity system planners must meet demand whenever it occurs and not on average. Where a technology is assessed with regard to its ability to supply peak load, the *capacity credit* describes the fraction of average capacity that is reliably available during peak demand. Capacity credit is also referred to in the literature as *demand capacity* (Pavlak 2008), *capacity value* (Milligan and Porter 2008), or *moderation factor* (Lund 2005). The difference between the average capacity and capacity credit is proportional to the time when wind power cannot meet (peak) demand because of a lack of wind. For example, provided a filled reservoir, the capacity credit of hydropower is virtually equal to its average capacity, but this is not the case for wind power because of its variability and uncertainty. Some generators assign zero capacity credit to wind; however, this is unrealistic (Diesendorf 2007). Wind can achieve up to 40 % capacity credit when penetration is low and times of

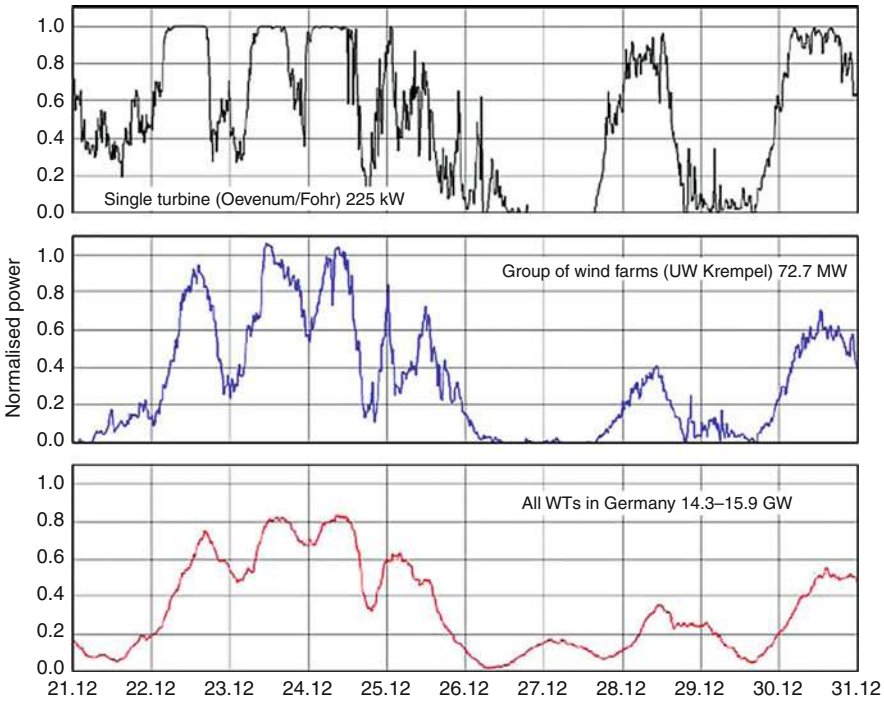

Fig. 6 Normalized power output from a single wind turbine (*top*), and group of turbines (*middle*), and all turbines in Germany (*bottom*; after Focken and Lange)

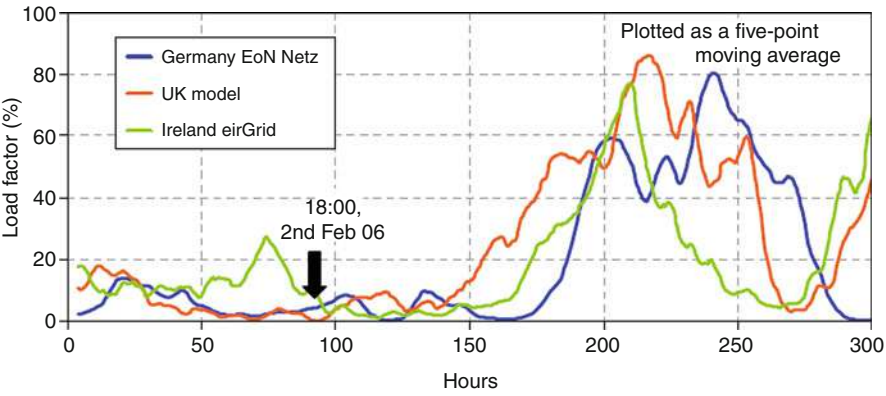

Fig. 7 Variability and correlation of wind loads across Ireland, the UK, and Germany (After Oswald et al. (2008)). On February 2, the electricity demand in Britain reached its peak for 2006

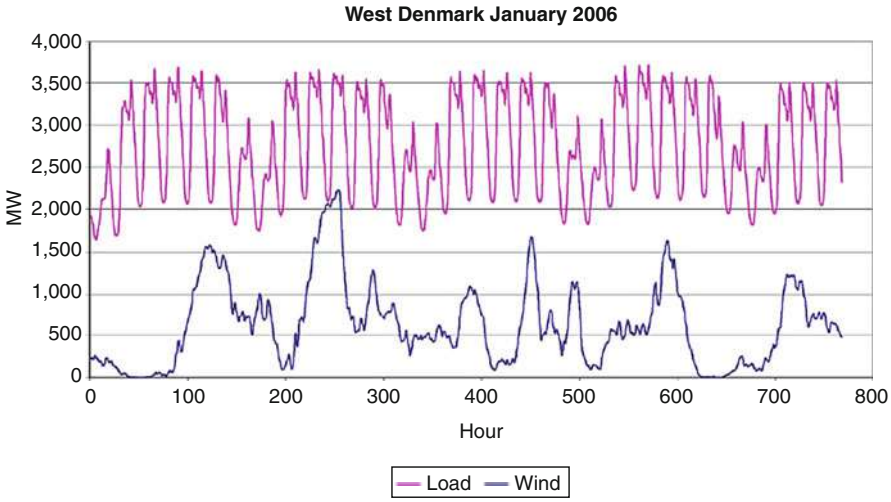

Fig. 8 Wind power output and load in West Denmark (After Söder et al. (2007), © 2007 IEEE)

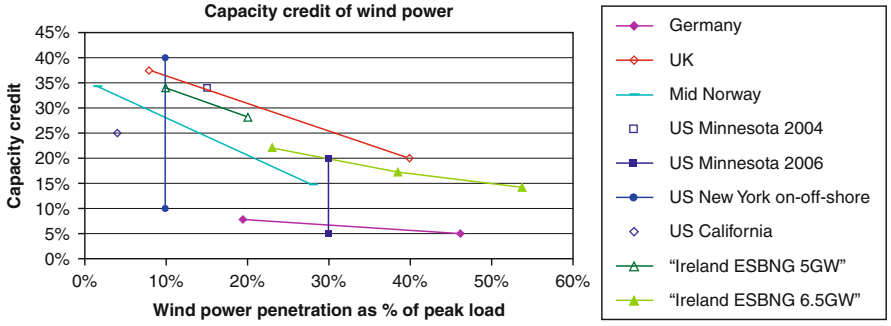

Fig. 9 Capacity credit of wind power as a function of wind penetration (After Holttinen et al. (2009)). Note that as penetration approaches 20 %, the capacity credit starts to fall consistently below wind power's average capacity factor. The results from Mid-Norway show that geographical dispersion improves capacity credit. Decreasing capacity credits have been confirmed theoretically, for example, by Martin and Diesendorf (1980)

ample wind coincide with times of high demand (Holttinen et al. 2009). In general, however, the higher the penetration of wind power in a system, and the more uncorrelated wind output with demand load, the lower its capacity credit (see Fig. 11 in Strbac et al. (2007) and Fig. 9).

Capacity credit is usually measured by applying probability calculus to hourly data on load, generation capacity, ramp rates, and planned or forced outages and applying merit orders in which technologies that avoid fuel costs are recruited first (Milligan and Porter 2008). The *loss-of-load probability* $\mathrm{LOLP}_i = \mathrm{Prob}(\sum_j C_j < L_i)$, with C_j being the capacity of generator j in the grid and L_i the load at hour i, is the probability that a supply system is not able to meet demand in hour i. Integrating

LOLP overall operating hours results in the*loss-of-load expectation* LOLE $= \sum_i$ LOLP$_i$, which is expressed in units of hours/year, or days/10 years, and provides a measure of system reliability. A common system LOLE target is 1 day/10 years, in which case the system has to import capacity from elsewhere. This corresponds to a $1 - 1/(10 \times 365) = 99.97$ % probability that the system will be able to meet demand without having to import capacity.

A power supply system is usually made up of a technology mix. A measure that allows characterizing the incremental contribution of any one component to the reliability of the system is the *effective load-carrying capability*ELCC, which is the new firm (i.e., zero-variance) load that can be added to the system including the incremental capacity increase, without deteriorating the system's reliability. Adding a new generator G as well as a hypothetical firm load ELCC to a system, hourly LOLP becomes LOLP$_i$ = Prob($\sum_j C_j + G < L_i +$ ELCC). ELCC is a hypothetical firm (i.e., zero-variance) load that can be added to a system as a result of the addition of a non-firm (i.e., variable) capacity G that would not change the system's LOLE. ELCC is hence calculated by solving $\sum_i$ Prob($\sum_j C_j < L_i$) = $\sum_i$ Prob($\sum_j C_j + G < L_i +$ ELCC).

ELCC depends critically on the ability of a generator to meet demand at top-ranking LOLP hours, which, in the case of wind, is determined by the correlation of wind output with top-ranking LOLP hours. *Capacity credit* is the ratio of ELCC and rated capacity. Defined as such, capacity credit values are around or lower than the average capacity (Fig. 9). However, capacity credit has at times been measured as the ratio of ELCC and average power (Martin and Diesendorf 1980), in which case it varies between 0 % and 100 %. As a result, where grid operators are required to meet demand at usual loss-of-load expectations, reserve load-carrying capacity or storage has to be secured (Pavlak 2008, Fig. 10).

Similarly, operators also strive to avoid having to curtail surplus wind power at times of high wind, raising different management issues again (Holttinen 2008). Geographical dispersion of wind turbines can help to reduce variability as well as increase predictability of output (Holttinen et al. 2008). Even during a rapidly passing storm front, power from dispersed capacity will take a few hours to change (Söder et al. 2007). Depending on the characteristics of the power system, that is, composition and diversity of technologies, demand management, size, demand profile, and degree of interconnection, low capacity credit poses barriers to the degree of integration of wind energy. In general, the more flexible, load-following capacity there is in the existing grid, the higher the potential penetration of wind power. However, operators run either the risk of not meeting demand by committing too much cheap slow-start capacity or the risk of overrunning cost by committing too much expensive fast-start capacity (DeCarolis and Keith 2006).

Grid integration issues have largely been studied theoretically, except for some European regions. For example, while Denmark receives on average more than 20 % of its electricity from wind, it sometimes receives much higher percentages and sometimes very little, in which case Denmark exports or imports electricity from the European grid and thus relies on other generation technology for load balancing (Pavlak 2008; Østergaard 2003), in particular Norwegian, Swedish, and Finnish hydro reservoirs and idle peaking plants in Denmark (Sovacool et al. 2008).

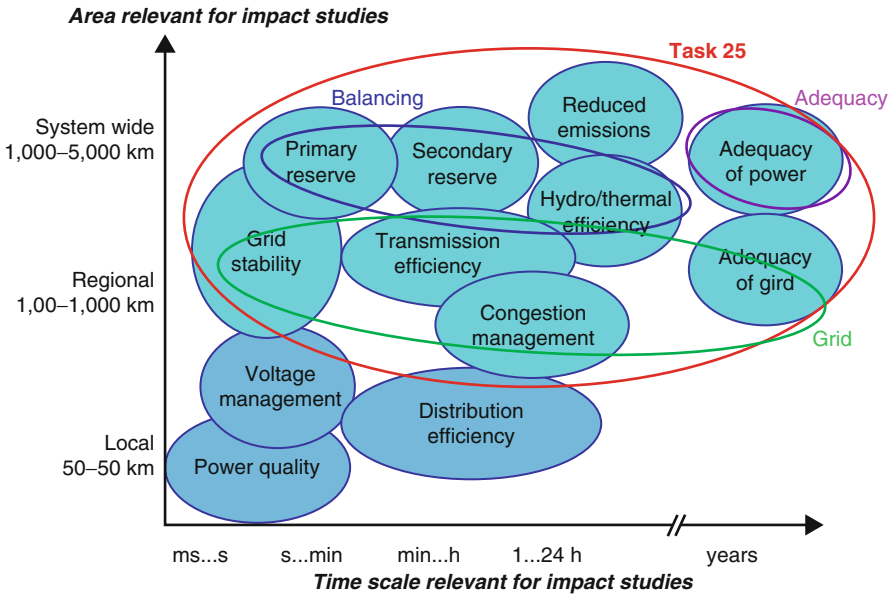

Fig. 10 Typology of grid impacts of wind power across temporal and spatial scales (After Holttinen et al. (2009)). *Balancing* reserves deal with short-term variability in the order of up to 24 h. *Adequacy* in peak-load situations (i.e., low LOLE) has to be secured long term and requires load-carrying reserves to compensate for shortfalls in capacity credit

For higher degrees of integration, the management and/or export of excess wind loads become(s) an issue (DeCarolis and Keith 2006). Söder et al. (2007) report results from four regional systems with high wind penetration, among which two are connected to a larger outside system, and two are not. Management of wind power variability involves the requirement for flexible interconnection capacity and the ability to curtail wind power production, respectively. Hoogwijk et al. (2007) (Fig. 9) find that – subject to supply and load correlation – the amount of electricity that has to be discarded grows strongly for penetrations in excess of 20–30 %. Lund (2005) investigates a scenario for expansion of wind power to cover 50 % of Danish demand and concludes that supply–demand balancing problems would become severe. Similarly, penetration of less than 20 % can lead to instabilities if a grid is not well interconnected with other grids, such as in the case of Spain (Hoogwijk et al. 2007).

Life-Cycle Characteristics

Lenzen and Munksgaard (2002) review and analyze a large body of literature on the life cycle of wind energy converters, comparing bottom-up component analyses with top-down input–output analyses. In their multiple regressions, these authors take into account not only technical features such as scale, vintage year, and load factor but also scope and methodology of the analysis (Fig. 11).

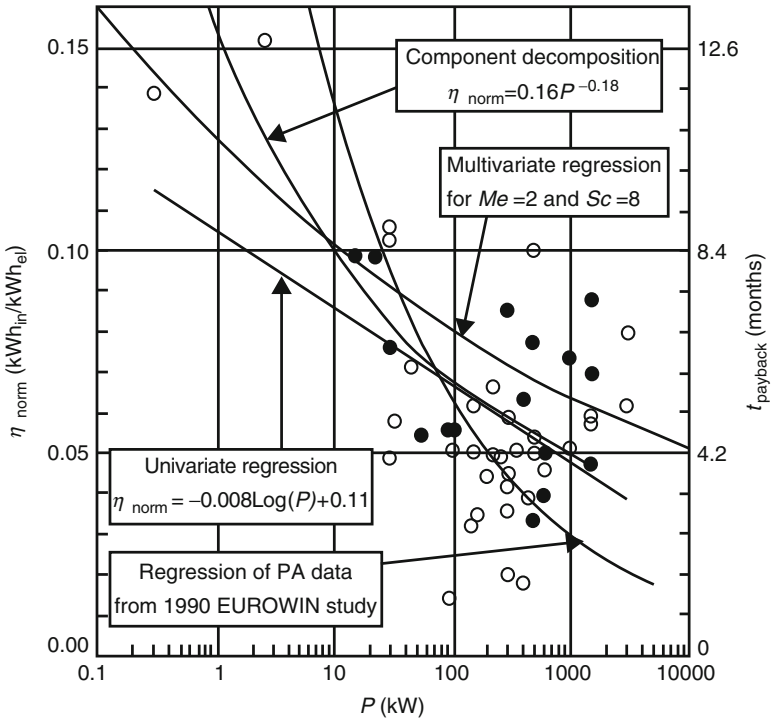

Fig. 11 Cumulative energy requirements of wind energy converters as a function of rated power (After Lenzen and Munksgaard (2002)). The multivariate regression line takes into account different scopes and methodologies adopted in case studies. 0.05 kWh_{th}/kWh_{el} is found to be realistic for modern large turbines

A more recent study by Wagner and Pick (2004) confirms the energy payback times between 3 and 7 months, which – assuming a turbine lifetime of 20 years – corresponds to cumulative energy requirements between 0.035 and 0.075 kWh_{th}/kWh_{el}. The cumulative energy requirement η is related to the energy payback time, that is, the time it takes the wind turbine (lifetime T) to generate the primary-energy equivalent of its energy requirement, via $t_{payback} = \eta \cdot T \cdot \varepsilon_{fossil}$. ε_{fossil} is the conversion efficiency (assumed to be 35 %) of conventional power plants that are to be displaced by wind turbines.

Lenzen and Munksgaard (2002) found greenhouse gas intensities for the larger, modern turbines to be about 10 g/kWh_{el}, ranging among the lowest values for all electricity generation technologies. Lenzen and Wachsmann (2004) found large variations of specific life-cycle emissions of wind turbines between countries where turbine components were produced.

Roth et al. (2005) and Pehnt et al. (2008) take the reduced capacity credit of wind into account in their systems LCA and conclude that CO_2 emissions arising from the need of additional reserves add between 35 and 75 g CO_2/kWh, thus outweighing CO_2 emissions from the turbine life cycle. However, these values depend strongly on the technology mix of the overall power system.

Noise and impacts on birds are likely to be small from wind farms, compared to other impacts (GWEC 2008). Snyder and Kaiser (2009) provide a detailed account of possible ecological impacts from offshore wind farms.

The mitigation potential of wind in a power system represents an optimization problem, because the higher the penetration of wind power, the higher the emission reductions, and also the higher the variability cost.

Current Scale of Deployment

Due to large economies of scale, the scale of single wind energy converters has been increasing steadily (Fig. 12), featuring taller towers and larger rotors. Larger turbines with ratings above 3.5 MW are usually dedicated to offshore power generation, while onshore installations are usually rated between 1.5 and 3 MW (GWEC 2008). In early 2009, the French manufacturer Areva deployed 5 MW turbines for operation 45 km offshore of the German North Sea island of Borkum (Jha 2009). Five-megawatt turbines are also installed at the Beatrice site (40 m depth) off the Moray Firth east of Scotland (http://www.repower.de/index.php?id=369). In 2007, the average size of operating turbines was 1.5 MW.

Contribution to Global Electricity Supply

In 2008, the global capacity of wind energy converters was 121 GW, generating about 260 TWh of electricity or about 1.5 % of global electricity production (WWEA 2008). Most of the capacity (Fig. 1) is installed in the USA (25 GW, 1 % of electricity generation) and in the EU (about 65 GW, 3.7 %), followed by China

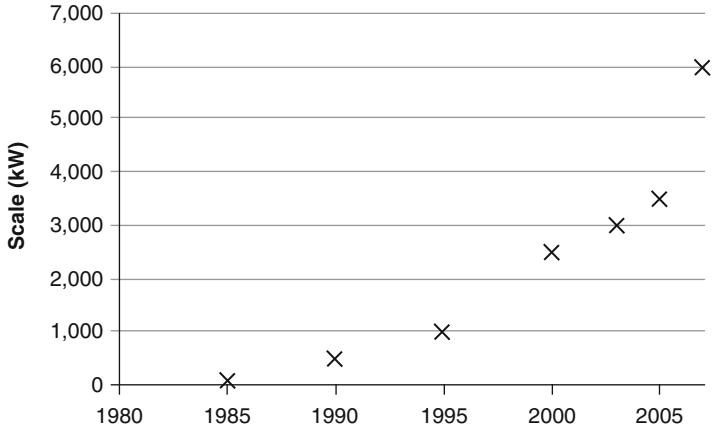

Fig. 12 Maximum scale of wind energy converters over time (Compiled after Hoogwijk et al. (2004), GWEC (2008), Joselin Herbert et al. (2007))

(12 GW) and India (10 GW). However, regional shares of wind power can be much higher in some countries: Denmark (21 %), Spain (12 %), Portugal (9 %), Ireland (8 %), and Germany (7 %). However, it is worth noting that Denmark at times receives much higher percentages of its electricity from wind and sometimes very little, in which case Denmark exports or imports electricity from the European grid and thus relies on other generation technology for load balancing (Pavlak 2008; Sovacool et al. 2008).

Wind energy deployment has been increasing rapidly throughout the past decade, recording growth rates of around 30 % since 1996 (Fig. 2). More than half of the 2008 additions occurred in the USA and in China (Fig. 3), with the USA overtaking Germany as the leader in installed wind capacity (WWEA 2008). In the USA, wind power has represented 40 % of 2007 national capacity growth (Bolinger and Wiser 2009).

Most of the wind generation is onshore; only about 1.1 GW is presently installed offshore, mainly located in Denmark (420 MW), the UK (300 MW), Sweden (135 MW), and the Netherlands (130 MW) (IEA 2008b, www.ieawind.org/Annex_XXIII.html). A further 8 GW were planned in early 2009 (Jha 2009).

Cost of Electricity Output

Capital costs make up about 80 % of total wind energy cost, with the remainder for operation and maintenance, since the wind turbine does not require any fuel input. Blanco (2008) presents a detailed breakdown of these costs; in onshore installations, the turbine covers 70 % of capital cost, with the remainder for grid connection, civil works, taxes, permits, etc. Within the turbine, the tower and blades make up for half of the costs. Electricity costs vary with site conditions: assuming a 20-year plant life, 5–10 % discount rate, and 23 % average capacity factor, Blanco (2008) states a levelized cost range for electricity from European 2 MW wind turbines between 6.5 and 13 US¢/kWh. Welch and Venkateswaran (2008) and Snyder and Kaiser (2009) report US cost estimate between 3 and 5 US¢/kWh and DeCarolis and Keith (2006) between 4 and 6 US¢/kWh.

Levelized electricity cost is the constant (discounted to present values) real wholesale price of electricity that recoups owners' and investors' capital costs, operating costs, fuel costs, income taxes, and associated cash flow constraints. They exclude costs for transmission and distribution. Levelized cost may differ from sales prices, because of profits or losses. The figures reported here are averages over plant types and vintages and over locations with varying resource endowments and demand profiles. Actual cost for particular plants may be different from the cost given here. Levelized electricity costs are strongly determined by the competitive landscape, in particular the extent and nature of regulation, subsidization and taxation, primary fuel (coal, gas, uranium) prices, and future carbon pricing. While under government regulation operators are able to transfer costs and risk to consumers and taxpayers, this is not the case in deregulated electricity markets, where high interest rates lead to investors favoring less capital-intensive and therefore less

risk-prone power options. Electricity cost figures reported here refer to the financial and regulatory environment at the time of publication of the various references.

Civil works and especially the foundations are much more expensive in offshore installations, where they represent 20 % of capital cost, leading to higher levelized cost of 9–16 US¢/kWh. This is confirmed in an estimate of 10 US¢/kWh by Snyder and Kaiser (2009). However, technological learning can bring these costs down in the future (IEA 2008b; Smit et al. 2007).

Wind energy costs have increased during the past 3 years, mainly driven by supply tightness and price hikes of raw materials (IEA 2008b), which is difficult to control by government fiscal policy. Bolinger and Wiser (2009) provide a detailed analysis of most recent upward cost trends. Yet, the analysis of learning curves for the industry suggests that levelized costs will come down through increased efficiency, by about 10 % for every doubling of capacity (Blanco (2008); compare Fig. 14 in UNDP (2004)). As with other nonfossil electricity generation technologies, wind plant operators expect the competitive landscape to change in favor of wind power, once carbon is adequately priced (GWEC 2008; DeCarolis and Keith 2006). In the future, wind energy is also expected to benefit more from not being affected by fuel price volatility.

However, depending on the penetration of a power system with variable wind energy, additional indirect costs arise for maintaining LOLE, because wind energy will not be able to meet demand at its average capacity factor but at a generally reduced rate depending on its capacity credit (DeCarolis and Keith 2006). In addition, the presence of wind power in a power supply system introduces short-term variability and uncertainty and therefore requires balancing reserve scheduling and unit commitment. Grid operators need to meet peak demand to certain statistical reliability standards even when wind output falls relative to load. During these periods, which range from minutes to hours, electricity markets need to recruit demand-following units (such as gas, hydro, or storage), which at times of sufficient wind remain idle, so that costs arise essentially for two redundant systems (Pavlak 2008; Benitez et al. 2008) and for inefficient fuel use during frequent ramping (see p. 903 in Hoogwijk et al. (2007), Benitez et al. (2008), Smith et al. (2007)). Both adequacy and balancing cost (compare Fig. 10) are sometimes referred to as intermittency cost; however, in this chapter the term variability cost is used because strictly speaking wind energy is variable and not intermittent (Diesendorf 2007). Thus, wind energy reduces dependence on fuel inputs but does not eliminate the dependence on short-term balancing capacity and long-term reliable load-carrying capacity.

The impact of wind power on the power supply system is critically dependent on the technology mix in the remainder of the system, because the more flexible and load-following existing technologies, the less peak reserves are needed. It is also dependent on time characteristics of system procedures (frequency and duration of forecasts, etc.) and local market rules (Holttinen 2008). In general, the higher the wind penetration, the higher the variability in the supply system, and the more long-term reserve and short-term balancing capacity has to be committed (Fig. 13) on short-term balancing only. The corresponding cost increases are only partly offset by

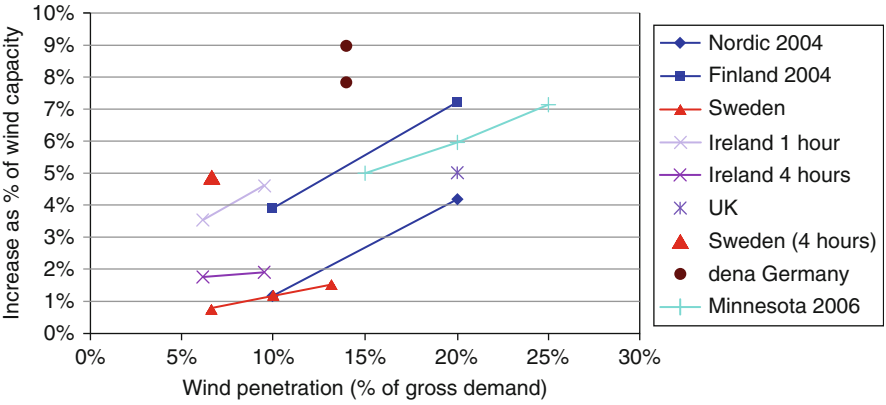

Fig. 13 Increase in short-term balancing requirement as a percentage of wind power as a function of wind penetration (After Holttinen et al. (2009))

a smoothing out of wind variability when many turbines are dispersed and interconnected over a wide geographical area (Hirst and Hild 2004), but they are more than offset by reduced fuel and operating cost. In specific applications, the cost of additional wind power also depends on the relative locations of turbines, load, and existing transmission lines and on whether sufficient load-carrying reserve exists in the grid or has to be built.

As expected, variability costs scatter significantly depending on a large array of parameters. They cannot be derived from capacity credit estimates, since these do not contain any information about to what extent cheap base load and expensive peak load are being displaced by wind (Martin and Diesendorf 1982). Variability costs are difficult to disentangle from overall cost in real-world grids (DeCarolis and Keith 2006), so that they have largely been estimated for theoretical settings, using statistical models for resource and load fluctuations and least-cost-optimizing generation and reserve scheduling under given output limits, startup and shutdown cost, ramp-rate restrictions, planned outages, fuel cost, and day-ahead forecasts (Holttinen et al. 2008; Hirst and Hild 2004). They have been quoted between 0.2 and 0.4 US¢/kWh for existing installations (Snyder and Kaiser 2009; GWEC 2008) and also higher at 1–1.8 US¢/kWh (DeCarolis and Keith 2006; Benitez et al. 2008; Ilex and Strbac 2002) for larger degrees of wind penetration. In a more up-to-date survey, Holttinen (2008), Strbac et al. (2007), and Smith et al. (2007) report on recent findings about increases in balancing requirements due to the presence of wind, ranging widely between 0.05 and 0.5 US¢/kWh (Fig. 14). Hence, at penetrations of up to 20 %, variability cost can be expected to be about equal or less than 10 % of generation cost.

Hoogwijk et al. (2007) (see Fig. 15) run numerical experiments at large-scale penetration rates of up to 45 % and find that beyond 30 % penetration the cost incurred by discarded excess electricity becomes comparable to base cost (6 US¢/kWh).

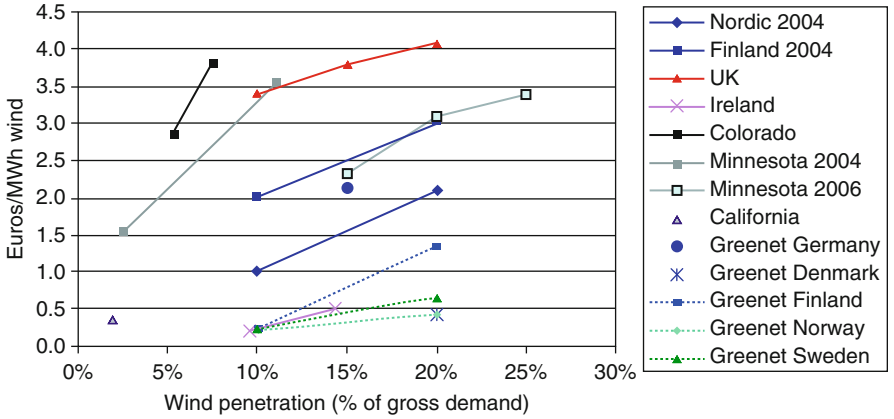

Fig. 14 Increase in balancing requirements per kWh of wind power as a function of wind penetration (After Holttinen et al. (2009))

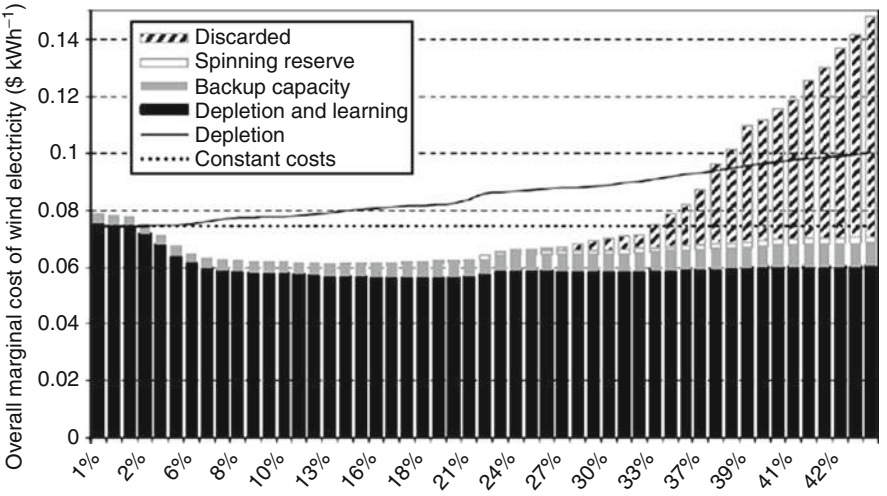

Fig. 15 Marginal cost of wind electricity at varying degrees of penetration (After Hoogwijk et al. (2007))

The market for wind turbine manufacturing is diverse and competitive, with manufacturers spread across many countries. However, large corporations are entering the market, sometimes assimilating smaller entities (GWEC 2008). During the recent wind market boom, and the shift to larger turbines, the industry faced a number of supply chain bottlenecks related to gearboxes and large bearings (Blanco 2008), leading to waiting times for turbines of up to 30 months (Sovacool et al. 2008).

Future Directions

Wind energy faces a number of technical future challenges. The variable and distributed nature of wind energy requires specific grid infrastructure in order to ensure grid stability, congestion management, and transmission efficiency. Significant investment in grid infrastructure has to occur in order to allow for substantial global penetration of wind energy (GWEC 2008). One of the most significant challenges is hence the integration of wind power into a large grid and the theoretical modeling of power system behavior at high penetration rates of wind. Recent efforts are also aimed at improving short-term forecasting of wind, which is still less accurate than forecasting of load (Holttinen et al. 2009). With increasing interconnection and geographical dispersion, forecasting errors are expected to decrease (see Fig. 16).

Some researchers suggest directing wind power to where it can be most competitive or where its variability does not create problems. Some industrial applications and also combined heat and power plants can – within limits – adjust their demand to supply (Østergaard 2003). Dedicated load-leveling applications such as desalination, aluminum smelting, space and water heating, or chargeable hybrid vehicle fleet can deal with hourly variations in wind power since they only require a certain amount of energy over a period of many hours (Kempton et al. 2007; Pavlak 2008). For example, large-scale vehicle-to-grid technologies can significantly reduce excess wind power at large wind penetration and replace a significant fraction of regulating capacity, but as Lund and Kempton (2008) show in a study for Denmark, electric vehicles would not nearly eliminate excess power and CO_2 emissions, even if they had long-range battery storage.

Tavner (2008) and Smith et al. (2007) list improvements in resource, turbine and systems modeling and forecasting, capital cost reduction, lifetime extension, transmission upgrading, and system integration as the main future research challenges for wind power. Joselin Herbert et al. (2007) review past developments and present

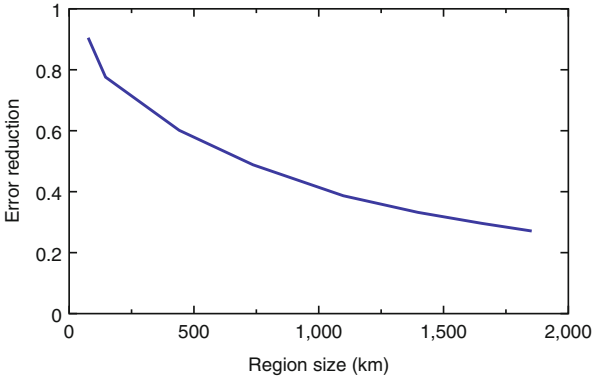

Fig. 16 Measured forecast error as a function of spatial range of interconnection (After Rohrig). The error reduction plotted on the y-axis is the ratio of the root-mean-square error (*RMSE*) of prediction at a regional scale and the single-site prediction RMSE

research needs for wind technologies, such as for resource assessment, site selection, turbine aerodynamics, wake effects, and turbine reliability. Offshore wind deployment faces technical challenges in the form of extreme wind conditions that exceed tolerances of current onshore turbines (Snyder and Kaiser 2009; Smit et al. 2007). The IEA Wind Offshore subgroup's tasks include research on ecological issues and deepwater installation. In order to reduce offshore wind costs, turbine concepts, submerged structures and cabling, and remote operation and maintenance will need to undergo further research (Blanco 2008). Many of the above issues are approached through theoretical modeling, be it turbine structure, system control and balancing, wind conditions, or reliability (Tavner 2008). Surprisingly, offshore wind power generation shares many of large hydropower and nuclear power's challenges regarding public opinion. Firestone and Kempton (2007) report a case study where the majority of survey respondents opposed offshore wind power development for environmental reasons and that many of the beliefs were "stunningly at odds" with the scientific literature. Perceived landscape changes also feature in a survey by Zoellner et al. (2008), but economic considerations more strongly influenced acceptance.

Summary

Wind energy deployment has witnessed a rapid increase throughout the past decade, with annual growth rates around 30 %, generating now about 1.5 % of global electricity. The technology is mature and simple, and decades of experience exist in a few countries. Due to strong economies of scale, wind turbines have grown to several megawatts per device, and wind farms have now been deployed offshore. In recent years, wind power has become competitive without subsidies, in markets without carbon pricing. The global technical potential of wind exceeds current global electricity consumption; however, taking into account the temporal mismatch and geographical dispersion of wind energy and demand loads and requirements for supply–load balance and grid stability, the maximum economic potential appears to be in the order of 20 % of electricity consumption. At such rates of wind energy penetration, and without storage and supply matched demand, the integration of wind power into electricity grids and long-distance transmission begins to present significant challenges for system reliability and loss-of-load expectation. The main issue for future deep penetrations of wind on a global scale is hence how wind plants can be integrated across very large geographical scales and with other variable power sources. For example, there are popular proposals for integrating parts of North African solar power for output smoothing of large wind supply in Europe. Some commentators remark that these proposals may be difficult to implement because of political and supply security issues; others are more optimistic. Finally, the life-cycle greenhouse gas emissions from wind power are some of the lowest among all electricity-generating technologies, but depending on the remainder of the power supply system, emissions arise because of the use of conventional technologies for supply–demand balancing.

References

Ackermann T, Söder L (2002) An overview of wind energy – status 2002. Renew Sustain Energy Rev 6:67–128

Archer CL, Jacobson MZ (2003) Spatial and temporal distributions of U.S. winds and wind power at 80 m derived from measurements. J Geophys Res 108:1–20

Archer CL, Jacobson MZ (2005) Evaluation of global wind power. J Geophys Res 110:1–20

Archer CL, Jacobson MZ (2007) Supplying baseload power and reducing transmission requirements by interconnecting wind farms. J Appl Meteorol Climatol 46:1701–1717

AWEA (2009) Wind energy basics. American Wind Energy Association. www.awea.org/faq/wwt_basics.html

Benitez LE, Benitez PC, Van Kooten GC (2008) The economics of wind power with energy storage. Energy Econ 30:1973–1989

Blanco MI (2008) The economics of wind energy. Renew Sustain Energy Rev 13:1372–1382

Bolinger M, Wiser R (2009) Wind power price trends in the United States: struggling to remain competitive in the face of strong growth. Energy Policy 37:1061–1071

Carolin Mabel M, Fernandez E (2008) Growth and future trends of wind energy in India. Renew Sustain Energy Rev 12:1745–1757

Changliang X, Zhanfeng S (2009) Wind energy in China: current scenario and future perspectives. Renew Sustain Energy Rev 13:1966–1974

DeCarolis JF, Keith DW (2006) The economics of large-scale wind power in a carbon constrained world. Energy Policy 34:395–410

Diesendorf M (2007) The base-load fallacy. www.energyscience.org.au

Firestone J, Kempton W (2007) Public opinion about large offshore wind power: underlying factors. Energy Policy 35:1584–1598

Focken U, Lange M. German forecasting company. Energy & Meteo systems. Accessed on 23 March 2015. www.energymeteo.de

Golding EW (1997) The generation of electricity by wind power. E & FN Spon, London

GWEC (2008) Global wind energy outlook. Global Wind Energy Council, Brussels

Hirst E, Hild J (2004) The value of wind power as a function of wind capacity. Electr J 17:11–20

Holttinen H (2008) Estimating the impacts of wind power on power systems – summary of IEA wind collaboration. Environ Res Lett 3:1–6

Holttinen H, Milligan M, Kirby B, Acker T, Neimane V, Molinski T (2008) Using standard deviation as a measure of increased operational reserve requirement for wind power. Wind Eng 32:355–378

Holttinen H, Meibom P, Orths A, van Hulle F, Lange B, Malley MO, Pierik J, Ummels B, Olav Tande J, Estanqueiro A, Matos M, Gomez E, Söder L, Strbac G, Shakoor A, Ricardo J, Charles Smith J, Milligan M, Ela E (2009) Design and operation of power systems with large amounts of wind power, VTT research notes, 2493. VTT Technical Research Centre of Finland, Espoo

Hoogwijk MM, De Vries BJM, Turkenburg WC (2004) Assessment of the global and regional geographical, technical and economic potential of onshore wind energy. Energy Econ 26:889–919

Hoogwijk MM, Van Vuuren D, De Vries BJM, Turkenburg WC (2007) Exploring the impact on cost and electricity production of high penetration levels of intermittent electricity in OECD Europe and the USA, results for wind energy. Energy 32:1381–1402

IEA (2008a) Energy technology perspectives. International Energy Agency, Paris

IEA (2008b) Wind renewable energy essentials. OECD/IEA, Paris

Ilex X, Strbac G (2002) Quantifying the system cost of additional renewables in 2020. Ilex Energy Consulting, Oxford

Jha A (2009) Brawny wind turbines set for German offshore debut. The Guardian Weekly, 30 Jan 2010

Joselin Herbert GM, Iniyan S, Sreevalsan E, Rajapandian S (2007) A review of wind energy technologies. Renew Sustain Energy Rev 11:1117–1145

Kempton W, Archer CL, Dhanju A, Garvine RW, Jacobson MZ (2007) Large CO_2 reductions via offshore wind power matched to inherent storage in energy end-uses. Geophys Res Lett 34:1–5
Lenzen M (2010) Current state of development of electricity-generating technologies: a literature review. Energies 3(3):462–591
Lenzen M, Badcock J (2009) Current state of development of electricity-generating technologies – a literature review. Centre for Integrated Sustainability Analysis, The University of Sydney, Sydney. www.aua.org.au/Content/Lenzenreport.aspx
Lenzen M, Munksgaard J (2002) Energy and CO_2 analyses of wind turbines – review and applications. Renew Energy 26:339–362
Lenzen M, Wachsmann U (2004) Wind energy converters in Brazil and Germany: an example for geographical variability in LCA. Appl Energy 77:119–130
Lund H (2005) Large-scale integration of wind power into different energy systems. Energy 30:2402–2412
Lund H, Kempton W (2008) Integration of renewable energy into the transport and electricity sectors through V2G. Energy Policy 36:3578–3587
Martin B, Diesendorf M (1980) Calculating the capacity credit of wind power. In: Proceedings of the Fourth Biennial Conference of the Simulation Society of Australia, Brisbane, 27-29
Martin B, Diesendorf M (1982) Optimal mix in electricity grids containing wind power. Electr Power Energy Syst 4:155–161
Milligan M, Porter K (2008) Determining the capacity value of wind: an updated survey of methods and implementation. In: Conference paper, NREL/CP-500-43433. National Renewable Energy Laboratory, Golden
NREL (2001) The history and state of the art of variable-speed wind turbine technology. Technical report, NREL/TP-500-28607. National Renewable Energy Laboratory
NREL (2006) Wind turbine design cost and scaling model. Technical report, NREL/TP-500-40566. National Renewable Energy Laboratory
Østergaard PA (2003) Transmission grid requirements wit scattered and fluctuating renewable electricity-sources. Appl Energy 76:247–255
Østergaard PA (2008) Geographic aggregation and wind power output variance in Denmark. Energy 33:1453–1460
Oswald J, Raine M, Ashraf-Ball H (2008) Will British weather provide reliable electricity? Energy Policy 36:3212–3225
Pavlak A (2008) The economic value of wind energy. Electr J 21:46–50
Pehnt M, Oeser M, Swider DJ (2008) Consequential environmental system analysis of expected offshore wind electricity production in Germany. Energy 33:747–759
Peterson EW, Hennessey JP (1978) On the use of power laws for estimates of wind power potential. J Appl Meteorol 17:390–394
Resch G, Held A, Faber T, Panzer C, Toro F, Haas R (2008) Potentials and prospects for renewable energies at global scale. Energy Policy 36:4048–4056
Rohrig K. Fraunhofer Institut für Windenergie und Energiesystemtechnik. IWES. www.iwes.fraunhofer.de
Roth H, Brückl O, Held A (2005) Windenergiebedingte CO_2-Emissionen konventioneller Kraftwerke, lfE-Schriftenreihe, Heft 50. Lehrstuhl für Energiewirtschaft und Anwendungstechnik, München
Sahin AD (2004) Progress and recent trends in wind energy. Prog Energy Combust Sci 30 (5):501–543
Sesto E, Casale C (1998) Exploitation of wind as an energy source to meet the world's electricity demand. J Wind Eng Ind Aerodyn 74–76:375–387
Shackleton J (2009) World first for Scotland gives engineering student a history lesson. The Robert Gordon University. www.rgu.ac.uk/pressrel/BlythProject.doc
Smit T, Junginger M, Smits R (2007) Technological learning in offshore wind energy: different roles of the government. Energy Policy 35:6431–6444

Smith JC, Milligan M, DeMeo EA, Parsons B (2007) Utility wind integration and operating impact state of the art. IEEE Trans Power Syst 22:900–908
Snyder B, Kaiser MJ (2009) Ecological and economic cost-benefit analysis of offshore wind energy. Renew Energy 34:1567–1578
Söder L (2004) On limits for wind power generation. Int J Global Energy Issues 21:243–254
Söder L, Hofmann L, Orths A, Holttinen H, Y-h W, Tuohy A (2007) Experience from wind integration in some high penetration areas. IEEE Trans Energy Convers 22:4–12
Sovacool BK, Lindboe HH, Odgaard O (2008) Is the Danish wind energy model replicable for other countries? Electr J 21:27–28
Strbac G, Shakoor A, Black M, Pudjianto D, Bopp T (2007) Impact of wind generation on the operation and development of the UK electricity systems. Electr Power Syst Res 77:1214–1227
Tavner P (2008) Wind power as a clean-energy contributor. Energy Policy 36:4397–4400
Thresher R, Dodge D (1998) Trends in the evolution of wind turbine generator configurations and systems. Wind Energy 1:70–85
U.S. Department of Energy, Black & Veatch and AWEA (2008) 20 % Wind energy by 2030. DOE/GO-102008-2567, U.S. Department of Energy, Oak Ridge
UNDP (2004) World energy assessment: 2004 update. United Nations Development Programme, New York
Wagner H-J, Pick E (2004) Energy yield ratio and cumulative energy demand for wind energy converters. Energy 29:2289–2295
Weigt H (2008) Germany's wind energy: the potential for fossil capacity replacement and cost saving. Appl Energy 86:1857–1863
Welch JB, Venkateswaran A (2008) The dual sustainability of wind energy. Renew Sustain Energ Rev 12(9):2265–2300
WWEA (2008) World wind energy report. World Wind Energy Association, Bonn. www.wwindea.org
Wyatt A (1986) Electric power: challenges and choices. Book Press, Toronto
Zoellner J, Schweizer-Ries P, Wemheuer C (2008) Public acceptance of renewable energies: results from case studies in Germany. Energy Policy 36:4136–4141

Wave Power: Climate Change Mitigation and Adaptation

Gregorio Iglesias and Javier Abanades

Contents

Abstract

Wave energy has a great potential in many coastal areas thanks to a number of advantages: the abundant resource, with the highest energy density of all renewables, leading to higher availability factors than, e.g., wind or solar energy, and the low environmental and particularly visual impact, not least in the case of

G. Iglesias (✉) • J. Abanades
School of Marine Science and Engineering, University of Plymouth, Plymouth, UK
e-mail: gregorio.iglesias@plymouth.ac.uk; javier.abanadestercero@plymouth.ac.uk

W.-Y. Chen et al. (eds.), *Handbook of Climate Change Mitigation and Adaptation*,
DOI 10.1007/978-3-319-14409-2_81

offshore floating wave energy converters (WECs). In addition, a novel advantage will be investigated in this work: the possibility of a synergetic use for carbon-free energy production and coastal protection. All in all, these advantages make wave energy a promising alternative to conventional energy sources. In this chapter the fundamentals of the wave resource and its characterization are outlined. The technologies for wave energy conversion are classified according to three criteria, the most representative WECs are presented, and the technological challenges discussed. Next, the environmental impacts of wave energy extraction are analyzed, with a focus on the reduction of coastal erosion.

If there are two main strategies to cope with climate change, mitigation and adaptation, wave farms participate on both. Indeed, wave energy contributes to mitigating climate change by two means, one acting on the cause, the other on the effect: (i) by bringing down carbon emissions (cause) through its production of renewable energy and (ii) by reducing coastal erosion (effect). Given that one of the causes of climate change is precisely coastal erosion – through sea-level rise and increased storminess – the contribution of wave farms to its mitigation is indeed welcome. As for adaptation, wave farms – which typically consist of floating WECs – adapt naturally to sea-level rise; this is a major advantage relative to conventional coastal defense schemes, based on fixed structures (seawalls, detached breakwaters, groynes, etc.)

Introduction

The adverse effects brought about by the world's reliance on fossil fuels are well known: (i) greenhouse gas emissions that exacerbate climate change, (ii) diminished reserves of carbon fuels, and (iii) geopolitical wrangling over the control of the oil and gas reserves, which has led to many conflicts and all-out wars in the last decades. In addition, the variability in oil and gas prices has a deleterious effect on the global economy. These arguments, and the international treaties and protocols signed to foster the efforts against climate change, call for the development of renewable energy sources.

Among renewable energies, the potential for development of marine renewable energy[1] (MRE) is widely recognized (Bahaj 2011; Iglesias and Carballo 2009), so much so that it is poised to become a fundamental pillar in the EU energy policy (cf. SET-Plan European Commission 2007). The MRE industry has a target for 2050 of 188 and 460 GW of installed capacity for ocean energy (wave and tidal) and offshore wind, respectively (EU-OEA 2010; Jeffrey and Sedgwick 2011; Moccia et al. 2011). The figures for 2020 are 3.6 and 40 GW for ocean and offshore wind energy, respectively (EWEA et al. 2012). In view of these values, it is obvious

[1]Marine renewable energies include both ocean energy and offshore wind energy. Ocean energy comprises essentially wave and tidal energy, but also Ocean Thermal Energy Conversion (OTEC) and salinity gradient energy.

that a relevant breakthrough is necessary for these targets to be attained. In the case of wave energy, single WECs will not be able to supply the amounts of energy that are required; therefore, arrays of devices, also known as wave farms, are to be deployed. As indicated above, these wave farms can serve not only to generate carbon-free energy and thus meet the previous targets but also to protect coastal sections experiencing erosion, flooding, or both.

Different types of waves exist in the ocean: (1) wind-generated waves, (2) tsunamis (seismic disturbance waves), and (3) tidal waves. In the following the terms "wave energy" or "wave power" are used to denote the energy and power of wind waves, respectively. Winds are caused by the differential heating of the Earth's atmosphere by the Sun, which in turn gives rise to waves through a complex energy transfer. In the transformation of solar energy into wind and, subsequently, wave energy, a concentration process occurs which augments power density. Thus, whereas the power density supplied by the Sun is of the order of 1.70×10^2 Wm^{-2}, the average wind power density is approx. 5.80×10^2 Wm^{-2} at a latitude of 15 °N or 15 °S, and the average wave power density is approx. 8.42×10^3 Wm^{-2}. It follows that wave energy can be considered a concentrated form of solar energy.

Wave energy presents a number of advantages relative to other renewables: the abundance and high density of the resource in many coastal areas, leading to high availability values (approx. 90 % vs. 30 % in the case of wind or solar energy), and, importantly, the low environmental and, in particular, visual impact of wave energy converters. On the downside, the cost of wave energy is often alluded to, and the levelized cost of energy (LCOE) of wave energy has been the object of recent studies, e.g., Astariz and Iglesias (2015). In this respect it is important to mention that the externalities of wave energy are often neglected in the analysis; these enhance economic viability of wave energy and should be accounted for – not least in public policy making (Astariz and Iglesias 2014). Moreover, the economies of scale that will occur once the rhythm of WEC production increases will contribute to lowering the costs of wave energy, much as in the case of offshore wind or, more generally, any nascent technology, from automobiles to computers.

The structure of this chapter is as follows. The fundamentals of the wave resource are summarized in section "Fundamentals of the Wave Energy Resource." For this resource to form the basis of a fully fledged renewable and thus contribute significantly to the energy mix, it is necessary to work along three lines: (i) the spatial and temporal variability of the resource must be assessed, the areas with potential determined, and their potential quantified (section "Wave Resource Characterization"); (ii) the existing technologies must be developed into reliable and efficient WECs (section "Wave Energy Conversion"); and (iii) the environmental effects of wave energy extraction must be investigated and in particular the effectiveness of wave farms as coastal protection means (section "Wave Farms"). On these grounds, future directions for wave energy are outlined (section "Future Directions") and conclusions drawn (section "Conclusions") as to the effectiveness of wave power to combat climate change, with a focus on the mitigation of its

effects on the double front of its roots (greenhouse gas emissions) and its consequences (sea-level rise and increased storminess).

Fundamentals of the Wave Energy Resource

In the following ocean waves and the wave resource are presented (section "Waves and the Wave Resource"), followed by a brief summary of their mathematical treatment, with references for the reader interested in further details (section "Mathematical Aspects of Ocean Waves").

Waves and the Wave Resource

The process of wind wave generation, whereby energy is transferred from the wind to the sea surface, is controlled by the wind speed under a quadratic relationship – meaning that, although stricto sensu any wind is capable of generating waves, in practice it is only the strong (storm) winds that generate wave fields of relevant power for energy conversion. This occurs primarily in the high seas, far from the coast. The waves thus generated travel over thousands of miles of open ocean in an extraordinarily efficient process of energy transmission – with very small energy losses – until they eventually reach a coastline. In approaching the shoreline, waves leave deep water, propagating over intermediate and, subsequently, shallow water. Whereas waves in deep water do not interact with the seabed, in intermediate water they start interacting ("feeling") the seabed, and this interaction intensifies as water depths decrease, consisting of two fundamental processes, refraction and shoaling, which modify wave properties.

Ultimately, waves reach the shoreline, where they are extinguished, their energy being in part dissipated through breaking and in part reflected back. In areas sheltered by natural or man-made structures (headlands or breakwaters and groynes, respectively), another process is to be added to the former: diffraction. As a result of these nearshore processes, wave patterns in intermediate and shallow water are generally more complex than offshore – all the more so where the bottom contours are irregular. Indeed, an uneven bathymetry typically leads to wave energy concentrations in certain areas (Fig. 1) – the so-called nearshore hotspots (Iglesias and Carballo 2010a) – and areas where the resource is comparatively very weak (e.g., bays). The typical spatial extent of nearshore hotspots is $O(10^2–10^3$ m), and therefore a detailed study (usually involving numerical modeling) must be carried out to determine the optimum locations for a wave farm (Carballo and Iglesias 2012; Veigas et al. 2014).

The complexity of the wave energy resource stems not only from its spatial variability but also from its temporal fluctuations, which occur at different time scales (Carballo et al. 2015). At the shortest (wave) time scale, an individual wave is generally different from the next, only some seconds later; at longer time scales (monthly, seasonal), the wave resource will typically differ markedly, with values

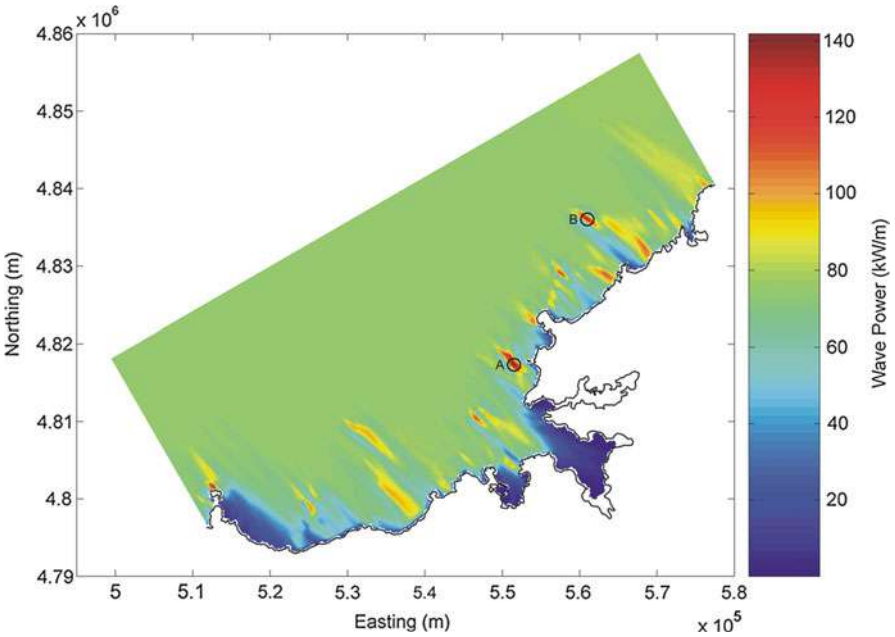

Fig. 1 Nearshore hot spots off the coast of NW Spain (Iglesias and Carballo 2009)

in winter bearing little resemblance to those in summer (Fig. 2); at even longer time scales (hyperannual), oscillations (Iglesias and Abanades 2014) such as ENSO (El Niño-Southern Oscillation) or NAO (North Atlantic Oscillation) must be taken into account.

In view of the variability of the wave resource – spatial and temporal – a fundamental requirement for its exploitation is a detailed assessment of this variability in the areas or regions of interest. The variability of the wave climate has long been investigated for other purposes, including navigation, port and coastal engineering, offshore engineering, and naval architecture – incidentally, fields in which wave energy is a source of concern (of loading, in technical terms) rather than a benefit. For this reason, the outcome of previous work, albeit informative, is often insufficient for purposes of assessing the wave resource, and an ad hoc characterization of the wave resource is necessary.

The areas with realistic potential for the development of wave energy present average power values above 20 kWm^{-1} and tend to be located in the mean and high latitudes owing to the global atmospheric circulation. Furthermore, the seasonal variability of the wave resource is typically lower in the Southern Hemisphere than in the Northern. On this basis, many coastal areas of South America, Africa, and Australia would be particularly attractive for wave energy exploitation – with the downside of their distance to the energy consumption centers.

The characterization of the wave resource has been undertaken recently in a number of areas with potential (Fig. 3) for the development of wave energy areas

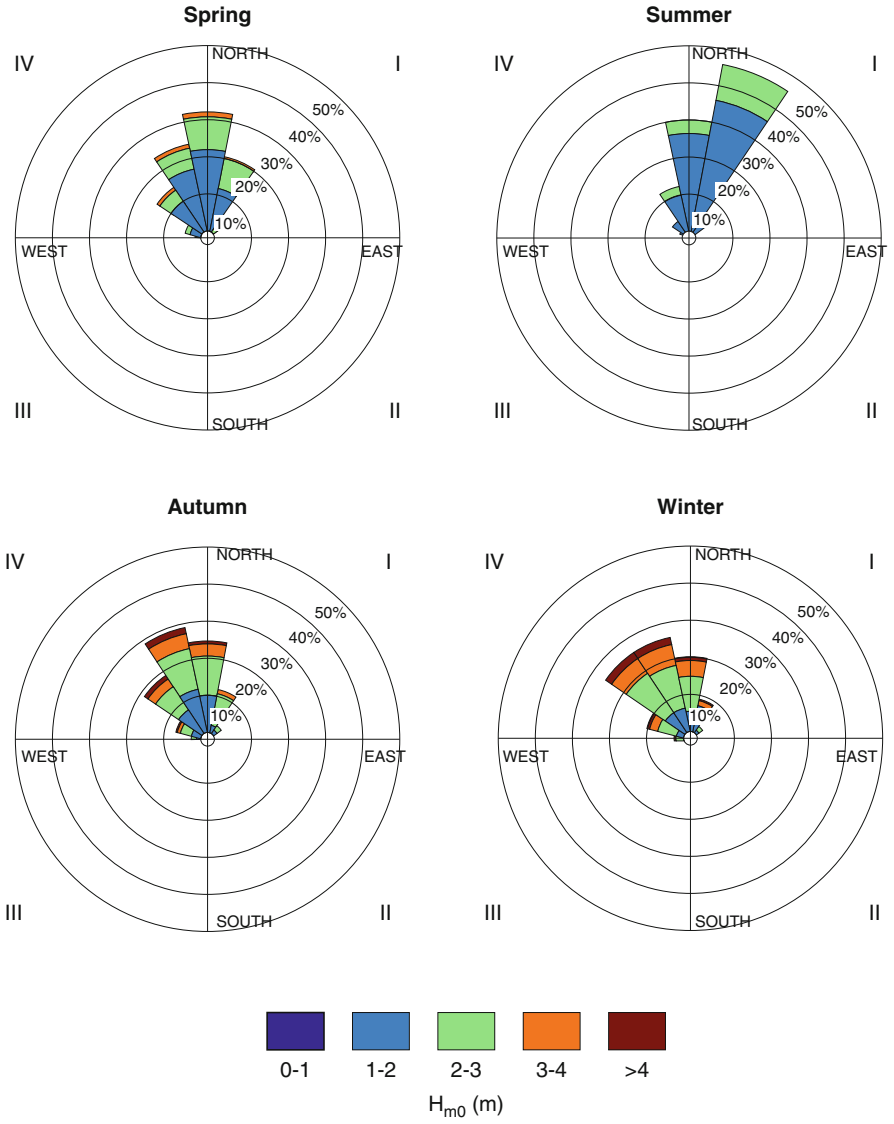

Fig. 2 Seasonal wave height roses at La Isla Bonita in the Island of La Palma (Iglesias and Carballo 2010b) (H_{m0}, significant wave height)

(Bernhoff et al. 2006; Defne et al. 2009; Folley and Whittaker 2009; Gonçalves et al. 2014; Iglesias and Carballo 2009, 2010a, c, 2011; Lenee-Bluhm et al. 2011; Pontes et al. 1998; Rusu and Guedes Soares 2012; Stopa et al. 2011; Thorpe 2001; Vicinanza et al. 2013). However, much work remains to be done in the small-scale characterization of the nearshore variability of the wave resource in the areas of interest.

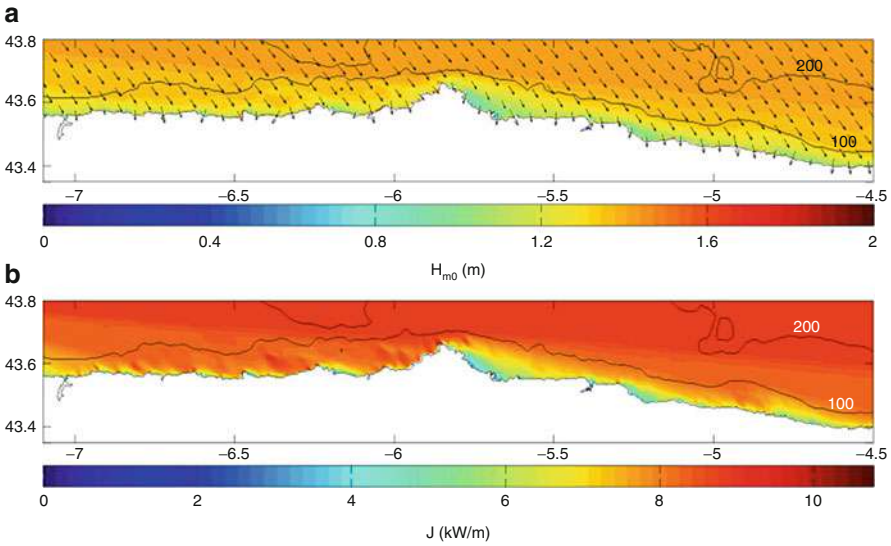

Fig. 3 Wave patterns: significant wave height and direction (**a**) and wave power (**b**) in the North Coast of Spain for the following deepwater wave conditions on 13/04/2009 at 03:00 UTC: significant wave height, 1.5 m; energy period, 10.0 s; mean wave direction, 315° (Iglesias and Carballo 2010c)

This characterization is typically carried out through numerical models, ideally calibrated and validated with wave data from wave buoys or other sources (Iglesias and Carballo 2009, 2010c; Iglesias et al. 2009). The following section summarizes the main principles of the characterization of the wave resource. For additional details the interested reader is referred to Carballo and Iglesias (2012).

Mathematical Aspects of Ocean Waves

Ocean waves consist of a superposition of a very large number of individual sinusoidal (harmonic) waves, each with its own amplitude, frequency, and direction. This superposition is expressed mathematically as a Fourier series, which can represent any sea state (Holthuijsen 2007). The Fourier series, a time domain concept, has its counterpart in the frequency domain in the wave energy density spectrum, usually referred to for brevity as the wave spectrum, which quantifies the distribution of wave energy over the different frequencies. Often, the directional information is contained in the spectrum, which is then a directional spectrum.

On the basis of the directional wave energy spectrum, it is possible to compute the wave parameters of interest, some of which are presented below for convenience; further details on irregular wave theory may be found in Holthuijsen (2007).

If the directional wave energy density is denoted by $S(f, \theta)$, with f the wave frequency, the spectral moments may be defined as

$$m_n = \int_0^{2\pi}\int_0^{\infty} f^n S(f,\theta)df\,d\theta, n = 0,1,2\ldots \tag{1}$$

The significant wave height is then given by

$$H_s = 4m_0^{1/2} \tag{2}$$

and the peak wave period may be computed as the inverse of the frequency at the spectral peak (f_p),

$$T_p = \left(f_p\right)^{-1} \tag{3}$$

Wave power, or wave energy flux, is given by

$$P = \rho g \int_0^{2\pi}\int_0^{\infty} c_g(f,h)S(f,\theta)df\,d\theta \tag{4}$$

where ρ is the seawater density, g is the gravitational acceleration, and c_g is the group celerity, i.e., the velocity at which wave energy propagates, which is a function of the wave frequency and water depth (Eq. 19). Seawater density depends on salinity and temperature, which vary in time and space; an average value was taken for this work, $\rho = 1025$ kg/m^3.

Equation 6 yields the wave power per unit width of wave front; if a certain wave energy converter (WEC) captures the energy of a width b of wave front, the corresponding power is

$$P_{WEC} = Pb \tag{5}$$

Naturally the actual power output will depend on the converter efficiency. The mean wave direction may be obtained from the directional wave energy spectrum through

$$\theta_m = \arctan \frac{\int_0^{2\pi}\int_0^{\infty} S(f,\theta)\sin\theta\,df\,d\theta}{\int_0^{2\pi}\int_0^{\infty} S(f,\theta)\cos\theta\,df\,d\theta} \tag{6}$$

In many cases, the detailed shape of the spectrum is unknown, and only some of the characteristic wave parameters are given. In this case, the wave power, also known as wave energy flux, can be computed from the following approximation:

$$J = \frac{\rho g^2}{64\pi} T_{m01} H_s^2 \tag{7}$$

where ρ is the water density, g is the acceleration due to gravity, H_s is the significant wave height (m), and T_{m01} (s^{-1}) the wave energy period:

$$T_{m01} = \frac{m_0}{m_1} \tag{8}$$

Wave Resource Characterization

The characterization of the wave resource is usually carried out by means of numerical wave models, which are introduced in section "Wave Models." The main points for their practical application to characterize the wave resource are explained in section "Methodology."

Wave Models

In characterizing the wave resource, it is necessary to assess not only the average values of wave power or the total annual resource but also the variability of the resource in terms of sea states or, in other words, the characteristics of the waves (significant wave height, peak period, mean direction, etc., or even more accurately, the directional wave spectrum) behind the resource.

This characterization is customarily carried out with numerical models of coastal wave propagation (e.g., SWAN, Simulating WAves Nearshore). There are many types of models, each type solving a specific equation that applies to certain conditions. A review of existing wave models is outside the scope of this chapter, and the interested reader is referred to Folley et al. (2012). A brief summary is presented in the following.

Coastal wave models can be classified into phase-resolving and phase-averaged (spectral) wave models. In turn, each of these categories comprises many models, solving different equations or variants of equations. Many phase-resolving models are based on Berkhoff's *mild-slope equation* (Berkhoff 1974), in its fully fledged (elliptical) version or in its parabolic and hyperbolic incarnations. Alternatively phase-resolving models may be based on Boussinesq's equation, e.g., Johnson (1997), which is adept at modeling nonlinear energy transfer in shallow water and has been recently extended to intermediate water depths. As for phase-averaged models, usually referred to as spectral models, they typically solve the spectral wave action balance equation (Hasselmann 1971; Holthuijsen et al. 1989; Longuet-Higgins and Stewart 1961) and are often the preferred choice in characterizing the wave resource, for their ability to model wave generation and propagation over large domains efficiently.

Spectral models solve the spectral wave action balance equation without a priori assumptions on the shape of the wave spectrum. The wave field is described by the two-dimensional wave action density spectrum, $N(\omega,\theta)$, where ω is the angular wave frequency and θ is the wave direction. The wave action density spectrum is used in lieu of the energy density spectrum, for action density is conserved in the presence of currents whereas energy density is not; in any case, the wave energy spectrum may be computed from the wave action spectrum.

The spectral wave action balance equation reads

$$\frac{\partial N}{\partial t}+\frac{\partial(c_x N)}{\partial x}+\frac{\partial\left(c_y N\right)}{\partial y}+\frac{\partial(c_\omega N)}{\partial \omega}+\frac{\partial(c_\theta N)}{\partial \theta}=\frac{F}{\omega} \tag{9}$$

The first term on the left-hand side represents the local rate of change of wave action density in time; the second and third terms stand for the propagation of wave action over geographical space, with propagation velocities c_x and c_y in the x and y directions, respectively; the fourth term quantifies the shifting of the relative frequency due to variations in depths and currents, with propagation velocity c_ω in the ω direction; finally, the fifth term represents the effects of refraction induced either by depth variations or by currents, with propagation velocity c_θ in the θ direction. The expressions of the above propagation velocities are derived from linear wave theory. As for the right-hand side of Eq. 9, F is the source term representing the effects of generation, dissipation, and nonlinear wave-wave interactions.

Wave power is then computed as

$$J_x=\int_0^{2\pi}\int_0^{360}\rho g c_x E(\sigma,\theta)d\sigma d\theta \tag{10}$$

$$J_y=\int_0^{2\pi}\int_0^{360}\rho g c_y E(\sigma,\theta)d\sigma d\theta \tag{11}$$

where $E(\sigma, \theta)$ is the directional spectral density, which specifies how the energy is distributed over frequencies (σ) and directions (θ). The wave power magnitude is then calculated as

$$J=\left(J_x^2+J_y^2\right)^{\frac{1}{2}} \tag{12}$$

Methodology

In practice, the detailed characterization of the resource for the purposes of wave energy exploitation is of interest in nearshore areas, for it is in these areas that wave farms can be deployed. Indeed, the water depths and lengths of submarine

connections (cables) quickly place a practical limit on the distances to the coastline at which it is economically feasible to build a wave farm. Thus, it is the nearshore resource that is of practical interest.

First, the offshore wave resource must be properly characterized as a prerequisite, for offshore wave conditions are required to prescribe the boundary conditions. The characterization of the offshore wave resource can be carried out using: (i) deepwater wave buoy data, where available; (ii) numerical models that account for wave generation and propagation in deep water (e.g., WAVEWATCH III); (iii) remote sensing (satellite, HF-RADAR, etc.); (iv) hindcast datasets; or a combination of the above.

The primary factors that produce the spatial distribution of the wave resource in the nearshore are the deepwater wave resource and the bathymetry. The typical source of bathymetric data is nautical charts. In some areas, however, it may be advisable to complement existing charts with ad hoc surveys, in particular of the area of interest. Therefore, the second consideration in characterizing the nearshore resource is that the bathymetry file must have a good spatial resolution in the area of interest, ideally $O(10^1$ m), for the model to be able to calculate wave propagation accurately. Nevertheless, this fine spatial resolution is not necessary throughout the computational domain, and medium and even coarse resolutions – which are normally available from off-the-shelf nautical charts – can be acceptable from deep water to the area of interest, depending on the level of accuracy required (Fig. 4).

Third, the geometry of the computational grid should be chosen based on the geometry of the coastline and the area of interest. Cartesian, curvilinear, or combined grids may be used (Fig. 5) (Carballo and Iglesias 2012; Iglesias and Carballo 2009). It is important to bear in mind that numerical disturbances often arise at the boundaries, so these must be set far enough from the study area for model results not to be polluted.

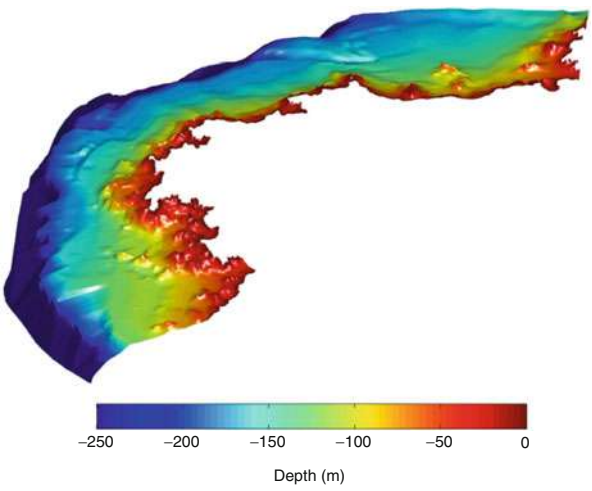

Fig. 4 Perspective view of the bathymetry used for the characterization of the nearshore wave resource (Iglesias and Carballo 2009)

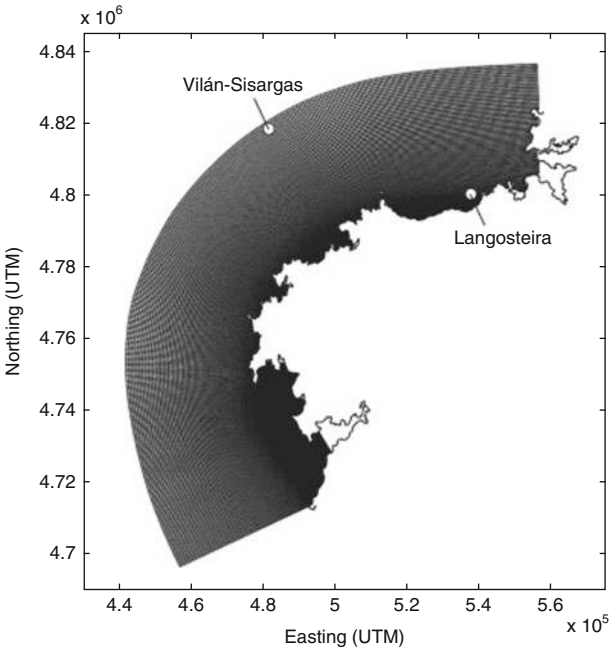

Fig. 5 Curvilinear grid for the characterization of the nearshore wave resource (Iglesias and Carballo 2009)

Fourth, the computational grid must have sufficient resolution, not least in the study area, which usually encompasses the lee of the wave farm up to the shoreline and the wave farm itself. The optimum resolution may be established through a sensitivity analysis, in which the grid is progressively refined until no significant differences can be detected in the results. A fine grid in the area of interest is often nested into a coarser grid with a view to limiting the computational cost of the model. Alternatively, a variable size mesh can be adopted, with increasing resolution toward the area of interest.

Last, but not least, the numerical model ought to be calibrated and validated. The model should ideally be driven with offshore data from wave buoys and calibrated and validated by comparing numerical results with observations from coastal wave buoys located within the computational domain. Time series of relevant wave parameters can be used to compare the model results with the coastal wave buoy data, and statistical indicators (e.g., R^2, RMSE, NMSE) can be applied to quantify the goodness of fit. It is well known that goodness of fit can decrease significantly under storm conditions. Furthermore, wave buoys are in the habit of failing in heavy storms; consequently, storm values are typically underrepresented in the dataset, which may lead to biased (and not conservative) assessments of goodness of fit.

Wave Energy Conversion

Wave energy conversion is a relatively young technology, and intensive research efforts have been devoted over the last years to the development of WECs (Carballo and Iglesias 2012). These technologies were reviewed by a number of authors (Clément et al. 2002; Drew et al. 2009; Falcão 2010; Falnes 2007; Iglesias et al. 2010; McCormick 1981; Thorpe 1999). At present no single technology can be deemed to be the definitive technology. A number of crucial aspects – from the energy performance to survivability under storm conditions – require further investigation. In addition to the existing technologies, new patents continue to appear. This interest in the sector is driven by the fact that the global wave resource is vast and more than sufficient to set wave energy on a par with other renewables such as hydropower or wind energy.

Historical Perspective

Although research and development of wave energy conversion did not gain momentum until 1973, with the world economy under the effects of the first oil crisis, the potential of wind waves for energy generation has long been acknowledged. Indeed, the first attempt to harness the wave resource dates back to the eighteenth century: the Girard brothers' patent registered in France in 1799. There is little information on the device in question, but it is known that in the late eighteenth century, it was tentatively applied in England to elevate seawater and subsequently using the energy thus stored as potential energy. This was followed by the tests carried out in Algeria by the French engineer M. Fursenot in the first decades of the nineteenth century with a device that captured wave oscillation and transformed it into energy by means of cams and gears.

Historically buoyant systems oscillating on the free surface feature prominently in the development of wave energy conversion, as in the case of the mechanism invented by P. Wright and patented in March of 1898 under the name "Wave Motor." In the following year, a new development came out, the Ocean Grove; based on an intake plate which, united to the shafts of a series of pumps, raised water to a group of elevated tanks, this WEC was designed so as to facilitate the subsequent use of the potential energy of the stored water. A device with a similar concept was in operation at the Oceanographic Museum of Monaco for 10 years, pumping seawater to the aquarium using wave energy. This WEC was ultimately destroyed by wave action.

The French scientist Montgolfier developed a "compliant flap" and installed it in a pilot plant in the Black Sea in 1917. With a nominal power of 10 kW, it was based on the dynamic pressures exerted by the movement of water particles. Its operating principle was very simple: a flexible sheet was placed perpendicular to the direction of wave propagation, thereby absorbing wave energy.

However, major efforts to convert wave power into energy did not begin in earnest until the oil crisis of 1973. A great deal of concepts for wave energy

conversion were put forward, many of which were patented; however, only a few progressed to the testing stages, and even fewer managed to actually produce energy. These first-generation converters laid the foundations for the current technologies.

It was also in the context of the oil crisis in the 1970s that studies aimed at a better understanding of wave mechanics were undertaken, often in connection with oil platforms. In the same decade research was carried out on cavity resonance devices, including the work by Yoshio Masuda at the Japan Marine Science and Technology Center and by R. M. Ricafranca at the RMR Research and Engineering Services in the Philippines. Working separately, they created the first two commercial WECs, belonging to the category that would later be called OWCs, or Oscillating Wave Columns.

The operating principle of OWCs is the oscillation of a water column inside a chamber connected with the ocean through an opening below the surface. The oscillating water column acts like a piston for the air in the upper part of the chamber, alternately compressing and decompressing it. The upper part of the chamber is connected with the exterior through a conduit in which the power take-off (PTO) system is installed – a bidirectional air turbine connected to a generator. When the water column rises, the air is compressed and expelled from the chamber, thereby driving the PTO. In the next half cycle, when the water column falls, the air pressure in the chamber decreases and air is absorbed from outside, also driving the PTO.

A British project carried out by the National Engineering Laboratory (Glasgow) capitalized on the knowledge acquired in the preceding years to improve on Masuda's WEC. However, this work did not progress beyond the prototype phase. Instead, Masuda was able to develop his device, a floating OWC named "Kaimai," into operation. Mounted on a barge and with a rated power of 1.3 MW, Kaimai was deployed off the coast of Japan.

In those years no less than £13 M were allocated for development and research in the field of marine energies by the British government. Stephen Salter, an engineer with the University of Edinburgh, presented the so-called Salter Duck in the 1980s. Rocking under wave action, its elements pumped a hydraulic fluid which in turn drove a generator. The project eventually stalled due to high operating costs (estimated). A recent reexamination of this WEC produced cost figures ten times lower than those initially estimated.

Also in the UK (in Southampton) Christopher Cockerell worked in the development of a WEC based on the relative movement of plates connected by hinged joints. Waves cause a relative movement between the plates, which pumps a high-pressure hydraulic fluid that drives a turbine connected to a generator. In 1974 the company Wave Power Limited was founded in order to commercialize the work and patents held by Cockerell's research group. The first of these devices was huge, measuring 50 m wide and 100 m long. Experiments with unidirectional waves and plates of different lengths were undertaken to determine the optimum configuration; when the prototypes were subjected to real operating conditions, they proved to be rather inefficient.

In Oxford Robert Russell, director of the Hydraulics Research Station at Wallingford, designed a device that would operate in shallow waters. The system, called the HRS Rectifier, was an anchored structure that breached through the surface of the water, with sluice gates closing off two tanks.

Although these WECs did not pass the experimental phase or, when they did, were not deemed efficient enough to warrant further development, they did form the knowledge basis upon which many of today's devices are built.

Classification of WECs

Wave energy converters can be classified according to different criteria: (i) installation site, (ii) dimensions relative to the wave length, and (iii) principle of operation. The latter is arguably the most usual and will be developed in more detail.

Classification According to the Installation Site

Three types of WECs can be distinguished according to this criterion:

(i) Onshore WECs, located entirely on land.
(ii) Onshore-offshore WECs, which capture wave energy in the nearshore and transform it into electricity in an onshore facility.
(iii) Offshore WECs, which are deployed in the sea. This group may be further divided according to whether the WECs are floating or resting on the seabed.

Classification According to the Dimensions Relative to Wave Length

This criterion distinguishes between two types of WECs: point absorbers and line absorbers. The dimensions of point absorbers are at least one order of magnitude smaller than the wave length, whereas the predominant dimension of line absorbers is of the same order of magnitude as the wave length. Line absorbers can be orientated transversally or longitudinally to the incoming wave direction.

Classification According to the Principle of Operation

There are three categories within this classification:

(i) Overtopping devices, based on waves overtopping a barrier, and the overtopping flow rate being stored at a reservoir and subsequently used to drive a turbine
(ii) Wave-activated bodies, which capture wave energy through the heaving motion of a floater
(iii) Oscillating Water Columns (OWCs), which – as indicated above – use a water column as a piston to create an air flow which in turn drives a turbine-generator group

Based on the principle of energy capture, they can be classified into: OWC, oscillating bodies, and overtopping devices. A short description of the three types is provided below.

WEC Technologies

Having put forward different criteria on which WEC technologies can be classified, in this section the state of the art is reviewed through notable WECs. The first criterion of classification (installation site) is followed to systematize the review.

Onshore WECs

As explained above, this group encompasses WECs that have both the energy capture and electricity generation systems onshore. Also known as first-generation devices, their technology is the most mature within the field. Indeed, some WECs in this category have already been in operation for a number of years. They are characterized by their relatively simple and inexpensive maintenance, a result of both their good accessibility as onshore devices and the fact that they are less exposed to the harsh marine environment than the other categories. Another substantial advantage is the absence of a submarine cable – unlike offshore devices. As a disadvantage, the wave resource that onshore WECs can exploit is smaller due to bottom friction and depth-induced wave breaking. A further disadvantage is the occupation of land and the corresponding environmental impact on the coastline, which can be more or less significant depending on the type of shoreline and the actual design of the device.

Within the onshore category, the oscillating water column (OWC) is the most advanced technology. The water column is housed in a semi-submerged concrete or (less commonly) steel chamber connected to the sea by an underwater opening. The lower part of the chamber is flooded with seawater, and its upper part contains air. The oscillation of the water inside the chamber (the "water column") induced by the waves outside causes the alternate compression and decompression of the air above, which is used to drive a bidirectional air turbine coupled to an electrical generator. There are currently several OWCs in operation (Falcão 2000; Torre-Enciso et al. 2009), e.g., Mutriku (Fig. 6 – Spain) or Pico (Acores, Portugal).

Civil works are the most important chapter in the cost of an OWC plant. In order to minimize this cost, OWCs have been installed on breakwaters, using the breakwater caissons to accommodate the chamber and its incumbent mechanical and electrical parts. Moreover, installation on a breakwater reduces not only the construction cost of the OWC itself, but also that of its road access and electricity connection. Maintenance costs are also reduced due to the easy access. Examples of OWCs installed on breakwaters are Sakata (Japan) and Mutriku (Spain), the latter with 16 chambers, each connected to a Wells turbine with a nominal power of 0.75 MW. Another project, finally not carried out, was envisaged at the recently built jetty at the Foz do Douro (Porto, Portugal). At present there are plans to install

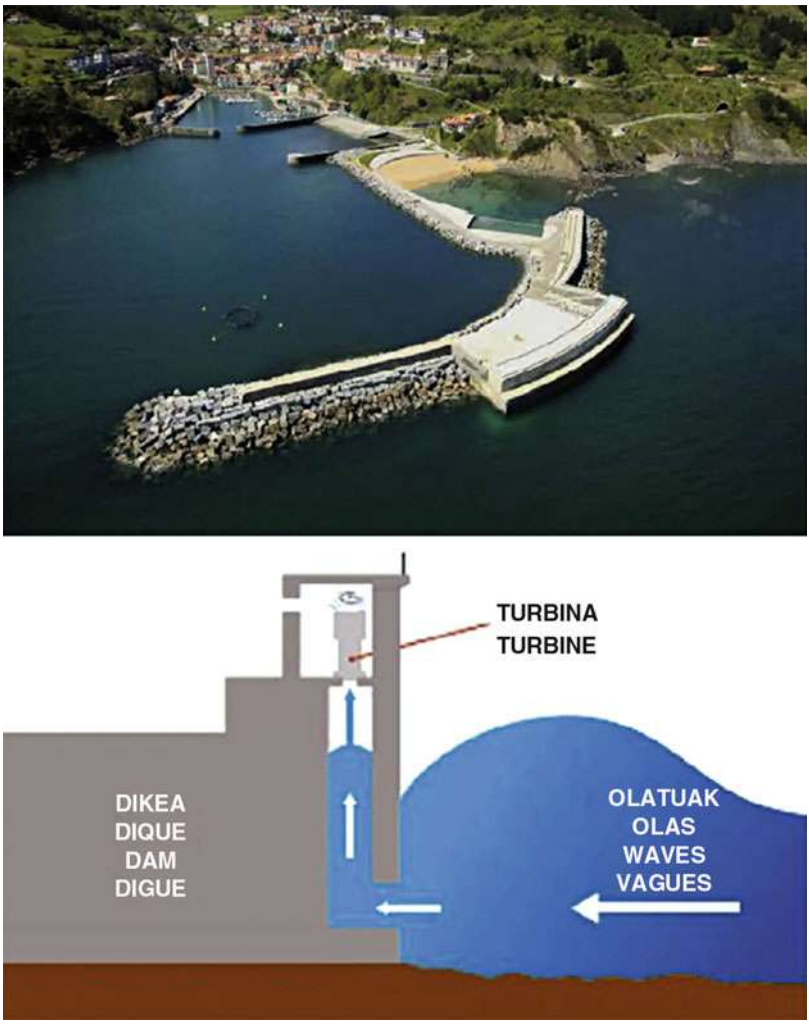

Fig. 6 Mutriku breakwater-mounted OWC (*top*) and schematic of the system (*bottom*) (Courtesy of EVE (2014))

the so-called U-OWC (Arena et al. 2013), an OWC with a U-shaped chamber, in the caisson breakwater of Civitavecchia (Italy).

Another group within this category consists of WECs whose principle of operation is wave overtopping, e.g., the Tapchan (Mehlum 1986) and the Seawave Slot-Cone Generator (Vicinanza and Frigaard 2008; Vicinanza et al. 2008). The former consists of a funneled-shape channel concentrating waves and directing their run-up toward an elevated reservoir. The difference in elevation between the water in this reservoir and the sea surface is used to drive the PTO. The volume of the reservoir can be large enough to store energy as potential energy, so that it is

only transformed into electricity when the demand arises. On the minus side, its disadvantages are related to the installation site, first, the very extension of the littoral area that it occupies; second, the environmental impact; third, the need for a relatively deep nearshore area for waves to reach the shoreline (and the entrance to the channel) without breaking and thus losing their energy; and, finally, the requirement of a microtidal range at the installation site (under 1 m), or else the efficiency would be considerably reduced. Tapchan was installed in Toftestallen, Øygarden (near Bergen, Norway), in 1985 and subsequently decommissioned.

In the Seawave Slot-Cone Generator, wave run-up over a sloping ramp (in principle on a rubble-mound breakwater) is captured through horizontal slots at three different levels, each connected with a reservoir. The outlets of the three reservoirs are connected to a multistage turbine, itself coupled with either an electrical generator or a hydrogen generation system.

The capture system of WaveStar (Denmark) consists of a number of hemispheric floaters, each connected to a hydraulic pump. The floaters are accommodated on a platform supported by two steel piles and oriented so that they are aligned perpendicular to the prevailing wave direction. Although the WaveStar platform is not strictly speaking on the shoreline, it was connected when installed to the shoreline by a catwalk; on these grounds, WaveStar is classified here as an onshore WEC. A 1:10 model installed at sea was recently tested (Kramer et al. 2011; Marquis et al. 2010).

Onshore-Offshore WECs

Onshore-offshore WECs can be regarded as a variant of onshore WECs in that the electricity generation occurs onshore; the difference with purely onshore WECs is that the capture system is in the sea.

This concept attempts to combine the advantages of onshore and offshore systems. The greater resource and smaller environmental impact of offshore WECs are achieved (to a certain extent), and the easier access and cheaper maintenance of onshore WECs are also attained (in part).

Oyster (Cameron et al. 2010) is one of the better known examples within this category. Its structure, with floating elements, is hinged at a base on the seabed and made to oscillate by waves. The oscillation around its vertical (rest) position drives a seawater piston that pumps water through a high-pressure flow line to an onshore hydroelectric power conversion plant. In order to minimize the cost of the line and bring friction losses down, the point absorber should not be far from the onshore part of the installation, which places a limit on the water depth at which the wave energy capture system can be installed – a downside shared by all the WECs in this category. Moreover, the nearshore installation of the capture system is not without a non-negligible environmental impact, including, not least, a visual impact.

The CETO III point absorber (Fig. 7), an evolution of the CETO I, consists of a number of submerged spheres that move back and forth with the waves (Mann 2011). These spheres are connected to pumps which drive high-pressure water to the onshore PTO, consisting of a Pelton turbine and an electrical generator.

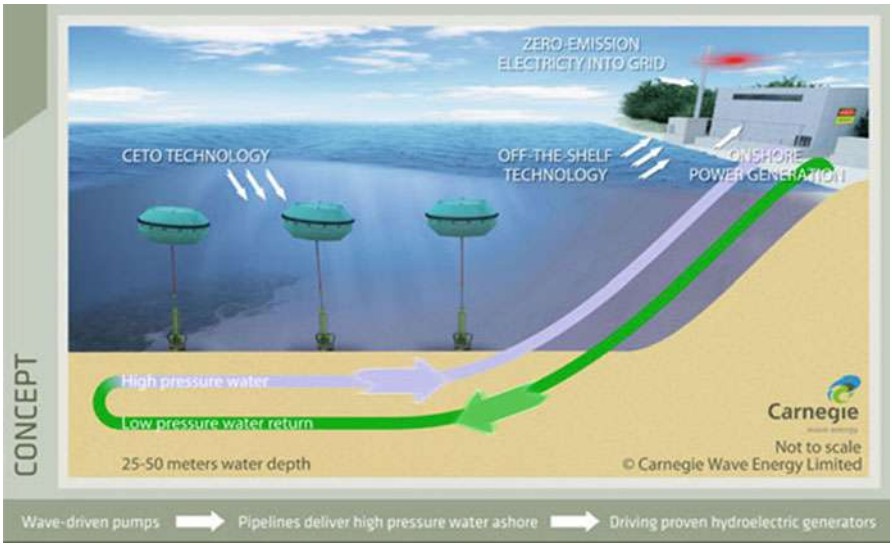

Fig. 7 Examples of onshore-offshore converters: the CETO wave energy converter (Courtesy of Carnegie Wave Energy)

Alternatively, the pumped water could be used to obtain freshwater using inverse osmosis.

Seadog is a point absorber device consisting of a floatation element that moves up and down inside a chamber with the passage of waves. This motion is used to propel a pump which pressurizes seawater; the high-pressure water is driven to the onshore installation, where it is used to power a turbine-generator module or a desalination plant. Several Seadog devices can be connected in parallel or in series. A water reservoir is part of the onshore facility, so the energy can be stored as potential energy and the generation of electricity can be accommodated to the demand – much as in the Tapchan.

Waveberg is a line absorber device consisting of a series of interconnected floaters. The joints between the floaters are activated with the passing waves, and their motion is used to propel piston-type pumps that drive high-pressure water to the shoreline part of the system, consisting of a turbine-generator group. The recommended water depth for the capture system is of the order of 50 m.

Finally, the wave-powered diaphragm pump is a point absorber system that exploits the oscillating movement generated by waves. At present it is an idea that has not yet been put into practice. The base of this device is a box-shaped concrete structure, full of rocks, designed to maintain the WEC stable on the ocean floor. The upper part of this base is an octagonal structure of steel housing 16 cylindrical columns. Within each one of these is a pump, separated from the other 15 through the use of used tires with cylindrical separators. All of these pumps are, in turn, housed in a large cylinder suspended in a raft measuring 32 m in diameter, which provides the buoyancy necessary to lift it when wave crests pass.

To transport the water from the capture system to the onshore generation system, piping is used to which the 16 pumps are connected using nonreturn valves. Once the fluid has been transferred onshore, it can be made to descend through a conventional hydraulic turbine connected to an electrical generator, or it may be stored in a reservoir for use when required. As in the case of Waveberg, the wave-powered diaphragm pump is designed to work at depths of approximately 50 m.

Offshore WECs

Offshore WECs are possibly the most prolific branch of wave energy conversion technology and can be classified into floating and fixed devices.

Floating Devices

The following WEC designs, Wave Dragon and WaveCat (Fig. 8), are based on wave overtopping (Fernandez et al. 2012; Iglesias et al. 2008; Kofoed et al. 2006; Tedd and Kofoed 2009). Overtopped water is collected in one or several reservoirs above the sea level. The water in these reservoirs is driven back to sea through one or several Kaplan turbines, much as in a conventional hydropower scheme. In the case of Wave Dragon, overtopping occurs at a ramp perpendicular to the direction of the incoming waves. In order to capture a wave front length larger than the ramp itself, two deflectors protrude from the ramp sides; they focus the waves toward the ramp, thereby enhancing wave height. Overtopping water is collected in a reservoir above the sea level; the difference in elevation between the water in the reservoir and the outside (sea) water is used to propel an ultra-low head Kaplan turbine. Freeboard and draft are varied according to the wave conditions. Wave Dragon is one of the heaviest WECs, with a structure around 30,000 t. This requires a substantial mooring system.

The WaveCat differs from the Wave Dragon in its structure and in the way overtopping occurs. Like a catamaran – from which it takes its name – WaveCat consists of two hulls. Unlike a catamaran, however, the hulls are convergent rather than parallel, so that from above they form a wedge. With a single-point mooring system (e.g., CALM, catenary anchor leg mooring), WaveCat swings so that it is always orientated in the direction of the incoming waves, which propagate into the wedge. As a wave crest advances between the two hulls, the wave height is enhanced by the tapering channel until, eventually, the inner hull sides are overtopped. Unlike Wave Dragon, in which the overtopping wave crest impinges normally on a ramp, in the case of WaveCat the overtopping crest impinges obliquely on the hull side. Overtopping water is collected in three reservoirs on each hull, at different levels – all above the mean sea level. The difference in elevation with respect to the exterior (sea) level is used to drive a turbine for each reservoir as the water is let out back to sea. Freeboard and draft, as well as the wedge angle, can be varied according to the sea state.

The advantages are threefold. First, overtopping occurs along the hull sides, so the WEC motions do not significantly affect the overtopping volumes but merely shift the point along the hull where overtopping starts. Second, the oblique overtopping signifies that the wave loads on the structure are considerably lower

Fig. 8 Overtopping wave energy converters: Wave Dragon (*top*) and WaveCat (*bottom*) (Courtesy of Wave Dragon AS (2005) and the COAST Research Group at Plymouth University and Fernandez et al. (2012))

than in the case of normally incident waves. Last, but not least, the wedge between the hulls can be closed so WaveCat becomes a conventional (monohull) ship – a useful survivability strategy. Maintenance costs are expected to be low, similar to those of a ship, and the fact that it can be towed to a dry dock in its closed configuration (monohull) and repaired using the same installations is an added advantage.

Pelamis (Fig. 9) belongs to another category of onshore WECs (wave-activated bodies). It is a semi-submerged device composed of four cylindrical sections held together by Cardan joints. As waves pass, the cylinders are displaced up and down by the buoyancy force, thereby activating the joints. These are equipped with a hydraulic system that takes advantage of the joint motions to pressurize an oleo

Fig. 9 Examples of oscillating body converters: Pelamis II (*left*) and PowerBuoy (*right*) (Courtesy of Pelamis Wave Power (2014) and Ocean Power Technologies Inc (2014))

hydraulic fluid. This pressure is used to propel a turbine-generator module. Pelamis is conceived for deployment at intermediate water depths, at distances from the coastline between 5 and 10 km. For complex repair operations, the Pelamis must be towed to a nearby port (Henderson 2006).

Another device that oscillates perpendicularly to the wave front is the Anaconda (Chaplin et al. 2007), which consists of a submerged flexible tube made of plastic materials and filled with seawater at low pressure; the tentative dimensions of the system are 5 m (diameter) and 150 m (length). It is moored at a single point so that it swings when the wave direction changes; thus, it is always head to sea. The tube is filled with seawater under low pressure. As a wave passes along the tube, a pressure bulge is excited and then moves down the tube in front of the crest, continuously capturing energy from the wave. At the stern is a turbine, which is driven by the flow resulting from the periodical pressure bulges. The turbine is coupled to an electrical generator. Among its advantages is its null visual impact (for it is submerged).

The next group of devices within the offshore category is composed of floatation elements oscillating on the sea surface. Among these is WET EnGEN, a point absorber consisting of a floating element that moves up and down along a steel mast with the passage of wave crests. The mast is inclined at an angle of 45° relative to the quiescent sea surface and swivels freely around its base with the purpose of being aligned to the wave direction. As the float moves up and down with the sea surface, it pulls on a cable housed within the mast, which conveys the energy to a rotational generator installed within the foundation.

The Aegir Dynamo WEC is another point absorber with an internal cylinder and an external, floating ring. The cylinder is anchored by means of cables or chains to deadmen laying on the seabed so that it remains practically stationary. The external, floating ring moves vertically with the sea surface. The cylinder houses a rotational generator that is driven continuously by the alternating motion of the external ring through a transmission system that transforms the ring's vertical motion into rotational motion.

Another subgroup within the offshore category is floating platform WECs, which have in common two main characteristics: they float and all their essential systems are above sea level – the mooring excepted. A representative of this subgroup is FO3, which takes advantage of the motion of the sea surface under waves by means of buoys mounted in rows and connected to the platform. The buoys drive pumps that pressurize an oleo hydraulic fluid, which in turn drives an electrical generator.

Finally, another line of development in floating offshore WECs is floating OWC devices (López and Iglesias 2014; López et al. 2014), e.g., Oceanlinx MK1 and Sperboy. The principle of operation of the OWC itself is the same as for onshore OWCs.

The Oceanlinx MK1 has a large rectangular chamber housed in a substantial structure. The turbine is designed so as to increase the energy efficiency of the device taking into account the prevailing wave frequency. Soft start systems powered by the electricity network are also included for the turbine to gain velocity faster.

The Sperboy is a vertical cylinder with hollow walls for flotation; within the cylinder is the chamber, connected to the sea through the cylinder bottom, which is open. While the lower part of the chamber is inundated, its upper part is filled with air, as in all OWCs. On the top of the device are four horizontal ducts through which air leaves and enters the chamber, driven by the alternating ascent and descent of the water surface within the chamber. The alternating air flow propels four Wells turbines (one in each duct), which in turn drive electrical generators.

The MAWEC converter, developed by Leancon, has a number of features in common with OWCs but also some differences – among which, the fact that the flow driving the turbine is recirculated. The device in plain view has a V shape. Each arm of the "V" has the transverse section of an inverted channel. The upper section is connected to two rows of vertical pipes, each with 30 pipes. The principle of operation is based on the fact that the length of the device is greater than the average wave length. When a wave reaches the end of the channel, it creates high- and low-pressure zones situated in front and behind the wave crests, respectively. The high pressure in front of the wave crest drives air flow through the corresponding tubes to a turbine, which drives a generator. The circuit is closed when the air expelled by the turbine is absorbed by the tubes under low pressure behind the wave crest. Valves are fitted to the ends of the low-pressure tubes to ensure that the flow occurs always in the same direction, i.e., the tubes are closed when they are in front of the wave crest. This conception allows for conventional turbines to be used rather than the far more expensive Wells turbines typical of OWCs.

Submerged Devices

Submerged offshore WECs are less common than floating ones, the reason being that underwater components add a new level of complexity. Designs are mostly at an early stage of development, and some of the most developed eventually failed.

The Archimedes Wave Swing WEC (Fig. 10) is composed of two cylinders measuring 9.5 m in diameter (de Sousa Prado et al. 2006; Valério et al. 2007).

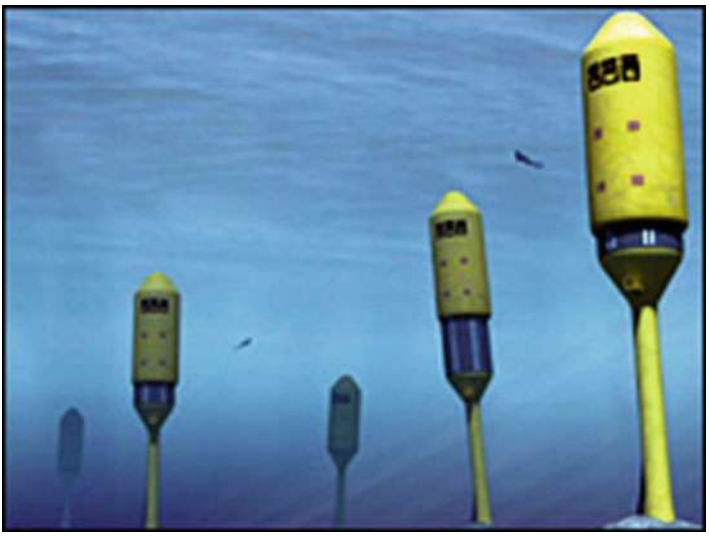

Fig. 10 Archimedes wave swing (Picture courtesy of AWS Ocean Energy (2015))

One of the cylinders is anchored to the seabed by means of a concrete structure. The other is located outside the first, at a higher elevation and full of air. When the crest of the wave passes over, the airbag is compressed, pressing the float downward. Conversely, when the trough of the wave passes over, the air expands, and the cylinder rises again. Magnets located in the upper cylinder generate electricity when they move relative to the coil inside the lower cylinder. This device cannot be seen on the surface of the sea, for it is located at a depth of 6 m – which reduces its visual impact. It does not have any hydraulic fluids, so there will be no leaks leading to contamination. On the other hand, the maintenance of this device is relatively complex, as all the equipment is underwater. However, this is advantageous in terms of survivability under storms. The device must be refloated in order to perform maintenance work. The manufacture of this WEC is of intermediate difficulty, given that it is a very large structure which requires significant resources in order to transport it to its anchoring site.

The Stellenbosch Wave Energy Converter is one of the first ideas for wave energy conversion, which did not materialize. The device's collector is installed on the seabed, forming a "V," and the power take-off is located at the tip of the V. It can be classed in the group of point absorbers. A bag of air is placed in a cavity at the top of the structure. As the crest of the wave passes over, the trapped air is compressed, thereby opening the high-pressure valves and allowing the air to flow toward a series of high-pressure pipes. When the trough of the wave passes, the pressure inside the bag drops and the low-pressure valves open. This yields a continual, one-way flow of air. In order to exploit this flow, on the converter is placed a one-way turbine between the low- and high-pressure collection tubes. The environmental impact of this device would be classified as intermediate, given that

it is a large apparatus occupying a large amount of space on the seabed. Nevertheless, it has no moving parts and does not interfere with marine life.

The wave rotor device represents a class of WECs that exploit the movement of the water as waves pass to drive a series of turbines. It employs two types of turbines: Darrieus and Wells. The rotors are used to generate electricity from upward and downward currents. The device is based on the same principle as wind turbines, which may also be installed on top of the WEC, taking advantage of the structure necessary for the wave energy converter. These systems can be quite efficient, as they feature no intermediate phases of energy transfer. The environmental impact of this type of device is intermediate, due to its visual impact and the existence of moving parts. Maintenance is relatively simple, but the fact that most of their components are underwater does complicate servicing. This type of device is constructed of familiar materials that are widely known but subjected to particular stresses. This converter is currently in a computational model and partial-scale design phase.

Finally, the BioWAVE device moves in the same way as a seaweed when a wave passes over it. This swaying motion is converted into electricity through the use of a specially developed generator called the O-Drive^{TM}, which is found at the point of articulation on the bottom of the device. If a storm approaches, the device protects itself by lying down on the seabed. Its environmental impact is thought to be minimal, as it has no high-speed parts which could harm marine life, and the anchoring system will also have only a slight impact. The maintenance difficulty of this device will be intermediate, as this type of apparatus has all its important mechanisms underwater. The manufacture of this converter is of intermediate complexity. Although the mast is easy to manufacture, the production of the energy absorption point is fraught with more difficulties.

Wave Farms for Coastal Protection

Introduction

A very significant proportion of the world's population (44 %) live within 150 km of the coast, and eight of the ten major cities are located on the coast (Oceans 2011), transforming the littoral into an extended hub for socioeconomic activity. This creates a substantial pressure on the coastal environment, with demands of use arising from fishing and aquaculture to residential, transport, industrial, or recreational purposes. This pressure is exerted on the single most sensitive, dynamic environment on the planet – the littoral. The resulting complex picture is further compounded by climate change, which can affect the coast chiefly through two main effects: sea-level rise and increased storminess.

In view of the large population of coastal areas throughout the world, it follows that climate change is likely to have one of its main impacts – in terms of socioeconomic consequences – through its effects on the coast. For example, in the case of the UK (Fig. 1), a significant portion of the coastline (17 %) is threatened by erosion; in the case of England and Wales, erosion rates exceed 10 cm per year

along approximately 28 % of the coastline (~1040 km) (EUROSION 2004). These figures are set to increase as a result of sea-level rise and increased storminess due to climate change, e.g., Pugh (2004), Chini et al. (2010), and Wadey et al. (2014) (Fig. 11).

It is hard to overstate the economic and environmental consequences of coastal erosion and flooding: loss or damage to property and infrastructure, disruption to the transport chain, losses through decreased revenues in the tourist and recreational sectors, etc. – hence, the importance of coastal defense. Almost half of the coastline (44 %) of England and Wales is protected by structures or artificial beaches (Huthnance and Mieszkowska 2010), and substantial investment (over £3.2 billion from April 2010 to March 2015) is undertaken by the Department for Environment, Food & Rural Affairs (DEFRA) in flood and coastal erosion risk management (DEFRA 2015).

The conventional approach to defending the coast against flooding and erosion involves coastal structures – this is the so-called "hard engineering" approach. The downsides of this approach are well known, not least its visual impact (armored coastlines) and, in the context of transition coasts, the inability of structures to adapt to sea-level rise. Indeed, there have been recently many cases of coastal structures failing to cope with the increased pressures of climate change (Castelle et al. 2015; Kendon and McCarthy 2015; Senechal et al. 2015; Sibley et al. 2015; Slingo et al. 2014; Spencer et al. 2015). A case in point is the failure of the Dawlish seawall (Devon, England) in the winter 2013/2014 – the stormiest period of the past 60 years, compounded by the highest sea-level of the past 100 years (Haigh et al. 2015) – which led to the destruction under massive overtopping of a critical section of railway and consequently the disruption to the rail link between SW England and the rest of the country for 3 months (Fig. 1). Other examples include the failure of the La Coruna seawall (Spain), the collapse of the Aberystwyth seawall (Wales), and the dramatic erosion affecting many beaches throughout

Fig. 11 Coastal infrastructure and property at risk

Fig. 12 Consequences of increased storminess in Soulac-sur-Mer (France) after winter 2013/2014

Europe, from Spain (e.g., Aviles, Barreiros) to France (e.g., Truc Vert, Biscarrosse) to the UK (e.g., Chesil, Perranporth, Isle of Man), which in some cases resulted in the demolition of buildings due to the great volumes of erosion that affected the foundations, such as in Soulac-sur-Mer (France – Fig. 12).

These examples of failures of coastal structures – due to either structural collapse or excessive overtopping – expose the dramatic consequences of the inadequacy of many of the existing structures in the current transition scenario. The conventional approach to solving this problem entails upgrading the existing structures or building new ones, in both cases at a large cost. The downsides of this approach are related to the difficulty of fixed coastal structures in dealing with the transition conditions, notably sea-level rise, and more generally to the environmental, and particularly visual, impact of these structures on the littoral.

The advent of marine renewable energy, particularly wave energy, posits wave farms as an alternative to coastal defense that presents numerous advantages, not least in the current transition environment. Wave farms, or arrays of wave energy converters (WECs), extract energy from the waves. Recent research has proven that nearshore wave farms lead to not only milder wave climates in their lee (Carballo and Iglesias 2013; Iglesias and Carballo 2014; Millar et al. 2007; Palha et al. 2010; Reeve et al. 2011; Rusu and Guedes Soares 2013; Vidal et al. 2007) but, importantly, reduced beach erosion under storm and post-storm conditions (Abanades et al. 2014a, b, 2015a, b; Mendoza et al. 2014; Zanuttigh and Angelelli 2013), which amounts to effective coastal protection – much as that provided by a conventional coastal structure. However, nearshore wave farms present three main advantages relative to coastal structures. First, by providing renewable, carbon-free energy, wave farms contribute to decarbonizing the energy supply and thereby combating the man-made causes of climate change. Second, the environmental impact of wave farms on the littoral – the single most sensitive

environment in the planet – is considerably lower than that of coastal structures. Last, but not least, wave farms consisting of floating WECs (e.g., WaveCat, Wave Dragon, DEXA) adapt naturally to sea-level rise and therefore can cope well with the main impact on the littoral of climate change. Thus, rather than resorting to the conventional approach (more structures) to fix obsolete, underperforming structures, deploying wave farms to generate carbon-free energy as their main purpose and, in synergy with it, defend the coastline against erosion and flooding is a new alternative that warrants consideration. Incidentally, their application to coastal defense would enhance their economic viability through the savings achieved in conventional defense schemes.

This alternative to conventional coastal defense schemes (based on structures such as groynes, detached breakwaters, etc.) is in fact a new paradigm to mitigating climate change and confronting two global challenges: the environmental repercussions of the current energy model and the risks to properties and infrastructure posed by coastal erosion. As explained, these two challenges are connected, for climate change is set to exacerbate coastal erosion through its effects of sea-level rise and increased storminess.

The effects of wave farms on coastal processes and, in particular, their effectiveness for coastal protection are investigated through a case study: Perranporth, a beach in Cornwall (SW England) that has experienced significant erosion over the last years, not least during the harsh winter 2013/2014. Indeed, the Shoreline Management Plan has identified the area as subject to significant erosion risk, and a number of options are being assessed to confront this challenge (CISCAG 2011).

The case study is analyzed through a suite of state-of-the-art process-based models, combined for the first time for this purpose – a third-generation spectral wave model and a coastal processes model. The evolution of the beach with and without the nearshore wave farm is studied in different scenarios, involving wave farms deployed at different locations and distances from the shoreline, plus the baseline scenario (without the farm). The response of the coastal system is analyzed at different time scales, from the short (days) to the medium (months) term, with the long-term study as future work. A set of ad hoc indicators is defined to quantify the effects of wave energy absorption by the farm on coastal processes and, in consequence, the degree of protection afforded by the wave farm in the different scenarios.

Case Study: Perranporth Beach (UK)

The effectiveness of wave farms in mitigating dune erosion on the beach was analyzed by means of a case study: Perranporth Beach (Fig. 13). The selection of this case study is motivated by two reasons: (i) the erosion experienced by the beach over the last years, particularly under the cluster of heavy storms (Fig. 14) of February 2014 (CISCAG 2011), and (ii) the interest of the area for wave energy development, as shown, e.g., by the nearby

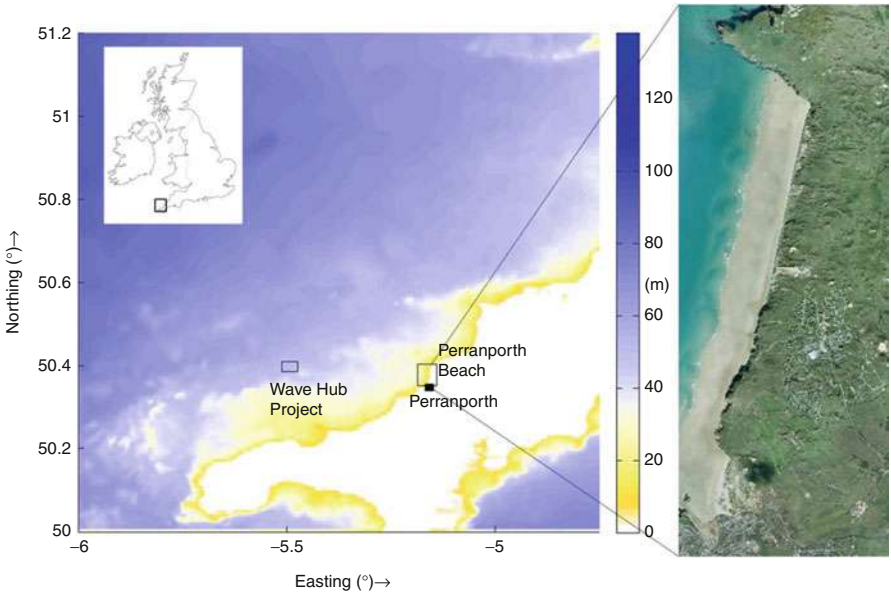

Fig. 13 Location of Perranporth Beach and the Wave Hub in SW England (*left*; water depths in m) and aerial photo of the beach (*right*; courtesy of Coastal Channel Observatory)

Fig. 14 Damages at Perranporth Beach after storms in winter 2013/14. Courtesy of West Briton

Wave Hub – a grid-connected offshore facility for WEC testing (Gonzalez-Santamaria et al. 2013; Reeve et al. 2011).

For this work wave buoy data were used alongside hindcast (numerical modeling) data. Half-hourly data were obtained from the directional wave buoy off Perranporth, in approximately 10 m of water, operated by the Coastal Channel Observatory. The analysis of these data reflects the exposure of the area to heavy swells generated by the long Atlantic fetch, as well as to locally generated wind seas. The average significant wave height (H_s), peak period (T_p), and peak direction (θ_p) in the period covered by the wave buoy data (2006–2012) were 1.79 m, 10.36 s, and 280°, respectively.

Hindcast data were obtained from WaveWatch III, a third-generation offshore wave model that is run on global and regional (nested) grids, the latter with a resolution of 0.5° (Tolman 2002). These values were prescribed at the outer boundaries of the wave model.

In addition to these large-scale hindcast wave data, three-hourly wind data obtained from the Global Forecast System (GFS) weather model were used to drive the wave model. The mean wind speed at a height of 10 m above the sea surface was $u_{10} = 9.5\ \mathrm{ms}^{-1}$ during the study period; the strongest winds, from the NW, had u_{10} values over $20\ \mathrm{ms}^{-1}$.

SW England is subjected to a semidiurnal tidal regime and a large tidal range (macrotidal), with a mean spring value of 6.3 m at Perranporth. The tide was accounted for in the modeling, with constituents obtained from the TPXO 7.2 global database (Egbert et al. 1994).

A 4 km long beach with a nearly flat intertidal area ($\tan \beta = 0.015$–0.025), Perranporth (Austin et al. 2010; Masselink et al. 2005) has medium sand size ($D_{50} = 0.27$–0.29 mm). The bathymetry (Fig. 15), kindly provided by the Coastal Channel Observatory, showed elevation values between −20 and 25 m relative to the local chart datum (LCD). A submarine bar is present between −5 and −10 m and has a bearing on behavior of the beach; under energetic waves and increased offshore sediment transport, it grows at the expense of the intertidal beach face. Overall, profile changes at Perranporth affect primarily the lower intertidal and subtidal active regions (Scott et al. 2011). In addition to the aforementioned submarine bar, Perranporth is characterized by a well-developed dune system.

Suite of Process-Based Numerical Models

Wave Propagation Model

Wave propagation is calculated with a third-generation numerical model, SWAN (Simulating WAves Nearshore), described in section "Wave models." This model was successfully applied in a number of works (Abanades et al. 2014b; Carballo and Iglesias 2013; Iglesias and Carballo 2014; Millar et al. 2007; Palha et al. 2010; Smith et al. 2012) to model wave farm effects on nearshore wave conditions.

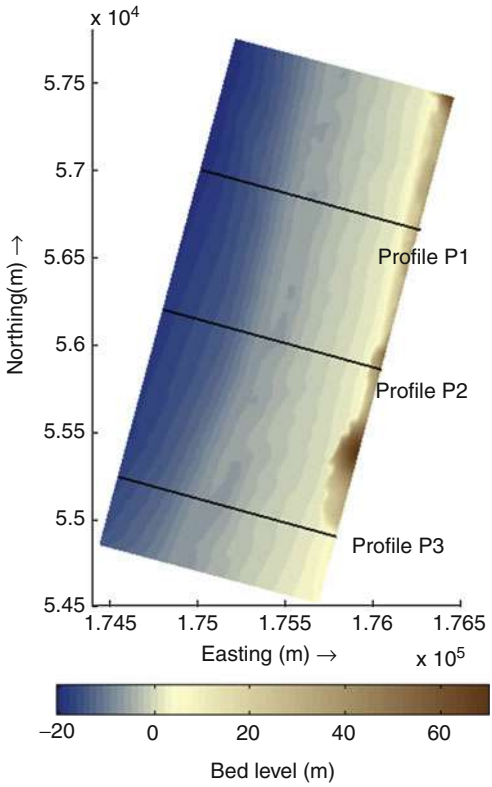

Fig. 15 Computer-modeled bathymetry at Perranporth Beach, including profiles P1, P2, and P3 (Water depth in m)

Two computational grids (Fig. 16) were used to obtain a high-resolution results in the area of interest without compromising computational efficiency, as follows: (i) a large-scale grid covering approx. 100 × 50 km with a resolution of 400 × 200 m and (ii) a small-scale (nested) grid focused on Perranporth Beach, covering an area of approx. 15 × 15 km with a resolution of 20 × 20 m. Thanks to the fine resolution of the nested grid, the individual WECs in the farm could be demarcated and their individual wakes modeled with accuracy – a prerequisite to establishing the wave farm effects on the beach profile (Carballo and Iglesias 2013). The offshore and nearshore bathymetric information – obtained from the UK data center Digimap and the Coastal Channel Observatory, respectively – was interpolated onto these grids (Fig. 17).

Based on the review of WEC technologies (section "WEC Technologies"), WaveCat, a floating overtopping WEC for offshore deployment, was selected. The wave farm considered consisted of 11 WaveCat WECs arranged in two rows (Fig. 18) – the same layout as in Carballo and Iglesias (2013), with a distance between devices of 90 m (equal to the distance between the twin bows of a single WaveCat WEC). Wave-WEC interaction was characterized on the basis of ad hoc laboratory tests (Fig. 18) reported by Fernandez et al. (2012).

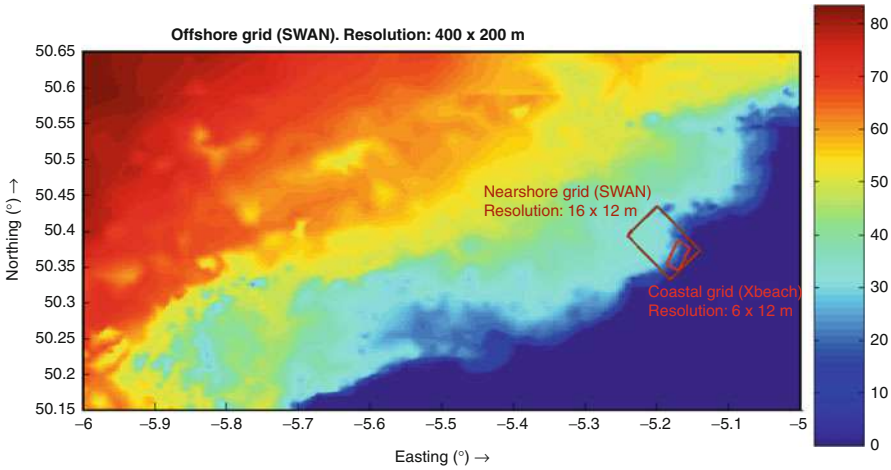

Fig. 16 Boundaries of the three levels computational grids used by the wave propagation and coastal processes models (SWAN and XBeach, respectively) (water depths in m)

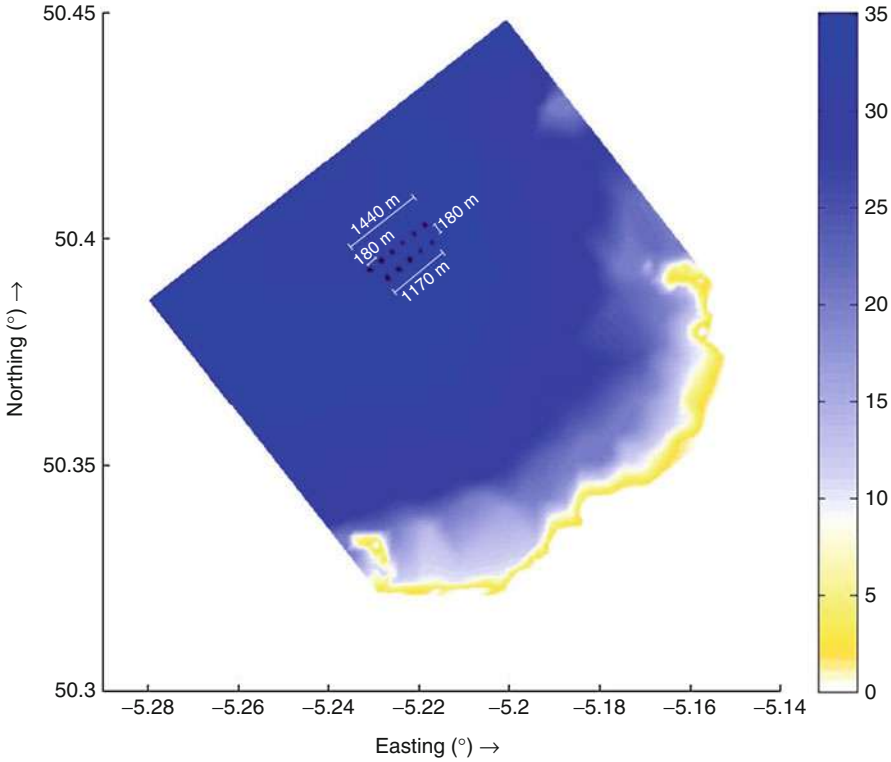

Fig. 17 The array of WECs, or *wave farm*, off Perranporth (water depths in m)

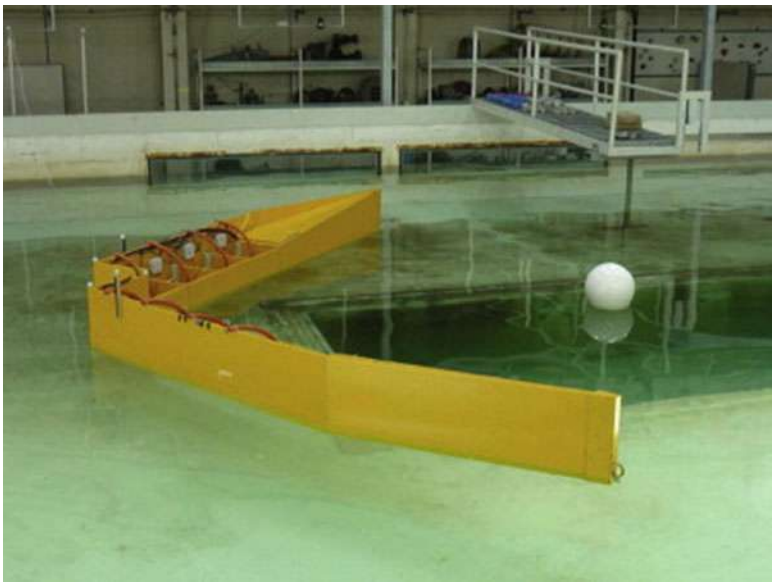

Fig. 18 Physical model tests of WaveCat (Carballo and Iglesias 2013)

Coastal Processes Model

A two-dimensional model for wave propagation, long waves and mean flow, sediment transport, and morphological changes of the nearshore area, beaches, dunes, and back barrier during storms, XBeach solves the time-dependent short wave action balance, the roller energy equations, the nonlinear shallow water equations of mass and momentum, sediment transport formulations, and bed update on the scale of wave groups concurrently. A full description of XBeach can be found in Roelvink et al. (2006) or Roelvink et al. (2009).

The input conditions for XBeach, the coastal processes model were obtained from the output of the SWAN wave propagation model. Sediment transport is modeled with the following depth-averaged advection-diffusion equation (Galappatti and Vreugdenhil 1985):

$$\frac{\partial(hC)}{\partial t}+\frac{\partial(hCu^E)}{\partial x}+\frac{\partial}{\partial x}\left(D_s h\frac{\partial C}{\partial x}\right)+\frac{\partial(hCv^E)}{\partial y}+\frac{\partial}{\partial y}\left(D_s h\frac{\partial C}{\partial y}\right)=\frac{hC_{eq}-hC}{T_s} \tag{14}$$

where C represents the depth-averaged sediment concentration, which varies on the wave-group time scale, D_s is the sediment diffusion coefficient, the terms u^E and v^E represent the Eulerian flow velocities, T_s is the sediment concentration adaptation time scale that depends on the local water depth and the sediment fall velocity, and C_{eq} is the equilibrium concentration, thus representing the source

term in the sediment transport equation. The sediment transport formula defined by Van Thiel de Vries (2009) was used to determine the sediment equilibrium concentration.

For this case study, the model was applied in one and two dimensions horizontal, 1DH (x,z) and 2DH (x, y, z), respectively. In the 1DH case the evolution of two profiles (Profiles P_1 and P_2 in Fig. 15) was investigated. In the 2DH case the entire Perranporth Beach was studied, with a computational grid that extended 1250 m across shore and 3600 m alongshore with a resolution of 6.25 and 18 m, respectively. In both cases the model was driven by spectral parameters obtained from the nearshore wave propagation model, the root-mean-square wave height, H_{rms}; mean absolute wave period, T_{m01}; mean wave direction, θ_{m}; and directional spreading coefficient, s; these were used to construct time series of wave amplitudes, including wave groups – of relevance in beach behavior under erosive conditions (Baldock et al. 2011).

Impact Factors

A set of ad hoc impact indicators recently developed were used to analyze impacts of the wave farm on the beach morphodynamics. Three impact indicators developed by Abanades et al. (2014a) were applied to the results of the coastal processes model (XBeach): (i) bed level impact (*BLI*), (ii) beach face eroded area (*FEA*), and (iii) nondimensional erosion reduction (*NER*).

The bed level impact (*BLI*), with units of m in the S. I., represents the change in bed level caused by the wave farm, calculated as

$$BLI(x,y) = \zeta_f(x,y) - \zeta_b(x,y) \tag{16}$$

where $\zeta_f(x, y)$ and $\zeta_b(x, y)$ are the seabed level in the presence or absence of the farm, respectively, at a generic point of the beach. The y-axis is aligned with the general coastline orientation, and the x-axis is positive away from the sea. $BLI > 0$ or $BLI < 0$ signify that the wave farm leads to a higher or lower seabed level relative to the baseline (no farm) scenario, respectively.

The beach face eroded area (*FEA*), with units of m^2 in the S. I., is a profile function that quantifies the storm-induced erosion in the beach face. Unlike the preceding parameter, which compared the farm and baseline (no farm) scenarios, the *FEA* index is defined separately for both scenarios, baseline (FEA_b) and wave farm (FEA_f):

$$FEA_b(y) = \int_{x_1}^{x_{\max}} [\zeta_0(x,y) - \zeta_b(x,y)]\,dx, \tag{17}$$

$$FEA_f(y) = \int_{x_1}^{x_{\max}} [\zeta_0(x,y) - \zeta_f(x,y)]\,dx, \tag{18}$$

where $\zeta_0(x, y)$ is the initial bed level at the point of coordinates (x, y), and x_1 and x_{max} are the values of the x-coordinate at the seaward end of the beach face and landward end of the profile, respectively.

A second profile function is the nondimensional erosion reduction (*NER*), given by

$$NER(y) = 1 - (x_{max} - x_1)^{-1} \int_{x_1}^{x_{max}} [\zeta_0(x,y) - \zeta_f(x,y)][\zeta_0(x,y) - \zeta_b(x,y)]^{-1} dx, \quad (19)$$

which quantifies the change in the eroded area of a generic profile (y) caused by the wave farm as a fraction of the total eroded area of the same profile. $NER > 0$ and $NER < 0$ signify a reduction or increase in the eroded area.

Medium-Term Impacts

Based on the wave buoy data from November 2007 to October 2008, the wave propagation model was validated. An excellent agreement between model results and wave buoy observations was achieved (Fig. 19), with a coefficient of correlation (R) and root-mean-square error of 0.97 and 0.38 m, respectively.

Upon validation, the numerical model was applied to compare the wave patterns with and without the wave farm, and to establish the wave conditions that were to be the input to the coastal processes model. The effects of the wave farm on the nearshore wave patterns are clear, for instance, in Fig. 20, corresponding to a storm peak. The significant wave height goes down by over 30 % in the direct wakes of the WECs – a reduction that is less marked on the beach itself, as a result of wave energy diffracted from the sides of the farm into its lee. This reduction of wave height is particularly apparent in the northern section of the beach owing to the deepwater wave direction (approx. WNW).

As explained, wave power on the beach was reduced by the presence of the farm. To quantify the effects of this reduction, the profiles P1 and P2 were followed from November 2007 to April 2008. The coastal processes model was forced with the spectra generated by the wave propagation model run with and without the wave farm.

In the presence of the wave farm (Fig. 21), the evolution of the profiles from the initial conditions to 3 months into the simulation is characterized by erosion concentrated on the beach face – the section exposed to wave uprush – with the eroded sediment depositing on lower sections.

In Fig. 22 the comparison between the farm and no farm scenarios is presented for profile P2. The energy extracted by the farm leads to a substantial reduction (approx. 3 m) in the erosion of the dune, which displaces the landward extreme of the eroded area more than 10 m toward the sea. This displacement can be of particular relevance in cases such as Soulac-sur-Mer (Fig. 12), where some

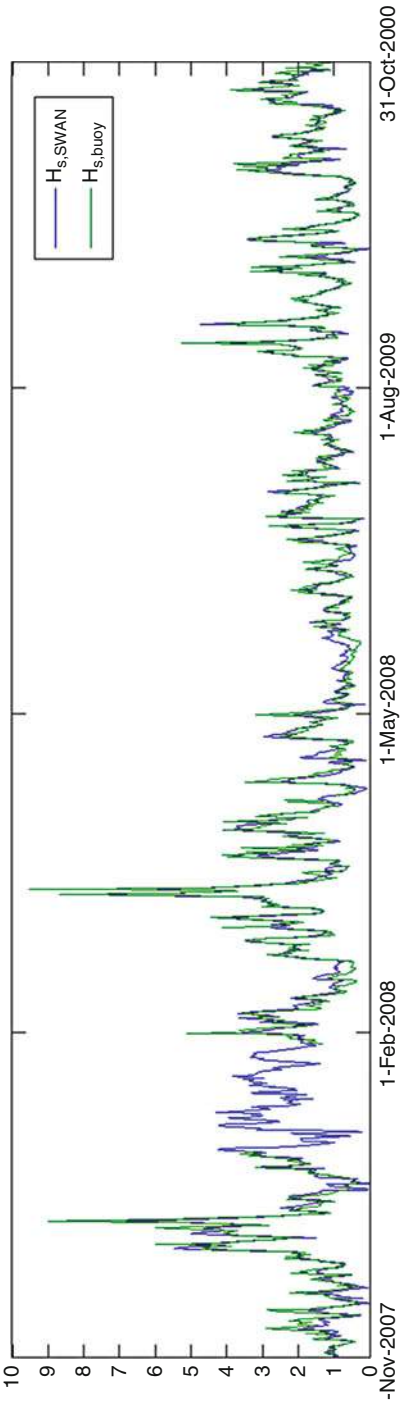

Fig. 19 Time series of modeled ($H_{s,\ SWAN}$) vs. observed ($H_{s,\ buoy}$) significant wave height

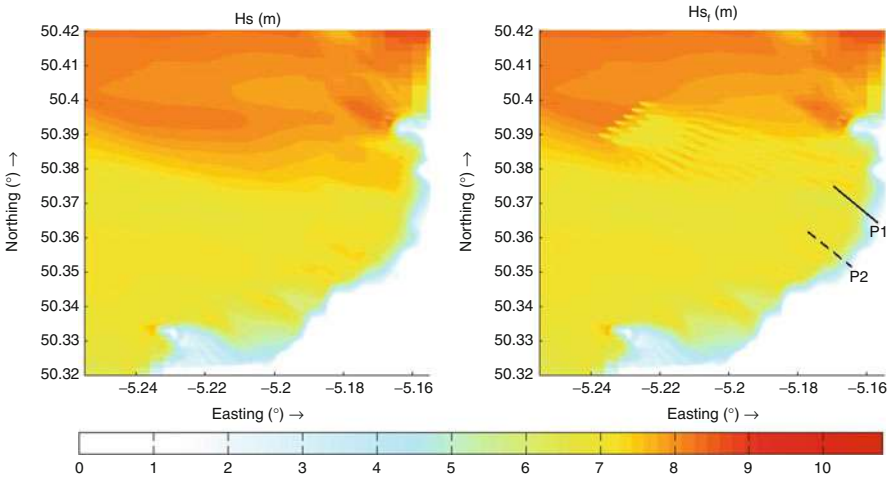

Fig. 20 Significant wave height in the no farm or baseline scenario (*Hs*, *left*) and in farm scenario (*Hsf*, *right*) at the storm peak on 10 Mar 2008, 18:00 UTC (deepwater wave conditions: $H_{s0} =$ 10.01 m, $T_p = 15.12$ s, $\theta_p = 296.38°$). Profiles P1 and P2 are delineated for reference

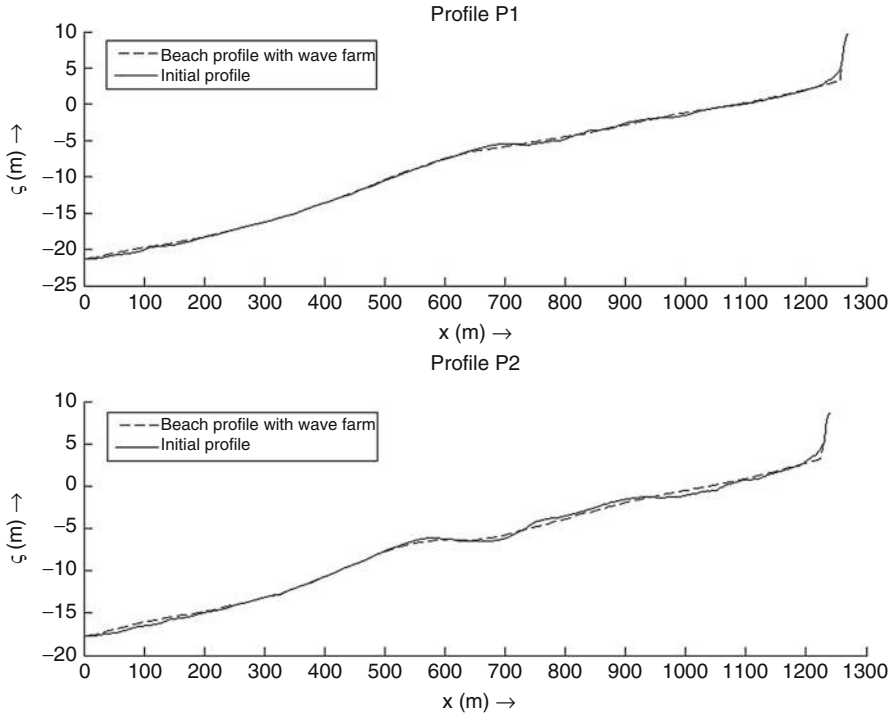

Fig. 21 Bed level at Profiles P1 and P2: initial (1 Nov 2007, 0000 UTC) and after 3 months, in the presence of the wave farm (22 Jan 2008, 15:47 UTC)

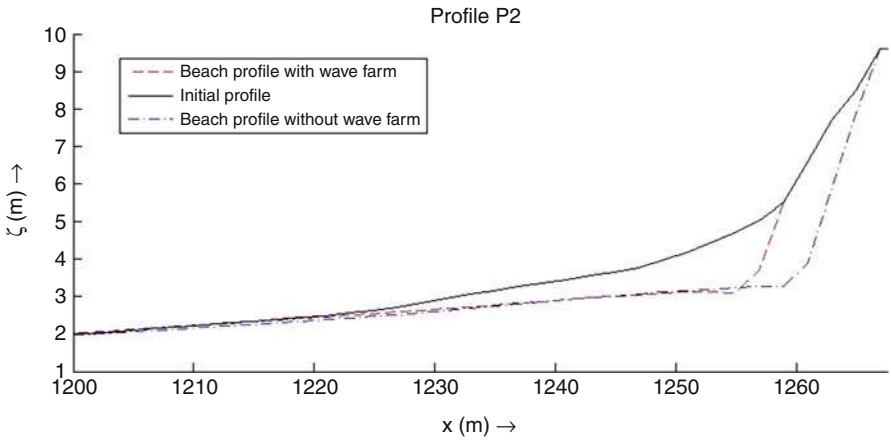

Fig. 22 Beach face level at Profile P2: initial (1 Nov 2007, 0000 UTC) and after 3 months with and without the wave farm (22 Jan 2008, 15:47 UTC)

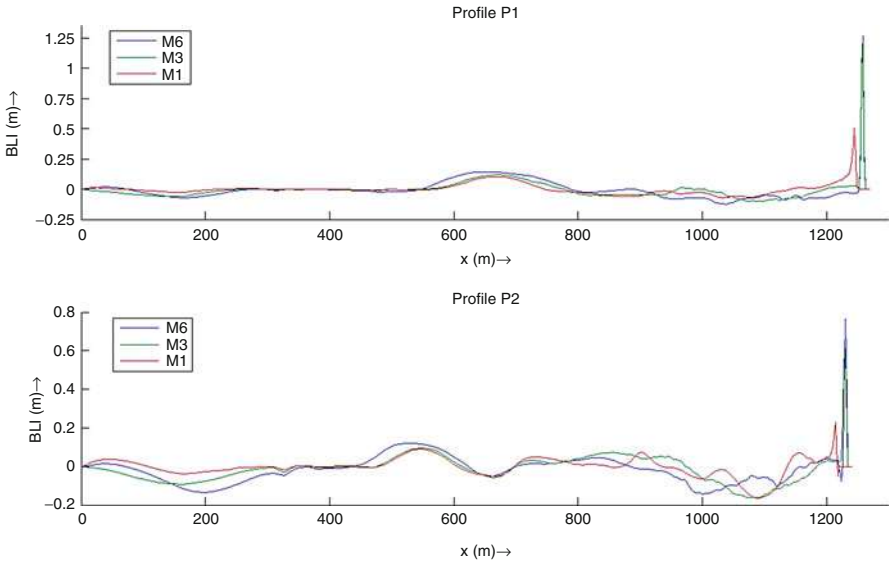

Fig. 23 *BLI* values along Profiles P1 and P2 at different points in time: 1 month (*M1*), 3 months (*M3*), and 6 months (*M6*) into the study period

buildings were at risk due to storm-induced erosion at the toe of the foundations. Had a wave farm been deployed off that section of the coast, the demolition of many a building would be avoided.

The impact of the wave farm on the beach profile was analyzed through the parameters defined in section "Suite of Process-Based Numerical Models." The *BLI* parameter along Profiles P1 and P2 (Fig. 23) was analysed for three different points

Table 1 *FEA* and *NER* factors for Profiles P1 and P2 at different points in time: 1 month (*M1*), 3 months (*M3*), and 6 months (*M6*) after the beginning of the study period

	M1			*M3*			*M6*		
Profiles	FEA_b (m^2)	FEA_f (m^2)	*NER* (%)	FEA_b (m^2)	FEA_f (m^2)	*NER* (%)	FEA_b (m^2)	FEA_f (m^2)	*NER* (%)
Profile P1	20.53	14.11	31.27	16.3	10.42	36.07	23.85	18.66	21.76
Profile P2	15.69	12.91	*17.72*	21.31	16.85	*20.93*	25.53	21.42	*16.10*

in time: 1 month (*M1*), 3 months (*M3*), and 6 months (*M6*) into the study period. A significant reduction of the erosion on the beach face and the submarine bar ($x \sim 600$ m) is apparent. Given that the bar is an essential element of the beach response to storms, its reinforcement thanks to the wave farm clearly increases the resilience of the system. This effect strengthens over time, as *BLI* values soar over the submarine bar.

The *BLI* values for both profiles were similarly non-negligible on the beach face, indicating that the wave farm reduces the erosion also in this section of the profile. To quantify these effects, the *FEA* and *NER* indicators were computed (Table 1). Comparing the two profiles, the effectiveness of the wave farm is more apparent in the northern section of the beach (Profile P1). The comparison between the FEA_b and FEA_f values and the nondimensional values of *NER* reflect the effectiveness of the wave farm in reducing storm-induced erosion and in maintaining this reduction over the medium term (M6 values, after 6 months). The relatively smaller reduction in proportional terms (*NER*) after 6 months is due to the fact that the later part of this period is not particularly stormy (March and April) – with fewer storms and less erosion, the reduction in storm-induced erosion is quantitatively smaller. Nevertheless, *NER* values after 6 months are still relevant.

The results in Table 1 showed a significant reduction of the erosion along profiles P1 and P2, which may indicate some degree of coastal protection owing to the presence of the wave farm nearshore. However, these results must be corroborated by means of a 3D study of the beach – and this is the main aim of the following section.

Short-Term Impacts

Having studied the medium-term effects of the wave farm on the beach profile, this section focuses on the response of the system in the short term during the storm, from 5 December 2007 0000 UTC to 10 December 2007 0600 UTC. The mean values of significant wave height, peak period, and peak direction were $H_s = 4.2$ m, $T_p = 12.1$ s, and $\theta_p = 295°$, respectively.

Based on the results of the wave propagation model, the coastal processes model was applied to determine how the modification of the nearshore wave conditions

affected the coastal processes and, consequently, the beach morphology. As in the previous section, the impact was quantified by means of the indicators defined in section "Suite of Process-Based Numerical Models."

The reduction of the erosion was particularly apparent on the dune, with values of *BLI* over than 4 m (Fig. 24) – the outcome of wave energy extraction by the wave farm. Similarly, the submarine bar experienced reduced erosion, particularly in water depths between 5 and 10 m and in the middle area of the beach, where the *BLI* parameter reached 0.5 m. The material that was eroded from the dune deposited primarily on lower sections of the profile, between the bar and the dune, leading to negative values of *BLI*, of the order of –0.5 m.

The beach face eroded area (*FEA*) values confirmed the effect of the wave farm in reducing erosion (Fig. 25). The most drastic erosion occurred in the southernmost end of the beach ($y \sim 0$ m) and in its northern section, the reason being that the former is not backed by the dune system, and the latter is exposed to larger waves. As regards the mid-south area of the beach, the *NER* factor presented a large variability in the section 500 m $< y <$1500 m, owing to the small values of baseline erosion (small values of the denominator in the expression of *NER*). The wave farm proved to be more effective in countering erosion in the northern area of the beach, in the direct lee of the WECs. The nondimensional erosion reduction (*NER*) confirmed this effectiveness, with values over 30 % along more than 1000 m of beach (Fig. 26).

Future Directions

At this point wave energy is generally considered as an expensive form of renewable. This is due, in part, to the early stage of development of the technology and, in part, to the difficulties posed by the harsh marine environment. In any case, for wave energy to truly take off, its costs must decrease substantially.

Over time it may be expected that, as the technologies develop, a proper chain of production for wave energy components is established, and manufacturing of WECs assumes an industrial scale, economies of scale will ensue which will lead to cost reductions. The process whereby the development of an incipient technology, improvements by practice, and economies of scale lead to savings is exemplified by the so-called learning curve. The greatest opportunities for cost reduction in wave energy as a stand-alone energy source at present are related to the installation and construction processes (Astariz and Iglesias 2015) and the optimization of WEC design.

In addition to the previous options, two "strategic" approaches for reducing the cost are (i) using wave farms for coastal defense in synergy with their main function of generating carbon-free energy (section "Wave Farms") and (ii) combining wave energy with other forms of marine renewable – notably, offshore wind (Astariz et al. 2015a, b, c; Perez Collazo et al. 2014; Stoutenburg et al. 2010).

The application of wave farms to coastal protection was investigated in section "Wave Farms." Its advantages are twofold: enhanced economic viability through

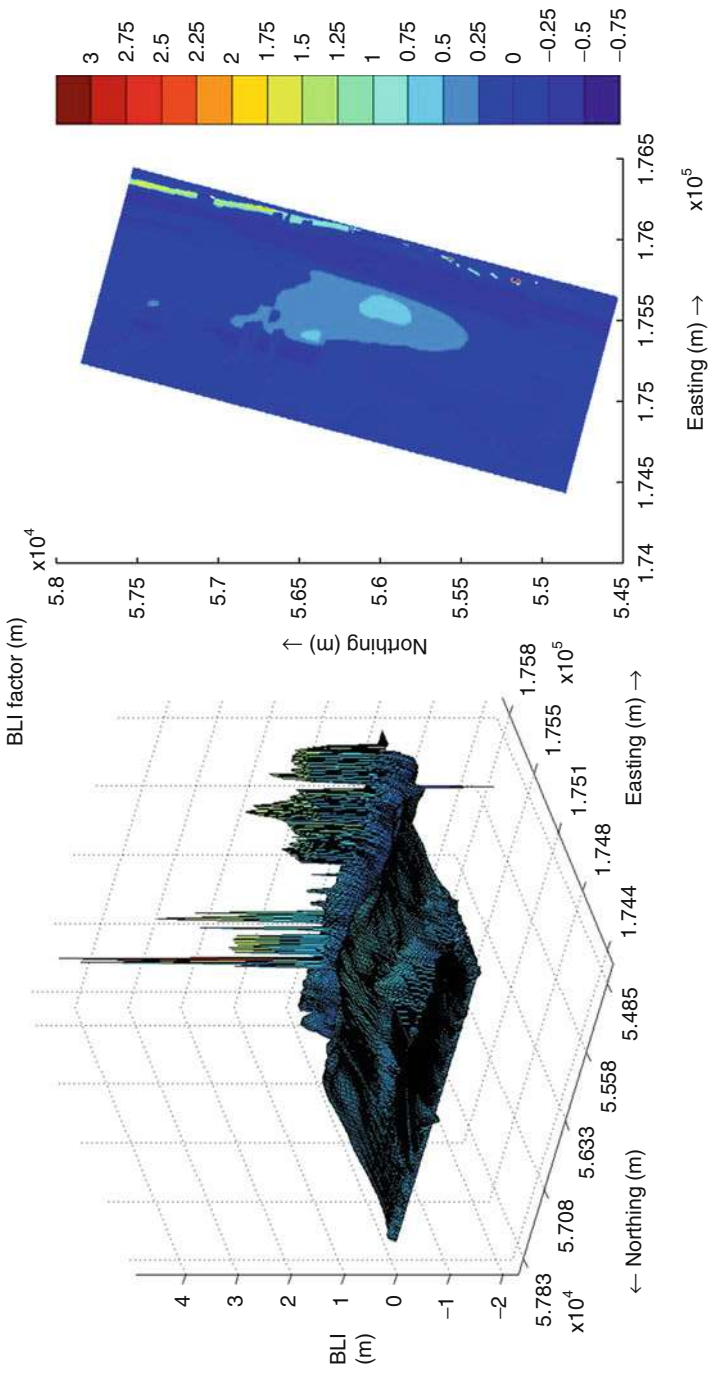

Fig. 24 Bed level impact (*BLI*) at the end of the study period

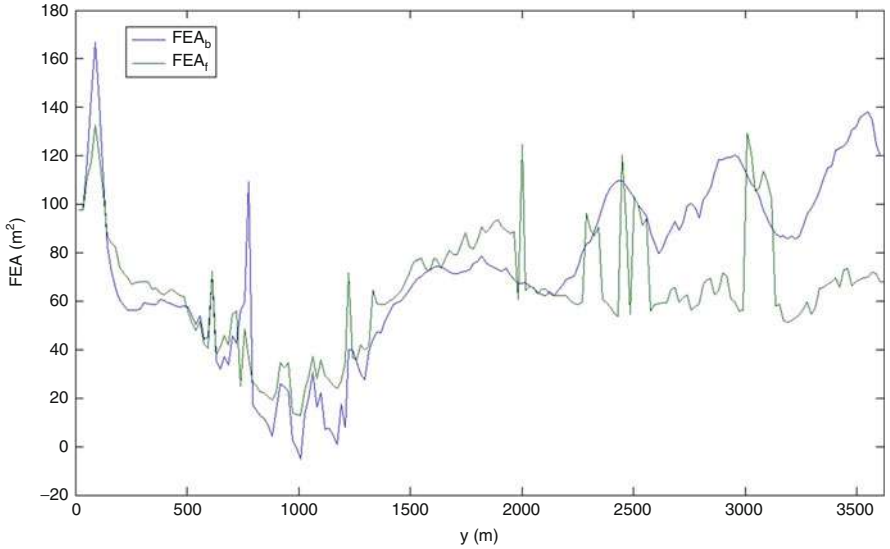

Fig. 25 Beach face eroded area in the baseline (FEA_b) and wave farm (FEA_f) scenarios at the end of the study period

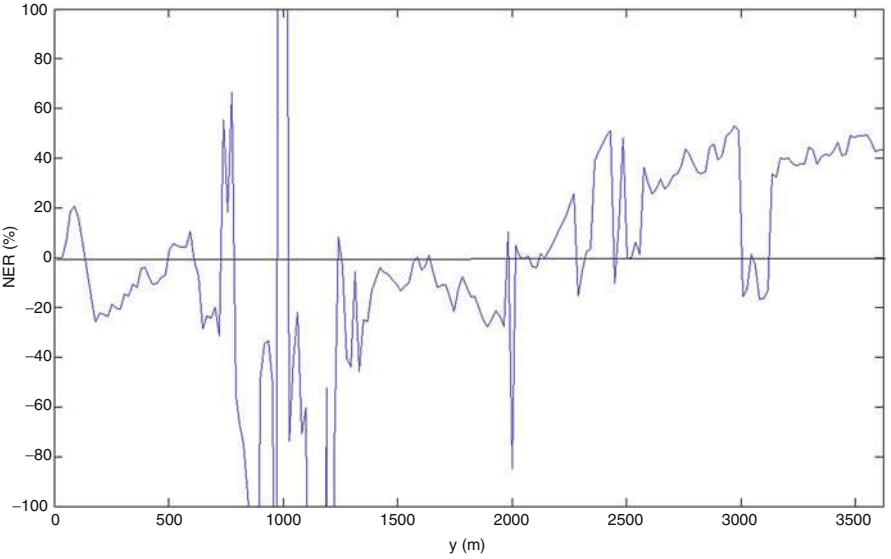

Fig. 26 Nondimensional erosion reduction (*NER*) on the beach face at the end of the study period

savings in conventional defense schemes and adaptability to effects of climate change such as sea-level rise (unlike conventional coastal defense schemes based on structures). So far the effectiveness of wave farms for coastal protection has been established in the short and medium term. The multidecadal response of the coastal

system must be studied in order to establish their long-term efficiency. In addition, further research is necessary to accurately predict the savings that could ensue.

Combined wave-offshore wind energy brings down costs through shared electrical infrastructure (cables, substation, grid connection), foundations and substructures (hybrid systems) or moorings, and maintenance (crews, boats, and other equipment). These items represent a substantial portion of the total cost, and therefore sharing them with an offshore wind farm would be effective in improving the economic viability of wave energy. Additional advantages of combined offshore wind and wave energy are (i) optimized use of the scarce marine space, with an enhanced energy yield per unit area; (ii) smoother power output; and (iii) a less energetic wave climate within the offshore wind farm, which will reduce the loads on foundations and, importantly, increase the weather windows for maintenance, which will in turn reduce downtime (Astariz et al. 2015b; Pérez-Collazo et al. 2015).

Research into these two avenues for reducing costs – the synergetic application of wave farms to coastal protection and combined wave-offshore wind farms – is currently under way by means of numerical modeling, laboratory work, and fieldwork. Laboratory and field data are necessary to improve the understanding of wave-WEC interaction, hence of the effects of wave farms on their environment, not least on the littoral. They constitute the means for calibrating and validating numerical models, which are instrumental in optimizing WEC design and modeling wave propagation through the wave farm and coastal processes in its lee.

Conclusions

In this chapter a review of wave energy was presented, from the wave resource to the technologies to harness it to its application to coastal defense or in combination with offshore wind. As regards the wave resource (section "Wave Resource Characterization"), its fundamentals were explained, and the procedure to characterize its temporal and spatial variability by means of numerical modeling and field data was outlined. This characterization is essential in: (i) selecting optimum wave farm locations; (ii) predicting the energy output of a wave farm; (iii) assessing its downtime, which may be due to extreme sea states, insufficient wave height, or maintenance (scheduled or unscheduled, after breakdowns); and (iv) determining the installation and maintenance costs. In sum, the characterization of the wave resource is fundamental to analyzing the viability of a wave energy project and to selecting the wave energy conversion technology that is most appropriate to a given site.

The different technologies for wave energy conversion (section "Wave Energy Conversion") were classified according to three criteria: installation site, dimensions relative to wave length, and principle of operation. Next, representative WECs of each category were briefly reviewed. Nowadays no single technology can be said to have gained overall acceptance, and it remains to be seen which concept will prevail. What is certain at present is that the two factors that are most

likely to influence the outcome of this natural selection process are economic viability and reliability, both of which depend on the performance (energy efficiency, i.e., capture width ratio) and survivability.

Wave farms were shown to be an efficient method to protect the coast in the short and medium term (section "Wave Farms") – with research into their long-term efficiency included into the future research lines (section "Future Directions"). In this regard, their advantages relative to conventional coastal protection means (based on structures: detached breakwaters, groynes, etc.) in terms of adaptation to sea-level rise and low environmental (particularly visual) impact are noteworthy. Promising quantitative results were obtained in the study case, with reductions over 50 % in storm-induced erosion.

The objectives of greenhouse gas reduction established by the Kyoto protocol and other treaties can only be attained by means of a very substantial increase in the proportion of renewables in the energy mix. This can only be possible through the expansion of consolidated renewables (e.g., offshore and onshore wind, solar, hydropower) and the development of nascent renewables (e.g., wave, tidal). In the case of wave energy, this development is taking place, with intensive research into a number of technologies, and new opportunities through combinations with other renewables (offshore wind) and the synergetic application to coastal protection. This chapter showed that wave energy is emerging as a promising renewable capable of tackling climate change on the double front of its causes (through reduced carbon emissions) and effects, particularly on the coast (erosion).

References

Abanades J, Greaves D, Iglesias G (2014a) Coastal defence through wave farms. Coast Eng 91:299–307

Abanades J, Greaves D, Iglesias G (2014b) Wave farm impact on the beach profile: a case study. Coast Eng 86:36–44

Abanades J, Greaves D, Iglesias G (2015a) Wave farm impact on beach modal state. Mar Geol 361:126–135

Abanades J, Greaves D, Iglesias G (2015b) Coastal defence using wave farms: the role of farm-to-coast distance. Renew Energy 75:572–582

Arena F, Fiamma V, Laface V, Malara G, Romolo A, Viviano A, Sannino G, Carillo A (2013) Installing U-OWC devices along Italian coasts. In: ASME 2013 32nd international conference on ocean, offshore and arctic engineering. American Society of Mechanical Engineers, pp V008T009A061-V008T009A061

Astariz S, Iglesias G (2014) Wave energy vs. other energy sources: a reassessment of the economics. Int J Green Energy, (in press)

Astariz S, Iglesias G (2015) The economics of wave energy: a review. Renew Sustain Energy Rev 45:397–408

Astariz S, Perez-Collazo C, Abanades J, Iglesias G (2015a) Towards the optimal design of a co-located wind-wave farm. Energy 84:15–24

Astariz S, Perez-Collazo C, Abanades J, Iglesias G (2015b) Co-located wind-wave farm synergies (operation & maintenance): a case study. Energy Convers Manag 91:63–75

Astariz S, Perez-Collazo C, Abanades J, Iglesias G (2015c) Co-located wave-wind farms: economic assessment as a function of layout. Renew Energy 83:837

Austin M, Scott T, Brown J, Brown J, MacMahan J, Masselink G, Russell P (2010) Temporal observations of rip current circulation on a macro-tidal beach. Cont Shelf Res 30(9):1149–1165
AWS Ocean Energy (2015) AWS Ocean Energy web page
Bahaj AS (2011) Generating electricity from the oceans. Renew Sustain Energy Rev 15 (7):3399–3416
Baldock TE, Alsina JA, Caceres I, Vicinanza D, Contestabile P, Power H, Sanchez-Arcilla A (2011) Large-scale experiments on beach profile evolution and surf and swash zone sediment transport induced by long waves, wave groups and random waves. Coast Eng 58 (2):214–227
Berkhoff J (1974) Computation of combined refraction-diffraction. Delft Hydraulics Laboratory, Delft
Bernhoff H, Sjöstedt E, Leijon M (2006) Wave energy resources in sheltered sea areas: a case study of the Baltic Sea. Renew Energy 31(13):2164–2170
Cameron L, Doherty R, Henry A, Doherty K, Van't Hoff J, Kaye D, Naylor D, Bourdier S, Whittaker T (2010) Design of the next generation of the Oyster wave energy converter. In: 3rd international conference on ocean energy
Carballo R, Iglesias G (2012) A methodology to determine the power performance of wave energy converters at a particular coastal location. Energy Convers Manag 61:8–18
Carballo R, Iglesias G (2013) Wave farm impact based on realistic wave-WEC interaction. Energy 51:216–229
Carballo R, Sánchez M, Ramos V, Fraguela J, Iglesias G (2015) The intra-annual variability in the performance of wave energy converters: a comparative study in N Galicia (Spain). Energy 82:138
Castelle B, Marieu V, Bujan S, Splinter KD, Robinet A, Sénéchal N, Ferreira S (2015) Impact of the winter 2013–2014 series of severe Western Europe storms on a double-barred sandy coast: beach and dune erosion and megacusp embayments. Geomorphology 238:135–148
Chaplin J, Farley F, Rainey R (2007) Power conversion in the ANACONDA WEC. In: Proceedings of the 22nd international workshop on water waves and floating bodies
Chini N, Stansby P, Leake J, Wolf J, Roberts-Jones J, Lowe J (2010) The impact of sea level rise and climate change on inshore wave climate: a case study for East Anglia (UK). Coast Eng 57 (11):973–984
CISCAG (2011) Shoreline management plan Cornwall and Isles of Scilly Coastal Advisory Group. Available
Clément A, McCullen P, Falcão AFdO, Fiorentino A, Gardner F, Hammarlund K, Lemonis G, Lewis T, Nielsen K, Petroncini S, Pontes MT, Schild P, Sjöström B, Sørensen HC, Thorpe TW (2002) Wave energy in Europe: current status and perspectives. Renew Sustain Energy Rev 6 (5):405–431
de Sousa Prado MG, Gardner F, Damen M, Polinder H (2006) Modelling and test results of the Archimedes wave swing. Proc Inst Mech Eng Part A J Power and Energy 220(8):855–868
Defne Z, Haas KA, Fritz HM (2009) Wave power potential along the Atlantic coast of the southeastern USA. Renew Energy 34(10):2197–2205
DEFRA (2015) Central government funding for flood and coastal erosion risk management in England. Available
Drew B, Plummer AR, Sahinkaya MN (2009) A review of wave energy converter technology. J Power Energy 223(8):887–902
Egbert GD, Bennett AF, Foreman MG (1994) TOPEX/POSEIDON tides estimated using a global inverse model. J Geophys Res Oceans (1978–2012) 99(C12):24821–24852
EU-OEA (2010) Oceans of energy. European ocean energy roadmap 2010–2050. European Ocean Energy Association, Bietlot, 36 pp. Available at: http://www.eu-oea.com/wp-content/uploads/2012/02/EUOEA-Roadmap.pdf
European Commission (2007) A European Strategic Energy Technology Plan (SET-Plan)–towards a low-carbon future. 723
EUROSION (2004) EUROSION. [Online]. Available at: http://www.eurosion.org
EVE (2014) Ente Vasco de la Energia

EWEA, ECN, 3E, SOW (2012) Delivering offshore electricty to the EU. Spatial planning of offshore renewable energies and electricity grid infrastrutures in an integrated EU maritime policy. 80 pp. Available at: www.seanergy2020.eu
Falcão AdO (2000) The shoreline OWC wave power plant at the Azores. In: Proceedings of the fourth European wave energy conference, Aalborg, pp 42–48
Falcão AFO (2010) Wave energy utilization: a review of the technologies. Renew Sustain Energy Rev 14(3):899–918
Falnes J (2007) A review of wave-energy extraction. Mar Struct 20(4):185–201
Fernandez H, Iglesias G, Carballo R, Castro A, Fraguela JA, Taveira-Pinto F, Sanchez M (2012) The new wave energy converter WaveCat: concept and laboratory tests. Mar Struct 29(1):58–70
Folley M, Whittaker T (2009) Analysis of the nearshore wave energy resource. Renew Energy 34 (7):1709–1715
Folley M, Babarit A, Child B, Forehand D, O'Boyle L, Silverthorne K, Spinneken J, Stratigaki V, Troch P (2012) A review of numerical modeling of wave energy converter arrays. In: International conference on ocean, offshore and arctic engineering (OMAE 2012). ASME, pp 1–11
Galappatti G, Vreugdenhil C (1985) A depth-integrated model for suspended sediment transport. J Hydraul Res 23(4):359–377
Gonçalves M, Martinho P, Guedes Soares C (2014) Wave energy conditions in the western French coast. Renew Energy 62:155–163
Gonzalez-Santamaria R, Zou Q-P, Pan S (2013) Impacts of a wave farm on waves, currents and coastal morphology in south west England. Estuar Coasts 38(1):1–14
Haigh ID, Wadey MP, Gallop SL, Loehr H, Nicholls RJ, Horsburgh K, Brown JM, Bradshaw E (2015) A user-friendly database of coastal flooding in the United Kingdom from 1915–2014. Sci Data 2:150021
Hasselmann K (1971) On the mass and momentum transfer between short gravity waves and larger-scale motions. J Fluid Mech 50(01):189–205
Henderson R (2006) Design, simulation, and testing of a novel hydraulic power take-off system for the Pelamis wave energy converter. Renew Energy 31(2):271–283
Holthuijsen LH (2007) Waves in oceanic and coastal waters. Cambridge University Press, Cambridge
Holthuijsen L, Booij N, Herbers T (1989) A prediction model for stationary, short-crested waves in shallow water with ambient currents. Coast Eng 13(1):23–54
Huthnance J, Mieszkowska N (2010) Charting progress 2 feeder report: ocean processes. The Scottish Govt., Edinburgh, (UK)
Iglesias G, Abanades J (2014) Characterisation of the wave resource: the crucial points. In: RENEW 1st international conference on renewable energies offshore, Lisbon
Iglesias G, Carballo R (2009) Wave energy potential along the Death Coast (Spain). Energy 34 (11):1963–1975
Iglesias G, Carballo R (2010a) Wave energy and nearshore hot spots: the case of the SE Bay of Biscay. Renew Energy 35(11):2490–2500
Iglesias G, Carballo R (2010b) Wave power for la isla bonita. Energy 35(12):5013–5021
Iglesias G, Carballo R (2010c) Offshore and inshore wave energy assessment: Asturias (N Spain). Energy 35(5):1964–1972
Iglesias G, Carballo R (2011) Choosing the site for the first wave farm in a region: a case study in the Galician Southwest (Spain). Energy 36(9):5525–5531
Iglesias G, Carballo R (2014) Wave farm impact: the role of farm-to-coast distance. Renew Energy 69:375–385
Iglesias G, Carballo R, Castro A, Fraga B (2008) Development and design of the WaveCat™ energy converter. Coast Eng:3970–3982
Iglesias G, López M, Carballo R, Castro A, Fraguela JA, Frigaard P (2009) Wave energy potential in Galicia (NW Spain). Renew Energy 34(11):2323–2333

Iglesias G, Alvarez M, García P (2010) Wave energy converters. In: Encyclopedia of life support systems (EOLSS). UNESCO, Paris
Jeffrey H, Sedgwick J (2011) ORECCA. European offshore renewable energy roadmap. 201 pp. Available at: http://www.orecca.eu/
Johnson R (1997) A modern introduction to the mathematical theory of water waves, vol 19. Cambridge University Press, Cambridge
Kendon M, McCarthy M (2015) The UK's wet and stormy winter of 2013/2014. Weather 70 (2):40–47
Kofoed JP, Frigaard P, Friis-Madsen E, Sørensen HC (2006) Prototype testing of the wave energy converter. Renew Energy 31(2):181–189
Kramer M, Marquis L, Frigaard P (2011) Performance evaluation of the wavestar prototype. In: The 9th European wave and tidal energy conference: EWTEC 2011
Lenee-Bluhm P, Paasch R, Özkan-Haller HT (2011) Characterizing the wave energy resource of the US Pacific Northwest. Renew Energy 36(8):2106–2119
Longuet-Higgins MS, Stewart R (1961) The changes in amplitude of short gravity waves on steady non-uniform currents. J Fluid Mech 10(04):529–549
López I, Iglesias G (2014) Efficiency of OWC wave energy converters: a virtual laboratory. Appl Ocean Res 44:63–70
López I, Pereiras B, Castro F, Iglesias G (2014) Optimisation of turbine-induced damping for an OWC wave energy converter using a RANS–VOF numerical model. Appl Energy 127:105–114
Mann LD (2011) Application of ocean observations & analysis: the CETO wave energy project. In: Operational oceanography in the 21st century. Springer, Heidelberg, pp 721–729
Marquis L, Kramer M, Frigaard P (2010) First power production figures from the wave star roshage wave energy converter. In: Proceedings of the international conference on ocean energy (ICOE)
Masselink G, Evans D, Hughes MG, Russell P (2005) Suspended sediment transport in the swash zone of a dissipative beach. Mar Geol 216(3):169–189
McCormick ME (1981) Ocean wave energy conversion. Wiley-Interscience, New York
Mehlum E (1986) Tapchan. In: Hydrodynamics of ocean wave-energy utilization. Springer, Heidelberg, pp 51–55
Mendoza E, Silva R, Zanuttigh B, Angelelli E, Lykke Andersen T, Martinelli L, Nørgaard JQH, Ruol P (2014) Beach response to wave energy converter farms acting as coastal defence. Coast Eng 87:97–111
Millar DL, Smith HCM, Reeve DE (2007) Modelling analysis of the sensitivity of shoreline change to a wave farm. Ocean Eng 34(5–6):884–901
Moccia J, Arapogianni A, Wilkes J, Kjaer C, Gruet R (2011) Pure power. Wind energy targets for 2020 and 2030. European Wind Energy Association, Brussels, 97 pp. Available at: http://www.ewea.org
Ocean Power Technologies Inc (2014) OPT web page
Oceans U. A. o. t. (2011) Human settlements on the coast [Online]. Available at: http://www.oceansatlas.org/servlet/CDSServlet?status=ND0xODc3JjY9ZW4mMzM9KiYzNz1rb3M. Accessed 21 May 2015
Palha A, Mendes L, Fortes CJ, Brito-Melo A, Sarmento A (2010) The impact of wave energy farms in the shoreline wave climate: Portuguese pilot zone case study using Pelamis energy wave devices. Renew Energy 35(1):62–77
Pelamis Wave Power (2014) Pelamis wave power web page
Perez Collazo C, Astariz S, Abanades J, Greaves D, Iglesias G (2014) Co-located wave and offshore wind farms: a preliminary case study of an hybrid array. In: International conference in coastal engineering (ICCE)
Pérez-Collazo C, Greaves D, Iglesias G (2015) A review of combined wave and offshore wind energy. Renew Sustain Energy Rev 42:141–153
Photobrooks (2014) Photobrooks web page

Pontes M, Athanassoulis G, Barstow S, Bertotti L, Cavaleri L, Holmes B, Mollison D, Pires H (1998) The European wave energy resource. In: 3rd European wave energy conference, Patras
Pugh D (2004) Changing sea levels: effects of tides, weather and climate. Cambridge University Press, Cambridge
Reeve DE, Chen Y, Pan S, Magar V, Simmonds DJ, Zacharioudaki A (2011) An investigation of the impacts of climate change on wave energy generation: the Wave Hub, Cornwall, UK. Renew Energy 36(9):2404–2413
Roelvink J, Reniers A, Van Dongeren A, Van Thiel de Vries J, Lescinski J, McCall R (2006) XBeach model description and manual. In: UNESCO-IHE Institute for Water Education. (Accessed: Roelvink J, Reniers A, Van Dongeren A, Van Thiel de Vries J, Lescinski J, McCall R)
Roelvink D, Reniers A, van Dongeren A, van Thiel de Vries J, McCall R, Lescinski J (2009) Modelling storm impacts on beaches, dunes and barrier islands. Coast Eng 56 (11–12):1133–1152
Rusu L, Guedes Soares C (2012) Wave energy assessments in the Azores islands. Renew Energy 45:183–196
Rusu E, Guedes Soares C (2013) Coastal impact induced by a Pelamis wave farm operating in the Portuguese nearshore. Renew Energy 58:34–49
Scott T, Masselink G, Russell P (2011) Morphodynamic characteristics and classification of beaches in England and Wales. Mar Geol 286(1–4):1–20
Senechal N, Coco G, Castelle B, Marieu V (2015) Storm impact on the seasonal shoreline dynamics of a meso- to macrotidal open sandy beach (Biscarrosse, France). Geomorphology 228:448–461
Sibley A, Cox D, Titley H (2015) Coastal flooding in England and Wales from Atlantic and North Sea storms during the 2013/2014 winter. Weather 70(2):62–70
Slingo J, Belcher S, Scaife A, McCarthy M, Saulter A, McBeath K, Jenkins A, Huntingford C, Marsh T, Hannaford J (2014) The recent storms and floods in the Met. Office, Exeter (UK)
Smith HCM, Pearce C, Millar DL (2012) Further analysis of change in nearshore wave climate due to an offshore wave farm: an enhanced case study for the Wave Hub site. Renew Energy 40 (1):51–64
Spencer T, Brooks SM, Evans BR, Tempest JA, Möller I (2015) Southern North Sea storm surge event of 5 December 2013: water levels, waves and coastal impacts. Earth Sci Rev 146:120–145
Stopa JE, Cheung KF, Chen Y-L (2011) Assessment of wave energy resources in Hawaii. Renew Energy 36(2):554–567
Stoutenburg ED, Jenkins N, Jacobson MZ (2010) Power output variations of co-located offshore wind turbines and wave energy converters in California. Renew Energy 35(12):2781–2791
Tedd J, Kofoed JP (2009) Measurements of overtopping flow time series on the Wave Dragon, wave energy converter. Renew Energy 34(3):711–717
Thorpe TW (1999) A brief review of wave energy. Harwell Laboratory, Energy Technology Support Unit, Oxford (UK)
Thorpe T (2001) The wave energy programme in the UK and the European wave energy network
Tolman HL (2002) User manual and system documentation of WAVEWATCH-III version 2.22
Torre-Enciso Y, Ortubia I, López de Aguileta L, Marqués J (2009) Mutriku wave power plant: from the thinking out to the reality. In: Proceedings of the 8th European wave and tidal energy conference, pp 319–329
Valério D, Beirão P, da Costa JS (2007) Optimisation of wave energy extraction with the Archimedes Wave Swing. Ocean Eng 34(17):2330–2344
Van Thiel de Vries J (2009) Dune erosion during storm surges. PhD thesis, Delft University of Technology
Veigas M, López M, Iglesias G (2014) Assessing the optimal location for a shoreline wave energy converter. Appl Energy 132:404–411
Vicinanza D, Frigaard P (2008) Wave pressure acting on a seawave slot-cone generator. Coast Eng 55(6):553–568

Vicinanza D, Margheritini L, Contestabile P, Kofoed JP, Frigaard P (2008) Seawave slot-cone generator: an innovative caisson breakwaters for energy production. In: The international conference on coastal engineering, pp 3694–3705

Vicinanza D, Contestabile P, Ferrante V (2013) Wave energy potential in the north-west of Sardinia (Italy). Renew Energy 50:506–521

Vidal C, Méndez Fernando J, Díaz G, Legaz R (2007) Impact of Santoña WEC installation on the littoral processes. In: Proceedings of the 7th European wave and tidal energy conference, Porto

Wadey M, Haigh I, Brown J (2014) A century of sea level data and the UK's 2013/14 storm surges: an assessment of extremes and clustering using the Newlyn tide gauge record. Ocean Sci Discuss 11(4):1995–2028

Wave Dragon AS (2005) Wave Dragon web page

Zanuttigh B, Angelelli E (2013) Experimental investigation of floating wave energy converters for coastal protection purpose. Coast Eng 80:148–159

Geothermal Energy

Hirofumi Muraoka

Contents

Abstract

While most renewable energies are, directly or indirectly, derived from the sun, geothermal energy originates in the interior of the earth. Geothermal energy is the most stable of the renewable energies because it can be utilized constantly, regardless of weather or season. Geothermal energy can be used not only for power generation but also for direct heat application. The development of geothermal power generation entered a phase of rapid growth in 2005, and its total installed capacity worldwide reached 10.7 GW_e in 2010. The capacity of 10.7 GW_e appears small when compared with solar and wind power generation; however, the high-capacity factor of geothermal power plants, which is 0.7–0.9, provides several times greater electricity from the same installed capacity than

H. Muraoka (✉)
North Japan Research Institute for Sustainable Energy, Hirosaki University, Aomori, Japan
e-mail: hiro@hirosaki-uc.jp

W.-Y. Chen et al. (eds.), *Handbook of Climate Change Mitigation and Adaptation*,
DOI 10.1007/978-3-319-14409-2_35

photovoltaic and wind plants. Direct heat application can be used almost anywhere on land. Geothermal resources are classified into two categories: hydrothermal convection resources and thermal conduction resources. Today's geothermal power capacity is mainly hydrothermal-based and unevenly distributed in volcanic countries. As a borehole is drilled into deeper formations, formation temperature becomes higher but permeability becomes lower. Hydrothermal convection resources have a limit depth. Rock's brittle-plastic transition gives a bottom depth to permeability, and it is the absolute limit depth for the hydrothermal convection resources. Enhanced or engineered geothermal systems (EGS), in which fractures are artificially created in less-permeable rocks and heat is extracted by artificially circulating water through the fractures, are still at a demonstration stage, but they will extend geothermal power generation to thermal conduction resources and to depths even deeper than the brittle-plastic transition. Assessment of worldwide geothermal resource potential is still under study. However, an estimate shows that potential is 312 GW_e for hydrothermal resources for electric power generation to a depth of 4 km, 1,500 GW_e for EGS resources to a depth of 10 km, and 4,400 GW_{th} for direct geothermal use resources. Were 70 % of hydrothermal resources, 20 % of EGS resources, and 20 % of direct-use resources to be developed by 2050, it could reduce carbon dioxide emission by 3.17 Gton/year, which is 11 % of the present worldwide emission.

Introduction

While most kinds of renewable energy available are, directly or indirectly, derived from the sun, geothermal energy originates in the interior of the earth. This makes geothermal energy distinct from other kinds of renewable energy, giving its use merits as well as demerits.

Geothermal energy is the most stable energy among a variety of renewable energies. The capacity factor, a ratio of working time of the facility, of geothermal power plants is as high as those of thermal power plants, qualifying geothermal power generation as a base load electricity source. Geothermal energy can be supplied constantly from the earth's interior regardless of time of the day or night, weather, or season.

Assessment of the resource potentials of most kinds of renewable energy, such as the wind velocity and solar radiant energy, is not very difficult because they can be directly observed. Assessment of geothermal resource potential is not as easy, however, because geothermal resources are stored in the earth's crust. This makes the initial investment risk for geothermal energy developments higher.

For many years, geothermal energy development was only undertaken in volcanic countries such as Italy, New Zealand, Japan, the USA, the Philippines, Iceland, and Indonesia. More recently, however, less volcanic countries, such as Germany, Australia, France, and Switzerland, have begun enthusiastically developing geothermal power plants under a new concept of the enhanced or engineered geothermal

system (EGS). Innovation in geothermal energy utilization technology currently aims at a goal that every country can use geothermal energy.

Heat in the Earth's Interior

Enormous heat is stored in the earth's interior. The simplified thermal structure of the earth's interior is illustrated in Fig. 1. The deepest hole ever drilled was the SG-3 well in Kola Peninsula, Russia, that reached a depth of 12,262 m in 1989

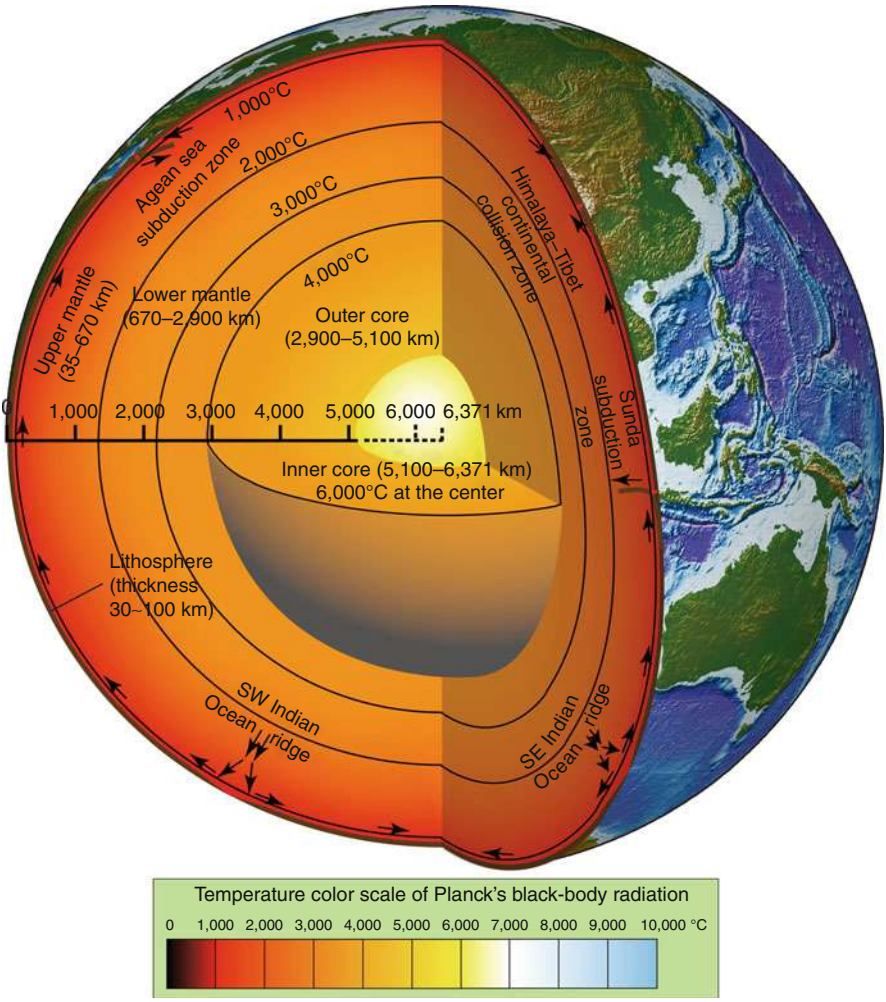

Fig. 1 Simplified thermal structure of the earth's interior (Topographic data are taken from Lindquist et al. (2004) and drawing is made with GMT by Wessel and Smith (1998))

(Fuchs et al. 1990). The hole reached only 0.2 % of the radius of the earth, suggesting that direct temperature measurement of the earth's interior would be difficult. The temperature of the earth's interior is estimated from the transmissibility and velocity of seismic waves, high-temperature and high-pressure experiments for mineral phase changes, a model calculation of temperature increases by the adiabatic compression of mineral phases, a model calculation of electric conductivity of mineral phases, and many other methods. All of these are indirect estimates and inevitably yield a large opportunity for error. The temperature at the center of the earth is commonly estimated to be 6,000 °C, but that may easily yield an error ±1,000 °C (Fig. 1).

Seismological observation delineates that the outer core of the earth consists mainly of molten state iron and nickel, and the mantle of the earth consists of solid state peridotite (ultramafic rocks mostly composed of olivine, Ca-poor pyroxene, and Ca-rich pyroxene). When the melting point temperatures of these are considered at the given pressure, the core-mantle boundary is estimated to be about 4,000 °C (Kanamori 1978). The abrupt change of the velocity of seismic waves at a depth of 670 km in the lower and upper mantle boundary is ascribed to the phase changes from γ phase of spinel to perovskite + magnesiowüstite at 1,600 °C (Tajika 1996). The thickness of the lithosphere, a rigid plate, is less than 30 km near the axis of ocean ridges and increases to 100 km away from the ridge. Low-velocity zones of the seismic waves or asthenosphere underlie the rigid plate at a depth between 70 and 250 km. This zone is partially fused and probably reaches 1,000 °C because of the wet solidus temperature of peridotite. Therefore, only a thin veneer of the earth's surface is less than 1,000 °C, and the 93 % volume of the earth's interior exceeds 1,000 °C (Fig. 1). Thus, the earth is some sort of a thermal engine.

The derivation of the heat is mainly attributed to the accretion heat from bombardment of unsorted micro-planet materials and the heat from gravitational differentiation and compression in the initial stage of the earth's formation history some 4.6 billion years ago (Takahashi 1996). The earth is gradually losing the initial heat with time. Nevertheless, abundant heat is still stored in the earth's interior, 4.6 billion years after its incipiency. The thermal life of the earth is prolonged by the additional heat generation in radioactive decay. Based on the past 4.6 billion years, the earth's heat will be probably preserved for another 4.6 billion years. Thus, the earth is some sort of a semipermanent thermal engine.

Quantity of Thermal Energy Supplied from the Earth's Interior

The earth's interior constantly supplies heat to the surface. This heat transportation phenomenon is called "terrestrial heat flow." Terrestrial heat flow can be measured in wells at a depth from 0.3 to 3 km on shore, where the solar radiant heat does not reach. Terrestrial heat flow can be measured in shallower wells on the ocean floor because of no disturbance by solar radiant heat. Terrestrial heat flow is calculated from the observed thermal gradient multiplied by the thermal conductivity of the constituent rocks. An average terrestrial heat flow is 65 ± 1.6 mW/m^2 onshore and 101 ± 2.2 mW/m^2 offshore (Tajika 1996). The value of the terrestrial heat flow

observed on shore consists of not only heat flow from the earth's interior but also heat flow from radioactive decay of elements such as uranium, thorium, and potassium predominantly concentrated in the continental crust. About half of the terrestrial heat-flow value on shore may be derived from radioactive decay. The value of the terrestrial heat flow observed offshore has a negative correlation with the geological age of the ocean floor. The younger ocean floor tends to yield the higher terrestrial heat flow (Tajika 1996).

Including both continental and oceanic regions, a global average terrestrial heat flow is $87 \pm 2.0\ \mathrm{mW/m^2}$. This value $2.1 \times 10^{-6}\ \mathrm{cal/cm^2 \cdot s}$ ($87\ \mathrm{mW/m^2}$) multiplied by the entire global area is converted to the annual value, yielding an annual global terrestrial heat-flow energy $E_{hf} = 1.3 \times 10^{21}$ J/year or 3.2×10^{20} cal/year (Mizutani and Watanabe 1978). This heat-flow energy causes a variety of the earth's internal dynamics, such as mantle convection, plate tectonics, earthquakes, and magma generation. Thermal energy of lava flow and volcanic ash that erupted from global volcanoes is estimated to be $E_e = 3 \times 10^{19}$ J/year or 7×10^{18} cal/year (Mizutani and Watanabe 1978). This energy is one or two orders of magnitude lower than the terrestrial heat-flow energy that causes it. Many active volcanoes form high-level magma chambers that heat up ground water to discharge fumaroles (natural vents of steam and volcanic gas) and hot springs. The discharge energy of fumaroles and hot springs on the earth is estimated to be $E_w = 2 \times 10^{18}$ J/year or 5×10^{17} cal/year (Mizutani and Watanabe 1978). This energy is also one magnitude lower than the volcanic eruption energy that causes it.

The earth seems to be an almost semipermanent thermal engine, where abundant terrestrial heat flow is always being lost from the earth's surface. Therefore, artificial utilization of the terrestrial heat flow does not seriously affect the dynamic equilibrium of the earth. This is a concept of the environment-friendly geothermal energy utilization.

Direct Use of Geothermal Energy

Since the early history of human beings, hot springs and steaming grounds were utilized for a variety of purposes such as bathing, cooking, balneology, and healing. Direct use of geothermal energy thus has a long history over the last few millenniums. The direct use of geothermal energy is currently extended to the hot-water supply, swimming pools, space heating, snow melting, drying foods or materials, condensing sugar, greenhouse cultivation, and fish cultivation. Geothermal heat pumps for heating and cooling of buildings and houses are rapidly spreading in the world. Methods of direct use of geothermal energies are briefly described here.

Bathing is one of the most traditional direct uses of geothermal energy. For example, as of March 2010, there are 27,825 hot-spring sources in Japan (Ministry of the Environment and Japan 2011), most of which were developed by drillings for bathing in hot-spring resort hotels. In China, since the China Western Development policy was launched in 2000, many hot springs were developed by 3,000-m class deep drillings to the porous Ordovician limestone strata (Zheng 2004).

In New Zealand, the Maori people have traditionally cooked foods in steaming grounds in Rotorua and Taupo. Large-scale flower cultivation greenhouses heated by hot springs are found in Monte Amiata, Italy. Shrimp cultivation by hot water from the geothermal power plant is famous in Wairakei, New Zealand. In Iceland, approximately 90 % of residences are heated by hot water from geothermal power plants and hot-spring wells. Thus, Iceland has become an almost energy-independent nation.

Use of geothermal heat pumps, a direct use of geothermal energies, has increased rapidly because they do not require any geothermal anomaly areas and can be utilized almost everywhere on land. The equivalent number of the 12 kW units (typical of US and Western European homes) reached 2.94 million in 2010, over double the number of units in 2005 (Lund et al. 2010). Temperature is constant underground. This can be experienced in limestone caves, which feel warm in winter and cool in summer. Only the atmospheric temperature changes from day to night and due to seasonal variation of solar radiant energy. Solar radiant energy reaches the shallower part of the ground, to a depth of 10, 20, or 30 m, depending on the rock species of strata, but does not reach the deeper formations. Therefore, heat can be wasted through a well as shallow as 50 or 100 m underground by a heat pump in summer and can be extracted in winter. Geothermal heat pumps resemble air conditioners (air-sourced heat pumps), but air conditioners waste heat to the atmosphere in summer, causing the heat island phenomenon. Increasing use of geothermal heat pumps for heating and cooling of buildings and houses will effectively mitigate the global warming and the heat island phenomena.

Geothermal Power Generation

Geothermal power generation has a relatively short history, beginning only in the last century. Geothermal power-generation experiments were successfully initiated at Larderello in Tuscany, Italy, in 1904 (Dickson and Fanelli 2004). Since then, a variety of methods of geothermal power generation have been developed. These methods are briefly described here.

Geothermal power generation is classified into two categories: steam flash power generation from high-temperature hydrothermal resources of 150–370 °C and binary cycle power generation from low-temperature hydrothermal resources of 50–200 °C (Fig. 2). In the 1970s, geothermal fluids less than 150 °C could not have been economically utilized for electric power generation. The only available method of geothermal power generation in those days was conventional-type steam flash power generation, which uses the conventional steam turbine directly rotated by the natural steam from the geothermal production wells (Fig. 3). Even if the subsurface natural fluid is a liquid state under the high-pressure geothermal reservoirs at a depth, a pressure release by the drill hole makes the fluid boil and the steam ascends to the surface automatically. This phenomenon is called “borehole flash” and requires the temperature of water to be at least 150 °C (Fig. 3). Therefore, the temperature threshold of 150 °C used to be important. This situation changed with the development of binary cycle power-generation technology in the 1980s. The binary cycle

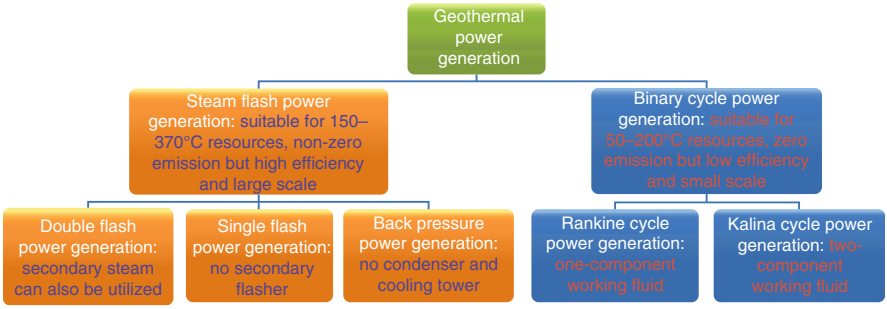

Fig. 2 Classification of geothermal power generation

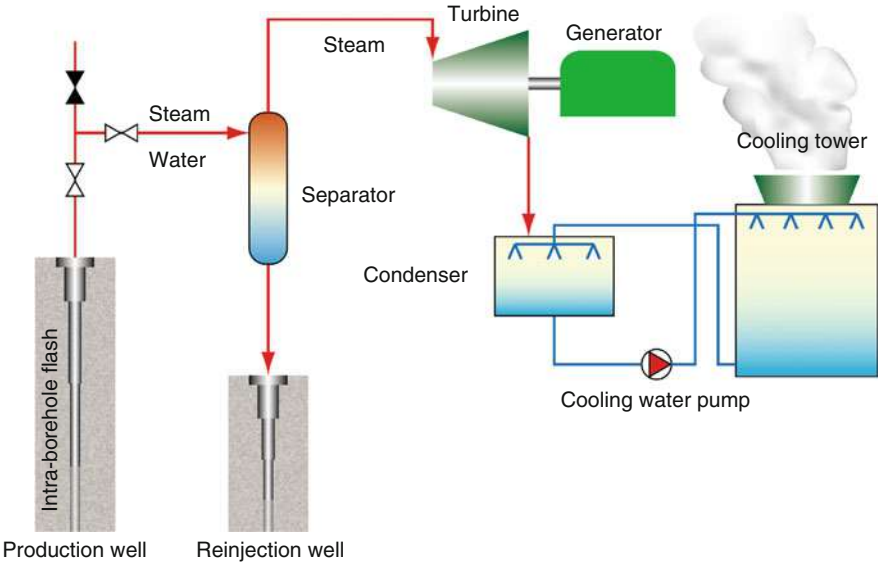

Fig. 3 Illustration of a plant of the single flash geothermal power generation (Modified from Dickson and Fanelli (2004))

power-generation method uses a secondary working fluid, such as pentane or ammonia, that has a low boiling-point temperature (Fig. 4). When the temperature of subsurface water is around 150 °C or lower, the water is not easy to flash. Then, subsurface hot water is pumped up from the production wells. The subsurface water is only used as a heat source for the secondary working fluid. Today, binary cycle power-generation technology enables use of moderate- (150–90 °C) to low-temperature (<90 °C) geothermal fluids (Fig. 4).

The most common type of binary cycle power generation is Rankine cycle power generation, which uses one-component working fluid with the fixed boiling-point temperature under a constant pressure. When a hydrocarbon is used for the working

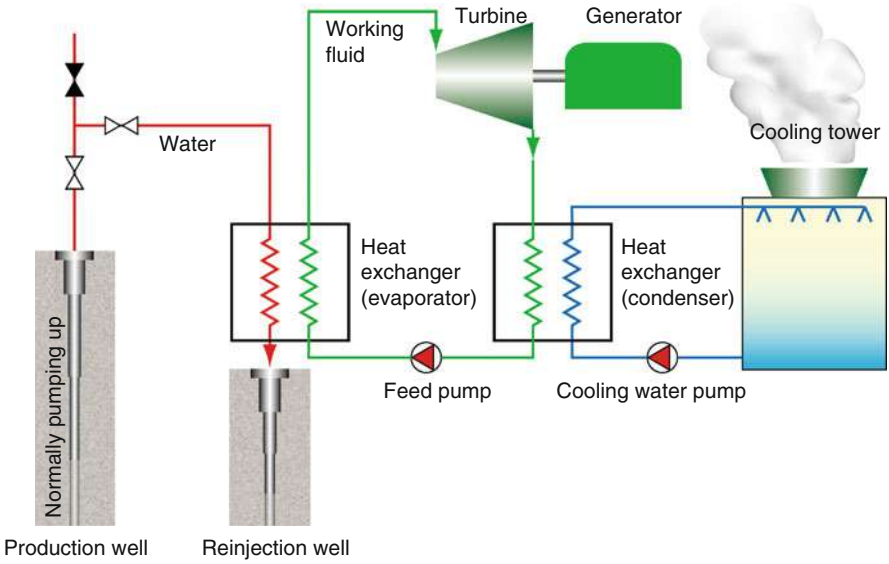

Fig. 4 Illustration of a plant of the binary cycle geothermal power generation (Modified from Dickson and Fanelli (2004))

fluid, such as pentane and butane, the system is called an organic Rankine cycle (ORC). In 1980, Aleksandr I. Kalina invented a binary cycle power-generation system that uses a two-component working fluid of ammonia and water. This system is called Kalina cycle power generation. The boiling-point temperature is continuously changed with the ratio of two components under a constant pressure so that the thermal efficiency is higher than that of the Rankine cycle. The original Kalina cycle is specific to binary cycle power generation with the ammonia-water working fluid, but it seems more useful to extend it to binary cycle power generation with a two-component working fluid (Fig. 2).

The most efficient existing cycle of thermal engines converting a given amount of thermal energy into work is expressed by the Carnot cycle. The Carnot cycle is a particular thermodynamic cycle proposed by Nicolas Léonard Sadi Carnot in 1824, and this theorem contributed to establish the second law of thermodynamics. The most efficient cycle of thermal engines is expressed as follows:

$$\eta = \frac{Q_H - Q_L}{Q_H} \tag{1}$$

where η is the efficiency of the thermal engine, Q_H is the thermal energy given from the high-temperature heat source to the working fluid, and Q_L is the thermal energy wasted from the working fluid to the low-temperature heat source. Any excellent thermal engine cannot exceed the idealistic efficiency expressed by Eq. 1. Equation 1 indicates that the temperature difference between high- and low-temperature heat

sources is critically important for the efficiency of thermal engines regardless of any species of materials of working fluid. It can be easily estimated from Eq. 1 that the ideal thermal efficiency of high-temperature steam flash power generation might be close to 0.5 but that of the low-temperature binary cycle power generation might be close to 0.2. In addition, low-temperature binary cycle power generation has large amounts of energy loss in the heat exchangers so that the available thermal efficiency is normally close to half of the ideal efficiency, as low as 0.1.

From the environmental point of view, steam flash power generation releases small amounts of natural steam from the cooling tower that contains small amounts of carbon dioxide. Hence, subsurface hot water in binary cycle power generation is only used as heat sources for the working fluid, and it can be totally recharged into shallower crust by reinjection wells. Zero-emission operation by a closed-loop system is possible in binary cycle power generation. Therefore, binary cycle power generation is more environmentally friendly, even if the thermal efficiency is low. When high-temperature hydrothermal fluid is unusually high in carbon dioxide, water binary cycle power generation, where relatively pure water is used as the secondary working fluid, is a possible option for zero-emission operation instead of the conventional steam flash power generation.

Category of Geothermal Resource Base

The assessment of a geothermal resource requires economic feasibility criteria, the same as other resources. Geothermal resources are one of the "invisible" resources stored in the earth's interior. Therefore, the confirmation of geothermal resources requires geological assurance processes such as exploration, drilling, and production tests. Based on factors of economical feasibility and geological assurance, geothermal resources are defined on a so-called McKelvy diagram, as shown in Fig. 5 (Muffler and Cataldi 1978).

In 1978, an economically feasible depth for geothermal power developments was considered to be about 3 km (Brook et al. 1979). There were not any geothermal wells deeper than 3 km at that time. Today, deep wells, at depths of 3.58 km at Unterhaching, Germany; 4.42 km at Cooper Basin, Australia; and 5 km at Soultz, France, are commonly utilized for geothermal power generation (Kaieda 2009). Likewise, the extent of geothermal resources is rapidly enlarging with time and technological innovation (Fig. 5).

The geothermal resource base, including future geothermal resources, is considered here (Fig. 5). A geothermal resource base is classified into three categories by the kind of the heat transportation medium: hydrothermal convection system, thermal conduction system, and high-level magma system (Fig. 6). The hydrothermal convection system is, in a narrow sense, a traditional geothermal resource. Conventional geothermal power generation includes steam flash-type power generation and binary cycle power generation using hydrothermal convection resources. The thermal conduction system is a next-generation geothermal resource and is economically marginal at this time. The high-level magma system is a remote future geothermal

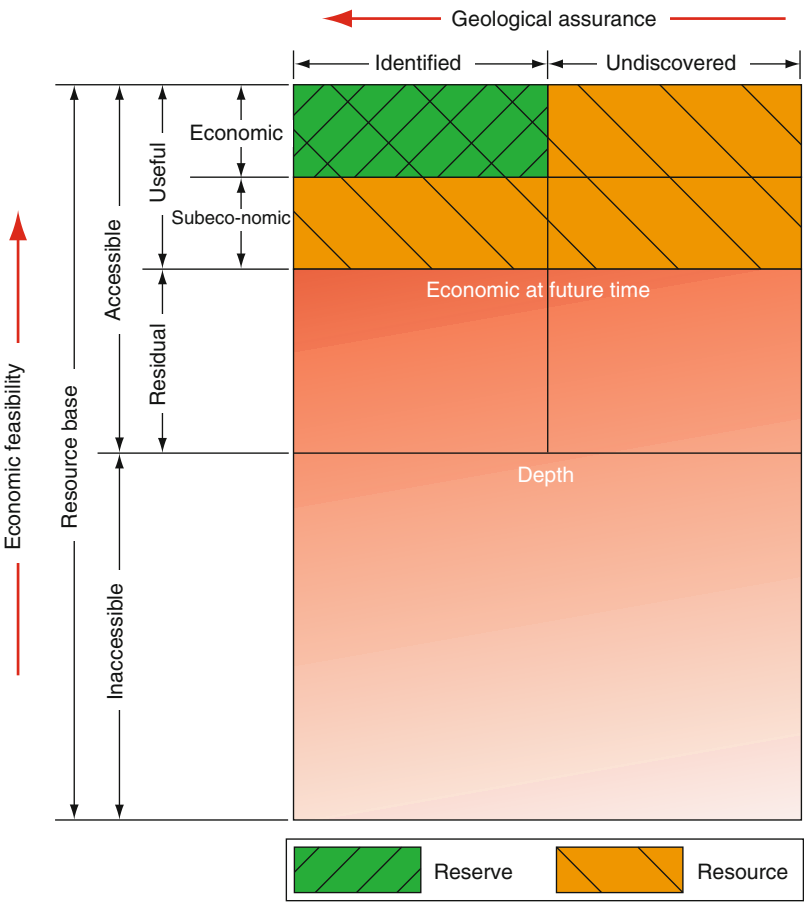

Fig. 5 Definition of geothermal resources on the so-called McKelvy diagram (Muffler and Cataldi 1978)

resource. However, the high-level magma systems have already played an important role of sub-volcanic heat sources to form hydrothermal convection systems.

Three representative thermal gradients are shown in Fig. 3, where their curvatures arise from the heat generation of radioactive decay mostly generated in the upper granitic crust. The geothermal gradient labeled "Continent" shows an average trend about 30 °C/km on the continental regions, "Volcanic zone" shows the higher trend about 40 °C/km on active volcanic zone, and "Older continent" shows the lower trend about 18 °C/km on the coldest region. In any geothermal gradient regions, if a hole is drilled deeper and deeper, the formation temperature can be higher and higher. Therefore, the greater depth is promising, with more abundant geothermal energy in terms of the temperature regime.

However, the permeability of crustal rocks is known to rapidly decrease with increasing depth of the crust (Fig. 6; Manning and Ingebritsen 1999). Permeability is

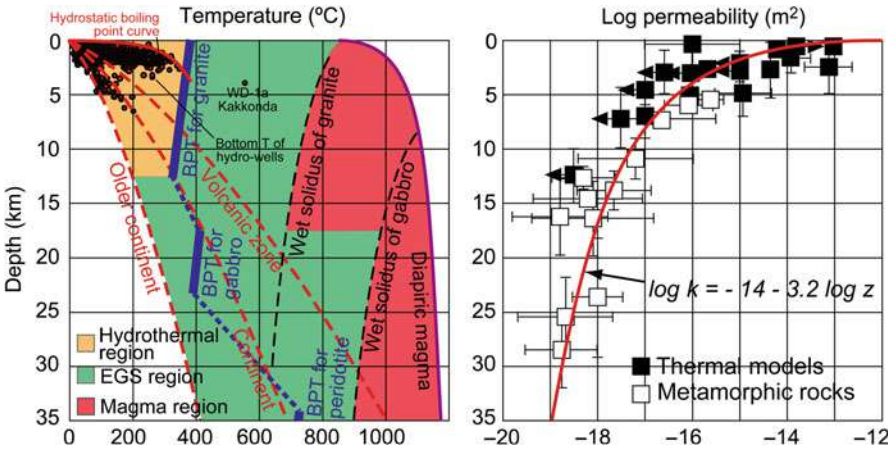

Fig. 6 Temperature (*left*) and permeability (*right*) with a depth of earth's crust. In the *left* diagram, *red dots* show 6,522 bottom hole temperatures from Japanese wells (Muraoka et al. 2007) and BPT indicates the brittle-plastic transition. The *right* diagram is redrawn from Manning and Ingebritsen (1999)

hydrological flow efficiency of water or water-dominated fluids in crustal rocks. This parameter depends not only on the porosity of rocks but also on the density of fractures of the macroscopic rock strata. The depth dependency of permeability indicates that the velocity of hydrothermal convection dramatically decreases with increasing depth of crust. Therefore, hydrothermal reservoirs become rarer with increasing depth of the crust. This is a continuous model on the permeability-depth relationship. There is another constraint on the permeability-depth relationship: the concept of the brittle-plastic transition. All rocks will lose permeability at the depth of the brittle-plastic transition below which all fractures and pores will be closed by the viscous behavior of rocks (Fournier 1991). Schematic models of the brittle-plastic transitions on upper granitic crust, lower gabbroic crust, and upper peridotite mantle are shown in Fig. 6. The WD-1a well drilled to the depth of 3,729 m in Kakkonda, northeastern Japan, penetrated the brittle-plastic transition at a depth of 3,100 m (Muraoka et al. 1998). The brittle-plastic transition on the upper peridotite mantle may coincide with the bottom of the lithosphere. This is a discontinuous model on the permeability-depth relationship. The continuous model (Manning and Ingebritsen 1999) and discontinuous model (Fournier 1991; Muraoka et al. 1998) on the permeability-depth relationship are probably compatible with each other. When the crust is observed statistically, the continuous model will be valid. When the crust is observed in some specific locality, the discontinuous model is obtained.

Based on both continuous and discontinuous models, the permeability-depth relationships suggest that all hydrothermal convection resources have a limit depth. As a borehole is drilled into deeper formations, the formation temperature becomes higher but permeability becomes lower. Therefore, hydrothermal convection resources have a limited depth. Particularly, the brittle-plastic transition of rock property gives a bottom depth to permeability and it gives the absolute limit depth

for the hydrothermal convection resources. As a result, the region of the hydrothermal system is confined to the low-temperature and shallow region, as schematically shown in Fig. 6.

Enhanced or engineered geothermal systems (EGS), in which fractures are artificially created in less-permeable rocks and heat is extracted by artificially circulating water through the fractures, are still at a demonstration stage. However, they will extend geothermal power generation to the thermal conduction region to a broad depth range even greater than the brittle-plastic transition and to a broad temperature range even higher than the brittle-plastic transition (Fig. 6). Even if the given depth is a plastic region, artificial circulation of water makes the local domain brittle and attains artificial fracturing. Therefore, the EGS technology will open the next generation of geothermal power generation that can be applied anywhere on land (Tester et al. 2006).

Sub-solidus Magma Penetrated by Well WD-1a in Kakkonda, Japan

The exploration well WD-1a was drilled to a depth of 3,729 m in the Kakkonda geothermal field, northeast Japan, using efficient borehole cooling techniques in July 1995 (Fig. 7; Muraoka et al. 1998; Muraoka 2005). The well penetrated an

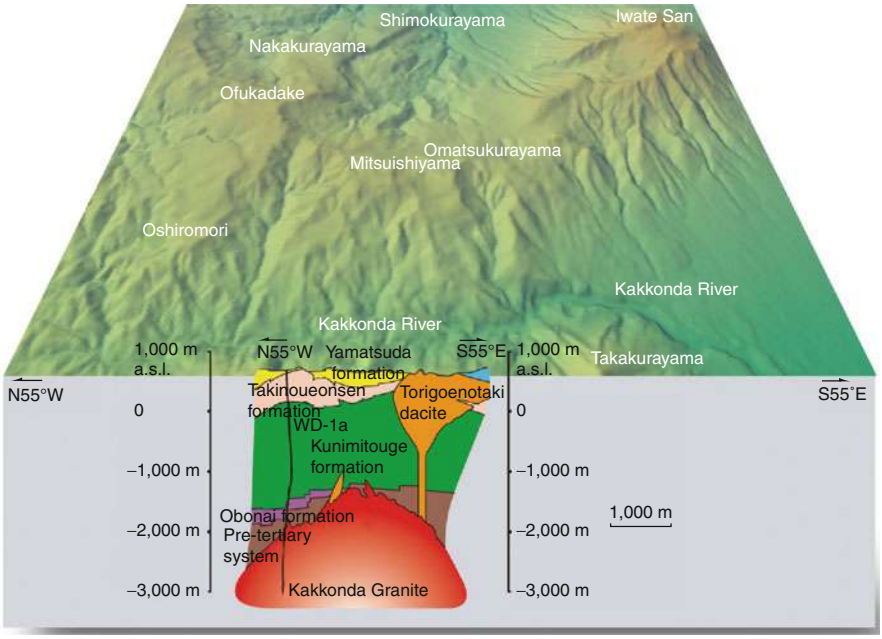

Fig. 7 The Kakkonda geothermal field, Iwate Prefecture, Japan, and the well WD-1a (Muraoka et al. 1998; Muraoka 2005)

entire shallow hydrothermal convection zone, an entire contact metamorphic aureole, and part of a young granitic intrusion called the Kakkonda Granite. The recovered temperature of the well indicates a boiling-point-controlled profile up to 380 °C to a depth of 3,100 m, and a conduction-controlled profile with a very high gradient from 3,100 m to the bottom of the hole, where the temperature is 500 °C (Fig. 8; Muraoka et al. 1998; Muraoka 2005). The well WD-1a may be the first geothermal well that encountered 500 °C, which exceeds the conventional hydrostatic boiling-point curve (Fig. 6). An inflection point of the temperature-depth profile at 3,100 m and about 380 °C reflects the brittle-plastic boundary (Fig. 8). The brittle-plastic boundary constrains the maximum depth of fracture formation, and the fracture distribution constrains the maximum depth of hydrothermal convection.

The theory of lithosphere strength can be applied to the well WD-1a. The theory consists of Byerlee's law in a brittle region and a power law creep equation in a plastic region (Fig. 9). The Byerlee's law in a brittle region is expressed by the following equation (Brace and Kohlstedt 1980):

$$\begin{aligned} \overline{\sigma}_1 &\cong 5\overline{\sigma}_3, \quad \overline{\sigma}_3 < 110\,\text{MPa} \\ \overline{\sigma}_1 &\cong 3.1\overline{\sigma}_3 + 210, \quad \overline{\sigma}_3 > 110\,\text{MPa} \end{aligned} \tag{2}$$

where

- σ_1 = the maximum principal stress
- σ_3 = the minimum principal stress

Figure 9 is only constrained by the upper equation. The power law creep is expressed by the following equation (Brace and Kohlstedt 1980):

$$\dot{\epsilon} = A(\sigma_1 - \sigma_3)^{\mathrm{n}} \mathrm{e}^{\left(\frac{-\mathrm{H}}{\mathrm{RT}}\right)} \tag{3}$$

where

- $\dot{\epsilon}$ = strain rate, s^{-1}
- A = material constant specified to the rock or mineral species
- n = stress exponent
- H = activation enthalpy, J mol^{-1}
- R = gas constant, J K-1 mol^{-1}
- T = temperature, K

Most of these parameters are reasonably determined on the well WD-1a. The strain rate $\dot{\epsilon}$ is given to be 10^{-12} s^{-1} because of the active compressive tectonic region (Fournier 1991). Taking the data from quartz diorite close to the Kakkonda Granite, the stress exponent n is given to be 2.4, and activation enthalpy H is given to be 219 kJ mol^{-1}. The temperature T is given by the temperature profile of the well WD-1a in Fig. 8. The material constant A varies from 10^{-19} to 10^{49} according to the

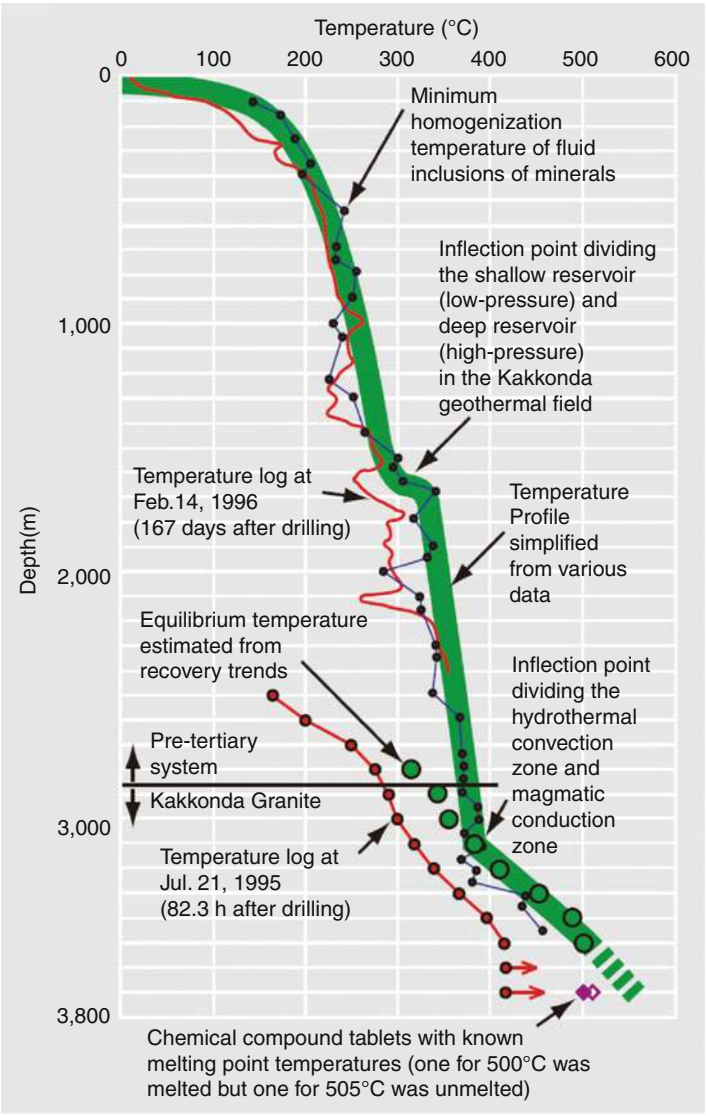

Fig. 8 Temperature profile of the well WD-1a in the Kakkonda geothermal field, Japan (Muraoka et al. 1998; Muraoka 2005)

given material, and only this parameter cannot be reasonably determined. However, the inflection point of the strength curve by the temperature inflection in the plastic region should coincide with the depth of 3.1 km, restricting the material constant A to be $10^{-0.85}$. Then, the strength curve on the plastic field is drawn as shown in Fig. 9 (Muraoka et al. 1999).

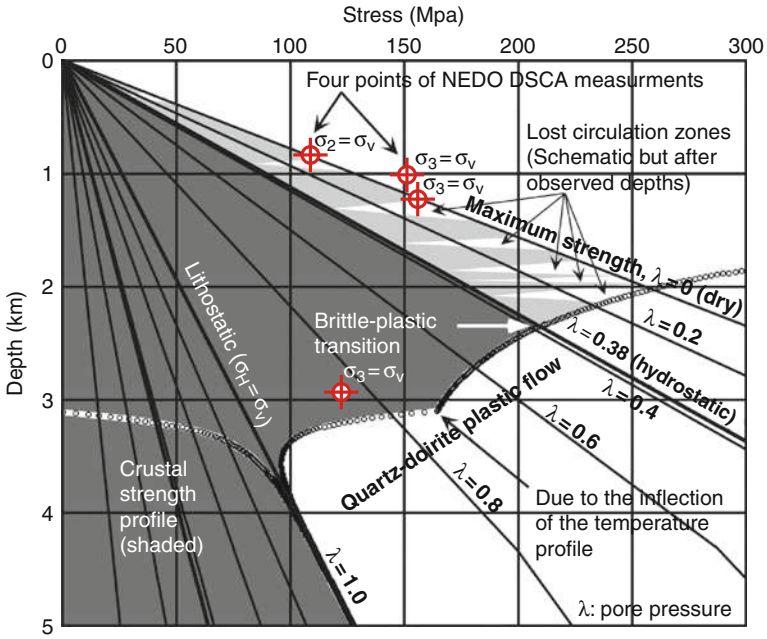

Fig. 9 Crustal strength-depth relation along the well WD-1a in the Kakkonda geothermal field, Japan (Muraoka et al. 1999)

The four points of stress ratio measurements of the differential strain curve analysis (DSCA) on the core samples (New Energy and Industrial Technology Development Organization 1996) are well explained by the model of the strength profile drawn by the Byerlee's law and the power law creep equation as shown in Fig. 9. Particularly, closure of σ_1 value to σ_3 at the deepest DSCA stress ratio measurement indicates that the dramatic strength weakening occurred as being accommodated by the plastic field as shown in Fig. 9. Three points of DSCA stress ratio measurements in the brittle field are close to the dry line ($\lambda = 0$). This is also reasonable because the sampling of cores could have been only performed from impermeable zones with no lost circulation. These observations strongly support that the well WD-1a actually penetrated the brittle-plastic transition (Muraoka et al. 1998; Muraoka 2005).

The brittle-plastic transition may primarily be expected in the temperature inflection point at the depth of 3,100 m and the temperature 380 °C (Muraoka et al. 1998). However, the graphical representation makes it clear that the brittle-plastic transition in a strict sense probably lies at a shallower depth, like 2,400 m, where the maximum strength is attained at 360 °C (Fig. 9). A zone of very high concentration of low-angle fractures is observed in the depth interval from 1,770 to 2,860 m (Fig. 10; Muraoka and Ohtani 2000). This fracture zone likely reflects the maximum strength zone of the bottom of the brittle layer because this zone may play a role of the dehydration front and dehydration-induced weakening front (Muraoka and Ohtani 2000).

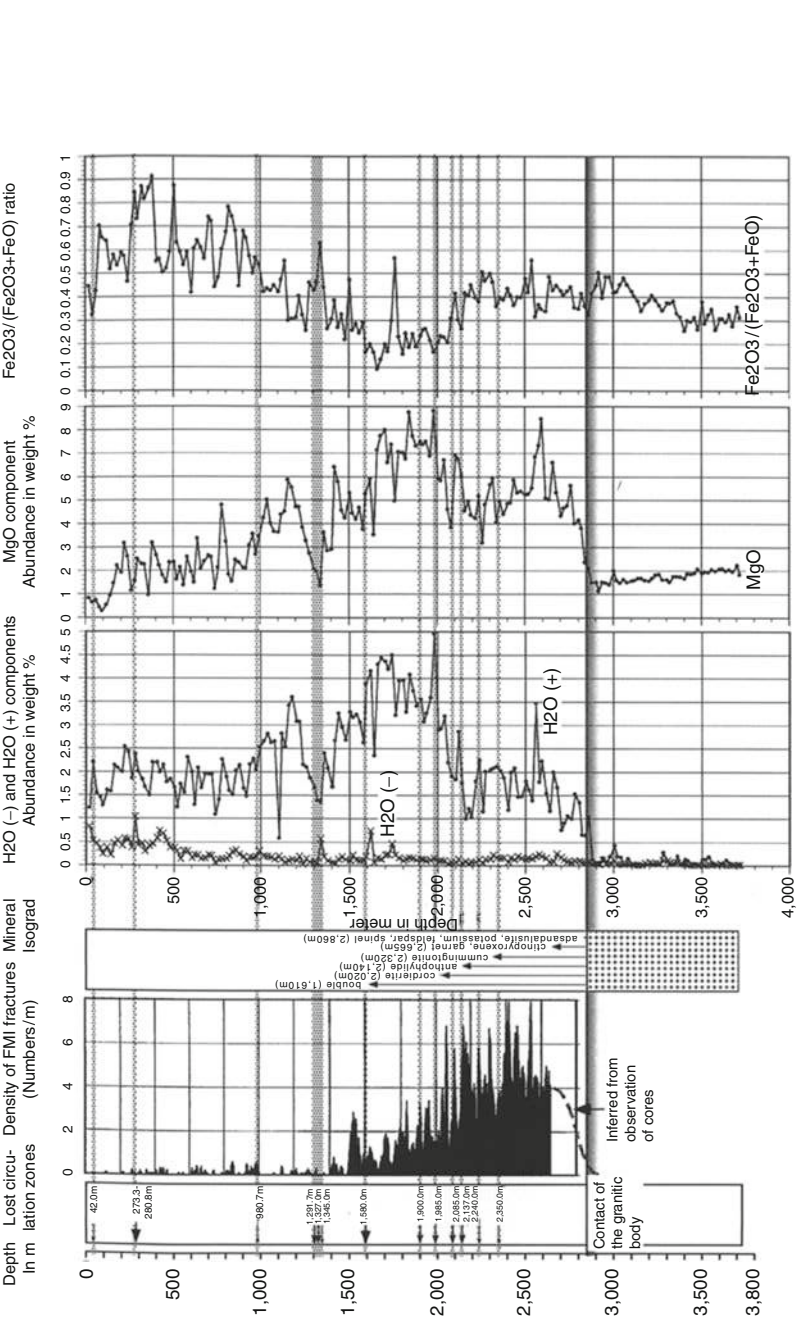

Fig. 10 Chemistry of cutting samples from the contact metamorphic aureole of the Kakkonda Granite and high concentration of low-angle fractures (Muraoka and Ohtani 2000)

Distribution of Geothermal Resources in the World

High-temperature hydrothermal resources (>150 °C) are unevenly distributed in the world. Figure 11 shows global topography, global bathymetry (topography of ocean floors), plate boundaries, active volcanoes (Siebert and Simkin 2002), and representative geothermal power plants. High-temperature hydrothermal resources that are hot enough for the steam flash-type power generation are associated with active volcanic zones so that most of the geothermal power plants are developed in active volcanic zones. This is because sub-volcanic magma chambers or their sub-solidus equivalents (hot intrusive bodies) are serving for geothermal heat sources for the high-temperature hydrothermal reservoirs. Actually, young plutonic bodies are often penetrated by geothermal wells not only in the Kakkonda geothermal field, Japan, as described in the preceding section, but also in other geothermal fields such as The Geysers, in California, USA; Tongonan and Palinpinon, in the Philippines; and Mutnovsky, in Russia (Muraoka 1993).

Active volcanic zones are associated with two types of plate boundaries: spreading and convergent. A typical spreading plate boundary is mid-ocean ridges. In Fig. 11, mid-ocean ridges are not represented as volcanoes, but they are the largest volcanoes on the earth that are lineally continued. Their geothermal development has been difficult so far because of the high cost of submarine exploitations. As a result, most of the geothermal power plants are built in the volcanic zones of the convergent plate boundaries. One exception is the Great Rift Valley in the eastern Africa, where spreading plate boundaries appear on shore. The other exception is the Salton Sea and Cerro Prieto geothermal fields in the western North America, where spreading plate boundaries or their transform faults appear on shore. The last exception is Iceland, which is situated on the mid-Atlantic ridge where the ridge appears above sea level because of the strong volcanic activity in the hot spot.

Most of geothermal power plants are developed in the volcanic zones of subduction zones. Particularly, the largest subduction zones are found in the circum-Pacific regions. Although the first geothermal power generation was accomplished in Italy in 1904, the largest geothermal power country is currently the USA, the second is the Philippines, and the third is Indonesia. All of these are situated along the circum-Pacific regions. Geothermal electricity plays a very important role in Central America, where 10 % or higher ratios of electricity are supplied from geothermal power generation in many countries. It seems curious that very few geothermal power plants have been developed in South America, in spite of the huge geothermal potential in the Andes. The Copahue geothermal power plant used to operate in Argentina, but it has been terminated. No geothermal power plant is currently operating in South America. In other words, South America has reserved a large potential for geothermal power development in the near future.

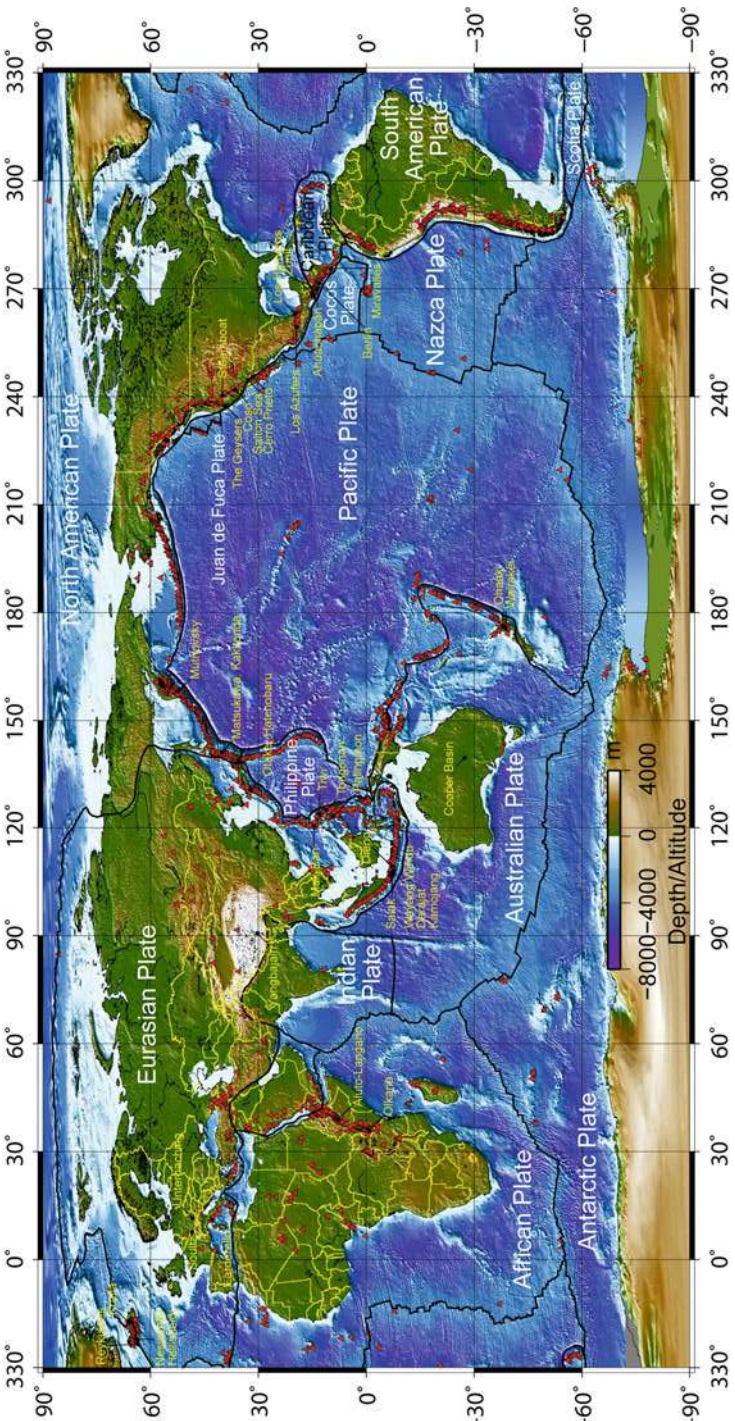

Fig. 11 Global topography, global bathymetry, plate boundaries, active volcanoes, and representative geothermal power plants (Topographic data are taken from Lindquist et al. (2004), drawing is made with GMT by Wessel and Smith (1998), and active volcanoes are taken from Siebert and Simkin (2002))

Global Geothermal Resource Potentials

Assessment of global geothermal resource potentials is hard to accomplish because subsurface exploration data with uniform accuracy are seldom available on a global scale. However, a rough estimate is possible by analogical reasoning. Hydrothermal power resources, EGS power resources, and direct-use resources are estimated here by analogical reasoning.

Stefansson (Stefansson 2005) estimated world geothermal assessment based on well-known data on active volcanoes (Siebert and Simkin 2002). Hydrothermal resources high enough in the temperature for the steam flash-type power generation are normally associated with active volcanoes, and therefore, his method is an excellent analogical reasoning by use of well-known data. Although the size of the active volcano varies from the 100-km-long Toba caldera in Indonesia to 0.6-km-long maars (explosion of volcanic craters without remarkable tuff rings in its surroundings) such as Megata in Japan, these size differences might cancel one another by using statistical data. Here, modification is made from the original paper because some data have been updated. Table 1 and Fig. 12 show a relationship between the numbers of active volcanoes and assessed hydrothermal power resources in eight representative countries modified from the original paper (Stefansson 2005). A number of active volcanoes are taken from the catalog (Siebert and Simkin 2002), where submarine volcanoes are excluded. Assessed hydrothermal power potentials are taken from each reference described in Table 1. A regression equation is obtained between numbers of active volcanoes and estimated hydrothermal power resources in eight representative countries:

Table 1 Number of active volcanoes and estimated geothermal potential for electrical generation in eight representative countries. The number of active volcanoes is taken from Siebert and Simkin (2002) where submarine volcanoes are excluded

Country	Number of active volcanoes	Assessed hydrothermal power potentials (MW)	References
USA	163	39,090	William et al. (2008)
Indonesia	137	27,140	Darma et al. (2010)
Japan	93	23,470	Muraoka et al. (2008)
Philippines	46	6,000	Wright (1999)
Mexico	39	6,000	Mulas de Pozo et al. (1985)
Iceland	27	5,800	Palmason et al. (1985)
New Zealand	12	3,650	Lawless (2002)
Italy	12	1,500	Buonasorte et al. (2007)

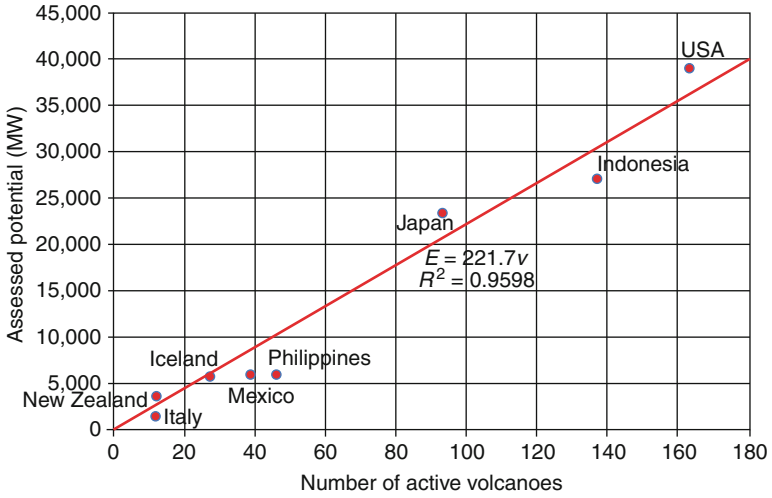

Fig. 12 Correlation between the number of active volcanoes and estimated geothermal potential in eight representative countries slightly modified from Stefansson (2005). The number of active volcanoes is taken from Siebert and Simkin (2002), where submarine volcanoes are excluded

$$E = 221.7\,\nu \tag{4}$$

where

- E = hydrothermal resource potential for geothermal power generation (MW_e)
- ν = a number of active volcanoes without submarine volcanoes

The maximum exploitation depth of Eq. 4 is not strictly defined in the different assessment condition in each country, but it is roughly assumed to be a depth of 4 km. Equation 4 is useful to estimate hydrothermal resource potentials when the subsurface exploration data are not fully available. If a number of global active volcanoes, 1,406 excluding submarine volcanoes, are input into this equation, about 312 GW_e are obtained as a hydrothermal resource potential for geothermal power generation in the world.

Only a few countries estimated the EGS resources. The EGS resources are, however, almost proportional to the width of the given area. Therefore, an estimate in the USA (Tester et al. 2006) can be used as teacher data, and it can be extrapolated to the world according to the area ratio. Tester et al. (2006) estimated EGS resources to be at least 100 GW_e in the USA for the exploitation to a depth of 10 km. The widths of the land area of the world and the USA are 148,890,000 km^2 and 9,826,635 km^2, respectively. Then, 1,500 GW_e was obtained as a global EGS resource potential.

Assessment of direct-use resources is far more difficult to attain because of the variety of uses: baths, swimming pools, snow melting, hot-water supply, space heating, greenhouses, and drying foods. Therefore, it needs some simplification.

Stefansson (2005) estimated hydrothermal resources lower than 130 °C for direct use to be 4,400 GW_{th} based on the resource frequency distribution like a power function.

This seems an excellent estimate, because the number is almost 10 % of the annual global terrestrial heat-flow energy. As described in the earlier section, an annual global terrestrial heat-flow energy $E_{hf} = 1.3 \times 10^{21}$ J/year, and 10 % is 1.3×10^{20} J/year, which is equivalent to 4,120 GW_{th}. Therefore, the estimate for direct-use resources of 4,400 GW_{th} seems reasonable.

Present State of Geothermal Development in the World

The present state of geothermal development in the world is briefly described for geothermal power generation (Bertani 2010) and on direct use (Lund et al. 2010). The installed capacity of geothermal power generation in the world is 10,715 MW_e as of 2010, and the growth rate during the last 5 years was the second greatest, after the early 1980s, as shown in Fig. 13. The produced electricity during the year 2010 was 67,246 GWh (Bertani 2010). The capacity factor, a ratio of working time of the facility, of geothermal power plants is 0.72 throughout the world. This capacity factor is amazingly high compared with not only other renewable electricity sources but also thermal or nuclear power sources. The five largest geothermal power-generation countries – the USA, the Philippines, Indonesia, Mexico, and Italy – account for about 75 % of the world geothermal power capacity (Table 2).

The installed geothermal energy facilities for direct utilization at the end of 2009 were 50,583 MW_{th}, and the thermal energy used was 438,071 TJ/year (121,696 GWh/year) as shown in Fig. 14 (Lund et al. 2010). Again, the growth rate during the last 5 years was rapid compared to the past. The capacity factor of direct use was 0.27 at the end of 2009, and it was decreasing with passing time. This is because

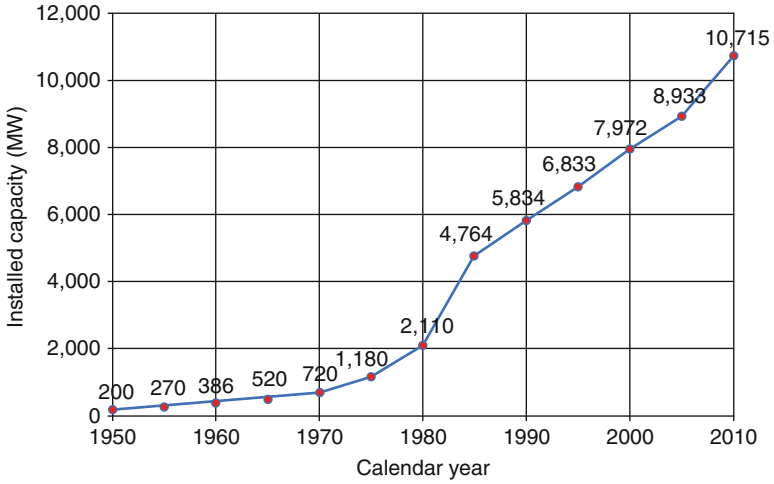

Fig. 13 Growing installed geothermal power capacity in the world (Bertani 2010)

Table 2 Installed geothermal power capacity and electricity production in the world (Bertani 2010)

Country	Installed in 2005 (MW)	Energy in 2005 (GWh)	Installed in 2010 (MW)	Energy in 2010 (GWh)
Argentina	0	0	0	0
Australia	0.2	0.5	1.1	0.5
Austria	1.1	3.2	1.4	3.8
Canada	0	0	0	0
Chile	0	0	0	0
China	28	96	24	150
Costa Rica	163	1,145	166	1,131
El Salvador	151	967	204	1,422
Ethiopia	7.3	0	7.3	10
France	15	102	16	95
Germany	0.2	1.5	6.6	50
Greece	0	0	0	0
Guatemala	33	212	52	289
Honduras	0	0	0	0
Hungary	0	0	0	0
Iceland	202	1,483	575	4,597
Indonesia	797	6,085	1,197	9,600
Italy	791	5,340	843	5,520
Japan	535	3,467	536	3,064
Kenya	129	1,088	167	1,430
Mexico	953	6,282	958	7,047
Nevis	0	0	0	0
New Zealand	435	2,774	628	4,055
Nicaragua	77	271	88	310
Papua New Guinea	6	17	56	450
Philippines	1,930	9,253	1,904	10,311
Portugal	16	90	29	175
Romania	0	0	0	0
Russia	79	85	82	441
Spain	0	0	0	0
Slovakia	0	0	0	0
Thailand	0.3	1.8	0.3	2
Netherlands	0	0	0	0
Turkey	20	105	82	490
USA	2,564	16,840	3,093	16,603
Total	8,933	55,709	10,715	67,246

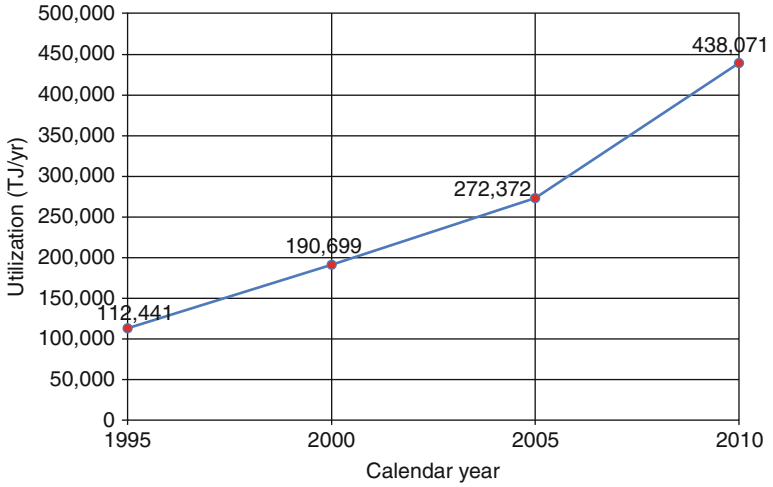

Fig. 14 Growing direct geothermal use in the world (Lund et al. 2010)

geothermal heat pumps are rapidly spreading among a variety of direct utilization methods, and the capacity factor of geothermal heat pumps is normally less than 0.2. Almost all countries are utilizing geothermal heat directly (Table 3). Countries in colder regions tend to use more geothermal heat.

Geothermal Cascade Utilization Technology

To date, geothermal resources tend to be used for a single utilization purpose, and the spent resources have been wasted into reinjection wells or rivers, in the case of low-temperature direct use. However, a more efficient utilization is repeated consumption of energy such as a cascade from the high-temperature resources to the low-temperature resources as shown in Fig. 15. This can be called geothermal cascade utilization.

A typical example is seen in Iceland, where voluminous hot water spent in geothermal power plants is transported by pipelines, more than 25 km long, to a tank on the hill of Reykjavik City. Then, the hot water is distributed to each residence for space heating. This is a typical example of the geothermal cascade utilization.

More efficient cascade utilization is possible with steam flash-type power generation, binary cycle power generation, space heating, and snow melting in descending order as shown in Fig. 15. Cascade utilization makes geothermal resources several times more efficient. However, for the development of the geothermal cascade utilization, heat exchange technology and scale-inhibition technology are critically important.

Table 3 Direct geothermal utilization in the world (Lund et al. 2010)

Country	Capacity (MWt)	Annual use (TJ/year)	Annual use (GWh/year)	Capacity factor
Albania	11.48	40.46	11.20	0.11
Algeria	55.64	1,723.13	478.70	0.98
Argentina	307.47	3,906.74	1,085.30	0.40
Armenia	1.00	15.00	4.20	0.48
Australia	33.33	235.10	65.30	0.22
Austria	662.85	3,727.70	1,035.60	0.18
Belarus	3.42	33.79	9.40	0.31
Belgium	117.90	546.97	151.90	0.15
Bosnia and Herzegovina	21.70	255.36	70.90	0.37
Brazil	360.10	6,622.40	1,839.70	0.58
Bulgaria	98.30	1,370.12	380.60	0.44
Canada	1,126.00	8,873.00	2,464.90	0.25
Caribbean islands	0.10	2.78	0.80	0.85
Chile	9.11	131.82	36.60	0.46
China	8,898.00	75.348.30	20,931.80	0.27
Columbia	14.40	287.00	79.70	0.63
Costa Rica	1.00	21.00	5.80	0.67
Croatia	67.48	468.89	130.30	0.22
Czech Republic	151.50	922.00	256.10	0.19
Denmark	200.00	2,500.00	694.50	0.40
Ecuador	5.16	102.40	28.40	0.63
Egypt	1.00	15.00	4.20	0.48
El Salvador	2.00	40.00	11.10	0.63
Estonia	63.00	356.00	98.90	0.18
Ethiopia	2.20	41.60	11.60	0.60
Finland	857.90	8,370.00	2,325.20	0.31
France	1,345.00	12,929.00	3,591.70	0.30
Georgia	24.51	659.24	183.10	0.85
Germany	2,485.40	12,764.50	3,546.00	0.16
Greece	134.60	937.80	260.50	0.22
Guatemala	2.31	56.46	15.70	0.78
Honduras	1.93	45.00	12.50	0.74
Hungary	654.60	9,767.00	2,713.30	0.47
Iceland	1,826.00	24,361.00	6,767.50	0.42
India	265.00	2,545.00	707.00	0.30
Indonesia	2.30	42.60	11.80	0.59
Iran	41.61	1,064.18	295.60	0.81
Ireland	152.88	764.02	212.20	0.16
Israel	82.40	2,193.00	609.20	0.84

(*continued*)

Table 3 (continued)

Country	Capacity (MWt)	Annual use (TJ/year)	Annual use (GWh/year)	Capacity factor
Italy	867.00	9,941.00	2,761.60	0.36
Japan	2,099.53	25,697.94	7,138.90	0.39
Jordan	153.30	1,540.00	427.80	0.32
Kenya	16.00	126.62	35.20	0.25
Korea (South)	229.30	1,954.65	543.00	0.27
Latvia	1.63	31.81	8.80	0.62
Lithuania	48.10	411.52	114.30	0.27
Macedonia	47.18	601.41	167.10	0.40
Mexico	155.82	4,022.80	1,117.50	0.82
Mongolia	6.80	213.20	59.20	0.99
Morocco	5.02	79.14	22.00	0.50
Nepal	2.72	73.74	20.50	0.86
Netherlands	1,410.26	10,699.40	2,972.30	0.24
New Zealand	393.22	9,552.00	2,653.50	0.77
Norway	3,300.00	25,200.00	7,000.60	0.24
Papua New Guinea	0.10	1.00	0.30	0.32
Peru	2.40	49.00	13.60	0.65
Philippines	3.30	39.58	11.00	0.38
Poland	281.05	1,501.10	417.00	0.17
Portugal	28.10	386.40	107.30	0.44
Romania	153.24	1,265.43	351.50	0.26
Russia	308.20	6,143.50	1,706.70	0.63
Serbia	100.80	1,410.00	391.70	0.44
Slovak Republic	132.20	3,067.20	852.10	0.74
Slovenia	104.17	1,136.39	315.70	0.35
South Africa	6.01	114.75	31.90	0.61
Spain	141.04	684.05	190.00	0.15
Sweden	4,460.00	45,301.00	12,584.60	0.32
Switzerland	1,060.90	7,714.60	2,143.10	0.23
Tajikistan	2.93	55.40	15.40	0.60
Thailand	2.54	79.10	22.00	0.99
Tunisia	43.80	364.00	101.10	0.26
Turkey	2,084.00	36,885.90	10,246.90	0.56
Ukraine	10.90	118.80	33.00	0.35
UK	186.62	849.74	236.10	0.14
USA	12,611.46	56,551.80	15,710.10	0.14
Venezuela	0.70	14.00	3.90	0.63
Vietnam	31.20	92.33	25.60	0.09
Yemen	1.00	15.00	4.20	0.48
Total	50,583.12	438,070.66	121,695.90	0.27

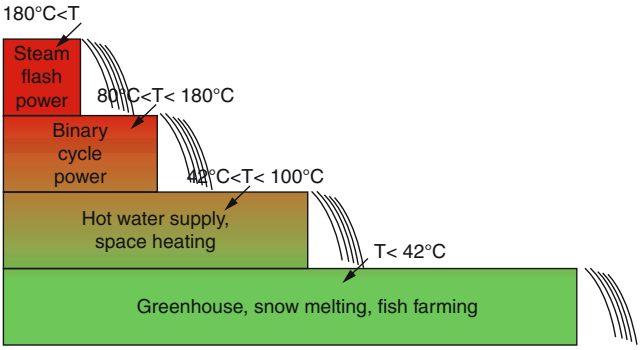

Fig. 15 A concept of the cascade utilization of geothermal energy

Mitigation of Global Warming by Geothermal Development

If 70 % of hydrothermal power resources and 20 % of EGS resources are developed by 2050, these capacities would be 218 GW_e and 300 GW_e, respectively, and their total installed capacity would be 518 GW_e. When the capacity factor is assumed to be 0.72 and the unit reduction of carbon dioxide emission by the replacement from the oil thermal power to geothermal power is assumed to be 817 g-CO_2/kWh (Mongillo 2005), it could reduce carbon dioxide emission by 2.67 Gton/year.

If 20 % of direct-use geothermal resources are developed by 2050, its installed capacity would be 880 GW_{th}. When the capacity factor is assumed to be 0.27 and the reduction unit of carbon dioxide emission by the replacement from the oil fuels to geothermal energy is assumed to be 409 g-CO_2/kWh (Mongillo 2005), it could reduce carbon dioxide emission by 0.50 Gton/year. Both geothermal electricity and direct use could reduce carbon dioxide emission by 3.17 Gton/year, which is 11 % of the present worldwide emission.

Future Directions

Available geothermal energy could commonly increase with increasing depth of drill holes in any geothermal gradient regions. The deepest hole ever drilled was the SG-3 well in Kola Peninsula, Russia, that reached a depth of 12,262 m, only 0.2 % of a radius of the earth (Fuchs et al. 1990). There still remain voluminous unexploited crust and upper mantle, and new technology will open a variety of techniques to utilize the enormous heat in the earth's interior. Many researchers thought that only volcanic countries enabled geothermal power generation in the 1970s. However, today, less volcanic countries such as Germany, Australia, France, and Switzerland are leading the EGS technology development for geothermal power generation. A 1.5-MW_e pilot power plant for the EGS has been operating in Soultz, France, since

June 2008. Geothermal utilization technology thus may achieve the goal of the EGS, where every country can use geothermal energy.

References

Bertani R (2010) Geothermal power generation in the world 2005-2010 update report. In: Proceedings of world geothermal congress 2010 (CD-ROM), Bali, 41 p

Brace WF, Kohlstedt DL (1980) Limits on lithospheric stress imposed by laboratory experiments. J Geophys Res 85(B11):6248–6252

Brook CA, Mariner RH, Mabey DR, Swanson JR, Guffanti M, Muffler LJP (1979) Hydrothermal convection systems with reservoir temperature ≥90°C. In: Assessment of geothermal resources of the United States – 1978, vol 790, Circular. U.S. Geological Survey, Oak Ridge, pp 18–85

Buonasorte G, Cataldi R, Passaleva G (2007) Geothermal development in Italy: from present to future. In: Proceedings of European geothermal congress 2007 (CD-ROM), Unterhaching, 9 p

Darma S, Harsoprayitno S, Setiawan B, Hadyanto, Sukhyar R, Soedibjo AW, Ganefianto N, Stimac J (2010) Geothermal energy update: geothermal energy development and utilization in Indonesia. In: Proceedings of world geothermal congress 2010 (CD-ROM), Bali, 13 p

Dickson MH, Fanelli M (2004) What is geothermal energy? http://www.geothermal-energy.org/314,what_is_geothermal_energy.html

Fournier RO (1991) The transition from hydrostatic to greater than hydrostatic fluid pressure in presently active continental hydrothermal systems in crystalline rock. Geophys Res Lett 18:6248–6252

Fuchs K, Kozlovsky EA, Krivtsov AI, Zoback MD (1990) Super-deep continental drilling and deep geophysical sounding. Springer, Berlin, 436 p

Kaieda H (2009) Hot dry rock geothermal power technology. In: Kaieda H et al (eds) Geothermal power generation. Thermal and Nuclear Power Engineering Society, Tokyo, pp 117–126 (in Japanese)

Kanamori H (1978) Chapter 2: structure of the earth. In: Uyeda S, Mizutani H (eds) Iwanami earth science lecture course 1: earth. Iwanami-Shoten, Tokyo, pp 45–98 (in Japanese)

Lawless J (2002) New Zealand's geothermal resources revised. In: Proceedings of the New Zealand geothermal association seminar, Taupo

Lindquist KG, Engle K, Stahlke D, Price E (2004) Global topography and bathymetry grid improves research efforts. EOS Trans AGU 85(19):186

Lund JW, Freeston DH, Boyd TL (2010) Direct utilization of geothermal energy 2010 worldwide review. In: Proceedings of world geothermal congress 2010 (CD-ROM), Bali, 23 p

Manning CE, Ingebritsen SE (1999) Permeability of the continental crust: implications of geothermal data and metamorphic systems. Rev Geophys 37:127–150

Ministry of the Environment, Japan (2011) State of utilization of hot springs in the fiscal year 2009. 1 p (in Japanese). http://www.env.go.jp/nature/onsen/data/index.html

Mizutani H, Watanabe T (1978) Chapter 4: geothermal science. In: Uyeda S, Mizutani H (eds) Iwanami earth science lecture course 1: earth. Iwanami-Shoten, Tokyo, pp 169–223 (in Japanese)

Mongillo MA (2005) Saving factors for geothermal energy utilization. International Energy Agency (IEA) – Geothermal Implementing Agreement (GIA), 4 p

Muffler LJP, Cataldi R (1978) Methods for regional assessments. Geothermics 7:53–89

Mulas de Pozo P, Gómez DN, Holland FA (1985) Developments in geothermal energy in Mexico – part one: general considerations. Heat Recovery Syst 5:277–283

Muraoka H (1993) A scope of the picture of future geothermal resources in the viewpoint from magma. Chinetsu (Geothermal) 30:100–126 (in Japanese)

Muraoka H (2005) The blessings of volcanoes: the front line of the utilization of geothermal heat. AIST Today 16:16

Muraoka H, Ohtani T (2000) Profiling of the Kakkonda geothermal system by the bulk rock chemical analyses of the well WD-1a. Rept Geol Surv Jpn 284:35–55 (in Japanese with English abstract)

Muraoka H, Uchida T, Sasada M, Yagi M, Akaku K, Sasaki M, Yasukawa K, Miyazaki S-I, Doi N, Saito S, Sato K, Tanaka S (1998) Deep geothermal resources survey program: igneous, metamorphic and hydrothermal processes in a well encountering 500°C at 3729 m depth, Kakkonda, Japan. Geothermics 27:507–534

Muraoka H, Tateno M, Okubo Y (1999) Brittle-plastic transition penetrated by the well WD-1a beneath the Kakkonda geothermal field, Japan. In: Proceedings of the GSJ workshop "Fault Rocks and Seismic Process", Geol. Surv. Japan Interim Report, no. EQ/99/1, pp 66–68

Muraoka H, Sakaguchi K, Tamanyu S, Sasaki M, Shigeno H, Mizugaki K (2007) Atlas of hydrothermal systems in Japan. Geological Survey of Japan, AIST, Tsukuba, 110 p (in Japanese with English abstract)

Muraoka H, Sakaguchi K, Komazawa M, Sasaki S (2008) 2008 assessment of hydrothermal resources potentials in Japan. In: Abstracts of 2008 meeting of Geotherm. Res. Soc. Japan, Kanazawa, B01 (in Japanese)

New Energy and Industrial Technology Development Organization (1996) FY 1995 report of the deep geothermal resources survey program. 887 p (in Japanese)

Palmason G, Johnsen GV, Torfason H, Saemundsson K, Ragnars K, Haraldsson GI, Halldorsson GK (1985) Assessment of the geothermal resources of Iceland. Orkustofnun Report OS-85076/JHD-10, 134 p (in Icelandic)

Siebert L, Simkin T (2002) Volcanoes of the world: an illustrated catalog of holocene volcanoes and their eruptions. Smithsonian Institution, Global Volcanism Program, Digital Information Series, GVP-3. http://www.volcano.si.edu/world/

Stefansson V (2005) World geothermal assessment. In: Proceedings of world geothermal congress 2005 (CD-ROM), Antalya, 6 p

Tajika E (1996) Chapter 2: composition of the earth. In: Matsui T et al (eds) Iwanami earth science lecture course 1: introduction to earth and planetary sciences. Iwanami-Shoten, Tokyo, pp 47–100 (in Japanese)

Takahashi E (1996) Chapter 3: differentiation. In: Matsui T et al (eds) Iwanami earth science lecture course 1: introduction to earth and planetary sciences. Iwanami-Shoten, Tokyo, pp 111–161 (in Japanese)

Tester JW, Anderson BJ, Batchelor AS, Blackwell DD, DiPippo R, Drake EM, Garnish J, Livesay B, Moore MC, Nichols K, Petty S, Toksöz MN, Veatch RW Jr (2006) The future of geothermal energy – impact of enhanced geothermal systems (EGS) on the United States in the 21st century. Massachusetts Institute of Technology, Cambridge, MA, 358 p

Wessel P, Smith WHF (1998) New, improved version of the generic mapping tools released. EOS Trans AGU 79:579

Williams CF, Reed MJ, Mariner RH, DeAngelo J, Galanis SP Jr (2008) Assessment of moderate- and high-temperature geothermal resources of the United States. Fact Sheet 2008-3082, U.S. Geological Survey, 4 p

Wright PM (1999) Summary of worldwide geothermal resources. Lecture given at the United Nations University Geothermal Training Programme

Zheng K (2004) Newest statistics of geothermal development in China. In: Proceedings of 6th Asian geothermal symposium, Daejeon, pp 85–90

Hydropower

Jingsheng Jia, Petras Punys, and Jing Ma

Contents

J. Jia (✉)
International Commission on Large Dams (ICOLD), Paris, France
e-mail: jiajsh@iwhr.com

P. Punys
Water Management Department, Water and Land Management Faculty, Lithuanian University of Agriculture, Kaunas-Akademija, Lithuania
e-mail: punys@hidro.lzuu.lt

J. Ma
China Institute of Water Resources and Hydropower Research, Beijing, China
e-mail: jingma@iwhr.com

W.-Y. Chen et al. (eds.), *Handbook of Climate Change Mitigation and Adaptation*,
DOI 10.1007/978-3-319-14409-2_36

Abstract

Climate change is regarded as the most severe challenge for the human being. The view on accelerating hydropower development and ensuring adequate water storage infrastructure to mitigate and adapt climate change has been widely accepted by the international community. Based on the challenge induced by climate change and the advantages on energy consumption and GHGs emission, the current development status, this chapter describes the importance and significance on development hydropower and ensuring adequate water storage facility for world sustainable development, mitigating, and adapting climate change. And it also points out the path on developing water and energy in a reliable, cheap, and environment-friendly way.

Introduction

The world is changing. Population growth and economic development turn to be the prime driving power that stimulates the ever-increasing demand for resources and energy, while the environment and resources are the biggest bottleneck that restricts human development today. Global climate change is the most outstanding expression of this constraint. As proven by physical, political, and economic studies with respect to climate change, the issue of global climate change is one of the largest, most extensive, and most profound challenges ever experienced by man up to now, and also one of the most important factors relating to future socioeconomic development of the world and reconstitution of the global political and economic pattern.

Necessary action is needed to be taken in adapting global climate change. On the one hand, the adjustment of the structure of energy supply should be actively pushed forward, as to change the leading role of hydrocarbon energy in the structure and reduce greenhouse gas emissions; on the other hand, security measures against the consequence of global climate change should be adopted, to enlarge the stock and improve the regulation capacity. To store water is actually to store energy.

The international community has realized that the lack of adequate water storage facilities will weaken man's response to changes and directly hinder the fulfillment of development objectives in the years to come. Thus, hydropower development to ensure adequate water storage facilities is important for dealing with climate change and solving the problem of energy.

Overview of Global Hydropower and Dam Development

Overview of Hydropower Development in the World

As the most technically mature and reliable source of renewable energy, hydropower plays an important role in the global supply of energy. Global hydropower theoretical reserve is 39,097 TWh/year with a technical availability about 14,653 TWh/year and an economic availability about 8,728 TWh/year. Except Antarctica, hydropower distributes everywhere in the world (Table 1, Fig. 1).

In 2007, there was an installed capacity of 848,400 MW and an output of 2,045,000 GWh/year on the globe, taking up about 20 % of power supply. The degree of hydropower development reached 35 % if based on the output as percentage of the economic availability, with 11 % in Africa, 25 % in Asia, 45 % in Oceania, 71 % in Europe, 65 % in North America, and 40 % in South America, respectively (Table 1).

The global total volume of water resources is about 55 trillion m^3. Due to the uneven distribution in time and space, the total availability is about 9 trillion m^3 only. According to the definition given by the International Commission on Large Dams, more than 50,000 large dams (higher than 15 m or 5–15 m, storage capacity larger than 3 million m^3) have been built in the world up to date. These dams control about 3.5 trillion m^3 water resources, about 38 % of the total volume available on the globe, and play an important role in comprehensive water utilization and management. Many dams in the world serve the function of power generation. For instance, 44 out of the reservoirs with a storage capacity over 25 billion m^3 on the globe serve the function of power generation, including 16 for the sole objective of power generation. These 44 reservoirs provide a total storage capacity of 2.5 trillion m^3 (about 37 % of the world total) and an annual output over 500 TWh/year, taking up about 18 % of the world hydropower generation. In 2007, out of the 370 dams higher than 60 m under construction in the world, 217 were designed for the primary or only function of power generation.

According to the statistical data of 2008, there were 16 countries depending upon hydropower for over 90 % energy supply, for example, Norway and Albania, 49 for over 50 %, including Brazil, Canada, Switzerland, and Sweden; and 57 for over 40 %, including most South American countries. The average degree of hydropower development in developed countries was higher than 60 %, up to 90 % in France, and ever over 90 % in Italy (Table 2).

Table 1 Profile of global hydropower development

	Theoretical reserve (GWh/year)	Technical availability (GWh/year)	Economic availability (GWh/year)	Installed capacity (MW)	Hydropower output (GWh/year)	Degree of development (%)
Africa	2,590,234	1,303,246	848,434	21,486	94,124	11
Asia	19,701,583	7,654,565	4,487,377	329,737	1,107,622	25
Oceania	633,384	195,987	88,644	13,470	40,259	45
Europe	2,900,767	1,120,541	752,348	178,814	530,999	71
North America	7,574,535	1,763,478	1,014,910	167,042	664,244	65
South America	5,696,000	2,615,299	1,536,197	137,908	607,577	40
Total	39,096,600	14,653,115	8,727,911	848,456	3,044,825	35

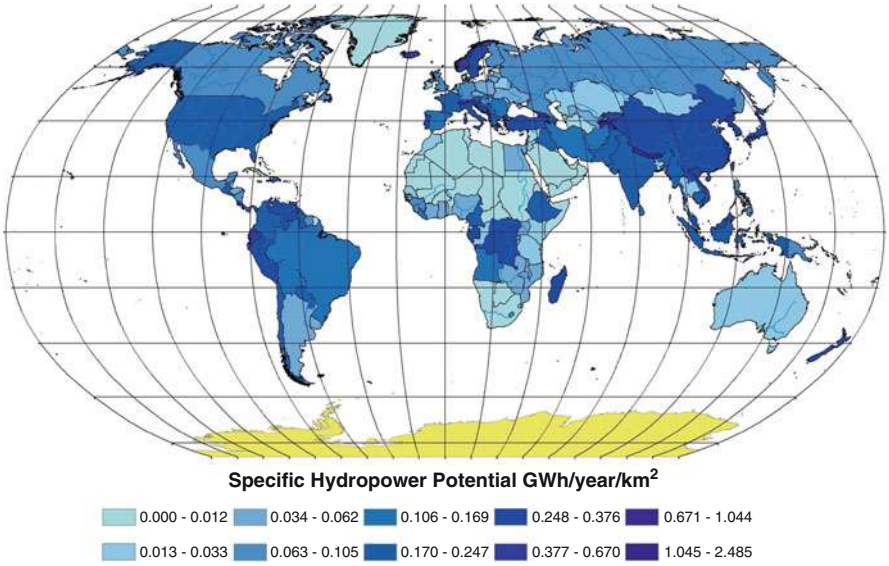

Fig. 1 Global hydro power density (GWh/year/km^2)

The 50,000 large dams in operation are distributed geographically as follows: 59.7 % in Asia, 21.1 % in North America, 12.6 % in Europe, 3.3 % in Africa, 2.0 % in South America, and 1.3 % in Australia.

There were 5,443 dams higher than 30 m in China in 2009 and 4,685 in 2003, taking up 38 % of the world total base on the data of 2003, the largest number of all countries. With regard to the number of built and ongoing dams higher than 30 m in 2003, the following countries were in the second to the seventh places, respectively: USA with 1,533; Japan with 1,075; Spain with 517; India with 504; Turkey with 376; and Italy with 322. By the function of reservoirs, statistics from the International Commission on Large Dams indicated that among 33,105 registered dams single-purpose dam accounts for 72 % and the rest of 28 % is for multipurpose. For single purpose dams, the distribution for each purpose lead to the following results: 48.6 % for irrigation, 17.4 % for hydropower, 12.7 % for water supply, 10 % for flood control, 5.3 % for recreation, 0.6 % for navigation and fish farming, and 5.45 for others. For multipurpose dams, the distribution for majority purpose lead to the following results: 24.6 % for irrigation, 18.7 % for hydropower, 16.3 % for water supply, 18 % for flood control, 12.2 % for recreation, 6.4 % for navigation and fish farming, and 3.8 % for others.

In order to have a better understanding of dam construction in the world, dams and reservoirs are tabulated below by number, height, storage capacity, and power output. With minor change over the recent years, the data are based on the statistical report published by the International Commission on Large Dams and the typical data produced by Chinese National Committee on Large Dams in 2005 (Tables 3, 4, 5, and 6).

Table 2 Hydropower development by countries in 2008

Country	Economic availability (TWh/year)	Hydropower output (TWh/year)	Percentage in economic availability (%)	Hydropower installed capacity (MW)	Total installed capacity (MW)	Storage capacity (10^9 m^3)
China	1,753	565.5	22.9	172,600	792,730	692.4
United States	376	270.0	71.8	78,200	687,000	1,350
Canada	536	350.0	65.3	72,660	114,950	650
Brazil	763.5	331.7	43.4	83,752	88,620	568
Russia	852	170.0	20.0	47,000	224,240	793
India	442	121.7	27.5	37,000	112,060	213
Japan	114.3	92.5	80.9	22,000	268,280	20.4
France	72	64.6	89.7	25,200	111,200	7.5
Norway	205.1	121.8	59.4	29,040	27,890	62
Italy	54	51.3	95.0	17,460	98,626	13
Spain	37	23.3	63.0	18,450	62,300	45.5

Table 3 Countries with more large dams higher than 100 m

Country	Number of dams >100 m	Maximum height	Name of highest dam
China	130	305	Jinping-I Dam
Japan	106	186	Kurobe No IV Dam
United States	86	234	Oroville Dam
Spain	51	202	Almendra Dam
Turkey	51	282	Keban Dam
Iran	47	315	Bakhtyari arch dam
India	30	260.5	Tehri Dam
Italy	28	262	Vaiont Dam
Switzerland	25	285	Grande Dixence Dam
Brazil	23	205	Irape Dam
Mexico	21	261	Chicoasen Dam
Romania	18	167.7	Gura Apelor Dam
Russia	17	245	Sayano-Shushenskaya
France	15	180	Tignes Dam
Vietnam	14	170	A Luoi Dam
Canada	14	244	Mica Dam
Colombia	14	250	Guavio Dam
Australia	13	180	Dartmouth Dam
Austria	13	200	Kolnbrein Dam
Argentina	11	170	Piedra Del Aguila

Table 4 First 10 built and on-going large dams

No	Name of dam	Dam height (m)	Purpose	Country
1	Jinping-I	305	HC	China
2	Nurek	300	IH	Tajikistan
3	Xiaowan	294.5	HCIN	China
4	Xiluodu	285.5	HCN	China
5	Grande Dixence	285	H	Switzerland
6	Keban	282	H	Turkey
7	Kambarazin Hydropower Station-1	275	H	Kyrgyzstan
8	Inguri	271.5	HI	Georgia
9	Vajont	262	H	Italy
10	Chicoasen	261	H	Mexico
11	Manuel m. Torres	261	H	Mexico
12	Tehri	261	IS	India

H hydropower, *I* irrigation, *C* flood control, *N* navigation, *S* water supply

Overview of Hydropower and Dam Development by Continents

Europe

In the early 1920s, most of the large dams in Europe were built in UK (220 in total). At the end of 2006, more than 5,280 large dams were registered in Europe, with the first numbers in Spain (1,188), France, and UK, over 500, respectively.

Table 5 First 10 built and ongoing reservoirs

No	Name of dam	Storage capacity (10^8 m^3)	Objective	Country
1	Kariba	1,806	H	Zimbabwe/ Zambia
2	Bratsk	1,690	HNS	Russia
3	High Aswan Dam	1,620	IHC	Egypt
4	Akosombo	1,500	H	Ghana
5	Daniel Johnson (manic 5)	1,419	H	Canada
6	Guri	1,350	H	Venezuela
7	Bennett w.a.c	743	H	Canada
8	Krasnoyarsk	733	HN	Russia
9	Zeya	684	HNC	Russia
10	LG Deux Principal cd-oo	617	H	Canada

H power generation, *I* irrigation, *C* flood control, *S* water supply, *N* navigation

Table 6 Top 10 built and ongoing hydropower stations

No	Name of dam	Time of completion	Installed capacity (MW)	Annual power output (GWh)	Country
1	Three Gorges	2009	22,500	84,000	China
2	Itaipu	1991	12,600	90,000	Brazil/ Paraguay
3	Xiluodu	2010	12,600	57,120	China
4	Guri	1986	10,000	52,000	Venezuela
5	Tucurui	1984	8,370	21,400	Brazil
6	Sayano-Shushenskaya	1990	6,400	22,800	Russia
7	Xiangjiaba	UC	6,000	30,747	China
8	Krasnoyarsk	1967	6,000	19,600	Russia
9	Longtan (in Guangxi)	2001	5,400	18,710	China
10	Bratsk	1964	4,500	22,500	Russia

UC under construction

The first objective of dams in Europe is power generation, which is followed by irrigation and water supply. In the European countries, the usage (and importance) of reservoirs varies considerably, particularly in the aspect of hydropower generation. This variation reflects the difference in topography, rainfall, and government policy. Many reservoirs designed for hydropower purposes are often located in mountainous areas and north European countries, obviously different from those for irrigation and water supply. The latter are relatively small in scale, generally in lowland countries and south European countries. About a quarter of the dams in Europe are designed for multipurpose operation. In several countries, hydropower contributes more than a half to the national power supply, for example, 97 % in Albania, 70.1 % in Iceland, 70 % in Latvija, and even up to 99 % in Norway.

In 1960, dam construction and hydropower development reached the climax in many parts of Europe. However, the focus today is to maintain and repair existing dams as required by new acts and regulations. In 2006, the installed capacity of hydropower stations under construction in Europe was about 4,733.2 MW, which was distributed in 20 countries, including Germany, Greece, Iceland, Italy, Macedonia, Portugal, Slovenia, and Ukraine.

Asia

Asia has being reached the climax of hydropower development. Most of the under constructed large dams higher than 60 m are distributed in Asia, 276 in total. The International Commission on Large Dams listed a total number of 35,070 large dams in Asia in 2006. Most of the dams in Asia are built for the purpose of irrigation, and then power generation, flood control, and water supply. At present, the first objective of dams in Asia varies from one country to another, including irrigation in India and Turkey, flood control, irrigation, and power generation (including pumped storage stations) in China, flood control and pumped storage in Japan, and irrigation and power generation in Iran. There are nine Asian countries where hydropower takes over 50 % of the national power supply. As shown by statistical data of the International Commission on Large Dams, this percentage is 14 % in China (based on the power output in 2007), 17.1 % in India (2007), 18 % in Russia, and 25.4 % in Turkey.

Generally, China, India, Turkey, Japan, and Iran are most vigorous in dam construction. The climax of dam construction in Asia appeared in the period of 1970–1980, with more than 200 dams built each year. In 2006, the installed capacity in progress was larger than 189,010 MW, mostly in China, and also in India, Iran, and Russia.

India has a large population, but the water availability per capita is about 1,829 m^3/year only, less than 30 % of the world average, representing water shortage. The number of dams in operation in India is 4,083, with a total installed capacity of 213 billion m^3. The dams in India are 90 % earth and rock fill ones, including 2,600 higher than 15 m. The national installed capacity of hydropower is 37,000 MW. Tehri Dam, the highest rock-fill dam, 260.6 m, has been completed.

Russia saddles the European and Asian continents, sharing long borders with China. There is a total annual mean precipitation of about 9.348 trillion m^3 and runoff of 4.262 trillion m^3, representing very rich water resources. At present, there are 101 dams in operation in the country, including 58 rock fill and 43 concrete ones, with a total storage capacity as large as 793 billion m^3 and an installed capacity about 47,000 MW. There are 85 hydropower stations with an installed capacity over 10 MW. In addition, about 7,000 MW is under construction. The planned installed capacity is about 12,000 MW. Bureya Dam, a concrete gravity dam with a height of 140 m and a storage capacity of 3.5 billion m^3, is the highest dam under construction.

North America and Central America

According to statistical data of the International Commission on Large Dams, there were 8,252 large dams in North America and Central America in 2006, including

some 6,510 in the USA. 4 countries out of 15 in the region, the hydropower generation is over 50 % of national power supply. They are Canada, Costa Rica, Haiti, and Panama. The hydropower output of Canada is the largest in North America, the third place in the world, and that of the USA is in the fourth place. The sum of these two countries takes up more than one-fifth of the world total. Flood control, power generation, irrigation, water supply, and recreation are the primary objectives of the large dams in the USA.

After the Second World War, the number of dams built and put into operation boosted in this part. In the USA, the number of dams put out of operation exceeds the number of dams newly registered and constructed each year.

The large dams under construction in Central America provide an installed capacity of about 3,047.1 MW (including Mexico). By the end of 2006, Mexico had built 668 large dams, with an annual output of 25,000 GWh. The installed capacity in progress is about 2,250 MW.

South America

In 2006, there existed 799 large dams in South America, including almost half of them in Brazil (387 in total). The first objective is power generation and flood control. Now, there are many high dams under construction in South America, mostly in Brazil, Venezuela, and Ecuador, with a total installed capacity of 11,327 MW distributed in nine countries. Proposed projects will provide another installed capacity of 62,956 MW.

Brazil is most active in hydropower development, which accounts for 76.6 % of the national power output. Other countries keen on hydropower development include Paraguay (99.99 %), Columbia (78 %), Peru (65 %), Venezuela (73.3 %), French Guiana (60 %), Chile (43.5 %), and Ecuador (43.5 %).

In 2007, there was a total installed capacity of about 11,327 MW under construction in 13 South American countries.

Africa

Africa is less capable in developing and regulating water resources. As suggested by the statistical data of the International Commission on Large Dams, there were 1,815 built large dams in Africa, including over 80 % in South Africa (1,166), Zimbabwe (250), and Morocco (120). In 2006, more than 20 African countries were developing hydropower resources, but the number of dams higher than 60 m was not large, only 13. There was a total installed capacity of 7,489 MW in progress in 17 countries in 2007, including 3 countries with an installed capacity larger than 1,000 MW, namely, Ethiopia (1,277 MW), Guinea (1,291 MW), and Sudan (1,300 MW). In the arid and semiarid north and south parts of Africa, dams are built mainly for irrigation. In the middle and other humid parts, the first objective is power generation.

The “Southern Africa Power Pool” has done something in investing in future power infrastructures here. In Africa, the percentage of hydropower in 22 countries takes up more than 50 % of the national power supply, and even more than 90 % in 5 countries including Zambia, Mozambique, and Namibia.

Oceania

There are altogether 621 large dams here, mostly in Australia (541) and New Zealand (67). Dams are first for the objective of water supply, but also for power generation and irrigation as well. There are three countries where hydropower constitutes over 50 % of the national power supply, namely, Fiji (50 %), New Zealand (60 %), and Papua New Guinea (65 %).

In Australia and New Zealand, the climax of dam construction was witnessed in 1980 (about 10 dams on the average each year). In 1990, the speed was slowed down. Now, there is only one 60 m high dam under construction in Australia, where the focus is shifted to small hydropower and water supply facilities.

Small Hydropower (SHP) Development

Small Hydropower

Under favorable circumstances, small hydropower (SHP) represents one of the cheapest methods of electricity generation. Of all the renewable energy sources, small hydro (large as well) represents the highest density of resource. For a long time, small hydro has been generally overshadowed and confused with large hydropower (LHP). The focus over the years in many developing countries (for instance, in some countries of Africa, Asia, and Latin America) has been large-scale hydropower schemes. SHP has attracted relatively little attention from entrepreneurs, equity investors, and project financiers in recent years in emerging economies with the exception of some of them. However, given the current global context, the cost competitiveness of the technology and the size of the remaining resource, investment analysts believe that small hydro has the potential to enjoy rapid expansion, particularly in emerging economies. Economically viable and proven small-scale hydropower technologies have been commercially developed and are available for generating both electrical and mechanical power for rural industrialization and development. In continents like Africa and Asia, small hydropower development is an adequate measure for electrification in rural areas.

In industrialized countries (e.g., European Union), SHP development followed a very specific way (Pelikan 2005):

- Phase 1: decentralized energy demand by industry (up to 1940/1950)
- Phase 2: economic-driven decrease until 1970
- Phase 3: energy crisis and boom until 1990
- Phase 4: decrease driven by environmental concerns up to present

Thousands of small hydroelectric plants were abandoned in Europe and North America during the period from the 1950s to the early 1980s. In 1990s, small hydropower plants virtually ceased to exist in the Former Soviet Union and Central and Eastern Europe.

However, in the EU, there is a good hope that the last phase will change its trend due to a recently enacted legally binding targets for increasing renewable energy use by 20 % by 2020. Actually, in some European countries (for instance, Balkan region/South Eastern Europe), there is ongoing boom of constructing new SHP plants.

Similarly, small hydropower development is actually booming in the USA. Driven by federal incentives, the market continues to grow and SHP is now recognized as one of the most cost effective and environmentally friendly forms of renewable power. Similar trends can also be seen in other countries, in particular in Brazil, Canada, and China.

SHP Versus Large Hydropower (LHP)

Major attributes of small (SHP) and large hydropower (LHP) are given in Table 7. It is important to realize that SHP is not simply a reduced version of a large hydropower plant. Specific equipment is needed to meet the fundamental requirements of simplicity, high-energy output, environmental measures, and maximum reliability.

A comparison of data from Fig. 2 representing small and large hydropower utilization, shows that in all continents, with the exception of Europe, small hydro has big untapped resources that may be utilized in the future, with Europe having realized close to 50 % of its potential.

Classification of Small Hydropower Plants

A common classification of hydropower plants according to installed power capacity is shown in Fig. 3.

Hydropower plants are often subdivided into “large” hydro (LHP) that usually involve dams, and small hydro (SHP), involving mini, micro, and pico schemes that are normally run-of-river systems and have little or no water storage capacity.

There is currently no agreement in the international community as to the definition of small hydropower. The upper limit is generally regarded to be 10 MW in capacity that suggests still minimal negative impact on environment. However, small hydro in the USA can refer to projects between 1 and 30 MW, in Canada between 1 and 50 MW, while in China it is as high as 50 MW (Table 8).

This classification can be supplemented by hydraulic head, operational mode (run-of-river, pondage/reservoir type), applicable turbine technology, etc.

Small hydro systems can either be connected to the grid and provide power to the grid or they can be used for independent and stand-alone applications in isolated remote areas. Micro, Mini, and even small hydro plants may provide power only to an isolated community or a single home.

Pico-Micro hydroschemes are generally stand-alone systems, that is, are not connected to the electricity grid. They are used for domestic electricity applications such as lighting, TV/radio, and battery-charging. It is becoming a mature technology which should now be considered as part of the menu of alternatives to grid extension,

Table 7 Major attributes of small (SHP) and large (LHP) hydropower

Positive			Negative		
	SHP	LHP		SHP	LHP
Emissions-free, with virtually no CO_2, NO_x, SO_x, hydrocarbons, or particulates	+	+	Frequently involves impoundment of large amounts of water with loss of habitat due to land inundation. Freshwater reservoirs might emit GHGs emissions.	–	+
Proven and reliable technology, indigenous resource, resistant to inflation	+	+	Altering river flows and natural flooding cycles, sedimentation/silting	–/+	+
Renewable resource with high conversion efficiency to electricity (90+%)	+	+	Variable output – dependent on rainfall and snowfall	+	+/–
Dispatchable with storage capability	–	+	Impacts on river flows, water quality, aquatic ecology, including fish migration and oxygen depletion	–/+	+
Usable for base load, peaking, improves grid stability	–/+	+	Social impacts of displacing indigenous people	–	+
Attractive energy pay-back ratio, low operating and maintenance costs	+	+	Health impacts in developing countries	–	+
Long lifetime – 50+ years typical, up to 100 years	+	+	High initial capital costs	+	+
Technology suitable for rural electrification notably in developing countries, output is consumed near the source	+	–/+	Long lead time in construction of mega-sized projects	–	+
Promotes multipurpose uses (irrigation, navigation, flood defense, recreation)	+	+	Structural dam failure risks	–/+	+

diesel generators, solar PV systems, and other energy systems presently being used in rural areas, especially developing countries. In comparison to these options, pico-hydro can be installed at a lower cost for the same energy output and in the markets where it has become established, subsidies have not been required.

Current Status of SHP

Overview of SHP Development of the World

As indicated in Table 9, global installed SHP capacity in 2008 was 53.7 GW representing TWh/year generation in electricity. Roughly 10 % of global economically feasible SHP potential has been exploited up to now. The biggest exploitation rate is observed in Europe – 46 %, whereas African continent have a long way to go – less than 2 %.

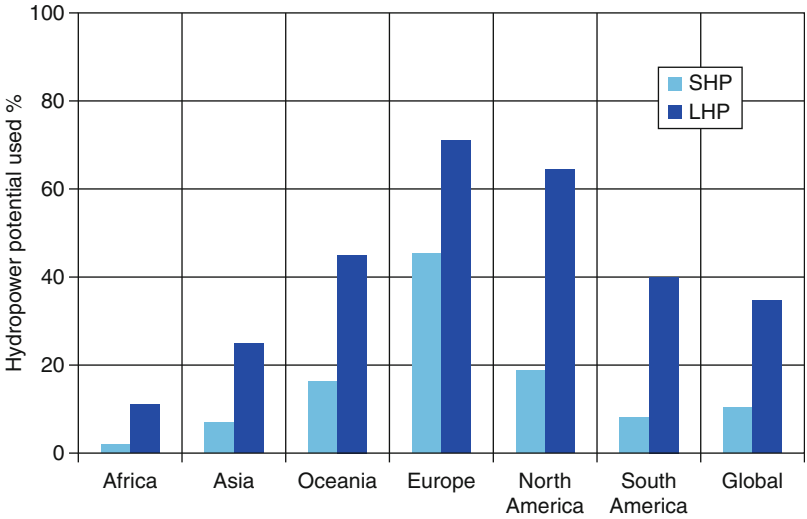

Fig. 2 Proportion of the small and large hydropower currently used to the economically feasible potential in each region

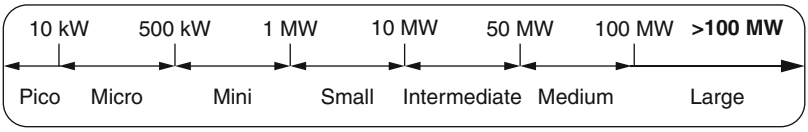

Fig. 3 Common classification of various hydropower schemes according to installed power capacity

Russia is attributed to Asian continent.

Economically feasible potential is subject to considerable fluctuations (due to economic competitiveness among power options, the status of energy, and environmental legislation). This issue is more problematic in emerging economies where data on SHP are scarce.

Global small hydro contribution to the gross electricity mix is insignificant – around 1 % and it is of a similar scale to the other renewable energy sources. Despite this, it should not be neglected though, because there is an even much larger market potential in Asia, South America, and Africa. SHP share to the global hydropower generation is more than 6 %. It is quite clear that SHP is the second largest renewable energy source after large hydropower in all contents. But in Europe electricity generation from wind energy is currently surpassing SHP.

There are, of course, many ways to look at global SHP players. Table 10 shows the 10 top countries with the highest share of SHP installed capacity and electricity generation, with China on top.

Small hydropower sector is represented according to country's SHP plant size limit.

Table 8 SHP definition and classification in selected countries

Continent/organization	Major attributes of classification
Africa	Guinea, Kenya, Nigeria, South Africa (<10 MW), Lesotho (<15 MW), Madagascar (<20 MW), Mozambique (<25 MW)
Asia	Nepal, Philippines (<10 MW), India (<25 MW), Russia (<30 MW)
	China (<50 MW). According to the scale of installed capacity, it can be divided into four grades: 0.5–5 MW, 5–10 MW, 10–25 MW, and 25–50 MW. It also can be divided into three types: run-of-river SHP, adjustable SHP, and irrigation SHP
Europe, ESHA (European Small Hydro Association), the European Commission and the UNIPEDE (International Union of Producers and Distributors of Electricity)	The European Union has no uniform classification criteria for SHP. As a rule, the installed power capacity is the main classification criterion (units up to 10 MW). However, this limit is set at 3 MW in Italy, 8 MW in France, and 5 MW in the UK, 2 MW in Latvia
	For the statistical purposes there is a common division between two groups of hydro schemes: less than 1 MW and between 1 and 10 MW
North and Central America	Small hydropower limit is often high
	In Canada, there are three categories recognized under small hydro: Micro hydro (less than 100 kW); Mini hydro (100 kW–1 MW) and Small hydro (1–50 MW)
	In the USA small hydro refers to hydropower potential $\geq$1 MW and $\leq$30 MW, and low power refers to hydropower potential <1 MW
	Mexico: small (1< P <30 MW)
South America	This continent is mostly dominated by large SHP capacity limit, more often up to 30 MW
	Brazil small hydropower sector is represented by two distinct classes: Mini hydropower plants (P $\leq$1 MW) and small hydropower plant (1 MW < P $\leq$30 MW) and Argentina (<30 MW), Chile, Columbia, Peru (<20 MW), Bolivia (<10 MW)
Australia and New Zealand	In Australia small hydro is divided into three categories: micro (less than 100 kW), mini (100 kW to <1 MW) and small (1 MW to <10 MW)
	New Zealand: 20 MW
UNIDO (United Nations Industrial Development Organization)	Micro <100 kW; Mini 101–2,000 kW; Small 2–10 MW
IN-SHP (International Network on Small Hydropower), International Small-hydro Atlas	Micro <100 kW; Mini 101–500 kW; Small 0.5–10 MW
	Small Hydro: 50 kW < P <10 MW installed capacity

Table 9 Profile of small hydropower (installed capacity <10 MW/site) development by continents

Continent	Economically feasible (realizable) SHP potential (TWh/year)	Installed capacity (MW)	SHP generation (TWh)	Degree of development (%)	SHP contribution in total hydropower electricity generation (%)	% of global SHP installed capacity
Africa	135	776	2.5	1.9	2.69	1.4
Asia	1,198	23,752	82.4	6.9	7.44	44.3
Oceania	7	277	1.1	16.3	2.76	0.5
Europe	118	15,931	54.0	45.7	10.18	29.7
North America	219	10,869	41.0	18.7	6.17	20.3
South America	111	2,054	8.9	8.1	1.47	3.8
Total	1,787	53,658	190.0	10.6	6.24	100.0

Table 10 SHP development by countries (top 10 by SHP installed capacity)

Country	Economically feasible SHP potential (GWh/year)	SHP generation (GWh/year)	SHP installed capacity (MW)	Degree development (%)	Number of SHP plants	Average size of power plants (MW)	SHP contribution in gross electricity mix (%)	SHP contribution in total hydropower electricity generation (%)
China	422,400	110,000	35,000	26.0	45,000	0.8	3.7	20.6
USA	145,760	26,718	7,087	18.3	2,050	3.5	0.6	9.9
Japan	24,478	18,796	3,509	76.8	1,335	2.6	1.8	20.4
Canada	53,600	12,818	3,400	23.9	200	17.0	2.1	3.6
Italy	11,000	8,538	2,468	77.6	1,799	1.4	2.9	19.0
Germany	10,000	7,996	1,714	80.0	8,000	0.2	1.3	39.2
Norway	25,000	6,751	1,521	27.0	852	1.8	5.0	5.6
Brazil	45,000	6,700	1,429	14.9	570	2.5	1.6	1.9
France	10,000	6,383	2,473	63.8	1,717	1.4	1.2	10.1
India	60,000	6,138	2,046	10.2	420	4.9	0.8	5.3

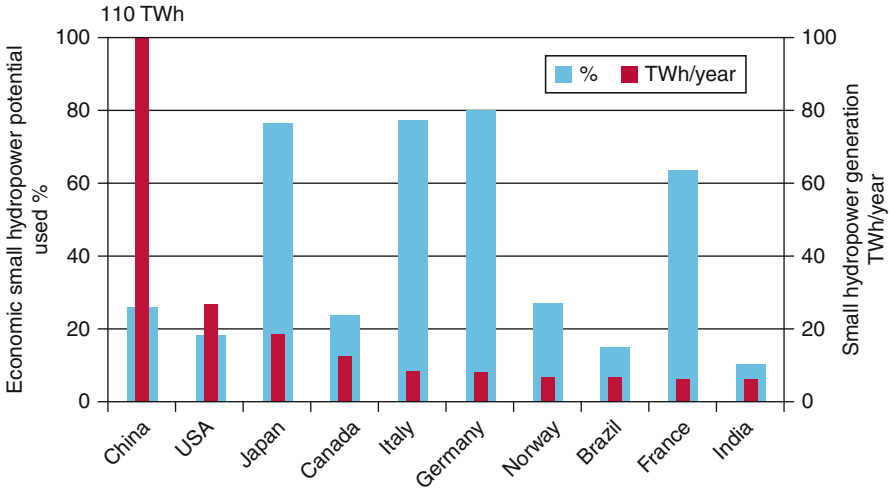

Fig. 4 Economic small hydropower potential that is currently utilized in selected countries (% and TWh/year)

Not surprisingly, countries with large mass and river drainage basins, including China, the USA, India, Canada, Brazil, and Japan, with the exception of hydro-rich country Russia, appear on the list. Another measure would be to look at SHP contribution to their overall electric energy generation. In this case, Norway (5 %), China (3.7 %), Italy (2.9 %), and Canada (2.1 %) are on the top.

In the cases of Japan, Italy, and Germany, for example, nearly 80 % of the economically viable small hydro resources have already been tapped, whereas large countries such as China, Canada, the USA, Brazil, and India having huge SHP potential have a long way to go (Fig. 4).

Overview of SHP Development by Continents

Africa

The African Continent is endowed with enormous hydropower potential that needs to be harnessed. The focus over the years in many African countries has been large-scale hydropower schemes. Recent studies have shown that electricity generation through small hydropower is gaining market share owing to its short gestation period, low investment, and least environmental impacts (Hydropower resource assessment of Africa. In: Ministerial conference on water for agriculture and energy in Africa: the challenges of climate change et al. 2008).

The current level of utilization of SHP potential is very low in the continent with regard with other continents. Total installed capacity of these plants exceeds 770 MW with power generation of 135 TWh/year in the continent. Small hydro is not popular in the individual countries either: in the majority of them, total installed capacity of SHP plants rarely exceeds a few dozen megawatts.

However, the assessed SHP economically feasible potential in a larger number of countries is quite high: Congo Democratic Republic, 33.7 TWh/year; Madagascar, 18 TWh/year; Angola, 15 TWh/year; Ethiopia, 16.2 TWh/year; Guinea, 12 TWh/year; and Cameroon, 11.5 TWh/year.

Europe

More than 24,000 SHP plants (units up to 10 MW) with total installed capacity of 16 GW and annual production of nearly 55 TWh/year operate in Europe. (Small hydropower sector of the European part of Russia is shortly represented under Asia continent.)

In the European Union (EU), the potential for medium and large-scale hydropower projects is already exploited to a high degree (some 80 %), small hydropower projects become the subject of increased development. In 2006, there were nearly 21,000 SHP plants with total installed capacity of 13 GW and total electricity generation of 41,000 GWh in the EU (ESHA and SERO 2008). More than 80 % is concentrated in the following six countries: Austria, France, Germany, Italy, Spain, and Sweden. In addition, Switzerland and Norway have a high SHP capacity followed Bulgaria, the Czech Republic, Poland, and Romania.

About 1.2 % of the total electricity generated as well as 9 % of all renewable energy in EU came from SHP. On average, a statistic SHP plant in the EU had a capacity of 0.6 MW and produced about 2.0 GWh in 2006.

Oceania

The continent's installed capacity of SHP is 280 MW with power generation of 1.1 TWh/year, against an estimated potential of 6.8 TWh/year. SHP hydro schemes are popular in New Zealand (P = 108 MW; E = 509 GWh/year), Australia (P = 70 MW; E = 255 GWh/year), and French Polynesia (P = 47 MW; E = 164 GWh/year). Small hydro plants are not developed in the remaining countries.

Asia

In China, small hydropower refers to such SHP project whose installed capacity is not more than 50 MW.

There are abundant and widely distributed SHP resources in China; SHP supplies some 30 % of the renewable energy electricity in China and constitutes the main electricity supplier in nearly half of the territory, one-third of the counties, and one quarter of the total population in China (Zhou et al. 2009). In 2004, China's total installed capacity of SHP is 34.66 GW and its generation is 97.79 TWh, the highest one in the world. The number of SHP stations operating in the country exceeds 45,000. There are abundant SHP resources in China, and the potential installed capacity is 128 GW (or 422.4 TWh/year) in technology, ranking first in the world.

Japan is the second largest after China with regard to the total installed capacity of small hydro schemes (P = 3,509 MW, E = 18.8 TWh/year). Nearly 80 % of the economically feasible potential has been harnessed so far.

Russia has the second highest level of mean annual river runoff in the world, after Brazil. The bulk of the stream flow is concentrated in the eastern part of the country.

The European part of Russia accounts for less than 25 % of the country's water resources (IEA 2003). The economic potential of small-scale hydropower can be estimated at 493 TWh/year, including more than 100 TWh/year in the European part of country. Before 1980s, some 7,000 small hydropower plants with a total capacity of 1,500 MW operated in the country, but later on due to commissioning of large power plants almost all of them were abandoned. Currently, there are plans to refurbish and develop some 3,000 MW in small-scale hydropower capacity.

India's total SHP capacity amounts to 2,046 MW (power generation 6.2 TWh/year).

Micro-hydro installations are especially widespread in Asia, where there is a significant resource potential for further development (Vietnam, Nepal, Korea DPR, Sri Lanka, Thailand, and Laos).

South America

Nearly 950 small hydropower plants with total installed capacity of 2,055 MW and annual power production of 8.9 TWh/year operate in the continent. Only a minor part of the economically feasible potential has been tapped so far (some 8 %).

In the past, Brazil favored large hydropower schemes, largely ignoring small hydropower (less than 30 MW). But as most of the economically feasible large dams have already been built, the attention is now shifting to small-scale hydropower, particularly in rural areas. Actually there is biggest number of hydro plants 570, with total installed capacity of 1,429 MW and electricity generation of 6.7 TWh/year. Brazil is followed by Peru and Argentina (installed capacity 237 and 92 MW, and electricity generation 1.0 and 0.34 TWh/year, respectively).

North and Central America

There are currently about 1,100 MW of installed small hydro capacity with power production of 41 TWh/year in the region. Some 19 % of economically feasible potential has been developed so far.

The USA is the first with regard number of plants in operation (2,050), installed capacity (7,087 MW), and electricity production (26.7 TWh/year). Canada is the second largest SHP producer in the region having an installed capacity of 3,400 MW and generating 12.8 TWh/year. The remaining countries' SHP capacities are significantly smaller: Mexico – 109 MW and 480 GWh/year, Costa Rica – 77 MW and 306 GWh/year, Honduras – 60 MW and 276 GWh/year.

Central America has outstanding potential for hydropower development. Costa Rica, Nicaragua, Guatemala, Panama, and Honduras are especially active in developing SHP plants.

SHP Prospects and Future Potential

Long-term challenges for small hydropower development are the following:

- Capture the low-head, run-of-river hydro resource in a sustainable manner using new technology
- Fish passage and fish friendly turbines
- Minimal water impoundment
- Minimal impacts on aquatic ecology
- No sediment buildup or depletion beyond normal levels

It is difficult to make forecast of global small hydropower due to the many uncertainties. Analysis of currently published studies, reports, papers, and information existing in available data bases shows there are no reliable SHP future development figures and scenarios. By contrast with large hydropower, where comprehensive and reliable data bases are available, statistics of small hydro are very scarce, incomplete, or event incompatible with different data providers. This is true even for developed countries; the figures of small hydropower economic or technical potential are seldom available.

At the time the World Energy Council (WEC) (2004) estimated that, under current policies, installed capacity of small hydro would increase to 51 GW by 2020, with the largest increase coming in China. Under the WEC's favorable case scenario, installed capacity increases to about 75 GW by 2020. All regions of the world are experiencing significant increases in small hydro capacity, with China again showing the largest increase (Small Hydropower Fact Sheet 1999).

Projections made by Zhou et al. (Zhou et al. 2009) show that in China by 2015, the installed capacity of SHP will be 63 GW (49.4 % of the total potential), 79 GW (61.5 %) by 2020, and 103 GW by 2030. SHP in the European Union will expand also impressively. Following BAU (Business As Usual – is based on projections of future emission if no action is taken) scenario, SHP installed capacity (<10 MW/site) will increase from 13 GW up to 16 GW by 2020. If optimal conditions for developing SHP (barriers are not an obstacle, the support system are well designed for SHP, etc.) are established, then the total installed capacity could reach 20 GW.

A recent study of estimation of small hydropower resources in the USA has shown that 41 states distributed around the country have sufficient potential to increase their generation by at least 50 % (US Department of Energy 2006). This means, that SHP installed capacity could be increased from the current 7.1 GW to more than 10 GW.

Relationship Between Hydropower and Water Storage Development and Socioeconomic Development

Hydropower Enables Multipurpose Utilization of Water and Hydroenergy Resources

Water represents fundamental natural resources, strategic economic resources, and a key environmental element. Subsequent to population growth, economic development, and urbanization, the water demand of human being is increasing at the speed

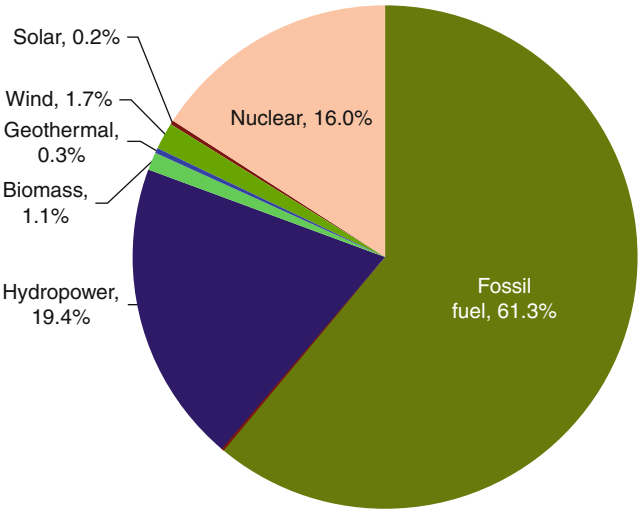

Fig. 5 Power generation by type

of 64 billion m^3/year. It is estimated that 47 % of the total population on the globe will live in places with a desperate water shortage (UNESCO 2009). Global climate change has caused profound evolution of water circles and water resources, obviously expressed by the increased variation of rainfall and water resources in time and space, significant change of hydrological process, and frequent occurrence of extreme weather events. All these have aggravated the imbalance between water supply and demand in water-deficit areas, increased the degree of difficulty in water resources development and utilization, and caused more difficulties in disaster alleviation and relief.

During the past century, multipurpose dams and reservoirs have provided an opportunity for drought protection, flood mitigation, water provision for rural and urban need, navigation, recreation, as well as energy. Moreover, its comprehensive advantage on water and energy utilization is popped out gradually with successive occurrence on energy crisis, water crisis, food crisis, and climate change.

Water storage is energy storage. It has played an important role in modern power systems. Currently, hydropower generation accounts for approximate 20 % of world electricity (EIA 2008), which is the second dominating power after fossil fuel (Fig. 5).

Large water storage facilities built for hydropower development are generally used for multiple purposes, such as flood control, water supply, navigation, power generation, irrigation, environmental protection, and recreation. Many of them act as the engine to increase the regional capability of integrated and well-coordinated development and become the landmark of countries where they are located. For instance, the Three Gorges Project in China is the world largest hydropower station, with an installed capacity of 22,500 MW, equivalent to a cumulative reduction of 34 million ton standard coal, 74.8 million ton CO_2 and 0.68 million ton SO_2. Clean energy is supplied for Central China, East China, South China, and Chongqing. Secondly, the

resultant reservoir serves the most important function of flood control in the world, directly protecting the fertile Jiang-Han plain, Wuhan and other major cities in the downstream area. Thirdly, the project is furnished with the world's largest shiplock, which will greatly improve the navigability of the Yangtze mainstream that has long been known as a "golden watercourse," with the annual volume of cargo transport increased to 300 million ton and the transport cost reduced by 35–37 %. Fourthly, the reservoir replenishes the lower reach in the dry season using its huge storage capacity to mitigate the imbalance between water supply and demand. Owing to the function of flood control, power generation, navigation, and water supply, the Three Gorges Project has secured the safety of the Yangtze River, which goes through China from west to east, and played an important role in promoting well-coordinated development in the middle, east, and west parts of China. There are many projects like this in the world, for example, Itaipu Hydropower Station in Brazil and Hoover Dam in the USA. They have turned out an indispensable and important part of the infrastructures in their countries and an engine to push forward regional sustainable economic, social, and environmental development.

Relationship Between Hydropower and Water Storage Facility Construction and Socioeconomic Development

Geographically, hydropower development in the world is extremely imbalanced. The hydropower resources in Asia and Africa account for 61 % of the world total economic availability, but the output takes up 39 % of the world total only. With regard to the degree of hydropower development, there is a global average of 35 %, but only 25 % in Asia and 11 % in Africa (Figs. 6 and 7).

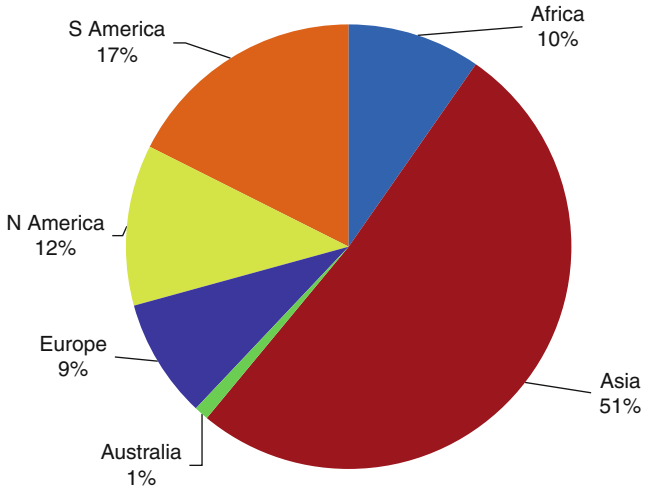

Fig. 6 Distribution of hydropower economic availability in the world

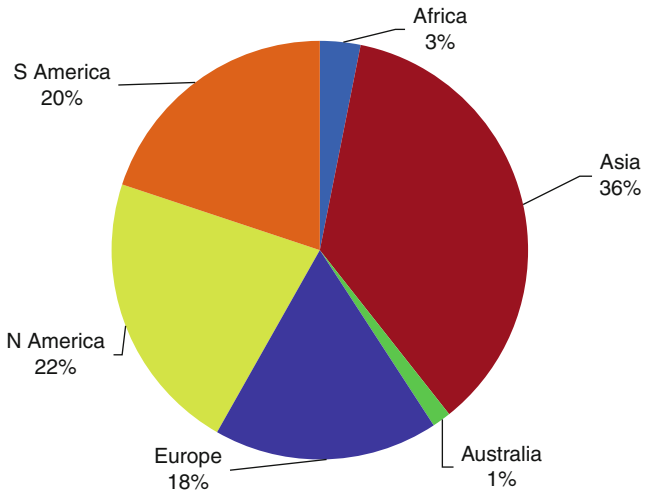

Fig. 7 Distribution of hydropower production by continent (in 2007)

Not only the comprehensive advantages that the dam has, but also the tight relation it has with socioeconomic development. This idea initiated from Berga (Berga 2008), the former president of ICOLD (International Commission on Large Dams). He thought the per capita storage capacity possessed by the country was closely related to the socioeconomic development. Follow this idea, the entry compares and analyzes per capita storage capacity index and the human development index (HDI) about more than 50 countries. The result clearly indicates how dam/reservoir development is related to socioeconomic development.

HDI, the weighted average of the per capita GDP, health and education which reflect the quality of life, is an overall index used to measure the level of socioeconomic development in the UN member countries. This index avoids the shortcoming that the per capita GDP is used as the sole index for measuring human development. HDI is a value ranging from 0 to 1, the closer it is to 1, the higher the human development level is. The countries with HDI higher than 0.9 are mostly developed countries, for example, Australia (0.970), USA (0.956), UK (0.947); those with HDI in the range of 0.8–0.9 are relatively developed countries, for example, Argentina (0.866), Russia (0.817), Brazil (0.813); while those with HDI below 0.5 are mostly less developed Asian and African countries, e.g., Rwanda (0.46), Burkina Faso (0.389), and Afghanistan (0.352).

As shown by the human development and dam/reservoir development data of over 50 countries in 2007, the countries with HDI above 0.9 had an average per capita storage capacity of 3,184 m^3, those with HDI in the range of 0.8–0.9 had 2,948 m^3, those with HDI in the range from 0.7 to 0.8 had 541 m^3, those with HDI in the range of 0.6–0.7 had 208 m^3, and those with HDI in the range of 0.5–0.6 had 125 m^3 only (Figs. 8 and 9). As seen from this fact, developed countries have a solid ground for securing water safety and coping with the changing water storage

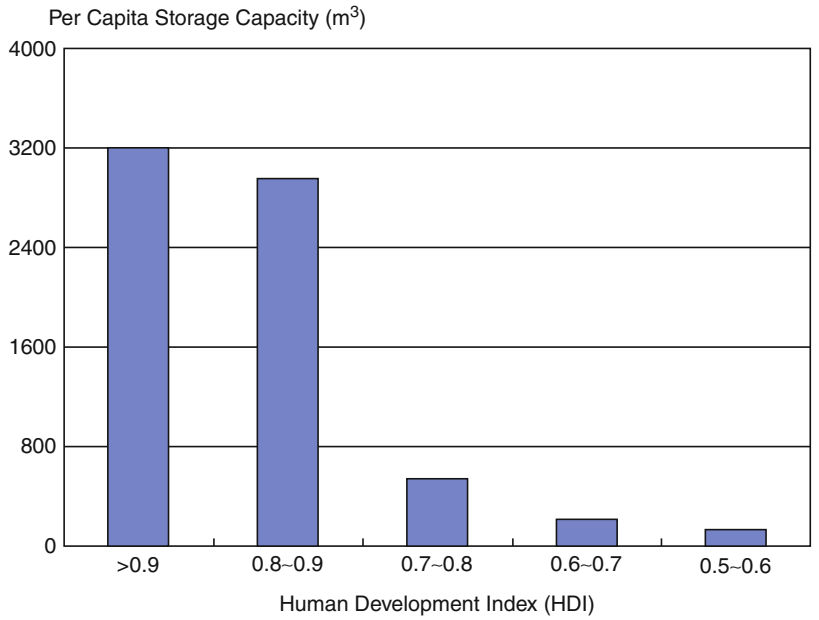

Fig. 8 Relationship between average per capita storage capacity and HDI

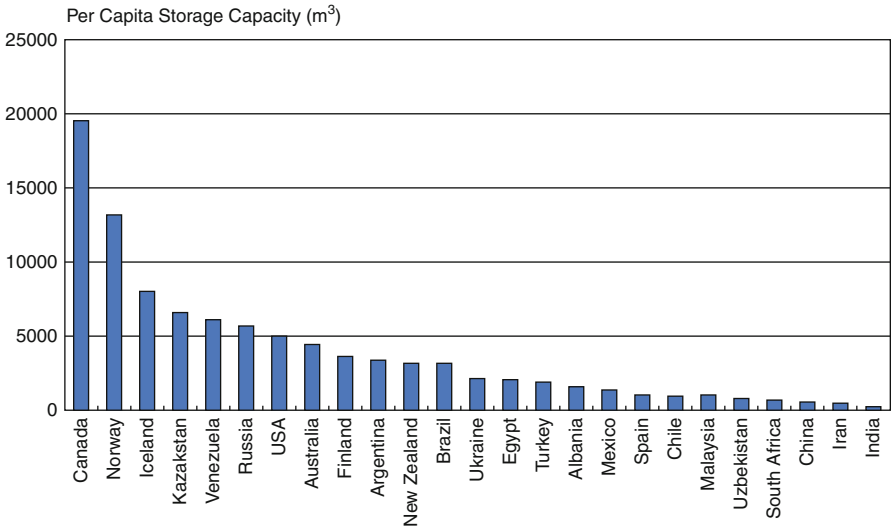

Fig. 9 Per capita storage capacity of typical countries

facilities, but developing countries still have a long way to go as limited by financial, technical, and human resources. As for a given country, despite exceptions, for example, Israel with HDI of 0.935 and a per capita storage capacity of 27 m^3, and Zambia with 0.481 and 1,072 m^3 respectively, the level of dam development in a country or region is directly proportional to the level of human development. The UN human development report also pointed out that "the distribution of global water infrastructures is reversely proportional to the distribution of global water risks."

Due to the varying extent effect, climate change represents different impacts and consequences to countries in different stages of development. Blair pointed out in his report: "the groups least responsible for climate change, i.e., the poor and vulnerable groups, are subject to the most adverse effects." Likewise, the poor or undeveloped countries that have not caused, are not causing, and will not cause significantly more greenhouse gas emissions are responsible for the cost of climate change. They are most easily subject to the effect of climate change and their adaptability is the most vulnerable. Countries in different stages of development have different objectives and priorities of water storage facilities, and also different concerns. For less developed countries, the consequence of global climate change is often catastrophic to the extent that, due to the inadequate storage capacity, subsequent extreme weather events occur frequently and bring about worse disasters. The construction of water storage facilities is a crucial matter relating to their surviving and getting rid of poverty. Just as stated in the World Declaration on Hydropower (2008) Development (Africa), water and electricity are materials to save life in less developed African countries. These countries are in desperate need of energy and water. With the dual benefit of water storage and power generation, multipurpose dams/reservoirs are critical for improving safe water supply. Also, they greatly mitigate the impacts posed on Africa by extreme weather events. Thus, the development of water and hydroenergy resources is of special significance for developing countries, especially the African countries, and one of the most urgent tasks to improve the livelihood.

To Accelerate Water Storage Infrastructure and Hydropower Development are a Common View of the International Community Today

Observed Impacts on Water and Future Changes in Water Demand and Availability

The IPCC (IPCC 2007a) has identified changes in a number of components of the hydrological cycle and systems which include: changing precipitation patterns; intensity and extremes; increasing melting of snow and glaciers; increasing atmospheric water vapor; and changes in soil moisture and runoff. These changes are consistent with the observed climate warming despite the fact that the components of the hydrological cycle and systems usually demonstrate a significant natural variability over various timescales.

Table 11 Climate-related observed trends of various components of the global freshwater systems (Modified from Table 1.3, Chap. 1. WGII of the IPCC AR4 (IPCC 2007a; IPCC 2007b))

Parameter	Observed changes	Period	Location/ catchment	Comments
Runoff/ streamflow	Annual increase of 5 %, winter increase of 25–90 %	1935–1999	Arctic drainage basin (Ob, Lena, Yenisei and Mackenzie)	Large impact of winter melting and thawing of permafrost. Summer has very little impact
	Onset of streamflow peaks 1–2 weeks earlier than before	1936–2000	Western North America, New England, Canada, and northern Eurasia	Early onset of spring
Increased runoff in the glacial basins in Peru	23 % increase in glacial melt	2001–2004	Yanamarey	Increased warming
	143 % increase	1953–1997	Llanganuco	
	169 % increase	2000–2004	Artesonraju	
Floods	Increasing catastrophic flood frequency (100–200 year flood)	Last few years	Russian Arctic rivers	Caused by earlier breakup of river ice accelerated by warming and heavy rainfall events
Hydrological droughts	29 % decrease in annual maximum streamflow	1847–1996	Southern Canada	Rise in temperature and increased streamflow
Water temperature	0.1–1.5 °C increases in lakes	40 years	Europe, North America, and Asia (100 stations)	Caused by atmospheric warming

Although there are regional variations (increasing or decreasing) in runoff changes, at the global scale, Milly et al. (Milly et al. 2005) have identified a coherent pattern of change in an annual runoff (Table 11).

Future changes in water demand and availability will arise from two fronts. First, main climatic parameters such as precipitation, temperature, and evaporation changes will drive water availability as well as demand. In the snow- and glaciers-melt-dependent rivers or water bodies, temperature is very important. Thermal expansion plays a major role in the process of sea level rise, which could affect surface water in the coastal areas.

Second, non-climatic drivers that would play major roles include population increase, food demand, increased income through economic development, lifestyle changes, and ecological water demand.

Major changes can be expected in flooding and droughts. In northern latitude countries, flooding from rain is projected, as most of the precipitation would be in the form of rain rather than snow. The timing of flooding will also change – early spring flooding could occur. If flood waters can be stored, this could be beneficial for

Table 12 Regional impacts on water resources (IPCC 2007b)

Region	Impacts of water
Africa	By 2020, between 75 and 250 million of people are projected to be exposed to increased water stress due to climate change
	By 2020, in some countries, yields from rain-fed agriculture could be reduced by up to 50 %
	By 2080, an increase of 5–8 % of arid and semiarid land in Africa is projected under a range of climate scenarios
Asia	By the 2050s, freshwater availability in Central, South, East, and South-East Asia, particularly in large river basins, is projected to decrease. Coastal areas, especially heavily populated megadelta regions in South, East, and South-East Asia, will be at greatest risk due to increased flooding from the sea and, in some megadeltas, flooding from the rivers
Australia and New Zealand	By 2030, water security problems are projected to intensify in southern and eastern Australia and, in New Zealand, in Northland and some eastern regions
Europe	Negative impacts will include increased risk of inland flash floods and more frequent coastal flooding and increased erosion (due to storminess and sea level rise)
	Mountainous areas will face glacier retreat, reduced snow cover (in some areas up to 60 % under high emissions scenarios by 2080)
	In southern Europe, climate change is projected to worsen conditions (high temperatures and drought) in a region already vulnerable to climate variability, and to reduce water availability, hydropower potential, summer tourism and, in general, crop productivity
Latin America	Changes in precipitation patterns and the disappearance of glaciers are projected to significantly affect water availability for human consumption, agriculture, and energy generation
North America	Warming in western mountains is projected to cause decreased snowpack, more winter flooding and reduced summer flows, exacerbating competition for over-allocated water resources
Small Islands	By mid-century, climate change is expected to reduce water resources in many small islands, e.g., in the Caribbean and Pacific, to the point where they become insufficient to meet demand during low-rainfall periods

hydropower and other uses. Droughts will result from low rainfall and high temperature. Table 12 below summarizes regional impacts of climate change of water.

Energy Consumption and Greenhouse Gas Emission Characteristics of Hydropower

Water storage means energy storage. Hydropower often pays for water storage. In addition, hydropower is a kind of energy with lower energy consumption and GHGs emission which is more important under the circumstance of global attention on climate change.

Energy Payback Ratio of Hydropower

The construction and operation of energy facilities also consume energy. The concept of energy payback ratio provides a way to better measure the overall benefits of different modes of energy development and better understand the advantage of hydropower in conserving energy, reducing emission dealing with climate change.

The use of energy payback emerged with the oil crisis occurred in the early 1970s. After the oil crisis, the energy agenda began to change significantly, resulting in issues like energy independence, air quality, and later climate change (Gagnon 2008). Many countries started to explore oil substitutes. One of the key problems that became apparent was the selection of efficient energy options for growing future demand. To identify appropriate solutions, policy-makers need to consider life-cycle assessments before taking decisions. Such life-cycle assessments must include energy payback as a central component. Energy payback may be a somewhat indirect measure of overall impact, and it provides a useful perspective on the origins of the real-world impacts. Therefore, the concept of energy payback was used to evaluate energy options in the form of Net Energy Analysis (NEA) by comparing the "net energy" for different energy options on a life-cycle basis.

One way to compare different energy options is to calculate the so-called life cycle Energy Payback Ratio (EPR). This is the ratio of total energy produced during that system's normal lifespan to the energy required to build, maintain, and fuel the system. The Energy Payback Ratio of a power plant is defined as the total energy produced over the lifetime of the plant divided by the energy needed to build, operate, fuel, and decommission it. White and Kulcinski (White and Kulcinski 1999) proposed a simple equation for calculating the Energy Payback Ratio, EPR,

$$\mathrm{EPR} = \frac{\mathrm{E_{nL}}}{(\mathrm{E_{matL}} + \mathrm{E_{conL}} + \mathrm{E_{opL}} + \mathrm{E_{decL}})}$$

in which, E_{nL} is the net electrical energy produced over a given plant lifetime L; E_{matL} is the total energy invested in materials used over a plant lifetime L; E_{conL} is the total energy invested in construction for a plant with lifetime L; E_{opL} is the total energy invested in operating the plant over the lifetime L; and E_{decL} is the total energy invested in decommissioning a plant after it has operated for a lifetime L. A high ratio indicates a good performance.

According to Gagnon (Gagnon 2005), the energy payback ratio of different modes of energy development is about 208–280 for hydropower with reservoir, 170–267 for hydropower run-of-river, 18–34 for wind power, 3–5 for biological energy, 3–6 for solar energy, 14–16 for nuclear energy, 2.5–5.1 for traditional thermal power, and only 1.6–3.3 for thermal power in CO_2 capture or storage technology (Fig. 10).

Greenhouse Gas Emission of Hydropower

Hydropower is a source of energy causing the least greenhouse gas emission. The unit CO_2 emission per MW is about 941–1,022 t for traditional thermal power,

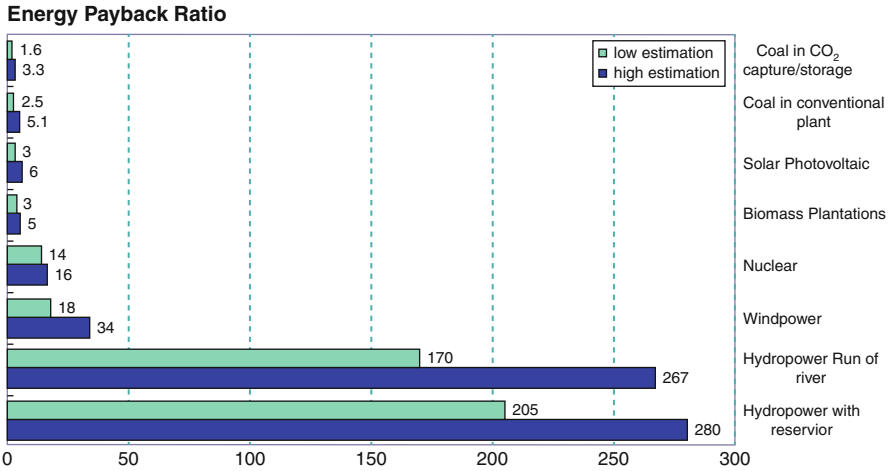

Fig. 10 Energy payback ratio by type

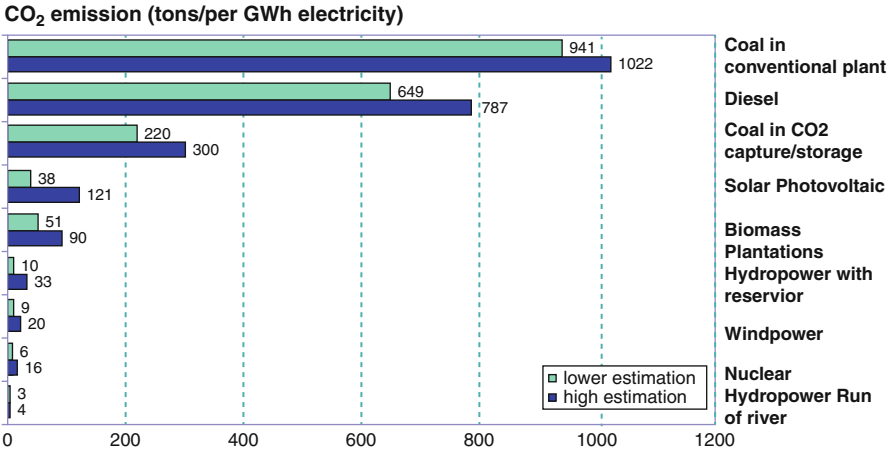

Fig. 11 Greenhouse gas emission by types

649–787 t for diesel power, 220–300 t for thermal power applying carbon recovery technology, 38–121 t for solar energy, 51–90 t for biological energy, 10–33 t for reservoir-type hydropower, 9–20 t for wind energy, 6–16 t for nuclear energy, and 3–4 t for runoff-river power, the least emission (Fig. 11).

Among various types of energies, hydropower has the highest energy pay back and lowest green house gas emission.

A Consensus on the Role of Hydropower and Dam in Adapting Climate Change has been Conducted in Wide Range by International Community

The world is faced with the problem of ever-increasing water shortage and also the problem of inadequate energy for economic development and domestic demand. For developing and undeveloped countries, which take up the majority of the world, the first task is to promote economic development and alleviate poverty. Just as Smt. Indira Gandhi (the late Prime Minister of India) said: "poverty is the worst enemy of the environment." There are 2 billion people without access to modern energy supply in the world today, 1.1 billion people without safe drinking water, 2.4 billion people in the lack of health facilities, and up to 211 million people affected by natural disasters each year. Hydropower is a source of energy renewable and capable of commercial development on a large scale. Under many circumstances, it is also an economically affordable option for poor areas to solve the issue of power supply. Large reservoirs with benefit of hydropower development are important facilities to secure safe water supply and mitigate flood/drought disasters effectively. In the twenty-first century, the world is confronted with worsening problems in sustainable development: soaring oil price, obvious consequence of climate change, and more urgent need to secure safe drinking water supply and power supply. Therefore, the demand of seek engineering solutions, for example, accelerated hydropower development and more reservoirs/dams, remains the most effective measure. To develop and utilize water and hydroenergy resources is an irresistible trend of development.

Having reviewed the issue of hydropower development again, relevant organizations in the world have raised the understanding of hydropower development to a new level at several summits and seminars of milestone significance.

The Johannesburg World Summit on Sustainable Development from August 26 to September 4, 2004 endorsed two important documents, the "Plan of Implementation" and the "Johannesburg Declaration on Sustainable Development," setting forth the indicators and timetable of renewable energy sources on the globe. This document includes:

Article 9: Take actions and improve efforts to work together at all levels to improve access to reliable and affordable energy services for sustainable development sufficient to facilitate the achievement of the Millennium development goals, including the goal of halving the proportion of people in poverty by 2015, and as a means to generate other important services that mitigate poverty.

Article 20: Develop and disseminate alternative energy technologies with the aim of giving a greater share of the energy mix to renewable energies, improving energy efficiency and greater reliance on advanced energy technologies, including cleaner fossil fuel technologies.

And the sustainable use of traditional energy resources, which could meet the growing need for energy services in the longer term to achieve sustainable development.

Diversity energy supply by developing advanced, cleaner, more efficient, affordable and cost-effective energy technologies, including fossil fuel technologies and renewable energy technologies, hydro included, and their transfer to developing countries on concessional terms as mutually agreed. With a sense of urgency, substantially increase the global share of renewable energy sources with the objective of increasing its contribution to total energy supply, recognizing the role of national and voluntary regional targets as well as initiatives, and ensuring that energy policies are supportive to developing countries' efforts to eradicate poverty.

At the conferences on drinking water, energy, health, agriculture, biodiversity, and other topics, attention is given to renewable energy likewise. It is emphasized by many that the renewable energy sources will take up 10 % of various energies by 2010 or 2015.

In October 2004, the UN Symposium on Hydropower and Sustainable Development was held successfully in Beijing and attended by the government organizations, nongovernment green environmental protection organizations, and resettler representatives from 44 advanced and developing countries, the relevant UN organizations, the World Bank, and other financial institutions. The seminar passed the "Beijing Declaration on Hydropower and Sustainable Development," which confirmed the strategic importance of hydropower to sustainable development and highlighted the sustainability of hydropower development in economic, social, and environmental aspects. This is the first discussion and summarization of the hot topics in hydropower development over the past two decades, greatly directive to hydropower development in the world.

In November 2008, the ICOLD, IHA, ICID, AU and other international organizations published the World Declaration on Hydropower (2008) (Africa) in Paris, France, stressing the importance of dam and hydropower development to the sustainable development in Africa, appealing to grasp the opportunity of hydropower development, causing the organizations which have signed the Declaration to fulfill their commitments, and assisting the African continent in joint efforts for hydropower development.

In March 2009, the Fifth World Water Forum in Istanbul adopted the Ministerial Declaration, stating that, in consideration of the difficulty in energy, food security, and poverty eradication, all countries unanimously agreed to support various water-related development projects instructed by countries to construct new infrastructures on a large scale, repair, rehabilitate, and improve existing facilities, and ensure economic feasibility, environmental sustainability and social equality, to meet various demands for water storage, irrigation, power generation, navigation, and disaster alleviation.

Prospect of Hydropower Development

Hydropower Will Play a Fundamental Role in Adapting Climate Change

Up to February 2010, approximately 57 countries, including the 23-nation European Union have set a voluntary target for reducing emissions. To fulfill the ambitious target, hydropower is regarded as the priority as long as the country still has the potential hydropower which is available to be developed. For instance:

- China will cut its carbon intensity (CO_2 emissions per unit of gross domestic product (GDP)) by 40–45 % below 2005 levels by 2020. By then, renewable energy will account for more than 15 % in primary energy. Therefore, China's efforts to increase its hydropower installed capacity to 300–350 GW in 2020 as hydropower is sole clean, renewable, and economical energy, which can be developed on large scale and from technical aspect (Shucheng 2010).
- India has pledged carbon intensity (CO_2 emissions per unit of gross domestic product (GDP)) cuts of 20–25 % by 2020 based on 2005 level. As reported, India prepares to stably increase its hydropower generation to an appropriate proportion – 40 % in national power generation (currently the proportion of hydropower is 25 %).
- Brazil has pledged absolute emissions cuts of emissions by 36–39 % from BAU by 2020. This translates to a 15–18 % reduction from 2005 level (Fransen 2009). Besides the measure to slow deforestation, abundant potential hydropower is another effective way to reach its goal.
- The EU has pledged to reduce emissions 20 % below 1990 levels by 2020. Of which, Norway is the first developed country whose CO_2 emission reduction target is line with the stipulation of Kyoto Protocol. Prime Minister Jens Stoltenberg (Stoltenberg 2007) announced to the Labor Party annual congress that Norway's GHG emissions would be cut by 10 % more than its Kyoto commitment by 2012, and that the government had agreed to achieve emission cuts of 30 % by 2020. He also proposed that Norway should become carbon neutral by 2050, and called upon other rich countries to do likewise. The country has courage to stipulate so ambitious target, mainly because 99 % of its power is from hydroelectric plant.

Prospect of Hydropower Development in the World

Against the background of striving for development and dealing with climate change, dam and hydropower development meets an exceptional opportunity and will have a new spring. All countries include hydropower development and water storage facility construction in the priority of infrastructure construction, which increases the global total amount of investment considerably. For example, the USA and China invest large amounts in rehabilitating risky reservoirs, to stimulate domestic demand and economic development while completing infrastructures. Many countries consider hydropower as a priority target of development, with ambitious development plans provided to this effect. According to the statistical data of 2007, there was a total installed capacity under construction up to 158 GW and a proposed installed capacity of 344∼461 GW in the world (Table 13).

As judged from the distribution of installed capacities by continent, the hot spot of future hydropower development is Asia, and then South America and Africa. These three continents take up 95 % of the global installed capacity under construction and 86 % of the proposed global installed capacity (Figs. 12 and 13).

Table 13 Proposed hydropower development in the world Unit (MW)

	Africa	Asia	Oceania	Europe	North America	South America	Total
Hydro capacity under construction	7,489	130,479	160	2,408	5,940	11,327	157,803
Planned hydro capacity	24,236–84,048	224,368–241,699	416–2,489	11,029–13,820	18,435–43,645	65,693–75,556	344,176–461,257

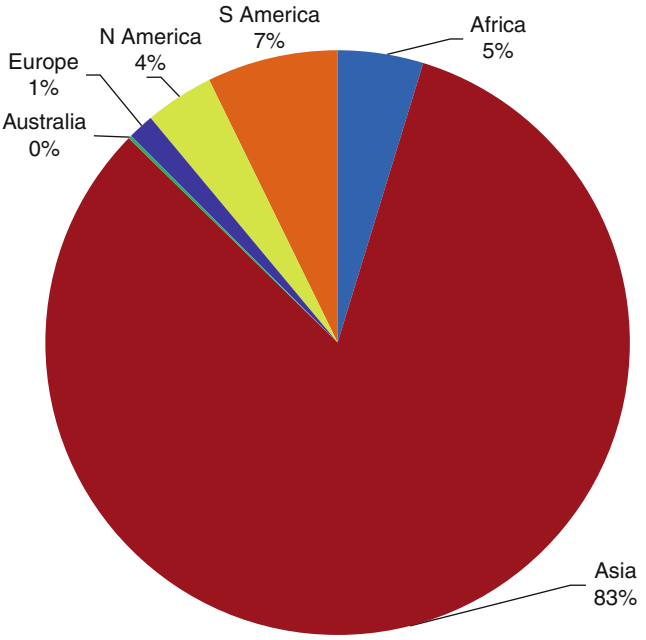

Fig. 12 Distribution of hydropower installed capacity in 2007

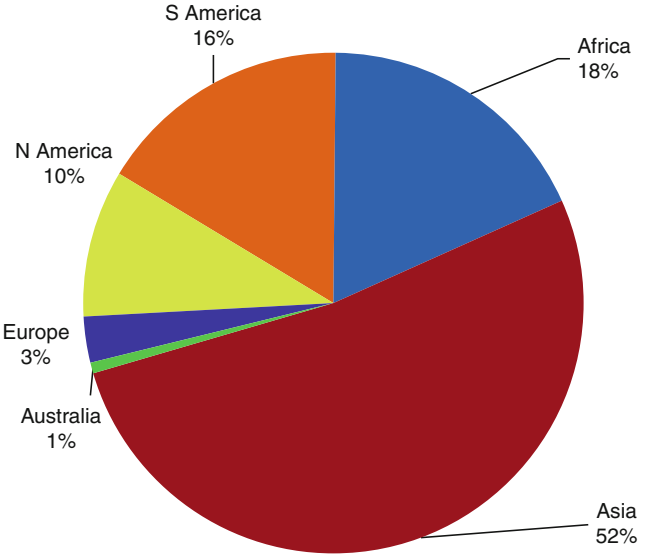

Fig. 13 Distribution of proposed installed capacity

Developing Country is Facing Tough Work to be Forehead in Adapting Climate Change

Due to the varying extent effect, climate change represents different impacts and consequences to countries in different stages of development. As Blair (Blair and Climate Group 2008) pointed out in his report, the change in climate is the same whether the emissions originate in New York or Shanghai. And of course, the most vulnerable to the impact of climate change live in the poorest area of the world. Likewise, the poor or undeveloped countries that have not caused, are not causing, and will not cause significantly more greenhouse gas emissions are responsible for the cost of climate change. They are most easily subject to the effect of climate change and their adaptability is the most vulnerable. Countries in different stages of development have different objectives and priorities of water storage facilities, and also different concerns. For less developed countries, the consequence of global climate change is often catastrophic to the extent that, due to the inadequate storage capacity, subsequent extreme weather events occur frequently and bring about worse disasters. The construction of water storage facilities is a crucial matter relating to their surviving and getting rid of poverty. Just as stated in the World Declaration on Hydropower Development (2008), a reliable electricity supply, taken for granted in many parts of the world, can be a life-saving commodity in the less developed African nations. In general, both energy and water needs are critical in these nations, so the obvious multiple benefits of hydro schemes (particularly when storage reservoirs are included) are of special significance in Africa. The effects of extreme climatic conditions (large-scale floods and regular droughts) that Africa suffers from can be vastly mitigated by dam/reservoir schemes. Naturally, the supply of clean drinking water and irrigation water to enhance food security are major additional benefits of hydro schemes. Thus, the development of water and hydropower resources is of special significance for developing countries, especially the African countries, and one of the most urgent tasks to improve the livelihood.

To Accelerate Hydropower Development Needs New Concepts

At the Session on Water Storage Facilities during the Fifth World Water Forum in March 2009, water security was defined as to maintain necessary hydrological conditions and water storage facilities for maintaining a healthy ecosystem in the climate change, ever-increasing regional socioeconomic demand (including energy demand), and other conditions. In the country with a relatively high level of water security, the problem of water will not cause any major impacts on the poor. To maintain a healthy and robust water ecosystem is greatly significant for ensuring the water security of the poor and the vulnerable groups. Therefore, one needs to know "why to do this?" "how to do," and "for whom (equality)" while constructing water infrastructures. The construction of new water storage facilities should follow the principle of sustainable development. However, the approval, investment, and implementation of new schemes should consider the protection of endangered

species, provision of information for the public and sharing of benefits by all stakeholders, including downstream ecosystem users. This definition reflects the international community's re-recognition of water security against the background of global climate change, and shows their concern about equality, poverty reduction, and other water-relating social issues in the present new situation.

Hydropower development is a practice involving water security and energy security. In the past decade or so, however, hydropower development, especially the construction of subsequent large-scale water storage facilities was subject to incisive criticism from all walks of life, and the reply and response to such criticism was still pale. As the voice of striving for development and coping with climate change runs higher and higher in the world, the voice against dam construction is weakened to some extent. This change helps creating a good international opinion for the development of water and hydroenergy resources. Nevertheless, in the twenty-first century, the construction and operation of a dam and reservoir can no longer be considered as a purely scientific and technical matter. A wide range of other aspects are involved: economic, social, and environmental. While it is clear today that water and energy schemes can be built to be safe, economic, and in harmony with the environment, mitigating environmental pacts remains a high priority for the profession, and must continue to be so. Water storage infrastructure construction must be speeded up in a sustainable way, and joint actions should be taken to minimize the adverse impacts caused by the development, and base water development and management on new concepts, to make a greater progress in maintaining man harmonious with water and man harmonious with nature. In the light of this, the following four points are critical:

First of all, the attitude to nature should shift away from simply exploiting natural resources and adopting restoration measures, but should aim to protect the natural environment at an early stage of planning;
Second, decision making should not only be based on technical and economic feasibility, but also on social equity and environmental requirement.
Third, project operation and management should not only involve traditional techniques to ensure safety, but should also play a role in protecting the ecosystem. Examples are ensuring minimum flows, and appropriate operation of reservoirs.

Finally, benefit-sharing should be more inclusive, rather than just relating to a region or state. All stakeholders should be involved. One should remember that the members related to the project have the right to benefit from a project.

Joint Efforts are Expected in a Better and Sustainable Way for Hydropower and Dam Development

The international community has made unremitting efforts and fruitful achievements in pushing forward the sustainable utilization of water and hydroenergy resources on the globe. For example, the ICOLD has issued the World Declaration on

Hydropower (Africa) (2008) together with the AU, UPDEA, IHA, ICID, and WEC. This declaration is intended to call on all the stakeholders of dam and hydropower development to engage themselves into speeding up hydropower development in Africa while being faced with the tremendous potential and the golden opportunity in Africa. Being confronted with the great potential, the ICOLD is preparing for the World Hydropower Declaration to ally all forces of the international community to push forward the course of hydropower development in Asia.

It was hardly imaginable that the supporters and opposers of dams could discuss the issue of global development peacefully. The common view regarding hydropower development on a big scale fully reflects that the demand of development is the ground of the main and common view today. Due to the complicated and global issue of climate change, the process of water and hydroenergy resources development and utilization involves numerous stakeholders. In the new century, no country or organization can meet the challenge by itself. Better communication and cooperation are needed to cope with global climate change by making great efforts to hydropower development.

Strategies of Hydropower Sector in Adapting Climate Change

Water storage infrastructure has advantages on comprehensive utilization of water and energy. The practice in many countries especially in the developing world shows water and energy development plays an important role in the context of poverty mitigation and driving socioeconomic development. The experience all over world demonstrates that water and energy can be developed in a reliable, cheap, and environmental-friendly way (Araujo et al. 2010). However, hydropower can be an effective measure to anti-climate change on the one hand; it is also sensitive and vulnerable in front of the climate change on the other as hydropower is a sector which is highly subject to the natural condition such as landform, river runoff, etc. Therefore, analyzing possible impacts and set adapting strategies are urgently needed either for energy saving and GHGs emission reduction or its own development.

Possible Impacts on Hydropower

Possible Impacts Scenarios of Climate Change on Hydropower Sector

It is certain future climate changes will pose some challenges to the hydropower industry. Depending on rate and magnitude of climate change, future impacts on the hydropower industry could be mixed. In some regions, the industry will benefit, but in some others it is likely to be adversely impacted. In both cases, the hydropower industry has to adapt to the changed climatic conditions. Three potential climate change scenarios could emerge (Mirza 2008):

- Increased frequency and magnitude of drought
- Increased frequency and magnitude of flood
- Both above

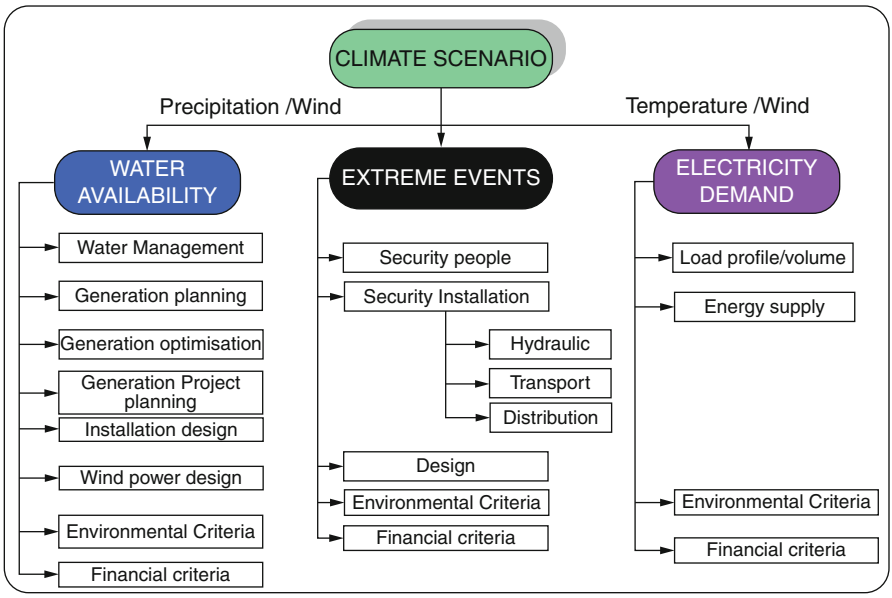

Fig. 14 Most important fields of activities in the hydropower sector that might be affected by climate change (Roy and Desrochers 2002)

In analyzing the impact of climate change on hydroelectric supply, Roy and Desrochers (Roy and Desrochers 2002) first identified the most important activities that might be affected by climate change (Fig. 14). Generally, three climate parameters, precipitation, temperature, and wind, are highly related to hydropower generation. Increases in temperature (and wind as well) result in higher evaporation, which reduce inflow and increase water losses from reservoirs.

All three factors point to less (or, at least, less flexible) hydroelectric capacity at existing powerhouses. Reduced flows in rivers and higher temperatures reduce the capabilities of thermal electric generation; high temperatures also reduce transmission capabilities.

The fields of activities can be arranged in three different groups (first-level concerns) according to the anticipated affects related to the modification of:

- The hydrological regime → water availability
- The thermal regime → electricity demand
- The occurrence of extreme events

Possible Impacts on Hydropower by Continents

The consequences will include modifications in flow seasonality and consequently hydropower. The changes in temperatures and precipitations will thus have impacts

on the runoff, which will increase by 10–40 % from 2050 in the high latitudes, and decrease by 10–30 % in the mid-latitudes (IPCC 2007a).

Changes in the average climate may not have serious impacts on hydropower for short and medium term, but extreme weather events will eventually affect hydropower generation. In the past few decades, extreme weather events have caused significant impacts on hydropower production around the world, especially in the countries of South America.

Africa

In 2007, the water level of Lake Volta, the largest man-made lake in West Africa, which normally supplies 60 % of Ghana's energy needs, was at an all times low (which is 71.65 m) 1.5 m below the critical minimum, as a result of low rainfall. The lack of water in the lake created a 300 MW power shortfall. Similar episodes were also reported in 1993 and 1994 (Mirza 2008).

Europe

Possible changes in hydropower in Europe are mixed. By the 2070s, potential may decline by 6 % overall or by 20–50 % around the Mediterranean. However, increases of 15–20 % are projected in Northern and Eastern Europe, while stable patterns are projected for Western and Central Europe (Alcamo et al. 2007).

According to the study performed by Lehner et al. (Lehner et al. 2005), the results show that, following moderate climate and global change scenario assumptions, severe future alterations in discharge regimes have to be expected, leading to unstable regional trends in hydropower potentials with reductions of 25 % and more for southern and south-eastern European countries.

The results of the analysis of the consequences of probable climate changes for the Nordic (Scandinavia) electricity system demonstrate that climate change leads to a considerable increase in hydro inflow during the winter season as well as reduced demand for heating (Mo et al. 2006). Almost all of the increase in inflow can be utilized by the hydro production system.

Australia and New Zealand

Flows in New Zealand's larger mountain-fed rivers are likely to increase benefiting hydroelectricity generation and irrigation supply (Hennessy et al. 2007).

From the early 2000s, Hydro Tasmania, operating on six major catchments on island (Australia) and having over 30 storages in these catchments has been pursuing greater insight into climate change and its potential impacts on its operations. These storages have a fill and empty cycle of approximately a decade and are used to support the hydro generation system during periods of drought and associated low inflows (Brewster et al. 2008). A review of the existing 80 years of hydrological records has shown a decline in yields especially over the past 30 years. There was a change in inflows around the 1950s with a drier period post 1950s (historical record 1924–2000).

A further catalyst to starting to explore climate change was the recent decline in inflows to the Perth water supply system in Western Australia. The records showed a

significant reduction (i.e., 38 % of long-term average) in the mid-1970s and a further reduction (70 % of long-term average) around the mid-1990s.

Asia

China's climate has witnessed significant change over the past 50 years. These changes include increased average temperatures, rising sea levels, glacier retreat, reduced annual precipitation in north and northeast China, and a significant increase in southern and northwestern China. Extreme weather and climatic events are projected to become more frequent in the future, and water resource scarcity will continue across the country. The case study of the Chaobai river in the Hai river basin, used to supply water to Beijing, demonstrated that the inflow to the Miyum reservoir had been decreasing as a result of rainfall changes and human activities in recent years. The overall runoff in the basin from 2000 to 2005 has decreased by about 66 %. Climate change projections using SRES A2 and B2 scenarios suggest that average annual temperature may increase by 2.4–2.8 °C and precipitation may increase around 4–5 % by 2050, increasing average annual inflow into the reservoir. While climate change projections indicate increased reservoir inflow in the long term, inflows may continue to decline in the medium term, according to SRES A2 scenario, necessitating adaption measures to assure adequate water supply for Beijing city (Jun 2010).

Based on the analysis of three hydropower projects in India, Sri Lanka, and Vietnam, the resulting impact on hydropower projects was indentified (Iimi 2007). Water streams discharges tend to increase with rainfall and decrease with temperature. The rainy season would likely have higher water levels, but in the lean season water resources would become even more limited. The amount of energy generated would be affected to a certain extent, but the project viability may not change so much. Comparing the three cases, it is suggested that having larger installed capacity and some storage capacity might be useful to accommodate future hydrological series and seasonality.

Tajikistan, with economically feasible hydropower potential amounts to 263 TWh/year may experience significant impact on its power output as a result of changes in river basin runoff (Cruz et al. 2007).

South America

Over the next decades, Andean intertropical glaciers are very likely to disappear, affecting water availability and hydropower generation in South America. Runoff changes from precipitation variability will also affect hydropower generation in many Latin American countries (Magrin et al. 2007). Hydropower is the main electrical energy source for most countries in Latin America, and is vulnerable to large-scale and persistent rainfall anomalies due to El Niño and La Niña, for example, in Colombia, Venezuela, Peru, Chile, Brazil, Uruguay, and Argentina. On the other hand, increased energy demand, combined with drought, caused a virtual breakdown in hydroelectricity generation in most parts of Brazil in 2001, contributing to a GDP reduction of 1.5 % or about US$10 billion.

However, the results found are fundamentally dependent on the climate projections which, in turn, are still highly uncertain with respect to the future evolution

of greenhouse gas emissions, greenhouse gas concentrations in the atmosphere, and global climate change (GCC) (Pereira de Lucena et al. 2009).

North and Central America

In the USA, hydropower yields in the Colorado River will likely decrease significantly. Diminished snowmelt runoff could lead to a decrease in the potential hydropower production, which now comprises about 15 % of California's in-state electricity production. If temperature rises to the medium warming range and precipitation decreases 10–30 %, hydropower output may be reduced up to 30 %. It has to be noted, there is uncertainty in future precipitation projections. It is also possible that precipitation may increase and expand hydropower production potential (California Climate Center (CCC) 2006).

In 2001, prolonged droughts caused the water levels in the Great Lakes to fall, resulting in significant reduction in hydropower generation at both the Niagara and Sault St. Marie power stations in Canada (Field et al. 2007). A similar low flow in 1965 caused a 20 % decrease in generation (Mirza 2004, 2008). In the Columbia river basin, runoff required for hydropower generation in the summer will likely conflict with other environmental needs.

Prognosis for the Pacific Northwest (PNW) hydropower supply under climate change has been worse than anticipated (Markoff and Cullen 2008). Differences between the predictions of individual climate models are found to contribute more to overall uncertainty than do divergent emissions pathways. Uncertainty in predictions of precipitation change appears to be more important with respect to impact on PNW hydropower than uncertainty in predictions of temperature change.

The management adaptation potential of the Peribonka River water resource system (Quebec, Canada) is investigated in the context of the evolution of climate change. The main results indicate that annual mean hydropower would decrease by 1.8 % for the period 2010–2039 and then increase by 9.3 % and 18.3 % during the periods 2040–2069 and 2070–2099, respectively. Overall, the reliability of a reservoir would decrease and the vulnerability increase as the climate changes (Minville et al. 2009).

Hydropower generation will be affected by changes in water availability, particularly in snowmelt-dominated basins, where impacts have already been reported. Hydropower production at facilities that are operated to meet multiple objectives (e.g., flood-risk reduction, irrigation, municipal and industrial water supply, navigation, in-stream flow augmentation, and water quality) may be especially vulnerable to changes (Brekke et al. 2009).

Adapting Strategies

In this context, adaption (Fig. 15) of the hydropower industry to climate change may not be simple and straightforward.

Many hydropower reservoirs and their operating criteria have been built based on the largest single observed or modeled event. But in the future, both magnitude and

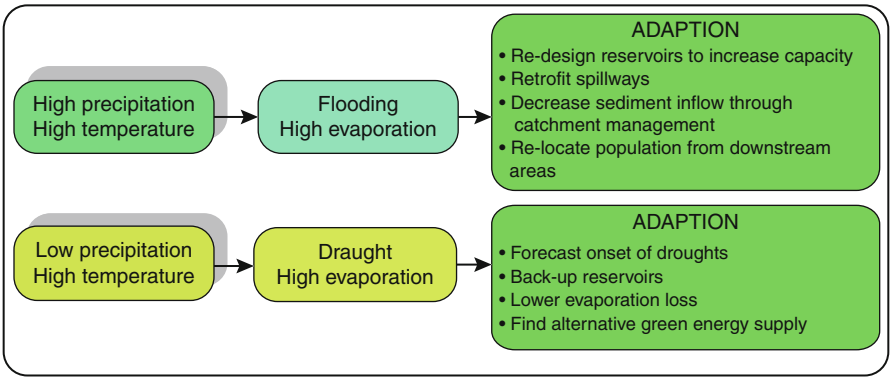

Fig. 15 Possible future scenarios and adaption options (Mirza 2008)

frequency of extreme events is likely to increase. So hydropower reservoirs may not be able to hold extra water or be able to generate electricity in the case of a rapid drop in water level caused by a drought triggered by the failure of rainfall. Retrofitting of spillways or redesigning reservoirs to increase capacity may be possible options. However, in many cases, retrofitting could be expensive and therefore not feasible. The economic and engineering lifecycles of many hydropower projects either recently built or under construction are within the time lines of climate change.

Another major potential obstacle is mainstreaming climate change into policy planning. Hydropower planners often talk about the uncertainty of scenarios projected by the climate models. Many studies of climate change impacts use the output of one or several global climate models (GCM) to project future climate. GCM temperature and precipitation output and historical records are used as input to a hydrologic model to derive stream flow. For instance, if the river is a managed system with reservoirs, a water management or optimization model may be used to model reservoir operating rules. Figure 16 is a schematic of this methodology.

Those modeling climate agree with uncertainty of scenarios, but that does not mean the planners should not act until the level of uncertainty becomes smaller than at present. For future adaption, one solution could be to use a range of scenarios to capture the uncertainty.

The hydropower sector usually relies on historical hydrometeorological time series for operational strategies and future investment planning. Potential global warming affects global precipitation patterns and enhances melting of glaciers, which in turn affect seasonal runoff. Assuming future flows as stationary extension of measured runoff series is no longer a probable scenario in a warming climate. There is need for developing mechanisms for adjustment of historical time series based on historical and possible future climate trends. These adjustments need to take into account the time frame of possible scenarios or planning horizons. Different methods for sophisticated risk analysis accounting for climate change must be explored and extensively used (Sveinsson et al. 2008).

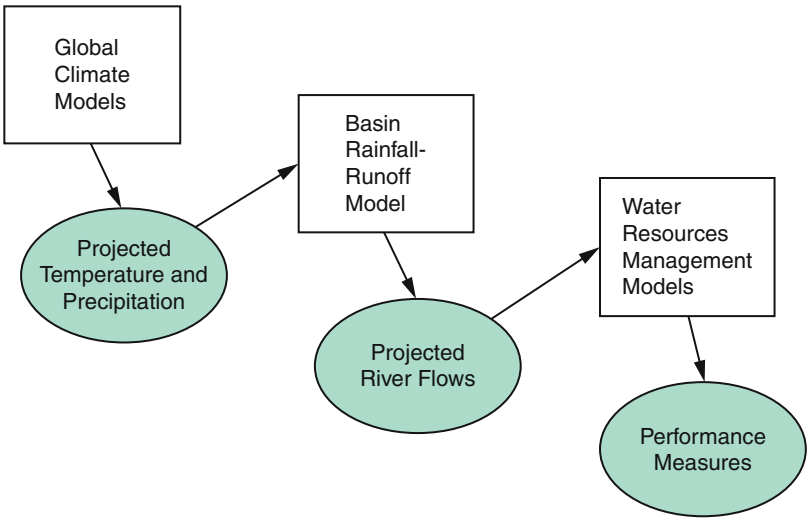

Fig. 16 Schematic for climate change impact studies for water resources (Western States Water Council (WSWC) 2009)

New Emerging Hydropower Technologies

The studies and the values of the World Energy Council (2004), the International Hydropower Association, and the European Small Hydropower Association clearly show us that the usage of hydropower will certainly change within the next 20–50 years. Some countries will increase their amount of hydroelectricity produced, whereas in other countries less water will be available. Therefore, new hydropower technologies are being actively tested in a number of countries.

There are many small dams in the world and the majority of them do not have a hydropower component. While this is not always an economic option, there is a significant market niche of this "sleeping" hydro potential in this area. Energy potential can be recovered by installing hydropower plants in irrigation, drinking water networks or even water treatment, and navigation waterways infrastructure. For such schemes, electricity generation is not the first priority, but the second (ESHA 2010).

Electric power is also being developed from nontraditional water sources (also called "hydrokinetics"), including river and ocean currents. The basic concept behind hydrokinetic power is not new. For centuries, people have harnessed the power of river currents by installing water wheels of various sorts to turn shafts or belts. River current energy conversion systems are electromechanical energy converters that convert kinetic energy of river water into other usable forms of energy. Over the past few decades, a number of reports on technical and economic feasibility of this technology have emerged (Khan et al. 2008). Installation of instream (kinetic) turbines directly in rivers, without a dam or other impoundment may provide an effective alternative means for generating power. Such systems would potentially

require little or no civil work, cause less environmental impact, and may possess significant economic value. However, the potentials of this technology as an effective source of alternative energy have not yet been explored to a great extent.

Ocean or marine energy using offshore plants also can also be attributed to hydropower. There are five main technologies, such as tidal power plants, current power plants, wave power plants, sea warmth power plants, and osmotic power plants, which could be used in future to produce electricity.

The data on hydrokinetic potential worldwide are still very preliminary. Estimates in the USA have ranged from minimums of 23 GW to maximums of 400 GW (Kosnik 2008). An independent market assessment estimated the worldwide potential of ocean wave energy economic contribution in the electricity market to be in the order of 2,000 TWh/year and is comparable to the amount of electricity currently produced worldwide by large-scale hydroelectric projects. According to Pike Research's study, "Hydrokinetic and Ocean Energy" (2009), in the best scenario case, the ocean energy industry could yield global power generation capacity of up to 200 GW by 2025.

In 2009, the USA had installed hydrokinetic generation capacity of less than 1 megawatt (MW), as compared to more than 77,000 MW of conventional hydroelectric generation capacity. Many hydrokinetic development projects are underway in the USA – as of 2009, the Federal Energy Regulatory Commission (FERC) has issued 146 preliminary applications to study development of 9,000 MW of proposed hydrokinetic generation capacity. Most of them are inland river projects and around half are designated to hold free flow power on the Missouri and Mississippi Rivers (Center 2009).

Any potential power will be located primarily along the coasts, where current wave and tidal prototypes are being employed, but future hydrokinetic technologies will also take advantage of the wave power in streams and rivers. This will benefit many of the inland states. First commercial projects of wave energy have been recently commissioned in Portugal, Scotland, and other countries.

Conclusion and Future Directions

Climate change is regarded as the most severe challenge for the human being. The view on accelerating hydropower development and ensuring adequate water storage infrastructure to mitigate and adapt climate change has been widely accepted by international community. In view of water storage capacity or hydropower development, a developed country has well conducted a complete network whereas developing country is facing tough work to be forehead. Many countries stipulate ambitious plan to accelerate hydropower development in order to fulfill their voluntary target for reducing emissions. It can be expected that hydropower development will have a great leap forward in the future.

However, in the new century, the construction and operation of a dam, reservoir, or a hydro plant can no longer be considered as a purely scientific and technical matter on the one hand and become more open and transparent on the other. The

inquiry and criticism on large-scaled water infrastructure are kept receiving from various paths, whereas the response on it is inadequate. To eliminate the misunderstanding and get support for further development at global scope, cooperation among various stakeholders, government authorities, knowledge institutions, business companies, civil societies, and local communities is the key to the development and implementation of effective and sustainable water solutions.

References

Alcamo J, Moreno JM, Nováky B, Bindi M, Corobov R, Devoy RJN, Giannakopoulos C, Martin E, Olesen JE, Shvidenko A (2007) Europe. In: Parry ML, Canziani OF, Palutikof JP, van der Linden PJ, Hanson CE (eds) Climate change 2007: impacts, adaptation and vulnerability. Contribution of working group II to the fourth assessment report of the intergovernmental panel on climate change. Cambridge University Press, Cambridge, pp 541–580

Araujo JL, Rosa LP, Silva NF (2010) Hydroelectricity: future potential and barriers. In: Sioshansi F (ed) Generating electricity in a carbon-constrained world. Elsevier, San Diego, pp 324–344

Berga L (2008) Dam for sustainable development. In: Proceedings of high-level international forum on water resources and hydropower, Beijing, pp 1–6

Blair T, Climate Group (2008) Breaking the climate deadlock: a global deal for our low-carbon future. The Climate Group, London

Brekke LD, Kiang JE, Olsen JR, Pulwarty RS, Raff DA, Turnipseed DP, Webb RS, White KD (2009) Climate change and water resources management – a federal perspective. US Geological Survey Circular 1331, 65 pp. http://pubs.usgs.gov/circ/1331/

Brewster M, Ling F, Connarty M (2008) Climate change response from a renewable electricity business. In: Proceedings of the international conference HYDRO 2008. The International Journal on Hydropower and Dams, 6–8 Oct 2008, Slovenia

California Climate Center (CCC) (2006) Our changing climate. Assessing the risks to California. A summary report. California. http://meteora.ucsd.edu/cap/pdffiles/CA_climate_Scenarios.pdf

Cruz RV, Harasawa H, Lal M, Wu S, Anokhin Y, Punsalmaa B, Honda Y, Jafari M, Li C, Huu Ninh N (2007) Asia. In: Parry ML, Canziani OF, Palutikof JP, van der Linden PJ, Hanson CE (eds) Climate change 2007: impacts, adaptation and vulnerability. Contribution of working group II to the fourth assessment report of the intergovernmental panel on climate change. Cambridge University Press, Cambridge, pp 469–506

EIA (2008) Energy Information Administration international statistics database. http://www.eia.doe.gov/

ESHA, MHylab (2010) Energy recovery in existing infrastructures with small hydropower plants. Multipurpose schemes – overview and examples. The 6th EU Framework Programme for Research and Technological Development, SHAPE project. http://www.esha.be/index.php?id=97

ESHA, LHA, SERO (2008) Strategic study for development of Small Hydropower in the European Union. SHERPA project. Intelligent Energy Europe. http://www.esha.be/index.php?id=80

Field CB, Mortsch LD, Brklacich M, Forbes DL, Kovacs P, Patz JA, Running SW, Scott MJ (2007) North America. In: Parry ML, Canziani OF, Palutikof JP, van der Linden PJ, Hanson CE (eds) Climate change 2007: impacts, adaptation and vulnerability. Contribution of working group II to the fourth assessment report of the intergovernmental panel on climate change. Cambridge University Press, Cambridge, pp 617–652

Fransen T (2009) Brazil pledges ambitious emissions reductions. http://www.wri.org/stories/2009/11/brazil-pledges-ambitious-emissions-reductions

Gagnon L (2005) Energy payback ratio. Hydro-Québec, Montreal

Gagnon L (2008) Civilisation and energy payback. Energy Policy 36(9):3317–3322

Hennessy K, Fitzharris B, Bates BC, Harvey N, Howden SM, Hughes L, Salinger J, Warrick R (2007) Australia and New Zealand. In: Parry ML, Canziani OF, Palutikof JP, van der Linden PJ, Hanson CE (eds) Climate change 2007: impacts, adaptation and vulnerability. Contribution of working group II to the fourth assessment report of the intergovernmental panel on climate change. Cambridge University Press, Cambridge, pp 507–540

Hydropower resource assessment of Africa. In: Ministerial conference on water for agriculture and energy in Africa: the challenges of climate change, Sirte, Libyan Arab Jamahiriya, 15–17 Dec 2008

IEA, OECD (2003) Renewables in Russia – from opportunity to reality. The International Energy Agency (IEA), Paris

Iimi A (2007) Estimating global climate change impacts on hydropower projects: applications in India, Sri Lanka and Vietnam. Policy Research working paper 4344. Sustainable Development Network Finance, Economics, and Urban Development Department, The World Bank

IPCC (2007) Summary for policymakers. In: Parry ML, Canziani OF, Palutikof JP, van der Linden PJ, Hanson CE (eds) Climate change 2007: impacts, adaptation and vulnerability. Contribution of working group II to the fourth assessment report of the intergovernmental panel on climate change. Cambridge University Press, Cambridge, pp 7–22

IPCC (2007) Climate change 2007. Synthesis report. An assessment of the intergovernmental panel on climate change

Jun X (2010) Screening for climate change adaption: impacts and challenges for China. Int J Hydropower Dams 17(2):78–81

Khan MJ, Iqbal MT, Quaicoe JE (2008) River current energy conversion systems: progress, prospects and challenges. Renew Sustain Energy Rev 12:2177–2193

Kosnik L (2008) The potential of water power in the fight against global warming in the US. Energy Policy 36:3252–3265

Lehner B, Czisch G, Vassolo S (2005) The impact of global change on the hydropower potential of Europe: a model-based analysis. Energy Policy 33(7):839–855

Magrin G, Gay García C, Cruz Choque D, Giménez JC, Moreno AR, Nagy GJ, Nobre C, Villamizar A (2007) Latin America. In: Parry ML, Canziani OF, Palutikof JP, van der Linden PJ, Hanson CE (eds) Climate change 2007: impacts, adaptation and vulnerability. Contribution of working group II to the fourth assessment report of the intergovernmental panel on climate change. Cambridge University Press, Cambridge, pp 581–615

Markoff MS, Cullen AC (2008) Impact of climate change on Pacific Northwest hydropower. Clim Change 87:451–469

Milly PCD, Dunne KA, Vecchia AV (2005) Global pattern of trends in streamflow and water availability in a changing climate. Nature 438(7066):347–350

Minville M, Brissette F, Krau S, Leconte R (2009) Adaptation to climate change in the management of a Canadian water-resources system exploited for hydropower. Water Resour Manag 23 (14):2965–2986

Mirza MMQ (2004) Climate change and the Canadian Energy sector. Report on vulnerability, impacts and adaption. Adaptation and Impacts Research Group (AIRG), Environment Canada, Toronto

Mirza MMQ (2008) Climate change, water and implications for hydropower. Int J Hydropower Dams 15(1):85–89

Mo B, Doorman G, Grinden B (2006) Climate change consequences for the electricity system. Analysis of the Nord Pool system. Climate and Energy Report CE-5. 159 pp. Hydrological Service, Norden Nordic Energy Research, Reykjavik

Pelikan B (2005) SHP engineering: a new approach and a key for the future. Int J Hydropower Dams 12(3):57–60

Pereira de Lucena AF, Salem Szklo A, Schaeffer R, Rodrigues de Souza R, Borba BSMC, Leal V, da Costa I, Olimpio Pereira A, Ferreira da Cunha SH (2009) The vulnerability of renewable energy to climate change in Brazil. Energy Policy 37:879–889

PEW Center (2009) Hydrokinetic electric generation. Climate TechBook. http://www.pewclimate.org/technology/factsheet/Hydrokinetic

Roy R, Desrochers G (2002) Hydro-Quebec coping with climate change anticipated effects. Interim Thematic Report for the Dialogue on Water and Climate, Quebec

Shucheng W (2010) China needs more hydropower projects to fight climate change. http://news.xinhuanet.com/english2010/china/2010-02/27/c_13190972.htm

Stoltenberg J (2007) Speech to the congress of the Labour Party. http://www.regjeringen.no/en/dep/smk/Whats-new/Speeches-and-articles/statsministeren/statsminister_jens_stoltenberg/Speech-at-Trafalgar-Square-London/Speech-to-the-congress-of-the-Labour-Par.html?id=463749

Sveinsson OGB, Elíassson EB, Linnet Ú (2008) The hydropower sector and climate change adaptation. In: Proceedings of the international conference HYDRO 2008. The International Journal on Hydropower & Dams, 6–8 Oct 2008, Slovenia

UNESCO (2009) The United Nations world water development report – water in a changing world. UNESCO, New York

US Department of Energy (2006) Feasibility assessment of the water energy resources of the United States for new low power and small hydro classes of hydroelectric plants. http://hydropower.inl.gov/resourceassessment/index.shtml

Western States Water Council (WSWC) (2009) Western States. Climate change and reservoir rule curves. www.westgov.org/wswc/appendices/appendix%20e_climate%20c

White SW, Kulcinski GL (1999) "Birth to Death" analysis of the energy payback ratio and CO_2 gas emission rates from coal, fission, wind and DT fusion electrical power plants. UWFDM-1063. University of Wisconsin-Madison

World Declaration Dams & Hydropower (2008) Paris

World Energy Council (2004) Comparison of energy systems using life cycle assessment: a special report for world energy council. World Energy Council, London

Zhou S, Zhang X, Liu J (2009) The trend of small hydropower development in China. Renew Energy 34:1078–1083

Nuclear Energy and Environmental Impact

K. S. Raja, B. Pesic, and M. Misra

Contents

K.S. Raja (✉) • B. Pesic
Chemical and Materials Engineering, University of Idaho, Moscow, ID, USA
e-mail: ksraja@uidaho.edu; raja.echem@gmail.com; pesic@uidaho.edu

M. Misra
Department of Metallurgical Engineering, University of Utah, Salt Lake City, UT, USA
e-mail: misra@unr.edu

W.-Y. Chen et al. (eds.), *Handbook of Climate Change Mitigation and Adaptation*,
DOI 10.1007/978-3-319-14409-2_30

Abstract

Nuclear energy is attracting revived interest as a potential alternate for electric power generation in the event of increased concerns about global warming. Compared to energy produced by combustion of a carbon atom in coal, fission of a U-235 atom will produce about 10 millions times more energy. However, storage of the nuclear waste is an environmental issue. This chapter has four sections with a major focus on introduction of nuclear power plants and reprocessing of spent nuclear fuels. Different nuclear fuel cycles and nuclear power reactors are introduced in the first section, and the cost–benefits of different energy sources are compared. Fuel burnup and formation of fission products are discussed along with operational impacts and risk analyses in the second section. The third section discusses design of nuclear structural components and various degradation modes. Section four discusses reprocessing issues of nuclear spent fuels. Reprocessing of spent nuclear fuel may be an economically viable option and reduces high-radioactive load in the nuclear waste repositories as well. However, there is a concern about proliferation of weapons-grade plutonium separated during reprocessing. Containment of radionuclides in different waste forms is also discussed in this section.

Introduction to Nuclear Energy

Radioactive decay of heavy metals such as uranium, plutonium, thorium, etc., can be converted into a useful energy form. Radioactivity occurs by emission of charged particles (such as α and β) and electromagnetic waves (γ ray). For heavier nuclei (elements with atomic number>40), more neutrons are required for a stable configuration so that the electrostatic repulsion force between the protons can be overcome (Jevremovic 2005). When the nucleus has too many or too few neutrons, it will be in a nonequilibrium condition. In order to reach a stable configuration, the nucleus undergoes a spontaneous transformation by rearranging its constituent particles. This is accomplished by the emission of an alpha particle, a beta particle (either β− or β+), a neutron, or a proton. Depending on the energy conservation, gamma radiation may or may not be present during the radioactive decay. In brief, when atoms containing nuclei in the nonequilibrium condition try to reach stable condition, the excess energy of the nuclei is emitted as radiation. In this process, the material disintegrates. According to Einstein's principle ($E = mc^2$), the disintegrated matter is converted into energy. For example, burning of 1 kg of uranium in a nuclear reactor results in conversion of 0.87 g of matter into energy which amounts to $(0.8 \times 10^{-3}\ \text{kg}) \times (3.0 \times 10^{8}\ \text{m/s})^2 = 7.8 \times 10^{13}$ J. For comparison, combustion of 1 kg of gasoline will release only 5×10^{7} J of energy, six orders of magnitude smaller than 1 kg of uranium (Murray 2001). In addition to high specific energy, the nuclear energy has an advantage of not releasing carbon dioxide into the atmosphere. Combustion of 1 kg of gasoline will release about 3.2 kg of carbon dioxide to the environment. An anthracite coal–based power plant will release about 1.2 kg of CO_2

for every KWh electricity generated, whereas the lifetime CO_2 emission of nuclear power plants, considering the electricity used for mining and processing operations from fossil fuel power plants, will be 100–140 g of CO_2 /kWh electricity generated (Storm van Leeuwen and Smith 2005).

The major advantages of nuclear energy are:

High specific energy
No CO_2 emission
Spent fuel can be reprocessed and reused, thus conserving natural resources
Possibility to produce more nuclear fuel than consumed by using fast breeder reactors
Lower operating cost in terms of fuel cost compared to fossil fuel power plants

Disadvantages are:

- Large capital cost and longer construction time of power plants
- Long-term storage of nuclear waste which is an issue
- Exposure to radioactivity in case of accidents
- Potential proliferation of weapons-grade fuel during reprocessing

Nuclear power plants attract more safety and environmental concerns from the public than other power plants. This chapter addresses some of the environmental issues associated with nuclear power generation. The first three sections introduce nuclear fuel cycles, nuclear power reactors, and issues on operational safety. Information on nuclear spent fuels reprocessing, waste management, and long-term storage is given in the last section.

Nuclear Fuel Cycles

Conversion of nuclear energy can be achieved by fission or fusion reactions. Most of the commercial nuclear power reactors operate based on nuclear fission reaction. The average energy of neutrons used for power generation is about 0.1 eV, which are called thermal neutrons. Neutrons that have energy in the order of 2 MeV are called fast neutrons. Uranium is the most common fissile material used in the nuclear reactors. Naturally mined uranium has 99.24 % U-238, 0.72 % U-235, and 0.0054 % U-234. U-235 is a fissile isotope. Fissile isotopes are the ones that undergo fission reaction upon absorption of slow neutrons (neutrons having energy <0.4 eV). When a neutron is absorbed by U-235, the isotope gains extra energy and transforms to U-236 in an excited state (Murray 2001):

$$^{235}_{92}U + ^{1}_{0}n \rightarrow ^{235}_{92}U* \quad (1)$$

Since the excited U-236 has a higher mass than U-236 in ground state, the difference in mass is converted into energy of 6.54 MeV. Each fission of U-235 yields about

190 MeV of useful energy. This energy is used for further fission reaction. A continuous and self-sustaining fission chain reaction is required for nuclear power generation. This is achieved by containing a critical mass of uranium, which is about 50 kg of U-235 in the nuclear reactor. For each megawatt-day of thermal energy, 1.3 g of U-235 is consumed (Knief 1992).

The natural isotope U-235 and artificial isotopes such as Pu-239 and U-233 require only slow (thermal) neutrons to induce fission. On the other hand, U-238, which is abundant in nature, can only be activated by fast neutrons of at least 0.9 MeV to initiate fission. If the fission occurs by thermal or slow neutrons, the material is considered as "fissile." If a material is converted into a "fissile" material by irradiation, then that material is classified as a "fertile" material. For example, fertile materials such as U-238 and Th-232 can be used for generating "fissile" materials such as Pu-239 and U-233, respectively, by the following neutron reactions (Murray 2001):

$$^{238}_{92}U + {}^{1}_{0}n \rightarrow {}^{239}_{91}U \rightarrow {}^{239}_{93}Np + {}^{0}_{-1}e \rightarrow {}^{239}_{94}Pu + {}^{0}_{-1}e \tag{2}$$

$$^{232}_{90}Th + {}^{1}_{0}n \rightarrow {}^{233}_{90}Th \rightarrow {}^{233}_{91}Pa + {}^{0}_{-1}e \rightarrow {}^{233}_{92}U + {}^{0}_{-1}e \tag{3}$$

Nuclear fuel cycle describes different stages of preparation, use, safe storage, and reprocessing of the spent fuel. The fuel cycle starts by mining of fuel ore and ends by reprocessing. If reprocessing is not carried out, then it is called as once-through nuclear cycle. The fuels that can be used in the nuclear power reactors are uranium, plutonium, minor actinides, and thorium. Most of the commercial nuclear reactors use uranium as a fuel with different levels of enrichment depending on the type of reactor. Thorium is also used in some countries at a small scale. This section will focus on only these two fuels.

Uranium Fuel Cycle

Mining and Extraction: Uranium ore is mined in several forms, most notably as uranite (UO_2), pitchblende ($UO_3 + U_2O_5$), coffinite ($U(SiO_4)_{1-x}(OH)_{4x}$), brannerite (UTi_2O_6), davidite ($REE(Y,U)(Ti,Fe)_{20}O_{38}$; REEs = rare earth elements), and thucolite (U-containing pyrobitumen) (Dahlkamp 1993). Uranium mining process is similar to mining of other metals such as copper, gold, etc. The mines can be of open-pit or underground type. In some cases, in situ leaching of ore is carried out without deep excavating of the earth. Lower-grade ores are concentrated by using a heap leaching process. The excavated ores are collected as heaps and a leaching agent (mostly low concentration of sulfuric acid) is sprayed on the heaps and drained through the ore collection. In this process, uranium is preferentially leached out of the oxide ore and carried by the draining leaching agent. This solution is further processed.

In situ leaching process is used by some mining companies. In this process, the surface of the earth is not disturbed by drilling or excavating operations. Instead, a leaching agent (mild acid/alkaline solution containing oxidizers such as hydrogen peroxide) is pumped through the porous surface of the ore deposits. The solution

passing through the ore will leach out the uranium. The uranium-containing solution is collected for further processing.

During heap leaching and in situ leaching processes, the surrounding groundwater is continuously monitored for any contamination. Even after shutdown of the mining operation, the monitoring continues. Recent international mining laws require that the mining companies set aside required amount of funds for reclamation of the environment in the neighborhood of the mining operation. This fund will be in place for the required environmental remediation even if the company goes out of business.

The uranium-rich ore from mill, U_3O_8, often called as yellow cake though the actual color is khaki, is purified further either by a solvent extraction or by an ion exchange process. The U_3O_8 is dissolved in nitric acid to form uranyl nitrate ($UO_2(NO_3)_2$), which is then treated with ammonia to produce ammonium diuranate ($(NH_4)_2U_2O_7$). This compound is then reduced in a hydrogen atmosphere to form uranite (UO_2). It should be noted that this UO_2 is not the final form of fuel that can be used in the reactor. It requires enrichment of U-235 isotope to more than 3.5 % from 0.7 %. In order to accomplish the enrichment process efficiently, the material needs to be in the form of a gas. Therefore, UO_2 should be first converted to uranium hexafluoride gas (UF_6), get enriched, and converted back to UO_2. In order to form UF_6, UO_2 is treated with HF, which results in UF_4. Further fluorination of UF_4 renders UF_6. Now the UF_6 is taken for enrichment process (Morss et al. 2006).

Enrichment of Uranium

U-235 is a fissile material that utilizes thermal neutrons, which is only 0.7 % in the natural uranium source. Stable operation of a critical reactor requires fissile nuclei. Therefore, the ratio between fissile (U-235) and nonfissile (U-238) should be high in a reactor for stable power generation. Typically, the U-235 content in a fuel should be more than 3.5 %. This can be achieved by the following enrichment methods (Krass et al. 1983):

- Gaseous diffusion
- Gas centrifuge
- Jet nozzle/aerodynamic separation
- Electromagnetic separation

Gaseous Diffusion

Separation of U-235 isotope by gaseous diffusion process occurs because of the difference in velocity of the gas molecules. The rate of diffusion of a gas through an ideal porous medium is inversely proportional to the square root of the molecular weight of the gas. Therefore, when UF_6 is passed through a porous tube, lighter U-235 isotopes will escape the porous container faster than their U-238 counterparts and thus be collected separately. Figure 1 schematically illustrates the working principle of a gas diffusion separator. In this arrangement, compressed UF_6 gas is contained in a large vessel under pressure and allowed to pass through a porous channel that acts as a diffusion barrier layer. The porous layer is an essential

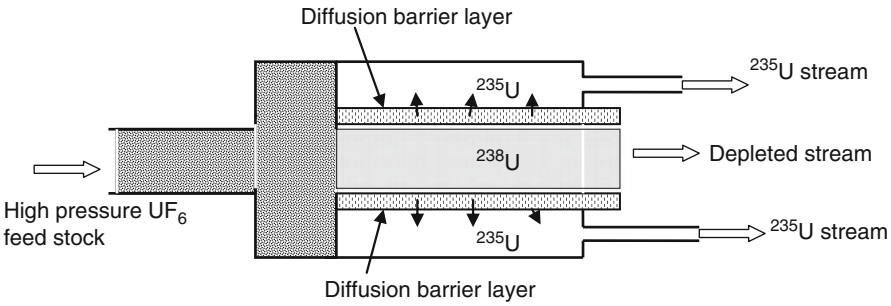

Fig. 1 Uranium enrichment by gaseous diffusion process

component of the diffusion separator because the efficiency of the U-235 enrichment process in the UF_6 stream is determined by the ability of the porous layer permeating the gas molecules. The barrier layer has to withstand the working pressure and be stable in the corrosive UF_6 atmosphere, and the pores should be tiny, in the order of 30–300 times the diameter of a single U atom, around 10 nm, and uniformly distributed in the order of billions per square centimeter area. The barrier layer thickness is around 5–6 mm. The material of construction is a classified information because enrichment of U-235 to more than 80 % becomes a weapons-grade material. Plasma-sprayed Zr, Ta, and Mo coatings of required thickness and porosity can be used as diffusion layer. Silver–zinc alloy pipes after selective etching with HCl also could serve as a diffusion barrier (Makhijani et al. 2004).

Since the velocity of diffusion varies only by 0.4 % between U-238 and U-235, multiple stages of gas passage are required to achieve the required enrichment for commercial reactors. In the diffusion cascade, the outlet of the depleted stream is bifurcated by redirecting 50 % of the depleted stream back to the previous stage and the remaining 50 % to the inlet of the next stage. This way one may require 4000 diffusion stages to obtain 99 % $^{235}UF_6$.

Gas Centrifuge

In this process, UF_6 is passed through rapidly spinning cylinders in series. The centrifugal action drives the heavier $^{238}UF_6$ molecules to the wall of the rotating container. Lighter $^{235}UF_6$ molecules are retained closer to the center of the container. Circulation of the gas from bottom to top helps separate the heavier and lighter molecules and pass to next separation stages. Figure 2 schematically illustrates the gas centrifuge (Olander 1978).

The cylinders are heavy in order to impart very high kinetic energy to the gas molecules and rotated at very high speed, in the order of 100,000 revolutions per minute. The linear velocity may approach the speed of sound in the material of construction. Therefore, the centrifuges are very sturdy. Nevertheless, this process requires 40–50 times less energy than the gaseous diffusion process to achieve the same level of enrichment. The diffusion process will consume about 4–5 % of the energy that the enriched fuel will generate in its cycle time. Furthermore, amount of

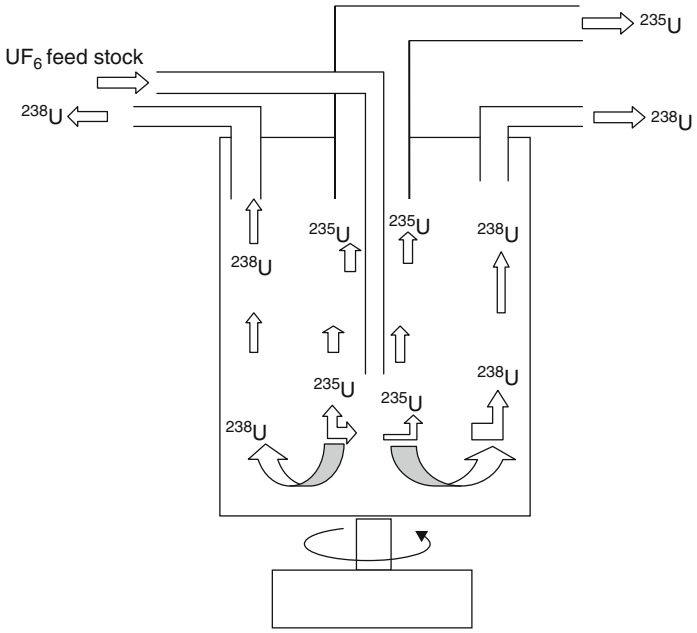

Fig. 2 Schematic of gas centrifuge for enrichment of U-235

waste heat generated during UF_6 compression for the diffusion process is much higher. This results in utilization of a significant amount of coolants such as Freon-12, etc., in order to cool the gas in the intermediate compression stages. Gas centrifuge process is more advantageous than gas diffusion process considering aforementioned issues.

Electromagnetic Isotope Separation

This process can be used as a stand-alone method for enriching uranium from the feedstock of natural uranium or in tandem with the gaseous diffusion process for producing highly enriched uranium from the low-enriched stream. It should be noted that commercial reactors do not require highly enriched uranium. The electromagnetic separator works on the principle that the radius of the trajectory of a particle traveling in a magnetic field is determined by its mass. The heavier the particle, the larger will be the radius, provided that the particles have the same charge and travel at the same speed. In this process, UCl_4 plasma is generated by heating a solid UCl_4 material and bombarding it with high-energy electrons. This process ionizes uranium. The uranium ions are then accelerated through a strong magnetic field. When these ions complete a half circle, the lighter U-235 ions are nearer to the inside wall of the semicircle channel, and heavier depleted U-238 ions are separated at the outer wall of the circular channel. This process requires a large amount of energy to maintain a high magnetic field. However, the rate of U-235 separation is lower than the other processes (Knief 1992).

Jet Nozzle/Aerodynamic Separation

In this process, UF_6 is pressurized with helium or hydrogen gas and sent through a bank of small circular pipes. The curved pipelines ensure that the heavier molecules stay at the outer surface and lighter U-235 stay at the inner surface of the circular path. This process is again energy intensive because compressing lighter gases such as He and H requires more energy. The compression process will be carried out at multiple stages with intercoolers in order to increase the thermal efficiency of the system. Therefore, the entire process results in generation of a significant amount of waste heat and utilization of a large amount of coolants/refrigerants, and both these outcomes lead to environmental concerns (Olander 1978).

Conversion of UF_6 to UO_2

The enriched UF_6 gas stream with 3.5 % U-235 is taken for fuel rod preparation. The first step is conversion of UF_6 back to UO_2. Oxide fuel is preferred because of its high melting point that shows resistance for meltdown. Metallic fuels (in the form of U or its alloys such as U–Mo, U–Si, U-Zr, etc.) have been used in some experimental fast breeder reactors. Most of the commercial reactors use oxide fuels such as UO_2 or mixed oxide fuels such as a blend of Pu-239 and depleted uranium (Galkin et al. 1982).

UF_6 can be converted to UO_2 using three different chemical routes such as:

1. UF_6 is reacted with hydrogen and steam to form UO_2.
2. UF_6 is sent through water and thus hydrolyzed. NH_4OH is added to this hydrolyzed solution to precipitate ammonium diuranate. This precipitate is then reduced in hydrogen at 820 °C to form UO_2.
3. In this method, a gaseous mixture of CO_2 and NH_3 is hydrolyzed in water to form ammonium uranyl carbonate. This precipitate is then treated with steam and hydrogen at 500–600 °C to form UO_2.

The UO_2 is then purified by several washing cycles, dried, and mixed with an organic binder to press as cylindrical pellets. The compacted pellets are sintered at high temperature (1400–1700 °C). The solid UO_2 pellets are machined by fine grinding operation to final dimensions which are typically about 1 cm in diameter and 1.5 cm in length depending on the type of reactor (boiling water or pressurized water).

Fuel Rod Assemblies

The cylindrical fuel pellets are stacked in a fuel-clad tube with a nominal diameter of 1 cm and length of 3.6 m. Then the tubes are backfilled with helium at about three atmospheres to improve the thermal conductivity and heat transfer. The fuel rods are bundled with a thin encasing tube to prevent density variation that may affect the thermohydraulics of the reactor core. In a typical BWR fuel bundle, there are about 96 fuel rods. The BWR reactor core contains about 360–800 fuel assemblies depending on the capacity of the nuclear reactor. In PWR reactors, the fuel assembly contains a matrix of 14 × 14 and 17 × 17 fuel rods. The PWR bundles are about

4 m long. The reactor core contains about 120–193 bundles, depending on the capacity of the reaction. In case of heavy water reactions, U-235 enrichment is not required. Natural uranium (U-238) is loaded into the fuel bundles that have 380 tubes (Knief 1992).

Thorium

The isotope ^{232}Th is about 3–4 times more abundant on earth than uranium. This fertile isotope can be used for producing fissile ^{233}U isotopes. The neutron absorption cross section of ^{232}Th is also about three times that of U-238 (7.4 barns vs. 2.7 barns, where 1 barn = 10^{-24} cm^2). The number of neutrons liberated per neutron absorbed is greater than 2.0 over a wide range of thermal neutron spectrum for U-233. Therefore, the ^{232}Th–^{233}U fuel cycle can operate in wide spectra of neutrons such as fast, epithermal, and thermal. Thorium oxide is chemically more stable than UO_2 and has a low fission product release rate. ThO_2 also has a better thermal conductivity than UO_2. Furthermore, (Th, Pu)O_2 mixed oxide fuel is more attractive than (U, Pu)O_2 fuel because Pu is not bred in the (Th, Pu)O_2 and the presence of ^{232}U makes the spent fuel more proliferation resistant (Thorium fuel cycle).

Some of the limitations of ThO_2 fuel are as follows: Melting point of ThO_2 is 3350 °C. Therefore, the sintering temperature is higher than 2000 °C. Reprocessing requires heavy shielding because of the presence of remitting ^{232}U with 73.6 years of half-life. Because of its high chemical stability, ThO_2 cannot be easily dissolved in HNO_3 for reprocessing. It requires addition of .005 M HF to 13 M HNO_3, which makes the stainless steel containers used in reprocessing more prone to corrosion attack even after adding 0.1 M $Al(NO_3)_3$ as inhibitor.

Fuel Burnup

Fuel burnup gives information about the fuel utilization as how much energy has been extracted from the fuel as a nuclear fuel source. It is expressed as megawatt-days per metric ton (MWd/ton). The generation (II) commercial reactors were designed for a burnup of 40 GWd/ton. During nuclear fission, fission products build up and poison the sustainability of the chain reaction. For example, xenon-135 (cross section 2 million barns), samarium-149 (75,000 barns), and Gd-157 (200,000 barns) poison the reactor core which is a serious problem (Knief 1992).

In order to operate the reactor for longer time/cycle, between shutdown for fuel change, excess fuel is added. This high reactivity of the excess fuel needs to be balanced by neutron-absorbing materials in addition to control rods. These are called burnable poisons. Compounds of B and Gd act as burnable poison whose neutron absorption capacity decreases with fuel burnup. By using neutron poison, the burnup of fuel in a modern reactor can achieve a burnup of 60 GWd/t (Murray 2001; Knief 1992).

Higher-enriched fuel in the advanced light water reactors can achieve a burnup rate of 90 GWd/t. Since the fast neutron reactors can handle fission product accumulation without affecting its performance, the burnup rate can be around 200 GWd/t. The deep burn modular helium reactor that utilizes ceramic-coated plutonium-based fuel can achieve a burnup rate of around 500 GWd/t (Rudling et al. 2008).

Types of Nuclear Reactors

Depending on the coolant and moderator, the reactors can be classified as:

Light water reactor
- Boiling water reactor
- Pressurized water

Heavy water moderated reactor
- CANDU
- Advanced heavy water reactors

Graphite-moderated reactors

Thermal breeder reactors
- Molten salt breeder reactor
- Light water breeder reactor

Fast neutron reactors
- Liquid metal fast breeder reactor
- Gas-cooled fast breeder reactor

Boiling Water Reactors

The original design was developed by the General Electric Company. Figure 3 schematically illustrates the major components of a BWR system. Different power generation capabilities are 200 MW_e, 650 MW_e, and 1250 MW_e. Here, the subscript "e" in the MW_e represents electrical energy as the output. The capacity is also expressed in terms of thermal energy as output. The efficiency of converting thermal energy into electrical energy is around 30 %. Therefore, for a given MW_e output, the corresponding thermal energy will be at least three times higher. It should be noted

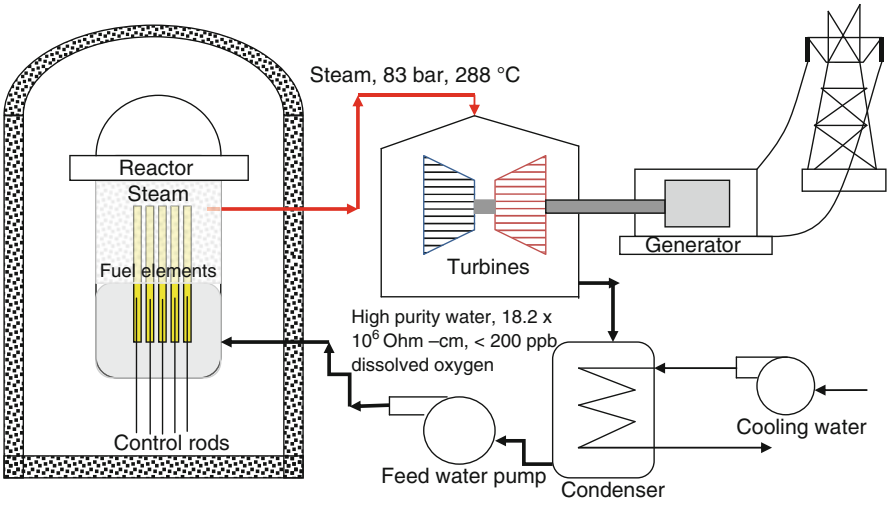

Fig. 3 Schematic diagram of system flow in a boiling water nuclear reactor. Only critical components are shown

that feedwater enters the reactor vessel at a pressure of about 70–85 bar and leaves as steam at 288 °C to run the steam turbines. The active core height is about 3–8 m that is placed in a reactor vessel of 22 m height. The bottom of the vessel is occupied by the control rod and drive mechanism. The space above the reactor core is occupied by the steam separator–dryer system components. The inner diameter of the vessel is about 6.4 m (for 1250 MW_e reactor). The wall of the reactor is made of 15 cm thick carbon steel clad with stainless steel. The stainless steel surface is exposed to the water/steam phases (Murray 2001; Knief 1992). Since a single coolant loop is used for heat transfer and steam generation, the water used in the BWR system is of ultrahigh purity with an electrical resistance of 18.2 megohm-cm. In order to minimize corrosion, the dissolved oxygen in the water is controlled below 200 parts per billion (ppb) by purging with ultrahigh-purity argon or hydrogen. The dissolved oxygen content of water exposed to ambient atmosphere is around 8 parts per million (ppm). Purging with nitrogen could lead to formation of NO_x-related compounds by radiolysis. Very high electric resistance of the water and low oxygen content result in low corrosion rates of the pressure boundary components.

Pressurized Water Reactors

Developed by Westinghouse Electric Company, they are based on the experience of nuclear submarine reactors. The power generation capability of PWR ranges from 60 MWe to 1450 MWe. Figure 4 schematically illustrates the major components of the PWR system. The PWR has two coolant circulation loops. The primary loop that removes heat from the reactor core is contained within the reactor vessel and used for transferring heat to a secondary coolant loop. Steam formation takes place in the secondary loop which runs the steam turbine for power generation. The water of the

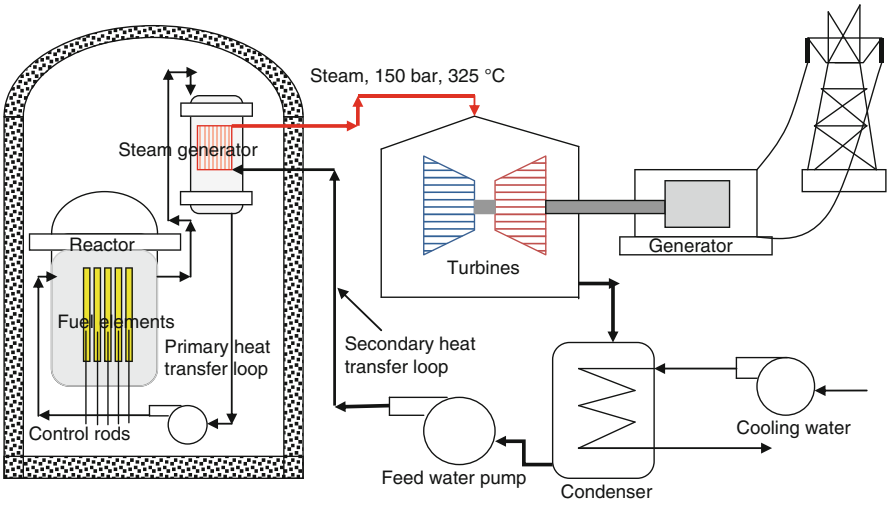

Fig. 4 Schematic diagram of system flow in a pressurized water nuclear reactor. Only critical components are shown

primary loop contains 1200–1800 ppm boron in the form of boric acid. Boron is added as moderator/neutron absorber. In order to balance the acidic pH due to boric acid, LiOH is added in the water to maintain a neutral pH at room temperature. The addition of boron and lithium compounds increases the ionic conductivity of the primary loop water. This may lead to increased corrosion rate. Since oxygen reduction reaction is the cathodic reaction in most of the corrosion mechanisms, the dissolved oxygen of the primary water is reduced to less than 5 ppb by purging with ultrahigh-purity hydrogen.

The primary loop contains lithiated and borated water at a pressure of about 150 bar (atmospheres). The core outlet temperature of the primary loop water is at about 350 °C. This primary loop heats the water in the secondary loop to above 290 °C and 70–85 bar. The secondary loop conditions are identical to that of BWR steam conditions. The main difference between the PWR and BWR is that the steam entering the turbines of PWR does not contain any radioactivity. A typical PWR reactor vessel is about 13 meters tall and 6.2 meters in diameter. The wall of the vessel is made of 23 cm thick ferritic–bainitic steel with 3 mm stainless steel clad that is exposed to the water/steam environment. The secondary loop, also called the steam generator, is 21 meters high and 4.5 meters in diameter (Murray 2001; Knief 1992).

Heavy Water Moderated Reactors

In light water reactors, the water is used as a moderator and coolant. An ideal moderator will have low mass, high neutron scattering cross section, and low neutron absorption cross section. Light water more rapidly moderates neutrons than heavy water. Therefore, fissile material such as U-235 is required for sustaining the chain reaction. In case of heavy water moderated reactors, high-energy neutrons are available for fission of U-238. Therefore, enrichment of U-235 is not required. However, preparation of heavy water is also a tedious process since deuterium is available in nature with a ratio of 1:7000 along with regular hydrogen in water. The separation of deuterium from water is an energy-intensive process.

In CANDU-PHW system, the primary heavy water coolant is pumped through a series of pressure tubes that also housed the fuel rods. The heavy water is contained in a vessel called calandria, which is about 7.6 m in diameter and about 4 m tall. There are about 380 calandria tubes. Each calandria tube contains one pressure tube through which the coolant flows (CANDU Reactors).

Graphite-Moderated Reactors

These reactors are fueled by natural uranium and moderated by graphite, and the coolant is an inert gas. Advanced gas-cooled reactors use helium as a heat transfer medium. Helium flows through the reactor core and exits at 740 °C with a pressure of about 50 bar. The heated gas is fed through the steam generator which produces superheated steam at 510 °C under a pressure of 170 bars. The reactor vessel is of prestressed concrete strengthened with vertical and circumferential prestressing steel cables. The dimensions of the vessel are 28 m high × 30 m in diameter. The reactor

core size is about 6.3 m × 8.5 m. There are six sets of helium loops and steam generators that produce about 1160 MWe power. Running the generators by gas turbines using the helium is possible (Murray 2001; Knief 1992).

Nuclear Reactor Safety

Radiation Effect

Three types of radiation damage can occur when high-energy particles impinge on a target. These are (Shapiro 1990):

- Transmutation of the constituent atoms of the target to new atoms of new material
- Displacement of atoms from their normal lattice positions in the structure of materials
- Ionization–removal of electrons of atoms that are present in the trajectory of the charged particles and formation of ion pairs

Alpha and beta particles have only low penetrating power and can be stopped by very thin layer of materials. Alpha particles produce a linear path of specific ionization per unit length of travel because of its high mass and charge. Smaller path and charge of particles result in a nonlinear path and very low specific ionization. Gamma rays have higher penetrating power than the alpha and beta particles. Therefore, a heavy shielding is required to stop gamma radiation.

Accumulation of fission products in the core of the nuclear reactor poses a potential safety threat among the public. Therefore, integrity of the fuel is important throughout the operating cycle. A set of specified operating parameters limits is determined for every reactor to assure safety of operation. These limits are generally the upper limitation on total reactor power which determines the maximum reactor core temperature that will not result in a meltdown. Fuel integrity is ensured by avoiding hot spots in the core. This is carried out by controlling the ratio of peak power to average power. The other important parameters that control the safe operation of the nuclear reactor core are the limit on the control rod position, difference between the power generation in the bottom half of the core and the top half, symmetry of power generation across the core, maximum reactor coolant temperature, minimum coolant flow, and maximum system pressure.

Under normal operating conditions, a negligible amount of radioactivity will get into the coolant (Murray 2001). Since abnormal conditions can exist, a design basis accident is postulated. In this hypothetical accident condition, a loss of coolant is assumed. Loss of coolant can occur either by a breakage of coolant piping or a failure of jet pumps supplying the coolant. Loss of coolant would result in an increase in the temperature of the nuclear core. When the temperature exceeds the melting point of fuel and cladding, the fuel tubes will be damaged and fission products will be released. The reactors are provided with safety measures such as safety rods and

emergency core cooling system (ECCS) to safeguard the reactor against loss of coolant accident. The safety rods reduce the reactor power immediately upon loss of coolant flow through the reactor core. The emergency core cooling system consists of auxiliary pumps that supply cooling water to bring down the temperature.

In order to minimize the effect of radiation, the nuclear plant is normally located several kilometers away from any population centers. The fission products that might be released, in case of an accident, will be contained within the steel-reinforced concrete reactor building. The concrete building can withstand high internal pressures and is designed to have a very minimal rate of leak.

Loss of Pressure Faults: If there is a leak in the PWR system, the vessel pressure may drop from nominal 2250 psi to lower values. The safe system in the PWR is activated which pumps water from the borated water storage tank. A large rupture in the coolant system will significantly decrease the vessel pressure and increase the concrete containment pressure. When the vessel pressure drops to 600 psi, water from the core flooding tank will be pumped to the core by a pressurized nitrogen gas stream. If the primary loop pressure drops below 500 psi, then water from the borated water storage tank is pumped to the core by the low-pressure injection pumps (Knief 1992).

Probabilistic Risk Assessment (PRA)

One objective of PRA is to find the chance of an undesired event occurring in a nuclear reactor and analyze its potential causes (Fullwood and Hall 1988). The event can be damage in the core, breach of containment, release of radioactivity, etc. The first step in the risk assessment is to investigate all of the possible failure modes of equipment and/or processes. Event trees are constructed to study the process flow. Fault trees are constructed using the principles of Boolean algebra that trace causes of failures and their effects mathematically. The ultimate objective of the probability risk assessment is to determine risks to people by calculating using the relation

$$\text{Risk} = \text{frequency} \times \text{consequences},$$

where frequency is the number of times per year of operation of a reactor that an undesired incident is expected to occur and consequences refers to quantifications of fatalities related directly or indirectly to the event.

Each nuclear power plant and the local government are required to have plans in place for emergency, in case of accidents occurring, and there is a potential for release of radioactivity. Mock accident drills are carried out periodically that resemble actions to be taken in a real accident. Many organizations also involve in such drills to make a coordinated effort to safeguard the life of residents in case of an accident. These organizations include radiation protection staff, police and fire departments, highway patrol, public health officers, and medical response personnel.

If the members of the public suffer loss due to accidents involving reactors or transportation of fuel, they are then compensated by nuclear insurance. The nuclear utilities pay the insurance premium to private insurances to cover any accidents to the public.

Nuclear Accidents

Safety goals are set either by regulatory authorities or by the utilities for safe operation of nuclear power plants.

The probabilistic design targets for LWR nuclear power plants are (IAEA 2001):

- A frequency of occurrence of severe core damage that is below about 10^{-4} events per plant operating year for existing nuclear plants
- Achievement of an improved goal of not more than 10^{-5} severe core damage events per plant operating year for future reactors
- Practical elimination of accident sequences that could lead to large early radioactive releases

In spite of strict safety regulations, there were accidents in the nuclear power plants. Postaccident analyses of accidents clearly indicated that these accidents were the results of severe violations of specifications and regulatory instructions.

Three Mile Island

A nuclear reactor at the Three Mile Island (TMI) facility failed on March 28, 1979, due to an accident. The accident was considered as the result of a combination of design deficiencies, equipment failure, and operation error. The accident was first triggered by a valve failure in the feedwater system. Since the feedwater system malfunctioned, the turbine generator automatically tripped, and the control rods were driven into the reactor to reduce its power. At this stage, water could have been supplied to the reactor by three backup feedwater pumps. However, there was an operator error as the valve to the steam generator was left closed by mistake. Therefore, the steam generators went dry increasing the temperature and the pressure of the primary water coolant to 2355 psi. This increase in the pressure set the relief valve on. This valve was stuck open due to a mechanical failure. The open valve let the coolant drain off from the primary system that led to a series of malfunctions and the meltdown of the core. The escape of the coolant water also resulted in spillage of some radioactivity. However, it was estimated that the highest possible dose of exposure was only 100 mrems or 1 millisievert, where 1 sievert is equivalent to 1 J/kg of energy release. It should be noted that a person taking a flight from the East Coast to the West Coast in the USA will have a radiation dose of 5 mrems due to cosmic rays.

The Chernobyl Accident

The Chernobyl accident occurred not because of operational abnormality but because of gross violation of operating rules and regulations. People who were in the vicinity of the damaged reactor received a radiation dose of 100 to 1500 rems. More than 135,000 people were evacuated from a 30 km zone.

Design Considerations and Life Prediction of Nuclear Components

In nuclear reactors, passive components such as pressure vessels and piping systems show very low failure probabilities. Therefore, failures of these components only have limited contributions to plant risk. On the other hand, components within a reactor core must tolerate high-temperature water, stress, vibration, and an intense neutron field. Degradation of materials in this environment can adversely affect the performance and in some cases lead to sudden failure. Degradation of materials in a nuclear power plant is very complex. There are over 25 different metal alloys within the primary and secondary systems. In addition, there are additional systems with complex nature such as the concrete containment vessel, instrumentation and control, and other support facilities. The combination of diverse set of materials, complex and harsh environment, and load conditions makes the degradation process very complicated.

The service failures of passive components occur because of the following mechanisms:

- Corrosion fatigue
- Thermal fatigue
- Stress corrosion cracking
- Corrosion attack
- Erosion and cavitation
- Flow-accelerated corrosion – i.e., erosion corrosion
- High-cycle vibration fatigue
- Water hammer

The in-core components are subjected to radiation-assisted failure mechanisms such as radiation-induced segregation, swelling, radiation creep relaxation, radiation-induced hardening, etc. The degradation of materials by radiation is considered first.

Fuel and Fuel Cladding

The fuel cladding helps contain the radioactive fission products. If the integrity of the cladding is maintained intact without cracking, rupturing, or melting during a reactor

transient, the radioactive fission products are contained within the fuel rod. Transients in reactor operation or hypothetical accidents could weaken the cladding because of a temperature increase, embrittlement by oxidation, or overstressing by swelling of the fuel because of mismatch in thermal expansion (pellet–clad mechanical interaction) or high fission gas pressure. These events alone or in combination can cause cracking or rupture of the cladding and release of the radioactive products to the coolant. The fuel cladding failure models consider several mechanisms such as cracking due to hydride formation, swelling of the clad because of differential pressure between the fuel rod gap and the coolant, thermal expansion of the fuel and clad, elastic and plastic straining of the clad, interference between adjacent ballooning rods, the effect of grids and azimuthal variations in temperature and straining caused by pellet eccentricity, and stress corrosion cracking induced by pellet–clad interaction in the presence of corrosive fission products such as iodine.

Zirconium-Based Alloys

Zirconium alloys are widely used in nuclear reactors as fuel cladding and other core internals because of their low thermal neutron absorption cross section and high corrosion resistance (Grobe et al. 2009; Choo et al. 1995). Zircaloy-2 (Zr-2) and Zircaloy-4 (Zr-4) are used in low-burnup fuel cladding applications. Modern Zr alloys such as ZIRLO^{TM} (Zr–1Sn–1Nb–0.1Fe) and M5^{TM} (Zr–1Nb–0.05Fe–0.015Cr) are candidate materials for high-burnup fuel claddings. During *in-reactor* irradiation, the Zr alloys undergo a number of changes. Most notable is corrosion by reaction with coolant water and subsequent formation of a thick oxide layer and hydrogen intake in solid solution. A large volume of data is available on the corrosion, creep, high-temperature oxidation, and hydride formation behaviors of Zircaloys that are used in the low-burnup fuel cladding application (Shoesmith 2006). On the other hand, only a limited amount of data is available on the oxidation and degradation behaviors of the modern Zr–Nb alloys intended for high-burnup application.

The available data for Zircaloy-2 and Zircaloy-4 cannot be directly correlated with ZIRLO^{TM} (Zr–1Sn–1Nb–0.1Fe) and M5^{TM} (Zr–1Nb–0.05Fe–0.015Cr) because of distinctly different microstructures. The Zircaloy-2 and Zircaloy-4 contain α-solid solution (hcp structure) at the normal operating and dry storage temperatures, whereas the Zr–Nb alloys show a mixture of α(Zr) + β(Nb) phases at the normal operating and dry storage conditions. The presence of the β(Nb) phase significantly alters the oxidation rate of the Zr–1Nb alloys, especially at the phase boundaries (Kiran Kumar et al. 2010). However, a detailed mechanism of the oxidation kinetics at the Nb-rich phase and phase boundary (where depletion of Nb is anticipated) is not available. It should be noted that thermodynamically Nb has a lower affinity to oxygen than Zr. Zr–1Nb alloy (M5) will have lower creep strength than Sn-containing alloys. It was postulated that the mechanical strength would be drastically increased upon irradiation in the reactor (Holt 1974). Furthermore, Zr alloy is capable of dissolving oxygen up to 29 at% during the oxidation process according to the zirconium–oxygen phase diagram reported by Domagala and McPherson (Domagala and McPherson 1954). Inspection of phase diagram of the

Zr–O binary indicates high amount of oxygen in the solid solution. The dissolved oxygen in Zr would act as an α-phase stabilizer and also impart creep resistance by solid solution strengthening. Yilmazbahyan et al. (2006) reported the Zr alloy–oxide interface enriched with oxygen up to its solid solution limit (29 at%) for a depth of 160–560 nm inside the metal substrate. Recently Ni et al. (2011) reported the presence of a suboxide layer in addition to an oxygen-rich region at the metal/oxide interface of the ZIRLO during the pretransition steam oxidation stage (prior to breakaway oxidation). The suboxide contained 50 at% oxygen for a thickness of 130 nm, and the metal beneath the suboxide contained 29 at% oxygen for a layer thickness of about 150 nm. Mechanical behavior of the oxygen-rich regions was not reported in detail in any of the literature; however, it is anticipated that these localized solid solution strengthened layers play a significant role in the integrity of the fuel cladding. Furthermore, the presence of a layer with oxygen concentration gradient across the metal/oxide interface greatly improves the adherence of the oxide layer. During temperature spikes, as experienced in the accidental conditions, the oxide layer and the Zr-alloy substrate undergo phase transformations. Volume changes associated with the phase transformations result in residual stresses that cause breakdown of the oxide. The presence of a graded layer would be beneficial since a large strain can be accommodated by this layer. Zr alloys that showed breakaway oxidation essentially had sharp oxygen profiles across the metal/oxide interface without any concentration gradient.

Silicon Carbide

Recent accidents in the Fukushima nuclear reactors of the Tokyo Electric Power Company, Japan, and associated worldwide concerns about the safe operation of nuclear power plants have reignited the interest in developing fuels that can contain fission products under meltdown conditions. Development of a passive LWR design that can withstand loss of coolant condition without replenishing the primary coolant, as occurred in the Fukushima nuclear power plant (I), requires substantial changes in the configuration of the reactor core geometry (Hejzlar et al. 1997). However, such design changes are very expensive and cannot be implemented easily in the existing LWRs. Recently, high-melting reactor core design based on sintered silicon carbide encasement of the UO_2 pellets within the Zircaloy cladding has been proposed (Lippmann et al. 2001). Since the proposed design changes occur only within the standard Zircaloy cladding, application of such modifications in the nuclear reactors that are already in service will be viable and less expensive.

Silicon carbide is a candidate material for one of the four coating layers of tristructural isotropic (TRISO) fuel particles to be used in high-temperature gas reactors. Among various polymorphs of SiC, β-SiC, having a cubic (zinc blende) lattice structure with two interpenetrating fcc lattices, one of carbon and the other of Si displaced by ¼<111>, is considered for various nuclear applications because of its refractoriness, low activation, good mechanical properties, and resistance to radiation damage (Henager et al. 2008). SiC is also considered as a fuel cladding material for Generation III light water reactors (LWRs), specifically by Westinghouse Electric Company. The Westinghouse concept for SiC-based cladding has a

monolithic SiC tube wound with SiC fiber tows. The SiC fibers are infiltrated with SiC deposited using chemical vapor infiltration (CVI) (Hallstadius et al. 2012). Silicon carbide is a ceramic material that has a good thermal conductivity (120 Wm^{-1} K^{-1}), a high sublimation point, and a high bending strength up to 1873 K. It is resistant to oxidation in steam and air up to 1300 °C and stable under neutron irradiation (Bloom 1998; Senor et al. 1996). In order to contain the fission products (especially the gases) under aggressive service conditions, the SiC overlay needs to be gas tight. The manufacture of UO_2 pellet encased with a thin SiC layer is complicated because enough space in between the SiC and UO_2 should be provided in order to accommodate the fission products and minimize the interaction between SiC and UO_2 at high off-normal temperatures.

The SiC-based fuel cladding is considered to be superior to Zr-based cladding because of the following advantages:

- SiC absorbs 25 % less thermal neutrons than the Zr alloy.
- No hydrogen pickup by SiC during normal operation.
- Superior mechanical properties such as SiC retains its mechanical strength even at very high temperatures (1100 °C), failure temperature in excess of 2000 °C, much slower degradation, and no meltdown.

All these factors make this material tolerant to loss of coolant accident (LOCA) conditions. However, stability of SiC in high-temperature water relevant to the LWR conditions should be demonstrated before deploying this material for commercial Generation III water reactor applications.

In high-temperature environments relevant to the very high-temperature gas-cooled reactors, the oxidation of SiC is limited by oxygen concentration and formation of a protective SiO_2 layer by following the reaction (Opila and Hann 1997):

$$2SiC + 3O_2(g) \rightarrow 2SiO_2 + 2CO(g) \tag{4}$$

However, in water vapor–containing environments, in addition to the oxidation reaction (2), a simultaneous volatilization reaction (3) was considered in order to estimate the steady-state oxide layer thickness (Opila 2003):

$$SiC + 3H_2O(g) \rightarrow SiO_2 + 3H_2(g) + CO(g) \tag{5}$$

$$SiO_2 + 2H_2O(g) \rightarrow Si(OH)_4(g) \tag{6}$$

The oxidation rate was limited by the transport of water vapor through the SiO_2 layer, and the thickness of the SiO_2 was a function of water vapor pressure. Since water availability is not a limiting factor in the light water reactors, the stability of the protective SiO_2 layer on the SiC surface in high-temperature water should be investigated in detail. Corrosion behavior of SiC in oxygenated and deoxygenated water at 290 °C was reported by Hirayama et al. (1989) in 1989, as a function of pH. The corrosion rate in oxygenated high-pH conditions was observed to obey a linear

rate law indicating absence of a protective film on the SiC surface. On the other hand, formation of amorphous, graphitic, and diamond-like carbon films was observed (Kraft et al. 1998; Gogotsi et al. 1996) on the chemical-vapor-deposited (CVD) SiC exposed to water at 100–200 MPa and 400–800 °C. Formation of a protective silica scale was not observed under the supercritical water oxidation conditions. In the oxygenated high-temperature water, the following reactions can occur (Dahlkamp 1993):

$$SiC + 2H_2O + 1/2O_2(\text{dissolved}) \rightarrow SiO_2 + CO + 2H_2 \quad (7)$$

$$SiC + 2H_2O + O_2(\text{dissolved}) \rightarrow SiO_2 + CO_2 + 2H_2 \quad (8)$$

$$SiC + 2H_2O + 2O_2 \rightarrow Si(OH)_4 + CO_2 \quad (9)$$

$$SiO_2 + H_2O \rightarrow 2H^+ + SiO_3^{2-} \quad (10)$$

$$CO_2 + H_2O \rightarrow 2H^+ + CO_3^{2-} \quad (11)$$

In the deoxygenated high-temperature water, the proposed surface reactions are

$$SiC + 2H_2O \rightarrow SiO_2 + CH_4 \quad (12)$$

$$SiC + 4H_2O \rightarrow Si(OH)_4 + CH_4 \quad (13)$$

$$Si(OH)_4 \rightarrow H_2SiO_4^{2-} + 2H^+ \quad (14)$$

The above reactions indicate that the corrosion rate of SiC is determined by the kinetics of the formation of a protective SiO_2 layer and its dissolution. Formation of gaseous phases like CH_4, CO, and CO_2 affects the morphology and defect structure of the surface layer that in turn detrimentally affects the protectiveness of the SiO_2 layer. Furthermore, corrosion resistance of the SiC is affected by the physical and chemical properties of the grain boundaries in addition to the purity and microstructure of the material. High-purity CVD SiC showed higher corrosion resistance than sintered SiC in distilled water at 360 °C (Kim et al. 2003). Localized corrosion was reported (Tan et al. 2009) on the SiC samples exposed to supercritical water at 500° C and deoxygenated high-purity water at 300 °C. The localized corrosion in supercritical water was attributed to high-intensity residual strains present in the small grains. Low-angle grain boundaries (Σ3, coincidence site lattices) showed better corrosion resistance than the general boundaries. The pit formation in deoxygenated (and subsequently hydrogenated) water at 300 °C during long exposure times was attributed to soluble silicon hydroxides and loss of silicon. The pits disappeared after reexposure of the samples to the test solution. Therefore, the pitting could be a transition corrosion mechanism of SiC exposed to hydrogenated water for an extended period of time (>4000 h).

It is well established by molecular dynamics simulations and experimental results that at room temperature water (both in gas and liquid phases) adsorbs preferentially on Si sites by a dissociative chemisorption process (Cicero et al. 2004; Liu

et al. 2012). The reactivity of Si-terminated SiC surface with water manifests into a corrosion process (by formation of Si–H and Si–OH bonds, reactions 10 and 11). Recently, nanocrystalline 3C–SiC has been used as electrodes for high-efficiency electrochemical hydrogen evolution (He et al. 2012). On the other hand, water dissociation on the C-terminated surface is reported to be energetically unfavorable even at high temperature (Liu et al. 2010). The relaxed H. . .H distance between H_3^+O and Si–H site is reported to be 0.125 nm, whereas for C–H site the corresponding distance of H. . .H is 0.275 nm. The larger H_2O–SiC distance of the C-terminated surface and relatively small binding energy (<0.05 eV) result in physic-sorption or no bonding at all (Shen and Pantelides 2013). Therefore, it is possible to improve the corrosion resistance of the SiC by having only the C-terminated surface. However, it should be noted that the structure of carbon is important in determining its activity toward water. For example, if the carbon is present as diamond form, then water adsorption by dissociative chemisorption is a possibility (Okamoto 1998). Furthermore, atomic hydrogen will etch both graphitic and diamond forms of carbon. The reaction of water with Si-terminated surface is associated with the interaction of lone pair of electrons of O atom in the H_2O with the *3-d* orbitals of the nearest Si atoms (as electron acceptors). Therefore, the corrosion resistance of SiC could be improved by tying the oxygen with an oxide-forming element that will have more stability in the PWR conditions, for example, Ti. Li et al. (2013) reported that, based on the ab initio calculations, Ti–C bonds are thermodynamically more stable than Ti–Si bonds and the β-SiC (111)/α-Ti(0001) interface shows large work of adhesion. Both titanium silicon carbide and titanium carbide showed better resistance to hydrothermal corrosion than SiC (Zhang et al. 2010; Shimada et al. 2006).

Irradiation Effects

Irradiation-assisted stress corrosion cracking (IASCC) has been drawing more attention over the years and has become potentially a critical phenomenon for core internals in light water reactors (LWRs). Alloys of iron and nickel base and oxygen-free copper are the materials found to be affected by IASCC. It is widely recognized that IASCC is a result of the interaction of irradiation, material, environment, temperature, and stress. The complexity of IASCC arises from the fact that irradiation has an impact on all the other variables listed above so that the knowledge available on SCC of materials in unirradiated environmental conditions is not sufficient to solve the IASCC problem. Because irradiation can alter the microstructure and microchemistry of the material, can affect the aggressiveness of the environment by water radiolysis, can increase the temperature of the parts by gamma heating, and can change the component stresses through relaxation of creep or by radiation hardening, interpretation of wide range of issues influencing IASCC requires specialized knowledge covering fracture mechanics, electrochemistry, physical metallurgy, and core neutronics. IASCC may have a higher potential to occur in fusion reactor components because of the higher dose rate of neutron

irradiation than in LWRs. Components of the blanket and first wall cooling system, divertor cooling system, and vacuum vessel cooling system are potential problem sites where IASCC could occur. Though the mechanism of IASCC is not fully understood, factors affecting it are well documented, especially the effect of radiation on the environment and on material properties. Among the radiation effects, some are fluence dependent and some are flux dependent, while both fluence and flux cause joint effects. Radiation-induced segregation (RIS), radiation-induced microstructures, and radiation creep relaxation are fluence dependent, while radiolysis and to some extent RIS are flux dependent. The ratio of thermal to fast neutron flux affects transmutation.

Environment-Assisted Cracking (EAC) of Austenitic Stainless Steel in High-Temperature Water

EAC of stainless alloys in high-temperature water occurs due to the synergistic interaction of stress, environment, and material. Generally, active path corrosion cracking and hydrogen cracking are the mechanisms involved in EAC. Crack initiation and crack propagation are two distinct events, which are controlled by environmental, mechanical, and material variables. Water chemistry and microchemistry of the material play a vital role in initiating the SCC. Dissolved oxygen and CO_2 and the presence of Cl^- and SO_4^{2-} are deleterious from an environmental point of view, and inclusions such as MnS, segregation of Si and P, sensitized microstructure, and the presence of secondary phases such as sigma, laves, chi, etc., are detrimental from a material point of view.

EAC of Unirradiated Ferritic/Martensitic Steels

Ferritic stainless steels (>17 % Cr) are considered to have better SCC resistance than austenitic stainless steels. This is true only when the Ni, Cu, and Co contents are below certain levels (Bond and Dundar 1977). However, 8–12 % Cr steels are subjected to both SCC and hydrogen embrittlement. Apart from the environmental factors such as dissolved oxygen, presence of sulfate and chloride ions, etc., microstructural condition of the material also controls the cracking behavior. Untempered martensite and acicular bainite phases are found to be more prone to hydrogen cracking than tempered martensite and bainite + ferrite phases (Kerr et al. 1987). Generally it is observed that pitting is associated with the initiation of SCC or corrosion fatigue in this type of material. Mostly intergranular cracking is observed along the prior austenite grain boundaries. However, it is not very clear why only the prior austenite grain boundaries are the most preferred site for cracking and not other boundaries such as interlath boundaries or interfaces between two martensite packets. Probably certain solute elements segregated in the austenite grain boundaries may have more affinity to hydrogen, as discussed by Leslie (1977). But, Auger electron spectroscopy carried out on these fracture surfaces did not throw much light

on this aspect. Hydrogen cracking resistance of ferritic/martensitic steel is significant for fusion wall application because direct transmutation, water–lithium interactions, radiolysis of water, and corrosion could charge hydrogen into the steel. Hydrogen cracking could be enhanced by other irradiation damage mechanisms such as RIS, increased defect density, etc.

Environmental Aspect

Radiolysis

Radiolysis is a complex issue affected by water chemistry, neutron flux (not fluence), flow rate, temperature, etc. Radiation causes decomposition of water into many species which affect the corrosion potential. At high hydrogen levels (>1 ppm), radiolysis is sufficiently suppressed so that it has very little effect on changing the corrosion potential (Maziasz and McHargue 1987). The interior of the cracks was not found to be polarized by radiation, as the corrosion potentials of cracks and tight crevices were not altered.

Flux Dependence

The structural materials are exposed to temperatures of 290–350 °C in water reactors. In the case of a BWR, the temperature is constant at 288 °C, whereas in a PWR, the temperature varies with location to a maximum of 400 °C in the baffle plates. The fast flux in a BWR is around 7×10^{17} n/m^2 s (E > 1 MeV), and in a PWR, it is 20–30 % higher than in a BWR. Radiation damage in materials is quantified in terms of displacements per atom (dpa) as calculated by approved methods. Empirically 1.4 dpa per 10^{25} neutrons (n)/m^2 (E > 1 MeV) is used for LWRs. From this, the fast flux can be back calculated to be 10^{-7} dpa/s in the core of LWRs and 1.5–4 $\times$ 10^{-7} dpa/s in test reactors. In fast reactors, the fast flux is given approximately as 10^{-6} dpa/s, and the temperature also is higher (>370 °C) in fast reactors. So, the data generated in fast reactors cannot be compared with those of LWRs. The thermal to fast flux ratio also is an important issue. The thermal neutrons are those which are in thermal equilibrium with neighboring atoms and with energies below 0.5 eV.

Radiation Water Chemistry and Corrosion Potential

Radiation causes breakdown of water into primary species (H^+, e^-_{aq}) and molecules such as H_2O_2, O_2, H_2, etc. The concentration of species is proportional to the square root of the radiation flux. Fast neutron radiation has a stronger effect on water chemistry than other types of radiation such as thermal neutrons, beta particles, and gamma radiation (Suzuki et al. 1991). This feature is because of the higher linear energy transfer (LET) and the higher neutron flux of fast neutrons.

It is generally believed that the corrosion potential has more influence than the concentration of oxidizing and reducing species in controlling SCC. The initial concentrations of oxygen and hydrogen are found to be important in determining the final corrosion potential after irradiation. Though a large increase in

concentration of some species occurs after irradiation, the change in corrosion potential is not drastic. When hydrogen is present at more than 200 ppb and at 0 ppb O_2, there is no radiation-induced elevation of corrosion potential, whereas the presence of H_2O_2 increases the corrosion potential.

Crack Initiation and Propagation

It is generally observed that SCC initiation preferentially occurs at sites like pits and second phase particles. Preferential dissolution of secondary phases or inclusions creates a crevice where the local electrolyte chemistry and local strain level become more favorable for SCC initiation by a slip dissolution mechanism. In the case of IASCC, irradiated microstructural features (like Cr depletion, Si and P segregation, etc.) and the presence of hard phases such as oxides make the crack initiation process much easier. Oxide particles effectively participate in IASCC initiation by two proposed mechanisms as follows: (1) Oxides are hard to deform. So, under load, the shear stress at the interface of the oxide matrix increases to very high levels as the ductile matrix around the particle deforms. This results in failure in the bonding, creating a crevice where the local chemistry of the electrolyte changes to more a conducive condition for promoting SCC. (2) Alternately, the oxide could fracture creating a microcrack which can either extend into the matrix or create a very high stress intensity for easy SCC initiation.

Strain at crack initiation (SCI) was proposed as the definition for IASCC initiation in slow strain rate tensile testing (SSRT) at 10^{-7} s^{-1} strain rate. It was defined as the strain at which the stress–strain curve of SSRTs began to depart from that of tensile tests, when plotted using the same coordinates. Higher SCI means SCC initiation starts at higher strain. Though the intergranular (IG) fracture ratio decreases with decreasing dissolved oxygen (DO), it increases inversely below 10 ppb of DO. These phenomena may indicate the continuum of initiation of IASCC from BWR conditions to PWR conditions.

Crack Propagation: Gamma ray irradiation is not expected to affect the microstructure or microchemistry of the material. However, it decomposes water into many kinds of radiolytic products of which hydrogen peroxide (H_2O_2) is very important to IASCC. In the 288 °C BWR environment, gamma irradiation accelerated the crack growth to varying degrees depending on the water chemistry, flux, etc. For example, the average crack growth rates in unirradiated, irradiated with gamma ray for fluxes of 5×10^6, and 9×10^6 R/h were 7.2×10^{-10}, 1×10^{-9}, and 1.3×10^{-9} m/s, respectively. From these values, the crack growth rates in low-conductivity pure water could be observed to be marginally affected by gamma ray irradiation.

The effect of dissolved oxygen (DO) on crack velocity with additions of Na_2SO_4 is similar in both irradiated and unirradiated test conditions. Addition of sulfate ions showed more effect in accelerating the crack growth than did irradiation. DO also had a similar effect. Suppressing the DO content decreased the crack growth rate. Though crack velocity increased with sulfate ions as in the case of the unirradiated

condition, DO had a major effect in controlling the crack behavior in the irradiated condition also. Nitrate additions were found to be less aggressive than sulfate additions in a BWR environment for 304 SS. Dissolved hydrogen showed greater beneficial effect in suppressing crack growth. The mechanism of crack growth mitigation by hydrogen injection could be explained by analyzing the corrosion potential of the system. The presence of molecules like H_2O_2 and O_2 increases the free corrosion potential which falls into the cracking range, and hence, the crack velocity is enhanced following the slip dissolution model and Faraday's law. Whereas when hydrogen is introduced into the environment, it helps the recombination of species and thus reduces the corrosion potential well below the cracking range. IASCC tests were carried out on irradiated stainless steel samples under BWR condition using the slow strain rate testing method. They presented average crack growth data by dividing the maximum crack depth by total test duration. The maximum crack growth rate divided by the test time was suppressed by hydrogen water chemistry (HWC) below 3×10^{21} neutrons (n)/cm^2, but not above 3×10^{21} n/cm^2. It was observed that variations in either fluence level (3×10^{20}–9×10^{21} n/cm^2; $E > 1$ MeV) or flux level (1.5×10^{13}–7.6×10^{13} n/cm^2 s) did not affect the crack velocity drastically (a maximum of a factor of two).

Critical Issues on Selection of Candidate Materials for Advanced Nuclear Reactors

Advanced systems selected for Generation IV reactors require high operating temperatures in the range of 500–1000 °C, depending on the coolant and longer service life. The fuels of the advanced reactors will have very high-burnup capabilities and fast neutron spectra. The construction materials of Generation IV reactors will be exposed to severe environmental conditions in combination with increased radiation damage. Therefore, selection of structural materials for advanced reactors requires a thorough understanding of materials' behavior in the extreme service conditions.

The structural materials of advanced nuclear reactors will undergo degradation primarily due to three factors, viz., (1) exposure to high temperature and service stresses (high-temperature degradation), (2) irradiation damage, and (3) interaction with service environments. The first two factors are common among all the types of reactors, and therefore, the data generated at high temperatures and irradiation levels relevant to the service conditions can be used for material qualification for different type of reactors, as the operating temperature of most of the advanced reactors is in the range of 500–800 °C. However, the third factor, interaction with environment, is reactor specific. The material should possess higher resistance to corrosion attack in the service environment. Among the various types of advanced reactors, liquid metal (particularly liquid sodium and lead–bismuth eutectic)-cooled fast reactors are considered in this study. Some of the critical issues pertaining to each major degradation modes will be discussed in this presentation.

The materials considered for advanced reactor structural applications can be classified into three major categories viz., (1) ferritic–martensitic-type Fe–Cr alloys,

(2) austenitic alloys (stainless steels and Ni–Cr–Mo alloys), and (3) oxide dispersion strengthened (ODS) alloys. Refractory metal-based alloys are not considered in this work. Merits and disadvantages of the first two categories of the materials will be analyzed based on the critical degradation issues.

High-Temperature Degradation

Major Issues and Temperature Limits

The major issues of high-temperature degradation are phase stability, oxidation, and creep–fatigue interaction. It is widely believed that thermal effects will offset the irradiation effects at high temperatures because of increased diffusivities and stress relaxation effects. This may be true for annihilation of point defects. However, effect of radiation-induced segregation could be aggravated at high temperatures.

Available literature data indicate that the maximum service temperatures of different alloys are limited by chemistry and microstructure. For example, ferritic/martensitic steel with a maximum Cr content of 12 % can service up to 650 °C and austenitic stainless steels up to 800 °C, nickel-based alloys up to 900 °C, and ODS alloys up to 1050 °C. The interaction of creep–fatigue is considered to be of primary importance.

Fatigue, Creep, and Creep–Fatigue Interaction

Creep or creep–fatigue interaction of structural materials at elevated temperatures over a long period of time in advanced reactor environments is a critical issue. High temperature and the temperature gradient during start-ups, in-services, and shut-downs induce both static and cyclic thermal stresses. These constitute the stress factors that generate creep and creep–fatigue interaction. In addition, components such as thread roots in steam turbine casing bolts, pipe, and branch connections in reactors endure multiaxial stresses.

The earlier studies (Brinkman and Korth 1973) investigated the effect of heat-to-heat variation on fatigue and creep–fatigue resistance of type 304 stainless steel at 593 °C. Carbide precipitation was considered as the reason of increasing low-cycle fatigue (LCF) resistance. Additionally, a fairly uniform distribution of inter- and intragranular carbides $M_{23}C_6$ was considered to increase the resistance to the tensile hold time effect. Generally, zero hold time tests revealed transgranular fracture surfaces, while intergranular features were obtained even with hold times as short as 0.01 h. This is also illustrated by the studies of Schaaf (1988) (Fig. 5). The creep–fatigue failure can be categorized into three modes: fatigue-dominated failure with almost transgranular features, creep–fatigue interaction (both transgranular and intergranular), and creep-dominated failure with mainly intergranular cracks.

In recent years, creep–fatigue properties of liquid metal fast breeder reactor (LMFBR) candidate structural materials, such as austenitic 304 L, 304NG, 316LN, and AISI 321, were investigated at 600 °C (Rho and Nam 2002; Nilsson 1988; Min and Nam 2003). It was observed that nitrogen addition improved fatigue life under creep–fatigue condition. The density of Cr-rich carbides formed at the grain boundary of 304NG (0.08 % N) was lower than that of 304 L (0.03 % N). Planar slip planes

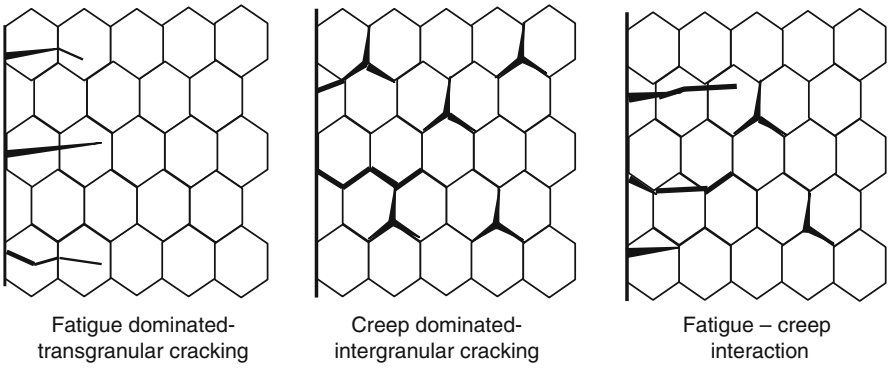

Fig. 5 The three failure modes: fatigue dominated (*left*), creep–fatigue interaction (*left*), creep dominated (*middle*) (Van Der Schaaf 1988)

of 316LN initiated under creep–fatigue interaction probably enhanced stress concentration immediately next to grain boundaries and promoted intergranular fatigue fracture. In the case of AISI 321, it was observed that the creep–fatigue life of TiC-aged specimen was 40 % longer than that of $Cr_{23}C_6$ aged, although the two carbide densities at grain boundaries were similar. It is suggested that the interfacial free energy between TiC and grains is lower than that between $Cr_{23}C_6$ and grains in AISI 321.

In addition, irradiation creep accumulates in reactor materials. It is known that irradiation creep has very weak temperature dependence. However, creep remains high at temperatures as low as 60 °C (Grossbeck et al. 1990). It is postulated that migration of vacancies and migration of interstitials are two independent mechanisms of irradiation creep. The effect of irradiation is to lower the endurance of plastic strain range.

So far, most of the experimental studies on creep–fatigue interaction were conducted by using low-cycle fatigue tests with and without tensile strain hold in air at temperatures ranging from 400 to 600 °C. The accumulated data in simulated reactor environments at high temperature up to 800 °C is inadequate for a better understanding of the creep–fatigue interaction mechanism. For example, oxidation and solubility of alloying elements in high-temperature liquid metal have to be considered as possible factors affecting creep–fatigue behavior. Also, carbide precipitation at component weld joints and heat-affected zone (HAZ) may have different behaviors from base metals.

Creep–Fatigue Life Prediction

In this section, selected creep–fatigue life prediction methods are reviewed without considering the irradiation effects.

Suauzay et al. (2004) analyzed their experimental results of creep–fatigue behavior of 316LN at 500 °C using linear damage accumulation model. This model is based on Miner's rule, expressed as

$$\frac{N_F}{N_F^{pf}} + \frac{t_F}{t_F^{relax}} = 1 \tag{15}$$

N_F: number of cycles to failure for a t_h hold time ($t_n > 0$)
N_F^{Pf}: number of cycles to failure in pure fatigue, based on the Coffin–Manson relation ($t_n = 0$)
$t_F = N_F t_h$
t_F^{creep}: failure time in pure creep condition given as
$t_F^{creep} = H / \sigma^r$, where H and r are creep coefficients

$$t_F^{relax} = N_F \int_0^{t_h} \frac{dt}{t_F^{creep}\sigma(t)} \tag{16}$$

Tsuji and Nakajima (1994) evaluated the damage accumulation of Hastelloy-XR in HTGR environment at 700–950 °C by applying the life fraction rule and ductility exhaustion rule. The creep damage during strain holding time was given as

$$D_{cL} = \sum_i \left(\Delta t_i / \Delta t_{Ri}\right)^n \tag{17}$$

D_{CL}: creep damage by life fraction rule
Δt_i: strain holding period for particular temperature and stress
t_{Ri}: rupture time based on the Larson–Miller parameter
n: number cycles for failure in the experimental condition with trapezoidal strain wave form (fatigue–creep components)

The ductility-exhaustion rule is given as

$$D_{cd} = \sum_i \left(\dot{\varepsilon}_{\min} \Delta t_i / \varepsilon_{Ri}\right)^n \tag{18}$$

D_{cd}: creep damage by ductility exhaustion rule
Δt_i: strain holding period for particular temperature and stress
$\dot{\varepsilon}_{\min}$: minimum creep rate calculated from the Larson–Miller parameter
ε_{Ri}: strain at rupture

It was observed that the ductility exhaustion rule predicted the fatigue life under the effective creep condition more successfully than the life fraction rule.

Most of the creep–fatigue life prediction models are based on phenomenology of failures. For example, ferritic/martensitic steels and nickel-based superalloys showed damage accumulation at the crack tip or crack process zones. In these materials even compressive stress hold times were found to affect the damage accumulation. In case of austenitic stainless steels, creep–fatigue damage occurs by grain boundary cavitation, and tensile hold time is considered to be more

important. The proposed damage accumulation function based on grain boundary cavitation phenomenon is given as (Nam 2002)

$$D_{C-F} = \Delta\varepsilon_p^m \left\{ \frac{\exp\left(-Q_g/RT\right)}{T} \int_0^t \sigma(t)dt \right\}^{2/3} \tag{19}$$

$\Delta\varepsilon_p$: plastic strain range
m: strain exponent
Q_g: activation energy for grain boundary diffusion
R: gas constant
T: temperature

When the damage function is plotted against experimental creep–fatigue life, as shown in Fig. 6, a linear relationship was observed with a slope of −1.66. Consideration of creep–fatigue life of different types of austenitic stainless steels at 600–700 °C revealed that the slope varies from −1.62 to −1.66. Therefore, the proposed damage function can be used for life prediction in the given experimental conditions.

It should be noted that most of the life prediction methodologies are based on the data generated using smooth tensile specimens. In these cases, the events of crack initiation and crack propagation were not distinguished. In service conditions, inspection and monitoring methods require data on crack initiation time and crack velocity to evaluate the integrity of the components.

Yokobori (Yokobori and Yokobori 2001) considered the crack initiation and crack propagation issues for creep–fatigue interaction based on critical notch opening displacement criterion. According to these authors, the crack initiation event is complete when the defect size reaches 5 μm, a dimension that can be resolved by optical microscopy. Crack initiation is considered to occur when a critical strain is

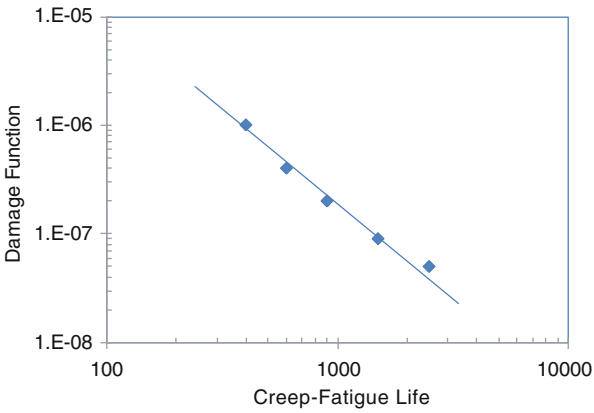

Fig. 6 Normalized Coffin–Manson plot for AISI 316 stainless steel (Nam 2002)

reached by some atomistic rearrangement by time-dependent plastic flow. This process in creep–fatigue interaction is thermally activated and aided by stress field. Based on these considerations, the time for crack initiation was given as

$$1/t_i = \frac{A_1}{\varepsilon_c} \exp\left(\frac{-\Delta H - \Phi(\sigma_g)}{RT}\right) \tag{20}$$

t_i: time for crack initiation
ε_c: critical strain required for crack initiation
A_1: material constant
ΔH: activation energy for plastic flow

$$\Phi(\sigma_g) = \Delta f \ln\left(\frac{K_I}{G\sqrt{b}}\right) \tag{21}$$

Δf: energy coefficient
K_I: stress intensity factor $= \alpha\, a^{1/2} \sigma_g$
G : modulus of rigidity
b: burgers vector

Similar expressions can also be written for crack propagation. The expression for crack propagation is

$$\frac{da}{dt} = B\sigma_g^m K_I^n \left[\frac{-\left\{\Delta H_g - \Delta f \ln\left(\frac{K_I}{G\sqrt{b}}\right)\right\}}{RT}\right] \tag{22}$$

The major advantage of the above approach is its ability to take various boundary conditions, such as environmental degradation (reduction in ΔH_g due to liquid metal) and irradiation effects, into account.

Radiation Damage

Radiation Damage of Microstructure

Among the radiation effects, some are fluence dependent and some are flux dependent, while both fluence and flux cause joint effects. Radiation-induced segregation (RIS), radiation-induced microstructures, and radiation creep relaxation are fluence dependent, while RIS is flux dependent to some extent.

Figure 7 illustrates schematically the collision of an energetic particle (either a neutron, an electron, or a proton) with a lattice atom generating radiation damage (Maziasz 1993). If the energy transfer of the elastic collision is greater than the displacement threshold (E_d), a primary knock-on atom (PKA) is generated. PKA can displace additional atoms through the lattice if it has sufficient energy until the energy of all the atoms has been reduced below E_d (Capdevila et al. 2008).

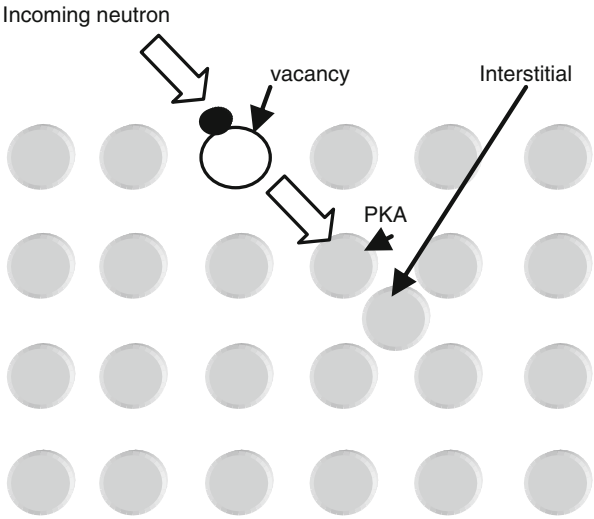

Fig. 7 Schematic illustration of generation of a primary knock-on atom (PKA) (Maziasz 1993)

The Frenkel pair, consisting of a vacancy and self-interstitial atom (SIA), could be considered as the fundamental component of radiation damage (Fullwood and Hall 1988).

The extent of radiation damage is a function of temperature. Several extensive reviews on microstructural evolution in irradiated austenitic stainless steels are available, which report a transition of microstructural damage approximately at 300 °C. At high temperatures (>300 °C), vacancy clusters in austenitic stainless steels become thermally unstable. The presence of voids and swelling is observed at higher temperatures. Under certain conditions small gas-filled bubbles can grow to form voids, referred to as swelling, as the volume of material increases beyond the size limitation dictated by the thermodynamic equilibrium of gas. Both hydrogen and helium play an important role in swelling of a material. A swelling rate of 1 % per dpa is maintained at temperatures above 425 °C. The lower limit of temperature for swelling is observed to be affected by displacement rate.

Radiation-Induced Microchemistry

In austenitic stainless steels, depletion of Cr and Fe and enrichment of Ni have been observed. The Cr and Fe have higher diffusivity than Ni. Therefore, they migrate away from the interface, enriching the boundary with Ni. This could be attributed to the inverse Kirkendall segregation. Segregation of Si and P at grain boundaries is observed by an uphill diffusion process. Along with Cr and Fe, minor alloying elements such as Mn, Ti, and Mo also get depleted at grain boundaries. Mn levels drop to 0.5 at% at grain boundaries in type 304 SS. In type 316 SS, more than 50 % depletion of Mo after irradiation to 3 dpa has been reported (Cookson and Was 1995). For the same level of irradiation, enrichment of Si occurred to levels of about 6–8 at%. Nickel-silicide precipitation also has often been reported to form at dislocation loops at temperatures >380 °C and at higher doses (>20 dpa) (Kimura

et al. 1996). At higher doses (PWR relevant, >10 dpa) sulfur segregation can be expected due to the burnup of Mn in MnS inclusions and subsequent release of S. Radiation-induced Cr depletion could retard carbide formation at grain boundaries. Radiation-induced segregation of Ni and Si could lead to formation of γ' or G phase at higher temperatures (Shiba et al. 1996).

Mechanical Properties

In general, it is observed that with increases in irradiation dose, the yield strength of the material increases. The ultimate tensile strength also increases, but the increase is not as great as for the yield strength. Formation of higher densities of vacancies and interstitials is attributed as the cause for this increase. Suzuki et al. (Holt 1974) reported increases in strength for various grades of austenitic stainless steels with increase in neutron fluence as shown in Fig. 8. However, a saturation level is reached at the 3×10^{25} n/m^2 fluence level (E > 1 MeV) beyond which no significant increase in strength could be observed. The increase in yield strength ($\Delta\sigma$) of the 304 SS irradiated in BWR environment at 288 °C showed a relation of $\Delta\sigma = 1.1 \times 10^{-3} \times$ (neutron fluence, n/m^2)$^{0.27}$. It was observed that type 304 SS was more prone to irradiation hardening than was type 316. Composition has two effects, viz., (1) certain alloy elements help nucleate Frank loops and (2) stacking fault energy (SFE) is altered. Low SFE results in more hardening. Also a low SFE can lead to nucleation of twins as an alternative deformation mechanism to dislocation glide. Alloying elements such as Ni, Mo, and C increase the SFE in austenitic stainless steel, and Cr, Si, Mn, and N tend to decrease the SFE.

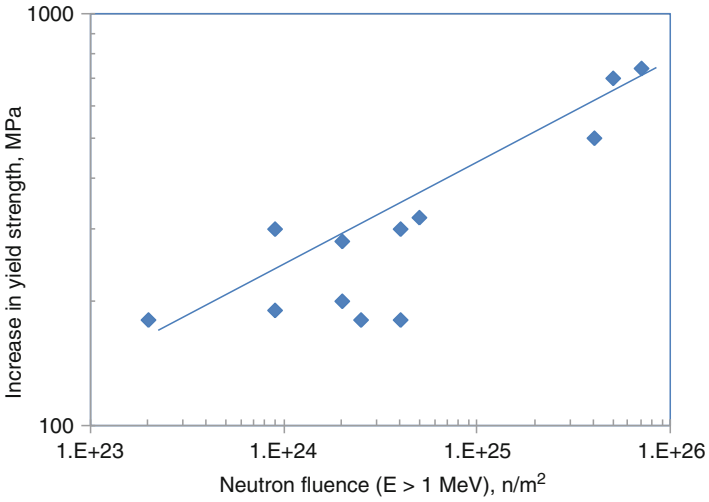

Fig. 8 Typical relation between the increase of the 0.2 % yield stress of austenitic stainless steels and neutron fluence (E > 1 MeV) after irradiation in BWR environment at 288 °C (Koyama et al. 2007)

Loss of work hardening and uniform elongation is observed after irradiation. The elongation decreases significantly with increasing dose. This kind of loss in work hardening and hence uniform ductility could be attributed to the irradiated microstructure, where annihilation of barriers occurs due to their interaction with dislocation. Interacting with obstacles, dislocations multiply in unirradiated material which results in development of back stresses and hence work hardening of the material. However, in irradiated conditions, the obstacles such as loops and voids can be destroyed when they interact with moving dislocations, resulting in work softening. This behavior causes flow localization, and hence, the slip band spacing increases, ultimately reducing the macroscopic deformation. At higher temperatures (above 600 °C), the ductility is observed to be severely affected by He embrittlement. When a large void population develops near 400 °C, the fracture mode is observed to be transgranular channel. The reduction of fracture toughness of irradiated SS can be attributed to the higher population of voids so that fracture occurs at an early stage by dislocation channeling or highly heterogeneous deformation–decohesion ahead of the crack tip[23]. RIS of Ni at voids also results in brittle behavior of a material. This preferential segregation of Ni at voids results in matrix depletion of Ni and hence destabilizes the austenite. The strain-induced martensite transformation, possible in the destabilized austenite, acts as low-energy path for crack propagation [24]. This mechanism for cracking resulted in quasi-cleavage fracture with an overall fracture toughness of 80 MPa $m^{1/2}$ after the austenitic material has been irradiated to high dose (1.6×10^{23} n/cm^2) at 425 °C.

Irradiation hardening and softening are important factors in determining the fusion reactor life limits as creep properties are affected by these changes. In ferritic steels, the irradiation hardening is attributed to the formation of small defect clusters and dislocation loops, with associated precipitation of small carbides such as M_2C, M_6C, etc. Kimura et al. (1996) studied the irradiation hardening behavior of 9Cr-2 WV steel and reported saturation of irradiation hardening at a dose level of about 10–15 dpa. Irradiating at above 430 °C resulted in softening at dose levels of 40–60 dpa. Swelling was found to be associated only with hardening, in this study.

Shiba et al. (1996) investigated the response of F82H steel to irradiation at low damage levels (<1 dpa) for 300–500 °C. They observed hardening only at 300 °C. However, no softening was observed when irradiated at 520 °C. Interestingly for these test conditions, no change in DBTT was observed between irradiated and unirradiated Charpy impact tested samples. However, the upper shelf energies were lower for irradiated samples.

Klueh and Alexander (1996) conducted a detailed study on Charpy impact toughness of different types of low-activation steels irradiated at 0–24 dpa. They observed that 9Cr-2 W-type steels were least affected by irradiation. In terms of microstructure, they found that steels with 100 % martensitic structure showed superior impact toughness properties after irradiation than steels with dual microstructures such as bainite + ferrite or martensite + ferrite. By changing the composition and microstructure, the effect of irradiation on toughness could be favorably modified.

Typical 12 % Cr steel shows very little void swelling (only 0.1 % volume change for a dose of 90 dpa at 400 °C). It is generally observed that 9 % Cr steel shows better impact toughness and DBTT values after irradiation than 12 % Cr steel. However, by controlling the phase content (either 100 % martensite or at least less than 20 % delta ferrite) and with uniform distribution of carbide/carbonitride phases, much improved mechanical properties could be achieved. In the case of 9 % Cr steel, the volumetric swelling was around 0.1 % at 100 dpa and 400 °C which is similar to that for 12 % Cr steel. After 90–100 dpa, the rate of swelling of 9 % Cr steel was reported to be approximately 0.01 %/dpa.

Irradiation Creep

Two groups of mechanisms have been proposed for irradiation creep, viz., (1) irradiation-induced creep and (2) irradiation-enhanced creep.

Irradiation-Induced Creep. Depending on the nucleation and growth of dislocation loops, two types of mechanisms are observed, viz.:

1. Stress-induced preferred nucleation (SIPN)
2. Stress-induced preferential absorption (SIPA)

For the case of SIPN, interstitial loops are assumed to nucleate preferentially on planes perpendicular to the tensile stress, and vacancy loops nucleate preferentially on the planes parallel to the applied stress.

For the SIPA mechanism, interstitials are preferentially absorbed by the loops oriented perpendicular to the tensile stress so that there is an elongation in the direction of stress.

Irradiation-Enhanced Creep. It is postulated that irradiation accelerates the thermal creep by producing excess vacancies and interstitials and thus facilitating the easier dislocation movements. For example, jogs in the form of nonglissile edge dislocation segments on a screw dislocation can be moved by the point defects produced by irradiation, otherwise not possible.

Fretting

Fretting results from low-amplitude motion between the tube and the support plates of the steam generators in the nuclear power plants. These flow-induced, low-amplitude vibrations occur during the normal operation of steam generator, in spite of the use of anti-vibration supports, wherein two fluids are flowing in countercurrent manner. Several parameters including fluid flow, vibration frequency, and impact force affect fretting. The flow-induced vibrations also lead to cyclic loading that will be random in nature. As per the US Nuclear Regulatory Commission, the USA has 27 nuclear power plants that use Inconel Alloy 600 (Ni, >72 %; Cr, 14–17 %; and Fe, 6–10 % form major constituents) and 42 that use Alloy 690 (Ni, >58 %; Cr, 27–31 %; and Fe, 7–11 % form major constituents) as tubing material. To improve mechanochemical properties, these materials are subjected to

mill annealing (Alloy 600) or thermal treatment (Alloy 600 or 690), which forms the important factor, other than the alloy composition, in determining its degradation. The tube support plates are typically fabricated using 405 ferritic stainless steels. While the primary reason for degradation and failure of the tubes used to be thinning of tubing material due to water flow, the recent failures and inspections indicate that accelerated degradation is becoming an issue of concern. At the center of this is the failure of steam generator tubes in January 2012, after less than 3 years of operation, at the San Onofre plant in California which led to the leakage of radioactive material from inside the tubes to the outside water. While the migration from Alloy 600 to 690 was primarily conducted due to improved corrosion resistance of Alloy 690 (provided by higher chromium content), the mechanical properties of Alloy 690 are not superior to that of Alloy 600. Therefore, Alloy 690 would be expected to be more susceptible to mechanically induced failure such as fretting and fatigue. Moreover, since the steam generator transfers excess heat from reactor core to outside, these tubes are exposed to extreme temperatures and (~320 °C) and pressures (~150 bar). Preliminary reports from the San Onofre nuclear plant indicated that the accelerated degradation was in part due to increased fretting from flow-induced vibration. This type of cyclic loading, in addition to the normal load (contact stress) due to fretting conditions, results in damage accumulation beneath the contacting surface of Alloy 690. The mechanism of fretting in LWR environments is complex because the failure occurs due to a combination of several synergistic processes such as fretting fatigue, fretting corrosion, and fretting wear. The material removal occurs in the following stages: (1) formation of highly plastic deformed surface layer, (2) fracture of the work-hardened layer, and (3) removal of wear debris and propagation of cracks in the deformed subsurface. The localized material loss due to fretting has two consequences in the LWR environment, namely, (1) accelerated corrosion of small worn-out areas that become anodes and large unaffected areas that act as cathodes and (2) fatigue crack initiation from the worn-out area that acts as a stress concentrator. Another important aspect is the microstructure of the alloy. Greater resistance to wear was observed with the large grain structures and coarse carbides along the grain boundaries of nickel-based alloys. Carbide morphology also influenced the wear resistance. Continuous grain boundary carbides showed increased propensity to crack formation (and hence low wear resistance) as compared to discrete grain boundary carbides.

Cast Stainless Steel Components

Cast stainless steels are extensively used in light water reactors (LWRs) as alloys for coolant piping and auxiliary piping components such as pump casings, valve bodies and fittings, elbows, and nozzles. Similar to the weld microstructure of austenitic stainless steels, the cast microstructure also contains delta ferrite. The ferrite content varies from 3 % to 12 % in welds and up to 40 % in cast austenitic stainless steel components. The delta ferrite is required to mitigate hot cracking

during solidification and control the intergranular corrosion. Mechanical strength and stress corrosion cracking resistance are improved by the ferrite phase present in the austenite matrix. Depending on the chemical composition, the primary solidification phase could be austenite or ferrite. When the primary solidification phase is austenite, the ferrite is present as interdendrites. Partitioning of the solute elements occur in the interdendritic regions that affect the chemical and mechanical properties when compared to the equiaxed wrought microstructures. The heterogeneity in the chemical composition also results in detrimental microstructural changes such as spinodal decomposition and precipitation of topologically close packed (TCP) phases during long time exposures to service temperatures that lead to thermal embrittlement.

The popular grades of cast austenite + ferrite duplex structure stainless steels in nuclear service are the CF3 and CF8 series of alloys. Among these, the CF3, CF3A, CF3M, CF8, CF8A, and CF8M are the most widely used alloys (equivalents of 304 and 316 wrought grades). These alloys typically have 17–21 wt% Cr and 8–13 wt% Ni. The digit following the letters CF refers to the carbon content of the alloys "3" for 0.03 % and "8" for 0.08 %. The fourth letter "A" denotes higher ferrite control which raises strength above that of the normal CF grades, and the letter "M" denotes addition of Mo to the nominal compositions of CF grade alloys. The macroscopic cast structure is generally divided into two categories depending on the casting process, namely, (1) static cast structure which contains columnar grain structure at the ends and equiaxed (randomly speckled) grains at the center (Calonne et al. 2004) and (2) centrifugally cast structure which contains long columnar grains at the outer wall and a mixture of equiaxed and columnar structures in the inner regions (Anderson et al. 2007).

Embrittlement due to thermal aging of cast stainless steels at service conditions in the temperature range of 280–320 °C has been a major concern (Chung and Leax 1990). The main transformations are the spinodal decomposition of α into α and a chromium-rich phase α′, precipitation of a G phase ($Ni_{16}Ti_6Si_7$), ε, and π (a nitride phase). Primarily, the formation of Cr-rich α′ (martensite) phase strengthens ferrite and decreases the toughness. With increased temperature (>550 °C), other embrittling phases such as σ, χ, η, $M_{23}C_6$ carbide, and γ_2 austenite are form aided by the presence of the ferrite/austenite interfaces. Sigma phase is a tetragonal crystal composed of $(Cr,Mo)_x$ $(Ni,Fe)_y$. The chi (χ) phase is a body-centered cubic with a typical composition of $Fe_{36}Cr_{12}Mo_{10}$. The typical stoichiometry of the Laves (η) phase is Fe_2Mo with a hexagonal structure. These topologically close packed (TCP) phases have large lattice parameters and large number of atoms in a lattice that show directional properties. Since these TCP phases nucleate at the high surface energy sites (grain boundaries and phase boundaries), cohesive strength of the grains is significantly reduced and brittle failure is often observed. It is important to note that the cold working accelerates the formation of the TCP phases by increased diffusion. Therefore, formation of Laves phase in cold-worked structure can be a high possibility even at reactor service temperatures.

Corrosion fatigue data for cast stainless steels in water containing 200 ppb and 8 ppm of dissolved oxygen (DO) at 289 °C have been generated and compiled by

Shack and Kassner of the Argonne National Laboratory (Shack and Kassner). In general, the corrosion fatigue crack growth rate is assumed to be related to the air fatigue crack growth through a power law given as

$$(da/dt)_{env} = A\,(da/dt)^{m}{}_{air} \tag{23}$$

For stress ratio R $<$ 0.9, A $= 4.5 \times 10^{-5}$ for DO $=$ 200 ppb, and A $= 1.5 \times 10^{-4}$ for DO $=$ 8 ppm, m $=$ 0.5.

Kawaguchi et al. (1997) studied the thermal embrittlement behavior of centrifugally cast CF8M duplex stainless steel after aging at 300–450 °C for up to 40,000 h. The aging treatment was quantified by a temper parameter denoted as P and given as $P = \log(t) + 0.4343(Q/R)(T_1{}^{-1} - T_2{}^{-1})$, where t = aging time, Q = activation energy for the embrittlement (typically 100 kJ/mol), T = temperature, and R = gas constant. The ferrite content of the samples varied from 15 % to 17.5 %. Spinodal decomposition of δ-ferrite to Cr-rich α′ phase (size, 5 nm) was observed after the following aging conditions: 300 °C for 10^4 h, 350 °C for 3000 h, and 450 °C for 300 h. The precipitation of larger (~50 nm) G phase was observed only at longer aging times than that required for spinodal decomposition and at higher temperatures. For example, aging at 300 °C for 40,000 h did not show the presence of G phase. Thermal aging at 350 °C for 10^4 h and 450 °C for 3000 h showed occurrence of the G phase. Spinodal decomposition was considered the main reason for the thermal embrittlement behavior of the CF8M cast stainless steel based on the Charpy V-notch energy of 230 J that decreased from the 300 J of the as-cast samples.

The use of subsize CT samples for the evaluation of the fracture toughness and the validation of the results with 1 T-CT samples was investigated by Jayet-Gendrot et al. (1998). Mini-CT specimens (5 mm thick) were extracted from the skin of the cast stainless steel elbows of a PWR unit that underwent 86,898 h of service at around 323 °C. The J-integral values of the mini-CT specimens (82 kJ/m^2 at 0.2 mm of Δa offset) were observed to be in good agreement with those derived from the 1 T-CT specimens. The effect of thermal aging on the low-cycle fatigue (LCF) behavior of the cast stainless steel in room temperature air was evaluated by Kwon et al. (2001). The samples were evaluated in as-cast and aged conditions (430 °C for 300 and 1800 h), and the LCF behavior was described by the relation

$$\frac{\Delta\varepsilon_t}{2} = \left[\frac{\sigma_f'}{E}\right] N_f^b + \varepsilon_f' N_f^c \tag{24}$$

where $\Delta\varepsilon_t$ = total strain range, σ_f' = fatigue strength coefficient, E = Young's modulus, b = Basquin's exponent, ε_f' = fatigue ductility coefficient, c = fatigue ductility exponent, and N_f = cycles to failure. The values of (σ_f'/E), $(-b)$, (ε_f'), and $(-c)$ of the 300 h aged samples were higher than that of un-aged samples. However, increasing the aging time to 1800 h resulted in lower values than that of the un-aged samples.

Jeong et al. (2009) evaluated the effect of strain hardening on the environmental fatigue behavior of CF8M under PWR conditions. The material was taken in the

as-cast condition with 25 % ferrite. The tests were carried out at 316 °C and 15 MPa with 30 ml of dissolved hydrogen per kg of H_2O and < 5 ppb of DO. Cyclic hardening was observed during the initial 200 cycles that showed peak loads which increased with increase in the strain amplitude. The fatigue test data points were scattered within the ASME design curve and the ASME mean curve. The same group also evaluated the effect of strain rate on the fatigue behavior (Jeong et al. 2011). The strain rate was varied from 0.004 % s^{-1} to 0.04 % s^{-1}. The number of cycles to failure increased with increase in the strain rate almost by an order of magnitude. The increase in the strain amplitude from 0.4 % to 0.8 % decreased the number of cycles to failure (from 2750 to 150 cycles at 0.004 % s^{-1} and from 13,500 cycles to 1500 cycles at 0.04 % s^{-1} strain rate).

Cicero et al. (2009) analyzed a CASS CF8M component (motor-operated valve of the reactor water cleanup (RWCU) system of a BWR unit) that was in service for 40 years using FITNET-FFS procedure and the ASME code. The ferrite content of the component was about 15 %. If the ferrite content was more than 10 %, the aging effect due to service temperature was needed to be considered for structural integrity analysis. The RWCU system was subjected to more than 60 major thermal cycles in the temperature range of 30–300 °C and a stable operating temperature of ~250 °C in 14 years. There were other minor temperature excursions at around 250 °C. The maximum service stress calculated at the neck of the valve was about 86 MPa, and the critical flaw size was much larger than that could be detected by inspection techniques. Wang et al. (2010) used nano-indentation technique to evaluate the thermal aging damage mechanism of the CASS. The specimens were aged at 400 °C for 100–3000 h representing service life of 0.7–21.48 years according to the corresponding Arrhenius relation. Dislocation pileup at the Cr-rich clusters of α′ spinodal decomposed phase was attributed to the observed embrittlement.

Cost–Benefit Analysis

Nuclear power is highly competitive with other forms of power generation such as fossil fuel power and renewable energy-based power generation. The cost of fuel is much less than that of fossil fuels. However, the capital cost is high because of increased margin of safety precautions and cost involved toward storage of spent fuels. While calculating the cost of nuclear power, the cost involved in waste management and decommissioning cost are fully considered (Economics of Nuclear Power).

In 2010, the cost of 1 kg of uranium as UO_2 reactor fuel is calculated as $ 2555. At 45,000 MW-day/ton burnup, 360,000 kWh electrical energy can be generated per kg of fuel. Therefore, the fuel cost per kWh energy is 0.77 cent. The US electricity production cost using different fuel sources in the year 2008 is given in Table 1. This includes cost of fuel, operation, and maintenance. Capital cost is not considered.

Table 1 Cost comparison of electricity generation in the USA using different fuel sources (for the year 2008)

Fuel source	Cost ($/kWh)
Oil	0.18
Gas	0.082
Coal	0.033
Nuclear	0.02

Table 2 Typical composition of nuclear fuel and spent nuclear fuel

	Fresh nuclear fuel	Spent nuclear fuel
235 U	3.3	0.81
238 U	96.7	94.30
236 U	–	0.51
239 Pu	–	0.52
240 Pu	–	0.21
241 Pu	–	0.10
242 Pu	–	0.05
Fission product	–	3.5

The capital cost includes:

- Bare plant – engineering, procurement, and construction (EPC)
- The owner's cost (land, cooling infrastructure, administration and associated buildings, site works, switch yard, transmission, project management, license, etc.)
- Cost escalation due to increased labor and materials
- Inflation
- Financing and interest of financing

The typical construction period of a nuclear power plant is about 48–54 months. Decommissioning cost is about 9–15 % of initial capital cost, which is about 0.1–0.2 cent per kWh of energy generated in the USA. The EPC cost in the year 2008 was about $ 3000/kW.

Spent Fuel and Reprocessing

When the spent fuel assembly is removed from the reactor, it is stored at the reactor site and allowed to cool before reprocessing or disposal. Typical compositions of fresh and spent fuels are listed in Table 2.

Most of the commercial reactor spent fuels are in water-filled swimming-pool-type structures. This type of arrangement is chosen because water is inexpensive, has good heat transfer coefficient by convection, and provides shielding, and visibility in water gives an opportunity to detect undesired events, if any. The limitation of water as a cooling medium in spent nuclear fuel is that water is a neutron monitor and active electrolyte for corrosion reactions.

The typical PWR operating cycle is about one year when 1/3 of the core is replaced with new fuel. After one year of operation, the fuel assembly, which weighs about 1300 lbs, is removed from the core and transferred to an interim storage facility. The radiation levels of the unshielded fuel assembly are more than millions of rems per hour.

The spent fuel assemblies are placed in vertical stainless steel racks. In order to prevent reaching critical conditions of the spent nuclear fuel assemblies, these are stored in well-separated conditions. Furthermore, neutron-absolving materials such as boron carbide or boron rods are inserted to inhibit neutron multiplication. The pool storage facility is designed only for interim storage – until the spent fuel is cooled down to low temperature. The remnant radioactive decay has subsided. Afterward the spent fuel will be taken for reprocessing or, in the absence of reprocessing, to a long-term storage facility.

Dry Storage

As an alternate to wet pool storage, dry storage using metal casks and concrete modules is practical. The heat generated during radioactive decay of the spent fuel is removed by the force convection of air, in case of modular concrete vault storage. Metal casks are provided with fins for faster heat transfer. These metal casks, if properly designed, can also be used for transportation of spent nuclear fuels.

For transportation of spent nuclear fuel, the metal casks are provided with (1) protection against direct radiation exposure to workers and the public, (2) provision for radioactive heat removal, and (3) neutron absorbers to prevent criticality. The metal casks can contain about 7 PWR assemblies or 18 BWR assemblies. The body of the cask is made of stainless steel of 5 m long and 1.5 m wide. Shielding is provided by depleted uranium or lead metal. It has an outer stainless steel shell and a corrugated stainless steel jacket that circulates water as neutron shielding fins are provided for external air forced cooling and minimal impact damage.

The spent fuel casks for transportation are constructed so sturdily that it can withstand the impact of being dropped from a height of 10 m onto an unyielding surface (metal anvil) and pass the crash test of a 130 km/h locomotive crash on a stationary cask-loaded tractor-trailer rig. It can also withstand fire for up to a 125 min burn in JP-4 fuel at 980–1150 °C.

Transmutation

Transmutation of transuranic elements such as plutonium, neptunium, americium, and curium can be conducted by irradiating with fast neutrons. In this process, the original actinide isotopes are transformed to radioactive and nonradioactive fission products. This process is important for nuclear waste management, since the isotopes of actinides have half-lives of thousands of years and alpha emitters. Transmuting these isotopes to short-lived fission products helps eliminate the radioactive hazardous associated with long-lived radionuclides.

Reprocessing

The spent fuel contains about 3.5 % fission products that predominantly contain neutron poisons such as Xe^{135} and I-137. Accumulation of fission products and depletion of fissile U-235 in the nuclear fuel make the sustainability of the nuclear chain reaction very difficult. Therefore, the nuclear fuel is removed from the reactor core. Currently, about 10,500 tons (of heavy metal) of spent fuel is disposed every year from nuclear reactors. The purpose of reprocessing is to separate the actinides from the fission products so that it can be reused as nuclear fuel. This decreases the burden on uranium mining and results in a more sustainable use of nuclear energy as a renewable energy source. Reprocessing can be carried over using aqueous or nonaqueous processes.

Aqueous Reprocessing

The aqueous process is based on the solvent extraction. Figure 9 illustrates the process flow. First, the spent nuclear fuel is dissolved in nitric acid. The Zircaloy cladding is removed separately. The aqueous solution containing dissolved spent fuel is taken for the solvent extraction in an organic solution of kerosene containing tributyl phosphate (TBP). When the aqueous solution comes in contact with the organic TBP, hexavalent uranium (U^{6+}) and tetravalent plutonium (Pu^{4+}) are

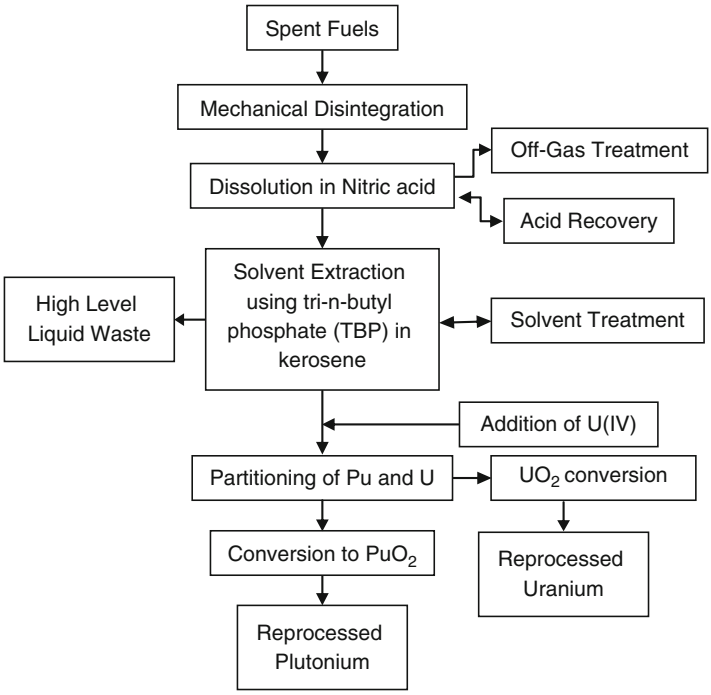

Fig. 9 Flow diagram of PUREX process of reprocessing spent nuclear oxide fuels

extracted by TBP. Almost all the fission products remain in the nitric acid solution which is extracted as high-level liquid waste. In the solvent extraction partitioning step, Pu^{4+} is reduced to Pu^{3+} by adding Li^{+} as a reductant. The Pu^{3+} is removed by dissolving in nitric acid solution. The recovered Pu can be used as a raw material for fast breeder reactor fuels in the future. The uranium species remaining in the solution can be recovered by processing through a series of scrubbing columns and purification columns. The purified uranium can be enriched and used as a fuel after converting to UO_2. The ability to separate plutonium from uranium is considered a potential proliferation concern. Therefore, modifications are made in the PUREX process to avoid separation of plutonium.

In the modified processes, uranium is separated while keeping Pu, minor actinides, and fission products in the waste solution. Later, the actinides are separated as a group. Another modification of the PUREX process is coprocessing. If the intent of reprocessing of spent fuel is to use the recovered actinides for producing mixed oxide fuel (MOX), then coprocessing is the right method. In this process, partitioning of U or Pu does not take place. Therefore, proliferation of Pu for weapon is not a concern. In the coprocessing method, 30 vol.% TBP in n-dodecane is used as solvent and a 2.5 M HNO_3 solution is used as scrub solution. The aqueous feed solution containing 4.2 M HNO_3, 2 M UO_2, + Pu, and 1.25 M FP is fed through solvent extraction column of TBP in n-dodecane. Uranium and plutonium are complexed with the TBP, and thus, fission products are separated. The U + Pu complexed with organic phase is washed with dilute nitric acid. The resulting nitrate solution of U + Pu is treated with peroxides or oxalates to form precipitates of U + Pu peroxide or oxalate. These oxalate precipitates are calcined to form UO_3 or U_3O_8 and reduced in hydrogen atmosphere to form UO_2. There are several variations in the PUREX process. Table 3 lists these modified PUREX processes.

Pyroprocessing

Pyrochemical or pyrometallurgical processing using LiCl–KCl molten salt systems is considered one of the most feasible alternatives to the PUREX process for safe and proliferation-resistant recovery of nuclear fuel elements from the spent fuels. This technology may also be useful for separating actinides from the high-level waste generated by the PUREX process. Pyrometallurgical process is preferred because of the stability of the molten salts to high radiation and shorter cooling times (OCDE/NEA Report). Reprocessing of metallic fuels involves separation of actinides from the fission products by electro-transport in a molten salt electrolyte. Since rare earth elements (as part of fission products) have similar chemical properties as that of actinides and show neutronic poison effect, separation of fission products is important for efficiently recycling the actinides. Spent oxide fuels also can be reprocessed by the pyrometallurgical electrorefining method. In this case, the spent oxide fuel is reduced to metal form by lithium (Koyama et al. 2007) or chlorinated in the presence of a reductant such as carbon (Yang et al. 1997) before anodic dissolution or direct dissolution in the presence of an oxidizer such as $CdCl_2$ into the molten salt (Koyama et al. 1997).

Table 3 Variations of aqueous–organic reprocessing of nuclear spent oxide fuels (Adopted from the Nuclear Technology Review Supplement, International Atomic Energy Agency, Vienna, 2008)

Process	Purpose	Special aspects
DIAMEX	Extraction of minor actinides and lanthanides from HLLW	**Diam**ide **ex**traction process solvent based on amides as alternate to phosphorous reagent generates minimum organic waste as the solvent is totally combustible
TOGDA	Ditto	**T**etra-**o**ctyl-**di**g**l**ycol-**a**mide Amide similar to DIAMEX
TRUEX	**Tr**ansuranic (**TRU**) element **ex**traction from HLLW	Extraction by using **c**arbamoyl **m**ethyl **p**hosphine **o**xide (CMPO) together with TBP
SANEX-N	**S**elective **a**cti**n**ide **ex**traction process for group separation of actinides from lanthanides	Process for separating actinides from lanthanides from HLLW by using neutral N-bearing extractants, viz., bis-triazinyl-pyridines (BTPs)
SANEX-S	Ditto	Use of acidic S-bearing extractants, for example, synergistic mixture of Cyanex-301 with 2,2-bipyridyl
TALSPEAK	Ditto	**T**rivalent **a**ctinide–**l**anthanide **s**eparation by **p**hosphorus reagent **e**xtraction from **a**queous **k**omplexes. Use of HDEHP as extractant and DRPA as the selective actinide complexing agent
ARTIST	Ditto	**A**mide-based **r**adio-resources **t**reatment with **i**nterim **s**torage of **t**ransuranics. This process is made up of (1) phosphorus-free **b**ranched **a**lkyl **m**ono**a**mides (BAMA) for separation of U and Pu, (2) TOGDA for actinide and lanthanide recovery, and (3) N-donor ligand for actinide–lanthanide separation
SESAME	**S**elective **e**xtraction and **s**eparation of **a**mericium by **m**eans of **e**lectrolysis	Process for separating Am from Cm by oxidation of Am to A (VI), subsequent extraction with TBP for separation from Cm
CSEX	**Cs e**xtraction	Using calix-crown extractants
CCD-PEG	Extraction of Cs and Sr from raffinate	**C**hlorinated **c**obalt **di**carbollide and **p**oly**e**thylene **g**lycol (CCD-PEG) in sulfone-based solvent is planned for extraction of Cs and Sr from UREX raffinate
SREX	**Sr ex**traction	Using dicyclohexano-18-crown-6 ether
GANEX	Uranium extraction + other processes for further separation	A series of five solvent extraction flow sheets that perform the following operations: (1) recovery of Tc and U (UREX); (2) recovery of Cs and Sr (CCD-PEG); (3) recovery of Pu and Np (NPEX); (4) recovery of Am, Cm, and rare earth fission products (TRUEX); and (5) separation of Am and Cm from the rare earth fission products (Cyanex-301)

The major advantages of the pyroprocessing spent fuel are as follows:

- The process is proliferation resistant since Pu is not separated from minor actinides.
- Interim storage of spent nuclear fuel may not be required since the pyroprocessing is capable of handling spent fuels in hot conditions as the process takes place in temperatures greater than 500 degrees Celsius.
- No liquid wastage is generated for disposal. Therefore, waste management becomes easy.
- The process can be adopted for in-line reprocessing at the reactor site.
- This process can accept several forms of fuel such as uranium oxide, carbide, nitride, mixed oxides, and pure heavy metals.
- Very short turnaround time results in cost saving.
- Generation of minimum transuranic waste.

The limitations of the process are requirements of facilities with oxygen- and moisture-free environment, arid construction materials that withstand very high temperature, and highly corrosive molten halide environment.

Reprocessing of Spent Metallic Fuel

Metallic fuels are used in experimental fast breeder reactors with liquid sodium as coolant. Reprocessing of this spent fuel (U–Zr, U–Pu + Zr alloys) is carried on by first chopping them into small pieces, loaded onto an anode basket made of SS, and dissolving them by applying anodic potential in an electrorefining cell. The electrolyte is typically an eutectic of LiCl–KCl at 500 °C. By applying an anodic potential to the stainless steel basket containing the chopped fuels, the pellets are oxidized and dissolved in the molten salt. Dissolved actinides are present as chlorides in the molten salt. Lanthanides in the fission product are converted to lanthanide chlorides and dissolved in the molten salt. Addition of $CdCl_2$ to the LiCl–KCl mixture helps transfer most of the actinides and lanthanides as chlorides in the molten salt bath. Gaseous fission products are out-gased. Undissolved cladding materials and noble fission products will be recovered as solids from the reprocessing cell.

During the electrorefining process, uranium is recovered from the molten salt by application of a constant cathodic current density to a steel cathode in a shape of a cylindrical rod, as shown in Fig. 10. The resultant cathodic potential is just sufficient to electrodeposit only uranium onto the steel cathode. After depositing uranium, when the ratio of plutonium to uranium is greater than 2 (Pu/U $>$ 2), now the electrodeposition process is continued with liquid cadmium as cathode. In this step, plutonium is recovered along with americium (Am) in the form of Pu–xAmxCd6 compound. More than 10 wt% of Pu is collected using this method. A high separation factor between actinides and rare earths within a MClx–LiCl–KCl system has also been reported when liquid bismuth is used as liquid cathode. After the actinide recovery, the molten salt is solidified and scrubbed to remove fission products through a zeolite column.

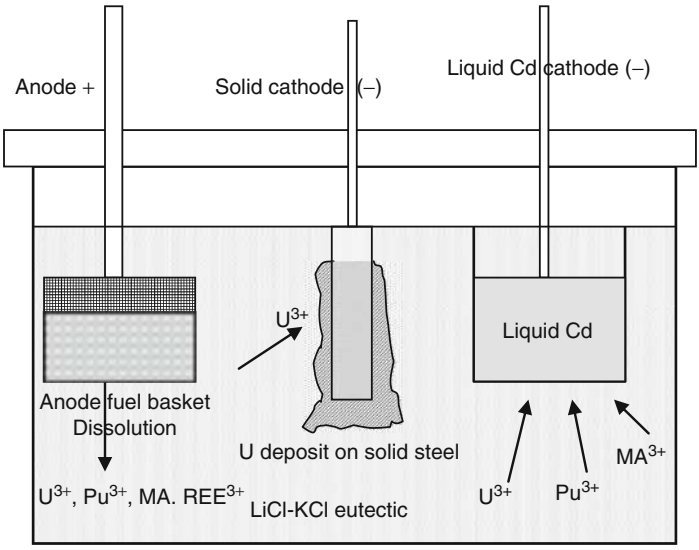

Fig. 10 Schematic arrangement of electrorefining cell for pyroprocessing of spent nuclear fuel in molten LiCl–KCl

Table 4 Redox potentials and activity coefficients of actinides in LiCl–KCl eutectic melt at different temperatures (Roy et al. 1996, pp 2487–2492)

	Potential at different temperatures of LiCl–KCl (V vs. Cl^-/Cl_2) (γ = activity coefficient)			
Actinide system	673 K	723 K	773 K	823 K
U(III)/U	−2.53 ($\gamma = 2 \times 10^{-3}$)	−2.49 ($\gamma = 3.1 \times 10^{-3}$)	−2.45	−2.42
Pu(III)/Pu	−2.845 ($\gamma = 1 \times 10^{-3}$)	−2.808 ($\gamma = 2.3 \times 10^{-3}$)	−2.775 ($\gamma = 4.1 \times 10^{-3}$)	–
Am(II)/Am	–	−2.843	–	–

The redox potentials of actinides and lanthanides are given in Tables 4 and 5, respectively. The lanthanides show more negative potentials than actinides. Among the actinides, uranium shows less negative reduction potential than plutonium and americium. Therefore, under a sufficient cathodic polarization, uranium will be reduced first. Electrodeposition of the uranium on the solid steel cathode decreases the concentration of the uranium (III) ions in the melt. Therefore, the redox potential of U(III) will move to more negative potentials with continuation of the electrorefining process. The electrorefining process is switched to liquid cadmium cathode because of the following reasons: (1) Liquid cadmium as cathode decreases the activity of actinides other than uranium as shown in Table 6; (2) the lower activity coefficient brings the redox potentials of all actinides closer so that these elements can be deposited together; and (3) recovery of Pu along with other minor actinides gives better proliferation resistance.

Table 5 Redox potentials of lanthanides dissolved in LiCl–KCl eutectic at 450 °C

Redox couple	Reduction potential at 450 °C, V vs. Cl^-/Cl_2
La^{3+}/La	−3.1 (Kuznetsov et al. 2005)
Ce^{3+}/Ce	−3.26 (Castrillejo et al. 2002)
Nd^{3+}/Nd	−3.02 (Hamel et al. 2004)
Dy^{3+}/Dy^{2+}	−3.32 (Castrillejo et al. 2005a)
Dy^{2+}/Dy	−3.36 (IAEA 2001)
Gd^{3+}/Gd	−3.15 (Caravaca et al. 2007)
Pr^{3+}/Pr	−3.41 (Castrillejo et al. 2005b)

Table 6 Activity coefficients of actinides in liquid cadmium at 450 °C

Element	Activity coefficient in liquid cadmium at 450 °C
U	15
Np	2.8×10^{-3}
Pu	3.1×10^{-5}
Am	1.1×10^{-4}

The five orders of magnitude smaller activity coefficient of Pu as compared to that of U could be attributed to formation of $PuCd_6$ compounds in the liquid Cd cathode (Shirai et al. 2000). When Pu is electrodeposited onto liquid cadmium cathode, the reduction potential is shifted by 0.3 V in the positive direction as compared to the electrodeposition onto a solid surface. This shift in the positive direction brings the reduction potential of Pu closer to the reduction potential of U(III). The shift in the reduction potential of PU(III) in liquid cadmium cathode can be explained by using the Nernst equation:

$$Pu^{3+} + 3\,e^- \rightarrow Pu \tag{25}$$

$$E^1 = E^0 + \frac{2.3RT}{3F}\log\frac{[Pu^{3+}]}{[\gamma Pu]} \tag{26}$$

Since the value of γ is 3.1×10^{-5} in the liquid cadmium, the redox potential is shifted almost by 0.25 V in the positive direction. Sustained operation of the electrometallurgical reprocessing cell results in accumulation of fission products in the electrolyte and depletion of the uranium ions in the salt. The variation in composition of the electrolyte could potentially alter the operating conditions of the cell because of the significant changes in the thermophysical properties and interfacial electrochemical behavior of the molten salt systems. For better process control, a detailed database of the electrochemical properties of the molten salt system is required. When multiple fission product elements are present in the electrolyte, the reduction behavior of the actinides could significantly be altered because of possible underpotential reduction of lanthanides and slower diffusion kinetics of actinides. This is important for determining limits on the use of the molten salt electrolyte before it needs to be purified or disposed.

Thermodynamic and transport properties of binary LnX_3–MX systems have been investigated widely (Gaune-Escard et al. 1994; Takagi et al. 1997; Gong et al. 2005) where Ln = La, Ce, Pr, Nd, Gd, Tb, and Eu; M = Li, L, Na, Cs, and Rb; and X = F, Cl, I, and Br. Addition of lanthanide chloride to alkali metal chloride results in formation of a variety of stoichiometric compounds such as M_3LnCl_6, MLn_2Cl_7, M_2LnCl_5, $M_3Ln_5Cl_{18}$, etc. Formation of compounds and complexes in the molten salt system affects the electrical conductivity and other thermophysical properties. Stoichiometric compounds show minimum electrical conductivity. Structural disordering increases the number of current carriers and improves the conductivity. The specific electrical conductivity of $LnCl_3$ ranged from 0.11 to 0.4 Sm^{-1} at 1000–1250 K. The activation energy for electrical conduction was about 28–30 kJ/mol. Polymerization of the melt was reported to play a significant role in increasing the electrical conductivity of the molten salt system[2]. Existence of octahedral complex anions of $LnCl_6^{3-}$ in the $LnCl_3$ melts and formation of dimers have been proposed by the following reaction (Ikeda et al. 1988):

$$2LnCl_6^{3-} \rightarrow Ln_2Cl_{11}^{5-} + Cl^- \tag{27}$$

Since free Cl^- ions are produced by the above dimerization reaction, the conductivity of the melt increases. Both polymerization of melt and presence of free chloride ions could affect the activity and mobility of the cations, and in turn the separation kinetics could be altered.

Standard potentials of actinides in LiCl–KCl eutectic salt and separation of the actinides from rare earths by electrorefining have been widely reported by many research groups (Sakamura et al. 1998; Roy et al. 1996; Serrano and Taxil 1999). Recently, Castrillejo and coworkers (2005c) reported electrochemical behavior of a series of lanthanide elements in LiCl–KCl eutectic melt in the temperature range of 400–550 °C.

Cyclic voltammetry results of binary, ternary, and quaternary $LnCl_3$-$(LiCl–KCl)_{Eutectic}$ systems at 500 °C indicate that the incipient potentials of cathodic reduction waves shifted to less negative values with increased additions of lanthanide components. The positive shift in the potential of reduction wave is, in general, associated with two phenomena, viz., (1) under potential deposition, the interaction of reducing species (R) with the substrate (S) is energetically more favorable than the species–species (R-R) interaction, and (2) when two species (A and B) are present in the electrolyte, formation of a compound (A_nB_m) is more favorable by having a negative free energy ($-\Delta G$), and the deposition potential is positively shifted from the redox potential of the more negative species by an amount ($-\Delta G/nF$) (Cohen 1983). The CV results of binary system (single component lanthanide addition) do not show any underpotential deposition of pure lanthanide elements. However, in this investigation, addition of more than one lanthanide chloride in the LiCl–KCl eutectic resulted in considerable shift in the incipient potential of the cathodic wave. According to Hume-Rothery principles, atoms having similar size (size difference <15 %) and electronegativity will preferentially form solid solutions and not compounds. Therefore, elements of lanthanide series will not form compounds

within them but can form solid solutions. The commercially available mischmetal is such an extended solid solution of various lanthanide elements that is separated from naturally occurring monazite mineral. Easy formation of solid solution of lanthanide elements indicates that this is a thermodynamically more favorable process. Therefore, any change in the free energy of formation of solid solution will be reflected in shifting the cathodic wave potential to positive direction with reference to the individual elements' reduction potential.

The other possible reason for the positive shift in the reduction potential of multicomponent lanthanide system could be because of lowered stability of the lanthanide clusters in the molten alkali salt. Generally, solvation of Ln(III) in LiCl–KCl eutectic mixture forms clusters of $[Ln(KCl)_n]^{3+}$ and $[Ln(LiCl)_n]^{3+}$, with the coordination number, n, varying from 4 to 9. The presence of a single lanthanide component in the alkali molten salt results in coordination numbers 6–9. Model calculations of Hazebroucq et al. (2005) indicated that the stable coordination number for Gd (III) was 6 and for La (III) it was 7–8. When multiple lanthanide components are present, the coordination of the solvated clusters is significantly affected and their stability is reduced. Therefore, the positive shift in the reduction potential for multicomponent system could be attributed to the change in stability of the solvated clusters in the molten salt.

Recovery of Rare Earth Elements (REEs) from Fission Products

Rare earth elements are part of strategic materials used in various important energy and defense applications. Separation of rare earth elements from fission products could help reduce the burden on nuclear waste management and reduce the impact on the environment during mining operation of extraction of these strategic materials. Rare earth elements such as neodymium and samarium are used in producing high-strength permanent magnets that are used in various applications such as motors and electronic components. Rare earth oxides are used in laser applications. Almost 38 % of REEs find application as phosphors and solid-state lighting device. Mischmetals are used for manufacturing AB5-type nickel–cobalt hydrides that are used as cathodes for metal hydride batteries and hydrogen storage for electric vehicle applications. Rare earth oxides are extensively used as catalysts for various chemical processes such as methane reformation, fluid cracking, oil refining, and water–gas shift reactions. Furthermore, rare earth oxides are used in fuel cell and high-temperature battery applications as catalysts and membranes. Rare earth elements are used in thermal barrier coatings and strategic alloys as well. Therefore, separation of lanthanide elements from fission products is important from both strategic and environmental points of view.

It is observed that addition of multicomponent lanthanides (more than 5 wt%) to the LiCl–KCl eutectic shifted the reduction potential to less negative values which might hinder the effective separation of actinides from the lanthanides. One possible way of minimizing this effect is to remove the lanthanides as the electrorefining progresses so that accumulation of lanthanide is minimized. Separation of lanthanide can be made possible by using a bipolar cell and a bipolar membrane that has a high diffusion coefficient to lanthanide series. The design of the cell is given in Fig. 11.

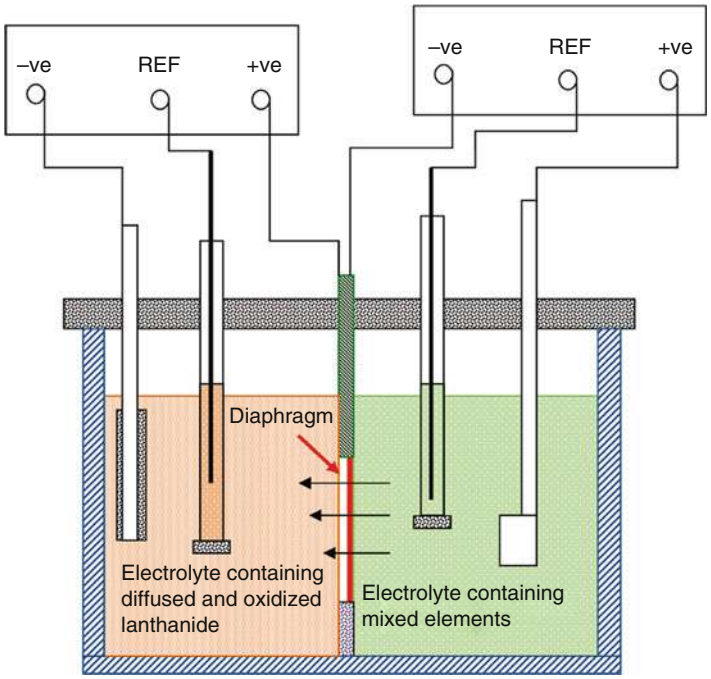

Fig. 11 Schematic of bipolar cell with metal diaphragm that preferentially alloys with select lanthanide(s) and allows diffusion of lanthanide elements to the other side

Working Principle of the Bipolar Cell for Separation of Lanthanides: Figure 11 schematically illustrates the construction of the bipolar cell. Two compartments are connected by a thin metal diaphragm. This metal diaphragm will preferentially alloy with a particular lanthanide element, for example, neodymium. The right-side compartment will contain molten salt of multicomponent additions that needs to be electrolyzed. The diaphragm as a cathode, an inert electrode as an anode, and Ag/AgCl as a reference electrode will complete the electrical circuit. Depending on the applied potential, a particular lanthanide element that has a higher alloying affinity with the diaphragm metal will deposit onto the diaphragm and diffuse out to the left compartment because of a concentration gradient and a small electric field across the diaphragm. In the left compartment, the diaphragm is connected to a positive terminal of another electric circuit. Therefore, depending on the anodic potential applied to the diaphragm, the diffused lanthanide element will dissolve into the electrolyte of the left-side compartment. The oxidized lanthanide species will get reduced at the cathode of the left-side compartment and thus separated from the other species.

The main issue of this design is construction of a stable diaphragm that is thin enough to allow a required flux of the lanthanide. Aluminum diaphragms can be used for separating Nd. Nickel diaphragm also can be used. A thin diaphragm of Ni can be prepared by electroless deposition onto an organic substrate.

Pyroprocessing of Spent Oxide Fuels

Spent nuclear oxide fuels also can be reprocessed using molten salt refining technique as that of metal oxide fuels. The electroreduction technique used for directly reducing uranium oxide to uranium is similar to the technique of the FFC Cambridge process proposed for directly reducing TiO_2 to Ti (Chen et al. 2000). Alternately, the oxide fuels can be reduced by using lithium. The first step in chemical reduction of UO_2 is to convert the material to U_3O_8. Similarly, PuO_2 is also converted to Pu_2O_3 before reacting with lithium. The proposed reactions are

$$U_3O_8 + 16\,Li \rightarrow 3U + 8Li_2O \qquad \Delta G = -871.8\ kJ \tag{28}$$

$$Pu_2O_3 + 6\,Li \rightarrow 2\,Pu + 3\,Li_2O \qquad \Delta G = 18.8\ kJ \tag{29}$$

$$Am_2O_3 + 6\,Li \rightarrow 2\,Am + 3\,Li_2O \qquad \Delta G = 23.18\ kJ \tag{30}$$

Mixed oxide spent fuels can be electrochemically reduced more easily than UO_2 in a LiCl bath at 650 °C. In the uranium oxide electroreduction cell as presently conceived, a platinum (Pt) wire is used as the anode.[1] The Pt wire is slowly etched away as the electrolytic reduction proceeds because of the highly oxidizing conditions and attack by lithium (Li). The cell is operated at 650 °C with a LiCl–Li_2O electrolyte. The overall cell reaction is as follows:

$$UO_2 \rightarrow U\,(\text{cathode}) + O_2 \uparrow (\text{anode}) \tag{31}$$

The Li_2O content varies from 1 to 8 wt% for the Li-assisted chemical reduction of UO_2 by participating in the following reactions:

$$2Li_2O \rightarrow 4Li + O_2 \uparrow \tag{32}$$

$$4Li + UO_2 \rightarrow U + 2Li_2O \tag{33}$$

Although the reduction of Li_2O to Li increases the reduction rate of the spent oxide fuel, the Li diffuses through the salt electrolyte and attacks Pt, thereby degrading the anode. To decrease degradation of the Pt anode, a secondary electric circuit is provided to oxidize the Li to Li(I). Provision of a more refractory anode that withstands the highly oxidizing conditions and attack by Li would greatly simplify operation of the cell.

Therefore, finding an alternative anode material is vital before the electrolytic cell is put into production. Platinum metal is highly resistant to oxidation under normal conditions, but not under high anodic potential at 650 °C in a corrosive Li containing molten chloride electrolyte. Several materials are worthy of consideration as inert anodes. Various nickel-based super alloys such as Haynes 263, Haynes 75, Inconel 718, Inconel X-750, Inconel 713 LC, Inconel MA 754, Nimonic 80A, and Nimonic 90 have been investigated by KAERI.[2] It was noted that increasing the chrome (Cr) contents of the above alloy increased the stress on the surface layer and

increased the corrosion rate. Elements such as aluminum (Al) and titanium (Ti) improved the corrosion resistance by forming a more protective layer. It should be pointed out that these test conditions did not include metallic Li in the electrolyte. The solubility of Li in LiCl was more than 0.6 mol%. Oxidizing environment was created by purging argon + 10 % O_2 gas into LiCl + 3 wt% Li_2O electrolyte at 650 °C. Boron-doped diamond as a potential anode material has also been reported (Storm van Leeuwen and Smith 2005).

Inert anode material for electrolytic reduction of the spent fuel in LiCl + Li_2O electrolyte should satisfy the following requirements:

- The material should have comparable electrical conductivity to that of platinum.
- The material should not be consumed by the electrochemical/chemical reaction so that the dimensions remain stable throughout the electrolytic process without altering the cell voltage significantly.
- The material should be resistant to corrosion by lithium in the molten salt.
- The protective oxide layer of the material must not dissolve in the basic flux of Li_2O present in the molten salt.
- The material must be stable in the highly oxidizing potentials encountered at ~650 °C in LiCl + Li_2O electrolyte.
- The material should possess sufficient mechanical properties (such as creep strength and fracture toughness) in order to withstand thermal shock and service-related stresses.

The material fulfilling the above requirements can be a metal or an alloy with high electronic conductivity. The material can also be a composite (cermet) or made of metal/alloy coated with external oxide/carbide/nitride. This article describes the investigation of inert anode materials for use in an electrochemical cell by simulating the corrosive environment of the spent nuclear fuels with LiCl and LiCl + Li_2O molten mixtures.

Containment of Radionuclide

Development of next-generation nuclear waste forms capable of reliable and safe immobilization of radionuclide is a significant challenge that limits the imminent nuclear renaissance to meet the energy demands. Among the nuclear wastes, Cs and Sr are considered critical because of the high activities of ^{134}Cs (half-life, 2 years), ^{137}Cs (half-life, 30.17 years), and ^{90}Sr (half-life, 28.8 years). Removal of these isotopes will significantly reduce the radioactive load on a geological repository (Wigeland et al. 2006). These radionuclides are separated from the low-level nuclear wastes using an ion-exchange process and combined with high-level waste fraction and then immobilized in a glass or ceramic form. The following transmutation reactions take place during radioactive decay of ^{137}Cs and ^{90}Sr:

$$^{137}\mathrm{Cs} \rightarrow ^{137}{*}\,\mathrm{Ba} + \beta(\text{half life}: 30.17\ \text{years}) \rightarrow ^{137}\mathrm{Ba} + \gamma(2.55\ \text{min}) \quad (34)$$

$$^{90}\mathrm{Sr} \rightarrow ^{90}\mathrm{Y} + \beta(\text{half life}: 30.17\ \text{years}) \rightarrow ^{90}\mathrm{Zr} + \beta(64.1\ \text{h}) \quad (35)$$

The decay of ^{137}Cs emits beta particles with energy ranging from 0.089 to 1.454 MeV and gamma rays with 0.475–1.168 MeV energy (Lide 1997). The beta and gamma decays of the radionuclides could detrimentally affect the stability of the host material. Furthermore, formation of the transmuted elements in the host materials alters the electronic structure and chemical composition of the waste form. Most of the investigations so far have concentrated on the effect of radiation damage such as swelling, bubble formation, and leachability on the structural stability of the waste form. Very little attention has been paid on the effect of electronic structure changes during the decay of constituent radioisotopes in the waste form. For example, when the Cs^+ transmutes to $Ba^{2+} + e^-(\beta) + \gamma$, the single valent Cs is replaced with divalent Ba. Therefore, the host material should be able to accommodate the valence and associated ionic radius changes. Recently, Jiang et al. (2009) from LANL reported for the first time the modeling of the chemical evolution of CsCl to BaCl due to radioactive decay using ab initio calculations. In the modeling calculations, these authors considered CsCl crystal as a representative waste form.

Crystalline silicotitanate (CST) and (Ba,Cs) hollandite ceramics are considered potential candidates for the specific immobilization of Cs. The sodium silicotitanate ($Na_2SiTi_2O_7$. $7H_2O$) is ion-exchanged to form hydrogen crystalline silicotitanate ($H_2SiTi_2O_7.1.5H_2O$). This material effectively sequesters both Cs and Sr (Celestian et al. 2008). The hollandite for Cs sequestration has a formula of $(Ba_xCs_y)(M_{2x+y}Ti_{8-2x-y}O_{16})$, where M is trivalent cations such as Fe^{3+}, Al^{3+}, and Ti^{3+} and $x + y < 2$. Celestian et al.[4] showed that selective ion exchange of Cs in the H-crystalline silicotitanate (H-CST) is achieved by repulsive forces between the Cs^+ and H_2O dipole that lead to a series of events at the molecular-scale level such as rotation of H_2O by 159° followed by bending away of hydroxyl group by 0.055 nm displacement which makes TiO_6 to rotate about 5.6°. The rotation of the TiO_6 columns results in a structural transformation that changes the initial $P4_2/mbc$ space group of the H-CST to $P4_2/mcm$ of Cs-CST. During this transformation, an initial elliptical eight-membered ring (8MR) channel becomes a circular one that opens up a new site for Cs^+ occupancy at the center of the channel (known as Cs1 site) in addition to the initial Cs2 site which is outside the 8MR window. A minimum occupancy of 0.15 at the Cs2 site is required to initiate the structural transformation and formation of the new Cs1 sites. The above hypothesis for the selective ion-exchange mechanism of Cs in the H-CST material indicates that the interaction of Cs^+ and H_2O dipole/hydroxyl groups is very important not only for the site selectivity but also for the stability of the Cs-CST structure. It is not clear how the radioactive transmutation of Cs^+ to Ba^{2+} will affect the stability of the Cs-CST structure over an extended period of time. In case of the hollandite, structural transformation from tetragonal to monoclinic at

room temperature is reported with increased Ba occupancy in $Ba_xFe_{2x}Ti_{8-2x}O_{16}$ (Carter 2004).

Nuclear Waste Management

All types of radioactive waste can be disposed of if the disposal method provides protection for the health and safety of people and the environment. Members of the European Union (EU) produce about 7000 m^3 of high-level waste from 143 nuclear power plants. Disposal in deep underground engineered facilities is considered the best solution for managing high-level and long-lived radioactive wastes. High-level waste is mixed with glass and vitrified. The vitrified waste is stored for 30–50 years and allowed to cool. After cooling, the waste is placed in an iron shell container. The iron container is placed inside a copper shell, which is evacuated and backfilled with an inert gas and sealed. The copper canister is buried in a deep permanent repository with engineered barriers. Swedish and Finnish nuclear waste repository models are based on copper canisters, since copper is considered to be stable in clay environments devoid of oxygen. Several countries plan to use this approach of permanent storage of the high-level radioactive waste.

When the amounts of radioactive waste in surface storage increase, the sustainability of storage in the long term and the associated safety and security implications are of concern. Geological disposal promises to provide containment and isolation of radioactive waste from the human environment for the very long periods required. Safety concerns due to possible human intrusion into the waste are very much reduced as compared to surface storage, owing mainly to the significant depths under the surface at which geological repositories will be located. In the USA, long-term storage of nuclear waste in Yucca Mountain was considered an option. The Yucca Mountain repository was based on different layers of engineered barriers to nuclear waste storage such as a 300 m deep geological barrier, a Ti-alloy drip shield to prevent water seeping through rock faults falling on the canister surface, an outer wall of canister made of Ni–22Cr–13Mo–3Fe alloy, and a thicker inner wall of canister made of type 304 stainless steel. Recently the US Department of Energy filed a motion with the Nuclear Regulatory Commission to withdraw the license application for a high-level nuclear waste repository at Yucca Mountain. Therefore, the spent fuel assemblies from the nuclear power plants will be stored on-site in the utility facilities for longer time.

Future Direction

Meltdown of the nuclear core is considered the severest form of nuclear accident, since the probability of release of radioactivity is high in this condition. In order to prevent core meltdown, Western nuclear power plants are provided with two or four emergency core cooling systems (ECCS). This system consists of

high-pressure coolant injection system, depressurization system, low-pressure coolant injection system, core spray system, containment spray system, isolation cooling system, and emergency electrical system. The emergency electrical system consists of diesel generators, motor generator flywheels, and batteries. In case of an emergency situation, the control rods are moved completely inside the reactor core and the power is reduced considerably. Any loss of coolant will trigger the ECCS. There are two or four ECCS in a reactor to ensure that at least one will respond and meltdown will be avoided. However, if all ECCS fail as in the case of Fukushima nuclear plants in March 11, 2011, meltdown of the core is initiated. It should be noted that the Fukushima nuclear disaster is not due to operator error or gross violation of safety regulations unlike the accidents reported in the Three Mile Island or Chernobyl. The plant suffered a major damage because of an earthquake of 9.0 in a Richter scale. The reactors were designed for a maximum ground acceleration of 0.18 g (1.74 m/s^2), whereas the earthquake caused a ground acceleration of 0.35 g (3.43 m/s^2). Therefore, the reactors were shut down automatically. This would have triggered the insertion of control rods and ECCS. However, a tsunami of 20 m tall waves followed the earthquake and flooded the power plant. The plant was designed only for a tsunami of 5.7 m. The flooding situation knocked down the emergency power and prevented any assistance reaching the power plant. The batteries provided in the emergency electrical system were not adequate to pump the required volume of coolant to the core. The power required for running coolant pumps or other electrical systems triggered a cascade of accidents in the Fukushima nuclear plant that released radioactive gases into the environment causing displacement of several thousand people living around the power plant.

In order to cool the core, several measures were taken by the Fukushima power plant officials. Adding water to the degraded core can result in several consequences such as (Kuan and Hanson 1991):

- Hydrogen production
- Change in the geometry of core
- Pressurization of the system due to high rate of steam generation
- Steam explosion
- Re-criticality of the core when enough neutron absorbers are not present

The core damage occurs in several stages as explained below (Cookson and Was 1995):

Pre-damage Stage: If the core is not fully immersed in water, then the upper portion of the core will be exposed to steam in the reactor. Now the core will start to heat up at a rate of 0.3–1 °C/s.

Ballooning and Bursting of Fuel Rods: When the temperature reaches > 1100 K, the Zircaloy cladding will balloon up because of the rapid heating and burst. This altered geometry of the fuel rod will affect the geometry of the coolant flow channels in the core. Some locations will have restricted access to the coolant

because of the ballooning effect. If sufficient water is added, core damage can be suppressed at this stage.

Rapid Oxidation: This stage is initiated at 1500 K. When Zircaloy reacts with steam, hydrogen is produced as given by the following reaction and a large amount of heat is released:

$$Zr + 2H_2O \rightarrow ZrO_2 + 4H_2 + 6.5\ MJ/kg\ of\ Zr$$

If water is added at sufficient rate and volume, the core will be quenched and progression of damage could be stopped. If the water is not sufficient or the rate of heat removal is less than the rate of heat generated, the damage propagates to the next stage.

Debris Bed Formation: When the temperature reaches 1700 K, the molten control materials will flow to the lower part of the core (which is submerged in the water) where the temperature is low and solidify. At 2150 K melting of Zircaloy occurs. Molten Zircaloy along with dissolved UO_2 may flow downward and solidify at the lower portion of the core. These solidified debris will form a cohesive bed leading to restricted flow of coolant in the lower region of the core.

Relocation of Lower Plenum: When molten core materials (which are experiencing 1500–2150 K) fall to the lower region of the core which is at ~550 K, steam is generated rapidly leading to occurrence of steam explosion. Furthermore, this steam oxidizes any unoxidized molten Zircaloy which generates hydrogen at a faster rate. These reactions lead to overpressurization of the system. Re-criticality also may occur in the relocated core debris when the control materials are not present in the required concentration.

Understanding of the sequence of core damage is necessary to design preventive measures of core meltdown. Future work on nuclear safety should concentrate on a reliable ECCS that can be operated even in the worst-case scenario as experienced in the Tohoku Tsunami. Future work also should focus on a reliable system, with public acceptance, for a long-term safe storage of nuclear spent fuel.

Future Fuel Cladding Materials: Zr–Sn alloys such as Zircaloy-2 and Zircaloy-4 are currently used as fuel cladding tubes in the current light water reactors because of their low neutron absorption cross sections for thermal neutrons, reasonable creep resistance, and corrosion resistance in high-temperature high-pressure water (Wray and Marra 2011). These cladding materials perform well under normal operating conditions and give a reasonable safety margin under design basis accident (DBA) scenarios. However, under beyond design basis accident (BDBA) conditions, such as a loss-of-coolant accident event that occurred in the Fukushima Daiichi power plant, zirconium-based cladding materials undergo severe degradation because the peak clad temperature (PCT) exceeds the design limit of 1204 °C (Charit and Murty 2008). When the Zr-alloy cladding is exposed to high-temperature steam environment, an exothermic Zr-steam reaction generates more heat than that of radioactive decay which in turn oxidizes the entire cladding material. The current US design regulation (10 code of Federal Regulation 50.46) limits the equivalent cladding reacted (ECR)

thickness to 17 % of the initial cladding thickness under DBA conditions. Furthermore, copious amount of hydrogen is generated during the steam oxidation reaction of zirconium that may result in explosion. Therefore, one of the goals of the Fuel Cycle R&D program is to develop high-performance LWR fuel and cladding materials that are resistant against different severe accident scenarios. In addition to the enhanced safety margin, the next-generation fuel clads should have the required properties to perform under high-burnup operating conditions (> 40 MWd/kg of U). At a high level of burnup, high fission gas pressures are realized along with higher creep deformation. In addition, neutron damage to the cladding makes it more susceptible to failure. There could be situations of fuel cladding chemical interaction (FCCI) involving fuel constituent redistribution (Carmack et al. 2009). Hence, improved cladding and matrix materials for pin-type and dispersion-type fuels with low FCCI potential, high strength, radiation tolerance, and high-temperature oxidation resistance are highly desirable for accident-tolerant fuel cladding materials.

Recently, renewed interest has emerged in aluminum-bearing ferritic alloys despite the neutronic penalty in LWR applications. For example, the APMT alloy (nominal composition, Fe-22 Cr-5 Al-3 Mo- < 0.05C, wt%) is being considered for its extreme high-temperature oxidation resistance even beyond 1200 °C due to the protective nature of alumina-based scale (Terrani et al. 2013). This alloy is conventionally used in high-temperature furnace elements. While the alloy has shown promise in terms of oxidation resistance at elevated temperatures, this alloy has not been adequately assessed for advanced fuel cladding applications. Furthermore, addition of "reactive" elements such as Y, Hf, Zr, etc., has been considered to improve the oxidation resistance of alumina-forming alloys (Guo et al. 2014). The details of growth stresses during steam oxidation of alumina layers and the effect of reactive elements on the diffusion and electronic behavior of the oxide layers are not studied in detail. Such an understanding is pertinent for the design of new FeCrAlRE cladding materials that show improved LOCA resistance. In addition to FeCrAl alloys, other materials such as Mo (Nelson et al. 2013) and ferritic ODS alloys (Klueh et al. 2005) are also actively investigated for fuel cladding applications. The design of the new cladding alloy will be based on the following considerations (Knief 1992; Pint et al. 2013):

- The target mechanical properties under unirradiated conditions:
  - The tensile strength at room temperature will be greater than 600 MPa.
  - The yield strength at 1200 °C will be about 100 MPa (versus ~50 MPa of the Zr-4 alloy at 800 °C).
  - A 100 h creep rupture strength at 1200 °C will be about 50 MPa (versus 5 MPa at 800 °C of the Zr-4 alloy).
  - Elastic modulus ~100 GPa at 1200 °C.
- Understanding irradiation effects:
  - Formation of dislocation loops and α′ phase; phase stability.
  - Fracture toughness after irradiation to 20 dpa level is ~50 MPa√m (compared to 12–15 MPa√m of Zr alloy); dimensional changes <1 % at 20 dpa.

- Understanding of corrosion behavior:
  - Cr-rich oxide layer that is expected to impart resistance to aqueous corrosion
  - Al_2O_3 layers associated with the high-temperature oxidation resistance (>600 °C)
  - Effect of reactive elements (actinides, Zr, Hf, Sc, etc.) on the diffusivity of Al^{3+}, $V_{Al}{}^{3-}$ $V_O{}^{2+}$, and O^{2-} and adhesion of oxide layer
  - Understanding the origin of oxide growth stresses during steam oxidation, electronic properties, and the stability of oxide layer under LOCA condition

It is well documented (Lim et al. 2013) that higher concentration of Cr in ferritic steel leads to Cr-rich α′ and σ phase formation during thermal aging between 350 °C and 550 °C. Since the normal operating temperature of the LWR falls in the embrittling temperature range, the effect of spinodal decomposition should be considered. It is observed that Al partitions to Fe-α phase and the partitioning factor increases with the aging time in Fe–20Cr–5Al ODS alloy (Capdevila et al. 2008). Under the LOCA condition, the α′ phase would be dissolved in the matrix, and therefore, spinodal decomposition may not be an issue. Since the formation of α′ does not affect the distribution of scale-forming Al, high-temperature oxidation resistance of the alloy may not be impaired by the embrittlement aging at low temperatures. However, ductility will be severely affected. The low-temperature (up to ~350 °C) corrosion resistance of the FeCrAlRE alloys will be imparted by a Cr-rich oxide layer in the high-temperature high-pressure water under normal operating conditions. The required oxidation resistance under LOCA conditions could be attributed to the formation of an impervious α-Al_2O_3 film which is stable at temperatures above 1040 °C. Transient aluminum oxides such as γ-Al_2O_3 and δ or θ-Al_2O_3 are stable at temperature ranges 500–800 °C and 800–1040 °C, respectively. The transformation of transient oxides into α-Al_2O_3 is accompanied by a 10 % volume contraction that results in accumulation of tensile stresses. If the oxide scale contains multiple oxide phases, the mismatch in the coefficient of thermal expansion again leads to build up of stresses. When starvation of oxygen occurs during high-temperature exposure, generation of oxygen vacancies ($V_O{}^{2+}$) is expected at the expense of oxygen sublattice ($O_O{}^x$) following the reaction:

$$O_O{}^x \rightarrow \tfrac{1}{2}\, O_2 + V_O{}^{2+} + 2e^- \tag{36}$$

Similarly, under oxygen-rich conditions, aluminum ion vacancies could be generated by incorporating the oxygen atoms into the lattice from the adsorbed oxygen molecule following the reaction:

$$\tfrac{1}{2}\, O_2 \rightarrow O_O{}^x + 2/3\, V_{Al}{}^{3-} + 2h^+ \tag{37}$$

These cation and anion vacancies are important in the formation of oxide layer through the reaction

$$2V_{Al}{}^{3-} + 3V_O{}^{2+} + 2Al_{Al}{}^x + 3O_O{}^x \rightarrow Al_2O_3 \tag{38}$$

However, when the concentration of the vacancies reaches a nonequilibrium condition, the stability of the oxide layer is affected by forming porosity either at the oxide/atmosphere interface due to condensation of oxygen vacancies or at the oxide/metal interface due to condensation of cation vacancies. Since grain boundaries act as short circuit diffusion paths for the transportation of atoms and ions, the presence of aliovalent ions in the oxide layer and reactive elements at the grain boundaries of the alloy could significantly alter the diffusivities of both oxygen and aluminum species. Hindering the diffusion of species that form an oxide will significantly decrease the oxidation rate. In addition to affecting the diffusivities, the RE can also modify the electronic states of the oxide layer and thereby affect the oxidation kinetics (Heuer et al. 2011).

References

Anderson MT, Crawford SL, Cumblidge SE, Denslow KM, Diaz AA, Doctor SR (2007) NUREG/CR-6933, PNNL-16292, March 2007
Bloom EE (1998) J Nucl Mater 263:7
Bond AP, Dundar HJ (1977) In: Staehle RW, Hochmann J, MdRight RD, Slater RE (eds) Stress corrosion cracking of ferritic stainless steels. NACE, Houston, p 1136
Brinkman CR, Korth GE (1973) Heat-to-heat variations in the fatigue and creep–fatigue behavior of AISI type 304 stainless steel at 593°C. J Nucl Mater 48(3):293–306
Calonne V, Gourgues AF, Pineau A (2004) Fatigue Fract Eng Mater Struct 27:31–43
CANDU Reactors, Information from: http://www.aecl.ca/Reactors.htm
Capdevila C, Miller MK, Russell KF, Chao J, Gonzalez-Carrasco JL (2008) Phase separation in PM 2000 Fe-base ODS alloy. Mater Sci Eng A 490:277–288
Caravaca C, De Cordoba G, Tomas MJ, Rosado M (2007) Electrochemical behavior of Gd in molten LiCl-KCl. J Nucl Mater 360:25–31
Carmack WJ et al (2009) Metallic fuels for advanced reactors. J Nucl Mater 392(2):139–150
Carter ML (2004) Mater Res Bull 39:1075
Castrillejo Y, Bermejo MR, Pardo R, Martinez AM (2002) Use of electrochemical techniques for study of solubilization of cerium compounds in molten chloride. J Electroanal Chem 322:124–140
Castrillejo Y et al (2005a) Electrochemistry of Dy in LiCl-KCl. Electrochim Acta 50:2047–2057
Castrillejo Y et al (2005b) Electrochemical behavior of Pr(III) in molten chlorides. J Electroanal Chem 575:61–74
Castrillejo J et al (2005c) Electrochim Acta 50:2047; (2006) 51:1941; (2008) 53:5106; (2005) J Electroanal Chem 575:61–74
Celestian AJ et al (2008) J Am Chem Soc 130:11689
Charit I, Murty KL (2008) Creep behavior of niobium-modified zirconium alloys. J Nucl Mater 374(3):354–363
Chen GZ, Fray DJ, Farthing TW (2000) Nature 407(6802):361–364
Choo KN, Pyun SI, Kim YS (1995) J Nucl Mater 226:9–14
Chung HM, Leax TR (1990) Mater Sci Technol 6:249–262
Cicero G, Catellani A, Galli G (2004) Phys Rev Lett 93:016102
Cicero S, Setien J, Gorrochategui I (2009) Nucl Eng Des 239:16–22
Cohen U (1983) J Electrochem Soc 130:1480
Cookson JM, Was GS (1995) Proceedings of the seventh international conference on environmental degradation of materials in nuclear power systems water reactors, NACE, Breckenridge, p 1109
Dahlkamp F (1993) Uranium ore deposits. Springer, Berlin. ISBN 3540532641

Domagala RF, McPherson DJ (1954) Trans AIME 200:238
"Economics of Nuclear Power" reported in http://www.world-nuclear.org/info/inf02.html
Fullwood RR, Hall RE (1988) Probabilistic risk assessment in the nuclear power industry: fundamentals and applications. Pergamon Press, Oxford
Galkin NP, Veryatin UD, Yakhonin IF, Lugonov AF, Dymkov YM (1982) The conversion of uranium hexafluoride to dioxide. At Energ 52(1):36–39
Gaune-Escard M, Bogacz A, Rycerz L, Szczepaniak W (1994) Thermochim Acta 236:67–80
Gogotsi YG et al (1996) J Mater Chem 6:595–604
Gong W, Gaune-Escard M, Rycerz L (2005) J Alloys Compd 396:92–99
Grobe M, Lehmann E, Steinbruck M, Kuhne G, Stuckert J (2009) J Nucl Mater 385:339–345
Grossbeck ML, Ehrlich K, Wassilew C (1990) An assessment of tensile, irradiation creep, creep rupture, and fatigue behavior in austenitic stainless steels with emphasis on spectral effects. J Nucl Mater 174(2–3):264–281
Guo H, Wang D, Gong S, Xu H (2014) Effect of reactive elements on oxidation behavior of β-NiAl at 1200 °C. Corros Sci 78:369–377
Hallstadius L, Johnson S, Lahoda E (2012) Prog Nucl Energy 57:71–76
Hamel C, Chamelot P, Taxil P (2004) Nd cathode process in molten fluoride. Electrochim Acta 49:4467–4476
Hazebroucq S, Picard GS, Adamo C (2005) A theoretical investigation of Gd(III) salvation in molten salts. J Chem Phys 122:224512
He C, Wu X, Shen J, Chu PK (2012) Nano Lett 12:1545–1548
Hejzlar P, Mattingly BT, Todreas NE, Driscoll MJ (1997) Nucl Eng Des 167:375–392
Henager CH et al (2008) J Nucl Mater 378:9–16
Heuer AH, Hovis DB, Smialek JL, Gleeson B (2011) Alumina scale formation: a new perspective. J Am Ceram Soc 94:S146–S153
Hirayama H, Kawakubo T, Goto A (1989) J Am Ceram Soc 72:2049–2053
Holt RA (1974) J Nucl Mater 51: 309; (1974) 50: 207
IAEA (2001) Safety assessment and verification for nuclear power plants – a safety guide. Safety standards series, No. NS-G-1.2. ISBN 92-0-101601-8
Ikeda M, Miyagi Y, Igarashi K, Mochinaga J, Ohno H (1988) The 20th symposium on molten salt chemistry, C303, Yokohama, 10 Nov 1988
Jayet-Gendrot S, Ould P, Meylogan T (1998) Nucl Eng Des 184:3–11
Jeong I-S, Ha G-H, Jun H-I (2009) J Loss Prev Process Ind 22:879–883
Jeong IS, Kim W, Kim TR, Jeon HI (2011) Nucl Eng Tech 43:83–88
Jevremovic T (2005) Nuclear principles in engineering. Springer, New York
Jiang C et al (2009) Phys Rev B 79:132110
Kawaguchi S, Sakamoto N, Takano G, Matsuda F, Kikuchi Y, Mraz L (1997) Nucl Eng Des 174:273–285
Kerr R, Solana F, Bernstein IM, Thompson AW (1987) Metall Trans A 18A:1011
Kim WJ, Hwang HS, Park JY, Ryu WS (2003) J Mater Lett 22:581–584
Kimura A et al (1996) Irradiation hardening of reduced activation martensitic steels. J Nucl Mater 233–237(Pt A):319–325
Kiran Kumar M, Aggarwal S, Kain V, Saario T, Bojinov M (2010) Nucl Eng Des 240:985–994
Klueh RL, Alexander DJ (1996) Impact behavior of reduced-activation steels irradiated to 24 dpa. J Nucl Mater 233–237(Pt A):336–341
Klueh RL, Shingledecker JP, Swinderman RW, Hoelzer DT (2005) Oxide dispersion-strengthened steels: a comparison of some commercial and experimental alloys. J Nucl Mater 341:103–114
Knief RA (1992) Nuclear engineering: theory and technology of commercial nuclear power. Hemisphere Publishing Corporation, Washington DC
Koyama T, Iizuka M, Shoji Y, Fujita R, Tanaka H, Kobayashi T, Tokiwai M (1997) An experimental study of molten salt reprocessing. J Nucl Sci Tech 34(4):384–393
Koyama T, Hijikata T, Usami T, Inoue T, Kitawaki S, Shinozaki T, Myochin M (2007) Integrated experiments on electrometallurgical processing using PuO_2. J Nucl Sci Tech 44(3):382–392

Kraft T, Nickel KG, Gogotsi YG (1998) J Mater Sci 33:4357–4364
Krass AS, Boskma P, Elzen B, Smit WA (1983) Uranium enrichment and nuclear weapon proliferation. Taylor and Francis, London
Kuan P, Hanson DJ (1991) INL report EGG-M-91375
Kuznetsov SA, Hayashi H, Minato K, Gauno-Escard M (2005) Determination of U and RE metals separation coefficients in LiCl-KCl melt. J Nucl Mater 344:169–172
Kwon J, Woo S, Lee Y, Park J, Park Y (2001) Nucl Eng Des 206:35–44
Leslie WC (1977) Stress corrosion cracking and hydrogen embrittlement of iron base alloys. NACE, Houston, p 52
Li J, Yang Y, Li L, Lou J, Luo X, Huang B (2013) J Appl Phys 113:023516
Lide DR (1997) Handbook of chemistry and physics, 78th edn. CRC Press, Boca Raton
Lim J, Hwang IS, Kim JH (2013) Design of alumina forming FeCrAl steels for lead cooled fast reactors. J Nucl Mater 441:650–660
Lippmann W, Knorr J, Nöring R, Umbreit M (2001) Nucl Eng Des 205:13–22
Liu Y, Su KH, Wang X, Wang Y, Zeng QF, Cheng LF, Zhang LT (2010) Chem Phys Lett 501:87–92
Liu Y, Su KH, Zeng QF, Cheng LF, Zhang LT (2012) Theor Chem Acc 131:1101
Makhijani A, Chalmers L, Smith B. Uranium Enrichment, Institute for Energy and Environmental Research, 15 Oct 2004. http://www.ieer.org/reports/uranium/enrichment.pdf
Maziasz PJ (1993) Overview of microstructural evolution in neutron-irradiated austenitic stainless steels. J Nucl Mater 205:118–145
Maziasz PJ, McHargue CJ (1987) Int Metal Rev 32:190
MIN KS, Nam SW (2003) Correlation between characteristics of grain boundary carbides and creep-fatigue properties in AISI 321 stainless steel. J Nucl Mater 322:91–97
Morss LR, Edelstein NM, Fuger J (eds) (2006) The chemistry of the actinide and transactinide elements, 3rd edn. Springer, Dordrecht
Murray RL (2001) Nuclear energy: an introduction to the concepts, systems, and applications of nuclear processes. Butterworth Heinemann, Woburn
Nam SW (2002) Assessment of damage and life prediction of austenitic stainless steel under high temperature creep-fatigue interaction condition. Mater Sci Eng A322(1–2):64–72
Nelson AT, Sooby ES, Kim YJ, Cheng B, Maloy SA (2013) High temperature oxidation of molybdenum in water vapor environments. J Nucl Mater 448(1–3):441–447
Ni N, Lozano-Perez S, Sykes J, Grovenor C (2011) Ultramicroscopy 111:123–130
Nilsson JO (1988), ASTM STP 942, 543, American Society for Testing Materials, Philadelphia
OCDE/NEA report: accelerator-driven systems (ADS) and fast reactors (FR) in advanced nuclear fuel cycles. A comparative study, (2002) 1
Okamoto Y (1998) Phys Rev B 58:6760
Olander DR (1978) The Gas Centrifuge. Scientific American, August 1978, p 37
Opila EJ (2003) J Am Ceram Soc 86:1238–1248
Opila EJ, Hann RE Jr (1997) J Am Ceram Soc 80:197–205
Pint BA, Terrani KA, Brady MP, Cheng T, Keiser JR (2013) High temperature oxidation of fuel cladding candidate materials in steam-hydrogen environments. J Nucl Mater 440:420–427
RHO BS, Nam SW (2002) Heat effects of nitrogen on low-cycle fatigue properties of Type 304L austenitic stainless steels tested with and without tensile strain hold. J Nucl Mater 300:65–72
Roy JJ et al (1996) J Electrochem Soc 143:2487
Rudling P, Adamson R, Cox B, Garzarolli F, Strasser A (2008) High burn-up fuel issues. Nucl Eng Technol 40(1):1–8
Sakamura Y et al (1998) J Alloys Compd 271–273:592–596
Senor DJ, Youngblood GE, Moore CE, Trimble DJ, Newsome GA, Woods JJ (1996) Fusion Technol 30:943
Serrano K, Taxil P (1999) J Appl Electrochem 29:505
Shack WJ, Kassner TF (1994) Review of Environmental Effects on Fatigue Crack Growth of Austenitic Stainless Steels, NUREG/CR-6176, ANL-94/1, U.S. Nuclear Regulatory Commission, Washington, DC, NRC FIN L2424

Shapiro J (1990) Radiation protection, 3rd edn. Harvard University Press, Cambridge, MA
Shen X, Pantelides ST (2013) J Phys Chem Lett 4:100–104
Shiba K et al (1996) Irradiation response on mechanical properties of neutron irradiated F82H. J Nucl Mater 233–237(Pt A):309–312
Shimada S, Onuma T, Kiyono H (2006) J Am Ceram Soc 89:1218–1225
Shirai O, Iizuka M, Iwai T, Suzuki Y, Arai Y (2000) J Electroanal Chem 490:31–36
Shoesmith DW (2006) Corrosion 62:703–722
Storm van Leeuwen JW, Smith P (2005) Nuclear power: the energy balance. http://www.stormsmith.nl/
Suauzay M et al (2004) Creep-fatigue behaviour of an AISI stainless steel at 550°C. Nucl Eng Des 232:219–236
Suzuki S, Saito K, Kodama M, Shima S, Saito T (1991) SmiRt 11 transactions, vol. D, August 1991, Tokyo
Takagi R, Rycerz L, Gaune-Escard M (1997) J Alloys Compd 257:134–136
Tan L, Allen TR, Barringer E (2009) J Nucl Mater 394:95–101
Terrani KA, Zinkle SL, Snead LL (2013) Advanced oxidation-resistant iron-based alloys for LWR fuel cladding. J Nuc Mater 448:374–379
Thorium fuel cycle–potential benefits and challenges, International Atomic Energy Agency, Vienna, IAEA-TECDOC-1450, May 2005
Tsuji H, Nakajima H (1994) Creep-fatigue Damage Evaluation of a Nickel-base Heat-resistant Alloy Hastelloy XR in Simulated HTGR Helium Gas Environment. J Nucl Mater 208:293–299
Van Der Schaaf B (1988) The effect of neutron irradiation on the fatigue and fatigue-creep behaviour of structural materials. J Nucl Mater 155–157:156–163
Wang ZX, Xue F, Guo WH, Shi HJ, Zhang GD, Shu G (2010) Nucl Eng Des 240:2538–2543
Wigeland RA et al (2006) Nucl Technol 154:95
Wray P, Marra J (2011) Materials for nuclear energy in the post-Fukushima era. Am Ceram Soc Bull 90(6):24–28
Yang YS, Kang YH, Lee HK (1997) Estimation of optimum experimental parameters in chlorination of UO_2 with Cl_2 gas and carbon for UCl_4. Mater Chem Phys 50:243–247
Yilmazbahyan A, Breval E, Motta AT, Comstock RJ (2006) J Nucl Mater 349:265–281
Yokobori T, Yokobori AT Jr (2001) High temperature creep, fatigue and creep-fatigue Interaction in engineering materials. Int J Press Vessel Pip 78:903–908
Zhang H et al (2010) J Am Ceram Soc 93:1148–1155

Part IV

Climate Change Mitigation: Advanced Carbon Conversion Sciences and Technologies

Reducing Greenhouse Gas Emissions with CO_2 Capture and Geological Storage

J. Marcelo Ketzer, Rodrigo S. Iglesias, and Sandra Einloft

Contents

J.M. Ketzer (✉)
IPR – Institute of Petroleum and Natural Resources, Pontifical Catholic University of Rio Grande do Sul, Porto Alegre, Brazil
e-mail: marcelo.ketzer@pucrs.br

R.S. Iglesias
FENG – Engineering Faculty, Pontifical Catholic University of Rio Grande do Sul, Porto Alegre, Brazil
e-mail: rodrigo.iglesias@pucrs.br

S. Einloft
FAQUI – Faculty of Chemistry, Pontifical Catholic University of Rio Grande do Sul, Porto Alegre, Brazil
e-mail: einloft@pucrs.br

W.-Y. Chen et al. (eds.), *Handbook of Climate Change Mitigation and Adaptation*,
DOI 10.1007/978-3-319-14409-2_37

Abstract

CO_2 capture and geological storage (CCS) is one of the most promising technologies to reduce greenhouse gas emissions and mitigate climate change in a fossil fuel-dependent world. If fully implemented, CCS may contribute to reduce 20 % of global emissions from fossil fuels by 2050 and 55 % by the end of this century. The complete CCS chain consists of capturing CO_2 from large stationary sources such as coal-fired power plants and heavy industries and transport and store it in appropriate geological reservoirs such as petroleum fields, saline aquifers, and coal seams, therefore returning carbon emitted from fossil fuels (as CO_2) back to geological sinks.

Recent studies have shown that geological reservoirs can safely store for many centuries the entire greenhouse gas (GHG) global emissions. In this chapter, we present a comprehensive summary of the latest advances in CCS research and technologies that can be used to store significant quantities of CO_2 for geological periods of time and therefore considerably contribute to GHG emission reduction.

Introduction

CO_2 capture and geological storage (CCGS or simply CCS) is the integrated process where carbon dioxide is captured and separated at stationary sources, transported to an adequate storage site, and injected into the porous space of deep

underground rock formations. Given the world's current dependence on fossil fuels, which is expected to last for no less than a century, the storage of carbon dioxide in geological reservoirs is a recognized viable mitigation option, with potential to be applied in a worldwide scale and therefore having a measurable impact on the reduction of the escalating emissions of greenhouse gases. The latest assessment report from the Intergovernmental Panel on Climate Change (IPCC), published in 2014, recognizes the importance of CCS technologies to reduce the lifecycle of greenhouse gas emissions from fossil fuel power plants, in order to keep the global temperature rise below 2 °C by 2100 (IPCC 2014). Since the increase in carbon dioxide concentration in the atmosphere is the outcome of continuous burning of fossil fuels extracted from the subsurface, the underlying motto of CO_2 geological storage is to "put the carbon back to the ground," hopefully reestablishing the equilibrium of this unbalanced carbon cycle (Greenhouse Gas R&D Programme 2001).

It is common ground that the reduction and stabilization of greenhouse gas emissions can only be achieved through a portfolio of solutions, including renewable sources, nuclear power, improved energy efficiency and fuel switching at power generation and end-use level, and carbon capture and storage, with increasing contributions at different levels (Pacala and Socolow 2004; IPCC 2005; IEA 2008a). From a recent assessment from the International Energy Agency (IEA) published in 2012, CCS is expected to contribute with at least one-sixth of the emission reduction (14 % of the cumulative emission reduction between 2015 and 2050) in a scenario where the global temperature rise is limited to 2 °C by 2050 (Fig. 1) (IEA 2012). Scenarios that exclude CCS would result in a cost increase to achieve emission stabilization in 2050 by at least 40 % (IEA 2012).

CO_2 sources that are suitable for CCS projects must be large stationary facilities, usually venting more than 100,000 metric tons of CO_2 per year (IPCC 2005). These usually include power-generation facilities (e.g., gas- or coal-fired power plants), natural gas processing plants, refineries, ethylene plants, hydrogen-producing plants from CH_4 reform and coal gasification, and cement and steel industries, among others. Depending on the type of source, costs, and technology maturity, CO_2 can be captured and separated from other gases using post-combustion, precombustion, or oxy-combustion technological routes. These systems will be further explained in detail in this chapter. Following separation, CO_2 may be transported using pipelines and/or ships to a storage site, where it is compressed and injected in the subsurface through wells (Rubin 2008). Transportation distances are an important factor to be evaluated in CCS projects, due to the elevated cost of pipelines. Most countries that are willing to develop CCS projects have been carrying out surveys to map their large stationary sources of CO_2 and the potential geological storage sites. This will provide an optimized source-sink match, in order to reduce transportation of CO_2 from the capture source to storage site.

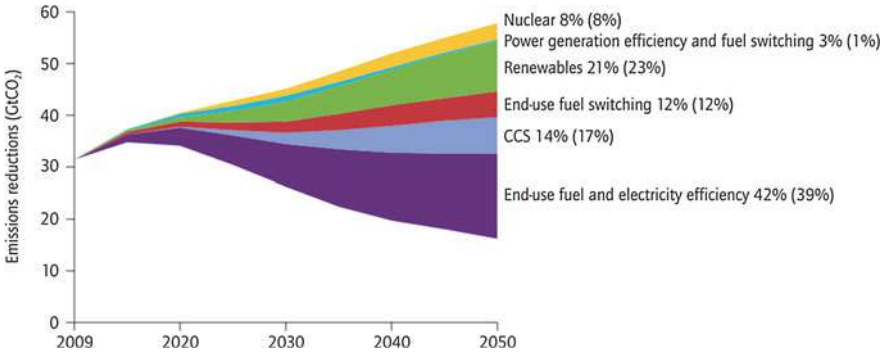

Fig. 1 CO_2 emission reduction scenario from the IEA for the twenty-first century: lower limit of the graphic corresponds to the 2DS scenario – reduction of CO_2 emissions to approximately half of the emissions in 2009, in order to limit the global temperature rise to 2 °C by 2050 – relative to the baseline 6DS scenario, or "business as usual" (upper limit), where global temperature could rise up to 6 °C. *IEA Energy Technology Perspectives* © OECD/IEA, 2012 (IEA 2012)

The most appropriate geological reservoirs for CO_2 storage are sedimentary units such as oil and gas fields, deep saline aquifers, and coal deposits. These types of formations have large storage capacity in their porous space and are evenly distributed worldwide (Bachu 2003). Estimated capacities for oil and gas fields range between 675 and 900 billion metric tons (Gt) of CO_2; for saline aquifers between 1,000 and 10,000 Gt; and coal beds between 3 and 200 Gt (IPCC 2005). These estimations are still highly uncertain, as they depend on selection criteria for validating a potential storage site (which may vary significantly for each assessment) and the methodology employed to calculate the effective pore volume available for storage (Bradshaw et al. 2007; Bachu et al. 2007). These methods and criteria will be further discussed in this chapter. Nevertheless, it is worth noting that even considering the lowest capacity estimations, storage volume of geological reservoirs is enough to contain 10 times the accumulated global emissions until 2050 (ca. 155 Gt CO_2) (IEA 2009).

CCS in geological media is in its early stages of worldwide deployment. Currently (as of 2015), there are 13 large-scale CCS projects in operation, although only three of those are dedicated geological storage operations. In the other projects, CO_2 is used for enhanced oil recovery purposes (EOR, see following sections), with questionable emission reduction results. Nine projects are under construction and expected to be operational in 2016 (IEA 2013). An up-to-date status of CCS projects worldwide (operating and planned) can be found on the Global CCS Institute (GCCSI) website (Large Scale CCS Projects 2015).

The first and most notorious large-scale CCS project was started in 1996, in the Sleipner gas field in the North Sea, operated by Norway-based oil company Statoil. In order to avoid a government-imposed tax for offshore greenhouse gas emissions,

Statoil started to strip CO_2 from the natural gas extracted in this field, reinjecting it in the Utsira formation, a saline aquifer 800 m below the sea floor and hundreds of meters above the Sleipner gas field. Approximately 1 million metric tons (Mt) of CO_2 are injected in this formation each year. The project is still ongoing, and its success has been a benchmark for CCS development (Korbøl and Kaddour 1995; Torp and Gale 2004). In 2004, Statoil and BP (British Petroleum) started a similar project in the In Salah gas field, in Algeria, reinjecting stripped CO_2 from natural gas below the gas-water contact in the same formation, 1800 m below the surface. The injection was suspended in 2011, and future operations are under review (IEA 2008a). The Snøhvit natural gas field in the Barents Sea is another asset operated by Statoil with dedicated geological storage. The company started capturing CO_2 from the produced gas in 2008 and injecting it offshore, through a submarine pipeline approximately 160 km from the Norwegian coast. In this project, 0.7 Mt of CO_2 are captured and stored each year (Snøhvit 2015). One of the most relevant CO_2-EOR projects is the Weyburn-Midale, a transnational operation (USA/Canada) where CO_2 is captured at the Great Plains Synfuels Plant and transported through a 320 km pipeline to the city of Weyburn, in the province of Saskatchewan (Canada), where it is injected into the mature Weyburn-Midale oil field for enhanced oil recovery (Greenhouse Gas R&D Programme 2004). In 2014, an important milestone was reached in CCS development – the first demonstration project in the power sector went operational, with the inauguration of the new capture plant in the Boundary Dam coal-fired power station in Canada. The plant captures CO_2 using a post-combustion process (see next section), which is transported and injected in the previously mentioned Weyburn oil field, supplementing the existing supply from the Great Plains plant. When fully operational, the project is expected to capture and store one million tons of CO_2 per year (Boundary Dam Carbon Capture Project 2015).

In total, the existing 13 CCS projects presently (2014) inject more than 27 million tons of CO_2 per year (Large Scale CCS Projects 2015). Current global emissions of CO_2 amount to *ca.* 36 *billion* metric tons per year (data from 2013), of which ca. 60 % (22 Gt) come from large-scale stationary sources (Le Quéré et al. 2014). This means that approximately 800 times the current storage ratio will be necessary to deal with the present emissions. From these numbers it would appear to be an overwhelming task, but the deployment of CCS projects, both in commercial or demonstration scale, has been steadily increasing in number in the past years, as well as the injection rates.

The aim of this chapter is to present an overview of the main technologies and processes employed to capture and separate CO_2 from stationary sources. Subsequently, storage options will be presented in detail, describing the main reservoirs and the methods employed to estimate their volumetric capacity. Safety issues and potential risks for human health and the environment derived from CO_2 storage will also be covered. The trapping mechanisms of CO_2 in a reservoir and the methods employed to investigate and monitor its interaction with the reservoir are described next. The last section will discuss the current knowledge gaps and requirements in

CCS research that still need to be addressed in order to achieve the expected goals in CO_2 emission reduction perspectives.

CO_2 Capture

CO_2 capture from industrial processes is well known and in use in different applications such as natural gas processing and chemical production (Markewitz et al. 2012). The separated CO_2 is however vented to the atmosphere, as, for example, in natural gas processing. The main purpose of CO_2 capture applied to geological storage is to produce a concentrated CO_2 stream (normally >90 %) to transport and inject in an adequate site.

To obtain CO_2 for storage purposes, it is necessary to separate this gas from a mixture of gases and pressurize it to permit transport and storage, requiring energy. There is currently no mature process for removing CO_2 from large sources, as, for example, power plants (Markewitz et al. 2012; Li et al. 2013). This process adds cost and reduces overall energy efficiency to no less than 25 %, e.g., in a coal-fired power plant, depending on the efficiency of the facility (IEA 2008b). With the current typical amine separation process, a cost of ca. 80 % in the electricity will be added in a new pulverized coal plant and ca. 35 % for a new advanced gasification power plant (Li et al. 2013).

CO_2 capture systems can be divided in three main technological routes, depending on the technology used and its applications (Fig. 2). The following sections will describe each of these systems in more detail.

Post-combustion System

In post-combustion, CO_2 is removed from flue gas, separating CO_2 from conventional diluted flue gas stream (N_2, O_2, H_2O, NO_x, and SO_x). The latter two are produced by combustion of fossil fuel or biomass, and their concentration also must be reduced to avoid solvent degradation (Blomen et al. 2009; Feron 2010; Kothandaraman et al. 2009). In this process, air is used for combustion, resulting in flue gas at nearly atmospheric pressure with a low CO_2 concentration (3–15 % by volume) (IPCC 2005; Figueroa et al. 2008; Yang et al. 2008). Different techniques can be used to capture CO_2 from post-combustion flue gas, such as absorption by a chemical sorbent, separation by membranes, adsorption in solids, and cryogenic separation. Absorption technology, using ammonia-based solvents such as monoethanolamine (MEA), plays a dominant role in the present and probably will continue to do so in the near future (IEA 2008b; Blomen et al. 2009; Zhao et al. 2008). Conventional aqueous amine process is a high-energy intensive approach, and their use for CO_2 capture will decrease power plant efficiency, so the improvement of known technologies and the development of new ones are imperative for the success of post-combustion capture processes (Bara et al. 2009a).

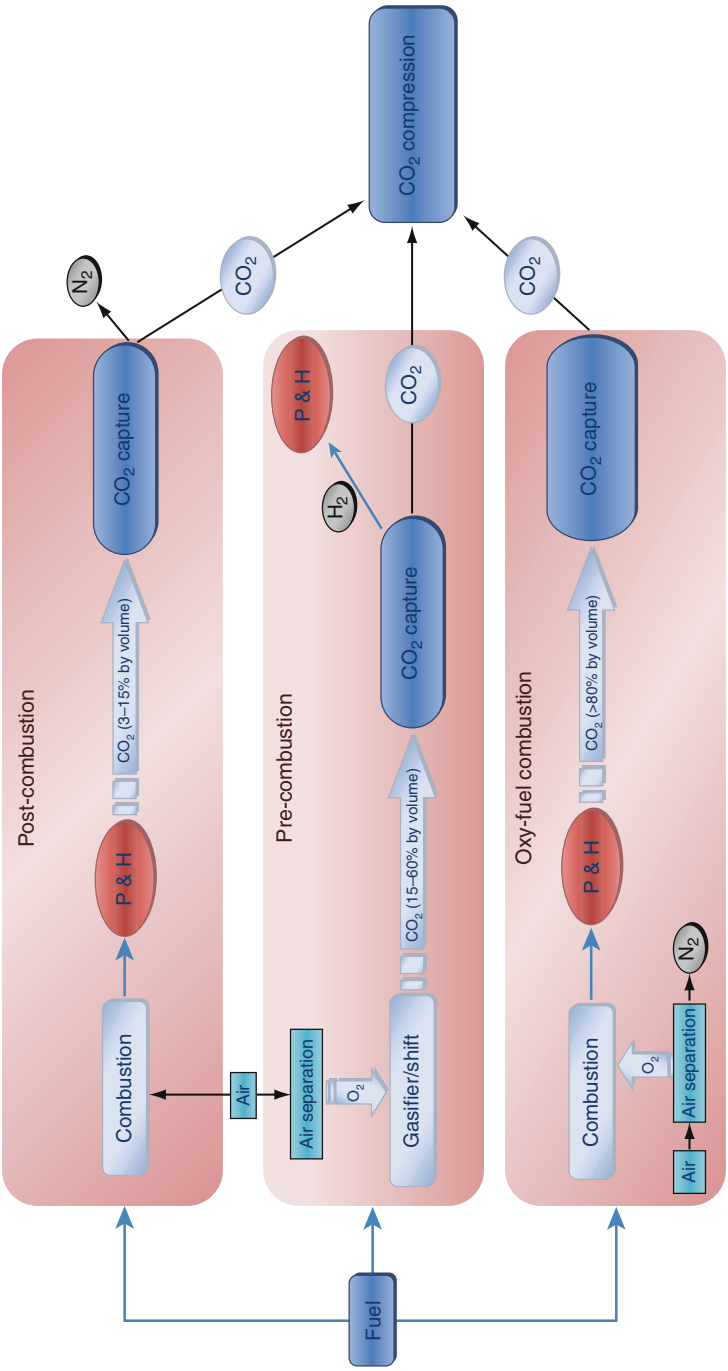

Fig. 2 Diagram illustrating CO_2 capture routes in power generation using fossil fuels (P&H: power and heat)

Precombustion System

In the precombustion system, CO_2 is separated from H_2, which is used as a fuel. Initially, coal, biomass, or natural gas is reacted with steam or oxygen in a gasification process to decompose the fuel in synthesis gas (*syngas*, mainly composed of CO + H_2) which is reacted in a water-gas shift reactor producing CO_2 and more H_2 (Blomen et al. 2009; Kanniche et al. 2010). The shift conversion produces a stream with a high CO_2 concentration (15–60 % by volume), resulting in higher partial pressure of CO_2 making it easier to separate, when compared to the post-combustion system, allowing the use of different solvents with lower regeneration energy requirements.

CO_2 can be separated by a physical or a physical/chemical absorption process, which is the most utilized technology. Membrane and solid sorbents can also be used, as well as cryogenic separation (IPCC 2005; Blomen et al. 2009). The disadvantage of precombustion methods is the total capital costs of the generating facility, which is very high (Sabouni et al. 2014).

Oxy-combustion System

In oxy-combustion, the oxygen is initially separated from air in an air separation unit, commonly through low-temperature cryogenic separation, and used in fuel combustion, producing a flue gas with a high CO_2 concentration (>80 %). Reacting fuel with almost pure oxygen results in a high-temperature flue gas containing mainly CO_2 and water that can be recycled to the burner to control the temperature (IPCC 2005; Blomen et al. 2009). The main advantage of oxy-combustion is the significant increase of the CO_2 partial pressure (Kanniche et al. 2010). CO_2 can be easily separated from the flue gas, for example, by cryogenic methods.

Chemical Looping

The chemical looping system can be considered as a variant of oxy-combustion system (IEA 2008b). In this process, oxygen is supplied for the fuel combustion/oxidation without direct contact with air, using a metal oxide as an oxygen carrier (Abad et al. 2006; Corbella et al. 2005; De Diego et al. 2005). The flue gas contains only water and CO_2. Water may be condensed and CO_2 compressed for transport and storage (Fig. 3).

Technological Options for CO_2 Separation

In the whole carbon capture and storage-integrated process, the CO_2 separation stage contributes with 70–80 % of the costs, so the possibility of reducing operating costs

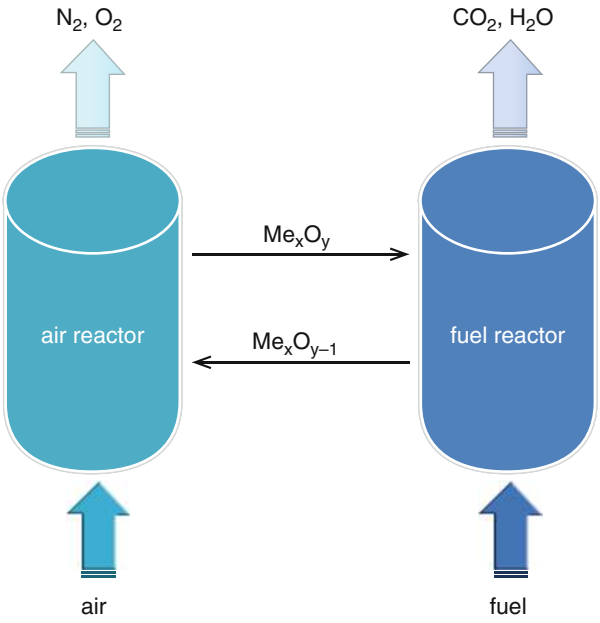

Fig. 3 A simplified scheme of the chemical looping process

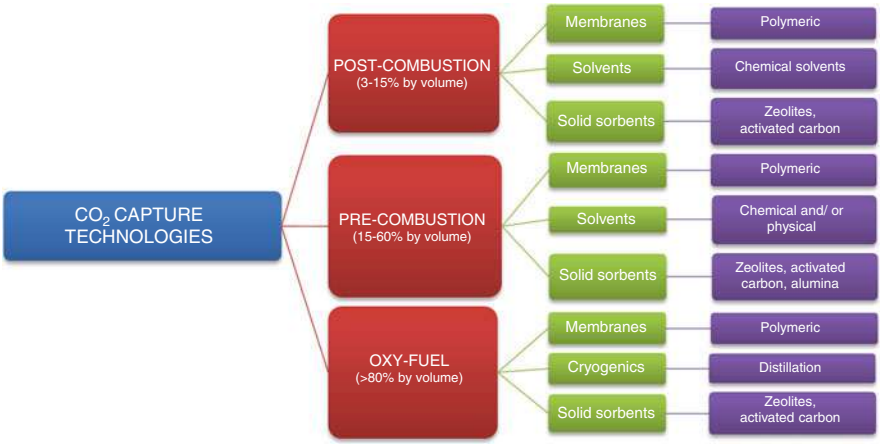

Fig. 4 Available technologies for CO_2 capture and separation

of CO_2 capture is an important issue to make CCS viable (Blomen et al. 2009; Feron & Hendriks 2005). Another important aspect to investigate is the environmental impact of CCS implementation. A critical study of all available and in development technologies is imperative to the carbon capture aiming the CO_2 long-term storage. Figure 4 presents a scheme of the technologies available for CO_2 capture.

Solvents

To capture CO_2 from a stream, it is possible to use solvents that may interact with CO_2 either by chemical or physical absorption. The choice of the solvent depends on the characteristics of the flue gas, like CO_2 partial pressure and concentration. The chemical absorption is independent of the CO_2 pressure due to the chemical character of the interaction solvent CO_2 and can be used even in low CO_2 pressure and concentration. On the other hand, when compared to physical solvents, chemical solvents need thermal energy to release CO_2, while physical solvents release CO_2 by flash desorption. In post-combustion technologies, amines are the most used chemical solvent, and in precombustion technology both chemical and physical solvents can be employed or a mixture of both. Membranes and solid sorbents can be used in post-combustion, precombustion, and oxy-fuel routes, but a technological improvement is needed to transform these options in attractive alternatives from both technological and economical point of view.

Amines

The use of aqueous amine solutions in CO_2 separation is the most mature technology and has been used in the industry for decades (IPCC 2005; IEA 2008b).

The absorption by amines in water is a well-known commercial technology of CO_2 separation: for example, in natural gas, CO_2 and H_2S are removed via an amine-based scrubber, capturing the acid gases by a chemical reaction with amines and releasing the natural gas. The acid gases are then driven off by heating the amine solution, which is regenerated. This process is energy intensive (Bara et al. 2009b; Pennline et al. 2008; Hicks et al. 2008). Figure 5 presents a typical cyclic process of the use of aqueous amine solutions in CO_2 capture. In the first vessel occurs the chemical absorption, and in the second vessel CO_2 undergoes heat-induced desorption followed by the solvent recuperation.

In addition to energy penalty, it is known that *N*-methyldiethanolamine (MDEA) and diethanolamine (DEA) used for gas treatment and monoethanolamine (MEA) used for CO_2 post-combustion separation decompose causing environmental problems due to generated waste (IPCC 2005; Pannocchia et al. 2007; Lepaumier et al. 2009; Ramdin et al. 2012).

Despite being used for a long time, the search for a better understanding of the chemistry involved in amine-CO_2 interactions is crucial to find an optimal formulation to lower the costs. In this sense, a study presented the results for CO_2 absorption capacity for seventy-six different amine solutions indicating that there are still possibilities to improve the CO_2 absorption capacity of aqueous amine solutions. Seven amines were found to exhibit significant absorption capacity, most of them comparable to the industry standard monoethanolamine (MEA). Most of the selected amines, one primary, three secondary, and three tertiary, have a number of structural features in common like steric hindrance and hydroxyl functionality 2 or 3 carbons from nitrogen (Puxty et al. 2009). These results indicate that there are

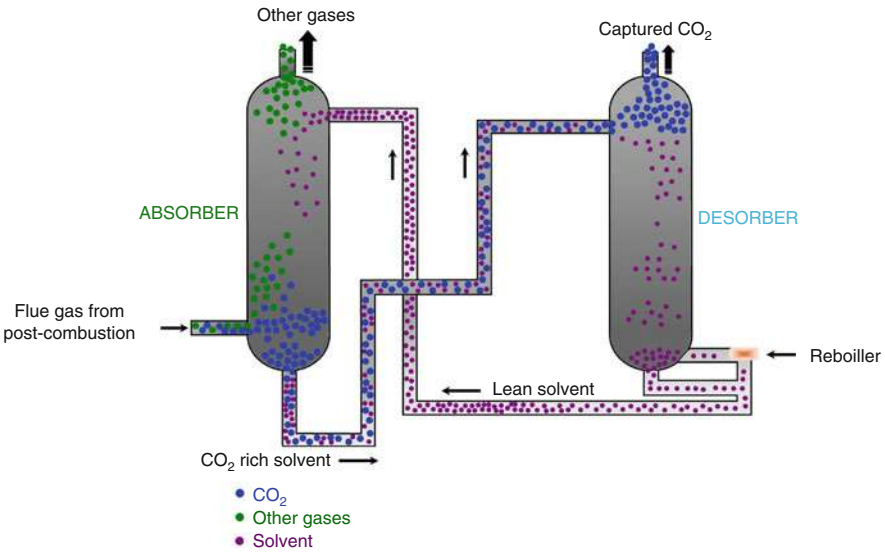

Fig. 5 Process of CO_2 capture using an aqueous amine solution

still possibilities to improve the CO_2 absorption capacity of aqueous amine solutions. The main issues regarding new amine research and development are related to reduction of energy requirements, minimizing corrosion of scrubbers, allowing higher amine concentration, and improving regeneration procedures (Figueroa et al. 2008). The advances in the development of CO_2 capture technologies utilizing absorption by aqueous amine solvents or new absorption systems need an accurate understanding of the chemical process occurring during the absorption/desorption steps (Perinu et al. 2014).

Physical Solvents

Physical solvents are so called for promoting a weaker bond between the solvent and carbon dioxide, when compared to chemical solvents. In this case, CO_2 is absorbed without a chemical reaction, so this class of solvent is suitable for CO_2 removal from flue gas with a higher CO_2 partial pressure. Current state-of-the-art physical solvents are glycol-based solvents like Selexol and methanol-based Rectisol (Blomen et al. 2009) as well as propylene carbonate (fluor process) (Figueroa et al. 2008). The main advantage of the physical solvents over amine solutions is the lower energy requirements for CO_2 absorption. However, these solvents present also some drawbacks, such as low CO_2 absorption capacity when compared to chemical solvents, the capacity of absorb significant quantity of hydrocarbon, and the need of high circulation rates resulting in high capital and operating expenses (Kumar et al. 2014).

Solid Sorbents

Solid sorbents can be used to react with CO_2 in a two-step process. Initially, a stable compound is produced, followed by releasing of CO_2 in the subsequent step, with regeneration of the original compound. These materials can overcome the amine drawback, energy penalty, and solvent decomposition, because of their lower energy requirements, cost advantage, and easiness of applicability over a relatively wide range of temperatures and pressures (Xu et al. 2003). A great number of physical adsorbent materials can be considered for CO_2 capture such as zeolites and zeolite-like materials, activated carbons, metal-organic frameworks, and aerogel-based materials (Sabouni et al. 2014; Kong et al. 2014). Several important criteria should be satisfied for a material before then can be considered as a suitable adsorbent for CO_2 capture from flue gas and compete with the present technologies: high adsorption capacity, high selectivity for CO_2, adequate adsorption/desorption kinetics, sorbent regeneration, stability during repeated adsorption/desorption cycling, mechanical strength, and low cost (Sabouni et al. 2014; Samanta et al. 2011; Wang et al. 2014). These attributes will rarely be fitted for one single adsorbent but are desirable for an ideal solid physisorbent material. However, a useful adsorbent should capture CO_2 from flue gas stream economically and effectively (Samanta et al. 2011).

Zeolites

Zeolitic materials comprise the largest group of the oxide molecular sieves and are used for many applications, as catalysis, gas separation and purification, and ion exchange. Zeolites X, Y, A, ZSM, and chabazites have been widely studied to be used in the field of adsorbents (Zhang et al. 2008). Zeolites have high thermal, mechanical, and chemical stability characteristics that, allied with the porous size and stable crystal structure, make these materials good candidates to be used in CO_2 adsorption processes and are among the most investigated in literature for adsorption and separation (Sabouni et al. 2014; Walton et al. 2006; García-Pérez et al. 2007).

Metal-Organic Frameworks

Metal-organic frameworks (MOFs) represent a new emerging class of crystalline porous materials formed by metal-based nodes (e.g., Al^{3+}, Cr^{3+}, Cu^{2+}, Zn^{2+}) with well-defined coordination geometry and organic bridging ligands (e.g., carboxylate, pyridyl). These structures offer advantages for CO_2 absorption: ordered structure, high storage capacity possible with low energy penalty for CO_2 recovery, high thermal stability, adjustable chemical functionality, and extra-high porosity, among others (Figueroa et al. 2008; Sabouni et al. 2014; Millward and Yaghi 2005; Wang et al. 2011a).

Membranes

Membranes are being used in many industrial separations and are currently dominated by polymeric membranes offering the advantage of cheap production on large scale when compared to metallic proton-conducting or ceramic membranes (IEA 2008b; Yang et al. 2008; Franz and Scherer 2010). Nevertheless, the membranes are low-cost options for processes that do not require a high-purity gas stream. Besides that, there are some other points related to the performance of membranes that limit their uses in carbon capture. For example, the low concentration of carbon dioxide in the flue gas indicates that a large volume of gases needs to be processed; the membranes are not resistant to temperature, demanding flue gas cooling prior the membrane separation; and extra power is required to create a pressure difference across the membrane (IEA 2008b; Powell and Qiao 2006).

Membranes are a promising technology in future for carbon capture but are still in a research and development phase, necessary to make their costs and performance attractive. The technology presents as main drawback the lack of stability under the reforming environment (Sabouni et al. 2014).

Ionic Liquids and Poly(ionic Liquids)

Room temperature ionic liquids (RTILs) are liquid salts at room temperatures (Scovazzo et al. 2004; Shin and Lee 2008). The several possible combinations of cations and anions allow designing more efficient solvents for process and products (Carvalho et al. 2009). Due to the excellent properties of RTIL like negligible vapor pressure at room temperature, a stable liquid range of over 300 K, the great CO_2 solubility, and the density greater than water, there is a growing interest to use this kind of solvents in gas separation (Shin and Lee 2008; Raeissi and Peters 2008).

As mentioned before, these compounds may combine good physical and chemical characteristics and the ability of selective dissolution of different organic and inorganic compounds by varying the composition of the ionic liquid being good candidates to be used in industrial applications (Bara et al. 2009b). The main problem with the RTIL is the costs. However, considering the small scale on which these solvents are produced, certainly the increased consumption would make the price lower. The capacity of reuse of these solvents must also be taken into account, as well as the energy save and the possibility of producing a specific and optimized ionic solvent for a particular reaction or application. Even if RTILs are more expensive when compared to common organic solvents, their unique properties allied to appropriated engineering designs can offset the costs (Bara et al. 2009b). Nevertheless, the CO_2 solubilities in conventional ILs are still too low to compete with amines in a post-combustion process (Ramdin et al. 2012; Kumar et al. 2014).

Table 1 presents some of the commonly used cations and anions in the RTIL synthesis.

The anion exchange in RTIL makes possible to alter significantly the ionic liquid properties. The cation is responsible for the ionic compound existence in the liquid

Table 1 Most commonly employed anions and cations in ionic liquid synthesis

Some cations and anions for ionic liquid synthesis			
Cations			
 N,N-Dialkylpiperidinium	 1,2-Dialkylpyrazolium	 N-Alkyl-thiazolium	 Trialkylsulfonium
 1,1-Dialkylpyrolidinium	 Tetraalkylammonium	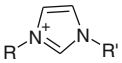 N,N-Alkyl-imidazolium	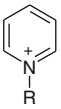 N-Alkylpyridinium
Anions			
 Hexafluorophosphate	 Tetrafluoroborate	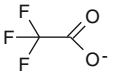 Trifluoroacetate	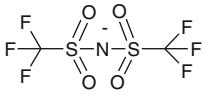 bis-trifluoromethylsulfonylimide

state at room temperature, but it is the anion that controls properties such as solubility and stability (Welton 2004). The alkyl side chain in the cation may play a role in the CO_2 solubility, increasing alkyl chain increases CO_2 solubility; however, the effect is not as important as the substitution of the anion (Raeissi and Peters 2008; Muldoon et al. 2007). Ionic liquids can be tailored to act as a chemical solvent reacting with the CO_2. The CO_2 absorption capacity was greatly improved by functionalizing conventional ILs with an amine moiety (Ramdin et al. 2012). Ionic liquids can absorb CO_2 by an equimolar capture mechanism. In this case it is possible to tune the ILs stability, absorption capacity, and absorption enthalpy by varying the anions with different pKa values (Wang et al. 2011b).

To find new materials for the purpose of CO_2 separation, it is important to study the solubility of CO_2 in these solvents and understand the solvent-CO_2 interaction. It was pointed out that CO_2 presents high solubility in imidazolium-based ionic liquids even in low pressures (Shin and Lee 2008; Blasig et al. 2007; Tang et al. 2005a). Several works related the behavior of the solubility of different gases in 1-*n*-butyl-3-methyl imidazolium hexafluorophosphate [bmim]PF_6 ionic liquids showing that CO_2 presents a superior solubility when compared to other gases like ethane, propane, and oxygen, while carbon oxide, nitrogen, and hydrogen showed solubilities below the detection method (Anthony et al. 2005). The role of the anion was studied by comparing the solubility as a function of both pressure and temperature for a series of gases in 1-*n*-butyl-3-methyl imidazolium tetrafluoroborate [bmim]BF_4, 1-*n*-butyl-3-methyl imidazolium

hexafluorophosphate [bmim]PF_6, and 1-*n*-butyl-3-methyl imidazolium bis(trifluoromethylsulfonyl)imide [bmim]Tf_2N. The latter had the largest affinity for CO_2 in all experimental conditions (Raeissi and Peters 2008; Anthony et al. 2005).

Besides the imidazolium cation, methyl-tributylammonium, butyl-methyl pyrrolidinium, and tri-isobutyl-methyl phosphonium p-toluenesulfonate were tested using Tf_2N as anion which, independent of the cation, had the largest affinity to CO_2, suggesting that the nature of the anion has the strongest influence on the gas solubility (Anthony et al. 2005).

A solubility study of SO_2 and CO_2 was carried out in 1-n-hexyl-3-methyl imidazolium bis(trifluoromethylsulfonyl)imide [hmim]Tf_2N, showing that SO_2 presents a larger solubility in this ionic liquid when compared to CO_2 (Anderson et al. 2006).

Quaternary ammonium polyethers manufactured by Evonik Degussa GmbH company, TEGO IL K5, TEGO IL P9, and TEGO IL P51P, were screened as potential solvents for CO_2 capture. The selection of these ionic liquids was based on the NETL and University of Pittsburgh idea of an "ideal" physical solvent for CO_2 capture (Pennline et al. 2008). Besides the characteristics like low vapor pressure, thermal stability, nonproduction of unwanted by-products, adequate viscosity, density, and ability to dissolve CO_2 at different temperatures and pressures, these solvents were evaluated according to Pearson's "hard and soft acid-base principles" aiming to maximizing the CO_2 solubility. CO_2 is a Pearson "hard acid" having a strong affinity with Pearson "hard bases," in this case the selected ionic liquids (Pennline et al. 2008).

Tang and coworkers first reported that making the ionic liquids in the polymeric form (poly(ionic liquid) – PLI) significantly increases the ability of CO_2 sorption when compared to ionic liquids. Poly(ionic liquids) synthesized from ammonium-based monomers present a CO_2 sorption capacity of 6.0–7.6 times higher than the RTIL (Tang et al. 2005a; Tang et al. 2005b). Besides that the CO_2 sorption and desorption are faster and completely reversible indicating that PLI are more suitable for industrial CO_2 capture and conversion when compared to ILs. These interesting results increased the research in PLI gas separation and sorption, and the related studies are among the most active in PLI field (Yuan et al. 2013). Poly(ionic liquids) based on tetraalkylammonium and a poly(p-vinylbenzyl trimethylammonium hexafluorophosphate) were studied, and the latter presented the highest CO_2 absorption capacity as well as a high selectivity for CO_2 in CO_2/N_2 mixtures. Both materials can be reused several times (Supasitmongkol and Styring 2010). The tetraalkylammonium-based PLIs present higher CO_2 sorption capacities than the imidazolium ones (Yuan and Antonietti 2011). New poly(ionic liquids) were obtained from melt condensation reaction of the imidazolium-based ionic liquids with symmetrical ester and hydroxyl groups. The results indicated that PLIs present higher CO_2 sorption capacity than IL except for the ionic liquid containing the hydroxyl group. This result is probably due to the association of the CO_2 with the anion and the hydrogen-bonding interactions between the hydroxyl groups of the IL and CO_2 (Xiong et al. 2012). A series of PLIs based on poly(urethane) structures were synthesized and presents a good performance when compared to ILs and

traditional solvents used in precombustion process as well as PLIs presented in literature. It is worth to note that these PLIs are based on poly(urethane), a versatile low-cost material (Magalhaes et al. 2014). The studies performed on PLIs for CO_2 capture demonstrated that the effects of anion, cation, and backbone were much different from those of room temperature ionic liquids. Cation seems to play a major role unlike IL, and the CO_2 sorption capacity decreases from ammonium > pyridinium > phosphonium > imidazolium (Yuan et al. 2013).

CO_2 Storage

Storing CO_2 in the subsurface is technologically feasible but far from a trivial endeavor. A large effort of multidisciplinary research is needed before any large-scale injection operation is started. Selection of a storage site is usually aided by a source-sink matching survey, which will limit the viable region for injection to those located close to large stationary CO_2 sources. Geological criteria will then determine whether a given formation in the selected area is suitable for injection. These criteria are basically related to the reservoir storage capacity, the containment capability, and the injectivity of CO_2. Geological characterization methods, such as those used in the oil industry, will be required for this evaluation, often being an expensive and time-consuming step.

Even if a suitable site is found, environmental and regulation issues must be assessed as well to ensure that the storage complex will operate within local safety standards and legislation. Furthermore, site operations must have a positive public acceptance, especially by local communities in the vicinity of the storage complex.

This section will review some of the technical aspects related to the injection of CO_2 and the characteristics of the geological media for storage and containment.

Technical Aspects

CO_2 is injected in a reservoir through an injection well, which is in many aspects similar to oil and gas production wells. However, wellbore materials have to be carefully selected. Cement and steel commonly employed for completion of production wells may experience corrosion by wet CO_2 (an acid media that reacts strongly with cement, leaching components resulting in structural damage) (Scherer et al. 2005). Steel casings may also be corroded by this media.

CO_2 needs to be compressed in the surface to reach the reservoir. Ideally, it should be stored underground in a supercritical phase – a state where CO_2 has gas-like viscosity (therefore with high mobility) and high density, which is advantageous for maximizing storage per pore volume. This state is reached when both temperature and pressure of CO_2 are both above 31.1 °C and 73.9 bar, respectively. Since there is an increase in pressure and temperature with depth in the Earth's crust (geothermal and hydrostatic gradients, averaging *ca.* 30 °C and 100 bar per kilometer, respectively), at approximately 800 m depth, CO_2 is likely to be found

in a supercritical state. One ton of CO_2 occupies 509 m^3 at surface conditions, and the same amount occupies only 1.39 m^3 at 1000 m depth (temperature of 35 °C and pressure of 102 bar) (Bentham and Kirby 2005).

Description of the Geological Media

The geological media used to store CO_2 are similar in many ways to a petroleum system. A storage system is composed of a reservoir and a caprock and may or may not contain a trap (Holt et al. 1995). A geological reservoir is a porous and permeable rock (commonly a sedimentary rock) that contains fluids such as water, oil (liquid hydrocarbons) and natural gas (light hydrocarbons), CO_2, or H_2S, among others, and can be used to safely store CO_2. Porosity is the space within rock matrix (e.g., in between sand grains) and/or rock fractures that contains fluids, which will be partly occupied by CO_2 during storage. A reservoir is preferentially a sedimentary rock (e.g., sandstone, limestone, coal) or less commonly a fractured metamorphic or igneous rock (e.g., basalts). Other less known (in terms of operation and performance) target reservoirs include oil shales, gas hydrates within marine sediments, and engineered salt caverns (IPCC 2005). These options are less investigated and will not be discussed here.

CO_2 stored in common geological conditions is typically found in a gas or supercritical phase, with density lower than water (*ca.* 600–800 kg/m^3) (Fig. 6), and therefore, it will tend to move upward in the reservoir and overburden sequence, until it seeps on the surface (Gunter et al. 2004). To ensure that the CO_2 will be

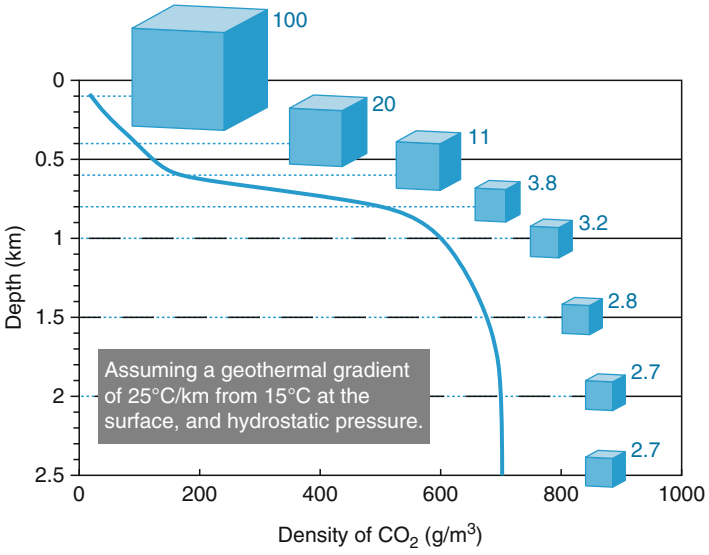

Fig. 6 Variation of CO_2 density with depth, assuming hydrostatic pressure and a geothermal gradient of 25 °C/km from 15 °C at the surface (IPCC 2005)

retained after injection, it is necessary that the reservoir be sealed with an overlying impermeable caprock (with permeability typically lower than 0.1 mD). This caprock will prevent migration of CO_2 out of the reservoir and allow other trapping mechanisms starting to operate (see following sections). Impermeable caprocks are commonly sedimentary rocks such as mudstones, limestones, or evaporites.

Injectivity

Injectivity is the ability of CO_2 to flow from the well into the reservoir and is directly related to the reservoir permeability, which is a measure of the degree of connection between the rock pores. This property is not easily predicted, as different techniques can be employed to evaluate it (using core samples, interpretation of well log data, and well testing), often resulting in conflicting data. Also, it is susceptible to minimum heterogeneities of the reservoir and is highly anisotropic (it varies significantly with the direction of measurement).

Ideally, a permeability higher than 100 mD is required to provide good injectivity. However, in some cases, the reservoir is not sufficiently permeable to allow high rates of CO_2 inflow, and it may require an artificial enhancement through well stimulation (by injection of chemicals or induction of fractures) to improve injectivity. The number and array of wells is also important to optimize injection rates.

In the next section, the most important geological reservoirs for CO_2 storage will be described in more detail.

Reservoir Options

As mentioned previously, there are three main groups of reservoirs that are more likely to be used in a CO_2 storage operation: petroleum fields, saline aquifers, and coal deposits (Fig. 7). The first two are already in their commercial phase, and the

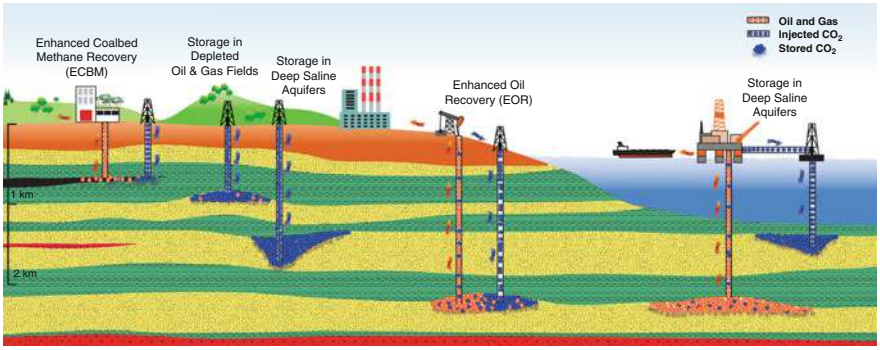

Fig. 7 Scheme of the possible reservoir options for CO_2 storage

latter, although proven in pilot scale, still needs to be demonstrated in larger scale (Van Bergen et al. 2004).

Oil and Gas Fields

Petroleum reservoirs are appealing targets for CO_2 storage, for several reasons. First, the trapping efficiency within these reservoirs is endorsed by the fact that they were capable of holding hydrocarbons for millions of years. Also, these formations are often well studied by oil companies, with plenty of data available. Finally, the injection of CO_2 has been already carried out in many oil fields (especially in the USA) for several years, to increase the pressure in the reservoir and improve the oil/gas recovery rates (a method known as *enhanced oil recovery* – EOR) (Gozalpour et al. 2005). CO_2 injection, often alternated with water, will mix with the residual oil forming a single phase (depending on reservoir pressure and temperature and oil properties) or, eventually, displace the petroleum and water phases to occupy pore space within the structural trap of the field. Mixing CO_2 with oil within a reservoir typically reduces oil viscosity and increases oil recovery by 8–15 % of the residual oil left after primary and secondary (water injection) recovery (NETL 2010; Blunt et al. 1993). Immiscible EOR with CO_2, i.e., related to the physical displacement of oil with CO_2, is also possible, but in this case recovery factors are typically lower than miscible EOR (Taber et al. 1997a, b).

Enhanced oil recovery using CO_2 is a proven technique that has been carried out by the oil industry since the 1970s to maximize oil exploration in mature fields, with approximately 140 projects in operation in 2010, the majority located in the Permian Basin in west Texas (USA) (IEA 2013; Gozalpour et al. 2005). In 2013, the first offshore CO_2-EOR project was started by the Brazilian oil company Petrobas, in the Lula field, one of the major ones in the Pre-Salt area in the south Atlantic Ocean (GC Institute 2014).

Unfortunately, the net emission reductions associated with an EOR project most likely will not be quite significant, as more fossil fuels are produced in the process, which will be consumed, generating additional CO_2. Furthermore, in many EOR projects currently running in the USA, CO_2 is not captured from anthropogenic sources but instead extracted from natural accumulations in the Colorado and New Mexico states and transported through an extensive pipeline network.

It is difficult to estimate how much CO_2 will remain stored in EOR projects, as it depends on the field structure, the recovery rates and injection methods, and the operation strategy after CO_2 breaks through in the production wells. To maximize CO_2 storage in EOR projects, the CO_2 produced together with oil must be separated and reinjected in the same or other reservoir.

Until 2010, approximately 560 Mt of CO_2 have been injected in petroleum fields by EOR projects in the USA only. Currently, ca. 60 Mt of CO_2 are injected every year in that country (NETL 2010). Despite its arguable benefits for emission reductions, CO_2 EOR is an activity with significant potential for CCS development. It is estimated that up to 80 % of oil reservoirs worldwide might be suitable for CO_2

injection based upon oil recovery criteria alone (Taber et al. 1997a, b), with an overall capacity between 675 and 900 Gt CO_2 (IPCC 2005).

Saline Aquifers

Saline aquifers are formations that are geologically similar to oil and gas fields, save for the fact that its pores are filled mostly with highly saline water (brine). Salinity of these formation waters should be above levels that make them unsuitable for human consumption, which usually means concentrations higher than 10 g/L. Usually, only aquifers with salinity higher than seawater (35 g/L) are considered suitable for storage projects.

As already mentioned, an ideal reservoir should be deeper than *ca*. 800 m, for a higher likelihood of CO_2 being in a supercritical phase, with a high density and gas-like viscosity, therefore maximizing pore-volume filling and mobility within the reservoir (Pruess and Garcia 2002). Both porosity and permeability of the reservoir should be sufficiently high so as to ensure constant injection of CO_2 for the time duration of the project (usually a few years, at least). Since the CO_2 injected will displace the original fluid, a low permeability may cause clogging and reservoir overpressures that may result in hydraulic fractures of the reservoir. Physicochemical interactions between CO_2 and reservoir rock and fluids should not deteriorate reservoir quality close to injection wells during injection phase (this topic will be described in greater detail further in the chapter).

To be eligible for CO_2 storage, a saline aquifer must present an overlying caprock with low permeability, being continuous and with minimum amounts of faults and fractures over the range of the estimated storage area. Moreover, this formation must resist the hydraulic overpressure imposed during the injection phase.

The great advantage of saline aquifers over other storage reservoirs is their enormous theoretical capacity and worldwide availability, with uniform distribution. On the other hand, there is much less information and data available for saline aquifers, since the economic incentive for their study is nearly absent. Therefore, global storage capacity estimations for deep saline formations have been roughly estimated thus far, between 1,000 and 10,000 Gt CO_2 (IPCC 2005).

Coal Fields

Coalbeds are able to trap CO_2 by adsorption (see next section), and most of the world coal resources are unminable (usually because of high depths), therefore being potential targets for CO_2 storage. Like in oil fields, storage in coalbeds may be economically interesting, as the injected CO_2 can be adsorbed by the coal matrix, displacing the naturally occurring methane from coal, which can be produced through wells – a technique known as *enhanced coalbed methane recovery* (ECBM). A key issue for storage in coal is the identification of suitable coalbeds. A detailed characterization of the coal is necessary to evaluate composition, rank, nonorganic material

content, permeability, and adsorption capacity, providing the necessary information for site selection. In addition, technical limitations related to coal permeability, which is typically lower than in common conventional reservoirs, have to be considered. The injection of CO_2 is known to cause coal swelling, which further decreases permeability and, consequently, injectivity (Day et al. 2010). Reactivity of coal with CO_2 and/or formation water is another issue that requires investigation, since the interactions of coal macerals (organic matter) with CO_2 are largely unknown and may lead to alterations that modify the coal matrix and its adsorption behavior toward CO_2, methane, and other gases (Reeves and Schoeling 2001).

Due to these limitations, CO_2 storage in coalbeds is still in the early stages of development, compared to the other reservoir options, with a few ECBM demonstration projects currently deployed. ECBM tests and demonstrations have been carried out in the USA, in the San Juan Basin (Colorado), where many commercial coalbed methane (CBM) operations are in place (Gale and Freund 2001; Stevens et al. 2001). An ECBM pilot project was started in 2009 in southern Brazil (Carbometano/Porto Batista project) to evaluate the potential for methane recovery and CO_2 storage of the coal reserves in this country (Beck et al. 2011).

Trapping Mechanisms of CO_2 in Geological Media

There are at least six trapping mechanisms that can keep CO_2 confined in a storage complex for long periods of time. These mechanisms, discussed in detail in this section and depicted in Fig. 8, may vary significantly with time and space within the reservoir (IPCC 2005).

Structural and Stratigraphic Trapping

CO_2 may fill "closed" structural or stratigraphic traps in a similar fashion that oil and gas do in petroleum fields. In this case, CO_2 will be accommodated within the reservoir below the caprock, and after equilibrium, it will be stored as an immiscible and immobile plume underneath the caprock. CO_2 may occupy the entire pore volume of the reservoir within the trap from the top until its spill point, minus the volume of irreducible water (and oil and gas). This is the most important mechanism in the early stages of an injection operation, as CO_2 tends to migrate upward through the reservoir in only a few years, accumulating below the caprock.

Hydrodynamic and Residual Trapping

CO_2 injected in an "open" reservoir, i.e., a reservoir with a caprock without a closure or trap, may form an immiscible plume that will migrate upward and up dip, due to density differences between the CO_2 and water (or oil) phases. Forces acting

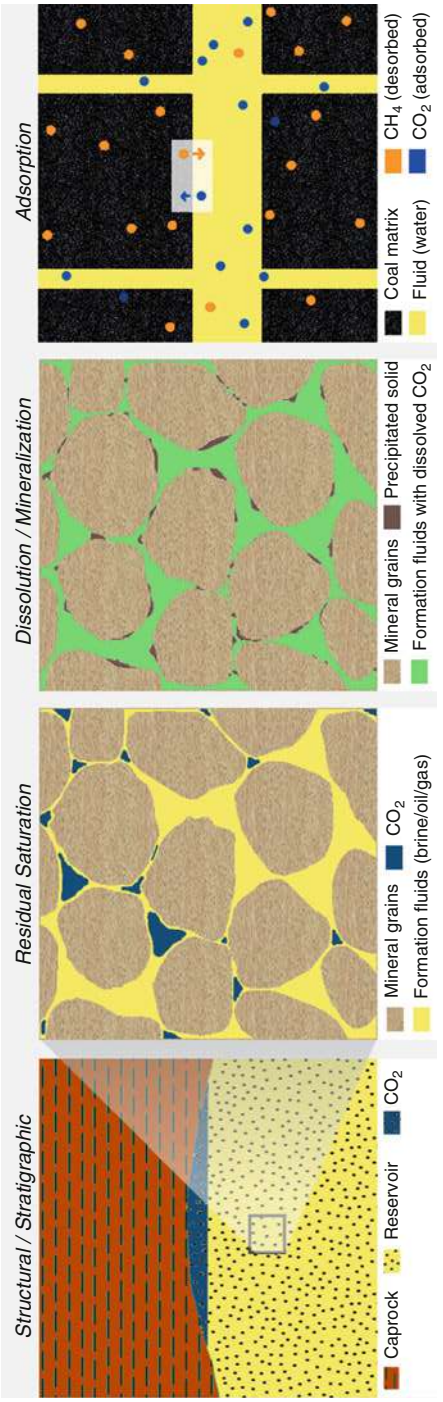

Fig. 8 Trapping mechanisms of stored CO_2 in geological reservoirs

against the displacement of CO_2 will retard plume movement and trap CO_2 within the reservoir for a certain period of time. The displacement of this plume will leave a CO_2 "tail" behind, in which storage occurs in pore space as residual gas at irreducible gas saturation (i.e., the minimum saturation of a fluid to be displaced in water media). As with the structural trapping, these mechanisms will also operate soon after CO_2 injection in a reservoir.

Dissolution and Mineralization Trapping

After injection, CO_2 will start to dissolve in formation water, and depending on factors like pH, a different proportion of dissolved species will form: H_2CO_3 (carbonic acid), HCO_3^- (bicarbonate), and CO_3^{2-} (carbonate). Once dissolved, CO_2 will be trapped within the reservoir aqueous phase as a dissolved species until geochemical conditions are changed (and proportion of dissolved species modified) or the fluids are displaced. Dissolved CO_2 may change drastically geochemical conditions of the media, mostly by increasing acidification of the aqueous phase, which in general enhances drastically the rate of dissolution of minerals present in the reservoir and caprock. Furthermore, the aqueous phase tends to be dried out in the vicinity of the CO_2-water interface, as the supercritical CO_2 absorbs water, leading to a more saturated brine (Kaszuba et al. 2003). This may set off the precipitation of minerals in this region, such as halite (NaCl). Dissolved CO_2 species and cations originated from dissolution of minerals or present in water may interact to form carbonates such as calcite ($CaCO_3$), magnesite ($MgCO_3$), and siderite ($FeCO_3$), among others. The type of carbonate formed will depend on pressure, temperature, and pH conditions, particularly on the activity of the cations dissolved in water and kinetics of reactions. Once in a solid phase, CO_2 will be stored within the reservoir until unlikely (in a period of $<$1,000 years) changes in pore water chemistry are drastic enough to dissolve carbonates and remove significant amounts of carbon off the storage complex.

Adsorption Trapping

Adsorption occurs when a gas molecule is bound to a solid surface by van der Waals forces. This is the main mechanism for trapping CO_2 in coal. CO_2 injected in a coal seam will migrate through its fracture network (denominated *cleat* system) as a free gas and diffuse through the coal matrix, being adsorbed in the microporous walls in coal. Binding strength is dependent on the pressure and temperature, with higher pressure and lower temperature favoring adsorption. Pressure and temperature will also control, together with the presence of other fluids (e.g., H_2S, H_2O), the quantity of CO_2 adsorbed in coal. CO_2 adsorption in coal may result in desorption of CH_4 owing to the lesser chemical affinity of the latter with coal. The desorbed methane is released as free gas to the cleat system and can be produced through wells (see Reservoir Options section above). After equilibrium,

and depending on conditions, ca. 5 % of the mass of CO_2 stored in coal will remain as free gas in the cleat system (and retained below an impermeable caprock) and 95 % as adsorbed CO_2. CO_2 will remain stored in coal if pressure and temperature conditions are unchanged. Changing pressure and temperature can only occur in a period smaller than 1,000 years by human intervention, through conventional mining, underground coal gasification, or depressurization of the seam as in coalbed methane production activities.

Storage Capacity Assessment

Estimating CO_2 storage capacity of a geological reservoir depends strongly on the methodology employed in calculations. Global capacity estimations available are largely inaccurate and conflicting, as they tend to be based on extrapolations of sparse data or erroneous assumptions (Bradshaw et al. 2007). A quick glance at some of these published assessments even reveals some world estimates that are lower than regional values. Many studies extrapolate values from a local or regional site to basin or continental scales, but the enormous geological variations that occur in storage complexes even within the same sedimentary basin make it nearly impossible for this upscaling to be precise.

Furthermore, capacity assessments were carried out using various approaches and methodologies. Recognizing these difficulties, the Carbon Sequestration Leadership Forum (CSLF), an international consortium for the development of CCS, launched in 2004 a task force to review and develop a standard methodology for storage capacity estimation. A comprehensive review of this methodology was presented by Bachu and Bradshaw in 2007 and is briefly explained in this section (Bradshaw et al. 2007; Bachu et al. 2007).

In this methodology, the different levels of capacity estimations are categorized in a resource pyramid (Fig. 9) (Bradshaw et al. 2007).

The first level, occupying the whole pyramid, is the *theoretical capacity* and represents the physical limit of what the storage system can accept. It can be either interpreted as the whole pore space available or pore space minus displaceable original fluids (water, oil, etc.) Either way, it represents the maximum upper limit to a capacity estimate. When technical cutoffs due to geological and/or engineering constraints are applied to the theoretical capacity assessment, an *effective capacity* upper limit is defined. Further restrictions due to legal and regulatory, infrastructure or economic barriers to storage result in a *practical capacity* subset. A final *matched capacity* estimation can be obtained by considering the previously mentioned source-sink matching assessment, taking into account proximity to stationary sources, injectivity, and supply rates of CO_2.

As this organization is more conceptual, it is unlikely that a capacity estimation assessment will result in precise values for each different category. In effect, the "resolution" of the data will depend largely on the scale considered. Estimations focused on a given site or local scale will probably give a higher level of resolution, while at larger scales (regional, basin, or country), this level of detail tends to decrease

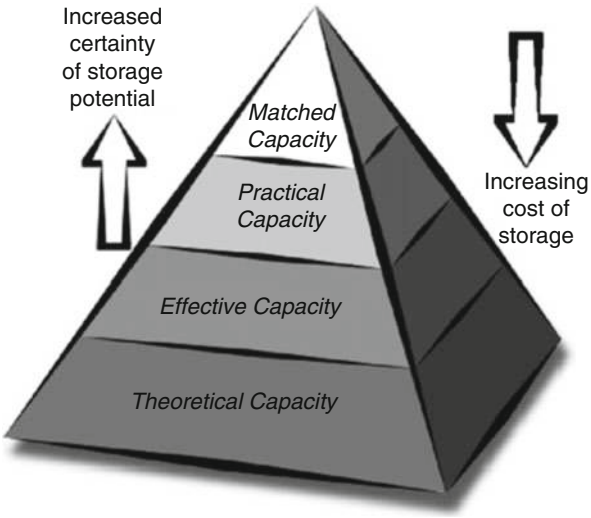

Fig. 9 Capacity estimation resource pyramid (Bachu et al. 2007)

significantly. Assessments at basin or country scale are more likely to be conducted by governments, while estimations at site or local scale will probably be run by project operators. Increasing resolution will usually result in higher costs of data acquisition. Next, a brief description of capacity estimation methods (and their current gaps and difficulties) for each main reservoir option is presented (Bradshaw et al. 2007; Bachu et al. 2007).

Petroleum Fields

Estimation of storage capacity in oil or gas fields is the most straightforward of all potential targets, as the oil industry gathers plenty of data from these reservoirs before and during exploration, to establish the precise amount of petroleum reserves and resources. Furthermore, oil and gas fields are discrete volumes with fairly well-defined boundaries, which allow for a more precise assessment.

On the other hand, petroleum production history and methods in a reservoir will influence directly the available storage space for CO_2. Secondary or tertiary recovery techniques (injection of water or other substances for improved production) can reduce the available space. Also, if the reservoir is in hydrodynamic contact with underlying aquifers, water may flood the reservoir during oil/gas production, occupying the previously oil-filled space. Injection of CO_2 can partially displace the water, although not all of the original oil-saturated volume will be available for storage, due to residual saturation or viscous fingering effects. It is assumed that injection of CO_2 in a petroleum field will be carried out until the original reservoir pressure is restored. However, this is not always possible, as the oil and gas exploration may damage the formation and/or caprock, limiting the maximum pressure. In other cases, injection can be performed beyond the original pressure,

as long as it does not compromise the safety of containment by the caprock, exceeding the rock-fracturing threshold or capillary entry pressure of this formation.

Theoretical capacities for petroleum reservoirs can be calculated based on geometrical parameters (reservoir area and thickness), physical and hydrodynamic properties such as CO_2 density and water saturation, and other data gathered from exploration activities, such as recovery factors, injected and produced water volumes. The *effective* storage capacity can then be obtained by applying a capacity coefficient (<1), which is dependent on buoyancy, mobility, heterogeneity, water saturation, and aquifer strength. These phenomena are site specific and the contribution to this coefficient is widely varied and difficult to estimate, usually being based on reservoir simulations (Bradshaw et al. 2007; Bachu et al. 2007).

Saline Aquifers

Capacity estimations for aquifers are difficult to estimate. The various trapping mechanisms that operate in these reservoirs have different capacities that are interrelated, and since these mechanisms act over different time intervals, the storage capacity associated with each one will also be time dependent. Considering a reservoir filling down to the spill point, the theoretical volume available will be dependent on the geometric volume (trap area and average thickness), porosity, and irreducible water saturation (the amount of water that is unable to move from the rock pores). The *effective* storage volume can be obtained applying a capacity coefficient (<1) to the theoretical volume, that for trap heterogeneity, CO_2 buoyancy, and sweep efficiency. This coefficient is highly site specific and can only be obtained by reservoir simulations (Bradshaw et al. 2007; Bachu et al. 2007).

Coalbeds

Storage capacity in coal can be estimated by analogy with CBM (coalbed methane) reserve estimation, which implies the determination of *initial* gas in place (IGIP) and *producible* gas in place (PGIP) for a given coal seam. The initial gas in place (IGIP) is usually calculated from the coalbed average thickness and area, bulk coal density, and gas content, subtracting the weight fractions of mineral and moisture contents. The gas content, in turn, is related to the adsorption capacity of coal, which depends on pressure, temperature, and coal characteristics, following a pressure-dependent isotherm that has to be determined in each case.

For estimation of storage capacity, it is assumed that CO_2 replaces the original gas content (primarily methane), due to the higher affinity with the coal matrix. The *theoretical* capacity for storage would then be equivalent to the IGIP, as if all the coal is accessed by CO_2, adsorbing at 100 % saturation. The *effective* capacity will be equivalent to the estimated *producible* gas in place (PGIP), in the case of gas production from coal seams. This producible content is a fraction of the IGIP, obtained by multiplying it by a recovery factor and a completion factor (which

represent actual fractions that can be produced and effective regions of the coal that contribute to gas production, respectively) (Bradshaw et al. 2007; Bachu et al. 2007).

Predicting the Fate of CO_2 Stored in Reservoirs: Experimental and Numerical Modeling

Several physicochemical alterations in the storage complex are triggered by massive injections of CO_2 into a geological reservoir, affecting both reservoir and caprock for large distances and long periods of time.

These phenomena and the complex interplay among them are not yet fully understood and have been extensively investigated ever since CCS started to develop worldwide. It involves the study of the geochemistry of the CO_2-water-rock interactions and the flow behavior of the different phases in the porous and fractured media present in the storage complex, as well as their impact on the geomechanical properties. This research ultimately aims to estimate the partition of the injected CO_2 among the different trapping mechanisms in a given time period (injection phase, earlier years, and geological time frames) and to unravel reservoir and caprock changes during injection and thousands of years later. To carry out these investigations, it is necessary to rely on both experimental and numerical modeling tools (Gaus 2010; Ketzer et al. 2009). By means of laboratory experiments, the conditions in the geological media can be simulated using actual reservoir and caprock samples, which are then analyzed for mineralogical changes following reactions with carbon dioxide and formation fluids. As experiments are limited by time constraints, complementary numerical simulations can be employed, by running kinetic and flow models spanning several years. The next sections will describe these methods with more detail.

Experimental Modeling

Laboratory experiments aim to simulate the interactions between CO_2 and the formation fluids and minerals (either reservoir or caprock), in similar conditions as those found in the geologic media (Kaszuba et al. 2013). In a straightforward approach, experiments can be carried out in static conditions, in which the reactants (CO_2, fluid, and rock samples) are introduced in a pressurized vessel and held at constant pressure and temperature for a certain period of time, usually ranging from hours to months (depending on the sample mineralogy). Pressure and temperature conditions for the experiments are usually set to replicate the reservoir environment, although more reactive conditions may be employed, in order to increase the chemical reactivity of the system reducing the time for the experiment (Kaszuba et al. 2003). Experiments with more reactive conditions should be taken carefully, as they may lead to flawed results, since the dissolution and precipitation kinetics of each mineral in a rock sample have a different dependence on temperature (Lasaga

1984). It is important for the quality of the results that the reactants are well characterized before and after the experiment. Ideally, for longer experiments, fluid samples should be collected from time to time from the reactor and analyzed. Characterization of the fluid phase is usually carried out through standard water analysis techniques such as chromatography and atomic absorption for quantification of ions, as well as pH and conductivity measurements. The mineral phase characterization often relies on imaging techniques such as scanning tunneling microscopy (STM), which provides a qualitative analysis of texture and crystalline habit, and optical microscopy for determination of sample mineralogy. Other techniques such as X-ray diffraction (useful for clay minerals) and, more recently, X-ray micro- and nanotomography, for 3D pore/channel structure visualization, may be employed. Materials employed for the vessel construction are an important issue, as they may suffer corrosion during the experiment. Stainless steels are well suited for experiments with distilled water or solutions with very low salinity, but more resistant alloys (such as titanium nitride or Hastelloy©) are needed for experiments with higher salinity brines, especially for longer experiments.

The methodology for batch experiments may vary significantly and is not a consensus among researchers on this field. Several key parameters are likely to be varied in the experiment design, such as the water/rock/vessel volume ratio, the rock sample physical aspect (crushed or unbroken), the depressurization procedure, and the pretreatment of products for characterization (addition of chemicals for solution conservation and carbon content fixation, filtration and desiccation of solid material, etc.) at the end of the experiment.

A more sophisticated approach, and possibly a more realistic simulation, consists of flow-through experiments, in which a core plug sample of the reservoir rock is placed in a tubular sealed reactor and subjected to a high-pressure continuous flow of either pure CO_2 or a saline solution saturated with CO_2 (Luquot and Gouze 2009). Ideally, the sample should be also submitted to radial and/or axial confining pressures during the experiment, using a Hassler-type cell (a similar tubular reactor, in which a radial load is applied to the sample). This results in a more realistic simulation of the overburden pressures existing in a geologic reservoir. With this design it is also possible to evaluate the rock permeability and its variations with mineral dissolution and precipitation. Using computerized X-ray tomography with proper resolution, it is possible to evaluate changes in porosity after a flow-through experiment, placing the reactor cell in the tomography scanner at selected time intervals.

A wide range of experiment designs are possible for this method, by changing the flowing phases, flow rates, fluid-mixing method, core size, and form of placement in the reactor, among others. Characterization techniques employed for both solution and minerals are essentially the same as used in batch experiments.

Numerical Modeling

Numerical simulations play an important role in the investigation of the interactions between carbon dioxide and the reservoir. It is the only method that allows to

estimate the consequences of a large-scale CO_2 injection to the reservoir and caprock in a geological timescale, thus being complementary to the laboratory experiments (Tsang et al. 2007).

However, the complexity of this natural system makes it nearly impossible for it to be simulated with high accuracy taking into account all the physicochemical transformations involved – multiphase flow of the different fluids, transport of mass and heat, geomechanical alterations, surface and interface interactions, and geochemical and biogeochemical reactions.

Fully coupled modeling tools capable of dealing with every possible phenomenon simultaneously and at different scales (from pore to basin) are not available so far and are not likely to be in the short term. Several existing numerical codes are able to partially integrate the simulation of these phenomena, and the choice for the appropriate code must take into account the reservoir and caprock properties, as well as the time and spatial scales of interest for the investigation.

In the early stages of injection of CO_2, simulations must target potential injectivity issues such as clogging by obstruction of pore throats or fracturing near the well by excessive pressure. For this, geomechanical and pore-scale flow models would be well suited. However, chemical reactions may also play an important role in this stage, especially with more reactive storage sites such as carbonatic or carbonate-rich reservoirs, which dissolve fast with increased acidification of the brine by CO_2 dissolution. Rapid dissolution may benefit CO_2 injectivity by increasing porosity and permeability, but an extensive dissolution of carbonate cement might be a risk, as it could induce fractures and activate faults in both reservoir and caprock. Another known effect is the brine desiccation caused by supercritical CO_2-absorbing water from the aqueous phase. In highly saline reservoirs, this may cause rapid precipitation of salts such as halite or anhydrite, affecting injectivity by clogging the pores. Hence, geochemical simulation tools may also be necessary to model the possible mineral dissolution and precipitation processes in the vicinity of injection wells.

In the long-term, large-scale reservoir simulations that take into account the sedimentary deposition environment which leads to heterogeneities in the formations will help to determine the CO_2 phase displacement in the reservoir. Accurate models for the calculation of CO_2 solubility and the chemical reaction kinetics of less reactive silicate minerals are also important, to estimate the amount of carbon trapped by dissolution in the aqueous phase, or safely stored in a solid phase by mineralization, after several years.

Geochemical modeling of CO_2-water-rock interactions is often divided in two approaches. One is the determination of the thermodynamic state of equilibrium of the CO_2-water-rock system, considering every chemical reaction involved within the water phase (speciation) and its equilibrium with the gas (CO_2) and solid (minerals) phases. This is accomplished by solving a system of equations involving the equilibrium constants for every chemical process involved and the activities for each species – which in turn requires a model for calculating activity coefficients. From this kind of model, it is possible to estimate the solubility of CO_2 in the formation fluid (if an appropriate equation of state for CO_2 at the reservoir pressure

and temperature conditions is used), as well as mineral saturation states at equilibrium, i.e., the tendency for a mineral to precipitate or dissolve in order to reach thermodynamic equilibrium.

A second approach is to model the kinetics of dissolution and precipitation of the reservoir and caprock minerals with time. Usually, a generic rate law for these processes is employed for all minerals, which depends on a rate constant, the specific reactive surface of the mineral, temperature, pH, and deviation from the equilibrium state. Unfortunately, very few kinetic studies have been carried out at the usual pressure and temperature conditions of storage reservoirs; therefore, existing data are often not accurate enough. Furthermore, the reactive surface of a mineral is another major source of errors – it may vary considerably for a given mineral depending on crystalline structure, chemical environment, depositional and diagenetic processes, coating by inert materials, etc. Usually, geometric estimations of the mineral surface are employed, as they have been found to be well correlated to measured values (using BET gas adsorption isotherms).

Geochemical calculations as described above are *static* models, as they do not consider the displacement of fluids (CO_2, water, oil/gas) and transport of mass and heat. The step-up on simulating approaches is to incorporate the geochemical transformations in fluid flow and transport models based on the Darcy equation for flow in porous media, coupled with advective, dispersive, and diffusive mass and heat transport. This coupling of flow and transport equations with chemical reactivity results in so-called *reactive transport* models (Steefel et al. 2005) and are possibly one of the most employed tools for numerical simulations in CO_2 geological storage research.

A wide range of numerical codes have been used in simulation studies applied to CO_2 geological storage. The US Geological Survey's PHREEQC (Parkhurst and Appelo 1999) is among the most employed ones. This code is capable of performing thermodynamic equilibrium calculations, both in aqueous phase and with the inclusion of mineral and gas phases. Kinetics of mineral dissolution and precipitation can also be included, introducing user-customizable rate laws. One-dimensional reactive transport simulations are also possible with this code. For more elaborate flow and reactive transport modeling studies, the current state-of-the-art code is TOUGHREACT, a modification of the TOUGH2 code (a 3D multiphase flow model for porous and fractured media, developed at the Lawrence Berkeley National Laboratory) (Xu et al. 2006) that couples chemical reactivity with the multiphase flow equations. Many other programs have been used in CCS studies though, and several others are under development. The strongest efforts are focused in the inclusion of geochemical and geomechanical effects into existing reservoir simulators.

Another important issue that also needs to be addressed by investigations in this area is the lack of reliable thermodynamic data and kinetic parameters in the specific conditions for CO_2 storage. Thermodynamic constants of aqueous and mineral phase equilibria have been used for decades through the available databases included in commercial codes without much regard for its origins. Current databases date from the 1980s and are far from accurate, as the initial missing entries

were in many cases completed through fittings and extrapolations from a few existing values at the time, and little effort has been put later to improve this situation. As for kinetics of dissolution and precipitation of minerals, rate laws and constants available so far have been mostly obtained at ambient conditions and extrapolated for use in numerical simulations at reservoir conditions. Furthermore, rate constant values are difficult to reproduce among experiments, for several reasons. First, the very slow rates of dissolution of some minerals make them difficult to determine experimentally. Experimental methodologies and settings are not standardized and may reflect on the values obtained. Rates may also vary significantly depending on the sample source, heterogeneities, and available reactive surface. One approach that has been adopted to minimize these issues was to fit several existing data into a general rate law (Palandri and Kharaka 2004).

Despite the existing knowledge of water-rock interactions, it is clear that the inclusion of carbon dioxide in this system requires a great research effort in developing both experimental and numerical methodologies and instruments, in order to improve the means to better understand the fate of CO_2 in a storage reservoir.

Safety of Geological Storage

Storage safety is a key issue for CCS projects. Carbon dioxide is a noncombustible low-toxicity gas, present in small concentrations in the atmosphere (0.04 % in volume), but in higher concentrations, it can be dangerous to human health and the environment. Until now, a single lethal event of major proportion has been registered caused by leakage of CO_2 from the subsurface and was due to natural causes. In 1986, 1.6 Mt of carbon dioxide were released abruptly from the bottom of the volcanic crater lake Nyos, in Cameroon. The gas was released overnight, and the plume descended over a valley, displacing air and suffocating over 1700 people and thousands of livestock in a nearby village. However ominous it may seem, the incident was very singular and highly unlikely to be repeated in nature, not to mention in engineered storage reservoirs, but it serves as a reminder of the hazards of high CO_2 concentrations.

Therefore, in any CCS project, safety measures and risk assessments must be carefully performed to evaluate potential sources of CO_2 leakages or seepages away from the storage complex, with indications of remediation actions in case of containment failures (Wilson and Gerard 2007). Figure 10 presents the most important escape routes for stored CO_2 that have to be evaluated in a risk assessment.

Once injected in a reservoir, CO_2 can be considered safely stored if at least 99 % of the injected quantity is retained in the reservoir for at least 1,000 years (Benson and Cole 2008).

Large engineered storage sites for gases or waste are not new concepts. In Europe and the USA, underground facilities have been used for decades to store natural gas during low-demand periods (summer seasons), many of which are located near urbanized localities (Katz and Tek 1981). Underground repositories for long-lived radioactive waste from nuclear power plants are employed and under

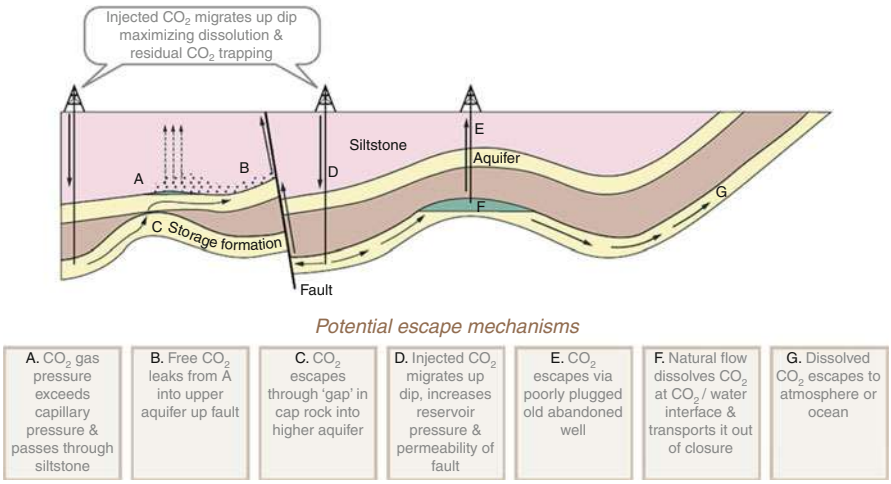

Fig. 10 Potential escape pathways for stored CO_2 in a geological formation (IPCC 2005)

construction. Research in this area has consolidated a considerable know-how on geological storage and containment of these materials for long periods of time (NEA 2008).

The safety of subsurface storage can also be vowed by the several existing natural accumulations of carbon dioxide, which can be used to gather further knowledge on containment conditions (Baines and Worden 2004). These natural CO_2 fields range from shallow (100 meters) to deep (up to 5 km) reservoirs, with high-purity (>90 %) carbon dioxide accumulations around the world that can be used as analogs to investigate the consequences of long-term storage of CO_2 in both limestone and sandstone lithologies (Pearce 1996). Many of these natural occurrences are exploited and primarily used for enhanced oil recovery (EOR) projects (see Reservoir Options section), particularly in the USA. The McElmo Dome in southwestern Colorado is the best documented natural CO_2 reservoir and the world's largest supply of commercial carbon dioxide, with 1.6 Gt of original carbon dioxide in place. A large part of the 14.6 Mt of CO_2 produced annually is transported to the Permian Basin by an 800 km long pipeline since 1984. There is no episode of CO_2 leakage from the field to the surface detected by an alarm system installed on the surface since the beginning of its exploration in 1976 (Stevens et al. 2000).

Monitoring Stored CO_2

The deployment of any CO_2 storage project will most likely require, by regulating organisms, a constant monitoring and verification of the storage complex, usually operated during the injection phase and in the first years or decades following site abandonment (depending on specific regulations). Most monitoring techniques rely

on proven technology which has already been in use for years in many applications, including oil and gas exploration, natural gas underground storage, and waste disposal. The choice for the appropriate monitoring methods and instruments will depend on the storage complex characteristics and regulatory requirements.

Among the most important techniques for monitoring CO_2 in the reservoir are geophysical methods such as seismic, electromagnetic, and gravity imaging, which allow to track the CO_2 plume displacement in the host formation. Other important methods include geochemical monitoring, which relies on measuring changes in formation water (and/or gas) composition, collected in observation wells to evaluate changes caused by the injection of CO_2, and atmospheric and surface monitoring, for detecting leakages and seepages of CO_2 in the air and soil, in the surrounding areas of the storage complex (Arts and Winthaegen 2005).

Monitoring activities differ according to the stage in which a CCS project is found. The first stage is the site selection and characterization, where the monitoring role is to gather enough data to establish accurate baseline conditions, to be compared with upcoming measurements. During the operational phase, usually taking place over a period of 30–50 years, monitoring is focused on ensuring operational safety and assessing injection well conditions, tracking migration of injected CO_2, and updating storage performance predictions, usually comparing with data from simulations, laboratory experiments, and previous field tests. After operations are finished (when injection of CO_2 is stopped), a closure phase ensues. In this stage that may last years or decades (depending on the project or regulations), injection wells are plugged and abandoned and must be monitored for a certain period of time. Most monitoring activities should also be continued during this period in order to demonstrate storage safety and performance. In a post-closure stage, the storage complex will most likely be handed to regulatory authorities, who would maintain data records. Further monitoring would no longer be needed, except in case of ongoing leakages or legal disputes or in case additional data is required for future projects (Benson 2007).

Future Directions

CCS is a transition technology to an alternative energy future, possibly based on renewable sources. Optimism for its success is based on industrial experience – many of the technologies needed for implementation of CCS projects in commercial scale are already available and mature. But even proponents acknowledge that there are several issues that need to be dealt with before it can achieve widespread application with a significant impact in reducing emissions of greenhouse gases, especially when those regarding integration, cost-reduction, and scaling up of known technologies in large-scale commercial projects. Nevertheless, CCS is the only available technology with potential to ensure the protection of climate, while preserving the value of fossil fuel reserves and of the existing infrastructure, guaranteeing a sustainable use of these resources whenever necessary. Furthermore, CCS is only viable option for reducing large-scale CO_2 emissions from industrial

sectors such as cement, steel, chemical, and refining, which represent one-fifth of global emissions (IEA 2013).

CCS has been progressing steadily, although at a slower pace than would be desired to meet the expectations and emission reductions required (IEA 2013). As mentioned earlier, the current amount of CO_2 stored in large-scale demonstration or commercial projects is approximately 27 million tons per year, roughly 0.1 % of the global emissions from large stationary sources that can be captured and stored. While it is very unlikely that all the emissions from these sources will be captured and stored, it is expected that by 2050 this number is multiplied 100-fold, with CCS operations routinely used in all applicable process, storing over 7000 Mt annually, according to the latest technology road map for CCS from the IEA (released in 2013) (IEA 2013). Most of the existing CCS projects are in the oil and gas production and refining sectors, operated by petroleum companies, the majority of them for EOR purposes. It was not until recently, in 2014, that the first long-expected integrated CCS project in the power generation sector started operating, at demonstration scale (the Boundary Dam project in Canada, operated by SaskPower energy company). Other industrial areas have shown nearly absent advances in actions to integrate CCS in their activities (only two demonstration projects at iron and steel plants and one in coal-to-liquid process are in planning stages) (IEA 2013).

The latest progress report from the Global CCS Institute (released in February 2014) indicates that there are 60 large-scale projects worldwide (more than 1 $MtCO_2$/year) integrating capture and storage – 13 in operation and 47 in different planning stages (identification, evaluation, definition) (GCSSI 2014). Unfortunately, recent history has shown that many of the planned operations ended up being canceled at the final investment decision, mostly due to the elevated costs associated with a CCS project. Indeed, the absence or uncertainty of an economic sustainable model for this activity is possibly one of the main reasons for the slow pace of CCS deployment so far. Governments are expected to contribute in these initial efforts, funding research and demonstration projects (and even funding pipeline networks, since they could be shared by more than one project), but it is widely accepted that an economic driver has to be established to stimulate the private sector to participate in CCS initiatives. With the current conditions, commercial power plants and industrial facilities will not invest in CCS owing to the elevated costs and reduced efficiency and energy outputs. CCS coupled to coal-fired power generation increases the costs between 40 % and 60 % (yet the end cost would still be comparable or less than that from photovoltaic of offshore wind generation costs). Injection of CO_2 in deep saline aquifers, which are possibly the most suitable reservoirs for storage, has no economic return by itself and requires some form of incentive to be deployed, as was the case in the Sleipner project, with Norway's government taxes imposed over CO_2 emissions offshore. The inclusion of CO_2 geological storage in the UN Framework Convention on Climate Change Clean Development Mechanism (CDM) is one solution that has been advocated strongly by many governments and stakeholders, as a means to establish an economic driver for CCS projects. The CDM is a mechanism established in the

Kyoto Protocol that provides means for companies and countries to offset their CO_2 emissions by investing in projects with proved emission reductions (such as CCS operations) in developing countries. Following many years of negotiations, CCS has finally been accepted to be included in the CDM in 2011, although many issues still need to be worked out before it starts going operative (UNFCCC 2011).

More recently, the utilization of CO_2 in activities that could provide it with some economic value has been proposed. While it has been used in several applications for many years, the amounts involved are too small to add a significant contribution to an effective reduction of emissions. Between 80 Mt and 120 Mt of CO_2 are sold commercially each year for many applications, with the majority (more than 60 Mt) being used for enhanced oil recovery (EOR) (IPCC 2005; IEA 2013; GCCSI 2011).

In the chain of a CCS integrated operation, the major bottleneck in the total cost is the capture and separation of CO_2 from the stationary source, being responsible for approximately 70 % of the global cost in a project. Capture and separation technologies have long been used in the industry to remove CO_2 from flue gas streams; however, there is still a strong need to develop and test new technologies (especially in view of the large scales required for CCS projects). In particular, the main challenges in capture technologies at the moment include: (i) diminishing costs of post-combustion capture, which are mainly related to energy penalty required for regeneration of solvents and (ii) developing novel, promising technologies such as oxy-combustion via chemical looping and ionic liquids.

While storage costs are usually much lower than those of capture and separation, the challenge remains in terms of the long time frame – usually 5–10 years – that is necessary for the site selection and characterization phases that are necessary for a given project.

Another important issue for the full-scale deployment of storage is related to scaling up the rate of CO_2 that must be injected per storage site. Even though CCS has been demonstrated in commercial scale (storage >1 Mt/year) by the projects mentioned earlier, future storage projects will have to increase this rate several times. It is agreed that CO_2 injection must reach rates at least comparable to those of oil and gas extraction (IEA 2013).

The peculiar characteristics of CO_2 and its interaction with each part of the CCS chain require continuous research to improve existing technologies and materials, such as new CO_2-resistant cements for injection wells, development of high-pressure compressors adapted for CO_2, and corrosion-resistant pipelines for transport, among others.

Demonstrating safety of storage is also a key point in the development of this technology. This requires the improvement of existing and developing new monitoring techniques, which in turn can only be achieved through field testing in pilot- and demonstration-scale sites of injection. Successful demonstration of storage and monitoring techniques will further improve public perception of CCS as well. Geologic storage of CO_2 is a relatively new concept to which most of the population is very unfamiliar overall. Communicating and introducing this technology to general public is a challenging task that has to be carefully addressed in order to succeed.

The recognition of CCS as an important technology for greenhouse gas emission reductions resulted in a prompt effort by several countries' administrations in developing regulatory marks and legislations for this activity. However, the majority of nations (mostly non-OECD) still require regulations for this activity to be introduced in their legal system, and this presents a series of difficulties. First, the categorization of CO_2 in a CCS project is a matter of discussion – it is usually unclear whether it should be treated as waste, commodity, or other nature. Legal responsibilities over environmental damage due to leakages need to be properly defined by regulators, for which a clear distinction of the storage complex boundaries is imperative. Liability for stored CO_2 over the years is another issue that requires careful analysis, since storage periods are likely to be much longer than the lifetime of a site operator.

For all the potential that CCS in geological reservoirs has in becoming an important solution for the climate crisis, it was patently shown that many issues and gaps in this integrated technology are yet to be resolved to achieve this objective. And as with most of the challenges mankind has faced, this will probably hardly succeed if not through a global determination in solving it, mostly through the combined efforts of academia, industry, and government sectors.

References

Abad A, Mattisson T, Lyngfelt A, Rydén M (2006) Chemical-looping combustion in a 300 W continuously operating reactor system using a manganese-based oxygen carrier. Fuel 85:1174–1185. doi:10.1016/j.fuel.2005.11.014

Anderson JL, Dixon JK, Maginn EJ, Brennecke JF (2006) Measurement of SO_2 solubility in ionic liquids. J Phys Chem B 110:15059–15062. doi:10.1021/jp063547u

Anthony JL, Anderson JL, Maginn EJ, Brennecke JF (2005) Anion effects on gas solubility in ionic liquids. J Phys Chem B 109:6366–6374. doi:10.1021/jp046404l

Arts R, Winthaegen P (2005) Monitoring options for CO_2 storage. In: Benson SM (ed) Carbon dioxide capture for storage in deep geologic formations: results from the CO_2 capture project, vol 2. Elsevier, Amsterdam, pp 1001–1014

Bachu S (2003) Screening and ranking of sedimentary basins for sequestration of CO_2 in geological media in response to climate change. Environ Geol 44:277–289

Bachu S, Bonijoly D, Bradshaw J et al (2007) CO_2 storage capacity estimation: methodology and gaps. Int J Greenh Gas Control 1:430–443

Baines SJ, Worden RH (2004) The long-term fate of CO_2 in the subsurface: natural analogues for CO_2 storage. In: Baines SJ, Worden RH (eds) Geological storage on carbon dioxide. Geological Society, London, pp 59–85

Bara JE, Camper DE, Gin DL, Noble RD (2009a) Room-temperature ionic liquids and composite materials: platform technologies for CO_2 capture. Acc Chem Res 43:152–159. doi:10.1021/ar9001747

Bara JE, Carlisle TK, Gabriel CJ et al (2009b) Guide to CO_2 separations in imidazolium-based room-temperature ionic liquids. Ind Eng Chem Res 48:2739–2751. doi:10.1021/ie8016237

Beck B, Cunha P, Ketzer M et al (2011) The current status of CCS development in Brazil. Energy Procedia 4:6148–6151. doi:10.1016/j.egypro.2011.02.623

Benson S (2007) Monitoring geological storage of carbon dioxide. In: Wilson EJ, Gerard D (eds) Carbon capture and sequestration: integrating technology, monitoring, regulation. Blackwell, Ames, pp 73–100

Benson SM, Cole DR (2008) CO_2 sequestration in deep sedimentary formations. Elements 4:325–331

Bentham M, Kirby G (2005) CO_2 storage in saline aquifers. Oil Gas Sci Technol L Inst Fr Du Pet 60:559–567

Blasig A, Tang J, Hu X et al (2007) Magnetic suspension balance study of carbon dioxide solubility in ammonium-based polymerized ionic liquids: Poly(*p*-vinylbenzyltrimethyl ammonium tetrafluoroborate) and poly([2-(methacryloyloxy)ethyl] trimethyl ammonium tetrafluoroborate). Fluid Phase Equilib 256:75–80. doi:10.1016/j.fluid.2007.03.007

Blomen E, Hendriks C, Neele F (2009) Capture technologies: improvements and promising developments. Energy Procedia 1:1505–1512. doi:10.1016/j.egypro.2009.01.197

Blunt M, Fayers FJ, Orr FM Jr (1993) Carbon dioxide in enhanced oil recovery. Energy Convers Manag 34:1197–1204. doi:10.1016/0196-8904(93)90069-m

Boundary Dam Carbon Capture Project. (2015) http://www.saskpowerccs.com/ccs-projects/boundary-dam-carbon-capture-project/. Accessed 22 Jan 2015

Bradshaw J, Bachu S, Bonijoly D et al (2007) CO_2 storage capacity estimation: issues and development of standards. Int J Greenh Gas Control 1:62–68

Carvalho PJ, Álvarez VH, Machado JJB et al (2009) High pressure phase behavior of carbon dioxide in 1-alkyl-3-methylimidazolium bis(trifluoromethylsulfonyl)imide ionic liquids. J Supercrit Fluids 48:99–107. doi:10.1016/j.supflu.2008.10.012

Corbella BM, de Diego L, García-Labiano F et al (2005) Characterization and performance in a multicycle test in a fixed-bed reactor of silica-supported copper oxide as oxygen carrier for chemical-looping combustion of methane. Energy & Fuels 20:148–154. doi:10.1021/ef050212n

Day S, Fry R, Sakurovs R, Weir S (2010) Swelling of coals by supercritical gases and its relationship to sorption. Energy & Fuels 24:2777–2783. doi:10.1021/ef901588h

De Diego LF, Gayan P, Garcia-Labiano F et al (2005) Impregnated CuO/Al_2O_3 oxygen carriers for chemical-looping combustion: avoiding fluidized bed agglomeration. Energy & Fuels 19:1850–1856. doi:10.1021/ef050052f

Feron PHM (2010) Exploring the potential for improvement of the energy performance of coal fired power plants with post-combustion capture of carbon dioxide. Int J Greenh Gas Control 4:152–160. doi:10.1016/j.ijggc.2009.10.018

Feron PHM, Hendriks CA (2005) Les différents procédés de capture du CO_2 et leurs coûts. Oil Gas Sci Technol – Rev IFP 60:451–459

Figueroa JD, Fout T, Plasynski S et al (2008) Advances in CO_2 capture technology – The U.S. Department of Energy's Carbon Sequestration Program. Int J Greenh Gas Control 2:9–20. doi:10.1016/s1750-5836(07)00094-1

Franz J, Scherer V (2010) An evaluation of CO_2 and H_2 selective polymeric membranes for CO_2 separation in IGCC processes. J Memb Sci 265:9. doi:10.1016/j.memsci.2010.01.047

Gale J, Freund P (2001) Coal-bed methane enhancement with CO_2 sequestration worldwide potential. Environ Geosci 8:210–217

García-Pérez E, Parra JB, Ania CO et al (2007) A computational study of CO_2, N_2, and CH_4 adsorption in zeolites. Adsorption 13:469–476. doi:10.1007/s10450-007-9039-z

Gaus I (2010) Role and impact of CO_2-rock interactions during CO_2 storage in sedimentary rocks. Int J Greenh Gas Control 4:73–89. doi:10.1016/j.ijggc.2009.09.015

GC Institute (2014) Petrobras Lula oil field CCS project. http://www.globalccsinstitute.com/project/petrobras-lula-oil-field-ccs-project. Accessed 22 Jan 2015

GCCSI (2011) Accelerating the uptake of CCS: industrial use of captured carbon dioxide. Global CCS Institute, Canberra

GCSSI (2014) The global status of CCS. Global CCS Institute, Canberra

Gozalpour F, Ren SR, Tohidi B (2005) CO_2 EOR and storage in oil reservoirs. Oil Gas Sci Technol L Inst Fr Du Pet 60:537–546

Gunter WD, Bachu S, Benson S (2004) The role of hydrogeological and geochemical trapping in sedimentary basins for secure geological storage of carbon dioxide.

In: Baines SJ, Worden RH (eds) Geological storage of carbon dioxide. Geological Society, London, pp 129–145

Hicks JC, Drese JH, Fauth DJ et al (2008) Designing adsorbents for CO_2 capture from flue gas-hyperbranched aminosilicas capable of capturing CO_2 reversibly. J Am Chem Soc 130:2902–2903. doi:10.1021/ja077795v

Holt T, Jensen JI, Lindeberg E (1995) Underground storage of CO_2 in aquifers and oil reservoirs. Energy Convers Manag 36:535–538

IEA (2008a) Energy technology perspectives: scenarios and strategies to 2050. International Energy Agency, Paris

IEA (2008b) CO_2 capture and storage: a key carbon abatement option. International Energy Agency, Paris

IEA (2009) Technology roadmap – carbon capture and storage. International Energy Agency, Paris

IEA (2012) Energy technology perspectives. International Energy Agency, Paris

IEA (2013) Technology roadmap – carbon capture and storage. International Energy Agency, Paris

IEA Greenhouse Gas R&D Programme (2001) Putting carbon back into the ground. In: Davidson J, Freud P, Smith A (eds). IEA Greenhouse Gas R&D Programme, Paris

IEA Greenhouse Gas R&D Programme (2004) IEA GHG Weyburn CO_2 monitoring & storage. Petroleum Technology Research Centre, Regina, Canada

IPCC (2005) Special report on carbon dioxide capture and storage. Cambridge University Press, Cambridge, UK

IPCC (2014) Climate change 2014: mitigation of climate change. Contribution of Working Group III to the Fifth Assessment Report of the Intergovernmental Panel on Climate Change. Cambridge University Press, Cambridge, UK/New York

Kanniche M, Gros-Bonnivard R, Jaud P et al (2010) Pre-combustion, post-combustion and oxy-combustion in thermal power plant for CO_2 capture. Appl Therm Eng 30:53–62. doi:10.1016/j.applthermaleng.2009.05.005

Kaszuba JP, Janecky DR, Snow MG (2003) Carbon dioxide reaction processes in a model brine aquifer at 200°C and 200 bars: implications for geologic sequestration of carbon. Appl Geochemistry 18:1065–1080. doi:10.1016/s0883-2927(02)00239-1

Kaszuba J, Yardley B, Andreani M (2013) Experimental perspectives of mineral dissolution and precipitation due to carbon dioxide-water-rock interactions. Rev Mineral Geochemistry 77:153–188

Katz DL, Tek MR (1981) Overview of underground storage of natural gas. J Pet Technol 33:943–951

Ketzer JM, Iglesias R, Einloft S et al (2009) Water-rock-CO_2 interactions in saline aquifers aimed for carbon dioxide storage: Experimental and numerical modeling studies of the Rio Bonito Formation (Permian), southern Brazil. Appl Geochemistry 24:760–767. doi:10.1016/j.apgeochem.2009.01.001

Kong Y, Jiang G, Fan M et al (2014) A new aerogel based CO_2 adsorbent developed using a simple sol–gel method along with supercritical drying. Chem Commun 50:12158–12161. doi:10.1039/C4CC06424K

Korbøl R, Kaddour A (1995) Sleipner vest CO_2 disposal – injection of removed CO_2 into the utsira formation. Energy Convers Manag 36:509–512

Kothandaraman A, Nord L, Bolland O et al (2009) Comparison of solvents for post-combustion capture of CO_2 by chemical absorption. Energy Procedia 1:1373–1380. doi:10.1016/j.egypro.2009.01.180

Kumar S, Cho JH, Moon I (2014) Ionic liquid-amine blends and CO_2BOLs: prospective solvents for natural gas sweetening and CO_2 capture technology – a review. Int J Greenh Gas Control 20:87–116. doi:10.1016/j.ijggc.2013.10.019

Large Scale CCS Projects. (2015) http://www.globalccsinstitute.com/projects/large-scale-ccs-projects. Accessed 22 Jan 2015

Lasaga AC (1984) Chemical kinetics of water-rock interactions. J Geophys Res 89:4009–4025. doi:10.1029/JB089iB06p04009

Le Quéré C, Moriarty R, Andrew RM et al (2014) Global carbon budget 2014. Earth Syst Sci Data Discuss 7:521–610. doi:10.5194/essdd-7-521-2014

Lepaumier H, Picq D, Carrette PL (2009) Degradation study of new solvents for CO_2 capture in post-combustion. Energy Procedia 1:893–900. doi:10.1016/j.egypro.2009.01.119

Li B, Duan Y, Luebke D, Morreale B (2013) Advances in CO_2 capture technology: a patent review. Appl Energy 102:1439–1447. doi:10.1016/j.apenergy.2012.09.009

Luquot L, Gouze P (2009) Experimental determination of porosity and permeability changes induced by injection of CO_2 into carbonate rocks. Chem Geol 265:148–159. doi:10.1016/j.chemgeo.2009.03.028

Magalhaes TO, Aquino AS, Vecchia FD et al (2014) Syntheses and characterization of new poly (ionic liquid)s designed for CO_2 capture. RSC Adv 4:18164–18170. doi:10.1039/C4RA00071D

Markewitz P, Kuckshinrichs W, Leitner W et al (2012) Worldwide innovations in the development of carbon capture technologies and the utilization of CO_2. Energy Environ Sci 5:7281–7305. doi:10.1039/C2EE03403D

Millward AR, Yaghi OM (2005) Metal−Organic frameworks with exceptionally high capacity for storage of carbon dioxide at room temperature. J Am Chem Soc 127:17998–17999. doi:10.1021/ja0570032

Muldoon MJ, Aki SNVK, Anderson JL et al (2007) Improving carbon dioxide solubility in ionic liquids. J Phys Chem B 111:9001–9009. doi:10.1021/jp071897q

NEA (2008) Moving forward with geological disposal of radioactive waste. Nuclear Energy Agency, Paris

NETL (2010) Carbon dioxide enhanced oil recovery [internet]. Available from: http://www.netl.doe.gov/file library/research/oil-gas/CO2_EOR_Primer.pdf

Pacala S, Socolow R (2004) Stabilization wedges: solving the climate problem for the next 50 years with current technologies. Science 305:968–972

Palandri JL, Kharaka YK (2004) A compilation of rate parameters of water-mineral interaction for application to geochemical modeling. U.S. Geological Survey, Menlo Park, CA

Pannocchia G, Puccini M, Seggiani M, Vitolo S (2007) Experimental and modeling studies on high-temperature capture of CO_2 using lithium zirconate based sorbents. Ind Eng Chem Res 46:6696–6706. doi:10.1021/ie0616949

Parkhurst DL, Appelo CAJ (1999) User's guide to PHREEQC (version 2)–A computer program for speciation, batch-reaction, one-dimensional transport, and inverse geochemical calculations. U.S. Geological Survey Water Resources Investigations

Pearce JM (1996) Natural occurrences as analogues for the geological disposal of carbon. Fuel Energy Abstr 37:305. doi:10.1016/0140-6701(96)82690-7

Pennline HW, Luebke DR, Jones KL et al (2008) Progress in carbon dioxide capture and separation research for gasification-based power generation point sources. Fuel Process Technol 89:897–907. doi:10.1016/j.fuproc.2008.02.002

Perinu C, Arstad B, Jens K-J (2014) NMR spectroscopy applied to amine–CO_2–H_2O systems relevant for post-combustion CO_2 capture: a review. Int J Greenh Gas Control 20:230–243. doi:10.1016/j.ijggc.2013.10.029

Powell CE, Qiao GG (2006) Polymeric CO_2/N_2 gas separation membranes for the capture of carbon dioxide from power plant flue gases. J Memb Sci 279:1–49. doi:10.1016/j.memsci.2005.12.062

Pruess K, Garcia J (2002) Multiphase flow dynamics during CO_2 disposal into saline aquifers. Environ Geol 42:282–295. doi:10.1007/s00254-001-0498-3

Puxty G, Rowland R, Allport A et al (2009) Carbon dioxide postcombustion capture: a novel screening study of the carbon dioxide absorption performance of 76 amines. Environ Sci Technol 43:6427–6433. doi:10.1021/es901376a

Raeissi S, Peters CJ (2008) Carbon dioxide solubility in the homologous 1-alkyl-3-methylimidazolium bis(trifluoromethylsulfonyl)imide family. J Chem Eng Data 54:382–386. doi:10.1021/je800433r

Ramdin M, de Loos TW, Vlugt TJH (2012) State-of-the-art of CO_2 capture with ionic liquids. Ind Eng Chem Res 51:8149–8177. doi:10.1021/ie3003705

Reeves SR, Schoeling L (2001) Geological sequestration of CO_2 in coal seams: reservoir mechanisms, field performance, and economics. In: Williams DJ, Durie RA, McMUllan P, et al (eds) Fifth international conference greenhouse gas control technologies. CSIRO Publishing, Cairns, pp 593–598

Rubin ES (2008) CO_2 capture and transport. Elements 4:311–317

Sabouni R, Kazemian H, Rohani S (2014) Carbon dioxide capturing technologies: a review focusing on metal organic framework materials (MOFs). Environ Sci Pollut Res 21:5427–5449. doi:10.1007/s11356-013-2406-2

Samanta A, Zhao A, Shimizu GKH et al (2011) Post-combustion CO_2 capture using solid sorbents: a review. Ind Eng Chem Res 51:1438–1463. doi:10.1021/ie200686q

Scherer GW, Celia MA, Prévost J-H et al (2005) Leakage of CO_2 through abandoned wells: role of corrosion of cement. In: Carbon dioxide capture for storage in deep geologic formations: results from the CO_2 capture project, vol 2. Elsevier, Amsterdam, pp 827–848

Scovazzo P, Kieft J, Finan DA et al (2004) Gas separations using non-hexafluorophosphate [PF6]-anion supported ionic liquid membranes. J Memb Sci 238:57–63. doi:10.1016/j.memsci.2004.02.033

Shin E-K, Lee B-C (2008) High-pressure phase behavior of carbon dioxide with ionic liquids: 1-alkyl-3-methylimidazolium trifluoromethanesulfonate. J Chem Eng Data 53:2728–2734. doi:10.1021/je8000443

Snøhvit. (2015) http://www.statoil.com/en/TechnologyInnovation/NewEnergy/CO_2CaptureStorage/Pages/Snohvit.aspx. Accessed 22 Jan 2015

Steefel CI, DePaolo DJ, Lichtner PC (2005) Reactive transport modeling: an essential tool and a new research approach for the earth sciences. Earth Planet Sci Lett 240:539–558. doi:10.1016/j.epsl.2005.09.017

Stevens SH, Fox CE, Melzer LS (2000) McElmo Dome and ST. Johns natural CO_2 deposits: analogs for carbon sequestration. GHGT-5

Stevens SH, Kuuskraa VA, Gale J, Beecy D (2001) CO_2 injection and sequestration in depleted oil and gas fields and deep coal seams: worldwide potential and costs. Environ Geosci 8:200–209

Supasitmongkol S, Styring P (2010) High CO_2 solubility in ionic liquids and a tetraalkylammonium-based poly(ionic liquid). Energy Environ Sci 3:1961–1972. doi:10.1039/C0EE00293C

Taber JJ, Martin FD, Seright RS (1997a) EOR screening criteria revisited – part 1: introduction to screening criteria and enhanced recovery field projects. Soc Pet Eng Res Eng 12(3):9

Taber JJ, Martin FD, Seright RS (1997b) EOR screening criteria revisited – part 2: applications and impact of oil prices. Soc Pet Eng Res Eng 12(3):6

Tang J, Sun W, Tang H et al (2005a) Enhanced CO_2 absorption of poly(ionic liquid)s. Macromolecules 38:2037–2039. doi:10.1021/ma047574z

Tang J, Tang H, Sun W et al (2005b) Poly(ionic liquid)s: a new material with enhanced and fast CO_2 absorption. Chem Commun 5:3325–3327

Torp TA, Gale J (2004) Demonstrating storage of CO_2 in geological reservoirs: the sleipner and SACS projects. Energy 29:1361–1369. doi:10.1016/j.energy.2004.03.104

Tsang C-F, Doughty C, Rutqvist J, Xu T (2007) Modeling to understand and simulate physico-chemical processes of CO_2 geological storage. In: Wilson EJ, Gerard D (eds) Carbon capture and sequestration: integrating technology, monitoring, regulation. Blackwell, Ames, pp 35–72

UNFCCC (2011) CDM: Carbon dioxide capture and storage in geological formations as CDM project activities. http://cdm.unfccc.int/about/ccs/index.html. Accessed 22 Jan 2015

Van Bergen F, Gale J, Damen KJ, Wildenborg AFB (2004) Worldwide selection of early opportunities for CO_2-enhanced oil recovery and CO_2-enhanced coal bed methane production. Energy 29:1611–1621. doi:10.1016/j.energy.2004.03.063

Walton KS, Abney MB, Douglas LeVan M (2006) CO_2 adsorption in Y and X zeolites modified by alkali metal cation exchange. Microporous Mesoporous Mater 91:78–84. doi:10.1016/j.micromeso.2005.11.023

Wang Q, Luo J, Zhong Z, Borgna A (2011a) CO_2 capture by solid adsorbents and their applications: current status and new trends. Energy Environ Sci 4:42–55. doi:10.1039/C0EE00064G

Wang C, Luo X, Luo H et al (2011b) Tuning the basicity of ionic liquids for equimolar CO_2 capture. Angew Chemie Int Ed 50:4918–4922. doi:10.1002/anie.201008151

Wang J, Huang L, Yang R et al (2014) Recent advances in solid sorbents for CO_2 capture and new development trends. Energy Environ Sci 7:3478–3518. doi:10.1039/C4EE01647E

Welton T (2004) Ionic liquids in catalysis. Coord Chem Rev 248:2459–2477. doi:10.1016/j.ccr.2004.04.015

Wilson EJ, Gerard D (2007) Risk assessment and management for geologic sequestration of carbon dioxide. In: Wilson EJ, Gerard D (eds) Carbon capture and sequestration: integrating technology, monitoring, regulation. Blackwell, Ames, pp 101–126

Xiong Y-B, Wang H, Wang Y-J, Wang R-M (2012) Novel imidazolium-based poly(ionic liquid)s: preparation, characterization, and absorption of CO_2. Polym Adv Technol 23:835–840. doi:10.1002/pat.1973

Xu X, Song C, Andrésen JM et al (2003) Preparation and characterization of novel CO_2 "molecular basket" adsorbents based on polymer-modified mesoporous molecular sieve MCM-41. Microporous Mesoporous Mater 62:29–45. doi:10.1016/s1387-1811(03)00388-3

Xu TF, Sonnenthal E, Spycher N, Pruess K (2006) TOUGHREACT – a simulation program for non-isothermal multiphase reactive geochemical transport in variably saturated geologic media: applications to geothermal injectivity and CO_2 geological sequestration. Comput Geosci 32:145–165. doi:10.1016/j.cageo.2005.06.014

Yang H, Xu Z, Fan M et al (2008) Progress in carbon dioxide separation and capture: a review. J Environ Sci 20:14–27. doi:10.1016/s1001-0742(08)60002-9

Yuan J, Antonietti M (2011) Poly(ionic liquid)s: polymers expanding classical property profiles. Polymer (Guildf) 52:1469–1482. doi:10.1016/j.polymer.2011.01.043

Yuan J, Mecerreyes D, Antonietti M (2013) Poly(ionic liquid)s: an update. Prog Polym Sci 38:1009–1036. doi:10.1016/j.progpolymsci.2013.04.002

Zhang J, Singh R, Webley PA (2008) Alkali and alkaline-earth cation exchanged chabazite zeolites for adsorption based CO_2 capture. Microporous Mesoporous Mater 111:478–487. doi:10.1016/j.micromeso.2007.08.022

Zhao L, Riensche E, Menzer R et al (2008) A parametric study of CO_2/N_2 gas separation membrane processes for post-combustion capture. J Memb Sci 325:284–294. doi:10.1016/j.memsci.2008.07.058

Chemical Absorption

Mengxiang Fang and Dechen Zhu

Contents

Abstract

Chemical absorption is one of the most effective methods for CO_2 separation. This chapter first explains the principle of chemical absorption. Amine-based systems, carbonate-based systems, aqueous ammonia, membranes, enzyme-based systems,

M. Fang (✉) • D. Zhu
Institute for Thermal Power Engineering, Zhejiang University, Hangzhou, Zhejiang, China
e-mail: mxfang@zju.edu.cn; zhudechen@zju.edu.cn

W.-Y. Chen et al. (eds.), *Handbook of Climate Change Mitigation and Adaptation*,
DOI 10.1007/978-3-319-14409-2_38

and ionic liquids-based system are discussed as the typical and emerging state of the art for chemical absorption. Furthermore, new solvent selection, novel reactors, and system intergradation have been analyzed. The key issues to hinder the application of chemical absorption are discussed, such as water-consumption-related issues, environmental effects, and economical factors. Finally, some industry applications and future directions are discussed.

Principle of Chemical Absorption

Introduction

Chemical absorption is one of the most effective methods for CO_2 separation and capture nowadays. Being of low equipment cost, high removal efficiency, stable operation conditions, and mature technology background, chemical absorption has already been widely applied to chemical engineering, food industry, and other fields.

Chemical absorption is based on the solubility difference between CO_2 and the other gas components in mixed gases. The difference between chemical absorption and physical absorption is whether CO_2 reacts with the absorbent during the absorption process. Chemical absorption can be classified into nonrecycling processes and recycling processes. For the former processes, the rich CO_2 solution cannot be regenerated. While for the latter processes, the absorbent can be recovered by the cycle of absorption and regeneration.

Mechanism of Chemical Absorption

During the chemical absorption process, the CO_2 solubility depends on the physical solubility in the absorbent, the chemical reaction equilibrium constant, the chemical equivalent ratio, and other factors. In addition, in cases where the chemical absorbent solution is a strong or weak electrolyte, dilute solution theory does not fit. Solubility of gases in the chemical absorbent is characterized by a uniform solubility increase with pressure. The higher the pressure, the lower the solubility enhancement is. In that case, the relationship between partial pressure and gas solubility is more complex than that of physical absorption.

A vapor–liquid equilibrium under the following conditions is the simplest chemical absorption balance.

It is assumed that:

1. Only one chemical reaction happens in the system.
2. The activity coefficient does not relate to the composition of the components, and it is considered to be one in the simplest case.
3. The physical solubility of gas x_{ph} is negligible relative to the chemical solubility of gas x_{ch}, that is to say, the total solubility can be written as follows:

$$X = X_{ph} + X_{ch} \approx X_{ch} \tag{1}$$

The chemical reaction equation can be written in the following form:

$$nA + mB = kC + 1D + \cdots \tag{2}$$

or

$$A + \frac{m}{n}B = \frac{k}{n}C + \frac{l}{n}D + \ldots \tag{3}$$

In the formula,

A – dissolved gas
B – chemical absorbent
C, D – reaction products
n, m, k, l – stoichiometric coefficients

According to assumption Eq. 2, the equilibrium constant can be viewed as the function of the concentrations of the reaction components. If reactant A is consumed for x mol and the initial concentration of chemical absorbent B is B_0, when the system reaches another equilibrium state

$$K_p = \frac{\left(\frac{k}{n}x\right)^{\frac{k}{n}}\left(\frac{1}{n}x\right)^{\frac{1}{n}}\ldots}{x_\phi\left(B_o - \frac{m}{n}x\right)^{\frac{m}{n}}} = i\frac{x^h}{x_\phi(B_o - jx)^j} \tag{4}$$

In the formula,

$$i = (k/n)^{\frac{k}{n}}(l/n)^{\frac{1}{n}}\cdots, h = (k + l + \cdots)/n$$

$j = m/n$ – the ratio of the stoichiometric reaction coefficients between dissolved gas and consumed absorbents.
h is the total mole number or ions number of reaction products generated per mole gas.
j is the mole number of consumed chemical absorbents per mole gas. If the first condition is correct, then the coefficients of i, h, and j are all integers.

Equation 4 can be turned into the equation expressed in gas-phase equilibrium form by equilibrium constant of physical solubility.

$$X_{ph} = \frac{P_A}{K_{ph}} = \frac{P_A}{K_H} \tag{5}$$

P_A is the partial pressure of gas A, K_{ph} is physical equilibrium constant of gas A, and K_H is Henry equilibrium constant

$$P_A = K_{ph}\frac{ix^h}{K_P(B_0 - jx)^j} = K\frac{x^h}{(B_o - j_x)^j} \tag{6}$$

Under these assumptions, K only relates with the temperature. What's more, K reflects the state of gas–liquid phase physical equilibrium and chemical equilibrium.

$$K_{ph} = A_1 e^{\frac{-\Delta H}{RT}} \text{ and } K_P = A_2 e^{\frac{-\Delta H}{RT}} \tag{7}$$

ΔH_1 and ΔH_2 are the enthalpy change during the process of physical dissolution and chemical reactions, respectively. A_1 and A_2 are deviation coefficients.

$$K = i\frac{K_{ph}}{K_P} = (A_1 - A_2)e^{\frac{-\Delta H}{RT}} \tag{8}$$

ΔH – the total enthalpy change during the gas dissolution process with chemical reactions.

Here, the utilization efficiency of chemical absorbent is defined as $\alpha = x/B_0$. T also reflects the state of chemical reactions. Equation 6 can be written as

$$P_A = K\frac{(\alpha B_o)^h}{(B_o - j\alpha B_o)^j} = KB_o^{h-j}\frac{\alpha^h}{(1 - j\alpha)^j} \tag{9}$$

Thus, no less than three constants were introduced into the vapor–liquid equilibrium equations. These constants can be measured by individual methods or obtained from a chemical solubility database.

According to Eqs. 6 and 9, the chemical equivalents affect the curvature of the balance curve greatly, when K is equal to B_0. Hence, the chemical absorbent of high h value, of which h is above 1, is hard to regenerate with a decrease of pressure. However, this absorbent is easy to regenerate with a decrease of pressure under the condition of purification or lower gas partial pressure.

Derived from Eq. 6, the increase of the initial absorbent concentration causes a drop of the gas partial pressure above the absorbent when the gas concentration in the solution stays constant. As Eq. 9 shows, the effect of the absorbent concentration is different only judged by $(h - j)$ when α stays constant.

If $x \to 0$, Eq. 6 can be written in the following form:

$$P_A = \frac{iK_{ph}}{K_P} \cdot \frac{X^h}{B_0^j} = K_{ch}x^h \tag{10}$$

Equation 9 can be written in the following form:

$$P_A = KB_0^{h-j}a^h \tag{11}$$

According to Eq. 11, during the process of chemical absorption, if $x \rightarrow 0$, the Henry law can be applied only when h equals 1. That is to say, one mole gas involved in the chemical reactions can produce only one mole product.

In many cases, the experimental data can be described by Eq. 6. The coefficients i, h, and j are all integers in the equation. For more complicated processes, such as two or more continuous and parallel reactions occurring during the process, the coefficients i, h, and j can be fractions, and they relate with x_{ph}. However, the meaning of the coefficients does not change at every case, and it reflects the relative relationship between chemical equivalents.

Equation 6 can be used for calculation only when the relationship between $K\,ph/K\,P$ and the components of the solution is considered. The reason is that for Eqs. 4 and 6, the concentration of the solution should be replaced by the activity of the solution.

The equation for a real solution is

$$K_{P,T} = \frac{\left(\frac{k}{n} a_C\right)^{k/n} \left(\frac{l}{n} a_D\right)^{l/n}}{a_{ph} (a_B)^{m/n}} \tag{12}$$

$K_{P,T}$ – equilibrium thermodynamic constant.

As a$i = \gamma i Xi$, hence

$$P_A = \frac{K_{ph} i}{K_P} \cdot \frac{x_{ch}^h}{(B_0 - jx)^j} \cdot \frac{\gamma_n^k \gamma_n^l}{\gamma_B^j} = \frac{K_{ph} K_\gamma}{K_P} \cdot \frac{X_{ch}^h}{(B_0 - jx)^j} \cdots \tag{13}$$

The coefficient related with chemical products and the activity of the absorbent.

By comparison of Eqs. 6 and 13, the two equations are consistent with each other when the change of the activity of solution components is mutually compensated, that is to say, $\gamma \neq 1$ and K_γ stay constant.

Both the relationship between K_{ph} and x and the relationship between K_{ph} and B have additional effects on the gas dissolution for chemical absorption processes.

$$K_{ph} = K_H e^{(ax + bB)} \tag{14}$$

In this equation, a and b are constants, x is solubility, and B is the concentration.

Figure 1a shows the relationship between gas solubility and partial pressure above the surface. Curve 1 and curve 2 describe the chemical absorption process. Curve 3, curve 4, and curve 5 are descriptions of the physical absorption process.

Figure 1b shows the relationship between gas partial pressure above the solution surface and temperature.

When the reaction between the absorbent and the gas is completed, that is to say ($j\alpha \rightarrow 1$), the gas solubility only depends on the physical absorption process. Hence, with the increase of operation pressure, the gas solubility increases at this time.

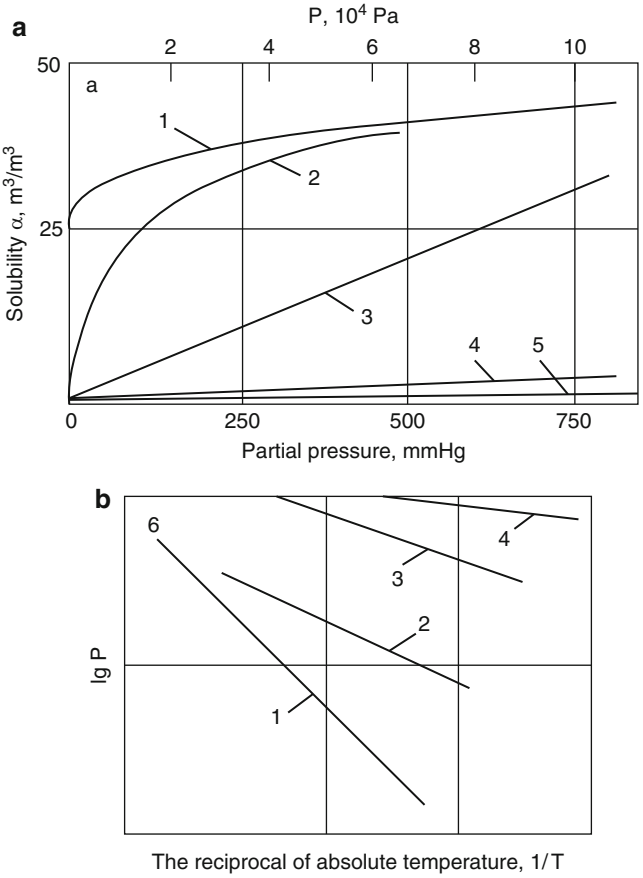

Fig. 1 The equilibrium pressure and temperature curve in the gas–liquid system. The meanings of the curves in the figures are listed as follows: (*1*) When the temperature is 20 °C, CO_2 is injected into the MEA (monoethanolamine) solution of 2.5 mol/L (chemical absorption). (*2*) When the temperature is 60 °C, CO_2 is injected into the solution of 25 % K_2CO_3 + 10 % DEA (diethanolamine), (chemical absorption). (*3*) When the temperature is 25 °C, C_2H_2 is injected into the *N*,*N*-dimethylformamide solution (physical absorption). (*4*) When the temperature is 25 °C, C_2H_2 is injected into the propylene carbonate solution (physical absorption). (*5*) When the temperature is 25 °C, C_2H_2 is injected into the water (physical absorption) (Semeonova and Lieyijiesi 1982)

Chemical absorption is different from physical absorption that the solution heat during the chemical absorption process is rather huge; even reaches 83.3 ∼ 125.8 kJ/mol. Hence, the gas solubility is affected strongly by the temperature. The lower the concentration of gas absorbed, the more the solution heat per gram of gas. The gas concentration above the surface of a regenerated absorbent solution is usually low, and the partial pressure above the surface of the solution

increases with the temperature. Compared to physical absorption, chemical absorption is fit for fine purification.

The operation pressure has little effect on the absorption capacity of an absorbent. Chemical absorption is particularly good for the case that the absorption gas concentration is not high.

Above all, the best method to regenerate an absorbent is to raise the operation temperature. The decrease of operation pressure is not a good choice. It is especially suitable for a strong absorbent, that is to say, ΔH and $K P$ are large. With the decrease of ΔH and $K P$, the characteristics of a chemical absorbent are more like those of a physical absorbent, and the process setup needs to vary with that change.

Typical Chemical Absorption System

Amine-Based Systems

The idea of separating CO_2 from flue gas streams started in the 1970s, not with concern about the greenhouse effect, but as a potentially economic source of CO_2, mainly for enhanced oil recovery (EOR) operations. All the early plants capture CO_2 with processes based on chemical absorption using amine-based solvents.

Typical amine-based absorbents can be classified into three categories by the number of active hydrogen atoms adjacent to the nitrogen atom, primary amine with two hydrogen atoms, secondary amine with one hydrogen atom, and tertiary amine without hydrogen atom. Judged by the number of active nitrogen atoms, the amine-based absorbents can be classified into monoamine and multi-amines. The reaction mechanism between alkanolamines and CO_2 can be expressed by the following description (Blauwhoff et al. 1984):

1. Reaction mechanism between CO_2 and primary amines or secondary amines
   When a primary amine and secondary alkanolamines are chosen to be the absorbents, the so-called zwitterions are formed at first due to the reaction between CO_2 and amines. After that, the zwitterions will react with alkanolamine and form carbamate. The detailed reactions are listed as follows, where R is an alkyl and R′ is H for primary amines and an alkyl for secondary amines (Industrial Development Bureau 2002):

$$\mathrm{RR'NH} + \mathrm{CO_2} \rightleftharpoons \mathrm{RR'NH^+COO^-}\,(\text{zwitterion}) \tag{15}$$

$$\mathrm{RR'NH} + \mathrm{RR'NH^+COO^-} \rightleftharpoons \mathrm{RR'NCOO^-}\,(\text{carbamate}) + \mathrm{RR'NH_2^+} \tag{16}$$

   The total reaction is

$$2\mathrm{RR'NH} + \mathrm{CO_2} \rightleftharpoons \mathrm{RR'NCOO^-} + \mathrm{RR'NH_2^+} \tag{17}$$

According to the total reaction, due to the restrictions of thermodynamics, the maximum CO_2 absorption capacity is 0.5 mol CO_2/mol absorbent. However, some amino acid root may be hydrolyzed into free amine.

$$RR'NCOO^- + H_2O \rightleftharpoons RR'NH + HCO_3^- \tag{18}$$

Hence, sometimes the maximum CO_2 absorption capacity exceeds 0.5 mol CO_2/mole absorbent. The characteristics for CO_2 absorption in amine solution are high reaction rate and low CO_2 absorption capacity.

2. Reaction mechanism between CO_2 and tertiary amines
There is no excess hydrogen atom adjacent to the nitrogen atom for tertiary amines so that no zwitterions are produced in the following process. The reaction mechanism can be depicted by the following equations, where R, R′, and R″ are alkyls (Industrial Development Bureau 2002):

$$RR'R''N + H_2O + CO_2 \rightleftharpoons RR'R''NH^+ + HCO_3^- \tag{19}$$

According to the above equation, there is no thermodynamic restriction for tertiary amines. The maximum CO_2 absorption capacity is 1 mol CO_2/mol absorbent. However, the absorption rate is rather low for tertiary amines.

3. Reaction mechanism between CO_2 and sterically hindered amines
The huge functional groups adjacent to the nitrogen atom can hinder the binding of CO_2 and alkanolamine so as to reduce the stability of the amino acid root. Hence, the maximum absorption capacity for sterically hindered amines is the same as for tertiary amines. What's more, the absorption rate is close to that of primary and secondary amines. Take AMP (aminomethylpropanol) as an example: The reaction mechanism of CO_2 and AMP can be described by the following equation, where R is $C(CH_3)_2CH_2OH$ (Mandal and Bandyopadhyay 2006a):

$$CO_2 + RNH_2 + H_2O \rightleftharpoons RNH_3^+ + HCO_3^- \tag{20}$$

A continuous scrubbing system is used to separate CO_2 from the flue gas stream. As illustrated in Fig. 2, the flue gas is transported into the absorber after removing the dust and other air pollutants, especially SO_2 and NO*x*. If necessary, the flue gas should also go through some cooling process and pressure enhancement process before it is sent to the absorber by the blower. Flue gas enters into the bottom of the packed column and contacts with the lean CO_2 absorbent injected from the top of the absorber directly and in counterflow. CO_2 in the flue gas reacts with the chemical absorbent and forms some weak salts so that CO_2 is separated from the flue gas by the absorber. The rich CO_2 solution is pumped to the regenerator, which is also called stripper. However, the rich CO_2 solution needs to pass a lean/rich solution heat exchanger before it enters into the regenerator. The lean/rich solution heat exchanger aims to optimize the heat cycle of the whole process. It can heat the rich CO_2 solution to a higher temperature that is closer to the stripping temperature. It can also decrease the

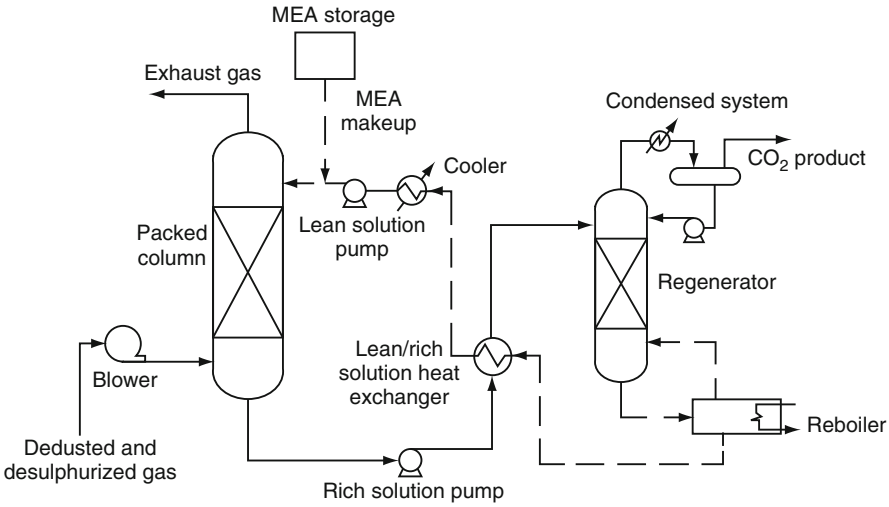

Fig. 2 Flow sheet for CO_2 capture from flue gases using amine-based systems (Rubin and Rao 2002)

lean CO_2 solution to a temperature which is much closer to the absorption temperature. CO_2 is regenerated in the stripper due to diverse reactions occurring at the higher temperature. The heat of the stripper is supplied by the reboiler. Then, the gas at the top of the stripper should be cooled to separate vapor from CO_2. The solution regenerated at the bottom of the stripper is sent back to the absorber.

Although amines have been used for many years, particularly in the removal of acid gases from natural gas, there is still enough space for process improvement. Amines are available in three forms (primary, secondary, and tertiary), each with its advantages and disadvantages as a CO_2 solvent. In addition to options for the amine, additives can be used to improve system performance. Furthermore, design optimization is possible to decrease capital costs and reduce energy consumption.

Past studies have shown that amine-based CO_2 absorption systems are the most suitable ones for combustion-based power plants for the following reasons:

- These systems are effective for dilute CO_2 streams, such as coal combustion flue gases, which typically contain only about 10–12 % CO_2 by volume.
- Amine-based CO_2 capture systems are a proven technology that is commercially available and in use today.
- Amine-based systems are similar to other end-of-pipe environmental control systems used at power plants. These units are operated at ordinary temperature and pressure.
- A major effort is being made worldwide to improve this process in the light of its potential role in CO_2 abatement. Thus, one can anticipate future technology advances.

However, the amine systems used at low partial pressure conditions encountered with carbon dioxide in flue gases have inherent disadvantages:

- High heat of reaction which leads to the need for expensive cooling systems
- High regeneration energy needs which require large quantities of low-pressure steam and correspondingly large stripper column reboilers
- The need for large volume absorbers with expensive packings to provide adequate mass transfer surface for the carbon dioxide absorption and reaction
- The need to circulate large quantities of amine solvents because of practical limitations of carbon dioxide loadings
- A high parasitic power loss caused by the need to overcome the pressure drops in the large absorbers

These factors combined result in relatively high capital costs for the capture plant and high operating costs and consequential efficiency losses in host power plants where the capture plant is integrated. Furthermore, due to the viscosity of the amines, problems such as entraining, channeling, bubbling, and overflowing may happen. The amine-based systems also have problems with equipment corrosion.

Improvements to amine-based systems for post-combustion CO_2 capture are being pursued by a number of process developers. Some of them are Fluor, Mitsubishi Heavy Industries (MHI), and Cansolv Technologies, Inc. Fluor's Econamine FG Plus™ is a proprietary acid gas removal system that has demonstrated larger than 95 % availability with natural gas-fired power plants, specifically on a 350 t/day CO_2 capture plant in Bellingham, MA. It is currently the state-of-the-art commercial technology baseline. MHI has developed a new absorption process, referred to as KS series absorbents. An innovative factor in this development is the utilization of a new amine-type solvent for the capture of CO_2 from flue gas (America 2005). Cansolv Technologies, Inc. proposes to reduce costs by incorporating CO_2 capture in a single column with processes for capturing pollutants, such as SO_2, NO*x*, and Hg. DC1031 tertiary amine solvent has demonstrated fast mass transfer and good chemical stability with high capacity – a net of 0.5 mol of CO_2/mol of amine per cycle compared to 0.25 mol/mol for monoethanolamine (MEA) (Hakka 2007, Cansolv Technologies Inc., private communication).

R&D pathways to improved amine-based systems include modifying tower packing to reduce pressure drop and increase contacting area, increasing heat integration to reduce energy requirements, using additives to reduce corrosion and allow higher amine concentrations, and improving regeneration procedures.

Carbonate-Based Systems

Carbonate systems are based on the ability of a soluble carbonate to react with CO_2 to form bicarbonate, which can be heated to release CO_2 and revert to a carbonate. A major advantage of carbonates over amine-based systems is the

significantly lower energy required for regeneration. The University of Texas at Austin has been developing a K_2CO_3-based system in which the solvent is promoted with catalytic amounts of piperazine (PZ). The K_2CO_3/PZ system (5 M K; 2.5 M PZ) has an absorption rate 10–30 % faster than a 30 % solution of MEA and favorable equilibrium characteristics. A benefit is that oxygen is less soluble in K+/PZ solvents; however, piperazine is more expensive than MEA, so the economic impact of oxidative degradation will be about the same (Resnik et al. 2004). Analysis has indicated that the energy requirement is approximately 5 % lower with a higher loading capacity of 40 % versus 30 % for MEA. System integration studies indicate that improvements in structured packing can provide an additional 5 % energy savings, and multi-pressure stripping can reduce energy use by 5–15 % (Rochelle 2006, private communication).

The reaction mechanism between CO_2 and PZ can be expressed as follows:

$$\mathrm{PZ} + \mathrm{CO_2} + \mathrm{OH^-} \longleftrightarrow \mathrm{PZCOO^-} + \mathrm{H_2O} \tag{21}$$

$$\mathrm{PZ} + \mathrm{CO_2} + \mathrm{H_2O} \longleftrightarrow \mathrm{PZCOO^-} + \mathrm{H_3O^+} \tag{22}$$

$$\mathrm{PZ} + \mathrm{CO_2} + \mathrm{PZ} \longleftrightarrow \mathrm{PZCOO^-} + \mathrm{PZH^+} \tag{23}$$

$$\mathrm{PZ} + \mathrm{CO_2} + \mathrm{CO_3^{2-}} \longleftrightarrow \mathrm{PZCOO^-} + \mathrm{HCO_3^-} \tag{24}$$

$$\mathrm{PZ} + \mathrm{CO_2} + \mathrm{PZCOO^-} \longleftrightarrow \mathrm{PZCOO^-} + \mathrm{H^+PZCOO^-} \tag{25}$$

$$\mathrm{PZCOO^-} + \mathrm{CO_2} + \mathrm{H_2O} \longleftrightarrow \mathrm{PZ(COO^-)_2} + \mathrm{H_3O^+} \tag{26}$$

$$\mathrm{PZCOO^-} + \mathrm{CO_2} + \mathrm{PZ} \longleftrightarrow \mathrm{PZ(COO^-)_2} + \mathrm{PZH^+} \tag{27}$$

$$\mathrm{PZCOO^-} + \mathrm{CO_2} + \mathrm{CO_3^{2-}} \longleftrightarrow \mathrm{PZ(COO^-)_2} + \mathrm{HCO_3^-} \tag{28}$$

$$\mathrm{PZCOO^-} + \mathrm{CO_2} + \mathrm{PZCOO^-} \longleftrightarrow \mathrm{PZ(COO^-)_2} + \mathrm{H^+PZCOO^-} \tag{29}$$

$$\mathrm{CO_2} + \mathrm{OH^-} \longleftrightarrow \mathrm{HCO_3^-} \tag{30}$$

$$\mathrm{PZ} + \mathrm{CO_2} + \mathrm{H_2O} \longleftrightarrow \mathrm{PZH^+} + \mathrm{HCO_3^-} \tag{31}$$

$$\mathrm{PZCOO^-} + \mathrm{CO_2} + \mathrm{H_2O} \longleftrightarrow \mathrm{H^+PZCOO^-} + \mathrm{HCO_3^-} \tag{32}$$

The K+/PZ solvent was introduced by Cullinane as an alternative to the widely used MEA. According to Cullinane, the K+/PZ solvent has a higher CO_2 capacity than MEA because PZ is a secondary amine and potassium carbonate increases the absorption capacity. Furthermore, the rate of absorption was increased due to the presence of secondary amine groups in PZ, the high pK_a, and the large quantity of carbonate/bicarbonate. He reported a CO_2 absorption rate 1.5–3 times faster than with 30 wt% MEA.

The flow sheet of carbonate-based systems is similar to that of an amine-based system. Although the K+/PZ system has several advantages over amine-based systems, the technology is still not mature. Lots of experimental data on this idea is still lacking. The pros and cons of this system still need to be tested.

Ammonia-Based Systems

Ammonia-based wet scrubbing is similar in operation to amine systems. Ammonia and its derivatives react with CO_2 via various mechanisms, one of which is the reaction of ammonium carbonate (AC), CO_2, and water to form ammonium bicarbonate (ABC). The gas–liquid chemical reactions can be expressed by the following reaction equation:

$$NH_3(l) + CO_2(g) + H_2O(l) \longleftrightarrow NH_4HCO_3(s) \tag{33}$$

However, the actual steps of the chemical reaction are complex and must pass through several intermediate reaction steps:

$$2NH_3(g) + CO_2(g) \longleftrightarrow NH_2COONH_4(s) \tag{34}$$

The formed NH_2COONH_4 is further hydrolyzed:

$$NH_2COONH_4(s) + H_2O(l) \longleftrightarrow NH_4HCO_3(s) + NH_3(g) \tag{35}$$

Then, the NH_3 reacts with H_2O to form NH_4OH:

$$NH_3(g) + H_2O(l) \longleftrightarrow NH_4OH(l) \tag{36}$$

The hydrolyzed product NH_4HCO_3 of reaction reacts with NH_4OH to form $(NH_4)_2CO_3$:

$$NH_4HCO_3(s) + NH_4OH(l) \longleftrightarrow (NH4)_2CO_3(s) + H_2O(l) \tag{37}$$

The $(NH_4)_2CO_3$ then absorbs CO_2 to form ammonium bicarbonate:

$$(NH_4)_2CO_3(s) + H_2O(l) + CO_2(g) \longleftrightarrow 2NH_4HCO_3(g) \tag{38}$$

All the reaction equations are reversible. This reaction has a significantly lower heat of reaction than amine-based systems, resulting in energy savings, provided the absorption/desorption cycle can be limited to this mechanism. Ammonia-based absorption has a number of other advantages over amine-based systems, such as the potential for high CO_2 capacity, lack of degradation during absorption/regeneration, tolerance to oxygen in the flue gas, low cost, and potential for regeneration at high pressure. There is also the possibility of reaction with SO*x* and NO*x* – critical pollutants found in flue gas – to form fertilizer (ammonium sulfate and ammonium nitrate) as a salable by-product. Figure 3 gives the typical flow sheet for CO_2 capture from flue gases using aqueous ammonia systems (Resnik et al. 2006).

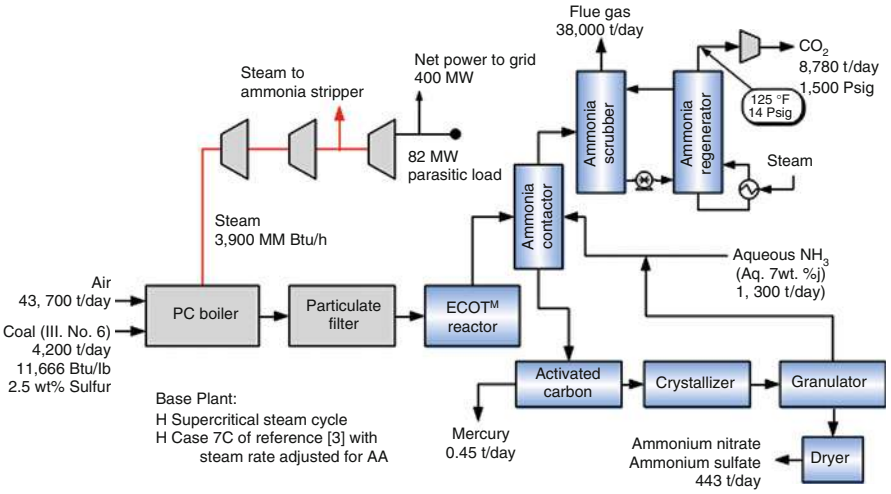

Fig. 3 Flow sheet for CO_2 capture from flue gases using aqueous ammonia systems (NETL 2007)

A few concerns are related to ammonia's higher volatility compared to that of MEA. One is that the flue gas must be cooled to the 288 ∼ 300 K range to enhance the CO_2 absorptivity of the ammonia compounds and to minimize ammonia vapor emissions during the absorption step. Additionally, there is concern over ammonia losses during regeneration, which occurs at elevated temperatures. R&D process improvements include process optimization to increase CO_2 loading and the use of various engineering techniques to eliminate ammonia vapor losses from the system during operation (Resnik et al. 2004, 2006; Yeh et al. 2005).

Another ammonia-based system, under development by Alstom, is the chilled ammonia process (CAP), which was first tested in a 5-MW pilot test in 2007 at We Energies Pleasant Prairie Power Plant. It was also tested in mid-2008 on AEP's 1,300-MW Mountaineer Plant in New Haven, WV, as a 30-MW (thermal) product validation with up to 100,000 t of CO_2 being captured per year. This process uses the same AC/ABC absorption chemistry as the aqueous system described above but differs in that no fertilizer is produced and a slurry of aqueous AC and ABC and solid ABC is circulated to capture CO_2 (Black 2006). The process operates at near-freezing temperatures (273–283 K), and the flue gas is cooled prior to absorption using chilled water and a series of direct contact coolers. Figure 4 gives the schematic of the chilled ammonia process. Technical hurdles associated with the technology include cooling the flue gas and absorber to maintain operating temperatures below 283 K required to reduce ammonia slip and achieve high CO_2 capacities and, for AC/ABC cycling, mitigating the ammonia slip during absorption and regeneration, achieving 90 % removal efficiencies in a single stage, and avoiding fouling of heat transfer and other equipment by ABC deposition as a result of absorber operation with a saturated solution. Both the aqueous and chilled ammonia

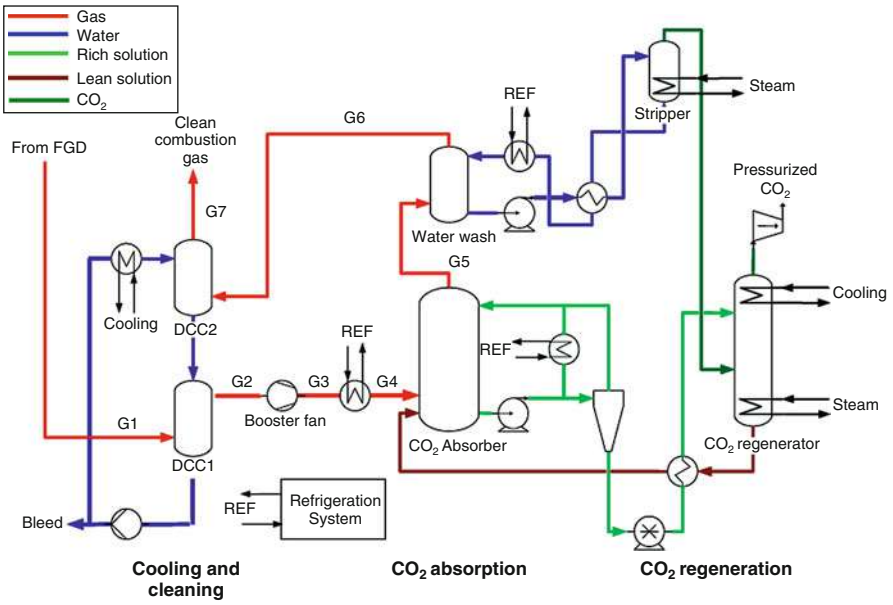

Fig. 4 Schematic of the chilled ammonia process (PT/PE Sector – Communications – November 2006, Chilled Ammonia Process for CO_2 Capture – content owner: Sean Black)

processes have the potential for improved energy efficiency over amine-based systems, if the hurdles can be overcome.

Membrane Absorption Systems

Membrane contactors have been considered a promising alternative to traditional packed columns for CO_2 capture in recent years. Membrane absorption technology combines the advantages of both membrane separation and chemical absorption, which has high specific surface area and high CO_2 selectivity. It can effectively reduce the equipment size and investment costs. Zhang and Cussler (1985a, b) firstly proposed using hollow fiber membrane contactors to replace the traditional packed tower for acid gases CO_2, H_2S removal. Membrane contactors are gas–liquid reactor to provide a barrier between the gas and liquid phases. The membranes do not offer selectivity, and the driving force for gas separation is a concentration gradient. As shown in Fig. 9, usually the gas phase (flue gas) flows in the shell side of the membrane contactor, while the liquid phase (aqueous CO_2 absorbent) flows in the tube side. The CO_2 molecules can pass through the membrane pores and react with the absorbent; however, the liquid absorbent could not permeate into the pores due to the membrane's high hydrophobic. Figure 5a shows the principle of membrane absorption for the CO_2 capture process. Figure 5b gives the true structure of a hollow fiber membrane, and Fig. 6 gives the experimental schematic of membrane absorption.

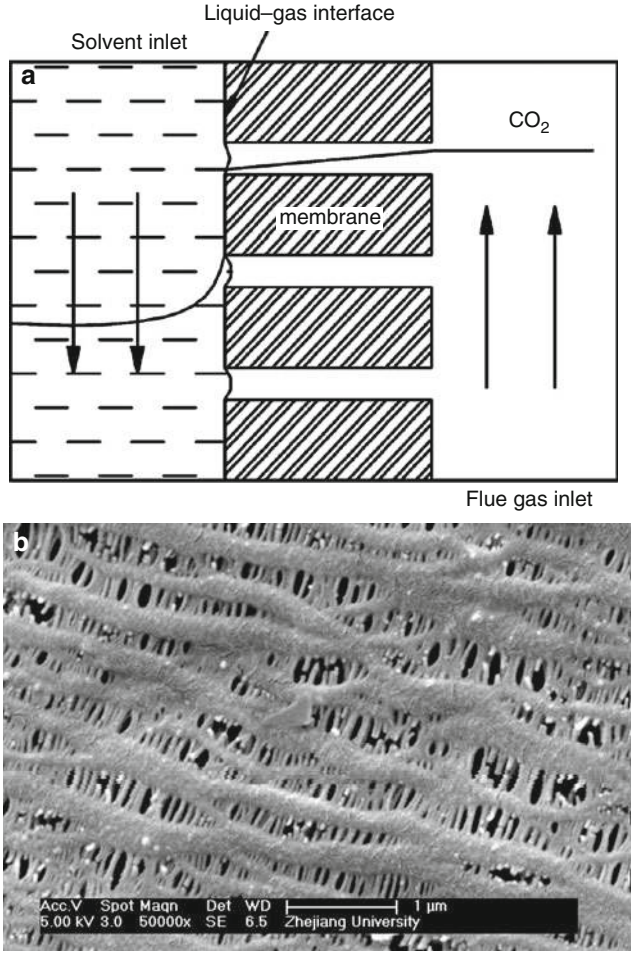

Fig. 5 (**a**) The principle of membrane absorption. (**b**) Typical structure of a hollow fiber membrane

Comparing with the traditional absorption contactors, membrane contactors have the following major advantages:

1. High specific surface area. The effective specific surface area of membrane contactor can be 1,500–3,000 m^2/m^3, which is much larger than that of packed column (100–800 m^2/m^3) [182].
2. Operational flexibility. Since the liquid phase and gas phase flow independently in the membrane contactors, the operating problems in packed columns can be avoided.
3. Linear scale-up. The modularity of membrane contactors makes it easy to scale up.

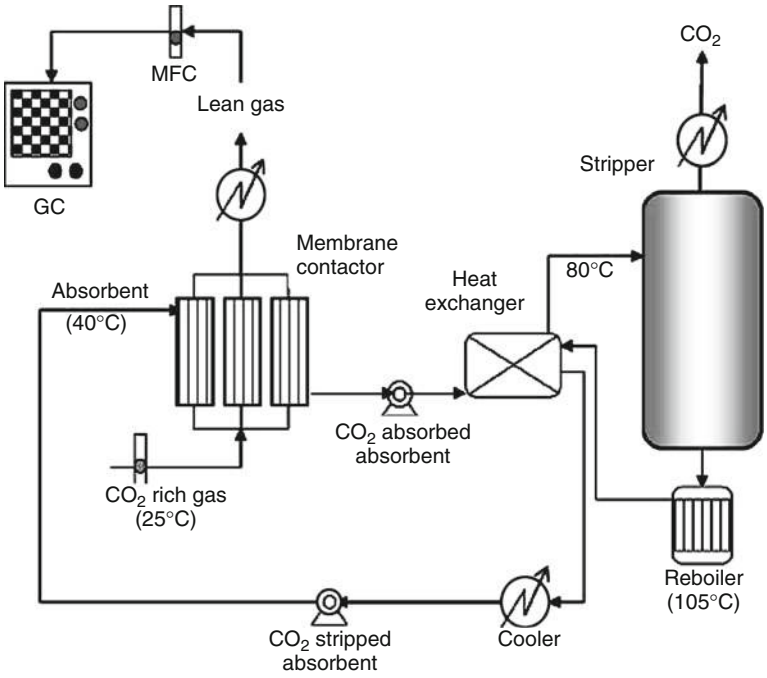

Fig. 6 Experimental schematic of CO_2 capture from flue gas by membrane absorption (Yeon et al. 2005)

4. Easy prediction. The gas–liquid contact area is constant for a membrane contactor, and it has no relationship to the operating conditions.

However, membrane contactors also have some disadvantages. First, the presence of membrane adds extra mass transfer resistance, which will result in a reduction in the overall mass transfer rate. But this negative impact can be potentially eliminated by the advantage of large interfacial mass transfer area. The main challenge for membrane contactor is the issue of membrane wetting, which leads to the deterioration of CO_2 absorption flux in long-term operation and limits its large-scale commercial application. In order to solve this problem, a number of studies have been conducted, including the selection of membrane materials, mechanism of membrane wetting, and prevention of membrane wetting (Pederson et al. 2000).

Enzyme-Based Systems

Biologically based capture systems are another potential avenue for improvements in CO_2 capture technology. These systems are based upon naturally occurring reactions of CO_2 in living organisms. One of these possibilities is the use of enzymes. An enzyme-based system, which achieves CO_2 capture and release by mimicking the

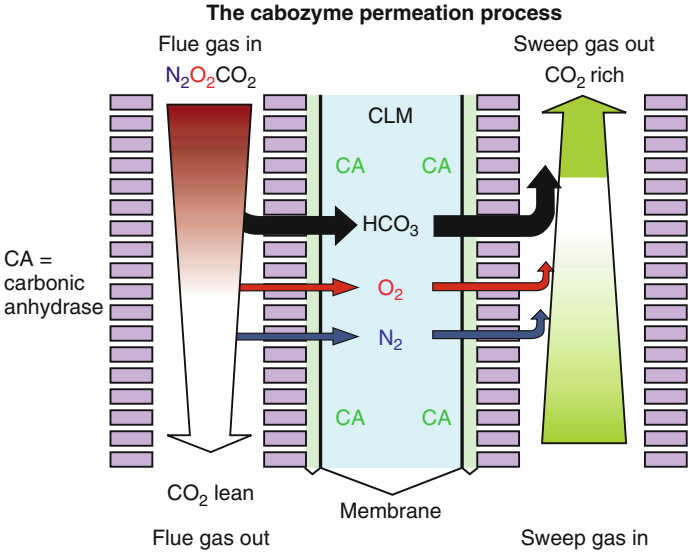

Fig. 7 Schematic of the carbozyme permeation process (Figueroa et al. 2008)

mechanism of the mammalian respiratory system, is under development by Carbozyme (see Fig. 7). The process, utilizing carbonic anhydrase (CA) in a hollow fiber contained liquid membrane, has demonstrated at laboratory scale the potential for 90 % CO_2 capture followed by regeneration at ambient conditions. This is a significant technical improvement over the MEA temperature swing absorption process. The CA process has been shown to have a very low heat of absorption that reduces the energy penalty typically associated with absorption processes.

The rate of CO_2 dissolution in water is limited by the rate of aqueous CO_2 hydration, and the CO_2-carrying capacity is limited by the buffering capacity. Adding the enzyme CA to the solution speeds up the rate of carbonic acid formation; CA has the ability to catalyze the hydration of 600,000 molecules of carbon dioxide per molecule of CA per second compared to a theoretical maximum rate of 1,400,000 (Trachtenberg et al. 1999). This fast turnover rate minimizes the amount of enzyme required. Coupled with a low makeup rate, due to a potential CA life of 6 months based on laboratory testing, this biomimetic membrane approach has the potential for a step change improvement in performance and cost for large-scale CO_2 capture in the power sector. Although the reported laboratory and economic results may be optimistic, the "carbozyme biomimetic process can afford a 17-fold increase in membrane area or a 17 times lower permeance value and still be competitive in cost with MEA technology" (Yang and Ciferno 2006). The idea behind this process is to use immobilized enzyme at the gas/liquid interface to increase the mass transfer and separation of CO_2 from flue gas. Technical challenges exist before this technology can be pilot tested in the field. These limitations include membrane boundary

layers, pore wetting, surface fouling (Boa and Trachtenberg 2006), loss of enzyme activity, long-term operation, and scale-up.

Key Technologies of Chemical Absorption Systems

Absorbent

The absorbent is one of the most important factors to affect the process of chemical absorption. The type of absorbent and the rational weight concentration/mixing weight ratio are the main characteristic parameters of chemical absorption technologies. An absorbent of high absorption rate and absorption capacity can help to minimize the equipment size and decrease the loss of absorbent, while an absorbent of lower regeneration energy consumption can basically decrease the total energy consumption of the whole process. The optimal choice of absorbent can make the chemical absorption technology more challenging than the other methods. What is more, the capital cost of absorbent, the physical and environmental properties of absorbent, and whether degradation reactions can occur with the other component in the flue gas are also important factors to be considered.

Properties of the Absorbent

The chemical absorbent for CO_2 capture should meet some basic requirements.

Absorption Capacity

Absorption capacity is the CO_2 solubility in the absorbent. The temperature and pressure effect on the solubility are the most important properties for an absorbent. The main index for the process such as circulation rate of absorbent, heat consumption and electricity consumption for regeneration process, operation conditions for regeneration, and the equipment size all depends on the solubility.

The Selectivity of Absorbent

The selectivity of absorbent refers to the ratio between the CO_2 solubility α_2 and the solubility α_1 of the other gas component which is closest to CO_2.

$$C = \frac{\alpha_2}{\alpha_1} = \frac{K_{ph,1}}{K_{ph,2}} \tag{39}$$

Among the equation,

C – selectivity coefficient
$K_{ph,\,i}$ – solubility coefficient of less dissolved component i

During the whole absorption process, the consumption of less dissolved gas, the possibility of complete separation of the mixed gases, the characteristics of the process, and many coefficients are related to the selectivity of the absorbent.

Saturated Vapor Pressure

In order to avoid the loss of absorbent during the operation, the vapor pressure under the absorption temperature should be low and the boiling point of the absorbent should be high enough. The requirement for the saturated vapor pressure depends on the pressure of the absorption process and the weight concentrations of the absorbent solution.

In some cases, an easily volatile absorbent like ammonia may be employed. However, it seems to be operated during the process that absorption temperature is low and operation pressure is high.

Boiling Point

To some extent, once the requirement for the saturated vapor pressure is met, the optimal boiling point for the absorbent should be generally above 423 K. In many cases, the boiling point of the absorbent is not expected to be high, that is to say, a low saturated vapor pressure is the ideal condition. It is necessary to carry out distillation when the by-products accumulate in the circulated solution. If the boiling point of the solution is too high, the distillation temperature has to be raised rather high to meet the requirements of energy consumption. Otherwise, the distillation should be carried out under high vacuum conditions. Factually, the boiling point of the absorbent is usually between 443 and 473 K. The saturated vapor pressure is usually up to 13.33 Pa at 303 K.

Freezing Point

The freezing point is also an important factor. Both the choice of the operation temperature and the storage condition depend on the freezing point. The mixed solution of absorbent, which usually refers to mixed solution composed of the absorbent and water, should not to be frozen easily.

Density

The density of the absorbent seldom affects the application of the absorbent. However, the density of the absorbent is better to be low when the other properties are the same.

Viscosity

The viscosity of the absorbent affects the heat transfer rate and mass transfer rate. Hence, it affects the size of the according equipment. It also has effects on the electricity consumption for solution transfer. Above all, the viscosity of the absorbent is better to be small when the other properties are the same.

Thermochemical Stability

The residence time of the absorbent in the system should be long. It usually needs to be completely changed every 6–18 months. Therefore, the thermochemical stability should be guaranteed. Even the degradation such as oxidizing which occurs very slowly should be considered during the choice of absorbent.

Another requirement for the absorbent is that the corrosion rate should be low and the market price should be not too high.

Absorbents for CO_2 Capture

Industry Used Absorbent

Until now, alkanolamines solution, alkali solution, and hot caustic potash solution have been widely used in many industries to separate CO_2 by chemical absorption methods, such as in the food industry, fertilizer industry, and so on. Table 1 lists the physical properties of the commonly used alkanolamines.

Maddox proposed a method to choose the absorbent (Maddox 1985). The CO_2 partial pressure and the CO_2 volume ratio before/after the chemical absorption process are considered to be the key factors. When the CO_2 partial pressure is no more than 103.4 kPa, the alkanolamine solutions are the best choices. In chemical absorption processes, the CO_2 partial pressure can be lower than 34.5 Pa. When the CO_2 partial pressure is 103.4–689.5 kPa, both the alkanolamine solutions and hot potassium carbonate solutions can decrease the CO_2 partial pressure to be lower than 6.9 kPa. When the CO_2 partial pressure is above 689.5 kPa, even the physical absorbent can decrease the CO_2 partial pressure to be 6.9–20.7 Pa.

According to Maddox's method on the selection of absorbent, alkanolamine solutions are the best choices for coal-fired power plants. The reason is that the coal-fired flue gas is usually of low CO_2 partial pressure, high volume, and high removal efficiency requirement of CO_2. Aqueous solutions of alkanolamines are the most commonly used chemical absorbents for the removal of acidic gases (CO_2 and H_2S) from natural, refinery, and synthesis gas streams. Among them, aqueous monoethanolamine (MEA) as a primary amine has been used extensively for this purpose, especially for removal of CO_2. It has several advantages over other commercial alkanolamines, such as high reactivity, low solvent cost, low molecular weight, and, thus, high absorbing capacity on a mass basis and reasonable thermal stability and thermal degradation rate. Generally speaking, MEA solution is currently the most widely used absorbent in fossil power plants.

To have a better understanding of the role played by MEA in the CO_2 capture process, the simple analysis on MEA is given according to the index raised above. Table 2 shows the evaluation for the conventional solvents MEA and MDEA (Kohl and Nielsen 1997).

Absorption and Regeneration Characteristics of CO_2 in MEA Solutions

A large number of studies have already been carried out in this field. Here is a brief introduction of absorption/regeneration characteristic data for MEA solutions.

The absorption rate and maximum net cycle capacity of several amines are given in Fig. 8.

Regeneration heat needs for the system are usually hard to measure. Generally speaking, the heat required to regenerate the solution in the desorber column of the CO_2 capture process (reboiler heat duty) can be described as the sum of three terms:

Table 1 The physical properties of commonly used alkanolamines (Kohl and Nielsen 1997)

Item	Monoethanolamine (MEA)	Diethanolamine (DEA)	Triethanolamine (TEA)	Methyldiethanolamine (MDEA)	Diisopropanolamine (DIPA)	Diethylene glycolamine (DGA)
Molecular formula[a]	R-NH_2	R_2-NH	R_2-N	R_2-NCH_2	R_2-NH	ROC_2H_4-NH
Molecular weight	61.09	105.14	149.19	119.17	133.19	105.14
Density (g/cm^3) (20 °C)	1.0179	1.0919	1.1258	1.0418	0.9890	1.0550
Boiling point (°C) (1.013×10^5 Pa)	171	269	360	247	249	221
Freezing point (°C)	10.5	28.0	21.2	−21.0	42	−95
Vapor pressure (Pa) (20 °C)	48.0	1.33	1.33	1.33	1.33	1.33
Solubility in the water (wt%, 20 °C)	100	96.4	100	100	87	100
Viscosity (cps)	24.1 (20 °C)	380 (30 °C)	1,013 (20 °C)	101 (20 °C)	198 (45 °C)	26 (24 °C)
Evaporation heat (kJ/kg) 1.013×10^5 Pa	825.6	669.8	534.9	518.6	429.1	509.5
Estimated price ($/kg)	1.036	1.058	1.08	2.138	0.97	1.499

[a]In the molecular formulae,

$$R = -CH_2CH_2OH$$

$$R' = -CH_2\underset{\displaystyle CH_3}{\underset{|}{C}}HOH$$

Table 2 Comparison of MEA and MDEA in the CO_2 capture process

Monoethanolamine (MEA)	Methyldiethanolamine (MDEA)
+ Fast reaction	− Slow reaction
+ Low molecular weight → high solution capacity on a weight basis	− High molecular weight
− Low net (cyclic) capacity	+ High net (cyclic) capacity
− High heat of reaction with CO_2 (due to carbamate formation)	+ Low heat of reaction with CO_2
− High corrosion	+ Low corrosion
− Irreversible reaction products with carbonyl sulfide (COS) and carbon disulfide (CS_2)	+ Low degradation
− High vapor pressure	+ Low vapor pressure
+ Yellow chemical (good biodegradability)	− Red chemical (low biodegradability)
+ Low cost (+)	− High cost

$$q_{reb} = q_{sens} + q_{vap,H_2O} + q_{abs,CO_2} \tag{40}$$

where q_{sens} is the sensible heat to raise the solvent from the temperature downstream the rich-lean heat exchanger (RLHX) to the reboiler temperature, $q_{vap,\ H2O}$ is the heat of evaporation required to produce that part of the stripping steam in the reboiler which does not condense on its way up in the column and which is ultimately being condensed in the overhead condenser, and $q_{abs,\ CO2}$ is the overall heat required to desorb the CO_2 from the solution. The third term ($q_{abs,\ CO2}$) corresponds to the heat of absorption of the solvent with the CO_2. The same amount of heat that is being released in the exothermic reactions in the absorber column must be provided in the desorber column to reverse the absorption process and to drive out the CO_2. The heat of absorption consists of three terms (Kim et al. 2009):

1. Nonideal mixing
2. Dissolution of gas into the liquid
3. Chemical reaction

Heat must therefore be provided in the reboiler to break up the CO_2/solvent complex formed during the absorption process (heat of reaction) and to desorb the dissolved molecular CO_2 from the solution (heat of dissolution). Figure 9a shows the comparison of stripping heat needs for different absorbents, and Fig. 9b gives the distribution of energy associated in reboiler heat duty for different absorbents. Generally speaking, when the actual CO_2 loading is around 0.2 mol CO_2/mol MEA for the absorption/desorption process, the regeneration heat consumption is around 3.9–4.5 $MJ_{th}/kgCO_2$, which equals to ~1.6 $MJ_e/kgCO_2$ (Desideri and Paolucci 1999; Okabe et al. 2008). The heat of evaporation occupies the main energy consumption. Hence, it is meaningful to reduce the evaporation heat consumption for the MEA scrubbing process.

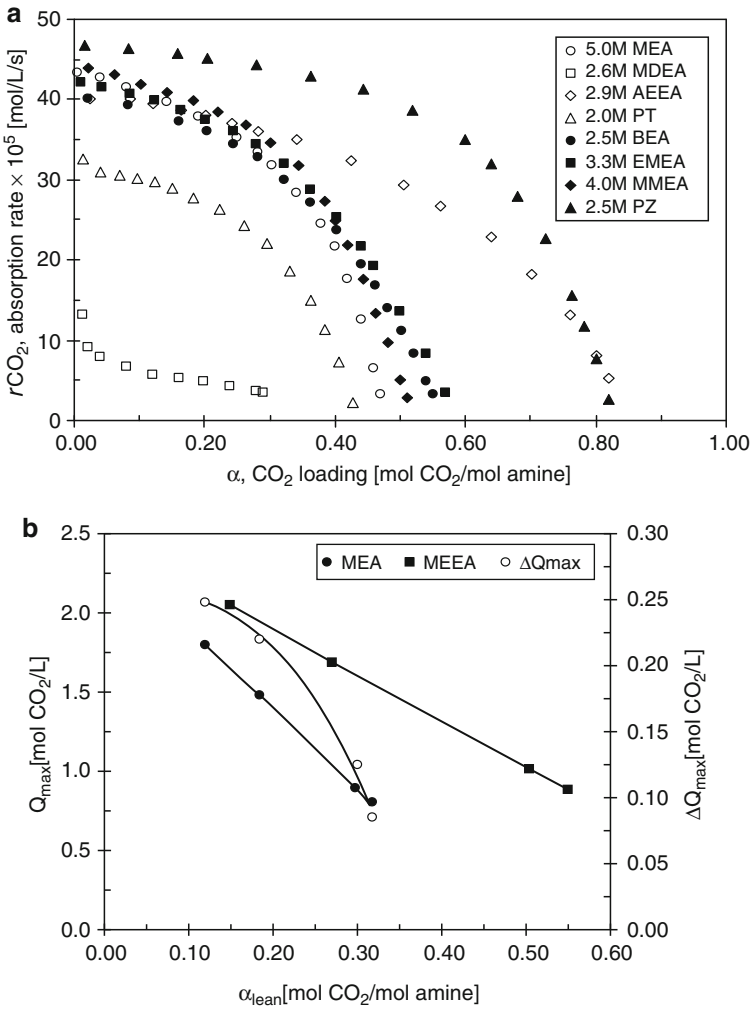

Fig. 8 (**a**) Absorption rate of CO_2 in amine-based solvent at 313 K. (**b**) Comparison of maximum net cycle capacity in 5 M MEA and 2.9 M AEEA (Mamun et al. 2007)

Degradation of MEA

The degradation of MEA in the flue gas is rather complicated. It may be caused by the following three main reasons: thermal degradation, oxidation degradation, and the formation of heat-stable salts. The detailed mechanisms are discussed here:

- Thermal degradation
- CO_2-induced degradation
- Degradation caused by COS and CS_2

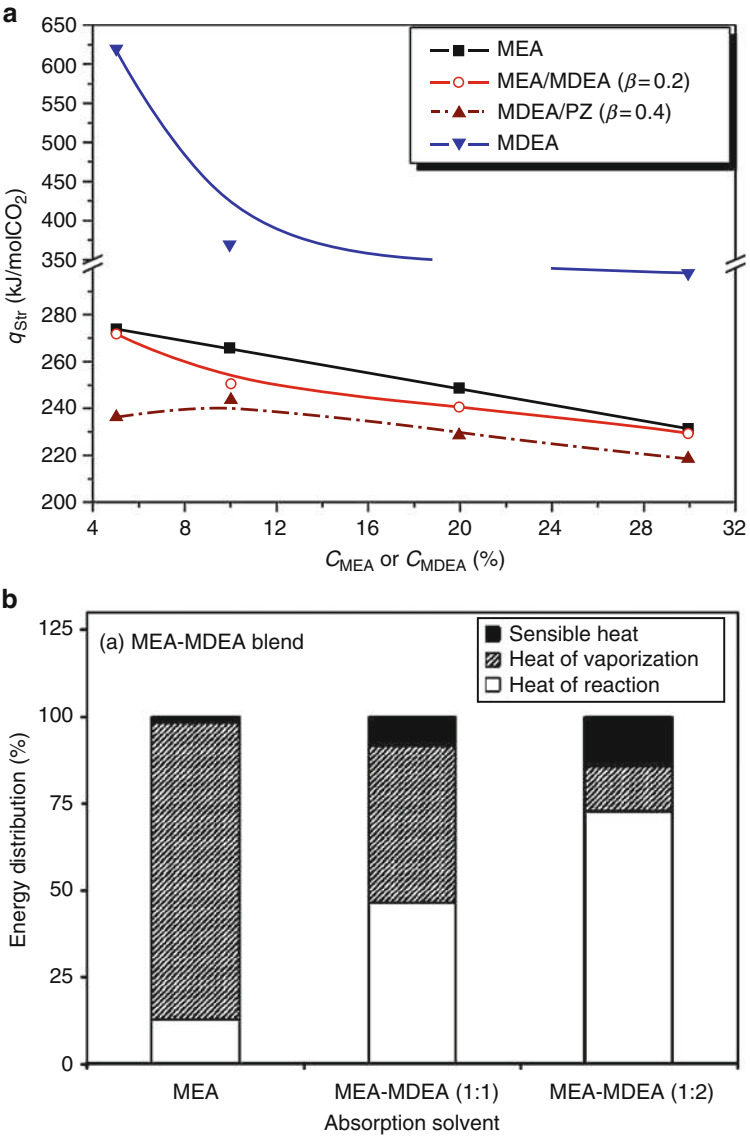

Fig. 9 (**a**) Stripping energy needs in solutions of different weight concentration. (**b**) Distribution of energy associated in reboiler heat duty for different absorbents (Sakwattanapong et al. 2005)

- Degradation caused by CO
- Formation of heat-stable salts and reaction of amines with strong acids
- Oxidation
- Sulfur and polysulfide degradation

Thermal Degradation

Polderman (Polderman et al. 1955) describes the mechanism for thermal degradation of MEA by carbamate polymerization. In the absorber, MEA associates with CO_2 to form MEA carbamate as illustrated below.

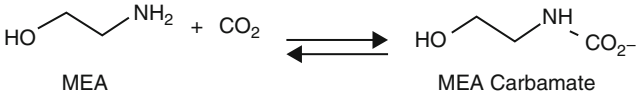

(41)

This reaction is normally reversed in the stripper, but in some cases the MEA carbamate will cyclize to form 2-oxazolidone, which is also a reversible reaction, as shown below:

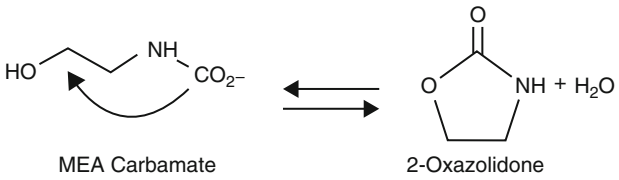

(42)

Yazvikova (Yazvikova et al. 1975) found that MEA carbamate can also react with a free MEA molecule and irreversibly dehydrolize to form *N*,*N*′-di(2-hydroxyethyl) urea.

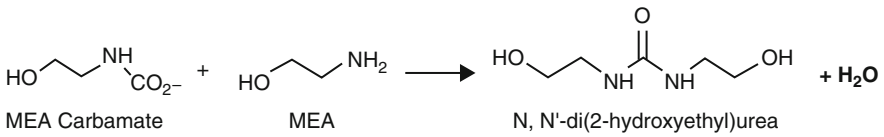

(43)

The former product, 2-oxazolidone, can then react with another molecule of MEA to form 1-(2-hydroxyethyl)-2-imidazolidone, which is sometimes referred to as HEIA.

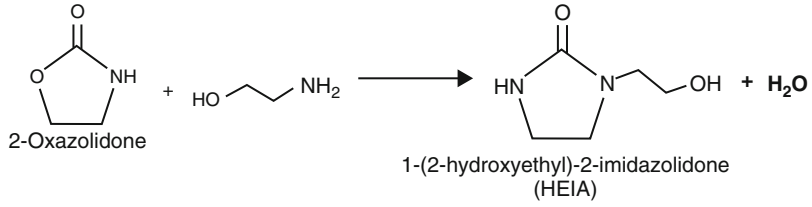

(44)

HEIA can then be hydrolyzed to form *N*-(2-hydroxyethyl)-ethylenediamine or HEEDA.

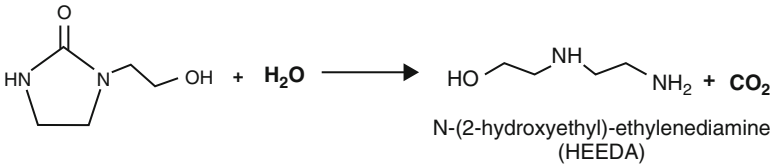

(45)

These four species (2-oxazolidone, dihydroxyethylurea, HEIA, and HEEDA) plus further polymerization products are believed to be the main products of thermal degradation. The rate of formation of these products is a function of temperature (faster kinetics), CO_2 loading (more carbamate present), and MEA concentration.

Oxidation Degradation

The use of amines for CO_2 capture from flue gases involves one distinct difference and challenge from traditional amine acid gas capture: the presence of dioxygen (O_2) and its role in the oxidative degradation of the amine.

It is important to realize that degradation conditions will vary within the gas-treating plant. Different mechanisms may be involved in different parts of the plant. For instance, the highest O_2 concentration and the lowest temperature will occur within the absorber while the highest temperature and lowest O_2 content will be found in the reboiler.

Oxidation of most stable organic compounds is sluggish at room temperature and occurs readily only at high temperature. Obviously, the amines in flue gas capture applications experience a higher temperature but are still low relative to pyrolysis conditions. This low kinetic reactivity of dioxygen can be explained by considering spin conservation requirements. The ground state for O_2 is a triplet (a biradical). Most stable organic compounds and the dioxygen reduction products, H_2O and H_2O_2, are singlet molecules. The direct reaction of a triplet molecule with a singlet to give singlet products is a spin-forbidden process. This means that the reaction between dioxygen and a substrate should occur at a very low rate, which is determined by the time required for spin inversion to occur. This is generally a slow process except at elevated temperatures.

In reported studies of amine autoxidation, combinations of high O_2 partial pressures, higher than ambient process temperatures, and long reaction times (often several weeks) had to be employed to see substantial degrees of reaction. Metal ion spiking resulted in much faster reactions. The metal ions may directly react with amines, but in the presence of dioxygen, they may act as catalysts to activate the dioxygen. Metal complexes, due to their abilities to act as radicals with varied spin multiplicities, can provide spin-allowed pathways for reaction. Thus, the reaction of dioxygen and amines is spin-allowed if the number of electrons on a ternary complex (metal ion + amine + O_2) remains constant throughout the reaction.

- Dioxygen complex intermediates as oxidants. Amine complexes of Fe(II), Cu(I), and other metal ions have been shown or proposed to form dioxygen complexes, both stable and short-lived (Rubin and Rao 2002; Yeon et al. 2005). Oxidation of amines via dehydrogenation of the C–N bond has been demonstrated via Co

(II) dioxygen complexes, though the reaction was limited to amines with aromatic groups that could form conjugated imine products. Aliphatic amines such as tetraethylenepentamine did not oxidize in these cobalt systems, and the amine ligand/Co(II) system was well known to form stable dioxygen complexes (Schwartz 1982). Other metal complex dehydrogenations of coordinated amines which may proceed via short-lived O_2 complex intermediates include autoxidation of ethylenediamine (dehydrogenation of both C–N bonds) with Ru(II) (Lente and Fabian 1998; Van Eldik et al. 1992) and Os(II) (Goff and Rochelle 2006), macrocyclic amines with Fe(II) (Hakka and Ouimet 2006), and peptides with Co (II) (Liu et al. 1995). Whether or not dioxygen complexes are involved, dehydrogenation reactions (imine formation and subsequent imine products) of amines should be considered when in the presence of transition metal ions and dioxygen.

- Free radical pathways for autoxidation. In studies of the iron chelate hydrodesulfurization degradation, it was noticed that long (several days) exposure to air sparging at room temperature did not cause degradation. This was consistent with the predicted slow amino acid hydrolysis and oxidation by Fe(III). It was only after introducing the reducing agent H_2S that ligand degradation was detected. Iron chelates, synthesized with Fe(II) and converted to Fe(III) with air, also exhibited degradation. This chemistry can be explained in terms of dioxygen reduction products such as superoxide, peroxide, and hydroxyl radical.

It should be remembered that these reduction intermediates are weak acids and may exist in two protonation states in amine solutions. As shown by the pK_a values in Fig. 10, superoxide should exist in the anionic form and peroxide in both mono- and diprotonated forms, and the hydroxyl radical can also exist as the oxide radical anion. For example, with pK_a values of 11.7 and 11.8 (values at 298 K), both oxide radical anions and hydroxyl may exist in an unloaded (lean) amine solution, while high CO_2 loadings will lower the pH enough so that hydroxyl will predominate. The rate constant for reaction of the glycine anion has been reported to be ten times higher for hydroxyl than for the oxide radical ion.

For the amino acid chelants, it was noted that the most reactive species was the hydroxyl radical (HO·). Compilations of reaction rates show that compounds such as

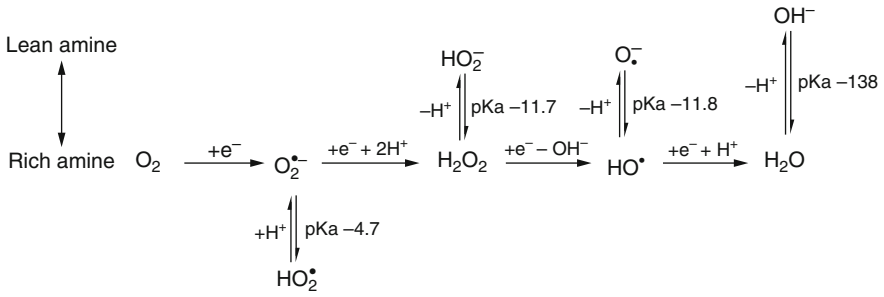

Fig. 10 Primary dioxygen reduction species at amine process conditions (Bedell 2009)

EDTA, NTA, HEDTA, and glycine have reaction rate constants of 10^9–10^{10} L/mol/s. Products that were seen to build up in solution had lower reactivities toward hydroxyl. For instance, the rate constant for oxalate (which can build up to problem levels in the process) was only 7.7×10^5. It was also shown that additives which had high hydroxyl radical rate constants (such as thiosulfate and sulfite) could act as hydroxyl radical scavengers. Because the rate constants were close to diffusion limitations and because of the high substrate concentrations, these additives could only act as competitive scavengers and not totally eliminate the degradation.

Data on reactivity of amines with dioxygen reduction intermediates are harder to find, but some of the results shown in Table 3 support the highest reactivity for hydroxyl. It should be mentioned that alternatives to the hydroxyl radical have been proposed to account for some subtle differences between Fe (II)/H_2O_2/O_2 reactions and reactions of hydroxyl produced via pulse radiolysis. For purposes of this discussion, it is easiest to consider the chemistry in terms of the hydroxyl radical.

Once the reaction has been initiated by formation of the carbon-based radicals, subsequent reaction with dioxygen should be extremely rapid, as shown by representative rate constants presented in Table 4. Figure 11 shows the reaction proposed for the dioxygenation of a MEA radical.

The further reaction of the organic peroxy radical involves abstraction of a hydrogen atom from another amine molecule in a scheme similar to what is often proposed in hydrocarbon autoxidations. This provides a potential chain step to

Table 3 Rate constants for dioxygen reduction intermediates at 298 K (Bedell 2009)

Reaction	Rate (L/mol/s)
Dioxygen: RH + O_2 → products	Slow
N-Propylpyrrolidine + O_2	1.1×10^{-3}
Superoxide: RH + $O_2^{\bullet -}$ → R · + HO_2^-	
$(HOCH_2)_3CNH_2$ + $O_2^{\bullet -}$	<0.42
Glycine + $O_2^{\bullet -}$	48.6
Glycine + HO_2^-	<0.001
Peroxide: RH + HO_2^- → R · + HO · + H_2O	Slow
Hydroxyl: RH + HO · → R · + H_2O	$10^8 - 10^{11}$
Ethylenediamine + HO	5.5×10^9
Ethylamine + HO	5.1×10^9
Triethylamine + HO	1×10^{10}
TEA + HO	8×10^9
$TEAH^+$ + HO	2×10^9

Table 4 Reaction of dioxygen with organic radicals (Bedell 2009)

Radical	pH	K (L/mol/s)
$H_2NCHCO_2^-$ (glycine)	7.9	1×10^9
$O_2CCH_2NHCHCO_2^-$ (IDA)	7	8×10^8
$CHOHCH(NH_2)CO_2^-$	7	2.4×10^9
$CH_2N(CH_3)_2$	10.4	3.5×10^9

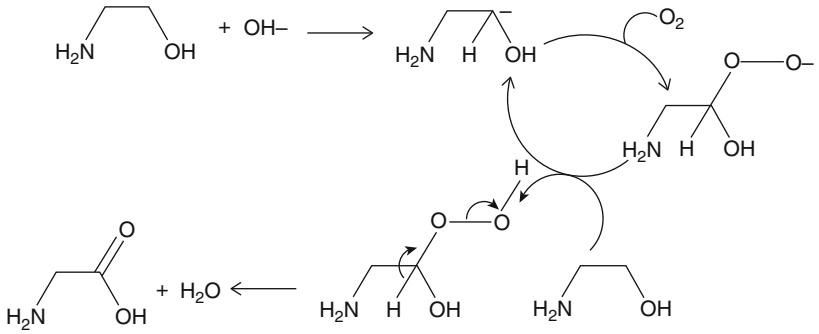

Fig. 11 Proposed reaction pathway for production of glycine from MEA (Bedell 2009)

sustain further oxidation. Though glycine (the product shown above) has been noted as an MEA oxidation product, radical formation on the carbon adjacent to the nitrogen would be expected to yield glycolamide which has not been reported as a product. It is possible that glycolamide would hydrolyze to form glycolic acid and ammonia, both of which have been noted as MEA oxidation products. In the hydrodesulfurization chelant degradation chemistry, species such as a keto intermediate were detected by mass spectral analysis in freshly degraded solutions, though only oxalate and R′RNH (the expected hydrolysis products) were noted after several days as shown in the equation below:

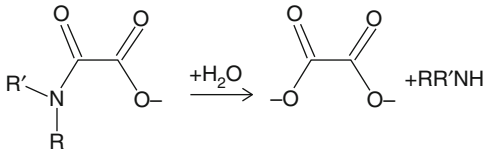

(46)

Figure 12 summarizes the different radical chemistries. There are three potential pathways to form the organic radical:

1. The direct one-electron oxidation by a metal ion. As a high-temperature reaction, this is most likely to occur at reboiler conditions and of course requires the introduction of an appropriate metal ion by corrosion or fly ash leaching. Reoxidation of the metal ion can result in hydroxyl radical formation. The reoxidation process is expected to be faster than the reduction by reaction with the amine. Thus, in an oxygen-rich environment, metal ion reduction could be a limiting factor. The SO_2-derived sulfite ion is known to reduce metal ions such as Fe(III) and Co(III).
2. Abstraction of hydrogen atoms by hydroxyl radicals. This abstraction as well as the dioxygen reduction which produces it should proceed at low (absorber) temperatures.

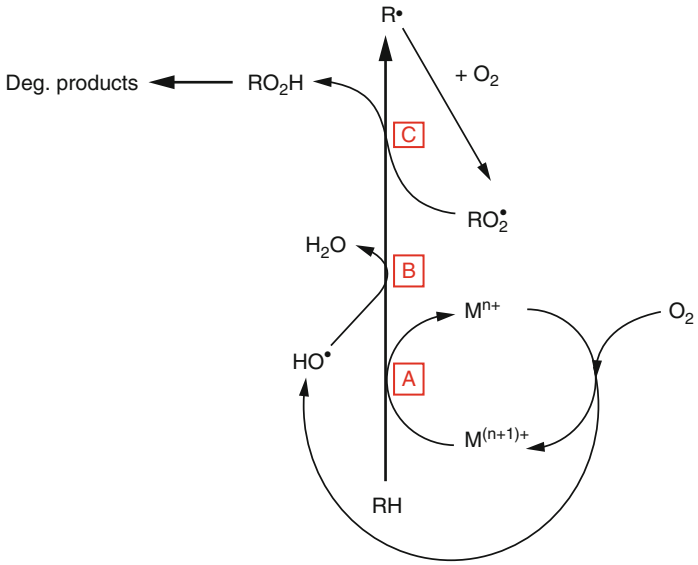

Fig. 12 Amine autoxidation routes (Bedell 2009)

3. Abstraction of hydrogen atoms by the organoperoxy radical.

The autoxidation mechanisms shown above all depend on initiation by metal ions. This underscores the need for good fly ash removal upstream of an amine scrubber. Corrosion, the other means for introducing metal ions, should be, for the most part, autocatalytic with respect to the formation of corrosive degradation products. Use of thermally stable amines and those amines not susceptible to degradation via CO_2 reactions should greatly reduce the corrosion rate and hence the amine autoxidation rate.

Additives to Reduce Degradation

Various types of additives have been proposed to reduce amine degradation.

1. Control of metal ions with chelating agents such as EDTA. Though some inhibition was noted, the effect was short-lived, possibly due to EDTA degradation. The use of iron chelates in hydrodesulfurization, however, showed that the ferrous EDTA chelates were very potent Fenton catalysts (activating intermediate peroxide as well as dioxygen toward hydroxyl radical format ions). Additionally, EDTA would be expected to increase the degree of metal ion solubilization from contaminant fly ash and could also be corrosive toward protective films formed on mild steels.
2. The use of potential hydroxyl radical scavengers. A recent patent claims the use of sulfite and thiosulfate to reduce amine consumption, though no examples were

given which quantified the effect on amine consumption. As discussed above, there is reason to believe that additives, which are capable of reducing hydroxyl radicals, may also be able to reduce metal ions and assist in their redox cycling to produce more degradation.

3. Formation of heat-stable salts and reaction of amines with strong acids. The existence of SO*x* and NO*x* in the flue gases may cause big problems for amine-based solvents. The reason is that the simultaneous existence of SO*x*/NO*x* and vapor in the flue gas has the possibility to form strong acids. The amine-based solvents will react with strong acids first. These reactions are much faster than the reactions between amines and CO_2. The salts formed in these reactions are generally heat stable.

However, the removal of heat-stable salts is usually very difficult. A schematic diagram, which simply describes the principles of HSS removal from MDEA solution using a three-compartment electrodialyzer, is shown in Fig. 13. As shown in Fig. 14, the feed solutions of NaOH and MDEA were added to compartments I and II, respectively. Two electrodes are positioned, one on either side parallel to the membranes. Applying a voltage to the electrodes generates an electric field. It is well known that the anion-exchange membrane permits the passage of anions only while

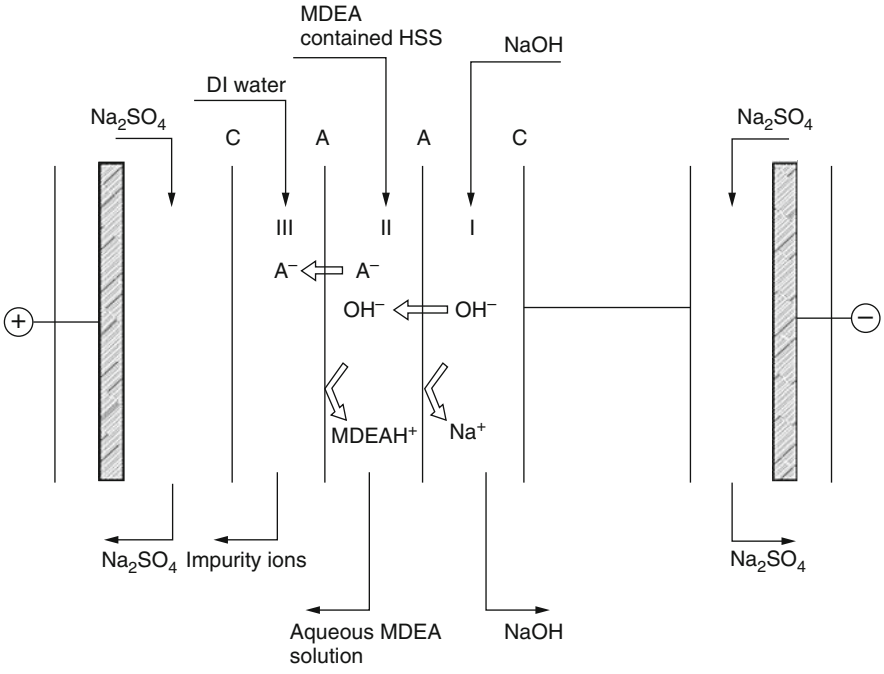

Fig. 13 Principles of HSS removal from aqueous solution of MDEA using a three-compartment ED (Meng et al. 2008)

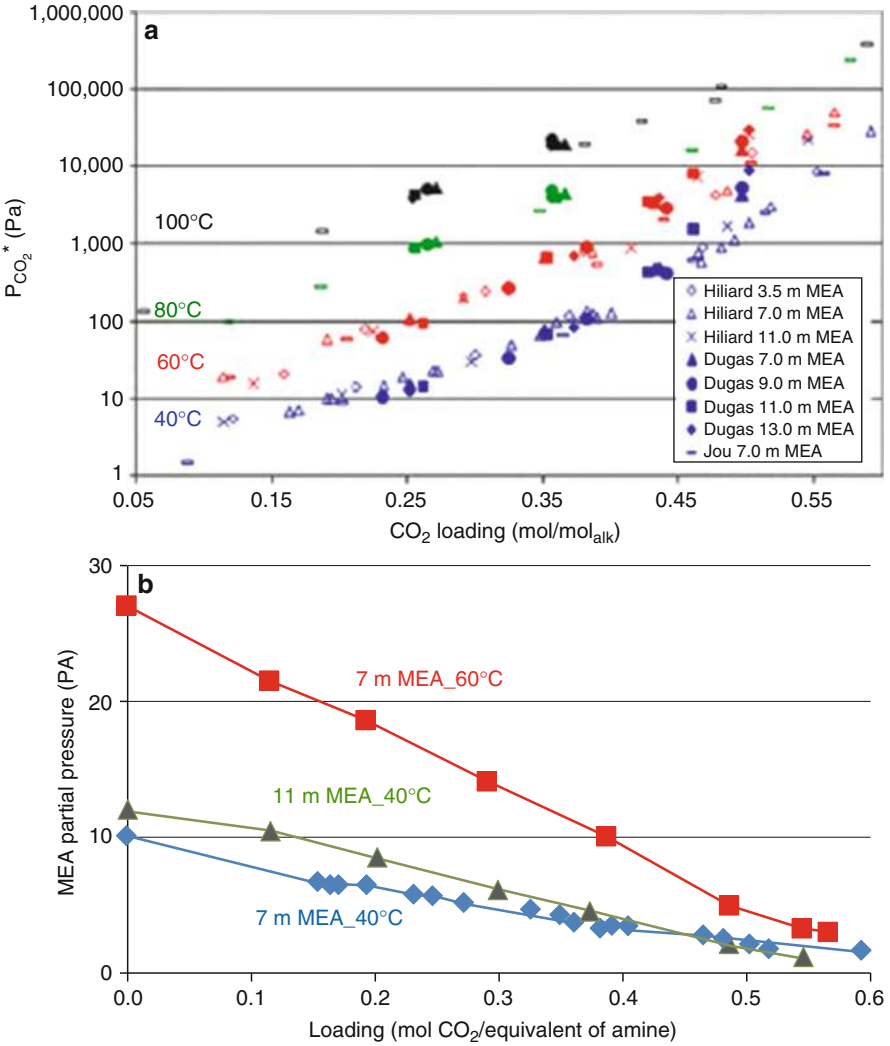

Fig. 14 (**a**) MEA–CO_2–H_2O system: CO_2 solubility comparison between FTIR technique and other methods. (**b**) MEA partial pressure in 7 and 11 m MEA systems for 313 and 333 K (Nguyen et al. 2010)

the cation-exchange membrane permits the passage of cations only. Therefore, OH^- in compartment I migrates through the anion-exchange membranes and then reacts with binding amine ($MDEAH^+ A^-$), as shown in Eq. 47:

$$OH^- + MDEAH^+A^- \rightarrow A^- + MDEA + H_2O \tag{47}$$

where A^- symbolizes impurity anions such as Cl^-, SO_4^{2-}, SCN^-, $HCOO^-$, H_3CCOO^-, and $H_3CH_2CCOO^-$. Once impurity anions such as Cl^-, SO_4^{2-}, SCN^-, $HCOO^-$, H_3CCOO^-, and $H_3CH_2CCOO^-$ were replaced by OH^- in compartment II, they would pass through anion-exchange membrane (AEMs) and reach compartment III under the action of DC electric field. The $[MDEAH]^+$ ions were kept and purified in compartment II. The same more matrixes could be settled in an electrodialysis apparatus according to the abovementioned arrangement principle.

Corrosion and Polarization Behavior of MEA

All amine-treating plants have experienced corrosion problems (Kohl and Nielsen 1997). Corrosion occurs in the forms of general, galvanic, crevice, pitting, intergranular, selective leaching, erosion, and stress corrosion cracking. The plant areas susceptible to corrosion are the bottom of absorbers, regenerators, reboiler bundles, pumps, and valves where the acid gas loading and temperatures are high (DuPart et al. 1993). According to a survey conducted for refinery plants (Rampin 2000), the process equipments that are frequently out of service due to severe corrosion problems are reboiler, rich amine exchanger, regenerator, condenser, absorber, and amine cooler. Although a number of factors contribute to severe corrosion, the major causes reported are poor plant design and operation, such as high flow velocity in pipelines, high operating temperature in reboiler and insufficient steam for solvent regeneration, and the presence of process contaminants.

Corrosion problems essentially lead to substantial expenditure in addition to the process costs. According to CC Technologies and NACE International (Koch 2001), in 1998, the plant expenditure due to corrosion in the USA was estimated at $276 billion while that for petroleum refining alone was $3.7 billion. Of this total, the maintenance-related expenses were estimated at $1.8 billion, the vessel turnaround expenses were at $1.4 billion, and the fouling-related costs were approximately $0.5 billion annually. This reflects a significant impact of corrosion problems in plant operations.

The corrosion mechanism at the interface between the carbon steel surface and the CO_2-loaded MEA aqueous solution was examined using the obtained results and previous work published in the literature. Let us consider chemical reactions taking place in the bulk solution due to CO_2 absorption (Eqs. 48, 49, 50, 51, and 52), possible electrochemical reactions due to corrosion (Eqs. 53, 54, 55, and 56), and possible chemical reactions due to formation of corrosion products (Eqs. 57 and 58; Veawab and Aroonwilas 2002).

Dissociation of water:

$$2H_2O \longleftrightarrow H_3O^+ + OH^- \tag{48}$$

Hydrolysis of CO_2:

$$2H_2O + CO_2 \longleftrightarrow H_3O^+ + HCO_3^- \tag{49}$$

Dissociation of bicarbonate ion:

$$H_2O + HCO_3^- \longleftrightarrow H_3O^+ + HCO_3^{2-} \tag{50}$$

Dissociation of protonated amine:

$$RNH_3^+ + H_2O \longleftrightarrow RNH_2 + H_3O^+ \tag{51}$$

Carbamate reversion:

$$RHNCOO^- + H_2O \longleftrightarrow RNH_2 + HCO_3^- \tag{52}$$

Iron dissolution:

$$Fe \longleftrightarrow Fe^2 + 2e^- \tag{53}$$

Reduction of hydronium ion:

$$2H_3O^+ + 2e^- \longleftrightarrow 2H_2O + H_2(g) \tag{54}$$

Reduction of bicarbonate ion:

$$2HCO_3^- + 2e^- \longleftrightarrow 2CO_3^{2-} + H_2(g) \tag{55}$$

Reduction of undissociated water:

$$2H_2O + 2e^- \longleftrightarrow 2OH^- + H_2(g) \tag{56}$$

Formation of ferrous hydroxide:

$$Fe^{2+} + 2OH^- \longleftrightarrow Fe(OH)_2 \tag{57}$$

Formation of ferrous carbonate:

$$Fe^{2+} + CO_3^{2-} \longleftrightarrow FeCO_3 \tag{58}$$

Essentially, corrosion occurs due to electrochemical reactions comprising anodic and cathodic reactions. The anodic reaction is iron dissolution (Eq. 53) while the cathodic reactions are reductions of oxidizers available in the solution. In the absence of O_2, some possible oxidizers in this system are H_3O^+, undissociated H_2O, and HCO_3^-. According to Veawab and Aroonwilas (Veawab and Aroonwilas 2002), undissociated H_2O and HCO_3^- are major oxidizers whereas H_3O^+ plays a minor role. As such, possible primary corrosion reactions are Eqs. 53, 55, and 56.

Previous studies show that factors listed below affect the corrosion and polarization behavior of MEA solution to different extent. Table 5 summarizes some of them: pH, conductivity, electrochemical parameters, and corrosion rate for uninhibited MEA-H_2O-CO_2 system.

Table 5 Summary of pH, conductivity, electrochemical parameters, and corrosion rate for an uninhibited MEA–H_2O–CO_2 system (Soosaiprakasam 2008)

Experimental condition	pH	σ (mS/cm^2)	β_a (mV/decade)	β_c (mV/decade)	E_{corr} (mV Ag/AgCl)	i_{corr} (μA)	E_{pp} (mV Ag/AgCl)	i_{crit} (μA)	i_{pass} (μA)	E_b (mV Ag/AgCl)	Corrosion rate (mm/year)
0.00 kPa O_2, 5.0 kmol/m^3 MEA											
80 °C, α = 0.20	9.06 ± 0.02	23.18 ± 0.33	72.92 ± 0.78	106.93 ± 1.11	−853.00 ± 3.50	8.02E + 01 ± 7.63E + 00	−662.00 ± 1.50	−9.44E + 00 ± 3.25E − 01	−8.45E + 01 ± 4.5E + 00	522.00 ± 4.50	0.31 ± 0.03
40 °C, α = 0.20	10.19 ± 0.00	20.29 ± 0.02	92.88 ± 0.00	101.71	−846.00	2.82E + 01	−686.00	−1.42	−15.00	580.00	0.11
80 °C, α = 0.55	7.95 ± 0.07	43.68 ± 2.17	88.00 ± 4.80	113.11 ± 1.045	−775.00 ± 4.00	1.75E + 02 ± 2.41E + 01	−573.00 ± 36.00	−2.52E + 01 ± 1.82E − 00	−2.55E + 02 ± 1.5E + 01	635.00 ± 26.00	0.67 ± 0.09
1,000 rpm, α = 0.20, 80 °C	9.23 ± 0.13	21.81 ± 1.85	97.67 ± 8.96	122.35 ± 1.71	−826.86 ± 8.59	3.15E + 02 ± 3.90E + 01	−634.00 ± 10.00	−1.4E + 01 ± 1.79E + 00	−4.72E + 02 ± 4E + 00	604.00 ± 19.00	1.21 ± 0.15
2,000 rpm, α = 0.20, 80 °C	9.25 ± 0.11	22.48 ± 2.69	110.25 ± 1.77	127.81 ± 8.65	−815.13 ± 5.83	3.66E + 02 ± 1.05E + 01	−583.00 ± 6.00	−1.42E + 01 ± 5.25E − 01	−7.25E + 02 ± 2.5E + 01	708.00 ± 31.00	1.43 ± 0.07
10.13 kPa O_2, 5.0 kmol/m^3 MEA											
80 °C, α = 0.20	9.14 ± 0.02	22.99 ± 0.46	76.00 ± 10.00	134.50 ± 8.50	−833.00 ± 7.00	1.99E + 02 ± 3.41E + 00	−673.00 ± 4.00	−8.94E + 00 ± 7.25E − 01	−2.60E + 01 ± 0.00E + 00	448.00 ± 4.00	0.43 ± 0.03
40 °C, α = 0.20	10.50 ± 0.57	19.69 ± 1.00	-	175.00	−356.00	2.12E + 01	-	-	−1.40E + 01	−408.00	0.08
80 °C, α = 0.55	8.17 ± 0.11	46.24 ± 1.38	76.00	113.00	−788.00	1.41E + 02	−507.00	−2.52E + 01	1.41E + 01	705.00	0.55
10.13 kPa O_2, α = 0.55, 80 °C											
7 kmol/m^3 MEA, α = 0.55	8.52 ± 0.04	32.62 ± 3.16	105.90	120.90	−795.00	1.87E ± 02	−507.00	−2.60E + 04	−7.80E + 01	699.00	0.72
9 kmol/m^3 MEA, α = 0.55	8.32 ± 0.00	21.89 ± 0.52	117.00	150.42	−795.00	2.74E + 02	−501.00	−2.04E + 04	−7.10E + 01	699.00	1.06
5.07 kPa O_2, 5.0 kmol/m^3 MEA											
80 °C, α = 0.20	9.13 ± 0.03	23.36 ± 0.58	76.85 ± 3.15	136.00 ± 5.00	−839.00 ± 1.00	1.59E + 02 ± 4.5E + 01	−653.00 ± 1.00	−1.59E + 02 ± 4.5E + 00	−2.56E + 01 ± 0.26E + 00	481.00 ± 23.00	0.37 ± 0.01
10.13 kPa O_2, 5.0 kmol/m^3 MEA, 80 °C, α = 0.20											
7 days	9.15 ± 0.06	23.03 ± 0.03	63.49	135.8	−780.00	2.07E + 02	−648.00	−8.05E + 03	−1.96E + 02	528.00	0.80
14 days	9.14 ± 0.07	23.31 ± 0.31	99.34	116.64	−789.00	4.74E + 02	−653.00	−7.59E + 03	−1.04E + 03	523.00	1.83
28 days	9.10 ± 0.12	24.04 ± 0.36	84.63	152.16	−790.00	8.31E + 02	−642.00	−1.31E + 04	−2.83E + 03	546.00	1.94

σ conductivity, β_a anodic Tafel slope, β_c cathodic Tafel slope, E_{corr} corrosion potential, i_{corr} corrosion current density, E_{pp} primary passivation potential, i_{crit} critical current density, i_{pass} passivation current density, E_b breakdown potential, α CO_2 loading (mol/mol)

- Increasing the O_2 partial pressure accelerates corrosion due to the increasing oxidizer concentration in the solution. Dissolved O_2 is required for the corrosion control that raises the system potential to passivation where a passive film of hematite ($\gamma - Fe_2O_3$) is established on the metal surface.
- A greater solution velocity causes a higher corrosion rate due to the enhancement of the transport rates of corroding agents between metal surface and bulk solution.
- Raising the solution temperature enhances the corrosion rate. This is the result of the increases in rates of iron dissolution and oxidizer reduction during the corrosion process.
- An increase in CO_2 loading in solution causes corrosion rate to increase. This is due to the increase in concentrations of corroding agents (HCO_3^- and H^+), which causes rates of oxidizer reduction to increase.
- An increase in amine concentration makes a solution more corrosive due to the increase in HCO_3^- available in the solution, which induces a greater rate of iron dissolution.
- The precorroded carbon steel corrodes faster than the nonprecorroded steel due to the faster rates of both iron dissolution and oxidizer reduction reactions.

Volatility of MEA

Amine volatility is a key screening criterion for amines to be used in CO_2 capture. Excessive volatility may result in significant economic losses and environmental impact. It also dictates the capital cost of the water wash.

There are several publications on the VLE (vapor–liquid model) of the binary MEA-H_2O system, but only few data on directly measured MEA volatility, more specifically the vapor-phase mole fraction of MEA. Lenard et al. (Harris et al. 2009) measured the gas-phase composition of MEA in binary aqueous solution (343 and 363 K) using gas chromatography. These data were represented using a three-parameter Redlich–Kister expansion. Cai et al. (1996) measured isobaric VLE at 101.3 and 66 kPa (373–443 K) using the standard curve of refraction index versus mole fraction of the binary mixture at 20 °C. The liquid phase activity coefficients were calculated with the UNIFAC group contribution model as published by Larsen et al. (1987). These data are in the high-temperature range. At temperatures relevant to absorption–stripping, McLees (2006) directly measured the volatility of MEA in a binary system (3.5, 7.0, 23.8 mMEA) as well as in blends having piperazine (PZ) as a promoter. PZ volatility was also measured for 0.9, 1.8, 2.5, and 3.6 m PZ. The data was obtained by hot gas Fourier transform infrared spectroscopy (FTIR). Efforts were also made to model the experimental data in terms of binary interaction parameters by utilizing the NRTL model within Aspen Plus®.

There have also been other thermodynamic measurements of MEA-H_2O. Touhara et al. (1982) measured the total pressure of this system at 298 and 308 K. Nath and Bender (1983) measured total pressure for pure substances as well as binary and ternary mixtures of alcohols, alkanolamines, and water from 60 °C to 95 °C in a vapor-recycle equilibrium cell. Specifically, the MEA-H_2O system was studied at 60 °C, 78 °C, and 91.7 °C. Activity coefficients for each system were calculated

Table 6 Amine volatilities and enthalpies for various systems at nominal lean loadings (Nguyen et al. 2010)

Solution	Loadings (mol CO_2/mol solvent)	Volatility (ppm)	$\Delta H_{apparent}^{\sim,excess}$ (kJ/mol)	ΔH^{vap} (kJ/mol)
7 m MDEA/ 2 m PZ	0.1	6/2	27/87	102/135
8 m PZ	0.29	8	37	85
12 m EDA	0.44	9	40	108
7 m MEA	0.45	31	33	55
5 m AMP	0.25	112	10	75

using the Wilson and UNIQUAC equations and were seen to have negative deviations from an ideal solution (Table 6).

New Type of Absorbent

Although MEA is considered to be the most reliable absorbent for CO_2 capture in power plants nowadays, there still exist a lot of inherent problems. The disadvantages of MEA include high enthalpy of reaction with CO_2, leading to higher regeneration energy consumption, the formation of a stable carbamate and also the formation of degradation products with COS or oxygen bearing gases, inability to remove mercaptans, vaporization losses because of high vapor pressure and more corrosiveness than many other alkanolamines, and, thus, the need for corrosion inhibitors when used in higher concentration. In addition, the market price of MEA is relatively high. Based on the analysis above, nowadays the laboratory research generally sets MEA as a base absorbent.

1. Aqueous ammonia

In 1997, Bai proposed to replace traditional amine solutions by aqueous ammonia solutions to capture CO_2 from coal-fired flue gas. The aqueous ammonia solutions have been testified to possess several advantages over MEA, such as higher absorption capacity, lower market price, and weaker erosion-degradation effects. With the efforts of worldwide researchers in recent years, understandings of the CO_2 capture by aqueous ammonia become much deeper and clearer.

Reaction Mechanism

- Reaction equations

Reactions described as follows, which are respectively proposed by Brooks and Audrieth (1946) Singh et al. (2007), Hatch and Pigford (1962), Thitakamol et al. (2007), Bai and Yeh (1997), Camacho et al. (2005), are widely accepted.

Reaction between NH_3 and CO_2:

$$2NH_3 + CO_2 \leftrightarrow NH_2COONH_4 \tag{59}$$

Hydrolysis of NH_2COONH_4:

$$NH_2COONH_4 + H_2O \leftrightarrow NH_4HCO_3 + NH_3 \quad (60)$$

Hydrolysis of NH_3:

$$NH_3 + H_2O \leftrightarrow NH_4OH \quad (61)$$

Reaction between products of hydrolysis (Eqs. 60 and 61):

$$NH_4HCO_3 + NH_4OH \leftrightarrow (NH_4)_2CO_3 + H_2O \quad (62)$$

$(NH_4)_2CO_3$ reacts with CO_2 and H_2O:

$$(NH_4)_2CO_3 + CO_2 + H_2O \leftrightarrow 2NH_4HCO_3 \quad (63)$$

The overall reaction of CO_2 absorption by aqueous ammonia can be usually expressed as the following equation:

$$NH_3 + CO_2 + H_2O \leftrightarrow NH_4HCO_3 \quad (64)$$

- Reaction products, process, and roles

In general, reactions among aqueous ammonia, carbon dioxide, and their derivates are extremely sensitive to the reaction time and controlled reaction conditions, e.g., concentration, temperature, pressure, and PH. However, during the whole reaction process, a stage has the great potential to appear, during which NH_2COO^-, HCO_3^-, and CO_3^{2-} coexist in the solution. The possible distribution of chemical species in three-phase system is illustrated in Fig. 15.

Recent studies show that carbamate formation dominates the early stage of absorption process due to the presence of excess ammonia. With the advancement of the reaction, CO_2 is introduced into the reaction system with a fixed flow rate while ammonia available to react decreases gradually. The bicarbonate formation hence becomes to act the major role in the later stage of the absorption process (Kim et al. 2008; Teramoto et al. 2004). The reaction steps are also understood as: formation of carbamate, formation of bicarbonate, release of protons, and conversion of carbamate into bicarbonate (Park et al. 2008; Vaidya and Kenig 2007). The ammonia is regarded as multiple roles, e.g., reactant, catalyst, base, and controller. It affects both the carbamate formation and carbonate formation.

Reaction Kinetics

The reaction rate constant for NH_3–CO_2 reaction system can be simply determined by Arrhenius equation:

$$\ln k = \ln \frac{A - E_a}{RT} \quad (65)$$

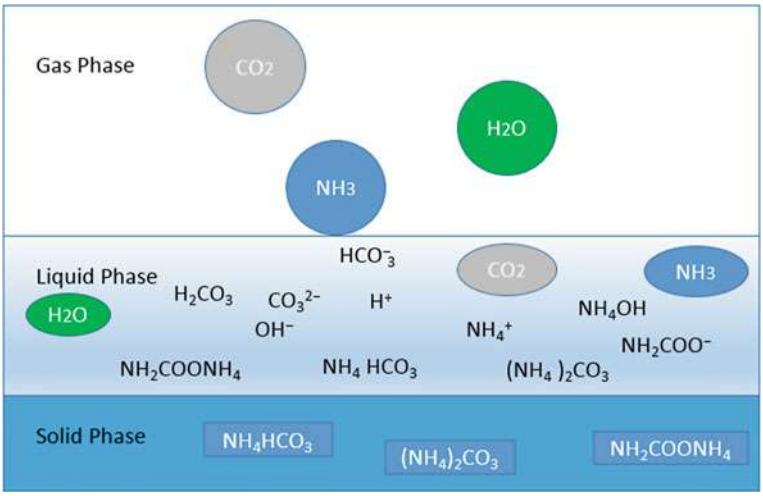

Fig. 15 Chemical species in the NH_3–CO_2–H_2O three-phase system

where A is the pre-exponential factor (s^{-1}) and E_a is the activation energy (kJ/mol).

However, as described from Eqs. 59, 60, 61, 62, 63, and 64, the actual reaction may contain several multistep reaction kinetic parameters rather than the overall reaction rate constant (Puxty et al. 2010; Rinker et al. 1995). A certain number of investigations have been carried out based on various mechanisms, e.g., single-equation mechanism, two-equation mechanism (Astarita, 1967; Horng and Li 2002), eight-equation mechanism(Wang et al. 2011; Ma'mun et al. 2006), zwitterionic mechanism (Caplow 1968; Derks et al. 2005; Danckwerts 1979; Aroonwilas and Veawab 2004; Derks and Versteeg 2009; Kumar et al. 2003), and termolecular mechanism (Crooks and Donnellan 1989; Harris et al. 2009). During the proposed mechanism for kinetics study, the single-equation mechanism is relatively easy to understand and widely studied. Some kinetic rate constants of CO_2 absorption by aqueous ammonia under different reaction conditions are summarized in Table 7.

Vapor–Liquid Equilibrium

Precise vapor–liquid equilibrium data is required parameters to design carbon capture processes using ammonia. Previous studies showed that the Extended UNIQUAC model was consistent with experimental data in terms of accuracy at the temperature range from 0 °C to 110 °C and at pressures up to 100 bar.

Figures 16 and 17, respectively, show the correlation between NH_3 partial pressure and solution CO_2 loading and the relationship between CO_2 partial pressure and solution CO_2 loading. Both of them are deserved from experiments at the temperature of 20 °C under ambient pressure. During these experiments, the amount of ammonia is constant while the amounts of carbon dioxide are various. It can be obtained from Figs. 16 and 17; NH_3 partial pressure decreases with the increase of

Table 7 Kinetic parameters of CO_2 absorption by ammonia based on single-equation mechanism

Equations	Reactor	Temperature	Specification	lnA	Ea (KJ/mol)	References
$NH_3 + CO_2 + H_2O \leftrightarrow NH_4HCO_3$	Disk column	20 ~ 30 °C	K_1	25.8580	43.073	Andrew (1954) (Oyenekan and Rochelle 2009)
	Mixing Chamber	0 ~ 40 °C	K_1	25.6278	48.529	Pinsent et al. (1956) (Weiyang 2005)
	Stirred tank	25–50 °C	K_1	25.556	48.000	Hus (2003) (Yan et al. 2007)
	Sieve-plate tower	28–43 °C	K_1	12.3884	26.730	Diao et al. (2004) (Ramshaw and Mallinson 1981)
	Stirred tank	5–30 °C	K_1	9.4867	28.093	Rivera-Tinoco (2010) (Yan et al. 2009)

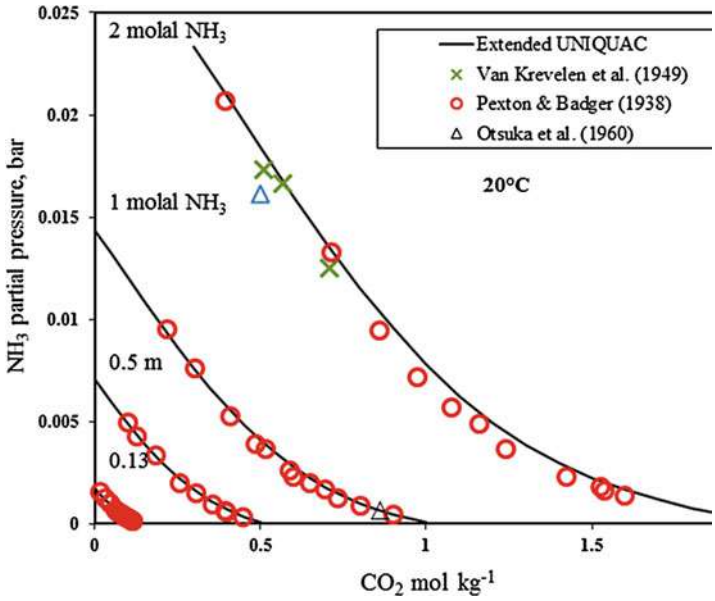

Fig. 16 NH_3 partial pressure versus CO_2 loading

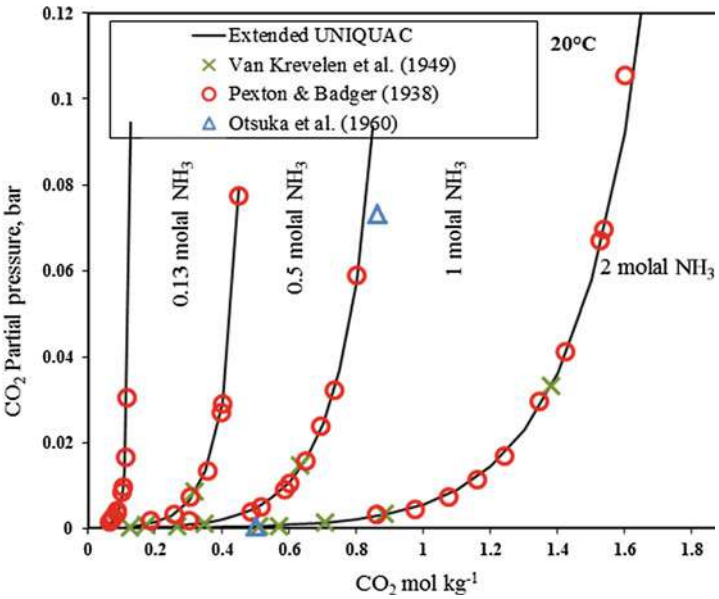

Fig. 17 CO_2 partial pressure versus CO_2 loading

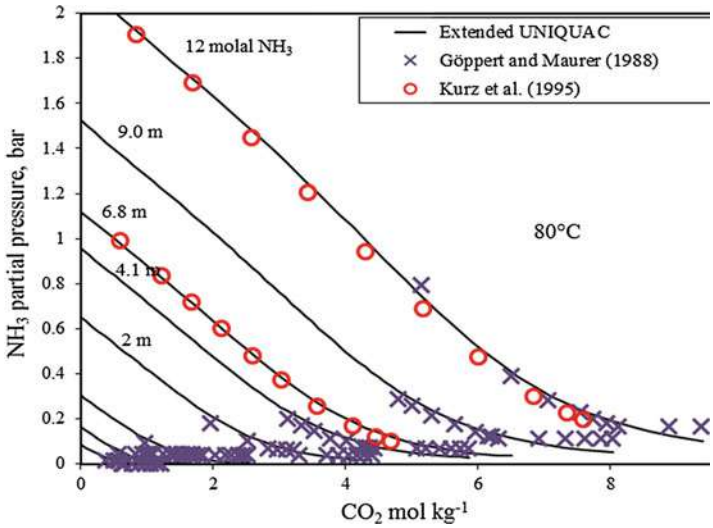

Fig. 18 NH_3 partial pressure versus CO_2 loading

CO_2 loading while CO_2 partial pressure exhibits an adverse changing tendency. When the solution CO_2 loading reaches 1 mol of CO_2 per mole of NH_3, the partial pressure of NH_3 almost vanishes while the partial pressure of CO_2 increases rapidly. It implies that NH_4HCO_3 might be the eventual product of these complicated chemical reactions.

To get a better understanding of vapor–liquid equilibrium at a higher temperature, the experimental results tested at the temperature of 80 °C under ambient pressure are shown in Figs. 18 and 19. The difference between the vapor liquid of lower temperature and that of higher temperature is the magnitude of partial pressure. Obviously, with the increase of temperature, both partial pressure of ammonia and that of carbon dioxide increase. Moreover, the partial pressure of carbon dioxide has been even increased 50–100 times that of deserved at the temperature of 20 °C. It implies that the temperature of 80 °C does facilitate the regeneration process of carbon dioxide.

Solid–Liquid Equilibrium

Solid–liquid equilibrium is less concerned; however, the data of solid–liquid equilibrium is rather important and helpful for the design and operation of aqueous ammonia-based CO_2 capture process. It allows us to determine the appropriate operational conditions to adjust the products. Figure 20 presents the correlation between CO_2 loading and temperature. It can be easily observed that when the loading exceeds 0.6 mole of CO_2 per mole of NH_3, the major product in the solution is ammonium bicarbonate. With the increase of temperature, the possibility to form ammonium carbamate sharply decreases.

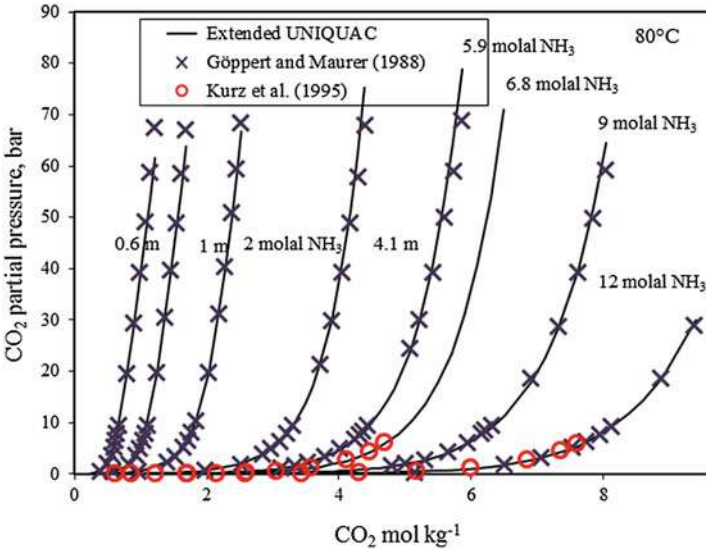

Fig. 19 CO_2 partial pressure versus CO_2 loading

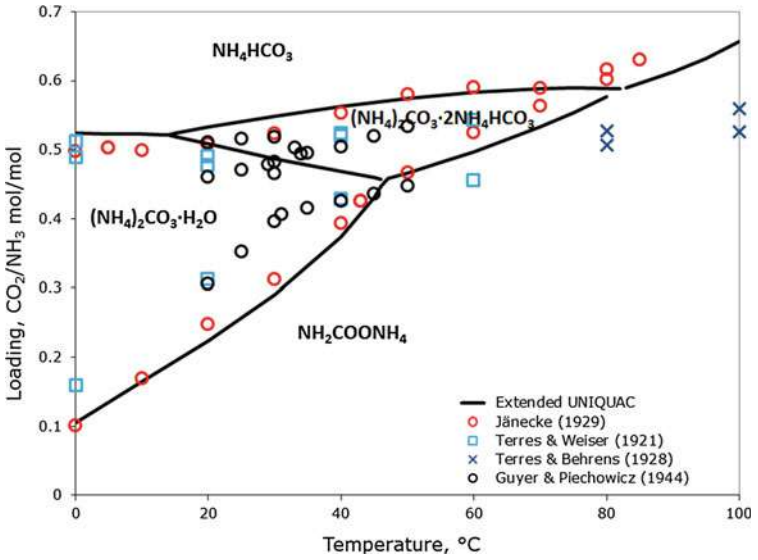

Fig. 20 The correlation between CO_2 loading and temperature

Effect of Reaction Parameters on Absorption Efficiency

During the process of CO_2 absorption into aqueous ammonia, a certain number of controlled conditions have significant impact on CO_2 absorption performance by aqueous ammonia. The concentration of aqueous ammonia, concentration of CO_2 in

the mixed gas, aqueous ammonia flow rate, flue gas flow rate, reaction temperature, controlled pressure, and reactors are discussed to the most extent.

Ammonia concentration

The relationship between aqueous ammonia concentration and CO_2 absorption efficiency is depicted in Fig. 21. It can be easily deserved that, with the increment of aqueous ammonia concentration, the CO_2 absorption efficiency gradually rises. However, for all cases published in the former literature, whenever the aqueous ammonia concentration reaches some specific value for the detailed experimental condition, the CO_2 absorption efficiency cannot be enhanced any further.

The maximum CO_2 removal efficiency can reach 99 %, and the absorption capacity is up to 1.20 kg CO_2/kg NH_3. Under the consistent experimental conditions, the maximum CO_2 removal efficiency is 94 %, and the absorption capacity is 0.40 kg CO_2/kg NH_3 (Bai 1997; Chen 2002).

CO_2 concentration

The effects of CO_2 concentration on its absorption efficiency are similar to that of ammonia concentration. It is easy to understand because increasing CO_2 concentration does good to enhance the mass transfer in gas-film side and promote CO_2 absorption efficiency only when the molar ratio of NH_3–CO_2 excesses its equivalent ratio (Ahn et al. 2011; Chen 2006). The published research results are given in Fig. 22.

Liquid and gas flow rates

The effects of aqueous ammonia (liquid) and flue gas flow rates on CO_2 absorption efficiency are illustrated in Figs. 23 and 24, respectively.

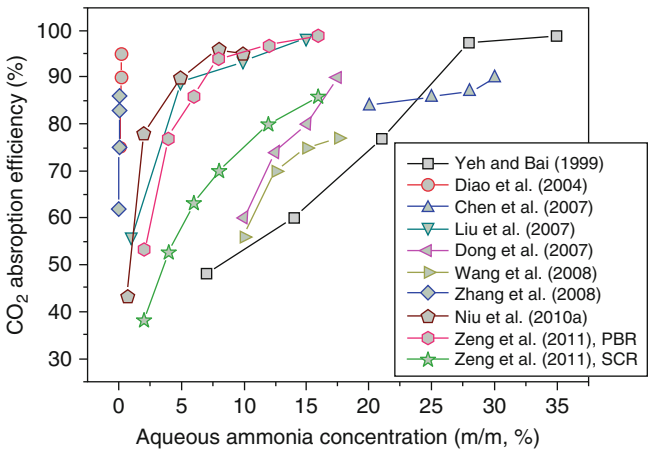

Fig. 21 Relationship between aqueous ammonia concentration and CO_2 absorption efficiency (1 bar, 35 °C, various gas–liquid ratios, various reactors)

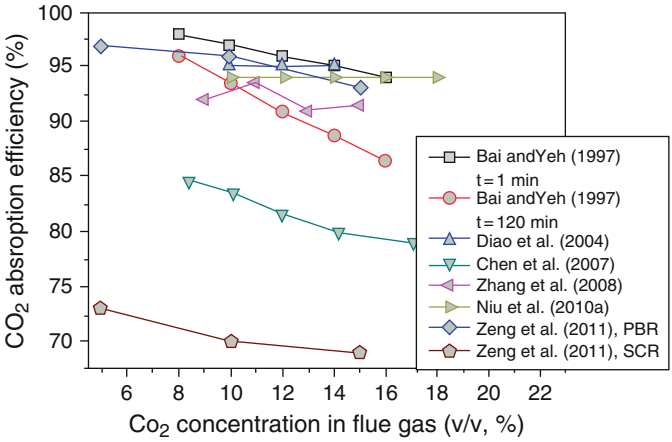

Fig. 22 Relationship between CO_2 concentration and CO_2 absorption efficiency (1 bar, 35 °C, various gas–liquid ratios, various concentrations of absorbent, various reactors)

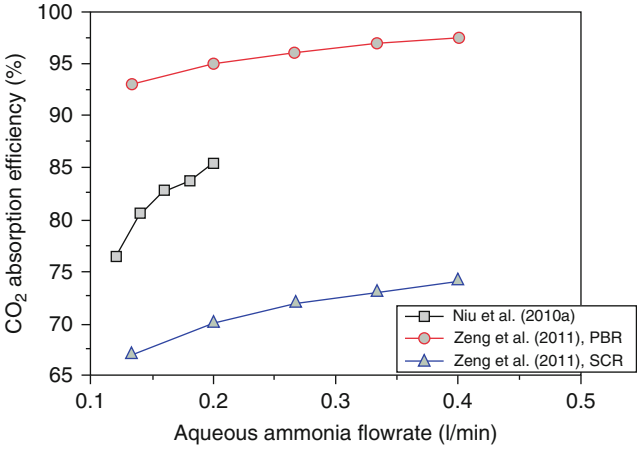

Fig. 23 Effect of aqueous ammonia (1 bar, 35 °C, various reactors)

It can be concluded from Figs. 23 and 24 that with the increment of aqueous ammonia flow rate, the CO_2 absorption efficiency can be improved, but only to a slight extent. However, the effect of flue gas flow rate is more influential than that of aqueous ammonia flow rate. With the increment of flue gas flow rate, the absorption efficiency is reduced sharply. On the whole, the absorption efficiency could be improved when the liquid–gas ratio is increased by either increasing the flow rate (volume) of aqueous ammonia or decreasing flue gas flow rate.

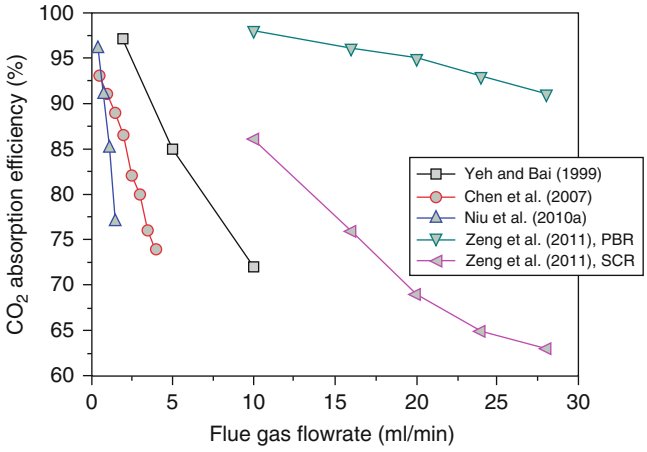

Fig. 24 Effect of flue gas (1 bar, 35 °C, various reactors)

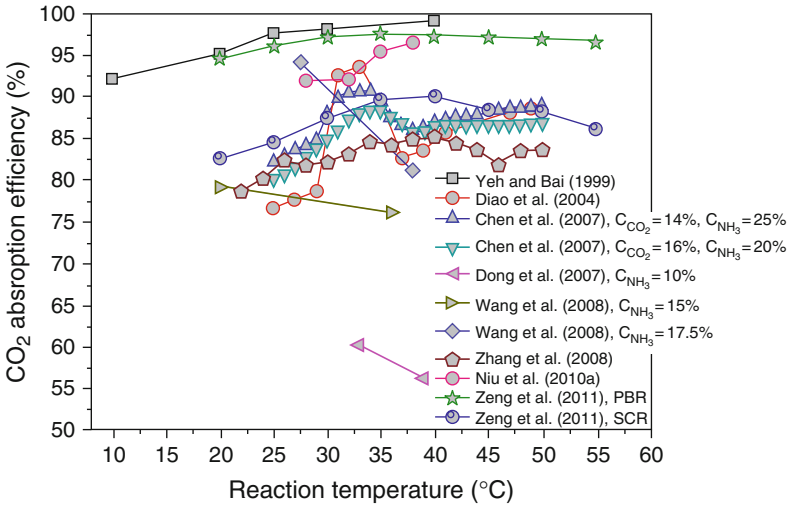

Fig. 25 Relationship between reaction temperature and CO_2 absorption efficiency

Reaction temperature

The effect of reaction temperature on CO_2 absorption efficiency is illustrated in Fig. 25.

Due to the reversibility of ammonia CO_2 reaction, the effect of temperature on the CO_2 absorption efficiency by ammonia is relatively complex with a non-monotonic relationship.

It is related to the reactor structure and other operating conditions. The previous work suggested that the CO_2 absorption reactions are dominant at room

temperature (Shale et al. 1971) while the CO_2 regeneration reactions occur in the temperature range of XX–60 °C (Pelkie et al. 1992). This relationship is also partially reflected by the experimental data. It is observed that most experimental data presented the optimal critical temperature. The absorption efficiency increased as the temperature increased when it was lower than the critical temperature, which indicated that the forward reaction was dominant. When the temperature exceeded the critical temperature, an opposite trend was presented. Note that very few experimental data showed that the absorption efficiency increased as temperature increased in high-temperature range. In addition, some experimental data indicated that absorption efficiencies monotonously decreased with increasing temperature.

Overall, the optimal reaction temperature could only be determined on the basis of a comprehensive consideration of absorption reactor, reaction conditions, and even regeneration energy consumption. According to the experimental results showed in Fig. 25, the optimal reaction temperature should be controlled in the range of 30–40 °C in order to obtain a relatively high absorption efficiency.

Improvement of Aqueous Ammonia

The most concerned inherent problems for aqueous ammonia are its high vitality and low absorption rate. The thermal regeneration method makes the slipperiness of aqueous ammonia become more severe and then leads to much heavier secondary pollution problems. Furthermore, it is essential to find a solution to enhance the reaction rate of aqueous ammonia.

Previous studies show that adding functional chemical additives into aqueous ammonia solution can considerably enhance the reaction rate and reduce the slipperiness of ammonia. Both organic additives, e.g., MEA, DEA, TEA, MDEA, AMP, PZ, AMP, AMPD, AEPD, and THAM, and inorganic additives, which refer to salt of strong acid and weak base such as $Na_3PO_4 \cdot 12H_2O$ and $Na_2B_4O_7 \cdot 10H_2O$ (Amitava 2011; Zhang et al. 2011; Fisher et al. 2005; Jassim and Rochelle 2006), have been studied.

Related experiment suggested that adding 1–3 % (w/w) AMP into ammonia could enhance the CO_2 absorption and control the slip of ammonia in the absorption process. However, it is found that the enhanced effects of 5 % AMP are not as significant as that of 3 % AMP. This demonstrates that when the additive AMP concentration is increased to a certain critical value, continuing addition of AMP is not much effective (Zhu et al. 2011; Teramoto et al. 2003). In essence, research showed that the major effect of organic additives was most of them could effectively reduce the surface tension of the aqueous ammonia and then promote the reaction between ammonia and CO_2 (Cheng et al. 2006; Matsumiya et al. 2005). Other organic additives to improve absorption performance are usually considered to have stronger affinity and faster reaction rate with CO_2 than ammonia (He et al. 2004; Mimura et al. 1998). For instance, when piperazine (PZ) reacts with CO_2 by the zwitterionic mechanism (Caplow 1968; Danckwerts 1979; Yan et al. 2008; Kang et al. 2002), its second-order reaction rate constant is much larger than that of ammonia by an order of magnitude (Puxty et al. 2010; Bougie et al. 2009; Shuster 2010; Kvamsdal and Rochelle 2008), suggesting that it can effectively improve the absorption reaction

process. Additionally, some additives can reduce the loss of ammonia by vaporization and slightly improve the CO_2 absorption efficiency. It was attributed to the interactions between ammonia and additives or absorbents and CO_2 via hydrogen bonding (You et al. 2008; Kvamsdal et al. 2010).

Unlike the mechanism of action of organic additives, inorganic additives indirectly promote the forward reaction through increasing the OH^- concentration or pH value in the solution by their hydrolysis and eventually promote the CO_2 absorption reaction.

However, the inorganic salt additive will reduce the solubility of CO_2 in the solvent, resulting in decreased absorption efficiency (Zhang et al. 2011); You et al. 2008; Eide-Haugmo et al. 2009; Chapel et al. 1999). Therefore, the enhanced effect of absorption efficiency depends on the additive load.

2. Ionic liquids (ILs)

Ionic liquid is regarded as a potential green alternative for the existing CO_2 absorbents, due to its unique characteristics, i.e., wide liquid range, thermal stability, negligible vapor pressure, tunable physicochemical character, and high CO_2 solubility. Blanchard et al. (1999; Schnell 2004) firstly reported that CO_2 is highly soluble in ionic liquid of 1-butyl-3-methylimidazolium hexafluorophosphate ($[C_4mim][PF_6]$). After that, considerable effort has been focused on seeking a sort of suitable ionic liquids as the alternatives for traditional absorbents. High viscosity and expensive material cost are major drawbacks for ionic liquid.

In general, ionic liquids are a category of compounds which are entirely composed of positive-charge ions and negative-charge ions. They tend to be liquid over a wide range of temperature, with a liquid range from −90 °C to 300 °C. It is estimated that the number of ionic liquids can even reach 10^{18}.

Some Key Physical Parameters

- Density
  Densities of ionic liquids are commonly between 0.80 and 2.10 g/cm^3. It has been demonstrated that densities of ionic liquids increase with an increase of the molecular weight of anion when the cation moiety is same. However, densities of ionic liquids decrease with an increase in the length of the alkyl chain in the cation when the anion is fixed.
- Viscosity
  Viscosities of ionic liquids range from 7 to about 1800 mPa s at ambient conditions. Obviously, this property brings trouble to the application of ionic liquids. In this context, a small number of investigations have ever been carried out. The studies lead to the following conclusions.
  1. For ILs with the same anion, the viscosity increases with increasing of the alkyl chain length (Seddon et al. 2002; Haslegrave et al. 1992). Moreover, the more asymmetrical cations have lower viscosity.

2. For ILs with the same cation, the chlorinated and fluorinated anions have higher viscosities than other anions, e.g., [I] > [Cl] > [PF_6] > [BF_4] ~[NO_3] > [Tf_2N]. In general, the effect of cation on viscosity is not that evident as changing the nature of anion (Endresand El Abedin 2006; McMahon and Harrop 1995).

- Heat capacity
  Deserved from a review by Paulechka (2010; Crognale 1999), specific heat capacities of 17 kinds of imidazolium-based ionic liquids are ranging from 1.29 to 1.93 J K^{-1} g^{-1} at the temperature of 298 K and under ambient pressure. Smaller specific heat capacities of ionic liquids relative to that of pure water provide the possibility to reduce the regeneration energy. During the past decade, the data of heat capacity for more than 100 aprotic ionic liquids were reported. However, these data are too less to satisfy the researchers' needs.
- Vapor pressure
  Vapor pressure is nearly negligible even when the environmental temperature is rather high. It might be mainly attributed to their chemical and thermal stability. The characteristic of ionic liquids leads to less consumption of the absorbent and much insignificant environmental hazard. However, ionic liquids can be designed to be volatile while required. Earle et al. (2006; Bacon and Demas 1987) reported that [$C_n$mim][Tf_2N] could be distilled without decomposition at the temperature of 300 °C and 0.1 mbar.
- Toxicity
  Imidazolium-based ionic liquids have been testified to possess a wide range of toxicities for some specified bioassays. Toxicity of ionic liquid correlates directly with the length of the *N*-alkyl substituent in the methyl imidazolium cation. It has been observed an increasing toxicity trend when the alkyl chain length substituent in imidazolium ionic liquids increases. On the other hand, minimal effects on toxicity are observed varying the anion of the methyl imidazolium salts. To avoid the potential contamination of the environment, it is important to minimize the opportunities of exposing ionic liquids to the aquatic media. The treatment and recycle apparatuses must be secured to install and operate normally.

Structure of Ionic Liquids

Figure 26 shows the structure of commonly used cations and anions. It can be easily deserved that the structure of ionic liquid is rather complex. Generally speaking, imidazolium-based ionic liquid is the most often employed category to capture CO_2 due to its high solubility.

Progress in the CO_2 Capture with Ionic Liquids

During the past decade, research into CO_2 capture by ionic liquid-based absorbents can be classified into the following directions, which can be further understood as four classes of ionic liquids with various structures.

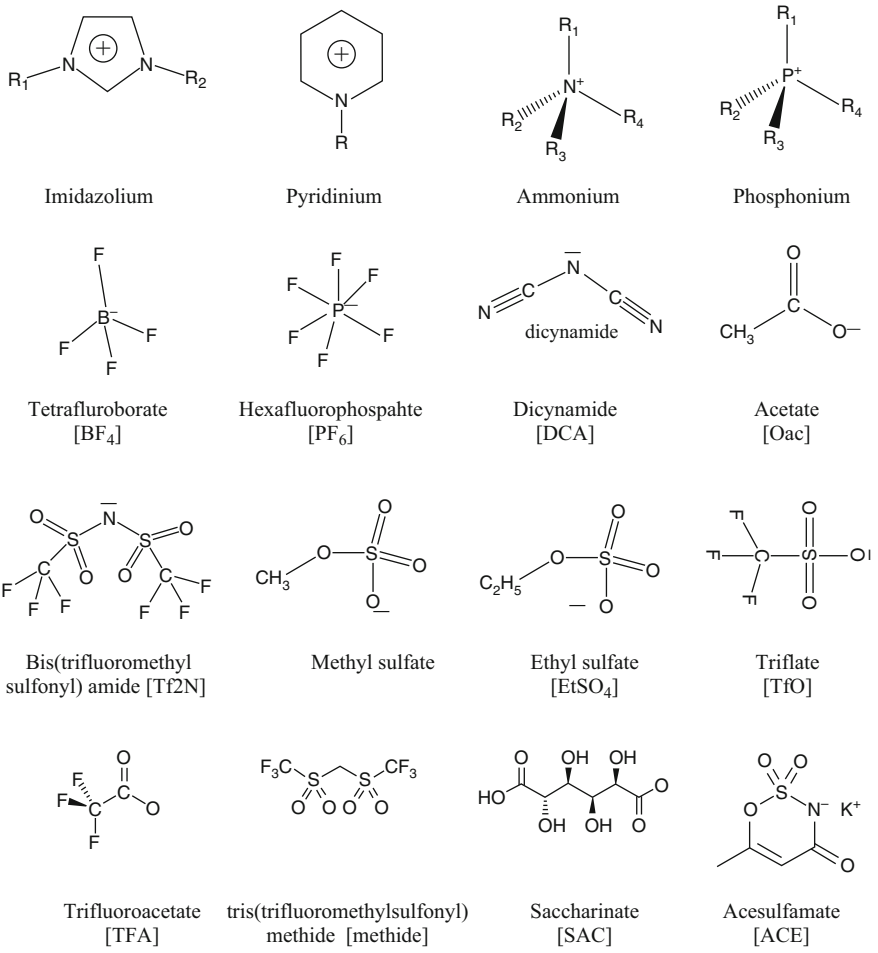

Fig. 26 Structure of commonly used cations and anions

- CO_2 capture with conventional ionic liquids

At the beginning of the study, most researchers focused on the CO_2 solubility of room-temperature ionic liquids due to their easy accessibility. However, with more understandings in this field, people noticed that the conventional ionic liquids absorb and separate CO_2 efficiently only by a mechanism of physical absorption. The absorption rate and capacity are therefore severely limited by this mechanism, e.g., the solubility of CO_2 in $[C_4mim][PF_6]$ is 2.65 mol kg^{-1} at 319 K and 5.73 MPa. In the previous studies, it is found that the anion dominates the interactions with the CO_2, with the cation playing a secondary role. Replacing the acidic hydrogen on the C_2 carbon of the [bmim] cation with a methyl group leads to a reduction in the

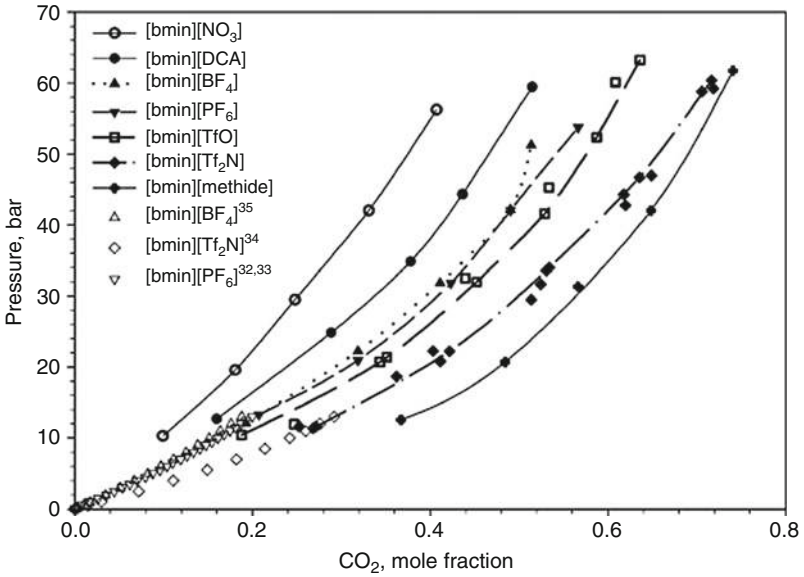

Fig. 27 Anion effect on the solubility of imidazolium-based ionic liquids at 25 °C

experimental enthalpy of absorption by about 1–3 kJ/mol. Figure 27 shows the correlation between pressure and CO_2 mole fraction. It can be seen that the solubility of CO_2 in [bmim] cation-based ILs at 25 °C increases in the following order: $[NO_3] < [DCA] < [BF_4] < [PF_6] < [TfO] < [Tf_2N] <$ [methide].

Some major findings in the field of conventional ionic liquids are summarized as follows (Table 8):

- CO_2 capture with functionalized ionic liquids

As discussed above, the dissolution of CO_2 in the conventional ionic liquid is through physical absorption mechanism, and the CO_2 absorption capacity can be further improved by functionalization of ionic liquid with a suitable moiety, such as the amino group and the other functional groups. Overall, two techniques are usually utilized by functionalizing the anion with alkaline group-NH_2 and attaching the functional group to the anion.

Bates et al. (2002; Thitakamol et al. 2007) firstly synthesized [NH_2p-bim][BF_4] consisting of an imidazolium ion to which a primary amine moiety is covalently bonded and gave the proposed reaction mechanism between FIL and CO_2, similar to the reaction between traditional organic amine and CO_2. The reaction mechanism between CO_2 and [NH_2p-bim][BF_4] is presented in Fig. 28. Experimental results show that the ultimate CO_2 absorption capacity of [NH_2p-bim][BF_4] can reach 0.5 mol CO_2 per mol IL and CO_2 can be regenerated by heating IL to 80 ~ 100 °C. There was no obvious loss of efficiency when the ionic liquid was recycled for five

cycles. After that, more attempts have been performed and superior results are obtained. A brief summary of the related work is presented in Table 9 (Fig. 29).

- CO_2 capture with supported ionic liquids membranes

It is well known that the ionic liquid has a relatively better performance in terms of thermal/chemical stability and essentially negligible volatility. Meanwhile, membrane can enhance the contact between gas and absorbents and further to cope with the limitations caused by ionic liquid. Above all, a certain number of researchers have carried out some work to explore the prospects of supported ionic liquid membranes involving CILs or FILs or both in CO_2 capture. Previous studies show that supported ionic liquids may prove a better choice in CO_2 separation from flue gases. Although several drawbacks, such as the thick membrane and inapplicability in separating CO_2 from the flue gases at high pressures, still hinder the application of supported IL membrane, it is already regarded as a potential technology for CO_2 capture. More researches will focus on the role of anion/cation in optimization of molar volume of constituent ILs and the structure of the support materials to develop more stable, more permeable, but thinner membranes (Table 10).

- CO_2 capture with polymerized ionic liquids

There is an inherent drawback for SILM. Once the pressure drop surpasses the liquid stabilizing forces within the matrix, the liquid may leach through membrane pores which may dramatically affect the mass transfer process. To avoid this phenomenon, Tang et al. (2005a; Mogul 1999) firstly proposed transforming ILs into polymeric form which could apparently increase the CO_2 sorption capacity compared with conventional ILs. Experimental results showed that both CO_2 sorption capacity and sorption rate of the polymers of tetraalkylammonium-based ILs are superior to those conventional ILs, e.g., CO_2 sorption capacity of poly (p-vinylbenzyl) trimethylammonium tetrafluoroborate (P[VBTMA][BF_4]) is 7.6 times that of [C_4mim][BF_4]. The selectivity of polymers is also testified to be rather satisfying. When the experimental conditions are set as 78.97 kPa and 22 °C, Tang et al. (2005b; Soosaiprakasam and Veawab 2008) found that it could selectively absorb CO_2 from N_2/CO_2 mixed gas without any absorption toward N_2 or O_2. Hu et al. (2006; Lenard et al. 1990) reported that the CO_2-selective membranes with thermal, chemical, and mechanical stability could be prepared by grafting polyethylene glycol (PEG) onto ionic polymers, such as P[VBTMA][BF_4]. Bara et al. (Mimura et al. 1998) found the solubility, permeability, and diffusion of CO_2 in both types of poly-CIL increased dramatically, and the sorption/desorption was completely reversible, which made these poly-ILs very promising as sorbent and membrane materials for CO_2 separation.

Tang et al. (Yan et al. 2008; Kang et al. 2002; Shuster 2010; Kvamsdal and Rochelle 2008; Kvamsdal et al. 2010) studied the CO_2 solubility in an ammonium-type ionic and other types of polymers and probed the structure effects on the CO_2 sorption. They showed the CO_2 sorption capacities of the PILs with different cations

Table 8 A brief summary of conventional ionic liquids studies

Ionic liquid	Findings	Conclusions	References
[Bmim][PF_6]	CO_2 solubility (8 MPa)	A large quantity of CO_2 was found to dissolve in the ionic liquid phase, while no visible amount of IL solubilized in the CO_2 phase	Blanchard et al. (1999)
[C_4mim][PF_6] **[C_8mim][PF_6]** **[C_8mim][BF_4]** **[C_4mim][NO_3]** **[C_2mim][$EtSO_4$]** **[N-bupy][BF_4]**	Solubility (high pressure)		Blanchard et al. (2010)
[C_3mim][Tf_2N],[C_4mim][Tf_2N] **[C_6mim][Tf_2N],[C_8mim][Tf_2N]** **[C_8F_{13}mim][Tf_2N],[C_3mim][PF_6]** **1,4-dibutyl-3-phenylimidazolium bis [trifluoromethylsulfonyl]amide** **1-butyl-3-phenylimidazolium bis [trifluoromethylsulfonyl]amide**	Henry's constants, (25 °C, CO_2 pressure ~1 bar)	CO_2 solubility was found to be lower in the ionic liquid containing PF_6^- than for the corresponding liquid with Tf_2N^- anion	Baltus et al. (2004)
[C_4mim][PF_6] **TMGL**	Solubility (297–328 K, 0–11 MPa)	Solubilities of CO_2 in TMGL are slightly higher than those in [C_4mim][PF_6]	Zhang et al. (2005)
[hmim][Tf_2N]	Selectivity toward gases CO_2, C_2H_4, C_2H_6, CH_4, O_2 and N_2	The CO_2 solubility increases as the numbers of fluorine in the alkyl side chain, but this tendency is not very visible	Anderson et al. (2007)
[hmim][Tf_2N], [hmmim][Tf_2N] **[bmim][TFA], [bmim][$C_7F_{15}CO_2$]** **[b_2-Nic] [Tf_2N], [hmpy] [Tf_2N]** **[hmim][eFAP], [hmim][pFAP]** **[$p_5$mim][bFAP], [N_{4444}][doc]** **[$C_6H_4F_9$mim][Tf_2N]** **[$C_8H_4F_{13}$mim][Tf_2N]** **Ecoeng 500, Ecoeng 41 M** **[hmim][SAC], [hmim][ACE]**	Solubility (10 °C, 25 °C, 60 °C, P <13 bar, 13 < P <150 bar)	Ionic liquids containing increased fluoroalkyl chains on either the cation or anion do improve CO_2 solubility	Muldoon et al. (2007)

(*continued*)

Table 8 (continued)

Ionic liquid	Findings	Conclusions	References
$[Et_3NBH_2mim][Tf_2N]$ **[choline][Tf_2N], $[N_{4111}][Tf_2N]$** **[hmim][PF_6], [bmim][Tf_2N]** **[bmim][methide]**			
[emim][Tf_2N], [emmim][Tf_2N] **[bmim][PF_6], [bmmim][PF_6]** **[bmim][BF_4], [bmmim][BF_4]**	Solubility, density, dissolved enthalpies, and entropies	The anion dominates the interactions with the CO_2	Cadena et al. (2004)
[bmim][BF_4] **[bmim][TfO]** **[bmim][methide]** **[bmim][DCA]** **[bmim][PF_6]** **[bmim][NO_3]** **[bmim][Tf_2N]** **[hmim][Tf_2N]** **[omim][Tf_2N]** **[hmmim][Tf_2N]**	Solubility (25 °C, 40 °C, 60 °C)	At 25 °C, the solubility of CO_2 in [bmim] cation-based ILs increases in the following order: $[NO_3] < [DCA] < [BF_4]$ $[PF_6] < [TfO] < [Tf_2N] < [methide]$	Aki et al. (2004)

[Bmim][PF_6]: 1-butyl-3-methylimidazolium hexafluorophosphate
[C_4mim][PF_6]: 1-*N*-butyl-3-methylimidazolium hexafluorophosphate
[C_8mim][PF_6]: 1-*N*-octyl-3-methylimidazolium hexafluorophosphate
[C_4mim][NO_3]: 1-*N*-butyl-3-methylimidazolium nitrate
[C_2mim][$EtSO_4$]: 1-ethyl-3-methylimidazolium ethylsulfate
[N-bupy][BF_4]: *N*-butylpyridinium tetrafluoroborate
[C_3mim][Tf_2N]: 1-methyl-3-propylimidazolium bis[trifluoromethylsulfonyl]amide
[C_4mim][Tf_2N]: 1-*N*-butyl-3-methylimidazolium bis[trifluoromethylsulfonyl]amide
[C_6mim][Tf_2N]: 1-*N*-hexyl-3-methylimidazolium bis[trifluoromethylsulfonyl]amide
[C_8mim][Tf_2N]: 1-methyl-3-*N*-octylimidazolium bis[trifluoromethylsulfonyl]amide
[C_8F_{13}mim][Tf_2N]: 1-methyl-3-(3,3,4,4,5,5,6,6,7,7,8,8,8-tridecafluorooctyl)-imidazolium bis[trifluoromethylsulfonyl]amide
TMGL: 1,1,3,3-tetramethylguanidium lactate
[hmim][Tf_2N]:1-hexyl-3-methylimidazolium bis(trifluoromethylsulfonyl)imide

[hmmim][Tf_2N]: 1-hexyl-2,3-dimethylimidazolium bis(trifluoromethylsulfonyl)imide
[bmim][TFA]: 1-butyl-3-methylimidazolium trifluoroacetate
[bmim][$C_7F_{15}CO_2$]: 1-butyl-3-methylimidazolium pentadecafluorooctanoate
[b_2-Nic] [Tf_2N]: 1-butyl-nicotinic acid butyl ester bis(trifluoromethylsulfonyl)imide
[hmpy] [Tf_2N]: 1-hexyl-3-methylpyridinium bis(trifluoromethylsulfonyl)imide
[hmim][eFAP]: 1-hexyl-3-methylimidazolium tris(pentafluoroethyl)trifluorophosphate
[hmim][pFAP]: 1-hexyl-3-methylimidazolium tris(heptafluoropropyl)trifluorophosphate
[$p_5$mim][bFAP]: 1-pentyl-3-methylimidazolium tris(nonafluorobutyl)trifluorophosphate
[N_{4444}][doc]: tetrabutylammonium docusate
[$C_6H_4F_9$mim][Tf_2N]: 1-methyl-(3,3,4,4,5,5,6,6,6-nonafluorohexyl)imidazolium bis(trifluoromethylsulfonyl)imide
[$C_8H_4F_{13}$mim][Tf_2N]: 1-methyl-(3,3,4,4,5,5,6,6,7,7,8,8,8-tridecafluorooctyl)imidazolium bis(trifluoromethylsulfonyl)imide
Ecoeng 500: PEG-5 cocomonium methylsulfate
Ecoeng 41 M: 1-butyl-3-methylimidazolium 2-(2-methoxyethoxy) ethylsulfate
[hmim][SAC]: 1-hexyl-3-methylimidazolium saccharinate
[hmim][ACE]: 1-hexyl-3-methylimidazolium acesulfamate
[Et_3NBH_2mim][Tf_2N]: (1-methylimidazole)(triethylamine) boronium bis(trifluoromethylsulfonyl)imide
[choline][Tf_2N]: choline bis(trifluoromethylsulfonyl)imide
[N_{4111}][Tf_2N]: N,N,N,N-trimethylbutylammonium bis(trifluoromethylsulfonyl)imide
[hmim][PF_6]: 1-hexyl-3-methylimidazolium hexafluorophosphate
[bmim][Tf_2N]: 1-butyl-3-methylimidazolium bis(trifluoromethylsulfonyl)imide
[bmim][methide]: 1-butyl-3-methylimidazolium tris(trifluoromethylsulfonyl) methide
[bmim][TfO]: 1-butyl-3-methylimidazolium triflate
[bmim][DCA]: 1-butyl-3-methylimidazolium dicyanamide
[omim][Tf_2N]: 1-octyl-3-methylimidazolium bis(trifluoromethylsulfonyl)imide

decreased in the order: ammonium > pyridinium > phosphonium > imidazolium, and those of the PILs with different anions were in the sequence of BF_4^- > PF_6^- > Tf_2N^-. P[VBTMA][BF_4] with a polystyrene backbone had a higher CO_2 absorption capacity than P[MATMA][BF_4] with a polymethylmethacrylate backbone.

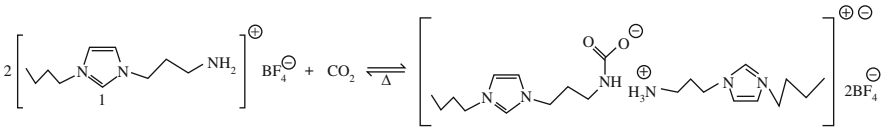

Fig. 28 Reaction mechanism between CO_2 and [NH_2p-bim][BF_4]

Table 9 A brief summary of functional ionic liquids studies

Ionic liquid	Performance	References
Functionalization of the anion of IL with alkalinegroup-NH_2		
[$P(C_4)_4$][AA]	Absorption capacity is 0.5 mol CO_2/mol IL	Zhang et al. (2006a, b) (Source: IPCC special report on carbon dioxide capture and storage 2005; Hu 2009)
[APMIM][BF_4]	The calculated kinetic constants (k1,1) of the reaction of CO_2 and [APmim]BF_4 vary between 32.4 and 87.6 L mol s^{-1}	Sanchez et al. (2011) (Agar et al. 2008)
[Choline][Pro] [Choline][Pro]/(PEG200)	The absorption process is exothermic, absorption capacity is 0.5 mol CO_2/mol IL	Li et al. (2008a, b) (Mandal and Bandyopadhyay 2005; Mandal and Bandyopadhyay 2006b)
[aP_{4443}][AA], [aP_{4443}][Gly] [aP_{4443}][leu], [aP_{4443}][Ala], [aP_{4443}][Val], [hmim]) [FEP]	Absorption capacity is 1 mol CO_2/mol IL within 80 min	Zhang et al. (2009a, b) (Mandal et al. 2001; Mandal et al. 2004)
[aemmim][Tau]	The CO_2 absorption capability of this IL was 0.9 mol CO_2/mol IL at 303.15 K and 0.1 MPa	Xue et al. (2011) (Rochelle et al. 2006)
Attach the anion of IL with functional group		
[P_{66614}][Pro], [P_{66614}][Met] [P_{66614}] [Gly], [P_{66614}][Ala], [P_{66614}][Sar], [P_{66614}][Val], [P_{66614}][Leu], [P_{66614}][Ile]		Gurkan et al. (2010) (Lin et al. 1990)
[P_{66614}][Pro]	The heat of absorption is −63 kJ•mol^{-1} CO_2 for the 1:1 reaction of CO_2 with [P_{66614}][Pro]	Goodrich et al. (2011) (Oyenekan and Rochelle 2007)

(*continued*)

Table 9 (continued)

Ionic liquid	Performance	References
$[C_1C_4Im][LEV]$ $[C_1C_4Pyrro][OAc]$	Mole fraction absorption of carbon dioxide in $[C_1C_4Im]$ [LEV] and $[C_1C_4Pyrro]$ [OAc] was equal to 0.93×10^{-2} and 1.10×10^{-2} at 303.15 K and 89.2 kPa and 353.15 K and 67.1 kPa, respectively	Stevanovic et al. (2013) (Oyenekan and Rochelle 2006)

$[P(C_4)_4][AA]$: tetrabutyl phosphonium amino acid
$[APMIM][BF_4]$: 1-(3-aminopropyl)-3-methylimidazolium tetrafluoroborate
[Choline][Pro]: (2-hydroxyethyl)-trimethyl-ammonium (S)-2-pyrrolidine-carboxylic acid salt
PEG200: polyethylene glycol 200
[aP4443][AA]: (3-aminopropyl)tributylphosphonium amino acid salts
[hmim]) [FEP]: 1-*N*-hexyl-3-methylimidazolium tris(pentafluoroethyl)trifluorophosphate
[aemmim][Tau]: 1,2-dimethylimidazolium taurine

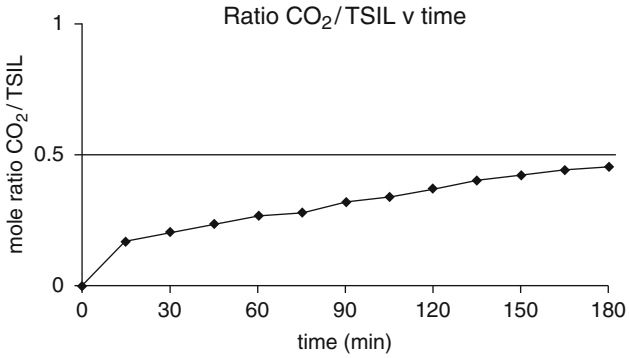

Fig. 29 Absorption performance of $[NH_2p\text{-}bim][BF_4]$

Long alkyl substituents on the cation and cross-linking decreased the CO_2 sorption capacity.

Bara et al. (Mimura et al. 1998; Eide-Haugmo et al. 2009) tethered oligo(ethylene glycol) or nitrile-terminated alkyl substituents to CIL monomers, and these polymer membranes were found to exhibit 50 % greater CO_2/N_2 and CO_2/CH_4 separation factors than those with comparable length *N*-alkyl substituents but with similar CO_2 permeability. The OEG-functionalized poly-CIL exhibited several times higher permeability than those with CnCN functional groups. They mixed CIL and poly-CIL as a composite gas separation membrane to absorb CO_2 and showed that by incorporating an appropriate amount of CIL and introducing free ion pairs into the polymer membrane, the CO_2 permeability and CO_2/N_2 selectivity increased up to 300–600 % and with 25–33 %, respectively, relative to the analogous poly-CIL membrane lacking any free ion pairs.

- CO_2 capture with mixture solvent of ionic liquids and molecular solvents

The viscosities of ionic liquids or their mixtures are usually much thicker than common amines, especially the viscosities of FILs. Furthermore, the reaction rate of ionic liquid is relatively lower than that of the most concerned commercial amine-based absorbents. In this context, some researcher proposed forming novel absorbents through mixing ionic liquids with molecular solvents. Generally speaking,

Table 10 A brief summary of supported ionic liquids membranes studies

Ionic liquid + membrane	Performance	References
Supported ionic liquids membranes based with conventional IL		
[emim][Tf_2N] [emim][CF_3SO_3] [emim][dca] [thtdp][Cl] PES	The performance of the tested RTIL-membranes is competitive or superior to existing membrane materials with their ideal-selectivity versus permeability ratios being above the Robeson upper bound for polymers	Scovazzo et al. (2004) (Polderman et al. 1955)
[C_4min][Tf_2N] Al_2O_3	An ionic liquid-based separation in a membrane separator with a 12-μm ionic liquid film with the same thermodynamic and transport characteristics as [C_4min][Tf_2N] is $27/metric ton of CO_2 removed, a cost 18 % lower than Simbeck's estimate for amine scrubbing	Baltus et al. (2005) (Yazvikova et al. 1975)
[C_4mim][PF_6] TiO_2/SiC	The CO_2 removal efficiency is over 80 % at 0.1 MPa, 40 °C	Moriya et al. (2007) (Davis and Rochelle 2009)
[C_4min][BF_4] PVDF	The selectivity of CO_2/CH_4 and H_2S/CH_4 was found to be 25–45 and 130–260	Park et al. (Rooney et al. 1998)
[C_4MIM][PF_6], [C_8MIM][PF_6] [C_4MIM][BF_4], [C_{10}MIM][BF_4] Vericel (Pall Corporation) Millipore (Millipore Corporation)	The selectivity of CO_2/CH_4 decreased with the increasing temperature	Neves et al. (Suzuki 2007)
[C_2mim][Tf_2N] polymeric hollow fiber	The structure of the support has a large impact on membrane stability, and the spongelike structure has higher stability than a fingerlike one	Kim et al. (Korendovych et al. 2007)
224 ILs	The ILs that may improve the CO_2/N_2 selectivities in SILMs, such as [SCN−]-based ILs, are those with generally low gas solubilities but capable of increasing the CO_2 solubility	Gonzalez-Miquel et al. (Buxton 1988)
Supported ionic liquids membranes based with FIL		
[C_3NH_2mim][Tf_2N] [C_3NH_2mim][CF_3SO_3] [C_4mim][Tf_2N] PTFE	The ionic liquid worked not only as the liquid membrane phase but also as a CO_2 carrier. The prepared SLM showed high selectivity and high stability for CO_2 separation from the gas mixture	Gurkan et al. (Bedell and Myers 1994)

(*continued*)

Table 10 (continued)

Ionic liquid + membrane	Performance	References
[hmim][Tf_2N]	The CO_2 permeability of the membranes increases from 744 to 1200 barrer as the temperature increases from 37 °C to 125 °C. The CO_2/He selectivity decreased from 8.7 to 3.1 over the same temperature range	Ilconich et.al. (Lalevee et al. 2002)

[emim][Tf_2N]: ethylmethylimidazolium bis(trifluoromethanesulfonyl)amide
[emim][CF_3SO_3]: ethylmethylimidazolium trifluoromethanesulfone
[emim][dca]: ethylmethylimidazolium dicyanamide
[thtdp][Cl]: trihexyltetradecylphosphonium chloride
PES: porous hydrophilic polyethersulfone
PVDF: polyvinylidene fluoride
[C_3NH_2mim][Tf_2N]: *N*-aminopropyl-3-methylimidazolium bis(trifluoromethylsulfonyl)imide
[C_3NH_2mim][CF_3SO_3]: *N*-aminopropyl-3-methylimidazolium trifluoromethanesulfone
[C_4mim][Tf_2N]: 1-butyl-3-methylimidazolium bis(trifluoromethylsulfonyl)imide
PTFE: porous hydrophilic polytetrafluoroethylene membrane

researchers have mixed water/methanol, alkanolamines, superbase, or other organic solvents into various ionic liquids to create an absorbent of better overall performance.

ILs Plus Amines

The primary purpose of this idea is to merge the eco-friendly features of ILs with the high reaction rate of amines. Another highlight for this idea is the economic performance in terms of both capital cost and operational cost. When amines of appropriate portions are introduced into ionic liquids, both the lower material price and lower pump energy consumption caused by relatively less viscosity of absorbents are favorable.

Camper et al. (2008) have demonstrated that RTILs and alkanolamines can be mixed in a proficient and effective manner for CO_2 gas capture, which exceeds those amine functionalized TSILs.

Zhang et al. (2010b, c) blended tetramethylammonium glycinate ([N_{1111}][Gly]), tetraethylammonium glycinate ([N_{2222}][Gly]), tetramethylammonium lysinate ([N_{1111}][Lys]), and tetraethylammonium lysinate ([N_{2222}][Lys]) with MDEA to form absorbents for CO_2 separation. Experiments show that addition of amino acid IL into MDEA could evidently improve the CO_2 absorption performance of MDEA. Moreover, the regeneration performances of IL + MDEA aqueous blends varied with the cations: ([N_{1111}] [Gly]) > ([N_{1111}][Lys]) > ([N_{2222}] [Gly]) > ([N_{2222}] [Lys]). The ultimate CO_2 regeneration efficiency of aqueous blend of 15 % ([N_{1111}] [Gly]) + 15 % MDEA even reached 98 %.

Based on the experimental research into the proposed absorbents such as amines-IL-H_2O, IL-H_2O, and amines-H_2O at temperature ranging from 303.15 to 343.15 K with different IL mass fractions, Zhao et al. (2010) concluded that the absorbent of amines-IL-H_2O shows the best performance on CO_2 capture. In the successive study, Zhao et al. (2011a) investigated the solubilities of CO, H_2, N_2, O_2, and CO_2 in IL,

[MDEA][Cl] when the pressure varies from 1.22 to 8.62 MPa and the temperature changes from 313.15 to 333.15 K. Experiments showed that the solubility of CO_2 was further superior to the other gases. Zhao et al. (2011b) also found that the absorption capacity of MCHP (MDEA-[MDEA][Cl]-H_2O-PZ) at 303.15 K and 1.50 MPa was approximately 0.1584 g of CO_2 per gram of MCHP. When the ionic liquid was replaced by [MDEA][PF_6], the absorption capacity of MCHP was 0.15 g of CO_2 per gram solvent of MCHP (MDEA-[MDEA][PF_6]-H_2O-PZ).

Ahmady et al. (2011) obtained the data for CO_2 loading in mixture of 4.0 mol/L aqueous MDEA and three types of imidazolium-based ionic liquids, [bmim][BF_4], [bmim][Ac], and [bmim][DCA], at temperature ranging from 303 to 333 K and CO_2 partial pressure ranging from 100 to 700 kPa. It is concluded that the CO_2 loading in mixtures increased with the rising of CO_2 partial pressure while decreased with an increase of temperature or ILs concentration increases.

Lu et al. (2012) investigated a mixed absorbent composed of MEA and [Bmim]BF_4 with the optimum mole ratio of MEA to [Bmim]BF_4 7:3. Experimental results showed that the absorption capacity of the mixed absorbent was significantly higher than pure MEA aqueous, approaching 0.6XX mol of CO_2 per mol of MEA.

In order to discover the influence of temperature, solution composition, and pressure on CO_2 absorption in aqueous solutions of MDEA and [N_{1111}][Gly], Gao et al. (2013) carried out the equilibrium absorption under a wide range of pressure (0–300 kPa) at three temperatures in a dual-vessel absorption equilibrium system. It was derived that with the increase of ILs or MDEA concentration, the solution density grows slightly, while the viscosity rises dramatically.

Baj et al. (2013) investigated the impact of blends of MEA and eight kinds of ILs. The presence of water was having a determinant effect on the volume of CO_2 that can be absorbed. The addition of water to [BMIM][OAc] decreased the amount of absorbed CO_2. Thus, CO_2 absorption capacity was not linearly dependent on the mass fraction of the water/ILs/MEA system. However, the absorption rate was increased with an addition of water; it was due to the lowering of viscosity.

ILs plus superbase or other organic solvents

Recently, a new class of solvent called binding organic liquids (BOLs) or switchable solvents has been discovered which can be formed and used in the presence of water. If water is in significant quantities, undesirable bicarbonate salts may be formed; however, these salts can be broken down more efficiently than in MEA systems due to the anticipated lower specific heat of CO_2 BOLs than water.

Jessop et al. (2005a) designed DBU, which is the first CO_2 BOL. Absorption capacities of CO_2 BOL are 2–3 times higher than those of aqueous alkanolamines. And then Wang et al. combined bicyclic amidine (DBU) with hydroxyl modified IL as a superbase to trap the proton produced during sorption process of CO_2, which proved to be an effective way in achieving an equimolar of sorption.

Zhang et al. (Oyenekan and Rochelle 2006) mixed IL 1-butyl-3-methylimidazolium chloride ([C4mim][Cl]) with chitin or chitosan as a mixed solvent to capture CO_2. Chitin has two hydroxyl groups in the cellulose-like polymeric structure, whereas chitosan has an additional amine group. For the chitosan/IL mixture, the measured absorption capacity exceeds the theoretical capacity due to the physical

absorption of CO_2 in these liquids. Physical absorption is also observed for the chitin/IL mixture. Although this approach cannot provide as high absorption capacities as pure FIL, it really has the advantage of bringing a fully recyclable, less corrosive, and nonvolatile CO_2 absorbent.

In summary, the viscosity of this kind of solvent is lower than that of pure ILs and easier to regenerate than the traditional alkanolamines. So it maybe another potential option to CO_2 capture in the future.

Future research should be focused on the following issues:

1. Understanding the mechanism of the CO_2 capture with ILs combing molecular simulation and experimental characteristics and revealing the relationships between structures of IL and the performance of CO_2 capture;
2. Developing the new ILs with low cost, low viscosity, and high absorption capacity with high selectivity, which will reduce the absorption rate and decrease the energy demand for desorption. The CO_2 desorption process is also crucial with respect to the energy consumption required by industries;
3. Studying the transport phenomena which will be very important for the suitable design and operation of industrial unit, especially at low pressure and high temperature (like flue gas from coal-fired power plants) used for CO_2 capture with ionic liquids.

Though there are lots of problems in using ILs to capture CO_2, we believe all the problems will be resolved one by one with in-depth investigation, and then it is possible to use ILs to capture CO_2 on large scales in the future.

3. Mixed amines

A single absorbent to satisfy all the requirements for a CO_2 separation process seems hard to find. Some researchers try to combine the advantages of several amines (Polderman et al. 1955). The new types of mixed amines are expected to have high CO_2 absorption capacity, high CO_2 loading, and low regeneration energy consumption. Generally speaking, monoethanolamine and diethanolamine have the advantage of high absorption rate, while triethanolamine has the advantage of low energy consumption. Based on the analysis above, mixed amines have become a new research direction nowadays. Although sterically hindered amines seem to be rather expensive, they have also become a research object because of high absorption capacity and absorption rate. For example, the mixed absorbents developed by MHI which are called KS-1/KS-2 and KS-3 employ sterically hindered amines as a component of the absorbent. The KS serial absorbent has already been verified to be better than the standard, single MEA solution. The energy consumption is reported to be reduced by 40 % compared to that of a MEA process. Zhejiang University developed MEA/MDEA and MDEA/PZ mixed amine absorbents, and the test result shows that they can decrease regeneration energy consumption by over 5–10 %.

Piperazine (PZ) is a cyclic diamine which has been studied as an advanced solvent for CO_2 capture. Because of its rapid formation of carbamate with CO_2, piperazine is used to be a promoter in blends for CO_2 capture with small concentrations. It is established that 8 m PZ (40 wt% PZ) has superior performance than conventional solvent 30 wt% MEA for CO_2 capture. Under process conditions, 8 m PZ has twice absorption rate and higher cyclic CO_2 capacity than 30 wt% MEA (Rochelle et al. 2011). Freeman has demonstrated that PZ is more stable at high temperature up to 150 °C and less prone to oxidation than MEA (Freeman and Rochelle 2011). The expected energy required for PZ system is 220 kwh/t CO_2 with optimized process design, 10–20 % less than MEA (Freeman et al. 2010). However, PZ has limited solubility window where solid precipitation occurs at both low and high CO_2 loading. It is a proper way to solve the problem by using PZ in blends with other highly performing amines. In this context, PZ blends with MEA, hexamethylenediamine (HMDA), diaminobutane (DAB), bis(aminoethyl)ether (BAE), aminoethylpiperazine (AEP), and 2-amino 2-methyl-propanol (AMP) have been investigated (IPCC 2005). Most of them have better solubility window than 8 m PZ, and the absorption rate in concentrated PZ blends is 1.5–2 times higher than 30 wt% MEA. However, the effect for degradation rate is different in various PZ blends. Combination of AMP and PZ catalyzes the degradation of each other, but for MDEA and PZ blends, the degradation rates are slower than their individual ones.

4. Phase transitional solvent

Phase transitional absorbent has attracted more and more attentions due to its great potential in reducing energy penalty for CO_2 capture. Rather than considering liquid–liquid phase separation and precipitation as drawbacks, some researchers regard it as a good property to reduce cost for CO_2 capture (Zhang et al. 2011).

French Institute of Petroleum (IFP) has developed DMXTM solvents in which the CO_2 captured concentrates in one of the two phases, and only a portion of the total flow rate has to be sent to the stripper. The DMXTM process proposed by Raynal can remarkably reduce the heat duty of reboiler to 2.3 GJ/t CO_2 (Raynal et al. 2011). Tan investigated kinetics and thermodynamic of the lipophilic amine blend of DPA and DMCA and found the cyclic loading of this solvent can reach up to 0.7 mol CO_2/mol amine (Tan 2010). Zhang did research on thermomorphic phase transitional solvents (TBS) and found a new ternary blended solvent DMCA + MCA + AMP which has successfully met the desired phase change temperatures, remained a high net CO_2 loading (>3.5 mol/kg), and exhibited a remarkable chemical stability against degradation. Moreover, the energy consumption of TBS process in which agitation, nucleation, and phase split are employed is only less than 2.0 GJ/t CO_2 (Zhang et al. 2013). Hu investigated a phase transitional absorption which was composed of 80 % solvent B and 20 % activated agent A. After absorption, the two liquid phases were separated and only 20 % of the absorbent was forwarded to regeneration (Hu 2009). Xu found 2 M 1,4-butanediamine (BDA) blended with 4 M 2-(diethylamino)-ethanol (DEEA) has 48 % higher cyclic capacity and 46 % higher

cyclic loading than 5 M MEA. Moreover, the separation mechanism of the phase transitional solvent was found due to the limited solubility of DEEA in the reaction products of BDA with CO_2 and the fast reaction rate of BDA with CO_2 (Zhang et al. 2013). Brennecke proposed phase change ionic liquids to remove CO_2 from flue gas (Dame UON). They discovered solid ionic materials with high CO_2 uptake would form a liquid upon reacting with CO_2. In the regeneration step, the heat of fusion of the salt would supply part of the heat needed to desorb the CO_2 from the absorbent, and the heat of regeneration would be significantly reduced.

Phase transitional absorbent is a novel concept for CO_2 capture which has great potential in reducing energy penalty. However, the new technology still meet challenges such as viscosity of rich solvent, pressure drop, and liquid holdup which means the design and modification of convention absorption column are required, and further investigations should be done for industrialized application.

Absorber

Packed Tower

A packed tower is a common choice in the traditional chemical absorption process to remove CO_2. The technology of the packed tower is mature, and it has already developed a huge market although there are still some problems. Low speed in mixing and mass transfer would lead to the big size of equipment and huge investment. The direct contact of gas and liquid would lead to such problems as entraining, channeling, bubbling, and overflowing. Hence, strengthening the mass transfer in reaction equipment and solving the operation problems in the contact of gas and liquid are the key points to reduce the tower size as well as the investment.

1. Packing

Packing is used to increase the gas–liquid contact time and surface area during CO_2 absorption and desorption process. Mainly, there are two kinds of packing, random packing and structured packing. In recent years, the performance of various packings are widely reported, and properties of structured and random packing like surface area and void fraction are compared in the review paper by Tan et al. (2012), as listed in Table 11. Structured packings are favored for they can provide a much higher overall mass transfer coefficient and lower pressure drops than random packings. Recent studies show that the development of new packing and the improvement of inner attachment structure inside of the packed columns would strengthen mass transfer so as to reduce the size of equipment. The new packing can lower the system resistance and strengthen the mass transfer capacity. As a result, the performance of the equipment will be improved. Figure 30 shows the typical structure of a packed tower and some new packing.

Table 11 Properties of structured and random packing (Tan et al. 2012)

Type of packing	Name of packing	Surface area (m^2/m^3)	Void fraction (%)
Structured	Flexipac 1Y	453	91
	Flexipac 2Y	223	95
	Flexipac 3Y	115	96
	Gempak 1A	115	95
	Gempak 2A	223	96
	Gempak 4A	446	92
	Mellapak 500Y	500	91
	Mellapak 500X	500	91
	Mellapak 350Y	351	95
	Mellapak 250Y	250	95
	Mellapak 250X	250	95
	Sulzer-BX	492	90
	Sulzer-DX	900	78
	Sulzer-EX	1710	86
	Optiflow	210	98
	Montz-Pak B1-200	200	98
	Montz-Pak B1-250	245	98
	Montz-Pak B2-300	300	93
Random	1 in. Pall Rings	205	94
	1.5 in. Pall Rings	130	95
	2 in. Pall Rings	115	96
	Raschig Super-Rings 0.5	236	96
	Raschig Super-Rings 0.7	176	97
	Raschig Super-Rings 1	156	98
	IMTP #25	230	97
	IMTP #40	154	97
	IMTP #50	98	98
	1 in. Intalox Saddles	256	72
	1.5 in. Intalox Saddles	194	73
	2 in. Intalox Saddles	118	75
	1 in. Raschig Rings	190	68
	1.5 in. Raschig Rings	121	72
	2 in. Raschig Rings	95	83
	1 in. Berl Saddles	250	68
	1.5 in. Berl Saddles	150	71
	2 in. Berl Saddles	105	72

2. Liquid distributors

Generally, fluid distribution in packed columns is not uniform, especially in the liquid phase. Maldistribution of fluids is always responsible for a significant reduction in the transfer efficiency. Normally, liquid distribution depends on the

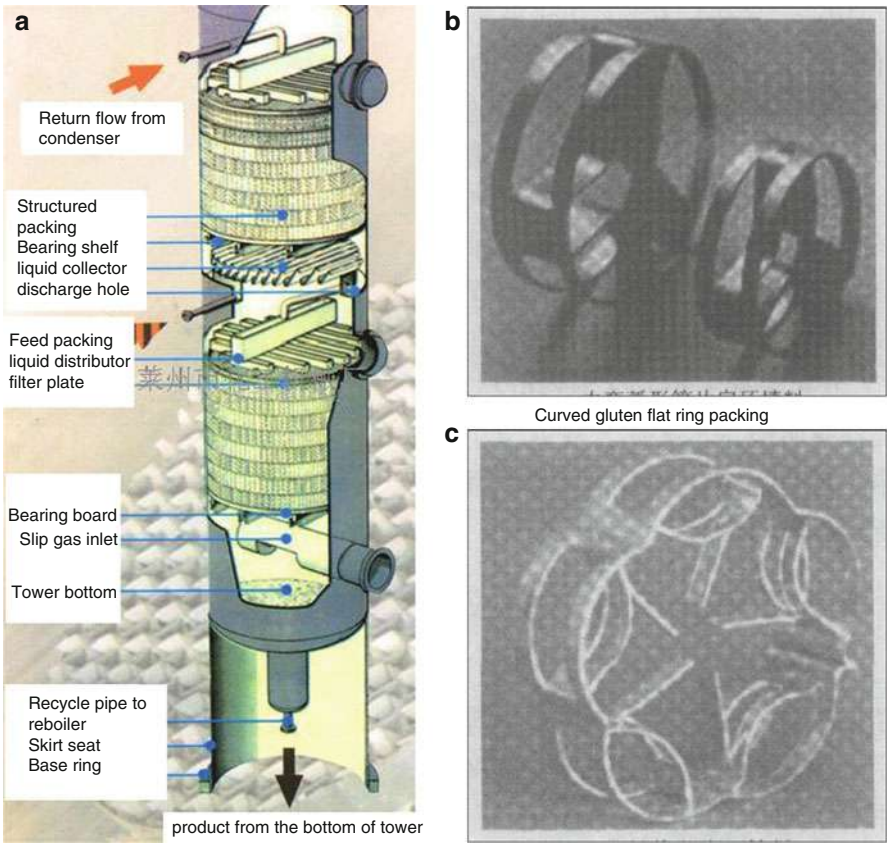

Fig. 30 Packed tower and some packing (Weiyang 2005)

distributors and the packing that is adopted in the column. Thus, liquid distributors are significantly meaningful to the packing column of high mass transfer efficiency. Liquid distributors are complex and expensive elements which are aimed to uniformly distribute the liquid over the packing. Their main parameters are the drip point density and their structure with regard to the underlying packing (Bozzano et al. 2014). The use of well-designed distributors coupling with the packing is a key point to achieve a best performance of the packing column. However, the study of liquid distributors and particularly their interactions with the beneath packing column are still a relatively unexplored area. In principle, the design of the liquid distributor should fulfill the following requirements (Spekuljak and Monella 1994): (1) the largest number of liquid distribution points in the column cross-section; (2) operating flexibility, without sacrificing the other requirements; (3) to be mechanically robust and easy to install into and remove from the column shell; (4) to minimize the distributor height; and (5) easy to clean and maintain.

Hollow Fiber Contactor

Many researchers hope to find a new CO_2 absorption equipment to reduce the equipment size. A hollow fiber contactor is one type of new absorption equipment widely studied now (Yan et al. 2007).

In a hydrophobic hollow fiber contactor (Fig. 31), gas and the absorbent solution flow in different sides of the hollow fiber. Gas and liquid contact indirectly, and absorbent entraining, channeling, bubbling, and overflowing can be avoided. At the same time, a hollow fiber's large surface area (1,000–3,000 m^2/m^3) can reduce the volume of the equipment effectively. Studies show that using hollow fiber contactor can reduce the size of an absorption and regeneration tower by 63 % compared with a packed tower.

However, membrane contactors also have some disadvantages. First, the presence of membrane adds extra mass transfer resistance, which will result in a reduction in the overall mass transfer rate. But this negative impact can be potentially eliminated by the advantage of large interfacial mass transfer area. The main challenge for membrane contactor is the issue of membrane wetting, which leads to the deterioration of CO_2 absorption flux in long-term operation and limits its large-scale commercial application. In order to solve this problem, a number of studies have been conducted, including the selection of membrane materials and mechanism of membrane wetting and prevention of membrane wetting.

Super-Gravity Rotating Bed

To solve the size problem of the common packed tower, Ramshaw (Ramshaw and Mallinson 1981) put forward the concept of a super-gravity rotating bed. High-speed rotation of the central axis can cause centrifugal super gravity, which can strengthen the transfer, mixing, and reaction process. Studies show that the mass transfer rate of such a super-gravity rotating bed is 10–1,000 times that of common packed tower. Therefore, the volume of the reactor can be greatly reduced.

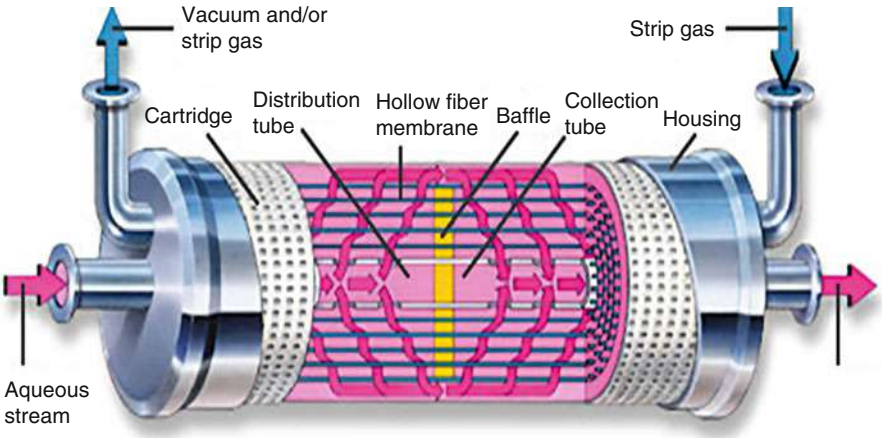

Fig. 31 Illustration of typical hollow fiber contactor (Yan et al. 2009)

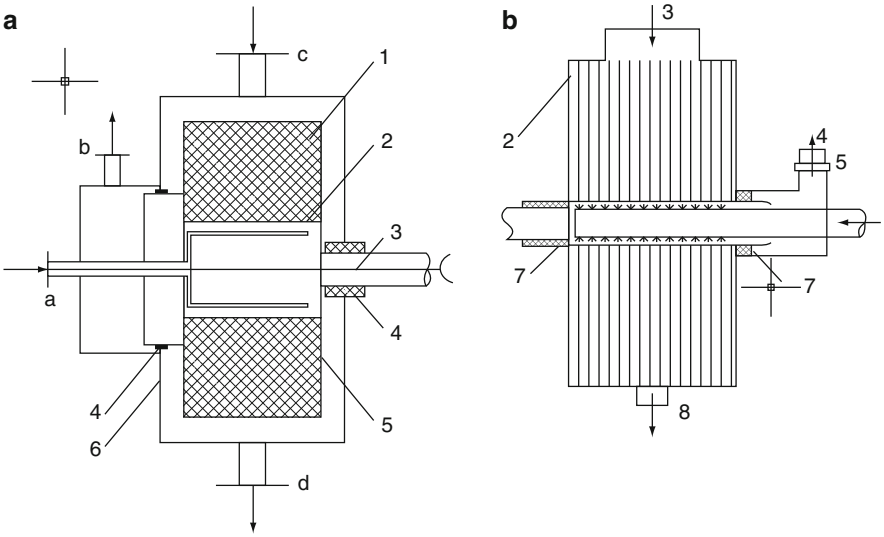

Fig. 32 Two kinds of rotating bed for CO_2 capture. (**a**) Structure of a wire packing rotating bed (*1*, packing; *2*, rotor; *3*, shaft; *4*, seal; *5*, liquid distributor; *6*, shell; *a*, liquid inlet; *b*, gas outlet; *c*, gas inlet; *d*, liquid outlet). (**b**) Structure of a disk packing rotating bed (*1*, shaft; *2*, concentric ring wave disk packing; *3*, gas inlet; *4*, gas outlet; *5*, separator of gas and liquid; *6*, spray tube; *7*, filler; *8*, liquid outlet with seal) (Chen 2002)

Some researchers have studied the CO_2 removal process of rotating beds and obtained the effect on CO_2 absorption characteristics of related operation and design parameters. Chen Minggong (2006) proposes the rotating disk super-gravity bed which has some improvements to traditional rotating packing beds, as shown in Fig. 17. Recently, studies of super-gravity rotating beds are mainly carried out in the chemical industry. The knowledge of inside flow fluid structure with high gas flow, mass transfer strengthening of flue gas decarbonization, and the adaptability of real gases are lacking (Fig. 32).

Integration and Optimization of the Process

As one of early chemical absorption processes, amine-based CO_2 scrubbing process was proposed by Bottoms in 1930. Based on its rationality and formerly applied occasions, during the following 70 years after this invention, few researchers tried to modify this process. However, when people realize the correlation between climate change and CO_2 emissions, things are changed. The energy consumption of this process is deemed to be unacceptable, especially to those occasions of high gas flow rate and lower CO_2 partial pressure, e.g., coal-fired power plants.

In this context, a sharp increase of patents related to process modification appeared in the past decade. It is widely considered that integration and optimization

of the process is one of the most effective ways to further reduce the energy consumption for chemical absorption method. In general, integration and optimization of the process can be understood or interpreted as two distinct meanings. One understanding refers to process modification and heat integration toward various components inside of carbon capture plant itself, while the other recognition is the integration between carbon capture plants with the other system. According to the components for integration, modifications to amine scrubbing process can be classified into two categories, integration with other system and optimization of itself.

Process Optimization by Coupling with Other System

- Integration of steam cycle and the boiler
  For amine scrubbing, thermal energy is needed for amine regeneration, electricity consumption for CO_2 compression, and cooling necessities for refrigeration. An important consideration to select steam quality for the stripper is the steam pressure. It is widely accepted that the reboiler temperature should not exceed 122 °C, or else degradation of MEA and corrosion of the equipment will be intolerable. In general, the temperature difference between the high-temperature side and low-temperature side ranges from 10 °C to to 15 °C in the reboiler, which means that the steam conditions of the saturation temperature amounts to 132–137 °C. Saturation pressure at this temperature is 2.8–3.4 bar. This thermal energy can be supplied from either an auxiliary boiler or from a power plant steam extraction. Finding the optimum way to extract this steam becomes essential in order to get the less power plant energy penalty. One potential form of the simplified CO_2 capture steam extraction system is shown in Fig. 33. Two evident characteristics for this process are that the steam is extracted from IP/LP crossover pipe for amine solvent regeneration and a throttling regulating valve in the LP turbine inlet should be installed to make the pressure stable. Although the operating requirements of CO_2 capture system can be achieved, the efficiency of LP section will reduce to some extent.

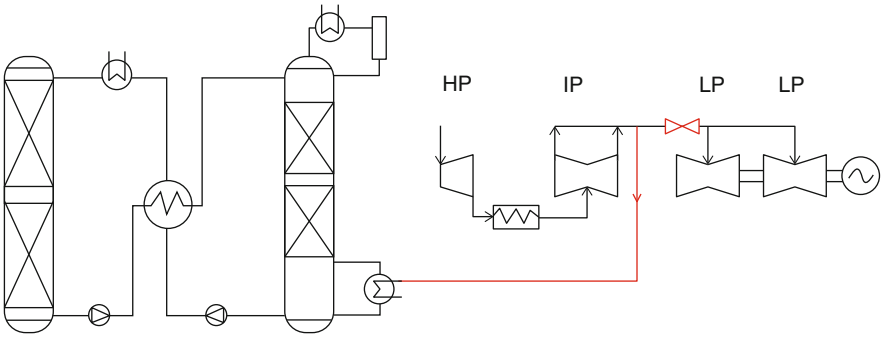

Fig. 33 Coupling between the steam cycle and the stripper's boiler

In addition to the process given in Fig. 33, there are a large number of variants of coupling between the amine scrubbing system and power plants, e.g., extracting steam from other parts of the steam cycle, integrating the condensate system of amine scrubbing with a power plant.

- Integration of flue gas and amine scrubbing
  Flue gas after removing SOx and NOx is usually of high temperature. In order to obtain a relatively stronger thermodynamic driving force, flue gas needs to be cooled before it is sent to the CO_2 absorber. Usually a pretreatment column is set to cool down the flue gas to the required temperature. However, it is not wise to waste this part of heat in the flue gas. Due to this reason, some researchers proposed adding a heat exchanger to utilize the heat of flue gas. A potential form to utilize the heat from flue gas is illustrated in Fig. 34. A heat exchanger is set up to replace the pretreatment column. The waste heat of flue gas can be used to raise the temperature of the rich solution.
- Integration of DeSOx and amine scrubbing
  In addition to the waste heat in the flue gas, remaining contaminants should also be concerned. In the one hand, remaining components, which refer to SOx, NOx, and particle matters, may affect the performance of carbon capture system, such as CO_2 removal efficiency and treatment of heat-stable salts. In the other hand, it is possible to integrate the desulfurization and carbon capture into one tower so as to reduce the capital cost of the equipment and save the space for power plants.

  Reddy et al. (2007) propose using a two-stage quench scrubber in place of the standard flue gas pretreatment column. Their modification refers to pretreatment systems where an alkali wash is utilized to remove SOx/NOx components in the flue gas. Hakka and Ouimet (2007) use a similar approach as indicated above for the sequential removal of SO_2 and CO_2 from a gas stream (Fig. 35), thus avoiding the generation of heat-stable salts. The cooled gas stream then passes through a

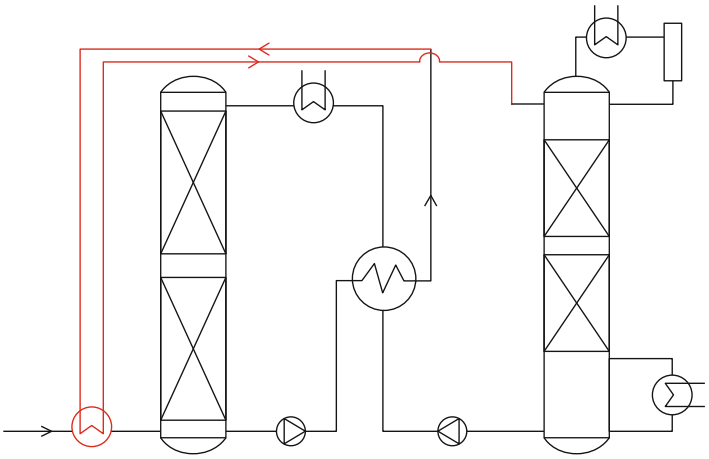

Fig. 34 Utilization of flue gas heat

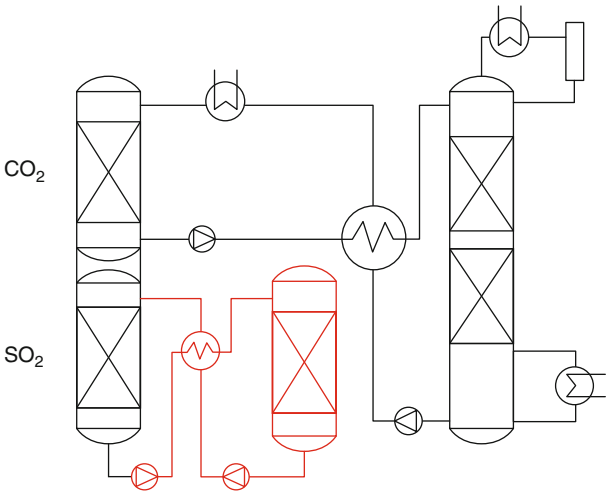

Fig. 35 Integration of DeSOx and amine scrubbing

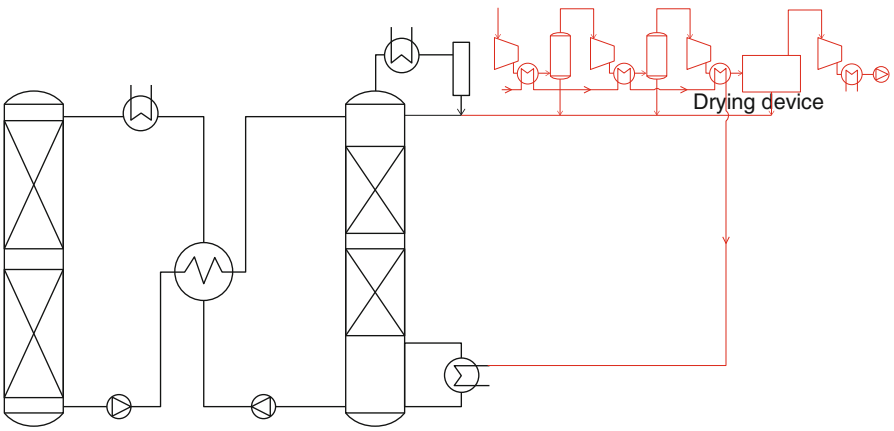

Fig. 36 Integration of compressors and amine scrubbing

SO_2 scrubbing section, followed by a CO_2 scrubbing section. Both the SO_2 and CO_2 scrubbing sections use sorbents that can be regenerated. Shaw (2009) also suggests a similar method for integrating the SO_2 and CO_2 capture processes.

- Integration of Compressors and amine scrubbing
  Once CO_2 is captured from flue gas, it will be sent to the transportation system or storage tanks after compression and dehydration. During the CO_2 compression, a large number of heat would be generated. One potential form is shown in Fig. 36. The heat of compression is utilized by heat transfer with fluids, and the working fluids are sent to the reboiler. Vapor recompression in the overhead of the stripper can be also regarded as a variant of this method.

Process Optimization by Modifications of Reactors and the Original Process

Process optimization illustrated in this section refers to the modifications toward the process itself. It is intended to seek a balance between kinetics and thermodynamics in the aspect of reactors. It also attempts to manage and improve the heat transfer between the process flow components. Yann et al. (2014) classified these modifications into three classes and 20 subclasses. Three major classes are absorption enhancement, heat integration, and heat pumps. This classification is partially based on the component inside of the process. The drawback for this method is that it brings trouble to understand the widely accepted and discussed modification concepts.

Process optimization is introduced concept by concept in this chapter. Once you figure out the nature of each concept, its derivations and compounds with other concepts will be easy for you to understand and manipulate. Until now, the most discussed concepts include interstage temperature control (particularly intercooling), split flow, vapor recompression, multi-pressure stripping, and heat integration.

- Interstage temperature control (intercooling and inter-heating)

It is a known fact that the chemical reaction between CO_2 and absorbent is usually exothermic and spontaneous. The exothermic effect can result in an increase in the temperature of the solvent pumped into the absorber. This will limit the driving force for absorption and hence lower the absorption capacity of the solvent system. In the aspect of thermodynamics, CO_2 absorption reactions favor lower temperatures, while higher temperatures facilitate reaction kinetics. The higher temperature will lead to the reduction of viscosities and the increase of diffusion coefficients, therefore obtaining higher mass transfer coefficients. These two effects always fight with each other in an adiabatically operated absorber.

Intercooling is to withdraw a fraction of the solvent in the lower section of the absorber, to cool down the solvent and send it back to the adjacent area of the absorber. The simplified process is shown in Fig. 37. The reason to do this is that at the lower section of the absorber the mass transfer driving force of solvent becomes weaker with the increase of CO_2 loading and temperature. To decrease the temperature of solvent is obviously beneficial to enhance the mass transfer driving force. The modification of inter-heating is similar to that of intercooling. The modification is usually installed at the top section of the absorber. At that section, reaction rate is the most concerned thing. To increase the temperature in this section facilitates to improve the kinetics performance of solvent.

Experimental validation of Knudsen et al. (2011) shows no clear effect of intercooling modification for MEA and a reduction of boiler duty of 7 % for activated AMP. The multiple intercooled column (Sanpasertparnich et al. 2011) leads to approximately 20 % reduction of the reboiler duty. The effect of inter-heating has not been validated by experimental studies.

There are a certain number of variants of interstage temperature control. Interstage temperature control can be also applied to the regenerator. Aroonwilas et al. (2007) proposed a process to adjust the temperature distribution in the absorber

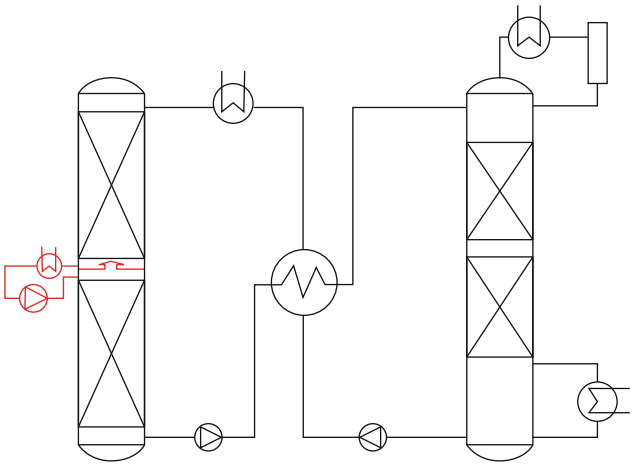

Fig. 37 Schematic of interstage temperature control process

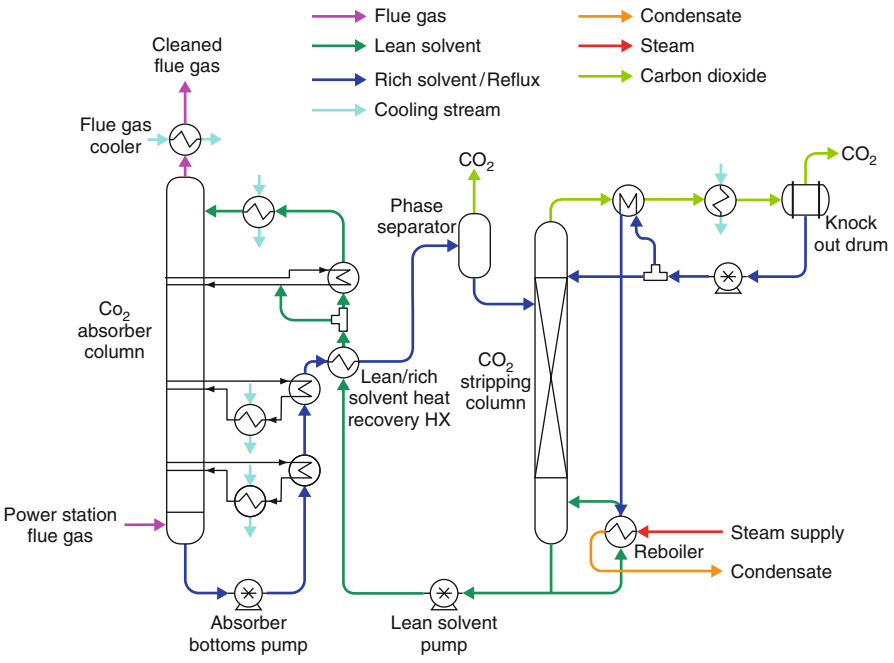

Fig. 38 Example of interstage temperature control process proposed by Aroonwilas

which is outlined in Fig. 38. The patent uses heating in the top section of the absorber to enhance the kinetically limited mass transfer in this section. Interstage cooling is then used to provide thermodynamically driven mass transfer in the lower stages of the absorber by maintaining a higher loading of CO_2 in the solvent. This process is

similar to concepts published by Leites et al. (2003). Aroonwilas and Veawab (2007) also suggest the incorporation of some heat recovery. Part of the condensate removed from the CO_2 leaving the stripper is used to cool the vapor upstream of the separator. The heated condensate is then used as feed for the reboiler.

- Split-flow process

There is no identical definition for split-flow process. A basic principle of this method is that either the flow in a pipe or the flow in the reactors should be split or divided into two or more parts. The splitting may occur at any position of the typical process, and the only purpose is to save energy or reduce the cost.

In 1934, the concept of split-flow process was firstly put forward by Shoeld, which is considered as one of the first methods proposed for addressing temperature problems in the absorber. During this process, both the absorber and stripper are split into two or more stages. Compared with the typical base process, partially used/regenerated solvents are introduced to recycle between the middle stages of absorber and those of stripper. The whole process is outlined in Fig. 39.

Shoeld declared that a 50 % reduction in steam usage within the stripping column could be achieved compared to processes using a single-stage absorber and stripper. The results were based on the comparison of a typical set of operating data for single-stage and split-flow systems using a sodium phenolate solution to capture the acid gas. However, Shoeld did not point out the applicable specific pressures.

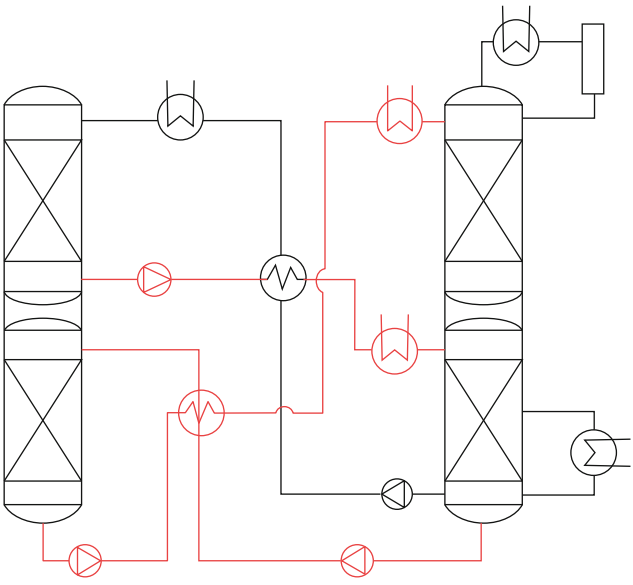

Fig. 39 Schematic of split-flow process proposed by Shoeld

Although the split-flow process was testified to be rather effective and feasible, researchers also noticed the drawbacks for this method. Towler et al. (1997) presented a comprehensive overview of the shortcomings of the standard split-flow process. They demonstrated that variation in the solvent concentration within the split loop might lead to thermodynamic inefficiencies.

Generally speaking, it is easier to strip solvents that are more concentrated in the active component. Towler et al. investigated split-flow process using TSWEET® and HYSIM®. Results show that the condensation mostly appears in the first few trays below the inlet of the rich solvent stream. Meanwhile, the chemical solvent in the upper section of the stripping column is generally dilute. Condensate steam at the overhead condenser returns to the stripping column as reflux to cool the exiting vapor stream, decrease the condenser duty, and maintain the water balance of the system. Moreover, the reflux further dilutes the solvent in the upper section of the stripper. It implies that solvent withdrawn from the stripper midsection will be much more dilute than solvent extracted from the stripper bottom section. Hence, to achieve the specified carrying capacity, the solvent flow rate needs to be increased which will bring more energy consumption.

In order to overcome the drawbacks of the standard split-flow process, Towler et al. suggested adding a second reboiler on the side draw from the stripping column, allowing the concentration of the solvent in this stream to match that leaving from the bottom of the column. Returning the reflux stream to the lowest point possible in the stripper (i.e., the reboiler) avoids dilution of the solvent in the stripping column while maintaining the water balance of the system. On the basis of their modeling results, Towler et al. claim that their improved split-flow process reduces the energy requirement of the stripping column by 70 % over that of the standard split-flow process (Fig. 40).

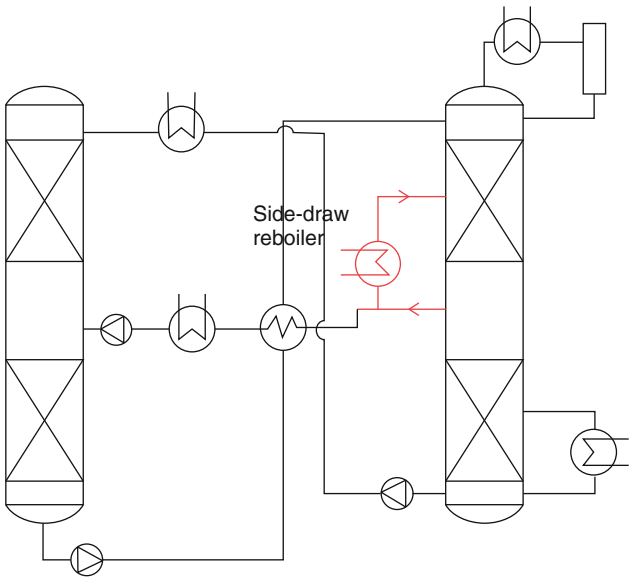

Fig. 40 Schematic of split-flow process with side-draw reboiler

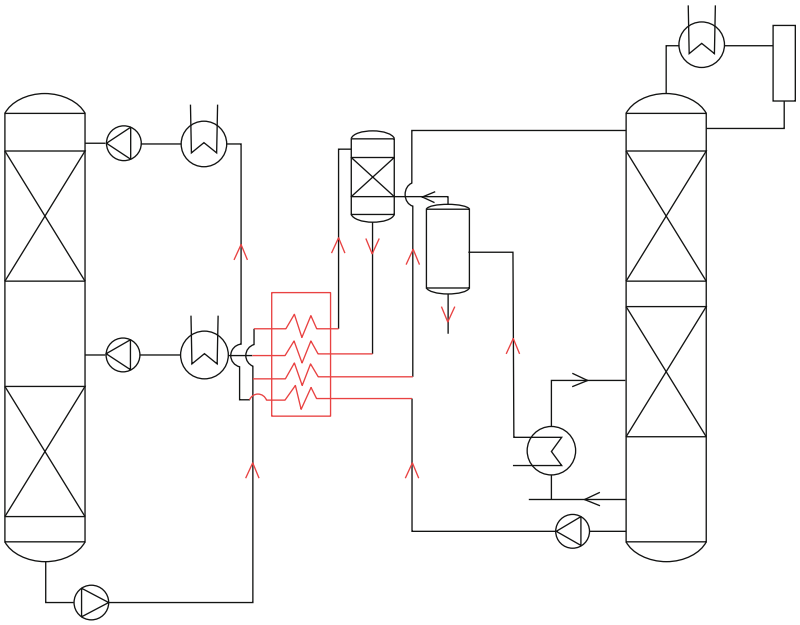

Fig. 41 Schematic of split-flow process with rich solution splitting

Reddy et al. (2004) pointed out similar problems of the standard split-flow process, and they brought forward a totally different method to overcome these problems (Fig. 41). They split the rich solvent into two parts. One portion of the rich solvent passing through cross-heat exchanger is fed to a conventional stripping column which produces a lean solvent. The lean solvent is then recycled to the top portion of the absorber. The other portion of the rich solvent stream is fed to a second stripping column. Heating from the lean/rich heat exchange is used to provide the energy needed to regenerate a semi-lean amine in this column. In addition, further stripping is achieved by adding steam flashed from the condensate from the conventional stripping column reboiler. This semi-lean amine is recycled to the absorber midsection. Interstage cooling between the two sections of the absorber is also recommended.

Mak (2006) proposed a more complex transformation of split-flow process in patent No.CA2605649 (Fig. 42). The components include both two separate stripping columns and a single two-stage stripping column, which are used to produce both lean and ultra-lean regenerated absorption solvents. Frankly speaking, this process is similar with the process proposed by Reddy. However, there are two evident differences between them. One difference is that in Mak's patent, one portion of the CO_2-rich solvent is sent to the stripper without heating. The other difference is that the stripper for Mak's process is a two-stage stripper.

As described by Mak, utilizing this process can effectively reduce the regenerator reboiler and condenser duties even if stripping is performed at higher temperatures than standard. It also declares that the reduction of amine recirculation rate can be

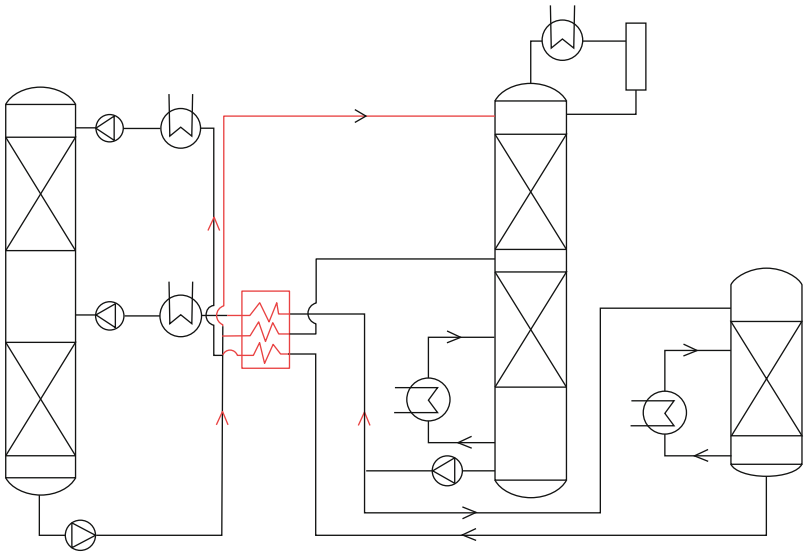

Fig. 42 Schematic of split-flow process proposed by Mak

achieved with the dual absorption and regeneration. It can be easily understood that once the circulation rate has been reduced, the pump energy required to operate the system will be much lower. Moreover, the lower circulation rate also leads to the minimizing of equipment size and savings in capital costs.

Eisenberg and Johnson (1979, Fig. 9) invented a simplified split-flow process with the idea of splitting the rich stream and using an unheated portion in the top section of the stripping column (Fig. 43). It is claimed that the overall energy requirement of the system can be reduced by maximizing the recovery of heat from the hot lean absorbent, as well as from the stripping vapors in the stripping column. However, there is a potential problem for this system. The problem is that the lean loading recycled to the absorber column may be slightly higher than that of standard process, which is caused by the relatively lower ratio of steam to liquid at the bottom of the column.

- Vapor recompression

Heat of steam vapor in the overhead separator of the stripper is generally wasted. The vapor recompression process is therefore put forward to address this problem. In this method, steam is extracted from one part of the stripping column, recompressed and either condensed with the heat of condensation providing part of the reboiler duty, or reintroduced into the column to provide additional stripping steam.

Woodhouse (2008) put forwarded a possible form to integrate vapor recompression method with CO_2 capture processes. In the system proposed by

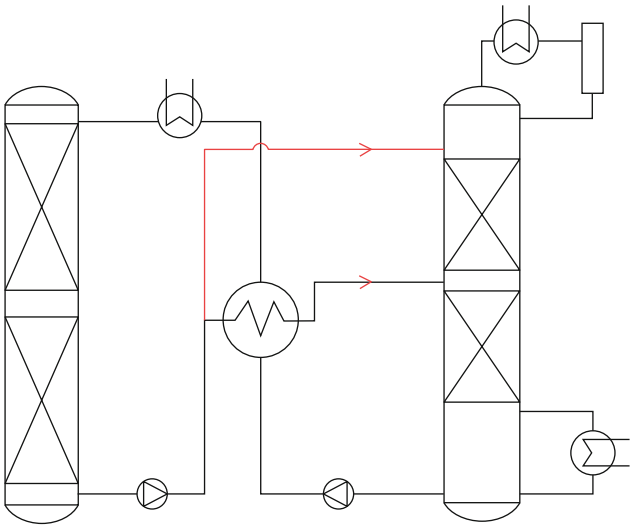

Fig. 43 Schematic of split-flow process proposed by Eisenberg and Johnson

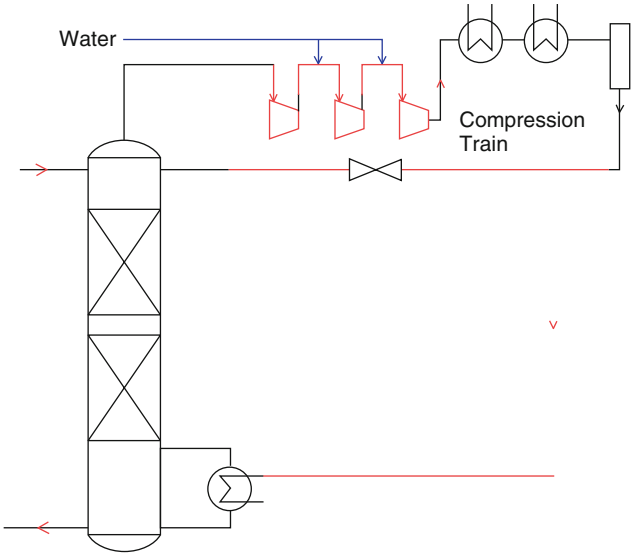

Fig. 44 Schematic of vapor recompression process proposed by Woodhouse

Woodhouse (Fig. 44), stripper overhead vapors are compressed to 2–5 times the operating pressure of the stripping column before being separated in a multistage compressor. An important feature of this system is that additional water is injected between compression stages to cool and saturate the vapor stream. The hot

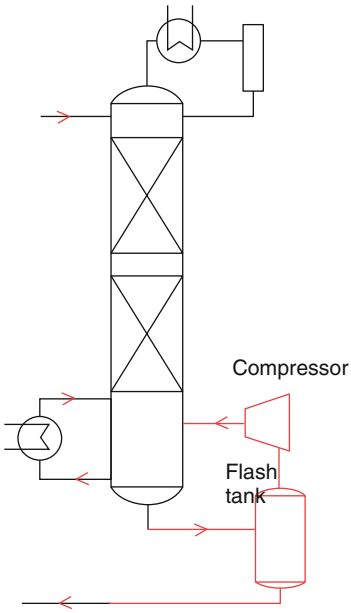

Fig. 45 Schematic of vapor recompression process proposed by Reddy

compressed vapor is then used to provide heat for other processes. It is considered as a potential substitute for the stripping column reboiler. According to his simulation results, this modification may lead to a reduction of 24 % of the duty for the stripping column reboiler. It should be pointed out that this process is rather similar to the concepts proposed by Jassim and Rochelle (Rochelle et al. 2006). The evident difference is that there is additional water injection between the compression stages used in this patent. However, the issue of water balance should be further studied due to the introduction of additional water.

Reddy et al. (Reddy 2007) showed the other transformation of process integrated with vapor recompression (Fig. 45). In this process, the hot lean stream leaves the stripping column and then is sent to a flash drum where the vapors are released due to the descending pressure. After that, the vapors (mainly steam) are compressed and reinjected back into the column to enhance the mass transfer of stripping process. Compared with Woodhouse's idea, there is no water loss or water makeup in this process, which makes it much easier to be accepted. According to Reddy et al.'s model, the net energy requirement of the system can be decreased although the compressing the flashed vapors requires additional electric power. Other benefits bringing forward by this modification include the reduction of the cooling water consumption and shrinking of the size of the stripping (Fig. 46).

It can be easily found that Woodhouse added the compressor at the overhead of the stripper and Reddy installed the compressor at the bottom of the stripper. In this context, Oyenekan and Rochelle (2006) set the compressors at the midsection of the stripper, which exhibits a form of the multi-pressure (or multiflash) stripper (Oyenekan

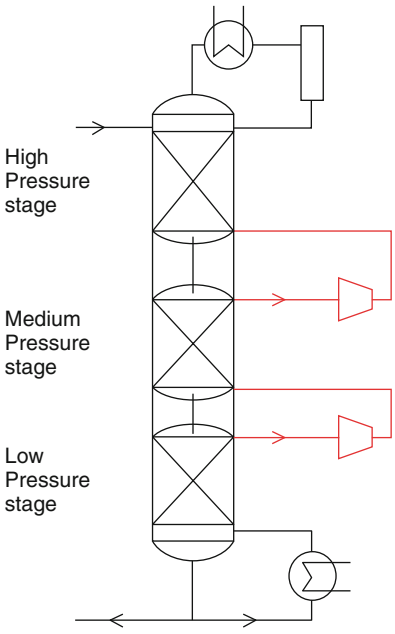

Fig. 46 Schematic of vapor recompression process proposed by Oyenekan and Rochelle

and Rochelle 2007). The feature of this process is that the stripper is divided into separate stages and the controlled operating pressure of each stage is gradually increasing from the bottom to the top of the stripper. The vapor from a lower pressure stage is compressed and subsequently used as stripping medium in a higher pressure stage. Multi-pressure stripping provides the possibility to recover the latent heat of water so as to decrease reboiler duties. Another benefit of this process is that the pressure at the top of the stripper is relatively higher than the standard stripper which is helpful for the final CO_2 compression to sequestration pressures. Oyenekan and Rochelle (2007) report that the reboiler duty is reduced by 20–27 % (depending on rich CO_2 partial pressure). Moreover, they claim an 8 % saving in equivalent work for the multi-pressure stripper compared to the "base case" (30%MEA).

- Matrix stripping

Matrix stripping virtually can be regarded as a transformation of vapor recompression process. As a further extension of the multi-pressure stripper, Rochelle and Oyenekan (Rochelle et al. 2006) call it matrix stripping. A number of strippers operating at different pressures in a matrix pattern are included in this process which is outlined in Fig. 47.

In this configuration, the rich solvent from the absorber is split into three streams and then enters the top of each stripping column, respectively. The flow direction of the regenerated solvent is from the stripper of higher pressure subsequently to the stripper of lower pressure. The vapor venting out from the top of each column is cooled and sent

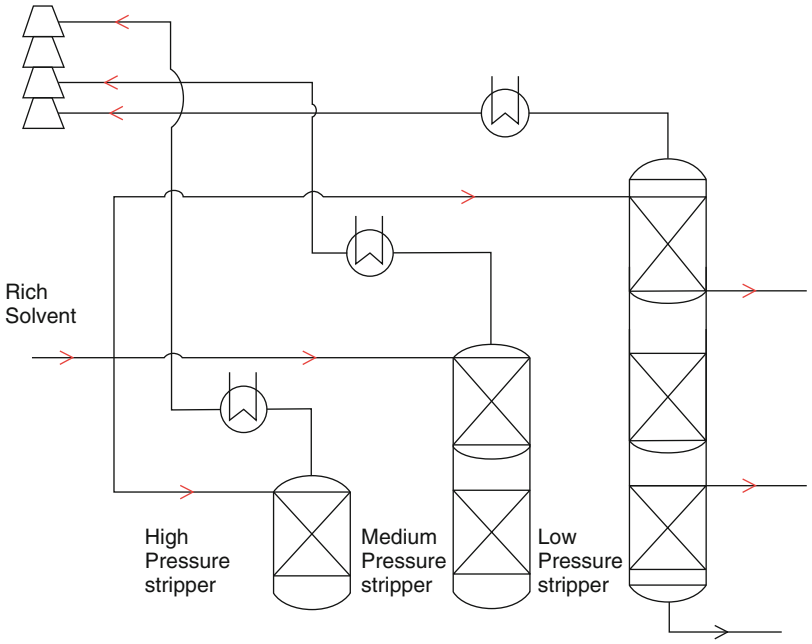

Fig. 47 Schematic of matrix stripping process

to the corresponding stage of the compression train. The multi-pressure stripper addresses the problem of utilization of the latent heat of the water vapor. It is claimed by simulation results that reductions in stripping energy requirements of 15–30 % can be achieved.

- Heat integration

It is well known that in a standard chemical absorption process, there are a number of heat exchangers to cool or heat the working fluids. To reduce the energy consumption, some researchers attempt to recover part of the wasted heat during the process. Kamijo et al. (Kamijo 2006) proposed recovering the waste heat of hot flue gas in the upper stream. The schematic of his idea is shown in Fig. 48. This configuration claims a 6.77 % reduction in reboiler heat duty, with a slight increase in condenser duty (~1 %).

The flue gas cooling stage is separated into two aspects: (1) indirect heating of the fluid from the stripper and (2) use of a heat pump to provide heat for the reboiler. Heat released from the CO_2 compression stage can also be used to supplement the heat pump. This patent claims that most or all of the energy needed for desorption can be obtained from the flue gas cooling stage/heat pump. In addition, as the stripper energy comes from the heat pump, integration with the power plant steam cycle is not required.

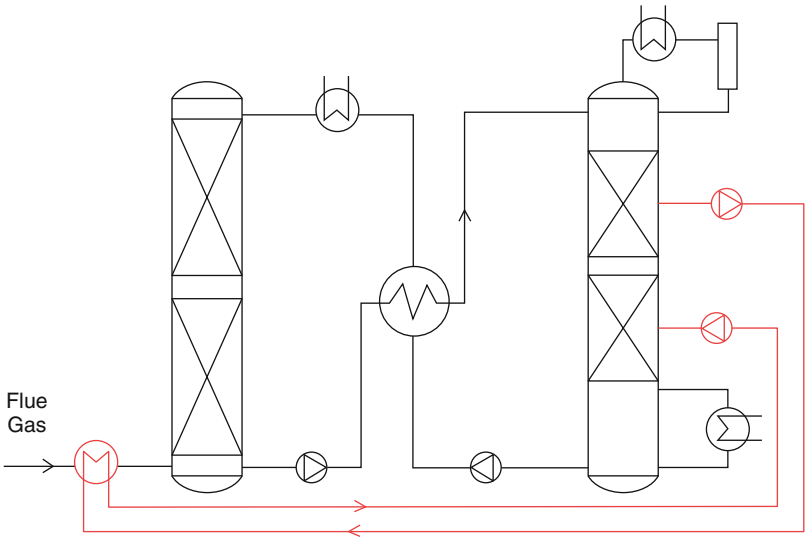

Fig. 48 Schematic of heat integration process proposed by Kamijo

Environmental and Economic Issues

Water Issue

Introduction

Carbon capture technologies could increase the water demand on thermoelectric power plants. It is important to estimate and explore the possible effects CO_2 mitigation will have on water demands. Current carbon capture technologies under development for coal-based power generation require large amounts of water. This analysis assumes that aggressive carbon mitigation policies will be put in place in the near future that would require all new and existing PC (pulverized coal) plants with scrubbers and IGCC (integrated gasification and carbon capture) plants to utilize carbon capture technologies by 2030. The water requirements, at full load, for PC and IGCC plants with and without carbon capture derived from the detailed performance study and used in this analysis are shown in Fig. 49. All additional cooling systems required for the retrofits and all new PC and IGCC capture ready plants are assumed to be recirculating systems based on current regulations and concerns with once-through systems.

It is astonishing that water needs may hinder the application of CCS (carbon capture and storage) technologies. As an Australian report states, coal-fired power plants incorporating carbon capture and storage could be one-quarter to one-third more water intensive. However, the addition of CO_2 capture and compression even

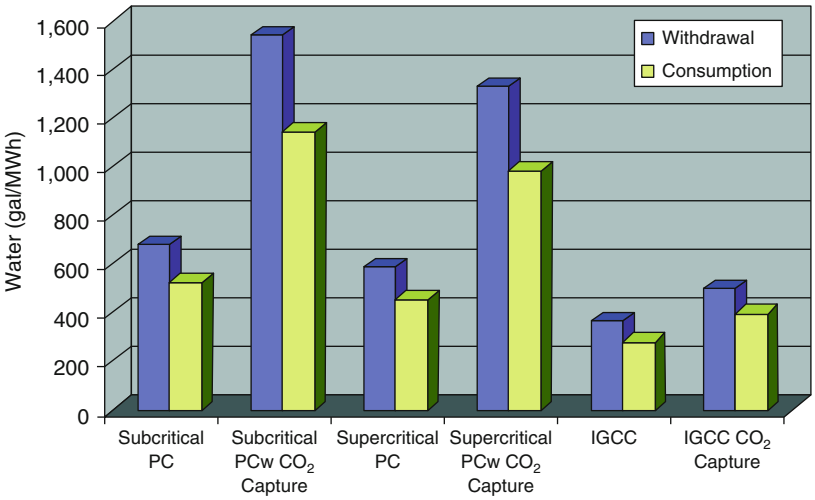

Fig. 49 Water requirements at full load for PC and IGCC plants with and without carbon capture (Shuster 2010)

increases water consumption by 50–90 %, which is indicated in the latest NETL (National Energy Technology Library) report. Whichever the value is in absolute numbers, it seems to be rather unacceptable as the basic water requirement for coal-fired plants is huge. Especially, it is unacceptable for places which are short of water, such as the Western USA and Western China.

Water Balance Strategy for Power Plants with CO_2 Capture

When considering a mode of operation which requires no makeup water, a subset of interrelated factors affecting the water balance should be assessed, such as:

- Flue gas temperature, absorber inlet and outlet: Due to the increased degradation of the amine by an increase in temperature, it is recommended to precool the flue gas to a temperature below at least 80 °C.
- Temperature profile within the absorption section of the absorber: As the CO_2 is absorbed into the solvent, the temperature of the downflowing solvent will increase due to the exothermic absorption reaction, and, thus, some water will inevitably be vaporized. Toward the top part of the column, the colder solvent will recover parts of the water vapor via condensation, and the temperature at the top section will determine the extent of this recovery. The resulting temperature profile along the column shows a pronounced bulge, the size and position of which depend on various factors including solvent flow rate and gas inlet CO_2 content (Kvamsdal and Rochelle 2008). For the optimal design case described later, the peak temperature occurs at the top of the column. The driving force of

mass transfer decreases with an increasing temperature in contrast to the reaction rate which increases. Consequently, the temperature bulge results in less favorable driving forces, although the kinetics becomes faster. If the former dominates, it may be of interest to provide methods that increase the thermodynamic driving forces by reducing the temperature bulge, which can be done by removing heat either within the absorber by intercooling or, prior to the absorber, by means of precooling.

- Absorber inlet lean amine temperature specification: The solvent temperature at the top of the absorption section will influence the absorber outlet gas temperature, thereby determining the amount of condensed water in the absorber section, though this effect is reasonably small.
- Washing sections in the top of the absorber and desorber: The main purpose of the washing section is to reduce the loss and emission of amine into the atmosphere. Thus, the process water fed to the top of the washing section must be almost free of amine.

In addition, the temperature of the cleaned flue gas before being released into the atmosphere (and thus its water content) is largely dependent on the temperature of the large recycling of water around the lower water wash section. These factors imply the establishment of a fine balance in order to keep the net water buildup or loss to a minimum, that is, close to zero on average. On this basis, a control strategy including the following steps was proposed (Fig. 50):

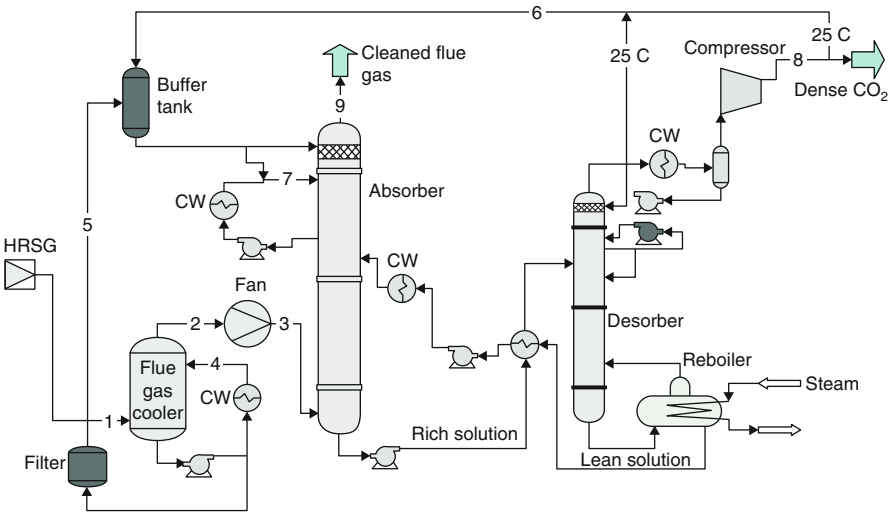

Fig. 50 The absorption system with a water-balancing strategy (indicated with *bold* streams) (Kvamsdal et al. 2010)

1. Precooling the flue gas prior to the absorption column
   - By reducing the temperature of the flue gas slightly below its dew point, some excess water will be produced in the direct contact precooler (DCC). This water is filtered and routed to a buffer tank (stream 5 in Fig. 50), which serves as the makeup water source for the water wash section of the upper part of the absorber, while also securing a proper water balancing during the transient conditions of the plant. The amount of excess water produced will be a trade-off between the cost of the cooling water requirement due to an increase in the size of the fresh cooling water recycling (stream 4 of Fig. 50) and possibly of the precooler and the possibility of a lower desorber reboiler duty and live steam demand, which is discussed later.
2. Water recycling
   - As the content of the amine in the water separated from the compression section and retrieved from the desorber condenser is almost negligible, these water sources (stream 6 of Fig. 50) can be utilized in the water wash section in the upper part of the absorber. Therefore, a bleed stream from the desorber reflux stream can be recycled to the absorber water wash section. The rest can be used in the desorber water wash section, in conjunction with a locally cooled water recycling circuit.
3. Gas cooling upon leaving the absorption column
   A temperature adjustment in the water wash section is required in order for the cleaned flue gas to leave the column at a desired humidity level, which corresponds to the amount of inlet water. Possible solutions could be:
   - Temperature measurement at the top of the absorber and adjustment of the cooling duty in the lower water wash section (stream 7 of Fig. 50) to approach the dew point (i.e., the dew point of the flue gas accounted for the CO_2 removal). This is accomplished by controlling the temperature of the cooler outlet in the lower water wash circulation. The advantage of doing it in this manner is that the temperature is easily measured and the accuracy becomes higher than with other online measurements. The drawback of this solution is that the inlet gas dew point varies as the flue gas concentration changes.
   - Online measurement of moisture in both the flue gas from the HRSG (heat recovery steam generator) unit and the cleaned flue gas effluent. An adjustment is then made by controlling the temperature in the water of the cooler outlet of the lower water wash circulation. One drawback of doing it this way may be obtaining incomplete measurements of the moisture if the samples are not properly heated since accurate online moisture measurements are generally difficult to achieve.

Environmental Effect

Environmental Assessment of the Alkanolamines

Amine-based processes have been used commercially for removal of acid gas impurities from process gas streams, and they are currently the most popular way

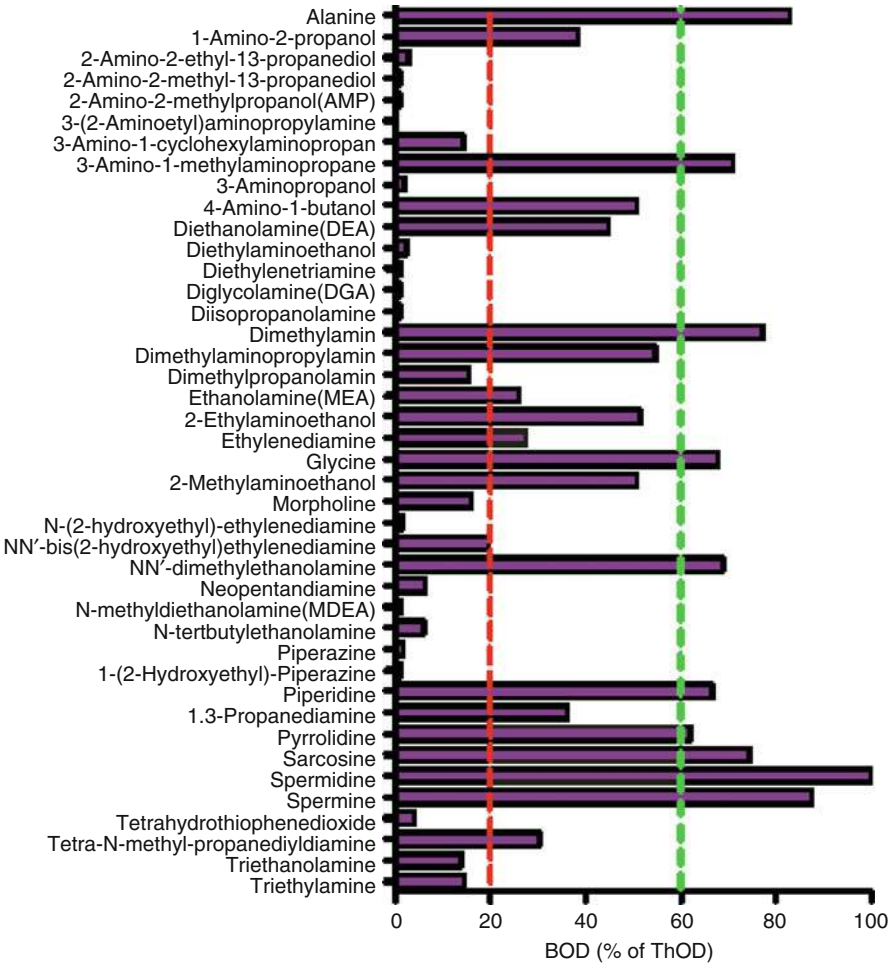

Fig. 51 The biodegradability of all the chemicals tested, results shown as percent degraded with regard to the theoretical oxygen demand (ThOD). The *red line* shows the lowest acceptable value for a chemical to be released in the marine environment, while the *green line* is the lower limit for a chemical to be released independent of the ecotoxicity (Eide-Haugmo et al. 2009)

to remove CO_2 in industry. For natural gas sweetening operations, typically alkanolamines like monoethanolamine (MEA), diethanolamine (DEA), and *N*-methyldiethanolamine (MDEA), as well as mixtures of alkanolamines, are used. Capture by absorption relies on large-scale use of chemicals, and emissions of the solvent may occur through the cleaned exhaust gas as degraded solvent and as accidental spills. It is thus important that the chemicals used have low or no environmental effect. Figures 51 and 52 show chemical test and ecotoxicity testing results of different absorbents based on EC-50.

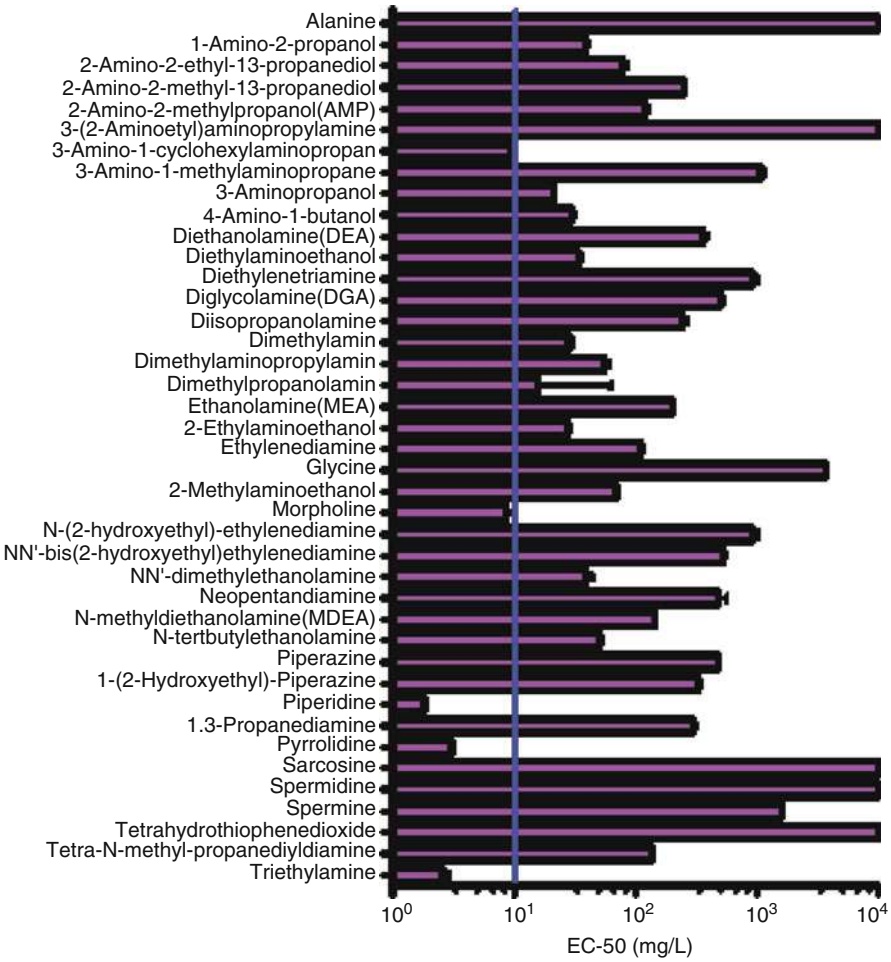

Fig. 52 Results of the ecotoxicity testing, shown as concentration where compounds inhibited algal growth by 50 % (EC-50). The blue line shows the lowest acceptable value (10 mg/L) for a chemical to be released in the marine environment (Eide-Haugmo et al. 2009)

Emission and Its Impact on the CO_2 Capture Process

Pollutant emissions potentially harming human health and the environment essentially stem from two sources in CO_2 capture processes: point of discharge and fugitive emissions. The emissions from the point of discharge are intentional, predictable, and quantifiable based on plant operating conditions. Such emissions are the treated gas released from the absorber top and the waste of process solution released from solution reclamation or other purification units. Fugitive emissions are unintentional releases from process equipment and piping during plant operation. Details of these emissions are given below.

Point Discharge of Treated Gas

A CO_2 capture unit releases the treated gas from the absorber top to the atmosphere on a continuous basis. The treated gas is basically composed of the flue gas with a reduced CO_2 content and vapors of process solution. The flue gas entering the CO_2 capture unit contains a great number of substances. Most of these substances, by themselves, have significant impacts on human health and the environment, and they are currently controlled under the environmental laws and regulations. Most gaseous components, including CO, HCl, HF, NO*x*, and SO*x*, are toxic. From MSDS (material safety data sheets), the organic compounds resulting in detrimental carcinogenic damage include benzo(a) anthracene, benzo(a)pyrene, benzo(b) fluoranthene, benzo(k)fluoranthene, chrysene, naphthalene, acetaldehyde, benzene, benzyl chloride, bis(2-ethylhexyl)phthalate, chlorobenzene, chloroform, 2,4-dinitrotoluene, dimethyl sulfate, ethyl benzene, ethyl chloride, ethylene dichloride, ethylene dibromide, formaldehyde, isophorone, methyl bromide, methyl chloride, methyl hydrazine, methyl tert-butyl ether, methylene chloride, tetrachloroethylene, styrene, and vinyl acetate. In addition, trace metals, such as arsenic, beryllium, cadmium, chromium, cobalt, lead, and nickel, are toxic and also carcinogenic.

Despite their adverse impacts, flue gas substances are not considered to be contributors to any environmental impacts caused by the CO_2 capture unit integrated into a power plant. This is because these flue gas substances are intrinsically and originally produced from the coal combustion regardless of the installation of a CO_2 capture unit. Vapors of process solution are, however, considered to be the actual emissions resulting from the CO_2 capture unit.

The emission of process solution vapors greatly depends on the operating conditions of the absorber top and the thermodynamic properties (i.e., vapor pressure) of the chemicals contained in the process solution. As an example, the vapor pressure of MEA is a function of absorber temperature (at the top) and chemical concentration (i.e., it increases with increasing MEA concentration and temperature). Any substance with high vapor pressure tends to vaporize and leave the top of the absorber very easily with the treated gas. A water wash and/or a well-designed mist eliminator are commonly installed at the top section of the absorber to reduce such entrainment and volatility loss.

According to the vapor pressures, for each chemical, besides water vapor, vapors of certain absorption solvents and degradation products can be released from the absorber top, but the release of corrosion inhibitors is considered negligible due to the extremely low partial pressure of the compounds. The primary amine MEA tends to cause greater solvent volatility loss than other alkanolamines but still less than methanol. On average, the entrainment can lead to the emission of up to 8.5 mg amine/Nm^3 of treated gas (Veldman 1989), and the total solvent loss is about up to 1.6 kg solvent/t CO_2 for gas-fired flue gas (Chapel et al. 1999). The entrained vapors of absorption solvents should cause low toxicity to human health and the environment due to their diluted concentrations in the atmosphere. The level of exposure depends on many factors, including environmental, geographic, and atmospheric conditions, which can affect the distribution and dispersion of pollutants from the

source of discharge into the air. The US laws regulate MEA by OSHA (Occupational Safety Health Administration) and DEA by NESHAP (National Emission Standards for Hazardous Air Pollutants), while the Canadian laws control DEA as "need to be declared" in NRPI. The other solvents are not enforced by any laws yet.

The degradation products, including formic acid, 1-propanamine, 2-butanamine, acetone, ammonia, butanone, and ethoxyethene, also have a tendency to vaporize and entrain with the treated gas, since their vapor pressures are higher than the vapor pressure of water at 20 °C. It was found that 2-butanamine, ammonia, and ethylamine are fairly toxic and can affect human health through skin burns and irritation. From its MSDS, 2-butanamine is also reported to be very harmful to aquatic organisms. However, 2-butanamine, ammonia, and ethoxyethene are currently not regulated under any laws, while the rest are enforced by US laws. Formic acid and butanone are controlled under Canadian laws.

According to general practice for gas-treating processes, a side stream of process solution must be purified to remove suspended solids, degradation products, and other process contaminants so that the concentration of active absorption solvents can be maintained. The solution purification is carried out through continuous adsorption, using mechanical and activated carbon filtration, and periodic thermal reclaiming. The filtration removes solid contaminants and large molecules of degradation products. As such, it results in routine disposal of wastes in the form of filter sludge/filter waste products, filter bag, cartridge, suspended solids, and used activated carbon. The thermal reclaiming is in operation to remove heat-stable salts, nonvolatile organics, and suspended solids via a side stream of 0.5–2 % of the process solution (Kohl and Nielsen 1997). The reclaiming operation will be performed when the content of heat-stable salt anions in the process reaches 1.2 wt% of the solution (CCR Technologies Inc.) or when the degradation product exceeds 10 wt% of active alkanolamine solvents (Kohl and Nielsen 1997). This generates a reclaimer waste comprising mostly heat-stable salts and solid precipitates and also small amounts of absorption solvents, corrosion inhibitor, and other additives. As an example, approximately 0.003 m^3 of reclaimer waste/t of CO_2 captured was produced in a commercial FG Econamine process (Chapel et al. 1999). Examples of reclaimer waste samples and their concentrations obtained from the IMC Chemical Facility in Trona, CA, in 1998 are summarized (Strazisar et al. 2003; Schnell 2004).

Among the chemicals present in the reclaimer wastes, heavy-metal corrosion inhibitors make the process waste toxic to humans and the environment. According to the US Environmental Protection Agency (EPA), corrosion inhibitors containing vanadium, antimony, and cyanide compounds are considered hazardous substances, and they are priority/toxic pollutants under the CAA (Clean Air Act) and also considered hazardous wastes under RCRA (Resource Conservation and Recovery Act). In Canada, uses of toxic substances, including several inorganic heavy metals, are controlled under CEPA (Canadian Environmental Protection Act). Many countries and regions around the world are introducing a series of controlling regulations to provide guidelines on the use and discharge of these toxic substances, especially inorganic salts and salts of heavy metals. In Europe, for example, the European

Union (EU) has charged the Paris Commission (PARCOM) with providing a framework for legislation (Haslegrave et al. 1992; McMahon and Harrop 1995). Other highlighted regulations include the Emergency Planning and Community Right to Know Act of 1986, regulations adopted by the US Occupational Safety and Health Administration (OSHA) in 1993, and adoption of the Chemical Hazard Assessment and Risk Management (CHARM) model in the UK and other European countries (Singh and Bockris 1996). Because of the adopted regulations, the use of toxic corrosion inhibitors makes disposal of the industrial waste difficult and costly (Kohl and Nielsen 1997; Singh and Bockris 1996). Restriction on the use of other heavy-metal inhibitors can be anticipated in the near future. Arsenic is a good example of the corrosion inhibitors; it was used effectively in gas-treating plants but is now banned from industrial applications due to its high toxicity and impacts on the environment.

Some degradation products, especially heat-stable salts and cations, are being regulated under laws and regulations. Their impacts are mostly irritation and burns. However, there are no regulations to control the emissions of such degradation products with high toxicity as 1H-imidazole, 2-butanamine, and 2-methylpropanenitrile.

The process wastes are generally disposed of by incineration and landfilling. Incineration involves the supply of energy and the phase change of wastes either from solid to liquid or gas or from liquid to gas. As a result, burning the process wastes produces ashes of both degradation products and additives together with vapors of amine solvents. Some of these products are harmful to humans and the environment, as described previously. To reduce the release of trace metals, a posttreatment of incineration (i.e., wet scrubber) should be used. In contrast to incineration, placing the process wastes in landfills does not result in a phase change of wastes, thus minimizing the emission of vapors of any toxic substances. Nevertheless, the process wastes should be neutralized prior to disposal in landfills.

Fugitive Emissions

Fugitive emissions also contribute to environmental impacts in addition to the above point-source emissions. During plant operation, the process fluids can be unintentionally released from the CO_2 capture unit mainly through leaks, which are usually a consequence of deterioration of process equipment and pipes, corrosion, impact damage, and vibration. Such emissions are unpredictable, random, and intermittent and can occur everywhere on the site, such as at pumps, valves, flanges, connectors, pressure relief devices, sampling connections, open-ended lines, instruments, vents, drains, and meters. According to the European Sealing Association (ESA) (2005), for any commercial plant, valves, especially control valves, contribute to the greatest extent to leakage losses (50–60 %), followed by relief valves (15 %), tanks (10 %), pumps (10 %), and flanges (5 %).

Apart from leakage losses, working and breathing losses also account for some fugitive emissions. Working loss occurs when the storage tanks of absorption solution are being filled. The quantity of solution vapor released from the tanks depends on temperature, vapor pressure of the solution, and pumping rate. Breathing

losses are caused by thermal expansion of the solution vapor in the tanks as a result of temperature increase during daytime. Regardless of their sources, fugitive emissions release certain amounts of process fluids and materials, including untreated flue gas, treated gas, absorption solvents, corrosion inhibitors, degradation products, and chemical additives, whose impacts to humans and the environment were previously discussed. The importance of fugitive emission has been recognized in environmental laws and regulations.

Accidental Release

Accidental release is a large release, spill, or discharge of process fluids as a result of accidents and emergency operations. The quantities of such releases are much larger than those of the fugitive emissions. According to the American Petroleum Institute (API) (2001), accidental release can be caused by failures of process equipment due to physical erosion, wear and tear, corrosion, malfunctions of process controls and instrumentation that lead to overpressure, overheating, and liquid overflow, as well as improper operations that lead to foaming, pluggings, or blockage of process equipment and piping.

Management of Pollutant Releases and Their Impacts

Although the impacts of a CO_2 capture unit integrated to the power plant are not severe, an environmental management system (EMS) should be practiced to control pollution, minimize waste production, ensure progress toward an environmental goal, and provide safety plans for normal plant operation and accidents. The EMS requires a commitment from top management to establish a corporate environmental management policy and educate employees on the policy (Crognale 1999). Proper operation, monitoring, and maintenance of process equipment, piping, and instrument and control systems play a key role in reducing emissions of hazardous substances from process points of discharge, fugitive sources, and accidental events. Pipeline and tube bundles in the heating elements should be regularly monitored, due to deterioration by corrosion. Trays or packings in both absorber and regenerator should be kept clean from sludge deposit. The amounts of heat-stable salts or any particulates in the process solution must be kept low to avoid foaming problems, which are a primary cause of entrainment at the absorber top. Repair, replacement, and modification of the existing equipment must be done promptly when the damage is identified. Several publications provide guidelines for amine plant operations. Bacon and Demas (1987) recommended tests on lean and rich amine solution loadings, total heat-stable salts, anion and cation assay, soluble iron content of solutions, degradation products, and foaming tendency (Bacon and Demas 1987). Pauley (1991) suggested that the amine solution should be sampled and tested regularly for organic acids, heat-stable salts, amine concentration, soluble metal content, iron sulfide content, liquid hydrocarbon content, and water content (Pauley 1991). Nielsen et al. (1995) provided a set of maximum concentrations of heat-stable salts that should be kept to prevent severe corrosion (e.g., 250 ppm for oxalate; 500 ppm for formate, glycolate, malonate, sulfite, and sulfate; 1,000 ppm for succinate; and 10,000 ppm for thiosulfate) (Nielsen and Lewis 1995). The

Table 12 Equipment modifications for control of equipment leak (European Sealing Association (ESA), 2005) (Thitakamol et al. 2007)

Equipment	Modification
Valves	Sealless design
	Avoid using valves with rising stem (gate valves and globe valves)
	Install the rupture disks before the safety valve to damp small pressure fluctuation
Pump seals	Sealless design
	Closed-vent system
	Dual mechanical seal with barrier fluid maintained at a higher pressure than the pumped fluid
Flanges and connectors	Weld together
	Correct selection and installation of the gasket and regular maintenance
	Minimize the number of flanged connection
Pressure relief devices	Closed-vent system
	Rupture disk assembly
Open-ended lines	Blind, cap, plug, or second valve

recommendations for leakage reduction from these process components are summarized in Table 12.

Standard plans for the worst and the most likely emergency scenarios should also be developed to effectively and immediately mitigate accidental release. Such plans must at least provide proper procedures for handling the release and cleanup of hazardous pollutants and must be distributed to and well understood by both plant employees and local authorities, such as local police, fire fighters, and hospitals.

Economical Factors of Chemical Absorption Systems

Economic considerations of chemical absorption systems are another key factor to affect the application of the capture technology. All the commercial technology seems hard to satisfy the requirement of power plants due to the problem of high cost. Figure 53a–c, respectively, shows different CO_2 capture technology on COE (cost of electricity), thermal efficiency, and CO_2 capture cost (NETL Report 2008).

It is easily derived from the above charts that these technologies are still rather expensive to be applied. More research needs to be performed to cut the energy consumption and capital cost so as to meet the economical requirements.

Above all, although chemical absorption is considered to be the most mature technology nowadays for CO_2 capturing, there is still a long way to go to put it into practice in large-scale power plants. Chemical solvent scrubbing processes are expected to improve between now and 2020. Improvements will be made by a combination of design optimization in a competitive market and technology developments, such as new solvents. Combustion power generation processes

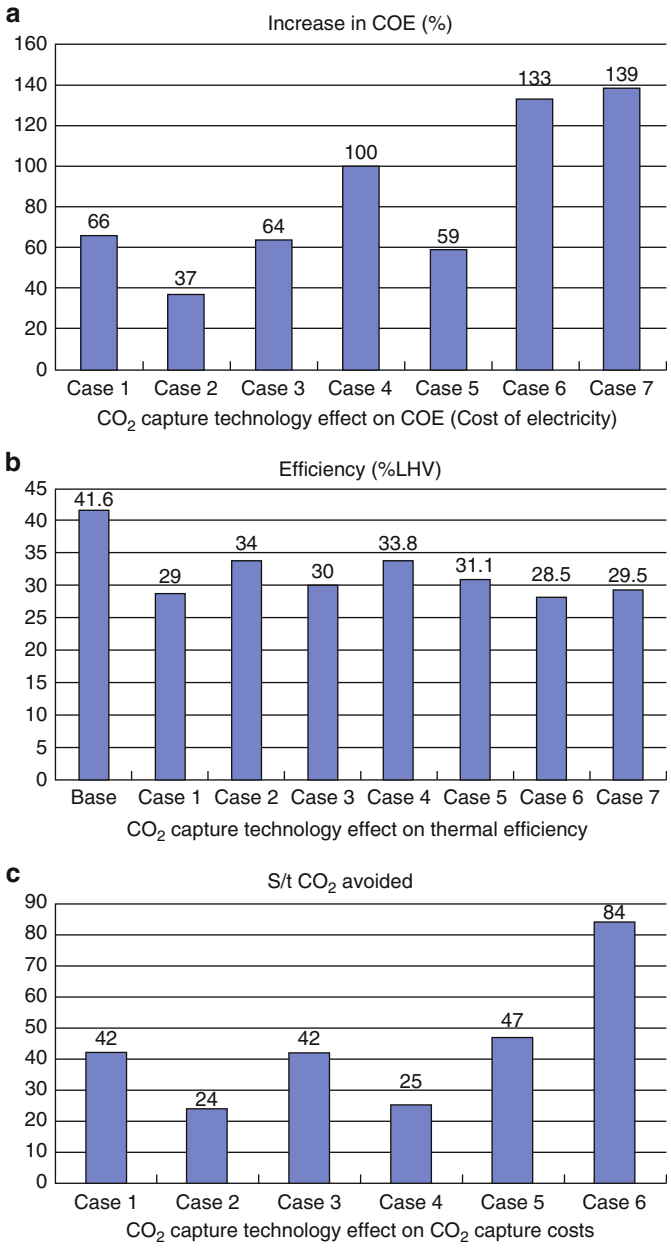

Fig. 53 CO_2 capture technology economy. *Base* refers to the standard pulverized coal power plant; *Case 1* refers to conventional MEA scrubbing technology; *Case 2* refers to aqueous ammonia scrubbing technology; *Case 3* refers to oxy-fuel combustion technology; *Case 4* refers to IGCC technology; *Case 5* refers to membrane separation technology; *Case 6* refers to pressure swing adsorption technology; *Case 7* refers to temperature swing adsorption technology

are also expected to improve, and these improvements will contribute to an overall improvement in the economics of power plants with post-combustion CO_2 capture.

Industry Application and Future Direction

Industry Application

Introduction

To assess the potential of CCS as an option for reducing global CO_2 emissions, the current global geographical relationship between large stationary CO_2 emission sources and their proximity to potential storage sites has been examined. Globally, emissions of CO_2 from fossil fuel use in the year 2000 total about 23.5 Gt CO_2. Of this, close to 60 % was attributed to large (>0.1 Mt CO_2/year) stationary emission sources. Table 13 lists the profile by process or industrial activity of worldwide large stationary CO_2 sources with emissions of more than 0.1 Mt CO_2/year.

The most promising near-term strategy for mitigating CO_2 emissions from these facilities is the post-combustion capture of CO_2 using chemical absorption with subsequent geologic sequestration. While MEA absorption of CO_2 from coal-derived flue gases on the scale proposed above is technologically feasible, MEA absorption is an energy-intensive process and especially requires large quantities of low-pressure steam. It is the magnitude of the cost of providing this supplemental energy that is currently inhibiting the deployment of CO_2 capture with MEA absorption as means of combating global warming. Hence, all governments are rather cautious to make a plan of CO_2 mitigation. Table 14 lists some CCS projects for power plants, which are related to chemical absorption. Table 15

Table 13 Profile by process or industrial activity of worldwide large stationary CO_2 sources with emissions of more than 0.1 Mt CO_2/year (Source: IPCC special report on carbon dioxide capture and storage 2005)

Process	Number of sources	Emissions($MtCO_2$/year)
Fossil fuels		
Power	4,942 (62.66 %)	10,539 (78.38 %)
Cement production	1,175	932
Refineries	638	798
Iron and steel industry	269	646
Petrochemical industry	470	379
Oil and gas processing	N/A	50
Other sources	90	33
Biomass		
Bioethanol and bioenergy	303	91
Total	7,887	13,466

Table 14 Some CCS projects for power plants related to chemical absorption

Pilot CCS projects – completed							
Project name	**Leader**	**Location**	**Feedstock**	**Size MW**	**Solvents**	**CO_2 fate**	**Status**
ECO2 Burger	Powerspan	USA	Coal	1	Ammonia	Vented	Operated
							2008–2010
Pleasant Prairie	Alstom	USA	Coal	5	Ammonia	Vented	Operated
							2008–2009
AEP Mountaineer	AEP	USA	Coal	30	Ammonia	Saline	Operated
							2009–2011
Karlshamn	E.ON	Sweden	Oil	5	Ammonia	Vented	Operated
							2009–2010
Ferrybridge CCSPilot100+	SSE	UK	Coal	5	Amine	Vented	Operated 2012–2013
Aberthaw	RWE	Wales, UK	Coal	3	Amine	N/A	Operational January 2013–2014
Pilot CCS projects – operating							
Project name	**Leader**	**Location**	**Feedstock**	**Size MW**	**Solvents**	**CO_2 fate**	**Status**
Shidongkou	Huaneng	China	Coal	0.1 Mt/ year	Amine	Commercial use	Operational 2011
Brindisi	Enel and Eni	Italy	Coal	48	Various chemicals	EOR	Operational March 2011
Wilhelmshaven	E.ON	Germany	Coal	3.5	Amine	Vented	Operational October 2012
Mongstad	Statoil	Norway	Gas	0.1 Mt/ year	Ammonia + Amine	Saline	Operational May 2012
Plant Barry	Southern Energy	AL, USA	Coal	25	Amine	Saline	Operational August 2012

Jingbian	Yanchang	China	Chemicals	40 Kt/year	N/A	EOR	2013
Boryeong Station	KEPCO	South Korea	Coal	10	Amine	N/A	Operational May 2013
E.W. Brown	University of Kentucky	KY, USA	Coal	2 MW	N/A	N/A	Under construction
Tomakomai	JCCS	Japan	Hydrogen production	0.1 Mt/year	Amine	Saline	Planning
Pikes Peak	Husky Energy	SA, Canada	Coal	15 t/day	Enzyme	EOR	Planning
Big Bend Station	Siemens	FL, USA	Coal	1	Amino acid salt	Vented	Planning

Table 15 List of worldwide large-scale power plant CCS projects based on chemical absorption

Project name	Leader	Location	Feedstock	Size MW	Solvents	CO_2 fate	Status
USA							
WA Parish Petra Nova	NRG Energy	Texas	Coal	250	Amine	EOR	Under construction
Canada							
Boundary Dam	SaskPower	Saskatchewan	Coal	110	Amine	EOR	Operational October 2014
Bow City	BCPL	Alberta	Coal	1000	Amine	EOR	Planning
European Union							
ROAD	E.ON	Netherlands	Coal	250	N/A	Depleted oil or gas	Planning
Peterhead	Shell and SSE	UK	Gas	385	Amine	Depleted gas	Planning
Norway							
Longyearbyen	Unis CO_2	Norway	Coal	N/A	N/A	Saline	Planning
Rest of the world							
Shengli Oil Field EOR	Sinopec	China	Coal	101–250	Amine	EOR	Planning
Taweelah	Masdar	UAE	Gas	2 Mt/year	N/A	EOR	Planning

gives a list of worldwide large-scale power plant CCS projects based on chemical absorption.

Typical CO_2 Capture Projects

CCS Projects in the USA

Although CCS experiences a number of challenges and several projects are canceled due to the instability of policies, America is still one of the most developed countries in the CCS field. Chemical absorption is widely accepted in the demo plants nowadays. Alstom has a total of four demonstration projects operating or completing, which are respectively based on chilled ammonia, advanced amine, and oxy-combustion. Powerspan also develops some post-combustion CO_2 capture pilot plants. The major projects are listed in Table 14.

- SECARB Plant Barry CCS Project

The capture facility (Fig. 54), located at Alabama Power Company's Plant Barry, is equivalent to 25 megawatts (MW) and utilizes post-combustion amine capture

Fig. 54 SECARB Plant Barry CCS project

technology licensed by Mitsubishi Heavy Industries America (MHIA). CO_2 captured at the plant is transported 12 miles via dedicated pipeline for underground storage in a deep, saline geologic formation within the Citronelle Dome. **This project is one of the first and the largest fully integrated commercial prototype coal-fired carbon capture and storage projects in the USA.** The CO_2 capture rate of this plant is over 500 tons per day with a removal efficiency of more than 90 %. According to the operation history, the steam consumption is 0.98 t of steam per ton of carbon dioxide.

Europe

CCS development in Europe is rather optimistic due to the wide broadcast of CCS knowledge and public acceptance in CCS technologies. The UK, Norway, Italy, Germany, and the Netherlands are among the promoting countries in the world. A typical CCS project in the UK is presented below.

- Ferrybridge CCS Pilot Plant

The Doosan Babcock, SSE (Scottish and Southern Energy), and Vattenfall consortium successfully completed a 2–year test program on the post-combustion carbon capture (PCC) pilot plant at SSE's Ferrybridge Power Station in December 2013. The 100 ton CO_2/day (15MWt, 5MWe equivalent) CCPilot100+ PCC pilot plant (Fig. 55), using Doosan Babcock's PCC technology, was the first of its size to be integrated into a live power plant in the UK. 90 % CO_2 capture was successfully demonstrated at 100 ton CO_2 capture per day on MEA and up to 120 ton CO_2

Fig. 55 Ferrybridge CCS Pilot100+

capture per day on RS-2TM. The MEA baseline regeneration energy was 3.5 GJ/ton CO_2, which is in agreement with MEA performance results from other pilot plants.

CCS Projects in China

More than ten large-scale demo plants have been put into operation in China since 2007. Meanwhile, a certain number of CCS projects are on schedule.

- Huaneng Gaobeidian CCS Pilot Plant

As the first post-combustion carbon capture pilot plant in Beijing of China, Huaneng Gaobeidian Power Plant got the most concern in 2008. The pilot plant was put into operation in June 2008. Amine-based scrubbing technology is chosen to capture CO_2 from coal-fired flue gas stream. The CO_2 capture rate for the pilot plant is greater than 85 %, and the CO_2 capture capacity is over 3,000 tons per annum. The captured CO_2 is further purified to food grade and is reused in the beverage industry in the Beijing area. Huang et al. (2010) declared that the solvent is composed by MEA of 18–22 wt%, antioxidant of 0.15–0.25 wt%, inhibitor of 0.08–0.15 wt%, and water of 78–82 wt%. According to the operational experiences, the consumptive cost recovery for 1 t of CO_2 (99.7 %, 30 °C, 40 kPa) is about 25.3 US$. In order to capture CO_2, the COE will increase by 0.02 US$/kW • h, which increases the electricity purchase price by 29 %. At 2010, Huaneng group erected another 120 kt/a CO_2 capture demonstration project at Huaneng Shanghai Shidongkou Power Plant, which is the largest CO_2 post-combustion capture project in China at that time (Fig. 56).

CCS Projects in Canada

Canada government and industry give a great support to CCS project, and several large-scale CCS projects have been erected in recent years in which the largest one is Boundary Dam CCS project.

Boundary Dam CCS Project

The Boundary Dam Integrated Carbon Capture and Storage Project (Stéphenne 2013) is the world's first and largest commercial-scale CCS project of its kind, which is located in Saskatchewan, Canada. The project was fully put into operation on October of 2014. It transforms the aging Unit 3 at Boundary Dam Power Station into a reliable, long-term producer of 110 MW of base-load electricity with a CO_2 capture rate over 90 % and a CO_2 capture capacity exceeding one million metric tons of CO_2 per year. The resulting captured CO_2 emissions are compressed and transported through pipelines to Cenovus Energy who uses the CO_2 for enhanced oil recovery activities in the Weyburn oil field. Meanwhile, all the sulfur dioxide (SO_2) present in the flue gas is recovered and used for production of sulfuric acid which is subsequently sold as a valuable by-product to offset a part of the operational costs.

Fig. 56 Huaneng Gaobeidian CCS pilot plant

The carbon capture technology which is supplied by Shell Cansolv uses regenerable amines to capture both SO_2 and CO_2. Figure 57 presents the schematic of Cansolv process for the Boundary Dam Project. In order to decrease the steam requirement of carbon capture process, Cansolv employs both selective heat integration and innovative combined SO_2/CO_2 capture system. With this approach, the capture plant steam requirement is significantly reduced.

Future Directions

Introduction

Post-combustion capture involves the removal of CO_2 from the flue gas produced by combustion. Existing power plants use air, which is almost four-fifths nitrogen, for combustion and generate a flue gas that is at atmospheric pressure and typically has a CO_2 concentration of less than 15vol %. Thus, the thermodynamic driving force for CO_2 capture from flue gas is low (CO_2 partial pressure is typically less than 15 kPa creating a technical challenge for the development of cost-effective advanced capture processes. In spite of this difficulty, post-combustion carbon capture has the greatest near-term potential for reducing GHG emissions, because it can be retrofitted to existing units that generate two-thirds of the CO_2 emissions in the power sector. Figure 58 indicates that as innovative CO_2 capture and

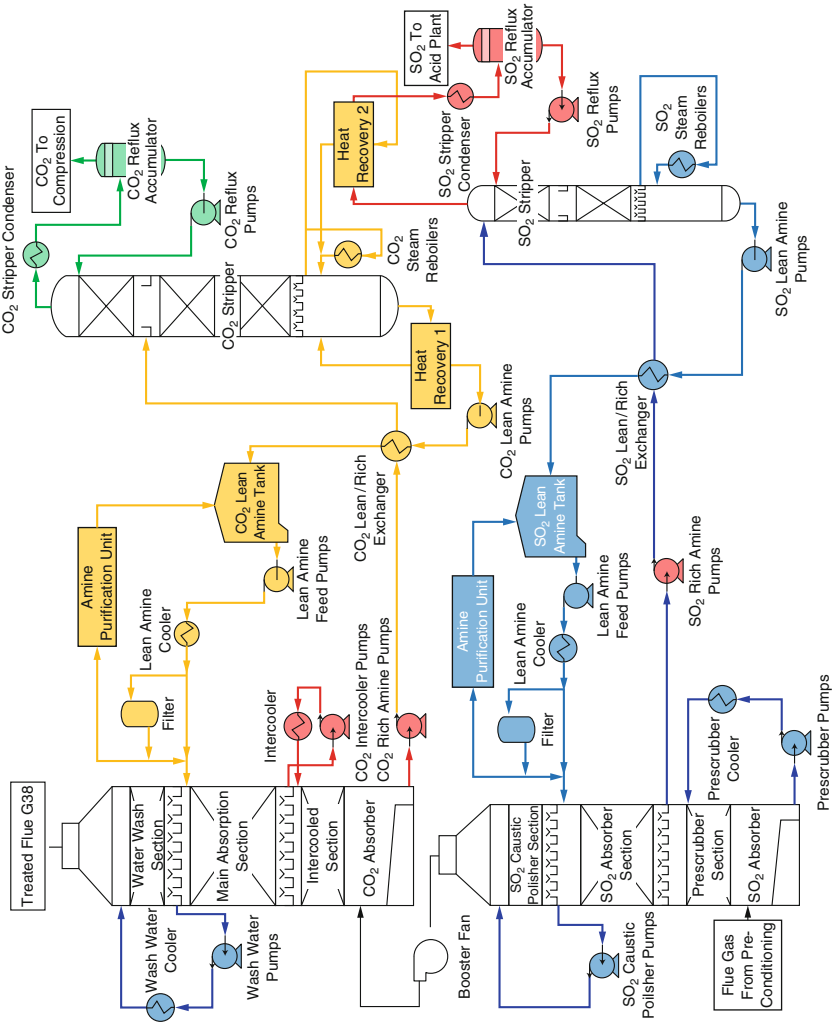

Fig. 57 Process lineup of the Boundary Dam CCS project

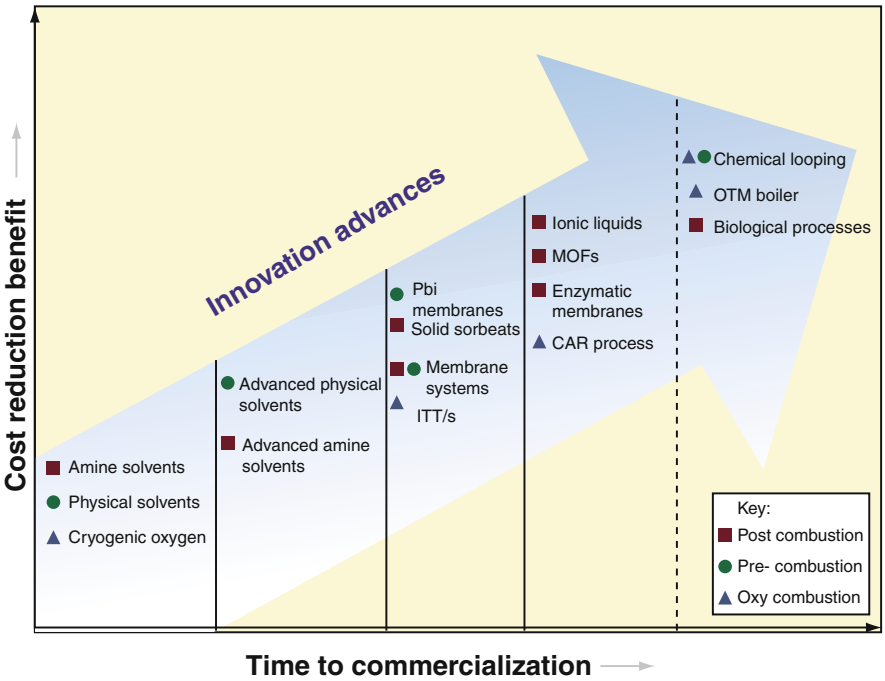

Fig. 58 Innovative CO_2 capture technologies – cost reduction benefits versus time to commercialization (Figueroa et al. 2008)

Table 16 Pros and cons of current CO_2 separation technologies

CO_2 capture technology	Pros	Cons
Amine scrubbing	Applicable to CO_2 partial pressures	Process consumes considerable energy
	Recovery rates of up to 95 % and product purity >99 vol.% can be achieved	Solvent degradation and equipment corrosion occur in the presence of O_2
		Concentrations of SO *x* and NO *x* in the gas stream combine with the amine to form irregenerable, heat-stable salts
		Rectisol™ refrigeration costs can be high
Ammonia process	Lower heat of regeneration than MEA	Ammonium bicarbonate decomposes at 140_F (use Kelvin), so temperature in the absorber must be lower than 140_F (use Kelvin)

(*continued*)

Table 16 (continued)

CO_2 capture technology	Pros	Cons
	Higher net CO_2 transfer capacity than MEA	Ammonia is more volatile than MEA and often provides an ammonia slip into the exit gas
	Stripping steam not required	Ammonia is consumed through the irreversible formation of ammonium sulfates and nitrates as well as removal of HCl and HF
	Offers multi-pollutant control	
Membrane technology	No regeneration energy is required	Membranes can be plugged by impurities in the gas stream
	Simple modular system	Preventing membrane wetting is a major challenge
	No waste streams	Technology has not been proven industrially

Table 17 Future directions of chemical absorption technologies for CO_2 capture

Technology for CO_2 capture	Future direction
Amine scrubbing	Absorbent studies
	1. Set an evaluation criterion for the selection of amines
	2. Mixed amines
	3. Ionic liquid
	4. New solvents
	Absorber column studies
	1. New packings
	2. High-efficiency reactors
	Process integration and optimization
	1. Heat integration
	2. Water balance
Ammonia process	Optimization of regeneration process
	Slippery control of ammonia
	Selection of additives for ammonia solution
Membrane technologies	Plugging mechanism of membrane and control measures
	Wetting mechanism of membrane and control measures
	Selection and pretreatment of membrane
	Optimization of process

separation technologies advance, significant cost reduction benefits can potentially be realized once they are commercialized. Obviously, as a method of post-combustion capture, chemical absorption is the most likely technology in the upcoming years. Table 16 shows the pros and cons of current CO_2 separation technologies.

Future Directions of Chemical Absorption Technologies for CO_2 Capture

To predict the future directions of chemical absorption technologies is a hard task. Every technology occupies its own advantages and disadvantages. The predictable truth is that the improvement of the chemical absorption technologies is the future work. Whatever the novel technology turns out, the technology should occupy the basic elements such as absorbent, absorber, and cyclic process. Hence, the future direction must have great improvement on the related problems. Some potential directions for the existing technologies are analyzed in Table 17.

References

Agar DW, Tan YH, Hui ZX (2008) Separation CO_2 from gas mixtures. Patent WO 2008/015217

BP America (2005) CO_2 capture project technical report DEFC26-01NT41145, National Energy Technology Laboratory

Aroonwilas A, Veawab A (2004) Integration of CO_2 capture unit using single- and blended-amines into supercritical coal-fired power plants: implications for emission and energy management. Int J Greenhouse Gas Control 1:143–150

Bacon JR, Demas JN (1987) Determination of oxygen concentrations by luminescence quenching of a polymer-immobilized transition-metal complex. Anal Chem 59(23):2780–2785

Bedell SA (2009) Oxidative degradation mechanisms for amines in flue gas capture. Energy Procedia 1:771–778

Bedell SA, Myers J (1994) Chelating agent formulation for hydrogen sulfide abatement. US Patent 5,338,778, 16 Aug 1994

Black S (2006) Chilled ammonia scrubber for CO_2 capture. MIT Carbon Sequestration Forum VII, Cambridge, MA

Blauwhoff PMM, Versteeg GF, Van Swaaij WPM (1984) A study on the reaction between CO_2 and alkanolamines in aqueous solutions. Chem Eng Sci 39:207–225

Boa L, Trachtenberg MC (2006) Facilitated transport of CO_2 across a liquid membrane: comparing enzyme, amine, and alkaline. J Membr Sci 280:330–334

Bozzano G, Dente M, Manenti F, Corna P, Masserdotti F (2014) Fluid distribution in packed beds. Part 1. Literature and technology overview. Ind Eng Chem Res 53:3157–3164

Buxton GV (1988) Critical review of rate constants for reactions of hydrated electrons, hydrogen atoms and hydroxyl radicals (OH radical dot/O radical dot-) in aqueous solution. J Phys Chem Ref Data 17:513

Cai Z, Xie R, Wu Z (1996) Binary isobaric vapor-liquid equilibria of ethanolamines + water. J Chem Eng Data 41:1101–1103

Camacho F, Sánchez S, Pacheco R, Sánchez A, La Rubia MD (2005) Absorption of carbon dioxide at high partial pressures in aqueous solutions of di-isopropanolamine. Ind Eng Chem Res 44:7451–7457

Chapel DG, Mariz CL, Ernest J (1999) Recovery of CO_2 from flue gases: commercial trends. http://www.netl.doe.gov/publications/proceedings/01/carbon_seq/2b3.pdf

Chen J (2002) Super-gravity technology and its application. Chemical Industry Press, Beijing

Chen M (2006) Super-gravity absorption reactors for CO_2 removal from flue gas. CN 2829861Y

Crognale G (1999) Environmental management strategies: the 21st century perspective. Air and Waste Management Association, Sewickley

Dame UON. CO_2 capture with ionic liquids involving phase change. http://www.arpae-summit.com/em_reporting/exhibitor_detail?exhibitor_id=4238

Davis J, Rochelle GT (2009) Thermal degradation of monoethanolamine at stripper conditions. Energy Procedia 1:327–333
Derks PWJ, Dijkstra HBS, Hogendoorn JA, Versteeg GF (2005) Solubility of carbon dioxide in aqueous piperazine solutions. AIChE J 51:2311–2327
Desideri U, Paolucci A (1999) Performance modelling of a carbon dioxide removal system for power plants. Energ Convers Manag 40:1899–1915
DuPart MS, Bacon TR, Edwards DJ (1993) Understanding corrosion in alkanolamine gas treating plants. Part 2. Case histories show actual plant problems and their solutions. Hydrocarb Process 75–80
Eide-Haugmo I et al (2009) Environmental impact of amines. Energy Procedia 1:1297–1304
Ermatchkov V, Kamps AP-S, Speyer D, Maurer G (2006) Solubility of carbon dioxide in aqueous solutions of piperazine in the low gas loading region. J Chem Eng Data 51:1788–1796
Figueroa JD, Fout T, Plasynski S, McIlvried H, Srivastava RD (2008) Advances in CO_2 capture technology – the U.S. Department of Energy's carbon sequestration program. Int J Greenhouse Gas Control 2:9–20
Fisher KS, Beitler C, Rueter C, Searcy K, Rochelle GT, Jassim M (2005) Integrating MEA regeneration with CO_2 compression and peaking to reduce CO_2 capture costs. US: final report of work performed under grant no: DE-FG02-04ER84111, 09 June 2005
Freeman SA, Rochelle GT (2011) Thermal degradation of piperazine and its structural analogs. Energy Procedia 4:43–50
Freeman SA, Dugas R, Van Wagener DH, Nguyen T, Rochelle GT (2010) Carbon dioxide capture with concentrated, aqueous piperazine. Int J Greenhouse Gas Control 4:119–124
Goff GS, Rochelle GT (2006) Oxidation inhibitors for copper and iron catalyzed degradation of monoethanolamine in CO_2 capture processes. Ind Eng Chem Res 45:2513
Hakka LE, Ouimet MA (2006) US Patent 7,056,482, 6 June 2006
Harris F, Kurnia KA, Mutalib MIA, Thanapalan M (2009) Solubilities of carbon dioxide an densities of aqueous sodium glycinate solutions before and after CO_2 absorption. J Chem Eng Data 54:144–147
Haslegrave JA, Hedges WM, Montgomerie HTR, O'Brien TM (1992) The development of corrosion inhibitors with low-environmental toxicity. In: SPE annual technical conference and exhibition, 4–7 Oct 1992, Washington, DC
Horng CT, Li M (2002) Bottom spin valves with continuous spacer exchange bias. US Patent, 6,466,418
Hu L (2009) Phase transitional absorption method. US Patent 7,541,011
Huang B, Xu S, Gao S, Liu L, Tao J, Niu H et al (2010) Industrial test and techno-economic analysis of CO_2 capture in Huaneng Beijing coal-fired power station. Appl Energ 87:3347–3354
Jassim MS, Rochelle GT (2006) Innovative absorber/stripper configurations for CO_2 capture by aqueous monoethanolamine. Ind Eng Res 45:2465–2472
Kamijo TIMM (2006) Apparatus and method for CO_2 recovery. Mitsubishi Heavy Industries, Kansai Electric Company
Kang MS, Moon SH, Park YI, Lee KH (2002) Development of carbon dioxide separation process using continuous hollow-fiber membrane contactor and water-splitting electrodialysis. Sep Sci Technol 37:1789–1806
Koch G (2001) Corrosion cost preventive strategies in the Unites States. CC Technologies & NACE international (Sponsored by Office of Infrastructure and Development Federal Highway Administration)
Kohl AL, Nielsen R (1997) Gas purification, 5th edn. Gulf Publishing Company, Houston
Korendovych IV, Kryatov SV, Rybak-Akimova EV (2007) Dioxygen activation at non-heme iron: insights from rapid kinetic studies. Acc Chem Res 40:510
Kumar PS, Hogendoorn JA, Feron PHM, Versteeg GF (2003) Equilibrium solubility of CO_2 in aqueous potassium taurate solutions: part 1. Crystallization in carbon dioxide loaded aqueous salt solutions of amino acids. Ind Eng Chem Res 42:2832–2840

Kvamsdal HM, Rochelle GT (2008) Effects of temperature in CO_2 absorption from flue gas by aqueous mono-ethanolamine. Ind Eng Chem Res 43(3):867–875

Kvamsdal HM et al (2010) Maintaining a neutral water balance in a 450 MWe NGCC-CCS power system with post-combustion carbon dioxide capture aimed at offshore operation. Int J Greenhouse Gas Control 4:613–622

Lalevee J, Allonas X, Fouassier J-P (2002) NH and α (CH) bond dissociation enthalpies of aliphatic amines. J Am Chem Soc 124:9613

Larsen BL, Rasmussen P, Fredenslund A (1987) A modified UNIFAC group contribution model for prediction of phase equilibria and heats of mixing. Ind Eng Chem Res 26:2274–2286

Lenard J, Rousseau R, Teja A (1990) Vapor-liquid equilibria for mixtures of 2-aminoethanol + water. AIChE Symp Ser 86(279):1–5

Lente G, Fabian I (1998) The early phase of the iron(III)-sulfite ion reaction. Formation of a novel iron(III)-sulfito complex. Inorg Chem 37:4204

Lin C-C, Liu W-T, Tan C-s (1990) Removal of carbon dioxide by absorption in a rotating packed bed. Ind Eng Chem Res 29:917

Liu X, Sawyer DT, Bedell SA, Worley CM (1995) Ligand degradation in the iron/dioxygen-induced dehydrogenation of H_2S. Paper presented at the seventh sulfur recovery conference, Austin, 24 Sept 1995

Ma'mun S, Jakobsen JP, Svendsen HF (2006) Experimental and modeling study of the solubility of carbon dioxide in aqueous 30 mass % 2-((2-aminoethyl)amino)ethanol solution. Ind Eng Chem Res 45:2505–2512

Maddox RN (1985) Gas conditioning and processing, vol 4, Gas and liquid sweetening. Campbell Petroleum Series, Norman

Mamun S et al (2007) Selection of new absorbents for carbon dioxide capture. Energy Conv Manag 48:251–258

Mandal BP, Bandyopadhyay SS (2005) Simulation absorption of carbon dioxide and hydrogen sulfide into aqueous blends of 2-amino-2-methyl-1-propanol and diethanolamine. Chem Eng Sci 60:6438–6451

Mandal BP, Bandyopadhyay SS (2006a) Absorption of carbon dioxide into aqueous blends of 2-amino-2-methyl-1-propanol and monoethanolamine. Chem Eng Sci 61:5440–5447

Mandal BP, Bandyopadhyay SS (2006b) Simultaneous absorption of CO_2 and H_2S into aqueous blends of *N*-methyldiethanolamine and diethanolamine. Environ Sci Technol 40:6076–6084

Mandal BP, Guba M, Biswas AK, Bandyopadhyay SS (2001) Removal of carbon dioxide by absorption in mixed amines: modeling of absorption in aqueous MDEA/MEA and AMP/MEA solutions. Chem Eng Sci 56:6217–6224

Mandal BP, Kundu M, Padhiyar NU, Bandyopadhyay SS (2004) Physical solubility and diffusivity of N_2O and CO_2 into aqueous solutions of (2-amino-2-methyl-1-propanol + diethanolamine) and (*N*-methyldiethanolamine + diethanolamine). J Chem Eng Data 49:264–270

Matsumiya N, Teramoto M, Kitada S, Matsuyama H (2005) Evaluation of energy consumption for separation of CO_2 in flue gas by hollow fiber facilitated transport membrane module with permeation of amine solution. Sep Purif Technol 46:26–32

McLees JA (2006) Vapor-liquid equilibrium of monoethanolamine/piperazine/water at 35–70 °C. MSE thesis, The University of Texas at Austin, Austin

McMahon AJ, Harrop D (1995) Green corrosion inhibitors: an oil company perspective. In: CORROSION 95, Houston

Meng H et al (2008) Removal of heat stable salts from aqueous solutions of *N*-methyldiethanolamine using a specially designed three-compartment configuration electrodialyzer. J Membr Sci 322:436–440

Mimura T, Suda T, Honda A, Kumazawa H (1998) Kinetics of reaction between carbon dioxide and sterically hindered amines for carbon dioxide recovery from power plant flue gases. Chem Eng Commun 170:245–260

MOEA Industrial Development Bureau (2002) The technique manual on the recovery of carbon dioxide by absorption, Taiwan
Mogul MG (1999) Reduce corrosion in amine gas absorption columns. Hydrocarb Process 78 (10):47–56
Nath A, Bender E (1983) Isothermal vapor-liquid equilibria of binary and ternary mixtures containing alcohol, alkanolamine, and water with a new static device. J Chem Eng Data 26:370–375
Nguyen T et al (2010) Amine volatility in CO_2 capture. Int J Greenhouse Gas Control 4(5):707–715
Okabe K, Mano H, Fujioka Y (2008) Separation and recovery of carbon dioxide by a membrane flash process. Int J Greenhouse Gas Control 2:485–491
Oyenekan BA, Rochelle GT (2006) Energy performance of stripper configurations for CO_2 capture by aqueous amines. Ind Eng Chem Res 45(8):2457–2464
Oyenekan BA, Rochelle GT (2007) Alternative stripper configurations for CO_2 capture by aqueous amines. AIChE J 53(12):3144–3154
Oyenekan BA, Rochelle GT (2009) Rate modeling of CO_2 stripping from potassium carbonate promoted by piperazine. Int J Greenhouse Gas Control 3:121–132
Pederson O, Dannstrom H, Gronvold M, Stuksrud D, Ronning O (2000) Gas treating using membrane gas/liquid contactors. In: Fifth international conference on greenhouse gas control technologies, Cairns
Polderman LD, Dillon CP et al (1955) Why monoethanolamine solution breaks down in gas treating service. In: Proceedings of the gas conditioning conference, pp 49–56
Rampin P (2000) Amine units: results of a survey on structural reliability. In: Proceedings of international conference corrosion in refinery, petrochemical and power generation plants, Venezia, pp 18–19
Ramshaw C, Mallinson RH (1981) Mass transfer process. US Patent 4,283,255
Raynal L, Alix P, Bouillon P, Gomez A, de Nailly MLF, Jacquin M et al (2011) The DMX™ process: an original solution for lowering the cost of post-combustion carbon capture. Energy Procedia 4:779–786
Reddy SGJF (2007) Integrated compressor/stripper configurations and methods. Fluor Technologies Corporation
Resnik KP, Yeh JT, Pennline HW (2004) Aqua ammonia process for simultaneous removal of CO_2, SO_2 and NO_x. Int J Environ Technol Manage 4(1/2):89–104
Resnik KP, Garber W, Hreha DC, Yeh JT, Pennline HW (2006) A parametric scan for regenerative ammonia-based scrubbing for the capture of CO_2. In: Proceedings of the 23rd annual international Pittsburgh coal conference, Pittsburgh
Rinker EB, Ashour SS, Sandall OC (1995) Kinetics and modelling of carbon dioxide absorption into aqueous solutions of *N*-methyldiethanolamine. Chem Eng Sci 50:755–768
Rochelle G, Chen E, Dugas R, Oyenakan B, Seibert F (2006) Solvent and process enhancements for CO_2 absorption/stripping. In: 2005 annual conference on capture and sequestration, Alexandria
Rochelle G, Chen E, Freeman S, Van Wagener D, Xu Q, Voice A (2011) Aqueous piperazine as the new standard for CO_2 capture technology. Chem Eng J 171:725–733
Rojey A, Cadours R, Carrette P-L et al (2007) Process for deacidification of a gas by means of an absorbent solution with fractionated regeneration by heating. Patent WO 2007/104856
Rooney PC, DuPart MS, Bacon TR (1998) Oxygen's role in alkanolamine degradation. Hydrocarb Process 77(7):109–113
Rubin ES, Rao AB (2002) A technical economic and environmental assessment of amine-based CO_2 capture technology for power plant greenhouse gas control. Annual Technical Progress Report
Sakwattanapong R et al (2005) Behavior of reboiler heat duty for CO_2 capture plants using regenerable single and blended alkanolamines. Ind Eng Chem Res 44:4465–4473
Schnell I (2004) Dipolar recoupling in fast-MAS solid-state NMR spectroscopy. Chem Inform 35. doi:10.1002/chin.200451274

Schwartz HA (1982) Chain decomposition of aqueous triethanolamine. J Phys Chem 86:3431
Semeonova TA, Lieyijiesi ИЛ (1982) Purification of industrial gas. Research Institute of Nanjing Chemical Industrial Corporation Translation. Chemical Industry Press, Beijing
Shuster E (2010) Estimating freshwater needs to meet future thermoelectric generation requirements, DOE/ NETL-400/2010/1339, pp 7–14
Singh D, Croiset E, Douglas PL, Douglas MA (2002) Economics of CO_2 capture from a coal-fired power plant – a sensitivity analysis. In: Proceedings of the sixth conference on greenhouse gas control technologies (GHGT-6), Kyoto
Singh P, Niederer JPM, Versteeg GF (2007) Structure and activity relationships for amine based CO_2 absorbents – I. Int J Greenhouse Gas Control 1:5–10
Soosaiprakasam IR (2008) Corrosion and polarization behavior of carbon steel in MEA2 based CO_2 capture process. Int J Greenhouse Gas Control 2(4):553–562
Soosaiprakasam IR, Veawab A (2008) Corrosion and polarization behavior of carbon steel in MEA-based CO_2 capture process. Int J Green House Gas Control 2:553–562
Source: IPCC special report on carbon dioxide capture and storage, 2005
Spekuljak Z, Monella H (1994) A new design concept of structured packing column auxiliaries. Chem Eng Technol 17:61–66
Stéphenne K (2013) Start-up of world's first commercial post-combustion coal fired CCS project: contribution of Shell Cansolv to SaskPower Boundary Dam ICCS project. Energy Procedia
Suzuki M (2007) Ligand effects on dioxygen activation by copper and nickel complexes: reactivity and intermediates. Acc Chem Res 40:609
Svendsen HF, Tobiesen FA, Mejdell T et al (2007) Method and apparatus for energy reduction in acid gas capture processes. Patent WO 2007/001190
Tan MSYH (2010) Study of CO_2-absorption into thermomorphic lipophilic amine solvents
Tan LS, Shariff AM, Lau KK, Bustam MA (2012) Factors affecting CO_2 absorption efficiency in packed column: a review. J Ind Eng Chem 18:1874–1883
Teramoto M, Ohnishi N, Takeuchi N, Kitada S, Matsuyama H, Matsumiya N, Mano H (2003) Separation and enrichment of carbon dioxide by capillary membrane module with permeation of carrier solution. Sep Purif Technol 30:215–217
Teramoto M, Kitada S, Ohnishi N, Matsuyama H, Matsumiya N (2004) Separation and concentration of CO_2 by capillary-type facilitated transport membrane module with permeation of carrier solution. J Membr Sci 234:83–94
Thitakamol B, Veawab A, Aroonwilas A (2007) Environmental impacts of absorption-based CO_2 capture unit for post-combustion treatment of flue gas from coal-fired power plant. Int J Greenhouse Gas Control 1(3):318–342
Touhara H, Okazaki S, Okino F, Tanaka H, Ikari K, Nakanishi K (1982) Thermodynamic properties of aqueous mixtures of hydrophilic compounds 2-aminoethanol and its methyl derivatives. J Chem Thermodyn 14:145–156
Trachtenberg MC, Tu CK, Landers RA, Wilson RC, McGregor ML, Laipis PJ, Paterson M, Silverman DN, Thomas D, Smith RL, Rudolph FB (1999) Carbon dioxide transport by proteic and facilitated transport membranes. Life Support Biosph Sci 6:293–302
Vaidya PD, Kenig EY (2007) Absorption of CO_2 into aqueous blends of alkanolamines prepared from renewable resources. Chem Eng Sci 62:7344–7350
Van Eldik R, Coichev N, Bal Reddy K, Gerhard A (1992) Metal ion catalyzed autoxidation of sulfur (IV) oxides: redox cycling of metal ions induced by sulfite. Ber Bunsenges Phys Chem 96:478
Veawab A, Aroonwilas A (2002) Identification of oxidizing agents in aqueous amine-CO_2 systems using a mechanistic corrosion model. Corros Sci 44:967–987
Weiyang F (2005) Liquid effective velocity in a column containing corrugated metal sheet packing. Chem Ind Eng Process 24:1–4
White CM, Strazisar BR, Granite EJ (2003) Separation and capture of CO_2 from large stationary sources and sequestration in geological formations: coalbeds and deep saline aquifers. J Air Waste Manag Assoc 53(6):645–715
Woodhouse SRP (2008) Improved absorbent regeneration. Aker Clean Carbon

Yan S, Fang M et al (2007) Experimental study on the separation of CO_2 from flue gas using hollow fiber membrane contactors without wetting. Fuel Process Technol 88(5):501–511
Yan S, Fang M et al (2008) Comparative analysis of CO_2 separation from flue gas by membrane gas absorption technology and chemical absorption technology in China. Energy Convers Manage 49:3188–3197
Yan S, Fang M et al (2009) Regeneration of CO_2 from CO_2-rich alkanolamines solution by using reduced thickness and vacuum technology: regeneration feasibility and characteristic of thin-layer solvent. Chem Eng Process 48:515–523
Yang WC, Ciferno J (2006) Assessment of carbozyme enzyme-based membrane technology for CO_2 capture from flue gas. DOE/NETL 401/072606
Yazvikova NV, Zelenskaya LG et al (1975) Mechanism of side reactions during removal of carbon dioxide from gases by treatment with monoethanolamine. Z Prik Khim 48(3):674–676
Yeh JT, Resnik KP, Rygle K, Pennline HW (2005) Semibatch absorption and regeneration studies for CO_2 capture by aqueous ammonia. Fuel Process Technol 86(14–15):1533–1546
Yeon SH, Lee KS, Sea B, Park YI, Lee KH (2005) Application of pilot-scale membrane contactor hybrid system for removal of carbon dioxide from flue gas. J Membr Sci 257:156–160
Zhang Q, Cussler EL (1985a) Microporous hollow fibers for gas-absorption. 1. Mass-transfer in the liquid. J Membr Sci 23:321–332
Zhang Q, Cussler EL (1985b) Microporous hollow fibers for gas-absorption. 2. Mass-transfer across the membrane. J Membr Sci 23:333–345
Zhang J, Agar DW, Zhang X, Geuzebroek F (2011) CO_2 absorption in biphasic solvents with enhanced low temperature solvent regeneration. Energy Procedia 4:67–74
Zhang J, Qiao Y, Wang W, Misch R, Hussain K, Agar DW (2013) Development of an energy-efficient CO_2 capture process using thermomorphic biphasic solvents. Energy Procedia 37:1254–1261

CO_2 Capture Using Solid Sorbents

Yao Shi, Qing Liu, and Yi He

Contents

Abstract

Global warming and climate change due to the emission of greenhouse gases, especially CO_2, has become a widespread concern in the recent years. Capturing CO_2 is one of the major approaches to tackle this issue. Among the currently available CO_2 capture technologies, adsorption processes using solid sorbents capable of capturing CO_2 have shown many advantages. In

Y. Shi (✉) • Q. Liu • Y. He
Department of Chemical and Biological Engineering, Institute of Industrial Ecology and Environment, College of Chemical and Biological Engineering, Zhejiang University, Hangzhou, Zhejiang, People's Republic of China
e-mail: shiyao@zju.edu.cn; 11228048@zju.edu.cn; yihezj@zju.edu.cn

W.-Y. Chen et al. (eds.), *Handbook of Climate Change Mitigation and Adaptation*,
DOI 10.1007/978-3-319-14409-2_83

the past few years, many groups have been engaged in the development of new solid sorbents for CO_2 capture with superior performance and desirable economics. The main purpose of this chapter is to provide a bridge between detailed technical reports and broad resource and economic assessments on CO_2 capture using solid sorbents. The fundamental aspects of solid sorbents for CO_2 capture are firstly discussed, which include both the selection and the evaluation of sorbents. The following characteristics of solid sorbents are covered: the equilibrium adsorption capacity, selectivity, adsorption/desorption kinetics, multicycle durability, mechanical properties, hydrothermal and chemical stability, and energy consumption of regeneration. Typical families of solid sorbents such as activated carbonaceous materials, polymeric materials, zeolites, silica, metal–organic frameworks (MOFs), and alkali-metal carbonate loaded with or without functionality for the adsorption of CO_2 are then reviewed, respectively. In addition, a brief review on technical challenges and pilot plant developments are presented. Finally, a few recommendations are provided for further research efforts on CO_2 capture with solid sorbents.

Introduction

Growing concerns for global warming and climate change in recent years have motivated research activities toward developing more efficient and improved processes for carbon dioxide (CO_2) capture and sequestration (CCS) from large point sources, such as coal-fired power plants, natural gas processing plants, and cement plants (Samanta et al. 2012). The development of efficient technologies for the capture and sequestration of carbon dioxide produced by existing point sources will prove vital in controlling the environmental impact of anthropogenic emissions. In order for these technologies to be economically viable, CCS systems must curb the energy penalty associated with CO_2 capture and sorbent regeneration and operate effectively in realistic conditions. The search for materials that fulfill the criteria of an efficient CO_2 sorbent has been proceeding with urgency (Sumida et al. 2012).

Processes based on aqueous amine absorbents represent the currently available and practically applied technology for CO_2 capture. They include an energy penalty of roughly 30 % on top of the power generation of the plant (Rochelle 2009). An alternative approach to reduce the energy penalty is by using solid sorbents as they have comparatively lower heat capacities. This chapter is devoted to the fundamentals of the solid adsorbents for CO_2 capture and the present status and prospect of their applications. The adsorption of CO_2 can be classified as physical adsorption (adsorption enthalpy $<$20–40 KJ/mol), chemical adsorption (adsorption enthalpy $>$20–40 KJ/mol), or both. These two types of adsorption differ from each other in many ways. The major difference is briefly discussed as follows.

The solid adsorbents for CO_2 capture can be various solid materials, including porous carbonaceous materials, zeolites, alumina, silica, and metal–organic frameworks (MOFs). For physisorption, the mechanism of CO_2 capture can be explained with the selective adsorption of CO_2, which is caused by van der Waals interaction between the CO_2 and adsorbent, as well as by pole–ion and pole–pole interactions between the quadruple of CO_2 and the ionic and polar sites of the sorbent surface (Samanta et al. 2012).

Most of the conventional physisorbents suffer from poor selectivity for CO_2 and low CO_2 adsorption capacities, especially at a relatively low CO_2 partial pressure. In order to increase CO_2 adsorption capacity and to keep high selectivity for CO_2, chemical modifications are often performed on the surface of the porous materials by incorporating basic groups which are capable of interacting efficiently with acidic CO_2. Amine is one of the commonly used functional groups for this purpose. Amine-based adsorbents can be classified into three classes (Li et al. 2010; Jones 2011):

- **Class 1**: This class of supported sorbents is prepared by physically loading monomeric or polymeric amine species onto or into the micro-/mesoporous support (impregnation).
- **Class 2**: The amine, mainly amine-containing silane, is covalently tethered to a solid support. This is accomplished by binding amines to oxides via the use of silane chemistry or via preparation of polymeric supports with amine-containing side chains. This provides covalently tethered amine sorbents which possess the potential to be completely regenerable through multicycle adsorption/desorption processes.
- **Class 3**: These adsorbents are based on porous supports upon which amino-polymers are polymerized in situ. This class of sorbents can be considered a hybrid of the first two classes (Li et al. 2010).

The structures of commonly used amines for sorbent functionalization were given in Table 1.

CO_2 adsorption using amine-functionalized sorbents involves chemical reaction. Therefore, it is essential to know how the nature of amine influences the adsorption capacity and the rate of adsorption. The zwitterion mechanism originally proposed by Caplow (1968) is often used to explain the reaction of primary/secondary amines and CO_2. The mechanism involves two steps: (1) formation of zwitterion and (2) deprotonation of zwitterion. The overall reaction can be written as:

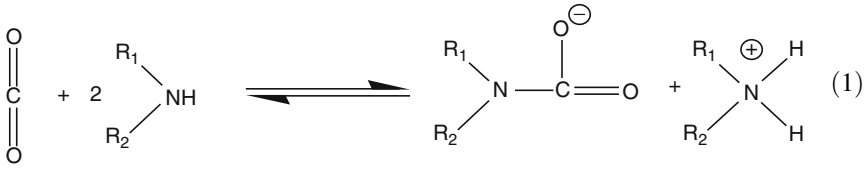

where $R_2 = H$ for the primary amine.

Table 1 Structure of widely used amines for sorbent functionalization (Samanta et al. 2012)

Name	Structure	Name	Structure
Amines		Silanes	
Monoethanolamine (MEA)		3-aminopropyltrimethoxysilane (APTS)	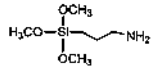
Diethanolamine (DEA)	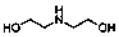	3-aminopropyltriethoxysilane (APTES)	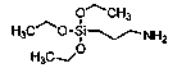
Triethanolamine (TEA)	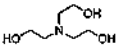	N-[3-(trimethoxysilyl)propyl]-ethylenediamine (AEAPTS)	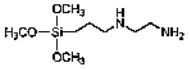
Polyethyleneimine (PEI)	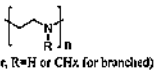 (R=H for linear, R=H or CH_2 for branched)	N-[3-(trimethoxysilyl)propyl]-diethylenetriamine (DAEAPTS)	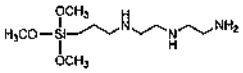
Diethylenetriamine (DETA)	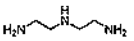	Ethylhydroxyl-aminopropyl-trimethoxysilane (EHAPTS)	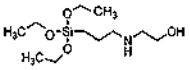
Tetraethylenepentamine (TEPA)	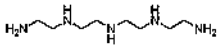	Diethylhydroxyl-aminopropyl-trimethoxysilane (DEHAPTS)	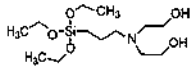
		Cyclic	
Tetraethylenepentamine-acrylonitrile (TEPAN)	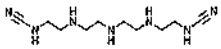	Aziridine	
Pentaethylenehexamine (PEHA)	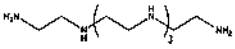	1,8-diazabicyclo[5.4.0]undec-7-ene (DBU)	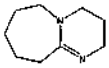
2-Amino-2-methyl-1,3-propanediol (AMPD)	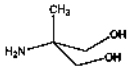	1,5-diazabicyclo [4.3.0]non-5-ene (DBN)	
2-(2-Aminoethylamino)ethanol (AEAE)	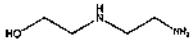	N-methyltetrahydropyrimidine (MTHP)	

If we consider the amine as a base, the equilibrium CO_2 adsorption capacities of primary/secondary amines are restricted by the overall stoichiometry to 0.5 mol (mol of amine)$^{-1}$.

The important reaction between CO_2 and the sterically hindered primary or secondary amine would be the formation of bicarbonate, as shown by reaction 2, similar to the case of tertiary amines. The stoichiometry for this reaction allows a CO_2 loading of up to 1 mol (mol of amine)$^{-1}$ for hindered primary or secondary amine.

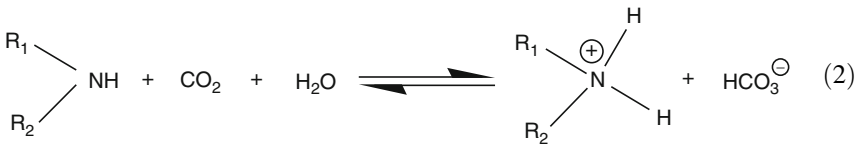

(2)

The reaction of CO_2 with moderately hindered amines includes the formation of a carbamate, as in the case of no hindered amines (reaction 1), the stoichiometry of which allows a CO_2 loading of up to 0.5 mol (mol of amine)$^{-1}$. Instead, the reaction produces protonated amine and bicarbonate ion in the presence of moisture, leading to a higher capacity for CO_2 up to 1.0 mol (mol of amine)$^{-1}$. The mechanism of this reaction is suggested to be base-catalyzed hydration of CO_2, as given previously in reaction 2 (Donaldson and Nguyen 1980). Generally, the formation of bicarbonate allows a high equilibrium capacity, but the kinetics is very slow. The primary and secondary amines can react directly with CO_2, while tertiary amines cannot directly react with CO_2. They lack the free proton needed in the deprotonation step.

Fundamentals of CO_2 Adsorption Using Solid Sorbents

Criteria for Selecting Sorbents

The selection of solid sorbents for CO_2 capture largely depends on the scenario where a solid sorbent is used. Capturing CO_2 from a flue gas stream and a biogas stream demands significant different criteria as these streams have dissimilar characteristics in composition, temperature, etc. The selection of sorbents for CO_2 capture must satisfy important criteria to be both economical and operational, as well. Here, we listed few most important criteria as below (Samanta et al. 2012; Yong et al. 2002; Sayari et al. 2011):

- **Adsorption capacity for CO_2**: The equilibrium adsorption capacity of a sorbent material is of great importance to the capital cost of a CO_2 capture system, as it dictates the amount of adsorbent to be used in an adsorption column and its size. Working capacity, which is an effective capacity in an adsorption/desorption cycle, is preferred to be used in place of equilibrium capacity in practice. To enhance the competitiveness of solid sorbents with existing monoethanolamine (MEA) scrubbing system, the CO_2 working capacity should be in the range of 3–4 mmol/g of sorbent (Gray et al. 2008). Because the study of CO_2 adsorbents is in its early stage, most of the CO_2 capture capacity reported in this review are lower than this criterion.
- **Selectivity for CO_2**: The selectivity, which is defined by the ratio of the CO_2 capacity to that of another component, has a direct influence to the purity of CO_2 captured. The purity of CO_2 has impacts on transportation and sequestration. It plays a vital role in the economics in CO_2 sequestration. Desired sorbent materials should exhibit high CO_2 selectivity over other bulk gas components. In addition, it is important that solid sorbents also show high capacity for CO_2 in the existence of significant amounts of water vapor.
- **Adsorption/desorption kinetics**: Fast adsorption/desorption kinetics for CO_2 under the operating conditions is extremely essential. The cycle time of a CO_2

Table 2 Physical parameters of gases relevant to carbon dioxide capture processes (Sumida et al. 2012; Li et al. 2009)

Molecule	Kinetic diameter (Å)	Polarizability (10^{-25} cm^{-3})	Dipole moment (10^{-19} esu^{-1} cm^{-1})	Quadrupole moment (10^{-27} esu^{-1} cm^{-1})
H_2	2.89	8.04	0	6.62
N_2	3.64	17.4	0	15.2
O_2	3.46	15.8	0	3.9
CO	3.76	19.5	1.10	
NO	3.49	17.0	1.59	
H_2O	2.65	14.5	18.5	
H_2S	3.60	37.8	9.78	
CO_2	3.30	29.1	0	43
NO_2		30.2	0	

adsorption system is controlled by the kinetics of adsorption and desorption. Fast kinetics yields a sharp CO_2 breakthrough curve, while slow kinetics provides a distended breakthrough curve. The overall kinetics of CO_2 adsorption onto a functionalized solid sorbent is influenced by the intrinsic reaction kinetics of CO_2 with the functional group present, as well as the mass transfer or diffusional resistance of the gas phase through the sorbent structures. The structures of porous support functionalized also can be tailored. The faster an adsorbent can adsorb CO_2 and be desorbed, the less of it will be needed to capture a given volume.

- **Mechanical strength of sorbent particles**: During multicycle between the adsorption and desorption steps, the sorbent must ensure microstructure and morphological stability and retain the CO_2 adsorption capacity. It is crucial to have microstructure and morphological stability of tailored regenerable sorbents in multicycle operation to maintain high kinetics. Operating conditions, such as high volumetric flow rate, vibration, and temperature, should not give rise to appreciable disintegration of the sorbent particles. This could also happen via abrasion or crushing. Therefore, adequate mechanical strength of sorbent particles is critical to minimize the sorbent makeup rate, as well as to keep CO_2 capture process cost-effective.
- **Chemical stability/tolerance to impurities**: Solid sorbents for CO_2 capture – in particular, amine-functionalized sorbents – should be stable in an oxidizing environment and be resistant to common gas contaminants. It is likely that contaminants such as SO_x, NO_x, and heavy metals should be removed, as they unfavorably affect the CO_2 adsorption process of the sorbent materials. Table 2 lists physical parameters of gases relevant to CO_2 capture processes.
- **Regeneration of sorbents**: The heat of adsorption, which is a measure of the energy required for regeneration, should be substantially low. The sorbent should be regenerable through a suitable pathway while maintaining efficient CO_2 adsorption capacity during repeated adsorption/desorption cycles.

Table 3 List of adsorption isotherm models

Isotherm	Form	Parameter meaning	References
Langmuir	$q_e = \frac{q_m}{1/K_L + C_e}$	q_e amount of CO_2 adsorbed at equilibrium (mmol/g); q_m maximum adsorption capacity of CO_2 (mmol/g); C_e CO_2 concentration at equilibrium (vol%); K_L Langmuir isotherm constant (1/vol.%)	(Crini et al. 2007)
Freundlich	$q_e = K_F C_e^{1/n}$	K_F Freundlich isotherm constant ((mmol/g)/(vol%)$^{1/n}$); n Freundlich constant	(Crini et al. 2007)
Langmuir–Freundlich	$q_e = \frac{q_m (K_L C_e)^n}{1 + (K_L C_e)^n}$		(Nestle and Kimmich 1996)
Temkin	$q_e = B\ln(K_T C_e)$	K_T Temkin equilibrium binding constant (mmol/g); B heat of adsorption constant	(Monazam et al. 2013)

Additionally, the ease of regeneration of the CO_2 sorbent will also help to reduce the cost of capture.

- **Sorbent costs**: These represent perhaps the most subtle characteristics. A cost of \$5/kg sorbent leads to a very good scenario, while a cost of \$15/kg sorbent is not economical. Therefore, to be more economical, the cost of the CO_2 adsorption sorbent should be in the range of approximately \$10/kg.

The attributes mentioned above are desirable for an ideal adsorbent. However, rarely will a single adsorbent be optimal in all these attributes. Therefore, useful adsorbents will be those that effectively and economically capture CO_2.

Thermodynamics of CO_2 Adsorption

The equilibrium adsorption isotherm is essential for the design of adsorption systems, which is usually described by an isotherm equation characterized by certain parameters whose values express the surface properties and affinity of the sorbent. The adsorption isotherms, in fact, describe the equilibrium relationships between adsorbent and adsorbate and the ratio between the amount adsorbed and that left in the reactant at a fixed temperature at equilibrium. Several commonly used adsorption models, such as Langmuir, Langmuir–Freundlich, Freundlich, and Temkin isotherms, were applied to evaluate feasibility of CO_2–adsorbent interaction (Table 3).

Isosteric heat of adsorption (Q) (adsorption enthalpy, $\triangle H$) is commonly defined as the enthalpy change of adsorption. Values of Q for the adsorption of CO_2 onto adsorbent were calculated from adsorption data obtained at different temperatures using the Clausius–Clapeyron equation:

Table 4 Kinetic adsorption models

Kinetic model	Equation	Differential form	References
Pseudo-first order	$q_t = q_e\left(1 - e^{-k_1 t}\right)$	$\frac{\partial q_t}{\partial t} = k_1(q_e - q_t)$	(Serna-Guerrero and Sayari 2010)
Pseudo-second order	$q_t = \frac{q_e}{\frac{1}{k_2 q_e} + t}$	$\frac{\partial q_t}{\partial t} = k_2(q_e - q_t)^2$	(Ho and McKay 1999)
Avrami's fractional order	$q_t = q_e\left(1 - e^{-(k_A t)^{n_A}}\right)$	$\frac{\partial q_t}{\partial t} = k_A^{n_A} t^{n_A - 1}(q_e - q_t)$	(Serna-Guerrero and Sayari 2010)
Sayari's fractional order	$q_t = q_e - \frac{1}{\left[\frac{(n-1)k_n t^m}{m} + \frac{1}{q_e^{n-1}}\right]^{\frac{1}{n-1}}}$	$\frac{\partial q_t}{\partial t} = k_n t^{m-1}(q_e - q_t)^n$	(Heydari-Gorji and Sayari 2011)

$$\left[\frac{\partial(\ln P)}{\partial(1/T)}\right]_q = -\frac{Q}{R} \tag{3}$$

where P is CO_2 partial pressure (Pa), T is the absolute temperature (K), and R denotes the universal gas constant, 8.3145 J/mol · K.

Kinetics of CO_2 Adsorption

CO_2 adsorption/desorption kinetics are critical characteristics for the performance of sorbents (Zhao et al. 2013). The kinetics determined the amount of the time required for one adsorption/desorption cycle. They are closely related to the size of adsorption/desorption columns, as well.

The kinetics can be described with various models, which are available in literatures. Because of the complexity involved in the prediction of kinetic parameters, a typical approach consists of fitting experimental data to a series of established models and selecting the one that provides the best fit. In recent years, however, several researchers attempted to rationalize some of the most popular kinetic models, making it possible to deduce information regarding the adsorbent–adsorbate interactions. Table 4 shows the list of equations associated with the kinetic models explored in this work, where t is the time elapsed from the beginning of the adsorption process, q_t is the amount adsorbed at a given point in time, and q_e represents the amount adsorbed at equilibrium.

To investigate the kinetics of CO_2 adsorption onto adsorbent, the following four models are often considered:

(i) Pseudo-first-order kinetic model: The Lagergren's pseudo-first-order model was the first adsorption rate equation described for sorption of liquid/solid system and one of the most commonly used adsorption rate models. It is represented by Eq. 1:

$$\frac{\partial q_t}{\partial t} = k_1(q_e - q_t) \tag{4}$$

where q_e and q_t are the adsorption capacity at equilibrium and at time t, respectively, and k_1 is the pseudo-first-order adsorption rate constant. For the boundary conditions $q_t = 0$ at $t = 0$ and $q_t = q_e$ at $t = \infty$, the integrated form of the Eq. 1 becomes

$$q_t = q_e\left(1 - e^{-k_1 t}\right) \tag{5}$$

(ii) Pseudo-second-order kinetic model: This model was put forward by Ho et al. (Ho and McKay 1999). It assumes that the adsorption capacity is proportional to the number of active sites occupied on the sorbent. It has been applied for analyzing chemisorption kinetics from liquid solutions (Ho and McKay 1999). This model is expressed by Eq. 3:

$$\frac{\partial q_t}{\partial t} = k_2(q_e - q_t)^2 \tag{6}$$

where k_2 is the pseudo-second-order adsorption rate constant. The integrated form for the abovementioned boundary conditions is

$$q_t = \frac{q_e}{\dfrac{1}{k_2 q_e} + t} \tag{7}$$

(iii) Avrami's fractional-order kinetic model: This model was recently developed based on Avrami's kinetic model to simulate phase transition and crystal growth of materials (Lopes et al. 2003). It has been applied to describe the adsorption of CO_2 on amine-functionalized adsorbents (Serna-Guerrero and Sayari 2010). The general form of the model is as follows:

$$\frac{\partial q_t}{\partial t} = k_A^{n_A} t^{n_A - 1}(q_e - q_t) \tag{8}$$

where k_A is the Avrami kinetic constant and n_A is the Avrami exponent. The Avrami exponent, n_A, is a fractionary number, which reflects mechanism changes that may take place during the adsorption process (de Menezes et al. 2012). The n_A is the dimensionality of growth of adsorption sites: $n_A = 2$ for one-dimensional growth, $n_A = 3$ for two-dimensional growth, and $n_A = 4$ for three-dimensional growth (Benedict and Coppens 2009). For a homogeneous adsorption in which the probability of the adsorption to occur is equal for any region for a given time interval, $n_A = 1$ (Avrami 1939, 1941). An Avrami exponent of exactly 2 indicates perfect one-dimensional growth from adsorption sites which form continuously and at a constant rate (Benedict and Coppens 2009). The integrated form for the abovementioned boundary conditions is

$$q_t = q_e\left(1 - e^{-(k_A t)^{n_A}}\right) \tag{9}$$

(iv) Fractional-order kinetic model: Heydari-Gorji and Sayari (2011) recently proposed this general semiempirical kinetic equation to describe the adsorption rate of CO_2 on amine-functionalized PE-MCM-41 adsorbents. In this mode, the adsorption rate is assumed to be proportional to the nth power of the driving force and mth power of the adsorption time. This kinetic model is represented by Eq. 7 as follows:

$$\frac{\partial q_t}{\partial t} = k_n t^{m-1}(q_e - q_t)^n \tag{10}$$

where k_n, m, and n are the constants for the fractional-order kinetic model. Since the fractional-order kinetic model represents the complexity of the reaction mechanism that may involve more than one reaction pathway (Lopes et al. 2003; Cestari et al. 2006), the parameter k_n could be an overall parameter that may couple various adsorption-related factors (Zhao et al. 2013). Integrating Eq. 7 for the abovementioned boundary conditions gives

$$q_t = q_e - \frac{1}{\left[\frac{(n-1)k_n t^m}{m} + \frac{1}{q_e^{n-1}}\right]^{\frac{1}{n-1}}} \tag{11}$$

The temperature dependence of the kinetic constant k_A may be described by the Arrhenius equation:

$$k_A = Ae^{-(E_a/RT)} \tag{12}$$

where A is the Arrhenius pre-exponential factor, E_a is the activation energy, R is the universal ideal gas constant, and T is the absolute temperature.

Typical Processes for CO_2 Capture

Based on how adsorbents are regenerated after each adsorption cycle in a CO_2 capture process, processes for CO_2 capture can be classified as temperature swing adsorption (TSA), pressure swing adsorption (PSA), vacuum swing adsorption (VSA), or a combination of these three basic processes. In all of these processes, the solid adsorbents will be packed into a large column, and CO_2 will be desorbed by increasing the temperature (for TSA) or reducing the pressure (for PSA and VSA) of the bed.

Among the three typical processes, TSA is particularly promising as it can use low-grade heat from the power plant as a source of energy for regeneration (Merel et al. 2008; Berger and Bhown 2011). In a TSA cycle (Fig. 1, left), the saturated adsorbent is heated from ambient temperature to the optimal desorption temperature of the adsorbent. As the temperature is increased, CO_2 desorbs from the adsorbent. Then the increased gas pressure drives the desorbed gases from the

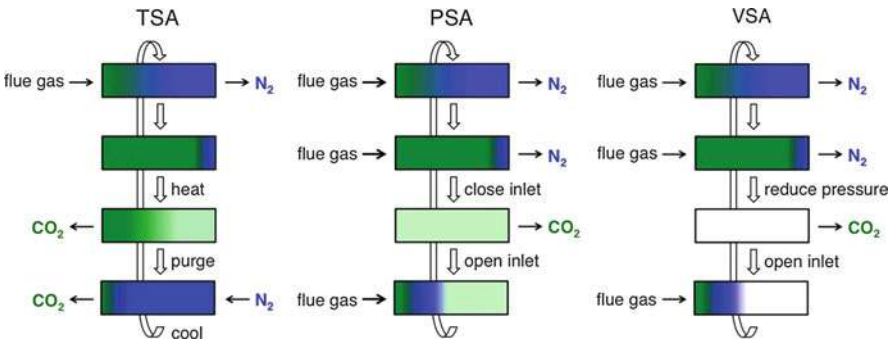

Fig. 1 Schematic diagrams of idealized TSA, PSA, and VSA processes for regenerating solid adsorbent in a fixed-bed column (Sumida et al. 2012)

column. Once equilibrium is reached at the maximum desorption temperature and no more adsorbed gas elutes from the column, a purge is used to push off any desorbed gases that fill the void spaces of the bed until the purity of eluted gas falls below a desired level. Finally, the bed is cooled and prepared for the next adsorption cycle.

For a PSA (Fig. 1, center) or VSA (Fig. 1, right) regeneration process, the column pressure is lowered after adsorption in order to desorb the adsorbed gas. For PSA, the inlet gas is pressurized by compression during adsorption and flowed through the column until saturation. Once the inlet valve is closed, the column pressure decreases toward ambient pressure. The pressure drop desorbs significant quantities of CO_2 from the adsorbent. Similarly, VSA lowers the pressure of the column to subatmospheric pressure after adsorption at a higher pressure. The vacuum applied to the column removes the CO_2 from the pores.

Since post-combustion flue gas is released near ambient pressure, compressing or applying a vacuum to such a large volume of gas is difficult; therefore, TSA might represent the most viable process. For pre-combustion capture, a PSA cycle is expected to be most appropriate because the gas stream is inherently pressurized after the conversion reactions (Mason et al. 2011; Herm et al. 2011).

The possibility of optimizing the parameters in each of these regeneration cycles and of combining multiple processes presents the option of tailoring the regeneration process to match the properties of a given adsorbent (Ishibashi et al. 1996; Mulgundmath and Tezel 2010). Primarily, regeneration strategies must be designed to minimize the total cost of capturing CO_2; therefore, there will be a trade-off between maximizing the working capacity and minimizing the energy required for regeneration (Berger and Bhown 2011; Rubin et al. 2007; House et al. 2009). Detailed analysis of the energy and economic optimization issues in CO_2 capture is crucial in directing the optimization of real-world CO_2 capture processes.

Typical Solid Sorbents for CO_2 Capture

Activated Carbon-Based Sorbents

Inorganic carbon is available in various forms, such as porous activated carbons (ACs), carbon nanotubes (CNTs), graphenes, etc. Adsorption behaviors of CO_2 on commercial and synthesized activated carbon-based sorbents have been widely studied experimentally and theoretically by a number of research groups from low to very high pressure. The structural properties and adsorption capacities are summarized in Table 5. As shown in Table 5, by incorporating certain functional groups into its porous surface, the CO_2 adsorption capacity of carbonaceous materials could be significantly enhanced.

ACs are widely used as adsorbents in various industrial fields (water treatment, gas purification) due to wide availability and the low cost of raw materials. ACs are low-cost materials with fast adsorption kinetics and require low regeneration energy. However, the predominance of ACs still fails to offset the drawbacks of physical adsorption processes. The CO_2 adsorption capacity using ACs decreases as the temperature increases (see Fig. 2) (Berlier and Frere 1996; Do and Wang 1998). At low partial pressures of CO_2, ACs exhibit lower adsorption capacity and selectivity than zeolites due to their unfavorable adsorption isotherms (Chue et al. 1995). The presence of water vapor may negatively affect the CO_2 capacity of ACs because of competitive adsorption between CO_2 and water vapor (Wang et al. 2008a). Additionally, other components or contaminants also have a detrimental impact on the CO_2 adsorption process.

Przepiorski et al. (2004) found significant improvement of CO_2 adsorption with commercial AC treated with ammonia at high temperatures (>473 K). The sorbent treated with ammonia at 673 K showed the adsorption capacity of 1.73 mmol/g. This improvement was ascribed to the introduction of nitrogen-containing groups to carbon structure. Pevida and his group (Pevida et al. 2008) made a conclusion that the CO_2 adsorption capacity is not directly related to the total nitrogen content of sorbents but rather to specific nitrogen functionalities that are responsible for increasing the CO_2–adsorbent affinity. Alesi et al. (2010) studied CO_2 adsorption and regeneration conditions of tertiary amidine derivatives supported on AC from 302 to 323 K. It was found that CO_2 adsorption on the amidine-modified AC only occurred in the existence of moisture. Adsorption of water vapor on the hydrophilic AC support limits the CO_2 capture capacities.

Maroto-Valer et al. (2005; Tang et al. 2004; Zhang et al. 2004; Zhong et al. 2004) found that anthracite coal with 2 h of activation at 1163 K achieved a CO_2 adsorption capacity of 1.49 mmol/g (Maroto-Valer et al. 2005). The feasibility of a high-surface-area sorbent from low-cost anthracites was also investigated (Zhong et al. 2004; Maroto-Valer et al. 2005). The adsorption capacity of polyethylenimine (PEI)-impregnated deashed anthracite sorbent was ~2.13 mmol/g at 348 K (Zhong et al. 2004). In another study, they observed a decrease in adsorption capacity of activated anthracites impregnated with PEI with increasing adsorption temperature (Maroto-Valer et al. 2005).

Table 5 CO_2 adsorption capacity of carbonaceous solid sorbents

Sorbent	Pore size (nm)	Pore volume (cm^3/g)	BET surface area (m^2/g)	Temperature T (K)	Pressure p (atm)	Capacity (mmol/g)	References
AC				298	1	2.07	(Kikkinides et al. 1993)
AC				298	1	2.45	(Chue et al. 1995)
AC				298	0.2	0.75	(Do and Wang 1998)
AC	1.5–2.2	0.6–0.8	1300	298	1	3.23	(Na et al. 2001)
AC				298	1	2.61	(Siriwardane et al. 2001)
Anthracite-based AC			540	303	1	1.49	(Maroto-Valer et al. 2005)
SWNT			1617	308	1	2.07	(Cinke et al. 2003)
AC	2	0.48	954	298	0.1	0.57	(Lu et al. 2008)
Ammonia-treated AC				309.15	1	1.73	(Przepiorski et al. 2004)
Ammonia-treated AC	2.79	0.831	1190	298	1	1.91	(Pevida et al. 2008)
Ammonia-treated char	1.98	0.28	653	298	1	2.20	(Plaza et al. 2009)

(*continued*)

Table 5 (continued)

Sorbent	Pore size (nm)	Pore volume (cm^3/g)	BET surface area (m^2/g)	Temperature T (K)	Pressure p (atm)	Capacity (mmol/g)	References
Amine-enriched fly ash				298	0.1	2.05	(Gray et al. 2004)
PEI-impregnated fly ash				348	1	1.02	(Arenillas et al. 2005)
APTS-modified CNT				293	0.15/0.5	0.98/2.59	(Su et al. 2009)
PEI-functionalized SWCNTs				300	1	2.1	(Dillon et al. 2008)
Graphene				195	1	0.8	(Ghosh et al. 2008)
CMS	0.70	0.603	1725	303	1	2.43	(Burchell et al. 1997)
APTES-grafted CNTs				293	0.15	1.32	(Hsu et al. 2010)
APTS-grafted CNTs	8.9	0.91	198	298	0.1	0.93	(Lu et al. 2008)
TEPA-impregnated CNTs	19.04	0.056	8.9	313	0.02	3.56 3.87 (humid)	(Ye et al. 2012)
TEPA-impregnated CNTs	25.47	0.108	17	343	0.1	3.09	(Liu et al. 2014a)

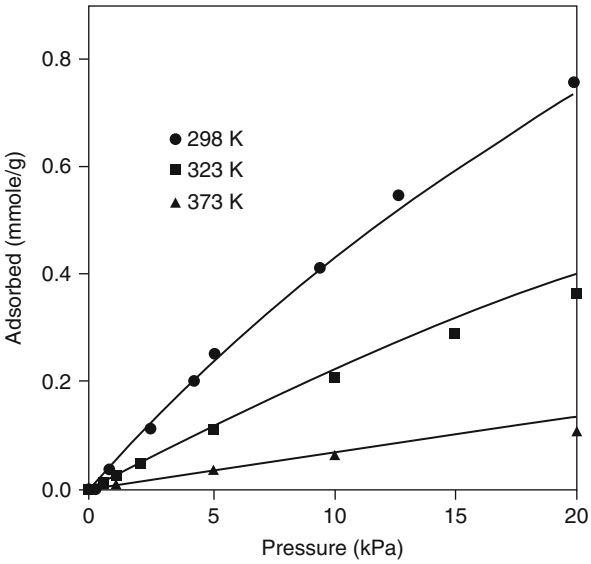

Fig. 2 Isotherm for adsorption of CO_2 on activated carbon (Do and Wang 1998)

Carbon-enriched fly ash concentrates treated with various amines were developed by Gray et al. (2004), Maroto-Valer et al. (2008; Zhang et al. 2004), and Arenillas et al. (2005). A typical comparison of CO_2 adsorption capacities of activated fly ash carbon and its alkanolamine-modified counterparts at various temperatures was reported by Maroto-Valer and others (Maroto-Valer et al. 2008). It was found that activation by steam before impregnation could successfully increase the pore volume and surface area, consequently resulting in the increase of CO_2 capture capacity (Zhang et al. 2004; Maroto-Valer et al. 2008). The impregnation with PEI could significantly enhance the adsorption capacity of this class of sorbents up to 2.13 mmol/g at 348 K, which is much higher than that without impregnation (0.22 mmol/g at 348 K) (Zhang et al. 2004). Arenillas et al. (2005) achieved the CO_2 adsorption capacity of ~1.02 mmol/g at 348 K using activated fly ash-derived sorbents impregnated with PEI (Zhang et al. 2004; Arenillas et al. 2005). Fly ash impregnated with PEI and its blend with poly (ethylene glycol) (PEG) was also investigated. The addition of PEG into the PEI-loaded sorbents improves the CO_2 adsorption capacity and kinetics, which could be attributed to the bicarbonate formation reaction in the presence of PEG (attracts more water).

CNT can act as a suitable candidate for CO_2 capture by choosing the appropriate pore size and optimum conditions (Huang et al. 2007; Razavi et al. 2011). Considerable experimental research and theoretical modeling efforts are being devoted to investigate the adsorption of CO_2 on CNTs. Cinke et al. (2003) reported CO_2 adsorption on purified single-walled carbon nanotubes (SWCNTs) in the temperature range from 273 to 473 K (see Fig. 3). The CO_2 adsorption capacity of SWCNTs was twice that of AC. Lu et al. (2008) reported CO_2 capture by CNT and its modification. After functionalization, CNT showed a significant enhancement in

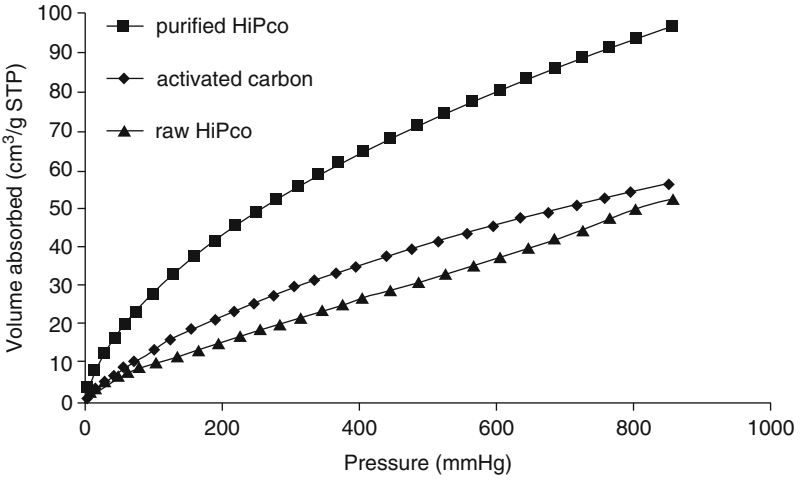

Fig. 3 Comparison of CO_2 adsorption capacities of high-pressure CO conversion (HiPco) single-walled nanotubes (SWNTs) and activated carbon (AC) at 308 K (Cinke et al. 2003)

CO_2 adsorption capacity. CNTs modified by APTES were also tested for their CO_2 adsorption potential at various temperatures by Su et al. (2009). The CO_2 adsorption capacities of CNTs and CNTs (APTS) increased with water content, and decreased with temperature, indicating the exothermic nature of adsorption process. The CO_2 adsorption capacity of CNT (APTS) was ~2.59 mmol/g at 293 K. The potential application of CNT as the support for amine-impregnated sorbents has been studied by Fifield et al. (2004). In order to increase the affinity of the carbon structure, pyrene methyl picolinimide (PMP) was introduced as anchors. Dillon et al. (2008) synthesized and characterized PEI-functionalized SWNTs. A maximum adsorption of 2.1 mmol/g was reported for PEI (25000)-SWNT at 300 K. Hsu et al. (2010) proposed that a combination of thermal and vacuum desorption of CNT (APTES) at 393 K could reduce the regeneration time. The adsorption capacities and physicochemical properties were preserved after 20 cycles of adsorption/regeneration.

Industrial-grade multi-walled carbon nanotubes (IG-MWCNTs) impregnated with tetraethylenepentamine (TEPA) were systematically investigated for CO_2 capture by Liu et al. (2014a, b). TEPA-impregnated IG-MWCNTs were shown to have high CO_2 adsorption capacity comparable to that of TEPA-impregnated P-MWCNTs (Ye et al. 2012). The adsorption capacity of IG-MWCNT-based adsorbents was in the range of 2.145–3.088 mmol/g, depending on adsorption temperatures. The isosteric heat of adsorption for CO_2 decreased with the increase in CO_2 loading (Fig. 4). The high heat of adsorption in the lower loading region was due to the reaction of CO_2 with the active sites of TEPA. The process of IG-MWCNTs-50 adsorption of CO_2 was partly physical and partly chemical adsorption. The adsorption/desorption kinetics of CO_2 on TEPA-impregnated

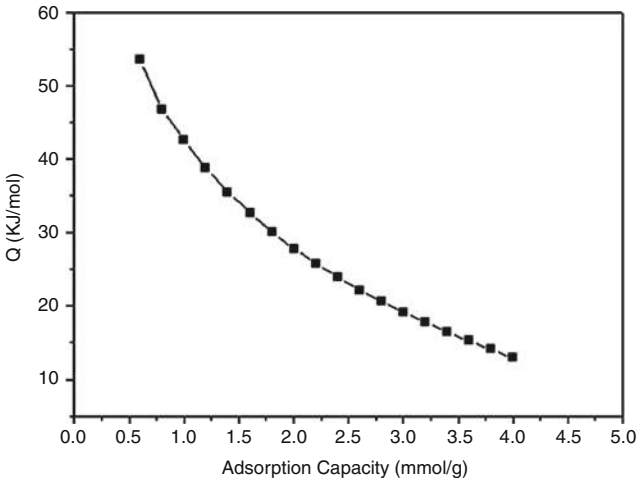

Fig. 4 Isosteric heats of adsorption of CO_2 for IG-MWCNTs-50 in a binary mixture of CO_2 and N_2 (Liu et al. 2014a)

IG-MWCNTs was investigated to obtain insight into the underlying mechanisms on the fixed bed. Avrami's fractional-order kinetic model provided the best fitting for the adsorption behavior of CO_2. In order to find the optimal regeneration method, three desorption methods were evaluated for the regeneration of solid sorbents. The activation energy E_a of CO_2 adsorption/desorption was calculated to evaluate the performance of the adsorbent. The effect of gas contaminants on the adsorption behavior of adsorbents for CO_2 was also studied. H_2O and NO had a minimal impact on CO_2 adsorption capacity, while the effect of SO_2 on CO_2 adsorption was influenced by adsorption temperature and SO_2 concentration.

Skoulidas et al. (2006) carried out simulations to analyze the adsorption and transport diffusion of CO_2 and N_2 in SWCNTs at room temperature. They reported that transport diffusivities for CO_2 in nanotubes with diameters ranging from $\sim$1 to $\sim$5 nm are approximately independent of pressure. The observed diffusion mechanism is not Knudsen-like diffusion. Based on Monte Carlo simulations, Huang et al. (2007) showed that CO_2 adsorption in the range of 4–9 mmol/g is an increasing function of the diameter of the CNTs. Additionally, CNTs demonstrated a higher selectivity toward CO_2 than other sorbents, such as ACs, zeolite 13X, and MOFs. Razavi et al. (2011) also concluded that CNTs exhibited a higher selectivity of CO_2 over N_2, compared to other carbon-based materials, for the separation of CO_2/N_2 mixture.

In summary, the impregnation of amines for carbonaceous materials is found to be effective to enhance CO_2 adsorption capacity. However, the impregnation also caused a significant decrease of the surface areas and pore volume. Although the exact mechanism of these changes is still not well understood, it is believed that the size and molecular structure of amines play an important role.

Polymer-Based Sorbents

Polymeric amine sorbents have been used for years to capture CO_2 in closed environments, such as aircraft, submarine, and space shuttles, under the concentrations of CO_2 <1 % (Satyapal et al. 2001). However, the cost of these sorbents is too high for large-scale applications in the industry. Table 6 shows the CO_2 adsorption capacity of polymer-based solid sorbents (Choi et al. 2009).

Satyapal et al. reported on a proprietary adsorbent HSC+ (consisting of PEI bonded to a high-surface-area, solid polymethylmethacrylate (PMMA) polymeric support coated with PEG). PEG was used to enhance the cyclic capacity of the sorbent. CO_2 adsorption capacity of the HSC+ sorbent was ~0.91 mmol/g at ambient pressure and 313 K, and the heat of adsorption was estimated to be -94 ± 8 kJ/mol. A variety of ethanolamines and their mixtures were impregnated with PMMA beads with high surface areas by Filburn et al. (2005). The results showed the advantage of secondary amines over other amine types in adsorbing low levels of CO_2, using a PSA process (Filburn et al. 2005). In their further studies, MEA, modified TEPA (TEPAN), and a mixture of ethyleneimine (E-100), reaction-modified ethyleneimine with acrylonitrile (E-100AN), etc. were used to functionalize PMMA (Lee et al. 2008a). TEPAN- and E-100AN-functionalized PMMA revealed remarkably higher cyclic CO_2 capacities and reproducibility.

Gray et al. immobilized Michael addition reaction products of ethylenediamine and TEPA with acrylonitrile within the pores of PMMA beads. The average CO_2 adsorption capacities of the sorbent were in the range of 3.4–6.6 mmol/g over four adsorption/desorption cycles. Furthermore, DBU was immobilized in PMMA beads in order to achieve the higher CO_2 capture capacity (Gray et al. 2008). With a DBU loading of 29 wt%, the modified sorbent showed an adsorption capacity of 3.43 mmol/g at room temperature under 10 % CO_2 and 2 % H_2O in He gas. However, the CO_2 capacity decreased significantly to 2.34 mmol/g as the temperature increased to 338 K, which is contrary to that observed for amine-impregnated mesoporous inorganic sorbents. Besides PMMA, other supports such as silicon dioxide (CARiACT) and polystyrene (macronet) were also compared (Gray et al. 2009). The CARiACT- and PMMA-supported PEI sorbents showed CO_2 capture capacities of 2.5–3.5 mmol/g under humid conditions and stability in the temperature range of 298–378 K for ten cycles.

Li et al. (2008a, b) reported the development of fibrous sorbents for CO_2 capture by coating PEI onto commercial glass fiber matrix with high surface area, using epoxy resin (EP) (Li et al. 2008a) and epichlorohydrin (ECH) (Li et al. 2008b) as a cross-linking agent. The CO_2 adsorption capacities were 6.30 mmol/g for PEI cross-linked with EP-coated fiber and 4.12 mmol/g for PEI cross-linked with ECH-coated fiber at 303 K, 1 atm and under humid conditions. Both modified fibrous adsorbents could be completely regenerated at 293 K. However, these modified glass fibrous adsorbents were most efficient at room temperature. At a higher temperature of 323 K, the adsorption capacity decreases drastically. In addition, Yang et al. (2010) synthesized an amine-containing fibrous adsorbent (PAN-AF) by grafting copolymerization of allylamine onto polyacrylonitrile

Table 6 CO_2 adsorption capacity of polymer-based sorbents

Sorbent	Pore size (nm)	Pore volume (cm^3/g)	BET surface area (m^2/g)	Temperature T (K)	Pressure p (atm)	Capacity (mmol/g)	References
HSC^+				313	1	0.91	(Satyapal et al. 2001)
TEPA-impregnated PMMA				343	0.15	14.03(humid)	(Lee et al. 2008a)
DBU-impregnated PMMA	20.3	0.58	94	298 338	0.1	3.0(humid) 2.34(humid)	(Gray et al. 2008)
PEI-impregnated PMMA				318	0.1	2.40 3.53(humid)	(Gray et al. 2009)
PEI cross-linked with EP-coated fiber				303	1	6.30(humid)	(Li et al. 2008a)
PEI cross-linked with ECH-coated fiber				303	1	4.12	(Li et al. 2008b)
Allylamine-grafted PAN fiber	3.08	0.0051	6.57	295	0.15	6.22	(Yang et al. 2010)

(PAN) fiber. The CO_2 adsorption capacity of 6.22 mmol/g with a grafting degree of 60.0 wt% was reported. Regeneration of PAN-AF is suggested to be carried out by heating PAN-AF in boiled water.

Zeolite-Based Sorbents

Zeolites are widely used in the field of gas separation and purification. Conventional zeolites are based on silicate frameworks wherein substitution of some of the Si with Al (or other metals) results in a negative charge on the framework or with cations (usually Na or other alkaline or alkaline-earth metals) within the pore structure. These cations can be exchanged to the adsorption characteristics or fine-tune the pore size. Owing to their defined crystalline structures, these sorbents have uniform pore sizes in the range of 0.5–1.2 nm, which is a property that allows them to separate molecules via the molecular sieving effect. Separation of gases by the zeolite adsorbents can also occur through the mechanism of selective adsorption of those molecules that have a relatively large energetic dipole and quadruple. The gases that have high quadrupole moment, such as CO_2 (Table 2) (Coriani et al. 2000), interact strongly with the electric field created by the structural cations of zeolites, and this favors their adsorption. Separation of gases in zeolites depends on the following factors: structure and composition of the framework, cationic form, purity, size and shape of the molecules, and molecular polarity. The typical physical properties of the zeolites are summarized in Table 7.

Zeolites have demonstrated promising results for the separation of CO_2 from gas streams. There is plenty of published literature concerning CO_2 adsorption over different types of zeolites, such as zeolites A, X, and Y, and other natural zeolites, such as chabazites, clintopiles, ferrierites, mordenites, etc. Table 7 lists the various zeolites for application of CO_2 separation from gas mixtures.

Earlier, a study of adsorption of CO_2 on various synthetic zeolites (4A, 5A, and 13X) and natural zeolites (mordenite, ferrierite, clinoptilolite, and chabazite) showed 13X and chabazite, among the synthetic and natural zeolites, respectively, to be better adsorbents for CO_2 separation from N_2 (Inui et al. 1988). The work by Siriwardane et al. (2003) indicated that natural zeolite with the highest surface area and highest sodium content showed the highest CO_2 adsorption capacity and highest rates of adsorption. A wide-ranging screening study of ~13 synthetic zeolites, including 5A, 13X, NaY, ZSM-5, and HiSiV-3000 (based on ZSM-5 structure with a silica-to-alumina ratio (Si/Al >1000), was conducted by Harlick and Tezel (2004) for the capture of CO_2 from flue gas. Adsorption capacities of the adsorbents increased in the following order (in the pressure range of ~0–2 atm):13X (Si/Al = 2:2) > NaY (Si/Al = 5:1) > H-ZSM-5-30 (Si/Al = 30)> HiSiv3000 > HY-5 (Si/Al = 5) (Fig. 5). It might be on account of a low Si/Al ratio with cations (sodium) in the structure that show strong interactions with CO_2. Zukal et al. (2010) investigated CO_2 adsorption on six high-silica zeolites (SiO_2/Al_2O_3 > 60): TNU-9, IM-5, SSZ-74, ferrierite, ZSM-5, and ZSM-11. TNU-9 and IM-5 were found to have the highest CO_2 adsorption capacity, attaining 2.61 and 2.42 mmol/g at the pressure of 100 kPa, respectively.

Table 7 CO_2 adsorption capacity of zeolites

Sorbent	Pore size (nm)	Pore volume (cm^3/g)	BET surface area (m^2/g)	Temperature T (K)	Pressure p (atm)	Capacity (mmol/g)	References
Zeolite 13X NaY H-ZSM-5-30 HiSiv 3000 HY-5				295	1	4.61 4.06 1.9 1.44 1.13	(Harlick and Tezel 2004)
Ferrierite ZSM-5 ZSM-11 TNU-9 IM-5 SSZ-74		0.118 0.163 0.131 0.165 0.134 0.123		293	0.1	2.03 2.30 2.17 2.61 2.42 1.92	(Zukal et al. 2010)
NaY Cs-treated NaY	1.54 1.58	0.46 0.21	811 483	473	1	0.46 0.80	(Diaz et al. 2008)
Na-ZSM-5				303	1	0.75	(Katoh et al. 2000)
13X MEA-modified 13X	11 11	0.34 0.059	615.5 9.15	303	0.15	1.25 0.78	(Jadhav et al. 2007)
13X MEA-modified 13X	11 11	0.34 0.059	615.5 9.15	393	0.15	0.18 0.63	(Jadhav et al. 2007)
TEPA-modified Y-type zeolite				333	0.15	2.54 4.27 (water)	(Su et al. 2010)
TEPA-impregnated beta zeolite			680	303	0.1	2.08	(Fisher et al. 2009)

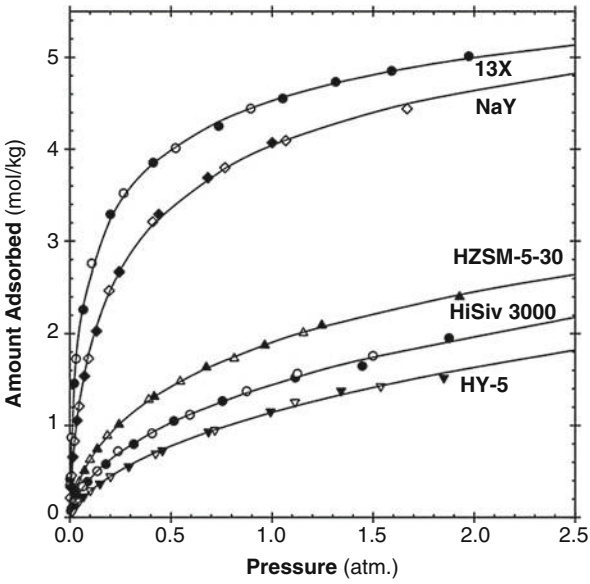

Fig. 5 Comparison of CO_2 adsorption isotherms for fresh zeolites at 295 K (Harlick and Tezel 2004). The *filled* symbols were obtained by regenerating the fresh adsorbent at 200 °C for 12 h followed by the adsorption study. The *open* symbols were obtained as a repeat of 200 °C regeneration for 12 h followed by adsorption without changing the adsorbent sample

To enhance the adsorption capacity of CO_2, the modification of zeolites via the introduction of electropositive and polyvalent cations was concentrated. Khelifa et al. (2004) concluded that NaX (Si/Al = 1.21) zeolite exchanged with Ni^{2+} and Cr^{3+} showed a decrease in CO_2 adsorption capacity, compared to that of the parent NaX zeolite, due to a weak CO_2–sorbent interaction. NaX and NaY and those resulting from ions exchanged with Cs, since it is the most electropositive metal of the periodic table, were tested regarding the adsorption of CO_2 by Diaz et al. (2008). Cs-treated zeolites performed better and were more active for adsorption at higher temperatures (373 K). Zhang et al. (2008a) prepared chabazite (CHA) zeolites (Si/Al < 2.5) and exchanged them with alkali cations (e.g., Li, Na, and K) and alkaline-earth cations (e.g., Mg, Ca, Ba) to evaluate their potential for CO_2 capture from flue gas by VSA below 393 K. From the adsorption isotherm, it was found that the NaX zeolite shows superior performance at relatively low temperatures, while NaCHA and CaCHA hold comparative advantages for high temperature (>273 K) CO_2 separation. According to the research of the selectivity of ion-exchanged ZSM-5 zeolites by Katoh et al. (2000), M-ZSM-5 (M = Li, Na, K, Rb, and Cs) might be attributed to the fact that almost all CO_2 molecules strongly adsorbed on the cation sites, while N_2 interacted with the wall of the H-ZMS-5.

There is a detrimental effect of water vapor on CO_2 adsorption for zeolite, due to its preferential adsorption from the gas mixture (Brandani and Ruthven 2004; Li et al. 2008c). Trace amounts of water vapor could significantly decrease the CO_2 adsorption capacity, because it gets competitively adsorbed on the zeolite surface and blocks the access for CO_2 (Brandani and Ruthven 2004). It was demonstrated by another study that the adsorption of CO_2 is considerably inhibited by H_2O as CO_2 and water vapor adsorption on zeolite 13X (Li et al. 2008c).

Zeolites with large surface area and pore volume present a potential option for CO_2 adsorption. However, CO_2 adsorption capacity on zeolites decreases significantly as the temperature increases. The capacity will also be very low in the existence of moisture. Therefore, a few researches (Table 7) synthesized aminated zeolites as alternative sorbents.

Zeolite 13X was modified with MEA by Jadhav et al. (2007) by impregnation method. Compared with unmodified zeolite, a higher capacity at 293 K was obtained with MEA loading of 50 wt%, despite reduced pore volume and lower surface area resulted from impregnation. The chemical interaction between CO_2 and amine probably played a significant role in adsorption of CO_2 at 293 K. Similarly, Su et al. (2010) dispersed TEPA into commercially available Y-type zeolite (Si/Al = 60). They obtained a CO_2 adsorption capacity of 4.27 mmol/g at 333 K in the presence of 15 % CO2 and 7 % water vapor in gas stream. In another study, Fisher et al. (2009) employed β-zeolite as a solid support for TEPA impregnation and compared it with TEPA-impregnated silica and alumina. The TEPA-modified β-zeolite exhibited a CO_2 adsorption capacity up to 2.08 mmol/g at 303 K under the 10 % CO_2/90 % argon flow, outperforming TEPA/SiO_2 and TEPA/Al_2O_3 sorbents. TEPA/β-zeolite maintains its CO_2 capture capacity for more than 10 adsorption/regeneration cycles. Their study suggests that the higher capacity of TEPA/β-zeolite can be related to zeolite's high surface area.

Silica-Based Sorbents

Impregnated Silica-Supported Sorbents

The first amine-impregnated silica used to capture CO_2 was reported by Song and others (Xu et al. 2002), and they used wet impregnation of hydrothermally synthesized MCM-41 with PEI to create an adsorbent in terms of a "molecular basket" (Xu et al. 2002, 2003, 2005a, b). In their further study, Xu et al. (2003) reported the highest CO_2 adsorption capacity of 3.02 mmol/g with MCM-41-PEI at a PEI loading of 75 wt% under a pure CO_2 atmosphere and at 348 K. As expected, increased PEI loadings led to higher adsorption of CO_2. Compared with the chemical adsorption for higher PEI loadings, the physical adsorption on the unmodified pore wall of MCM-41 (and the capillary condensation in the mesopore) is negligible. Additionally, a synergetic effect of MCM-41 and PEI for CO_2 adsorption was hypothesized (Xu et al. 2003). When the mesoporous pores were loaded with ~50 wt% PEI, the highest synergetic adsorption gain was obtained. MCM-41 impregnated with PEI exhibited an increase in adsorption capacity with increasing temperature, in comparison to ACs and zeolites. Xu et al. (2003) assumed that low adsorption rate caused by kinetic limitations results in the low adsorption capacity at low temperature. Therefore, the overall process is kinetically controlled.

Song and his groups also studied a series of performance and stability using a MCM-41-PEI sorbent to capture CO_2 from simulated flue gas, flue gas from a natural gas-fired boiler, and simulated humid flue gas using a packed-bed

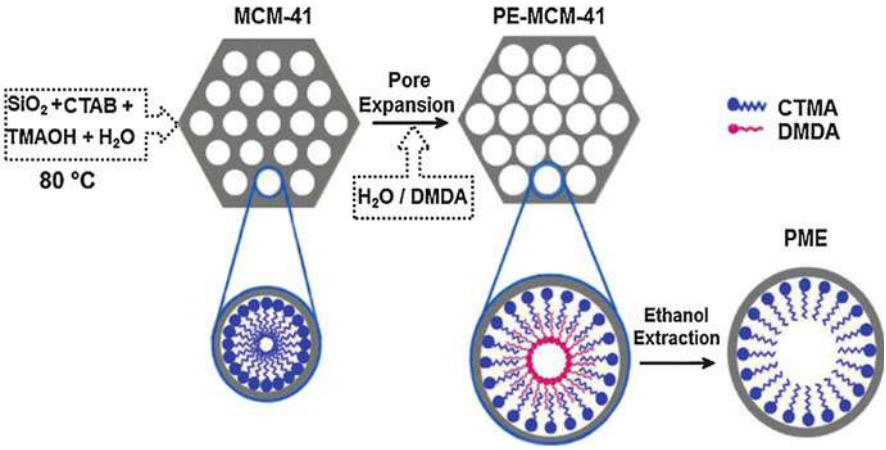

Fig. 6 Schematic representation of the synthesis of PME (Heydari-Gorji and Sayari 2011)

adsorption column (Xu et al. 2005a, b). The adsorbent showed a separation selectivity of ~180 for CO_2/O_2 and >1000 for CO_2/N_2. The adsorbent was stable at 348 K after ten cycles of adsorption/desorption process, while it was not stable when the operation temperature was >373 K. The observation of NO_x to be adsorbed simultaneously with CO_2 indicates the need for preremoval of NO_x from flue gas (Xu et al. 2005a, b). In addition, the CO_2 adsorption capacity was enhanced when the moisture concentration is lower than that of the CO_2, which could be due to the formation of bicarbonate ion (reaction 2) during the chemical interaction between PEI and CO_2 in the presence of moisture.

To enhance the CO_2 adsorption capacity of MCM-41-PEI, PEI supported on pore-expanded (PE) MCM-41 was studied by Heydari-Gorji et al. (2011). The adsorption capacity exhibits as high as 4.68 mmol/g at 348 K for 55 wt% PEI loading due to the well-dispersed PEI inside the PE-MCM-41 pores (Heydari-Gorji and Sayari 2011) (Fig. 6). As an alternative strategy to further improve efficiency for CO_2 adsorption, Yue et al. (2008a) impregnated TEPA into as-prepared MCM-41 that had been prepared with the ionic surfactant cetyltrimethylammonium bromide (CTAB). The as-prepared MCM-41 impregnated with 50 wt% TEPA exhibited a CO_2 adsorption capacity of 4.16 mmol/g in 5 % CO_2, probably owing to better amine distribution using ionic surfactant templates (Yue et al. 2008a). The type, amount, and distribution of the surfactant in the pores of MCM-41 all have significant influences on adsorption process. However, their studies showed that the adsorbent required only 1.5 min to reach the adsorption halftime but 140 min to reach close to equilibrium adsorption capacities.

SBA-15-supported sorbent loaded with 50 wt% PEI was developed by Ma et al. (2009). The CO_2 adsorption capacity of 3.18 mmol/g was obtained at 348 K under a CO_2 partial pressure of 15 kPa. The CO_2 adsorption capacity was ~50 % higher than that of their previously reported MCM-41-PEI sorbent, probably due to the higher pore diameter and pore volume of SBA-15. This allows the PEI-modified

sample prepared from SBA-15 to have a higher surface area for the same PEI loading. The significant role of the distribution of the amine groups impregnated in the porous materials has been confirmed by Zhu and his group (Yue et al. 2006). As-prepared mesoporous SBA-15 occluded with an organic template (Pluronic P123) was used to impregnate TEPA. The CO_2 adsorption capacity of the modified SBA-15 with a TEPA loading of 50 wt% was higher than that of the calcined SBA-15. The presence of the template enhanced the accessibility of CO_2 to TEPA because of a better dispersion and distribution of amines. Furthermore, Yue et al. (2008b) also synthesized as-prepared SBA-15-supported sorbents through dispersing amine blends of TEPA and DEA. The hydroxyl group in DEA is found to significantly improve the CO_2 adsorption. Hydroxyl group facilitates the formation of the carbamate zwitterion; therefore, equilibrium CO_2 loadings of amine can reach 2 mol CO_2 (mol amine)$^{-1}$.

Ahn and coworkers (Son et al. 2008) synthesized a series of PEI-loaded (50 wt%) ordered mesoporous silica supports, namely, MCM-41, MCM-48, SBA-15, SBA-16, and KIT-6, to evaluate their CO_2 adsorption performance. All impregnated sorbents showed substantially higher CO_2 sorption capacities and stability, as well as faster adsorption kinetics, than that of pure PEI. The CO_2 adsorption capacities were in the following order: KIT-6 ($d_p = 6.5$) > SBA-15 ($d_p = 5.5$) ≈ SBA-16 ($d_p = 4.1$) > MCM-48 ($d_p = 3.1$) > MCM-41 ($d_p = 2.1$), where d_p is the average pore diameter (nm). The adsorption performance was proposed to be influenced by the pore diameter and pore arrangement of mesoporous silica materials. Bulky PEI is assumed to be introduced to the pore easily as the pore size in the support increases. Goeppert et al. (2010) studied nanostructured fumed silica impregnated with various organoamines, namely, PEI, MEA, DEA, TEPA, and PEHA, as well as 2-amino-2-methyl-1-3-propanediol (AMPD), 2-(2-amino-ethylamino)ethanol (AEAE), etc. Simple amines such as MEA, DEA, AEAE, etc. are not suitable for impregnation, due to amine leaching problems at higher temperature.

As shown in Table 8, amine-impregnated silica sorbents can effectively adsorb CO_2 with relatively higher working capacity. The modification of pore size of silica support can further enhance the adsorption capacity. The adsorption capacity of amine-impregnated silica sorbents is not sensitive to the presence of moisture (in many cases, moisture helps to obtain higher capacity). However, the durability and regeneration kinetics of the amine-impregnated solid sorbents have not been tested adequately. Their desorption kinetics is still slow. In addition, considerable loss of amines is a major drawback for impregnated amine-functionalized sorbents.

Grafted Silica-Supported Sorbents

The synthesis and characterization of amine-grafted mesoporous silica sorbents (Class 2 category) for CO_2 capture were reported by many groups. In this case, amine, mainly aminosilane, is covalently tethered to the silica support (Choi et al. 2009). Three methods have been used for the grafting of amine onto a silica support: post-synthesis grafting, direct synthesis by co-condensation, and anionic template synthesis with the help of the interaction between the cation head in

Table 8 CO_2 adsorption capacity of silica solid sorbents

Sorbent	Pore size (nm)	Pore volume (cm^3/g)	BET surface area (m^2/g)	Temperature T (K)	Pressure p (atm)	Capacity (mmol/g)	References
MCM-41 PEI(50 wt%)-impregnated MCM-41	2.75 0.4	1.0 0.011	1480 4.2	348 348	1 0.1	0.195 2.05	(Xu et al. 2002)
PEI(50 wt%)-impregnated MCM-41				348	0.13	3.08 (humid)	(Xu et al. 2005a)
PE-MCM-41	2–3	2.03	917				
DEA(77 wt%)-impregnated PE-MCM-41				298	0.05	2.93	(Franchi et al. 2005)
MCM-41 PEI(50 wt%)-impregnated MCM-41 MCM-48 PEI(50 wt%)-impregnated MCM-48 SBA-15 PEI(50 wt%)-impregnated SBA-15 SBA-16 PEI(50 wt%)-impregnated SBA-16 KIT-6 PEI(50 wt%)-impregnated KIT-6	2.8 – 3.1 – 5.5 – 4.1 – 6.0 5.3	0.85 0.01 1.17 0.10 0.94 0.04 0.75 0.02 1.22 0.18	1042 4 1162 26 753 13 736 23 895 86	348	1	2.52 2.89 2.93 2.70 3.07	(Son et al. 2008)
PEI(65 wt%)-impregnated monolith				348	0.05	3.75	(Chen et al. 2009)
TEPA(50 wt%)-impregnated MCM-41		0.03	16	348	0.05	4.54	(Yue et al. 2008a)
MCM-41 PEI(50 wt%)-impregnated MCM-41	2.7 –	1.15 0.03	1229 11	348	0.15	0.14 2.02	(Ma et al. 2009)
SBA-15 PEI(50 wt%)-impregnated SBA-15	6.6 6.1	1.31 0.2	950 80	348 348	0.15 0.15	0.11 3.18	(Ma et al. 2009)
TEPA(50 wt%)-impregnated SBA-15	–	0.02	7	348	0.05	3.23	(Yue et al. 2006)

TEPA(30 wt%) + DEA(20 wt%)-impregnated SBA-15	–	0.01	3.9	348	0.05	3.61	(Yue et al. 2008b)
PEI(40 wt%)-impregnated mesoporous silica		0.704	125	348	1	2.4	(Goeppert et al. 2010)
TEPA(83 wt%)-impregnated MC400/10	3.6	0.016	6.16	348	0.1	5.57	(Qi et al. 2011)
APTES-grafted silica gel				323	1	0.89	(Leal et al. 1995)
APTS-grafted HMS	19.0	0.67	1125	293	0.9	1.59	(Knowles et al. 2005)
DAEAPTS-grafted HMS	18.6	0.46	926	293	0.9	1.34	(Knowles et al. 2006)
APTES-grafted SBA-15 AEAPS-grafted SBA-15 DAEAPTS-grafted SBA-15		0.54 0.40 0.29	374 250 183	333	0.15	0.66, 0.65 (humid) 1.36, 1.51 (humid) 1.58, 1.80 (humid)	(Hiyoshi et al. 2005)
APTES-grafted SBA-15				298	0.04	0.4	(Gray et al. 2005)
DAEAPTS-grafted PE-MCM-41	10	2.21	950	298	0.05	2.65	(Harlick and Sayari 2007)
DAEAPTS-grafted PE-MCM-41	9.6	1.05	429	343	0.05	2.28	(Serna-Guerrero et al. 2010a)
Aziridine polymer-grafted SBA-15				348 298	0.1	1.98 (humid) 3.11 (humid)	(Hicks et al. 2008)

(*continued*)

Table 8 (continued)

Sorbent	Pore size (nm)	Pore volume (cm^3/g)	BET surface area (m^2/g)	Temperature T (K)	Pressure p (atm)	Capacity (mmol/g)	References
AEAPTS-grafted SBA-16		0.54	715	300	1	1.4	(Knofel et al. 2007)
APTES-grafted SBA-12 APTES-grafted MCM-41 APTES-grafted SBA-15	37 9 52 38 55 28		1347 310 1506 239 687 134	298	0.1	1.04 0.57 1.53	(Zelenak et al. 2008)

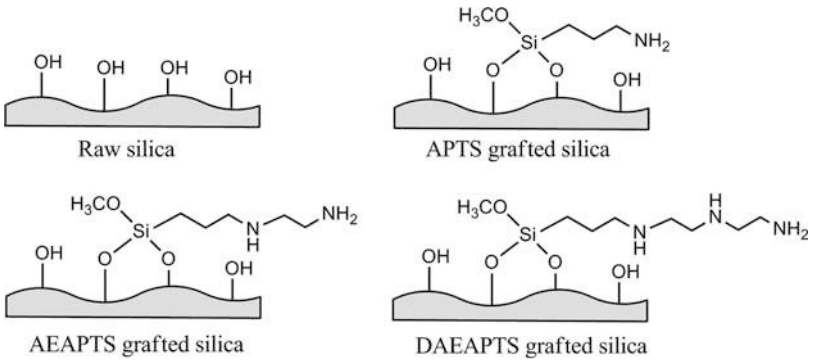

Fig. 7 Modified hexagonal mesoporous silica (*HMS*) materials (Chaffee et al. 2002)

aminosilane and anionic surfactants (Chew et al. 2010). The mesoporous nature of the silica permits high diffusivity of organic amine into the pore structure and, following functionalization, easy diffusion for CO_2 to enter and leave the pores. A wide variety of aminosilanes (see Table 8) have been grafted onto the surface of porous silica for the investigation of the impact of amine type and loadings on the CO_2 adsorption capacity.

Leal et al. (1995) first investigated the chemisorption of CO_2 onto APTES-grafted surface of silica gel. However, the CO_2 adsorption capacity of this sorbent was far below the requirement for industrial application of the sorbents. Afterward, a series of aminopropyl-grafted hexagonal mesoporous silica (HMS) compounds was prepared and characterized by Chaffee's group to enhance CO_2 adsorption. The grafted HMS materials, as shown in Fig. 7, were developed by Delaney et al. (Chaffee et al. 2002) using 3-aminopropyl-trimethoxysilane (APTS), aminoethyl-aminopropyl-trimethoxysilane (AEAPTS), and N-[3-(trimethoxysilyl) propyl) diethylenetriamine (DAEAPTS), ethylhydroxyl-aminopropyl-trimethoxysilane (EHAPTS), and diethylhydroxyl-aminopropyl-trimethoxysilane (DEHAPTS) (see Table 8). The modified silica supports showed high surface area with varied concentrations of surface-bound amine and hydroxyl functional groups. The modified HMS sorbents were also shown to reversibly adsorb significantly more CO_2 than modified silica gel, as reported by Leal et al. (1995). The ratio of CO_2 molecules adsorbed per available N atom was ~0.5 for HMS-APTS, HMS-AEAPTS, and HMS-DEAPTS, which is consistent with the carbamate formation mechanism, as presented by reaction 1. For HMS-DEHAPTS, the ratio was ~1. Because tertiary amines cannot form stable carbamates, it was proposed that the hydroxyl groups may serve to stabilize carbamate-type zwitterions.

Based on a systematic investigation on CO_2 adsorption on different mesoporous silica substrates and their amine-functionalized hybrid product, Knowles et al. (2005, 2006; Chaffee 2005) also pointed out that the extent of surface functionalization is found to be dependent on substrate morphology (e.g., available surface area, pore geometry, and pore volume), diffusion of reagents to the surface, as well as the silanol concentration on the substrate surface. The higher nitrogen

content of the tether caused a higher CO_2 adsorption capacity. The CO_2 adsorption performance of hybrid materials exhibited highest CO_2 capacity of ~1.66 mmol/g at 293 K in dry 90 % CO_2/10 % argon mixture, and good adsorption kinetics, reaching equilibrium within 4 min.

Hiyoshi et al. (2004, 2005) revealed the potential application of aminosilane-modified mesoporous silica for the separation of CO_2 from gas streams in the presence of moisture. In their subsequent research (Hiyoshi et al. 2005), DAEAPTS-SBA-15 showed enhanced CO_2 adsorption capacity after SBA-15 was treated with boiling water for 2 h, followed by the grafting of aminosilanes. The CO_2 adsorption capacity reached 1.58 and 1.80 mmol/g in the absence and presence of moisture, respectively. The efficiencies of the aminosilanes at identical amine surface density were in the following order: APTES > AEAPTS > DAEAPTS. Gray and coworkers (Gray et al. 2005; Chang et al. 2003; Khatri et al. 2005, 2006) also prepared a series of amine-grafted SBA-15 sorbents for CO_2 adsorption. Enhanced CO_2 adsorption capacity was observed in the presence of H_2O because of the formation of carbonate and bicarbonate (Chang et al. 2003) confirmed by Khatri et al. (2006). Khatri et al. (2006) and Zheng et al. (2004) studied the thermal stability of several grafted SBA-15 and found these to be stable up to 523 K. Furthermore, the SO_2 adsorption on APTES-SBA-15 led to a sharply decrease of CO_2 adsorption capacity, indicating the necessity of SO_2 removal before amine-based CO_2 adsorption (Khatri et al. 2006).

Sayari and coworkers (Harlick and Sayari 2006, 2007; Sayari et al. 2005; Serna-Guerrero et al. 2008, 2010a, b, c; Belmabkhout et al. 2010; Belmabkhout and Sayari 2010; Sayari and Belmabkhout 2010) developed pore-expanded MCM-41 mesoporous silica (PE-MCM-41) grafted with amine. The DAEAPTS-grafted PE-MCM-41 support with aminosilane loading of 5.98 mmol (N)/g showed an adsorption capacity of 2.05 mmol/g at 298 K and 1.0 atm for a dry 5 % CO_2 in N_2 feed mixture (Harlick and Sayari 2006). The amine surface density of the sorbent had a strong impact on the adsorption capacity. However, the existence of moisture did not significantly improve the performance of the amine-impregnated PE-MCM-41 sorbents. Subsequently, Harlick and Sayari (2007) found that, compared with dry grafting procedure, wet grafting via the co-addition of water at 358 K showed an increase in the total amine content, resulting in a 90 % overall improvement. The sorbent exhibited good stability over 100 cycles with an average working adsorption capacity of 2.28 mmol/g for pure CO_2 through regeneration under a vacuum at 343 K (Serna-Guerrero et al. 2010a), while the temperature swing regeneration process was suitable only at >393 K (Serna-Guerrero et al. 2010b). In addition to thermal stability, it also showed extremely high selectivity for CO_2 over N_2 and O_2 (Serna-Guerrero et al. 2010b, c; Belmabkhout et al. 2010; Belmabkhout and Sayari 2010). It was also confirmed by Belmabkhout and Sayari (2010) that SO_2 has an adverse effect for CO_2 capture (Khatri et al. 2006). In addition, this group noted that their sorbent underwent over 700 cycles without any loss of capacity when adsorption and regeneration was carried out using a humid gas with ~7.5 % relative humidity at 343 K. Furthermore, experimental data of CO_2 uptake as a function of time at temperatures between 298 and 373 K were fit to a series of kinetic models, namely, Lagergren's pseudo-first- and pseudo-second-order and

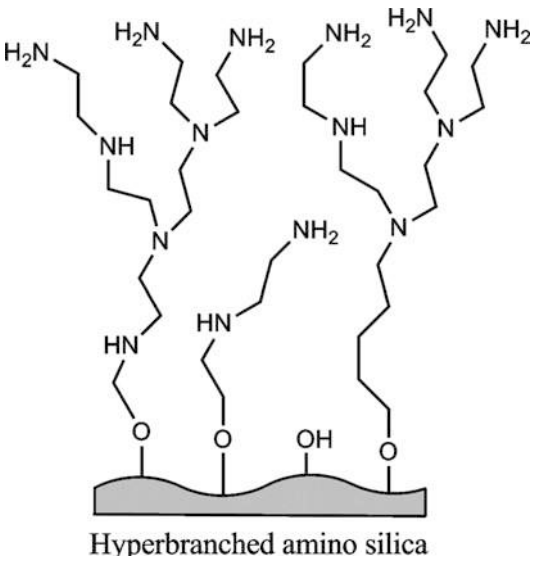

Fig. 8 Hyperbranched amino silica (Drese et al. 2009)

Avrami's kinetic models. The adsorption kinetics of CO_2 on amine-functionalized PE-MCM-41 was successfully described using Avrami's kinetic model with a reaction kinetic order of 1.4, which has been associated with the occurrence of multiple adsorption pathways (Serna-Guerrero and Sayari 2010).

Jones and his coworkers developed a covalently tethered hyperbranched aminosilica (HAS) sorbent (Fig. 8) with high amine content capable of capturing CO_2 reversibly from flue gas. They also compared it with other covalently supported solid sorbents (Hicks et al. 2008; Drese et al. 2009). HAS was synthesized via a one-step surface polymerization reaction of aziridine monomer inside SBA-15 pores (Drese et al. 2009). The HAS sorbent had an amine loading of 7.0 mmol N/g and CO_2 adsorption capacity of 3.08 mmol/g when tested in a packed-bed reactor under a flow of 10 % CO_2/90 % argon saturated with water at 298 K. It was stable over 12 cycles with regeneration temperature at 403 K. In another study, Drese et al. (2009) proposed modification of the HAS synthesis conditions, such as the aziridine-to-silica ratio and the solvent to further tune the sorbent's composition, adsorbent capacity, and kinetics. They found that higher amine loadings contributed to a better adsorption capacity.

The comparison of three APTES-grafted mesoporous silica materials, namely, MCM-41 ($d_p = 3.3$), SBA-12 ($d_p = 3.8$), and SBA-15 ($d_p = 7.1$), was made by Zelenak et al. (2008). The sorbent capacity was consistent with the order of pore size and amine surface density, similar to that observed in the amine-impregnated mesoporous silica sorbents. Kim et al. (2008) developed and tested a series of amine-functionalized mesoporous silica sorbents via anionic surfactant-mediated synthesis method for CO_2 adsorption at room temperature. As expected, higher amine loading on the mesoporous structure was the governing factor to achieve high CO_2 adsorption.

Table 8 lists the CO_2 adsorption capacity of various amine-grafted adsorbents. Although the functionalization of mesoporous silicas with amine functional groups significantly enhances the CO_2 adsorption capacity of silica substrate, the reported equilibrium CO_2 adsorption capacities are not as high as those reported with amine-impregnated mesoporous silicas. Moreover, the low thermal stability of mesoporous silicas, in the presence of water vapor at elevated temperature, is still one of the major concerns.

Metal–Organic Frameworks

MOFs are network solids composed of metal ion or metal cluster vertices and organic linkers. The ability to freely incorporate and vary organic linkers in MOFs translates to abundant options to control pore shape, pore size, and the chemical potential of the adsorbing surfaces and, consequently, their capacity, selectivity, and kinetics. MOFs have two important features: (i) their syntheses can be modular, and (ii) the solids are crystalline. Because the bonding (coordinate covalent) is weaker than those in metal oxides, solvated pores are not sure to necessarily exist if the solvent is removed. Indeed, these compounds can be classified into three generations due to this fact: first generation, those that collapse irreversibly and are not porous; second generation, those that retain their structures and show reversible gas sorption isotherms; third generation, a category where the material behaves more like a sponge and changes structure reversibly with guest sorption (Kitagawa et al. 2004).

Many of the MOFs show large CO_2 adsorption capacities at pressures at and above 1 bar, due to their high surface areas. However, the adsorption capacities at lower CO_2 pressures are often not directly reported, and these have been carefully estimated for CO_2 (0.15 bar) and N_2 (0.75 bar) and are listed in Table 9. Table 9 also lists the calculated selectivity values for CO_2 over N_2 at 298 K for selected MOFs, using the molar ratio of the CO_2 uptake at 0.15 bar and the N_2 uptake at 0.75 bar. The direct measurement of multicomponent isotherms, which has not been performed for CO_2/N_2 mixtures, is necessary in order to evaluate the accuracy of selectivity factors predicted from single-component isotherms and ideal adsorbed solution theory (IAST).

Surface Functionalization of MOFs

It is essential to tune the affinity of the framework functionalities toward CO_2 for optimization of the adsorptive properties. The various kinds of functionalities to enhance CO_2 capture performance are discussed in the following sections, including amines, strongly polarizing organic functionalities, and exposed metal cation sites.

- **Pores Functionalized by Nitrogen Bases**. MOFs functionalized with basic nitrogen-containing organic groups have been widely investigated for the CO_2 adsorption. The dispersion and electrostatic forces due to the interaction between

Table 9 CO_2 and N_2 uptake in selected MOFs

Material chemical formula	Common names	CO_2 uptake at 0.15 bar (mmol/g)	N_2 uptake at 0.75 bar (mmol/g)	Selectivity	Temperature (K)	References
Mg_2(dobdc)	Mg-MOF-74, Mg-CPO-27	4.68 4.30 3.80 3.30	0.65 0.5 0.39 0.31	44 52.3 58.8 61.1	303 313 323 333	(Mason et al. 2011)
Ni_2(dobdc)	Ni-MOF-74, CPO-27-Ni	3.84	0.76	30	298	(Dietzel et al. 2009; Yazaydin et al. 2009b)
Co_2(dobdc)	Co-MOF-74, CPO-27-Co	3.23			298	(Yazaydin et al. 2009b)
Zn_2(dobdc)	Zn-MOF-74, CPO-27-Zn	1.73			296	(Caskey et al. 2008)
$Cu_3(BTC)_2$	HKUST-1	2.64	0.15	101	293	(Aprea et al. 2010)
$H_3[(Cu_4Cl)_3(BTTri)_8(mmen)_{12}]$	mmen-Cu-BTTri	2.15	0.07	165	298	(McDonald et al. 2011)
$Zn_2(ox)(atz)_2$		1.89			293	(Vaidhyanathan et al. 2009)
$Pd(\mu\text{-F-pymo-}N^1,N^3)_2$		1.48			293	(Navarro et al. 2007)
$Cu_3(TATB)_2$	CuTATB-60	1.32	0.29	24	298	(Kim et al. 2011)
$Co_2(adenine)_2(CO_2CH_3)_2$	bio-MOF-11	1.23	0.1	65	298	(An et al. 2010)
$Fe_3[(Fe_4Cl)_3(BTT)_8(MeOH)_4]_2$	Fe-BTT	1.20	0.34	18	298	(Sumida et al. 2010)
$Al(OH)(bpydc)\bullet 0.97Cu(BF_4)_2$		0.91	0.12	39	298	(Bloch et al. 2010)
Zn(nbIm)(nIm)	ZIF-78	0.75	0.13	30	298	(Phan et al. 2010; Banerjee et al. 2009)
Al(OH)(2-amino-BDC)	NH2-MIL-53 (Al), USO-1-Al-A	0.70			298	(Arstad et al. 2008b)

(*continued*)

Table 9 (continued)

Material chemical formula	Common names	CO_2 uptake at 0.15 bar (mmol/g)	N_2 uptake at 0.75 bar (mmol/g)	Selectivity	Temperature (K)	References
$H_3[(Cu_4Cl)_3(BTTri)_8]$	Cu-BTTri	0.66	0.06	19	298	(Demessence et al. 2009)
$Zn_2(bpdc)_2(bpee)$		0.48	0.01	44	298	(Demessence et al. 2009)
$Ni_2(2\text{-amino-BDC})_2(DABCO)$	USO-2-Ni-A	0.48			298	(Wu et al. 2010)
$Cu_3(BPT(N_2))_2$	UMC-150(N)2	0.43			298	(Yazaydin et al. 2009b; Park et al. 2011)
$Cu_3(BPT)_2$	UMCM-150	0.41			298	(Yazaydin et al. 2009b; Park et al. 2011)
$Zn_2(BTetB)$		0.41	0.11	19	298	(Bae et al. 2009)
Al(OH)(BDC)	MIL-53(Al), USO-1-A	0.39			298	(Arstad et al. 2008b)
$Zn_2(bmbdc)_2(4,4'\text{-bpy})$		0.32			298	(Henke and Fischer 2011)
$Ni_2(BDC)_2(DABCO)$	USO-2-Ni	0.27			298	(Arstad et al. 2008b)
$V^{(IV)}O(BDC)$	MIL-47	0.25			298	(Yazaydin et al. 2009b)
Al(OH)(bpydc)	MOF-253	0.23	0.13	9	298	(Bloch et al. 2010)
$Zn_{20}(cbIm)_{39}(OH)$	ZIF-100	0.23	0.05	22	298	(Wang et al. 2008b)
$Zn_4O(NO_2\text{-BDC})_{1.19}((C_3H_5O)2\text{-BDC})_{1.07}\text{-}((C_7H_7O)_2\text{-BDC})_{0.74}$	MTV-MOF-5-EHI	0.23			298	(Deng et al. 2010)
$Zn_2(BTetB)(py\text{-}CF_3)_2$		0.20	0.02	50	298	(Bae et al. 2009)
$Zn(MeIM)_2$	ZIF-8	0.14			298	(Yazaydin et al. 2009b)
$Zn_4O(BDC\text{-}NH_2)_3$	IRMOF-3	0.14			298	(Millward and Yaghi 2005; Yazaydin et al. 2009b)
$Zn_4O(BTB)_2$	MOF-177	0.14	0.14	4	298	(Mason et al. 2011)
$Zn_4O(BDC)(BTB)_{4/3}$	UMCM-1	0.11			298	(Yazaydin et al. 2009b)
$Zn_4O(BDC)_3$	MOF-5, IRMOF-1	0.11			298	(Yazaydin et al. 2009b)
$Co_4(OH)_2(doborDC)_3$		0.11	0.03	18	298	(Bae et al. 2010)

the quadrupole moment of CO_2 and localized dipoles generated by heteroatom incorporation are typically responsible for the enhanced CO_2 adsorption performance. In some cases, acid–base-type interactions of the lone pair of nitrogen with CO_2 have also been observed. The degree to which nitrogen incorporation improves CO_2 adsorption depends significantly on the properties of the functional group. Three major classes of nitrogen-functionalized MOFs have been synthesized: heterocycle (i.e., pyridine) derivatives (Stylianou et al. 2011; An and Rosi 2010; An et al. 2010), aromatic amine (i.e., aniline) derivatives (Millward and Yaghi 2005; Zhao et al. 2009a; Arstad et al. 2008a; Stavitski et al. 2011; Couck et al. 2009), and alkylamine (i.e., ethylenediamine) bearing frameworks (McDonald et al. 2011; Demessence et al. 2009; Hwang et al. 2008).

- **Other Strongly Polarizing Organic Functional Groups**. In addition to the nitrogen-based functionalities, organic linkers with heteroatom functional groups (other than amines) have also been examined on the CO_2 adsorption behavior (Phan et al. 2010; Banerjee et al. 2008, 2009; Deng et al. 2010). These functional groups contain hydroxy, nitro, cyano, thio, and halide groups, and the degree to which CO_2 adsorption capacity is improved in these cases depends primary upon the extent of ligand functionalization and the polarizing strength of the functional group. Generally, strongly polarizing groups will influence CO_2 adsorption favorably.
- **Exposed Metal Cation Sites**. The generation of structure types bearing exposed metal cation sites on the pore surface is another way that has been used to enhance the affinity and selectivity of MOFs toward CO_2 (Mason et al. 2011; Chui et al. 1999; Bordiga et al. 2007; Vishnyakov et al. 2003; Caskey et al. 2008; Bloch et al. 2010). $Cu_3(BTC)_2$ (HKUST-1) is one of the most studied materials featuring such binding sites (Chui et al. 1999). It shows a cubic, twisted boracite topology constructed from dinuclear Cu^{2+} paddlewheel units and triangular 1,3,5-benzenetricarboxylate linkers. The as-synthesized form of the framework has bound solvent molecules on the axial coordination sites of each Cu^{2+} metal center, which can be subsequently removed in vacuo at elevated temperatures to create open binding sites for guest molecules. The open metal cation sites serve as charge-dense binding sites for CO_2, which is adsorbed more strongly at these sites due to its greater quadrupole moment and polarizability.

Application for MOFs in Harsh Environment

Understanding the effects of the contaminants (water vapor, SO_2, NO_x, et al.) is critical to properly evaluate MOFs in a realistic CO_2 capture process. Here, we discuss a number of researches that have aimed to study the performance of MOFs under more realistic conditions.

- **Stability to Water Vapor**. Although partial dehydration of the effluent may be possible, it is costly and most likely not feasible on a large scale to dry the gas completely prior to adsorbing CO_2 (Granite and Pennline 2002; Lee and Sircar 2008). In evaluating MOFs for applications in CO_2 capture processes, it is significant to consider not only the stability of the framework to water vapor but also the effect of water vapor on the adsorption of CO_2.

Regarding water stability, the metal–ligand bond is typically the weakest point of a MOF, and hydrolysis can cause the displacement of bound ligands and collapse of the framework structure (Low et al. 2009). This was first observed in MOF-5, which is water sensitive and begins to lose crystallinity when exposed to small amounts of water vapor.

It was found that the basic zinc acetate clusters characteristic of most zinc carboxylate MOFs, such as MOF-177 and the IRMOF series, are most susceptible to hydrolysis (Cychosz and Matzger 2010). The trinuclear chromium clusters found in many of the MIL series of frameworks are the most stable, while the copper-paddlewheel carboxylate clusters found in HKUST-1 exhibit intermediate stability.

One way to increase the water stability of MOFs is to use azolate-based linkers rather than the typical carboxylate linkers (Demessence et al. 2009). The azolate linkers can bind metals with a similar geometry to carboxylate ligands, but their greater basicity typically results in stronger M–N bonds and greater thermal and chemical stability. The relative M–N bond strengths can be predicted based on the pK_a values associated with the deprotonation of the free ligand. Therefore, stability typically decreases with the pK_a: pyrazole ($pK_a = 14.4$) linkers exhibit the greatest stability, imidazole ($pK_a = 10.0$) and triazole ($pK_a = 9.3$) are intermediate, and tetrazole ($pK_a = 4.6$) linkers are the most labile (Fig. 9).

An alternative strategy for increasing the metal–ligand bond strength in MOFs is through the use of trior tetravalent metal cations (Low et al. 2009). Generally, frameworks containing Cr^{3+}, Al^{3+}, Fe^{3+}, and Zr^{4+} cations exhibit a high degree of stability in water. Specifically, MIL-53 (M(OH)(BDC), M = Cr^{3+}, Fe^{3+}, Al^{3+}) is a flexible framework that expands or contracts based on the absence or presence of water (Serre et al. 2002; Whitfield et al. 2005; Loiseau et al. 2004). The overall framework scaffold remains intact upon repeated exposure to water, due to the reversibility of the structural transition. MIL-100 and MIL-101 are rigid trivalent frameworks built from trinuclear metallic clusters that have shown a high stability in both boiling water and steam. On the contrary, the zirconium(IV)-based UiO-66, which contains extremely robust $Zr_6O_4(OH)_4(CO_2)_{12}$ cluster units (Fig. 10), exhibits their high solubility in water (Cavka et al. 2008).

There have been several researches of MOF stability in liquid water, but few regarding different levels of humidity. HKUST-1 was initially focused on understanding the effect of water on CO_2 capture in MOFs. The effect of water coordination on the CO_2 adsorption performance of HKUST-1 was tested (Yazaydin et al. 2009a). Near 5 mmol/g of CO_2 was adsorbed for the dehydrated form, compared with less than 1 mmol/g at 1 bar in the fully hydrated form. This is in agreement with a similar research, which found that HKUST-1 shows a decrease in CO_2 uptake to about 75 % of its original value and a concurrent loss of some crystallinity after exposure to 30 % relative humidity (Liu et al. 2010). In a similar study, CO_2 adsorption isotherms were measured at different water loadings for HKUST-1 and Ni_2(dobdc) (Liu et al. 2010). Both MOFs retained some adsorption capacity for CO_2 at low water loadings but exhibited essentially no capacity above 70 % relative humidity. Significantly, water adsorption caused a much faster decrease in CO_2 adsorption for zeolites 5A and NaX than for either MOF.

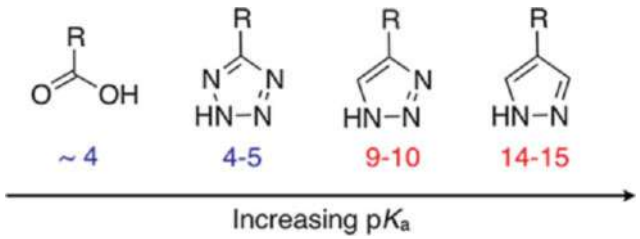

Fig. 9 The general trend of increasing pK_a for ligands built from carboxylic acids, tetrazoles, triazoles, and pyrazoles. The metal–ligand bond is expected to be stronger as the pK_a increases (Sumida et al. 2012)

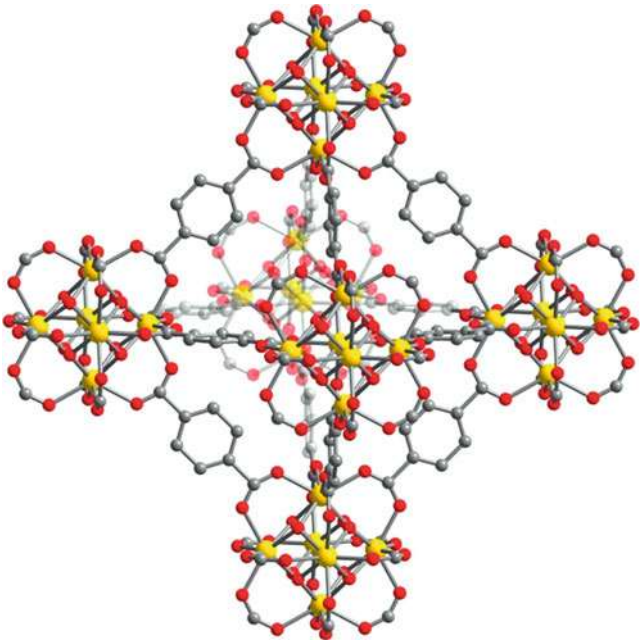

Fig. 10 A portion of the crystal structure of the high-stability metal–organic framework UiO-66 (Cavka et al. 2008). *Yellow*, *gray*, and *red spheres* represent Zr, C, and O atoms, respectively. H atoms are omitted for clarity

In order to evaluate their CO_2/N_2 separation performance, the effects of water vapor on the performance of the M_2(dobdc) (M = Zn, Ni, Co, and Mg) series of MOFs were studied (Fig. 11) (Kizzie et al. 2011). Although Mg_2(dobdc) has the highest reported adsorption capacity for CO_2 at low pressures, it performed the worst out of the series with a recovery of only 16 % of its initial capacity after regeneration. Ni_2(dobdc) and Co_2(dobdc) performed far better with recoveries of

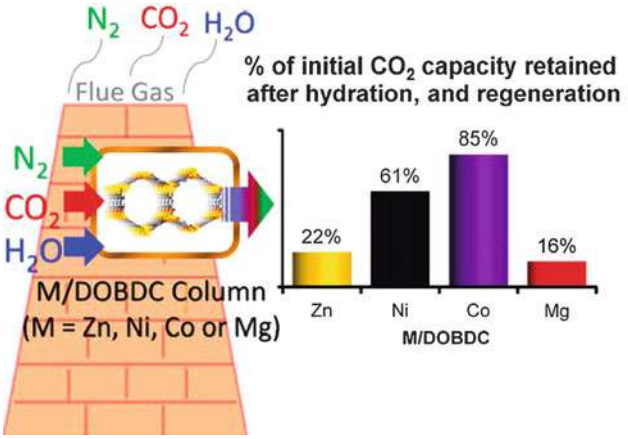

Fig. 11 Comparison of the flow-through CO_2 capacities, as determined from breakthrough experiments using a 5:1 N_2/CO_2 mixture, for pristine M_2(dobdc) and regenerated M_2(dobdc) after exposure to 70 % RH (Kizzie et al. 2011)

61 % and 85 % of their initial CO_2 capacity, respectively. This is in consistent with a similar study that found Ni_2(dobdc) could maintain its CO_2 capacity after steam conditioning and long-term storage, while Mg_2(dobdc) suffers a significant loss in capacity (Liu et al. 2011).

Some flexible MOFs exhibit promising CO_2 adsorption properties in the existence of water vapor (Cheng et al. 2009). In one report, water induced structural changes in MIL-53 that promoted a higher selectivity for CO_2 over CH_4 (Llewellyn et al. 2006). The breakthrough CO_2 adsorption of the flexible framework NH_2-MIL-53(Al) in the presence of 5 % water vapor was also investigated (Stavitski et al. 2011). Interestingly, CO_2 is selectively retained by the framework even in the presence of water.

While the abovementioned experiments are crucial for the initial assessment of MOFs for CO_2 capture, multicomponent adsorption isotherms are of high priority for evaluating and understanding the performance under conditions likely to be encountered in an actual capture system (Keskin et al. 2010).

- **Other Minor Components**. The exact amount of each species present in actual gas varies based on the specific configuration of a given plant. Particularly, in order to research the influence of flue gas contaminants, MIL-101(Cr) was selected as the focal point by Liu (Liu et al. 2013). CO_2 adsorption capacity of MIL-101(Cr) was able to maintain a high level of performance in trace gas-contaminated environments as well as after multiple cycles of adsorption and mild-condition regeneration. The addition of H_2O, SO_2, and NO to a 10 vol. % CO_2/N_2 feed flow was found to have only a minor effect on adsorption capacity. Under feed flow conditions of 10 vol.% CO_2, 100 ppm SO_2, 100 ppm NO, and 10 % RH, MIL-101(Cr) preserved greater than 95 % of its adsorption capacity after 5 cycles of adsorption/desorption.

Regenerable Alkali-Metal Carbonate-Based Sorbents

Due to the low operating temperature (<473 K), chemical adsorption of CO_2 with a dry regenerable alkali-metal carbonate-based solid sorbent (M_2CO_3, where M = K, Na, Li) is being considered for a period of time for CO_2 capture. In the adsorption process (carbonation, reaction 9), CO_2 and H_2O react with the carbonate sorbent in the range of 333–383 K and form alkali-metal bicarbonate. Heat treatment of the bicarbonate in the range from 373 to 473 K regenerates alkali-metal carbonate, releasing the CO_2 (decarbonation; reaction 10). The maximum theoretical capacity of Na_2CO_3 is 9.43 mmol/g.

Carbonation:

$$M_2CO_3 + H_2O + CO_2 = 2MHCO_3 \tag{13}$$

$\triangle H = -135$ kJ/mol, M = Na; $\triangle H = -141$ kJ/mol, M = K

Decarbonation:

$$2MHCO_3 = M_2CO_3 + H_2O + CO_2 \tag{14}$$

Hayashi et al. (1998) developed a TSA and a regeneration cyclic process for CO_2 capture using K_2CO_3 supported on AC. K_2CO_3 performs the best out of the three carbonates, as shown in Fig. 12. It has a wide carbonation temperature range where the sorbent efficiency is 100 %. In addition, there was an optimum loading of K_2CO_3 on AC support. Above the optimum loading, excess K_2CO_3 blocks micropores of AC, restricting CO_2 diffusion to the active reaction sites, leading to the reduction of working adsorption capacity and adsorption kinetics.

Seo et al. (2007; Lee et al. 2008b) investigated the effect of water vapor pretreatment on Na_2CO_3-based sorbent system in a bubbling fluidized-bed reactor

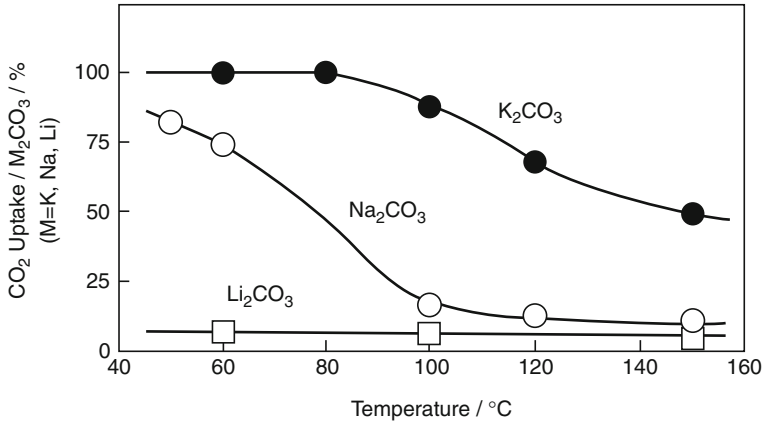

Fig. 12 Effect of temperature on the efficiency of CO_2 capture by alkali-metal carbonates. Feed gas composition: 13.8 % CO_2, 10 % H_2O, and balance He (Hayashi et al. 1998)

and found that, out of six types of spray-dried sorbent systems, three samples had better CO_2 adsorption capacity than MEA. Okunev et al. (2000, 2003; Sharonov et al. 2004) studied the impact of a porous support matrix on the CO_2 adsorption of K_2CO_3. Both hydrophilic (silica gel, alumina, vermiculite) and hydrophobic (AC) materials were used for support. The porous alumina/K_2CO_3 sorbent system possesses the highest dynamic capacity initially, but it decreases immediately after the first cycle. A completely reversible regeneration was observed in the case of an AC-impregnated sorbent system. The sorbent system dynamic capacity decreases in the following sequence: alumina > AC > vermiculite > silica gel.

To identify the best sorbent support system, some researchers (Lee et al. 2006a; Lee and Kim 2007) have prepared several K_2CO_3-based sorbents by impregnating it on various supports, such as AC, TiO_2, Al_2O_3, MgO, SiO_2, and zeolites. CO_2 adsorption capacities of K_2CO_3/AC, K_2CO_3/TiO_2, K_2CO_3/MgO, and K_2CO_3/Al_2O_3 (with an active phase loading of ~30 wt%) were ~2.0, 1.9, 2.7, and 1.9 mmol/g, respectively. However, the CO_2 adsorption capacities of K_2CO_3/Al_2O_3 and K_2CO_3/MgO decreased after regeneration at ≤473 K , because of the formation of $KAl(CO_3)_2(OH)_2$, $K_2Mg(CO_3)_2$, and $K_2Mg(CO_3)_2 \cdot 4(H_2O)$ phases during carbonation, which were not completely converted to the original K_2CO_3 phase. However, in the case of K_2CO_3/AC and K_2CO_3/TiO_2 sorbent systems, regeneration was not a problem in the temperature range of 403–423 K. "KZrI30" (30 wt% K_2CO_3/ZrO_2 sorbent system) was developed in 2009. The CO_2 adsorption capacity of the sorbent was ~96 % of the theoretical value in the presence of 1 % CO_2 and 9 % H_2O at 323 K, and it almost remained the same in multicycle operation (Lee et al. 2009). It is reported that the enhanced CO_2 capture capacity can be obtained by converting the entire $K_2CO_3 \cdot 1.5H_2O$ phase to the $KHCO_3$ phase if the sorbents are fully activated with excess water (Lee et al. 2006b). Lee et al. (2011) reported a new regenerable modified Al_2O_3 support for K_2CO_3 sorbent for CO_2 adsorption below 473 K. The CO_2 adsorption capacity of the 48 wt% K_2CO_3-loaded sorbent was ~2.9 mmol/g and did not decrease over five cycles.

Zhao et al. (2009b, c) found that K_2CO_3 with hexagonal crystals has superior carbonation kinetics over monoclinic K_2CO_3, because of the crystal structure similarities between K_2CO_3 (hexagonal) and $KHCO_3$. Table 10 summarizes the literature data on alkali carbonate sorbents for CO_2 capture.

In summary, the high CO_2 capture capacity of Na_2CO_3 (9.43 mmol/g) and K_2CO_3 (7.23 mmol/g) and favorable carbonation/regeneration temperature between 333 K and 473 K suggest that they are potentially excellent adsorbents for CO_2 capture. Moreover, they have the additional advantage of being relatively inexpensive. However, to be commercially viable, the long-term stability and persistence performance of these sorbents under real flue gas conditions of post-combustion applications have yet to be established.

The above discussion clearly indicates that several chemisorbents, such as amine-functionalized sorbent (both impregnated and grafted), have shown promise to meet the desired working capacity target in simulated flue gas conditions. Mostly, chemisorbents are found to have higher CO_2 selectivity. Amine-functionalized polymer-based sorbents showed very high adsorption capacity, but

Table 10 Alkali carbonate sorbents for CO_2 capture

Active phase	Support	Temperature of operation (K)	wt% active phase	Gas composition	Capacity (mmol/g)	References
K_2CO_3	AC, activated coke, and silica	Ads.: 373 Reg.: 423	~35 wt% in AC	Simulated flue gas and actual flue gas in slipstream	~2.1 (Ads. efficiency ~80 %)	(Hayashi et al. 1998)
Na_2CO_3	Ceramic supported sorbents	Ads.: 333–343 Reg.: 393–413	10–40 wt%	Simulated flue gas and actual flue gas	~0.5–3.2	(Samanta et al. 2012)
Na_2CO_3	Ceramic supported sorbents	Ads.: 323–343 Reg.: >408 (in N_2)	35 wt%	10 % CO_2, 12.2 % H_2O, and 77.8 % N_2	~2.6 (~80 % efficiency with a 35 % active phase)	(Seo et al. 2007)
Na_2CO_3	Ceramic supported sorbents	Ads.: 323–343 Reg.: 393 (in N_2)	20–50 wt%	Simulated flue gas: 14.4 % CO_2, 5.4 % O_2, 10 % H_2O, and 70.2 % N_2	~2.3 (>80 % sorbent efficiency with a 30 % active phase)	(Lee et al. 2008b)
K_2CO_3	AC, TiO_2, Al_2O_3, MgO, ZrO_2, CaO, SiO_2, and zeolites	Ads.: 333–373 Reg.: 403–673 (Moisture up to 9 % and balance N_2)	30 wt%	1 % CO_2, 0–11 % H_2O, and N_2 balance	~1.1–2.7	(Lee et al. 2006a, b, 2009; Lee and Kim 2007)
K_2CO_3	"Sorb KX35" (proprietary recipe)	Ads.: 333–373 Reg.: 393–493 (in N_2)	35 wt%	Simulated flue gas: (dry basis)12 % CO_2 and 88 % N_2; 7–30 % moisture	~2.1 (~96 % sorbent efficiency)	(Yi et al. 2007)
K_2CO_3	"Sorb A" (proprietary recipe)	Ads.: 343–363 Reg.: g150 (in N_2)	35 wt%	Slipstream coal-fired flue gas: 7–9 % CO_2 (dry basis), 10–19 % H_2O	CO_2 >85 % (capacity not available)	(Park et al. 2009)
K_2CO_3	AC, silica gel, activated Al_2O_3	Ads.: 333 Reg.: 473 (in N_2)	~25 wt%	15 % CO_2, 15 % H_2O, and N_2 balance	~0.34–1.7	(Zhao et al. 2009d)
K_2CO_3	Modified Al_2O_3 support $KAl(CO_3)(OH)_2$	Ads.: 343–363 Reg.: 403 (in N_2)	~28–48 wt%	1 % CO_2, 9 % H_2O, and N_2 balance	~2.9 (~48 wt% K_2CO_3 loading)	(Lee et al. 2011)

there is not adequate information regarding other selection criteria. Impregnated mesoporous silica sorbents showed improved capacity in the presence of water vapor, whereas grafted silica showed good thermal stability at high temperature (<473 K). However, a considerable amount of time is required to regenerate these sorbents via thermal swing cycling, and it is found that SO_2 has an adverse effect on CO_2 removal, and its removal is required prior to CO_2 adsorption. Moreover, all of the identified sorbents are in the early development stage and require further investigation.

Technical Challenges and Pilot Plant Developments

Technical Challenges

Compared to conventional aqueous amine absorption/regeneration processes, an efficient and cost-effective sorption technique using a solid sorbent could produce certain technical and economic advantages. It appears that there are some potentially attractive solid sorbents that exhibit better CO_2 adsorption capacities and lower regeneration energy than conventional aqueous amine-based absorbents on the basis of the ongoing both experimental and theoretical studies. However, the efficient use of the solid sorbent in a particular contactor type is a key point and will ultimately determine whether the sorbent-based technology can actually be economical for CO_2 capture. The knowledge of key engineering data such as equilibrium CO_2 adsorption capacity under given conditions of pressure, temperature, and concentration, kinetic data for adsorption and desorption, mass transfer and diffusional effects, effects of moisture, effects of flue gas contaminants, the heat of adsorption and desorption, particle/bed characteristics of solid sorbents, etc. are essential for candidate sorbents being developed and for the design of CO_2 capture system. All of these characteristics are not available up to now. Process design and economic analysis are limited because of the lack of sufficient data on solid sorbent performance in various contactor configurations.

The process technologies frequently explored for a continuous CO_2 capture process are the cyclic processes, such as PSA, VSA, and TSA. Ho et al. (2008a) investigated the economic feasibility of PSA for CO_2 capture from power plant flue gas, using zeolite 13X with a working capacity of 2.2 mmol/g and a CO_2/N_2 selectivity of 54. They reported that the use of vacuum regeneration reduces the capture cost from US$57 to US$51 per ton of CO_2 captured. This cost is comparable to the cost of MEA absorption (Ho et al. 2008b). On the basis of experimental data and economic analysis on VSA process for CO_2 capture from flue gas, Zhang et al. (2008b) found that the operating capture costs vary significantly with process configuration and operating parameters, such as feed gas temperature, feed concentration, and evacuation pressure, which have significant influence on power consumption and CO_2 capture cost. For example, for CO_2 capture from a 500 MW coal-fired power plant flue gas stream using zeolite 13X sorbents, the estimated operating capture costs for a six-step VSA cycle without purge is

US$12–$35 per ton CO_2 captured, and the costs for a nine-step VSA cycle with purge are US$18–$32 per ton CO_2 captured.

The bed configuration for sorbent system also has strongly influence on techno-economic analysis. The possible configurations for contacting CO_2 streams with solid sorbents are fixed bed, fluidized bed, and moving bed. Fluidized-bed contactors is likely to be superior to the fixed-bed adsorber, due to some inherent advantages, such as (i) excellent gas–solid contact due to vigorous agitation of sorbent particles, (ii) minimum diffusional resistance, (iii) uniformity of temperature, and (iv) faster overall kinetics over fixed-bed contactors. For the sorbents that withstand fluidized-bed conditions, their operation shortcomings in fixed beds introduce can be overcome. Circulating-bed and fast-fluidized-bed, transport-bed, and other innovative contactor configurations will be the subject of future search for an optimal contactor configuration to meet the design constraints of CO_2 capture. Moreover, there is considerable scope for process optimization, because of the variety of cycle configurations, process conditions, and adsorbent types available (Zhang et al. 2008b).

Pilot Plant Developments

A few pilot-scale demonstrations are investigating the effectiveness of low-temperature adsorbents for CO_2 adsorption. One of the first pilot plant projects was the CO2CRC H3 project (Qader et al. 2011) lignite-fired power plant based at International Power's Hazelwood Power Station, which was commissioned in 2009 at Latrobe Valley, Victoria, Australia, and completed in 2011. The performance of CO_2 adsorbents was investigated with a three-bed multilayered VSA process at high humidity levels in the presence of SO_x and NO_x. Multilayered adsorbents were used to remove the water firstly and subsequently SO_x/NO_x from the flue gas. A layer of CO_2-selective sorbents was then added. A purity of ~71 % and a recovery of ~60 % were achieved after continuous running of the process with a simple six-step cycle (without purge) for a week.

The capture and concentration of CO_2 from a dry flue gas by VSA process has been experimentally demonstrated in a pilot plant by Krishnamurthy (Krishnamurthy et al. 2014). The pilot plant has the provision for using two coupled columns that are each packed with approximately 41 kg of Zeochem zeolite 13X (Fig. 13). With the cycle configuration, CO_2 was concentrated to 95.9 $\pm$ 1 % with a recovery of 86.4 $\pm$ 5.6 %. To enhance the process performance, a four-step cycle with light product pressurization (LPP) using two beds was investigated. This cycle was able to achieve 94.8 $\pm$ 1 % purity and 89.7 $\pm$ 5.6 % recovery. The energy consumptions in the pilot plant experiments were 339–583 $\pm$ 636.7 kWh ton^{-1} CO_2 captured, and they were significantly different from the theoretical power consumptions obtained from isentropic compression calculations. The productivities were 0.87 ~1.4 $\pm$ 0.07 ton CO_2 m^{-3} adsorbent day^{-1}.

CO_2 capture from the real flue gas was performed in an existing coal-fired power plant by Li's group (Fig. 14) (Liu et al. 2012; Wang et al. 2013a, b). The pilot-scale

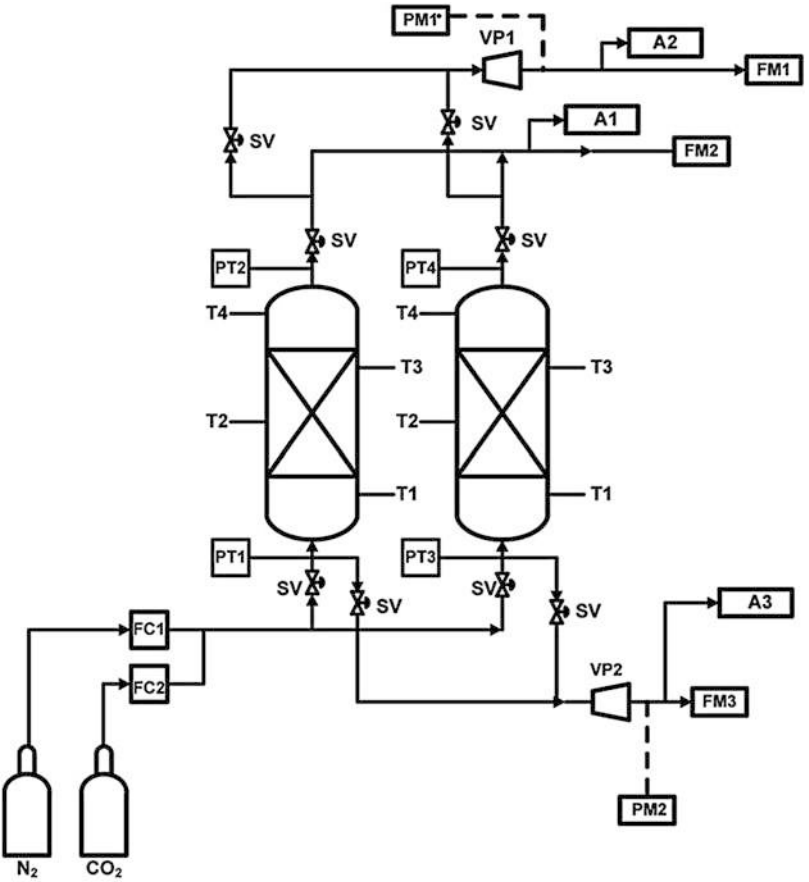

INSTRUMENT	BRAND	RANGE	MANUFACTURER REPORTED ERROR
PT1-PT4	GE UNIK 5000	0-10 bar	±0.04% FS
T1-T4	LAB FACILITY PT-100	-100 to 450°C	±1°C
A1	QUANTEK INSTRUMENTS 906	0-5%	±1% FS
A2	QUANTEK INSTRUMENTS 906	0-50%	±1% FS
A3	QUANTEK INSTRUMENTS 906	0-100%	±1% FS
FC1	BROOKS 5850E	0-1250 SLPM	±1% FS
FC2	BROOKS 5850E	0-250 SLPM	±1% FS
FM1	TELEDYNE HFM 305	0-1800 SLPM	±1% FS
FM2	TELEDYNE HFM 200	0-250 SLPM	±1% FS
PM1,PM2	LUTRON DW 6093	10-600 V	±0.5%

Fig. 13 Schematic of the pilot plant. SV solenoid valve, PT pressure transducer, FM flow meter, FC flow controller, A1–A3–CO_2 analyzers, T1–T4 thermocouples, VP1 and VP2 vacuum pumps. The instrument specifications are also listed here

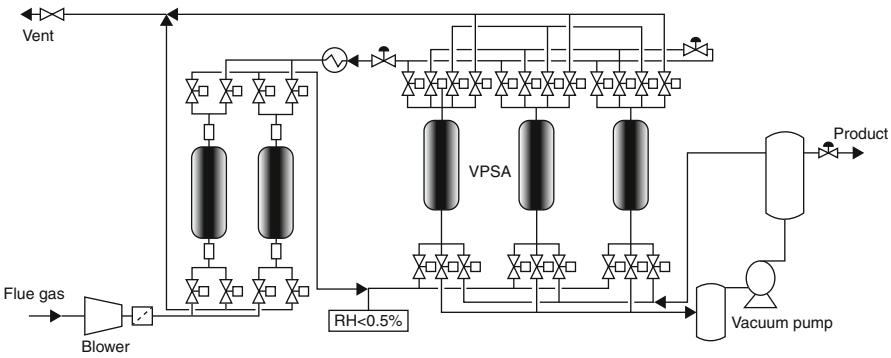

Fig. 14 Schematic diagram of pilot-scale carbon capture plant consisting of a dehumidifying unit and a CO_2 capture unit

CO_2 capture plant consisted of a CO_2 capture unit and a dehumidifying unit. The dehumidifying unit received the desulfurized flue gas from the power plant at a controlled flow rate and supplied the dehumidified flue gas (15.5–16.5 % CO_2, less than 0.5 % relative humidity) for the CO_2 capture unit. The three-bed eight-step vacuum pressure swing adsorption (VPSA) process was employed in the CO_2 capture unit, where two types of adsorbent materials were tested, zeolite 5A and 13XAPG done. 85–95 % CO_2 is recovered from the flue gas with 73–82 % purity in product gas. With the three-bed eight-step VPSA process CO_2 adsorption, the power consumption of a blower and a vacuum pump is measured onsite as 1.79–2.14 MJ/kg CO_2. However, the actual power consumption of vacuum pump accounts for two third of the total power consumption and is greater than the theoretically predicted value by the conventional adiabatic pump-down calculation.

Inventys claims that their VeloxoTherm^{TM} process can capture CO_2 for US$15/t. The technology involves an intensified TSA process with structured adsorbent and steam regeneration in a rotating adsorbent wheel. ETI announced the award of £20 million funding for a 5 MW project that can be used for a new-build CCGT or retrofitted onto one. The initial stage of the project is lab-scale studies, while the final aim is to have a commercial technology by 2020.

The ATMI/SRI BrightBlack microporous carbon was tested at a coal-fired steam production facility carried out by the University of Toledo in Ohio, USA. The material exceeded the DOE targets of >90 % CO_2 capture with >90 % CO_2 purity during tests with 200 standard l min^{-1} of flue gas. In addition, the column operated for approximately 7000 adsorption/regeneration cycles with no signs of adsorbent degradation and no loss in process or adsorbent performance. The project partners are now looking at scaling up to pilot-scale testing.

Due to the early stages of development, not much information is available currently on the pilot plants; the availability of data on these projects in the future will represent a crucial step toward the deployment of adsorption processes at commercial scale.

Future Directions

Compared to conventional liquid amine processes, solid sorbents for capture CO_2 are advantageous in regeneration energy cutback, corrosion prevention, and cost reduction. However, as discussed previously, solid sorbents also have limitations and challenges to be addressed before they can be applied commercially. The following are three recommendations for further research:

- Synthesis and modification of the potential solid sorbents to enhance the adsorption performance, such as working capacity, selectivity, and multicycle durability
- Comparison of some of the most promising solid sorbents, based on techno-economic assessment of the system including thermal integration
- Performance study of the potential solid sorbents under actual gas conditions using various bed configurations, such as fixed bed, fluidized bed, moving bed, and circulating bed

References

Alesi WR, Gray M, Kitchin JR (2010) CO_2 adsorption on supported molecular amidine systems on activated carbon. Chemsuschem 3(8):948–956

An J, Rosi NL (2010) Tuning MOF CO_2 adsorption properties via cation exchange. J Am Chem Soc 132(16):5578–5579

An J, Geib SJ, Rosi NL (2010) High and selective CO_2 uptake in a cobalt adeninate metal-organic framework exhibiting pyrimidine- and amino-decorated pores. J Am Chem Soc 132(1):38–39

Aprea P, Caputo D, Gargiulo N, Iucolano F, Pepe F (2010) Modeling carbon dioxide adsorption on microporous substrates: comparison between Cu-BTC metal-organic framework and 13X zeolitic molecular sieve. J Chem Eng Data 55(9):3655–3661

Arenillas A, Smith KM, Drage TC, Snape CE (2005) CO_2 capture using some fly ash-derived carbon materials. Fuel 84(17):2204–2210

Arstad B, Fjellvåg H, Kongshaug KO, Swang O, Blom R (2008a) Amine functionalised metal organic frameworks (MOFs) as adsorbents for carbon dioxide. Adsorption 14(6):755–762

Arstad B, Fjellvag H, Kongshaug KO, Swang O, Blom R (2008b) Amine functionalised metal organic frameworks (MOFs) as adsorbents for carbon dioxide. Adsorption J Int Adsorption Soc 14(6):755–762

Avrami M (1939) Kinetics of phase change I – general theory. J Chem Phys 7(12):1103–1112

Avrami M (1941) Granulation, phase change, and microstructure – kinetics of phase change. III. J Chem Phys 9(2):177–184

Bae YS, Farha OK, Hupp JT, Snurr RQ (2009) Enhancement of CO_2/N-2 selectivity in a metal-organic framework by cavity modification. J Mater Chem 19(15):2131–2134

Bae YS, Spokoyny AM, Farha OK, Snurr RQ, Hupp JT, Mirkin CA (2010) Separation of gas mixtures using Co(II) carborane-based porous coordination polymers. Chem Commun 46(20):3478–3480

Banerjee R, Phan A, Wang B, Knobler C, Furukawa H, O'Keeffe M, Yaghi OM (2008) High-throughput synthesis of zeolitic imidazolate frameworks and application to CO_2 capture. Science 319(5865):939–943

Banerjee R, Furukawa H, Britt D, Knobler C, O'Keeffe M, Yaghi OM (2009) Control of pore size and functionality in isoreticular zeolitic imidazolate frameworks and their carbon dioxide selective capture properties. J Am Chem Soc 131(11):3875–3877

Belmabkhout Y, Sayari A (2010) Isothermal versus non-isothermal adsorption-desorption cycling of triamine-grafted pore-expanded MCM-41 mesoporous silica for CO_2 capture from flue gas. Energy Fuel 24:5273–5280

Belmabkhout Y, Serna-Guerrero R, Sayari A (2010) Adsorption of CO_2-containing gas mixtures over amine-bearing pore-expanded MCM-41 silica: application for gas purification. Ind Eng Chem Res 49(1):359–365

Benedict JB, Coppens P (2009) Kinetics of the single-crystal to single-crystal two-photon photodimerization of alpha-trans-cinnamic acid to alpha-truxillic acid. J Phys Chem A 113(13):3116–3120

Berger AH, Bhown AS (2011) Comparing physisorption and chemisorption solid sorbents for use separating CO_2 from flue gas using temperature swing adsorption. 10th international conference on greenhouse gas control technologies, vol 4, pp 562–567

Berlier K, Frere M (1996) Adsorption of CO_2 on activated carbon: simultaneous determination of integral heat and isotherm of adsorption. J Chem Eng Data 41(5):1144–1148

Bloch ED, Britt D, Lee C, Doonan CJ, Uribe-Romo FJ, Furukawa H, Long JR, Yaghi OM (2010) Metal insertion in a microporous metal-organic framework lined with 2,2′-bipyridine. J Am Chem Soc 132(41):14382–14384

Bordiga S, Regli L, Bonino F, Groppo E, Lamberti C, Xiao B, Wheatley PS, Morris RE, Zecchina A (2007) Adsorption properties of HKUST-1 toward hydrogen and other small molecules monitored by IR. Phys Chem Chem Phys 9(21):2676–2685

Brandani F, Ruthven DM (2004) The effect of water on the adsorption of CO_2 and C_3H_8 on type X zeolites. Ind Eng Chem Res 43(26):8339–8344

Burchell TD, Judkins RR, Rogers MR, Williams AM (1997) A novel process and material for the separation of carbon dioxide and hydrogen sulfide gas mixtures. Carbon 35(9):1279–1294

Caplow M (1968) Kinetics of carbamate formation and breakdown. J Am Chem Soc 90(24):6795–6803

Caskey SR, Wong-Foy AG, Matzger AJ (2008) Dramatic tuning of carbon dioxide uptake via metal substitution in a coordination polymer with cylindrical pores. J Am Chem Soc 130(33):10870–10871

Cavka JH, Jakobsen S, Olsbye U, Guillou N, Lamberti C, Bordiga S, Lillerud KP (2008) A new zirconium inorganic building brick forming metal organic frameworks with exceptional stability. J Am Chem Soc 130(42):13850–13851

Cestari AR, Vieira EFS, Vieira GS, Almeida LE (2006) The removal of anionic dyes from aqueous solutions in the presence of anionic surfactant using aminopropylsilica – a kinetic study. J Hazard Mater 138(1):133–141

Chaffee AL (2005) Molecular modeling of HMS hybrid materials for CO_2 adsorption. Fuel Process Technol 86(14–15):1473–1486

Chaffee AL, Delaney SW, Knowles GP (2002) Hybrid mesoporous materials for carbon dioxide separation. Abstr Pap Am Chem Soc 223:U572–U573

Chang ACC, Chuang SSC, Gray M, Soong Y (2003) In-situ infrared study of CO_2 adsorption on SBA-15 grafted with gamma-(aminopropyl)triethoxysilane. Energy Fuel 17(2):468–473

Chen C, Yang ST, Ahn WS, Ryoo R (2009) Amine-impregnated silica monolith with a hierarchical pore structure: enhancement of CO_2 capture capacity. Chem Commun 24:3627–3629

Cheng Y, Kondo A, Noguchi H, Kajiro H, Urita K, Ohba T, Kaneko K, Kanoh H (2009) Reversible structural change of Cu-MOF on exposure to water and its CO_2 adsorptivity. Langmuir 25(8):4510–4513

Chew TL, Ahmad AL, Bhatia S (2010) Ordered mesoporous silica (OMS) as an adsorbent and membrane for separation of carbon dioxide (CO_2). Adv Colloid Interface Sci 153(1–2):43–57

Choi S, Drese JH, Jones CW (2009) Adsorbent materials for carbon dioxide capture from large anthropogenic point sources. Chemsuschem 2(9):796–854

Chue KT, Kim JN, Yoo YJ, Cho SH, Yang RT (1995) Comparison of activated carbon and zeolite 13x for Co_2 recovery from flue-gas by pressure swing adsorption. Ind Eng Chem Res 34(2):591–598

Chui SSY, Lo SMF, Charmant JPH, Orpen AG, Williams ID (1999) A chemically functionalizable nanoporous material [Cu-3(TMA)(2)(H2O)(3)](n). Science 283(5405):1148–1150

Cinke M, Li J, Bauschlicher CW, Ricca A, Meyyappan M (2003) CO_2 adsorption in single-walled carbon nanotubes. Chem Phys Lett 376(5–6):761–766

Coriani S, Halkier A, Rizzo A, Ruud K (2000) On the molecular electric quadrupole moment and the electric-field-gradient-induced birefringence of CO_2 and CS2. Chem Phys Lett 326(3–4):269–276

Couck S, Denayer JFM, Baron GV, Remy T, Gascon J, Kapteijn F (2009) An amine-functionalized MIL-53 metal-organic framework with large separation power for CO_2 and CH_4. J Am Chem Soc 131(18):6326–6327

Crini G, Peindy HN, Gimbert F, Robert C (2007) Removal of CI basic green 4 (Malachite Green) from aqueous solutions by adsorption using cyclodextrin-based adsorbent: kinetic and equilibrium studies. Sep Purif Technol 53(1):97–110

Cychosz KA, Matzger AJ (2010) Water stability of microporous coordination polymers and the adsorption of pharmaceuticals from water. Langmuir 26(22):17198–17202

de Menezes EW, Lima EC, Royer B, de Souza FE, dos Santos BD, Gregorio JR, Costa TMH, Gushikem Y, Benvenutti EV (2012) Ionic silica based hybrid material containing the pyridinium group used as an adsorbent for textile dye. J Colloid Interface Sci 378:10–20

Demessence A, D'Alessandro DM, Foo ML, Long JR (2009) Strong CO_2 binding in a water-stable, triazolate-bridged metal-organic framework functionalized with ethylenediamine. J Am Chem Soc 131(25):8784–8786

Deng H, Doonan CJ, Furukawa H, Ferreira RB, Towne J, Knobler CB, Wang B, Yaghi OM (2010) Multiple functional groups of varying ratios in metal-organic frameworks. Science 327 (5967):846–850

Diaz E, Munoz E, Vega A, Ordonez S (2008) Enhancement of the CO_2 retention capacity of Y zeolites by Na and Cs treatments: effect of adsorption temperature and water treatment. Ind Eng Chem Res 47(2):412–418

Dietzel PDC, Besikiotis V, Blom R (2009) Application of metal-organic frameworks with coordinatively unsaturated metal sites in storage and separation of methane and carbon dioxide. J Mater Chem 19(39):7362–7370

Dillon EP, Crouse CA, Barron AR (2008) Synthesis, characterization, and carbon dioxide adsorption of covalently attached polyethyleneimine-functionalized single-wall carbon nanotubes. ACS Nano 2(1):156–164

Do DD, Wang K (1998) A new model for the description of adsorption kinetics in heterogeneous activated carbon. Carbon 36(10):1539–1554

Donaldson TL, Nguyen YN (1980) Carbon-dioxide reaction-kinetics and transport in aqueous amine membranes. Ind Eng Chem Fundam 19(3):260–266

Drese JH, Choi S, Lively RP, Koros WJ, Fauth DJ, Gray ML, Jones CW (2009) Synthesis-structure–property relationships for hyperbranched aminosilica CO_2 adsorbents. Adv Funct Mater 19(23):3821–3832

Fifield LS, Fryxell GE, Addleman RS, Aardahl CL (2004) Carbon dioxide capture using amine-based molecular anchors on multi wall carbon nanotubes. Abstr Pap Am Chem Soc 227:U1089

Filburn T, Helble JJ, Weiss RA (2005) Development of supported ethanolamines and modified ethanolamines for CO_2 capture. Ind Eng Chem Res 44(5):1542–1546

Fisher JC, Tanthana J, Chuang SSC (2009) Oxide-supported tetraethylenepentamine for CO_2 capture. Environ Progr Sustain Energy 28(4):589–598

Franchi RS, Harlick PJE, Sayari A (2005) Applications of pore-expanded mesoporous silica. 2. Development of a high-capacity, water-tolerant adsorbent for CO_2. Ind Eng Chem Res 44(21):8007–8013

Ghosh A, Subrahmanyam KS, Krishna KS, Datta S, Govindaraj A, Pati SK, Rao CNR (2008) Uptake of H-2 and CO_2 by graphene. J Phys Chem C 112(40):15704–15707

Goeppert A, Meth S, Prakash GKS, Olah GA (2010) Nanostructured silica as a support for regenerable high-capacity organoamine-based CO_2 sorbents. Energy Environ Sci 3(12):1949–1960

Granite EJ, Pennline HW (2002) Photochemical removal of mercury from flue gas. Abstr Pap Am Chem Soc 223:U523–U524

Gray ML, Soong Y, Champagne KJ, Baltrus J, Stevens RW, Toochinda P, Chuang SSC (2004) CO_2 capture by amine-enriched fly ash carbon sorbents. Sep Purif Technol 35(1):31–36

Gray ML, Soong Y, Champagne KJ, Pennline H, Baltrus JP, Stevens RW, Khatri R, Chuang SSC, Filburn T (2005) Improved immobilized carbon dioxide capture sorbents. Fuel Process Technol 86(14–15):1449–1455

Gray ML, Champagne KJ, Fauth D, Baltrus JP, Pennline H (2008) Performance of immobilized tertiary amine solid sorbents for the capture of carbon dioxide. Int J Greenhouse Gas Control 2(1):3–8

Gray ML, Hoffman JS, Hreha DC, Fauth DJ, Hedges SW, Champagne KJ, Pennline HW (2009) Parametric study of solid amine sorbents for the capture of carbon dioxide. Energy Fuel 23:4840–4844

Harlick PJE, Sayari A (2006) Applications of pore-expanded mesoporous silicas. 3. Triamine silane grafting for enhanced CO(2) adsorption. Ind Eng Chem Res 45(9):3248–3255

Harlick PJE, Sayari A (2007) Applications of pore-expanded mesoporous silica. 5. Triamine grafted material with exceptional CO(2) dynamic and equilibrium adsorption performance. Ind Eng Chem Res 46(2):446–458

Harlick PJE, Tezel FH (2004) An experimental adsorbent screening study for CO_2 removal from N-2. Microporous Mesoporous Mater 76(1–3):71–79

Hayashi H, Taniuchi J, Furuyashiki N, Sugiyama S, Hirano S, Shigemoto N, Nonaka T (1998) Efficient recovery of carbon dioxide from flue gases of coal-fired power plants by cyclic fixed-bed operations over K_2CO_3-on-carbon. Ind Eng Chem Res 37(1):185–191

Henke S, Fischer RA (2011) Gated channels in a honeycomb-like zinc-dicarboxylate-bipyridine framework with flexible alkyl ether side chains. J Am Chem Soc 133(7):2064–2067

Herm ZR, Swisher JA, Smit B, Krishna R, Long JR (2011) Metal-organic frameworks as adsorbents for hydrogen purification and precombustion carbon dioxide capture. J Am Chem Soc 133(15):5664–5667

Heydari-Gorji A, Sayari A (2011) CO_2 capture on polyethylenimine-impregnated hydrophobic mesoporous silica: experimental and kinetic modeling. Chem Eng J 173(1):72–79

Heydari-Gorji A, Belmabkhout Y, Sayari A (2011) Polyethylenimine-impregnated mesoporous silica: effect of amine loading and surface alkyl chains on CO_2 adsorption. Langmuir 27(20):12411–12416

Hicks JC, Drese JH, Fauth DJ, Gray ML, Qi GG, Jones CW (2008) Designing adsorbents for CO (2) capture from flue gas-hyperbranched aminosilicas capable, of capturing CO(2) reversibly. J Am Chem Soc 130(10):2902–2903

Hiyoshi N, Yogo K, Yashima T (2004) Adsorption of carbon dioxide on amine modified SBA-15 in the presence of water vapor. Chem Lett 33(5):510–511

Hiyoshi N, Yogo K, Yashima T (2005) Adsorption characteristics of carbon dioxide on organically functionalized SBA-15. Microporous Mesoporous Mater 84(1–3):357–365

Ho YS, McKay G (1999) Pseudo-second order model for sorption processes. Process Biochem 34(5):451–465

Ho MT, Allinson GW, Wiley DE (2008a) Reducing the cost of CO_2 capture from flue gases using pressure swing adsorption. Ind Eng Chem Res 47(14):4883–4890

Ho MT, Allinson GW, Wiley DE (2008b) Reducing the cost of CO_2 capture from flue gases using membrane technology. Ind Eng Chem Res 47(5):1562–1568

House KZ, Harvey CF, Aziz MJ, Schrag DP (2009) The energy penalty of post-combustion CO_2 capture & storage and its implications for retrofitting the US installed base. Energy Environ Sci 2(2):193–205

Hsu SC, Lu CS, Su FS, Zeng WT, Chen WF (2010) Thermodynamics and regeneration studies of CO_2 adsorption on multiwalled carbon nanotubes. Chem Eng Sci 65(4):1354–1361

Huang LL, Zhang LZ, Shao Q, Lu LH, Lu XH, Jiang SY, Shen WF (2007) Simulations of binary mixture adsorption of carbon dioxide and methane in carbon nanotubes: temperature, pressure, and pore size effects. J Phys Chem C 111(32):11912–11920

Hwang YK, Hong DY, Chang JS, Jhung SH, Seo YK, Kim J, Vimont A, Daturi M, Serre C, Ferey G (2008) Amine grafting on coordinatively unsaturated metal centers of MOFs: consequences for catalysis and metal encapsulation. Angew Chem Int Ed 47(22):4144–4148

Inui T, Okugawa Y, Yasuda M (1988) Relationship between properties of various zeolites and their CO_2-adsorption behaviors in pressure swing adsorption operation. Ind Eng Chem Res 27(7):1103–1109

Ishibashi M, Ota H, Akutsu N, Umeda S, Tajika M, Izumi J, Yasutake A, Kabata T, Kageyama Y (1996) Technology for removing carbon dioxide from power plant flue gas by the physical adsorption method. Energy Convers Manage 37(6–8):929–933

Jadhav PD, Chatti RV, Biniwale RB, Labhsetwar NK, Devotta S, Rayalu SS (2007) Monoethanol amine modified zeolite 13X for CO_2 adsorption at different temperatures. Energy Fuel 21(6):3555–3559

Jones CW (2011) CO_2 capture from dilute gases as a component of modern global carbon management. Annu Rev Chem Biomol Eng 2(2):31–52

Katoh M, Yoshikawa T, Tomonari T, Katayama K, Tomida T (2000) Adsorption characteristics of ion-exchanged ZSM-5 zeolites for CO_2/N-2 mixtures. J Colloid Interface Sci 226(1):145–150

Keskin S, van Heest TM, Sholl DS (2010) Can metal-organic framework materials play a useful role in large-scale carbon dioxide separations? Chemsuschem 3(8):879–891

Khatri RA, Chuang SSC, Soong Y, Gray M (2005) Carbon dioxide capture by diamine-grafted SBA-15: a combined Fourier transform infrared and mass spectrometry study. Ind Eng Chem Res 44(10):3702–3708

Khatri RA, Chuang SSC, Soong Y, Gray M (2006) Thermal and chemical stability of regenerable solid amine sorbent for CO_2 capture. Energy Fuel 20(4):1514–1520

Khelifa A, Benchehida L, Derriche Z (2004) Adsorption of carbon dioxide by X zeolites exchanged with Ni2+ and Cr3+: isotherms and isosteric heat. J Colloid Interface Sci 278(1):9–17

Kikkinides ES, Yang RT, Cho SH (1993) Concentration and recovery of CO_2 from flue-gas by pressure swing adsorption. Ind Eng Chem Res 32(11):2714–2720

Kim SN, Son WJ, Choi JS, Ahn WS (2008) CO_2 adsorption using amine-functionalized mesoporous silica prepared via anionic surfactant-mediated synthesis. Microporous Mesoporous Mater 115(3):497–503

Kim J, Yang ST, Choi SB, Sim J, Kim J, Ahn WS (2011) Control of catenation in CuTATB-n metal-organic frameworks by sonochemical synthesis and its effect on CO_2 adsorption. J Mater Chem 21(9):3070–3076

Kitagawa S, Kitaura R, Noro S (2004) Functional porous coordination polymers. Angew Chem Int Ed 43(18):2334–2375

Kizzie AC, Wong-Foy AG, Matzger AJ (2011) Effect of humidity on the performance of microporous coordination polymers as adsorbents for CO_2 capture. Langmuir 27(10):6368–6373

Knofel C, Descarpentries J, Benzaouia A, Zelenak V, Mornet S, Llewellyn PL, Hornebecq V (2007) Functionalised micro-/mesoporous silica for the adsorption of carbon dioxide. Microporous Mesoporous Mater 99(1–2):79–85

Knowles GP, Graham JV, Delaney SW, Chaffee AL (2005) Aminopropyl-functionalized mesoporous silicas as CO_2 adsorbents. Fuel Process Technol 86(14–15):1435–1448

Knowles GP, Delaney SW, Chaffee AL (2006) Diethylenetriamine[propyl(silyl)]-functionalized (DT) mesoporous silicas as CO_2 adsorbents. Ind Eng Chem Res 45(8):2626–2633

Krishnamurthy S, Rao VR, Guntuka S, Sharratt P, Haghpanah R, Rajendran A, Amanullah M, Karimi IA, Farooq S (2014) CO_2 capture from dry flue gas by vacuum swing adsorption: a pilot plant study. AICHE J 60(5):1830–1842

Leal O, Bolivar C, Ovalles C, Garcia JJ, Espidel Y (1995) Reversible adsorption of carbon dioxide on amine surface-bonded silica gel. Inorg Chim Acta 240(1–2):183–189

Lee SC, Kim JC (2007) Dry potassium-based sorbents for CO_2 capture. Catal Surv Asia 11(4):171–185

Lee KB, Sircar S (2008) Removal and recovery of compressed CO_2 from flue gas by a novel thermal swing chemisorption process. AICHE J 54(9):2293–2302

Lee SC, Choi BY, Lee TJ, Ryu CK, Soo YS, Kim JC (2006a) CO_2 absorption and regeneration of alkali metal-based solid sorbents. Catal Today 111(3–4):385–390

Lee SC, Choi BY, Ryu CK, Ahn YS, Lee TJ, Kim JC (2006b) The effect of water on the activation and the CO_2 capture capacities of alkali metal-based sorbents. Korean J Chem Eng 23(3):374–379

Lee S, Filburn TP, Gray M, Park JW, Song HJ (2008a) Screening test of solid amine sorbents for CO_2 capture. Ind Eng Chem Res 47(19):7419–7423

Lee JB, Ryu CK, Baek JI, Lee JH, Eom TH, Kim SH (2008b) Sodium-based dry regenerable sorbent for carbon dioxide capture from power plant flue gas. Ind Eng Chem Res 47(13):4465–4472

Lee SC, Chae HJ, Lee SJ, Park YH, Ryu CK, Yi CK, Kim JC (2009) Novel regenerable potassium-based dry sorbents for CO_2 capture at low temperatures. J Mol Catal B Enzym 56(2–3):179–184

Lee SC, Kwon YM, Ryu CY, Chae HJ, Ragupathy D, Jung SY, Lee JB, Ryu CK, Kim JC (2011) Development of new alumina-modified sorbents for CO_2 sorption and regeneration at temperatures below 200 degrees C. Fuel 90(4):1465–1470

Li PY, Zhang SJ, Chen SX, Zhang QK, Pan JJ, Ge BQ (2008a) Preparation and adsorption properties of polyethylenimine containing fibrous adsorbent for carbon dioxide capture. J Appl Polym Sci 108(6):3851–3858

Li PY, Ge BQ, Zhang SJ, Chen SX, Zhang QK, Zhao YN (2008b) CO_2 capture by polyethylenimine-modified fibrous adsorbent. Langmuir 24(13):6567–6574

Li G, Xiao P, Webley P, Zhang J, Singh R, Marshall M (2008c) Capture of CO_2 from high humidity flue gas by vacuum swing adsorption with zeolite 13X. Adsorption J Int Adsorption Soc 14(2–3):415–422

Li JR, Kuppler RJ, Zhou HC (2009) Selective gas adsorption and separation in metal-organic frameworks. Chem Soc Rev 38(5):1477–1504

Li W, Choi S, Drese JH, Hornbostel M, Krishnan G, Eisenberger PM, Jones CW (2010) Steam-stripping for regeneration of supported amine-based CO_2 adsorbents. Chemsuschem 3(8):899–903

Liu J, Wang Y, Benin AI, Jakubczak P, Willis RR, LeVan MD (2010) CO_2/H_2O adsorption equilibrium and rates on metal-organic frameworks: HKUST-1 and Ni/DOBDC. Langmuir 26(17):14301–14307

Liu J, Benin AI, Furtado AMB, Jakubczak P, Willis RR, LeVan MD (2011) Stability effects on CO_2 adsorption for the DOBDC series of metal-organic frameworks. Langmuir 27(18):11451–11456

Liu Z, Wang L, Kong XM, Li P, Yu JG, Rodrigues AE (2012) Onsite CO_2 capture from flue gas by an adsorption process in a coal-fired power plant. Ind Eng Chem Res 51(21):7355–7363

Liu Q, Ning LQ, Zheng SD, Tao MN, Shi Y, He Y (2013) Adsorption of carbon dioxide by MIL-101(Cr): regeneration conditions and influence of flue gas contaminants. Sci Rep 3:2916

Liu Q, Shi Y, Zheng SD, Ning LQ, Ye Q, Tao MN, He Y (2014a) Amine-functionalized low-cost industrial grade multi-walled carbon nanotubes for the capture of carbon dioxide. J Energy Chem 23(1):111–118

Liu Q, Shi JJ, Zheng SD, Tao MN, He Y, Shi Y (2014b) Kinetics studies of CO_2 adsorption/desorption on amine-functionalized multiwalled carbon nanotubes. Ind Eng Chem Res 53(29):11677–11683

Llewellyn PL, Bourrelly S, Serre C, Filinchuk Y, Ferey G (2006) How hydration drastically improves adsorption selectivity for CO_2 over CH4 in the flexible chromium terephthalate MIL-53. Angew Chem Int Ed 45(46):7751–7754

Loiseau T, Serre C, Huguenard C, Fink G, Taulelle F, Henry M, Bataille T, Ferey G (2004) A rationale for the large breathing of the porous aluminum terephthalate (MIL-53) upon hydration. Chem Eur J 10(6):1373–1382

Lopes ECN, dos Anjos FSC, Vieira EFS, Cestari AR (2003) An alternative Avrami equation to evaluate kinetic parameters of the interaction of Hg(11) with thin chitosan membranes. J Colloid Interface Sci 263(2):542–547

Low JJ, Benin AI, Jakubczak P, Abrahamian JF, Faheem SA, Willis RR (2009) Virtual high throughput screening confirmed experimentally: porous coordination polymer hydration. J Am Chem Soc 131(43):15834–15842

Lu CY, Bai HL, Wu BL, Su FS, Fen-Hwang J (2008) Comparative study of CO_2 capture by carbon nanotubes, activated carbons, and zeolites. Energy Fuel 22(5):3050–3056

Ma XL, Wang XX, Song CS (2009) "Molecular Basket" sorbents for separation of CO_2 and H_2S from various gas streams. J Am Chem Soc 131(16):5777–5783

Maroto-Valer MM, Tang Z, Zhang Y (2005) CO_2 capture by activated and impregnated anthracites. Fuel Process Technol 86(14–15):1487–1502

Maroto-Valer MM, Lu Z, Zhang Y, Tang Z (2008) Sorbents for CO_2 capture from high carbon fly ashes. Waste Manag 28(11):2320–2328

Mason JA, Sumida K, Herm ZR, Krishna R, Long JR (2011) Evaluating metal-organic frameworks for post-combustion carbon dioxide capture via temperature swing adsorption. Energy Environ Sci 4(8):3030–3040

McDonald TM, D'Alessandro DM, Krishna R, Long JR (2011) Enhanced carbon dioxide capture upon incorporation of N, N′-dimethylethylenediamine in the metal-organic framework CuBTTri. Chem Sci 2(10):2022–2028

Merel J, Clausse M, Meunier F (2008) Experimental investigation on CO_2 post-combustion capture by indirect thermal swing adsorption using 13X and 5A zeolites. Ind Eng Chem Res 47(1):209–215

Millward AR, Yaghi OM (2005) Metal-organic frameworks with exceptionally high capacity for storage of carbon dioxide at room temperature. J Am Chem Soc 127(51):17998–17999

Monazam ER, Shadle LJ, Miller DC, Pennline HW, Fauth DJ, Hoffman JS, Gray ML (2013) Equilibrium and kinetics analysis of carbon dioxide capture using immobilized amine on a mesoporous silica. AICHE J 59(3):923–935

Mulgundmath V, Tezel FH (2010) Optimisation of carbon dioxide recovery from flue gas in a TPSA system. Adsorption J Int Adsorption Soc 16(6):587–598

Na BK, Koo KK, Eum HM, Lee H, Song HK (2001) CO(2) recovery from flue gas by PSA process using activated carbon. Korean J Chem Eng 18(2):220–227

Navarro JAR, Barea E, Salas JM, Masciocchi N, Galli S, Sironi A, Ania CO, Parra JB (2007) Borderline microporous-ultramicroporous palladium(II) coordination polymer networks. Effect of pore functionalisation on gas adsorption properties. J Mater Chem 17(19):1939–1946

Nestle NFEI, Kimmich R (1996) NMR imaging of heavy metal absorption in alginate, immobilized cells, and kombu algal biosorbents. Biotechnol Bioeng 51(5):538–543

Okunev AG, Sharonov VE, Aristov YI, Parmon VN (2000) Sorption of carbon dioxide from wet gases by K_2CO_3-in-porous matrix: influence of the matrix nature. React Kinet Catal Lett 71(2):355–362

Okunev AG, Sharonov VE, Gubar AV, Danilova IG, Paukshtis EA, Moroz EM, Kriger TA, Malakhov VV, Aristov YI (2003) Sorption of carbon dioxide by the composite sorbent of potassium carbonate in porous matrix. Russ Chem Bull 52(2):359–363

Park YC, Jo SH, Ryu CK, Yi CK (2009) Long-term operation of carbon dioxide capture system from a real coal-fired flue gas using dry regenerable potassium-based sorbents. Greenhouse Gas Control Technol 1(1):1235–1239

Park TH, Cychosz KA, Wong-Foy AG, Dailly A, Matzger AJ (2011) Gas and liquid phase adsorption in isostructural Cu-3[biaryltricarboxylate](2) microporous coordination polymers. Chem Commun 47(5):1452–1454

Pevida C, Plaza MG, Arias B, Fermoso J, Rubiera F, Pis JJ (2008) Surface modification of activated carbons for CO(2) capture. Appl Surf Sci 254(22):7165–7172

Phan A, Doonan CJ, Uribe-Romo FJ, Knobler CB, O'Keeffe M, Yaghi OM (2010) Synthesis, structure, and carbon dioxide capture properties of zeolitic imidazolate frameworks. Acc Chem Res 43(1):58–67

Plaza MG, Pevida C, Arias B, Fermoso J, Rubiera F, Pis JJ (2009) A comparison of two methods for producing CO(2) capture adsorbents. Greenhouse Gas Control Technol 1(1):1107–1113

Przepiorski J, Skrodzewicz M, Morawski AW (2004) High temperature ammonia treatment of activated carbon for enhancement of CO_2 adsorption. Appl Surf Sci 225(1–4):235–242

Qader A, Hooper B, Innocenzi T, Stevens G, Kentish S, Scholes C, Mumford K, Smith K, Webley PA, Zhang J (2011) Novel post-combustion capture technologies on a lignite fired power plant – results of the CO_2CRC/H3 capture project. 10th international conference on greenhouse gas control technologies, vol 4, pp 1668–1675

Qi GG, Wang YB, Estevez L, Duan XN, Anako N, Park AHA, Li W, Jones CW, Giannelis EP (2011) High efficiency nanocomposite sorbents for CO_2 capture based on amine-functionalized mesoporous capsules. Energy Environ Sci 4(2):444–452

Razavi SS, Hashemianzadeh SM, Karimi H (2011) Modeling the adsorptive selectivity of carbon nanotubes for effective separation of CO_2/N-2 mixtures. J Mol Model 17(5):1163–1172

Rochelle GT (2009) Amine scrubbing for CO_2 capture. Science 325(5948):1652–1654

Rubin ES, Chen C, Rao AB (2007) Cost and performance of fossil fuel power plants with CO_2 capture and storage. Energy Policy 35(9):4444–4454

Samanta A, Zhao A, Shimizu GKH, Sarkar P, Gupta R (2012) Post-combustion CO_2 capture using solid sorbents: a review. Ind Eng Chem Res 51(4):1438–1463

Satyapal S, Filburn T, Trela J, Strange J (2001) Performance and properties of a solid amine sorbent for carbon dioxide removal in space life support applications. Energy Fuel 15(2):250–255

Sayari A, Belmabkhout Y (2010) Stabilization of amine-containing CO_2 adsorbents: dramatic effect of water vapor. J Am Chem Soc 132(18):6312–6314

Sayari A, Hamoudi S, Yang Y (2005) Applications of pore-expanded mesoporous silica. 1. Removal of heavy metal cations and organic pollutants from wastewater. Chem Mater 17(1):212–216

Sayari A, Belmabkhout Y, Serna-Guerrero R (2011) Flue gas treatment via CO_2 adsorption. Chem Eng J 171(3):760–774

Seo Y, Jo SH, Ryu CK, Yi CK (2007) Effects of water vapor pretreatment time and reaction temperature on CO_2 capture characteristics of a sodium-based solid sorbent in a bubbling fluidized-bed reactor. Chemosphere 69(5):712–718

Serna-Guerrero R, Sayari A (2010) Modeling adsorption of CO_2 on amine-functionalized mesoporous silica. 2: kinetics and breakthrough curves. Chem Eng J 161(1–2):182–190

Serna-Guerrero R, Da'na E, Sayari A (2008) New insights into the interactions of CO(2) with amine-functionalized silica. Ind Eng Chem Res 47(23):9406–9412

Serna-Guerrero R, Belmabkhout Y, Sayari A (2010a) Influence of regeneration conditions on the cyclic performance of amine- grafted mesoporous silica for CO_2 capture: An experimental and statistical study. Chem Eng Sci 65(14):4166–4172

Serna-Guerrero R, Belmabkhout Y, Sayari A (2010b) Further investigations of CO_2 capture using triamine-grafted pore-expanded mesoporous silica. Chem Eng J 158(3):513–519

Serna-Guerrero R, Belmabkhout Y, Sayari A (2010c) Triamine-grafted pore-expanded mesoporous silica for CO_2 capture: effect of moisture and adsorbent regeneration strategies. Adsorption J Int Adsorption Soc 16(6):567–575

Serre C, Millange F, Thouvenot C, Nogues M, Marsolier G, Louer D, Ferey G (2002) Very large breathing effect in the first nanoporous chromium(III)-based solids: MIL-53 or Cr-III(OH) center dot{O2C-C6H4-CO2}center dot{HO2C-C6H4-CO2H}(x)center dot H2Oy. J Am Chem Soc 124(45):13519–13526

Sharonov VE, Okunev AG, Aristov YI (2004) Kinetics of carbon dioxide sorption by the composite material K_2CO_3 in Al_2O_3. React Kinet Catal Lett 82(2):363–369

Siriwardane RV, Shen MS, Fisher EP, Poston JA (2001) Adsorption of CO_2 on molecular sieves and activated carbon. Energy Fuel 15(2):279–284

Siriwardane RV, Shen MS, Fisher EP (2003) Adsorption of CO(2), N(2), and O(2) on natural zeolites. Energy Fuel 17(3):571–576

Skoulidas AI, Sholl DS, Johnson JK (2006) Adsorption and diffusion of carbon dioxide and nitrogen through single-walled carbon nanotube membranes. J Chem Phys 124, 054708

Son WJ, Choi JS, Ahn WS (2008) Adsorptive removal of carbon dioxide using polyethyleneimine-loaded mesoporous silica materials. Microporous Mesoporous Mater 113(1–3):31–40

Stavitski E, Pidko EA, Couck S, Remy T, Hensen EJM, Weckhuysen BM, Denayer J, Gascon J, Kapteijn F (2011) Complexity behind CO_2 Capture on NH2-MIL-53(Al). Langmuir 27(7):3970–3976

Stylianou KC, Warren JE, Chong SY, Rabone J, Bacsa J, Bradshaw D, Rosseinsky MJ (2011) CO_2 selectivity of a 1D microporous adenine-based metal-organic framework synthesised in water. Chem Commun 47(12):3389–3391

Su FS, Lu CS, Cnen WF, Bai HL, Hwang JF (2009) Capture of CO_2 from flue gas via multiwalled carbon nanotubes. Sci Total Environ 407(8):3017–3023

Su FS, Lu CY, Kuo SC, Zeng WT (2010) Adsorption of CO_2 on amine-functionalized Y-type zeolites. Energy Fuel 24:1441–1448

Sumida K, Horike S, Kaye SS, Herm ZR, Queen WL, Brown CM, Grandjean F, Long GJ, Dailly A, Long JR (2010) Hydrogen storage and carbon dioxide capture in an iron-based sodalite-type metal-organic framework (Fe-BTT) discovered via high-throughput methods. Chem Sci 1(2):184–191

Sumida K, Rogow DL, Mason JA, McDonald TM, Bloch ED, Herm ZR, Bae TH, Long JR (2012) Carbon dioxide capture in metal-organic frameworks. Chem Rev 112(2):724–781

Tang Z, Maroto-Valer MM, Zhang YZ (2004) CO_2 capture using anthracite based sorbents. Abstr Pap Am Chem Soc 227:U1089

Vaidhyanathan R, Iremonger SS, Dawson KW, Shimizu GKH (2009) An amine-functionalized metal organic framework for preferential CO_2 adsorption at low pressures. Chem Commun 35:5230–5232

Vishnyakov A, Ravikovitch PI, Neimark AV, Bulow M (2003) Nanopore structure and sorption properties of Cu-BTC metal-organic framework. Abstr Pap Am Chem Soc 226:U683

Wang YX, Zhou YP, Liu CM, Zhou L (2008a) Comparative studies of CO_2 and CH_4 sorption on activated carbon in presence of water. Colloids Surf Physicochem Eng Aspects 322 (1–3):14–18

Wang B, Cote AP, Furukawa H, O'Keeffe M, Yaghi OM (2008b) Colossal cages in zeolitic imidazolate frameworks as selective carbon dioxide reservoirs. Nature 453(7192):207–211

Wang L, Yang Y, Shen WL, Kong XM, Li P, Yu JG, Rodrigues AE (2013a) Experimental evaluation of adsorption technology for CO_2 capture from flue gas in an existing coal-fired power plant. Chem Eng Sci 101:615–619

Wang L, Yang Y, Shen WL, Kong XM, Li P, Yu JG, Rodrigues AE (2013b) CO_2 capture from flue gas in an existing coal-fired power plant by two successive pilot-scale VPSA units. Ind Eng Chem Res 52(23):7947–7955

Whitfield TR, Wang XQ, Liu LM, Jacobson AJ (2005) Metal-organic frameworks based on iron oxide octahedral chains connected by benzenedicarboxylate dianions. Solid State Sci 7(9):1096–1103

Wu HH, Reali RS, Smith DA, Trachtenberg MC, Li J (2010) Highly selective CO_2 capture by a flexible microporous metal-organic framework (MMOF) material. Chem Eur J 16(47):13951–13954

Xu XC, Song CS, Andresen JM, Miller BG, Scaroni AW (2002) Novel polyethylenimine-modified mesoporous molecular sieve of MCM-41 type as high-capacity adsorbent for CO_2 capture. Energy Fuel 16(6):1463–1469

Xu XC, Song CS, Andresen JM, Miller BG, Scaroni AW (2003) Preparation and characterization of novel CO_2 "molecular basket" adsorbents based on polymer-modified mesoporous molecular sieve MCM-41. Microporous Mesoporous Mater 62(1–2):29–45

Xu XC, Song CS, Miller BG, Scaroni AW (2005a) Influence of moisture on CO_2 separation from gas mixture by a nanoporous adsorbent based on polyethylenimine-modified molecular sieve MCM-41. Ind Eng Chem Res 44(21):8113–8119

Xu XC, Song CS, Miller BG, Scaroni AW (2005b) Adsorption separation of carbon dioxide from flue gas of natural gas-fired boiler by a novel nanoporous "molecular basket" adsorbent. Fuel Process Technol 86(14–15):1457–1472

Yang Y, Li H, Chen S, Zhao Y, Li Q (2010) Preparation and characterization of a solid amine adsorbent for capturing CO_2 by grafting allylamine onto PAN fiber. Langmuir 26(17):13897–13902

Yazaydin AO, Benin AI, Faheem SA, Jakubczak P, Low JJ, Willis RR, Snurr RQ (2009a) Enhanced CO_2 adsorption in metal-organic frameworks via occupation of open-metal sites by coordinated water molecules. Chem Mater 21(8):1425–1430

Yazaydin AO, Snurr RQ, Park TH, Koh K, Liu J, LeVan MD, Benin AI, Jakubczak P, Lanuza M, Galloway DB, Low JJ, Willis RR (2009b) Screening of metal-organic frameworks for carbon dioxide capture from flue gas using a combined experimental and modeling approach. J Am Chem Soc 131(51):18198–18199

Ye Q, Jiang JQ, Wang CX, Liu YM, Pan H, Shi Y (2012) Adsorption of low-concentration carbon dioxide on amine-modified carbon nanotubes at ambient temperature. Energy Fuel 26 (4):2497–2504

Yi CK, Jo SH, Seo Y, Lee JB, Ryu CK (2007) Continuous operation of the potassium-based dry sorbent CO_2 capture process with two fluidized-bed reactors. Int J Greenhouse Gas Control 1 (1):31–36

Yong Z, Mata V, Rodrigues AE (2002) Adsorption of carbon dioxide at high temperature – a review. Sep Purif Technol 26(2–3):195–205

Yue MB, Chun Y, Cao Y, Dong X, Zhu JH (2006) CO_2 capture by As-prepared SBA-15 with an occluded organic template. Adv Funct Mater 16(13):1717–1722

Yue MB, Sun LB, Cao Y, Wang Y, Wang ZJ, Zhu JH (2008a) Efficient CO_2 capturer derived from as-synthesized MCM-41 modified with amine. Chem Eur J 14(11):3442–3451

Yue MB, Sun LB, Cao Y, Wang ZJ, Wang Y, Yu Q, Zhu JH (2008b) Promoting the CO_2 adsorption in the amine-containing SBA-15 by hydroxyl group. Microporous Mesoporous Mater 114(1–3):74–81

Zelenak V, Badanicova M, Halamova D, Cejka J, Zukal A, Murafa N, Goerigk G (2008) Amine-modified ordered mesoporous silica: effect of pore size on carbon dioxide capture. Chem Eng J 144(2):336–342

Zhang YZ, Maroto-Valer MM, Zhong Z (2004) Microporous activated carbons produced from unburned carbon in fly ash and their application for CO_2 capture. Abstr Pap Am Chem Soc 227: U1090

Zhang J, Singh R, Webley PA (2008a) Alkali and alkaline-earth cation exchanged chabazite zeolites for adsorption based CO_2 capture. Microporous Mesoporous Mater 111(1–3):478–487

Zhang J, Webley PA, Xiao P (2008b) Effect of process parameters on power requirements of vacuum swing adsorption technology for CO_2 capture from flue gas. Energy Convers Manage 49(2):346–356

Zhao ZX, Li Z, Lin YS (2009a) Adsorption and diffusion of carbon dioxide on metal-organic framework (MOF-5). Ind Eng Chem Res 48(22):10015–10020

Zhao CW, Chen XP, Zhao CS, Liu YK (2009b) Carbonation and hydration characteristics of dry potassium-based sorbents for CO(2) capture. Energy Fuel 23:1766–1769

Zhao CW, Chen XP, Zhao CS (2009c) Effect of crystal structure on CO_2 capture characteristics of dry potassium-based sorbents. Chemosphere 75(10):1401–1404

Zhao CW, Chen XP, Zhao CS (2009d) CO_2 absorption using dry potassium-based sorbents with different supports. Energy Fuel 23:4683–4687

Zhao A, Samanta A, Sarkar P, Gupta R (2013) Carbon dioxide adsorption on amine-impregnated mesoporous SBA-15 sorbents: experimental and kinetics study. Ind Eng Chem Res 52(19):6480–6491

Zheng F, Tran DN, Busche B, Fryxell GE, Addleman RS, Zemanian TS, Aardahl CL (2004) Ethylenediamine-modified SBA-15 as regenerable CO_2 sorbents. Abstr Pap Am Chem Soc 227:U1086–U1087

Zhong T, Zhang YZ, Maroto-Valer MM (2004) Study of CO_2 adsorption capacities of modified activated anthracites. Abstr Pap Am Chem Soc 227:U1090

Zukal A, Mayerova J, Kubu M (2010) Adsorption of carbon dioxide on high-silica zeolites with different framework topology. Top Catal 53(19–20):1361–1366

CO_2 Capture by Membrane

Teruhiko Kai and Shuhong Duan

Contents

Abstract

Among various CO_2-capture technologies, membrane separation is considered as one of the promising solutions because of its energy efficiency and operation simplicity. Many research and development are conducted for the (1) CO_2/N_2 (CO_2 separation from flue gas), (2) CO_2/CH_4 (CO_2 separation from natural gas), and (3) CO_2/H_2 (CO_2 separation from integrated gasification combined cycle (IGCC) processes). In this section, recent research and development of various types of membranes (polymeric membranes, inorganic membranes, ionic liquid membranes, facilitated transport membranes) for these applications are reviewed, as well as future prospects of membrane separation technologies.

T. Kai (✉) • S. Duan
Research Institute of Innovative Technology for the Earth (RITE), Kizugawa-shi, Kyoto, Japan
e-mail: kai.te@rite.or.jp; shduan@rite.or.jp

W.-Y. Chen et al. (eds.), *Handbook of Climate Change Mitigation and Adaptation*,
DOI 10.1007/978-3-319-14409-2_84

Introduction

Carbon dioxide (CO_2) capture and storage (CCS) is generally considered as an option for climate change mitigation. There are three principal pathways to capture CO_2 from large emission sources: (1) CO_2/N_2 (CO_2 separation from flue gas), (2) CO_2/CH_4 (CO_2 separation from natural gas), and (3) CO_2/H_2 (CO_2 separation from integrated gasification combined cycle (IGCC) processes).

For practical application of the CCS technology, cost-effective methods for CO_2 capture are required. Many studies have focused on the development of effective CO_2-capture and CO_2-separation technologies. Among them, membrane separation is one of the promising solutions because of its energy efficiency and operation simplicity.

In the case of CO_2 separation from flue gas, more than half of the cost of membrane separation goes toward powering the vacuum pump to evacuate the permeate side of the membrane. In addition, the costs of the membrane module and piping are high because the pressure ratio between the feed and the permeate side is low, and a large membrane area is needed. Therefore, high CO_2 permeability is more important than high selectivity to reduce the cost of the membrane modules.

On the other hand, in the case of CO_2 separation in IGCC processes, a significant reduction in the CO_2-capture cost is expected via the use of membrane technology, because a vacuum pump is not needed for high-pressure gas separations. In this case, both CO_2 permeability and CO_2/H_2 selectivity are important to separate CO_2 effectively.

A schematic diagram of the IGCC process with membrane separation is shown in Fig. 1. Coal is gasified into synthesis gas and is then converted into H_2 and CO_2 via the water-gas shift reaction. Here, the gas composition is roughly 60 % H_2 and 40 % CO_2 at pressure of 2–4 MPa. Therefore, it is expected that membrane separation can reduce the cost of CO_2 capture from IGCC. However, it is very difficult to separate CO_2 from H_2, which has a smaller molecular size. Therefore, it is very important to develop CO_2-selective membranes with high CO_2/H_2 selectivity. In this section, research and development on CO_2-selective membranes using various types of materials is reviewed.

CO_2-Separation Membrane

Principle of Membrane Gas Separation

The early membrane separations were osmosis described by Nollet in 1748, electroosmosis described by Reuss in 1803, and dialysis described by Graham in 1861. These observations laid the scientific milestone of the beginning of membrane separation (Mulder 1996). Research on membrane gas separation using O_2, N_2, CO_2, CH_4, SO_2, etc. started around 170 years ago. However, the application of membrane gas separation started relatively recently. In 1979, Monsanto Company in the United States developed membrane modules for O_2/N_2 separation

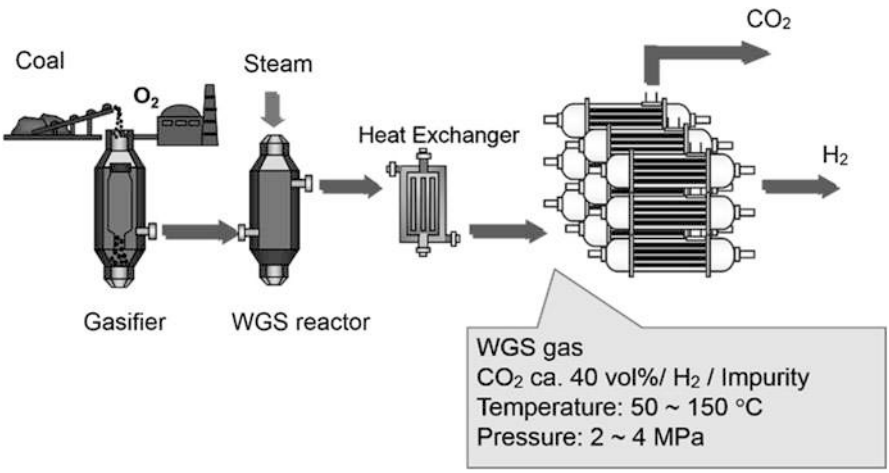

Fig. 1 Schematic diagram of IGCC with CO_2 capture

(Nakagama 1989). Membranes were known to have the potential to separate gas mixtures long before 1960, but the technology to fabricate high-performance membranes and modules economically was lacking. The development of high-flux asymmetric membranes and large-surface-area membrane modules for reverse osmosis applications occurred in the late 1960s and early 1970s. The innovative concept of high-flux asymmetric membranes was reported and prepared by Loeb and Sourirajan in 1961 initially for reverse osmosis and then adapted to gas separation, as shown in Fig. 2 (So et al. 1973). An acetone solution of 20 % (w/v) cellulose acetate was cast on a glass plate and dried for about 2 min for forming the surface dense layer and then immersed in water. Phase separation of water and acetone resulted in pore formation in the inner membrane. Hence, asymmetric membrane with porous layer and skin dense layer was prepared, and high flux was obtained.

Milestones in the development of membrane gas separation are shown in Fig. 3 (Adapted from (Baker 2002; Li et al. 2006; Ismail and David 2001)). It is considered that the first plant with polysulfone hollow fiber membranes for gas separation was performed by Permea PRISM® membranes in 1980 for H_2/N_2 separation. The first plant for CO_2/CH_4 separation with cellulose triacetate membranes was produced by Separex in 1982. The first commercial vapor separation plants were installed by MTR, GKSS, and Nitto Denko in 1988. The largest membrane plant for natural gas processing (CO_2/CH_4 separation) was installed in Pakistan in 1994 with spiral wound modules, which was a clear example of the easy scale-up of membrane technology. LTA zeolite membranes were commercialized by MES for dehydration in 1997. The development of membrane materials was investigated from conventional polymers to nanoporous materials (zeolite, carbon, silica, MOF, TR polymer, etc.).

With the development of industry, separation of carbon dioxide from gas mixture has become very important. CO_2 gas separation can be used for many industrial

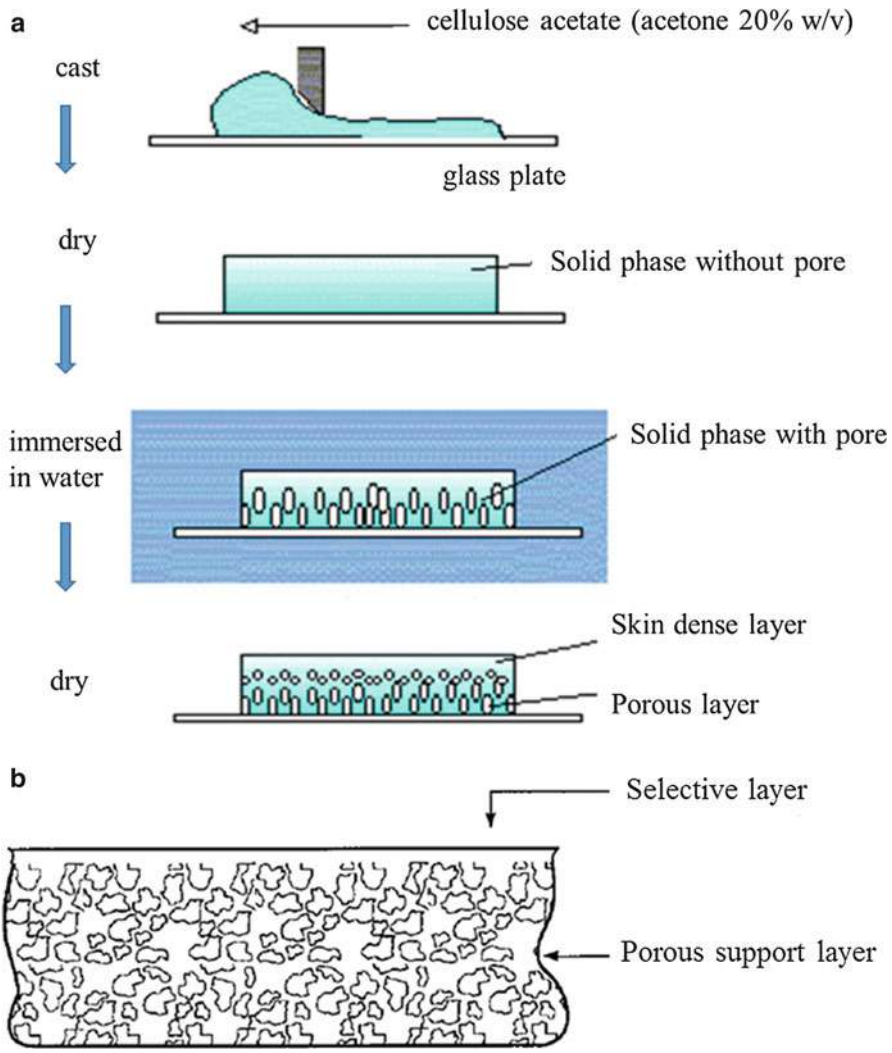

Fig. 2 Diagram of high-flux asymmetric membranes prepared by Loeb and Sourirajan (Preparation of asymmetric 1973). (**a**) Diagram of membrane preparation. (**b**) Loeb and Sourirajan anisotropic phase separation membrane

fields, such as natural gas or land fill gas recovery process, enhanced oil recovery (EOR), upgrading of methane (CO_2/CH_4 separation) generated by the decomposition of biological wastes, and integrated gasification combined cycle (IGCC) processes (CO_2/H_2). And, CO_2 membrane separation will play an important role in CCS.

The membrane can be considered as a permselective barrier or interface between two phases as shown in Fig. 4a. Phase 1 is usually considered as the feed or upstream side phase while phase 2 is considered as the permeate side or downstream side phase. The membrane has the ability to transport one component from

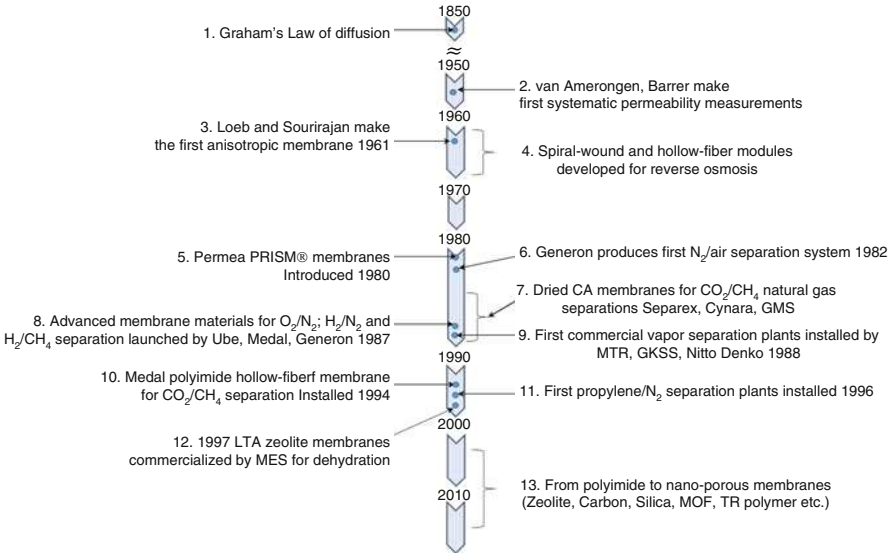

Fig. 3 Milestones in the development of membrane gas separation (Baker 2002; Li et al. 2006; Ismail and David 2001)

the feed mixture more readily than any other component or components because of differences in physical or chemical properties between the membrane and the permeating components. Transport through the membrane takes place as a result of a driving force acting on the components in the feed. In many cases, the permeation rate through the membrane is proportional to the driving force.

The two phases divided by a membrane are different for various membrane separation processes as depicted in Fig. 4b. Driving force can be gradients in the pressure, concentration, and temperature. Membrane separation processes can be classified according to their driving force as in Table 1.

Most of membranes used for gas separation have been nonporous polymer membranes, such as cellulose acetate (Yan 1996), silicone rubber polysulfone (Hao Jihao and Wang Shichang 1998; Ismail and Shilton 1998; Borisov et al. 1997), and polyimide (Li and Teo 1998; Thundyil et al. 1999; Staudt-Bickel and Koros 1999). Recently, microporous inorganic membranes, such as zeolite membranes (Wang et al. 1998; Poshusta et al. 1999; Aoki et al. 1998), nanoporous carbon membranes (Hernandez-Huesca et al. 1999), and ceramic membranes (Paranjape et al. 1998), have also been developed.

Mechanism of membrane gas separation has been proposed depending on the properties of both the permeant and the membranes, as shown in Fig. 5. Different mechanisms may be involved in the transport of gases across a porous membrane included Poiseuille flow, Knudsen diffusion, and the molecular sieve effect as shown in Fig. 5(1). When membrane has pore sizes much larger than the dimension of gas molecules, Poiseuille flow takes place. Knudsen diffusion is the predominant transport mechanism in small pores at low pressures and high

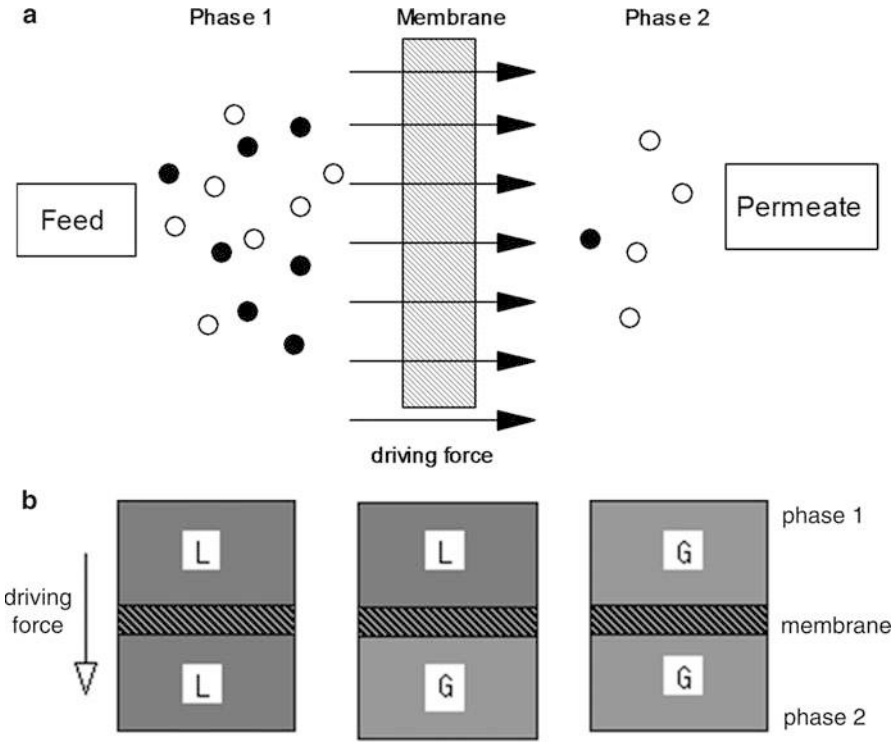

Fig. 4 Schematic drawings of membrane separation. (**a**) Two phases separated by a membrane with driving force such as ΔP, ΔC, ΔT, and ΔE. (**b**) Schematic representation of phases divided by a membrane. *L* liquid, *G* gas

Table 1 Driving force for various membrane separation processes. *L* liquid, *G* gas

Driving force	Phase 1	Phase 2	Membrane process
1. Pressure	L	L	Reverse osmosis Nanofiltration Ultrafiltration Microfiltration
2. Partial pressure	G G L	G G G	Gas separation Vapor permeation Pervaporation
3. Concentration	L L	L L	Dialysis Membrane extraction
4. Electrical potential	L L	L L	Electrodialysis Membrane Electrodialysis

temperatures. When membrane has pore sizes close to the dimension of gas molecules, the molecular sieve will be effective. In some cases, affinity between gas molecules (e.g., CO_2) and membrane materials can play an important role in high separation performance.

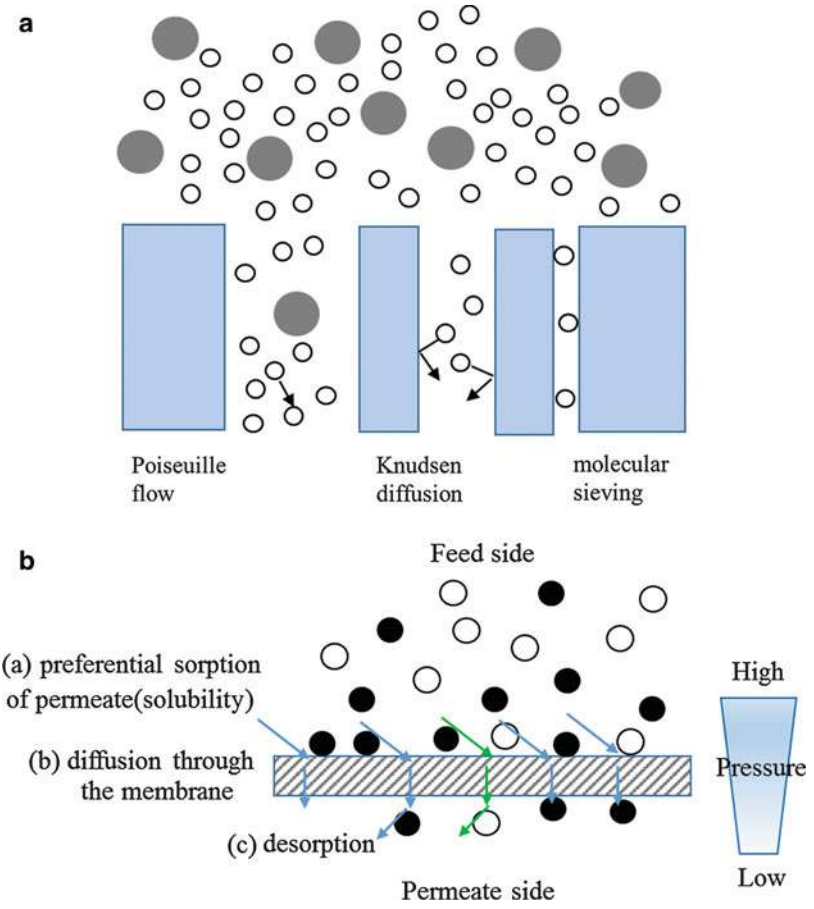

Fig. 5 Mechanism of membrane gas separation. (*1*) Mechanisms for gas flow though a microporous membrane. (2) Mechanisms for gas flow though a nonporous polymeric membrane

The solution–diffusion model is used for transport mechanism for the permeation of gases through nonporous polymeric membranes, as shown in Fig. 5(2). The solution—diffusion model describes the transport of gases through a membrane as a three-step process: (a) preferential sorption of the gas into the membrane at the feed side, (b) diffusion through the membrane due to an applied concentration gradient (e.g., partial pressure), and (c) desorption of the gas from the permeate side of the membrane.

Gas Transport Through Porous Membrane

Up to now a lot of work has been done in modeling the gas transport through membranes including porous and nonporous membranes.

The models of gas permeation through porous membrane began with a comparison of the mean free path of the gas molecules and the mean membrane pore size. If the mean free path of the gas molecules is very small relative to the pore

diameter, gas transport takes place by viscous or Poiseuille flow, and no separation is achieved. The volume flux through these pores may be described by the Hagen–Poiseuille equation (Mulder 1996):

$$J = \frac{\varepsilon r^2 \Delta P}{8\eta\tau l} \tag{1}$$

where J is the volume flux through the pores, ε is the porosity, r is pore radius, ΔP is pressure difference across a membrane of thickness l, η is viscosity, and τ is pore tortuosity.

If the mean free path of the gas molecules is much greater than the pore diameter, gas transport takes place by Knudsen flow, and separation is achieved. Mass transfer may be expressed by the following equation (Mulder 1996):

$$J = \frac{\pi n r^2 D_K \Delta P}{RT\tau l} \tag{2}$$

where n is the number of pores and r is the pore radius. D_k, the Knudsen diffusion coefficient, is given by

$$D_K = 0.66 r \sqrt{\frac{8RT}{\pi M_W}} \tag{3}$$

T and M_w are the temperature and molecular weight, respectively. Equations 2 and 3 show that the flux is proportional to the driving force, i.e., the pressure difference (ΔP), across the membrane and inversely proportional to the ratio of the square root of the molecular weights of the gases.

If the pore size of membrane used in separation is close to the mean free path of the gas molecules, the transport of gases and vapors falls in the transition between Knudsen and Poiseuille flow. Schofield et al. (1990) developed the transport model of gas and vapor for the transition region between Knudsen and Poiseuille flow in a simple and effective semiempirical relationship. The flux was expressed as follows:

$$J = aP^b \Delta P \tag{4}$$

where a is membrane permeation constant and b is 0 for Knudsen diffusion and 1 for Poiseuille flow.

Gas Transport Through Nonporous Polymeric Membrane

The transport of gases through a dense, nonporous membrane is expressed in terms of a solution–diffusion model, as described above (Fig. 5b). The relationship between permeability, solubility, and diffusivity is expressed as follows:

$$\text{Permeability}(P) = \text{Solubility}(S) \times \text{Diffusivity}(D) \tag{5}$$

The ability of a membrane to separate two molecules, A and B, is expressed as the ratio of their permeability (the selectivity, α):

$$\alpha = P_A/P_B \tag{6}$$

For a binary gas mixture, the selectivity can also be determined from a molar concentration of the two gases in feed and permeate:

$$\alpha = y(1-x)/x(1-y) \tag{7}$$

where y is the permeate concentration of the fast permeating gas and x is its feed concentration.

The simplest way to describe the transport of gases and vapors through nonporous membrane is by Fick's first law (Mulder 1996):

$$J = -D\frac{dc}{dx} \tag{8}$$

The flux J of a component through a plane perpendicular to the direction of diffusion is proportional to the concentration gradient dc/dx. The proportionality constant D is called the diffusion coefficient.

If it is assumed that the diffusion coefficient is constant, the change in concentration as a function of distance and time is given by Fick's second law (Mulder 1996):

$$\frac{\partial c}{\partial t} = -D\frac{\partial^2 c}{\partial x^2} \tag{9}$$

Gas Transport Through Facilitated Transport Membrane

Facilitated transport membranes, a type of liquid membranes, were developed for gas separation with high selectivity, especially at low gas partial pressure. Facilitated transport membranes selectively permeate specific gases (e.g., CO_2) by means of a reversible reaction between the gases and the membrane. Other gases such as H_2, N_2, and CH_4 do not react with the membrane and can only permeate by a solution–diffusion mechanism.

The model of gas transport through a carrier membrane is described as follows.

First, component A molecules form a complex AC with the carrier, and AC diffuses through the membrane. Second, dissolved gas A diffuses across the membrane with normal Fickian diffusion (shown in Fig. 6). The total flux of component A will then be the sum of the two contributions, i.e.,

$$J_A = \frac{D_A}{l}\left(C_{A,o} - C_{A,l}\right) + \frac{D_{AC}}{l}\left(C_{AC,o} - C_{AC,l}\right) \tag{10}$$

The first term on the right-hand side of Eq. 10 represents permeant diffusion according to Fick's law, where D_A is the diffusion coefficient of the uncomplexed

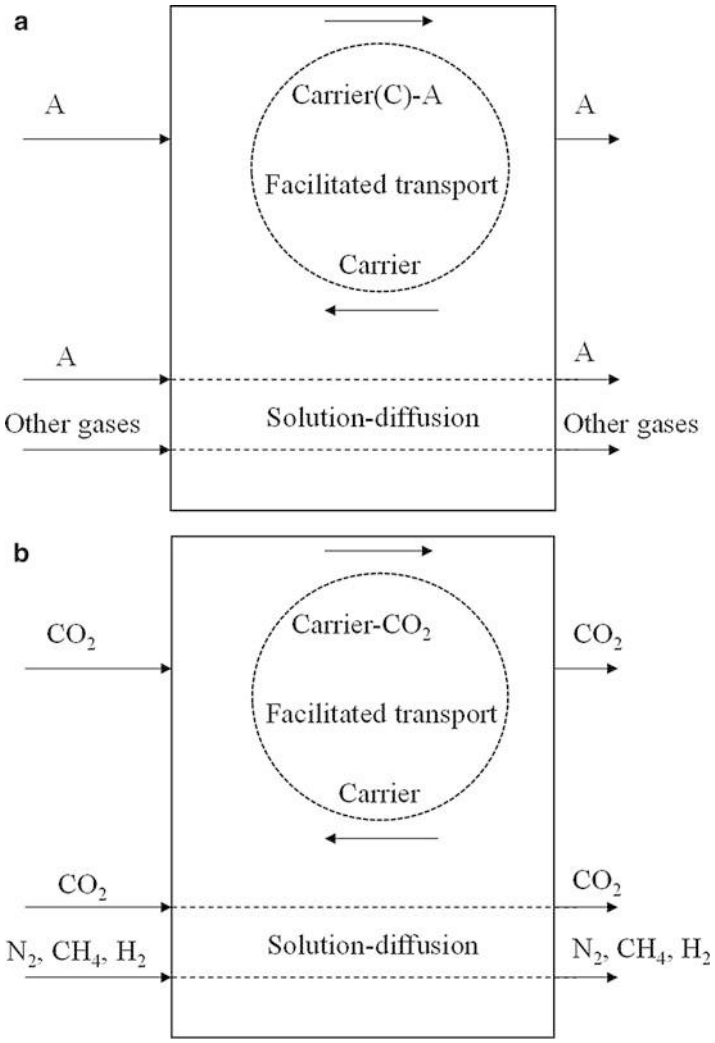

Fig. 6 The mechanism of a facilitated transport membrane. (**a**) The scheme of a facilitated transport membrane. (**b**) The scheme of a facilitated transport membrane for CO_2

component inside the liquid membrane, while $C_{A,o}$ is the concentration of component A just inside the liquid membrane at the feed side and is equal to the solubility of the liquid of A when thermodynamic equilibrium occurs at the interface. The second term represents carrier-mediated diffusion with the flux being proportional to the driving force, which in this case is the concentration difference of complex across the liquid membrane. D_{AC} is the diffusion coefficient of the complex, and $C_{AC,o}$ is the concentration of the complex at the feed side. The following limiting cases can be observed:

1. $C_{A,o} \gg C_{AC,o}$
   When the concentration of the complex *AC* is much lower than the concentration of *A*, the first term, i.e., Fickian diffusion, is rate determining.
2. $C_{A,o} \ll C_{AC,o}$
   When the concentration of the complex *AC* is much greater than the concentration of *A*, the second term, i.e., diffusion of the complex, is rate determining.
3. $C_{A,o} \approx C_{AC,o}$
   When the concentration of the complex *AC* is close to the concentration of *A*, both Fickian diffusion and the diffusion of the complex are rate determining.

Facilitated transport membranes for CO_2 separation were originally prepared by impregnating pores of microporous support membranes or polymer matrices with carrier solutions such as amines and alkali metal carbonates, which have chemical affinity to CO_2. Figure 6b shows the conceptual diagram of CO_2-facilitated transport membranes (Matsuyama et al. 1996). As shown in Fig. 6b, CO_2 carrier incorporated membrane can react selectively and reversibly with CO_2. The CO_2 permeation rate can be facilitated because CO_2 carrier of the reaction product can transport through the membrane, in addition to CO_2 transport membrane of physical solution–diffusion mechanism. On the other hand, other gases, such as N_2, CH_4, and H_2, transport through the membrane only by solution–diffusion mechanism. As a result, the CO_2 selectivity of facilitated transport membranes can be extremely high at low CO_2 partial pressures.

If amine is used as CO_2 carrier, the reaction of carrier and CO_2 is expressed as follows:

$$2CO_2 + 2RNH_2 + H_2O \rightleftharpoons RHNCOOH + RNH_3^+ + HCO_3^- \tag{11}$$

The weak basic amino group will initiate the reaction. However, considering that amino groups are not consumed during the reversible reactions, they are taking the role of catalysts for the reversible CO_2 hydration reactions; the final reactions can therefore be demonstrated with Eq. 12:

$$H_2O + CO_2 \overset{+NH_2}{\rightleftharpoons} H^+ + HCO_3^- \tag{12}$$

It is suggested that the high CO_2 selectivity and permeability can be obtained by the reversible reaction above.

An Overview in the Development of CO_2 Membrane Separation Material

Polymeric Membranes

Many studies have reported CO_2-selective polymer membranes for the separation of CO_2/CH_4 and CO_2/N_2 gas mixtures. On the other hand, there are comparatively few polymeric membranes that can be utilized for the selective recovery of CO_2

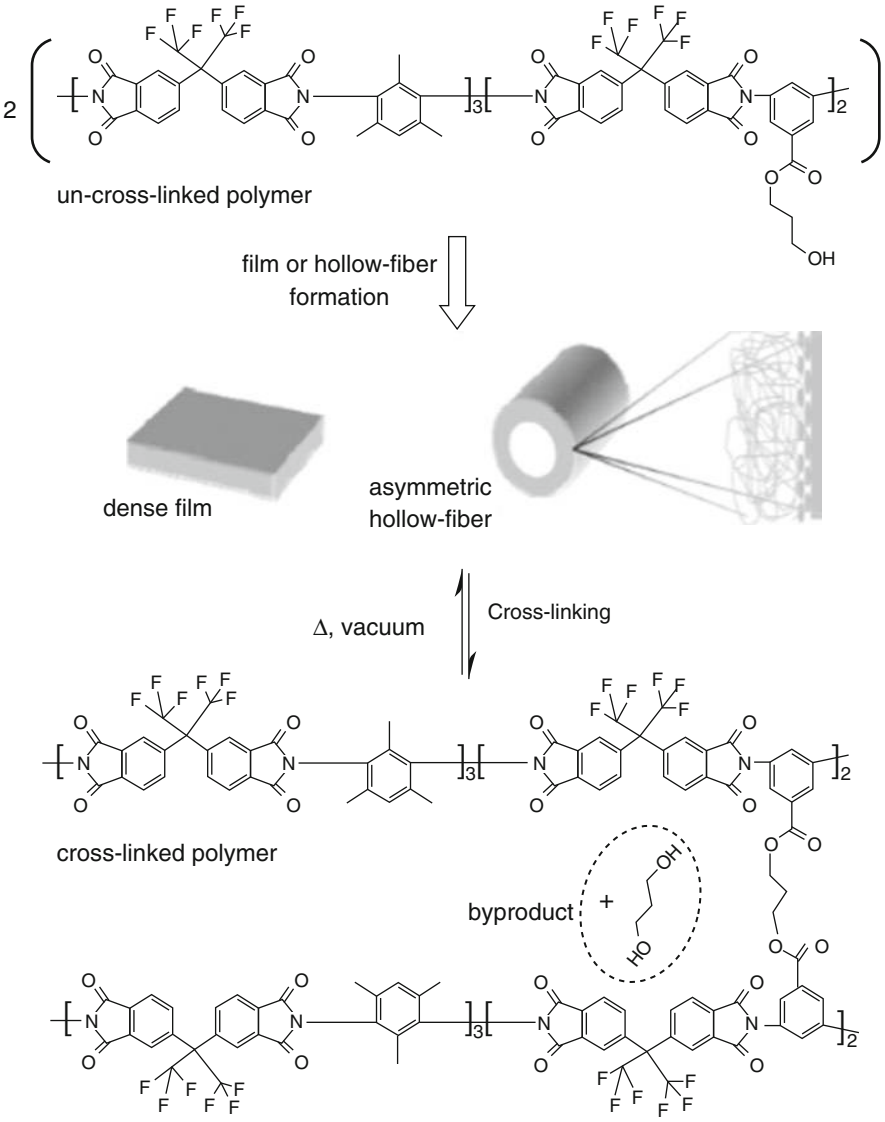

Fig. 7 Illustration showing the cross-linked polyimide (propane-diol monoesterified) membrane formation (Omole et al. 2010)

over H_2. Polymeric membranes made from glassy polymers such as cellulose acetate and polyimide have exhibited practical use in selective CO_2 separation from CO_2/CH_4 gas mixtures. However, CO_2/CH4 separation greatly decreases under high CO_2 partial pressures due to CO_2-induced plasticization. Koros et al. reported that cross-linked polyimide membranes exhibited enhanced resistance to CO_2 plasticization, as shown in Figs. 7 and 8 (Omole et al. 2010).

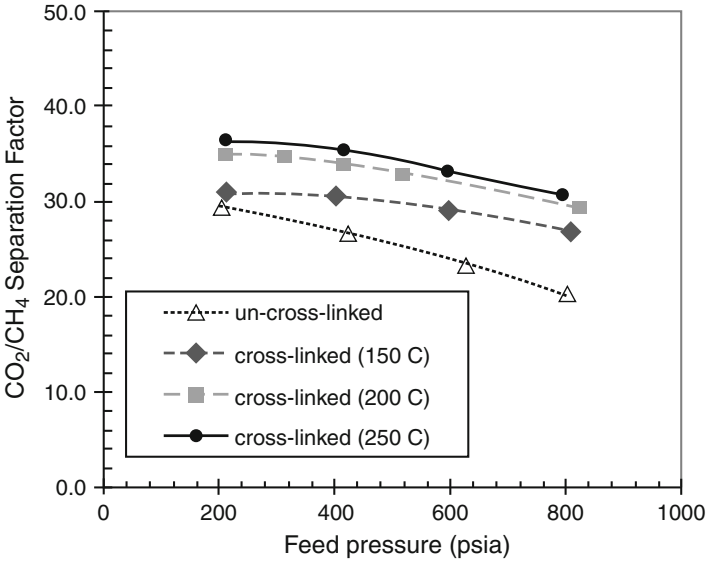

Fig. 8 Effect of cross-linking temperature on CO_2/CH_4 separation factor (Omole et al. 2010)

The structure of polyimide consisted of the following three monomer units: (1) 4, 4′-(hexafluoroisopropylidene) diphthalic anhydride (6FDA), (2) 2,4,6-trimethyl-1,3-diaminobenzene (DAM), and (3) 3,5-diaminobenzoic acid (DABA), in the ratio 5:3:2. The DABA groups were used as sites for cross-linking at 150, 200, and 250 °C for 2 h under vacuum, as shown in Fig. 2. The effect of cross-linking temperature on CO_2/CH_4 separation factor using a mixed-gas feed with 50 % CO_2 was shown in Fig. 3. 200 and 250 °C cross-linked fibers showed higher selectivities than the un-cross-linked and 150 °C cross-linked counterparts. Due to scale-up considerations for using lower cost conventional ovens, lower temperatures are referred commercially. Considering these aspects, 200 °C cross-linking temperature would be useful to pursue.

Robeson reported that there was a trade-off relationship between separation factor and the gas permeability for polymeric membranes. This upper-bound relationship for CO_2/CH_4 is shown in Fig. 9 (Robeson 2008). In recent years, the development of new membrane materials has been studied to produce both high permeability and high selectivity. Among of them, thermally rearranged polymers (TR polymers) are a novel polymer material in which the molecular sizes of the interchains are controlled by heat treatment. The outstanding performance of TR polymer membrane results from largely unique cavity formation with the size of angstrom order during thermal molecular rearrangement (Park et al. 2007). In the case of TR polymer, free-volume structure and distribution are suitable for gas transport (formation of cavity with size, distribution, and shape for a preferred CO_2 transport) in contrast with conventional polymers. For comparative investigation, mixed-gas separation of CO_2/CH_4 by TR polymer and carbon molecular sieve

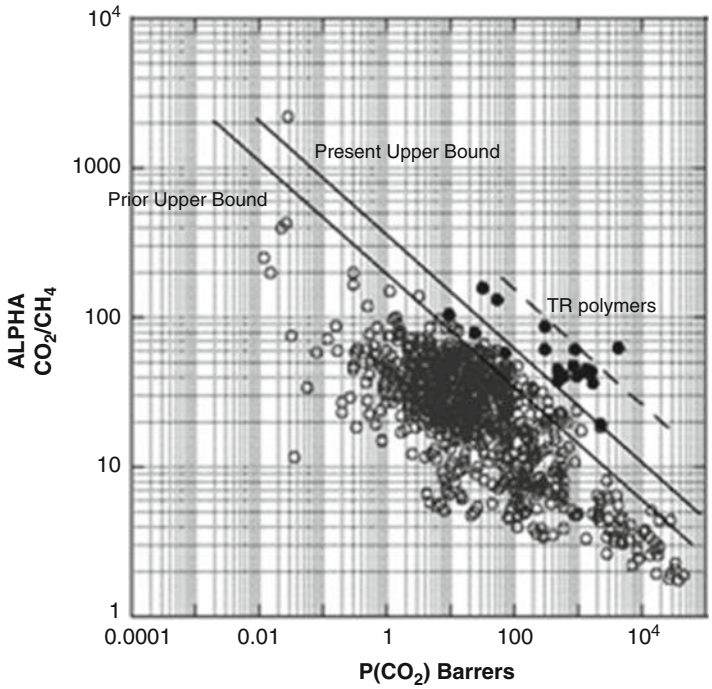

Fig. 9 Upper-bound correlation for CO_2/CH_4 separation (Robeson 2008)

membranes derived from a polyimide of intrinsic micro porosity was reported. High CO_2/CH_4 separations by TR polymer membranes were maintained under high pressures because of its high free volume and enhanced resistance to plasticization (Swaidan et al. 2013). Chung et al. reported that thickness, durability, and plasticization of membrane with TR polymer from ortho-functional polyimide based on 2,2′-bis-(3,4-dicarboxyphenyl) hexafluoropropane dianhydride (6FDA) and 3,3-dihydroxy-4,4-diamino-biphenyl (HAB) for CO_2 permeability was studied. Long-term exposure of the TR films to CO_2 showed that the CO_2 permeability of the thick TR films (15–20 μm) did not show significant decline at 32 atm for over 500 h (Wang et al. 2014). Lee et al. reported on physical properties, cavity size, and transport behavior of TR-PBO membranes by precursor hydroxypolyimide (Calle et al. 2013). Freeman et al. investigated on TR poly(benzoxazole)/polyimide-blended membranes for CO_2/CH_4 separation and showed that blending a-hydroxy-polyimides with non-TR polyimides was a feasible strategy to produce films with improved mechanical strength that retain the high gas separation performance of the TR polymer alone (Scholes et al. 2014a, b). It was also reported that MOP (microporous organic polymer) membranes with high affinity to CO_2 displayed excellent CO_2 separation, the same as TR polymer (Du et al. 2011; Xu and Hedin 2014). In addition, the directions for new membrane material design have been investigated to obtain high CO_2 gas selectivity and permeability. And more

research and investigation are carried out actively to introduce the molecular sieve ability with angstrom order size (Gin and Noble 2011; Hudiono et al. 2011).

Poly(ethylene glycol) (PEG) has a high physical affinity toward CO_2 and was expected to be a viable CO_2-separation membrane material. However, pure PEG exhibited very low CO_2 permeability, owing to its crystallization. Freeman et al. developed cross-linked PEG membranes in order to prevent this crystallization. The cross-linked PEG membranes exhibited favorable interactions with CO_2, which enhanced the solubility of CO_2 over that of H_2 and showed a CO_2/H_2 selectivity of about 10 at 35 °C and 25 at −20 °C (Lin et al. 2006). Wessling et al. developed a PEG block copolymer membrane and obtained a CO_2/H_2 selectivity of 10 at 35 °C (Husken et al. 2010). Peinemann et al. also developed a PEG block copolymer with CO_2 affinity and obtained a CO_2/H_2 selectivity of 10.8 at 30 °C (Car et al. 2008).

As stated in introduction, CO_2 separation from flue gas using membranes is performed under low pressure ratio between the feed and the permeate side, and the improvement in CO_2 permeability is important in terms of flowering the system cost and membrane area. It is also important to improve the separation process. Merkel et al. proposed a new system to obtain a CO_2 partial pressure difference between the feed and the permeate side using air as a sweep gas to reduce the energy cost. In addition, a membrane module with high CO_2 permeability (Polaris TM membrane) was developed (Merkel et al. 2010). Huang et al. investigated on pressure ratio between feed side and permeate side and its impact on membrane gas separation processes. They reported that the optimum membrane processes may not correlate with the highest selectivity because of limited pressure ratio (Huang et al. 2014). Hägg et al. reported similarly that the optimization of the operating conditions is important for membrane gas separation process, by investigating the influences of the operating parameters such as temperature, pressure, and stage-cut using the carbon membrane (He and Hagg 2011).

Inorganic Membranes

As for inorganic membranes, zeolite membranes and carbon membranes, among others, have been reported for CO_2 separation. Inorganic membranes have appropriate-sized pores that can act as molecular sieves to separate gas molecules by their effective size. In addition, inorganic membranes with strong CO_2 affinities show high CO_2 selectivity over N_2 and CH_4.

Noble et al. reported that zeolite SAPO-34 membrane showed a high CO_2/CH_4 separation performance (Zhang et al. 2010). Zhou et al. reported preparation for silica MFI membranes with a thickness of 0.5 μm on analumina support membrane. The membrane showed a separation selectivity of 109 for CO_2/H_2 mixtures and a CO_2 permeance of 51×10^{-7} mol m^{-2} s^{-1} Pa^{-1} at −35 °C (Zhou et al. 2014).

Sub-nanoporous carbon membranes are prepared through precursor polymer thermolysis and carbonization in several hundred degrees or more by heat treating. Polyimide, polyacrylonitrile, cellulose, phenolic resin, etc. are used as precursors. Carbon membranes prepared from a precursor polyimide based on 6FDA-mPDA/DABA (3:2) by thermolysis under 550 °C showed CO_2 permeability as high as

14750 Barrer with CO_2/CH_4 selectivity of approximately 52. Even 800 °C pyrolyzed carbon membranes still showed high CO_2 permeability of 2610 Barrer with high CO_2/CH_4 selectivity of approximately 118 (Qiu et al. 2014).

Inorganic membranes show high gas separation performance and high stability and durability at high temperature. On the other hand, they have the disadvantages of high membrane cost, compared with polymeric ones. To combine the benefits of both polymeric and inorganic materials, mixed-matrix membranes (MMMs), a type of organic/inorganic composite membranes, have also been studied. Many studies have been reported on gas separation membranes using ZIF (zeolitic imidazolate frameworks), a type of MOF (metal-organic framework), as inorganic nanoparticles. Bae et al. reported that MMMs prepared by incorporating MOF (ZIF-90) into a polymeric matrix showed a high CO_2/CH_4 separation performance (Bae et al. 2010). MMMs prepared by incorporating ZIF-108 nanoparticles into polysulfone (PSf) matrix showed CO_2/N_2 selectivity of 227 (Ban et al. 2014). Hägg et al. developed ZIF-8/PEBAX-2533 MMMs for CO_2 capture. MMMs from PEBAX-2533/ZIF-8 with 25 % ZIF-8 loading showed CO_2 permeability of 1129 Barrer with CO_2/N_2 selectivity of 31 (Nafisi and Hagg 2014). Because CO_2 separation by inorganic membranes is mainly carried out via molecular sieving, a high selectivity is obtained for CO_2/CH_4 and CO_2/N_2 separation but generally not for CO_2/H_2 separation.

Ionic Liquid Membranes

Ionic liquid (IL) membranes have received increasing interest and have been studied in recent years because of their low vapor pressures and stability at high temperatures. Polymerized IL membranes were prepared for the separation of CO_2/N2, CO_2/CH_4, etc. by Noble et al. (Bara et al. 2007). Amino-containing ILs were investigated for the separation of CO_2/H_2 by Myers et al. (2008), and a CO_2/H_2 selectivity of 15 was obtained at 85 °C. Matsuyama et al. reported amino-containing IL membranes for the separation of CO_2/CH_4, and the membrane showed constant separation abilities for 260 days ($\alpha_{CO2/CH4}$ = ca. 60) (Hanioka et al. 2008). Nagai et al. reported impregnating IL and ZSM-5 into PI matrix for improvement of IL composite membrane stability. The resulting membrane exhibited CO_2/CH_4 selectivity of 31 with CO_2 permeability of 4509 Barrer (Shindo et al. 2014). IL monomer was polymerized to improve pressure durability of IL membranes by Wessling et al. The resulting membrane showed CO_2/CH_4 selectivity of 22 with CO_2 permeability of 18 Barrer at 40 °C, CO_2 (50 vol.%)/CH_4 (50 vol.%) of feed mixed gas under 40 atm total pressure (Simons et al. 2010).

Facilitated Transport Membranes

Facilitated transport membranes for CO_2 separation were originally prepared by impregnating pores of microporous support membranes or polymer matrices with carrier solutions such as amines and alkali metal carbonates, which have chemical affinity to CO_2. Figure 10 shows the conceptual diagram of CO_2-facilitated transport membranes (Zou and Ho 2006). As shown in Fig. 5, CO_2 carrier incorporated membrane can react selectively and reversibly with CO_2. The CO_2 transport membrane rate can be facilitated because CO_2 carrier of the reaction product can transport through the

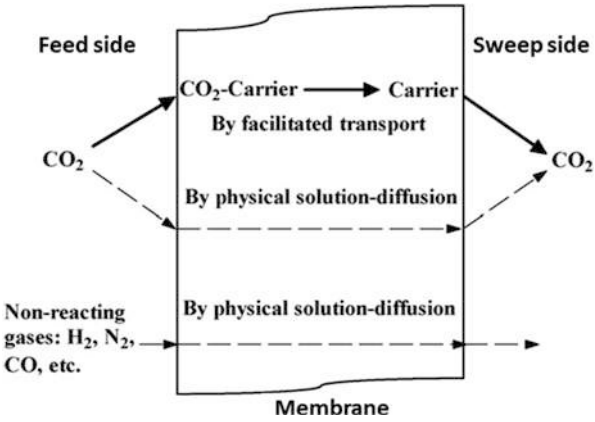

Fig. 10 The conceptual diagram of CO_2-facilitated transport membrane (Zou and Ho 2006)

membrane, in addition to CO_2 transport membrane of physical solution–diffusion mechanism. On the other hand, other gases, such as N_2, H_2, and CO, transport membrane only by solution–diffusion mechanism. As a result, the CO_2 selectivity of facilitated transport membranes can be extremely high at low CO_2 partial pressures.

Facilitated transport membranes for CO_2 separation have been studied since the 1960s. Ward and Robb immobilized an aqueous bicarbonate–carbonate solution into a porous support and obtained a CO_2/O_2 separation factor of 1500 (Ward and Robb 1967). Immobilized liquid membranes impregnated with carbonate and bicarbonate solutions were studied by Jung and Ihm (1984), Bhave and Sirkar (1986) and Yamaguchi et al. (1996). Apart from carbonate or bicarbonate ions as the reactive carrier, amines were other chemicals that can facilitate CO_2 transport. Aqueous solution of diethanolamine (DEA) was used for facilitating CO_2 transport (Guha et al. 1990) (Matsuyama et al. 1996). The transport of acid gases through an ion-exchange membrane was facilitated with a diamine carrier (Quinn et al. 1997). The membrane which acted as a fixed carrier membrane for CO_2-facilitated transport was prepared by plasma grafting 2-(N, N-dimethyl) aminoethyl methacrylate (Matsuyama et al., 1996) (Neplembroek et al. 1992). The membranes based on the polyelectrolyte, poly(vinylbenzyl trimethyl ammonium fluoride), exhibited high permselective properties for CO_2/CH_4 (Quinn et al. 1997; Kemperman et al. 1997).

Although the immobilized liquid membranes have quite high permselectivity, they have a shortcoming of instability. Some methods were proposed to improve membrane stability under a pressurized condition or in a vacuum. For example, polymer gel was used to retain CO_2 carriers in membrane (Neplembroek et al. 1992; Kemperman et al. 1997; Matsumiya et al. 2004, 2005) or the surface of support membrane was treated by chemical method and liquid membrane layer was formed on the pretreated support membrane (Ito et al. 1997), etc.

Ho et al. developed facilitated transport membranes by blending amines with poly(vinyl alcohol) (PVA) (Zou and Ho 2006). These membranes showed a CO_2/H_2 selectivity of 300 at 110 °C and 100 at 150 °C, as shown in Fig. 11. Matsuyama et al. reported facilitated transport membranes prepared by the immobilization of

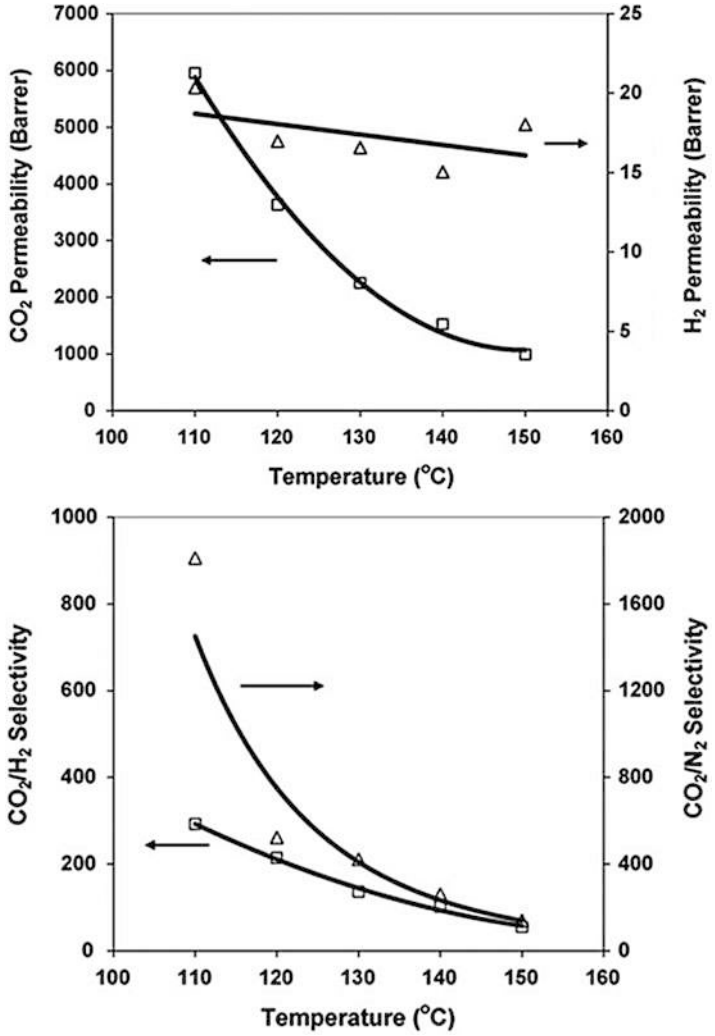

Fig. 11 CO_2/H_2-separation properties of facilitated transport membranes prepared by blending amines with poly(vinyl alcohol) (PVA) (Zou and Ho 2006)

2,3-diaminopropionic acid and cesium carbonate in a PVA/poly(acrylic acid) copolymer matrix, and the resulting membrane showed a CO_2/H_2 selectivity of 432 at 160 °C, as shown in Fig. 12 (Yegani et al. 2007). Hägg et al. developed a CO_2/N_2-separation membrane by blending PVA and poly(vinyl amine) (PVAm). The composite membrane with a selective layer thickness of 0.3 μm was prepared by casting a solution of PVA/PVAm on a polysulfone (PSf) support membrane (Sandru et al. 2010). A model of CO_2-facilitated transport membrane mechanism was shown in Fig. 13. In this model, the bicarbonate ion is considered as CO_2 carrier and plays an important role for CO_2 permeation.

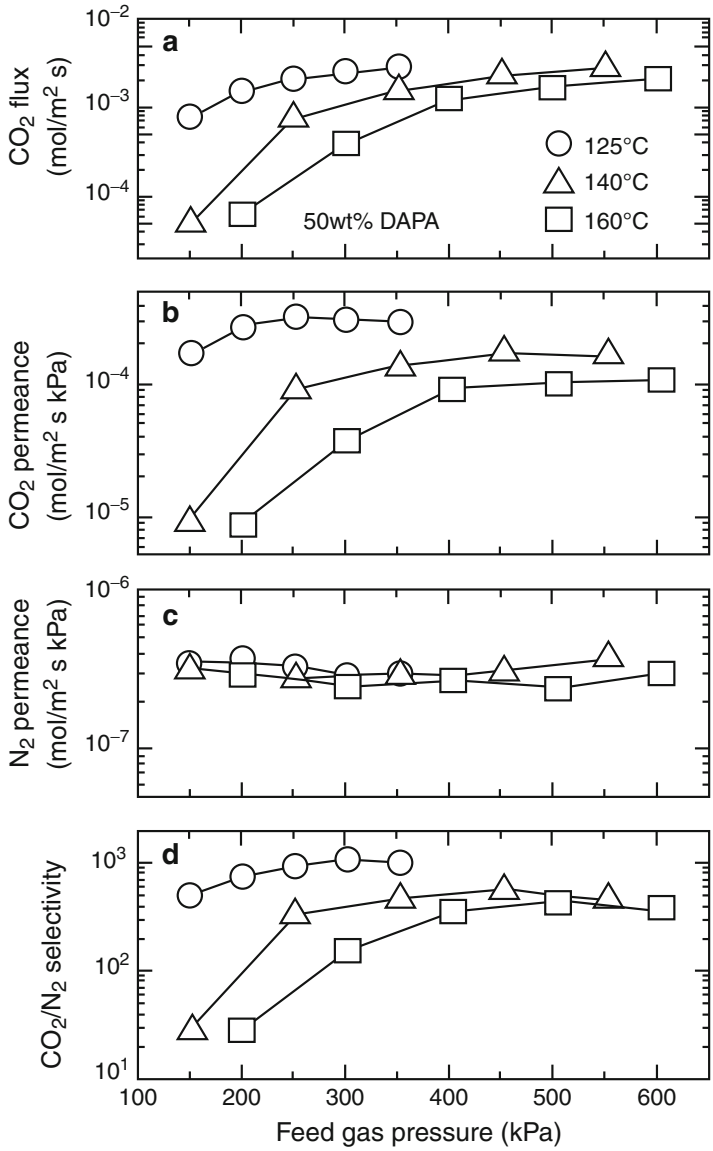

Fig. 12 CO_2/N_2-separation properties of facilitated transport membranes prepared by the immobilization of 2,3-diaminopropionic acid and cesium carbonate in a PVA/poly(acrylic acid) copolymer matrix (Yegani et al. 2007)

Myers et al. reported that amino-containing IL membrane showed CO_2-facilitated transport for dry CO_2/H_2 mixed-gas separation (Myers et al. 2008). Matsuyama et al. developed amino acid IL-based facilitated transport membranes for CO_2 separation. A tetrabutylphosphonium proline as amino acid IL membrane showed

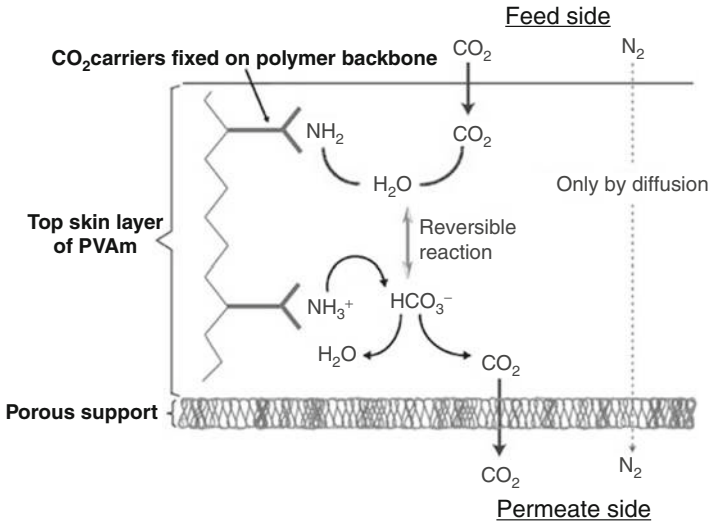

Fig. 13 CO_2-facilitated transport membrane mechanism by bicarbonate (Sandru et al. 2010)

an excellent CO_2 permeability of 14,000 Barrer with CO_2/N_2 selectivity of 100 at 373 K under dry conditions and 10 kPa CO_2 partial pressure (Kasahara et al. 2012). CO_2 partial pressure and temperature significantly influenced CO_2 permeability and CO_2/N_2 selectivity (Kasahara et al. 2014a, b).

Svec et al. developed polymer hybrid CO_2-facilitated transport membrane by photopolymerization based on polyaniline and 2-hydroxyethylmethacrylate. The resulting hybrid membranes showed a CO_2 permeability of 3460 Barrer with CO_2/CH_4 selectivity of 540 under 8.3 kPa CO_2 partial pressure (Blinova and Svec 2012). Sirkar et al. reported excellent CO_2/N_2 selectivity using a viscous and nonvolatile poly(amidoamine) (PAMAM) dendrimer as an immobilized liquid membrane under isobaric and saturated water vapor test conditions (Kovvali et al. 2000). In the integrated coal gasification combined cycles with CO_2 capture and storage (IGCC-CCS), CO_2-separation membranes will play an important role for reducing CO_2-capture costs. In Japan, PAMAM dendrimer/polymer hybrid membranes were developed for CO_2 separation from flue gas (CO_2/N_2) (Duan et al. 2006; Kai et al. 2008) and from IGCC process (CO_2/H_2) (Taniguchi et al. 2008; Duan et al. 2012; RITE today (annual report 2015).

Membrane Module Design and Manufacturing for CO_2 Membrane Separation

Industrial membrane plants for gas separation often require hundreds to thousands of square meters of membrane to perform the separation. It is very important to provide a large surface area to deal with large quantity of flue gas or fuel gas.

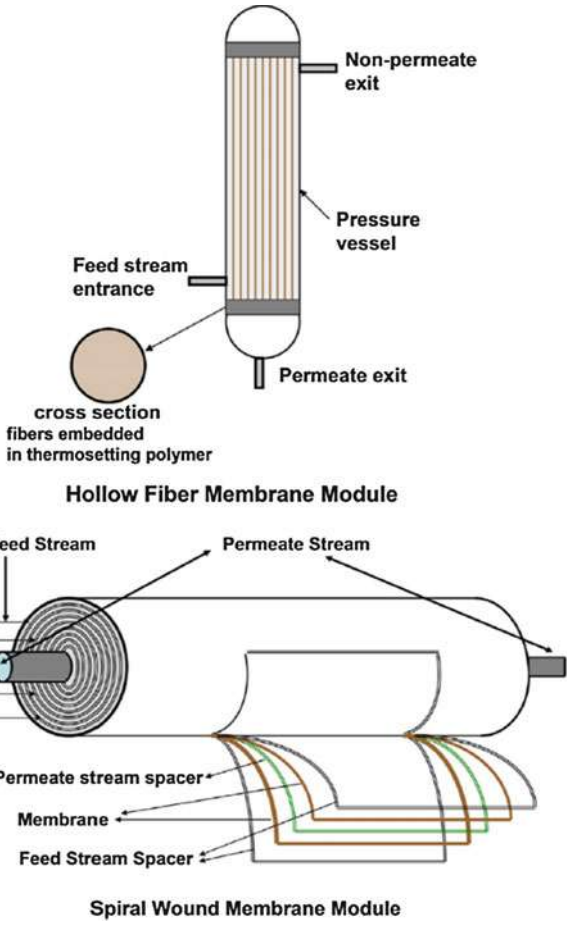

Fig. 14 Modular constructions employed for gas separation processes (Sanders et al. 2013)

Hence, it is very important to design and produce membrane modules. There are several ways to economically and efficiently package membranes for high surface area and economical module for gas separation. These packages are called membrane modules. The examples of membrane modules are shown in Fig. 14 (Sanders et al. 2013).

1. Hollow Fiber Membrane Modules
   A typical hollow fiber bundle contains on the order of 10^5 hollow fibers which are tightly packed (packing fractions on the order of 50 % are common) with both ends embedded in a thermosetting epoxy polymer (Coker et al. 1998). A hollow fiber bundle would then be housed in a polymeric or metal pressure vessel, depending on the pressure that the system was expected to encounter during operation. Feed gas can be introduced into the bore side or the shell side of a hollow fiber module, depending on the application.

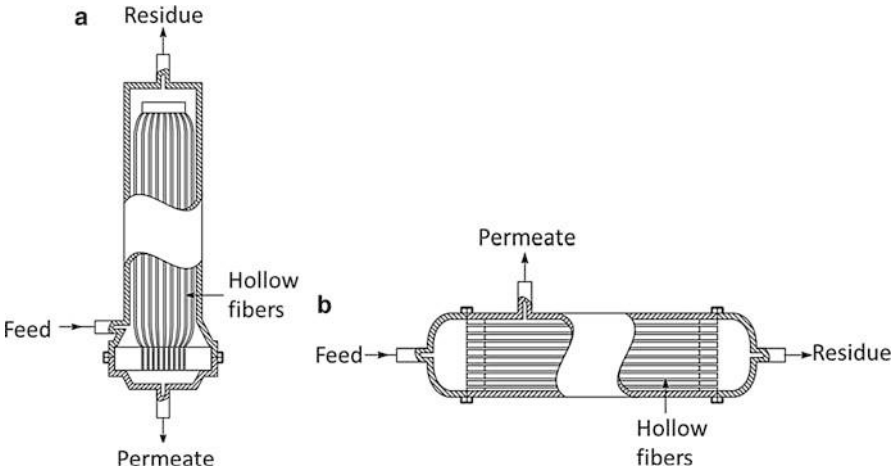

Fig. 15 Hollow fiber membrane module. (**a**) Countercurrent flow. (**b**) Cocurrent flow

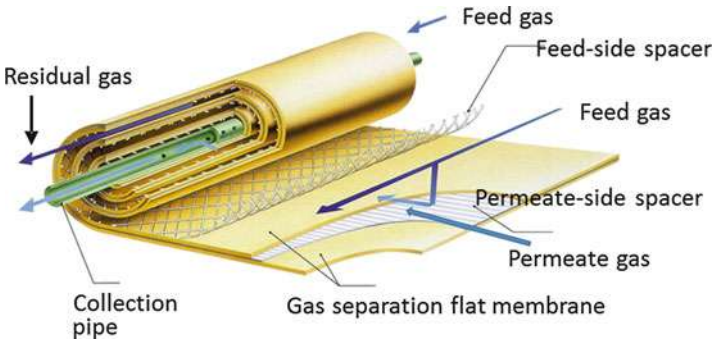

Fig. 16 Cross section constructions of spiral wound membrane module for gas separation

Two basic shapes of hollow fiber membrane module are shown in Fig. 15: (a) countercurrent flow and (b) cocurrent flow. Countercurrent shape module has the shell-side feed design with a loop of fibers contained in a pressure vessel. The system is pressurized from the shell side, and the permeate passes through the fiber wall and exits through the open fiber ends. It is easy to make very large membrane areas, thick wall, and small diameter to stand the pressure for used in-gas separation.

In cocurrent shape module, fibers are open at both ends, and the feed fluid is circulated through the bore of the fibers. Large diameter is needed to minimize pressure drop (Δp) for in-gas separation at $p < 10$ bar.

2. Spiral Wound Membrane Modules

The spiral wound membrane module configuration as shown in Fig. 16 includes some layers of flat sheet asymmetric membranes with porous spacers between

the membrane sheets. The feed gas passes axially down the module across the membrane envelope. The permeate gas spirals toward the center and exits through the collection pipe.

Demonstration (Field Test)

In the United States, the US Department of Energy (DOE) sponsored CO_2-capture technology projects of three primary technology areas (post-combustion, precombustion, and advanced combustion systems), and various stages of development (lab scale, bench scale, and pilot scale) are conducted. CO_2-capture technologies include absorption, adsorption (solid sorbent), and membrane separations Achievement of the projects is reported in the annual NETL CO_2 Capture Technology meeting. In the NETL CO_2 Capture Technology meeting in 2015, latest results of more than 50 projects were reported (http://www.netl.doe.gov/events/conference-proceedings/2015/2015-co2-capture-technology-meeting).

In some of the projects above, field test has been conducted in the National Carbon Capture Center (NCCC) (2014–2019). Realistic syngas and flue gas for performance verification are used for membranes supplied by various membrane companies, universities, and research institute (http://www.nationalcarboncapturecenter.com/).

For post-combustion, CO_2-selective membranes, such as polymeric membranes by MTR and Air Liquide and polymeric/inorganic hybrid membranes by the Ohio State University are tested.

For MTR CO_2 membrane process, primary CO_2 removal with cross-flow module and selective recycle of CO_2 with countercurrent/air sweep module to increase overall capture are combined. Combustion air sweep provides driving force that lowers the capture energy. In addition, pre-concentrated CO_2 decreases membrane area and power required. So far, 0.05 MW bench-scale unit was operated successfully.

In MTR, bench-scale hybrid membrane-absorption CO_2-capture processes (series and parallel systems) are also developed.

Ho et al. (Ohio State University) reported membranes composed of selective amine polymer layer/zeolite nanoparticle layer/polymer support.

For pre-combustion, H_2 selective membranes, such as Pd–alloy membranes by WPI, carbon molecular sieve (CMS) membranes by MPT, and polymeric membranes by MTR, are tested. CO_2-selective membranes by MTR are also tested.

Summary and Future Prospects

As described above, over the past three decades, membrane gas separation in industry application has become widely used for a variety of industrial application. From a commercial point of view, three steps of membrane material, membrane module design, and manufacturing, system design, and engineering are very important for the application of CO_2 capture by membrane (Fig. 17; Bernardo and Clarizia 2013).

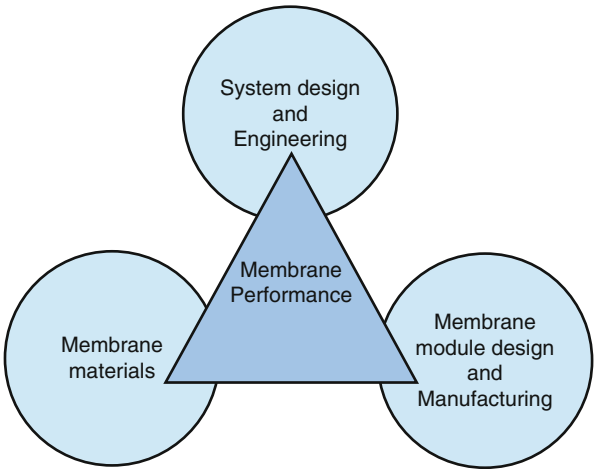

Fig. 17 Main points in membrane performance development (Bernardo and Clarizia 2013)

So far, various types of CO_2-selective membranes have been developed using both organic and inorganic materials. As for polymeric membranes, research using PEG-based materials and microporous polymer membranes using TR polymer, MOP, etc. are reported. As for IL membranes, novel IL-containing amino group and their fabrication into polymeric membranes are reported. As for inorganic membranes, zeolite membranes and carbon membranes among others have been reported in the selective separation of CO_2. Mixed-matrix membranes (MMMs), a type of organic/inorganic composite membranes, combining the benefits of both polymeric and inorganic materials have also been studied extensively. As for facilitated transport membranes, novel membranes using ILs, amines, etc. are reported.

In the case of CO_2 separation from flue gas (post-combustion), it is pointed out that the CO_2 permeability is more important than CO_2/N_2 selectivity because pressure ratio between feed side and permeate side is small. On the other hand, in the case of CO_2 separation from IGCC process (precombustion), both CO_2 permeability and CO_2/H_2 selectivity are important to separate CO_2 effectively. It is also important to consider the difference of properties of membrane materials. System analysis as well as field test using membrane modules using real flue gas or real syngas would be also very important to make membrane module and membrane system more reliable and feasible.

References

Aoki K, Kusakabe K, Morooka S (1998) Gas permeation properties of A-type zeolite membrane formed on porous substrate by hydrothermal synthesis. J Membr Sci 141:197–205

Bae T-H, Lee JS, Qiu W, Koros WJ, Jones CW, Nair S (2010) A high-performance gas-separation membrane containing submicrometer-sized metal-organic framework crystal. Angew Chem Int Ed 49:9863–9866

Baker RW (2002) Reviews: future directions of membrane gas separation technology. Ind Eng Chem Res 41:1393–1411

Ban Y, Li Y, Peng Y, Jin H, Jiao W, Liu X, Yang W (2014) Metal-substituted zeolitic imidazolate framework ZIF-108: gas-sorption and membrane-separation properties. Chem Eur J 20:11402–11409

Bara JE, Lessmann S, Gabriel CJ, Hatakeyama ES, Noble RD, Gin DL (2007) Synthesis and performance of polymerizable room-temperature ionic liquids as gas separation membranes. Ind Eng Chem Res 46:5397–5404

Behave RR, Sirkar KK (1986) Gas permeation and separation by aqueous membranes immobilized across the whole thickness or in a thin section of hydrophobic microporous celgard films. J Membr Sci 27:41

Bernardo P, Clarizia G (2013) 30 years of membrane technology for gas separation. Chem Eng Trans 32:1999–2004

Blinova NV, Svec F (2012) Functionalized polyaniline-based composite membranes with vastly improved performance for separation of carbon dioxide from methane. J Membr Sci 423–424:514–521

Borisov S, Khotimsky VS, Slovetsky AI, Pashunin YM (1997) Plasma fluorination of organosilicon polymeric films for gas separation applications. J Membr Sci 125:319–329

Calle M, Doherty CM, Hill AJ, Lee YM (2013) Cross-linked thermally rearranged poly(benzoxazole-co-imide) membranes for gas separation. Macromolecules 46:8179–8189

Car A, Stropnik C, Yave W, Peinemann K-V (2008) PEG modified poly(amide-b-ethylene oxide) membranes for CO_2 separation. J Membr Sci 307:88–95

Coker DT, Freeman BD, Fleming GK (1998) Modeling multicomponent gas separation using hollow-fiber membrane contactors. AIChE J 44(6):1289–1302

Du N, Park HB, Robertson GP, Dal-Cin MM, Visser T, Scoles L, Guiver MD (2011) Polymer nanosieve membranes for CO_2-capture applications. Nat Mater 10:372–375

Duan S, Kouketsu T, Kazama S, Yamada K (2006) Development of PAMAM dendrimer composite membranes for CO_2 separation. J Membr Sci 283:2–6

Duan S, Taniguchi I, Kai T, Kazama S (2012) Poly(amidoamine) dendrimer/poly(vinyl alcohol) hybrid membranes for CO_2 capture. J Membr Sci 423–424:107–112

Gin DL, Noble RD (2011) Designing the next generation of chemical separation membranes. Science 332:674–676

Guha AK, Majumdar S, Sirkar KK (1990) Facilitated transport of CO_2 through an immobilized liquid membrane of aqueous diethanolamine. Ind Eng Chem Res 29:2093–2100

Hanioka S, Maruyama T, Sotani T, Teramoto M, Matsuyama H, Nakashima K, Hanaki M, Kubota F, Goto M (2008) CO_2 separation facilitated by task-specific ionic liquids using a supported liquid membrane. J Membr Sci 314:1–4

Hao Jihao, Wang Shichang (1998) Development of membrane for separation of CO_2/CH_4. Huaxue Gongcheng (Xi'an, People's Repub. China) 26(1):33–35, 38

He X, Hagg M-B (2011) Optimization of carbonization process for preparation of high performance hollow fiber carbon membranes. Ind Eng Chem Res 50:8065–8072

Hernandez-Huesca R, Diaz L, Aguilar-Armenta G (1999) Adsorption equilibria and kinetics of CO_2, CH_4 and N_2 in natural zeolites. Sep Purif Technol 15:163–173

Huang Y, Merkel TC, Baker RW (2014) Pressure ratio and its impact on membrane gas separation processes. J Membr Sci 463:33–40

Hudiono YC, Carlisle TK, La Frate AL, Gin DL, Noble RD (2011) Novel mixed matrix membranes based on polymerizable room-temperature ionic liquids and SAPO-34 particles to improve CO_2 separation. J Membr Sci 370:141–148

Husken D, Visser T, Wessling M, Gaymans RJ (2010) CO_2 permeation properties of poly(ethylene oxide)-based segmented block copolymers. J Membr Sci 346:194–201

Ismail AF, David LIB (2001) A review on the latest development of carbon membranes for gas separation. J Membr Sci 193:1–18

Ismail AF, Shilton SJ (1998) Polysulfone gas separation hollow fiber membranes with enhanced selectivity. J Membr Sci 139:285–286

Ito A, Sato M, Anma T (1997) Permeability of CO_2 through chitosan membrane swollen by water vapor in feed gas. Angew Makromol Chem 248:85–94

Jung YW, Ihm SK (1984) Facilitated transport of carbon dioxide through alkaline solutions. Int Chem Eng 24:74

Kai T, Kouketsu T, Duan S, Kazama S, Yamada K (2008) Development of commercial-sized dendrimer composite membrane modules for CO_2 removal from flue gas. Sep Purif Technol 63:524–530

Kasahara S, Kamio E, Ishigami T, Matsuyama H (2012) Effect of water in ionic liquids on CO_2 permeability in amino acid ionic liquid-based facilitated transport membranes. J Membr Sci 415–416:168–175

Kasahara S, Kamio E, Matsuyama H (2014a) Improvements in the CO_2 permeation selectivities of amino acid ionic liquid-based facilitated transport membranes by controlling their gas absorption properties. J Membr Sci 454:155–162

Kasahara S, Kamio E, Otani A, Matsuyama H (2014b) Fundamental investigation of the factors controlling the CO_2 permeability of facilitated Transport membranes containing amine-functionalized task-specific ionic liquids. Ind Eng Chem Res 53:2422–2431

Kemperman AJB, Damink B, Boomgaard TVD, Strathann H (1997) Stabilization of supported liquid membranes by gelation with PVC. J Appl Polym Sci 65(6):1205–1216

Kovvali AS, Chen H, Sirkar KK (2000) Dendrimer membranes: a CO_2-selective molecular gate. J Am Chem Soc 122:7594–7595

Li K, Teo WK (1998) Use of permeation and absorption methods for CO_2 removal in hollow fibre membrane modules. Sep Purif Technol 13:79–88

Li Y, Chena H, Liu J, Yang W (2006) Microwave synthesis of LTA zeolite membranes without seeding. J Membr Sci 277:230–239

Lin H, Wagner EV, Freeman BD, Toy LG, Gupta RP (2006) Plasticization-enhanced hydrogen purification using polymeric membranes. Science 311:639–642

Matsumiya N, Matsufuji S, Nakabayashi M, Okabe K, Mano H, Teramoto M (2004) Separation of CO_2 from model flue gas by facilitated transport membrane with hydrogel. Membrane 29 (1):66–72

Matsumiya N, Matsufuji S, Okabe K, Mano H, Matsuyama H, Teramoto M (2005) Facilitated transport of CO_2 through Gel-coated liquid membranes using 2, 3-diaminopropionic acid as carrier. Membrane 30(1):46–51

Matsuyama H, Teramoto M, Sakakura H (1996) Selective permeation of CO_2 through poly{2-(N, N-dimethyl)aminoethyl methacrylate} membrane prepared by plasma-graft polymerization technique. J Membr Sci 114:193–200

Merkel TC, Lin H, Wei X, Baker R (2010) Power plant post-combustion carbon dioxide capture: an opportunity for membranes. J Membr Sci 359:126–139

Mulder M (1996) Basic principles of membrane technology, 2nd edn. Kluwer, Academic Publishers, pp 1–16

Myers C, Pennline H, Luebke D, Ilconich J, Dixon JK, Maginn EJ, Brennecke JF (2008) High temperature separation of carbon dioxide/hydrogen mixtures using facilitated supported ionic liquid membranes. J Membr Sci 322:28–31

Nafisi V, Hagg M-B (2014) Development of dual layer of ZIF-8/PEBAX-2533 mixed matrix membrane for CO_2 capture. J Membr Sci 459:244–255

Nakagama T (1989) Current status of gas membrane separation. Recent chemical Engineering 41, Membrane separation engineering – the present situation and the application on engineering–, kagaku kogyo sha, p109

Neplembroek AM, Bargeman D, Smolders CA (1992) Supported liquid membranes: stabilization by gelation. J Membr Sci 67:147–165

Omole IC, Adams RT, Miller SJ, Koros WJ (2010) Effects of CO_2 on a high performance hollow-fiber membrane for natural gas purification. Ind Eng Chem Res 49:4887–4896

Paranjape M, Clarke PF, Pruden BB, Parrillo DJ, Thaeron C, Sircar S (1998) Separation of bulk carbon dioxide-hydrogen mixtures by selective surface flow membrane. Adsorption 4:355–360
Park HB, Jung CH, Lee YM, Hill AJ, Pas SJ, Mudie ST, Van Wagner E, Freeman BD, Cookson DJ (2007) Polymers with cavities tuned for fast selective transport of small molecules and ions. Science 318:254–258
Poshusta JC, Noble RD, Falconer JL (1999) Temperature and pressure effects on CO_2 and CH_4 permeation through MFI zeolite membranes. J Membr Sci 160:115–125
Qiu W, Zhang K, Li FS, Zhang K, Koros WJ (2014) Gas separation performance of carbon molecular sieve membranes based on 6FDA-mPDA/DABA (3:2) polyimide. ChemSusChem 7:1186–1194
Quinn R, Laciak DV, Pez GP (1997) Polyelectrolyte-salt blend membranes for acid gas separations. J Membr Sci 131:49–60
RITE today (annual report, 2015). http://www.rite.or.jp/en/results/today/pdf/rt2015_all_e.pdf
Robeson LM (2008) The upper bound revisited. J Membr Sci 320:390–400
Robeson LM (2012) Polymer membranes. In: Matyjaszewski K, Möller M (eds) Polymers for advanced functional materials. Polymer science: a comprehensive reference, vol 8. Elsevier, Amsterdam, pp 325–347
Sanders DF, Smith ZP, Guo R, Robeson LM, McGrath JE, Paul DR, Freeman BD (2013) Energy-efficient polymeric gas separation membranes for a sustainable future: a review. Polymer 54:4729–4761
Sandru M, Haukebo SH, Hagg M-B (2010) Composite hollow fiber membranes for CO_2 capture. J Membr Sci 346:172–186
Schofield RW, Fane AG, Fell CJD (1990) Gas and vapor transport through microporous membranes. I. Knudsen-Poiseuille transition. J Membr Sci 53:159–172
Scholes CA, Ribeiro CP, Kentish SE, Freeman BD (2014a) Thermal rearranged poly (benzoxazole)/polyimide blended membranes for CO_2 separation. Sep Purif Technol 124:134–140
Scholes CA, Ribeiro CP, Kentish SE, Freeman BD (2014b) Thermal rearranged poly (benzoxazole-co-imide)membranes for CO_2 separation. J Membr Sci 450:72–80
Shindo R, Kishida M, Sawa H, Kidesaki T, Sato S, Kanehashi S, Nagai K (2014) Characterization and gas permeation properties of polyimide/ZSM-5 zeolite composite membranes containing ionic liquid. J Membr Sci 454:330–338
Simons K, Nijmeijer K, Bara JE, Noble RD, Wessling M (2010) How do polymerized room-temperature ionic liquid membranes plasticize during high pressure CO_2 permeation? J Membr Sci 360:202–209
So MT, Eirich FR, Strathmann H, Baker RW (1973) Preparation of asymmetric loeb-sourirajan membranes (1973) Polym Lett Ed 11:201–205. Wiley
Staudt-Bickel C, Koros WJ (1999) Improvement of CO_2/CH_4 separation characteristics of polyimides by chemical crosslinking. J Membr Sci 155:145–154
Swaidan R, Ma X, Litwiller E, Pinnau I (2013) High pressure pure-and mixed-gas separation of CO_2/CH_4 by thermally-rearranged and carbon molecular sieve membranes derived from a polyimide of intrinsic microporosity. J Membr Sci 447:387–394
Taniguchi I, Duan S, Kazama S, Fujioka Y (2008) Facile fabrication of a novel high performance CO_2 separation membrane: immobilization of poly(amidoamine) dendrimers in poly(ethylene glycol) networks. J Membr Sci 322:277–280
Thundyil MJ, Jois YH, Koros WJ (1999) Effect of permeate pressure on the mixed gas permeation of carbon dioxide and methane in a glassy polyimide. J Membr Sci 152:29–40
Wang D, Li K, Teo WK (1998) Preparation and characterization of polyetherimide asymmetric hollow fiber membranes for gas separation. J Membr Sci 138:193–201
Wang H, Chung T-S, Paul DR (2014) Physical aging and plasticization of thick and thin films of the thermally rearranged ortho-functional polyimide 6FDA–HAB. J Membr Sci 458:27–35
Ward WJ, Robb WL (1967) Carbon dioxide-oxygen separation: facilitated transport of carbon dioxide across a liquid film. Science 156:1481–1484

Xu C, Hedin N (2014) Microporous adsorbents for CO_2 capture – a case for microporous polymers? Mater Today 17:397–403

Yamaguchi T, Koval CA, Noble RD, Bowman CN (1996) Transport mechanism of carbon dioxide through perfluorosulfonate ionomer membranes containing an amine carrier. Chem Eng Sci 51 (21):4781–4789

Yan Feng (1996) A study on vapor permeability and pervaporation through polymer membranes, Doctor of philosophy thesis, Graduate School of Science and Technology Niigata University, pp 1–9

Yegani R, Hirozawa H, Teramoto M, Himei H, Okada O, Takigawa T, Ohmura N, Matsumiya N, Matsuyama H (2007) Selective separation of CO_2 by using novel facilitated transport membrane at elevated temperatures and pressures. J Membr Sci 291:157–164

Zhang Y, Tokay B, Funke HH, Falconer JL, Noble RD (2010) Template removal from SAPO-34 crystals and membranes. J Membr Sci 363:29–35

Zhou M, Korelskiy D, Ye P, Grahn M, Hedlund J (2014) A uniformly oriented MFI membrane for improved CO_2 separation. Angew Chem Int Ed 53:3492–3495

Zou J, Ho WSW (2006) CO_2-selective polymeric membranes containing amines in crosslinked poly(vinyl alcohol). J Membr Sci 286:310–321

CO_2 Geological Storage

Masao Sorai, Xing Lei, Yuji Nishi, Tsuneo Ishido, and Shinsuke Nakao

Contents

M. Sorai (✉) • X. Lei • Y. Nishi • T. Ishido • S. Nakao
National Institute of Advanced Industrial Science and Technology (AIST), Geological Survey of Japan, Tsukuba, Ibaraki, Japan
e-mail: m.sorai@aist.go.jp; xinglin-lei@aist.go.jp; y.nishi@aist.go.jp; ishido-t@aist.go.jp; sh-nakao@aist.go.jp

W.-Y. Chen et al. (eds.), *Handbook of Climate Change Mitigation and Adaptation*,
DOI 10.1007/978-3-319-14409-2_85

Abstract

Carbon dioxide (CO_2) geological storage is the last process in carbon dioxide capture and storage (CCS). Technical issues to conduct it safely are firstly introduced. Geophysical and geochemical trapping mechanisms to store CO_2 within the reservoir, geophysical monitoring and modeling, and geomechanical modeling are then described as key issues. Finally, future directions are discussed.

Introduction

Carbon dioxide capture and storage (CCS) is a key technology for reducing the amount of carbon dioxide (CO_2) emitted into the atmosphere to mitigate climate change. It consists of several processes: separating and capturing CO_2 from large-scale emission sources, such as thermal electric power plants and steel mills, transportation, and then storing and isolating it underground or under-seabed geological formations for long periods of time. CO_2 geological storage (CGS) can be conducted using deep saline aquifers, depleted oil, and gas reservoirs as well as coal seam fixing. CO_2 injection has been also utilized for enhanced oil recovery (EOR) and enhanced gas recovery (EGR).

Since the Intergovernmental Panel on Climate Change (IPCC) published their special report on CCS in 2005 (IPCC 2005), CCS has received attention as an option in the portfolio of mitigation actions for stabilization of atmospheric greenhouse gas concentrations. Each process of CCS, however, has been developed individually, and CCS can be recognized as a combination to be practical these existing techniques as a climate change countermeasure. Drilling technologies similar to those used for the exploration and production of petroleum and gas can be applied to CGS, and CO_2 injections have been performed for enhanced oil recovery (EOR) since the 1970s (Blunt et al. 1993). Furthermore, storage in saline aquifers (Koide et al. 1992) and coal seams (Gunter et al. 1997) has been proposed.

Technical Issues

Let us consider technical challenges regarding CGS into a deep saline aquifer along the lines of life cycle of a large-scale demonstration or commercial-scale storage project. First, we need to select candidate reservoirs that seem to be suitable for the storage project. It might be onshore or offshore sites. The technical suitability criteria, such as sufficient storage capacity of reservoirs, injectivity, seal integrity, and other geological

features, should be carefully examined using wide variety of site-specific geological, geophysical, and geochemical data and numerical modeling techniques. Further studies should be necessary regarding economics, risk, and environmental aspects. How to estimate the reservoir capacity for CO_2 storage is also one of the important issues.

After the site screening process, the project proceeds to further assessment using investigation well drilling, baseline survey of geophysical monitoring, and reservoir simulation to check whether the site meets the required criteria; then an overall plan for CO_2 injection will be developed.

Once full-scale CO_2 injection is started, monitoring techniques play key roles whether stored CO_2 remains within the reservoir as expected quantitatively, which is also very important in putting CCS into practical use. Available monitoring tools are well logging using injection and observation wells, seismic reflection, gravity method, and so forth. In order to measure and verify the amount of injected CO_2 quantitatively and predict the further reservoir performance, construction of precise reservoir model, history matching using the monitoring data, and revise of the reservoir model are inevitable. Numerical simulation of subsurface changes and geophysical observables can be used to find an appropriate combination and layout of geophysical measurements for the CCS project and to detect discrepancies between actual and simulated subsurface changes, which provide a clue to find unexpected CO_2 leakage or to improve reservoir model. Monitoring, not only in operation phase, yet after operation ends should be sometimes carried out, so that cost reduction of monitoring methods is the issue to be considered. It is also an important task to quantitatively investigate how injected CO_2 is physically and chemically trapped (retained) in the structure, strata, and formation water.

By any chance, a small amount of CO_2 leakage might be occurred in the vicinity of the seafloor or shallow tapped water aquifer. To this end, evaluation of environmental impact is also indispensable. Underground stress change due to CO_2 injection is also a concern to induce micro-earthquakes. To avoid them, the appropriate injection rates and the characteristics of the reservoir are sufficiently assessed in advance and during injections. Real-time seismicity monitoring is important with high-accuracy seismic network. For earthquake-prone countries like Japan, there is a possibility that a natural earthquake occurs around. In preparation for such a situation, it is also necessary to evaluate the robustness of the reservoir in advance.

We will first discuss sealing mechanisms of CGSs and then proceed to describe state of the art of geophysical and geomechanical reservoir modeling and geophysical monitoring tools.

Evaluation of the Sealing Performance of Caprocks

Introduction

To implement the CGS technology, it is necessary to verify that the reservoir layer such as deep saline aquifer can safely store CO_2 for a long time. For this, evaluating the sealing performance of potential CO_2 leakage pathways (e.g., abandoned wells,

faults, and caprocks) is needed (e.g., IPCC 2005). In particular, the sealing performance of a caprock itself is important in terms of the: (1) leakage of CO_2, (2) CO_2 storage potential, and (3) upper pressure limit at the time of CO_2 injection.

In this paper, the author first discusses capillary pressure theory and measurement methods that describe the sealing performance of rocks. Following this, current research dealing with the evaluation of the safety of CGS is reviewed. It is important to estimate the range of variations in capillary pressures, especially in rocks. Thus, the author introduces new approaches for evaluating the sealing performance of rocks in which artificial samples, with controlled internal structures, are used to design empirical models.

Capillary Pressure Theory

Sealing Mechanisms of Porous Medium

When an immiscible non-wetting phase (mainly gas and nonaqueous liquid) permeates a porous medium (rocks such as caprocks) that has pore space filled with water, the capillary pressure P_c acting on a curved interface (meniscus) between two fluids is defined as the following Laplace equation (Washburn 1921):

$$P_c = \frac{2\sigma\cos\theta}{r} \tag{1}$$

Therein, σ is the interfacial tension between the wetting phase and non-wetting phase, θ is the contact angle of the wetting phase on the solid surface, and r is the pore throat radius within a solid.

The sealing performance of a porous medium against a non-wetting phase is determined by the magnitude relationship of P_c and the difference in the pressures of non-wetting phase and wetting phase (P_{nw} and P_w). In other words, when $P_{nw}-P_w < P_c$, the porous medium functions as a seal and prevents penetration of the non-wetting phase; however, when $P_{nw}-P_w > P_c$, penetration of the non-wetting phase occurs. In fact, there are pores (i.e., pore spaces with relatively large diameter forming between particles) and pore throats (i.e., the narrowest point of a tube connecting pores) of various sizes within the target porous medium. Therefore, even if $P_{nw}-P_w > P_c$ for a certain pore or pore throat diameter, penetration of CO_2 (breakthrough) does not occur immediately, and the non-wetting phase is blocked by the next throat of the flow path with a smaller diameter. The first breakthrough occurs when the continuous flow path for the non-wetting phase is formed between both ends of the porous medium. The flow path of the non-wetting phase at this point occupies an insignificant fraction of total pore space (i.e., the water saturation S_w is high). A further increase in the difference of P_{nw} and P_w enables the penetration through pore throats with a smaller diameter, which results in the expansion of the flow path volume of the non-wetting phase.

In contrast, a reduction of the difference between P_{nw} and P_w after the breakthrough of the non-wetting phase leads to re-imbibition of the wetting phase,

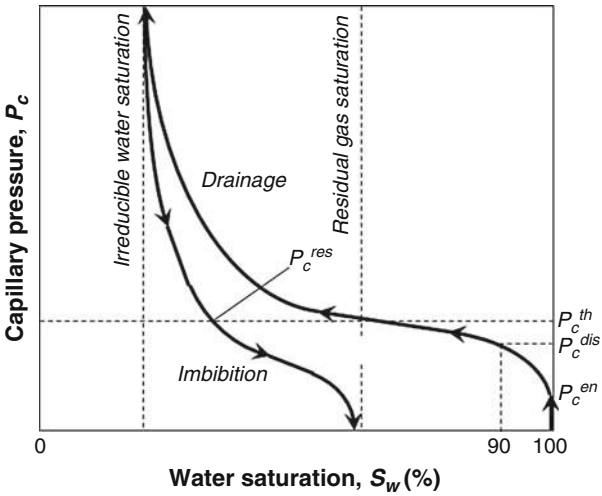

Fig. 1 Relationship of each P_c term characterizing the sealing performance (P_c^{en}, P_c^{dis}, P_c^{th}, and P_c^{res}) with the P_c–S_w curve

starting with the smallest pores and proceeding successively to larger pores (Hildenbrand et al. 2002). As a result, the connected flow path becomes blocked; the permeability k of the non-wetting phase decreases. Ultimately, the flow path in the largest pore throats is shut off, and the penetration of the non-wetting phase stops.

The drainage and imbibition process of the wetting phase within the porous medium presents a P_c-S_w curve (Fig. 1). Generally, the P_c in the imbibition process is smaller than that of the drainage process on the equal S_w. Therefore, the P_c-S_w curve between the two produces large hysteresis.

Definition of P_c

On the P_c-S_w curve, the P_c value changes with penetration of the non-wetting phase into the porous medium. However, depending on its processes, various terms are defined to characterize the sealing performance. These terms include the entry pressure P_c^{en}, displacement pressure P_c^{dis}, threshold pressure P_c^{th}, and residual capillary pressure P_c^{res}. Here, Fig. 1 presents their general definitions and relationships with P_c-S_w curve.

The P_c^{en} is the pressure when the non-wetting phase first comes in contact with the target porous medium. It is an index of the diameter of pores or maximum pore throat exposed at the porous medium surface. In this case, however, the throat does not need to be connected to the opposite end of the porous medium. The P_c^{en} is easy to identify experimentally, but the structures of pores and pore throats exposed on the surface are dependent on the effects of sample size and heterogeneity. Thus, the physical meaning of measured P_c^{en} is not necessarily clear (Pittman 1992).

Based on a breakthrough experiment of mercury in sandstone, limestone, and silty shale rocks, Schowalter (1979) defined the P_c at a mercury saturation of 10 % as the P_c^{dis}. Although these samples had a wide pore throat diameter distribution,

the non-wetting phase saturation necessary to build connected flow paths was limited to a narrow range of 4.5–17 %. Thus, it is concluded that breakthrough of non-wetting phase occurs in many rocks when S_w is approximately 90 %.

The P_c^{th} is a particularly ambiguous measure of sealing performance, and its definition has varied in past research. Generally, it refers to the difference of P_{nw} and P_w at both ends of porous medium, when building a connected flow path for the non-wetting phase in the porous medium. Experimentally, it is measured as the differential pressure when the non-wetting phase initially penetrates the porous sample. The magnitude of P_c^{th} is defined by the P_c at the maximum pore throat diameter. Katz and Thompson (1986, 1987) considered that the pressure at which mercury forms a connected pathway within the sample is equivalent to the inflection point at which the $P_c{-}S_w$ curve becomes convex upward and defined this pressure as P_c^{th}. In connection with this, Thomeer (1960) and Swanson (1981) both showed by numerical analysis and experiments, respectively, that a pore system with a good connectivity forms within rocks at the vertex of a hyperbola (i.e., a point where the slope of the tangent is 45°) obtained when the $P_c{-}S_w$ curve is expressed in a double logarithmic diagram.

Along with P_c in these drainage processes, the P_c in imbibition process is also defined. If the flow path of the non-wetting phase is completely blocked in the imbibition process of the wetting phase, residual pressure difference is generated at both ends of the porous medium and defined as the P_c^{res} (Hildenbrand et al. 2002).

Measurement Methods for P_c

Commonly, P_c is measured by mercury intrusion or gas sorption (mainly using nitrogen). The results are then converted to the P_c in the target system. In the former method, a throat diameter of several nm to several hundred μm is the target, while the throat diameter of approximately 0.1–100 nm is the target for the latter method. In either method, the principle of analysis is the same. For example, conversion to the CO_2–water system using the mercury intrusion method is conducted as follows (Purcell 1949):

$$(P_c)_{c-w} = \frac{\sigma_{c-w} \cdot \cos\theta_{c-w}}{\sigma_{m-a} \cdot \cos\theta_{m-a}} \cdot (P_c)_{m-a} \tag{2}$$

where subscripts $c{-}w$ represents the CO_2–water system and $m{-}a$ represents the mercury–air system. Specifically, the relationship between the volume of injected mercury and pressure is measured, and $(P_c)_{m-a}$ is obtained from the shape of the $P_c{-}S_w$ curve. At this point, σ_{m-a} (480 dynes/cm) and θ_{m-a} (40°) are both known; thus by using σ_{c-w} and θ_{c-w} under the target condition as the input parameters, $(P_c)_{c-w}$ is determined.

There are several methods that use the actual target fluid to determine P_c. The most common is the step-by-step approach, where the pressure of the non-wetting phase is slowly increased in steps and the P_c is obtained based on the flow rate

changes of the injected non-wetting phase and effluent wetting phase. The step-by-step approach corresponds to the measurement under static conditions in conformity with the definition of the seal; thus, it is considered to be the optimum method. However, to eliminate the dynamic effect, injection of the non-wetting phase at an extremely slow flow rate is required. As a result, it takes a few days to up to several weeks or more to measure the breakthrough of non-wetting phase (e.g., Liu et al. 1998).

In contrast with these drainage processes, the P_c^{res} is measured for imbibition processes (Hildenbrand et al. 2002). In this method, under the condition of constant volume for the whole system, the non-wetting phase is injected instantaneously at the same or higher pressure than the predicted P_c^{th}. Following this, the upstream pressure in the sample decreases, while the downstream pressure increases. By measuring pressure changes in the non-wetting phase at both ends of the sample, P_c^{res} is obtained from the difference in the final residual pressure. However, the P_c^{res} measured in experiments possibly becomes lower when re-imbibition of the wetting phase is prevented because the flow path volume is different between at drainage and imbibition process. In fact, Hildenbrand et al. (2002) confirmed that in samples with $k > 100$ nD, P_c^{res} becomes smaller than the P_c^{th} in drainage process.

To replace above static or quasi-static measurement methods, Egermann et al. (2006) proposed a dynamic measurement method, in which the non-wetting phase is injected applying a constant overall pressure drop, above P_c^{th}, across the sample. This method stands on the following mechanism. Before the non-wetting phase reaches to the sample surface, the drainage rate of the wetting phase depends on the pressure drop over the whole sample. However, once the non-wetting phase starts to penetrate within the sample, the generation of P_c^{th} at its front decreases the drainage rate of the wetting phase. From the experiments with a brine–nitrogen system, they showed that for fine-grained sandstone, carbonates, and chalk rocks with $k \geq 1$ μD, the dynamic measurement method has a similar accuracy as the step-by-step approach, and measurements can be conducted in the same time as the P_c^{res} method (Egermann et al. 2006). However, it is noteworthy that the P_c^{th} measured in this method is influenced by the flow. In other words, under dynamic conditions, the interface between the wetting and non-wetting phase takes a shape defined by the receding contact angle against the wetting phase; thus, for rocks with poor wettability (i.e., θ of the wetting phase $> 0°$), there is a possibility that θ becomes different from the equilibrium contact angle corresponding to static conditions. In such a case, P_c^{th} may be overestimated (Egermann et al. 2006).

Evaluation of Sealing Performance Under CGS Conditions

Previous Works

The sealing performance of systems for CGS is evaluated with two types of methods: a method that converts from mercury's P_c (e.g., Dewhurst et al. 2002; Bachu and Bennion 2008) and the direct measurement using CO_2 (Hildenbrand et al. 2004; Li et al. 2005; Plug and Bruining 2007; Wollenweber et al. 2010). As shown clearly in

Eq. 1, P_c depends on the type of fluid; thus, the latter method is more desirable in order to reduce uncertainties. However, the number of studies is currently limited.

As one example, Li et al. (2005) measured the P_c^{th} of N_2, CH_4, and supercritical CO_2 in anhydrite ($CaSO_4$) (a simulated sample of the caprock) using the step-by-step approach. It was shown that the P_c^{th} of CO_2 is lower than those of CH_4 and N_2, which reflects the fact that P_c^{th} is proportional to σ between gas and brine. In contrast, after injecting CO_2 with a constant flow in unconsolidated sand samples under the condition of various temperatures and pressures, Plug and Bruining (2007) kept the CO_2 pressure constant to cause the imbibition of water with a constant flow. As a result, they indicated that an increase of CO_2 pressure, which causes a decrease of σ, decreases the P_c in both drainage and imbibition processes. Hildenbrand et al. (2004) measured the P_c^{res} of N_2, CH_4, and CO_2 in argillaceous rocks from changes in the differential pressure for imbibition. In addition to the derivation of the relational expression of k and P_c^{res}, they also analyzed the pore size distribution based on P_c. In a similar manner, Wollenweber et al. (2010) conducted an experiment with limestone and marl as the target. By repeatedly injecting CO_2, a decrease in P_c^{res} was observed, which was attributed to the dissolution and re-precipitation of carbonates.

Modeling of the Correlation Between P_c^{th} and k

Generally, rocks in nature can differ greatly from their P_c^{th} because penetration depends on the flow path structure in individual samples. Therefore, from the perspective of stable CO_2 containment, it is necessary to ascertain the range of variation of caprock's P_c^{th} by measuring numerous samples instead of a single one. Moreover, the sealing performance over a widespread area must be evaluated especially for grand-scale CGS. However, the core samples that one can realistically obtain from a storage site are numerically restricted. Moreover, samples are not necessarily available over the whole site.

Because of these problems, the authors have proposed a method to represent P_c^{th}'s variation using artificial samples of which the internal structure is intergraded from a simple to a more complicated one (Sorai et al. 2014a). This methodology enables the prediction of the range of variation of rocks' P_c^{th} without repeated measurements of numerous rock samples. As a first step, the authors prepared sintered compacts of uniform spherical silica particles with diameters of 0.1–10 μm. Manufactured sintered compacts were made available for measurements of k and P_c^{th}. Specifically, P_c^{th} was measured in supercritical CO_2–water system under conditions of 1,000 m depth (10 MPa and 40 °C). The CO_2 in this condition corresponds to the supercritical phase. The CO_2 pressure at the sample bottom was increased to higher than 10 MPa in steps of 10 kPa, but the water pressure at the upper side of the sample was maintained 10 MPa. The authors determined P_c^{th} of a sample based on differential pressure at the instant when the CO_2 breakthrough was observed through a sample cell observation window.

Figure 2 shows a breakthrough image of supercritical CO_2 from the upper surface of the sample, taking the 0.1 μm particle sample, for example (Sorai et al. 2014a). Initially the CO_2 was not able to penetrate into the sample because

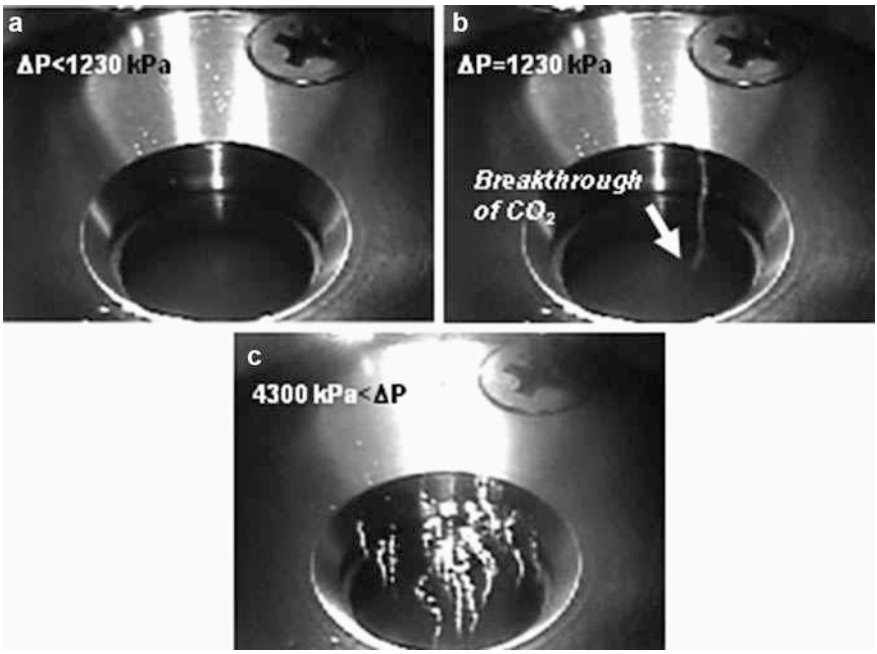

Fig. 2 Breakthrough image of supercritical CO_2 from an upper surface of a sample (Modified after Sorai et al. 2014a): (**a**) immediately before breakthrough; (**b**) breakthrough started from a specific point; and (**c**) finally the entire surface was covered with numerous breakthrough points

of a capillary effect (Fig. 2a), but a further increase of differential pressure caused CO_2 seepage from the upper surface. The breakthrough started from a specific point even though particles were packed homogeneously in the interior of a sample. The CO_2 flow passing through this point increased with increasing differential pressure (Fig. 2b). An additional rise of the differential pressure gradually increased the number of breakthrough points. Finally, the entire surface was covered with numerous breakthrough points (Fig. 2c).

Figure 3 presents the correlation between P_c^{th} and k for sintered compacts. The closest-packing structure of uniform spherical particles is defined theoretically as a line on a double logarithmic plot. Here, it is noteworthy that sintered compacts scatter around the closest-packing line because of their random packing (Sorai et al. 2014a). This variation is enhanced on lower k. Moreover, results suggest that samples with inhomogeneous particle packing are above the line, but samples in which particles are packed homogeneously overall, with inhomogeneous structures such as cracks included locally, are below the line. Figure 3 also shows experimentally obtained results for various sedimentary rocks. The P_c^{th} of rock samples, which is shifted downward further distant from the closest-packing line, seems to be lower than that of sintered compacts. This is due to the diverse sizes, shapes, and mineral compositions of the particles contained in rocks. In other words, the rock's P_c^{th} can vary greatly due to such factors.

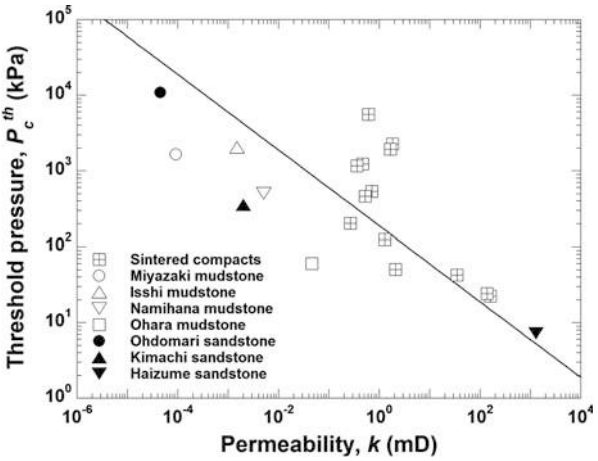

Fig. 3 Correlation between P_c^{th} and k of sintered compacts and various sedimentary rocks. The *straight line* represents calculated values for a case in which the closest packing of spherical particles is assumed

To what extent does such variation of P_c^{th} affect the predictions of the spread of CO_2 plumes after injection? For this problem, the migration of a CO_2 plume was numerically simulated for a case, where a 100 m thick alternating sandstone and mudstone layer was set as the site, and one million ton of CO_2 was injected annually into a sandstone stratum at 950–1,050 m depth for 50 years (Sorai et al. 2014b). The simulation compared the experimentally obtained upper (1.2 MPa) and lower limit (150 kPa) for the P_c^{th} of mudstone stratum, assuming the k of each stratum in the vertical direction to be 10 mD (millidarcy) and 0.1 mD respectively. The result revealed a significant impact on the spread of the CO_2 plume, particularly during the period following the completion of the injection. When P_c^{th} was increased, almost all of the CO_2 remained within the injection stratum over a longer period of time (Fig. 4a). However, when P_c^{th} decreased, CO_2 moved upward through the mudstone stratum due to its buoyancy, even after the injection had completed and reached the sandstone stratum located one layer above after 1,000 years (Fig. 4b). The magnitude of P_c^{th}, therefore, has a significant impact on the predictions of CO_2 behavior after storage. Determining the variation range of rock's P_c^{th} will be an issue tackled in the future. As the next step, the authors are investigating the impact of particle configuration and mineral composition on P_c^{th}, in addition to the effect of particle size distribution arising from mixtures of particles with various sizes.

Conclusion of This Section

With respect to the sealing performance of rocks, fundamental theory, measurement and analytical methods, and the application of obtained data have been well studied, particularly in the field of petroleum exploration. The acquired knowledge is directly useful in evaluating the safety of CGS. However, some questions remain regarding CGS, which were not necessary for consideration in petroleum exploration, such as the interaction of the non-wetting phase (CO_2) and wetting phase

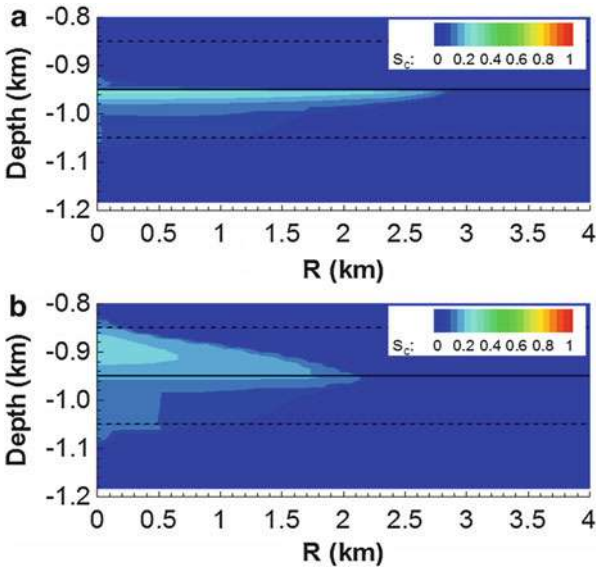

Fig. 4 Impact of difference in P_c^{th} of mudstone stratum on CO_2 plumes (After Sorai et al., 2014b). The *solid line* represents the upper edge of the sandstone stratum, while the *dotted lines* represent the *upper* edge of the mudstone stratum. The P_c^{th} of the mudstone stratum corresponds to (**a**) 1.2 MPa and (**b**) 150 kPa, respectively

(formation water) and the phase change of non-wetting phase itself. Moreover, even for existing evaluation methods, many issues remain such as the development of an accurate and efficient measurement method and the establishment of a theory that can be applied to rocks with complex internal structures. Future work should hopefully involve new approaches, such as modeling of P_c^{th} using artificial samples with controlled internal structures, which can further develop the methods for the evaluation of sealing performance for CGS.

Evaluation of Geochemical Processes

Introduction

Implementing the CGS requires the quantitative evaluation of the behavior and effects of the injected CO_2. Regarding this, the focus is generally on physical processes, such as CO_2 migration, starting immediately after CO_2 injection. This leaves many unknowns in the long term ($\geq$1,000 years) (IPCC 2005) such as the effect of geochemical interactions. For instance, in storage aquifers in which the highest storage potential is expected, active geochemical processes are expected to occur due to the acidification of formation water caused by dissolution of CO_2. The time scale for this process is expected to be long term, e.g., ranging from several hundred years to several tens of thousands of years. However, some processes may start immediately after CO_2 injection in areas near injection wells and in rocks containing highly reactive carbonate minerals.

In this paper, the author presents the target processes and the methods for understanding geochemical processes related to CGS in aquifers. The author focuses on numerical simulations as the essential approach for the evaluation of long-term geochemical processes. To improve model reliability, the author examined conditions and issues to improve the accuracy of input parameters. The paper also includes an example of reaction rate measurements for carbonates at hot springs.

Approach to Evaluation of Geochemical Processes

On CGS in aquifers, geochemical processes on various temporal and spatial scales are predicted to occur in components of the storage system, such as reservoirs, sealing layers, cracks, faults, wellbores, and upper aquifers. These processes include the dissolution of CO_2 in formation water, reactions of acidified water with surrounding rocks, pore-filling materials, and cement, carbonation of CO_2 through reaction with mafic or ultramafic rocks, evaporation of formation water (dry-out), formation of CO_2 hydrate, groundwater pollution, etc. These processes are directly related to the evaluation of important issues associated with implementing CGS. These issues include: the storage potential (geochemical trapping) based on long-term mechanisms; CO_2 injectivity in reservoirs; leakage risks from caprock, cracks, faults, and wellbores; and environmental effects on shallow groundwater.

Four types of approaches are applied for the evaluation of the abovementioned issues: field tests, laboratory experiments, natural analogue studies, and simulation studies. Each method targets a different temporal and spatial scale. Laboratory experiments have significant constraints on the temporal and spatial scales, yet conditions can be strictly controlled. Thus, laboratory experiments are suitable for elucidating mechanisms and the acquisition of parameters for each fundamental process. In contrast, natural analogue studies make it possible to understand phenomena occurring on the geological time scale. However, the transitional history of the environmental conditions is not always clear; thus, these are not suitable for acquisition of quantitative data related to reaction kinetics. On the other hand, simulation studies can deal with phenomena of all scale and play a crucial role in complementing other approaches. Especially in recent years, a three-dimensional reactive transport simulation is becoming mainstream with drastic advances in computing power (e.g., Xu et al. 2003; Johnson et al. 2004; White et al. 2005). However, as will be later discussed, there are many issues regarding the reliability of calculation results.

Field tests are quite efficient for conducting quantitative analysis of CO_2 behavior in underground conditions. Starting with the Norwegian Sleipner Project in 1996 for the study of CGS in aquifers, demonstration projects of various scales are currently in progress around the world. However, geochemical approach mainly bases on ex situ analyses of brine and rock samples. In other words, there is no effective tool for in situ monitoring of geochemical processes.

The Role and Directionality of Simulation Studies

Geochemical processes are phenomena that occur on an extremely long time scale. Thus, the ultimate evaluation of these processes must rely on numerical simulations. However, as previous studies have indicated, current simulations are based on many assumptions with various uncertainties and unknown parameters. Thus, for the long-term evaluation of CGS, these uncertainties must be reduced in order to increase the accuracy of simulation results. Here, to improve the prediction accuracy of geochemical processes, the author examined the parameters that are especially important for simulation studies including contributions from each of the abovementioned approaches.

Equilibrium Parameters

Equilibrium parameters include the density, solubility, and enthalpy in the CO_2–water system and so forth (Gaus et al. 2008). For these parameters, it is necessary to formulate as a function not only of temperature, pressure, and salinity but also of the effect of impurities and acidic gases other than CO_2.

Interfacial tension and wettability that regulate capillary pressure of CO_2 in rocks are also important parameters to which geochemical processes indirectly contribute. As for interfacial tension, a relatively large number of measurements have already been made for the CO_2–water system (e.g., Bachu and Bennion 2009), and in part, expansion into multicomponent systems such as a mixed gas of CO_2 and H_2S is underway (Shah et al. 2008). Wettability is difficult to evaluate due to its complex behavior depending on the surface conditions; thus, subsurface minerals are often assumed as a condition of the surface being completely saturated with water (i.e., contact angle of 0°). However, some of the recent studies showed that contact angles of mica and quartz change in the presence of CO_2 (e.g., Chiquet et al. 2007). Therefore, additional data from laboratory experiments are desired.

Kinetic Parameters

Generally, the rate formula for the mineral reaction is expressed as the following Eq. 3 (e.g., Lasaga 1998):

$$\text{Rate} = kA\exp(-E/RT)\,\Pi a_i^{n_i} f(\Delta G_r), \tag{3}$$

where k is the rate constant, A signifies the reactive surface area, E is the activation energy, R denotes the gas constant, T is the absolute temperature, a_i is the activity of chemical species i, and n_i stands for the reaction order for a_i. The last term $f(\Delta G_r)$ corresponds to a function related to the Gibbs free energy change, which is expressed as a function of the degree of saturation:

$$\Delta G_r = RT\ln\left(Q/K_{eq}\right), \tag{4}$$

where Q signifies the activity product and K_{eq} is the equilibrium constant. As shown clearly in Eq. 3, the reaction rate is calculated as the product of each parameter;

thus, just one inaccurate parameter can reduce the overall reliability of the calculated results.

The US Geological Survey (USGS) compiled the value of k, E, and n for H^+, in acidic, neutral, and alkaline ranges, based on the dissolution rate data for all the important minerals (Palandri and Kharaka 2004). This is currently one of the most useful reaction rate database, but these values are not always measured under conditions consistent with those in CGS. As a result, reaction rates may change due to differences in reaction mechanisms.

The A has long been discussed as the parameter with the highest uncertainty (e.g., Lasaga 1998). Especially when obtaining A, there is no agreement on whether the commonly used BET method – based on the amount of adsorbed inert gas – expresses the actual reactive surface areas. In addition, natural mineral surfaces are different from fresh cleavage planes often used in laboratory experiments and may be influenced by adhesion of clay minerals, coating of secondary products precipitated from leaching components, etc. (Blum and Stillings 1995; White and Brantley 2003). These effects of surface conditions also should be investigated further.

The $f(\Delta G_r)$ have mostly been overlooked in numerical simulations until now, as the knowledge of dissolution mechanism is especially limited. As a result, it was often approximated as a linear function of Q/K_{eq} based on the transition state theory (e.g., Xu et al. 2005). However, based on dissolution experiments of feldspars in recent years, it has been shown that $f(\Delta G_r)$ follows a sigmoidal curve, or an irregular shape is produced in response to the difference in dissolution mechanisms (Burch et al. 1993; Lüttge 2006; Hellmann and Tisserand 2006; Sorai and Sasaki 2010). On the other hand, the function form of the ΔG_r in the precipitation should incorporate the nucleation process prior to the growth. Most simulations assume that secondary minerals precipitate immediately after the solution becomes supersaturated (i.e., $Q/K_{eq} > 1$). In fact, however, nucleation first occurs when a certain critical supersaturation is achieved. In addition, rates differ in homogeneous nucleation in free space and heterogeneous nucleation on the wall. Especially the heterogeneous nucleation rate is predicted to change significantly depending on the property of the wall surface.

A factor that has not been considered much in previous numerical simulations is the activity of various impurities other than H^+, i.e., promotion and inhibition effects of the reaction. It is unrealistic to examine the effects of all chemical species dissolved in the formation water for each mineral in this regard. However, for example, in the precipitation of calcite – the most important CO_2 fixing mineral – it has been known for a long time that divalent cations such as Mg^{2+} function as inhibitory factors (e.g., Morse et al. 2007). Therefore, given the fact that the formation water generally includes these ions, effects of impurities should be taken into account at least in such reactions that relate to the nature of geochemical processes.

Setting Conditions

Simulation results are strongly influenced by the setting of primary and secondary minerals. Primary minerals can reflect the analysis of the rock samples from the site, but generated secondary minerals cannot be determined based on thermodynamically stable relationships only. In other words, when conducting an analysis from a kinetics perspective, in addition to the setting of a metastable phase as an intermediate product, the deviation from the thermodynamically stable region caused by changes in environmental conditions must also be considered (Gaus et al. 2008).

The simulation of CGS into sandstone aquifers often assumes that the CO_2 is mineralized into dawsonite. However, both thermodynamic and kinetic properties of dawsonite are not fully understood yet, except for some thermodynamic parameters (Bénézeth et al. 2007). Regarding this, the dawsonite dissolution rate measured at 80 °C and pH range of 3–10 indicates that dawsonite is in a stable phase only under high CO_2 pressure conditions; it dissolves rapidly as the CO_2 pressure decreases and mainly precipitates as kaolinite (Hellevang et al. 2005). Therefore, to avoid the overestimation of mineral trapping, care should be taken when assuming dawsonite. Similar issues exist for dolomite and magnesite, for which the precipitation mechanism is still unknown.

Measurement of Reaction Rates of Carbonates at Hot Springs

The CO_2 stored in aquifers dissolves in formation water to become carbonic acid, which in turn dissolves mineral components in rocks over a long period of time. Reaction rates of minerals are ordinarily extremely slow, but carbonates such as calcite or aragonite (calcium carbonate in both cases) are exceptions as they have high reactivity. When carbonates dissolve within alternating sandstone and mudstone layers, particularly in cases where the thicknesses of respective strata are thin, it can potentially lead to the formation of a leakage path to upper strata. In contrast, precipitation of carbonates can also occur when cations reaching from minerals in a sandstone stratum combine with bicarbonate or carbonate ions. In such cases, sealing performance would be enhanced due to the clogging of the sandstone stratum. The reaction of carbonates is, therefore, one of the most important geochemical processes associated with CGS, and knowing its rate is essential for geochemical simulations of CGS.

It has been pointed out that mineral reaction rates measured in laboratories are completely different from those in nature because of the effects of various factors, such as reaction time, surface area, surface conditions (defects and coatings), pore water compositions, mass transfers, and biological activities (Blum and Stillings 1995; White and Brantley 2003). For this problem, the authors attempt to obtain carbonate reaction rates at carbonated and bicarbonated springs in various regions of Japan, regarding these sites as the natural analogue field of CGS. Selected sites

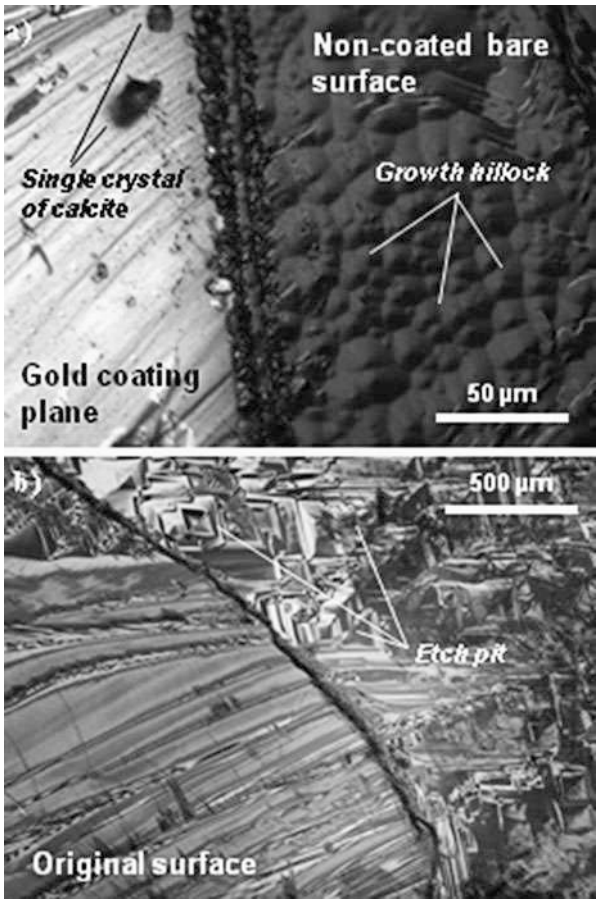

Fig. 5 Differential interference microscope images for reacted calcite surface: (**a**) growth experiment at Masutomi Hot Springs (30 min after the start of the reaction) and (**b**) dissolution experiment at Shichirida Hot Springs (336 h after the start of the reaction)

contain either undersaturated or supersaturated waters with respect to carbonates. At each site, cleaved single crystals of various carbonate species were immersed in the spring water for up to 1 month. Each sample was taken out at prescribed times for surface observations. A part of the sample surface was covered with a sputtered gold thin film or a silicon rubber for an inert reference area.

Figure 5a shows the calcite cleavage plane reacted in the supersaturated water at Masutomi Hot Springs in Yamanashi, Japan, as viewed with a differential interference microscope. Numerous pyramidal-shaped pattern, referred to as growth hillocks, formed immediately after the start of experiment. These growth hillocks grew in size and repeatedly combined with the progress of reaction. It is noteworthy that calcite single crystals in the shape of rhombohedron formed on a gold coating plane. This signifies that the solute flux applied uniformly on the sample was directly incorporated on a non-coated bare calcite surface to form growth hillocks, but the heterogeneous nucleation of calcite occurred on a gold coating plane, since solutes were not incorporated into gold. In contrast, Fig. 5b corresponds to the sample

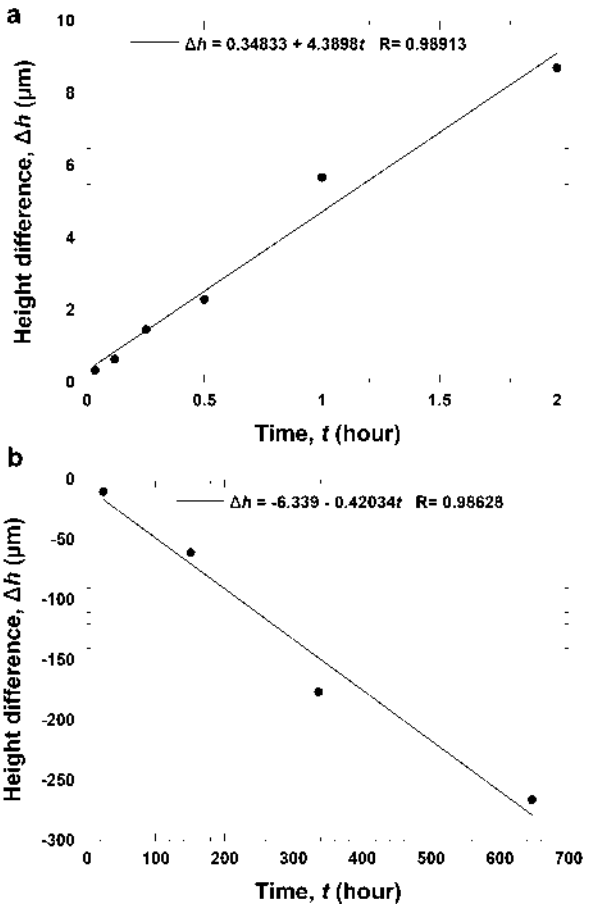

Fig. 6 The temporal profile of the height difference between the reacted and reference surface (gold coating or original surface): (**a**) growth experiment at Masutomi Hot Springs and (**b**) dissolution experiment at Shichirida Hot Springs

reacted in the undersaturated water at Shichirida Hot Springs in Oita Prefecture. The length scale of the image is different from that of Fig. 5a, since the change of surface configuration was greater due to the long duration of the experiment. The undersaturated water produced numerous etch pits in the shape of inverted pyramids, a pattern of dissolution. These etch pits were expanded and combined with the progress of reaction.

A phase shift interferometer with a nanoscale vertical resolution and a laser microscope were used to take measurements of the height difference Δh between coated and non-coated areas of these calcite cleavage planes (Sorai and Sasaki 2010). Figure 6 presents the time-course change of the Δh, corresponding to the experiments shown in Fig. 5 (Sorai et al. 2014b). The Δh for the former was expressed as a positive value, being growth from the reference plane, while the latter was expressed as a negative value, being regression from the reference plane. The growth and dissolution rates were estimated to be 3.3×10^{-5} and

3.2×10^{-6} mol m^{-2} s^{-1}, respectively, from the slope of a fitting line to the temporal profile. However, the growth and dissolution rates derived based on the USGS database described above were 4.5×10^{-5} mol m^{-2} s^{-1} and 2.9×10^{-6} mol m^{-2} s^{-1}, respectively, under identical temperature and pH conditions (Palandri and Kharaka 2004), showing that the experimentally obtained values, particularly with regard to the growth rate, were smaller by almost 30 %. Regarding this, the USGS database defines the reaction rate as a function of temperature, pH, and the degree of saturation, with no consideration given to the effects of impurities contained in the solution. Therefore, it is possible that the growth rate was reduced by trace dissolved components, primarily magnesium ions, in the field experiment. On the other hand, the effect of impurities on the dissolution process of calcite is presumably small because the actually measured and calculated values are practically identical for the dissolution rate.

Conclusion of This Section

Geochemical processes improve the safety of a reservoir by stabilizing and changing the form of CO_2 on geological time scales; however, geochemical processes can also result in negative effects such as increased leakage risks near injection wells and lowered injectivity. Evaluation of these geochemical processes tends to rely on numerical simulations owing to the long time scales involved. However, the author highlights that many previous studies point out the lack of sufficient knowledge on reaction kinetics, especially compared to the equilibrium theory. Therefore, to improve the reliability of simulation studies, data with high uncertainties and assumptions should be examined on a case-specific basis while referencing appropriate monitoring results of demonstration tests, laboratory experiments, natural analogue studies, etc.

Geophysical Monitoring and Modeling

Introduction

In CO_2 geological storage projects, monitoring is indispensable for verification of CO_2 storage. Various techniques are used to monitor the location of CO_2 injection and volumetric extent of CO_2 migration and detect possible leaks of CO_2 at faults and seals. Monitoring is required to implement for long time, beginning with the survey and development of a site, continuing throughout the CO_2 injection period, and even after the site is closed. Therefore, it is essential to develop monitoring technology that is cost-effective. In order to make CO_2 geological storage (CGS) projects acceptable to society, consideration of long-term cost is also very important.

Monitoring technologies for CGS are divided into four main categories: (1) atmospheric monitoring tools, (2) near-surface monitoring tools, (3) subsurface

monitoring tools, and (4) data integration and analysis technologies (Litynski et al. 2012). Here we describe geophysical monitoring and modeling technologies concerning the latter two categories.

Seismic Monitoring

Geophysical exploration methods that detect the two- or three-dimensional distribution of physical properties from the ground surface/sea surface are used as effective monitoring methods that can supplement well data (which provide direct information of the deep underground, but consist only of linear or point measurements). Among them representative one is seismic monitoring using active seismic methods such as seismic reflection, vertical seismic profiling (VSP), and cross-hole seismic tomography. Seismic monitoring is considered to be the standard monitoring method in CGS worldwide (e.g., Eiken et al. 2011). In these methods, an elastic wave emitted from multiple source points by a moving artificial hypocenter is received by a multichannel seismometer array spread across the wellbores or on the ground surface/seabed and then analyzed to estimate the elastic properties of the medium (e.g., elastic wave velocity and attenuation) through which the elastic wave propagates. The underground structure and physical state are estimated based on the results. Since it is believed that the outline of the underground area where injected CO_2 has spread (a CO_2 plume) can be detected through this process, active seismic exploration method, especially seismic reflection, is considered to be an extremely useful method for CO_2 monitoring.

In active seismic exploration, a "snapshot" that captures the underground CO_2 plume at a given time is obtained. This process of taking a snapshot is repeated over appropriate time intervals to detect temporal variations of the snapshots. In the seismic reflection, a method that obtains a "three-dimensional snapshot" using sources and geophones distributed on the ground surface is called three-dimensional (3D) reflection method. It is also called 4D reflection method since a time axis is added in monitoring. However, such seismic reflection surveys are expensive, in particularly expensive to conduct surveys in the ocean, where a ship is used for the deployment of sources and geophones. Since sources and geophones are spread over a wide area, negotiations with local people and officials in the survey area are also required, which can influence social receptivity to CGS. Therefore, it is desirable to decrease the number of 3D seismic reflection survey when monitoring needs to be conducted regularly. There are also the following fundamental limits: seismic waves can only detect elastic properties, and the detectable structures and resolution can change depending on the frequency, energy, and source location of the elastic wave. Considering these limitations, it is worthwhile to take into account the use of other geophysical methods, in particular passive exploration methods, which can supplement seismic methods and reduce overall monitoring cost.

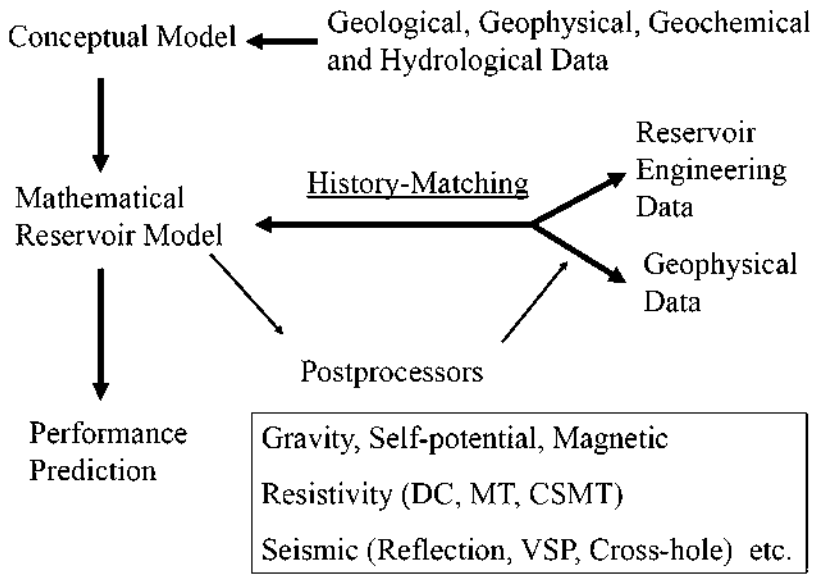

Fig. 7 Geophysical postprocessors. Various computational postprocessors permit the user to calculate temporal changes that are likely to be observed if geophysical surveys of an operating and/or closed CO_2 injection site are repeated from time to time. Results may be used to supplement conventional reservoir engineering measurements in history-matching studies undertaken during reservoir model development

Geophysical Modeling

To appraise the utility of geophysical techniques in monitoring of CO_2 injected into deep aquifers, Ishido et al. (2011) carried out numerical simulations using the so-called geophysical postprocessors. The geophysical postprocessors calculate temporal changes in geophysical observables that result from changing underground conditions computed by reservoir simulations (e.g., Pritchett et al. 2000; Ishido et al. 2011, 2015). The purpose of the development is to enable us to use monitoring data from repeat and/or continuous geophysical measurements in history-matching studies (Fig. 7). The name, postprocessor, comes from the fact that there is no need to couple and solve governing equations for geophysical phenomena with governing equations for reservoir simulations to calculate changes in geophysical observables; rather, they can be solved using the results of a reservoir simulation (snapshots) "afterwards." For example, electrokinetic phenomena handled by the self-potential postprocessor (Ishido and Pritchett 1999) are current flows coupled with fluid flow within the pores of rocks. It handles a phenomenon in which the potential difference (streaming potential) is created proportional to the pore pressure difference. The streaming potential leads to secondary pressure difference due to an electroosmotic effect at the same time, but the secondary pressure difference is extremely small and can be neglected.

Thus, governing equations for electrokinetic phenomena do not need to be solved at the same time as the governing equations for reservoir simulations. A simulation that couples "G" (geophysical observables) to a reservoir simulation, which is a TH coupled simulation in which governing equations for the transport of T (heat) and H (fluid/chemical species) are coupled and solved simultaneously, is generally not required. However, when calculating underground stress changes and/or ground surface deformation due to pressure or temperature changes, a THM coupled simulation that includes M (mechanics) should be performed if changes in porosity and permeability due to stress changes are important.

In the applications to CGS, the geophysical postprocessors can be used for the following purposes:

1. Planning of an appropriate monitoring system: Effective methods and way of monitoring can be chosen based upon prediction of changes in geophysical observables, which are calculated from underground flow models and potential risks associated with vertical faults, openings in the caprock, etc.
2. Quick understanding of the underground conditions: Whether or not injected CO_2 is stored as predicted can be judged by comparing the monitoring data obtained from actual geophysical measurements with predicted changes. If the behavior that is different from the predictions possibly arises from potential risks, the selection and deployment of effective monitoring methods can be examined.
3. Verification of the storage model: If the measured changes in geophysical observables are different from the predictions, the underground flow model is improved so as to reproduce the measured changes (history matching). The calibrated flow model provides a basis for reliable long-term predictions.

Flow Simulation Based Upon Tokyo Bay Model

Here, illustrative computations which have been carried out using various geophysical postprocessors are described, based upon the results of numerical simulations of CO_2 injection into an aquifer system underlying a portion of the Boso Peninsula/Tokyo Bay area and calculations of the temporal changes in geophysical observables caused by changing underground conditions as computed by the reservoir simulation.

The Tokyo Bay area in the southern Kanto plain is a representative industrial area in Japan. A number of large-scale CO_2 emission sources surround the Tokyo Bay. From a geological point of view, sedimentary strata underlying the Tokyo Bay area are believed to be suitable for open aquifer CO_2 storage (e.g., Okuyama et al. 2009). Late Pliocene to Middle Pleistocene Kazusa Group sediments are found below several hundred meters depth, comprising an alternation of turbidite sandstone and pelagic to hemipelagic mudstone. The sandstone is poorly consolidated with high porosity and permeability. The mudstone, on the other hand, is well consolidated, having fairly high porosity but very low permeability. Below the Boso Peninsula, the Kazusa Group sediments are more than 2,000 m thick, almost undeformed, and dip to the west toward Tokyo Bay at very low angles (less than 10°).

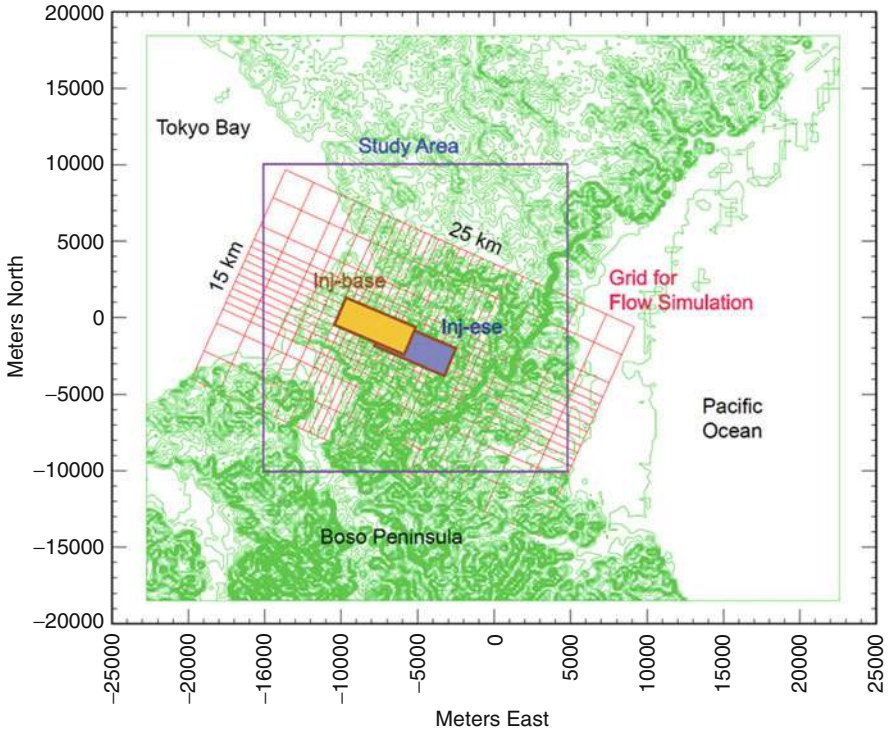

Fig. 8 Study area (in the Boso Peninsula, Japan) considered in the numerical simulation. Also shown is a top view of the computational grid blocks used for flow simulations. "Inj-base" and "Inj-ese" indicate the location of CO_2 injection site for the base and the ESE injection scenarios, respectively

A three-dimensional model is covering a 25 × 15 km^2 area (Fig. 8) and representing 2,500 m of alternating sandstone- and mudstone-dominated formations based broadly upon the geological structure underlying the Tokyo Bay area (Fig. 9). In the base-case model, the horizontal and vertical permeabilities are simply assumed as 50 and 10 mD (1 mD = 10^{-15} m^2), respectively, for the sandstone-dominated (aquifer) formations, and 10 and 1 mD, respectively, for the mudstone-dominated (seal) formations. In view of the relative thinness of individual mudstone layers compared to the vertical size of the computational grid blocks (=100 m), they assumed a relatively high average permeability for the mudstone-dominated seal formations. The porosity is assumed to be 0.2 for all formations. Relative permeability models for CO_2 gas and liquid water are represented by Corey-type curves (with 0.1 residual saturation) and van Genuchten-type curves (with 0.2 residual saturation), respectively (Fig. 10). Capillary pressure (gas or liquid CO_2 phase vs. aqueous phase) is represented by a van Genuchten-type model, and the capillary pressure magnitude is 3.58 kPa when the water saturation is ∼0.8 in the base model (Fig. 11).

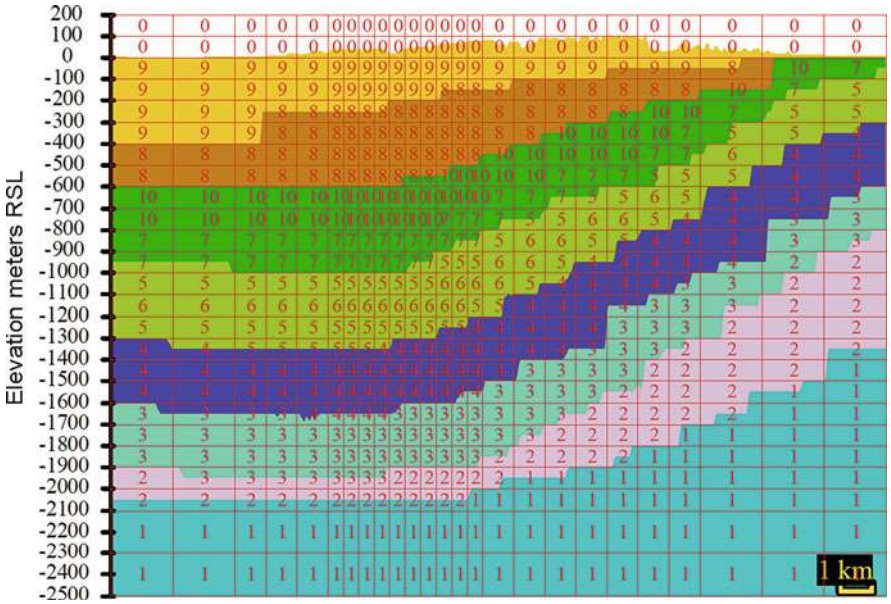

Fig. 9 Distribution of rock formations in the WNW-ESE section (x-z plane) at j = 8. The Umegase formation is indicated by the *dark blue* color.

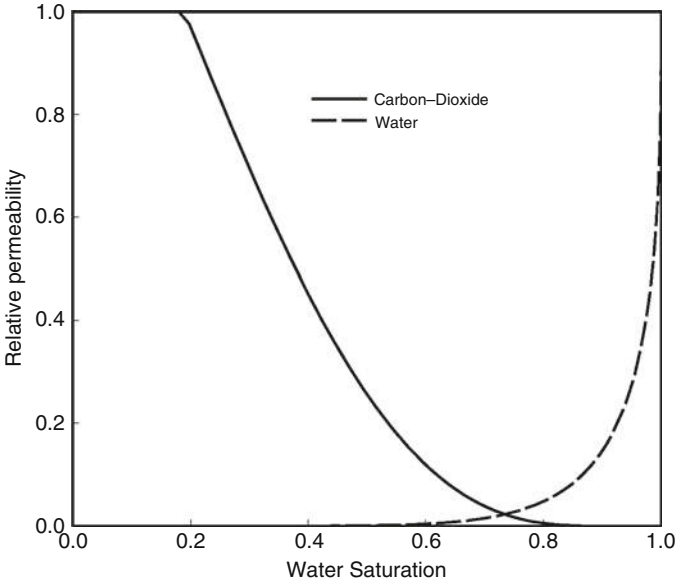

Fig. 10 Relative permeabilities for the non-wetting (carbon-dioxide gas, liquid carbonate) and wetting (water) phases. Residual saturation for the wetting (non-wetting) phase is 0.2 (0.1)

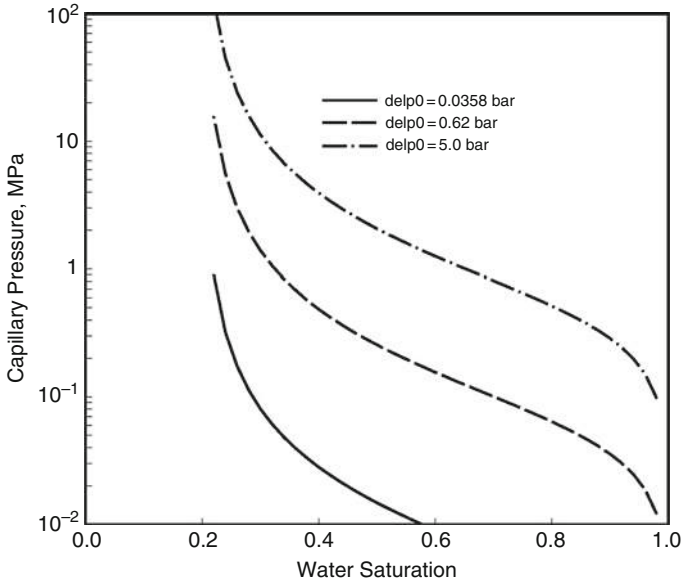

Fig. 11 Van Genuchten capillary pressure curves parameterized by delp0 (capillary pressure magnitude when the water saturation is ~0.8)

In the initial state, all of the pore space within the computational grid is full of motionless liquid H_2O (with small amount of dissolved CO_2). At the outer lateral boundaries, the fluid pressure distribution is maintained at the initial (hydrostatic) value. At the top boundary, the pressure and temperature are maintained at 1 bar and 15 °C, respectively. The bottom boundary is impermeable, and its temperature varies between 40 °C at x = 0 km and 60 °C at x = 25 km.

In the numerical simulations, the "STAR" reservoir simulation code (Pritchett 1995, 2002) was used with the "SQSCO2" fluid constitutive module (Pritchett 2008) which represents the thermodynamics and thermophysical properties of H_2O–NaCl–CO_2 mixtures over the range from liquid-CO_2 to supercritical-CO_2 conditions including the three-phase region. (For test problem #3 in a code intercomparison project (Pruess et al. 2002), the STAR/SQSCO2 gave almost the same results (dry-out region development, disolved CO_2 mass fraction, etc.) as those given by the TOUGH2/ECO2N simulation (Pruess 2005). See Fig. 12) Similar to the TOUGH2/ECO2M (Pruess 2011), the STAR/SQSCO2 can describe all possible phase conditions for brine–CO_2 mixtures, including transitions between super- and subcritical conditions and phase change between liquid and gaseous CO_2.

Simulations were carried out for 50 years of injection (at a rate of ten million tons of CO_2 per year) into a sandstone-dominated layer at 1,400 m depth (the Umegase formation) at the grid blocks (i = 10, 11; j = 8, 9; k = 9; "Inj-base" shown in Fig. 8) followed by 1,000 years of shut-in. The internal energy of the injected

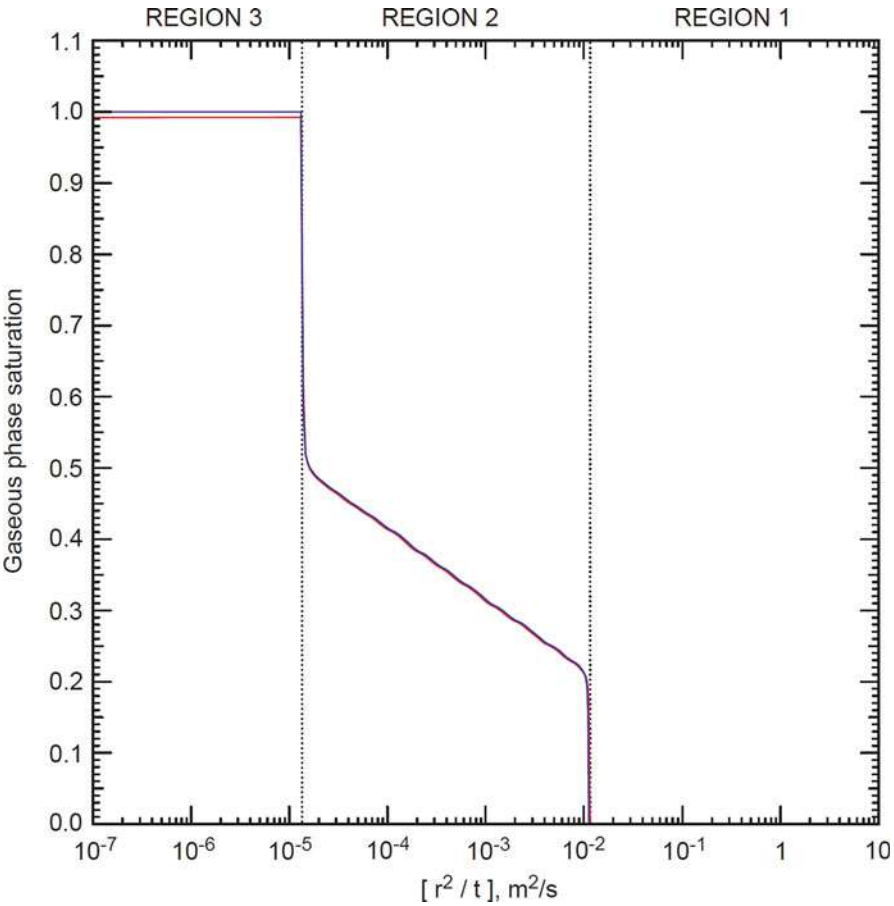

Fig. 12 A result of the "STAR/SQSCO2" application to test problem #3 in a code intercomparison project (Pruess et al. 2002). Computed distribution of gaseous-phase saturation as a function of the similarity variable ξ ($= r^2/t$) for freshwater (blue) and seawater (red) cases (after Pritchett 2008)

CO_2 corresponds to a temperature and pressure of ~34 °C and ~144 bars (same as in situ conditions prior to injection). Here the results for two variants of the base case model: "*L-k*" and "*H-k*" models are presented, in which the horizontal/vertical permeabilities of the Umegase formation are 50 mD/ 10 mD and 500 mD/ 100 mD, respectively. Figure 13 shows the distribution of pressure, temperature, and phase saturations at t = 50 years (when injection ceases) and 1,050 years (after 1,000 years of shut-in) for the "H-h" model. At t = 50 years, the injected CO_2 remains as a supercritical free phase with the saturation 0.2 or more within the sandstone-dominated layers (the Umegase and underlying Otadai formations). After injection ceases, the CO_2 density decreases (and its volume increases) due to pressure release. The supercritical CO_2 then gradually migrates upward for hundreds of

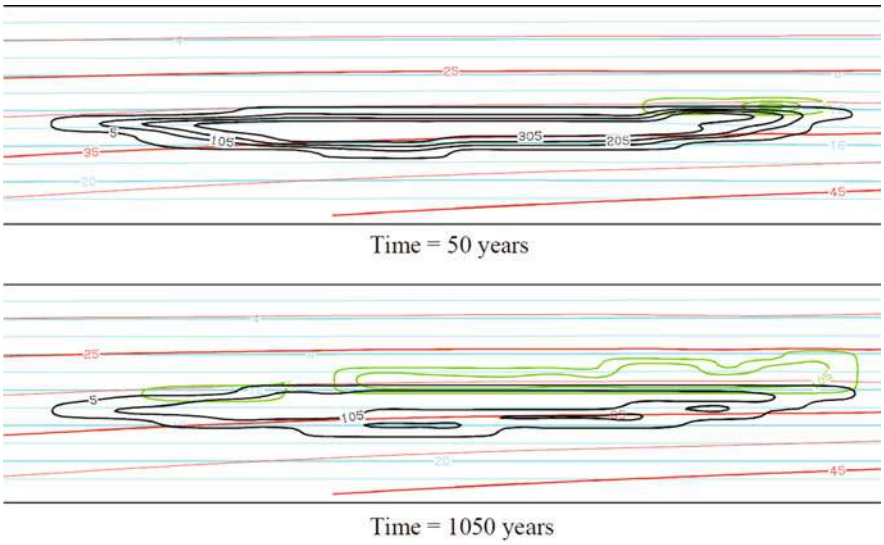

Fig. 13 "*H-k*" model: pressure (*cyan*), temperature (*red*), liquid CO_2 (*green*) and gas (*black)* saturation contours in x-z plane at j = 8 at t = 50 and 1050 years. Contour interval is 2 MPa for pressure and 5 °C for temperature. Liquid CO_2 and gas saturation contour labels are 0.005, 0.105, 0.205 and 0.305. The region shown in the figure extends 2500 m in the vertical (z) direction and 10,000 m (i = 3, . . ., 19) in the x-direction

years due to buoyancy and penetrates into the overlying seal layer (the Kokumoto formation). However, the rising gaseous CO_2 is then densified at shallower levels as the temperature decreases below the critical temperature at sufficiently deep levels and becomes relatively immobile liquid CO_2 condensate. As shown in Fig. 14, at t =1,050 years about 17 % of the CO_2 is trapped as immobile CO_2 condensate at near residual saturation, and the remaining CO_2 is trapped as dissolved CO_2 in the aqueous phase (41 %) and supercritical residual gas below the seal layer (42 %). Other similar calculations have shown that if a much lower permeability (i.e., 0.1 mD) or a larger capillary pressure is assumed for the seal layer than in the base-case model, CO_2 intrusion into the seal layer in the postinjection period will become negligible.

Prediction of Changes in Geophysical Observables

Next, various "geophysical postprocessors" were used to calculate time-dependent earth-surface distributions of seismic observables (from reflection, VSP, or tomography surveys), microgravity, electrical self-potential (SP), and apparent resistivity (from either DC or MT surveys). The temporal changes are caused by changing underground conditions (pressure, temperature, gas saturation, concentrations of dissolved species, flow rate, etc.), as computed by the reservoir simulations.

Figures 15 and 16 show seismic sections calculated by applying the seismic (reflection survey) postprocessor (Stevens et al. 2003) to the reservoir simulation

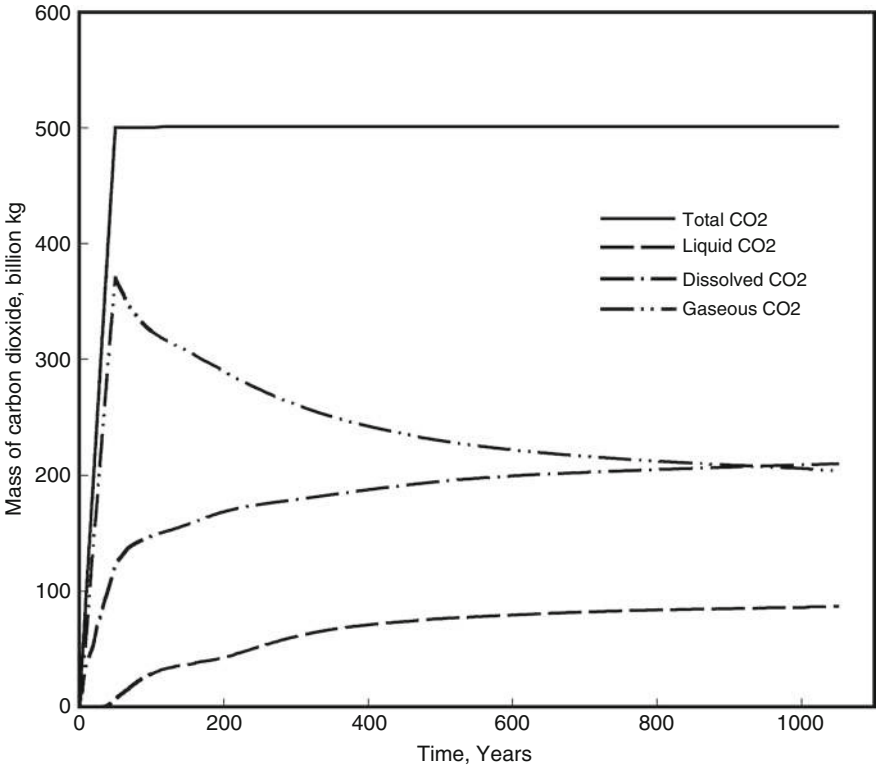

Fig. 14 "*H-k*" model: total mass of carbon-dioxide, mass of liquid CO_2, mass of CO_2 dissolved in water, and mass of gaseous (and supercritical) CO_2 in the computational grid

results. The reflected waves correspond to the upper and lower boundaries of regions containing CO_2 gas around the injection wells. In this case, the seismic postprocessor calculated the seismic velocity and Q factor in the water/gas two-phase regions using a "patchy saturation" model (e.g., Mavko et al. 2009). In this model, the low-frequency and high-frequency limiting bulk moduli are given by Gassmann's relation and by Hill's relation, respectively. The "standard linear solid" is applied to predict the velocity dispersion and attenuation with the characteristic frequency, which is inversely proportional to the square of liquid cluster size which depends on the liquid-phase saturation. The reflection events for the "*H-k*" model (Fig. 15) corresponds to the CO_2 gas region at t=50 year shown in Fig. 13. Compared with this, the seismic events for the "*L-k*" model (Fig. 16) remains in a narrower region, which corresponds to a less horizontal expansion of CO_2 gas region due to lower permeabilities of the injection aquifer (the Umegase formation) assumed for the "*L-k*" model.

Figure 17 shows "sounding results" calculated by using the magnetotelluric (MT) postprocessor for the "*L-k*" model. In this calculation the postprocessor assumes that the pore fluid salinity is homogeneous at 0.01 below the upper surface

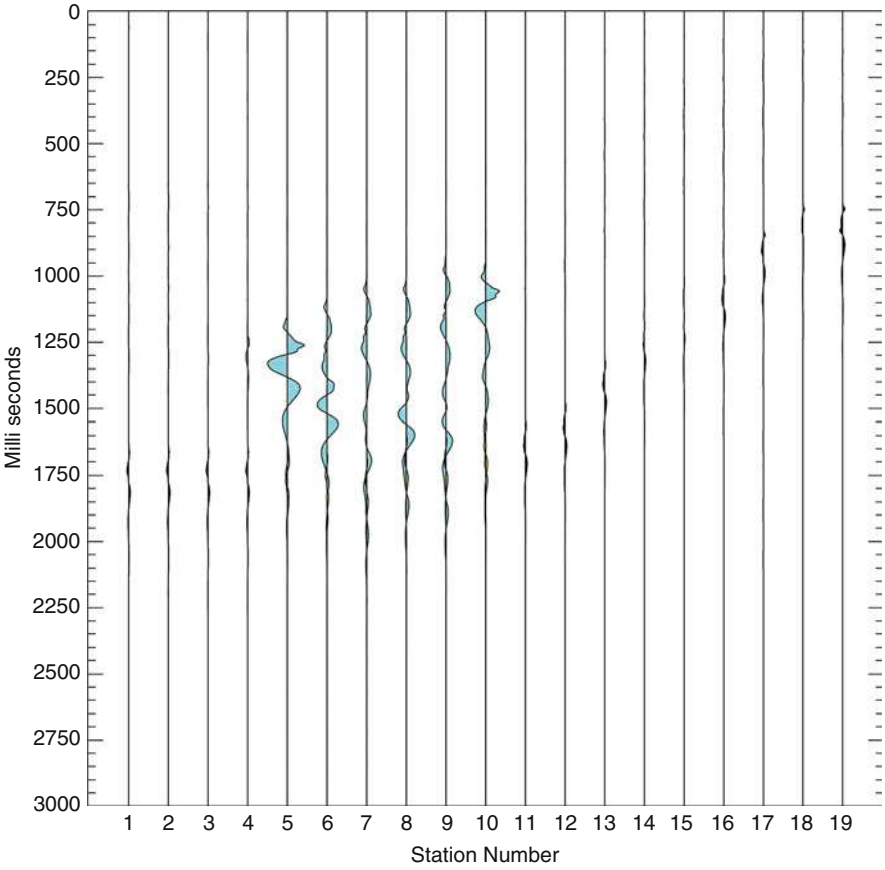

Fig. 15 "*H-k*" model: comparison of time-series results (*blue*) calculated for a seismic reflection survey after 50 years of CO_2 injection with those for an initial survey (*yellow*) across the center of the study area (along 24 km-long A–A′ line shown in Fig. 18). The results overlapped with each other are shown by *black color*

of the seal layer (the Kokumoto formation), which gives ~2.5 S/m pore fluid conductivity around the injection level. Change in the pore fluid conductivity (σ) due to CO_2 injection is given so as that σ is proportional to the square of the aqueous-phase saturation. In shallower levels than the seal layer, the bulk conductivity of rock–fluid mixture is fixed at 0.01 S/m to represent freshwater regions. As seen in Fig. 17, although the apparent resistivity of the CO_2-saturated region does not change very rapidly, it has increased by 15 % or more after 50 years.

Figure 18 shows changes in earth-surface gravity at t = 50 years for the "*H-k*" model. The maximum decrease, which appears just above the injection zone, is about 75 μGal. The gravity disturbance grows almost linearly with time during the 50 year of injection interval (Fig. 19). After shut-in, further gravity decrease takes place up to about t = 55 years arising from the upward buoyant migration of the

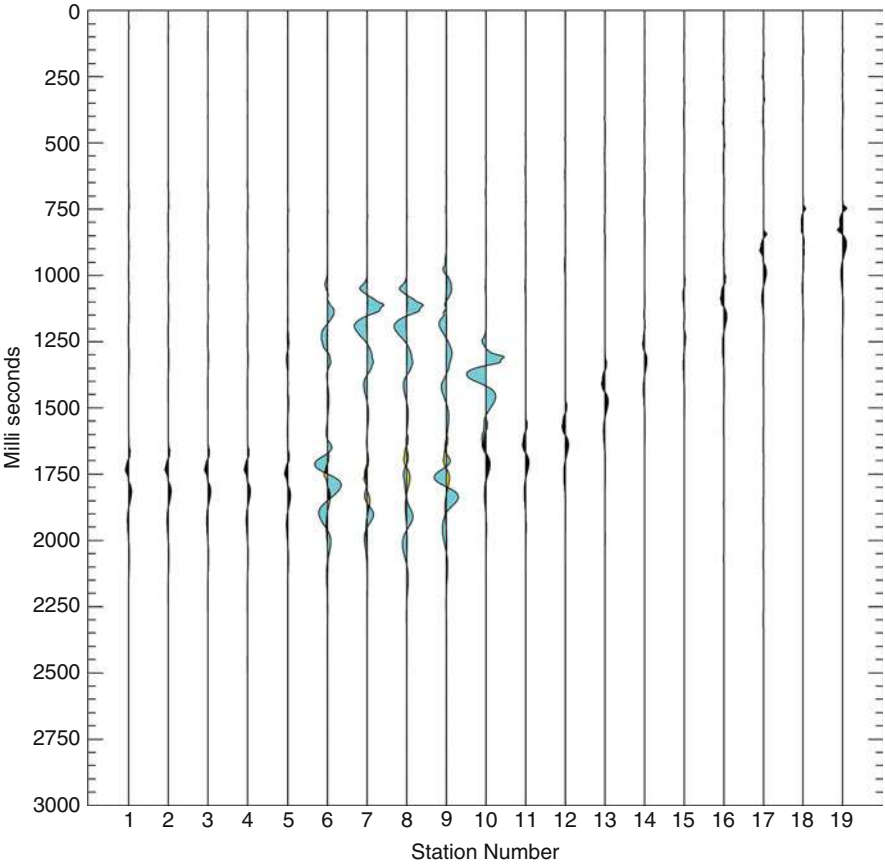

Fig. 16 "*L-k*" model: comparison of time-series results (*blue*) calculated for a seismic reflection survey after 50 years of CO_2 injection with those for an initial survey (*yellow*) across the center of the study area (along 24 km-long A–A′ line shown in Fig. 18). The results overlapped with each other are shown by *black color*

CO_2 (Fig. 19). However, the rate of further gravity change becomes very small after $t = 60$ years although the upward migration continues for hundreds of years after shut-in. This is because the supercritical CO_2 entering the Kokumoto seal layer is densified by condensation as the temperature decreases below the critical temperature at sufficiently deep levels and the upward movement slows down. As for the "*H-k*" model, gravity increase and decrease continue at stations 1 and 2 respectively after $t = 55$ years. This slight change reflects CO_2 gas movement from the injection location to peripheral regions.

Figure 20 shows downhole borehole-gravity response at stations 1 and 2 (see Fig. 18 for the locations) for the "*H-k*" model. At the injection location (station 1), pronounced gravity changes appear even as early as $t = 5$ years, corresponding to the thickness of the CO_2 plume. At station 2, the change in earth-surface gravity is

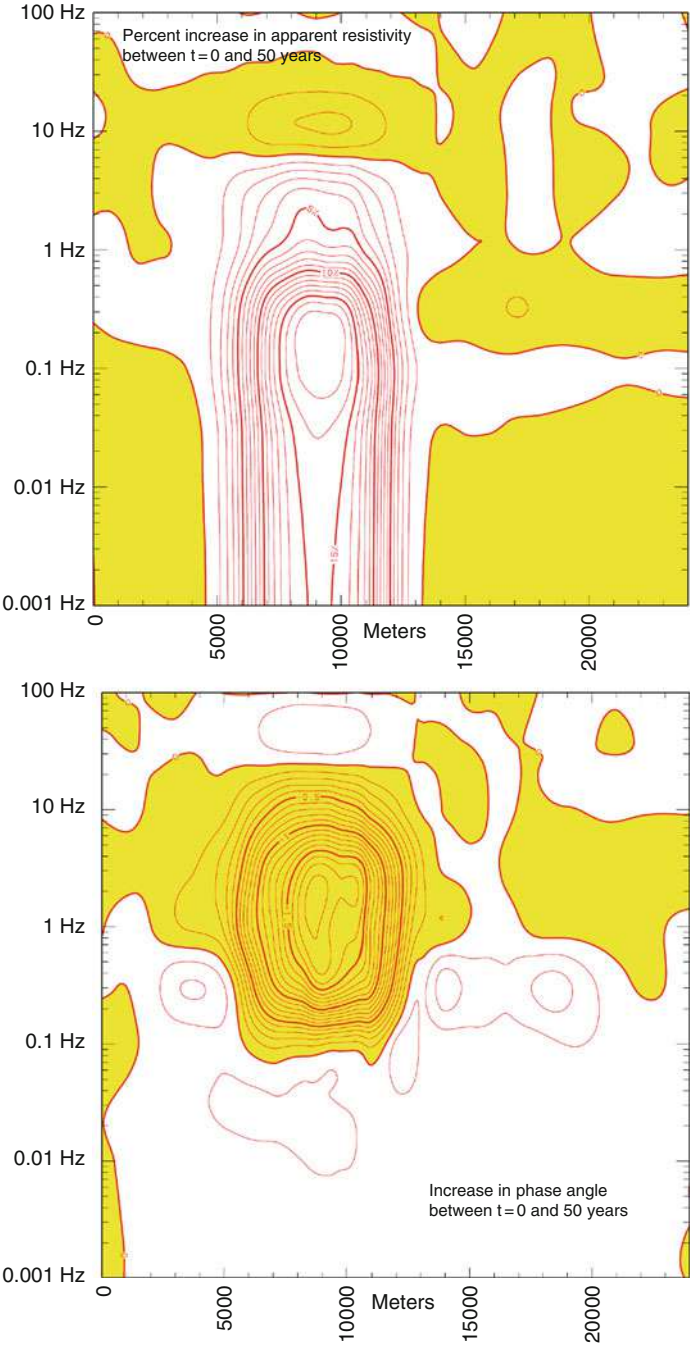

Fig. 17 Percentage apparent resistivity increase (*upper*) and phase angle increase (*lower*) as a function of frequency between t=0 and 50 years along 24 km long A–A0 line shown in Fig. 18

small even at t = 50 years (Fig. 19), but the borehole response is very apparent particularly after 25 years or so when the expanding CO_2 plume engulfs the borehole location.

Figure 21 shows change in self-potential (SP) at t = 5 years for the "*H-k*" model; the maximum increase, which appears just above the injection zone, is more than 40 mV. The self-potential postprocessor calculates changes in subsurface electrical potential induced by pressure disturbances through electrokinetic coupling (Ishido and Pritchett 1999). Since the permeability of the seal layer (the Kokumoto formation) is relatively large in the present model, a pressure disturbance propagates to shallower levels where a transition zone between the shallower fresh and deeper saline water is assumed to be present as in the MT calculations. This transition zone acts as an interface between regions of different streaming potential coefficient. Pressure increases about 2 bars around this interface, which is located at a depth of ~1,000 m at the injection location, bringing about a positive change of 40 mV at the earth surface (see the vertical section in Fig. 21). This obvious SP change develops rapidly with pressure increase for the first several years and persists until shut-in at t = 50 years. After shut-in, SP disturbance gradually declines as pressures return to their original levels. As seen in Fig. 22, more pronounced SP disturbance appears for the "*L-k*" model, which corresponds to larger pressure buildup (about 5 bars) due to CO_2 injection into the lower permeability formation.

Summary

Of course, the applicability of any particular method is likely to be highly site specific, but the calculations described here indicate that none of these techniques should be ruled out altogether. In addition to seismic methods (especially reflection surveys, e.g., Chadwick et al. 2009), microgravity surveys appear to be suitable for characterizing long-term changes, and SP measurements are quite responsive to short-term disturbances.

The computed gravity changes suggest that microgravity monitoring can be used to characterize the subsurface flow of CO_2 injected into underground aquifers. Gravity monitoring results are sensitive to the lateral migration of the CO_2-rich phases (both liquid condensate and particularly gaseous CO_2). Gravity monitoring may also be useful for assessing the suitability of particular disposal aquifers for CO_2 sequestration. If the geothermal gradient is low as is observed in a portion of the Tokyo Bay area, the predicted decrease in gravity is quite small considering the relatively large injection rate. Even if the (supercritical) gaseous CO_2 gradually migrates upward for hundreds of years after injection, the gaseous CO_2 will be densified as the temperature decreases below the critical temperature at sufficiently deep levels and become relatively immobile liquid condensate, which is much less likely to escape the aquifer than highly buoyant, low-viscosity CO_2 gas. When this occurs, the gravity change is very slight during the 1,000-year postinjection period. Considering the current advanced technology for field measurements (e.g., Nooner et al. 2007; Alnes et al. 2008; Sugihara and Ishido 2008; Sugihara et al. 2013), microgravity monitoring is thought to be a very promising technique for evaluating CO_2 geological storage.

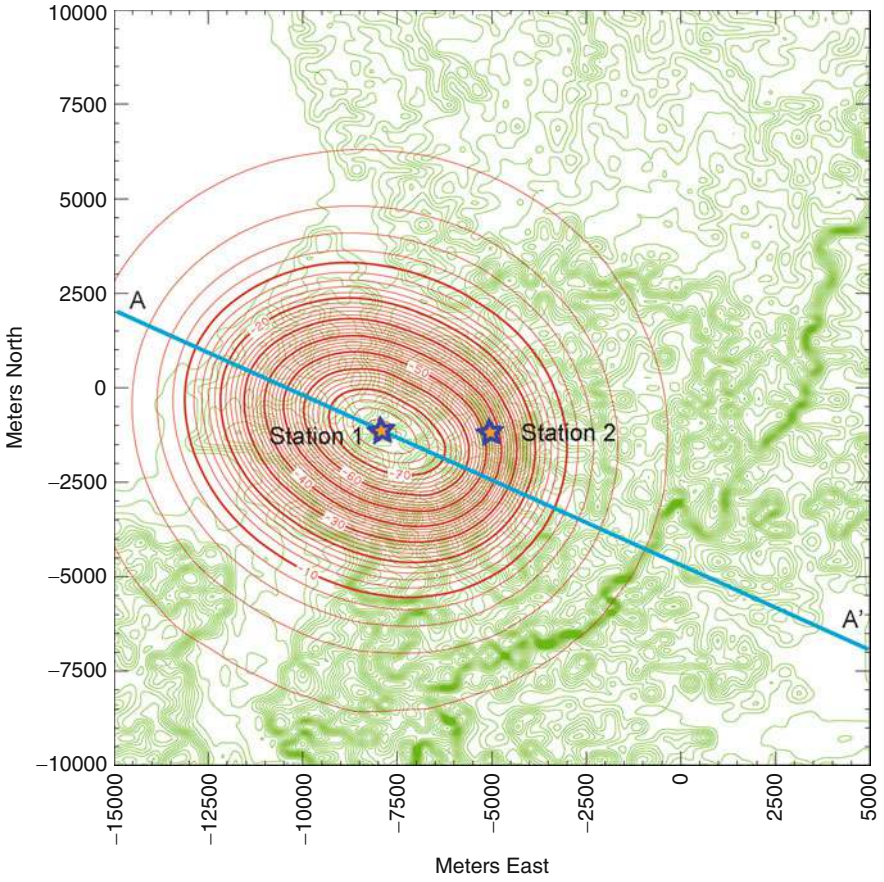

Fig. 18 Distribution of gravity change between t = 0 and 50 years in the study area shown in Figure 8 (extending from −15 km to 5 km in the east-west direction and from −10 km to 10 km in the northsouth direction). Maximum decrease is ∼75 μGal near the injection site centered at −8 km east and −1 km north

The self-potential postprocessor calculates changes in subsurface electrical potential induced by pressure disturbances through electrokinetic coupling. If the permeability of the seal layer overlying the injection zone is not too small, substantial SP changes will appear at the earth surface during the first few years of injection. At least in coastal and estuarine environments, this large change is produced by a pressure increase of several bars at the interface between the shallower fresh and deeper saline water layers, which acts as an interface between regions of different streaming potential coefficient. If a discontinuity of streaming potential coefficient is present, SP monitoring can be an effective technique for monitoring pressure changes near the interface at depth.

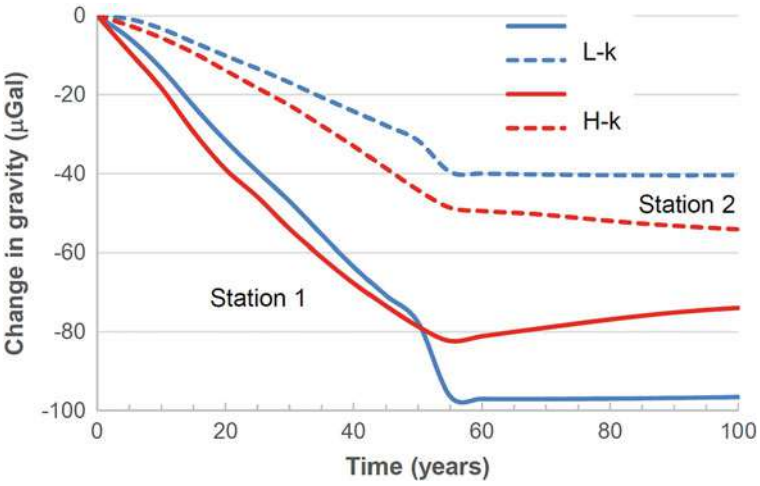

Fig. 19 Change in gravity from t = 0 to 100 years for the "*H-k*" and "*L-k*" models at two stations 1 and 2, the locations of which are shown in Fig. 18

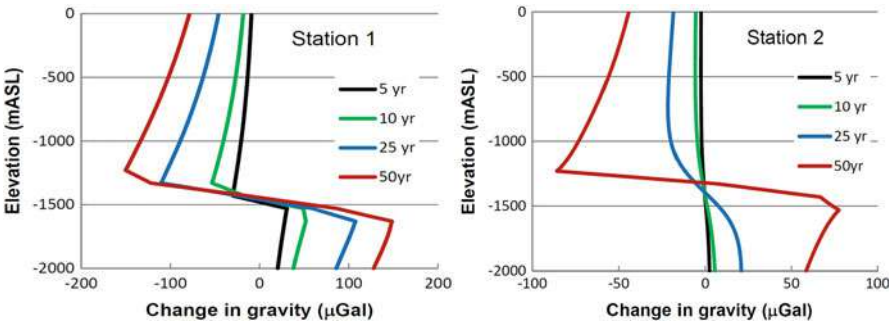

Fig. 20 Borehole gravity response for the "*H-k*" model at selected times at stations 1 and 2, the locations of which are shown in Fig. 18

Geomechanical Modeling

Introduction

When any kind of fluid like CO_2 is pressure injected into an underground reservoir as is done for geological CO_2 storage, the pressure (pore pressure) of the fluids underground increases, and the stress distribution underground may change. Stress redistribution within and surrounding the reservoir and caprock system may lead to geophysical changes, microseismicity, and fault reactivation and may even trigger

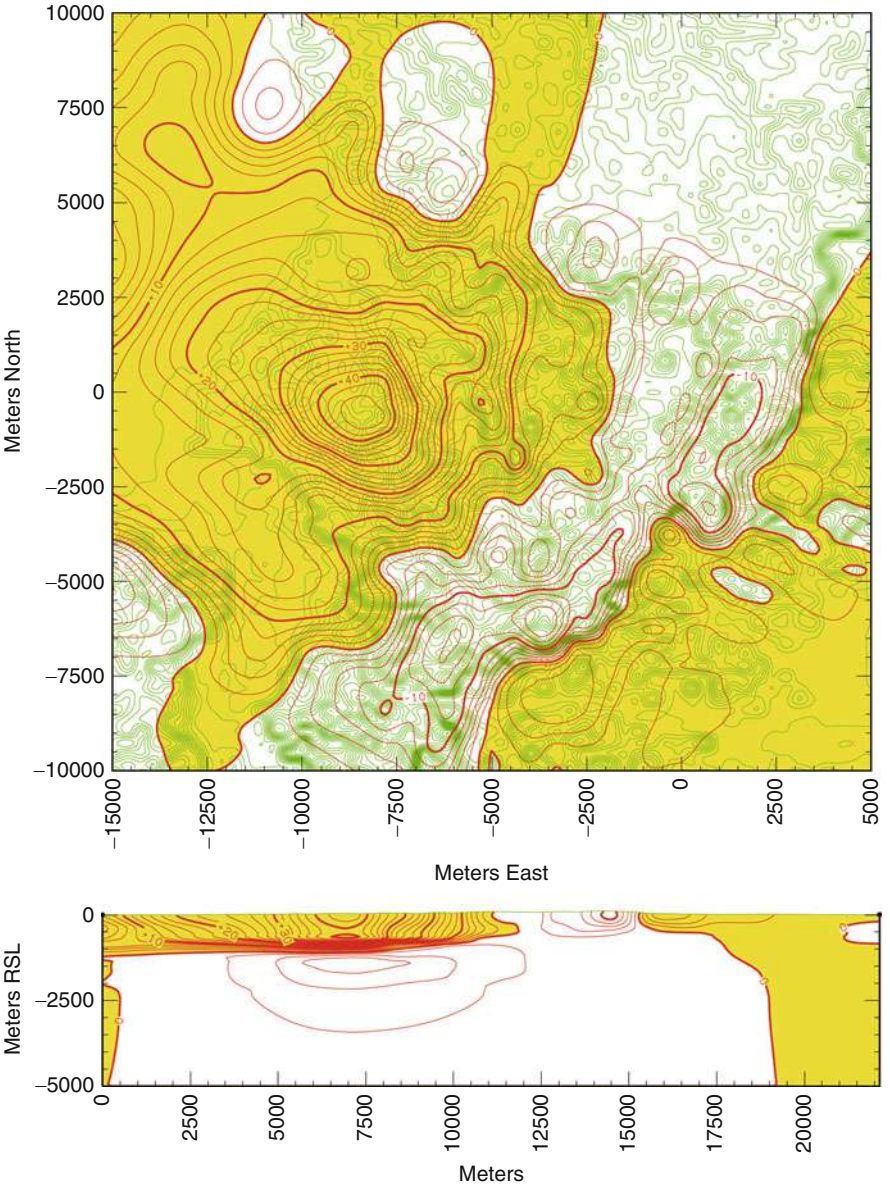

Fig. 21 Distribution of self-potential at the earth's surface (*upper*) and a vertical section (*lower*) for the "*H-k*" model at t = 5 years. The area represented is the same as that of Fig. 18. Contour interval is 5 mV, and the *yellow color* denotes positive SP

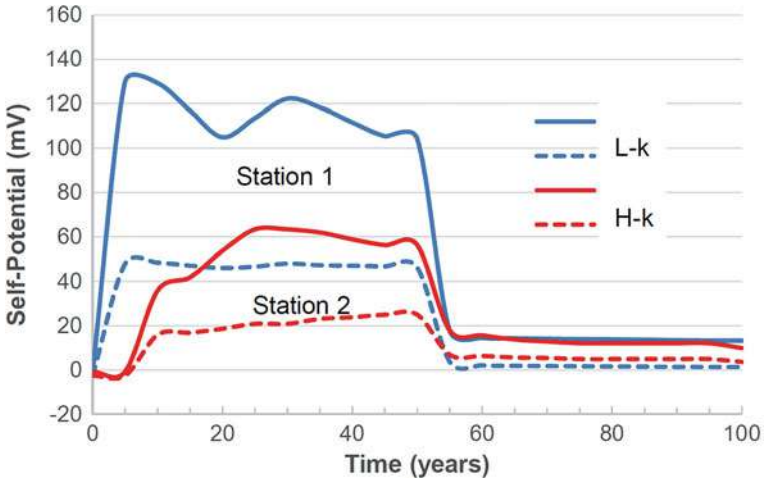

Fig. 22 Temporal variations of self-potential from t = 0 to 100 years for the "*H-k*" and "*L-k*" models at two stations 1 and 2, the locations of which are shown in Fig. 18

large earthquakes (Giammanco et al. 2008; Lei et al. 2008; Miller et al. 2004; Yamashita and Suzuki 2009). For example, at a gas field in In Salah, Algeria, where CO_2 is pressure injected to enhance natural gas production, synthetic aperture radar observations from a satellite have indicated a ground uplift rate of about 1 cm/year around the CO_2 pressure injection wells, along with a similar amount of subsidence around the gas production wells (Onuma and Ohkawa 2009). In some gas fields in the Sichuan Basin, China, following injection of unwanted water into depleted gas reservoirs, a number of seismic sequences have been observed with sizable earthquakes ranging up to M4 $\sim$ 5 (Lei et al. 2008, 2013). In recent years, following the rapid increase of applications in which fluids are intensively pressed into the deep formations of the Earth's crust, such as the enhanced geothermal system (EGS), fracking of shale gas, and geological sequestering of CO_2, injection-induced earthquakes and other risks related to injection-induced rock deformation and failure have attracted growing attention (Ellsworth 2013; Lei et al. 2013; Zoback et al. 2013; Zoback and Gorelick 2012).

Indeed, geophysical changes and microseismicity are useful in the monitoring and management required during and after a large-scale injection project. However, the risks related to fluid leakage and earthquakes that can be felt may give rise to strong social impacts. The issue of noticeable or damage-causing earthquakes induced by artificial operations is controversial and has been the cause of delays and threatened cancelation of some projections such as the EGS (enhanced geothermal system) project at Basel (Deichmann and Giardini 2009). To carry out geological CO_2 storage safely and for this technology to be accepted not only by the

inhabitants around the storage sites but also by the society as a whole, technological developments that address such public concerns are essential. In addition, there is a strong desire to be able to control or predict the occurrence of damaging earthquakes. In this regard, geophysical/geomechanical modeling is key in site selection, injection operation, and postinjection management.

The purpose of the following subsections is to provide a general framework for geophysical/geomechanical modeling and microseismicity analysis. Section "A General Framework of Geophysical/Geomechanical Modeling" introduces a general framework for modeling. Then, section "Numerical Simulation for THM Coupling Analysis" introduces the numerical simulation technology used in the coupled THM (heat transferring, fluid flow, rock mechanics) analysis. Postprocessing for history matching and fault stability analysis is presented in section "Fault Stability Analysis: Coulomb Failure and Slip Tendency." A case study of a natural analogue is introduced in section "An Example of a Natural Analogue: The Matsushiro Seismic Swarm Driven by CO_2-Quality Fluid Activity." Finally, section "Data Processing and Analysis of Injection-Induced Seismicity" introduces some key technologies for data processing and analyzing of injection-induced seismicity.

A General Framework of Geophysical/Geomechanical Modeling

Figure 23 shows a schematic flowchart of modeling with coupled THM simulation and history matching using a geophysical postprocessor (see section "Geophysical Monitoring and Modeling" for details). Firstly, existing geological and geophysical data should be integrated to build a conceptual geological model of a reservoir system. Then the mechanical and petrological properties of the major rocks in the geological model must be sufficiently investigated to create a numerical model. Additional laboratory experiments might be required to collect data on specified rocks to improve the reliability of the numerical analysis. Finally, history matching is applied to refine the numerical model of a reservoir to reproduce observed data. All data obtained through geophysical exploration methods, such as microgravity measurements, seismic exploration, electrical or electromagnetic exploration, etc., can be used in history matching to improve the accuracy of future forecasts. Geophysical postprocesses are used to convert changes in pressure, temperature, salinity, CO_2 saturation, etc., calculated by reservoir simulation into changes in geophysical observables (Ishido et al. 2011, section 5). Since there are uncertainties in many aspects of the numerical model, such as small-scale inhomogeneity and upscaling, uncertainty analysis is necessary for a probability-based prediction.

In geomechanical modeling, discontinuous structures including joints, fractures, and faults have a governing role in fluid flow and rock stability. Studies on water injection-induced seismicity in depleted gas/oil reservoirs show that earthquakes of relatively greater magnitude (M3 or greater) are mostly related to the reactivation of preexisting faults, favorably or unfavorably oriented, within or

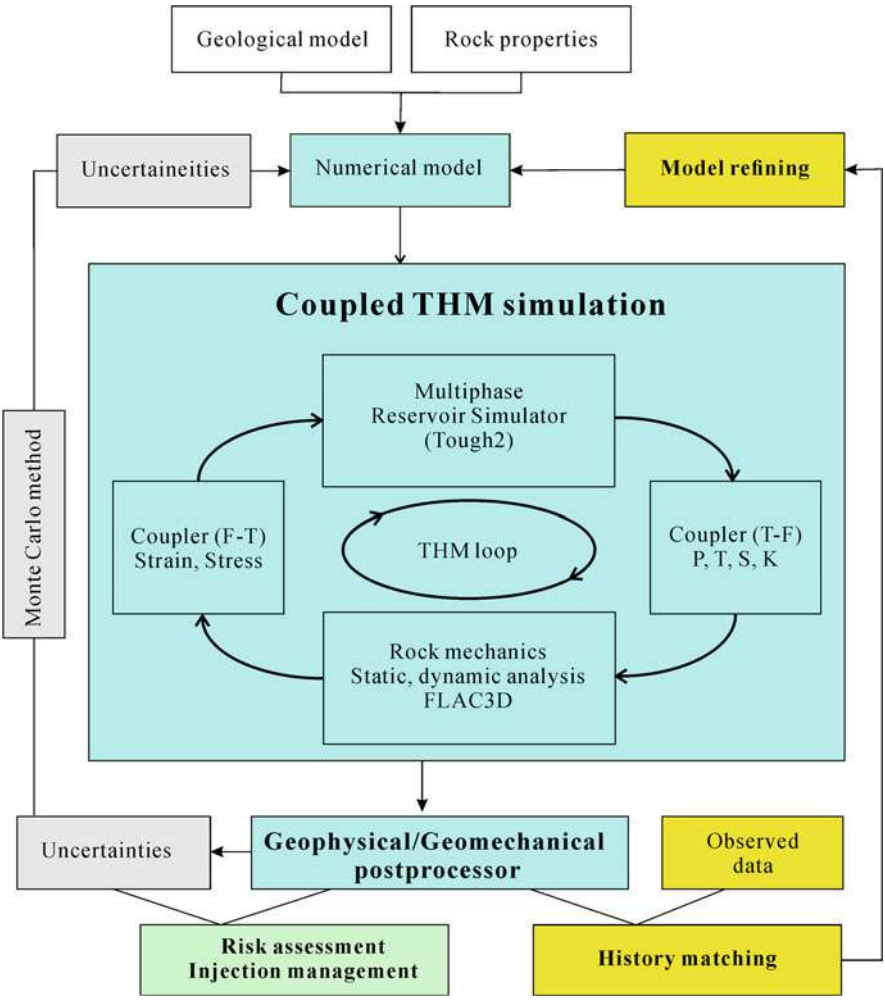

Fig. 23 Flowchart of modeling with coupled THM simulation and history matching using a geophysical postprocessor

surrounding the reservoir (Lei et al. 2008, 2013). Therefore, estimating fault stability and sustainable fluid pressures for underground storage of CO_2 is an important issue in geomechanical modeling (Rutqvist et al. 2008; Streit and Hillis 2004). Known major faults in or near target aquifers can be avoided during site screening. Since a fault of a dimension of a few hundreds/thousands of meters is sufficient to produce $\sim$ M3/M5 earthquakes as indicated by the empirical relationship between source dimension and earthquake magnitude (Utsu 2002), faults that are not resolvable by geophysical surveys must also be properly addressed (Mazzoldi et al. 2012).

Numerical Simulation for THM Coupling Analysis

There is a current focus on coupled THM analysis as a budding technology. This technology is used to predict injection-induced changes in rock properties, formation deformation, stress redistribution, and fracture/fault stability. Although the simulation technology is still in development, there are a number of choices of research-oriented or commercial software for reservoir simulation and/or stress analysis, such as TOUGH2 and FLAC3D. TOUGH2 is a multiphase reservoir simulation program developed by the Lawrence Berkeley National Laboratory (LBNL) in the US FLAC-3D (Itasca 2000) and is a commercial software for stress analysis. As a promising combination, the "TOUGH-FLAC" approach with couplers developed by Rutqvist et al. (2002) has proven useful in the analysis of deformation accompanied with fluid flow within hard and soft rocks in geothermal studies (Todesco et al. 2004), in CCS studies (Funatsu et al. 2013; Rinaldi and Rutqvist 2013; Rutqvist et al. 2008), and in natural analogues (Cappa et al. 2009).

A schematic of the couplers and physical quantities handled by the TOUGH-FLAC approach is shown in the center of Fig. 23. A reservoir is presumably a porous medium filled with formation water. If a fluid (CO_2 in CGS) is pressure injected into this reservoir, the pore fluid pressure increases, and there is flow between the formation water and the pressure-injected fluid. Changes in pore fluid pressure lead to small changes in the reservoir rock. In addition, if there is a temperature difference between the reservoir and the pressure-injected fluid, as the fluid flows and spreads, heat is transported, and the temperature change causes rock deformation. The fluid flow simulator TOUGH2 calculates changes in the pore fluid pressure, temperature, degree of saturation, etc., and sends the results to the rock mechanics simulator in FLAC3D. The rock mechanics simulator then calculates the solid deformation and sends the changes in porosity, permeability, and capillary pressure back to the fluid flow simulator. The couplers are some built-in functions in TOUGH2 and FISH codes in FLAC3D (Rutqvist et al. 2002). Such coupling approaches, termed sequential coupling, work well for problems in which coupling is relatively weak.

In the THM coupling simulation, the following parameters and models are required and should be investigated through laboratory experiments: (1) parameters governing the deformation and fracturing behaviors of a given rock; (2) petrophysical models linking porosity, intrinsic permeability, relative permeability, and effective confining pressure; and (3) permeability of fracture as a function of effective confining pressure. Rock properties and mechanical behaviors strongly depend on individual rock types and structures within the rock. Thus, individual rocks of a target reservoir system should be fully investigated to obtain reliable parameters. If a typical rock of the reservoir system has not been investigated by earlier studies, additional experimental study is required. Further, laboratory experimentation has a twofold role in geomechanical modeling. On one hand, it is the only way to get the physical/mechanical/hydraulic properties of a given rock and the constitutive laws required for conducting numerical models (Lei and Xue 2009; Lei et al. 2011a). On the other hand, a well-designed experiment is

useful for verifying and improving a related numerical model by matching the numerical results with the experimental results (Lei et al. 2015).

Permeability might change greatly due to deformation and fracturing (Zhang et al. 2007). In brittle rocks, fault rupturing can lead to a 2-order-of-magnitude permeability increase as estimated by in situ testing (Ohtake 1976) and laboratory experiments (Alam et al. 2014). Thus, permeability as function of deformation should be properly considered. In the TOUGH-FLAC approach, permeability is revised within Tough2 in every time step by built-in functions. In some previous works, permeability has been expressed as a function of volumetric strain (ε_v) or shear strain (ε_s) (Cappa et al. 2009; Cappa and Rutqvist 2011; Chin et al. 2000):

$$k = k_0(1 + \beta\Delta\varepsilon_s) \tag{5}$$

$$k = k_0\left(\frac{\phi}{\phi_i}\right)^n, \varphi = 1 - (1 - \varphi_i)e^{-\varepsilon_v} \tag{6}$$

where ϕ and k are porosity and permeability, respectively, with ϕ_i and k_i being the initial values. A β on the order 10^4 or n of ~30 results in a 2-order-of-magnitude permeability increase for a fully reactivated fault (Fig. 24). As seen from Fig. 24, Eqs. 5 and 6 result in quite different behaviors. This should be examined in future studies.

Fault Stability Analysis: Coulomb Failure and Slip Tendency

In most cases, the stress tensor is not fully defined or is badly defined, so rock failure analysis based on absolute stress tensors may lead to incorrect results. The earth's crust is considered to be critically stressed; thus, a small change in stress may trigger earthquakes. The amplitude thresholds of the Coulomb failure stress change (ΔCFS) required to trigger earthquakes has been estimated to range from 0.01 to 0.03 MPa (Brodsky and Prejean 2005; Cochran et al. 2004; King et al. 1994; Lockner and Beeler 1999; Stein 1999). Based on Coulomb failure law, the critical condition for rupturing on a preexisting fault is

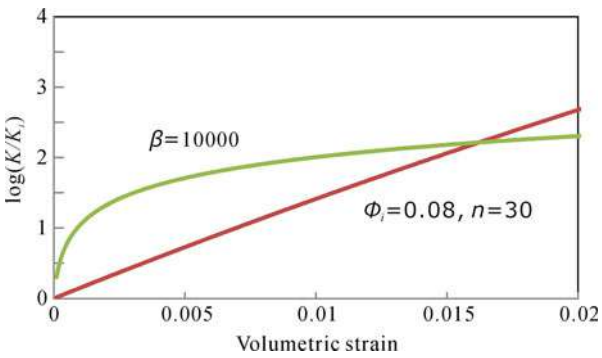

Fig. 24 Rock permeability as a function of volumetric strain for two different models

$$\tau = \mu\sigma_e = \mu\left(\sigma - P_f\right) \tag{7}$$

where τ and σ are shear and normal stresses acting on the fault plane, respectively, σ_e is effective normal stress, P_f is pore pressure, and μ represents the sliding friction of the fault plane. A change in Coulomb failure stress (ΔCFS) is defined as

$$\Delta CFS = \Delta\tau - \mu\Delta\sigma_e \tag{8}$$

The tendency of a planar discontinuous structure such as a fault to undergo slip under a given stress pattern depends on the frictional coefficient of the surface and the ratio of shear to normal stress acting on the plane. The slip tendency of the fault is defined as the ratio of the shear stress and normal stress (Morris et al. 1996) and thus equals the friction coefficient:

$$Ts = \tau/\sigma_e \tag{9}$$

Slip-tendency analysis is a technique that visualizes the stress tensor in terms of its associated slip-tendency distribution and the relative likelihood and direction of slip on interfaces at all orientations (Morris et al. 1996). It can be used in assessing the risks of geological CO_2 storage (Kano et al. 2014).

Under a uniform regional stress field, the most optimally oriented fault has the maximum slip tendency, as faults with greater slip tendency values are easier to rupture.

Under the principal stress coordinate system (s1, s2, s3), the shear and normal stresses on a surface of given direction cosines (l, m, n) can be calculated from the three principal stress magnitudes (σ_1, σ_2, σ_3) as:

$$\begin{aligned} \tau^2 &= (\sigma_1 - \sigma_2)^2 l^2 m^2 + (\sigma_2 - \sigma_3)^2 m^2 n^2 + (\sigma_3 - \sigma_1)^2 n^2 l^2 \\ \sigma^2 &= {\sigma_1}^2 l^2 + {\sigma_2}^2 m^2 + {\sigma_3}^2 n^2 \end{aligned} \tag{10}$$

In some cases, only the direction of the principal stresses and the stress difference ratio (R), or equivalently the shape ratio (ϕ), are given (Etchecopar et al. 1981; Gephart and Forsyth 1984):

$$R = \frac{(\sigma_1 - \sigma_2)}{(\sigma_1 - \sigma_3)} \tag{11}$$

$$\phi = 1 - R = \frac{(\sigma_2 - \sigma_3)}{(\sigma_1 - \sigma_3)} \tag{12}$$

In addition, $\sigma_1 - \sigma_3$ is not well constrained and can be expressed as an unknown parameter k. By further assuming that the frictional sliding envelope is tangential to the (σ_1, σ_3) Mohr circle, then the principal stresses are given by

$$\begin{aligned}\sigma_1 &= k(1/\sin(\phi)+1)/2\\ \sigma_2 &= \sigma_1 - kR\\ \sigma_3 &= \sigma_1 - k\end{aligned} \tag{13}$$

where $\tan\varphi = 1/\tan(2\theta) = \mu$. Inserting Eq. 13 into Eq. 10 leads to the following equations for shear stress and normal stress:

$$\begin{aligned}\tau &= k\left[(1-\phi)^2 l^2 m^2 + \phi^2 m^2 n^2 + n^2 l^2\right]^{1/2}\\ \sigma &= k\left(\frac{\csc(\varphi)+1}{2} - (1-\phi)m^2 - n^2\right)\end{aligned} \tag{14}$$

Thus, the slip tendency is independent of the choice of the unknown parameter k, and we can get a slip tendency normalized by the maximum. For such a partially defined stress field, we can draw the 3-D Mohr circles for shear and normal stresses normalized by k or the maximum shear stress.

It is convenient to define an overpressure coefficient λ for fluid pressure (Terakawa et al. 2013):

$$\lambda = \frac{(P_f - P_0)}{(P_{\max} - P_0)} \tag{15}$$

where P_0 is the critical pore pressure required to initiate rupture on the optimally oriented fault for a given friction coefficient, $P_{\max}$ ($=\sigma_3$), which is the maximum pore pressure above which hydrofracture occurs.

In the geophysical/geomechanical modeling approach, one can develop a postprocessor to calculate ΔCFS and slip tendency. It can be done within Flac3D by writing a simple FISH program. ΔCFS and slip tendency are especially useful for analyzing the effect of injection to preexisting nearby faults that have not been involved in the numerical model. Figure 25 shows an example of slip tendency analysis for a location where only the direction of the principal stresses and the stress difference ratio R ($=0.6$) are given. Faults having a strike and dip in the red zones have relatively greater probability of being reactivated.

An Example of a Natural Analogue: The Matsushiro Seismic Swarm Driven by CO_2-Quality Fluid Activity

In geological CO_2 storage, it is important to clarify the mechanisms and geomechanical conditions of worst-case events, such as damaging earthquakes and reservoir leakage, so that they can either be avoided or mitigated. It is most desirable to use an actual CGS site in which such events have actually occurred and have been well monitored. However, many pilot projects are sited in places with

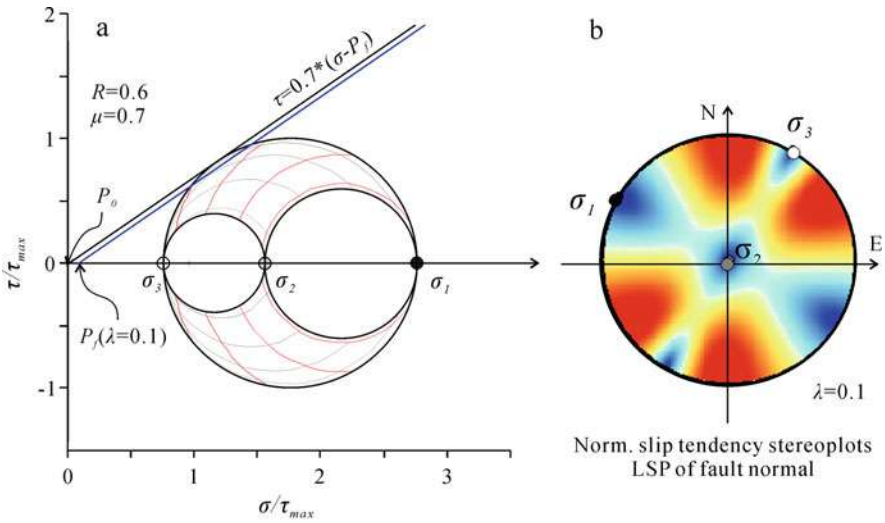

Fig. 25 (**a**) 3D Mohr circles and (**b**) normalized slip tendency stereoplots (*LSP* lower sphere projection) under an over pore pressure constant of 0.1 and a local stress field in which only the direction of the principal stresses and the stress difference ratio *R* are given

good conditions for safely pressing CO_2 into the reservoir. Thus, it is valuable to carry out "natural analogue research," analyzing similar phenomena caused by the activity of a natural CO_2-quality fluid to examining the modeling technology. Here, we make a brief review of studies on the fluid-driven earthquake swarm in Matsushiro, central Japan, as a natural analogue of seismicity induced by fluid injection.

In the Matsushiro area, which is located in the central and northern part of Nagano Prefecture, a series of more than 700,000 earthquakes occurred over a 2-year period (1965–1967). This swarm, termed the Matsushiro swarm, resulted in ground surface deformations (uplifts as large as 75 cm), cracking of the topsoil, enhanced spring outflows with changes in chemical compositions, and CO_2 degassing. Ten million tons of CO_2-rich saltwater was estimated to have seeped out from underground along the cracks (Ohtake 1976). Thus, the Matsushiro swarm is believed to have been triggered and driven by high-pressure CO_2-rich fluid from deep sources. Data observed during the Matsushiro swarm can therefore be used as a natural analogue for examining THM coupling analysis (Cappa et al. 2009; Funatsu et al. 2013). In Matsushiro and surrounding areas, subsurface geophysical surveys have been frequently conducted since the occurrence of earthquake swarms, and underground data, such as seismic wave velocity structure data, are abundant. In addition, the surface geology is relatively well understood. The geological model was developed based on these existing data. Here, a new Matsushiro model is used, which is basically an improved model modified from earlier studies (Cappa et al. 2009; Funatsu et al. 2013). In the new model, the

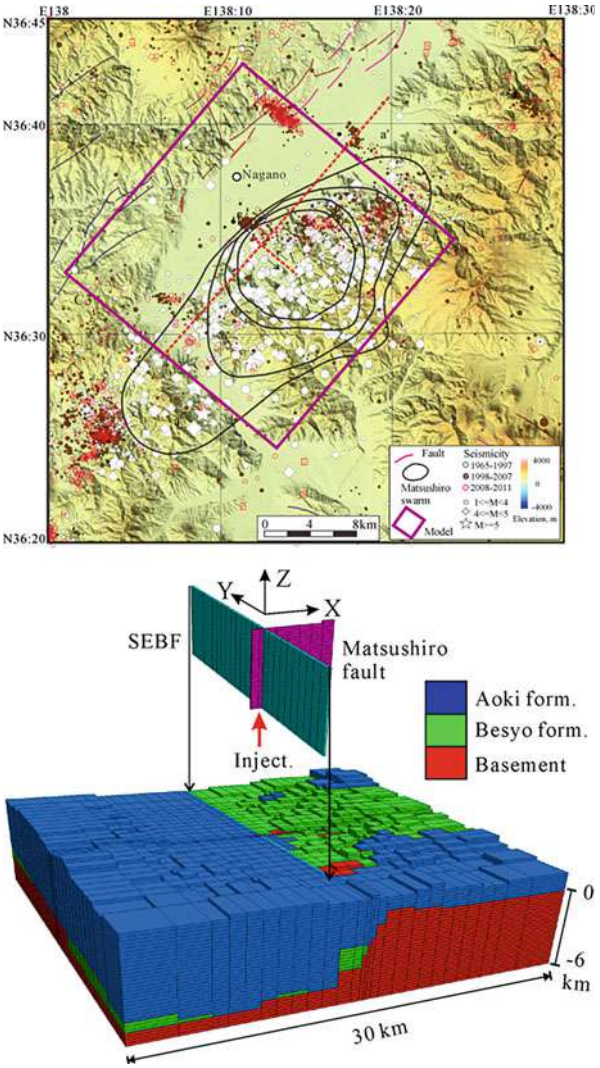

Fig. 26 Map showing basic features around the Matsushiro earthquake swarm. The model area is shown on the topographic map. *Red dotted lines* indicate the Matsushiro fault and the Southeast Boundary Fault (SEBF) of the Nagano basin. Contours show earthquake swarm migration (Modified from Hagiwara and Iwata 1968). The *right plot* shows a 3D model for numerical analysis viewed from the southwest

boundaries along all four sides are enlarged to limit the effect of boundary conditions. It covers a $50 \times 50 \times \sim 6$ km area with a focus dimension of $24 \times 24 \times 6$ km centered at the intersection of the Matsushiro fault and SEBF (Fig. 26). In addition, the topography is also involved in the new model to simulate subsurface ground water flow. In order to better represent the deep structure in the area, a geological model of three lithology groups was constructed, considering the seismic profiles obtained so far. Two vertical faults that intersect at the center of the model are assumed. The faults are modeled as narrow zones of a new group termed "fault." The regional stress field has its maximum compression axis in the east–west direction, and its minimum compression axis in the north–south direction. This

Table 1 Mechanical properties

Property	Aoki	Besyo	Basement	Fault/fault inters.
Bulk modulus (GPa)	1.96	4.42	7.85	3.16
Shear modulus (GPa)	1.55	3.49	6.20	2.42
Cohesion (MPa)	–	–	–	1.5
Ten. strength (MPa)	–	–	–	0.0
Friction angle (°)	–	–	–	28.8
Dilation angle (°)	–	–	–	20
Biot's coefficient	0.9	0.8	0.8	0.6
Ini. Perm.(k_0), (m^2)	1e−17	1e−18	1e−18	1e−15/5e−15
	$k = k_0(1 + \beta\Delta\varepsilon_s), \beta = 30,000$			
Porosity	0.05	0.01	0.01	0.05

model is divided into grids by steps so that the fault zone is split in small parts, while the surrounding matrix becomes coarser as the distance from the fault increases (depth, however, is equally split at 500 m intervals). The total number of elements is 9,248. Mechanical properties, which are set similar to those in Cappa et al. (2009), are listed in Table 1, and the geometry of the model is shown in Fig. 26. After failure, in order to incorporate strain softening behavior into the model, we decreased the cohesion and tensile strength with strain following two linear paths to given values. After failure, the friction angle and dilation angle also change with the shear strain. The associated parameters are listed in Table 1.

Note that some parameters used this, and former studies differ significantly from laboratory-derived data for intact rocks. For instance, the values of Young's modulus used in the numerical model appear too low. As we know, the real crust contains fractures and faults at all scales. It is impossible to represent all individual fractures and small faults in a model, so we have to adjust some properties, such as the bulk and shear moduli, as an upscaling technique. Similar techniques are used in core-scale simulation to account for preexisting microcracks in rock samples (Lei et al. 2015).

The calculated horizontal displacements and uplifts at the ground surface are shown in Fig. 27. The maximum uplift, 66 cm, is obtained at the point where the faults cross 1 year after from the beginning of fluid injection. This value is close to the observed maximum value of 75 cm. The uplift pattern becomes asymmetric to the SEBF, which concurs with observations. Left-lateral slip along the two faults is also identified. Results of the new model match observed values better than previous studies. The uplift gradually stretches away from the intersection of the two faults along their extensions in a skewed rhombic pattern, indicating a fault-controlled pore pressure diffusion process.

Figure 28 compares the Matsushiro earthquake swarm migration and a calculated distribution of ruptured zones along the Matsushiro and east Nagano earthquake faults 180 and 720 days after injection began. Except for fractures at the surface, all fractures demonstrate shear mechanisms. Surface fractures show tensile modes. Calculated surface uplift is plotted in Fig. 29. For comparison, some data

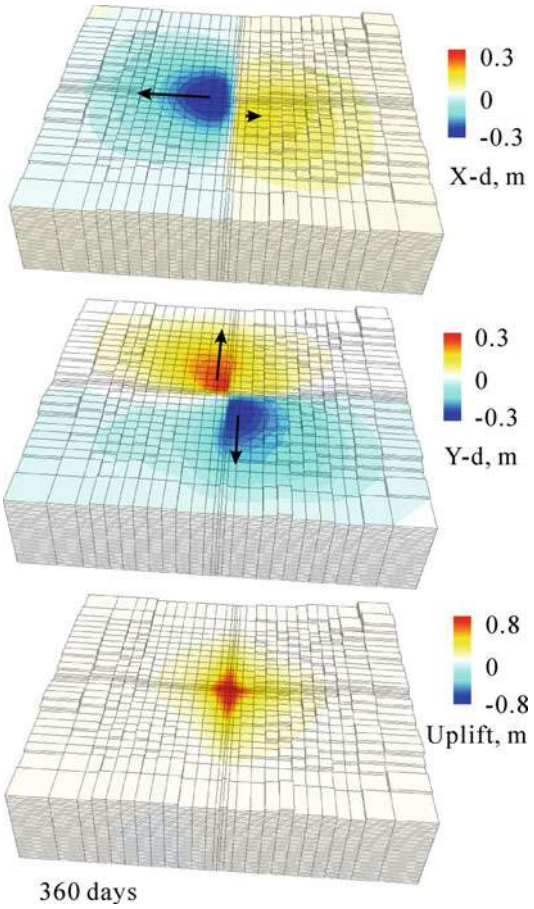

Fig. 27 Calculated distributions of X- and Y-displacement and uplift of the ground surface 360 days after injection began

estimated from field observations (Kasahara 1970; Tsukahara and Yoshida 2005) are also plotted.

In conclusion, the numerical model and coupled THM analysis using the TOUGH-FLAC3D approach successfully represent major characteristics of observed phenomena associated with the CO_2-rich fluid-driven Matsushiro earthquake swarm.

Data Processing and Analysis of Injection-Induced Seismicity

Statistical Properties of Injection-Induced Seismicity Based on ETAS Modeling

It is well known that an earthquake triggers aftershocks following modified Omori's law. In the case of injection-induced seismicity, it is important to be able to discriminate induced activity from background seismicity and statistically

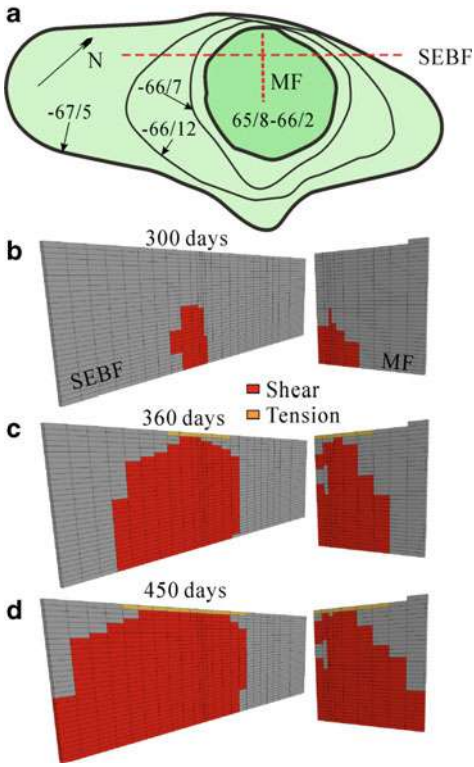

Fig. 28 A comparison of the Matsushiro earthquake swarm's migration and calculated distribution of ruptured zones at 300, 360, and 450 days after injection began along the Matsushiro and east Nagano earthquake faults

separate fluid-induced and Omori-law-type aftershock triggering. The epidemic-type aftershock sequence (ETAS) model (Ogata 1992), which incorporates Omori's law by assuming that each earthquake has a magnitude-dependent ability to trigger its own Omori-law-type aftershocks. The ETAS model is an appropriate tool for testing the significance of changes in seismic patterns (Ogata 1992, 2001), detecting minor stress changes (Helmstetter et al. 2003), and extracting a fluid signal from seismicity data (Hainzl and Ogata 2005). Thus, it is particularly useful for analyzing injection-induced seismicity (Lei et al. 2008, 2013). In the ETAS model, the total occurrence rate is described as the sum of the rate triggered by all preceding earthquakes and a forcing rate λ_0(t) that represents the background activity:

$$\lambda(t) = \lambda_0(t) + \nu(t), \nu(t) = \sum_{\{i:t_i<t\}} K_0 e^{\alpha(M_i - M_c)} (t - t_i + c)^{-p} \tag{16}$$

where M_c is the low cut-off magnitude of the catalogue and α is a constant that specifies the degree of magnitude dependence. For injection-induced seismicity, the background activity consists of tectonic background and injection-induced activities. The injection-induced activity forcing rate is somewhat dependent on injection

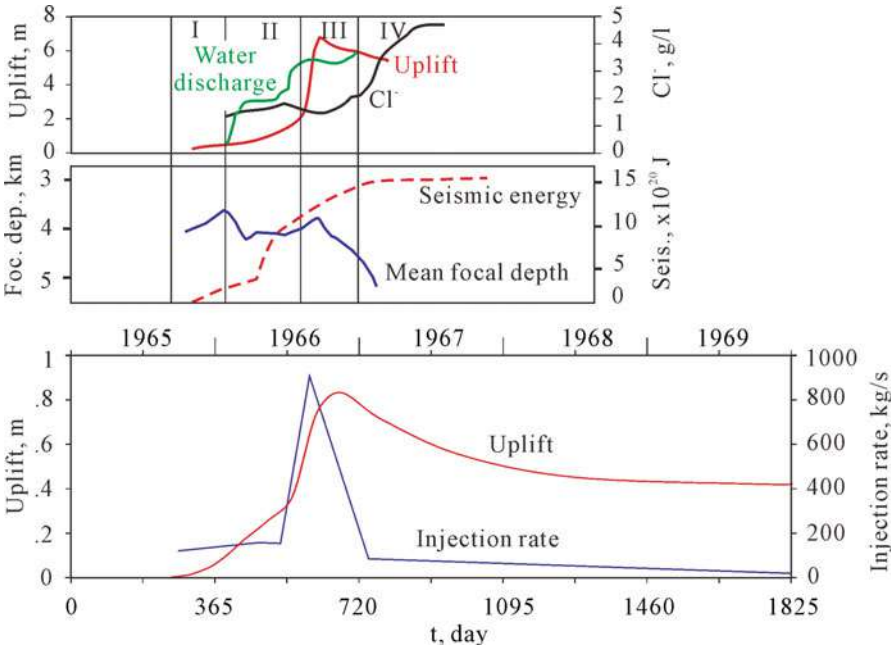

Fig. 29 Calculated maximum surface uplift with given injection rate against time. As a comparison, some data, including uplift, water discharge, concentration of Cl^-, accumulated seismic energy, and mean focal depth, estimated from observations (Kasahara 1970; Tsukahara and Yoshida 2005) are also plotted

parameters such as injection rate, total volume so far injected, well head pressure, fluid temperature, and so on. The sophisticated algorithm inspired by Zhuang et al. (Marsan et al. 2013; Zhuang et al. 2002) is very powerful for use in estimating the time-dependent forcing rate and other parameters of injection-induced seismicity (Lei et al. 2013).

It is well-documented that injection-induced seismicity demonstrates (1) smaller α values ($<\sim 1.5$), (2) varying forcing rates correlated with injection pressure or other factors, and (3) forced seismicity takes on a major component and shows strong correlation with injection factors such as injection rate and volume injected so far (Lei et al. 2008, 2013). These characteristics are similar to seismic swarms observed in geothermally active areas (Lei et al. 2011) but significantly different from tectonic background seismicity, which has greater a values ($> \sim 2$) and a minor component of forced activity.

Lessons from Some Significant Cases of Injection-Induced Seismicity

In many cases, fluid injection induces only small earthquakes ($M < 3$). But there are increasing cases in which damaging earthquakes of a magnitude greater than $4 \sim 5$ are observed. Although the injected fluid, in most cases, is not CO_2 but

water, the major mechanism of inducing earthquakes is similar. Therefore, insights gained from such worst cases may also provide a better understanding of why damaging events occur so that they can be avoided or mitigated. The injection-induced seismic activity in the Sichuan Basin in southwest China has proven to be a significant example. During the past decades, a number of seismic sequences have been observed with sizable earthquakes ranging up to M4 $\sim$ 5 (Lei et al. 2008, 2013; Lei and Ma 2013). Statistical models of their timing, location, and occurrence patterns convincingly suggest that these sequences were induced by water injected into deep wells in the gas fields in this region. Event rates fluctuated following changes of injection rates and tapered after injection was shut down. Most events show shear fracturing mechanisms, which, together with hypocenter location data, demonstrate that preexisting faults, known or unknown, in the formations have a governing role in controlling the hypocenter distribution of the induced earthquakes (Lei et al. 2013). In some cases of long-term injection, there are clear phases of deeper events that mirror the reactivation of underlying faults. Faults of a relative larger scale have a twofold role: working as a bounding interface for horizontal fluid flow and a leakage path for vertical fluid flow.

In agreement with other cases, the injection-induced seismic sequences in the Sichuan Basin demonstrate following general features. (1) Injection-induced seismicity is more swarm-like, characterized by smaller α values (normally $1 \sim 1.5$ or less) in the ETAS model. (2) Most events occurred due to reactivation of preexisting planar structures including faults, fractures, joints, and bedding surfaces. (3) During the earlier stages of injection, the total fraction of Omori-law-type aftershocks is also important, indicating that the stress in the formations is critical or subcritical and seismic triggering and injection forcing are both important for earthquake occurrence. (4) As a natural implication of (2), the maximum magnitude of potential earthquakes is determined primarily by the size of preexisting faults in which the pore pressure may be raised during injection. (5) It is commonly observed that the forced earthquake rate increases with injection time. (6) A uniform regional stress field is insufficient to interpret all focal mechanism solutions, indicating the local stress field on the scale of the reservoir is inhomogeneous.

Results of rock fracture experiments on rock samples collected from the Sichuan Basin shed some light on the question of why injection-induced seismicity is so significant there (Lei et al. 2014). Major Pre-Triassic sedimentary rocks in this region, including dolomite, shale, and dolomitic limestone, are strong and demonstrate brittle deformation/fracturing behaviors. Such properties are necessary conditions for maintaining high-level reservoir stress and lead to seismic fracturing. In general, critically or subcritically stressed faults of a dimension of a few kilometers are sufficient to allow M $\sim$ 5 class earthquakes. Such faults are distributed widely in the reservoir system in this region. Lessons from the Sichuan Basin tell us that it is important to investigate the basic rock properties and the size and location of preexisting faults in assessing the risks of a candidate CO_2 storage site.

Future Directions

There are 13 large-scale CCS-related projects in operation as of October 2014, and the same number of projects is scheduled to begin operations by 2015 (Global CCS Institute 2014). The first offshore commercial-scale project that is not an EOR is the Sleipner gas field operated by STATOIL in the North Sea since 1996. Approximately 1 $MtCO_2$ is separated annually from the produced natural gas and injected into the deep saline aquifer located approximately 800 m to 1,000 m depth formations below the seabed. Monitoring by seismic reflection method, to gain an understanding of the behavior of the stored CO_2, as well as gravity monitoring using seafloor gravity meters, is being performed (Arts et al. 2004).

Other than the 13 sites currently in operation, about 42 sites are being planned for CCS-related projects, and they are not limited to EOR- and EGR-related projects. These include projects that use aquifers as the storage site (Global CCS Institute 2014). However, there is an emerging shift to EOR-related projects, in which economic incentives are in effect, mainly in the United States and other countries. On the other hand, a technical committee known as the TC265 was established at the ISO (International Standardization Organization) in October 2011, and examination for the international standardization of CCS begins.

Abovementioned technical issues regarding CGS should be examined by applying the techniques to the individual site-specific geological storage site, and then the techniques will be expected to brush up, supporting practical realization of CGS over the world.

References

Alam A, Niioka M, Fujii Y, Fukuda D, Kodama J (2014) Effects of confining pressure on the permeability of three rock types under compression. Int J Rock Mech Min Sci 65:49–61

Alnes H, Eiken O, Stenvold T (2008) Monitoring gas production and CO_2 injection at the Sleipner field using time-lapse gravimetry. Geophysics 73:WA155–WA162

Arts R, Eiken O, Chadwick A, Zweigel P, Van del Meer B, Kirby G (2004) Seismic monitoring at the Sleipner underground CO_2 storage site (North Sea). In: Baines SJ, Worden RH (eds) Geological storage of carbon dioxide, vol 233, Special publications. Geological Society, London, pp 181–191

Bachu S, Bennion DB (2008) Effects of in-situ conditions on relative permeability characteristics of CO_2-brine systems. Environ Geol 54:1707–1722

Bachu S, Bennion DB (2009) Interfacial tension between CO_2, freshwater, and brine in the range of pressure from (2 to 27) MPa, temperature from (20 to 125) °C, and water salinity from (0 to 334 000) mg · L^{-1}. J Chem Eng Data 54:765–775

Bénézeth P, Palmer DA, Anovitz LM, Horita J (2007) Dawsonite synthesis and reevaluation of its thermodynamic properties from solubility measurements: implications for mineral trapping of CO_2. Geochim Cosmochim Acta 71:4438–4455

Blum AE, Stillings LL (1995) Feldspar dissolution kinetics. In: White AF, Brantley SL (eds) Chemical weathering rates of silicate minerals, vol 31, Reviews in mineralogy. Mineralogical Society of America, Washington, DC, pp 291–351

Blunt M, Fayers FJ, Orr FM Jr (1993) Carbon dioxide in enhanced oil recovery. Energy Convers Manage 34:1197–1204

Brodsky EE, Prejean SG (2005) New constraints on mechanisms of remotely triggered seismicity at long valley caldera. J Geophys Res Solid Earth (1978–2012) 110(B4), B04302, doi:10.1029/2004JB003211

Burch TE, Nagy KL, Lasaga AC (1993) Free energy dependence of albite dissolution kinetics at 80°C and pH8.8. Chem Geol 105:137–162

Cappa F, Rutqvist J (2011) Modeling of coupled deformation and permeability evolution during fault reactivation induced by deep underground injection of CO_2. Int J Greenhouse Gas Control 5(2):336–346

Cappa F, Rutqvist J, Yamamoto K (2009) Modeling crustal deformation and rupture processes related to upwelling of deep CO_2-rich fluids during the 1965–1967 Matsushiro earthquake swarm in Japan. J Geophys Res 114(B10), B10304, doi:10.1029/2009jb006398

Chadwick RA, Noy D, Arts R, Eiken O (2009) Latest time-lapse seismic data from Sleipner yield new insights into CO_2 plume development. Energy Procedia 1:2103–2110

Chin L, Raghavan R, Thomas L (2000) Fully coupled geomechanics and fluid-flow analysis of wells with stress-dependent permeability. SPE J 5(01):32–45

Chiquet P, Broseta D, Thibeau S (2007) Wettability alteration of caprock minerals by carbon dioxide. Geofluids 7:112–122

Cochran ES, Vidale JE, Tanaka S (2004) Earth tides can trigger shallow thrust fault earthquakes. Science 306(5699):1164–1166

Deichmann N, Giardini D (2009) Earthquakes induced by the stimulation of an enhanced geothermal system below Basel (Switzerland). Seismol Res Lett 80(5):784–798

Dewhurst DN, Jones RM, Raven MD (2002) Microstructural and petrophysical characterization of Muderong Shale: application to top seal risking. Petrol Geosci 8:371–383

Egermann P, Lombard J-M, Bretonnier P (2006) A fast and accurate method to measure threshold capillary pressure of caprocks under representative conditions. In: SCA2006-07, presented at the 2006 SCA international symposium, Trondheim, 18–22 Sept

Eiken O, Ringrose P, Hermanrud C, Nazarian B, Torp TA, Høier L (2011) Lessons learned from 14 years of CCS operations: Sleipner, In Salah and Snøhvit. Energy Procedia 4:5541–5548

Ellsworth WL (2013) Injection-induced earthquakes. Science 341(6142):1225942

Etchecopar A, Vasseur G, Daignieres M (1981) An inverse problem in microtectonics for the determination of stress tensors from fault striation analysis, Journal of Structural Geology, 3 (1), 51–65

Funatsu T, Okuyama Y, Lei X, Uehara S, Nakashima Y, Fujii T, Nakao S (2013) Assessing the geomechanical responses of storage system in CO_2 geological storage: an introduction of research program in the national institute for advanced industrial science and technology (AIST). Energy Procedia 37:3875–3882

Gaus I, Audigane P, André L, Lions J, Jacquemet N, Durst P, Czernichowski-Lauriol I, Azaroual M (2008) Geochemical and solute transport modeling for CO_2 storage, what to expect from it? Int J Greenhouse Gas Control 2:605–625

Gephart JW, Forsyth DW (1984) An improved method for determining the regional stress tensor using earthquake focal mechanism data: application to the San Fernando earthquake sequence, Journal of Geophysical Research: Solid Earth (1978–2012), 89(B11), 9305–9320.

Giammanco S, Palano M, Scaltrito A, Scarfi L, Sortino F (2008) Possible role of fluid overpressure in the generation of earthquake swarms in active tectonic areas: the case of the Peloritani Mts. (Sicily, Italy). J Volcanol Geotherm Res 178(4):795–806

Global CCS Institute (2014) Status of CCS project database. http://www.globalccsinstitute.com/data/status-ccsproject-database

Gunter WD, Gentzis T, Rottenfusser BA, Richardson RJH (1997) Deep coalbed methane in Alberta, Canada: a fuel resource with the potential of zero greenhouse gas emissions. Energy Convers Manage 38:217–222

Hagiwara T, Iwata T (1968) Summary of the seismographic observation of the Matsushiro swarm earthquakes. Bull Earthq Res Inst 46:485–515

Hainzl S, Ogata Y (2005) Detecting fluid signals in seismicity data through statistical earthquake modeling. J Geophys Res Solid Earth (1978–2012) 110(B5), B5S07, doi:10.1029/2004JB003247

Hellevang H, Aagaard P, Oelkers EH, Kvamme B (2005) Can dawsonite permanently trap CO_2? Environ Sci Technol 39:8281–8287

Hellmann R, Tisserand D (2006) Dissolution kinetics as a function of the Gibbs free energy of reaction: an experimental study based on albite feldspar. Geochim Cosmochim Acta 70:364–383

Helmstetter A, Sornette D, Grasso JR (2003) Mainshocks are aftershocks of conditional foreshocks: how do foreshock statistical properties emerge from aftershock laws. J Geophys Res Solid Earth (1978–2012) 108(B1), B012046, doi:10.1029/2002JB001991

Hildenbrand A, Schlömer S, Krooss BM (2002) Gas breakthrough experiments on fine-grained sedimentary rocks. Geofluids 2:3–23

Hildenbrand A, Schlömer S, Krooss BM, Littke R (2004) Gas breakthrough experiments on pelitic rocks: comparative study with N_2, CO_2 and CH_4. Geofluids 4:61–80

IPCC (2005) Underground geological storage. In: Metz B, Davidson O, Coninck H, Loos M, Meyer L (eds) IPCC special report on carbon dioxide capture and storage. Cambridge University Press, New York, pp 195–276

Ishido T, Pritchett JW (1999) Numerical simulation of electrokinetic potentials associated with subsurface fluid flow. J Geophys Res 104:15247–15259

Ishido T, Tosha T, Akasaka C, Nishi Y, Sugihara M, Kano Y, Nakanishi S (2011) Changes in geophysical observables caused by CO_2 injection into saline aquifers. Energy Procedia 4:3276–3283

Ishido T, Pritchett JW, Nishi Y, Sugihara M, Garg SK, Stevens JL, Tosha T, Nakanishi S, Nakao S (2015) Application of various geophysical techniques to reservoir monitoring and modeling. In: Proceedings, World Geothermal Congress, Melbourne

Itasca F (2000) Fast Lagrangian analysis of continua. Itasca Consulting Group, Minneapolis

Johnson JW, Nitao JJ, Knauss KG (2004) Reactive transport modeling of CO_2 storage in saline aquifers to elucidate fundamental processes, trapping mechanisms and sequestration partitioning. In: Baines SJ, Worden RH (eds) Geological storage of carbon dioxide. The Geological Society, London, pp 107–128

Kano Y, Funatsu T, Nakao S, Kusunose K, Ishido T, Lei X, Tosha T (2014) Analysis of changes in stress state and fault stability related to planned CO_2 injection at the Tomakomai offshore site. Energy Procedia 63:2870–2878

Kasahara K (1970) The source region of the Matsushiro swarm earthquakes. Bull Earthq Res Inst Tokyo Univ 48:581–602

Katz AJ, Thompson AH (1986) Quantitative prediction of permeability in porous rock. Phys Rev B 34:8179–8181

Katz AJ, Thompson AH (1987) Prediction of rock electrical conductivity from mercury injection measurements. J Geophys Res 92:599–607

King GC, Stein RS, Lin J (1994) Static stress changes and the triggering of earthquakes. Bull Seismol Soc Am 84(3):935–953

Koide HG, Tazaki Y, Noguchi Y, Nakayama S, Iijima M, Ito K, Shindo Y (1992) Subterranean containment and long-term storage of carbon dioxide in unused aquifers and in depleted natural gas reservoirs. Energy Convers Manage 33:619–626

Lasaga AC (1998) Kinetic theory in the earth sciences. Princeton University Press, Princeton

Lei X, Ma S (2013) Insights gained from the injection-induced seismicity in the southwestern Sichuan Basin, China. In: Ito T (ed) 6th international symposium on in-situ rock stress, Sendai, pp 176–187

Lei X, Xue Z (2009) Ultrasonic velocity and attenuation during CO_2 injection into water-saturated porous sandstone: measurements using difference seismic tomography. Phys Earth Planet In 176(3–4):224–234

Lei X, Yu G, Ma S, Wen X, Wang Q (2008) Earthquakes induced by water injection at ~ 3 km depth within the Rongchang gas field, Chongqing, China. J Geophys Res 113(B10), B10310, doi:10.1029/2008jb005604

Lei X, Tamagawa T, Tezuka K, Takahashi M (2011a) Role of drainage conditions in deformation and fracture of porous rocks under triaxial compression in the laboratory. Geophys Res Lett 38 (24), L24310, doi:10.1029/2011gl049888

Lei X, Xie C, Fu B (2011b) Remotely triggered seismicity in Yunnan, southwestern China, following the 2004mw9.3 Sumatra earthquake. J Geophys Res 116(B8), B08303, doi:10.1029/2011jb008245

Lei X, Ma S, Chen W, Pang C, Zeng J, Jiang B (2013) A detailed view of the injection-induced seismicity in a natural gas reservoir in Zigong, southwestern Sichuan Basin, China. J Geophys Res Solid Earth 118(8):4296–4311

Lei X, Li X, Li Q (2014) Insights on injection-induced seismicity gained from laboratory AE study – fracture behavior of sedimentary rocks. In: Shimizu N, Kaneko K, Kodama J (eds) 8th Asian rock mechanics symposium. Japanese Committee for Rock Mechanics, Sapporo, pp 947–953

Lei X, Funatsu T, Ma S, Liu L (2015) A laboratory acoustic emission experiment and numerical simulation of rock fracture driven by a high-pressure fluid source. J Rock Mech Geotech, doi:10.1016/j.jrmge.2015.02.010 (In press, Available online 4 June 2015)

Li S, Dong M, Li Z, Huang S, Qing H, Nickel E (2005) Gas breakthrough pressure for hydrocarbon reservoir seal rocks: implications for the security of long-term CO_2 storage in the Weyburn field. Geofluids 5:326–334

Litynski J, Rodosta T, Brown B (2012) Best practices for monitoring, verification, and accounting of CO_2 stored in deep geologic formations – 2012 update. NETL, Albany OR USA

Liu YP, Hopmans JW, Grismer ME, Chen JY (1998) Direct estimation of air-oil and oil–water capillary pressure and permeability relations from multi-step outflow experiments. J Contam Hydrol 32:223–245

Lockner DA, Beeler NM (1999) Premonitory slip and tidal triggering of earthquakes. J Geophys Res Solid Earth (1978–2012) 104(B9):20133–20151

Lüttge A (2006) Crystal dissolution kinetics and Gibbs free energy. J Electron Spectrosc Relat Phenom 150:248–259

Marsan D, Prono E, Helmstetter A (2013) Monitoring aseismic forcing in fault zones using earthquake time series. Bull Seismol Soc Am 103(1):169–179

Mavko G, Mukerji T, Dvorkin J (2009) The rock physics handbook, 2nd edn. Cambridge University Press, Cambridge

Mazzoldi A, Rinaldi AP, Borgia A, Rutqvist J (2012) Induced seismicity within geological carbon sequestration projects: maximum earthquake magnitude and leakage potential from undetected faults. Int J Greenhouse Gas Control 10:434–442

Miller SA, Collettini C, Chiaraluce L, Cocco M, Barchi M, Kaus BJ (2004) Aftershocks driven by a high-pressure CO_2 source at depth. Nature 427(6976):724–727

Morris A, Ferrill DA, Brent Henderson DB (1996) Slip-tendency analysis and fault reactivation. Geology 24(3):275

Morse JW, Arvidson RS, Lüttge A (2007) Calcium carbonate formation and dissolution. Chem Rev 107:342–381

Nooner SL, Eiken O, Hermanrud C, Sasagawa GS, Stenvold T, Zumberge MA (2007) Constraints on the in situ density of CO_2 within the Utsira formation from time-lapse seafloor gravity measurements. Int J Greenhouse Gas Control 1:198–214

Ogata Y (1992) Detection of precursory relative quiescence before great earthquakes through a statistical model. J Geophys Res Solid Earth (1978–2012) 97(B13):19845–19871

Ogata Y (2001) Increased probability of large earthquakes near aftershock regions with relative quiescence. J Geophys Res Solid Earth (1978–2012) 106(B5):8729–8744

Ohtake M (1976) A review of the Matsushiro earthquake swarm. Kagaku (Jpn) 46:306–313

Okuyama Y, Sasaki M, Nakanishi S, Todaka N, Ajima S (2009) Geochemical CO_2 trapping in open aquifer storage – the Tokyo Bay model. Energy Procedia 1:3253–3258

Onuma T, Ohkawa S (2009) Detection of surface deformation related with CO_2 injection by DInSAR at In Salah, Algeria. Energy Procedia 1(1):2177–2184
Palandri JL, Kharaka YK (2004) A compilation of rate parameters of water-mineral interaction kinetics for application to geochemical modeling. U.S. Geological Survey, open file reports, 2004–1068
Pittman ED (1992) Relationship of porosity and permeability to various parameters derived from mercury injection – capillary pressure curves for sandstone. AAPG Bull 76:191–198
Plug W-J, Bruining J (2007) Capillary pressure for the sand-CO_2-water system under various pressure conditions. Application to CO_2 sequestration. Adv Water Resour 30:2339–2353
Pritchett JW (1995) STAR – a geothermal reservoir simulation system. In: Proceedings, World Geothermal Congress, Florence, pp 2959–2963
Pritchett JW (2002) STAR user's manual version 9.0. SAIC-02/1055, San Diego
Pritchett JW (2008) New "SQSCO2" equation of state for the "STAR" code. SAIC, San Diego
Pritchett JW, Stevens JL, Wannamaker P, Nakanishi S, Yamazawa S (2000) Theoretical feasibility studies of reservoir monitoring using geophysical survey techniques. In: Proceedings, World Geothermal Congress, Kyushu/Tohoku, pp 2803–2808
Pruess K (2005) ECO2N: a TOUGH2 fluid property module for mixtures of water, NaCl, and CO_2. LBNL-57952, Berkeley
Pruess K (2011) ECO2M: a TOUGH2 fluid property module for mixtures of water, NaCl, and CO_2, including super- and sub-critical conditions, and phase change between liquid and gaseous CO_2. LBNL-4590E, Berkeley
Pruess K, García J, Kovscek T, Oldenburg C, Rutqvist J, Steefel C, Xu T (2002) Intercomparison of numerical simulation codes for geologic disposal of CO_2. LBNL-51813, Berkeley
Purcell WR (1949) Capillary pressures — their measurement using mercury and the calculation of permeability therefrom. AIME Pet Trans 186:39–48
Rinaldi AP, Rutqvist J (2013) Modeling of deep fracture zone opening and transient ground surface uplift at kb-502 CO_2 injection well, In Salah, Algeria. Int J Greenhouse Gas Control 12:155–167
Rutqvist J, Wu Y-S, Tsang C-F, Bodvarsson G (2002) A modeling approach for analysis of coupled multiphase fluid flow, heat transfer, and deformation in fractured porous rock. Int J Rock Mech Min Sci 39(4):429–442
Rutqvist J, Birkholzer J, Tsang C-F (2008) Coupled reservoir–geomechanical analysis of the potential for tensile and shear failure associated with CO_2 injection in multilayered reservoir–caprock systems. Int J Rock Mech Min Sci 45(2):132–143
Schowalter TT (1979) Mechanics of secondary hydrocarbon migration and entrapment. AAPG Bull 63:723–760
Shah V, Broseta D, Mouronval G, Montel F (2008) Water/acid gas interfacial tensions and their impact on acid gas geological storage. Int J Greenhouse Gas Control 2:594–604
Sorai M, Sasaki M (2010) Dissolution kinetics of anorthite in a supercritical CO_2–water system. Am Mineral 95:853–862
Sorai M, Fujii T, Kano Y, Uehara S, Honda K (2014a) Experimental study of sealing performance: effects of particle size and particle-packing state on threshold pressure of sintered compacts. J Geophys Res. doi:10.1002/2014JB011177
Sorai M, Sasaki M, Fujii T, Kano Y, Uehara S (2014b) Evaluation of sealing performance of alternated sandstone and mudstone layers on CO_2 geological sequestration (in Japanese). GSJ Chishitsu News 3:153–156
Stein RS (1999) The role of stress transfer in earthquake occurrence. Nature 402(6762):605–609
Stevens JL, Pritchett JW, Garg SK, Ishido T, Tosha T (2003) Prediction of seismic observables from geothermal reservoir simulations. Geotherm Resour Counc Trans 27:841–846
Streit JE, Hillis RR (2004) Estimating fault stability and sustainable fluid pressures for underground storage of CO_2 in porous rock. Energy 29(9–10):1445–1456
Sugihara M, Ishido T (2008) Geothermal reservoir monitoring with a combination of absolute and relative gravimetry. Geophysics 73:WA37–WA47

Sugihara M, Nawa K, Nishi Y, Ishido T, Soma N (2013) Continuous gravity monitoring for CO_2 geo-sequestration. Energy Procedia 37:4302–4309

Swanson BF (1981) A simple correlation between permeabilities and mercury capillary pressures. J Petrol Tech 33:2488–2504

Terakawa T, Hashimoto C, Matsu'ura M (2013) Changes in seismic activity following the 2011 Tohoku-oki earthquake: effects of pore fluid pressure. Earth Planet Sci Lett 365:17–24

Thomeer JHM (1960) Introduction of a pore geometrical factor defined by the capillary pressure curve. J Petrol Tech 12:73–77

Todesco M, Rutqvist J, Chiodini G, Pruess K, Oldenburg CM (2004) Modeling of recent volcanic episodes at phlegrean fields (italy): Geochemical variations and ground deformation. Geothermics 33(4):531–47

Tsukahara H, Yoshida N (2005) Origin of groundwater which caused the Matsushiro earthquake swarm. Chikyu 27(6):453–460

Utsu T (2002) Statistical features of seismicity. Int Geophys Ser 81(A):719–732

Washburn EW (1921) Note on a method of determining the distribution of pore sizes in a porous material. Proc Natl Acad Sci 7:115–116

White AF, Brantley SL (2003) The effect of time on the weathering of silicate minerals: why do weathering rates differ in the laboratory and field? Chem Geol 202:479–506

White SP, Allis RG, Moore J, Chidsey T, Morgan C, Gwynn W, Adams M (2005) Simulation of reactive transport of injected CO_2 on the Colorado Plateau, Utah. USA Chem Geol 217:387–405

Wollenweber J, Alles S, Busch A, Kroos BM, Stanjek H, Littke R (2010) Experimental investigation of the CO_2 sealing efficiency of caprocks. Int J Greenhouse Gas Control 4:231–241

Xu T, Apps JA, Pruess K (2003) Reactive geochemical transport simulation to study mineral trapping for CO_2 disposal in deep arenaceous formations. J Geophys Res 108(B2):2071. doi:10.1029/2002JB001979

Xu T, Apps JA, Pruess K (2005) Mineral sequestration of carbon dioxide in a sandstone-shale system. Chem Geol 217:295–318

Yamashita T, Suzuki T (2009) Quasi-static fault slip on an interface between poroelastic media with different hydraulic diffusivity: a generation mechanism of afterslip. J Geophys Res 114(B3), B03405, doi:10.1029/2008jb005930

Zhang J, Standifird W, Roegiers J-C, Zhang Y (2007) Stress-dependent fluid flow and permeability in fractured media: from lab experiments to engineering applications. Rock Mech Rock Eng 40(1):3–21

Zhuang J, Ogata Y, Vere-Jones D (2002) Stochastic declustering of space-time earthquake occurrences. J Am Stat Assoc 97(458):369–380

Zoback MD, Gorelick SM (2012) Earthquake triggering and large-scale geologic storage of carbon dioxide. Proc Natl Acad Sci U S A 109(26):10164–10168

Zoback M, Kohli A, Das I, McClure M (2013) The importance of slow slip on faults during hydraulic fracturing stimulation of shale gas reservoirs, paper presented at SPE Americas Unconventional Resources Conference, 5-7 June, Pittsburgh, Pennsylvania USA

Conversion of CO_2 to Value Added Chemicals: Opportunities and Challenges

Arun S. Agarwal, Edward Rode, Narasi Sridhar, and Davion Hill

Contents

A.S. Agarwal (✉) • E. Rode • N. Sridhar
Materials Program, Strategic Research and Innovation, DNV GL, Dublin, OH, USA
e-mail: arun.agarwal@dnvgl.com; edward.rode@dnvgl.com; narasi.sridhar@dnvgl.com

D. Hill
Energy and Materials, DNV GL, Dublin, OH, USA
e-mail: davion.m.hill@dnvgl.com

W.-Y. Chen et al. (eds.), *Handbook of Climate Change Mitigation and Adaptation*,
DOI 10.1007/978-3-319-14409-2_86

Abstract

The world is likely to emit almost 40 Gt/year of CO_2 into the atmosphere. Even if only a small fraction of the globally emitted CO_2 is captured, there will be a large quantity of CO_2 available to society for use in a variety of ways. Thus, CO_2 should not be regarded as a waste product, but as an asset that, with human ingenuity, could be used in a sustainable way. Since sustainability is at the intersection of environmental, economic, and intergenerational stewardship, the selection of a CO_2 utilization process must offer net CO_2 and waste reductions compared to conventional methods of producing the same end product, must be economical, and must not leave any additional problems for future society to solve. The criteria for selection may involve a variety of local considerations, such as government incentives, the availability of suitable renewable energy source, availability of water and other chemicals, land use, local demand for a specific product, etc. Therefore, CO_2 utilization is a locally sustainable solution, rather than a one-size-fits-all approach. Utilization of CO_2 may involve mostly physical processes, such as in enhanced oil recovery (EOR), solvent use, and beverage industry, where the CO_2 is essentially retained in its original valence state, or chemical processes, where its valence state undergoes a change (Fig. 1). We will focus in this chapter on chemical conversion, which broadly includes thermochemical and electrochemical processes. The critical technology development parameters as well as the barriers for adoption of utilization technologies are also discussed.

Introduction

The utilization of CO_2 to make a variety of end products can be potentially transformational because it enables the valorization of CO_2 using thermochemical, biochemical, and electrochemical processes (Fig. 1). The utilization technologies will vary in the volume of CO_2 utilized, the economic value of the end product (i.e., value added), and the time of fixation of CO_2 (Fig. 2). Carbon capture and storage (CCS) can potentially store and theoretically fix large volumes of CO_2 in geological media for hundreds of years but without any monetary value (unless

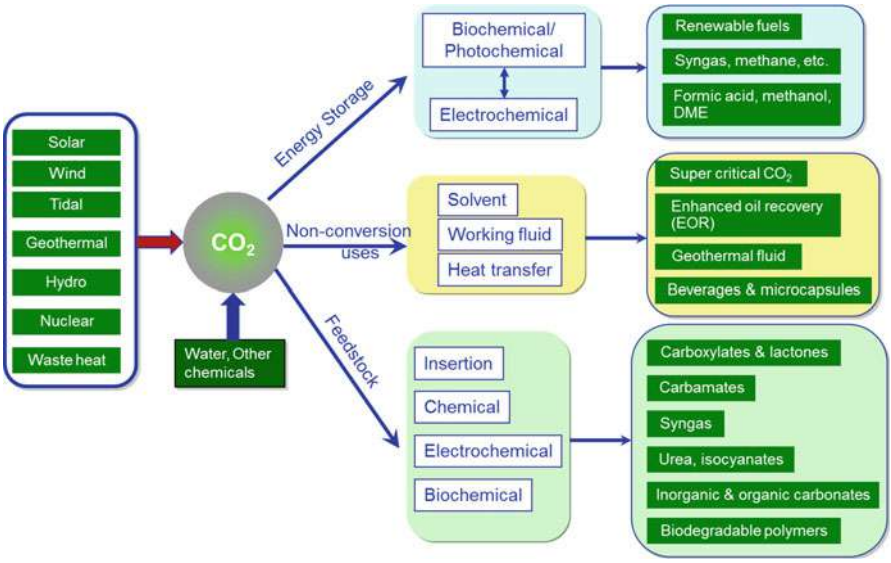

Fig. 1 Different ways in which CO_2 can be used to create value and the energy sources needed for sustainable use (Peters et al. 2011; Wu et al. 2007; Tao 2008; Zaelke et al. 2011; Pew Charitable Trusts 2012; Global CCS Institute 2012; Al-Musabbeh et al. 2006; Moats et al. 2008)

enhanced oil recovery (EOR) is done). Cements and minerals made from CO_2 can provide some value, while being able to convert relatively large volumes of CO_2. On the other hand, specialty chemicals can have attractive economic value, but are in limited quantities, and fix CO_2 over a limited period of time. Plastics, in principle, can be stable for many decades, but will eventually biodegrade. Fuels have a very short fixation time, emitting CO_2 as soon as they are burned. However, they add significant value because they contribute to energy storage from renewable power and provide energy security to those countries that are dependent on foreign sources of fuel. It is already recognized that biofuels from photosynthetic plants and organisms have the potential to substantially reduce net life cycle CO_2 emissions. However, photosynthetic biofuels, including sugar cane, cellulosic, and algae-based biofuels, require significant land use.

An example of a novel pathway is the conversion of formic acid and methanol into ethanol. The traditional corn-based ethanol process emits about 2.6 mol of CO_2 per mole of ethanol (or about 70 g of CO_2 equivalent/MJ). This does not include the CO_2 emitted upon use in the internal combustion engine. In contrast, the electro-biochemical route of ethanol from CO_2 and methane could involve a net consumption of CO_2 of the order of three million ton per year even using fossil-based power. The net reductions can be increased if greater percentage of renewable power is used.

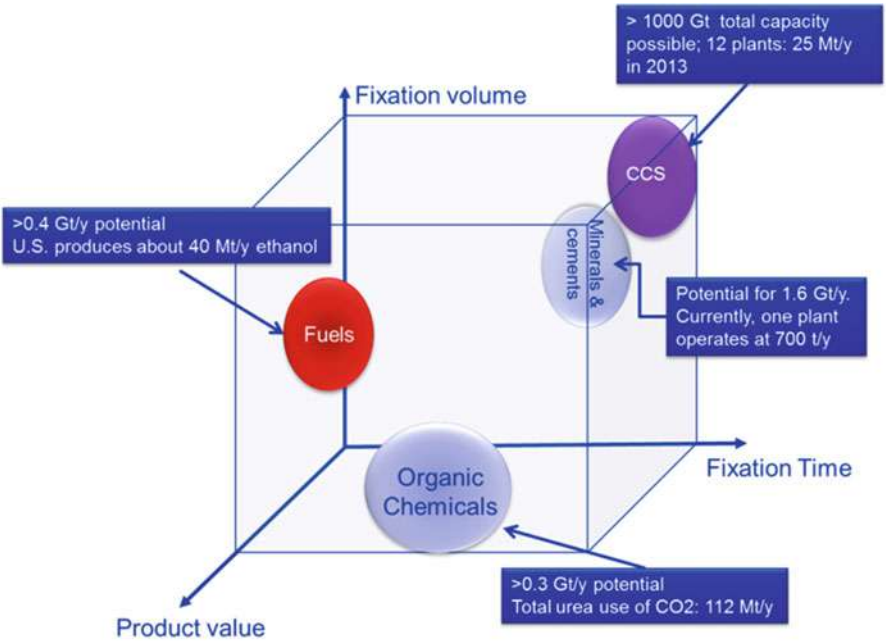

Fig. 2 CO_2 utilization value for different products (Peters et al. 2011; Wu et al. 2007; Tao 2008; Zaelke et al. 2011; Pew Charitable Trusts 2012; Global CCS Institute 2012; Al-Musabbeh et al. 2006; Moats et al. 2008; Hu et al. 2013)

Thermochemical Methods

Chemical fixation of CO_2 to useful products might represent an attractive way of reducing emissions of CO_2 to air. Using CO_2 as a feedstock also has the potential of replacing fossil feedstock such as natural gas, carbon monoxide, syngas, methanol, and even higher hydrocarbons (Fig. 3). The main challenge in utilizing CO_2 as a chemical feedstock is its unfavorable thermodynamics.

Figure 3 summarizes the major CO_2 to chemical routes which will be discussed. This is by no means an all-inclusive representation. These routes were chosen from the many options based on the relative maturity of the technologies as well the sizeable market volumes the chemical can support. For some chemicals, such as formic acid, the direct market is relatively small (<1 MM tpy), but the market can be expanded by employing it as a base chemical to manufacture other large volume chemicals.

There are numerous reviews and books which provide descriptions of reactions, products, and markets derived from CO_2 chemistry (Peters et al. 2011; Quadrelli et al. (2011); Wu et al. 2007; Hu et al. 2013; Quadreilli et al. 2011; Centi and Perathoner 2009; Ratnasamy and Wagner 2009).

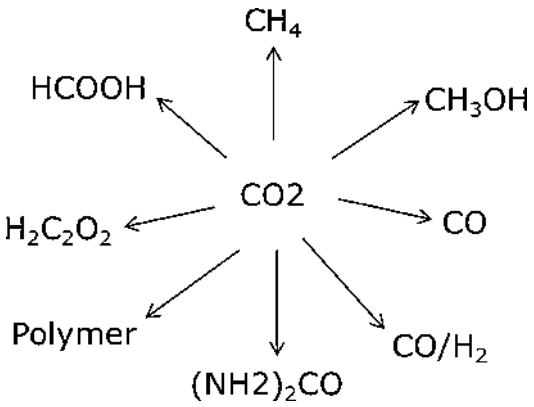

Fig. 3 CO_2 conversion to chemicals

Hydrogen Supply

The interesting observation about the various paths in Fig. 3 is the hydrogen requirement for all products except carbon monoxide. So while the main problem being addressed for the CO_2 utilization is obviously the CO_2 itself, the problem can in large part be restated to be a "hydrogen problem." The next section discusses the requirements to supply the hydrogen as dihydrogen (H_2).

Steam methane reforming (SMR) is the most common method of producing commercial bulk hydrogen. Other hydrocarbons may be used, such as propane or naphtha. Hydrogen is used in the industrial synthesis of ammonia and other chemicals. At high temperatures (800–1000 °C) and 20–30 atm in the presence of nickel-based catalyst, steam reacts with methane to yield carbon monoxide and hydrogen (Olah 2005):

$$CH_4 + H_2O \rightleftharpoons CO + 3H_2 \quad (1)$$

Additional hydrogen can be recovered by a lower-temperature water-gas shift (WGS) reaction with the carbon monoxide produced. The reaction is summarized by

$$CO + H_2O \rightleftharpoons CO_2 + H_2 \quad (2)$$

Carbon dioxide is a substantial waste product from these processes. SMR emits a mole of CO_2 per mole of methane (2.75 kg CO_2 per kg of methane) reacted in the scheme above. The gas is then fed to a gas separation system, such as pressure swing adsorption, which can provide hydrogen at a range of purities, such as 99.5–99.995 % H_2. Impurities such as CO, which acts as a poison for most precious metal catalysts, can be minimized to less than 10 ppm.

Because of the concurrent emission of CO_2 from SMR, lower CO_2-emitting processes need to be used for H_2 supply. The predominant renewable method for H_2 production is via electrolytic water splitting. The electrical energy for this process needs to be from renewable sources, or a non-carbon-emitting source, such as wind, solar, nuclear, or hydroelectric. These methods are described elsewhere (Utgikar 2006).

Table 1 LCA-based CO_2 emissions for various production methods

Hydrogen production method	Kg CO_2/kg H_2	Mole CO_2/mol H_2
Biomass	2.9	0.23
Hydroelectric/elect.	2	0.09
Solar photovoltaic	6	0.27
Wind/elect.	1.5	0.045
Steam reforming	12	0.55
High-temp electrolysis	4	0.18

Utgikar and Thiesen report the life cycle assessment of the various hydrogen production methods (Utgikar 2006). They reported the mass of CO_2 emitted per mass of H_2 produced by various means. Hydrogen from SMR emits roughly 0.55 mol CO_2/mol H_2 produced. Wind-generated electricity supplying a water electrolysis unit is the lowest in the study, at ~0.045 mol CO_2/mol H_2. Table 1 provides a summary of various H_2 generation technologies along with the respective carbon balances.

The key message from the life cycle assessment (LCA) results is that CO_2 emissions are generated from even the "clean" sources of H_2. But there is a wide range – fossil fuel systems being the worst emitter.

Carbon Monoxide and Synthesis Gas Production

Catalytic Hydrogenation

By reversing the water-gas shift reaction (2), one can produce carbon monoxide from carbon dioxide and hydrogen (Ratnasamy and Wagner 2009; Whitlow and Parish 2003; Edwards and Maitra 1995):

$$CO_2 + H_2 \rightarrow CO + H_2O \tag{3}$$

Depending on the reaction conditions, the equilibrium for the water-gas shift can be pushed in either the forward or reverse direction with temperature and pressure adjustments. The reversibility of the WGSR is important in the production of ammonia, methanol, and Fischer–Tropsch synthesis, where the ratio of H_2/CO is critical. Many industrial processes exploit the reverse water-gas shift (RWGS) reaction as a source of the synthetically valuable CO from cheap CO_2. Typically, it is done using a copper on alumina catalyst.

Reforming with CO_2

Dry reforming refers to the production of synthesis gas ($CO + H_2$) from natural gas, petroleum or coal, and CO_2. By contrast to SMR above, there is no water introduced in this process. CO_2 is the soft oxidant (Logan 1997; Song and Pan 2004; Ted Oyama et al. 2012). For natural gas, the reaction is

$$CO_2 + CH_4 \rightarrow 2CO + 2H_2 \tag{4}$$

The syngas can then be converted to chemical products and hydrocarbons. However, Oyama points out that this reaction has limited utility due to the consumption

of the hydrogen generated by the reverse water-gas shift reaction (Ted Oyama et al. 2012). This point is missed in many studies due to operation at low pressures. At pressures above 5 atm, the RWGS takes over. That is, H_2 is further converted to H_2O according to reaction (3). This reduces the H_2/CO ratio to less than one, an unfavorable composition if the desire is to upgrade the CO/H_2 to higher hydrocarbons. The system is also plagued by rapid catalyst deactivation as a result of coke formation. So while attractive on paper, the system has yet to be successfully commercialized.

A second option for syngas production is a combination of the steam methane reforming reaction (1) and dry reforming reaction. The net reaction in this case is

$$CH_4 + H_2O \rightarrow CO + 3H_2 \tag{5}$$

$$CO_2 + CH_4 \rightarrow 2CO + 2H_2O \tag{6}$$

$$\text{Net} : 3CH_4 + \ + CO_2 \rightarrow 4CO + 6H_2 \tag{7}$$

This bi-reforming gives a molar CO:H_2 ratio of 1:1.5, the stoichiometry required for methanol synthesis (Goeppert et al. 2014). The presence of steam reduces the tendency to form coke, and the system has shown good stability at low pressures and, with different catalysts, at elevated pressures (Wittcoff et al. 2013).

Yet another option is tri-reforming of methane, a novel concept for catalytic production of industrially useful synthesis gas with desired H_2/CO ratio (Ted Oyama et al. 2012). The proposed tri-reforming process is a synergetic combination of CO_2 reforming, steam reforming, and partial oxidation of methane in a single reactor for effective production of industrially useful synthesis gas (syngas). Power plant emissions flue gas typically contains a small amount of oxygen. The oxygen is typically a poison for water-gas shift catalysts and needs to be removed if RWGS is to be used. However, the tri-forming does not need this removal and allows for effectively an autothermal oxidation of methane. Another key feature is the ability to adjust feed composition to CO:H_2 ratio in the product, preferably into the 1:2–3 range needed for conversion to methanol or hydrocarbons via Fischer–Tropsch. These options are discussed extensively in recent reviews (Quadreilli et al. 2011; Logan 1997; Song and Pan 2004).

Methanol Synthesis

Renewably produced methanol has been actively promoted as an alternative fuel and chemical to the traditional energy and petrochemicals markets based on oil and natural gas. The methanol market is well established with a global consumption of 58 million tons in 2008 and 83 % of the product going to chemicals production (Olah et al. 2011).

Catalytic hydrogenation of mixture of CO_2 and CO is at the basis of syngas processes. These syngas processes make it possible to produce a variety of chemical

products, including methanol. Chemical reactions involved for methanol production are

$$CO + 2H_2 \rightarrow CH_3OH \tag{8}$$

$$CO_2 + 3H_2 \rightarrow CH_3OH + H_2O \tag{9}$$

Methanol production can hence be enhanced by injecting CO_2 (Wittcoff et al. 2013; Olah et al. 2009; http://www.carbonrecycling.is/). Both reactions (8) and (9) are exothermic and favored by high pressures. The standard operating conditions (for low-pressure synthesis) are 50–80 bar pressure and 210–290 °C temperature (reactor inlet/outlet).

Methanol production has trended toward very large plants with daily capacity at 3000–5000 t. This trend has been largely due to the economies of scale and the lower production costs. The Middle East, Latin America, and Asia produce 80 % of the market. With recent increases of shale gas in the USA, some methanol production is returning to the USA (http://www.carbonrecycling.is/).

In order to capitalize on renewable energy and point sources of CO_2, carbon-neutral synthesis of methanol plants will need to be significantly smaller than the megaplants. Carbon Recycling Inc (CRI) is one of the first companies to demonstrate industrial solutions in power-to-methanol production, by capturing carbon dioxide (CO_2) from flue gas, large-scale conversion of renewable energy to hydrogen, and reacting hydrogen and carbon dioxide to produce methanol. CRI's power-to-methanol production plant in Iceland, which has been operating since 2012, produces ultra-low carbon intensity methanol that is used for biodiesel manufacturing and gasoline blending. The plant has recently been expanded to 4000-t/year production capacity (Pontzen et al. 2011).

Methanol can be used in various sectors, and if CO_2 comes from the atmosphere in the beginning, the methanol is then considered CO_2 neutral when burned in an internal combustion engine or when used in a direct methanol fuel cell (DMFC), for instance. This is the basis for the so-called "methanol" economy where methanol replaces fossil fuels and is used as an energy carrier (Olah 2005).

Production of higher hydrocarbons from methanol is a well-established technology as well. For example, methanol to olefins and methanol to gasoline technology is well known. Another possibility is the formation of dimethyl ether (DME) from methanol (Tao 2008). This reaction is also exothermic (Utgikar 2006; http://etogas.com/fileadmin/documents/datasheets/ETOGAS_Hydrogen-to-SNG_Datasheet_EN_Rev1.pdf):

$$2CH_3OH \rightarrow CH_3OCH_3 + H_2O \quad \Delta H = -21.25\ \text{kJ/mol} \tag{10}$$

DME has many advantages: its fuel characteristics are similar to LPG, it is relatively environmentally friendly, and it is nontoxic and noncarcinogenic.

Methanation

The methanation of carbon dioxide, also known as the Sabatier reaction, allows producing methane from carbon dioxide and hydrogen and is a strongly exothermic reaction:

$$CO_2 + 4H_2 \rightarrow CH_4 + 2H_2O \quad \Delta H = -165\ \text{kJ/mol} \tag{11}$$

The methane produced can then be used for many purposes, and again if the CO_2 comes from the atmosphere and if the hydrogen is produced from renewable sources, the methane is also considered CO_2 neutral.

The methanation reaction is also referred to as "power to gas" in some instances. This is attractive in some geographies which do not have natural gas readily available. Domestically produced renewable gas successively permits the displacement of fossil gas, thus reducing dependence on gas imports (Quadreilli et al. 2011).

While this synthetic natural gas is equivalent to natural gas and can be fed into the gas grid without limitations, the produced gas will be limited by the amount of unreacted hydrogen remaining.

As a CO_2 mitigation strategy, this should be pursued only when the CO_2 storage capacity is completely utilized. Natural gas itself can store CO_2; however, it is typically consumed via combustion for heat and power purposes.

The German company ETOGAS designs and builds multi-megawatt power-to-gas (PtG) turn-key systems based on its proprietary technology portfolio, comprising high-pressure alkaline electrolyzers and methanation systems as well as balance of plant components. ETOGAS has designed and installed and operates the world's largest commercial 6.3 MW power-to-SNG system in Werlte, Germany, for customer Audi AG (Ledgard et al. 2011).

Urea

The production of urea is a large consumer of CO_2. The process consists of two main equilibrium reactions, with incomplete conversion of the reactants. The first is carbamate formation: the fast exothermic reaction of liquid ammonia with gaseous carbon dioxide (CO_2) at high temperature and pressure to form ammonium carbamate ($H_2N\text{-}COONH_4$):

$$2NH_3 + CO_2 \rightleftharpoons H_2N\text{-}COONH_4 \tag{12}$$

The second is urea conversion: the slower dehydration is an endothermic decomposition of ammonium carbamate into urea and water:

$$H_2N\text{-}COONH_4 \rightleftharpoons (NH_2)_2CO + H_2O \tag{13}$$

The overall conversion of NH_3 and CO_2 to urea is exothermic, the reaction heat from the first reaction driving the second (Quadreilli et al. 2011). The overall enthalpy of reaction of urea formation from CO_2 and NH_3 is −133.6 kJ/mol.

Table 2 Net CO_2 mol emitted for various H_2 sources (negative is CO_2 reducing)

	SMR	Biomass	Solar	Wind
Emissions (mol CO_2/mol H_2)	0.55	0.23	0.27	0.045
$CO_2 + H_2 \leftrightarrow CO + H_2O$	−0.45	−0.77	−0.73	−0.96
$CO_2 + 3H_2 = CH_3OH + H_2O$	0.65	−0.31	−0.19	−0.87
$CO_2 + 4H_2 = CH_4 + 2H_2O$	1.2	−0.08	0.08	−0.82

Ammonia is typically produced by the reaction of H_2 and N_2, where the H_2 is supplied by the SMR-WGS-PSA route. Legard et al. reported an LCA on urea production and delivery to New Zealand. They show the production of urea can vary from 0.73 kg CO_2/kg urea in the case of Middle East from natural gas for H_2 source to 2.14 kg CO_2/kg urea for material produced in China where the H_2 is derived from 80 % coal/20 % natural gas (Halmann and Steinberg 1999).

Net CO_2 Reduction

Table 2 shows the net CO_2 emissions for some of the reactions discussed accounting for various H_2 production methods. The table values are derived by using the reaction stoichiometry for H_2 required and the amount of CO_2 emitted per hydrogen consumed. Positive values are a net increase in CO_2 emissions. The results show that with biomass, solar photovoltaic, and wind-generated H_2, there is a net CO_2 reduction. Admittedly this is not a completely rigorous CO_2 accounting since the complete LCA is not performed on the conversion process. But it does provide some scale of the differences.

Electrochemical Conversion of CO_2 to Value-Added Chemicals

The electrochemical method of utilizing carbon dioxide (CO_2) includes two generic categories (Sanchez-Sanchez et al. 2001): (1) electrocarboxylation, which involves the coupling of CO_2 to electrochemically reduced organic molecules, and (2) direct electrochemical reduction of CO_2 to hydrocarbons, alcohols, or other fuels. CO_2 cannot be used widely by category 1 because electrocarboxylation is mostly used to synthesize chemicals that are of pharmaceutical interests whose amount needed is limited. Therefore, we only focus on the second category in this section because the wider applications of the products from the direct electrochemical reduction of CO_2 may significantly reduce net CO_2 emissions.

The investigation of electrochemical conversion of CO_2 in gaseous and liquid phases has been carried out with a variety of catalysts, electrolytes, electrode potential, pressure, and temperature ranges. Different reduction products can be formed via different reaction pathways including carbon monoxide (CO), formaldehyde (CH_2O), formic acid (HCOOH) or formate ($HCOO^-$) in basic solution, oxalic acid ($H_2C_2O_4$) or oxalate ($C_2O_4^{2-}$) depending on the pH of the solution, methane

(CH_4), ethylene (CH_2CH_2), and many others. Solid oxide fuel cells (SOFCs) were employed for CO_2 conversions at high temperatures usually permitting a higher selectivity (Spinner et al. 2012). Transition metal-based electrodes in conventional electrochemical cells constitute the low-temperature systems (Spinner et al. 2012) which provide a broader range of products. Low-temperature CO_2 conversions in liquids require large overpotentials leading to large energy and power demands.

Electrochemical conversion of CO_2 is a very promising method for reversing CO_2 to a reduced form such as fuels or other useful chemicals. Compared with other CO_2 conversion/reduction methods, electrochemical methods have the following advantages:

1. Extensive studies on electrochemical CO_2 conversion have been conducted for more than 50 years, with greater focus in the last 25 years. Heterogeneous catalysts with high activity and selectivity for various useful products such as CO, formic acid, methane, ethylene, and methanol have been found for aqueous reaction systems. Heterogeneous catalyst can be easily separated from the products, unlike in the homogeneous catalytic chemical CO_2 conversion in either aqueous or nonaqueous solutions.
2. Most electrochemical conversion processes can be performed at room temperature and ambient pressure, while most chemical conversion processes require high temperature and high pressures which could lead to corrosion, material failure, and accidental release.
3. Unlike chemical or combustion type reactions, electrochemical processes are not limited by traditional thermochemical cycles, thereby being capable of providing significantly higher energy efficiencies.
4. In electrochemical processes, the electrode potential can be manipulated to a desired value to obtain the optimal reaction rate and catalyst selectivity, with such precise adjustments being difficult in other processes.
5. Electrons flowing as current may be regarded as one of the reagents thereby simplifies requirements for commercial production. In fact, by careful selection of the proper reaction schemes, most electrochemical CO_2 conversion processes will not generate any environmentally harmful "by-products" or waste solutions. Also, if the supporting electrolytes are fully recycled, the overall chemical consumption can be minimized to just water or waste water.
6. Any source of electricity can be used to drive electrochemical CO_2 conversion processes, including solar, wind, hydro, geothermal, tidal, and atomic power. Therefore this method can also be used as an off-peak electricity or renewable energy storage vehicle; it converts the electrical energy to chemical energy by producing fuels from CO_2, and the stored energy can be released later for end use by oxidization of the fuels through fuel cells or normal fuel-burning engines.
7. Electrochemical reaction system is modular and easy for scale-up application. At the same time, the benefits of economy of scale are less for electrochemical processes than other processes.
8. Electrochemical processes require relatively small spatial footprint. There is significant experience base in industrial scale electrochemistry through chlor-alkali production.

Table 3 Half-cell reactions for the electroreduction of carbon dioxide. E^0 versus normal hydrogen electrode (NHE) at 298 °K in aqueous solutions and pH = 0

(a)	$2CO_2 + 2H^+ + 2e^- \rightarrow H_2C_2O_4$	$E^0 = -0.500$ V
(b)	$CO_2 + 2H^+ + 2e^- \rightarrow HCOOH$	$E^0 = -0.250$ V
(c)	$CO_2 + 2H^+ + 2e^- \rightarrow CO + H_2O$	$E^0 = -0.106$ V
(d)	$CO_2 + 4H^+ + 4e^- \rightarrow HCHO + H_2O$	$E^0 = -0.070$ V
(e)	$CO_2 + 6H^+ + 6e^- \rightarrow CH_3OH + H_2O$	$E^0 = +0.016$ V
(f)	$CO_2 + 8H^+ + 8e^- \rightarrow CH_4 + 2H_2O$	$E^0 = +0.169$ V

Low-Temperature Direct Electrochemical Pathways

Electrochemical reduction of CO_2 generates a wide variety of products through various reaction pathways or combinations of several pathways. These pathways critically depend on experimental conditions, such as the nature of the catalyst, electrode potential, electrolyte chemistry, pH, temperature, and CO_2 concentration. The details of the proposed pathways can be obtained elsewhere (Spinner et al. 2012; Saeki et al. 1995; Magdesieva et al. 2002; Ikeda et al. 1987; Li and Prentice 1997). In this chapter, the discussion is framed around the end products of the CO_2 conversion.

In Table 3, the standard equilibrium potentials, E^0 (the standard equilibrium potentials are related to free energy change associated with the reaction by $\Delta G = -nFE$ where "n" is the number of electrons involved in the reaction and F is the Faraday's constant = 96,485 C/mol. equivalent) indicate only the thermodynamic propensity and do not indicate the knowledge of the mechanism which are much more complicated. The kinetics of these reactions are sluggish even with presence of catalysts and require significant overpotential (i.e., potential more negative than the equilibrium potentials) to obtain useful product for detection and could be more to achieve sufficient production rates.

There are relatively few effective electrocatalysts for electrochemical conversion of CO_2, although a number of other catalysts may produce some products (Fig. 4).

Major Products

Carbon Monoxide (CO)

Carbon monoxide is the major product from CO_2 electrochemical conversion on Au, Ag, Zn, Pd, and Ga electrode; the selectivity on these metals can reach as high as 90–100 %. CO can also be generated in smaller amount on other metals such as Cu and Ni under optimized operation conditions. CO is considered a more versatile starting material than CO_2 as chemical feedstock. Carbon monoxide can be used in a host of organic syntheses, but it is best known as a component of synthesis gas (syngas), which is an important feedstock in the chemical industry for making hydrocarbons via Fischer–Tropsch (FT) reactions. Some research efforts have been pursued on the electrochemical reduction of CO_2 to syngas with certain ratio of

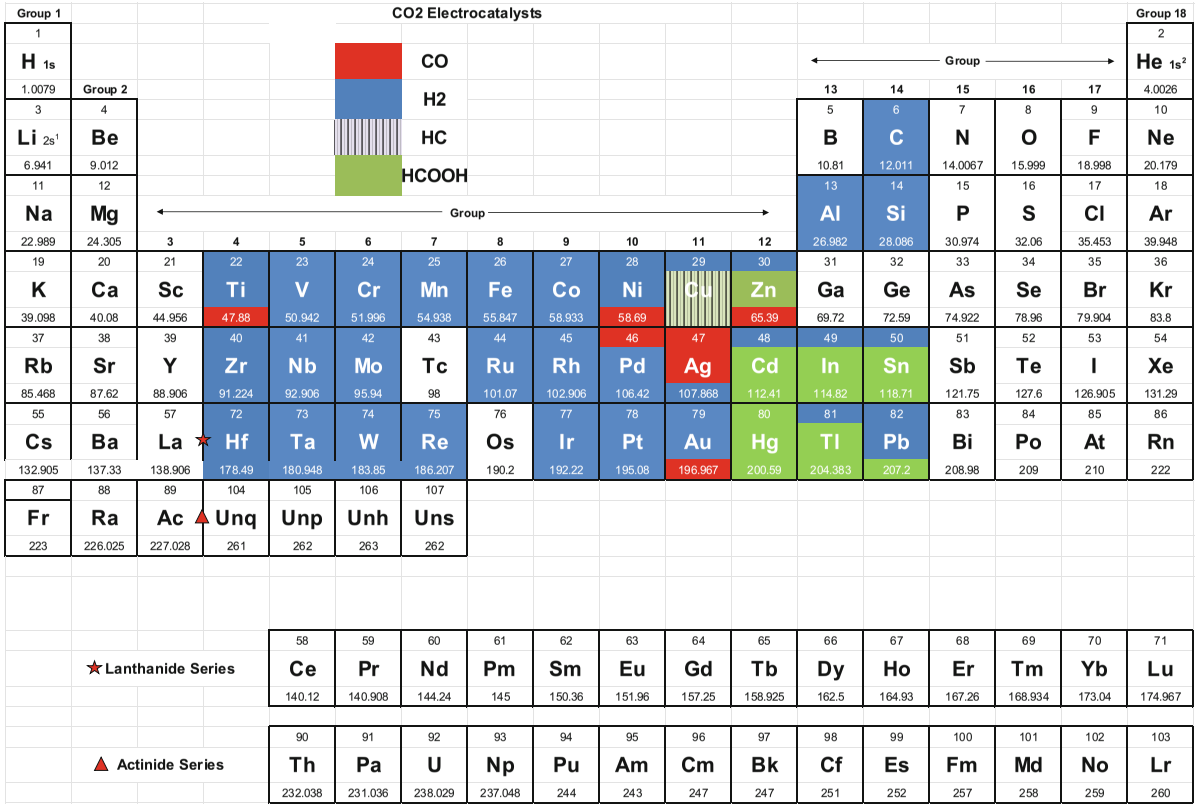

Fig. 4 Periodic table indicating metals for electrochemical CO_2 to specific products

CO/H_2 on metal electrodes such as Ag which favors both CO and H_2 evolution kinetically (Hori et al. 2003; Yamamoto et al. 2002; Delacourt et al. 2008).

Formic Acid

Formic acid appears as an energy storage medium that is being considered both as a fuel for direct formic acid (DFA) fuel cells and as a source of H_2 for hydrogen fuel cells. Formic acid is now manufactured by thermochemical processes based on the carbonylation of methanol in sodium hydroxide and by the oxidation of hydrocarbons, all of which have negative environmental consequences. High selectivity of formic acid from electrochemical reduction of CO_2 is found on metals with high hydrogen overpotential such as indium (In), lead (Pb), mercury (Hg), and tin (Sn) (selectivity ranges from 65 % to 100 % depending on the metals, CO_2 pressure, and electrolytes (Jitaru et al. 1997a)). Tin may be the most practical candidate for production of formic acid as it has been studied extensively in the literature, as well as its availability, cost, and low toxicity to humans. A number of studies using Sn as a catalyst have been conducted (Udupa et al. 1971; Mahmood et al. 1987; Todoroki et al. 1995; Akahori et al. 2004; Agarwal et al. 2011; Chen and Kanan 2012; Furuya et al. 1997; Hinogami et al. 2012).

Hydrocarbons and Alcohols

Copper electrode uniquely reduces CO_2 to methane, ethylene, and alcohols at high current densities (0.05–0.1 kA/m^2) in aqueous electrolytes (Gattrell et al. 2006; Hori et al. 1997; Tang et al. (2012); Li and Kannan 2012; Schouten et al. 2012). These products are particularly of interest in transportation applications as a way to convert renewable or nuclear power to carbon-based energy. Besides the mass transfer limitation as that for CO and formate/formic acid products, high overpotentials and low selectivity are two additional issues for these products. Some work has been done to address the selectivity problem. For example, it is found that selectivity is affected by CO_2 pressure, stirring conditions, and current density (Hara et al. 1994). Particularly, on a gas–liquid–solid (GLS) three-phase Cu electrode, the main product is ethylene (Yano et al. 2002a; Ogura 2003; Ogura et al. 2003), while on flat electrodes, it is methane. The selectivity issue has to be addressed in the practical applications as selectivity may change with position in a larger electrolysis reactor due to pressure drop, intermediates product (CO) accumulation and conversion, nonuniform potential distributions, etc.

Critical Technology Development Factors for Electrochemical Methods

Economic viability is the key for any technology to be accepted commercially even if there is a significant environmental benefit. The economic feasibility is a trade-off between operating and capital expenditure along with the market factors affecting product salability, as depicted in Fig. 5. The cost of operation is mostly dependent on energy cost and consumption, consumable chemicals, long-term stability, and also the replacement and/or recycling of reactor components. The process infrastructure would decide the capital expenditure. Product pricing, demand/availability, and its ease of utility in broader applications are the major factors affecting the

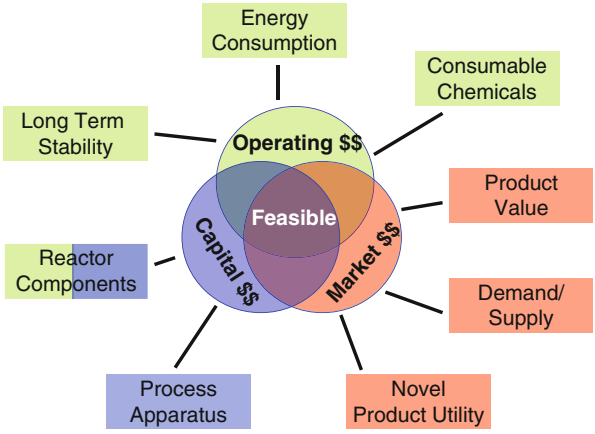

Fig. 5 Critical factors that together determine economic feasibility

market value. Only when sufficient knowledge of all these components is available can a comprehensive economic and value chain analysis be performed and the commercial feasibility of the process assessed with high confidence.

Typical requirements for a commercial electrochemical process are continuous (or on demand) operation, high product selectivity and rate of generation, long-term stable operation, and preferably operating close to ambient temperature and pressure. Catalysts should be able to favorably convert CO_2 to the desired product, i.e., display high selectivity. To reduce the size of the electrochemical reactor, it is also required to have high reactivity or product generation rate, which depends on the current density. Degradation of catalyst with time, limiting use of consumable chemicals, and decrease of electrical energy requirement by proper catalyst selection are critical for stable long-term operation. Continuous processing is essential for large-scale CO_2 utilization. Hence, optimal processing conditions for stable long-term operation need to be evaluated. Although considerable development has occurred in these different areas, as will be discussed in this section, gaps still exist. There are also limited efforts in developing and operating near commercial size reactors to solve issues related to long-term stable continuous operation.

Catalysts Activity and Selectivity

Specific energy indicates how much energy is consumed for each unit amount of CO_2 that is reduced. It is proportional to cell voltage and inversely proportional to the Faradic efficiency or selectivity. Therefore by decreasing the overall cell voltage and improving the selectivity, lower specific energy can be achieved. Both cell voltage and FE depend on current density or reaction rate; typically at larger current density (which is preferred for faster CO_2 reduction rate), higher cell voltage and worse selectivity will be observed.

Cell voltage is the summation of the difference of equilibrium electrode potential between anode and cathode, overpotential of anode, overpotential of cathode, and solution potential drop through membrane and electrolyte. Not many reports have been found giving specific energy except Oloman's work on electrochemical

reduction of CO_2 to formate on Sn electrode where 340 kWh/kmol was obtained at 3.1 kA/m^2 (probably when cell voltage is 4.3 V). High overpotential of cathode can be mitigated by the use of transition metal complex or photoelectrochemical process but stability of the electrodes is a big issue for these electrodes. Choosing anode materials with low overpotential and finding a membrane with high conductivity can also help lower the overall cell voltage. Relatively lower energy consumption is expected for CO and formic acid products from electrochemical reduction of CO_2.

One currently studied application involving the electrochemical reduction of CO_2 on Cu electrode is to adjust the selectivity of the gaseous products mix (hydrogen, methane, ethylene, and CO) such that it has close fuel properties to "hythane," a clean burning hydrogen/natural gas blend that has been promoted as an alternative fuel for existing vehicles (Gattrell et al. 2006, 2007; Gupta et al. 2006). Gattrell's group (Gattrell et al. 2007) specifically studied using this electrolysis process to upgrade biogases to a fuel mix that can be directly used by existing engines with minimal modifications. Assuming a total cell voltage of 3 V (−1.5 V for cathode, 1.2 V for anode-IrO_2, and IR drop of 0.3 V at 0.5–1 kA/m^2), the energy efficiency would be around 40 %.

As shown in Table 3, electrochemical reduction of CO_2 to hydrocarbons and alcohols is a multielectron transfer reaction which requires catalysts with high electron density. Noble metal nanoclusters are expected to be suitable as such catalysts because large percentage of metal atoms lying on the surface can provide high electron density. Moreover, the electrons in nanoclusters are confined to spaces that can be as small as a few atom widths across, giving rise to quantum size effects. Some preliminary research result is reported on utilizing Pd and Pt nanoclusters deposited on carbon nanotubes (CNT) or carbon nanofibers (CNF) to electrochemically reduce CO_2 to hydrocarbons and alcohols at room temperature (Perathoner et al. 2007). With Nafion membrane, after 30 min electrolysis at applied potential of −1.99 V, the main products are C1−C3 hydrocarbons (CH_4, C_2H_6, C_3H_6) and alcohols (CH_3OH, CH_3CH_2OH). However, selectivity and current density are not analyzed in their report. Also adsorptions of heavier products on the gas diffusion cathode (GDE) after longer time of electrolysis (30 min) deactivate the electrodes.

Work by Jaramillo et al. identified and explained the mechanism of hydrocarbon product formation using a flow cell with a Cu-based cathode (Kuhl et al. 2012). Numerous other studies showed that modifying copper surfaces lowers the overpotential and increases the selectivity for hydrocarbon formation (Tang et al. 2012; Li and Kanan 2012; Schouten et al. 2012). Tang et al. showed that by covering a Cu electrode with Cu nanoparticles, a higher selectivity toward hydrocarbons was achieved due to a greater abundance of under-coordinated sites (Tang et al. 2012). Li et al. annealed Cu foil in air and employed these modified Cu electrodes which provided a stable electrode that lowered the overpotential by 0.5 V compared to polycrystalline Cu (Li and Kanan 2012). Schouten et al. observed two different mechanisms for ethylene formation on the two single crystal copper electrodes (Schouten et al. 2012).

Ag catalysts have been extensively pursued for CO production, with reported current densities as high as 91 mA/cm^2 (Jhong et al. 2013a). Use of ionic liquids in the aqueous electrolyte has been shown to decrease the overpotential for CO generation on Ag. The work by Rosen et al. decreased the overpotential for CO production to 0.17 V by using an aqueous ionic liquid solution, in which the 1-ethyl-3-methylimidazolium ($EMIM^+$) cation serves as a cocatalyst, in combination with Ag nanoparticles immobilized on the electrode (Rosen et al. 2011). The current densities were less than 5 mA/cm^2. Tornow et al. showed that the use of diaminotriazole-based organometallic silver catalysts decreased Ag loading by a factor of 20, while keeping similar performance (Tornow et al. 2012). They also suggested a cocatalyst role of the ionic liquid species. Salehi-Khojin et al. observed that the optimal activity of Ag particles on CO_2 reduction is at an average size of 5 nm (Salehi-Khojin et al. 2012). Chen et al. reported highly selective reduction of CO_2 to CO at overpotentials of about 0.14 V with Au nanoparticles synthesized by reduction of Au oxide films (Chen et al. 2012).

Metal oxides (Chen and Kanan 2012), alloys (Agarwal et al. 2011; Furuya et al. 1997), and MOF catalysts (Hinogami et al. 2012) have been employed as active electrocatalysts for HCOOH production. Work by Chen et al. showed that a Sn/SnOx catalyst displays higher current density and faradaic efficiency for HCOOH unlike SnO that seems to mostly produce H_2 (Chen and Kanan 2012), suggesting the role of SnOx in CO_2 conversion mechanism. Agarwal et al. employed Sn alloy catalysts that provided higher faradaic efficiencies than pure Sn at lower polarization (Agarwal et al. 2011). Copper rubeanate metal organic framework catalysts (CR-MOF) developed by Hinogami et al. decreased the potential for onset of CO_2 reduction by 0.2 V compared to a plain Cu electrode (Hinogami et al. 2012).

Cathode Current Density

Any practical electrochemical reactor for CO_2 reduction must also deal with the issue of mass transfer of CO_2 to the cathode surface. Relatively low solubility of CO_2 in aqueous solutions (ca. 70 mM at STP) creates a mass transfer constraint on reaction rate to a maximum current density of 0.1 kA/m^2 under 1 atm and 25 °C for formic acid production, while a superficial current density greater than 1 kA/m^2 is desired for practical operations. Current density may be increased by using a gas diffusion cathode (GDE) or using a fixed-bed cathode while providing a "three-phase interface" for the reaction by sparging the cathode chamber with CO_2 gas or high CO_2 pressure or activated carbon fibers simulating high pressure by "nanospace effect" (Yamamoto et al. 1998, 2000). For example, Hara and Skata (Hara and Sakata 1997) reported a total current efficiency of 50 % (five products) at 6 kA/m^2 on a Pt GDE under 2000 kPa(abs) CO_2 pressure. Nanostructured electrode (Perathoner et al. 2007) is claimed to be able to "simulate" the high-pressure effects to obtain large current density with the confinement effects inside the nanopores. However, two issues with the use of GDE and/or nanostructured electrodes are the temporal stability and the potential for accumulation of liquid phase reaction products in the pores of the electrode.

The use of organic solvent instead of water is also considered because higher solubility of CO_2 in organic solvents may increase the current density. Furthermore,

the competition from hydrogen evolution can be suppressed in organic electrolytes. Methanol is especially actively explored because CO_2-saturated methanol from industrial absorbers (the Rectisol process) is readily available (Kaneco et al. 2002, 2007). (However, methanol used in Rectisol process absorbs not only CO_2 but also H_2S.)

Li and Oloman (Oloman and Li 2008) developed a scaled-up, continuous reactor using tin as the cathode catalyst to generate formic acid/formate as the reduction product of CO_2. They demonstrated that a reactor can operate for relatively extended periods of time (up to 200 min) and produce significant current efficiency ranging from 91 % to 67 %. Under a reactor current of 3.1 kA/m^2 ($\sim CO_2$ reduction rate of 0.025 t/m^2.h), a formate product concentration of 1 M was obtained in a single pass resulting in a specific energy of 340 kWh/kmol of formate. A trickle-bed cathode consisting of a 3-mm thick sandwich of approximately 0.3 mm tin granules was used to obtain a high CO_2 mass transfer capacity in two-phase flow with adequate gas space velocity. The work also pointed to three problems that could prevent commercial development of electrochemical reduction of CO_2 to formate/formic acid, specifically, (1) temporal stability of the cathode; (2) crossover of formate, through the cation membrane, from cathode to anode; and (3) two-phase fluid distribution in the cathode. Commercialization of this technique is sought by Mantra Venture Group (www.mantraenergy.com).

Electrode Structure Affecting Current Density

The performance and durability of electrodes is critical for all heterogeneous electrochemical reactions. These are dependent on the processes occurring at the electrode–electrolyte interface and within the electrode of the electrochemical reactor. The electrodes usually consist of a complex structure with a catalyst layer on top of a backing or substrate layer. The backing layer delivers reactant gas, CO_2, from flow-field channels to the catalyst layer, and transports product from the catalyst layer into flow channels or to the electrolyte/membrane. It also acts as the current distributor for the catalyst layer and should possess a low resistance to avoid large potential variations to be applied to the catalyst layer (Hori et al. 2003; Hara et al. 1994). All these transport processes require optimization for maximizing the electrode and, consequently, the reactor performance.

There have been limited efforts to understand electrode geometrical effects (Delacourt et al. 2008; Yano et al. 2002a; Jhong et al. 2013a; Hori et al. 1994, 2005). CO_2 reduction reaction on planar metal electrodes (Cu, Au, Ag, Zn, Pd, Ga, Pb, Hg, In, Sn, Cd, Tl, Ni, Fe, Pt, Ti) used by Hori et al. in the early work resulted in low current densities of about 5 mA/cm^2 (Hori et al. 1994). Apart from the low surface area of planar electrodes, the low CO_2 concentrations in due to the limited CO_2 solubility in the aqueous electrolytes are responsible for low current density. Metal (Ag, Cu) mesh cathodes were employed by Yano et al. in a modified H-type cell where CO_2 reduction takes place at a three-phase gas–liquid–solid interface by delivery of gaseous CO_2 from a gas chamber (Hori et al. 1997; Yano et al. 2002a). However, current density data was not reported, probably owing to difficult in determining the geometric electrode area in the multiphase system.

Delacourt et al. developed electrodes by spray-painting Ag catalyst ink on gas diffusion layers (GDLs), similar to those prepared for polymer electrolyte membrane fuel cells, cathodes with a Ag loading of 8–10 mg/cm^2, and Ag particle sizes of about 1 μm (Delacourt et al. 2008). Current densities as high as 20 mA/cm^2 were obtained with product selectivities comparable to the findings by Hori et al. (1994) and Yano et al. (2002a). Kenis et al. developed gas diffusion electrodes (GDE) covered with a catalyst layer of Ag nanoparticles (particle size of 70 nm) (Jhong et al. 2013a) and obtained a current density as high as 91 mA/cm^2 in combination with 94 % faradaic efficiency for CO and 46 % energetic efficiency. Deposition of a very thin, crack-free catalyst layer (Ag loading of only 0.75 mg/cm^2) using a fully automated airbrushing method was critical for the high current density achieved. Salehi-Khojin et al. observed that the optimal activity of Ag particles on CO_2 reduction is at an average size of 5 nm (Salehi-Khojin et al. 2012).

Electrolyte

Electrolyte composition is another parameter that has a significant effect on current density and product selectivity of electrochemical CO_2 reduction (Hori et al. 1989; Murata and Hori 1991; Wu et al. 2012). Supporting electrolytes in varying concentrations, such as salts comprising of alkali cations (e.g., Na^+, K^+), halide anions (e.g., Cl^-), bicarbonate (HCO_3^-), or hydroxide (OH-) (Hori et al. 1989, 1994; Murata and Hori 1991; Wu et al. 2012), are employed generally to minimize the ohmic potential loss by keeping the electrolyte conductivity high. Protons in the electrochemical CO_2 reduction process are provided by water (Hori et al. 1994; Peterson et al. 2010). For example, Hori et al. showed that the choice of cation for bicarbonate (HCO_3^-) electrolytes affects the distribution of product formed on copper (Cu) electrodes (Murata and Hori 1991). Another study by Hori et al. showed that anions (i.e., Cl^-, ClO_4^-, SO_4^{2-}, HCO_3^-, $H_2PO_4^-$) affected product distribution by changing local pH at Cu electrodes, which in turn affects the reaction kinetics (Hori et al. 1989). Wu et al. observed similar electrolyte effects on activity and selectivity of tin (Sn) electrodes (Wu et al. 2012). Thorson et al. reported that larger cations in electrolyte salts favor CO production and suppress H_2 evolution (Thorson et al. 2013). Use of ionic liquids, in combination of aqueous solutions, can increase the solubility of CO_2 and reduce mass transfer limitations (Rosen et al. 2011; Tornow et al. 2012). Jingjie Wu et al. (2012) evaluated electrolyte effects on the selectivity and activity for the electrochemical reduction of CO_2 on the Sn electrode. They found that SO_4^{2-} anion and Na^+ cation favor higher faradaic and energy efficiencies while HCO_3^- and K^+ produce formate at a faster rate. Cs^+ containing electrolytes showed the lowest faradaic efficiency. As the electrolyte is diluted, faradaic efficiency was seen to increase, while the current density decreased. Na_2SO_4 and $KHCO_3$ were found to be most optimal.

Cathode Catalyst Stability and Life

For commercial viability, it is imperative that electrodes in an electrochemical reactor can be used for up to several thousands of hours without significant loss in activity or selectivity. Currently, for most applications reviewed above, there exists a big gap between the reported lifetime of the electrodes/catalysts and the desired ones.

Production of formate/formic acid can be highly selective at the beginning of an electrochemically CO_2 reduction process; however, the longest tested operation time before substantial deactivation of the electrodes is for a few days, far less than the required several thousands of hours lifetime for the electrodes.

Deactivation of the Cu electrode (Jitaru et al. 1997b; Chaplin and Wragg 2003) (for hydrocarbons and alcohols), of Pb and Sn (Koleli et al. 2003) (for formate/formic acid), and of Ag electrode (Yano et al. 2002b) (for CO) have been reported. Several "poisoning" mechanisms are proposed:

1. Poisoning of the electrodes occurs due to graphitic carbon deposition at the electrode formed by further reduction of CO (Yano et al. 2002b; Ishimaru et al. 2000; Lee and Tak 2001)
2. Organic adsorbates, such as formaldehyde HCHO (Kostecki and Augustynski 1994) and formic acid which form complexes (Li and Oloman 2007)
3. Presence of Fe and Zn impurities in the electrolyte, which deposit at the electrode surface and progressively induce a change in product selectivity (Hori et al. 2005)

In order to suppress this poisoning effect, some authors have proposed the use of pulse techniques, aimed at desorbing the intermediates before they can further be reduced into a "poison" by shifting periodically the potential to a less negative value (Ishimaru et al. 2000; Yano and Yamasaki 2008) or reverse the polarity of applied current (Li and Oloman 2007). As to the last possible poisoning mechanism, a pre-electrolysis of the electrolyte is performed to reduce the concentration of metallic impurities (Hori et al. 2005).

Jingjie Wu et al. studied the stability of the Sn electrode for CO_2 reduction as a function of electrolytes such as $KHCO_3$ and Na_2SO_4 (Wu et al. 2012). Deposition of Zn on Sn cathode from the impurities present in the catholyte leads to obstruction of the CO_2 reduction with Sn, and rapid loss in faradaic efficiency was observed during the initial 10-h operation in both Na_2SO_4 and $KHCO_3$ electrolytes. L. Chiacchiarelli et al. (2012) studied the cathodic degradation mechanisms of pure Sn in a nitrogen atmosphere as a function of rotation rate, time, current density, electrolyte concentration, grain size, and orientation. Anawati et al. (2014) studied the degradation of Sn catalyst used for CO_2 reduction to formate in 2 M KCl solution using a rotating disk electrode. Optimum faradaic efficiencies were obtained at −1.8 VSCE. Two types of degradation were observed after cathodic polarization using SEM/EDS and XPS. Cathodic corrosion of Sn at higher cathodic potentials leads to a crystallographic type of etching morphology near and at the grain boundaries. Intermetallic colloidal deposits of KSn were observed on the Sn cathode causing an increase in total current due to excessive hydrogen evolution. It is imperative to develop a technique to avoid or remove the alkali metal deposit for sustained stable performance.

The pulse techniques proved to be useful to counteract the poisoning. However, in most research work, the pulse techniques were applied to a rather small size of electrode (0.28 or 1.0 cm^2), and it is unknown whether these methods are applicable

on a practical scale. Evaluation on how the electric charge consumed during the anodic polarization is lacking in the estimation of energy efficiency. Furthermore, in the repeated anodic polarization techniques, anodic dissolution of the electrode may occur and shorten the life of the electrode. Hence, poisoning of the electrodes should be prevented by means of some chemical methods without using any anodic treatment. In situ deposition of catalyst to the electrode by adding salts like $AgNO_3$ was shown to improve the lifetime of Ag electrode (Yano et al. 2002b). Sn catalyst can be regenerated by washing used catalysts with dilute hydrochloric acid and potassium hydroxide (Li and Oloman 2007). It is found that the GLS (gas–liquid–solid) interface (Yano et al. 2002a) and lower pH of the electrolyte (Yano et al. 2002b) would suppress the deposition of poisoning species.

Electrolyzer

Majority of the work on CO_2 conversion involves the setup of a half cell for the study of cathodic electrode behavior. However, the evaluation of the performance of an electrochemical reactor requires a full-cell setup which consists of cathode, anode, cathodic and anodic chambers for holding and distributing electrolytes, membranes for ionic transport, electrolyte conductivities, and corrosivity (Jhong et al. 2013b). The selection of materials for anodes, electrolytes, and membranes plays a significant role in terms of improving the energy efficiency (by decreasing the overall cell voltage) and maintaining long-time stable operation. Compatibility of materials needs to be considered. In the case of low one-pass conversion rate, recirculation of the reactants (both CO_2 gas and electrolytes) may be needed to improve the overall efficiency of the process. A microfluidic flow cell design has been employed by researchers to study the performance of a full cell, where the geometric surface area of the electrode surface is of the order of 10 cm^2 (Delacourt et al. 2008; Agarwal et al. 2011; Wu et al. 2013). Chlor-alkali industry, an established manufacturing technology, employs electrochemical reactors with single cells spanning an electrode area of about 2 m^2. Few groups are looking to advance the full cell design of reactors to such sizes (http://llchemical.com/technology; http://www.dioxidematerials.com/co2.html; Zhai et al. 2015). The scaling-up of reactors brings in new challenges such as fluid flow distribution both within and between the cells of a multicell stack, distribution of concentration, electrode potential, pressure drop, etc. that needs to be optimized. Reactor modeling may speed up the analysis on the effects of process variables (concentrations and flow rates, cell potential, current, pressure, pH, temperature, materials) and their optimization.

Anode Performance

In the methods for CO_2 electroreduction discussed above, very little attention is given to the anodic process. The overall energy efficiency can be significantly improved by optimizing the anodic process specifically complementing the electroreduction of CO_2.

Anodes used in cases where formic acid/formate ion is the primary product, such as carbon (Mahmood et al. 1987) and stainless steel (Oloman and Li 2008), do not exhibit the optimum catalytic behavior for oxygen evolution reaction, while

platinum-coated mesh (Li and Oloman 2007) might be expensive or prone to rapid poisoning. Ni foam anodes employed for (CO + H_2) synthesis (Yamamoto et al. 2002) showed variable behavior depending on the type of the cathode catalysts.

Significantly improved anode catalysts for oxygen evolution reaction have been proposed for the generation of pure hydrogen by water electrolysis, few of which are discussed in Table 4. Although the development of these catalysts is not specifically aimed at ERC of CO_2, these systems can be applied for optimizing the electroreduction process.

The advantages of employing anode catalysts developed for PEM and alkaline water electrolyzers are:

- Oxygen evolution at the anode using nickel catalyst (fairly inexpensive, good corrosion resistance in alkaline medium) or mixed oxide noble metal (similar to dimensionally stable anodes (DSAs) in acidic media) is well characterized.
- Cationic exchange membrane to separate the anodic and cathodic chambers, similar to the ERC of CO_2.
- Industrial scale reactors have been developed and employed over long times, indicating excellent durability and low likelihood of poisoning.

Other Electrochemical Methods

Photoelectrochemical Reduction of CO_2

The photoelectrochemical method for the conversion and reduction of CO_2 is of interest because it employs direct solar energy conversion to fuels/chemicals and can be regarded as an artificial photosynthesis. Many investigations have been conducted on the photoelectrochemical reduction of CO_2 on p-type semiconductor electrodes including p-GaP, p-CdTe, p-GaAs, p-InP, p-SiC, and p-Si and its diamond coats. Most recent reports on the progress of photoelectrochemical reduction of CO_2 involves the use of methanol as the solvent in electrolyte because the solubility of CO_2 in methanol is approximately five times higher than in water at room temperature. Kaneco et al. (2006a, b) studied the photoelectrochemical reduction of CO_2 at p-type semiconductor electrodes, p-GaAs and p-InP, in the methanol-based electrolyte. The main products from CO_2 were carbon monoxide and formic acid. The onset potentials of the photocathodic current in the methanol-based electrolyte were around -1.2 and -0.8 V versus Ag/AgCl with p-GaAs and p-InP electrodes, respectively. Compared to potentials with normal metallic electrodes (in the same methanol-based electrolyte), the photo-aided electrolysis can reduce the total voltage by about $0.3 - 1.0$ V. The maximum current efficiency for CO ($FE = 41.5$ %) was obtained at -2.4 V for the p-InP photocathode. Another research group at Princeton University (Barton et al. 2008) showed a high selectivity of methanol as the product (nearly 100 %) from photoelectrochemical

Table 4 Characteristics of anode catalysts for oxygen evolution employed in hydrogen generators

	Catalyst/electrolyte and temperature/reference	Salient features			Physical characteristics/ electrode construction
Polymer electrolyte membrane (PEM) electrolyzers for hydrogen generation					
1.	Ru, RuO_2, Ir, IrO_2/ acidic (0.5 M H_2SO_4) at RT/(Shidong et al. 2008)	IrO_2 – high stability, 20 h at 0.3 A/cm^2 for cell potential ~1.55 V for 500 nm thick layer 0.2 mg/cm^2 loading			BET sp. area 10–200 m^2/g/catalyst coated on cation exchange membranes
2.	IrO_2 on Ti/C/acidic Nafion type at 90 °C/(Labou et al. 2008)	High uniform surface area with low metal deposit negligible C substrate oxidation			Magnetron-assisted Ir sputtering on Ti-coated carbon/ catalyst-coated Nafion membrane
		1 A/cm^2 at 1.51 V for 0.2 mg/cm^2 loading			
3.	Mixed oxide, noble metals/acidic Nafion type at 90 °C/(Grigoriev et al. 2006)	**Catalyst composition**	**Loading mg/cm^2**	**Cell potential (V) at 1 A/cm^2**	Commercial/catalyst-coated Nafion membrane
		Ir	2.4	1.75	
		RuO_2 (30 %) – IrO_2 (32 %) – SnO_2 (38 %)	2.0	1.7	
		RuO_2(50 %) – IrO_2(50 %)	2.0	1.65	
		Cathode – Pt30/C, 2 mg/cm^2			
	Alkaline water electrolyzers for hydrogen generation				
4.	Sintered Ni/30 % KOH at 25 °C/ (Dyer 1985)	Reduction in overpotential by 200 mV as compared to unactivated Ni (measured at 250 mA/cm^2)			Sintered Ni avg. porosity 77.5 %, mean pore size 12.7 μm with activation by AC cycling (125 mA at 0.25 Hz in 1 M KCl) to form uniform Ni $(OH)_2$/Ni mesh
		<1 mV change in overpotential per hr in 6 h test			
5.	Raney Ni + Co_3O_4 on Ni substrate/30% KOH, 40–80 °C/ (Schiller et al. 1998)	300 mA/cm^2 at cell voltage ~1.6 V			Vacuum plasma spraying of NiAl (50 %) and Co_3O_4 (50 %) on porous Ni substrate, heat 700 °C, cold roll, activation/Al leaching at 80 °C in 30 % KOH+ K–Na tartrate tetrahydrate/Ni mesh
		Intermittent operation 1500 h			
		Negligible degradation of 600 cm^2 area electrodes			

(*continued*)

Table 4 (continued)

Catalyst/electrolyte and temperature/reference	Salient features	Physical characteristics/ electrode construction
6. Composite Ni + Mo, Ni + Mo + Si/5 M KOH, 25 °C (Kubisztal and Budniok 2008)	High surface area of deposited catalysts lead to high current densities at low overpotentials	Co-deposition of Ni with Si and Mo powders suspended in Ni bath, modified by leaching out Si/carbon steel substrate
	Overpotentials for a current density of 10 mA/cm^2: Ni = 354 mV, Ni + Mo = 273 mV, Ni + Mo + Si = 254 mV	

reduction of CO_2 on p-GaP electrode at low potentials of −0.2 V to −0.7 V (SCE). However, the current density was very low, less than 0.01 kA/m^2.

Another type of direct solar energy electrochemical conversion of CO_2 is the use of n-type semiconductor such as TiO_2 as anode in the electrolysis cell to act as an electron donor for the reduction of CO_2. The photoelectrocatalytic (PEC) reactor concept was originally proposed by "Hitachi Green Center" researchers (Doi et al. 1995; Ichikawa and Doi 1996). Photosensitizers such as complexes containing 2,20-bipyridine (bipy) are used with transition metals for the reduction of CO_2 under irradiation in both aqueous and nonaqueous electrolytes (Kitamura and Tazuke 1983; Lehn and Ziessel 1982, 1990).

On the anode side a photocatalyst (nanostructured titania (TiO_2)) photodissociates water to produce protons and electrons which are used on the cathode side of a membrane to reduce CO_2 to hydrocarbons. The membrane is a proton-conductive membrane such as Nafion 117. Development of efficient photocatalysts for anode, electrocatalysts for cathode, and integration in the PEC device are required for practical application. The development of the anode side may benefit from the improvement on the photocatalysts for water splitting. The construction, characteristics, and materials (apart the photocatalytic side) of the PEC reactor are those of PEM fuel cells. There is no solvent on the cathode side and therefore there is no need to recover the products from a liquid phase (a main problem in the conventional CO_2 photo- and electroreduction), and there are no problems of solubility of CO_2. Electrodes based on nanostructured carbon is suggested for the cathode in order to use the confinement effect inside the nanopores to create a virtual higher pressure of the reactant (CO_2) at the electrocatalyst surface and thus favor the chain growth. The use of nanostructured carbon would also favor a high mobility of hydrogen radicals that are important in the reaction mechanism.

General problems of photoelectrochemical reduction of CO_2 are low current density due to high resistances of the semiconductor electrodes, long-term stability of the electrodes, the requirement of high purity semiconductor electrodes, and low energy efficiency when sunlight is used as light source.

High-Temperature Electrochemical Conversion Using Solid Oxide Electrolyzers

Electrochemical syngas (CO and H_2) production using solid oxide fuel cell-based electrolyzers (SOFCs) is developing into a potentially viable method due to high

current densities and its potential to co-generate power, as compared to low-temperature electrochemical processes that are generally highly power intensive. Solid oxide electrolyzers (SOEs) are essentially solid oxide fuel cells (SOFCs) operated in reverse and are capable of higher efficiencies for water electrolysis and CO_2 reduction to CO compared to solution-based electrolysis cells. This is because of the higher operating temperatures (>925 K) that significantly lower the electrode potential by lowering the thermodynamic (Nernst) potential (Parkinson 2006). In SOEs the electrolyte membrane conducts oxygen anions, rather than protons in low-temperature, solution-based electrolyzers. Yttria-stabilized zirconia, YSZ, with its oxygen-anion conduction and electronic insulation properties is most commonly used as the electrolyte.

The cathodic or the fuel-side reaction is the electrochemical reduction of water to produce H_2 and O^{2-} anions and (Eq. 2) CO_2 reduction to CO and O^{2-} anions:

$$H_2O + 2e^- \rightarrow O^{2-} + H_2 \tag{14}$$

$$CO_2 + 2e^- \rightarrow O^{2-} + CO \tag{15}$$

The anodic or the air-side reaction is the recombination of the oxygen ions to O_2:

$$O^{2-} \rightarrow 2e^- + 1/2O_2 \tag{16}$$

Nernst potentials for the electrolysis of H_2O and CO_2 are similar (Sanchez-Sanchez et al. 2001). There are a few reports for the electrochemical reduction of CO_2 to CO in SOEs (Yamamoto et al. 2002; Sridhar and Vaniman 1997; Tao et al. 2004). Idaho National Laboratory developed a syngas generation electrolyzer (called "Syntrolysis") from CO_2 and H_2O by using solid oxide electrolyzer which operates at high temperature of 830 °C (http://www.inl.gov/factsheets/docs/syntrolysis.pdf). The cell design is based on solid oxide fuel cell (SOFC). This novel technique is claimed to be very promising in recycling CO_2 to fuels (through Fischer–Tropsch processes of the syngas) if it is integrated into carbon-free nuclear energy production facilities where process heat and electricity from an advanced nuclear reactor can be used for the electrolysis. Some research focused on O_2 production for space missions employ CO_2 to CO reaction at the cathode (Yamamoto et al. 2002; Sridhar and Vaniman 1997; Tao et al. 2004). The use of expensive bulk Pt electrodes make these SOEs less practical for large-scale CO_2 electrolysis where the intent is sustainable chemical and fuel (CO) production. Furthermore, Pt electrodes displayed higher overpotentials leading to low overall efficiency for CO_2 reduction. Dry reforming (CH_4 reforming with CO_2 rather than steam) is less energy intensive and could produce syngas with more favorable H_2/CO ratios (Belyaev et al. 1998; Kim et al. 2002). An yttria-stabilized zirconia (YSZ)-based electrolyte or tube with various metal and/or mixed metal catalysts at the anode and cathode is typically employed in such cells (Belyaev et al. 1998; Choudhary et al. 1995). SOFCs using nickel-based catalysts, such as ceria-doped nickel-YSZ or nickel oxide–calcium oxide-mixed metal electrodes have been employed for CH_4 reforming (Kim et al. 2002; Choudhary et al. 1995). Bidrawn et al. demonstrated direct CO_2

electrolysis to CO without utilizing CH_4 (Eq. 15) with high current densities of the order of 1 A/cm^2 (Bidrawn et al. 2008). Furukawa et al. utilized H_2 fuel with CO_2 at lower temperatures (500 °C) with nickel/zeolite and silver electrodes to generate CH_4 at yields as high as 80 % (Furukawa et al. 1999):

$$CO_2 + 4H_2 \rightarrow CH_4 + 2H_2O \tag{17}$$

Electrode degradation due to prolonged usage at high temperature and deactivation due to coke formation and deposition (via CH_4 decomposition and CO disproportion) are major impediments to the long-term usage of SOFCs. Inclusion of small fractions of metal or metal oxide phases such as CeO_2, gadolinia-doped ceria (GDC), copper, palladium, and $Ce_{0.48}$ $Zr_{0.48}$ $Y_{0.04}$ (CZY) to SOFC electrodes could lead to reduced electrode coking and better overall cell performance and stability (Kim et al. 2002; Bidrawn et al. 2008; Huang and Chou 2009).

Metal-Free Catalysts

There is an upcoming trend for CO_2 conversion processes using metal-free electrocatalysts that can be obtained by relatively inexpensive means, do not use noble metals, and show comparable catalytic activities relative to the metal-containing electrocatalysts described above. These consist of conducting polymers, pyridinium derivatives, radical anions, and heteroatom-doped carbon materials (Mao and Alan Hatton 2015).

In the case of homogeneous catalysts (i.e., pyridinium derivatives and radical ions), the electrode type is critical due to its direct contact with the electrolyte solution, thus affecting the faradaic efficiencies and product selectivity. Seshadri et al. (1994) employed pyridium in a Pd-catalyzed scheme to reduce CO_2 to methanol at a faradaic efficiency of 30 % in an aqueous solution with a pH value of 5.4, 200 mV overpotential, 40 mA/cm^2 current density, and stable life of 19 h, with the rest of the product being hydrogen. The Bocarsly group developed important mechanistic understanding of pyridinium ion-based systems (Cole et al. 2010; Morris et al. 2011). They showed that the electrochemical reduction of carbon dioxide did not occur in presence of an inert electrode that does not catalyze hydrogen evolution. Also, carbon dioxide rather than bicarbonate was reduced during electrolysis with a pyridinium/Pt system, suggesting that carbon dioxide reduction proceeds by a first-order surface-active rate-limiting step with respect to both pyridinium and carbon dioxide. Selectivity was seen to increase significantly with a semiconducting electrode, combined with the pyridinium-based homogeneous catalytic system (Barton et al. 2008). A faradaic efficiency of almost 100 % was achieved by Barton et al. for CH_3OH from CO_2 reduction using the pyridinium/p-GaP system under illumination. However, the low solar-to-fuel quantum efficiencies obtained in this case is not feasible for commercialization. Nonetheless, this photoelectrochemical process is of great interest due to its very low overpotentials and extremely high faradaic efficiency for methanol production from CO_2.

Heterogeneous conducting polymer catalysts are usually prepared from monomers (e.g., aniline and pyrrole) that are electrochemically polymerized onto conductive

substrates (i.e., electrodes). Since the electrode is usually covered completely by the resulting polymer film avoiding its contact with the electrolyte solution, the nature of the electrode has negligible effects on the catalytic performance. Lack of stability due to degradation and reduced catalysis efficiencies because of morphological changes in the polymer structure during long-term electrolysis, however, is an issue. Stability can be improved by hybridization of conducting polymers with other materials such as graphene and carbon nanotubes. Heteroatom-doped carbons appear to be quite stable during electrocatalysis. Another advantage is the ability of being employed in nonaqueous solutions such as ionic liquids which eliminates the hydrogen evolution side reaction and thereby significantly improves faradaic efficiencies of desired products. Along with these materials, established strategies for modulating the electronic properties of carbon materials could be employed for improving the catalytic performance. A potential issue could be the overall carbon footprint of these electrodes if they are made in large scale since most of these materials are derived from fossil fuel sources. Aydin et al. (Aydin and Koleli 2004) employed a polypyrrole electrode in a methanol/$LiClO_4$/H_2O/H^+ (pH = 1) electrolyte at a potential of −0.4 V versus Ag/AgCl to obtain a mixture with the majority products being HCOOH, HCHO, and CH_3COOH, with a decrease in FE with time. Electrolysis under high CO_2 pressures, ranging from 5 to 20 bar, improved the faradaic efficiencies for HCOOH and HCHO, while that of CH_3COOH remained unchanged. A polyaniline-based electrode was developed by Koleli et al. (2004) for electrocatalytic reduction of carbon dioxide under ambient conditions, using methanol as the solvent. In this case the maximum faradaic efficiencies observed were for the formic acid (12 %) and acetic acid (78 %). Kumar et al. (2013) developed polyacrylonitrile (PAN)-based heteroatomic carbon nanofiber (CNFs) for reducing carbon dioxide to carbon monoxide in 1-ethyl-3-methylimidazolium tetrafluoroborate (EMIN-BF4) with a high FE of 98 %.

Novel CO_2 Electro-biochemical Pathways

One of the challenges for CO_2 utilization revolves around balancing the energy required (or costs) to produce a chemical with a large market volume and high value. The conversion of CO_2 to chemicals such as formic acid that are less energy intensive to make and have a high selling price are more likely to reach commercialization. However, such chemicals have a smaller worldwide market demand (1–10 million t/year). It would be desirable to convert CO_2 to chemicals that can be directly employed as fuels since they have a much larger demand and hence can make a bigger impact on reducing CO_2 emissions. However, the energy-intensive nature of such direct CO_2 conversion processes (e.g., electrochemical synthesis of methane; the primary component of natural gas requires four times the electrical energy per mole as compared to formic acid) makes them significantly less economical.

A combination of electrochemical and biochemical pathways has been proposed that addresses these issues. Photosynthesis converts solar energy into stored chemical energy in plants, which is the biomass that is converted into biofuels. However, current biomass processing methods for biofuel production require large areas of land and sunlight, conditions that are not widely available. Developing microorganisms that can circumvent the low efficiency photosynthesis and directly utilize

energy and nutrients from chemicals produced from CO or CO_2 have been receiving greater attention recently. The use of bacteria for large-scale chemical production is not new and has been successfully employed in processes such as bioethanol production via fermentation. Bulk of the cutting-edge research in this field is focused on genetically modifying these microorganisms for greater efficiency and liquid fuel choice. The advantages include:

- Much greater energy efficiencies than photosynthetic routes
- Ability to operate in the dark
- Independent of geographic limitations
- Reduced land usage
- No competition to food
- The process can use any renewable energy source
- The processes can be scaled to different needs

The Advanced Research Projects Agency-Energy (ARPA-E), which is a part of the US Department of Energy, has funded several projects based on this concept under the "electrofuels" initiative (http://arpa-e.energy.gov/?q=arpa-e-programs/electrofuels). Researchers at EASEL, one of the recipients, have been engineering bacteria to convert CO_2 with electricity to higher carbon chain compounds that can be directly used as fuel. It is a two-step process, where CO_2, with the aid of electricity, is first converted to formate ion and then the bacteria in the vicinity of the electrode, where formate is generated, converts formate into biofuels (http://www.easelbio.com/technology/). Another recipient of the ARPA-E award, Ginkgo Bioworks, worked on incorporating the genes responsible for CO_2 metabolism in *E. coli* for production of liquid fuels (http://arpa-e.energy.gov/?q=arpa-e-programs/electrofuels). They found that mass transfer limitations owing to low solubility of the reactants CO_2 and H_2 that need to be fed to the microorganisms in aqueous solution could be bypassed by providing formate salts/formic acid directly as a source of carbon and hydrogen. This new hybrid process consisted of production of formic acid via electrochemical reduction of CO_2 based on the technology developed by DNVGL which is then further processed by genetically engineered autotrophic bacteria by Ginkgo Bioworks yielding liquid fuels, such as ethanol, butanol, and isoprenol (http://www.dnv.com/press_area/press_releases/2012/dnv_and_gingko_bioworks_with_potentially_game_changing_technology_for_utilizing_co2.asp) (Fig. 6).

Technical Barriers to Adoption of CO_2 Utilization

Energy Reduction

The first technical challenge is to reduce the energy required for activation of CO_2 molecule so that it reacts with protons or other molecules. CO_2 is a relatively stable molecule, although it is not the most stable product of carbon – carbonates and

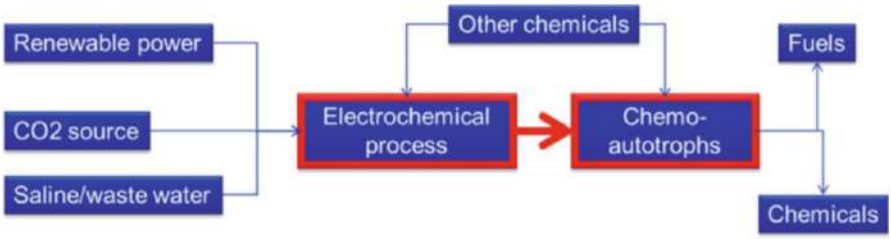

Fig. 6 Combination of electrochemical and biochemical pathways for fuels from CO_2

oxalic acid are even more stable. The Gibbs free energy for formation is an indicator of the energy hill we have to climb to make a product from CO_2. It requires far less energy in theory (0.24 MWh/t) to convert CO_2 to formic acid compared to other products we experience in daily life, but practical considerations require us to expend more energy to speed up the process. For example, at the current state of technology, the energy required to convert CO_2 to formic acid at a reasonable production rate is about 6 MWh/t. In comparison, polysilicon for a solar panel is produced from quartz at an energy penalty of about 60 MWh/t of Si (Tao 2008). Single crystal silicon for semiconductors requires a much greater energy penalty of about 350 MWh/t (Fig. 7).

Renewable Energy

Renewable energy is needed because the use of fossil energy would negate the benefit of CO_2 utilization. Because renewable energy, with the exception of hydro-electric energy, is variable in nature, CO_2 utilization processes must operate intermittently, which will make it expensive due to idling capital equipment during the time renewable power is not available. Additionally, when the process is not operating, provisions to mitigate equipment/catalyst damage due to corrosion must be made. In places where geothermal energy is readily available, such as Iceland, CO_2 conversion processes using renewable energy are being demonstrated. In addition to well-known renewable energy sources, energy harvesting from heat (a relatively low efficiency process using current thermoelectric technologies), ocean currents, or salinity differences at estuarine areas may be used in selected places.

Consumable Chemicals

As the energy usage is optimized, the cost of consumable chemicals can affect the overall profitability of the process and must be minimized. The lack of ready availability of some consumables may also render a process unattractive. For

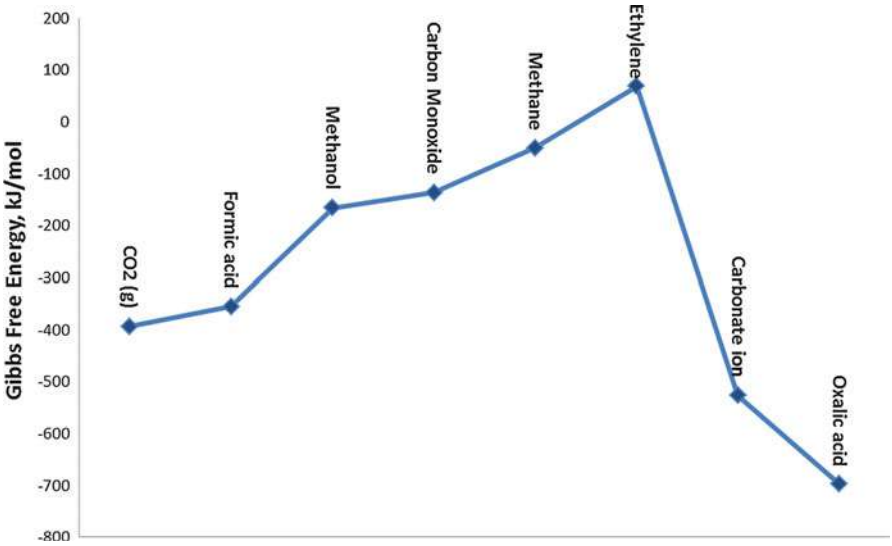

Fig. 7 Gibbs free energy for various products of interest from CO_2 conversion

example, Calera's cement manufacturing from CO_2 pilot plant in Latrobe Valley power plant in Australia had to be canceled partly due to the lack of proper brine chemistry available at the site and partly due to inadequate carbon pricing. In this regard, CO_2 utilization processes should be regarded as an integrated synthesis operation, where the products from one process can be used as inputs in another process.

CO_2 Purity

Conventional capture processes using absorption technologies are highly energy and capital intensive. Some CO_2 utilization processes, such as cement manufacturing, may be able to use low concentration exhausts directly from the stack, but most CO_2 utilization processes require a high concentration CO_2 source to be economical. Therefore, significant improvements in capture technologies are necessary for the overall system to be economical. Capture technologies involving adsorbents impregnated on porous solids may be economical and less energy intensive, but they have not been sufficiently tested at scale. Issues related to long-term (50,000 cycles or longer) degradation of adsorbents and substrates need to be addressed. Initial results from more limited duration testing appear to be promising. Alternatively, relatively pure CO_2 streams can be obtained from biofuel fermentation processes. Avoiding the need for compression reduces the energy consumption in capture processes significantly.

Material Degradation

Material degradation can contribute both to Capex (e.g., need to design more expensive alloys) and Opex (e.g., more frequent replacement of catalysts). Many CO_2 utilization processes have not been operated sufficiently long to understand material degradation issues.

Integration into Existing Systems

Integrating the rate of utilization with the rate of production is a significant challenge, even for EOR which uses significant amounts of CO_2. For example, EOR typically requires large quantities of CO_2 at the beginning of oil production and then tapers off its use, whereas a power plant expects CO_2 to be used at a relatively steady rate. Similarly, integrating renewable power with a CO_2 utilization process and a fossil plant producing CO_2 can be a challenge. Significant process engineering is required to ensure that mismatches in the production rates, thermal loads, and impurities do not adversely affect both the power production and CO_2 utilization processes. Furthermore, power plants are culturally attuned to producing electricity, not chemicals.

As mentioned before, a single CO_2 conversion process may not be economically viable. Therefore, CO_2 utilization should be considered as an integrated synthesis plant making a number of products. Integrating a number of processes is a technical challenge that can be met using a variety of simulation tools.

Product Quality Acceptance

Although product acceptance is generally a market issue, the production method may affect product acceptability. This was an issue for cement material produced from CO_2 and could be an issue for other materials, such as polymers and fuels. Significant time and process evolution may be required to meet current product specifications or change these specifications.

Life Cycle Analysis

LCA is necessary for CO_2 utilization processes to be accepted. LCA requires significant input on process parameters which may be lacking for new processes. However, LCA can also help modify process chemistry and improve CO_2 footprint.

Economic/Social/Environmental Barriers

Unlike CCS, CO_2 utilization does not face adverse public opinion. This is because recycling waste has become a cultural norm in most societies and CO_2 is regarded

as another example of waste recycling. This is evident in the interviews of public perception regarding CCS, where many participants suggested CO_2 utilization as an alternative to be explored. However, products from CO_2 utilization have to compete in the market place with products from fossil sources.

The large volume of CO_2 that can be converted to various products will saturate the local and global market. This is especially true for specialty chemicals and materials that can bring higher profitability at current market prices. For example, formic acid currently sells at approximately $1200 per ton. This provides a reasonable profit margin under current electrochemical production routes of this chemical from CO_2. However, the global annual market for formic acid is approximately 0.5 M tons. Lowering the cost can expand its market, but it is unlikely to expand it to levels that can meet the production volumes from reasonable use of CO_2. In terms of fuels, the volumes can be large, but the prices are relatively low. For example, isoprene produced from CO_2 through the formic acid has to compete with current gasoline prices of about $4 per gallon ($1300 per ton). The current biochemical process using genetically modified organisms yields 0.11 t of isoprene per ton of formic acid, thus requiring extremely low cost of production of formic acid.

Distributed Production of Fuels and Chemicals

If local sources of renewable energy and captured CO_2 (e.g., from air capture technologies or locally available CO_2 sources) are used to produce fuels and chemicals for local markets, the distribution costs can be lowered. On the other hand the advantages of centralized production in terms of scale and the use of resources available in one location can be lost. There may be greater difficulty in enforcing safety and environmental practices in a distributed manufacturing infrastructure. Electrochemical processes have a near linear cost with scale. Thus a large centralized plant brings no big cost advantage over several smaller-scale plants. The distributed production of chemicals and fuels may be useful for remote communities or in developing nations.

Policy Barriers

Green technologies, as a whole, require consistent policies to help them grow and become established. A recent research by Pew Research Center showed that in the USA, where periodic policy shifts occurred, wind energy market suffered 76–94 % drop whenever production tax credits expired. At present, CO_2 utilization is not as well recognized as CCS as a way of GHG mitigation. This has resulted in significant underfunding of efforts to develop utilization methods, other than EOR. The total government funding of large-scale CCS demonstration projects globally was approximately $9 billion in 2014. In contrast, the level of government funding for CO_2 utilization projects (other than EOR) amounted to about $50 million. Increased visibility of CO_2 utilization through government or international policies will encourage innovation and help bridge the funding gaps.

Subsidizing emerging CO_2 utilization processes or products will be necessary to help establish these technologies. At present traditional energy production (oil and gas, nuclear, etc.) receive significant government subsidies. Traditional biofuels from agricultural products also receive subsidies, although these are being phased out. Unlike these industries, the CO_2 utilization technologies lack an industry voice that can help educate policymakers and the public and promote the common goals of various technologies.

The market price of CO_2 is extremely low or nonexistent. Many of the analyses of CO_2 utilization processes assume that there will be no price for carbon. However, there is a gap in understanding between those who emit CO_2 and those who would like to utilize CO_2 regarding the price of carbon.

Future Directions

The barriers for adoption of CO_2 utilization technologies discussed above can be reduced with the following strategies:

Improved Electrochemical Reaction Kinetics Technology

As mentioned previously, for long-term viability of CO_2 utilization technologies using the electrochemical approach, improved catalyst performance is essential. This included significantly increased catalyst life, increased current densities, and increased impurity tolerance. Although significant progress has been made in the first two of these issues, the last issue has not been adequately addressed. Novel high surface area catalysts can further increased current densities, but they have to be balanced by increased life. The reactor design is another area that can be significantly improved. High-pressure operations could benefit the overall economics. Improved hydrodynamics is another area that needs further development.

Improved Biochemical Processes

The current biochemical technologies have relatively low yields requiring large land area. Furthermore, the requirements for CO_2 are somewhat low and the purity issues need further improvement.

Value Chain Analysis

An important aspect of reducing technical barriers is to set metrics for success in selected technologies. These metrics should be based on a full techno-economic (value chain) analysis, considering the uncertainties involved in many of the parameters. The characterization of uncertainties and their effects on the resultant

delivery of results is an important first step in managing the risk from these technologies. The value chain analysis enables setting technology development targets shown in the figure above on the right. In order to conduct value chain analysis, process modeling tools need to be developed in a modular fashion so that different processes can be combined in various ways to determine outputs. The value chain analysis can also be used for comparing different options and their energy, environmental, and economic consequences. Value chain analyses require significant process data that is often not available due to proprietary considerations or the early stage development of processes.

Formation of Networks: Improved Communication and Influence

Many CO_2 utilization networks have now been formed to provide venues for exchange of knowledge and capabilities. Sites, such as CO_2 Chem Network (http://co2chem.co.uk), provide a forum for technical information exchange. Focused conferences and workshops are also taking place to highlight the developments in this area and develop roadmaps for the future.

Ways to Bring Technologies to Market

Many different funding models are being tried to bring forward CO_2 utilization technologies. Venture capital has been provided in a number of cases. It has been seen that the timeline for process development is typically much too long for VC firms, who like to see a substantial return on investment within 2–3 years. Furthermore, the risk in green technologies is high as many of these technologies depend on government subsidies. When these technologies hit the valley of death, VC firms often seem to lose interest.

Governments can provide long-term support to high-risk technologies and can potentially carry these technologies through the valley of death. But, the funding is often subject to the vagaries of politics, especially in the Western countries.

Open innovation model is championed in some areas. However, proprietary technologies are barriers to open innovation because the intellectual property behind many component technologies is often unknown and the effort required to cross-license various technologies become a significant barrier. A patent pooling model, wherein all the participants in a technology with complementary patents can pool technologies that are required to work together, has been successful in consumer electronics area.

Another mechanism for bringing technologies to market is through a prize. Historically, prizes have helped spur innovation. For example, method to determine longitude was discovered through a prize scheme as were soda manufacturing and transatlantic flight. More recently private space flight was realized through the X Prize Foundation.

References

Agarwal AS, Zhai YM, Hill D, Sridhar N (2011) The electrochemical reduction of carbon dioxide to formate/formic acid: engineering and economic feasibility. ChemSusChem 4:1301–1310

Akahori Y, Iwanaga N et al (2004) New electrochemical process for CO_2 reduction to from formic acid from combustion flue gases. Electrochemistry 72(4):266–270

Al-Musabbeh MA et al (2006) Enhancing methanol production by CO_2 injection. Saudi Methanol Co. April 2006. http://www.co2management.org/proceedings/Abdulatif_Al_Musabbeh_Final.pdf

Anawati NS, Frankel GS, Agarwal A, Sridhar N (2014) Degradation and deactivation of Sn catalyst used for CO_2 reduction as function of overpotential. Electrochim Acta 133(1):188–196

Aydin R, Koleli F (2004) Electrocatalytic conversion of CO_2 on a polypyrrole electrode under high pressure in methanol. Synth Met 144:75–80

Barton EE, Rampulla DM et al (2008) Selective solar-driven reduction of CO_2 to methanol using a catalyzed p-GaP based photoelectrochemical cell. J Am Chem Soc 130:6342–6344

Belyaev V, Galvita V, Sobyanin V (1998) Effect of anodic current on carbon dioxide reforming of methane on pt electrode in a cell with solid oxide electrolyte. React Kinet Catal Lett 63:341

Bidrawn F, Kim G, Corre G, Irvine JTS, Vohs JM, Gorte RJ (2008) Efficient reduction of CO_2 in a solid oxide electrolyzer. Electrochem Solid-State Lett 11(9):B167–B170

Centi G, Perathoner S (2009) Opportunities and prospects in the chemical recycling of carbon dioxide to fuels. Catal Today 148:191–205

Chaplin RPS, Wragg AA (2003) Effects of process conditions and electrode material on reaction pathways for carbon dioxide electroreduction with particular reference to formate formation. J Appl Electrochem 33(12):1107–1123

Chen YH, Kanan MW (2012) Tin oxide dependence of the CO_2 reduction efficiency on tin electrodes and enhanced activity for tin/tin oxide thin-film catalysts. J Am Chem Soc 134:1986–1989

Chen Y, Li CW, Kanan MW (2012) Aqueous CO_2 reduction at very low overpotential on oxide-derived Au nanoparticles. J Am Chem Soc 134:19969–19972

Chiacchiarelli L, Zhai Y, Frankel G, Agarwal AS, Sridhar N (2012) Cathodic degradation mechanisms of pure Sn electrocatalyst in a nitrogen atmosphere. J Appl Electrochem 42(1):21–29

Choudhary V, Rajput A, Prabhakar B (1995) Energy efficient methane-to-syngas conversion with low H_2/CO ratio by simultaneous catalytic reactions of methane with carbon dioxide and oxygen. Catal Lett 32:391

Cole EB, Lakkaraju PS, Rampulla DM, Morris AJ, Abelev E, Bocarsly AB (2010) Using a one-electron shuttle for the multielectron reduction of CO_2 to methanol: kinetic, mechanistic, and structural insights. J Am Chem Soc 132:11539–11551

Delacourt C, Ridgway PL, Kerr JB, Newman J (2008) Design of an electrochemical cell making syngas (CO + H-2) from CO_2 and H_2O reduction at room temperature. J Electrochem Soc 155: B42–B49

Doi R, Ichikawa S et al (1995) Japanese Patent 08296077, Japan

Dyer CK (1985) Improved nickel anodes for industrial water electrolyzers. J Electrochem Soc 132 (1):64–67

Edwards JH, Maitra A (1995) The chemistry of methane reforming with carbon dioxide and its current and potential applications. Fuel Process Technol 42:269–289

Furukawa S, Okada M, Suzuki Y (1999) Isolation of oxygen formed during catalytic reduction of carbon dioxide using a solid electrolyte membrane. Energy Fuel 13:1074

Furuya N, Yamazaki T, Shibata M (1997) High performance Ru–Pd catalysts for CO_2 reduction at gas-diffusion electrodes. J Electroanal Chem 431:39–41

Gattrell M, Gupta N et al (2006) A review of the aqueous electrochemical reduction of CO_2 to hydrocarbons at copper. J Electroanal Chem 594(1):1–19

Gattrell M, Gupta N et al (2007) Electrochemical reduction of CO_2 to hydrocarbons to store renewable electrical energy and upgrade biogas. Energy Convers Manag 48(4):1255–1265

Global CCS Institute (2012) The Global Status of CCS 2012, Canberra, Australia http://hub.globalccsinstitute.com/sites/default/files/publications/47936/global-status-ccs-2012.pdf
Goeppert A, Czaun M, Jones J-P, Surya Prakash GK, Olah G (2014) Recycling of carbon dioxide to methanol and derived products – closing the loop. Chem Soc Rev 43:7957–8194
Grigoriev SA, Porembsky VI et al (2006) Pure hydrogen production by PEM electrolysis for hydrogen energy. Int J Hydrogen Energ 31(2):171–175
Gupta N, Gattrell M et al (2006) Calculation for the cathode surface concentrations in the electrochemical reduction of CO_2 in $KHCO_3$ solutions. J Appl Electrochem 36(2):161–172
Halmann MM, Steinberg M (1999) Greenhouse gas carbon dioxide mitigation science and technology. Lewis Publishers, Boca Raton
Hara K, Sakata T (1997) Electrocatalytic formation of CH_4 from CO_2 on a Pt gas diffusion electrode. J Electrochem Soc 144(2):539–545
Hara K, Tsuneto A et al (1994) Electrochemical reduction of CO_2 on a cu electrode under high-pressure – factors that determine the product selectivity. J Electrochem Soc 141(8):2097–2103
Hinogami R, Yotsuhashi S, Deguchi M, Zenitani Y, Hashiba H, Yamada Y (2012) Electrochemical reduction of carbon dioxide using a copper rubeanate metal organic framework. ECS Electrochem Lett 1:H17–H19
Hori Y, Murata A, Takahashi R (1989) Formation of hydrocarbons in the electrochemical reduction of carbon-dioxide at a copper electrode in aqueous-solution. J Chem Soc Faraday Trans 1 85:2309–2326
Hori Y, Wakebe H, Tsukamoto T, Koga O (1994) Electrocatalytic process of CO selectivity in electrochemical reduction of CO_2 at metal–electrodes in aqueous-media. Electrochim Acta 39:1833–1839
Hori Y, Takahashi R et al (1997) Electrochemical reduction of CO at a copper electrode. J Phys Chem B 101(36):7075–7081
Hori Y, Ito H et al (2003) Silver-coated ion exchange membrane electrode applied to electrochemical reduction of carbon dioxide. Electrochim Acta 48(18):2651–2657
Hori Y, Konishi H et al (2005) "Deactivation of copper electrode" in electrochemical reduction of CO_2. Electrochim Acta 50(27):5354–5369
Hu B, Guild C, Sui S, Suib S (2013) Thermal, electrochemical, and photochemical conversion of CO_2 to fuels and value added products. J CO2 Util 1:18–27
Huang T, Chou C (2009) Electrochemical CO_2 reduction with power generation in SOFCs with Cu-added LSCF–GDC cathode. Electrochem Commun 11:1464
Ichikawa S, Doi R (1996) Hydrogen production from water and conversion of carbon dioxide to useful chemicals by room temperature photoelectrocatalysis. Catal Today 27(1–2):271–277
Ikeda S, Takagi T, Ito K (1987) Selective formation of formic-acid, oxalic-acid, and carbon-monoxide by electrochemical reduction of carbon-dioxide. Chem Soc Jpn B 60:2517–2522
Pew Charitable Trusts (2012) Research & Analysis Innovate, Manufacture, Compete: A Clean Energy Action Plan, Philadelphia, PA. http://clean-economy.org/wp-content/uploads/2013/01/Innovate-Manufacture-Compete.pdf
Ishimaru S, Shiratsuchi R et al (2000) Pulsed electroreduction of CO_2 on Cu-Ag alloy electrodes. J Electrochem Soc 147(5):1864–1867
Jhong HR, Brushett FR, Kenis PJA (2013a) The effects of catalyst layer deposition methodology on electrode performance. Adv Energy Mater 3(5):589–599
Jhong H-RM, Ma S, Kenis PJA (2013b) Electrochemical conversion of CO_2 to useful chemicals: current status, remaining challenges, and future opportunities. Curr Opin Chem Eng 2:191–199
Jitaru M, Lowy DA et al (1997a) Electrochemical reduction of carbon dioxide on flat metallic cathodes. J Appl Electrochem 27(8):875–889
Jitaru M, Lowy DA et al (1997b) Electrochemical reduction of carbon dioxide on flat metallic cathodes. J Appl Electrochem 27(8):875–889
Kaneco S, Iiba K et al (2002) High efficiency electrochemical CO_2-to-methane conversion method using methanol with lithium supporting electrolytes. Ind Eng Chem Res 41(21):5165–5170

Kaneco S, Katsumata H et al (2006a) Photoelectrocatalytic reduction of CO_2 in LiOH/methanol at metal-modified p-InP electrodes. Appl Catal B-Environ 64(1-2):139–145
Kaneco S, Katsumata H et al (2006b) Photoelectrochemical reduction of carbon dioxide at p-type gallium arsenide and p-type indium phosphide electrodes in methanol. Chem Eng J 116 (3):227–231
Kaneco S, Iiba K et al (2007) Electrochemical reduction of high pressure carbon dioxide at a Cu electrode in cold methanol with CsOH supporting salt. Chem Eng J 128(1):47–50
Kim T, Moon S, Hong S (2002) Internal carbon dioxide reforming by methane over Ni-YSZ-CeO_2 catalyst electrode in electrochemical cell. Appl Catal A 224:111
Kitamura N, Tazuke S (1983) Photoreduction of carbon dioxide to formic acid mediated by a methylviologen electron relay. Chem Lett 12:1109
Koleli F, Atilan T et al (2003) Electrochemical reduction of CO_2 at Pb- and Sn-electrodes in a fixed-bed reactor in aqueous K_2CO_3 and $KHCO_3$ media. J Appl Electrochem 33(5):447–450
Koleli F, Ropke T, Hamann CH (2004) The reduction of CO_2 on polyaniline electrode in a membrane cell. Synth Met 140:65–68
Kostecki R, Augustynski J (1994) Electrochemical reduction of CO_2 at an activated silver electrode. Ber Bunsen Phys Chem 98(12):1510–1515
Kubisztal J, Budniok A (2008) Study of the oxygen evolution reaction on nickel-based composite coatings in alkaline media. Int J Hydrogen Energ 33(17):4488–4494
Kuhl KP, Cave ER, Abram DN, Jaramillo TF (2012) New insights into the electrochemical reduction of carbon dioxide on metallic copper surfaces. Energy Environ Sci 5:7050–7059
Kumar B, Asadi M, Pisasale D, Sinha-Ray S, Rosen BA, Haasch R, Abiade J, Yarin AL, Salehi-Khojin A (2013) Renewable and metal-free carbon nanofibre catalysts for carbon dioxide reduction. Nat Commun 4:2819. doi:10.1038/ncomms3819
Labou D, Slavcheva E et al (2008) Performance of laboratory polymer electrolyte membrane hydrogen generator with sputtered iridium oxide anode. J Power Sources 185:1073–1078
Ledgard SF, Boyes M, Brentrup F (2011) Life cycle assessment of local and imported fertilisers used on New Zealand farms. http://www.massey.ac.nz/~flrc/workshops/11/Manuscripts/Ledgard_2011.pdf
Lee J, Tak Y (2001) Electrocatalytic activity of Cu electrode in electroreduction of CO_2. Electrochim Acta 46(19):3015–3022
Lehn J, Ziessel R (1982) Photochemical generation of carbon monoxide and hydrogen by reduction of carbon dioxide and water under visible light irradiation. Proc Natl Acad Sci U S A 79:701
Lehn J, Ziessel R (1990) Photochemical reduction of carbon dioxide to formate catalyzed by 2,2′-bipyridine- or 1,10-phenanthroline-ruthenium(II) complexes. J Organomet Chem 382:157
Li CW, Kanan MW (2012) CO_2 reduction at low overpotential on Cu electrodes resulting from the reduction of thick Cu_2O films. J Am Chem Soc 134:7231–7234
Li H, Oloman C (2007) Development of a continuous reactor for the electro-reduction of carbon dioxide to formate – Part 2: scale-up. J Appl Electrochem 37(10):1107–1117
Li JW, Prentice G (1997) Electrochemical synthesis of methanol from CO_2 in high-pressure electrolyte. J Electrochem Soc 144:4284–4288
Logan DA (1997) Estimating physical properties for control equipment design. Environ Prog 16:237–244
Magdesieva TV, Zhukov IV, Kravchuk DN, Semenikhin OA, Tomilova LG, Butin KP (2002) Electrocatalytic CO_2 reduction in methanol catalyzed by mono-, di-, and electropolymerized phthalocyanine complexes. Russ Chem Bull 51:805–812
Mahmood MN, Masheder D et al (1987) Use of gas-diffusion electrodes for high-rate electrochemical reduction of carbon-dioxide. 1. Reduction at lead, indium-impregnated and tin-impregnated electrodes. J Appl Electrochem 17(6):1159–1170
Mao X, Alan Hatton T (2015) Recent advances in electrocatalytic reduction of carbon dioxide using metal-free catalysts. Ind Eng Chem Res 54:4033–4042

Moats MS, Miller JD, Zmierczak WW (2008) Chemical utilization of sequestered carbon dioxide as a booster of hydrogen economy. In: Neelameggham N, Reddy RG (eds) Carbon dioxide reduction metallurgy. The Minerals, Metals, and Materials Society, Warrendale, pp 19–23

Morris AJ, McGibbon RT, Bocarsly AB (2011) Electrocatalytic carbon dioxide activation: the rate-determining step of pyridinium- catalyzed CO_2 reduction. ChemSusChem 4:191–196

Murata A, Hori Y (1991) Product selectivity affected by cationic species in electrochemical reduction of CO_2 and CO at a Cu electrode. Bull Chem Soc Jpn 64:123–127

Ogura K (2003) Electrochemical and selective conversion of CO_2 to ethylene. Electrochemistry 71(8):676–680

Ogura K, Yano H et al (2003) Catalytic reduction of CO_2 to ethylene by electrolysis at a three-phase interface. J Electrochem Soc 150(9):D163–D168

Olah GA (2005) Beyond oil and gas: the methanol economy. Angew Chem Int Ed Engl 44 (18):2636–2639. Loker Hydrocarbon Research Institute and Department of Chemistry, University of Southern California, Los Angeles

Olah GA, Goeppert A, Prakash GKS (2009) Chemical recycling of carbon dioxide to methanol and dimethyl ether: from greenhouse gas to renewable environmentally carbon neutral fuels and synthetic hydrocarbons. J Org Chem 74:487–498

Olah GA, Surya Prakash GK, Goeppert A (2011) Anthropogenic chemical carbon cycle for a sustainable future. J Am Chem Soc 133:12881–12898

Oloman C, Li H (2008) Electrochemical processing of carbon dioxide. ChemSusChem 1 (5):385–391

Parkinson G (2006) Chem Eng Prog 102:7

Perathoner S, Gangeri M et al (2007) Nanostructured electrocatalytic Pt-carbon materials for fuel cells and CO_2 conversion. Kinetics Catal 48(6):877–883

Peters M et al (2011) Chemical Technologies for Exploiting and Recycling Carbon Dioxide into the Value Chain. ChemSusChem 4:1216–1240

Peterson AA, Abild-Pedersen F, Studt F, Rossmeisl J, Norskov JK (2010) How copper catalyzes the electroreduction of carbon dioxide into hydrocarbon fuels. Energy Environ Sci 3:1311–1315

Pontzen F, Leibner W, Gronemann V, Rothaemelm M, Ahlers B (2011) CO_2-based methanol and DME – efficient technologies for industrial scale production. Catal Today 171:242–250

Quadreilli EA, Centi G, Duplan J-L, Perathoner S (2011) Carbon dioxide recycling: emerging large scale technologies with industrial potential. ChemSusChem 4:1194–1215

Quadrelli EA et al (2011) ChemSusChem 4:1194–1215

Ratnasamy C, Wagner JP (2009) Water gas shift catalysis. Catal Rev 51(3):325–440

Rosen BA, Salehi-Khojin A, Thorson MR, Zhu W, Whipple DT, Kenis PJA, Masel RI (2011) Ionic liquid-mediated selective conversion of CO_2 to CO at low overpotentials. Science 334:643–644

Saeki T, Hashimoto K, Kimura N, Omata K, Fujishima A (1995) Electrochemical reduction of CO_2 with high-current density in a CO_2 plus methanol medium. 2. CO formation promoted by tetrabutylammonium cation. J Electroanal Chem 390:77–82

Salehi-Khojin A, Jhong H-RM, Rosen BA, Zhu W, Ma S, Kenis PJA, Masel RI (2012) Nanoparticle silver catalysts that show enhanced activity for carbon dioxide electrolysis. J Phys Chem C 117:1627–1632

Sanchez-Sanchez CM, Montiel V et al (2001) Electrochemical approaches to alleviation of the problem of carbon dioxide accumulation. Pure Appl Chem 73(12):1917–1927

Schiller G, Henne R et al (1998) High performance electrodes for an advanced intermittently operated 10-kW alkaline water electrolyzer. Int J Hydrogen Energ 23(9):761–765

Schouten KJP, Qin Z, Gallent EP, Koper MTM (2012) Two pathways for the formation of ethylene in CO reduction on single-crystal copper electrodes. J Am Chem Soc 134:9864–9867

Seshadri G, Lin C, Bocarsly AB (1994) A new homogeneous electrocatalyst for the reduction of carbon-dioxide to methanol at low overpotential. J Electroanal Chem 372:145–150

Shidong S, Huamin Z et al (2008) Electrochemical investigation of electrocatalysts for the oxygen evolution reaction in PEM water electrolyzers. Int J Hydrogen Energ 33:4955–4961

Song C, Pan W (2004) Tri-reforming of methane: a novel concept for catalytic production of industrially useful synthesis gas with desired H_2/CO ratios. Catal Today 98:463–484

Spinner NS, Vega JA, Mustain WE (2012) Recent progress in the electrochemical conversion and utilization of CO_2. Catal Sci Technol 2:19–28

Sridhar KR, Vaniman BT (1997) Oxygen production on Mars using solid oxide electrolysis. Solid State Ion 93:321

Tang W, Peterson AA, Varela AS, Jovanov ZP, Bech L, Durand WJ, Dahl S, Norskov JK, Chorkendorff I (2012) The importance of surface morphology in controlling the selectivity of polycrystalline copper for CO_2 electroreduction. Phys Chem Chem Phys 14:76–81

Tao M (2008) Inorganic photovoltaic solar cells: silicon and beyond, The electrochemical society's interface. Winter 17(4):30

Tao G, Sridhar KR, Chan CL (2004) Study of carbon dioxide electrolysis at electrode/electrolyte interface: Part II. Pt-YSZ cermet/YSZ interface. Solid State Ion 175:621

Ted Oyama S et al (2012) Dry reforming of methane has no future for hydrogen production: comparison with steam reforming at high pressure in standard and membrane reactors. Int J Hyd Energy 37(13):10444

Thorson MR, Siil SI, Kenis PJA (2013) Effect of cations on the electrochemical conversion of CO_2 to CO. J Electrochem Soc 160:F69–F74

Todoroki M, Hara K et al (1995) Electrochemical reduction of high-pressure CO_2 at Pb, Hg and in electrodes in an aqueous Khco3 solution. J Electroanal Chem 394(1–2):199–203

Tornow CE, Thorson MR, Ma S, Gewirth AA, Kenis PJA (2012) Nitrogen-based catalysts for the electrochemical reduction of CO_2 to CO. J Am Chem Soc 134:19520–19523

Udupa KS, Subraman G et al (1971) Electrolytic reduction of carbon dioxide to formic acid. Electrochim Acta 16(9):1593

Utgikar VT (2006) Life cycle assessment of high temperature electrolysis for hydrogen production via nuclear energy. Int J Hydrogen Energ 31(7):939–944

Whitlow JE, Parish CF (2003) Operation, modeling and analysis of the reverse water gas shift process, AIP Conference Proceedings, 654:1116–1123

Wittcoff HA, Reuben BG, Plotkin JS (2013) Industrial organic chemicals, 3rd edn. Wiley, Hoboken

Wu M et al (2007) Argonne National Lab report, ANL-ESD-07-10, Nov 2007

Wu JJ, Risalvato FG, Ke FS, Pellechia PJ, Zhou XD (2012) Electrochemical reduction of carbon dioxide I. Effects of the electrolyte on the selectivity and activity with Sn electrode. J Electrochem Soc 159(7):F353–F359

Wu J, Risalvato FG, Sharma PP, Pellechia PJ, Ke F-S, Zhou X-D (2013) Electrochemical reduction of carbon dioxide II. Design, assembly, and performance of low temperature full electrochemical cells. J Electrochem Soc 160(9):F953–F957

Yamamoto T, Hirota K et al (1998) Electrochemical reduction of CO_2 in microspores. Chem Lett 8:825–826

Yamamoto T, Tryk DA et al (2000) Electrochemical reduction of CO_2 in the micropores of activated carbon fibers. J Electrochem Soc 147(9):3393–3400

Yamamoto T, Tryk DA et al (2002) Production of syngas plus oxygen from CO_2 in a gas-diffusion electrode-based electrolytic cell. Electrochim Acta 47(20):3327–3334

Yano J, Yamasaki S (2008) Pulse-mode electrochemical reduction of carbon dioxide using copper and copper oxide electrodes for selective ethylene formation. J Appl Electrochem 38 (12):1721–1726

Yano H, Shirai F, Nakayama M, Ogura K (2002a) Efficient electrochemical conversion of CO_2 to CO, C_2H_4 and CH_4 at a three-phase interface on a Cu net electrode in acidic solution. J Electroanal Chem 519(1-2):93–100

Yano H, Shirai F et al (2002b) Electrochemical reduction of CO_2 at three-phase (gas/liquid/solid) and two-phase (liquid/solid) interfaces on Ag electrodes. J Electroanal Chem 533 (1-2):113–118

Zaelke D et al (2011) Scientific synthesis of Calera carbon sequestration and carbonaceous by-product applications. Consensus findings of the scientific synthesis team, January 2011, University of California, Santa Barbara

Zhai Y, Guan S, Sridhar N, Agarwal AS (2015) Method and apparatus for the electrochemical reduction of carbon dioxide. US Patent App. 9,145,615, 2015

General Reading References

Aresta M (ed) (2010) Carbon dioxide as a chemical feedstock. Wiley, New York

Halmann MM, Steinberg M (1999) Greenhouse gas carbon dioxide mitigation science and technology. Lewis Publishers, Boca Raton

Olah GA (2005) Beyond oil and gas: the methanol economy. Angew Chem Int Ed Engl 44 (18):2636–2639. Loker Hydrocarbon Research Institute and Department of Chemistry, University of Southern California, Los Angeles

Styrin P, Quadrelli EA, Armstrong K (2015) Carbon dioxide utilisation: closing the carbon cycle. Elsevier, Amsterdam

Oxy-Fuel Firing Technology for Power Generation

Edward John (Ben) Anthony

Contents

Abstract

In order to generate pure streams of CO_2 suitable for sequestration/storage, various routes are possible, involving either precombustion strategies such as the use of gasification technology combined with shift reactors to produce H_2 or alternatively post-combustion strategies such as CO_2 scrubbing with, for example, amine-based carriers. One of the more direct approaches is to carry out the

E.J.B. Anthony (✉)
CanmetENERGY, Natural Resources Canada, Ottawa, ON, USA
e-mail: EdwardJohn.Anthony@NRCan-RNCan.gc.ca

W.-Y. Chen et al. (eds.), *Handbook of Climate Change Mitigation and Adaptation*,
DOI 10.1007/978-3-319-14409-2_39

combustion in pure or nearly pure oxygen-oxy-fuel combustion to produce primarily CO_2 and H_2O in the combustion gases, resulting in almost complete CO_2 capture. Until recently, the primary avenue for deploying this technology was with conventional pulverized fuel-fired boilers, and there is already one large demonstration plant operating in Europe with more being planned in the future. However, more recently oxy-fired fluidized bed combustion (FBC) has also become increasingly important as a potential technology, offering as it does fuel flexibility and the possibility of firing local or indigenous fuels, including biomass in a CO_2-neutral manner. Both oxy-fuel combustion technologies have been examined here, considering factors such as their economics and potential for improvement, as well as challenges to the technology, including the need to generate CO_2 streams of suitable purity for pipeline transport to available sequestration sites. Finally, the emission issues for both classes of the technology are discussed.

Introduction

The idea that anthropogenic CO_2 could cause significant global warming was first presented over 114 years ago by Svante Arrhenius (1896); by 1907, the use of fossil fuels as a potent cause of CO_2 emissions had also been clearly spelled out: "The enormous combustion of coal by industrial establishments suffices to increase the percentage of carbon dioxide in the air to an appreciable amount" (Arrhenius 1907), albeit that Arrhenius saw global warming as a potential benefit. Unfortunately, it has taken a further 60 or more years for the potential for damage due to these phenomena to be universally recognized (Houghton 2004; Edwards 2010). Against this background, world populations have been burgeoning, and the use of fossil fuels to meet mankind's energy needs has increased and shows no signs of stopping in the near future. To further complicate the picture, many countries have aging thermal power plants, most of which will have to be replaced in the next couple of decades.

At this point the major hope for continuing to use fossil fuels for widespread power generation in an environmentally benign manner lies in the technology known as carbon capture and sequestration (CCS), as renewable and nuclear technologies would not be able to quickly fill the gap if fossil fuels were simply abandoned. In practice, this means that the norm may well be to build thermal power plants to incorporate back-end technologies for CO_2 capture following a carbon-capture-ready philosophy (Irons et al. 2007). Thus, if "new" technologies are to be introduced on a wide scale, they had best either be already commercialized, such as gasification, or in a near-market-ready state. Fortunately, for oxy-fuel combustion technology, in which the fuel is converted in a stream of nearly pure oxygen (90–95 % plus) using pulverized fuel (PF) or pulverized coal (PC), research is now well underway with various larger pilot-scale demonstrations either completed or under construction, as will be seen later in this chapter. The oxy-fuel technology, in its currently typical configuration, is presented in a

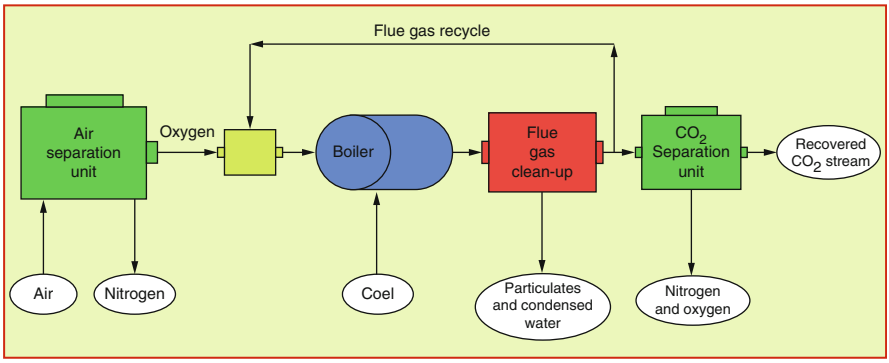

Fig. 1 Schematic of generic oxy-fired boiler configuration

schematic in Fig. 1. As an alternative there is also the possibility of retrofitting existing boilers, and here too oxy-fuel technology can potentially meet this challenge in an economically attractive fashion when compared with other CO_2-neutral options (Farley 2006). Finally, it should also be added that there are side benefits of oxy-fuel combustion, the most obvious being that thermal NO_x levels are expected to be significantly reduced, since N_2 in air is largely absent from the oxidant.

This chapter focuses on oxy-fuel PF and circulating fluidized bed (CFB), and it will not discuss oxy-fuel technology in which water is used instead of CO_2 to moderate flame temperatures, as any such technology is much further from commercialization than oxy-fuel technology with flue gas recycle (FGR) and/or may pose excessive technical challenges at the present time (Zheng et al. 2009). Nor will this chapter consider hybrid systems combining, for instance, amine scrubbing and oxy-fuel, although they have been proposed (Doukelis et al. 2008), for the same reason, namely, that such concepts are probably significantly further removed from commercialization than "conventional" oxy-fuel technology.

Oxy-Fuel Pulverized Fuel Technology

Oxy-fuel work in PF systems traces its origins to pioneering research carried out by Argonne National Laboratory in the 1980s (Weller et al. 1985). Subsequently, in the 1990s, significant oxy-fuel research and development (R&D) work was initiated elsewhere, with a number of small pilot plant programs, including CanmetENERGY (Canada), Air Liquide (USA), and the International Flame Research Foundation (IFRF) R&D program in Ijmuiden (The Netherlands) looking initially at natural gas firing (Buhre et al. 2005). In addition to the early small-scale pilot plant work, there were various economic evaluations of the technology versus back-end scrubbing, primarily for natural gas-fired systems, and there are now at least three major reviews in the open literature available to describe such developments (Buhre et al. 2005;

Toftegaard et al. 2010; Davidson and Stanley 2010). The economic studies often suggested that oxy-firing was not a preferred technology or, if so, only slightly better, with efficiencies in the mid-40 % range and costs somewhat higher than back-end capture of CO_2 for natural gas, and there has been vigorous debate about the results of such evaluations. The paper of Kvamsdal et al. (2007) is typical of such studies, looking at nine potential concepts and ranking oxy-firing of natural gas as only of moderate performance, while noting the significant energy losses associated with the cryogenic separation of air (6.6 % in that study with a further loss of 2.4 % for compression, when expressed in percent of the net plant efficiency, based on the fuel's lower heating value).

More recent studies also confirm efficiency losses of 8–10 % (on the same basis) for both natural gas- and coal-fired systems (Liszka and Ziębik 2010). Studies, which tend to focus more on coal, seem to show a fairly similar picture in terms of overall economics, that is, that oxy-fuel PC looks comparable to PC technology with back-end CO_2 capture. Thus, Bouillon et al. (2009) came to the conclusion that the penalties for both post-combustion and oxy-fuel combustion-integrated processes were around 44 €/t CO_2. In a later study, Hadjipaschalis et al. (2009) carried out an analysis for a 500 MW steam plant, with assumed efficiency of 33.5 %, a generation capacity factor of 85 %, and 90 % CO_2 capture rate. The results of their study indicate that the oxy-fuel combustion plant represents a competitive technology, which currently seems to be the most economical having the lowest electricity costs and lower CO_2 avoidance costs. Similarly, a major Canadian study done for the Canadian Clean Power Coalition (CCPC) in 2007 (Xu et al. 2007) came to the following conclusions:

- The oxy-fuel combustion technology was found to have technical and environmental benefits comparable to post-combustion capture, and it was the most economic option in one of the cases studied, which was based on a greenfield site in Alberta utilizing low-S coal, where flue gas desulfurization (FGD) was not required for oxy-fuel but was for post-combustion capture. The assumption in this case was that most SO_2 emissions would be captured in the CO_2 compression phase. In the two other sites studied (Saskatchewan and Nova Scotia), the amine-based post-combustion options were found to be more economic, but the difference was marginal.
- It was also found that parasitic energy losses directly related to CO_2 capture were the largest single cost item, closely followed in most cases by capital charges. These costs were similar for both oxy-fuel and amine-based capture if FGDs were present in both cases. The capital and operating costs of the air separation unit (ASU) represent a major problem for oxy-fuel economics, and improvements in this area will have major benefits.
- Operating and maintenance (O&M) costs were found to make up a relatively minor portion of the total charges.
- The CCPC study also found that oxy-fuel combustion was expected to capture slightly more CO_2 than post-combustion technology, which tended to help its cost-per-tonne-captured figures.

- Retrofits based on oxy-fuel were found to be significantly more expensive compared to back-end retrofits that left the existing boiler plant intact.

Finally, Farley (2006) also quotes costs which suggest that post-combustion capture and oxy-fuel technologies are comparable, but in apparent contrast to the 2007 CCPC (Xu et al. 2007) study, suggesting that a significant advantage lies in the fact that oxy-fuel technology can be retrofitted to existing plants (Farley 2006).

From the above citations, it is clear that the oxy-fuel combustion concept is comparable with post-combustion capture in terms of cost, and it represents a midterm solution with considerable potential for commercialization, as opposed to many of the schemes evaluated where scale-up presented significant uncertainties. It is also clear that very significant economic gains can be made if oxygen could be produced more cheaply.

Buhre et al. (2005) summarized some key conclusions about oxy-firing as follows:

- Typically 31 % oxygen, rather than 21 % for air-fired boilers, must be used to achieve a similar adiabatic flame temperature, and to achieve this level, it requires recycle of about 60 % of the flue gas.
- The much higher CO_2 and H_2O proportions in the flue gases result in increased emissivity, so a retrofitted boiler will have similar radiative heat transfer to an air-fired boiler for an O_2 proportion of 30 %.
- Gas flows will be reduced to about 80 % of those in the air case.
- Emissions of minor species such as SO_2 and NO will be higher in the recycled gases, unless they are removed in the recycle process.

Such conclusions are useful but are dependent on case-specific factors such as how much air leakage there is into the boiler (1 % or less is desired) and details concerning auxiliary systems. The choice of whether flue gas recycle should be wet or dry is also important. Zheng et al. (2009) suggest that, as an approximate guideline, coals with less than 1 % sulfur content are suitable for wet flue gas recycle, while coals with higher sulfur levels are not, because of concerns over corrosion associated with high SO_x levels. Zhou and Moyeda (2010) suggest that typical wet flue gas recycle should be in the range of 70–75 %. Wet flue gas recycle lowers the adiabatic flame temperature of the gas, while dry recycle allows higher flame temperatures but reduces the overall gas velocity. Table 1 gives an expected comparison for air-fired and oxy-fuel combustion with wet flue gas recycle taken from Zhou and Moyeda (2010).

These authors also note that the efficiency of such a plant is less than that of a conventional plant without carbon capture but greater than that of an air-fired plant fitted with an amine system, and this is a conclusion on which there is considerable debate, as noted above.

Finally, a last comment to be made on such plants is that since the oxygen used has to be produced cryogenically, and hence is expensive, excess oxygen levels should ideally be kept as low as possible.

Table 1 Comparison of burner gas compositions (wt%) (From Zhou and Moyeda 2010)

Composition	Conventional air fired	Oxy-fuel with wet FGR
O_2	3.2	3.1
CO_2	14.7	69
H_2O	5.85	27.5
NO_x (ppm)	154	82

Emissions: SO_x, NO_x, and Other Micro-pollutants

As PC firing is the ranking coal combustion technology, dating back to at least the 1940s when early attempts were made to use pulverized coal in fire-tube boilers, it is not surprising that an enormous amount is known about the emissions from such systems (Gunn and Horton 1989). The obvious differences between air firing and oxy-firing (with FGR) using pulverized coal are the high levels of CO_2 (of the order of five times or more) and water (of the order of two to three times more) and the somewhat smaller flue gas volumes that will tend to concentrate the emissions of micro-pollutants in the flue gas stream. Other differences would include the effect of somewhat higher oxygen levels in the burner of around 30 %, which together with the lower flue gas levels allows a similar exit oxygen content to the air-fired case (Table 1), and possible effects on fuel devolatilization and char combustion due to the differences in the gaseous environment.

Also, absolute emissions might well vary if the flame length and its temperature and/or the gas concentrations change, and it has been shown, for instance, that at high flue gas recycle ratios, flame temperatures may fall by as much as 100 °C or more (Smart et al. 2010). This affects the combustion process itself and reduces flame stability, although such effects are lower for high-volatile coals, in line with the results of earlier work (Buhre et al. 2005). Much of the early work was done in thermogravimetric analyzers (TGAs) and other laboratory-scale devices, with low heating rates, which are atypical of pulverized fuel firing. However, there is now more information from systems with realistic heating rates. Thus, for instance, wire mesh tests done with two coals in an oxy-fuel environment (30 % O_2/70 % CO_2) showed evidence of a small rise in ignition temperature of around 20 °C for the coals used in this study (Qiao et al. 2010).

Experiments were done in an entrained flow reactor (0.08 m diameter and 2 m length) with a bituminous coal but failed to find any evidence of char–CO_2 gasification reactions (Brix et al. 2010). In addition, unlike earlier studies this one found no significant change in volatile production between air firing and oxy-firing, but char burned faster in air than in oxy-fuel conditions, suggesting that the CO_2 is important in reducing the burning rate when external mass transfer dominates the combustion process, which is also in agreement with other earlier work (Shaddix and Molina 2008).

NO_x Production

The production of nitric oxides can occur in combustion systems by means of three mechanisms:

- Prompt NO_x – where hydrocarbon radicals in the flame front react with the nitrogen in the combustion gases
- Thermal NO_x – where oxygen reacts at temperatures above about 1,000 °C to form NO_x (the so-called Zeldovich mechanism)
- Fuel nitrogen reactions

Prompt NO_x is more important in gaseous hydrocarbon flames, while thermal NO_x would reasonably be expected to be substantially reduced by a factor of about 20 due to the effective removal of nitrogen from the oxidant, but fuel nitrogen mechanisms can still be expected to be important and give rise to significant NO_x production.

In a recent study using a quartz flow reactor, high CO_2 levels were shown to compete for H atoms (the main source of chain branching and hence radical production) and thus reduce the rate of oxidation of HCN (Giménez-López et al. 2010). Similar arguments concerning the change of OH/H radical concentrations in methane oxy-fuel flames have also been advanced from measurements and modeling done by Mendiara and Glarborg (2009). Since HCN is an important intermediate for the production of NO, this implies that the elevated CO_2 levels in oxy-fuel combustion should also decrease NO formation from fuel nitrogen. These results are interesting in that they are in contradiction to an earlier study which stated that the influence of CO_2 on NO_x was negligible (Okazi and Ando 1997). However, both measurements (Tan et al. 2006; Hjärtstam et al. 2009) and modeling (Cao et al. 2010) have shown reduced NO_x levels, even without flue gas recycle, which itself also causes a reduction in NO_x production.

Another difference between the air and oxy-fuel cases is that the CO levels can be higher for oxy-fuel systems, depending on flame temperature and the degree of recycle. However, in measurements of CO profiles when burning lignitic fuels in a small oxy-fuel combustor, Hjärstam et al. (2009) showed that this did not necessarily reflect in emissions of either CO or NO leaving the boiler.

SO_x Production

Sulfur in fossil fuel combustion is released as SO_2 and SO_3, and except in the case of, for example, ashes with very high Ca contents (e.g., the French Gardanne lignite, which has an extremely high natural Ca/S molar ratio in its ash), more than 90 % of the S in the fuel will typically be found as SO_2 in the flue gas (Smoot and Pratt 1979). Flue gas recycle will tend to concentrate micro-pollutants and Fig. 2, in a

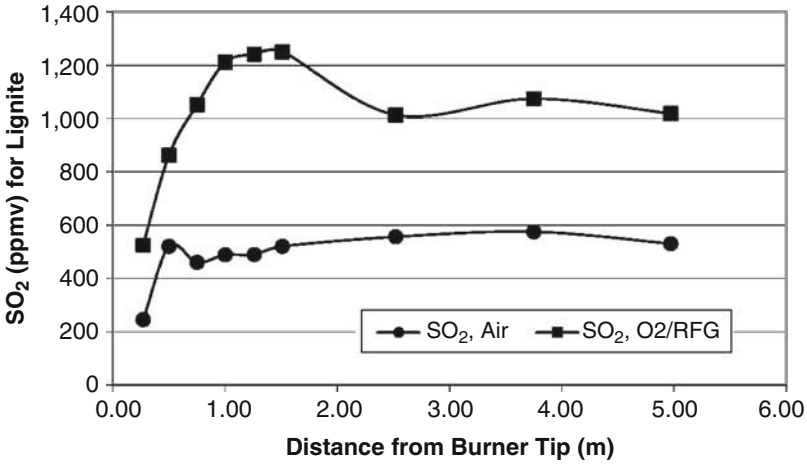

Fig. 2 SO_2 emissions from CanmetENERGY oxy-fired pilot plant (oxy-fuel case at 35 % O_2)

CanmetENERGY small-scale pilot plant study at high temperatures appropriate to suspension firing shows SO_2 levels for oxy-fuel with recycled flue gas versus the air-firing case. SO_2 is the dominant sulfur form, as even at lower temperatures oxidation of SO_2 to SO_3 tends to be very slow and dependent on the presence of catalytic reactions. However, higher SO_2 levels mean that fly ash components will tend to react more readily if they can sulfate (Sturgeon et al. 2009).

In early studies, both Hu et al. (2000), who carried out experiments in a small flow reactor burning coal (1.1 % sulfur), and Croiset and Thambimuthu (2001), operating the CanmetENERGY oxy-fuel combustor with an Eastern US bituminous coal (1 % sulfur), reported a decrease in sulfur release for oxy-fuel combustion, ranging from 75 % without flue gas recycle to 65 % with recycle. Hu et al. (2000) suggested that the reduced SO_2 levels they experienced were due to ash reactions, the possible formation of other sulfur compounds (COS and/or H_2S), or retention of sulfur in the char. The reaction of ash with sulfur in pulverized coal-fired systems is well established, especially for lignites and Western US coals (Smoot and Pratt 1979), although the ash content of the coal used in their experiments was only 2 %. The possibility that some of the sulfur is retained in the char is also reasonable for a small flow reactor, but suggestions of other sulfur compounds do not seem likely if oxidizing conditions prevail. Croiset and Thambimuthu (2001) ruled out capture in the ash and significant losses of SO_2 in condensate from the flue gas recycle for their experiments and instead postulated the production of elevated SO_3 levels.

Subsequent experiments have not, however, suggested such dramatic reductions in SO_2 releases, at least where Ca levels in the ash are not high, but elevated levels of SO_3 are indeed found. Thus, Tan et al. (2006) found that SO_3 concentrations could be up to three or four times higher for oxy-fuel with wet flue gas recycling than for the corresponding air-fired situation, with levels consistently around 5 %, whereas normal levels would vary in the range of 1–5 %, depending on the sulfur content of

Table 2 Average measured SO_2/SO_3 concentrations in ppm (From Maier et al. 2008)

Firing mode	SO_2 (ppm)	SO_3 (ppm)
Air	733	8
Oxy-fuel	1,758	85

the fuel, air/fuel mixing patterns, and excess air in the furnace. This picture for SO_3 levels has also been confirmed in later experiments. Thus, Maier et al. (2008) found an elevated level of SO_3 and indicated that the average SO_3 concentrations for their experiments were in the range of 36–121 ppm, for an average SO_2 concentration of 1,791 ppm, and flue gas moisture of 28.9 vol.%. Table 2 gives average SO_2 and SO_3 levels for their experiments (note that SO_2 levels are also elevated, as expected).

However, it is clear that an increase in SO_3 up to about 5 % may occur, which is sufficient to cause the acid dew point to be raised, leading to a real potential for enhanced corrosion, if flue gases go below that temperature. Based on their data, Maier et al. (2008) predict an increase in the acid dew point of around 30 °C for oxy-fuel conditions, from 138 °C for air to 169 °C for oxy-fuel. Ahn et al. (2010) have also noted that SO_3 levels are likely to be elevated, based on their experiments with a small pilot-scale combustor at the University of Utah, and that on average the SO_3 levels under oxy-fuel-fired conditions are about four times higher than in the air-fired situation. Both of these studies are in agreement with the work of Fleig et al. (2009), who explored the SO_3 levels to be produced for the oxy-fuel combustion of lignite for wet recycling and indicated that they should be about four times higher than in the air-fired case, with a resulting rise in the acid dew point of 20–30 °C.

As a result of these higher SO_2 and SO_3 levels, there are concerns about corrosion and deposition on boiler walls and surfaces; however, research is still in its early days. Nonetheless, the large boiler companies have initiated research programs to generate information on these potential problems, and it can be expected that significant results will be produced in the next several years (Kung and Tanzosh 2008; Bordenet et al. 2008). It should also be added that on the positive front, air pollution control (APC) devices may be reduced in size, leading to some cost reductions, and this is especially true for FGD if wet flue gas recycle is used. Concerning the use of FGD equipment, while there were questions initially on the effect of high CO_2 concentrations on limestone effectiveness in FGD, Vattenfall's experience showed that SO_2 removal rate and limestone usage are the same for air and oxy-fuel cases (Strőmberg et al. 2009). For a very detailed analysis of the issues relating to sulfation in oxy-fired PF systems, the interested reader is referred to a very recent review article by Stranger and Wall (2011).

Major Pilot Plant Developments

There are now a large number of major pilot plant and pre-commercial demonstration projects worldwide, and these include:

- Germany – 30 MW_{th} demonstration unit (Strőmberg et al. 2009, 2010; Vattenfall 2010)
- USA – Jupiter Oxygen Corporation, 15 MW_{th} burner test facility, National Energy Technology Laboratory (NETL) (Ochs et al. 2009; NETL 2010); Demonstration of a 30 MW_{th} oxy-fired unit (the Clean Environmental Development Facility in Alliance, Ohio), Babcock & Wilcox Power Generation Group, Inc. (B&W PGG) and Air Liquide (McDonald et al. 2008; Air Liquide Press 2008)
- United Kingdom – 40 MW_{th} Doosan Babcock Demonstration unit (Hesselmann et al. 2009)
- France – 30 MW_{th} Lacq Project, Total, in partnership with Air Liquide (Total 2010)
- Australia – Callide Oxy-fuel Project (30 MW unit) and various other projects (Cook 2009)

Another possibility also exists that of retrofitting older conventional power plants to operate in an oxy-fuel mode (Tigges et al. 2009). Moreover there is considerable research underway to develop cheaper methods of oxygen production, such as membrane technologies, which have the potential to make oxy-fuel technologies even more attractive, either by themselves (especially for smaller-scale applications) (Carbo et al. 2009) or possibly by first carrying out a first-stage air separation, prior to the cryogenic separation, thus reducing the size of the unit and the energy used in making oxygen at 90 % + purity (Burdyny and Struchtrup 2010). However, for now at least it is also clear that the classic approach of cryogenic air separation can, in principle, meet the needs of a new generation of oxy-fuel power plants (Allam et al. 2005), and the use of this technology is generally assumed in this chapter.

Other Issues for Oxy-Fuel Firing in Pulverized Fuel Combustion Systems

Biomass Firing in Oxy-Fuel Combustion Systems

The idea of using biomass in pulverized coal blends is well established, and there are efforts in most countries to supplement the coal fuel supply with biomass (a carbon-neutral fuel), as an approach to the reduction of carbon emissions. In Canada, for instance, trials have been undertaken with up to 100 % biomass firing in the 227 MW_e Atikokan Generating Station in Ontario (Marshall et al. 2010). Unfortunately, there are a number of issues, the first, and probably most important, being that there is usually insufficient biomass in a given area to supply a commercial-scale power plant. Second, the properties of biomass differ from coal, and so torrefaction or pelletization, before the fuel is then pulverized, is effectively essential if such fuels are to be used directly, and modifications of the fuel feed system are necessary. On this point, it is instructive that the Atikokan unit had a dust explosion in its coal feeding system during preparations for further biomass trials (Marshall et al. 2010).

One ingenious suggestion is that biomass, which typically has high moisture, might be co-fired with coal, thus providing an alternative method to flue gas recycle; however, as noted above the problem with such an approach would be the need to obtain sufficient biomass for such a concept to be applied (Haykir-Acma et al. 2010). Another issue for biomass is fouling, and depending on the nature of the coal ash (i.e., does it contain sufficient Ca in the form of CaO that it can carbonate), it is evident that the fouling and deposit behavior of an ash might be different in an oxy-fuel environment compared to that in an air-fired one. Fryda et al. (2010) carried out some experiments in a drop tube using biomass blends and a Russian and South African coal. They report some small changes in K, Na, and Ca in the deposits depending on operating conditions and speculate that the "lower char temperature" in oxy-fuel combustion may be producing such effects. At the present time, it appears that general conclusions are probably premature, but it seems likely the greatest barrier to using biomass in oxy-fuel combustion is probably simply insufficient supply, although other issues such as the inhomogeneity of biomass, potentially high alkali metal content for some types of biomass, and the cost of good quality biomass, especially if the biomass must be pelletized before pulverization, are also potential concerns.

Oxy-Fuel CFBC Combustion

Oxy-fuel combustion has been thoroughly studied for pulverized coal combustion, but to date there has been relatively little attention paid to oxy-fuel circulating fluidized bed combustion (CFBC), although the concept was examined over 30 years ago for bubbling FBC (Yaverbaum 1977). More recently the boiler companies, Alstom and Foster Wheeler, have explored the oxy-fuel CFBC concept using pilot-scale tests (Eriksson et al. 2007; Stamatelopoulos and Darling 2008). Alstom's work included tests in a unit of up to 3 MW_{th} in size but did not involve recycle of flue gas (Liljedahl et al. 2006). Foster Wheeler's work (Eriksson et al. 2007) also involved pilot-scale testing, using a small (30–100 kW) CFBC owned and operated by VTT (Technical Research Centre of Finland), and this work along with CanmetENERGY's work with its own 100 kW CFBC appears to be the first in which units were operated with oxy-fuel combustion using flue gas recycle. Foster Wheeler is currently developing its Flexi-burn™ technology, which would allow a CFBC boiler to operate either in air- or oxy-firing conditions (Eriksson et al. 2009).

The advantages of the CFBC technology are already well known in terms of its ability to burn a wide range of fuels, both individually and co-fired, to achieve relatively low NO_x emissions, because temperatures are too low for significant thermal NO_x production, and to accomplish SO_2 removal by limestone (Grace et al. 1997). Another advantage of CFBC technology, in the context of oxy-fuel firing, is the fact that hot solids are kept in the primary reaction loop by means of a hot cyclone. This solid circulation potentially provides an effective means, in conjunction with the recycle of flue gas, to control combustion and effectively extract heat during the combustion process, thus allowing either a significant

reduction of the amount of recycled flue gas or, alternatively, permitting the use of a much higher oxygen concentration in the combustor. These factors allow the economics of oxy-fired CFBC to be significantly improved over PC or stoker firing by reducing the size of the CFBC boiler island by as much as 50 % (Liljedahl et al. 2006). In considering the scale-up of CFBC units above 300 MW_e, both Foster Wheeler and Alstom are now offering much larger units, and Foster Wheeler has in operation a 460 MW_e supercritical CFBC boiler (Stamatelopoulos and Darling 2008; Hotta et al. 2008).

Advantages more difficult to quantify for the technology relate to: the possibility of co-firing biomass, so that in conjunction with CCS, the overall combustion process may potentially result in a net reduction of anthropogenic CO_2 and the potential for this technology to be used with more marginal fuels, as premium fossil fuel supplies wane. The co-firing option offers a potentially interesting advantage of CFBC technology, since it is well established that CFBC can burn biomass and fossil fuels at any given ratio ranging from 0 % to 100 %, thus offering the possibility of using local and seasonally available biomass fuels in a CO_2 "negative" manner.

The ultimate availability of premium coal for a period of hundreds of years has also recently been called into doubt with suggestions that coal production may peak well before the end of this century. Thus, Mohr and Evans (2009), for example, have developed a model which suggests that coal production will peak in 2034 on a mass basis and 2026 on an energy basis. A good general discussion of these ideas can also be found in Wikipedia (2010). In the event of such solid fuel shortages, fluidized bed combustion is ideally suited to exploit the many marginal coals and hydrocarbon-based waste streams available worldwide.

Currently R&D on oxy-fired CFBC technology is being undertaken in numerous countries, including Canada, Finland, Poland, China, and the USA among others. However, to date most test work has been done at small scale (in the $<$100 kW range) and/or using bottled gases to supply a suitable combustion gas, instead of recycling flue gas to achieve the necessary gas velocity and solid circulation rate in terms of heat transfer requirements. CFBC systems can potentially accommodate recycling of less flue gases than a PC boiler, despite the inherently low temperature of the combustion process, required to avoid ash softening or melting and to achieve better in-bed sulfur capture. This situation arises because the hot solids that are recycled in a CFBC can also be used to produce steam, thus cooling the fluidized bed, and hence less flue gases need to be recycled than for a suspension-fired boiler. However, the minimum amount of flue gas recycling is governed by the need to maintain sufficient fluid velocity in the fluidized bed while ensuring that enough water/steam-cooled surface area is available to provide adequate internal and external solid heat transfer.

Probably the most important developments in the area of oxy-fuel FBC are the construction and operation of an increasing number of pilot-scale test facilities. This section will concentrate on the CanmetENERGY work, because it appears to be the most detailed and well reported of such studies that exist. CanmetENERGY has two pilot plants which are capable of being operated in the oxy-fuel mode, with full flue gas recycle: a nominal 75 kW unit and a larger 0.8 MW_{th} unit. However, it is the

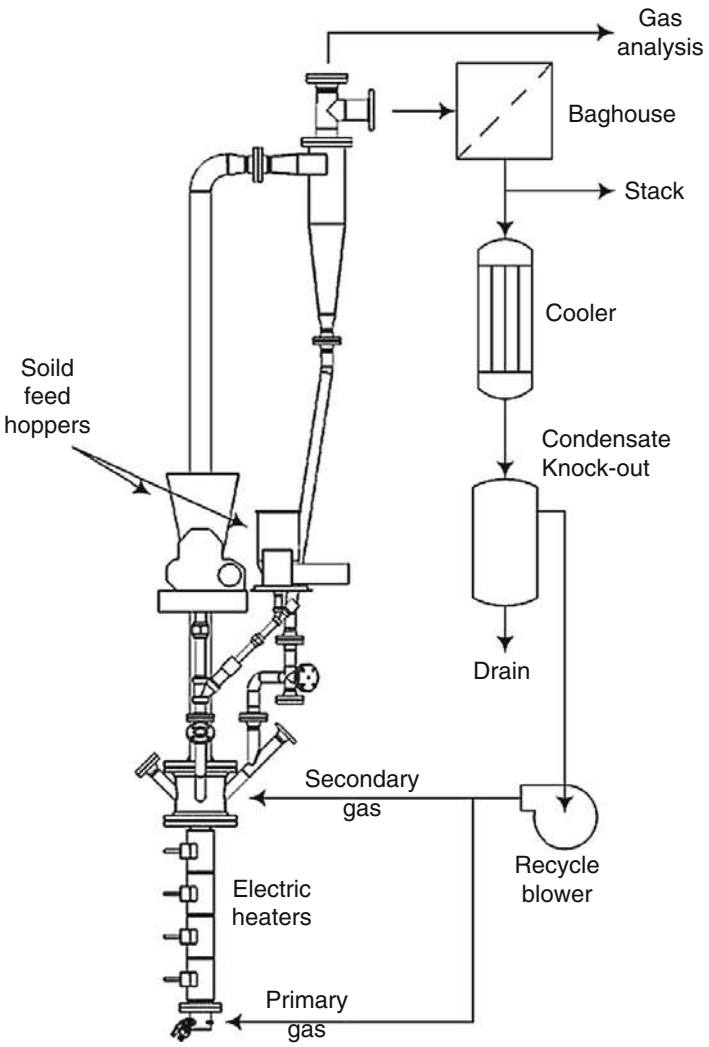

Fig. 3 CanmetENERGY's 5.5 m high, 100 mm diameter minibed oxy-fired CFBC

smaller unit which will be discussed in detail in this section. This unit (Fig. 3) was first described in 2006, for the tests carried out by Hughes et al. (2006). However, that initial work was marred by the fact that the unit still had significant air leaks, and, as a consequence, high CO_2 levels were not produced in the off-gases, which is a typical problem for this type of unit. Completely successful results from the unit were first presented in 2007 (Jia et al. 2007).

CanmetENERGY's mini-CFBC consists of a 0.1 m inside diameter stainless steel riser (Fig. 3) covered with 100 mm of insulation. Independent feed augers can supply multiple fuel types and a sorbent, with solid fuel feed rates of up to 15 kg/h. Oxygen,

Table 3 Analysis of fuels

	Eastern bituminous coal (EB)	Kentucky coal	Highvale coal	Petroleum coke
Proximate analysis (wt%) (dry)				
Moisture (wt%) (as analyzed)	1.08	2.01	10.39	0.66
Ash	8.86	11.31	19.17	1.00
Volatile matter	35.78	37.35	33.76	11.46
Fixed carbon	55.56	51.34	47.076	86.97
Ultimate analysis (wt%) (dry)				
Carbon	77.81	74.05	59.78	86.91
Hydrogen	5.05	5.06	3.49	3.22
Nitrogen	1.49	1.62	0.79	1.83
Sulfur	0.95	1.56	0.22	5.88
Ash	8.86	11.31	19.17	1.00
Oxygen (by difference)	6.04	6.40	16.58	1.16
Heating value (MJ/kg)	32.51	30.93	23.27	34.71

Table 4 Analysis of limestones

	Havelock	Katowice	Cadomin
CaO	53.99	54.32	54.59
MgO	0.59	0.48	<0.20
SiO_2	1.23		1.20
Al_2O_3	<0.38	0.04–0.09	0.41
Fe_2O_3	<0.55	0.08–0.11	0.17
Na_2O	<0.17	0.01–0.03	<0.20
K_2O	<0.08	0.02–0.04	0.05
MnO	0.08		
TiO_2	<0.04		
Cr_2O_3	<0.01		
P_2O_5	<0.02		
SO_3	0.20	0.08	
V_2O_5	<0.02		
SrO	0.02		
BaO	0.02		
NiO	0.01		
Loss on fusion	43.34	42.70	43.6
SUM	99.48		99.83

CO_2, and recycled flue gas flow rates are controlled by a combination of mass flow controllers and rotameters. Bed temperature is in the range of 750–950 °C, which is the typical range for fluidized bed combustion. Superficial gas velocity can be varied up to 8 m/s, although the unit is more normally operated at around 4 m/s.

Fuels and limestones primarily tested to date are given in Tables 3 and 4, respectively.

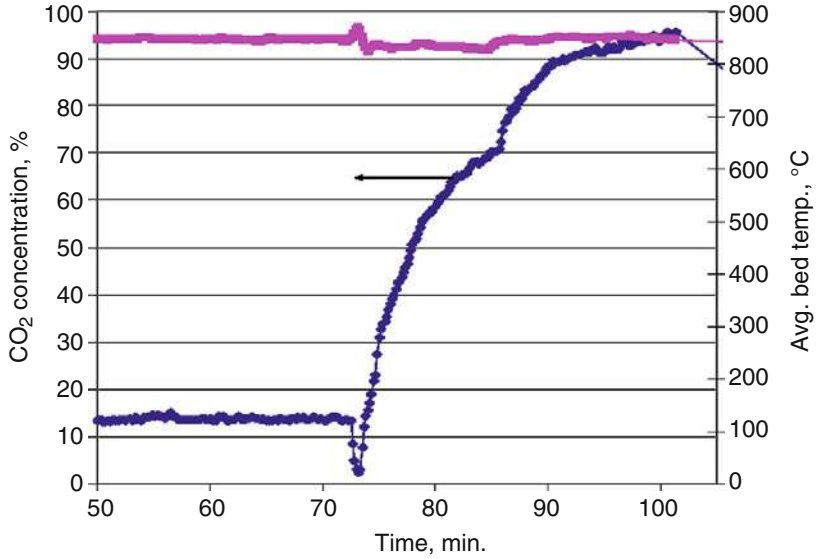

Fig. 4 Transition from air firing to oxy-fuel firing in CanmetENERGY's mini-CFBC during second Highvale coal test

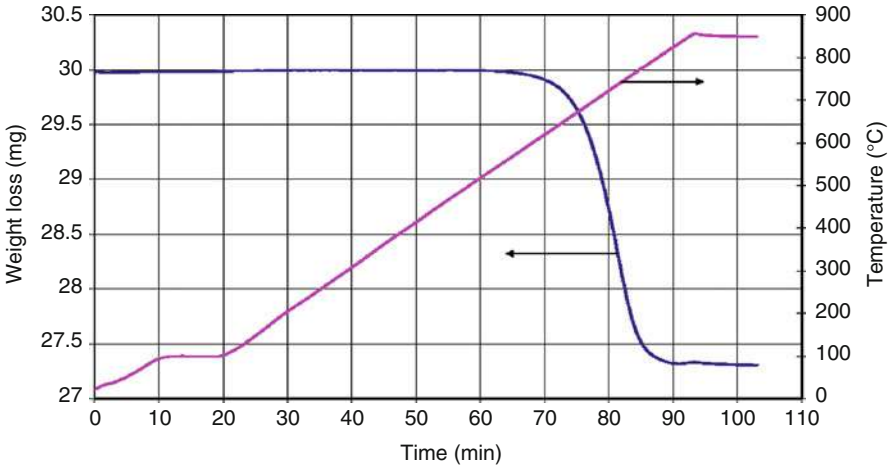

Fig. 5 TGA analysis of bed ash generated in oxy-fuel CFBC combustion with Eastern bituminous coal

Jia et al. (2007, 2010) have reported that it was easy to change from air-fired to oxy-fired mode, at least with the pilot-scale units, and Fig. 4 shows a typical result. Another important, albeit anticipated, result was that $CaCO_3$ was stable at typical bed temperatures (850 °C), as is indicated in Fig. 5, which means that sulfation can be expected to proceed via direct reaction (see section "SO_2 Emissions").

CO Emissions

In the initial work done by Hughes et al. (2006), CO was elevated with levels of up to 0.75 %, and it was speculated that this might be due to elevated CO_2 levels, based on equilibrium considerations. However, more careful work later with much higher CO_2 levels failed to establish such behavior and instead showed that CO levels were extremely sensitive to cyclone temperature (see Fig. 6) (Jia et al. 2007), which is also in good agreement with work by Knöbig et al. (1998).

NO_x Emissions

A series of oxy-fuel combustion trials (Jia et al. 2007, 2010) indicated that fuel nitrogen conversions were always lower or comparable with those in air firing, as indicated by Table 5.

Two tests done with petroleum coke at a nominal 950 °C showed, if anything, a very similar level of fuel nitrogen conversion of 3.3 % and 3.7 % with Havelock and Katowice limestone, respectively, despite the fact that this temperature meant that the limestone must have calcined and, therefore, might be expected to influence fuel nitrogen conversion via catalytic processes, as suggested early on by Lyngfelt and Leckner (1989).

SO_2 Emissions

Sulfur capture is an important issue, because one of the main reasons for using this technology under air-firing conditions is the ability to capture SO_2 in situ with limestone addition. An important difference between oxy-fuel combustion and air

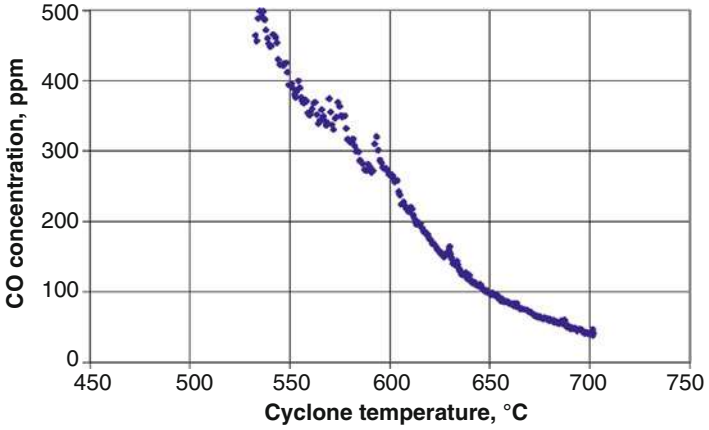

Fig. 6 Effect of cyclone temperature on CO concentration, Highvale coal

Table 5 Fuel nitrogen conversions at a nominal bed temperature of 850 °C

Limestone	Highvale coal	EB coal	Kentucky coal	Petroleum coke
None	6.64 [6.61][a]			
Havelock		2.83 [6.64]	3.51 [4.53]	
		1.54		
Katowice		1.76 [6.22]	1.14 [3.78]	3.35

[a][ ] represents data for air firing

Table 6 Ca utilizations (%) for Ca/S molar ratios of 2–3

	EB coal	Kentucky coal	Petroleum coke	Petroleum coke
Limestone	Nominal bed temperature of 850 °C			Nominal bed temperature of 950 °C
Havelock	20 [34][a]	21 [27]		
	26			43
Katowice	22 [25]	23 [27]	22	29

[a][ ] represents data for air firing

firing is that, at least until a temperature of around 900 °C (depending on the partial pressure of CO_2), sulfation can be expected to occur with $CaCO_3$ (i.e., the limestone will not calcine) (Reaction 1), instead of the indirect mechanism, which is the normal route for atmospheric pressure FBC systems (Reactions 2 and 3).

$$CaCO_3 + SO_2 + 1/2O_2 = CaSO_4 + CO_2 \quad (1)$$

$$CaCO_3 = CaO + CO_2 \quad (2)$$

$$CaO + SO_2 + 1/2O_2 = CaSO_4 \quad (3)$$

Table 6 gives Ca utilizations for various oxy-fuel tests. Unfortunately, these results do not agree with the only comparable set of studies done by VTT, which showed much higher Ca utilizations (more than double) (Eriksson et al. 2007; Hotta et al. 2008), and instead, all tests done to date at CanmetENERGY have continued to show these rather low utilizations for limestone at typical Ca/S molar ratios (2–3:1) for sulfur capture. The exception here is with petroleum coke at higher temperatures, where indirect sulfation would prevail, and the sulfur capture was somewhat better, if not exceptional; a typical result can be seen in Fig. 7. It is interesting to note that, in small-scale tests (in a 40 mm diameter, electrically heated fluidized bed reactor) directed at studying attrition under oxy-fired conditions, Scala and Salatino (2010) have also found a much lower conversion rate than would be expected in air firing.

To understand these results, there is substantial literature on direct sulfation conditions for pressurized fluidized bed (PFB) combustion, where sulfation normally occurs directly with $CaCO_3$. However, even here it is clear that the mechanisms for direct sulfation are still not completely understood (Hu et al. 2006).

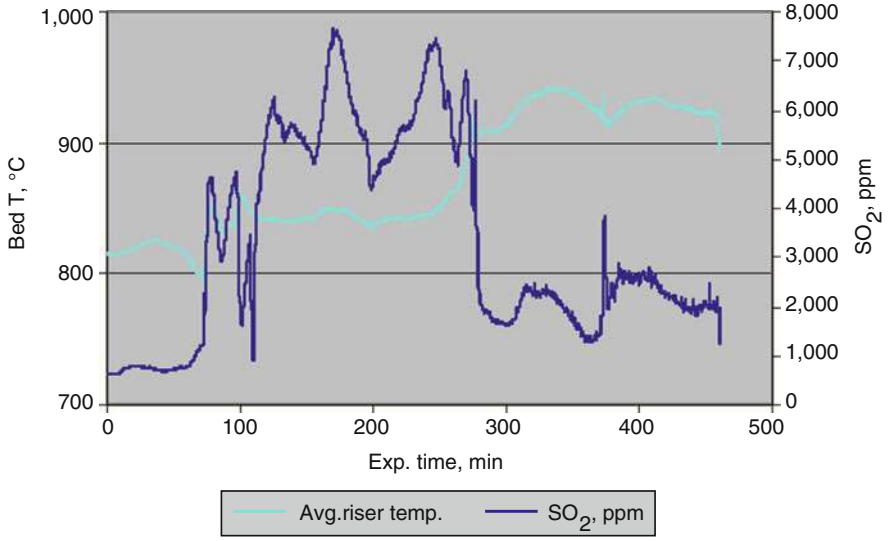

Fig. 7 Profiles of SO_2 concentration and average bed temperature for petroleum coke

Very early work by Snow et al. (1988) and Hajaligol et al. (1988) suggested that direct sulfation might be more effective than indirect sulfation, and an explanation was advanced that counter-diffusion of CO_2 allowed improved sorbent performance. Similar results were produced much later by Liu et al. (2000), who studied limestone sulfation using two limestones at atmospheric pressure with different concentrations of CO_2 in the sulfation gases in a fixed bed reactor. Interesting findings from that study are that indirect sulfation is faster at low degrees of Ca conversion (<0.3), but thereafter direct sulfation becomes faster, and that sintering was much reduced in direct sulfation, so that at higher conversions direct sulfation was faster than indirect sulfation. Very similar arguments have been put forward recently by Chen et al. (2009), who again note the earlier literature concerning almost complete conversion of $CaCO_3$ and mention the back-diffusion argument by CO_2. Like Liu and his coworkers (2000), they found that direct sulfation becomes faster at fractional conversions of 0.4, for limestone samples sulfated in a TGA. In this context, it is worth noting that while Hu and his colleagues agree with the observation that the sulfate layer is porous, they argue that this is not due to back diffusion of CO_2, but instead due to the way the product crystal grains form on the calcite surface, and local porosity (Hu et al. 2007). However, to add a note of caution, it is worth remarking that results from pilot-scale and commercial PFBC units tend to show comparable performance to air-fired FBC (Cuenca and Anthony 1995) and not the superior performance reported from fixed beds and TGA tests for which most of the studies have been done to date. This is not altogether surprising, given the various additional factors that must pertain to a real system, such as oxidizing/reducing conditions, particle loss due to attrition, etc.

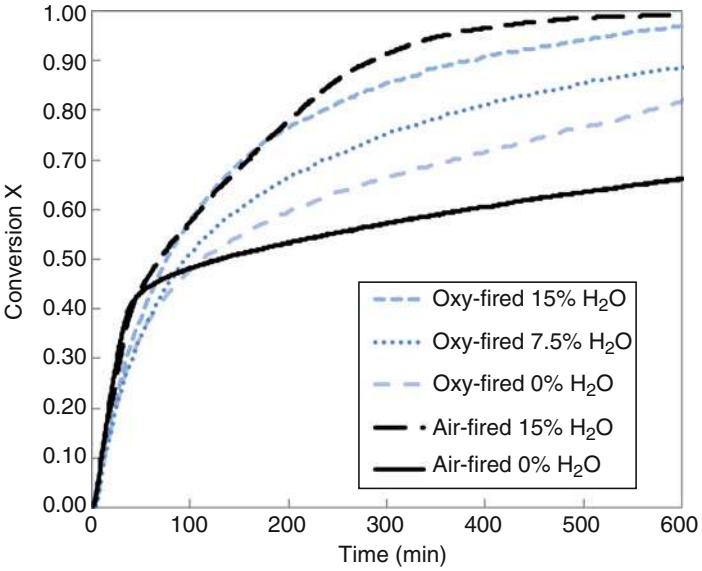

Fig. 8 Sulfation conversion profiles under oxy-fired conditions for varying concentrations of H_2O, with air-fired profiles overlaid

The studies of Hu et al. (2006, 2007, 2008) noted that high partial pressures of both CO_2 and H_2O might cause significant sintering of the $CaCO_3$, thus impairing overall sulfation performance. In a TGA study done in a fixed bed laboratory reactor at temperatures ranging from 500 °C to 700 °C, a concentration of 7.5 % H_2O produced an enhancement of sulfation behavior (Hu et al. 2007). In practice, depending on the fuel used, one would always expect H_2O to be present in a pilot-scale combustor at levels greater than that, and calculations indicate, for the CanmetENERGY work, water concentrations varying from 5.8 to almost 19 %.

In a series of sulfation tests reported by Stewart et al. (2010), Cadomin limestone samples sized 75–115 μm were sulfated in a TGA under varying concentrations of water and CO_2 over the course of 10 h to simulate CFB conditions. Figure 8 shows that the indirect sulfation reaction is greatly enhanced in the presence of water for sulfation beyond the initial regime. In 10 h, 100 % conversion is achieved, and the addition of 15 % H_2O is responsible for an increase in conversion of nearly 45 %. Figure 8 shows the conversion profiles for tests performed under both air-fired (indirect) and oxy-fired (direct) conditions (15 % and 85 % CO_2, respectively). In the tests performed without water, oxy-fuel conditions led to more rapid reaction rates for conversion levels >0.45, a level that is dependent on particle size and is thus comparable to the findings of Liu et al. (2000) and Chen et al. (2009) for direct sulfation.

Stewart et al. (2010) have also argued that it is important to note that the bench-scale studies showing the direct sulfation reaction is more rapid at conversions >0.3 do not include the effects of water in this determination. Figure 8 shows that water

greatly enhances the direct sulfation reaction; however, the effects only become apparent after initial sulfation (~0.40 conversion). Furthermore, it appears that the indirect sulfation reaction is just as rapid as the direct sulfation reaction for conversions >0.3 in the presence of 15 % water, contrary to previous findings for the reaction without water. The effects of water observed here also have an implication on increasing the sulfur capture performance of FBCs firing high-rank/low-moisture fuels such as petroleum coke. It is conceivable that the simple addition of water into the bed at or above concentrations of 15 % would result in enhanced calcium utilization.

Other Issues for Oxy-Fuel Firing in CFBC Systems

If oxy-fuel CFBC is used primarily with high-sulfur fuels, as tends to be the case for the larger air-fired atmospheric boilers, there are several possible issues relating to fouling and to ash disposal or utilization where limestone is used for sulfur capture. In the event that the boiler is operated under conditions such that direct sulfation occurs (Reaction 1), then the ash is expected to show similar characteristics to that produced by PFBC ash (Anthony et al. 1997). In particular, it can be expected to have low free lime content, and this will give it a number of advantages.

Normally, ash from air-fired CFBC boilers using limestone can have up to 20–30 % free lime content. This means that, prior to its disposal, it must first be conditioned (reacted with water), which entails significant water losses due to evaporation. When it is subsequently compacted in the landfill, it can be expected to show significant expansive behavior due to the formation of Ca alumino-sulfate compounds such as ettringite. In practice this means that a landfill that may have the permeability of a clay liner after suitable compaction will after several weeks have the permeability of sandy soil, potentially producing three or more orders of magnitude of high-pH (12–13) leachate with high total dissolved solids (mostly Ca^{2+} and SO_4^{2-} ions), which most regulators will require to be treated before discharge. The high carbon and sulfate contents, along with this expansive behavior, have also meant that such ashes have found very limited use in construction applications, while the heavy metal content from the coal ash-derived fraction means that they have also found relatively little traction for use as soil amendment agents or for agricultural use (Anthony et al. 1995). By contrast, such ashes produced from an oxy-fired CFBC operating with direct sulfation might have much lesser issues with the production of a high pH content (due to its low free lime content). Therefore, they might be expected to show fewer problems in the landfill and might even find more use in construction applications because of the absence of ettringite formation, even though the high carbon and sulfate content would continue to pose a problem. Currently, the only study on oxy-fuel CFBC ash is due to Wu et al. (2008), looking at ashes from the CanmetENERGY pilot plant, and this seems to support the analysis presented above. However, if the combustor is operated at higher temperatures and indirect sulfation prevails, then the ash disposal behavior and potential for use should be very similar to those for the air-fired case.

There is one other issue that deserves to be mentioned for the indirect sulfation case (Reaction 3). CaO, the product of calcination, can react very readily with CO_2 at appropriate conditions, and this is the basis of the so-called Ca looping technology. In early work, Nsakala et al. (2004) identified recarbonation as a potential issue for flue gas fluidized bed heat exchangers (FBHE), which are cooled to below about 650 °C, and if this recarbonation was sufficiently great, it might be enough to defluidize the FBHE. Unfortunately, such a unit cannot easily be fluidized with air, since N_2 is likely to find its way into the combustion stream, thus reducing its purity. The alternatives in this case appear to be to fluidize with steam or replace such units, and Nsakala et al. (2004) proposed the use of a moving bed heat exchanger.

Another possibility that they identified was fouling in the convective pass due to the formation of $CaCO_3$ (Nsakala et al. 2004), which could potentially be a problem. If the sulfation performance in such units is significantly worse, requiring more limestone use than for the air-fired case as suggested by Jia et al. (2007, 2010), then this situation might be exacerbated, as Anthony et al. (1998, 2000, 2001a, b) have shown that both sulfation and carbonation of lime, in situations where there is relatively little fuel-derived ash, are potential problems for CFBC boilers.

Wang et al. (2008) have suggested that such carbonation effects are likely to be enhanced by water over a wide range of temperatures from 800 down to 300 °C, with such effects becoming more pronounced at lower temperatures. This finding has also been recently reiterated in a study by Manovic and Anthony (2010) of the effect of water on carbonation for Ca looping cycles for nine different limestones at water concentrations from 10 % or more, which are typical of most hydrocarbon fuels. The implication of this work is that there is a potential for enhanced fouling due to carbonation in situations where indirect sulfation is employed, which may be problematic for oxy-fuel FBC systems firing fuels with high sulfur levels.

A possible issue is that of gas mixing in fluidized beds. Although solids mixing in FBC systems are excellent, the same is not true of the fluidizing gases, especially for larger boilers (Grace et al. 1997), and this opens the possibility of maldistribution of oxidant and fuel. This could potentially be important if the amount of recycled flue gas was reduced by applying high oxygen concentration to take advantage of the possibility of using hot solids for heat removal in external heat exchangers, thus allowing the construction of physically smaller boilers for a given thermal power capacity. According to Johnsson (2010, Department of Energy and Environment, Chalmers University of Technology, Gothenburg, personal communication) and Seddighi et al. (2010), this could result in local hot spots. This is possible because the dense bottom bed in a CFB furnace of industrial size is typically characterized by large fluctuations in gas flow with high-velocity (oxygen rich) bubbles passing the bed (Svensson et al. 1996a, b). In the case of oxy-fuel firing with high primary oxygen concentration, this may result in high-temperature flame combustion within the bubbles, and this need requires further investigation in order to determine if this is a potential problem which can lead to phenomena such as agglomeration. Another possible problem when applying high oxygen concentrations is that since a majority of the heat most likely has to be extracted from external heat particle coolers, this will require high external solid flux (Gs), which could cause erosion. Commercial

air-fired CFB boilers have rather low Gs, less than 10 kg/m^2 s, whereas an oxy-fuel-fired CFB boiler applying low recycle flue gas flows may require 30–50 kg/m^2 s in order to close the heat balance (Seddighi et al. 2010).

Flue Gas Issues and Conditioning for Oxy-Fuel Technology

Ultimately, the goal of all oxy-fuel combustions, whether pulverized fuel or fluidized bed, is to produce a stream of CO_2 suitable for transportation and sequestration. A few key factors will determine what that stream looks like, while the pressures for piping and storage will be set by practical requirements for those technologies, which are quite independent of boiler conditions or operation. Another factor that will help in the development of the technology is smaller flue gas volumes for oxy-fuel PF technology (perhaps by 20–30 %) and oxy-fuel FBC technology (perhaps by 30–50 % from the air-fired case). Ultimately, it must also be remembered that at this time there is no firm agreement on the purity requirements for the gases to be either transported or stored, whether they are used in enhanced oil recovery (EOR) or simply sequestered (Pipitone and Bolland 2009).

In particular, the oxygen purity used will help determine what the final gases to be treated and sequestered look like, regardless of whether oxy-fuel PF or FBC is employed, even if air leaks can be minimized to a low level. Almost certainly, it is simply too expensive to produce pure or nearly pure O_2, and instead oxygen with 90–95 % purity will be used, and this in turn will mean that the flue gases produced will contain 3 % or 4 % N_2 and about 1 % Ar. In a recent modeling study of oxy-fuel PF technology, the N_2/Ar ratio was predicted to vary from 1 to 3 depending on oxygen purity, and O_2 concentrations were predicted to vary from 3 % to 5 % depending on combustion stoichiometry, with water concentrations from 10 % to 40 % dependent on fuel properties and the partitioning between dry and wet flue gas recycles (Liu and Shao 2010).

The other important factor is of course the micro-pollutants, SO_2, SO_3, NO_x (mainly NO), CO, possibly HCl, and Hg. Their levels will be set by two factors, namely, what the technology itself produces and the perceived cleanup necessary for both transport and ultimate storage. Here it seems that there could be a difference between the two technologies, namely, SO_2 can be scrubbed by means of in situ limestone addition and NO_x levels are likely to be comparable or even lower from oxy-fuel FBC, although in both cases NO_x levels will be lower than in the air-fired cases. If there is a possibility of co-capture of SO_2 along with CO_2 (for co-sequestration), this could offer significant cost reductions and might preclude treatment altogether, providing it did not raise significant corrosion issues for piping, for example. In an early IEA study (Report 2004), it was estimated that the gas to be sequestered might in that case have 2–3 % SO_2 content that might produce savings of the order of $12–25/t CO_2. This point has been again discussed in a more recent paper by Pehnt and Henkel (2009), which makes a comparison between oxy-fuel and precombustion CO_2 capture and notes that co-capture would make oxy-fuel a more attractive choice than precombustion options. Alternatively, White and his

colleagues (2009) have suggested that, with suitable conditions, SO_x and NO_x can be removed with the water if sufficient pressure (around 3 MPa) is employed, and the development of such technologies might also make significant changes to the economics of oxy-fuel technology. However, at this point probably the most important developments are a firmer regulatory framework, in the jurisdictions that might employ CCS, and agreement as to the purity levels required for CCS, rather than likely emissions from oxy-fuel boilers. Pending the outcome of these regulations, low-NO_x burner design is still an important area for the oxy-fuel PF and possibly the CFBC case and/or the use of selective catalytic reduction (SCR) and selective non-catalytic reduction (SNCR). Also, depending on the APC technologies used, Hg capture may be easier in the oxy-fuel case, in part due to lower flue gas volumes as well as chemical factors, and this may lead to cost reductions.

Larger-Scale Tests and Future Industrial Plans

Oxy-Fuel CFBC

Foster Wheeler has recently commissioned 8 months of oxy-fuel combustion trials at CanmetENERGY using the larger 0.8 MW_{th} unit. Figure 9 provides an example of the CO_2 emissions over a 2½-day trial under oxy-fuel conditions, indicating that it is possible to maintain excellent control on CO_2 levels and combustion conditions; these tests are briefly described in a recent paper by Kuivalainen et al. (2010). To date performance has been excellent, which is a very positive sign for the further development of the technology.

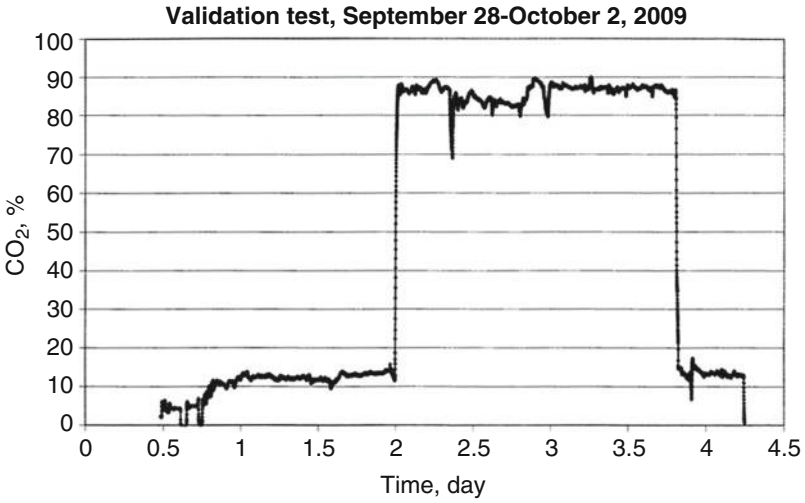

Fig. 9 Tests on oxy-fired combustion using CanmetENERGY's 0.8 MW_{th} CFBC

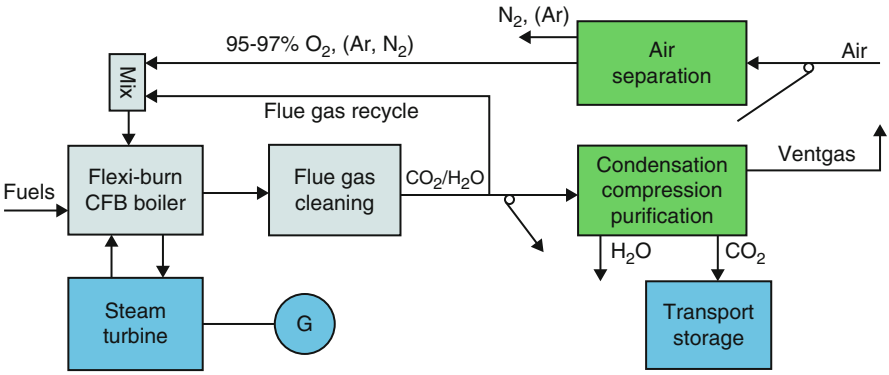

Fig. 10 Schematic of a Flexi-burn™ CFB power plant (With permission of the Foster Wheeler North America Corporation)

Foster Wheeler is also the first company to commercialize supercritical CFBC technology (Lagisza Power Plant, Poland), and with this as the basis, it is now working with the power company ENDESA on the development of a 500 MW_e supercritical Flexi-burn™ CFBC (Fig. 10 provides a general schematic of the technology). The predicted CO_2 capture for the Flexi-burn CFBC technology is 90 % of emissions, and it is anticipated that it could be available by 2020 (Eriksson et al. 2009). Ultimately, Foster Wheeler believes that it could offer such technology at the 600–800 MW_e size with 600 °C steam temperature.

Following the extensive tests at CanmetENERGY in Canada, demonstration tests are scheduled to start in 2010 at the 30 MW_{th} CIUDEN pilot CFB facility, which will provide a full experimental CCS platform for the demonstration and validation of the flexible air/oxy-fuel CFB combustion. Finally, it must be noted that Alstom has also announced its intention of carrying out a 100 MW_e oxy-fuel CFB demonstration, although at the time of writing no further information appears to be available in the open literature (Suraniti et al. 2009). At this point in time it appears that oxy-fired CFBC technology is making major strides to enter the commercial arena, and there seems little doubt that before the end of the decade it will also be available as a commercial and competitive CCS technology along with oxy-fuel PF technology.

Oxy-Fuel Retrofit Plans

The US DOE's FutureGen program, which for the first 7 years of its existence had the objective of constructing, operating, and demonstrating a gasification plant with hydrogen production and carbon capture and sequestration, was recently and somewhat surprisingly refocused as an oxy-fuel retrofit and is now referred to as FutureGen 2 (Flavelle-While 2010). At present, the plan is to retrofit the existing pulverized coal-fired Ameren 200 MW_e Unit 4 in Meredosia, Illinois, with oxy-fuel technology, but if this does not proceed, the project will look for a new site

(http://www.futuregenalliance.org/). If a retrofit is chosen, this will require a new boiler, ASU, and CO_2 purification and gas compression unit. About 90 % CO_2 is to be captured and transported by a new pipeline to a storage site yet to be determined. US DOE has committed US $1 billion to the project partners (State of Illinois, Ameren, Babcock & Wilcox, American Air Liquide, and the FutureGen Alliance). Construction is set to begin in 2012.

Conclusions

Oxy-fuel PF represents an advanced technology suitable for power generation with high levels of CO_2 capture (90 % plus). At this point in time, there has been more than 20 years of research done in this area, and the first large-scale demonstration units (30 MW_{th}) are already operating. There appear to be no major barriers to implementation other than the capital costs, and it seems likely that full-scale demonstration units will be operating by the end of the next decade (and in the case of retrofit installations, much earlier than that). By contrast oxy-fuel FBC technology is far less developed, and the first few pilot-scale units with flue gas recycle are only now being operated. Nonetheless, again there seem to be no major barriers to the technology, and Foster Wheeler, for example, is predicting that there will be full-scale demonstrations operating by 2020.

Acknowledgments The author gratefully acknowledges the assistance and advice of Dr. David Granatstein (Granatstein Technical Services/CanmetENERGY) and Drs. Yewen Tan and Murlidhar Gupta (CanmetENERGY), for a number of valuable discussions during the preparation of this chapter, as well as suggestions for various amendments and improvements, and he would also like to thank Professor Filip Johnsson of Chalmers University, Sweden, for valuable suggestions about potential problems for oxy-fuel CFBC.

References

Ahn J, Overacker D, Okerlund R et al (2010) SO_3 formation during oxy-coal combustion. In: 35th Clearwater clean coal conference, Clearwater, 6–10 June 2010

Air Liquide Press Release (2008) Reducing carbon dioxide using oyxfuel combustion processes. Paris

Allam R, White V, Ivens N, Simmonds M (2005) The oxyfuel baseline: revamping heaters and boiler to oxyfuel by cryogenic air separation and flue gas recycle. In: Thomas DC, Bensen SM (eds) Carbon dioxide for storage in deep geological formations, vol 1. Elsevier, Amsterdam

Anthony EJ, Ross GG, Berry EE et al (1995) Characterization of solid wastes from circulating fluidized beds. J Energy Resour Technol 117:18–23

Anthony EJ, Iribarne AP, Iribarne JV (1997) The characterization of solid residues from PFBC boilers. Can J Chem Eng 75:1115–1121

Anthony EJ, Preto F, Jia L, Iribarne JV (1998) Agglomeration and fouling in petroleum coke-fired FBC boilers. J Energy Resour Technol 120:285–292

Anthony EJ, Talbot R, Jia L, Granatstein DL (2000) Agglomeration and fouling in three FBC boilers. Energy Fuels 14:1021–1027

Anthony EJ, Iribarne AP, Iribarne JV et al (2001a) Agglomeration in a 160 MW_e FBC boiler. Fuel 80:1009–1014
Anthony EJ, Jia L, Laursen K (2001b) Agglomeration of high-sulfur fuels. Can J Chem Eng 79:356–366
Arrhenius S (1896) On the influence of carbonic acid in the air upon the temperatures of the ground. Philos Mag J Sci 41:237–276
Arrhenius S (1907) Worlds in the making: the evolution of the universe (trans: Borns H). Harper & Brothers, London/New York
Bordenet B, Kluger F, Goodstine S (2008) Boiler materials behavior in oxy-firing environments. In: 33rd international conference on coal utilization and fuel systems, Clearwater, 1–5 June 2008
Bouillon P-A, Hennes S, Mahieux C (2009) ECO_2: post-combustion or oxyfuel – a comparison between coal power plants with integrated CO_2 capture. GHGT-9. Energy Procedia 1:4015–4022
Brix J, Jensen PA, Jensen AD (2010) Coal devolatilization and char conversion under suspension fired conditions in O_2/N_2 and O_2/CO_2 atmospheres. Fuel 28:3373–3380
Buhre BJP, Elliot LK, Sheng CD et al (2005) Oxy-fuel combustion technology for coal-fired power generation. Prog Energy Combust Sci 31:283–307
Burdyny T, Struchtrup H (2010) Hybrid membrane/cryogenic separation of oxygen from air for use in the oxy-fuel process. Energy 35:1884–1897
Cao H, Sun S, Liu Y, Wall TF (2010) Computational fluid dynamics modelling of NO_x reduction mechanisms in oxy-fuel combustion. Energy Fuels 24:131–135
Carbo M, Jansen D, Hendriks C et al (2009) Opportunities for CO_2 capture through oxygen conducting membranes at medium-scale oxyfuel coal boilers. GHGT-9. Energy Procedia 1:487–494
Chen C, Zhao C, Liu S, Wang C (2009) Direct sulphation of limestone based on oxy-fuel combustion technology. Environ Eng 22:1481–1488
Cook PJ (2009) Demonstration of carbon dioxide capture and storage in Australia. GHGT-9. Energy Procedia 1:3859–3866
Croiset E, Thambimuthu KV (2001) NO_x and SO_2 emissions from O_2/CO_2 recycle coal combustion. Fuel 80:2117–2121
Cuenca MA, Anthony EJ (eds) (1995) Pressurized fluidized beds. Blackie Academic and Professional, London
Davidson RM, Stanley SO (2010) Oxyfuel combustion of pulverized coal. IEA Clean Coal Centre Report CCC/168, June
Doukelis A, Vorrias I, Grammelis P et al (2008) Partial O_2-fired coal power plant with post-combustion CO_2 capture: a retrofitting option for CO_2 capture ready plants. Fuel 88:2428–2468
Edwards PN (2010) A vast machine: computer models, climate data and the politics of global warming. MIT Press, Cambridge
Eriksson T, Sippu O, Hotta A et al (2007) Oxyfuel CFB boiler as a route to near zero CO_2 emission coal firing. Power-Gen Europe, Madrid, 26–28 June 2007
Eriksson T, Sippu O, Hotta A et al (2009) Development of Flexi-burn^{TM} CFB technology aiming at fully integrated CCS demonstration. Power-Gen Europe, Cologne, 26–28 May 2009
Farley M (2006) Developing oxyfuel capture as a retrofit technology. Mod Power Syst 26:20
Flavelle-While C (2010) FutureGen 2 to showcase low-emission coal: oxyfuel retrofit rather than IGCC wins the day. tcetoday News, 9 Aug, http://www.tcetoday.com/tcetoday/newsdetail.aspx?nid=13022
Fleig D, Normann F, Andersson K et al (2009) The fate of sulphur during oxy-fuel combustion of lignite. GHGT-9. Energy Procedia 1:383–390
Fryda L, Sobrino C, Cieplik M, van de Kamp WL (2010) Study on ash deposition under oxyfuel combustion of coal/biomass blends. Fuel 89:1889–1902
Giménez-López J, Millera A, Bilbao R, Alzueta MU (2010) HCN oxidation in an O_2/CO_2 atmosphere: an experimental and kinetic study. Combust Flame 157:267–276
Grace JR, Avidan AA, Knowlton TM (eds) (1997) Circulating fluidized beds. Blackie Academic and Professional, London

Gunn D, Horton D (1989) Industrial pollutants. Longman Scientific and Technical, New York
Hadjipaschalis I, Kourtis G, Poulikkas A (2009) Assessment of oxyfuel power generation technology. Renew Sustain Energy Rev R13:2637–2644
Hajaligol MR, Longwell JP, Sarofim AF (1988) Analysis and modeling of the direct sulfation of $CaCO_3$. Ind Eng Chem Res 27:2203–2210
Haykir-Acma H, Turan AZ, Kucukbayrak S (2010) Controlling the excess heat from oxy-combustion of coal by blending with biomass. Fuel Process Technol 91:1569–1575
Hesselmann G, Cameron ED, Sturgeon DW et al (2009) Oxyfuel firing and lessons learned from the demonstration of a full-sized utility scale 40 MW oxycoal^{tm} combustion system. In: South African carbon capture and storage conference, Johannesburg, 29–30 Sept 2009
Hjärtstam S, Andersson K, Johnsson F, Leckner B (2009) Combustion characteristics of lignite-fired oxygen fuel flames. Fuel 88:2216–2224
Hotta A, Nuorimo K, Eriksson T et al (2008) CFB technology provides solutions to combat climate change. In: Werther J, Nowak, W, Wirth K-E, Hartge E-U (eds) Proceedings of the 9th international conference on circulating fluidized beds, in conjunction with 45th international VGB workshop, operating experience with fluidized bed systems, Hamburg, 13–16 May 2008, pp 11–17
Houghton J (2004) Global warming: the complete briefing, 3rd edn. Cambridge University Press, Cambridge
Hu Y, Naito S, Kobayashi N, Hasatani M (2000) CO_2, NO_x and SO_2 emissions from the combustion of coal with high oxygen concentration gases. Fuel 79:1925–1932
Hu G, Dam-Johansen K, Wedel S, Hansen JP (2006) Review of the direct sulfation of limestone. Prog Energy Combust Sci 32:386–407
Hu G, Dam-Johansen K, Wedel S (2007) Direct sulphation of limestone. AIChE J 53:948–960
Hu G, Shang L, Dam-Johansen K et al (2008) Indirect kinetics of the direct sulphation of limestone. AIChE J 54:2663–2673
Hughes R, Jia L, Tan Y, Anthony EJ (2006) Oxy-fuel combustion of coal in a circulating fluidized bed combustor. In: Proceedings of the 19th international conference on FBC, Vienna, 2006
IEA Report (2004) Impact of impurities on CO_2 capture, transport and storage. Report No. PH4/32, Aug
Irons R, Sekkapan G, Panesar R et al (2007) CO_2 capture ready plants. IEA Technical Report No. 2007/4, May
Jia L, Tan Y, Wang C, Anthony EJ (2007) Experimental study of oxy-fuel combustion and sulphur capture in a mini CFBC. Energy Fuels 21:3160–3164
Jia L, Tan Y, Anthony EJ (2010) Emissions of SO_2 and NO_x during oxy-fuel CFB combustion tests in a mini-CFBC. Energy Fuels 24:910–915
Knöbig T, Werther J, Åmand L-E, Leckner B (1998) Comparison of large- and small-scale circulating fluidized bed combustors with respect to pollutant formation and reduction for different fuels. Fuel 77:1635–1642
Kuivalainen R, Eriksson T, Hotta A et al (2010) Development and demonstration of oxy-fuel CFBC technology. In: 35th international technical conference on clean coal & fuel systems, Clearwater, 6–10 June 2010
Kung SC, Tanzosh JM (2008) Investigation of fireside corrosion in oxy-coal combustion systems. In: 33rd international conference on coal utilization and fuel systems, Clearwater, 1–5 June 2008
Kvamsdal H, Jordal K, Bolland O (2007) A quantitative comparison of gas turbine cycles with CO_2 capture. Energy 32:10–32
Liljedahl GN, Turek DG, Nsakala NY et al (2006) Alstom's oxygen-fired CFB technology development status for CO_2 mitigation. In: 31st international technical conference on coal utilization and fuel systems, Clearwater, 21–25 May 2006
Liszka M, Ziębik A (2010) Coal-fired oxy-fuel power unit – process and system analysis. Energy 35:943–951
Liu H, Shao Y (2010) Prediction of the impurities in the CO_2 stream of an oxy-fuel combustion plant. Appl Energy 87:3162–3170

Liu H, Katagiri S, Kaneko U, Okazaki K (2000) Sulfation behaviour of limestone under high CO_2 concentrations in O_2/CO_2 coal combustion. Fuel 79:945–953

Lyngfelt A, Leckner B (1989) The effect of reductive decomposition of $CaSO_4$ on sulphur capture in fluidized bed boilers. In: Proceedings of the 10th international conference on fluidized bed combustion, Boston, 1989, pp 675–684

Maier J, Dhungel B, Mőnckert P et al (2008) Impact of recycled gas species (SO_2, NO) on emission behaviour and fly ash quality during oxy-coal combustion. In: 33rd international conference on coal utilization and fuel systems, Clearwater, 1–5 June 2008

Manovic V, Anthony EJ (2010) Carbonation of CaO-based sorbents enhanced by steam addition. Ind Eng Chem Res 49(19):9105–9110

Marshall L, Fralick C, Gaudry D (2010) OPG charts moving from coal to biomass. http://www.powermag.com/coal/OPG-Charts-Move-from-Coal-to-Biomass_2570_p6.html, Apr

McDonald DK, Flyn TJ, DeVault DJ (2008) 30 MW_{th} clean environmental development oxy-coal combustion test program. In: 33rd international conference on coal utilization and fuel systems, Clearwater, 1–5 June 2008

Mendiara T, Glarborg P (2009) Reburn chemistry in oxy-fuel combustion of methane. Energy Fuels 23:3563–3572

Mohr SH, Evans GM (2009) Forecasting coal production until 2100. Fuel 88:2059–2067

NETL (2010) http://www.netl.doe.gov/technologies/carbon_seq/core_rd/capture/41147.html

Nsakala N, Liljedahl GN, Turek DG (2004) Greenhouse gas emissions control by oxygen firing in circulating fluidized bed boilers: phase II – pilot scale testing and updated performance and economics for oxygen fired CFB with CO_2 capture: final technical report. PRL Report No. PPL-04-CT-25, Oct 2004

Ochs T, Oryshchyn D, Woodside R et al (2009) Results of initial operation of the Jupiter Oxygen Corporation oxy-fuel 15 MW_{th} burner test facility. GHGT-9. Energy Procedia 1:511–518

Okazi K, Ando T (1997) NO_x reduction mechanisms in coal combustion with recycled CO_2. Energy 22:207–215

Pehnt M, Henkel J (2009) Life cycle assessment of carbon dioxide capture and storage for lignite power plants. Int J Greenh Gas Control 2:49–66

Pipitone G, Bolland O (2009) Power generation with CO_2 capture: technology for CO_2 purification. Int J Greenh Gas Control 3:528–534

Qiao Y, Zhang L, Binner E et al (2010) An investigation of the causes of the difference in coal particle temperatures between combustion in air and in O_2/CO_2. Fuel 89:3381–3387

Scala F, Salatino P (2010) Flue gas desulphurization under simulated oxyfiring fluidized bed combustion conditions: the influence of limestone attrition and fragmentation. Chem Eng Sci 65:556–561

Seddighi S, Pallarès D, Johnsson F (2010) One-dimensional modeling of oxy-fuel fluidized bed combustion for CO_2 capture. In: Proceedings of the fluidization XIII, Gyungju (Report)

Shaddix CR, Molina A (2008) Effect of O_2 and high CO_2 concentrations on PC char burning rates during oxy-fuel combustion. In: 33rd international conference on coal utilization and fuel systems, Clearwater, 1–5 June 2008

Smart J, Lu G, Yan Y, Riley G (2010) Characterisation of an oxy-coal flame through digital imaging. Combust Flame 157:1132–1139

Smoot LD, Pratt T (1979) Pulverized coal combustion and gasification: theory and applications for continuous flow processes. Plenum, New York

Snow MJH, Longwell JP, Sarofim AF (1988) Direct sulfation of calcium carbonate. Ind Eng Chem Res 27:268–273

Stamatelopoulos GN, Darling S (2008) Alstom's CFBC technology. In: Werther J, Nowak W, Wirth K-E, Hartge E-U (eds) Proceedings of the 9th international conference on circulating fluidized beds, in conjunction with 45th international VGB workshop, operating experience with fluidized bed systems, Hamburg, 13–16 May 2008, pp 11–17

Stewart M, Jia L, Tan Y et al (2010) Oxy-fuel combustion in a circulating fluidized bed pilot plant. In: Impacts of fuel quality on power production and the environment, Lapland, 29 Aug–3 Sept 2010

Stranger R, Wall T (2011) Sulphur impacts during pulverized coal combustion in oxy-fuel for carbon capture and storage. Prog Energy Combust Sci 37:69–88

Strőmberg L, Lindgren G, Jacoby J et al (2009) Update on Vattenfall's 30 MW_{th} oxyfuel pilot plant in Schwarze Pumpe. GHGT-9. Energy Procedia 1:581–589

Strőmberg L, Lindgren G, Anheden M et al (2010) Vattenfall's R&D program on CO_2 capture technology in support of scale-up and commercialisation of oxyfuel, postcombustion and precombustion technology. In: 35th international technical conference on clean coal & fuel systems, Clearwater, 6–10 June 2010

Sturgeon DW, Cameron ED, Fitzgerald FD (2009) Demonstration of an oxyfuel combustion system. Energy Procedia 1:471–478

Suraniti SL, Nsakala NY, Darling SL (2009) Alstom oxyfuel CFB boilers: a promising option for CO_2 capture. GHGT-9. Energy Procedia 1:543–548

Svensson A, Johnsson F, Leckner B (1996a) Bottom bed regimes in a circulating fluidized bed boiler. Int J Multiphase Flow 22:1187–1204

Svensson A, Johnsson F, Leckner B (1996b) Fluidization regimes in non-slugging fluidized beds: the influence of pressure drop across the air distributor. Powder Technol 86:299–312

Tan Y, Croiset E, Douglas MA et al (2006) Combustion characteristics of coal in a mixture of oxygen and recycled flue gas. Fuel 85:507–512

Tigges K-D, Klauke F, Bergins C et al (2009) Conversion of existing coal-fired power plants to oxyfuel combustion: case study with experimental results and CFD simulations. GHGT-9. Energy Procedia 1:549–556

Toftegaard MB, Brix J, Jensen PA et al (2010) Oxy-fuel combustion of solid fuels. Prog Energy Combust Sci 36:581–625

Total (2010) http://www.total.com/en/special-reports/carbon-dioxide-capture-and-geological-storage/lacq-project-940768.html

Vattenfall (2010) http://www.vattenfall.com/en/ccs/oxyfuel-combustion.htm

Wang C, Jia L, Tan Y, Anthony EJ (2008) Carbonation of fly ash in oxy fuel CFB combustion. Fuel 87:1108–1114

Weller AE, Rising BW, Boiarski AA et al (1985) Experimental evaluation of firing pulverised coal in a CO_2/O_2 atmosphere. Argonne National Laboratory Report No.: ANL/CNSV-TM-168

White V, Torrente-Murciano L, Sturgeon D, Chadwick D (2009) Purification of oxyfuel-derived CO_2. GHGT-9. Energy Procedia 1:399–406

Wikipedia (2010) http://en.wikipedia.org/wiki/Peak_coal

Wu Y, Jia L, Tan Y, Anthony EJ (2008) Characterization of ashes from oxy-fuel combustion in a pilot-scale circulating fluidized bed. In: Proceedings of the 9th international conference on circulating fluidized beds, Hamburg, 13–16 May 2008

Xu B, Stobbs RA, White V et al (2007) Future CO_2 capture options for the Canadian market. Report No. Coal R309 BERR/Pub URN 07/12251, Mar

Yaverbaum L (1977) Fluidized bed combustion of coal and waste materials. Noyes Data Corporation, Park Ridge

Zheng L, Clements B, Tan Y, Pomalis R (2009) Flue gas recycle strategies in oxy-coal combustion. In: 34th international technical conference on clean coal & fuel systems, Clearwater, 1–4 June 2009

Zhou W, Moyeda D (2010) Process evaluation of oxy-fuel combustion with flue gas recycle in a conventional boiler. Energy Fuels 24(3):2162–2169

Gasification Technology

Lawrence J. Shadle, Ronald W. Breault, and James Bennett

Contents

Abstract

Gasification is an enabling technology for the cleanup of fossil and biomass fuels for energy production. A history of gasifier development is told from the perspective of a technology evolving to meet the ever-changing market needs. The chemistry and physics of coal conversion include pyrolysis, combustion, gasification, mineral transformations, as well as a discussion of the materials

L.J. Shadle (✉) • R.W. Breault • J. Bennett
U. S. Department of Energy, National Energy Technology Laboratory, Morgantown, WV, USA
e-mail: LShadl@NETL.DOE.GOV; Ronald.Breault@netl.doe.gov; James.Bennett@NETL.DOE.GOV

W.-Y. Chen et al. (eds.), *Handbook of Climate Change Mitigation and Adaptation*,
DOI 10.1007/978-3-319-14409-2_40

developed to meet the most challenging gasifier applications. Integrated gasification and combined cycle processes are discussed with respect to electrical power production. The distinguishing features for different types of gasifiers are described including fixed-bed, fluidized-bed, entrained-flow, and transport gasifiers. The twelve major gasifiers being marketed today are described. The hydrodynamics and kinetics of each are reviewed along with salient differences in performance, such as gas composition, when using a variety of fuels under different conditions. Critical operational features that are discussed include oxidizing media, air, or oxygen blown; the system pressure; fuel feedstock; and downstream cleanup. Thermal integration is discussed with respect to its impact on the gasifier performance. Gas cleanup is also considered with respect to the removal of potential pollutants and the shifting to environmentally benign transportation and process fuels.

Introduction

History of Gasification

The concept of progress has changed dramatically over the past century. The development of new industry was considered progress regardless of the impact on the environment. From the first time man could see images of the fragile planet earth, he has become increasingly aware that one must learn how to not only tap the earth's natural riches but also how to preserve and serve as guardians of her most common resources – air and water. Coal was one of the critical natural resources leading to the industrialization that allows man the luxury of planning the planet's future. As the world emerged into the Industrial Age, coal provided more than just the fuel for heat and industry. Coal gas also played a key role in the innovative development of tools, materials, and lighting. In 1609, Jean-Baptiste van Helmont first heated and observed the release of gas from coal. He wrote how the coal "did belch forth a wild spirit or breath . . . not susceptible of being confined in vessels, nor capable of being reduced to a visible body." Helmont surely wondered about this spirit and called it "gas" as derived from the Dutch word "geest" for ghost (Massey 1979). The first coal gasifier was used by Fontana in 1780 when he directed a flow of water (steam) over red-hot, or incandescent, coal that was partially burned in air. The process can be described using two reactions. Heat was provided by combustion of coal with air, and then the air was replaced with steam to gasify the hot char and produce synthesis gas, a combustible mixture of carbon monoxide and hydrogen. Fontana called the resulting coal gas "blue water gas," because it produced a pale blue flame when burned in air (Probstein and Hicks 1979).

Coal gasification supplied lighting and heating for industrializing America and Europe beginning in the early 1800s. The first public street lighting with coal-derived gas was in Pall Mall, London, on January 28, 1807. This was where coal-derived fuel gas became commonly known as "town gas." Town gas was a

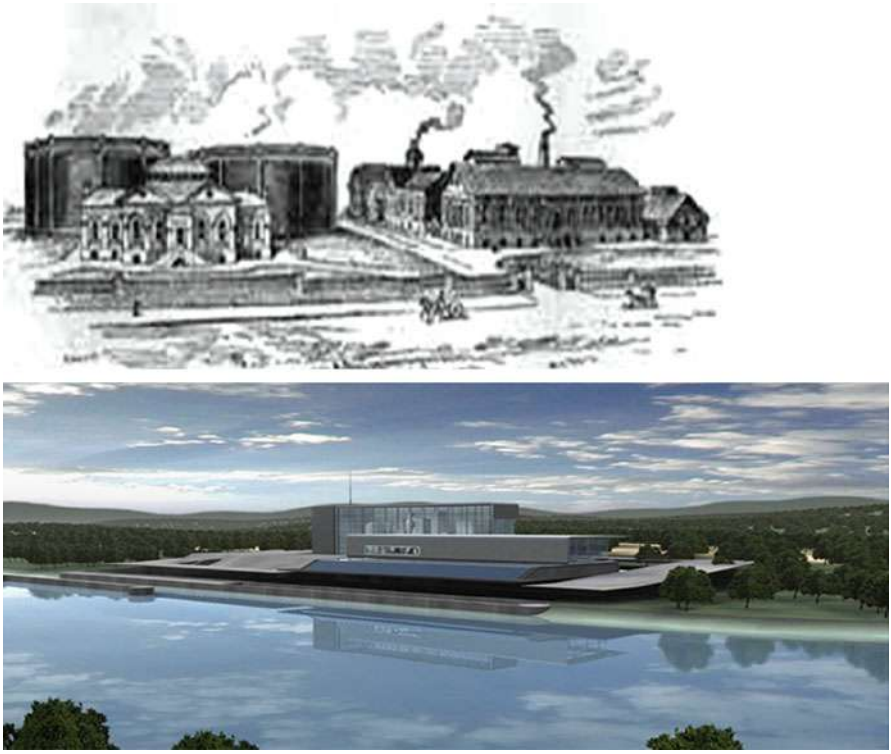

Fig. 1 Artists' view of Baltimore's Bayard Street Station (*on left*) from "Progressive Magazine" of 1889 picturing the plant prior to 1850 and a FutureGen power plant (*on right*) depicting a modern, green-field, zero-emission integrated gasification combined cycle (IGCC) plant

gaseous product from coal, containing nearly 50 % hydrogen, with the remainder made up of methane and carbon dioxide, and 3–6 % carbon monoxide. Not long after that, Baltimore, Maryland, began the first commercial gas lighting of residences, businesses, and streets in 1816. A typical town gas plant for the era is shown in Fig. 1 and contrasted to today's vision of a FutureGen power plant. Both images represent progress to different generations.

Gasification was the leading energy source in many industries in need of process fuel gas since the early 1800s. The light bulb was not discovered by Thomas Edison until late in the nineteenth century, 1879. The first electric power plant was not built until nearly two decades after the American Civil War in 1882. However, as early as 1792, Murdock, a Scotch engineer, used Fontana's process to produce a fuel gas and light his house. James Watt, the inventor of the steam engine, employed Murdock to light one of his foundries with this newly discovered coal gas (Shindman 1945). By 1875, every medium- and large-sized city in America and Europe developed coal gasworks and distribution networks. Gasworks were a large

number of batch gasifiers set up in series so that a continuous stream of fuel could be supplied to residential and industrial users.

The "blue water gas" produced from cyclic gas generators of the type used by Fontana was not directly usable for street or household lighting. While the heating value was high enough to sustain combustion, the blue flame was not bright enough. Early developers learned that the coal gas needed to add "illuminates," i.e., C_{2+} hydrocarbons, to provide a bright luminous yellow flame. However, too many or the wrong types of higher hydrocarbons would produce condensable species like tars and naphthalene, and the gas would eventually foul and plug the pipelines. Noxious and poisonous gases, such as hydrogen sulfide, hydrogen cyanide, and ammonia, were also produced. It was soon found that the undesirable components could be separated and cleaned from the coal gas. Cooling with a direct water spray and filtering of the gases were usually effective in removing the condensables and noxious impurities.

By the mid-1800s, there were two main types of coal gasifier cyclic gas generators similar to those first used by Fontana and gas producers. The cyclic gas generators produced a high-quality fuel gas. This high heat value is accomplished by collecting only the products during the steam blast and venting the products of combustion during the air blast. The carbureted gasifier produced "town gas" which was particularly well suited for lighting. The original cyclic gas generators were ideal industrial fuels used in kilns, boilers, brick ovens, and curing materials particularly where particulate impurities were to be avoided. These batch units were typically loaded by hand, and more importantly, the glowing hot ash or coke also had to be removed by hand – often with nothing more than a shovel.

In addition to the obvious benefits to gas workers of the time, many economic advantages were possible by making this cyclic process continuous. Gas manufacturers learned that they could improve both the rate and efficiency of gas making by introducing steam and air together into the coal. In this way the steam was available to gasify the carbon at the same time that heat was being produced from coal combustion. The result was the ability to substantially increase the overall conversion of coal to gas. This led to the development of the fully continuous gasifier of today with respect to both coal and air/steam. Thus, the modern gas producers were developed.

The development of gas producers did not, however, displace the cyclic gas generators. By 1936, the Federal Trade Commission reported that there were 3,800 machine-fed and still about 1,000 hand-fed gas producers in the USA (Wen and Dutta 1979). By firing air and steam simultaneously, the product gas in these producers now contained the unreactive, or inert, nitrogen that is present in the airstream fed to the gasifier. Air is, in fact, 79 % N_2 and only 21 % O_2 by volume. This added nitrogen is merely a diluent and plays no role in the combustion or gasification reactions. To make matters worse, this diluent must be heated both during the gasification process and later as the fuel is burned. As a result, the producer gas is only about one-half of the heating value compared to "town gas." There are several process ramifications when using this low-quality gas fuel. Economic transportation of producer gas is limited to a short distance.

Upon combustion the flame is longer, cooler, and more luminous. Still many industrial applications could take advantage of the peculiar flame properties of this low heating value fuel. For instance, the relatively low temperatures and long flame are useful to avoid hot spots and nonuniformities in glassmaking.

In contrast to traditional coal combustion, coal gasification processes can be thought to include: pyrolyzers, cokers, cyclic gas generators, and gas producers. All of these processes are heated with substoichiometric air, i.e., insufficient oxygen to completely convert the coal to the final products of combustion. The products of all of these processes are a solid fuel, condensable hydrocarbons and tars, and flammable gases. Both the quality and quantity of these products depend upon how the coal is heated, the gas atmosphere used during the process, and the temperature. The product distribution generated from these coal technologies is presented in Table 1. As is still true today, the coal gas in those early gasifiers was produced in several different reactors depending on the desired products and end use.

Gasification technology development has had its ups and downs. It is worthwhile to note some of the high points. Gasification was the foundation for modern chemical industry. In 1920 Fischer and Tropsch developed a catalyst to convert the hydrogen and carbon monoxide from coal gasifier gas to hydrocarbon liquids. By the mid-1930s, nearly two million liters of gasoline and oil per year were produced in German gasification plants. Individual reactors in the early Fischer-Tropsch plants yielded only about 5000 l of gasoline per day. Literally, 100 such gasifiers were used in these first plants. During the World War II, this coal-derived oil was one source of synthetic fuel for the German war machine. Gasification technology has been a mainstay in the refining industry for the production of synthesis gas from coal, heavy residual oils, and petroleum coke since the 1950s.

After World War II, South Africa required their own independent sources of oil and gas, when international economic sanctions cut off their access to world petroleum supplies in protest to their social policies of apartheid. While South Africa had no domestic oil and gas supplies, it had ample coal reserves. Gasification technology was chosen to supply the needed liquid transportation fuels, and the South African Coal, Oil, and Gas Company (SASOL) employed the Fischer-Tropsch process. The SASOL coal gasification plant has been operated since 1955 producing liquid fuels from coal. The individual reactors in these plants are 100 times larger than the plants used in Germany during the World War II.

SASOL operations were increased tenfold by their expansions in 1977 and 1982. Today SASOL has the largest gasification capacity in the world. By 1982, SASOL had a capacity of nearly 2.5 million gallons of oil and gasoline per day using Lurgi fixed-bed gasifiers. The SASOL plants remain the largest collection of coal gasifiers in the world today and include 80 Lurgi gasifiers with no spares (80 + 0) producing Fischer-Tropsch (FT) liquid transportation fuel as the product (Table 2).

Gasification has been used extensively in the last 50–60 years to convert coal and heavy oil into hydrogen – for the production of ammonia/urea fertilizer. The chemical industry and the refinery industry applied gasification in the 1960s and 1980s, respectively, for feedstock preparation. In 1984, the USA responded to pressure from oil-producing exporting countries to control oil prices by developing

Table 1 Operating conditions and product distribution for various coal conversion processes using bituminous (bit.) and subbituminous (subbit.) coal (Massey 1979; Van Der Hoeven 1945)

Product composition	Blue water gas	Town gas	Gas producers Fixed-fluid bed		Entrained gasifier		Coke oven
Oxidant	Steam	Steam	Air, steam	Oxygen, steam	Air, steam	Oxygen, steam	None
Fuel	Bit. coal	Bit. coal	Bit. coal	Brown coal	Subbit. coal	Bit. coal	Bit. coal
Exit temp., K	–	–	415	755	1366	1366	1255
Gases, %wt							
H_2	50.5	40.5	14.5	36.0	12.9	35.8	46.5
CO	38.5	34.0	25.0	44.4	23.5	50.7	6.3
CH_4	1.0	10.2	3.1	1.6	0.02	0.1	32.1
Illuminates[a]	–	8.0	–	0	0	0	0.31
N_2	52.7	0.5	52.7	0.8	60.3	0.2	0.95
CO_2	4.7	2.9	4.7	15.7	3.1	13.1	0.9
Tars[b], wt. %	–	–	–	0	0	0	–
Char, wt %			19.5	20.0	11.8	11.4	75
Gas HV[c], kJ/m^3	11,178	20,493	6,222	9,948	4,359	10,432	21,760

[a]Noncondensable gases consisting of hydrocarbons with carbon chains between C_2 and C_4
[b]Condensable liquids consisting of hydrocarbons with carbon chains greater than C_{5+}
[c]Gas HV is the heating value of the gas

Table 2 Twenty-five largest operating gasification plants worldwide (Higman 2014)

	Gasification plant	Country	Gasifier	Year	MWthOut	Fuel	Product	No. of gasifiers + spares
1	Sasol Chemical Ind. (Pty.)	South Africa	Lurgi	1977	14096	Bit. coal	FT liquids	80 + 0
2	Pearl GTL	Qatar	Shell	2011	10936	Natural gas	FT liquids	18 + 0
3	Datang Ningxia SNG	China	SEDIN	2015	7125	Lignite	SNG	45 + 3
4	CHNG Xinjiang SNG	China	TPRI	2014	6450	Coal	SNG	7 + 1
5	Jamnagar Gasification	India	E-Gas	2015	5000	Petcoke	Electricity-syngas chemicals	6 + 2
6	Yulin Methanol	China	GE	2015	3383	Coal	Methanol	10 + 4
7	Shenhua Ningxia II	China	SEDIN	2014	2500	Coal	Methanol-propylene	14 + 2
8	Shenhua Ningxia I	China	Siemens	2011	1912	Coal	Methanol-propylene	5 + 0
9	Great Plains Synfuels	USA	Lurgi	1984	1900	Lignite	SNG and $C0_2$	12 + 2
10	Shenhua Baotou	China	GE	2011	1750	Coal	Methanol-olefins	5 + 2
11	Hexigten	China	SEDIN	2012	1670	Coal	SNG	12 + 2
12	Rongxin, Inner Mongolia	China	ECUST	2014	1400	Coal	Methanol	2 + 1
13	SARLUX IGCC	Italy	GE	2001	1271	Visbreaker residue	Electricity, H_2, and steam	3 + 0
14	ISAB Energy	Italy	GE	1999	1203	ROSE asphalt	Electricity, H_2, and steam	2 + 0
15	Sanwei Neimenggu MeOH	China	GE	2011	1167	Coal	Methanol	4 + 2
16	Edwardsport IGCC	USA	GE	2011	1150	Coal	Electricity	2 + 0
17	Tianjin Chemical	China	Shell	2010	1124	Coal	Syngas chemicals	2 + 0
18	Henan Jinkai	China	HT-Lurgi	2012	1120	Coal	Ammonia	4 + 0
19	Yunnan MeOH and DME	China	BGL	2011	1120	Coal	Methanol	4 + 1
20	Bintulu GTL Plant	Malaysia	Shell	1993	1032	Natural gas	FT liquids	6 + 0

(*continued*)

Table 2 (continued)

	Gasification plant	Country	Gasifier	Year	MWthOut	Fuel	Product	No. of gasifiers + spares
21	Long Lake Integrated Upgrading	Canada	Shell	2008	1025	Asphalt	Hydrogen	4 + 0
22	Leuna Methanol	Germany	Shell	1985	984.3	Visbreaker residue	H_2, methanol, and electricity	6 + 0
23	Sasol Chemical Ind. (Pty.)	South Africa	Lurgi	1955	970.6	Bit. coal	FT liquids	15 + 2
24	Shenhua Erdos DCL H_2 Plant	China	Shell	2008	861	Coal	Hydrogen	2 + 0
25	Fujian Refinery Ethylene Project	China	Shell	2009	858	Asphalt	Hydrogen and electricity	2 + 1

the synthetic natural gas (SNG) plant in North Dakota known as the Great Plains Gasification Plant. Like SASOL, this large-scale demonstration selected fixed-bed technologies developed by Lurgi and Synthane. Coal gasifiers were also built in the late 1970s using entrained- (Texaco and Dow) and fluidized-bed gasifiers (U-GAS®) primarily in oil refineries and chemical plants.

In 1977, the USA passed the Clean Air Act Amendments which identified the concept of benchmarking technologies with respect to the best available control technology (BACT). This drove an interest in integrated gasification combined cycle (IGCC). Several utility-scale IGCC power trains were built in the 1990s as demonstration plants using entrained gasifiers including the Tampa Electric's TECO plant using 2 Texaco (now GE Energy) gasifiers and the Wabash plants using 2 E-Gas (now ConocoPhillips) gasifiers.

Coal-based plants using today's gasification technology are efficient and clean. Gasification has been demonstrated to be superior to conventional utility power systems in response to tightening environmental regulations and as a result of the development of the highly efficient gas turbines or the combined power cycles and the relative ease and level of maturity of the associated gas cleanup technology. However, the technology still lacks the experience base in the power sector and so has had difficulty to raise the large capital investments required. Technologies have been developed for gasifiers to shift the product stream from carbon dioxide to clean-burning hydrogen gas. When coupled with the well-proven acid gas removal technology, carbon dioxide can be removed and concentrated for market applications or to be sequestered. Gasification is posed to be a leading technology capable of addressing the challenges to global climate change.

Basics: Chemistry and Physics

Gasification has been around for more than 200 years, so why the interest in it now? There are many reasons, but the two most significant are the continuing high price of natural gas and highway transportation fuels. Granted that these prices are moderated occasionally. However, the price of gasoline has fluctuated widely over the past decade. The second significant reason is the need for energy independence. In other words, the use of domestic energy sources such as coal is needed not only for electricity production but also for synthetic natural gas (SNG) and liquids for transportation.

Gasification is a technology for converting coal to a gaseous product often called synthesis gas or fuel gas depending on the application. The product gas can literally be converted to almost anything, other than electrons, and can potentially be competitive even there (U.S. Department of Energy 2009). Gasification is often considered the baseline technology and foundation for developing many advanced carbon-based fuels and chemicals. For example, gasification is the key conversion step for converting coal to H_2, synthetic natural gas (SNG), liquid fuels, and the capture of CO_2 for sequestration. Gasification has excellent environmental performance such that some states' public utility commissions have identified integrated

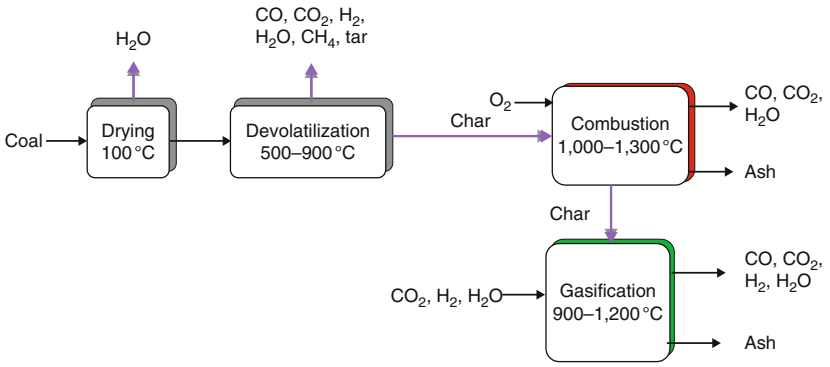

Fig. 2 Simplified schematic of reaction pathways contributing to coal conversion in a gasifier

gasification combined cycle (IGCC) plants for power generation as the best available control technology (BACT). In addition, the uncertainty of carbon management requirements and the potential suitability of IGCC for CO_2 controls make it an ideal choice for power.

So, what is gasification? Strictly speaking, gasification is the reaction of carbon with steam to produce carbon monoxide and hydrogen. Because this reaction is highly endothermic and because coal and biomass are not simply carbon, gasification technology is more complex than that. As compared to combustion, gasification is the conversion of organic matter to carbon monoxide and hydrogen by reaction of substoichiometric mixtures of the solid fuels and oxygen usually in the presence of excess water or steam. It is useful to consider the conversion processes involved in solid fuel gasification individually. Coal undergoes a series of chemical and physical changes as shown in Fig. 2.

As the coal is heated, most of the moisture is driven out when the particle temperature is about 105 °C. Drying is a rapid process and is essentially complete when the temperature exceeds the boiling temperature of water.

Devolatilization and Coal Dependence

A large percentage of coal weight is lost during devolatilization or pyrolysis. Pyrolysis occurs rapidly as the coal heats up above 300 °C and continues up to temperatures required for gasification. If the heating rate is slow, pyrolysis can reach completion at temperatures as low as 450 °C, but for rapid heating processes, pyrolysis continues as the coal heats up to 700–1000 °C required for gasification. Given and others (Given 1984; Given et al. 1986) describe the organic matter in coal as a macromolecular network with varying contents of lower molecular structures and components which are mobile but entrapped within that solid structure. During pyrolysis, mobile components evolve. Labile bonds are broken producing lower molecular weight fragments. Fragments and low molecular weight components vaporize and escape from the coal particle forming light gases and tar. The more reactive or higher molecular weight fragments with low vapor pressure

can remain in the coal under typical devolatilization conditions and reattach to the coal's macromolecular network. This can be thought of as the precursor to char. The devolatilization gases that do not condense at room temperature and pressure are called light or fixed gases and consist mainly of CO, CO_2, CH_4, H_2, and H_2O. The portion of the volatile matter that condenses at room temperature and pressure is called tar. Tar is a mixture of hydrocarbons with an average molecular weight ranging from 200 to 500 amu (Fletcher et al.). The yield and chemical nature of tar depend upon the coal rank; in general, higher-rank coal produces lower amounts of tar. The solid product left over from devolatilization is char. Devolatilization alters the coal porosity from 2 % to 20 %, typical of coal, to over 80 % in the char. The surface area increases from 10–20 m^2/g (coal) to 200–400 m^2/g as measured by with nitrogen gas in a BET (Brunauer-Emmett-Teller) apparatus (Gan et al. 1972; Walker 1981). This increased surface area increases the rate of subsequent combustion and gasification reactions.

The volatile yield, its composition, and the residual char reactivity depend upon the coal petrology, degree of geologic maturation, and process conditions (van Krevelen 1993; Chitsora et al. 1987; Hecht et al. 2010). Coal rank is the relative measure of the extent of maturation for an organic sediment due to exposing the deposited organic detritus to elevated pressures and temperatures during the geologic eras required for its burial, subsidence, and compaction (Teichmuller 1982). Organic materials increase in level of maturity from:

$$\text{BIOMASS} < \text{PEAT} < \text{LIGNITE} < \text{SUBBITUMINOUS} < \text{BITUMINOUS} < \text{ANTHRACITE}.$$

Maturation processes are characterized by first the loss of water and oxygen functionality, followed by increase in polymeric molecular size, and finally the condensation of aromatic structures.

Classification for low-rank coals, subbituminous coals, and lignites is based upon the inherent moisture content and their calorific value (ASTM D3172 07a). Low-rank coal volatiles contain a large proportion of the fixed gases and the tars produced are low molecular weight. Their tars are typically limited to one- and two-ring aromatic structures, but contain a wide variety of heteroatomic functionality. Chars produced from heating low-rank coals are open and exhibit a greater degree of disorder and more heteroatomic functionality (H, O, N, and S) than their higher-rank counterparts. As a result these chars have high gasification reactivities (Radovic et al. 1985; Mahajan et al. 1978). It is the potential for the reactive oxygen functional groups such as the carboxyl groups to chelate exchangeable cations that can atomically disperse catalytic species such as Ca, K, and Na to dramatically enhance gasification rates (Jenkins and Morgan 1986; Morgan and Jenkins 1986a, b).

Coals which are higher in rank than subbituminous have lower oxygen contents, but still substantial volatile matter. Reactive oxygen functionalities such as esters, carbonyl, and carboxyl groups are gone in the bituminous rank coals, but phenols, furan cyclic oxygen, and ether linkages persist [11]. The volatile matter consists of

less fixed gases, but higher molecular weight aromatic hydrocarbons with less heteroatomic functionality than the lighter counterparts formed from lower-rank coals. Bituminous coals are differentiated by their volatile matter content being classified as high-, medium-, or low-volatile bituminous coals. These high molecular weight compounds, when combined with the residual macromolecular network during heating, form what is known as metaplast (Fletcher et al.). The quantity, volatility, and solubility characteristics of tars in bituminous coals are favorable to dissolve or melt the coal's macromolecular network which makes up the bulk of organic matter in this rank coal. During metaplast formation, the particle traps evolving gases and swells to an extent which depends on its composition and the heating conditions. When rapidly heated in drop-tube reactors, bituminous coals produce char cenospheres often greater than three times the size of the feed coal (Maloney et al. 1982). A cenosphere is a remarkably spherical char structure which is essentially hollow formed when these coals are heated reaching a plastic stage while still evolving volatile gases. The residual chars formed after devolatilizing bituminous coal are more highly ordered carbons consisting largely of condensed polynuclear aromatic structures. Thus, in spite of their lower density and extremely high porosities, bituminous coal chars are inherently less reactive than their lower-rank counterparts.

Low-volatile bituminous coals can be distinguished from anthracite by the relative hydrogen to carbon content which decreases as the rank increases due to the condensation of aromatic rings into highly condensed and unreactive polynuclear aromatic structures. Tar yields from these high-rank coals are quite small and fixed gases evolved consist mainly of CO, H_2, and CH_4.

Process conditions also influence devolatilization and the products volatiles and char. Key parameters include heating rate, final temperature, and pressure. At slow heating rates (less than 1 K/s), the volatile yield is relatively low. It is under these conditions that the total volatile yield will be equal to the volatile matter content determined from the ASTM (American Society for Testing and Materials) proximate analysis, which is an analysis done at a slow heating rate. Under rapid heating rate (500–10^5 K/s), the volatile yield is 20–40 % more than that at slow heating rates (Wen and Dutta 1979). At any given temperature only a certain fraction of the volatiles is released. Significant devolatilization begins when the coal temperature is about 500 °C. As the temperature is increased, more volatiles are released. The maximum volatile yield occurs when the temperature is above 900 °C, the temperature at which ASTM proximate analysis is conducted. Higher gasifier temperature also reduces the amount of tar in the gasifier products because of increased cracking rate of tar into lighter gases.

The amount of tar also decreases with increasing pressure and decreasing heating rates. The predominant source of CH_4 in the gasifier product gas is the devolatilization process, and its production is favored by low temperature and high pressure. Therefore, the amount of methane in the product of moving-bed gasifiers, which operate at a low temperature, is higher than that in typical fluidized-bed and entrained-bed gasifiers (Moreea-Taha 2000).

As such it is apparent that predicting the early stages of gasification, devolatilization for coal is quite complex. While the rate is rapid and can be simulated as being coincident with coal heating, the yields, stoichiometry, physical characteristics, and resulting reactivity of the products are dependent upon many factors. One common, simple, and expedient approach is to scale the devolatilization yield with temperature based upon the ultimate yield determined in the ASTM proximate analysis (Syamlal and Bissett 1992). This provides a relative distribution of volatile matter in the gas phase that is dependent on the coal feedstock which can then be modeled to react further to produce fixed gases, depending on the thermal environment in the gasifier. The more rigorous two-stage pyrolysis model is often employed to explain the effects of heating rate and pressure on tar yields (Kobayashi et al. 1977). In this model primary tars are produced initially within the coal particle followed by their subsequent cracking and release via a second reaction. Thus, if the heat rate is fast enough to raise the particle temperature sufficiently for vaporization, the high molecular weight primary tars are released into the gas phase before they can reattach to the char. However, at lower heat rates or higher pressures, these low-volatile primary products stay longer within the particle and crack there to form lighter volatile products which can escape as well as fixed carbon which reattaches to the char.

Anthony et al. (1976) have demonstrated that thermal decomposition of the complex coal macromolecular structure can be modeled by a series of parallel reaction pathways in which the reaction progresses along the most favorable one which can be described by distributed activation energies. The activation energies increase as the extent of conversion increases. Another more rigorous approach is to characterize the evolution rates of these individual gas species themselves dependent on precursor species as identified by more detailed characterization of the cross-linked nature of coal. Such approaches have included the use of infrared (Solomon et al. 1990, 1993a; Solomon and Serio 1994; Solomon et al. 1991) and NMR spectroscopic analysis (Solomon et al. 1993b; Fletcher et al. 1991). These methods have been further refined through the development of volatile percolation models such as FLASHCHAIN (Niksa 1986; Niksa and Lau 1993; Niksa et al. 2003) and CPD (Coal Percolation and Devolatilization) (Fletcher et al.; Solomon et al. 1993b; Fletcher et al. 1991) to account for the variations in thermal and mass transfer during volatile release due to variations in process pressure, heating rates, and particle sizes. NETL's C3M efforts are designed to incorporate all of these models in a platform that can be used with various models (Van Essendelft et al. 2014).

Combustion

Char in an oxygen atmosphere undergoes combustion. In gasifiers partial combustion occurs in an oxygen-deficient or reducing atmosphere. Gasifiers use 20–30 % of the oxygen theoretically required for complete combustion to carbon dioxide and water. Carbon monoxide and hydrogen are the principal products, and only a fraction of the carbon in the coal is oxidized completely to carbon dioxide. The combustion reaction is written in a general form as follows:

$$(1+\lambda)\,C\ +\ O_2 \rightarrow 2\lambda\ CO\ +\ (1-\lambda)\,CO_2 \quad \Delta H^0_{298K} = \begin{array}{l} 172.5\lambda \\ -393.5\ \text{kJ/mol} \end{array}$$

where λ varies from 0 (pure CO_2 product) to 1 (pure CO product). The value of λ depends upon the gasification conditions and is usually close to 1. This is quite important since the ratio of CO/CO_2 determines how much of the carbon in the char is converted to gas. Computational models for coal oxidation under these conditions are quite common, but vary in the manner that they treat the value of λ. Arthur conducted tests on various carbons often cited to model the temperature dependence for this stoichiometric coefficient (Arthur 1951). As the temperature of reaction increases, carbon monoxide is favored. Wen (Wen and Dutta 1979; Wen and Chaung 1979) incorporated this concept by including a particle size dependence such that larger particles with greater thermal mass have a greater tendency to reach higher temperatures and higher values for λ and yield greater proportions of CO. Monazam et al. (1998) and Shadle et al. 2001) have employed Arthur's temperature dependence directly into plug flow and stirred-tank models.

The carbon-oxygen reaction is quite fast and highly exothermic. Under typical gasifier conditions, the carbon-oxygen reaction rate is controlled by the rate of the diffusion of oxygen to the particle surface. For a particle size of 50 μm, the diffusion rate is the rate-limiting step for temperatures above 750 K. For smaller particles the diffusion of O_2 into the particle becomes dominant only at a higher temperature (e.g., 1600 K for 20 μm particles). The heat released by the partial combustion provides the bulk of the energy necessary to drive the endothermic gasification reactions.

Gasification

As a result of these rapid oxidation kinetics, all oxygen is rapidly consumed in a combustion zone, near the injection of oxidant. Further conversion of char occurs through the much slower, reversible gasification reactions with CO_2, H_2O, and H_2.

$$C\ +\ CO_2 \leftrightarrow 2\,CO \quad \Delta H^0_{298K} = 172.5\ \text{kJ/mol}$$

$$C + H_2O \leftrightarrow CO + H_2 \quad \Delta H^0_{298K} = 131.3\,\text{kJ/mol}$$

$$C + 2H_2 \leftrightarrow CH_4 \quad \Delta H^0_{298K} = -74.8\ \text{kJ/mol}$$

The rate of gasification reactions depends upon the char properties and the gasification conditions. Typical orders of magnitude of the relative reaction rates for various oxidants are provided in Table 3.

In general, gasification rates increase with temperature according to the Arrhenius expression. The kinetic parameters reported by Wen et al. (Wen and Dutta 1979; Wen and Chaung 1979) are commonly used to model the kinetics of coal gasification. This is used by Syamlal et al. (1996) in MFIX (Syamlal et al. 1993) and by Slezak et al.(2010). During combustion and gasification, the particle mass and

Table 3 Relative gasification rates at 10 kPa and 800 °C

Reaction	Relative rate
$C + O_2$	10^5
$C + H_2O$	3
$C + CO_2$	1
$C + H_2$	10^{-3}

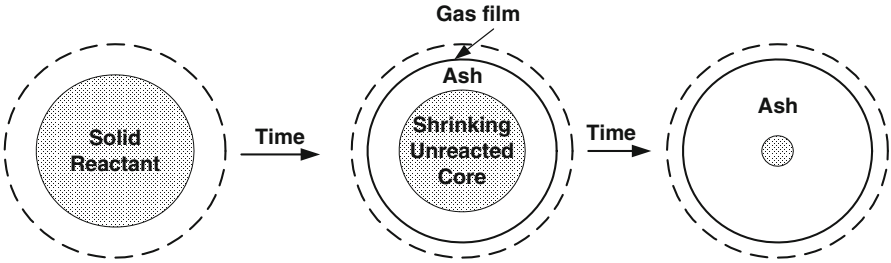

Fig. 3 Shrinking core model for the combustion of coal

temperature are governed by the following reactions developed from the mass and energy balances for a reacting coal particle:

$$\frac{dm_p}{dt} = -Rate$$

$$m_p C_p \frac{dT_p}{dt} = hA_p\left(T_\infty - T_p\right) + \frac{dm_p}{dt} h_{reac} + \varepsilon A_p \sigma\left({\theta_R}^4 - {T_p}^4\right)$$

where m_p is the reacting particle mass, C_p its heat capacity, T_p its temperature, A_p its area, h the gas-solid heat transfer coefficient, T_∞ the bulk process gas temperature, h_{reac} the heat of reaction, ε the voidage, σ the view factor, and θ_R the refractory wall temperature. The refractory wall is a corrosion- and heat-resistant brick often used to line the gasifier walls. The term on the left of the latter equation represents the change in the sensible heat in the particle during the coal conversion. At any instant in time, this is equal to the heat transferred between the gas and the particle (1st term on the right), plus the heat gained or lost due to the heat of reaction (2nd term on the right), plus the radiant heat transfer. The combustion reaction is normally modeled as a shrinking core model graphically shown in Fig. 3 where the coal particle is depicted initially, after the reaction front has progressed in time so that a coal ash layer has built up and when the reaction has progressed to nearly completion. In coal this is complicated by potential coal swelling initially. The initial gas-char reactions involve fast surface combustion of oxygen. These reactions occur at the surface because the processes are limited by the relatively slow diffusion of oxygen into the porous coal char at these temperatures. This is the shrinking particle and constant density stage of the process. After the oxygen is depleted, the gasification of char becomes relatively slow as compared to diffusion,

and so gasification reactions are kinetically limited. This second stage of heterogeneous gas-char reactions takes place uniformly throughout the particle volume and results in decreasing particle density and constant diameter.

The reaction rate (per unit area) for combustion and gasification is obtained from comparing the relative reaction rates associated with gas-solid film diffusion, chemical reaction, and diffusion through the reacted char layer:

$$rate = \frac{1}{\frac{1}{k_{diff}} + \frac{1}{k_r Y^2} + \frac{1}{k_{dash}}\left(\frac{1}{Y} - 1\right)} (P_i - P_i^*)$$

where k_{diff} is the gas film diffusion constant, k_r is the Arrhenius rate constant, k_{dash} is the ash film diffusion constant, Y is the char conversion factor defined as the ratio of the unreacted core radius to the initial radius of the particle, P_i is the partial pressure of reactant i, and P_i^* is the back reaction equilibrium pressure of reactant i (Wen and Chaung 1979).

Variations in the relative rates are normally accounted for by adjusting the frequency factor or pre-exponential term. Differences in char reactivity as a result of degree of disorder of the carbon structure are also treated by adjusting this pre-exponential factor (Monazam et al. 1998; Shadle et al. 2001). Differences in the degree of disorder in the char are due to differences in heat treatment history, number of imperfections due mainly to heteroatoms (i.e., organic O, S, and N), and degree of condensation in the aromatic structure (due to level of maturity in the sediment). In addition, it is important to note that elevated pressures increase the partial pressure of the oxidant and thus increase the gasification rate relative to the absolute increase in overall pressure (Monazam et al. 1998; Shadle et al. 2001).

Another important chemical reaction in a gasifier is the water-gas shift reaction:

$$CO + H_2O \leftrightarrow CO_2 + H_2 \quad \Delta H^0_{298K} = -41.2\,\text{kJ/mol}$$

The relatively low heat of this reaction contributes to the low activation energy and quick approach to equilibrium. As a result the gasifier product distribution can often be estimated from the conversion and the equilibrium constant for this reaction. However, this equilibrium constant if dependent on temperature and the equilibrium will be frozen at the process or downstream temperature depending on the effective quench rates in the various processes. Thus, the equilibrium temperature for a different process configuration must be experimentally established. Detailed computational modeling has the potential to incorporate all of these complex reaction pathways to provide insight into how to predict changes in this effective equilibrium temperature and thus how modifications will alter gasifier product distributions.

Mineral matter in the coal catalyzes this gas-phase reaction. Other gas-phase reactions are the combustion of CO, H_2, and CH_4 and tar cracking. One intermediate product from these gas-phase reactions in a gasifier is the formation and further conversion of soot. This can play a pivotal role in determining the performance, reliability, and efficiency of the downstream cleanup process units as well as determining the overall process performance.

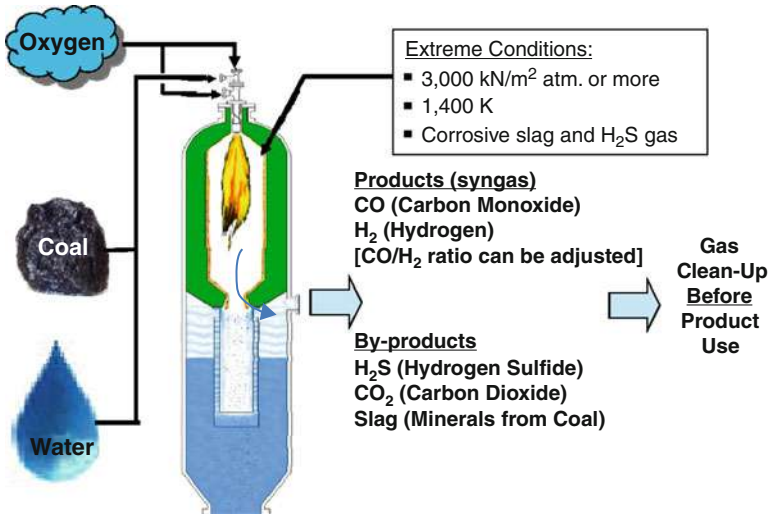

Fig. 4 Gasification process basics

Gasification turns any carbon-containing material into synthesis gas as depicted in Fig. 4. Carbon reacts with water, in the form of steam, and oxygen at relatively high pressure, typically greater than 3000 kN/m^2, and at temperatures typically reaching 1,500 K to produce raw synthesis gas or syngas. Syngas is a mixture composed primarily of carbon monoxide and hydrogen and some minor by-products. The by-products are removed to produce a clean syngas that can be used as a fuel to generate electricity and steam. Syngas is the basic chemical building block for a large number of uses in the petrochemical and refining industries. Syngas production is the first step in the efficient manufacture of the clean-burning hydrogen fuel. Gasification adds value to low- or negative-value feedstocks by converting them to marketable fuels and products.

There are a number of previous reviews and extended writings on gasification available to get a deeper understanding of the process and various gasification technologies. These include the book by Higman (Higman and van der Burgt 2008), the Gasification Technologies Council website http://www.gasification.org/, the DOE Gasification website http://www.netl.doe.gov/technologies/coalpower/gasification/index.html, and numerous conferences including Gasification Technologies Annual Conference, the Clearwater Conference, and the Pittsburgh Coal Conference.

Coal Minerals and Their Transformations

Coal is a sedimentary deposit comprising mainly the remains of swampy forest plants that accumulated and subsided beneath the soil to escape the carbon cycle. As such it is a combination of the organic matter from biological source, as well as inorganic matter depending on the geological formation in which it was deposited.

The coals that we find in the ground today have matured to different levels depending on its age, depth of burial, and associated geology. Up until now we have considered primarily the organic matter in coal; however, the processes that use coal are often affected in very important ways by the amount and type of minerals in it.

The coals in the USA have low mineral contents (often <10 % wt.), and those minerals often occur in discrete particles that can be readily separated from the organics. Eastern US geological basins are older and more mature, being from the Carboniferous age, than their Western counterparts which are from the Cretaceous age. As a result the Western coals have alkaline earth metals in the form of ion-exchangeable cations associated with oxygenated functionality in the coal that catalyze many thermal conversion processes. The most common minerals in US coals are clays, but the Eastern coals often have sulfur in the form of pyrite due to the brackish depositional environment in which they were deposited. The depositional environments in the Western coals were more variable, and besides clays, the coals may have quartz and calcite but pyrite is more rare. By contrast, coals in the Southern hemisphere, often referred to as Gondwanaland coals after the supercontinent that once encompassed all of the land masses there, are characterized by the high inorganic content (40–80 % wt.) distributed uniformly creating a coal that is not amenable to physical separation or beneficiation.

The mineral composition of the coal will influence its thermal behavior. Upon heating in air, coal yields ash in which the pyrite is converted to hematite, and carbonates are calcined producing metal oxides. By contrast, a gasifier will produce reduced metal ash, forming pyrrhotite from pyrite and forming sulfides or reduced metal oxides depending on the presence of sulfur. The clays are dehydrated in either case. The composition of the ash will determine its thermal behavior: melting temperature and slag viscosity. Gasifiers are generally categorized according to how they handle the mineral waste.

Gasifiers which operate at high temperature, melting the minerals, are referred to as slagging gasifiers. Slagging gasifiers operate at temperatures high enough that mineral or organic impurities in the carbon feedstock become molten, and if contact is made with other particles or the gasification chamber sidewalls, coalescence can occur to form slag. Dry bottom gasifiers handle the mineral matter waste by either operating at temperatures below the melting temperature or by extracting the heat from the combustion zone to resolidify any slag that is formed. Both types of gasifiers use refractory to improve performance and maintain reactor vessel integrity.

Slagging gasifiers operate at temperatures between about 1325–1575 °C, a temperature determined by the fluidity of the slag contacting the gasifier sidewall that must flow from the gasifier. If the slag is not fluid enough to flow from the gasifier (high viscosity), it will build up on the gasifier sidewalls or in the solid waste exit, causing gas flow to become restrained, with either higher gasification temperatures used to remelt slag so it flows from the gasifier or shutdown of the gasifier occurs so solidified slag can be physically removed from the gasifier. Note that if high temperatures are needed to cause build up slag to flow from the gasifier,

Table 4 Range of ash chemistry found in over 300 Eastern coals and 9 petcoke carbon feedstock found in the USA due to mineral and metal-organic impurities (Vassilev et al. 2002; Conn 1995; Bryers 1995)

	Coal (wt pct)			Petcoke (wt pct)		
Compound	Avg.	Std. dev.	High to low	Avg.	Std. dev.	High to low
SiO_2	43.6	16.4	68.5–7.1	14.1	8.7	18.9–3.1
Al_2O_3	25.2	10.2	38.6–4.1	4.8	2.8	9.4–0.5
Fe_2O_3	17.0	11.2	69.7–2.1	7.2	9.3	36.1–1.2
CaO	5.8	6.6	45.1–0.5	5.4	3.8	11.9–2.0
MgO	1.2	1.1	8.0–0.1	1.0	1.6	5.1–0.3
K_2O	1.4	0.7	3.5–0.2	0.5	0.4	0.7–0.3
Na_2O	0.9	0.6	6.5–0.3	0.8	0.8	2.3–0.1
TiO_2	1.4	0.8	3.7–0.4	0.3	0.2	0.6–0.2
NiO	NL	NL	NL	8.4	3.2	11.4–2.9
V_2O_5	NL	NL	NL	57.0	19.5	79.4–30.2

NL not listed

corrosive wear of the refractory liner in the gasifier increases, shorting the service life of those materials. The amount of solid waste removed from a gasifier can be high, representing the mineral matter content of the fuel feedstock, highlighting the importance of a smoothly operating system. Slag fluidity (viscosity in poise) must be low enough so it can flow from the gasifier, but not so high that refractory wear becomes excessive. Gasifier operators typically target a viscosity range between two temperature values, t_{100} and t_{250}, although other values can be used. The t_{100} temperature is higher, and produces a fluid slag, while the t_{250} temperature produces a thicker slag that takes more time to flow a specific distance. Viscosity values higher than t_{250} become too thick to flow from the gasifier, while viscosity values lower than t_{100}, as mentioned previously, involve temperatures that accelerate refractory wear and increase the likelihood that syngas cooler fouling will occur and will occur faster than at lower temperatures. Gasifier operators prefer carbon feedstock that will produce a wide temperature range between t_{100} and t_{250} viscosity values, giving them a greater degree of operational flexibility. A carbon feedstock viscosity can be altered by blending different materials or by using additives (typically mineral) to produce slag viscosities in a desired temperature range. A viscosity versus temperature curve for a synthetic slag mixture of an average Eastern coal (Table 4) evaluated under a gasification condition of 10–8 atm oxygen partial pressure is shown in Fig. 5.

The two most commonly used slags in slagging gasifiers are coal, petcoke, or mixtures of them. The chemistry ranges of average coal and petcoke ashes found in the USA are shown in Table 4. Coal averages about 10 wt% mineral impurities, although quantities can be lower or higher, depending on where the coal was mined. The major impurities in coal are minerals high in oxides of Si, Al, Fe, and Ca, although other elements can be high depending on the coal source. Petcoke averages about 1 % impurities which are typically metal-organic compounds high in V, Ni, Si, and Al. Examples of impurities found in coal and petcoke are given in

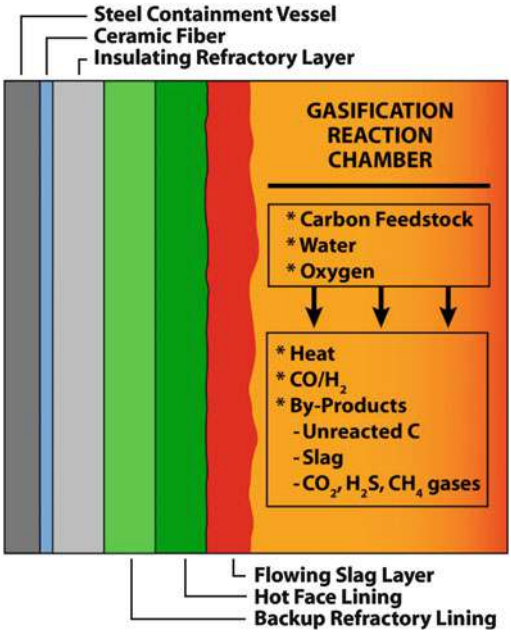

Fig. 5 Sidewall of a refractory-lined slagging gasifier

Table 4. Petcoke is the solid by-product from oil refinery operations derived from the thermal treatment (coking) of the higher molecular weight fractions of petroleum. In general, petcoke slags are considered by gasifier operators to have similar refractory liner behavior to coal slags. It is worth noting that on a microscopic level, differences between coal and petcoke slag interactions with refractories do exist. Limited thermodynamic information exists, however, on vanadium slags formed under the high temperature and low oxygen partial pressures of gasification, limiting modeling of petcoke slags. Work done by Nakano (Vassilev et al. 2002) on synthetic vanadium slags has indicated that V_2O_3 is the stable phase in the low oxygen partial pressure of gasification at high temperatures. This phase is important because when a slag is saturated with it, the amount of vanadium phase existing as crystalline material impacts slag viscosity.

Materials for Slagging Gasifiers

Because of the extremely harsh environment, high temperatures, and reducing environment, slagging gasifiers present unique design and material challenges. Because of the high temperatures, the walls are either cooled by air or water. Both require refractory lining to sustain the gasifier metal wall integrity and strength. A highly cooled gasifier (water cooling) produces a colder interior wall where a slag layer deposits and builds up or sloughs off depending on the operating conditions. However, these heat losses result in reducing the process thermal efficiency and so must be balanced with process operability and reliability. The alternative is to use less cooling (air-cooled wall) with higher temperature

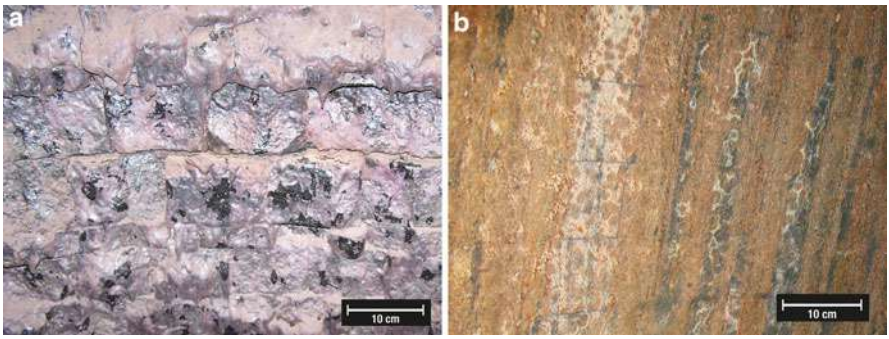

Fig. 6 Air-cooled slagging gasifier refractory wear as seen from the gasifier interior. (**a**) Typical surface wear on conventional refractory materials caused by slag and (**b**) refractory wear in newly developed liner materials

refractory-lined walls, which reduce heat losses, thereby increasing process efficiencies, but require maintenance and servicing. Examples of both types of technologies are available (see below).

The failure of a refractory lining in a slagging gasifier causes gasifiers to be shut down for repair or replacement, a process that can take 1–3 weeks, depending on the extent of repairs needed. Failure can be one or more bricks and occurs because of excessive heat transfer to the steel containment vessel (see Fig. 5). Much of the focus of laboratory research has been on the air-cooled slagging gasifiers because of the shorter service life of refractory liner materials versus the longer life of the cooling screen design materials (about 3 years of service life versus approximately 8 years for cooling screen designs). Examples of the refractory lining wear in air-cooled gasifier refractory lining are shown in Fig. 6. Note the cobbled or rough surface appearance on the hot face refractory surfaces in the gasification chamber that occurs on the surface of traditionally used refractory materials (Fig. 6a) versus the smoother surface of newer formulations of refractory materials being put into service (shown in Fig. 6b). The rough surface is caused by slag penetration into the porous refractory materials leading to a process called spalling, where surface sections of the refractory material spall off in chunks, accelerating material wear. Spalling wear causes the rough surface visible in Fig. 6a and has nearly been eliminated by newer types of refractories, as shown in the image in Fig. 6b. Spalling in a cross section of a refractory is shown in Fig. 7a and is caused by slag penetration into refractory pores, with thermal cycling or continued slag penetration leading to thermal expansion mismatches, causing stress cracking of the refractory to occur parallel to the hot face. It is a repetitive process that removes portions of the refractory lining surface, as shown in Fig. 7b, accelerating refractory wear caused by refractory dissolution.

The general types of refractory liner materials used in slagging gasifiers are shown in Table 5, with newly developed spalling-resistant materials containing phosphate additives. It is worth noting that refractory wear is not caused by one or two material interactions, but can be caused by a number of issues, as shown in

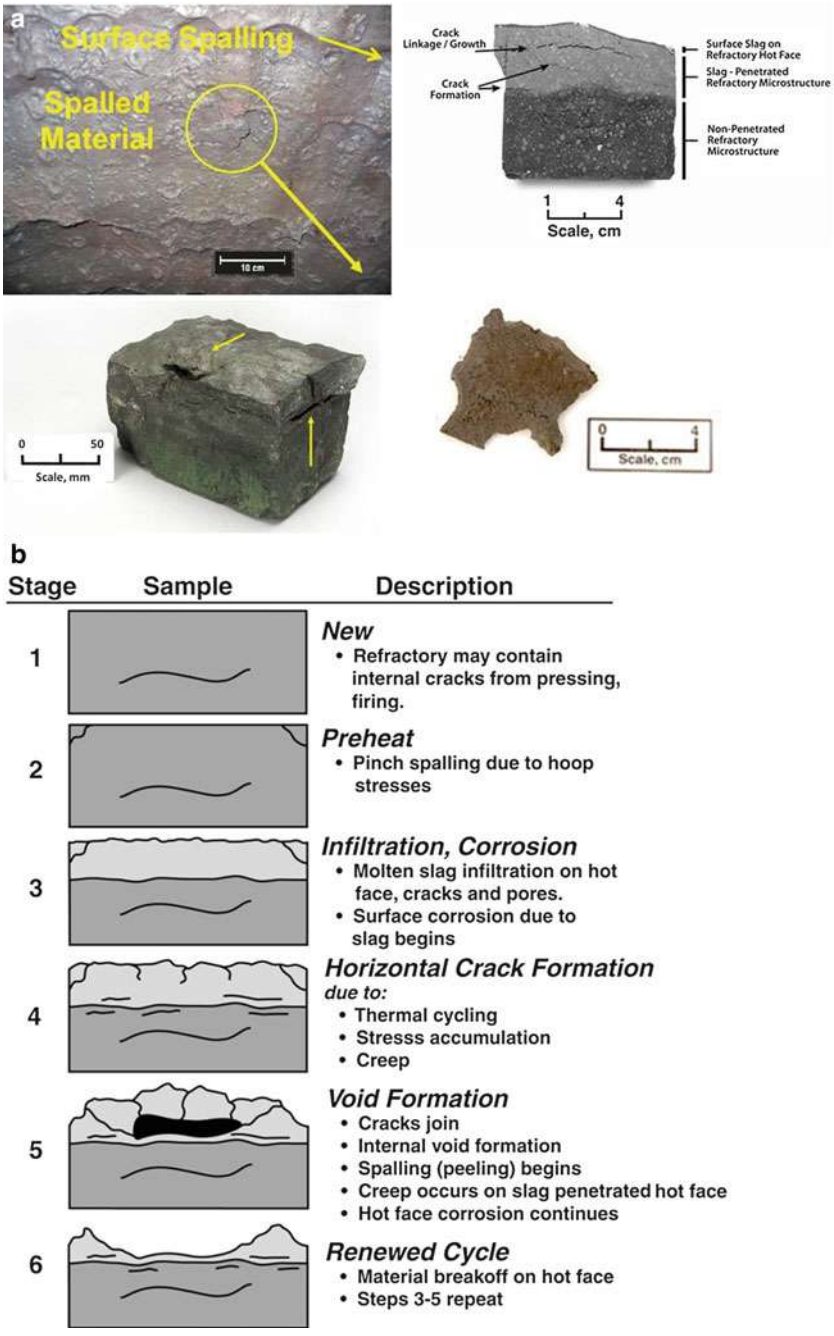

Fig. 7 Refractory spalling occurring within a used refractory brick (**a**) and an illustration as to how the process reoccurs during gasifier operation (**b**)

Table 5 Chemical and physical properties of gasifier refractory materials used in the highest wear area of a gasifier

Chemistry (wt %)[a]	Brick type		
	A	B	C
Cr_2O_3	89.0	87.3	92.0
Al_2O_3	10.2	2.5	4.7
ZrO_2	NR	5.2	NR
P_2O_5	NR	NR	3.3
Bulk density[a] (gm/cm^3)	4.21	4.07	4.23
Porosity[a] (vol %)	16.7	16.5	15.0
CCS[a] (MPa)	48.3	66.9	51.7

NR not reported, *CCS* cold compressive strength
[a]Data from manufacturer's technical data sheets

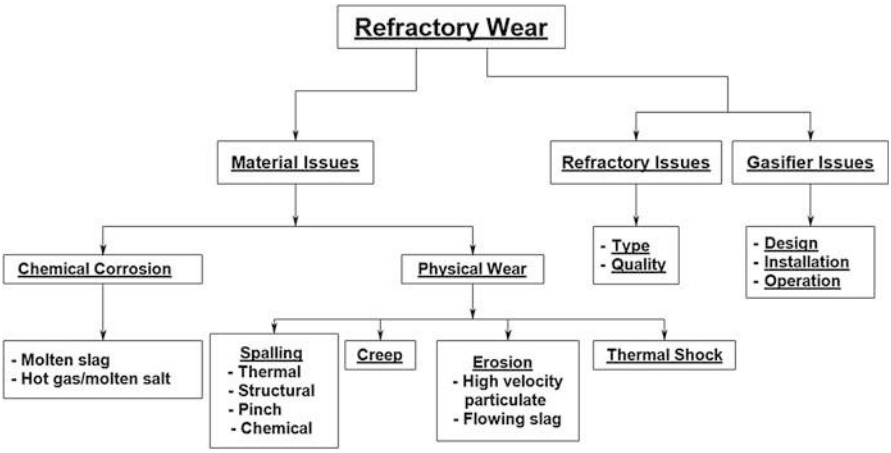

Fig. 8 A breakdown as to the possible causes of refractory wear during carbon feedstock gasification

Fig. 8. Along with spalling, chemical dissolution of a refractory material is also a major cause of refractory liner wear and leads to the gradual dissolution of a refractory lining into the slag flowing on the brick surface. Interactions between the slag and the refractory can lead to mineral phases being created on the refractory surface, which impact and slow the dissolution process. Because chrome oxide forms high-melting mineral phases with oxide components such as iron in slag, the dissolution of a high chrome oxide lining into slag occurs slowly compared to most other materials considered for use in a gasifier. Phases that form on a refractory surface when exposed to a coal slag are shown in Fig. 9 and are the core reason why chrome oxide has superior performance over other refractory oxides in the gasification environment. Note the solid solution spinel layer of $(Fe,Mg)(Al,Cr)_2O_4$ on the refractory surface and the formation of $(Fe,Mg)(Cr,Al)_2O_4$ forming on the surface of the chrome oxide grain. Both materials have high melting points and slow dissolution in the slag. These changes in mineral compositions at different

a

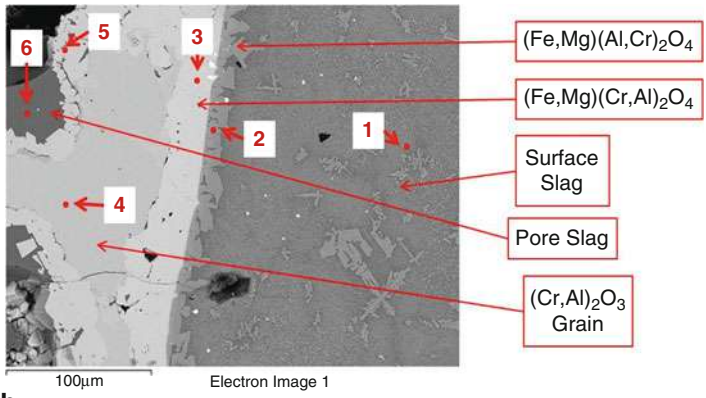

b

Point	Element (wt %)							
	Si	Al	Cr	Fe	Ca	Mg	K	P
1	23.8	7.9	ND	20.8	3.1	0.3	2.2	ND
2	0.2	24.5	7.1	33.6	ND	1.6	ND	ND
3	ND	2.1	37.3	30.7	ND	0.5	ND	ND
4	ND	3.7	57.5	ND	ND	ND	ND	ND
5	ND	4.8	35.0	31.1	ND	0.7	ND	ND
6	33.8	9.2	ND	1.2	0.8	ND	5.1	0.9

ND = Not Detectable

Fig. 9 Surface interactions between a high chrome oxide refractory and a coal slag during gasification as analyzed by SEM in backscatter mode (**a**) and elemental analysis by EDAX (**b**) for points indicated in (**a**)

locations can be discerned using the powerful combination of scanning electron microscopy (SEM) and energy-dispersive spectroscopy (EDS).

Besides ways to reduce refractory wear through the development of new or improved performance materials, research is evaluating how to control slag chemistry to reduce refractory wear. Slag chemistry can be managed by blending carbon feedstock, using of additives such as MgO, or changing the refractory liner to be more chemically compatible with the slag. The impact of changing slag chemistry must take into consideration viscosity changes, which has made this approach difficult.

Gasification Versus Combustion

Gasification and combustion can essentially be considered as two ends of a continuum for reactions of coal and oxygen, where water can be added as a reactant to

Table 6 Gasification and combustion chemistry

Reaction process	Chemical formula	Change in enthalpy
Gasification with oxygen	$C + ½O_2 \rightarrow CO$	−9,123 kJ/kg C
Combustion with oxygen	$C + O_2 \rightarrow CO_2$	−32,822 kJ/kg C
Gasification with carbon dioxide	$C + CO_2 \rightarrow 2CO$	14,577 kJ/kg C
Gasification with steam	$C + H_2O \rightarrow CO + H_2$	11,048 kJ/kg C
Gasification with hydrogen	$C + 2H_2 \rightarrow CH_4$	−6,215 kJ/kg C
Water-gas shift	$CO + H_2O \rightarrow CO_2 + H_2$	−1,512 kJ/kg CO
Methanation	$CO + 3H_2 \rightarrow CH_4 + H_2O$	−7,399 kJ/kg CO

increase the H_2 content of the products. Table 6 is a list of the most significant reactions and the enthalpy change associated with each of these reactions with respect to weight of carbon or carbon monoxide. Looking at the first two reactions in the table, it is seen that coal denoted here with a C for carbon is reacted with one oxygen atom denoted here as 1/2 O_2 to get carbon monoxide and with two oxygen atoms (2) to get carbon dioxide. In reality, this second reaction is not a one-step process as the solid-phase carbon reacts with one oxygen atom to produce carbon monoxide which then reacts with the second oxygen atom to form carbon dioxide. All of the reactions in the table are exothermic except the two reactions identified as gasification with steam and gasification with carbon dioxide. These two endothermic reactions are the reactions that are most often referred to as gasification, where the solid carbon is turned into a reactive gas through a reaction with a "nonreactive" gas (H_2O or CO_2). In addition to these two reactions being endothermic, they also require high temperatures to proceed.

In Table 7 combustion and gasification are compared and contrasted. Combustion is referred to as full oxidation and gasification as partial oxidation. Combustion occurs in an oxidizing (excess oxygen) environment, and gasification occurs in a reducing (oxygen-depleted) environment. For power production, gasification using a gas turbine is more efficient and has lower emissions and competitive capital costs compared to combustion. With respect to the competitiveness of the cost, it is the cost of electricity that is nearly the same for both technologies; the higher capital cost of gasification is offset by the improved efficiency. Combustion is the dominant power-producing technology in the world and as such has lower risk with demonstrated reliability.

Integrated Gasification Combined Cycle

IGCC plants as shown in Fig. 10 convert carbonaceous fuels/materials into electricity and could be considered first-generation plants – those not requiring CO_2 separation or sequestration. In these plants, the carbon-containing material is fed to the gasifier along with oxygen and steam to produce the raw syngas. The raw syngas is cleaned of particulate matter and sulfur. The clean syngas is fed to the

Table 7 Contrasts between combustion and gasification (U.S. Department of Energy 2009)

	Combustion	Gasification
Chemical process	Full oxidation	Partial oxidation
Chemical environment	Excess oxygen (air) – oxidizing	Oxygen starved – reducing
Primary product	Heat (e.g., steam)	Syngas (CO and H_2)
"Downstream" products	Electric power	Electric power, pure H_2, liquid fuels, chemicals
Current application	Dominates coal-fired power generation worldwide	Mostly chemicals and fuels, power generation demonstrated
Efficiency	35–37 % (HHV[a])	39–42 % HHV[a]
Emissions	~NSPS[b]	~1/10 NSPS[b]
Capital cost	$1,000–1,150 /kW	Competitive
Maturity/risk	High experience, low risk	Reliability needs to be improved

[a]HHV is the high heating value or gross calorific value as determined by bringing all the products of combustion back to the original precombustion temperature and condensing any water vapor produced
[b]NSPS is the new source performance standards

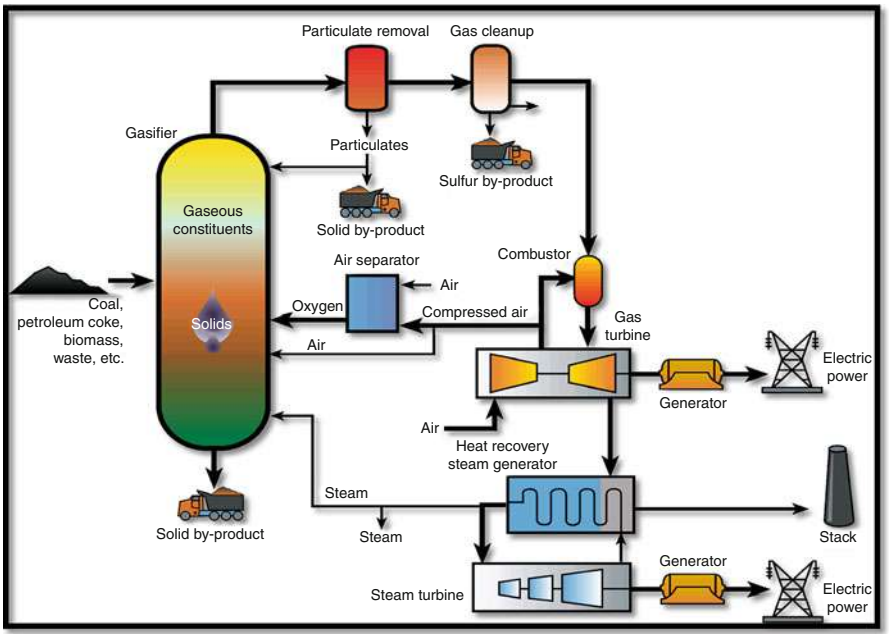

Fig. 10 IGCC system without carbon capture (U.S. Department of Energy 2009)

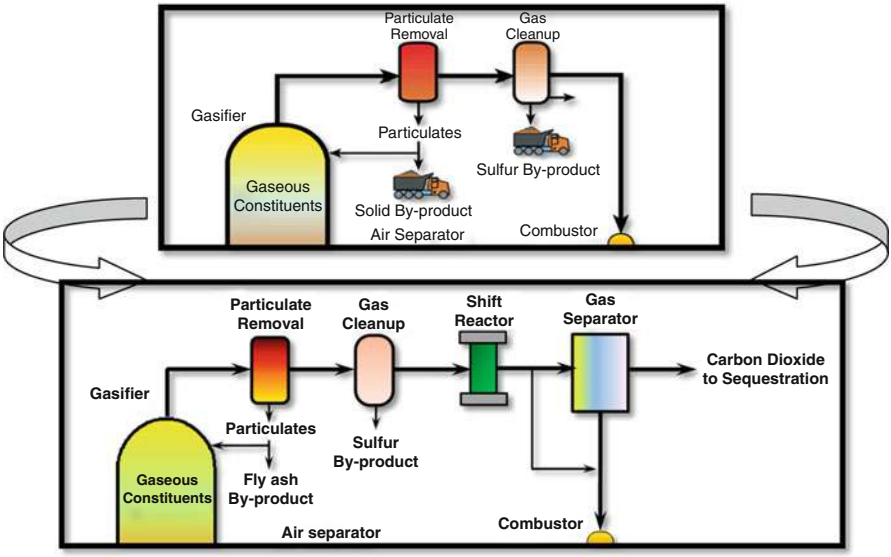

Fig. 11 Changes in the downstream IGCC process flow schematic with carbon capture (U.S. Department of Energy 2009)

combustion turbine with the products going to a heat recovery steam generator and steam turbine.

IGCC systems with carbon capture (Massey 1979) are similar to IGCC systems without carbon capture as can be seen by comparing Figs. 10 and 11. In Fig. 11 the IGCC system is shown with precombustion capture of the carbon for sequestration. The primary difference between the two processes is that the clean syngas passes through a shift reactor and an absorption tower to remove the carbon in the form of carbon dioxide. The shift reactor converts the CO in the syngas by reacting it with water over a catalyst to form H_2 and CO_2 with the latter going to sequestration.

A conceptual poly-generation IGCC plant (one that generates multiple products) is depicted in Fig. 12. In this concept, the clean syngas is shifted to change the CO/H_2 ratio. A partial shift adjusts the ratio to be comparable to the end hydrocarbon product being synthesized. If power is being made as the product, the gas stream will undergo a full shift.

Gasification Processes

Gasifiers fall into four primary configurations: moving bed, fluidized bed, entrained flow, and transport as shown in Fig. 13. Each of these is defined based upon how the reactor brings about contact with the coal and the reactive gas. The gas and solid (coal particle) temperature differs dramatically as they traverse through the gasifier. In a typical moving-bed gasifier designed for coal, the solids are loaded into the top

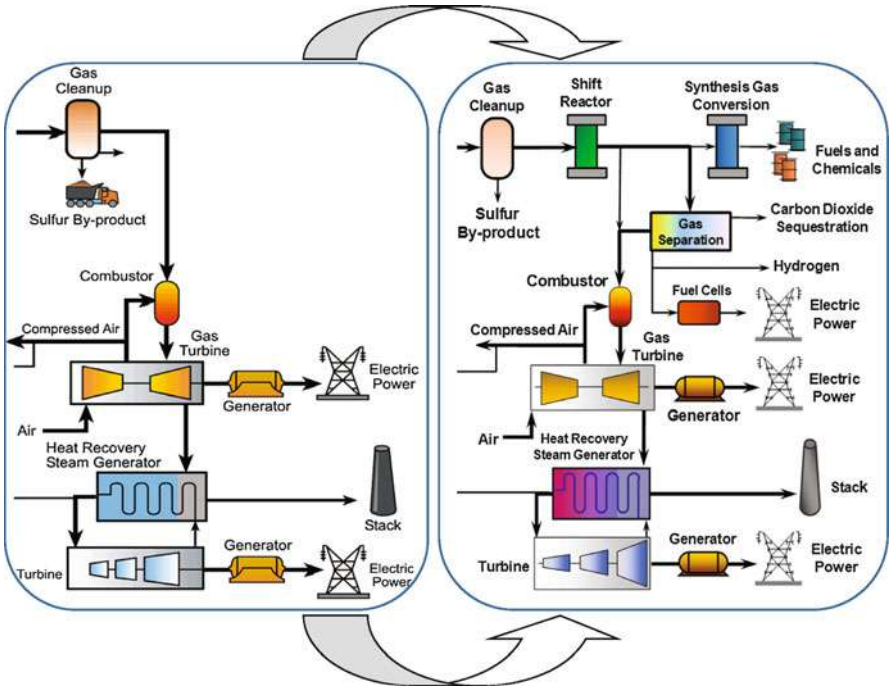

Fig. 12 Changes in the downstream IGCC process flow schematic for a poly-generation plant (U.S. Department of Energy 2009)

of the gasifier and move slowly down in a packed moving bed as the coal below is consumed and converted to gas. The oxidant gas is introduced in the bottom of the gasifier gases and the settling coal char and ash. After gasification reactions slow due to dropping gas temperatures, the product gas still holds sufficient sensible heat to pyrolyze, dry, and preheat the coal before it exits the reactor at a relatively low temperature. The sensible heat is the heat absorbed or evolved by a substance solely due to a change in temperature. The greatest part of time in the moving-bed gasifier is spent in this drying, heat-up, and pyrolysis region of the gasifier as is apparent by the long thermal heat up portrayed in Fig. 13. The volatile matter released during devolatilization undergoes a vaporization and condensation depending on the volatility of the tars which results in some secondary cracking but ultimately results in the production of significant quantities of tars in the product stream.

For very high-volatile matter coals and biomass, an alternative cocurrent configuration is often preferred to reduce the quantity of complex tar products. In this configuration the oxidizing gases are primarily introduced along with the coal at the top of the gasifier and product gas withdrawn at the bottom along with the solid waste. The result is twofold: the tars must traverse through the combustion zone and are cracked and partially combusted, and the product gas temperature is relatively high similar to the fluidized-bed gasifiers.

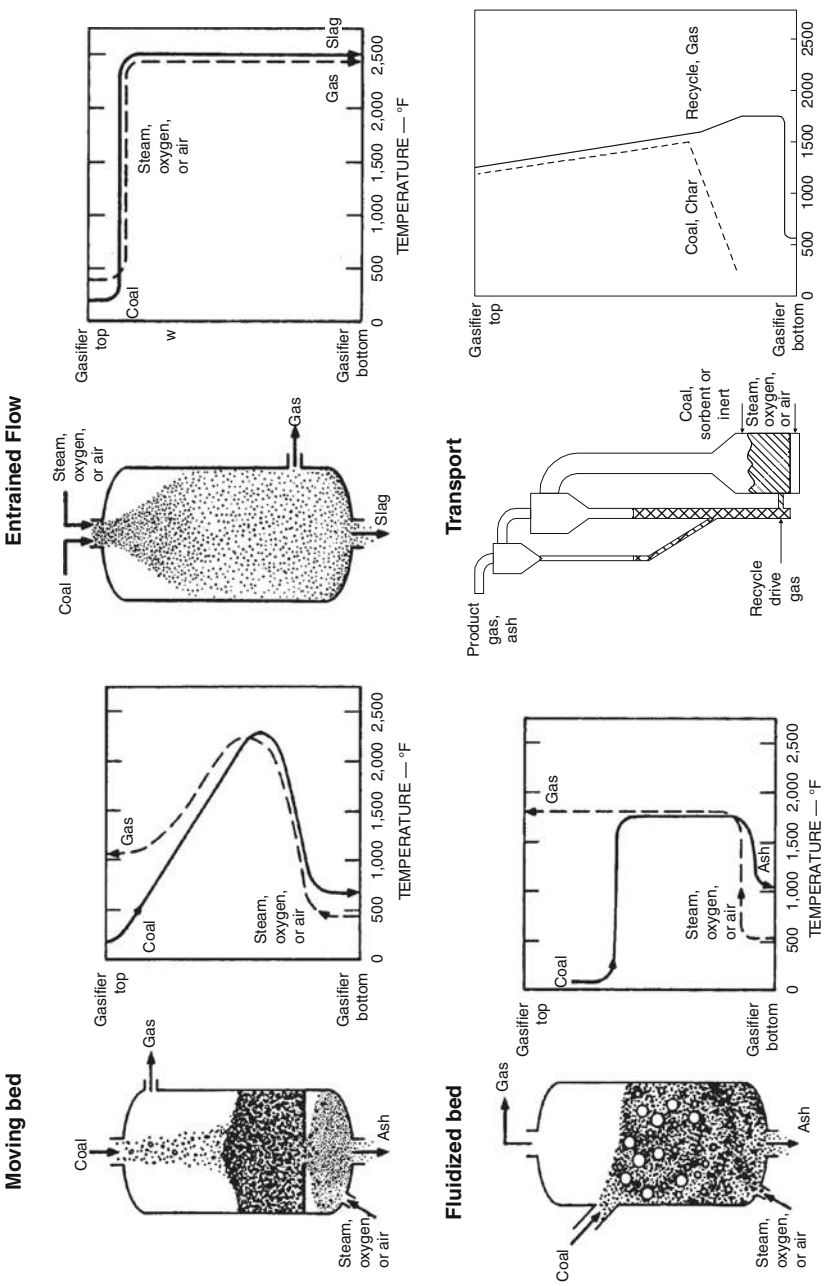

Fig. 13 Four basic coal gasifier types (U.S. Department of Energy 2009)

In a fluidized-bed gasifier, the oxidant gas is introduced at the bottom with sufficient flow and velocity to support the weight of the entire inventory of coal, char, and ash or sorbents. The coal may be introduced at the top or deeper into the fluidized bed to reduce the amount and vapor pressure of tars. Both are heated rapidly to gasification temperatures near 1000 °C and mixed thoroughly approaching the performance of a stirred-tank reactor. The inventory is sufficient to obtain 10–30 min solid residence time. Pyrolysis, combustion, and gasification reactions take place throughout the reactor. The solids may be taken off either through an overflow stream or an underflow removal system depending on process concept goals. The product gas is removed off of the top at process temperature and must be cooled and any entrained fines removed. Due to the mixing, large solid surface area, and relatively low temperatures, the product gases are richer in hydrocarbons from the cracking of tars and relatively high CO/CO_2 ratio. The solids are withdrawn at low temperatures below mineral melting temperatures, dry, either from the top of the reactor to be sent to a combustor for complete conversion or from the bottom as a mineral enriched solid waste as shown in Fig. 13.

An entrained gasifier may be upflow or downflow, but it is dilute cocurrent flow with both coal and oxidant gas moving in the same direction rapidly approaching 1500 °C (Fig. 13). The coal spends less than 10 s residence time, and all minerals are melted and removed from the gasifier as molten slag. In that time the coal particle must be dried, heated, pyrolyzed, and then combusted and gasified in essentially a plug flow reactor. The product gas exits the gasifier at these high reaction temperatures and must be quenched either directly or indirectly in order to further clean by removing particulates and then sulfur and other acid gases.

The transport gasifier is a blending of the fluidized-bed and entrained-bed gasifiers with the oxidant entering the gasifier at the very bottom with recycle solids and unreacted coal char. The concept is to deplete all the oxygen prior to adding the coal. The coal is rapidly dried, heated, and pyrolyzed and gasified with steam. The product gas exits the gasifier after 3–10 s, but the tars are cracked over the high loading of hot mineral surface area. The char and inert minerals in the transport gasifier experience internal mixing spending 10–50 s residence time. These solids are captured using two stages of disengagers and/or cyclones, excess solids are extracted and cooled, but the bulk of the solids are recycled back into the transport reactor to maintain process temperature, avoid agglomeration, and assist cracking of low-volatile hydrocarbons.

A comparison of the four basic gasifier types is presented in Table 8. The moving-/fixed-bed gasifier category refers to the Lurgi Mark IV (dry bottom) and the British Gas/Lurgi (slagging) with both having dry coal feed systems. These are both countercurrent flow systems which operate principally as plug flow reactors. There are three principal entrained-flow gasifiers produced by ConocoPhillips, General Electric, and Shell. The Shell unit is a dry feed gasifier whereas the ConocoPhillips and the General Electric are slurry-fed gasifiers. The moving-bed gasifiers utilize coarsely crushed coal and require the long residence times as a result, while the entrained-flow reactor uses finely crushed coal and the residence

Table 8 Comparison of salient features for each of the four different gasifier types

	Moving bed		Fluidized bed		Entrained flow	Transport flow
Ash condition	Dry	Slagging	Dry	Agglomerate	Slagging	Dry
Coal Feed	~2 in	~ 2 in	~ ¼ in	~ ¼ in	100 mesh	~ 1/16 in
Fines	Limited	Better than dry ash	Good	Better	Unlimited	Better
Coal rank	Low	High	Low	Any	Any for dry feed	Any
Oxidant req.	Low	Low	Moderate	Moderate	High	Moderate
Steam req.	High	Low	Moderate	Moderate	Low	Moderate
Issues	Fines and hydrocarbon liquids		Carbon conversion		Raw gas cooling	Control carbon inventory and carryover

times are correspondingly short. On the other hand, the fluidized-bed and the transport gasifiers are dry fed and non-slagging gasifiers. These are well-mixed reactors operating with lower peak temperatures than the plug flow reactors. These gasifiers have coal residence intermediate between the moving-bed and the entrained gasifier and thus utilize intermediate particle sizes. Each of these four gasifier types has process options which make it possible to gasify any coal types. The moving bed is the most efficient and thus requires the least oxidant, while the entrained gasifier has the greatest coal throughput (feed rate per cross-sectional area). The transport gasifier was developed in order to maximize coal throughput while utilizing lower-quality feedstocks which are unattractive in entrained gasifiers. The issues associated with each gasifier type are also listed in Table 8.

Fixed-/Moving-Bed Gasifiers

A sketch of the fixed-/moving-bed gasifiers is shown in Fig. 14. Lurgi produces the non-slagging unit of this type, while British Gas designed the slagging version of this technology, often referred to as the British Gas/Lurgi (BGL). These units are both countercurrent flows and are characterized by very high combustion zone temperatures and low gas and solid exit temperatures. The high combustion temperatures provide the thermal energy required to drive the highly endothermic gasification reactions located immediately above. The reactor configuration effectively recoups the sensible energy in the gas by exchanging the heat with the incoming coal in the devolatilization and coal drying zones giving these gasifiers the highest cold gas efficiency of any of

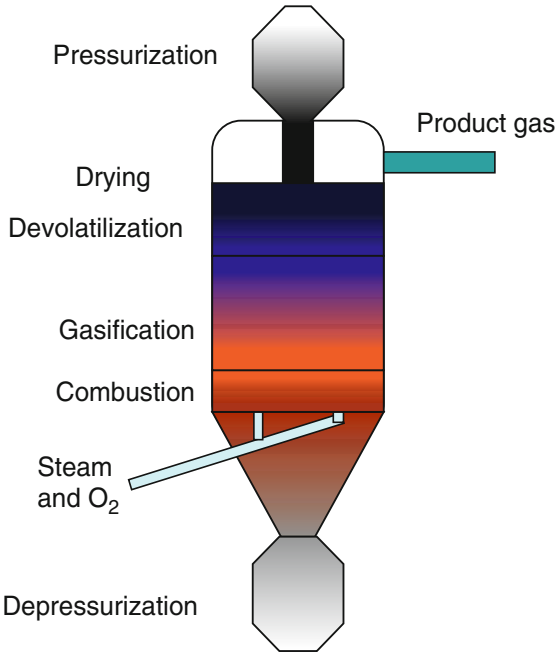

Fig. 14 Typical configuration for dry and slagging moving bed

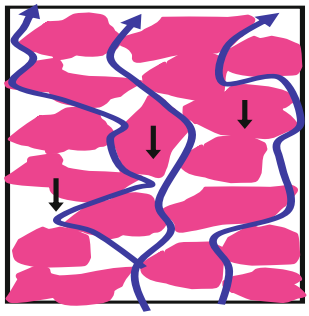

Fig. 15 Moving-bed gas-solid flow patterns

the gasifier types. As a result, however, the product gas contains hydrocarbons, tar, and water released in the devolatilization and drying zones of the gasifier.

Hydrodynamically, the reactors resemble flow through a porous medium as shown in Fig. 15. Although in this gasifier, the continuous (gas) and the discrete (solids) phases flow countercurrently, i.e. the solids move down while gas moves up. These types of reactors can be problematic due to nonuniform flow which may be a result of particles agglomerating and overpacking with fines. All of these issues lead to poor interphase mixing, unreacted carbon, hot spots, and lower conversion.

Kinetically, the moving bed is a low-temperature reactor operating in the kinetically controlled shrinking core reaction mode pictured in the sketch shown

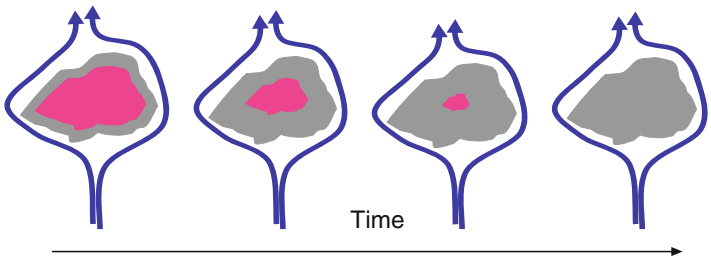

Fig. 16 Particle time history in moving bed showing the progressive conversion of unreacted coal (*red*) into char and ash (*gray*)

in Fig. 16. The burnout time or conversion time for a particle fed to the top of the gasifier is

$$\tau = \frac{2\rho_B R}{kC_{O_2}}$$

where: τ is the time for complete conversion, ρ_B is the coal particle density, 2 is 1/stoichiometric coefficient for O_2, R is the particle radius, k is the combined kinetic and mass transfer rate constant, and C is the concentration of O_2 (Levenspiel 1998).

Table 10 presents typical product gas compositions for air-blown operation of the Lurgi dry bottom configuration for subbituminous and bituminous coals. Lower-rank coals produce more CO_2 and hydrocarbons because of their lower heating value and higher volatile content. More process energy is required to provide sensible and latent heat for the lower-quality fuel, thereby driving the combustion reaction further to completion. Lower-rank coals have inherently greater oxygen content and release more carbon dioxide directly from pyrolysis. In addition, the lower-rank coal char is more reactive and thus reacts faster and so maintains a lower process temperature producing a greater relative proportion of CO_2/CO.

Typical product compositions are provided in both Tables 9 and 10.

A study of the relative impact of different process parameters for a moving-bed gasifier was reported by Monazam and Shadle (Monazam et al. 1998; Shadle et al. 2001). A plug flow model was developed including mass and energy balances for the major gas and solid product streams during devolatilization, gasification, and combustion of coal. Then a sensitivity study was conducted on each of the operating and design parameters for the gasifier when operated under a given coal feed rate. The base conditions are presented in Table 11. The average responses and normalized response factors are summarized for each independent parameter in Table 12. As expected from review of the kinetic equations above, increased process pressures and gas velocities (air/coal) were the two most significant factors influencing (increasing) the rate of conversion or burning rate. Increased particle size resulted in slower conversion. Steam/air ratio was the most critical parameter impacting the temperature and gas composition over the range tested. Only variations in the efficiency factor had significant impact on the gas product quality.

Table 9 Typical product compositions for oxygen-blown moving-bed gasifiers (Lowry 1963; Elliot 1981; Stultz 1992)

Oxygen blown					
	Dry bottom moving bed				Slagging moving bed
Coal type	*Brown/lignite*	*Subbit*	*Bit*	*Anth*	*Bit*
Pressure, atm	up to 92	25	24–100	~	21.0–32.0
Gas composition (dry)					
CO	17.4–19.7	15.1	15.2–19.5	22.1	55.0–61.2
CO_2	30.4–32.2	30.4	28.9–32.4	30.8	2.4–3.5
H_2	37.2–37.2	41.1	38.3–42.3	40.7	28.1–31.5
N_2	0.5–0.5	1.2	0.5–1.6	0.4	3.3–3.3
CH_4	11.8–12.1	11.7	8.6–10.1	5.6	5.0–8.3
H_2S	0.1	0.5	0.8–1.1	~	1.3–1.3

Table 10 Typical product compositions for air-blown moving-bed gasifiers (Lowry 1963; Huang et al. 2003)

Air blown		
Dry bottom moving bed		
Coal type	Subbit	Bit
Pressure, atm	20	1
Gas composition (vol % dry)		
CO	17.1–17.4	22.7–27.8
CO_2	14.8–14.8	5.9–6.3
H_2	23.3–23.3	16.2–16.6
N_2	38.5–38.5	48–50.5
CH_4	5.1–5.8	1.7–3.6
H_2S	0.2–0.2	0–0

Table 11 Base conditions used for the sensitivity study (Monazam et al. 1998; Shadle et al. 2001)

P	Pressure, kPa	2850
d_p	Particle size, cm	0.5
S/A	Steam/air ratio	0.2
T_o	Initial temperature, K	920
T_{og}	Inlet gas temperature, K	590
V_g	Gas superficial velocity, cm/s	3.0
D	Bed diameter, cm	30
L	Bed depth, cm	66

Examples of Fixed-Bed Gasifiers

British Gas/Lurgi (BGL)

The British Gas/Lurgi gasifier shown in Fig. 17 is a "slagging" version of Lurgi gasifier. The BGL gasifier was developed by British Gas during the period from

Table 12 The relative importance (dimensionless) of each of the operating parameters on performance variables in the gasifier general linear model (Monazam et al. 1998; Shadle et al. 2001)

Independent parameters:		V_g (cm/s)	Inlet T^o_g(K)	Stm./air	D_p(cm)	ε	L(cm)	η	P (kPa)
Range:		1.5–4.6	533–645	0.1–0.4	0.35–0.8	0.4–0.6	33–132	0.5–100	1400–4300
Dep. var.	**Base:**	3.0	589	0.2	0.48	0.5	66.0	1.0	2860
CO (%V)	25.7	−0.06	0.09	−0.77	−.083	−0.027	0.11	0.13	0.0
CO_2 (%V)	7.3	0.0	−.153	1.48	0.0	0.04	−0.044	−0.13	0.0
H_2 (%V)	14.8	−0.105	0.041	0.59	−0.067	−0.027	0.135	0.18	−0.078
H_2O (%V)	4.4	0.46	−0.23	2.96	0.28	0.114	−0.57	−0.07	0.26
Burning rate (kg/h)	31.1	0.86	−0.065	0.0	−0.25	−0.05	0.0	0.0	0.89
Comb. length (cm)	30.5	1.0	−0.17	0.18	1.5	0.2	0.0	0.190	0.91
$T_{s,Max.}$ (K)	1352	−0.007	0.03	−0.21	−.069	0.004	0.0	−0.21	−0.064
$T_{g,Out}$ (K)	1106	0.133	−0.004	−0.114	0.04	0.014	−0.132	−0.2	0.092

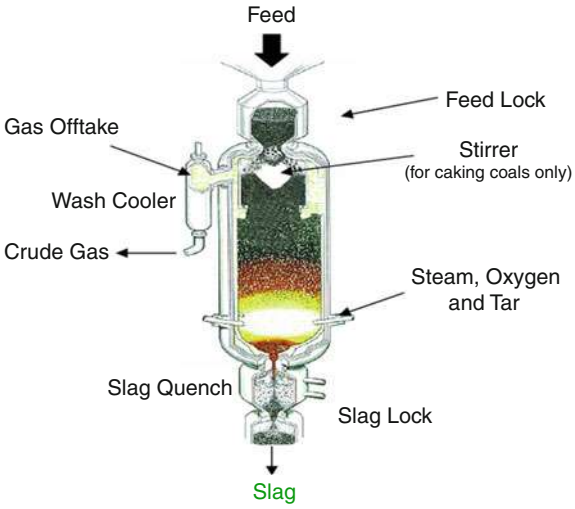

Fig. 17 British Gas/Lurgi gasifier (U.S. Department of Energy 2009) where ASC/SVC-type feed system was that developed by Allied Syngas Corporation (ASC) at the Sekundarrohstoff-Verwertungszentrum Schwarze Pumpe (SVZ) waste recycle plant in Saxony, Germany

1958 to 1965 at the Gas Council Midlands Research Station where it operated 4 m gasifier, 380 kg/h (Seed et al. 2007). It is a dry feed, oxygen-blown, refractory-lined gasifier. It is good for a wide range of coals including opportunity fuel blends with RDF (refuse derived fuel), tires, and wood waste. It is a modular design by Allied Syngas which will build, own, and operate it in North America. A 19,000 kg/h demonstration plant operated from 1986 to 1990. And the first commercial plant at Schwarze Pumpe operated 2000–2005.

Multipurpose Gasifier (MPG)

Lurgi developed the MPG technology shown in Fig. 18 based on its fixed-bed gasification process. It is an oxygen-blown, down-fired, refractory-lined gasifier good for a wide range of feedstocks including petroleum coke (petcoke) and coal slurries as well as waste. It operates in a quench configuration for coal/petcoke feedstocks. Lurgi demonstrated a "reference plant" at Schwarze Pumpe which has been in operation since 1968.

Lurgi Mark IV Gasifier

The Lurgi Mark IV gasifier is an extension of the original proven moving-bed Lurgi gasifier. As shown in Fig. 19, it has a dry feed system with lock hoppers to provide the pressure seal. It is an oxygen-blown, dry bottom gasifier. There is extensive experience worldwide with low-rank coals. There are eight plants operating worldwide including one in North Dakota producing 18,600 MW_{th} syngas in 14 gasifiers. The plant has two trains of seven gasifiers each. It was originally designed to have one unit as a spare in each train. Operating all seven gasifiers has improved the plant's economic performance.

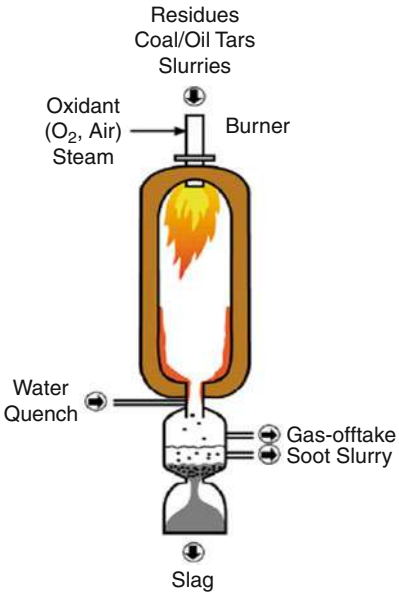

Fig. 18 Lurgi multipurpose gasifier (U.S. Department of Energy 2009)

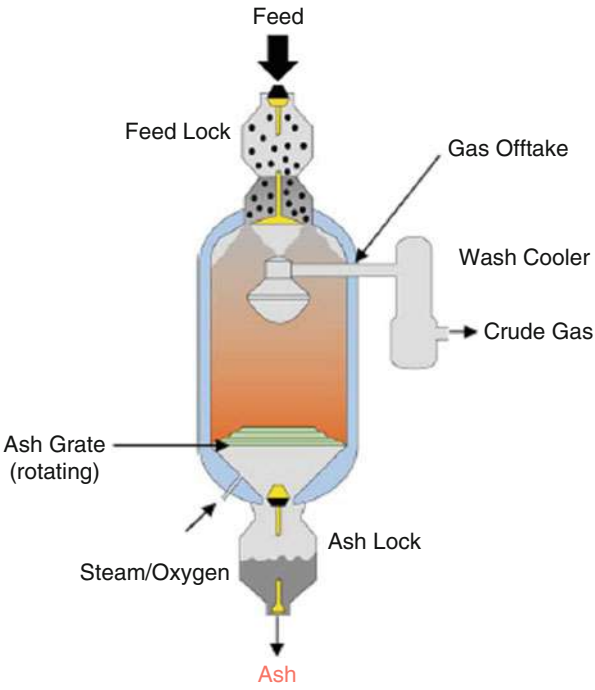

Fig. 19 Lurgi Mark IV gasifier (U.S. Department of Energy 2009)

Plasma Gasification

Plasma gasification is an electrically heated gasifier utilizing a plasma, generated by passing air through electric arcs in plasma torches, to create a very high-temperature (~5,000 °C) gasification environment. Figure 20 depicts an example, Westinghouse Plasma Corporation's plasma gasifier (Summary of Qualifications and Westinghouse Plasma Gasification Technology 2013). Feedstock (coal, biomass, solid water, etc.) is added to the gasifier along with air or oxygen, which descends through the vessel essentially in a moving-bed configuration, reaching an injected plasma zone. The extremely high temperatures and relatively long residence time allow complete conversion of the feedstock, even otherwise difficult to convert materials such as high-moisture biomass feedstocks and sludge, and municipal and industrial wastes containing high amounts of inerts such as glass and metal. The high operation temperatures produce syngas devoid of tars and hydrocarbons and convert inerts into slag, similar to the results of entrained-flow gasifiers. Furthermore, this is accomplished without the strict requirements on feedstock preparation and quality associated with entrained-flow gasifiers.

Many commercial instances of plasma gasification involve destruction of hazardous wastes. Unlike conventional incineration, hazardous constituents are completely converted in the extreme gasification conditions, making this an effective option for these and other more difficult to manage municipal, commercial, industrial, and medical wastes. Plasma gasification's great versatility to handle almost any type of carbonaceous feedstock with little or no pretreatment is

Fig. 20 Westinghouse plasma corporation gasifier (Summary of Qualifications and Westinghouse Plasma Gasification Technology 2013)

considered its main advantage. On the other hand, plasma gasifiers have high operating costs (due to electricity use) and initial capital investment. Also, these gasifiers are operated at ambient or slightly negative pressure, which may be considered a limitation in some process contexts.

Fluidized-Bed Gasifiers

Figure 21 represents a typical configuration of a fluidized-bed gasifier. Operating in the fluidized-bed mode, these reactors are very well mixed. All processes take place simultaneously throughout the bed. Lime, limestone, or dolomite can be added for in-bed sulfur removal. The requirement to capture sulfur can limit the maximum temperature in these gasifiers to about 1273 K or less which also keeps the ash from slagging. Gasification kinetics determines bed volume and the fluidization velocity determines cross-sectional area such that the bed height is fixed. Tar is cracked in freeboard. The Gas Technology Institute's (GTI's) U-GAS® process and Winkler gasifier are examples of fluidized-bed gasifiers.

Hydrodynamically, fluidized beds are more complicated than fixed-bed reactors where bubbles of excess gas induce and promote mixing as shown in Fig. 22. The better mixing of gas and solids leads to better interphase transport and better

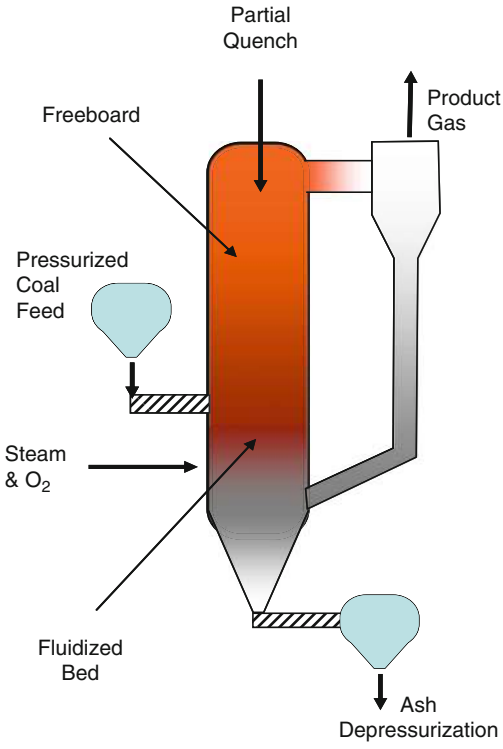

Fig. 21 Fluidized-bed gasifier concept

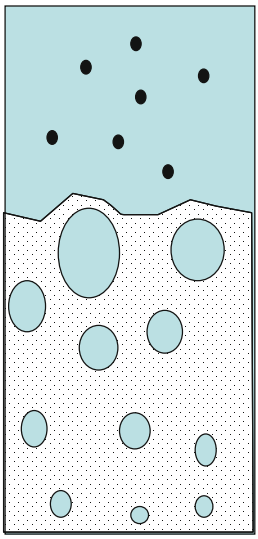

Fig. 22 Bubbling fluidized-bed hydrodynamics showing bubbles rising through denser emulsion phase and splashing particles and cluster in the freeboard

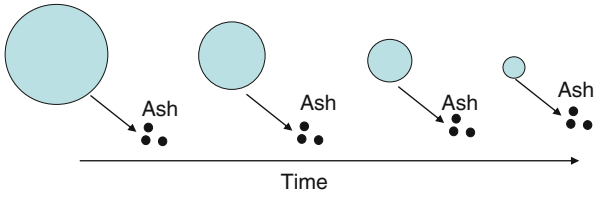

Fig. 23 Particle time history in fluidized bed depicting the reduction in size of a coal particle and release of ash due to mixing as conversion proceeds with time

conversion of the coal. In addition, the mechanical movement of the solids against each other essentially scrubs the ash from particles. Fluidized-bed gasifiers have been conceived with indirect heating due to the high heat transfer rates with heat exchange surfaces; however, the most successful processes have been directly heated. The reactors' performance approaches that of a continuous stirred process.

Kinetically, because of the scrubbing of the reacted layer, the burnout or conversion follows a shrinking particle as pictured in Fig. 23. The conversion time can be calculated from the equation

$$\tau = \frac{2\rho_B R}{kC_{O_2}}$$

where τ is the time for complete conversion, ρ_B is the cal particle density, 2 is 1/stoichiometric coefficient for O_2, R is the particle radius, k is the combined kinetic and mass transfer rate constant, and C is the concentration of O_2 (Levenspiel 1998).

Table 13 Gas composition for oxygen-blown fluidized-bed gasifiers (Lowry 1963; Elliot 1981; Stultz 1992; Huang et al. 2003)

Coal type	Lig	Bit
Pressure, atm	1.0–30.0	30.0
Gas composition (dry)		
CO	31–53.0	52.0
CO_2	6.7–19.5	5.3
H_2	32.8–40.0	37.3
N_2	0.3–1.7	0.3
CH_4	0.3–3.1	3.5
H_2S	0.44	

Table 14 Gas composition for air-blown fluidized-bed gasifiers (Elliot 1981; Stultz 1992; Huang et al. 2003)

Coal type	Lig	Bit
Pressure, atm	1	5–30
Gas composition (dry)		
CO	22.5	12.54–30.7
CO_2	7.7	6.4–14.47
H_2	12.6	14.4–28.56
N_2	55.7	47–54.3
CH_4	0.8	0.2–3.59
H_2S		

These units have moderate cold gas efficiencies and they accept a broad range of coals. Typical gas compositions are presented in Table 13 for oxygen-blown gasification in a fluidized bed when using lignite and bituminous coal. Table 14 presents air-blown gas composition data for the same coal types.

Examples of Fluidized-Bed Gasifiers

U-GAS®

The U-GAS(® process is a fluidized-bed gasifier incorporating a dry feed system as shown in Fig. 24. It can operate on all coals and coal/biomass blends. It is highly efficient in either the air- or oxygen-blown configuration producing a non-slagging/bottom ash. There is presently a 30-year license agreement with Synthesis Energy Systems (SES) in place. There is 20+ years of experience including plants in Shanghai, Finland, and Hawaii. Two plants are presently in operation producing 520 MW_{th} syngas.

High-Temperature Winkler Gasifier

The high-temperature Winkler gasifier, shown in Fig. 25, is a fluidized-bed gasifier utilizing a dry feed and operating either in the oxygen- or air-blown modes. It produces a dry bottom ash. It was developed to utilize lignite coal but is capable of efficiently gasifying a broad range of feedstocks. The R&D is complete and has been marketed for waste materials as the Uhde PreCon process. A demonstration

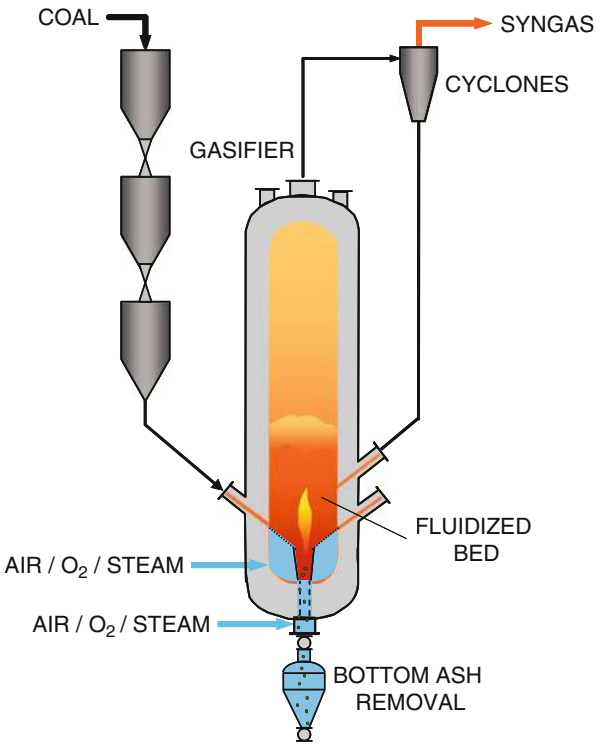

Fig. 24 U-GAS process (U.S. Department of Energy 2009)

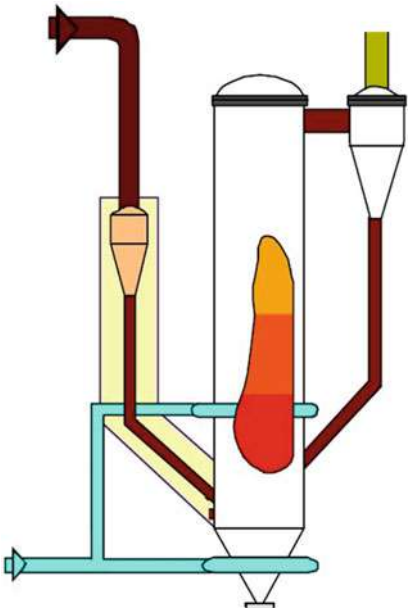

Fig. 25 High-temperature Winkler gasifier (U.S. Department of Energy 2009)

plant shut down in 1997. It under went 20 years of testing for 67,000 operating hours gasifying 1.6 million metric tons dry lignite to produce 800,000 metric tons methanol.

Entrained-Flow Gasifiers

There are seven entrained-flow gasifiers in the marketplace at this time. These are the ConocoPhillips E-Gas, GE (formerly Texaco), Shell, PRENFLO™, MHI, Siemens, and MPG gasifiers. A general sketch of these units is depicted in Fig. 26. In these gasifiers, widely dispersed very fine particles are radiantly heated to high temperature for slagging and rapid gasification. Some of the issues are obtaining uniform feed, slurry drying, and separation of gas production from the heat recovery. The volume is determined from conversion time for average particle. These units have a relatively low cold gas efficiency and high O_2 demand.

Hydrodynamically, entrained-flow gasifiers are quite simple with respect to the conversion of the coal particle and the reacting gas. They operate in a cocurrent manner with the solids and gas moving either in upflow or downflow as shown in Fig. 27 and are characterized as plug flow processes. The solid concentrations are less than 2 or 3 % by volume and they spend less than 10 s in the reactor. Nonuniform flow can occur which can lead to poor bulk mixing, unreacted carbon, and hot spots.

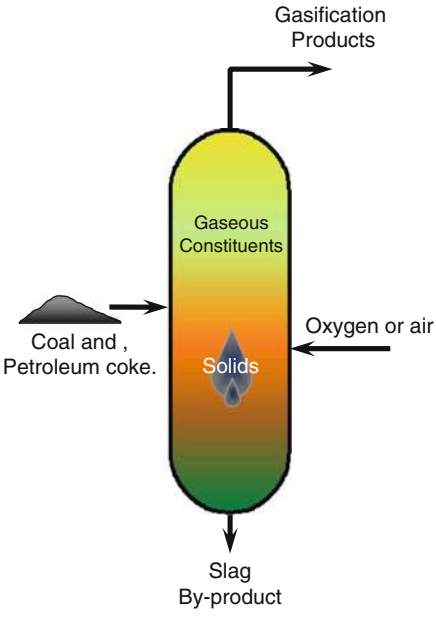

Fig. 26 Typical entrained-flow gasifier (U.S. Department of Energy 2009)

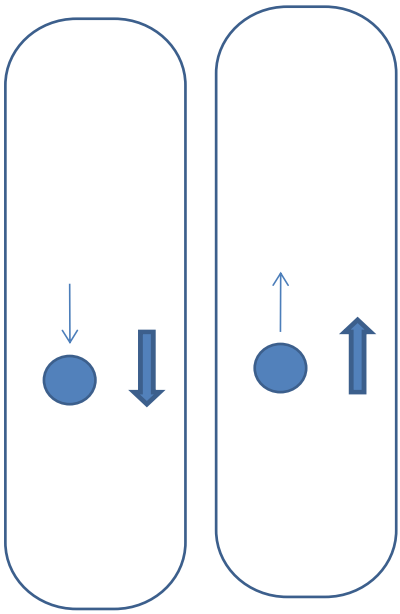

Fig. 27 Hydrodynamics for entrained-flow gasifiers showing coflow and countercurrent configurations

The conversion of a coal particle in an entrained-flow gasifier is shown in Fig. 28. The kinetic model to predict the burnout or total conversion of a coal particle in an entrained-flow gasifier is

$$\tau = \frac{2\rho_B R}{3k_g C_{O_2}}$$

where τ is the time for complete conversion, ρ_B is the coal particle density, 2 is the reciprocal of the stoichiometric coefficient for O_2, k_g is the mass transfer rate constant, and C is the concentration of O_2 (Levenspiel 1998).

These gasifiers can burn a fairly wide range of fuels when operated with a dry feed but are more limited when firing the fuel as a slurry since a large amount of energy is required to vaporize the water in the slurry. Typical gas compositions for these gasifiers are presented in Table 15.

The majority of particles flow from an entrained gasifier as slag; however, some portion remains airborne within the syngas and flows into the syngas coolers. Most large particulate material ends up in the quench chamber, where it is broken into small particulates and periodically removed from the gasifier. It is worth noting that the portion of the particulate remaining airborne during gasification flows with the raw syngas, where it can build up on the radiant or convective syngas cooler surfaces, solidifying on cooling surfaces and leading to a condition called fouling. Two types of entrained-flow slagging gasifiers using air-cooled sidewalls and syngas coolers are shown below in Figs. 31 and 32. Fouling from gasifier solid by-products in the radiant and convective syngas coolers caused by carbon

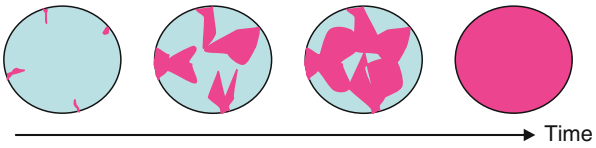

Fig. 28 Bulk diffusion-controlled conversion in entrained-flow gasifiers in which oxidant (*red*) penetrates through macropores and diffuses through the solid or coal matrix (*blue*)

Table 15 Typical gas composition for entrained-flow gasifiers (Stultz 1992; Huang et al. 2003)

Oxygen blown				
Gasifier	Dry entrained			Slurry entrained
Coal type	Brown/lignite	Subbit	Bit	Bit
Pressure, atm	30	30	25–30	42
Gas composition (dry)				
CO	62.01	64.48	61.53–64.97	49.46
CO_2	6.88	1.33	0.81–1.63	12.30
H_2	30.42	33.37	30.61–32.08	35.95
N_2	0.34	0.51	0.51–4.80	0.97
CH_4	0.00	0.00	0.00–0.00	0.36
H_2S	0.23	0.31	1.33–1.42	1.33

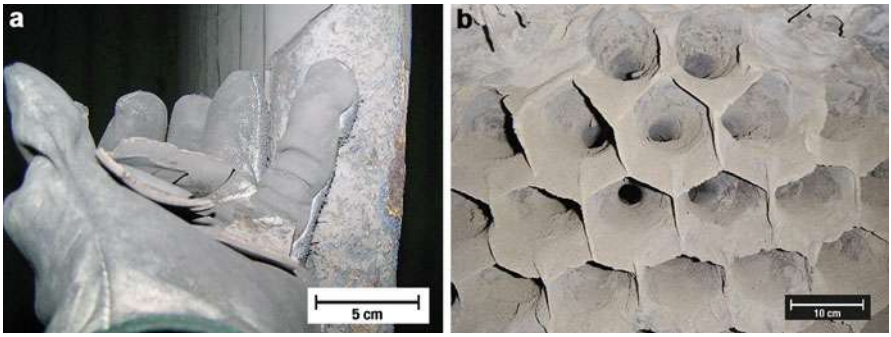

Fig. 29 Examples of fouling buildup caused by molten ash/slag and carbon char in the radiant (**a**) and convective (**b**) syngas coolers

feedstock in these types of convective coolers is shown in Fig. 29. Waste solid by-products for the most part do not remain airborne, instead flowing as slag or dropping from the syngas stream as large particles that are collected in the quench chamber where they are granulated and periodically removed from the gasifier. The appearance of that granulated waste is shown in Fig. 30 and is a mixture of ash, slag, and unburned carbon (called char).

There are two general types of entrained-bed gasifiers: those used in air-cooled systems (GE gasifier and CB&I design) and those using water cooling screen

Fig. 30 Solid waste (mixture of ash, slag, and carbon char) removed from an entrained-flow slagging gasifier during operation

designs (Shell, Siemens, MHI, and PRENFLO). Differences exist in each of the gasifier designs, but in general, those that are air cooled are slightly more efficient (Vassilev et al. 2002) than the water cooling screen designs. The refractory liners in air-cooled gasifiers are typically sintered brick that are high in oxides of chrome and aluminum and, depending on how the gasifier is operated, last from about 6–36 months, although in some gasifier types with newer materials such as those containing phosphates, the service life could be longer. Slagging gasifiers designed around cooling screens depend on the high conductivity of the refractory lining to limit refractory wear and maximize refractory service life, which can be 8 years or more. Lining material could be castable or plastic ram mixtures of SiC particles and alumina, which with water cooling on one side, would cause slag to solidify on the refractory surface, protecting it from corrosive wear. Linings of this type can operate 8 years or more before a lining needs replacement unless the refractory material separates from the cooling coils or the studs holding the refractory break, causing refractory material to rapidly fail.

Examples of Entrained-Bed Gasifiers

GE Energy

The GE Energy gasifier shown in Fig. 31 was initially developed by Texaco which became the Chevron-Texaco gasifier upon the merger of those two companies which eventually sold the technology to GE. The technology is a coal-water slurry-fed, oxygen-blown, entrained-flow, refractory-lined slagging gasifier. Two versions of the gasifier have been offered: gasifier with radiant cooler and a full-quench gasifier with the latter taking precedence currently. The gasifier is good for bituminous coal, petcoke (petroleum-derived coke), or blends of petcoke/low-rank coals. Commercially, GE Energy provides gasification technology in an EPC

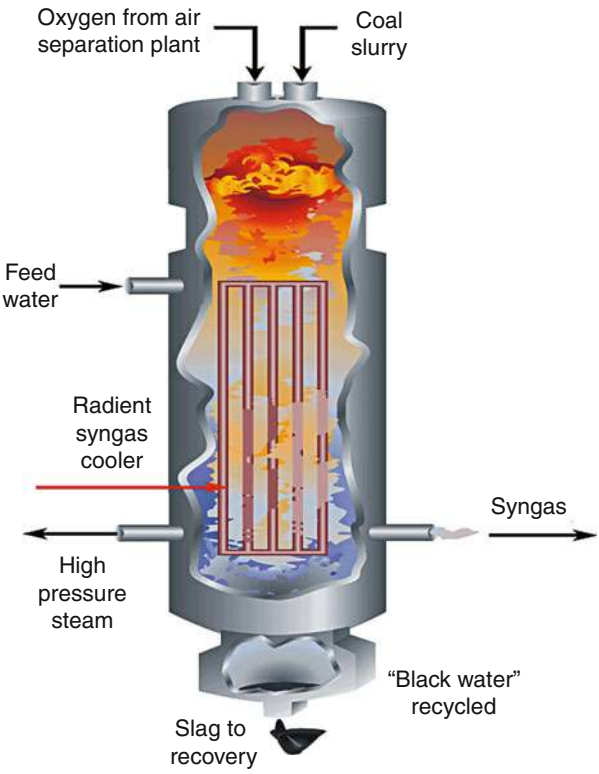

Fig. 31 GE Energy gasifier (U.S. Department of Energy 2009)

(engineer-procure-construct) alliance with Bechtel for guarantees on total IGCC plant. Presently, there are 64 plants operating, producing more than 15,000 MW_{th} syngas. There are six plants in the planning phases.

ConocoPhillips E-Gas

The ConocoPhillips E-Gas gasifier shown in Fig. 32 was originally developed by DOW Chemicals and demonstrated at the Louisiana Gasification Technology Inc. (LGTI) from 1987 through 1995. It is a two-stage gasifier with 80 % of feed to first stage (lower). The gasifier is coal-water slurry-fed, oxygen-blown, refractory-lined gasifier with continuous slag removal system and dry particulate removal. The E-Gas process is good for a wide range of coals, from petcoke to Powder River Basin (PRB) subbituminous coal to bituminous coal and blends. Commercially, ConocoPhillips provides gasification technology and process guarantee. Project-specific EPC and combined cycle supplier alliances provide balance of plant components and guarantees. There is one 590 MW_{th} syngas plant operating and six plants in planning.

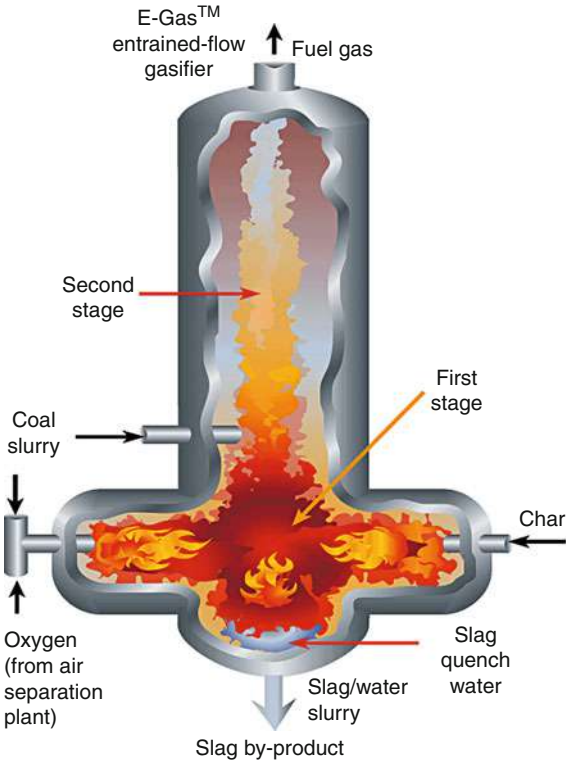

Fig. 32 CB&I ConocoPhillips E-Gas (U.S. Department of Energy 2009)

Shell

The Shell gasifier has its roots dating back to 1956 leading to their first demonstration facility in 1974 (Mark et al. 2009). In the Shell gasification process, coal is crushed and dried and then fed into the Shell gasifier as a dry feed. The gasifier, as shown in Fig. 33, is an oxygen-blown, waterwall gasifier eliminating refractory durability issues. It is good for a wide variety of feedstocks, from petcoke to low-rank coals, and has been run on biomass as well. Commercially, Shell provides the gasification technology and has alliances with both Black & Veatch and Uhde to provide the EPC. There are 26 plants operating producing 8,500 MW_{th} syngas. There are 24 plants in planning.

Siemens

The Siemens gasifier was initially developed in 1975 for low-rank coals and waste by Deutsches Brennstoffinstitut in Freiberg, Germany, and was first demonstrated at Schwarze Pumpe in 1984 at a thermal rating of 200 MW (Higman and van der Burgt 2008). The technology was marketed under the name GPS by the Noell Group and later under the name Future Energy until purchased by Siemens in 2006. The gasifier, as shown in Fig. 34, is a dry feed, oxygen-blown, top-fired reactor with a waterwall screen in the gasifier. It is good for a wide variety of feedstocks, from

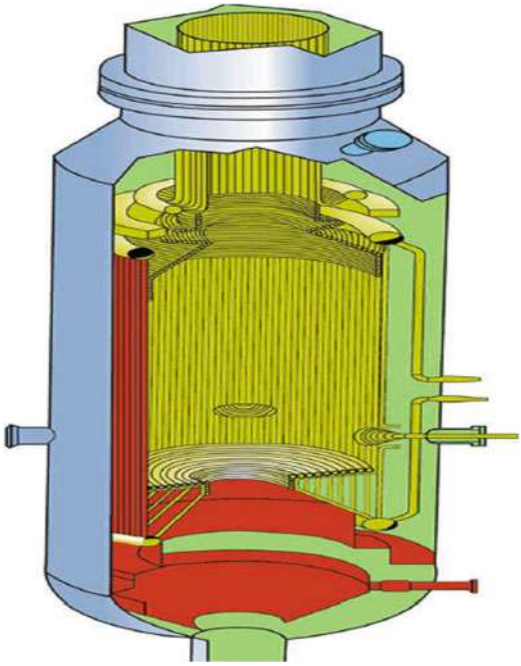

Fig. 33 Shell gasifier (U.S. Department of Energy 2009)

bituminous to low-rank coals. Siemens provides the gasification island and power block. They recently were awarded $39 million contract for two gasifiers 500 MW each for China's Shenhua DME (dimethyl ether) Project. Presently, there is one plant operating producing 787 MW_{th} syngas and they have one plant in planning.

MHI Gasifier

The Mitsubishi Heavy Industries (MHI) gasifier is based upon the Combustion Engineering air-blown slagging gasifier and codeveloped between Combustion Engineering (and its subsequent owners) and MHI. As shown in Fig. 35, it has a dry feed system, suitable for low-rank coals having high moisture contents. It is an air-blown two-stage entrained-bed slagging gasifier utilizing membrane waterwall construction. There is one demonstration plant in operation producing 250 MW_e and located in Nakoso, Japan. It started operations in September of 2007.

PRENFLO™ Gasifier/Boiler (PSG)

The PRENFLO™ gasifier/boiler is a pressurized entrained-flow gasifier with steam generation being marketed by Uhde. As shown in Fig. 36, it is an oxygen-blown, dry feed, membrane wall gasifier that is able to gasify a wide variety of solid fuels including hard coal, lignite, anthracite, refinery residues, etc. A demonstration plant in Fürstenhausen, Germany, gasified 48 t/day. The technology is used in the world's largest solid-feedstock-based IGCC plant in Puertollano, Spain.

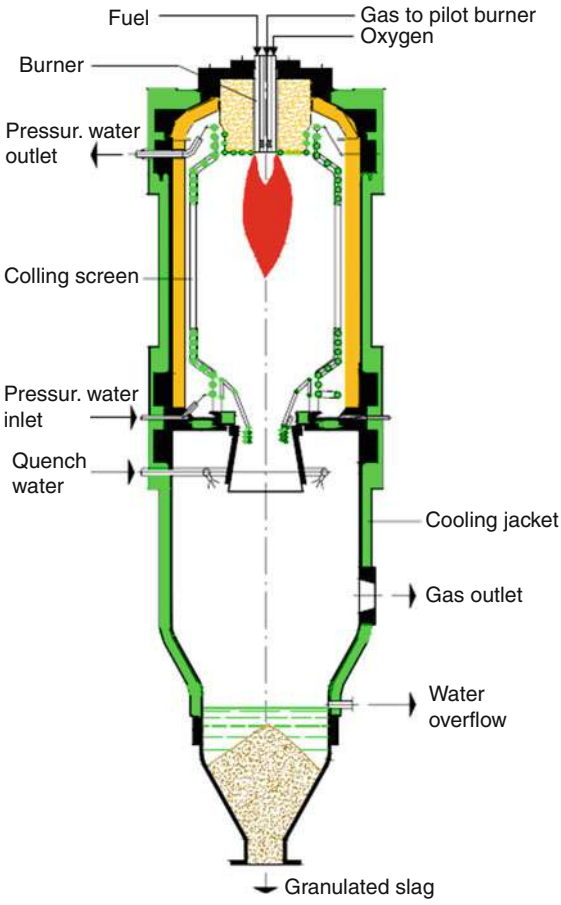

Fig. 34 Siemens gasifier (U.S. Department of Energy 2009)

Transport Gasifier

Kellogg, Brown, and Root (KBR) has developed the transport gasifier at the Department of Energy's (DOE's) Power Systems Development Facility at Southern Company Services, Wilsonville, Alabama, plant (Ariyapadi et al. 2008). The transport gasifier (Fig. 37) is based upon the hydrodynamic flow field that exists in KBR's catalytic cracking technology. It has excellent gas-solid contact and very low mass transfer resistance between gas and solids. It has a highly turbulent atmosphere that allows for high coal throughput and high heat release rates at a low temperature that avoids problems with slag handling and liner erosion.

Hydrodynamically, transport reactors are circulating fluidized beds which have more complicated hydrodynamics than fixed-bed reactors or bubbling fluidized beds have. In this type of reactor both excess gas and excess solids are fed to the reactor where the high gas velocity carries the solids upward. The excess solids tend to form clusters which act like large particles and fall back into the lower riser

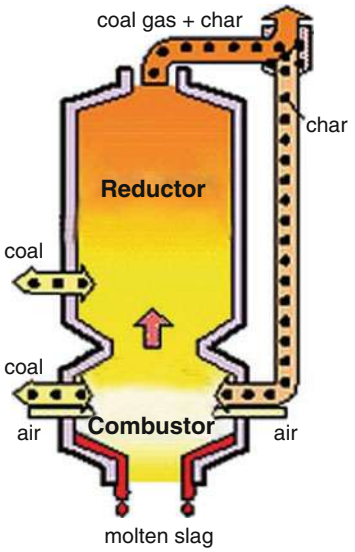

Fig. 35 MHI gasifier (U.S. Department of Energy 2009)

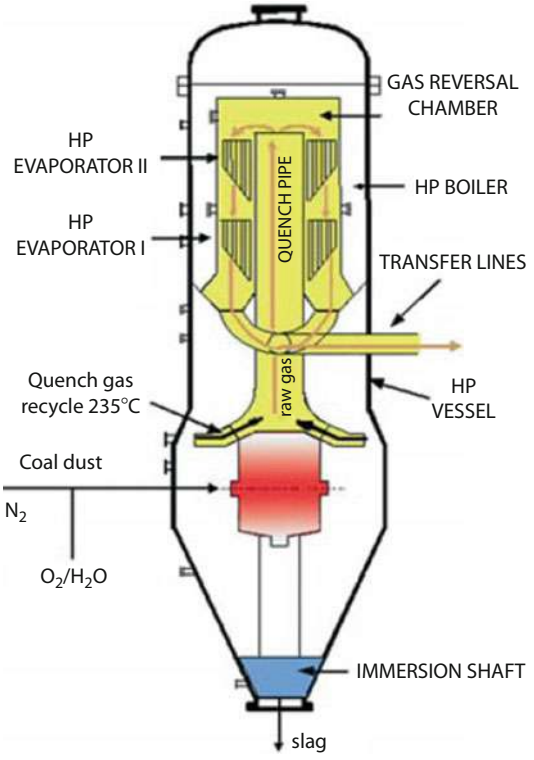

Fig. 36 PRENFLO™ (U.S. Department of Energy 2009)

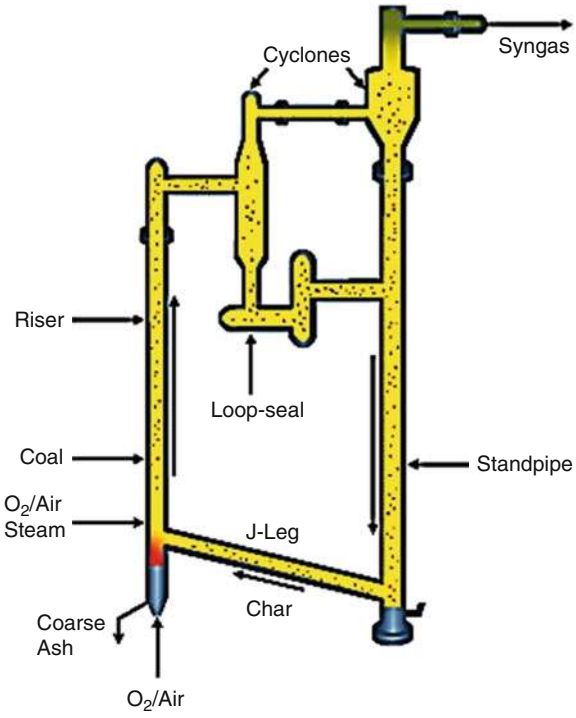

Fig. 37 KBR transport gasifier. The gas-solid separators include dual cyclones with nonmechanical valves designed to transfer solids but provide resistance to gas flows

where they break up and start to rise again. The results of an Eulerian-Eulerian simulation of the process is presented in Fig. 38 where the deep blue is a gas void and the yellow and red areas are clusters moving down while the other solids are moving up. These reactors have better mixing of gas and solids which leads to better interphase transport and better conversion of the coal. In addition, the mechanical movement of the solids against each other essentially scrubs the ash from particles.

Kinetically, because of the scrubbing of the reacted layer, the burnout or conversion follows a shrinking particle as pictured in Fig. 23. The conversion time can be calculated from the equation

$$\tau = \frac{2\rho_B R}{kC_{O_2}}$$

where τ is the time for complete conversion, ρ_B is the coal particle density, 2 is 1/stoichiometric coefficient for O_2, R is the particle radius, k is the combined kinetic and mass transfer rate constant, and C is the concentration of O_2 (Levenspiel 1998). These units have moderate cold gas efficiencies and they accept a broad range of

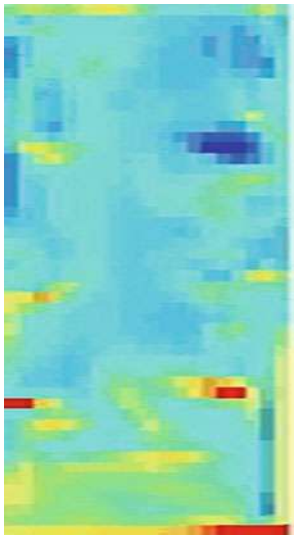

Fig. 38 A two-dimensional view of clustering in a 30 cm diameter riser of a circulating fluidized-bed hydrodynamics depicting the solid fraction where *red* pixels represent solid fraction of 0.6 and *navy blue* is a solid fraction of 0

Table 16 Typical gas analysis from the transport gasifier pilot plant (Smith 2007)

Coal type	Subbituminous		Lignite		Bituminous	
Mode	Air	Oxygen	Air	Oxygen	Air	Oxygen
Pressure, atm	30	30	30	30	30	30
Gas composition (dry)						
CO	23.7	39.1	18.8	37.9	13.3	25.5
CO_2	7.6	19.9	11.7	21.8	13.4	28.6
H_2	11.8	36.2	14.8	37.4	15.7	41.9
N_2	54.3	0.1	53.2	0.1	55.6	0.1
CH_4	2.6	4.8	1.6	2.9	2.0	3.9

coals. Typical gas compositions for thee different coals from the experimental facility are presented in Table 16.

KBR Transport Gasifier

The KBR transport gasifier operates in either oxygen- or air-blown configurations. For power generation it is operated air blown, but it can be fired using oxygen for liquid fuels and chemicals. It has a high reliability design based on years of designing and building FCC (fluidized catalytic cracking) units for the petroleum industry. It is a non-slagging gasifier with no burners and utilizing a coarse, dry low-rank coal feed. Presently, there is a 560 MW_e IGCC with a 2 × 1 combined cycle to be owned by the Mississippi Power Company in Kemper County, MS, in design.

Carbon Capture Technologies

Conventional Acid Gas Control Technologies

Acid gas control technologies remove the sulfur and CO_2 from the syngas. There are a number of commercial technologies that can be classified as physical sorbents, chemical sorbents, and single-species processes. Physical sorbent processes are known by their commercial names: Rectisol™, Selexol™, Purisol™, and Morphysorb™. Chemical sorbents are represented by MDEA (methyldiethanolamine) and other amines. There are two commercial single-species processes: CrystaSulf™ for sulfur control and Fluor Solvent™ for CO_2 control. A general schematic of an IGCC power plant with a desulfurization-decarbonization process is shown in Fig. 39 (Carbon Capture Technology Research and Breakthrough Concepts). This particular configuration is the preferred configuration when using one of the physical sorbents like Selexol™ as shown and a sour shift. The advanced warm desulfurization technologies being developed by DOE are more efficient, use a sweet-shift process, and then finally remove the CO_2. There are many configurations that can be assembled to achieve a site-specific optimum design.

The plant configuration in Fig. 39 utilizes an oxygen stream of 95 % purity produced from a cryogenic air separation unit (ASU), no air extraction from the syngas combustion turbine. It produces 122.5 Atm., 537 K superheated steam with a single 535 K reheat. The CO_2 is captured at high pressure from a relatively low syngas volume and produces CO_2 at high pressure which is then boosted to 15,200 kN/m^2 for sequestration.

Physical Sorbent Processes

The physical sorbent processes are known by their commercial names: Rectisol™, Selexol™, Purisol™, and Morphysorb™. These systems operate at low temperature with Rectisol™ operating at −40 °C. As one would expect, there is a large heat penalty paid for using these processes, but the level of purity achievable warrants and pays for that expense – particularly when producing high-value chemicals.

Rectisol™

The Rectisol™ is a physical acid gas removal process using an organic solvent (methanol) at subzero temperatures, nominally −40 °C. It can purify synthesis gas down to very low total sulfur and CO_2 levels. The main advantages of the process are the rather low utility consumption figures for regeneration as compared to the chemical sorbents, the use of a cheap and easily available solvent, and the flexibility in process configurations. With regard to performance, the Rectisol™ process is capable of achieving total sulfur (H_2S + COS) in the 0.1–1 ppm range and CO_2 levels in the 10–50 ppm range and limits the H_2S in CO_2 by-product to levels on the order of 5 ppm. Further detail can be found in review articles (RECTISOL® Wash; Hochges 1970; Newman 1985; Burr and Lyddon 2008; Acid Gas Removal and Sulfur Recovery).

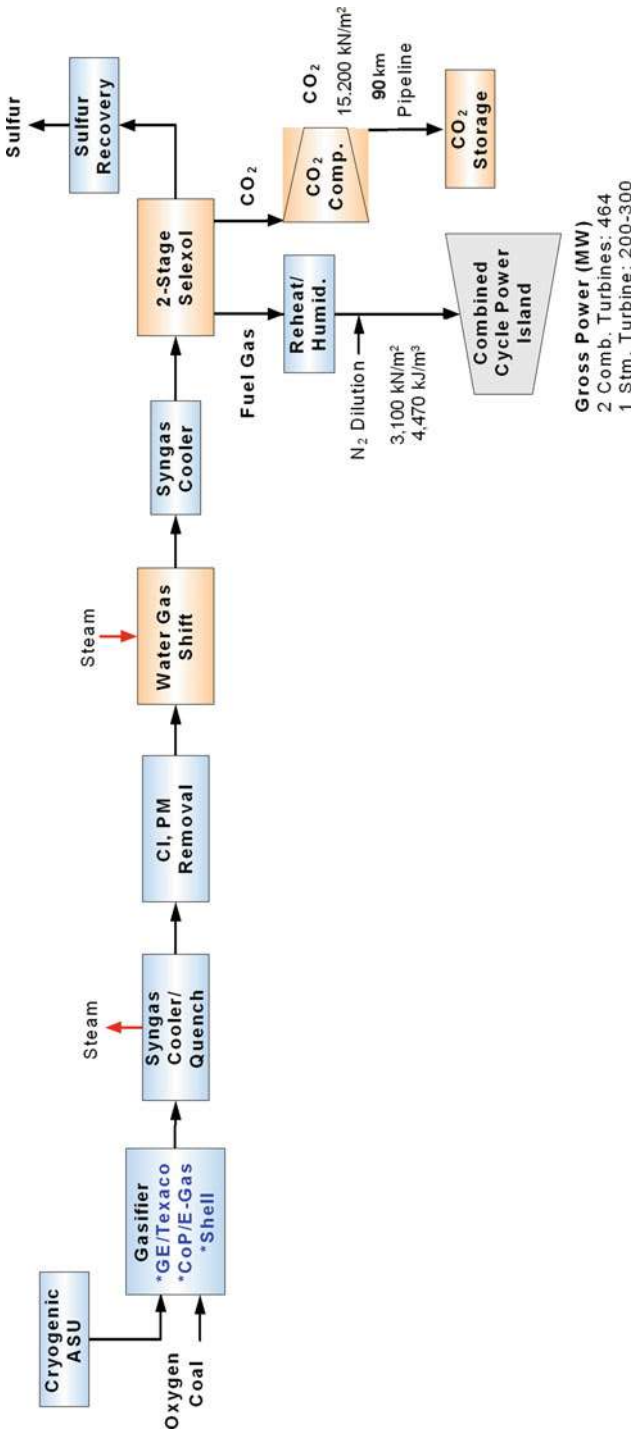

Fig. 39 Precombustion current technology IGCC power plant with CO_2 scrubbing (Adapted from Smith 2007)

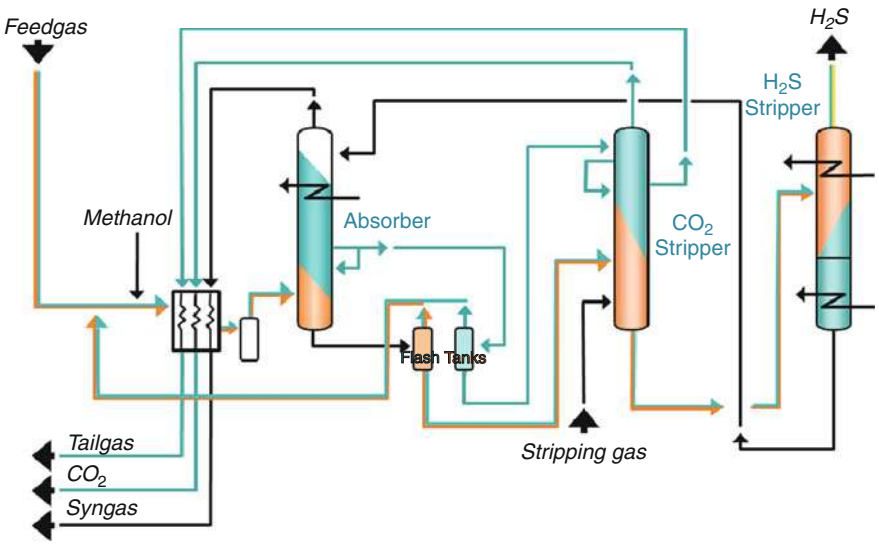

Fig. 40 Basic flow diagram/process scheme for Rectisol™ (Adapted from Carbon Capture Technology Research and Breakthrough Concepts)

The simple process flow diagram is displayed in Fig. 40. The syngas is mixed with methanol and enters the absorber column where H_2S, COS, and CO_2 are absorbed. The pure or cleaned syngas leaves the top of the column where it passes through a heat exchanger to cool the incoming syngas and methanol mixture. The CO_2 and sulfur compounds are removed in separate fractions as the solvent flows through a two-stage stripper. A pure CO_2 product is recovered from the top of the first stripper after passing through a heat exchanger to help cool the incoming syngas and methanol mixture. An H_2S/COS enriched Claus gas fraction is recovered from the top of the second stripper and passes through a heat exchanger to help cool the incoming syngas and methanol mixture.

CO_2 capture with Rectisol™ scrubbing is based on low temperature (refrigerated methanol ~ -40 °F or C) which is capable of deep total sulfur removal as well as CO_2 removal. It is the most expensive AGR process giving the deepest cleaning. It is predominantly used in chemical synthesis gas applications where total sulfur requirements are less than 0.1 ppmv. It has been proposed for use in IGCC for CO_2 removal but no published cost studies presently exist.

Selexol™

The Selexol™ process uses a physical solvent to remove acid gas from streams of synthetic or natural gas. The process may be regenerated either thermally, by flashing, or by stripping gas. The Selexol™ process is ideally suited for the selective removal of H_2S and other sulfur compounds or for the bulk removal of CO_2. The Selexol™ process uses Union Carbide's Selexol™ solvent, a physical solvent made of a dimethyl ether of polyethylene glycol (DPG or DEPG or

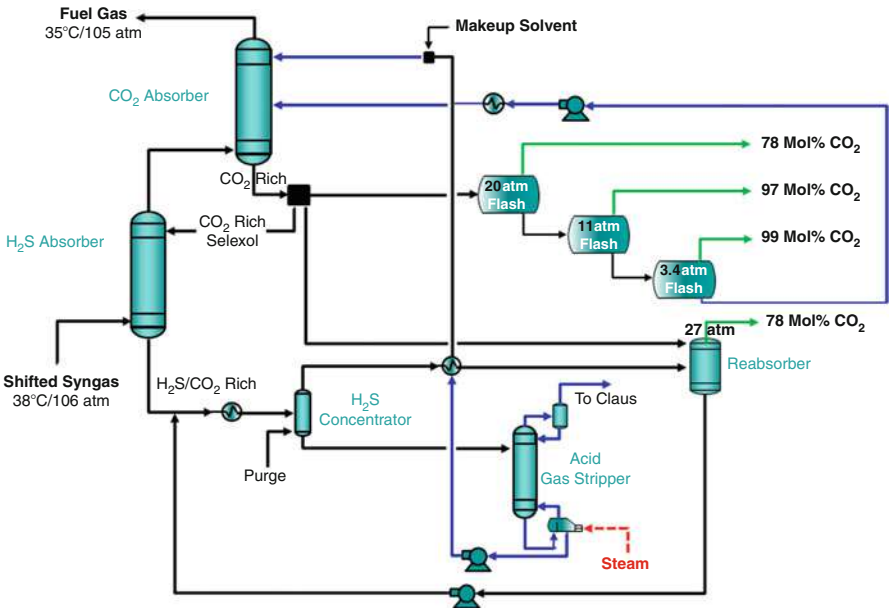

Fig. 41 Selexol™ process flow chart (Adapted from Acid Gas Removal and Sulfur Recovery)

DMPEG). The Selexol™ solvent is chemically inert and is not subject to degradation. The Selexol™ process also removes COS, mercaptans, ammonia, HCN, and metal carbonyls. This process allows for construction of mostly carbon steel due to its nonaqueous nature and inert chemical characteristics (Hochges 1970; Newman 1985; SELEXOLTM PROCESS; SELEXOL™solvent; 2009).

The Selexol™ process can be tailored for either bulk or trace acid gas removal. Because of the staged separation of acid gases (Fig. 41), Selexol™ is primarily used in the following applications and markets:

1. Selective removal of H_2S and COS in integrated gasification combined cycle (IGCC), with high CO_2 rejection to product gas (85 % +) and high sulfur (25–80 %) feed to the Claus unit
2. Selective removal of H_2S/COS plus bulk removal of CO_2 in gasification for high-purity H_2 generation for refinery or fertilizer use
3. Treatment of natural gas to achieve either LNG or pipeline specification with dew-point reduction

The Selexol™ process was introduced over 30 years ago. It has been and continues to be the dominant acid gas removal system selection in gasification project awards within the past several years.

A process flow diagram for a Selexol process for a gasification plant to remove CO_2 is shown in Fig. 42. It has two absorber tower stages. The first stage is for removing H_2S and the second is for removing the CO_2. The H_2S is separated from

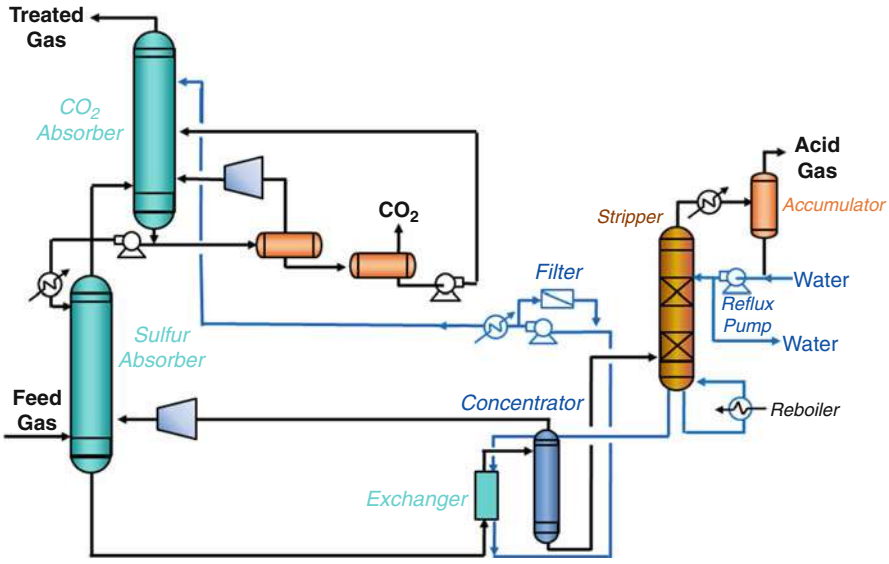

Fig. 42 Selexol™ scrubbing for CO_2 capture (Adapted from SELEXOL™solvent)

the solvent in an acid gas stripper column, while the CO_2 is removed from the solvent in a series of flash drums.

Selexol™ has a number of beneficial properties. It is a physical liquid sorbent, capable of having high loadings at high CO_2 partial pressure levels. It is highly selective for H_2S and CO_2 such that there is no need for a separate sulfur capture system. A big advantage of Selexol™ and other physical sorbents is that there is no heat of reaction (ΔH_{rxn}) with only a small heat of solution. The Selexol™ sorbent is chemically and thermally stable and has a low vapor pressure – keeping losses to a minimum. There is 30+ years of commercial operating experience on 55 plants worldwide. Selexol™ does have a couple of disadvantages. Namely, it requires gas cooling to about 35 °C (~100 °F), and it requires considerable heat for CO_2 regeneration by flashing.

Purisol™

The Purisol™ process is a second acid gas removal process developed by Lurgi. It uses normal methyl pyrrolidone or NMP as the solvent. Its operating conditions and overall process configuration are similar to that of Selexol™; however, it is not as widely used. Additional information can be found elsewhere (RECTISOL® Wash; Hochges 1970).

Morphysorb™

Morphysorb™ is a proprietary solvent CO_2 removal process developed by GTI and owned by both GTI and Uhde. It uses *N*-formyl morpholine/*N*-acetyl morpholine mixtures (see Fig. 43). It can be used for both bulk or trace removal of acid gas

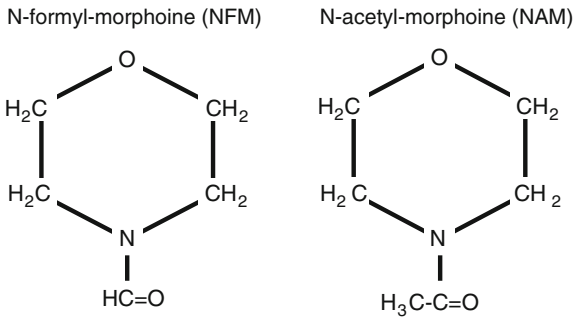

Fig. 43 Morphysorb™ chemicals

components in subquality natural gas upgrading to either pipeline or LNG specification, selective removal of H_2S from natural/synthesis gas for generation of acid gas stream suitable for Claus plant feed, and selective removal of H_2S, CO_2, COS, CS_2, mercaptans, and other components from coal/oil gasification syngas at IGCC facilities (Lippin; Kowalsky et al. 2003).

Morphysorb™ offers a number of benefits relative to chemical and some other physical sorbents. It has higher solvent loading which leads to either lower circulation or higher throughput. It has lower co-absorption of hydrocarbons which translates into fewer losses or, in other words, less recycle gas flow for recovery of these hydrocarbons. It has lower CO and H_2 absorption. It assists in the hydrolysis of COS. It is low in corrosivity and, thereby, low environmental hazard as well as low capital and operating costs.

There is one natural gas commercial application owned by Spectra Energy™ Transmission which was started in late 2002. It processes 450 MMscfd after a plant expansion of 50 %. The solubility of the mophysorb sorbent is presented in Fig. 44.

Chemical Sorbents

There are a number of chemical sorbents that have been used for acid gas control. All of these fall into the chemical category called amines. Primary, secondary, and tertiary amines have all been used (Fig. 45). Primary amines are monosubstituted ammonia like monoethanolamine (MEA). Secondary amines are bi-substituted ammonia like diethanolamine (DEA). Tertiary amines are trisubstituted ammonia like methyldiethanolamine (MDEA).

The process flow diagram for a typical amine-based process is shown in Fig. 46. The absorption of acid gases (H_2S, SO_2, CO_2) in amine solution is conducted with a two-column operation. The acid gas is absorbed in the first column. The second column is used to regenerate the amine. The process relies on countercurrent flow to achieve optimum mixing. A lean solution (low acid gas) enters the top of the absorber and flows to the bottom while acid gas enters the bottom of the absorber tower and bubbles to the top. The rich amine (high acid gas) liquid enters the stripper where the acid gases are released and the "clean" amine is returned to the absorber. The acid gases exit from the top of the stripper. The MEA/DEA/MDEA is

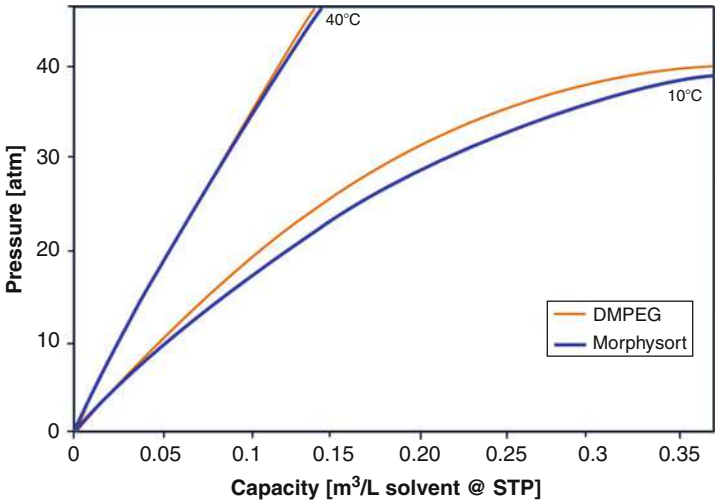

Fig. 44 Morphysorb™ CO_2 solubility (2009)

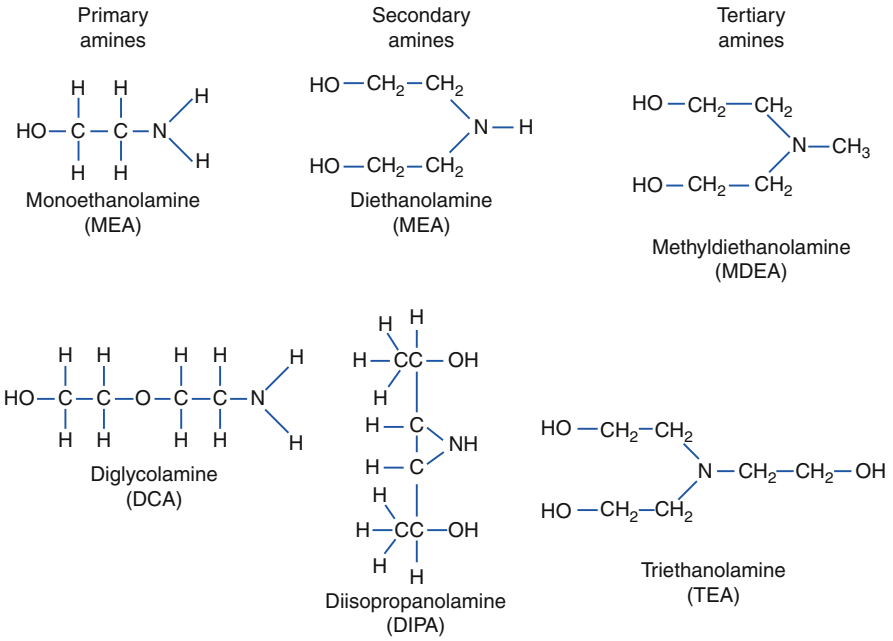

Fig. 45 Commonly used amine-based chemical sorbents

regenerated in the stripper column. It is beneficial to be sure the amine concentration is at proper level in order to optimize the H_2S, SO_2, and CO_2 removal. The final amine concentration can be controlled by the adding amine makeup. Additional information can be found online (Burr and Lyddon 2008).

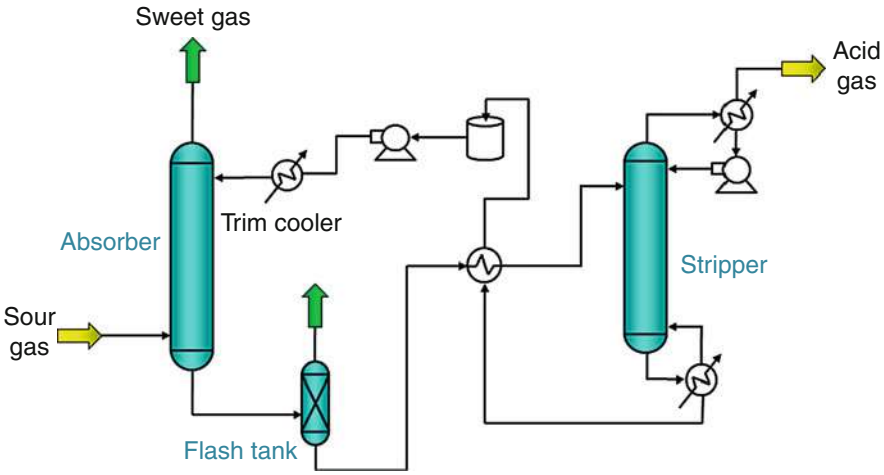

Fig. 46 Process flow diagram of a typical amine treating process used in industrial plants

Single-Species Processes

CrystaSulf™: Sulfur Control

The CrystaSulf™ process for direct treatment of sour gas can be used for recovering sulfur from gas streams that contain as little as 0.2–25 LPD of sulfur which have historically been problematic. In this size range, the operating costs of throwaway H_2S scavenging chemicals are too high, and traditional amine/Claus approaches are unwieldy and capital intensive. Aqueous-iron redox systems showed promise in this range, but often proved unacceptable because of their operating problems. Therefore, the new breakthrough sulfur recovery technology, CrystaSulf™, can remove sulfur economically without the operating problems of aqueous-iron systems for plants of this size. Using a gentle SO_2 oxidant, CrystaSulf™ converts inlet H_2S to elemental sulfur. Elemental sulfur is soluble in the CrystaSulf™ solution; thus, there is no danger of sulfur plugging high-pressure equipment that plagues aqueous-iron systems. Meeting pipeline H_2S specifications is easy, and CO_2 has been shown to have no effect on the CrystaSulf™ process (Rueter et al. 2002).

The process has a number of advantages, particularly for these medium-scale systems. It has lower capital cost, lower overall treatment cost, and much lower maintenance and cleanout costs. It can directly treat high-pressure streams with a solid-free solution which is easy to pump and requires a very low circulation rate. The nonaqueous solvent has high solubility for elemental sulfur and therefore has no sulfur particles in circulating liquor and needs no sulfur settling additives or surfactants. It avoids problems of foaming and plugging associated with aqueous-iron redox system. It produces large sulfur particles in a crystallizer that separates and purifies easily, yielding a much higher sulfur purity product than possible with aqueous-iron redox systems. A process flow diagram for the process is shown in Fig. 47.

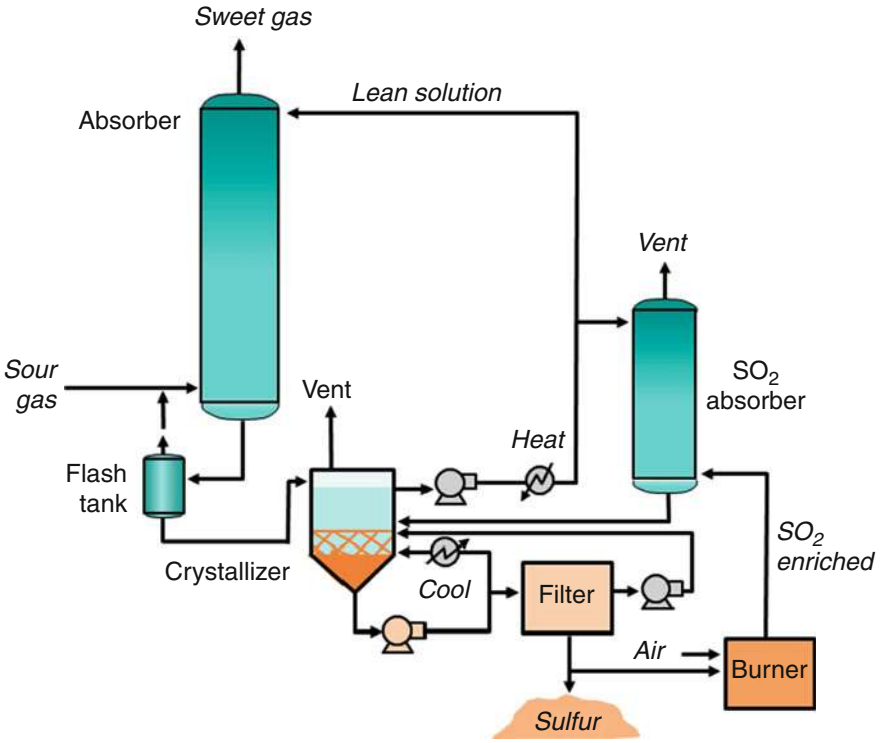

Fig. 47 Process flow diagram for CrystaSulf™ process

Fig. 48 Fluor solvent chemical structure

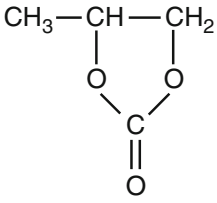

Fluor Solvent: CO_2 Control

The Fluor Solvent process has significant advantages over an amine treating process in an offshore environment when treating large gas volumes where the CO_2 partial pressure is high. The Fluor Solvent process configuration is much simpler. It requires no heat for solvent regeneration. It requires no makeup water. It produces a dry product gas. The solvent is minimally corrosive, resistant to foaming, and biodegradable. The chemical structure is shown in Fig. 48.

Figure 49 shows the configuration of the Fluor Solvent process for low to medium CO_2 content applications (Mak et al. 2003). The process consists of an absorber and two flash drums. A pressurized flash drum with low-, medium-, and

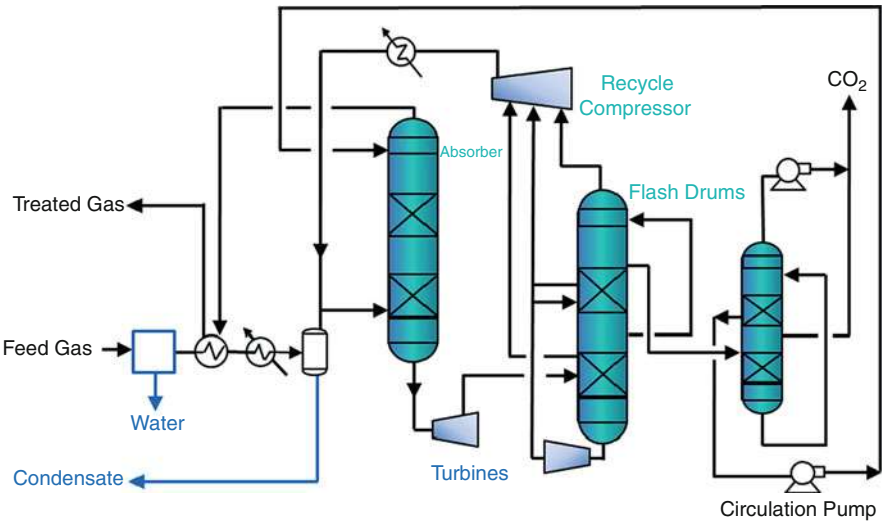

Fig. 49 Fluor Solvent process schematic (Adapted from Rueter et al. 2002)

high-pressure zones and a vacuum flash drum with zones at atmospheric pressure and at vacuum.

Future Directions in Research and Development

Recent Gasification Systems Studies

The use of advanced gasification power systems was identified as the most favorable coal alternative for reducing carbon dioxide emissions (Klara 2007). The cost of capturing 90 % of the carbon dioxide from a coal gasifier was compared with coal combustion in both conventional and new ultra-supercritical steam systems and natural gas-fired power systems. The capital, operating, and maintenance costs were evaluated for a green field 640 MW_e power plant based upon reasonable process design alternatives for each. Without carbon capture, both IGCC and pulverized coal (PC) combustion can achieve 39 % efficiency based upon the high heating value (HHV) for bituminous coals. Available commercial capture technology can remove 90 % of CO_2, but at significant increase in COE. The total IGCC plant cost was found to be ~20 % higher than PC, but with carbon capture and sequestration, the total for PC exceeded that of IGCC. With carbon capture and sequestration, IGCC was the lowest coal-based option (in 2007 dollars) (Klara 2007):

- Natural Gas Combined Cycle: 96 mills/kWh
- IGCC: 105 mills/kWh (average)
- PC: 116 mills/kWh (average)

where 1 mill is equal to 0.001 USD. This indicates that when considering the capital, operating, and maintenance costs and including carbon management systems, IGCC has a lower relative cost of producing electricity than PC power plants. The gas cleanup system is smaller for gasifiers because they have lower product fuel gas volume as compared to the flue gas from coal and natural gas combustors.

The carbon footprint for various coal gasification scenarios has been considered using a life cycle analysis (Reed 2007). Life cycle analysis considers the energy and costs required from cradle to grave including mining, mine reclamation, transportation, mineral preparation, processing, waste disposal, sequestration, and monitoring of the wastes. Coal biomass mixtures were considered in various power systems and compared against a baseline natural gas power system. Gasification with biomass coal co-firing was found to be able to match natural gas performance. It was found that a combination of gasification and biomass co-firing when used with shift cleanup and sequestration could dramatically reduce the carbon footprint relative to natural gas.

Gasification R&D

The US Department of Energy is involved in a wide range of research, development, and demonstration (RD&D) activities to improve the fuel and product versatility, process efficiency, and system. The challenge is to achieve widespread market penetration in the most large-scale markets including power generation, chemical processing, and gas and liquid synthesis. The program goals are to improve gasifier efficiency and process control; improve process train reliability, reducing downtime and expenses from redundant process components; and improve the flexibility of gasification processes to handle a wider variety of grades and types of feedstocks. Research is being funded on the capture and sequestration of carbon dioxide (CO_2). The DOE's Office of Fossil Energy conducts the Gasification Technologies Research and Development (R&D) Program. The focus of the Advanced Power Systems Program is on electricity production, and its intent is to foster public-private partnerships and provide technology to utilize the extensive US fossil fuel resource. Having collaborated with industry over the decades of the 1980s and 1990s to bring coal gasification to commercial-scale demonstration plants, the emphasis is now shifting to refining and expanding gasification potential to bring the technology to its potential as a near-zero-emission clean coal technology. The Gasification Technologies R&D Program consists of four distinct areas: (1) adaption of gasification technologies to a range of coal feedstock varieties, better control of gasifier performance and gas production, and improved overall efficiency; (2) cleanup of produced gases to meet increasingly stringent environmental standards; (3) better separation of product gases and oxygen from air to improve economics and efficiency and facilitate gas cleanup; and (4) identification of economic and infrastructure issues with various gasification applications (http www netl doe gov technologies coalpower gasification gasifipedia 8 research).

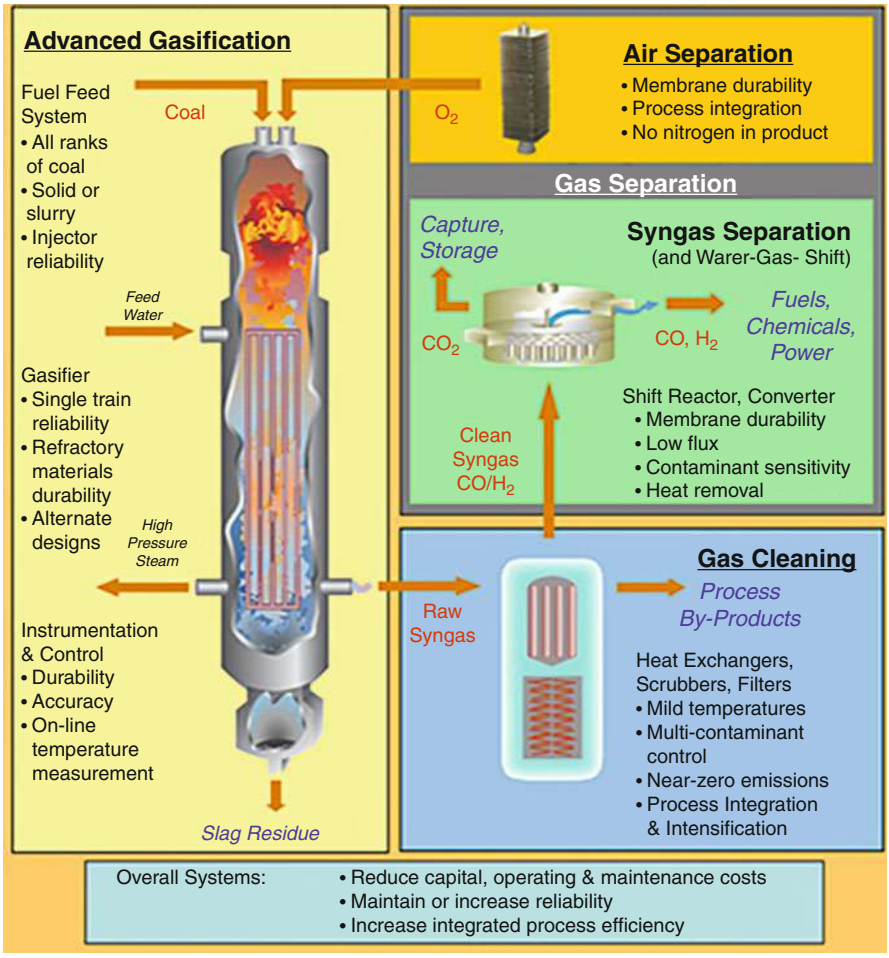

Fig. 50 Gasification research and development areas and major technology issues

The key issues identified in the US DOE's programs are listed in each of these research areas in Fig. 50. Gasifiers need to be able to be efficient operating on lower-grade fuel feedstocks including low rank, high mineral contents, and biomass. In order to be efficient in using these resources, utilities must be able to introduce these lower-quality fuels into gasifiers without using quantities of water in excess to what is required for rapid gasification. Otherwise, the large latent heat of water vaporization will increase the inefficiencies due to unrecoverable heat losses. The reliability of the solid fuel feed system has historically been the single most frequent cause for unplanned shutdown in coal-fired systems. The lack of reactor availability due to downstream fouling, refractory failures, and loss of the solid fuel feed systems is being addressed by research on fly-ash formation,

refractory durability, alternative gasifier concepts, as well as improved diagnostics, instrumentation, and control systems.

Gas Cleanup and CO_2 Capture Research

Gas cleaning systems research funded by the US DOE includes improving heat exchangers, scrubbers, and filter technologies. For example, researchers at the Power System Development Facility have demonstrated improvements in particulate filtration reliability and filter element durability and developed fail-safe devices to insure removal of particulate matter to protect downstream turbines and cleanup systems (Dahlin and Landham 2008; Guan et al. 2005). One research goal is to intensify and better integrate cleaning processes by taking steps where possible to develop multicomponent cleanup systems, thereby reducing the number of process units. Alternative gasifiers such as the transport reactor employ milder temperatures which reduce the severity of the environment with which the process materials must survive. These milder temperatures allow the use of more robust cleanup technologies.

Research is being supported on gas separations in order to remove, capture, and sequester CO_2. Commercial cryogenic air separation units have the greatest share of the oxygen production from air separation; however, the energy-intensive nature of this process has targeted this process operation as having a high potential for improvement. In addition to developments in cryogenics, leading alternatives include pressure swing absorption and membranes. Gas separations are also critical to gas cleanup and to tailor the product distribution. In a zero-emission gasifier power plant, the product syngas is shifted to CO_2 and H_2, and the CO_2 must be separated from the mixture. Shift reactors utilize the water-gas shift reaction (see above) and catalytically convert the product distribution in the direction desired. Shift reactors employed in gasifier facilities such as the Great Plains Gasification facility in North Dakota are required to alter the H_2/CO ratio from ~1.5:1 produced in the gasifier to 3:1 to optimize production of synthetic natural gas (CH_4, methane). The process demands (selectivity and yields) are different to produce H_2 as a clean-burning fuel. Research is also needed to improve the separation systems at the elevated temperatures and pressures consistent with water-gas shift catalyst operations. Contamination of membranes and other separation systems are potential poisons potentially damaging sorbents and catalysts. A recent review of some novel methods for CO_2 separations includes electrochemical pumps, membranes, and chemical looping (Granite and O'Brien 2005).

Chemical looping is a process in which the oxidant in a combustor or gasifier is supplied from an oxygen-carrying particle such that the products of combustion or gasification are separated from the nitrogen in the air. The chemical looping process is shown in Fig. 51. Beginning with the air reactor or oxidizer, the reduced or oxygen-depleted carrier is reacted with air to fully oxygenate it by essentially burning the carrier particles through the exothermic reaction. The air reactor produces a vitiated airstream (i.e., air partially depleted in oxygen) and hot oxygenated

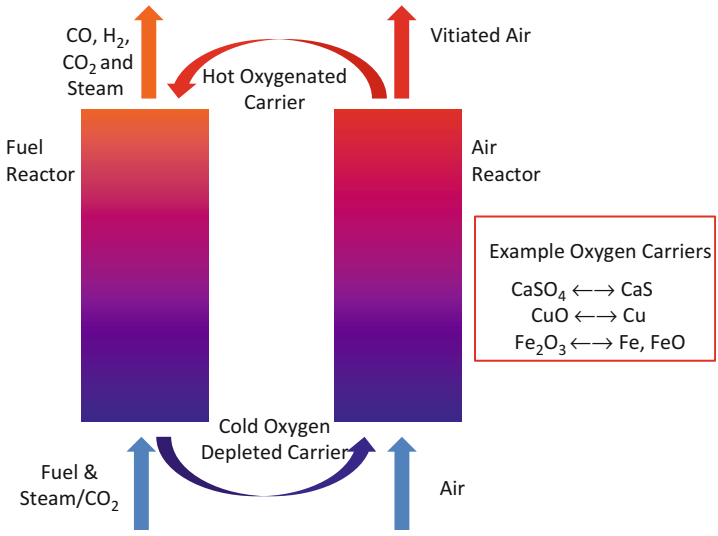

Fig. 51 Chemical looping concept

particle that convey heat and oxygen to the fuel reactor. The carrier particles are thereby reduced by reaction with the hydrocarbon fuel. After oxidizing the fuel, the reduced carrier is transferred to an air reactor where it is reoxidized – completing the loop. Depending on the stoichiometry, the gaseous product from the fuel reactor is CO_2 and water when excess oxygen is supplied by the carrier (combustion) or syngas when excess fuel is supplied to the reactor relative to the oxygen in the carrier (gasification). The result is a gas from the fuel reactor without nitrogen. A variety of carriers have been proposed: metal oxides such as nickel, iron, and copper and sulfates such as calcium sulfate. Technical and economic analyses have indicated very promising results (Yu et al. 2003; 2013).

Increasing regulatory limits on the release of CO_2 could give gasification a competitive advantage in future markets. Gasification has a distinct economic advantage over competing technologies in capturing and sequestering CO_2 from process streams. Acid gas cleanup systems presented above have been traditionally used to remove trace pollutants such as sulfur, but the scale required to remove one of the principal gases, i.e., CO_2, from utility-scale gas streams elevates the need to significantly increase the efficiency and reduce the cost of the process. The US Department of Energy's research goals keep the cost of removing 90 % of the carbon from the product gas stream to less than 30 % increase over the cost without carbon capture. What was considered acceptable energy costs when removing trace pollutants becomes onerous when scrubbing out 15 % of the gas stream. CO_2 sorbent or solvents operate by absorbing carbon dioxide at low temperature, transferring the sorbent to a regenerator and releasing the carbon dioxide by increasing the temperature. This is known as a temperature swing absorption and regeneration process. Amines form an ionic bond with acid gases such as carbon

dioxide. Traditional scrubbing is conducted in aqueous or methanol solutions; however, these liquid processes lose significant quantities of latent heat of vaporization of these liquids. Methods to improve heat integration, increase heat exchange, and reduce latent and sensible heat losses are under investigation. Low-volatile ionic liquids (mostly amines) and solid-supported amines are being developed to optimize these processes. After surveying the performance in terms of capacity and absorption rates of over 100 solid-supported sorbents, several very promising sorbents were identified for use in flue gas. The sorbent capacity target of over 2 mol of CO_2 per kg of sorbent (Fisher and Keller 2006) was achieved using a polyamine bonded to a mesoporous silica developed at NETL (Monazam et al. 2013, 2014). This sorbent is currently being evaluated in a circulating fluidized-bed process at a 1 kW scale on a utility slipstream.

Acknowledgments The authors would like to express their gratitude to the US Department of Energy in making resources and the time available to prepare this manuscript. In addition we would also like to extend appreciation to Peter Smith, Ranjani Siriwardane, Esmail Monazam, Tom O'Brien, and Mehrdad Shahnam for their contributions.

References

Acid Gas Removal and Sulfur Recovery, Website, available on line, http://www.linde-engineering.de/process_plants/gas_processing/acid_gas_sulfur.php

Anthony DB, Howard JB, Hottel HC, Meissner HP (1976) Rapid devolatilization and hydrogasification of bituminous coal. Fuel 55(2):121–128

Ariyapadi S, Shires P, Bhargava M, Ebbern D (2008) KBR's Transport Gasifier (Trig™) – an advanced gasification technology for SNG Production from low-rank coals, twenty-fifth annual international Pittsburgh Coal Conference Pittsburgh, Sept 29 – Oct 02, 2008

Arthur JR (1951) Reactions between carbon and oxygen. Trans Faraday Soc 47(2):164–178

ASTM Standard D3172 - 13 Standard practice for proximate analysis of coal and coke. ASTM International, West Conshohocken, PA, 2013, DOI: 10.1520/D3172, www.astm.org

Bryers RW (1995) Utilization of petroleum coke and petroleum coke/coal blends as a means of steam raising. Fuel Process Technol 44:121–141

Burr B, Lyddon L (2008) A comparison of physical solvents for acid gas removal, Bryan Research & Engineering, Bryan. GPA 2008. http://www.bre.com/support/technical-articles/gas-treating.aspx

Carbon Capture Technology Research and Breakthrough Concepts, Website, available on line http://www.netl.doe.gov/technologies/carbon_seq/refshelf/overviews/Carbon%20Capture%20Technology%20Research%20and%20Breakthrough%20Concepts.pdf

Chitsora CT, Mühlen HJ, van Heek KH, Jüntgen H (1987) The influence of pyrolysis conditions on the reactivity of CHAR in H_2O. Fuel Process Technol 15:17–29

Conn RE (1995) Laboratory techniques for evaluating ash agglomeration potential in petroleum coke fired circulating fluidized bed combustors. Fuel Process Technol 44:95–103

Dahlin RS, Landham EC Jr (2008) Factors affecting dustcake drag in a hot-gas filter system collecting coal gasification ash. Powder Technol 180:45–50

Elliot M (ed) (1981) Chemistry of coal utilization, 2nd Supl Vol. Wiley, New York

Final Report: ALSTOM's Chemical looping combustion prototype for CO_2 capture from existing pulverized coal-fired power plants, DOE/NETL Cooperative Agreement No. DE-NT0005286, Dec 2013

Fisher D, Keller G (2006) Process analyses and R&D plans forward for dry-sorbent-based processes for removal of CO_2 from power plant flue gas, Contract Report to US DOE NETL, pp 74
Fletcher TH, Kerstein AR, Pugmire RJ, Solum M, Grant D A chemical percolation model for devolatilization: Summary, http://www.et.byu.edu/tom/cpd/CPD_Summary.pdf
Fletcher TH, Solum MS, Grant DM, Critchfield S, Pugmire RJ (1991) Solid state ^{13}C and ^{1}H NMR studies of the evolution of the chemical structure of coal char and tar during devolatilization. Symp (Int) Combust 23(1):1231–1237
Gan H, Nandi SP, Walker PL Jr (1972) Nature of the porosity in American coals. Fuel 51(4):272–277
Given PH (1984) Concepts of coal structure in relation to combustion behavior. Prog Energy Combust Sci 10:149–155
Given PH, Marzec A, Barton WA, Lynch LJ, Gerstein BC (1986) The concept of a mobile or molecular phase within the macromolecular network of coals: a debate. Fuel 65:155–163
Granite EJ, O'Brien T (2005) Review of novel methods for carbon dioxide separation from flue and fuel gases. Fuel Process Technol 86:1423–1434
Guan X, Gardner B, Martin RA, Spain J (2005) Demonstration of hot-gas filtration inAdvanced coal gasification system, 6th international symposium on gas cleaning at high temperatures, Osaka, Oct 20–22
Hecht ES, Shaddix CR, Molina A, Haynes BS (2010, in press) Effect of CO_2 gasification reaction on oxy-combustion of pulverized coal char. In: Proceedings of the combustion institute, Corrected Proof, doi:10.1016/j.proci.2010.07.087
Higman C (2014) State of the gasification industry: worldwide gasification database 2014 update, Gasification Technologies Conference, Washington, DC, p 14. http://www.gasification.org/uploads/downloads/GTC_Database_2014.pdf
Higman C, van der Burgt M (2008) Gasification. Elsevier Science & Technology Books, London
Hochges G (1970) Rectisol and purisol. Ind Eng Chem 62(7):37–43
http://www.netl.doe.gov/technologies/coalpower/gasification/gasifipedia/8-research/
Huang J, Fang Y, Chen H, Wang Y (2003) Coal gasification characteristics in a PFB. Energy Fuels 17:1474–1479
Jenkins RG, Morgan ME (1986) Pyrolysis of a lignite in an entrained flow reactor: 3. Pyrolysis in reactive atmospheres of air, carbon dioxide and wet nitrogen. Fuel 65(6):769–771
Klara J (2007) Cost and performance Ba seline for fossil energy plants: volume I, DOE/NETL-2007/1281, r ev. 1, Aug 2007
Kobayashi H, Howard JB, Sarofim AF (1977) Coal devolatilization at high temperatures. Symp (Int) Combust 16(1):411–425
Kowalsky G, Leppin D, Palla R, Jamal A, Hooper HM (2003) Morphysorb® applied to de-bottlenecking of gas treating system. GasTIPS, Winter 2003, pp 28–32
Levenspiel O (1998) Chemical reaction engineering, 3rd edn. Wiley, New York
Lippin D, Personal communication
Lowry HH (ed) (1963) Chem of coal utilization, Supl Vol. Wiley, New York
Mahajan OP, Yarzab R, Walker PL Jr (1978) Unification of coal-char gasification reaction mechanisms. Fuel 57(10):643–646
Mak J, Wierenga D, Nielsen D, Graham C, Viejo A (2003) New physical solvent treating configurations for offshore high pressure CO_2 removal, In Proceedings of Offshore Technology Conference, 5-8 May, Houston, Texas, Society of Petroleum Engineers, paper OTC 15354, http://dx.doi.org/10.4043/15354-MS
Maloney DJ, Jenkins RG, Walker PL (1982) Low-temperature air oxidation of caking coals. 2. Effect on swelling and softening properties. Fuel 61(2):175–181
Mark M (2009) Delivering performance in Chinese operations. In: Proceedings of the gasification technologies conference, Colorado Springs
Massey LG (1979) Coal Gasification for High and Low Btu Fuels. In: Wen CY, Lee ES (eds) Coal conversion technology. Addison-Wesley Publishing, Reading, pp 313–427

Monazam ER, Shadle LJ (1998) Predictive tool to aid design and operations of pressurized fixed bed coal gasifiers. Ind Eng Chem Res 37(1):120–130
Monazam ER, Shadle LJ, Miller DC, Pennline HW, Fauth DJ, Hoffman JS, Gray ML (2013) Equilibrium and kinetics analysis of carbon dioxide capture using immobilized amine on a mesoporous silica. AIChE J 59(3):923–935
Monazam ER, Spenik J, Shadle LJ (2014) CO_2 desorption kinetics for immobilized polyethylenimine (PEI). Energy Fuels 28:650–656. doi:10.1021/ef401879z
Moreea-Taha R (2000) Modeling and simulation for coal gasification, Report CCC/42, IEA Coal Research, London, UK
Morgan ME, Jenkins RG (1986a) Pyrolysis of a lignite in an entrained flow reactor: 2. Effect of metal cations on decarboxylation and tar yield. Fuel 65(6):764–768
Morgan ME, Jenkins RG (1986b) Pyrolysis of a lignite in an entrained flow reactor: 1. Effect of cations on total weight loss. Fuel 65(6):757–763
Newman SA (ed) (1985) Acid and sour gas treating processes. Gulf Publishing Company, Houston
Niksa S (1986) The distributed-energy chain model for rapid coal devolatilization kinetics. Part II: transient weight loss correlations. Combust Flame 66(2):111–119
Niksa S, Lau C-W (1993) Global rates of devolatilization for various coal types. Combust Flame 94(3):293–307
Niksa S, Liu G-S, Hurt RH (2003) Coal conversion submodels for design applications at elevated pressures. Part I. devolatilization and char oxidation. Prog Energy Combust Sci 29(5):425–477
Probstein RF, Hicks RE (1979) Synthetic fuels. McGraw-Hill Book, New York, pp 1–256
Radovic LR, Steczko K, Walker PL Jr, Jenkins RG (1985) Combined effects of inorganic constituents and pyrolysis conditions on the gasification reactivity of coal chars. Fuel Process Technol 10(3):311–326
RECTISOL® Wash, Website, available on line, http://www.linde-engineering.com/en/process_plants/hydrogen_and_synthesis_gas_plants/gas_processing_plants/rectisol_wash/index.html
Reed M (2007) Systems studies, NETL/DOE report 2007/1255
Rueter C (2002) CrystaSulf® process fills mid-size niche for sulfur recovery in multiple applications, GasTips, Winter 2002, pp 8–12
Seed MA, Williams AR, Brown DJ, Hirschfelder H (2007) Application of slagging gasification technology to as received Lignite in China. In: Proceedings of the third international conference on clean coal technologies for our future, Cagliari, May 2007
SELEXOLTM PROCESS, website available online, http://www.uop.com/objects/97%20Selexol.pdf
SELEXOL™ solvent, website available online, http://www.dow.com/PublishedLiterature/dh_0043/0901b803800430d0.pdf?filepath=gastreating/pdfs/noreg/170-01432.pdf&fromPage=GetDoc
Shadle LJ, Monazam ER, Swanson ML (2001) Coal gasification in a transport reactor. Ind Eng Chem Res 40(13):2782–2792
Shnidman L (1945) Utilization of Coal Gas, In: Lowry HH (ed) Chemistry of coal utilization, vol II. Wiley, New York, pp 1252–1286
Slezak A, Kuhlman JM, Shadle LJ, Spenik J, Shi S (2010) CFD simulation of entrained-flow coal gasification: coal particle density/size fraction effects. Powder Technol 203(1):98–108
Smith P (2007) Personnel communication for test results. Kellogg, Brown and Root, Houston
Solomon PR, Serio MA (1994) A characterization method and model for predicting coal conversion behaviour. Reply to Herod, A. and Kandiyoti, R. Fuel 1993, 72, 469. Fuel 73(8):1371–1371
Solomon PR, Hamblen DG, Yu Z-Z, Serio MA (1990) Network models of coal thermal decomposition. Fuel 69(6):754–763
Solomon PR, Serio MA, Carangelo RM, Bassilakis R, Yu ZZ, Charpenay S, Whelan J (1991) Analysis of coal by thermogravimetry – fourier transform infrared spectroscopy and pyrolysis modeling. J Anal Appl Pyrolysis 19:1–14
Solomon PR, Hamblen DG, Serio MA, Yu Z-Z, Charpenay S (1993a) A characterization method and model for predicting coal conversion behaviour. Fuel 72(4):469–488

Solomon PR, Fletcher TH, Pugmire RJ (1993b) Progress in coal pyrolysis. Fuel 72(5):587–597
Stultz SC (ed) (1992) Steam, 40th ed. Babcock and Wilcox, Barberton
Summary of Qualifications, Westinghouse Plasma Gasification Technology (2013) Westinghouse plasma corporation, a division of Alter NRG Corp. http://www.westinghouse-plasma.com/wp-content/uploads/2013/08/WPC-SoQ-August-2013-NDA-Not-Required-Final.pdf
Syamlal M, Bissett LA (1992) METC Gasifier Advanced Simulation (MGAS) Model, Technical Note, DOE/METC-92/4108, NTIS/DE92001111, National Technical Information Service, Springfield
Syamlal M, Rogers WA, Brien TJO (1993) MFIX documentation, theory guide. In: Technical Note, DOE/METC-94/1004, NTIS/DE94000087, National Technical Information Service, Springfield
Syamlal M, Venkatesan S, Cho SM (1996) Modeling of coal conversion in a carbonizer. In: Ciang S-H (ed) Proceedings of thirteenth annual international Pittsburgh coal conference, vol 2. University of Pittsburgh, Pittsburgh, 3–7 Sept 1996, pp 1309–1314
Teichmuller M (1982) Coal petrology. GebruderBorntraeger, Berlin, 535 p.
U.S. Department of Energy (2009) Overview of DOE's gasification program, Gasification Technologies Website, available on line: http://www.netl.doe.gov/technologies/coalpower/gasification/pubs/pdf/DOE%20Gasification%20Program%20Overview%202009%2009-03%20v1s.pdf. Accessed 20 Sept 2009
UOP Selexol technology applications for CO_2 capture. In: 3rd annual Wyoming CO_2 conference, 23–24 June 2009. http://eori.uwyo.edu/downloads/CO2_Conf_2009/Presentation%20PDF/Mike%20Clark%20REVISED%20Selexol_Wyoming_Conference.pdf
Van der Hoeven BJC (1945) Producers and Producer Gas, In: Lowry HH (ed) Chemistry of coal utilization, vol II. Wiley, New York, pp 1586–1672
Van Essendelft D, Li T, Nicoletti P, Jordan T (2014) Advanced chemistry surrogate model development within C3M for CFD Modeling, Part 1: methodology development for coal pyrolysis. Ind Eng Chem Res 53:7780–7796. doi:10.1021/ie402678f
van Krevelen DW (1993) Coal – typology, physics, chemistry, constitution, 3rd edn. Elsevier, New York, xxi, 979 p
Vassilev SV et al (2002) Low cost catalytic sorbents for NOx reduction – 1. Preparation and characterization of coal char impregnated with model vanadium components and petroleum coke ash. Fuel 81:1281–1296
Walker PL Jr (1981) Structure of coals and their conversion to gaseous fuels. Fuel 60(9):801–802
Wen CY, Chaung TZ (1979) Entrainment coal gasification modeling. Ind Eng Chem Process Dev 18:684–695
Wen CY, Dutta S (1979) Rates of coal pyrolysis and gasification reactions. In: Wen CY, Lee ES (eds) Coal conversion technology. Addison-Wesley, Reading Mass, pp 57–170
Yu J, Corripio AB, Harrison DP, Copeland RJ (2003) Analysis of the sorbent energy transfer system (SETS) for power generation and CO_2 capture. Adv Environ Res 7:335–345

Conversion of Syngas to Fuels and Chemicals

Steven S. C. Chuang and Long Zhang

Contents

Abstract

This chapter examines the reaction pathways and the selectivity of the catalysts for the conversion of syngas to liquid hydrocarbons and ethanol fuels. Rh is by far the most active catalyst for ethanol synthesis. Co- and Fe-based catalysts exhibit excellent activity for hydrocarbon fuel synthesis from high H_2/CO and low H_2/CO ratio syngas, respectively. Regardless of the differences in the catalyst selectivity, all of these CO hydrogenation catalysts produce methane as one of the major products. So far, no approaches are effective in suppressing CH_4 formation. Development of a cost-effective liquid-fuel process from syngas with a low net fuel cycle CO_2 emission requires consideration of (1) the overall

S.S.C. Chuang (✉)
First Energy Advanced Energy Research Center, Department of Chemical and Biomolecular Engineering, The University of Akron, Akron, OH, USA
e-mail: schuang@uakron.edu

L. Zhang
Department of Polymer Science, The University of Akron, Akron, OH, USA
e-mail: leonard.lzhang@gmail.com; long.zhang@zips.uakron.edu

W.-Y. Chen et al. (eds.), *Handbook of Climate Change Mitigation and Adaptation*,
DOI 10.1007/978-3-319-14409-2_41

system, including the source of raw materials and by-products and (2) analysis of carbon footprint of each step from raw materials to the desired products and undesired by-products.

Introduction

Synthesis gas (syngas), a mixture of CO and H_2, has long been recognized as an important building block for manufacturing a wide range of chemicals and liquid fuels (Anderson 1983; Keim 1983). Figure 1 illustrates the pathways from raw materials (i.e., coal, natural gas, and biomass) to syngas and syngas to liquid fuels. Syngas can undergo the water-gas shift reaction to produce high-purity H_2 and the reversed water-gas shift reaction to produce high-purity CO. Individual CO and H_2 are important precursor for a number of reaction processes such as ammonia synthesis, carbonylation, and hydrogenation.

The driving force for the development of syngas to liquid fuel and chemicals has been mainly from the cost of crude oil and natural gas. Growing concerns on the effect of CO_2 on climate changes and the potential for stringent regulations on CO_2 emission demand consideration of the carbon footprint (i.e., a measure of the total quantity of all greenhouse gases emitted by a specific entity or process over a period of 1 year) of producing, distributing, and using liquid fuels. Liquid hydrocarbon fuel is the dominant form of the transportation fuel of which combustion produces more than 19 lb of CO_2 per gal of the fuels (Treptow 2010). It is very unlikely that a cost-effective approach could be developed for capture of CO_2 produced from the use of transportation liquid fuels. The use of coal- and natural gas-derived transportation fuels will lead to a net fuel cycle CO_2 emission. In contrast, the use of biomass, which is produced from the photosynthesis reaction of CO_2 with H_2O, has been expected to lower the net fuel cycle CO_2 emission, given similar level of carbon footprint of producing the liquid fuels (Larson et al. 2010).

The key differences in raw materials (i.e., coal, natural gas, and biomass) and their usage include the hydrogen to carbon ratio, contaminants, and cost. These different characteristics have a significant impact on the net fuel cycle CO_2 emission. Biomass is generally considered as an environmentally benign fuel; biomass has also been misconstrued as a fuel with zero net fuel cycle CO_2 emission. However, biomass suffers from low energy density and the diversity of its sources. The latter introduces the complexity of preprocessing steps which require the sophisticated control of gasification and syngas cleanup processes. The extent of

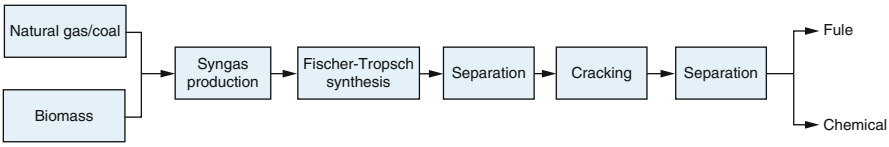

Fig. 1 Syngas production and conversion pathways

lowering carbon footprint of using biomass-derived fuel can only be determined from careful analysis of the energy usage in collection, preprocessing, syngas generation, and cleanup. A recent study has shown that coupling use of coal and biomass as a feedstock with (1) electricity and liquid-fuel production and (2) CO_2 capture and storage could be a promising approach for the production of liquid fuels with a low net fuel cycle CO_2 emission (Larson et al. 2010).

The primary use of syngas has been in methanol synthesis and Fischer-Tropsch (FT) synthesis. Methanol can serve as a fuel or a precursor for the synthesis of many industrial chemicals. Hydrocarbons and oxygenates from the FT synthesis can serve as an excellent clean fuel – an alternative to petroleum-based fuel because it is free of sulfur and nitrogen compounds commonly present in the petroleum-based fuels. This chapter will focus on direct synthesis of hydrocarbons and oxygenates from synthesis gas on heterogeneous catalysts.

Direct synthesis of hydrocarbons and oxygenates from syngas has been a subject of extensive studies due to its importance in the production of liquid transportation fuels. The syngas reaction process (i.e., CO hydrogenation) was first reported on nickel catalysts, producing methane at 1 atm (0.1 MPa) and 200–300 °C (473–573 K) (Keim 1983). Increasing reaction pressure and replacing Ni with Co leads to the formation of liquid hydrocarbons. Further increasing reaction pressure and temperature to 150 atm and 450 °C on alkalized Fe catalysts leads to the formation of oxygenates. Extensive studies have shown that Group VIII metals and some of their sulfides are active catalysts for CO hydrogenation (Wender 1996; Chuang et al. 1985a; Chuang 1990; Vannice 1975a; Burtron and Davis 2009; Dry 1981a). FT synthesis, methanol synthesis, and ethanol synthesis involve the use of the same reactants, CO and H_2. Each of these syntheses is a subclass of CO hydrogenation reactions. The development of the synthesis process such as CO hydrogenation reaction generally involves a sequence: thermodynamics, catalyst preparation, mechanistic study on a molecular scale, kinetics studies on a micro-reactor, scale-up of the reactor on a macroscale, and system integration, shown in Fig. 2. An effective catalyst development strategy must take both physical and chemical characteristics of the catalytic process into account, considering the active sites, reaction pathways, catalyst shape, pore structure, and the reactor type. The thermodynamics of the synthesis reaction can be easily calculated and have widely been reported (Ertl et al. 2008). The reactions for producing hydrocarbons and oxygenates are highly thermodynamically favorable, except for methanol. ΔG, the change in Gibbs free energy for the formation of C_n product (i.e., the species containing *n* number of carbon atoms), decreases as the product carbon number increases. Most scientific literature on this synthesis reaction can be classified into three areas: (1) mechanistic studies for elucidation of catalytic reaction mechanisms, i.e., reaction pathways and the nature of active sites (Ichikawa and Fukushima 1985); (2) catalyst preparation, characterization, and reaction kinetics studies (Underwood and Bell 1986); and (3) reactor modeling (Hedrick and Chuang 2003). The catalytic reaction steps have been shown to occur in sec scale (Balakos and Chuang 1995); the reactor process in min scale depends on the

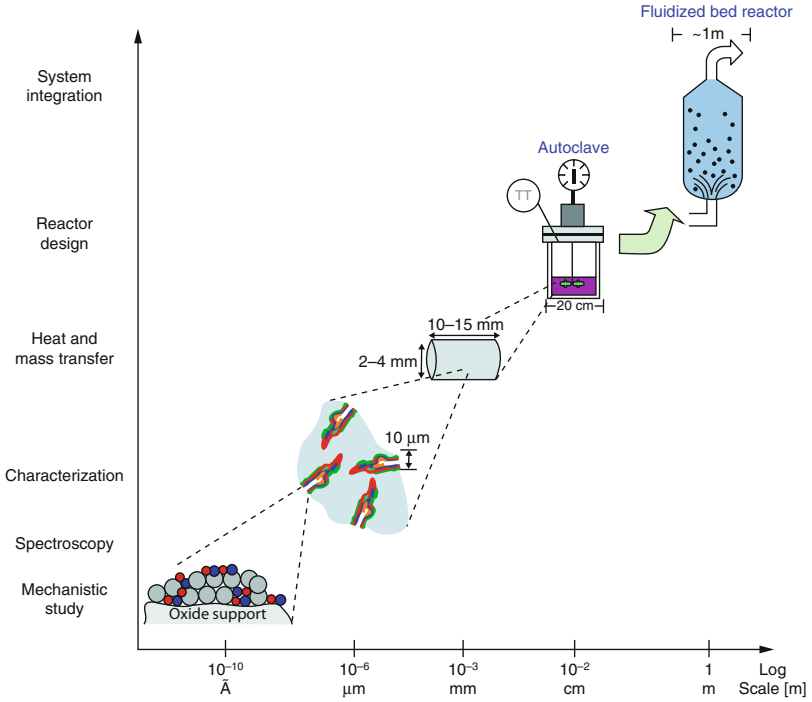

Fig. 2 The relationship among different levels of catalytic process research and development

reactant residence time. This chapter will elaborate on our current understanding of the reaction mechanism, discuss the approach for preparation of durable catalysts, and touch on the reactor modeling and scaling up issues.

Reaction Pathway

The reaction pathway and selectivity for hydrocarbon and oxygenate formation from the CO hydrogenation are governed by reaction conditions and catalyst compositions. A summary of these catalysts and a description of their typical selectivities are given in Table 1.

The reason for the formation of a wide range of C_1 to C_n products (i.e., C_1, methane and methanol; C_2, ethylene, ethane, ethanol, and acetaldehyde; C_3, propylene, propane, propanol, propionaldehyde, and acetone, C_n, species containing n number of carbon atoms) can be traced to the polymerization and network characteristics of the reaction which consists of a large set of parallel and series reaction pathways, shown in Fig. 3.

Depending on the types of metals and metal oxides, listed in Table 1, as well as their surface state and structure, these catalysts are able to catalyze each rate of the steps in the reaction network to a certain extent.

Table 1 Typical product selectivity of various CO hydrogenation catalysts

Key catalyst component	Selectivity
I. Group VIII metals	
Fe and Co	Linear and branched hydrocarbons: alkanes/alkenes and oxygenates: 1-alcohols, aldehydes, esters, ketones (Dry 1981b; Soled et al. 2003; Rao and Gormley 1982)
Ru	Methane, hydrocarbons, and polyethylene at high pressures (Kellner and Bell 1981)
Ni and Pt	Methane, low carbon-number hydrocarbons
Rh	C_2 oxygenates, including ethanol, acetaldehyde, and acetic acid (Underwood and Bell 1988a; Chuang and Pien 1992a)
Pd	Methanol (Poels and Ponec 1983)
II. Mixed oxides	Stroch et al. 1951
Zn oxide	Promotes methanol and ethanol formation on Rh
Cr oxide	Methanol and branched alcohols (C_4)
Th oxide	Hydrocarbons: branched alkanes and oxygenates: methanol $(CH_3)_2O$, branched alcohols
Cu-Zn Oxide	Methanol
Alkali – Cu-Zn oxide	Methanol and higher alcohols (Nunan et al. 1989)
$CuCoCr_{0.8}\ K_{0.09}O_x$ (an IFP catalyst)	Branched higher alcohols
III. Coprecipitated Ni-based catalysts	Chuang and Pien 1991
Na-Ni	Methane
Alkali-Mn-Na	Methane, acetaldehyde (Chuang et al. 1991)
IV. Mo-based catalysts	Tatsumi et al. 1986
Mo	Hydrocarbons
Alkali-Mo sulfide	C_1–C_5 linear, primary alcohols
Alkali-K-Co-Mo	C_1–C_4 alcohols (Li et al. 1998)

$$\text{CO dissociation: } {}^*\text{CO} \rightarrow {}^*\text{C} + {}^*\text{O} \tag{1}$$

*CO: adsorbed CO; *C: surface carbon; *O: adsorbed oxygen

$$\text{Hydrogenation: } {}^*\text{C} + x{}^*\text{H} \rightarrow {}^*\text{CH}_x \tag{2}$$

$$ {}^*\text{CO} + x{}^*\text{H} \rightarrow {}^*\text{CH}_x\text{O} \tag{3}$$

$x = 2$ or 3. $^*CH_2$: adsorbed methylene; $^*CH_3$: adsorbed methyl; *H: adsorbed hydrogen.

$$\text{Chain growth: } {}^*\text{CH}_x + {}^*\text{CH}_3 \rightarrow {}^*\text{C}_2\text{H}_{x+3} \tag{4}$$

$$ {}^*\text{CH}_x\text{O} + {}^*\text{CH}_3 \rightarrow {}^*\text{C}_2\text{H}_{x+3}\text{O} \tag{5}$$

$^*C_2H_{x+3}$: adsorbed ethylene or ethyl; $^*C_2H_{x+3}O$: adsorbed C_2 oxygenated species.

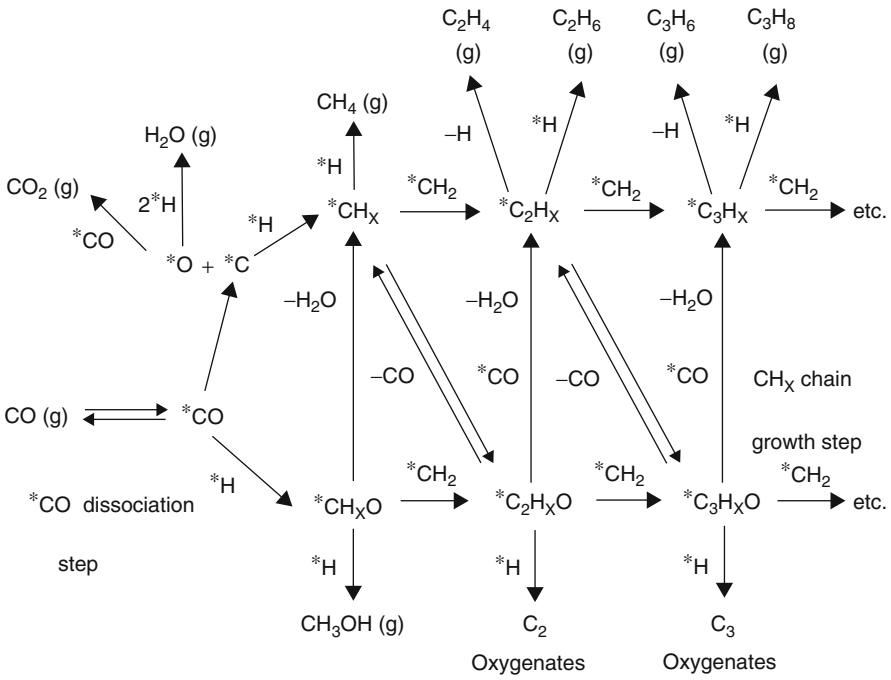

Fig. 3 The CO hydrogenation

$$\text{CO insertion: } {}^{*}\text{CH}_x + {}^{*}\text{CO} \rightarrow {}^{*}\text{C}_2\text{H}_x\text{O} \tag{6}$$

$$\text{Dehydeation: } {}^{*}\text{C}_2\text{H}_x\text{O} \rightarrow {}^{*}\text{C}_2\text{H}_{x-2+}\text{H}_2\text{O} \tag{7}$$

The first set of steps in the overall CO hydrogenation reaction network is adsorption of reactants, H_2 and CO. All of the CO hydrogenation catalysts must possess the ability to chemisorb hydrogen dissociatively, $H_2 + 2^* \rightarrow 2H^*$ (2^*: two empty sites) and chemisorb CO in either a dissociative or non-dissociative form. Group VIII metals have shown such a capability of adsorbing H_2 and CO. A surface science study shows the ability of metals to dissociate CO which is related to their position in the periodic table (Table 2) (McCash 2001).

This relationship is a result of the difference in the Fermi energy, E_f, reflecting in the ability of the metal in electron back donation to the $2\pi^*$ vacant orbital of CO, as illustrated in Fig. 4 (McCash 2001). This back donation would weaken the CO bond and stabilize the M-C bond. Metals such as Fe on the left-hand side of the ambient temperature line that possess E_f above the level of the $2\pi^*$ orbital tend to dissociate adsorbed CO. In contrast, metal on the right-hand side of 200–300 °C (473–573 K) line such as Pd, Pt, and Cu exhibit activity for chemisorbing CO non-dissociatively. Metals between these two lines would possess moderate CO dissociation ability and produce both adsorbed CO and adsorbed carbon on their surface. Although the practical catalysts containing supports and additives are significantly more complex

Table 2 Adsorption of CO metal surface

Dissociative					Non-dissociative
Cr	Mn	Fe	Co	Ni	Cu
Mo	Tc	Ru	Rh	Pd	Ag
W	Rc	Os	Ir	Pt	Au

Ambient temperature line (┈┈)

200–300°C (437–537 K) line (—)

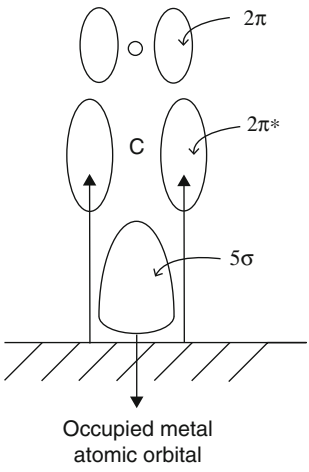

Fig. 4 Interaction of CO with metal surfaces

than the simple metal surface, the relationship in Table 2 holds for a number of SiO_2-supported catalysts. The CO dissociation activity decreases in the order: $Ni/SiO_2 > Ru/SiO_2 > Rh/SiO_2 > Pd/SiO_2$. The ranking of CO dissociation activity is consistent with the prediction by the above theoretical mode of electron back donation from the metal surface to the $2\pi^*$ empty orbital of adsorbed CO and the Fermi level of metals.

The most direct impact of the CO dissociation activity is on the selectivity of the reaction. High CO dissociation activity favors the formation of adsorbed carbon which can further hydrogenate to form CH_x, leading to the formation of hydrocarbons such as CH_4. In contrast, poor CO dissociation activity allows adsorbed CO to be hydrogenated to methanol. Metals such as Rh in the forms of either single-crystal or supported catalysts with moderate CO dissociation activity exhibited good selectivity toward C_2 oxygenates (Watson and Somorjai 1982). This observation is consistent with the proposed C_2 oxygenate formation mechanism that C_2 oxygenates are produced from both dissociatively and non-dissociatively adsorbed CO (Chuang et al. 2005).

The Nature of Active Sites

The active sites responsible for CO dissociation have been shown to be the reduced metal ensemble sites which consist of a number of surface atoms. Chain growth step involves more than two CH_xO or CHx species and would be expected to occur on the ensemble sites. In contrast, CO insertion has been demonstrated to occur on a single Rh site. Results of Rh single-crystal studies indicated that oxidized Rh sites catalyze for CO insertion (Watson and Somorjai 1981; Castner et al. 1980); the observation that sulfided Rh catalyzes the formation of propionaldehyde from ethylene hydroformylation further confirms that the Rh^+ site is an active site for catalyzing CO insertion (Konishi et al. 1987). Rh^0 and Rh^+ sites chemisorb CO in various forms which yield specific infrared bands as shown in Fig. 5. Due to the low tendency for electron back donation from Rh^{2+} and Rh^{3+}, these sites chemisorb CO, giving high-wave number IR bands in the 2,120–2,145 cm^{-1} range (McKee and Worley 1988). The structure of chemisorbed CO and its wave number are closely related to the nature of the sites it resides on. From the position of the IR band of adsorbed CO, information about the site that it is adsorbed onto can be inferred. For example, observation of vibrational bands corresponding to bridged CO on Rh implies that surface sites are in a reduced state as well as that the sites exist as an ensemble (i.e., not isolated). Similarly, from the position of linear CO, the oxidation state of the metal site can be deduced as well (i.e., Rh^0, Rh^+, Rh^{2+}, etc.). It is interesting to note that adsorbed CO on Rh-based catalysts exhibits infrared bands with excellent resolution and intensity. In contrast, infrared spectra of adsorbed CO on Fe- and Co-based catalysts have been vague and seldom reported in the literature. This may be due to the difficulty in keeping Fe and Co in the reduced state during in situ infrared study of CO adsorption.

The formation of high carbon-number products involves C-C bond formation steps which have been shown to occur via CH_x chain growth steps specifically on Rh/SiO_2 catalysts, as illustrated in Fig. 3. This reaction pathway consists of a subset of the overall CO hydrogenation reaction network, where (1) higher hydrocarbon intermediates, C_nH_x species, are produced from chain growth; (2) high hydrocarbon products, C_nH_{2n} and C_nH_{2n+2}, are produced from hydrogenation of C_nH_x; and (3) higher oxygenates are produced from the insertion of adsorbed CO into C_nH_x species. Chain growth resembles radical propagation, while hydrogenation and CO insertion correspond to chain termination steps of the polymerization kinetics and mechanism. Both methylene ($^*CH_2$) and methyl ($^*CH_3$) species have been proposed to serve as precursors for the chain growth (Underwood and Bell 1986; Hedrick and Chuang 2003; Balakos and Chuang 1995). Due to a lack of experimental techniques for in situ studies of such adsorbed intermediate species, the exact structure of chain growth precursor (i.e., x for CH_x) remains to be determined.

Owing to the polymerization characteristics of the reaction, carbon-number (C_n) distribution in hydrocarbon and oxygenated products generally follows the Anderson-Schulz-Flory (ASF) distribution in which the concentration of C_n product is inherently greater than that of C_{n+1} product (Biloen and Sachtler 1981). Variations in reaction conditions and catalyst composition allow adjustment of the chain

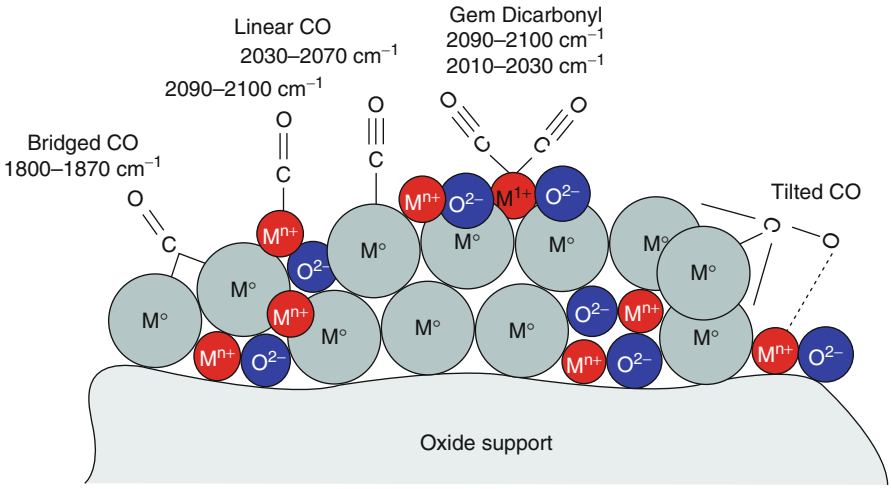

Fig. 5 Adsorbed CO on supported Rh catalysts

growth probability parameter, $\alpha(\alpha = k_1/(k_1 + k_2 + k_3)$: chain growth probability – k_1, the rate constant for chain growth; k_2, the rate constant for hydrogenation; and k_3, the rate constant for CO insertion). High temperature (i.e., temperatures above 300 °C) and 1 atm pressure shift the product distributions toward CH_4 and lower hydrocarbon products; intermediate temperature (230–275 °C) and pressure (10–50 atm) shift the products toward higher oxygenates.

Ni-, Ru-, Fe-, and Co-based catalysts exhibit excellent activity for the synthesis of higher hydrocarbons. Ru is the most active catalyst which produced primarily long chain hydrocarbons via the CH_x chain growth pathway. The reaction pathways on Fe- and Co-based catalysts have been studied extensively by probe molecules and isotope tracing techniques. Results of ^{14}C-tracing studies suggest that the chain growth proceeds primarily via oxygenated intermediates, $C_n H_x O$ on Fe-based catalysts and partially on Co-based catalysts (Davis 2001). In this pathway, oxygen dissociates from the $C_n H_x O$ intermediate in the chain termination. Mixed oxide catalysts catalyze methanol as a major product and higher alcohols (i.e., ethanol, propanol, and various isomers of C_4 alcohols) as minor products through the $CH_x O$ chain growth pathway, shown in Fig. 3. Mo-based catalysts also follow the same $CH_x O$ pathway to produce higher yields of higher alcohols than the mixed oxide catalysts, but require operating at very high pressure (>200 atm).

Circumventing Fischer-Tropsch Chain Growth Kinetics

The most significant challenge in the investigation and development of FT synthesis chemistry is the selective synthesis of C_{2+} hydrocarbons or oxygenates without producing methane. Voluminous work has been done on circumventing this

selectivity limitation of ASF. Various approaches, including (1) unsteady-state operation, (2) use of shape-selective supports, (3) interception of intermediate products, and (4) addition of olefins to the reactant stream, have been studied.

While unsteady-state operation can skew the product distribution to a certain extent, it inherently produces methane and significantly increases the difficulty in reactor operation and control. The use of shape-selective supports such as zeolites was expected to limit the chain growth through either geometric or diffusional constraints. However, the shape-selective effects have been shown to be temporary or the results of errors in data analysis. At present, no definite evidence to support the lasting shape-selective modification of the ASF has been reported. The approach of intercepting reaction intermediates utilized either multifunctional catalysts or multistep processes for catalyzing the secondary reaction processes such as isomerization and hydrocracking. FT/zeolite catalysts use metals such as Co, Fe, or Ru to catalyze the formation of FT products and the acidic function of zeolites to isomerize and crack FT products. Two-step processes with two different reactors are used if conditions for the cracking, isomerization, or other processes are significantly different from those of the FT synthesis. Addition of an olefin to the CO/H_2 feed stream has been shown to increase the higher hydrocarbon yields through chain incorporation. This approach is not economically viable due to the cost of the added olefin and the high tendency of olefin hydrogenation.

All of these attempts have failed to produce steady-state product distributions that deviate significantly from the ASF kinetics. Methane and methanol (C_1 products) have always been produced with higher yields than C_2 or higher carbon-number products. An alternative to higher hydrocarbon synthesis is the selective synthesis of C_2 oxygenates from syngas. C_2 oxygenates may be produced with high selectivity since they share the common precursor, CHx, with methane. Theoretically, both C_2 oxygenates and methane should be considered as C_1 products in the ASF kinetics. In fact, a high C_2 oxygenate selectivity (up to 75 % carbon efficiency) has been achieved on promoted Rh catalysts at 573 K and 10 MPa (Chuang et al. 2005). This selectivity is significantly higher than the maximum selectivity of 25 % for C_2 products predicted by ASF distribution, further supporting the theoretical basis of considering C_2 oxygenates as a C_1 product in ASF. Nevertheless, high hydrogenation activity of Rh leads to methane formation.

Improved control of the chain termination and chain growth steps are needed to circumvent ASF distribution of the FT synthesis. A number of studies have shown that different types of adsorbed hydrogen are responsible for the chain termination (i.e., hydrogenation of alkyl species) and chain growth steps (Stroch et al. 1951; Nunan et al. 1989; Chuang and Pien 1991; Chuang et al. 1991; Tatsumi et al. 1986; Li et al. 1998). Results from these studies suggest the possibility of controlling ASF distribution by manipulating the hydrogen reactivity. Examination of the FT mechanism in Fig. 3 shows that the suppression of termination requires inhibition of both hydrogenation and CO insertion. If the site for hydrogenation of surface carbon to form CH_x is the same as that for hydrogenation of CH_x to form methane, inhibition of hydrogenation could suppress the CH_x formation, decreasing the FT synthesis rate. A great deal of work has shown that alkali promoters enhance higher

hydrocarbon formation and decrease methane/paraffin formation, indicating that the site for CH_x formation is not the same as that for hydrogenation of CH_x (Stroch et al. 1951; Nunan et al. 1989; Chuang and Pien 1991; Chuang et al. 1991; Tatsumi et al. 1986). NMR studies show that the suppression of methane/paraffin formation is a result of limited migration of adsorbed hydrogen brought about by potassium promoters (Chuang et al. 2005). Although complete suppression of methane formation may never be achieved, it remains to be determined what extent of methane suppression can be achieved through limiting migration of adsorbed hydrogen. The challenge is to suppress methane formation and enhance CO insertion for further improving C_2 oxygenate selectivity.

Ethanol Synthesis Catalysts

Ethanol is one of the oxygenated products (i.e., alcohols, aldehydes, and acids) synthesized from CO hydrogenation (i.e., the reaction of CO with H_2). The catalytic synthesis of C_{2+} oxygenates (ethanol, propanol, and higher alcohol; acetaldehyde, propionaldehyde, and higher aldehydes; acetic acid, propanoic acid, and higher acids) has been a subject of intensive interest because of their high value-added and versatile applications (Anderson 1983; Biloen and Sachtler 1981). The early developments of C_{2+} oxygenates synthesis from CO hydrogenation took place in Germany. In 1913, BASF discovered that cobalt and osmium catalysts produced a mixture of oxygenates, including alcohols, aldehydes, ketones, and acids at pressures above 20 MPa and temperatures up to 673 K (Schindeler 1989). Since that time, a significant amount of work has been done to determine the activity, selectivity, and durability (i.e., deactivation characteristics) of catalysts for the higher oxygenate and Fischer-Tropsch (FT) synthesis (Chuang et al. 1985a; Davis 2001; Klier et al. 1988; Vannice 1975b).

Most studies on the effect of additives on C_{2+} oxygenate synthesis have been focused on Rh/SiO_2 (Nonneman et al. 1990; Yoneda 1989), which give a moderate selectivity toward acetaldehyde and ethanol as compared to Rh/La_2O_3 and Rh/TiO_2. Additives such as Mn (Boffa et al. 1994), Na (Dry 1981b), Sc, Ti, and La enhanced CO dissociation; Ag, Cl, Zr, Zn, S (Chuang 1990), Ti, La (Underwood and Bell 1988b), and V promoted CO insertion (Ichikawa and Fukushima 1985; Ichikawa et al. 1985); alkali species promoted CO dissociation and suppressed hydrogenation.

With the knowledge of the specific additive effect and extensive catalyst screening studies, Rh-Mn-Fe-Li (1:1:0.1:0.1 in the atomic ratio)/SiO_2 catalyst with a 4.5 wt% Rh loading emerged as one of the most active and selective catalyst for C_2 oxygenate synthesis, exhibiting ethanol selectivity up to 44 % and a total C_2 oxygenate selectivity of 56 % with about 0.178 mol/Kg-h in the ethanol production rate at $CO/H_2 = 0.5$, 50 atm, 270 °C, SV (space velocity) = 12,000 h^{-1} in the Japanese C_1 chemistry program in the 1980s (Yoneda 1989). Note that SV is defined as the ratio of the reactor volume to the inlet volumetric flow rate at room temperature. Researchers in China have rediscovered the high activity and

selectivity of the Rh-Mn-Fe-Li (1:1:0.075:0.05 in the weight ratio) with a 1 wt% Rh loading showing 27 % in ethanol and 56 % in C_2 oxygenate selectivity and 9.1 mol/kg-h in the C_2 oxygenate production rate at $CO/H_2 = 0.5$, 30 atm, 320 °C, SV (space velocity) = 12,000 h^{-1} (Yin et al. 2003). The best C_2 oxygenate selectivity obtained in our laboratory with a Rh-Ag (1:1 in the atomic radio)/SiO_2 with a 3 wt% Rh loading was 59 % with a 0.25 mol/kg-h in C_2 oxygenate production rate at $CO/H_2 = 1$, 20 atm, 240 °C, SV (space velocity) = 11,000 h^{-1} (Chuang and Pien 1992a). This Rh-Ag catalyst showed negligible activity toward ethanol. These results are summarized in Table 3 for comparison. While it is difficult to compare the results of these studies due to the use of different conditions, the rate data at various temperatures can be further adjusted with the activation energy of 23 kcal/mol-K, the average value found from literature (Chuang et al. 1985b), to the rate at 280 °C. The production rates at 280 °C show that the C_2 oxygenate rate on these promoted catalysts are in the range of 0.23–2.2 mol/kg-h which are close to the rates of higher hydrocarbon formation in the Fischer-Tropsch synthesis (Dry 1981b). The results of the rate comparison suggest that the size of pilot or commercial scale ethanol synthesis reactors should be in the same range of the Fischer-Tropsch synthesis reactors. Although the results of the study by Yin et al. are significantly higher than those of others, further verification is needed (Yin et al. 2003).

Studies on the effect of reaction conditions show increasing temperature and pressure increased the rate of C_2 oxygenate formation and further increasing temperature above 320 °C can shift the reaction selectivity toward methane and cause a rapid catalyst deactivation. This is the reason why the long-term pilot scale study is conducted at 280 °C in the Japanese C_1 chemistry program (Yoneda 1989). Use of a 200 cm^3 (about 400 g) of Rh-Mn-Li/SiO_2 and 200 cm^3 of Cu-Zn/SiO_2 catalyst mixture in a pilot scale unit showed that the mixed catalysts produced 0.14 mol/kg-h in the ethanol production rate with 70 % ethanol selectivity at $CO/H_2 = 0.5$, 40 atm, 280 °C, SV (space velocity) = 16,000 h^{-1} decayed less than 15 % of its activity in a period of 1 year. The results of this study are the only pilot scale data available in the literature. Examination of the catalyst preparation procedures and their characterization results showed that the activity, selectivity, and durability of the Rh-based catalysts for ethanol synthesis can be further improved with adjusting the following catalyst characteristics:

Control of Rh particle size. The average Rh particle size of 3.5 nm has been shown to give the highest selectivity for C_2 oxygenate synthesis (Yoneda 1989). The single reduced Rh site chemisorbing linear CO has been demonstrated to be active for CO insertion (Chuang and Pien 1992b); Rh ensemble sites (i.e., a group of surface Rh atoms) are active for CO dissociation. 3.5 nm Rh particle appears to contain the appropriate ratio of the sites for CO dissociation and CO insertion to give the highest C_2 oxygenate selectivity.

Fine-tuning promoter composition. On the basis of the mechanistic information and results of previous studies, the optimum catalysts for ethanol synthesis will be a multicomponent catalyst which consists of 3.5 nm Rh particle size and appropriate

Table 3 Comparison of Rh-based catalyst activities and selectivities

Catalyst	Experimental conditions	C_2 oxygenate/ethanol selectivity (%)	C_2 oxygenate production rate (mol/kg-h)	C_2 oxygenate production rate at 280 °C (mol/kg-h)	Reference
Rh-Mn-Fe-Li	Pressure: 50 atm	56/44	0.23	0.23	Yoneda 1989
1:1:0.1:0.1	Temperature: 543 K				
4.5 wt% Rh	SV: 12,000 h^{-1}				
	$CO/H_2 = 0.5$				
Rh-Mn-Fe-Li	Pressure: 30 atm	56/27	9.1	2.2	Yin et al. 2003
1:1:0.075:0.05	Temperature: 593 K				
Rh-Ag	Pressure: 20 atm	59/–	0.25	1.25	Chuang and Pien 1992a
1:1	Temperature: 513 K				
	SV: 11,000 h^{-1}				
	$CO/H_2 = 1$				

amount of each promoter to enhance CO dissociation and CO insertion and to balance hydrogenation of C and CH*x*. The role of each promoter based on our and other studies discussed above is summarized below:

- Ag: Suppress CO dissociation and promote CO insertion.
- Mn: Enhance CO dissociation and CO insertion.
- Li: Suppress hydrogenation.
- Fe: Promote CO insertion.
- Cu: Promote hydrogenation of acetaldehyde and acetic acid to ethanol without promoting hydrogenation of CH_x species (Yoneda 1989). Cu-based catalysts, which lack CO dissociation activities, are not able to accommodate CH*x* species and catalyze hydrogenation of CH_x to the undesired methane (i.e., CH_4). Cu-based catalysts will be especially useful to promote ethanol formation from Rh-Ag catalysts which showed high C_2 oxygenate selectivity, but low ethanol selectivity. Although the specific role of each promoter has been identified, it remains unclear about the optimum composition of the promoters for enhanced ethanol synthesis.

Hydrocarbon Synthesis Catalysts

The above ethanol synthesis catalysts serve as an excellent example to illustrate the importance of identifying the role of each component in a multicomponent catalyst. In fact, almost all of practical heterogeneous catalysts consist of multicomponents. The FT′s Fe- and Co-based catalysts consist of more than four components (Davis and Occelli 2009).

The traditional FT Fe catalysts are either in the formed fused iron oxides or coprecipitated catalysts. The fused Fe catalysts prepared at 1,500 °C contain K_2O as chemical promoter and MgO or Al_2O_3 as the structural promoters. These structural promoters can atomically disperse in the Fe oxide phase and serve as the spacers between metal crystallite after reduction of Fe oxides. The coprecipitated catalyst is prepared by coprecipitation of Fe and Cu nitrate solution with Na_2CO_3. The concentration of catalyst precursors, the precipitation temperature, and the pH govern the final catalyst form, i.e., the types of oxides, the surface area, and the porosity. Prior to the reaction, the fused catalyst has to be activated by hydrogen reduction; the coprecipitated catalysts are activated by syngas. Removal of reduced product, H_2O, from reduction is necessary to avoid sintering of reduced metals and accelerate the activation process. It is interesting to note that the commonly used impregnation method is not used because a large fraction of the chemical promoters could end up adsorbing on or reacting with the support.

In contrast to Fe-based catalysts, cobalt-based catalysts are prepared by impregnation on high surface area supports with a low cobalt loading, i.e., 20 wt% or less. Co-based catalysts may contain Cu or noble metals to facilitate the reduction of cobalt oxide particles; oxidic promoters such as lanthanide, thorium, cerium, titania, and zirconium oxides to stabilize the Co dispersion on the support; and Mn to suppress hydrogenation and to enhance chain growth.

Both Fe-based and Co-based catalysts show increase in the selectivity toward high hydrocarbon at low temperature and H_2/CO ratios. Selection of either Fe- and Co-based catalysts requires further consideration of issues of cost, deactivation, the CO/H_2 ratio of syngas gas, and the overall net fuel cycle CO_2 emission. Co-based catalyst is less sensitive to H_2O deactivation. The cost of Co-based catalyst is significantly higher than that of Fe-based catalysts. In addition to the cost and H_2O sensitivity issues, Co catalysts produced H_2O and do not have the water-gas shift activity; Fe catalysts produced CO_2 with a high water shift activity. Thus, Fe catalysts are used for the low H_2/CO ratio syngas from coal; Co catalysts are considered for the high H_2/CO ratio syngas from natural gas.

Reactor Issues

CO hydrogenation is a highly exothermic reaction releasing 140–150 kJ/mol of the heat per CH_2 added onto the C_n products or 165–180 kJ/mol CO converted. Rise in reactor temperature will lead to catalyst deactivation and the enhanced formation of

undesired methane. Commercial FT reactors include multitubular fixed bed, slurry bubble column bed, fixed fluidized bed, and entrained fluidized bed. These reactors are designed for maximum heat removal to avoid catalyst deactivation. The fixed bed reactor possesses the advantage of simplicity and low cost as well as the disadvantage of difficulty in controlling the reaction temperature. Slurry bubble reactors contain high heat capacity inert media which facilitate the removal of the reaction heat; however, it may cause complications due to attrition of the catalyst particles. Ethanol synthesis from syngas is also a highly exothermic process. So far, ethanol synthesis has only been reported to be carried out in the fixed bed reactor.

Future Directions

Almost every element in the periodic table has been tested as promoter for both hydrocarbon and ethanol syntheses. The effects of concentration of promoters generally follow a trend: increasing the promotion effect in the low concentration range and decreasing the promotion effect in the high concentration range. Without gaining an in-depth understanding of the promoter-metal, metal-support, and promoter-support interaction, as well as the effect of these interactions on the nature of active sites for the rate-determining step, further variation in the concentration of promoters and the addition of different sequences and combinations of promoters are unlikely to generate the breakthrough results in catalyst selectivity and durability. The emphasis on the basic research should be placed on in situ studies since the nature of the catalyst surface is strongly influenced by the reaction environment where both reactants and products are present. The rate-determining step can be identified by careful design and use of transient techniques. The use of transient techniques coupling with isotope tracer has been shown to be highly effective in determining the rate-determining step (Chuang and Guzmanm 2009). In addition to determining the effects of the promoters on the catalyst activity, selectivity, and durability, the focus should be placed on the promoter effects on the rate-determining step.

Catalyst development deals with catalyst activity, selectivity, and deactivation resistance. The deactivation usually resulted from sintering and sulfur poisoning. Sintering of metal crystallite may be addressed by addition of the nanoscale spacer to serve as the barrier for the migration of small reduced metal crystallite. Sulfur compounds bind strongly on the reduced metal sites. Instead of modifying metal surface site to impart the sulfur resistance, it may be more effective if a cost-effective approach can be developed to remove sulfur compounds and sulfur content of the syngas to the ppb level.

The global emphasis on development of the low carbon dioxide emission technologies shifted the focus from the use of coal-based syngas to biomass-based syngas. The challenge in the biomass routes will lie at the cost of biomass gasification and purification of its syngas. The issues such as the cost of shipping and pretreating are common for all of biomass-related conversion processes. Syngas conversion to fuel processes has to be examined by considering the overall system, including the life cycle of each species in the process and the energy efficiency of each processing step.

References

Anderson RB (1983) Fischer Tropsch and related synthesis. Academic, New York

Balakos MW, Chuang SSC (1995) Dynamic and LHHW kinetic analyses of heterogeneous catalytic hydroformylation. J Catal 151(2):266–278

Biloen P, Sachtler WMH (1981) Mechanism of hydrocarbon synthesis over Fischer-Tropsch catalysts. Adv Catal 30:165–216

Boffa A et al (1994) Promotion of CO and CO_2 hydrogenation over Rh by metal oxides: the influence of oxide Lewis acidity and reducibility. J Catal 149(1):149–158

Burtron H, Davis MLO (2009) Advances in Fischer-Tropsch synthesis, catalysts, and catalysis. CRC Press, Boca Raton

Castner DG, Blackadar RL, Somorjai GA (1980) Carbon monoxide hydrogenation over clean and oxidized rhodium foil and single crystal catalysts. Correlations of catalyst activity, selectivity, and surface composition. J Catal 66(2):257–266

Chuang SSC (1990) Sulfided group VIII metals for hydroformylation. Appl Catal 66(1):L1–L6

Chuang SSC, Guzmanm F (2009) Mechanistic investigation of heterogeneous catalysis by transient infrared methods. Top Catal 52:1448–1458

Chuang SSC, Pien SI (1991) Synthesis of aldehydes from synthesis gas over sodium-promoted manganese-nickel catalysts. J Catal 128(2):569–573

Chuang SSC, Pien SI (1992a) Role of silver promoter in carbon monoxide hydrogenation and ethylene hydroformylation over rhodium/silica catalysts. J Catal 138(2):536–546

Chuang SSC, Pien SI (1992b) Infrared study of the carbon monoxide insertion reaction on reduced, oxidized, and sulfided rhodium/silica catalysts. J Catal 135(2):618–634

Chuang SC et al (1985a) The use of probe molecules in the study of carbon monoxide hydrogenation over silica-supported nickel, ruthenium, rhodium, and palladium. J Catal 96(2):396–407

Chuang SC, Goodwin JG Jr, Wender I (1985b) The effect of alkali promotion on carbon monoxide hydrogenation over rhodium/titania. J Catal 95(2):435–446

Chuang SSC et al (1991) Carbon monoxide hydrogenation over sodium-manganese-nickel catalysts: effects of catalyst preparation methods on the C_{2+} oxygenate selectivity. Appl Catal 70 (1):101–114

Chuang SSC, Stevens RW Jr, Khatri R (2005) Mechanism of C_{2+} oxygenate synthesis on Rh catalysts. Top Catal 32(3–4):225–232

Davis BH (2001) Fischer-Tropsch synthesis: current mechanism and futuristic needs. Fuel Process Technol 71(1–3):157–166

Davis BH, Occelli ML (eds) (2009) Advances in Fischer-Tropsch synthesis, catalysts, and catalysis, vol 128, Chemical industries. CRC Press, Boca Raton, 403 pp

Dry ME (1981a) The Fischer-Tropsch synthesis. Catal Sci Technol 1:159–255

Dry ME (1981b) The Fischer-Tropsch synthesis. In: Anderson JR, Boudart M (eds) Catalysis – science and technology, vol 1. Springer, Berlin/Heidelberg/New York, pp 159–255

Ertl G, Knözinger H, Schüth F, Weitkamp J (2008) Handbook of heterogeneous catalysis, vol 6. Wiley, Weinheim

Hedrick SA, Chuang SSC (2003) Modeling the Fischer-Tropsch reaction in a slurry bubble column reactor. Chem Eng Commun 190(4):445–474

Ichikawa M, Fukushima T (1985) Mechanism of syngas conversion into C_2-oxygenates such as ethanol catalyzed on a silica-supported rhodium-titanium catalyst. J Chem Soc Chem Commun 6:321–323

Ichikawa M et al (1985) Selective hydroformylation of ethylene on rhodium-zinc-silica. An apparent example of site isolation of rhodium and Lewis acid-promoted carbonyl insertion. J Am Chem Soc 107(24):7216–7218

Keim W (1983) Catalysis in C1 chemistry: catalysis by metal complexes, vol 4. Springer, Berlin

Kellner CS, Bell AT (1981) Synthesis of oxygenated products from carbon monoxide and hydrogen over silica- and alumina-supported ruthenium catalysts. J Catal 71(2):288–295

Klier K et al (1988) Mechanism of methanol and higher oxygenate synthesis. Stud Surf Sci Catal 36:109–125. Methane Conversion, Proceedings of a Symposium on the Production of Fuels and Chemicals from Natural Gas

Konishi Y, Ichikawa M, Sachtler WMH (1987) Hydrogenation and hydroformylation with supported rhodium catalysts: effect of adsorbed sulfur. J Phys Chem 91(24):6286–6291

Larson ED et al (2010) Co-production of decarbonized synfuels and electricity from coal + biomass with CO_2 capture and storage: an Illinois case study. Energy Environ Sci 3(1):28–42

Li X et al (1998) Higher alcohols from synthesis gas using carbon-supported doped molybdenum-based catalysts. Ind Eng Chem Res 37(10):3853–3863

McCash EM (2001) Surface chemistry. Oxford University Press, New York

McKee ML, Worley SD (1988) A theoretical study of rhodium/carbonyl species. J Phys Chem 92 (13):3699–3700

Nonneman LEY et al (1990) Role of impurities in the enhancement of C_2-oxygenates activity: supported rhodium catalysts. Appl Catal 62(2):L23–L28

Nunan JG et al (1989) Higher alcohol and oxygenate synthesis over cesium-doped copper/zinc oxide catalysts. J Catal 116(1):195–221

Poels EK, Ponec V (1983) Formation of oxygenated products from synthesis gas. Catalysis 6:196–234

Rao VUS, Gormley RJ (1982) Catalyst for converting synthesis gas to light olefins. (United States Dept. of Energy, USA). Application: US, 5 pp

Schindeler HD (1989) Coal liquefaction – a research and development needs assessment, vol II. US Department of Energy, McLean

Soled SL et al (2003) Control of metal dispersion and structure by changes in the solid-state chemistry of supported cobalt Fischer-Tropsch catalysts. Top Catal 26(1–4):101–109

Stroch HH, Golumbic N, Anderson RB (1951) The Fischer-Tropsch and related syntheses. Wiley, New York

Tatsumi T et al (1986) Effects of molybdenum precursors on the activity of alkali-promoted molybdenum catalysts for alcohol synthesis from carbon monoxide-hydrogen. Polyhedron 5 (1–2):257–260

Treptow RS (2010) Carbon footprint calculations: an application of chemical principles. J Chem Educ 87(2):168–171

Underwood RP, Bell AT (1986) Carbon monoxide hydrogenation over rhodium supported on silicon oxide, lanthanum oxide, neodymium oxide, and samarium(III) oxide. Appl Catal 21 (1):157–168

Underwood RP, Bell AT (1988a) Lanthana-promoted rhodium/silica. I. Studies of carbon monoxide and hydrogen adsorption and desorption. J Catal 109(1):61–75

Underwood RP, Bell AT (1988b) Lanthana-promoted rhodium/silica. II. Studies of carbon monoxide hydrogenation. J Catal 111(2):325–335

Vannice MA (1975a) Catalytic synthesis of hydrocarbons from molecular hydrogen/carbon monoxide mixtures over the group VIII metals. III. Metal-support effects with platinum and palladium catalysts. J Catal 40(1):129–134

Vannice MA (1975b) Catalytic synthesis of hydrocarbons from hydrogen-carbon monoxide mixtures over the group VIII metals. I. Specific activities and product distributions of supported metals. J Catal 37(3):449–461

Watson PR, Somorjai GA (1981) The hydrogenation of carbon monoxide over rhodium oxide surfaces. J Catal 72(2):347–363

Watson PR, Somorjai GA (1982) The formation of oxygen-containing organic molecules by the hydrogenation of carbon monoxide over a lanthanum rhodate catalyst. J Catal 74(2):282–295

Wender I (1996) Reactions of synthesis gas. Fuel Process Technol 48(3):189–297

Yin H et al (2003) Influence of iron promoter on catalytic properties of Rh-Mn-Li/SiO_2 for CO hydrogenation. Appl Catal A 243(1):155–164

Yoneda Y (1989) Progress in C1 chemistry in Japan. Kodansha/Elsevier, Tokyo

Chemical Looping Combustion

Edward John (Ben) Anthony

Contents

Abstract

Chemical looping combustion (CLC) and looping cycles in general represent an important new class of technologies, which can be deployed for direct combustion as well as be used in gasification applications. In this type of system, a solid carrier is used to bring oxygen to the fuel gas, so that it can be subsequently released as a pure CO_2 stream suitable for use or, more likely, for sequestration.

E.J.B. Anthony (✉)
CanmetENERGY, Natural Resources Canada, Ottawa, ON, USA
e-mail: EdwardJohn.Anthony@NRCan-RNCan.gc.ca

W.-Y. Chen et al. (eds.), *Handbook of Climate Change Mitigation and Adaptation*,
DOI 10.1007/978-3-319-14409-2_42

The solid is then regenerated in a reactor using air, so that the technology effectively achieves oxygen separation from air without the use of a cryogenic process or membrane technology. In a sense, cycles using liquids, such as amine scrubbing, could also be regarded as a type of looping cycle, the key being that the carrier must be regenerated and reutilized for as long as possible. However, this chapter will restrict itself to considering the uses of solid carriers only and, more specifically, those in which oxygen is transported and not CO_2 as is the case for calcium looping. Particular focuses of this chapter will be on the use of this technology for H_2 production and gasification applications, as well as its use with solid fuels. Another issue that will be discussed is high-pressure cycles, which are ultimately necessary if such systems are to be integrated into high-efficiency electrical energy cycles.

Introduction

Chemical looping combustion (CLC) was first suggested by Lewis, Gilliland, and Reed in a paper published in *Industrial and Engineering Chemistry* (Lewis et al. 1949). In this paper, they carried out an experimental investigation of the use of CuO to oxidize methane to CO and H_2 using a small fluidized bed reactor at a temperature of 925 °C to avoid both the use of oxygen and high net heat requirements normally required in the reforming process. Subsequently, these workers proposed the use of this approach for the production of pure CO_2 from a hydrocarbon gas (Lewis and Gilliland 1954). Later, the idea of using a metal oxide to combust a gaseous hydrocarbon was again proposed as a method of achieving "controlled combustion" by Richter and Knoche (1983), who explored the Ni system and proposed the Cd system based on a theoretical analysis (although, since Cd has a low melting point of around 321 °C, this would seem to preclude its use, even if its noted toxicity did not). Although the work of Richter and Knoche clearly references the earlier work of Lewis and his colleagues in 1949, the contribution of Lewis and his colleagues in proposing the basic ideas of CLC seems to have been largely ignored in subsequent developments. In subsequent work Richter emphasized the potential benefits of employing such a cycle in combination with a solid oxide fuel cell and stressed the potential benefits of producing three separate fluid streams, namely, CO_2, H_2O, and N_2 (when air is used to oxidize the carrier) (Harvey and Richter 1994). In a thermodynamic study done by Jerndal et al. (2006), 27 possible systems were examined, based on the potential of an oxide to achieve complete or near-complete conversion of CH_4, H_2, and CO. Factors like stability in air and melting temperatures were also examined, and metal oxides based on Ni, Cu, Fe, Mn, Co, W, and sulfates of Ba and Sr were shown to offer possible chemical looping systems, although for some reason the sulfate of Ca was not considered. However, it is to the Ni-, Cu-, and Fe-based systems that most of this chapter will be devoted.

Early experimental work was done extensively in either thermogravimetric analyzers (TGAs) or subsequently in fixed bed reactors in Japan by various workers including, most notably, Ishida and his coworkers (Ishida and Jin 1994a, b), using

primarily Ni-based carriers, all of which demonstrated that the reaction was fast enough to be employed in practice and that soot formation or carbon deposition on the particles did not appear to be a major problem if the oxidation reaction was carried out at a high enough temperature (Hatanak et al. 1997). This work uses the term chemical looping combustion and also clearly identifies the benefits of such an approach in terms of producing a pure stream of CO_2 for sequestration after water has been removed. Subsequent research has been heavily directed to pilot plant studies, using fluidized beds, and has been carried out most notably in places like Chalmers University, Sweden, with a major focus on developing practical systems (Lyngfelt et al. 2001). These developments will be discussed in considerable detail below since it is the practical application of these technologies and their demonstration at the industrial scale in the next several decades that is key to their contribution to a carbon-constrained world.

Chemical Looping Combustion Concept

Until quite recently, when efforts have been made to use these cycles with solid fuels, nearly all of the proposed cycles involved reaction of a gaseous hydrocarbon with a metal oxide that is taken from a higher to a lower state of oxidation, following the global reaction scheme:

$$(2n+m)\mathrm{M}_y\mathrm{O}_x + \mathrm{C}_n\mathrm{H}_{2m} = (2n+m)\mathrm{M}_y\mathrm{O}_{x-1} + m\mathrm{H}_2\mathrm{O} + n\mathrm{CO}_2 \quad (1)$$

Alternatively, if a reforming step is being considered, the amount of oxidant is reduced to allow for the production of CO and H_2, as in the original concept of Lewis et al. (1949):

$$n\mathrm{M}_y\mathrm{O}_x + \mathrm{C}_n\mathrm{H}_{2m} = n\mathrm{M}_y\mathrm{O}_{x-1} + m\mathrm{H}_2 + n\mathrm{CO} \quad (2)$$

In the case of combustion (Rx. 1), after the water produced from hydrocarbon oxidation is removed, the flue gas stream contains an effectively pure stream of CO_2 suitable for sequestration. The metal oxide is regenerated in a separate reactor by reaction with air (Rx. 3), and the regenerated solid can be transferred back for further reaction with the fuel gas (Fig. 1):

$$\mathrm{M}_y\mathrm{O}_{x-1} + \mathrm{Air} = \mathrm{M}_y\mathrm{O}_x \quad (3)$$

Typically, the oxidation reaction is strongly exothermic and the reduction step is not (an exception is the CuO/Cu cycle in which both oxidizing and reducing cycles are exothermic (Chuang et al. 2008)), so that overall, the system yields the heating value of the fuel. Such a cycle represents an elegant way of oxidizing a fuel gas by effectively achieving air separation, without using cryogenic or membrane technology, and, in addition, avoiding or minimizing the formation of fuel-NO_x. In practice,

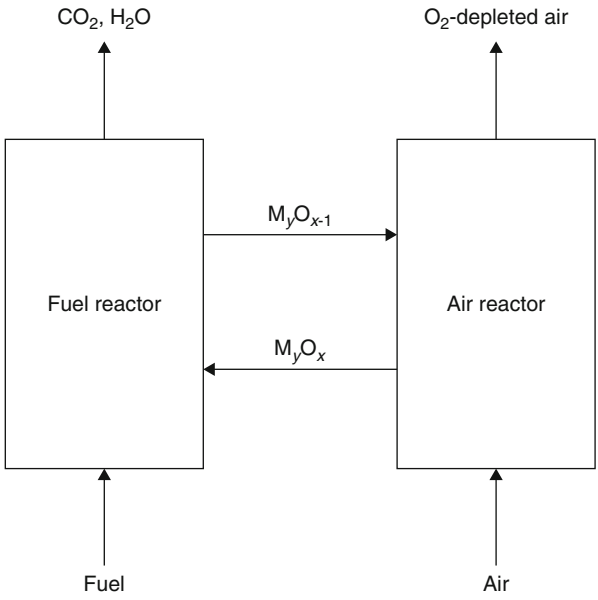

Fig. 1 Typical metal oxide looping cycle

these cycles typically operate at temperatures in the range of 800–1,200 °C, which normally ensures that the reactions occur at a sufficient rate to be compatible with a fluidized bed system and to ensure that agglomeration and sintering are minimized. In principle, they can be run either at atmospheric or high pressure, although the vast bulk of the research done to date has been at atmospheric pressure. It should also be noted that Rx. 1 and 2 are idealized since many oxides permit multiple oxidation states, and complete conversion of the oxide need not necessarily occur in either Rx. 1, 2, 3 to ensure effective use of the chemical looping reagent (Bohn et al. 2008).

Choices of Oxide Carriers

Any given oxide system will have a carrying capacity, which can be defined as

$$\mathrm{Rx} = (m_{\mathrm{ox}} - m_{\mathrm{red}})/m_{\mathrm{ox}} \tag{4}$$

where m_{ox} is the mass of the fully oxidized sample and m_{red} is the mass of the reduced sample. The values of m_{ox} for the common systems (Fe_2O_3/Fe_3O_4, Ni/NiO, Cu/CuO) are 0.03, 0.22, and 0.24, respectively, and the oxidation reactions are of the type shown below:

$$3Fe_2O_3 + CO/H_2 = 2Fe_3O_4 + CO_2/H_2O \tag{5}$$

$$CuO + CO/H_2 = Cu + CO_2/H_2O \quad (6)$$

$$NiO + CO/H_2 = Ni + CO_2/H_2O \quad (7)$$

Other systems of course exist, such as the Mn_3O_4/MnO and CoO/Co systems:

$$Mn_3O_4 + CO/H_2 = 3MnO + CO_2/H_2O \quad (8)$$

$$CoO + CO/H_2 + CO + CO_2/H_2O \quad (9)$$

which have received limited investigation (Johansson et al. 2006a). There is one notable nonmetallic system, the $CaSO_4$/CaS system, that has the highest carrying capacity of all, at 0.47, and this system will be discussed later. It should also be mentioned that there has been some success in preparing oxygen carriers with mixed oxide systems, which together show better overall performance. For example, the addition of small amounts of Ni was shown to improve the performance of various oxygen carriers, and it is suggested that this arises because Ni^0 can catalyze methane conversion by methane pyrolysis and steam reforming (Johansson et al. 2006b).

In practice, it is more usual and useful to consider the carrying capacity of the particles themselves, since they contain an inert substrate to support the active component and the oxygen-carrying capacity figures will be lower and depend on the formulation of the particle itself. Also, in some instances, the carrier itself will form a compound with the support material that is itself inert, an example of this being Al_2O_3 with Ni, which forms a Ni spinel ($NiAl_2O_4$) that is not itself active as an oxygen carrier and consumes some of the Ni otherwise available for reaction (Gayán et al. 2009). Thus, for instance, Abad et al. (2007a) give figures for three oxygen carriers based on Fe, Ni, and Cu, showing that their actual carrying capacities are 0.013, 0.084, and 0.02, respectively.

While the carrying capacity of the material and the particles made from it will be of major significance, there are obviously a number of other factors that must be considered. Kinetics is clearly one, and based on an evaluation of 600 different oxygen carriers (i.e., predominantly the Ni, Cu, and Fe systems with different inert substrates), Johansson concluded that Ni and Cu were the most reactive (Johansson 2007). Another potential concern is the melting point of the active material since sintering will be significantly enhanced if the carrier must be operated near its melting point for kinetic reasons. Here, the material with the lowest melting point of those commonly considered for chemical looping cycles is Cu, which has a melting point of 1,083 °C, and since operation of chemical looping systems is normally in the range of 700–1,000 °C, this has been somewhat of a concern for the copper system; however, extensive experimentation has shown that Cu-based chemical looping systems can be operated satisfactorily with Cu at a temperature range of up to 950 °C (Johansson 2007). Another issue is thermodynamic limitations for the oxidation cycle; thus, the Ni/NiO cycle cannot convert a hydrocarbon completely to CO_2 and H_2O, having a conversion of 98.8 %, for instance, at 1,000 °C, with higher conversions at lower temperatures. In the case of CoO/Co,

the thermodynamics are even less favorable with a conversion of 93 % at 1,000 °C (Johansson 2007).

Finally, there are the issues of toxicity and availability. Ni is a known carcinogen, and Co would be considered as toxic in other than trace amounts, at which levels it is a micronutrient. Copper also has minor toxicity issues. However, the factors that are more likely to limit the use of such materials are their availability, cost, and reactivity. In this situation, there will always be a tendency to prefer iron-based systems if their reactivity can be increased sufficiently for practical applications, since iron-based materials are always likely to be more available, less costly, and less toxic than any other metal/metal oxide system. Unfortunately, the iron-based systems have a rather low carrying capacity and are the least reactive of the common systems being considered, that is, Ni, Cu, and Fe systems. Nonetheless, as will be seen below, because of their relatively low costs and essential lack of toxic or environmental concerns, iron-based systems continue to receive considerable attention.

Preparation of Chemical Looping Particles and Related Issues

In a detailed analysis of the cost limits for looping cycle materials, Abanades et al. (2007) noted that:

A makeup flow of sorbent is required to compensate for the natural decay of activity and/or sorbent losses during many sorption/desorption cycles. It must be emphasized that this decay is to some extent always unavoidable because of [a] wide range of chemical and physical interactions of the sorbent inside the reactor and transport lines and the sorbent losses associated with gases leaving the system.

In consequence, in the analysis of Abanades et al. (2007), they stressed that in order for costs to be kept to a reasonable limit, it is necessary to reduce the amount of makeup of expensive sorbents by increasing the number of reaction cycles to a figure approaching tens of thousands.

Unfortunately, unlike, say, Ca looping for CO_2 capture or the $CaS/CaSO_4$ looping cycles, where one can envisage using natural limestones or natural anhydrite materials, respectively, nearly all of the earlier efforts at making chemical looping reagents envisage using relatively expensive materials that have to be prepared in the form of synthetic particles, an exception being the use of natural ilmenite ($FeTiO_3$) (Prőll et al. 2009). This issue was apparent with the pioneering work of Lewis et al. (1949), who noted that CuO itself did not work well due to a rapid growth in particle sizes and instead used Cu on supports including silica gel, alumina gel, and kaolin, with the carriers ground to the required size and the metal deposited on it. In the work of Lewis et al. (1949), a copper nitrate solution was mixed with the carrier and the copper deposited on the particles by thermal decomposition in an oven. Variants of this approach include the so-called dissolution method adopted by Japanese workers, a typical recipe for which is as follows:

$Ni(NO_3)_2 \cdot 6H_2O$ and $Al(NO_3)_3 \cdot 9H_2O$ were dissolved into a mixture of distilled water and 2-propanol, and the solution dried at 100 °C for 3 h, at 150 °C for

Table 1 Synthesis of a CLC particle

The oxygen carrier particle was prepared by freeze-granulation and was composed of 40-wt% active material of CuO and 60 % ZrO_2
A water-based slurry was prepared by mixing CuO (Panreac No. 141269) and ZrO_2 (Sigma-Aldrich No. 24.403-1)
This mixture was ball milled for 24 h A small amount of dispergent was also added to this mixture in order to improve slurry characteristics
After milling, an organic binder was added to the slurry to keep the particles intact during later stages in the production process, that is, freeze-drying and sintering
Spherical particles were produced by freeze-granulation, that is, the slurry is pumped to a spray nozzle where passing atomizing air produces drops, which are sprayed into liquid nitrogen where they freeze instantaneously
The frozen water in the resulting particles is then removed by sublimation in a freeze-drier operating at a pressure that corresponds to the vapor pressure over ice at 10 °C
After drying, the particles were sintered at 950 °C for 6 h using a heating rate of 5 °C/min

5 h, and finally at 500 °C for 3 h. Subsequently, the agglomerates were crushed in a ball mill and water slurry introduced into a spray dryer. The resulting particles were then baked in an oven for 10 h, during which baking a $NiAl_2O_4$ support is produced on which the active Ni component is maintained (Ishida et al. 2002).

An alternative approach also used in some of the earlier Japanese work was to grind the oxide together with the carrier after wetting (for periods of up to 2 days) and then sinter the particles for 10–12 h, after which they were sieved and held in a desiccator (Ishida et al. 2005). More recently, freeze-dry granulation has been explored at Chalmers University in Sweden (e.g., Johansson 2007; Mattisson et al. 2009), and an example of the procedure employed is found in Table 1.

Yet another approach, the so-called sol–gel method, is also being developed and involves the formation of a colloidal suspension (sol) and gelation of the sol to form a wet gel, which after drying forms a "dry gel" state (xerogel), which is then processed to make sorbent particles (Zhao et al. 2008). However, the procedure of producing the carrier outlined by these workers is of considerable complexity to that outlined in Table 1. Numerous other efforts are under way, such as efforts to develop a cheap wet impregnation method (Gayán et al. 2009). Very recently, Jerndal et al. (2010) have reported considerable success in producing suitable particles by means of spray drying, which is a technology that could be used to scale up the production to make the large amount of carrier particles needed by an industrial unit at a reasonable cost. This must be regarded as a very positive, if early, result, although spray drying produced a high degree of cenospheric particles.

What is clear from the above is that, while making reactive materials is important for any practical applications, their longevity, especially if they are used in fluidized bed systems, which transport materials from one vessel to another (oxidizer, regenerator), will be critical, and there will be major pressure to reduce the cost of such carriers for large-scale applications such as what will be required if CLC is to be employed in thermal power generation. To date, such tests as have been done in

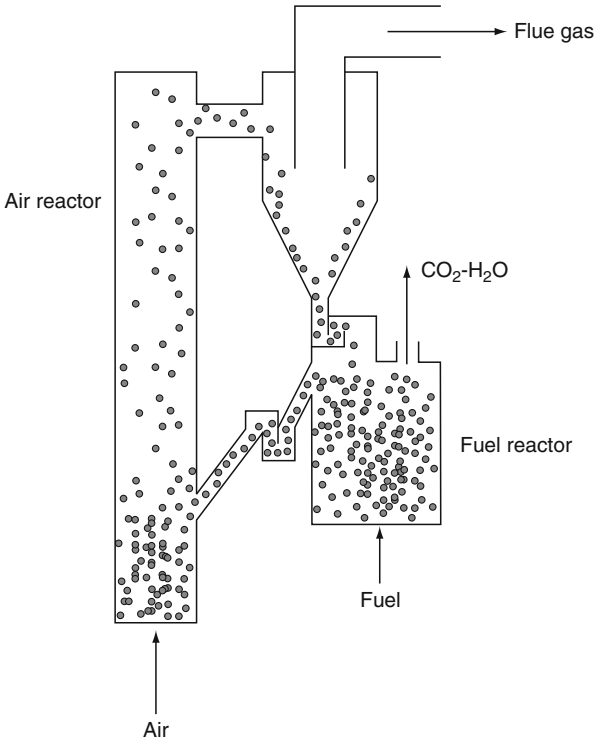

Fig. 2 Schematic of Grace 10-kW chemical looping reactor

pilot-scale equipment, supplemented with crush tests to measure the individual strength of particles under ambient conditions, have suggested that the best particles produced are strong enough to survive extremely well in the small-scale units that have been studied (Lyngfelt et al. 2004; De Diego et al. 2005, 2007). Thus, De Diego et al. (2005) suggest that a loss of 0.01 % per cycle is reasonable based on their experimental work, implying a lifetime of particles of 10,000 cycles (5,000 h in their tests), which they suggest is equivalent to a particle cost of less than 1 €/t of CO_2 captured. Similarly, in a later paper, De Diego et al. (2007) suggested a loss of 0.04 wt%/h, with a particle lifetime of approximately 2,400 h, or replacement of the bed inventory 3.4 times per year. Very similar conclusions were reached by Lyngfelt et al. (2004) for the Grace Reactor (Fig. 2) where these workers suggested that particle lifetimes of 40,000 h were possible. The same workers studying the $NiO/NiAl_2O_4$ particles in a 1,016-h test using their 10-kW reactor reported that the largest decrease of fines occurred in the first 100 h and estimated that a particle lifetime of 33,000 h could be achieved with these particles (Linderholm et al. 2009).

Nonetheless, as large demonstrations and early efforts at commercialization are being developed, the production of large quantities of such materials by less complicated and, hence, less expensive methods will continue to be a priority as

will verifying the fact that such materials can withstand full-scale operation with minimal carrier loss, especially if they are used directly with solid fuels.

$CaS/CaSO_4$ System

As noted above, the $CaSO_4$/CaS system has the highest carrying capacity of all, at 0.47, and is also unique in that it employs a nonmetallic system. Coupled to the very high carrying capacity, it has another obvious advantage in that anhydrite ($CaSO_4$) and gypsum are available in large quantities in the natural environment and can, therefore, be obtained at relatively low cost. CaS itself might be more problematic in that it can react with water to release H_2S, but otherwise this system seems at first sight particularly promising. Unfortunately, there are some obvious problems, firstly, that the system can lose SO_2 via direct oxidation of CaS:

$$CaS + 3/2C_2 = CaO + SO_2 \tag{10}$$

as well as the well-known reaction:

$$CaS + 3CaSO_4 = 4 \quad CaO + 4SO_2 \tag{11}$$

which occurs in the temperature region above 900 °C (Partington 1939), where one might expect to operate a chemical looping system, which means that unless conditions are carefully controlled, the active system will lose sulfur in the form of SO_2. Secondly, one can reasonably expect such natural materials to sinter and to lose activity rapidly as is the case, for example, with natural limestone in Ca looping cycles, where CaO is used to remove CO_2 from hot flue gases (Blamey et al. 2010). In addition, one would expect the attrition from such systems to be relatively high when compared with other chemical looping carriers unless synthetic materials are prepared, in which case the system loses some of its obvious advantages.

The loss of SO_2 was demonstrated in studies done by the researchers of Southeast University in China, who used a natural anhydrite (94.4 % pure), with an oxygen capacity of around 0.444, which they tested in a fixed bed reactor (24-mm dia.) (Song et al. 2008a). They found that conversion of natural gas was low unless temperatures were in the range of 950 °C but that high temperatures were associated with a loss of SO_2 from the reactor of up to 6 % in the flue gases. These workers also noted that there was a small loss of SO_2 even at 850 °C. In addition, there was some agglomeration of particles at higher temperatures. These workers also explored the performance of this system for simulated syngases, again using the same natural anhydrite, but this time in a small fluidized bed reactor (25-mm dia.), and found that the mass conversion rate for this system was considerably less than the metal oxide systems. They also noted that CaO became the main component after the 20th oxidation cycle, due to the loss of SO_2 (Song et al. 2008b, c). In a study by Shen

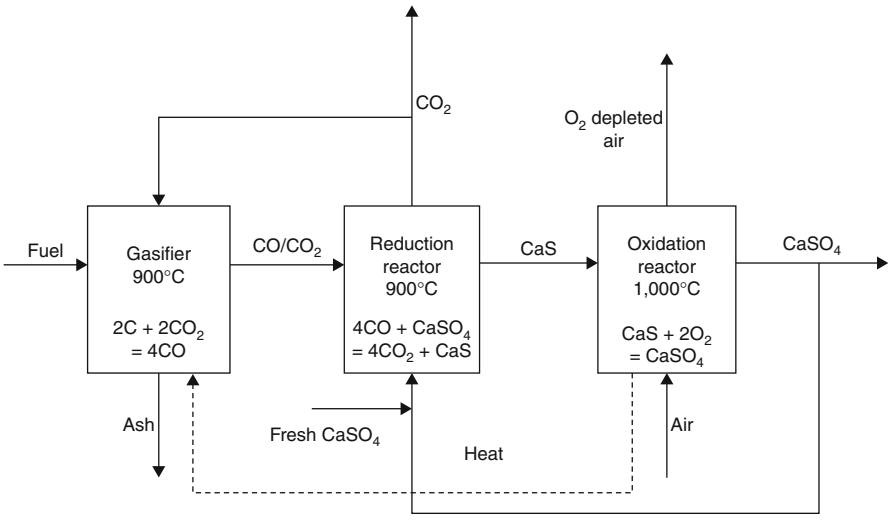

Fig. 3 Schematic of chemical looping process for combustion of solid fuels using the $CaSO_4$/CaS system (From Wang and Anthony (2008))

et al. (2008), Rx. 11 was identified as the main cause of sulfur loss from the system, and these workers recommend recapturing the SO_2 by feeding a small amount of limestone into the system. They further recommend that the air reactor should be between 1,050 °C and 1,150 °C, while the fuel reactor should be operated between 900 °C and 950 °C.

These problems with this system might well suggest that it would not be the first to be explored despite its obvious advantages. However, it is clear that a more detailed examination of other sources of the natural oxidizers could be explored or that one could consider making synthetic carriers such as sulfating dolomite, in the hope that the magnesium component might reduce sintering, and/or adding a guard bed to capture any SO_2 escaping the system, perhaps in the form of CaS or $CaSO_4$ so that the material could be recycled back to the reactor. Wang and Anthony (2008) also proposed such a system (Fig. 3) in which syngases from a material like petroleum coke are oxidized by $CaSO_4$, which is then regenerated in a separate reactor that can be used to generate heat and power, and supported their ideas with an ASPEN™ simulation. In this system, any loss of SO_2 will occur together with the oxidized syngas stream and must be separated from the CO_2 stream or sequestered with it. They also proposed the possible use of dolomites if reactivity issues were significant and made similar points to that of Song et al. (2008c) who discussed the use of this cycle with solid fuel. They stated that these materials are intrinsically cheap and so, having a fairly high makeup rate, may be acceptable for this system, whereas it would most certainly not be for a more expensive carrier. In the work by Song et al. (2008c), they suggest that complete separation of carrier and ash might not be problematic, because for a really cheap natural sorbent, even if there are ash-sorbent interactions, sintering issues, or losses of SO_2 leading to high losses of

sorbent/carrier, it may still be possible to operate economically with such a cycle, although this clearly would not be ideal. Yet another suggestion for dealing with the problem of loss of SO_2 comes from the work of Tian and Guo (2009), whose research noted that the amount of SO_2 released was also dependent on the partial pressure of CO and suggested that in a pressurized system the release rate of SO_2 could be minimized if the partial pressure of CO was high enough, even at 1,000 °C.

This brings us to the final reason for considering this system, and that is that it was proposed by Alstom Ltd., as part of a $4-million US Department of Energy Program from the National Energy Technology Laboratory (NETL) Existing Plants Program, aimed at demonstrating the conversion of solid fuels in a specially designed 3-MW_{th} pilot plant (Andrus et al. 2010). The system considered by Alstom has a number of looping cycles working together: a $CaSO_4$–CaS cycle, a $CaCO_3$–CaO cycle for CO_2 removal, and a thermal loop involving bauxite. This system is evidently of considerable complexity as has been critically noted by Wang and Anthony (2008) but apparently has very attractive potential costs for avoided CO_2 ($11–13/ton of CO_2) (Andrus 2007). The pilot plant is expected to be running sometime in 2010–2011, and interested readers can follow developments for this system via the US DOE website (US DOE 2010).

Cu System

The copper system was the first chemical looping system to be explored with the groundbreaking work of Lewis et al. (1949), and it was also used to provide an example of a chemical looping process in the paper by Richter and Knoche (1983). Copper is attractive because it can be used to make extremely reactive oxygen carriers and is in addition a reasonably inexpensive material with relatively low toxicity. In addition, it has one interesting feature, namely, that both the oxidation and reduction are exothermic; this property can feed into a number of schemes, the most obvious of which is a fuel reactor that does not need to be supplied with heat, as is the case for other systems. However, its tendency to agglomerate with the potential to cause defluidization in fluidized bed systems is still an important consideration (Chandel et al. 2009). This is also the view presented in two reviews carried out on chemical looping in 2006 and 2008; based on the available literature, both stress the tendency of copper carriers to agglomerate and the need to avoid higher temperatures. In the first review, Tan et al. (2006) suggest that Cu-based carriers are restricted to relatively low temperatures because of a tendency to agglomerate above 800 °C, while in a review published 2 years later, Hossain and de Lasa (2008) explicitly state that "Cu also has a relatively low melting point (1,085 °C) and as a consequence cannot be used above 900 °C."

An early exception to these views can be found in the work of De Diego et al. (2005) who note that, under proper conditions, it is possible to produce Cu-based carriers with high reactivity and low attrition rates, which also do not agglomerate in a fluidized bed, thus negating the main reason to avoid such carriers. In this paper, they also note that they have carried out tests for 20 cycles at 950 °C in

a fluidized bed reactor without evidence of problems. Moreover, it can be argued, however, that the more recent literature suggests a somewhat more positive picture, although temperatures above 900 °C are generally still avoided. Thus, a number of workers have reported good success with CuO supported on Al with trials of up to 200 h in a 10-kW reactor, showing very little signs of agglomeration, albeit that the temperatures were around 800 °C (De Diego et al. 2007; Adánez et al. 2006a), and these workers note that theirs is the first demonstration of good performance exhibited by a Cu-based material operating at high temperature in a continuous chemical looping process. Equally, Chuang et al. (2008) have argued that coprecipitated CuO–Al_2O_3 carriers perform better than wet-impregnated carriers and show no sign of copper redistribution in the carrier or agglomeration in the temperature range of 800–900 °C, while Tian et al. (2008) report excellent performance of nanostructured Cu–BHA (barium hexa-aluminate) carriers over the temperature range of 700–900 °C. Finally, Mattisson et al. (2009) have argued that, based on the work of Adánez and his coworkers (De Diego et al. 2005; Adánez et al. 2006a, b, De Diego et al. 2004), it should be possible to manufacture Cu-based oxygen carriers that do not agglomerate at higher temperatures. This is important for the work Mattisson et al. (2009) are discussing, because they are interested in using copper oxide systems for a process they call chemical looping with oxygen uncoupling, in which the metal oxide releases gaseous oxygen. This phenomenon is potentially valuable in gasification schemes for solids, which are otherwise rate-limited by the reaction rate of H_2O or CO with the solid, and this will be discussed in more detail later in this chapter. It is interesting to note in the experiments described by Mattisson et al. (2009) that the copper carrier (CuO/ZrO_2) is regenerated at temperatures of 905 °C and 955 °C. Finally, it is worth remarking that Cao et al. (2006) suggested that the Cu/CuO system was particularly suited for the conversion of solid fuels due to its exceptional reactivity, based on thermogravimetric and differential scanning calorimetry experiments (Cao et al. 2006). The subject of solid fuel conversion will be discussed later on.

Fe System

As noted earlier, this is the least reactive of the common systems (i.e., Ni, Cu, and Fe); however, it is the most environmentally benign, and potentially it is also the cheapest. There has as a result been considerable interest in this system, and work has been done both on synthetic and natural hematite carriers (Fe_2O_3) (Mattisson et al. 2001) and natural ilmenite ($FeTiO_3$) (Prőll et al. 2009; Leion et al. 2008a, b). Early work in a fixed bed reactor using hematite showed that the particles developed cracks, and the authors suggested that a binder would probably be desirable in manufacturing a synthetic carrier (Mattisson et al. 2001), and later work was almost exclusively focused on systems using a carrier; thus, for instance, in his list of studies (Tables 1–5 of his work), Johansson (2007) lists 7 studies with Fe_2O_3 and 38 for Fe_2O_3 with various carrier materials. In a study of an Al_2O_3-supported carrier with

40 % Fe_2O_3, Abad et al. (2007b) carried out tests for 40-h duration at temperatures ranging from 800 °C to 950 °C in a 300-W fluidized bed reactor. They noted that there was no sign of agglomeration under conditions examined but that the conversions of CH_4 were relatively low with combustion efficiencies reaching 94 %, as compared to 99 % with syngas, which reflects the general realization that iron-based oxygen carriers can be expected to be less reactive. Experiments done in a fixed bed reactor at 900 °C with an iron-based carrier supported on titania prepared by a wet impregnation method showed that the Fe reacted with the TiO_2 to form ilmenite. Although the amount of active carrier was reduced, reasonable performance with CH_4 was achieved, but the reactivity of the Fe-based carrier was less than what would have been expected for Cu- or Ni-based carriers (Son and Kim 2006; Corbella and Palacios 2007). An interesting method of dealing with the reactivity problems associated with the iron system is to add Ni at a low level, and Rydén et al. (2008a, b) report that by adding 10 % NiO/$MgAl_2O_4$ they were able to produce a material with similar behavior to a pure NiO/$MgAl_2O_4$ carrier. In later work, they report that addition of the equivalent of 5 wt% of a NiO material changed the combustion efficiency in a small fluidized bed operated at 900 °C from 76 % to 90 % for the conversion of CH_4 (Rydén et al. 2010).

Pröll and his colleagues (2009) have carried out experiments with ilmenite in a 120-kW dual fluidized bed system and reported what they describe as reasonable fuel conversions (between 60 % and 90 %) at 950 °C for syngas (mixtures of CO and H_2) but much more limited performance with CH_4, around 30–40 %. They also found that low load was associated with poorer conversion and the addition of natural olivine, at a level of 18 % of the bed material, helped to achieve a moderate increase in CH_4 conversion. These results are fairly similar to those obtained earlier by Leion et al. (2008a), who carried out tests in a small fluidized bed reactor (22-mm dia.) at a nominal 950 °C, in which they looked at either pure methane or syngas (50 % CO and 50 % H_2) conversion; again they report good conversion of syngas but much poorer conversion of CH_4.

It is also interesting that, unlike Cao et al. (2006), Rubel et al. (2009) who carried out experiments on a beneficiated high-carbon coal gasification char, using a thermal analyzer–differential scanning calorimeter–mass spectrometer system, recommended Fe-based carriers as the best for solid fuel conversion. In particular, they noted that their experiments showed that Fe_2O_3 and an iron-based catalyst remained more durable through multiple oxidation/reduction cycles.

Finally, it is interesting to note that some research has recently been done on syngas production from mixed cerium–iron systems with natural gas (He et al. 2009; Li et al. 2010). Both the cerium and iron are considered to contribute to oxidation in the fuel reactor, and in the work of He et al., the Cu and Mn oxide systems were also explored. Ce/Fe molar ratios of greater than 1 were found to perform best by He et al. (2009), and similar results were obtained by Li et al. (2010). Perhaps the only negative comment that can be made is that any benefits of price in terms of using the iron system must be compromised for such systems, even allowing for the fact that cerium is the most abundant of the rare earth elements.

Ni System

The vast majority of chemical looping research work has concentrated on using Ni-based carriers, and, thus, as an example of the 105 studies recorded by Johansson (2007) (Tables 1–5 of his work), 67 of them employed Ni-based carriers. It also appears to be extensively addressed in the early work of Ishida's group in Japan (Ishida and Jin 1994a, b; Ishida et al. 2002; Jin et al. 1999). Despite the concerns with the cost of Ni and potential toxicity problems as discussed earlier, and the fact that the reaction does not go to completion with CH_4 (conversions of 99 % at 1,000 °C) (Jerndal et al. 2006), its excellent performance and stability on suitable inert matrices, such as Al_2O_3 and YSZ (yttria-stabilized zirconia) in particular at temperatures up to 1,000 °C, have meant that it is the preferred candidate for research work at least. Numerous other inert matrices have been explored such as titania-supported nickel oxide (Corbella and Palacios 2007; Corbella et al. 2006); bentonite (Siriwardane et al. 2007), with MgO as an additive to Al_2O_3 and $NiAl_2O_4$ to prevent agglomeration under reducing conditions (Kuusik et al. 2009) and $NiAl_2O_4$ acting as the inert matrix in $NiO/NiAl_2O_4$ particles (Redman et al. 2006; Mattisson et al. 2008); SiO_2; and sepiolite ($Mg_4Si_6O_{15}(OH)_2 \cdot 6H_2O$) (Ksepko et al. 2010), and all of these have been reported as successful, although it appears that Al_2O_3 and YSZ are probably the most successful and commonly used and there appear to be some problems with SiO_2 as an inert matrix (Ksepko et al. 2010; Zafar et al. 2005). $NiAl_2O_4$ is an interesting carrier in that it can also, in principle, react with CH_4, but in the presence of NiO in the particle, it is assumed to be inert (Redman et al. 2006; Mattisson et al. 2008). Work has also been done on the use of Ni with a lanthanum-modified γ-Al_2O_3 inert substrate (Hossain et al. 2009). These workers noted that the lanthanum addition improved the reducibility of the oxygen carrier and speculated that the lanthanum inhibits nickel aluminate formation.

Very recently, an interesting suggestion has been made to reduce the cost of a Ni-based carrier, and that is to combine it with ilmenite, and based on a limited set of experiments done in a 120-kW_{th} dual fluidized bed reactor, it has been suggested that the performance of a properly designed NiO-based carrier will be close to that of the NiO-based carrier with up to 90 % ilmenite (Mayer et al. 2010). However, an overall conclusion that can be drawn from the literature is that at least to date the Ni/NiO oxide system is preferred for most research work; whether that translates into the commercial scale of course waits to be demonstrated.

Pilot Plant Research

In a review article published in 2006, Johansson et al. (2006c) list 11 studies carried out in 10-W, 40-W, 300-W, and 1-kW reactors using the NiO, Fe_2O_3, Co_3O_4, Mn_3O_4, and CuO systems with different stabilizers and test durations ranging from 3 to 60 h. Nearly all of the research was done with natural gas, although one study was done with CH_4 and another with a synthetic gas mixture. Since that date, there has been considerable focus on achieving longer trials in larger reactors, albeit that

reactor sizes at university laboratories at least are generally limited for practical reasons. More importantly, it is now commonplace to carry out trials for several hundred hours, and the Grace Project (Lyngfelt et al. 2004) carried out at Chalmers University, in Sweden, and tests done by Adánez et al. (2009a) on a 500-W_{th} chemical looping system using an impregnated Ni-based oxygen carrier, this time built and operated at the Instituto de Carboquímica, in Spain, are two examples of this type of facility and longer-duration testing. Equally impressive, the operation of a 10-kW_{th} unit using the copper system (CuO–Al_2O_3 carrier) has been demonstrated with no evidence of significant agglomeration (De Diego et al. 2007; Adánez et al. 2006a), and tests of 1,016-h duration have been achieved with a Ni-based system, carried out again at Chalmers University, Sweden, in their 10-kW unit (Linderholm et al. 2009). From the point of view of duration, these tests give as much reasonable assurance as one could ask that it is possible to operate these systems indefinitely.

Finally, it should be remarked that implicit in this discussion is the idea that dual fluidized bed reactors are likely to be used for commercial-scale operation, and this is, for example, the assessment of Hossain and de Lasa (2008) in their review of the literature. However, it is worth noting that some workers are considering the possibility of building industrial-scale fixed bed systems (Kimball et al. 2010). Arguments they make against dual fluidized bed systems include concerns that the gas-particle separation cyclones required between the two reactors are likely to be very expensive for commercial-scale systems and will also be associated with damage to the oxygen carrier particles and that attrition of fines will be a problem for gas turbines, something which has been an issue for pressurized fluidized bed systems, for instance (Cuenca and Anthony 1995).

Use of Natural Gas in Chemical Looping Systems

A fairly obvious caveat that can be raised about nearly all CLC R&D until 2008 or 2009 is that it depends on the use of natural gas and/or syngas and, moreover, it is somewhat limited in temperature to around 1,000 °C due to the sintering of the solid carriers. This point was made strongly by Tan et al. (2006), who noted that at the time of writing, the technology was only suitable for use with gaseous fuels. They also expressed concerns about the carryover of char if the technology was used with gasification. However, they did note that it appeared to offer significant flexibility for use with industrial boilers, gas turbines, and even fuel cells. This limitation is obviously considerable for thermal power systems because natural gas by itself is an ideal fuel, offering extremely high efficiencies and the cheapest power generation. What the technology clearly offers is very effective CO_2 removal, and it is interesting to explore what other advantages it might have with natural gas.

The group of Professor Bolland, at the Norwegian University of Technology and Science, has carried out significant work performing simulations of CLC plants. In 2004, it carried out a simulation of a CLC power station, using the NiO system, with a circulating fluidized bed for the oxidation or regeneration and a fluidized bed

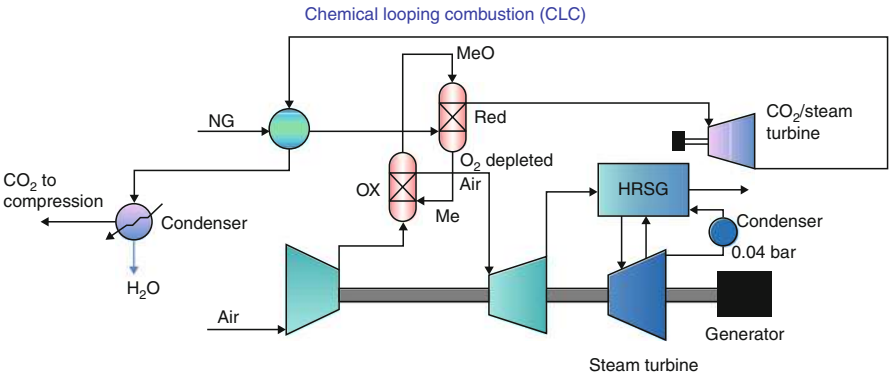

Fig. 4 Natural gas-fired chemical looping scheme (Taken with permission of Professor Bolland, Norwegian University of Science and Technology, from the paper by Kvamsdal et al. (2007)). *NG* natural gas, *HRSG* heat recovery steam generator

(bubbling) for the fuel reactor. The simulation demonstrated that the oxidation reactor exhaust temperature and the oxidation reactor air inlet temperature were very significant, but making various assumptions, the work indicated an optimum efficiency of 55.9 %. In an examination of the effect of part load on plant efficiency, for a natural gas-fired power cycle using CLC, Naqvi et al. (2007) noted a drop of 2.6 % in efficiency when reducing the load down to 60 % for a CLC concept but stated that this system performed better than a conventional combined cycle system. The same group subsequently looked at nine concepts for natural gas firing, including six oxy-fuel and two precombustion capture systems (Kvamsdal et al. 2007), and concluded that chemical looping technology showed among the best results, with a plant efficiency of 55.1 %, exceeded only by an advanced zero-emissions power plant and a solid oxide fuel cell integrated with a gas turbine. Figure 4 shows the scheme considered by these workers. However, they noted that CLC and other advanced concepts might not be realized at the scale of the analysis.

Wolf et al. (2005) made a comparison of the nickel- and iron-based systems for power generation with natural gas with CO_2 capture and concluded that overall efficiencies of almost 53 % were achievable for a natural gas combined cycle incorporating a chemical looping system, provided that the temperature of the air reactor could be kept at 1,200 °C. Here, they considered two interconnected pressurized fluidized beds. However, they did note that this efficiency strongly depended on the exit temperature of the air reactor being only 1,000 °C, and the system did not look any better than conventional technology with backend CO_2 removal.

Consonni et al. (2006) carried out an analysis of a chemical looping cycle for a utility-scale application using natural gas and came to the conclusion that employing chemical looping combustion should not pose a significant problem when using commercially available gas turbine technology, an important consideration because, as they note, unless CLC becomes the technology of choice for power generation, it is unlikely that manufacturers will ever offer a gas turbine

specifically designed to operate at the optimum conditions for an integrated chemical looping combined cycle system. In their simulations, unfired configurations with maximum process temperatures were able to reach net efficiencies of 43–48 %, while fired configurations, where the temperature is raised from 850 °C to 1,200 °C by supplementary firing, could achieve 52 % net efficiency. A possible limitation is that a preliminary economic analysis indicated that the cost of CO_2 avoided by integrated chemical looping combined cycle plants with a maximum CLC temperature of 850 °C is about 50 €/t for both fired and unfired concepts. The authors of this study note that this compares unfavorably with the cost of alternative technologies; however, considerable caution should be exercised about such conclusions given that no practical carbon capture and sequestration technology currently exists at the utility scale. Finally, it is of interest that Damen et al. (2006) made a detailed study of various schemes for electricity and hydrogen production with CO_2 capture and suggested that chemical looping combustion was promising and that net electric efficiencies might reach between 50 % and 55 % for CO_2 capture of 85–100 % for CLC systems.

Solid Fuels in Chemical Looping Combustion

The use of solid fuels is evidently an extremely desirable goal. Unfortunately, syngas must first be made, albeit that it is likely to be very reactive as has been demonstrated in fluidized bed experiments (Dueso et al. 2009), while natural gas represents a premium fuel, with the lowest greenhouse gas potential of any fossil fuel even if burned in a conventional cycle. Unfortunately, the direct use of such fuels evidently poses significant problems. If fluidized beds are to be used, there is the issue of making sure that a significant amount of char carbon does not enter the air reactor, reducing the benefit of the inherent separation, although this is perhaps not as much of a problem as has been occasionally suggested, since even amine scrubbing is likely to be operated with only 80–85 % CO_2 removal for large-scale units (Rao and Rubin 2006). In addition, choices will have to be made in terms of the amount of steam and/or CO_2 to be used for fluidization in the fuel reactor.

Another problem of course is the potential of ash interaction with the oxygen carrier, which, as has been seen here, is likely to be expensive unless an iron-based natural ore can be used; in short, it will very strongly and adversely affect the economics of a chemical looping system if the makeup of an expensive carrier becomes excessive (Abanades et al. 2007). However, by far the biggest problem is that direct solid–solid reactions are not favored in this system. After the solid fuel (presumed to be coal but could be petroleum coke) has devolatilized, CO_2 and H_2O in the system must first gasify the resulting char by Rx. 12 and 13, and this process is inherently slow in fluidized bed environments, at least for most coals (a possible exception is lignite), which is why coal gasification is normally done at high temperatures and pressures with fine particles in entrained flow systems (Higman and van der Burgt 2008):

$$C + H_2O = CO + H_2 \quad (12)$$

$$C + CO_2 = 2CO \quad (13)$$

It should be noted that Siriwardane et al. (2010) have proposed that if there is sufficient contact between the fuel carbon and the carrier, genuine solid–solid reactions are possible, and they call this mechanism "fuel-induced oxygen release." Furthermore, they have demonstrated this by work with pure carbon and CuO. Specifically, they suggest that reaction of CuO in the bulk of the particle may proceed by carbon–CuO contacts produced by surface melting of metallic copper at temperatures as low as 500–600 °C, and they note that the Tammann temperature for copper (i.e., half the absolute melting point of the substance, which is the temperature at which bulk diffusion becomes rapid in a solid) is particularly low (406 °C).

Nonetheless, it seems most unlikely that this process by itself could achieve or explain the good conversions in a fluidized bed of char carbon by copper oxide recently reported by Dennis and Scott (2010). They used relatively large particles (+600 mm, −1190 mm) of porous alumina, impregnated with copper, so that the direct contact between the copper and the char was relatively limited. They proposed (Dennis and Scott 2010) that the conversion of the char by the chemical looping agent, when the bed was fluidized by nitrogen, was in fact mediated by gaseous CO_2 (produced by the reaction itself), reacting with the char to produce an intermediate of CO, which was then rapidly converted to CO_2 via reaction with the oxygen carrier. Unfortunately, their model was not able to fully account for the conversion seen. Subsequent work using an iron-based oxygen carrier (Brown et al. 2010) was able to account for the conversion of the char in a bed fluidized by nitrogen, without the need to invoke a solid–solid reaction. In this case, a model that only incorporated the Boudouard reaction and the combustion of the CO intermediate by the oxygen carrier was sufficient to quantitatively account for the observed conversions. The model was found to be very sensitive to the kinetics of conversion of the char by CO_2, which may explain, in part, the difficulties encountered by Dennis and Scott (2010).

It is difficult to rule out some contribution from a direct solid–solid reaction between the oxygen carrier and the char, and the controlling mechanism may depend on temperature, the metal oxide, and the degree of contact between the char and the oxygen carrier. This problem was previously of interest for the reduction of iron oxides, and the idea that the reaction may proceed by gaseous intermediates and the Boudouard reaction under some conditions (e.g., higher temperatures, more reactive chars) and direct reduction under others (e.g., vacuum, lower temperatures) is not new (see, e.g., Srinivasan and Lahiri 1975). The experiments of Dennis and Scott (2010) and Brown et al. (2010) were carried out at temperatures high enough for the Boudouard reaction to be significant, with reactive chars, while those by Siriwardane et al. (2010) used finer particles and observed some reaction at temperatures at which the Boudouard reaction can be neglected.

This mechanism does, however, appear to offer an explanation for the finite rate of reaction reported by Dennis and Scott (2010) in the following words: "However,

the observation of finite rates of conversion in a bed of active carrier, fluidized by nitrogen is a curiosity, which we have not been able to explain satisfactorily."

Despite the potential problems, the idea of using solid fuels in a chemical looping cycle was explored over a decade ago, and the work of Lyon and Cole (2000) provides an extremely interesting example of this early attention. These workers called the concept unmixed combustion and looked at the possibility of using the Cu/CuO, FeO/Fe_2O_3, and Ni/NiO systems with the oxygen carriers supported on γ-Al_2O_3 for a number of applications including a dual fluidized bed combustion scheme working at elevated pressure. To support this work, they also carried out a limited series of tests in batch mode with coal and Fe_2O_3 in a small fluidized bed, as well as a number of other experiments with methane, and concluded that the chemical looping approach had considerable promise for a range of applications including solid fuel conversion.

In 2007, Chalmers University started a series of experiments on petroleum coke (Leion et al. 2008b, 2007; Berguerand and Lyngfelt 2008a). Petroleum coke, unlike most coals, normally has extremely high carbon contents (~80 % plus), low ash (~1 % or less), high sulfur (5–8 %), low volatiles (5–10 %), and elevated V (a potential agglomerating agent in fluidized beds) in the ash. Furthermore, it is a relatively unreactive fuel for fluidized bed applications, and primarily its high energy value and low price are the driving force for its use (Anthony 1995). Hence, success with this fuel would be a very positive result for the application of chemical looping technology for solids under standard fluidized bed conditions. The first reported set of experiments was conducted in a small quartz fluidized bed, using 20 g of oxygen carrier (60 % Fe_2O_3/40 % $MgAl_2O_4$) at a nominal temperature of 950 °C, and the carrier was subjected to 100 cycles (~100 h). This work showed that conversions were sensitive to the amount of steam in the fluidizing gas and rose with the addition of SO_2, which, as noted by Lyon and Cole (2000), can effectively oxidize char carbon.

In a second series of tests, this time using a 10-kW_{th} chemical looping combustor, an 11-h operation was logged, at a nominal temperature of 950 °C, using ilmenite as the oxygen carrier (Berguerand and Lyngfelt 2008a), and the resulting carbon conversions were in the range of 60–75 %. While these are low figures, the authors commented that improved reactor design would enhance performance, and it must be remarked that the oxygen carrier is known to be one of the less reactive carriers.

More recently, the same group has looked at petroleum coke combustion, this time using a CuO carrier for a temperature range of 850–950 °C in a batch fluidized bed (Mattisson et al. 2009). Here, the carrier actually releases oxygen in a process that can be described in the following manner:

$$Me_xO_y = Me_xO_{y-2} + O_2 \tag{14}$$

and this process, which the authors call chemical looping with oxygen uncoupling (CLOU), allows much faster rates of reaction, rather than depending on the gasification reactions Eqs. 12 and 13. In the case of Cu, the overall global reaction is

$$4CuO + C = 2Cu_2O + CO_2 \quad (15)$$

and the use of this reaction with solid fuels is also discussed much earlier in the patent of Lewis and Gilliland (1954).

In work with a South African coal, again using their 10-kW_{th} fluidized bed facility and ilmenite as the oxygen carrier, Berguerand and Lyngfelt (2008b) report solid fuel conversions in the range of 50–80 %, and they stress the problems associated with loss of carbon fines from their cyclone and suggest various ways in which performance could be improved. These workers have also carried out a more extensive series of trials on petroleum coke and five different coals (South African, Chinese, Indonesian, Taiwanese, and French) using a quartz fluidized bed reactor and two oxygen carriers, a synthetic iron-based carrier ($Fe_2O_3/MgAl_2O_4$) and ilmenite (Leion et al. 2008a), at a temperature of 950 °C. This work again confirmed the importance of steam levels for high conversions and found that the two carriers performed similarly. These workers have also recently developed a model for residence time analysis of the CLC of solid fuels, which can give the mass-based reaction rate for chars from the batch tests (Markström et al. 2010).

The NiO oxide system with $NiAl_2O_4$ inert (77 %) has also been examined at Southeast University in China for a bituminous coal from Inner Mongolia using a small, electrically heated fluidized bed and 1 g (nominal) of coal samples (Gao et al. 2008). These workers noted that the gasification rate was slow compared with syngas, and they suggested that 100 % steam as a gasification agent would improve the performance; they found that the best performance was achieved at the highest temperature they explored, 900 °C. A small amount of Ni-containing material was found in the cooler designed to remove water vapor, and they suggested that in a commercial system, a nitric acid treatment of these "ashes" might be used to recover the Ni. In a more recent paper, the same group explored the use of a dual fluidized bed system consisting of a spouted fluidized bed fuel reactor and a fast fluidized bed as the air reactor (Shen et al. 2009) using the same bituminous coal as in previous studies. Again they used the NiO system with a very similar amount of $NiAl_2O_4$ inert (67.3 %). As with previous studies, carbon conversions were somewhat limited, and in these experiments it reached only 92.8 %, even at a temperature of 970 °C in the fuel reactor.

These workers at Southeast University have also studied the use of $CaSO_4$ as an oxidizing agent for coal in a small, electrically heated fluidized bed (Zheng et al. 2010). This work showed that increasing the steam/CO_2 ratio improved the gasification of coal and overall performance, but again they had problems with loss of SO_2 from the system. Another problem was that sintering of the natural anhydrite became worse at 950 °C, effectively negating the benefits of operating at higher temperatures.

Chemical looping has also been considered for use with lignite and lignitic char (Dennis and Scott 2010; Brown et al. 2010; Scott et al. 2006; Dennis et al. 2006), which, because of their low rank, provide the most reactive coals with the highest volatile content and, thus, might be a particularly good choice of solid fuel for chemical looping. In their first study on lignite (Hambach, Germany)

and its char, they explored the possibility of a process in which the coal is fed batchwise for a limited period into the reactor, its feed is then stopped until the char content in the bed is sufficiently small, and then air is reintroduced into the system to regenerate the solid oxide carrier (Scott et al. 2006). Their first experiments were done with a small bubbling bed quartz reactor, using Fe_2O_3 as the oxygen carrier at a nominal temperature of 900 °C, fluidized with N_2 and CO_2 mixtures or steam or air, and while they note that the process was not optimized in their experiments, the initial results were sufficiently encouraging to suggest that this approach offered a potentially interesting process. These workers subsequently carried out more detailed work with the same system operating at temperatures of 800–900 °C with fluidizing gases consisting of mixtures of nitrogen, air, CO, and CO_2 as desired (Brown et al. 2010). They note that combustion of char also occurred when the bed was fluidized only with nitrogen, and they suggest that this is most unlikely to be due to a solid–solid reaction, but rather by small amounts of residual oxygen forming CO and CO_2. In their most recent paper, these workers have also looked at the copper system and again found a reaction when the bed is fluidized with N_2, which they also suggest cannot be due to a solid–solid reaction. These experiments were done at 900 °C for up to 20 cycles and showed no significant deterioration in the performance of the CuO carrier.

Given the challenges of solid fuel conversion, Xiang et al. (2006) suggest that "direct reaction between the coal and oxygen carrier in the CLC is not expected to be feasible because the reaction rate is likely to be too slow." They also note that coal ash interactions with carriers may reduce the reactivity of the carrier and raise the issue of carbon bypassing to the air reactor, all of which they suggest will cause the advantages of easy CO_2 separation to be lost. Instead, they suggest that coal slurry should be fed through the air reactor and the resulting syngases used to reduce the carrier in the fuel reactor. In this way, this concept was supported by an ASPEN™ simulation, and the authors suggest this is a particularly promising route, although they do note that there are some issues with "pipe gasification."

Xiao et al. (2010a, b) have examined the performance of a Chinese bituminous coal in a small fixed bed reactor at pressures up to 0.6 MPa, with an iron ore-based oxygen carrier using a laboratory-scale fixed bed reactor. In this work, the cycle responsible for providing oxygen was assumed to be Fe_2O_3/Fe_3O_4. The primary focus of these studies was to determine what effect pressure had on performance rather than reactor design or scale-up, and therefore, issues such as the amount of carrier required per MW_{fuel} were not examined in these studies. In the initial study by Xiao et al. (2010a), these workers looked at three to five reaction cycles and found that increasing the pressure up to about 0.5 MPa enhanced the reduction of the oxygen carrier but that slightly lower conversions were obtained at 0.6 MPa, which was the highest pressure examined in this work. In a subsequent study, experiments were carried out for up to 20 cycles (Xiao et al. 2010b). Interesting results from this study included: no evidence of agglomeration or the formation of large grains, a high stable average CO_2 production (96 %), and no evidence of deterioration of the oxygen carrier.

Effects of Sulfur

Fairly recently the potential effects of sulfur have started to receive attention (Ksepko et al. 2010; Adánez et al. 2009b; Foero et al. 2010; Shen et al. 2010). Sulfur may be reasonably expected in natural gas prior to cleaning, in various industrial gases, and, of course, in coal syngas. Concerns expressed for the effects of sulfur include possible poisoning of the oxygen carrier, release of sulfur compounds in the gases from the air and fuel reactor, and, in the case of Ni, the possibility of melting and agglomeration phenomena due to the low melting point of Ni_3S_2 (melting point 791 °C). In a study of a Ni-based carrier with alumina inert support, Adánez et al. (Adánez et al. 2009b) looked at the behavior of methane, ethane, and propane, as well as performed experiments with H_2S addition in their 500-W_{th} unit. Without H_2S they obtained excellent performance with high hydrocarbon conversion and no evidence of carbon formation, which was a concern especially for the higher hydrocarbons (these tests showed no signs of agglomeration or carbon formation, with or without the addition of H_2S), but there was deterioration in the performance of the oxygen carrier when H_2S was added to the system and sulfur compounds were found in emissions from both the air and fuel reactors. What is an extremely positive result from this work is that the oxygen carrier fully recovered its activity after the carrier was oxidized in the air reactor, suggesting that sulfur compounds do not do damage to the long-term performance of such carriers. However, it is the conclusion of these workers that high concentrations of sulfur should best be avoided in a chemical looping system operating with a Ni carrier.

Ksepko et al. (2010) have also recently done tests on the NiO system using a range of inert supports including sepiolite (a complex magnesium silicate), SiO_2, ZrO_2, and TiO_2, with simulated coal-derived synthesis gas in a thermogravimetric analyzer, including tests in which 4,042 ppm of H_2S was added. This work also supported the work of Adánez et al. (2009b) in showing the formation of nickel sulfide compounds, and again they showed that sulfur in these compounds was released in the oxidation stage. Another such study has been performed by Shen et al. (2010) using a Ni-based oxygen carrier prepared by a coprecipitation method, with Al_2O_3 as a support using both a thermogravimetric analyzer and a small 1-kW_{th} reactor consisting of a spouted fluidized bed as the fuel reactor and a fast fluidized bed operating as the air reactor. This work takes a very detailed look at possible reaction mechanisms with sulfur and also produces similar findings to the two other studies reported here on the Ni system. Finally, the group of Adánez has now looked at the Cu system with γ-Al_2O_3 as the inert support with their 500-W_{th} reactor for reaction with CH_4 with H_2S addition (Foero et al. 2010). Here, the fuel reactor was operated at 800 °C and 900 °C, and the compound of concern is Cu_2S, although with a melting point of 1,130 °C, it seems unlikely that it would perform worse than Cu (1,085 °C), other than by the formation of eutectic mixtures. Overall, their results were extremely positive with no evidence of impairment of combustion efficiency, even with H_2S levels at 1,300 vppm, or agglomeration; the majority of the sulfur compounds were found in the emissions from the fuel reactor with very little being

released from the air reactor, except at low equivalence ratios (Ø) of less than 1.5, where there was evidence of Cu_2S formation. (Here Ø is defined as the oxygen requirement of the fuel, divided by the potential oxygen release from the carrier, with a value of 1 being equivalent to the complete conversion of the fuel to CO_2 and H_2O.) One interesting result was that in experiments done to explore a possible regeneration of the carrier, where the H_2S feeding to the air reactor was suspended and the fuel feed was decreased to achieve an equivalence ratio of 1.9, there was a sudden release of SO_2 (3,300 ppm) and the gas composition returned to values corresponding to normal combustion for this system. These workers attribute this to a solid–solid reaction:

$$Cu_2S + 2CuO = 4Cu + SO_2 \tag{16}$$

and these results can reasonably be interpreted to be in agreement with the work of Siriwardane et al. (2010), who suggest that the copper system is capable of significant solid–solid reaction at standard chemical looping conditions.

Hydrogen Production and Reforming

Applications Relating to Hydrogen Production

The production of H_2 is important for many reasons, some of them being longer term, such as introducing the H_2 economy, possibly with the use of fuel cells, and encompassing the transportation industry (McGlashan 2010), rather than just stationary power sources or industrial processes, as are the bulk of examples considered in this chapter. However, H_2 itself is an important chemical, produced in very large amounts (of the order of 65 million t/a (Harrison 2009)), and is of profound interest to some national economies, such as in the case of Canada for oil sand upgrading, where current needs are around one million t/a, but have been predicted to rise to 7.7 million t/a by 2030 (Larsen et al. 2004). Thus, cheap methods of producing H_2 are desired, especially if this can be produced in a CO_2-neutral manner, since about 48 % of H_2 is produced from natural gas while another 48 % comes from oil or coal, with electrolysis supplying the rest (Harrison 2009).

The idea of using H_2 to fuel CLC was considered early on by Jin and Ishida (2001), but reasonably most of the research and development has been concentrated on various schemes for H_2 production (Zafar et al. 2005; Chiesa et al. 2008; Go et al. 2009; Xiang et al. 2010). Thus, Zafar et al. (2005) looked at the possibility of integrated hydrogen and power production for the CuO, Mn_2O_3, NiO, and Fe_2O_3 systems with SiO_2 as a support. For their experimental work, they used a small quartz fluidized bed reactor and they looked at performance for the fuel-rich situation. The concept they proposed was that methane is first converted into CO_2 and H_2 and then shifted in a separate reactor; in particular, they were interested in the potential performance of the oxygen carriers, which they ranked in the order of decreasing reactivity as $NiO/SiO_2 > CuO/SiO_2 > Mn_2O_3/SiO_2 > Fe_2O_3/SiO_2$.

An interesting study has been performed by Chiesa et al. (2008), which envisages the use of three reactors using the iron system and natural gas. Here, in the fuel reactor, hematite (Fe_2O_3) is reduced primarily to Wüstite ($Fe_{(1-y)}O$ where $0.05 < y < 0.17$ (Bohn et al. 2008)) by oxidizing the natural gas; in the steam reactor, most of the reduced FeO reacts with steam to form magnetite (Fe_3O_4), and finally, in the third reactor, the Fe_3O_4 is reoxidized to Fe_2O_3. Among the interesting points about such a scheme is that, unlike most chemical looping schemes, it involves the metal in more than two oxidation states, and the result of the simulation performed suggested that it was economically preferable simply to produce H_2, rather than H_2 and electricity. This study suggested that the economics of such a scheme were comparable with those of other approaches but that the environmental benefits in terms of 100 % CO_2 capture were better, given that the best alternative would at most achieve no more than 80 % CO_2 capture.

A fairly similar scheme, again with an iron-based carrier, has also been explored using coal as the fuel source by Xiang et al. (2010) for the simultaneous production of hydrogen and electricity, again with three reactors, using an ASPEN™ plus simulation. For the system considered by the authors, they note that the costs of such a system are high but the environmental benefits are significant. One limitation they see in a scheme producing both H_2 and electricity is that it is not possible to greatly vary the ratio of hydrogen production to electricity because this is dependent on the circulation rates for the oxygen carrier and hence the heat balance for the three reactors. The iron system with H_2 production from coal syngas, using an ASPEN™ simulation based on bench-scale results, is also explored by Fan et al. (2008), again with a very positive evaluation.

This scheme has also been explored experimentally, but this time using mixtures of CO, CO_2, and N_2 as the fuel source, in a small packed bed reactor (dia. 103 mm), by workers at the University of Cambridge (Bohn et al. 2008) whose work supported the general feasibility of such a scheme for producing very pure H_2. In 2009, these same workers carried out simulations of the same scheme, looking at steam pressures of 0.1 and 1 MPa, and showed that it was possible to achieve the necessary heat integration (Cleeton et al. 2009). Finally, this scheme has also been explored experimentally using a lignitic coal and its chars (Yang et al. 2008) and a small fluidized bed reactor using batches of hematite or Fe_2O_3 and demonstrated successful reduction of the hematite with potassium carbonate-promoted chars, production of H_2 via the reaction of water with the FeO, Fe produced by reaction with char, and final oxidation of the resulting magnetite (Fe_3O_4) to hematite (Fe_2O_3) by reaction with air.

Reforming

The chemical looping process can be utilized for reforming by using the oxygen carrier to supply heat to drive reactions such as

$$CH_4 + CO_2 + = 2CO + 2H_2 \tag{17}$$

or the more familiar

$$CH_4 + H_2O = CO + 3H_2 \quad (18)$$

Alternatively, chemical looping can be used simply to make a syngas containing CO and H_2 directly (as in Rx. 2; i.e., an autothermal scheme), which was the subject of the first published paper on chemical looping using the copper system (Lewis et al. 1949). A detailed review of R&D in Europe within the framework of the CACHET project was produced by Rydén et al. (2008a). This evaluation, which looks at results from thermogravimetric analyzers, and various batch and continuous fluidized bed facilities (up to a scale of 140 kW_{th}), including a semicontinuous pressurized facility (with reforming pressures up to 1 MPa), has suggested that autothermal reforming is feasible with the standard metal oxide systems (NiO, Fe_2O_3, Mn_3O_4, and CuO) with syngas compositions close to those expected on thermodynamic grounds and that carbon formation can be avoided provided that the fuel is diluted with around 30 % by volume of steam. The work reported in this study suggests that adding Ni to Fe- and Mn-based carriers is a promising approach to improve the performance of these systems, with Ni also acting as a catalyst to promote the formation of CO and H_2 from CH_4. The work at elevated pressure was also successful, with no adverse pressure effects or evidence of carbon formation over the range of conditions examined. With respect to carbon formation, Rydén et al. (2008c) make the interesting point that any carbon formation in the fuel reactor is not necessarily problematic since it can be converted to CO_2 in the air reactor and this could be seen as another benefit of the chemical looping process.

Recently, De Diego et al. (2009) have carried out reforming trials of up to 40-h duration using a Ni-based carrier and a 900-W_{th} continuous atmospheric chemical looping reforming pilot plant with a temperature in the air reactor of 950 °C and in the fuel reactor ranging from 800 °C to 900 °C. They report excellent CH_4 conversions of greater than 98 %. The product gases are strongly dependent on the oxygen carrier circulation rate, and these workers recommend a NiO-reacted/CH_4 molar ratio of around 1.25. In this work, no deterioration of the carrier, agglomeration, or defluidization issues were detected and the attrition rate was negligible. In recent tests done in a 140-kW reactor using two different NiO-based carriers (with $NiAl_2O_4$ and $MgAl_2O_4$ as inerts), excellent performance has been reported (Pröll et al. 2010). No carbon formation occurred for global air/fuel ratios larger than 0.4, even though the steam/carbon ratio was less than 0.4, and no CO_2 emissions were detected from the air reactor.

An unusual choice, the $CaSO_4$ system has also been analyzed for propane reforming (as an analog for liquefied propane gas, LPG) by Kale et al. (2010). They suggested that at a recommended temperature of about 700 °C, significant carbon or methane formation should be avoided, and they also noted that sulfur release is unlikely below about 780 °C. Unfortunately, there is no experimental work to support this analysis, and issues with the kinetic rate for reaction and sintering of a natural form of $CaSO_4$ could reasonably be expected to be problematic, in line with

the work done so far for use of this system in combustion. This work also suggests that, by using the CO_2 and H_2O for reforming with more propane, the "risks" of carbon sequestration are eliminated; however, any benefits of CO_2 reduction depend entirely on the subsequent fate of the syngas.

Pressurized Chemical Looping Systems

The use of pressure is of interest for a number of reasons. For thermal power, the dominant reason is the possibility of high-efficiency cycles via combined cycle operation and, in addition, depending on the pressure of operation, less or no energy would be needed to compress the CO_2 to levels necessary for pipeline transportation for final sequestration. This approach has had its most notable commercial successes with gasification and integrated gasification combined cycle operation (Higman and van der Burgt 2008). However, pressurized fluidized bed technology, although it has been developed to the 350-MW_e demonstration size, has not had the same success, and the largest of such unit will shortly be closed down because of poor availability and other problems (Shimuzu 2010). In general, problems with access to the equipment due to the existence of the pressure vessel (which translate into availability problems) and, above all, the need to operate with expensive ruggedized turbines have meant this technology could reasonably be considered moribund at this point. However, given the very low attrition rates observed, as discussed earlier in this chapter, from hot beds of oxygen carriers, it is to be hoped that for gaseous fuels at least, pressurized applications might have less problems.

Normally, in pressurized gasification and combustion applications, it is the oxidant (either air or oxygen) that is compressed; in the case of pressurized chemical looping cycles, the fuel gas must be pressurized, and this will mean that the amounts of solid oxide carrier to be circulated to the fuel reactor must be significantly increased.

A very early examination of the effect of pressure on the Ni system, using a thermogravimetric analyzer (Jin and Ishida 2001) for H_2 conversion, showed that increased pressure (up to 909 kPa) reduced the temperature for the commencement of both reduction and oxidation (by about 50 °C) and that the oxidation rate was nearly independent of pressure. In a subsequent study, looking at $NiO/NiAl_2O_4$ and CoO-NiO/YSZ particles in a TGA, with simulated coal gas, the same workers found evidence of methanation and carbon deposition, but the carbon deposition could be resolved by increasing the H_2O/CO ratio from 0.5 to 1 at elevated pressure (up to 909 kPa) (Jin and Ishida 2004). They also reported that the overall reaction rate increased with increasing pressure.

However, a later study using a pressurized thermogravimetric analyzer (PTGA), carried out with pressures up to 3 MPa using H_2/N_2 and $CO/CO_2/N_2$ mixtures, showed that increasing total pressure reduces the reaction rate of the oxygen carriers examined, and it was speculated that increasing pressure might affect the internal structure of the oxygen carrier (Garcia-Labiano et al. 2006). In analyzing this study to map the range of operation conditions for Cu-, Fe-, and Ni-based carriers

(Abad et al. 2007a), the same group notes that there will be a need for higher solid inventories than expected due to the increase in gas concentrations at higher pressure and suggests that even at 1 MPa the iron system might present problems because of the upper limit for transport capacity of solids in the riser.

Siriwardane et al. (2007) looked at the behavior of a nickel oxide (60 % by wt) oxygen carrier supported on bentonite, using a high-pressure flow reactor operating at 101–690 kPa, and showed a rather more complicated picture for this system, with improved reaction at the highest pressure. However, the same workers also examined a copper oxide carrier using bentonite with a tapered-element oscillating microbalance, at pressures up to 690 kPa, and concluded that reaction pressure has a negative effect on reaction rates (Adánez et al. 2006b), in agreement with work by Garcia-Labiano et al. (2006).

Future Directions

What is now missing in the development of CLC are the first commercial- or near-commercial-scale demonstrations of the technology, similar to those being developed, for instance, by the US DOE for the $CaSO_4$ system (US DOE 2010). In a related effort, Tobias Pröll of the Technical University of Vienna has informed the author that they have developed a process flow sheet and design criteria for a 10-MW_{th} demonstration plant firing natural gas. For this work, the overall efficiency estimated is only 36 %, but it is suggested that this is reasonable considering the size of the plant. It is the practical application of these technologies and their demonstration at the industrial scale in the next several decades that are key to their contribution to a carbon-constrained world.

Although this chapter is devoted to considering primarily fossil fuels, or syngas derived from them, and focuses in particular on CH_4, syngas, and coal, there are of course numerous other possible applications for chemical looping processes. Examples include the synthesis of methanol from methane with a reduced carbon footprint (Zeeman and Castaldi 2008), a novel methanol power system using chemical looping with low-temperature reduction of methanol (Zhang et al. 2008), and a number of schemes involving chemical looping including coal to liquids, as explored by Professor Fan's group at Ohio State University (Fan et al. 2008). No attempt to consider these in detail is made here; they are noted simply to indicate the vast range of possibilities associated with the future of this technology.

Conclusions

Chemical looping is a relatively new technology, which had its beginnings some 60 years ago. However, it only began to receive major attention in the last 25 years or so. Major strides have been made taking the technology from work primarily involving fixed beds and thermogravimetric analyzers to numerous small pilot-scale fluidized bed reactors, with trials achieving upward of 1,000 h. In addition,

numerous possible systems have been explored, although the bulk of research has focused on Ni-, Cu-, and Fe-based carriers together with a vast number of possible inert substrates. Straight combustion of natural gas and, more recently, solid fuels has been explored including various schemes for the production of hydrogen. There has also been significant development in the area of reforming using this technology. What is currently lacking are larger-scale demonstration units, and the development of such facilities is urgently needed if the technology is to progress. However, for now, this technology can be seen as one of the most interesting and promising, available for use in a future carbon-constrained world.

Acknowledgments The author gratefully acknowledges the assistance and advice of Dr. David Granatstein (Granatstein Technical Services/CanmetENERGY) and Dr. Stuart Scott (Lecturer in Sustainable Energy, Department of Engineering, University of Cambridge) for a number of valuable discussions during the preparation of this chapter as well as for suggesting various amendments and improvements.

References

Abad A, Adánez J, García-Labiano F et al (2007a) Mapping of the range of operational conditions for Cu-, Fe-, and Ni-based oxygen carriers in chemical-looping combustion. Chem Eng Sci 62:533–549

Abad A, Mattisson T, Lyngfelt A, Johansson M (2007b) The use of iron oxide as oxygen carrier in a chemical looping reactor. Fuel 86:1021–1035

Abanades JC, Rubin ES, Anthony EJ (2007) Sorbent cost and performance in CO_2 capture systems. Ind Eng Chem Res 43:3462–3466

Adánez J, Gayán P, Celaya J et al (2006a) Chemical looping in a 10 kW_{th} prototype using a CuO/Al_2O_3 oxygen carrier: effect of operating conditions on methane combustion. Ind Eng Chem Res 45:6075–6080

Adánez J, Gayán P, Celaya J et al (2006) Behaviour of a $CuO\text{-}Al_2O_3$ oxygen carrier in a 10 kW chemical looping combustion plant. In: Nineteenth international conference on fluidized bed combustion, Vienna, 21–24 May 2006

Adánez J, Dueso C, de Diego LF et al (2009a) Methane combustion in a 500 W_{th} chemical looping combustion system using an impregnated Ni-based oxygen carrier. Energy Fuels 23:130–142

Adánez J, García-Labiano F, Gayán P et al (2009b) Effects of gas impurities on the behavior of Ni-based oxygen carriers on chemical-looping combustion. GHGT-9. Energy Procedia 1:11–18

Andrus H (2007) Chemical looping combustion: R&D efforts of Alstom. In: Second workshop, oxy-combustion research network, Windsor, 25–27 Jan 2007

Andrus HE, Thibeault PR, Chui JH, Lani BW (2010) Calcium oxide chemical looping with CO_2 capture for the power industry. In: Ninth annual conference on carbon capture and sequestration, Pittsburgh

Anthony EJ (1995) Fluidized bed combustion of alternative solid fuels: status, successes and problems of the technology. Prog Energy Combust Sci 21:239–268

Berguerand N, Lyngfelt A (2008a) The use of petroleum coke as fuel in a 10 kW_{th} chemical-looping combustor. Int J Greenhouse Gas Control 2:169–179

Berguerand N, Lyngfelt A (2008b) Design and operation of a 10 kW_{th} chemical-looping combustor for solid fuels – testing with South African coal. Fuel 87:2713–2726

Blamey J, Anthony EJ, Wang J, Fennell PS (2010) The calcium looping cycle for large-scale CO_2 capture. Prog Energy Combust Sci 36:260–279

Bohn CD, Muller CR, Cleeton JP et al (2008) Production of very pure hydrogen with simultaneous capture of carbon dioxide using the redox reactions of iron oxide in packed beds. Ind Eng Chem Res 47:7623–7630

Brown TA, Dennis JS, Scott SA et al (2010) Gasification and chemical-looping combustion of a lignite char in a fluidized bed of iron oxide. Energy Fuels 24:3034–3048

Cao Y, Casenas B, Pan W-P (2006) Investigation of chemical looping combustion by solid fuels. 2. Redox reaction kinetics and product characterization with coal, biomass, and solid waste as solid fuels, and CuO as an oxygen carrier. Energy Fuels 20:1845–1854

Chandel MK, Hoteit A, Delebarre A (2009) Experimental investigations of some metal oxides for chemical looping combustion in a fluidized bed reactor. Fuel 88:898–908

Chiesa P, Lozza G, Malandrino A et al (2008) Three-reactors chemical looping process for hydrogen. Int J Hydrogen Energy 33:2233–2245

Chuang SY, Dennis JS, Hayhurst AN, Scott SA (2008) Development and performance of Cu-based oxygen carriers for chemical looping combustion. Combust Flame 154:109–121

Cleeton JPE, Bohn CD, Dennis JS, Scott SA (2009) Clean hydrogen production and electricity from coal via chemical looping: identifying a suitable operating regime. Int J Hydrogen Energy 34:1–12

Consonni S, Lozza G, Pelliccia G et al (2006) Chemical looping combustion for combined cycles with CO_2 capture. J Eng Gas Turbine Power 128:525–534

Corbella BM, Palacios JM (2007) Titania-supported iron oxide as oxygen carrier for chemical-looping combustion of methane. Fuel 86:113–122

Corbella BM, de Diego F, García-Labiano F et al (2006) Performance in a fixed bed reactor of titania-supported nickel oxide as oxygen carrier for the chemical-looping combustion of methane in multicycle tests. Ind Eng Chem 45:157–165

Cuenca MA, Anthony EJ (eds) (1995) Pressurized fluidized beds. Blackie Academic and Professional, London

Damen K, van Troost M, Faaij A, Turkenburg W (2006) A comparison of electricity and hydrogen systems with CO_2 capture and storage: part A: review and selection of promising conversions and capture systems. Prog Energy Combust Sci 32:215–246

De Diego LF, García-Labiano F, Adánez J et al (2004) Development of Cu-based oxygen carriers for chemical looping combustion. Fuel 83:1749–1757

De Diego LF, Gayán P, García-Labiano F et al (2005) Impregnated CuO/Al_2O_3 oxygen carriers for chemical looping combustion: avoiding fluidized bed agglomeration. Energy Fuels 19:1850–1856

De Diego LF, García-Labiano F, Gayán P et al (2007) Operation of a 10 kW_{th} chemical-looping combustor during 200 h with a $CuO\text{-}Al_2O_3$ oxygen carrier. Fuel 86:1036–1045

De Diego LF, Ortiz M, García-Labiano F et al (2009) Synthesis gas generation by chemical-looping reforming using a Ni-based oxygen carrier. GHGT-9. Energy Procedia 1:3–10

Dennis JS, Scott SA (2010) In situ gasification of a lignite coal and CO_2 separation using chemical looping with a Cu-based oxygen carrier. Fuel 89:1623–1640

Dennis JS, Scott SA, Hayhurst AN (2006) In situ gasification of coal using steam with chemical looping: a technique for isolating CO_2 from burning a solid fuel. J Energy Inst 79:187–190

Dueso C, García-Labiano F, Adánez J et al (2009) Syngas combustion in a chemical-looping combustion system using impregnated Ni-based oxygen carrier. Fuel 88:2357–2364

Fan L, Li F, Ramkumar S (2008) Utilization of chemical looping strategy in coal gasification processes. Particuology 6:131–142

Foero CR, Gayán P, García-Labiano F et al (2010) Effect of gas composition in chemical-looping combustion with copper based oxygen carriers: fate of sulphur. Int J Greenhouse Gas Control 4 (5):762–770

Gao Z, Shen L, Xian J et al (2008) Use of coal as fuel for chemical-looping combustion with Ni-based oxygen carrier. Ind Eng Chem Res 47:9279–9287

Garcia-Labiano F, Adánez J, de Diego LF et al (2006) Effect of pressure on the behavior of copper-, iron-, and nickel-based oxygen carriers for chemical-looping combustion. Energy Fuels 20:26–33

Gayán P, Dueso C, Abad A et al (2009) NiO/Al_2O_3 oxygen carrier for chemical looping combustion prepared by impregnation and deposition-precipitation methods. Fuel 88:1016–1023
Go KS, Son SR, Kim SD et al (2009) Hydrogen production from two-step steam methane reforming in a fluidized bed reactor. Int J Hydrogen Energy 34:1301–1309
Harrison DP (2009) Private communication. University of Louisiana, Lafayette
Harvey SP, Richter HJ (1994) A high-efficiency gas turbine power generation cycle with solid oxide fuel cell technology and chemical looping fuel combustion. ASME Thermodyn Des Anal Improv Energy Syst Symp AES 33:66–71
Hatanak T, Matsuda S, Hatano H (1997) A new concept gas-solid combustion system "Merit", for high combustion efficiency, and low emissions. In: Proceedings of the 23rd energy conversion engineering conference, vol 2, Denver, pp 994–948
He F, Wei Y, Li H, Wang H (2009) Synthesis gas generation by chemical-looping reforming using Ce-based oxygen carriers modified with Fe, Cu and Mn oxides. Energy Fuels 23:2095–2102
Higman C, van der Burgt M (2008) Gasification, 2nd edn. Gulf Professional Publishing, Elsevier/Oxford
Hossain MM, de Lasa HI (2008) Chemical looping combustion (CLC) for inherent CO_2 separations – a review. Chem Eng Sci 63:4433–4451
Hossain M, Lopez D, Herrera J, de Lasa HI (2009) Nickel on lanthanum-modified γ-Al_2O_3 oxygen carrier for CLC: reactivity and stability. Catal Today 43:179–186
Ishida M, Jin H (1994a) A novel combustor based on chemical looping reactions and its reaction kinetics. J Chem Eng Jpn 27:296–301
Ishida M, Jin H (1994b) A new advanced power-generation system using chemical-looping combustion. Energy 19:415–419
Ishida M, Yamamoto M, Ohba T (2002) Experimental results of chemical looping combustion with $NiO/NiAl_2O_4$ particle circulation at 1200 °C. Energy Convers Manage 43:1469–1478
Ishida M, Takeshita K, Suzuki K, Ohba T (2005) Application of Fe_2O_3-Al_2O_3 composite particles as solid looping materials of the chemical-loop combustor. Energy Fuels 19:2514–2518
Jerndal E, Mattisson T, Lyngfelt A (2006) Thermal analysis of chemical looping combustion. Chem Eng Res Des 84:795–806
Jerndal E, Mattisson T, Thijs I et al (2010) Investigation of $NiO/NiAl_2O_4$ oxygen carriers for chemical-looping combustion produced by spray-drying. Int J Greenhouse Gas Control 4:23–35
Jin H, Ishida M (2001) Reactivity study on a novel hydrogen fueled chemical-looping combustion. Int J Hydrogen Energy 26:889–894
Jin H, Ishida M (2004) A new type of coal gas fueled chemical looping combustion. Fuel 83:2411–2417
Jin H, Okamato T, Ishida M (1999) Development of a novel chemical-looping combustion: synthesis of a solid looping material of $NiO/NiAl_2O_4$. Ind Eng Chem Res 38:126–132
Johansson M (2007) Screening of oxygen carrier particles based on iron, manganese, copper and nickel oxides for use in chemical looping technologies. PhD thesis, Chalmers University, Sweden
Johansson M, Mattisson T, Lyngfelt A (2006a) Investigation of Mn_3O_4 with stabilized ZrO_2 for chemical looping combustion. Chem Eng Res Des 84:807–818
Johansson M, Mattisson T, Lyngfelt A (2006b) Creating a synergy effect by using mixed oxides of iron and nickel in the combustion of methane in a chemical-looping combustor reactor. Energy Fuels 20:2399–2407
Johansson M, Mattisson T, Rydén M, Lyngfelt A (2006) Carbon capture via chemical looping combustion and reforming. In: International seminar on carbon sequestration and climate change, Rio de Janeiro, 24–26 Oct 2006
Kale GR, Kulkarni BD, Joshi AR (2010) Thermodynamic study of combining chemical looping combustion and combined reforming of propane. Fuel 89:3141–3146
Kimball E, Geerdink P, Huisinga A et al (2010) Fixed bed chemical looping combustion experiment based design. In: Proceedings of the 35th international technical conference on clean coal and fuel systems, Clearwater, 6–10 June 2010

Ksepko E, Siriwardane RV, Tian H et al (2010) Comparative investigation on chemical looping combustion of coal-derived synthesis gas containing H_2S over supported NiO oxygen carrier. Energy Fuels 24(8):4206–4214
Kuusik R, Trikkel A, Lyngfelt A, Mattisson T (2009) High temperature behavior of NiO-based oxygen carriers for chemical looping combustion. Energy Procedia 1:3885–3892
Kvamsdal HM, Jordal K, Bolland O (2007) A quantitative comparison of gas turbine cycles with CO_2 capture. Energy 32:10–24
Larsen R, Wang M, Santini D et al (2004) Might Canadian oil sands promote hydrogen production technology for transportation. Argonne National Laboratory Presentation, Chicago, IL, 20(Apr 2004)
Leion H, Mattisson T, Lyngfelt A (2007) The use of petroleum coke as fuel in chemical-looping combustion. Fuel 86:1947–1958
Leion H, Lyngfelt A, Johansson M et al (2008a) The use of ilmenite as an oxygen carrier in chemical-looping combustion. Chem Eng Res Dev 86:1017–1026
Leion H, Mattisson T, Lyngfelt A (2008b) Solid fuels in chemical-looping combustion. Int J Greenhouse Gas Control 2:180–193
Lewis WK, Gilliland ER (1954) Production of pure carbon dioxide. US patent no 2,665,972
Lewis WK, Gilliland ER, Reed WA (1949) Reaction of methane with copper oxide in a fluidized bed. Ind Eng Res 41:1227–1237
Li K, Wang H, Wei Y et al (2010) Syngas production from methane and air via a redox process using Ce-Fe mixed oxides as oxygen carriers. Appl Catal B 97:361–372
Linderholm C, Mattisson T, Lyngfelt A (2009) Long-term integrity testing of spray-dried particles in a 10-kW chemical-looping combustor using natural gas as fuel. Fuel 88:2083–2096
Lyngfelt A, Leckner B, Mattisson T (2001) A fluidized-bed combustion process with inherent CO_2 separation: application of chemical looping combustion. Chem Eng Sci 56:3101–3113
Lyngfelt A, Kronberger B, Adanez J et al (2004) The Grace Project development of oxygen carrier particles for chemical looping combustion, design and operation of a 10 kW chemical looping combustor. http://uregina.ca/ghgt7/PDF/papers/peer/132.pdf
Lyon RK, Cole JA (2000) Unmixed combustion: an alternative to fire. Combust Flame 121:249–261
Markström P, Berguerand N, Lyngfelt A (2010) The application of a multistage-bed model for residence-time analysis in chemical-looping combustion of solid fuel. Chem Eng Sci 65 (18):5055–5066
Mattisson T, Lyngfelt A, Cho P (2001) The use of iron oxide as an oxygen carrier, in chemical-looping of methane with inherent separation of CO_2. Fuel 80:1953–1962
Mattisson T, Johansson M, Jerndal E, Lyngfelt A (2008) The reaction of Ni/$NiAl_2O_4$ particles with alternating methane and oxygen. Can J Chem Eng 86:756–767
Mattisson T, Leion H, Lyngfelt A (2009) Chemical-looping with oxygen uncoupling using CuO/ZrO_2 with petroleum coke. Fuel 88:683–690
McGlashan NR (2010) The thermodynamics of chemical looping combustion applied to the hydrogen economy. Int J Hydrogen Energy 35:6465–6474
Mayer K, Prőll T, Hofbauer H (2010) Performance of mixtures of natural minerals and a nickel based material as oxygen carriers in chemical looping combustion in a 120 kW pilot plant. In: 1st international conference on chemical looping, Lyon, 17–19 Mar 2010
Naqvi R, Wolf J, Bolland O (2007) Part-load analysis of a chemical looping combustion (CLC) combined cycle with CO_2 capture. Energy 32:360–370
Partington JR (1939) A text book of inorganic chemistry, 5th edn. MacMillan, London
Prőll T, Mayer K, Bolhàr-Nordenkampf J et al (2009) Natural minerals as oxygen carriers for chemical looping combustion in a dual circulating fluidized bed system. Energy Procedia 1:27–34
Pröll T, Bolhàr-Nordenkampf J, Kolbitsch P, Hofbauer H (2010) Syngas and a separate nitrogen/argon stream via chemical looping reforming – a 140 kW pilot plant study. Fuel 89:1249–1256

Rao AB, Rubin ES (2006) Identifying cost-effective CO_2 control levels for amine-based CO_2 capture. Ind Eng Chem Res 45:2421–2429

Redman JE, Olafsen A, Smith JB, Blom R (2006) Chemical looping combustion using $NiO/NiAl_2O_4$: mechanisms and kinetics of reduction-oxidation (Red-Ox) reactions from in situ powder X-ray diffraction and thermogravimetric experiments. Energy Fuels 20:1382–1387

Richter HJ, Knoche K (1983) Reversibility of combustion processes. ACS Symp Ser 235:71–85

Rubel A, Liu K, Neathery J, Taulbee D (2009) Oxygen carriers for chemical looping combustion of solid fuels. Fuel 88:876–884

Rydén M, Lyngfelt A, Schulman A et al (2008a) Developing chemical-looping steam reforming and chemical-looping autothermal reforming. In: Thomas DC, Bensen SM (eds) Carbon dioxide capture for storage in deep geological formations, vol 3. CPL Press, Berks

Rydén M, Lyngfelt A, Mattisson T et al (2008b) Novel oxygen carrier materials for chemical looping combustion and chemical-looping reforming La x Sr1 − x Fe y Co1 − y, O3-δ perovskites and mixed-metal oxides of NiO, Fe_2O_3, and Mn_3O_4. Int J Greenhouse Gas Control 2:21–36

Rydén M, Lyngfelt A, Mattisson T (2008c) Chemical-looping combustion and chemical-looping reforming in a circulating fluidized-bed reactor using Ni-based oxygen carriers. Energy Fuels 22:2285–2297

Rydén M, Johansson M, Cleverstam E et al (2010) Ilmenite with addition of NiO as oxygen carrier for chemical-looping combustion. Fuel 89(11):3523–3533

Scott SA, Dennis JS, Hayhurst AN, Brown T (2006) In-situ gasification of a solid fuel and CO_2 separation using chemical looping. AIChE J 52:3325–3328

Shen L, Zheng M, Xiao J, Xiao R (2008) A mechanistic investigation of a calcium based oxygen carrier for chemical looping combustion. Combust Flame 154:489–506

Shen L, Wu J, Xiao J (2009) Experiments on chemical looping combustion of coal with a NiO based oxygen carrier. Combust Flame 156:721–728

Shen L, Gao Z, Wu J, Xiao J (2010) Sulfur behavior in chemical looping combustion with NiO/Al_2O_3 oxygen carrier. Combust Flame 157:853–863

Shimuzu T (2010) Open communication at 60th IEA FBC meeting. Gothenburg, Sweden(May 2010)

Siriwardane R, Poston J, Chaudhari K et al (2007) Chemical looping combustion of simulated synthesis gas using nickel oxide oxygen carrier supported on bentonite. Energy Fuels 21:1582–1591

Siriwardane R, Tian H, Miller D et al (2010) Evaluation of reaction mechanism of coal-metal oxide interaction in chemical looping combustion. Combust Flame 157:2198–2208

Son SR, Kim SD (2006) Chemical looping combustion with NiO and Fe_2O_3 in a thermobalance and circulating fluidized bed reactor with double loops. Ind Eng Chem Res 45:2689–2696

Song Q, Xiao R, Deng Z et al (2008a) Chemical looping combustion of methane with $CaSO_4$ oxygen carrier in a fixed bed reactor. Energy Convers Manage 40:3178–3187

Song Q, Xiao R, Deng Z et al (2008b) Multicycle study on chemical-looping combustion of simulated coal gas with a $CaSO_4$ oxygen carrier in a fluidized bed reactor. Energy Fuels 22:3661–3672

Song Q, Ziao R, Deng Z et al (2008c) Effect of temperature on reduction of $CaSO_4$ oxygen carrier in a chemical-looping combustion of simulated coal gas in a fluidized bed reactor. Ind Eng Chem 47:8148–8149

Srinivasan NS, Lahiri AK (1975) On the mechanism of iron oxide reduction by carbon. Metall Trans B 6(2):269–274

Tan R, Santos S, Spliethoff H (2006) Chemical looping combustion for fossil fuel utilization with carbon sequestration. International flame foundation study report document no G 23/y/s

Tian H, Guo Q (2009) Investigation into the behavior of reductive decomposition of calcium sulfate by carbon monoxide in chemical looping combustion. Ind Eng Chem Res 48:5624–5632

Tian H, Chaudhari K, Simonyi T et al (2008) Chemical looping combustion of coal derived synthesis gas over copper oxide oxygen carriers. Energy Fuels 22:3744–3755

US DOE (2010) http://www.netl.doe.gov/technologies/coalpower/ewr/co2/oxy-combustion/prototype.html
Wang J, Anthony EJ (2008) A process for clean combustion of solid fuels. Appl Energy 85:73–79
Wolf J, Anheden M, Yan J (2005) Comparison of nickel- and iron-based oxygen carriers in chemical looping combustion for CO_2 capture in power generation. Fuel 84:993–1006
Xiang W, Wang S, Di T (2006) Investigation of gasification chemical looping combustion combined cycle performance. Energy Fuels 22:961–966
Xiang W, Chen S, Xue Z, Sun X (2010) Investigation of coal gasification hydrogen and electricity co-production with three-reactors chemical looping process. Int J Hydrogen Energy 35 (16):8580–8591
Xiao R, Song Q, Song M et al (2010a) Pressurized chemical-looping combustion of coal with an iron ore-based oxygen carrier. Combust Flame 157:1140–1153
Xiao R, Song S, Zhang S et al (2010b) Pressurized chemical-looping combustion of Chinese bituminous coal: cyclic performance and characterization of iron-ore based oxygen carrier. Energy Fuels 24:1449–1463
Yang J, Cai N-S, Li Z-S (2008) Hydrogen production from the steam-iron process with direct reduction of iron oxide by chemical looping combustion of coal char. Energy Fuels 22:2570–2579
Zafar Q, Mattisson T, Gevert B (2005) Integrated hydrogen and power production with CO_2 capture using chemical-looping reforming-redox reactivity of particles of CuO, NiO and Fe_2O_3 using SiO_2 as a support. Ind Eng Chem Res 44:3485–3496
Zeeman F, Castaldi M (2008) An investigation of synthetic fuel production via chemical looping. Environ Sci Technol 42:2723–2727
Zhang X, Han W, Hong H, Jin H (2008) A chemical intercooling turbine cycle with chemical looping combustion. Energy 34:2131–2136
Zhao H, Liu L, Wang B et al (2008) Sol-gel derived NiO/$NiAl_2O_4$ oxygen carriers for chemical-looping combustion by coal char. Energy Fuels 22:898–905
Zheng M, Shen L, Xiao J (2010) Reduction of $CaSO_4$ oxygen carrier with coal in chemical-looping combustion: effects of temperature and gasification intermediate. Int J Greenhouse Gas Control 4(5):716–728

High Temperature Oxygen Separation Using Dense Ceramic Membranes

Jaka Sunarso, Kun Zhang, and Shaomin Liu

Contents

Abstract

Mixed ionic–electronic conducting (MIEC) ceramic membrane has rapidly become an attractive alternative technology to conventional cryogenic distillation for oxygen separation from air. Given the heat integration opportunity in most energy generation processes, this technology offers lower cost and energy penalty due to its capability to produce pure oxygen at high temperature

J. Sunarso (✉)
Department of Chemistry, University of Waterloo, Waterloo, ON, Canada
e-mail: barryjakasunarso@yahoo.com; jsunarso@uwaterloo.ca

K. Zhang • S. Liu (✉)
Department of Chemical Engineering, Curtin University, Perth, WA, Australia
e-mail: kun.zhang@curtin.edu.au; shaomin.liu@curtin.edu.au

W.-Y. Chen et al. (eds.), *Handbook of Climate Change Mitigation and Adaptation*,
DOI 10.1007/978-3-319-14409-2_94

(>800 °C). Using pure oxygen for combustion in turn facilitates the production of concentrated carbon dioxide gas downstream which can be easily captured and handled to mitigate the greenhouse gas effect. This chapter overviews and discusses all essential aspects to understand oxygen selective MIEC ceramic technology. The basics behind the formation of defects responsible for high-temperature ionic transport are explained together with the transport theory. Two major family structures, e.g., fluorite and perovskite, which become the building blocks of most MIEC materials are discussed. Specific structure and properties as well as the advantages and the drawbacks of each family are explained. Some important structural considerations, e.g., crystal structure packing and Goldschmidt tolerance factor, are elaborated due to its strong relationship with the properties. Two additional concepts, e.g., dual-phase membrane and external short circuit, are given to address the drawbacks associated with fluorite and perovskite MIEC materials. Various geometries and types of MIEC membranes can be prepared, e.g., disk, tube, hollow fiber, or flat plate, each of which fits particular application. A short paragraph is presented at the end of the chapter on another possible application of this technology to facilitate a particular reaction to synthesize value-added products.

Introduction

Oxygen plays a vital role in industry with applications in almost every industry sector such as steel and aluminum or other metals manufacturing, chemicals, pharmaceuticals, petroleum, glass, cement, ceramics, pulp and paper, metal cutting and welding, waste treatment, rocket fuel, medical, and healthcare and other life support systems. The annual global oxygen production is predicted to reach hundreds of millions of tons from air separation and contributes to the largest section in the industrial gases market with the kept rising global demand foreseen to reach US$6 billion in 2018 (http://www.prweb.com/releases/2013/11/prweb11347927.html). As we are transferring the energy infrastructure from fossil fuel-based energy technology to a cleaner and more sustainable technology, oxygen has been recognized as an important component in the mitigation of greenhouse gas emission.

In current oxygen market, steel industry alone accounts for more than 50 % of the consumption where oxygen is used to enhance blast furnace iron production. In contrast, energy generation industry only uses 4 %. With increased attention and stricter regulations toward environmental compliance, the oxygen will also be used in clean energy generation technologies such as integrated gasification combined cycle (IGCC) and oxy-fuel projects. These technologies require pure oxygen or a mixture of oxygen and carbon dioxide as the feed gas. It is estimated that by 2040, the energy sector will occupy 60 % shares of the market, translating to approximately two million tons of oxygen per day (http://www.world-nuclear.org/info/energy-and-environment/-clean-coal–technologies/). While oxygen is available free of cost directly from air, obtaining it at a concentration higher than 21 % entails cost and energy penalty associated with the enrichment or separation

processes. At the moment, industrial tonnage oxygen is produced at a lower purity (<93 %) on an intermediate scale by pressure swing adsorption or at a high purity (>93 %) on a large scale (>1000 t per day) by cryogenic distillation. Both processes are capital and energy intensive. In particular, cryogenic distillation is a quite old technology which has been used for more than a century, therefore leaving no space for improvement.

Recently, a more efficient alternative technology relying on gas separation through membrane has emerged which also facilitates easy carbon capture and storage (CCS). This less mature technology offers higher energy efficiency and less capital cost. Several different types of membranes are available. Polymeric membranes have restricted applications due to their low selectivity and permeability as well as their organic nature which hinders operation to high temperature. Inorganic porous membranes, the so-called "molecular sieving" membranes such as zeolite, silica, and carbon membranes, provide good selectivity and permeability, but they are difficult to be scaled up. Thus far, dense mixed ionic–electronic conducting (MIEC) ceramic membranes have attracted the largest attention from research communities, industries, and governments of developed countries given their absolute selectivity and robustness in addition to the capability to operate at high temperature (>800 °C) and harsh conditions. For example, starting from 1997, Air Products and Chemicals and US Department of Energy (US DOE) have initiated one of the longest and biggest investments worth US$150 million to advance this technology, referred as ion-transporting membrane (ITM) technology (Foster 2008). Research in this topic actually began in the early 1980s with the current efforts directed more toward improving materials stability in reducing acidic gas in the atmosphere (Sunarso et al. 2008; Teraoka et al. 1985). The availability of stable materials with high oxygen permeability is expected to favor a wide application of MIEC technology for energy sector and industries.

The objective of this chapter is to provide an introductory overview of important aspects of MIEC ceramic membrane technology which is not covered (or detailed) in the more comprehensive reviews elsewhere (Sunarso et al. 2008; Zhang et al. 2011). Some overlaps with these reviews exist but nonetheless are included to make this chapter an independent reading for the beginners in this topic.

Transport Theory

Transport Mechanisms

Oxygen transport through MIEC ceramic membrane is made possible by the formation of substantial amount of defects, e.g., oxygen vacancies or oxygen interstitials at high temperatures (>800 °C). Even at a room temperature, numerous oxides readily exhibit defects due to "nonstoichiometry," where the cation and anion have different effective charges. This has been manifested in some cations and/or anions emptied from the lattice for the charge neutrality to be maintained in the compound (Kingery et al. 1976; Tilley 2013).

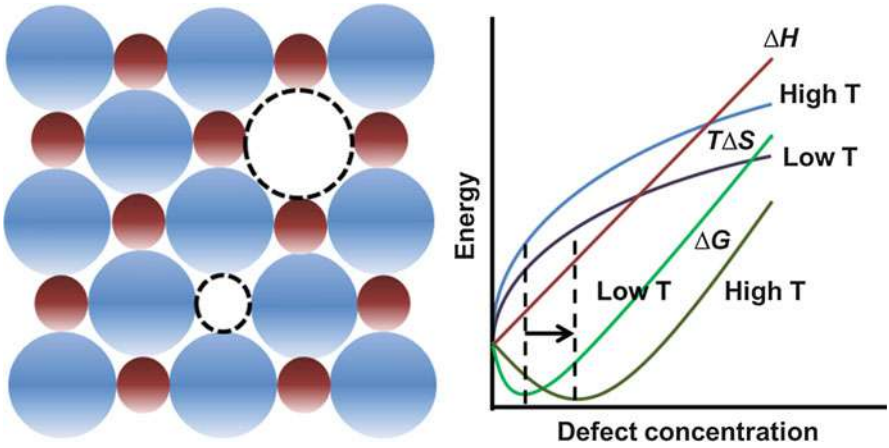

Fig. 1 Typical defects represented by Schottky defect (*left*) and relative Gibbs energy versus defect concentration at low and high temperature (*right*)

In general, defects form as a consequence of the lowering of Gibbs energy obtained from increased entropy, e.g., the vacancies of some cations or anions allow more possibility of distinct arrangements within the crystal lattice (Kingery et al. 1976). Typical defect formation is depicted in Fig. 1 (left) which shows that one cation and one anion are missing, e.g., Schottky defect. Other defect types are also available which are not discussed here (Kingery et al. 1976; Tilley 2013). Gibbs energy is represented by

$$\Delta G = \Delta H - T\Delta S \tag{1}$$

Figure 1 (right) illustrates the relative Gibbs energy for low- and high-temperature scenarios. At a certain temperature, a minimum energy is achieved when an optimum amount of defects form. Increasing temperature results in the increased $T\Delta S$ for every concentration, and therefore the minimum energy is also shifted to larger defect concentration. Simply put, increasing temperature favors larger defect concentration.

In MIEC compound, the presence of defects, e.g., oxygen vacancies, provides a pathway for oxygen ionic diffusion (where oxygen ion hops from one empty site to another empty site) and is the main contributor to its oxygen ionic conductivity. In addition, electronic conductivity also exists due to the presence of transition metal in the oxides framework (mostly in perovskite compounds without ruling out fluorite compounds). Notably, transition metals can have more than one oxidation state during reduction and oxidation reaction. The formation of oxygen vacancies at increasing temperature is often accompanied by the reduction of the transition metal components (mostly in perovskite oxide) simultaneously accompanied by electron transfer reactions (Feldhoff et al. 2009; Arnold et al. 2009).

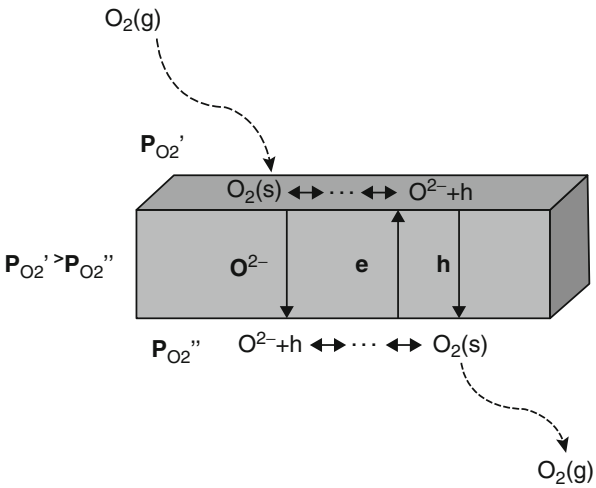

Fig. 2 Schematic diagram of oxygen transport through mixed ionic–electronic conducting (MIEC) ceramic membrane (Reproduced from Zhang et al. (2011))

The existence of this simultaneous ionic and electronic conductivity defines its "mixed ionic–electronic conducting" name (Sunarso et al. 2008; Zhang et al. 2011). During membrane operation, a driving force is established normally through oxygen partial pressure difference between two different membrane sides. Figure 2 provides the schematic of the process. Oxygen gas on high partial pressure side of the membrane approaches the surface of the membrane, adsorbed on the surface (in some cases), and, upon receiving electron, becomes an oxygen ion. This oxygen ion then diffuses through the membrane (via the oxygen vacancies throughout the membrane), the process of which is accompanied by simultaneous electron transfer (or hole) in the opposite direction (same direction) to maintain the charge balance. The oxygen ion arrives at the other side of the membrane and, upon releasing electron, becomes an oxygen gas again. The first and the third processes are defined as surface exchange reactions, while the second process is defined as bulk diffusion. In the absence of any mechanical defect and assuming a perfect sealing, dense MIEC membrane permeates only oxygen to the other side, thus achieving an absolute selectivity in such system.

Limiting Steps

The oxygen transport rate through the membrane, i.e., the flux, is limited by the slowest step, either bulk diffusion or surface exchange reaction (Sunarso et al. 2008). Consequently, thickness of the membrane becomes an important variable. For a relatively thick membrane, bulk diffusion tends to dominate, and as the thickness is reduced, surface exchange reaction becomes more prevalent.

The incorporation of oxygen from the atmosphere (high oxygen potential) into the lattice and the subsequent release of lattice oxygen back to the atmosphere (low oxygen potential) can be described by two simple surface reactions:

$$\frac{1}{2}O_2 + V_{\ddot{o}} + 2e' \rightarrow O_O^x \text{ (high } O_2 \text{ potential)} \tag{2}$$

$$O_O^x \rightarrow \frac{1}{2}O_2 + V_{\ddot{o}} + 2e' \text{ (low } O_2 \text{ potential)} \tag{3}$$

Here, O_2, $V_{\ddot{o}}$, e', and $O_O{}^x$ represent molecular oxygen, oxygen vacancy, electron, and lattice oxygen, respectively. Albeit their oversimplicity to address the complexity of the real surface reactions, they can be used as a starting point. The consequence of oxygen incorporation into the lattice and the release of lattice oxygen back to the atmosphere is the generation of chemical potential gradient across the membrane (when one side is exposed to low oxygen potential), and because of the mobility of the charge carrier species, a net flux of oxygen will occur toward the lower potential side.

Bulk Diffusion

If bulk diffusion is predominant, oxygen flux can normally be described using Wagner equation as a function of the conductivity of the charge carrier species and the oxygen partial pressure (Wagner 1975):

$$J_{O_2} = \frac{RT}{4^2F^2L}\int_{\ln P'_{o_2}}^{\ln P''_{o_2}} \frac{\sigma_{el}\sigma_{ion}}{\sigma_{el}+\sigma_{ion}} d(\ln P_{O_2}) \tag{4}$$

Here, σ_{el}, σ_{ion}, P_{O2}, R, F, and L represent electronic conductivity, ionic conductivity, oxygen partial pressure, ideal gas constant, Faraday constant, and membrane thickness, respectively.

If the oxygen vacancies are proportional to the ionic conductivity (i.e., if all vacancies do not associate among each other), an assumption which is valid at low vacancy concentration, the ionic conductivity can be expressed by Nernst–Einstein equation:

$$\sigma_{ion} = \frac{4F^2[V_{\ddot{o}}]D_V}{RTV_m} \tag{5}$$

Here, D_V is the vacancy diffusion coefficient and V_m is the molar volume of the oxide. This relationship implies that the electronic conductivity is not limiting, e.g., when it is substantially higher than the ionic conductivity. Therefore, Eq. 4 simplifies into

$$J_{O_2} = \frac{D_V}{4V_mL}\int_{\ln P'_{o_2}}^{\ln P''_{o_2}} [V_{\ddot{O}}] d(\ln P_{O_2}) \tag{6}$$

The vacancy diffusion coefficient can be determined via experimental measurement of chemical diffusion coefficient and tracer diffusion coefficient, e.g., via ^{18}O–^{16}O isotope exchange experiments. The oxygen vacancy concentration can be derived as a function of oxygen partial pressure at low concentration of defects

which leads to simplification. More details on the various simplifications pertaining to different special cases can be found elsewhere (Sunarso et al. 2008).

Surface Exchange Reaction

Surface exchange reaction normally involves a series of steps with each one may become the limiting step. The possible steps are adsorption from the gas phase, charge transfer reaction between the adsorbed species and the bulk, and surface diffusion of intermediate species (Sunarso et al. 2008). Further additional steps are possible when every other gas impurity components such as CO, CO_2, and CH_4 which are exposed to the surface are taken into account. Oxygen flux equation can be derived theoretically by assuming the slowest step among the proposed reaction steps and using the law of mass action related to the oxygen partial pressure or empirically, examples of which can be found elsewhere (Sunarso et al. 2008).

An important variable defined as L_c, i.e., a characteristic thickness, signifies the membrane thickness below which surface exchange dominates while above it, bulk diffusion dominates. It is quite accurate to say that at L_c, oxygen transport is equally determined by surface exchange and bulk diffusion (Bouwmeester et al. 1994). L_c however is not an intrinsic property as it generally depends on the surface morphology and the operating conditions such as oxygen partial pressure and temperature (Sunarso et al. 2008).

Membrane Developments, Limitations, and Improvements

Fluorite

Oxide compounds with fluorite structure are often used as an ionic conductor (an electrolyte) due to its predominant ionic conductivity at a certain temperature range. The ideal fluorite structure is illustrated in Fig. 3. Fluorite compounds have a general formula of AO_2, exemplified by calcium fluoride (CaF_2). In such structure,

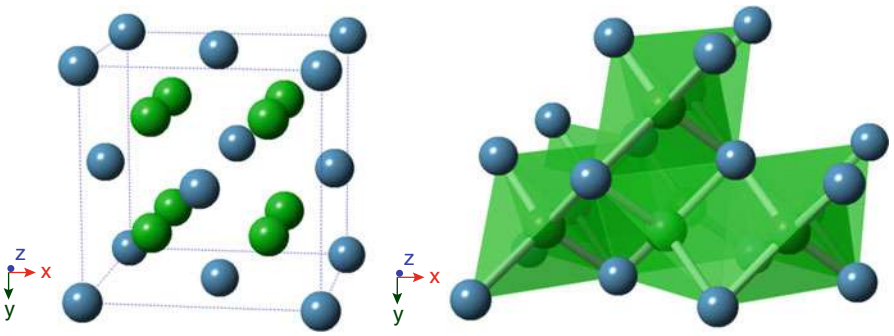

Fig. 3 Ideal fluorite structure for AO_2 compounds represented by CaF_2 (*left*) and its packing (*right*). *Blue* atoms, A (Ca); *green* atoms, O (F)

the A cations form cubic close packing and occupy the face-centered cubic positions, while the O anions occupy the tetrahedral interstices (Megaw 1973).

Zirconia (ZrO_2) represents the classical example of oxides with fluorite structure which forms an important family of electrolytes in conventional solid oxide fuel cells. It requires temperature above 700 °C to have substantial conductivity. Zirconia exhibits phase transition from monoclinic to tetragonal between 1100–1200 °C and tetragonal to cubic at 2300 °C (Aldebert and Traverse 1985). The cubic phase can be stabilized to room temperature by (about 10 mol%) Zr^{4+} substitution with lower valence cations, e.g., Ca^{2+}, Mg^{2+}, and Ln^{3+} (lanthanides). The tetragonal phase can also be stabilized using a less amount (about 3 mol%) of specific dopant such as Y^{3+}. The drawback of using zirconia lies on the very high temperature required to achieve substantial oxygen ionic conductivity which is closely related to the structure. The ionic conductivity of the monoclinic ZrO_2 is negligible, i.e., 10^{-7}–10^{-6} S cm^{-1} which is improved for its tetragonal phase to 10^{-3}–10^{-2} S cm^{-1} and reaches 10 S cm^{-1} for cubic ZrO_2 beyond 2100 °C. Higher conductivity can also be obtained at lower temperature by partially substituting ZrO_2 with CaO, resulting in a conductivity value close to 10^{-1} S cm^{-1} at 1300 °C.

An attractive alternative to zirconia is bismuth oxide. Bismuth oxide also experiences phase transition from monoclinic (α-phase) to cubic (δ-phase) at 730 °C prior to melting at 825 °C (Sammes et al. 1999). The cubic δ-phase of Bi_2O_3 has fluorite structure with ordered defects in the oxygen sub-lattice and is attractive in terms of its 1–2 orders of magnitude higher conductivity than yttria-doped zirconia, i.e., 1 S cm^{-1} at 650 °C. This superior ionic conductivity is attributable to the vacancy of a quarter of oxygen sites in the lattice, the electronic configuration of Bi^{3+} comprising $6s^2$ lone pair electrons which leads to the high polarizability of the cation (and high oxide ion mobility) and Bi^{3+} ability to accommodate highly disordered surroundings (Sammes et al. 1999). The cubic phase can be stabilized to room temperature by partially substituting Bi with Dy, Er, Gd, Ho, Lu, Tb, Tm, Y, and Yb (despite existing dispute on the resultant structure), among which Dy-, Er-, Ho-, and Tb-doped ones show the highest conductivity of 0.1–0.4 S cm^{-1} between 650 °C and 700 °C.

Another fluorite compound of interest is ceria (CeO_2). Pure CeO_2 is actually a mixed conductor showing almost similar ionic and electronic conductivities (Inaba and Tagawa 1996). This is quite consistent with the fact that cerium can change its oxidation state depending on the oxygen partial pressure, i.e., Ce^{4+} may be reduced to Ce^{3+} under reducing atmosphere (and the opposite) (Kuharuangrong 2007). The ionic conductivity of the ceria can be made predominant by partially substituting Ce with other metal cations having lower and fixed valence. The interest on ceria-based materials comes from its high oxygen ionic conductivity, i.e., its conductivity at 750 °C is similar to that of yttria-doped zirconia at 1000 °C. Despite the superior conductivity of Bi_2O_3-based materials, they are not stable and can be reduced easily in reducing atmosphere. In contrast, ceria-based materials are quite stable and therefore have been largely used to replace yttria-doped zirconia as an electrolyte for lower temperature operation (<800 °C) (Inaba and Tagawa 1996). A relatively high oxygen ionic conductivity of 10^{-2} S cm^{-1} at 500 °C is reported for

gadolinium-doped ceria, $Ce_{0.9}Gd_{0.1}O_{1.95}$. In spite of variations in the conductivity values reported as well as various possible dopants, e.g., Ba, Ca, Dy, Gd, Ho, La, Mg, Nd, Sm, Sr, Y, and Yb, to improve the conductivity, generally Gd- and Sm-doped cerias provide the highest conductivity values (Inaba and Tagawa 1996; Eguchi et al. 1992). Sm-doped ceria, $Ce_{0.8}Sm_{0.2}O_{1.9}$, particularly is the most attractive one to replace yttria-doped zirconia given its lowest reducibility among the doped ceria compounds (Eguchi et al. 1992).

As a trend, the oxygen fluxes of the fluorite compounds are lower by two to three orders of magnitude with respect to the perovskite compounds due to its limited electronic conductivity. Multivalent cations can be incorporated as a dopant although the improvement of the electronic conductivity is marginal and therefore does not contribute substantially to the resultant oxygen flux (Sunarso et al. 2008). The compilation of the oxygen fluxes for fluorite compounds is available elsewhere (Sunarso et al. 2008).

Perovskite

Research and development of MIEC materials have been heavily focused on perovskite compounds due to their high ionic and electronic conductivity. The ideal perovskite structure is schematized in Fig. 4. Perovskite compounds have a general ABO_3 formula and contain two different metal cations with different sizes. Typical compound with this structure is $SrTiO_3$. Perovskite framework consists of corner-shared BO_6 octahedra where the large A cation sits in the center of the cavity between 8 octahedra (Megaw 1973). In perovskite, each B cation is surrounded by 6 O anions forming 6 equidistant B–O bonds and likewise each A cation is surrounded by 12 O anions forming 12 equidistant A–O bonds. The effective valence state of A and B may vary as exemplified by the formula of $A^{2+}B^{4+}O_3$ or

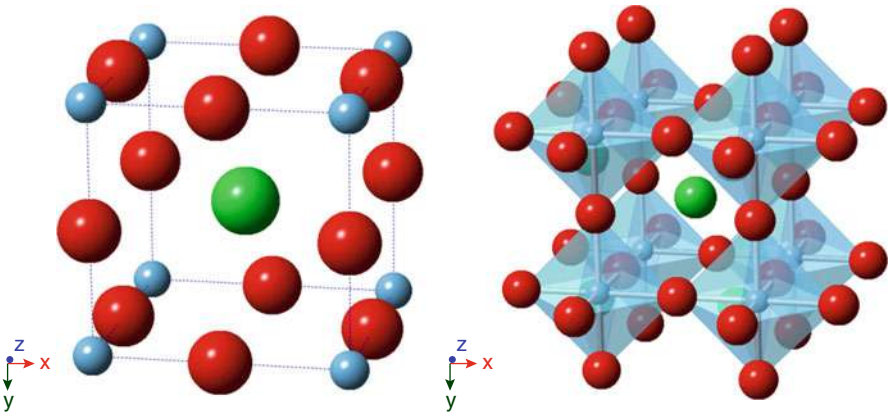

Fig. 4 Ideal perovskite structure for ABO_3 compounds represented by $SrTiO_3$ (*left*) and its packing (*right*). *Green* atoms, A (Sr); *light blue* atoms, B (Ti); *red* atoms, O (O)

$A^{1+}B^{5+}O_3$ or $A^{3+}B^{3+}O_3$. In general, A cation and B cation can have ionic radius between 1.1–1.8 Å and 0.62–1 Å, respectively (Bhalla et al. 2000). A-site cation can be lanthanides, e.g., La, Pr, and Gd, or alkaline earth metals, e.g., Ba and Sr, while B-site cation can be transition metals, e.g., Mn, Co, Ni, Cr, and Fe, or non-transition metals, e.g., Al and Ga (Sunarso et al. 2008).

Perovskite represents one of the best examples for "nonstoichiometry" mentioned above. Depending on the effective valence states of A and B cations, O anions may be missing. This manifests in a formula of $ABO_{3-\delta}$. The δ represents the nonstoichiometry parameter which is enhanced by the incorporation of metal cations having low valence value, e.g., A^{2+}.

Within a cubic structure, A and B cations fulfill a simple geometric relationship where A cation can be viewed to touch B cation and vice versa. For the cube shown in Fig. 4, the edge is equal to twice the sum of ionic radius of B cation and ionic radius of O anion, while the face diagonal is equal to twice the sum of ionic radius of A cation and ionic radius of O anion. Pythagorean theorem can be used here to relate the face diagonal to the edge, resulting in

$$R_A + R_O = \sqrt{2}(R_B + R_O) \tag{7}$$

$$1 = \frac{R_A + R_O}{\sqrt{2}(R_B + R_O)} \tag{8}$$

$$t = \frac{R_A + R_O}{\sqrt{2}(R_B + R_O)} \tag{9}$$

Ionic radius values for A, B, and O should comply with Eq. 7 for the cubic structure to form. This equation can then be modified into Eq. 8, where a value of 1 is obtained for the ratio of the sum of ionic radius of A and O to root square of 2 multiplied by the sum of ionic radius of B and O. This ratio (Eq. 9) is defined as Goldschmidt tolerance factor (due to the contact criterion between A and B cations) which is very useful as a predictor (whether cubic structure will form) but not to rationalize structure. The empirical ionic radius value for metal cation is available; the most widely used ones have been compiled by Shannon and Prewitt (1969).

The interest to perovskite MIEC compounds is derived from the perovskite capability to host numerous metal oxides represented by $A_{1-x-y}A'_xA''_yB_{1-x-y}B'_xB''_yO_{3-\delta}$. As such, the structure and properties of the resultant perovskite can be adjusted by compositional tailoring to fit particular applications to obtain high ionic conductivity, electronic conductivity, or catalytic activity. When MIEC properties are desired, oxygen vacancies (nonstoichiometry) and electronic conductivity can be promoted by incorporating metal cation with low valence into A site so that the total valence of the cation is substantially less than 6 and incorporating transition metal elements into B-site. If electronic conductivity is to be eliminated, non-transition metal can be chosen such as Ga. $LaGaO_3$, for example, is as an excellent ionic conductor (Ishihara et al. 1994).

Development of MIEC perovskite membranes has been largely concentrated on the compositional tailoring since the initial report by Teraoka and coworkers (1985). They reported that the oxygen flux through $La_{1-x}Sr_xCo_{1-y}Fe_yO_{3-\delta}$ increases with the Sr or Co content. A very high flux of 1.79×10^{-6} mol cm^{-2} s^{-1} (equal to 2.4 ml cm^{-2} min^{-1}) at 850 °C was obtained for 1-mm-thick $SrCo_{0.4}Fe_{0.6}O_{3-\delta}$ membrane (Teraoka et al. 1985). Later on, they also reported that for $La_{0.6}Sr_{0.4}Co_{0.8}B_{0.2}O_{3-\delta}$ compounds, oxygen flux decreases in the order of B = Cu, Ni, Co, Fe, Cr, and Mn (Teraoka et al. 1988). Likewise, for $La_{0.6}A_{0.4}Co_{0.8}Fe_{0.2}O_{3-\delta}$, flux decreases in the order of A = Ba, Ca, Sr, Na, and La, while for $A_{0.6}Sr_{0.4}Co_{0.8}Co_{0.2}O_{3-\delta}$, flux decreases in the order of A = Gd, Sr, Nd, Pr, and La. A cation instead of B cation has more substantial effect to the onset permeation temperature. $SrCoO_{3-\delta}$ is also quite attractive although it does not exhibit cubic structure at room temperature. Rather, it undergoes phase transition from hexagonal to cubic at 900 °C. $SrCo_{0.8}$(Cr,Cu,Fe)$_{0.2}O_{3-\delta}$ also experiences such "order–disorder" transition (Kruidhof et al. 1993). Oxygen permeation through $Sr_{0.7}$(La,Nd,Sm,Gd)$_{0.3}CoO_{3-\delta}$ was reported to decrease in the order of La, Nd, Sm, and Gd. This trend is explained by the reduction of the A cation radius (Kovalevsky et al. 1998). Partial substitution of Sr with Ba in $SrCo_{0.8}Fe_{0.2}O_{3-\delta}$ can stabilize the cubic structure into room temperature, therefore retaining the high oxygen flux to lower temperature (Shao et al. 2000a).

The performances of the most commonly studied perovskite MIEC materials are listed in Table 1 to provide some pictures on the flux magnitudes (Teraoka et al. 1985, 1988; Shao et al. 2000b; Tsai et al. 1998; Ten Elshof et al. 1995). A more comprehensive list is also available elsewhere (Sunarso et al. 2008).

A trade-off occurs between the oxygen permeability and the structure stability. Perovskite compounds with large nonstoichiometry tend to provide high oxygen fluxes with the drawback of low structure stability. The cubic phase of $Ba_{0.5}Sr_{0.5}Co_{0.8}Fe_{0.2}O_{3-\delta}$ (BSCF), for example, is unstable below 850–900 °C. After 10-day annealing at 750 °C, the cubic phase of BSCF partially converts into lower symmetry hexagonal phase (Švarcova et al. 2008). Perovskite compound

Table 1 Summary of perovskite membrane materials and performances

Material	Thickness (mm)	$\mathbf{J(O_2)} \times 10^6$ (mol cm^{-2} s^{-1})	Temp. (°C)	Note	Ref.
$BaBi_{0.5}Co_{02}Fe_{0.3}O_{3-\delta}$	1.50	0.55	925	Disk	(Shao et al. 2000b)
$Ba_{0.5}Sr_{0.5}Co_{0.8}Fe_{0.2}O_{3-\delta}$	1.80	1.56	900	Disk	(Shao et al. 2000a)
$La_{0.6}Sr_{0.4}CoO_{3-\delta}$	1.00	0.38	870	Disk	(Teraoka et al. 1985)
$La_{0.6}Sr_{0.4}Co_{0.8}Fe_{0.2}O_{3-\delta}$	1.50	0.46	860	Disk	(Teraoka et al. 1988)
$La_{0.4}Sr_{0.6}Co_{0.2}Fe_{0.8}O_{3-\delta}$	0.55	0.08	900	Disk	(Tsai et al. 1998)
$La_{0.9}Sr_{0.1}FeO_{3-\delta}$	1.00	0.02	1000	Disk	(Ten Elshof et al. 1995)

with low nonstoichiometry and low fluxes such as $La_{0.6}Sr_{0.4}Co_{0.2}Fe_{0.8}O_{3-\delta}$ is generally more stable for long-term operation (Schlehuber et al. 2010). Alkaline-earth metal containing perovskite is also prone to acidic gases such as CO_2. CO_2 readily reacts with the alkaline metal to form carbonate, leading to the deterioration of the original structure (Klande et al. 2013; Chen et al. 2011).

Dual-Phase Membrane

The limited electronic conductivity of the fluorite compounds can be resolved by adding another phase with predominant electronic conductivity as depicted in Fig. 5. The advantage of this strategy is that the stability of the fluorite compounds in reducing and acidic atmosphere is also imparted to the final composite. This composite concept was brought forward by Mazanec et al. to provide internal short circuit to electrolyte material, i.e., (8 mol%) yttria-doped zirconia utilizing Pd-, Pt-, and B-doped $MgLaCrO_x$ and InPr (Mazanec et al. 1992). For the dual-phase membrane to work, both the ionic and electronic conductor phases should have continuous (or percolative) networks which extend from one side to the other side of the membrane. The minimum content of electronic phase required for this phase to form a continuous network is called the percolative threshold. The percolative threshold can be determined by measuring the electrical conductivity of the composite as a function of the electronic phase content. Furthermore, the thermomechanical properties of both phases should be compatible with each other to obtain high density and avoid cracks formation and structure deterioration during thermal cycling. In most cases, fluorite compounds are used as an ionic conductor, while metal or perovskite compounds can be used as an electronic conductor.

Lee et al. prepared Ag-$(Bi_2O_3)_{0.8}(BaO)_{0.2}$ composite with different Ag vol.% from 0 % to 45 %. They found that the conductivity increased significantly at 17 vol.% of Ag which indicated this composition as the percolative threshold. Above this threshold, all membranes showed comparable (similar or slightly

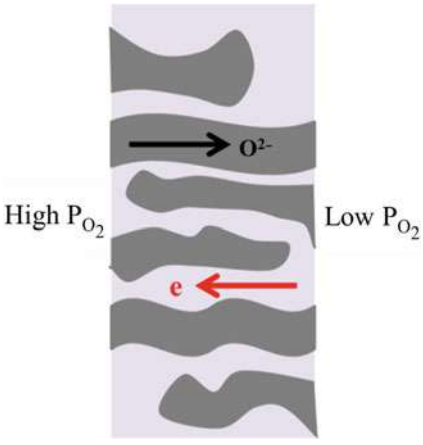

Fig. 5 Dual-phase membrane; *dark gray* matrix is the oxygen ionic conductor phase and light purple matrix is the electronic conductor phase

improved) oxygen fluxes (Lee et al. 2000). Chen and Burggraaf reported oxygen permeability of composite of Ag (or Au – 40 vol.%) with erbium-doped bismuth oxide made by mixing (and grounding) the powders and sintering using low heating and cooling rate. They found that the electrical resistance at the room temperature for composite was very low which suggested the formation of percolative electronic phase network. The silver-based composite has an order of magnitude higher flux than the gold-based composite due to the higher catalytic activity for silver (Chen and Burggraaf 1999). Wu et al. measured the oxygen flux through Ag-$(Bi_2O_3)_{0.74}(SrO)_{0.26}$ composite (Wu et al. 2001). Kim and Lin synthesized Ag (30 and 40 vol.%) and $Bi_{1.5}Y_{0.3}Sm_{0.2}O_3$ composites. The electronic conductor phase in the 30 vol.% composite was not percolative while that in the 40 vol.% was percolative. This was confirmed by energy dispersive X-ray analysis and four orders of magnitude higher electrical conductivity for the 40 vol.% composite (relative to the 30 vol.% composite). The 40 and 30 vol.% composite showed flux improvement by a factor of 50 and 10, respectively, relative to the $Bi_{1.5}Y_{0.3}Sm_{0.2}O_3$ membrane. Despite its non-percolative electronic phase, the 30 vol.% composite benefited from the presence of Ag which increased the surface reaction rate (Kim and Lin 2000).

Recently, doped ceria becomes more attractive as the ionic conductor phase. The fact that Ce can be reduced in reducing atmosphere may contribute toward electronic conductivity enhancement. Samson et al. combined $Ce_{0.9}Gd_{0.1}O_{1.95}$ ionic conductor with electronic conductor material, e.g., Ag–CuO (promising for low temperatures), and various perovskite MIEC materials, e.g., $LaCoO_3$, $La_{0.6}Sr_{0.4}CoO_{3-\delta}$, and $(La_{0.6}Sr_{0.4})_{0.99}Co_{0.2}Fe_{0.8}O_{3-\delta}$ (for applications between 1 and 10^{-3} atm) or $La_{0.6}Sr_{0.4}FeO_{3-\delta}$ and $La_{0.75}Sr_{0.25}Cr_{0.97}V_{0.03}O_{3-\delta}$ (for applications down to 10^{-19} atm) (Samson et al. 2014). Among these materials, they found that $Ce_{0.9}Gd_{0.1}O_{1.95}$-$La_{0.6}Sr_{0.4}CoO_{3-\delta}$ (52 vol.%) composite showed the highest oxygen flux despite the micro-crack formation due to the large mismatch between the thermal expansion coefficients of the two phases (Samson et al. 2014). Kim et al. prepared dual-phase membrane of $Ce_{0.9}Gd_{0.1}O_{2-\delta}$-$Sr_{0.95}Co_{0.5}Fe_{0.5}O_{3-\delta}$ (50 vol.%) and found that the perovskite MIEC phase was stable under the condition where it normally undergoes phase transformation as a single phase (Kim et al. 2014). The stability of $Ce_{0.9}Nd_{0.1}O_{2-\delta}$-$Nd_{0.6}Sr_{0.4}FeO_{3-\delta}$ (40 wt%) composite under CO_2 was confirmed by the reversibility of oxygen flux when the sweep gas was changed between He and CO_2 (Luo et al. 2014). Li et al. prepared dual-phase hollow fiber of $Ce_{0.8}Sm_{0.2}O_{2-\delta}$-$La_{0.8}Sr_{0.2}MnO_{3-\delta}$ (38 wt%) and found that the flux decreased slightly using CO_2 as a sweep gas with respect to that obtained using He (Li et al. 2009a). Dual-phase disk membrane of $Ce_{0.8}Sm_{0.2}O_{2-\delta}$ with $Sm_{0.6}Ca_{0.4}CoO_{3-\delta}$ and $Sm_{0.6}Ca_{0.4}FeO_{3-\delta}$ was reported by Li et al., the fluxes of which were stable for 100 h of operation using CO_2 as a sweep gas (Li et al. 2014). As a comparison, yttria-doped zirconia ($Zr_{0.84}Y_{0.16}O_{1.92}$)–lanthanum strontium manganite ($La_{0.8}Sr_{0.2}MnO_{3-\delta}$, 43 wt%) hollow fiber composite was also prepared. The oxygen flux of the fiber at 950 °C was not changed when the sweep gas was changed from helium to high concentration of CO_2 (Li et al. 2009b).

Table 2 lists the performances of some of the dual-phase membranes which include the electronic phase from metals and perovskite MIEC materials (Lee

Table 2 Summary of dual-phase membrane materials and performances

Ionic conductor phase	Electronic conductor phase	Ratio	Thickness (mm)	$J(O_2) \times 10^6$ (mol cm^{-2} s^{-1})	Temp. (°C)	Note	Ref.
$(Bi_2O_3)_{0.8}(BaO)_{0.2}$	Ag	45 vol.% El. phase	1400	0.06	680	Disk	(Lee et al. 2000)
$(Bi_2O_3)_{0.75}(Er_2O_3)_{0.25}$	Ag	40 vol.% El. Phase	1600	0.16	850	Disk	(Chen and Burggraaf 1999)
$(Bi_2O_3)_{0.75}(Er_2O_3)_{0.25}$	Au	40 vol.% El. phase	1000	0.06	850	Disk	(Chen and Burggraaf 1999)
$(Bi_2O_3)_{0.74}(SrO)_{0.26}$	Ag	40 vol.% El. phase	1000	0.05	700	Disk	(Wu et al. 2001)
$Bi_{1.5}Y_{0.3}Sm_{0.2}O_3$	Ag	40 vol.% El. phase	1300	0.58	850	Disk	(Kim and Lin 2000)
$Ce_{0.9}Gd_{0.1}O_{1.95}$	Ag–CuO	11 vol.% El. phase	1000	0.21	890	Disk	(Samson et al. 2014)
$Ce_{0.9}Gd_{0.1}O_{1.95}$	$LaCoO_3$	50 vol.% El. phase	1000	0.18	924	Disk	(Samson et al. 2014)
$Ce_{0.9}Gd_{0.1}O_{1.95}$	$La_{0.6}Sr_{0.4}CoO_3$	52 vol.% El. phase	1000	0.42	941	Disk	(Samson et al. 2014)

$Ce_{0.9}Gd_{0.1}O_{1.95}$	$La_{0.6}Sr_{0.4}FeO_3$	46 vol.% El. phase	1000	0.23	931	Disk	(Samson et al. 2014)
$Ce_{0.9}Gd_{0.1}O_{1.95}$	$(La_{0.6}Sr_{0.4})_{0.99}Co_{0.2}Fe_{0.8}O_3$	54 vol.% El. phase	1000	0.32	931	Disk	(Samson et al. 2014)
$Ce_{0.9}Gd_{0.1}O_{1.95}$	$La_{0.75}Sr_{0.25}Cr_{0.97}V_{0.03}O_3$	30 vol.% El. phase	1000	0.10	943	Disk	(Samson et al. 2014)
$Ce_{0.9}Gd_{0.1}O_{2-\delta}$	$Sr_{0.95}Fe_{0.5}Co_{0.5}O_{3-\delta}$	50 vol.% El. phase	1000	0.38	1000	Disk	(Kim et al. 2014)
$Ce_{0.9}Nd_{0.1}O_{2-\delta}$	$Nd_{0.6}Sr_{0.4}FeO_{3-\delta}$	40 wt% El. phase	600	0.19	950	Disk	(Luo et al. 2014)
$Ce_{0.8}Sm_{0.2}O_{2-\delta}$	$La_{0.8}Sr_{0.2}MnO_3$	38 wt% El. phase	300	0.32	950	Hollow fiber	(Li et al. 2009a)
$Ce_{0.8}Sm_{0.2}O_{1.9}$	$Sm_{0.6}Ca_{0.4}CoO_{3-\delta}$	33 wt% El. phase	500	0.41	950	Disk coated with porous layer	(Li et al. 2014)
$Ce_{0.8}Sm_{0.2}O_{1.9}$	$Sm_{0.6}Ca_{0.4}FeO_{3-d}$	25 wt% El. phase	500	0.33	950	Disk coated with porous layer	(Li et al. 2014)
$Zr_{0.84}Y_{0.16}O_{1.92}$	$La_{0.8}Sr_{0.2}MnO_3$	43 wt% El. Phase	200	0.21	950	Hollow fiber	(Li et al. 2009b)

et al. 2000; Chen and Burggraaf 1999; Wu et al. 2001; Kim and Lin 2000; Samson et al. 2014; Kim et al. 2014; Luo et al. 2014; Li et al. 2009a, b 2014). Dual-phase membranes generally have oxygen flux values between that of fluorite and perovskite MIEC membranes. Recent efforts on the development of dual-phase membranes exclude metals as a component due to its high cost.

External Short-Circuit Concept

An alternative to dual-phase membrane was devised recently where external short circuit is applied to compensate the inability to conduct electrons through the membrane (Zhang et al. 2012). Rather than using the classical configuration depicted in Fig. 6 (left) where an external metal wire is employed as an electron pathway, metal layer can simply be pasted over the disk circumferential surface as an electron pathway (Fig. 6 (right)). This circumferential metal layer is continuously connected with the metal layers over the top and bottom of the disk to ensure efficient electron collections on the high oxygen potential side and the low oxygen potential side.

This concept was demonstrated using $Sm_{0.2}Ce_{0.8}O_{1.9}$ disk membrane where by itself showed zero oxygen fluxes at 500–800 °C. Ag (35 wt%)-$Sm_{0.2}Ce_{0.8}O_{1.9}$ dual-phase disk membrane exhibited a very low fluxes only above 700 °C which reaches a maximum of 0.022×10^{-6} mol cm^{-2} s^{-1} (equal to 0.03 ml cm^{-2} min^{-1}) at 800 °C. Using configuration shown in Fig. 6 (left) with Ag layers over the top and bottom of $Sm_{0.2}Ce_{0.8}O_{1.9}$ disk, the oxygen flux was improved to 0.02×10^{-6}–3.87×10^{-6} mol cm^{-2} s^{-1} (equal to 0.027–0.52 ml cm^{-2} min^{-1}) between 600 °C and 800 °C. These oxygen fluxes were comparable to the fluxes obtained using simplified configuration displayed in Fig. 6 (right), denoting the feasibility of this concept which offers less complexity than using external wire or preparing dual-phase

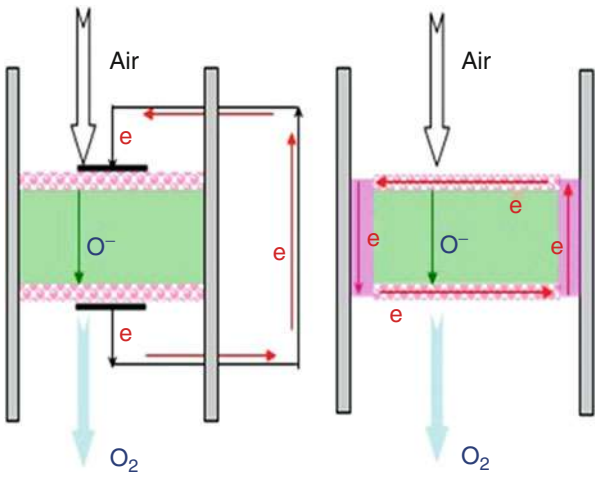

Fig. 6 Short-circuit concept. (*Left*) Metal layers over the *top* and *bottom* disk surfaces and external electron circuit and (*right*) metal layers over the *top* and *bottom* disk surfaces and metal (paste) layer over the disk circumferential surface

membrane (Zhang et al. 2012). The external short-circuited $Sm_{0.2}Ce_{0.8}O_{1.9}$ disk membrane was also tested in terms of CO_2 stability where it was subjected to 10 % CO_2 in helium (as a sweep gas) for 500 h. Upon switching back to helium, the original flux value was recovered.

It is also possible to use perovskite MIEC materials for short-circuiting layers as reported by Wang et al. (2013), and Imashuku et al. (2013). The external short-circuit concept can also be extended to internal short-circuit by inserting metal wires within the membrane as detailed elsewhere (Zhang et al. 2013).

Membrane Type and Preparation

Oxygen selective mixed ionic–electronic conducting (MIEC) ceramic membranes have been prepared in different types depending on the application purpose.

Dense Disk Membranes

This membrane configuration represents the most universal configuration found in numerous research papers used particularly for screening purpose in the laboratory and fundamental research studies (Sunarso et al. 2008). Disk membrane is the easiest one to fabricate. Its fabrication involves synthesizing ceramic oxide powder precursor through solid-state, co-precipitation, sol–gel, or other synthesis routes followed by the calcination of the powder (at 700 °C or below) to remove the organic content and, in some cases, also to form the structure of interest. The powder is then poured into and fitted within the pellet press die set or mold where following this (a hydraulic or an isostatic or a uniaxial) pressure is applied onto the powder, resulting in the so-called green disk. This "green disk" is finally sintered at a temperature substantially higher than the initial calcination temperature (at least 1000 °C) to obtain a pore-free disk membrane (Sunarso et al. 2009). The sintering process can be observed using the high-temperature microscope and quantified by the density measurement (Itoh et al. 1994). The formation of dense body is indicated by the attainment of a final density of at least 90 % of the theoretical density. The sintering temperature normally depends on the particle size and the specific preparation route of the powder. Smaller particle size provides larger surface area and therefore is favorable toward acquiring higher density and sinterability. The effects of sintering temperature, dwell time, and pressure to the final density and grain size of typical disk membrane are discussed by Asadi et al. (2012). Temperature generally has the most influence followed by dwell time while pressure has the least influence. Nevertheless, optimum values always exist for these variables which vary for different system.

Given the relatively high thickness of the disk membrane, its oxygen ionic transport is often limited by the bulk diffusion process. While theoretically the oxygen fluxes can be improved by reducing the thickness to submicron thickness, decreasing the disk membrane thickness to below 1 mm is considered impractical

from the mechanical strength perspective. Another drawback of this configuration is its very low surface to volume ratio (Luyten et al. 2000).

Porous Substrate Supported Thin-Film Disk Membranes

To overcome the thickness limitation without compromising mechanical integrity, an asymmetric structure can be developed by combining porous substrate with a thin dense layer. The porous layer provides the mechanical strength while allowing gas transport through its porous channels. Most of these studies are also performed in disk geometry. The suitable porous substrate has several required characteristics (Watanabe et al. 2008a, b):

(i) Similar thermal expansion coefficient to that of the thin dense layer to prevent structure cracking during sintering
(ii) Adequate gas diffusion flow to supply oxygen gas to the dense layer (minimum permeance is claimed as 6×10^{-4} cm^3 min^{-1} Pa^{-1} cm^{-2})

To ensure the thermal expansion properties of the dense layer matches that of the porous layer, same material is usually used on both layers. Watanabe et al. utilized simple slurry dropping method to form a 10-μm-thick dense layer of $La_{0.6}Ca_{0.4}CoO_3$ (LCC) on top of a 2-mm-thick porous disk of LCC (Watanabe et al. 2008a, b). Ethanol-based slurry containing 1 wt% of LCC powder was dropped onto the porous support followed by sintering. A simpler technique such as a three-stage uniaxial compaction procedure was also used to fabricate three-layer asymmetric disk membrane of $Ba_{0.5}Sr_{0.5}Co_{0.8}Fe_{0.2}O_{3-\delta}$ (BSCF), the final structure of which consisting 1.05-mm-thick porous and 30–300-μm-thick porous layers sandwiching a 170-μm-thick dense layer (Kovalevsky et al. 2011). For the first layer, a pore former was added into the powder followed by compaction at 100 MPa. The process is similar for the second layer except that a pore former was excluded to facilitate a dense layer formation. Accordingly, for the last layer, pore former was also included. A substantially higher pressure of 300 MPa was used during the last compaction process. Nonetheless, the oxygen permeation fluxes were only improved by 1.5 times relative to 1-mm-thick dense disk membrane which highlights the inability of such process to provide optimized porous structure with favorable gas diffusivity. A more complicated procedure was reported by Araki et al. (2012). To synthesize hierarchical structure, they prepared three identical compositions of $Ca_{0.8}Sr_{0.2}Ti_{0.7}Fe_{0.3}O_{3-\delta}$ (CSTF) powders made from different routes, e.g., solid-state route, citrate method, and supercritical hydrothermal route. Solid-state CSTF powder was used to form the porous disk substrate onto which the citrate CSTF powder was applied as a buffer layer by spin coating followed by drying and sintering. In the final step, hydrothermal CSTF powder was deposited. Such systematic and precise procedure involves the usage of powder with gradually reduced particle size (from that of the substrate) upon each additional step and enabled the fabrication of a defect-free 20-μm-thick asymmetric

membrane allowing high flux. In addition, tape casting was employed to prepare asymmetric BSCF membrane containing 20-μm-thick dense layer and 0.9-mm-thick porous substrate (Li et al. 2013). The resultant oxygen permeability under vacuum pressure (in the permeate side) is very high, reaching a maximum of 24.10 $\times 10^{-6}$ mol cm^{-2} s^{-1} (equal to 32.5 ml cm^{-2} min^{-1}) at 900 °C. Serra et al. made a $La_{0.6}Sr_{0.4}Co_{0.2}Fe_{0.8}O_{3-\delta}$ asymmetric disk membrane by tape casting (Serra et al. 2013). The membrane which has 30-μm-thick dense layer and 630-μm-thick layer of porous support showed a maximum flux of 8.83 $\times 10^{-6}$ mol cm^{-2} s^{-1} (equal to 11.87 ml cm^{-2} min^{-1}) at 1000 °C.

The performances of several asymmetric disk membranes are summarized in Table 3 (Watanabe et al. 2008a, b; Kovalevsky et al. 2011; Araki et al. 2012; Li et al. 2013; Serra et al. 2013).

Tubular and Hollow Fiber Membranes

The interest on the tubular and hollow fiber membranes is associated with the need to enlarge the surface to volume ratio when industrial application is envisaged. Dense tubular membranes with uniform dense structure throughout the cross-section can be made using isostatic pressing method and plastic extrusion method. The plastic extrusion method is usually more widely reported where the calcined powder precursor is mixed with solvent, dispersant, binder, and plasticizer to form viscous liquid mixture which can be extruded into a tube to form "green tubular membrane." The "green tubular membrane" is then sintered to obtain dense body (Wang et al. 2002). The typical sintered tube geometry has an outside and inside diameter of 8 mm and 5 mm, respectively, and length of 30 cm, all of which can be modified by changing the extruder tube size and length. Despite the marginal improvement in the oxygen flux (maximum value of 2.31 $\times 10^{-6}$ mol cm^{-2} s^{-1} (equal to 3.1 ml cm^{-2} min^{-1}) at 900 °C) relative to the dense disk membrane, this membrane allows the application of compressed air on the shell side and vacuum on the inner channel side due to its robust structure. As such, the driving force is effectively increased so that higher fluxes can be achieved.

A better alternative to tubular dense membrane is hollow fiber membrane. Such fiber can be prepared using a phase inversion technique and sintering (Luyten et al. 2000; Liu et al. 2001, 2004; Sunarso et al. 2011). Analogous with the tubular membrane, the calcined powder precursor is mixed with polymeric binder, e.g., polyethersulfone or polyetherimide, and solvent, e.g., 1-methyl-2-pyrrolidone (NMP). Polyvinylpyrrolidone can be added to adjust the viscosity of the solution mixture. After degassing, the mixture is then spun through a tube-in-orifice spinneret with typical orifice diameter and inner tube diameter of 2 mm and 0.72 mm, respectively. The inner and outer coagulant can be chosen to adjust the phase inversion process. Normal coagulant during the spinning process is water which favors fast coagulation and results in dense layer formation. If slower coagulation is preferred to facilitate the porous layer formation, either on the outer or inner circumferential side of the fiber, NMP can be added as an outer or inner coagulant

Table 3 Summary of asymmetric disk membrane materials and performances

Dense layer		Porous layer		$J(O_2) \times 10^6$ (mol cm^{-2} s^{-1})	Temp. (°C)	Note	Ref.
Material	Thickness (mm)	Material	Thickness (mm)				
$La_{0.6}Ca_{0.4}CoO_3$	10	$La_{0.6}Ca_{0.4}CoO_3$	2000	1.24	930	Slurry dropping	(Watanabe et al. 2008a; Watanabe et al. 2008b)
$Ba_{0.5}Sr_{0.5}Co_{0.8}Fe_{0.2}O_{3-\delta}$	170	$Ba_{0.5}Sr_{0.5}Co_{0.8}Fe_{0.2}O_{3-\delta}$	30–300 and 1050	1.05	950	Three-stage uniaxial compaction/2 porous layers and 1 dense layer	(Kovalevsky et al. 2011)
$Ca_{0.8}Sr_{0.2}Ti_{0.7}Fe_{0.3}O_{3-\delta}$	20	$Ca_{0.8}Sr_{0.2}Ti_{0.7}Fe_{0.3}O_{3-\delta}$	500	2.50	950	Spin coating using powders from citrate and hydrothermal route	(Araki et al. 2012)
$Ba_{0.5}Sr_{0.5}Co_{0.8}Fe_{0.2}O_{3-\delta}$	20	$Ba_{0.5}Sr_{0.5}Co_{0.8}Fe_{0.2}O_{3-\delta}$	900	24.10	900	Tape casting/permeation under vacuum pressure	(Li et al. 2013)
$La_{0.6}Sr_{0.4}Co_{0.2}Fe_{0.8}O_{3-\delta}$	30	$La_{0.6}Sr_{0.4}Co_{0.2}Fe_{0.8}O_{3-\delta}$	630	8.83	1000	Tape casting	(Serra et al. 2013)

Fig. 7 (*Top left*) Typical sintered disk membrane (*bottom*), sintered hollow fiber (*middle*) and green hollow fiber (*top*), (*top right*) tube-in-orifice spinneret to synthesize hollow fiber and (*bottom*) hollow fiber membrane module consisting of 889 fibers

component. As is known, phase inversion process involves the polymer transformation from the initial liquid state to solid state upon contacting non-solvent (also referred as coagulant) at the same time as the solvent diffuses from polymer solution to water. Due to the different polymer precipitation rate, the asymmetric cross-sectional structure is formed on the hollow fiber precursor just like the morphology of polymeric membranes. The asymmetric structure where the dense middle layer is sandwiched by two porous layers is commonly attained when water is used as the internal and external coagulants. The "green fiber" shrinks during the sintering process due to the removal of organic materials and densification, but their original structure is normally retained.

For the sake of comparison, disk membrane and hollow fiber membrane are depicted in Fig. 7 (top left). The spinneret used during the hollow fiber synthesis is also displayed in Fig. 7 (top right). A perovskite membrane module consisting of 889 $La_{0.6}Sr_{0.4}Co_{0.2}Fe_{0.8}O_{3-\delta}$ hollow fibers which can be operated for more than 1167 h with the maximum oxygen production rate of 3.1 L min^{-1} and the lowest purity of 99.4 % between 960 °C and 1070 °C was developed recently and is depicted in Fig. 7 (bottom) (Tan et al. 2010).

Other configurations such as multiple planar cell stack and monolith are available. In fact, the flat-plate multicell stack design was already developed by Air Products and Chemicals and Ceramatec to separate oxygen from air (Dyer et al. 2000). Monolithic structure, albeit its potential to provide large surface area

and has been used largely for catalytic reactors, has problems associated with complex manifold and sealing of different gas streams due to its large number of channels (Kapteijn et al. 2001).

Other Important Applications

Oxygen selective MIEC membrane enables simultaneous separation and reaction to be carried out, e.g., as a membrane reactor for chemical synthesis (Balachandran et al. 1995, 1997; Tsai et al. 1997; Jin et al. 2000; Ishihara and Takita 2000). This is beneficial, for example, toward syngas production from methane (CH_4). There is a high interest to convert methane into liquid petroleum products such as methanol, formaldehyde, and/or alkenes given the abundant amount of methane as well as higher price and higher practical value of the products (the latter, e.g., can be easily transported and contained). Two options are available for the conversion, i.e., via direct conversion process of methane to liquid products which is not efficient due to the low selectivity since the products are more reactive than the reactants or via indirect conversion processes which involve either steam reforming (Reaction 1 – Eq. 10) or partial oxidation of methane to form syngas (Reaction 2 – Eq. 11) followed by Fischer–Tropsch or methanol synthesis to convert syngas to liquid products:

$$CH_4 + H_2O \rightarrow CO + 3H_2 \quad \Delta H\,(25\,^{o}C) = 49.2\ \text{kcal mol}^{-1} \tag{10}$$

$$CH_4 + \tfrac{1}{2}O_2 \rightarrow CO + 2H_2 \quad \Delta H\,(25\,^{o}C) = -8.5\ \text{kcal mol}^{-1} \tag{11}$$

Steam reforming requires operating at 15–30 atm pressure and 850–900 °C temperature in the presence of Ni/Al_2O_3 catalyst due to its endothermic nature. Partial oxidation on the other hand can be carried out at 13 atm pressure with no external energy supply due to its exothermic nature, therefore providing a more economical alternative. While air (79 % N_2 and 21 % O_2) can be used in Reaction 2, the resultant separation of nitrogen (N_2) from the gas products (i.e., N_2 should be removed for downstream reactions) would entail high energy penalty and cost especially if conventional technology such as cryogenic distillation is employed. Oxygen selective MIEC membrane technology offers several advantages here, i.e., high product selectivities, exclusion of N_2 and thus the absence of NO_x, less flame formation risk since the oxygen input rate is diffusion-limited, and reduced cost associated with gas compression for downstream process.

Balachandran et al. prepared tubular $SrCo_{0.5}FeO_x$ membrane through plastic extrusion technique for partial oxidation of CH_4 (Balachandran et al. 1995, 1997). They operated the membrane reactor at 850 °C for 70 h in the presence of Rh-based reforming catalyst during which the reactor provided methane conversion efficiency of >98 %, CO selectivity of ~90 %, and H_2 yield twice that of CO. Tsai et al. reported the same reaction using disk $La_{0.2}Ba_{0.8}Fe_{0.8}Co_{0.2}O_{3-\delta}$ membrane incorporating $Ni/\alpha\text{-}Al_2O_3$ catalyst where they observed during 500-h operation the

increasing CH_4 conversion from 17 % to 80 % in conjunction with constant CO selectivity of ~99 % and H_2/CO ratio of 2 (Tsai et al. 1997). Beyond 500 h up to 700 h, the conversion remained constant while CO selectivity decreased slightly to ~95 %. Jin et al. utilized tubular $La_{0.6}Sr_{0.4}Co_{0.2}Fe_{0.8}O_{3-\delta}$ membrane (made by isostatic pressing) and Ni/γ-Al_2O_3 catalyst and observed CH_4 conversion larger than 96 % with CO selectivity larger than 97 % (at low CH_4 feed concentration) between 825 °C and 885 °C (Jin et al. 2000). Ishihara and Takita reported partial oxidation of CH_4 using disk $La_{0.8}Sr_{0.2}Ga_{0.6}Fe_{0.4}O_3$ membrane with the presence of Ni and $La_{0.6}Sr_{0.4}CoO_3$ catalysts where they obtained CH_4 conversion of 30.6 %, CO yield of 29.2 %, and H_2 yield of 30.2 % at 1000 °C (Ishihara and Takita 2000). Membrane reactor for industrial scale applications requires membrane materials which can tolerate harsh conditions, i.e., operate under reducing and acidic gas atmosphere such as CH_4, H_2, and CO_2 at high temperatures (>800 °C). In this context, perovskite MIEC membranes have very limited applicability. Fluorite MIEC membranes, on the other hand, show more potential (Zhang et al. 2014).

Future Directions

Substantial advances in the oxygen selective MIEC ceramic membrane technology have been demonstrated over the past decades as represented by systematic and multitude approaches and concepts which leads to several orders of magnitude improvement of oxygen fluxes relative to those obtained in the 1980s. These aspects were reviewed throughout this chapter. In terms of oxygen production, the MIEC perovskite membranes are successful with the operation mode of high pressurized air as the feed gas as these perovskite membranes have sufficient material stability under such gas atmosphere. However, in many cases of clean energy applications, pure oxygen is not required. For example, to continuously use the existing power generation infrastructure under the oxy-fuel concept (one of the clean energy schemes), an O_2/CO_2 mixture for combustion with not very high flame temperature is required to get highly CO_2-concentrated flue gas. In such case, air separation via these MIEC membranes operated by sweep gas mode using part of the flue gas (CO_2) instead of high pressurized feed gas mode will be more economical. The prerequisite for such operation is the robust membrane stability under acidic gases at high temperatures. Thus, future directions of this technology will be placed on materials development with improved operational stability under severe gas atmospheres containing CO_2, CH_4, H_2, SOx, and so on. Once there is a breakthrough, the applications of such MIEC ceramic membranes will be expanded from the field of air separation to chemical synthesis like syngas production from methane partial oxidation with much savings in capital investment and operation cost.

Acknowledgment The authors acknowledge the research funding provided by the Australian Research Council (FT120100178).

References

Aldebert P, Traverse J-P (1985) Structure and ionic mobility of zirconia at high temperature. J Am Ceram Soc 68:34–40

Araki S, Yamamoto H, Hoshi Y, Lu J, Hakuta Y, Hayashi H, Ohashi T, Sato K, Nishioka M, Inoue T, Hikazudani S, Hamakawa S (2012) Synthesis of $Ca_{0.8}Sr_{0.2}Ti_{0.7}Fe_{0.3}O_{3-\delta}$ thin film membranes and its application to the partial oxidation of methane. Solid State Ion 221:43–49

Arnold M, Xu Q, Tichelaar FD, Feldhoff A (2009) Local charge disproportion in a high-performance perovskite. Chem Mater 21:635–640

Asadi AA, Behrouzifar A, Mohammadi T, Pak A (2012) Effects of nano powder synthesis methods, shaping and sintering conditions on microstructure and oxygen permeation properties of $La_{0.6}Sr_{0.4}Co_{0.2}Fe_{0.8}O_{3-\delta}$ (LSCF) perovskite-type membranes. High Temp Mater Proc 31:47–59

Balachandran U, Dusek JT, Mieville RL, Poeppel RB, Kleefisch MS, Pei S, Kobylinski TP, Udovich CA, Bose AC (1995) Dense ceramic membranes for partial oxidation of methane to syngas. Appl Catal A 133:19–29

Balachandran U, Dusek JT, Maiya PS, Ma B, Mieville RL, Kleefisch MS, Udovich CA (1997) Ceramic membrane reactor for converting methane to syngas. Catal Today 36:265–272

Bhalla AS, Guo R, Roy R (2000) The perovskite structure – a review of its role in ceramic science and technology. Mater Res Innov 4:3–26

Bouwmeester HJM, Kruidhof H, Burggraaf AJ (1994) Importance of the surface exchange kinetics as rate limiting step in oxygen permeation through mixed-conducting oxides. Solid State Ion 72:185–194

Chen CS, Burggraaf AJ (1999) Stabilized bismuth oxide-noble metal mixed conducting composites as high temperature oxygen separation membranes. J Appl Electrochem 29:355–360

Chen W, Chen C-s, Winnubst L (2011) Ta-doped $SrCo_{0.8}Fe_{0.2}O_{3-\delta}$ membranes: phase stability and oxygen permeation in CO_2 atmosphere. Solid State Ion 196:30–33

Dyer PN, Richards RE, Russek SL, Taylor DM (2000) Ion transport membrane technology for oxygen separation and syngas production. Solid State Ion 134:21–33

Eguchi K, Setoguchi T, Inoue T, Arai H (1992) Electrical properties of ceria-based oxides and their application to solid oxide fuel cells. Solid State Ion 52:165–172

Feldhoff A, Martynczuk J, Arnold M, Myndyk M, Bergmann I, Šepelak V, Gruner W, Vogt U, Hähnel A, Woltersdorf J (2009) Spin state transition of iron in $(Ba_{0.5}Sr_{0.5})(Fe_{0.8}Zn_{0.2})O_{3-\delta}$ perovskite. J Solid State Chem 182:2961–2971

Foster T (2008) Air products, air separation technology – ion transport membrane (ITM). Allentown, Air Products and Chemicals, Inc. http://www.google.co.id/url?sa=t&rct=j&q=&esrc=s&source=web&cd=1&ved=0CBsQFjAAahUKEwjc3Nnr7LTIAhXCPo4KHTeeANU&url=http%3A%2F%2Fwww.airproducts.com%2F~%2Fmedia%2FFiles%2FPDF%2Fproducts%2FLiterature_Cryogenic-Air-Separation-ITM-28007017GLB.pdf&usg=AFQjCNFRV-JKBokHQHOTDJ_cT8y 2qO1lIw&sig2=–imzHgHoQUQmghFVOhHew&bvm=bv.104615367,d.c2E

Imashuku S, Wang L, Mezghani K, Habib MA, Shao-Horn Y (2013) Oxygen permeation from oxygen ion-conducting membranes coated with porous metals or mixed ionic and electronic conducting oxides. J Electrochem Soc 160:E148–E153

Inaba H, Tagawa H (1996) Ceria-based solid electrolytes. Solid State Ion 83:1–16

Ishihara T, Takita Y (2000) Partial oxidation of methane into syngas with oxygen permeating ceramic membrane reactors. Catal Surv Jpn 4:125–133

Ishihara T, Matsuda H, Takita Y (1994) Doped $LaGaO_3$ perovskite type oxide as a new oxide ionic conductor. J Am Ceram Soc 116:3801–3803

Itoh N, Kato T, Uchida K, Haraya K (1994) Preparation of pore-free disk of $La_{1-x}Sr_xCoO_3$ mixed conductor and its oxygen permeability. J Membr Sci 92:239–246

Jin W, Li S, Huang P, Xu N, Shi J, Lin YS (2000) Tubular lanthanum cobaltite perovskite-type membrane reactors for partial oxidation of methane to syngas. J Membr Sci 166:13–22

Kapteijn F, Nijhuis TA, Heiszwolf JJ, Moulijn JA (2001) New non-traditional multiphase catalytic reactors based on monolithic structures. Catal Today 66:133–144

Kim J, Lin YS (2000) Synthesis and oxygen permeation properties of ceramic-metal dual-phase membranes. J Membr Sci 167:123–133

Kim SK, Shin MJ, Rufner J, Van Benthem K, Yu JH, Kim S (2014) $Sr_{0.95}Fe_{0.5}Co_{0.5}O_{3-\delta}$-$Ce_{0.9}Gd_{0.1}O_{2-\delta}$ dual-phase membrane: oxygen permeability, phase stability, and chemical compatibility. J Membr Sci 462:153–159

Kingery WD, Bowen HK, Uhlmann DR (1976) Introduction to ceramics. Wiley, Toronto

Klande T, Ravkina O, Feldhoff A (2013) Effect of A-site lanthanum doping on the CO_2 tolerance of $SrCo_{0.8}Fe_{0.2}O_{3-\delta}$ oxygen transporting membrane. J Membr Sci 437:122–130

Kovalevsky AV, Kharton VV, Tikhonovich VN, Naumovich EN, Tonoyan AA, Reut OP, Boginsky LS (1998) Oxygen permeation through $Sr(Ln)CoO_{3-\delta}$ (Ln = La, Nd, Sm, Gd) ceramic membranes. Mater Sci Eng B 52:105–116

Kovalevsky AV, Yaremchenko AA, Kolotygin VA, Snijkers FMM, Kharton VV, Buekenhoudt A, Luyten JJ (2011) Oxygen permeability and stability of asymmetric multilayer Ba0.5Sr0.5Co0.8Fe0.2O3–δ ceramic membranes. Solid State Ion 192:677–681

Kruidhof H, Bouwmeester HJM, Van Doorn RHE, Burggraaf AJ (1993) Influence of order–disorder transitions on oxygen permeability through selected non-stoichiometric perovskite-type oxides. Solid State Ion 63–65:816–822

Kuharuangrong S (2007) Ionic conductivity of Sm, Gd, Dy and Er-doped ceria. J Power Sources 171:506–510

Lee TH, Yang YL, Jacobson AJ (2000) Electrical conductivity and oxygen permeation of $Ag/BaBi_8O_{13}$. Solid State Ion 134:331–339

Li W, Tian T-F, Shi F-Y, Wang Y-S, Chen C-S (2009a) $Ce_{0.8}Sm_{0.2}O_{2-\delta}$-$La_{0.8}Sr_{0.2}MnO_{3-\delta}$ dual-phase composite hollow fiber membrane for oxygen separation. Ind Eng Chem Res 48:5789–5793

Li W, Liu J-J, Chen C-S (2009b) Hollow fiber membrane of yttrium-stabilized zirconia and strontium-doped lanthanum manganite dual-phase composite for oxygen separation. J Membr Sci 340:266–271

Li X, Kerstiens T, Markus T (2013) Oxygen permeability and phase stability of $Ba_{0.5}Sr_{0.5}Co_{0.8}Fe_{0.2}O_{3-\delta}$ perovskite at intermediate temperatures. J Membr Sci 438:83–89

Li H, Zhu X, Liu Y, Wang W, Yang W (2014) Comparative investigation of dual-phase membranes containing cobalt and iron-based mixed conducting perovskite for oxygen permeation. J Membr Sci 462:170–177

Liu S, Tan X, Li K, Hughes R (2001) Preparation and characterisation of $SrCe_{0.95}Yb_{0.05}O_{2.975}$ hollow fibre membranes. J Membr Sci 193:249–260

Liu S, Tan X, Li K, Hughes R (2004) Preparation of $SrCe_{0.95}Yb_{0.05}O_{2.975}$ perovskite for use as a membrane material in hollow fibre fabrication. Mater Res Bull 39:119–133

Luo H, Klande T, Cao Z, Liang F, Wang H, Caro J (2014) A CO_2-stable reduction-tolerant Nd-containing dual phase membrane for oxyfuel CO_2 capture. J Mater Chem A 2:7780–7787

Luyten J, Buekenhoudt A, Adriansens W, Cooymans J, Weyten H, Servaes F, Leysen R (2000) Preparation of $LaSrCoFeO_{3-x}$ membranes. Solid State Ion 135:637–642

Mazanec TJ, Cable TL, Frye JG Jr (1992) Electrocatalytic cells for chemical reaction. Solid State Ion 53–56:111–118

Megaw HD (1973) Crystal structures: a working approach. WB Saunders Company, Philadelphia

Sammes NM, Tompsett GA, Näfe H, Aldinger F (1999) Bismuth based oxide electrolytes – structure and ionic conductivity. J Eur Ceram Soc 19:1801–1826

Samson AJ, Søgaard M, Hendriksen PV (2014) (Ce, Gd)O2-δ-based dual phase membranes for oxygen separation. J Membr Sci 470:178–188

Schlehuber D, Wessel E, Singheiser L, Markus T (2010) Long-term operation of a $La_{0.58}Sr_{0.4}Co_{0.2}Fe_{0.8}O_{3-\delta}$-membrane for oxygen separation. J Membr Sci 351:16–20

Serra JM, Garcia-Fayos J, Baumann S, Schulze-Küppers F, Meulenberg W (2013) Oxygen permeation through tape-cast asymmetric all-$La_{0.6}Sr_{0.4}Co_{0.2}Fe_{0.8}O_{3-\delta}$ membranes. J Membr Sci 447:297–305

Shannon RD, Prewitt CT (1969) Effective ionic radii in oxides and fluorides. Acta Cryst B25:925–946

Shao Z, Yang W, Cong Y, Dong H, Tong J, Xiong G (2000a) Investigation of the permeation behavior and stability of $Ba_{0.5}Sr_{0.5}Co_{0.8}Fe_{0.2}O_{3-\delta}$ oxygen membrane. J Membr Sci 172:177–188

Shao Z, Xiong G, Cong Y, Yang W (2000b) Synthesis and oxygen permeation study of novel perovskite-type $BaBixCo_{0.2}Fe_{0.8-x}O_{3-\delta}$ ceramic membranes. J Membr Sci 164:167–176

Sunarso J, Baumann S, Serra JM, Meulenberg WA, Liu S, Lin YS, Diniz da Costa JC (2008) Mixed ionic–electronic conducting (MIEC) ceramic-based membranes for oxygen separation. J Membr Sci 320:13–41

Sunarso J, Liu S, Lin YS, Diniz da Costa JC (2009) Oxygen permeation performance of $BaBiO_{3-\delta}$ ceramic membranes. J Membr Sci 344:281–287

Sunarso J, Liu S, Lin YS, Diniz da Costa JC (2011) High performance BaBiScCo hollow fibre membranes for oxygen transport. Energy Environ Sci 4:2516–2519

Švarcova S, Wiik K, Tolchard J, Bouwmeester HJM, Grande T (2008) Structural instability of cubic perovskite $Ba_xSr_{1-x}Co_{1-y}Fe_yO_{3-\delta}$. Solid State Ion 178:1787–1791

Tan X, Wang Z, Meng B, Meng X, Li K (2010) Pilot-scale production of oxygen from air using perovskite hollow fibre membranes. J Membr Sci 352:189–196

Ten Elshof JE, Bouwmeester HJM, Verweij H (1995) Oxygen transport through $La_{1-x}Sr_xFeO_{3-\delta}$. I. Permeation in air/He gradients. Solid State Ion 81:97–109

Teraoka Y, Zhang H, Furukawa S, Yamazoe N (1985) Oxygen permeation through perovskite-type oxides. Chem Lett 14:1743–1746

Teraoka Y, Nobunaga T, Yamazoe N (1988) Effect of cation substitution on the oxygen semipermeability of perovskite-type oxides. Chem Lett 17:503–506

Tilley RJD (2013) Understanding solids – the science of materials. Wiley, Chichester

Tsai C-Y, Dixon AG, Moser WR, Ma YH (1997) Dense perovskite membrane reactors for partial oxidation of methane to syngas. AIChE J 43:2741–2750

Tsai CY, Dixon AG, Ma YH, Moser WR, Pascucci MR (1998) Dense perovskite, $La_{1-x}A_xFe_{1-y}Co_yO_{3-\delta}$ (A = Ba, Sr, Ca), membrane synthesis, applications, and characterizations. J Am Ceram Soc 81:1437–1444

Wagner C (1975) Equations for transport in solid oxides and sulfides of transition metals. Prog Solid State Chem 10:3–16

Wang H, Cong Y, Yang W (2002) Oxygen permeation study in a tubular $Ba_{0.5}Sr_{0.5}Co_{0.8}Fe_{0.2}O_{3-\delta}$ oxygen permeable membrane. J Membr Sci 210:259–271

Wang L, Imashuku S, Grimaud A, Lee D, Mezghani K, Habib MA, Shao-Horn Y (2013) Enhancing oxygen permeation of electronically short-circuited oxygen-ion conductors by decorating with mixed ionic-electronic conducting oxides. ECS Electrochem Lett 2:F77–F81

Watanabe K, Yuasa M, Kida T, Shimanoe K, Teraoka Y, Yamazoe N (2008a) Preparation of oxygen evolution layer/$La_{0.6}Ca_{0.4}CoO_3$ dense membrane/porous support asymmetric structure for high-performance oxygen permeation. Solid State Ion 179:1377–1381

Watanabe K, Yuasa M, Kida T, Shimanoe K, Teraoka Y, Yamazoe N (2008b) Dense/porous asymmetric-structured oxygen permeable membranes based on $La_{0.6}Ca_{0.4}CoO_3$ perovskite-type oxide. Chem Mater 20:6965–6973

Wu K, Xie S, Jiang GS, Liu W, Chen CS (2001) Oxygen permeation through $(Bi_2O_3)_{0.74}(SrO)_{0.26}$-Ag (40% v/o) composite. J Membr Sci 188:189–193

Zhang K, Sunarso J, Shao Z, Zhou W, Sun C, Wang S, Liu S (2011) Research progress and materials selection guidelines on mixed conducting perovskite-type ceramic membranes for oxygen production. RSC Adv 1:1661–1676

Zhang K, Shao Z, Li C, Liu S (2012) Novel CO_2-tolerant ion-transporting ceramic membranes with an external short circuit for oxygen separation at intermediate temperatures. Energy Environ Sci 2:5257–5264

Zhang K, Liu L, Shao Z, Xu R, Diniz da Costa JC, Wang S, Liu S (2013) Robust ion-transporting ceramic membrane with an internal short circuit for oxygen production. J Mater Chem A 1:9150–9156

Zhang K, Liu L, Sunarso J, Yu H, Pareek V, Liu S (2014) Highly stable external short-circuit-assisted oxygen ionic transport membrane reactor for carbon dioxide reduction coupled with methane partial oxidation. Energy Fuels 28:349–355

Part V

Climate Change Mitigation: Advanced Technologies

Photocatalytic Water Splitting and Carbon Dioxide Reduction

Nathan I. Hammer, Sarah Sutton, Jared Delcamp, and Jacob D. Graham

Contents

Abstract

Photocatalytic water splitting, which involves the simultaneous reduction and oxidation of water-producing hydrogen and oxygen gas, provides a means of harnessing the sun's power to generate an energy source in a clean and renewable fashion. Photocatalytic reduction of carbon dioxide to form hydrocarbons such as methane not only promises reduced emission of an important greenhouse but also a new source of fuel. Concerns over the effects of global climate change and the eventual demise of fossil fuels make the search for clean alternative energy sources a top priority. This chapter details the progress in these two increasingly important areas: hydrogen production by photocatalytic water splitting and photocatalytic carbon dioxide reduction.

N.I. Hammer (✉) • S. Sutton • J. Delcamp
Department of Chemistry and Biochemistry, The University of Mississippi University, Oxford, MS, USA
e-mail: nhammer@olemiss.edu; scsutton@go.olemiss.edu; delcamp@olemiss.edu

J.D. Graham
Johns Hopkins University, Baltimore, MD, USA
e-mail: jdgraham@jhu.edu

W.-Y. Chen et al. (eds.), *Handbook of Climate Change Mitigation and Adaptation*,
DOI 10.1007/978-3-319-14409-2_46

Introduction

It is an understatement to say that the consumption of energy is a critical requirement for modern human civilization. The rapid industrialization and technological progress that permeate every facet of life would not be possible without the cheap and abundant energy sources enjoyed by mankind today. Annual worldwide energy consumption reached 497 exajoules in 2006, and with current conditions, energy demands are expected to grow 44 % by the year 2030 (Energy Information Administration and International Energy 2009). Currently, fossil fuels provide the vast majority of this energy as they are easily obtainable, abundant, and energetically dense. In order to keep up with this pace, society's reliance on fossil fuels will grow dramatically in the coming years if alternative sources of energy are not developed.

It is now well accepted in society that human dependence on fossil fuels presents a number of problems. Competition for fossil fuel-based sources of energy will have destabilizing geopolitical effects as the supply of these valuable resources declines. However, the most publicized consequences of the continued use of fossil fuels come in the form of environmental pollution. Sulfur dioxide, nitrogen oxides, cadmium, and mercury are all released as a result of burning fossil fuels, with coal being the largest contributor. Under the right conditions, these pollutants produce easily visible results in the form of acid rain and smog, while other combustion products, such as carbon dioxide, may not appear to have an immediately visible effect. Although CO_2 can generally be considered harmless (at least physiologically to plants and animals – including humans), the quantities released annually into the atmosphere (about six billion tons) could possibly result in climate-altering effects. Concerns over "global warming" and, more recently, "global climate change" have captivated the attention of world governments and are currently transforming society in areas ranging from concern over automobile emissions to managing carbon footprints (Hansen and Sato 2004; Fischer et al. 1999; Luthi et al. 2008; McMichael and Woodruff 2004; Jackson and Schlesinger 2004; Schimel et al. 2000; Armaroli and Balzani 2007; Caetano et al. 2008; Zhang et al. 2007).

Certain atmospheric gases such as CO_2 are thought to trap long wavelength, thermal radiation in the Earth's atmosphere through the "greenhouse effect" and CO_2 itself is considered a greenhouse gas. Other important greenhouse gases include water, methane (CH_4), nitrous oxide (N_2O), and ozone (O_3). The historical development of the greenhouse effect is rather quite interesting and dates back to the nineteenth century and scientists including Svante Arrhenius (Arrhenius 1896). The basic mechanism behind the greenhouse effect is depicted in Fig. 1. Radiation from the sun is absorbed by the Earth and is converted to heat. This heat is radiated back into space but some wavelengths of radiation corresponding to the vibrational normal modes of greenhouse gases are absorbed by these gases. This energy is then reemitted in all directions, including back toward the Earth, rather than into space. The overall effect is a "trapping" of heat energy in the atmosphere.

Ice core samples possess trapped gaseous bubbles that reveal atmospheric CO_2 concentrations dating back as far as 800,000 years (Fischer et al. 1999; Luthi et al. 2008). They have shown a correlation between higher CO_2 concentration and

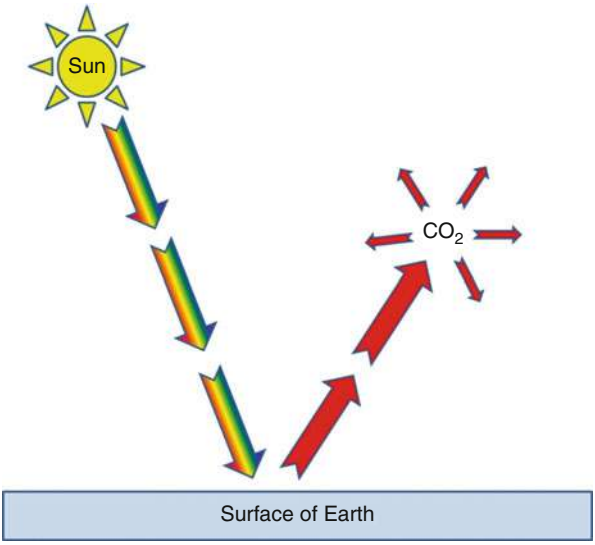

Fig. 1 Various wavelengths of solar radiation are absorbed by the Earth's surface and transformed into heat, which is eventually reradiated back into space. Greenhouse gases, such as CO_2, absorb some of this infrared radiation and reemit it in all directions, including back toward the Earth's surface

higher average global temperatures. However, this correlation is delayed from the effect of the oceans and other buffer systems (Hansen and Sato 2004). With current conditions, an eventual average global temperature increase of several degrees Celsius is possible. Along with sea level rise, acidification of the oceans, and glacial melt, the rise in average temperature could destabilize much of the Earth's current ecology with altered fauna migration and flowering times. These circumstances also would likely diminish food supplies as environmental conditions change.

Although the dangers of global climate change have been in public thought for decades, solutions remain elusive for technical and economic reasons (Keith 2009). The possible solutions to global warming are numerous and varied, but most can be divided into two avenues of approach: removing sources of CO_2 or capturing released CO_2. An example of a geoengineering form of the latter would be injecting CO_2 underground. Groundwater is the major sink for CO_2 injected underground, and the possibility of long-term containment is difficult to predict (Gilfillan et al. 2009). While removing CO_2 from the atmosphere would help in reversing the trend of global warming, replacing current fossil fuel-dependant energy sources with non-CO_2-emitting energy sources is a more long-term solution. Of all the 6 billion tons of CO_2 released annually, 80 % is due to the burning of fossil fuels. Nuclear, geothermal, wind, hydroelectric, and solar methods of energy production emit no CO_2 and are much cleaner sources of energy than fossil fuels. A geothermal, wind, or hydroelectric energy supply is renewable and clean but has limited implementation in specific areas. Nuclear energy is a very real alternative to fossil fuels but is not renewable, and fissile materials will eventually be depleted. Solar-derived energy has the most potential as a permanent replacement for fossil fuels and as a means by which to transform one form of energy into another, and photovoltaics have emerged as perhaps the most promising avenue for that capture and conversion.

Although the development of solar energy as an alternative energy source seems like the perfect solution to society's energy needs, long-term storage and realistic energy density are obstacles. Many have touted hydrogen gas as an attractive alternative to fossil fuels as an energy carrier (Barreto et al. 2003; Crabtree et al. 2004; Dunn 2002; Moriarty and Honnery 2009). Hydrogen's reaction with oxygen yields only water and heat, and this heat can easily be used as a source in automobiles or generators (Crabtree et al. 2004). Hydrogen storage in tanks involves high-pressure or cryogenic storage (Schlapbach and Zuttel 2001; Zuttel 2004). Other methods involve hydrogen adsorption onto certain specialized surfaces with metal hydrides having the highest hydrogen storage density (Zuttel 2004). Currently, most hydrogen production is dominated by steam reformation of natural gas (Crabtree et al. 2004). An efficient, cheap, and renewable method of hydrogen production would allow hydrogen gas to become the primary energy carrier in automobiles and in stationary applications. Coupling the storage and transportation potential of hydrogen gas with solar energy-based production would allow for the creation of an inexpensive and highly useful source of energy.

It is often noted in reviews and by advocates of solar energy that the sun provides many thousands of times the annual energy consumption of the Earth, and harnessing only a fraction of this energy would be adequate. Shown in Fig. 2 is a solar emission spectrum obtained on the campus of the University of Mississippi. This emission mimics a blackbody curve, and it is readily apparent that most of the light from the Earth's yellow sun that reaches the Earth's surface is in the visible region of the electromagnetic spectrum. The number of photons reaching the Earth's surface drops dramatically as ultraviolet (UV) wavelengths are approached. Dips in the spectrum correspond to absorption by different atmospheric gases such as water vapor. Various methods exist for harvesting solar energy, but the use of photocatalysts provides perhaps the most viable option with their reversible

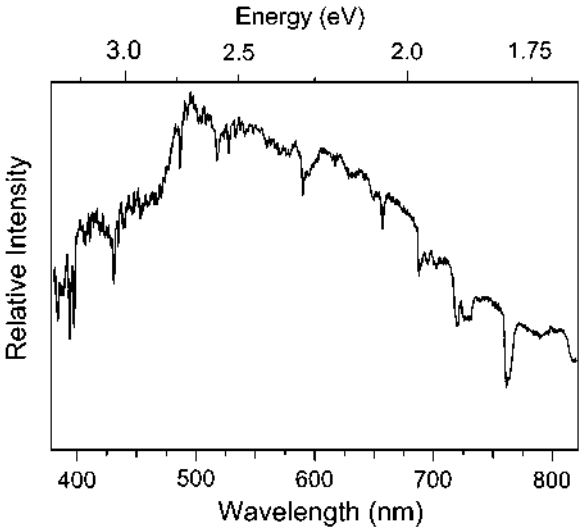

Fig. 2 Solar emission spectrum obtained at the University of Mississippi

oxidation–reduction capabilities. Photocatalytic water splitting, which involves the simultaneous reduction and oxidation of water-producing H_2 and O_2, provides a means of harnessing the sun's power to generate an energy source in a clean and renewable fashion. Besides the production of an alternative to fossil fuels, photocatalytic processes can turn the tide against global climate change in a more direct way. Photocatalytic materials can reduce carbon dioxide to form hydrocarbons such as methane and ethanol, essentially taking exhaust and turning it back into fuel. This chapter details the progress in these two increasingly important areas: hydrogen production by photocatalytic water splitting and photocatalytic carbon dioxide reduction.

Photocatalytic Processes

A photocatalytic process relies on a semiconductor's adsorption of light to create stored energy and the use of that energy to do some form of useful work – in this case, serving as a catalyst for the production of a desired reaction product. In semiconductors, groups of closely spaced electronic energy levels form bands, namely, the conduction and valence bands, as shown schematically below in Fig. 3. When incident light has energy that is greater than that of the band gap of the semiconductor material, electrons in the valence band of the material are excited to the conduction band. At the same time, holes are created in the valence band. Photocatalytic reactions then occur on the surface of the semiconductor, where these newly generated electrons and holes are located. Many important considerations go into the engineering of a useful photocatalyst. A few of these include matching the band gap to the radiation wavelength (or frequency/energy) to be employed, the suppression of the recombination of electron–hole pairs, and appropriate sensitization by other materials.

The conduction band is higher in energy and less populated with electrons than the valence band, and the energy separation of these two bands is commonly referred to as the band gap. This band gap limits the minimum energy (or wavelength) of incident photons able to be absorbed. Photons that are absorbed promote electrons (e^-) across the band gap from the filled valence band into the empty conduction band creating a hole (h^+) in the valence band. Thermal relaxation of the electron–hole pair to the band edge can occur or recombination of the electron–hole pair can result, although this takes longer to occur (on a picosecond timescale). While the electron–hole pair exists, the photocatalyst can perform useful reduction and oxidation reactions by accepting electrons into its valence band or donating the promoted electrons in its conduction band. When an electron moves to the surface of the photocatalyst and has the correct potential, anion radicals (A^- in Fig. 3) are produced, while cation radicals (B^+ in Fig. 3) are produced from electron holes at the surface.

As mentioned above, there are a number of design considerations to keep in mind in order to create a useful photocatalytic material. Suppression of the recombination of electron–hole pairs in a photocatalyst is essential to improving its efficiency

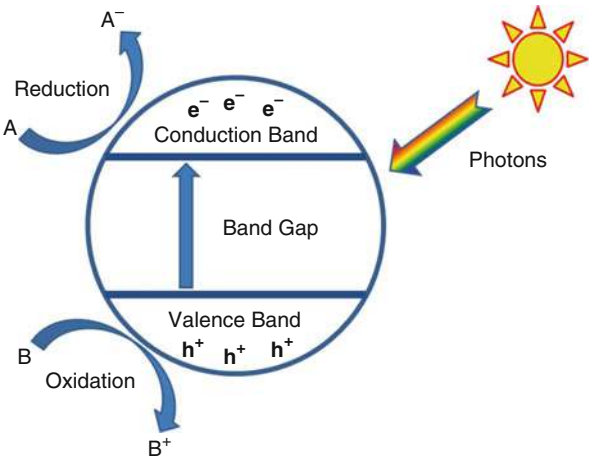

Fig. 3 In a semiconductor, electrons (e^-) are promoted from the valence band to the conduction band when photons of light are absorbed. Electron holes (h^+) are created with the excitation of electrons. The creation of this electron–hole pair allows for the reduction and oxidation of other species

(Hurum et al. 2005; Mohapatra et al. 2008; Fox and Dulay 1993; Colombo and Bowman 1996; Kaneco et al. 1998). Trapping of a promoted electron, hole, or both impedes the detrimental recombination process. An example of electron–hole trapping would be using a sacrificial reagent to donate electrons to a photocatalyst after excitation. Electrons donated into the valence band provide a longer lifetime for the excited electron in the conduction band. Oxygen and several inorganic oxidizing species have been shown to serve as good recombination inhibitors (Fox and Dulay 1993). Sensitization of semiconductors by dye molecules is another important design element employed to both increase the excitation rate and extend the excitation wavelength window (Fox and Dulay 1993; Younpblood et al. 2009). Photoelectrons are provided by a photosensitive dye that is in contact with the semiconductor material, and charge separation occurs at the surfaces between the dye, semiconductor, and electrolyte. The semiconductor serves primarily as the charge carrier, rather than the source of electrons and holes.

Physically adsorbing the molecules to be reduced or oxidized (A and B, respectively, in Fig. 3) by the photocatalyst is another important design element that is essential to successful catalytic activity (Fox and Dulay 1993; Li et al. 2008). This is because of the fact that the recombination of photogenerated electrons and holes is very fast. There is no time for diffusion of the charge acceptor to the site of oxidation or reduction. Electron transfer is kinetically competitive only when the donor or acceptor molecule is adsorbed before the reaction of interest is to take place (Fox and Dulay 1993). Doping of other atoms and molecules into semiconductor photocatalysts to modify the electronic structure is also an important area of research in recent years that will be discussed in the later sections of this chapter (Fox and Dulay 1993; Yeredla and Xu 2008; Bhattacharyya et al. 2008; Choi et al. 1994; Yan et al. 2005; Wang et al. 2000; Bae et al. 2008; Livraghi et al. 2008; Jagadale et al. 2008; Graciani et al. 2008; Kesselman et al. 1997; Fang et al. 2008; Varghese et al. 2009; Gai et al. 2009; Hong et al. 2005; Hidalgo et al. 2009; Usubharatana et al. 2006; Osterloh 2008; Domen et al. 2000; Kudo and Miseki 2009).

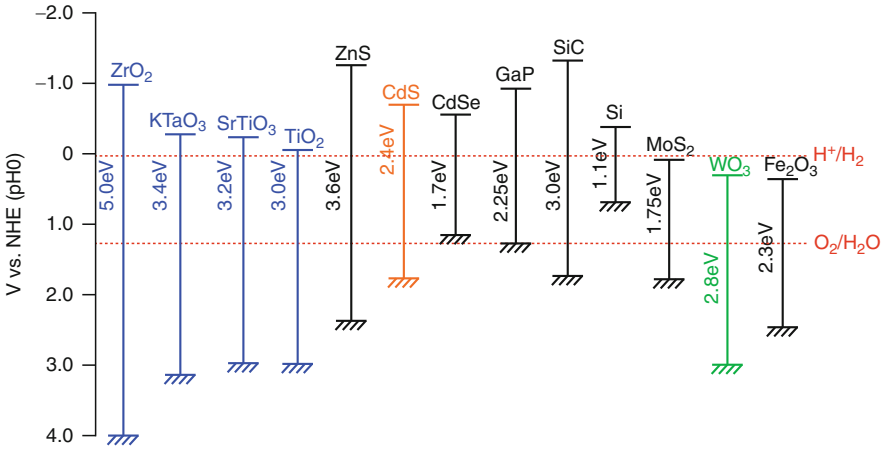

Fig. 4 Band structures of common semiconductor photocatalysts relative to NHE. Note that in this representation, the valence band is at the bottom and the *conduction band is on the top* (Reproduced with permission from Kudo and Miseki (2009))

The number of photocatalysts developed for water splitting and carbon dioxide reduction increases more each year and many of these materials are cataloged below in the following two sections of this chapter. Important considerations already mentioned above in creating an effective photocatalyst include suppressing electron–hole recombination and achieving effective charge separation. Another important consideration is the selection of the best semiconductor for the desired photocatalytic reaction. The choice of semiconductor material and the other species that are incorporated into it such as sensitizers and dopants are critical in achieving the optimal overlap of band gap with the wavelengths of light. Shown in Fig. 4 are the band structures of a few representative semiconductor photocatalysts relative to the normal hydrogen electrode (NHE) at pH = 0 (Kudo and Miseki 2009). In the NHE, hydrogen's standard electrode potential is defined as zero ($2H^+ + 2e^- \rightarrow H_2$, E = 0.0 V), and the potential of all other electrode reactions are defined as relative to hydrogen. To effectively use the abundant visible solar radiation shown in Fig. 2, the band gap (the height of the bar in Fig. 4) needs to be less than about 3 eV. This energy corresponds to photons of about 400 nm, right at the visible edge of the solar emission spectrum. However, to be effective in water splitting or carbon dioxide reduction, the location of the top and bottom of the band gap is also very important.

Photocatalytic materials have promising and practical uses in many areas as wide ranging as organic synthesis (Fox and Dulay 1993; Kudo and Miseki 2009) and the degradation of hazardous waste (Bahnemann 2004; Hoffmann et al. 1995). Here, the interest is in the application of semiconductor photocatalysts to the splitting water to create a new source of hydrogen gas and the reduction of carbon dioxide to useful forms. In the following two sections, the application of photocatalytic semiconductor materials for these purposes is discussed and many examples of recently developed materials are listed.

Photocatalytic Water Splitting

Water splitting is the simultaneous reduction and oxidation of water to produce H_2 and O_2. In the early 1970s, the Honda–Fujishima effect was reported, in which water splitting was achieved with a TiO_2 electrode under ultraviolet (UV) irradiation (Fujishima and Honda 1971, 1972). In their configuration, which is illustrated in Fig. 5, a platinum electrode and a TiO_2 electrode are connected through an external load and immersed in water. When irradiated with UV light, current flows from the platinum electrode to the TiO_2 electrode. Oxidation proceeds at the TiO_2 electrode, while reduction proceeds at the platinum electrode. These processes are given by:

$$\text{Oxidation} : 2h^+ + H_2O \rightarrow \frac{1}{2}O_2 + 2H^+ \tag{1}$$

$$\text{Reduction} : 2e^- + 2H^+ \rightarrow H_2 \tag{2}$$

where h^+ are electron holes. The overall chemical equation for this process is thus:

$$H_2O \rightarrow \frac{1}{2}O_2 + H_2 \tag{3}$$

Not all semiconductor materials are appropriate for the photocatalytic splitting of water. As mentioned above, it is important to choose a semiconductor material that exhibits a band gap appropriate for the desired photochemical reaction. In the case of water, the top level of the valence band must be more positive than the oxidation–reduction potential of Eq. 1 – the oxidation of water to form oxygen gas and two protons. This reaction occurs at 1.23 V relative to NHE. The lower level of

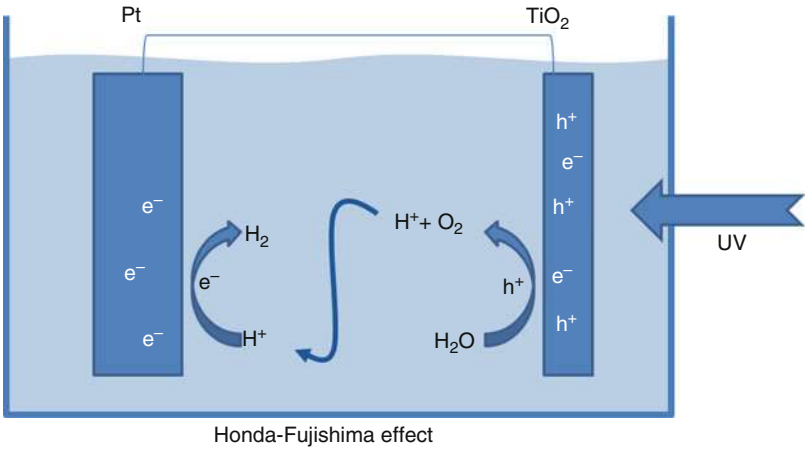

Fig. 5 Cartoon schematic of the photocatalytic water splitting setup employed by Fujishima and Honda (1971, 1972)

the conduction band must be more negative than the oxidation–reduction potential of Eq. 2, the reduction of the hydrogen cation, to create the desired product hydrogen gas. This, as all freshman chemistry students can attest to is 0 V relative to NHE. Honda and Fujishima's choice in their original paper was TiO_2. As evident from Fig. 4, the band gap for TiO_2 is approximately 3.2 eV (different sources report 3–3.5 eV, depending if the TiO_2 is in the rutile or anatase form), requiring photons with wavelengths less than about 400 nm. This energy requirement is right on the edge of usable visible light and therefore either violet or ultraviolet photons are required to mobilize electron–hole pairs in TiO_2. This is unfortunate since most photons hitting the Earth are longer in wavelength as illustrated from Fig. 2. For this reason, there have been many attempts to improve on the efficiency of the photocatalytic water splitting process.

Since Honda and Fujishima's initial discovery, a number of architectures for achieving efficient photocatalytic water splitting using both ultraviolet and visible light have been developed. However, the overall quantum efficiencies of these architectures have been less than stellar (less than 10 % for catalyzing Eq. 3) (Osterloh 2008), and wide-scale utilization has still not been achieved. For solar-based water splitting to be practical, several goals must be met. One is that the photocatalyst must efficiently adsorb solar radiation. TiO_2, for example, requires UV light, while most of the sun's photons have energy in the visible region of the electromagnetic spectrum (or longer wavelengths) as shown in Fig. 2. The band gap of the photocatalyst must also be tuned so that both the reduction and oxidation processes necessary for water splitting are energetically possible. This requirement is indicated in Fig. 4 with dotted lines intersecting the various photocatalyst materials for these two processes. Another consideration is that these reduction and oxidation reactions be spatially separated to prevent recombination of the freshly produced H_2 and O_2. This last requirement needs clever engineering of the photocatalytic material and is one reason for the large number of publications in this area each year.

Excellent reviews summarize the extensive literature that has been amassed over the past few decades on the subject of photocatalytic water splitting. These reviews detail the various photocatalytic materials employed and the clever architectures that have been engineered to improve the efficiency of this process. Table 1 catalogs a number of the reports described in detail in these literature reviews (Osterloh 2008; Kudo and Miseki 2009; Yang et al. 2005; Navarro et al. 2009; Zong and Wang 2014; Vaneski et al. 2014; Abe 2010; Hernández-Alonso et al. 2009; Kudo et al. 2004; Xie et al. 2013; Zhang and Guo 2013; Janáky et al. 2013). The band gap of the photocatalyst material and the light source employed to mimic solar radiation in most cases are listed. Also included in Table 1 are the H_2 and O_2 activities reported from these studies. High-powered mercury (Hg) and xenon (Xe) arc lamps are commonly employed as the light sources in experiments that test the photocatalytic ability of newly developed materials. It is not feasible to use actual solar radiation in experiments to test for photocatalytic activity because a constant flux of a known range of wavelengths is desired so that the photocatalytic responses of different materials can be directly compared. Hg lamps are useful for high-powered, short-wavelength UV excitation, and Xe lamps cover both longer-wavelength UV and are

Table 1 Materials for photocatalytic water splitting

Photocatalyst	Band gap (eV)	Cocatalyst	Light source	H_2 activity (μmol/h)	O_2 activity (μmol/h)
Sulfide-based photocatalysts					
CdS		Pt	150 W Hg	1–10 per 5 mg	
CdS		Pt/RuO_2	450 W Xe	2.8 mL/44 h/2.75 mg	1.4 mL/44 h/2.75 mg
CdS–ZnS	2.35		300 W Hg	250	
Pt/CdS	2.4		500 W Hg	40	
Pt/CdS:Ag	2.35		900 W Xe	11,440	
CdS quantum dots–titanate nanosheets hybrid	2.9		300 W Xe	1,000 per g	
CdS/alumina				41.3–180.8	
CdS/CNT		Pt		819	
CdS/CNT particles and nanotubes				92.5	
CdS/Ag_2S nanosheets and nanorods		Pt		874	
CdS/Al-HMS particles		Ru		825.9	
CdS/colloidal rhodium		Rh		Low	
CdS/ETS-4				175	
CdS–glass nanosystem				3,570	
CdS-cluster-decorated graphene nanosheets		Pt		56,000	
CdS-incorporated special glass				1,549	
CdS/$LaMnO_3$ particles				595	
CdS/M-MCM-41				47.11	
CdS/Ti–MCM-41 particles and nanotubes				250	
CdS/Ti–MCM-41 particles and nanotubes		Pt		875	
CdS/MgO particles		Pt		290	
CdS/MoO_3 core (MoO_3)–shell(CdS)				5,250	
CdS/Ni/NiO/$KNbO_3$ particles				150	
CdS/pani particles				299.1	
CdS/silicas rod-like				33	
CdS/SrS particles				615	
CdS/TiO_2		Pt		8.4	

(*continued*)

Table 1 (continued)

Photocatalyst	Band gap (eV)	Cocatalyst	Light source	H_2 activity (μmol/h)	O_2 activity (μmol/h)
CdS/TiO_2 nanowires and nanoparticles				~107	
CdS/TiO_2 particles				4,224–9,800	
CdS/(Pt-TiO_2) particles				2,670	
CdS/TiO_2NTs nanoparticles and nanotubes				12.7	
CdS/TiO_2NTs nanoparticles and nanotubes		Pt		2,680	
CdS/$Na_2Ti_2O_2(OH)_2$ nanoparticles and nanotubes		Pt		~1,080	
CdS/zirconium titanium phosphate particles		Pt		2,300	
CdS/zeolite		ZnS		2,455	
CdS/ZnO				1,805	
CdS/ZnO core-shell nanorods		Pt		3,870	
CdS/ZnO		RuO2		~6,200	
CdS–ZnO–CdO		Ru		~75	
CdS/N-doped graphene nanoparticles and nanosheets				1,050	
In-doped CdS on ZrO_2 particles		Pd		~800	
$Cd_{1-x}Zn_xS$ particle				~850–16,320	
$Cd_{1-x}Zn_xS$ particle with nanotwins				17,900	
$Cd_{1-x}Zn_xS$ nanoparticles				2,640	
$Cd_{0.1}Zn_{0.9}S$ nanoparticles and microspheres				403.75	
$Cd_{0.1}Zn_{0.9}S$ nanospheres				21,850	
$Cd_{0.2}Zn_{0.8}S$ particles				965–1,260	
$Cd_{0.2}Zn_{0.8}S$ particles				2,290–3,200	
$Cd_{0.5}Zn_{0.5}S$		Pt		~350	
CdZnS (containg Ag_22S)		Pt		39062.5	

(*continued*)

Table 1 (continued)

Photocatalyst	Band gap (eV)	Cocatalyst	Light source	H_2 activity (μmol/h)	O_2 activity (μmol/h)
$Cd_{0.1}Zn_{0.9}S$–CNT particles				1563.2	
$Cd_{0.5}Zn_{0.5}S$/TNTs particles and nanotubes				13,200	
$Cd_{0.8}Zn_{0.2}S/HNbWO_6$		Pt		~625	
$Cd_{0.8}Zn_{0.2}S/HNbWO_7$		Pt		536	
$Zn_xCd_{1-x}S$–CuS nanospheres				2,080	
$Zn_xCd_{1-x}S$–CuS nanoparticles nanosheets		Pt		2466.7	
Reduced graphene oxide–$Zn_xCd_{1-x}S$ particles				1,824	
CdS QDs-sensitized $Zn_{1-x}Cd_xS$				2,128	
CdS–ZnS				2283.9	
CdS–ZnS	2.35		300 W Hg	250	
CdS/ZnS/n-Si				1584.8	
CdS–ZnS/silica particles				~268	
[Pt/(CdS/n-Si)]/ZnS		Pt		647.3	
Sr-doped CdS–ZnS nanoparticles				~500	
Ba-doped $Cd_{0.8}Zn_{0.2}S$ nanoparticles				~700	
$ZnIn_2S_4$		Pt		257	
$ZnIn_2S_4$ nanoplates and nanotips				10,574	
$ZnIn_2S_4$ floriated microspheres		Pt		8,420	
$ZnIn_2S_4$ microsphere		Pt		562.25–612.5	
$ZnIn_2S_4$ nanosheet flower-like microspheres				766.8	
$ZnIn_2S_4$ microspheres (petals/sheets)		Pt		692	
$ZnIn_2S_4$ flowering-cherry sphere		Pt		136.5	
$ZnIn_2S_4$ with irregular lumps		Pt		~55	
$ZnIn_2S_{3+m}$ microspheres		Pt		159.5	

(*continued*)

Table 1 (continued)

Photocatalyst	Band gap (eV)	Cocatalyst	Light source	H_2 activity (μmol/h)	O_2 activity (μmol/h)
$ZnIn_2S_4$/MWCNTs				6,840	
$ZnIn_2S_4$/fluoropolymer particles and fibers				~398.3	
$ZnIn_2S_4$ microspheres with transition metals		Pt		4,000	
Cu-doped $ZnIn_2S_4$ microspheres		Pt		757.5	
Ni-doped $ZnIn_2S_4$ petals		Pt		~45	
$CdIn_2S_4$ nanopetals and nanotubes				6,960	
$CdIn_2S_4$ nanopetals				6,476	
$Cd_xIn_2S_4$-$Zn_{1-x}In_2S_4$ particles				590	
$CuInS_2$ microsphere built by flakes		Pt		59.4	
$CuGa_3S_5$ particles				300	
$CuGa_3S_5$ particles		Rh		800	
$CuGa_3S_5$ particles		NiS		1,000	
$AgGaS_2$ particles		Pt		~3,000	
$AGa_2In_5S_8$ (A = Cu or Ag)		Cu: Rh		10,666.70	
$AGa_2In_5S_8$ (A = Cu or Ag)		Ag; Rh		3,433.30	
$AgIn_5S_8$		Pt		59.4	
$(CuIn)_xCd_{2(1-x)}S_2$ microspheres				649.9	
$(CuIn)_xCd_{2(1-x)}S_2$ microspheres		Pt		2,456	
$(CuIn)_xCd_{2(1-x)}S_2$ microspheres				274.5	
$(CuIn)_xCd_{2(1-x)}S_2$ microspheres		Pt		1172.5	
$AgInZn_7S_9$		Pt		3,133	
$Zn_{1-x}Cu_xS$				~370	
Cu-doped ZnS shell structure particles				~210	
$(CuIn)_xZn_{2(1-x)}S_2$ microspheres		Ru		990.45	
$(CuIn)_xZn_{2(1-x)}S_2$ particles with hexagonal plane		Pt		2,280	

(*continued*)

Table 1 (continued)

Photocatalyst	Band gap (eV)	Cocatalyst	Light source	H_2 activity (μmol/h)	O_2 activity (μmol/h)
$(CuIn)_xZn_{2(1-x)}S_2$ particles with nanosteps structure				320	
$(CuIn)_xZn_{2(1-x)}S_2$ particles with nanosteps structure		Pt		1413.3	
ZnS-coated $ZnIn_2S_4$ microspheres and rod-like grains		Pt		103	
ZnS–$CuInS_2$–$AgInS_2$ particles		Ru		7733.3	
ZnS–$CuInS_2$–$AgInS_2$ platelike particles		Ru		1,208	
$(CuxAg_{1-x})_2ZnSnS_4$ particles		Ru		~750	
ZnS			125 W Hg	22 per 12 mg	
ZnS	3.1	Pt	200 W Hg	13,000	
ZnS, with $AgInS_2$ or $CuInS_2$		Pt or Ru	300 W Xe		
ZnS:Cu	2.5		300 W Xe	450	
ZnS:Ni	2.3		300 W Xe	280	
ZnS:Pb, Cl	2.3		300 W Xe	40	
Tungsten-based photocatalysts					
$(AgBi)_{0.5}WO_4$	3.5	Pt		0.1	5.8
Ag_2WO_4	3.1	Pt			
$AgBiW_2O_8$	2.8	Pt			
$AgInW_2O_8$	3.1	Pt, NiO_x			
$BiWO_4$					
$BiYWO_6$	2.7	RuO_2 Cr_2O_3-Pt			
Ca_2NiWO_6	3.0, 2.6	Pt			
$CsTaWO_6$	3.8				
$HNbWO_6$	3.1	Pt			
$HTaWO_6$	3.1	Pt			
$KInW_2O_8$	3	Pt			
$Li_2CoW_2O_8$	1.6, 2.6	Pt			
$LiCrW_2O_8$	3.3, 2.5, 1.9	Pt			
$LiInW_2O_8$	3.5	Pt			
$MNgWO_6$ (M: Rb, Cs)	2.4, 2.9	NiO_x			
$MTaWO_6$ (M: Rb, Cs)	3.8	NiO_x			
$NaBiW_2O_8$	3.5	Pt			

(*continued*)

Table 1 (continued)

Photocatalyst	Band gap (eV)	Cocatalyst	Light source	H_2 activity (μmol/h)	O_2 activity (μmol/h)
$NaInW_2O_8$	3.6	Pt			
$PbWO_4$	3.9	RuO_2	200 W Hg–Xe	24	12
$SnWO_4$	1.6, 2.7	Pt			
WO_3	2.8	Pt for H_2			65
WO_3		Pt	300 W Xe		
WO_3 in presence of Fe^{3+} or Ag^+			500 W Xe		1,220 per g
WS_2			1,000 W Xe	0.05 mL/h/10 mg	
$ZnWO_4$	3.3	RuO_2/Pt			
$ZrW_2O_7(OH)_2$	3.9	Pt			
ZrW_2O_8	4	Pt			
Titanium oxides					
$AgLi_{1/3}Ti_{2/3}O_2$	2.7	Pt for H_2			24
B/Ti Oxide	3.2	Pt	400–450 W Hg	22	11
$BaBi_4Ti_4O_{15}$	3.1	Pt		8.2	3.7
Ba:$La_2Ti_2O_7$	3.8	NiO_x	450 W Hg	5,000 per g	
$BaLa_4Ti_4O_{15}$	3.85	NiO_x	450 W Hg	4,600 per g	
$BaTi_4O_9$		RuO_2	200 W Hg–Xe	33	16
$Bi_4Ti_3O_{12}$	3.1			0.6	3
$Ca_{0.25}La_{0.75}TiO_{2.25}N_{0.75}$	2	Pt for H_2, IrO_2 for O_3		5.5	230
$CaTiO_3$:Rh		Pt for H_2		8.5	
Cr/Ta:$SrTiO_3$		Pt	300 W Xe	0.21	0.11
$Cs_2La_2Ti_3O_{10}$	3.4–3.5	NiO_x	400–450 W Hg	700	340
$Cs_2Ti_2O_5$	4.4	None		500	
$Cs_2Ti_5O_{11}$	3.75	None		90	
$Cs_2Ti_6O_{13}$	3.7	None		38	
$Gd_2Ti_2O_7$	3.5	NiO_x	400–450 W Hg	400	198
H^+-$Cs_2Ti_2O_5$		None		852	
$H_2Ti_4O_9$			100 W Hg	560	
$K_2La_2Ti_3O_{10}$	3.4–3.5	NiO_x	400–450 W Hg	2,186	1,131
$K_2LaTi_3O_{10}$		Ni, Pt, RuO_2	450 W Hg		
$K_2LaTi_3O_{10}$-Au		Pt	450 W Hg	841 per g	Not significant

(*continued*)

Table 1 (continued)

Photocatalyst	Band gap (eV)	Cocatalyst	Light source	H_2 activity (μmol/h)	O_2 activity (μmol/h)
$K_2Ti_2O_5$		Pt		34.7	
$K_2Ti_4O_9$		Pt		4.8	
$K_4Nb_6O_{17}$–TiO_2 intercalated			450 W Hg		
$KLaZr_{0.3}Ti_{0.7}O_4$	3.91	NiO_x	400–450 W Hg	230	116
$LaTiO_2N$	2.1	Pt for H_2, IrO_2 for O_2	300 W Xe	30	41
La_2TiO_5		NiO_x	400–450 W Hg	442	Stoich
$La_2Ti_3O_9$		NiO_x	400–450 W Hg	386	Stoich
$La_2Ti_2O_7$, doped with Fe, Cr		Pt	500 W Hg	<15 per g	
$La_2Ti_2O_7$:Ba		NiO_x	400–450 W Hg	5,000	
$La_2Ti_2O_7$:Cr	2.2	Pt for H_2		15	
$La_2Ti_2O_7$:Fe	2.6	Pt for H_2		10	
$La_2Ti_2O_7$	3.8	NiO_x	400–450 W Hg	441	152 per 0.5 g
$La_4CaTi_5O_{17}$	3.8	NiO_x	400–450 W Hg	499	Stoich
$M_2Ti_6O_{13}$ (M = Na, K, Rb)		RuO_2	400 W Xe	17 per g for Na	8 per g for Na
$Na_2Ti_3O_7$		Pt		19	
$Na_2Ti_6O_{13}$		RuO_2	200 W Hg/Xe	7.3	3.5
Nb_2O_5:TiO_2 (anatase)		Pt and RuO_2	450 W Xe	200–222 per 0.1 g	Stoich
N-doped $H_2Ti_4O_9$	2.8		420 nm Xe	6	
N-doped $K_2Ti_4O_9$, $KTiNbO_5$			500 W Xe	1.2	
N-doped TiO_2		Pt	450 W Xe		21 per g
$PbBi_4Ti_4O_{15}$		Pt	450 W Xe	11.2 per 0.3 g	422 per 0.3 g
$PbTiO_3$		Pt	450 W Xe	13.6 per 0.3 g	523 per 0.3 g
Pt/$SrTiO_3$:Cr,Ta				16	8
Pt/$SrTiO_3$:Rh				19	8.9
Pt/$SrTiO_3$:Rh				7.8	4
Pt/TiO_2			1,000 W Xe	182	
Pt/TiO_2			300 W Xe	210	
Pt/TiO_2			300 W Xe	156	

(*continued*)

Table 1 (continued)

Photocatalyst	Band gap (eV)	Cocatalyst	Light source	H_2 activity (μmol/h)	O_2 activity (μmol/h)
$Rb_2La_2Ti_3O_{10}$	3.4–3.5	NiO_x	400–450 W Hg	869	430
SiO_2-pillared $K_2Ti_4O_9$	3.17	Pt		560	
SiO_2-pillared N-doped $H_2Ti_4O_8$	2.9		300 W Xe	6	
$Sm_2Ti_2O_5S_2$	2	Pt for H_2	300 W Xe	22	30
Sn^{2+}-doped $K_2Ti_4O_9$, $K_2Ti_2O_5$, $KTiNbO_5$	2.5–2.8		300 W Xe	54	4
$Sr_3Ti_2O_7$	3.2	NiO_x	400–450 W Hg	144	72
$Sr_4Ti_3O_{10}$	3.2	NiO_x	400–450 W Hg	170	
$SrTiO_3$		NiO	450 W Hg	100 per g	
$SrTiO_3$		Ru	1,000 W Xe/Hg	159 μmol L/h/0.05 g	
$SrTiO_3$:Cr/Sb	2.4	Pt for H_2		78	0.9
$SrTiO_3$:Cr/Ta	2.3	Pt for H_2		70	
$SrTiO_3$:Ni/Ta	2.8	Pt for H_2		2.4	0.5
$SrTiO_3$:Rh	2.3	Pt for H_2		117	
TiO_2	3.2	Rh	400–450 W Hg	449	
TiO_2	3.2	NiO_x	400–450 W Hg	6	2
TiO_2	3.2	Pt	400–450 W Hg	568	287
TiO_2	3.2	Pt	400–450 W Hg	106	53
TiO_2			500 W Xe	0.9	
TiO_2			360 W Hg	1.16 per 0.2 g	0.55 per 0.2 g
TiO_2		Pd	500 W Xe	284 per 0.3 g	
TiO_2		Pt	200 W Hg	0.1 per 0.250 g	Stoich
TiO_2		Pt	200 W Hg		
TiO_2 (anatase and rutile)		Pt	400 W Hg	180 per 0.5 g	90 per 0.5 g
TiO_2:Cr/Sb	2.2	Pt for H_2		0.06	31.5
TiO_2:Ni/Nb	2.6	Pt for H_2			7.6
TiO_2:Rh/Sb	2.13	Pt for H_2			16.9
$Y_2Ti_2O_7$	3.5	NiO_x	400–450 W Hg	850	420
Other photocatalysts					
$(AEP)_6In_{10}S_{18}$			300 W Xe	20 per 0.25 g	

(*continued*)

Table 1 (continued)

Photocatalyst	Band gap (eV)	Cocatalyst	Light source	H_2 activity (μmol/h)	O_2 activity (μmol/h)
$(AgBi)_{0.5}MoO_4$	3	Pt		0	10.7
$AgGaS_2$					
$AgLi_{1/3}Sn_{2/3}O_2$	2.7	Pt for H_2			53
$AgNbO_3$	2.86	Pt for H_2		8.2	37
$AgTaO_3$	3.4	NiO_x	400–450 W Hg	21	10
Ag_3VO_4	2	Pt for H_2	300 W Xe		17
$Ba_2In_2O_5$		NiO, Pt	Hg/Xe		
$BaCeO_3$	3.2	RuO_2	400–450 W Hg	59	26
$BaTaO_2N$	2	Pt for H_2		15	
$BaTa_2O_6$	4.1	NiO	400–450 W Hg	629	303
$Ba_5Nb_2O_{15}$	3.85	NiO_x	400–450 W Hg	2,366	1,139
$Ba_5Ta_4O_{15}$		NiO	400–450 W Hg	2,080	910
$BiVO_4$	2.4	Pt for H_2	300 W Xe		421
Bi_2LaTaO_7			400 W Hg	41.8 per g	20.5 per g
Bi_2MNbO_7 (M = Al, Ga, In),M_2BiNbO_7 (M = Ga, In)			400 W Hg		
Bi_2MoO_6	2.7	Pt for H_2			55
$Bi_2Mo_2O_9$	3.1				1.8
$Bi_2Mo_3O_{12}$	2.88	Pt for H_2			8
Bi_2S_3			500 W Xe	0.011 mL/h/ 0.001 g	
Bi_2WO_6	2.8	Pt for H_2	450 W Hg	1.6 per g	3
$Bi_2W_2O_9$	3	Pt	450 W Hg	18	281
Bi_2YTaO_7			400 W Hg		
Bi_3TiNbO_9	3.1	Pt	450 W Hg	33	31
$BiCu_2VO_6$	2.1	Pt for H_2			2.3
$BiZn_2VO_6$	2.4	Pt for H_2			6
Carbonate-intercalated Zn/Cr LDH			400 nm Hg	577.33	
$CaIn_2O_4$		RuO_2	400 W Xe or 200 W Hg/Xe	21	10
$CaSb_2O_6$	3.6	RuO_2	200 W Hg/Xe	1.5	0.2
$CaNbO_2N$	1.9	Pt for H_2		1.5	46
$CaTa_2O_6$	4	NiO_x	400–450 W Hg	72	32

(*continued*)

Table 1 (continued)

Photocatalyst	Band gap (eV)	Cocatalyst	Light source	H_2 activity (μmol/h)	O_2 activity (μmol/h)
$CaTO_3$	3.5	NiO_x	400–450 W Hg	30	17
$CaTaO_2N$	2.5	Pt for H_2		15	
$Ca_2Nb_2O_7$	4.3	NiO_x	400–450 W Hg	101	
$Ca_2Nb_4O_{11}$			400 W Hg	1.7 mmol/h/ 0.5 g	0.8 mmol/ h/0.5 g
Ca_2NiWO_6		Pt	300 W Xe	4.21 per 0.5 g	0.38 per 0.5 g
$Ca_2Sb_2O_7$	3.9	RuO_2	200 W Hg/Xe	3	1
$Ca_2Ta_2O_7$	4.4	NiO	400–450 W Hg	170	83
CeO_2			500 W Xe		2.5 per 0.8 g
CeO_2:Sr		RuO_2	400–450 W Hg	110	55
$CeTaO_4$		NiO	400 W Hg	Not significant	Not significant
$CoTa_2O_6$			400 W Hg	Trace	
Cr:$PbMoO_4$	2.26	Pt for H_2	300 W Xe		120 per 0.5 g
$CrTaO_4$			400 W Hg	Trace	
$Cs_2Nb_4O_{11}$	3.7	NiO_x	400–450 W Hg	1,700	800
$CsLa_2Ti_2NbO_{10}$	3.4–3.5	NiO_x	400–450 W Hg	115	50
$CuAlO_2$	3.01, 1.87				
$CuInS_2$			400 W Xe	0.3	
$CuIn_5S_8$			400 W Xe	1.8	
Cu_2O			300 W Xe at >460 nm	1.7 per 0.5 g	0.9 per 0.5 g
$Ca_2Nb_3O_{10}/K^+$		Pt		550	
Fe-doped Mg/Al LDH	1.9–2.8		125 W Hg	301	
$FeTaO_4$			400 W Hg	Trace	
$(Ga_{0.88}Zn_{0.12})(N_{0.88}O_{0.12})$	2.6	$Rh_{2-x}Cr_xO_3$	450 W Hg	800	400
$Ga_{1.14}In_{0.8}6O_3$	3.7	Pt		30	30
Ga_2O_3	4.6	NiO		46	23
Ga_2O_3:Zn	4.6	Ni		4,100	2,200
GaN	3.4	$Rh_{2-x}Cr_xO_3$	450 W Hg	19	9.5
GaN:Mg	3.4	RuO_2	450 W Hg	730	290

(*continued*)

Table 1 (continued)

Photocatalyst	Band gap (eV)	Cocatalyst	Light source	H_2 activity (μmol/h)	O_2 activity (μmol/h)
GaN:ZnO		RuO_2	450 W Hg and 300 W Xe	1 mmol/h/0.3 g	0.29 mmol/h/0.3 g
GaN:ZnO		Cr/Rh oxide	450 W Hg and 300 W Xe		
Gd_3TaO_7		NiO	400 W Hg		
Ge_3N_4	3.6	RuO_2	450 W Hg	1,400	700
H^+-$CsCa_2Nb_3O_{10}$		Pt		8,300	10
$H^+CsLaNb_2O_7$		Pt		2,200	3
H^+-$KCa_2NaNb_4O_{13}$		Pt		18,000	39
H^+-$KCa_2Nb_3O_{10}$		Pt		19,000	8
H^+-$KLaNb_2O_7$		Pt		3,800	46
H^+-$KSr_2Nb_3O_{10}$		Pt		4,300	30
H^+-$RbCa_2Nb_3O_{10}$		Pt		17,000	16
H^+-$RbLaNb_2O_7$		Pt		2,600	2
$H_{1.8}Sr_{0.81}Bi_{0.19}Ta_2O_7$	3.88	None	400–450 W Hg	250	110
$H_2K_2Nb_6O_{17}$		Pt	500 W Hg–Xe	0.4	
$H_2La_{2/3}Ta_2O_7$	4	NiO_x	400–450 W Hg	940	459
$H_4Nb_6O_{17}$			100 W Hg	220	
$HCa_2Nb_3O_{10}$		Pt		19 mmol/h/g	
$HCa_2Nb_3O_{10}$		Pt	750 W Hg	78 per 0.1 g	None
$In_2O_3(ZnO)_3$	2.6	Pt for H_2	300 W Xe	1.1	1.3
In_2O_3/Cr:In_2O_3		NiO, Pt	Hg/Xe		
InP		Pt	250 W Hg	2–5 per 30 mg	
$K_{0.5}La_{0.25}Bi_{0.25}Ca_{0.75}Pb_{0.75}Nb_3O_{10}$		Pt	450 W Xe	Trace amounts	168 per 0.3 g
$KBa_2Ta_3O_{10}$	3.5	NiO_x	400–450 W Hg	170	
$KCa_2Nb_3O_{10}$		Pt	450 W Hg	100 per g	None
$KCa_2Nb_3O_{10}$		RuO_x	450 W Hg	96 per 0.3 g	47 per 0.3 g
KNb_3O_8, $KTiNbO_5$, $CsTi_2NbO_7$		Pt	500 W Hg/Xe	<0.2 per 0.1 g	
$KTaO_3$	3.6	Ni	400–450 W Hg	6	2
$KTaO_3$ doped with Ti		NiO	500 W Xe	100 per 0.1 g	30 per 0.1 g

(*continued*)

Table 1 (continued)

Photocatalyst	Band gap (eV)	Cocatalyst	Light source	H_2 activity (μmol/h)	O_2 activity (μmol/h)
$KTaO_3$:Zr	3.6	NiO_x	300–500 W Xe	9.4	4.2
$KTiNbO_5$	3.6	NiO_x	400–450 W Hg	30	10
$K_2PrTa_5O_{15}$	3.8	NiO	400–450 W Hg	1,550	830
$K_2SrTa_2O_7$	3.9	None	400–450 W Hg	374	192
$K_2Sr_{3/2}Ta_3O_{10}$	4.1	RuO_2	400–450 W Hg	100	39.4
$K_2Ta_2O_6$	4.5	NiO	400–450 W Hg	437	226
$K_3Ta_3Si_2O_{13}$	4.1	NiO	400–450 W Hg	390	200
$K_3Ta_3B_2O_{12}$	4	None	400–450 W Hg	2,390	1,210
$K_4Nb_6O_{17}$	3.4	NiO_x	400–450 W Hg	1,837	850
La:$NaTaO_3$		NiO	400 W Hg	19.8 per g	9.7 per g
$LaTaO_4$	3.9	NiO_x	400–450 W Hg	116	52
$LaInO_3$	4.1	RuO_2	400 W Xe or 200 W Hg/Xe	1	0.5
$LaTaO_2N$	2	Pt for H_2		20	
$La_{1/3}TaO_3$		NiO	400 W Hg	35 per 0.5 g	7.9 per g
La_3TaO_7	4.6	NiO_x	400–450 W Hg	164	80
La_3NbO_7	3.9	NiO_x	400–450 W Hg	35	17
La–In oxysulfide	2.6	Pt for H_2, IrO_2 for O_2		10	7
$LiCa_2Ta_3O_{10}$	4.2–4.3	NiO_x	400–450 W Hg	708	333
$LiTaO_3$	4.7	None	400–450 W Hg	430	220
$LiInGeO_4$	4.4	RuO_2		26	13
$M_3(PO_4)_4$ (M = Ti, Zr)		Pt	300 W Xe		
Mg–Ta Oxide		NiO	400–450 W Hg	102	51
$MnTa_2O_6$			400 W Hg	Trace	
MTa_2O_6			400 W Hg	Trace	

(*continued*)

Table 1 (continued)

Photocatalyst	Band gap (eV)	Cocatalyst	Light source	H_2 activity (μmol/h)	O_2 activity (μmol/h)
$MTaO_3$ (M = Li, Na, K)		NiO	400 W Hg	1,940 per g	1,000 per g
N-doped $CsCa_2Ta_3O_{10}$	2.1		300 W Xe		72
N-doped $CsCa_2Ta_3O_{10}$ nanosheet	2.1		500 and 300 W Xe	<1	<1
N-doped $K_4Nb_6O_{17}$, $KCa_2Nb_3O_{10}$			500 W Xe	1.2	
$Na_{0.5}Bi_{1.5}VMoO_8$	2.5	Pt for H_2			74
$(NaBi)_{0.5}MoO_4$	3.1	Pt		0.6	58
$(NaBi)_{0.5}WO_4$	3.5	Pt		7	1.3
$NaCa_2Nb_3O_{10}$		RuO_2	400–450 W Hg	118	56
$NaInO_2$	3.9	RuO_2		0.9	0.3
$NaInS_2$	2.3	Pt	303 W Xe	470	
$NaSbO_3$		RuO_2	200 W Hg/Xe	1.8 per 0.25 g	Stoich
$NaTaO_3$	4	NiO	400–450 W Hg	2,180	1,100
$NaTaO_3$:La	4.1	NiO	400–450 W Hg	19,800	9,700
$NaTaO_3$:Sr	4.1	NiO	400–450 W Hg	9,500	4,700
$Na_2Ta_2O_6$	4.6	NiO	400–450 W Hg	391	195
$[Na_5(H_2O)_6]^{5+}$ $[SIn_4(SIn_4)_{6/2}]^{5-}$	3.2		300 W Xe	2.4	
$Na_2W_4O_{13}$	3.1	Pt	400 W Hg	21	9
$Na_{10}In_{16}Cu_4S_{35}$	2		300 W Xe	9	
$NbSbO_3$	3.6	RuO_2		1.7	0.8
$NdTaO_4$		NiO	400 W Hg	Not significant	Not significant
$Ni/K_4Nb_6O_{17}$			300 W Xe	56	
Ni:$InTaO_4$, $InTaO_4$		RuO_2 or NiO	400 W Hg and 300 W Xe	16.6 per 0.5 g	8.3 per 0.5 g
Ni/Ti and Cu/Ti LDHs			400–700 nm Ze		8.167 and 5.167
Ni-Zn/Cr LDH			400 nm Hg	1,915	
$NiTa_2O_6$	3.7	None	400–450 W Hg	11	4
Pb:ZnS			300 W Xe	15 per g	
$PbBi_2Nb_2O_9$	2.88	Pt for H_2		3.2	520
$PbBi_2Nb_2O_9$		Pt	450 W Xe	7.6 per g	520 per g

(*continued*)

Table 1 (continued)

Photocatalyst	Band gap (eV)	Cocatalyst	Light source	H_2 activity (μmol/h)	O_2 activity (μmol/h)
$PbMoO_4$	3.31	Pt	200 W Hg	1.9	12.8
$PrTaO_4$		NiO	400 W Hg	Not significant	Not significant
Pt(in)/$H_4Nb_6O_{17}$			300 W Xe	94	
Pt/$AgGa_{0.9}In_{0.1}S_2$	2.4		450 W Hg	250	
Pt/$AgIn_5S_8$	1.8		400 W Xe	60	
Pt/$AgInZn_7S_9$	2.4		300 W Xe	940	
Pt/$BaTaO_2N$			300 W Xe	24	12
Pt/$CaTaO_2N$				6.6	3.3
Pt/$CaTaO_2N$				4	2
Pt/$Cu_{0.09}In_{0.09}Zn_{1.82}S_2$	2.35		300 W Xe	1,200	
Pt/[In(OH)ySz]:Zn	2.2		300 W Xe	67	
Pt/$NaInS_2$	2.3		300 W Xe	470	
Pt/TaON				3	1.5
Pt/TaON				15	7.2
Pt/$ZnIn_2S_4$	2.3		300 W Xe	77	
Pt/ZnO			500 W Xe	80.4	
$Rb_2La_2Ti_2Nb_2O_{10}$		Pt	450 W Hg	79 per g	Stoich
$Rb_4Nb_6O_{17}$	3.4	NiO_x	400–450 W Hg	936	451
$RbLaTa_2O_7$			450 W Hg		
$RbNdTa_2O_7$	3.9	NiO_x	400–450 W Hg	117	59
$RbPb_2Nb_3O_{10}$	2.5	Pt for H_2	500 W Xe	4	1.1
$RbPb_2Nb_3O_{10}$, $HPb_2Ng_3O_{10}$	2.5		420 nm Xe	15	1.1
$RbPrTa2O_7$			450 W Hg		
$RbWNbO_6$	3.6	NiO *x*	400–450 W Hg	11.4	4.3
$RbWTaO_6$	3.8	NiO *x*	400–450 W Hg	69.7	34.5
$Rb_4Ta_6O_{17}$	4.2	NiO	400–450 W Hg	92	46
Restacked ex-$Ca_2Nb_3O_{10}$/Na+		Pt		880	
Rh-doped $HCa_2Nb_{3-x}Rh_xO_{10-d}$ and $Ca_2Nb_{3-x}Rh_xO_{10-d}$			500 W Xe		
Rh/$AgGaS_2$	2.6		300 W Xe	1,340	
Rose Bengal-sensitized Mg/Al LDH			300 W Xe		

(*continued*)

Table 1 (continued)

Photocatalyst	Band gap (eV)	Cocatalyst	Light source	H_2 activity (μmol/h)	O_2 activity (μmol/h)
Ru/ $Cu_{0.25}Ag_{0.25}In_{0.5}ZnS_2$	2		300 W Xe	2,300	
RuP^{+2}-sensitized $HCa_2Nb_3O_{10}$			300 W Xe	7.1	
SiO_2-pillared $K_2Ti_{2.7}Mn_{0.3}O_7$		None		320	
SiO_2-pillared $KCa_2Nb_3O_{10}$		Pt		10,800	
$SmTaO_4$		NiO	400 W Hg	Not significant	Not significant
Sn^{2+}-doped $K_4Nb_6O_{17}$, $CsTi_2NbO_7$	2.5–2.8		300 W Xe	54	4
$SnNb_2O_6$	2.3	Pt for H_2, IrO_2 for O_2	300 W Xe	14.4	62.8
$SnTa_2O_6$		Pt	400 W Hg	2.1 per 0.3 g	
$SrIn_2O_4$	3.6	RuO_2	400 W Xe or 200 W Hg/Xe	7	3
$SrTaO_2N$	2.1	Pt for H_2		20	
$SrTa_2O_6$	4.4	NiO	400 W Hg	960 per g	490 per g
$Sr_2Nb_2O_7$		NiO	450 W Hg	110 per g	36 per g
$Sr_2Sb_2O_7$	4	RuO_2	200 W Hg/Xe	8	3
Sr_2SnO_4		RuO_2	400 W Hg	5	2.5
$Sr_2Ta_2O_7$	4.6	NiO	400–450 W Hg	1,000	480
$Sr_4Ta_2O_9$		NiO	401 W Hg	32 per 0.5 g	2 per 0.5 g
$Sr_5Ta_4O_{15}$	4.75	NiO	400–450 W Hg	1,194	722
Ta_3N_5	2.1	Pt for H_2		10	420
Ta_3N_5		Pt	300 W Xe	1.8 per 0.2 g	100 per 0.2 g
TaON	2.5	RuO2 for H_2	300 W Xe	120	380
Ta_2O_5	4	NiO_x	400–450 W Hg	1,154	529
$TiSi_2$	3.4–1.5		Halogen lamp	1,000 per g	
$Ti_{1.5}Zr_{1.5}(PO_4)_4$	3.8	Pt		11.8	
$TiN_x O_y F_z$	2.2				30
$Y_2Ta_2O_5N_2$	2.2	Pt–Ru for H_2		250	140

(*continued*)

Table 1 (continued)

Photocatalyst	Band gap (eV)	Cocatalyst	Light source	H_2 activity (μmol/h)	O_2 activity (μmol/h)
$Y_2Ta_2O_5N_2$			300 W Xe	250 per 0.3 g	140 per 0.3 g
Y_3TaO_7		NiO	400 W Hg	Trace	
Yb_3TaO_7		NiO	400 W Hg	Trace	
$Y_x\ In_{2-x}\ O_3$	4.3	RuO_2		8	4
Zn/Ti, Zn/Ce, Zn/Cr LDHs			400 nm Xe		
Zn/Cr LDH nanosheet hybrid	2.9		450 W Xe	1,200 per g	
$Zn:Lu_2O_3/Ga_2O_3$		NiO	400 W Hg	50.2 per 0.25 g	26.7 per 0.25 g
$Zn_{1.44}GeN_{2.08}O_{0.38}$		RuO_2	450 W Hg	54.3 per 0.2 g	27.5 per 0.2 g
$ZnGa_2O_4$	4.2	RuO_2	200 W Hg/Xe	10	4
Zn_2GeO_4	4.6	RuO_2	Hg/Xe	22	10
Zn_2GeO_4		RuO_2	Hg/Xe	22	10
$Zn_3V_2O_8$	2.92	Pt for H_2			10.2
ZnNb2O6	4	NiO_x	400–450 W Hg	54	21
$ZnNb_2O_6$		NiO	400–450 W Hg	54 per g	21 per g
$Zr:NaTaO_3$		Pt	500 W Xe	57 per 0.1 g	28 per 0.1 g
ZrO_2		$NaHCO_3$	400 W Hg	309 per g	167 per g
ZrO_2	5	None	400–450 W Hg	72	36
β-Ga_2O_3	4.6	Pt		50	7

good mimics for the visible solar spectrum. Later, in the section of this chapter describing carbon dioxide reduction, a photograph of a photocatalytic setup employing a 450 W Xe arc lamp is shown.

The materials in Table 1 are grouped as best as possible into categories based on the photocatalytic material. These include materials based off of Honda and Fujishima's original choice, TiO_2, or materials that incorporate tungsten or sulfides. Mixed materials with multiple metals are evident with such combinations changing not only the band gap of the photocatalyst but also the crystal structure and geometry of the photocatalyst surface. Such considerations are important when trying to develop a photocatalyst that not only has the correct electronic properties but also allows for effective charge separation. In addition to metal oxides, both CdS and ZnS have proven to be successful photocatalytic materials for water splitting. Of these two, CdS offers the added benefit of access to visible regions of the electromagnetic

spectrum with a band gap of only 2.4 eV, which corresponds to the green (~515 nm) region of the spectrum. Unfortunately, however, these materials exhibit instability due to photoanodic corrosion. One of the most popular new building blocks for photocatalytic water splitting is graphene oxide (Xie et al. 2013).

Photocatalytic CO_2 Reduction

The facile conversion of carbon dioxide to usable forms such as methane or ethanol would solve two important problems simultaneously. Not only would there be an outlet for the ever-growing supply of CO_2 gas, but concerns over dwindling energy supplies would also be partially mediated. The process for the photocatalytic reduction of carbon dioxide resembles that of water splitting, but rather than having just one reactant (two water molecules) and one set of products (H_2 and O_2), multiple reactants and a variety of products can be obtained. The resulting products depend upon the use of specific semiconductor materials and the choice of reductant. Possible products include carbon monoxide, alkanes, alcohols, aldehydes, ketones, and carboxylic acids.

The photoreduction of carbon dioxide in aqueous solution was first demonstrated by Inoue et al. in 1979 using mercury and xenon arc lamps for excitation. In that report, formaldehyde (HCHO), formic acid (HCOOH), methanol (CH_3OH), and methane were produced using water as the reductant. The authors compared a number of photocatalysts that included TiO_2, WO_3, ZnO, CdS, GaP, and SiC. The band structures of most of these materials are shown in Fig. 4. Equations 4, 5, 6, 7, 8, 9, 10, 11, and 12 detail the important reactions that lead to the various observed organic products in this and later studies:

$$\text{Initial Oxidation} : 2h^+ + H_2O \rightarrow \frac{1}{2}O_2 + 2H^+ \tag{4}$$

$$\text{Initial Reduction} : e^- + H^+ \rightarrow {}^\bullet H \tag{5}$$

$$\text{Initial Reduction} : e^- + CO_2 \rightarrow {}^\bullet CO_2^- \tag{6}$$

$$\text{Subsequent Reactions} : {}^\bullet CO_2^- + 8{}^\bullet H + h^+ \rightarrow CH_4 + 2H_2O \tag{7}$$

$${}^\bullet CO_2^- + 6{}^\bullet H + h^+ \rightarrow CH_3OH + H_2O \tag{8}$$

$${}^\bullet CO_2^- + 2{}^\bullet H + h^+ \rightarrow CO + H_2O \tag{9}$$

$${}^\bullet CO_2^- + 2{}^\bullet H + h^+ \rightarrow HCOOH \tag{10}$$

$${}^\bullet CO_2^- + 4{}^\bullet H + h^+ \rightarrow HCHO + H_2O \tag{11}$$

$${}^\bullet CO_2^- + 12{}^\bullet H + 2h^+ \rightarrow C_2H_5OH + 3H_2O \tag{12}$$

Heterogeneous CO_2 Reduction

Shown in Fig. 6 is a photograph of a setup employed at the University of Mississippi for the photocatalytic reduction of carbon dioxide (Chen et al. 2012). A 450 W Xe arc lamp is employed as a substitute for solar radiation. The light is directed using a high-reflection focusing mirror into a flask containing the reaction solution. This solution contains the photocatalyst (such as TiO_2), gaseous CO_2, water, and other reductants. After irradiation for an extended period of time (6–10 h), the resulting hydrocarbon products can be determined using quantitative and qualitative analytical methods. Compared to water splitting, photocatalytic carbon dioxide reduction is much less developed in the literature. Since Inoue's first report, a number of new photocatalytic materials have been developed in attempts to improve upon both the conversion efficiency of carbon dioxide to hydrocarbons and the variety of hydrocarbon products possible. A number of excellent reviews summarize this work and Table 2 lists a number of these studies (Usubharatana et al. 2006; Hernández-Alonso et al. 2009; Habisreutinger et al. 2013; Izumi 2013; de Richter et al. 2013; Dhakshinamoorthy et al. 2012; Liu et al. 2012; Tahir and Amin 2013; Roy et al. 2010; Kondratenko et al. 2013; Kočí et al. 2008; Navalón et al. 2013).

As in the case of photocatalytic water splitting, TiO_2-based materials dominate the carbon dioxide reduction literature. This includes pure TiO_2 with varying choice of reductants or TiO_2 doped with other species such as copper (Cu) that aid in red-shifting the absorption profile more into the visible region of the electromagnetic spectrum. The reasons for the dominance of TiO_2 in both water splitting and carbon dioxide reduction include TiO_2's good photoactivity, inertness, ready availability,

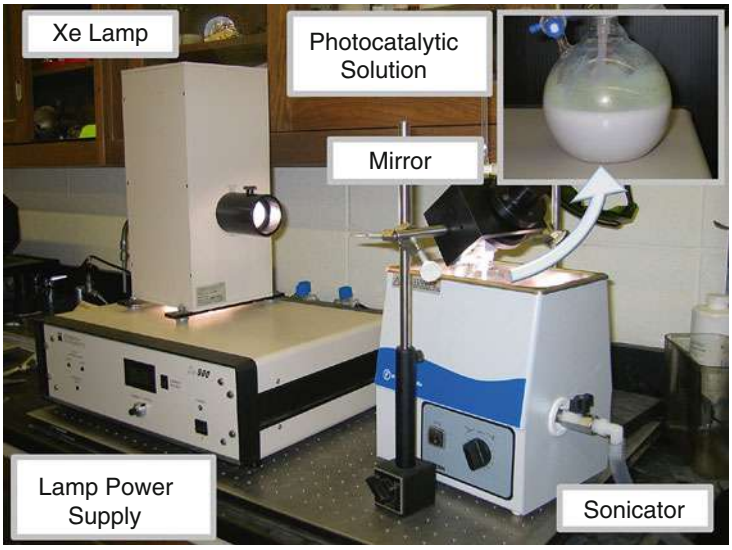

Fig. 6 Photograph of a setup employed at the University of Mississippi for the photocatalytic reduction of carbon dioxide

Table 2 Materials for photocatalytic carbon dioxide reduction

Photocatalyst	Band gap (eV)	Reductants	Light source	Products
TiO_2-based photocatalysts				
Ag–$BaLa_4Ti_4O_{15}$			400 W HP Hg	CO, HCOOH
Ag–$CaLa_4Ti_4O_{15}$			400 W HP Hg	CO, HCOOH
Ag–$SrLa_4TiO_{15}$			400 W HP Hg	CO, HCOOH
Ag–TiO_2			8 W Hg	CH_4, CH_3OH
Ag–TiO_2 (Nafion membrane)			990 W Xe	CH_3OH, HCOOH
AgBr–TiO_2			150 W Xe	CH_3OH, CH_2H_3OH, CH_4, CO
$Ag/ALa_4Ti_4O_{17}$ (A: Ca,Sr,Ba)				CO, HCOOH, H_2, O_2
$BaTiO_3$	3.2			HCOOH, HCHO
C-doped TiO_2				HCOOH
C-doped TiO_2			175 W Hg	HCOOH
CdSe-Pt/TiO_2			300 W Xe	CH_4, CH_3OH
0.5 wt % CeO_2 over TiO_2			Visible light	H_2, CH_4
CeO_2–TiO_2			300 W Xe arc lamp	CO, CH_4
Co-Pc/TiO_2			500 W W halogen	HCOOH
Cr-doped multifilm layers of TiO_2			Xe	CO, CH_4, C_2H_6
Cu/CdS–TiO_2/SiO_2			125 W Hg ultrahigh pressure	CH_3COCH_3
Cu–Fe/TiO_2			150 W Hg	H_2, CH_4
Cu–N–TiO_2NT			Sun	CH_4
Cu/TiO_2	3.2	Water	450 W Xe	CH_4, C_2H_4
Cu/TiO_2	3.2	Water	Hg	CH_3OH
Cu/TiO_2, sol–gel prepared	3.2	NaOH solution	Hg	CH_3OH
Cu/TiO_2, sol–gel prepared Cu/P-25		NaOH solution	Hg	CH_3OH, O_2
1.2 % Cu/TiO_2			16 W/cm^2 Hg	CH_3OH
2 % Cu/TiO_2			8 W Hg	CH_3OH
3 % CuO/TiO_2			2,450 uW/cm^2	CH_3OH
Iodine-doped TiO_2			450 W Xe	CO
$K_2Ti_6O_{13}$	>3.0			CH_4
N–Ni–TiO_2			15 W UV	CH_3OH
Nd(0.2 wt %)/TiO_2			UV	CH_3OH
PbS–Cu/TiO_2			300 W Xe	CO, CH_4

(*continued*)

Table 2 (continued)

Photocatalyst	Band gap (eV)	Reductants	Light source	Products
Pd-loaded TiO_2			500 W Hg	CH_4
Pt-loaded exchanged TiO_2–Y zeolite			Hg	CH_4, CH_3OH
Pt–TiO_2 (nanorods)			300 W Xe	CH_4
Pt–TiO_2 (nanotubes)			Sunlight	CH_4
Rh/TiO_2	3.2		500 W HP Hg	CO, CH_4
Rh/WO_3–TiO_2			500 W HP Xe	HCOOH
Rh/WO_3–TiO_2 (reduced)			500 W HP Xe	CH_3OH
Ru/RuOx/TiO_2				CH_4
$SrTiO_3$	3.2			CH_4
TiO_2	3.2	CH_3OH, ethanol, 2-propanol, and nitric, hydrochloric, and phosphoric acids	0.96 kW Xe	HCOOH
TiO_2	3.0–3.5	Water	75 W Hg	CH_4, CH_3OH, CO
TiO_2	3.2	Water	75 W Hg	CH_4, CH_3OH, CO
TiO_2	3.0	Water in NaOH solution	4.5 kW Xe	HCOOH, CH_3OH, CH_3CH_2OH, CH_4, C_2H_6, C_2H_4
TiO_2	3.0	2-propanol	4.2 kW Xe	CH_4, HCOOH
TiO_2	3.2	Water	Hg	CH_4
TiO_2	3.2	Water	Hg	CH_4, H_2, CO
TiO_2	3.2	Water	Hg	CH_4, CHOOH, CH_3CH_2OH
TiO_2 in liquid CO_2	3.0	Water	990 W Xe	HCOOH
TiO_2/Cu–TiO_2	3.3	NaOH solution	Hg	CH_3OH
TiO_2/zeolite	3.2	Water	75 W Hg	CH_4
TiO_2/zeolite, TiO_2/ molecular sieves	3.2	Water vapor	Hg	CH_3OH
TiO_2 nanocrystals in SiO_2	3.9	2-propanol	500 W Hg	CO, $HCOO^-$
TiO_2-SiO_2	3.6	Acetyl acetone	Solar 6.35 mW/cm^2	CH_4
TiO_2-SiO_2 with Cu and Fe	3.6	Acetyl acetone	Solar 2.05 mW/cm^2	CH_4, C_2H_4
TiO_2 supported on SiO_2			1,000 W Hg	H_2, HCOOH, CH_4, CH_2O, CH_3OH
TiO_2 nanocrystals in SiO_2	3.9	Lithium nitrate in 2-propanol	500 W Hg	CO, $HCOO^-$, NH_3, $(NH_2)_2CO$
TiO_2 with MWCNTs			UV	CH_2CH_3OH, HCOOH, CH_4

(*continued*)

Table 2 (continued)

Photocatalyst	Band gap (eV)	Reductants	Light source	Products
Ru-TiO_2/SiO_2	3.2	Water	1,000 W Hg	HCOOH, CH_2O, H_2, CH_4, CH_3OH
Rh/TiO_2	3.2	Hydrogen	Hg	CO, CH_4
TiO_2/Pd/Al_2O_3,TiO_2/Pd/SiO_2 CuO/ZnOand Li_2O/TiO_2 supported over MgO, Al_2O_3		Water	Hg	$(CH_3)_2CO$, CH_4, C_2H_6, HCHO, HCOOH, CH_3OH, C_2H_5OH
Pd/RuO_2/TiO_2, Pd/TiO_2		Aqueous Na_2SO_3 and NaOH	450 W Xe	$HCOO^-$
Pt/$K_2Ti_6O_{13}$ with Fe-based catalyst		Water	300 W Xe and 150 W Hg	H_2, CH_4, HCHO, HCOOH, CH_3OH, C_2H_5OH
Y-doped TiO_2			300 W Hg	HCHO
Zn–Pc/TiO_2			500 W W halogen	HCOOH
Sulfides				
Bi_2S_3/CdS	1.28			CH_3OH
CdS	2.4			CO
CdS	2.4			$C_2O_4O^{-2}$
CdS surface modified by DMF	2.4	Triethylamine	300 W halogen tungsten	Not reported
CdS surface modified by thiol	2.4	Propanol	500 W Hg	$HCOO^-$, CO, H_2, $(CH_3)_2CO$
Cu_2ZnSnS_4	1.5			HCOOH
CuxAgyInzZnkSm	1.4			CH_3OH
MnS	3			HCOOH
ZnS	3.66			HCOOH
ZnS	3.66			HCOOH
CdS-montmorillonite			8 W Hg	CH_4
Bi_2S_3/CdS:Bi_2S_3			500 W Xe	CH_3OH
$Rh_{1.32}Cr_{0.66}O_3$/Cu_xAg_y/In_2Zn_kSm			1,000 W/m^2 Xe	CH_3OH
ZnS–MMT			8 W Hg	CH_3OH,CH_4,CO, H_2,O_2
ZnS microcrystal			UV Hg	CH_3OH
ZnS nanocrystal			Hg	HCOOH
Oxides				
Bi_2WO_6	2.75			CH_4
$BiVO_4$	2.24			C_2H_5OH
$BiWO_6$			300 W Xe arc	CH_4
$Ce_{0.97}Ru_{0.03}O_2$				CH_4
Cu_2O/SiC:Cu_2O			500 W Xe	CH_3OH

(*continued*)

Table 2 (continued)

Photocatalyst	Band gap (eV)	Reductants	Light source	Products
Cu-$BaLa_4Ti_4O_{15}$			400 W HP Hg	CO
$CuGaO_2$	2.6			CO
Cu–ZnO			500 W Xe arc	CO
α-Fe_2O_3	2.2			
Ga_2O_3			300 W Xe	CO, H_2, C_2H_6
α-Ga_2O_3			500 W Xe arc	CO
β-Ga_2O_2			200 W Hg–Xe	CO
β-Ga_2O_3	4.9			CO
HNb_3O_8	3.66			CH_4
$In_2Ge_2O_7$	3.98			CO
$InNbO_4$	2.5			CH_3OH
$InTaO_4$	2.6			CH_3OH
$KNbO_3$	3.1			CH_4
MgO			500 W Hg ultrahigh	CO, H_2
MgO_2			500 W HP Hg	CO
N-Ta_2O_5	2.4			HCOOH
$NaNbO_3$	3.29			CH_4
Ni@NiO/N-doped $InTaO_4$			Xe	CH_3OH
N-$InTaO_4$	2.28			CH_3OH
NiO				CH_3OH
NiO(1 wt %)/$InTaO_4$			500 W halogen	CH_3OH
NiO(2.6 wt %)/ $InTaO_4$			300 W Xe	C_2H_4O
NiO/$InNbO_4$;Co_3O_4/ $InNbO_4$			500 W halogen lamp	CH_3OH
NiO/$InTaO_4$ (Optical fiber)			100 W halogen lamp	CH_3OH
Pd–Mg/SiO_2				CH_4
Pd–Ni/SiO_2				CH_4
Pt/meso-ZNGO			300 W Xe	CH_4
Pt/$NaNbO_3$			300 W Xe	CH_4
Pt–$K_2Ti_6O_{13}$				H_2,HCOOH, CH_2O, CH_4, CH_3OH
Pt–$NaNbO_3$			300 W Xe arc	CH_4
RuO_2			1,000 W m-2 Xe	CH_3OH
RuO_2–Pt–Zn_2GeO_4				CH_4
RuO_2–$Zn_{1.7}GeN_{1.8}O$			300 W Xe	CH_4

(*continued*)

Table 2 (continued)

Photocatalyst	Band gap (eV)	Reductants	Light source	Products
RuO_2–Zn_2GeO_4				CH_4
V_2O_3	2.7			
$W_{18}O_{49}$	2.7			CH_4
$W_{18}O_{49}$			300 W Xe	CH_4
WO_3	2.79			CH_4
$Zn_{1.7}GeN_{1.8}O$	2.6			CH_4
Zn_2GeO_4	4.5			CH_4
Zn_2GeO_4	4.65			CO
Zn_2SnO_4	3.87			CH_4
$Zn_2Ga_2O_4$				
$Zn_2Ga_2O_4$;RuO_2/$ZnGa_2O_4$			300 W Xe	CH_4
ZnGaNO-modified $Pt/ZnAl_2O_4$			300 W Xe	CH_4
ZnGaNO-modified $Pt/ZnAl_2O_4$			300 W Xe	CH_4
ZnO				CH_3OH
ZnO on activated carbon	3		Xe	CO, H_2
$Zn_xGe_yO_zN_k$	2.7			CH_4
ZrO_2			500 W HP Hg	CO
Phosphides				
GaP	2.3			CH_3OH
GaP			500 W Xe/HP Hg	CH_2O
Inp	1.35			HCOOH
Other photocatalysts				
Au or Pt/carbon nanoparticles			Visible light	HCOOH
$BaLa_4Ti_4$	3.8			CO
$Co(bpy)_3^{2+}$ sensitized with $Ru(bpy)_3^{2+}$		DMF/TEOA, DMF/H_2O/TEOA	Xe	CO, H_2
Cu-p-SiC			Hg	CH_4
MgO	8.7	Hydrogen	500 W Hg	CO
10Ni–CZ				CH_4
Ni–MCM-41				CH_4
$Pt/K_2Ti_6O_{13}$ $^+$Fe-Cu-K-DAY			Sunlight	CH_4, HCOOH, CH_3OH, CH_3CH_2OH, H_2CH_3OH, HCHO, HCOOH, H_2

(*continued*)

Table 2 (continued)

Photocatalyst	Band gap (eV)	Reductants	Light source	Products
[*fac*-Re(bpy)-$(CO)_3$(4-Xpy)]$^+$		TEOA/DMF	500 W Hg	CO, H_2
[*fac*-Re(bpy)-$(CO)_3$Cl]		Et3N/DMF	500 W Hg	CO, H_2
[*fac*-Re(bpy)-$(CO)_3$P$(O^iPr)_3$]$^+$		TEOA/DMF	500 W Hg	CO, H_2
Ru-bipyridine-Co (II) chloride			Visible light	CO
Ti-containing mesoporous silica thin film	4.0–5.0	Water vapor	100 W Hg	CH_4, CH_3OH
Ti–MCM-41 and Ti–MCM-48	4.0–5.0	Water vapor	Hg	CH_4, CH_3OH
Ti–PVG			UV	CH_4
Ti–PVG			75 W HP Hg	CH_4
Ti-SBA-15			100 W HP Hg	CH_4, CH_3OH
Ti-SBA-15			120 W HP Hg	C_2H_6, CH_4, C_2H_4
Ti/Si-h-c			100 W Hg high pressure	CH_3OH, CH_4
Ti–Y zeolite			HP Hg	CH_4, CH_3OH
Ti-β zeolite	4.75–6.0	Water vapor	100 W Hg	CH_4, CH_3OH
Ti silicalite molecular sieve	4.0–5.0	CH_3OH	266-nm Nd: YAG laser	HCO_2H, CO, HCO_2CH_3
ZrO_2	5.0	Hydrogen	500 W Hg	CO
ZrO_2	5.0	Hydrogen	500 W Hg	CO
ZrO_2	5.0	CH_4	500 W Hg	CO
ZnO on activated carbon	3.0		Xe	CO, H_2

processability, abundance, resistance to corrosion, and low cost (Kočí et al. 2008). Newer materials based on materials such as WO_3 offer alternatives to TiO_2, but to date, titanium dioxide remains the most successful and widely employed material. For carbon dioxide reduction, using water as a reductant is a cheap and effective option that would be ideal for widespread adoption of this technology. However, the solubility of carbon dioxide in water is low, and the reduction of CO_2 in water has to compete with the formation of hydrogen gas (H_2) and hydrogen peroxide (H_2O_2). For these reasons, other reductants and mixtures of various reductants in different conditions have been investigated. In particular, the use of basic solution offers advantages over pure water with hydroxide ions acting as hole scavengers and extending the recombination time of the electron–hole pairs (Kočí et al. 2008; Tseng et al. 2002).

Homogeneous CO_2 Reduction

Homogeneous catalysis offers the opportunity to relatively simply and precisely tune catalyst structures leading to changes in properties such as product selectivities and catalyst photoreduction rates. Homogeneous photocatalytic reduction of CO_2 has received less attention than the heterogeneous counterpart and is in a relatively early stage of development with initial reports in molecular catalysis dating to circa 1980. Currently, the homogeneous photocatalysis field is undergoing a resurgence in activity which has led to several excellent reviews (Reithmeier et al. 2012; Benson et al. 2009; Xiaoding and Moulijn 1996; Morris et al. 2009; Savéant 2008; Mikkelsen et al. 2010; Schneider et al. 2012).

Several major challenges face homogeneous catalysis including catalyst lifetimes, catalytic rates, and electron/proton sources. Ideally, the stability of semiconductor-based photocatalysts and the selectivity of photocatalyst systems could be combined to give long-lasting selective photocatalytic systems. Several noteworthy examples have arisen exploring this concept with highly encouraging catalyst lifetime improvements (Kumar et al. 2012; Anfuso et al. 2012; Linsebigler et al. 1995; Wang et al. 2011; Sekizawa et al. 2013; Ha et al. 2014; Kou et al. 2014; Ettedgui et al. 2011). This chapter will focus on various molecular catalyst systems, which have been explored in fully homogenous reactions.

The single-electron reduction of CO_2 is highly unfavorable and occurs near -1.90 V versus normal hydrogen electrode (NHE). The lowest energy pathways to CO_2 reduction involve simultaneous multiple electron and proton transfers which are detailed below versus NHE.

$$CO_2 + e^- \rightarrow {}^{\bullet}CO_2^- \quad E^o = -1.90 \text{ V} \tag{13}$$

$$CO_2 + 2H^+ + 2e^- \rightarrow CO + H_2O \quad E^o = -0.53 \text{ V} \tag{14}$$

$$CO_2 + 2H^+ + 2e^- \rightarrow HCO_2H \quad E^o = -0.61 \text{ V} \tag{15}$$

$$CO_2 + 4H^+ + 4e^- \rightarrow HCHO + H_2O \quad E^o = -0.48 \text{ V} \tag{16}$$

$$CO_2 + 6H^+ + 6e^- \rightarrow CH_3OH + H_2O \quad E^o = -0.38 \text{ V} \tag{17}$$

$$CO_2 + 8H^+ + 8e^- \rightarrow CH_4 + H_2O \quad E^o = -0.24 \text{ V} \tag{18}$$

One of the key challenges in molecular photocatalysis is the storage of electrons to deliver to CO_2 in the presence of H^+ sources. This is in stark contrast to homogeneous semiconductor catalysts where large numbers of available electrons are often readily available in the semiconductor conduction band. However, the practical restrictions (i.e., number of reduction potentials) on the number of electrons which may be "stored" with molecular catalysts are in part responsible for the excellent selectivities of homogeneous catalysts for the formation of CO and HCO_2H. These products are at the balance between the *number* of electrons needed for reduction versus reduction potential. The selectivity for these products and the ease of

separation from one another (gas–liquid separation) has in part fueled the recent boom in molecular catalysis. Either product is highly desirable with the potential conversion into synthetic fuels via processes such as the *Fischer–Tropsch synthesis*.

A second concern in homogeneous photocatalysis is many of the catalysts and photosensitizers used are commonly soluble in organic solvents with low solubility and stability in H_2O. This has led to the common use of organic proton and electron sources and restricted available solvents to those with high solubilities for CO_2 such as DMF and H_2O. However, care must be taken when using solvents such as DMF, which have the potential to decompose to CO and HCO_2H under UV irradiation or in the presence of Lewis acids. *DMF as a solvent* in particular has led to a desire for careful background reaction measurements, *light source cutoff filters, and* ^{13}*C-labeling studies to* verify the carbon source for the products. The use of an organic electron and proton source has enabled the exploration of molecular photocatalysts, but has come with the cost of threatening practicality in generating a carbon-based waste during the reduction of CO_2 to desirable products (such as fuels) at a tremendous scale. Ideally, the electron and proton source should be derived either directly or indirectly from H_2O. To date, a single homogeneous catalyst system has emerged, which does not generate a carbon-based wasted during CO_2 reduction. The rhenium polyoxometalate-based catalyst developed by Neumann (Ettedgui et al. 2011) has demonstrated the potential for a homogeneous catalyst which undergoes a reverse water–gas shift (rWGS) reaction, as shown in Fig. 7.

This catalyst uses H_2 as a proton and electron source for the reduction of CO_2 to CO and H_2O. While this catalyst is a novel step toward practicality in terms of starting material conversion to desirable products for large-scale applications, it is limited in turnover numbers (TON, ~22) and turnover frequency (TOF, ~1.5/h) before the catalyst is rendered inactive.

The remaining catalyst examples shown in Figs. 8 and 9 will focus on systems, which use common organic amine proton and electron sources such as triethylamine (TEA) and triethanolamine (*TEOA*) in solvent quantities (Fig. 9). Table 3 summarizes the properties of these systems.

Very few catalysts have been demonstrated to operate effectively in the absence of a photosensitizer. The added demand of light absorption to CO_2 reduction processes limited catalyst variability to Re-pyridyl, Ru-pyridyl, Ir-pyridyl, and porphyrin-based complexes along with a few organic catalysts. The most well-

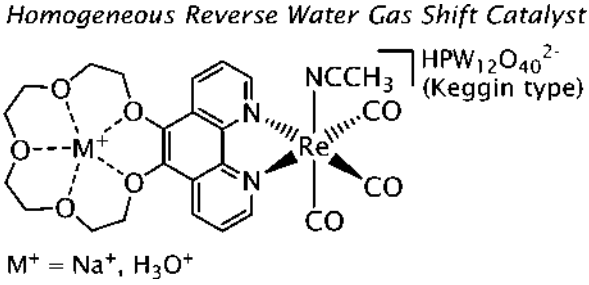

Fig. 7 Homogeneous *reverse water–gas shift* catalyst

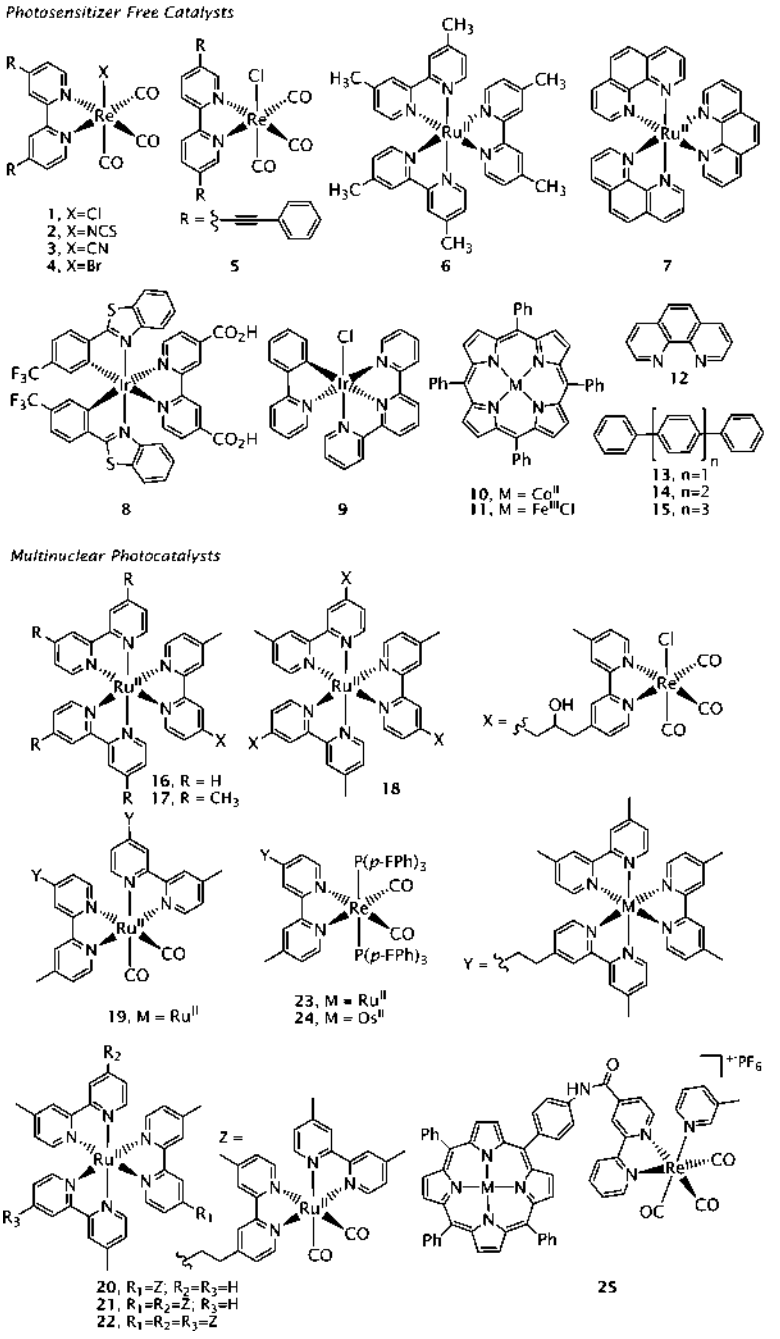

Fig. 8 Materials for homogeneous photocatalytic carbon dioxide reduction: photosensitizer-free catalysts and multinuclear photocatalysts

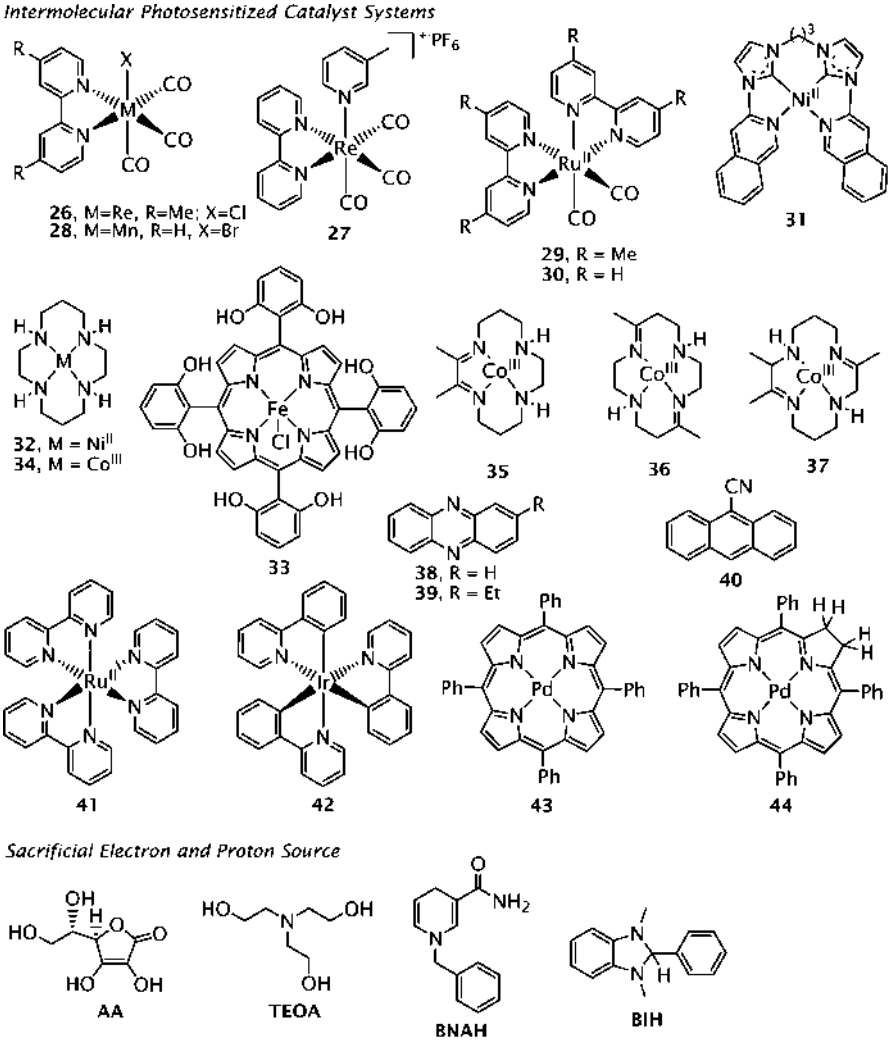

Fig. 9 Materials for homogeneous photocatalytic carbon dioxide reduction: intermolecular photosensitized catalyst systems, sacrificial electron, and proton source

studied molecular catalysts for CO_2 reduction are based on rhenium bipyridyl analogues, which are highly selective for CO product formation. The first example of this catalyst was discovered in the early 1980s (Takeda et al. 2008)and has been explored as a standard for comparison as well as a common catalyst for developing multinuclear as well as semiconductor-bound novel systems. The initial *Re catalyst* (**1**) has a coordinated chlorine atom and operates for 15 turnovers in the presence of *TEOA* with a 500 W Hg lamp. Exchange of the anionic ligand $^{-}$NCS (**2**) led to a doubling of the TON while introduction of a $^{-}$CN (**3**) ligand rendered the catalyst

Table 3 Materials for homogeneous photocatalytic carbon dioxide reduction

CO_2 red. catalyst	Photosensitizer	Electron, proton, additive source	Light	CO (TON)	HCO_2H (TON)	Solvent	φ	References
Photosensitizerfree catalysts								
1	–	TEOA	500 W Hg	15	–	DMF	–	(Takeda et al. 2008)
1	–	TEOA	250 W	27	–	DMF	–	(Hawecker et al. 1983)
1	–	TEOA, NEt_4Cl	250 W	48	–	DMF	–	(Hawecker et al. 1983)
2	–	TEOA	500 W Hg	30	–	DMF	–	(Takeda et al. 2008)
3	–	TEOA	500 W Hg	0	–	DMF	–	(Takeda et al. 2008)
4	–	TEOA	250 W	20	–	DMF	–	(Hawecker et al. 1983)
5	–	TEOA	>360 nm	~1.2	–	DMF	–	(Portenkirchner et al. 2012)
6	–	TEOA, BNAH	480 nm	3	25	DMF	–	(Takeda et al. 2014)
6	–	TEOA, BNAH	480 nm	2	14	MeCN	–	(Takeda et al. 2014)
7	–	AA, pyridine	LED	–	9[b]	H_2O	0.003	(Boston et al. 2013)
7	–	AA, pyridine, KCl	LED	–	76[b]	H_2O	0.025	(Boston et al. 2013)
7	–	AA, pyridine, KCl	LED	–	76[b]	H_2O	0.025	(Boston et al. 2013)
8	–	Water	>420 nm	80 ppm	–	water	–	(Yuan et al. 2011)
9	–	TEOA	>410 nm	80	–	MeCN	–	(Sato et al. 2013)
10	–	TEA	300 W Xe	80	–	MeCN	–	(Behar et al. 1998)
11	–	TEA	300 W Xe	70	–	DMF	0.05	(Grodkowski et al. 1997)
$CoCl_2$*12	–	TEA, H_2O	1,000 W Xe	0.5[a]	–	MeCN	–	(Lehn and Ziessel 1982)
$CoCl_2$*12	–	TEOA, H_2O	1,000 W Xe–Hg	2.6	–	MeCN	–	(Lehn and Ziessel 1982)
13°	–	TEA	>290 nm	0.1	4.0	DMF	0.07	(Matsuoka et al. 1992)
13	–	TEA	>290 nm	trace	2.0	MeCN	–	(Matsuoka et al. 1992)
13	–	TEA	>290 nm	0.1	1.0	DMF	–	(Matsuoka et al. 1992)
14	–	TEA	>290 nm	0.3	2.8	DMF	0.08	(Matsuoka et al. 1992)
15	–	TEA	>290 nm	0.1	0.7	DMF	–	(Matsuoka et al. 1992)
Multinuclear photocatalysts								
16	Bound	TEOA, BNAH	Hg	50	–	DMF	0.120	(Gholamkhass et al. 2005)

17	Bound	TEOA, BNAH	Hg	170	–	DMF	–	(Gholamkhass et al. 2005)
18	Bound	TEOA, BNAH	Hg	240	–	DMF	0.093	(Gholamkhass et al. 2005)
19	Bound	TEOA, BNAH	500 W Xe	–	562	DMF	0.04	(Tamaki et al. 2012a)
19	Bound	TEOA, BNAH-OMe	500 W Xe	–	671	DMF	0.06	(Tamaki et al. 2012a)
20	Bound	TEOA, BNAH	500 W Xe	13	315	DMF	0.04	(Tamaki et al. 2012a)
21	Bound	TEOA, BNAH	500 W Xe	315[d]	353[d]	DMF	0.03	(Tamaki et al. 2012a)
22	Bound	TEOA, BNAH	500 W Xe	358[d]	234[d]	DMF	0.02	(Tamaki et al. 2012a)
23	Bound	BNAH, TEOA	>500 nm	207	–	DMF	0.15	(Tamaki et al. 2012b)
23	Bound	BIH, TEOA	>500 nm	3,029	–	DMF	0.45	(Tamaki et al. 2013a)
24	Bound	BIH, TEOA	>620 nm	1,138	–	DMF	0.12	(Tamaki et al. 2013b)
25	Bound	TEA	>420 nm	1	–	DMF	–	(Schneider et al. 2011)
25	Bound	TEA	>420 nm	1	–	DMF	–	(Schneider et al. 2011)
Intermolecular photosensitized catalyst systems								
$CoCl_2$	13	TEA, MeOH	UV*	–	–	MeCN	–	(Matsuoka et al. 1993; Ogata et al. 1995a)
$CoCl_2$	41	TEOA, H_2O	1,000 W Xe	0.8[a]	–	MeCN	–	(Lehn and Ziessel 1982)
$CoCl_2$*12	41	TEOA, H_2O	1,000 W Xe	0.2[a]	–	MeCN	–	(Lehn and Ziessel 1982)
$CoCl_2$*12	41	TEOA	250 W	4	–	DMF	–	(Hawecker et al. 1983)
10	13	TEA	300 W Xe	6	5	MeCN	–	(Dhanasekaran et al. 1999)
11	13	TEA	300 W Xe	4	5	MeCN	–	(Dhanasekaran et al. 1999)
26	6	TEOA, BNAH	Hg	101	–	DMF	0.062	(Gholamkhass et al. 2005)
27	41	TEA	>420 nm	10	–	DMF	–	(Schneider et al. 2011)
27	43	TEA	>420 nm	3	–	DMF	–	(Schneider et al. 2011)
27	44	TEA	>420 nm	9	–	DMF	–	(Schneider et al. 2011)
28	6	TEOA, BNAH	480 nm	12	157	DMF	–	(Takeda et al. 2014)
28	6	TEOA, BNAH	480 nm	40	78	MeCN	–	(Takeda et al. 2014)
28	41	TEOA, BNAH	480 nm	12	149	DMF	–	(Takeda et al. 2014)
29	6	TEOA, BNAH	500 W Xe	113[d]	316[d]	DMF	–	(Tamaki et al. 2012a)
30	–	TEOA	300 W Hg	–	–	DMF	–	(Ishida et al. 1990)

(*continued*)

Table 3 (continued)

CO_2 red. catalyst	Photosensitizer	Electron, proton, additive source	Light	CO (TON)	HCO_2H (TON)	Solvent	φ	References
30	41	TEOA	300 W Hg	–	158	DMF	–	(Ishida et al. 1990)
30	41	BNAH, H_2O	300 W Hg	~120	158	DMF	–	(Ishida et al. 1990)
30	41	BNAH	300 W Hg	<10	<10	DMF	–	(Ishida et al. 1990)
31[c]	42	TEA	AM 1.5	98,000	–	MeCN	–	(Thoi et al. 2013)
31	42	TEA	AM 1.5	1,500	–	MeCN	0.01	(Thoi et al. 2013)
32	13	TEA, MeOH	UV*	–	–	MeCN	–	(Matsuoka et al. 1993; Ogata et al. 1995a)
33	42	TEA	>420 nm	140	–	MeCN	–	(Bonin et al. 2014a)
33	40	TEA	>420 nm	~55	–	MeCN	–	(Bonin et al. 2014a)
34	13	TEA, MeOH	UV*	4.8	2.4	MeCN	–	(Matsuoka et al. 1993; Ogata et al. 1995a)
34	13	TEOA, MeOH	UV*	10	6.0	MeCN	–	(Matsuoka et al. 1993; Ogata et al. 1995a)
34	13	TIPOA, MeOH	UV*	13	3.5	MeCN	–	(Matsuoka et al. 1993; Ogata et al. 1995a)
34	38	TEA, MeOH	500 W Hg	0.3	4.8	MeCN	–	(Yanagida et al. 1995)
34	39	TEA, MeOH	500 W Xe	0.3	5.6	MeCN	0.07	(Ogata et al. 1995b)
35	13	TEA, MeOH	UV*	5.6	3.6	MeCN	–	(Matsuoka et al. 1993; Ogata et al. 1995a)
36	13	TEA, MeOH	UV*	5.6	3.6	MeCN	–	(Matsuoka et al. 1993; Ogata et al. 1995a)
37	13	TEA, MeOH	UV*	5.0	2.6	MeCN	–	(Matsuoka et al. 1993; Ogata et al. 1995a)

*Visible Light Not Confirmed TON are per molecule, not per catalytic site where applicable
[a]significant H_2 produced
[b]significant MeOH produced
[c]low concentration
[d]estimated

inactive (Takeda et al. 2008). With a lower wattage lamp (250 W), a higher TON for (**1**) was observed (TON = 27), and this number could be near doubled though the addition of tetraethylammonium chloride to give a TON of 48 (Hawecker et al. 1983). A bromine complex (**4**) was also evaluated and yielded slightly lower reactivity. Substitution on the bipyridyl ligand with phenylacetylene was found to yield substantially lower reactivities despite an enhanced absorption in the visible wavelength range (Portenkirchner et al. 2012).

Ruthenium-based photocatalysts**6** and **7** are known to give good selectivities for formate formation (Takeda et al. 2014; Boston et al. 2013) *with turnover numbers as* high as 76. **7** is also one of the only reported molecular catalysts to form MeOH during photolysis. Both the ruthenium catalysts **6** and **7** along with iridium-based catalyst **8** are effective photocatalysts in water as solvent (Yuan et al. 2011). The highest TON catalyst which operates in the absence of a photosensitizer is Ishitani's iridium-based catalyst (**9**) (Sato et al. 2013).There are examples of first-row transition metal catalyst known to function as photon-absorbing and CO_2-reducing catalysts based on porphyrin (**10** and **11**) and phenanthroline (**12**) (Behar et al. 1998; Grodkowski et al. 1997; Lehn and Ziessel 1982). The porphyrin catalysts demonstrated comparable TONs to **9** while the cobalt chloride in situ complexed with **12** gave relatively few turnovers in an early report (~3). Although few studies have focused on homogeneous organic photocatalysts, some early reports indicate oligophenyl structures can reduce CO_2 to selectively give formate albeit in modest TONs (1–4) (Matsuoka et al. 1992).

Covalently linked multinuclear photocatalysts have shown incredibly high TON values of >3,000 for a *Re–Ru*-linked polypyridyl catalyst **23** and demonstrated the use of red visible light to reduce CO_2 with a *Re–Os-linked catalyst***24** (Gholamkhass et al. 2005; Tamaki et al. 2012b, 2013a, b). These structures likely benefit from a close proximity of the photosensitizer to a CO_2 reduction catalyst to allow for efficient electron transfer. In these cases, the CO_2 reduction catalyst does not need to absorb photons, but only needs a reduction potential below that of the reduced photosensitizer. Currently, $Ru(bpy)_3$ analogues are ubiquitous covalently linked photosensitizers although osmium (**24**, TON = 1,138) and porphyrin (**25**, TON = 1)-based photosensitizers have also been reported (Schneider et al. 2011). In these systems, the selectivity among CO_2 reduction products is largely determined by the catalyst appended to the photosensitizer, whereas Re-based reduction catalyst typically gives CO selectively and Ru-based reduction catalyst typically gives HCO_2H. It is noteworthy that the highest quantum-yielding (ϕ) photocatalyst system (**23**) reached efficiencies of 45 %. This is dramatically higher than other observed good quantum yields of 8–5 % for non-covalently linked catalysts.

A diverse array of catalysts known to be active electrocatalysts for CO_2 reduction has been studied in photocatalytic systems with a variety of added photosensitizers (**38**–**44**). While Re and Ru complexes similar to those studied as covalently linked multinuclear photocatalysts have been studied, reactivity commonly decreases significantly (~twofold in many cases) when the linking tether is removed. However, these systems still typically perform an order of magnitude better with regard to TON when compared with mononuclear systems. The use of non-linked photosensitizers

has enabled the recent rapid evaluation of several noteworthy electrocatalysts in photocatalytic systems including those based on manganese (**28**) (Takeda et al. 2014), nickel (**31** and **32**) (Thoi et al. 2013), iron porphyrins (Bonin et al. 2014a), and cobalt cyclams (**32**, **35**–**37**) (Yanagida et al. 1995; Ogata et al. 1995b). Manganese complex **28** paired with ruthenium photosensitizer **6** demonstrated an unusual switch in CO_2 product selectivity from CO under electrocatalytic conditions to HCO_2H under photocatalytic conditions with a dramatic increase in TON (from 13 to 149). Perhaps one of the most important developments in these non-covalently bound systems is the recent use of $Ir(ppy)_3$ (**42**) which has been paired with electrocatalysts **31** and **33. 42** has a remarkably high-energy reduction potential (near −1.9 V vs. NHE) which allows for pairing with many electrocatalysts with higher reduction potentials than that of $Ru(bpy)_3$ photosensitizers (reduction potential near −1.1). For that case of **42** paired with **31** record TON values of 98,000 were observed under very dilute conditions. With more common concentrations, high TONs were still observed (~1,500). In this system, the photosensitizer was found to decompose over time whereas the addition of fresh **42** led to reactivity rates near that *at the start of photolysis*. **33** is a known efficient electrocatalyst which was recently paired with **42** to give good TON values >100. Interestingly, **33** was also paired with anthracene **40** to give the highest TON values observed with an organic sensitizer. It should be noted that **33** was recently shown to operate as a photocatalyst independent of a photosensitizer for 30 TON (Bonin et al. 2014b).

With the exception of Neumann's RWGS reaction catalyst, the above systems have used an organic electron and proton source. These are often present in solvent quantities as amine additives (TEA and TEOA, typically 1:5 with the listed solvent). However, several researchers have noted that addition of a second electron/proton source has resulted in substantially higher reactivities. These additional sources are often suggested to be a co-catalyst which received electrons from the stoichiometric amine reductant and delivers them efficiently to the photosensitizer or catalyst. The most commonly observed sources are ascorbic acid (**AA**), 1-benzyl-1,4-dihydronicotinamide (**BNAH**), and most recently, 1,3-dimethyl-2-phenyl-2,3-dihydro-1H-benzo[d]imidazole (**BIH**). Care must again be taken concerning the background reactions associated with **AA** which can decompose to CO. **BIH** has been shown to directly lead to a >10x increase in catalyst turnover numbers and a threefold increase in already high ϕ values (Tamaki et al. 2012b, 2013a). **BIH** has led to some of the highest quantum yields and TONs to date and will likely find utility in further studies.

Future Directions

Photocatalytic water splitting and photocatalytic carbon dioxide reduction each offer the promise of cheap and plentiful sources of energy for society's future. In addition, the transformation of carbon dioxide from a harmful waste product to usable energy source is a win/win proposition. However, the development of efficient

photocatalytic materials that make either of these processes viable on large scales has not been realized. With such a clear and potentially substantial payoff, many synthetic chemists have been attracted to this problem. In this very active field, advances are constant as the search for an ideal photocatalyst continues.

References

Abe R (2010) Recent progress on photocatalytic and photoelectrochemical water splitting under visible light irradiation. J Photochem Photobiol C 11:179–209

Anfuso CL, Xiao D, Ricks AM et al (2012) Orientation of a series of CO_2 reduction catalysts on single crystal TiO_2 probed by phase-sensitive vibrational Sum frequency generation spectroscopy (PS-VSFG). J Phys Chem C 116:24107–24114

Armaroli N, Balzani V (2007) The future of energy supply: challenges and opportunities. Angew Chem Int Ed 46:52–66

Arrhenius S (1896) On the influence of carbonic acid in the air upon the temperature of the ground. Philos Mag A 41:237–276

Bae ST, Shin H, Kim JY et al (2008) Roles of MgO coating layer on mesoporous TiO_2/ITO electrode in a photoelectrochemical cell for water splitting. J Phys Chem C 112:9937–9942

Bahnemann D (2004) Photocatalytic water treatment: solar energy applications. Sol Energy 77:445–459

Barreto L, Makihira A, Riahi K (2003) The hydrogen economy in the 21st century: a sustainable development scenario. Int J Hydrog Energy 28:267–284

Behar D, Dhanasekaran T, Neta P et al (1998) Cobalt porphyrin catalyzed reduction of CO_2. Radiation chemical, photochemical, and electrochemical studies. J Phys Chem A 102:2870–2877

Benson EE, Kubiak CP, Sathrum AJ et al (2009) Electrocatalytic and homogeneous approaches to conversion of CO_2 to liquid fuels. Chem Soc Rev 38:89–99

Bhattacharyya K, Varma S, Tripathi AK et al (2008) Effect of vanadia doping and its oxidation state on the photocatalytic activity of TiO_2 for gas-phase oxidation of ethene. J Phys Chem C 112:19102–19112

Bonin J, Robert M, Routier M (2014a) Selective and efficient photocatalytic CO_2 reduction to CO using visible light and an iron-based homogeneous catalyst. J Am Chem Soc 136:16768–16771

Bonin J, Robert M, Routier M (2014b) Homogeneous photocatalytic reduction of CO_2 to CO using iron(0) porphyrin catalysis: mechanism and intrinsic limitations. ChemCatChem 6:3200–3207

Boston DJ, Xu C, Armstrong DW et al (2013) Photochemical reduction of carbon dioxide to methanol and formate in a homogeneous system with pyridinium catalysts. J Am Chem Soc 135:16252–16255

Caetano MAL, Gherardi DFM, Yoneyama T (2008) Optimal resource management control for CO_2 emission and reduction of the greenhouse effect. Ecol Model 213:119–126

Chen W-Y, Shi G, Hailey AK et al (2012) Photocatalytic conversion of carbon dioxide to organic compounds using a green photocatalyst: an undergraduate research experiment. Chem Educ 17:166–171

Choi WY, Termin A, Hoffmann MR (1994) The role of metal-ion dopants in quantum-sized TiO_2 – correlation between photoreactivity and charge-carrier recombination dynamics. J Phys Chem 98:13669–13679

Colombo DP, Bowman RM (1996) Does interfacial charge transfer compete with charge carrier recombination? A femtosecond diffuse reflectance investigation of TiO_2 nanoparticles. J Phys Chem 100:18445–18449

Crabtree GW, Dresselhaus MS, Buchanan MV (2004) The hydrogen economy. Phys Today 57:39–44

de Richter RK, Ming T, Caillol S (2013) Fighting global warming by photocatalytic reduction of CO_2 using giant photocatalytic reactors. Renew Sustain Energy Rev 19:82–106

Dhakshinamoorthy A, Navalon S, Corma A et al (2012) Photocatalytic CO_2 reduction by TiO_2 and related titanium containing solids. Energy Environ Sci 5:9217–9233

Dhanasekaran T, Grodkowski J, Neta P et al (1999) p-terphenyl-sensitized photoreduction of CO_2 with cobalt and iron porphyrins. Interaction between CO and reduced metalloporphyrins. J Phys Chem 103:7742–7748

Domen K, Kondo JN, Hara M et al (2000) Photo- and mechano-catalytic overall water splitting reactions to form hydrogen and oxygen on heterogeneous catalysts. Bull Chem Soc Jpn 73:1307–1331

Dunn S (2002) Hydrogen futures: toward a sustainable energy system. Int J Hydrog Energy 27:235–264

Ettedgui J, Diskin-Posner Y, Weiner L et al (2011) Photoreduction of carbon dioxide to carbon monoxide with hydrogen catalyzed by a rhenium(I) phenanthroline-polyoxometalate hybrid complex. J Am Chem Soc 133:188–190

Fang J, Wang F, Qian K et al (2008) Bifunctional N-doped mesoporous TiO_2 photocatalysts. J Phys Chem C 112:18150–18156

Fischer H, Wahlen M, Smith J et al (1999) Ice core records of atmospheric CO_2 around the last three glacial terminations. Science 283:1712–1714

Fox MA, Dulay MT (1993) Heterogeneous photocatalysis. Chem Rev 93:341–357

Fujishima A, Honda KB (1971) Electrochemical evidence for the mechanism of the primary stage of photosynthesis. Bull Chem Soc Jpn 44:1148–1150

Fujishima A, Honda K (1972) Electrochemical photolysis of water at a semiconductor electrode. Nature 238:37–38

Gai YQ, Li JB, Li SS et al (2009) Design of narrow-gap TiO2: a passivated codoping approach for enhanced photoelectrochemical activity. Phys Rev Lett 102:036402

Gholamkhass B, Mametsuka H, Koike K et al (2005) Architecture of supramolecular metal complexes for photocatalytic CO_2 reduction: ruthenium − rhenium Bi- and tetranuclear complexes. Inorg Chem 44:2326–2336

Gilfillan SMV, Lollar BS, Holland G et al (2009) Solubility trapping in formation water as dominant CO_2 sink in natural gas fields. Nature 458:614–618

Graciani J, Nambu A, Evans J et al (2008) Au – N synergy and N-doping of metal oxide-based photocatalysts. J Am Chem Soc 130:12056–12063

Grodkowski J, Behar D, Neta P et al (1997) Iron porphyrin-catalyzed reduction of CO_2. Photochemical and radiation chemical studies. J Phys Chem A 101:248–254

Ha E-G, Chang J-A, Byun S-M et al (2014) High-turnover visible-light photoreduction of CO_2 by a Re(I) complex stabilized on dye-sensitized TiO2. Chem Commun 50:4462–4464

Habisreutinger SN, Schmidt-Mende L, Stolarczyk JK (2013) Photocatalytic reduction of CO_2 on TiO_2 and other semiconductors. Angew Chem Int Ed 52:7372–7408

Hansen J, Sato M (2004) Greenhouse gas growth rates. Proc Natl Acad Sci U S A 101:16109–16114

Hawecker J, Lehn J-M, Ziessel R (1983) Efficient photochemical reduction of CO_2 to CO by visible light irradiation of systems containing $Re(bipy)(CO)_3X$ or $Ru(bipy)_3^{2+}$-Co^{2+} combinations as homogeneous catalysts. J Chem Soc Chem Commun 536–538

Hernández-Alonso MD, Fresno F, Suárez S et al (2009) Development of alternative photocatalysts to TiO_2: challenges and opportunities. Energy Environ Sci 2:1231–1257

Hidalgo MC, Maicu M, Navio JA et al (2009) Effect of sulfate pretreatment on gold-modified TiO_2 for photocatalytic applications. J Phys Chem C 113:12840–12847

Hoffmann MR, Martin ST, Choi WY et al (1995) Environmental applications of semiconductor photocatalysis. Chem Rev 95:69–96

Hong YC, Bang CU, Shin DH et al (2005) Band gap narrowing of TiO_2 by nitrogen doping in atmospheric microwave plasma. Chem Phys Lett 413:454–457

Hurum DC, Gray KA, Rajh T et al (2005) Recombination pathways in the Degussa P25 formulation of TiO_2: surface versus lattice mechanisms. J Phys Chem B 109:977–980

Inoue T, Fujishima A, Konishi S et al (1979) Photoelectrocatalytic reduction of carbon dioxide in aqueous suspensions of semiconductor powders. Nature 277:637–638

Ishida H, Terada T, Tanaka K et al (1990) Photochemical CO_2 reduction catalyzed by Ru $(bpy)_2(CO)_2^{2+}$ using triethanolamine and 1-benzyl-1,4-dihydronicotinamide as an electron donor. Inorg Chem 29:905–911

Izumi Y (2013) Recent advances in the photocatalytic conversion of carbon dioxide to fuels with water and/or hydrogen using solar energy and beyond. Coord Chem Rev 257:171–186

Jackson RB, Schlesinger WH (2004) Curbing the US carbon deficit. Proc Natl Acad Sci U S A 101:15827–15829

Jagadale TC, Takale SP, Sonawane RS et al (2008) N-doped TiO_2 nanoparticle based visible light photocatalyst by modified peroxide sol–gel method. J Phys Chem C 112:14595–14602

Janáky C, Rajeshwar K, de Tacconi NR et al (2013) Tungsten-based oxide semiconductors for solar hydrogen generation. Catal Today 199:53–64

Kaneco S, Shimizu Y, Ohta K et al (1998) Photocatalytic reduction of high pressure carbon dioxide using TiO_2 powders with a positive hole scavenger. J Photochem Photobiol A 115:223–226

Keith DW (2009) Why capture CO_2 from the atmosphere? Science 325:1654–1655

Kesselman JM, Weres O, Lewis NS et al (1997) Electrochemical production of hydroxyl radical at polycrystalline Nb-doped TiO_2 electrodes and estimation of the partitioning between hydroxyl radical and direct Hole oxidation pathways. J Phys Chem B 101:2637–2643

Kočí K, Obalová L, Lacný Z (2008) Photocatalytic reduction of CO_2 over TiO_2 based catalysts. Chem Pap 62:1–9

Kondratenko EV, Mul G, Baltrusaitis J et al (2013) Status and perspectives of CO_2 conversion into fuels and chemicals by catalytic, photocatalytic and electrocatalytic processes. Energy Environ Sci 6:3112–3135

Kou Y, Nakatani S, Sunagawa G et al (2014) Visible light-induced reduction of carbon dioxide sensitized by a porphyrin – rhenium dyad metal complex on p-type semiconducting NiO as the reduction terminal end of an artificial photosynthetic system. J Catal 310:57–66

Kudo A, Miseki Y (2009) Heterogeneous photocatalyst materials for water splitting. Chem Soc Rev 38:253–278

Kudo A, Kato H, Tsuji I (2004) Strategies for the development of visible-light-driven photocatalysts for water splitting. Chem Lett 33:1534–1539

Kumar B, Smieja JM, Sasayama AF et al (2012) Tunable, light-assisted co-generation of CO and H_2 from CO_2 and H_2O by Re(bipy-tbu)$(CO)_3$Cl and p-Si in non-aqueous medium. Chem Commun 48:272–274

Lehn J-M, Ziessel R (1982) Photochemical generation of carbon monoxide and hydrogen by reduction of carbon dioxide and water under visible light irradiation. Proc Natl Acad Sci U S A 79:701–704

Li GH, Dimitrijevic NM, Chen L et al (2008) Role of surface/interfacial Cu^{2+} sites in the photocatalytic activity of coupled CuO-TiO_2 nanocomposites. J Phys Chem C 112:19040–19044

Linsebigler AL, Lu G, Yates JT (1995) Photocatalysis on TiO_2 surfaces: principles, mechanisms, and selected results. Chem Rev 95:735–758

Liu G, Hoivik N, Wang K et al (2012) Engineering TiO_2 nanomaterials for CO_2 conversion/solar fuels. Sol Energy Mater Sol Cells 105:53–68

Livraghi S, Chierotti MR, Giamello E et al (2008) Nitrogen-doped titanium dioxide active in photocatalytic reactions with visible light: a multi-technique characterization of differently prepared materials. J Phys Chem C 112:17244–17252

Luthi D, Le Floch M, Bereiter B et al (2008) High-resolution carbon dioxide concentration record 650,000–800,000 years before present. Nature 453:379–382

Matsuoka S, Kohzuki T, Pac C et al (1992) Photocatalysis of ollgo(p-phenylenes). Photochemical reduction of carbon dloxlde with trlethylamlne. J Phys Chem 96:4437–4442

Matsuoka S, Yamamoto K, Ogata T et al (1993) Efficient and selective electron mediation of cobalt complexes with cyclam and related macrocycles in the p-terphenyl-catalyzed photoreduction of CO_2. J Am Chem Soc 115:601–609

McMichael A, Woodruff R (2004) Climate change and risk to health. Br Med J 329:1416–1417

Mikkelsen M, Jørgensen M, Krebs FC (2010) The teraton challenge. A review of fixation and transformation of carbon dioxide. Energy Environ Sci 3:43–81

Mohapatra SK, Raja KS, Mahajan VK et al (2008) Efficient photoelectrolysis of water using TiO_2 nanotube arrays by minimizing recombination losses with organic additives. J Phys Chem C 112:11007–11012

Moriarty P, Honnery D (2009) Hydrogen's role in an uncertain energy future. Int J Hydrog Energy 34:31–39

Morris AJ, Meyer GJ, Fujita E (2009) Molecular approaches to the photocatalytic reduction of carbon dioxide for solar fuels. Acc Chem Res 42:1983–1994

Navalón S, Dhakshinamoorthy A, Álvaro M et al (2013) Photocatalytic CO_2 reduction using non-titanium metal oxides and sulfides. ChemSusChem 6:562–577

Navarro RM, Sanchez-Sanchez MC, Alvarez-Galvan MC et al (2009) Hydrogen production from renewable sources: biomass and photocatalytic opportunities. Energy Environ Sci 2:35–54

Ogata T, Yanagida S, Brunschwig BS et al (1995a) Mechanistic and kinetic studies of cobalt macrocycles in a photochemical CO_2 reduction system: evidence of Co-CO_2 adducts as intermediates. J Am Chem Soc 117:6708–6716

Ogata T, Yamamoto Y, Wadaj Y et al (1995b) Phenazine-photosensitized reduction of CO_2 mediated by a cobalt-cyclam complex through electron and hydrogen transfer. J Phys Chem 99:11916–11922

Osterloh FE (2008) Inorganic materials as catalysts for photochemical splitting of water. Chem Mater 20:35–54

Portenkirchner E, Oppelt K, Ulbricht C et al (2012) Electrocatalytic and photocatalytic reduction of carbon dioxide to carbon monoxide using the alkynyl-substituted rhenium(I) complex (5,5-′-bisphenylethynyl-2,2′-bipyridyl)Re$(CO)_3$Cl. J Organomet Chem 716:19–25

Reithmeier R, Bruckmeier C, Rieger B (2012) Conversion of CO_2 via visible light promoted homogeneous redox catalysis. Catalysts 2:544–571

Roy SC, Varghese OK, Paulose M et al (2010) Toward solar fuels: photocatalytic conversion of carbon dioxide to hydrocarbons. ACS Nano 4:1259–1278

Sato S, Morikawa T, Kajino T et al (2013) A highly efficient mononuclear iridium complex photocatalyst for CO_2 reduction under visible light. Angew Chem Int Ed 52:988–992

Savéant J-M (2008) Molecular catalysis of electrochemical reactions. Mechanistic aspects. Chem Rev 108:2348–2378

Schimel D, Melillo J, Tian HQ et al (2000) Contribution of increasing CO_2 and climate to carbon storage by ecosystems in the United States. Science 287:2004–2006

Schlapbach L, Zuttel A (2001) Hydrogen-storage materials for mobile applications. Nature 414:353–358

Schneider J, Vuong KQ, Calladine JA et al (2011) Photochemistry and photophysics of a Pd (II) metalloporphyrin: Re(I) tricarbonyl bipyridine molecular dyad and its activity toward the photoreduction of CO_2 to CO. Inorg Chem 50:11877–11889

Schneider J, Jia H, Muckerman JT et al (2012) Thermodynamics and kinetics of CO_2, CO, and H^+ binding to the metal centre of CO_2 reduction catalysts. Chem Soc Rev 41:2036–2051

Sekizawa K, Maeda K, Domen K et al (2013) Artificial Z – scheme constructed with a supramolecular metal complex and semiconductor for the photocatalytic reduction of CO_2. J Am Chem Soc 135:4596–4599

Tahir M, Amin NS (2013) Advances in visible light responsive titanium oxide-based photocatalysts for CO_2 conversion to hydrocarbon fuels. Energy Convers Manag 76:194–214

Takeda H, Koike K, Inoue H et al (2008) Development of an efficient photocatalytic system for CO_2 reduction using rhenium(l) complexes based on mechanistic studies. J Am Chem Soc 130:2023–2031

Takeda H, Koizumi H, Okamoto K et al (2014) Photocatalytic CO_2 reduction using a Mn complex as a catalyst. Chem Commun 50:1491–1493

Tamaki Y, Morimoto T, Koike K et al (2012a) Photocatalytic CO_2 reduction with high turnover frequency and selectivity of formic acid formation using Ru(II) multinuclear complexes. Proc Natl Acad Sci U S A 109:15673–15678

Tamaki Y, Watanabe K, Koike K et al (2012b) Development of highly efficient supramolecular CO_2 reduction photocatalysts with high turnover frequency and durability. Faraday Discuss 155:115–127

Tamaki Y, Koike K, Morimoto T et al (2013a) Substantial improvement in the efficiency and durability of a photocatalyst for carbon dioxide reduction using a benzoimidazole derivative as an electron donor. J Catal 304:22–28

Tamaki Y, Koike K, Morimoto T et al (2013b) Red-light-driven photocatalytic reduction of CO_2 using Os(II)-Re(I) supramolecular complexes. Inorg Chem 52:11902–11909

Thoi VS, Kornienko N, Margarit CG et al (2013) Visible-light photoredox catalysis: selective reduction of carbon dioxide to carbon monoxide by a nickel N – heterocyclic carbene – isoquinoline complex. J Am Chem Soc 135:14413–14424

Tseng IH, Chang W-C, Wu JCS (2002) Photoreduction of CO_2 using sol–gel derived titania and titania-supported copper catalysts. Appl Catal B Environ 37:37–48

Usubharatana P, McMartin D, Veawab A et al (2006) Photocatalytic process for CO_2 emission reduction from industrial flue gas streams. Ind Eng Chem Res 45:2558–2568

U.S. Energy Information Administration, International Energy Outlook 2009 Document #DOE/EIA-0484 (2009)

Vaneski A, Schneider J, Susha AS et al (2014) Colloidal hybrid heterostructures based on II–VI semiconductor nanocrystals for photocatalytic hydrogen generation. J Photochem Photobiol C 19:52–61

Varghese OK, Paulose M, LaTempa TJ et al (2009) High-rate solar photocatalytic conversion of CO_2 and water vapor to hydrocarbon fuels. Nano Lett 9:731–737

Wang YQ, Cheng HM, Zhang L et al (2000) The preparation, characterization, photoelectrochemical and photocatalytic properties of lanthanide metal-ion-doped TiO_2 nanoparticles. J Mol Catal A Chem 151:205–216

Wang C, Xie Z, DeKrafft KE et al (2011) Doping metal-organic frameworks for water oxidation, carbon dioxide reduction, and organic photocatalysis. J Am Chem Soc 133:13445–13454

Xiaoding X, Moulijn JA (1996) Mitigation of CO_2 by chemical conversion: plausible chemical reactions and promising products. Energy Fuel 10:305–325

Xie G, Zhang K, Guo B et al (2013) Graphene-based materials for hydrogen generation from light-driven water splitting. Adv Mater 25:3820–3839

Yan XL, He J, Evans DG et al (2005) Preparation, characterization and photocatalytic activity of Si-doped and rare earth-doped TiO_2 from mesoporous precursors. Appl Catal B Environ 55:243–252

Yanagida S, Ogata T, Yamamoto Y et al (1995) A novel CO_2 photoreduction system consisting of phenazine as a photosensitizer and cobalt cyclam as a CO_2 scavenger. Energy Convers Manag 36:601–604

Yang YH, Chen QY, Yin ZL et al (2005) Progress in research of photocatalytic water splitting. Prog Chem 17:631–642

Yeredla RR, Xu HF (2008) Incorporating strong polarity minerals of tourmaline with semiconductor titania to improve the photosplitting of water. J Phys Chem C 112:532–539

Younpblood WJ, Lee SHA, Kobayashi Y et al (2009) Photoassisted overall water splitting in a visible light-absorbing dye-sensitized photoelectrochemical cell. J Am Chem Soc 131:926–927

Yuan Y-J, Yu Z-T, Chen X-Y et al (2011) Visible-light-driven H_2 generation from water and CO_2 conversion by using a zwitterionic cyclometalated iridium(III) complex. Chem Eur J 17:12891–12895

Zhang K, Guo L (2013) Metal sulphide semiconductors for photocatalytic hydrogen production. Catal Sci Technol 3:1672–1690

Zhang PD, Jia G, Wang G (2007) Contribution to emission reduction of CO_2 and SO_2 by household biogas construction in rural China. Renew Sustain Energy Rev 11:1903–1912
Zong X, Wang L (2014) Ion-exchangeable semiconductor materials for visible light-induced photocatalysis. J Photochem Photobiol C 18:32–49
Zuttel A (2004) Hydrogen storage methods. Naturwissenschaften 91:157–172

Simultaneous CO_2 and H_2S Sequestration by Electrocatalytic Conversion for Chemical Feedstock Synthesis

Nosa O. Egiebor and Jonathan Mbah

Contents

Abstract

This paper addresses the development of an innovative ionic membrane consisting of electrocatalysts and electrolyte assembly that can be used in an electrochemical cell to produce useful chemicals via simultaneous splitting of hydrogen sulfide (H_2S) and carbon dioxide (CO_2) content feedstock. The cell consists of an endurance membrane electrode assembly (MEA) material with CO_2 and H_2S feedstock and operates near 120–145 °C. Thus, a benign method of CO_2 mitigation is achieved, and at the same time useful chemicals are produced from two pollutant gases. We have successfully conducted a preliminary study in

N.O. Egiebor
Department of Chemical Engineering and Division of Global Engagement, The University of Mississippi, Oxford, MS, USA
e-mail: negiebor@olemiss.edu

J. Mbah (✉)
Department of Chemical Engineering, Florida Institute of Technology, Melbourne, FL, USA
e-mail: jmbah@fit.edu; joneschinwe2003@yahoo.com

W.-Y. Chen et al. (eds.), *Handbook of Climate Change Mitigation and Adaptation*,
DOI 10.1007/978-3-319-14409-2_88

our laboratory. The overall Gibbs energy, ΔG, of the process is (−49.27 kcal/mol), with a net energy output of about +1.06 V per mole. The instability of the cathode electrode due to the poisoning of electrode materials, corrosive aqueous media, and the chemistry nature of the electrode kinetics can be addressed by implementing electrocatalyst design scheme, which takes into consideration the location of the active ingredients and support materials of the electrocatalyst in order to enhance activity, stability, and selectivity. The aim is to research, formulate, and design anode and cathode electrocatalyst materials which are not susceptible to degradation in corrosive aqueous environment. Solid electrolytes from cesium hydrogen sulfate and from Nafion^{TM} family that conducts only hydrogen protons with added nanoscale hygroscopic oxide (silica) to maintain their integrities were studied. Operation at high pressures ensured that the membrane remained hydrated. Proper positioning of active and support materials during catalyst impregnation will eliminate any catalytic poisoning of active materials.

Introduction

Carbon dioxide (CO_2) and hydrogen sulfide (H_2S) are both greenhouse gases and pose a challenge to the modern society where environmental pollution has to be minimized to an acceptable level. CO_2 reduction over aqueous media in electrochemical cells has been reported in many literatures (Fujita 1999; Gattrell and Gupta 2006), but to date no report on simultaneous oxidation and reduction techniques for H_2S and CO_2 containing gases using solid media is available. There are so many disadvantages inherent with using aqueous media, for example, solubility issue of CO_2 with decrease in temperature is a major drawback with aqueous systems. This project tends to propose a novel technique of simultaneously splitting CO_2 and H_2S containing gases into useful chemicals via a solid membrane. Since both H_2S and CO_2 often occur together in petroleum and natural gas resources and are major by-products of integrated gasification combined cycle (IGCC) power plants, a technique that can simultaneously split both gases and at the same time produce a valuable energy fuel resource is certainly very desirable. Such a technical advancement will invariably contribute significantly to CO_2 sequestration, and toxic H_2S gas utilization for clean energy production. The concentrations of H_2S present in natural gas generally range from trace amounts to more than 80 %. Caldeira et al. (2003), while CO_2 is the main end product of fossil hydrocarbon combustion for energy. Currently, CO_2 and H_2S are separated using a double-absorber Selexol process which preferentially removes H_2S as product leaving CO_2 as a separate product stream.

Sequestration of CO_2 in geological formations includes deposition in oil and gas reservoirs, unmineable coal seams (due to seam thickness, depth, and structural integrity), and deep saline reservoirs, such as in oceans. This approach takes into consideration that many of the large emitters of CO_2 are sited near geological formations that can be tailored into storage facilities. In the case of oil and gas

reservoirs, additional revenue can be generated from enhanced oil recovery with carbon dioxide injection. Given the perspective of this program, this method will provide a low net cost as a result of the enhanced oil recovery. However, the studies are still being conducted to understand the utility of the technique for carbon dioxide sequestration and the behavior of injected CO_2 over time in these depleted oil wells. Such studies have included the determination of the extent to which the CO_2 moves within the geological formation, and what physical and chemical changes occur to the formation when CO_2 is injected (Wise et al. 2009).

The adsorption of CO_2 in coal beds to displace methane due to its higher adsorptivity than methane provides another possible technical alternative to CO_2 sequestration, but limited researches have been conducted in this area (Grimes 2005). which are not sufficient to justify this approach since sequestration capacities of these basins are yet to be quantified. Similar to the enhanced oil recovery, the recovered methane provides a value-added product stream to the CO_2 sequestration process. In comparison, the saline formations do not generate any value-added by-products but do have higher storage capacity for injected CO_2. The key issues in these programs are the safety of CO_2 storage in saline formations and perhaps potential and emerging environmental problems (Clarkson et al. 1997; Bachu and Adams 2003).

Despite the modest successes recorded by these programs, minimizing CO_2 air pollution and emission is still a major concern because the long-term effects of these methods are not yet clear. Rock layers may be weakened as a result of formation of carbonaceous acid if CO_2 happens to react with underground water. The recent recorded events of oil spillages in our high seas and oceans, worldwide, is a reminder that we ought to be cautious of the adverse effect that may proceed from the enhanced oil recovery and other nondestructive CO_2 sequestration approaches. The electrochemical approach proposed here, and described in the sections that follow, has the potential to avoid the major drawbacks associated with current approaches for carbon dioxide sequestration.

Electrochemical carbon dioxide sequestration method has also been considered by many researchers (Pérez-Rodríguez et al. 2011; Kaneco et al. 2006a). Some of the electrochemical approaches make use of aqueous media while others consider solid media. The use of electrochemical conversion to split CO_2 has shown to produce carbon monoxide and formic acid in aqueous solution in the presence of most flat metallic electrodes (Kaneco et al. 2006b). Nevertheless, it has been proven that only copper is a suitable electrode for the formation of hydrocarbons such as methane and ethylene, which can be used as fuel gases (Lee et al. 2011; Li and Oloman 2007; Chang et al. 2009). High current yields were only achieved with large overpotentials (-1.5 V vs. SCE). Some of the Faradaic yields exceeded 90 %. The primary reduction intermediate was proposed to be CO, while weakly adsorbed onto the Cu electrode, interfered with the cathodic hydrogen production reactions. The adsorbed CO was thus reduced to hydrocarbons and alcohols, with the yields increasing with more negative potentials. However, the temperature of operation must be low enough to obtain significant product efficiencies since the solubility of CO_2 decreases with increasing temperature. Owing to the freezing temperature of

water, few reports have dealt with the electrochemical reduction of CO_2 in an aqueous solution at less than 273 K. As a result of the relatively low solubility of CO_2 in aqueous solutions, methods for increasing its solubility have to be sought. A possible solution is to perform the electroreduction at high pressures or in nonaqueous solutions.

Formation of methane, methanol, CO, and formic acid has been reported by electroreduction of CO_2 with H_2. This process requires an enormous amount of overvoltage. It has been hypothesized that using hydrogen radicals instead of hydrogen molecules to react with CO_2 will circumvent this problem of overvoltage encountered. Hydrogen radicals are very reactive and can easily attack CO_2 to form methane. The use of oxygen selective membranes has also been applied to split CO_2 into C and O_2 or partial conversion to CO and $½O_2$ by noncatalytic and catalytic means (e.g., thermal, electrochemical, radiolytic, etc.), followed by subsequent removal of carbon deposits in the reactor (Bockris 2005; Toyir et al. 2001; Ordorica-Garcia et al. 2006). Reverse water gas shift and Fischer Tropsch reactions were also considered using bimetallic catalyst. In this approach, the first catalyst initiates the conversion of CO_2 to CO, and the second catalyst facilitates the conversion of CO to organic compound (Hoek et al. 1985) through Fischer-Tropsch synthesis.

It is worthy to note that electricity generation accounts for 42 % (2397.3 millions of metric tons) of the total CO_2 emissions in the USA alone excluding emissions from US territories in 2007 (Rayne 2008). The two IGCC power plants in the USA each have a capacity of 250 MW. Currently, CO_2 and H_2S are separated using a double-absorber Selexol process which preferentially removes H_2S as product leaving CO_2 as a separate product stream (Gomberg et al. 1984; Ku et al. 2005). These two by-products can subsequently be utilized as feedstock to an electrochemical cell system for useful chemical synthesis. Although the cost of electricity (COE) is less for an IGCC plant with CO_2 and H_2S cocapture compared to those IGCC plants that capture 80 % CO_2 and H_2S separately (5.48 and 6.67 US¢/kWh) respectively, the sale of methane and sulfur will eventually close this gap (Klara and Wimer 2007; Hockstad and Cook 2009). Based on the review of the available options, the chemistry provided by simultaneous splitting of H_2S and CO_2 can provide a cost-effective solution, provided the electrode kinetics can be achieved at low cost. Our starting electrochemical feedstock will be procured from CO_2 and H_2S vendors.

Electrochemical CO_2 Reduction

Aspen Plus™

Varieties of commercially available process simulators, such as Aspen Plus™, can ease the analysis of an electrochemical system. Electrochemical system may include feed preprocessors, heat exchangers, turbines, bottoming cycles, etc., all of which can be very effectively modeled in process simulation software

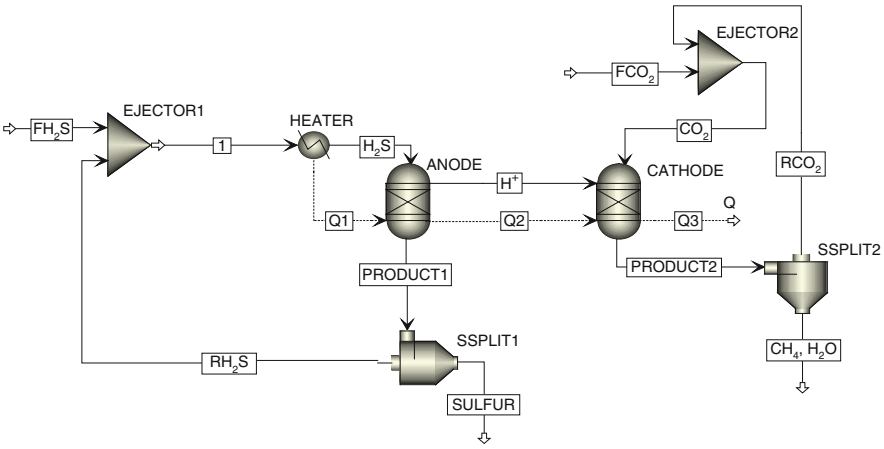

Fig. 1 Aspen Plus™ electrochemical cell model flowsheet. *Dotted lines* represent energy streams. The process involves passing H_2S through the anode compartment of the electrochemical cell to generate H^+ and electron. At the cathode compartment, CO_2 is reduced in the presence of the electron and H^+ to product

(Campanari 2001; Ersoz et al. 2006; Aspen Plus™ 2010). The concept is shown in Fig. 1. Fresh H_2S (FH2S) and unreacted H_2S (RH2S) from the anode chamber are mixed in the block called EJECTOR 1 and fed to the anode compartment where it contacts the catalytic anode and hydrogen proton selective membrane. The H_2S then split into hydrogen protons, electrons, and elemental sulfur. The sulfur flows out of the anode chamber as a low-viscosity fluid at temperature of operation (120–145 °C). The solid membrane is impermeable to the electrons which are then forced through the external circuit as a heat duty (*Q3*) via the electrode. The hydrogen protons migrate through the solid membrane as hydronium ion and at the catalytic cathode combine with the electrons and fresh CO_2 (FCO2) feed that was mixed with unreacted CO_2 (RCO2) from the block called EJECTOR 2 to form methane and water. The heat duty, *Q3*, appears as available energy which is used to drive the system since the process is highly exothermic. The overall Gibbs energy, ΔG, of the process is (−49.27 kcal/mol), with a net energy output of about +1.06 V per mole, as shown in Eq. 1, because of the favorable thermodynamics of water formation.

$$\begin{aligned} 4H_2S + CO_2 \rightarrow CH_4 + 2H_2O + 4S_{(l)}(2\text{Faradays})@\Delta G \\ = -49.27 \ \text{Kcal/mol@400 K} \end{aligned} \quad (1)$$

The outcome of the process simulation using AspenPlus™ package whose schematic is shown in Fig. 1 provides viable information on the proposed approach. One of the benefits of using the developed Aspen Plus™ model is that sensitivity analyses can be performed in an easy and time-saving manner, which helps to understand the effects of variations of the operating parameters on the

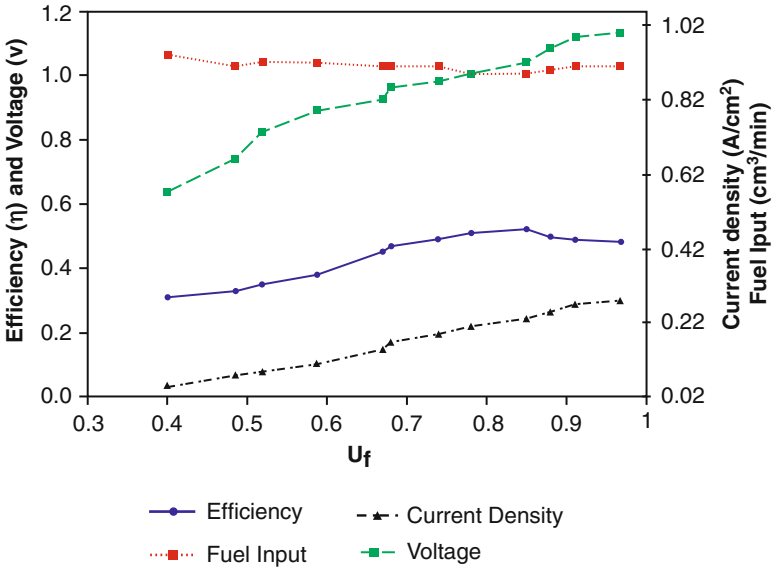

Fig. 2 Aspen Plus™ simulation: effect of fuel utilization factor (U_f) on the cell current density, cell efficiency, and fuel input for the simultaneous splitting of CO_2 and H_2S feedstock. This is based on 4:1 H_2S to C content feed

electrochemical cell's performance. Figure 2 illustrates the results of sensitivity analyses performed using Aspen Plus™. The utilization factor (U_f) is one of the most important operating parameters for most electrochemical cells and has significant effects on the cell voltage and efficiency. The utilization factor is defined as $U_f = v_{\text{H2S, consumed}}/v_{\text{H2S,equivalent}}$, where $v_{\text{H2S, consumed}}$ is the volumetric flow rate of H_2S consumed in the electrochemical reaction at the anode compartment. However, this analysis is based on 4:1 molar ratio of H_2S to C consumed. This is the preferred possible ratio for a galvanic process to proceed based on reaction Eq. 1. The electrode design will help balance the cost-effectiveness of the overall process. The effects of fuel utilization on the cell voltage, cell efficiency, current density, and required fuel input for H_2S/CO_2 splitting electrochemical cell are shown. Current density is a direct measure of the rate of electrode kinetics. If U_f is increased from 0.4 to 0.95, the cell voltage will increase because the fuel is more depleted. The current density will increase, which can be realized by increasing the CO_2 flow at the cathode, resulting in more H_2S being consumed.

Three major requirements for the success of this operation are identifiable:

1. The issue pertaining to cathodic electrode degradation needs to be resolved before meaningful progress is made.
2. Designing good electrode configurations for the cathode such that CO_2 can easily be activated and be selective to the desired end products is another issue that needs to be addressed.

3. Fabrication of an effective membrane electrode assembly (MEA) system that has good mechanical integrity, fast electron transport, and a good ionic conductivity.

Membrane Electrode Assembly

These requirements can be fulfilled by (a) considering the effect of electrocatalyst design, which considered the location of the active ingredients and support materials during electrocatalyst formulation and their composition ratios in order to enhance activity, stability, and selectivity; (b) utilizing a solid electrolyte with good ionic conductivity (Nafion@ families ~0.1 S/cm around room temperature) or cesium hydrogen sulfate, $CsHSO_4$; and (c) an innovative MEA which will consist of an anode with added nanoscale hygroscopic oxide (silica), a cathode either with or without added nanoscale hygroscopic oxide, with the solid electrolyte sandwiched between them as shown in Fig. 3. The nanosilica particles also play a role in water adsorption. When the water produced by electrochemical reaction at the cathode back-diffuses from cathode to anode, the silica, which has hygroscopic property, will adsorb the water. The water back-diffusion process also lends benefits by hydrating the membrane. As a result of the formation of strong absorption bonds between the water molecules and silica due to Van Der Waals forces, elevated temperatures cannot desorb the water adsorbed onto silica (Miyake et al. 2001). The silica at the cathode tends to retain the water which subsequently keeps the membrane from dehydrating. This self-hydrating membrane electrode assembly technique will enhance the system performance without external humidification. At our temperature of operation (120–145 °C), sulfur is a low-viscous fluid and can flow out of the electrolytic cell without hindrance.

The electrochemical system will employ solid-state electrolyte that transports only hydrogen proton or hydronium ions at operating temperature. Their ionic conductance is based on H^+ protons being transported as hydronium (H_3O^+) ions

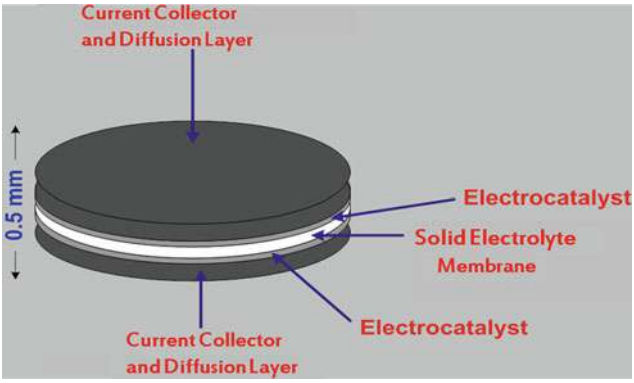

Fig. 3 Schematic of membrane electrode assembly (MEA) for CO_2 and H_2S splitting

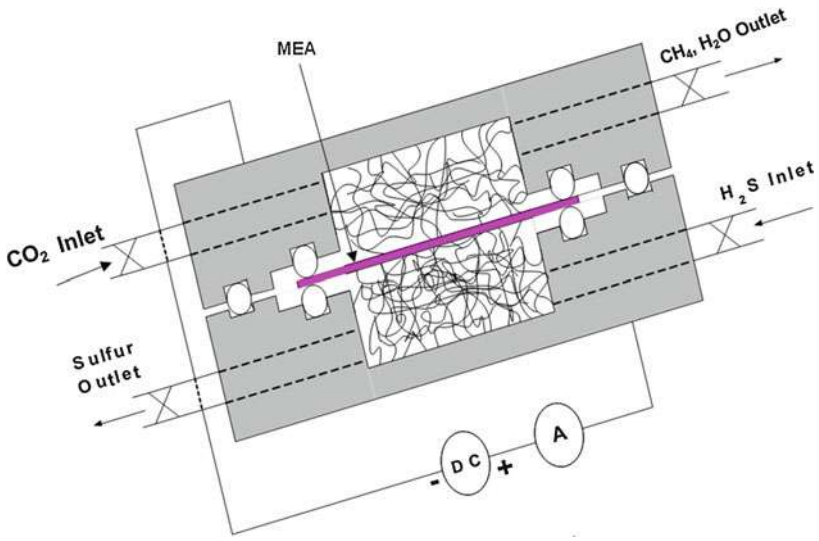

Fig. 4 Schematic of electrochemical cell

and have been tested for their good ionic conductivities. Membrane surfaces are modified with nanoscale hygroscopic oxide (silica) to prevent H_2O product from back-diffusing from cathode to anode with added advantage of keeping the membrane hydrated for easy transport of H_3O^+ ions.

The electrochemical cell schematic is shown in Fig. 4 and the experimental setup for the simultaneous splitting of H_2S and CO_2 in Fig. 5. Besides the membrane, the MEA is composed of two electrodes as electrocatalytic layers and two gas diffusion layers (GDL) made of carbon materials (see Fig. 3).

Design and Stability Study of Cathode Electrocatalysts

The electrocatalytic materials for the cathode can be selected to mimic what is obtainable in photosynthesis in plants where CO_2 is converted into organic compounds in the presence of H_2O using the energy from the sun; the hydrogen is split into its protons and electrons and used to generate chemical energy. In photosynthesis, the CO_2 molecule is initially bonded to nitrogen atoms, making reactive compounds called carbamates (Gust and Moore 1989). These less stable compounds can then be broken down, allowing the carbon to be used in the synthesis of other plant products, such as sugars and proteins.

In the electrochemical cell, the overall cell reaction potential will supply the energy that splits the CO_2 while sunlight provides the energy during photosynthesis in plants. In the electrochemical process, the electrical potential provides the driving force necessary to convert CO_2 into methane and water at the cathode compartment by using the hydrogen protons and electrons generated from H_2S split

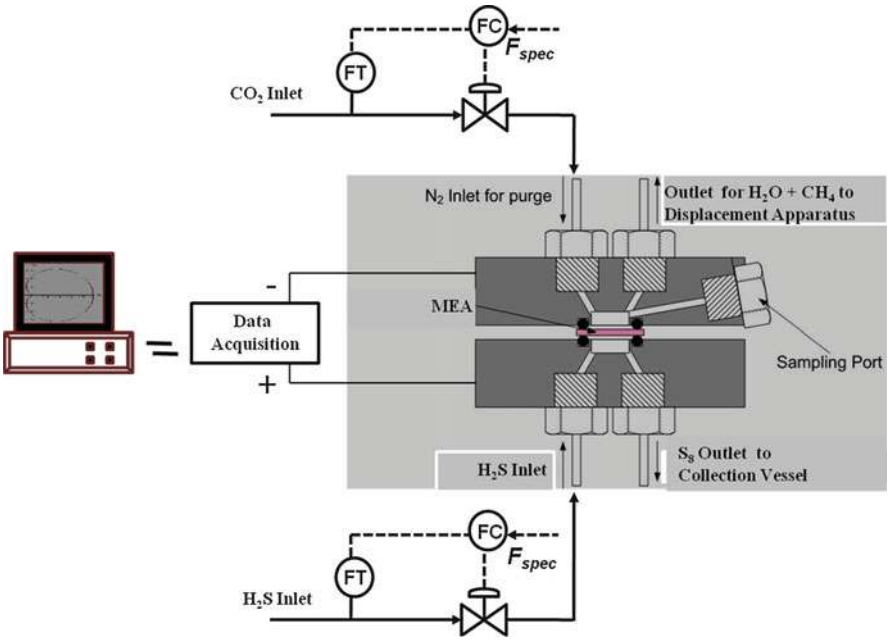

Fig. 5 Experimental setup of CO_2 and H_2S splitting system

Table 1 Postulated cathodic reaction mechanism for methane synthesis

$M_1 \rightarrow {M_1}^{x+} + xe^-$	(1)
$x\mathrm{H_2O} \rightarrow x\mathrm{H}^x + x\mathrm{OH}^-$	(2)
$xe^- + x\mathrm{H}^+ \rightarrow x\mathrm{H}^*$	(3)
$M_2 + x\mathrm{H}^* \rightarrow xM_2 - \mathrm{H}$	(4)
$\mathrm{CO_2} + xM_2 - \mathrm{H} \rightarrow \mathrm{CH_4} + 2\mathrm{H_2O} + xM_2 - \mathrm{H}$	(5)
$M_1 + M_2 + x\mathrm{H_2O} \rightarrow \mathrm{CH_4} + 2\mathrm{H_2O} + xM_2 - \mathrm{H}$	(6)

at the anode compartment in the presence of highly active bimetallic electrocatalysts (M1 and M2). The postulation is that in a first step, the catalyst enabled the CO_2 to form a reactive carbon monoxide (CO) species and oxygen atom. The catalyst's next useful step is to enable the hydrogen protons to grab the very highly reactive CO species from the CO_2 split, producing methane. The oxygen atom from the split reacts with other protons to produce H_2O. Thus CO_2 is used as a source of chemical synthesis. We have in Table 1 postulated a mechanism for CO_2 conversion to methane at the cathode as pertaining to our electrochemical synthesis.

A bimetallic catalyst (M_1 and M_2), in which one metal acts as the electron donor for the production of hydrogen radical while the other acts as a catalyst for the reduction of CO_2, was formulated using impregnation method to serve as the cathode electrocatalyst. At the cathode, metal M_1 converts the migrated hydronium

ion from the anode reaction to hydrogen with subsequent conversion to hydrogen radical. The hydrogen radical is adsorbed locally onto another metal (M_2) of known catalytic activity toward CO_2 hydrogenation. The advantage is that other intermediates formed will be reduced by the highly active hydrogen radical/metal hydride formed. Electrocatalyst M_1 will be chosen such that it can form a galvanic couple with electrocatalyst $M_{2;}$ in that case, the reaction rates would further be enhanced since the process would circumvent the need for an external electric field. Certain transition metals have these capabilities. Depending on the electrode design, the end product may be methanol or methane or other hydrocarbons. The challenge is to design a suitable electrode system that is compatible with electrolyte membrane and selective toward the production of methane and water and not susceptible to degradation in corrosive aqueous environment.

The solubility of CO_2 in water decreases with increase in temperature which implies that at the temperature of operation water produced will not be in solution with CO_2. More also, the hydration equilibrium constant is small (1.7×10^{-3}), hence CO_2 remains as molecules, given that the rate constants are 0.039 s^{-1} for the forward reaction ($CO_2 + H_2O \rightarrow H_2CO_3$) and 23 s^{-1} for the reverse reaction ($H_2CO_3 \rightarrow CO_2 + H_2O$). The water produced will be used to hydrate the membrane instead.

At the anode, the electrolytic splitting of H_2S occurs very easily since H_2S possesses a very low Gibbs energy of formation ($\Delta G = 8.9$ kcal/mol @ 145 °C), so a small amount of electrical energy can split it into elemental sulfur and hydrogen proton (Mbah et al. 2008). This initial energy demand is subsequently compensated by the overall Gibbs free energy of the process ($\Delta G = -49.27$ kcal/mol). While the primary means of splitting H_2S and CO_2 in this application appears to be electrochemical, the elevated temperatures at the membrane interface where CO_2 is adsorbed and subsequently reacts also appears to be indicative of potential thermal catalytic processes.

Cost Analysis of Electrochemical Process

Electrolytic splitting of the extracted CO_2 and H_2S can yield sulfur, methane, and water. This process is illustrated in Figs. 1 and 2. The value of the methane makes the system more profitable. The energy benefit of electrolytic splitting of the CO_2 and H_2S is shown in Eq. 1. The energy costs required to do it electrochemically are significantly low when compared to other electrochemical methods. As a result, this is potentially such a cost-effective procedure that it can have a positive influence on the cost-effectiveness of IGCC energy. This is illustrated by the conceptual economic analysis in Table 2 for IGCC energy (Krakow et al. 2006) initially developed for hydrogen production but modified herein for methane production. It considers the plant capital cost and life, the operating and maintenance costs, and the offsetting revenue from the sale of sulfur to determine the cost of methane.

The cost of $137/t of sulfur for performing the Claus process exceeds the $63/t market value of the sulfur. The $74/t difference is a penalty that operators currently

Table 2 Economic analysis of hydrogen sulfide/carbon dioxide splitting in an IGCC power plant

Power plant parameters	
IGCC Plant capacity (Gross MW)	315
On line (Days/year)	335
Coal consumption (Tons/day)	63
Coal sulfur content (%)	2.5
Electrochemical plant investments	
Apparatus to remove carbon dioxide	$ 1,350,000
Electrolyzer	$ 6,460,000
Balance of plant	$ 3,325,000
Total electrochemical plant investments	$ 11,135,000
Annual capital and O&M costs	
Annualized capital costs	$ 1,500,000
Labor	$ 525,000
Catalysts, water and other operating costs	$ 40,000
Electricity	$ 2,500,000
Total annual capital and O&M costs	$ 4,565,000
Methane production costs	
Costs to produce 1 Ton of S + 125 lb. of H_2	$ 215
Avoided cost of claus process/Ton of S	$ 137
Net production cost of 1 lb. of H_2	($ 0.63)
Net production cost of 1 lb. of CH_4 Gas	($ 0.63)
Market price of sulfur ($/LB)	$ 2.50
Market price of CH_4 ($/LB)	$ 0.08
Cost of electricity US$/kWh	($ 0.07)
Gross profit ($/LB.)	$ 1.25

pay to get rid of the hydrogen sulfide by-product gas. This penalty would be avoided by using the electrochemical/electrolytic process where the total value of the two products (sulfur and methane) exceeds the cost of the electrochemical processing. Methane costs will vary based on location and also by the quantity. The $1.25/lb. profit on the methane and sulfur increases the cost-effectiveness of IGCC energy by over $1/MWh. This is achieved without claiming any economic credit for purifying the CO_2 in the acid gas to make it more suitable for splitting.

Splitting of H_2S Over a Solid Membrane

The electrochemical system is operated near (120–145 °C) using a solid electrolyte membrane. Natural separation of the H_2S gas, CO_2, liquid sulfur, CH_4, and H_2O occurs in such a system. Hydrogen sulfide introduced at the anode compartment is electrolyzed at the surface of the solid electrolyte producing hydronium ions that pass through the electrolyte and liquid sulfur that pools at the bottom of the positive compartment from which it is withdrawn through a drain. The pool of liquid sulfur

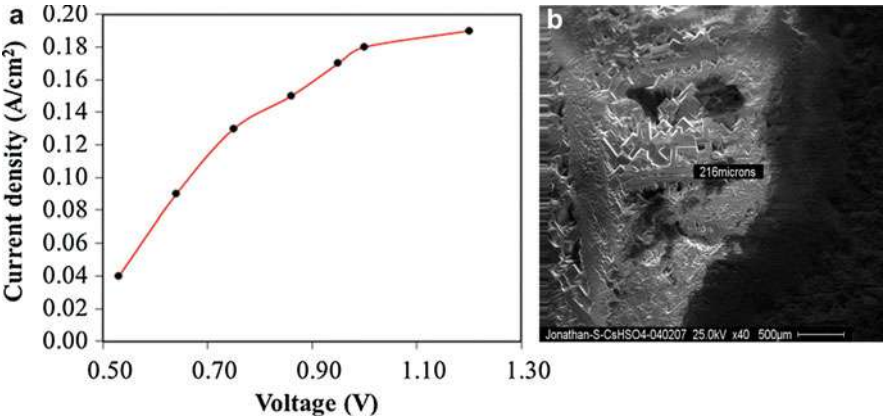

Fig. 6 (**a**) Current density versus voltage generated, (**b**) SEM image (25.0 kV × 40 500 pm) of electrolyzed pellet of $CsHSO_4$ membrane with layers of 65 wt% sulfur deposit

forms a barrier that keeps H_2S away from the drain. Figures 6a, b show the current density/voltage relationship and the resulting SEM spectrogram of electrolyzed sulfur by wt% in the electrochemical splitting of H_2S to elemental sulfur over a solid membrane using anodic electrocatalysts comprising of ruthenium (IV) oxide/ cesium hydrogen sulfate/pt black/ p-Dichlorobenzene and cathodic electrocatalyst comprising of platinum black/p-Dichlorobenzene.

The oxidation of H_2S to H^+ and sulfur ($H_2S \rightarrow 2H^+ + 2e^- + \frac{1}{8}S_8$) over a supported metal component is an important step involved in the splitting system. Most noble metal catalysts such as Pt, Pd, Ru, and Ir have high selectivity toward H_2S splitting. Noble catalysts are expensive, so augmentation is carried out by formulating metal composite using more of the less expensive materials from other groups to serve as the support materials and less of the expensive materials as the active ingredients. If dispersion of the active materials is carried out effectively during impregnation, then less quantity of more expensive materials can be utilized compared to using bulk active materials. Nevertheless, choice eletrocatalytic materials must have high density of catalytic active sites and not susceptible to poisoning.

Other potential electrocatalysts can be selected from both non-noble and noble transition metals and their bimetallic alloys and base metals. For the anode configuration, electrocatalyst precursors could consist of noble and non-noble metals of transition elements or their compounds and base metals. In some cases, main group elements and their compounds may be included. Impregnation technique is used in electrocatalyst synthesis from these precursors because it enables proper control of electrocatalyst design parameters – activity, stability, regenerability, and selectivity. These precursors include salt solutions of $CuSO_4 \cdot 5H_2O$, $RuC1_3$, H_2PtC1_6, hydrated copper chloride, hydrated zinc oxide, $Pd(NO_3)_2$, NaOH solution, $PdO{\cdot}nH_2O$, aluminum oxides, hydrated nickel chloride, iridium (III) chloride hydrate, p-Dichlorobenzene, ruthenium (IV) oxide, and hydrated cobalt chloride.

These materials have proven to possess excellent catalytic properties toward H_2S oxidation and/or CO_2 reduction. Electrocatalyst formulation using these precursors focuses on increasing the catalytic active sites and altering of the surfaces of the materials, harnessing their properties to products that have good mechanical strength at operating conditions since material integrity is an issue as discussed in the previous section. The resulted electrocatalysts after impregnation and calcinations provide the required activity, selectivity, and stability needed for both the cathode and anode reactions. It has been shown that even though copper electrode is suitable for the formation of hydrocarbons such as methane and ethylene from CO, it lacks stability. Thus, improving the stability of copper using this formulation method is desirable.

Design and Composition Ratios of Supported Electrocatalyst

Stability of the cathodic compartment is of utmost priority in this design since this is where major degradation is most prominent due to poisoning of active sites. In using impregnation techniques, it is essential to have an understanding of both chemical and physical properties of the support and the chemistry of the impregnating solution in order to control the physical properties of the finished catalyst. Loading of active metals and support materials should be varied in order to obtain optimum dosage. However, trade-off between catalyst activity and stability should be expected. Changes in selectivity can also arise from changes in intrinsic chemical activity of the active component. Typically this can be affected by use of multicomponent catalysts in which case the location of the difference components ideally should be the same.

Poisoning of the catalyst by impurities introduced with the reactants can often be minimized by placing the active material deep within the catalyst support structure, and since most catalyst supports are also good absorbents, poisons frequently can be selectively removed by such absorption before reaching the active surface. A catalyst design modification would be the deposition of a poison-resistant catalyst component close to the surface and a poison-sensitive component deep within the support. The poison resistance location of the active component becomes a critical factor in proper catalyst design. The use of electron probe microanalysis (EPMA) will provide information on the location not only of active materials but also potential catalyst poisons. Blockage of the support-pore structure is critically dependent upon the pore-size distribution of the support. Normally a correct balance of large and small pores is required; the former to aid reactant transport and the latter to provide the large surface necessary for the optimal dispersion of the active components. Porous carbon material with high activated carbon content as a support material serves this purpose. Characterization of supported catalyst species, particularly with regard to metal-support and metal-metal interactions, should be carried out possibly using temperature-programmed reduction/oxidation (TPR/O) equipment.

The techniques of catalyst preparation involves two simple steps, dispersing the active material in a liquid form and immobilizing this dispersed material as it is

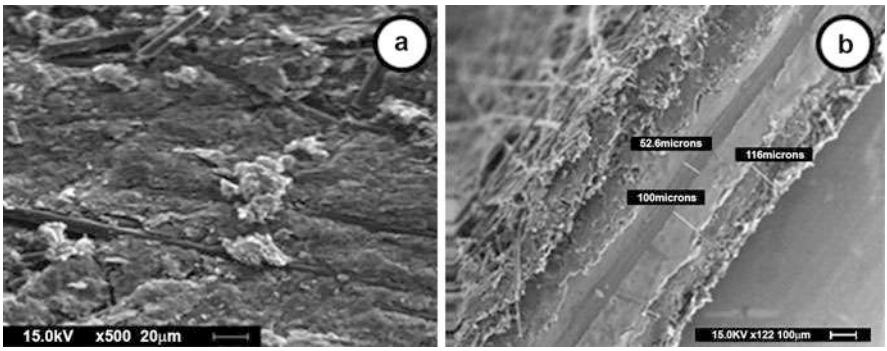

Fig. 7 (**a**) Dispersion observed for formulated cathode electrocatalyst (Cu/RuO_2) using catalyst design approach; (**b**) cross sectional view of MEA comprising of the designed electrocatalyst formulated

reconverted to an insoluble solid form. One way of doing this is to allow the material to react with the insoluble support surface. This implies that support surface should be reactive with the soluble active material. This becomes a drawback since the support material is carbon, which has peculiar and variable properties tending to form charge-transfer complexes as an electron donor, but it also can act as a weak cation exchanger by virtue of acidic surface oxide groups. Interactions between the active materials and support in terms of immobilizing the active ingredients on the support surface are either the cationic or anionic exchange with protons or hydroxyl groups on the surface. To enhance the supports cationic exchange, the carbon with γ-alumina together with bonding agents such as alumina, silica, etc. are washcoated before impregnation which then provides the necessary reactive surface for the active ingredients. In this way atomic dispersion of active ingredients is in principle possible. The proton or hydroxyl group is provided by the γ-alumina. Temperature-programmed reduction and oxidation will provide valuable guides to the thermal treatment and reduction stages of electrocatalyst preparation.

As previously mentioned, copper is a good reduction cathode electrocatalyst but suffers severely from thermal instability at elevated temperature and in corrosive environment. Stability will be improved by supporting it in a high surface material such as high-carbon porous material. Catalyst retention on support materials, regenerability, stability, activity, and selectivity is very important. Cyclic voltammetry potential sweep test should be applied to evaluate the stability of synthesized catalysts. Of equal importance is the weight lost by thermogravimetric analysis using simultaneous DSC-TGA instrument. This is very important since some materials have the tendencies to lose their integrity in the presence of sulfur and corrosive environments as was found. Furthermore, by evaluating the responses of each electrocatalytic material the catalyst loading required and the partial pressures of component gases that provide the best reactivity can easily be found.

Figure 7a is a surface morphology view of cathode electrocatalyst formulated by applying catalyst design scheme where poison-sensitive Cu component is

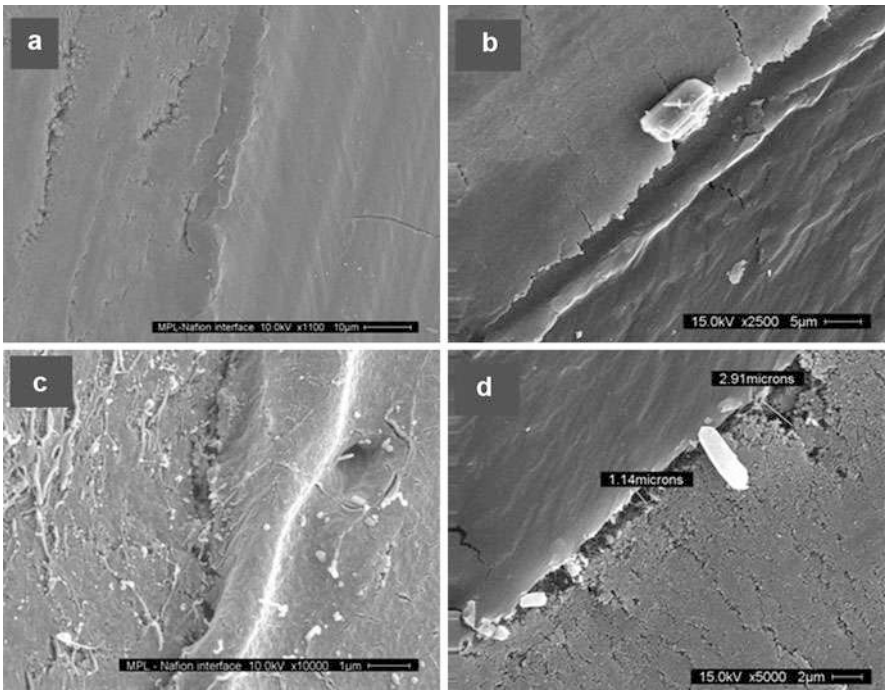

Fig. 8 (**a**) Control MEA – interface ×1100; (**b**) MEA with no catalyst design approach nterface ×2500; (**c**) a– interface ×10,000; (**d**) b – interface ×5,000

embedded deep within carbon support while poison-resistant component ruthenium (IV) oxide, RuO_2, is close to the surface. Figure 7b illustrates a typical MEA fabricated from this electrocatalyst (see also Fig. 3); the cross-sectional view was analyzed for any apparent separation or tearing of the individual layers after several cycles. The image has been annotated to indicate the approximate thickness of each of the layers of assembly, namely, Gas Diffusion Layer ∼ 116 μm; Micro Porous Layer ∼ 100 μm; Proton Exchange Layer ∼ 52.6 μm. At higher magnification, no delamination was observed in MEA fabricated using the designed electrocatalyst. The results of this investigation are summarized in Fig. 6.

Mesoporous investigation is shown in Fig. 8. Figure 8a shows the interface between the microporous (electrocatalyst) and proton exchange (Nafion) layers of an MEA which electrocatalyst layer was formulated using impregnation design approach with the noble metal-based catalyst 4 wt% (RuO_2) on the surface and 1.6 wt% active Cu embedded deep on the support (control membrane). At lower magnification of 1100×, no apparent gap or tearing of the interface was observed at 125 °C and varying cell pressures. Figure 8b depicts the same interface in the MEA which electrocatalyst layer was formulated using impregnation method but with no catalyst design approach. This image shows a more pronounced division between the two layers. This feature was very clear when we look at these membrane

microstructures at higher magnifications, 10,000×. Figure 8c shows the control membrane's interface at 10,000x magnification. A relatively smooth transition is still seen between the layers even at this magnification. In contrast, Fig. 8d shows a distinct channel dividing the two layers at half the magnification. This channel would be enough to increase the ohmic proton exchange resistance of the membrane.

This indicates that catalyst design, if monitored properly, provides good promise in eliminating cathode electrode degradation currently faced in many electrochemical applications. Different electrode/electrolyte attachments should be tested since this is a major issue in electrochemical applications that utilize solid electrolyte where delamination of membrane increases the cell ohmic resistances: as interfacial delamination width and area fraction increases, the ohmic resistance increases. Characterization of MEA may include the use of X-ray diffractometer (XRD), scanning electron microscopy (SEM), simultaneous differential calorimetry-thermogravimetric analysis (DSC-TGA), cyclic voltammeter, Quantachrome instruments (BET for specific surface, pore sizes), and electrochemical impedance spectroscopy (EIS).

Conclusion

Carbon dioxide and hydrogen sulfide are both greenhouse gases and pose a challenge to the modern society, where environmental pollution has to be minimized to an acceptable level. Since both H_2S and CO_2 often occur together in petroleum and natural gas resources, and are major by-products of integrated gasification combined cycle (IGCC) power plants, a technique that can simultaneously split both gases is desirable. The advantages offered by electrochemical approach using CO_2 and H_2S as feedstock to reduce air pollution and at the same time conduct carbon dioxide sequestration cannot be overemphasized, thereby providing a vista to the long-sought method of CO_2 mitigation. Currently, CO_2 and H_2S are separated using a double-absorber Selexol process which preferentially removes H_2S as product leaving CO_2 as a separate product stream. These two separate streams can be channeled into an electrochemical cell apparatus for production of useful chemicals. This approach is useful in the integrated gasification combined cycle power plants (IGCC), which currently extract sulfur from the process stream as hydrogen sulfide using the Claus Process along with unsequestered CO_2 stream. Our process is cost effective and overcomes the energy barrier associated with previous electrochemical processes. At the temperature range of operation (120–145 °C), sulfur is a low-viscosity liquid and can flow out of the electrolytic cell without hindrance. Although, the COE is less for an IGCC plant with CO_2 and H_2S cocapture compared to those IGCC plants that capture 80 % CO_2 and H_2S separately (5.48 and 6.67 US¢/kWh) respectively, the sale of methane and sulfur will eventually close this gap.

Future Directions

Electrochemical reduction of CO_2 into value-added chemicals using renewable energy is one approach to help address CO_2 emission as it will recycle "spent" CO_2 (carbon neutral cycle) and it provides a method to store or utilize otherwise wasted excess renewable energy from intermittent sources, both reducing our dependence on fossil fuels. Current electrolysis cells accomplish either high Faradaic yield (often >95 % selectivity) for a desired product or reasonable current density, whereas both need to be high for a commercial process.

Catalysts for the selective reduction of CO_2 into different interesting products have been developed, but catalysts that simultaneously exhibit overpotentials (e.g. <0.2 V) and current densities (e.g. >100 mA/cm^2) needed for commercial applications are still lacking. The quest for such catalysts could be aided by more fundamental studies focusing on elucidation of reaction mechanisms for distinct catalysts, an area in which reports are few. Novel catalysts have both low overpotential and high activity for CO_2 reduction reactions.

Few efforts to date have focused on the effects of electrolyte composition on electrochemical CO_2 reduction, despite the fact that electrolytes have been known to affect almost every electrochemical process. Electrolyte choice has profound effects on current density, product selectivity, and energetic efficiency in CO_2 reduction. More also, CO_2 electrolysis is much more sensitive to the structure and composition of the microporous layer. Significant strides will be made to enhance catalyst activity while reducing overpotential. Such efforts will greatly benefit from fundamental mechanistic studies, as well as modeling of new classes of catalytic materials. Fine-tuning the electrolyte composition for a given catalyst offers a further opportunity for performance enhancement. A key opportunity resides in optimization of electrode structure and/or composition.

References

Aspen Plus™ 11.1 (2010) Users guide. Aspen Tech Ltd, Cambridge

Bachu S, Adams JJ (2003) Sequestration of CO_2 in geological media in response to climate change: capacity of deep saline aquifers to sequester CO_2 in solution. Energy Convers Manag 44(20):3151–3175

Bockris B (2005) Method and device for dissociating carbon dioxide molecules. United States Patent Application 2006/0213782 A1

Burt K, Eric W, George M, Lee S (2006) Hydrogen production by electrochemical dissociation of hydrogen sulfide in refineries, University of South Florida Clean Energy Research Center, ACS Proceeding, National Mtg Atlanta, 26–30 Mar 2006

Caldeira K, Jain AK, Hoffert MI (2003) Climate sensitivity uncertainty and the need for energy without CO_2 emission. Science 299(5615):2052–2054

Campanari S (2001) Thermodynamic model and parametric analysis of a tubular SOFC module. J Power Sources 92:26–34

Chang T, Liang R, Wu PW, Chen J, Hsieh Y (2009) Electrochemical reduction of CO_2 by Cu_2O-catalyzed carbon clothes. Mater Lett 63(12):1001–1003

Clarkson CR, Bustin RM, Levy JH (1997) Application of the mono/multilayer and adsorption potential theories to coal methane adsorption isotherms at elevated temperature and pressure. Carbon 35:1689–1705

Ersoz A, Olgun H, Ozdogan S (2006) Reforming options for hydrogen production from fossil fuels for PEM fuel cells. J Power Sources 154(1):67–73

Fujita E (1999) Photochemical carbon dioxide reduction with metal complexes. Coord Rev 185–186:373–384

Gattrell M, Gupta N (2006) A review of the aqueous electrochemical reduction of CO_2 to hydrocarbons at copper. J Electroanal Chem 594(1):1–19

Gomberg HJ, Lewis JG, Powers JE (1984) Radiolytic dissociative gas power conversion cycles. United States Patent Re. 31697. Reissued Oct

Grimes W (2005) Evaluating the risk of encountering non-hydrocarbon gas contaminants (CO_2, N_2, H_2S) using gas geochemistry. OilTracers L.L.C Copyright © 199

Gust D, Moore TA (1989) Mimicking photosynthesis. Science 244:35–41

Hockstad L, Cook B (2009) Inventory of U.S. greenhouse gas emissions and sinks: 1990 – 2009. U.S. Environmental Protection Agency, EPA 430-R-11-005

Hoek A, Martin FM, Minderhoud KJ, Lednor PW (1985) Process for the preparation of a Fischer-Tropsch catalyst and preparation of hydrocarbons from syngas, United States Patent 4499209

Kaneco S, Iiba K, Katsumata H, Suzuki T, Ohta K (2006a) Electrochemical reduction of high pressure CO_2 at a Cu electrode in cold methanol. Electrochim Acta 51(23):4880–4885

Kaneco S, Katsumata H, Suzuki T, Ohta K (2006b) Photoelectrocatalytic reduction of CO_2 in LiOH/methanol at metal-modified p-InP electrodes. Appl Catal Environ 64(1–2):139–145

Klara JM, Wimer JG (2007) Cost and performance baseline for fossil energy plants, vol. 1. DOE/NETL-2007/1281

Ku AYC, Ruud JA, Manoharan M, Kool LB, Martins-Loureiro SP, Blohm ML, Norman BG (2005) Reactor for carbon dioxide capture and conversion. United States Patent Application 2007/0149392 A1

Lee M, Ren M, Zhang Z, Sprunger PT, Kurtz RL, Flake JC (2011) Electrochemical reduction of CO_2 to CH_3OH at copper oxide surfaces. J Electrochem Soc 158(5):E45–E49

Li H, Oloman C (2007) Development of a continuous reactor for the electro-reduction of carbon dioxide to formate – Part 2: scale-up. J Appl Electrochem 37:1107–1117

Mbah J, Krakow B, Stefanakos E, Wolan J (2008) Electrolytic splitting of H_2S using $CsHSO_4$ membrane. J Electrochem Soc 155(11):E166–E170

Miyake N, Wainright JS, Savinell RF (2001) Evaluation of a Sol–gel derived Nafion/Silica hybrid membrane for proton electrolyte membrane fuel cell applications: I. Proton conductivity and water content. J Electrochem Soc 148(8):A898–A904

Ordorica-Garcia G, Douglas P, Croiset E, Zheng L (2006) Technoeconomic evaluation of IGCC power plants for CO_2 avoidance. Energy Convers Manag 47:2250–2259

Pérez-Rodríguez S, García G, Calvillo L, Celorrio V, Pastor E, Lázaro MJ (2011) Carbon-supported Fe catalysts for CO_2 electroreduction to high-added value products: a DEMS study: effect of the functionalization of the support. Int J Electrochem, volume 2011:13. http://dx.doi.org/10.4061/2011/249804

Rayne (2008) Thermal carbon dioxide splitting: A summary of the peer-reviewed scientific literature. Available from nature precedings. http://dx.doi.org/10.1038/npre..2008.1741.2

Toyir J, Ramirez de la Piscina P, Llorca J, Fierro G, Homs N (2001) Methanol synthesis from CO_2 and H_2 over gallium promoted copper-based supported catalysts. Effect of hydrocarbon impurities in the CO_2 source. Phys Chem Chem Phys 3:4837–4842

Wise M, Calvin K, Thomson A, Clarke L, Bond-Lamberty B, Sands R, Smith SJ, Janetos A, Edmonds J (2009) Implications of limiting CO_2 concentrations for land use and energy. Science 324(5931):1183–1186

Power-to-Gas

Michael Sterner

Contents

This chapter was originally published in M. Sterner, I. Stadler, Energiespeicher – Bedarf, Technologien, Integration- 2009. Published with kind permission of Springer-Verlag Berlin Heidelberg.

M. Sterner (✉)
Forschungsstelle Energienetze und Energiespeicher (FENES), Fakultät für Elektro- und Informationstechnik, OTH Regensburg, Regensburg, Germany
e-mail: michael.sterner@oth-regensburg.de

W.-Y. Chen et al. (eds.), *Handbook of Climate Change Mitigation and Adaptation*,
DOI 10.1007/978-3-319-14409-2_89

Abstract

This chapter provides an overview on the storage technology power-to-gas for the decarbonization of all energy sectors. Other than "negative emissions" with CCS or biomass, which have clear limits in potentials, costs and environmental benefits, storage and energy conversion technologies like power-to-gas and power-to-x enable the decarbonization by neutralizing the CO_2 footprint of all energy services. Via the conversion of renewable electricity into chemical energy carriers like renewable hydrogen or renewable hydrocarbons, the existing fossil infrastructure with vast and sufficient storage and transport capacities can be used with carbon neutral renewable energy. After showing the demand for storage technologies, the technology components of power-to-gas are described, building the basis for the storage system power-to-gas itself that is described in detail, including efficiency, potential, CO_2 emissions, and costs. In conclusion, a technical pathway of decarbonization including costs is described for the industrial nation of Germany and necessary policy frameworks are derived.

Introduction

No energy system can do without storage. Storage is essential for energy security. Each energy transition needs also a storage transition. Storage will be an essential part of decarbonization worldwide. As several international summits pointed out, we need to complete decarbonization in industrialized nations by 2050. That means the exit of fossil energy carriers such as coal, oil, and natural gas. The good news is that this is actually doable: there is enough renewable energy potential, to shift completely to renewable and clean energy sources. The storage technologies also exist and are ready to be deployed. Decarbonization is possible without CCS and large-scale deployment of biomass by using vastly available wind and solar resources, transformed in biomass-like energy carriers. The technological and economical dimension of the storage technology power-to-gas in a decarbonization scenario is described in the following chapter.

The Need for a Storage Transition in Energy Transition

Storage in the Context of Energy Transition and Flexibility Options

No energy system can do without storage. Storage is essential for energy security. Each energy transition needs also a storage transition. Storage will be an essential part of decarbonization worldwide. As several international summits pointed out, we need to complete decarbonization in industrialized nations by 2050. That means the exit of fossil energy carriers such as coal, oil, and natural gas. The good news is that this is actually doable: there is enough renewable energy potential, to shift completely to renewable and clean energy sources (Sterner and Stadler 2014).

Among renewable energy technologies, wind and solar power have proven to be the most cost- and land-use-efficient technologies to harvest the energy that is in our environment. The downside is of course the intermittency of wind and solar power, but there are solutions to this:

- Flexible generation (e.g., flexible gas turbines and gas CHPs [combined heat and power])
- Flexible consumption (e.g., demand side integration)
- Network expansion
- Storage

In electricity supply, the exact matching of generation and consumption (loads) is essential for a stable supply. The chain consists of generation, transport via networks, and consumption. First of all, not all electricity from wind and solar generators must be integrated into the electricity system. It is economically not feasible to include the "last" kilowatt-hour, since some power peaks are rather high and the energy contained in those peaks is not enough to refinance the respective flexibility option.

Flexible Generation

The conventional generation capacities need to be flexibilized: fast ramping will become mandatory to include cheap wind and solar power, which does not follow any market command but is as naturally available as nature is. Fast ramping can be done by gas turbines and gas CHPs but not at the required scale by lignite coal or nuclear plants. The latter require a very high utilization rate over the years to cover their investment-intensive capital cost. Gas turbines are not capital-intensive. So both technically and economically, gas technologies offer the best "fossil" solution for backing up wind and solar. Hydropower and biomass electricity can do the same, but they are as well rather capital-intensive and limited in potential.

Flexible Demand: Demand Side Integration

Flexibilizing the power consumption is being done for demand side integration, as a combination of demand side response and demand side management, since the 1970s in the form of night heating systems and flexible tariffs. In Germany, there were state subsidies for night heating systems; in Belgium, highways were lit during the night. France shifted the major share of its heating system towards electricity. The goal in each case was to increase the utilization rate of nuclear power plants. Nowadays, demand side flexibility potentials exist at the GW scale, but they need to be market stimulated. It will be mandatory for new electricity consumers like electromobility and heat pumps. These new devices need to be connected and controlled via smart grid technologies in order to stabilize and not destabilize power network operation. The largest advantage of demand side management is the very low investment cost, since the major process is financed separately and demand side management is just an additional function. However, this potential is

also limited, since the manufacturing of products or consumer needs can be delayed by some minutes or hours, but not for days, if there is no wind and solar power for longer periods. Also, for a safe and stable network operation, a nearly 100 % availability and reliability is necessary. This availability is a challenge for demand side management in industrial applications that follow a different major function rather than the additional function demand side management.

Network Expansion
The expansion of electricity networks is another flexibility option, which is so far the most efficient integration option in terms of economy and technology, as long as a total underground cabling is not necessary. Wide area networks, like a pan European network, are therefore an essential element of future energy systems. But network expansion also has its limits: it can balance the spatial component of fluctuating wind and solar power but not the temporal component. In addition, public acceptance is not always given. The temporal balancing can only be done by storage.

Storage
Storage is needed as a flexibility option – today and tomorrow. The stability of today's system is based on stored fossil energy: coal piles, gas caverns, and so on. This functionality has to be provided also in future energy systems, since wind and solar power may be increased infinitely, due to weather conditions, still up to 80 % of the peaking power of a nation is required as backup capacity. This will be achieved by gas power plants, using the existing gas infrastructure, that offer what has been missing in the power sector: immense storage capacities.

Power-to-Gas in the Context of Energy Storage

A storage system consists of three parts:

1. Charging
2. Storing
3. Discharging

These three parts can be in one system (e.g., batteries), several parts in one system (e.g., pumped hydro), or even distributed parts over several various sectors (intersectoral energy storage, e.g., Power-to-Gas), as shown in Table 1.

These storage technologies can be classified again in different ways:

– Technology
  - Electrical
  - Electrochemical
  - Chemical
  - Mechanical
  - Thermal

Table 1 Three parts of energy storage in various applications for electricity storage

	Lithium-ion battery	Pumped hydro	Power-to-Gas
Charging	Internally fixed energy and power units	Water pumps	Electrolysis (and methanation)
Storing		Two reservoirs	Gas storage
Discharging		Water turbine	Gas turbine/vehicle/heating system

– Temporal balancing
  • Short-term storage
  • Long-term storage

Thermal energy storage is still the cheapest option to store energy and is being used widely, but it is not suitable for electricity storage, since the conversion step is "one way" from power to heat. The reconversion of heat to power is very inefficient and thus not feasible. The focus of the following part is electricity storage.

Pumped Hydro, Batteries, and Compressed Air as Short-Term Storage
Among electricity storage, pumped hydropower plants is an old, established technology that is very efficient for power storage. It is, however, a classical short-term storage technology, and its expansion is limited to geography, ecological impact in the form of land use, and public acceptance in general. The second option is batteries. Electromobility gives an impressive drive on this technology, which has been used in power plants for ages. Battery power plants are also feasible for electricity grid stabilization: they can react much faster than conventional power plants and therefore balance wind and solar in no time. In combination with renewables, stationary battery systems can take over the stability services of conventional power plants and replace them. There has been a misbelief in the past that the increase of renewables in the electricity grid is limited to 30 %. This is, from an electric engineering perspective, not true: all technologies are available to operate an electric grid even at 100 % renewables. The third option is compressed air, but compared to pumped hydro and batteries, it is not feasible and only two plants in Huntorf, Germany (60 MW charging power), and in McIntosh, USA (50 MW), are in operation worldwide. Pumped hydro and batteries offer a feasible and highly efficient short-term storage option. The drawback is the high cost for capacity and the self-discharging over time in the case of batteries. There is therefore the need for a long-term storage facility, and the gas infrastructure offers this. One standard gas cavern can fuel a gas power plant with 800 MW rated capacity for 3 months. The question remains: how can we use this infrastructure for wind and solar power? The answer is Power-to-Gas.

Power-to-Gas as Long-Term Storage and Decarbonization Technology
Power-to-Gas is a new storage technology that interlinks the power with the gas sector. It allows in the first step to split water into hydrogen and oxygen via

electrolysis and the use of renewable power. In the second step, hydrogen is combined with CO_2 to form a substitute for natural gas (SNG, synthetic natural gas), which is 100 % compatible with the natural gas infrastructure. The access for renewable energy is then given to millions of households with a gas network connection. The renewable gas (windgas, solargas) can then fuel the necessary backup gas power plants. For short-term balancing, pumped hydro and batteries offer of course much cheaper storage services with double efficiency, but when it comes to long-term storage, Power-to-Gas is the most cost-efficient option: a kilowatt-hour storage capacity costs 200–300 € for batteries and only 0.2–0.3 € for gas storage. With Power-to-Gas, a decarbonization of mobility and nonenergetic use of fossil resources in the chemical industry is possible.

A short overview of sectoral and cross-sectoral energy storage units is shown in, embedding the described different pathways and applications of Power-to-Gas within the energy system.

This promising new technology is described in the following:

Technology Components of Power-to-Gas

Power-to-Gas is an energy storage system that consists of various technologies. The systems are described in section "The Storage System Power-to-Gas" and the necessary technologies in this part. The main part of Power-to-Gas is the charging unit, which contains water electrolysis (section "Charging Technology Water Electrolysis") and optionally methanation (section "Charging Technology Methanation"). The storage and discharging unit are usually the conventional existing technology parts: salt caverns, aquifers, gas turbines, CHPs, heating units, and CNG (compressed natural gas) cars and hence not described in detail in this chapter but in the main book *Energy Storage – Demand, Technologies, Integration* at Springer-Editors (Sterner and Stadler 2014).

Chemical energy storage is the backbone of the conventional energy supply. Solid (wood & coal), liquid (crude oil), and gaseous (natural gas) energy carriers are different types of energy storage themselves. Also in the energy transition, chemical energy storage plays an important role, especially in its function as long-term storage for the electricity sector but also as a distributor of fuel for mobility and heat. This chapter will, besides the conventional storage technologies, take a deep look into the storage of renewable energies in the form of gaseous (Power-to-Gas) energy carriers.

Charging Technology Water Electrolysis

There are three different technologies available for water electrolysis, which are of technical relevance and differ in function, operating conditions, and stage of development:

– Alkaline electrolysis (AEL)
– Proton exchange membrane electrolysis (PEM)
– High temperature electrolysis of steam (HTES) or solid oxide electrolysis (SOE)

These different electrolysis technologies can be implemented as an atmospheric or a pressurized electrolysis system in various stack designs and plant peripheries, which are described in Sterner and Stadler (2014).

Alkaline Electrolysis (AEL)

The alkaline electrolysis of water is a widely proven and well-established large-scale technology. Realized sites were constructed nearby large power plants because of the continuously required power for the electrolysis unit. The largest atmospheric alkaline electrolysis unit in the world with 156 MW nominal power is situated at the Assuan retaining dam in Egypt, with a hydrogen production rate of 33,000 standard cubic meter per hour. The technology is proven and commercially available since many decades. Nevertheless, there is a need for optimization and adoption to the new requirements of fluctuating renewable energies in terms of dynamics and efficiencies.

Figure 1 shows the schematic construction and the function of an alkaline electrolysis cell.

Water circulates through both halves of the cell, which are separated by an ion-conducting membrane. Potassium hydroxide (KOH) 20–40 % by weight is added to the water to increase its conductivity. Thus, the inner resistances in the cell decrease and the conversion efficiency rises. Porous electrodes with a large surface are located on both sides near the membrane. The decomposition voltage of

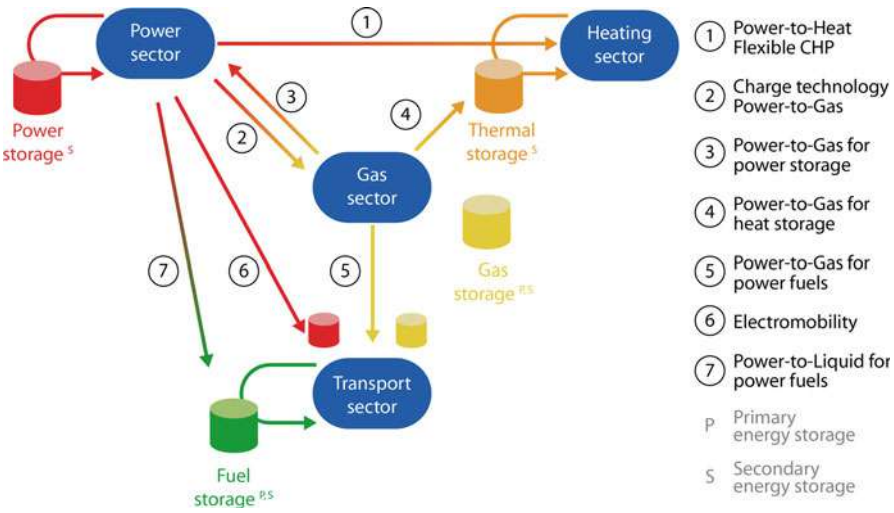

Fig. 1 Sectoral and cross-sectoral energy storage units within the energy system (Source: Sterner and Stadler 2014)

water is 1.23 V. If an ideally equal or realistically higher voltage is applied to these electrodes, the water on the side of the cathode is split into atomic hydrogen and hydroxide ions (HO^-), as described by the cathode reaction (Eq. 1).

$$2H_2O(l) + 2e^- \rightarrow H_2(g) + 2OH^- \quad (1)$$

The generated atomic hydrogen reacts to molecules, rises, and is separated from the electrolyte. At the same time, hydroxide ions pass through the membrane and react to water and atomic oxygen in the anodic reaction (Eq. 2), releasing an electron.

$$2OH^- \rightarrow {}^1\!/_2O_2(g) + H_2O(l) + 2e^- \quad (2)$$

The generated oxygen molecules are separated from the electrolyte and extracted. The consumed water has to be refilled, the electrolyte is recycled. Two electrons are required in each half of the cell for the whole reaction (Eq. 3). They are provided by the power source and transported via the closed electrical circuit.

$$H_2O(l) \rightarrow H_2(g) + {}^1\!/_2O_2(g) \quad (3)$$

The cell frame seals the cell against external influences, isolates the electrons from each other, and serves as a carrier for the membrane. The circulation of the electrolyte and hence the homogenous load distribution is ensured by the flow of rising gas bubbles at low loads. At higher loads, an active agitation has to be implemented.

Membrane Electrolysis (PEM)

The membrane electrolysis (also called Proton exchange membrane or PEM electrolysis) originates from the fuel cell technology and is based on the inverted processes of a fuel cell. It is better suited for a dynamic and pressurized operation than the alkaline electrolysis and needs less space, but to present, it has only been realized in a rather small kW-scale.

A PEM electrolysis cell (Fig. 2) consists of a proton conducting membrane, which is usually permanently fixed on both sides with the electrodes to the so-called membrane electrode assembly (MEA). A solid polymer electrolyte (SPE) like Nafion™ is coated on the electrodes. It is highly porous and accomplishes on one hand the current flow from the bipolar plates to the electrode and on the other hand the transport of water and product gases.

The bipolar plates conduct water via engraved canals to the anode and permit the withdrawal of product gases. In addition, they serve to supply a uniform current density distribution over the electrolyte.

The PEM electrolysis cell differs fundamentally from the alkaline electrolysis cell in its function. Water is supplied to the anode and split to atomic oxygen and two protons in the anode reaction (Eq. 4) with the decomposition voltage applied.

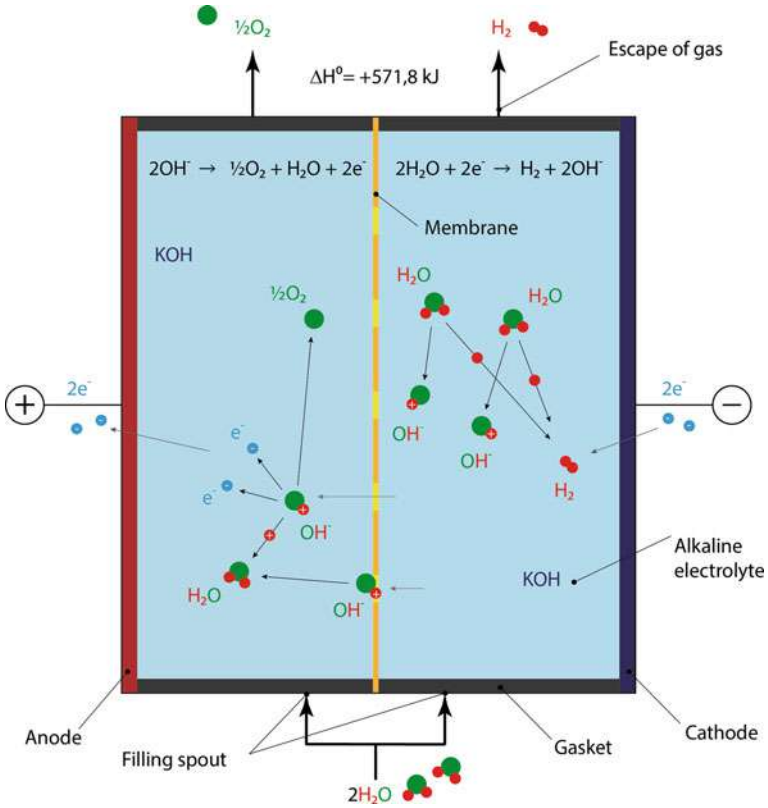

Fig. 2 Function of the alkaline electrolysis (Source: Sterner and Stadler 2014)

$$H_2O(l) \rightarrow {}^{1}/_{2}O_2(g) + 2H^+ + 2e^- \tag{4}$$

The oxygen is withdrawn whereas the protons pass through the membrane and react in the cathode reaction (Eq. 5) with two electrons to form hydrogen.

$$2H^+ + 2e^- \rightarrow H_2(g) \tag{5}$$

Hence, only the anode side is flushed with water. In theory, hydrogen is only produced in the cathode side of the cell. In reality, this side contains high humidity. Compared to the alkaline electrolysis, where partially residues have to be washed out of the electrolyte, the resulting hydrogen contains far less waste materials and has a higher purity. Therefore, the need for hydrogen purification and treatment after the cell is less in the PEM technology, but it is currently still twice as expensive as the alkaline technology.

High Temperature Electrolysis of Steam (HTES)

In the high temperature electrolysis of steam (HTES), a part of the energy for water splitting is supplied by high calorific heat in the range of 850–1,000 °C. The cell voltage can be reduced by 0.5 V to less than 1 V compared to PEM, and alkaline electrolysis and high efficiencies can be realized.

The function of the HTES is based on the reverse reaction of the solid oxide fuel cell (SOFC) (Fig. 3). Both halves of the cell are separated by an oxygen ion conducting solid electrolyte, on which the electrodes are applied on both sides.

Overheated steam is fed to the cathode and reacts with two electrons to form hydrogen and oxygen ions on the cathode side (Eq. 6). Hydrogen can be extracted, and the oxygen ions diffuse through the electrolyte to the anode, where they react to atomic oxygen, releasing two electrons (Eq. 7).

$$H_2O + 2e^- \rightarrow H_2 + O^{2-} \tag{6}$$

$$O^{2-} \rightarrow 2e^- + \tfrac{1}{2}O^{2-} \tag{7}$$

Overall reaction equation:

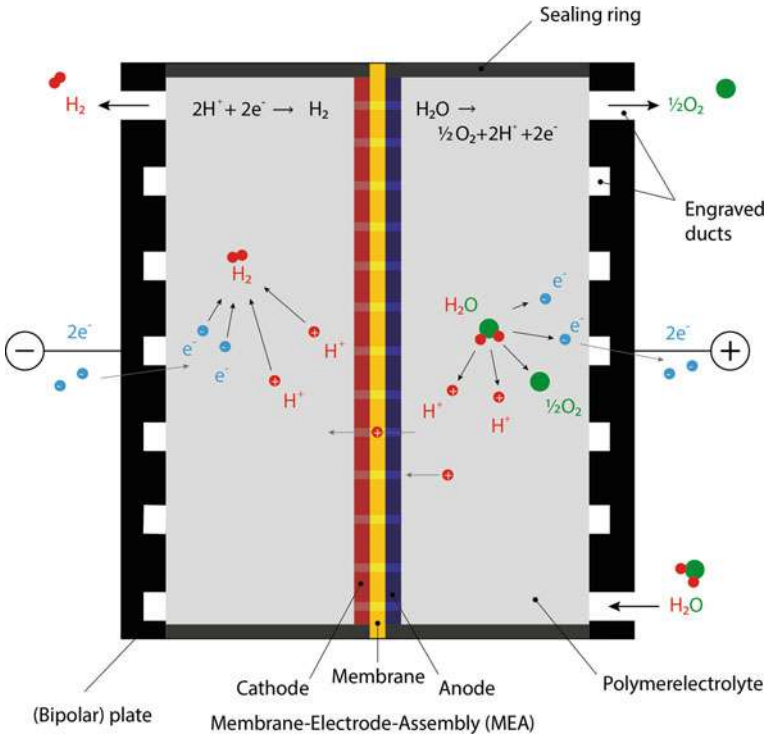

Fig. 3 Function of the membrane electrolysis (Source: Sterner and Stadler 2014)

$$H_2O \rightarrow H_2 + {}^{1}/_{2}O_2 \quad (8)$$

All of these three different approaches of electrolysis technologies have their reason and application. The AEL is the most proven one, inexpensive and well established, but needs a lot of space and has not the best efficiencies. The PEM electrolysis is efficient in conversion and space but rather expensive. The HTEL (high temperature electrolysis) is the most efficient technology, using surplus heat from other processes. However, it is also the most complex technology in terms of lifetime and technology readiness level.

Charging Technology Methanation

It is possible to transform the electrolytically produced hydrogen with the use of CO_2 to gaseous or liquid hydrocarbons. To generate methane, which is chemically the main constituent of and almost identical to natural gas, the methanation synthesis is used.

As hydrogen integration in the existing energy infrastructure is limited, further processing with an additional expenditure is appropriate. By processing hydrogen with the following technologies, it is easier to store, transport, and use it.

Chemical Versus Biological Methanation

There are two ways of methanation: the chemical and the biological way. The different parameters are described in Table 2.

The Sabatier Process

Already in 1902, the French chemist Paul Sabatier discovered the transformation of carbon dioxide to methane via a chemical synthesis. Hence, the scientist is the eponym to this chemical reaction, the "Sabatier process."

Table 2 Different parameters of the chemical and the biological methanation (Sterner and Stadler 2014)

	Chemical methanation	Biological methanation
Operating temperature in °C	200–600	40–60
Pressure in bar	5–80	1–3
Overall reaction	$4H_2 + CO_2 \rightarrow CH_4 + 2H_2O$	
Plant size	Large plants up to more MW	kW scale (up to single digit MW scale possible)
CO_2 gas quality	High syngas quality and gas upgrading necessary; H_2 temporary storage	No requirements
Rate of production	Up to 325 m^3/h (Audi e-gas plant, Werlte)	Up to 540 l per day and liter pure culture

The industrial breakthrough of the CO-methanation succeeded during the oil crisis in the 1970s. In this period, oil prices rose sharply and through the linked price natural gas became more expensive as well. This put a burden on the economy of industrial nations, which were forced to find different solutions. Besides the expansion of nuclear energy, one approach was the production of "synthetic natural gas" (SNG) by gasifying coal to syngas and converting it via methanation to SNG. Especially brown coal was used because of its cheap price and its abundance in industrial nations. The produced gas mixture had a relatively low content of methane and needed to be upgraded before feeding it into the natural gas network.

Chemical Reactions

The chemical methanation consists of two chemical reactions that run at the same time: the methanation of carbon monoxide (CO) and the water gas shift reaction (WGSR).

CO-methanation is state of the art for decades already to gasify coal and was enhanced during the 1960s as explained before. Its chemical reaction proceeds as described by Eq. 9:

$$3H_2 + CO \rightarrow CH_4 + H_2O \qquad \Delta H_R = -206\ \mathrm{kJ/kg} \tag{9}$$

The WGSR produces water and carbon monoxide (Eq. 10):

$$H_2 + CO_2 \rightarrow CO + H_2O \qquad \Delta H_R = 41.5\ \mathrm{kJ/kg} \tag{10}$$

The resulting reaction is described in Eq. 11:

$$4H_2 + CO_2 \rightarrow CH_4 + 2H_2O \qquad \Delta H_R = -164.5\ \mathrm{kJ/kg} \tag{11}$$

The negative sign of the molar reaction enthalpy indicates that the reaction is highly exothermic and thus sets energy free, respectively heat. A thermal management, which reliably dissipates the released energy, is necessary to provide an uninterrupted operation. To accelerate the reaction, a catalyst is used.

Operation pressure and temperature may vary according to the applied reactor concept, though general conditions of 200–300 °C and 20 bar can be assumed.

Sources of CO_2

CO_2 has to be provided as reactant gas. The following three sources are basically accessible:

1. Extraction from air
2. Fossil sources (coal power plants)
3. Renewable sources (biogas facilities)

Theoretically, any exhaust mass flow from industry or any energy supply station as well as ambient air could be used. However, the source has to fulfill the demands of a certain degree of purity as well as being able to provide the necessary quantity.

Purity is the determining factor, as, e.g., sulfur degrades the catalyst of the methanation. The CO_2 flow is mixed with hydrogen in the methanation reactor, and thus, the degree of purity has to be even higher than the CO_2 reactant gas flow.

The origin of CO_2 is relevant due to ecological reasons. Taken from a coal power plant, the plant will improve its carbon footprint, which is good on the one hand. On the other, it is contradictory to the aim of the energy transition, which implies the decrease of fossil energy carriers in favor of an increase of renewable energy carriers. Considering this, the exhaust mass flow from biogas facilities is excellently suitable. The CO_2 originates from plants, which collected it during recent years. By contrast, fossil CO_2 had been safely stored for thousands of years and thus would additionally pollute the environment. Biomass itself is a low-carbon CO_2 source as long as the associated land use is carbon neutral and does not provoke new greenhouse gas emissions by direct and indirect land-use changes. Thus, residual biomass or residues are the ideal biogenic CO_2 sources.

To separate CO_2 from air today is technically complicated and expensive. There are very good starting points at the research and development sides, which will become more attractive in future. Therefore, this is also a considerable eco-friendly source of CO_2, as it closes the carbon cycle as well.

More details on the origin and use of CO_2 are described in section "Power-to-Gas Methane."

Use of Exhaust Heat

Methanation is an exothermic reaction as described in section "The Sabatier Process." It is recommended to use the exhaust heat of the process to increase efficiency, cost-effectiveness, and improve the carbon footprint. Heat is also generated in the upstream electrolysis; hence, an overall heat management is appropriate.

Generated heat can be used for:

1. Internal process heat (purification of gas)
2. Power generation (Organic ranking cycle – ORC)
3. Integration of a heat sink (district heating)

The most obvious use is to cover the internal heat demand of the overall process, e.g., in the purification of reactant and resulting gas. However, the process heat also has the necessary temperature level to convert heat to electricity. This could be realized with the use of a conventional steam turbine or alternatively by an ORC or Kalina cycle.

However, the operating mode of the complete unit has to be considered. If the primary application of the unit is to store excessive electric energy in the gas network, the conversion of heat into electricity is counterproductive. Feeding the heat into the district heating would be an adequate solution in this case, but appropriate heat consumption throughout the whole year has to be guaranteed. If the district heating cannot continuously distribute and use the heat in summer, operational disruptions at the methanation unit could occur.

Reactor Concepts

Reactor concepts in general have to address two basic demands:

- Dissipation of heat (as explained above) to prevent hot spots
- A flexible operating method

A hot spot is a punctual overheating of the catalyst inside of the reactor. As a result, the catalyst can be deactivated or even profoundly damaged. In both cases, the operation mode is disturbed permanently.

The flexible operating mode is necessary to serve the future increase of power fluctuations in the power network, due to volatile renewable energy feed-in. This implies the operation at different levels of load. The reactor mass is critical in this context.

Fixed-Bed Reactor

In this concept, the gas usually passes through the reactor from the top to the bottom to avoid any swirling of the fixed-bed. The danger of hot spots is rather high compared to other technologies. They have to be eliminated by constant intercooling of the gas. This can be achieved by several heat exchangers placed inside the gas flow or by inserting cold reactant gas.

An advantage of this technology is its high availability and reaction time during a cool start, since only the walls of the reactor and the catalyst have to be heated to operating temperature. On the contrary, the process is very sensitive to fluctuations in its load due to a fast cooling down.

Fluidized-Bed Reactor

The fluid streams through the reactor with a relatively high velocity to swirl up the catalyst. In this way, a swirling layer with fluid-like properties is created.

The temperature distribution inside the reactor is homogenous, but the inner walls of the reactor tend to wear out with time due to the swirling layer. A low fluid flow is not able to swirl up the catalyst layer; on the other hand, when operating with high fluid flows, dwell time inside the reactor is too short and there is danger of removing particles from the catalyst. Both situations decrease the possibility of a flexible reactor operation.

Three-Phase Reactor

The reactor is filled with a fluid containing solid catalyst particles. This is also the reason for the name of the reactor: including the gaseous fluid flow, three states of matter are represented inside the reactor. The fluid is responsible for the thermal management. The main task is to dissipate generated process heat and thus to prevent hot spots. Moreover, heat can be applied in this way from outside to keep temperature on a constant level during operational interruption. However, this is only partly necessary, since the reactor mass is rather high due to a high fluid content. This allows to buffer short interruptions. A disadvantage results from the long warm-up time and therefore less flexibility.

Gas Storage Technologies

Already in the mid-nineteenth century, the construction of the gas infrastructure in Germany began – at first only for town gas – which, after the transition to natural gas in the 1970s, even in the twenty-first century is not finished. From the beginning, it was problematic to adapt the rather constant production of gas to the daily and seasonal fluctuations in the consumption. This was solved by developing gas storage facilities, at first with pressure-less gasometers via spherical gas tanks up to the underground storage with an enormous capacity, which dominates today.

In the transition from fossil to renewable energies, the development of storage technologies like Power-to-Gas congruently gains importance and will take its time, as it is still in its infancy.

Gas Holders Aboveground

The compressed gas containers explained in this section were developed for the storage of town gas. Only in individual cases they were also used for pure hydrogen. Any subsequent reference to mass storage is based on the requirements in the town gas era. Storage capacities in the future energy economy depending on renewable energies are required to be much bigger.

The first mass storage for town gas, the so-called gasometers, worked at a lower overpressure than constant pressure gasometers at a variable volume. A typical example is the liquid seal gasholder, which realized the gas sealing against the atmosphere by water. Later, telescope containers, as seen in Fig. 4, which work with the same basic principle allowed a significantly higher storage capacity.

The actual storage container was installed inside a supporting structure. After the telescope gasholder, the disk-type gasholder was established. In this technology, a piston in a cylinder created the storage volume at still low pressures.

Due to limitation to pressures insignificantly higher than ambient pressure, shortly an interest for pressure vessels emerged. In contrast to gasometers, pressure vessels operate at a constant volume but variable pressure between a minimum and a maximum value. The usable quantity of gas between these pressures is called working gas, and the quantity below the acceptable minimal pressure is called "cushion gas," while the proportion of working gas to cushion gas differs in the single pressure vessel technologies.

Spherical gas tanks, as seen in Fig. 5, allow significantly higher operational pressures and thus energy storage densities, due to their favorable geometry. This technology offers the lowest specific consumption of material for the container, which is a critical aspect, as investment costs depend on material costs in the first place (Table 3).

To date no storage technology for pure hydrogen is known.

Pipe storage facilities are gas pipelines installed in a meandering shape in the floor near the surface.

In contrast to underground storage in geological formations, these storage facilities can be installed in nearly any region. The usage of commercially available steel

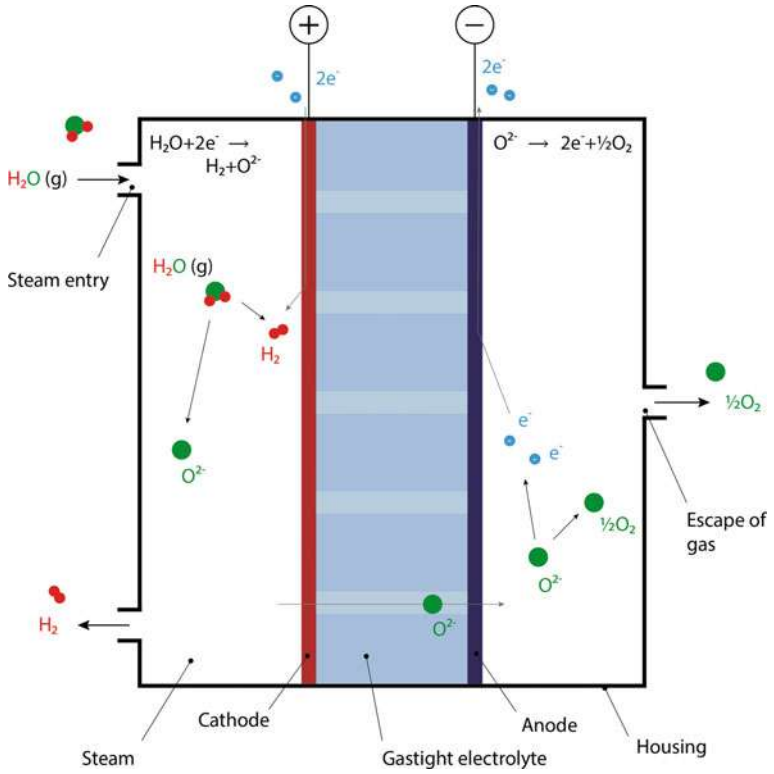

Fig. 4 Function of the high temperature electrolysis of steam (Source: Sterner and Stadler 2014)

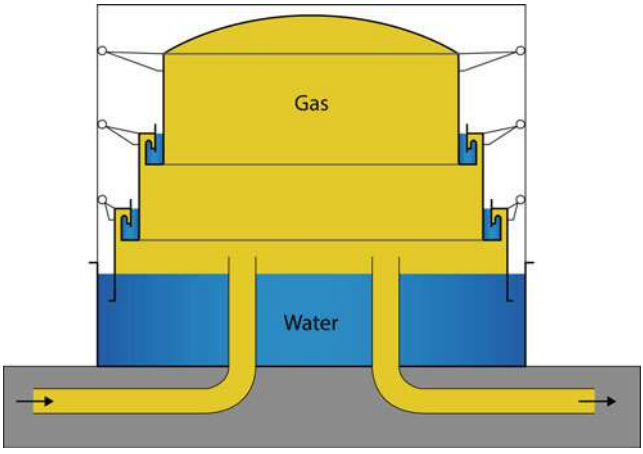

Fig. 5 Gasometer (telescope principle) (Source: Sterner and Stadler 2014)

Table 3 Typical dimensions of a spherical gas tank

Diameter of the sphere	40 m
Maximum pressure	10 bar
Storage capacity	335,000 m^2 (V_n – standard volume)

pipes allows an operation at significantly higher pressures in comparison to spherical gas tanks. The geometry of the long cylinder with a low diameter leads to a higher material consumption and thus higher specific investment costs. Therefore, also this storage technology is only used for small capacities and can only be applied to compensate minor consumption fluctuations.

Underground Gas Storage

The storage capacity of a holder aboveground is basically limited by the economically reasonable geometric volumes in combination with the desired storage pressure, whereas material costs are the predominant factor.

Big storage volumes at significantly lower area consumption can be realized in the geological underground. In addition, storage pressures of up to 200 bars and more are possible with increasing depth. As storage capacity depends on the product of volume and pressure in the first place, fundamentally bigger dimensions in capacity are possible in comparison to the storage aboveground. While the pressure vessels named above provide capacities of under one million m^3 (V_n – standard volume), the averaged capacity of German underground storage facilities is at nearly 500 million m^3 (V_n).

This is the reason why underground storage became the state-of-the-art technology for big amounts of gas.

Figure 6 shows the different types of underground storage. In the beginning, depleted deposits for hydrocarbons and porous aquifers were used as storage. Later they were complemented by artificially created salt caverns. To a low extent, porous formations and salt caverns were used for the storage of town gas, which comprises 50 % hydrogen. For many years, the storage of pure hydrogen takes place in specially equipped salt caverns.

All of the internationally installed underground gas storage facilities have in common:

1. The high safety against unintended escape of gas through the sealing rock layers of up to several hundred meters thickness – compared to the thin thickness of a few centimeters for overground containers
2. High storage capacity established by big geometric volumes and high operational pressures
3. Low surface usage overground
4. Low specific installation and maintenance costs compared to storage overground
5. Feasibility being coupled to the availability of suitable geological formations, which is a big limitation to a lot of regional cases

Fig. 6 Spherical gas tank in Gelsenkirchen (Source: Sterner and Stadler 2014)

6. Extensive positive experience in a lot of industrialized nations and therefore good conditions for the acceptance of future storage of hydrogen

Salt Caverns

Salt caverns are artificially created cavities in underground salt rock. If sufficiently big and homogenous salt rock formations are available, a drilling is sunk into the rock with a diameter of less than 1 m and sealed with a cemented steel pipe. Afterwards, the cavity is created by the so-called solution mining process. The big advantage of the further explained process is that for creating the cavern, neither an extensive tunnel has to be sunk nor a person or machine has to be transported underground. All work can be executed overground, which is a considerable advantage in costs and time compared to conventional mining.

To inject the required water for the solution process into the drilling, two concentric tubes are inserted into it at first, as seen in Fig. 7. Water is pressed through the inner tube, which dissolves the salt rock. Through the annular gap between the tubes, the evolving brine is brought overground and either used as a raw material or conducted into the sea environmentally friendly. Additionally, a protective fluid (blanket) is injected into the annular gap to prevent an uncontrolled rupture of the brine. The time-dependent spatial development of the cavern can be controlled by sonar measurements and thus applied to the requirements.

The aim is to create a cavity which effectively uses the available salt rock and which provides a safe long-term storage of gas. The unique creeping properties of salt rock make these caverns tight for gases, as long as the permitted operational pressure is maintained. Nevertheless, the creeping leads to a decreasing volume over time.

Fig. 7 Options for gas storage in the geological underground (Source: KBB UT)

As soon as the cavern obtained the required volume, tightness tests are executed, the cavern is modified for operation with gas, and the first gas is filled in. In the first step, the tightness of the drilling has to be proved – an important requirement for further approval as gas storage. Afterwards, the cavern is equipped with a casing for the exploration of gas as well as with a downhole safety valve. If the cavern head at the surface is damaged in the worst case, this valve prevents the blowout of gases from the cavern. The so-called brine removal string is inserted into the cavern and allows the displacement of the brine with the storage gas. Finally, the string is removed under pressure.

Summing up, there are sufficient technologies available for a safe and economic storage of gas.

The Storage System Power-to-Gas

The storage system Power-to-Gas (electricity to gas, PtG) is presented in this chapter. It is made out of the single conversion technologies, described in section "Technology Components of Power-to-Gas."

In general, two PtG concepts have to be differentiated based on the characteristics of their energy sources hydrogen (H_2) and methane (CH_4). Their deployment, as well as the extraction technologies used, make the main difference. In addition, there is the optional methanation stage. In the following, basic concepts of PtG are

explained. The specific application for decarbonization and some projects is presented in section "Decarbonization with Power-to-Gas."

The Beginnings of Power-to-Gas

Energy Storage Demand in Dynamic Simulations: Hydrogen and Biomass
In the course of expansion of renewable energies in Germany – mostly wind and photovoltaics – calls for energy storage grew ever louder since the early 2000s.

While it has been sufficient for a long time to consider the annual balance sheet, which is based on only one value for wind and solar power generation, dynamic simulations of a power system containing a large percentage of renewable energies have detected and revealed a large storage and balance demand. This demand could not be supplied by conventional German storage technologies, such as pumped hydro, battery power plants, or compressed air storage. Solely, caverns exclusively for hydrogen have been considered as solution (see Sauer 2006; VDE 2013). Since there is no infrastructure for hydrogen and a very limited potential for hydropower buildout, pure renewable energy systems depend on bioenergy as balancing energy.

The Combi Power Plant at the ISET Kassel, Now Fraunhofer IWES
In the 1990s, Enßin, Füller, Hahn, Rohrig, and their colleagues, at the Institute for Solar Energy Supply Technology (ISET) in Kassel, built a database for feed-in from wind turbines as part of the 250-MW measuring program. Since the early 2000s, this data has been used for wind forecasts and the construction of virtual power plant in the form of a wind turbine cluster (see Ernst et al. 2004; Ernst 2003; Enßlin et al. 1993). The project called "Combined Power Station" (see Fig. 8) resulted from their work and was able to prove that, at any point of time, power supply based on 100 % renewable energies was possible in Germany at a scale of 1–10,000, measured at the necessary energy supply and demand. To achieve this goal, wind turbines of Enercon GmbH, photovoltaic plants of Solarworld AG, and biogas plants of Schmack Biogas GmbH were combined and controlled in real time according to German load profile. Only power storage was simulated as the pump storage plant Goldisthal. That is how it was possible to rebut presumptions that purely renewable power systems were not able to provide a stable power supply (see Mackensen et al. 2008).

Reinhard Mackensen's analyzes showed that the expansion of renewable energies to the full extent would mainly be based on wind power and photovoltaics and thus require major balancing measures in the form of storage capacities or stored biomass. It is neither possible to provide these balancing measures by expanding pump storage plants nor can enough biomass be produced on the available areas (see Mackensen et al. 2008; Mackensen 2011). The core problem was to realistically upscale installed biomass and storage capacity by a factor of 10,000. One approach of the ISET was to interconnect the power and gas sector and thus be able to store wind and solar energy in the form of hydrogen in the natural gas grid. It would then

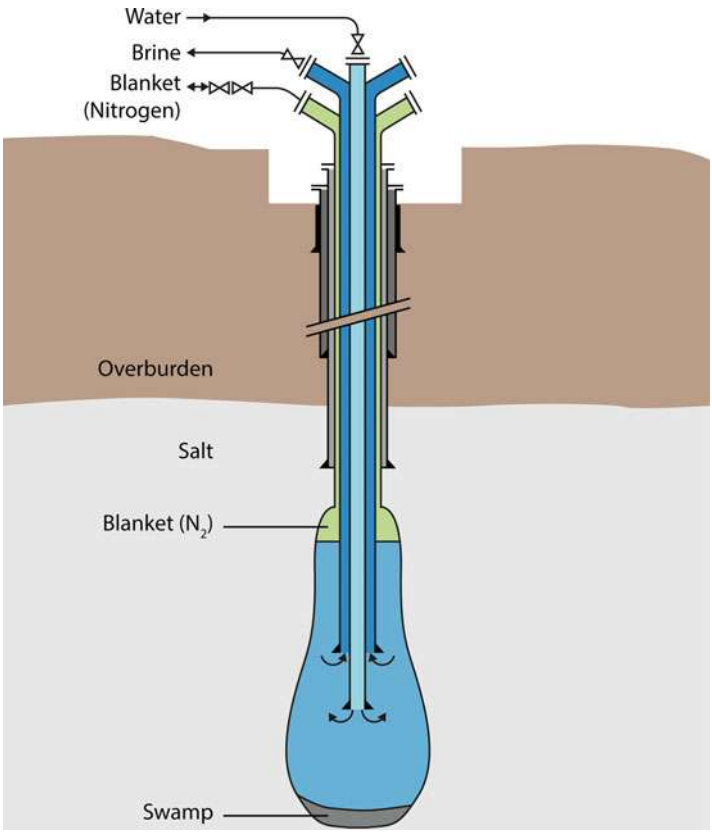

Fig. 8 The brine process – cavern creation in the salt rock (Source: KBB UT)

be possible to flexibly reconvert it into electricity via gas turbines and cogeneration plants (see WBGU 2008).

Methanol Production from CO_2 and Biomass Gasification at the ZSW Stuttgart
In the 1990s, Andreas Bandi, Thomas Weimer, Michael Specht, and their colleagues, at the Centre for Solar Energy and Hydrogen Research (ZSW) in Stuttgart, developed a synthesis to produce methanol from atmospheric CO_2 and solar energy. A small-scale pilot plant was set up, which extracts CO_2 from the air by means of adsorption and electro dialysis. It then chemically reacts the CO_2 to methanol using hydrogen from solar powered electrolysis. At this point, the technical feasibility of CO_2 recycling to produce methanol was successfully proven (see Bandi 1995; Specht 1998; Specht et al. 2000; Weimer 1996). In the 2000s, research at the ZSW concerning hydrogen and chemical energy sources focused on biomass gasification. They developed a process of their own (Absorption Enhanced Reforming Process) to produce a hydrogen-rich gas from biomass via two coupled fluidized bed reactors (see Weimer 1996; Specht et al. 2006, 2010).

The First Coupled Power and Gas Grid in the WBGU-Bioenergy Report

Until the middle of the 2000s, it became clear that the biomass potential is and will be limited. The increase in food prices in 2008 got the "food-versus-fuel debate" going and brought up the question to which degree biomass can and should be energetically used (see FAO 2008; Sachs 2008). The WBGU-Bioenergy Report shows that, while bioenergy is very well suited to balance fluctuating wind and solar energy, the necessary sustainable potential is not available. Both authors, Jürgen Schmid and Michael Sterner of the ISET Kassel, came to the conclusion that, because of its scarcity, bioenergy is best integrated into the existing natural gas grid via fermentation, gasification, and methanation (see WBGU 2008; Sterner and Schmid 2009). In this way, existing transport and storage capacities can be used and thus provide energy to all sectors via power plants, cogeneration plants, gas cars, and gas heating. In addition, it is possible on the one hand to separate CO_2 and establish an actual CO_2 sink and on the other hand to integrate fossil coal, which will last a long time, in a climate-friendly way.

In the end, this integrated energy system consisted of an electricity and a gas system, which were coupled via gas power stations and cogeneration plants on the one hand and an electrolyser, which produced hydrogen for fuel cells, on the other (see Fig. 9). Schmid and Sterner presented this system along with the combined power station at the

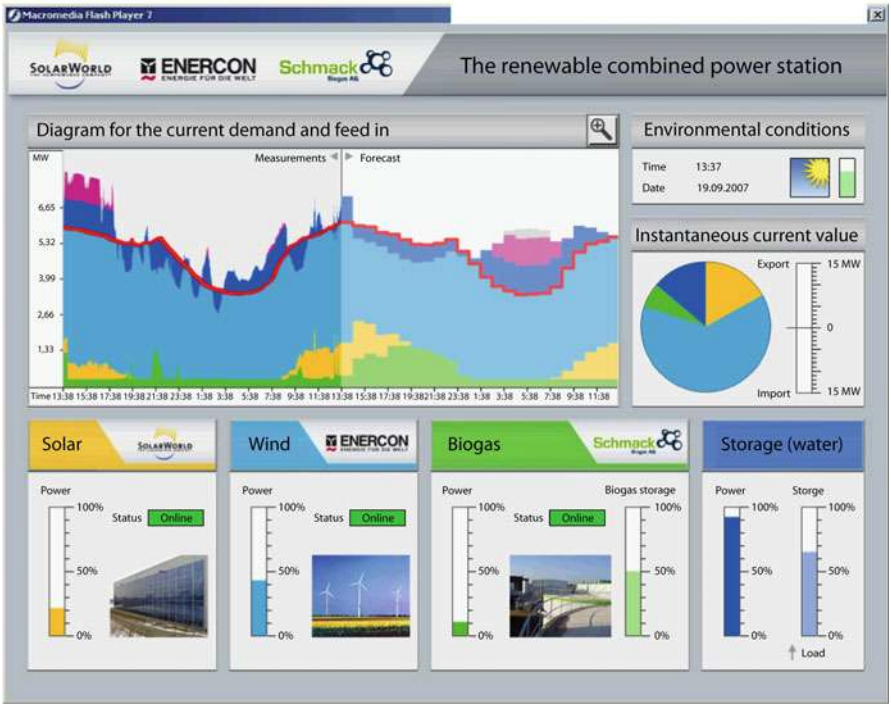

Fig. 9 Combined power station at the ISET (Source: Sterner and Stadler 2014)

16th European Biomass Conference (see Schmid and Sterner 2008; Sterner and Schmid 2008). Michael Specht and his colleagues from the ZWS Stuttgart presented their paper on chemical energy conversion of biomass (see Bandi 1995). Having the accordant background, he produced the idea to improve the possibility of integration of hydrogen into the natural gas grid by using the Sabatier reaction. As shown in Fig. 9, the syngas CO_2 from coal and biomass is used for methanation.

Patent, Studies, and Projects Concerning Power-to-Gas
At this point, both institute's preliminary work was merged together and the Power-to-Gas concept was elaborated. In 2009, this led to a patent application (see Specht et al. 2009) and a doctoral thesis on Power-to-Gas, which made the concept of chemically storing energy from wind and solar plants well known and put it into context with energy transition (see Sterner 2009). As another consequence, the first PtG plant for methanation of CO_2 in Germany was developed in Stuttgart by the order of Waldstein, the founder of SolarFuel GmbH (see Fichtner 2011; Specht et al. 2008).

In addition, different pilot projects were launched. While studies were carried out for E-On, Greenpeace Energy, and Audi AG in Kassel, hardware was refined in Stuttgart. Both activities paved the way for the realization of pilot projects and the publication of the new concept.

In energy economy, this concept was made well known by a number of associations: the research papers by the Fraunhofer IWES (formerly ISET) on which the long-term scenario of the Federal Environment Ministry (BMU) is based (see Nitsch et al. 2012), the report published by the German Advisory Council on the Environment (SRU, see SRU 2011), the Federal Environment Agency's "UBA Energy Goals 2050" (see UBA 2010), and the VDE ETG Storage Study (see VDE ETG 2012). So far, the greatest PtG project has been realized by Audi AG and fuels 1,500 vehicles with CO_2-neutral gas.

PtG Hydrogen

The storage system PtG hydrogen (PtG-H_2) uses electricity surplus from renewable energies to produce hydrogen. Hydrogen can potentially be used in several different ways, e.g., as an admixture in the natural gas grid or it can be used energetically at a different point of time and place if filled in a compressed hydrogen tube trailer. Following stages are passed through:

- Storing:
  Storing technologies
  - Alkaline electrolysis (AEL)
  - Proton exchange membrane electrolysis (PEMEL)
  - High temperature electrolysis (HTEL)
- Storage:
  Storage media
  - Gas grid

  - Cavern storage
  - Gas and oil deposits
  - Aboveground storage
- Extraction:
  Extraction technologies
  - Fuel cell
  - Gas turbine, combined cycle plant, cogeneration plant
  - Gas heating, gas hat pump, refrigeration machines
  - Fuel cell vehicles, rocket propulsion
  - Material use

Possible Plant Concepts

High-quality natural gas in Germany is composed of 96 % by volume methane, 1 vol % CO_2, 2 vol% nitrogen (N_2), and 1 vol% hydrocarbons, such as propane and butane (see Henel et al. 2013). According to the DVGW (German Technical and Scientific Association for Gas and Water), the admixture of 1.5 % hydrogen is possible. Higher blending quotas cause research needs and adjustment requirements for certain applications, such as gas turbines, porous storage, or natural gas tanks in vehicles, which are limited to 0–4 %. For this reason, PtG hydrogen storage systems differ in regard to the way hydrogen is used after electrolysis.

In this book, the use of hydrogen is distinguished between material (1) and energetic. Furthermore, energetic use can be divided into use in an infrastructure exclusively for hydrogen (2) and use in an already existing gas infrastructure (3). There is a clear presentation of how hydrogen can be used in Fig. 10.

Material Use

An industrial plant or a refinery with a great need for hydrogen can be attached directly to a PtG-H_2 plant (Fig. 11). Since most industrial applications need constant supply, the system includes hydrogen tank as buffer. Hence, requirements for PtG-H_2 systems are a location with great availability of renewable energy sources and a suitable consumer for the H_2.

> There is a great climate protection potential in the reduction of iron by applying the direct reduction process (DRP) rather than the CO_2-intensive blast furnace process. The DRP uses hydrogen to withdraw oxygen from the ore (Fe_2O_3). As a result of this reaction, there is pig iron and water. Another advantage of the DRP is that there is less than 1 % carbon in the pig iron. After the blast furnace process, up to several percent carbon has to be removed in order to meet DIN (German Institute for Standardization) norms, according to which pig iron, the staring product for steel, has to contain less than 2 % carbon.

Energetic Use via Hydrogen Infrastructure

When, in the future, a hydrogen economy has been established, it will be possible to use hydrogen directly in a hydrogen-only system (Fig. 12). Regions with already

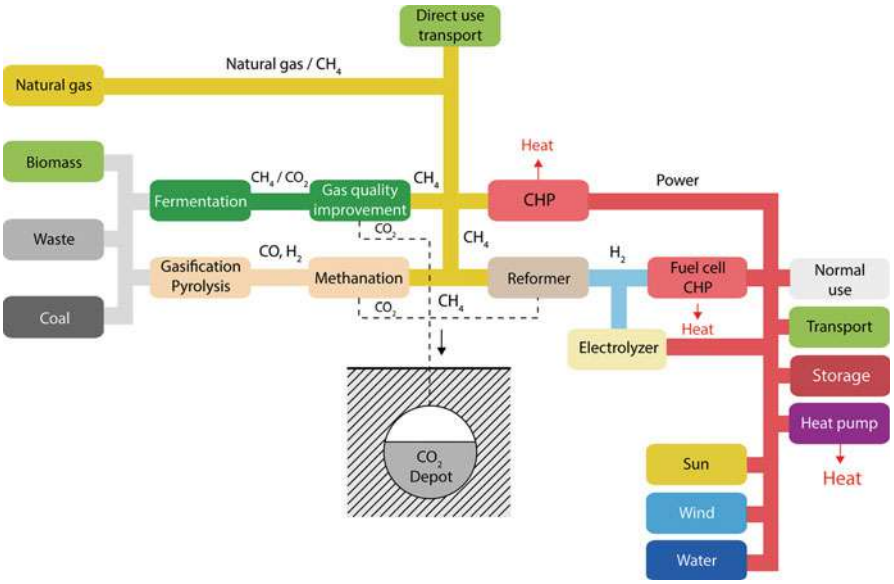

Fig. 10 Coupling of electricity and gas system via electrolysis in the WBGU Report on bioenergy (Source: WBGU 2008)

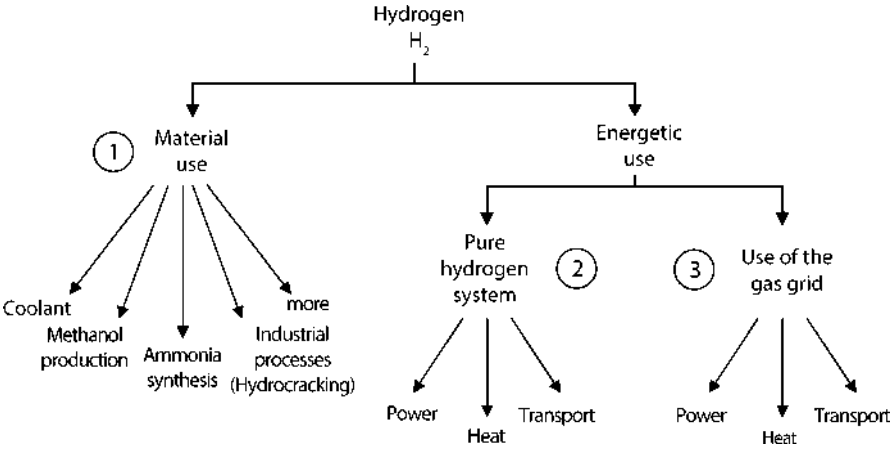

Fig. 11 Overview of the possible uses of hydrogen (Source: Sterner and Stadler 2014)

existing suitable hydrogen storage and lines are eligible starting points as well as regions with a high density of consumers in chemistry parks. This is researched in the course of the BMBF project "HYPOS" for eastern Germany, which examines wind-photovoltaic-hydrogen hybrid parks and hydrogen test fields including Germany's first hydrogen storage (see HYPOS 2014). Storage options for short-term storage are, along with hydrogen lines, aboveground H_2 tanks. Long-term

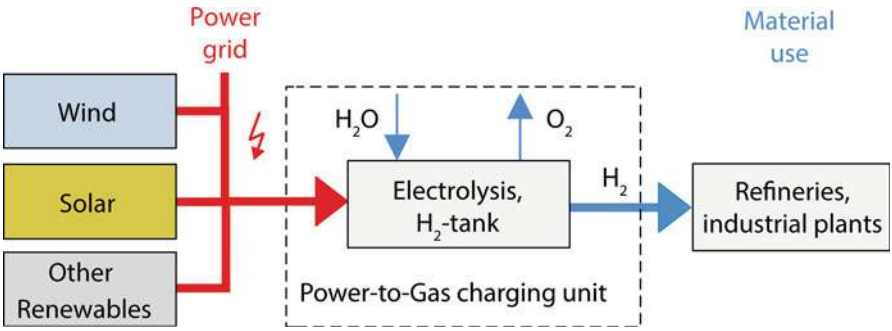

Fig. 12 Schematic representation of a PtG system for material use of hydrogen (Source: Sterner and Stadler 2014)

storage can be realized in gas caverns. Porous storage is not suitable for hydrogen storage because of microbiological hydrogen sulfide emergence, which results in corrosion.

In times of deficits due to fluctuating renewable energies, this system reconverts hydrogen to electricity via especially adapted gas turbines or fuel cells and thus acts as electricity storage. In this case, an independent hydrogen infrastructure provides seasonal balance for times of both low winds and sunshine hours.

In addition, hydrogen can be used for transport when sold at hydrogen stations or in the field of heat supply.

Realization is obstructed by high costs for the expansion of an independent hydrogen infrastructure and high prices for hydrogen extraction technologies, such as fuel cell vehicles, fuel cell cogeneration plants, and reconversion units.

Energetic Use via Admixture to Natural Gas and Use of Existing Gas Infrastructure

From today's point of view, an independent hydrogen infrastructure is only financially reasonable in some regions with a great demand for hydrogen, industrial consumers, and existing, suitable storage facilities, such as cavern storage.

Matters are different, when hydrogen is added to natural gas using the existing gas infrastructure. The gas grid is expanded over all of Germany and there are high-capacity cross-border interconnections. Furthermore, state-of-the-art consumers which only need slight adaptions to higher hydrogen percentage can be used in all energy sectors. These already existing technologies make development of new ones redundant.

The challenge here is hydrogen tolerance of specific components (Fig. 13). In this field, there are research needs and adjustment requirements to increase the technically possible blending quota of 1–2 vol% (see Henel et al. 2013).

In a PtG hydrogen storage system, surplus electricity is used for water splitting in an electrolyser (Fig. 13). In order to prepare hydrogen produced in this manner for feed-in to the gas infrastructure, it is fed to a gas storing unit including a compressor.

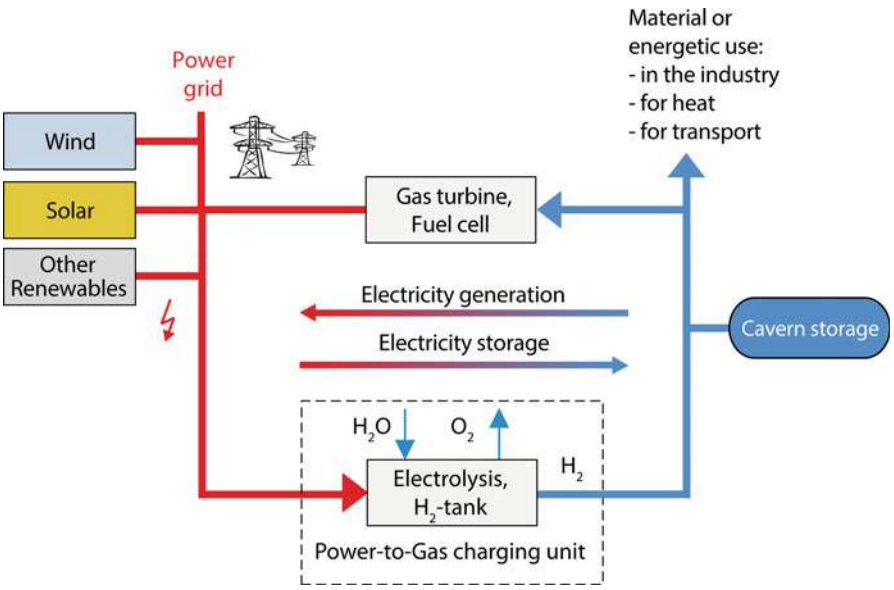

Fig. 13 Energetic use of hydrogen in a hydrogen-only infrastructure (Source: Sterner and Stadler 2014)

From that point on, usage is possible, in consideration of hydrogen tolerances shown in Fig. 22, in all kinds of ways: reconversion to electricity, heat, transport, or material use.

When used for seasonal balancing, the mixture of hydrogen and natural gas can be stored, other than pure hydrogen, in all gas storages up to a blending quota of 1 % hydrogen. Along with salt cavities, porous storage is an option. Buffering on a short-term scale is possible in aboveground gas storages. Furthermore, the gas mixture can be brought to all consumers in households, business, and industry via the gas grid. Among others, possible applications are gas engines, condensing gas boilers, gas heat pumps, gas stoves, gas tools, gas base materials, or reconversion to electricity for peak-load supply.

Power-to-Gas Methane

In addition to electrolysis, there is another storing technology, methanation, in the Power-to-Gas methane (PtG-CH_4) storage system. Hydrogen and carbon dioxide (CO_2) are reacted biologically or chemically to methane (CH_4) and water (H_2O) (see Sterner 2009).

Main advantages of this system are easier compressibility, storage, transport, and usage, due to higher energy density of methane. Disadvantages result from the additional procedural step, which needs CO_2, causes waste heat and therefore

reduces efficiency of the overall process. Among others, intelligent heat concepts can compensate for this disadvantage by using waste heat for vaporization in high temperature electrolysis (section "Efficiency, Potentials, CO_2 Emissions and Costs").

A PtG-CH_4 system can be composed of the following components:

- Storing:
  Storing technologies
  - Electrolysis
    - Alkaline electrolysis (AEL)
    - Proton exchange membrane electrolysis (PEMEL)
    - High temperature electrolysis (HTEL)
  - Methanation
    - Chemical methanation
    - Biological methanation
- Storage:
  Storage media
  - Gas grid
  - Cavern storage
  - Gas and oil deposits
  - Aboveground storage
- Extraction:
  Extraction technologies
  - Fuel cell
  - Gas turbine, combined cycle plant, cogeneration plant
  - Gas heating, gas hat pump, refrigeration machines
  - Gas vehicles, ships, airplanes
  - Material use

Possible Plant Concepts

In the field of PtG-CH_4, there are different concept categories, which are all based on the concept shown in Fig. 14 (see Sterner 2009).

Bidirectional interconnection of power and gas grid in order to store renewable energies is the general idea of Power-to-Gas (section "The Beginnings of Power-to-Gas"). Electricity surpluses power water splitting. In the process of methanation, thus produced hydrogen and CO_2 are reacted to methane. This requires one of several different possible sources of CO_2, such as Carbon Dioxide Capture and Storage (CCS), biogas plants, sewage plants, atmospheric CO_2, industrial processes, or conventional power plants. Renewable methane can be temporarily stored in gas storage or fed into the gas grid. Once there, it can be reconverted to electricity via gas turbines, cogeneration plants, etc., or be used in the heat and transport sector.

What differs between each concept from another is the CO_2 sources and how it is integrated into the process of methanation.

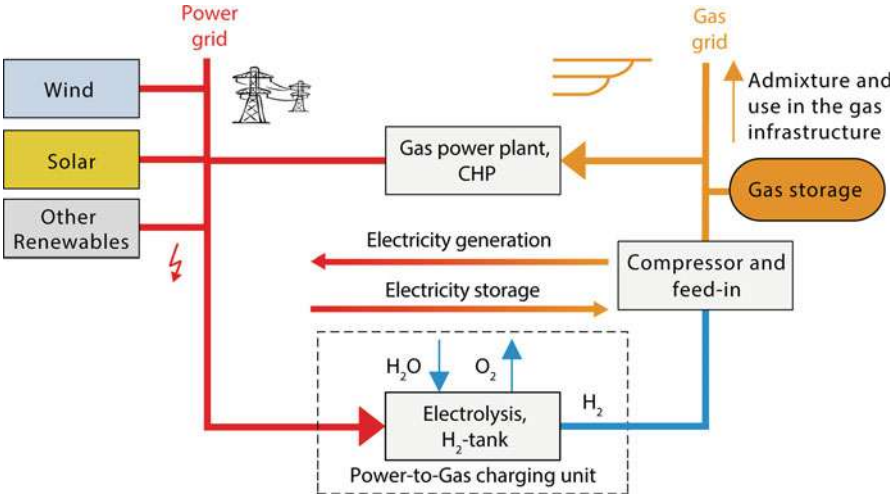

Fig. 14 Schematic representation of hydrogen use in the existing gas infrastructure (Source: Sterner and Stadler 2014)

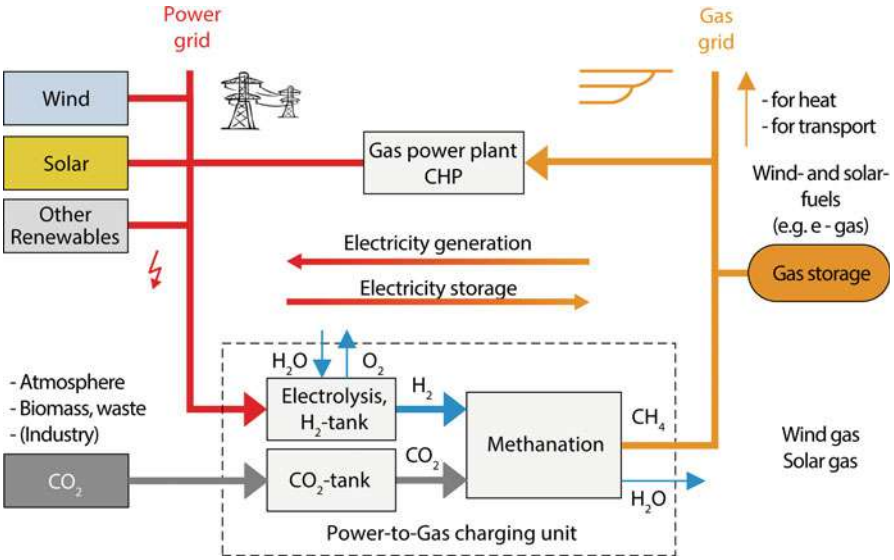

Fig. 15 Basic concept of PtG methane (Source: Sterner 2009)

Atmospheric CO_2

Methane produced with atmospheric CO_2 and renewable electricity is CO_2 neutral (Fig. 15). It is possible to decrease the content of CO_2 in the atmosphere by connecting the combustion process with a CCS system.

There are different ways to extract CO_2 from the air:

1. Adsorption
2. Absorption
3. Condensation
4. Membrane separation

Since the concentration of CO_2 in the atmosphere is only ca. 400 ppm or 0.4 ‰, every one of these processes is energy-intensive. Therefore, pure CO_2 sources should be used in order to increase efficiency and profitability of PtG plants.

This system is given its raison d'être by regions worldwide which offer a great potential of renewable energies but are far from consumers. Since air is the only source of CO_2 in these regions, this system makes it possible to use their potential and decrease their dependence on natural gas imports (see Sterner 2009).

Two of the four abovenamed extraction technologies are very energy-intensive: Condensation requires considerable cooling of the air; membrane separation requires a very high pressure to extract CO_2 from the air. These processes are standardly applied in air separation units (ASU) for industrial extraction of nitrogen, oxygen, and noble gases, such as argon (see Specht et al. 2000). From today's point of view, with respect to effort and losses, technologies based on absorption and adsorption are favored.

Absorption Process

An alkaline solution, such as sodium hydroxide (NaOH), potassium hydroxide (KOH), or calcium hydroxide ($Ca(OH)_2$), absorbs CO_2 from the air and reacts to a carbonate like sodium carbonate (Na_2CO_3). Now, an acid can dissolve CO_2 from the carbonate.

In order to restore acid and alkaline solution, an electrodialysis with bipolar membranes is carried out. In this electrochemical process, protons (H^+) and hydroxide ions (OH^-) are being separated by an electric field. These ions are produced by splitting water, which in turn is activated by a bipolar membrane.

According to tests in the laboratories of ZSW Stuttgart, absorption and electrodialysis put together require 2.28 MWh per ton CO_2 (see Bandi 1995; Specht et al. 2000). In practice, this value is higher.

Adsorption Process

The adsorption process uses a batch procedure, in which first CO_2 is adsorbed and then emitted and thus made available, when supplied with low calorific heat. Adsorption processes, such as the pressure swing adsorption (PSA), are standard in gas preparation and purification technologies. The advantage is that low temperature heat from different processes (e.g., electrolysis, CHP, possibly synthesis) can be used for desorption.

The Climeworks company produces and runs a commercially available demonstration plant capable of extracting atmospheric CO_2. One cycle takes some 6 h.

First of all, air is conducted through the adsorption chamber, where CO_2 adheres to cellulose granulate. It takes 3 h before enough CO_2 is accumulated. After another 3 h at 95 °C and reduced pressure, the desorption phase has completed the cycle. Under these conditions, it is possible to extract 99.5 % pure CO_2 from the cellulose with a vacuum pump. It is possible to extract 80 % of all CO_2 molecules from the air with this plant using a sorbent. In absolute numbers, this means 800 m^3/h air and 4 kg/d respectively 1,000 kg/a CO_2 (see Gebald et al. 2011, 2013; Wurzbacher et al. 2011).

In the future, ca. 1,000 t CO_2/a with a composition of 99.9 % CO_2, 30 ppm O_2, and 20 ppm H_2O will be achievable on a 100 m^2 area. Energy input is between 200 and 300 kWh electricity per ton CO_2 mainly for the fan and between 1,500 and 2,000 kWh/t CO_2 for low calorific heat (supply temperature: 105 °C, return temperature: 95 °C) mainly for desorption. Costs for extraction are expected to decrease in the future to some 200 €/t from today ca. 800 €/t with an expenditure of ca. 30 €/t for electricity and heat (see Gebald 2013).

This demonstration plant was installed at the beginning of 2013 and proved its suitability for daily use under different environmental conditions. It is planned to cooperate with Audi, which provides CO_2 for the PtG plant in Werlte (see Audi 2014).

CO_2 from Biogas Treatment Plants

Principle

This concept's base material for CO_2 is biomass or waste, which is being fermented in a digester. Depending on dwelling time and the kind of digester, the purified biogas can contain up to 45 % CO_2. For a lot of technical applications, the inert CO_2 is obstructive, which is why biogas is purified to natural gas quality (>96 % CH_4) prior to feed-in into the natural gas grid. For this reason, the purified biogas is called biomethane and can be stored, distributed, and used in all fields of application via gas grid. Using the existing gas infrastructure has many advantages: already existing technology can be applied and, contrarily to on-site conversion to electricity, waste heat can be used more specifically. This makes exploitation of biogas more efficient. Processes for gas separation are adsorption, absorption, chemical absorption, membrane separation, or cooling (see Beil 2008).

In combination with PtG, thus extracted very pure CO_2, which is normally blown into the atmosphere, can be used for methanation. Together with electricity surpluses and hydrogen it is reacted to methane. When there is no sufficient electricity surplus for hydrogen production or hydrogen buffers are empty, CO_2 can simply be stored and used when needed (Fig. 16).

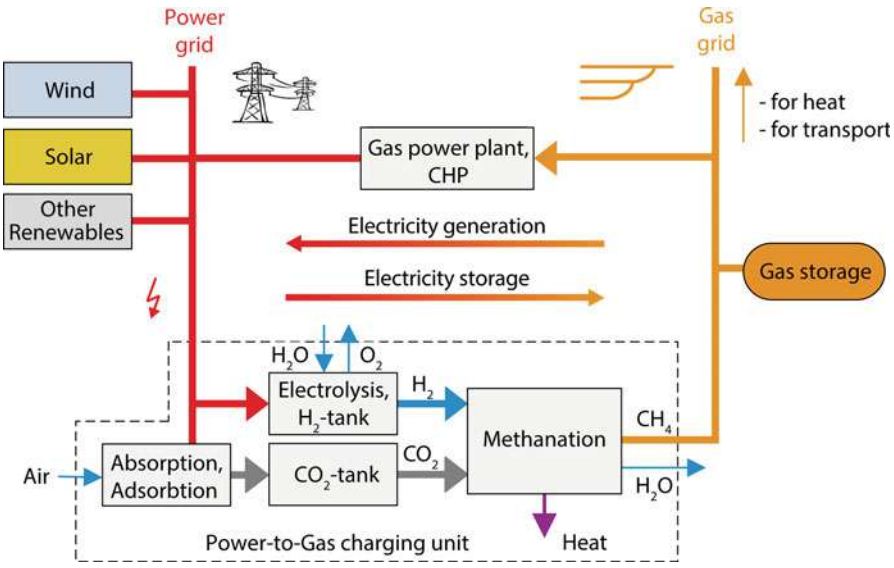

Fig. 16 PtG methane using atmospheric CO_2 (Source: Sterner 2009)

Advantages

The great advantage of coupling these processes is a more efficient use of resources and energy: in this system, waste heat produced by methanation can entirely be used for the fermentation or treatment procedures. By using CO_2, a naturally bound resource, methane production of a biogas treatment plant can almost be doubled if PtG is applied. Additionally, the climate-damaging methane slip of treatment plants can be avoided.

Biomass Gasification Variant

Instead of a digester, a gasification plant can be used for solid biomass. When supplied with heat and oxygen, carbon hydrate compounds are split into CO, H_2, H_2O, CH_4, and CO_2. This gas mixture is catalytically reacted to methane after purification and conditioning. A PtG plant can provide this process with oxygen and hydrogen and increase its gas yield by using surplus electricity.

CO_2, a Component of Gas from Biogas and Gas Purification Plants

Principle

Direct methanation of biogas or sewage gas is possible even without previous CO_2 separation (Fig. 17). Both gases consist of 50–60 % methane and 40–50 % CO_2 and small amounts of accompanying substances. This gas is conducted from the digester to methanation, where CO_2 from biogas or sewage gas and renewable hydrogen can react to high percentage methane.

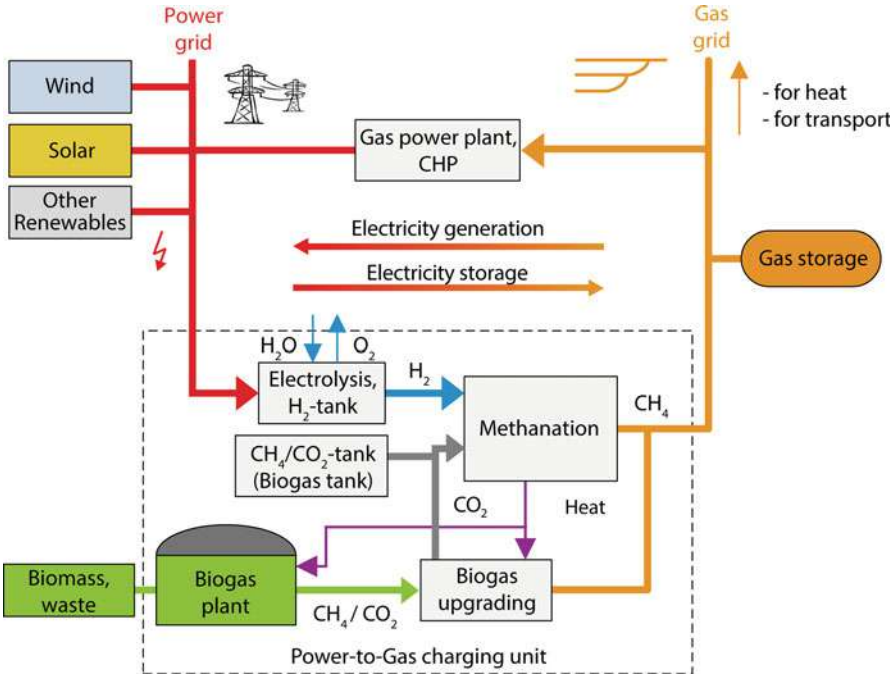

Fig. 17 PtG methane using CO_2 from biogas treatment or biomass gasification (Source: Sterner 2009)

By connecting a biogas plant to a PtG system, which also eliminates the additional energy expenditure for biogas treatment, it can produce twice as much methane.

Advantages of Biological Methanation

This process can be realized both chemically and biologically. Especially biological methanation seems suitable in this case, because the necessary bacterial strains are already contained in biogas and sewage treatment plants. Additionally, parts of the infrastructure of already existing biogas and sewage treatment plants can be used and thus save investment cost. This includes premises, electrical installations, and, if applicable, biogas or sewage gas utilization (conversion to electricity, gas grid, etc.). Especially in combination with municipal infrastructure (e.g., transport fleet), on-site PtG at a sewage treatment plant is very promising.

Along with integration into existing biogas or sewer-gas plants, another possibility is methanation in pure cultures. This has the advantage of increasing conversion rate at reduced dwelling time, because bacterial strains can be treated more specifically.

CO_2 from Flue Gas Emitted by Coal Power Stations

Principle

The main shortcoming of today's coal usage is its CO_2 emission. In the light of worldwide coal reserves, concepts for separation, sequestration, and storage (carbon capture and storage – CCS) are developed and put to the test (see Sterner 2009). It is far more realistic, to use CO_2 from coal power stations energetically or materially (carbon capture and use – CCU), rather than store it in potentially leaky formations underground. There are different processes for separating carbon dioxide from waste gases of combustion processes: In a downstream separation of waste gas after combustion, during the gasification stage before combustion for combined cycle plants using coal gasification, or during combustion in a pure oxygen atmosphere (oxyfuel combustion process, Fig. 18).

Oxyfuel Combustion Process

Since one product of water electrolysis is pure oxygen, latter process seems most attractive. If electrolysis cannot provide enough oxygen, an air separation unit can. This is more energy intensive and decreases the overall system's efficiency. Taking

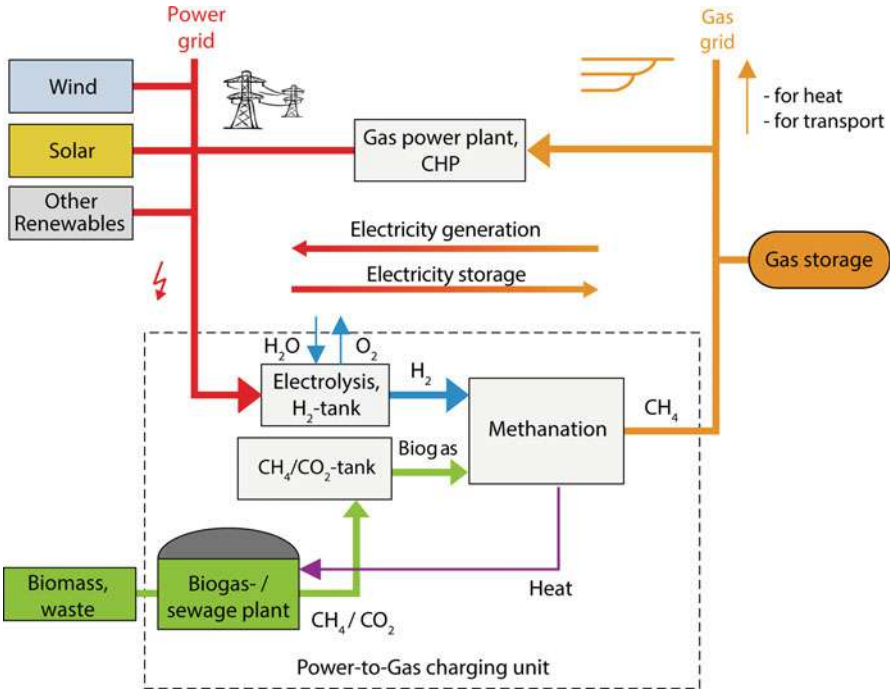

Fig. 18 PtG methane directly reacting a CH_4/CO_2 mixture from biogas or gas purification plants (Source: Sterner 2009)

everything into account, this process may still be more advantageous than energy-intensive downstream separation.

Allocation of Emissions
The allocation of CO_2 emissions is quite a challenge. On the one hand, CO_2 is disposed of by the power plant, on the other hand it is not emitted until the combustion of methane, whose production is based on renewable energies. For this reason, the concept is climate neutral at best. Clear allocation of emissions to coal power stations or gas consumers is required. Otherwise, emissions can be outsourced from the power sector to the heat and transport sector, where the emissions trading law does not apply. So-called green washing of coal power plants is to be avoided.

It is of great importance for this concept that coal power stations are not operated above their must-run limit when methanation is in progress in times of great wind and solar feed-in. In this way, energetically pointless conversion of a chemical energy source to an electrical one and following reconversion (so-called chemical short circuit) can be avoided. Renewable feed-in is mainly there to replace fossil power plants. Electrolysis must not be supplied with electrical energy by fossil power plants.

CO_2 Recycling from Gas Power Stations and Other Sources

Principle
In order to create a closed carbon cycle, the oxyfuel combustion process can be applied to combustion of thus produced methane in gas power stations. This requires spatial proximity of storing and extraction technology, because pure oxygen from electrolysis is needed for clean burning, whose only product gases are carbon dioxide and water. Thus produced CO_2 can be recycled to methane; therefore, the carbon cycle is closed, and the use of CO_2 is climate neutral.

Other Sources
Another possibility is the use of fossil CO_2 from energy-intensive industrial plants, such as steel works, paper mills, or cement plants. They supply their high energy consumption for process heat (possibility of waste heat integration) by combustion of fossil energy sources. This source of CO_2 is very favorable, because they also allow reduction of material, nonenergetic CO_2 emissions. Further sources are waste gases from engine test benches or special industrial processes.

Efficiency, Potentials, CO_2 Emissions, and Costs

Efficiency Increases Because of Integration of High Temperature Electrolysis

Irrespective of which specific process is applied to produce a specific end product, all production variants for synthetic carbon hydrates have one thing in common: while

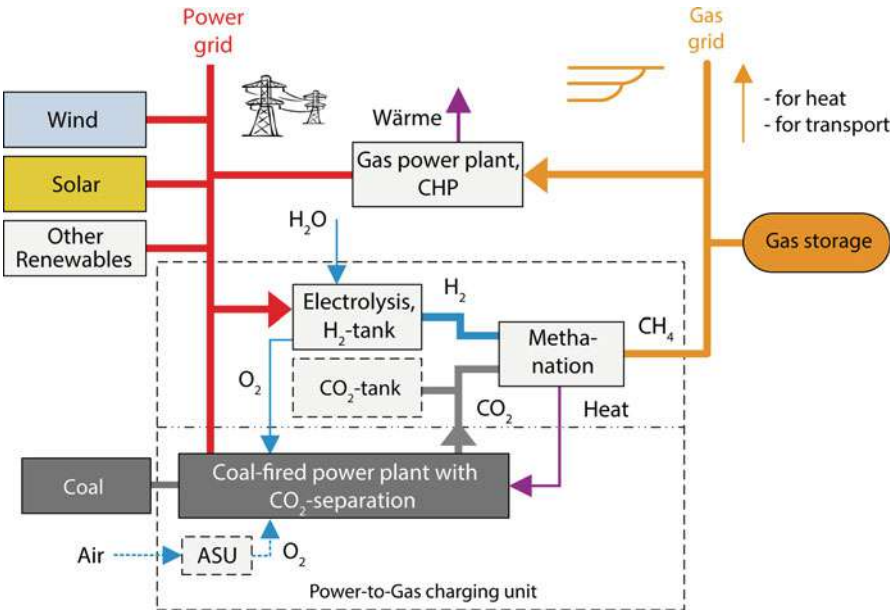

Fig. 19 PtG methane using CO_2 emitted by coal power stations via oxyfuel combustion process (Source: Sterner 2009)

production of hydrogen is an endothermic reaction at the beginning, during the exothermic synthesis of hydrogen and carbons to carbon hydrates, such as methane, methanol, gasoline, diesel, kerosene, or waxes, parts of previously supplied electrical energy are released in the form of heat.

It is this thermodynamic fundamental principle efficiency losses compared to pure hydrogen production are based upon for production of synthetic carbon hydrates. These losses can only be compensated for by reintegration of waste heat released during the process.

One way to achieve this is to vaporize feed water and supply thus produced vapor to steam electrolysis (HTEL). Now, electrical energy only has to supply the net calorific value (NCV) instead of the gross calorific value (GCV), which it has to provide for water electrolysis.

This thermodynamic saving of 16 % electrical energy by recuperating waste heat allows production of synthetic carbon hydrates with an efficiency similar to pure hydrogen production.

These two process chains are compared in Figs. 19 and 20. The thermodynamic maximum efficiency is 84 % for each one, which equals the difference between GCV and NCV of hydrogen (NCV_{H2}/GCV_{H2} – ratio). Efficiency rates expected in practice are between ca. 65 % and 79 %.

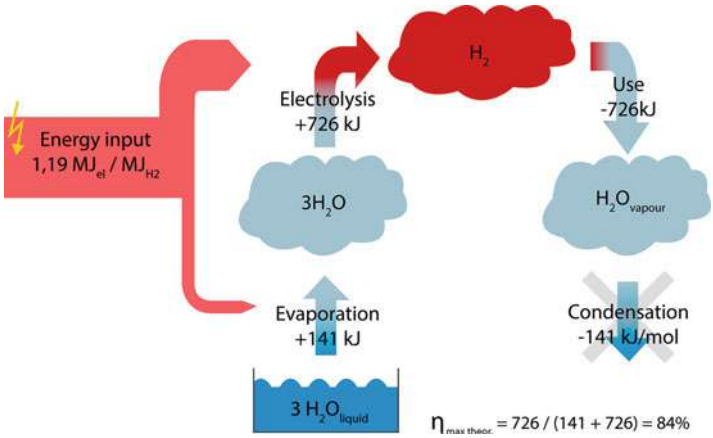

Fig. 20 High temperature electrolysis for hydrogen production from steam without recuperation of waste heat from syntheses (Source: Sterner and Stadler 2014)

Efficiency Rates of Power-to-Gas Systems

A complete PtG system contains

1. Transformer ($\eta = 90$ %)
2. Electrolyser ($\eta = 70$ %)
3. Methanation ($\eta = 82.5$ %)
4. Compression and gas storage ($\eta = 97$ %)
5. And an extraction technology, which can vary depending on the energy service

These average efficiency rates result in different overall efficiency rates (see Table 4). Efficiency of pure PtG hydrogen storage systems are some 5–12 % higher than systems with methanation, because of the missing interim step.

Potentials for Energy Storage

Other than the power grid, the gas grid offers enough transmission and storage capacity. In gas storage, there is a chemical respectively thermal storage capacity of 217 TWh with considerable potential for expansion. Thus stored gas can provide some 120 TWh electricity or 20 % of Germany's gross power consumption and fill all major gaps in renewable energy supply, if reconverted efficiently via sufficient combined cycle plants at an efficiency rate of 60 %.

For systems including methanation, this capacity is completely available. For feed-in of hydrogen, respective limits have to be considered. Assuming an average tolerance of 1–2 %, there is 2–4 TWh storage capacity for hydrogen. However, this value is purely theoretical, because it is based on the assumption that hydrogen is evenly distributed over Germany. Many gas grids' flows vary with the season. In reality, mainly hydrogen caverns are suited for hydrogen storage.

Table 4 Efficiency chains for different PtG storage systems (source: own depiction, based on (Sterner and Jentsch 2011), completed by recuperation of waste heat from synthesis for HTEL)

Path	Overall efficiency (%)	Boundary condition
Power-to-Gas		
Power to hydrogen	54–79	Compression to 200 bar (gas storage)
Power to methane	49–78	
Power to hydrogen	57–80	Compression to 80 bar (long-distance and transport lines)
Power to methane	50–78	
Power to hydrogen	64–84	No compression
Power to methane	51–79	
Power sector		
Power to hydrogen to power	34–51	Conversion to electricity via fuel cell
Power to methane to power	30–38	Combustion in combined cycle plant (60 %)
Transport sector		
Power to hydrogen to motor power	38–53	Use in fuel cell (60 %)
Power-to-gas to motor power	24–49	Reconversion via combined cycle plant and use of electric vehicle (80 %)
Power to methane to motor power	18–37	Combustion in gasoline engine (35 %)
Heat sector		
Power to methane to heat and power	43–68	CHP (45 % heat, 40 % power)
Power to methane to heat	53–84	Condensing boiler (105 %)

For comparison, pump storage plants have a storage capacity of 0.04 TWh. If, theoretically, all 42 M existing cars in Germany were electric vehicles with a capacity of 20 kWh each and on the grid at the same time, they could provide 0.42 TWh storage capacity. This calculation is realistically based on the assumption that half of the cars can be used to balance deficits. At a discharge rate of 60 GW, they could stabilize the power grid for some 7 h. Extraction of all gas storage would suffice, at the same rate, for 2,000 h or 3 months. This comparison makes clear what a huge storage potential Power-to-Gas has.

Along with storage capacity, the gas grid supplies a well expanded transport and distribution network. While typical transmission lines limit transmissions to 3.5 GW (two 380 kV three-phase systems), the long-distance trans-Europe natural gas pipeline can transport gas equal to some 70 GW.

This means the coupling of power and gas grid does not only make storage of great amounts of energy possible, it also allows their spatial separation of storing and usage of renewable methane. This is a unique selling proposition of PtG.

CO_2 Emissions of Power-to-Gas

Potential to Decrease CO_2 Emissions with Renewable Electricity Only

Two things are of importance for the climate impact of PtG storage systems: The source respectively supply of electricity and the substituted energy source.

In summary, it can be said that only renewable, CO_2-free electricity is environmentally friendly and has a decreasing effect on emissions. Gray electricity from coal or gas for hydrogen or methane production is not only energetically absurd but also causes many times over the emissions conventional hydrogen or methane do. This is revealed even by a simplistic greenhouse gas balance:

If cheap lignite electricity (1,161 g CO_2-eq./kWh) is conversed to methane at an efficiency of 60 % (1,935 g CO_2-eq./kWh) and reconverted to electricity via combined cycle plant at an efficiency of 60 %, storage electricity with 3,225 g CO_2-eq./kWh has been produced (see Table 5). This is almost eight times the amount of fossil power from natural gas.

The same applies for transport: at a thrifty consumption of 40 kWh/100 km (ca. 4 l diesel or 0.4 kWh/km) a vehicle fuelled by lignite PtG emits 774 g CO_2-eq./km, which is six times more than fossil diesel (126 g CO_2-eq./km).

In spite of this negative environmental balance, lignite electricity is in discussion to supply PtG, because it is currently the cheapest power on the market. At this point, opposing goals of economy and ecology, as discussed in section "The Need for a Storage Transition in Energy Transition", become clear.

Potential to Decrease CO_2 Emissions: Also a Question of Which Energy Source Is Substituted

The second point of climate impact of PtG is the question, in which order fossil energy sources are substituted. It is essential, if the federal government's goals are to be achieved and climate protection is to be further established, to substitute all fossil energy sources with renewable energies, renewable fuels, and energy storage in all sectors. First, the procedure of substitution should remove emission-rich energy sources, such as coal, subsequently low-emission energy sources, e.g., natural gas.

As shown in Table 5, substitution of lignite and hard coal in the power sector is the first choice from a climate protection point of view. In the first step, coal is replaced by wind, sun, and water power, and in the second step by energy storage, such as Power-to-Gas. Since PtG is only deployed in rare times of deficits of renewable energies, efficiency losses are acceptable.

Substitution of gasoline and diesel fuels makes sense, as long as they cannot be replaced by direct usage of renewable electricity in electric vehicles.

An extrapolation of the potential to decrease CO_2 emissions from one single plant to all of Germany is only possible, if surplus quantities are taken into account (section "The Storage System Power-to-Gas"). As a rule, it can be said that:

Table 5 Emissions of fossil energy sources and PtG storage systems in g CO_2-eq. per energy unit (kWh) and per energy service resp. in g CO_2-eq. per km mileage at a very moderate consumption of 40 kWh/100 km (ca. 4 l diesel/100 km); based on 100 % combustion, conversion losses included. Reference system 2010. Gray electricity mix emissions: 546 g CO_2-eq./kWh (Source: Icha 2013)

Energy source	g CO_2-eq./kWh_{th} combustible	g CO_2-eq./kWh energy service	g CO_2-eq./km mileage	Energy service
Fossil systems				
Lignite	404	1,161 ($\eta = 0.35$)		Power
Hard coal	339	902 ($\eta = 0.38$)		
Natural gas	202	411 ($\eta = 0.49$)		
Natural gas	202	224 ($\eta = 0.9$)		Heat
Heating oil	266	296 ($\eta = 0.9$)		
Diesel	266		106	Transport
Natural gas	202		81	
PtG systems (efficiency of electricity to gas: 60 %)				
Lignite – gas	1,935	3,949 ($\eta = 0.49$)		Power
Gray electricity – gas	950	1,857 ($\eta = 0.49$)		
Wind gas	33	68 ($\eta = 0.49$)		
Lignite – gas	1,935	2,050 ($\eta = 0.9$)		Heat
Gray electricity – gas	950	1,011 ($\eta = 0.9$)		
Wind gas	33	37 ($\eta = 0.9$)		
Lignite – gas	1,935		774	Transport
Gray electricity – gas	950		364	
Wind gas	33		13	

– The deployment of renewable electricity is a basic prerequisite
– The more CO_2 intensive a substituted energy source, the greater the reduction potential

Costs of PtG

Market Conditions

Hydrogen produced by steam reforming of natural gas causes production costs of 3–4 €-¢/kWh, natural gas costs 2–3 €-¢/kWh at the stock market, and gray electricity between 1 and 6 €-¢/kWh (see EEX 2014). Surplus electricity for even smaller prices is only available for a very small number of hours, which shows how difficult it is for PtG to competitively convert Power-to-Gas.

Economic Efficiency

PtG is a very young energy technology; today, it cannot be realized economically. Investment costs for new plants are between 2,500 and 5,000 €/kW; operating costs

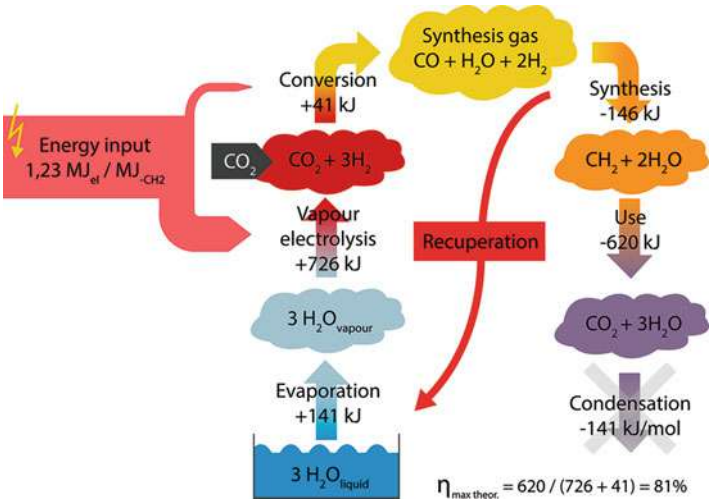

Fig. 21 High temperature electrolysis for carbon hydrate production from steam and CO_2 with recuperation of waste heat from syntheses for vaporization of water. Similar efficiency rates as pure hydrogen production (Source: Sterner and Stadler 2014)

are mainly subject to electricity prices, which vary between 0 €-¢/kWh (very rare) and 9 €-¢/kWh (average price for wind power).

Figure 21 shows results of elaborated cost calculation that were made in the course of the project "Energy Storage Concepts" for PRG hydrogen and PtG methane. These results are shown as a range from optimistic (low investment and operating costs, low interest rates, and low risk) to pessimistic expectations (high investment and operating costs, high interest rates, and high risk). All assumption can be seen in detail in Henel et al. (2013).

Economically competitive production of renewable hydrogen or methane requires more than 7,000 h electricity supply at 0 €-¢/kWh without further levies. From today's point of view, this scenario seems more than unlikely.

Only after a concept with electricity supply costs of 5 €-¢/kWh in base load operation (more than 7,000 h) has been developed, e.g., sail powered energy, it will be possible to supply hydrogen for 8–17 €-¢/kWh and methane for 13–24 €-¢/kWh. If levies for CO_2 or prices for natural gas were to increase, renewable gases could be an economical and sustainable alternative, even for higher costs.

It becomes clear that hydrogen can only be produced economically in the most optimistic case, which means almost constant electricity supply at stock market prices or below can be used. But this means that something else than surpluses of wind or solar energy are used, because they occur only very rarely and not on a constant basis. If gray electricity is used, the product gas is the same as fossil gas concerning disadvantages in the CO_2 balance and marketing. In many places in Germany, feed-in management is used to curtail surpluses. At the moment, the absolute value is within limits: in the past year, only ca. 1 ‰ of Germany's energy consumption has been curtailed.

A basic rule for PtG: only if electricity supply is mainly renewable (more than 80 %), the produced gas has the privilege to be equal to biogas. This simplifies the connection of the PtG plant to the gas grid and the gas' benchmark is increased from 2–3 €-¢/kWh (fossil natural gas) to 7–8 €-¢/kWh (bio-natural gas).

If the stored gas is reconverted to electricity via gas power station, thus generated power costs some two times more because of the complete electricity storage chain.

From today's point of view, market entry seems most likely in the field of fuels for transport or resources for the chemical industry, because the price level is higher in there than in the electricity and heat market.

Hydrogen Versus Methane

On the one hand, a PtG hydrogen storage system does not require a methanation unit and therefore saves efficiency and costs. On the other hand, costs are not assessable for the adaption of plants incompatible to hydrogen in the gas infrastructure or setting up a hydrogen infrastructure. For this reason, the exhaustion of hydrogen admixture quotas of 1–2 % including downstream methanation is favorable for long-term storage with PtG, from today's point of view. More information can be found in the gas grid development plans (see Netzentwicklungsplan Gas 2012).

Advantages and Disadvantages of Hydrogen and Methane

PtG Hydrogen

A PtG hydrogen storage system is favorable, for reasons of efficiency and costs, as long as admixture limits of hydrogen are not exceeded or hydrogen can be stored and used locally. It has to be preconceived that, for small natural gas flows, admixture limits are reached very quickly and storage has to be applied in order to level hydrogen feed-in.

Unlike for methane and natural gas, there are no comprehensive solutions suitable for the mass. While fuel cell technology is subject to research in auto industry and heat supply long since, technologies ready for the market are merely announced time and again. Furthermore, market entry is only possible, and even then merely in small quantities, if subsidized by companies or the public purse. It is also yet to be seen if fuel cells will come on top of e-mobility, conventional powertrains, electric heat pumps, and alternative renewable heating systems based on wood and sun.

When adding hydrogen to the natural gas, changing fuel properties of the gas mixture have to be taken into account. For one thing, the volumetric calorific value decreases by some 7 %, depending on the natural gas quality, if 10 % by volume hydrogen is added. This has to be compensated for by an increased quantity to be supplied, which in turn requires adaption of, for example, compressors.

The adaption of the natural gas infrastructure to higher admixture quotas is associated with the need for research and high costs.

Figure 22 shows which components are particularly affected and the existence of need for adaption and research.

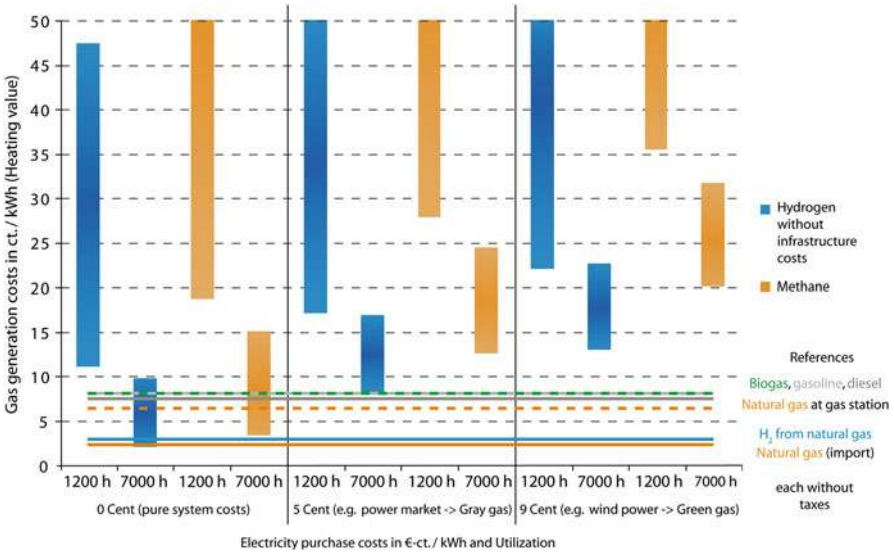

Fig. 22 Range of gas production costs in €-¢/kWh for PtG hydrogen and PtG methane for different electricity prices and full load hours in the DVGW project "Energy Storage Concepts." Hydrogen paths are represented in blue, methane in orange, each in a range from optimistic to pessimistic. Electricity supply is plotted from 0 €-¢/kWh (plant costs only) over an average value for stock market prices (5 €-¢/kWh) to electricity supply by a wind power plant (9 €-¢/kWh), each for different periods of use and utilization time (the year has 8,760 h). Reference costs for gases and fuels made with fossil and biogenic energy are depicted as dashed lines (Source: adapted from Henel et al. (2013))

In the transport sector, it has to be taken into account that natural gas must not contain more than 2 % by volume hydrogen, because higher concentrations may cause embrittlement of steel tanks in CNG vehicles. But also for reconversion to electricity, high shares of H_2 are problematic: gas turbines are only operational, as specified by the manufacturer, for admixture quotas between 1 % and 3 % by volume, because of changing combustion characteristics (increased flame velocity, different temperature, etc.). For this reason, even cogeneration plants which are, according to manufacturer's data, hydrogen-tolerant up to 25 % are in practice operated with only 15 %.

In general, it is assumed that the admixture limit for hydrogen in the natural gas grid is 1–1.5 %. High local feed-in of hydrogen may cause problems if the natural gas load flow is low, because limits are exceeded locally. Additionally, there are some industrial gas applications, which use gas as "flaming tool" (e.g., drying in the porcelain and glass industry). Fluctuating gas quality can have a strong influence on the product quality (see Henel et al. 2013).

Since conditions and requirements in long-distance and distribution gas grids vary strongly both locally and regionally, each possibility for the feed-in of the additive gas hydrogen has to be checked individually.

According to the FNB's (long-distance grid operators) gas grid development plans, increasing the admixture limit from today's 1–1.5 % to 10 % requires the replacement of all compressors, which costs 3.6 Bio. € in the long-distance grid alone (see Netzentwicklungsplan Gas 2012).

Advantages and disadvantages of feed-in of hydrogen into the gas grid versus PtG methane are compared in Fig. 23 and Table 6.

PtG Methane

The storage system PtG methane has certain advantages compared to the hydrogen system and other long-term storage systems but also disadvantages.

The systems advantages are obvious. It is possible to integrate renewable methane in today's energy infrastructure without any problem, since it has the same quality, it can fully replace natural gas ("replacement gas"). Unlike hydrogen, the use of renewable methane is uncritical regardless of admixture quotas for gas turbines, porous storage, distribution lines, seals, and applications, such as combustion engines or gas stoves.

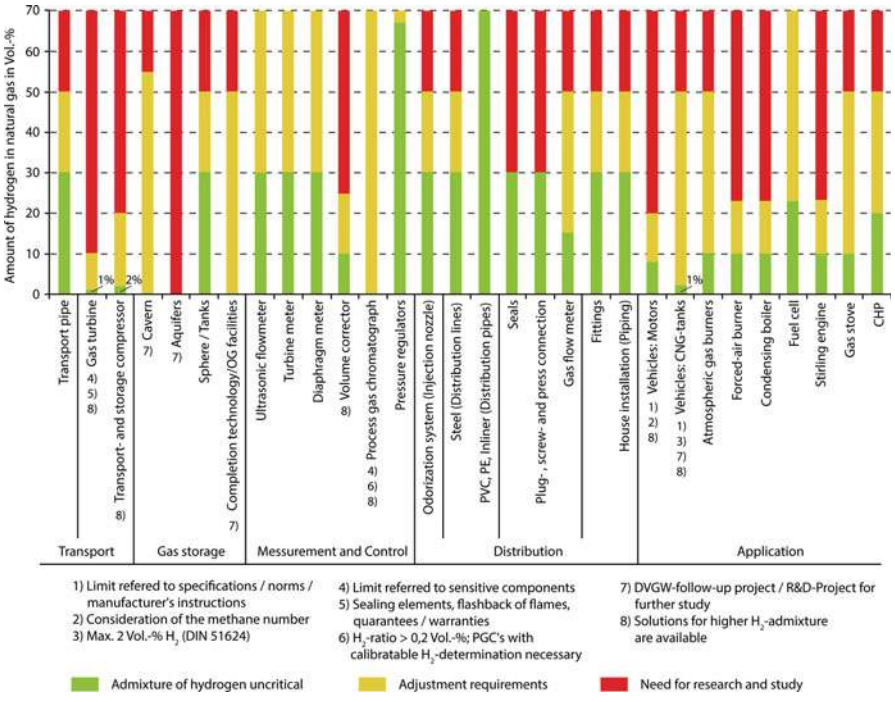

Fig. 23 Hydrogen tolerance of specific components of the gas infrastructure (Source: Henel et al. 2013)

Table 6 Advantages and disadvantages of a PtG storage system with hydrogen and methane

	Hydrogen		Methane	
	Advantages	Disadvantages	Advantages	Disadvantages
Efficiency				
Storing technology	54–84 %		Equal	49–79 %
Storage	Equal		Equal	
Extraction technology	Equal			
Feed-in into the gas grid	Equal	Additive gas: today's admixture limit 1–1.5 %; max. 2 % by Volume	Replacement gas: no limit	
Infrastructure		Largely nonexistent, no affordable and fully developed application technology	Existing infrastructure including application technologies, usable to the full extent	
Transport				
Storage				
Application				
Material demand, climate impact, and plant operation	Independent of CO_2, therefore more flexible siting (except for usage of atmospheric CO_2 for methanation)	Additional hydrogen storage necessary for fluctuating load flow of natural gas	Possible CO_2 sink if operated in CCS mode	Necessity of a CO_2 source, continuous methanation is based on upstream hydrogen production
Energy density (specific calorific value at 0 °C and 1.013 bar or space requirement for storage)		3.0 kWh/m³	10.0 kWh/m³ Three times more, smaller storage system possible	
Transformation costs	Cheaper than methane up to the admixture limit	Storing: Electricity – H_2 Storage Extraction: H_2 – electricity Transport, storage		Only storing and additional methanation and CO_2 supply versus hydrogen

Furthermore, there exists already a large and widely distributed infrastructure for energy transport, storage, and application technology. This means there are well-established state-of-the-art applications in every energy sector and in the chemical industry.

Another advantage is the higher volumetric energy density of methane compared to hydrogen, which makes smaller storage systems possible and saves cost and space. With reference to one standard cubic meter, the calorific value of methane is 3.3 times that of hydrogen.

The cost situation of this storage system requires a differentiated review. Up to the admixture limit of hydrogen, a system without methanation is more economical, because they operate without CO_2 supply and methanation units. As soon as that limit is reached, it is more cost-efficient to store renewable energy in the form of methane instead of adapting the German infrastructure to a higher admixture quota of hydrogen.

A disadvantage of PtG methane is its need for CO_2 supply. Efficiency losses of the overall process reflect the additional expenditure. But, on the other hand, the extraction and storage of atmospheric CO_2 is a possibility to reduce its concentration in the air by the energy system itself and in the long run, CO_2 extraction from air might become a necessity in fighting global climate change anyway and therefore cheaply available. In any way, it is important to operate PtG with a closed carbon cycle.

Decarbonization with Power-to-Gas

So far, the necessity for energy storage and the physical, economical, and ecological parameters of the technology of Power-to-Gas have been described in detail. Now, a brief outlook on the potential for decarbonization with Power-to-Gas is given in the context of the energy transition in Germany and more over is given.

Technical Pathway of Decarbonization

As seen, PtG can be very useful for the decarbonization of electricity and heat: It offers the required long-term storage for weeks of no wind and solar energy at reasonable cost and is a supplement/addition to biomass, geothermal energy, and solar energy for decarbonizing heating and cooling systems. The access is also given for mobility: although electric vehicles will be the most efficient way of using wind and solar power, their range is limited. Long-distance mobility, lorries, ships, and airplanes still demand energy carriers with high energy density. These can be hydrogen or SNG from Power-to-Gas or even wind kerosene or wind diesel from Power-to-Liquid. Biofuels will have their share also in heavy duty applications like tractors, but their potential is limited and not sufficient to cover all high energy density fuel demand (Sterner and Schmid 2009). A possible pathway towards decarbonization of the whole energy sector is given in Fig. 24.

Power-to-Gas or Power-to-X will also be required to decarbonize the chemical industry. This sector is also using large amounts of fossil fuels like oil and gas in a nonenergetic way. To decarbonize industrialized nations not only by 80 % (2 °C goal) but by 95 % (1.5 °C goal), Power-to-X will become a requirement, since there

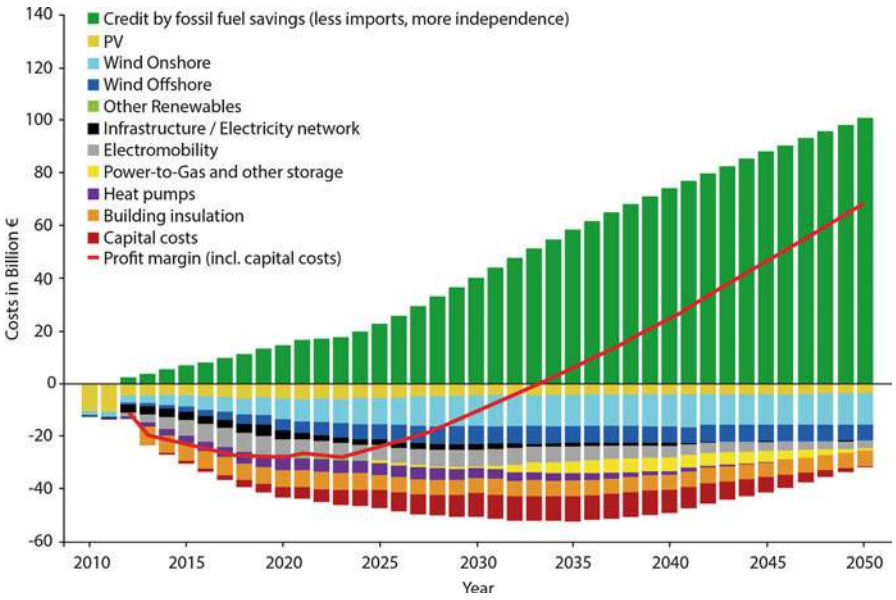

Fig. 24 Energy transition scenario for all energy sectors in Germany until 2050 – costs and savings in Mio. €/a (Source: Gerhardt et al. 2014)

are no other technologies left that can technically do this. As mentioned, biomass does not have the potential but chemical products from wind and solar do.

Costs of Decarbonization with Power-to-Gas

So technically, the energy transition and decarbonization is doable. And it is also feasibly regarding costs: wind and solar show generation costs below 10 €-cts/kWh and are therefore less expensive than new coal, gas, or nuclear power generation. What is missing is the cost for storage and balancing. The EU imports fossil energy carriers worth 400 Bio. € each year. If this money would be saved by the implementation of locally available renewable energy, it could refinance the necessary expensive infrastructure for networks and storage. There are calculations for Germany, that show a macroeconomic return of invest rate of 4–7 %, if a moderate increase of fossil fuels prices are assumed (see Fig. 25 and Gerhardt et al. (2014)).

Necessary Policy Framework

What is then left for decision makers in the EU and worldwide? First of all, remove subsidies for fossil energy. Second, a must for the energy transition is the interlinkage of electricity, gas, heat, and transport sectors. The technical possibilities are given and should be used (Fig. 26).

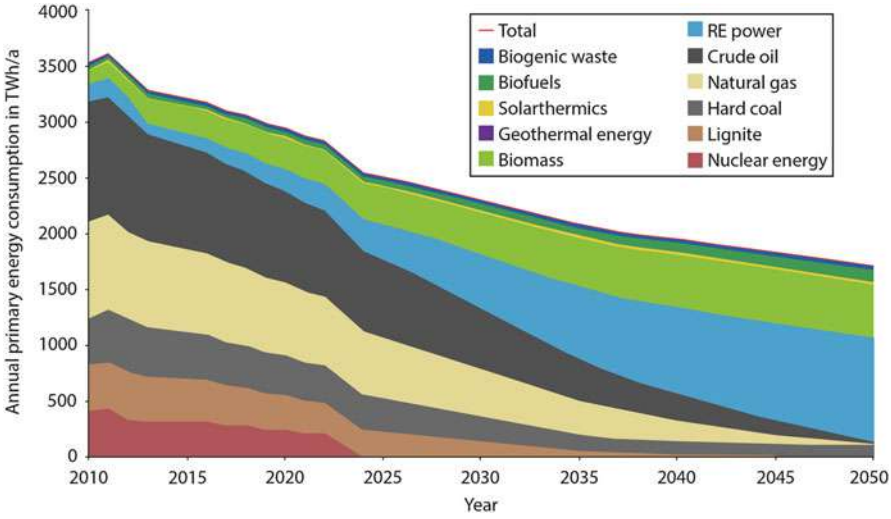

Fig. 25 Energy transition scenario for all energy sectors in Germany until 2050 – primary energy sources and demand in TWh/a (Source: Gerhardt et al. 2014)

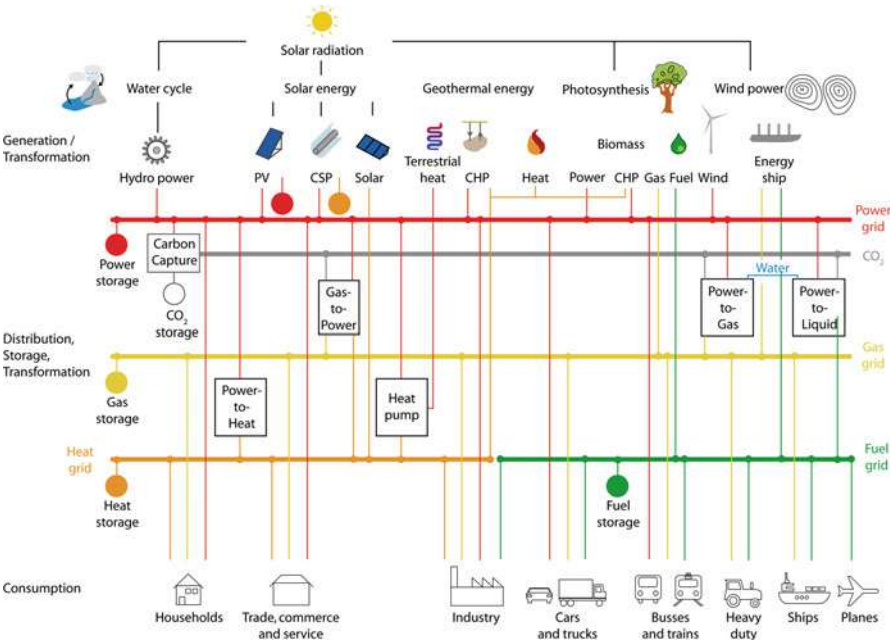

Fig. 26 Technical pathways of the decarbonization of energy sectors, mobility, and chemical industry via renewable energy and interlinked energy storage and transport infrastructure and Power-to-Gas/Heat/Fuels at the heart of the system (Source: Sterner and Stadler 2014)

Energy markets should be merged via energy storage and energy transmission. Power-to-Gas and Power-to-X are essential technologies that save costs by using existing storage and transmission infrastructure. Storage technologies should be developed in Europe to create jobs and values in the EU with these complex system technologies that would be needed worldwide at some point of time in future. But without framework conditions, we would not see a large-scale development of storage that is needed to bring costs down by mass production. To reduce import dependence, it is helpful to build up strategic "renewable reserves." The still cost-intensive technologies like storage or electromobility should be cross-financed by CO_2 funds, fossil fuel savings, and cheap renewables. To enable this transition, market barriers have to be removed. That includes better access of storage and renewables to control power markets, the avoiding of double taxing, and the implementation of limited tax exemptions. The storage problem is solved technically and global markets are ahead, but in history, no new energy technology did its way to the market without official support. Another requirement is the mandatory use of renewable power for storage, electromobility, and heat pumps. Otherwise, with fossil power, these new technology do not have the desired impact on climate change.

And last but not least: policy makers need to explain to people the need of this energy transition due to climate change, import dependency, and depleting fossil resources in an open, transparent, and decisive way. We can find nice technical, eco-friendly solutions that are economic, but if we don't convince society, we would implement decarbonization. Besides an energy transition, there is therefore also a strong need for the transition of storage and the transition of consciousness and awareness.

Concluding Remark

The chapter shows that BioCCS (Biomass and CCS) is not the only option to reach the 1.5 °C climate target and that storage systems are ready for decarbonization of all sectors

Changes in the Future

- Cost updates will be implemented.
- Eventually emission reduction scenarios will be integrated.

References

Audi (2014) Aus der Luft gegriffen. Available: http://audi-dialoge.de/magazin/technologie/01-2014/104-aus-der-luft-gegriffen. 10 Mar 2014

Bandi A (1995) CO_2 recycling for hydrogen storage and transportation: electrochemical CO_2 removal and fixation (ger). Energy Convers Manage 36(6/9):899

Beil M (2008) BiogasMAX: Biogasaufbereitung zu Biomethan. 6. Hanauer Dialog. Tagungsband. ISET – Institut für Solar Energieversorgungstechnik, Kassel/Hanau

EEX (2014) EEX ist die führende Energiebörse in Europa. Available: http://www.eex.com/de#/de. 14 Feb 2014

Enßlin C, Füller G, Hahn B, Hoppe-Kilpper M, Rohrig K (1993) The scientific measurement and evaluation programme in the German 250 MW wind programme: European wind energy conference. ISET – Institut für Solar Energieversorgungstechnik, Kassel

Ernst B (2003) Entwicklung eines Windleistungsprognosemodells zur Verbesserung der Kraftwerkseinsatzplanung. Dissertation, Universität Kassel, kassel university press, Kassel

Ernst B, Hoppe-Kilpper M, Rohrig K, Scheibe M (2004) Zeitreihen der Windeinspeisung und deren statistische Analyse – Zusatzuntersuchung im Rahmen der dena-Netzstudie: Energiewirtschaftliche Planung für die Netzintegration von Windenergie in Deutschland an Land und Offshore bis zum Jahr 2020. Kassel

FAO (2008) The state of food and agriculture 2008: biofuels – prospects, risks and opportunities. FAO, Rome

Fichtner N (2011) Aus Wind mach Gas mach Strom: Vor drei Jahren hatten zwei Wissenschaftler eine gute Idee. Bald könnte sie das deutsche Energiesystem revolutionieren. Financial Times Deutschland, 18 Jul, p 10

FNB (2014) Netzentwicklungsplan Gas 2012–2014. Available: http://www.fnb-gas.de/de/netzentwicklungsplan/netzentwicklungsplan.html. 13 Feb 2014

Gebald C (2013) CO_2 supply through direct air capture. Essen, Climeworks

Gebald C, Wurzbacher JA, Tingaut P, Zimmermann T, Steinfeld A (2011) Amine-based nanofibrillated cellulose as adsorbent for CO_2 capture from air. Environ Sci Technol 45(20):9101–9108

Gebald C, Wurzbacher JA, Tingaut P, Steinfeld A (2013) Stability of amine-functionalized cellulose during temperature-vacuum-swing cycling for CO_2 capture from air (en). Environ Sci Technol 47(17):10063–10070

Gerhardt N, Sandau F, Zimmermann B, Pape C, Bofinger S, Hoffmann C (2014) Geschäftsmodell Energiewende: Eine Antwort auf das "Die-Kosten-der-Energiewende"-Argument. "Herkulesprojekt Energiewende." Fraunhofer Institut für Windenergie und Energiesystemtechnik (IWES) Kassel, Kassel

Henel M, Köppel W, Mlaker H, Sterner M, Höcher T (2013) Entwicklung von modularen Konzepten zur Erzeugung, Speicherung und Entwicklung von modularen Konzepten zur Erzeugung, Speicherung und Einspeisung von Wasserstoff und Methan ins Erdgasnetz. Abschlussbericht DVGW-Projekt G1-07-10, Deutscher Verein des Gas- und Wasserfaches e.V. (DVGW e.V.), Leipzig

HYPOS (2014) Hydrogen power storage & solutions East Germany. Available: http://www.hypos-eastgermany.de/. 14 Mar 2014

Icha P (2013) Entwicklung der spezifischen Kohlendioxid-Emissionen des deutschen Strommix in den Jahren 1990 bis 2012: climate change 07/2013. UBA – Umweltbundesamt, Dessau-Roßlau

Mackensen R (2011) Herausforderungen und Lösungen für eine regenerative Elektrizitätsversorgung Deutschlands. Dissertation, Universität Kassel, Kassel

Mackensen R, Rohrig K, Emanuel H (2008) Das regenerative Kombikraftwerk: Abschlussbericht. ISET, Kassel

Nitsch J, Pregger T, Sterner M, Wenzel B (2012) Langfristszenarien und Strategien für den Ausbau der erneuerbaren Energien in Deutschland bei Berücksichtigung der Entwicklung in Europa und global: Schlussbericht BMU – FKZ 03MAP146. Deutsches Zentrum für Luft- und Raumfahrt/Fraunhofer-Institut für Windenergie und Energiesystemtechnik/Ingenieurbüro für neue Energien, Berlin

Sachs JD (2008) Surging food prices mean global instability: misguided policies favor biofuels over grain for hungry people (en). Scientific American Magazine, 2 May, 2008

Sauer D (2006) In: The demand for energy storage in regenerative energy systems: first international renewable energy storage conference (Eurosolar IRES I), Gelsenkirchen, Oct 2006

Schmid J, Sterner M (2008) Bioenergy in future energy systems (en). In: Proceedings of the international conference '16th European biomass conference & exhibition' of EUBIA in Valencia, vol 16

Specht M (1998) Comparison of the renewable transportation fuels, liquid hydrogen and methanol, with gasoline – energetic and economic aspects (ger). Energy Convers Manage 23(5):387–396

Specht M, Bandi A, Elser M, Heberle A, Maier CU, Schaber K, Weimer T (2000) CO_2-Recycling zur Herstellung von Methanol: Endbericht. ZSW Stuttgart, Stuttgart

Specht M, Marquard-Möllenstedt T, Sichler P, Zuberbühler U (2006) Der AER-Prozess: Neues thermochemisches Biomasse-Vergasungsverfahren mit flexiblen Edukt- und Produktströmen: Beiträge zur DGMK-Fachbereichstagung "Energetische Nutzung von Biomassen." ZSW – Zentrum fuer Sonnenenergie- und Wasserstoffforschung Baden-Wuerttemberg, Hamburg, Tagungsbericht/Deutsche Wissenschaftliche Gesellschaft für Erdöl, Erdgas und Kohle

Specht M, Zuberbühler U, Koppatz S, Pfeifer C, Marquard-Möllenstedt T (2008) Transfer of absorption enhanced reforming process (AER) from pilot scale to an 8 MW gasification plant in guessing, Austria (en). In: Proceedings of the international conference '16th European biomass conference & exhibition' of EUBIA in Valencia, vol 16

Specht M, Sterner M, Stuermer B, Frick V, Hahn B (2009) Renewable power methane – Stromspeicherung durch Kopplung von Strom- und Gasnetz – Wind/PV-to-SNG. Germany 10 2009 018 126.1

Specht M, Sterner M, Brellochs J, Frick V, Stuermer B, Zuberbühler U, Waldstein G (2010) Speicherung von Bioenergie und erneuerbarem Strom im Erdgasnetz: storage of renewable energy in the natural gas grid (en). Erdöl Erdgas Kohle 126(10):342–346

SRU (2011) Wege zur 100 % erneuerbaren Stromversorgung: Sondergutachten. Erich Schmidt, Berlin

Sterner M (2009) Bioenergy and renewable power methane in integrated 100% renewable energy systems: limiting global warming by transforming energy systems. Kassel University Press, Kassel

Sterner M, Jentsch M (2011) Energiewirtschaftliche und ökologische Bewertung eines Windgas-Angebotes: Gutachten für Greenpeace Energy. Fraunhofer IWES, Kassel

Sterner M, Schmid J (2008) Electromobility – an efficient alternative to conventional biofuels to put biomass on the road (en). In: Proceedings of the international conference '16th European biomass conference & exhibition' of EUBIA in Valencia, vol 16

Sterner M, Schmid J (2009) WBGU Gutachten – zukunftsfähige Bioenergie und nachhaltige Landnutzung. In: Faulstich M, Mocker M (eds) Biomasse & Abfall: Emissionen mindern und Rückstände nutzen, vol 5, Verfahren & Werkstoffe für die Energietechnik. Dorner PrintConcept GmbH, Sulzbach-Rosenberg, pp 23–38

Sterner M, Stadler I (2014) Energiespeicher – Bedarf, Technologien, Integration. Springer, Berlin

UBA (2010) 2050: 100 % erneuerbarer Strom: Energieziel 2050. Umweltbundesamt, Dessau-Roßlau

VDE ETG (2012) Energiespeicher für die Energiewende. Energietechnische Gesellschaft im VDE, Frankfurt am Main

VDE (2013) Energiespeicher in Stromversorgungssystemen mit hohem Anteil erneuerbarer Energieträger. Available: http://www.vde.com/de/fg/ETG/Arbeitsgebiete/V1/Aktuelles/Oeffentlich/Seiten/Energiespeicherstudie-Ergebnisse.aspx. 29 Dec 2013

WBGU (2008) Welt im Wandel: Zukunftsfähige Bioenergie und nachhaltige Landnutzung: Hauptgutachten 2008. WBGU, Berlin

Weimer T (1996) Methanol from atmospheric carbon dioxide a liquid zero emission fuel for the future (ger). Energy Convers Manage 37(6/8):1351–1356

Wurzbacher JA, Gebald C, Steinfeld A (2011) Separation of CO_2 from air by temperature-vacuum swing adsorption using diamine-functionalized silica gel (en). Energy Environ Sci 4(9):3584

Reduction of Greenhouse Gas Emissions by Catalytic Processes

Gabriele Centi and Siglinda Perathoner

Contents

Abstract

Catalytic technologies for the abatement of greenhouse gases (GHGs) can effectively limit the increasing tropospheric concentration of GHGs and reduce their contribution to global warming. After introducing the general possible applications of catalytic technologies for GHG abatement, two specific cases are discussed: (1) reduction of anthropogenic emissions of non-CO_2 GHGs (N_2O and CH_4) and (2) reduction or conversion of CO_2.

G. Centi (✉) • S. Perathoner
Dip. Ingegneria Elettronica, Chimica ed Ingegneria Industriale (DIECII), University of Messina, ERIC aisbl and CASPE-INSTM, Messina, Italy
e-mail: centi@unime.it; centi@live.it; perathon@unime.it

W.-Y. Chen et al. (eds.), *Handbook of Climate Change Mitigation and Adaptation*,
DOI 10.1007/978-3-319-14409-2_49

Combustion is one of the main options for controlling methane emissions. The use of catalytic combustion may yield economic benefits, due to the usually low concentration of methane in its emissions, and avoid the formation of by-products in traces like formaldehyde, which may be more harmful than methane itself. The types of catalysts, mechanism of action, and reactor options (regenerative catalytic combustion, reverse flow catalytic combustion, and catalytic combustion using a rotating concentrator) are discussed.

The catalytic control of N_2O emissions shows different specificities, because different types of emission sources are present. The catalytic abatement or reuse of N_2O from industrial emissions (particularly adipic and nitric acid production), the treatment of emissions from power plants or waste combustion, the alternatives of catalytic decomposition or reduction, and the role of the other gas components (O_2, NO_x, SO_x) are analyzed.

The problem of the catalytic conversion of fluorocarbons is also briefly discussed.

The case of carbon dioxide is different because, in this case, the issue is the development of cost- and energy-effective catalytic routes for its conversion to usable products. There are many catalytic routes for using CO_2 as a building block in organic syntheses to obtain valuable chemicals and materials. Attention has focused recently on the catalytic conversion of carbon dioxide to fuels. In this case as well, different options exist, such as hydrogenation to form oxygenates (e.g., methanol) and/or hydrocarbons, dry reforming with methane, reverse water gas shift, or, in a longer-term perspective, different methods using solar energy directly or indirectly (via bioconversion). Limitations and possible advantages of these different options are analyzed.

Introduction

The control of GHG emissions from anthropogenic sources is becoming a global challenge. In addition to regions such as Europe at the forefront of measures to reduce GHG emissions, there is a global trend to adopt advanced environmental political measures to reduce GHG emissions. EU leaders agreed on 23 October 2014 the domestic 2030 GHG reduction target of at least 40 % compared to 1990, following the roadmap on GHG emissions approved from the European Parliament for their reduction to 80 % with respect to 1990. On 11 November 2014, a historic US-China Joint Announcement on Climate Change reported that the USA and China joined the European Union in committing to new limits on GHG emissions. These three economic powerhouses emit about as much each year as the rest of the world combined, so their commitments have important implications for the world's ability to stay within its carbon budget. The USA will reduce GHG emissions 26–28 % from 2005 levels by 2025. China announced its intent to peak carbon dioxide emissions around 2030 (around ten billion metric tons per year, with respect to emissions leveling off between 2030 and 2040 at approximately 12–14 billion metric tons per year) and to strive to peak earlier by reducing carbon emissions per unit of GDP by

40–45 % from 2005 levels by 2020. The Cop 20 (UN climate change) conference (Lima, 1–12 December 2014) for the first time commits all countries – including developing nations – to cutting GHG emissions.

The IPCC Fifth Assessment Report, finalized in November 2014 (Pachauri and Meyer 2014), showed how the "warming of the climate system is unequivocal" and "continued emission of greenhouse gases will cause further warming and long-lasting changes in all components of the climate system, increasing the likelihood of severe, pervasive and irreversible impacts for people and ecosystems." The report also remarked that "without additional mitigation efforts beyond those in place today, and even with adaptation, warming by the end of the twenty-first century will lead to high to very high risk of severe, widespread, and irreversible impacts globally (high confidence)."

The implementation of the decisions taken at a political level coincides with the scientific indications deriving from the cited IPCC report that it is necessary to accelerate the measurer to reduce GHG emissions. Catalytic technologies offer effective cost-basis solutions for their control (Centi et al. 1999, 2003a). The "Technology Roadmap on Energy and GHG Reductions in the Chemical Industry via Catalytic Processes," prepared recently by the IEA and the ICCA in collaboration with Dechema (IEA 2013), evidences the role of catalysis to meet the objectives of GHG reduction in the chemical industry, with a potential impact on the reduction of energy intensity by 20–40 % as a whole by 2050. In absolute terms, such improvements could save as much as 13 EJ and 1 Gton of CO_2-eq. per year by 2050 versus a "business-as-usual" scenario. The white paper "Available and emerging technologies for reducing greenhouse gas emissions from the petroleum refining industry" prepared by US EPA (2010) shows the role of catalysis in reducing GHG emissions in refinery industry, one of the highest industrial consumers of energy.

Although catalysis has been associated traditionally to chemical production and refinery, except for the relevant cases of catalytic converters for mobile sources and DeNOx systems for the reduction of NOx emissions from stationary sources, catalytic technologies for GHG emissions have a broader area of applications, as discussed in this chapter. By including the potential role of converting CO_2 as a way to trade on a worldwide scale renewable energy (presented later), the potential is of several Gton CO_2-eq. Catalytic technologies have thus the potential, although still underestimated, to be one of the pillars to reach the political goals to reduce GHG emissions.

We may distinguish between direct and indirect roles of catalytic technologies in contributing to climate change goals. The direct role is associated to catalytic technologies for the conversion of GHG, either for direct conversion to not harmful products (e.g., conversion of N_2O to N_2) or having lower GWP (e.g., conversion of CH_4 to CO_2) or for reutilization of GHG (e.g., N_2O utilization as selective oxidation or utilization of CO_2 as raw material). In the latter case, it is important to distinguish when the utilization leads to an effective reduction of GHG impact on a LCA basis. For example, the reaction of CO_2 with high-energy molecules such as epoxides to form carbonate needs to account the impact on GHG of forming the epoxide but also the positive impact of producing an alternative material to those based on fossil fuels.

Therefore, the impact is not relative to utilization only of CO_2 as raw material but to the associated effect on LCA bases. It is possible to indicate an effectiveness factor (EF) to the various routes for reducing GHG emissions, for example, for carbon dioxide. Sequestration and storage (CSS) has an average EF value of around 0.5, because it is necessary to consider the energy necessary to capture and store CO_2. On the contrary, several of the routes for chemical utilization of CO_2 have an EF value higher than one, for the benefit in substituting other materials starting from fossil fuels only (Centi and Perathoner 2014; De Falco et al. 2013). When renewable energy is utilized in the process of converting CO_2 to valuable fuels, EF may be even larger than a decade on a timescale of 20 years. It is thus necessary to account this EF value in estimating the impact of the different routes of utilization of GHG and not only the direct amount of GHG utilized as raw material.

The indirect role of catalytic technologies in contributing to climate change goals is related to various aspects, from the role of catalysis to produce biofuels having lower GHG impact (on LCA bases) with respect to the equivalent fossil fuel-based ones to the role of catalysis in developing new production routes having a better efficiency of using raw materials and energy (Centi and Perathoner 2014). There are additional aspects more difficult to estimate in terms of positive impact on climate change goals. For example, enabling a new competitive catalytic route to produce polyurethane foams (using CO_2 as one of the feedstocks), in addition to a specific benefit (compared to production of conventional polyether polyols, the production of polyols with 20 wt% CO_2 allows for GHG reductions of 11–19 % as shown by von der Assen and Bardow 2014), allows further benefits related to the utilization of the foam to insulate buildings. We limit discussion here, however, to only routes related to the direct role of catalytic technologies in contributing to climate change goals.

A further necessary preliminary differentiation is between technologies for converting non-CO_2 greenhouse gases (NCGG) and those related to utilization of carbon dioxide (CO_2), due to the different types of sources and problems to address. In fact, NCGGs have typically a GWP (over a 20-year time horizon) significantly larger than CO_2, which is conventionally put equal to one: 72 for CH_4, 289 for N_2O, to values ranging from 3000 to over 16,000 for hydrofluorocarbon depending on the specific structure. The emissions of NCGGs are lower of those CO_2: in 2010, the sum of NCGG emissions was about 15 Gton CO_2-eq. with respect to about 35 Gton CO_2-eq. emissions of CO_2 from fossil fuel exploitation plus land use change (Montzka et al. 2011). On the average, NCGGs contribute to about 35–45 % of total climate forcing from all LLGHGs (range represents direct forcing to the sum of direct and indirect forcing). Climate or radiative forcing is the time-dependent responses of the warming influence. Cut NCGG emissions could substantially lessen future climate forcing, with additional ancillary benefits that include reduced costs for climate mitigation relative to CO_2-only approaches, improvements in air and water quality, reduced acid deposition, and decreased eutrophication of aquatic ecosystems (Montzka et al. 2011).

There is a tendency to increase NCGG emissions, for example, due to the increase of shale gas production (CH_4) and biofuels (N_2O, due to the larger use of fertilizers in monocultures).

Short Introduction to Catalytic Concepts, Materials, and Technologies

The reduction of GHG emissions by catalytic processes belongs to the general area often referred to as environmental catalysis or catalysis for environment protection, which is part of the broader area of catalysis for sustainable industrial production (Cavani et al. 2009). The largest part of catalytic technologies in this field is based on solid catalysts, because cost, pressure drop, effectiveness in a wide range of experimental conditions, low sensitivity to deactivation, and ease of management and handling are the critical aspects for these applications. Solid (heterogeneous) catalysts offer advantages over homogenous catalysts from these points of view and for this reason predominantly used in the area of environmental catalysis.

The term "solid or heterogeneous catalyst" indicates a material having one or both of the following characteristics:

- Increases the reaction rate (moles converted per unit time) of a chemical reaction, thus enhancing the conversion of a reagent, that is, the moles of a reactant converted with respect to inlet moles of the reactant
- Changes favorably the reaction rate of one reaction with respect to competing reactions, thus enhancing the selectivity, that is, the fraction of moles of the reagent(s) converted to the desired product

The catalyst itself does not undergo any permanent change, although it participates in the reaction mechanism providing an alternative reaction pathway, which modifies the energy associated with the pathways of reaction (activation energies of formation of reaction intermediates). However, the thermodynamics of the reaction (e.g., the net reaction enthalpy and free energy) do not change. The catalyst thus changes the kinetics, not the thermodynamics, of the reaction.

A catalyst may undergo a progressive modification with time, leading to an alteration of the catalytic behavior (usually associated with a loss in catalytic performance, that is, catalyst deactivation), even if formally the catalyst is not modified in the catalytic cycle. This is a consequence of chemical reaction and/or of external factors (e.g., other components of the feed, the reaction temperature, etc.). The three properties that characterize a catalyst are (1) activity, (2) selectivity, and (3) stability (i.e., no deactivation). However, there are a number of other aspects equally important for the choice of the catalyst, such as its texture (porosity) and shape, its macro- and microstructure, and its mechanical strength properties.

In defining the activity of the catalyst, differentiation must be made between the following aspects:

- *Intrinsic activity*, that is, the rate of reaction not affected by mass or heat transfer limitations (see below), which may refer to total weight or volume of the catalyst or to the amount of the active phase or component; the units of measure are moles per time and per mass or volume.

- *Effective activity*, that is, the measured rate of reaction (effective activity depends on the conditions of testing, because it can be influenced by mass or heat transfer limitations); the units of measure are the same as for intrinsic activity. The ratio between effective and intrinsic activity defines the effectiveness factor (η) of the catalyst.
- *Catalyst performances* and specifically the following quantities:
  1. *Conversion*: the ratio between the molar flow of reactant converted with respect to the inlet molar flow of the same reactant.
  2. *Selectivity*: the ratio between molar product flows at the outlet of the reactor with respect to the inlet molar flow of the reactant.
  3. *Yield*: the conversion multiplied by the selectivity.
  4. *Productivity*: the ratio between molar product flows at the outlet of the reactor and catalyst weight or volume. The units of measure are the same as those for the reaction rate, but the two concepts should not be confused.

Conversion, selectivity, and productivity depend on the integrated change in the reaction rate(s) along the reactor. Therefore, these parameters (often indicated as global activity parameters) are not intrinsic characteristics of the catalyst. When more than one reactant is present, conversion, yield, and selectivity should refer to the limiting reactant, that is, the reactant that may limit (also considering reaction stoichiometry) the conversion. However, these parameters (conversion, yield, and selectivity) also can refer to other reactants, and it is therefore a good practice to indicate the reference reactant.

While all these terms depend on the reaction conditions (reaction temperature and reactant composition), conversion, selectivity, yield, and productivity also depend on the type of reactor and space velocity (total volumetric flow of the reactants divided by the volume of the catalyst). The inverse of the space velocity is defined as the contact time, that is, the time required by the flow of reactants to fill the volume occupied by the catalyst. Sometimes, the space velocity refers to the apparent volume of the catalyst, that is, the total volume of the catalyst (this volume depends on the grain size and packing of the pellets) and sometimes to the specific catalyst volume, that is, considering the void fraction of the catalytic bed. For this reason, it is preferable to refer not to the catalyst volume but to the mass of catalyst. In this case, the units of measure of the space velocity (indicated also as space–time) are $g_{cat}s_{cat}mol^{-1}$, that is, the inverse of the units of measure of the reaction rate, although the two concepts are different. In gas–solid catalytic reactions, the space velocity is often defined as GHSV (gas hourly space velocity), which is exactly the same definition as that of space velocity, but the time unit is hours instead of seconds. In liquid–solid reactions, the equivalent definition is LHSV (liquid hourly space velocity).

In the discussed applications, the reactant(s) is typically present in one or more different phases (gas and/or liquid) with respect to the solid catalyst. The reactant (s) should thus diffuse to the catalyst surface before reacting. The reactant(s) diffuses across the boundary gas or liquid layer that surrounds the solid catalyst body (pellet, layer, or film) and diffuses inside the catalyst pore volume. These two steps are referred to below as external and internal diffusion. Often in environmental

applications, the rate of these steps is slower than the rate of the chemical reaction (s) occurring at the catalyst surface, and therefore the rate of the overall process becomes controlled by the mass transfer. Gradients in concentration through the boundary fluid layer and throughout the catalyst pore volume develop.

The heat transfer to or from the catalyst surface (due to the heat generated or consumed by the reaction) can also determine temperature gradients within the catalyst pellet or layer and through the fluid boundary layer. The magnitude of the effect depends on the effectiveness of internal and external heat transfer, which is a function of the rate of heat generation/consumption, the solid characteristics, and the fluidodynamics of the system.

The presence of thermal or concentration gradients influences considerably selectivity, activity, and/or stability. Therefore, proper reactor design integrated with catalyst design is critical to improving performances. Different types of reactors are used commercially in these reactions. The choice depends on various factors, such as the catalyst characteristics, mass and heat transfer limitations, scale-up, fluidodynamic and flow regimes, pressure drop, liquid holdup, etc. However, often there is a contrast between optimal conditions for efficient multiphase contact, high catalyst effectiveness and wetting efficiency, and low fouling/attrition and pressure drop. In these cases, new types of reactors based on structured catalysts are an attractive alternative to conventional reactors, due to low-pressure drop, the absence of a need for catalyst separation, and the large geometrical surface area.

Structured catalysts offer an efficient multiphase contact and minimize the influence on the reaction rate and selectivity of the reagents' diffusion and products' back-diffusion. They also offer some additional advantages: easy catalyst separation and handling, minimization of contamination of the solution by the catalyst, safer operation, improved heat supply and removal, and easier scale-up and technology manageability. The latter characteristics of the structured catalysts often are the critical factors for the selection of these technologies in environmental protection applications. Four main types of macrostructured catalysts can be distinguished: (1) monoliths, (2) foams, (3) cloths, and (4) membranes.

The main classes of catalysts used for the reduction of GHG emissions are metals (noble and not noble metals, typically supported), oxides (typically multicomponent metal oxides in the bulk or support form), and solid acids (clays, mixed oxides, and, in particular, ordered metal oxides: zeolite and mesoporous materials). Solid catalysts come in a multitude of forms and can be loose particles or small particles on a support. The support can be a porous powder, such as aluminum oxide particles, or a large monolithic structure, such as the ceramics used in some applications. The choice depends on many requirements, but the critical ones are the type of reaction and relative reaction conditions and the choice of the reactor to use. Industrial catalysts are generally shaped bodies of various forms, for example, rings, spheres, tablets, and pellets. Monolithic-type catalysts, similar to those in automobile catalytic converters, are also used.

The production of heterogeneous catalysts entails numerous physical and chemical steps. The conditions in each step have a decisive influence on the catalyst properties. Catalysts must therefore be manufactured under precisely defined and

carefully controlled conditions, including the control of the level of the impurities in raw materials, which may have a dramatic effect on the performances. Depending on their structure and method of production, solid catalysts can be divided into three main groups: (1) bulk catalysts, (2) supported catalysts, and (3) ordered porous structure catalysts.

Bulk catalysts are used when the active components are cheap, there are no specific diffusional limitations on the reaction rate under industrial relevant conditions, and other specific requirements (e.g., density and mechanical resistance for fluid-bed reactor applications) are absent. Supported catalysts are the class of catalysts most used industrially. They are used under the following circumstances:

- When expensive active components such as noble metals are employed and there is the need for their effective dispersion over a support that also provides the stabilization of these metal nanoparticles against their sintering
- When a modification of the properties of an oxide by supporting it over another oxide is necessary
- When the density of the catalyst and its mechanical properties are not suited for the specific reactor operation, as well as in other cases

The most common class of ordered porous structure catalysts are zeolites, but there are many more examples, from ordered mesoporous materials (e.g., mesoporous silica such as SBA-15 and MCM-41) to other class of inorganic or inorganic–organic hybrid materials. Zeolites are microporous crystalline solids with well-defined structures. Generally, they contain silicon, aluminum, and oxygen in their framework and cations, water, and/or other molecules within their pores. Many occur naturally as minerals, but the most used commercially are synthetic one due to their better reproducibility.

A defining feature of zeolites is that their frameworks are made up of four connected networks of atoms. These tetrahedra can then link together by their corners to form a rich variety of beautiful structures. The framework structure may contain linked cages, cavities, or channels, which are of the right size to allow small molecules to enter – that is, the limiting pore sizes are roughly between 3 and 10 Å in diameter. There are nearly 200 different types of framework structures prepared and identified, but the theoretical number is much larger. Zeolites have the ability to act as catalysts for chemical reactions taking place within the internal cavities.

Reduction of NCGG Emissions

Methane (CH_4)

Methane is the second most important long-lived GHG. Approximately 40 % of methane is emitted into the atmosphere by natural sources (e.g., wetlands and termites), and about 60 % comes from human activities (about 400 Mt/y) by different sources (Fig. 1).

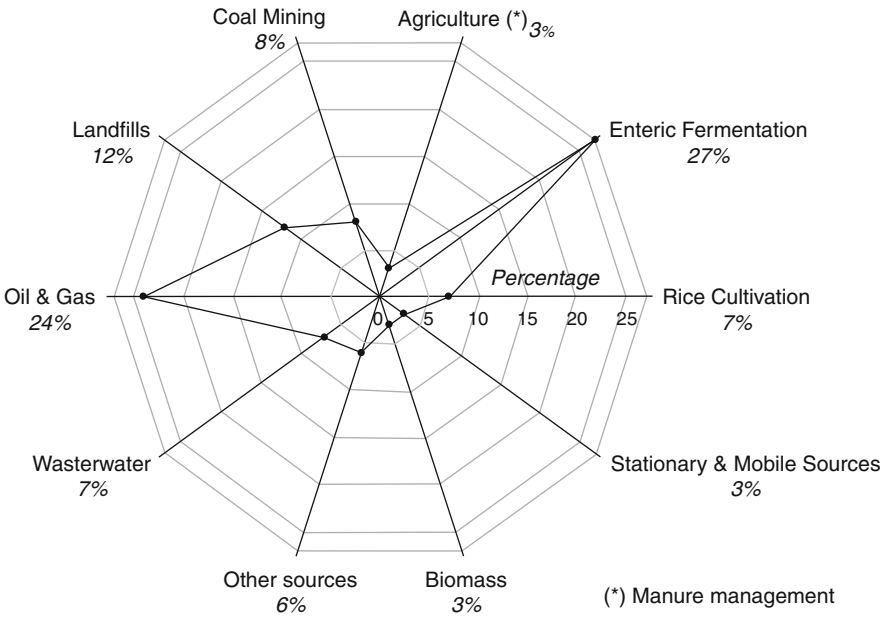

Fig. 1 Estimated global anthropogenic methane emissions by source, 2015

Atmospheric methane reached a new high of about 1,824 ppb in 2013, due to increased emissions from anthropogenic sources. Around half of methane emissions from anthropogenic activities derive from sewage disposal, rice cultivation, livestock, and burning of biomass. The remaining part is associated with production, transport and use of natural gas, coal mining, and disposal of solid waste. A considerable part of the methane emitted is converted to CO_2 and water in the troposphere by reaction with hydroxyl radicals, around 500 Mt/y. The total methane removed annually in all sinks is estimated to be about 600 Mton/year, but a large amount uncertainly exists in the balance of methane emissions. The current role of methane in global warming is large, contributing 1.0 W m^{-2} out of the net total 2.29 W m^{-2} of radiative forcing (Pachauri and Meyer 2014). The expected increase in shale gas production will further increase impact on climate changes, because the carbon footprint of shale gas (on average, integrated over 20 years) is higher than that of conventional natural gas and coal (about 51 gC per MJ with respect to about 38 and about 30, respectively).

Methane emissions from the oil and gas industry derive mainly from the venting of unused gas during oil production, the use of natural gas to purge or to operate pipeline equipment, and leakage from the gas distribution system. It is estimated that these emissions will nearly double in two decades (due to the increase in gas production and pipeline transport) unless abatement measures are taken. Coal measures contain methane, which will be released by mining. The methane is removed by drainage of the coal measures before and during mining; the rest is

removed in the ventilation air while mining is taking place. Drainage gas is high in methane concentration and can be used directly to generate electricity. The emissions associated to production and transport of coal is expected to increase in the future from the current value of about 22–33 Mton/year by year 2020 unless actions are taken.

A major source of methane emissions is the anaerobic decomposition of solid wastes in landfills, although the amount generated depends upon the method of dumping and on the composition of the waste and therefore vary considerably from country to country. It is expected that methane emissions from solid waste disposal will increase from the current 32–62 Mton/year by year 2025. Other anthropogenic sources of methane include sewage treatment, rice growing, livestock, and biomass burning. The large majority of these emissions are associated to developing countries. Methane emissions from sewage treatment are expected to increase from current 35 Mton/year value to 58 Mton/year, while those deriving from rice growing have leveled off in the last two decades. Livestock (mainly enteric fermentation in ruminants) contributes an estimated 49 Mton/year of methane emissions, but significant is also contribution from the anaerobic decomposition of manure. Biomass burning gives rise to direct emissions of methane, but has also the negative impact of reducing the ability of the soil to act as a sink. An increase of about 20–25 % of these emissions is estimated in two decades.

The increase in methane emissions should be contrasted by introducing highly efficient technologies to limit the emissions that can be reduced, because only a part of the global emissions of methane can be effectively controlled. The complexity of the problem derives from the very broad range of situations and type of emissions, e.g., various methodologies should be used and integrated.

It is possible to distinguish between two main types of sources: (i) confined, e.g., the gas is physically contained and can be managed with industrial process units, and (ii) diffused, e.g., methane is produced over a large land or aqueous area. The strategies for mitigation of the two cases are different (Stolaroff et al. 2012). For the latter case of diffuse sources, three general strategies of mitigation have been developed: suppressing methanogenesis, biocovers, and caps. The latter may be related to catalytic technologies, differently from the first two methodologies, although the first deals on enzymatic catalysis that however is not covered here. Caps are a typical method for controlling landfill emissions, being the land or manure ponds covered with an impermeable layer (a plastic sheet or layer of clay) and an array of wells and pipes to collect the gas then treated as discussed later. An alternative possibility is to use materials, such as liquid solvents and nanoporous zeolites, which can capture effectively the fugitive methane emissions (Kim et al. 2013). The methane stream produced during the regeneration of these capture materials can be then treated as discussed below.

Table 1 reports examples of typical concentrations of CH_4 in some relevant cases of methane sources. Concentrated streams (above about 40 %) can be used as chemical feedstocks, with syngas, methanol, and carbon black production among the main possibilities (but requiring typically further treatments to purify the gas and concentrate above about 95 %). In the concentration range 30–60 %, different

Table 1 Examples of typical concentrations of CH_4 in relevant cases of methane sources (Adapted from (Stolaroff et al. 2012))

Source	Methane concentration, vol fraction
Arctic air (current reference free air)	2–8 ppm (1.8 ppm)
Swine feeding or dairy milking ventilation air	10–300 ppm
Enclosed manure storage headspace	140–28,000 ppm (2.8 %)
US landfill, at surface	<500 ppm by regulation
Fugitive methane emissions at shale gas production wells	10–1000 ppm
Coal mine VAM	0.1–1 % typical, <1 % by regulation
Anaerobic digester gas	35–65 %
Landfill drainage gas	40–60 % at peak production
Coal postmining drainage gas	30–95 %
Coal premining drainage gas	60–95 %
Natural gas, at wellhead	75–99 %, typical

technologies are applied to coal mine drainage gas, landfill gas, and gas from anaerobic digesters. For lower concentrations, catalytic combustion is the main option, with commercial units able to handle methane concentrations as low as 0.1 % (1000 ppm). Bioreactors may be used to treat ppm and ppb (parts per billion) concentrations of methane, or alternatively very dilute methane streams can be used as air in combustion processes. Not yet developed, but a potentially interesting possibility, is the use of photocatalytic semiconductors such as TiO_2 to oxidize methane in the presence of sunlight. A modification of titania is required to activate methane.

Combustion is one of the main options in controlling methane emissions. The utilization of this methane, besides to contribute to the reduction of GHG impact, may be an opportunity in some cases for a sustainable energy source (Karakurt et al. 2011), as proposed for VAM (about 70 % of the methane emitted from coalmines). In general, however, incentives to mitigate VAM (carbon market or other regulatory drivers) are necessary to generate revenue from energy production. Some cost-effective solutions, as thermal reverse flow reactors (discussed later), may have a payback period of 3–6 years at a relatively modest carbon price (about $10/t-$CO_2$-eq.) (Stolaroff et al. 2012).

Due to the usually low concentration of methane in these emissions, the use of catalytic combustion is necessary and may avoid the formation of traces of harmful by-products like formaldehyde. Note that the combustion reduces the overall GWP of emissions, but produces CO_2 and water (combustion converts 1 kg of methane with a GWP of 21–2.75 kg of carbon dioxide with a GWP of 1 and 2.25 kg water). An additional benefit derives from the use of the heat of combustion in steam raising or electricity production, because it avoids the use of fuels for these purposes.

Autothermal methane combustion requires that methane concentration in the feed should be around 0.6–1.0 %. For lower concentration, the extra addition of fuel is necessary to sustain combustion. Using catalytic combustion, besides the much lower reaction and light-off temperature necessary for operations, different reactor/

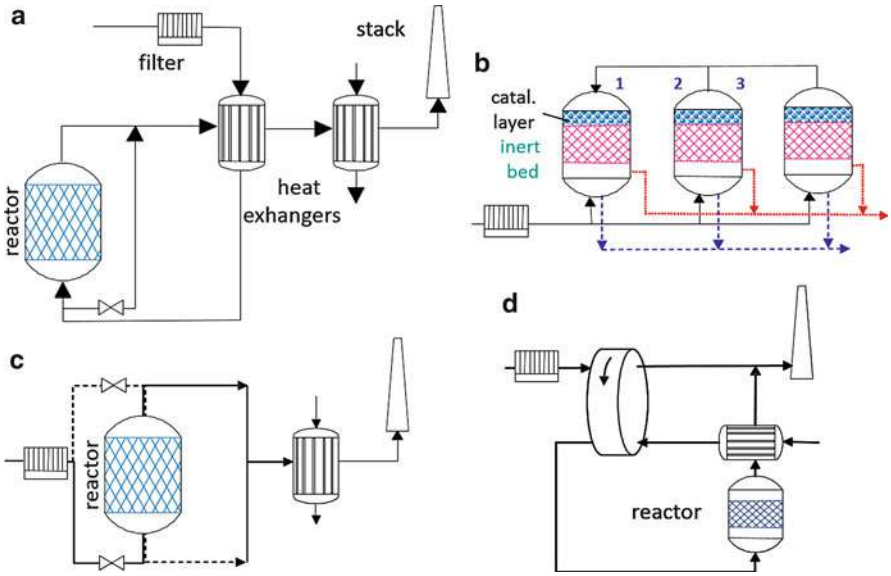

Fig. 2 Different reactor/process options for catalytic combustion of methane in diluted emissions: (**a**) recuperative catalytic combustion, (**b**) regenerative catalytic combustion, (**c**) reverse flow catalytic combustion, and (**d**) catalytic combustion using a rotating concentrator

process options are possible to operate it autothermally by using much lower methane concentrations in the feed:

- Regenerative catalytic combustion
- Reverse flow catalytic combustion
- Catalytic combustion using a rotating concentrator

Figure 2 shows the schematic flow sheet of the different options. Recuperative catalytic combustion (A) is the conventional option in which the reactor inlet is preheated from the reactor outlet and an eventual further heat exchanger allows further recovery of the heat before sending the gas to the stack. The regenerative catalytic combustion (B) allows better heat recovery efficiency and thus autothermal operations with lower methane concentrations. It involves cyclic operations: the ceramic layer preheats the gas to light-off temperature and the off-gas heats the ceramic layer of another reactor, while the third is under purging. When the ceramic layer has lost the capacity of gas preheating, the second reactor starts operations. The operations then continue in a cyclic way. Efficiency in heat recovery passes from about 70–75 % (case A) to 90–95 % (case B), but fixed costs are higher.

The reverse flow catalytic combustion (C) involves a periodical switch of the feed introduction from the bottom to the top of the reactor and vice versa. Fixed costs are lower than in case B, which heat recovery efficiency remains good. However, problems related to thermal shock and deactivation of the catalyst can occur.

Table 2 Fields of application of catalytic technologies for methane combustion (especially emissions containing diluted CH_4 concentration) and potential reduction of methane emissions which could be attained using catalytic combustion

Source		Emissions potentially reduced, Mt/y
Oil and gas supply chain	Fugitive emissions Process vents and flares	6–10
Coal mining	Underground ventilation and drainage	10–15
Shale gas production	Up- (well) and mid- (processing) stream	6–15
Solid waste	Landfill gas capture	4–8
Sewage treatment	Emissions from anaerobic digestion	7–12
Agricultural livestocks	Emissions from anaerobic digestion	3–5

The catalytic combustion using a rotating concentrator (D) may be applied also to very low methane concentrations. It is based on the concept of a rotating adsorption/desorption system. The part exposed to (cold) emissions adsorbs methane from the feed, while on the other part of the rotating element, the desorption of methane is induced by exposition to a hot air feed producing a concentrated stream which can be then sent to a catalytic combustor. The limit of the approach is given from the difficulty to find suitable adsorption materials, which can efficiently capture methane from the main stream in the presence of the typical, other gas-phase components (like water vapor). Other reactor options for the catalytic combustion of methane not shown in Fig. 2 include catalytic fluidized bed reactor, microchannel reactor, and catalytic membrane reactor (Wang et al. 2013), but these options are valuable mainly for concentrated streams of methane.

Catalytic combustion offers thus several opportunities to improve the economics in diluted methane emission control, although higher in fixed costs with respect to flame combustion. Some examples of possible specific applications are shown in Table 2 with also an indication of the potential reduction of methane emissions, which could be attained using catalytic combustion. As commented before, some economic incentives or regulatory drivers are necessary for the wider utilization of these technologies. Consequently, only for some specific application, such as coalmine methane (Özgen et al. 2011), commercial technologies are available. In general, catalysts should be further developed especially regarding their sensitivity to poisoning, being this one of the major problems in the treatment of the emissions, and low-temperature activity.

Table 2 evidences that coal mining is one of the main sources to control for methane. Coal measures contain methane, which will be released by mining (Özgen et al. 2011). The methane is removed by drainage of the coal measures before and during mining; the rest is removed in the ventilation air (VAM) while mining is taking place. Drainage gas is high in methane concentration (from 20 % to 90 %, depending on mine) and therefore can be used directly to generate electricity. VAM,

which carries around 70 % of the emissions, contains instead a very low CH_4 concentration (Table 1). Catalytic combustion using supported noble metals can be successfully employed to destroy all of the dilute emissions. The same technology could be applied to control methane fugitive emissions, process vents, and flares in the oil and gas supply chain.

CH_4 emissions from shale gas production are becoming a major issue of concern. Large emissions averaging 1.1 kton CH_4/y per well were observed (Caulton et al. 2014). The fraction of methane that is emitted ranges 0.6–7.7 % of the lifetime production of a well and 0.07–10 % emitted during "downstream" transmission, storage, and distribution to consumers (Weber and Clavin 2012). To note, a recent study (Alvarez et al. 2012) showed that the immediate net radiative forcing for natural gas use is worse than for coal (when used to generate electricity), if total CH_4 emissions are greater than approximately 3.2 % of production. Table 1 shows that fugitive methane emissions at wells for shale gas production are on the average more diluted than VAM. It would be thus necessary to develop improved (catalytic) technologies to utilize these low concentrations (around 200 ppm), in which development opens also a new range of applications (animal feedlots and manure storage), including the possible potential utilization for unconfined sources, Arctic or otherwise. A requisite is the development of efficient capture systems for methane, operating around room temperature or below (e.g., for Artic). Porous covalent–organic materials (Xiang and Cao 2013) are one of the interesting options to investigate further.

Disposal of solid waste on land is another significant source of methane. Given appropriate conditions, solid waste decomposes anaerobically with production of methane, which can be captured with existing technologies (low permeability barriers around the waste and capture of gas and leachate). Landfill gas can be burned, but the addition of fuel may be necessary because of its low quality. In this case, catalytic combustion is potentially preferable, although specific tailoring of catalyst characteristics may be necessary due to the possible presence of a number of poisoning elements. It is also possible to upgrade the gas so that it can be used as a substitute for natural gas, using the catalytic technologies commonly employed in the natural gas industry, although this option can be expensive. A third possibility is to use landfill gas for direct electricity generation with gas turbines. Gas cleanup using conventional catalytic technologies may be however necessary. Therefore, the basic catalytic technologies and knowledge are already available, but they must be adapted to the quality of the specific landfill gas. In addition, downsizing of the technology is necessary, because in most applications, small, compact, modular, and automatic equipment is required.

Sewage arises from both domestic and industrial sources, especially from the food processing, pulp/paper making, and chemical industries. In developed countries, most municipal and industrial wastewater is collected and treated in an integrated sewage system, in which an aerobic degradation step minimizes CH_4 emissions. In developing countries, integrated systems are not common, and thus collection of the gas from existing disposal sites and catalytic combustion is a feasible, cost-effective solution.

A special case may be considered, the conversion of residual methane in the emissions from NGVs (natural gas vehicles). Although the very limited diffusion of these vehicles do not allow to indicate this source as a major issue of methane emissions, the expected increase of these vehicles due to their lower environmental impact may determine a more serious problem in the future. In Germany, for example, Audi's e-gas plant, first announced in May 2011, is a first industrial step to push the conversion of CO_2 to methane using excess electrical energy produced during night by windmills and use this methane to fuel cars. The facility will generate enough e-gas to power 1,500 new Audi A3 Sportback TCNG vehicles for 9,320 miles every year. "Power-to-gas" (P2G) is the name given to an energy process and storage technology, which allows renewable electricity to be "stored" and distributed as chemical energy in the form of a gaseous fuel (methane), for which already an extended network of distribution and storage (e.g., in salt caverns) is available.

Although NG-fueled vehicles (NGV) are presented as a very clean solution, methane is not totally converted and emitted from the car, in the absence of suitable catalysts. The current legislation, Euro 6 in Europe, for example, puts limits for total hydrocarbons (THC) but does not differentiate, as in the past, non-methane hydrocarbon emissions (NMHC). It is necessary to use catalysts with a quite high content of noble metals (platinum, rhodium, and palladium, particularly the latter), around 2–4 g/L (from 4 to 10 times higher than conventional) to convert the THC emissions composed by more than 90 % of NMHC for NGV. In addition, the high presence of oxygen in the emissions does not allow converting NOx in the absence of a specific additional catalyst able to operate in lean-burn conditions, as for diesel vehicles emissions.

Lean-burn NGVs equipped with catalysts are commercially available in buses and other fleet service vehicles. Characteristics required for a catalyst for methane conversion in lean-burn NGVs are the following:

- Low light-off temperature (200–300 °C or below) at space velocities of 50,000 h^{-1} or above
- High efficiency using low methane concentrations (below 1000 ppm) and high oxygen concentrations (the air to fuel ratio in lean-burn engines is typically in the 20–27 range and thus residual oxygen in exhaust gases may be 8 % or higher)
- Stability (thermal and hydrothermal) in the presence of about 8 % O_2 and similar water concentration in the feed
- Resistance to deactivation by sulfur (low concentrations of sulfur compounds are present as impurities in the feed)

Pd-based catalysts show the best performances under the conditions outlined above, but are very sensitive to poisoning by H_2O and SO_2 (the latter as little as 1 ppm SO_x in the exhaust vehicle gases) which shifts the light-off curve to temperatures about 200 °C higher. Furthermore, high Pd loadings in the catalysts are necessary. The performances of the catalysts are thus still not satisfactory, and further improvements are necessary.

Three directions of research may be identified to improve performances:

- Identification of the reaction mechanism of methane activation as a tool to design improved catalysts
- Identification of the deactivation mechanism to identify how to prepare more resistant catalysts
- Development of alternative supports for palladium which may improve activity or stability

Supported noble metal catalysts are used in the largest part of commercial applications of methane combustion, especially when temperature of operation may be limited due to low methane concentrations in the stream. A large effort has been made in literature to find alternative catalysts not containing noble metals, like supported transition metals (e.g., CuO/alumina), spinel, and perovskite materials. They may find application when the presence of other components in the feed gives rise to deactivation of the noble metal catalysts, but usually the light-off temperature is around 500 °C or above and thus too high for the conversion of diluted methane containing emissions.

Often the choice of non-noble metal containing catalysts is motivated from the supposed lower cost of the catalyst. Structured type catalysts such as monoliths should be generally used in catalytic combustion. The cost of the active component (noble metal or other) in a monolith is typically only a fraction of the overall costs (10–30 %). If a non-noble metal catalyst has a reaction rate 50 % lower with respect to that of a noble metal catalyst, for example (often is even less), and a cost per active phase mass which is about a quarter of that of noble metal, the total cost of the monolith catalyst in order to have the same conversion is higher. The process cost (fixed + variable) is higher, if the reaction temperature should be 50 °C or higher with respect to the case of using noble metal-based catalysts. In conclusion, non-noble metal catalysts for methane conversion should be considered when (i) the rate of reaction is comparable, (ii) deactivation phenomena may dominate the behavior, or (iii) activity is not an issue due to the high temperatures of operations (e.g., using high methane concentrations).

Palladium is usually the most active noble metal in methane combustion. The resistance of palladium to thermal and hydrothermal sintering is also better than that of platinum, but its behavior in the presence of poisons such as sulfur-containing pollutants or lead is worse. Either supported Pd catalysts or Pd–zeolite catalysts are used in diluted methane combustion.

Some new direction is proposed. Gorte and collaborators (Cargnello et al. 2012) have developed nanomaterial that catalyzes methane combustion 30 times better than existing catalysts and at lower temperatures. Existing catalysts are usually composed of Pd nanoparticles deposited on oxides such as CeO_2, while Gorte and collaborators (Cargnello et al. 2012) use 1.8 nm Pd nanoparticles surrounded by a protective shell of 3 nm CeO_2 crystallites as their catalysts. Such small particles usually sinter together when heated, reducing catalyst activity, while the core–shell structure of these new catalysts (prepared by a self-assembly techniques) avoids

(or greatly limit) this sintering. However, it is still necessary to demonstrate the use of these catalysts in real applications.

The mechanism of low-temperature methane oxidation on supported Pd samples should be not generalized, because it depends on the specific catalyst. However, a typical mechanism is the following (Liu et al. 2012). The rate-determining step is the dissociative chemisorption of CH_4 on a site pair consisting of adjacent Pd surface vacancies and surface Pd–O species. The negative water effect is due to the inhibition of the formation of Pd–O species which block the water desorption during recombination of the surface hydroxyl groups. The stronger Pd–O bonds in small Pd–O clusters or incompletely oxidized PdO_x crystallites can lead to a lower surface density of vacancies and thus to lower methane oxidation turnover numbers. The mechanism of deactivation at temperatures below 450 °C is attributed to a water/hydroxyl inhibition effect (Schwartz et al. 2012). Hydroxyl accumulation occurs on the oxide supports during catalytic methane combustion, hindering oxygen exchange with the oxide support playing a relevant role in catalyst activity.

Nitrous Oxide (N_2O)

N_2O global emissions from natural sources (soils, oceans, and atmospheric chemistry) account for about 13 Mton N_2O per year, while those from anthropogenic activities about 7–8 Mton N_2O per year. The latter derives for about 50 % from agricultural practices (including use of fertilizers) and the remaining from various main sources: fuel and waste combustion (especially combustion of industrial N-containing waste in fluidized bed reactors), transport (this contribution is increasing much faster than the others), polluted surface water and wastewater (sewage) treatment plants, chemical production (nitric acid production and use), and biomass combustion (van Ham et al. 2000).

Control of N_2O emissions from agriculture is difficult to implement in a short term, due to the different types of diffuse sources and the limited number of existing options for the control. However, it is possible to utilize nitrification inhibitors to reduce nitrous oxide emissions. In general, global food system (fertilizers, manure, grazing animals, resides treatment, and waste) is a main source of N_2O, estimated at 4.1–4.4 Tg N_2O-N for 2010 (Oenema et al. 2014). Lowering this impact is possible by various (non-catalytic) mitigation strategies, such as improved crop and animal production, better manure management, improved food utilization, and lowering the animal-derived protein in human diets (Oenema et al. 2014). However, all these are long-term strategies.

The transport sector (mobile sources) is expected to increase rapidly in relevance especially with the expansion in the use of diesel and lean-burn engines. Their contribution was doubled in the last decade and was about 0.142 Tg N_2O-N/y in 2010 with the majority (≈55 %) of emissions resulting from catalytic emission control systems of light-duty vehicles (Wallington and Wiesen 2014). It is unlikely that N_2O emissions will be regulated, with attention being given to other priorities (NO_x, particulate). However, improvements in the emission control systems of

light-duty vehicles will reduce the emissions of N_2O from global transportation to about 0.108 Tg N_2O-N/y by 2030 (Wallington and Wiesen 2014).

N_2O from (uncontrolled) biomass combustion, being also widespread, cannot be reduced in short term. N_2O emissions that can be reduced in the short term are associated with chemical production, energy industry, waste combustion, and sewage treatment. The better premise for an economic and efficient reduction strategy is to eliminate N_2O in localized and large sources, such as from some chemical industry processes and from stationary combustion processes. Emissions from chemical industry mainly apply to adipic and nitric acid production plants, but significant emissions of N_2O are also present in plants for the production of caprolactam, glyoxal, and acrylonitrile and in general in all processes using nitric acid as oxidizing agent or involving ammonia oxidation (Lee et al. 2011).

The impact can be significant, even if in some countries voluntary actions have already significantly reduced nitrous oxide emissions. In China, however, industrial N_2O emissions grew by some 37-fold from 5.07 to 174 Gg (N_2O), with total accumulated emissions of 1.26 Tg from 1990 to 2012. The projected emissions are expected to continue growing rapidly from 174 to 561 Gg in 2020 under current policies and assuming no additional mitigation measures (Li et al. 2014). The total accumulated mitigation potential for this forecast period is about 1.54 Tg, the equivalent of reducing all the 2011 greenhouse gases from Australia or halocarbon ozone-depleting substances from China. Adipic acid production is the major industrial emission source and contributes nearly 80 % of the industrial N_2O emissions, e.g., about 96.2 % of the industrial mitigation potential.

Adipic acid production differs from the other cases, because N_2O concentration in the tail gas is quite high (typically 20–40 %). A number of adipic acid producers have voluntarily introduced technologies to reduce N_2O emissions, which passed from about 0.6 Mton/year in 1994 to about 0.1 Mton/year in 2000. Due to the exothermicity of the decomposition of N_2O to N_2 and O_2 (a feed containing 20 % N_2O would increase the adiabatic temperature of a reactor of more than 500 °C), activity of the N_2O decomposition catalyst is not a real critical issue for the effectiveness of the technology, but rather its stability. A number of different catalysts are active using high N_2O concentrations. The catalysts employed are based on noble (Rh) or non-noble (Cu, Co) transition metals supported on a structured matrix such as zeolites or hydrotalcites deposited on monoliths. However, the same kind of catalysts do not show enough activity when applied to the treatment of streams containing low concentration of N_2O (typically below 1 %) (Pérez-Ramírez et al. 2003; Sobolev and Pirutko 2013; Centi et al. 2003b).

When N_2O is present in high concentrations in the effluents, besides catalytic decomposition, other options are also possible, such as the recovery and use of N_2O as valuable reactant (see later, Solutia–Boreskov process) (Parmon et al. 2005). Thermal (non-catalytic) decomposition is also an effective possibility. However, most of N_2O emissions, which may be treated by catalytic technologies, are characterized from N_2O concentrations below about 1 % (Fig. 3). Furthermore, tail gas

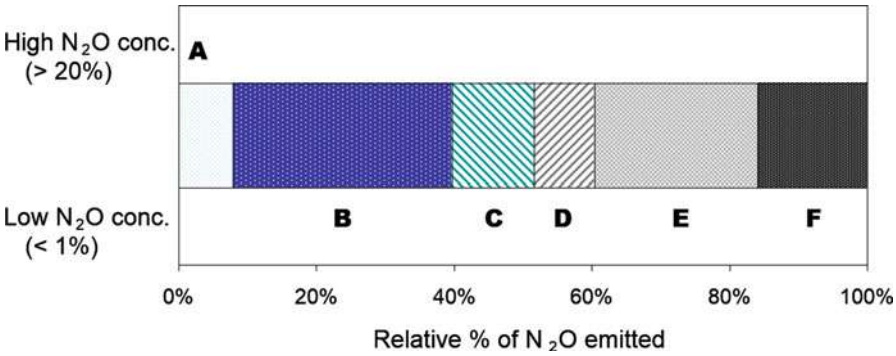

Fig. 3 Relative % of N_2O anthropogenic emissions, which may be treated by catalytic technologies: (**a**) adipic acid plants. (**b**) Nitric acid production. (**c**) HNO_3 use (no SO_2 in emissions). (**d**) HNO_3 use (the presence of SO_2 in the emissions). (**e**) Sludge and industrial waste combustion (fluidized bed combustion). (**f**) Municipal incinerators

differs in terms of temperature and composition (especially the presence of inhibitors for the catalyst such as O_2, H_2O, SO_2, and NO_x).

In Fig. 3, emissions derived from nitric acid use in chemical processes are differentiated between those containing and not containing SO_2, because N_2O abatement technologies may be different in the two cases (as discussed in the following sections). Figure 3 distinguishes also emissions having high (above 20 % v/v) or low (below 1 % v/v) concentrations of N_2O, because this also determines different N_2O abatement technologies. It may be further differentiated between emissions at low temperature (typically below 200 °C) (cases A–D) and emissions characterized by high temperatures (above 300 °C) (cases E–F), because in the former, catalysts active at low temperature are required for economic operations, similarly to what is discussed in the case of methane conversion.

For adipic acid plants, an interesting alternative to the N_2O catalytic or thermal abatement is the reuse of N_2O, which is a valuable chemical in some oxidation reactions of industrial interest such as the hydroxylation of (substituted) benzene to (substituted) phenol (Parmon et al. 2005). The relatively high cost of synthesis of N_2O (e.g., by ammonia selective oxidation) has prevented its practical application, but its recovery from industrial emissions can be economically interesting and avoids at the same time N_2O emissions.

This is the basic idea of the Solutia–Boreskov AlphOx process (Parmon et al. 2005; Notte 2000) to reuse nitrous oxide emissions from adipic acid plants, instead of eliminating them through catalytic decomposition. The process uses N_2O, formed as a by-product in the adipic acid process, to hydroxylate benzene to phenol on Fe-containing ZSM-5 catalysts. Phenol, after hydrogenation to cyclohexanone, is introduced in the adipic acid process thus closing the cycle. Figure 4 outlines the reaction scheme and reports a model of the reaction inside the zeolite channels of the catalyst. The key features of the process are the very high selectivity in benzene to phenol (over 98 %) and reuse of N_2O which eliminates the cost of its abatement

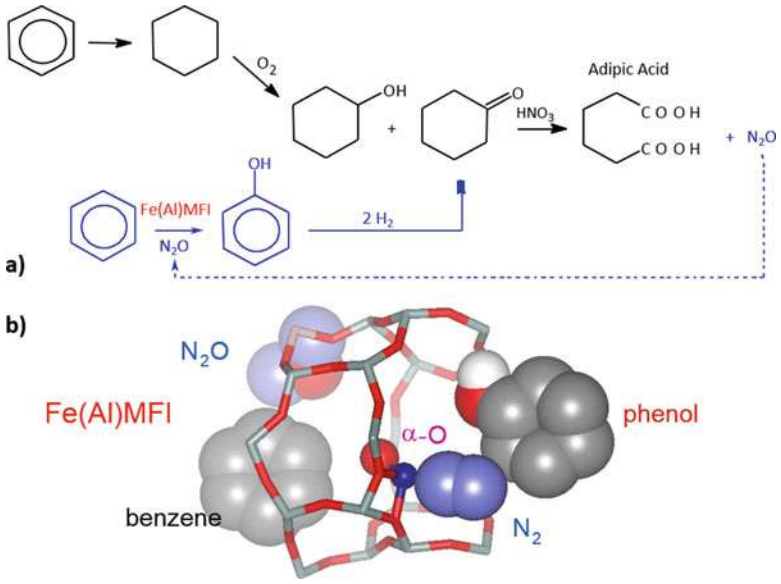

Fig. 4 Outline of the reaction network in the AlphOx process of recovery/reuse of N_2O in adipic acid production (**a**) and model of the reaction occurring at the active sites of Fe-containing MFI catalyst (**b**) (Modified from (Centi et al. 2005))

(although a purification step is necessary) and allows higher plant productivity, reduction of costs, and decrease in hydrogen consumption. The deactivation rate, however, still requires improvement.

This AlphOx process has been successfully tested in a pilot plant facility erected by Solutia in its adipic acid plant in Pensacola (USA). However, the process has not passed on commercial scale. Fe(Al)–MFI catalysts are used in the reaction of benzene hydroxylation with N_2O. No other classes of catalysts have been reported in the literature having comparable performances to Fe–MFI catalysts, although other Fe-zeolites also have been shown to be active in the reaction (Hensen et al. 2005; Centi et al. 2005). The proposed model of the reaction occurring at the active sites of Fe-containing MFI catalyst (Centi et al. 2005, 2006) is reported in Fig. 4b. The reason of the specific behavior, in addition to the stabilization of specific configurations for iron ions, is related to the large repulsive interaction of benzene with zeolite framework that can be greatly reduced when forming C–O bond (Yang et al. 2013). The otherwise repulsive adsorption on iron sites derives thus from the specific constrains induced from the zeolite cage. Adsorbents have nearly no migrations for proton-transfer steps to form phenol.

Due to the interest of N_2O as reactant, the possibility of its recovery is interesting also from emissions where it is present in low concentrations (below 1 %). A possibility of selective recovery is given by modified zeolites, which can selectively trap N_2O in the 25–80 °C temperature range, which is that of interest for a process of recovery of N_2O from a nitric acid plant. Ba-exchanged ZSM-5 zeolites, in

particular, show the best performances (Centi et al. 2000). Ba^{2+} due to its large ionic radius and electronic configuration creates a large local electrostatic field within the cavities of the zeolite and probably the enhanced adsorption behavior and the difference with respect to other analogous alkali and alkaline-earth elements can be attributed to this effect.

N_2O forms as a side product of ammonia oxidation in the synthesis of nitric acid (concentration 50–65 %) (Keller 2011), produced in large amounts worldwide (over 130 plants in Western Europe providing a total yearly capacity of approximately 22 million tons of 100 wt% nitric acid), which is being used to synthesize nitrogen fertilizers like ammonium nitrate and super phosphates, but also as reacting agent for the production of adipic acid and other chemicals. N_2O emissions from nitric acid plants can range from about 2–20 kg per ton of HNO_3 or up to 3,500 ppm concentration in the tail gas, depending on the nitric acid process and plant operating conditions. The process of nitric acid can be schematically differentiated in three main blocks:

- Catalytic oxidation of ammonia with air into nitric oxide
- Oxidation of nitric oxide into nitrogen dioxide
- Absorption of nitrogen dioxide in water to produce nitric acid

N_2O forms only in the first stage (ammonia combustion), but passes unchanged through the remaining parts of the plant and is emitted in the tail gases. Pt–Rh gauzes (typically 90 % Pt and 10 % Rh) are used for the ammonia oxidation. The selectivity to N_2O in this process depends on the reaction temperature (reaction temperatures below 1000 °C favor N_2O formation with respect to NO). Low linear velocities (below about 1 m/s) may also favor the secondary reaction of N_2O formation by reaction of NH_3 and NO in the gas phase. Although selectivity to N_2O is typically lower than 2 % in current plants, inhomogeneous flow distributions in the combustion chamber and aged catalysts may increase N_2O formation. Typical N_2O concentration in the tail gases ranges from 500 to 1,500 ppm. Depending on the burner design and reactor configuration, the kg N_2O produced per ton 100 % HNO_3 may vary from 2 (new plants) to 5–6 (usual value) up to 20 for the oldest plants.

In new nitric acid plants, N_2O emissions may be reduced by a better reactor design, improved geometry of Pt–Rh gauzes, or even using alternative (oxide-based) catalysts. Using extended chambers in the ammonia oxidation reactor, it is also possible to minimize N_2O formation, because upon increasing the residence time by 1–2 s in the reactor down to Pt–Rh gauzes, thermal decomposition of N_2O occurs resulting in a nitrous oxide level of about 200 ppm (from 50 % to 70 % abatement) in the tail gas. This technology was developed by Norsk Hydro. It suffers high capital costs and limited applicability to retrofit.

An alternative is the in-process use of a catalyst for selective decomposition of N_2O formed during ammonia oxidation (Fig. 5, position 1) (Pérez-Ramírez et al. 2003; Kapteijn et al. 1996). The catalyst can be introduced behind the Pt–Rh gauze pack and the recovery unit for the noble metals lost from the Pt–Rh catalyst, in substitution of the inert Raschig rings used as support for the Pt–Rh gauze. The main

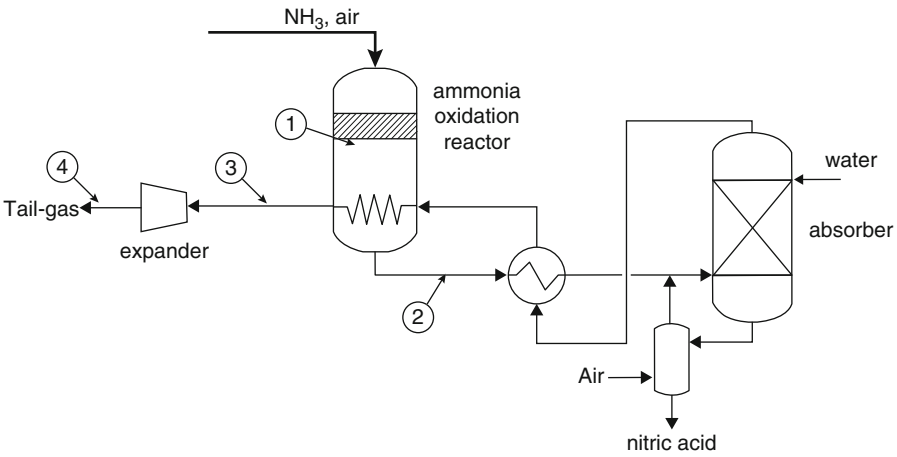

Fig. 5 Simplified flowsheet of a nitric acid plant with the indication of the potential locations of catalytic N_2O abatement systems (DeN_2O). See text regarding the description of "positions in the flow sheet"

problems in development of these in-process N_2O decomposition catalysts are associated to the necessity of minimizing possible NO decomposition and developing high hydrothermal and chemical stability related to the high temperatures of operations. This solution was proposed by BASF using first Cu–Zn–Al spinel catalysts and then CuO/Al_2O_3 in the shape of small pellets, which were also installed in two commercial plants in Ludwigshafen (Germany) and Antwerp (Belgium). A stable activity for 3 years and minimal NO decomposition (<0.5 %) were reported. N_2O decomposition efficiencies higher than 80 % were reported. However, a problem may arise from the possible loss of copper, because when it contaminates nitric acid used for fertilizers' production, severe safety problems can occur (copper catalyzes ammonium nitrate decomposition). Instead of decomposing N_2O to N_2 and O_2, it is preferable to oxidize N_2O to NO, because this solution would improve HNO_3 productivity. This reaction is endothermic, and although thermodynamically favorable, the equilibrium constant is very low at the ammonia oxidation reactor conditions.

An alternative to in-process location of the N_2O abatement catalyst (inside the ammonia oxidation reactor) is to put it downstream to the reactor (Fig. 5, position 2) in line with the absorption column. Iron-loaded zeolites with MFI or BEA structure have been proposed by Krupp UhDe to be used for this application. However, hydrothermal stability of these materials is unclear, taking into account the high steam content of emissions (typical 13 % vol.) and high temperature (above 500 °C). This location of the DeN_2O technology interferes with heat exchange series (simplified in Fig. 5), and therefore the advantage of simpler revamping of existing plants with respect to in-process solution is unclear.

In terms of simpler revamping of existing nitric acid plants, it is preferable to position the DeN_2O unit in the tail gas train upstream of the tail gas expander

(position 3 in Fig. 5). This configuration offers the great advantage of not influencing the heart of the nitric acid plant, i.e., the ammonia burner and the absorber, and therefore of greater flexibility in terms of reaction temperature with respect to previous options. Being present less space constraints on the volume of the catalytic bed, higher levels of N_2O removal (higher than 95 %) are possible. The decoupling of the DeN_2O unit from the ammonia burner is important, because the stop of the unit (e.g., to change the deactivated catalyst) may be independent on the main process operations. The tail gas leaves the absorber at temperatures close to room temperature, but then passes various heat recovery stages before reaching the expander where pressure decreases typically from 3 to 13 bar to near to 1 bar recovering energy. Depending on the exact position of the DeN_2O unit in the tail gas train, the temperature ranges from 250 °C to 500 °C. In modern nitric acid plants, the typical NOx concentration is around 0.02–0.04 %, N_2O concentration about 0.01–0.02 %, O_2 concentration about 2–3 %, and H_2O concentration at 0.5–1.0 %. Values may change depending on the nitric acid plant technology (low or high pressure, mono- or dual pressure).

Two catalytic options are possible to convert N_2O:

- Catalytic decomposition
- Selective catalytic reduction by adding a selective reductant for N_2O

Direct catalytic decomposition of N_2O without adding a reducing agent is the preferable option, if catalysts having suitable activity under realistic conditions of feed composition and space velocities can be found. Transition metals like Cu, Co, and Ni and noble metals (Pt, Rh, Pd) supported on oxides such as Al_2O_3, TiO_2, ZrO_2, and CeO_2 or mixed oxides (ZrO_2–Al_2O_3, ZrO_2–CeO_2, perovskites, Mg–Al hydrotalcites) are active in N_2O decomposition but generally very sensitive to the presence of other gases in the feed (O_2, NO_x, H_2O) which cause severe deactivation. N_2O decomposition process may be located also downstream of the tail gas expander before the stack (position 4 in Fig. 5). The main advantage of this solution is that this end-of-pipe technology does not require modifications in the tail gas expander in existing plants and is thus the simplest solution for revamping existing processes. However, temperature of the emissions is low (200–300 °C), and thus preheating is required. Furthermore, pressure is also lower (about one bar vs. 4–10 bar in the case of positioning before the tail gas expander). The increase of the pressure increases the reaction rate.

N_2O concentration in tail gases of nitric acid plants is too low to have autothermal operations. Therefore, if the temperature of the emissions is below the temperature necessary for achieving the necessary N_2O conversion in the catalytic decomposition reactor, the preheating of the stream, usually through a separate furnace, is necessary. Instead of using the fuel gas only for external heating of the tail gas in a furnace, it is preferable to add it directly to the feed and use both to in situ heating of the gas stream (due to its combustion) and as selective reductant for N_2O, when a suitable catalyst can be found. An economic estimation of the two competitive technologies, based on a temperature of 430 °C for decomposition operations and 380 °C for

selective reduction operations (by adding 0.2 % propane to the feed in the latter case) and a conversion of N_2O of 90 % or above in both cases, indicates nearly equal operating costs, but an advantage of the selective reduction technology in terms of fixed costs.

Ethane or propane are an interesting reductant for this purpose (Hevia and Perez-Ramirez 2008; Centi and Vazzana 1999), because they are inexpensive hydrocarbons, much more reactive than methane and preferable to ammonia, because it does not have the problems of safety, side pollution, and formation of deposits (ammonium bisulphate) of the latter. The main problem in searching for a catalyst able to reduce N_2O by ethane or propane in the presence of oxygen is that the catalyst reactivity toward propane oxidation to carbon oxides by O_2 must be lower than the catalyst activity in the reaction of alkane with N_2O (or atomic oxygen produced by N_2O dissociation). The largest majority of the catalysts active for N_2O decomposition are not promoted or are even deactivated in comparing the reactivity in N_2O decomposition (in the presence of O_2) with that observed when the alkane is also co-fed.

Propene, propane, ethane, methane, and ammonia have been used as the reductants. Criteria to consider in their evaluation are (i) de-N_2O activity and operation temperature; (ii) hydrocarbon utilization, i.e., the selectivity to react with N_2O in O_2 excess; (iii) emission of CO and CO_2; (iv) sensitivity to NO and NH_3; and (v) cost. Propene, due to the higher cost, is not a suitable reductant. Methane requires reaction temperatures higher than ethane and propane (about 100–150 °C higher), with the latter allowing the lowest reaction temperatures. Ammonia has a comparable activity of propane as reducing agent, but the cost is higher. Propane and ethane are the preferable reducing agent, but propane has the advantage of slightly lower reaction temperatures and especially an easier storage, although carbon efficiency is lower with respect to ethane.

The N_2O abatement unit can be located downstream of the tail gas expander (position 4 in Fig. 5). This *end-of-pipe* unit does not require modifications of the tail gas expander in the existing plant (therefore, may be well suited for revamping of existing plants), but due to the low temperature (typically below 250–300 °C), the gas must be preheated. Selective catalytic reduction seems the only feasible solution from the economic point of view in this case. Using propane as reductant and Fe–ZSM-5 catalysts, the efficiency for the reduction of N_2O could be better than 70 %. A start-up in-line burner is required to start the reaction and to correct for fluctuations in the tail- as flow and composition, while tail gas preheating is made using the heat generated in the catalytic reactor.

The evaluation of the different options to reduce N_2O emissions in nitric acid plants depends on several factors, which may vary from case to case, including regulations on emissions or incentives on lower emissions. The cost of N_2O abatement (per ton of CO_2 equivalent) is in the 0.2–3.0 € range, a cost which appears compatible with polities for the reduction of greenhouse gas emissions. Two main distinctions, which should be made in the selection of the preferable de-N_2O technology, are whether or not the technology should be applied to existing nitric acid plants and if in process gas (with respect to tail gas N_2O abatement) N_2O

decomposition is feasible. Catalytic N_2O decomposition directly after the ammonia oxidation catalyst in the converter is the less expensive option, but the loss of NO and the catalyst lifetimes are the crucial factors.

For new nitric acid plants, catalytic decomposition of N_2O upstream of the expander (with a cost in the 0.3–0.5 € per ton CO_2-eq.) is often preferable, but the plant should be designed in such a way that the temperature before the expander is around 500 °C to avoid sufficiently high reaction rates for the decomposition. In existing nitric acid plants, the temperature before the expander is too low and often no space in the ammonia oxidation reactor for catalyst placement is present. SCR upstream of the tail gas expander or downstream when space constraints do not allow location of the unit appears to be the preferable solution, although the cost is higher (in the 0.5–1.0 € per ton CO_2-eq.). However, if SCR of N_2O can be combined with elimination of also NO_x, the SCR technology will gain attractiveness.

Combined N_2O–NO_x removal from the emissions of nitric acid plants is an interesting opportunity, because NO_x emissions of a nitric acid plant range from 100 to 2000 ppm, with an average of 200 to 500 ppm. In order to comply with emission targets, a DeNOx SCR unit is used. Typically, ammonia is used as the reductant and supported vanadium oxide as the catalysts. The DeNOx unit is generally located upstream the expander in the tail gases of the plant, but N_2O emissions are not reduced from the conventional NH_3–DeNOx technology.

A less studied case of N_2O emissions is that of N_2O emissions from waste (industrial or municipal) combustion. N_2O forms in relatively high amounts (0.1–0.6 %), when combustion temperatures are lower than 1000 °C (e.g., using fluidized bed combustors). Temperature of the emissions is typically above 300 °C, but often SO_2 is present in the emissions, together with O_2, CO_2, CO, NO, N_2, H_2O, and other minor compounds. Ashes are also typically present. Deactivation of the catalyst is a main issue. N_2O decomposition catalysts typically deactivate quite fast in the reaction conditions of the emissions from waste combustion. Fe–ZSM-5 catalysts show good performances in the SCR of N_2O with propane, also in the presence of SO_2 in the feed (Centi and Vazzana 1999).

Fluorocarbons

Differently from methane and nitrous oxide, fluorocarbons, which include hydrofluorocarbons (HFCs), perfluorocarbons (PFCs), and sulfur hexafluoride (SF6), are generated exclusively by anthropogenic activities. Current atmospheric concentrations of these gases are small relative to other greenhouse gases, but their GWP is quite high. Halocarbons that contain chlorine and bromine, being implicated in depletion of the ozone layer, are controlled by the Montreal Protocol and its amendments. The uncertainly in the estimations of the emissions of fluorocarbons is high, due to unpredictable developments in the mix of substitutes for CFCs and halons, the presence of a mix of applications, lag times, etc. HFCs and PFCs have been introduced as alternatives to ozone-depleting substances (e.g., HFC-134a

($C_2H_2F_4$) is a substitute for CFC-12 (CCl_2F_2)), and thus their emissions are expected to increase dramatically in the coming years. IPCC evaluations (Pachauri and Meyer 2014) is that the replacement of CFCs and HCFCs, which are both ozone depleters and greenhouse gases, with HFCs (emissions of which are regulated under the Kyoto Protocol) is not expected to produce a runaway greenhouse effect. The effect of the fluorocarbons will remain constant or will decline over the coming century, both in absolute terms and relative to the other greenhouse gases.

Fluorocarbons are used in a variety of industrial processes, including the manufacture of semiconductors (plasma etching and cleaning tool chambers), refrigeration, and fire protection. There are also some emissions during their manufacture. For example, HFC-23 is emitted during the production of HCFC-22. PFCs are emitted during the aluminum smelting process (during primary aluminum production, CF_4 and C_2F_6 are emitted as by-products of the smelting process). Sulfur hexafluoride is mainly used in the electric power industry as a gas for electrical insulation, current interruption, and arc quenching in the transmission and distribution of electricity, because of its inertness and dielectric properties. SF_6 is used extensively in circuit breakers, gas-insulated substations, and switchgear. Other industrial applications include use in magnesium melting operations and as a gas tracer.

These emissions probably will decrease in the future, based on a voluntary program of the aluminum and magnesium industries, semiconductor manufacturers, HCFC-22 producers, and the electric power industry. In several cases, the fluorocarbons will be recovered from the emissions using conventional adsorbents and then reused, when possible. However, in some cases, their destruction will be necessary, but thermal incineration is expensive, and special care must be adopted to avoid the formation of harmful products, corrosion problems, etc.

There are limited studies on the catalytic conversion of fluorocarbons to inert chemicals, although a large number of studies deal with the catalytic conversion of CFCs to fluorocarbons as a consequence of the Montreal Protocol to find alternatives to CFCs responsible for the depletion of the ozone layer (Ertl et al. 1999; Manzer and Nappa 2001). Supported metal catalysts (Pd on alumina or carbon), AlF_3, and other oxides are active in the hydrodechlorination of CFCs to HFCs. In particular, the CCl_2F_2 (CFC-12) conversion to CH_2F_2 (HFC-32) has been studied (Yu et al. 2006), but the higher strength of the C–F bond makes the selective catalytic hydrodefluorination of fluorocarbons to form inert hydrocarbons (which then can be combusted safely) more difficult to realize. Some of the emerging ideas (Perutz 2008; Schwartsburd et al. 2014; Whittlesey and Peris 2014; Ahrens et al. 2013; Reade et al. 2009; Sabater et al. 2013) are difficult or costly to implement on an industrial scale, but some have a promising potential, although still to be fully demonstrated. Methane is formed with selectivities ca. 50 % as a side product in CFC-12 hydrodechlorination on supported Pd catalysts. The selectivity can be increased by tuning the operating conditions and catalyst composition. New homogeneous catalysts, based on silylium-carborane or ruthenium *N*-heterocyclic carbene (NHC) complexes, have been shown to be able to break the carbon–fluorine bond at room temperature. They were reported as highly promising for an effective disposal

of these pollutants, but the effective applicability to practical problems has to be demonstrated.

A different possibility is catalytic steam reforming for the effective destruction of halocarbons using nickel-based catalysts (Menini et al. 2000). The process has been demonstrated with conversion levels higher than 99.99 % for chlorocarbons (trichloroethane, trichloroethylene, perchloroethylene) but can be adapted to treat fluorocarbons. The process was found to be economically attractive over thermal incineration and catalytic combustion. Furthermore, in comparison with thermal combustion, catalytic combustion avoids the formation of harmful by-products in traces.

Catalytic Conversion of CO_2

The use of catalytic technologies for the reduction of CO_2 emissions is a different case from those discussed regarding methane and nitrous oxide emissions, due to the higher volume of emissions, different characteristics of the source, and different requirements for its transformation. In particular, while N_2O after transformation to an inert gas such as N_2 and CH_4 after conversion to CO_2 having about 30 times lower GWP can be emitted to the atmosphere, the problem with CO_2 is different. The possible options for CO_2 are the following:

- Recovery and storage underground or under the sea (CSS)
- Reaction with inorganic solids to form inorganic carbonate (disposed or eventually used as materials)
- Conversion to chemicals or fuels which are reused

Catalysis plays a central role in the third option. Large amounts of carbon dioxide, often already concentrated as side stream of many processes or CSS plants, are available at zero or even negative cost due to carbon taxes. There is thus increasing research attention on chemical, biological, and physical uses of CO_2 (Centi and Perathoner 2009, 2014; Aresta and Dibenedetto 2007; Sakakura et al. 2007; Schaefer et al. 2010; Darensbourg 2007; Dorner et al. 2010; Quadrelli et al. 2011; Aresta 2010). An emerging possibility as regards the use of the conversion of CO_2 to higher-energy products as a way to introduce renewable energy in the chemical production value chain (Quadrelli et al. 2011) is commented in a more detail below. This opportunity will also allow creating a worldwide base marked to trade and exchange renewable energy through the conversion of CO_2 to liquid fuels (Barbato et al. 2014), in order to enable a smooth and effective transition from current (largely based on liquid fuels) to the future energy system based on renewable (perennial) energy. The potential of this route is thus quite large, with a potential contribution in saving CO_2-eq. emissions of several Gtons.

Often the discussion on mitigation of GHG effect has been limited to consider long-term sequestration of CO_2, for example, CSS or mineralization, supposing that a short cycle time means that carbon is returned to the atmosphere quickly. However,

when renewable energy is introduced in the cycle of CO_2 to fuel conversion (thus storing renewable energy in the form of chemical energy), a short cycle time (e.g., when CO_2 is converted to methanol using the H_2 produced with renewable energy sources and then methanol is used as fuel) means that in every cycle, there is a minus delta in carbon emissions deriving from the substitution of fossil fuels with less carbon-intensive sources. On a certain timescale (e.g., 20 years), the long-term sequestration of CO_2 impacts once, while for short time cycles there is a cumulative effect. The exact value derives from a LCA analysis, but on average, the effect is at least one order magnitude higher in short time cycles with respect to long-term sequestration.

Carbon dioxide, in addition, is an excellent carbon source (Centi and Perathoner 2014), particularly when combined with the incorporation of renewable energy in CO_2 transformation. Recycle of CO_2 and incorporation of renewable energy in the production process will be between the driving elements reshaping the future of chemical production (Perathoner and Centi 2014a, b; Lanzafame et al. 2014a). In a longer term, a distributed conversion of CO_2 to chemicals/fuels will be possible by the development of artificial leaf-type devices, in which the development is raising interest (Bensaid et al. 2012). There is thus a progressive movement to a kind of CO_2 circular economy, which is schematically outlined in Fig. 6. Current economy is largely based on the use of fossil fuels, but as already at the stage of transformation of fossil fuels to the energy products or the raw materials used for chemical production, nearly half of the original energy content is lost in the form of CO_2, as indicatively shown in Fig. 6 (Ampelli et al. 2015). Various other losses are further present in downstream processes, before the utilization of the energy or chemical products. Even in the process of production of biofuels, large amounts of CO_2 are

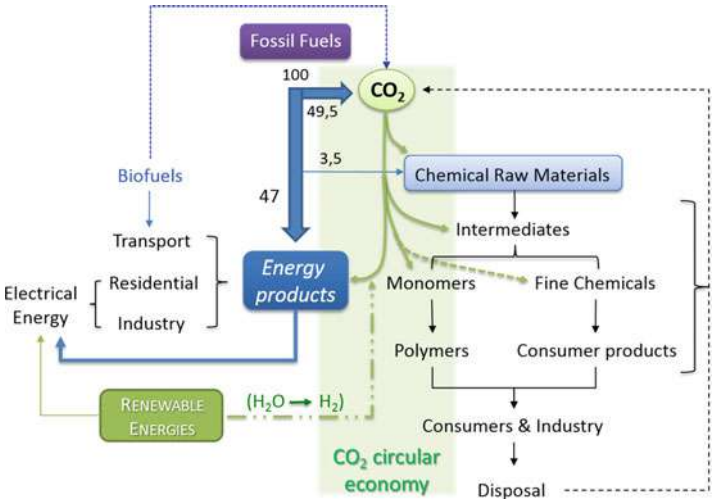

Fig. 6 Simplified model of CO_2 circular economy and its impact on chemical and energy value chain (Modified from (Ampelli et al. 2015))

formed (e.g., approx. 1 t CO_2 per ton of ethanol). Through the (re)use of CO_2, it is possible to rebalance this economy, allowing a more effective use of renewable energy (including a lower impact on environment and a better carbon footprint for biofuels), providing new raw materials for chemical production and especially preserving the actual value chain. The latter is a very important element because it allows to minimize the costs of transformation to new sustainable production system.

Although a number of organic syntheses using carbon dioxide are known, only a few were applied in industry, the main processes being the syntheses of urea and its derivatives and the production of organic carbonates, where phosgene ($COCl_2$) is increasingly being replaced by CO_2 as the C1 building unit. CO_2 is also used in the electrochemical Kolbe–Schmitt process for the production of salicylic acid. CO_2 is used industrially for fertilization in greenhouses and increasingly in photobioreactors (for breeding algae and microalgae), in enhanced gas or oil recovery processes and in refrigerant applications. All these uses account for about 110 Mtons/year, e.g., for less than 1 % of the worldwide carbon dioxide emissions. Although other industrial uses outlined below are still quite limited currently, this is a dynamic field with many emerging industrial initiatives. The concise technology roadmap outlined in Fig. 7 introduces the expected scenario for industrial utilization of CO_2 based on the analysis of the state of the art, including recent trends in patents (Ampelli et al. 2015). In a short-to-medium-term perspective, CO_2 utilization will continue its progression especially in areas that are technologically more advanced (e.g., CO_2-containing polymers, CO_2 hydrogenation). The use of CO_2 conversion to exploit

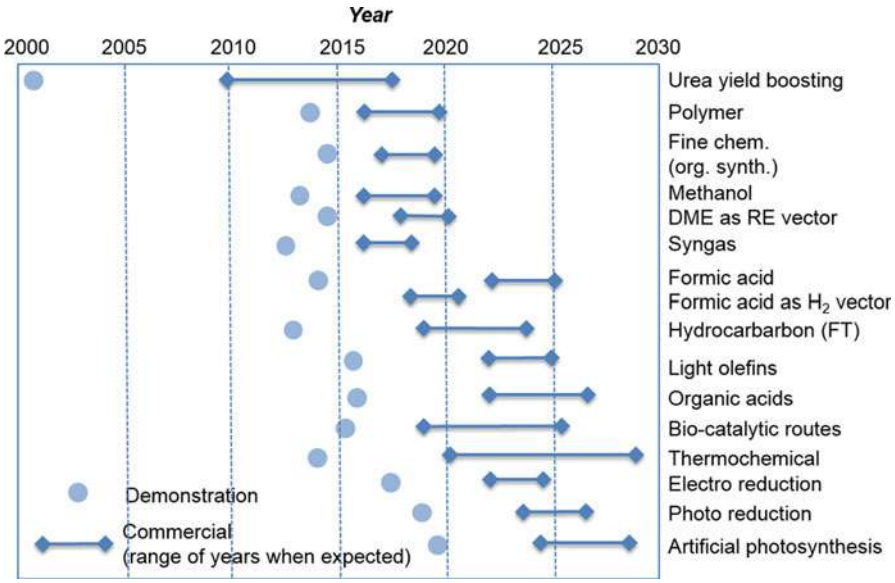

Fig. 7 Estimated technology roadmap for commercialization of CO_2 reuse paths (Modified from (Ampelli et al. 2015))

unused renewable energy resources or to mitigate instabilities on the grid (related to the discontinuous production of energy by renewable sources; chemical conversion is a way to store and distribute energy) will play a future relevant role.

In the long term, CO_2 utilization will become a key element of sustainable low-carbon economy in chemical and energy companies, combined with curbing consumption (Centi and Perathoner 2014; Perathoner and Centi 2014a). CO_2 will become especially a strategic molecule for the progressive introduction of renewable energy resources into the chemical and energy chain (Perathoner and Centi 2014a), thus helping to lessen fossil fuel consumption (expected to decrease by >30 % by year 2030). CO_2 utilization will become an important component of the strategy portfolio necessary for curbing CO_2 emissions (with an estimated potential impact of gigatons equivalent CO_2 emissions, similar or even superior to the impact of CCS and biofuels, but with lower cost for society (Barbato et al. 2014)). CO_2 utilization will thus be at the heart of strategies for sustainable chemical, energy, and process industries and for a resource and energy efficiency development.

Four main routes are predominantly investigated:

- Carboxylic acids and derivatives, e.g., novel CO_2-based routes to products essentially for the chemical market
- Alcohols, ethers, and hydrocarbons, e.g., CO_2 conversion to already well-established products for the chemical and energy market
- Organic carbonates and other monomers for CO_2-based plastics
- Urea and derivate, e.g., novel alternative or more sustainable (phosgene-free) routes to well-established chemical products

Figure 8 reports an overview of the different possible catalytic conversions of CO_2 to industrially relevant chemical products or components for fuels. Most of these routes are still not commercial, apart from urea and some organic carbonate. Their expected industrial application is summarized in Fig. 7. Some of them, such as acetic and acrylic acid or vinyl acetate from CO_2, are attracting, but the results are still far from the possible application.

Many valuable chemicals can be also produced by CO_2 fixation using homogeneous catalysis: lactones, pyrones, oxazolidinone, imidazolidinone, quinazoline, etc. Although interesting, the market for these products is quite limited, and thus the impact of these synthesis on the global carbon dioxide emissions is nearly negligible. CO_2, coordinated to metal centers, may be inserted into various metal–element bonds to give rise to various reactions, such as (i) C–C bond formation to produce acids, esters, lactones, and pyrones; (ii) C–N bond formation with production of carbamates and isocyanates; and (iii) C–O bond formation for the synthesis of linear or cyclic carbonates and poly(carbonates).

Some interesting examples of recent new routes for activating CO_2 using homogeneous catalysts are listed below:

- Hydrosilanes used to convert CO_2 into methane or methanol using zirconium phenoxide borane complexes or *N*-heterocyclic carbenes as catalysts

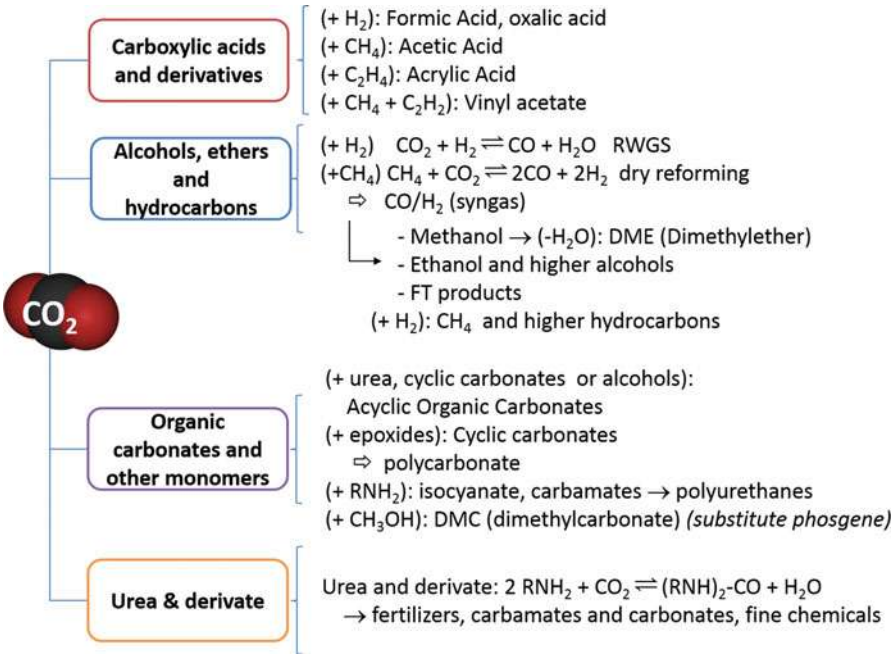

Fig. 8 Overview of the different possible catalytic conversions of CO_2 to industrially relevant chemical products or components for fuels

- Borane reduction of CO_2 to form boryl formats using nickel diphosphine complexes as catalysts
- Frustrated Lewis pairs for homogeneous hydrogenation of CO_2
- Nonmetal-mediated homogeneous hydrogenation of CO_2 to CH_3OH
- Indirect conversion of CO_2 to methanol based on the use of Ru pincer complexes as catalysts for the hydrogenation of carbonates, carbamates, and formats

Also in the area of the use of CO_2 in organic synthesis, a number of recent breakthroughs have been discovered. For example, in the area of carboxylation, the catalytic hydrocarboxylation of styrene and the copper-catalyzed hydrocarboxylation of alkynes using CO_2 in the presence of a hydrosilane may be cited. These reactions open new interesting perspectives for organic synthesis, but all these cases refer to low-volume productions.

Electrocatalysis is offering new possibilities, either to produce small organic molecules to be used in conjunction or integrated with solar devices (for artificial leaf-type systems) or as a valuable synthetic procedure. The number of new discoveries after years of stagnation is remarkable. There is the need to go beyond the conventional metal-type electrodes operating in liquid phase. Gas-phase or liquid-phase operations in the presence of molecular catalysts (such as pyridinium ions) are two promising directions to form either methanol or even long-chain alcohols, but

scientific effort in these areas is still too limited. The use of nonconventional electrolytes, such as ionic liquids, is another attractive direction. New electrocatalysts are also recently discovered, for example, a nanoporous silver electrocatalyst that is able to reduce CO_2 to carbon monoxide with approximately 92 % selectivity at a rate over 3000 times higher than its polycrystalline counterpart under moderate overpotentials (<0.50 V). Electrocatalytic carbonylation on novel catalysts (MOF) is another interesting possibility relevant for organic syntheses.

On short term, the following two are the catalytic routes with the higher potential impact to reduce the CO_2 emissions:

- The use of CO_2 to produce monomers for advanced material polymers, e.g., CO_2-containing polymers such as polycarbonate
- The hydrogenation of CO_2 to produce synthesis gas (syngas, a mixture of carbon monoxide and hydrogen) which can be subsequently transformed to compounds for energy/chemical market: (i) via Fischer–Tropsch process, a set of chemical reactions that convert syngas into liquid hydrocarbons, or (ii) via methanol/DME (dimethyl ether)

CO_2 Use to Produce Monomers for Advanced Materials Polymers

The incorporation of carbon dioxide into polymers is an active area of research for the interesting perspectives of application (Darensbourg 2007; Fukuoka et al. 2010). Examples are the synthesis of polycarbonates, polypyrones, lactone intermediates, and polyurethanes. There are various industrial initiatives in this sector, among which the production of polyols for polyurethane (Bayer) and the production of polypropylene carbonate (BASF and Novomer Inc.) (Centi et al. 2013).

Asahi Kasei Corporation was the first to succeed in industrializing the production of an aromatic polycarbonate (PC) using CO_2 as a starting material (Fukuoka et al. 2010). The carbonate group of PC links directly to the residual aromatic groups of the bisphenol. Until Asahi Kasei's new process was developed, all of carbonate groups of PC in the world were derived from CO as starting material. Furthermore, more than about 90 % of PC has been produced by the so-called phosgene process (phosgene is highly toxic and corrosive and derives from the reaction of CO with Cl_2), which besides safety issues, gives rise to a PC containing Cl impurities and large amounts of wastewater. The new CO_2-based process uses a safer reactant and contributes to reduce carbon dioxide emissions but also produces a higher quality PC and has a lower impact on the environment. Regardless of the many advantages, the higher cost of production has still significantly hindered the market introduction of this process.

The novel green Asahi Kasei process is based on the condensation of DPC and BPA in a melt-polymerization process including a pre-polymerization step (Fig. 9). The process is clean, producing valuable ethylene glycol as the by-product. The starting material is ethylene oxide (EO) (Step 1). The by-product of ethylene oxide manufacture, CO_2, is itself consumed in the process (173 t per 1000 t of BPC);

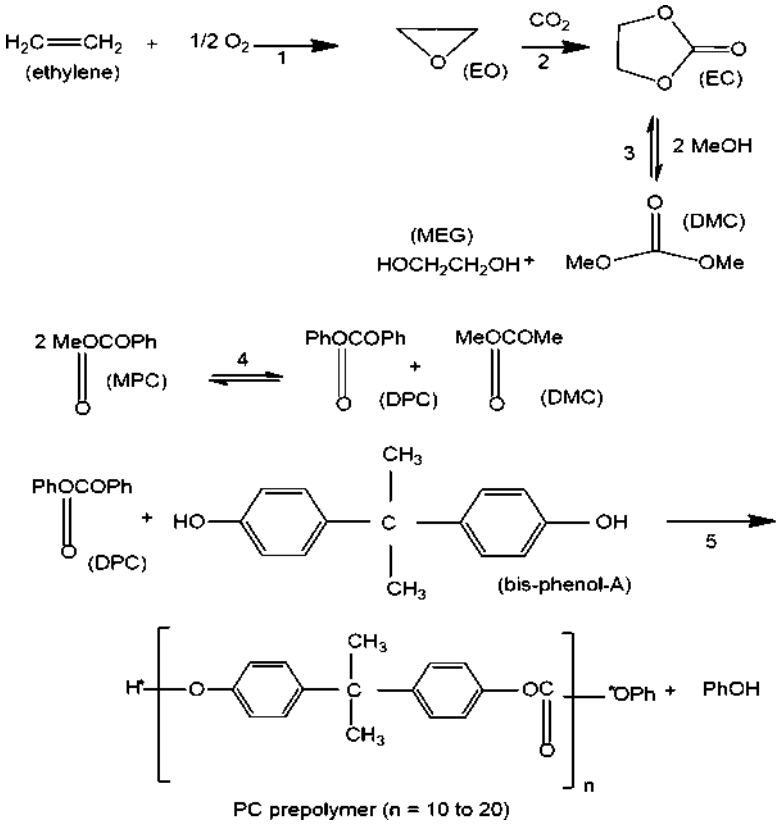

Fig. 9 Asahi Kasei process for polycarbonates

ethylene oxide is converted into ethylene carbonate (EC) by reaction with CO_2 (Step 2). Step 3 is the conversion of EC into DMC by reaction with methanol and the production of high purity monoethylene glycol (MEG).

Bayer has developed a process for polyether carbonates polyols (PPP) from CO_2 up to pilot/demo plant. The PPP resulting from the copolymerization of CO_2 with a starter molecule (mono-, di-, and polyols; alkoxylated oligomers of glycols) and an alkylene oxide are characterized by low molecular weight and terminal OH functionalities, available for further reaction with isocyanate to lead to urethane groups (Fig. 10). A key scientific breakthrough allowing industrialization of CO_2 polymerization to PPP was the development of a catalyst that is sufficiently stable and active under the process conditions (90 °C, 10 bar of CO_2), such as double metal cyanide catalyst.

Novomer has proposed a new catalytic process for the industrial production of aliphatic polycarbonates by reaction of CO_2 with epoxides. In particular, they have developed novel catalytic processes for the reaction of carbon dioxide with propene oxide or ethylene oxide to produce polypropylene carbonate and polyethylene

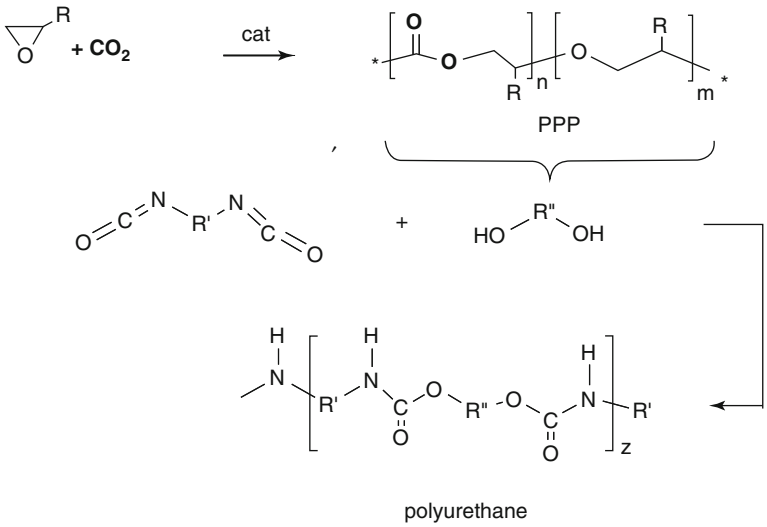

Fig. 10 Schematized Bayer route to polyurethane from the polyether polycarbonate polyols (PPP)

carbonate, respectively. Applications of these polymers range from packaging, coatings to electronics, and barrier layers. The processes, however, are not still on a commercial production scale (demonstration at an about 2 m^3 scale). The polymer has different properties – it can be hard, soft, transparent, or opaque – based on the type of epoxide used, and it is biodegradable.

There are other possible monomers for polymers produced using CO_2 in the step syntheses, directly or indirectly. Urea can be used as a "reactive CO_2" in the synthesis of carbamates and then carbonates.

$$H_2N - CO - NH_2 + ROH \rightarrow H_2N - CO - OR + NH_3 \quad (1)$$

$$H_2N - CO - OR + ROH \rightarrow RO - CO - OR + NH_3 \quad (2)$$

The separation/purification cost of the carbonate decreases with increasing number of carbon atoms in the chain of the alcohol. Hence, this technology is better suited for the synthesis of carbonates of higher alcohols. Urea has been used for the synthesis of cyclic carbonates by reaction with diols. The released ammonia can be recovered and recycled. The transesterification reaction can be used to convert one carbonate into another (Eq. 3). However, the alcohol coproduct must be recycled or have a market comparable to that of carbonates.

$$(RO)_2CO + 2R'OH \rightarrow (R'O)_2CO + 2ROH \quad (3)$$

Diphenyl carbonate is commercially produced by this way, using efficient catalysts, which have been recently developed, such as Cp_2TiCl_2, Pb and Zn double oxide, and V, Nb, and Ta.

Isocyanates are also industrially relevant compounds with applications in several fields, as starting materials for pesticides, dyes, detergents, and adhesives, as well as in the manufacture of resins and rubbery plastics. Furthermore, diisocyanates are the primary feedstock for the production of polyurethanes, with a global market of almost 5 Mtons/year. The direct synthesis of isocyanates from amines and CO_2 (Eq. 4) is a challenging task which requires to deoxygenate the cumulene bonds of CO_2; some Ti(IV) and U(V) organometallic complexes are capable of promoting such a transformation.

$$RNH_2 + CO_2 \leftrightharpoons RNCO + H_2O \tag{4}$$

New catalysts in combination with ionic liquids show promising results (Heyn et al. 2014).

CO_2 Hydrogenation

A main route of conversion of carbon dioxide is the hydrogenation to produce syngas, alcohols such as methanol or ether such as dimethyl ether, or hydrocarbons. The availability of renewable H_2 and/or renewable sources of energy is the critical element for this route. The alternative is to use methane as the source of H_2 in the so-called dry reforming reaction. This is an endothermic reaction occurring at high temperature and may be combined with the steam reforming (also the endothermic reaction between methane and water, to optimize the CO/H_2 ratio) and with the partial methane oxidation (an exothermic reaction between methane and O_2) in the so-called tri-reforming process. After this first step of formation of syngas (CO/H_2) different established routes are possible to produce chemicals or clean fuels. The alternative is to produce CO by breaking the C–O bond in carbon dioxide. This requires high reaction temperatures (>2000 °C), but the process could be assisted by redox metal oxides which reduce the temperature of operations to a range (around 1000 °C) compatible with concentrated solar furnaces. An alternative is the use of a photocatalytic or photoelectrocatalytic systems to convert directly CO_2 and H_2O at near room temperature using solar light.

Between the carboxylic acids, which can be obtained by hydrogenation of CO_2, formic acid is the more interesting. This reaction has been proposed as the basis for a "formic acid" economy, being possible to use formic acid in fuel cells (to store and transport H_2) and as chemical. However, formic acid has problems of toxicity and storage. Methanol economy (Olah et al. 2009a, b), which could be also based on CO_2 hydrogenation, has stronger fundaments.

Formic acid is the simpler chemical produced by hydrogenation of CO_2 and that requires less hydrogen:

$$CO_2 + H_2 \leftrightharpoons HCOOH \tag{5}$$

A consortium was formed within EPSRC (Engineering and Physical Sciences Research Council) activities in the UK to investigate formic acid synthesis from CO_2 and its use including as feedstock for fuel cells. A renewed interest on this reaction is also present in Japan after a significant improvement in the understanding of the active form of the catalyst and rate-determining step to convert CO_2 into formic acid using water as a green solvent. There is an active research on the synthesis of formic acid particularly using homogeneous catalysts. New opportunities have been also offered from ionic liquids.

Formate could be reduced to formic acid also in mild hydrothermal conditions using iron nanoparticles as the reductant and Ni as a catalyst. CO_2 may be also directly reduced in the presence of iron nanoparticles under mild hydrothermal conditions to form formic and acetic acid. Both these possibilities, however, still appear far from the application.

The enzyme formate dehydrogenase can be also used to convert CO_2 to formic acid. It may be also encapsulated in biomimetic hydroxyapatite–polysaccharide capsules to promote stability and operations (broader temperature and pH range). However, productivity should be improved.

Electroreduction of CO_2 (ERC) is the method used by the company Mantra up to pilot scale for producing formic acid. The reduction of CO_2 in methanol-based electrolyte (limited CO_2 solubility in water is an issue) gives rise to formic acid and CO using Zn particle-pressed electrodes, while the addition of Cu_2O particles to this electrode leads to the formation of also methane and ethylene. At high CO_2 pressure (to increase productivity) using Cu electrode and MeOH as electrolyte, the reduction products were formed in the order of CO, methane, formic acid, and ethylene. The use of microfluidic techniques to build microscale electrochemical reactors is identified to be highly promising to increase the electrochemical performance (Lu et al. 2014).

Formic acid, together with other products such as methanol, formaldehyde, and minor amounts of hydrocarbons (CH_4, ethylene), is the main product obtained in the photocatalytic reduction of CO_2 in water (Das and Wan Daud 2014). The recovery of the products in the photocatalytic reduction of CO_2 is energy-intensive and particularly critical due to the low productivity. To promote visible light activity, sensitizers could be used, but stability is still low. In the photoelectrochemical reduction of CO_2 at p-InP electrode, formic acid and carbon monoxide form by reaction of CO_2 with a photogenerated electron at the semiconductor surface. The $^{\bullet}CO_2^-$ adsorbed anion radical formed may react with a further electron and a proton to give either adsorbed CO or $HCOO^-$, but when copper particles are present in solution, methane and ethylene were also detected.

The coupling of two $^{\bullet}CO_2^-$ anion radicals formed by the addition of one electron to CO_2 can give rise to oxalate ion, particularly in some nonaqueous electrolyte. Oxalic acid is used as industrial cleanser especially to scour rust off metals. A dinuclear Cu^{I} complex that is oxidized in air by CO_2 rather than O_2 was discovered recently. The product is a tetranuclear Cu^{II} complex containing two bridging CO_2-derived oxalate groups. Treatment of the Cu^{II}–oxalate complex in acetonitrile with a soluble lithium salt results in quantitative precipitation of lithium

oxalate. The Cu^{II} complex can then be electrochemically reduced nearly quantitatively at a relatively accessible potential, regenerating the initial dinuclear Cu^{I} compound.

The direct synthesis of acetic acid by reaction of CO_2 with methane is potentially a very attractive reaction alternative to current method by methanol carbonylation (e.g., using CO). The methanol carboxylation (e.g., using CO_2) forms dimethyl carbonate (DMC), but acetic acid could be produced from the reaction of CO_2 and methane, using two powerful and widely available greenhouse gases:

$$CO_2 + CH_4 \rightarrow CH_3COOH \tag{6}$$

However, current results are still far from the possible application. Another attractive reaction is the carboxylation of alkenes with CO_2 using transition elements in a low oxidation state (Fe^0, Mo^0, Ni^0, and Rh^I) as catalysts. This reaction has been recently revisited for its potential for obtaining acrylic acid derivatives. The development of efficient catalysts is required to favor the acrylic acid or acrylate release. An alternative synthetic approach to acrylates is based on the formation of alkyl esters of acrylic acids' alkyl esters. The reaction involves a preformed Pd–COOMe moiety as a system for the insertion of ethene and propene into the Pd–C bond, followed by acrylate elimination. Actual data, however, are quite far from those necessary for the process to be in competition with the commercial process involving the selective (multistep) catalytic oxidation of propene.

The production of alcohols (methanol in particular or its products of dehydration dimethyl ether (DME)) or hydrocarbons (especially Fischer–Tropsch (FT) products) is actually the more interested route to hydrogenate CO_2 (Quadrelli et al. 2011). Pilot plant experimentation is available as well as stable catalysts. The possibility of commercialization is highly dependent on the need to use CO_2 as raw materials (e.g., due to carbon taxes) and the availability of H_2 sources from renewable or other nonfossil fuel (e.g., nuclear plants) energy sources.

Methanol is one of the most important commodity chemicals as it is used as a raw material in several intermediate chemicals and end uses. Methanol is commercially produced from synthesis gas (CO/H_2), but the presence of small amounts of CO_2 in the feed accelerates the reaction. However, pure CO_2 feed or even larger CO_2/CO ratios instead inhibit the reaction rate, essentially due to the poisoning effect of the water formed from the reverse water–gas shift (RWGS) reaction:

$$CO_2 + H_2 \leftrightharpoons CO + H_2O \tag{7}$$

The critical aspect for a process using a CO_2–H_2 feed is to improve current syngas–methanol catalysts in terms of both low-temperature activity and water tolerance. Current catalysts are based on Cu–Zn oxides containing various additives (ZrO_2, Ga_2O_3, and SiO_2) in addition to alumina (Behrens 2014). The best productivities were obtained with Ga_2O_3, but within the same support, the productivity to methanol was linearly dependent on the metallic copper surface area, as found in syngas to methanol reaction. Ga_2O_3 allows improving the specific activity for

methanol synthesis, while Al_2O_3, ZrO_2, or SiO_2 improves the dispersion of copper particles and the stability.

Due to the strong water inhibition, a new process for methanol from CO_2 should include also a continuous removal of water from the reactor. Possible solutions are the catalytic distillation and the use of inorganic water permselective membranes. The latter is a preferred solution, although no specific results have been reported in literature. Suitable and recoverable membranes are those based on hydrophilic nanopore zeolite (NaA) films over a ceramic tubular support and developed for pervaporation of water–ethanol solutions.

A new interesting area of development is based on the nonmetal-mediated homogeneous hydrogenation of CO_2 to methanol at low pressures (1–2 atm) using frustrated Lewis pairs (FLP). In FLP, the steric environment imposed on the donor and acceptor atoms by the substituents prevents a strong donor–acceptor interaction.

High faradaic efficiencies (up to 90 % and 96 % with 465 and 365 nm radiation, respectively) in the selective conversion of CO_2 to methanol at a p-GaP semiconductor electrode with a homogeneous pyridinium ion catalyst and an applied potential of about −0.2 to 0.3 eV have been reported (Barton et al. 2008). Quantum efficiencies were between 1 % and 10 %, but an inverse relationship between methanol formation and current density was observed. This indicates from the practical point of view that only very diluted solutions of methanol in water could be obtained, and thus the energy to recover methanol is greater than the advantage of using solar energy.

Ethanol is less toxic and a better intermediate for chemicals with respect to methanol, although its low-cost production by sugar fermentation makes less attractive its synthesis by CO_2 hydrogenation. The selective ethanol synthesis from CO_2 using supported $Rh_{10}Se/TiO_2$ catalysts is known for a long time. At 300–350 °C, a rate of ethanol formation from CO_2–H_2 of about $2–4 \cdot 10^{-3}$ mol/h · g_{cat} with a selectivity to ethanol in the 70–85 % range has been observed. The alternative routes are (i) to add centers (such as K^+) able to promote the C–C bond formation to catalysts for the synthesis of methanol from CO_2 and (ii) use homogeneous catalysts able to give the methanol homologation with CO_2–H_2 such as bimetallic ruthenium–cobalt carbonyl complexes. Both routes, studied around the years 1995–2000, were only partially successful and no longer explored recently.

Dimethyl ether (DME) is a clean and economical alternative fuel (high cetane number, but low boiling point). There are also several technology developments recently for selective production of olefins, especially propylene either from methanol or from DME. DME synthesis from CO_2–H_2 should be considered as an extension of methanol synthesis to shift the equilibrium by using hybrid catalysts.

$$2CH_3OH \leftrightharpoons CH_3OCH_3 + H_2O \tag{8}$$

Catalysts used are thus a combination of a catalyst for methanol synthesis from CO_2–H_2 and an acid catalyst, typically zeolite.

Higher alcohols (>C2) are valuable chemicals, solvents, and additives for fuels, but few data are available regarding their possible synthesis from CO_2.

Cyanobacteria (*Synechococcus elongatus PCC7942*) have been recently genetically modified (strain SA579) to consume carbon dioxide in a set of steps to produce a mixture of isobutyraldehyde (primarily) and isobutanol. The engineered strain remained active for 8 days and produced isobutyraldehyde at a higher rate than those reported for ethanol, hydrogen, or lipid production by cyanobacteria or algae.

A different approach is by electrocatalysis (Centi and Perathoner 2004, 2009, 2010). Using novel electrocatalysts based on metal particles carbon nanotubes and gas-phase operations, it is possible to form isopropanol as the main product, together with other alcohols (methanol, ethanol) and hydrocarbons (up to C8–C9). The rate of formation is roughly comparable to that of biocatalysis, but with the advantage in the case of electrocatalysis that the products form in the gas phase and are thus easily recovered. The electron and protons necessary to reduce the CO_2 electrocatalytically have to be supplied from water photoelectrolysis on the photo-anode side of a photoelectrocatalytic device, but the full apparatus has not been tested yet.

CO_2 hydrogenation to methane is the well-known Sabatier reaction. It proceeds in the presence of a Ni-based catalyst:

$$CO_2 + 4H_2 \rightarrow CH_4 + 2H_2O \tag{9}$$

On this reaction, indicated with the acronym P2G, there is strong R&D effort, particularly in Germany, in relation to the local storage of excess electrical energy (by wind) and the production of methane for automotive use (Audi e-gas process). A 6-MW P2G, located in the Lower Saxony city of Wertle, started the operations in 2013. Being methane as gas, storage and distribution are more difficult than that with methanol (even considering the large pipeline net; there are also issues of purity for introduction in the pipeline system), and chemical use is quite difficult, if not passing through syngas (but then direct production of syngas from CO_2 would be preferable).

Interest on this reaction also arises for the possibility to generate O_2 and fuels on Mars and for applications such as propellant production on Mars or air revitalization in the space habitat. Microchannel designs offer advantages for a compact reactor with excellent thermal control. A Ru–TiO_2-based catalyst was used for the microchannel reactor.

The Sabatier reaction can be viewed as the combination of CO methanation and RWGS reaction. Therefore, catalysts active in these reactions are also active on CO_2 methanation. The conversion of CO_2 in Sabatier reaction could be increased using a water permselective membrane. Using a membrane reactor integrated with a water vapor permselective membrane, the conversion was increased about 18 % in comparison to the case without the membrane.

From the application perspective, more interesting is the production of higher hydrocarbons via the Fischer–Tropsch (FT) synthesis (Davis and Occelli 2009). This reaction typically uses synthesis gas, e.g., CO/H_2 mixtures, as the raw materials, but a number of recent studies have been dedicated to the effect of CO_2 on FT synthesis. CO_2 can be activated by suitable promoter(s) for hydrocarbon synthesis at low temperature. Low K content is suitable for increasing hydrocarbon yield. The Fe

catalysts promoted by Zn and Cu have higher CO and CO_2 conversion and decreased CH_4 selectivity. FT synthesis could be useful to produce hydrocarbons from CO_2-rich syngas as those produced from biomass. In general, there is increased carbon utilization in FT synthesis using CO_2-rich syngas feeds.

A modification of the FT catalysts allows obtaining good selectivities to light alkenes and thus to use this process also to make chemicals. About 85 % selectivity to alkene in the C_2–C_4 fraction (about 40 % of the whole hydrocarbon fraction) could be obtained. There are problems of catalyst stability, however. Hydrocarbons may be obtained via conversion of methanol/DME on multifunctional catalysts instead of the FT mechanism. On Fe–Zn–Zr/HY catalyst, it is possible to maximize the selectivity to isoC4. The use of CO_2 instead of CO increases the formation of isoalkanes (iC_4 and iC_5). The selective synthesis of ethylene by electrocatalytic reduction of CO_2 has been also shown using copper electrodes. Up to 33 % faradaic efficiency to ethylene was observed with low amounts of methane (about 4 %).

Urea and Derivate

The industrial synthesis of urea from carbon dioxide and ammonia is one of the most important examples of the large-scale production processes where carbon dioxide is utilized as a raw material. The worldwide urea production is over 120 Mtons/year, being used as fertilizer and as monomer for the manufacture of thermosetting polymers/plastics, such as melamine and urea–formaldehyde resins. Urea is also used as an auxiliary material in the petroleum and pharmaceutical industries. Although urea synthesis is commercially made from already many years, still there is the need of improvements, particularly regarding the increase of carbon dioxide conversion and heat recovery, the minimization of the environmental impact, and the introduction of catalysts to optimize the process variables.

Urea boosting indicates the capture of an external current of fossil CO_2 for urea production in an integrated ammonia–urea manufacturing plant and the use of natural gas as a feedstock in the reforming process to produce CO_2 and NH_3. When natural gas is used as feedstock, an excess of NH_3 is produced. An external source of CO_2 can be delivered via pipeline to the urea plant and reacted with surplus ammonia to form urea. This solution gives various types of GHG emission mitigation action:

1. Feedstock switch (avoidance of the emission of a fossil CO_2 current through its capture and utilization as input for urea production)
2. Thermal energy savings (thermal energy savings through the reduction of fossil fuel combustion needed to produce the CO_2 input for urea production)

Disubstituted ureas are useful chemical intermediates in the synthesis of pharmaceuticals, agricultural chemicals, and in dye chemistry. They are also used as antioxidants in gasoline and additives in plastics. As an alternative to their synthesis by phosgenation or oxidative carbonylation, they can be synthesized by the reaction

of CO_2 with primary amines, with different catalytic systems. Basic ionic liquid (1-*N*-butyl-3-methylimidazolium hydroxide ([BMIM]OH)) could be also used as the catalyst.

The interaction of CO_2 with several N-nucleophiles (e.g., amines) has a great synthetic relevance as it is a key step toward the formation of N–C bonds, when the carbamic acids generated in situ react with electrophiles such as organic halides or alcohols (Eqs. 10 and 11), to obtain carbamates RHN–C(=O)OR′, R, and R′ = alkyl or aryl. The utilization of CO_2 for the synthesis of these derivatives is a safer alternative to toxic phosgene.

$$R_1R_2NH + CO_2 + R_3X + \text{Base} \rightarrow R_1R_2N - C(=O)OR_3 + HX(\text{Base}) \quad (10)$$

$$RNH_2 + CO_2 + R'OH \rightarrow RNH - C(=O)OR' + H_2O \quad (11)$$

Carbamates find a wide application in the chemical, pharmaceutical, and agrochemical industries, with a market of several Mtons/year.

Organic Carbonates

Linear and cyclic carbonates are industrially relevant chemicals, which incorporate CO_2 via catalytic routes. The most relevant chemicals are the following: dimethyl carbonate (DMC), diphenyl carbonate (DPC), ethylene carbonate (EC), and styrene carbonate (SC). The latter is useful intermediates for polycarbonate production, while DMC, EC, and propylene carbonate (PC) are widely used as nontoxic aprotic polar solvents and as electrolytes in Li-ion batteries. Moreover, linear carbonates are important alkylating and carbonylating agents (Sakakura et al. 2007). DMC is of interest as an additive to diesel fuel, increasing the octane number and reducing the particulate emissions from engines. Current DMC worldwide production is about 0.5 million tons/year, but if DMC will be used as gasoline additive, its market would reach the Mtons/year.

Traditional routes for the industrial production of linear carbonates, especially DMC, utilize either phosgene or carbon monoxide, causing problems due to toxicity or corrosion. The synthesis of linear carbonates by means of urea or cyclic carbonates, as well as by direct one-step CO_2 reaction with alcohols, is much safer and cleaner than other processes, although thermodynamically unfavorable.

The alcoholysis of urea has the potential to be integrated with a urea plant for optimizing ammonia recycling. The use of catalytic distillation can intensify the process. The formation of several side products, which results in poor selectivity, is one of the major drawbacks of using this reaction. The indirect transesterification route represents a method for achieving high purity in DMC and DPC production. The economic advantage of this method mainly relies on (i) reactant costs; (ii) enhancement of catalyst productivity, separation, and recycling; and (iii) higher conversion by a drift in thermodynamic constraints. The advantage of the direct reaction is that it does not depend on the demand and supply balance of the

coproducts formed in the indirect routes (ammonia or glycols). The key issue to advance this green process and related engineering will be either a proper choice of more stable, active, and selective catalytic systems or a new approach to eliminate water by pervaporation or separation technology with mesoporous silica, polyimide–silica, and polyimide–titania hybrid membranes.

Oxiranes and oxetanes undergo cycloaddition with CO_2 to give five- and six-membered cyclic carbonates. This synthesis is selective, but homo- and copolymerization can also take place. Synthesis of five-membered carbonates occurs by oxidative carboxylation of alkenes. In the presence of CO_2, the dehydration of 1,2-diols gives cyclic carbonates. A wide range of catalysts recently developed for the synthesis of cyclic carbonates from CO_2 and oxiranes can be classified as follows: (i) alkali metal halides (KCl, KI, LiBr, etc.), (ii) ammonium or phosphonium salts, (iii) metal *salen* complexes, and (iv) solid or immobilized catalysts (in particular, amine-functionalized silica catalysts) to facilitate recovery and recycling without affecting activity. Recently, the carboxylation of oxiranes was carried out in ionic liquids (i.e., imidazolium salts) as solvents and/or catalysts, resulting in deep effects on the reaction rate and product selectivity.

The oxidative carboxylation of carbon double bonds into five-membered cyclic carbonates has been tested on alkenes such as ethene, propene, and styrene, using different catalysts. This oxidative methodology has a great potential, starting from cheap and easily available reagents and would be inherently safer due to the presence of CO_2.

Cyclic carbonates are widely used as high-boiling point aprotic polar solvents, electrolytes in secondary batteries, precursors for polycarbonates and polyurethanes, and intermediates in the production of fine chemicals and pharmaceuticals (Fig. 11).

CO_2 in Reforming Reactions and as Selective Oxidant

Syngas, e.g., a mixture of CO/H_2, is one of the major petrochemical building blocks and is commercially produced by hydrocarbon (mainly methane) steam reforming, partial oxidation, or a combination of the two processes. An alternative route is to produce syngas by reforming methane with carbon dioxide. This process is indicated as “dry” reforming, in contrast to “wet” reforming by steam. Combination of “dry” and “wet” reforming and/or partial oxidation is instead indicated as “mixed” reforming.

$$CH_4 + CO_2 \leftrightharpoons 2CO + 2H_2 \tag{12}$$

$$CH_4 + H_2O \leftrightharpoons CO + 3H_2 \tag{13}$$

The CO/H_2 ratio produced in the dry reforming is 1, but the RWGS reaction occurs simultaneously, and thus the effective ratio is less than 1 and the CO_2 conversion greater than that of methane. The CO/H_2 ratio is appropriated for FT synthesis of alkanes (which requires a ratio between 0.5 and 1) and alkenes (ratio 0.5). This is a

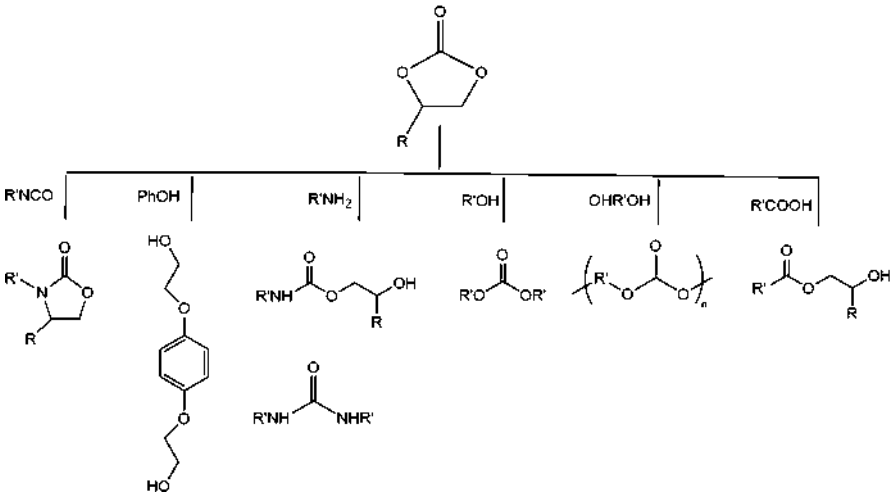

Fig. 11 Applications of cyclic carbonates in organic synthesis

clear advantage over the conventional production of syngas for FT reaction, which uses a combination of steam reforming and partial oxidation.

A further great advantage is that often CO_2 is present together with methane in natural gas deposits. Therefore, using dry reforming at or near wellhead coupled to FT would produce liquid hydrocarbons that are easy to transport from remote areas (stranded gas). The additional potential advantage is that the process converts two of the principal gases responsible for greenhouse effect. It should be remarked, however, that CO_2 is typically reintroduced in the well to increase the deposit exploitation. Biogas upgrading is another target application for dry reforming.

The dry reforming is a strong endothermic reaction and requires temperatures above 700 °C to have reasonable conversions. A key problem is how to supply the energy needed to sustain the reaction, which under industrial conditions is limited from this rate of heat transfer. A typical reactor configuration is to use packed tubes directly placed inside the furnace. Advances in this area regard mainly the reactor design to improve efficiency of this heat transfer.

In principle, catalysts that are active for steam reforming also work for dry reforming. However, since the steam-to-carbon ratio is lower for dry (or mixed) reforming than for steam reforming, the risk of carbon formation is considerably higher. As a result, research efforts have focused on catalysts, which show high activity to synthesis gas formation and are resistant to coking, thus displaying stable long-term operation. Especially the rare earth elements (in particular La and Ce) have been identified as suitable candidates for enhancing catalyst performance.

An important factor for catalyst reactivity and stability lies in the catalyst's resistance to carbon deposits, which could lead to active site blocking. Apart from directly altering the metal's properties by additives, an alternative route is to use a support, which suppresses carbon deposition. This can be achieved with so-called

oxy-transporters, such as ZrO_2 or CeO_2, which are capable of oxidizing deposited carbon. Additionally, because of their oxygen-conducting properties, these supports can actively participate in the catalytic reaction by oxidizing or reducing reaction intermediates.

Carbon is one of the principal mechanisms of catalyst deactivation, even if it should be considered that in dry reforming with respect to steam reforming, the carbon is more easily oxidized. Carbon derives from two main reactions:

$$\text{Methane decomposition} : CH_4 \rightarrow C(s) + 2H_2 \tag{14}$$

$$\text{CO disproportionation} : 2CO \rightarrow C(s) + CO_2 \tag{15}$$

To design a catalyst to be active and stable, it is necessary to consider both thermodynamic and kinetic aspects. The first aspect requires to optimize the key process variables, but within the constraints of economic feasibility. For example, low methane concentrations minimize Eq. 12 but also inhibit the main reforming reaction. For this reason, typical reaction conditions are those in which carbon formation is thermodynamically feasible. Therefore, it has to operate to minimize reactions 10 from the kinetic point of view. On Ni-based catalysts, carbon formation is minimized by adding small amounts of an alkali metal to the catalyst. Doping with MoO_3 also reduces the carbon formation. A special case is the carbon deposition inhibition by "controlled passivation" of the catalyst surface (noble metal) by sulfur, the basis for the Haldor Topsøe A/S SPARG process.

Sintering is a further important aspect determining the lifetime of the catalyst. The stability of nickel-based catalysts can be enhanced by addition of basic and rare earth metal-oxide promoters.

The tri-reforming process is a synergetic combination of endothermic CO_2 reforming (Eq. 11), steam reforming (Eq. 12), and exothermic partial oxidation of CH_4 (Eqs. 18 and 19) in a single reactor for effective production of industrially useful syngas (Song 2006):

$$CH_4 + CO_2 \rightarrow 2CO + 2H_2 \tag{16}$$

$$CH_4 + H_2O \rightarrow CO + 3H_2 \tag{17}$$

$$CH_4 + ½O_2 \rightarrow CO + 2H_2 \tag{18}$$

$$CH_4 + 2O_2 \rightarrow CO_2 + 2H_2O \tag{19}$$

Tri-reforming cannot only produce synthesis gas ($CO + H_2$) with desired H_2/CO ratios (1.5–2.0) but also could eliminate carbon formation, which is usually a serious problem in the CO_2 reforming of CH_4. These two advantages have been demonstrated by tri-reforming of CH_4. A fixed-bed flow reactor operating at 850 °C with supported nickel catalysts was used.

An area of emerging interest, particularly in patents, is the use of nonthermal plasma (NTP) to activate both CO_2 and CH_4 and produce syngas under quite mild

conditions. Plasma, i.e., ionized gas, is usually sustained in electrical discharges by the application of electric fields. The energy is transferred, in the first instance, to free electrons. It is subsequently distributed through collisions to the feedstock molecules (CO_2 and CH_4) and their decomposition products. The sum of all possible excitation mechanisms leads to the key aspect of NTP: the injected energy is not equally distributed across all the species and their degrees of freedom. In particular, heating of the gas can remain low (due to the large mass difference between the colliding electron and molecule), while certain molecular vibrations are highly excited. The latter will promote bond breaking and dissociation. It is possible to obtain up to 90 % energy efficiency in plasma chemical reduction of pure CO_2 (in the absence of CH_4) into CO. In the CO_2 reforming with methane, conversions typically lower than 50 % were obtained, in combination with catalysts such as supported Pd catalysts, nickel ferrite nanoparticles, and Ni-based supported catalysts. However, conventional-type catalysts have been used. The challenge is to develop specific catalysts tailored to operate optimally in synergy with the high reactive species present in the plasma.

The dissociation of CO_2 on catalyst surface could produce active oxygen species. Some heterogeneous chemical reactions can benefit from using CO_2 as a mild oxidant or as a selective source of "oxygen" atoms. Oxidative dehydrogenation (ODH) of alkanes is a relevant example. With respect to ODH with oxygen, the use of CO_2 allows forming CO as by-product and a better control of the heat of reaction but requires more severe reaction conditions:

$$C_nH_{2n+2} + CO_2 \rightarrow C_nH_{2n} + CO + H_2O \tag{20}$$

Ethane ODH is the most interesting application, for both the interest in producing ethylene, the need of high temperatures in ethane dehydrogenation due to thermodynamic limitations, and the low selectivities observed in ODH with oxygen. An ethylene yield of about 55 % at relatively mild reaction temperatures (650 °C) could be obtained using Cr_2O_3/SiO_2 catalysts modified by some acidic and basic oxides.

ODH of propane to propylene was also extensively studied. The equilibrium conversion of C_3H_8 in the presence of CO_2 is much higher than that without CO_2. The catalysts studied for this reaction were also mainly based on Cr.

Another relevant case of using CO_2 as a mild oxidant is the conversion of ethylbenzene to styrene. Styrene is an important monomer required for the production of polystyrene and copolymer blends. It is currently produced by the dehydrogenation of ethylbenzene over iron oxide catalysts (Fe_2O_3–K_2O–CeO_2 with additives) in the presence of large excess steam. This reaction suffers of many drawbacks, but the addition of CO_2 promotes the reaction. KRICT (Korea Research Institute of Chemical Technology) developed a novel process for dehydrogenation of ethylbenzene to produce styrene using carbon dioxide as soft oxidant, so-called KRICT-DECSO process. The dehydrogenation catalyst employed comprises oxygen-deficient iron oxide and many promoters with transition metal oxides. Chon International Co. developed SODECO$_2$ (Styrene from Oxidative Dehydrogenation via CO_2) technology based on KRICT studies. A Fe_2O_3–V_2O_5 supported on

Al_2O_3–ZrO_2 and doped with Mn (activity promoter), Mo and Sb (stability promoter), Ca and Mg (structural stabilizer) is used as the catalyst.

Also the liquid-phase air oxidation of p-xylene to terephthalic acid (PTA) (a large-scale chemical) using commercial Co/Mn/Br catalysts and acetic acid as the solvent (reaction temperature 195 °C) could be promoted by adding CO_2. Introduction of CO_2 in the O_2 feed increases both the yield and selectivity toward PTA, with also an increase of the product quality. This effect is more marketable when the catalyst is modified with an alkali and/or transition metal additives. The effect is probably related to the formation of a peroxocarbonate species [$CO_4^{=}$] which either participate in the selective oxidation or simple acts as reservoir to enhance the amount of dissolved oxygen in solution, improving the oxidation effectiveness.

The promotion effect of CO_2 on both activity and selectivity is also present in the liquid oxidation of other alkylaromatics, for example, in p-toluic acid oxidation to PTA, in ethylbenzene oxidation to acetophenone and benzoic acid, and in the oxidation of p-methylanisole.

CO_2 modifies the selectivity also in gas-phase oxidation. Using iron and molybdenum containing zeolite, the introduction of CO_2 in the feed increases both the conversion and the selectivity in the gas-phase selective oxidation of toluene, xylenes, and ethylbenzene to the corresponding aldehydes and acids.

CO_2 may thus have multiple roles in catalytic industrial processes. It is an interesting feedstock and a green solvent (supercritical CO_2) but may also have other uses. It may act as modifier of the catalytic behavior, it allows safer reaction conditions (as ballast to avoid explosive mixtures), it may be used to modify the properties of solvents (CO_2-expanded solvents (Subramaniam 2010)) and particularly O_2 solubility, it can tune and control the surface properties (oxidation state), and it can reduce the formation of carbonaceous species.

CO_2 Utilization in Biocatalytic Routes and to Reduce Impact of Bioprocesses

There are several emerging biocatalytic industrial routes for CO_2 valorization. Evonik is developing a CO_2-based acetone fermentation process using industrial waste gas streams that contain carbon monoxide (CO) and hydrogen (H_2) in addition to CO_2. They use genetically modified acetogens, e.g., bacteria strains (*Clostridium ljungdahlii*, *C. carboxidivorans*, and *C. aceticum*) that are able to utilize CO_2. The stage of development is the successful acetone production and the scale-up from flask into lab fermenter.

Bio-succinic acid from glucose and CO_2 is another interesting product derived from engineering strategies. At least five groups are developing (semi)commercial plants for bio-succinic acid. Bioamber is starting a facility in Pomacle, France, with an annual capacity of 2000 tons. Their process uses an *Escherichia coli* strain developed specifically to produce succinic acid, with wheat-derived glucose currently being used as the substrate. DSM (now Sabic) is also actively investigating the production of bio-succinic acid. In early 2008, DSM formed a partnership with

France's Roquette Frères to develop bio-succinic acid, and the two companies have been supplying kilo-scale samples for over a year from a pilot plant at Roquette's site (Lestrem, France). Myriant is building a commercial-scale facility in Louisiana using *E. coli* and unrefined sugar as a feedstock. BASF linked up with Purac subsidiary CSM is planning to produce bio-succinic acid using a BASF-developed bacterial strain (*Basfia succiniciproducens*) and glycerine or glucose as a feedstock. Finally, Mitsubishi Chem. Co. has also developed its own process for making bio-succinic acid from biomass.

Another interesting metabolic pathway is the production of longer-chain alcohols from CO_2. Mitsubishi Chemical Holdings Corporation is developing the original results of UCLA researchers on CO_2 conversion, in particular, for the production of butanol and hexanol by applying genetic manipulation techniques to modify algae. Liao at UCLA developed engineered bacteria to convert CO_2 into alcohols, in particular, genetically modified *E. coli* bacteria to produce various alcohols and modified cyanobacterium to produce isobutanol (Zhang et al. 2008). Using a nonnatural metabolic engineering approach, the branched-chain amino acid pathways are extended to produce abiotic longer-chain keto acids and alcohols by engineering the chain elongation activity of 2-isopropylmalate synthase and altering the substrate specificity of downstream enzymes through rational protein design.

An interesting possibility for CO_2 valorization is through syngas fermentation. Although industrial developments are still on the use of syngas (CO/H_2) rather than CO_2, the modification of the path could lead to direct use of CO_2. It is known that CODH from *C. thermoaceticum* (a Ni- and Fe-containing metalloenzyme) catalyzes the reversible oxidation of CO to CO_2. It is possible to couple this enzyme with a semiconductor such as TiO_2, which produces the electrons necessary for the reduction. A hybrid enzyme–nanoparticle system was used to achieve an efficient CO_2 to CO reduction using visible light as the energy source. In a different approach, several purple non-sulfur bacteria were used to convert CO to H_2 in a process similar to the WGS reaction. An alternative possibility is represented from coupling syngas fermentation to a plasma approach to convert CO_2 to CO or CH_4/CO_2 mixtures (e.g., deriving from biogas) to a mixture, which may be treated by syngas fermentation processes, which are at a semicommercial level. There are several microorganisms which can produce fuels and chemicals by syngas fermentation. These microorganisms are mostly known as acetogens including *C. ljungdahlii*, *C. autoethanogenum*, *Eurobacterium limosum*, etc. (Henstra et al. 2007). Most use the Wood–Ljungdahl pathway. The fermentation of syngas to ethanol by *C. ljungdahlii* was developed into a commercial process that combines biomass gasification, syngas fermentation, and distillation of ethanol from the reactor effluent. LanzaTech process of CO fermentation is currently applied on a 0.4 Ml demonstration facility (Shanghai, China) using steel mill off-gas from a working steel mill. INEOS Bio also began in 2011 the construction of their first commercial-scale plant, the Indian River BioEnergy Center in Florida.

The integration of CO_2 valorization routes in the frame of production schemes of biorefineries/biofactories (Perathoner and Centi 2014a; Lanzafame et al. 2014b) is a necessary direction to reduce the carbon footprint and environment impact of these

productions and increase their added value as well. Some of the possible routes have been discussed above, but further are possible in developing integrated solar biorefineries schemes (Lanzafame et al. 2014b), e.g., in production schemes integrating the use of waste and CO_2 to enhance the production and also through the use of solar light, for example, to convert CO_2 to valuable products such as methanol.

Introduction of Renewable Energy in the Chemical Production Chain Through CO_2 Utilization

An indirect, but relevant, way to address GHG emissions is to improve efficiency of use of resource and energy in production processes. Increasing the use of renewable resources is between the relevant goals for this objective, but the direct use of renewable energy is not effective, for example, in chemical industry, for two main reasons:

1. Most of renewable energy sources produce electrical energy, which accounts for only a small fraction (10–15 % typically) of the energy input in the actual chemical production.
2. These renewable energy sources are discontinuous, while a continuous input is necessary in process and chemical industries.

The most effective way is to produce raw materials (utilized in process industry) from the conversion of CO_2 utilizing renewable energy in the conversion process. The concept is exemplified in Fig. 12. The reaction of CO_2 catalytic hydrogenation to methanol with renewable H_2 is a possibility which has the potential to be used:

- As chemical, which may be introduced directly in the chemical production chain or after the eventual conversion to other building blocks for petrochemistry (light olefins, e.g., (Capoferri et al. 2011)); also note that these are products already in large use (drop-in products) and do not require large investments for their use differently from novel chemicals.
- As liquid energy carrier, which can be easily stored and distributed, bypassing the issue on renewable energy production intermittency and enabling the possibility to use unexploited remote sources or excess of renewable energy production; both these are current relevant targets for R&D in the area of renewable energy.

With respect to bio-routes, CO_2 utilization paths are not in opposition but in integration to move to a low-carbon economy, as commented in the previous section. Realizing a sustainable, resource-efficient, and low-carbon economy requires integrating in the chemical production chain other forms of renewable energy than those associated to the use of biomass.

Preliminary studies (Barbato et al. 2014; Perathoner and Centi 2014a) evidence how this is an economically feasible route. The concept of using reaction of CO_2 conversion to methanol to trade renewable energy (after incorporation in a suitable liquid chemical such as methanol) allows to exploit remote production of energy

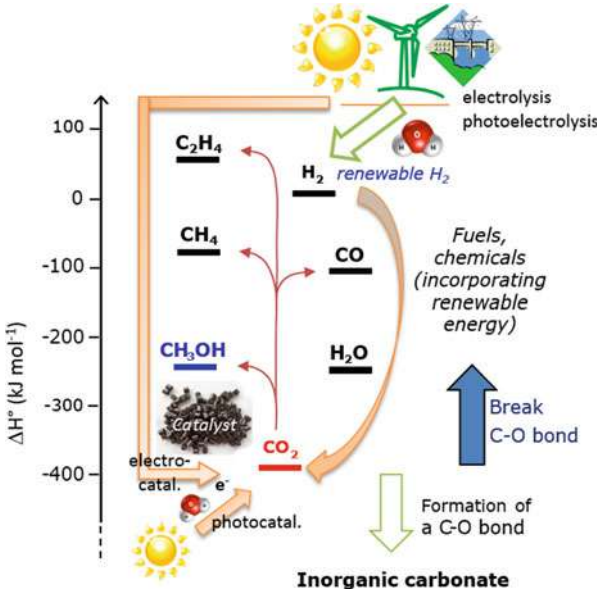

Fig. 12 Energy scale in some of the products of CO_2 conversion, with illustration of the different routes by which renewable energy could be introduced in the carbon dioxide molecule to produce fuels or chemicals

(by hydropower, solar, etc.), which otherwise cannot be utilized, thus promoting the transition to a new low-carbon economy. The technology can be considered nearly ready for commercialization, although scale-up aspects in electrolyzers have to be solved and improvements in CO_2 conversion catalysts and in stability of the electrolyzers, particularly under high-pressure operations, would be necessary. In a longer term (approximately 15 years), it will be possible to reduce the number of steps, realizing inverse fuel cells or directly solar fuels cells.

Future Directions

The effect of GHGs on global warming is becoming a problem of increasing relevance (Li et al. 2014), and there is thus an increasing need to find new and improved solutions to limit the anthropogenic emission of methane, nitrous oxides, and carbon dioxide, while for other very powerful greenhouse gases, such as fluorocarbons, some mitigation strategies are already in place.

This short overview on the reduction of greenhouse gas emissions by catalytic processes has demonstrated how these technologies can be an effective possibility for limiting the increasing tropospheric concentration of GHGs and reducing their contribution to global warming, but the more extensive use of these technologies depends on the environmental regulations that will be adopted to control GHG emissions from the variety of possible sources.

Catalytic technologies should be useful in the (1) reduction of anthropogenic emissions of non-CO_2 GHG (mainly N_2O and CH_4) and (2) reduction or conversion of CO_2. In the latter case, it was shown how a problem may be converted (reducing

CO_2 emissions) to an opportunity for more sustainable and innovative chemical and energy processes.

The challenge for methane and nitrous oxide control by catalytic technologies is the development of more active catalysts at low temperature in the presence of the other typical components of the emissions. Control of the characteristics of the support is a key step toward this objective of low-temperature activity.

Several opportunities exist for the conversion of carbon dioxide to chemicals, particularly polymers or organic intermediates. However, the challenge is the possibilities of the conversion to fuels, because the market for chemicals is two orders of magnitude lower with respect to that for fuels. It was shown how this path has a large potential, several Gtons of CO_2 eq., and is as a relevant pillar of the strategies to move to a low-carbon economy, as well as for the future of sustainable chemical production.

The requisites for these objectives are to (i) minimize as much as possible the consumption of hydrogen (or hydrogen sources), (ii) produce fuels that can be easily stored and transported, and (iii) use renewable energy sources. From this perspective, the preferable option is to produce liquid fuels using solar energy to produce the protons and electrons necessary for the reaction of CO_2 reduction. Integration between CO_2 use and bioeconomy, for example, in developing integrated solar biorefineries, is another relevant aspect to reach above objectives.

The conversion of CO_2 to methanol or syngas is already at a pilot plant scale and may thus be commercially implemented. The economy of the process will strongly depend on the value (or negative value) of CO_2 and the availability (and cost) of energy and hydrogen. These aspects will greatly depend on a number of variables.

Hydrogenation of CO_2 to form fuels is the most investigated area. By coupling conventional methanol process to RWGS, it is possible to feed even pure CO_2 to produce methanol. This reaction scheme has been implemented at a pilot plant level, and results are quite encouraging. A further step would be to use multifunctional catalysts to directly produce DME, which is a preferable energy carrier.

Hydrogenation of carbon dioxide to hydrocarbons is possible, but requires much higher consumption of H_2. Conversion of CO_2 to other oxygenates such as ethanol and DME is attractive, but further development of the catalysts is necessary. There is great interest in the conversion of carbon dioxide to formic acid, but a complicating factor is the availability of efficient technologies to use formic acid as energy carrier, as well as the toxic character of formic acid.

Dry reforming of methane with CO_2 is a known technology. Tri-reforming is an extension of the concept to operate autothermically and with the advantage of not requiring a pure CO_2 stream to operate. Pilot plant studies have shown stability of operations (using noble metals supported on MgO) for over 7000 h, although larger-scale demonstration could be necessary.

There are also various processes at an earlier stage, particularly biological and photo-/electrocatalytic processes, which need to be studied representing the future in medium to long term. Therefore, the area of carbon dioxide conversion to fuels and chemicals is a very active R&D sector and represents a challenging possibility for companies to develop complementary strategies to CCS to reduce greenhouse gas emissions.

References

Ahrens M, Scholz G et al (2013) Catalytic hydrodefluorination of fluoromethanes at room temperature by silylium-ion-like surface species. Angew Chem Int Ed 52:5328–5332

Alvarez RA, Pacala SW et al (2012) Greater focus needed on methane leakage from natural gas infrastructure. Proc Natl Acad Sci U S A 109:6435–6440

Ampelli C, Perathoner S, Centi G (2015) CO_2 utilization: an enabling element to move to a resource and energy-efficient chemical and fuel production. Phil Trans A. doi:10.1098/rsta.2014.0177

Aresta M (ed) (2010) Carbon dioxide as chemical feedstock. Wiley-VCH, Weinheim

Aresta M, Dibenedetto A (2007) Utilisation of CO_2 as a chemical feedstock: opportunities and challenges. Dalton Trans 28:2975–2992

Barbato L, Centi G et al (2014) Trading renewable energy by using CO_2: an effective option to mitigate climate change and increase the use of renewable energy sources. Energy Technol 2:453–461

Barton EE, Rampulla DM, Bocarsly AB (2008) Selective solar-driven reduction of CO_2 to methanol using a catalyzed p-GaP based photoelectrochemical cell. J Am Chem Soc 130 (20):6342–6345

Behrens M (2014) Heterogeneous catalysis of CO_2 conversion to methanol on copper surfaces. Angew Chem Int Ed 53:12022–12024

Bensaid S, Centi G et al (2012) Towards artificial leaves for solar hydrogen and fuels from carbon dioxide. ChemSusChem 5:500–521

Capoferri D, Cucchiella B et al (2011) Catalytic partial oxidation and membrane separation to optimize the conversion of natural gas to syngas and hydrogen. ChemSusChem 4:1787–1795

Cargnello M, Delgado Jaén JJ et al (2012) Exceptional activity for methane combustion over modular Pd@CeO2 subunits on functionalized Al2O3 Science 337:713–717

Caulton DR, Shepson PB et al (2014) Toward a better understanding and quantification of methane emissions from shale gas development. Proc Natl Acad Sci U S A 111:6237–6242

Cavani F, Centi G et al (2009) Sustainable industrial chemistry. Wiley VCH, Weinheim

Centi G, Perathoner S (2004) Heterogeneous catalytic reactions with CO_2: status and perspectives. Stud Surf Sci Catal 153:1–8

Centi G, Perathoner S (2009) Opportunities and prospects in the chemical recycling of carbon dioxide to fuels. Catal Today 148:191–205

Centi G, Perathoner S (2010) Towards solar fuels from water and CO_2. ChemSusChem 3:195–208

Centi G, Perathoner S (eds) (2014) Green carbon dioxide: advances in CO_2 utilization. Wiley, Hoboken

Centi G, Vazzana F (1999) Selective catalytic reduction of N_2O in industrial emissions containing O_2, H_2O and SO_2: behavior of Fe/ZSM-5 catalysts. Catal Today 53:683–693

Centi G, Perathoner S, Vazzana F (1999) Catalytic control of non-CO_2 greenhouse gases. ChemTech 29(12):48–55

Centi G, Generali P et al (2000) Removal of N_2O from industrial gaseous streams by selective adsorption over metal-exchanged zeolites. Ind Eng Chem Res 39:131–137

Centi G, Perathoner S, Rak ZS (2003a) Reduction of greenhouse gas emissions by catalytic processes. Appl Catal B Environ 41:143–155

Centi G, Arena GE, Perathoner S (2003b) Nanostructured catalysts for NOx storage-reduction and N_2O decomposition. J Catal 216:443–454

Centi G, Perathoner S et al (2005) Performances of Fe-[Al, B] MFI catalysts in benzene hydroxylation with N_2O. Catal Today 110:211–220

Centi G, Perathoner S et al (2006) Characterization and reactivity of Fe-[Al, B] MFI catalysts for benzene hydroxylation with N_2O. Appl Catal A Gen 307:30–41

Centi G, Quadrelli EA, Perathoner S (2013) Catalysis for CO_2 conversion: a key technology for rapid introduction of renewable energy in the value chain of chemical industries. Energy Environ Sci 6:1711–1731

Darensbourg DJ (2007) Making plastics from carbon dioxide: salen metal complexes as catalysts for the production of polycarbonates from epoxides and CO_2. Chem Rev 107:2388–2410
Das S, Wan Daud WMA (2014) A review on advances in photocatalysts towards CO_2 conversion. RSC Adv 4:20856–20893
Davis BH, Occelli ML (eds) (2009) Advances in Fischer-Tropsch synthesis, catalysts, and catalysis. CRC Press/Taylor & Francis Group, Boca Raton
De Falco M, Iaquaniello G, Centi G (2013) CO_2: a valuable source of carbon. Springer, London
Dorner RW, Hardy DR et al (2010) Heterogeneous catalytic CO_2 conversion to value-added hydrocarbons. Energy Environ Sci 3:884–890
EPA (US Environmental Protection Agency) (2010) Available and emerging technologies for reducing greenhouse gas emissions from the petroleum refining industry. EPA, Washington, DC
Ertl G, Knozinger H, Weitkamp J (eds) (1999) Environmental catalysis. Wiley-VCH, Weinheim
Fukuoka S, Fukawa I et al (2010) A novel non-phosgene process for polycarbonate production from CO_2: green and sustainable chemistry in practice. Catal Surv Asia 14:146–163
Hensen EJM, Zhu Q et al (2005) Selective oxidation of benzene to phenol with nitrous oxide over MFI zeolites. J Catal 233:123–135
Henstra AH, Sipma J et al (2007) Microbiology of synthesis gas fermentation for biofuel production. Curr Opin Biotechnol 18:200–206
Hevia MAG, Perez-Ramirez J (2008) Optimal hydrocarbon selection for catalytic N_2O reduction over iron-containing ZSM-5 zeolite. Environ Sci Technol 42:8896–8900
Heyn RH, Jacobs I, Carr RH (2014) Synthesis of aromatic carbamates from CO_2: implications for the polyurethane industry. Adv Inorg Chem 66:83–115
IEA (International Energy Agengy) (2013) Technology roadmap energy and GHG reductions in the chemical industry via catalytic processes. IEA, Paris
Kapteijn F, Rodriguez-Mirasol J, Moulijn JA (1996) Heterogeneous catalytic decomposition of nitrous oxide. Appl Catal B Environ 9:25–64
Karakurt I, Aydin G, Aydiner K (2011) Mine ventilation air methane as a sustainable energy source. Renew Sustain Energy Rev 15:1042–1049
Keller T (2011) Reducing N_2O emissions from nitric acid plants. Nitrogen + Syngas 313:33–35
Kim J, Maiti A et al (2013) New materials for methane capture from dilute and medium-concentration sources. Nat Commun 4:1694
Lanzafame P, Centi G, Perathoner S (2014a) Catalysis for biomass and CO_2 use through solar energy: opening new scenarios for a sustainable and low-carbon chemical production. Chem Soc Rev 43:7562–7580
Lanzafame P, Centi G, Perathoner S (2014b) Evolving scenarios for biorefineries and the impact on catalysis. Catal Today 234:2–12
Lee S-J, Ryu I-S et al (2011) A review of the current application of N_2O emission reduction in CDM projects. Int J Greenhouse Gas Control 5:167–176
Li L, Xu J, Hu J, Han J (2014) Reducing nitrous oxide emissions to mitigate climate change and protect the ozone layer. Environ Sci Technol 48:5290–5297
Liu W, Guo D, Xu X (2012) Research progress of palladium catalysts for methane combustion. China Pet Process Petrochem Technol 14:1–9
Lu X, Leung DYC et al (2014) Electrochemical reduction of carbon dioxide to formic acid. ChemElectroChem 1:836–849
Manzer LE, Nappa MJ (2001) The key role of catalysis in the phase-out of chlorofluorocarbons (CFCs). Appl Catal A Gen 121:267–274
Menini C, Park C et al (2000) Catalytic hydrodehalogenation as a detoxification methodology. Catal Today 62:355–366
Montzka SA, Dlugokencky EJ, Butler JH (2011) Non-CO_2 greenhouse gases and climate change. Nature 476:43–50
Notte PP (2000) The AlphOx process or the one-step hydroxylation of benzene into phenol by nitrous oxide. Understanding and tuning the ZSM-5 catalyst activities. Top Catal 13:387–394

Oenema O, Ju X et al (2014) Reducing nitrous oxide emissions from the global food system. Curr Opin Environ Sustain 9–10:55–64
Olah GA, Goeppert A, Surya Prakash GK (2009a) Beyond oil and gas: the methanol economy, 2nd edn. Wiley-VCH, Weinheim
Olah GA, Goeppert A, Prakash GKS (2009b) Chemical recycling of carbon dioxide to methanol and dimethyl ether: from greenhouse gas to renewable, environmentally carbon neutral fuels and synthetic. J Org Chem 74:487–498
Özgen KC, Ruiz FA et al (2011) Coal mine methane: a review of capture and utilization practices with benefits to mining safety and to greenhouse gas reduction. Int J Coal Geol 86:121–156
Pachauri RK, Meyer L (eds) (2014) Climate change 2014: synthesis report. Cambridge University Press, Cambridge/New York
Parmon VN, Panov GI et al (2005) Nitrous oxide in oxidation chemistry and catalysis: application and production. Catal Today 100:115–131
Perathoner S, Centi G (2014a) A new scenario for green & sustainable chemical production. J Chin Chem Soc 61:719–730
Perathoner S, Centi G (2014b) CO_2 recycling: a key strategy to introduce green energy in the chemical production chain. ChemSusChem 7:1274–1282
Pérez-Ramírez J, Kapteijn F et al (2003) Formation and control of N_2O in nitric acid production. Where do we stand today? Appl Catal B Environ 44:117–151
Perutz RN (2008) A catalytic foothold for fluorocarbon reactions. Science 321:1168–1169
Quadrelli EA, Centi G et al (2011) Carbon dioxide recycling: emerging large-scale technologies with industrial potential. ChemSusChem 4:1194–1215
Reade SP, Mahon MF, Whittlesey MK (2009) Catalytic hydrodefluorination of aromatic fluorocarbons by ruthenium N-heterocyclic carbene complexes. J Am Chem Soc 131:1847–1861
Sabater S, Mata JA, Peris E (2013) Hydrodefluorination of carbon-fluorine bonds by the synergistic action of a ruthenium-palladium catalyst. Nat Commun 4:3553–3560
Sakakura T, Choi JC, Yasuda H (2007) Transformation of carbon dioxide. Chem Rev 107:2365–2387
Schaefer M, Behrendt F, Hammer T (2010) Evaluation of strategies for the subsequent use of CO_2. Front Chem Eng Chin 4:172–184
Schwartsburd L, Mahon MF et al (2014) Mechanistic studies of the rhodium NHC catalyzed hydrodefluorination of polyfluorotoluenes. Organometallics 33:6165–6170
Schwartz WR, Ciuparu D, Pfefferle LD (2012) Combustion of methane over palladium-based catalysts: catalytic deactivation and role of the support. J Phys Chem C 116:8587–8593
Sobolev VI, Pirutko LV (2013) Catalysis for nitrous oxide abatement. Adv Chem Res 19:1–23
Song C (2006) Global challenges and strategies for control, conversion and utilization of CO_2 for sustainable development involving energy, catalysis, adsorption and chemical processing. Catal Today 115:2–32
Stolaroff JK, Bhattacharyya S et al (2012) Review of methane mitigation technologies with application to rapid release of methane from the arctic. Environ Sci Technol 46:6455–6469
Subramaniam B (2010) Gas-expanded liquids for sustainable catalysis and novel materials: recent advances. Coord Chem Rev 254:1843–1853
van Ham J, Baede APM et al (2000) Non-CO_2 greenhouse gases: scientific understanding, control and implementation. Springer/Kluwer, Heidelberg
von der Assen N, Bardow A (2014) Life cycle assessment of polyols for polyurethane production using CO_2 as feedstock: insights from an industrial case study. Green Chem 16:3272–3280
Wallington TJ, Wiesen P (2014) N_2O emissions from global transportation. Atmos Environ 94:258–263
Wang F, Fu R et al (2013) Reactors used for catalytic combustion of methane. Adv Mater Res 634–638:798–804
Weber CL, Clavin C (2012) Life cycle carbon footprint of shale gas: review of evidence and implications. Environ Sci Technol 46:5688–5695

Whittlesey MK, Peris E (2014) Catalytic hydrodefluorination with late transition metal complexes. ACS Catal 4:3152–3159
Xiang Z, Cao D (2013) Porous covalent-organic materials: synthesis, clean energy application and design. J Mat Chem A 1:2691–2718
Yang Z, Yang G et al (2013) The direct hydroxylation of benzene to phenol catalyzed by Fe-ZSM-5 zeolite: a DFT and hybrid MP2:DFT calculation. Catal Lett 143:260–266
Yu H, Kennedy EM et al (2006) A review of CFC and halon treatment technologies – the nature and role of catalysts. Catal Surv Asia 10:40–54
Zhang K, Sawaya MR et al (2008) Expanding metabolism for biosynthesis of non-natural alcohols. Proc Natl Acad Sci U S A 105:20653–20658

Integrated Systems to Reduce Global Warming

Preben Maegaard and Anna Krenz

Contents

P. Maegaard (✉) • A. Krenz
Nordic Folkecenter for Renewable Energy, Hurup Thy, Denmark
e-mail: pm@folkecenter.dk; annakrenz@folkecenter.dk

W.-Y. Chen et al. (eds.), *Handbook of Climate Change Mitigation and Adaptation*,
DOI 10.1007/978-3-319-14409-2_50

Abstract

A future of renewable energy as a primary source for the world's energy society can no longer be ignored. As fossil fuel supplies diminish and the cost of atomic energy continues to rise, while there is no safe and well-documented solution to the deposition of nuclear waste, renewable energy can step in to provide feasible alternatives to energy demands. Renewables do pose significant challenges especially in addressing the fluctuating power supply that is inherent in their nature. Robust, integrated solutions using available, mature technologies have proven to be the solution to the challenges that wind and solar energy causes. Denmark has in the past and continues to be a leader in integrated renewable energy solutions. By 2014, Denmark with its 5.65 million inhabitants still was on the world top 10 list measured by accumulated wind power capacity; 39 % of the electricity came from the wind. In particular, the use of combined heat and power systems and the implementation of district heating have proven successful for Denmark and can be transferred elsewhere. This chapter seeks to explore questions surrounding the implementation of sustainable integrated solutions very concretely in relation to energy in general and renewable energy in particular.

Introduction

Increasing populations, urbanization, and sustained economic growth have resulted in strong rise of the demand for energy services, not least in the developing countries. Also growing concerns over climate change and the environmental impact of fossil fuels are causing many nations and communities to seek low-emission options.

Rapid technological progress has made renewable energy increasingly viable and cost-effective while contributing to security of energy supply. Worldwide, over 100 GW of new renewable energy capacity has been added every year from 2011to 2014, which is the equivalent to the total installed generation capacity of Brazil. Renewable energy has contributed with more than half of net capacity of the global power sector since 2011, which means that more new renewable energy capacity is being installed than new capacity in fossil and atomic energy combined. In China, 2013 marked the first time that new renewable electricity capacity surpassed new fossil fuel and atomic energy additions while solar deployment outpaced wind for the first time IRENA (2014).

Global investment in renewable generating capacity has increased fivefold 2004–2014 and has exceeded investment in new fossil-based power generation capacity. The rapid expansion in deployment is stepped up by declining costs of renewable energy technologies. Renewable energy is often competitive with conventional power at utility scale, and while this becomes more widely recognized, markets will expand; due to mass production and increased competitions, costs are expected to fall further. Furthermore renewable energy increases energy supply security, diversifies national energy mixes, mitigates the impact of price fluctuations, and reduces impact of geopolitical risks.

Especially in the face of climate change and resource scarcity, the world's energy system is on the verge of a major transformation. In order to massively reduce CO_2 emissions, there is a need to build a new energy system that is based on a greatly expanded use of renewable energies. It is almost certain that in 20 or 30 years the world will have a very different energy system from the one that currently exists.

In discussions of climate change, it is frequently stated that it is urgent to reduce CO_2 emissions by 40 % below what were 1990 levels by the year 2020 and further still to 95 % by 2050. The technological building blocks for the transition to a sustainable energy future already exist in the form of hydropower, decentralized cogeneration plants, wind turbines, large and small biogas plants, geothermal energy, several types of solar energy, and numerous types of biomass for energy purposes. The primary task, therefore, is to integrate the various forms of renewable energy, sometimes in combination with natural gas, in order to achieve the maximum utilization of renewable energy sources and supplies (Fig. 1).

The necessity to combine and integrate technologies is the reality of renewable energy since no single renewable energy source can sufficiently stand alone. A comprehensive future conversion to renewable energy requires mobilization of all forms of renewable energy installations, including both large and small plants. It is not enough to base development on technologies which are currently the cheapest, as this could lead to a unilateral deployment of large wind turbines in particular. Electricity generation from renewable energy sources, especially solar and wind, has a fluctuating nature. As these sources will be more and more integrated into existing power grids in large quantities, the fluctuations will become a main technical challenge. While the share of wind and solar energy on power grids increases, electric utilities must find solutions of balancing large amounts of the fluctuating

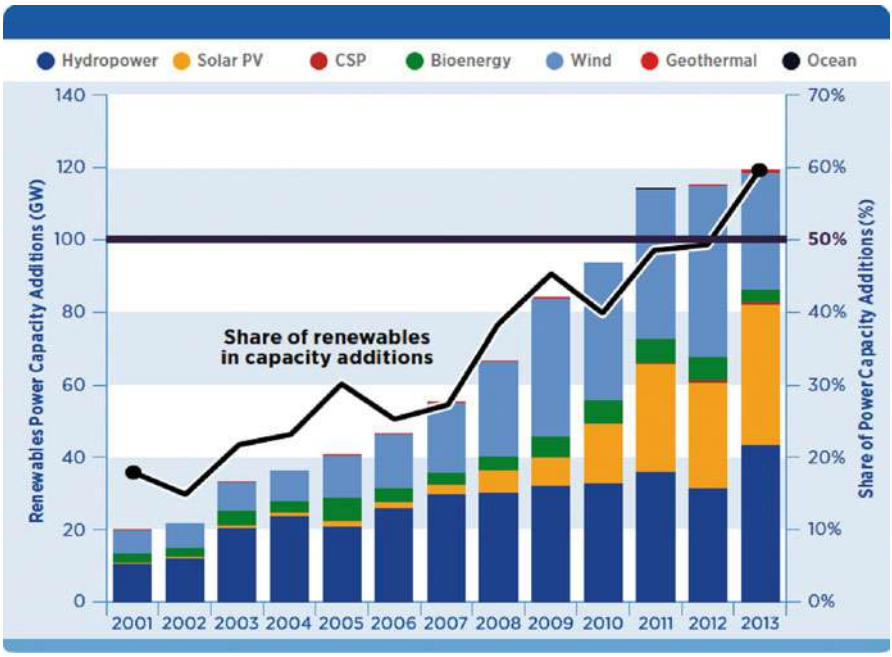

Fig. 1 Annual renewables capacity addition by technology (2001–2013) (Source: IRENA database)

renewables, in order to maintain grid balance and stability according to technical and regulatory tolerances (Fig. 2).

A persistent global attachment to the dominant fossil fuel-based energy system has limited the development of combined fluctuating solar and wind energies into coherent, autonomous systems. One consequence of this is that renewable energies, when generated in excess, remain unutilized or even wasted. Wind turbines in regions with high shares of wind energy may periodically be shut down when they produce too much power. Similarly, when combined heat and power (CHP) production coincides with excess wind energy, a surplus power capacity may occur. These problems will become increasingly frequent as more wind turbines feed power into the grid and more CHP systems are utilized. Electric boilers have proved to be a low-cost solution to capture excess energy, by using excess wind power in fuel-efficient combined heat and power systems.

A lack of balance between supply and demand of power means that there may periodically be an increasing problem of excess power from the combined supply from wind turbines, solar power, and CHP. The problem, however, needs not to exist but is caused by lack of political management and coordination.

"Renewables Global Futures Report 2013 (REN21)" registers six different types of measures within technology and operation for balancing fluctuating energy production and distribution.

Rank	State category SOLAR	P, W/c	State category WIND	P, W/c
1	Germany	445	Denmark	837
2	Liechtenstein	413	Spain	492
3	Italy	290	Sweden	463
4	Belgium	269	Portugal	451
5	Vatican City State	265	Ireland	443
6	Greece	239	Germany	429
7	Czech Republic	206	Canada	220
8	Luxembourg	182	Estonia	218
9	Australia	142	Austria	199
10	Bulgaria	140	USA	192
11	Slovenia	124	Cyprus	175
12	Spain	119	Greece	173
13	Japan	107	United Kingdom	167
14	Qatar	105	Netherlands	164
15	Slovakia	99	Norway	152
16	Denmark	93	Belgium	149
17	Switzerland	90	Italy	141
18	Austria	74	New Zealand	140
19	Malta	72	Australia	135
20	France	69	Romania	130
21	Romania	55	France	121
22	Israel	53	Luxembourg	106
23	United Kingdom	46	Dominica	101
24	Cyprus	41	Bulgaria	94
25	Netherlands	39	Lithuania	93
26	USA	38	Poland	88
27	Canada	35	Finland	83
28	Palau	33	Croatia	70
29	South Korea	29	China	57
30	Portugal	27	Cape Verde	51
31	New Zealand	27	Saint Kitts and Nevis	41
32	Lithuania	23	Turkey	39
33	Bahamas, The	22	Costa Rica	34
34	Tonga	21	Hungary	33
35	Serbia	21	Latvia	31
36	Cape Verde	20	Taiwan	26
37	Taiwan	17	Czech Republic	26
38	United Arab Emirates	14	Nicaragua	23
39	Barbados	14	Japan	21
40	Ukraine	14	Chile	20
41	China	14	Uruguay	18
42	Oman	13	Guyana	18
43	Thailand	12	Jamaica	18
44	Saint Kitts and Nevis	11	Brazil	18
45	Dominican Republic	10	Mongolia	17
46	Namibia	9	Mexico	17
47	Mauritius	9	India	17
48	Saudi Arabia	9	Morocco	15

Fig. 2 2014 global ranking of cumulative installed power (P) and Watt per capita (W/c) of wind and solar power in 48 nations. Exclusion of installed power waiting for grid connection (SolarSuperState Association)

Controlled Curtailment of Renewables

"Curtailment" is the prevailing strategy by many utilities to deal with excess amounts of wind power during periods of insufficient demand or uncurtailable generation from especially combined heat and power stations, CHP, with a commitment to supply of heating. In Denmark the share of CHP in electricity generation is up to 60 % which makes curtailment obsolete when electric boilers and heat pumps are installed and can use some of the excess power. In 2014, Denmark averaged about 39 % of its power generation from wind, with much higher peaks during some time periods, including a historic peak of 127 % of total national power demand at midnight on 22 December 2013 (Fig. 3).

Demand Response

"Demand response" covers a range of actions by utilities and the consumers to reduce power demand at specific times. It includes contracted load curtailment that is controllable by the utility within pre-established parameters and can also include time-of-use-based market prices to influence consumption decisions. Demand

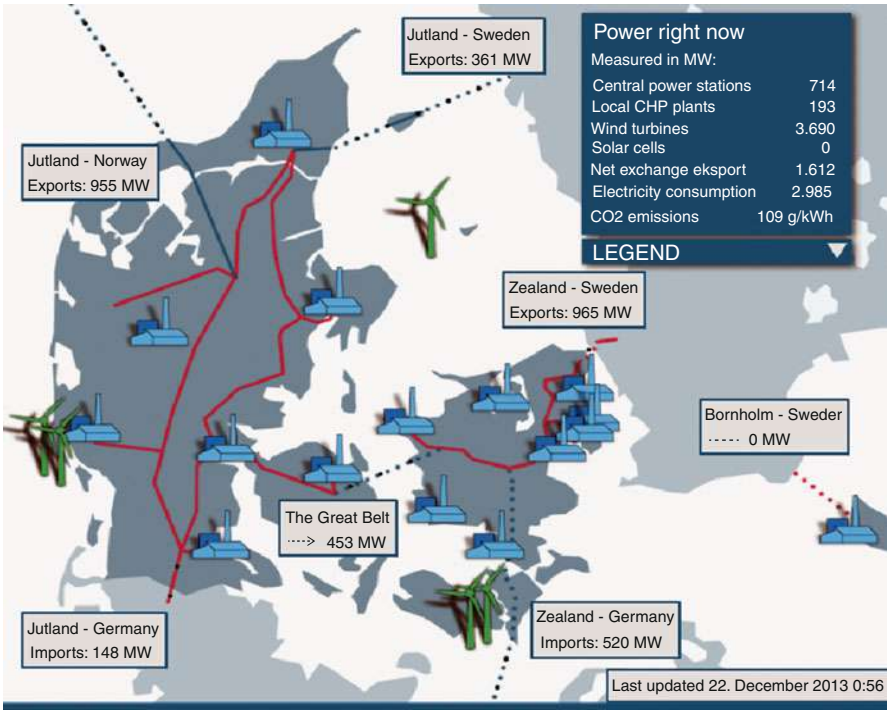

Fig. 3 Power right now – power production, exports and imports of energy in Denmark, 22 December 2013 (energinet.dk)

response in the chemical and metals industries can be integrated with process engineering as well as hydrogen production and water desalination, examples of which can be seen in China as derivatives of non-grid-connected wind power. Other examples are water pumping, air conditioning, and freezing, which can offer options for shifting demand when integrated with storage solutions.

Gas Turbines and Gas Motors (Peaking and Non-peaking)

Natural gas can be seen as a bridging fuel toward high-renewable shares. Advanced gas motors at CHP stations have electrical efficiencies around 44 % and included heating more than 90 %. They find a growing need for balancing grids, particularly for complementing wind power. Even if most gas engine CHP stations that exist today were not planned nor designed to operate on a variable regime, daily ramping up and down does not create lowering lifetimes and increasing maintenance costs. In Denmark up to 60 % of the electricity used to come from combined heat and power. CHP stations below 10 MW electrical capacity mostly are gas engines that are especially suited for power balancing.

Strengthened Transmission Capacity and Interconnection

Stronger transmission capacity is an important means to balance power flows and variable sources within a region, as well as to deliver renewable generation from remote locations. Some countries bury underground transmission to achieve a more robust grid at weather extremes and stronger balancing capability while mitigating social acceptance. In Denmark nearly all distribution up to 10 kV is already in underground cables and big share of new transmission will also be buried underground.

Also stronger two-way cross-border interconnections to transfer renewable power generated in one country to neighboring countries are increasing, not least in Northwestern Europe. However, with increased simultaneous amounts of fluctuating power from solar and wind, countries in the same region will try to export their excess power to each other. Asian countries are discussing an "Asian super grid," while in Europe the "Desertec" was envisioned to one-way transfer of especially solar power from Sahara to Europe.

Energy Storage

From a grid stability perspective, different storage technologies are suited for different balancing time frames, ranging from seconds to minutes, minutes to hours, and even to days or weeks. As seasonal storage from summer to winter or from windy to calm seasons, huge hot water covered ponds up to 90 °C are emerging in Denmark with its high share of district heating. Postponing combustion of

Fig. 4 Energy autonomous house in Freiberg, Germany. Gray battery electricity storage box and its own car charging station (Preben Maegaard/Nordic Folkecenter for Renewable Energy)

biomass (straw, wood chips, pellets) can be considered as a cheap and reliable season-to-season storage solution where solar and wind energy is the primary sources of supply while stored biomass is the primary backup fuel. Hydropower is a traditional form of large-scale energy storage on power grids, in the form of both conventional and pumped hydro. Grid-tied battery storage has made inroads and shows promise for the future both in the form of container size battery storage stations and distributed batteries at the millions of end users that have acquired residential photovoltaic installation. At the consumer level the self-supply ratio can be doubled from 30 % to over 60 %. In Germany household battery systems and controllers connected to domestic PV installations are commercialized products that are offered by several suppliers (Fig. 4).

Beyond hydro and batteries, concentrated solar thermal power (CSP) plants also offer storage capabilities. Currently operating CSP plants typically have 4–8 h of thermal storage that allows evening and morning peak period operation.

Ramping and Cycling of Conventional Plants

Conventional hydropower plants are routinely used to ramp and cycle. For other types of conventional power plants, however, ramping and cycling on a daily or hourly basis can reduce equipment lifetime and cause higher maintenance costs and stability of emission equipment.

Atomic power plants are primarily built for covering base loads and are not designed for cycles on a daily or even less than hourly basis which is needed to follow rapid changes in the supply of wind and solar electricity production. Denmark

early decided not to deploy atomic energy and therefore with over one third of the electricity by 2014 coming from wind power does not have the challenge to integrate technologies with conflicting operational modes. For backup capacity, the many gas engine-based CHP stations that allow start-ups within a few minutes are available and high-capacity, two-way cross-border power interconnections to Sweden, Norway, Germany, and Holland. Thus, centralized grids are still being developed to facilitate large-scale wind farms, including offshore wind along with large capacities of electricity-based electric boilers and heat pumps and new applications of fluctuating power together with strong interconnections to neighboring countries. Distributed generation will not necessarily seem like a revolution of the energy system as a whole but an evolution of current systems.

Appropriate forms of public management and control of supply seems best to solve problems associated with fluctuating and intermittent power production. What is required are political solutions with incentives for the wise use of this so-called surplus power to avoid selling it at very low prices, especially to neighboring countries, and the establishment of major new transmission lines and integrated systems to match with supply peaks when solar and winds are strong.

The various renewable forms of energy (solar, wind, biomass, etc.) can provide an alternative to fossil fuels when they are used in combination with one another. None of the renewable energy forms are capable of covering the need for electricity, heat, and transportation if they are used alone. There must be, however, a multiform effort involving many kinds of supply systems, energy storage, and saving mechanisms, as well as appropriate user-management strategies.

The constant expansion of renewable energy not only provides realistic potential but ultimately could lead to an end of the combustion of fossil fuels. The economic risks associated with investments in new conventional power plants will grow significantly, especially with increased uncertainties of fossil fuel prices in the future. Not least will be the growing risk of low utilization as their annual production is being marginalized by increased use of decentralized renewable energy forms.

Renewable energies will have the key role in the global push toward a CO_2-neutral future of energy production. Due to their in-principle unlimited potential, in comparison to the current global energy regime, they are treated in this chapter as the primary source of supply for meeting the future demand for electricity, heating, and mobility, irrespective of their intermittent character. In areas with high shares of wind or solar availability, these energies will more and more be seen as a base load that periodically covers the supply of power of 100 % and often more. Overall, a picture of power systems of the future emerges as a complex combination of on-site, minigrid, and centralized grid levels, with renewables and natural gas generation and energy storage at all levels and with all levels coordinated and interacting, according to a range of requirements for cost, reliability, flexibility, and service.

Because biomass functions as an ideal long-term storage solution, due to its limited availability, it is necessary that it be reserved for combustion in combined heat and power stations with efficiencies of 85 % or more. Their primary function is for balancing by upregulation when solar and wind energy cannot cover the demand loads.

Besides an electricity grid, in the future energy structure with extensive pipe networks for district heating and cooling will have ancillary functions. Due to their low efficiencies of 45 % or less, conventional condensation power stations will not have an appreciable role to play.

Some regions and even countries already have relatively high shares of fluctuating power supply. In 2014, Denmark saw 39 % of its demand for electricity from wind turbines, which by 2020 will grow to approximately 50 %. During periods of low peak power demand and high wind speeds, wind power can currently fully cover the consumption of electricity; at the local level, the share of wind power may even be 400 % of actual consumption. Interregional compensation with strong power line connections to neighboring countries plays an important role for upregulation and downregulation; it may be a short-term solution, however, as the present importers of excess power most likely in the future will be less interested in buying power as the deployment of fluctuating forms of renewable energy will only increase in neighboring countries as well. The reality is that new outlets for periodical overcapacities will be required locally.

There are solutions for providing a balanced energy supply from fluctuating renewable energy sources such as the use of biomass in combined heat and power (CHP) plants with embedded heat storage or locally variable operation of the CHP plant based on end users' demands, generation of hydrogen or synthetic gas from excess renewable electricity for injection into the natural gas grid (absorption on-demand), and centralized "smart grid" for charging increasing numbers of electric vehicles and appliances.

Since the first wind turbines were introduced in the 1980s, there has been much discussion and controversy about the level of variability from renewable energy sources that power grids are/will be able to support and integrate cost-effectively. The crucial issue of this debate is the percentage of a technical "upper limit" to integration, with conservative numbers such as 10 % or 20 % often cited. Practical experiences in Nordfriesland in northern Germany, the Jylland peninsular in Denmark, and other regions with similarly high shares of especially wind power demonstrate the potential to reach significantly higher shares with appropriate use of the various balancing measures.

In the pioneering regions, up to 100 % shares of variable renewables can be accommodated at the annual basis and peaks of 400 % compared to the actual demand for electricity without negative impact on power quality. As there are plans in the regions mentioned to even double the share of fluctuating power by 2025, further restructuring of the power system, also with the incorporation of non-grid-connected energy solution, which is being developed especially in China, may increase shares of variable renewable energies even more gradually leading to 100% renewable energy supply solutions.

Electricity storage will be an essential part of the integrated systems that see power supply, mobility, heating, and cooling as a whole together with existing possibilities such as demand-side management. These systems should be affordable, sustainable, and efficient.

By 2014, there exist many different energy storage systems, but only a few are functional and commercially available. Moreover, these technologies need to be compared by their investment volume, their losses, and their potential for centralized and decentralized applications. The storage solutions have to be discussed by their limits, environmental effects, geographical requirements, application focus, investment complexity, and efficiency. Furthermore, storage technologies have to be optimized in terms of size and capacity, responding time and flexibility, as well as their cost-effectiveness.

Worldwide, their role is still limited, but with the expected significantly increased use of intermittent and fluctuating energy forms, structural aspects including CHP connected to district heating and cooling are indispensable. The supplies of water, electricity, gas, heat, and energy for transportation have in common the fact that they are all daily necessities for domestic consumers, as well as for industry and public sector institutions. Therefore, it is the case in many countries that the same company, often a municipal-owned entity, may have supplied all these services for several decades, a process which has generally worked to everyone's satisfaction.

The following chapters will focus on increased applications of various forms of renewable energy and solutions for power-balancing technologies with references to pioneering countries that are already facing the need for new kinds of power management and its opportunities. Besides storage technologies, power production in combination with heating and cooling will be discussed as especially important ancillary solutions.

A Brief History of Energy Transition in Denmark

Denmark is internationally well known for its wind industry and the high share of electricity that is obtained from wind power. District heating, coupled with combined heat and power (CHP), may, however, in the long term prove to be even more important (Fig. 5). This transition represents the single most important initiative to reduce CO_2 emissions in Denmark. Moreover, the construction of CHP plants that already by 2001 supplied up to 60 % of electricity and 70 % of the demand for heat has created the necessary infrastructure to gradually transition entirely to renewable energy.

By 2007, 43 % of the 36 TWh of electricity used in Denmark came from independent power producers (IPPs) consisting of wind power operators and local, consumer-owner district heating companies. As a consequence, the central power utilities (owned by Vattenfall and DONG Energy) had their share of the electricity market reduced to little over 50 % of the domestic demand. The transition primarily took place in a 10-year period since 1990. Coincidently this is the amount of time it takes to build one nuclear power plant, or the equivalent of 1,200 MWel. Denmark has not and is not planning to build atomic power plants; this controversial source of supply was ultimately withdrawn from national energy plans in 1985.

Denmark has succeeded in stabilizing its primary energy supply during 30 years of economic growth. During this time, CHP plants and renewable energy

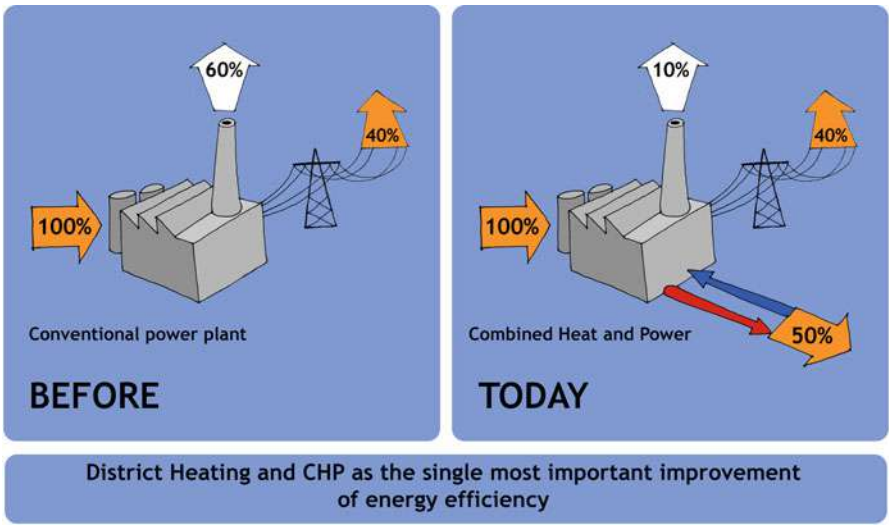

Fig. 5 It took 10 years to dramatically shift almost half of the power production from inefficient, centralized fossil fuel power supply to local, municipal, or consumer-owned companies. In conventional power plants, the loss is 60 % or more, whereas CHP may have efficiencies of 90 % (Anna Krenz/Nordic Folkecenter for Renewable Energy)

technologies were introduced extensively and supported by the state. In the period 1975–2000, fuel consumption for space heating was reduced by 30 %. In the same period, an almost 100 % oil-based primary energy supply in the year 1975 decreased to 40 % by means of diversification. The fuels used were a mixture of oil, coal, natural gas, and renewable energy Maegaard (2009).

During the whole period, the national gross energy consumption had a level of around 20 million tons of oil equivalents (TOE). The combination of energy conservation and district heating based on CHP was the most important single factor in improving overall energy efficiency. Insulation of buildings contributed to a 12 % decreased heat demand from 1975 to 2000, while at the same time the heated areas increased by 46 %. District heating increased by over 50 %, while CHP plants replaced conventional condensing power plants, which, during the 25-year period, decreased the consumption for heating per square meter by half. Approximately 40 % of this decrease was attributable to the implementation of new building codes that were important for the energy conservation that resulted from improved energy efficiencies and new CHP for the balance. Since 1980 permission has not been given to build new conventional condensing power stations, only for CHP with supply of district heating as main location factor. Coal was not accepted as fuel for new CHP stations built since 1990 Danish Energy Agency (2010).

During the 1990s, many hundreds of decentralized Danish CHP plants in sizes of 0.5 MWel to double-digit MWel capacity were mostly built in connection with district heating systems in towns and villages as small as 150 households. The

CHP plants contain one or more CHP units, peak load boilers, and heat storage systems. The CHP units are either engines, gas turbines, or in some cases steam turbines or combined cycle plants (Fig. 6).

Support for CHP has a long tradition in Denmark. In the past it has been mainly focused on the development of district heating based on large centralized or smaller decentralized plants. Bioenergy CHP is supported primarily by energy tax exemption. New installation on natural gas-based CHP is no longer promoted and has to face a highly complex energy taxation system.

Based on an energy agreement in the Danish Parliament in 2012, Denmark has set the target to reach an energy supply system based on 100 % renewable energy up to 2050 (Fig. 7). CHP with bioenergy has an important role to play. CHP in industries and greenhouses shall be promoted as well.

With a share of CHP in total power production of about 60 %, Denmark has the most developed CHP system in the European Union and in the world as such. With changing focus to the expansion of renewable energy, support for CHP has shifted to bioenergy which has been designated to take the role of coal, while natural gas CHP is not promoted anymore. There exist, however, still relevant potentials to switch from boiler firing to CHP in industry, housing, commercial companies, and public institutes situated in areas without district heat supply. Key proposal in Denmark is to take an active CHP expansion policy that the CHP electricity produced could be increased by 10 % up to 2030.

For some years it has been judged that Danish potential for installing cogeneration output is largely being exploited that the socioeconomic potential of cogeneration was found to be limited. Since 2012, new technologies and a change to the rest of the energy system may alter the picture in respect of both theoretical and economic potential.

The planned increase of wind power to 50 % share in total power production up to 2020 needs a further development of flexible backup capacities of fuel-based power production. Contrary to previous analysis, there is a need for growing CHP electric capacities. The additional amounts of wind power should not replace CHP electricity but the remaining production of condensing electricity, which covered still 26 % in 2011. Regarding Denmark's political objective of reaching a 100 % share of renewable energy in electricity and heat supply up to 2035, the state Energy Agency has carried out a study with four scenarios designed to reach the 100 % renewable energy target. The biomass scenario with a relative high share of bioenergy had the lowest total cost; also the cost of electricity grid construction measures had been taken into consideration.

With a growing share of bioenergy in heat production, either in district heating or individual housing with biomethane distributed over the existing natural gas grid, solid biomass and waste gasification offer the opportunity to replace the conventional steam turbine CHP plants with their relative low electric efficiency by high-efficiency CHP based on gas engines or combined cycle gas turbines.

The replacement of old low-efficiency coal-fired CHP by modern technologies with biogas, biomethane, gasified solid bioenergy, and waste could increase the electricity capacity and supply from CHP by an estimated 20–30 %. In the

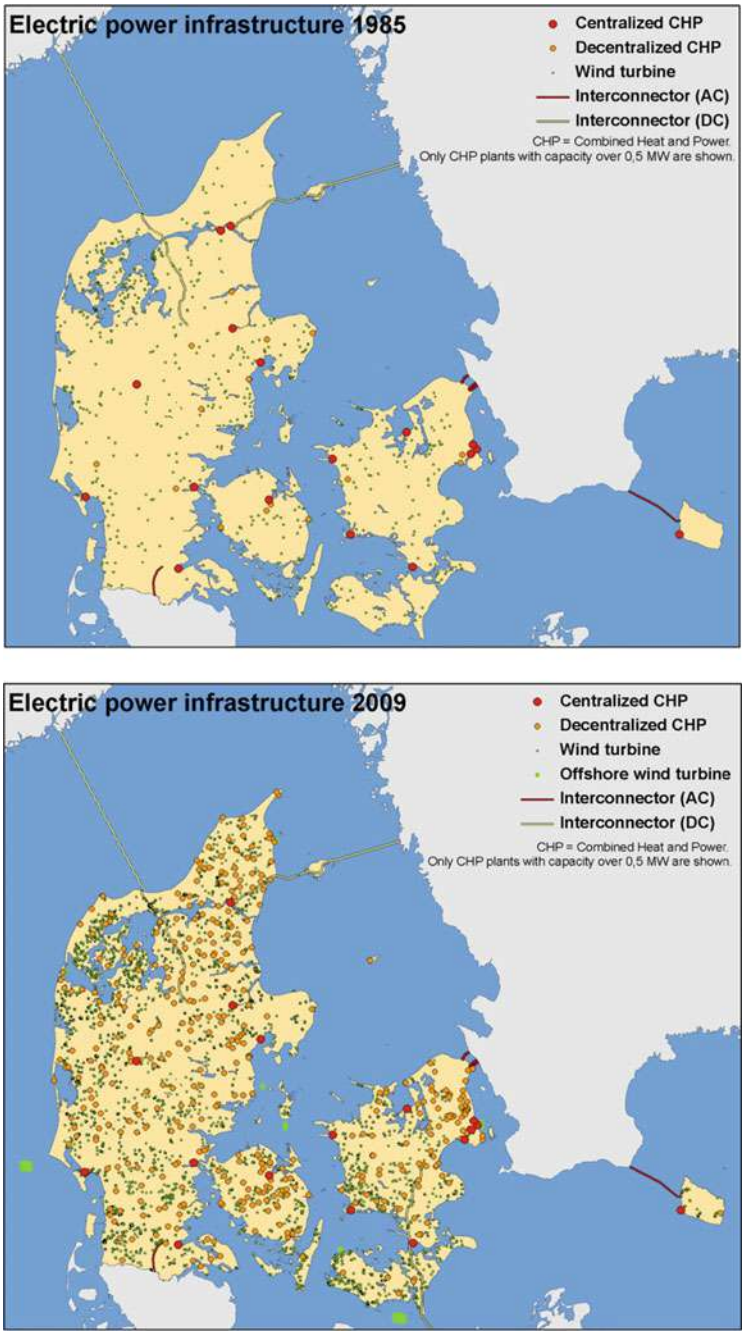

Fig. 6 (continued)

Government's targets	Results of „Our Future Energy" in 2020
100% renewable energy in 2050	A reduction of the total consumption of fossil fuels by 26% from 2010-2020 is a major leap towards total phasing-out of fossil fuels and the conversion to 100% renewable energy
100% renewable energy in electricity and heat supply by 2035	On track towards the target in 2035 by cutting consumption of fossil fuels for electricity and heat supply by 50% from 2010 to 2020
Coal phased-out in 2030	A large contribution to the target as coal consumption is reduced by 65% in 2020 in relation to today
Oil-fired boilers phased-out by 2030	Halving the number of oil-fired boilers in 2020 in relation to 2010 and a good start towards the effort to be done from 2020 to 2030
Half of electricity consumption supplied by wind in 2020	The share of wind power in electricity consumption will be 52% in 2020

Fig. 7 Danish Government Energy Plan of 22 March 2012

meantime, micro CHP systems are available on the market which offers good economic results for the users, and, combined with heat pumps, they additionally can contribute to a flexible smart electricity supply system. In the industry additional CHP potentials should be reconsidered by a revision of the energy taxation system and some financial incentives to switch from boiler fired process heat production to CHP.

Fluctuating Sources of Energy

The Consequences of Fluctuating Power Supply

On days with both a high demand for heat and high winds, combined heat and power plants, CHPs, and wind turbines together sometimes feed more power into the grid than needed by power consumers. On such occasions, the CHPs are not operating to cover a need for power but to supply heat through district heating systems, while the production of electricity can be seen as residual. Wind turbines deliver their electricity production to the grid in accordance to the prevailing wind speeds (Fig. 8).

Together, CHP plants and fluctuating wind and solar feed their production into the same grid. The early application of solar and wind to an existing power grid can be balanced without special problems. Once the share of wind energyexceeds 20 % or more, however, initiatives have to be taken. With 20 % of wind power at the annual basis, there will be hours and even days when wind power production can fully cover the actual need for power. In regions with a high concentration of wind power, they

Fig. 6 In 1985, Denmark's 14 central power stations and a small number of windmills covered the production of electricity in Denmark. By 2009, power production was decentralized with approximately 3,000 windmills and more than 700 CHP units over 0.5 MWel. Together, wind power and small CHP periodically can deliver 60 % of the annual demand for electricity (Danish Energy Agency)

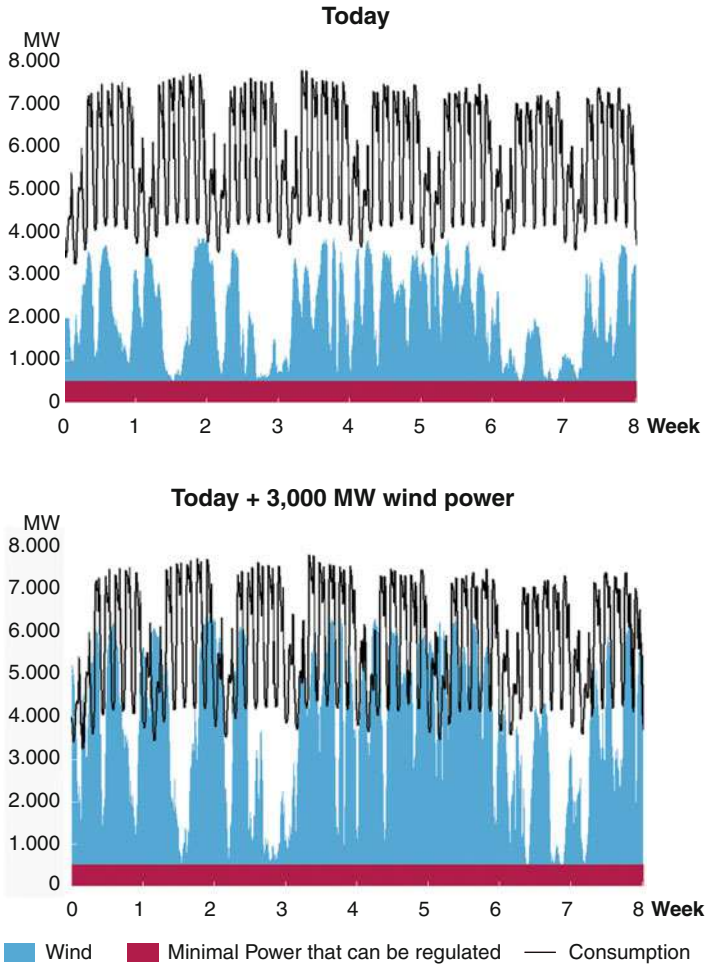

Fig. 8 Consumption of power and production of wind power during the first 8 weeks of 2007 (*left*); same consumption with the integration of 3,000 MW additional wind power (*right*). Security of supply should be maintained and the value of wind power should be maximized ecologically and economically (Danish District Heating Association)

can deliver most of the base load for power, but also periodically when wind speeds are high, they can even produce up to 400 % of actual power needs (Fig. 9). The structural and technological challenges involved in a transition from fossil fuels and atomic energy to renewable energy are obvious, considering that some countries have plans of 50 % wind and solar in their supply of power. In Denmark by 2020 wind energy will supply half of the demand for electricity Energy Policy Report (2013).

As an example of current fluctuating power management, on 2 January 2015, which was a windy day, out of total installed capacity of 5,000 MW of wind power in

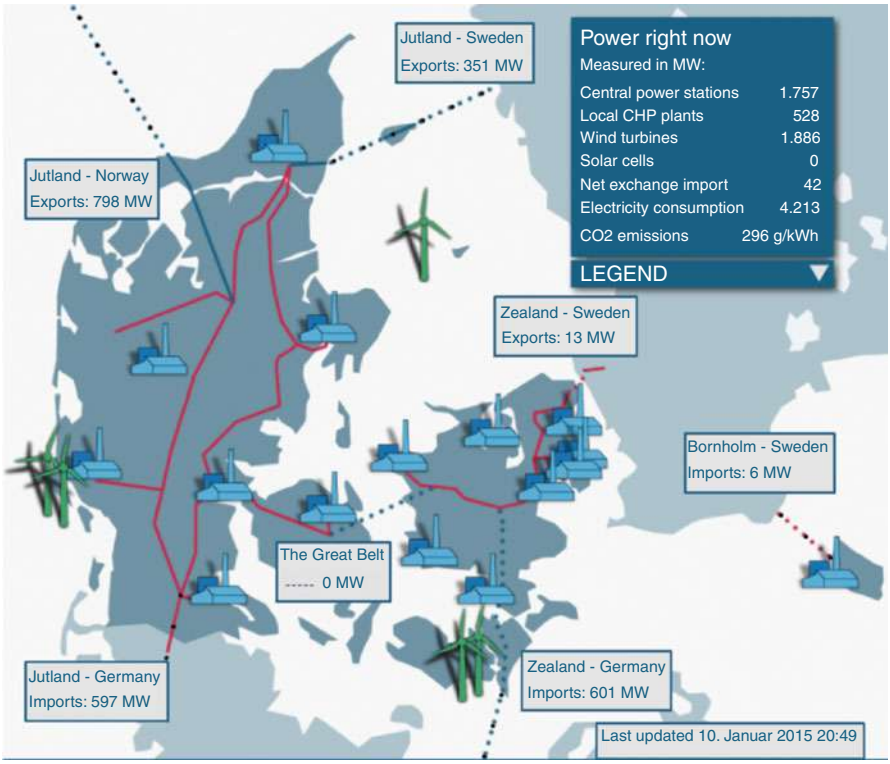

Fig. 9 "Power right now" from the system responsible state company, Energinet.dk. When high wind velocities were available in the evening on 10 January 2015, the wind turbine capacity of approx. 5,000 MW potentially should have been able to deliver the total demand of 4,213 MW. Wind turbines at the moment in question supply 1,886 MW only. There are various reasons. Many automatically stop when they are beyond cutout wind speeds; the demand for heating forces the CHP stations to operate at a minimum level, while strong wind over most of Northwestern Europe can cause negative electricity prices that encourage the wind turbine operators to curtail production

Denmark, 1,700 MW was sold at low or negative prices to Norway and Sweden, while simultaneously wind turbines of 1,200 MW capacity were simply stopped. The nationally unused power of 2,900 MW (58 % of total available capacity) could have delivered electricity and power-to-heat to consumers in Denmark, substituting fossil energy sources such as coal or natural gas, which at the same time delivered 1,700 MWel capacity into the CHP-based networks. The existing power system in Denmark by 2014 was not adapted to match big power capacities that allow it to absorb sufficient amounts of excess power from wind. Therefore, significant part of it was not utilized, stored, or commercialized in a rational manner. While the capacity for usage of excess power is lower than the wind power production peaks, the surplus is either sold to neighboring countries bringing no income or rather economic losses. Stopping windmills is the sign of an irrational approach to

wind energy. Denmark, like other countries, annually installs more and more wind power capacity, but is in the end not sufficiently considering the development of the total energy system to allow proper use of the produced energy. The challenge is to design and apply smart energy system concepts, which can absorb the excess power and balance different fluctuating renewable energy sources. Denmark is facing problems that other countries still have ahead; however, solutions have to be given high priority.

Some measures that can be taken to maintain a balance between supply and demand include:

- Store the electricity for use in periods with insufficient solar and wind.
- Temporarily stop the operation of some wind turbines.
- Export power to neighboring countries.
- Encourage demand-side power consumption.
- Find new applications of fluctuating electricity for industrial purposes and in the heating/cooling sector.

Special focus will be made at the use of fluctuating power in the heating/cooling sector and the infrastructural changes that it requires. Storage of electricity will be discussed separately, whereas discontinued operation of windmills is considered non-acceptable during periods when fossil fuels are being combusted. Export of power to neighboring countries involves heavy investments in long-distance transmission lines and is not a long-term realistic solution; period with high wind speeds is a transborder phenomenon and neighboring countries are often expanding their wind power capacity as well. With tariff differentiation and smart grids, industrial consumers and households may be encouraged as well to change the pattern of their electricity use by operating special machinery, using their washing machines at night, and charging-discharging future electric cars at periods according to the power supply situation (Fig. 10).

Experiences, however, indicate that changes of consumer behavior have their limits. Electric car owners, for instance, may prefer the benefit of leaving their home in the morning with a fully charged car instead of earning a few cents per kWh for delivering excess electricity to their utility company during peak consumption periods.

Supply and demand on windy days can be balanced with simple solutions such that excess wind and solar power can be used in electric boilers and heat pumps at combined heat and power stations. In the case of Denmark, with its many hundreds of CHP stations, it is possible to stop gas engines at periods when the wind and solar power is sufficient for both the actual supply of power and heat and hot water-based cooling. As the CHP stations already have large hot water storagetanks, additional excess power can be stored for some days of hot water supply with no electricity to water conversion loss.

As an example, the gas-based cogeneration in Denmark from around 600 decentralized CHP plants and more than 170 industrial auto producers can be stopped and started within minutes so that they match ideally with the fluctuating renewable energy supply. Conversely, conventional fossil fuel and in particular

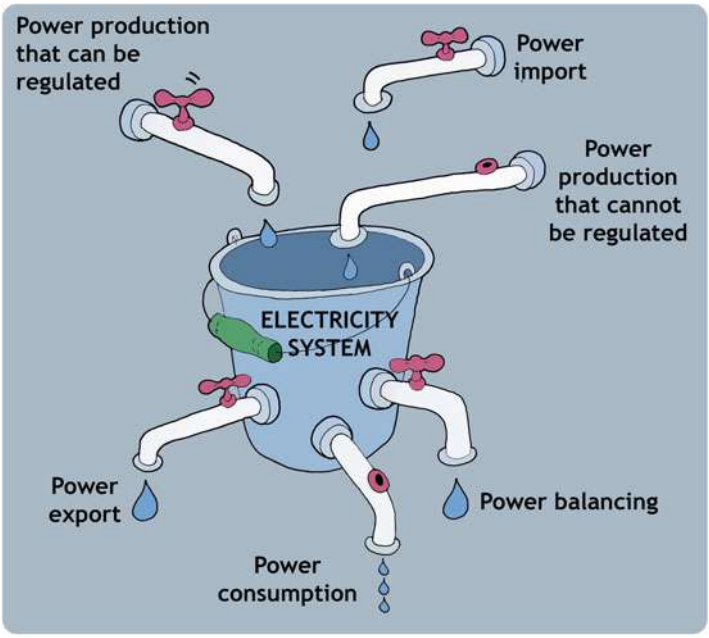

Fig. 10 An electrical system based on fluctuating sources – unlike conventional supply of energy that can be regulated – needs to be balanced according to the consumption. District heating stations with CHP plants can support by converting excess electricity to hot water that can cover the actual demand or stored for later use (Nordic Folkecenter for Renewable Energy)

atomic energy power plants have basic constraints in terms of curtailment and may need several hours or even a day for adjustment.

A decentralized power supply system will only work to further create a more robust power structure against national blackouts. Energinet.dk, the national enterprise responsible for Denmark's power system, announced to divide up the national supply system in cells with each 50,000–100,000 consumers in primarily self-supplying cells based on local wind and CHP to take advantage of the decentralized and diversified structure.

With its high share of wind electricity (in 2014, 39 %, and by 2020, 50 %) Denmark is the first country that experienced problems related to big amounts of fluctuating renewable energy supplies and, therefore, is especially focused for the quantification of the challenge (Lund 2010).

The challenge for the system operator is already and will increasingly continue in the future to further optimize the available resources even more. While Europe as a whole has 11 % of the efficient CHP in the energy system, the share in Denmark is the world's highest at about 60 %, which at the same time represents not only the problem mentioned but also its solution. Therefore, already existing challenges and solutions as they can be observed in Denmark will throughout the chapter be presented as examples of reference.

In principle, the experiences and solutions in the case of Denmark are generally transferrable and will hold true in other countries and regions as well. It should be mentioned that one of the authors of the chapter is a resident in a municipality of 46,000 inhabitants that since 1992 has basically received its supplies of heating and power from various local renewable forms.

It is often claimed in the media that with the expansion of wind energy, periods of a surplus of wind energy will become more and more frequent and contribute to instability in the power system. It is, however, as impossible to determine whether the wind or whether the heat-generated power causes the excess power as it is to separate cream from coffee. By combining and integrating CHPs with electric boilers, heat pumps, and hot water storage in combination with fluctuating energy forms of wind and solar, it will be possible to have much higher shares of solar and wind in the energy structure as a whole, without causing instability in the power system. With further integration of the mobility sector using cars with batteries and smart grids, additional possibilities of handling fluctuating power will become available.

Integration of fluctuating power production with the heating sector will gradually allow significantly higher future shares of wind and solar energy in the system because in a temperate climate, the demand for heat exceeds the need for electricity by a factor of 3 or so. With increased use of hot water for cooling when applying adsorption heat pumps that are driven by hot water, not only does it become realistic for more temperate climate regions, but a more general application is feasible when combining fluctuating power supply from solar and wind with local CHP. Thus, the need for heating, and cooling with hot water and adsorption chillers at the point of consumption, may become the largest single outlet for the disposal of power fluctuations from solar and wind. Furthermore, this can be achieved with low initial investments especially when a district heating/cooling network is already available. Building of new district heating structures will at the same time create the needed flexibility for the management of a 100 % renewable energy supply and is an affordable, highly efficient, and well-developed solution with a mature technology.

Following a decision by the EU Commission, the use of wind power for heat has become an attractive alternative. Previously, heavy taxation prior to 2007 did not make the excess energy economical. While excess electricity sometimes was sold at the spot market for €0.01 per kWh or less, it will at any time (when used for heating) have a value equivalent to the fuel that it replaces, €0.04–0.12 per kWh.

Technologies for Up- and Downregulation

Solar and wind cannot alone ensure a continuous supply of electricity. In a future supply scenario dominated by fluctuating energy forms based in full on renewables, three typical situations may occur to meet the actual demand for electricity:

(a) Solar and wind produce too much power; downregulation is required and some of the excess power can be converted, stored, or exported.
(b) Solar and wind produce too little power; upregulation is required and the stored energy will be used and power imported.
(c) Solar and wind produce no power; storageable supply and import is required and will cover the total demand.

Wind and photovoltaic (PV) power are cornerstones in future integrated renewable energy supply structures. They are, however, fluctuating which causes a need for adaptation by consumers and backup from other supply solutions or storage (Fig. 11).

With wind and solar as the primary sources of energy, biomass that is easy and cheap to store will be the ideal backup fuel (Fig. 12). On the other side, biomass should not be combusted when wind and solar is sufficient (Fig. 14). Environmentally and economically, the conversion of excess wind power for the local district heating supply and in their hot water reservoirs will have the per kWh value of the substituted combustible fuel (Fig. 13). Thus, it becomes an optimal solution instead of exporting the excess power to neighboring countries, sometimes at low or even negative spot market prices (Fig. 15).

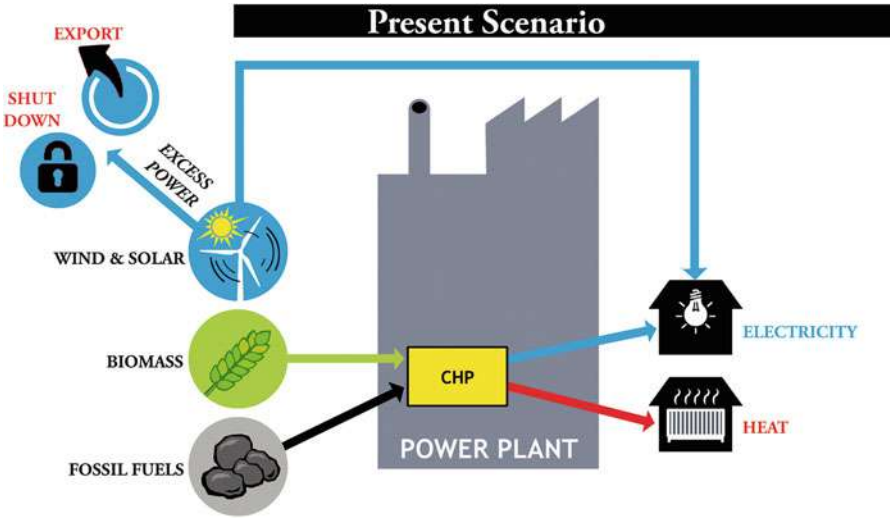

Fig. 11 Traditional CHP facility that combusts fossil fuel and/or biomass. The heat production is supplied to the heat consumers and the electricity to the grid. The power is supplied without considering to which extent wind power is available. The demand of heat must be satisfied and therefore the CHP is given priority to feed power into the grid. On windy days, excess power from wind is either exported or wind turbines are stopped. With increased fluctuating power capacity, excess power will appear more and more frequently (Anna Krenz/Nordic Folkecenter for Renewable Energy)

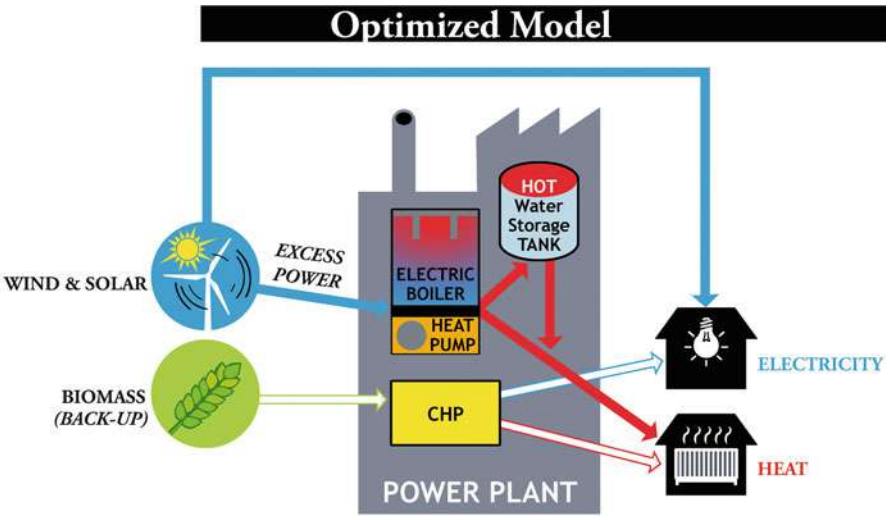

Fig. 12 In the alternative scenario, the solar and wind energy finds two kinds of applications: an electric boiler and heat pump have been installed in the CHP station. It will still be able to supply electric power into the grid when fluctuating power is not sufficiently available to fully cover the demand for heat. However, on days with strong wind and/or solar, excess power is fed into the electric boiler (or heat pump) at the CHP station. Now wind and/or solar power has the potential to cover the demand for heat as well and the CHP engine or turbine can be stopped. Thus combustible fuels can be saved (Anna Krenz/Nordic Folkecenter for Renewable Energy)

Energy Storage

A number of storage solutions are available. They are of very different character regarding technology, medium, and cost. Flexibility and response time are important requirements that the various types of energy storage will meet differently to match satisfactorily with the integrated supply of power, heat, and cooling.

A storage solution that converts the residual power from wind and solar may be chemical, gravity, heat, compression, etc. and suitable for either conversion back to electricity or heating/cooling. The need of storage may be for seconds, minutes, hours, or a few days. Seasonal storage is well developed for hot water but is rare for large-scale electricity storage (Fig. 15).

Electrolysis has been around for many decades and is widely used for the production of oxygen and hydrogen in the chemical industry, paper industry, hospitals, and for welding. For energy storage, hydrogen is still at the early stage of development. Initial costs are high due to prohibitive pressure and diffusion of hydrogen, while conventional gas storage equipment is not suitable. Losses of conversion in the process from electricity back to electricity may be 65–80 % accumulated by losses in rectifier, electrolyzer, compression, transmission, and the fuel cell.

*Compressed Air Storage for Energy*has been in operational use for several years in the USA and Germany. Excess fluctuating electricity is used for the compression

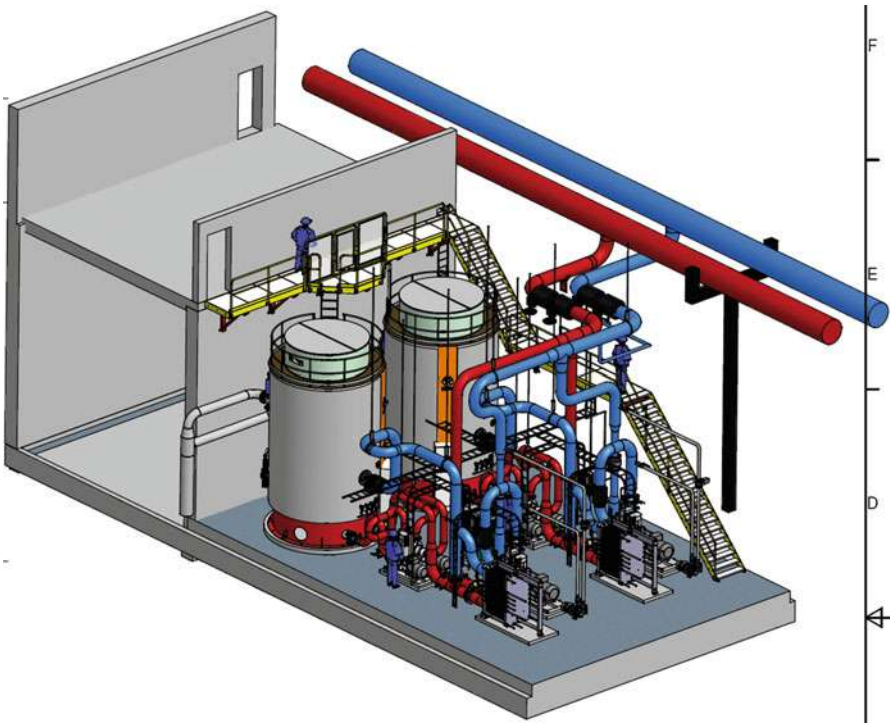

Fig. 13 A new scale of downregulation: 80 MW electric boiler that in March 2015 will start operation at the central power station to use excess wind power. The heat will be supplied to the city of Aarhus (Aarhus Municipality)

of atmospheric air into deep underground caverns of a type similar to natural gas storages. At the time of consumption, the process is reversed and the air drives a conventional-type turbine that instead of natural gas or steam uses compressed air. The turbine is connected to the generator. During compression, heat is produced while the reversal process occurs with decompression and the air expands so that the system can deliver cooling. The electric efficiency is around 50 %; the overall efficiency can be improved in case the heating and cooling potential is utilized.

Batteries for storage of electricity are widely used for many applications. For electric cars, a new generation of lithium batteries is being developed in many industrialized countries; they are expected gradually to be available for large-scale storages as well. For the hundreds of thousands of stand-alone PV installations in the developing countries, conventional car and truck batteries are used as well as batteries designed for frequent deep discharging and recharging. For regional and national supply structures, such batteries will have a limited application.

Water-pumped storages are installed in many countries to compensate for fluctuations in the demand for power. Pump storages have dual purposes. At times of downregulation, water is pumped from the lower to the higher reservoir; the process

Fig. 14 Biomass from agriculture and forests is a limited resource. Dry biomass is ideal for long-term and seasonal storage of energy when solar and wind energy is not available (Preben Maegaard/ Nordic Folkecenter for Renewable Energy)

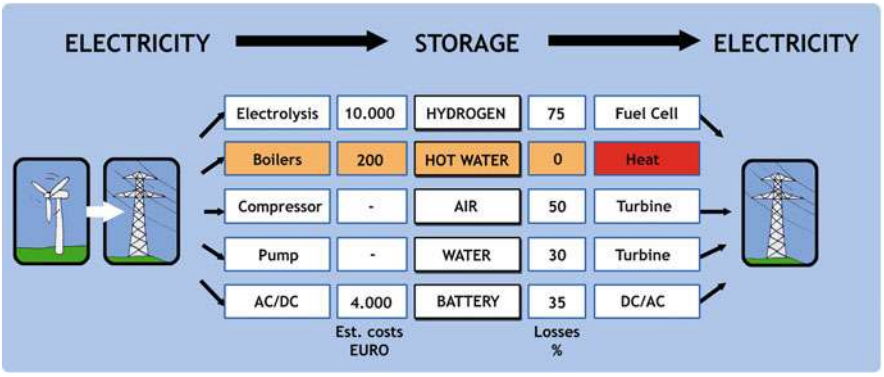

Fig. 15 Storage of electricity (Nordic Folkecenter for Renewable Energy)

is reversed for upregulation. Pumps/motors and turbines/generators are often of multimegawatt capacity. They match well with atomic power stations with constant power output. At nighttime and other off-peak periods, water is pumped to a higher-level reservoir and available for typical morning power peak periods. Their general application is limited by the topography; in Europe, most potential sites for pump storage have already been developed.

Other storage solutions can be mentioned as well. Molten salt is used for concentrated solar power storage. It can be used alone or combined with wind energy in utility size installations of 50 MW or larger as it is being demonstrated in southern Spain and in the USA (Fig. 16). With operational temperatures up to 400 °C, the storage medium can produce steam for conventional steam turbines

Fig. 16 The 150 MW Andasol solar power station (*Top*) is a commercial parabolic trough solar thermal power plant, located in Aldeire, Granada, Spain. The Andasol plant uses tanks of molten salt to store solar energy so that it can continue generating electricity even when the sun is not shining (BSMPS). (*Bottom*) Molten salt secondary battery (FIAMM SoNick) (Rudolf Simon)

combined with production of electricity. The process heat can be distributed by a district heating network for heating and for cooling by adsorption chillers. Flywheels with integrated motor/generation are one of many other forms of storage technologies that will be relevant in integrated energy systems (Boston Consulting Group 2010).

Special focus in this chapter will be made at hot water storage at temperatures below 100 °C at atmospheric pressure in insulated tanks made of steel or concrete. Hot water storage within this temperature range is not suitable for electricity production.

Considering that the amount of energy needed for space heating in temperate climate is about three times higher than the energy need for electricity, hot water supply and storage based on solar and wind peaks can find large-scale applications by replacing oil, natural gas, and coal for heating purposes and for cooling by adsorption chillers. In Denmark, several hundred hot water reservoirs are installed at local CHP; sizes range from 10 m^3 for short-term storage up to 200,000 m^3 for seasonal storage. The dimensioning criterium is mostly to cover the CHP station's need for supply to the district heating network during low peak power periods and weekends.

Compared to the earlier mentioned storage solutions, hot water storage involves an especially low initial investment. Compared to batteries and hydrogen for storage, the investment may be more than 90 % lower. In pumped storage, air compression, and flywheels, the conversion losses range between 30 % and 50 %, however, with initial costs significantly lower than with the hydrogen/fuel cell option.

Average investments per kW in new power generation based on fossil fuel and renewable energy are shown as well in the table. It will be seen that initial investment in the electric boilers for downregulation combined with decentralized natural gas CHP for upregulation (€900 per kW together) is less than investment costs of conventional fossil fuel power stations and significantly lower than atomic power where costs of long-term storage of radioactive waste have to be added. One objective to the preferred solution may be that costs of a district heating network should be added. Based on experiences of numerous installations in Denmark, the investment in a new district heating network is often similar to the costs of the CHP station that it is connected to (Fig. 17).

In case that conversion from electricity to hot water is made by an electric boiler, the conversion factor is 1:1. When conversion is by compression heat pumps, the conversion factor is significantly better and may be 1:2 up to 1:6 depending on the heat source available for the heat pump. A heat pump costs 5–8 times more than electric boilers in initial investment; therefore the annual hours of operation for heat pumps must be 3,000–5,000 h per year, whereas electric boilers will be profitable with much fewer operational hours per year.

District heating and cooling, CHP, and fluctuating energy forms from solar and wind energycan be combined and integrated to create truly autonomous systems. Pioneering projects demonstrate that a decentralized heat and power system using biomass and wind energy can be cost-effective and pave the way for a sustainable

Technology	STORAGE / Est. EUR/kW
Electrolysis/Fuel Cells	10.000
Electric Boilers	200
Electric Heat Pumps	1.800
Air Compression	-
Pumped Storage	-
Battery AC/DC/AC	4.000
Fly Wheel	3.000

Technology	GENERATION / Est. EUR/kW
Conventional Coal	1.500
Atomic Power	5.000
Wind Power	1.200
NG-Gas Engine	700
Biogas-CHP	2.000
Photovoltaic	2.200

Fig. 17 Cost estimates in EUR per kW capacity of a number of storage and generation technologies

energy supply. It has been demonstrated as well that conventional fossil fuel-based power production from big centralized power plants can be phased out with improved safety of supply and prevention of climate changes (Fig. 18).

The transition from a few large-scale centralized, fossil fuel-based power stations to thousands of wind turbines, solar installations for heat and electricity, and combined heat and power stations using biomass or natural gas will be a technological and structural challenge. As it was seen in Denmark, the shift to renewables takes some decades using a mix of conventional and renewable energy technologies. Denmark in 2013 had around 6,000 MW of centralized power plants, 2,500 MW independent combined heat and power, and 4,800 MW wind power that will increase to 6,000 MW or more by 2020. With more and more decentralized CO_2 neutral capacity, the centralized plants are being modified to combust biomass fuels (wood pellets and wood chips) (Figs. 19 and 20). Several units that used to burn coal have been phased out. The transition to renewable energy forms will stabilize consumer energy prices and fulfill international climate commitments.

A smart energy system strategy implies the development and integration of a wide range of supply and end-use technologies, markets, and control systems, including electric boilers and heat pumps in distributed generation, electric vehicles, mechanical and electrochemical storage systems, flexible demand mechanisms, and more.

According to *Coherent Energy and Environmental System Analysis* (*CEESA*) (Aalborg 2011), approximately 20–25 % of wind power on the grid can be integrated without significant changes to the energy system. With more than 20–25 % of wind

Fig. 18 Viborg CHP plant (*Top*) using natural gas turbine for the production of heat and electricity. The hot water storage is seen to the right of the turbine hall. The city of Odense (*Bottom*) with its 165,000 inhabitants was a pioneer within large urban CHP resulting in low heating costs. Fuels for the supply of steam to the turbines are straw, household waste, and natural gas (Preben Maegaard/ Nordic Folkecenter for Renewable Energy)

power, the analysis points to installation of large heat pumps in district heating plants in combination with the heat storages as the next needed step in integrating the heating and power systems. With wind power levels above 40–45 %, the transport sector also needs to be integrated with the electricity system. Integration with the transport sector will be a significant challenge in the coming years. Electric vehicles can be important in this integration, as they provide flexibility on the demand side. Exceeding 50–60 % fluctuation renewable energy in the system electrolysis becomes important as really large capacity.

Fig. 19 *Left*: Boiler for central heating at farm for full-size straw bales. *Right*: wood chips are being unloaded at the central heating station (Jane Kruse/Nordic Folkecenter for Renewable Energy)

Fig. 20 Large scale: Boiler for wood chips in district heating station for town with 4,000 residents (*left*). Small scale: Hertl boiler, capacity up to 145 KW_{th}, for the gasification of especially wood stems (*right*) (Jane Kruse/Nordic Folkecenter for Renewable Energy)

Wind Energy and Its Role in Power Production

By the end of June 2014, the accumulated installed wind power capacity in the world had reached 318 GW. Within less than a decade, a historic change has occurred to the wind power development of China. Takeoff for wind power in China was 2005. Five years later, in 2010, China became a country with the largest annual newly added installed capacity in the world. In 2013, the newly added wind-power installed capacity of China reached 16,000 MW, and the accumulated installed capacity of China reached 91,000 MW. Wind power generation output of China was 135 TWh, which made wind power the third biggest source of supply in China in the wake of thermal power and hydropower.

Being fluctuating power this in itself will cause a total restructuring of the whole energy sector. This most certainly will lead to the integration of the sectors for power,

heating, and mobility. Each represents about one third of the total national energy consumption and will gradually eliminate the use of oil and coal.

The problems associated to this have gradually emerged along with the increase of the percentage of wind power in the total electric power consumption. Comprehensive projects and programs for the development of new applications of renewable energy have been launched. The Chinese government has also made efforts and attempts in the development process of wind power to match with the new situation.

For many years, the efforts have been to explore exploring new concepts with renewable energy development to achieve high efficiency and low cost in the utilization of renewable energy resources at a large scale. Wind energy and other new energy resources are, however, by nature leading to significant fluctuations of their electric output. This is bringing very big challenges to the utilization of electric power which calls for innovation and new advanced concepts in various countries, including China.

In this process, professor Gu Weidong, Nanjing University, has conducted a Chinese national "973" research program and put forward the pioneering non-grid-connected development model (Fig. 21). He proposes that a smart grid system based on the non-grid-connected coordinated power supply of multiple and new energy resources should be set up. This new system succeeds in making power grid more flexible and intelligent, i.e., transforming high-energy-consuming industries into new intelligent loads which can carry out peak regulation for power-grid facilities (Maegaard 2010).

The theory has sparked a new field for the worldwide multiple application of large-scale wind and solar power for the manufacturing of basic industrial products and services for which there will a big demand in a post-fossil-fuel age as well. These research fields are unprecedented worldwide and open up for new ways of integrating very huge quantities of fluctuating power.

Examples of innovative use of solar and wind energy include:

- Large-scale non-grid-connected wind-power seawater desalination
- Large-scale direct wind-power hydrogen and oxygen production

Fig. 21 Water desalination based on non-grid-connected wind power is one of the technologies pioneered by Prof. Gu Weidong, Nanjing University, within the "973" research program (Preben Maegaard/Nordic Folkecenter for Renewable Energy)

- Nonferrous metallurgical industry
- Salt-chemical chlorine-alkali industry
- Wind/methane power-to-gas integration
- Wind/nickel-ferrite alloy smelting
- Wind/hydrogen reduction iron-making
- Pure-oxygen converter steel-making

Wind energy will be a cornerstone in future supply of electricity. Worldwide, wind energy capacity by end of June 2014 reached 336,000 MW, out of which 18,000 MW new capacity was added in the first half of that year.

Onshore wind power is fast approaching grid parity in terms of cost per kWh. Technical innovation and series production make onshore wind the cheapest source of new electricity in a range of markets in China, Germany, Italy, Spain, and the UK and has already attained parity in Brazil and Denmark.

Electricity from onshore wind energy is already significantly cheaper than new atomic energy with the British *Hinckley Point C* as a reference for 2014 and would also be cost competitive with natural gas and coal globally if health and environmental costs were included in prices. In 2014, the Danish Energy Agency informed that onshore wind was the cheapest of all new power producing technologies. Most of wind energy's competitiveness has been driven by the strong pace of technological development among the largest turbine manufacturers. Growth in the scale of the wind market has encouraged competition, driving down costs. The capital costs of wind turbines have also declined.

The wind energy sector in 2013 employed 834,000 persons worldwide and is expected for the first time to offer one million jobs a few years later. The *World Wind Energy Association* (WWEA) expects global wind power capacity to reach 500,000 MW by 2016 and that total global wind power capacity of around one million MW is possible by the year 2020, according to its *World Wind Energy Report 2013* (Fig. 22).

In 2013, for the first time in contemporary wind energy development, there was a decline of annual new installed capacity of wind power, as some countries leading within wind energy did not maintain their traditional policies in favour of renewable energy. In this regard, the Chinese and the Danish governments have set up positive examples for the world and will have special attention in this chapter as both countries have set ambitious targets (Figs. 23, 24, and 25).

The onshore wind resources available in most countries exceed the demand for electricity several times. An assessment by country for Europe indicates that utilization of a limited share of the wind resources available is sufficient to cover all present and future needs for power. To mention a few examples in the largest economy in Europe, Germany, onshore wind in principle can deliver seven times more than the total demand for electricity. For Sweden, Denmark, and the UK it will be factors of 40, 20, and 10, respectively (Fig. 26).

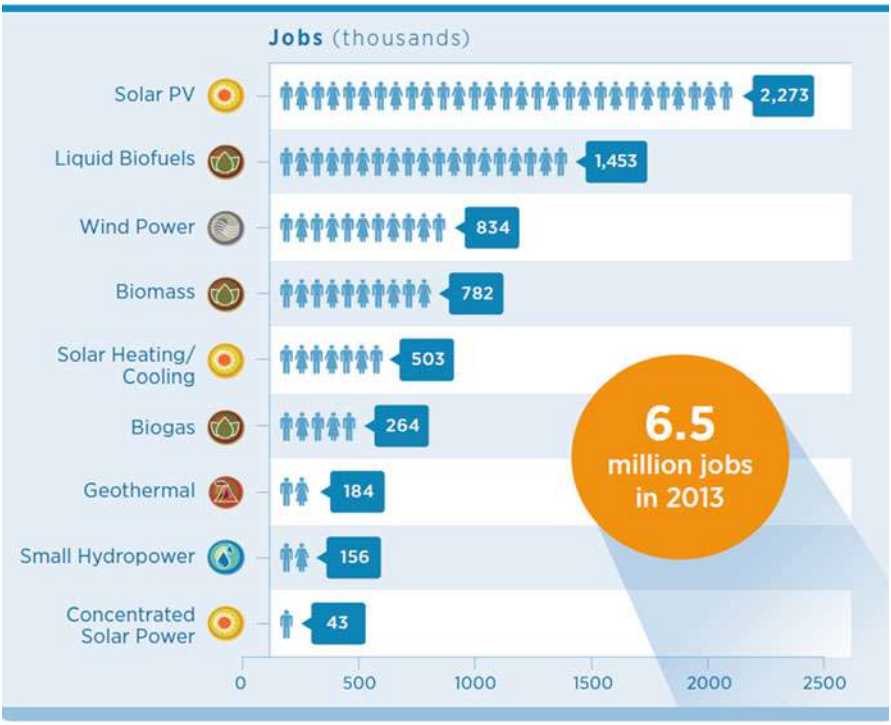

Fig. 22 Employment in thousands of persons in 2013 within various renewable energy sectors (Source: IRENA 2014)

Wind Energy Development in Denmark

Contemporary wind technology was born and came of age in Denmark. In the 1980s Denmark began to implement wind power at a commercial level and a dynamic production and implementation process evolved, resulting in the creation of a new industry.

Wind power during days with strong wind and low peak power consumption sometimes covers more than the total need for electricity in Denmark, while normal power quality standards are maintained. The wind power of Denmark accounted for 39 % in 2014 of its total electric power consumption of 36 TWh. The percentage is planned to reach 50 % by 2020. Further growth is expected from 5,000 MW of wind power in 2014 to 20,000 MW. This means that wind power within a decade or so will cover much more than the demand for electricity in 2014 (Fig. 27).

Even though wind power in Denmark was close to a standstill from 2002 to 2009, Denmark by 2014 was still the leading wind power country on a power percentage and per capita basis. By middle of 2014, 4,855 MW of wind capacity was installed in Denmark; with a population of 5.65 million, this is equivalent to 859 W per person

Position	Country	Total Capacity by June 2014 [MW]	Added Capacity H1 2014 [MW]	Total Capacity end 2013 [MW]	Added Capacity H1 2013 [MW]	Total Capacity end 2012 [MW]	Added Capacity H1 2012 [MW]	Total Capacity end 2011 [MW]
1	China	98'588	7'175	91'413	5'503	75'324	5'410	62'364
2	USA	61'946	835	61'108	1,6	59'882	2'883	46'919
3	Germany	36'488	1'830	34'658	1'143	31'315	941	29'075
4	Spain	22'970	0,1	22'959	122	22'796	414	21'673
5	India*	21'262	1'112	20'150	1'243	18'321	1'471	15'880
6	United Kingdom	11'180	649	10'531	1'331	8'445	822	6'018
7	France	8'592	338	8'254	198	7'499	320	6'877
8	Italy	8'586	30	8'551	273	8'144	650	6'640
9	Canada	8'526	723	7'698	377	6'201	246	5'265
10	Denmark	4'855	83	4'772	416	4'162	56	3'927
11	Portugal	4'829	105	4'724	22	4'525	19	4'379
12	Sweden	4'824	354	4'470	526	3'745	-	2'798
13	Brazil	4'700	1'301	3'399	281	2'507	118	1'429
14	Australia	3'748	699	3'049	475	2'584	-	2'226
15	Poland	3'727	337	3'390	310	2'497	-	1'616
	Rest of the World	31'506	2'042	29'451	1'761	24'660	3'026	16'493
	Total	**336'327**	**17'613**	**318'488**	**13'978**	**282'607**	**16'376**	**233'579**

Fig. 23 The top 15 countries worldwide in terms of installed wind energy capacity by June 2014 (World Wind Energy Association, WWEA)

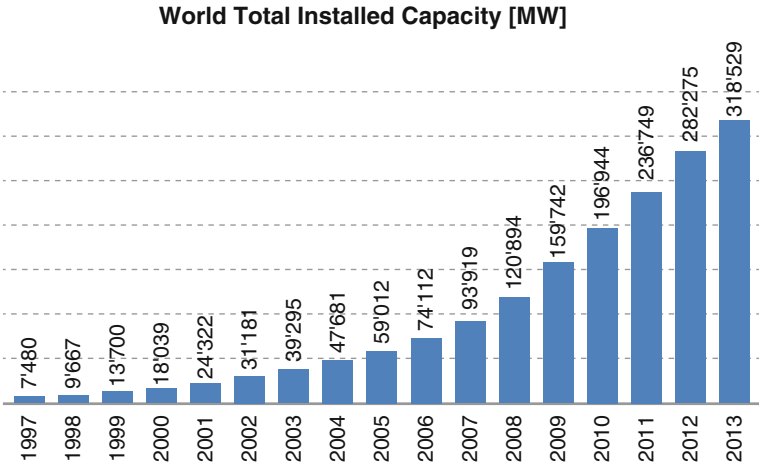

Fig. 24 World total installed capacity 1998–2013 (World Wind Energy Association, WWEA)

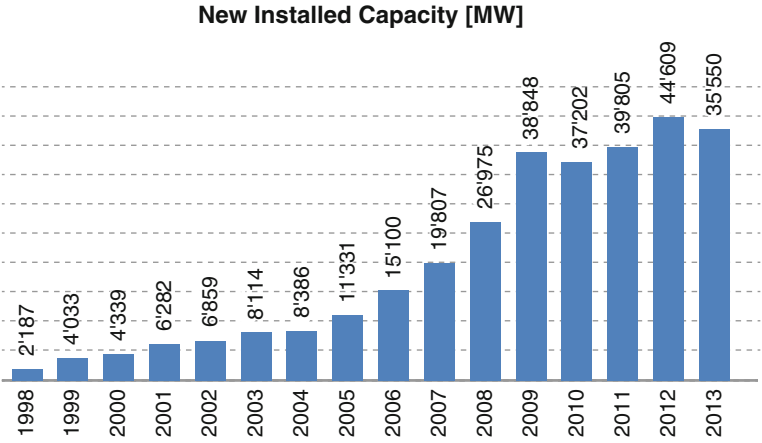

Fig. 25 New annually installed wind energy capacity 1998–2013 (World Wind Energy Association, WWEA)

(Fig. 28). As an extreme, the peninsular of Thy in Denmark with its 46,000 inhabitants, the 219 wind turbines' capacity of 125 MW results in 2,700 W per person, sufficient for 80 % of the demand for electricity coming from the wind. In Germany by middle of 2014, there were 36,488 MW and 82 million people, resulting in 445 W per person. On the other side, the UK, which has especially rich resources of wind, by middle of 2014 had 11,180 MW, meaning with a population of 64 million, 174 W per person. Even with 6 years of wind energy moratorium, Denmark has, by the middle of 2014, still obtained the number ten position on the world wind top 15 list.

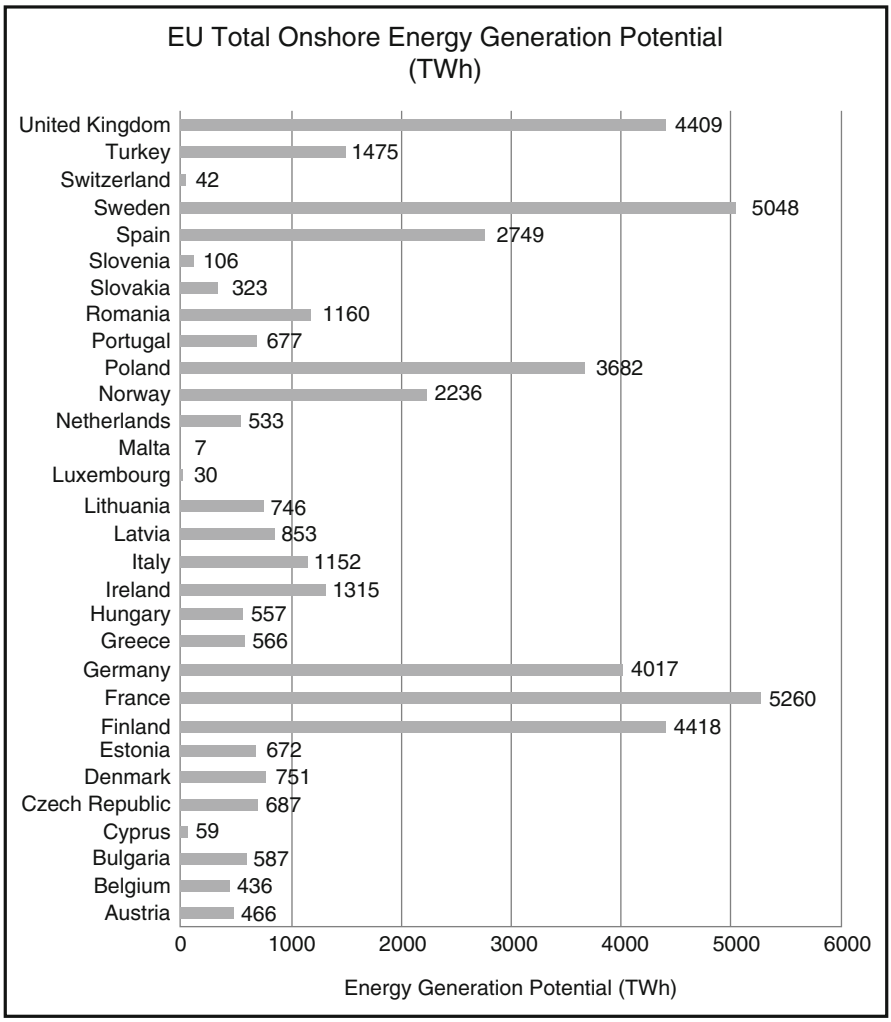

Fig. 26 EU total onshore energy generation potential (WWEA, World Wind Resource Assessment Report, 2014)

In the meantime, 2012 new targets have been set for wind energy in Denmark. The wind energy policy in 2014 consisted of targets that will be reached by 2020–2022 through the installation of 1,000 MW offshore wind farms, with one in the North Sea of 400 MW and another of 600 MW (called Kriegers Flak) in the Baltic Sea. Each 100 MW of new offshore wind power capacity will add some 1 % to wind energy's share of electricity in Denmark. Furthermore till 2020, 500 MW nearshore and 1,800 MW of onshore wind power will be installed while there will be repowering of some hundred MW of existing wind turbines. New multi-MW size offshore wind turbines will have capacity factors of 0.45–0.50, while onshore

Fig. 27 (*Left*) 25 KW solid wind of the new household wind turbine generation for single families and farms. Production: 40,000–80,000 kWh per year. (*Right*) Envision 3 MW wind turbine prototype during testing in Thyborøn, Denmark. Engineering and design by a Chinese company's R&D division in Denmark (Preben Maegaard/Nordic Folkecenter for Renewable Energy)

Year	2010	2011	2012	2013	2014*
Installed wind capacity (MW)	3,752	3,927	4,162	4,792	4,855
Electricity generated (TWh)	7.81	9.77	10.27	11.12	9.30
Wind power share in domestic electricity supply (%)	20.2	28.0	33.7	32.2	40.8

Fig. 28 Key figures for wind power in Denmark (energinet.dk/Danish Energy Agency)

capacity factor ranges between 35 % and 42 % on wind rich locations. With the newly decided offshore and onshore capacity, the adaptation of the entire power system to balancing the fluctuating energy forms is more urgent in Denmark than other countries (Maegaard et al. 2013).

Wind energy share of electricity demand in Denmark 2007 to 2030:

- **2007: 18 %**
- **2010: 25 %**
- **2013: 33 %**
- **2014: 39 % = 5,000 MW**

Type of wind power	Year/period	Installed capacity, MW	Costs/kWh/€-cents
Existing	End of 2011	3900	5-9
Offshore, Anholt	2013/14	400	14 (50 000 full load hours)
Onshore	2012-2020	1800	7,5 (22 000 full load hours)
Near shore (up to 3 km)	2013-2020	500	10,5 ?
Offshore	2017-2020	1000	12-15 (50 000 full load hours)
Community owned	*2012-2020*	-	*5-8*
TOTAL		6,600 MW	

Fig. 29 Electricity costs in Denmark by type of wind power (Danish Ministry of Energy, press release)

- **2020: 50 %**
- **2030: 150 % ? = 20,000 MW**

Denmark does not have a coherent feed-in tariff scheme. Biogas finds one solution, onshore wind a second that may be quite different from offshore. For PV household, small wind power, and mini CHP up to 6 kW installed capacity, net metering principle is the rule. The tariff for wind energy in Denmark depends on several variables: which year the turbine went into operation, how many full-load hours they already delivered, and whether they are offshore or onshore. The tariff comprises a market power price element, power-balance compensation, and a government subsidy.

New onshore wind turbines receive as a general rule a price premium of €0.03 per kWh for 22,000 full-load hours, which leads a total remuneration of €0.7 per kWh. In comparison, the most recent offshore wind farm, Anholt with 400 MW, 2013/2014, was installed by the central utility DONG Energy. A tendering process guarantees a price of €0.14 per kWh for 50,000 full-load hours, making offshore wind power at least two times more expensive than when placed onshore (Fig. 29).

The Ownership Model Behind Two Decades of Success

Nontechnical aspects are also of importance for a successful transition to renewable energy supply. The absence of financial investors made the wind sector in Denmark unique at an early stage compared to other countries. At the turn of the century, around 150,000 households were co-owners of a local windmill. The ownership model rather than the technology and tariff schemes were substantial for the success of wind energy in Denmark. It was the key factor behind the high public acceptance that wind power projects enjoyed during that time. It also enabled a much faster deployment, since large numbers of people were involved in the sector that provided the necessary goodwill (Fig. 30).

In 1992, the role of cooperatives shrank due to a change in planning procedures. In 1998, due to liberalization in the sector, the ownership model changed dramatically. The residential criteria for ownership were abolished and everyone was allowed to own any amount of windmills as they could get, building permission for anywhere in the country. The takeover bids began, resulting in a dramatic decrease in public involvement. As a result, in 2009 about 50,000 households

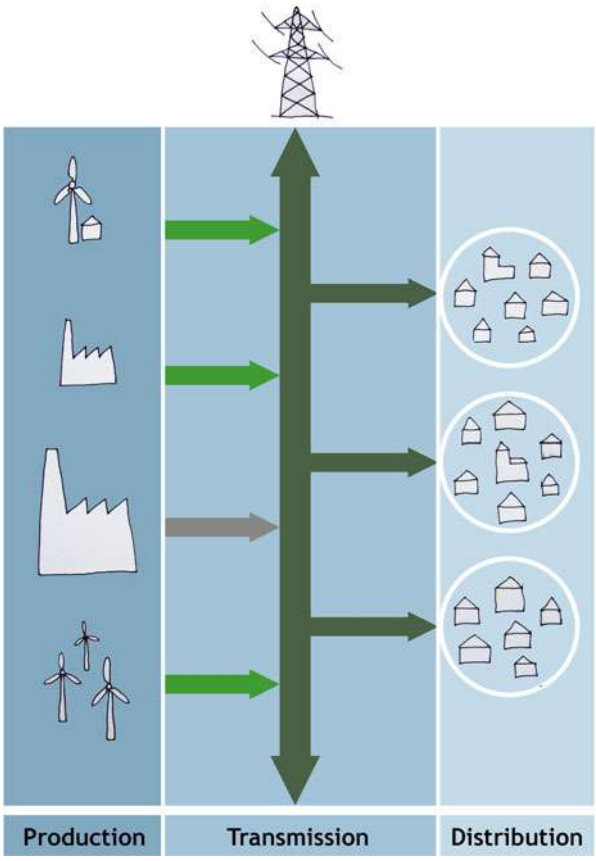

Fig. 30 Legislation in 2004 in Denmark resulted in separation of production of power, transmission, and distribution (Nordic Folkecenter for Renewable Energy)

were co-owners of windmills compared to 150,000 a decade earlier (Maegaard 2012).

Consequently, the attitude toward wind power suffered a reversal. The erection of a windmill often became a local drama and resulted in bitter conflicts that lead to long delays or cancellations. In 2008, a wind turbine neighbor compensation scheme was introduced that also caused local conflicts. The solution seems to be to "normalize" the wind energy sector so that wind power like district heating, CHP, and power distribution changed from investment to public supply, with municipalities and consumer-owned local companies as the future wind power owners. This would make wind power even more significantly cheaper.

Denmark already has hundreds of consumer-owned local energy supply companies for combined heat and power, district heating, and power distribution. New organizational structures and nonprofit ownership models to the direct benefit of the involved municipalities may prove to be the most realistic long-term solution for community wind power as well to again make it locally acceptable.

Integration of the Energy Supply by Public Ownership

Renewable energy is still young; technology and tariff problems have found reasonable solutions; however, generally acceptable organizational structures for decentralized ownership for the common good as well are part of the transition process.

The ownership and operation of large wind turbines for community supply should be a service provided by local public authorities as for CHP, supply of water, central district heating, public transport, and other parts of public infrastructure. It is the lesson from the past 100 years of practice that the state should promote public regulation in favor of local and collective ownership of basic public services, such as energy. This approach is in line with the protection and promotion of the common good in most democratic societies. Considering the size of order and complexity of the transition to 100 % renewable energy-based energy system, and its urgency, it is only realistic for public administrations to undertake this task.

The common good approach will make wind power a part of the public planning with expropriation of the necessary areas for wind turbines, as it is done with power pylons, waterworks, and similar areas of public interest. It is already standard practice to provide monetary compensation when areas are being designated for the common good. This would be a decisive contribution for attaining local acceptance and making wind energy more competitive. In Denmark, it could lead to a 30 % or more cost reduction, more than can be expected from improved technologies.

In several countries, new legislation mandates utility companies to buy electricity from renewable energy installations at a price determined by the government that is guaranteed for a period of 10–20 years. Such laws, based on guaranteed and differentiated feed-in tariffs, FIT, are used in the most successful wind energy countries. This would be a serious incentive for municipalities as well to actively be a part of the development of CHP combined with renewable energy either through municipal companies or existing and eventually new local renewable supply companies that can supply a full renewable energy package including wind power.

By making the establishment and operation of large wind turbines the responsibility of public supply companies, there would be significant savings due to cheaper sites for wind turbines, saved repowering fees, and cheaper long-term financing. Wind energy would then be more attractive for individual municipalities as well as at a national level and improve supply security, guaranty steady energy prices, and fulfill international agreements concerning CO_2 reduction as well.

Combined Heat and Power (CHP) and Its General Application

Cogeneration/CHP is the second cornerstone in future self-sustaining supply structures. CHP is the simultaneous production of electricity and heating/cooling from the same fuel which more than doubles traditional conversion efficiencies. This chapter focused on two aspects of CHP: its higher overall fuel efficiency and the important

role for power balancing in future energy systems with high shares of fluctuating power from wind and solar energy due to its generally local character with proximity to the places of consumption.

As a whole, the European Union generates 11 % of its electricity using cogeneration. However, there is large difference in the member states with variations of the share of CHP between 2 % and 60 %. The four countries with the Europe's most intensive cogeneration shares are Denmark, Latvia, Finland, and the Netherlands. The Danish CHP share varies from 43 % to 60 % with the lower share generated in years when export to neighboring countries of coal-based electricity from conventional power stations is high (Fig. 31).

Other European countries are also making efforts to increase their overall energy efficiency by increased use of CHP. Over 50 % of Germany's total electricity demand could be provided through cogeneration. Germany has set a target to double its electricity supply from cogeneration from 12.5 % of the country's demand to 25 % by 2020. Due to the advantages of combining the fluctuating renewable energy forms with CHP, Germany's ambitious wind and solar energy programs will not be in conflict with an increased share of CHP. On the contrary, with an extensive

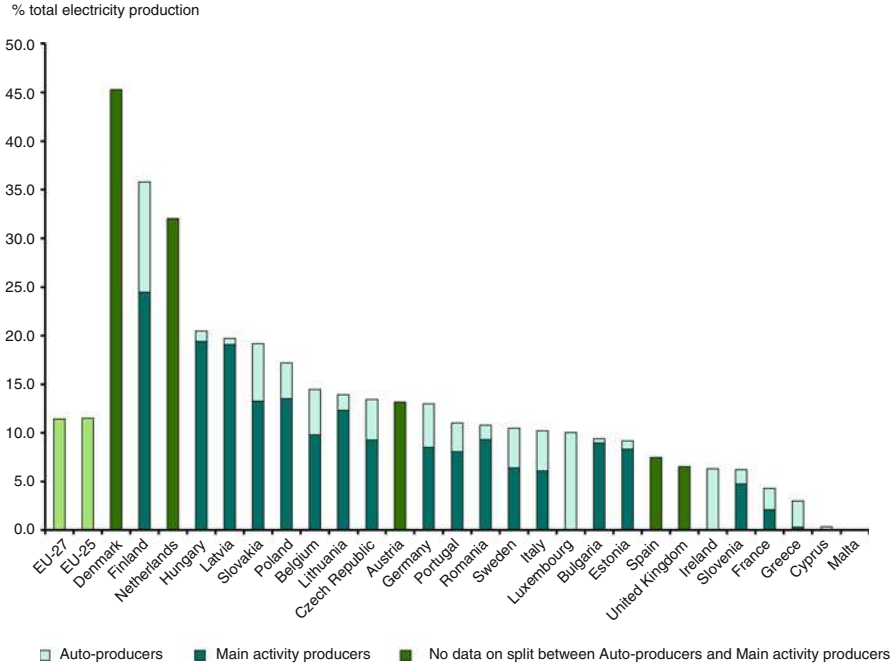

Fig. 31 Share of combined heat and power in gross electricity production in 2009. The share of electricity from combined heat and power in total gross electricity production in the EU-27 was 11.2 % in 2011, but 11.4 % in 2009, a growth from 2008 of 0.4 % and from 2005 of just 0.3 % points. CHP has seen modest progress in increasing the share of CHP in EU electricity generation (Eurostat, energy statistics)

increase of hot water-based district heating and cooling and the technologies properly integrated with electric boilers, heat pumps, and hot water storage, the CHP stations will pave the way so that significantly more solar and wind power can be installed in Germany. With high shares of wind power, some of it will, at periods with high wind, be available for the supply of heat. This will lead the way to 100 % renewable energy in the largest European economy. Using well-proven already existing technologies, investments per MW of new installed capacity of electricity and heating will be in the same size of order as conventional fossil fuel-based investments for similar power capacity.

Conventional power generation is based on burning fuel to produce steam. It is the pressure of steam that turns turbines and generates power in an inherently inefficient process. Because of a basic principle of physics in practice, a maximum of 40–45 % of the energy of the original fuel is converted to electricity. The European average is 35 % and the world average 30 % meaning that conventional condensation power plants represent an outdated technology.

Cogeneration, in contrast, recovers the heat for useful purposes. With efficiencies up to 90 % or higher, CHP is the ideal means of generating heat and electric power; at the same time from the same consumption of gas, oil, or biomass, it can double the supply of energy compared to conventional power generation (Fig. 32).

The favorable environmental implications of cogeneration stem not only from its inherent efficiency but also from its decentralized character. Because it is impractical to transport heat over long distances, cogeneration equipment must be located physically close to its heat application. A number of environmental benefits flow from this fact: power is generated close to its consumer, significantly reducing

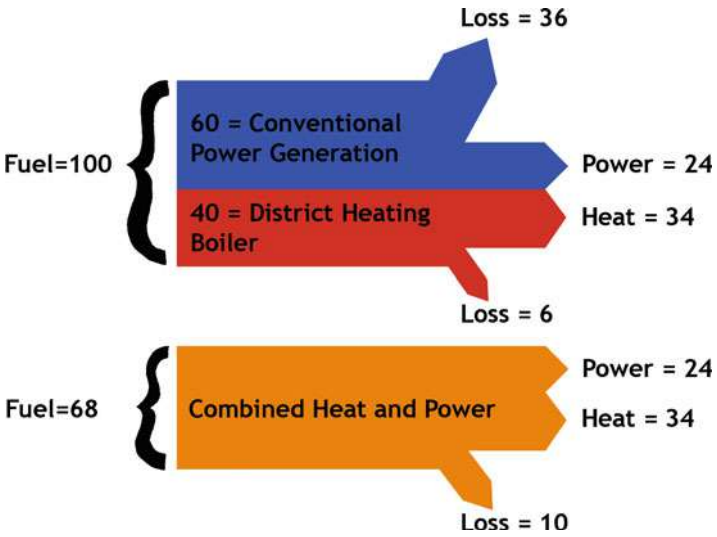

Fig. 32 For the same supply of heat and power, with the conventional solution with separated heat and power production, the consumption of fuel is 47 % higher (Nordic Folkecenter for Renewable Energy)

Fig. 33 Faaborg CHP plant (*left*) with its location close to the town center. It can supply its 7,000 inhabitants. The circular center building is for the hot water storage (*right*) (Jane Kruse/Nordic Folkecenter for Renewable Energy)

transmission losses and the need for distribution equipment. Cogeneration plants are usually smaller and owned and operated by smaller and more localized consumer companies than conventional power plants. Cogeneration is at the heart of district heating and cooling systems (Fig. 33).

Cogeneration units can be manufactured in series, similar to how truck and tractors are, which leads to low unit costs, while each individual conventional power station is unique so that similar cost reductions cannot be expected.

Due to international policies to reduce emissions of greenhouse gases, governments, municipalities, owners, and operators of industrial and commercial facilities are actively seeking ways to use energy more efficiently. Especially important is cogeneration that is the key technology in future integrated energy systems based on CO_2-neutral energy forms, solar, wind and biomass, to maintain continuous supply of electricity, cooling, and heating.

Combining a cogeneration plant with an adsorption refrigeration system for air conditioning and other needs for cooling allows utilization of seasonal excess heat. The hot water from the cogeneration plant can serve as drive energy for an adsorption chiller. Around 70 % of the thermal output of the cogeneration plant is thereby converted to chilled water. As the hot water replaces electricity for cooling needs, a well-balanced system with low losses can be designed. In this way, the year-round capacity utilization and the overall efficiency of the cogeneration plant can be increased significantly.

Cogeneration Technology

A typical cogeneration system consists of a gas engine, steam turbine, or gas turbine that drives an electrical generator. Heat exchangers recover the engine's cooling water, exhaust gas, lubrication oil, turbocharger, etc. to produce hot water.

An emerging technology that provides additional possibilities for cogeneration is the fuel cell. A fuel cell converts hydrogen or other fuels to electricity without combustion. Heat is also produced. Most fuel cells use natural gas (composed mainly of methane) as the source of hydrogen. Solid oxide fuel cells may be a potential source for cogeneration, due to the high temperature heat generated by their operation and high electrical efficiency of around 60 %.

Cogeneration Units

Cogeneration plants are the modules for combined production of electricity and heat.

CHP is characterized by:

- Low investment costs
- High efficiency rate, on average 85–90 %, of which electricity is 35–44 %
- Process automatic control
- 40,000 h of operation between major overhauls
- Rapid installation of 6 months or less
- Meets international emission standards

Main parts of a cogeneration unit are:

1. Internal combustion engine
2. Engine support frame
3. Alternator
4. Electricity control cabinet
5. Engine cooling system with heat exchangers for connection to the heating and cooling system

A CHP module including all components can be factory built on a frame or in a container ready for transport and installation. It can be designed for operating on natural gas, plant oil, biogas, or mixtures of gas. Its compact construction includes all the components of the CHP system, it can also contain additional facilities as heat pumps and electric boiler to match well with fluctuating energy forms like wind and solar (Fig. 34).

A CHP module can be built to industrial standards and meet the requirements of various national energy authorities. The modularized design ensures use of compatible technical components. Trouble-free and rapid commissioning of district heating stations and biogas plant using CHP is possible by using standardized equipment. Building time of conventional power stations may take 4–8 years. In contrast, CHP stations may be planned, installed, and commissioned between 4 and 8 months. The CHP module has already been tested and is ready to be connected when it is delivered. Only the cables and pipes for electricity and the heat supply must be connected as well as the source of fuel that can be natural gas,

Fig. 34 Ancillary equipment in a CHP station: the exhaust heat exchangers (*left*) convert the exhaust heat from the gas engines to hot water. The absorption heat pump (*right*) upgrades 20–40 °C water for use in district heating (Preben Maegaard/Nordic Folkecenter for Renewable Energy)

oil, biogas, and other gases. Consequently, the production of electricity and heat can begin within a short period of time.

Cogeneration Applications

Cogeneration systems have been designed and built for many different applications. Large-scale systems can be built on-site as a plant to supply a city or industry with district heating or steam. Cogeneration systems are also available to small-scale users of electricity. Small-scale packaged or "modular" systems are being manufactured for commercial and light industrial applications and in agriculture using biogas. Modular cogeneration systems, such as energy boxes, are compact and can in the future be manufactured like automobiles and other mass-produced equipment. These systems range in size from 6 kWel and up to several MWel capacities. It is usually best to size the systems to meet the hot water and heating needs. They can be operated continuously or only during peak load hours to benefit from peak demand tariffs. Cogeneration is inherently more energy efficient than using separate power and heat generating sources, making it an effective antipollution strategy.

Manufacturers of gas engines include GE Jenbacher, Caterpillar, Perkins, MWM, Scania, Cummins, Rolls-Royce, Wärtsilä, MTU, MAN, Yanmar, Kubota, and several other engine builders (Fig. 35). Engines can have spark plug ignition, which is the most common. Some have 4–10 % oil injection for compression ignition. The modern high-speed gas engine has higher efficiency (44 %) than gas turbines. The gas engines are intensively used in transcontinental compressor stations with proven long-time trouble-free operation without service and major overhauls. Most of the gas engines are based on a diesel engine platform that is converted.

Germany in particular uses a significant amount of small-size CHP that are based on natural gas, biogas, diesel oil, pure plant oil (PPO), wood pellets, or other fuels (Figs. 36 and 37). In the city of Freiburg, Germany, often described as Europe's renewable

Fig. 35 Snedsted CHP (*left*) with GE Jenbacher V20 3,500 KWel gas motor. Farm CHP (*right*) with MAN V12 375 kWel motor using biogas (Preben Maegaard/Nordic Folkecenter for Renewable Energy)

Fig. 36 Two types of small-scale CHP in Bavaria, Germany. KW Energie CHP (*left*) with Kubota 8 kWel/18 kWth engine for one family house using pure plant oil, PPO. Farm CHP (*right*) with 3 × 120 kWel (approx.) MAN engines using biogas (Preben Maegaard/Nordic Folkecenter for Renewable Energy)

Fig. 37 Three types of small-size CHP. The Ecopower using natural gas (*left*), the Sunmachine wood pellet-fueled Stirling CHP, and small farm CHP using biogas (Preben Maegaard/Nordic Folkecenter for Renewable Energy)

energy capital, a small CHP campaign for 1,000 CHP units was launched. They will be installed in Freiburg's old buildings in city quarters. Freiburg already has 55 % of its electricity coming from CHP consisting of a 40 MWel natural gas CHP of a chemical company and some CHP in public and family houses. The additional potential for CHP in Freiburg is more than 5,000 multifamily buildings and other buildings.

The CHP plants in Denmark already have considerable experience in optimizing their electricity production against the triple tariff which has existed since the early 1990s. Consequently, the plant operators know how to organize the production of the CHP units in order to optimize their income. Meanwhile, Denmark had a process of replacing such pricing conditions by market prices. Consequently, new methodologies and tools for the optimization of the daily operation of small CHP plants are needed. The new markets include upregulation and downregulation which meets short-term imbalances mostly caused by increased use of fluctuating and intermittent supply from solar and wind energy.

Case Study: CHP in Skagen, Denmark

District heating systems have a long history in Denmark – the very first system was established in the beginning of the 1900s in the city of Frederiksberg. Other cities followed the example and today there are about 500 district heating plants in the country, covering over 60 % of Denmark's demand for space and water heating.

Skagen Varmeværk started operating in 1964 with 535 cooperative society members. Today Skagen Varmeværk is responsible for operating district heating for the town of Skagen, the most northern town in Jutland, with 8,400 inhabitants. The Wärtsilä CHP plant (3 × W28SG) is equipped with efficient heat exchangers that reach total efficiencies of above 90 %. After some years of operation, the engines were upgraded to give a higher output and improved performance. In addition to its own production, a municipal waste incineration plant and a nearby industry are delivering heat to the common Skagen district heating network (Fig. 38).

Fig. 38 CHP power plant in Skagen (Jane Kruse/Nordic Folkecenter for Renewable Energy)

Table 1 Fact sheet – Skagen CHP power plant

3 × Wärtsilä gas engines	3 × 4.6 MWel/19.4 MWth
4 × Gas hot water boilers	46 MWth
1 × Electrical hot water boiler	11 MWth
Heat import from the waste incineration plant	Max. 6 MWth
Heat import from the neighboring industrial plant	Max. 6 MWth
Heat storage capacity/hot water accumulator	600 MWhth

The plant not only produces heat for the city and power for the distribution system operator but also actively participates in the Danish electricity regulating and primary reserve/frequency balancing markets. To handle these simultaneous production requirements effectively, very flexible operation, short start-up, and shutdown capability, as well as operator alertness, are essential. Besides the gas engines and in order to secure the production, the plant is equipped with hot water boilers operating on natural gas and prepared for the possible use of bio-oils and fuel oils, an electrical boiler operating in parallel with the gas engines and with heat storage accumulator. All these units allow very flexible and environmentally friendly operation (Table 1).

Heating of Communities

District Heating Networks

District heating systems are networks that supply hot water that is produced centrally, in one or several locations, to heating and cooling customers. Two-way pipes are used to distribute the hot water at a temperature of 60–90 °C that is returned at 30–50 °C after consumption.

The countries with the strongest growth in CHP capacity also had the strongest growth in district heating capacity. Operators that construct new district heating schemes often consider application of CHP a rational and viable solution or CHP may be a requirement by the local or national energy authorities as it improves energy efficiency significantly and makes it easier to meet CO_2emission reductions.

The same policies that have created a high penetration of district heating in Scandinavia have also created a high share of CHP with hot water storage connected to the district heating systems. This as well paves the way for increased use of the fluctuating energy from solar and wind leading to 100 % renewable energy. Presently, power peaks coming from wind and solar can be balanced in the local CHP stations as gas engines can respond within seconds or minutes to the variations in the productions of wind and power. In the long term, solar and wind can often cover power base load needs and at periods with maximum supply of solar and wind power, the fluctuating energy forms may even periodically cover both the need for electricity and the need for heating. This saves natural gas or biomass that will be available as backup fuel when solar and wind is not sufficient.

While some countries have opened up for decentralized energy structures with numerous operators and a diversity of energy drivers, the relatively low penetration of CHP in district heat production in, for instance, France, is an example of the obstacles decentralized producers face when entering an electricity market that is dominated by monopolies or oligopolies.

In practice, it is feasible for an ambitious national policy to reach, as in Finland, an almost 80 % share of district heating produced in combined production. The Finnish example shows that this can be reached by a diversified fuel input without depending on a single fuel type. In the future, the integration of large quantities of solar and wind can become included as well. Well-planned district heating and CHP offer an important potential for increased energy efficiency in the energy sector.

In Denmark, district heat is supplied by some 500 district heating companies and accounts for more than 60 % of Denmark's heat demand, compared to levels of 30 % in 1980. Most of the companies produce and supply the heat, but some purchase heat from the central power plants. The average consumer connection rate in district heating areas is 82 % and is still increasing. The district heating network supplies heat to large consumers, apartment blocks, offices, institutions, and to single-family houses. Danish district heating companies are owned either by the municipalities, particularly in the major cities, or by local consumer cooperatives (Fig. 39).

Between 43 % and 60 % of the electricity generation is from CHP, compared to just fewer than 20 % in 1980. Twelve of the 14 central power stations in Denmark deliver all or part of their excess heat to a district heating network. Nearly all large-scale power plants are located close to major cities. This and the fact that 80 % of the population lives in urban areas allowed the high shares of combined development of district heating and CHP. The first steps in the development of CHP were taken in Aarhus, Odense, and Aalborg, which are the second, third, and fourth largest cities in Denmark, respectively.

In 1904, the first CHP plant was commissioned, supplying heat and electricity to a hospital. By the mid-1930s, the Copenhagen district heating network was well established, even though heating was to a large extent still provided by small individual coal-fired boilers. The first plant specifically designed for CHP was commissioned in 1934. The heat planning legislation, initiated in 1979, aimed to increase the share of cogeneration in the district heating supply system and to promote use of natural gas. Through the heat plan, the cities and towns were divided into areas suitable for district heating and areas more suited for individual supply of natural gas. The heat plan shielded district heating from interfuel competition from natural gas and electric heating. The majority of district heating loops are owned by the inhabitants of the community (Fig. 40). This gives control to the residents and ensures that energy is distributed to the communities at the lowest possible prices. If

Fig. 39 Share of district heating supply for households only by ownership, Denmark, 2012/2013 (Energitilsynet)

Ownership	Share in %
Municipal	61
Consumer-owned	36
Commercial	4
Housing Associations	0,1

Fig. 40 Example of a district heating network (*left*). Vorupoer CHP (*right*) has two Jenbacher natural gas motors, each of 900 kWel. The electrical efficiency is 42 %. It serves 200 households, local business, and institutions with heat. The electricity is delivered to the public grid. The chimney is decorated by a local artist. In the background are two hot water storagetanks. The CHP and heating network is owned by the local consumers in a not-for-profit company. The staff consists of one person, a technician. In 2010 the plant was presented in the film documentary "The 4th Revolution" as an example of best practice (Jane Kruse/Nordic Folkecenter for Renewable Energy)

profits are made, they are given back to the energy consumers in the form of lower heating costs in the succeeding year.

Major cities have city-wide district heating systems where almost all of the heat (95–98 %) is produced in large coal-fired or gas-fired CHP plants and waste incineration plants, with a number of oil-fired or gas-fired heat-only boilers for peak load and emergency. Since the early 1980s, no new power plants have got permission for commissioning unless provided with the ability to use CHP and to supply heat to the district heating networks (Fig. 41). This was motivated by security of supply and environmental concerns encouraging energy efficiency. Construction of new electricity-generating capacity must be justified by the need for new heat-production capacity (Fig. 42).

In addition to the large-scale CHP and district heating units, a large number of small-scale CHP plants exist. Most of the plants range between capacities of 0.5–5 MW and supply heat to small communities and institutional buildings. Often, the plants consist of more than one CHP gas engine unit. Small-scale CHP plants, which are not connected to a district heating network, rarely exceed an electric capacity of 1 MW. Small-scale CHP plants are laid out to cover at least 90 % of the local heat demand.

The national power system responsible will purchase the electricity from all types of producers (Fig. 43). The electricity generated is sold to the public grid. The fuels used in small-scale CHP are natural gas and, to a lesser extent, biogas and other biomass (Fig. 44). In connection with the presentation of the Energy 2000 plan in 1990, a more ambitious program for small-scale CHP was put forward. To accelerate the establishment of small-scale CHP, a state subsidy was introduced in 1992 for power production from waste incineration, natural gas, and renewables. The subsidy originally amounted to €0.014 per kWh. With an implementation period of less than 10 years, the development of small-scale CHP peaked in the late 1990s. The capacity

Fig. 41 PU foam insulated pipes (*left*) for district heating for a small rural community (Preben Maegaard/Nordic Folkecenter for Renewable Energy). (*right*) Through well-insulated heating pipes (red), 60–90 °C water is circulated to every building. After cooling down to approximately 30–50 °C, the water returns (blue) to the CHP station (Jane Kruse/ Nordic Folkecenter for Renewable Energy)

Fig. 42 Hanstholm (*left*) and Hurup (*right*) district heating plants without CHP. Both are located in regions with high density of wind power. Hanstholm has been modified to substitute some of the present fuels with excess power from wind and solar energy (Jane Kruse/Nordic Folkecenter for Renewable Energy)

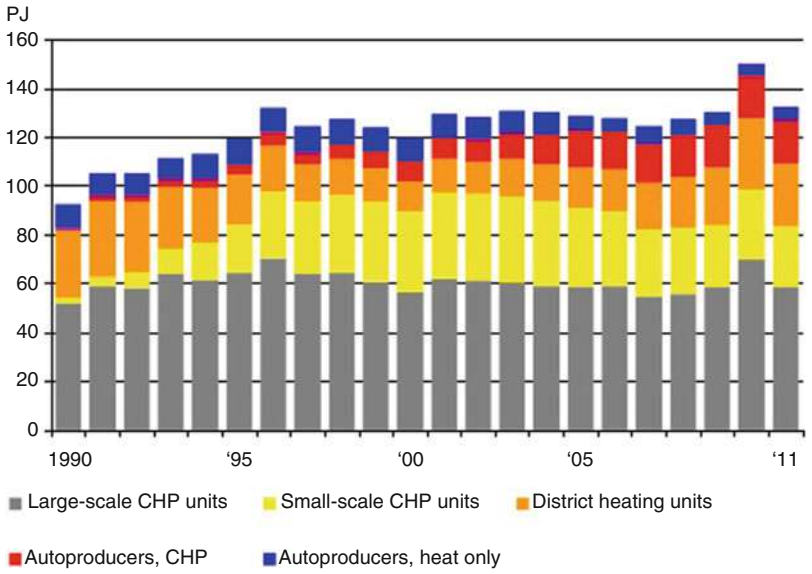

Fig. 43 District heating by type of producers (Nordic Folkecenter for Renewable Energy through Danish Energy Agency) (Source: Danish Energy Agency)

Fig. 44 Share of district heating supply (only for households) by primary fuel, in Denmark in 2013 (Energitilsynet)

Fuel	*Share in %*
Biofuels	29
Natural gas	21
Coal	21
Waste	19
Industrial surplus	7
Other	2

was sufficient to produce 25 % of the national demand for power. About 80 % of the installed capacity is based on natural gas engines. Sixteen percent are gas turbines and 4 % are biogas-fired engines. Most of the installed gas engines have an electric capacity in the range of 0.5–6 MWel, whereas gas turbine units typically range in capacity from 5 to 25 MWel.

The electricity from CHPs is fed into the national grid. The feed-in tariffs for CHP were based on a three-tier tariff system, with tariffs reflecting electricity demand patterns (low, medium, and peak tariff periods). After liberalization of the electricity sector, market principles were applied like in the other Nordic countries.

Industrial CHP is used in industries with high demand for process heat, especially the petrochemical, wood, malt, and paper industries. The food industry and greenhouses can also use low-pressure steam or hot water from CHPs. To illustrate the variety of applications, the national railway company gets hot water for cleaning its passenger trains from a medium-size CHP at the maintenance facility. In 2000, electricity production from industrial CHP was about 8 % of total power generation.

Technology for Decentralized District Heating

As mentioned earlier, the preferred CHP technology predominantly has been gas-powered engines. Stationary natural gas engines used in combined heat and power applications boast a factor 4 reduction in CO_2emission compared with conventionally generated thermal coal power for same produced power and individual supply of heat.

This is because:

1. The heat can be used if the system is placed in the community increasing the total efficiency of the system to over 85 % compared with the best thermal coal condensing power plant at around 45 % electrical efficiency.
2. Natural gas has a tenth of the SOx, half of the NOx, and a third of the CO_2 produced compared to the emission by the combustion of coal. The cost of removal of these pollutants in a coal-generation plant is significant.
3. The cost to install a gas engine is around 40 % lower per kWel installed than that of a coal plant and even cheaper if removal of the emissions from coal is included. Additionally, gas-fired engines can be installed in 6 months as opposed to 4–8 years for a thermal coal plant.
4. Gas engines are manufactured in series and are cheap, while central power plants are one-of-a-kind technology. The gas engines can be installed in existing or new buildings without any noise or visual impact for the neighborhood.

With these benefits, it became possible for local district heating companies owned by municipalities or consumers to build their own CHPs and offer cheaper heat to households. This became the primary driving force which encouraged a rapid change to local CHPs.

Natural gas used in a CHP is not renewable but local CHP creates the basis for a decentralized energy structure that later with modest investments can be changed to local renewable energy sources. Stationary gas engines can run on a variety of fuels which can be tailored to local fuel availability.

These local supply sources can be:

- Biodiesel
- Plant oil
- Biogas
- Gasified biomass
- Landfill gas
- Solar thermal installations
- Wind heat and power (WHP)

If these alternate fuel sources are not available, natural gas can be used as a transitional fuel, while the community determines which fuel can be utilized in the future. In essence, district heating with CHP provides the initial framework toward a renewable energy power and heat system.

Summarizing the Advantages of Local CHP

Advantages of community-based CHP units are significant, the main benefits being:

1. Reliability: Gas engines can be used where reliability is of the utmost importance. Typically these gas engines are installed in transcontinental gas compressor stations, drilling rigs, offshore oil platforms, and villages not served by the national power grid.
2. Community Autonomy: Having local CHP provides the local community with autonomy giving the "power to the people." This enables the community to ensure that the electricity is produced in an appropriate manner.
3. The Ability to Incorporate Renewable Energy in the Future: Having CHP with district heating opens opportunities to incorporate large shares of renewable energy in the form of biogas, solar thermal heating, wind for heat, biomass gasification, plant oil-based fuels, and combustion of locally grown biomass.
4. Scalability and Flexibility: Local CHP is scalable and flexile to operate. This makes it easy to increase capacity in the future and matches well with the incorporation of wind and solar power in the supply system.
5. High Efficiency: Medium-size stationary gas CHP units boast an electrical efficiency of around 44 %, and with heat recovery of the jacket water, exhaust, lube oil, and turbocharger, they can achieve an overall efficiency of over 85 % (power 44 % plus heat 43–48 %).
6. Cost-Effective Heat and Power: With high total efficiencies and two energy products from the same fuel source, cost of power and heat can be reduced. As an example, in 2007, Denmark according to Eurostat had the fifth lowest power prices (without taxes) for GWh consumers in Europe with Sweden, Norway, France, and Finland, all countries with old hydro and/or atomic energy, being lower.

Combining CHP and Wind, in Summary

On days with a high demand for heat combined with high wind, CHPs and wind turbines, as mentioned earlier, together periodically feed more power into the grid than needed by the consumers. The challenge for the system operator in some countries is already and will in the future be even more to optimize the available resources. While Europe as a whole has 11 % of the efficient combined heat and power (CHP) in the energy system, the share in Denmark is 43–60 %, the world's highest, which at the same time represents not only the problem mentioned but also its solution.

The combined high CHP and wind power production causes a potentially major problem in the power sector. However, supply and demand can be balanced by feeding on windy days the excess wind power into electric boilers and heat pumps at the combined heat and power stations, which makes 100 % renewable energy supply of heat and power realistic. The electric boilers and heat pumps make it possible to

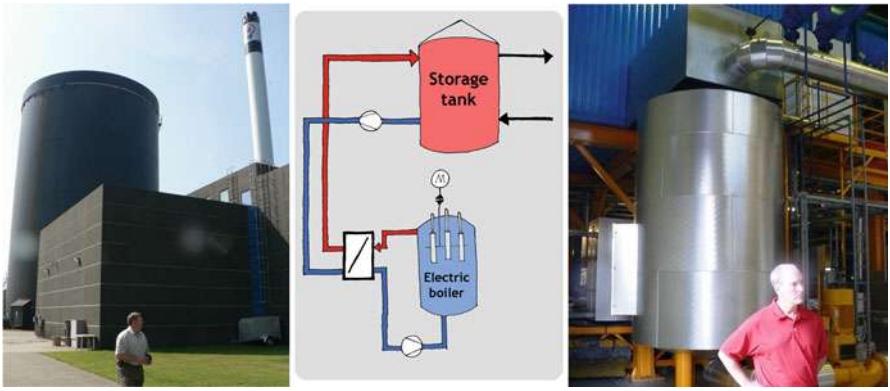

Fig. 45 Principle of downregulation using excess wind power at a CHP plant with 10,000 consumers. Storage for 2 days of heat supply (*left*) in Grindsted; 20 MW electric boiler (*right*) (Nordic Folkecenter for Renewable Energy)

stop the natural gas and biomass-fueled CHP units at periods with excess wind and solar energy. With increased renewable energy shares in the future, more and more often the fluctuating solar and wind energy will be sufficient to satisfy both the need for power and heat (Fig. 45).

Compared to other uses and storage of excess power, electric boilers and heat pumps cause no conversion loss. Heat pumps even boost the excess production of power by a factor of 2–6 depending on the energy source available. For the heat pumps, a low-quality source may be atmospheric air, soil, and water from the sea or rivers, which will result in a relatively low efficiency, while geothermal heat, air ventilated from buildings and industries, and other types of potential heat sources up to 40 °C will result in high efficiencies in the heat pumps. As they require substantial investments, the operation of heat pumps using excess wind and solar power for balancing the grid by downregulation should result in yearly operation of 3,000 h or more. This amount of excess power will in a more distant future be available at medium peak periods. As fluctuating solar and wind will always cause short-term high peaks, electric boilers will due to their low initial investment be the preferred solution to utilize the high peaks of solar and wind energy.

Therefore, it is not a relevant discussion whether electric boilers or heat pumps should be preferred. In the early stage of using fluctuating solar and wind in the heating system, electric boilers will be optimal, while increased amounts of fluctuating power will pave the way for heat pumps to convert the medium peak electricity into district heating while the electric boilers will take the high peaks (Fig. 46).

Like the transition from fossil fuels to renewable energy forms leads to zero emission, the modern power balancing is an integrated part of the change of the energy system. The natural gas-based cogeneration in district heating stations and the industrial autoproducers can be adjusted within seconds or minutes and ideally match the fluctuating renewable energy supply.

Fig. 46 Three sizes and types of electric boilers for power downregulation: 20 MW, 10 kV (*left*); 3,300 kW, 400 V (*middle*); and 45 kW, 400 V (*right*) (Nordic Folkecenter for Renewable Energy)

New taxation rules can make it economically beneficial to use fluctuating wind electricity for district heating according to a decision by the EU Commission. While excess electricity sometimes is being sold at the spot market for €0.01 per kWh or even at negative prices, it will at any time when used for heating have a value equivalent to the fuel that it replaces or €0.04–0.12 per kWh depending on the type of fuel and taxation.

Case Study: Thy, the Municipality of Thisted

In the Thy peninsular with its 46,000 inhabitants, the 219 windmills and other renewables cover 100 % of the annual need for electricity. The local energy production has become an important source of income. "In Thy people prefer to use renewable energy. That is the essence of the Thy model where people, economics and technology come together to create clean carbon neutral energy" (Thisted Municipality).

On days with strong wind, the wind turbines may even produce four times more than the actual consumption and the power quality still lives up to the highest standards. The local utility, Thy-Mors Energi, has demonstrated real-time management of such big quantities of wind energy to visitors from all parts of the world.

In the towns and villages in Thy, people get their heating from hot water pipelines in the streets. It is environmentally and economically the best solution to use the excess wind power for the actual supply and storage in the big hot water reservoirs of the local district heating suppliers instead of exporting the surplus power to neighboring countries sometimes at low-spot market prices (Fig. 47).

A new municipal energy foundation plans to own further windmills. In 2010, 80 MW of new capacity was in the planning process. The income of the discussed foundation may be up to €7 million per year earmarked for local energy initiatives which secures acceptance of the wind power and illustrates the benefits of change from investor policy to local supply (Table 2).

Fig. 47 (*Left*) Thisted combined heat and power for a town of 25,000 residents. Fuels used include household waste, straw, wood, solar thermal, and geothermal. (*Middle*) 6 MWel steam turbine. (*Right*) trucks discharge waste (Jane Kruse/Nordic Folkecenter for Renewable Energy)

Table 2 Thisted Municipality fact sheet for 2012

Electricity
Power production: 365 GWh Power consumption: 322 GWh Share of natural gas: 33 GWh (12 % of produced electricity available for "export")
100 % of power consumption was produced fossil-free: Wind: 297 GWh Waste: 20 GWh Biogas: 9 GWh Solar: 6 GWh Fossil-free total: 332 GWh Power consumption: 322 GWh (3 % surplus of produced electricity available for "export")
92 % of power consumption came from local windmills: Number of windmills: 219 Capacity: 113 MW Production: 297 GWh Power consumption: 322 GWh (92 % from wind)
Renewable energy total
84 % of energy consumption (heat and power) was fossil-free: Fossil-free production: 642 GWh Heating and power, total: 762 GWh

For the last 35 years, farmers, industry, utilities, and cooperatives in Thy have invested in and used renewable energy resources such as:

- Biomass for district heating
- Biogas, small and large CHP
- Geothermal heat
- Concentrated solar heating
- CHP waste incineration
- Wind power
- Wind energy management
- CHP and wind heat and power (WHP)

The further development of wind power will make it the primary source of electricity and heating, WHP. With an estimated 80 MW new additional wind power, peaks will be more frequent. The strong local support is crucial and is obtained by local ownership of windmills and biogas plants by several farmers. All the CHP plants and the district heating are not-for-profit consumer owned. Local surplus of wind electricity will in the future be used in combined heating and power plants and periodically replace natural gas and biomass. Biomass will function as backup storage when wind and solar energy is not sufficient to cover the need for electricity and heating. Solid and liquid biomass is easy and cheap to store. Biomass will only be used when solar and wind is not sufficient to cover the needs for heat and power.

In the peninsular of Thy, the local community owns/installs/operates the green power producing infrastructure; therefore the benefits from the infrastructure are reaped by the community. Local pollution and CO_2 reduction, job creation, business development, economic diversification, and skill building are of general interest for the community. Once a community has experience with community power, that skill can be transferred to other communities.

In 2007, the Thisted Municipality received the prestigious European Solar Prize. At the award ceremony in Berlin, mayor Erik Hove Olesen stated: "I am very proud and grateful that we today receive this award. Not us as authorities have the honour. Our 46,000 citizens, the energy centre, and our 1,700 local companies made the change. The many windmill owners, the farmers that have biogas plants and the community utilities, they have together made Thy self-sufficient with energy."

Case Study: Ringkøbing District Heating, Denmark

Ringkøbing Fjernvarmeværk, the Ringkøbing district heating, is an example of a successful integration of CHP (gas engine and gas turbine), solar thermal, electric boiler, natural gas boilers, and hot water storage making it an independent, attractive, and reliable source of cheap fossil-free heating with a high level service across the district heating consumers and with a remarkable ability to evolve following changing targets of sustainable energy supply since 60 years.

Ringkøbing Fjernvarmeværk is a private consumer-owned cooperative established in 1963. In the beginning the Ringkøbing plant was an oil-fired plant, and in 1980, following higher demand for heat, another coal-fired plant was built in Rindum (Fig. 48).

In 1989, the Ringkøbing plant converted from oil to a CHP with natural gas. A gas turbine of the Ruston Tornado class was installed with an output of 6.2 MWel and 12.5 MWth. In addition, two boilers were installed with a total power of 18 MWth.

In 1993, the Rindum plant also converted from coal to a CHP with natural gas. There a gas turbine of Siemens-Ruston Typhoon class was installed, and by the end of 2002, it was replaced by a Wärtsilä gas engine 20V34SG with an output of 8.8 MWel and 10.5 MWth (it produces almost twice as much electrical power as the

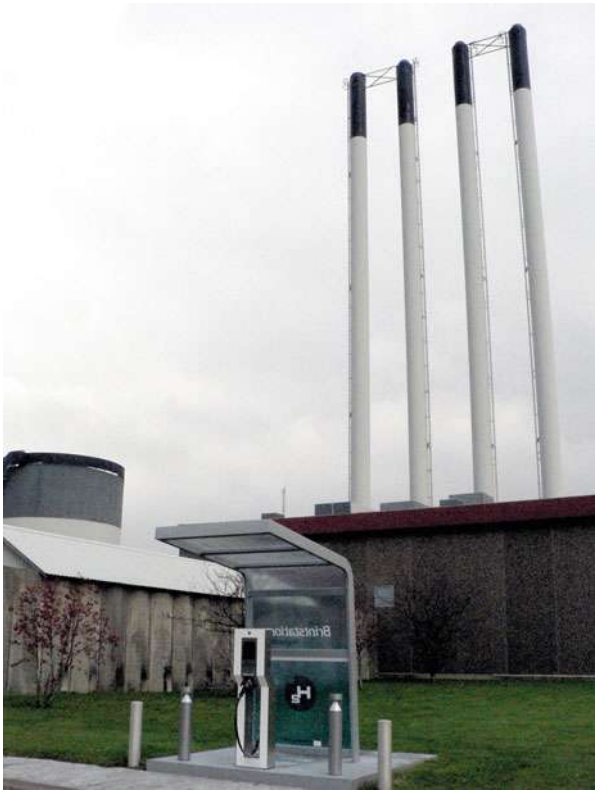

Fig. 48 The combined heat and power station in Rindum, Ringkøbing (Jane Kruse/ Nordic Folkecenter for Renewable Energy)

Table 3 Main specifications of CHP unit at the Rindum power plant

Heat capacity (total)	9,680 KWth
Electrical capacity (total)	7,861 kWel
Technology	Lean-burn gas engine
No. of units	1
Manufacturer	Wärtsilä
Type of fuel	Natural gas
Year of construction	2001
Investment	3.2 M EUR

replaced engine) and two gas/oil boilers were installed with a total power of 20 MWth (Table 3).

The electrical efficiency of the gas turbine was 27 %, while the efficiency of the Wärtsilä 20-cylinder gas engine is almost 44 %. The spark-ignited lean burn engine delivers heat to the town's 3,500 consumers and electricity to the local utility company RAH.

The operator was faced with tough environmental demands from the authorities to reduce the NO_X emissions from the gas turbine, in addition to which a major overhaul was scheduled for the gas turbine. The high total efficiency of the plant

Fig. 49 *Left*: Ringkøbing Fjernvarmeværk's power plant. To the right, hot water storage tank, in the background there are solar thermal panels; *Right*: Ringkøbing solar heating panels (Preben Maegaard/Nordic Folkecenter for Renewable Energy)

gives the owner maximum security in an open market where fuel and power prices are volatile. The cost of heat production from the Rindum plant has been reduced by 20 % compared with continuing operation of the gas turbine.

In 2010, the Rindum plant furthermore installed an electric boiler with power of 12 MW during periods of power from surplus production from wind turbines, converting electricity into cheap district heating.

In keeping with the focus on renewable clean energy, in 2010, a solar heating plant "Sol 1" of 15,000 m^2 was built. By that time, it was the world's second largest solar plant, with a maximum power of 11 MWth when weather conditions were optimal. Four years later, in 2014, the solar heating plant was extended by a further solar heating system, "Sol 2" of 15,000 m^2 (Fig. 49). Both plants currently supply around 14 % of the total district heating to Ringkøbing. The district heating pipeline network delivers heat to approximately 4,200 consumers.

Ringkøbing Fjernvarmeværk sets its goals following the Energy 2020 Plan, for the municipality to become self-sufficient in energy by 2020, and changing from gas to renewable energy supply considering various alternative solutions such as more solar heating, heat pumps, biomass, biogas, and geothermal energy.

Renewable Energy Sources for Integrated Systems

Focus: Biogas, Energy Source with Potential

Biogas will be an important component in the future combined and integrated energy systems. It can be produced where organic waste is available. Resources that basically are without value for other purposes can be digested – often in combination with energy crops to increase the yield. Biogas digesters are a well-developed technology and available in many varieties and sizes. Family-size biogas plants in developing countries may treat the dung from a few cattle, while big, advanced biogas plants can handle several hundred tons of slurry per day.

Anaerobic digestion (AD) involves the breakdown of organic waste by bacteria in oxygen-free environment. It is commonly used as a waste-treatment process but also produces a methane-rich biogas with 50–70 % being methane and the rest CO_2 and small quantities of other trace elements. Biogas can be used to generate heat and electricity.

AD equipment in a biogas plant consists, in simple terms, of an air-tight heated digester tank, a gasholder to store biogas, a gas-burning engine/generator, and a CHP unit if electricity is to be produced. The organic waste is fermented in the digester at temperatures between 25 °C and 55 °C.

The fermentation process is in itself unlike composting not able to produce heat. The rate of breakdown depends on the nature of the waste and the operating temperature. Biogas has a calorific value typically between 50 % and 70 % that of natural gas and can be combusted directly in modified natural gas boilers or used to run internal combustion engines. Apart from biogas, the process also produces a residue that may be separated into liquid and solid components. The liquid fraction can be used as a fertilizer and the solid element may be used as a soil conditioner or further processed to produce higher value organic compost.

Biogas has several applications of use: for direct combustion in boilers, for combustion in gas engines, and for transport. When upgraded by removal of CO_2, biogas can be fed into existing natural gas network. Compared to solar and wind power, biogas is fairly easy and cheap to store and can periodically fill the gap when solar and wind is not sufficient. When applying the Sabatier catalytic process, hydrogen will react with the CO_2 component in the biogas and it will have the same properties as natural gas.

Deployment of Biogas: Denmark as a Case Study

According to the Danish Energy Strategy 2050, biogas will play an essential role in the process of limiting and finally being independent of fossil fuels in Denmark. Biogas has the potential to balance fluctuating power generated from renewable energy sources like wind and solar by cogeneration. Also, produced biomethane can replace natural gas in the grid, reducing the country's dependence on imports of oil. As for the use of biogas for transportation, unlike in other countries, Denmark is in favor of electric vehicles and has rather limited infrastructure for gas vehicles. However, public and heavy transport is of increasing interest for more and more municipalities (Fig. 50).

Compared to its size, Denmark has the second biggest number of farms in the EU and the highest amounts of livestock per holding.

Production of biogas in Denmark can offer a solution to the manure problem the country is facing and support the development toward the goal of use 50 % of the raw manure for biogas production (as stated in the Government "Green Growth" program of 2009) and at the same time improve Denmark's energetic independence of oil, natural gas, or coal, offering a substitute to fossil fuels. Other advantages of biogas production are the reduction of evaporation in the atmosphere of methane and

Fig. 50 Farm biogas plant of the ComBiogas type during the inauguration. Through a network of pipes the slurry is pumped from the farms for digestion and returned back for spreading as fertilizer over the fields. The biogas is piped to the nearest CHP station (Jane Kruse/Nordic Folkecenter for Renewable Energy)

laughing gas from manure as well as transition of nitrogen in the manure to more accessible fertilizer for the crops.

By 2014, there were approximately 150 biogas plants in Denmark, producing 4.2 PJ of energy annually. In centralized biogas plants, heat is used in internal process and in district heating networks, based on two models:

- CHP unit is integrated in the biogas plant and then heat is sold to a district heating company.
- Biogas plant sells and transports biogas to a district heating CHP plant.

In the farm plants heat is used in internal process and in:

- District heating networks (when possible)
- Heating of houses, or stables, or other buildings on-site while surplus heat is ventilated to the atmosphere

The first biogas plants in Denmark were established in the 1970s; however, the development increased in the period of 1999 to 2003, doubling the number of plants from about 30 to 60. By 2003, total production of biogas accounted for 0.8 TWh_{el}. Since that time, the development of biogas production has been steadily but slowly increasing. In 2012, total production of biogas reached

1.14 GWh_{el}/a and 1.19 TWh_{el} in 2013. It is estimated that the production may increase to 2.77 TWh_{el} by 2020.

In 2012, the largest biogas plant in Denmark, and one of the biggest in the world, is the Maabjerg BioEnergy plant producing approximately 5MWel, followed by Lemvig plant of 2 MW while delivering biogas for other applications as well.

Historical Overview of Biogas Development

Biogas was first introduced in Denmark in the late 1970s. The first plants were by present standards rather primitive and built at farms by dedicated and enthusiastic individuals searching for alternatives to the fossil oil that was being imported from the Middle East. As a consequence of the precarious situation in 1974, the energy policy of Denmark became for almost three decades a concerted effort uniting normally divided parties in broad consensus with the primary purpose to reduce the dependency on oil.

In 1977, oil covered 95 % of the total energy consumption of Denmark. Twenty-five years later oil represents only 40 % of the energy consumption of 20 million TOE/year, followed by 36 % in 2012. In the meantime, there came significant improvements in energy efficiency combined with increased use of renewable energy sources and extensive application of central and decentral cogeneration solutions being the main elements in the energy policy. The result is energy consumption at nearly the same levels as in the 1980s.

The long-term benefits of the policy in 2010 were a renewable energy sector employing 30,000 people and an annual export value of €6 billion with around 75 % coming from the windmill industry. Further, Denmark is one of the first European countries which is targeting a complete independency from fossil fuels by 2050. The transition is supported by policies like the new Energy Agreement reached in March 2012, containing energy initiatives and large investments in renewable energy and energy efficiency that by 2020 approximately 50 % of electricity consumption should be delivered from wind power, and more than 35 % of final energy consumption should be supplied from renewable energy sources. Hardly any other countries have achieved similar industrial benefits by restructuring the energy sector Biogas in Denmark (2014).

In the early 1970s, renewable energy equipment based on wind, solar radiation, biomass, and similar natural resources could not be imported from abroad in the form of well-tested, documented, and reliable equipment. At the local-level teams of voluntary development, groups consisting of engineers, blacksmiths, farmers, architects, and others with practical skills were organized to invent concepts and build biogas plant prototypes that were installed and tested under real-life conditions.

Throughout the following decade, a broad variety of experiments and concepts emerged at the noncommercial level as a result of this bottom-up research and development process that is historically unique. Undoubtedly the success and efficiency also by conventional professional standards was significant, furthered by principles of local cooperation. Absence of patents and other forms of protection

of rights allowed exchange of knowledge between inventors, coordinators, potential consumers, and manufacturers. Experience and knowledge was exchanged at the informal level but also more systematically transferred in manuals and seminars organized by the emerging renewable energy organizations satisfying the need for best practice solutions. Around 1980, the first regular commercial initiatives of manufacturing and marketing of renewable energy equipment within wind power, solar thermal panels, wood stoves, and biogas installations were demonstrated. Apart from energy planners and a few physicists, professionals from universities in general did not see the development of the renewable energies as an earnest and promising effort by that time. However, the following development proved the opposite.

Origins of Three Farm Biogas Concepts

Biogas was initially used only for individual farms. Its specific development grew out of the process described above involving a broad variety of concepts and experiments. Especially three parallel development lines contributed to advance the technology:

(a) The first one came as a result of a state financed research and development program named Cooperation for Technological Development of Biogas Plants (STUB), initiated in 1978, that set up three extremely different digester concepts. None of which, however, became of commercial relevance. The aim was to combine theoretical skills, prototype building, capacity building at the farms, deployment of biogas in agriculture, and setting the standards for future biogas plants. Within the project, a number of reports mostly based on experiences and measurements from the prototypes were published.
(b) The second biogas development team, Højbogaard, was the combined efforts of a progressive farmer and the local blacksmith. They quickly obtained high gas yields from well-designed digesters in different versions made from steel plate and concrete by systematically investigating the biological process. Under the trade name of Bigadan, in 1982 they became suppliers of a scaled-up version for some of the first community biogas plants in Denmark. Today, Bigadan operates on large-scale biogas plants.
(c) The third significant biogas development initiative grew out from an effort of mobilizing the local human and technological potential in the region of Thy in northwestern Denmark. Funding from UNESCO made it possible quite early in the biogas implementation phase in 1977 to invite a few international biogas experts with proven knowledge and experiences within a new technology. It became an early and concrete example of international technology transfer within renewable energy, however, in the form of South-North cooperation.

This opportunity allowed consultancy and technology transfer from experts like Ram Bux Singh from India, former leader of the Gobar Gas Research Institute. He had the authority to set important standards in the early development process in

terms of valuable technology inputs by encouraging farmers in the region and stressing that comprehensive application of biogas was a long-term learning process and not merely a matter of hardware.

Materials and Technology in Biogas Construction

The suppliers of biogas plants in Germany and other countries are primarily using concrete digesters, whereas almost all biogas plants in Denmark manufactured are from steel plate. Concrete was also used in Denmark in the 1980s for digester tanks made from concrete prefabricated sections originally developed for liquid manure storage tank.

These tanks had a large diameter in comparison to the height (ratio 3:1) providing a wide span cover structure. Gas leaks, however, occurred and it was determined that gas molecules were diffused through the porous concrete. Therefore, steel became the preferred construction material for digesters irrespective of its higher costs. Steel tanks either were welded constructions or enamel steel plate elements bolted together with flexible sealing between the joints. Similar types of tanks are widely used for grain silos. In Denmark, three main categories of biogas plants are found:

- Community biogas plants, each 500–20,000 m^3, delivering electricity to the grid and heat to the town district heating network from 50 % to 70 % manure and 30 % to 50 % industrial waste
- Large, rather farm biogas plants using a concrete or steel tank digester with cogeneration and co-fermentation
- Smedemester (Blacksmith) farm biogas with steel digesters, 37–45 °C operating temperature, 150–1,000 m^3 digesters, 2–5 % fish waste oil co-fermentation, cogeneration units of 100–500 kW

The first community biogas plants were built in the early 1980s. This was part of a desire to supply villages and townships with biogas for cogeneration in regions that were not going to be supplied by the new Danish fossil gas distribution network. It was anticipated that daily operation of the community biogas plants would become the responsibility of well-trained staff with insight into the biogas process that individual farmers with an already wide variety of duties could not take.

After 1985, more stringent environmental legislation concerning storage and land application of animal manure was introduced. Nine months of storage capacity became a legal requirement for Danish farms. Quantities of nitrogen and phosphates applied per hectare of land also became subject to public regulation. This increased farmers' interest in centralized plants with manure storage capacity included in the concept. The centralized biogas plants all co-digest animal manure and organic waste primarily from the food industry. In 1991, a biogas production level of 30–35 m^3 of biogas per cubic meter of slurry was evaluated as being a necessary precondition for the economic viability of centralized biogas plant. This production

Fig. 51 Community biogas plant with CHP. The tanker truck (*left*) collects 400 t of liquid waste from farms daily. In the 7,000 m^3Bigadan digester (*middle*), the biogas is produced which the Jenbacher gas engine (*right*) converts into heat and electricity (Jane Kruse/Nordic Folkecenter for Renewable Energy)

could only be achieved by co-digesting animal manure with wastes from the food industry, normally by admixing 10–30 % organic wastes depending on the character, biogas potential, procurement costs, and availability of the waste.

The animal manure for community biogas plants is transported from a number of farms to the plants by tank trucks or pumped through slurry network from the farms. After digestion, the slurry is returned as a nutritionally defined fertilizer, partly to the farms that delivered the fresh manure and partly sold as organic manure to farms engaged in crop farming only.

The volume of animal manure and industrial wastes daily delivered into the community biogas digesters range from 50 to 500 t with resulting biogas production of 1,000 m^3 up to 15,000 m^3 per day (Fig. 51).

At farm biogas plants, the gas is normally combusted at the farm more or less independent of the energy requirements of the specific farm. In that respect siting of community biogas plants ensures that the biogas production can be utilized with high efficiency in cogeneration systems with a total efficiency up to 90 % when the heat is used for district heating of towns, villages, and rural communities.

When installing farm biogas plants, export of heat for district heating is generally not possible. Therefore, high overall efficiencies can only be obtained in the event case the biogas farm has the necessary requirements for utilization of the generated heat.

In the future, availability of surplus heat generation will certainly lead to Integrated Energy Farm (IEF), using biogas and other forms of renewable energy technologies, energy storage systems, and settlements for the occupants of the complex in innovative forms of zero emission, ecological villages depending on renewable resources of local origin.

Community biogas plants in their present form include environmental and agricultural benefits, investment savings for the farmers, improved fertilization efficiency, reduced greenhouse gas emissions, and cheap, environmentally sound waste recycling of organic material that is generally delivered from the agriculture or fishery to the food industry.

By returning the waste to the fields from which it originally came, it helps to maintain the humus balance of the top soil as well as substituting chemical fertilizers

Fig. 52 *Left*: Tank truck collects liquid manure at the farm (Preben Maegaard/Nordic Folkecenter for Renewable Energy). *Right*: Storage of maize silage for the production of biogas, Nieboell, northern Germany

produced from fossil fuels. The main disadvantage of centralized plants compared to farm biogas plants is the significant cost of manure transportation.

Admixing is predominantly considered a major advantage for both biogas plants and waste suppliers but has, however, also given rise to uncertainties. Often the long-term reliability of industrial waste supplies has been unpredictable.

There are important aspects related to spreading of diseases with community biogas plants not least a risk of pathogens from one farm being transferred to other farms by the trucks visiting several farms every day, and due to mixing of manure from many places of origin, pathogens from one farm can be spread to other farms (Fig. 52).

The veterinarian authorities are of course aware of such risks and have implemented regulations to prevent these problems, however, at considerable costs; every time a tank truck departs for collecting a new load of manure, it has to be carefully cleaned. In order to prevent pathogens passing through the community biogas plant without being killed, all the slurry passing through the plant is subject to heat treatment (70 °C) for a minimum of 1 h in order to kill pathogens. Since farm biogas plants do not have this kind of additional expenses, farm biogas plants will have significant investment and operational cost advantages.

Technological Development of Farm Biogas Plants

With regard to costs, efficiency, and reliability, new standards have been set with the Smedemester (Blacksmith) biogas technology. Two versions were developed, both with steel tanks:

1. Horizontal tanks manufactured in industrial workshops of sizes from 50 to 300 m^3
2. Vertical tanks built on-site in 500 and 1,000 m^3 sizes

Fig. 53 Biogas plant at farm in Denmark. The gear motor for the internal slow-moving agitator is seen on top the digester (Jane Kruse/Nordic Folkecenter for Renewable Energy)

For agitation, slowly rotating blades were preferred due to low energy consumption. The Folkecenter for Renewable Energy developed the technology and supported manufacturers in Denmark, Germany, Lithuania, and Japan. After 1988, European biogas experts were involved in the development process, thus transferring the experiences gained within the various national farm biogas sectors. Erwin Köberle especially provided essential inputs for the success of the Smedemester technology. Also Dr Anton Perwanger, Dr Arthur Wellinger, and Ekkehard Schneider made valuable contributions.

In terms of quantities, community biogas plants in general get their waste supply from nonagricultural suppliers. However, this is mostly waste with low-content fermentable material coming from the food industry (slaughterhouses, dairies, fish processing), pharmaceutical industry, kitchens in hospitals, hotels, etc. The farm biogas economy benefits significantly from the use of small quantities of high-grade waste oil from the food industry, consisting of fish oil and animal fats and other types of organic industrial waste. The waste oil used contains up to 700–1,000 m^3 of biogas per cubic meter of waste substrate (Figs. 53 and 54).

Legislation

The Danish government together with political parties has developed ambitious energy policy agreement on 22 March 2012, which sets the framework for green transition in the country.

Fig. 54 Biogas storage tanks at community plant (Preben Maegaard/Nordic Folkecenter for Renewable Energy)

Intermediate goals of the agreement are:

- Green biomass energy sector creating jobs for 4,000 people in 2013 and 2014 and for 6–7,000 people in 2015–2019
- Total phaseout of oil and coal for heating by 2030.
- Supply of 100 % renewable energy for heating and electricity by 2035.

Danish renewable energy policies are promising setting ambitious goals, whereas in Germany, Europe's biggest biogas producer and the market leader in biogas technology, after more than 20 years of rapid development and successful policies, situation has dramatically changed in 2014.

In the early 1990s, German government introduced *Law on ElectricityFeed* (StrEG), a law that guaranteed the producers of energy from renewable sources the feed into the public power grid, and the power companies were obligated to take all produced energy from independent private producers of renewable energy Scheer (2006).

The development of biogas and other renewable energy was rapid and successful in Germany (Fig. 55). By 2014, in Germany there were approximately 7,944 biogas power plants producing electricity fed to the public grid with total installed capacity of 3,859 MW, electricity supply of 27,55 TWh for 7.9 million households. Germany is the world leader for science and technology know-how in the biogas sector, with several billion of euros invested and over 40,000 jobs in the sector.

However, the amended Renewable Energy Act (EEG), approved by the German Parliament in June 2014, dramatically limited the development of energy produced from biogas (Fig. 56).

Fig. 55 Big farm biogas plant on the island of Rügen, Germany. In Germany there are several thousands of farm biogas plants with digestion of animal manure and energy crops. The biogas is normally combusted in gas engines on location (Preben Maegaard/Nordic Folkecenter for Renewable Energy)

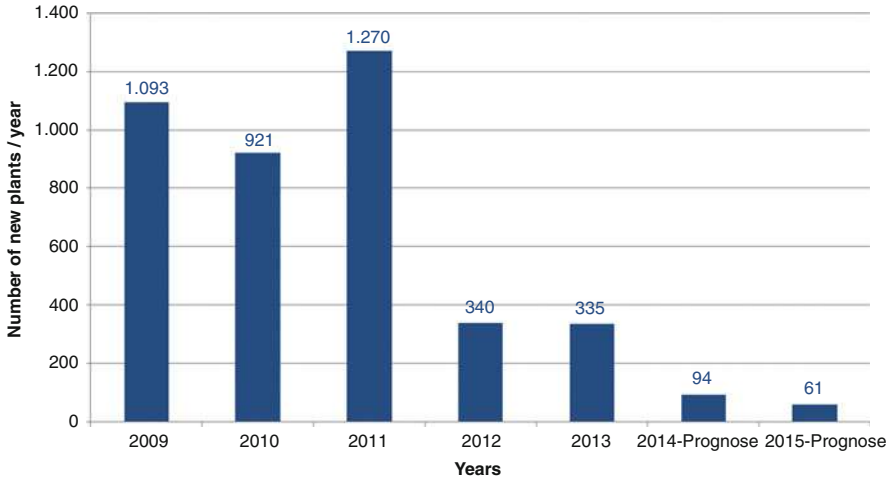

Fig. 56 Installation of new biogas plants in Germany on the yearly basis (data from 11/2014) (Fachverband Biogas e.V.)

Since 1980s, Denmark has been developing various policies supporting renewable energy. Some were more successful than others. For many years, the Danish biogas sector remained stagnating, due to insufficient framework. However, there are new policies favoring renewable energy sources, including biogas.

In 2012, the Agreement on Energy (VE-Lov) was updated and signed by the government, which increased feed-in tariffs not only for electricity production but

also enabled other biogas uses (injection, transport fuel, industrial processes) to be considered for the support scheme. Also, municipality-owned gas companies are now allowed to invest in production and a special Biogas Taskforce was established to support local authorities in implementing biogas projects in the period of 2012–2015.

The agreement changes focus from CHP production toward upgrade of biogas. By 2020, biogas production is expected to double and 75 % of produced biogas is expected to be upgraded for the gas grid and for transport. It is difficult to predict if these expectations are realistic, but Denmark is prepared for taking this challenge: the country has a well-developed natural gas grid, district heating networks in cities and towns, and many CHP plants, and the government and gas companies focus on the security of the grid to receive upgraded biogas.

Community-Owned Biogas Plants

In Denmark, by tradition, most biogas plants based on manure are owned privately: plants in farm scale by private farmers and larger plants by cooperatives. Publicly owned plants and investor-owned plants are lesser; however, in the recent years gas companies show increased interest in entering the biogas sector.

Case Study: Lemvig Biogas Plant

Since 1992, for 20 years, Lemvig Biogas has been the largest biogas plant in Denmark. The plant is owned by 69 local farmers in a farmer privately owned cooperative.

The plants receive and treat 615 t/day of slurry: 500 t (82 %) manure from approximately 75 farms and 115 t (18 %) organic waste to generate heat and power. The plant can process about 226,000 t of biomass per year, of which 183,000 t is animal manure and slurry and 43,000 t is suitable industrial waste. In 2011, biogas production was 8.5 million m^3 and, in 2012, 10.2 million m^3 on a yearly basis. There are four digesters with a total capacity of 14,300 m^3 (Fig. 57).

This simple exchange: manure and waste for electricity and heat is a good solution in terms of environment, reduction of pollution, but also economy, both for the biogas plant and households (consumers). Local farmers use the fermented slurry as fertilizer, as it performs positive values for farming and in the process of thermophilic digestion kills infectious species (bacteria, viruses, worms), reduces the smell, and inactivates plant seeds and weed. Compared to raw slurries, digestate has better balanced nitrogen-phosphorus content, is more homogenous which makes it easier to stir, and spread on the soil, not to mention social benefits. Biogas plants can contribute to better relations with the neighbors and form a positive perception of farming activities.

Lemvig Biogas Plant converts produced biogas into electricity and heat in a CHP unit (Jenbacher 316 gas engine of 836 kW_{el}, and since 2013 a new Caterpillar biogas engine of 1,560 kW_{el}). It generates over 21 million kWh/year of electricity from biogas, which is then sold to the local grid (Fig. 58).

Fig 57 Reactor tanks of 14,300 m^3 at the Lemvig Biogas Plant (Photo: lemvigbiogas.com)

Fig. 58 *Left*: Lemvig Biogas Plant (Jane Kruse/Nordic Folkecenter for Renewable Energy). *Right*: Slurry-to-slurry heat exchangers at Lemvig Biogas Plant reduce the demand for process energy for heating the digesters (Jane Kruse/Nordic Folkecenter for Renewable Energy)

Since 2011, part of the produced biogas is transported 8 km to the Klinkby district heating plant and combusted in a 889 kWel Jenbacher CHP unit. In 2012, 5.6 million kWhel was produced and used in about 300 households of Klinkby.

Transport of raw slurry from local farms to the biogas plant and in return, transport of digestate from the biogas plant to the farmers' storage tanks are carried out at the expenses of the biogas plant, which results in lower transportation costs for the farmers.

The plant can receive a variety of suitable wastes delivered by all kinds of vehicles such as articulated tip trailers, truck trailers, tankers and slurry trucks, as well as ships at Lemvig harbor or Thyborøn harbor.

Lemvig Biogas Plant besides the animal manure waste receives all types of waste like fish waste, slaughterhouse waste, organic household waste, feed waste/residues, pharmaceutical waste, soft drinks, beer, alcohol, even chemically or bacteriologically contaminated foods, and all organic matter with a high content of fat, protein, or sugar. However, recently organic farmers from the area consider a possibility to have their deep litter also treated in the biogas plant. To answer these needs, Lemvig Biogas plans a synergy with Lemvig Organic Biogas and builds a new organic plant nearby, which would use the gas processing, gas storage systems, and the same biogas pipeline as already existing plant. Biogas produced in both plants would be mixed and then delivered to CHP units in Klinkby and Nissum. The existing plant would supply excess process heat also to the organic plant.

Addressing future challenges, Lemvig Biogas together with the Center for Energy Technologies (AU), GreenHydrogen.dk, DTU Mechanical, and Elpatek is working on a new project called MeGa-Store (Methane Gas for the Storage of Renewable Energy).

Aim of the project is to develop a technology for upgrading biogas to natural gas quality by hydrogen produced by wind or solar energy. Upgraded biogas can then be sent directly and stored on the natural gas network. The technology is relevant for reduction of the use of fossil fuels (natural gas) and for solving the problem of storing of renewable energy sources such as wind and solar. There is a testing plant at the Lemvig Biogas for the MeGa-Store technology.

Biogas for Transport

Biogas consists of mainly methane CH_4 (40–75 %) and CO_2 (25–60 %), different proportions depend on substrate used for the production. Upgrading of biogas to content of CH_4 higher than 90 % means to remove carbon dioxide from its content and pressure it Luo and Angelidaki (2012).

The advantage is increased heating value of upgraded biogas as well as further use of it as renewable energy source, but most of all upgraded biogas can be an alternative to natural gas. Injection of upgraded biogas into the national gas grid gives the possibility to store it, which is practical and allows using biogas to balance fluctuating power from the wind. Upgraded biogas with natural gas quality can be used as fuel for vehicles (Fig. 59). It is also practical to use existing natural gas pipelines to transport upgraded biogas from rural areas where it is being produced to urban areas with more dense population. No extra pipeline network is neither needed, nor special transport.

According to a study from the Danish Energy Agency from 2010, upgraded biogas is one of the alternative fuels for transport with the lowest socioeconomic costs, despite its extra upgrading costs.

Biogas upgrading technology is relatively new in Denmark, but there are more and more projects dealing with this challenge. In 2011, the first biogas upgrading facility in the country was built in Fredericia with the capacity of 180 m^3/h. Following, there are a few other projects in a planning phase or under construction. DONG Energy, Denmark's biggest producer of renewable energy, signed a long-

Fig. 59 Neoplan biogas bus in Uppsala, Sweden, "for a better environment" *(Preben Maegaard/ Nordic Folkecenter for Renewable Energy)*

term agreement with the Swedish cleantech company Malmberg for building multiple biomethane plants in 2012. Malmberg already has built 40 gas pretreatment plants in Germany but also some in the UK or Norway.

From November 2014, Denmark's first regional buses on CO_2-neutral biogas have just started on the route Aalborg to Frederikshavn. The gas for the buses is provided by HMN Naturgas, which at the same time opens two biogas filling stations in Northern Jutland – in Aalborg and Frederikshavn. By early 2012, there were no gas buses in Denmark at all, but currently there are about 40 biogas buses around the country. They run as city buses in Fredericia, Holstebro, the Copenhagen area, and Skive. In neighboring countries, biogas is much more widely used for transportation, as biogas is a well-known and reliable technology for CO_2-neutral transport. In Denmark, biogas for transport is slightly more expensive than diesel.

Hydrogen and Biogas

There are various methods for upgrading biogas: chemical absorption, pressure swing adsorption, high pressure water scrubbing, membrane separation, physical and chemical technologies, high pressure, or chemical addition.

However, currently there are studies being carried in search for alternative solutions for biogas upgrading by hydrogenation of the biogas, which would transform most of the CO_2 (CO_2 is not combustible) from the biogas and hydrogen (H_2) to methane (CH_4) (Fig. 60).

Hydrogen used could be produced by electrolysis using excess energy from wind power. This option would provide more biogas for utilization.

$$4H_2 + CO_2 = CH_4 + 2H_2O$$

There are considerable advantages of this method: increased methane production without methane losses, minimal energy and chemical requirements in the process, and possibility of storage of fluctuating wind power as methane, which is easier to store and distribute. Simple and rational solutions are usually promising.

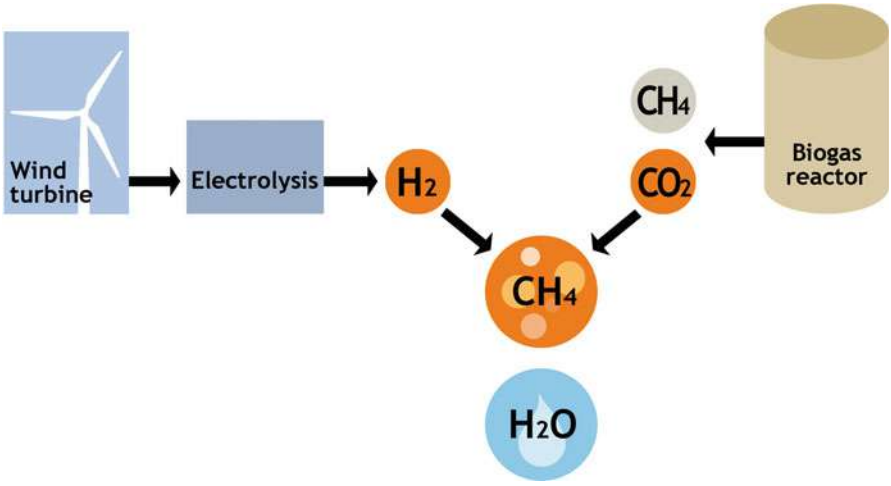

Fig. 60 Hydrogenation of methane by the use of hydrogen from wind power (Nordic Folkecenter for Renewable Energy)

European Union already develops R&D programs on the subject, and in other countries a combination of biogas and hydrogen as transport fuel is being researched. In Costa Rica, a team of researchers from the Ad Astra Rocket Company with Cummins Power Generation and EARTH University have successfully developed a new type of portable electric generator (Internal Combustion Engine) using a combination of hydrogen and biogas. This achievement has been implemented as a research prototype but is still in the process of testing.

Water electrolysis has been used industrially to produce hydrogen for more than a century. Earlier it was the preferred production method but later displaced by reforming of natural gas and other technologies. By 2014, some 5 % of hydrogen is produced by electrolysis. It has increased due to its potential to provide hydrogen from solar and wind and for load management in power grids CODE2 (2014).

Electrolyzers will have a role to operate when electricity generation is in excess of demand during periods of high solar irradiation and strong wind to reduce the need to curtail renewable electricity generation. The produced hydrogen can be stored locally or fed into the natural gas network for re-electrification in integrated energy systems (Fig. 61). Because the electrolyzers will need to respond to intermittent and fluctuating renewable power generation, the ability to operate dynamically is a requirement for electrolyzers to be integrated in fluctuating energy systems.

Water electrolysis can be expected to have a key role for the widespread use of hydrogen for mobility, industry, or energy storage. It is the most efficient and proven solution to hydrogen production from renewable electricity sources. Electrolysis also has the added advantage of being flexible where rapid changes of loads will be the normal in the future with increasing intermittent solar and wind energy. For balancing of power and storage of energy in integrated systems that are dominated by wind and solar energy, start-stop and dynamic operation and efficiency across

Fig. 61 H-TEC SYSREM PEM electrolyzer for decentralized production of hydrogen (*left*). A key technology for integration of wind, solar, and other renewable energies. (*right*) Pipe network for water, hydrogen, and oxygen of containerized H2 package (Preben Maegaard/Nordic Folkecenter for Renewable Energy)

Fig. 62 Fully integrated 150 m^3 per hour hydrogen production package (*left*). Includes water treatment, power supply, electrolyzer, and ancillary equipment; (*right*) 150 m^3 per hour electrolyzer in container (Preben Maegaard/Nordic Folkecenter for Renewable Energy)

much of the load curve will be basic operating parameters that will allow electrolyzers to interact with grids E4tech Sàrl and Element Energy Ltd (2014).

With increased amounts of fluctuating power, electrolyzers will play an important role in energy applications. The electrolyzers are technologically mature, but the industry is still rather small. Costs have not been reduced through mass production or supply chain optimization that is why the room for technology improvement is significant. Most present systems are designed for operation at full load and to run continuously (Fig. 62).

Alkaline electrolyzers are most mature, followed by polymer electrolyte membrane (PEM) electrolyzers and the solid oxide electrolyzer. Electrolyzers in the future will find widespread use in energy applications, leading eventually to

Fig. 63 (*Left*) London transport: hydrogen is widely used for urban mass transport. (*Right*) Hydrogen bus that has been in operation for many years in Hamburg, Germany (Preben Maegaard/Nordic Folkecenter for Renewable Energy)

Fig. 64 (*Left*) Fuel cell car at hydrogen filling station at major radial road, Berlin, Germany. (*Right*) Compact hydrogen filling station for cars and vans in Ringkøbing, Denmark. Developed by H2 Logic (Preben Maegaard/Nordic Folkecenter for Renewable Energy)

hundreds or thousands of megawatts of installed capacity within a pioneering period that may run till 2025.

The largest electrolysis plants of several thousands of m^3/h have historically been used in the fertilizer industry. Hydrogen from electrolysis can be found as well in making chemicals, food processing, metallurgy, glass production, electronics manufacturing, and power plant generator cooling. Only small amounts of hydrogen from electrolysis are used in energy applications, in sustainable transport program, and for renewable energy storage (Figs. 63, 64, and 65).

Case Study: Utsira Wind Power and Hydrogen Plant, Utsira Island, Norway

Utsira, a small island 20 km off the southwest coast of Norway, had an ambition to exploit wind resources and become self-sufficient with renewable energy. Utsira has

Fig. 65 *Left*: Standard car had the combustion engine converted into hydrogen by Professor Sun Baigang, BIT, Beijing, China. *Right*: The diesel engine of a Hamburg city bus is replaced by hydrogen fuel cells and storage (Preben Maegaard/Nordic Folkecenter for Renewable Energy)

the smallest population of all municipalities in Norway (about 235 inhabitants) and a total area of only 6.15 km^2.

In July 2004, Norsk Hydro (now StatoilHydro) and Enercon officially launched an autonomous wind/hydrogen energy demonstration project on the island. In the pilot project, 10 households are directly supplied by energy from wind turbines. Excess power from wind turbines is used to produce hydrogen in an electrolyzer, which is then compressed and stored. On days with low winds, a hydrogen engine and a fuel cell use stored hydrogen to produce the necessary electricity. This system ensures a continuous and reliable energy supply when wind power is not available and provides 2–3 days of full energy autonomy for 10 households on the island. Utsira plant is the first of its kind in the world.

The system consists of:

- 600 kW wind turbine
- Flywheel (5 kWh, 200 kWmax)
- Water electrolyzer (10 Nm3/h, 48 kW)
- Synchronous machine (100 kVA)
- Hydrogen gas storage (2,400 Nm3, 200 bar)
- Hydrogen engine (55 kW)
- PEM fuel cell (10 kW)
- Battery (50 kWh)

The plant's operation has been a success: for more than 18 months, the island was in a stand-alone mode, delivered power quality was very good, and the project contributed to local activities. There were no accidents and no complaints from customers. The project has been honored with the "Platt's Global Energy Award."

Case Study: Enertrag Hybrid Power Plant, Prenzlau, Germany

The Prenzlau power plant, commissioned in October 2011, is the world's first hydrogen-wind-biogas hybrid power plant. The plant is owned by companies: Enertrag AG, Vattenfall Europe, Total, and DB Energie.

The power plant consists of three Enercon E-82 E2 wind turbines, each of 2.3 MW capacity, and a 500 kW electrolyzer that uses the surplus electricity for hydrogen production. Two CHP units can be operated with a mixture of hydrogen and biogas. Both the CHP and wind turbines provide electricity that can be fed into the grid. Excess power can be used for electrolysis to produce water from oxygen and hydrogen, which is stored in high pressure tanks. These tanks are storage for windless times to meet the energy needs of consumers (Fig. 66).

Dike-Pond System with Comprehensive Integration

Full integration of crops for vegetable oil, fodder production, and biogas can be obtained in combination with the dike-pond system that is in itself an energy-neutral aquaculture system. The system combines production of domestic animals, plants, and fish in a balanced ecosystem where the waste from one level of organic production is the precondition of the following step. The water leaving the system has a low level of organic and mineral nutrients. It can be used as recycled water. Any stable biological system is based upon conservation of energy and matter. This means that the production is the surplus created by the system being the difference between the products leaving the system and the external supplies (Fig. 67).

All natural ecosystems tend to obtain an ecological balance where all organisms find a niche. A viable productive ecosystem adapted to certain nutrients and certain

Fig. 66 *Left*: Gas storage, Biogas plant and wind power at the Enertrag Hybrid Power Plant in Prenzlau, Germany (Molgreen); *Right*: Large-scale electrolyzer plant, at the Hybrid Power Plant in Prenzlau, Germany (Hanno Böck)

Fig. 67 Dike-pond system in the biodome, Nordic Folkecenter for Renewable Energy. The biodome is a unique greenhouse, which integrates water cycle, recycling of nutrients, insulation, and aquaculture (Anna Krenz/Nordic Folkecenter for Renewable Energy)

external conditions must follow the same basic principles including conservation of energy and matter. A successful system must be based upon well-adapted organisms in balanced niches and stable external conditions.

The dike-pond component of the integrated farm system has been derived by the experiences from the delta of the Pearl River in southern China. Here is an ancient system of cultivation consisting of ponds and dikes. It has high productivity, so it can provide a surplus of a wide range of products to the cities including fish, vegetables, fruits, pigs, eggs, and poultry. The production is obtained without any artificial external inputs in the form of chemical fertilizers and pesticides.

With carp ponds as the central element of this system, which integrates agriculture and freshwater aquaculture, this is considered one of the most productive cultivating systems in the world. The dike-pond system requires very little energy input. Since the waste originating from one production element is perpetually used as input resource for the next element, the system is virtually nonpolluting. The system is a complex chain of cultivation elements that is modeled on the cycles of nature. For this reason, the system gradually could become a model for the development of local complex cultivation structures in the industrial countries where monocultures and environmental problems make it obvious to seek solutions that respect the natural cycles and at the same time have high productivity.

It is calculated that the manure from one pig can yield 40 kg of carp meat per year and at the same time produce 20–30 % of the fodder for the pig. The food production per unit area is 4–5 times higher than in the traditional agriculture. This intensive biomass production is combined with water purification and energy production.

An advanced farm biogas plant can be connected directly to a greenhouse dike-pond system. This arrangement combines efficient systems of cultivation and energy production. One special advantage is the most efficient use of the nutrients in the manure without any transport. The clean water leaving the system may be used elsewhere on the farm or drained to supplement the groundwater resource.

Plant Oils

Agriculture and forestry are the primary production sectors which are directly based upon solar energy. This is done through production of various forms of biomass which can be used for food, directly and indirectly in the form of fodder, and for energy. From a general consideration of sustainability, it would be natural for agriculture to contribute a significant part of a country's energy supply bringing new income to farmers and to have a positive energy balance.

It would seem obvious to cover the agricultural sector's own energy consumption directly through biomass. As an element in this, the agricultural machinery can be operated on plant oil. This would also provide immediate environmental improvements in agriculture. Plants that produce high amounts of oil are known as oleaginous. Of these, only a few are used for commercial purposes. Each climatic region has its own particular oleaginous plants. Tropical regions are especially privileged by a larger variety of plants with higher yields. Most oleaginous plants are significant from an agricultural point of view and allow for crop rotation and crop combinations. Planting of oleaginous plants makes it possible to combat erosion, reclaim desert land, reforest, and manage soil – allowing a better water control and management.

The main by-product of vegetable oil is expeller cake. Sometimes the cake is the main commercial product and the oil becomes the by-product. The expeller cake is protein rich, can be used to feed humans and animals, and is highly valuable as a natural fertilizer.

Pure plant oil (PPO) helps the Integrated Energy Farm (IEF) to become self-sufficient in terms of energy through the use of vegetable oil. In temperate climates, the combined cultivation, harvesting, and supply of 1,000 l rape seed oil, expeller cake, and straw requires 140–160 l of oil, which can also be plant oil. The oil is physically extracted by means of an oil press (Bassam and Maegaard 2004).

The pressing is cold when the temperature does not exceed 60 °C. The simplicity of the process means that it can be on a large or small scale. The oil has to be cleaned by using a filter, centrifuge, or purifier. It is neither explosive nor flammable. It does not emit toxic, carcinogenic gases nor is it harmful to soil, water, animals, and humans in the event of accidental spillage.

The solid biofuels, such as straw of the oil plants, can be used for heat production in boilers. With the availability of more advanced biomass gasifier technology, straw from oil plants can fuel CHP. Liquid biofuels such as rape seed oil, biodiesel, and ethanol are the most versatile fuels because they can easily be used for heat production, CHP, and agriculture mobility purposes that can contribute to a more environmentally sound transport sector – that has shown a lack of positive environmental results and an increasing contribution to energy consumption and greenhouse effects. A breakthrough for plant oil can push this development.

Biodiesel can substitute fossil diesel right away. However, biodiesel presents health and fire hazards in itself, and it is polluting. The pressing and the following esterification comprise of an industrial process with relatively high energy consumption that requires needed costly infrastructure and production plants. In order to meet the requirements of diesel engines, vegetable oils can be modified into vegetable oil

ester (transesterification). The transesterification procedure includes the production of methylesters and glycerol (glycerine) by the processing of plant oils, alcohol, and catalysts. Biodiesel can replace diesel entirely or be mixed with it in different proportions for running diesel engines.

Folkecenter Autonomous Energy System

At the Nordic Folkecenter for Renewable Energy located in the Thisted Municipality, a prototype autonomous renewable energy system is installed. The energy system supplies heat and electricity to 2,000 m^2 of offices, meeting rooms, laboratories, workshops, and residential facilities. Sources of energy supply are wind turbines of 75 kWel and various 5–10 kWel wind turbines, 42 kWth electric boiler, 45 kWth wood pellet stoker with automatic start-up and stop, 8 kWel/20 kWth plant oil CHP unit with automatic start-up and stop, and 25 kWel PV and 50 m^2 solar thermal panels. Wind energy and solar energy are the primary sources for heat and electricity. Biomass (wood pellets and pure plant oil (PPO)) is used for backup (Fig. 68).

The overall operational strategy is:

- The power flow control (PFC) directs excess wind electricity through the thyristors to the electric boiler.
- When the electric boiler does not supply sufficient wind-generated heat, the wood pellet stoker is automatically activated.
- In case of no power from solar and wind, the CHP unit using plant oil is activated.

Excess production of solar and wind generated heat is stored in a 10 m^3 hot water storage.

The system is connected to the public grid. The overall principle is not-to-sell/not-to- purchase from the grid. The CHP unit, however, can operate in island mode in case of a power blackout. At summer nights with no wind and sufficiently stored solar-generated heat, the CHP unit will not start up; the grid will supply the need for power only, as there is no electric storage capacity in the system and the CHP-generated heat would be wasted. In practice, excess wind power covers 60 % of the annual demand for heat, with the balance coming from solar and biomass Maegaard (2010–2014).

The technology and strategy of the autonomous system was pioneered, developed, and implemented by the Folkecenter in 2007. For a 100 % supply of power and heat/cooling from renewable energies, the same principle and strategy should be applied at the regional and national level as well. The system delivers a realistic solution to questions often made about alternative energy sources.

The combined high CHP and wind power production causes a potentially major problem in the power sector. However, supply and demand can as demonstrated in the Folkecenter Autonomous Energy System be balanced by feeding on windy days the excess wind power into the electric boiler. The electric boiler makes it possible to

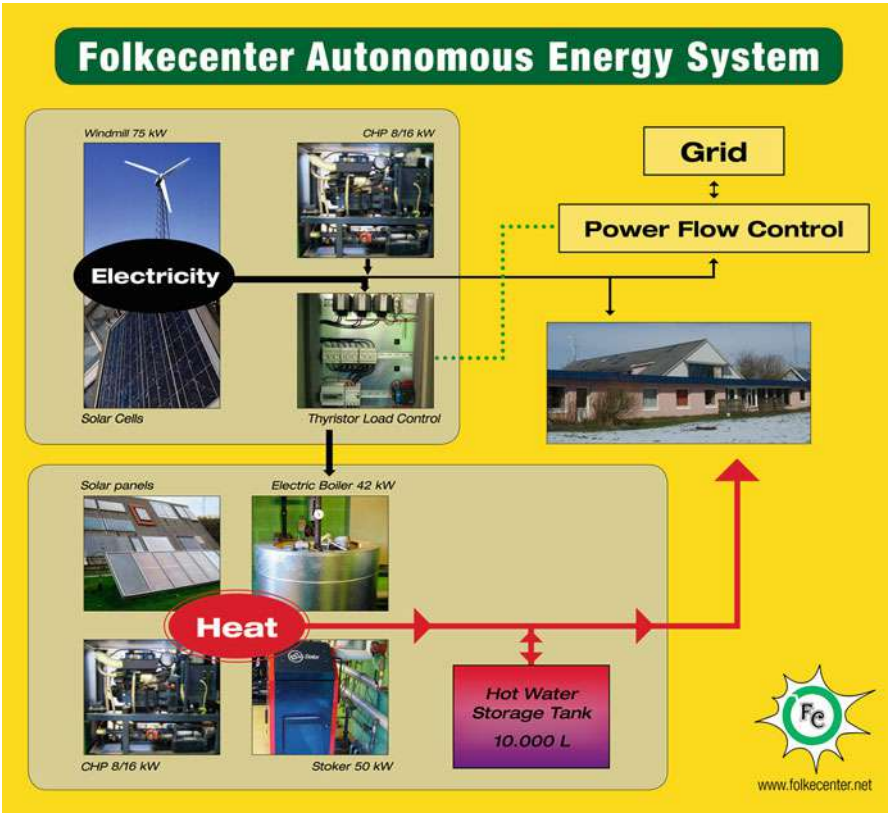

Fig. 68 Autonomous integrated energy supply system at the Folkecenter for Renewable Energy (Nordic Folkecenter for Renewable Energy)

avoid the combustion of wood pellets in the stoker and use of liquid biomass in the CHP unit at periods with excess wind and solar energy. With increased renewable energy shares in the future, more and more often fluctuating solar and wind energy will be sufficient to satisfy both the need for power and heat and can be given priority, while solid and liquid biomass is reserved for periods without sufficient wind and solar.

The Global Perspective

The necessity of sustainable development and the use of clean energy technologies are well recognized. Actions at national and international levels to tackle the problems of limited resources, environmental damage, and climate change are being developed, and these will require new directions for energy policy and technology. The scale and type of investment decisions in energy supply and

end-use systems will change. The "Rio Declaration on Environment and Development" in 1992 did, however, not recognize the intimate link between energy and development or the direct relation between environmental aspects and the use of conventional atomic and fossil fuel-based energy supply.

Conventional sources of power help populations live more comfortably than past generations, but while they meet new needs, they also carry the risk of irreversibly altering natural balances, both locally and globally. The fast-growing world population and the ever-increasing consumption of resources driven by the diffusion of lifestyles that have developed in industrialized societies are emulated in most of the world.

Under the conditions of nuclear and fossil energy use (as well as nonrenewable biomass), the target of a "sustainable development" cannot be reached. None of the pending and visible dangers can be overcome without substituting nuclear and fossil energy with renewable energies.

A great number of solar, wind, and biomass technologies for the production of fuel, heat, and electricity have become available or close to commercialization. They have been installed on a significant scale in both developed and developing countries. They are used in many different ways, stand-alone or integrated in conventional energy networks and grids. They are already providing energy services to individual homes, villages, and cities. Solar, wind, and biomass in some communities in the industrialized countries fully cover the need for power, heating, and cooling.

By 2013, wind energy production worldwide reached a level 510 TWh sufficient to cover the demand of electricity in Germany, the largest economy in Europe. By continuously increasing the rate of growth and applying the most advanced technology and principles of implementation, the wind industry will within a dozen years supply enough energy for a continent. However, when moving from examples to worldwide applications of renewable energy technologies in communities, cities, islands, and rural areas, society as a whole must demonstrate positive interest and provide its support. By applying appropriate legal framework, renewable energy infrastructure, whether installed in remote rural areas in a developing country or integrated within existing conventional infrastructure in a city in the developed world, needs to be better known, accepted, and given the necessary political support.

To increase the use of renewable energy and to spread it throughout the technologically advanced world to a needed extent – 50 % of world energy consumption by 2050 – it is necessary to involve many more renewable energy scientists and engineers, environmental scientists, entrepreneurs, financial experts, publicists, and architects. Above all, we will need many more politicians and civil servants who know the subject and are more courageous and determined. A new generation of renewable energy pioneers has to be nurtured, especially to work in local communities and industries.

The founding in 2009 of the International Renewable Energy Agency (IRENA) as an international governmental organization supports and advances the active utilization of renewable energies at a global scale. Since 1956, there has existed an international agency for the promotion of atomic energy, whereas the furthering of

renewable energies irrespective of their worldwide potential has been more random. These energies can, more than any other technologies, play a key role in the protection of the global climate and the environment, resource conservation, the fight against poverty in developing countries, and securing the long-term reliability of supplies.

IRENA has the status for promoting worldwide capacity building, best policy practice and technology transfer in connection with the renewable energies, and not least the necessary efficient and integrated utilization of energy to meet the most basic needs: decent homes, healthy food, clean water, health care, and education. If these legitimate and ever-growing needs are to be met, energy consumption must increase.

Development of a successful renewable energy sector will in the future make a useful long-term contribution to diversity, security, and self-sufficiency of energy supply, because in contrast to fossil fuels and atomic energy, they will not be depleted. Both in the industrialized countries and in the unserved areas with limited or no access to commercial energy supply, the transition to renewable energies will create new, labor-intensive, industrial sectors. The local and national economies will become less vulnerable to international conflicts and price fluctuations of fossil fuels.

Renewable energy exists everywhere, but has a weaker concentration or density of energy than fossil and nuclear sources. Using renewable energy will create a more balanced relationship with nature. A new culture of energy efficiency can lead to a more concerned, socially responsible use of all natural resources. The use of renewable energy – a local resource – can contribute to the preservation of local cultures and also promote new lifestyles and new concepts of prosperity and security that can help mankind meet the challenges of the twenty-first century.

A Promising Future for Renewables

In contrast to 2004, the application of renewable energy technologies to provide electricity, heating and cooling, and transportation 10 years later was widely spread across the globe; recent trends suggest sustained growth worldwide. At the turn of the century, renewables had a strong appeal to those who were interested in moving away from conventional fuels for environmental reasons. By 2014, renewables have demonstrated that, in addition to their environmental and climate benefits, they are also economic drivers, creating jobs, helping to diversify revenue streams, and stimulating new technological developments.

The share of renewables in global electricity generation continues to increase while the share of nuclear power has been declining. The idea of achieving very high shares of non-hydro renewable energy earlier was quite radical, yet today it is considered feasible by many governments and experts. Several local, regional, and national governments around the world have committed to 100 % renewable energy in one or more sectors within the coming decades.

Nonetheless, the renewable energy sector still faces numerous challenges. Enormous subsidies for fossil fuels and nuclear power persist, and they continue to vastly

outweigh financial incentives for renewables. Many countries are directing increasing resources toward the exploration and extraction of unconventional fossil resources, while most governments remain reluctant to internalize the external costs associated with the extraction and use of fossil fuels.

Further advances and investment in renewable energy, as well as improvements in energy efficiency, must continue if the increase in global temperature is to be limited to 2 °C. For this to happen, stable and predictable policy frameworks are key concerns. Integrated policy approaches that incorporate energy efficiency – considered as the low-hanging fruit on the path to sustainability – will further facilitate the global transition to renewable energy.

The development since 2000 has set the wheels in motion for this transition, but a concerted and sustained effort will be required to fully achieve it. With increasingly ambitious targets, innovative policies, and technological advances, renewables can continue to surpass expectations and foster a cleaner energy future.

References

Bassam N, Maegaard P (2004) Integrated renewable energy for rural communities, planning guidelines, technologies and applications. Elsevier, Amsterdam

Boston Consulting Group (2010) Electricity storage, making large-scale adoption of wind and solar energies a reality, Cornelius Pieper and Holger Rubel Cologne/Frankfurt

CEESA (2011) Coherent energy and environmental system analysis. Aalborg

CODE2, Cogeneration Observatory and Dissemination Europe (2014) D5.1 – final cogeneration roadmap, Denmark

Danish Energy Agency (2010) Heat supply: goals and means over the years, homepage

E4tech Sàrl and Element Energy Ltd (2014) Development of water electrolysis in the European Union, final report. Lausanne/Cambridge

El Bassam N, Maegaard P, Schlichting ML (2012) Distributed renewable energies for off-grid communities. Elsevier Science, New York

Energy Policy Report (2013) The Ministry of climate, energy and building to the Danish Parliament on Danish energy policy, Copenhagen

Hossain J (2014) WWEA World Wind Energy Assessment report, Bonn

IRENA (2014) REthinking Energy: Towards a new power system, report, Abu Dhabi

Lund H (2010) Renewable energy systems: the choice and modelling of 100 % renewable solutions. Academic, Burlington

Luo G, Angelidaki I (2012) Integrated biogas upgrading and hydrogen utilization in an anaerobic reactor containing enriched hydrogenotrophic methanogenic culture. In: Biotechnology and bioengineering magazine. Department of Environmental Engineering, Technical University of Denmark, Biotechnology and Bioengineering, Wiley Periodicals inc

Maegaard P (2009) Danish renewable energy policy (article). WCRE.org, Sept 2009

Maegaard P (2010) Wind energy development and application prospects of non-grid-connected wind power. In: Proceedings of 2009 world non-grid-connected wind power and energy conference. IEEE Press, Nanjing, 24–26 Sept 2009

Maegaard P (2010/2014) Thisted, 100 % renewable energy municipality. PPT, presented 2010/2014 at conferences/events in 50 cities in 18 countries

Maegaard P (2012) Integrated systems to reduce global warming. In: Handbook of climate mitigation. Springer Science, New York

Maegaard P, Palz W, Krenz A (2013) Power for the world. The emergence of wind energy, vols I–II. Pan Stanford, Singapore

Renewable Energy Policy Network for the 21st Century, REN21 (2014) Renewables global futures report 2013, ren21.net, Paris
Biogas i Danmark – status, barrierer og perspektiver (2014), Energi Styrelsen, Copenhagen
Scheer H (2006) Energy autonomy, the economic, social and technological case for renewable energy. Earthscan, London
www.ecotrinova.de/downloads/080610glfreeffstadtwettbewerb.pdf (article)

Thermoacoustics

Matthew E. Poese

Contents

Abstract

Thermoacoustic heat engines offer mechanically simple energy conversion that can utilize a wide variety of heat sources – including solar energy, biomass, and even the "waste" heat from internal combustion engines and industrial processes. This chapter will address the gas thermodynamics that enable such machines and discuss the practical elements that comprise thermoacoustic machines that act either as a converter of heat energy to another form of energy (such as electrical or mechanical energy) or as a heat pump that "moves" heat from a cold region to a warmer one. The distinction between the two topologies of thermoacoustic

M.E. Poese (✉)
Applied Research Laboratory, State College, PA, USA
e-mail: poese@psu.edu

W.-Y. Chen et al. (eds.), *Handbook of Climate Change Mitigation and Adaptation*,
DOI 10.1007/978-3-319-14409-2_48

machines, stack-based and regenerator-based, will also be clarified and the differences between the two made clear. Finally, the latter portion of the chapter will discuss existing and potential applications for thermoacoustic machines.

Introduction

At the end of the last century, the National Academy of Engineering created a list called the "Greatest Engineering Achievements of the Twentieth Century." On that list, two of the top ten achievements have a heat engine at their heart: the automobile (rated second) and air-conditioning/refrigeration (rated tenth). After nearly 100 years of widespread adoption and significant incremental improvements to each of these products that have greatly improved the quality of life, the automobile engine and the cooling machine have also been identified as causing a large fraction of the atmospheric pollution problems. As a result, there is a significant global research and development effort underway to not only improve the efficiency of both automobile/truck engines and cooling machines, but also design automobiles that do not use fossil fuels and refrigerators that do not require HFC/HCFC refrigerants that are 2,000–3,000 times more potent as a global warming gas than carbon dioxide. To address these challenges, novel heat engines are being developed that utilize thermoacoustic energy conversion.

Thermoacoustic energy conversion technology can be a part of a strategy to reduce global warming gas emissions for four primary reasons:

- The working fluid of these machines is typically an inert gas, like helium, which has no global warming potential (GWP).
- The efficiency is comparable with existing power conversion technology and has room for growth.
- The machines are fuel-flexible and do not require fossil-fuel based liquids.
- The machines are mechanically simple, which makes them an attractive target for commercialization.

Thermoacoustic machines belong to the closed-cycle class of heat engines and are subject to Carnot efficiency restrictions. They are similar in many ways with Stirling machines. The goal for the technology development has been to create a closed-cycle engine technology that is both efficient enough to present significant fuel savings (and therefore reduce emissions) while also being mechanically simple enough to meet price and reliability targets. A schematic of a thermoacoustic refrigerator compared to a vapor-compression machine is shown in Fig. 1

This technology has been under active development since the late 1970s with the work of Peter Ceperley (Ceperley 1979) and, independently, John Wheatley, Greg Swift, and collaborators (Wheatley et al. 1983). In the three decades that have elapsed since the foundations were laid, the physical understanding of the hydro- and thermodynamics in these devices have been well developed and codified largely by Greg

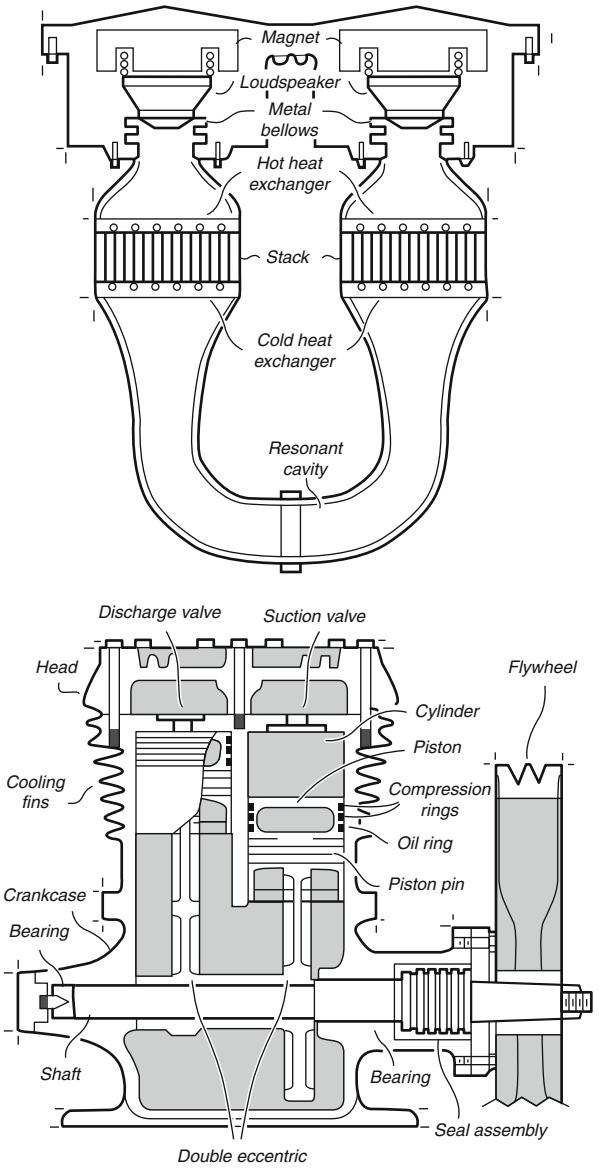

Fig. 1 The schematic of a thermoacoustic refrigerator is shown on the *left* which cooled radar electronics aboard the USS Deyo in 1995. A pair of linear motors convert electrical energy into a sound wave which fills the resonant cavity where cold heat exchangers allow heat from the cold radar electronics to enter the cavity and be pumped to the hot heat exchangers which exhaust that heat to the ambient temperature environment. The schematic of the thermoacoustic machine is somewhat mechanically simpler than the schematic of the vapor compression machine shown on the *right* which requires lubricated sliding/rotating seals and often relies on working fluids that have a high global warming potential (Artwork by Tom Dunne courtesy of The American Scientist, used with permission)

Swift in a textbook (Swift 2002) and, previously, in a comprehensive journal article (Swift 1988). This chapter will not attempt to recast or even improve upon this work; readers who have an interest in the detailed physics of thermoacoustic heat engines will find satisfaction in Swift's textbook treatment of the subject.

This chapter will provide an explanation of the two main types of thermoacoustic heat engines (stack-based and regenerator-based). Some of the applications to which

thermoacoustic technology has seen development efforts will be discussed followed by an outline of some of the challenges that have been discovered that pose hurdles to adoption on the scale that could have an impact on the mitigation of climate change.

Thermoacoustic machines can be broken into two broad application fields: machines that convert the flow of heat from a hot temperature to a colder one into sinusoidal oscillations in a gas (acoustic waves), and machines that use an acoustic wave as an input to "pump" heat from a cold temperature to a hotter one. Machines designed to accomplish the former are typically called engines, and they require some small oscillation of the gas to start an instability that grows and is sustained by the temperature difference and continuing flow of heat from hot to cold. In practice, the small oscillation required to trigger the instability occurs naturally from convection currents of the gas. Machines designed to utilize the energy in a sound wave to pump heat from a cold temperature to a warmer one are called alternately refrigerators, heat pumps and sometimes air-conditioners when targeted toward indoor climate control. In the case of the thermoacoustic heat pump, a source of sound is required: often this is accomplished using a transducer (e.g., linear motor) but the sound could also be provided by a separate (but coupled) thermoacoustic engine.

At the core of the machine is a pair of heat exchangers which bookend a slab of porous media. The working gas of the machine can flow through the heat exchangers and through the porous media between them. As the gas in thermal contact with these core elements experiences pressure and velocity changes with the correct phase, the desired effect (either amplification of the oscillations or heat pumping) is realized.

This core is mounted into a container of carefully designed dimensions so that the gas oscillations will be resonant, which not only sets the frequency of the gas oscillation, but provides an impedance (the ratio of the oscillating gas pressure to the oscillating gas velocity) enhancement favorable to the design and efficiency of the machine. From the standpoint of efficiency, a high impedance is preferable because the gas velocities are small for a given power flow (power in this case is the product of the oscillating pressure amplitude, the oscillating velocity amplitude, and the phase between them). The loss in the porous medium tends to be attributable more to drag than to non-adiabatic pressure oscillations since the pores have to be fairly small to get good thermal communication between the solid and the gas. Additionally, for heat pumps that are driven electromechanically, a high impedance means that a relatively small back-and-forth motion of the piston is enough to make large pressure swings: small piston motions can take advantage of many kinds of seals that do not require lubrication, like flexure seals or dry-fit clearance seals.

Thermoacoustic machines are also categorized on another criterion: the pore size of porous medium that is placed between the two primary heat exchangers mentioned above. One category uses a porous medium called a "stack," and the other category uses a medium called a "regenerator." The fundamental difference between the two is the size of the pores. This difference will be discussed later the chapter. The regenerator-based machines have the potential to be more efficient than the

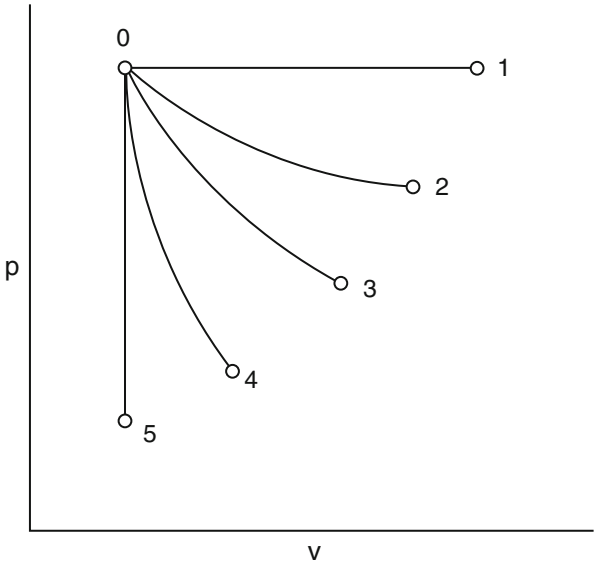

Fig. 2 The four special cases of polytropic state change are shown on a pV diagram. For an ideal gas, γ is the ratio of specific heats for the adiabatic case. When considering an ideal gas, there are no physically meaningful values of γ between the ratio of specific heats and ∞ (the constant volume case). The numbers correspond to the list of thermodynamic state change categories above

stack-based machines at the expense of slightly more complication. Each type of machine may have a role in particular applications.

A final element shared by many thermoacoustic machines is a transducer of some kind that either converts electricity to sound or the reverse, converting sound waves produced by an engine to electricity. A linear motor is a common device that can perform both of these functions; there are linear motors with moving magnets (Liu and Garrett 2005), which are typically preferred for reliability due to the coils being stationary. Moving coil designs have also been used, especially for research purposes (these are similar to a loudspeaker in design).

Heat Engine Cycles Background

A machine that either converts heat flow into mechanical work or forces heat to flow from a cold object to a hot one using mechanical work can be described in terms of the thermodynamic steps that make up one cycle of operation. The state of the working medium at the end of each step can be predicted (if the state before the change is known) using the expression $p_0 V_0^\gamma = p_n V_n^\gamma$, where γ is a variable that depends upon the details of the thermodynamic process by which the system changed state. Thermodynamic state change is commonly categorized in five ways listed below and shown on a *p-v* diagram in Fig. 2:

1. Isobaric (constant pressure, $\gamma = 0$)
2. Isothermal (constant temperature, $\gamma = 1$)
3. Polytropic ($1 > \gamma > c_p/c_v$)

Table 1 A chronological list of ten elementary heat engine cycles showing that the concept of a regenerator occurred early in the development of heat engines

Type of state change	Credit	Year
1 & 5, isobaric and isometric	Papin	1690
1 & 3, isobaric and polytropic	Cayley	1807
2 & 5, isothermal and isometric	Stirling	1816
2 & 4, isothermal and adiabatic	Carnot	1824
2 & 3, isothermal and polytropic	Reitlinger	1843
1 & 4, isobaric and adiabatic	Joule	1852
2 & 1, isobaric and isothermal	Ericsson	1853
4 & 5, adiabatic and isometric	Otto	1867
3 & 4, polytropic and adiabatic	Lorenz	1894
3 & 5, polytropic and isometric	Crossley	1896

4. Adiabatic (constant entropy, $\gamma = c_p/c_v$)
5. Isometric (constant volume, $\gamma = \infty$)

A heat engine cycle generally has four steps executed in succession. These four special cases of a polytropic process (and the generic case labeled "polytropic") can be combined to realize ten different heat engine cycles since only two unique processes can be included in a cycle. (One reason for the requirement that each process must occur twice per cycle is that a machine built to execute a heat engine cycle must repeat its motion; for example, if a machine executes a constant volume process during one-quarter of the cycle, it will (usually) mechanically execute another one to return to the initial state.) These five thermodynamic processes can be combined into ten identifiable elementary heat engine cycles, which are listed in Table 1 (Kolin 1995).

Rev. Robert Stirling's contribution in 1816 to the development of heat engines was to recognize the importance of the regenerator (he called it the "economizer") to increase efficiency, which was important as the price of coal had begun to rise steadily since the beginning of the Industrial Revolution (Urieli and Berchowitz 1984; Sier 1995).

How a Regenerator Is Utilized to Pump Heat Efficiently

Since regenerator-based thermoacoustic machines are the first choice for efficiency, it makes sense to lay out the phenomenological physics of how an acoustic wave passing within it pumps heat and how it relates to the Stirling cycle. Following Fig. 2, the pV diagram for the Stirling cycle is shown in Fig. 3. A schematic of a machine that can execute this cycle is shown in Fig. 4.

The schematic diagram of the alpha-Stirling refrigerator shown in Fig. 4 contains a regenerator sandwiched between heat exchangers with two pistons, one on either side of the regenerator (these will be referred to as the cold- and hot-side piston in this discussion). At steady state, the ideal regenerator has a linear temperature gradient across its length. The pistons are connected by some linkage that provides

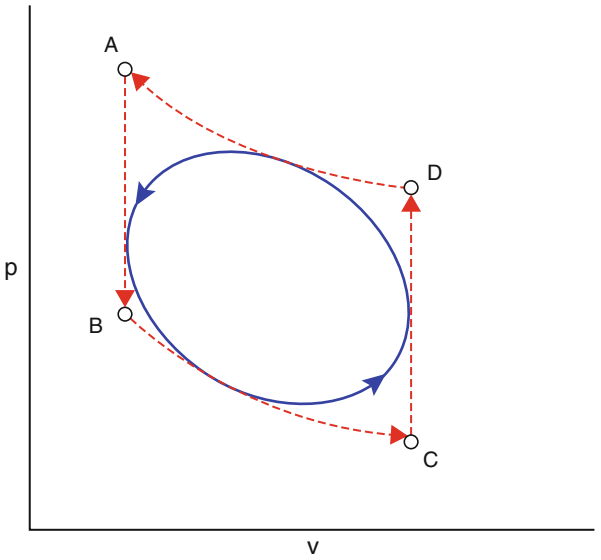

Fig. 3 A qualitative graph of pressure versus volume for an articulated Stirling cycle. The *oval* (*solid curve*) represents the cycle driven with sinusoidal pressure and velocity oscillations. The *outer curves* (*dotted*) represent an articulated cycle

for the correct relative motion of the pistons to make the machine function as a refrigerator or an engine (or nothing useful). One usual simplification is to suppose that each piston has the range of motion to be able to sweep out the entire volume of its cylinder, right up to the edge of the heat-exchanger/regenerator edge. The simplest view of the operation of this machine as a refrigerator contains four distinct strokes in the following order:

A-B Displacement: Both pistons move in concert to move the gas from the hot-side piston cylinder through the regenerator to the cold piston cylinder. The gas is cooled reversibly as it passes through the regenerator since the gas is assumed to be in perfect thermal contact with the regenerator material due to the porous design of the regenerator. Since the gas is colder, heat is (reversibly) absorbed by the regenerator from the gas. This movement through the regenerator is carried out so that the volume that the gas occupies is constant throughout the step. Since the temperature of the gas decreases at constant volume, the pressure of the gas must decrease during this step. Although no $p \cdot \Delta V$ work is done on or by the gas (since the volume did not change), the energy lost by the gas from thermal conduction can be expressed by the decrease in pressure at constant volume.

B-C Cooling: Now that the gas is at a low temperature, but at the starting volume, the cold-side piston moves away from the hot-side piston (the separation distance increases) which decreases the pressure of the gas even further. This expansion would cause the temperature of the gas to decrease to a temperature below the coldest temperature of the regenerator if the step were adiabatic. In the isothermal limit, during each differential step of this expansion stroke, the gas gets a differential amount colder which allows a differential amount of heat to move from the heat exchanger located at the cold end of the regenerator to the gas. The cold (or load) heat exchanger is assumed to have the same temperature as the cold end of the

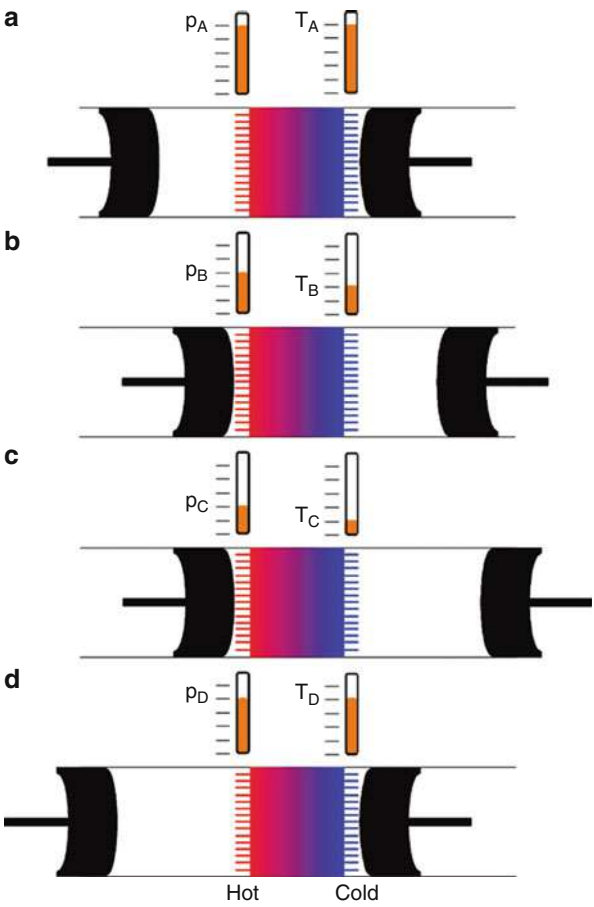

Fig. 4 This figure shows the piston motion in an alpha-Stirling refrigerator (the alpha configuration is where two distinct pistons are located in separate cylinders). The letter designations correspond to the *pV* diagram in Fig. 3, and the meters above each picture display the relative magnitudes of the gas pressure and average gas temperature

regenerator and, like the regenerator, this heat exchanger is in perfect thermal contact with the gas. Although the ideal Stirling refrigerator exhibits an isothermal expansion during this step, in real machines, this step is closer to an adiabatic expansion, as noted below. The job of the load heat exchanger is to move the heat from the thing to be cooled (e.g., ice-cream, medicine, foodstuffs) into the cold-side cylinder so that it can be transferred to the gas during this cooling step.

C-D Displacement: Following the cooling stroke, the pistons move together to drive the gas back through the regenerator toward the hot-side piston. During this constant volume displacement, the gas is reversibly warmed to the hot-side regenerator temperature. Since the warming occurs at a constant volume, the pressure of the gas increases during this step. It is during this step that the parcel of gas recovers the energy given to the regenerator from step *[A]–[C]*. It is in this reversible recovery of energy that the regenerator proves its worth; because of the regenerator, the expansion stroke only has to move heat *at the cold temperature* and does not have to cool the charge of gas from ambient temperature to the cold temperature

since the displacement stroke through the regenerator took care of that part. It is this idea of precooling and preheating the gas in preparation for heat transfer to or from a load that makes the Stirling cycle and other regenerative heat engine cycles useful. The fact that the regenerator can, in principle, do this precooling and preheating reversibly makes it efficient.

D-A Exhaust: Once all of the gas has been reversibly warmed to the hot-side temperature, the hot-side piston moves toward the cold-side piston compressing the gas that has been warmed. If isothermal, the amount of heat that was removed from the load exchanger plus the work done to remove it is absorbed by the exhaust heat exchanger. The job of the exhaust exchanger is to provide a path for that heat to leave the hot-side cylinder.

After reading this simplified step-by-step description of the operation some complications might be evident. First, a machine cannot produce such articulated motions to be able to easily mark, for example, the end of the cooling step and the beginning of the displacement step. In real machines, the pistons usually move in a sinusoidal motion (as shown in Fig. 3), which not only blurs the distinction between each of the four steps, but also reduces the power density of the machine for a given operating pressure range. This reduction in power density can easily be understood by appreciating that the area enclosed by the lines of the pV diagram is the amount of work required to move heat from material at the cold temperature to the environment. If a machine was operating at a constant efficiency, it would be able to move more heat for a specified pressure and volume oscillation amplitude if it could operate on the dotted curves in Fig. 3 (articulated piston motion) than it could if the pistons moved with sinusoidal motion as shown on the ellipse.

Secondly, it would be difficult to make a machine that could execute isothermal expansions and contractions in the cylinder spaces on the left and right of the regenerator in Fig. 4. If the relative scale of the schematic shown in Fig. 4 were used to build a machine, that machine would be better modeled with adiabatic compressions and expansions in place of the isothermal ones described above. These adiabatic compressions decrease performance below the Carnot limit since during the adiabatic pressure change, the gas gets measurably warmer or colder than the regenerator end-temperatures. Consequently, when this hotter or colder gas enters the regenerator (or heat exchangers), heat moves across a finite temperature difference, which is an irreversibility that decreases maximum theoretical performance below the Second Law limit. Also called the Carnot limit, the Second Law of Thermodynamics sets an upper limit for the amount of heat that can be moved from a mass at a cold temperature and exhausted to the environment at ambient temperature for a given amount of input work. This limit depends only upon the cold temperature, T_c, and the ambient temperature, T_0, and is expressed as $COP_C = Q_C/W = \frac{T_C}{T_0 - T_C}$, where Q_C is the amount of heat removed from the cold object and W is the amount of work required to move that heat (COP is an acronym that stands for coefficient-of-performance).

The Stirling cycle, as presented with isothermal compressions and expansions, is reversible (in the limit of zero viscosity) and, therefore, has the theoretical potential

to reach the Carnot limit of efficiency. In earlier days of Stirling machine design, assuming isothermal expansions and compressions made the analysis of potential designs tractable in closed form; the first published isothermal analysis of the machine was in 1871 by Gustav Schmidt, a professor at the German Polytechnical Institute at Prague. It was Schmidt, 50 years after the invention of the Stirling machine, who first represented the cycle with isothermal expansions and contractions because that model yielded a closed-form solution. Almost 100 years later, Finkelstein published the first analysis of a Stirling machine with non-isothermal expansions and compressions (Urieli and Berchowitz 1984).

The Function of the Regenerator and Its Advantages Compared to a Stack

The purpose of the regenerator in Stirling machines is to provide for the temporary storage of heat for the oscillating working gas. The gas must be brought to the cold temperature before the cooling (expansion) stroke is executed and then warmed before the exhaust (compression) is executed. The amount of heat removed to provide the cool gas for the expansion stroke is exactly the same amount of heat that must be returned to the gas in preparation for the exhaust stroke. The regenerator provides a place for the gas to temporarily store this heat; to do so, it must have enough heat capacity to be able to store the required heat to get the gas to the desired temperature and it also must be as thermally nonconducting as possible to reduce heat flow along its length, a heat flow that reduces the effectiveness of the regenerator. For this reason, many regenerators are made of stacked stainless steel screens, which provide plenty of heat capacity and a large array of pore size possibilities. Since each layer of screen has a significant amount of thermal contact resistance, heat conduction along the length is minimized to an acceptable level.

Stack-Based Thermoacoustics

In the last 20 years of the twentieth century, much research and design was dedicated to thermoacoustic machines that utilized an oscillating gas with nominally standing wave phasing (gas pressure and velocity 90° out of phase) in the presence of a "stack" of closely spaced, rather nonconducting plates (Swift 1988). This stack of plates was designed with a plate-to-plate spacing on the order of a few thermal penetration depths, or the acoustic thermal boundary layer thickness. This acoustic boundary layer is called a "penetration depth" because it is the distance that heat (or momentum, in which case, it is referred to as the viscous penetration depth) can diffuse in one acoustic cycle. The penetration depths are defined as

$$\delta_\kappa = \sqrt{\frac{2k}{\rho_m c_p \omega}}$$

$$\delta_v = \sqrt{\frac{2\mu}{\rho_m \omega}}$$

where ω is the angular frequency of the gas oscillation, ρ_m is the mean gas density, c_p is the gas specific heat at constant pressure, k is the thermal conductivity, and μ is the shear viscosity of the gas. Since the stack plate-to-plate spacing might be twice this thermal penetration depth, the rate of heat transfer between the plates and a gas parcel translating in a plane equidistant from two plates is not fast compared to an acoustic period, as it might be for a parcel of gas near to the plates. The lag of heat transfer with respect to the motion of the active gas parcels (those parcels that are not too near the plates) is what allows the gas to execute a useful heat engine cycle – one that either spontaneously converts heat input into sound energy or one that uses sound energy to move heat from a cold reservoir to an ambient temperature one.

This natural phasing idea, utilized by designing the stack with the proper plate spacing for a particular thermal penetration depth (which depends on working gas properties and frequency of oscillation), is considered an innovation since it rids a machine of any number of complicated methods to impose the required phase difference between heat transfer and gas motion. For example, in an automotive engine, each cylinder has at least two valves that must be opened and closed at the right time via the motion of rockers, cams, and pushrods. Most Stirling machines, as well as other air and gas engines, also have complicated linkages that impose the phasing of gas motion, pressure and heat input, and exhaust. However, the mechanical simplicity that comes with the exploitation of natural phasing brings with it a significant penalty in efficiency of the cycle. The fact that the thermal contact between the stack and the gas in the stack is not perfect (in order to get the right "natural" phasing) the heat that is exchanged between the stack and the gas is not exchanged in a reversible way (Wheatley et al. 1986). Since this heat transfer that occurs each cycle happens over a finite temperature difference, the *theoretical* limit in efficiency of the stack-based thermodynamic cycle is lower than the Second Law limit.

Regenerator-Based Thermoacoustics

As opposed to using a stack as the second thermodynamic medium, the use of a regenerator allows the theoretical thermodynamic efficiency to reach the Carnot limit. The function of a regenerator is slightly different than that of a stack. While both the stack and regenerator provide heat capacity for the temporary storage of heat, the details of how this heat is exchanged with the gas are different. In the stack, this exchange is irreversible because the active gas is one or a few thermal penetration depths away from the stack material (as explained above). It is this irreversibility that is the source of the natural phasing: a simplicity that can be desirable and worth the efficiency penalty. In a regenerator, the gas passage pores are much tighter. This ensures that all of the gas in the regenerator is well within a fraction of a thermal

penetration depth so that the thermal diffusion time is significantly shorter than an acoustic period. (A rule of thumb might be that the pore sizes are one fifth of the size of a thermal penetration depth.) Consequently, the transfer of heat between the regenerator and the gas is theoretically reversible which allows the efficiency to approach the Carnot limit. (However, since the pore size is small, the COP of any real incarnation of a regenerator-based heat engine will be limited by viscous loss in the regenerator, as well as other irreversibilities. In the comparison of stack-based to regenerator-based machines, it is somewhat arbitrary to compare the limiting case of a working fluid with zero viscosity since its effect is much bigger in the regenerator than the stack.) This gain in potential efficiency comes with the loss of the elegant natural phasing found within the pores of the stack. Therefore, the phasing of heat transfer and gas motion in the regenerator must be imposed by some other mechanism.

Using a Regenerator in an Acoustic Heat Engine

Since the natural phasing found in the stack is lost when taking advantage of the improved properties of the regenerator-based Stirling cycle, the correct phasing of heat transfer and gas motion must be imposed in some other way. In the late 1970s, Ceperley (1979) recognized that a traveling acoustic wave exhibits the correct phasing to force the oscillating gas to execute a Stirling cycle. This phasing, where oscillating pressure is in phase with the velocity of the gas, is enforced in conventional kinematic Stirling machines by way of the mechanical linkage. Ceperley built an acoustic-Stirling engine apparatus that included a regenerator inside of a pipe that was several wavelengths long, but his engines failed to produce acoustic energy. Although the regenerator was providing the needed energy storage, it also presented a significant viscous loss to the acoustic wave passing through the regenerator matrix. This attenuation, proportional to the square of the acoustic velocity, was much too large to allow any acoustic pressure oscillations to build in the tube; as the pressure would increase from the Stirling cycle taking place in the regenerator, the acoustic particle velocity would also increase, causing increased attenuation in the regenerator which robbed the wave of the power produced by phased heat transfer in the regenerator.

This is best understood by considering that the impedance (the complex quotient of oscillating pressure divided by the gas velocity) of the wave traveling along the tube that is several wavelengths long is simply the characteristic impedance of the gas in the tube: the product of density and sound speed. This impedance is relatively low compared to the impedance found near the closed end of a tube that is half of a wavelength long. In such a tube, the magnitude of the impedance near the closed end is large compared to the characteristic impedance of that gas; the oscillating pressure is large in magnitude compared to the relative magnitude of the gas velocity which becomes zero where the gas meets the capped end of the tube. This location would be a good place to locate a regenerator, except for the fact that in such a standing wave tube, the pressure is almost 90° out of phase with the gas velocity.

This preference for high impedance (ratio of driving potential to flow velocity) is also found in the electrical power transmission network. Electrical power (alternating current) is the real part of the product of the complex voltage (analogous to pressure) and complex current (analogous to acoustic velocity) in the form $\dot{E}_{\text{elec}} = \frac{1}{2}\Re\left[\tilde{e}\cdot\tilde{i}^{*}\right]$, where the asterisk represents the complex conjugate. The energy lost to Joule heating, which is the dominant loss mechanism in power transmission, is the product of the square of the current and the electrical resistance, $\dot{E}_{\text{loss}} = i^2R$, of the transmission line. Therefore, electrical power is transmitted at much higher voltage amplitudes than people like to use in their homes and at a significantly reduced current amplitude to reduce the resistive loss. Since power is the product of the potential and the flow, the amount of power transmitted can be maintained while the potential is increased and flow decreased proportionally to minimize losses.

In a regenerator-based acoustic machine, it is desirable to deliver a particular amount of power to the regenerator with the acoustic wave. The delivery of this power must have pressure and velocity in phase and at an acceptably large impedance so that viscous losses in the regenerator do not make the machine so inefficient as to be of no practical use. The first machines to successfully exploit this idea of an acoustic Stirling machine with the regenerator at a high impedance location was an engine built at Los Alamos by Scott Backhaus and Greg Swift (Backhaus and Swift 2000) and an engine of Kees de Blok and collaborators in the Netherlands (de Blok et al. 2001). Their pioneering concept for a thermoacoustic Stirling engine led the way for a new decade of thermoacoustic machine development that continues to this day.

The Acoustic Phasing Network

For successful utilization of a regenerator, several requirements must be met. First, pressure oscillations and velocity oscillations must be substantially in phase. The frequency of this oscillation must be low enough that the acoustic boundary layer thickness is several times larger than the average pore size of the regenerator matrix. The magnitude of the complex ratio of oscillating pressure to oscillating velocity must be relatively large in comparison to the characteristic impedance of the working gas. In addition to these elements, the energy flow in the machine is important.

In a Stirling refrigerator, the gas in the regenerator is a sink for mechanical (or acoustical) energy that passes from the exhaust (ambient temperature) side to the load (cold temperature) side. Energy in the form of mechanical work is supplied to the gas in the regenerator (see Fig. 5), and that gas absorbs some amount of this work in order to move heat against a temperature gradient from the cold end to the ambient (or hot) end of the regenerator. In a regenerator that transfers heat reversibly to a gas with no viscosity (this is a "perfect" regenerator and could also be thought of as one that generates no entropy), the remaining amount of work that flows out of the cold end of the regenerator is equal to the amount of heat removed from the load and pumped to ambient temperature. In this perfect regenerator, the amount of total

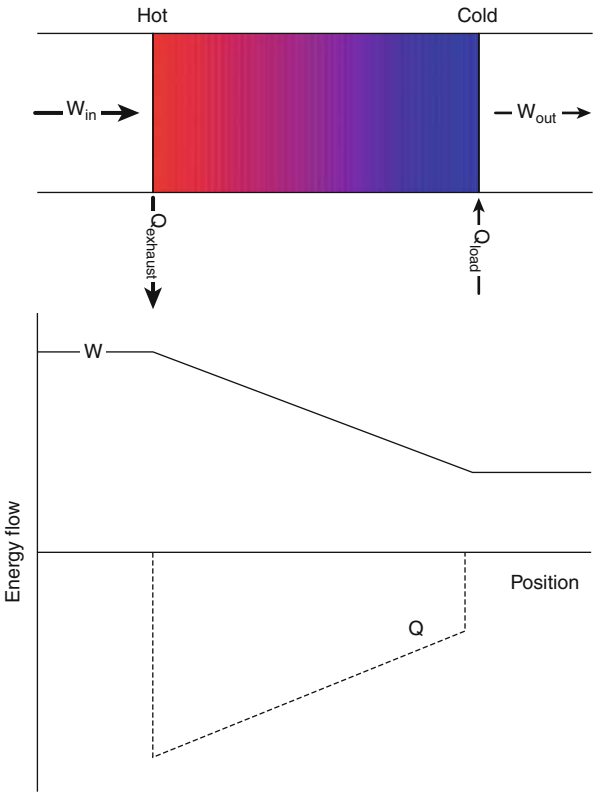

Fig. 5 This graph shows the energy flow through a regenerator that produces refrigeration. The *dotted line* represents the heat and the *solid line* shows the mechanical work. Note that everywhere in the regenerator, the sum of the heat and work is zero. The useful cooling capacity in an ideal regenerator is equal in magnitude to the amount of work that flows out of the regenerator at the cold (load) side

energy at any location along the regenerator's axis is zero. Since total energy or enthalpy, $\dot{H}_2$, is the sum of the work energy and the heat energy in the regenerator (and would include other types of energy if the magnitude was changing within the regenerator), the heat moving to the left ("up" the temperature gradient) is equivalent to the magnitude of work energy that is flowing to the right (the direction of propagation of the acoustic wave). In a machine with a perfect regenerator, in order to move an amount of heat, δQ per cycle some amount of work δW is absorbed per cycle in the regenerator as demanded by Carnot.

The work required by the Second Law of Thermodynamics to move an amount of heat δQ is related only to the temperatures between which the heat is moved T_0 and T_C: $\delta W = \delta Q \frac{T_0 - T_C}{T_C}$. In a real regenerator, the amount of work absorbed in the regenerator due to viscosity is greater than the Carnot minimum; since this work does not contribute to moving any useful heat, this extra work raises the total power in the regenerator to a value greater than zero. Likewise, since a real regenerator allows some conduction of heat from the ambient side to the cold (load) side and heat exchange in the real regenerator has irreversibility associated with it, the net amount of heat moved from the load to the ambient reservoir will not be as great as it could have been for the amount of work flowing into the regenerator. This reduction in the

useful amount of heat moved "up" the thermal gradient within the regenerator also increases the magnitude of total power in the regenerator above the ideal value of zero. The concept of total power allows a quantitative way to judge the "effectiveness" of the regenerator and allows the designer to know if a proposed change to the design of the machine or regenerator parameters will increase efficiency.

Within the Stirling community, machines are commonly classified into two major categories: kinematic and free-piston. In a kinematic machine, the two moving elements (either a piston and a displacer or two pistons) are connected together by a mechanical linkage and the motion of the two elements with respect to one another is completely defined by the mechanics of the linkage. Free-piston machines are a much more recent development, largely credited to Beale (1971), but could also be attributed to Ringbom (Sier 1995). The recognition that the mass of the displacer could be made to resonate against the stiffness of trapped gas in the machine created a renewed interest in Stirling machines in the early 1970s. Free-piston Stirling machines offer a more compact and mechanically simpler alternative to their kinematic brothers; however, these benefits come at the price of increased design complexity since the dynamics of the heat transfer directly impact the motion of the two moving elements which create the pressures – the pressures that dictate how much heat moves. In a kinematic machine, the motion of the piston/displacer is set mechanically and the thermodynamic events taking place in the machine cannot impact the displacement magnitude (or therefore, the pressure amplitude).

In either category, the free-piston or the kinematic, the energy flow in the device is the same; energy flows into the ambient temperature end (exhaust side) of the regenerator and out of the cold (load side). This amount of "left-over" energy that leaves the regenerator must be recycled to the front of the regenerator for the device to be efficient – this is another job of the mechanical linkage and flywheel of the kinematic Stirling machine, and in a free-piston machine, this energy is stored and released by the piston that resonates against the sealed volume of gas, that is, the "free" piston of the free-piston machine.

As shown in Fig. 6, the innovation of Beale (or Ringbom) was to recognize that the complicated and expensive linkages found in kinematic Stirling machines could be removed and replaced with a spring: either a mechanical spring or the stiffness formed by gas in a sealed chamber. The improvement made by Backhaus, Swift, and independently by de Blok et al. was to eliminate the piston that Beale left in his device. Backhaus and Swift substituted for the piston a "slug" of gas that has relatively more inertia than the rest of the gas in the cylinder that contains the regenerator.

The terms "inertance" and "compliance" are terms that describe sections of a gas-filled resonator that behave as acoustic analogs (in a complex impedance sense) to an electrical inductor and capacitor, respectively. A necked-down section of resonator has the effect of delaying the oscillating flow of gas through it in response to a pressure difference across the section. Once the gas is accelerated by this pressure difference, it continues to move even though the pressure difference has changed direction. In order to connote this function, the word "inertance" has both the sense of "inductor" and "inertia." A resonator section that has substantially more volume than the rest of the resonator acts like a capacitor because just as the

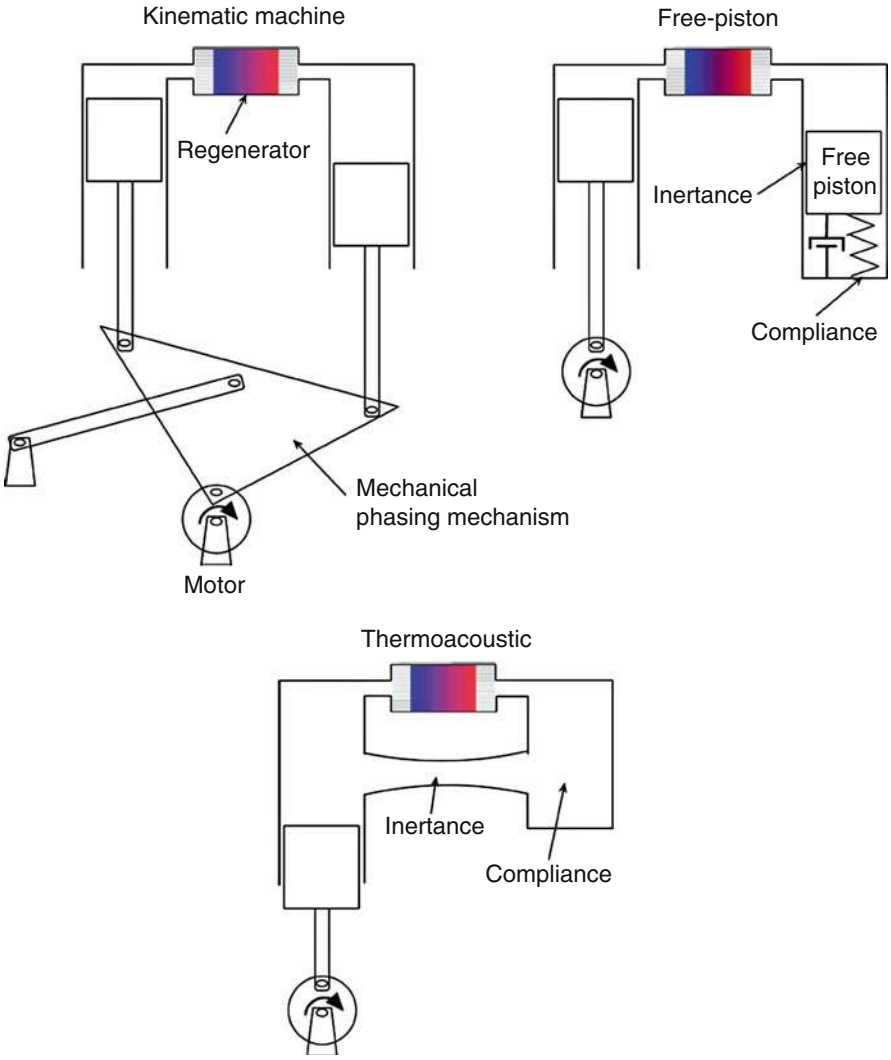

Fig. 6 The broad steps in the evolution of mechanisms to support a Stirling cycle are shown in this figure as refrigerators (these topologies are equivalent in the case of an engine). The kinematic machine, which was born in the early nineteenth century, has many forms and derivatives; only the simplest alpha configuration is shown here. The free-piston Stirling concept started to be developed in about 1970, and although the acoustic-Stirling idea was conceived of in the late 1970s, the first working prototypes were produced in the late 1990s by de Blok in the Netherlands and by Backhaus and Swift at Los Alamos National Laboratory

capacitor stores energy in the form of electrical charge temporarily, the compliance section of a resonator stores energy in the form of pressure. These pressure changes lag the flow of gas into or out of the section just like the voltage across a capacitor lags the flow of current. This equivalent circuit analog to acoustical systems is quite

convenient for the design of acoustic networks and is an established analytical tool in the field of acoustics (Beranek 1954).

The crux of Backhaus and Swift's 1999 engine is the concept of an acoustic phasing network that both delivers acoustic power to the regenerator at a high impedance and correct phase and then returns the power that is not utilized to move heat. (In the case of an engine, the amount of power that is not taken from the wave to do work on a load is returned to the regenerator.) The function of the phasing network is twofold: condition the impedance of the incoming acoustic energy so that it can be efficiently utilized by the regenerator and then return unutilized energy back to the regenerator.

Future Directions

Motivation for Development of Thermoacoustic Machines

Now that some historical and theoretical background has provided a context for thermoacoustic machines, it is important to describe the motivation for pursuing thermoacoustic-Stirling technology.

Thermoacoustic Machine Replacements to Vapor Compression Refrigerators

A candidate replacement technology for refrigeration equipment firmly established on the market must have at least three properties: increased effectiveness (efficiency), reduced cost (simplicity), or present less of a risk for legislative phaseout. In some sense, these three reasons all collapse to the issue of cost. In order for efficiency improvements to lead to lower lifecycle costs, the increase in acquisition cost must not be greater than the fuel savings due to increased efficiency. Legislation created to limit pollution is often driven by the high cost of cleanup associated with that pollution – this is the case for greenhouse gas emissions. Reducing the carbon dioxide in the atmosphere is either very costly or not even technically well understood (an understanding that might be attainable for a higher cost than society has been willing to spend).

Several thermoacoustic machines have been built to perform low-lift (small temperature difference) cooling. One such machine, pictured in Fig. 7, was built for Unilever's subsidiary Ben and Jerry's Homemade. This machine had a performance equivalent to the ice-cream storage cabinets that it was intended to replace but used helium as a refrigerant which has no global warming potential. The unit that it was designed to replace uses R134a (1,1,1,2-Tetrafluoroethane), which has a global warming potential (GWP) of greater than 1,400 over 100 years.

With that in mind, there are at least three considerations that can influence lifecycle cost:

Fig. 7 A view of the regenerator-based thermoacoustic ice-cream storage cabinet built at Penn State University with sponsorship from Unilever/Ben & Jerry's. The thermoacoustic cooler is the silver unit to the *right* of the off-the-shelf storage cabinet. Heat was moved out of the storage cabinet and to the oscillating helium in the thermoacoustic machine by circulating ethanol within the copper tubing of the cabinet that typically carries R134a refrigerant and into the thermoacoustic machine's internal load heat exchanger. The photo on the *right* shows the pump that moved the ethanol covered with ice from condensed water-vapor in the air. A thermocouple reader shows the temperature of the ethanol to be −19.8 °C (*Left* photo by Greg Grieco, used with permission)

- *Cost to Manufacture*: The commodity level vapor-compression refrigerator that is found in the kitchens of most homes in the industrialized world is inexpensive. However, since a thermoacoustic machine has a few moving parts, requires no exotic materials, and has no inherently close dimensional tolerances, a commodity thermoacoustic machine stands some chance of being manufactured as inexpensively as a vapor compression machine. It is true that thermoacoustic machines, as do all closed-cycle machines, require some secondary heat exchange mechanism on both the hot and cold sides. This subsystem does increase complexity, but for some applications like fountain beverage vending, this fluid loop is integral since it is the product delivery system. In grocery store display cases and geothermal heat pumps, secondary heat transfer systems are already in use with conventional compressor technology.
- *Cost to Operate*: The cost of energy purchased to operate the refrigeration machine is minimized by increasing its efficiency and reducing maintenance costs. Cost of energy is important for some applications where the energy is hard to transport to the location of the machine, or applications that demand significant amounts of cooling, and, therefore, reducing the energy demands of the machine saves a significant amount of money. On the other hand, the efficiency of a cooling machine is only a secondary metric for some applications; in the market of commercial ice-cream storage cabinets, the company who makes/markets the ice-cream usually provides a storage freezer to a grocery/convenience-store for no charge (as long as their product continues to sell at the store) and the shopkeeper pays the operating costs. In this case, efficiency may

be of secondary importance to the purchaser compared to acquisition cost. For large capacity applications, such as grocery stores and refrigerated warehouses, efficiency becomes more important since the energy and acquisition cost is borne usually by the same organization and the electrical power consumption is large. Thermoacoustic machines can be made to be competitively efficient and, like Stirling machines, may become competitive with vapor compression machines. However, vapor-compression refrigeration can be made to be quite efficient if cost is no object. Efficiency of vapor-compression machinery on the market is only constrained by the acquisition price tolerance of that market. Typically, reduced operating costs, even if that reduction makes the lifecycle costs smaller, do not offset a high acquisition cost as a priority driving the purchasing decision of many consumers in both the residential and commercial sectors.

- *Cost to Dispose*: Thermoacoustic machines use no environmentally harmful working fluids/gases. Consequently, disposal is inexpensive compared to vapor compression machines which currently utilize gases 2,000–3,000 times more potent as "greenhouse" gases than CO_2. Since the machine uses no lubricants, maintenance is expected to be small and lifetime should be long. Compared to large vapor compression machines which have compressors and rotating machinery that require maintenance and suffer breakdown of the seals, thermoacoustic technology with its linear motors and flexure or clearance seals can increase the useful lifetime of refrigeration equipment with decreases the costs of disposal and wasted material/labor.

Pitting thermoacoustic technology head-to-head with the established vapor compression technology (which is 100 years old) is daunting for as young of a technology as thermoacoustics, which has no established supplier base, a short design history and limited expertise. Vapor-compression is such a mature technology and the market has not yet found vapor compression to be deficient in the three categories above. However, if environmental legislation were to be enacted, either banning certain refrigerants or forcing consumers to pay a premium for buying and disposing of a machine that contains a global warming gas, thermoacoustic technology could become more attractive in the "cost to buy/manufacture" and the "cost to dispose" categories. As the direct cost of energy increases (direct cost is exclusive of the indirect costs such as those associated with natural resource depletion, military protection of oil prices, coal mine runoff and subsidence, etc.) due to pollution taxes or carbon credits as specified by the Kyoto Accords, thermoacoustics with its high inherent efficiency might also be attractive in the cost-to-operate category. Support for technologies that do not use global warming gases is much stronger in Europe at this time than it is in North America.

Thermoacoustic Machines as Power Generators

There are two primary applications for acoustic engines: those that convert the acoustic power to electricity or those that use the acoustic power to drive a

thermoacoustic refrigerator/heat pump (there is not much demand for energy in acoustic form, and the "one-note samba" of an acoustic machine is hard to dance to). Thermoacoustic machines that are built to convert heat energy to acoustic energy and then to electrical energy might be an attractive commercialization target for flexible-fuel, small-scale power generation between 5 and 500 kW of electrical output. In-home electrical generators that burn natural gas or fuel oil to provide both the electrical power for a home and heat the home and domestic water supply might allow a household to reduce the number of subscribed utilities by at least one and eliminate the significant transmission loss associated with electrical power delivery that is wasteful of the global natural resources.

Alternators for Power Generation

A significant component in a thermoacoustic machine that converts heat to electricity is the alternator that performs the conversion of the acoustic energy to electrical energy. Carefully engineered linear motors made for this purpose are commercially available today (QDrive Corporation in Troy, New York); these are the type employed to create the sound wave that powered the thermoacoustic ice-cream freezer shown above.

However, since the diameter of the thermoacoustic machine scales with power, at high powers, the linear alternator/motor and the pistons that attach to them will have to be large and heavy, which will create a challenge for high-frequency (and therefore high power density) operation. The recent invention of a piezoelectric alternator (Keolian et al. 2007) to enable power generation looks promising. Several advantages of an alternator of this design are that the piezoelectric material itself is robust, relatively inexpensive, and low maintenance. Since the design of the alternator allows the piezoelectric ceramic elements to be squeezed twice per cycle by the acoustic oscillation, the power density of the alternator is much higher than that of a linear motor. Figure 8 shows the bare alternator (left) and the alternator installed in a thermoacoustic engine generating 37 W of electricity. This photo was taken at an early stage of the development; this proof-of-concept alternator is capable of generating over 600 W of electricity.

This alternator was designed with the intention of including it in a system to capture the heat from the exhaust pipe on over-the-road trucks and convert it to electricity for use in the truck. A thermoacoustic electrical generator was designed and built at Los Alamos to power a space satellite (Backhaus et al. 2004). For that project, a specialized electrodynamic alternator was designed and built.

Engines Used to Drive Heat Pumps (Refrigerators)

A very compelling application for thermoacoustic technology is to utilize a heat source directly for heat pumping. This is especially elegant because a thermoacoustic machine to accomplish this is only comprised of heat exchangers and stack/regenerators – no moving parts or sliding/rotating seals are required. There are other technologies, like absorption refrigeration, that can have similar simplicity, but these

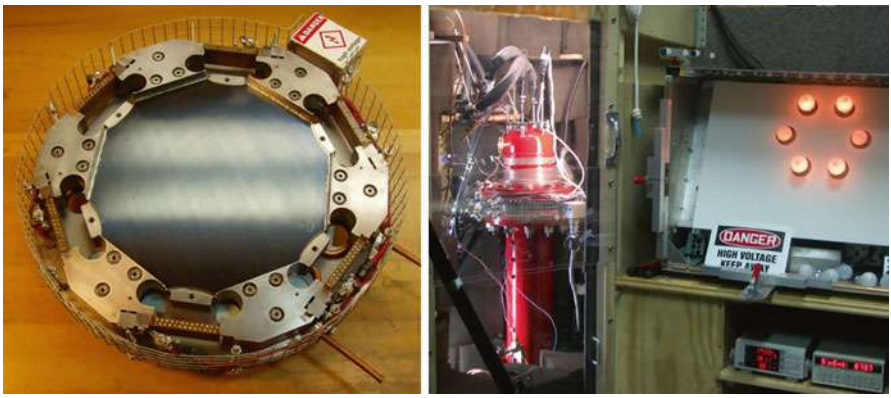

Fig. 8 Two photos show the piezoelectric alternator. On the *left*, the bare alternator is shown, and the piezoelectric elements are the six tan-colored rectangular prisms arrays on the perimeter of the alternator which has an overall diameter of 35 cm. As the oscillating pressure flexes the diaphragm, the piezoelectric elements are squeezed and produce electrical power. The diaphragm squeezes the piezoelectric elements when it moves up and down. On the *right*, the alternator is installed into a regenerator-based thermoacoustic engine (Bastyr 2004) and is powering six light bulbs with 37 W of electricity. This proof-of-concept alternator is capable of generating over 600 W of electricity (Photos by Robert Keolian, used with permission)

machines typically use chemicals like ammonia and hydrogen instead of helium. They also have to work around the phase change temperatures and pressures – phase change systems have a power density advantage over non-phase change systems, but this comes at some reduced flexibility for variable working temperatures.

Along with thermoelectrics and organic Rankine cycles, thermoacoustic machines are often considered as an option for reclamation of waste heat. In many industrial processes, there is low (100–200° C) and medium temperature (200–400° C) heat that is often allowed to escape to the atmosphere unutilized. Often, the heat is difficult to divert into some machine or storage mechanism, but there is also a lack of products available on the market that can accomplish the task in a cost effective way. The lower temperature waste heat reclamation is especially challenging because the size of a device to accomplish the task is large and the Carnot efficiency is low. Nevertheless, the simple combination of a thermoacoustic engine that powers a refrigerator offers one possibility of such a solution.

There are ongoing efforts at Los Alamos National Labs in New Mexico and Aster Thermoakoestische Systemen in the Netherlands to exploit this kind of opportunity. At Los Alamos, an extensive program was executed with the goal of utilizing stranded natural gas reserves – that is, natural gas that is hard to access with piping networks to carry the gas to market. Several systems were built in escalating size and efficiency to burn natural gas at remote well-heads to power a thermoacoustic system that would liquefy the remainder of the gas stream for easy transport from the remote area (Bayram et al. 2005). The largest of these systems is shown in Fig. 9. At Aster, a thermoacoustic heat-driven heat pump system was created to utilize waste heat

Fig. 9 A photo of the natural gas liquifier next to a six-foot (1.8 m) tall man shows the highest power thermoacoustic device ever built. At the *top* is a blower attached to the combustion chamber. The thermoacoustic engine is below the combustion chamber (the conical shaped component) and is connected via the wave tube to a vacuum can at the bottom next to John Wollan, one of the designers and builders of the machine. This device liquified 350 gal/day with a projected production efficiency of 70 % liquifaction and 30 % combustion of an incoming gas stream (Photo by Greg Swift, used with permission)

streams to pump the remainder of the heat to a higher temperature so that it could be utilized in another industrial process.

Cookstoves for Developing World Power Generation

There has long been an interest on the part of developed nations to enable developing nations to share in the technological bounty enabled by heat engines. In many of these countries, fuel for cooking and heating is biomass (mostly wood), collected daily or weekly and oftentimes at great distances from population centers. The relative scarcity of biomass in many places is exacerbated by the collection of it, so the distance of these daily/weekly journeys increases at alarming rates through difficult and/or dangerous terrain. Additionally, the relatively poor utilization of these fuels in stoves or open fires with incomplete combustion causes very poor indoor and outdoor air quality, and the health of women and children (who spend more time around the fires and in the house than men) suffers dramatically. Poor indoor air quality caused by inefficient cookstoves is as big of a health risk than any other in some developing countries, causing 1.9 million deaths each year and chronic illnesses such as low birth weight, acute pneumonia in children under 5, lung cancer, chronic obstructive pulmonary disease, and cardiovascular disease (Global Alliance

for Clean Cookstoves 2010). From the standpoint of global warming, the billions of inefficient, poorly constructed cookstoves in use today contribute to global warming through not only the CO_2, methane, and nitrous oxide present in the combustion products, but also the soot or black carbon emissions from these stoves. Particulate matter of elemental carbon is suspect as a major contributor to climate change and has an estimated GWP of 680 (Roden and Bond 2006).

It has been established (MacCarty et al. 2008) that a fan integrated into the combustion chamber of a stove can increase combustion efficiency and dramatically decrease particulate and black carbon emissions. Lowered emissions can improve atmospheric health in a very short timeframe, and increased efficiency translates to less deforestation and increased carbon sequestration in these areas. Since one way to power a fan is with electricity, there has been some interest to utilize a thermoacoustic electrical generator to provide this electricity using a small fraction of the heat produced by the stove's fuel. Cost is one of the dominant constraints for the successful adoption of technology in the developing world, and the mechanical simplicity of thermoacoustic machines, the lack of exotic materials, and no need for tight machining tolerances all make thermoacoustic technology a candidate for small-scale power generation in developing countries. The other likely technology to fill this niche, which has undergone more testing and commercialization for the application than thermoacoustics, is thermoelectric modules.

Aster Thermoakoestische Systemen has recently completed the testing of a prototype intended for this market with funding from the SCORE program at the University of Nottingham (SCORE stands for Stove for Cooking, Refrigeration and Electricity) and the FACT Foundation in Eindhoven, Netherlands. The topology of the thermoacoustic engine designed and built by Aster is novel (de Blok 2010) due to its planar geometry shown in Fig. 10, which allows integration to a stove by presenting a large heat exchange area to the hot gases above the fire. The thermoacoustic machine is a four-stage regenerator-based engine coupled to electro-dynamic alternators. Each of four regenerators is positioned on a set of ambient-side fins shown below on the left hand side of Fig. 10. The tubes connecting each of the four quadrants are part of the acoustic network. A similar finned plate is installed on the ambient plate which sandwiches the regenerators between the plates and making a series connection between each of the four stages of the machine. This ambient fin plate is shown immersed in the water bath on the right-side photo of Fig. 10, and the hot-side fin plate is facing the gas burner. In practice, the burner could be a three-stone fire or cookstove. The electrodynamic alternators for this design are still under-construction.

Commercialization Considerations

Direct competition with vapor compression technology may not be the only path toward commercialization of thermoacoustic cooling technology. There is surely an application for a machine that uses an environmentally benign working fluid, is quiet, efficient, has low moving mass, and can easily take advantage of proportional

Fig. 10 The ambient temperature heat exchange plate of the cookstove generator developed by Aster is shown on the *left-hand side*, and the full machine is shown on the *right* being fired by a natural gas burner. A pot of water serves as the exhaust-side sink; the device is intended to provide hot water and electricity for citizens of developing countries (Photo by Kees de Blok, used with permission)

control that could propel the technology to prominence even at a cost premium. Consequently, putting research efforts into increasing the power density, reducing cost, and increasing efficiency is not wasted – especially in light of the fact that thermoacoustic technology is functionally reversible. This means that knowledge gained by research into the machine as a refrigerator is directly transferable to the design of a machine that is built as an engine.

Now that a clear link has been established between the operation of thermoacoustic technology and Stirling machines, the next logical question is "Why spend money/time developing thermoacoustic machines in favor of developing Stirling machines?" Alternatively, this question could be asked of a developer of thermoacoustic technology: "What makes you think that thermoacoustic machines will be commercially feasible when Stirling machines have not reached a 'commodity status' during the nearly 200 year history of their development? " (Kinematic Stirling machines attained a brief "commodity status" at the start of the twentieth century as water pumps and compressors.) There are several clear advantages and some disadvantages of thermoacoustics when compared to Stirling (Fig. 11).

Mechanical Complexity: Stirling machines, and kinematic Stirling machines especially, are mechanically complex. A kinematic machine requires some mechanical means to link the pistons in such a way to create the correct phasing of pressure oscillation and gas displacement. In Fig. 6, two kinematic machines are shown that were made at the extremes of the twentieth century, and both are burdened with this linkage that requires lubrication, experiences wear, dissipates energy, and is costly to manufacture and maintain. Many Stirling machines, both kinematic and free-piston, have a piston (to create pressure oscillations) and a displacer (to move the gas through the regenerator at a roughly constant volume) that must move in the same bore. In many designs, this requires that the rod for the displacer penetrate the piston and sometimes that both of the connectors for these mechanical components penetrate the pressure vessel that contains the working fluid (usually helium).

Fig. 11 On the *left* is photograph of a Rider-Ericson engine produced in the late 1800s and early 1900s. Notice the complicated linkage that connects the flywheel to the piston rods that penetrate the *top* of the piston cylinder. On the *right* is a modern Stirling machine made by Whisper Tech (http://www.whispergen.com/) in 2002 that is used to generate electricity for residences, yachts, and motor-homes. Hidden in the stainless steel pressure vessel is a complicated linkage called a "wobble-yoke" (*left* photo in the public domain, *right* photo credit: Whispergen)

These dynamic seals, sometimes in the presence of either hot or cold temperatures, present a difficult engineering problem that is usually costly to implement due to close-tolerance manufacturing requirements that provide simultaneously low friction and low leakage. The most significant contribution of thermoacoustic technology to the development of regenerative heat engines is simplicity. By eliminating the displacer or second piston (and in a prime mover, by removing all moving metal) in favor of gas inertia and by exchanging a mechanical phasing mechanism for one that is executed using the compliance and inertia of the working fluid itself, a much simpler and consequently cheaper machine can be made. Thus far, this reduction of complexity has probably come at the price of power density. In the machines that are the subject of this chapter, the sliding seals that dominate Stirling machines have been replaced by flexure seals. These seals, while simple and low maintenance require careful design for "infinite" fatigue life. At this time, the metal bellows that are used are expensive.

Power Density: The power density of thermoacoustic machines tends to be neither as high as that of its Stirling "brothers" nor as high as either vapor compression refrigerators or internal combustion engines. The relatively low power density comes as consequence of relying on the stiffness (compliance) of gas trapped in the resonator to provide restoring force and moving gas to provide inertia. Compared to

a mechanical spring, gas springs are much bigger for a given stiffness and the density of gas is much lower than the density of metal or plastic used as pistons in traditional Stirling machines. That said, since the compliance of trapped gas is a function of the mean pressure in the gas $\left(C_g = V/\gamma p_m\right)$ and since density is also proportional to mean pressure, by increasing the mean pressure in a thermoacoustic machine, the power density can be improved, although the cost/weight/complexity of a stronger pressure vessel must be considered.

Moving Mass: The moving mass of thermoacoustic machines can be low for a given amount of cooling capacity (or power output if operating as an engine) compared to Stirling machines. This has advantages with respect to fatigue life as well as transmitted noise/vibration levels and radiated noise levels.

Resonance: One overarching advantage of thermoacoustic machines described herein is that since the energy storage medium is the working gas itself and the moving mass, there are no requirements for external energy storage elements (like flywheels) that are found in many traditional Stirling machines.

Limitations Imposed byHeat Exchangers: All closed-cycle engines suffer an efficiency penalty compared to open-cycle machines like internal combustion engines or vapor-compression refrigerators. This penalty comes from the extra heat-exchange step inherent in closed-cycle engines because the working gas does not directly contact the heat source and sink. In the internal-combustion engine, for example, the fuel enters the engine cylinder and explodes – the engine takes advantage of the very hot temperature of that explosion in the form of the expansion of the combustion products. Following that expansion, the hot gas is exhausted from the cylinder, whereupon a new charge of cool fuel/air mixture is injected. Because of this rapid exchange of hot gas with cool gas and the fact that the hottest temperature of the explosion only lasts for an instant, the metal of engine block does not have to sustain the high temperatures of which the engine gets to take advantage. Closed-cycle engines usually have to be designed for significantly lower temperatures due to material constraints, but they also suffer a temperature difference across the heat exchanger through which all of the heat that the engine uses must pass. As a result, the engine takes an efficiency penalty because it cannot utilize the highest temperature that the fuel is providing.

Temperature-related material constraints are not usually a factor in a heat pump application, but the same handicap arises due to the temperature drop on the heat exchangers that transfer heat from the cooling load and again out of the machine into the environment. Especially for low-lift applications (small temperature difference) like food refrigeration or air-conditioning, the temperature drop on the primary helium-to-secondary heat exchangers can be a significant fraction of the total temperature difference and therefore be the largest efficiency penalty in the system. In an open-cycle vapor compression system, where the refrigerant undergoes a phase change, the compressor effectively pumps the refrigerant between two heat exchangers that directly exchange heat with the load and exhaust. Consequently, these systems have half of the heat exchange steps than a closed-cycle machine (like one that utilizes thermoacoustics) would have. The designer of a thermoacoustic

machine that has to compete only in terms of efficiency has to carefully consider the primary (oscillating gas to secondary fluid) and secondary (secondary fluid to load/environment) heat exchangers. Ideas to eliminate the secondary heat exchange step have been explored with some success; for example, a design was tested at Los Alamos that acoustically pumped helium out of the resonator to the heat source/sink (Swift and Backhaus 2004). A flow-through design was also tested at Los Alamos that allowed a steady flow of air to move through the resonator; this machine used air at atmospheric pressure as the working gas and, therefore, was not particularly power dense in either weight or volume (Reid and Swift 2000).

References

Backhaus S, Swift GW (2000) A thermoacoustic-Stirling heat engine: detailed study. J Acoust Soc Am 107:3148–3166

Backhaus S, Tward E, Petach M (2004) Traveling-wave thermoacoustic electric generator. Appl Phys Lett 85:1085–1087

Bastyr KJ (2004) The design, construction, and performance of a high-frequency, high-power thermoacoustic-Stirling engine. Doctoral dissertation, The Pennsylvania State University

Bayram A et al (2005) Operation of thermoacoustic Stirling heat engine driven large multiple pulse tube refrigerators. In: Ross RG Jr (ed) Cryocoolers 13: proceedings of the 13th ICC held in New Orleans, Louisiana. Springer Science + Business Media, New York

Beale WT (1971) Stirling cycle type thermal device. US Patent 3,552,120

Beranek LL (1954) Acoustic elements, Chapter 5. In: Acoustics. Acoustical Society of America Through the American Institute of Physics, pp 116–143

Ceperley PH (1979) A pistonless Stirling engine – the traveling wave heat engine. J Acoust Soc Am 66(5):1508–1513

de Blok K (2010) Novel 4-stage traveling wave thermoacoustic power generator. In: Proceedings of ASME 2010 3rd Joint US-European fluids engineering summer meeting and 8th international conference on nanochannels, microchannels and minichannels, Montreal

de Blok, Maria C, Hendrikus NA, Van Rijt J (2001) Thermo-acoustic system. US Patent 6,314,740

Global Alliance for Clean Cookstoves (2010) National Institute of Environmental Health Science, National Institutes of Health. http://www.niehs.nih.gov/about/od/programs/cookstoves/index.cfm. Accessed 17 Mar 2011

Keolian RM, Wuthrich JW, Bastyr KJ (2007) Thermoacoustic piezoelectric generator. US Patent 77, 72, 746

Kolin I (1995) Thermodynamic theory for Stirling cycle machine designs: special lecture 1. In: Proceedings of the seventh international conference on Stirling cycle machines, Waseda University, Tokyo, pp 1–7

Liu J, Garrett SL (2005) Characterization of a small moving-magnet electrodynamic linear motor. J Acoust Soc Am 118(4):2289–2294

MacCarty N et al (2008) A laboratory comparison of the global warming impact of five major types of biomass cooking stoves. Energy Sust Dev 12:56–65

Reid RS, Swift GW (2000) Experiments with a flow-through thermoacoustic refrigerator. J Acoust Soc Am 108(6):2835–2842

Roden C, Bond T (2006) Emission factors and real-time optical properties of particles emitted from traditional wood burning cookstoves. Environ Sci Technol 40(21):6750–6757

Sier R (1995) Rev. Robert Stirling D. D.: inventor of the heat economiser and Stirling engine. Ipswich Book, Ipswich

Swift GW (1988) Thermoacoustic engines. J Acoust Soc Am 84(4):1145–1180

Swift GW (2002) Thermoacoustics: a unifying perspective for some engines and refrigerators. Acoustical Society of America, New York
Swift GW, Backhaus S (2004) A resonant, self-pumped, circulating thermoacoustic heat exchanger. J Acoust Soc Am 116(5):2923–2938
Urieli I, Berchowitz D (1984) Stirling cycle engine analysis. A. Hilger, Bristol
Wheatley JC, Swift GW, Migliori A (1983) Acoustical heat pumping engine. US Patent 4,398,398, 16 Aug 1983
Wheatley JC, Swift GW, Migliori A (1986) The natural heat engine. Los Alamos Sci 14:2–33, LAUR 86–2699

Hydrogen Production

Qinhui Wang

Contents

Abstract

Hydrogen (H_2) is mainly used in chemical industry currently. In the near future, it will also become a significant fuel due to advantages of reductions in greenhouse gas emissions, enhanced energy security, and increased energy efficiency. To meet future demand, sufficient H_2 production in an environmentally and economically benign manner is the major challenge. This chapter provides an

Q. Wang (✉)
Institute for Thermal Power Engineering, Zhejiang University, Hangzhou, Zhejiang, China
e-mail: qhwang@zju.edu.cn

W.-Y. Chen et al. (eds.), *Handbook of Climate Change Mitigation and Adaptation*,
DOI 10.1007/978-3-319-14409-2_29

overview of H_2 production pathways from fossil hydrocarbons, renewable resources (mainly biomass), and water. And high-purity H_2 production by the novel CO_2 sorption-enhanced gasification is highlighted. The current research activities, recent breakthrough, and challenges of various H_2 production technologies are all presented.

Fossil hydrocarbons account for 96 % of total H_2 production in the world. Steam methane reforming, oil reforming, and coal gasification are the most common methods, and all technologies have been commercially available. However, H_2 produced from fossil fuel is nonrenewable and results in significant CO_2 emissions, which will limit its utilization.

H_2 produced from biomass is renewable and CO_2 neutral. Biomass thermochemical processes such as pyrolysis and gasification have been widely investigated and will probably be economically competitive with steam methane reforming. However, research on biomass biological processes such as photolysis, dark fermentation, photo-fermentation, etc., is in laboratory scale and the practical applications still need to be demonstrated.

H_2 from water splitting is also attractive because water is widely available and very convenient to use. However, water splitting technologies, including electrolysis, thermolysis, and photoelectrolysis, are more expensive than using large-scale fuel-processing technologies and large improvement in system efficiency is necessary.

CO_2 sorption-enhanced gasification is the core unit of zero emission systems. It has been thermodynamically and experimentally demonstrated to produce H_2 with purity over 90 % from both fossil hydrocarbons and biomass. The major challenge is that the reactivity of CO_2 sorbents decays through multi-calcination–carbonation cycles.

Introduction

Fossil fuels (i.e., petroleum, natural gas, and coal), which meet most of the world's energy demand today, are being depleted fast. Also, it is now widely acknowledged that combustion of fossil fuels contributes to the buildup of CO_2 in the atmosphere, which in turn contributes to the greenhouse effect, causing the well-known global warming. Many engineers and scientists agree that the solution to this problem would be to replace the existing fossil system by the hydrogen energy system. The idea of a hydrogen economy with decarbonizing energy supply has merit. Additional drivers for the switch to a H_2 energy economy can include opportunities for increased energy security through greater diversity of resources for supply and greater efficiency and versatility with the mastery of hydrogen fuel cell technology.

Hydrogen is the simplest element known to man. It is also the most plentiful gas in the universe. Hydrogen gas is the lightest gas; thus, it rises in the atmosphere. Therefore, hydrogen as a gas (H_2) is not found by itself on earth. It is found only in compound form with other elements. Hydrogen combined with carbon forms

different compounds such as methane (CH_4), coal, and petroleum. Hydrogen combined with oxygen forms water. And hydrogen is also found in growing things – biomass. The amount of energy produced during hydrogen combustion is higher than released by any other fuel on a mass basis, with a lower heating value (LHV) 2.4, 2.8, and 4 times higher than that of methane, gasoline, and coal, respectively. The product of hydrogen combustion is only water, and thus, the utilization of hydrogen is pollutant zero emission.

About 38 Mt (5000 petajoules) of hydrogen is produced worldwide annually, a market valued at about $60 billion (Levin and Chahine 2010). An idyllic vision of a "hydrogen economy" is one in which H_2 and electricity are the sole energy carriers and both are produced without harmful emissions, from renewable resources. H_2 would be used in transport, industrial, commercial, and residential applications, where fossil fuels are currently used. As hydrogen is not an energy source, but a carrier, so it must be produced from other natural sources, not only fossil fuels but also biomass and water. Sufficient H_2 production to meet future demand is the major challenge in moving toward a H_2 energy economy.

Hydrogen Production from Fossil Fuel

At the present time, H_2 is mainly used in chemical industry, e.g., to upgrade crude oil and synthesize methanol and ammonia in the petroleum and chemical reactors. Fossil fuel is the major sources to produce hydrogen, which amounts to 96 % of total hydrogen production in the world. The mostly common hydrogen production methods are (1) steam methane reforming (SMR) (48 %), (2) oil reforming (30 %), and (3) coal gasification (18 %) (Ewan and Allen 2005). Although ammonia and methanol are also used for H_2 production, the proportion is minor. During the transition phase to a sustainable hydrogen economy, hydrogen from fossil fuel will continue to be paid large attention due to the need of considerable cost reduction and technology improvement throughout the entire hydrogen system (production, delivery, storage, conversion, and application).

Steam Methane Reforming (SMR)

The dominant industrial process used to produce hydrogen is the SMR process. About 59 % of hydrogen production comes from SMR of natural gas, but hydrogen production by SMR is responsible for the emission of about 30 million tonnes of CO_2 per year (Levin and Chahine 2010). The first industrial application of SMR was implemented in 1930 (Barelli et al. 2008). And it is a mature technology, which has been in use for several decades as an effective mean for hydrogen production. The SMR process is characterized by multiple-step and harsh reaction conditions. Typically, four steps are necessary, namely, (1) desulfurization, (2) steam reforming, (3) water–gas shift (WGS), and (4) H_2 purification. Figure 1 shows the diagram of a typical SMR process.

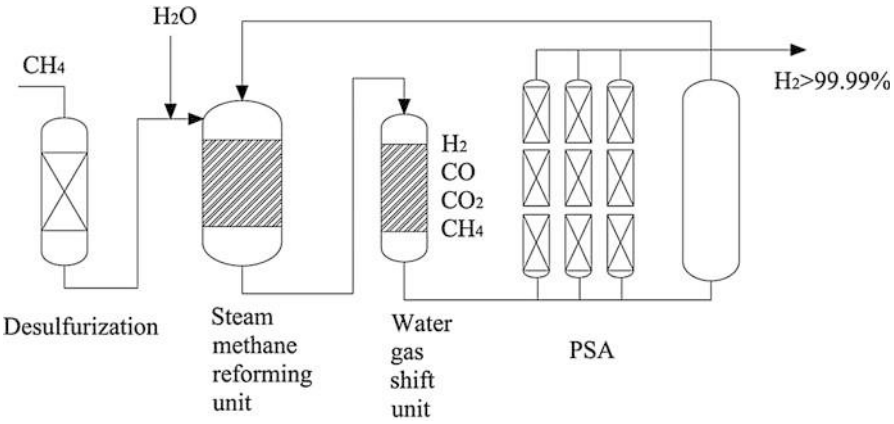

Fig. 1 A diagram of a typical SMR process

Desulfurization

Sulfur that contained in raw natural gas will lead to catalyst deactivation and facility destruction during H_2 production; thus, desulfurization from natural gas to keep the sulfur content being in a very low level is a primary and necessary procedure. Typically, the desulfurization proceeds by two steps.

The first step is wet desulfurization, which is usually performed by the natural gas provider. In this step, natural gas reacts with monoethanolamine (MEA) to remove most sulfur content. The reaction can be expressed by two equations:

$$2CH_3CH_2OHNH_2 + H_2S \rightleftarrows (CH_3CH_2OHNH_3)_2S$$

$$(CH_3CH_2OHNH_3)_2S + H_2S \rightleftarrows 2(CH_3CH_2OHNH_3)HS$$

The MEA solvent can be recovered through being heated to a higher temperature ($>$105 °C). After wet desulfurization, the sulfur concentration in the raw natural gas will be lowered to approximately 200 ppm.

The second step, dry desulfurization, is conducted just prior to the SMR reactor. The aim of dry desulfurization is to realize organic sulfur removal and reach a very low sulfur concentration ($<$0.1 ppm) in the raw natural gas. The typical approaches can be categorized as chemical reaction technologies and adsorptive technologies (Holladay et al. 2009). Chemical reaction approaches include hydrodesulfurization (HDS) and alkylation. Most commercial large-scale applications use HDS; although selective alkylation has the potential advantage of not requiring high-pressure hydrogen compared with HDS, but to date it has not been implemented on a large commercial scale, only pilot-scale demonstration is being conducted. The mechanism of HDS is shown in the following equations, where HDS catalysts partially or completely hydrogenate the sulfur-bearing molecules, resulting in a release of sulfur as inorganic H_2S:

$$R - SH + H_2 \rightarrow RH + H_2S$$

$$R - S - R' + 2H_2 \rightarrow RH + R'H + H_2S$$

$$R - S - S - R' + 3H_2 \rightarrow RH + R'H + 2H_2S$$

$$C_4H_4S + 4H_2 \rightarrow C_4H_{10} + H_2S$$

$$CS_2 + 4H_2 \rightarrow CH_4 + 2H_2S$$

Adsorptive approaches employ adsorbents for sulfur removal from the fuel. Most often, this is achieved by (1) adsorption of the entire sulfur-containing molecule in activated carbon, modified zeolites, or other materials such as zinc oxide (ZnO) or (2) adsorption onto metal surfaces such as nickel, wherein nickel sulfide is formed and the remainder of the hydrocarbon is recovered. The former approach is conceptually quite simple to operate, as it can in principle be carried out at ambient temperature and pressure using conventional fixed bed equipment. The other approach is more complicated, requiring a fluidized bed operating at elevated temperatures and pressures. The following equations show the adsorption of entire sulfur by using ZnO:

$$H_2S + ZnO \rightarrow ZnS + H_2O$$

$$C_2H_5SH + ZnO \rightarrow ZnS + C_2H_4 + H_2O$$

$$C_2H_5SH + ZnO \rightarrow ZnS + C_2H_5OH$$

Steam Reforming

Steam reforming is a catalytic process that involves a reaction between natural gas and steam. The product is a mixture of H_2, carbon monoxide (CO), carbon dioxide (CO_2), and water (H_2O). The effluent gas from the steam reformer typically contains about 76 % H_2 (mol.%), 13 % CH_4, 12 % CO, and 10 % CO_2 on a dry basis (Barelli et al. 2008). The following equations show the steam reforming reactions:

$$CH_4 + H_2O \rightarrow CO + 3H_2$$

$$CH_4 + 2H_2O \rightarrow CO_2 + 4H_2$$

These reactions are highly endothermic and a large amount of heat is provided by feeding supplemental natural gas to the furnace. These reactions are typically carried out at a temperature of 800–1000 °C and a pressure of 14–20 atm.

The key issue for steam reforming is to select high-efficiency catalyst, so as to avoid coke formation due to the high operation temperature. The catalysts can be divided into two types: non-precious metal (typically nickel) and precious metals from group VIII elements (typically platinum or rhodium based). For nickel-based catalyst, steam to carbon ratios that are higher than stoichiometry (2.5 or higher) are

required to gasify coke. Coke formation is much less over the noble group VIII metals and these metals, particularly Rh, are preferred since they exhibit much higher specific activities than nickel catalysts. However, the high cost of Rh is driving some researchers to develop alternative catalysts such as Co-based catalysts. In addition, promoters, such as magnesia or potassium or other alkaline components, can be added to the catalyst support to minimize the coke formation.

WGS

The steam reforming process produces a product gas mixture with significant amounts of carbon monoxide. To increase the amount of hydrogen, the product gas is passed through a water–gas shift reactor to decrease the carbon monoxide content while increasing the hydrogen content. The water–gas shift reaction can be expressed as the following:

$$CO + H_2O \rightarrow CO_2 + H_2$$

Typically, a high temperature is desired in order to achieve fast kinetics but results in high-equilibrium carbon monoxide selectivity and decreased hydrogen production due to the exothermic characteristic of water shift reaction. Therefore, the high-temperature WGS reactor is often followed by a low-temperature reactor to decrease CO content to 1 % or less. TeGrotenhuis et al. (2002) have demonstrated the potential of using microreactors to build a gradient-temperature WGS reactor that contains the high-temperature WGS and low-temperature WGS in a single unit for >2–3 kWe units. The most common catalyst for WGS is Cu based, although some interesting work is currently being done with molybdenum carbide, platinum-based catalysts, and Fe-Pd alloy catalysts.

To further reduce the carbon monoxide, a preferential oxidation (PrOx) reactor or a carbon monoxide selective methanation reactor can be used. The PrOx and methanation reactors each have their advantages and challenges. The preferential oxidation reactor increases the system complexity because carefully measured concentrations of air must be added to the system. However, these reactors are compact and if excessive air is introduced, some hydrogen is burned. Methanation reactors are simpler in that no air is required; however, for every molecule of carbon monoxide reacted, three hydrogen molecules are consumed. Also, the carbon dioxide reacts with the hydrogen, so careful control of the reactor conditions need to be maintained in order to minimize unnecessary consumption of hydrogen. Currently, preferential oxidation is the primary technique being developed. The catalysts for both these systems are typically noble metals such as platinum, ruthenium, or rhodium supported on Al_2O_3.

H_2 Purification

The effluent gas from WGS reactors still contains considerable amounts of CO_2, CO, and CH_4 gases. In order to obtain H_2 with purity higher than 99 %, pressure swing adsorption (PSA) processes are designed and conducted after WGS reactors. Production of pure hydrogen by using PSA processes has become the state-of-the-art

technology in the chemical and petrochemical industries. Several 100 PSA-H_2 process units have been installed around the world. In the PSA units, impurity gases with high boiling points are absorbed on the absorbent (zeolites or active carbon) bed at high pressures; however, H_2 can pass through the absorbent bed due to the fact that it has the lowest boiling point. The absorbents are then regenerated by lowering down the unit pressure to release the absorbed impurities. In this way, pure H_2 is separated from the impurities and fed into the plant's H_2 grid. The released impurities (tail gases) are recycled to the steam reformer burners to provide the necessary heat for the endothermic reforming reactions. Currently, the research goals consisted of developing new H_2-PSA processes for (a) increasing the primary and secondary product recoveries while maintaining their high purities and (b) reducing the absorbent inventory and the associated hardware costs. A considerable effort was also made to develop new absorbents or to modify existing absorbents in order to achieve these research goals. It became a common practice to use more than one type of absorbents in these PSA processes (as layers in the same absorbent vessel or as single absorbents in different vessels) in order to obtain optimum absorption capacity and selectivity for the feed gas impurities while reducing the coabsorption of H_2, as well as for their efficient desorption under the operating conditions of the PSA processes.

Oil Reforming

Oil reforming is another significant commercial H_2 production technology. Comparing with heavy oil, such as bitumen or residual oil, which is easier to suffer from coke formation resulting to catalyst deactivation, light oil with relatively low molecular weight is much favorable to produce H_2. Generally, four reforming techniques, namely, steam reforming, partial oxidation (POX), autothermal reforming (ATR), and pyrolysis, are used to produce hydrogen from oil (Holladay et al. 2009). In fact, these techniques can also use methane as raw material and all should proceed with the similar four steps as mentioned in steam methane reforming (section "Steam Methane Reforming (SMR)"): desulfurization, reforming (steam), water–gas shift (WGS), and purification (not necessary for pyrolysis). This section will mainly focus on the distinction among each technology.

Steam Reforming

Steam reforming is typically the preferred process for hydrogen production in industry, using either natural gas or oil. The mechanism can be expressed by the following equation:

$$C_mH_n + mH_2O \rightarrow mCO + \left(m + \frac{n}{2}\right)H_2$$

Oil steam reforming is an endothermic reaction and requires an external heat source. It has advantages of not requiring oxygen, having a lower operating temperature than

POX and ATR, and producing syngas with a high H_2/CO ratio (~3:1) which is beneficial for H_2 production. However, it does have the highest emissions of the three processes. The catalysts used for oil steam reforming are similar to those in the SMR process. Developing improved and economically available catalysts with high resistance to coke formation is the main research goal.

Partial Oxidation (POX)

Partial oxidation (POX) of hydrocarbons and catalytic partial oxidation (CPOX) of oil have been proposed for use in hydrogen production for automobile fuel cells and some commercial applications. It converts oil to hydrogen by partially oxidizing (combusting) the material with oxygen, as shown in the equation:

$$C_mH_n + \frac{m}{2}O_2 \rightarrow mCO + \frac{n}{2}H_2$$

Partial oxidation has advantages of minimal methane slip, higher sulfur tolerance, and beneficial H_2/CO ratio (1:1 to 2:1) favored for the feeds to hydrocarbon synthesis reactors such as Fischer–Tropsch. However, in order to reduce coke formation, the non-catalytic partial oxidation process needs operating at high temperatures (1300–1500 °C). Although catalysts can be added to the partial oxidation system to lower the operating temperatures, it is proving hard to control temperature because of coke and hot spot formation due to the exothermic nature of the reactions. Krummenacher et al. (2003) have had success using catalytic partial oxidation for decane, hexadecane, and diesel fuel. But the high operating temperatures (>800 °C and often >1000 °C) (Krummenacher et al. 2003) and safety concerns may make their use for practical, compact, portable devices difficult due to thermal management (Holladay et al. 2004). In addition, this process requires an expensive and complex oxygen separation unit in order to feed pure oxygen to the reactor.

Autothermal Reforming (ATR)

Autothermal reforming adds steam to catalytic partial oxidation (CPOX). The reaction mechanism can be expressed as:

$$C_mH_n + \frac{m}{2}H_2O + \frac{m}{4}O_2 \rightarrow mCO + \left(\frac{m}{2} + \frac{n}{2}\right)H_2$$

Autothermal reforming is typically conducted at a lower pressure than POX reforming and has a low methane slip. It consists of a thermal zone where POX or CPOX is used to generate the heat needed to drive the downstream steam reforming reactions in a catalytic zone. The heat from the POX negates the need for an external heat source, simplifying the system and decreasing the start-up time. A significant advantage for this process over steam reforming is that it can be stopped and started very rapidly while producing a larger amount of hydrogen than POX alone. There is some expectation that this process will gain favorability with the gas–liquids industry due to favorable gas composition for the Fischer–Tropsch synthesis, ATR's relative compactness, lower capital cost, and potential for economies of scale

(Wilhelm et al. 2001). However, for ATR to operate properly, both the oxygen to fuel ratio and the steam to carbon ratio must be properly controlled at all times in order to control the reaction temperature and product gas composition while preventing coke formation. Similar to POX, this process also needs an expensive oxygen separation unit.

Pyrolysis

Pyrolysis is another H_2 production technology where the raw oil is decomposed (without water or oxygen present) into hydrogen and carbon. The reactions can be written in the following form:

$$C_mH_n \rightarrow mC + \frac{n}{2} H_2$$

Since no water or air is present, no carbon oxides (e.g., CO or CO_2) are formed, eliminating the need for secondary reactors (WGS, PrOx, PSA, etc.). Thus, this process offers significant emission reduction. Among the advantages of this process are fuel flexibility, relative simplicity and compactness, clean carbon by-product, and reduction in CO_2 and CO emissions. One of the challenges with this approach is the potential for fouling by the carbon formed, but proponents claim this can be minimized by appropriate design (Guo et al. 2005). Pyrolysis may play a significant role in the future. In Norway, the Kvaerner Oil and Gas Company has developed an attractive technique to simultaneously produce carbon and H_2 by oil plasma pyrolysis. It is said that this technique has an energy efficiency of 1.1 kW h m^{-3} H_2, and the commercial operation is feasible now.

Coal Gasification

Coal is an abundant energy source in many parts of the world. H_2 production by coal gasification is considered to be a promising option before economical H_2 production pathways from renewable energy sources are developed. Coal gasification can be defined as the reaction of solid fuels with air, oxygen, steam, carbon dioxide, or a mixture of these gases at a temperature exceeding 700 °C to yield a gaseous product suitable for use either as a source of energy or as a raw material for the synthesis of chemicals, liquid fuels, or other gaseous fuels. Figure 2 shows the diagram of a typical gasification process. Coal gasification is currently used to produce H_2 as an intermediate for the synthesis of chemicals. However, large-scale H_2 production project mainly for power generation is also under development. A well-known example is the FutureGen project sponsored by the department of energy (DOE) in the USA, which is a 10-year, US$ 1 billion, demonstration project started from February 2003 (Collot 2006). This section shows not only the three main conventional coal gasification technologies – moving bed gasification, fluidized bed gasification, and entrained flow gasification – but also an alternative method, denoted underground coal gasification (UCG).

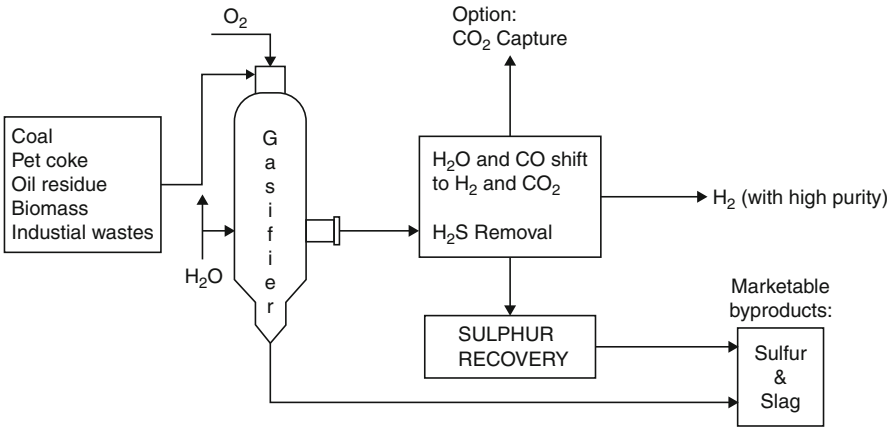

Fig. 2 A diagram of a typical gasification process

Moving Bed Gasification

Moving bed gasification is only suitable for solid fuels with a particle size in the range of 5–80 mm. Typically, a mixture of steam and oxygen is introduced at the bottom of the reactor and runs counterflow to the coal. Coal residence times in moving bed gasifiers are of the order of 15–60 min for high-pressure steam/oxygen gasifiers and can be several hours for atmospheric steam/air gasifiers. The pressure in the bed is typically of the order of 3 MPa for commercial gasifiers with tests realized at up to 10 MPa. Maximum temperatures in the combustion zone are typically in the range of 1500–1800 °C for slagging gasifiers and 1300 °C for dry ash gasifiers. Although moving bed gasifiers are presently less used than entrained flow gasifiers for the construction of new power plants, moving bed gasification presents the advantage of being a mature technology. The main requirement of moving bed gasifiers is good bed permeability to avoid pressure drops and channel burning that can lead to unstable gas outlet temperatures and composition as well as risk of a downstream explosion. A typical advanced moving bed technique is the British Gas/Lurgi (BGL) technology (Bailey 2001). It is said that this technology will be adopted in the Kentucky Pioneer Energy project, which is an Integrated Coal Gasification Combined Cycle (IGCC) project cosponsored by Global Energy Inc and DOE of USA. Table 1 shows the process characteristics of BGL technology.

Fluidized Bed Gasification

Fluidized bed gasification can only operate with solid crushed coals in the range of 0.5–5 mm. Coals are introduced into an upward flow of gas (either air or oxygen/steam) that fluidizes the bed of fuel while the reaction is taking place. The bed is either formed of sand/coke/char/sorbent or ash. Residence time of the feed in the gasifier is typically in the order of 10–100 s but can also be much longer, with the feed experiencing a high heating rate from the entry in the gasifier. High levels of

Table 1 Process characteristics of BGL technology (Collot 2006; Fc and Yf 2006)

Feeding mode and operating conditions	Lumped coal together with a flux is discharged at the top of the gasifier as a sequence of batches. A distributor plate slowly rotates to ensure even distribution of the coal
Gasifier	Double-walled cylindrical reactor surrounded by a steam jacket. O_2 and steam are added toward the bottom of the bed through tuyeres, resulting in high internal temperature within the gasifier (2000 °C)
Ash removal system	Slagging gasifier. Molten ash is tapped off and quenched with water
Cooling and cleaning modes	Tars, high-boiling-point hydrocarbons and particulates are removed in a quench vessel and reinjected in the bed near the tuyeres. The gas (450–500 °C) is cooled and cleaned by a water quench and scrubbed to remove H_2S
Remarks	It is a slagging gasifier modified from the Lurgi dry ash gasifier and not suitable for high reactive coals. O_2 consumption is higher than Lurgi dry ash gasifier. It is still difficult to develop very large commercial unit meeting the demand for large-scale industrial gasifier

back-mixing ensure a uniform temperature distribution in the gasifier. Fluidized bed gasifiers usually operate at temperatures well below the ash fusion temperatures of the fuels (900–1050 °C) to avoid ash melting, thereby avoiding clinker formation and loss of fluidity of the bed. The low operating temperatures may lead to incomplete carbon conversion of coal, but this can be overcome by char recirculation into the gasifier. Advanced fluidized bed gasifiers are also operated at elevated pressures. Among the main advantages of this type of gasifier are that they can operate at variable loads and more tolerant to coals with high sulfur content. But for fluidized bed gasification, it is necessary to process coals with a higher ash fusion temperature than the operating temperature of the gasifier to avoid ash agglomeration (which causes uneven fluidization in dry ash, fluidized bed gasifiers). Two types of fluidized bed gasification technologies have been operated at commercial scale. They are High-Temperature Winkler (HTW) and Kellogg Rust Westinghouse (KRW) gasification technologies, respectively, both of which can be used in IGCC plants. Table 2 gives the process characteristics of HTW and KRW technologies.

Entrained Flow Gasification

In entrained flow gasifiers, coal particles concurrently react at high speed with steam and oxygen or air in a suspension mode called entrained fluid flow. Short gas residence times (seconds) give them a high load capacity but also require coal to be pulverized. Coal can either be fed dry (commonly using nitrogen as a transport gas) or wet (carried in slurry water) into the gasifier. They usually operate at high temperatures of 1200–1600 °C and pressures in the range of 2–8 MPa. Although entrained flow gasifiers are the most widely used gasifiers, more critical operational requirements are needed compared to moving bed and fluidized gasifiers, such as

Table 2 Process characteristics of HTW and KRW technologies (Collot 2006; Fc and Yf 2006)

HTW	
Feeding mode and operating conditions	Coal dropped from a bin via a gravity pipe into the gasifier. Operating pressure is 1–3 MPa
Gasifier	Bed is formed of particles of ash, semicoke, and coal and is maintained at 800 °C
Ash removal system	Dry ash removal through a discharge screw
Cooling and cleaning modes	Using cyclone to remove particulates, water, or fire tube cooling system
Remarks	Plan to replace old Lurgi dry ash reactors at Vresova IGCC plant in Czech Republic. It is promising due to the elevated operation temperature and pressure compared to the conventional Winkler gasifier
KRW	
Feeding mode and operating conditions	Lock hoppers, operating pressure is up to 2 MPa
Gasifier	Coal partial combustion around the feed nozzle forming 1150–1260 °C high temperature zone
Ash removal system	Ash agglomerating to large particles then separated from the remaining coal char
Cooling and cleaning modes	Raw gas is cooled from 900 °C to 600 °C and enters a hot gas cleaning system. A portion of the gas is recycled to the gasifier
Remarks	Used in the Pinon Pine IGCC plant. Carbon content in the ash can be greatly lowered down

significant cooling of the raw syngas before being cleaned; controlling the coal/oxidant ratio within narrow limits through the entire operation in order to maintain a stable flame close to the injector tip; and strict requests on coal properties including a minimum ash content required for gasifiers with slag self-coating walls, a maximum ash content fixed for each type of entrained flow gasifier, ash composition (SiO_2, CaO, iron oxides) limitations to avoid the refractory cracking, optimum ash fusion temperature and critical temperature viscosity recommended for smooth slag tapping, etc. Entrained flow gasification is the most widely used technology. Table 3 shows the process characteristics of Texaco and Shell technologies, representing the wet feed and dry feed entrained flow gasification, respectively.

Underground Coal Gasification

Underground coal gasification does not need the construction of surface plants. In the process, injection and production wells are drilled from the surface and linked together in a coal seam. Once the wells are linked, air or oxygen is injected, and the coal is ignited in a controlled manner. Water present in the coal seam or in the surrounding rocks flows into the cavity formed by the combustion and is utilized in the gasification process. The produced gases (primarily H_2, CO, CH_4, and CO_2) can be used to generate electric power or synthesize chemicals after being cleaned. The

Table 3 Process characteristics of Texaco and Shell technologies (Collot 2006; Fc and Yf 2006)

Texaco	
Feeding mode and operating conditions	Slurry fed through burners at the top of the gasifier. Operate at temperatures in the range of 1250–1450 °C and 3–8 MPa pressures
Gasifier	Pressure vessel with refractory lining
Ash removal system	The molten slag flows out toward the bottom of the gasifier with the raw gas and is water quenched and removed through a lock hopper
Cooling and cleaning modes	Raw gas can either be cooled or cleaned from slag by water quenching or radiant cooler
Remarks	There are six Texaco-owned gasification facilities worldwide that produce power, chemicals, and H_2 from coal. It has wide applicability to various coal types
Shell	
Feeding mode and operating conditions	Coal powders are transported by N_2 gases, operation at 2–4 MPa, at 1500 °C and above
Gasifier	A carbon steel vessel enclosed by a non-refractory membrane wall
Ash removal system	Molten slag is removed through a slag tap and water quenched
Cooling and cleaning modes	Syngas is quenched with cooled recycled product gas and further cooled in a syngas cooler. Raw gas is cleaned in ceramic filters. Fifty percent gas is recycled to act as a quenching medium
Remarks	There are five gasification plants using the Shell gasification technology till 2006. Only the Nuon Power Buggenum IGCC plant in the Netherlands is fed with coal. More plants are planned to be built in China and the USA

former Soviet Union (FSU) performed intensive research on UCG from 1930s to 1960s, and over 15 Mt of coal has been gasified underground in the FSU, generating 50 Gm^3 of gas. Due to the discovery of extensive natural gas in Siberia in 1970s, FSU declined the usage of UCG. As a result of the increasing energy needs in recent years, interest in UCG has been rejuvenated all over the world (Shafirovich and Varma 2009). It is said that China is generally believed to have the largest UCG program currently underway. A pilot industrial UCG plant at the Gonggou coal mine, Wulanchabu, Northern Inner Mongolia Autonomous Region, is under construction. This $112 million project is a joint venture between the China University of Mining and Technology and Hebei Xin'ao Group. The UCG process has several advantages over surface coal gasification such as lower capital investment costs (due to the absence of a manufactured gasifier), no handling of coal and solid wastes at the surface (ash remains in the underground cavity), no human labor or capital for underground coal mining, minimum surface disruption, no coal transportation costs, and direct use of water and feedstock available in situ. In addition, cavities formed as a result of UCG could potentially be used for CO_2 sequestration. However, construction of a UCG process is quite complex as lots of criteria should be strictly considered, such as the coal seam conditions (thickness, depth, coal seam dip, coal amount and ranks), groundwater protection, and land-use restrictions.

Hydrogen Production from Biomass

Biomass comprises all the living matter present on earth. It is derived from growing plants including algae, trees, and crops or from animal manure. The biomass resources are the organic matters in which the solar energy is stored in chemical bonds. It generally consists of carbon, hydrogen, oxygen, and nitrogen. Sulfur is also present in minor proportions. Some biomass also consists of significant amounts of inorganic species. Biomass is the fourth largest source of energy in the world, accounting for about 12 % of the world's primary energy consumption in and about 22 % of the primary energy consumption in the developing countries in 2006 (Loo and Koppejan 2008). Since biomass is renewable and consumes atmospheric CO_2 during growth, it can have a small net CO_2 impact compared to fossil fuels. Biomass can be converted into useful forms of energy products using a number of different processes. Generally, there are two routes for biomass conversion into hydrogen-rich gas, namely, (i) thermochemical conversion and (ii) biochemical/biological conversion. The yield of hydrogen is low from biomass since the hydrogen content in biomass is low to begin with (approximately 6 % vs. 25 % for methane) and the energy content is low due to the 40 % oxygen content of biomass. Thus, hydrogen from biomass has major challenges. There are no completed technology demonstrations (Kalinci et al. 2009). However, biomass still has the potential to accelerate the realization of hydrogen as a major fuel of the future.

Thermochemical Conversions

Thermochemical conversion involves a series of cyclical chemical reaction for releasing hydrogen. There are main three methods for biomass-based hydrogen production via thermochemical conversions: (i) pyrolysis, (ii) conventional gasification, and (iii) SCWG (supercritical water gasification), respectively.

Pyrolysis

Pyrolysis is the heating of biomass at a temperature of 650–800 K at 0.1–0.5 MPa in the absence of air to convert biomass into liquid oils, solid charcoal, and gaseous compounds. Pyrolysis can be further classified into slow pyrolysis and fast pyrolysis. As the products are mainly charcoal, slow pyrolysis is normally not considered for hydrogen production. Fast pyrolysis is a high-temperature process, in which the biomass feedstock is heated rapidly in the absence of air to form vapor and subsequently condensed to a dark brown mobile bio-liquid. The products of fast pyrolysis can be found in all gas, liquid, and solid phases:

(i) Gaseous products include H_2, CH_4, CO, CO_2, and other gases depending on the organic nature of the biomass for pyrolysis.
(ii) Liquid products include tar and oils that remain in liquid form at room temperature like acetone, acetic acid, etc.

(iii) Solid products are mainly composed of char and almost pure carbon plus other inert materials.

Although most pyrolysis processes are designed for biofuel production, hydrogen can be produced directly through fast or flash pyrolysis if high temperature and sufficient volatile phase residence time are allowed as follows:

$$\text{Biomass} + \text{heat} \rightarrow H_2 + CO + CH_4 + \text{otherproducts}$$

Methane and other hydrocarbon vapors produced can be steam reformed for more hydrogen production:

$$CH_4 + H_2O \rightarrow CO + 3H_2$$

In order to increase the hydrogen production, water–gas shift reaction can be applied as follows:

$$CO + H_2O \rightarrow CO_2 + H_2$$

Besides the gaseous products, the oily products can also be processed for hydrogen production. The pyrolysis oil can be separated into two fractions based on water solubility. The water-soluble fraction can be used for hydrogen production while the water-insoluble fraction for adhesive formulation. Experimental study has shown that when Ni-based catalyst is used, the maximum yield of hydrogen can reach 90 %. With additional steam reforming and water–gas shift reaction, the hydrogen yield can be increased significantly.

Temperature, heating rate, residence time, and type of catalyst used are important pyrolysis process control parameters. In favor of gaseous products especially in hydrogen production, high temperature, high heating rate, and long volatile phase residence time are required. These parameters can be regulated by selection among different reactor types and heat transfer modes, such as gas–solid convective heat transfer and solid–solid conductive heat transfer. Fluidized bed reactor exhibits higher heating rates, and thus, it appears to be the promising reactor type for hydrogen production from biomass pyrolysis.

Some inorganic salts, such as chlorides, carbonates, and chromates, exhibit beneficial effect on pyrolysis reaction rate. As tar is difficult to be gasified, extensive studies on the catalytic tar elimination were carried out to converting more tar into product gases (Han and Kim 2008; Shen and Yoshikawa 2013). Effect of inexpensive dolomite and CaO on the decomposition of hydrocarbon compounds in tar has been conducted (Simell et al. 1997). The catalytic effects of other catalysts (Ni-based catalysts, Y-type zeolite, K_2CO_3, Na_2CO_3, and $CaCO_3$) and various metal oxides (Al_2O_3, SiO_2, ZrO_2, TiO_2, and Cr_2O_3) have also been investigated. Among the different metal oxides, Al_2O_3 and Cr_2O_3 exhibit better catalytic effect than the others. Among the catalysts, Na_2CO_3 is better than K_2CO_3 and $CaCO_3$. Although noble metals Ru and Rh are more effective than Ni catalyst and less susceptible to

carbon formation, they are not commonly used due to their high costs (Garcia et al. 2000).

In order to evaluate hydrogen production through pyrolysis of various types of biomass, extensive experimental investigations have been conducted in recent years. Agricultural residues; peanut shell; postconsumer wastes such as plastics, trap grease, mixed biomass, and synthetic polymers; and rapeseed have been widely tested for pyrolysis for hydrogen production. In order to solve the problem of decreasing reforming performance caused by char and coke deposition on the catalyst surface and in the bed itself, fluidized catalyst beds are usually used to improve hydrogen production from biomass-pyrolysis-derived biofuel. Yeboah et al. (2002) constructed a demonstration plant for hydrogen production from peanut shell pyrolysis and steam reforming in a fluidized bed reactor, and the production rates of 250 kg H_2/day was achieved. Padro and Putsche (1999) estimated the hydrogen production cost of biomass pyrolysis to be in the range of US$ 8.86/GJ to US$ 15.52/GJ depending on the facility size and biomass type. For comparison, the costs of hydrogen production by wind-electrolysis systems and PV-electrolysis systems are US$ 20.2/GJ and US$ 41.8/GJ, respectively. It can be seen that biomass pyrolysis is a competitive method for renewable hydrogen production. Demirbas (2006) carried out pyrolysis and gasification experiments in a self-designed device, and the highest yields (% dry and ash free basis) were obtained from the pyrolysis (46 %) and steam gasification (55 %) of wheat straw while the lowest yields from olive waste. Yang et al. (2006) studied on pyrolysis of palm oil wastes in a countercurrent fixed bed. The total gas yield was enhanced greatly while the temperature increased from 500 °C to 900 °C and reached the maximum value (∼70 wt.%, on the raw biomass sample basis) at 900 °C with big portions of H_2 (33.49 vol.%) and CO (41.33 vol.%). The optimum residence time (9 s) was found to get a higher H_2 yield (10.40 g/kg (daf)). The effect of adding chemicals (Ni, γ-Al_2O_3, Fe_2O_3, La/Al_2O_3, etc.) on gas product yield was investigated, and adding Ni showed the greatest catalytic effect with the maximum H_2 yield achieved at 29.78 g/kg (daf).

Gasification

Gasification is the conversion of biomass into a combustible gas mixture via the partial oxidation at high temperatures, typically varying from 800 °C to 900 °C. It is applicable to biomass having moisture content less than 35 %. Biomass is converted completely to CO and H_2 although in practice, some CO_2, water, and other hydrocarbons including methane in an ideal gasification. The char compositions occurring by the fast pyrolysis of biomass can be gasified with gasifying agents. Air, oxygen, and steam are widely used gasifying agents. Reaction conditions along with heating values are mentioned as follows:

(i) Oxygen gasification: It yields a better quality gas of heating value of 10–15 MJ/Nm^3. In this process, the temperatures between 1000 °C and 1400 °C are achieved. O_2 supply may bring a simultaneous problem of cost and safety.
(ii) Air gasification: It is most widely used technology as being cheap, single product is formed at high efficiency and without requiring oxygen.

A low-heating value gas is produced containing up to 60 % N_2 having a typical heating value of 4–6 MJ/Nm^3 with by-products such as water, CO_2, hydrocarbons, tar, and nitrogen gas. The reactor temperatures between 900 °C and 1100 °C have been achieved.

(iii) Steam gasification: Biomass steam gasification converts carbonaceous material to permanent gases (H_2, CO, CO_2, CH_4, and light hydrocarbons), char, and tar. This method has some problems such as corrosion, poisoning of catalysts, and minimizing tar components.

Hydrogen can be produced from the gasification gaseous products through the same procedure of steam reforming and water–gas shift reaction as discussed in the pyrolysis section. As the products of gasification are mainly gases, this process is more favorable for hydrogen production than pyrolysis. In order to optimize the process for hydrogen production, a number of efforts have been made by researchers to test hydrogen production from biomass gasification with various biomass types and at various operating conditions. Using a fluidized bed gasifier along with suitable catalysts, it is possible to achieve hydrogen production about 60 vol.%. Such high conversion efficiency makes biomass gasification an attractive hydrogen production alternative. In addition, the costs of hydrogen production by biomass gasification are competitive with natural gas reforming. Taking into account the environmental benefit as well, hydrogen production from biomass gasification should be a promising option based on both economic and environmental considerations.

One of the major issues in biomass gasification is to deal with the tar formation that occurs during the process. The unwanted tar may cause the formation of tar aerosols and polymerization to a more complex structure, which are not favorable for hydrogen production through steam reforming. Currently, three methods are available to minimize tar formation: (i) proper design of gasifier, (ii) proper control and operation, and (iii) proper additives/catalysts. The operation parameters, such as temperature, gasifying agent, and residence time, play an important role in the formation and decomposition of tar. It has been reported that tar could be thermally cracked at temperature above 1273 K (Milne et al. 1998). The use of some additives (dolomite, olivine, and char) inside the gasifier also helps tar reduction. When dolomite is used, 100 % elimination of tar can be achieved (Sutton et al. 2001). Catalysts not only reduce the tar content but also improve the gas product quality and conversion efficiency. Dolomite, Ni-based catalysts, and alkaline metal oxides are widely used as gasification catalysts. Researches on iron-based catalysts and the novel carbon-supported catalysts were reported recently (Xu et al. 2010). Process modifications by two-stage gasification and secondary air injection in the gasifier are also useful for tar reduction.

Another problem of biomass gasification is the formation of ash that may cause deposition, sintering, slagging, fouling, and agglomeration. To resolve the ash-associated problems, fractionation and leaching have been employed to reduce ash formation inside the reactor. Though fractionation is effective for ash removal, it may deteriorate the quality of the remaining ash. On the other hand, leaching can

remove biomass' inorganic fraction, as well as improve the quality of the remaining ash. More recently, gasification of leached olive oil waste in a circulating fluidized bed reactor was reported for gas production that demonstrated the feasibility of leaching as a pretreatment technique for gas production (Garcıa-Ibañez et al. 2004).

Supercritical Water Gasification (SCWG)

The properties of water displayed beyond critical point plays a significant role for chemical reactions, especially in the gasification process. Below the critical point, both the liquid and gas phases exhibit different properties, although it is apparent that these properties become increasingly alike as the temperature arises. Ultimately, when it reaches the critical point (temperature >374 °C, pressure >22 MPa), the properties of both liquid and gas become identical. Over the critical point, the properties of this SCW vary in between liquid-like or gas-like conditions. SCW is completely miscible with organic substance as well as with gases. When biomass has high moisture content above 35 %, it is likely to gasify biomass in a supercritical water condition, where biomass can be rapidly decomposed into small molecules or gases in a few minutes at a high efficiency. Supercritical water gasification is a promising process to gasify biomass with high moisture contents due to the high gasification ratio (100 % achievable), high hydrogen volumetric ratio (50 % achievable), and avoidance of biomass drying.

In the past 25 years, the US Pacific Northwest Laboratory, Hawaii Natural Energy Institute, Forschungszentrum Karlsruhe in Germany, National Institute for Resources and Environment in Japan, State Key Laboratory of Multiphase Flow in Power Engineering in China (Guo et al. 2007), and other research institutions have had some in-depth researches on the hydrogen production by SCWG of some organic compounds without catalysts. Studies covered glucose, methanol, cellulose, lignin, and some real biomass compounds and organic waste/water. As successful demonstrations have been accumulated, detailed reaction mechanism, kinetics, and thermodynamics have built a solid foundation for subsequent investigations (Guo et al. 2010). And in recent years, extensive research has been carried out to evaluate the suitability of various wet biomass gasification in supercritical water conditions. However, the works have been mostly on a laboratory scale and in an early development stage.

The solubility of biomass components in hot-compressed water has been first studied by Mok and Antal (1992). The results show that in hot-compressed waters, about 40–60 % of the biomass sample is soluble, though the reaction is maintained slightly below the critical water condition. Minowa et al. (1998) reported hydrogen production from cellulose gasification in hot-compressed water (subcritical) using nickel catalyst. Resende and Savage (2010) gasified cellulose and lignin in supercritical water, using quartz reactors, and quantified the catalytic effect of metals by adding them to these reactors in different forms. Yu et al. (1993) reported that the gasification of glucose at supercritical water condition, such as 873 K and 34.5 MPa, was different from the nonsupercritical water condition. One advantage is that, during gasification, neither tar nor char formation occurs. This early finding

stimulated extensive interests in supercritical water research. Using glucose as a model compound, hydrogen yield of more than 50 vol.% can be achieved with the use of proper catalysts in supercritical water condition. Tubular reactors are widely used in supercritical water gasification because of their robust structures to withstand high pressure. Calzavara et al. (2005) made an evaluation of the energy efficiency of biomass gasification, and results show that the energy efficiency from thermodynamic calculation reaches 60 % when considering hydrogen, carbon monoxide, and methane as valuable species in the ideal case. Including energy recovery from the water at 280 bar and 740 °C, the overall energy yield reaches 90 %, if the heat loss is ignored. Although supercritical water gasification is still at its early development stage, the technology has already shown its economic competitiveness with other hydrogen production methods. Spritzer and Hong (2003) have estimated the cost of hydrogen produced by supercritical water gasification to be about US$ 3/GJ (US$ 0.35/kg).

Hydrogen production from biomass thermochemical processes has already been shown to be attractive economically and demonstrated to be a feasible option. However, it should be noted that hydrogen gas is normally produced together with other gas constituents. Thus, separation and purification of hydrogen gas are required. Nowadays, several methods, such as CO_2 absorption, drying/chilling, and membrane separation, have been successfully developed for hydrogen gas purification. It is expected that biomass thermochemical conversion processes will be available for large-scale hydrogen production in the near future.

Biological Conversion

Another method for biomass-based hydrogen is biological conversions. These are summarized as photosynthesis process, fermentative hydrogen production, and hydrogen production by BWGS (biological water–gas shift reaction). All processes depend on hydrogen production enzymes.

Photosynthesis Process

Many phototropic organisms, such as purple bacteria, green bacteria, cyanobacteria, and several algae can be used to produce hydrogen with the aid of solar energy. Microalgae, such as green algae and cyanobacteria, absorb light energy and generate electrons. The electrons are then transferred to ferredoxin (FD) using the solar energy absorbed by photosystem. However, the mechanism varies from organism to organism but the main steps are similar.

Direct Biophotolysis

Direct biophotolysis of hydrogen production is a biological process using microalgae photosynthetic systems to convert solar energy into chemical energy in the form of hydrogen:

$$2H_2O \overset{\text{solar energy}}{\rightarrow} 2H_2 + O_2$$

Two photosynthetic systems are responsible for photosynthesis process: (i) photosystem I (PSI) producing reductant for CO_2 reduction and (ii) photosystem II (PSII) splitting water and evolving oxygen. In the biophotolysis process, two photons from water can yield either CO_2 reduction by PSI or hydrogen formation with the presence of hydrogenase. In green plants, due to the lack of hydrogenase, only CO_2 reduction takes place. On the contrary, microalgae, such as green algae and cyanobacteria (blue-green algae), contain hydrogenase and, thus, have the ability to produce hydrogen. In this process, electrons are generated when PSII absorbs light energy. The electrons are then transferred to the ferredoxin (Fd) using the solar energy absorbed by PSI.

Since hydrogenase is sensitive to oxygen, it is necessary to maintain the oxygen content at a low level under 0.1 % so that hydrogen production can be sustained. This condition can be obtained by the use of green algae *Chlamydomonas reinhardtii* that can deplete oxygen during oxidative respiration. However, due to the significant amount of substrate being respired and consumed during this process, the efficiency is low. Recently, mutants derived from microalgae were reported to have good O_2 tolerance and thus higher hydrogen production. The efficiency can be increased significantly using mutants for hydrogen production.

Benemann (1998) estimated the cost of direct biophotolysis for hydrogen production to be \$20/GJ assuming that the capital cost is about US\$ 60/m^2 with an overall solar conversion efficiency of 10 %. Hallenbeck and Benemann (2002) performed similar cost estimation and reported the capital cost of US\$ 100/m^2. However, in their estimation, some practical factors were neglected, such as gas separation and handling.

Indirect Biophotolysis

The concept of indirect biophotolysis involves the following four steps: (i) biomass production by photosynthesis; (ii) biomass concentration; (iii) aerobic dark fermentation yielding 4 mol hydrogen/mol glucose in the algae cell, along with 2 mol of acetates; and (iv) conversion of 2 mol of acetates into hydrogen. In a typical indirect biophotolysis, cyanobacteria are used to produce hydrogen via the following reactions:

$$12H\pm_2O + 6CO_2 \rightarrow C_6H_{12}O_6 + 6O_2$$

$$C_6H_{12}O_6 + 12H_2O \rightarrow 12H_2 + 6CO_2$$

Markov et al. (1997) investigated the indirect biophotolysis with cyanobacterium *Anabaena variabilis* exposed to light intensities of 45–55 A mol^{-1} m^{-2} and 170–180 A mol^{-1} m^{-2} in the first stage and second stage, respectively. Photoproduction of hydrogen at a rate of about 12.5 ml H_2/gcdw h (cdw, cell dry weight) was found. In the study on indirect biophotolysis with cyanobacterium *Gloeocapsa alpicola* by Troshina et al. (2002), it was found that maintaining the

medium at pH value between 6.8 and 8.3 yielded optimal hydrogen production. Increasing the temperature from 30 °C to 40 °C can increase the hydrogen production twice as much. The hydrogen production rate through indirect biophotolysis is comparable to hydrogenase-based hydrogen production by green algae. The estimated overall cost is US$ 10/GJ of hydrogen (Hallenbeck and Benemann 2002). However, it should be pointed out that indirect biophotolysis technology is still under active research and development. The estimated cost is subject to a significant change depending on the technological advancement.

Fermentative Hydrogen Production

Bio hydrogen production can be realized by anaerobic (dark fermentation) and photoheterotrophic (light fermentation) microorganisms using carbohydrate-rich biomass as a renewable resource. The first step is the acid or enzymatic hydrolysis of biomass to highly concentrated sugar solution which is further fermented by anaerobic organisms to produce volatile fatty acids (VFA), hydrogen, and CO_2. The organic acids are further fermented by the photoheterotrophic bacteria (*Rhodobacter* sp) to produce CO_2 and H_2 which is known as the light fermentation. Combined utilization of dark and photo-fermentations was reported to improve the yield of hydrogen formation from carbohydrates.

Dark Fermentation

Fermentation by anaerobic bacteria as well as some microalgae, such as green algae on carbohydrate-rich substrates, can produce hydrogen at 30–80 °C especially in a dark condition. Unlike a biophotolysis process that produces only H_2, the products of dark fermentation are mostly H_2 and CO_2 combined with other gases, such as CH_4 or H_2S, depending on the reaction process and the substrate used. With glucose as the model substrate, maximum 4 mol H_2 is produced per mole glucose when the end product is acetic acid:

$$C_6H_{12}O_6 + 2H_2O \rightarrow 2CH_3COOH + 4H_2 + 2CO_2$$

When the end product is butyrate, 2 mol H_2 is produced:

$$C_6H_{12}O_6 + 2H_2O \rightarrow CH_2CH_2CH_2OOH + 2H_2 + 2CO_2$$

However, in practice, the 4 mol H_2 production/mol glucose cannot be achieved because the end products normally contain both acetate and butyrate. The amount of hydrogen production by dark fermentation highly depends on the pH value, hydraulic retention time (HRT), and gas partial pressure. For the optimal hydrogen production, pH should be maintained between 5 and 6. Partial pressure of H_2 is yet another important parameter affecting the hydrogen production. When hydrogen concentration increases, the metabolic pathways shift to produce more reduced substrates, such as lactate, ethanol, acetone, butanol, or alanine, which in turn decrease the hydrogen production. Besides the pH value and partial pressure, HRT (hydraulic retention time) also plays an important role in hydrogen production. Ueno

et al. (1996) have reported that an optimal HRT of 0.5 day could affect maximum hydrogen production (14 mmol/g carbohydrate) from wastewater by anaerobic microflora in the presence of chemostat culture. When HRT was increased from 0.5 day to 3 days, hydrogen production rate was reduced from 198 to 34 mmol l^{-1} day^{-1}, while the carbohydrates in the wastewater were decomposed at an increasing efficiency from 70 % to 97 %. Due to the fact that solar radiation is not a requirement, hydrogen production by dark fermentation does not demand much land and is not affected by the weather condition. Hence, the feasibility of the technology yields a growing commercial value.

Photo-Fermentation

Photosynthetic nonsulfur (PNS) bacteria have the ability to convert VFAs to H_2 and CO_2 under anoxygenic conditions. PNS bacteria also have the ability to use carbon sources like glucose, sucrose, and succinate rather than VFA for H2 production. The most widely known PNS bacteria used in photo-fermentative H_2 production are *Rhodobacter sphaeroides* O.U001, *Rhodobacter capsulatus*, *R. sphaeroides-RV*, *Rhodobacter sulfidophilus*, *Rhodopseudomonas palustris*, and *Rhodospirillum rubrum* (Argun and Kargi 2011).

As presented in the equation below, theoretically 4 mol of H_2 can be produced from 1 mol of acetic acid when acetic acid is the only VFA present in fermentation medium:

$$CH_3COOH + 2H_2O \rightarrow 4H_2 + 2CO_2,\ \Delta G^{\circ} = +104\text{kJ}$$

Hydrogen can be produced by photo-fermentation of various types of biomass wastes. However, these processes have three main drawbacks: (i) use of nitrogenase enzyme with high-energy demand, (ii) low solar energy conversion efficiency, and (iii) demand for elaborate anaerobic photobioreactors covering large areas. Hence, at the present time, photo-fermentation process is not a competitive method for hydrogen production.

Design of photobioreactors enabling efficient H_2 production is still a challenge. Light distribution inside photobioreactors constitutes the most important parameter effecting H_2 production rate. Thus, optimization of light distribution with high reactor surface area was reported as an essential factor to enhance the light efficiency in photo-fermentation. Operating parameters also affect the photo-fermentation process efficiency. The concept of net energy ratio (NER) is used to determine the process efficiency which is the ratio of total energy produced to the energy required for plant operations like mixing, pumping, aeration, and cooling.

Biological Water–Gas Shift Reaction (BWGS)

The BWGS is a relatively new method for hydrogen production. Some bacteria (certain photoheterotrophic bacteria), such as *Rubrivivax gelatinosus*, are capable of performing water–gas shift reaction at ambient temperature and atmospheric pressure. Such bacteria can survive in the dark by using CO as the sole carbon source to

generate adenosine triphosphate (ATP) coupling the oxidation of CO with the reduction of H^+ to H_2:

$$CO + H_2O \leftrightarrow CO_2 + H_2,\ \Delta G^\circ = -20.1 kJ/mol$$

In equilibrium, the dominating products are CO_2 and H_2. Therefore, this process is favorable for hydrogen production. Organisms growing at the expense of this process are the gram-negative bacteria, such as *R. rubrum* and *Rubrivivax gelatinosus*, and the gram-positive bacteria, such as *Carboxydothermus hydrogenoformans*. Under anaerobic conditions, CO induces the synthesis of several proteins, including CO dehydrogenase, Fe–S protein, and CO-tolerant hydrogenase. Electrons produced from CO oxidation are conveyed via the Fe–S protein to the hydrogenase for hydrogen production.

Biological water–gas shift reaction for hydrogen production is still under laboratory scale and only few works have been reported. The common objectives of these works were to identify suitable microorganisms that had high CO uptake and to estimate the hydrogen production rate. Kerby et al. (1995) observed that under dark, anaerobic conditions in the presence of sufficient nickel, the doubling time of *R. rubrum* was less than 5 h by the oxidation of CO to CO_2 coupled with the reduction of protons to hydrogen. However, *R. rubrum* requires light to grow and hydrogen production is inhibited by medium CO partial pressure above 0.2 atm. An alternative new chemoheterotrophic bacterium *Citrobacter sp. Y19* was tested by Jung et al. (2002) for hydrogen production using water–gas shift reaction. The maximum hydrogen production activity was found to be 27 mmol/g cell h, which is about three times higher than *R. rubrum*.

Recently, Wolfrum et al. (2003) have conducted a detailed study to compare the biological water–gas shift reaction with conventional water–gas shift processes. Their analysis showed that biological water–gas shift process was economically competitive when the methane concentration was under 3 %. The hydrogen production cost from biological water–gas shift reaction ranged from US$ 1.75/kg (US$ 14.6/GJ) to around US$ 2.25/kg (US$ 18.8/GJ) for a methane concentration between 1 % and 10 %. Compared with thermochemical water–gas shift processes, the cost of biological water–gas shift processes is lower due to the elimination of reformer and associated equipment.

Hydrogen Production from Water

There is abundant water resource on the earth and it is widely available almost everywhere. Thus, hydrogen production from water is a convenient option and the amount can be boundless. Extensive research efforts have focused on this promising hydrogen production route. In fact, its commercial use dates back to the 1890s. Hydrogen production from water splitting consists of three categories: electrolysis, thermolysis, and photoelectrolysis.

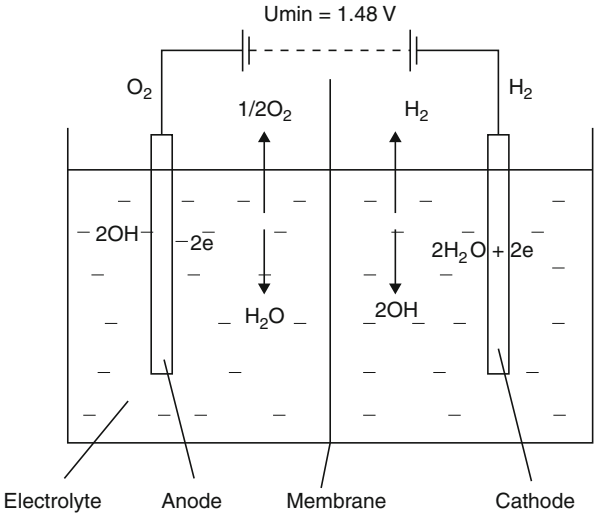

Fig. 3 A diagram of a typical water electrolysis process

Water Electrolysis

Water electrolysis is essentially the conversion of electrical energy to chemical energy in the form of hydrogen, with oxygen as a useful by-product. Figure 3 shows the diagram of a typical water electrolysis process. It is realized by an electrical current passing through two electrodes to break water into hydrogen and oxygen. The most common water electrolysis technology is alkaline based, but more proton exchange membrane (PEM) electrolysis and solid oxide electrolysis cell (SOEC) units are developing.

Alkaline Electrolyzer

Alkaline systems are the most developed and lowest in capital cost. They have the lowest efficiency so they have the highest electrical energy costs. Alkaline electrolyzers are typically composed of electrodes, a microporous separator, and an aqueous alkaline electrolyte of approximately 30 wt.% KOH or NaOH. In alkaline electrolyzers, nickel with a catalytic coating, such as platinum, is the most common cathode material. For the anode, nickel or copper metals coated with metal oxides, such as manganese, tungsten, or ruthenium, are used. The liquid electrolyte is not consumed in the reaction but must be replenished over time because of other system losses primarily during hydrogen recovery. In an alkaline cell, the water is introduced in the cathode where it is decomposed into hydrogen and OH^-. The OH^- travels through the electrolytic material to the anode where O_2 is formed. The hydrogen is left in the alkaline solution. The hydrogen is then separated from the water in a gas–liquid separation unit outside of the electrolyzer. The typical current density is 100–300 mA cm^{-2} and alkaline electrolyzers typically achieve efficiencies of 50–60 % based on the lower heating value of hydrogen. The overall reactions at the anode and cathode are:

Cathode:

$$2H_2O + 2e^- \rightarrow H_2 + 2OH^-$$

Anode:

$$2OH^- \rightarrow \frac{1}{2} O_2 + H_2O$$

Overall reaction:

$$H_2O \rightarrow H_2 + \frac{1}{2} O_2 \, \Delta H = -288 \text{kJ/mol}$$

PEM Electrolyzer

PEM electrolyzers build upon the recent advances in PEM fuel cell technology. They are more efficient than alkaline and do not have the corrosion and seal issues as SOEC but cost more than alkaline systems. PEM-based electrolyzers typically use Pt black, iridium, ruthenium, and rhodium for electrode catalysts and a Nafion membrane which not only separates the electrodes but acts as a gas separator. In PEM electrolyzers, water is introduced at the anode where it is split into protons and oxygen. The protons travel through the membrane to the cathode, where they are recombined into hydrogen. The O_2 gas remains behind with the unreacted water. There is no need for a separation unit. Depending on the purity requirements, a drier may be used to remove residual water after a gas–liquid separation unit. PEM electrolyzers have low ionic resistances, and therefore, high currents of >1600 mA cm^{-2} can be achieved while maintaining high efficiencies of 55–70 %. The reactions at the anode and cathode are:

Anode:

$$2H_2O \rightarrow O_2 + 4H^+ + 4e^-$$

Cathode:

$$4H^+ + 4e^- \rightarrow 2H_2$$

Overall reaction:

$$H_2O \rightarrow H_2 + \frac{1}{2} O_2 \, \Delta H = -288 \text{kJ/mol}$$

Solid Oxide Electrolysis Cells

Solid oxide electrolysis cells (SOEC) are essentially solid oxide fuel cells operating in reverse. These systems replace part of the electrical energy required to split water with thermal energy. The higher temperatures increase the electrolyzer efficiency by

decreasing the anode and cathode over potentials which cause power loss in electrolysis. It is said that an increase in temperature from 375 to 1050 K can reduce the combined thermal and electrical energy requirements by close to 35 % (Utgikar and Thiesen 2006). Another advantage of SOEC units is the use of a solid electrolyte which, unlike KOH for alkaline systems, is noncorrosive, and it does not experience any liquid and flow distribution problems. A SOEC operates similar to the alkaline system in that an oxygen ion travels through the electrolyte (typically ZrO_2) leaving the hydrogen in unreacted steam stream. The reactions are shown as follows:

Cathode:

$$2H_2O + 4e^- \rightarrow 2H_2 + 2O^{2-}$$

Anode:

$$2O^{2-} \rightarrow O_2 + 4e^-$$

Overall reaction:

$$H_2O \rightarrow H_2 + \frac{1}{2}O_2 \, \Delta H = -288 \text{kJ/mol}$$

SOEC electrolyzers are the most electrically efficient but are the least developed of the technologies. A major challenge of SOEC technology is that the high-temperature operation requires the use of costly materials and fabrication methods in addition to a heat source. The materials are similar to those being developed for solid oxide fuel cells (SOFC), yttria-stabilized zirconia (YSZ) electrolyte, nickel-containing YSZ anode, and metal-doped lanthanum metal oxides and have the same problems with seals which are being investigated.

Water Thermochemical Splitting

Water thermochemical splitting is also called water thermolysis, in which heat alone is used to decompose water to hydrogen and oxygen. It is well known that water will decompose at 2500 °C, but materials stable at this temperature and also sustainable heat sources are not easily available. Thus, chemical reagents have been proposed to lower the temperatures. Research in this area was prominent from the 1960s through the early 1980s. However, essentially all research and development stopped after the mid-1980s, until recently. There are more than 300 water splitting cycles referenced in the literature (Hydrogen 2005). All of the processes have significantly reduced the operating temperature.

In choosing the process, there are five criteria which should be met. (1) Within the temperatures considered, the ΔG (differential Gibbs free energy) of the individual reactions must approach zero. This is the most important criterion. (2) The number of

steps should be minimal. (3) Each individual step must have both fast reaction rates and rates which are similar to the other steps in the process. (4) The reaction products cannot result in chemical by-products, and any separation of the reaction products must be minimal in terms of cost and energy consumption. (5) Intermediate products must be easily handled.

Currently, there are several processes which meet the five criteria, such as the UT-3 process and the sulfuric acid decomposition process. The mechanisms of these two processes are shown as follows:

1. Iodine–sulfur process

$$2H_2O(l) + I_2(g) + SO_2(g) \rightarrow 2HI(l) + H_2SO_4(l)\,(100 \sim 120^{\circ}C,\ \text{exothermic})$$

$$2HI(g) \rightarrow H_2(g) + I_2(g)\,(400 \sim 500\ ^{\circ}C,\ \text{exothermic})$$

$$H_2SO_4(l) \rightarrow H_2O(g) + SO_2(g) + \frac{1}{2}O_2(g)\,(850\ ^{\circ}C,\ \text{endothermic})$$

Overall reaction:

$$H_2O \rightarrow H_2 + \frac{1}{2}O_2$$

Figure 4 gives the diagram of a typical water thermochemical splitting process for hydrogen production using the iodine–sulfur process.

2. UT-3 process

$$CaBr_2(s) + H_2O(g) \rightarrow CaO(s) + 2HBr(g)\,(700 \sim 750\ ^{\circ}C,\ \text{endothermic})$$

$$CaO(s) + Br_2(g) \rightarrow CaBr_2(s) + \frac{1}{2}O_2(g)\,(500 \sim 600\ ^{\circ}C,\ \text{exothermic})$$

$$Fe_3O_4(s) + 8HBr(g) \rightarrow 3FeBr_2(s) + 4H_2O(g) + Br_2(g)\,(200 \sim 300\ ^{\circ}C,\ \text{exothermic})$$

$$3FeBr_2(s) + 4H_2O(g) \rightarrow Fe_3O_4(s) + 6HBr(g) + H_2(g)\,(550 \sim 600\ ^{\circ}C,\ \text{endothermic})$$

Overall reaction:

$$H_2O \rightarrow H_2 + \frac{1}{2}O_2$$

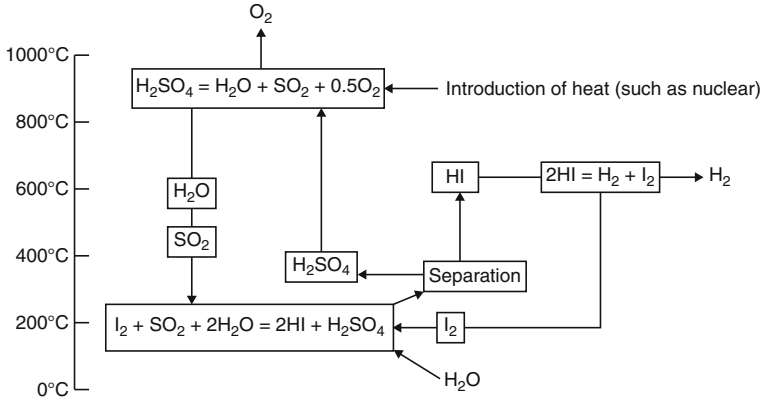

Fig. 4 A diagram of the iodine–sulfur water thermochemical splitting process

However, water thermochemical splitting is still not competitive with other hydrogen generation technologies in terms of cost and efficiency which is the major focus of research in those processes (Norbeck et al. 1996a). In addition, these processes require large inventories of highly hazardous corrosive materials. The requirements of high temperature, high pressure, and corrosion result in the need for new materials. The US DOE has active projects investigating several of these processes focused on improving materials, lowering cost, and increasing efficiency (Hydrogen 2005). Current research and development on hydrogen from water thermochemical splitting are ongoing in Canada on technologies that couple synergistically with Canada's present and future nuclear reactors. Also, several countries (Japan, USA, France) are currently advancing nuclear technology and corresponding thermochemical cycles. Sandia National Laboratories in the USA and CEA in France are developing a hydrogen pilot plant with a sulfur–iodine (S–I) cycle. The KAERI Institute in Korea is collaborating with China to produce hydrogen with the HTR-10 reactor. The Japan Atomic Energy Agency plans to complete a large sulfur–iodine plant to produce 60,000 m^3/h of hydrogen by 2020, an amount sufficient for about one million fuel cell vehicles.

It is believed that scaling up the processes may lead to improved thermal efficiency overcoming one of the principle challenges faced by this technology. In addition, a better understanding of the relationship between capital costs, thermodynamic losses, and process thermal efficiency may lead to decreased hydrogen production costs (Funk 2001). The current processes all use four or more reactions, and it is believed that an efficient two-reaction process as shown in the following equations may make this technology viable (Funk 2001):

$$\mathrm{ZnO(s)} \rightarrow \mathrm{Zn(g)} + \frac{1}{2}\mathrm{O_2}\,(2300\ \mathrm{K},\ \text{endothermic})$$

$$Zn(l) + H_2O \rightarrow ZnO(s) + H_2\,(700\ K,\ \text{exothermic})$$

Water Photoelectrolysis

Photoelectrolysis uses sunlight to directly decompose water into hydrogen and oxygen and uses semiconductor materials similar to those used in photovoltaics. In photovoltaics, two doped semiconductor materials, a p-type and an n-type, are brought together forming a p–n junction. At the junction, a permanent electric field is formed when the charges in the p- and n-type of material rearrange. When a photon with energy greater than the semiconductor material's bandgap is absorbed at the junction, an electron is released and a hole is formed. Since an electric field is present, the hole and electron are forced to move in opposite directions which, if an external load is also connected, will create an electric current. This type of situation occurs in photoelectrolysis when a photocathode, p-type material with excess holes, or a photoanode, n-type of material with excess electrons, are immersed in an aqueous electrolyte, but instead of generating an electric current, water is split to form hydrogen and oxygen.

The process can be summarized for a photoanode-based system as follows: (1) A photon with greater energy than the bandgap strikes the anode creating an electron–hole pair. (2) The holes decompose water at the anode's front surface to form hydrogen ions and gaseous oxygen, while the electrons flow through the back of the anode which is electrically connected to the cathode. (3) The hydrogen ions pass through the electrolyte and react with the electrons at the cathode to form hydrogen gas (Turner et al. 2008). (4) The oxygen and hydrogen gases are separated, for example, by the use of a semipermeable membrane, for processing and storage.

Current photoelectrodes used in PEC (photon-to-electron conversion) that are stable in aqueous solutions have a low efficiency for using photons to split water to produce hydrogen. The target efficiency is >16 % solar energy to hydrogen. This encompasses three material system characteristics necessary for efficient conversion: the bandgap should (i) fall in the range sufficient to achieve the energetics for electrolysis and yet allow maximum absorption of the solar spectrum (this is 1.6–2.0 eV for single photoelectrode cells and 1.6–2.0/0.8–1.2 eV for top/bottom cells in stacked tandem configurations), (ii) have a high quantum yield (>80 %) across its absorption band to reach the efficiency necessary for a viable device, and (iii) straddle the redox potentials of the H_2 and O_2 half reactions with its conduction and valence band edges, respectively. The efficiency is directly related to the semiconductor bandgap (Eg), i.e., the energy difference between the bottom of the conduction band and the top of the valence band, as well as the band edge alignments, since the material or device must have the correct energy to split water. The energetics are determined by the band edges, which must straddle water's redox potential with sufficient margins to account for inherent energy losses. Cost-efficient, durable catalysts with appropriate Eg and band edge positions must be developed. To achieve the highest efficiency possible in a tandem configuration,

"current matching" of the photoelectrodes must be done. Electron transfer catalysts and other surface enhancements may be used to increase the efficiency of the system. These enhancements can minimize the surface overpotentials in relation to the water and facilitate the reaction kinetics, decreasing the electric losses in the system. Fundamental research is ongoing to understand the mechanisms involved and to discover and develop appropriate candidate surface catalysts for these systems (Licht 2005).

In addition, it is possible to use suspended metal complexes in solution as the photochemical catalysts (Norbeck et al. 1996b). Typically, nanoparticles of ZnO, Nb_2O_5, and TiO_2 (the material of choice) have been used (Norbeck et al. 1996b). The advantages of these systems include the use of low-cost materials and the potential for high efficiencies. Current research involves overcoming the low light absorption and unsatisfactory stability in time for these systems.

Sorption-Enhanced H_2 Production with In Situ CO_2 Capture Using Carbon-Containing Resources

It is now widely acknowledged that "decarbonizing" energy supply will be essential in the near future due to the well-known global warming. Although utilization of H_2 is clean and no pollution, the production of H_2 from fossil fuels actually produces CO_2 emission. A typical SMR hydrogen plant with the capacity of one million m^3 of hydrogen per day produces 0.3–0.4 million standard cubic meters of CO_2 per day. If hydrogen is to be produced by coal gasification, the amount of CO_2 emissions would be doubled compared to SMR. Further, with regard to end-use applications of H_2, additional costs and process complexity are incurred for gas cleaning. Taking fuel cell applications, for example, the CO content in the product gas must be closely managed, a CO concentration of less than 10 ppm is required for low-temperature proton exchange membranes and alkaline fuel cells. The cost of separating H_2 from a H_2-rich gas with impurities, such as CO, CH_4, and tar, incurs major cost penalties. The increasing attentions on global warming and the demands for pure H_2 production together result in the great interest in the research on sorption-enhance gasification system where high-purity H_2 production and in situ CO_2capture can be realized in one single reactor. Figure 5 shows a simple diagram of the system.

It is seen that the core unit of the system is the dual gasification–regeneration reactors. And the system is apparently characterized by the addition of CaO additives to the gasifier. The corresponding introduced influences include the following: the water–gas reaction and the water–gas shift reaction are both enhanced to produce more hydrogen due to the CO_2 absorption by the CaO carbonation reaction, (ii) the necessary external energy consumption for hydrocarbons steam gasification can be partially substituted by the releasing heat of carbonation, and (iii) the formation of pyrolysis tars in the presence of CaO additives could be reduced. The reaction mechanisms of the system are as follows:

Reactions in the gasifier:

Water–gas reaction

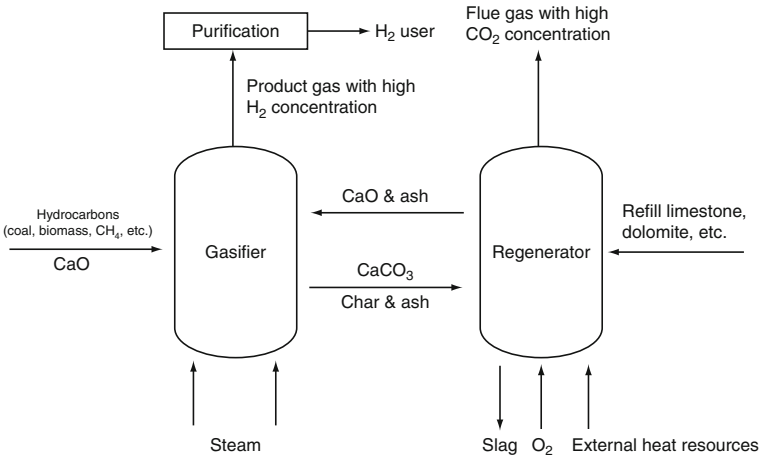

Fig. 5 A simple diagram of the sorption-enhanced gasification system

$$C(s) + H_2O(g) \rightarrow CO(g) + H_2(g) (\text{for coal})$$

$$CH_4(g) + H_2O(g) \rightarrow CO(g) + 3H_2(g) (\text{for natural gas})$$

$$CH_{1.5}O_{0.7}(s) + 0.3H_2O(g) \rightarrow CO(g) + 1.05H_2(g) (\text{for typical biomass})$$

Water–gas shift reaction

$$CO(g) + H_2O(g) \rightarrow CO_2(g) + H_2(g)$$

Carbonation reaction

$$CaO(s) + CO_2(g) \rightarrow CaCO_3(s)$$

The global reaction in the gasifier can be summarized as:

$$C(s) + 2H_2O(g) + CaO(s) \rightarrow CaCO_3(s) + 2H_2(g) (\text{for coal})$$

$$CH_4(g) + 2H_2O(g) + CaO(s) \rightarrow CaCO_3(s) + 4H_2(g) (\text{for natural gas})$$

$$CH_{1.5}O_{0.7}(s) + 1.3H_2O(g) + CaO(s) \rightarrow CaCO_3(s) + 2.05H_2(g) (\text{for typical biomass})$$

Reactions in the regenerator:

Combustion reaction

$$C(s) + O_2(g) \rightarrow CO_2(g)$$

Calcination reaction

$$CaCO_3(s) \rightarrow CaO(s) + CO_2(g)$$

It should be noted that beside Ca-based oxides, a number of candidate CO_2 sorbents have been also studied including potassium-promoted hydrotalcite (K-HTC) and mixed metal oxides of Li and Na (Harrison 2008). HTCs are members of the family of double-layered hydroxides that, when doped with K_2CO_3, can serve as high-temperature CO_2 sorbents. They react rapidly and the sorbent regeneration is possible with less external energy input. But HTCs have much lower CO_2 capacity than Ca-based sorbents and are also considerably more expensive. Mixed metal oxide sorbents of Li and Na such as Li_2ZrO_3, Li_4SiO_4, and Na_2ZrO_3 were spawned, on the one hand, by the desire to find a replacement for Ca-based sorbents that could be regenerated at lower temperature and, on the other hand, would have considerably higher CO_2 capacity than HTC. However, because of less favorable thermodynamic properties associated with these sorbents, the equilibrium CO_2 pressures are higher and product H_2 concentrations must be lower than can be obtained using Ca-based sorbents at equivalent reaction conditions. Anyway, Ca-based sorbents are considered to be the most promising option. As a result, current studies on sorption-enhanced H_2 production are mostly being conducted using CaO. This section also just discusses sorption-enhanced gasification using Ca-based sorbents. Different feedstocks including both solid fuels (coal, biomass) and natural gas are all summarized.

Sorption-Enhanced H_2 Production from Solid Fuels

A new near-zero emission coal (also biomass) utilization technology with combined gasification and combustion has been proposed by Zhejiang University in China (Qinhui et al. 2003; Wang et al. 2006; Guan et al. 2007; Han et al. 2010). Figure 6 displays the diagram of the system.

In this system, solid fuels are partly gasified with steam in a pressured circulation fluidized bed gasifier, producing H_2, CO, and CO_2. As CaO is used as the CO_2 acceptor to absorb CO_2 and release the heat for the gasification processes in the gasifier, CO is depleted from the gas phase by the water–gas shift reaction. The H_2-rich gas stream produced in the gasifier is oxidized in the solid oxide fuel cell. The remaining char with low reaction activity is transferred in a circulating fluidized bed combustor together with the carbonated $CaCO_3$. The char and the unreacted H_2, in the hot off-gas from the fuel cell, are oxidized with oxygen in the combustor to supply the heat for the $CaCO_3$ calcination. The CO_2-rich gas stream produced in the combustor is suitable for disposal after the heat is recovered by a gas–steam-combined cycle. The authors firstly examined the influences of gasifier operation temperature, pressure and fuel type (coal and biomass), and H_2O/C on hydrogen production based on chemical equilibrium calculation (Wang et al. 2006; Guan et al. 2007). The results showed that the increase of CaO addition can obviously

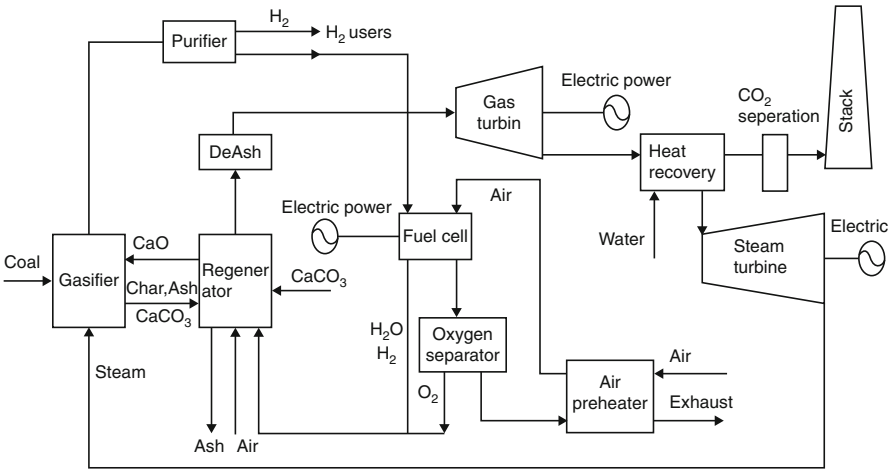

Fig. 6 The near-zero emission system proposed by Zhejiang University

increase H_2 mole fraction in C/H_2O reaction products. The process may achieve high conversion efficiency from coal energy to electrical energy (around 65.5 %) with near-zero gaseous emissions. Our study (Han et al. 2010) also showed that the CaO additives cannot only absorb CO_2 gases but also enhance the tar reduction reactions in biomass steam gasification with in situ CO_2 capture. Sorption-enhanced coal/biomass gasification in pressurized fluidized bed reactor is also being performed in Zhejiang University. Biomass and coal gasification experiments were carried out aiming to investigate the influences of operation variables such as CaO to carbon mole ratio (CaO/C), H_2O to carbon mole ratio (H_2O/C), reaction temperature (T), and pressure(P) on hydrogen (H_2) production(Han et al. 2010, 2013; Wang et al. 2014). Pressurized operation not only promoted gasification reactions but also apparently enhanced CaO carbonation. Within the experimental ranges investigated in the biomass gasification work, H_2 fraction and H_2 yield were both elevated with the increase in reaction pressure, CaO/C, H_2O/C, and T. Pressurized operation also increased the carbon conversion and cold gas efficiency for CaO sorption-enhanced sawdust gasification. A maximum H_2 output with a fraction of 67.7 % and a yield of 68 g/kg sawdust was achieved at CaO/C = 1.2, H_2O/C = 0.89, T = 680 °C, and pressure of 4 bar. In the case of Chinese bituminous coal as feedstock, the highest H_2 concentration of 77.98 vol.% was achieved under a condition of 4 bar(highest pressure condition the system can achieve), 750 °C, $[H_2O]/[C]$ = 2, and [Ca]/[C] = 1.

In Japan, the hydrogen production by the reaction-integrated novel gasification (HyPr-RING) process is under development (Lin et al. 2001). The mechanism of this process is very similar to the system proposed by Zhejiang University. HyPr-RING process has been conducted for both coal and biomass. For coal, conditions in the gasifier of 873–973 K and 3 MPa are reported to result in slightly over 50 % carbon

conversion with about 90 % H_2 in the product gas. The remainder of the product gas is predominantly CH_4 with less than 0.4 % ($CO + CO_2$). The regenerator operates at 1073 K and 0.1 MPa. For biomass, Lin et al. (Hanaoka et al. 2005) examined the H_2 production from woody biomass by steam gasification using CaO as a CO_2 sorbent. Firstly, it is said that in the absence of CaO, the product gas contained CO_2. On the other hand, in the presence of CaO ([Ca]/[C] = 1, 2, and 4), no CO_2 was detected in the product gas. And at a [Ca]/[C] of 2, the maximum yield of H_2 was obtained. Secondly, they reported that the H_2 yield and conversion to gas were largely dependent on the reaction pressure and exhibited the maximum value at 0:6 MPa, which indicated a much lower pressure compared to other carbonaceous materials such as coal (>12 MPa) and heavy oil (>4.2 MPa) in steam gasification using a CO_2 sorbent. As a result, they concluded that woody biomass is one of the most appropriate carbonaceous materials in H_2 production by steam gasification using CaO as a CO_2 sorbent, taking the reaction pressure into account. A further kinetic study conducted at 923 K and pressure of 6.5 MPa using a batch reactor with 50 cm^3 capacity also demonstrated the complete absorption of CO_2 from the gasification syngas (Fujimoto et al. 2007).

Another significant sorption-enhanced gasification process is the absorption-enhanced reforming (AER) developed within the frame of EU Project AER-Gas II. The atmospheric dual fluidized bed technology developed at Vienna University of Technology realizes the steam gasification through circulation of hot bed material. The technology has been realized in pilot plant scale of 100 kW fuel input (at Vienna University of Technology) as well as in industrial scale at the combined heat and power plant (CHP) guessing in an industrial scale of 8 MW fuel input in Austria. A comparison of dual fluidized bed gasification of biomass with and without selective transport of CO_2 from the gasification to the combustion reactor is performed by using the facility with 100 kW fuel input. In the case of convention gasification, the hydrogen content in the product gas of gasifier is about 40 vol.% (dry basis). However, in the case of carbonate addition to the bed material, much higher hydrogen content up to 75 vol.% (dry basis) can be achieved at lower gasification temperatures (Pfeifer et al. 2009). The first time application of the AER process on the 8 MW industrial facility also realizes the continuous CO_2 removal by cyclic carbonation of CaO and calcination of $CaCO_3$. Results obtained in the industrial facility are presented to be comparable with those obtained at pilot plant scale (Koppatz et al. 2009).

In addition, other similar sorption-enhanced gasification processes for solid fuels are also under development. One is the ZEC process developed at Los Alamos National Laboratory (Ziock et al. 2001). It is designed to first hydrogasified coal to produce CH_4, which is then reformed to H_2 using the calcium-based sorption-enhanced process. A system analysis performed by Nexant Corp. (Nawaz and Ruby 2001) estimated coal to electricity conversion efficiency on the order of 70 %. Research on this concept is continuing in a joint study at Cambridge University and Imperial College in the UK (Gao 2009). The other is the innovative fuel-flexible advanced gasification–combustion (AGC) process developed by

General Electric Energy and Environmental Research Corporation (GE EER) (Rizeq et al. 2001). The R&D on the AGC technology is being conducted under a Vision-21 award from the US DOE NETL with co-funding from GE EER, Southern Illinois University at Carbondale (SIU-C), and the California Energy Commission (CEC). The AGC technology converts coal and air into three separate streams of pure hydrogen, sequestration-ready CO_2, and high-temperature/high-pressure oxygen-depleted air to produce electricity in a gas turbine. The program integrates lab-, bench-, and pilot-scale studies to demonstrate the AGC concept. Besides, research on lab-scale H2 production from sorption-enhanced solid fuel gasification was also performed by Madhukar (Mahishi and Goswami 2007) and Wei et al. (2008). Fan et al. (2008) and his research group from Ohio State University developed the concept of Calcium Looping Process (CLP) for clean coal and biomass conversion and hydrogen production, and comprehensive simulations allow for a direct comparison of the CLP with other processes developed for post-combustion carbon dioxide removal. The comparison indicates that the CLP always provides a lower energy penalty under similar operating conditions.

Sorption-Enhanced H2 Production from Natural Gas

The effectiveness of both sorption-enhanced steam methane reforming (SE-SMR) and the use of calcium-based CO2 sorbents have been demonstrated in previous works. In particular, Rostrup-Nielsen (1984) reports that the first description of the addition of a CO2 sorbent to a hydrocarbon-steam-reforming reactor was published in 1868. Williams (1933) was issued a patent for a process in which steam and methane react in the presence of a mixture of lime and reforming catalyst to produce hydrogen. A fluidized bed version of the process was patented by Gorin and Retallick (1963). Brun-Tsekhovoi et al. (1988) published limited experimental results and reported potential energy saving of about 20 % compared to the conventional process. Recently, Kumar et al. (1999) reported on a process known as unmixed combustion (UMC), in which the reforming, shift, and CO2 removal reactions are carried out simultaneously over a mixture of reforming catalyst and CaO-based CO2 sorbent. In related work, Hufton et al. (2000) reported on H2 production through SE-SMR using a K2CO3-treated HTC sorbent, although the extremely low CO2 working capacity above was discussed. Average purity of H2 was about 96 % while CO and CO2 contents were less than 50 ppm. The methane conversion to H2 product reaches 82 %. The conversion and product purity are substantially higher than the thermodynamic limits for a catalyst-only reactor operated at these same conditions (28 % conversion, 53 % H2, 13 % CO/CO2). In an earlier work, Balasubramanian et al. (1999) showed that a gas with a H2 content up to 95 % (dry basis) could be produced in a single reactor containing reforming catalyst and CaO formed by calcination of high-purity CaCO3. The reported methane conversion was 88 %. Arstad et al. (2012) studied the continuous hydrogen production by SE-SMR using a CFB reactor with calcined natural dolomite as CO2

sorbent and Ni/NiAl2O4 as catalyst. The sorbent and catalyst materials we have used appear to have quite good mechanical properties at the time scale used (8 h), but only a fraction of the sorbent's CO2 capacity appears to be in use. Johnsen et al. (2006) use dolomite as CO2 sorbent in SE-SMR investigation, and a 100 mm-diameter bubbling fluidized bed reactor was operated alternating between reforming/carbonation conditions and higher-temperature calcination conditions to regenerate the sorbent. Equilibrium H2 concentration of above 98 % on a dry basis was reached at 600 °C and 1.013×10^5 Pa. Esther Ochoa-Fernández et al. (2007) compared the conventional steam reforming plus CO2 capture with the SE-SMR system, and SE-SMR resulted in competitive H2 yields and thermal efficiencies. The best efficiencies were obtained using CaO as acceptor due to its more favorable thermodynamics and high reaction rates, but the stability of CaO has to be improved, while Na2ZrO3 is a promising alternative due to the good kinetics for CO2 removal and the stability.

A large number of numerical study and simulation works on the SE-SMR are also carried out these years. Zhen-shan Li and Cai (2007) developed mathematical models of multiple cycles for SE-SMR and Ca-based sorbent regeneration in a fixed bed reactor, of which the results agree with experimental data. The effect of reactivity decay of dolomite, CaO/Ca12Al14O33, and limestone sorbents on sorption-enhanced hydrogen production and sorbent regeneration processes was studied. Jannike Solsvik and Jakobsen (2011) studied the performance of a combined catalyst/sorbent pellet design for the SE-SMR process. Different mathematical model complexities have been studied and parameter sensitivity analyses have been performed, which showed that the combined pellet performance is promising compared to the conventional two-pellet design. Reijers et al. (2009a, b) built a one-dimensional reactor model to describe the performance of an SE-SMR and water–gas shift reactor and verified using the results of an analytical solution for the increase of CH4 conversion over the bed and finally validated using the results of SE-SMR laboratory-scale experiments. Solieman et al. (2009) presented an analysis of the relation between different process conditions and parameters during both adsorption and desorption modes using Aspen Plus, and a relatively high (methane) reforming reaction conversion of 85 % could be achieved at 600 °C, 17 bar, and a steam to carbon ratio (S/C) of 3. Compared to Li2ZrO3 and BaO, CaO is the most suitable sorbent for achieving the targeted 85 % carbon capture ratio. Wang et al. (2011) developed a three-dimensional (3D) Eulerian two-fluid model with an in-house code to simulate the Ca-based SE-SMR process using such model combined with the reaction kinetics. Jakobsen and Halmøy (2009) built an SE-SMR reactor model which comprises simplified mathematical representation of the flow regime, differential equations for mass and heat transfer, sub-model for chemical reaction kinetics, and absorption equilibria. The model was used to investigate various operational modes for the reformer as well as for comparison of the reformer performance with use of various sorbents (Li4SO4, Na2ZrO3, CaO). Di Carlo et al. (2010) investigated the SE-SMR process numerically through computational fluid dynamics Eulerian–Eulerian Code. Dry hydrogen mole fraction of >0.93 is

predicted for temperatures of 900 K and a superficial gas velocity of 0.3 m/s with a dolomite/catalyst ratio >2. Fernandez et al. (2012) present a dynamic pseudo-homogeneous model to describe the operation of a packed bed reactor in which the SE-SMR reaction is carried out under adiabatic conditions. The results demonstrated that the SER process can yield a CH4 conversion and H2 purity of up to 85 % and 95 %, respectively, under operating conditions of 923 K and 3.5 MPa, a steam/carbon ratio of 5, and a space velocity of 3.5 kg/m^2 s.

One process that utilizes natural gas is designated Zero Emission Gas Power Project (ZEG) and is being led by the Institute of Gas Technology in cooperation with Christian Michelsen Research AS and Prototech AS in Norway. A brief discussion of the process may be found on the Internet, and an update on the status of the project was recently presented by Johnsen (2007). A number of candidate sorbents have been considered with Arctic dolomite, which does not require pretreatment for sulfur removal, receiving the most attention. H2 is to be used to produce electricity in a high-temperature solid oxide fuel cell with the exhaust heat used for sorbent regeneration. Electrical efficiencies from 50 % to 80 % based on the net power output (LHV) of four process configurations having varying degrees of heat integration are reported.

The other sorption-enhanced H2 production process from natural gas is the Pratt and Whitney Rocketdyne (PWR) process. It is now in the pilot stages. While few details have been released, the company claims a 90 % size reduction, 30–40 % reduction in capital costs, 5–20 % higher H2 yield, and reduced product purification requirements that will lead to a smaller PSA system. The comparisons are relative to a standard steam methane reforming process with PSA purification. Upon completion of the current pilot tests, PWR plans to construct a 5 MM scf/d commercial demonstration plant (Stewart PAE and WR, 2007, Personal Communication).

Reactivity of CaO Sorbents Throughout Cyclic Calcination–Carbonation (CC) Reactions

A critical challenge for applications of the sorption-enhanced gasification process is the activity durability (Florin and Harris 2008) of CaO sorbent. It is estimated that the CO2 capture process would not be economical unless the value of CaO conversion after 20 cycles increased to a value of at least 0.45. However, previous studies show that CaO sorbents lose activity dramatically during cyclic CC reactions, which would increase both consumption of fresh sorbents and storage of spent sorbent, consequently reduce process economic, and result in environmental problem.

Reasons that are responsible for the calcium-based sorbent reactivity loss can be summarized as: (i) Thermodynamic equilibrium limitation. Higher temperatures are favorable for H2 generation; however, increasing the temperature at a constant total pressure will limit the capture of CO2 by CaO sorbents. (ii) Tars and coke formation. Interaction between CaO and the tar and coke is expected to hamper CO2 capture (Delgado et al. 1996). There is a trade-off between the optimal temperatures for

eliminating tar and decomposing coke and maximizing CO2 capture by CaO. (iii) Sintering of sorbents. Sintering leads to a reduction in both surface area and pore volume, which in turn affects the rate and extent of gas–solid reactions. (iv) Decay in reactivity through multiple CO2 capture and release cycles. Abanades and Alvarez (2003) concluded that the decay in activity throughout CC cycles was due to a decrease in microporosity and an increase in meso-porosity. They proposed a simple equation to estimate the CaO conversion, XN, after the Nth CC cycles, claiming that values of fm = 0.77 and fw = 0.17 fit most experimental data of both previous researchers and themselves well:

$$X_N = f_m^N(1 - f_w) + f_w \tag{3}$$

In order to improve the reactivity of calcium-based sorbents, various methods have been proposed, including (i) using mild calcination conditions, (ii) steam/water hydration or addition, (iii) the use of nano-sized sorbent particles, and (iv) thermal pretreatment. Barker (1974) hypothesized that if the particle size (diameter) of CaO is smaller than the product layer thickness that may form on a single particle, then 100 % conversion could be achieved. Barker reported a conversion of 0.93 after 24 h of carbonation, maintained for 30 reaction cycles.

The use of mild calcination conditions, i.e., inert atmospheres (N2 or Ar) and low temperatures (700 °C), were reported to produce a more reactive sorbent (Hughes et al. 2004). However, it may be necessary to use steam as a diluent gas in the regenerator to lower down the CO2 partial pressure while simultaneously obtaining high-purity CO2 gases. The introduction of a water hydration step, or the utilization of steam as a "carbonation–catalyst," has been reported to enhance CO2 capture through multiple reaction cycles (Hughes et al. 2004; Kuramoto et al. 2003; Manovic and Anthony 2007). Rong et al. (2013) studied the effects of hydration temperature, steam concentration, and hydration frequency on the sorbent reactivity during 10 carbonation–calcination cycles using a pressurized thermogravimetric analyzer with reagent-grade CaCO3 used as a precursor under atmospheric pressure. In comparison to other steam reactivation strategies, such as the steam addition during the carbonation and calcination process, separate steam hydration after calcination has shown excellent reactivation performance.

In conclusion, the development of a CO2 sorbent, which is resistant to physical deterioration and maintains high chemical reactivity through multiple CO2 capture and release cycles, is the limiting step in the scale-up and commercial operation of the sorption-enhanced H2 production process.

Future Directions

Given the advantages inherent in fossil fuels, such as their availability, relatively low cost, and the existing infrastructure for delivery and distribution, they are likely to play a major role in energy and H2 production in the near to medium-term future.

However, H2 production from fossil fuels produces large CO2 emission to the atmosphere, which may diminish the environmental appeal of H2 as an ecologically clean fuel. As a result, H2 production from fossil fuels must consider the CO2 capture problem in long-term future.

Biomass is a potentially a reliable energy resource for hydrogen production. Biomass is renewable, abundant, and easy to use. Over the life cycle, net CO2 emission is nearly zero due to the photosynthesis of green plants. Although the yield of H2 is low from biomass since the hydrogen content in biomass is low to begin with (approximately 6 % vs. 25 % for methane) and the energy content is low due to the 40 % oxygen content of biomass, the thermochemical pyrolysis and gasification hydrogen production methods are economically viable and are said to become competitive with the conventional natural gas reforming method. Biological dark fermentation is also a promising hydrogen production method for commercial use in the future. With further development of these technologies, biomass will play an important role in the development of sustainable hydrogen economy.

Hydrogen production from water electrolysis has been commercially available. Regarding the CO2 emission, electricity produced from renewable resources (such as wind, solar, hydro, biomass, tidal, etc.) is favored to be used for water electrolysis. Thermochemical water decomposition is one alternative process competitive to water electrolysis. The nuclear power systems have a great potential to be integrated with H2 production from water decomposition. The Advanced High-Temperature Reactor (AHTR) concept, proposed for the US Department of Energy's Generation IV nuclear plant development program, is specifically designed for H2 production (via high-temperature water electrolysis or thermochemical cycles). Thermochemical water-splitting cycles, such as UT-3 cycle and sulfur–iodine cycle, can potentially produce higher overall energy efficiencies (around 50 %) compared to electrolysis-based systems (around 24 %). However, a major shift away from the negative public perception of nuclear energy would be necessary in order to base a long-term energy scenario on the nuclear–hydrogen option. In addition, H2 production by direct water splitting, using the solar photocatalysis route, could become favorable if conversion efficiencies were increased by a factor of 2–3. It is anticipated that the low-cost, environmentally friendly photocatalytic water splitting for hydrogen production will play an important role in the hydrogen production and contribute much to the coming hydrogen economy. However, it is still very far from practical utilization.

Sorption-enhanced H2 production with in situ CO2 capture and then CO2 sequestration in geologic formations (e.g., deep coal seams, depleted oil and gas reservoirs, and salt domes), the ocean, aquifers, terrestrial ecosystems, etc., provides a promising solution for the CO2 release during H2 production from fossil fuels. For the future development, challenges for CO2 sequestration such as bringing its cost down and understanding the reservoir options (e.g., size, permanence, and, most importantly, environmental effect) should also be paid significant attention, besides improving the CaO sorbent cyclic reactivity to be practical.

References

Abanades JC, Alvarez D (2003) Conversion limits in the reaction of CO2 with lime. Energy Fuel 17 (2):308–315

Argun H, Kargi F (2011) Bio-hydrogen production by different operational modes of dark and photo-fermentation: an overview. Int J Hydrog Energy 36(13):7443–7459

Arstad B, Prostak J, Blom R (2012) Continuous hydrogen production by sorption enhanced steam methane reforming (SE-SMR) in a circulating fluidized bed reactor: sorbent to catalyst ratio dependencies. Chem Eng J 189–190:413–421

Bailey R (2001) Projects in development Kentucky pioneer energy lima energy. Gasification Technologies

Balasubramanian B et al (1999) Hydrogen from methane in a single-step process. Chem Eng Sci 54 (15–16):3543–3552

Barelli L et al (2008) Hydrogen production through sorption-enhanced steam methane reforming and membrane technology: a review. Energy 33(4):554–570

Barker R (1974) The reactivity of calcium oxide towards carbon dioxide and its use for energy storage. J Appl Chem Biotech 24(4–5):221–227

Benemann JR (1998) Process analysis and economics of biophotolysis of water. IEA Hydrogen Program, Paris

Brun-Tsekhovoi A et al (1988) The process of catalytic steam-reforming of hydrocarbons in the presence of carbon dioxide acceptor. In: Hydrogen energy progress VII, Proceedings of the 7th world hydrogen energy conference

Calzavara Y et al (2005) Evaluation of biomass gasification in supercritical water process for hydrogen production. Energy Convers Manag 46(4):615–631

Collot A-G (2006) Matching gasification technologies to coal properties. Int J Coal Geol 65 (3–4):191–212

Delgado J, Aznar MP, Corella J (1996) Calcined dolomite, magnesite, and calcite for cleaning hot gas from a fluidized bed biomass gasifier with steam: life and usefulness. Ind Eng Chem Res 35 (10):3637–3643

Demirbas MF (2006) Hydrogen from various biomass species via pyrolysis and steam gasification processes. Energy Sources Part A 28(3):245–252

Di Carlo A et al (2010) Numerical investigation of sorption enhanced steam methane reforming process using computational fluid dynamics eulerian–eulerian code. Ind Eng Chem Res 49 (4):1561–1576

Ewan BCR, Allen RWK (2005) A figure of merit assessment of the routes to hydrogen. Int J Hydrog Energy 30(8):809–819

Fan LS, Li FX, Ramkumar S (2008) Utilization of chemical looping strategy in coal gasification processes. Particuology 6(3):131–142

Fc D, Yf Y (2006) Hydrogen production and storage technologies. Chemical Industry Press, Beijing

Fernandez JR, Abanades JC, Murillo R (2012) Modeling of sorption enhanced steam methane reforming in an adiabatic fixed bed reactor. Chem Eng Sci 84:1–11

Florin NH, Harris AT (2008) Enhanced hydrogen production from biomass with in situ carbon dioxide capture using calcium oxide sorbents. Chem Eng Sci 63(2):287–316

Fujimoto S et al (2007) A kinetic study of in situ CO2 removal gasification of woody biomass for hydrogen production. Biomass Bioenergy 31(8):556–562

Funk JE (2001) Thermochemical hydrogen production: past and present. Int J Hydrog Energy 26 (3):185–190

Gao L (2009) A study of the reaction chemistry in the production of hydrogen from coal using a novel process concept. Imperial College London

Garcia LA et al (2000) Catalytic steam reforming of bio-oils for the production of hydrogen: effects of catalyst composition. Appl Catal A Gen 201(2):225–239

Garcıa-Ibañez P, Cabanillas A, Sánchez JM (2004) Gasification of leached orujillo (olive oil waste) in a pilot plant circulating fluidised bed reactor. Preliminary results. Biomass Bioenergy 27 (2):183–194
Gorin E, Retallick WB (1963) Method for the production of hydrogen. US Patents. p. 3,108,857
Guan J et al (2007) Thermodynamic analysis of a biomass anaerobic gasification process for hydrogen production with sufficient CaO. Renew Energy 32(15):2502–2515
Guo Y, Fang W, Lin R (2005) Zhejiang daxue xuebao (gongxue ban). J Zhejiang Univ (Eng Sci) 39:538–541
Guo LJ et al (2007) Hydrogen production by biomass gasification in supercritical water: a systematic experimental and analytical study. Catal Today 129(3–4):275–286
Guo Y et al (2010) Review of catalytic supercritical water gasification for hydrogen production from biomass. Renew Sustain Energy Rev 14(1):334–343
Hallenbeck PC, Benemann JR (2002) Biological hydrogen production; fundamentals and limiting processes. Int J Hydrog Energy 27(11–12):1185–1193
Han J, Kim H (2008) The reduction and control technology of tar during biomass gasification/ pyrolysis: an overview. Renew Sustain Energy Rev 12(2):397–416
Han L et al (2010) Influence of CaO additives on wheat-straw pyrolysis as determined by TG-FTIR analysis. J Anal Appl Pyrolysis 88(2):199–206
Han L et al (2013) H2 rich gas production via pressurized fluidized bed gasification of sawdust with in situ CO2 capture. Appl Energy 109:36–43
Hanaoka T et al (2005) Hydrogen production from woody biomass by steam gasification using a CO2 sorbent. Biomass Bioenergy 28(1):63–68
Harrison DP (2008) Sorption-enhanced hydrogen production: a review. Ind Eng Chem Res 47 (17):6486–6501
Holladay JD, Wang Y, Jones E (2004) Review of developments in portable hydrogen production using microreactor technology. Chem Rev 104(10):4767–4790
Holladay JD et al (2009) An overview of hydrogen production technologies. Catal Today 139 (4):244–260
Hufton J et al (2000) Sorption enhanced reaction process (SERP) for the production of hydrogen. In: Proceedings of the 2000 US DOE hydrogen program review
Hughes RW et al (2004) Improved long-term conversion of limestone-derived sorbents for in situ capture of CO2 in a fluidized bed combustor. Ind Eng Chem Res 43(18):5529–5539
Hydrogen FC (2005) Infrastructure technologies program: multi-year research, development and demonstration plan. US Department of Energy, Energy Efficiency and Renewable Energy, Washington, DC
Jakobsen JP, Halmøy E (2009) Reactor modeling of sorption enhanced steam methane reforming. Energy Procedia 1(1):725–732
Johnsen K (2007) Sorption enhanced steam methane reforming- reactor configurations and sorbent development. In: The third international workshop on in-situ CO2 removal
Johnsen K et al (2006) Sorption-enhanced steam reforming of methane in a fluidized bed reactor with dolomite as -acceptor. Chem Eng Sci 61(4):1195–1202
Jung GY et al (2002) Hydrogen production by a new chemoheterotrophic bacterium *Citrobacter sp*. Y19. Int J Hydrog Energy 27(6):601–610
Kalinci Y, Hepbasli A, Dincer I (2009) Biomass-based hydrogen production: a review and analysis. Int J Hydrog Energy 34(21):8799–8817
Kerby RL, Ludden PW, Roberts GP (1995) Carbon monoxide-dependent growth of *Rhodospirillum rubrum*. J Bacteriol 177(8):2241–2244
Koppatz S et al (2009) H2 rich product gas by steam gasification of biomass with in situ CO2 absorption in a dual fluidized bed system of 8 MW fuel input. Fuel Process Technol 90 (7–8):914–921
Krummenacher JJ, West KN, Schmidt LD (2003) Catalytic partial oxidation of higher hydrocarbons at millisecond contact times: decane, hexadecane, and diesel fuel. J Catal 215(2):332–343

Kumar RV, Cole JA, Lyon RK (1999) Unmixed reforming: an advanced steam reforming process. In: Preprints of symposia, 218th. ACS national meeting
Kuramoto K et al (2003) Repetitive carbonation–calcination reactions of Ca-based sorbents for efficient CO2 sorption at elevated temperatures and pressures. Ind Eng Chem Res 42 (5):975–981
Levin DB, Chahine R (2010) Challenges for renewable hydrogen production from biomass. Int J Hydrog Energy 35(10):4962–4969
Li Z-S, Cai N-S (2007) Modeling of multiple cycles for sorption-enhanced steam methane reforming and sorbent regeneration in fixed bed reactor. Energy Fuel 21(5):2909–2918
Licht S (2005) Solar water splitting to generate hydrogen fuel – a photothermal electrochemical analysis. Int J Hydrog Energy 30(5):459–470
Lin SY et al (2001) Hydrogen production from hydrocarbon by integration of water-carbon reaction and carbon dioxide removal (HyPr-RING method). Energy Fuel 15(2):339–343
Loo SV, Koppejan J (2008) The handbook of biomass combustion and co-firing. Earthscan, London
Mahishi MR, Goswami DY (2007) An experimental study of hydrogen production by gasification of biomass in the presence of a sorbent. Int J Hydrog Energy 32(14):2803–2808
Manovic V, Anthony EJ (2007) Steam reactivation of spent CaO-based sorbent for multiple CO2 capture cycles. Environ Sci Technol 41(4):1420–1425
Markov SA et al (1997) Photoproduction of hydrogen by cyanobacteria under partial vacuum in batch culture or in a photobioreactor. Int J Hydrog Energy 22(5):521–524
Milne TA, Abatzoglou N, Evans RJ (1998) Biomass gasifier“ tars”: their nature, formation, and conversion. National Renewable Energy Laboratory, Golden
Minowa T, Zhen F, Ogi T (1998) Cellulose decomposition in hot-compressed water with alkali or nickel catalyst. J Supercrit Fluids 13(1–3):253–259
Mok WSL, Antal MJ (1992) Uncatalyzed solvolysis of whole biomass hemicellulose by hot compressed liquid water. Ind Eng Chem Res 31(4):1157–1161
Nawaz M, Ruby J (2001) Zero emission coal alliance project conceptual design and economics. In: 26th international technical conference on coal utilization & fuel systems, (The Clearwater Conference)
Norbeck JM et al (1996a) Hydrogen fuel for surface transportation, vol 160. SAE, Warrendale
Norbeck J et al (1996b) Hydrogen fuel for surface transportation. Society of Automotive Engineers, Warrendale
Ochoa-Fernández E et al (2007) Process design simulation of H2 production by sorption enhanced steam methane reforming: evaluation of potential CO2 acceptors. Green Chem 9(6):654–662
Padró CEG, Putsche V (1999) Survey of the economics of hydrogen technologies. National Renewable Energy Laboratory, Golden
Pfeifer C, Puchner B, Hofbauer H (2009) Comparison of dual fluidized bed steam gasification of biomass with and without selective transport of CO2. Chem Eng Sci 64(23):5073–5083
Qinhui W et al (2003) New near-zero emissions coal utilization technology with combined gasification and combustion. Power Eng 23(5):2711–2715
Reijers HTJ et al (2009a) Modeling study of the sorption-enhanced reaction process for CO2 capture. I model development and validation. Ind Eng Chem Res 48(15):6966–6974
Reijers HTJ et al (2009b) Modeling study of the sorption-enhanced reaction process for CO2 capture. II. Application to steam-methane reforming. Ind Eng Chem Res 48(15):6975–6982
Resende FLP, Savage PE (2010) Effect of metals on supercritical water gasification of cellulose and lignin. Ind Eng Chem Res 49(6):2694–2700
Rizeq R, Lyon R, Zamansky V (2001) Fuel-flexible AGC technology for H2, power, and sequestration-ready CO2. In: The proceedings of the 26th international technical conference on coal utilization & fuel systems, Clearwater
Rong N et al (2013) Steam hydration reactivation of CaO-based sorbent in cyclic carbonation/ calcination for CO2 capture. Energy Fuel 27:5332
Rostrup-Nielsen JR (1984) Catalytic steam reforming. Springer, Berlin

Shafirovich E, Varma A (2009) Underground coal gasification: a brief review of current status. Ind Eng Chem Res 48(17):7865–7875
Shen Y, Yoshikawa K (2013) Recent progresses in catalytic tar elimination during biomass gasification or pyrolysis – a review. Renew Sustain Energy Rev 21:371–392
Simell PA et al (1997) Catalytic decomposition of gasification gas tar with benzene as the model compound. Ind Eng Chem Res 36(1):42–51
Solieman AAA et al (2009) Calcium oxide for CO2 capture: operational window and efficiency penalty in sorption-enhanced steam methane reforming. Int J Greenhouse Gas Control 3 (4):393–400
Solsvik J, Jakobsen HA (2011) A numerical study of a two property catalyst/sorbent pellet design for the sorption-enhanced steam–methane reforming process: modeling complexity and parameter sensitivity study. Chem Eng J 178:407–422
Spritzer MH, Hong GT (2003) Supercritical water partial oxidation. In: Proceedings of the 2002 US DOE hydrogen program review. NREL/CP-570-30535
Sutton D, Kelleher B, Ross JRH (2001) Review of literature on catalysts for biomass gasification. Fuel Process Technol 73(3):155–173
TeGrottehuis W, King D, Brooks K (2002) Optimizing microchannel reactors by trading-off equilibrium and reaction kinetics through temperature management. In: 6th international conference on microreaction technology
Troshina O et al (2002) Production of H2 by the unicellular cyanobacterium *Gloeocapsa alpicola* CALU 743 during fermentation. Int J Hydrog Energy 27(11–12):1283–1289
Turner J et al (2008) Renewable hydrogen production. Int J Energy Res 32(5):379–407
Ueno Y, Otsuka S, Morimoto M (1996) Hydrogen production from industrial wastewater by anaerobic microflora in chemostat culture. J Ferment Bioeng 82(2):194–197
Utgikar V, Thiesen T (2006) Life cycle assessment of high temperature electrolysis for hydrogen production via nuclear energy. Int J Hydrog Energy 31(7):939–944
Wang Z et al (2006) Thermodynamic equilibrium analysis of hydrogen production by coal based on Coal/CaO/H2O gasification system. Int J Hydrog Energy 31(7):945–952
Wang Y, Chao Z, Jakobsen H (2011) Numerical study of hydrogen production by the sorption-enhanced steam methane reforming process with online CO2 capture as operated in fluidized bed reactors. Clean Techn Environ Policy 13(4):559–565
Wang Q et al (2014) Enhanced hydrogen-rich gas production from steam gasification of coal in a pressurized fluidized bed with CaO as a CO2 sorbent. Int J Hydrog Energy 39:5781
Wei LG et al (2008) Hydrogen production in steam gasification of biomass with CaO as a CO2 absorbent. Energy Fuel 22(3):1997–2004
Wilhelm DJ et al (2001) Syngas production for gas-to-liquids applications: technologies, issues and outlook. Fuel Process Technol 71(1–3):139–148
Williams R (1933) Hydrogen production. US Patents. p. 1,938,20
Wolfrum EJ, et al (2003) Biological water gas shift development. DOE hydrogen, fuel cell, and infrastructure technologies program review
Xu C et al (2010) Recent advances in catalysts for hot-gas removal of tar and NH3 from biomass gasification. Fuel 89(8):1784–1795
Yang H et al (2006) Pyrolysis of palm oil wastes for enhanced production of hydrogen rich gases. Fuel Process Technol 87(10):935–942
Yeboah Y et al (2002) Hydrogen from biomass for urban transportation. In: Proceedings of the US DOE hydrogen program review
Yu D, Aihara M, Antal MJ (1993) Hydrogen production by steam reforming glucose in supercritical water. Energy Fuel 7(5):574–577
Ziock H-J, Lackner KS, Harrison DP (2001) Zero emission coal power, a new concept. In: Proceedings of the first national conference on carbon sequestration

Low-Temperature Fuel Cell Technology for Green Energy

Scott A. Gold

Contents

S.A. Gold (✉)
Department of Chemical and Materials Engineering, University of Dayton, Dayton, OH, USA
e-mail: Scott.Gold@notes.udayton.edu

W.-Y. Chen et al. (eds.), *Handbook of Climate Change Mitigation and Adaptation*,
DOI 10.1007/978-3-319-14409-2_43

Abstract

Fuel cells convert chemical energy to electrical energy via an electrochemical reaction. They are more efficient than traditional heat engine-based power systems and can have zero or near-zero emissions during operation. A leading alternative green energy technology, fuel cells are finding applications in many areas, including transportation, portable power, and stationary power generation. These divergent uses have driven development of several different types of fuel cell technologies. A brief overview of these will be provided in this chapter; however, the focus will be on low-temperature proton exchange membrane (PEM) technologies predominant in portable power and automotive applications. Fuel cell operating principles will be reviewed, focusing on thermodynamics, efficiency, reaction kinetics, and transport phenomena in order to develop a framework for evaluating different fuel cells and comparing them with other power systems. Theoretically, much improvement in fuel cell performance is possible and is needed along with means of lowering economic costs in order for fuel cells to see more widespread use. Some of the major technical challenges in these regards are outlined along with approaches being investigated to meet these challenges. Life cycle assessment and its application to fuel cells will be discussed to evaluate environmental impacts associated with manufacturing, operation, and disposal.

Introduction to Fuel Cell Technology

Fuel cells are one of the leading alternative energy technologies for a variety of applications, including automobiles, portable electronics, and many others. These electrochemical power generators convert chemical energy to electrical energy, in a manner similar to that of batteries. Fuel is oxidized at the anode to produce electrons and mobile ions. The mobile ions pass through an electrolyte to reach the cathode, while the electrons pass through a circuit, providing electrical current power some external load before returning to the cathode. At the cathode, the mobile ions are reduced, completing the reaction. This basic description applies to the most common fuel cells for which protons or other positive ions are the mobile ions, including the most common low-temperature fuel cell, the hydrogen proton exchange membrane (PEM) fuel cell, in which hydrogen fuel is oxidized to form protons (the mobile ions) and electrons. The electrons pass through an external circuit, while the protons pass through the PEM. Oxygen (the oxidant) combines with the protons and electrons at the cathode to form water, completing the overall reaction. This process continues producing electricity so long as fuel and oxidant are supplied to the cell, whereas in a battery, the fuel and oxidant are contained in the electrode materials themselves.

There are many different varieties of fuel cells in addition to the hydrogen PEM fuel cell discussed above. These may be classified based on the type of materials used for the electrolyte, the type of fuel utilized, or typical operation temperature.

Table 1 Summary of types of fuel cells

Fuel cell type	Fuel	Mobile ion	Electrolyte	Operating temperature	Main applications
Alkaline (AFC)	Pure H_2	OH^-	KOH	50–200 °C	Space program (historical)
Proton exchange membrane (PEMFC)	Pure H_2 (tolerates CO_2)	H^+	Solid polymer (e.g., Nafion)	30–100 °C	Vehicles and mobile power
Direct methanol (DMFC), formic acid (DFAFC), and other liquid fuels	Methanol, formic acid, other alcohols	H^+	Solid polymer (e.g., Nafion)	20–90 °C	Portable electronics
Phosphoric acid (PAFC)	Pure H_2 (tolerates CO_2, ~1 % CO)	H^+	Phosphoric acid	~220 °C	~200-kW CHP systems
Molten carbonate (MCFC)	H_2, CH_4, other hydrocarbons (tolerates CO_2)	CO_3^{2-}	Lithium and potassium carbonate	~650 °C	Medium- to large-scale stationary combined heat and power (MW capacity)
Solid oxide (SOFC)	H_2, CH_4, other hydrocarbons (tolerates CO_2)	O^{2-}	Solid oxide (e.g., yttria-stabilized zirconia)	500–1,000 °C	All-size stationary combined heat and power systems (2-kW to multi-MW capacity)
Enzymatic biofuel cells	Sugars or alcohols	H^+	Solid polymer (e.g., Nafion) or biological fluid	20–40 °C	Bio-implants and energy scavenging (research)

Some of the most common varieties of fuel cell are described in Table 1. This chapter will be concerned with the most common types of low-temperature fuel cells which primarily utilize proton exchange membranes, or PEMS: hydrogen PEM fuel cells, direct methanol fuel cells (DMFCs), direct formic acid fuel cells (DFAFCs), and other direct liquid fuel cells. High-temperature technologies such as solid oxide and molten carbonate fuel cells will be covered in more detail in the next chapter as they have very different technical challenges and are being developed primarily for larger-scale power generation.

Chapter Overview

The goals of this chapter will be to provide context for the evaluation of fuel cell technology as a green energy alternative. A short history of the development of this technology will be provided, followed by a discussion of means of comparing fuel cells with other energy technologies. Technical background on the thermodynamic, reaction, and mass transfer processes occurring in a fuel cell is then provided along with a brief overview of each of the major low-temperature fuel cell technologies. A fuel cell is only one part of a total power system. Fuel storage and delivery, thermal management, and power management subsystems are among the many components of a total fuel cell power system. Key characteristics and design criteria for each of these will be reviewed. Fuel cell technology, while holding much promise, is only beginning to find its way into commercial applications. Some of the major technical challenges that are providing roadblocks to more widespread use of fuel cells will be highlighted along with a brief discussion of current research aimed at solving these problems. If only efficiency and emissions are considered, fuel cells are a truly "green" technology. Emissions are primarily water vapor and carbon dioxide, and in well-designed systems, a very high fraction of the usable energy in the fuel is converted to electricity. However, a more rigorous analysis that considers everything from mining of raw materials to final disposal is needed to compare the environmental impact of different energy technologies. Life cycle assessment of fuel cell technology will be reviewed as a means of evaluating how truly "green" fuel cell, or any technology, truly is. This chapter will conclude with some speculation on what the future might hold for fuel cell technology.

A Brief History of Fuel Cells

Sir William Grove is credited with demonstrating the first fuel cell in 1839, ironically at about the same time the first internal combustion engines were developed. For much of the next century, fuel cells essentially remained a curiosity studied by academics and hobbyists. Beginning in the 1930s, F. T. Bacon made great advances in alkaline hydrogen fuel cells (Srinivasan et al. 1999). Bacon's designs were adopted and further developed by Pratt and Whitney and later United Technologies and utilized for power generation in American space program (Srinivasan et al. 1999). Throughout the Apollo space program, alkaline fuel cells were used to provide onboard power for electrical systems. The high energy density (energy per unit weight or volume) of fuel cells made them ideal for this use where minimizing payload weight is crucial. This concern has also been one of the primary drivers of ongoing research and development of fuel cells for portable commercial electronics (e.g., laptop computers, cell phones, etc.). Since 2000, several electronics manufacturers, including Samsung, NEC, Casio, and LG, have introduced fuel cell power systems for portable electronic devices, though these have yet to reach any large markets (FCB 2003, 2005). In the 1990s, environmental and regulatory concerns as well as issues relating to the cost and supply of oil led automotive companies begin

to develop hydrogen fuel cell technology for electric vehicles in earnest. This work has begun to bear fruit as many different types of hydrogen vehicles have been introduced around the world by auto manufacturers. Iceland in particular has embraced the move toward a hydrogen economy (Oil Gas European Magazine 2001). Daimler-Benz began developing hydrogen-powered busses in the early 1980s, which are now being utilized in Australia (FCB 2004) and many cities in Europe through the Europe-wide Clean Urban Transport (CUTE) (Energy 2004). Honda has developed its FCX Concept vehicle utilizing a 100-kW hydrogen fuel cell, which began road testing in Japan in 2002 and was available for lease in 2007 in California (FCB 2007a). Similarly, both Ford and General Motors have been developing vehicles with hybrid fuel cell power system, some of which have been evaluated on North American roads (FCB 2007b). These are only a few examples of the many fuel cell vehicles under development and/or evaluation in recent years. If the progress of recent years is any indication, fuel cell technology has a very exciting future.

Fundamentals of Fuel Cell Operation

Performance Metrics for Comparing Fuel Cells and Other Energy Systems

The most obvious measures of fuel cell performance metrics include current, voltage, and power output as well as the lifetime of the cell before refueling is required. These are of somewhat limited value in comparing different fuel cells or fuel cells to other power sources however, as they are dependent on size. In comparing different fuel cells to one another, current and power should be compared on a per unit area basis. Voltage is not impacted by the area of the electrodes, but can be increased by connecting cells in series as is done in batteries. As the lifetime of a fuel reservoir is primarily dependent on the size of that reservoir, a better measure for comparing fuel cells is the fuel utilization efficiency or the fraction of fuel fed to the system that is converted to power.

The most common measures used to compare fuel cells to other energy systems are energy density and power density. These can both be measured gravimetrically (i.e., energy or power per unit mass) and volumetrically (i.e., energy or power per unit volume). Graphically, plots of energy density versus power density called Ragone plots are often utilized to compare energy sources, such as the one shown in Fig. 1. One of the more attractive features of fuel cells is that they provide a relatively high energy density. A driving factor in the development of new electronic devices is reducing size and weight. Currently, batteries comprise a large fraction of the weight of laptop and tablet computers, mobile phones, and other devices, motivating efforts to develop fuel cells for such systems. Weight reduction is also important in automotive applications, though less critical than for portable electronics. Various efficiency measurements are also utilized in comparing fuel cells to other energy systems. In general, these are based on thermodynamics; however, because of

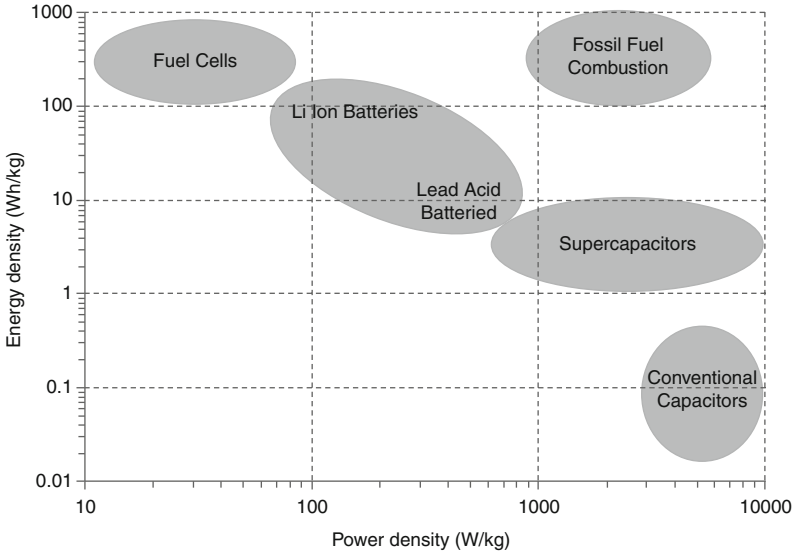

Fig. 1 A Ragone plot illustrating approximate energy and power densities of various energy technologies

fundamental differences in the mechanisms of operation, such measures often create more confusion than clarity. These measures will be discussed in greater detail later in this chapter.

Description of Basic Operation of a Fuel Cell

The hydrogen proton exchange membrane fuel cell (H_2 PEM FC) provides a chemically simple example to illustrate the fundamental principles for all types of fuel cells. In this type of cell, the hydrogen fuel is oxidized at the anode to form protons and electrons:

$$H_2 \rightarrow 2H^+ + 2e^- \tag{1}$$

An electrolyte acts to physically separate the two half-cell reactions and force the electrons to pass through a circuit where they can do electrical work before returning to the cathode while the mobile hydrogen ions pass through the electrolyte (see Fig. 2). The protons and electrons ultimately combine to reduce oxygen at the cathode and form water as a waste product:

$$\frac{1}{2}O_2 + 2H^+ + 2e^- \rightarrow H_2O \tag{2}$$

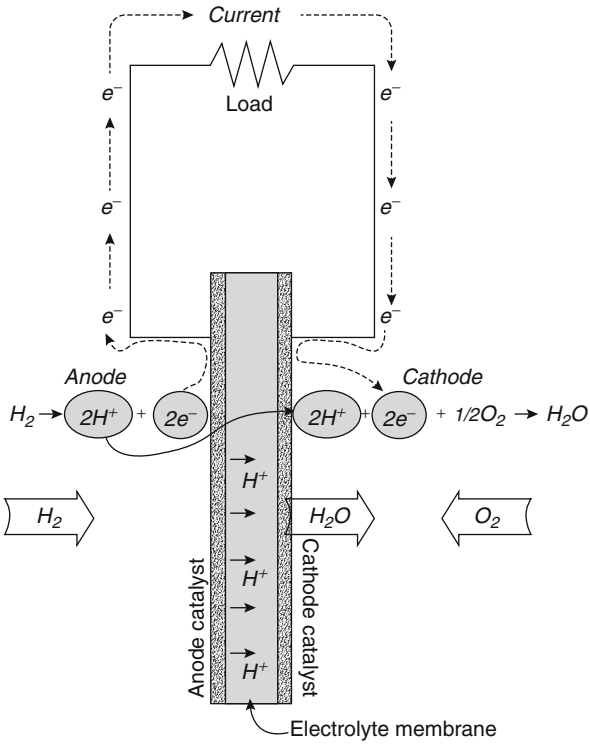

Fig. 2 Illustration of the basic operation of a hydrogen proton exchange membrane fuel cell

Thus, the overall reaction for a hydrogen fuel cell is

$$H_2 + O_2 \rightarrow H_2O \tag{3}$$

The various types of fuel cells outlined in Table 1 operate in the same general manner in that fuel is oxidized at the anode and electrons are forced through a circuit while mobile ions move through an electrolyte to combine at the cathode in a reduction reaction. They differ in the specific fuels, mobile ions, and typical operating conditions. As will become evident, each type of fuel cells has its own strengths and weaknesses, which determine the applications for which they are suitable.

In this section, some of the fundamental science and engineering principles of fuel cell operation will be reviewed, beginning with a discussion of thermodynamics in fuel cells. From thermodynamics, the maximum performance in terms of electrical potential that can be generated by a given fuel cell can be determined. This "ideal" limit also provides a means of evaluating the potential of a given fuel cell technology as well as providing important, but sometimes confusing, means of evaluating fuel cell efficiency. While thermodynamics provides theoretical limits on performance, practical limits are imposed by kinetic and transport processes. Reaction kinetics, particularly for oxygen reduction, significantly limit fuel cell performance driving

significant research to develop improved catalysts. An overview of these topics is provided in the following sections. For a more detailed discussion, the reader is referred to any of a number of fuel cell and electrochemistry texts (O'Hayre et al. 2009; Larminie and Dicks 2003; Hoogers 2003; Bockris et al. 1998; Bard and Faulkner 2001; Sawyer et al. 1995).

Thermodynamics and Efficiency

Fuel Cell Thermodynamics

For an isothermal, isobaric system, the maximum amount of work that can be done by the system is equal to the Gibbs free energy change for that system. In the case of a fuel cell, electrical work (W_{elec}) is of interest, and the Gibbs free energy change occurs as a result of the overall fuel cell reaction; thus, we can mathematically state:

$$W_{\text{elec}} = -\Delta G^0_{\text{rxn}} \tag{4}$$

where ΔG^0_{rxn} is the standard-state change in the Gibbs free energy of the reaction. The change in Gibbs free energy is related to the change in enthalpy of the reaction (H_{rxn}) by Eq. 5:

$$\Delta G = \Delta H - T\Delta S \tag{5}$$

where ΔS is the enthalpy of the reaction at absolute temperature T. The value $T\Delta S$ represents thermal energy unavailable for being converted to electrical work and places a fundamental limit on the efficiency of a given fuel cell. Electrical work is accomplished by moving charge carried by electrons through an electrical potential gradient ΔE; thus, electrical work can be expressed as the product of the total charge ($Q = nF$) and the field strength:

$$W_{\text{elec}} = \Delta EQ = nF\Delta E \tag{6}$$

where n is the number of moles of electrons produced in the fuel cell reaction and F is Faraday's constant. Combining Eqs. 4 and 6, we get ΔE_0, the maximum standard-state reversible voltage for the overall reaction in a fuel cell:

$$\Delta E^0 = -\frac{\Delta G^0_{\text{rxn}}}{nF} \tag{7}$$

Cell potential can be related to reactant and product concentrations at a given temperature by considering a general reaction of A and B to form products C and D:

$$\alpha\text{A} + \beta\text{B} \rightarrow \chi\text{C} + \delta\text{D} \tag{8}$$

The Gibbs free energy for such a reaction is familiar from basic thermodynamics as

$$\Delta G = \Delta G^0_{\text{rxn}} RT \ln\left(\frac{a_{\text{C}}^{\chi} a_{\text{D}}^{\delta}}{a_{\text{A}}^{\alpha} a_{\text{B}}^{\beta}}\right) \tag{9}$$

where a_{A}, a_{B}, a_{C}, and a_{D} are the activities of species A, B, C, and D, respectively, and R is the gas constant. The activities of course are dependent upon the physical state of the reactants or products. For an ideal gas, the activity of species i can be expressed:

$$a_i = \frac{P_i}{P^0} \tag{10}$$

where P_i is the partial pressure of species i and P^0 is the standard pressure (usually 1 atm). For an ideal solution, the activity of species i is expressed:

$$a_i = \frac{[i]}{[i]^0} \tag{11}$$

where $[i]$ and $[i]^0$ are the concentration and standard-state concentrations of species i. If the reactants and products for the generic reaction (Eq. 8) are presumed to be in an ideal solution, then Eq. 9 can be rewritten as

$$\Delta G = \Delta G^0_{\text{rxn}} RT \ln\left(\frac{[\text{C}]^{\chi}[\text{D}]^{\delta}}{[\text{A}]^{\alpha}[\text{B}]^{\beta}}\right) \tag{12}$$

Substituting Eq. 7 into Eq. 12 yields the familiar Nernst equation:

$$\Delta E = \Delta E^0 \left(\frac{RT}{nF}\right) \ln\left(\frac{[\text{C}]^{\chi}[\text{D}]^{\delta}}{[\text{A}]^{\alpha}[\text{B}]^{\beta}}\right) \tag{13}$$

relating the cell potential or emf, ΔE, to the standard-state potential and reactant concentrations at a given temperature. As this equation illustrates, the cell potential increases with the concentration of the reactants. The overall reaction in a fuel cell is of course the sum of two half-cell reactions, which often are studied separately. The total cell potential is expressed as a difference between the thermodynamic electrochemical potentials of the half-cell reactions at the cathode and anode, respectively:

$$\Delta E = E_{\text{cathode}} - E_{\text{anode}} \tag{14}$$

Thermodynamic Efficiency

As noted previously, the entropy of the overall fuel cell reaction places a fundamental limit on fuel cell efficiency. Thermodynamic efficiency is of course an important concept in evaluating fuel cells or any other system that converts energy to work. The standard definition of thermal efficiency, ε, for any system is

$$\varepsilon = \frac{W_{\text{out}}}{Q_{\text{in}}} \tag{15}$$

where W_{out} is the work done by the system and Q_{in} is the energy supplied to the system. For transportation applications where internal combustion engines are standard, it is useful to compare fuel cell efficiency to that of such heat engines. For a heat engine, the maximum efficiency is that of a reversible Carnot cycle. Applying the first law of thermodynamics to a completely reversible system requires that all thermal energy supplied to the system (Q_{in}) is either converted to work (W_{out}) or rejected to the surroundings (Q_{out}), so that Eq. 7 above can be expressed as

$$\varepsilon_{\text{Carnot}} = \frac{Q_{\text{in}} - Q_{\text{out}}}{Q_{\text{in}}} \tag{16}$$

where $\varepsilon_{\text{Carnot}}$ is the Carnot efficiency. This can also be expressed in the more familiar manner in terms of the low and high reservoir temperatures of the system:

$$\varepsilon_{\text{Carnot}} = 1 - \frac{T_{\text{low}}}{T_{\text{hi}}} \tag{17}$$

T_{hi} and T_{low} are the absolute temperatures of the respective thermal reservoirs in the heat engine. T_{low} is typically limited to the ambient temperature. As Eq. 17 illustrates, 100 % efficiency is approached as the temperature difference between the two reservoirs in a heat engine becomes very large. An internal combustion engine, however, is not a completely reversible Carnot engine. The combustion process introduces significant irreversibility to the system and serves to limit the achievable efficiency. Practical values for thermodynamic efficiency of heat engines are around 40 % (Wright 2004).

It is frequently noted that an advantage of fuel cells is that not being heat engines, they are not Carnot limited (O'Hayre et al. 2009; Larminie and Dicks 2003; Hoogers 2003). Fuel cells are often operated nearly isothermally and directly convert chemical energy to electrical work. Not surprisingly, Eqs. 16 and 17 are not valid or even meaningful for fuel cells. This does not mean that fuel cells are not thermodynamically limited as Eq. 15 above still determines the maximum thermodynamic efficiency possible. Neither should it be misunderstood that the theoretical limit of efficiency is higher for fuel cells than heat engines.

As shown in Eq. 7, the maximum amount of energy available to do work in a fuel cell is given by the Gibbs free energy of the overall fuel cell reaction, providing a limiting value for W_{out} in Eq. 15 when determining the maximum theoretical

thermodynamic efficiency of a fuel cell. It is common to assume that fuel cells are operating isothermally and in thermal equilibrium with the surroundings. Care should be taken before the latter of these assumptions is made, especially if the fuel cell operates at a temperature significantly above ambient (Haynes 2001).

The higher heating value of the fuel, or the enthalpy of combustion to a vapor phase product, ΔH_{HHV}, as shown in Eq. 18 is most commonly used for Q_{in}:

$$\varepsilon_{fC} = \frac{\Delta G_{\mathrm{rxn}}}{\Delta H_{\mathrm{HHV}}} \tag{18}$$

This is justified by the fact that fuel combustion is used to provide energy to a heat engine, thus providing a convenient means of comparison. Nonetheless, this choice presents some challenges that can lead to significant confusion. Equation 18 can also give efficiencies of greater than 100 % for some systems in which there is a positive entropy change on reaction. Lutz et al. proposed a modified solution to deal with this, noting that energy for a positive entropy change must be taken from the surroundings (Lutz et al. 2002):

$$Q_{\mathrm{in}} = \begin{cases} -\Delta H_{\mathrm{R}} & \text{if} \quad \Delta S_R \leq 0 \\ -\Delta H_{\mathrm{R}} + T\Delta S_{\mathrm{R}} & \text{if} \quad \Delta S_R < 0 \end{cases} \tag{19}$$

where ΔH_{R} and ΔS_{R} are the enthalpy and entropy of reaction, respectively.

In direct comparisons of the thermodynamic efficiencies of heat engines and fuel cells, conservation of exergy or availability, not energy, should be considered (Haynes 2001). For both an ideal fuel cell and a Carnot engine, exergy is completely conserved. However, when full systems are taken into account, the situation changes. An ideal heat engine is supplied with heat, not chemical fuel. Combustion irreversibility significantly limits the maximum efficiency of heat engine system, though not of the heat engine itself (Haynes 2001). Likewise, fuel processing and heat rejection by the fuel cell system should also be considered. A fair comparison would also use the same chemical fuel as a feed to both systems, though in practice such a situation may not be realistic.

Electrochemical Efficiency

Another measure of efficiency in fuel cells is the electrochemical efficiency, defined as the ratio of the actual cell voltage to the ideal cell voltage:

$$\varepsilon_{\mathrm{electrochem}} = \frac{\Delta E}{\Delta E^0} \tag{20}$$

The ideal potential was described previously in Eq. 6. The actual cell potential is inevitably reduced from the ideal value, due primarily to various cell polarization losses, which will be discussed in more detail later in this chapter. The primary value of this efficiency measure is in comparing fuel cells to one another. It is sometimes

referred to as the voltage or activation efficiency as it is closely related to limitations imposed by reaction kinetics, as will be discussed subsequently in this chapter.

Fuel Utilization Efficiency

Fuel utilization, mentioned previously, provides yet another type of efficiency measure for fuel cells. In practice, some fraction of the fuel supplied to a fuel cell remains unreacted. The fuel utilization efficiency can be thus defined as the ratio of the mass of fuel reacted in the cell to the mass fed to the cell:

$$\varepsilon_{\text{fuel}} = \frac{m_{\text{fuel}}^{\text{reacted}}}{m_{\text{fuel}}^{\text{fed}}} \tag{21}$$

By combining this measure with the electrochemical efficiency expressed in Eq. 20, yet another efficiency value can be defined, the total electrochemical efficiency:

$$\varepsilon_{\text{total}} = \varepsilon_{\text{fuel}} \frac{\Delta E}{\Delta E^0} \tag{22}$$

Summary

Thermodynamics are fundamental to understanding fuel cell operation. As shown above, the maximum achievable efficiency in a fuel cell is limited in that not all reaction enthalpy can be converted to work. Of course, this is true of any other type of system as well as some fraction of energy is inevitably lost to entropy. Several different measures of efficiency can be defined from thermodynamic considerations. Reported efficiency values are not always explicitly defined in the fuel cell literature, with further challenges introduced in comparing efficiency from different types of systems, requiring care on the part of anyone working with such values.

Kinetic Processes in Fuel Cells

Other limitations on fuel cell performance occur due to activation and ohmic and mass transfer effects (O'Hayre et al. 2009; Larminie and Dicks 2003; Hoogers 2003). The effect of these losses on a typical current–voltage curve for a fuel cell is shown in Fig. 3. Each of these will be described in more detail in this section.

Reaction Kinetics and Activation Polarization

Irreversible kinetic effect in the half-cell reactions of a fuel cell leads to activation losses in the observed voltage output. In terms of the current–voltage characteristic, activation losses are most evident under low current conditions. Often, the ideal open-circuit voltage is not observed due to these effects. The activation or voltage efficiency, described in Eq. 20, provides a measure of this loss term. A deeper look at the relationship between reaction kinetics and the current voltage characteristics of a

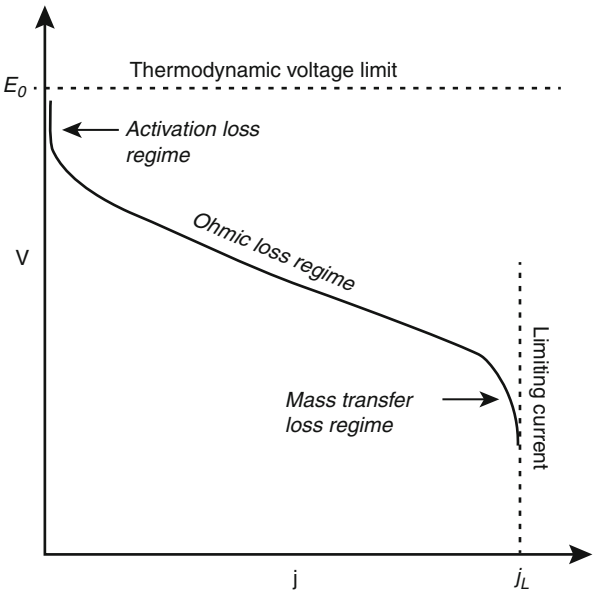

Fig. 3 Typical current–voltage characteristic curve illustrating major sources of voltage loss

fuel cell can provide some helpful insight into the source and means of preventing activation losses.

Equations 1 and 2 describe the reactions occurring at the anode and cathode of a hydrogen PEM fuel cell. More generally, an oxidation reaction where the reductant (Red) loses electrons occurs at the anode of a fuel cell:

$$\mathrm{Red} \rightarrow \mathrm{Ox} + ne^{-}, \tag{23}$$

while a reduction where the reactant, the oxidant (Ox), gains electrons occurs at the cathode:

$$\mathrm{Ox} + ne^{-} \rightarrow \mathrm{Red} \tag{24}$$

The overall reaction for a generic fuel cell can thus be expressed as

$$\mathrm{Ox} + ne^{-} \Leftrightarrow \mathrm{Red} \tag{25}$$

The activation barriers to these reactions determine the overall reaction rate, hence the rate at which electrons are generated and consumed at each electrode and how much current is supplied by the fuel cell. For simplicity, consider a single-step elementary reaction at each electrode. The rate of the half-cell reactions, R, can be expressed as

$$\begin{aligned} R_{\mathrm{Red}} &= k_{\mathrm{Red}}[\mathrm{Ox}]_{\mathrm{o}} \\ R_{\mathrm{Ox}} &= k_{\mathrm{Ox}}[\mathrm{Red}]_{\mathrm{o}} \end{aligned} \tag{26}$$

yielding a net reaction rate of

$$R = R_{\mathrm{Red}} - R_{\mathrm{Ox}} = k_{\mathrm{Red}}[\mathrm{Ox}]_{\mathrm{o}} - k_{\mathrm{Ox}}[\mathrm{Red}]_{\mathrm{o}} \tag{27}$$

where k_{Red} and k_{Ox} are the reduction and oxidation rate constants, while the [Red] and [Ox] are the surface concentrations of the reduced and oxidized species, respectively. The current density, j, at each electrode is related to reaction rate (R) by Faraday's constant for an n electron reaction:

$$j = RnF \tag{28}$$

so that the net current generated by the fuel cell is

$$j = j_{\mathrm{Red}} - j_{\mathrm{Ox}} = n\left(Fk_{\mathrm{Red}}[\mathrm{Ox}]_{\mathrm{o}} - Fk_{\mathrm{Ox}}[\mathrm{Red}]_{\mathrm{o}}\right) \tag{29}$$

The activation barriers for the anodic and cathodic reactions at the equilibrium potential can be defined as $\Delta G_{0a}^{\ddagger}$ and $\Delta G_{0c}^{\ddagger}$, respectively. In the presence of an electric field, E, the anodic activation energy for the oxidation reaction is decreased, and the cathodic activation energy for reduction increased by some fraction α of the applied field, as shown in Eqs. 30 and 31:

$$\Delta G_{a}^{\ddagger} = \Delta G_{0a}^{\ddagger} - n(1-\alpha)F\Delta\left(E - E^{0}\right) \tag{30}$$

$$\Delta G_{c}^{\ddagger} = \Delta G_{0c}^{\ddagger} + n\alpha F\Delta\left(E - E^{0}\right) \tag{31}$$

Rate constants can be expressed as a function of the Gibbs free energy of the reactions in an Arrhenius-type equation from transition state theory as

$$k_{\mathrm{Red}} = A_{\mathrm{Red}}\exp\left(\frac{-\Delta G_{\mathrm{c}}^{\ddagger}}{RT}\right) = A_{\mathrm{Red}}\exp\left(\frac{-\Delta G_{0\mathrm{c}}^{\ddagger}}{RT}\right)\exp\left(\frac{-\alpha F\left(E - E^{0}\right)}{RT}\right) \tag{32}$$

for the reduction reaction at the cathode and

$$k_{\mathrm{Ox}} = A_{\mathrm{Ox}}\exp\left(\frac{-\Delta G_{\mathrm{a}}^{\ddagger}}{RT}\right) = A_{\mathrm{Ox}}\exp\left(\frac{-\Delta G_{0\mathrm{a}}^{\ddagger}}{RT}\right)\exp\left(\frac{(1-\alpha)F\left(E - E^{0}\right)}{RT}\right) \tag{33}$$

for the oxidation reaction at the anode. At equilibrium, $E = E_0$ and the rate of the forward (reduction) and reverse (oxidation) reactions are equivalent, and the net current is zero. While the net current is zero, both half-cell reactions continue to occur and current does flow; however, the anodic and cathodic currents are equal and in opposite directions. This current is referred to as the exchange current density, j_0, defined in Eq. 34:

$$nFk_{\mathrm{Red}}^{0}[\mathrm{Ox}]_{\mathrm{o}} = nFk_{\mathrm{Ox}}^{0}[\mathrm{Red}]_{\mathrm{o}} = j_0 \tag{34}$$

Here, the standard rate constants are defined from Eqs. 35 and 36 for the case when $E = E_0$:

$$k^0_{\mathrm{Red}} = A_{\mathrm{Red}} \exp\left(\frac{-\Delta G^{\ddagger}_{0c}}{RT}\right) \tag{35}$$

and

$$k^0_{\mathrm{Ox}} = A_{\mathrm{Ox}} \exp\left(\frac{-\Delta G^{\ddagger}_{0a}}{RT}\right) \tag{36}$$

Exchange current is an indicator of catalyst activity; the more active the catalyst, the greater the exchange current. Substituting the rate constants from Eqs. 35 and 56 into Eq. 34 gives

$$j_0 = nFA_{\mathrm{Ox}} \exp\left(\frac{\Delta G^{\ddagger}_{0a}}{RT}\right)[\mathrm{Ox}]_{\mathrm{o}} = nFA_{\mathrm{Red}} \exp\left(\frac{\Delta G^{\ddagger}_{0c}}{RT}\right)[\mathrm{Red}]_{\mathrm{o}} \tag{37}$$

The Butler–Volmer equation describing the current density generated from a fuel cell is found by combining Eq. 29 with Eqs. 32, 33, and 37:

$$j = j_0 \left[\exp\left(\frac{-\alpha F\left(E - E^0\right)}{RT}\right) - \exp\left(\frac{(1-\alpha)F\left(E - E^0\right)}{RT}\right)\right] \tag{38}$$

The Butler–Volmer equation is considered one of the most important in electrochemistry and is presented with a variety of different forms with a more complete derivation in most electrochemistry and fuel cell texts (O'Hayre et al. 2009; Larminie and Dicks 2003; Hoogers 2003; Bockris et al. 1998; Bard and Faulkner 2001). The derivation presented here is only rigorously valid for a single-step reaction, though modifications can be made to account for more complex reaction mechanisms. Nonetheless, it still provides a good approximation of fuel cell kinetics and is instructive in describing key variables impacting reaction kinetics. The Tafel equation (39) describes an important limiting case of the Butler–Volmer equation for high overpotential, relating activation polarization, η_{act}, directly to the rate of an electrochemical reaction:

$$\eta_{\mathrm{act}} = E - E^0 = \left(\frac{RT}{\alpha nF}\right)\ln\left(\frac{j}{j_0}\right) \tag{39}$$

From the Butler–Volmer and Tafel equations, it is apparent that as more current is drawn from a fuel cell, a greater voltage loss is required. It also points the way toward how kinetic activity can be increased, namely, by increasing reactant

concentration, reducing the activation barrier to the reaction ($\Delta G_{0a}^{\ddagger}$), and/or increasing operating temperature (T).

Side reactions and catalyst poisoning are also important, acting to reduce the overall reaction rate in a fuel cell. Methanol and formic acid oxidations have more complex mechanisms than hydrogen oxidation, and the intermediates formed can impact reaction kinetics, in particular carbon monoxide, CO. Carbon monoxide poisoning is also an issue in hydrogen PEM fuel cells when the hydrogen comes from reformed hydrocarbons such as methane. These issues will be discussed further in the section on "Fundamentals of Fuel Cell Operation."

Charge Transport and Ohmic Losses

Ohmic losses are the result of resistance to charge transport in the system and include interconnect or electronic resistance ($R_{\text{interconnect}}$ or $R_{\text{electronic}}$) within the external circuit, contact resistances (R_{contact}) between different layers of the fuel cell associated with the transfer of electrons from the electrodes to the circuit or of ions from the electrocatalyst to the electrolyte (R_{anode} and R_{cathode}), and resistance to ionic motion in the electrolyte ($R_{\text{electrolyte}}$), illustrated in Fig. 4. The total ohmic resistance in the cell is described by Eq. 40:

$$\begin{aligned} R_{\text{ohmic}} &= R_{\text{interconnect}} + R_{\text{anode}} + R_{\text{cathode}} + R_{\text{electrolyte}} \\ &= R_{\text{electronic}} + R_{\text{contact}} + R_{\text{electrolyte}} \end{aligned} \tag{40}$$

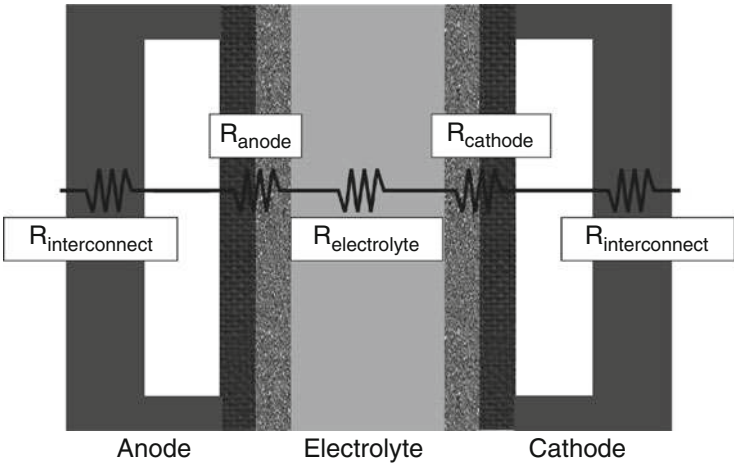

Fig. 4 Ohmic losses in a typical fuel cell result from resistances to current flow connected in series, including interconnect resistance ($R_{\text{interconnect}}$) due to the conductivity of the bipolar plate, electrode resistances (R_{cathode} and R_{anode}) in the catalyst and gas diffusion layers of the anode and cathode, respectively, and electrolyte resistance ($R_{\text{electrolyte}}$) due to the ionic conductivity of the electrolyte material

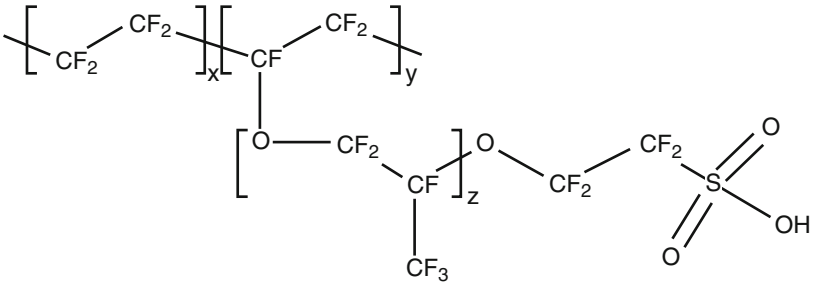

Fig. 5 Chemical structure of Nafion®

The different terms used here reflect the variation in the nomenclature found in the literature. Using Ohm's law, ohmic overpotential losses, η_{ohmic}, can be easily described:

$$\eta_{\text{ohmic}} = jR_{\text{ohmic}} \tag{41}$$

Generally, electronic transfer is rapid and contact resistance negligible, and thus have a minimal impact on fuel cell performance. The main source of ohmic loss is from the rate of ionic transport in the electrolyte. The slope of the linear region of the current–voltage plot in Fig. 3 at intermediate voltages is due largely to ohmic losses. In the presence of only an ohmic loss term, current density is directly proportional to the electric field driving the motion of the charge carrier, with the proportionality constant, σ, being the conductivity:

$$j = \sigma \frac{\mathrm{d}V}{\mathrm{d}x} \tag{42}$$

For an electrolyte of thickness L, the conductivity of interest is ionic:

$$j = \sigma_{\text{ionic}} \frac{V}{L} \tag{43}$$

Writing this expression in terms of the area of the electrolyte, we get the familiar expression for Ohm's law, where resistance is $\sigma A/L$:

$$i = \frac{A\sigma_{\text{ionic}} V}{L} = \frac{V}{R_{\text{ionic}}} \tag{44}$$

Equations 42, 43, and 44 make evident that it is desirable to maximize the ionic conductivity of the electrolyte as well as to minimize its thickness in order to minimize ohmic losses.

The most widely used electrolytes in hydrogen and other low-temperature fuel cells are solid sulfonated fluoropolymers, most notably DuPont's Nafion®, the general structure of which is illustrated in Fig. 5. Similar sulfonated fluoropolymer

membranes are marketed by 3M and Dow, among others. The fluoropolymer backbone of these materials provided a mechanically strong, chemically resistant structure, while the sulfonic acid groups lend both hydrophilicity and surface acidity that facilitate proton conduction. The performance of these membranes is a strong function of water content, with water acting as a vehicle to carry protons through the membrane (Choi et al. 2005). The phenomenon of water molecules being carried through the membrane by protons is referred to as electroosmotic drag. The production of water at the cathode in conjunction with electroosmotic drag creates a concentration gradient that leads to back diffusion of water. Total water transport is thus the sum of fluxes due to electroosmotic drag from anode to cathode and diffusion from cathode to anode (O'Hayre et al. 2009). The critical nature of water in proton transport limits the operating conditions of PEM-based fuel cells using Nafion®. At temperatures above ~80 °C and/or under conditions of low relative humidity, Nafion® can become dehydrated resulting in a loss of proton conductivity. At temperatures about ~120 °C, the polymer itself starts to degrade. As a consequence, practical operating temperatures are limited to below 80 °C, and humidification of hydrogen and airstreams is often necessary.

Mass Transfer and Concentration Polarization

In order for chemical reactions to occur at the respective electrodes, fuel and oxidant must reach the catalyst via mass transfer. Similarly, reaction products must be removed from the catalyst's surface. Under high current conditions, the fuel cell is limited by the rate of transport of fuel to the anode surface. Two regions are of interest in a fuel cell with regard to mass transport, the porous electrode surface where molecular diffusion is important and the flow field of the bipolar plate where bulk convective flow dominates.

The oxidation and reduction reactions occur at the catalyst surfaces on each respective side of the membrane electrode assembly. A concentration gradient develops as fuel and oxidant are consumed at the anode and cathode, respectively. The catalyst itself is on a support of microscale particles with nanoscale porosity; thus, diffusion is occurring both within the pores of the support and in the larger void spaces between catalyst particles. The rate of diffusive mass transfer of reactants in the catalyst layer provides a fundamental limit to fuel cell performance. Diffusive flux, J_{diff}, can be described by Fick's first law of diffusion, which for the case of steady state, one-dimensional diffusion in the x-direction in a planar catalyst layer becomes

$$J_{\text{diff}} = -D\frac{\mathrm{d}c}{\mathrm{d}x} = -D_{\text{eff}}\frac{c_R^* - c_R^0}{\delta} \tag{45}$$

where the diffusivity (D) and the concentration derivative in the x-direction ($\mathrm{d}c/\mathrm{d}x$) are expressed in terms of the surface and bulk concentrations of the reactant (c_{R}* and c_{R}^0, respectively), the effective diffusivity of the reactant in the catalyst layer (D_{eff}), and the diffusion length taken as the thickness of the catalyst layer (δ). The catalyst

layer is typically porous in order to maximize reactive surface area and on the order of 100–300-μm thick (O'Hayre et al. 2009). Effective diffusion coefficients in this layer are generally on the order of 10^{-2} cm^2 s^{-1} (O'Hayre et al. 2009). At steady state, the flux of reactants is equal to the rate of consumption of the reactant, which in turn determines the rate of current generation. The diffusion-limited current density can be related to the reactant flux using Faraday's constant:

$$j = nFJ_{\text{diff}} \tag{46}$$

Combining Eqs. 45 and 46, the current density due to diffusion can be expressed:

$$j = -nFD_{\text{eff}} \frac{c_{\text{R}}^{*} - c_{\text{R}}^{0}}{\delta} \tag{47}$$

A limiting current density, j_{L}, of the fuel cell would occur when the surface concentration reaches zero:

$$j_L = nFD_{\text{eff}} \frac{c_{\text{R}}^{0}}{\delta} \tag{48}$$

The higher j_{L} is, the greater the operating range of the fuel cell is. It is thus desirable to design catalyst layers and structures so as to minimize the diffusion length or layer thickness and to maximize the effective diffusivity. Combining the Nernst equation (Eq. 13) that describes the effect of concentration on voltage with the results described above from Fick's law yields an expression for the concentration polarization loss in a fuel cell, η_{conc}:

$$\eta_{\text{conc}} = \left(\frac{RT}{nF}\right) \ln\left(1 - \frac{j}{j_{\text{L}}}\right) \tag{49}$$

where j_{L} is the limiting current, as described by Eq. 48 where all of the reactant is consumed at the catalytic active site on the electrode surface.

The bulk concentration of reactants is determined by flow field design. Maximizing this value will also serve to maximize the limiting current as described by Eq. 48. With the exception of very small systems, most fuel cells are flow systems with multiple cells connected in series to supply sufficient voltage. In addition to collecting current from the fuel cells, flow field structures or bipolar plates serve to supply reactants to the cell through a series of channels machined into the plate. The channels may be arranged in any of a variety of complex patterns, some of the most common of which are illustrated in Fig. 6 including serpentine, parallel, and interdigitated designs. Critical dimensions of these channels are typically on the order of mm or cm. To date, no particular design enjoys consensus support as optimal. In addition to mass transfer, pressure drop and fuel utilization must also be considered in the design of flow fields, as well as material and manufacturing cost.

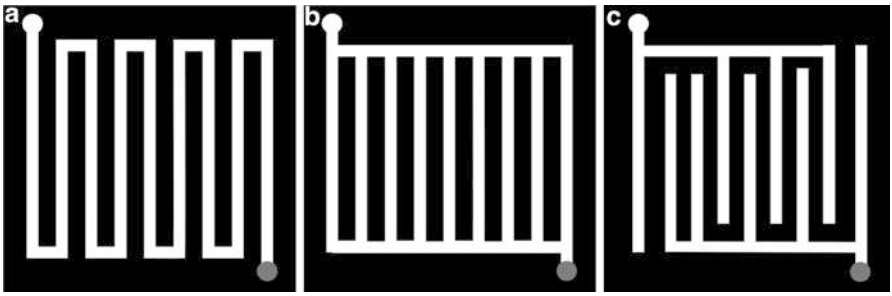

Fig. 6 Some common, simple flow field patterns, including (**a**) serpentine, (**b**) parallel, and (**c**) interdigitated channel designs

High flow rates favorable to mass transfer can result in incomplete fuel utilization and also result in a greater pressure drop, requiring more energy to move fuel and oxidant through the system. Analysis of flow field design using computational fluid dynamics continues to be an active area of fuel cell research (Nguyen et al. 2004).

Fuel Crossover Polarization

Ideally, a fuel cell electrolyte is impermeable to both fuel and oxidant. In practice, however, fuel crossover also presents challenges with Nafion, especially in direct methanol fuel cells (Heinzel and BarragÃn 1999; Jiang and Chu 2004; Neburchilov et al. 2007). Though not negligible, crossover is less of a concern in hydrogen (Cheng et al. 2007) and direct formic acid fuel cells (Rhee et al. 2003). The most obvious impact of crossover is in the reduction of fuel utilization efficiency. To quantify the effect of crossover, an internal current density, j_n, is defined:

$$j_n = v_{\text{fuel}}(nFA) \tag{50}$$

where v_{fuel} is the fuel crossover rate (mol s^{-1} cm^{-2}), n is the total number of the electrons participating in the reaction, F is Faraday's constant, and A is the area of the electrolyte membrane. Including this term in the expressions for activation and ohmic and concentration polarization losses (Eqs. 39, 41, and 49) illustrates the impact of crossover on each of these loss terms:

$$\eta_{\text{act}} = E - E^0 = \left(\frac{RT}{\alpha nF}\right)\ln\left(\frac{j + j_n}{j_0}\right) \tag{51}$$

$$\eta_{\text{ohmic}} = (j + j_n)R_{\text{ohmic}} \tag{52}$$

$$\eta_{\text{conc}} = \left(\frac{RT}{nF}\right)\ln\left(1 - \frac{j + j_n}{j_{\text{L}}}\right) \tag{53}$$

Activation overpotential can be further impacted by crossover if the fuel is oxidized at the cathode or acts as a poison to the cathode catalyst.

Summary of Electrode Polarization Effects

The major contributions to voltage loss in an operating fuel cell have been described in the preceding sections. These include activation and ohmic, concentration, and crossover polarization effects. The polarization losses at the anode and cathode are the result of activation and concentration polarization losses at each respective electrode:

$$\eta_{\text{anode}} = \eta_{\text{act},a} + \eta_{\text{conc},a} \tag{54}$$

and

$$\eta_{\text{cathode}} = \eta_{\text{act},c} + \eta_{\text{conc},c} \tag{55}$$

where activation and concentration polarization terms are described by either Eqs. 39 and 49 or Eqs. 51 and 53, depending on the relative importance of crossover. These overpotentials change the anode and cathode potentials from their theoretical values, as shown in Eqs. 56 and 57:

$$E_{\text{anode}} = E^0_{\text{anode}} + |\eta_{\text{anode}}| \tag{56}$$

and

$$E_{\text{cathode}} = E^0_{\text{cathode}} + |\eta_{\text{cathode}}| \tag{57}$$

The overall cell potential is then the difference between the cathode and anode potentials described above less ohmic polarization:

$$\Delta E_{\text{cell}} = E_{\text{cathode}} - E_{\text{anode}} - \eta_{\text{ohmic}} \tag{58}$$

where ohmic polarization is given by Eq. 40 or 52 depending on the importance of fuel crossover. Substituting Eqs. 56 and 57 into Eq. 58 yields

$$\Delta E_{\text{cell}} = \left(E^0_{\text{cathode}} - |\eta_{\text{cathode}}|\right) - \left(E^0_{\text{anode}} + |\eta_{\text{anode}}|\right) - \eta_{\text{ohmic}} \tag{59}$$

Rearranging terms and substituting the theoretical standard-state open-cell potential from Eqs. 7 and 14 yields

$$\Delta E_{\text{cell}} = \Delta E^0 - |\eta_{\text{cathode}}| - |\eta_{\text{anode}}| - \eta_{\text{ohmic}} \tag{60}$$

Equation 60 clearly illustrates how each of the polarization terms served to reduce the operating potential of a fuel cell from its theoretical maximum. Using basic concepts of thermodynamics, reaction kinetics, electrochemistry, and transport phenomena, we can see how relatively simple fundamental mathematical models of fuel cell performance can be developed, facilitating analysis of working cells, providing means of comparing research results, and enabling model-based control algorithms.

Low-Temperature Fuel Cell Technologies

One way of classifying fuel cell technologies is by the typical operating temperatures. As previously noted, this chapter will deal with low-temperature technologies. High-temperature fuel cells, including molten carbonate and solid oxide fuel cells, will be discussed in subsequent chapters. Proton exchange membrane or PEM fuel cells form the most widely studied category of fuel cells. These include hydrogen PEM fuel cells, direct alcohol cells such as the direct methanol fuel cell (DMFC), and direct formic acid fuel cells (DFAFCs). Alkaline and biological fuel cells will also be discussed briefly here, though these technologies are not currently of great importance for power generation.

PEM Fuel Cells

A key characteristic of these fuel cells is the proton exchange membrane, or PEM. The PEM is also sometimes referred to as a polymer electrolyte membrane as the most widely used materials are sulfonated perfluoropolymers such as Nafion®. This solid electrolyte serves as an electronic insulator, proton conductor, and the heart of the membrane electrode assembly, most notably for hydrogen PEM fuel cells but also for DMFCs and DFAFCs.

Hydrogen PEM Fuel Cells

In a hydrogen PEM fuel cell, hydrogen fuel is oxidized at the anode, while oxygen is reduced at the cathode in the reactions shown in Eqs. 1, 2, and 3. The mobile ion produced is the proton, H^+, with platinum on a carbon support serving as the catalyst at both the anode and cathode. The theoretical open-circuit voltage at 25 °C, assuming liquid water as the product, is 1.23 V (O'Hayre et al. 2009; Larminie and Dicks 2003; Hoogers 2003).

Hydrogen PEM fuel cells are without doubt the most widely studied and used today. This technology supplies power on NASA spacecraft and is the primary fuel cell technology being developed by the automobile industry. The low-temperature operation of hydrogen PEM fuel cells makes them suitable for portable applications as well.

Direct Alcohol Fuel Cells

Direct alcohol fuel cells utilize a proton exchange membrane in a manner similar to hydrogen PEM fuel cells. Methanol is the most common fuel for such cells (Wasmus and Küver 1999); however, significant research into ethanol has also been pursued. In these cells, protons are extracted directly from the alcohol, usually in a liquid state, at the anode. These are primarily being developed for portable power applications due to their high energy density and relative ease of fuel storage (O'Hayre et al. 2009; Larminie and Dicks 2003; Hoogers 2003).

By far, the most widely studied in this class of fuel cells is the direct methanol fuel cell, or DMFC. As the name implies, methanol is oxidized at the anode of a direct methanol fuel cell via the reaction shown below:

$$CH_3OH + H_2O \rightarrow 6H^+ + 6e^- + CO_2 \tag{61}$$

Oxygen is reduced at the cathode, similarly to a hydrogen cell:

$$\frac{3}{2}O_2 + 6H^+ + 6e^- \rightarrow 3H_2O \tag{62}$$

The overall reaction for a DMFC is then

$$CH_3OH + \frac{3}{2}O_2 \rightarrow 2H_2O + CO_2 \tag{63}$$

The theoretical open-circuit voltage of a DMFC is 1.18 V at 25 °C, though in practice, 0.6–0.8 V is more common due to kinetic limitations for both oxidation and reduction reactions. The slow oxidation kinetics are compounded by catalyst poisoning from carbon monoxide formed as an intermediate product in the oxidation mechanism (Wasmus and Küver 1999; Antolini et al. 2008). The other major limitation in DMFC performance is fuel crossover through the PEM (Heinzel and BarragÃn 1999; Jiang and Chu 2004; Neburchilov et al. 2007). This problem limits practical methanol concentrations to 1–2 M in working DMFCs. Despite these problems, DMFCs are one of the leading technologies being pursued for portable power generation.

Direct Formic Acid Fuel Cells

In recent years, direct formic acid fuel cells (DFAFCs) have emerged as a rival technology to DMFCs for portable power applications (O'Hayre et al. 2009; Yu and Pickup 2008). As the name implies, formic acid is oxidized at the anode:

$$HCOOH \rightarrow CO_2 + 2H^+ + 2e^- \tag{64}$$

As with hydrogen PEM fuel cells and DMFCs, oxygen is reduced at the cathode:

$$\frac{1}{2}O_2 + 2H^+ + 2e^- \rightarrow H_2O \tag{65}$$

The overall reaction in a DFAFC is thus

$$HCOOH + \frac{1}{2}O_2 \rightarrow H_2O + CO_2 \tag{66}$$

This cell gives a theoretical open-cell voltage of 1.48 V, much higher than that for either DMFCs or hydrogen PEM fuel cells (Yu and Pickup 2008). The leading catalysts for formic acid oxidation are palladium rather than platinum based, offering a potential cost advantage over DMFCs (Larsen et al. 2006; Liu et al. 2006a). The major drawback for formic acid is that its energy density is significantly lower than that of methanol (Yu and Pickup 2008). However, since formic acid crossover

through Nafion® is much lower than that of methanol, this problem can be compensated for by the use of higher fuel concentrations (Rhee et al. 2003; Yu and Pickup 2008). Progress with these fuel cells has been very rapid and they show much promise for the future.

Alkaline Fuel Cells

Hydrogen is utilized as the fuel in alkaline fuel cells; however, instead of protons, hydroxyl ions serve as the mobile ions in an alkaline electrolyte, most commonly potassium hydroxide. The anode and cathode reactions are given in Eqs. 67 and 68, respectively:

$$H_2 + 2OH^- \rightarrow 2H_2O + 2e^- \tag{67}$$

$$\frac{1}{2}O_2 + 2e^- + 2H_2O \rightarrow 2OH^- \tag{68}$$

Alkaline fuel cells hold a special place in fuel cell history as they were the first power systems demonstrated to be of practical use for power generation (Larminie and Dicks 2003; Perry and Fuller 2002). Francis Bacon is credited for pioneering development of these fuel cells in the 1940s and 1950s, and this technology was the one chosen by NASA to provide electrical power onboard its first spacecraft (Larminie and Dicks 2003; Perry and Fuller 2002). Alkaline fuel cells have several advantages over other fuel cell technologies, one of which is that the oxygen reduction reaction at the cathode occurs at a lower activation overvoltage than in acidic PEM fuel cells allowing the cells to operate higher voltages (up to 0.875 V) and consequently higher efficiency (O'Hayre et al. 2009; Larminie and Dicks 2003). Non-precious metal catalysts can also be utilized making these fuel cells very low in cost (O'Hayre et al. 2009; Larminie and Dicks 2003). In spite of these advantages, NASA and much of the fuel cell world began turning away from alkaline fuel cells in favor of PEM-based technology in the 1970s and 1980s, and today they receive far less research and development attention. The chief disadvantage of alkaline fuel cells is their sensitivity to CO_2, which reacts with the alkaline electrolyte to form carbonates and reduce the availability of hydroxyl ions as well as oxygen solubility in the electrolyte (O'Hayre et al. 2009; Larminie and Dicks 2003). The electrolyte must thus be sealed from the air to maintain a long cell life and very pure hydrogen must be utilized. Hydrogen reformed from hydrocarbon sources inevitably contains some degree of CO_2, which would have to be removed prior to use in an alkaline fuel cell. While this technology does have its challenges, they do not appear to be more substantially formidable than those associated with other technologies, as others have noted (Gülzow 1996; McLean et al. 2002). However, the limited research attention currently directed toward alkaline fuel cells makes it unlikely that they will surpass PEM fuel cell technology in importance or value in the near future.

Enzymatic and Other Biofuel Cells

Biological fuel cells utilize enzymes (either alone or with a microorganism) to catalyze the electrochemical reactions in a fuel cell (Bullen et al. 2006; Shukla et al. 2004; Barton et al. 2004; Heller 2004). As such, their operation is limited to conditions where the organisms can survive and/or the enzymes can remain stable and not denature, typically nearly neutral pH and from around 20–40 °C. Typical fuels include sugars and simple alcohols. A key advantage of these is their inherent selectivity as enzymes typically only catalyze very specific substrates. This selectivity, however, comes at a price as it is the result of a complex protein matrix surrounding the active center of a given enzyme where the reaction occurs. While conferring great selectivity on the enzyme, this matrix also serves in effect as an electrical insulator, reducing the transduction efficiency of electrons produced at the active center to an electrode where it can be collected. Poor transduction efficiency also plagues microbial fuel cells. Probably the greatest challenge associated with enzymatic fuel cells is the poor stability of the enzymes themselves. Currently, practical lifetimes of enzymatic fuel cells are limited to days or weeks as the enzymes denature in a working cell. Biofuel cells are not currently nor are they expected to be of major importance for power generation; however, they do have potential for some niche applications such as energy scavenging, biosensors, and in vivo power generation (Bullen et al. 2006; Shukla et al. 2004; Barton et al. 2004; Heller 2004).

Fuel Cell Systems

The fuel cell or fuel cell stack in and of itself is only part of a full power system. Specific requirements vary widely depending on the type of fuel cell and the application; however, several other systems and components are often necessary. These might include fuel delivery and fuel processing systems, thermal management systems, and power management systems (O'Hayre et al. 2009). These systems add cost to the total system and utilize a fraction of the energy produced. Accounting for these is important not just in cost and performance calculations but also in evaluating the environmental impact of a fuel cell.

Membrane Electrode Assembly, Flow Field, and Fuel Cell Stack

At the heart of a fuel cell is the membrane electrode assembly or MEA. This consists of up to five layers including the proton exchange membrane at the center, anode and cathode electrocatalyst layers on either side of the membrane, and gas diffusion layers, illustrated in Fig. 7. The proton exchange membrane is most commonly Nafion®, a perfluorocarbon polymer manufactured by DuPont. Gas diffusion layers are most commonly made from carbon paper or carbon fabric. The catalyst, most commonly platinum based, may or may not be supported on a high-surface area ($>75\ m^2\ g^{-1}$) conductive carbon support. Whether supported or pure metal, the

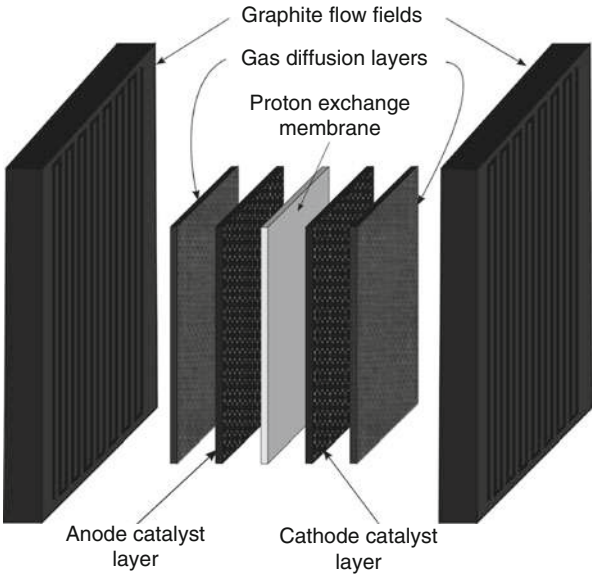

Fig. 7 Layers of a typical membrane electrode assembly and flow field

catalyst is used to make an ink with an appropriate solvent. Typically, a small amount of Nafion® is added to the catalyst ink. The ink may be applied to the proton exchange membrane or the gas diffusion layer via screen printing, spraying, ink-jet, or some similar technique (Ralph and Hogarth 2002). The layers are then bonded together, typically by hot pressing (Ralph and Hogarth 2002).

The MEA is in turn sandwiched between flow field plates which, often referred to as bipolar plates, also serve as current collectors. These are typically machined from graphite and contain flow channels to supply fuel and oxidant to the anode and cathode, respectively. As noted previously, a single fuel cell can supply a maximum, open-cell voltage of around 1 V, depending on the specific type of fuel cell being used. Practical operating voltages are usually around 0.6–0.7 V, where power output is maximized. Most applications, however, require anywhere from a few volts to several hundred volts. For this reason, fuel cells are commonly connected in series in vertical stack where a flow field plate serves as the anode for one cell and cathode for a neighboring cell, hence the name bipolar plate. Using a fuel cell stack in this manner allows the voltage requirements of any given application to be met.

Fuel Processing, Storage, and Delivery

One of the more challenging aspects of fuel cell design is providing fuel to the cell. The approach to solving this problem depends in large part on the type of fuel cell being employed and the needs of the target application. The approach to this design challenge has a major impact on the energy density of the overall fuel cell system. Trends in hydrogen storage research will be discussed in the subsequent section on "Hydrogen Storage."

Probably the simplest solution to the problem of fuel storage and delivery is that of liquid-powered fuel cells where the fuel is directly electrooxidized, such as in direct methanol and direct formic acid fuel cells. These types of fuel cells are of interest primarily for small-scale, portable power systems. While such fuels have high energy densities, kinetic and transport limitations limit fuel cell performance, imposed in part by the fuel delivery systems. For small-scale fuel cells, a passive fuel delivery system may be employed, placing the fuel reservoir in direct contact with the anode or using gravity, surface tension, evaporation, or a similar mechanism to supply fuel to the cell or stack. Such an approach helps to minimize the weight of the total system allowing a high system energy density to be achieved; however, it also can lead to mass transfer limitations. The use of a passive fuel delivery system is typically only sufficient for the smallest of fuel cells.

There are several fuel storage options for hydrogen PEM fuel cells. The most notable of these are direct hydrogen storage in the form of a compressed gas or cryogenic liquid, storage in the form of chemical hydrides, and the use of a hydrogen carrier such as methane or ammonia. Each of these involves a very different balance of plant requirements, as will be discussed below.

Current hydrogen vehicles utilize compressed hydrogen gas tanks for fuel storage. This approach is arguably the simplest and most straightforward. Tank pressures of up to 700 bar can currently be achieved. The safety of a high-pressure, explosive gas presents a significant concern in such systems. To safely maintain such high pressures requires the use of a heavy storage tank, as well as protective measures for lines, valves, regulators, etc. This weight dramatically reduces the overall energy density of the system, which has driven research efforts toward an alternative hydrogen storage methodology. Additionally, a significant amount of energy must be expended to pressurize the hydrogen. For fuel delivery, the pressure of the tank can in most cases provide a sufficient driving force to move hydrogen through the fuel cell stack. Liquid hydrogen presents similar, though magnified, challenges as even more energy is required to cool and liquefy the hydrogen and the cost and weight of a vacuum insulated storage tank are large.

One alternative approach to hydrogen storage and delivery that has attracted much attention is the use of solid-state, metal, or chemical hydrides or hydrogen adsorbents. Generally, these materials release hydrogen as they are heated; thus, thermal management is critical for a fuel delivery system using these materials. The hydrogen supplied in this manner can be extremely clean, lacking the performance-degrading impurities such as CO that are found in hydrogen obtained from hydrocarbons. There are still many challenges associated with solid-state hydrogen storage materials, including the need to further increase hydrogen capacity and to reduce the energy required for recharging the materials with hydrogen after use. To date, the use of these materials is still confined primarily to the research laboratory.

The use of hydrogen carriers provides another alternative for hydrogen storage and delivery in fuel cell systems. Common hydrogen carriers in fuel cell systems include organic hydrocarbons such as methane, methanol, formic acid, and even gasoline as well as inorganic compounds such as sodium borohydride and ammonia. These are attractive for many applications in that they provide greater gravimetric

and volumetric energy densities than hydrogen itself. They are also typically easier to store and transport, and often a supply chain infrastructure already exists for them. It should be noted that hydrogen gas is not naturally occurring and is most commonly derived from methane, natural gas, or some other source industrially. Hydrogen carriers are generally not able to be used directly by a fuel cell. Instead, they must be reformed or chemically processed to yield hydrogen. The need for fuel reforming or a fuel processing subsystem generally limits this hydrogen storage and delivery methodology to stationary power generation applications. Fuel reforming systems have an added advantage in that they can often be configured to run with multiple hydrogen carriers providing fuel flexibility.

Reforming of hydrogen carriers may occur internally within the fuel cell stack or more likely external to the fuel cell in a separate reforming subsystem. In either case, the carrier is chemically converted to hydrogen and by-products via a chemical reaction before it can be utilized by the fuel cell to provide power. Design goals for a fuel processing system include minimizing energy required by the system as well as the amount of impurities and pollutants produced (particularly CO and other catalyst poisons) and maximizing the hydrogen yield from the system. A common figure of merit for comparing different fuel sources is the carrier system effectiveness, defined as the ratio of the percentage of energy in the carrier converted to electricity to the percentage of energy in pure hydrogen converted to electricity in the same fuel cell. Care should be taken in using this or any other measure comparing fuel cell performance as often such calculations are reported based upon the fuel only, neglecting the energy used in the fuel processing step or other system components.

When using a hydrogen carrier, the required fuel processing subsystem is often extremely complex, which is why such systems are primarily of interest only for larger, stationary power systems. The major components of such a system include a fuel reformer or similar reactor to convert the carrier to hydrogen and by-products, a water gas shift reactor to increase the hydrogen to carbon monoxide ratio, and a hydrogen cleanup unit to remove carbon monoxide and any other impurities that may poison fuel cell catalysts or must otherwise be removed.

There are three common reforming reaction types for hydrocarbons: steam reforming, partial oxidation, and autothermal reforming. Operating temperatures for these reactions range from 600 to 1,000 °C depending on the fuel and type of process. Steam reforming involves the endothermic reaction of the hydrocarbon with steam, as the name implies:

$$\mathrm{C}_x\mathrm{H}_y + x\mathrm{H}_2\mathrm{O}(g) \Leftrightarrow x\mathrm{CO} + \left(\frac{1}{2}y + x\right)\mathrm{H}_2 \rightarrow \mathrm{CO}, \mathrm{CO}_2\mathrm{H}_2, \mathrm{H}_2\mathrm{O} \tag{69}$$

The endothermic reaction makes thermal management challenging in steam reforming reactors. This approach provides the highest hydrogen yield but also the least fuel flexibility. A generic partial oxidation reaction of a hydrocarbon is shown in Eq. 70:

$$C_xH_y\frac{1}{2}xO_2 \Leftrightarrow xCO + \frac{1}{2}yH_2 \tag{70}$$

Unlike steam reforming, this reaction is exothermic, simplifying thermal management and allowing for faster reactor start-up, though at a higher operating temperature. Partial oxidation provides a greater degree of fuel flexibility than steam reforming. Unfortunately, this approach to reforming provides the lowest hydrogen yield as well as the highest degree of pollutant emissions. Autothermal reforming combines aspects of both steam reforming and partial oxidation, as shown in the generic reaction for the process:

$$C_xH_y + zH_2O(g) + \left(x - \frac{1}{2}\right)O_2 \Leftrightarrow xCO + \left(z + \frac{1}{2}y\right)H_2 \rightarrow CO, CO_2H_2, H_2O \tag{71}$$

As both exothermic and endothermic reactions are combined in a single process, thermal management is somewhat simplified eliminating the need for heat exchangers and allowing a physically smaller system to be constructed. However, a more complex control system design is necessitated. Hydrogen yield from autothermal reforming is greater than with partial oxidation, though not as high as with steam reforming.

An alternative to reforming hydrocarbon fuels is production of hydrogen from solid carbonaceous material (e.g., coal) via gasification or from biomass through anaerobic digestion. A generic gasification reaction is shown in Eq. 72:

$$C + aO_2 + bH_2O \Leftrightarrow cCO_2 + dCO + eH_2 + \text{other species} \tag{72}$$

The full mechanism involves several elementary steps and varies depending on the carbon source. As with reforming, reaction temperatures are high, ranging from 700 °C to 1,400 °C. Common polluting by-products include sulfur and nitrogen oxides. Anaerobic digestion is attractive from an environmental standpoint in that it utilizes renewable biomass such as sewage, livestock waste (i.e., manure), plant matter, or food processing waste as the hydrogen carrier. Through a series of chemical reactions facilitated by bacteria, the biomass is converted to methane, CO_2, and subsequently to hydrogen. By-products include CO and CO_2 as well as hydrogen sulfide.

The hydrogen gas produced in the reforming, gasification, or anaerobic digestion stage cannot be fed directly to a fuel cell as it also contains by-products, notably carbon monoxide, which can poison fuel cell catalysts. Most hydrogen PEM fuel cell catalysts can withstand CO concentration levels no greater than about 100 ppm. Two processes are typically employed to clean up this hydrogen gas stream before it is sent to the fuel cell, a water gas shift reactor followed by a chemical separation/cleanup process. The reversible water gas shift reaction

$$CO + H_2O \Leftrightarrow CO_2 + H_2 \tag{73}$$

describes an equilibrium between water vapor and carbon monoxide with hydrogen and carbon dioxide. The goal in utilizing such a reaction is to maximize the hydrogen to carbon monoxide ratio in the product stream. Typically, CO content can be reduced to 0.2–1.0 mol% in this way.

The final cleanup of the hydrogen stream can be accomplished using any of several methods or a combination of methods. Chemically, selective methanation or selective oxidation of CO can be utilized. Unfortunately, both of these reactions also consume some amount of hydrogen. Physical separation processes, including adsorption and membrane processes, can also be employed. Adsorbents such as high-surface area carbon, silica, and zeolites can provide a great deal of selectivity and also consume very little power in an operating separation system. Palladium–silver alloy membranes can also be used as hydrogen diffuses through a membrane at a faster rate than other species.

Thermal Management

Not all energy from the fuel cell reactions is converted to electricity; some is lost as heat. A thermal management system serves to dissipate this heat in order to control the operating temperature of the fuel cell. The degree of thermal management required varies depending on the size and type of fuel cell system. For small portable systems, passive thermal management relying on natural convection is often sufficient as the amount of heat produced is small. However, for larger systems producing on the order of 100 W or more, significant heat can be produced, overheating the cell and/or creating significant thermal gradients. In such cases, active cooling is necessary. A common approach is to utilized forced convection with a fan, blower, or pump pushing air or cooling fluid through additional cooling channels within the bipolar plates. Liquid coolants with their high heat capacity are commonly used in automotive fuel cells. Liquid coolants create additional challenges in system design as their larger pressure drop requires greater energy to pump them through the system, and unlike ambient air, they are necessarily in limited supply onboard the system and must be recycled. A key figure of merit for an active thermal management system design is its effectiveness ratio, defined as the ratio of the heat removal rate to the electrical power consumption rate. The goal of system design is thus to minimize power consumed by fans, blowers, or pumps moving the cooling media through the system while maximizing the rate of heat dissipation. Typical values of effectiveness ratios for well-designed systems range from ~20 to 40 (O'Hayre et al. 2009). For systems that include a high-temperature fuel reformer and/or an afterburner to combust unused hydrogen leaving the fuel cell, employment of a heat recovery mechanism is necessary to maximize the overall efficiency of the system. Using one or more heat exchangers, heat emitted from the fuel cell or an afterburner that combusts unused hydrogen leaving the fuel cell can be used to supply energy to a fuel reforming subsystem.

Power Management

Power management is critical for any fuel cell-based power system and typically includes electrical circuitry for four tasks: (1) power regulation, (2) power inversion, (3) monitoring and control, and (4) power supply management (O'Hayre et al. 2009; Larminie and Dicks 2003). The power supplied by a fuel cell is not stable as the voltage varies with current load, environmental conditions (temperature, humidity, etc.), and other factors. Typically, DC/DC converters are utilized to convert fuel cell voltage output to a stable, specified value, forming the main component of a power regulation system. The DC power produced by the cell, however, must be converted to AC for many applications, such as supplying power to AC motors used in electric vehicles and other AC electric devices that traditionally might be powered from the electric grid. Power inversion serves to convert DC power to AC power. The total fuel cell system is essentially an electrochemical processing plant. Process monitoring tools such as thermocouple and pressure gauges provide inputs to feedback control loops. The process controls serve to adjust variables such as fuel feed flow rate and coolant flow rate in response to perturbations in the system to maintain steady performance of the system as a whole. Finally, power supply management is necessary to deal with rapid changes in load requirements. For example, a typical car would require ~25 kW of power on average, but as much as 120 kW at peak (e.g., during rapid acceleration). Fuel cells have a relatively slow response to rapid changes in power demands, on the order of seconds to hundreds of seconds, as pumps, compressors, and other components must respond in order for the power output to begin to change. Batteries and supercapacitors are the main components of the power supply management systems, acting as energy buffers to reduce response time to the order of milliseconds.

Technical Challenges and Current Research

Many technical challenges remain to be overcome if fuel cells are to be competitive both in terms of performance and economics with currently dominant technologies. The biggest of these are hydrogen storage, catalysis, electrolyte membrane, and bipolar plate materials. An overview of these issues will be provided here. References cited should provide a good starting point for the reader interested in a more in-depth study of these topics.

Hydrogen Storage

For automotive and other mobile applications, storage of hydrogen is one of the greatest technical challenges for fuel cell technology. High-pressure and cryogenic hydrogen storage, while conceptually simple, has an assortment of problems. An ideal hydrogen storage technology would have both high gravimetric and volumetric hydrogen density, be stable at temperature up to 50 °C, enable rapid delivery of

Table 2 Summary of DOE hydrogen storage goals

	2010	2015
Gravimetric system energy density (net useful energy/maximum system mass)	1.5 kW h kg^{-1}	3 kW h kg^{-1}
	6 wt% H_2	9 wt% H_2
Volumetric system energy density (net useful energy/maximum system volume)	1.5 kW h L^{-1}	2.7 kW h L^{-1}
	0.045 kg H_2 L^{-1}	0.081 kg H_2 L^{-1}
Storage system cost	4 $/kW·h net	2 $/kW·h net

hydrogen to the fuel cell, and be capable of being regenerated. The US Department of Energy has set targets in this regard as part of a National Hydrogen Energy Roadmap, some of which are summarized in Table 2 (US Department of Energy 2002). It should be noted that these targets are for hydrogen storage systems, not hydrogen storage materials. A number of materials are capable of meeting energy density goals, if only the material is accounted for.

Hydrocarbon materials meet DOE targets, but reforming of these fuels to produce hydrogen also yields CO_2 and catalyst-poisoning CO in addition to H_2. The reforming process is also energy intensive. As previously noted, this approach is generally seen as promising only for stationary power generation.

Solid-state hydrogen storage materials are currently a major research focus in fuel cell technology (US Department of Energy 2002; Hubert 2005; Züttel 2004). In general, solid-state hydrogen storage solutions can be grouped into two categories: hydrogen physisorption systems and chemical hydrides. The majority absorbents investigated for hydrogen physisorption are either various forms of carbon (e.g., graphene and carbon nanotubes) (Shiraishi et al. 2004; Thomas 2007; Yamanaka et al. 2004) or metal organic frameworks (Thomas 2007; Panella and Hirscher 2005), though these are certainly not the only materials under investigation. The advantages of physisorption systems are their low cost, simple design, and ability to adsorb hydrogen at low pressures (Züttel 2004). However, to date no absorbent material has been able to meet the DOE hydrogen density goals, much less system the hydrogen density goals for a full system. Further, they typically desorb hydrogen at near or slightly above room temperature, making them unattractive for many practical applications (Züttel 2004). Nonetheless, this approach continues to be widely investigated, and some new adsorbents, in particular metal organic frameworks, show promise.

Among the most promising solid hydrogen storage materials are metal and complex chemical hydrides. Metal hydrides of interest involve the lightest metals, such as Li, Be, Na, Mg, B, and Al, in order to meet hydrogen density goals (Züttel 2004; Van Den Berg and Areán 2008; Sakintuna et al. 2007). Some examples include $LiAlH_4$, $LiBH_4$, $LiNH_2$, $NaAlH_4$, $NaBH_4$, and MgH_2, among many, many others (Züttel 2004; Van Den Berg and Areán 2008; Sakintuna et al. 2007). Some of these advanced hydride materials can meet hydrogen density goals, but present a host of other system challenges. Many of these hydrides are unstable to the point of

explosion in the presence of air and/or water, requiring that they be sealed in a working system. Typically, hydrides are heated to release hydrogen, often in a highly exothermic reaction, leading to sintering of material; also there is typically a volume change on hydrogen discharge (Schüth et al. 2004). Heavier metals may be added to the system in small quantities as a catalyst to enhance dehydrogenation kinetics. Ball milling and other processes to create small particles, even nanostructured materials, are also commonly utilized as a means of enhancing reaction kinetics in metal hydrides (Bérubé et al. 2007). Rehydrogenation is accomplished by placing the used material in a pressurized hydrogen atmosphere, typically requiring an excessive amount of energy (Van Den Berg and Areán 2008; Sakintuna et al. 2007).

Among the most promising hydrogen storage materials are the chemical hydrides ammonia borane (NH_3BH_3) and related compounds (Stephens et al. 2007; Marder 2007). Ammonia borane (AB) is a stable power in air and readily soluble in a number of common solvents. Hydrogen is released in a three-stage process, shown below, with a 6.5 wt% hydrogen yield in the first stage, 13.1 wt% in the second, and 19.6 wt % in the third. A rehydrogenation process has not been perfected, but progress has been made on this front, and the reactions involved are all thermodynamically favorable (Hausdorf et al. 2008). As with the metal hydrides, improving reaction kinetics is a challenge as is the volume change on reaction. Enhanced kinetics have been observed with a number of metal catalysts as well as with ammonia borane incorporated into mesoporous matrices. A slightly acidic environment has been observed to considerably enhance dehydrogenation of AB.

Catalysis

Anode and cathode reactions in low-temperature fuel cells require catalysts to achieve reaction rates sufficient for fuel cells to be practical. Leading catalysts for fuel cells are based on expensive, precious metals such as platinum, palladium, and ruthenium. Sufficient progress has been made to reduce metal loading to the point that catalysts are often no longer the largest cost contributor to fuel cell systems. However, should fuel cell technology become more widespread, this may change as increasing demand for catalyst metals would be expected to drive up prices. The largest fraction of the environmental impact of fuel cell technology remains in the mining, processing, and transport of the catalyst material.

From a performance standpoint, the greatest activation losses occur at the cathode of hydrogen fuel cells in the oxygen reduction reaction. Not surprisingly, this is the focus of significant research and development efforts (Wang 2005). The complex mechanism of oxygen reduction provides insight into some of the challenges. The desired pathway for the reaction is the direct oxygen reduction shown in Eq. 74:

$$\frac{1}{2}O_2 + 2H^+ + 2e^- \rightarrow H_2O \tag{74}$$

However, the formation of hydrogen peroxide

$$O_2 + 2H^+ + 2e^- \rightarrow H_2O_2 \tag{75}$$

and various platinum oxides

$$Pt + H_2O \rightarrow PtO + 2H^+ + 2e^- \tag{76}$$

occurring at standard potentials of 0.68 and 0.88 V versus NHE at 25 °C, respectively, contributes to a reduction in the open-circuit voltage in the cell. The most active catalysts for oxygen reduction are platinum alloys, containing predominantly platinum (∼75 wt%, metal basis) (Ralph and Hogarth 2002). The stability of the alloy in contact with the acidic membrane surface is a key factor that must be considered, as the base metal in the alloy can dissolve into the membrane (Ralph and Hogarth 2002). Alloys that showed both high activity and stability included Pt–Cr, Pt–Zr, and Pt–Ti (Ralph and Hogarth 2002). Hydrogen peroxide produced at the cathode can also impact catalyst stability, especially for non-platinum catalysts (Lefévre and Dodelet 2003).

The considerable cost of platinum has also spurred research into cheaper catalyst materials (Wang 2005) though to date none has been found with sufficient activity and stability to supplant the platinum alloys. Iron- and cobalt-based catalysts have shown some promise, particularly in porphyrins and in the presence of pyrrole and pyridine structures (Feng and Alonso-Vante 2008; Bezerra et al. 2008). Metal-free carbon catalysts doped with nitrogen or nitrogen and boron have drawn considerable attention of late (Ikeda et al. 2008; Gong et al. 2009). Nitrogen appears to have some beneficial effect in each of these types of catalyst, though the mechanism is still a subject of investigation (Ikeda et al. 2008). Though the activity of these alternative catalysts is still not as good as that of platinum, the lower cost could justify their use in some applications.

A number of metals will catalyze the hydrogen oxidation reaction, though platinum is the most active. Activation losses at the anode of hydrogen fuel cells are generally quite small. The primary focus of research on hydrogen oxidation catalysis is related to poison resistance. Hydrogen is most commonly derived from natural gas reforming, which inevitably results in the formation of not only hydrogen but also CO and CO_2. CO in particular is a notorious catalyst poison (Camara et al. 2002). The most widely studied CO-resistant catalysts are Pt–Ru alloys, though others have been examined (Wee and Lee 2006).

Unlike with hydrogen oxidation, significant activation losses are associated with both the methanol and formic acid oxidation reactions in DMFCs and DFAFCs, respectively. Methanol oxidation catalysis research has been recently reviewed by several authors (Wasmus and Küver 1999; Wee and Lee 2006). As with hydrogen oxidation, improving resistance to carbon monoxide poisoning is one of the major challenges in improving methanol oxidation catalysts, though it is more critical as CO is formed through the electrooxidation reaction mechanism itself rather than appearing as an impurity in the fuel.

The electrooxidation of methanol occurs predominantly through an indirect pathway that is initiated by the adsorption of methanol (CH_3OH_{ad}) onto the catalyst,

a step that requires three to four adjacent metal atom sites arranged triangularly on the catalyst surface (Neurock et al. 2008):

$$CH_2OH \rightarrow CH_2OH_{ad} \tag{77}$$

This is followed by dehydrogenation of the adsorbed methanol on the surface of the catalyst, forming carbon monoxide (CO_{ad}) as a strongly adsorbed reaction intermediate (O'Hayre et al. 2009; Larminie and Andrew 2003; Parsons and VanderNoot 1988; Hogarth and Ralph 2002):

$$CH_2OH_{ad} \rightarrow CO_{ad} + 4H^+ + 4e^- \tag{78}$$

Subsequently, an activated hydroxyl, OH_{ad}, or similar activated hydrous intermediate is required for complete oxidation of the adsorbed carbon monoxide (O'Hayre et al. 2009; Neurock et al. 2008; Larminie and Andrew 2003; Parsons and VanderNoot 1988). The formation of this OH_{ad} species

$$H_2O_{ad} \rightarrow OH_{ad} + H^+ + e^- \tag{79}$$

is the rate-determining step for the overall methanol electrooxidation reaction. In the presence of the activated OH_{ad} complex, CO_{ad} is oxidized to carbon dioxide (CO_2), the final reaction product:

$$CO_{ad} + OH_{ad} \rightarrow H^+ + e^- + CO_2 \tag{80}$$

Summing Eqs. 78, 79, and 80 gives the overall electrooxidation reaction for methanol, shown previously in Eq. 61, which produces six protons and electrons per methanol molecule reacted. Platinum has the highest reactivity of any pure metal catalyst and is the predominant catalyst used for this reaction (O'Hayre et al. 2009; Parsons and VanderNoot 1988). Unfortunately, the rate-determining step for methanol electrooxidation, the dissociation of water to form an adsorbed active hydroxyl described in Eq. 79, occurs at well above the desired operation fuel cell anode voltages, requiring an overpotential greater than 0.6 V versus a reversible hydrogen electrode (RHE), well above the thermodynamic methanol electrooxidation potential of 0.03 V (O'Hayre et al. 2009; Neurock et al. 2008). Minimizing the overpotential required for active hydroxyl formation is key to improving anode electrocatalyst performance in DMFCs. The same challenge applies to improving CO tolerance in hydrogen oxidation catalysts.

Bimetallic Pt–Ru catalysts are the most widely used for enhancing CO tolerance for both hydrogen and methanol electrooxidation (O'Hayre et al. 2009; Wee and Lee 2006; Hogarth and Ralph 2002; Liu et al. 2006b). The overpotential required for the oxidation of water on Ru surfaces is significantly lower than on platinum at ~0.3 V versus RHE. While improving performance overall, ruthenium creates some additional problems with regard to its stability in a fuel cell environment (Piela et al. 2004) and high cost. The instability of multimetallic electrodes in general is

of concern due to metal dissolution in the acidic fuel cell environment and at excursion potentials typically experienced during start/stop cycling. Dissolved ruthenium from the anode has been shown to diffuse through the membrane and adsorb onto the cathode catalyst surface, negatively impacting the oxygen reduction reaction. Elimination of these problems and further improvement of the water electrooxidation overpotential limitation continue to drive research into alternative catalysts. A wide range of bimetallics and trimetallics combining platinum with an oxophilic cocatalyst have been explored (Hogarth and Ralph 2002; Liu et al. 2006b). In most cases, the mode of enhancement is via an electrocatalytic bifunctional mechanism, although some are thought to additionally experience to a lesser degree a ligand effect, reducing the strength of the Pt surface bond to the CO_{ad} reaction intermediate. Both enhancement mechanisms have been found in Pt–Ru catalysts. An interesting alternative to purely metallic catalysts, several groups have examined metal oxides as cocatalysts with platinum. These are believed to increase the availability of activated hydroxyl species for the bifunctional pathway through oxygen vacancies in the metal oxide structure (Bai et al. 2005; Song et al. 2008).

Formic acid oxidation catalysis has also drawn much attention in recent years, and the resulting reduction in activation losses has dramatically increased interest in direct formic acid fuel cells as an alternative to direct methanol cells (Yu and Pickup 2008). The best catalysts to date have been found to be Pd- and PdV-based materials (Yu and Pickup 2008; Larsen et al. 2006; Liu et al. 2006a). Resistance to CO poisoning is also a challenge with formic acid electrooxidation, though much less so than in methanol electrooxidation. Formic acid electrooxidation may proceed through one of three pathways: (1) through a formate intermediate

$$\mathrm{HCOOH} \rightarrow \mathrm{HCOO_{ad}} + \mathrm{H^+} + e^- \rightarrow \mathrm{CO_2} + \mathrm{H^+} + e^-; \tag{81}$$

(2) a direct pathway, shown above as Eq. 64; and (3) an indirect pathway through an adsorbed CO intermediate as seen in methanol electrooxidation

$$\mathrm{HCOOH} \rightarrow \mathrm{CO_{ad}} + \mathrm{H_2O} \tag{82}$$

where adsorbed CO is subsequently oxidized as illustrated in Eqs. 79 and 80 (Neurock et al. 2008). Poisoning due to impurities in formic acid, namely, acetic acid and methyl formate, has been shown to be a problem (Yu and Pickup 2008).

Electrolyte Membranes

The drawbacks of Nafion® and related ionomers have led to numerous efforts to develop new proton-conducting membrane materials. The greatest technical challenges associated with Nafion® and other related sulfonated fluoropolymers are poor performance at elevated temperatures and low humidity levels. The need for water as part of the proton conduction mechanism results in a practical limit of ~80 °C for the operating temperature in Nafion®-based fuel cells and leads to the requirement

that hydrogen and oxygen streams in hydrogen PEMS be humidified. Excessive methanol crossover is also a problem when using Nafion® in DMFCs. These shortcomings have led to innumerable efforts to develop alternative membrane materials. The characteristics of an ideal fuel cell membrane are outlined in Table 3. The relative importance of each of these is highly dependent on the application. For example, cost is of somewhat less importance for fuel cells targeting portable power applications as the cost per watt hour of current battery technologies remains quite high. Conversely, cost requirements are of great concern in automotive applications. One of the chief motivations for using fuel cells for portable power is to take advantage of their high theoretical energy density; therefore, it is desirable to utilize the highest fuel concentrations possible in these typically liquid-fed cells. The importance of resistance to fuel crossover is magnified by this desire to operate at high fuel concentrations, while the use of aqueous liquid fuels makes water retention concerns of much less significance. Despite much effort, sulfonated perfluoropolymer materials remain dominant for all PEM-type fuel cells today. Still, it is reasonable to expect that different classes of materials may eventually emerge from this ongoing research.

Several reviews of these efforts have been published recently (Hogarth et al. 2005; Kerres et al. 2003; Alberti and Casciola 2003; Kerres 2001; Knauth and Tuller 2002). New membrane materials that have been reported in the literature can be very broadly classified into four main groups: new ionomers, solubilized acids in a polymer matrix, composites of ionomers and insoluble solids, and inorganic solid acids and their composites. A significant number of ionomers have been investigated, the majority being sulfonated aromatic polymers and sulfonated fluorocarbons and perfluorocarbons with similar chemical functionality to Nafion®. Notable examples of the former include sulfonated polyetheretherketone (SPEEK) and sulfonated polyetherketone (SPEK). These have the advantage of low cost but tend to be less chemically and mechanically stable than sulfonated perfluorocarbons and do not provide significant advantages in proton conductivity (Kerres et al. 2003; Kerres 2001). Another approach has been to incorporate soluble acid species, most commonly a mineral acid such as phosphoric or sulfuric acid or a low molecular weight amphoter such as imidazole or pyrazole (Hogarth et al. 2005; Alberti and Casciola 2003; Kerres 2001). Examples of this approach include polybenzimidazole

Table 3 Summary of the ideal characteristics of an ideal proton exchange membrane. The relative importance of these is highly dependent upon the specific application

Ideal proton exchange membrane characteristics
High proton conductivity
Low electronic conductivity
Thermal stability
Water retention in dry environments
Low permeability to fuel
Low electroosmotic drag coefficient
Good mechanical properties
Chemical stability
Low cost

(PBI)/phosphoric acid membranes. The main problem with this approach is the tendency of the acid or amphoter to diffuse or leach out of the membrane (Hogarth et al. 2005; Alberti and Casciola 2003; Kerres 2001).

One of the most widely pursued approaches has been the development of composites of ionomers (most commonly Nafion® or SPEEK) and insoluble solid materials. This approach has shown promise, yielding moderate improvement in proton conductivity and water retention in comparison with ionomers alone (Hogarth et al. 2005; Alberti and Casciola 2001, 2003; Wang et al. 2002). The solids incorporated in these composites are typically chosen for their hydrophilicity and/or surface acidity and are most commonly incorporated as nanoparticles. Materials that have been incorporated into composites with Nafion® and/or SPEEK include alumina, silica, titania, zirconium phosphate, zirconia, and many others (Hogarth et al. 2005; Alberti and Casciola 2001, 2003; Arico et al. 2005). It has been speculated that proton conduction in ionomers with added ceramic nanoparticles is enhanced by proton transport along the surfaces of the nanoparticles (Hogarth et al. 2005; Alberti and Casciola 2001, 2003 Arico et al. 2005). The majority of the observed improvement is most likely due to increased water retention in these membranes (Hogarth et al. 2005; Arico et al. 2005). The perfluorocarbon backbone of Nafion® and related materials adds a degree of hydrophobicity contributing to their poor ability to retain water (Zawodzinski et al. 1993a, b). The addition of ceramic nanoparticles has been observed to enhance water retention in those membranes (Alberti and Casciola 2001, 2003; Arico et al. 2005), allowing the membranes to be effective at higher temperatures and lower relative humidity than ambient conditions.

Porous materials have been the subject of several recent studies, being used primarily as structural components in a PEM. One of the most notable examples of this approach is the GORE® membrane in which the pores of a porous Teflon® membrane are filled with Nafion® (Kerres 2001). Several other studies have utilized porous silicon, filling the pores with Nafion® and other ionomeric materials with some success. In a similar vein, porous alumina has been filled with solid acid materials for use as a PEM (Bocchetta et al. 2004; Park et al. 2004). Recent work has demonstrated that porous ceramics themselves may be viable as potential PEM materials. While metal oxides, clays, and other ceramics exhibit bulk proton conductivities several orders of magnitude lower than that of Nafion®, a fact which has led many to dismiss such materials from consideration as potential PEM materials, surface proton conductivities of these materials have been observed to approach or exceed that of Nafion® at the same temperatures (Vichi et al. 1999). A major advantage of ceramic materials is that they can readily be fabricated into very thin films; thus, the total proton conduction rate can be very rapid even if the conductivity of the material is low. This can be of particular value in microscale fuel cells being investigated for providing onboard power for computer chips, sensors, and similar small devices (Gold et al. 2004).

Recent work examining high-surface area, nanoporous metal oxide membranes has sought to take advantage of this rapid surface conduction, demonstrating membrane proton conductivities within less than an order of magnitude of Nafion® at

comparable temperatures (Vichi et al. 1999; Ioroi et al. 2004; Colomer and Anderson 2001). Thin, nanoporous metal oxide membranes have most commonly been formed by casting via a sol–gel process followed by a heat treatment to sinter the nanoparticles. Proton transport in such membranes at low temperatures is believed to be dominated by a surface mechanism. Anderson et al. when studying xerogel membranes of SiO_2, TiO_2, and Al_2O_3 noted that the proton conductivity of all three materials increased with temperature, but no correlation was found with water content of the ambient air (Vichi et al. 1999). The surface hydrophilicity of these materials combined with very large surface tensions in nanoscale pores should strongly enhance water retention and likely contribute to the observation of no correlation between proton conductivity and ambient humidity (Vichi et al. 1999). A strong correlation of proton conductivity with surface acidity was however seen (Vichi et al. 1999).

Bipolar Plate Materials and Manufacturing

Bipolar plates or flow fields are one of the largest contributors to the cost of fuel cell systems, contributing as much as a third of the total cost in some systems (Bar-On et al. 2002; Hermann et al. 2005; Cunningham and Baird 2006). Ideal materials for bipolar plate should be thermally and electrically conductive; chemically compatible with other fuel cell materials, reactants, and products; low in weight and volume; and mechanically strong enough to maintain high gas pressures when sealed (O'Hayre et al. 2009). The great challenge is finding materials that simultaneously meet performance requirements and can be easily and cheaply manufactured.

Graphite is most commonly used; however, its brittleness, porosity, and high cost of machining have led to research efforts to develop numerous alternatives. The brittleness and porosity of the material require relatively thick plates to be used, increasing the weight of the system. The difficulty and expense of machining graphite, however, present the greatest problem with using graphite for bipolar plates. Various metals have been suggested as alternative bipolar plate materials, including stainless steel, titanium, and aluminum (Tawfik et al. 2007). Machining costs remain a problem with metals; however, corrosion in a fuel cell environment provides the greatest barrier viability as the oxides of most metals are insulators. A number of different promising coatings to increase corrosion resistance of metal bipolar plates have been and continue to be studied (Tawfik et al. 2007).

Carbon/carbon materials have shown excellent performance properties as bipolar plates. These are manufactured by preforming a plate from a carbon fiber or graphite composite with phenolic resin. After the plate is formed, chemical vapor impregnation (CVI) is used to deposit carbon in the pores of the material providing a hermetic seal. The CVI process provides the main drawback of carbon/carbon materials as it utilizes methane as the carbon source and requires temperatures of 1,400–1,500 °C as well as long processing times (Cunningham et al. 2007). Warping of the material is also a common problem associated with the CVI process (Cunningham et al. 2007).

Polymer composites represent the most widely studied and promising alternative bipolar plate materials (Cho et al. 2004; Heinzel et al. 2004; Scholta et al. 1999; Kuan et al. 2004). Their chief advantage lies in the low-cost, rapid manufacturing techniques that can be employed, such as injection molding for thermoplastic composites and compression molding for thermoset composites (Cunningham and Baird 2006). Typical composites contain between 60 and 80 wt% graphite to supply sufficient electrical conductivity (Cunningham and Baird 2006). To enhance mechanical strength, small amounts of carbon or glass fiber are often added. Nonetheless, poor mechanical properties are the primary disadvantage of polymer composite bipolar plates (Cunningham and Baird 2006).

How Green Is My Fuel Cell or Life Cycle Analysis

Fuel cells offer many potential advantages, many of which have been highlighted here already, including very high thermodynamic efficiencies without directly using fossil fuels. While these are indicators of an environmentally friendly alternative energy technology, they can be deceiving. Life cycle assessment provides a means of systematically analyzing the environmental impact of energy systems or any device over the lifetime of that device, from raw materials to final disposal (Ayres 1995). This process goes by several different names, including life cycle analysis, cradle-to-grave analysis, and ecobalance. Procedures for this process are codified as part of the ISO 14000 environmental management standards (Finkbeiner et al. 2006). Life cycle analysis for fuel cells would involve both direct economic costs associated with the manufacturing and use of the fuel cell and environmental costs to society. While the process is useful and necessary, it is also complicated by a host of uncertainties associated with estimating each of these items and even determining what items to include. Some of these challenges have been reviewed recently by Reap et al. (2008a, b). Because fuel cells, as well as other energy technologies, are constantly evolving, it is important that life cycle assessment be a continual process, which will inevitably require some degree of forecasting until the technology matures (Pehnt 2003). Any change in the materials used or the manufacturing processes will impact the overall environmental impact.

Several life cycle assessment studies relating to fuel cells, especially for automotive applications, have been published in recent years which illustrate some of the challenges involved. As one might expect, the longer the lifetime of the fuel cell or any technology is, the less important the impact of the manufacturing process is. The manufacturing process for fuel cells is thus less important in long-lifetime cells used for stationary power generation than it is in cells used for transportation with shorter lifetimes (Pehnt 2003). Fuel cells offer definite environmental advantages in operation when compared to combustion engines. The impact of the manufacturing process, however, reduces this advantage significantly. A life cycle assessment of fuel cell manufacturing process by Pehnt compared impact of manufacturing to fuel cell use, accounting for production of graphite for the flow field, platinum mining and refining, and membrane production (Pehnt 2001). The biggest environmental

impacts were found to be from platinum metal production for catalyst; thus, recycling of these is important in minimizing environmental impact (Pehnt 2001).

If only economic factors are considered, fuel cells cannot yet compete with gasoline or hybrid gasoline/electric vehicles (Jeong and Oh 2002). However, Ogden et al. (2004) evaluating several different automotive engine and fuel technologies (hydrogen, internal combustion/hybrid, Diesel, Fischer–Tropsch liquids, etc.) concluded that hydrogen fuel cell vehicles offered the lowest "societal life cycle cost," which included vehicle first cost (assuming large-scale mass production), fuel costs (assuming a fully developed fuel infrastructure), externality costs for oil supply security, and damage costs for emissions of air pollutants and greenhouse gases calculated over the full fuel cycle. The assumptions employed here are a topic of some debate and an illustration of the challenges involved in life cycle analysis. It is likely that solid-state hydrogen would be supplied in the form of a replicable fuel cartridge or something similar.

Future Directions

The major technical challenges have been reviewed on the preceding pages, including hydrogen storage, catalysis, electrolyte membrane materials, and bipolar plate materials and manufacturing, among others. Progress in solving these technical challenges will certainly play a large role in determining the role of fuel cells in meeting future energy needs. In addition to progress on meeting technical challenges, the future of fuel cell technology and energy technology in general depends strongly on complex economic, political, and social factors. In order to achieve widespread use, fuel cells must be at a minimum cost competitive, though ideally offering a cost advantage, in comparison with the current dominant technology in a given market. Historically, interest in fuel cells and other alternative energy technologies has corresponded strongly with the price of oil and gasoline. Some have expressed concerns lithium prices may go up considerably as the use of advanced batteries becomes more widespread.

Beyond market considerations, energy prices are heavily impacted by government policies and geopolitical considerations. The world's largest oil reserves are also located in some of most politically volatile regions. Other energy technologies, including green technologies, are subject to such forces as well. Lithium used in advanced batteries is currently plentiful, but many of the world's largest reserves of this material are also found in volatile regions of the world. Fuel taxes, environmental regulations, and, in the USA, CAFE (corporate average fuel economy) standards are among the many governmental policies that impact the prices paid by consumers for energy. Research and development progress is also impacted by government funding priorities. For example, NASA's use of fuel cells in spacecraft beginning in the 1960s provided a major impetus to research and development efforts (Srinivasan et al. 1999). Some governments have also invested in green public transportation, including the use of hydrogen fuel cell-powered busses in Australia, Iceland, and the European Union (Oil Gas European Magazine 2001; FCB 2004; Energy 2004). In

2009, the Obama administration moved to eliminate Department of Energy funding for hydrogen fuel cell research, though this was ultimately restored by the Congress. Subsidies and rebates in various forms are also a way in which green energy technologies of one type or another have been advanced by governments.

Economically, it is reasonable to expect small-scale fuel cells for portable power applications to be the first to achieve widespread market penetration, likely in the very near future. Fuel cells can already produce power at costs per W/h close to those of current advanced battery technologies which dominate such markets. The importance of weight, volume, and lifetime in this market also provides a potential advantage to fuel cells with their high energy densities and the lack of a need for lengthy recharging cycles. Advances made for fuel cells in this market should help improve competitiveness of fuel cells in other markets, such as the automotive industry.

Though several major automotive companies are actively developing fuel cell vehicles, it will likely be some time before fuel cell vehicles become common on roadways, barring significant changes in economic conditions. Fuel cells and other electric vehicle technologies offer benefits in terms of lower emissions and fossil fuel usage, but are not currently cost competitive. Fuel cell vehicles currently in public use benefit from significant government subsidies. The key to fuel cell vehicles becoming a major force in the marketplace will be reducing their cost relative to internal combustion engines and competing electric vehicle technologies. Key technical challenges that impact the cost of fuel cells are discussed in the section on "Technical Challenges and Current Research" on the preceding pages. An additional challenge is posed by the need to develop infrastructure to support such vehicles. Currently, only a handful of hydrogen fueling stations exist in the USA, concentrated in California. Long term, it is likely that hydrogen will be stored in a solid-state form, as discussed in the section on "Hydrogen Storage." The nature of the infrastructure necessary to support vehicles using solid hydrogen storage materials is unclear.

Conclusion

Fuel cell technologies are among of the most promising green energy technologies for a number of applications. Their high energy density makes them a very attractive alternative to batteries for portable power applications. Unlike batteries, they need not be recharged, merely refueled. These characteristics along with having little or no emissions during operation and their high efficiency make fuel cell promising for transportation and stationary power generation.

That fuel cells are efficient and have minimal emissions should not be taken to mean they have no environmental impact. Fundamental thermodynamic considerations place a limit on the possible performance of a fuel cell, as they do with any energy technology. Kinetic and transport-related issues place practical limits on fuel cell performance. From life cycle analysis, however, it is found that the primary environmental impact of fuel cells occurs during manufacturing.

Fuel cell systems range from the very simple passive microscale and miniature power applications to complex stationary power systems. Subsystems making up the balance of plant, including fuel processing and delivery, thermal management, and power management, reduce the overall energy density of the system and add to the environmental impact of the overall system, requiring careful design.

There are currently only a few niche applications where fuel cells are widely used, though this can be expected to change in the near future. Many companies are actively developing fuel cells for an array of applications. The first to market will likely be for portable electronics. Automotive fuel cells are seeing use in public transportation and in some prototype vehicles, though it will likely be longer before roadways are filled with such vehicles. Improvement in the technology and its cost competitiveness is still needed in a number of areas for fuel cells to reach their full potential. Nonetheless, a number of indicators point to a hydrogen-based economy sometime in the future.

References

Alberti G, Casciola M (2001) Solid state protonic conductors, present main applications and future prospects. Solid State Ion 145:3–16

Alberti G, Casciola M (2003) Composite membranes for medium-temperature PEM fuel cells. Annu Rev Mater Res 33:129–154

Antolini E, Lopes T, Gonzalez ER (2008) An overview of platinum-based catalysts as methanol-resistant oxygen reduction materials for direct methanol fuel cells. J Alloys Compd 461:253–262

Arico AS, Bruce P, Scrosati B, Tarascon J-M, van Schalkwijk W (2005) Nanostructured materials for advanced energy conversion and storage devices. Nat Mater 4:366–377

Ayres RU (1995) Life cycle analysis: a critique. Resour Conserv Recycl 14:199–223

Bai Y, Wu J, Xi J, Wang J, Zhu W, Chen L, Qiu X (2005) Electrochemical oxidation of ethanol on Pt-ZrO_2/C catalyst. Electrochem Commun 7:1087–1090

Bard AJ, Faulkner LR (2001) Electrochemical methods: fundamentals and applications, 2nd edn. Wiley, New York

Bar-On I, Kirchain R, Roth R (2002) Technical cost analysis for PEM fuel cells. J Power Sources 109:71–75

Barton SC, Gallaway J, Atanassov P (2004) Enzymatic biofuel cells for implantable and microscale devices. Chem Rev 104:4867–4886

Bérubé V, Radtke G, Dresselhaus M, Chen G (2007) Size effects on the hydrogen storage properties of nanostructured metal hydrides: a review. Int J Energy Res 31:637–663

Bezerra CWB, Zhang L, Lee K, Liu H, Marques ALB, Marques EP, Wang H, Zhang J (2008) A review of Fe-N/C and Co-N/C catalysts for the oxygen reduction reaction. Electrochim Acta 53:4937–4951

Bocchetta P, Chiavarotti G, Masi R, Sunseri C, Di Quarto F (2004) Nanoporous alumina membranes filled with solid acid for thin film fuel cells at intermediate temperatures. Electrochem Commun 6:923–928

Bockris JOM, Reddy AKN, Gamboa-Aldeco M (1998) Modern electrochemistry 2A: fundamentals of electrodics, 2nd edn. Kluwer/Plenum, New York

Bullen RA, Arnot TC, Lakeman JB, Walsh FC (2006) Biofuel cells and their development. Biosens Bioelectron 21:2015–2045

Camara GA, Ticianelli EA, Mukerjee S, Lee SJ, McBreen J (2002) The CO poisoning mechanism of the hydrogen oxidation reaction in proton exchange membrane fuel cells. J Electrochem Soc 149:A748
Cheng X, Zhang J, Tang Y, Song C, Shen J, Song D (2007) Hydrogen crossover in high-temperature PEM fuel cells. J Power Sources 167:25–31
Cho EA, Jeon US, Ha HY, Hong SA, Oh IH (2004) Characteristics of composite bipolar plates for polymer electrolyte membrane fuel cells. J Power Sources 125:178–182
Choi P, Jalani NH, Datta R (2005) Thermodynamics and proton transport in Nafion. II. Proton diffusion mechanisms and conductivity. J Electrochem Soc 152:E123–E130
Colomer MT, Anderson MA (2001) High porosity silica xerogels prepared by a particulate sol–gel route: pore structure and proton conductivity. J Non Cryst Solids 290:93–104
Cunningham B, Baird DG (2006) The development of economical bipolar plates for fuel cells. J Mater Chem 16:4385–4388
Cunningham BD, Huang J, Baird DG (2007) Review of materials and processing methods used in the production of bipolar plates for fuel cells. Int Mater Rev 52:1–13
Energy World (2004) Zero-emission fuel cell buses for 10 European cities. Energy World 18
FCB (2003) NEC unveils fully integrated fuel cell notebook PC. Fuel Cells Bull 2003(8):1
FCB (2004) In brief: fuel cell buses operational in Perth. Fuel Cells Bull 7
FCB (2005) LG Chem commercializes portable fuel cell. Fuel Cells Bull 2005:5
FCB (2007a) Honda to start leasing fuel cell cars in US. Fuel Cell Bull 2007:6
FCB (2007b) In brief: ford, GM focused on contrasting records for their FCVs. Fuel Cell Bull 2007:11
Feng Y, Alonso-Vante N (2008) Nonprecious metal catalysts for the molecular oxygen-reduction reaction. Phys Status Solidi B 245:1792–1806
Finkbeiner M, Inaba A, Tan RBH, Christiansen K, Klüppel HJ (2006) The new international standards for life cycle assessment: ISO 14040 and ISO 14044. Int J Life Cycle Assess 11:80–85
Gold S, Chu K-L, Lu C, Shannon MA, Masel RI (2004) Acid loaded porous silicon as a proton exchange membrane for micro-fuel cells. J Power Sources 135:198–203
Gong K, Du F, Xia Z, Durstock M, Dai L (2009) Nitrogen-doped carbon nanotube arrays with high electrocatalytic activity for oxygen reduction. Science 323:760–764
Gülzow E (1996) Alkaline fuel cells: a critical view. J Power Sources 61:99–104
Hausdorf S, Baitalow F, Wolf G, Mertens FORL (2008) A procedure for the regeneration of ammonia borane from BNH-waste products. Int J Hydrog Energy 33:608–614
Haynes C (2001) Clarifying reversible efficiency misconceptions of high temperature fuel cells in relation to reversible heat engines. J Power Sources 92:199–203
Heinzel A, BarragÃn VM (1999) Review of the state-of-the-art of the methanol crossover in direct methanol fuel cells. J Power Sources 84:70–74
Heinzel A, Mahlendorf F, Niemzig O, Kreuz C (2004) Injection moulded low cost bipolar plates for PEM fuel cells. J Power Sources 131:35–40
Heller A (2004) Miniature biofuel cells. Phys Chem Chem Phys 6:209–216
Hermann A, Chaudhuri T, Spagnol P (2005) Bipolar plates for PEM fuel cells: a review. Int J Hydrog Energy 30:1297–1302
Hogarth MP, Ralph TR (2002) Catalysis for low temperature fuel cells. Part III: challenges for the direct methanol fuel cell. Platin Met Rev 46:146–164
Hogarth WHJ, Diniz da Costa JC, Lu GQ (2005) Solid acid membranes for high temperature (>140°C) proton exchange membrane fuel cells. J Power Sources 142:223–237
Hoogers G (2003) Fuel cell technology handbook. CRC Press, Boca Raton
Hubert M (2005) The grand challenge: hydrogen storage. Fuel Cell 5:20–22
Ikeda T, Boero M, Huang SF, Terakura K, Oshima M, Ozaki JI (2008) Carbon alloy catalysts: active sites for oxygen reduction reaction. J Phys Chem C 112:14706–14709
Ioroi T, Kuraoka K, Yasuda K, Yazawa T, Miyazaki Y (2004) Surface-modified nanopore glass membrane as electrolyte for DMFCs. Electrochem Solid-State Lett 7:A394–A396

Jeong KS, Oh BS (2002) Fuel economy and life-cycle cost analysis of a fuel cell hybrid vehicle. J Power Sources 105:58–65
Jiang R, Chu D (2004) Comparative studies of methanol crossover and cell performance for a DMFC. J Electrochem Soc 151:A69–A76
Kerres JA (2001) Development of ionomer membranes for fuel cells. J Membr Sci 185:3–27
Kerres J, Hein M, Zhang W, Graf S, Nicoloso N (2003) Development of new blend membranes for polymer electrolyte fuel cell applications. J New Mater Electrochem Syst 6:223–229
Knauth P, Tuller HL (2002) Solid-state ionics: roots, status, and future prospects. J Am Ceram Soc 85:1654–1680
Kuan HC, Ma CCM, Chen KH, Chen SM (2004) Preparation, electrical, mechanical and thermal properties of composite bipolar plate for a fuel cell. J Power Sources 134:7–17
Larminie J, Dicks A (2003) Fuel cell systems explained. Wiley, Hoboken
Larsen R, Ha S, Zakzeski J, Masel RI (2006) Unusually active palladium-based catalysts for the electrooxidation of formic acid. J Power Sources 157:78–84
Lefévre M, Dodelet JP (2003) Fe-based catalysts for the reduction of oxygen in polymer electrolyte membrane fuel cell conditions: determination of the amount of peroxide released during electroreduction and its influence on the stability of the catalysts. Electrochim Acta 48:2749–2760
Liu Z, Hong L, Tham MP, Lim TH, Jiang H (2006a) Nanostructured Pt/C and Pd/C catalysts for direct formic acid fuel cells. J Power Sources 161:831–835
Liu H, Song C, Zhang L, Zhang J, Wang H, Wilkinson DP (2006b) A review of anode catalysis in the direct methanol fuel cell. J Power Sources 155:95–110
Lutz AE, Larson RS, Keller JO (2002) Thermodynamic comparison of fuel cells to the Carnot cycle. Int J Hydrog Energy 27:1103–1111
Marder TB (2007) Will we soon be fueling our automobiles with ammonia-borane? Angew Chem Int Ed 46:8116–8118
McLean GF, Niet T, Prince-Richard S, Djilali N (2002) An assessment of alkaline fuel cell technology. Int J Hydrog Energy 27:507–526
Neburchilov V, Martin J, Wang H, Zhang J (2007) A review of polymer electrolyte membranes for direct methanol fuel cells. J Power Sources 169:221–238
Neurock M, Janik M, Wieckowski A (2008) A first principles comparison of the mechanism and site requirements for the electrocatalytic oxidation of methanol and formic acid over Pt. Faraday Discuss 140:363–378
Nguyen PT, Berning T, Djilali N (2004) Computational model of a PEM fuel cell with serpentine gas flow channels. J Power Sources 130:149–157
Ogden JM, Williams RH, Larson ED (2004) Societal lifecycle costs of cars with alternative fuels/engines. Energy Policy 32:7–27
O'Hayre R, Cha S-W, Colella W, Prinz FB (2009) Fuel cell fundamentals, 2nd edn. Wiley, Hoboken
Oil Gas European Magazine (2001) On road to world's first hydrogen economy. Oil Gas Eur Mag 27:9
Panella B, Hirscher M (2005) Hydrogen physisorption in metal-organic porous crystals. Adv Mater 17:538–541
Park Y-I, Nagai M, Kim J-D, Kobayashi K (2004) Inorganic proton-conducting gel glass/porous alumina nanocomposite. J Power Sources 137:175–182
Parsons R, VanderNoot T (1988) The oxidation of small organic molecules. A survey of recent fuel cell related research. J Electroanal Chem 257:9–45
Pehnt M (2001) Life-cycle assessment of fuel cell stacks. Int J Hydrog Energy 26:91–101
Pehnt M (2003) Assessing future energy and transport systems: the case of fuel cells. Part I: methodological aspects. Int J Life Cycle Assess 8:283–289
Perry ML, Fuller TF (2002) A historical perspective of fuel cell technology in the 20th century. J Electrochem Soc 149(7):S59–S67

Piela P, Eickes C, Brosha E, Garzon F, Zelenay P (2004) Ruthenium crossover in direct methanol fuel cell with Pt-Ru black anode. J Electrochem Soc 151:A2053–A2059
Ralph TR, Hogarth MP (2002) Catalysis for low temperature fuel cells. Part I: the cathode challenges. Platin Met Rev 46:3–14
Reap J, Roman F, Duncan S, Bras B (2008a) A survey of unresolved problems in life cycle assessment. Part 1: goal and scope and inventory analysis. Int J Life Cycle Assess 13:290–300
Reap J, Roman F, Duncan S, Bras B (2008b) A survey of unresolved problems in life cycle assessment. Part 2: impact assessment and interpretation. Int J Life Cycle Assess 13:374–388
Rhee YW, Ha SY, Masel RI (2003) Crossover of formic acid through Nafion® membranes. J Power Sources 117:35–38
Sakintuna B, Lamari-Darkrim F, Hirscher M (2007) Metal hydride materials for solid hydrogen storage: a review. Int J Hydrog Energy 32:1121–1140
Sawyer DT, Andrzej S, Julian LR Jr (1995) Electrochemistry for chemists, 2nd edn. Wiley, New York
Scholta J, Rohland B, Trapp V, Focken U (1999) Investigations on novel low-cost graphite composite bipolar plates. J Power Sources 84:231–234
Schüth F, Bogdanović B, Felderhoff M (2004) Light metal hydrides and complex hydrides for hydrogen storage. Chem Commun 10:2249–2258
Shiraishi M, Takenobu T, Kataura H, Ata M (2004) Hydrogen adsorption and desorption in carbon nanotube systems and its mechanisms. Appl Phys A 78:947–954
Shukla AK, Suresh P, Berchmans S, Rajendran A (2004) Biological fuel cells and their applications. Curr Sci 87:455–468
Song H, Qiu X, Li F (2008) Effect of heat treatment on the performance of TiO2-Pt/CNT catalysts for methanol electrooxidation. Electrochim Acta 53:3708–3713
Srinivasan S, Renaut M, Phillippe S, Christopher Y (1999) Fuel cells: reaching the era of clean and efficient power generation in the twenty-first century. Annu Rev Energy Environ 24:281–328
Stephens FH, Pons V, Baker RT (2007) Ammonia-borane: the hydrogen source par excellence? Dalton Trans 25:2613–2626
Tawfik H, Hung Y, Mahajan D (2007) Metal bipolar plates for PEM fuel cell – a review. J Power Sources 163:755–767
Thomas KM (2007) Hydrogen adsorption and storage on porous materials. Catal Today 120:389–398
US Department of Energy (2002) National hydrogen energy roadmap. US Office of Energy Efficiency and Renewable Energy, Washington, DC
Van Den Berg AWC, Areán CO (2008) Materials for hydrogen storage: current research trends and perspectives. Chem Commun 6:668–681
Vichi FM, Colomer MT, Anderson MA (1999) Nanopore ceramic membranes as novel electrolytes for proton exchange membranes. Electrochem Solid-State Lett 2:313–316
Wang B (2005) Recent development of non-platinum catalysts for oxygen reduction reaction. J Power Sources 152:1–15
Wang H, Holmberg BA, Huang L, Wang Z, Mitra A, Norbeck JM, Yan Y (2002) Nafion-bifunctional silica composite proton conductive membranes. J Mater Chem 12:834–837
Wasmus S, Küver A (1999) Methanol oxidation and direct methanol fuel cells: a selective review. J Electroanal Chem 461:14–31
Wee JH, Lee KY (2006) Overview of the development of CO-tolerant anode electrocatalysts for proton-exchange membrane fuel cells. J Power Sources 157:128–135
Wright SE (2004) Comparison of the theoretical performance potential of fuel cells and heat engines. Renew Energy 29:179–195
Yamanaka S, Fujikane M, Uno M, Murakami H, Miura O (2004) Hydrogen content and desorption of carbon nano-structures. J Alloys Compd 366:264–268
Yu X, Pickup PG (2008) Recent advances in direct formic acid fuel cells (DFAFC). J Power Sources 182:124–132

Zawodzinski TA Jr, Springer TE, Davey J, Jestel R, Lopez C, Valerio J, Gottesfeld S (1993a) A comparative study of water uptake by and transport through ionomeric fuel cell membranes. J Electrochem Soc 140:1981–1985

Zawodzinski TA Jr, Derouin C, Radzinski S, Sherman RJ, Smith VT, Springer TE, Gottesfeld S (1993b) Water uptake by and transport through Nafion 117 membranes. J Electrochem Soc 140:1041–1047

Züttel A (2004) Hydrogen storage methods. Naturwissenschaften 91:157–172

Solid Oxide Fuel Cells

Nigel M. Sammes, Kevin Galloway, Mustafa F. Serincan, Toshio Suzuki, Toshiaki Yamaguchi, Masanobu Awano, and Whitney Colella

Contents

N.M. Sammes (✉) • K. Galloway
Department of Metallurgical and Materials Engineering, Colorado School of Mines, Golden, CO, USA
e-mail: nsammes@postech.ac.kr; nsammes@mines.edu; kgalloway@mines.edu

M.F. Serincan
Department of Mechanical Engineering, University of Connecticut, Storrs, CT, USA

T. Suzuki • T. Yamaguchi • M. Awano
National Institute of Advanced Industrial Science and Technology (AIST), Nagoya, Japan
e-mail: toshio.suzuki@aist.go.jp

W. Colella
Sandia National Laboratories, Albuquerque, NM, USA
e-mail: wgcolel@sandia.gov

W.-Y. Chen et al. (eds.), *Handbook of Climate Change Mitigation and Adaptation*,
DOI 10.1007/978-3-319-14409-2_44

Abstract

This chapter describes the concept, electrochemical reactions, and fabrication of a solid oxide fuel cell (SOFC). It initially describes how SOFC systems differ from other electrical devices and how they differ from other types of fuel cells, for example, they are all solid state (ceramics), run at high temperature, and have the potential for directly running off hydrocarbon fuels. Then the basic principles of the fuel cell are studied and each of the components described in more detail (the anode, cathode, and electrolyte). The discussion then moves on to how single SOFC's can be stacked in a number of ways, to form systems, and what the advantages and disadvantages of each are. The chapter discusses one such SOFC system in more detail, that of the microtubular SOFC. Here, it examines how these microtubes are made, what they are made from, and how they have the potential for running at low temperature for small applications such as auxiliary power units (APU), for example. Then it deals with some micro- and macro-modeling on the microtubular SOFC, describing issues such as mass and thermal transport, the effect of altering a number of parameters, and how the modeling results compare to real data. Finally, the chapter concludes with some future directions on solid oxide fuel cells.

Introduction

Recent awareness of environmental protection and fast growth of the world's energy consumption has led the public, policy makers, entrepreneurs, technology developers, and scientists to search for alternative means to carry out and convert energy. Fuel cells are promising devices, potentially emerging as the substitutes for traditional energy converters, such as the internal combustion engine. Their improved environmentally friendly nature, and high efficiency, can potentially allow fuel cells to be employed from small portable applications, such as laptops and cell phones, to large-scale stationary applications for central heating facilities and electricity generation.

General Principles of a Fuel Cell

A fuel cell is an electrochemical energy conversion device that uses chemical energy to produce electricity. Similar to a battery, the electrodes are separated by an electrolyte in a fuel cell, and electricity is generated due to the electrochemical reaction going on inside the cell. However, reactants are stored inside the battery; thus, the performance of the battery decreases when the charge inside the battery

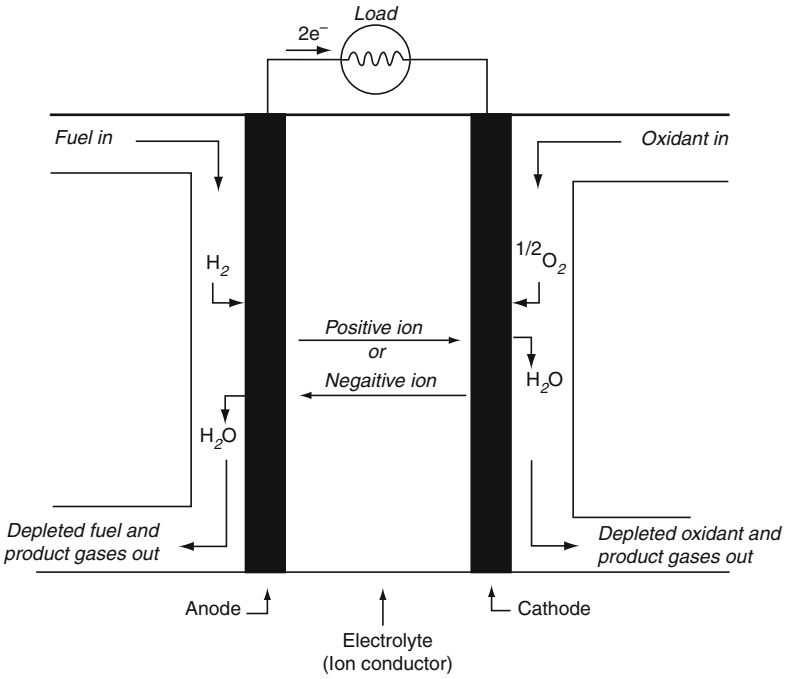

Fig. 1 Schematic of a generalized fuel cell

drops until it eventually goes dead and needs to be recharged. On the other hand, reactants flow into the fuel cell continuously and electricity is generated as long as the supply continues.

A general cross-sectional view of a fuel cell is depicted in Fig. 1. Fuel enters the negative electrode (anode) and oxidant enters the positive electrode (cathode) in a gaseous state. Porous electrodes that allow the reactant gases to pass through are separated by an electrolyte. The chemical reactions occur at the electrode-electrolyte interface often with the help of catalysts especially for the oxidation reaction. Fuel entering the anode is separated into electrons and ions, which are protons when the fuel is hydrogen. The ions pass through the electrolyte to the cathode side, while the electrons go through an external circuit connecting the anode and cathode providing electricity. At the cathode, ions combine with the oxidant and the electrons. To get a reasonable voltage and current output, cells are combined in parallel and series to form a fuel cell stack.

The types of fuel cells are defined by the electrolyte material. Though each type of fuel cell has different properties, they share some characteristics. The energy conversion process from the chemical reaction is common for all of them. Although other fuels such as methanol are used in fuel cells, hydrogen is used as the typical fuel. Finally, each type of fuel cell stack generates direct current (DC) electricity. The characteristics of fuel cells make them favorable over conventional energy

converters in many applications. These characteristics, which vary for the different types of fuel cells, determine the applications for which they can be employed.

Efficiency: Direct conversion of the chemical energy to electrical energy is not limited by the Carnot cycle efficiency; hence, fuel cell efficiencies are greater than heat engines. Depending on the fuel cell type, stack efficiency of up to 50–60 % is possible. If the surplus heat is utilized, an overall system efficiency of up to 80–90 % is realizable.

Power density: Higher power is maintained from a fuel cell that has the same size as that of most of the conventional energy conversion devices, such as internal combustion engines, partly owing to higher efficiency.

Low emissions: When pure hydrogen is used as the fuel, the fuel cell maintains a zero emission characteristic. However, in the case of utilizing hydrogen from carbon-rich fossil fuels, oxides of nitrogen, sulfur and carbon are released; yet the emissions values are far below those of conventional energy converters. Even when the hydrogen from natural gas is used as energy source, the higher conversion efficiency allows for the production of less CO_2.

Reliability and availability: Since the moving parts of a fuel cell system are in the auxiliary components and the fuel cell systems are relatively simple, the maintenance requirements are reduced, and the life of the fuel cells is generally longer than conventional systems, although there are a number of exceptions, depending on the material set utilized. Due to the low maintenance requirements, therefore, system availability is higher. It is reported that a PC25 (by UTC Power) fleet consisting of more than 200 units have demonstrated 90 % availability during four million operating hours. Also power is available 99.9999 % of the operating time.

Thermal output and cogeneration capability: Depending on the type of the fuel cell, product heat can be utilized by means of domestic hot water applications or space heating. Also, in case of higher thermal output, fuel cells can be used with other devices such as turbines to enhance the system efficiency.

Despite these positive characteristics, there are also a number of negative features of the fuel cells, such as high costs, insufficient infrastructure, and immaturity of the technology.

General Principles of an SOFC

The solid oxide fuel cell system will now be discussed in more detail. The SOFC consists of a ceramic electrolyte, usually yttria-stabilized zirconia (YSZ), with an air electrode (cathode) and a fuel electrode (anode) on either side, as described in Fig. 2. A solid oxide fuel cell (SOFC) is an all solid-state electrochemical device producing both electricity and waste heat directly from the electrochemical conversion of a fuel with an oxidant. Because it produces electricity by electrochemical means, there is no necessity to have any moving parts, and thus the SOFC overcomes the Carnot limitation inherent in all heat engines. Hence, the SOFC has high-energy efficiency, which can be further increased by using waste by-product heat in applications such

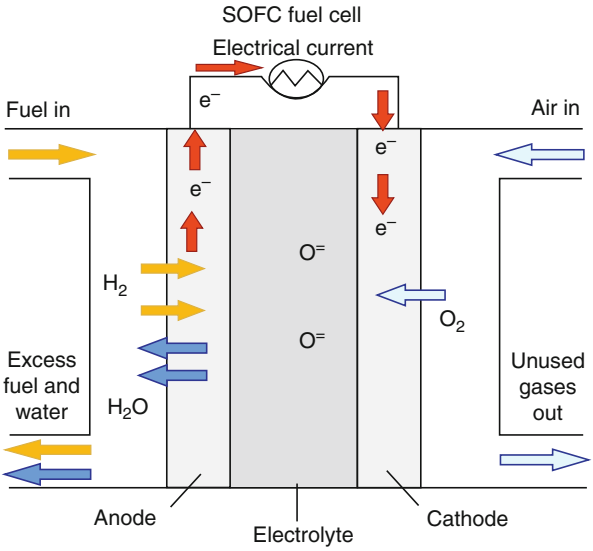

Fig. 2 Diagrammatic representation of the elements of the SOFC

as cogeneration (greater than 50 % electrical efficiency is possible, with efficiencies approaching 75 % with cogeneration).

The SOFC also has a number of advantages over conventional systems including its modularity whereby single units can be stacked, its flexibility, and its ability to use a number of different fuels. It has a number of disadvantages including cost (far greater than conventional systems/kW at the moment) and raw material availability (possibly a problem in the long term), and it has no real history, unlike the turbine engine. It should however be noted that the fuel cell was invented by Sir William Grove over 150 years ago, but was never commercialized possibly due to the invention of the turbine and its use and development in the turbine-driven aeroplane.

Now, as has already been stated, the SOFC system consists of a ceramic electrolyte, usually yttria-stabilized zirconia, with an air electrode (cathode) and a fuel electrode (anode) on either side. The electrolyte must be of a high percentage theoretical density so that the two fuels are physically separated and have no opportunity of mixing. The cell (anode/electrolyte/cathode) is operated at a high temperature primarily to allow the ionic conductivity of the electrolyte to be high enough to produce a reasonable current density, although other factors such as reaction kinetics must also be considered. Fuel (currently H_2, although other hydrocarbon fuels are being studied) is fed to the anode, where it undergoes an oxidation reaction and releases electrons to an external circuit. Oxidant (either air or pure oxygen) is fed to the cathode where it is reduced and accepts electrons from the external circuit. The flow of electrons around the external circuit produces DC electricity. The oxygen is transported as oxygen ions across the electrolyte via the vacancy mechanism. Figure 2 summarizes the SOFC operation.

As explained above, the electrolyte is usually based on yttria-stabilized zirconia, which is an oxygen ion conductor. Other oxygen ion conductors have been studied,

including doped-CeO_2 systems, perovskite-based systems, and doped-Bi_2O_3. Most of these other oxides, although they are superior oxygen ion conductors, are prone to reduction at low oxygen partial pressures (as found at the anode) and thus show n-type electronic conductivity, which reduces the efficiency of the overall system. Doped-$LaGaO_3$ is a new material that does show promise as an SOFC electrolyte, because it does not appear to be reduced at the anode. Much work is still necessary, as preliminary studies appear to show it to be mechanically weak.

Now it is important to study the reactions occurring in the SOFC cell. At the cathode (described in more detail below), reduction of oxygen occurs, via equation:

$$O_2 + 4e' = 2O^{2-}$$

The main function of the cathode is to provide reaction sites for the reduction reaction to take place.

At the anode, however, an oxidation reaction takes place, whereby the oxide ion is oxidized, releasing an electron.

$$2O^{2-} = O_2 + 4e'$$

Thus, the SOFC can be regarded as an oxygen concentration cell, and the electromotive force (EMF) is, therefore, dependent upon the oxygen partial pressure at the anode and the cathode. The oxygen partial pressure at the anode is based not upon oxygen being present, but upon the oxidation of the fuel. In this example, we will consider H_2. The oxidation of H_2 is given by

$$H_2 + \frac{1}{2}O_2 = H_2O$$

The oxygen partial pressure at the anode is, therefore, given by

$$P_{O_2} = \left[\frac{P_{H_2O}}{P_{H_2}K_{OX}}\right]^2$$

where K_{ox} is the equilibrium constant for the oxidation reaction described above. Substitution yields, where E^0 is the reversible voltage at the standard state, are given by

$$E = E^0 + \frac{RT}{4F}\ln P_{O_2} + \frac{RT}{2F}\ln\frac{P_{H_2}}{P_{H_2O}}$$

Under standard state conditions, E equals the reversible standard voltage at the standard state, E^0, and thus we can say that the following equation is applicable:

$$E^0 = \frac{RT}{2F}\ln K_{OX}$$

Now,

$$E^0 = -\frac{\Delta G^0}{4F}$$

where ΔG^0 is the Gibbs free energy of the reaction given in equation (at 1,250 K this is -178.2 kJ/mol). This value will differ for different combustion reactions, such as CO, CH_4, and CH_3OH.

Now, this reaction occurs at the anode, which, like the cathode, must perform under quite specific conditions. The reversible EMF produced by the reaction is approximately 1 V (0.924 V at 1,250 K and 0.997 V at 1,000 K). This EMF is of little practical benefit, and thus single cells are connected in electrical series in what is known as a stack. The height of the stack (or number of cells) varies depending on the design and the power output required. Many designs have been examined; however, the two most common ones today are the tubular and planar designs, described below.

Materials and Reactions

Electrolyte

The electrolyte must be fully dense so that the fuel and air are physically separated and have no opportunity of mixing. The cell (anode/electrolyte/cathode) is operated at a high temperature primarily to allow the ionic conductivity of the electrolyte to be high enough to produce a reasonable current density, although other factors such as reaction kinetics must also be considered. Fuel (such as H_2 or other hydrocarbons) is fed to the anode, where it undergoes an oxidation reaction and releases electrons to an external circuit. Oxidant (either air or pure oxygen) is fed to the cathode where it is reduced and accepts electrons from the external circuit. The flow of electrons around the external circuit produces DC electricity. The oxygen is transported as oxygen ions across the electrolyte via a vacancy mechanism.

The electrolyte is usually based on yttria-stabilized zirconia, which is an oxygen ion conductor. Other oxygen ion conductors have been studied including doped-CeO_2 systems, perovskite-based systems, and doped-Bi_2O_3. Most of these other oxides, although they are superior oxygen ion conductors, are prone to reduction at low oxygen partial pressures (as found at the anode) and thus show n-type electronic conductivity, which reduces the efficiency of the overall system, although this may not be such a problem for doped-ceria. Doped-$LaGaO_3$ is also a material that does show promise as a SOFC electrolyte, because it does not appear to be reduced at the anode.

Cathode

The cathode must be a good electronic conductor with a high surface area and catalytically active toward this reaction. The cathode must also have the following

requirements: stability at high temperature and under the oxidizing gas present, compatibility with the other cell components, similarity of thermal expansion coefficient to that of the other components (otherwise it is prone to peeling off the electrolyte), retention of its porosity (and thus the number of reaction sites) during the lifetime of the cell, and retention of its catalytic activity during the lifetime of the cell. Because of the high temperature and oxidizing environment, most metals cannot be used. Only noble metals will withstand the environments found at the cathode, but these materials are too expensive for a commercial system. Many oxide materials have a high electronic conductivity, but they are either incompatible with the electrolyte or have a thermal expansion coefficient very different to those of the other cell components. Doped-$LaMnO_3$ meets almost all the requirements of the cathode and is the most commonly used material. Traditionally, Sr-doped (on the A-site of the perovskite) is used, due to its good electronic conductivity. Sr enhances the electronic conductivity by increasing the Mn^{4+} content by substitution of La^{3+} by Sr^{2+}, as described in the equation below, and increases with increasing Sr content. At Sr contents greater than 20–30 mol%, metallic conduction is observed.

$$LaMnO_3 + xSr^{2+} \rightarrow La^{3+}{}_{1-x}Sr^{2+}{}_{x}Mn^{3+}{}_{1-x}Mn^{4+}{}_{x}O_3$$

Electronic conductivity occurs via the small polaron conduction mechanism. Ca doping has a similar effect to that of Sr doping, causing a significant increase in the electronic conductivity, with increasing Ca content.

Anode

The anode must provide the reaction sites for the electrochemical oxidation of the fuel gas to occur. Hence, the anode must be stable under the very reducing conditions of the fuel atmosphere, have sufficient electronic conductivity, have excellent catalytic activity for the reaction (and remain catalytically active during the lifetime of the cell), be chemically compatible with the other cell components, have a high surface area to allow a large reaction zone to occur (the anode must also remain with a high surface area and not degrade with time), have a similar thermal expansion coefficient to that of the other cell components, and be relatively low cost and easily fabricated. Because of the reducing environments, metals can be used, although the high temperatures limit these to Co, Ni, and noble metals. Electronically conducting ceramic materials can also be used (provided they do not reduce under the anode atmosphere). Currently, Ni is the anode of choice, primarily due to its good catalytic activity for hydrogen oxidation, its low cost, and its good stability. YSZ powder is added to the Ni metal in the form of a metal/ceramic composite for two reasons. Firstly, the YSZ inhibits the Ni coarsening during the operation, and secondly, the YSZ acts to lower the thermal expansion coefficient of the metal composite (which is much higher than the electrolyte) closer to that of the other cell components. The optimum amount of YSZ depends upon the percolation theory. Too much YSZ, and the sample does not electronically conduct (due to a minimal/no electron pathways);

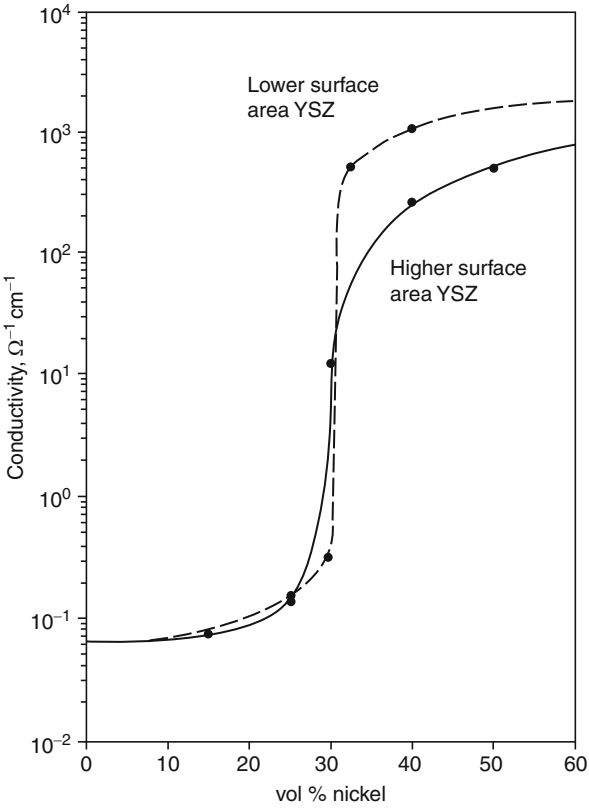

Fig. 3 The conductivity of Ni/YSZ as a function of Ni content, at 1,000 °C (After Dees et al. 1987)

too little YSZ, and the composite has too high a thermal expansion coefficient. The effect of Ni content on the electronic conductivity is shown in Fig. 3.

It is obvious that the percolation threshold is at approximately 30 vol% Ni. Most anodes have approximately 40–50 mol% Ni in the composite, which appears to produce a relatively stable system. However, all anodes are found to degrade with time, due to either slight oxidation of the Ni to NiO or due to sintering of the Ni particles.

Alternative anode systems are being studied, particularly in respect to internal reformation of hydrocarbons, rather than having to use H_2 as a fuel. Ni, although an extremely good catalyst for the oxidation of H_2, is also very good at cracking natural gas into C. The C is then liable to form whiskers which lift the anode from the electrolyte surface, thus greatly reducing its activity. Other catalytic electrode materials being studied do not cause methane (and other hydrocarbons to crack) and thus may allow for a direct internal reformation reaction to take place. These include doped-CeO_2-based systems and perovskites. Currently, however, there are still many problems to be solved when investigating alternative electrode materials, and the technology of today either externally reforms the hydrocarbon or uses a high steam to carbon ratio in the feed stream. Both of these are not totally acceptable, as large efficiency losses are observed.

Typically, the EMF produced by the reactions described above is of little practical benefit, and thus single cells are connected in electrical series in what is known as a stack. The height of the stack (or number of cells) varies depending on the design and the power output required.

Stacking and Types of SOFC

Many designs have been examined; however, the two most common ones today are the tubular and planar designs, shown in Fig. 4. The planar design consists of electrolyte components configured as thin (approximately 50 mm) planar plates or laid down on a cathode and, more typically, an anode support. On either side of these plates are the anode and cathode materials. Between each cell is what is known as an interconnect. The interconnect has two main purposes; it serves as a bipolar gas separator, contacting the anode and cathode of adjoining cells, and sometimes has ribs on both sides to form gas channels. The properties of the interconnect are quite tight, as it must be electronically conducting, stable in both reducing and oxidizing environments and at high temperatures, relatively cheap (as it is usually the thickest component), dense (for the same reasons as the electrolyte, so that the fuel and air gases do not mix), easy to fabricate, compatible with the other cell components, and possess a similar thermal expansion coefficient to those of the other cell components. The interconnect is usually based on the perovskite $LaCrO_3$. To increase the electronic conductivity, A-site (such as Ca or Sr) and B-site (such as Co or Fe) are added, which have the same effect as that of the Mn^{3+} in the cathode, to increase the amount of Cr^{4+} ions.

Once the stack has been fabricated, the system is sealed using a ceramic or glass ceramic seal with a similar thermal expansion coefficient as the cell, and gas manifolds are placed around it, similar to those shown in Fig. 5.

The tubular design, on the other hand, uses a very different concept. Here, an electrolyte tube (either anode or cathode supported or unsupported) has electrodes on the inside and outside. The Siemens design (which uses traditional SOFC materials) has an electrolyte that is typically electrovapor deposited (EVD) onto a porous cathode support tube (although other methods have been examined). On the outside of the electrolyte/cathode tube is placed the anode, using a dip-coating technique. The interconnect (Mg-doped $LaCrO_3$) is then added using EVD processing, and the

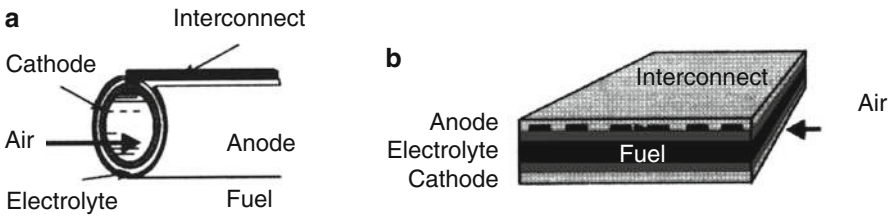

Fig. 4 The SOFC stack designs (**a**) tubular, (**b**) planar (After Kordesch and Simader 1996)

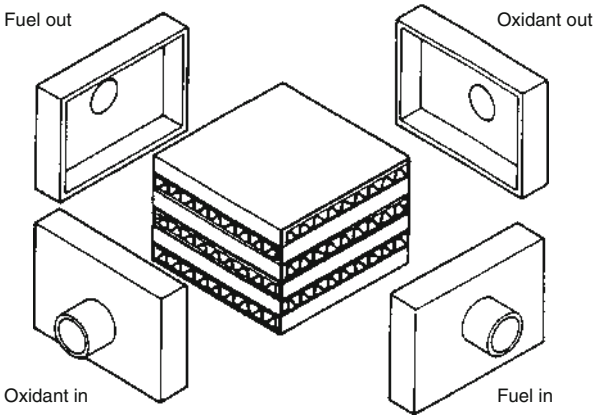

Fig. 5 Gas manifolding in the planar SOFC design (After Minh and Takahashi 1995)

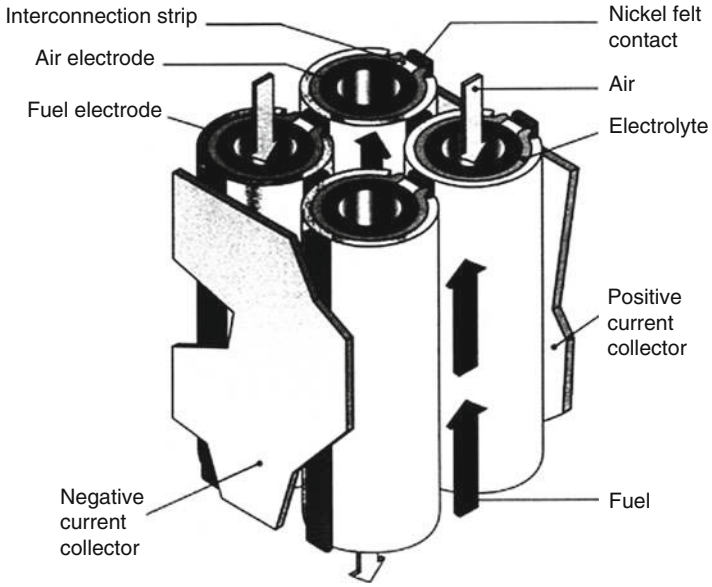

Fig. 6 Electrical connection in the tubular SOFC design (After Kordesch and Simader 1996)

tubular cells (which are closed at the bottom) are bundled together, using Ni-felt to connect the anode of one cell to the adjacent anode for parallel connection and to the Ni-plating on the interconnect for series connection as shown in (Fig. 6).

As the tubes are themselves already sealed, there is no requirement for a sealant, as required in the planar design. The gas manifolding is relatively straightforward with oxidant (air) being fed down the center of the tubes via an oxidant plenum. The fuel is fed from a fuel plenum at the bottom and up along the outside of the tubes, where the oxidation reaction takes place. The spent fuel flows through a porous ceramic barrier, enters the combustion chamber, and combines with the spent

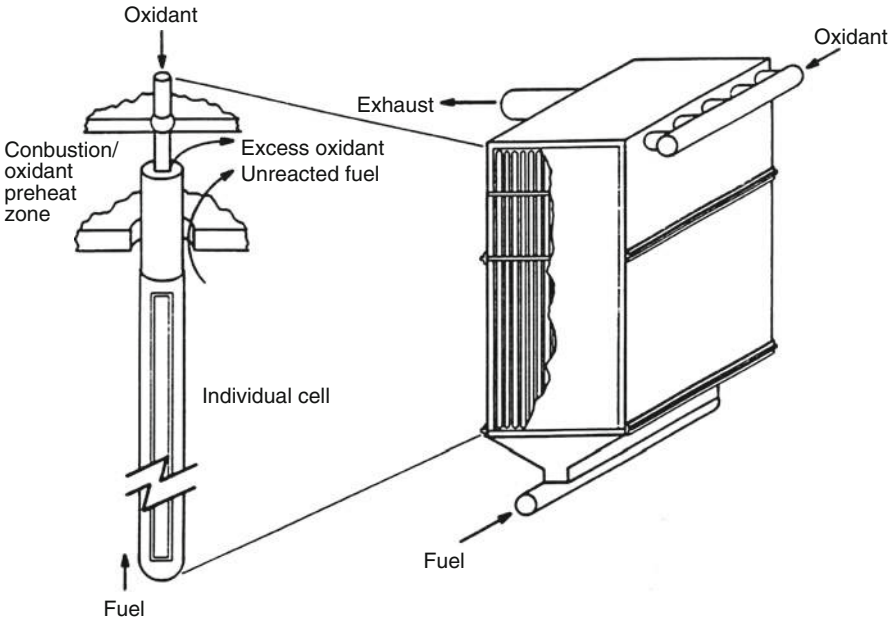

Fig. 7 Gas manifolding in the tubular design (After Singhal 1991)

oxidant. This heat is then used to preheat the oxidant entering the cell. The exhaust gases exit the generator at approximately 900 °C. The gas-manifolding concept is described in Fig. 7.

Power is obtained from the cell, or stack, by applying a load between the anode and cathode, and hence drawing current. The power output (P) is thus the product of the current drawn and the EMF across the cell, after the losses have occurred, namely, $P = I\,(E - R_{\mathrm{T}}I)$, where E is the thermodynamic EMF across the cell, and $R_{\mathrm{T}}I$ are the losses (R_{T} is the total resistance of the cell and I the current).

Power Output and System Efficiency

SOFC efficiency consists of a number of elements.

- *Thermodynamic efficiency.* This is given by the assumption that the Gibbs free energy of the cell reaction may be totally converted to electrical energy:

$$\epsilon_{\mathrm{therm}} = \frac{\Delta G}{\Delta H}$$

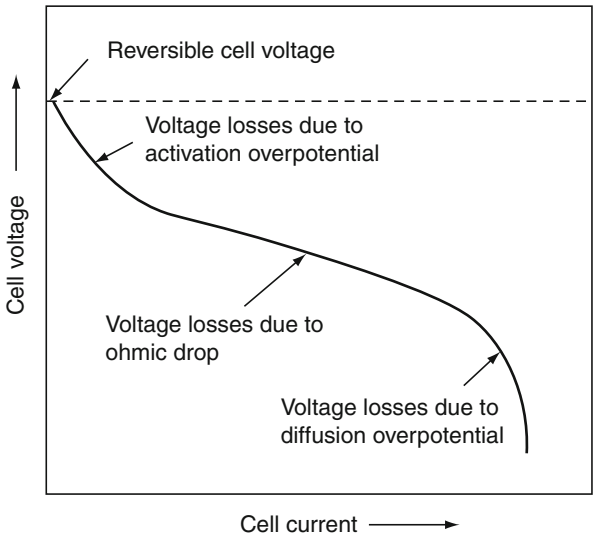

Fig. 8 Typical voltage losses in a running SOFC cell

- *EMF efficiency*. This is shown by the fact that the cell voltage, in an operating cell, is always less than the reversible voltage. As the current is drawn from the fuel cell, the cell voltage falls due to a number of losses, as described in Fig. 8. The EMF efficiency is given by the ratio of the operating cell voltage under load to the equilibrium cell voltage. This difference is due to a number of polarizations (or overpotentials), as described in the equation below, which shows that the total polarization losses (η) is the sum of a number of losses:

$$\eta = \eta_{\mathrm{a}} + \eta_{\mathrm{d}} + \eta_{\mathrm{r}} + \eta_{\mathrm{ohm}}$$

where the subscripts denote a = charge transfer polarization, d = diffusion polarization, r = reaction resistance, and ohm = ohmic losses.

Power is obtained from the cell, or stack, by applying a load between the anode and cathode and hence drawing current. The power output (P) is thus the product of the current drawn and the EMF across the cell, after the losses have occurred; $P = I\,(E - R_{\mathrm{T}}I)$, where E is the thermodynamic EMF across the cell, and $R_{\mathrm{T}}I$ are the losses (R_{T} is the total resistance of the cell and I the current).

New Concepts for SOFCs

Yttria-stabilized zirconia (YSZ) is the most common type of electrolyte material used in SOFC designs. However, due to its poor conductivity at lower temperatures, SOFCs using YSZ electrolytes operate at relatively higher temperatures, that is,

above 750 °C, to generate practical output power. This requires use of high quality alloy metal interconnects in order to prevent corrosion and increases the cost of these systems. On the other hand with the use of ceria-based rare earth oxides as electrolyte materials, which have high conductivities at lower temperatures, SOFCs running at intermediate temperatures (IT-SOFCs) possess desirable assets. Minimizing ionic interdiffusion between the electrode/electrolyte interfaces, mitigation of sintering problems seen at high temperature operation, use of inexpensive materials, and lower operating costs are the main advantages. Albeit providing these advantages, the common problem with ceria-based electrolytes is that they can be reduced under fuel cell operating conditions and become electronically conductive. As a result, the cell is short circuited and the performance decreases.

SOFC electrodes are designed to provide a good conductive medium for both ions and the electrons. Hence, they are typically compounds of metal and ceramic materials to serve as mixed ionic and electronic conductors (MIEC). Both anode and cathode are porous structures to supply reactants and remove by-products. However, the design of the porous structure should be carried out meticulously. An open network of pores must be maintained throughout the structure to utilize all the electrode volume. Also the porosity must be high enough to prevent mass transfer limitations; however, higher porosities may lead to structural instabilities. Thus, the supporting electrode is always less porous than the other.

One of the most important features of the electrode design is to maintain high catalytic activity. This is achieved by longer triple-phase boundaries (TPBs) where gas phase in the pores, ionic conductor, and electronic conductor regions in the electrodes has a common interface. TPBs are where the anode and cathode reactions take place. To have a high quality TPB distribution, the electrodes must possess an open network of pores as well as the electrode materials must be sintered well to provide good bonding between the metallic and the ceramic components.

Another important parameter for the SOFC design is the thermal expansion characteristics of the components. Using the electrolyte material in the anode and the cathode alleviates the mismatch between different layers. A common dilemma related to the cathode design is the trade-off between electronic conductivity, ionic conductivity, and the thermal expansion coefficient. The cathode design must be carried out taking into consideration all these three parameters simultaneously to optimize the cell performance while considering the structural stability.

Keeping all this in mind, SOFCs are still far from commercial viability, mainly due to problems such as cost targets, operating life, system optimization, and eventual integration with traditional devices in hybrid systems, aiming at maximizing the overall electrical efficiency.

Intermediate Temperature SOFCs

Solid oxide fuel cell applications have long been limited by the necessity to operate at high temperatures, causing prolonged start-up times and material constraints, among other cost-increasing constraints. Considerably, decreasing the operating

temperature of SOFCs seems an absolute necessity for efficient power production, specifically in mobile applications where start-up time and material cost is of increasing importance. Reducing the operating temperature of SOFCs below 650 °C can extend the lifetime of the SOFC stack, lower cost by allowing the use of metal materials, and can decrease the degradation of SOFC and stack materials. Tubular SOFC designs have been shown to be stable for repeated cycling under rapid changes in electrical load and in cell operating temperatures. However, tubular SOFC capital costs are very high. This is mainly due to their low power density and to the materials to be used for safe operation at the high temperatures typical of SOFC stacks. In this respect, microtubular SOFCs aim at solving both the problems affecting the typical tubular SOFC. In fact, their lower diameter and operating temperature promise to (1) reduce capital costs, (2) increase power density, (3) increase thermal shock resistance, and (4) reduce start-up and shutdown times. Microtubular SOFCs have also been shown to be able to endure the thermal stresses associated with rapid heating up to operating temperatures. In contrast to planar SOFC designs, when the diameter of tubular SOFC is decreased, it is possible to design SOFC stacks for high volumetric power densities.

However, the literature dealing with thermal, electrical, and electrochemical performance of microtubular SOFCs is scarce at best, since this is an emerging technology with respect to the tubular one. Here, one such microtubular SOFC technology will be discussed, that of the anode-supported microtubular SOFCs with a cermet anode of NiO and GDC (gadolinium-doped ceria), a GDC electrolyte, and a cathode in LSCF ($La_{0.6}Sr_{0.4}Co_{0.2}Fe_{0.8}O_{3-y}$). These cells were tested at operating temperatures ranging from 450 °C to 550 °C. Such experimental analysis was carried out varying cell temperature and fuel flow, in order to assess the effects of these two parameters on the electrochemical performance of the cell. To this scope, a parametric study is also presented.

Concept, Manufacture, and Results of the Microtubular SOFC

The microtubular SOFCs were fabricated using traditional extrusion and coating techniques. The anode slurry was prepared and consisted of NO powder, GDC powder, and cellulose as the binder. The anode components were mixed with water using an industrial mixer for 1–2 h and left to age overnight. Placing a vacuum over the anode mixture allowed for excess air to be removed. Anode tubes were extruded from the anode mixture using a ram extruder and a custom-made die. The anode tubes were allowed to dry, were cut to the desired length, then dip-coated in GDC electrolyte slurry, and allowed to dry. The GDC electrolyte slurry is composed of the same GDC powder described above and organic ingredients such as binder (polyvinyl butyral), dispersant (fish oil), and solvents (toluene and ethanol). The desired electrolyte thickness was achieved through multiple electrolyte coatings, and subsequently, the tubes were sintered at 1,450 °C for 6 h in air. Next, the electrolyte-coated anode tubes were dip-coated in cathode slurry consisting of the LSCF and GDC powder and organic ingredients similar with those of the electrolyte slurry. The

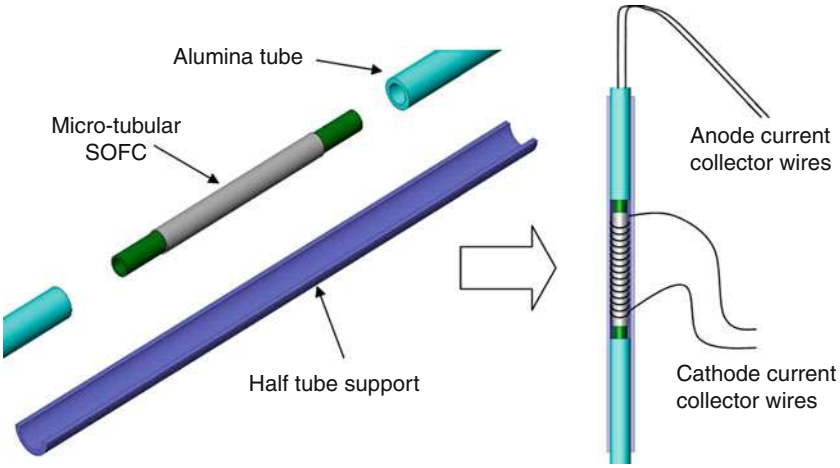

Fig. 9 Showing how the micro-SOFCs were supported for testing

cathode dip-coated tubes were dried in air and sintered at 1,000 °C for 1 h in air to complete the fuel cell fabrication.

An environmental scanning electron microscope (ESEM) was used to check the electrode and electrolyte microstructure. In order to carry out the experimental activities, measuring the fuel cell electrochemical performances, a specific support was also manufactured. Such a support is capable of sustaining the fuel cell when it is mounted in the furnace; it also allows the gas distribution on the anode and cathode sides and assures the electrical connection with the electrical load and potentiostat. Each tube was connected to two alumina tubes allowing the inner anode gas distribution, sustaining the cell in the furnace. The entire system was placed on an alumina half-tube support in order to yield stronger structure (Fig. 9). Figure 10 shows how each microtube was mounted for testing within a vertically mounted microtube furnace (Carbolite) and also shows a cross-sectional ESEM image of the fabricated microtubular SOFC, with porous electrodes and a dense electrolyte.

Cells were tested vertically as shown in order to ensure evenly distributed flow of fuel gas across the anode surface (horizontally oriented cells are subject to uneven fuel gas distribution due to gravity).

Each tube was equipped with four 0.5 mm silver sensor wires attached for collecting current for anode and cathode sides. The anode electrical connection was realized using two long silver wires fixed using nickel paste. A silver wire was wrapped around the tubular fuel cell (on the cathode), as a reel, and fixed with silver paste for the cathode electrical connection. The silver paste and nickel paste were brush painted on the cathode and anode surfaces to reduce the contact resistance between the silver sensor wires and the electrode surfaces. The pastes are porous enough at operating temperatures that fuel and oxygen are able to pass through them to arrive at their respective electrodes. Ceramabond 552 (Aremco)

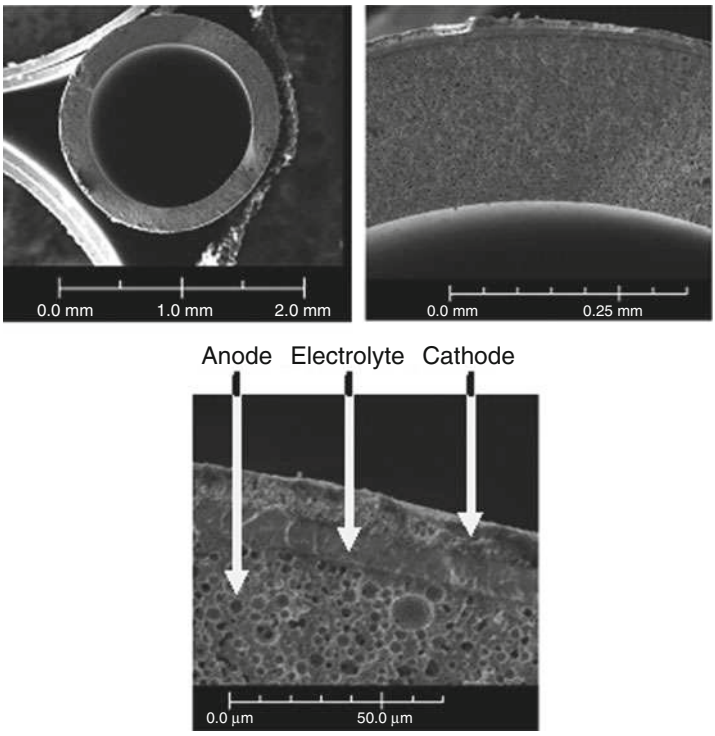

Fig. 10 Showing how the micro-SOFCs were mounted for testing

was used as a sealant between anode, alumina tubes, and alumina half-tube support. The four current collecting wires from the cell were connected to an impedance analyzer, and the electrical load at operating temperature ranges between 450 °C and 550 °C. Individual cells were run using humidified hydrogen gases (2–3 % of H_2O) as fuel to the anode side, while the cathode side (outside surface of tube) was exposed to atmospheric conditions. The microtubular SOFC was brought up to 450 °C at 3 °C/min from room temperature under atmospheric conditions with air exposed to both anode and cathode sides. After arriving at the operating temperature of 450 °C, the cell was exposed to 15 sccm-humidified H_2 (3 % H_2O by volume). The cell immediately began to reduce and produce a voltage as shown in Fig. 11. The cell voltage rose to 0.94 V after only 1 min and the cell continued to produce a voltage of 0.94 V thereafter. In order to understand whether the cell had fully reduced in this time, impedance measurements were taken in increments after the cell had started up. The start-up impedance information is shown in Fig. 12. The information gathered through the impedance analysis shows that the entire cell impedance decreases the longer the cell has been run. The ohmic impedance of the cell remains relatively constant at around 1 Ω; however, the electrode polarization resistances decrease with time until around 50 min where no further change in electrode polarization resistance is observed as a function of time. The electrode

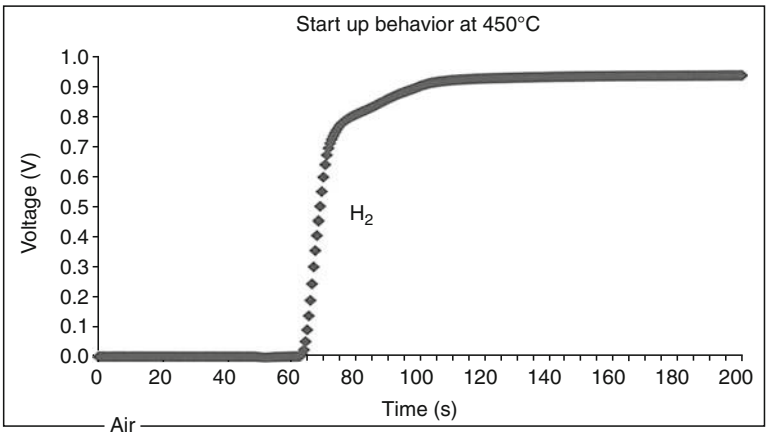

Fig. 11 *Microtubular* SOFC start-up behavior

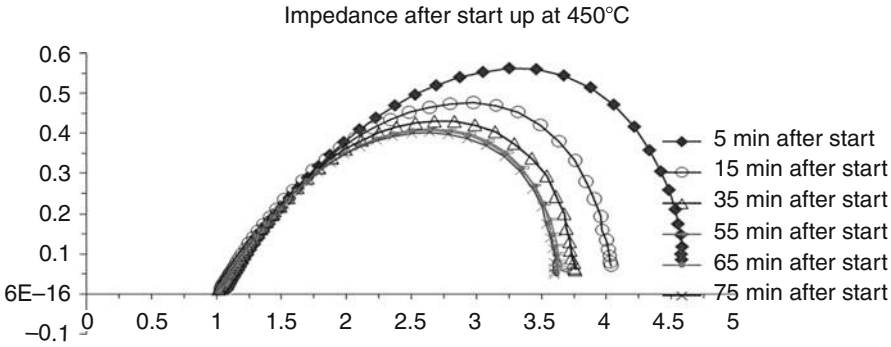

Fig. 12 Impedance spectra during the first 75 min of running

polarization resistance decreased by as much as 0.5 Ω in 10 min after the cell had started up. After start-up behavior analysis, the cell was held at 450 °C, and IV characterization of the cell was performed for varying flow rates of humidified H_2 (3 % H_2O by volume) through the cell. Figure 11a–c outlines the performance of the cell for varying fuel utilizations at 450 °C and concentration polarization losses are apparent in the IV curves shown. The fuel utilization was calculated from equation $U_f = i/(nFv)$, where the current drawn from the cell i), the number of electrons transferred in the reaction between H_2 and ½ O_2 ($n = 2$), the flow rate of fuel (v), and the inlet temperature of the fuel were used to calculate the fuel utilization (U_f) of the cell for the varying flow rates of fuel through the cell. The temperature of the inlet fuel stream is important because the density of H_2 entering the fuel cell is dependent on this parameter. As can be seen in Fig. 13a–c since at higher temperatures more current can be drawn from the cell, more hydrogen is necessary to drive the higher

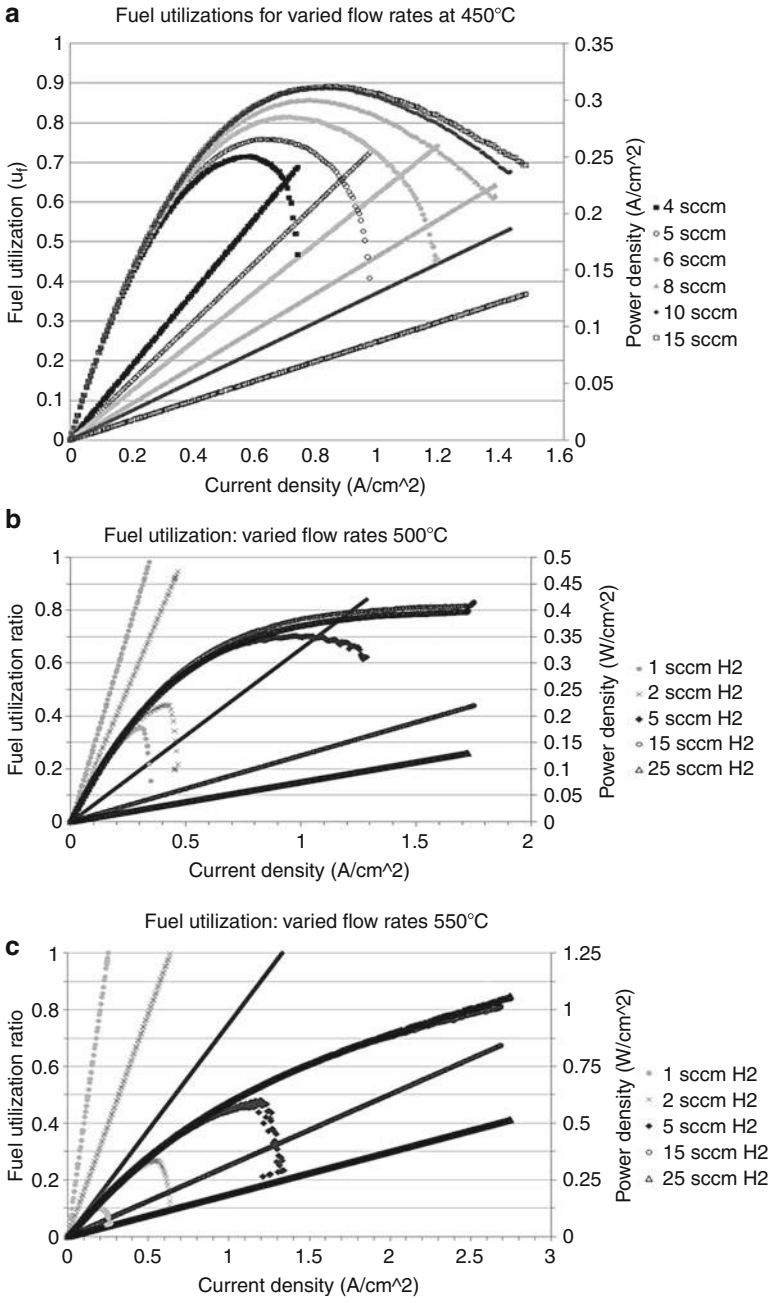

Fig. 13 (**a**–**c**) Fuel utilization and power density of the cells running at (**a**) 450 °C, (**b**) 500 °C, and (**c**) 550 °C

currents and fuel utilization values change for a specific flow rate. Thus, balancing fuel utilization with performance loss is an important issue when designing an efficient system since the performance of the cell is closely related to the fuel utilization.

Modeling of SOFC Systems

In modeling studies of solid oxide fuel cells, the common approach is to either model the cell isolated from its surrounding or to include some aspects of the surrounding environment by truncating the domain where the variables associated with the transport phenomena have not yet settled down to their "free stream" values. When large gradients (of these variables) are present, these approaches may lead to misrepresentation of the physics. For example, large differences in temperature or species concentration between the SOFC and its surroundings result in larger length scales for heat and mass transfer. Therefore, if a single cell is to be modeled with some portion of the physical domain, boundary conditions should be selected at the boundaries where truncation takes place; otherwise, a broader domain should be selected to cover spatial variations. However, selecting a larger domain requires further computational effort due to the mismatch between the aspect ratios of different parts of the computational domain.

Leakage Currents

There are a considerable number of studies to characterize the electron transfer process in the electrolyte. In early attempts, implicit relations of fuel cell electrochemical parameters were suggested as solutions to the electron transport equation in the electrolyte. Riess developed an explicit solution relating oxygen partial pressures and cell voltage to the electron flux across the electrolyte. His approach has been widely accepted in modeling studies. With some modifications to his derivation, some other forms of solutions also exist in the literature. Previously, Godickemeier developed a model to study the GDC electrolyte with the perspective of optimizing the cell design. Leah et al. developed a model to show that the use of MIEC electrolytes under certain conditions does not cause critical efficiency drops. Baron et al. further reported a reasonable fit of their model results to the experimental data when leakage currents were included.

Parametric Analysis

Although there are substantial works in modeling of SOFCs, few modeling studies have focused on the parametric analysis. Parametric analysis is an important method to understand the fuel cell behavior and compare the performance of the system affected by various factors. These factors can be related to either the cell geometry

and material properties or operational conditions. Changes in the geometry of the cell come along with uncertainties in the parameters related to reaction kinetics as the latter cannot be predicted without additional experiments. If the fuel cell performance is desired to be compared for two different cathode thicknesses, parameters related to reaction kinetics have to be updated for the new geometry as the distribution of the three-phase boundaries will change along with the percolation of the phases in the new geometry. Many of the modeling studies found in the literature carrying out parametric analyses of SOFCs focus on the geometrical aspects of the system. However, these studies neglect the abovementioned uncertainties arising with the change of the electrode geometry and are incapable of providing a precise tool to assess the effects of the geometrical parameters. Therefore, the effects of geometry on the fuel cell performance are not considered in this study. There are also studies focusing on the operational parameters such as utilization, flow rate, temperature, and pressure. Ni et al. developed a model to conduct parametric analysis to address the effects of operating conditions on the overpotentials. Their work constitutes a 1D model employing electrochemical relations and mass balances and does not include energy and momentum balances. Jiang et al. built a thermal and electrochemical model of a tubular SOFC to study the effects of operating conditions such as pressure, temperature, and flow rate. Their model is a lumped model and does not consider spatial distribution of the variables. Lisbona et al. analyzed an SOFC stack with the balance of plant to develop relations between cell performance and the operational parameters such as utilization, air flow rate, and inlet gas temperature. The developed model consists of only electrochemical relations, and the transport phenomena inside the stack are not considered. Colpan et al. developed a model employing thermodynamic calculations to identify the effects of utilization on cell output power and efficiency. Bove et al. carried out a utilization analysis for a tubular SOFC. Their model employs energy balance and electrochemical relations along with the simple algebraic relations for gas compositions. Although these models constitute significant contributions to the field, they either do not incorporate the sophisticated transport phenomena in the fuel cell rigorously or they underestimate the effects of spatial distributions of the transport variables.

Transient SOFC Modeling

While there are a number of significant modeling efforts, both in steady state and in transient, transient SOFC models typically are not as elaborate as steady-state models. Some of the transient models are lumped models neglecting all the spatial variations. They are mainly developed for control or to simulate the fuel cell as part of the larger system. Transient models incorporating transport phenomena vary from 1D to 3D models. 3D models are developed generally for planar SOFC, whereas exploiting the axial symmetry of the tubes, 2D models are preferred and most of the time sufficient to represent an SOFC with a tubular design.

Achenbach presented one of the first transient studies on SOFCs. He developed a 3D transient model to investigate the voltage responses of a planar SOFC to certain

load changes. Ioara et al. developed a 1D model for a planar direct internal reforming SOFC in which they concluded that neglecting the variation of the gas stream properties may lead to incorrect dynamic response predictions. Jia et al. provide detailed analysis of the effects of operating parameters on the steady state and transient performance of a tubular SOFC. Employing a 1D model, they represented the conservation laws with a control volume approach. In a recent study by Barzi et al., dynamic responses of a tubular SOFC are predicted during the start-up. Their 2D model incorporates mass, momentum, and species balances accompanied with a circuit representation of charge balances. Bhattacharyya et al. compared the dynamic behavior of the cell with the experiments in their 2D model of a tubular SOFC. Along with investigating dynamic response of the cell to the changes in voltage, they also predicted the response of the cell to the changes in hydrogen flow rate. Ota et al. compared transient characteristics of a standard tubular cell with a microtubular cell with a modeling framework presented therein. Their modeling framework is based on simplifications instead of taking into account full coupling of the sophisticated transport phenomena. They reported that timescales of a standard tubular cell to a specific voltage response are six times larger than that of a microtubular cell.

Another modeling study on microtubular SOFCs is presented by Nehter. In this study, he compared a common microtubular cell with a cascaded one. Although localized temperature and species concentrations are provided in his 2D axial symmetric model, momentum balance and multicomponent species transfer are not included. Mass balance is carried out in a simple way via algebraic equations describing the electrochemical and shift reactions.

Although there are many simplifications in the models of Ota et al. and Nehter, their studies are significant since, to the knowledge of the authors, they are the only modeling efforts emphasizing dynamics of microtubular SOFCs. Since the characteristics of a microtubular SOFC are very different than a standard tubular cell, there is still need for a rigorous model to study the dynamics of such a cell.

Thermal Fluid Model Description

The work performed by Serincan et al. employed two separate models to have a more accurate representation of the actual fuel cell test system: (1) a furnace model and (2) a fuel cell model. With the predictions from the former, boundary conditions were determined for the fuel cell model.

Figure 14 represents the geometrical domains for the furnace model and the fuel cell model. The model exploited the axial symmetry of the tubular geometry, therefore reducing the modeling domain into a 2D axisymmetric domain, assuming the anode and the cathode current collectors were uniformly distributed on the electrode surfaces. Figure 14 (not drawn to scale) also shows the cross section of the axisymmetric geometry.

The actual model geometry can be visualized by revolving this cross section around the symmetry axis, that is, centerline of the anode tube. Mass, species, and

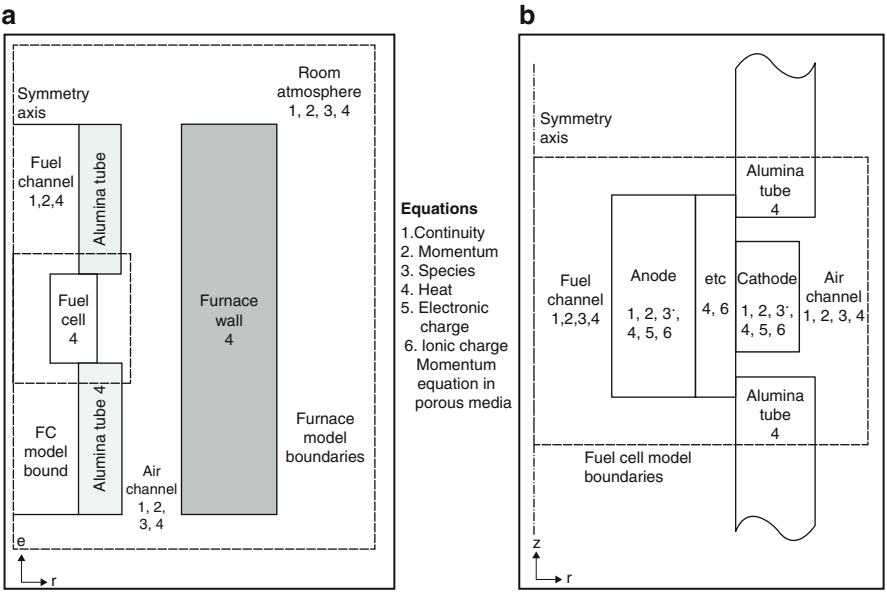

Fig. 14 (**a**) Furnace model domain. (**b**) Fuel cell model domain. Numbers represent the equations solved in each section of the domain

momentum conservation equations were solved in the gas channels and the porous electrodes, and energy conservation was applied for the entire domain. Ionic charge balance was applied in the anode, the electrolyte, and the cathode, whereas the electronic charge balance was applied in the anode and cathode.

The microtubular cells considered in this study were fabricated and characterized as described above. The anode-supported cells employed a GDC electrolyte coated on a NiO-GDC anode and (LSCF)-GDC cathode. It is well known that GDC electrolytes are prone to internal current leakages. GDC can reduce and become electronically conductive, especially at elevated temperatures. A fraction of the electrons generated at the anode can then be transferred to the cathode through the electrolyte. As a result, the cell is short circuited and a drop in the open circuit potential is experienced. The effect of current leakages becomes less significant at higher current densities, because they are inversely proportional to the ionic current density. In this work, the electronic current leakages were modeled as boundary conditions to the electronic charge equation at the electrolyte interfaces of anode and cathode while describing the boundary conditions. The furnace model was used to explicate the transport phenomena in the furnace and the surrounding room atmosphere and estimated the transport properties at the boundaries of the fuel cell model domain. Computational domain for furnace model was chosen by trying different dimensions until the gradients disappeared and/or not to have a significant effect on the distribution inside the furnace.

Results from Modeling

The furnace model consisted of the furnace, fuel cell as a whole, alumina tubes shown in (Fig. 9), air channel, and the surrounding room atmosphere. In the air channel and the room atmosphere species, momentum and heat equations were solved. In the fuel cell, these equations were modified accordingly to account for porous media transport. In the furnace walls and alumina tube, only heat equation was solved. The difference between the furnace temperature and the room temperature invokes natural convection, which transmits the air to the fuel cell. To implement natural convection in the model, a nonisothermal flow equation was used. Another approach could have been to apply a Boussinesq approximation to the Navier-Stokes equation, which would be based on linearization of density with respect to the changes in temperature and concentration. Further, Maxwell-Stefan equations coupled with heat and momentum equations were used to model the species balance.

On the other hand, the fuel cell model included truncated air and fuel channels, alumina tubes, anode, electrolyte, and cathode as is seen in Fig. 14. In the air and fuel channels, species, momentum, and heat equations were solved. In the anode and cathode, in addition to these equations that were modified for porous media, ionic and electronic charge equations were also solved. In the electrolyte ionic charge, equation was solved along with heat equation. In the alumina tubes, only heat equations were solved.

Maxwell-Stefan equations were used to model the multicomponent species balance instead of Fick's law, which is applicable only for binary mixtures. To model momentum transfer, nonisothermal flow equations were solved, with the nonisothermal continuity equation, to take into account the density changes with temperature and species concentration. In the porous electrodes, momentum equations were modified in the form of nonisothermal Brinkman equations. Darcy's law for momentum transfer in porous media was not chosen as it does not include stress tensors in its formulation. Heat equations were formulated in order to include enthalpy transfer. Heat transfer due to radiation was modeled as boundary conditions. Electronic and ionic charge balances were implemented in the form of Ohm's law throughout the anode, electrolyte, and the cathode domains.

The results of the furnace model described above showed that oxygen concentration at the boundaries strongly depend upon the fuel cell operation conditions and the importance of assigning the right boundary condition. The model results were also compared with experimental data, and related polarization curves show good agreement for a set of different operating temperatures. Having a good match with the same set of fitting parameters for three different polarization curves suggests the model captures the temperature dependence of the fuel cell electrochemistry well. Temperature distribution in the cell was evaluated and the average radial temperature gradient was calculated as 2.25 °C/mm, whereas the axial average gradient was

found to be 18 °C/mm. It was predicted that the temperature may rise by up to 120 °C for an SOFC operating at 0.2 V. This temperature rise is attributed to the ohmic heating due to the losses during fuel cell operation. It was further shown that it was a good assumption for a microtubular SOFC to lump all the losses at the anode due to the very small thickness of the tube.

Leakage currents were found to be the reason for an OCV drop of 0.18 V at 550 °C, and their effects diminish gradually until they vanish around cell voltages of 0.6 V. It was also shown that at higher operating temperatures, the internal current leaks associated with the electron transfer through the electrolyte were more significant. It was predicted that if the output current demand is 0.53 A/cm^2, the fuel cell has to generate an ionic current density of 0.65 A/cm^2 at 550 °C, as under this condition, the leakage currents sum up to 0.12 A/cm^2.

The dependency of current density on transport properties was also studied, and the effects of temperature and species concentration were shown on the current density profiles. Moreover, exchange current density as a measure of reaction rate was considered, and it was suggested from model results that anode thickness can be reduced to promote reactant diffusion to the active catalyst sites.

Effects of temperature, fuel flow rate, fuel composition, anode pressure, and cathode pressure on the SOFC performance were investigated. It was shown that increase in temperature results in better cell performance due to increase in catalytic activity, ionic conductivity, and decrease in mass transport losses. It was found that with higher flow rates, the performance of the cell increases; however, efficiency decreases due to the lower utilization. In conjunction with this, it was advised that the fuel flow rate should be chosen according to the desired operating range such as at midrange current densities lower flow rate as suggested because of the efficiency of the cell, and in the higher current density range, higher flow rate should be chosen (i.e., a stoichiometric flow control) because of the output power implications. It was also shown that the utilization of the fuel was not zero when the cell does not generate current because the reacted fuel is not enough to overcome the internal current leakages. When fuel composition was considered, higher hydrogen content was favorable for power output, efficiency, and thermal management. Increases in anode side and cathode side pressures have two distinct effects on cell performance: increase in pressure reduces reactant diffusivity but increases catalytic activity. However, the latter overwhelms the adverse effects of decreased mass transport and cell performance is always observed to improve with larger back pressure. When the effects of pressure on the anode and cathode sides are compared, it was seen that it was more sensitive to changes in the air pressure mainly due to the slow reaction kinetics of the cathode.

Response of the cell to a change in voltage was also investigated. An overshoot was observed in the current density response as a result of the combined effect of fast electrochemical reaction and slower dynamics of the mass transfer. It was predicted that timescales of a microtubular SOFC are in the order of 20 s governed by the dynamics of heat transfer.

Future Directions

Solid oxide fuel cells (SOFC) have tremendous potential for a number of applications from small mW to W scale, all the way up to MW scale systems. However, research around the world is concentrating in the development of suitable materials and fabrication processes to bring down the price of the SOFC to make it a commercially viable product. Programs are underway internationally to look at novel SOFC geometries utilizing cheaper materials that work at lower temperatures. The demonstration of a low-temperature SOFC running directly off methane or natural gas signals an important new opportunity for making simple, cost-effective power plants. Changes in cell composition and design have resulted in improved power densities, with higher power densities contributing to lower weight, size, and cost of the final fuel cell systems. This is the future direction that has to be optimized to allow these systems to become a reality.

References

Dees DW, Claar TD, Easler TE, Fee DC, M'razek FC (1987) J Electrochem Soc 134:2141
Kordesch K, Simader G (1996) Fuel cells and their applications. VCH, Weinheim
Minh NQ, Takahashi T (1995) Science and technology of ceramic fuel cells. Elsevier, Amsterdam
Singhal SC (1991) In: Grosz F, Zegers P, Singhal SC, Yamamoto O (eds) Proceedings of the 2nd international SOFC symposium, Athens. Commission of the European Communities, Luxembourg, p 25

Molten Carbonate Fuel Cells

Takao Watanabe

Contents

T. Watanabe (✉)
Central Research Institute of Electric Power Industry, Yokosuka, Kanagawa, Japan
e-mail: wata@criepi.denken.or.jp

W.-Y. Chen et al. (eds.), *Handbook of Climate Change Mitigation and Adaptation*,
DOI 10.1007/978-3-319-14409-2_45

Abstract

Molten carbonate fuel cell (MCFC) is a high-temperature fuel cell. Because of high-temperature operation, various fuel gases can be widely used and internal reforming of hydrocarbon fuel is also possible, resulting in improving fuel utilization and providing higher power generation efficiency. Many MCFC plants are being installed as the stationary cogeneration power supply using various fuels in various countries in the world, and among them, the world's largest fuel cell power plant has 2.8 MW electric capacity. The power generation efficiency of the systems including smaller 300 kW units reaches 47 % (LHV, net, same as above unless otherwise noted). In addition, the hybrid systems which contain both MCFC and gas turbine have been demonstrated, and a new carbon dioxide (CO_2) recovering hybrid system concept with extremely high value of 77 % efficiency is proposed. The advantage of MCFC is not only the use of city gas but also the use of digestion gas from the sewage disposal plant. In the future, it is expected to develop a large-scale centralized electric power generating plant using the coal gasification gas. The MCFC is one of the key technologies to reduce CO_2 emission for the future.

Introduction

The MCFC is a high-temperature fuel cell operated at approximately 600–650 °C. Along with the features of general fuel cells that are high power generation efficiency, capacity flexibility, and excellent environmental property, it has a lot of additional attractive features such as the variety of an applicable fuel and improvement of the power generation efficiency by a combination with the gas turbine and/or by the internal reforming. The MW class plants are already introduced, and its commercialization is just around the corner. This chapter outlines the features of MCFC, the principle, the basic performance, the configurations of cell/stack/system, and current development situations and issues. The future directions are also given.

Features

The MCFC uses carbonate which is in a molten state for an electrolyte, and the electrochemical reactions take place through carbonate ion. Besides the features of the general fuel cells such as high efficiency, capacity flexibility, and the superior environmental sustainability, the MCFC has additional features as follows.

High Efficiency

Because the operating temperature is around 600–650 °C, it can form the power generation systems combined with the gas turbine and the steam turbine by using the high-quality exhaust heat from the MCFC. It can attain much higher power generation efficiency.

Various Fuels

Due to high operating temperature, electrode reactions take place in fast speed, and thus expensive platinum (Pt) catalyst is unnecessary, resulting in avoiding carbon monoxide (CO) poisoning. Therefore, the application of the CO-containing gasification gases such as coal, biomass, and waste is also possible.

Internal Reforming

When methane-based fuel is in use, internal reforming can be applied using steam and heat generated inside the fuel cell. The internal reforming can be expected to improve the generation efficiency by increasing fuel utilization and lowering energy consumption for cooling the MCFC to maintain the operating temperature. The internal reforming can also simplify the system configuration by eliminating the external reformer.

CO_2 Concentration

Because the electrochemical reactions take place through carbonate ion, CO_2 is necessary for the cathode reaction. On the other hand, same amount of CO_2 is generated at the anode. Therefore, the CO_2 generated at the anode is generally circulated to the cathode side. It is called the CO_2 recycling. Because the generation of CO_2 at the anode increases the concentration of CO_2 at the anode exhaust, low concentration of the CO_2 at the cathode inlet can be increased at anode exhaust. For example, if low CO_2-containing flue gas from thermal power station is supplied to the MCFC cathode, we can obtain high CO_2-containing gas which can separate CO_2 easier.

Easier Manufacturing of Large Cells

The MCFC generally adopts a planar multilayered structure, using metal separators and sheets of active components manufactured by tape casting method. Therefore, it is rather easy to make it big and to be adopted by large-capacity power plants from the production viewpoint.

Principle

Figure 1 shows the principle of the MCFC operation (U.S. Department of Energy 2004). The electrolyte is a liquid that melts under the operating temperature. Hydrogen (H_2) supplied to the anode reacts with carbonate ion (CO_3^{2-}) in the electrolyte. The electron is discharged from the anode and steam (H_2O) and CO_2 are generated at the same time. Reacting with the electron, oxygen (O_2) and CO_2 supplied to the cathode generate CO_3^{2-}. These reactions are expressed as follows:

$$\text{Anode} : H_2 + CO_3^{2-} = H_2O + CO_2 + 2e^- \quad (1)$$

$$\text{Cathode} : CO_2 + 1/2O_2 + 2e^- = CO_3^{2-} \quad (2)$$

$$\text{Total} : H_2 + 1/2O_2 = H_2O \quad (3)$$

The electron is discharged from the anode and taken into the cathode through an external circuit in a series of reaction. Power generation by the fuel cell is achieved by flowing the electron. Because the operating temperature is high and nickel (Ni) is used for both electrodes, Ni acts as a catalyst and CO in the fuel gas (if there is any) supplies H_2 by the shift reaction ($CO + H_2O = H_2 + CO_2$) relating to the reaction of Eq. 1. The operating temperature of MCFC is high enough for the proceeding of

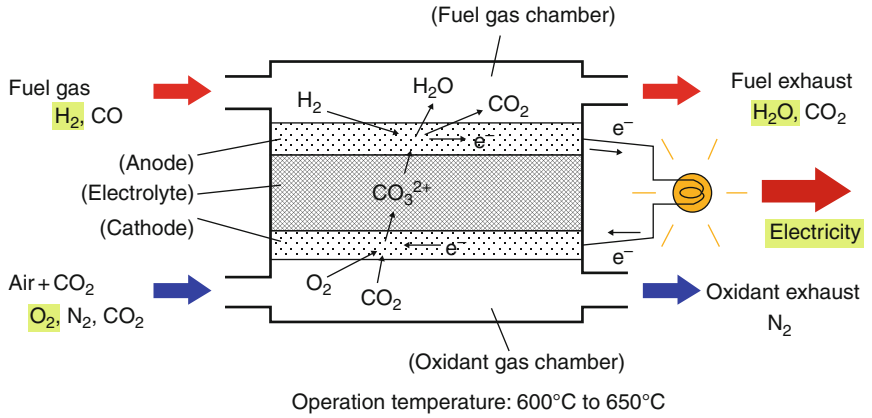

Fig. 1 Principle of the MCFC

the shift reaction. Therefore, it becomes possible to use the gasification gas of coal, biomass, and waste, which contain certain percentage of CO. In addition, a big characteristic of the MCFC is to have to contain CO_2 in the supplied oxidant gas, because the ion in the electrolyte that contributes to the reaction is CO_3^{2-}.

Cell Stack Configuration and Materials

The actual cell consists of the matrix sheet, the electrode (anode and cathode) sheets, and the metallic components that provide reactant gas passageway and current collection, as shown in Fig. 2. Then, the size of the cell is described.

Matrix and Electrodes

The matrix has a porous ceramic structure consisting of $LiAlO_2$. It is usually impregnated with the electrolyte liquid maintained by capillary force under the operating temperature. Mixed carbonate of Li_2CO_3 and K_2CO_3 or of Li_2CO_3 and Na_2CO_3 is used as the electrolyte. A γ type has been used for $LiAlO_2$ mainly, but the α type is examined recently from a point of the stability for carbonate. Moreover, the coarse particle or fiber of alumina (Al_2O_3) is mixed to keep the mechanical strength.

Both anode and cathode provide reaction places for the reactions (1 and 2) and are placed on the surface of the thin electrolyte film (matrix). Therefore, the electrodes are required to have high electric conductivity, optimal pore size, and porosity for providing sufficient active area (reaction places), adequate wettability for maintaining electrolyte stable, stable porosity structure, etc. Because mean pore sizes of the electrodes are larger than that of the matrix by single digit, capillary force in the matrix is stronger than that in the electrodes. Then, pores within the

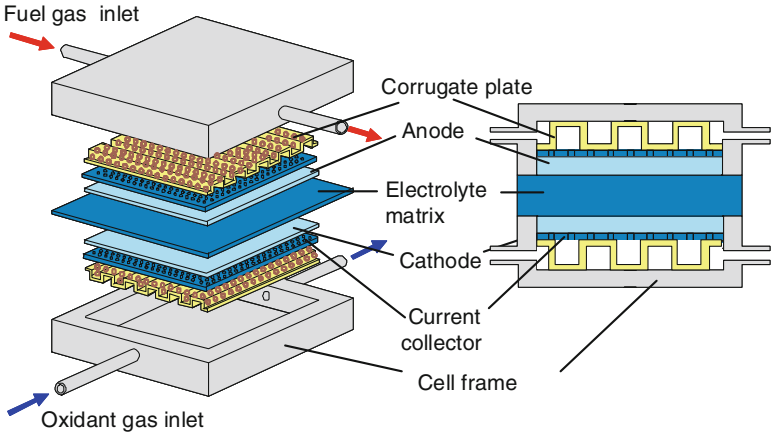

Fig. 2 Configuration of MCFC cell

matrix are firstly filled up and then excess electrolyte is impregnated in the pores within the electrodes. Matrix is usually filled up 100 % with electrolyte and the pores of the electrodes are filled by 20–40 % of the void volume.

1. Anode: The anode is required to have high corrosion resistance for melted carbonate under the fuel gas atmosphere. It also should be stable under steam and CO_2 generated at the anode. Therefore, the porous sheet sintered from fine nickel (Ni) particle is used. Chrome (Cr) and aluminum (Al_2O_3) are usually added for the improvement of creep resistivity at high temperature.
2. Cathode: The cathode is operated under a severe condition of oxidative atmosphere, and thus the metallic oxide is used. Typically, the porous media made of oxidized nickel particle is used. Nickel oxide (NiO) does not have sufficient electric conductivity; however, the electric conductivity is given by lithium in molten carbonate being doped in the cathode.
3. Manufacturing of the sheets: The electrodes and the matrix are made by the tape casting method and the formed sheets are cut for required sizes. The tape casting method is a useful process for simple, easy, quantitative, and cost-effective production. In the process, the slurry to the mixture of the fine particle of the raw material with the solvent is thinly spread by a doctor blade on a substrate sheet and dried. The spreadsheet is about 0.5 mm in thickness and about 1 m in width. The electrodes and matrix are called active components, and they are cut to have rectangular-shape-like PAFC.

Metallic Components

1. Gas flow channels: Gas flow channels for fuel and air (it is accurately called "oxidant gas" because it contains CO_2) are formed using the metallic end plates which sandwich active components. The outer periphery of the end plates touches the electrolyte matrix directly, and the wet seal covered with the liquid film of the impregnated electrolyte is formed and prevents gas leakage to the outside. Stainless steels such as SUS316L and SUS310S are machined or pressed for the end plate. The nickel clad steel is used as a center plate of the separator, which is exposed to both reducing and oxidizing condition on each side in consideration of corrosion resistance with the carbonate.
2. Current collector: Moreover, the current collector is placed within the gas flow channel for better electric contact between the electrode and the end plate. Perforated metal plates with same materials to the end plates are generally used.
3. Separator: Because the voltage of a single cell is about 0.7–0.8 V, it is necessary to obtain a high voltage of several 100 V or more to operate the power conditioner efficiently. Therefore, it is required to pile up the single cells through the metallic separator plates. This is called a stack. The separator has gas flow channels on both sides instead of the end plate for single cell, and it connects single cells in series electrically. The number of cells in the stack is usually 100–300.

4. Gas flow directions and manifolds: There are three ways for fuel and oxidant flow directions at a cell. These are cross flow, parallel flow, and co-flow. It is chosen in consideration of the operating temperature and the current distribution in the cell. There are also three ways for distributing reactant gases to each cell within a stack, which are external manifold, internal manifold, and hybrid manifold. External manifold is adopted in the PAFC stack. However, internal manifold which has a penetration hole through the cell is sometimes selected for MCFC stack. It is also chosen in consideration of reactant gas flow directions within the cell. External manifold is selected in the case of cross-flow-like PAFC. However, internal manifold could be adopted in the case of parallel flow and co-flow. There are both merits and demerits from the viewpoint of the manufacturing process, electrolyte migration in the stack, effective electrode surface area of the cell, etc.

Cell Size

The thickness of the single cell is several mm with the two electrodes and electrolyte matrix (active components). The size of stacked cell is slightly bigger than general PAFC, and the length is about 1 m on a side of the rectangular shape. The separator is produced using a metal part with about the same size. Table 1 shows a general specification of each material that composes the cell (U.S. Department of Energy 2004).

External and Internal Reforming

Either an external reforming or an internal reforming method is adopted for the supplying H_2 to the system as a reactant at the anode. Reforming reaction is expressed as follows:

Table 1 Specification of MCFC components

Component	Material	Thickness	Mean pore diameter (MPD), porosity, etc.
Anode	Ni–Al–Cr	0.7–1.0 mm	MPD: 4–6 μm
			Porosity: ca.60 %
Cathode	Lithiated Ni	0.3–0.8 mm	MPD: 8–10 μm
			Porosity: ca.80
Electrolyte support	γ-$LiAlO_2$, α-$LiAlO_2$	0.5–1.0 mm	Porosity: ca.60 %
			Specific surface: 15–20 m^2/g
Electrolyte	Li_2CO_3–K_2CO_3	–	–
	Li_2CO_3–Na_2CO_3		
Separator	SUS310S, SUS316L, Ni	–	–
	SUS316L-Ni clad		

$$CH_4 + H_2O = 3H_2 + CO \quad (4)$$

The external reforming is a method that the reformer is installed separately from the stack, same as the PAFC system, and H_2 is generated from natural gas outside the stack. In the internal reforming method, the reforming catalyst is loaded within the fuel flow channel of the cell and H_2 is generated in parallel with power generation. The MCFC can adopt the internal reforming method because of its high-temperature operation.

External Reforming

In the external reforming, natural gas and steam mixture are supplied to the separated reformer and H_2-rich gas is produced through a catalyst-loaded tube heated from outside. Reforming rate (methane conversion rate) is limited by the reforming condition, and the number of Balance of Plants (BOPs, equipments configuring the fuel cell system other than the fuel cell stack) is increased. The advantage of this method is that it can avoid undesirable effect of electrolyte on the catalyst (please see below) because the reformer is separated and located upstream of the stack.

Internal Reforming

The internal reforming enables a system compact, stack cooling load small, and to improve methane conversion rate and efficiency, because endothermic reforming reaction proceeds further by using both steam and heat, which are generated within the cell during consuming H_2 at the same time. On the other hand, the reforming catalyst is exposed to the electrolyte, which might cause damaging catalyst. Indirect internal reforming method is usually adopted to avoid this problem (http://www.fuelcellenergy.com). The exclusive reforming plates are sandwiched every several cells in the stack, and pre-reformed gas from the reforming plate is supplied to the cells.

Basic Performance

Current–Voltage (I–V) Characteristic

Basic performance of the fuel cell can be represented by the current–voltage characteristics which affect largely on the efficiency and cost of the plant. The current–voltage characteristic of the MCFC is expressed by a straight line as shown in Fig. 3. Because of high-temperature operation, voltage loss with electrode reaction is small. The cell voltage is generally over 1 V in no load and it becomes 0.7–0.8 V with load of 150 mA/cm^2 current density. The operating cell voltage of MCFC is higher than other types of fuel cells in the current density range

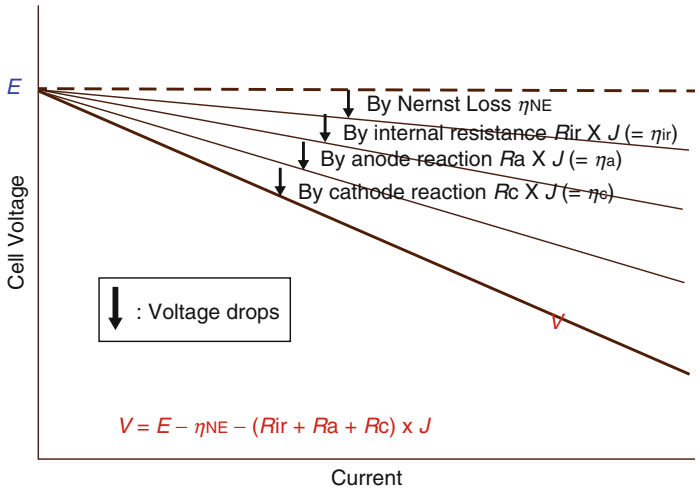

Fig. 3 Current–voltage performance

Fig. 4 Voltage decay pattern

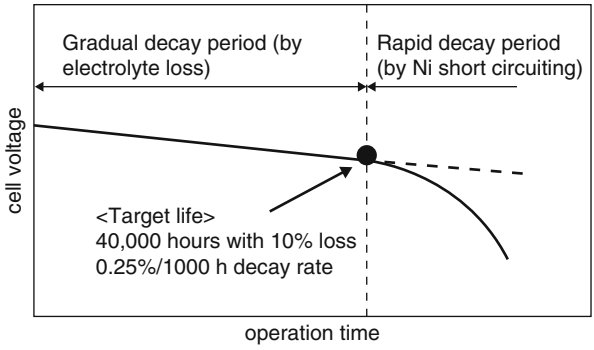

of 100–250 mA/cm^2. It is one of the appropriate MCFC operating conditions at this current density range.

Life Characteristic

To discuss the stability of the cell, voltage decay characteristic (life characteristic) is important. It affects on the efficiency change and eventually on the cost of electricity. Typical voltage decay pattern of the MCFC is shown in Fig. 4. In general, the cell voltage decays gradually and linearly until certain time and then drops rapidly after. The rapid drop is caused by "nickel short-circuiting" as described later. The voltage drop means not only the decrease of plant efficiency but also the change in relevant BOP's operating conditions. Because it is generally considered that the acceptable change of the operating conditions is about 10 %, practical MCFC life should be the

time when cell voltage decreased to the ca. 90 % level from the initial voltage during the linear decay range or the time when the rapid voltage drop started. The reason of the voltage decay will be described in the next section. For keeping high efficiency and reducing cost of electricity, it is important to control the voltage decay rate as small as possible and to delay the starting point of rapid voltage drop after the target lifetime. The current goal of life is generally considered about 30,000–50,000 h as same as other types of fuel cells.

Performance Improvements

Enhancement

Voltage-Determining Factors

There are several voltage-determining factors as shown in Fig. 5 (Morita et al. 1998; Morita et al. 2002). The voltage loss caused by internal resistance is relatively small, and the loss caused by electrochemical reaction at both anode and cathode is large. The electrolyte of the MCFC is the mixture of Li_2CO_3 and K_2CO_3 (Li/K) or the mixture of Li_2CO_3 and Na_2CO_3 (Li/Na). The reaction voltage loss is large using either electrolytes, and the reaction voltage loss at the cathode is larger than the one at the anode. Nernst loss means the decrease of theoretical voltage caused by the gas composition change by electrode reactions, and it is mainly caused by the anode reaction. The composition of fuel gas changes larger than that of oxidant because H_2O and CO_2 are produced at the anode with higher fuel utilization (about 80 % in natural gas-fueled system) which means that the concentration of H_2 is drastically reduced. Oxidant utilization is usually set at lower level (about 30–50 %), meaning higher flow rate, for stack cooling. This is the reason why the fuel-side Nernst loss is larger than the oxidant side.

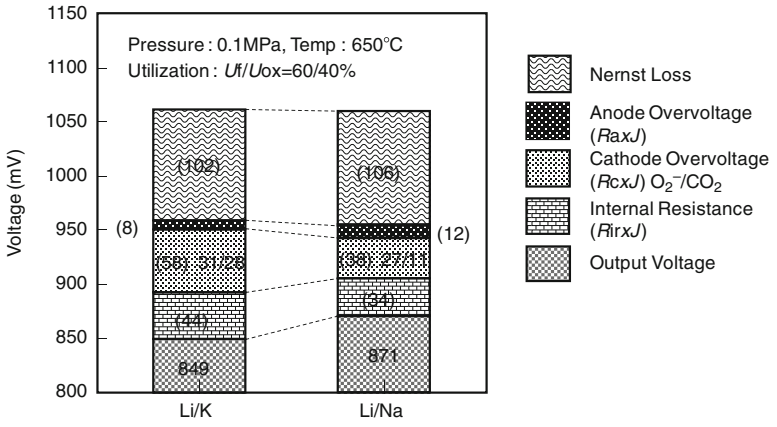

Fig. 5 Voltage-determining factors

Reducing Voltage Loss Factors

The MCFC is expected to replace the conventional centralized thermal power plants in the future. Such large-scale power plants are operated with very high efficiency; therefore, the MCFC power plant is required to be operated with much higher efficiency. If the fuel cell system generates electricity only by the fuel cell, the system efficiency is almost proportional to the cell voltage. Therefore, the fuel cell voltage should be maintained as high as possible, and it is important to reduce the voltage loss factors as can be seen from Fig. 5. It is effective to reduce the voltage loss, first of the cathode reaction and then of the anode reaction and the internal resistance. For the reaction loss reduction at the electrodes, it is important to realize adequate electrolyte distribution, designed by optimizing the microstructure and wettability of the electrodes. For the internal resistance reduction, higher ionic conducting electrolyte or thinner matrix is applied.

Pressurized Operation

Pressurized operation is another way to increase the cell voltage. Higher operation pressure increases theoretical voltage (Nernst potential) and reactant gas solubility which means the decrease of reaction voltage loss, and it can eventually provide higher plant efficiency. It corresponds to push up the voltage–current characteristic indicated in Figs. 3 and 6 shows the pressurized characteristic of the MCFC up to 5 MPa range (Yoshikawa et al. 1999). Regardless of electrolyte composition, the cell voltage increases in proportion to a logarithm of the pressure. However, above about 3 MPa, the cell voltage is suppressed or decreases in some cases. This is caused by the methanation reaction in which methane is produced from carbon and hydrogen elements in fuel gas, resulting in lowering hydrogen composition and decreasing theoretical voltage. The methanation reaction is described as follows:

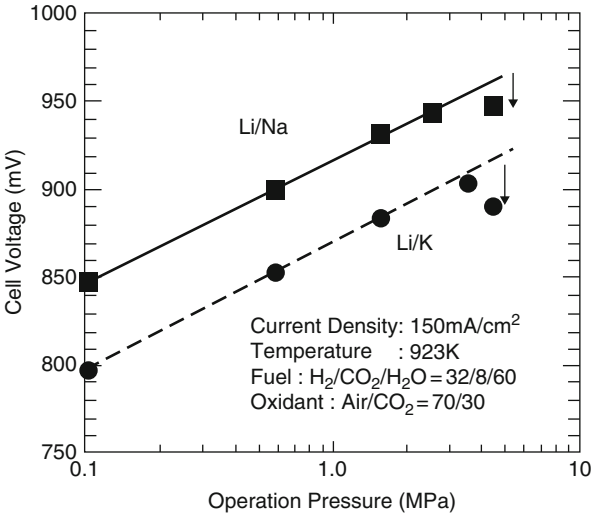

Fig. 6 Pressurized performance

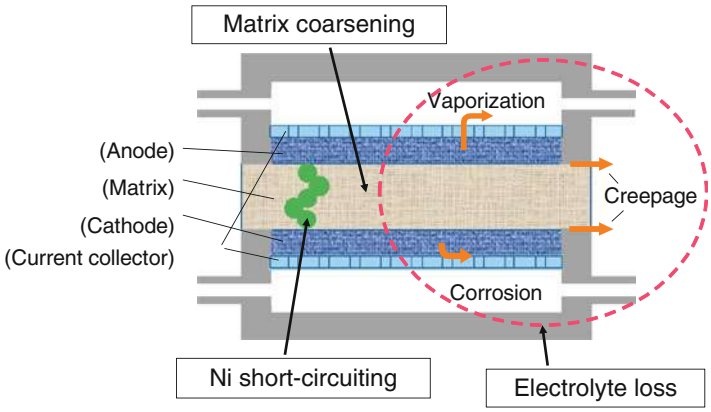

Fig. 7 Life-limiting issues

$$3H_2 + CO = CH_4 + H_2O \tag{5}$$

The reasonable operation pressure range might be up to about 3 MPa based on these data, and it is possible to use gas turbine for the existing combined cycle power plant, which pressure range is less than about 2 MPa.

Life Extension

The factors decreasing cell voltage during operation and determining MCFC life are electrolyte loss such as matrix pore coarsening and nickel short-circuiting, as described in Fig. 7.

Electrolyte Loss

Pores within the matrix are filled up with electrolytes. Excess electrolytes which cannot enter into the matrix are distributed to the anode and the cathode. The distribution ratio is determined by the balance of capillary forces between the anode and the cathode. High cell voltage is attained by adequate electrolyte distribution with proper amount within the electrodes. From its viewpoint, pore distributions determining capillary force and total electrolyte amount are important design factors which affect strongly on cell performance. Meanwhile, it is well known that the amount of electrolyte decreases with time by some reasons. Electrolyte loss changes the distribution to inadequate one and it leads to voltage drop. Most of the loss is caused by the corrosion reaction with metallic components of the cell, and the corrosion products with high electric resistance increase internal resistance. The electrolyte loss is also caused by vaporization and creepage. Usually, corrosion-resistant treatment is applied on the surface of the metallic components. In addition, electrolyte loss is controlled by reducing the number or the total surface area of the

metallic components. Current technology is considered to be able to control the loss that meets the present target life.

Matrix Pore Coarsening

Matrix pore coarsening is caused by dissolution and deposition of $LiAlO_2$ that is ceramic material constituting the matrix during longtime operation. The pore coarsening decreases electrolyte holding force and electrolyte moves out to the electrodes or leaks outside. The electrolyte distribution changes within the electrode and finally voltage decays. One of the solutions is the change of the phase of $LiAlO_2$ from γ to α.

Nickel Short-Circuiting

"The nickel short-circuiting" is a phenomenon that forms the internal short circuits between the anode and the cathode by metal nickel particles in the matrix. Figure 8 shows that NiO as cathode material dissolves as Ni^{2+} ion into the electrolyte by reacting with CO_2 in the oxidant gas, and metallic nickel particles are precipitated when Ni^{2+} ions react with dissolved H_2 from fuel gas. Those reactions are expressed as follows:

$$Ni^{2+} + H_2 + CO_3^{2-} = Ni + H_2O + CO_2 \tag{6}$$

$$NiO + CO_2 = Ni^{2+} + CO_3^{2-} \tag{7}$$

The nickel short-circuiting time can be expressed by the next equation (Mugikura et al. 1995; Yoshikawa et al. 2001):

$$t_s = APco_2^{\alpha} L^{\beta} \tag{8}$$

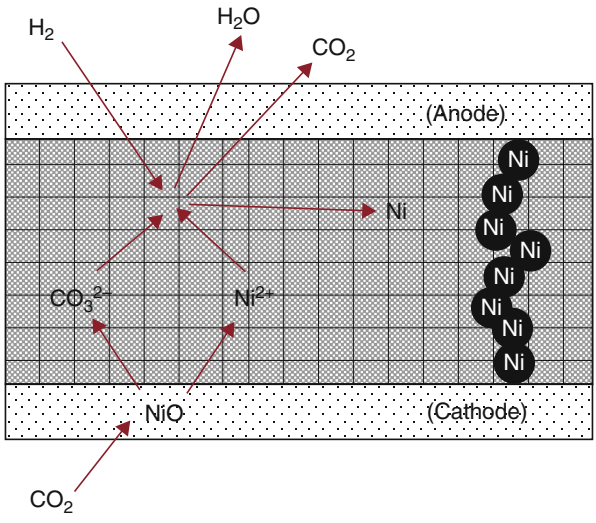

Fig. 8 Nickel short-circuiting phenomenon

Table 2 Comparison of Li/Na and Li/K electrolyte

		Li/KCO_3	$Li/NaCO_3$
Composition	mol%	62:38	53:47
Melting point	°C	488	495.8
Basicity	pO^{2-}	6.9	6.62
NiO solubility	mole frac. ($\times 10^{-6}$)	41.9	22
Surface tension[a]	N/m	0.22	0.24
Density[a]	g/m^3	1.93	1.97
Viscosity[a]	Ns/m^2	8.3×10^{-3}	8.1×10^{-3}
Vapor pressure[a]	g/m^3	-3.2×10^{-10}	-3.5×10^{-10}
Ionic conductivity[a]	1/(Wcm)	1.4–1.6	2.1–2.3
O_2 solubility	$Mol/(cm^3atm)$	3.3×10^{-7}[b]	1.8×10^{-7}

[a]650 °C
[b]Li/K = 50/50

where A is a coefficient, PCO_2 is a CO_2 partial pressure at cathode, L is an electrolyte thickness, and $\alpha \cong -1$ and $\beta \cong 2$.

As can be seen, this phenomenon occurs in a shorter time under higher CO_2 partial pressure in oxidant gas, and the occurrence time of the short-circuiting can be delayed by using thicker matrix. However, thick matrix increases internal resistance and decreases cell voltage. There are several trade-offs for cell stack design. The setting of the electrolyte thickness is an example of a typical trade-off to influence the cell voltage, and it is one of the essential design points from the nickel short-circuiting viewpoint. In order to avoid the nickel short-circuiting, the changes of electrolyte composition, matrix material, and operation condition with lower CO_2 partial pressure are attempted.

Recently, it is proposed as one of the solutions to use Li/Na electrolyte instead of conventional Li/K electrolyte. As for the Li/Na electrolyte, the solubility of the nickel is about a half compared with Li/K system as shown in Table 2, and it would be possible to delay the nickel short-circuiting behind. Moreover, this electrolyte can decrease internal resistance because the electric conductivity of the ion is higher as shown in Fig. 5 and can improve the voltage of the cell. It is concurrently tried to decrease nickel solubility by a small amount of additive to the electrolyte or to control the precipitation of nickel particles by the improvement of the matrix structure.

System Configurations

Basic Configuration

The MCFC power generation system is composed of the fuel processing system, the air supply system, the MCFC, the inverter, etc., so that fuel and air can be supplied to the stack in appropriate temperature conditions, same as the case of PAFC system. Because the MCFC can utilize various kinds of fuels, the fuel processing system is

different from the kind of fuel. It will contain a steam reformer for natural gas and a gasifier and a gas cleanup unit for coal, biomass, or wastes.

In addition, the shift converter which was applied to reduce CO in fuel gas in the case of PEFC and PAFC is unnecessary. Because the operation temperature of the MCFC is about 600–650 °C, the exhaust heat can be used for temperature control at the inlet gas of the stack and for reforming reaction at the reformer. In addition, it is possible to configure a hybrid power generation system including a gas expander and a steam turbine at MCFC downstream as a bottoming cycle.

The details of the natural gas or coal-fueled MCFC power generation systems are described below. The natural gas-fueled pressurized external reforming system or ambient pressure internal reforming system has already realized about 47 % efficiency. As for the future large-scale plants, simulation results show that the natural gas-fueled pressurized external reforming system with 1,000 MW capacity would be about 65 %, the pressurized internal reforming system with 700 MW capacity would be about 69 %, and the integrated coal gasification system (IGMCFC) with 600 MW capacity would be about 57 % efficiency (Watanabe 2001).

Natural Gas-Fueled External Reforming System

Configuration of the natural gas-fueled pressurized external reforming MCFC power generation system is shown in Fig. 9 (Krumpelt et al. 1982). In this system, natural gas mixed with steam is supplied to the reformer, converted to H_2 and CO, and used at MCFC. CO should be a certain lower level for low-temperature fuel cells. However, the MCFC has no catalyst which has poisoning problem like low-temperature fuel cells. Moreover, CO can be shifted to H_2 by fast shift reaction under high-temperature condition. Even in the case that H_2 is consumed for power generation, CO can shift to H_2 very fast. Therefore, CO can be considered as an

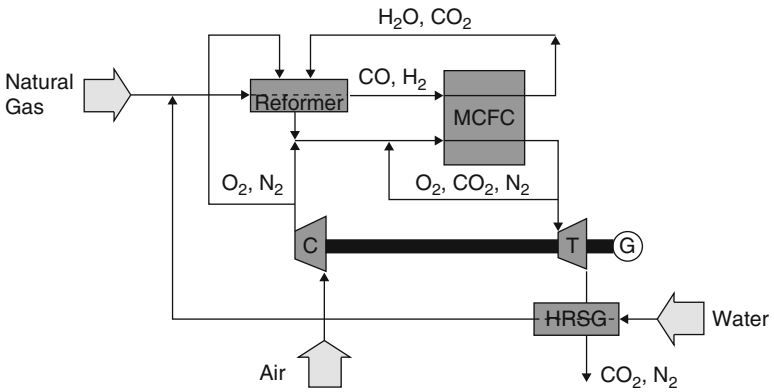

Fig. 9 Natural gas-fueled external reforming MCFC system

effective fuel in the MCFC. However, high-temperature condition also allows Boudouard reaction, which forms solid carbon from gaseous CO around fuel supply line. The Boudouard reaction is expressed as follows:

$$2\mathrm{CO(gas)} = \mathrm{C(solid)} + \mathrm{CO_2(gas)} \tag{9}$$

Thus, it is required that the fuel gas should be in a certain condition to avoid this reaction, and humidifying the fuel gas is one of the countermeasures.

MCFC exhaust gas from the anode contains combustible components, and they can be used as a heat source of an external reforming in the natural gas system. Actually, certain quantity of non-reacted fuel is necessary, and the quantity of H_2 and CO that can be utilized for anode reaction (fuel utilization) is decided from the calorific value required for reforming reaction.

Oxygen as one of the reaction species at the cathode is supplied from air compressor connected to the expander turbine at the same pressure to the fuel gas. Reaction specie, CO_2, is recycled from the anode exhaust, which contains the produced CO_2 at the anode. The amount of the produced CO_2 is same to the required amount for the cathode reaction. The fuel exhaust from the MCFC contains not only CO_2 but also unreacted flammable species, such as H_2, CO, and CH_4. It is supplied to the burner of the reformer to supply heat for reforming. The burner has another role to complete oxidizing the flammable species before supplying CO_2 mixed gas to the cathode. The combustion gas from the reformer combustor is mixed to the air from a compressor, and it is supplied to the cathode.

Heat is generated within the MCFC by the internal resistance or electrode reactions same as the PAFC. Therefore, it is necessary to control the MCFC temperature and to keep it at constant value. Because any liquid coolant such as water cannot be applied for cooling of high-temperature fuel cells, large quantity of the oxidant gas (cathode gas including O_2 and CO_2) is circulated through the cathode channel for cooling the MCFC. The inlet temperature of the circulated oxidant gas should be set around 600 °C, and the outlet temperature should be around 650 °C for adequate temperature operation. Therefore, the cathode gas recycling is adopted. The oxidant gas supplied to the cathode is a mixture of the combustion gas from the reformer, a part of cathode exhaust gas, and fresh air from outside. The generated heat in the stack is removed by the oxidant whose inlet and outlet temperatures are adjusted by controlling the flow rate of recycling gas and the fresh air from outside.

Finally, high-temperature pressurized exhaust gas from the cathode is led to the turbine expander and this recovers power for air compressor. In addition, the surplus power can generate electricity using a power generator connected to the expander, and this also contributes to enhance the entire system efficiency. The necessity H_2O (steam) for reforming reaction is supplied from the recovered water from the anode exhaust gas by condensing before supplying to the reformer.

Natural Gas-Fueled Internal Reforming System

As mentioned above, the internal reforming can be applied to the MCFC because of high-temperature operation (Krumpelt et al. 1982). The internal reforming can produce reaction specie H_2 from CH_4 within a stack. Therefore, the system can eliminate an external reformer. Conventional external reforming reaction has a limitation of the CH_4 conversion ratio by the equilibrium composition with given fuel composition, temperature, and pressure. In contrast, the internal reforming does not reach the equilibrium as long as electricity is generated; that is, H_2 is consumed at the anode. The reforming reaction proceeds further and eventually CH_4 conversion is approaching approximately to 100 %. This means that almost no residual CH_4 exists at the anode. As a result, the concentration of H_2 and the system efficiency increase. In addition, the heat generated from the stack can be used for reforming reaction, and the flow rate of the oxidant can be reduced so that the parasitic power for cathode recycling blower can be reduced. The operation temperature of the MCFC is 600–650 °C, which is slightly lower than the typical reforming temperature around 700–800 °C. Therefore, reforming catalyst must be placed inside the stack. On the other hand, there could be a problem regarding the catalyst performance decay caused by the electrolyte vapor, and therefore, pre-reforming plates are usually installed upstream and sandwiched between every several cells to avoid the problem. The internal reforming system is usually operated at ambient pressure condition for enhancing CH_4 conversion rate in the stack, and air blower can be utilized instead of using the expander turbine.

Integrated Coal Gasification MCFC Combined Cycle (IGMCFC)

Figure 10 shows the configuration of coal-fired power plant (Bonds et al. 1981). The high-temperature fuel cells, as described above, can use a fuel containing CO. The gasified coal gas containing mainly CO can be supplied directly to the MCFC after being purified. The coal gas contains trace impurities which adversely affect the performance, and therefore gas purification equipment is required. The stack has no upper limit of fuel utilization because there is no need to use anode exhaust as a heat source for reforming like natural gas-fueled system. Thus, the fuel utilization can be maximized to improve the efficiency as far as uniform fuel distribution to each cell is attained. Fuel exhaust from the stack contains CO_2, and it is recycled to supply to the cathode same as the natural gas-fueled system. Additional combustor is necessary instead of reformer burner to burn any flammable species contained in the anode exhaust with CO_2. The cathode exhaust gas is then fed to the heat recovery steam generator (HRSG) after recovering mechanical power and generating additional electricity at the expander turbine generator. The generated steam is supplied to the steam turbine with other generated steam at the stack or gasifier for producing additional electricity.

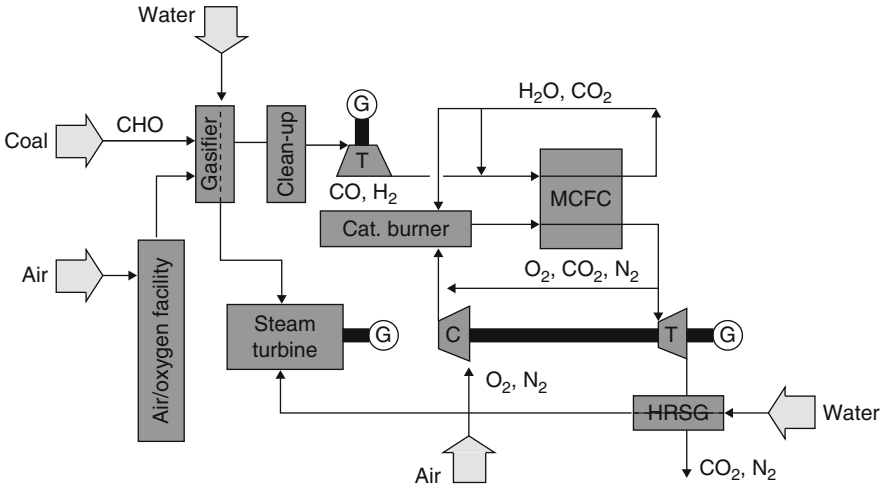

Fig. 10 Configuration of integrated gasification MCFC combined cycle

Development Status of MCFC in the World

Dawn of the Development

It is said that the development of MCFC started from the experiment by Baur of Germany using melted carbonate as electrolyte in 1921 at about 1,000 °C. The concept of the matrix where the electrolyte was impregnated was introduced in 1946 by Davtyan of the Soviet Union, and the porous nickel electrode was adopted in 1958 by the Netherlands Broers and others. The research was actively advanced for the combination of the electrolyte and the electrodes in the Netherlands and the USA. Meanwhile, the MgO matrix and the Fe, Ni, Co, Ag, and Zn electrodes have been attempted, and the current prototype was completed in around 1970 (Mamantov and Braunstein 1981).

Above fundamental research, results have been expanded in the USA since the late 1970s. The US ERDA (US Energy Research and Development Administration) started the national program in 1976 and the US DOE (Department of Energy) has taken over the program in 1978. Other countries such as the Netherlands, Japan, Italy, etc. have started their developments since around 1980 as if responding to the activities in the USA.

USA

The US DOE has promoted the development of MCFC in the USA. In the early 1970s, the final goal was set as a centralized power plants using coal. However, development focus has moved to the MW class small- or middle-sized distributed generators as a cogeneration plant since the 1990s.

The IGT (Institute of Gas Technology, presently GTI, Gas Technology Institute), UTC (United Technologies Co.), GE (General Electric Co.), etc. have developed and established basic technologies under the DOE's program. Afterward the venture companies such as the ERC (Energy Research Co., presently FuelCell Energy) and the MCP (MC Power Co.) have taken over the developments, and the governmental program for market introduction was continued focusing on the product development and performance improvement until 2003. Thereafter, getting a financial support from the government or the states, the systems as distributed generators are being introduced into the states which have great concern with the environmental issues in particular.

The main player of the development and the introduction is FCE Co. (FuelCell Energy) now (http://www.fuelcellenergy.com). FCE has a longtime development history in MCFC of the ambient pressure internal reforming type that is called DFC in the company. A 2 MW internal reforming system was demonstrated in 1997. FCE currently produces a lot of 300 kW commercial cogeneration systems (sub-MW system) with a Hot Module structure (horizontal stack) jointly developed with Germany MTU Onsite Energy Co. FCE now produces three different capacity models including two kinds of the MW system.

Sub-MW system (DFC300, 47 % net efficiency) has been installed about 70 units in total so far, mainly in the USA, Japan, and South Korea. MW class systems adopting FCE's own configuration are 1.4 and 2.8 MW system (DFC1500, DFC3000, respectively, both 47 % net efficiency) (Leo et al. 2007). These MW class plants are initially built by the combination of the sub-MW units. But now for lowering the cost, the module consisting of four vertical stacks in a container (one module in DFC1500, two modules in DFC3000) becomes a mainstream (Farooque et al. 2009). According to the company's report, the capacity of the base stack was initially about 250 kW (AC) around the year 2000, and it is increased to 300 kW in the year 2006. Now it is expected to be 350 kW shortly. The life of the stack was improved from 3 to 5 years, recently (Farooque et al. 2007). The plant's specifications of FCE are shown in Table 3 (http://www.fuelcellenergy.com).

Table 3 Specification of the MCFC plants (FCE)

Type		DFC300	DFC1500	DFC3000
Net output (kW)		300	1,400	2,800
Net efficiency (%, LHV)		47 ± 2		
Exhaust heat utilization	Temp. (°C)	121 (49)		
	Heat output (MJ/h)	506 (852)	2,338 (3,935)	4,677 (7,870)
Size (m) (L × W × H [chimney])		8.5 × 6.1 × 4.6	17.0 × 12.2 × 9.2	23.8 × 12.5 × 6.4
Total weight (t)		35	104	163
Noise (dB(A), @3 m)		72 (65)		
Exhaust (mg/MWh)		NOx: 4,500, SOx: 45, PM10: 0.009		

(): option

Europe

The MCFC has been developed as the distributed cogeneration in Europe. In Germany, MTU Onsite Energy is developing the Hot Module design from the viewpoint of low-cost BPOs (http://www.mtu-online.com/?L=1; Rolf 2006). The 250 kW stack made by FCE in the USA is introduced to the MTU's ambient pressure internal reforming 250 kW system. The Hot Module structure has a horizontal stack inside a cylindrical cathode gas-filled container. Cathode gas is circulated within the container for controlling stack temperature. The system has features such as less piping and compact. MTU Onsite Energy supplied the company's own 250 kW system (HM300) within Europe and is developing the larger HM400 system in recent years. Both systems can utilize biogas, digestive gas, methanol, and natural gas. In addition to these, the company's 320 kW stack was supplied to Wärtsilä Marine Inc. for the ship use demonstration project in Finland.

Italy developed 100 kW class stack (pressurized: 0.35 MPa, external reforming, external manifold, cross-flow type, and 0.75 $m^2 \times 150$ cells) and compact unit (CU) plants with Spain in the MOLCARE program in 1999. The compact unit contains the high-temperature modules including the stack and the reformer in the same pressure vessel. Based on the results, Ansaldo Fuel Cells Co. (AFCo) has been leading the development of the 500 kW modules with the twin-stack concept (http://www.ansaldofuelcells.com/en/index.htm). In this twin-stack concept, two stacks are integrated with catalytic combustor and reformer at the bottom of each stack (Marcenaro 2008). More than ten demonstrations were planned not only in Italy but also in Spain and Turkey, and about half were demonstrated. AFCo has developed a 200 kW stack until now.

Asia

In Japan, the development for energy conservation has been promoted as a national project in the earlier phase in the world in the late 1970s. In this project, the target was set especially for electric power company use, aiming immediate application as natural gas-fueled plant as well as considering the future coal-fueled plant. The 1,000 kW pressurized external reforming system was operated in 1999. Fuel was LNG and operation pressure was 0.5 MPa. The efficiency target of 45 % (HHV, gross) was attained (Nakayama 2000). Another 200 kW pressurized internal reforming system was demonstrated in parallel. These results were reflected in two 300 kW systems using fermentation digestion gas of the garbage and gasified wood biomass gas as part of the power supplies which constituted a microgrid at the world exposition at Aichi in EXPO 2005. The generation efficiency achieved 51 % (gross) at the maximum. Meanwhile, the longtime continuous operation over 66,000 h by a single cell was demonstrated. Its decay rate was less than 10 % per 40,000 h and met the present target. Also CO_2 concentration from the flue gas from the conventional coal-fired thermal plant was demonstrated by supplying the flue gas to the cathode side of 50 kW MCFC stack (Toyota and Dairaku 2009).

KEPRI (Korea Electric Power Research Institute) plays a key role to develop the pressurized external reforming system in Korea (Kim et al. 2008). Based on the fundamental researches in KIST (Korea Institute of Science and Technology), POSCO and RIST (Research Institute of Industrial Science and Technology) participate in the program. The 125 kW system developed with own technology was demonstrated in 2009. The internal reforming system is under development in parallel and its demonstration is planned in 2010.

Apart from these, POSCO Power has been promoting the introduction of MCFC plants (http://poscofuelcell.com/english/). Introducing the technology from FCE in the USA, the company built a new factory for BOPs with 50 MW annual productions in Korea in 2008. Mounted stacks have been supplied from FCE so far; however, POSCO Power has a plan to build another factory for stack assembling with cell components being supplied from FCE.

Development Issues

Cell Stack Issues

Not only applicable to the MCFC, it is necessary for a newly developed technology to achieve higher performance, longer life, and lower cost for accelerating the commercialization of MCFC. In MCFC, it is necessary to exceed above items of the existing power generation technology.

The basic cell and stack technology has been almost established to achieve the immediate objective except the cost. Among the remaining issues needed to be solved, a life extension issue is one of the most important ones. The nickel short-circuiting is the most important problem for the pressurized system aiming higher efficiency. Handling the impurities included in coal gasification gas should also be considered in the future. In addition, the stack design technology enabling lightening the weight of the stack, producing larger cells, and achieving uniform gas distribution for tall stack should be improved continuously.

The nickel short-circuiting is caused by the dissolution reaction of cathode NiO into the electrolyte, which needs to be avoided. The comprehensive measures are required from the viewpoint of the cathode material, the electrolyte composition, the operation condition, etc.

The effects of impurities in the fuel gas are not the urgent issue right now, but it must be resolved when gasified fuels, such as biomass, waste, and eventually coal, will be used on the way to promoting the expansion of application fields. These gasified fuels contain the sulfur compound, the halogenated compound, the nitrogenous substance, etc. These affect largely on the cell performance even though the concentration is ppm order. The effects are being clarified through every kind of actual cell test, and gas cleanup system that reduces impurity content to the acceptable level is under development. The maximum number of stacked cell is currently about 300, and it is expected to increase the number for efficient integration of the stack from the viewpoint of the entire plant. Thus, it is important to develop stacking

technology and to select an appropriate number of stacked cells, because the number of the cells in the stack is restricted by the gas distribution for each cell through the manifold.

Reducing the weight of the stack will become more important issue from the viewpoint of the economy or transportation in the future. Additionally, the improvement of the output power density is also important.

System Issues

It is thought that the development of the constitution apparatus was almost completed for the natural gas-fueled system. The plant operation method such as start/stop, load change, and emergency shutdown is considered to be almost established, because many natural gas units are shipped to the market from the USA and German manufacturers and much experience is being accumulated. The establishment of the operating method for the hybrid system and the pressurizing system combined with the gas turbine for higher efficiency will become important in the future. For the future system using biomass, waste, or coal, it is required to develop the technologies on gasification, gas cleanup, effective heat exchange, and system configuration including topping/bottoming cycle, operation of pressurized system including carbon deposition avoidance, etc.

Economy

About the economy, stack cost reduction is the most important at present. It could be attained by, for example, reducing the number of parts, reducing the amount of the material use, lightening weight, and increasing power density. A great decrease in the stack cost by mass production is necessary. The cost reduction of the BOP equipments is also important. It is said that the BOP cost occupies large part especially in sub-MW small-capacity system. FCE is developing multi-MW systems for this reason. In addition, not only fixed cost reduction but also variable cost reduction is important. Improving the system efficiency and accumulating operation experience, it is expected that the operation and maintenance cost will be greatly reduced in the future.

Fuel cell has shorter lifetime compared to the general power generation plants, so that the stack is expected to be replaced in the period corresponding to its lifetime. Replacing cost affects largely in the cost of electricity. Recently the tentative target of stack life is set around 30,000–50,000 h and it becomes achievable by technology developments except pressurized operation. However, there could be another increment of the cost to realize the target life. It is important to introduce the stepped performance targets based on the market introduction progress. In the initial market penetration phase, the plant price might be rather expensive, but initial market would be established. The stack production can be expected to increase dramatically and large cost reduction can be attained. Once an initial market is formed, the

introduction of a small system increases, reliability is confirmed, and the awareness level rises. It enters the cycle of the virtuous circle. Then it could be expected to lead to the application of a larger power plant.

Future Directions

Expansion of Market Introduction

The market introduction of the MCFC is pushed forward as a cogeneration system of the small or medium size mainly applying the internal reforming system developed in the USA or Germany now. However, it concentrates in the country and the state where the promotion plan of the subsidies and grant is well prepared. Therefore, the MCFC market can be understood to be never independent economically at present. As a future direction, fundamental developments such as high efficiency, long life, lower cost, etc. should be continued. Accumulating experience of more market introduction, it is required to reach the level of real competition to existing conventional technologies.

As mentioned above, the development of the following directions should be pushed forward:

- Addition of load following various operability functions to the abovementioned small power supply for load management
- Diversification of fuel that allows using waste and biomass, etc., for the community-based small power supply
- Enhancement of the efficiency higher than the existing large-scale thermal power plants, intending centralized natural gas-fueled MCFC plant
- Demonstration of high-efficiency integrated coal gasification MCFC combined cycle (IGMCFC)

Development of Power Generating Systems with Novel Function

In addition to the expansion of the abovementioned market introduction, the power generating system that has a new function to make the best use of a MCFC's inherent features has been proposed. Some of those systems have been demonstrated. It is possible to expand the application field much more by achieving those.

1. DFC/T (an internal reforming hybrid system)
   FCE proposed a highly efficient natural gas-fueled hybrid system that operates the internal reforming MCFC at ambient pressure and locates the gas turbine upstream. Figure 11 shows its configuration. The power generation efficiency of about 71 % is calculated in 20 MW class (Ghezel-Ayagh et al. 1999). In parallel to this, the company has applied DFC300 stack and micro-gas turbine to the system. Maximum output of 320 kW and 58 % power generation net efficiency were

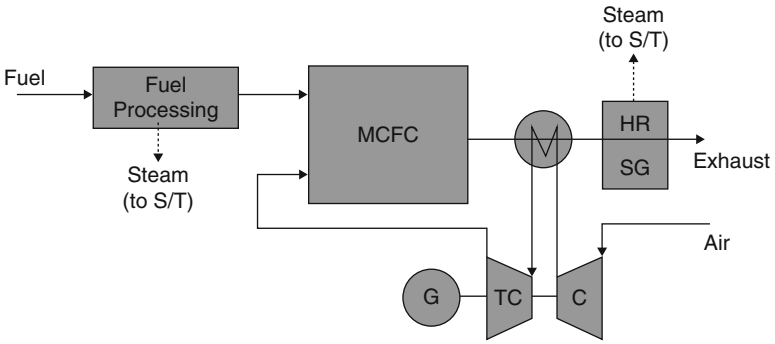

Fig. 11 Internal reforming hybrid system

achieved and approximately 8,000 h of operation was demonstrated (Ghezel-Ayagh et al. 2007). Based on current DFC3000, 3.4 MW scale has been engaged in system design (Ghezel-Ayagh et al. 2008); the first unit is planned to introduce a project underway in Connecticut.

2. DFC-ERG (a pipeline energy collection system)
   The DFC-ERG (Energy Recovery Generation) system is a highly effective hybrid system that applies the gas expander to the decompression process of the natural gas supplied by the gas pipeline in place of a conventional valve. It combines MCFC in addition and uses the rejection heat of MCFC for the preheating for preventing the gas temperature being decreased at the decompression process (http://www.fuelcellenergy.com/dfc-erg.php). FCE demonstrated the concept in the first 2.2 MW pilot plant set up in Toronto in 2009 and achieved average power generation efficiency 62.5 % and availability factor (uptime rate) 93 % during 1-year operation. In the latter half 6 months, the peak power generation efficiency was 70 % and availability was 96 % (http://www.fuelcellenergy.com).
3. DFC-H_2 (a trigeneration system)
   DFC-H_2 system is also being developed by FCE (Patell et al. 2009). Hydrogen aiming to be used for fuel cell vehicle can be generated as well as electricity and heat at the same time. This technology is to be built into hydrogen stations in California. The plan is underway to generate 300 kW of power and about 150 kg/day or more hydrogen, based on biogas generated in sewage treatment process.
4. CO_2 recovery system
   CRIEPI (Central Research Institute of Electric Power Industry) proposes the CO_2 recovery-type hybrid system using oxygen in place of air and showed the extremely high efficiency of 77 % in 300 MW class (Koda et al. 2006). Figure 12 shows its flow diagram. Only natural gas and oxygen are supplied with stoichiometric ratio to the system, and the final products are only H_2O (steam) and CO_2. CO_2 is easily recovered after condensing steam. In addition, O_2 and CO_2 with composition of 1:2 (noble gas) maximize the cathode potential and achieve the

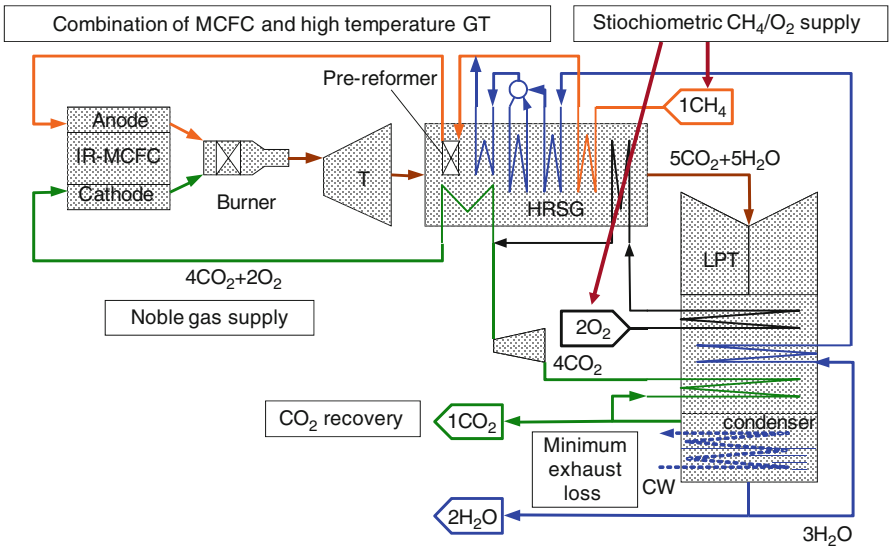

Fig. 12 Ultrahigh efficiency system with CO_2 recovery

high cell voltage. Moreover, no mixture of N_2 by not using air enables realizing minimum effluent gas flow and minimum exhaust heat quantity. It can also contribute to high efficiency.

References

Bonds T, Dawes M, Schnacke A, Spradlin L (1981) Fuel cell plant integrated systems evaluation. Electric Power Research Institute Final Report, EM-1670

Farooque M, Leo A, Pawlaczyk R, Rauseo A, Venkataraman R (2009) Direct fuel cell stack design evolution. Fuel Cell Semin Abst DEM33-1:140–143

Farooque M, Venkataraman R, Rauseo T, Carlson G, Berntsen G (2007) Direct fuel cell (DFC®) improvements based on field experience. Fuel Cell Semin Abstr 44–47

Ghezel-Ayagh H, Sanderson R, Leo A (1999) ultra high efficiency hybrid direct fuel cell/turbine power plant. Carbonate fuel cell technology V, PV99-20. The Electrochemical Society 297–305

Ghezel-Ayagh H, Walzak J, Junker S, Patel D, Michelson F, Adriani A (2007) DFC/T® power plant: from sub-megawatt demonstration to multi-megawatt design. Fuel Cell Semin Abstr 54–57

Ghezel-Ayagh H, Walzak J, Patel D, Jolly S, Lukas M, Michelson F, Adriani A (2008) Ultra high efficiency direct fuelcell systems for premium power generation. Fuel Cell Semin Abstr RDP33-2:150–153

http://poscofuelcell.com/english/

http://www.ansaldofuelcells.com/en/index.htm

http://www.fuelcellenergy.com/dfc-erg.php

http://www.fuelcellenergy.com/

http://www.mtu-online.com/?L=1

Kim S, Choi Y, Kuk S, Jun J, Lim H (2008) Status and recent progress of MCFC stack development in Korea. Fuel Cell Semin Abstr RDP33-3:154–157

Koda E et al. (2006) MCFC-GT hybrid system aiming At 70% thermal efficiency. ASME Turbo Expo 2006

Krumpelt M, Ackerman J, Herceg J, Zwick S, Slack C, Lwin Y (1982) Gas systems. Fuel Cell Semin Abstr 127–133

Leo T, Brdar D, Bentley C, Ludemann B, Farooque M, Oei P, Rauseo T (2007) Stationary DFC® power plants status. Fuel Cell Semin Abstr 50–53

Mamantov G, Braunstein J (eds) (1981) Advances in molten salts chemistry, vol 4. Plenum, New York, p 391

Marcenaro B (2008) Development and industrialisation of MCFC systems at ansaldo fuel cells. Fuel Cell Semin Abstr RDP33-1:145–149

Morita H, Mugikura Y, Izaki Y, Watanabe T, Abe T (1998) Model of cathode reaction resistance in molten carbonate fuel cells. J Electrochem Soc 145:A1511–A1517

Morita H, Komoda M, Mugikura Y, Izaki Y, Watanabe T, Masuda Y, Matsuyama T (2002) Performance analysis of molten carbonate fuel cell using Li/Na electrolyte. J Power Sources 112:509–518

Mugikura Y, Abe T, Yoshioka S, Urushibata H (1995) NiO dissolution in molten carbonate fuel cells: effect on performance and life. J Electrochem Soc 142:2971–2977

Nakayama T (2000) Current status of the fuel cell R&D program at Nedo. Fuel Cell Semin Abstr 9–13

Patell P, Lipp L, Jahnke F, Holcomb F, Heydorn E (2009) Co-production of renewable hydrogen and electricity: technology development and demonstration. Fuel Cell Semin Abstr COM43-1:373–376

Rolf S (2006) Operation Experience with MTU's Hot Module. Fuel Cell Semin Abstr 186

Toyota M, Dairaku M (2009) Development of CO2 capture system with MCFC. Fuel Cell Semin Abstr HRD33a-2:95–99

U.S. Department of Energy (2004) Fuel cell handbook, 7th edn. U.S. Department of Energy, West Virginia

Watanabe T (2001) Development of molten carbonate fuel cells in Japan – application of Li/Na electrolyte. Fuel Cells 1:1–7

Yoshikawa M, Mugikura Y, Watanabe T, Kahara T, Mizukami T (2001) NiO cathode dissolution and Ni precipitation in Li/Na molten carbonate fuel cells. J Electrochem Soc 148:A1230–A1238

Yoshikawa M, Mugikura Y, Watanabe T, Ohta T, Suzuki A (1999) The behavior of MCFCs using Li/K and Li/Na carbonates as the electrolyte at high pressure. J Electrochem Soc 146:2834–2840

Fusion Energy

Hiroshi Yamada

Contents

Abstract

Nuclear fusion is the power of the sun and all shining stars in the universe. Controlled nuclear fusion toward ultimate energy sources for human beings has been developed intensively worldwide for this half a century. A fusion power plant is free from concern of exhaustion of fuels and production of CO_2. Therefore it has a very attractive potential to be an eternal fundamental energy source and will contribute to resolving problems of climate change. On the other hand, unresolved issues in physics and engineering still remain. It will take another several decades to realize a fusion power plant by integration of advanced science

H. Yamada (✉)
Department of Helical Plasma Research, National Institute for Fusion Science, Toki, Gifu, Japan
e-mail: yamada.hiroshi@nifs.ac.jp

W.-Y. Chen et al. (eds.), *Handbook of Climate Change Mitigation and Adaptation*,
DOI 10.1007/978-3-319-14409-2_31

and engineering such as control of high-temperature plasma exceeding 100 million °C and breeding technology of tritium by generated neutrons. The research and development has just entered the phase of engineering demonstration to extract 500 MW of thermal energy from fusion reaction in the 2020s. The demonstration of electric power generation is targeted in the 2040s.

Introduction

Nuclear fusion is the power of the sun and all shining stars in the universe. An artificial sun on the Earth, that is, controlled nuclear fusion, has a very attractive potential to offer an environmentally friendly and intrinsically safe energy source. Tremendous efforts have been paid globally in these 50 years toward the realization of controlled nuclear fusion (Meade 2010; Braams and Stott 2002). Hereafter, *nuclear fusion* is simply referred as fusion. At this moment, there still remain unresolved issues for a fusion reactor even with state-of-the-art science and technology. It would be said that it will still take another 30 years to realize the first fusion reactor. Nonetheless, fusion is no longer a dream or a mirage and the targeted goal and a roadmap to reach the goal can be defined clearly. Symbolically, the construction of the International Thermonuclear Experimental Reactor (ITER) (http://www.iter.org/; Green 2003), which plans to produce more than 500 MW of heat by fusion, has been just started by international collaboration.

The fuel for nuclear fusion is isotopes of hydrogen: deuterium and tritium. Deuterium can be extracted from water and tritium can be transmuted from lithium, which is abundant, in a fusion reactor. Therefore fusion is an inexhaustible energy source. When these fuels are heated up beyond 100 million °C, fusion reaction occurs. At this extremely high-temperature state, fuels become plasma which is ionized gas consisting of ions and electrons (Eliezer and Eliezer 2001). High temperature means that ions and electrons have large kinetic energy. It is necessary to put nuclei (ions) sufficiently close to each other to drive fusion reaction. Large kinetic energy is required to overcome the repulsive force between nuclei with positive electric charge. The product of fusion reaction is helium. To control fusion reaction, it is required to integrate advanced science and technology such as deep understanding of complex plasma physics, development of materials against high heat and neutron loads, and critical engineering related to superconductivity, vacuum, and electricity.

Nuclear fusion was discovered in 1932, which is earlier than nuclear fission in 1939. Although the physics study was initiated almost at the same time, these two nuclear reactions have traced different history. Nuclear fission was used for an atomic bomb in 1942 when it was only 3 years later since its discovery. The fission reactor started power generation in 1951, and more than 400 fission power plants are operated to provide base load of electricity worldwide now. In contrast, nuclear fusion was used for a hydrogen bomb in 1952, and its peaceful use for power generation awaits for another couple of decades. These two nuclear reactions are quite different and consequently they contrast with each other from the aspect of their

engineering control. Nuclear fission occurs in heavy atoms such as uranium and plutonium. Some isotopes of these heavy atoms are unstable and break apart easily or spontaneously. Although purification of fuels of nuclear fission requires a huge facility and operating cost, it has been industrialized. The control of nuclear fission means suppression of runway of reactions. In contrast, nuclear fusion does not occur easily. Since the reaction occurs between light nuclei which have positive electric charge, extremely high energy is required to bring nuclei closely enough to fuse. This reaction only occurs naturally only in the sun and stars. The required temperature is in the millions of °C. Therefore the control of nuclear fusion means how to heat the fuels to this extremely high temperature and keep them. The scientific assessment of a fusion reactor has been almost completed by more than 50-year research, and the development stage is shifting to the assessment of engineering and technological feasibility. A fusion reactor is not a dream but a target within hailing distance.

While another couple of decades of research and development is necessary to realize fusion energy, its realization will be able to resolve global issues related to environment and energy and change social structure. Patient long-term research and development should be conducted with global social endorsement of this highly innovative technology. Then, steady progress will enable commercial reactors to deliver one million kW of electric power to the grid in 2050. The fusion power plant has a promising potential to provide the base load of electricity in the later half of this century.

Two methodologies which are magnetic confinement fusion (Lie et al. 2010) and inertia confinement fusion (Mima 2010) are being developed in parallel worldwide. This chapter is devoted to the present status and prospect of magnetic confinement fusion which is now stepping up to engineering demonstration from successful scientific demonstration.

Why Fusion for Global Warming Suppression?

Fusion is on the stage of research and development, and it will take another half century to commercialize a fusion reactor. Nonetheless, fusion offers attractive advantages to other energy sources in terms of waste, fuel, and safety.

1. Waste
   Fusion does not emit CO_2. The effect of power plants on global warming is assessed by CO_2 emission intensity with consideration of construction and operation of a plant, consumed fuel, and release of methane in digging, etc. Figure 1 shows the CO_2 emission intensity of thermal power plants, a fission reactor and a fusion reactor (Report of Japan Atomic Energy Commission in 2005). Coal-fired, oil-fired, and LNG-fired thermal stations emit much larger amount of CO_2 than other power stations. Although the CO_2 emission intensities are reduced to one third by employing CO_2 collection, they are still major players to emit CO_2. Fusion power plant does not emit CO_2 in operation, and its CO_2 emission intensity is a little bit larger than hydraulic and nuclear fission power plants.

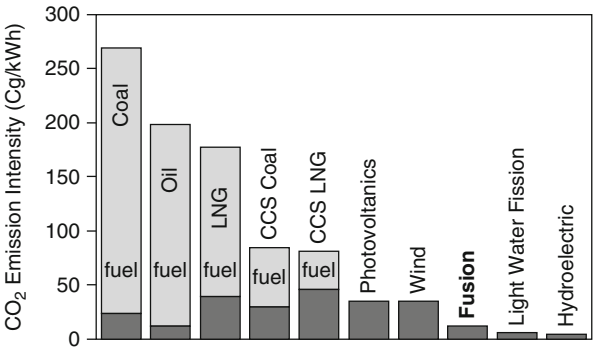

Fig. 1 Carbon dioxide emission intensity of fired (coal, oil, LNG), renewable (solar, wind), fusion, fission, and hydroelectric power plants. CCS stands for carbon capture and storage. Each bar is separated to the contributions from fuel and construction of a power plant

Fusion power is produced by nuclear reaction and fusion is not free from nuclear waste. However, a product of fusion reaction is helium, which is not radioactive at all, and nuclear waste is limited to structure materials with neutron-induced activation. Absence of very long-lived radioactive waste promises annihilation of radiotoxicity in the order of 100 years (see Fig. 2) (Jacquinot 2010). This property would ease the management of radioactive wastes compared with fission reactors. Hazard potential due to radioactivity of a fusion reactor is one thousandth of a fission reactor.

2. Fuel
   Fuels of fusion are abundant atoms: deuterium and lithium. They are substantially inexhaustible and widely distributed on Earth. Thirty-three grams of deuterium exists in 1 m^3 of water, which means 4.5×10^{13} t in oceans and is still a tiny amount of water itself. The amount of lithium as a mineral resource is estimated 940 million t and that in oceans is 230 billion t. Compared with these abundant fuels, a fusion power station producing one million kW of electricity only consumes 0.1 t of deuterium and 10 t of lithium a year. Readers can evaluate sustainability of fusion energy in terms of fuels easily.
3. Safety
   Fusion reaction occurs in very high-temperature gas; plasma and fuels are supplied to a reactor like a gas burner. Fuels do not stay for longer than a minute in a reactor core. The fusion reaction is intrinsically quenched by any accident to disturb the burning condition. Unlike the fission reaction, which is essentially a chain reaction in massive fuels, the fusion reaction does not run away in principle.

   Since fusion itself is completely unrelated to uranium and plutonium, it does not cause proliferation of nuclear weapons. Extreme temperature as high as 100 million °C is required to make fusion happen. Even if fuels of fusion (deuterium and tritium) are available, fusion does not take place. Therefore it is emphasized that fusion does not strictly adhere the nonproliferation treaty unlike fission. Also, it should be noted that there is a fusion-fission hybrid which utilizes neutrons generated by fusion reaction to drive fission reaction. This concept is not free from a proliferation issue.

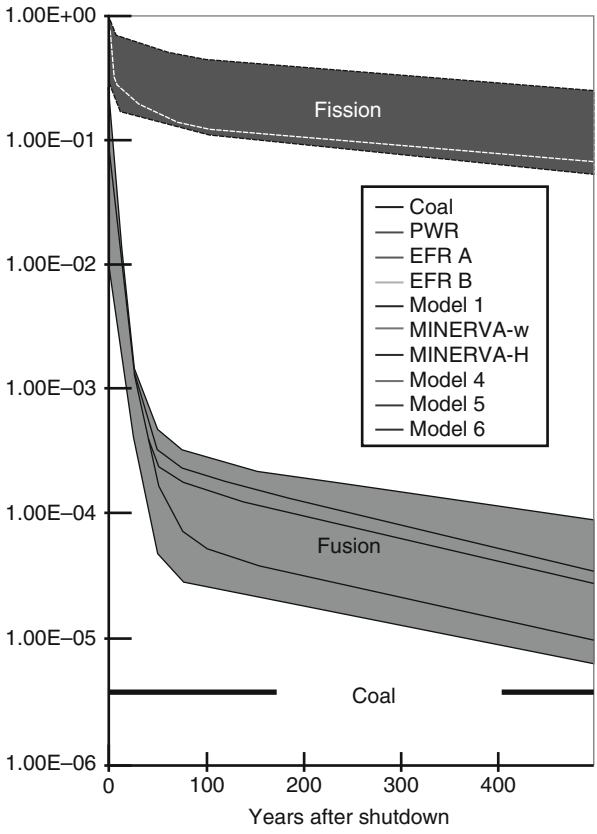

Fig. 2 Relative radiotoxicity of fission and fusion reactors versus time after shutdown. The bands correspond to differences in the fuel cycle (reprocessing) for fission and to the choice of structural material for fusion. The *bottom black line* is the radiotoxicity of coal (Reproduction of Fig. 1 in Jacquinot (2010))

What Is Fusion?

Fusion Reaction

Solar energy, which not only human kind but also almost all lives on the Earth enjoy, is delivered as light from the sun. The energy of light originates from fusion reaction taking place in the core of the sun. Four nuclei of hydrogen are fused into a nucleus of helium there. This fusion reaction has been taking place continuously, and the sun has been burning stably in these five billion years and will continue to burn in another five billion years. Physical process of this fusion reaction in the sun was identified in late 1930 after the establishment of quantum mechanics (Bethe and Peierls 1935). Studies to realize this reaction in a laboratory and utilize this reaction as energy source were launched soon after this discovery.

The special theory of relativity by Einstein gives the famous formula $E = mc^2$, where E, m, and c are energy, mass, and velocity of light, respectively. This formula means energy and mass are equivalent. It is known that the total rest mass of nuclei

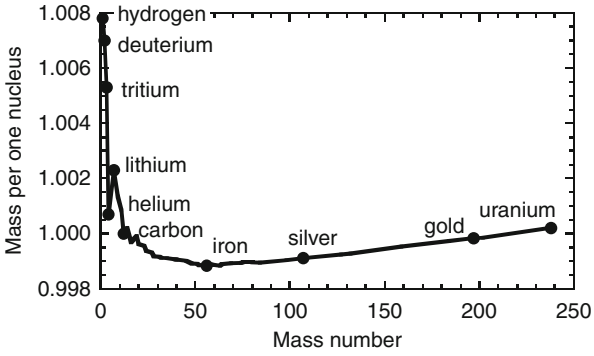

Fig. 3 Change of mass per one nucleus composing an atom

changes when the combination of nuclei is reorganized by nuclear reaction. If the rest mass after reaction is smaller than that before the reaction, loss of mass is transformed into energy. This relation is not only limited to nuclear reactions but also applicable to chemical reactions. However, while the loss of mass is usually amounted to one thousandth in the case of nuclear reaction, that in the case of chemical reaction is only in the order of 100 millionth. This is the reason why a nuclear reaction produces 100,000 to 1 million times larger power than a chemical reaction.

Figure 3 shows the mass per one nucleon (proton or neutron) which composes an atomic nucleus from the lightest element, hydrogen, to the heaviest element, uranium, in nature. Even at the nuclear reaction, the number of nucleon is conserved. Therefore, this figure indicates that mass is lost when combination (fusion) of lighter elements like hydrogen generates a heavier element like helium. Mass is also lost at the breakup of heavier elements like uranium to lighter elements. This is fission reaction has been already used in nuclear power plants. The mass of a composing nucleon is lightest as iron, thus the most stable element. In stars like the sun, fusion reaction proceeds stage by stage and ultimately generates iron. Heavier elements than iron are generated by another process, such as neutron capture at a supernova explosion. The fact that heavier elements than iron exist on the Earth means that the solar system is on and after the second generation which experienced a supernova explosion since the initiation of the universe.

There are a variety of fusion reactions and each has its own specific probability of reaction. Since this probability of nuclear reaction between particles has the dimension of area (m^2), it is referred to as cross section and expressed by σ. Probability of fusion reaction between two particles has been well investigated and quantified by various kinds of experiments using accelerators. The probability of the reaction of four hydrogen nuclei to a helium nucleus, which takes place in the core of the sun, is extremely low. The sun is so huge (100 times larger diameter than that of the Earth) that it can keep burning by this fusion reaction with very low probability. Therefore another fusion reaction of hydrogen isotopes (see Fig. 4) which has the largest probability is required to realize a fusion reaction in a plant size on the Earth. This reaction is the combination of D (deuterium) and T (tritium).

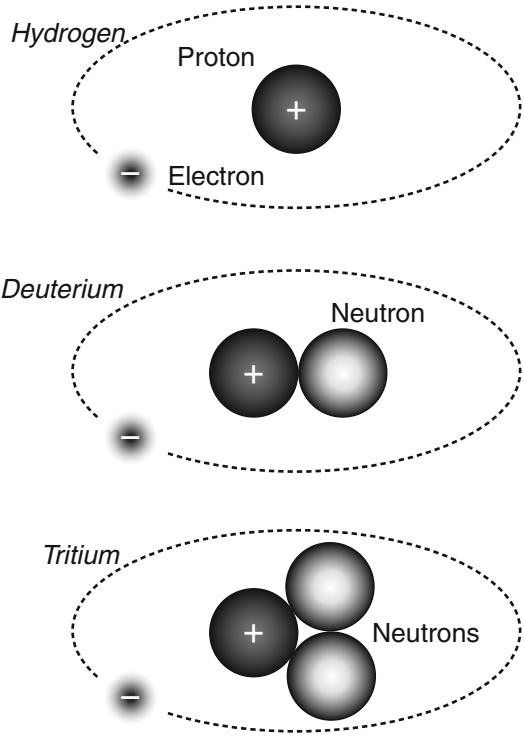

Fig. 4 Isotopes of hydrogen

In the case of the fusion reaction between D (deuterium) and T (tritium), the probability has the maximum at the relative speed of these two particles of 3×10^6 m/s. In order to use fusion reaction for energy production beyond a basic experiment of elementary particle physics by an accelerator, massive number of fusion reaction should be controlled. A cluster of particles with this speed forms very high-temperature gas: plasma. Then, the ensemble average of probability over distribution functions of all particles is more meaningful to evaluate released power. While the cross section is a function of the energy of particles, reaction rate (the number of reactions per unit volume and unit time) expressed by $< \sigma v >$ with the unit of m^3/s at the specific temperature is calculated by the integration of the cross section with regard to the velocity space. The reaction rate of representative fusion reactions is shown in Fig. 5 (Laby Online 2005). In the case of D (deuterium) and T (tritium), the cross section has the peak around several tens keV (1,000 million °C – note that 1 eV (electron volt) corresponds to 11,600 K).

Its rate equation is described as

$$\mathrm{D} + \mathrm{T} \rightarrow \mathrm{He} + \mathrm{n}$$

Consequently, helium and neutron are generated and simultaneously the energy of 17.6 MeV (2.8×10^{-12} J) is released. From the law of momentum conservation, the kinetic energy delivered to helium and neutron is 3.5 and 14.1 MeV, respectively.

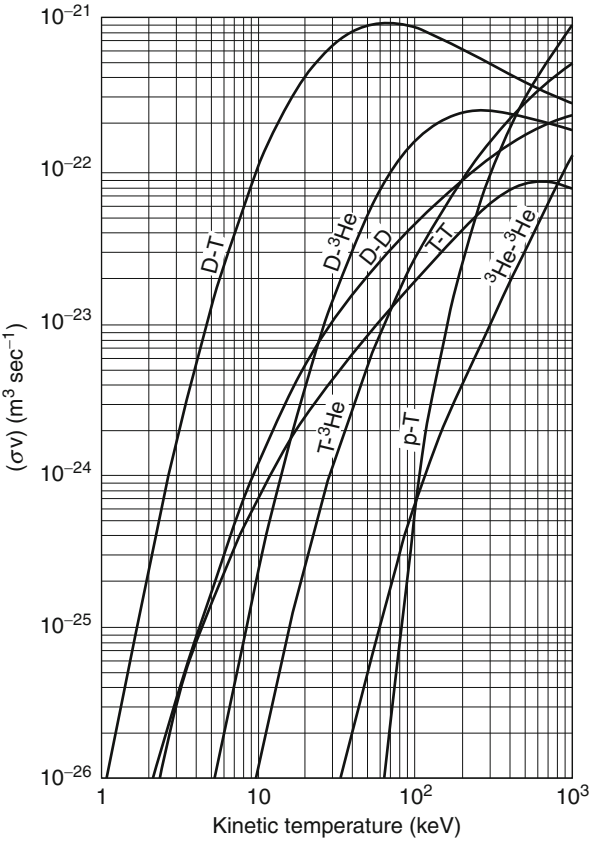

Fig. 5 Fusion reaction rate between light atoms (Reproduction from Laby Online (2005))

Fusion power density P_{fusion} is expressed by

$$P_{\text{fusion}} = n_D n_T \sigma v >_{DT} Q_{DT}, \tag{1}$$

where n_D, n_T, $<\sigma v>_{DT}$, and Q_{DT} are particle density of deuterium, particle density of tritium, rate of DT fusion reaction, and released energy by one DT fusion reaction (17.6 MeV = 3.5 MeV + 14.1 MeV), respectively. For example, a typical presumed condition of fusion reactor with $n_D = n_T = 1 \times 10^{20}/\text{m}^{-3}$ and the temperature of 20 keV (230 million °C) gives fusion power of 11 MW/m^3.

While deuterium exists as 1/7,000 (0.015 %) in hydrogen, abundance of tritium is quite low in nature. Therefore, a fusion reactor produces tritium in itself through the reaction of lithium with neutron which is generated by the following two reactions:

$$\text{n} + {}^6\text{Li} \rightarrow {}^4\text{He} + \text{T} + 4.8\text{MeV}$$

$$\text{n} + {}^7\text{Li} \rightarrow {}^4\text{He} + \text{T} + \text{n} - 2.5\text{MeV}$$

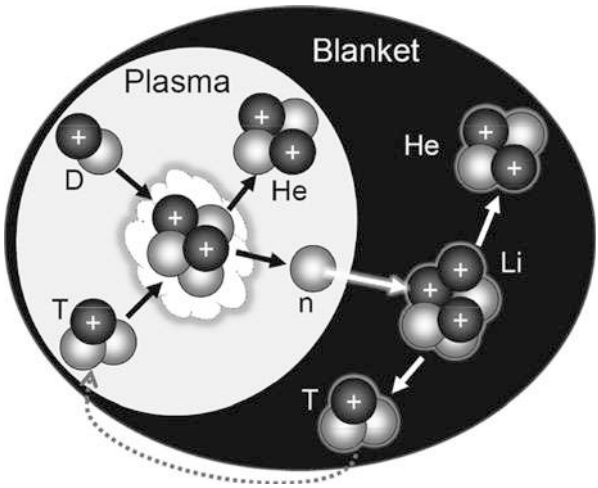

Fig. 6 Major nuclear reactions in a fusion reactor

Natural lithium is composed of 7.4 % ^{6}Li and of 92.6 % ^{7}Li. While the reaction between a neutron and ^{6}Li releases 4.8 MeV, the ^{7}Li reaction only occurs with neutron fast enough to absorb 2.5 MeV of energy. Therefore, enriched ^{6}Li to several tens% is placed around the fusion reactor core like a blanket to breed tritium (see Fig. 6). Various forms of breeding material have been proposed, such as ceramics like Li_2O and Li_2TiO_3, liquid metals like Li and LiPb, etc. Techniques for isotope separation of lithium have been established as the column exchange separation method which uses the difference in affinity for mercury and the vacuum distillation method which uses the difference in the mean free path of the evaporated isotopes.

Fuels from the amount of lithium in a single cellular phone (around 0.3 g) and deuterium extracted from only 3 l of ordinary water produce energy of 78,000 MJ which is equivalent to electricity of 22,000 kWh. A typical family in developed countries can be furnished with this electricity for a year.

A fusion power plant with electric power production of one million kW consumes 0.1 t of deuterium and 10 t of lithium a year as fuel. Needless to say, deuterium is truly abundant in seawater. Technology extracting heavy water (D_2O) is available as an industrial process. Since the fusion energy is one million times larger than the chemical binding energy, the cost for electrolysis of heavy water to get deuterium is easily recovered. Lithium is an abundant mineral resource and also available from seawater. Collection of lithium from seawater has not been industrialized yet; however, promising technologies are being developed. The increasing demand of lithium for batteries accelerates these technologies. Therefore, a fusion reactor is free from the issue of fuel.

Difference Between Fusion and Fission Reactors

While both fusion and fission accompany huge energy released by loss of mass at the change of nuclei, there exist contrasting features between them.

The first difference can be seen in the way how the reaction is controlled. The fission reaction that has been already employed in a power plant is driven by the absorption of neutrons into uranium-235. One fission reaction releases two or three neutrons, and consequently a chain reaction takes place. This means only one neutron can trigger a continuous and even explosive reaction within a certain amount of uranium-235, in principle. In a fission power plant, uranium fuel for several-yearlong operations is mounted on a reactor and burned gradually by applying the brake with control rods absorbing neutrons. In a fusion reactor, in contrast, hydrogen isotope fuel is fed continuously into a reactor like a gas burner. Therefore when the refueling is stopped, fusion reaction stops immediately. Burning takes place in plasma state which will be described in detail later. A very high temperature more than 100 million °C is required to give rise to a fusion reaction. This necessary condition is broken so easily since fusion is free from chain reaction in principle. For example, too much amount of fuel drops the temperature and quickly stops the fusion reaction since fusion power cannot keep the sufficiently high temperature of the inlet fuel.

The second difference is distinguished by products of reaction. In case of fission, elements with the mass number around 90–100, such as strontium and yttrium, and elements with the mass number around 130–140, such as iodine and barium, are produced as ash. Majority of these have large radioactivity and need a careful treatment as high-level radioactive waste. Also unburnable uranium-238 is converted to plutonium-239. While this plutonium can be used as fission fuel in a reactor, it is a long-lived radioactive element and has very high toxicity. Plutonium can be used to make nuclear weapons and must be controlled strictly under the Nuclear Non-Proliferation Treaty.

On the other hand, the product from fusion reaction is a stable element: helium. Simultaneously produced neutrons are used to make tritium by reacting with lithium in a surrounding blanket. Neutrons are also absorbed in peripheral components of a reactor and may activate them. Tritium is also a radioactive element with a half-life of 12 years and changes to helium-3 by the β-decay. Therefore, it should be noted that a fusion reactor is not free from issues related to radioactivity. However it is much mitigated. Its hazard potential can be compared by a potential radioactive risk factor. This factor assesses the risk of the maximum accident of reactors by how much air is required to dilute released radioactive elements to the tolerable level to human body. When iodine-131 and tritium, which are easily absorbed in the human body in fission and fusion reactors, respectively, are compared, the risk of a fusion reactor is less than that of a fission reactor by a factor of 1,500. The risk of a whole activated material of a reactor is about one hundredth at the operation, and the risk of fusion reactor decays quickly after shutdown since a majority of produced radioactive elements have short half-lives. The present material design of a fusion reactor aims at the reuse of materials after 100-year cooling phase.

Both fission and fusion power stations need fuel processing; however, the level of risks related to proliferation and radioactive wastes in the processing is much mitigated for a fusion power station. In the case of a fission power station, used fuels contain high-level radioactive wastes as a fission product, and plutonium is transformed from uranium-238. High-level radioactive wastes are hazardous and should be controlled safely for an extremely long time. Reprocessing of used fuels breeds fuels (plutonium), which is, in turn, concerned for proliferation. It should be also pointed out that this fuel processing is done in a fuel-cycle factory which is usually located apart from a fission power station. Tight security in transportation of used fuels and new fuels between a fission power station and a fuel-cycle factory should be in force. In the case of a fusion reactor, in contrast, tritium is bred in a fusion power station through the reaction between lithium and neutrons as described in the previous chapter. This process is confined in a fusion power station. Therefore, transportation of radioactive tritium outside a fusion power station is not required.

Core of Fusion Reactor: Burning Plasma

A schematic diagram of a fusion reactor is shown in Fig. 7. The energy source of a fusion reactor is the burning plasma in the core. In this chapter, the principle to confine the plasma leading to burning is described.

Characteristics of Plasma

The fusion reaction requires temperature beyond 100 million °C, which is higher than in the core of the sun by more than one order of magnitude. At this high

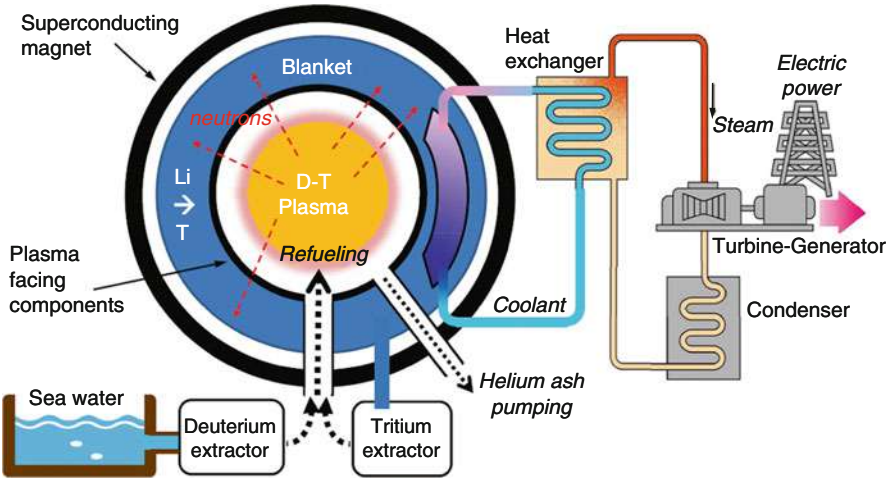

Fig. 7 Conceptual schematic view of a fusion power plant

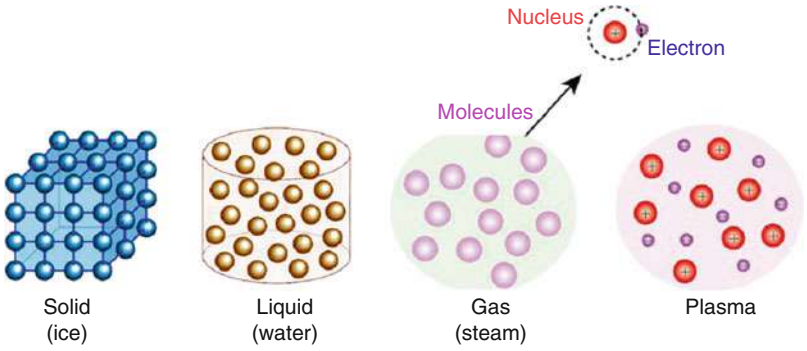

Fig. 8 Four states of matter

temperature, all materials become plasma, which is ionized gas. It is well known that the state of material has three phases: solid, liquid, and gas. And when material is heated to ten thousand °C, molecules composing gas dissociate into atoms and then electric restraint between nucleus with positive electric charge and electrons with negative electric charge is unbounded. This state is the fourth state of matter, plasma (see Fig. 8). All fixed stars shining in the sky including the sun are a mass of plasma. On the Earth, a flash of lightning and aurora are natural plasma, and plasma is used for neon lights and plasma displays.

It is necessary to confine high-temperature plasma to ignite fusion reaction and maintain burning. Here it should be noted that confinement does not mean absolute confinement so as not to release anything. To prevent fuel cooling, thermal insulation is needed like in a fireplace to keep burning. It is also necessary to supply new fuels continuously. Therefore, confinement here is defined as sustainment of the phase with sufficient condition of burning and continuous replacement of fuels. The temperature should be kept beyond 100 million °C. Usual materials such as metal used for a gas cylinder cannot withstand high temperature of plasma. In other words, plasma is cooled down by the cylinder wall.

In addition to temperature, appropriate density as high as 1×10^{14} ions per 1 cc (1×10^{20} ions/m^3) is also required to keep burning. This density is one over 200,000 of air, which means burning plasma is very rare. It should be noted, however, that the pressure of burning plasma reaches 10 atmospheres because of high temperature of 100 million °C. Balancing force against this pressure is required to confine the plasma. In the case of the sun, its own gravity balances the expansion due to the plasma pressure, since gravitation is, unfortunately, not large enough to realize the fusion burning condition by the same scheme on the Earth. There are two alternative potential concepts to realize and control fusion reaction, which are inertial confinement and magnetic confinement.

Very fast compression and heating of a small D/T fuel cell can be achieved by highly intensive laser reaching several hundred terawatt or even petawatt. This has been investigated to realize the required condition for fusion in very short timescale as long as the inertia confines the fuels (Atzeni and Meyer-Ter-Vehn 2004).

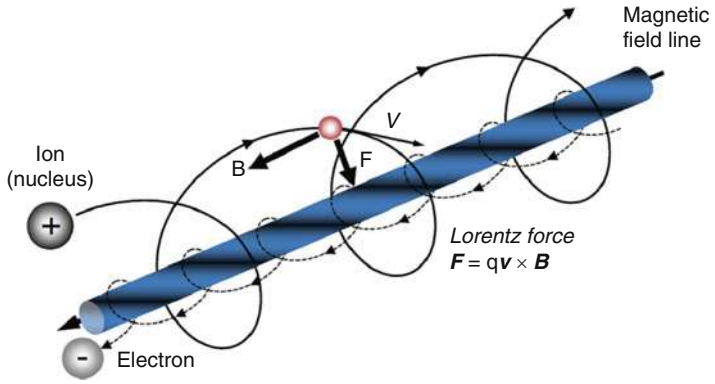

Fig. 9 Motion of an ion and an electron restricted by a magnetic field line

The outer layer of the fuel cell (typically a few millimeters in diameter) is heated by intensive laser itself or converted X-ray and explodes outward. This ablation produces the force to compress the inner part of the fuel cell. This implosion energy leads the D/T fuel to ignition.

The other method to keep the burning plasma is magnetic field confinement. Magnetic field forms invisible bottle to contain plasma apart from material wall in steady state. Since the plasma is composed of charged particles (ions and electrons), the invisible bottle made by magnetic field can confine the plasma. Charged particles rotate around the field line by the Lorentz force and consequently their motion is restricted by a magnetic field line as shown in Fig. 9. It should be noted that the rotating directions of positively charged ions and negatively charged electrons are opposite to each other. This is the principle of magnetic confinement of plasmas in a microscopic (particle) view. In a macroscopic (fluid) view, the expanding pressure of the plasma is pushed back by the pressure of magnetic field which is usually 20 times larger than the pressure of the plasma.

Magnetic Confinement of Plasma

If the magnetic field line intersects the material, the charged particles hit the material along the magnetic field line. Therefore, circulating magnetic field lines without end is required to avoid interaction with the material wall. Figure 10 shows the basic concept, where electric current on the major axis generates the circulating magnetic field lines. An important point here is that the strength of magnetic field is inversely proportional to the distance from the major axis. The charged particles rotate around the magnetic field lines and its rotating radius, which is called the Larmor radius, is inversely proportional to the strength of magnetic field. Therefore, the rotating radius becomes small in approaching the major axis and large in going away from the major axis. The combination of this change and rotating motion results in the vertical motion of particles. Remembering the difference of rotational direction of ions and

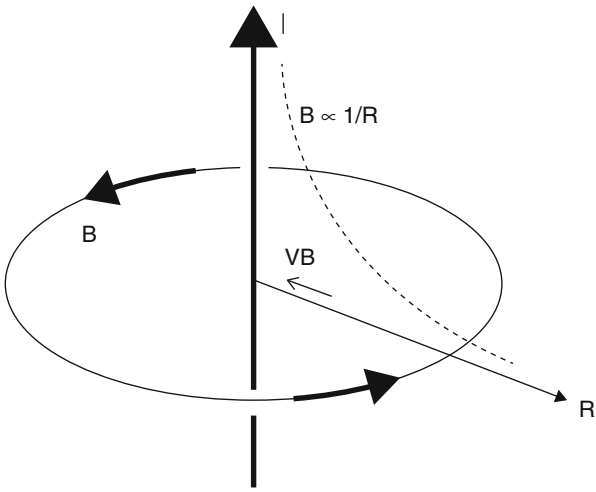

Fig. 10 Generation of circulating magnetic field line without an end. Electric current I generates magnetic field B

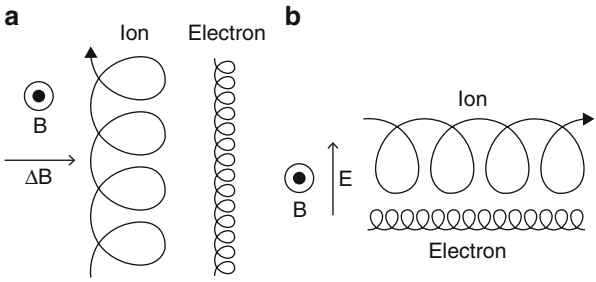

Fig. 11 Drift motion of charged particles in a nonuniform magnetic field. E and B denote an electric field and magnetic field, respectively. (**a**) A drift by the gradient of magnetic field. (**b**) A drift by resultant electric field due to the gradient of magnetic field

electrons, these two kinds of particles are separated upside down (see Fig. 11a). This separation of charged particles generates vertical electric field, which accelerates or decelerates the charge particles. Since the rotating radius is proportional to the velocity of the charged particle, rotating motion is affected by the electric field as shown in Fig. 11b. In this case, both ions and electrons go away from the major axis and are lost eventually. As a result, simple circulating magnetic field lines cannot confine charged particles.

By twisting magnetic field lines in a torus, the upper part and the lower part can be short-circuited and consequently unfavorable charge separation can be avoided. In reality, sophisticated modification of simple circulating magnetic field lines is required to keep high-temperature plasma stable. One element twists the magnetic field lines and another element forms nested magnetic surfaces composed of numerous turns around a doughnut. Most simply speaking, centrifugal force driven by the motion along the bended magnetic field line and electric field generated by charge separation are compensated by the geometrical arrangement.

There are two ways to form a magnetic bottle with fulfillments of these requirements. One is called "*tokamak*" (Wesson 2004) which was invented by Sakharov and Leontovitch (1961) and Tamm in the former Soviet Union in the 1950s. This concept

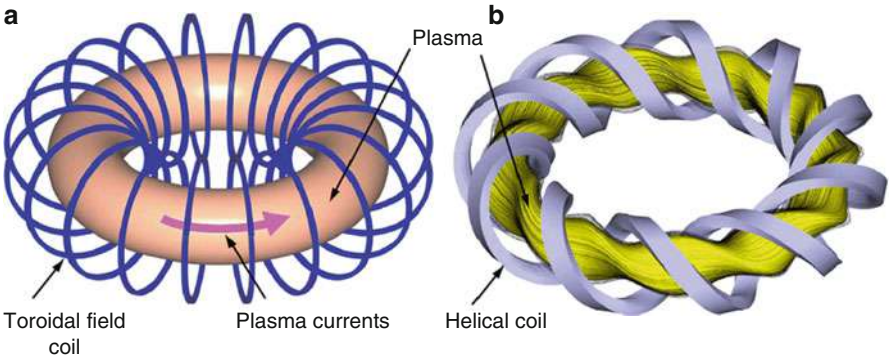

Fig. 12 Concepts of magnetic confinement fusion. (**a**) Tokamak and (**b**) helical system

is based on the combination of externally generated circulating magnetic field and the magnetic field generated by circulating currents in the plasma (Fig. 12a). Circulating magnetic field looking like a doughnut can hold the plasma apart from the material wall. A set of planar coils arranged around a doughnut generates simple circulating magnetic field and circulating currents in the plasma are driven by the principle of transformer. This concept is axisymmetric and simple in machine construction as well as theoretical analysis of plasma physics.

Another concept is a helical system. Only twisted (helical) coils generate the magnetic field to confine the plasma (see Fig. 12b). The American physicist Spitzer (1954) and the Japanese physicist Uo (1961) are pioneers in this concept. Their inventions are called stellarator and heliotron, respectively. A helical system does not require the currents in the plasma to generated twisted magnetic field. Therefore a helical system is free from issues related to the plasma currents, which are critical in a tokamak. A helical system has an intrinsic advantage of steady-state and stable operation. Although the complicated three-dimensional geometry has prevented the progress of this concept both experimentally and theoretically, the development is being accelerated by the first large-scale experiment (Large Helical Device: LHD (http://www.lhd.nifs.ac.jp/en/) in Japan) and large-scale simulations. Confinement capability has been proved to be equivalent to a tokamak.

Although the physical picture of particle confinement is well documented, plasma also behaves as a fluid. Dynamics of plasma is highly nonlinear and the modeling of plasma motion is still a challenging issue. Heat loss due to turbulence in the plasma has not been fully understood yet. The confinement capability of plasma is compared with the containment of water in a bucket with holes (see Fig. 13a). Supply of water from an external faucet P is balanced with the leak from holes L and consequently the water level W is kept. When the faucet is closed, the water level goes down exponentially with a specific time constant τ. In the case of fusion plasma, the plasma stored energy W is modeled by

$$dW/dt = P_{in} - W/\tau_E, \tag{2}$$

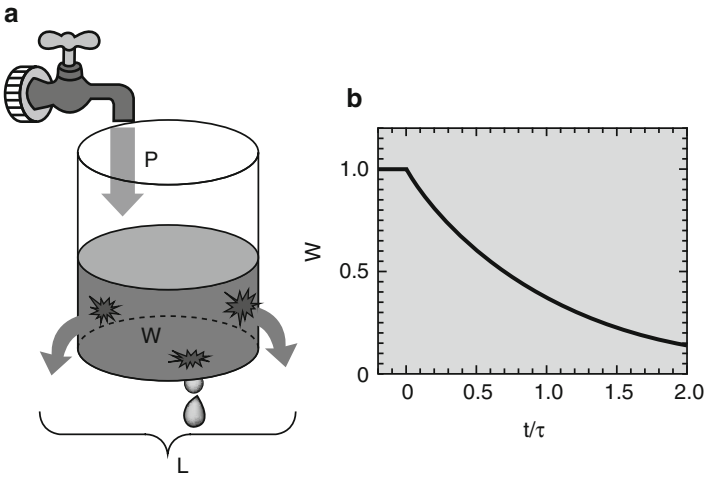

Fig. 13 (**a**) Concepts of confinement. Water is compared to energy. (**b**) Level (volume) of water decreases exponentially

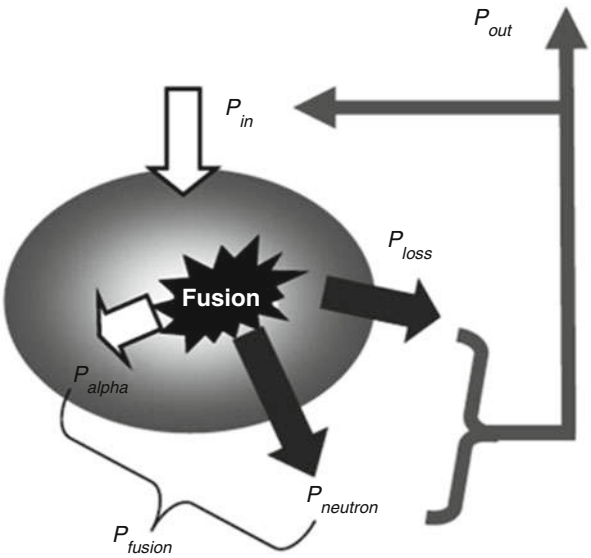

Fig. 14 Conceptual diagram of power balance in a fusion reactor

where P_{in} is input heating power and τ_{E} is called an energy confinement time. If there is no external heating, the plasma stored energy decays with $\exp(-t/\tau_{\mathrm{E}})$ as shown in Fig. 13b.

Power balance in a fusion reactor is schematically shown in Fig. 14. It should be noted that the fusion energy carried by fusion-producing helium contributes to heating of the plasma. Another fusion product, neutrons, is not confined by the

magnetic field because of no electric charge. The energy multiplication factor Q of a fusion reactor is defined based on this picture by

$$Q = P_{\text{fusion}}/P_{\text{in}} \tag{3}$$

This Q value should be larger than 50 to establish a fusion reactor as an energy source and the condition of $Q = 1$ is called breakeven. In steady state, Eq. 2. gives

$$P_{\text{in}} = W/\tau_{\text{E}}. \tag{4}$$

The combination of Eq. 1 in section "Fusion Reaction" and Eq. 4 yields

$$Q \propto n_D, n_T, \sigma v>_{DT}/(W/\tau_{\text{E}}), \tag{5}$$

where the bracket <> means the volume averaged value.

The cross section $< \sigma v >_{DT}$ can be approximated well by the temperature T squared in the targeted temperature range around 10 keV and n_D and n_T are ideally the same. Also the plasma stored energy W can be rephrased by $< nT >$, where n is the representative particle density. Consequently, Q is expressed approximately by $< n^2T^2 > / < nT > \tau_{\text{E}}$ and then $< n > < T > \tau_{\text{E}}$.

More simply, $nT\tau_{\text{E}}$ is called a fusion triple product and the most important parameter to describe the performance of fusion plasma. In early stage of fusion energy development, J. D. Lawson defined the condition to produce net energy (Lawson 1957) and indicated that the breakeven condition corresponds to 1×10^{21} m^{-3} keV s. More specifically, a typical target is simultaneous achievement of the density of 1×10^{20} m^{-3}, the temperature of 10 keV (around 120 million °C), and the energy confinement time of 1 s.

Although the plasma turbulence predominating the energy confinement has not been understood from the first principle yet, empirical scaling tolerable enough to foresee a reactor has been already available (Lawson 1957; ITER Physics Basis Editors 1999). The energy confinement time is described by the power laws with plasma and operational parameters, for example (ITER Physics Basis Editors 1999),

$$\tau_E = 0.0562 I^{0.93} B^{0.15} \overline{n}_{19}^{0.41} P^{-0.69} R^{1.39} a^{0.58} \kappa^{0.78} M^{0.19},$$

where I is the circulating current in tokamak plasma in MA, B is the magnetic field in T, $\overline{n}_{19}$ is the line averaged density in 10^{19} m^{-3}, P is the heating power in MW, R is the major radius of the torus in m, a is the minor radius of the torus in m, κ is the elongation of the poloidal cross section of the plasma (the plasma cross section is usually vertically elongated prolate shape and κ is the ratio of the height and the breadth of the plasma cross section), and M is the mass number (1 for hydrogen and 2 for deuterium). For helical systems, another scaling expression has been proposed (Dinklage et al. 2007) and both scaling expressions share large commonality in physics. As shown in Fig. 15, the scaling fits the experimental observation by a factor of 2 in 3 orders of magnitude.

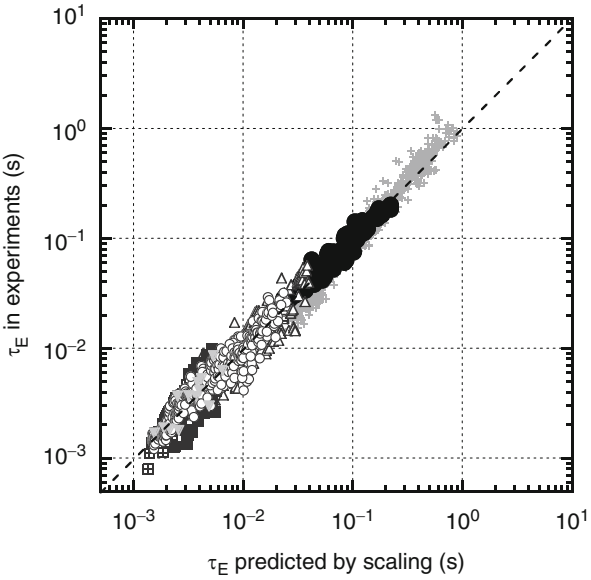

Fig. 15 Comparison of an energy confinement time in experiments with prediction from the scaling

Engineering Elements of Fusion Reactor

Structure of a Fusion Reactor

As shown in Fig. 7, fundamental components in the core are (1) confined plasma as energy source due to fusion reaction, (2) plasma-facing components surrounding the plasma, (3) blanket to receive neutrons and generate heat and tritium, and (4) superconducting magnets to generate confining magnetic field. Heat generated in the blanket is transferred by coolant like water. The consequent process of electric power generation is the same as a fission power plant and a thermal power plant. In addition, affiliate facilities which are not seen in other power plants are vacuum pumping system and heating system to bring the plasma to ignition.

A fusion reactor is basically a large-scale electromagnetic and nuclear device which requires extremely high-level integration of engineering and physics. Steady-state control of the plasma is a primary demand. Safety and materials are also key issues. Damage on plasma-facing components by high-energy (14 MeV) neutrons and helium irradiation should be assessed precisely to guarantee safety over their lifetime. For safe steady-state operation, peak heat loads exceeding 10 MW/m^2 should be managed safely. Also, an economically competitive power station must minimize the internal circulating power consumed in the plant. A fusion reactor needs a variety of large-scale electric facilities such as vacuum and cooling pumps, cryogenic system, magnets, and heating and control system. This internal circulating power in the present fission power station is only 3–4 % of the generated electric

power. If the circulating power becomes significantly large to operate a fusion reactor, a fusion reactor cannot gain economical attractiveness.

The abovementioned major three components besides the core plasma are explained in detail in the following sections.

Plasma-Facing Component and Structure Material

When the plasma is contaminated by impurities other than deuterium and tritium, radiation loss is enhanced to cool the plasma and fuels are diluted. Therefore, the plasma is generated in an airtight vacuum vessel. Although the plasma is held apart from the wall of the vacuum vessel by the magnetic field, a part of highly energetic particles and particles neutralized by the charge exchange process bombard the plasma-facing components located on the wall. Here it should be noted that the plasma with the pressure as high as 10 atmospheres is pressed down by the magnetic field and that the space between the plasma and the wall of the vacuum vessel is almost vacuum with very rare neutral gas.

While the temperature of the burning plasma exceeds 100 million °C, the direct interaction between the burning plasma and the plasma-facing component is avoided by the magnetic field. Even in this thermal insulation, the heat load to the plasma-facing component reaches 10 MW/m^2 due to radiation and the fluxes of neutrons and charge exchanged neutrals. The operational temperature of the plasma-facing component is evaluated up to 900° C, and the first planned material is tungsten which has high melting temperature (3,380° C). Although carbon is widely used as the plasma-facing component in the present fusion experiment devices, it is not compatible with the reactor condition due to large erosion and retention of tritium.

Neutrons generated by fusion reaction are not confined by the magnetic field and penetrate into the structure materials. Therefore, the plasma-facing components and structure materials are required to have sufficient tolerance against the heat and neutron loads. Relatedly, employed materials should have good heat removal property and reduced activation. Also it is preferable to keep sufficient tightness and mechanical strength during a lifetime of a plant. Alloys such as stainless steel have been usually used in the current experimental devices, but these alloys do not fulfill the requirement of a reactor. Ferritic steel is a promising material for the first generation of a reactor, and advanced materials using vanadium silicon carbide are being developed. In addition to heat and neutron loads, helium generates bubbles in the plasma-facing components and causes swelling and consequent blistering. Since falling flakes deteriorate plasma performance, materials should suppress this effect in addition to securing soundness of components themselves.

In general, materials show degradation of its properties, such as dimensional instabilities, yield strength, ductility, creep rate, fatigue life, and fracture toughness. Neutron radiation often accelerates this process (Zinkle 2005). The standard to assess irradiation damage is displacements per atom (dpa) (Norgett et al. 1975). The dose of 1 dpa corresponds to a 14 MeV neutron wall loading of 0.1 MW year/m^2

in steels. The structure component of a fusion power plant is expected to have a neutron dose of 100–150 dpa around temperatures of 500–600° C.

While stainless steel can be used in the experimental reactor level (ITER) where the neutron fluence is limited to 3 dpa, development of new material is prerequisite for a fusion reactor as a power plant. The promising material for the first generation of a fusion reactor is low-activation ferritic steel, which has been used in fuel tubes for a fast breeder fission reactor and evaluated to be used up to 40 dpa by 14 MeV neutron radiation. This tolerance corresponds to 1-year operation of a fusion reactor. Innovative and attractive materials such as vanadium alloy (V-4Cr-4Ti) (Muroga et al. 2002) and silicon carbide (SiC/SiC) (Katoh et al. 2007) are also under development.

In addition to mechanical properties, physical properties such as electric conductivity change due to neutron irradiation. These complicated phenomena depend on energy and dose of neutrons and operating temperature. A new neutron irradiation facility is planned to evaluate irradiation property of materials precisely for reliable design of a fusion reactor. This facility is called the International Fusion Materials Irradiation Facility (IFMIF) (Martone 1996) and simulates 14 MeV neutrons at the maximum capability of 50 dpa/year. The schematic view of IFMIF is shown in Fig. 16. The report of Martone (1996) defines the mission of IFMIF as to provide an accelerator-based, D-Li neutron source to produce high-energy neutrons at sufficient intensity and irradiation volume to test samples of candidate materials up to about a full lifetime of anticipated use in fusion energy reactors. IFMIF would also provide calibration and validation of data from fission reactor and other accelerator-based irradiation tests. It would generate an engineering base of material-specific activation

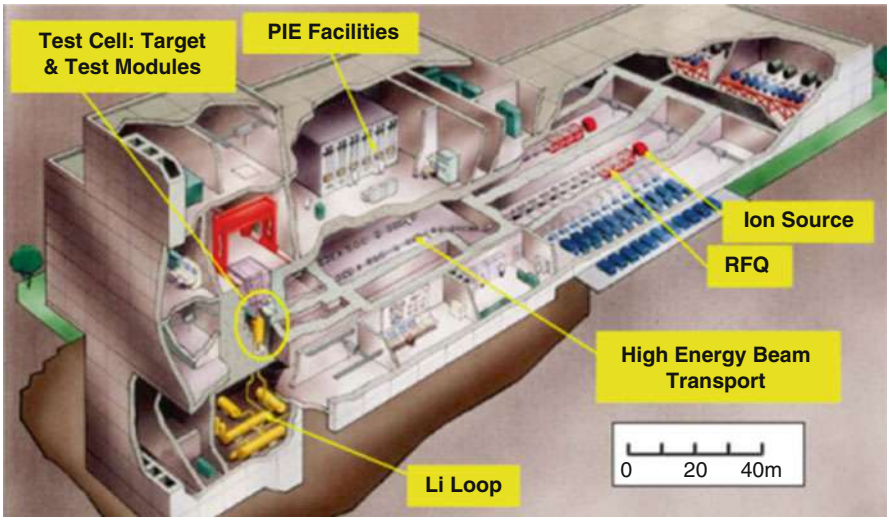

Fig. 16 Schematic view of the International Fusion Materials Irradiation Facility (*IFMIF*). PIE and RFQ stand for postirradiation examination and radio-frequency quadrupole, respectively

and radiological properties data as well as support the analysis of materials for use in safety, maintenance, recycling, decommissioning, and waste disposal systems. A deuterium beam with 40 MeV and 250 mA irradiates a lithium target and generates neutrons with the energy peak at 14 MeV through the D-Li stripping reaction. The Engineering Validation and Engineering Design Activities (EVEDA) for IFMIF are now being conducted by Japan-EU cooperation in Rokkasho, Japan (Garin et al. 2009).

Blanket

The blanket surrounds the plasma with protection by the plasma-facing components. The function of blanket is to produce tritium and extract heat from neutrons generated by the fusion reaction. Tritium breeding ratio (TBR) is a critical parameter for a fusion reactor. TBR is a measure of breeding capability of the blanket and is defined as

$$\text{TBR} = \text{rate of tritium production in the blanket} / \text{rate of burning tritium in the plasma}$$

Since the abundance of tritium in nature is tiny, a fusion reactor is required to produce more tritium than burned tritium, which means TBR >1.

The blanket consists of breeding material for tritium, multiplier of neutrons, and coolant which are designed to fulfill three major specifications: (1) sufficient tolerance against heat, neutrons, and electromagnetic forces due to confining magnetic field; (2) the tritium breeding ratio with more than 1; and (3) sufficiently high efficiency of heat removal.

Tritium breeding material produces more tritium than consumed tritium by using the reaction between lithium and neutron described in section "Fusion Reaction." There are two major categories in the form of lithium. One is a solid-breeding scheme in ceramic made of lithium and another is a liquid-breeding scheme of pure lithium(Li), lithium lead (LiPb), or molten salt (FLiBe). Solid breeding is progressing faster due to the advantages of easy handling and chemical stability. Liquid breeding has advantages of much reduction of radiation damage, simple design for easy maintenance, and potentially high TBR. However, liquid-breeding material is chemically active in general. In particular, careful attention should be paid to a chemical reaction with water which is the secondary coolant and corrosion of the cooling channel. Also liquid metal is an electrically conducting fluid and the electromagnetic force under the strong magnetic field prevents efficient flow. Therefore, research and development has been conducted to resolve these issues.

One neutron is generated by one fusion reaction between deuterium and tritium, and a fusion reactor must produce more than one tritium by this one neutron. Since some neutrons are absorbed in surrounding structure and lost, all neutrons cannot be used to breed tritium. Therefore, it is needed to multiply neutrons by the reaction using beryllium such as

$$^{9}Be + n \rightarrow 2n + 2^{4}He.$$

This kind of neutron multiplier is inserted between the plasma-facing component and tritium breeding material. Also the shield is located behind the breeding material to reflect neutrons back to use them efficiently and protect superconducting magnet located behind the breeding material.

Coolant should be compatible with tritium breeding material and have sufficient heat removal capability. The most conservative combination is to use solid breeding and water or helium as coolant. Operating temperatures are around 300° and up to 500° C for water cooling and helium gas cooling, respectively.

The blanket must hold a critical compound role in a fusion reactor. In addition, constraints due to configuration of magnets and economical viewpoints require the thickness of blanket limited to around 1 m.

In spite of limited availability of neutron fluence on ITER (around 3 dpa), the ITER project definition states that "ITER should test tritium breeding module concepts that would lead in a future reactor to tritium self-sufficiency and to the extraction of high-grade heat and electricity production" (Aymar 2001). Toward this goal, several fusion reactor-relevant Test Blanket Modules (TBM) (Giancarli et al. 2006) are proposed.

Superconducting Magnet

To confine the burning plasma described in "Core of Fusion Reactor: Burning Plasma," the strong magnetic field exceeding 10 T at the magnets is needed. Since the volume of the plasma is around 1,000 m^3, magnets produce this strong magnetic field with sufficient accuracy to cover the large volume. It is well known that Joule heating due to resistivity is accompanied by currents. The loss of this energy is critical in a fusion power plant. Therefore, superconducting magnets are inevitable since they are free from energy loss due to Joule heating because of no resistivity at cryogenic temperature. Superconducting magnets in a fusion power plant are characterized by large-scale, sufficient tolerance and preservation of accuracy against the large electromagnetic force and tolerance against nuclear heating and activation. Superconducting magnets using alloys such as NbTi and a compound such as Nb_3Sn have been developed to fulfill these specifications.

Figure 17 shows the development of large superconducting magnets in fusion devices (Yamada et al. 2009). The largest operating magnet system for fusion is the Large Helical Device (LHD) (Imagawa et al. 2010), and its magnetic stored energy is close to 1 GJ. The Large Hadron Collider (LHC) employs two large detectors with large-scale superconducting magnets, ATLAS and CMS, and each magnetic stored energy exceeds 1 GJ. The total stored magnetic energy of LHC reaches 15 GJ (Ross 2010). The stored magnetic energy of the superconducting magnet system in ITER is 50 GJ (Mitchell et al. 2010), which is well beyond the achievements so far.

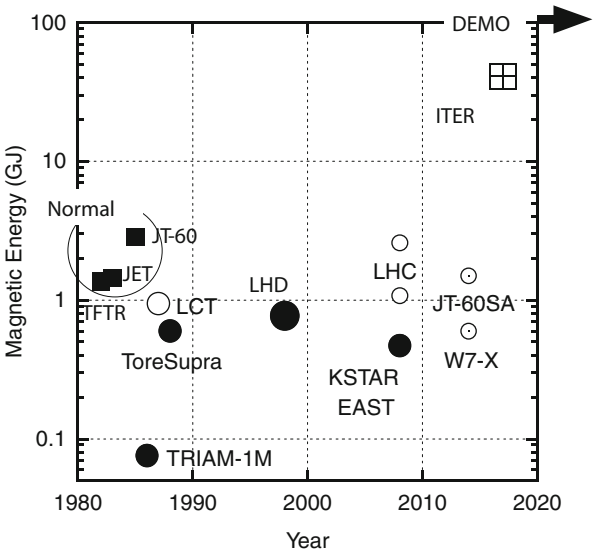

Fig. 17 Development of large-scale superconducting magnets in terms of magnetic energy. Three large tokamaks employing normal conductors and the superconducting magnets for the Large Hadron Collider (*LHC*) are also plotted as references (Reproduction of Fig. 4 in Yamada et al. (2009))

The specification of the magnets for ITER requires the mechanical tolerance against 1 GPa, the withstanding voltage of 10 kV, and irradiation dose on electric insulation of 10 MGy, which are the present technological limits. The prototype magnet employing Nb_3Sn conductors has demonstrated 13 T (Kato et al. 2001) and fabrication of real components has started. The specification required for a fusion reactor would be higher than that of ITER. The solution to the issue of Nb_3Sn having the critical current density that degrades by strain is inevitable to achieve higher magnetic field for a fusion reactor than in ITER. A strong candidate is Nb_3Al because of its outstanding property of critical current density against strain and magnetic field (Koizumi et al. 2005). Although basic engineering advantage has been already established for Nb_3Al, R&D to mitigate difficulty in mass production and cost is still required for its application to a fusion reactor.

Further development of conductors is being conducted to pursue capability to carry higher currents under higher magnetic field than these established conductors. In particular, a high-temperature superconductor which does not need cryogenic operation by liquid helium will have a big impact on a design of a fusion reactor.

Present Status and Future Direction of Nuclear Fusion

Fusion research was started as classified military research about 60 years ago. Then, global scientific research activity toward a peaceful use of fusion energy was launched by declassification at the second United Nations Conference on the Peaceful Uses of Atomic Energy in Geneva in 1958. Tabletop-sized experiments demonstrated proof of principle of physical ideas, and medium-sized experiments with the

major diameter of up to 3 m extended plasma parameters to the order of ten million °C. Then three large-scale tokamaks, TFTR (Hawryluk et al. 1998), JET (http://www.jet.efda.org/; Pamera and Solano 2001), and JT-60U (Ohyama et al. 2009), with the diameter of about 6 m and the plasma volume of several tens to more than 100 m^3 were constructed in the 1980s to demonstrate scientific feasibility of fusion. As an alternative line, a helical system is catching up with tokamak by large facilities, LHD (http://www.lhd.nifs.ac.jp/en/; Yamada et al. 2009; Komori et al. 2010) and Wendelstein 7-X (http://www.ipp.mpg.de/ippcms/eng/pr/forschung/w7x/; Bosch et al. 2010). In parallel with convergence to the first demonstration of burning plasma on ITER, a variety of experimental project are being conducted to resolve unresolved issues and create innovation by worldwide efforts as shown in Fig. 18.

Although the fusion power plant has not been realized like a fission power plant, the progress in these 50 years is remarkable (Meade 2010). For example, the most typical index to describe performance of fusion plasma, the fusion triple product of temperature, density, and energy confinement time, has been improved in the same speed as the density of an integrated circuit, which refers to the famous Moore's law (doubled in 18–24 months) (see Fig. 19) (Webster 2003). Figure 20 is the so-called Lawson diagram, which shows the performance of fusion plasmas on the plane of the product of central ion density and energy confinement time, and temperature. Recent experiments on JET (Team 1992) and JT-60U (Ishida et al. 1999) achieved the breakeven condition $Q = 1$ in the 1990s. It should be noted that the breakeven conditions have been equivalently satisfied by using only deuterium. Also more than 10 MW of real fusion power generation has been demonstrated using deuterium and tritium on TFTR (Bell et al. 1995) and JET (Gibson 1998) even for a short time period as long as a few seconds (see Fig. 21). These two major achievements, breakeven and DT burning, have motivated the next generation of a tokamak experimental reactor.

Based on accumulated achievements by worldwide tokamaks (Ikeda et al. 2007), fusion power development is stepping up the stage. Seven leading parties of fusion research, China, EU, India, Japan, Korea, Russia, and the USA, have jointly started construction of the International Thermonuclear Experimental Reactor (ITER) (http://www.iter.org/) in Cadarache, France. For this distinguished international project, the ITER Organization was formally established on October 24, 2007, after ratification of the ITER Agreement in each member party. ITER will be built largely (90 %) through in-kind contribution by the domestic agencies of seven parties. ITER is the largest tokamak ever built. Its plasma volume is close to 1,000 m^3 (see Fig. 22), and the total weight reaches 23,000 t. The goal of ITER is the demonstration of control of burning plasma and engineering feasibility of a fusion reactor. ITER plans to demonstrate 500 MW of fusion power production by DT fusion reaction at the temperature of 150 million °C for 500 s in the 2020s. This amount of fusion power is expected to be ten times larger than the external heating power put into the plasma, which means $Q = 10$. Figure 23 is the schedule of ITER (Ikeda 2010). The latest argument suggests an updated schedule that is a bit behind.

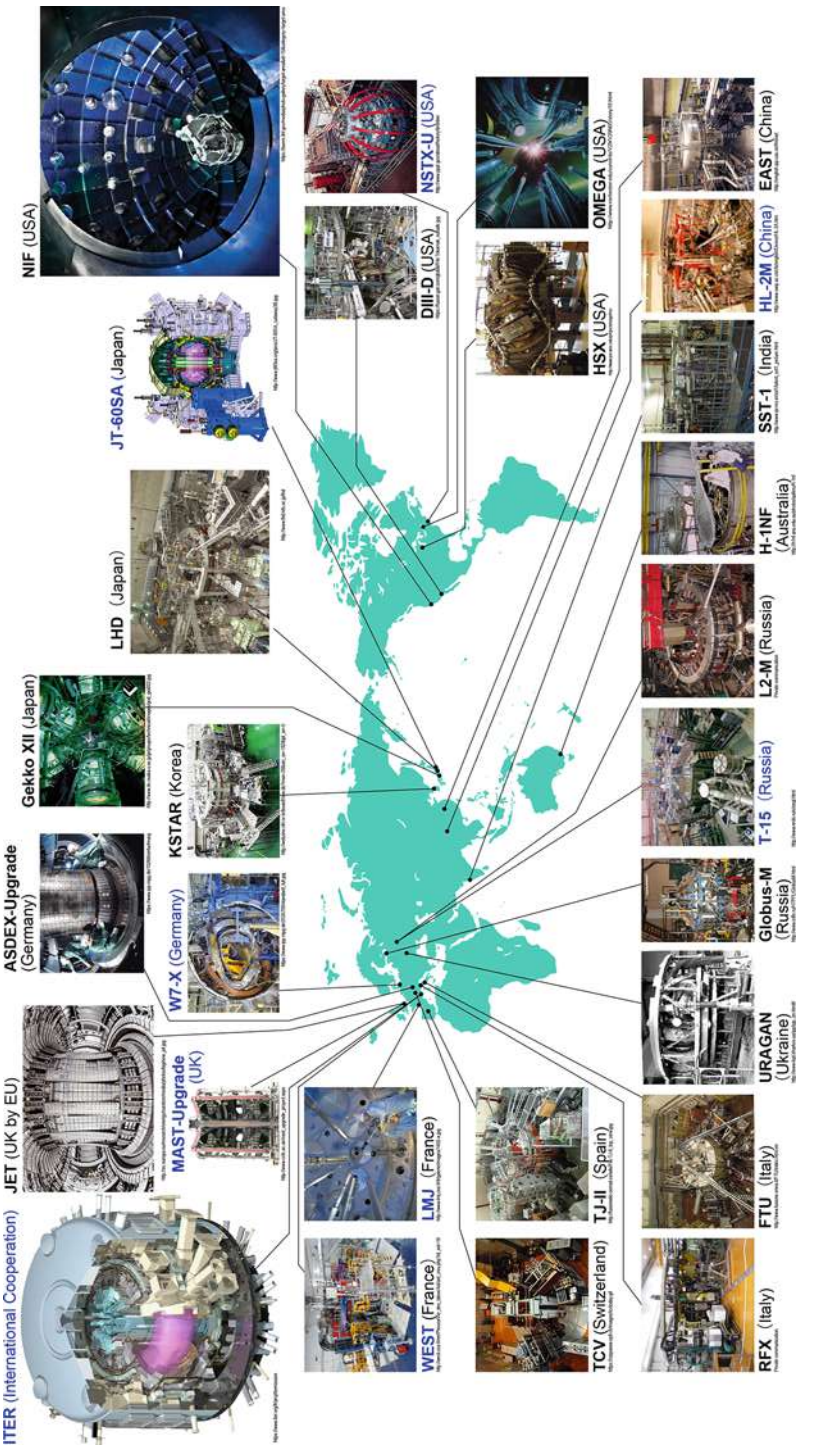

Fig. 18 Experimental facilities for magnetic confinement of fusion plasma in the world

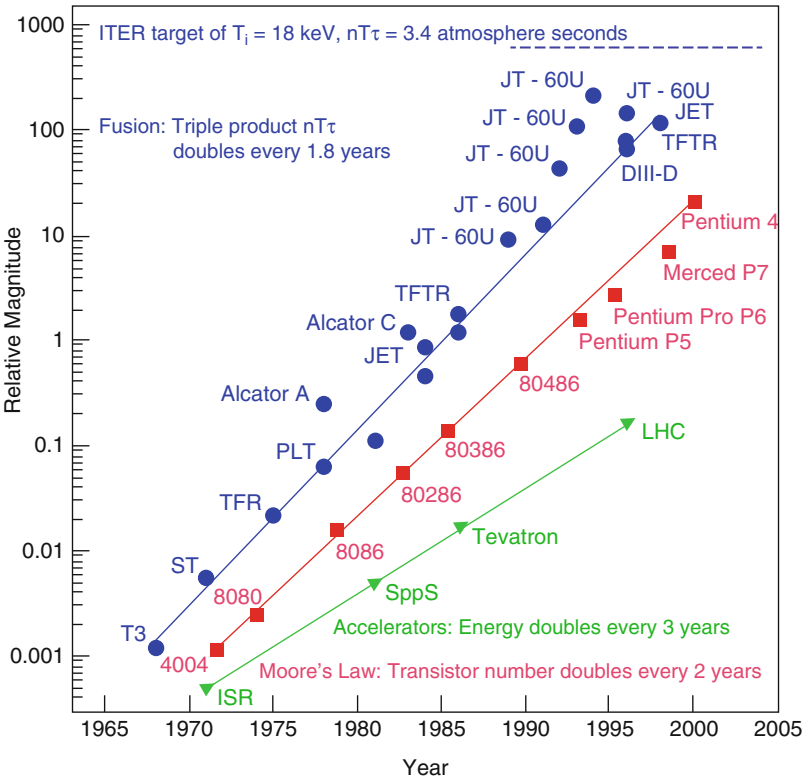

Fig. 19 The rapid progress toward harnessing fusion as a power source compares very favorably with progress in other high technologies such as computing performance and particle accelerators. This figure was originally produced by J. B. Lister, CRPP Lausanne (crpp www.epfl.ch), and M. Greenwald, MIT (www.psfc.mit.edu) (Reproduction of Fig. 3 in Webster (2003))

The first plasma with hydrogen is planned to be ignited in 2019, and the experimental campaign of DT burning will start in 2027.

ITER will also be a test bed for blanket technology as discussed in section "Blanket." The goal of ITER is defined as engineering demonstration of fusion energy. However, it should be noted that ITER does not have a plan to generate electric power. Then, a demonstration reactor which fulfills the requirement of a power plant including economical validity to some extent will come in the next. ITER is certainly the necessary condition to proceed to a demonstration fusion reactor but not sufficient for a demonstration fusion reactor. In particular, material development should be conducted by an intensive neutron irradiation facility (IFMIF) (Martone 1996) in parallel to assess property of materials, in particular lifetime.

ITER adopts the tokamak concept described in section "Magnetic Confinement of Plasma." Tokamak is the most promising concept to demonstrate controlled burning plasma from the presently available knowledge. However, when the system is

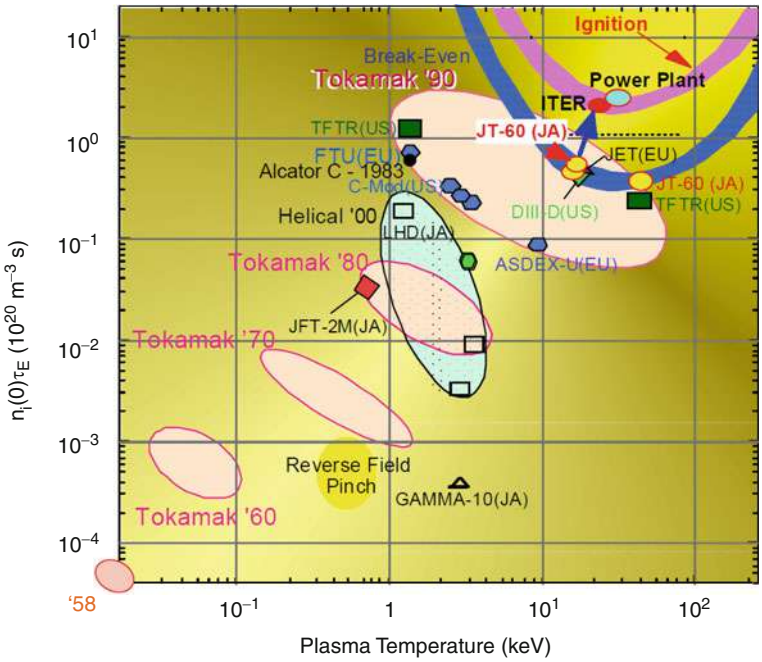

Fig. 20 Lawson diagram for magnetic fusion illustrating progress over 50 years (Courtesy of the Japan Atomic Energy Agency: Naka Fusion Institute. Reproduction of Fig. 10 in Meade (2010))

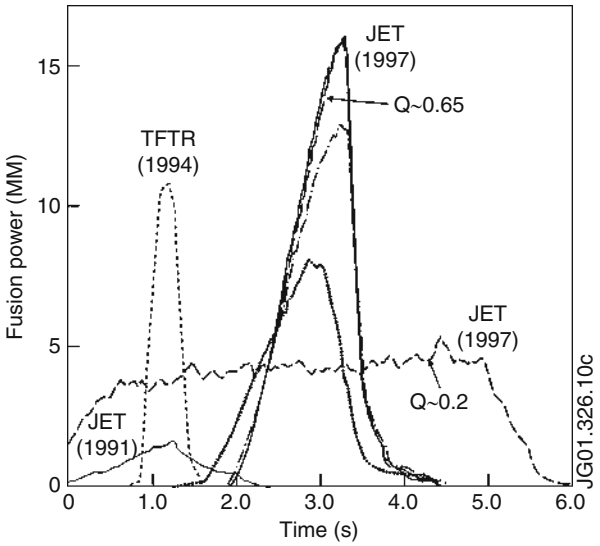

Fig. 21 Progress in fusion power and energy in time, from JET and TFTR which are capable of DT operation (Reproduction from http://figures.jet.efda.org/JG01.326-10c.eps)

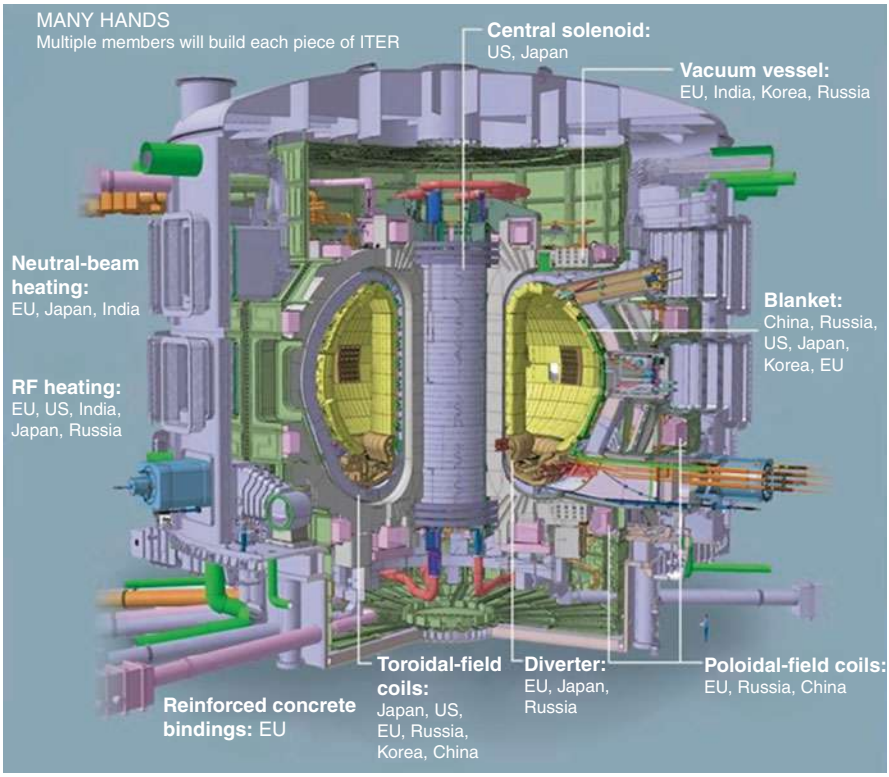

Fig. 22 A cutaway view of ITER (courtesy of the ITER Organization). The major diameter of a doughnut-shaped plasma is 12.4 m. Duplication from Nature 459: 488–489, 2009. Seven parties in the world share the responsibility of construction

assessed from the viewpoint of a fusion power plant, it is serious and critical to overcome the issues related to the control of huge currents in the plasma. In the case of ITER, electric current of 15 MA (1.5×10^7A) flows in very rare gas (plasma) with weight of less than 1 g. This plasma current should be stably held in steady state. This requirement poses two critical issues. One is avoidance of current disruption. Since a huge plasma current has huge electromagnetic energy, abrupt destruction of the plasma current called disruption occurs when the stability of the current is lost. This phenomenon happens in the order of 1 ms; huge transient electromagnetic forces are generated in the machine component. Therefore the control and mitigation of disruption is a prerequisite for a tokamak fusion reactor. Another requirement is current drive. In addition to transient induction as in a transformer, a reliable and efficient current-drive scheme should be established. Fortunately, to some extent, high-temperature plasma in a doughnut shape has a physical mechanism to drive the circulating currents spontaneously, called bootstrap currents. However these currents are not sufficient to sustain the burning plasma and an external source to drive the sufficient current. This means that some amount of produced electric power in a

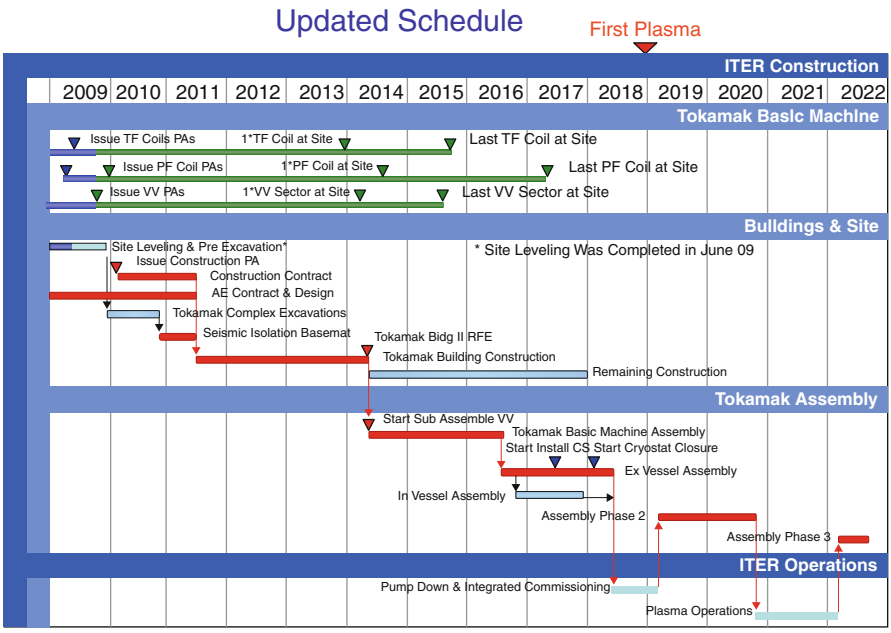

Fig. 23 Schedule of ITER (Reproduction of Fig. 13 in Ikeda (2010))

tokamak fusion power plant is consumed to drive the plasma currents. Simultaneous achievements of spontaneous current fraction of 70 % and efficiency of current drive from the plug of 50 % are required to deliver electric power to the grid economically. This requirement is very demanding, and ITER will not be able to resolve this issue. Therefore a new tokamak facility JT-60SA (Ishida et al. 2010) to explore the steady-state tokamak operation is now under construction by bilateral collaboration of EU and Japan.

Since a helical system which is alternative to a tokamak does not need plasma currents to confine the plasma and is free from challenging issues related to the plasma current, it is an extremely attractive concept of a steady-state stable reactor. Nonetheless, complex shape of magnets has caused troubles and difficulties in both experimental and theoretical approaches, and the progress of research and development lagged behind tokamak by one generation. However, the first large-scale helical device, LHD (see Fig. 24), has been in operation since 1998, and remarkable progress has been achieved recently (Komori et al. 2010). LHD employs superconducting magnets and has the capability of steady-state operation in both physics and engineering aspects. LHD has achieved the comparable plasma parameters such as temperature of 75 million °C and already demonstrated 1 h long operation of high-temperature plasma with 12 million °C. Another helical device, Wendelstein 7-X, is now under construction in Germany and will be operational in 2015 (Bosch et al. 2010).

Fig. 24 Photograph of the plasma vacuum vessel of *LHD*: the Large Helical Device (Courtesy of the National Institute for Fusion Science, Japan). The major diameter of a twisted doughnut-shaped plasma is 7.8 m

In the coming couple of decades, physical study and engineering demonstration of burning plasma will be conducted in ITER in parallel with research and development of steady-state operation by advanced tokamaks and helical systems. Reactor engineering, in particular material development, should be also pursued toward the establishment of an economical fusion reactor. Integration of all this knowledge will lead to the first demonstration fusion reactor which produces electric power of one million kW in the 2040s (see Fig. 25). The establishment of fusion as energy source is targeted in the mid of this century (Masionnier et al. 2005).

The National Ignition Facility (http://lasers.llnl.gov/) in the USA plans to demonstrate ignition by the completely different inertia confinement scheme in 2011. Operation is limited to a single-shot basis due to the availability of highly intensive laser, and the inertia confinement is in the stage of scientific demonstration.

Summary

Fusion is an energy source of the sun, and controlled fusion as an energy source for human beings has been developed intensively worldwide for this half a century. A fusion power plant is free from concern of exhaustion of fuels and production of CO_2 and has an advantage to a nuclear fission power plant in terms of high-level radioactive waste. Therefore it has a very attractive potential to resolve global warming and to be an eternal fundamental energy source. On the other hand, unresolved issues still remain. It will take another several decades to realize a fusion

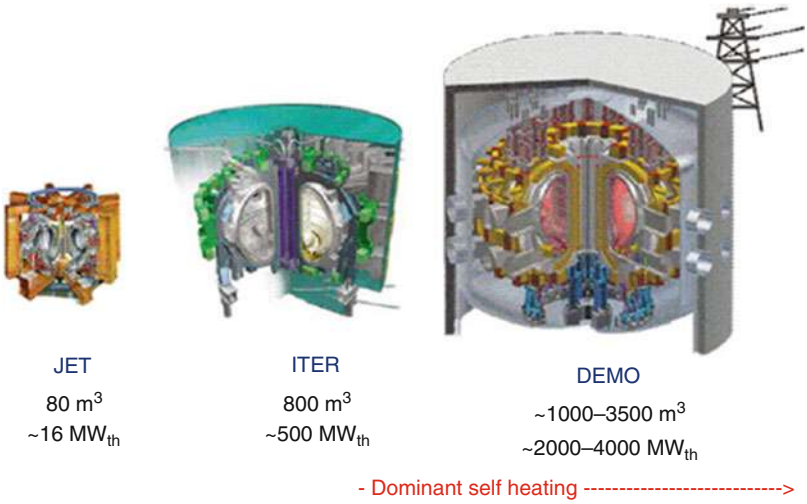

Fig. 25 The growth in scale of tokamak devices from JET, which produced the first DT fusion power, through ITER, aiming for Q = 10 at 500 MW thermal, to a DEMO reactor producing ~1GW electrical (Reproduction of Fig. 15 in Ikeda (2010))

power plant by integration of advanced science and engineering such as control of high-temperature plasma exceeding 100 million °C and breeding technology of tritium by generated neutrons. The research and development has just entered the phase to start the project to extract 500 MW of thermal energy from fusion reaction in the 2020s. The demonstration of electric power generation is targeted in the 2040s. Even the first-generation fusion demonstration reactor will produce electricity of one million kW.

Fusion reaction itself has been already demonstrated in an unpeaceful manner as a hydrogen bomb which is ignited by an atomic bomb. In peaceful use of fusion energy, a fusion power plant employs completely different principle that the fusion reaction in plasma is controlled stably in steady state. Since fusion energy is free from nuclear proliferation and unfair distribution of fuels, geopolitical issues can be much mitigated by its realization. Fusion energy, a sun on the Earth, has attractive and critical potential to resolve diversified issues related to energy and to change global social structure.

Lastly, the further sources about *fusion* can be found in books as cited by McCraken and Stott (2005), Stacey (2010), Kikuchi (2011), and Chen (2011).

References

Atzeni S, Meyer-Ter-Vehn J (2004) The physics of inertial fusion. Clarendon, Oxford
Aymar R (2001) Summary of the ITER final design report. ITER document G A0 FDR 4 01-06-28 R 0.2, Garching ITER joint work site, 9 July 2001

Bell M et al (1995) Overview of DT results from TFTR. Nucl Fusion 35:1429–1436
Bethe H, Peierls R (1935) Quantum theory of the diplon. Proc R Soc Lond A 148:146–156
Bosch HS et al (2010) Construction of wendelstein 7-X engineering a steady-state stellarator. IEEE Trans Plasma Sci 38:265–273
Braams CM, Stott PE (2002) Nuclear fusion: half a century of magnetic confinement fusion research. IOP, London
Chen FF (2011) An indispensable truth, how fusion power can save the planet. Springer, London
Dinklage A et al (2007) Physics model assessment of energy confinement time scaling in stellarators. Nucl Fusion 47:1265–1273
Eliezer S, Eliezer Y (2001) The fourth state of matter: an introduction to plasma science. IOP, London
Garin P et al (2009) Main baseline of IFMIF/EVEDA project. Fusion Eng Des 84:259–264
Giancarli L et al (2006) Breeding blanket modules testing in ITER: an international program on the way to DEMO. Fusion Eng Des 81:393–405
Gibson A (1998) Deuterium-tritium plasmas in the Joint European Torus (JET): behavior and implications. Phys Plasmas 5:1839–1846
Green BJ (2003) ITER: burning plasma physics experiment. Plasma Phys Cont Fusion 45:687–706
Hawryluk RJ et al (1998) Fusion plasma experiments on TFTR: a 20 year retrospective. Phys Plasmas 5:1577–1589
Ikeda K (2010) ITER on the road to fusion energy. Nucl Fusion 50:014002
Ikeda K et al (2007) ITER progress in the ITER physics basis. Nucl Fusion 47(E01):S1–S414
Imagawa S et al (2010) Overview of LHD superconducting magnet system and its 10-year operation. Fusion Sci Technol 58:560–570
Ishida S et al (1999) JT-60U high performance regime. Nucl Fusion 39:1211–1226
Ishida S et al (2010) Status and prospect of the JT-60SA project. Fusion Eng Des 85:2070–2079
ITER Physics Basis Editors (1999) ITER Physics Basis. Nucl Fusion 39:2137–2638
Jacquinot J (2010) Fifty years in fusion and the way forward. Nucl Fusion 50:014001
Kato T et al (2001) First test results for the ITER central solenoid model coil. Fusion Eng Des 56–57:59–70
Katoh Y et al (2007) Current status and critical issues for development of SiC composites for fusion applications. J Nucl Mater 367–370:659–671
Kaye and Laby Online (2005) Tables of physical & chemical constants, 16th edn. 2.1.4 Hygrometry version 1.0. Available at http://www.kayelaby.npl.co.uk/
Kikuchi M (2011) Frontiers in fusion research. Springer, London
Koizumi N et al (2005) Development of advanced Nb3Al superconductors for a fusion demo plant. Nucl Fusion 45:431–438
Komori A et al (2010) Goal and achievements of large helical device project. Fusion Sci Technol 58:1–11
Lawson JD (1957) Some criteria for a power producing thermonuclear reactor. Proc Phys Soc Sect B 70:6–10
Lie J, Zhang J, Duan X (2010) Magnetic fusion development for global warming suppression. Nucl Fusion 50:014005
Martone M (ed) (1996) IFMIF-international fusion materials irradiation facility conceptual design activity, final report. ENEA frascati report, RT/ERG/FUS/96/11
Masionnier D et al (2005) A conceptual study of commercial fusion power plants, final report of the European fusion power plant conceptual study (PPCS). European fusion development agreement, EFDA(05)-27/4.10. Available at http://www.efda.org/eu_fusion_programme/downloads/scientific_and_technical_publications/PPCS_overall_report_final.pdf
McCraken G, Stott P (2005) Fusion: the energy of the universe. Elsevier Academic, London
Meade D (2010) 50 years of fusion research. Nucl Fusion 50:014004
Mima K (2010) Inertial fusion development: the path to global warming suppression. Nucl Fusion 50:014006
Mitchell N et al (2010) Status of the ITER magnets. Fusion Eng Des 84:113–121

Muroga T et al (2002) Vanadium alloys – overview and recent results. J Nucl Mater 307–311:547–554
Norgett MJ et al (1975) A proposed method of calculating displacement dose rates. Nucl Eng Des 33:50–54
Ohyama N et al (2009) Overview of JT-60U results towards the establishment of advanced tokamak operation. Nucl Fusion 49:104007
Pamera J, Solano ER (2001) From JET to ITER: preparing the next step in fusion research. EFDA-JET-PR(01)16, EFDA, Culham Science Centre, Abington
Report of Japan Atomic Energy Commission in 2005. Japanese. Available at http://www.aec.go.jp/jicst/NC/senmon/kakuyugo2/siryo/kettei/houkoku051026/index.htm
Ross L (2010) Superconductivity: its role, its success and its setbacks in the large hadron collider of CERN. Supercond Sci Technol 23:034001
Sakharov AD, Leontovitch MA (eds) (1961) Plasma physics and the problem of controlled thermonuclear reactions, vol 1. Pergamon, London, p 21
Spitzer L Jr et al (1954) Problems of the stellarator as a useful power source, NYO-6047; PM-S-14, Princeton University, N.J. Project Matterhorn
Stacey WM (2010) Fusion: an introduction to the physics and technology of magnetic confinement fusion. Wiley-VCH, Weinheim
Team JET (1992) Fusion energy production from deuterium-tritium plasma in the JET tokamak. Nucl Fusion 32:187–203
Uo K (1961) The confinement of plasma by the heliotron magnetic field. J Phys Soc Jpn 16:1380–1395
Webster AJ (2003) Fusion: power for the future. Phys Educ 38:135–142
Wesson J (2004) Tokamaks, The international series of monographs on physics. Oxford University Press, Oxford
Yamada H et al (2009) 10 years of engineering and physics achievements by the large helical device project. Fusion Eng Des 84:186–193
Zinkle SJ (2005) Fusion material science: overview of challenges and recent progress. Phys Plasmas 12:058101

3rd-Generation Biofuels: Bacteria and Algae as Sustainable Producers and Converters

Maximilian Lackner

Contents

M. Lackner (✉)
Institute of Advanced Engineering Technologies, University of Applied Sciences FH Technikum Wien, Vienna, Austria
e-mail: maximilian.lackner@tuwien.ac.at

W.-Y. Chen et al. (eds.), *Handbook of Climate Change Mitigation and Adaptation*,
DOI 10.1007/978-3-319-14409-2_90

Abstract

Biofuels have been commercialized, predominantly bioethanol, biodiesel, and biogas. Mostly, they are based on edible feedstock such as corn, maize, or soybean (so-called 1st-generation (1G) biofuels). The arising competition over arable land with food crops has caused significant debate, as well as the net contribution to climate change mitigation, where it was found that sometimes 1G biofuels perform even worse than petroleum-based fuels, due to land use change, fertilizer usage, and process yields, for instance. Biofuel research has hence targeted lignocellulosic feedstock, which exists in abundance. Due to the stability of these biopolymers, cost-effective 2G biofuels are now only at the verge of commercialization. Processes to break up the biomass into fuels are thermochemical and biochemical, using enzymes. 3G biofuels have been envisioned, where microorganisms are deployed. For instance, since algae can form up to 200 times more biomass per area than terrestrial biomass, they hold great promise for future biofuel production on marginal land or in the ocean. In this chapter, 2G and particularly 3G biofuel concepts, where bacteria and algae are used to obtain biofuels, are discussed. Standard industrial processes, like ethanol fermentation through microorganisms for regular 1G biofuels, are not covered here. Alternative biofuels from bacteria and algae, such as biomethanol or biohydrogen, are also addressed.

Introduction

Bioenergy is energy of biological origin, derived from **biomass**, and **biofuels** are fuels produced from biomass or renewable energy sources (RESs). They can contribute to sustainable transportation and electricity production. **Sustainability** is defined as creating and maintaining *"the conditions under which humans and nature can exist in productive harmony, that permit fulfilling the social, economic and other requirements of present and future generations"* (EPA 2015).

Main biofuel feedstocks, which are all produced by sun energy, are the following:

- Wood (forest management residues and fuel timber)
- Crops (annual and perennial ones, such as rapeseed and *Miscanthus*)
- Wastes (e.g., straw and animal manure)
- Others (e.g., algae)

Biofuels are a means of climate change mitigation, since less net CO_{2eq} is emitted than from fossil fuels. CO_{2eq} (CO_2 equivalent) is the amount of CO_2 that corresponds to the same amount of radiative forcing caused by an emitted greenhouse gas (GHG) such as CH_4 or N_2O; it facilitates comparison.

Theoretically, biofuels close the carbon cycle (see Fig. 1 below).

Other positive aspects are, e.g., less dependency on (foreign) crude oil, local and rural value generation, and more stable fuel prices. Policy measures to support

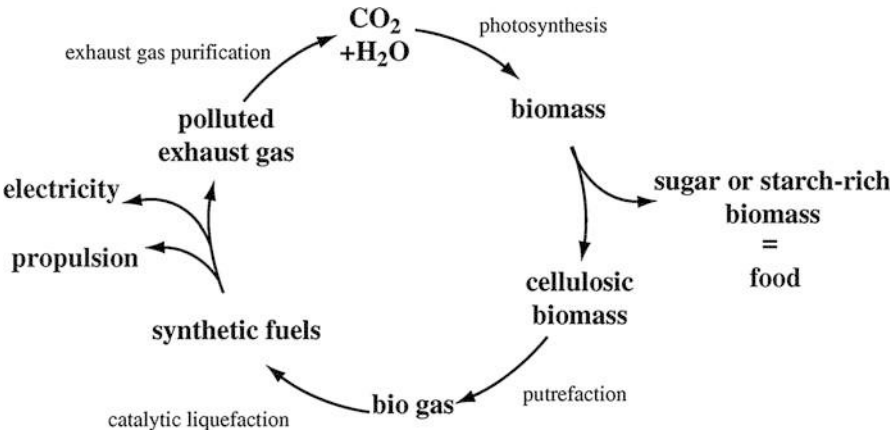

Fig. 1 A possible carbon cycle for synthetic fuel production from biomass (Source: Inderwildi and King 2009)

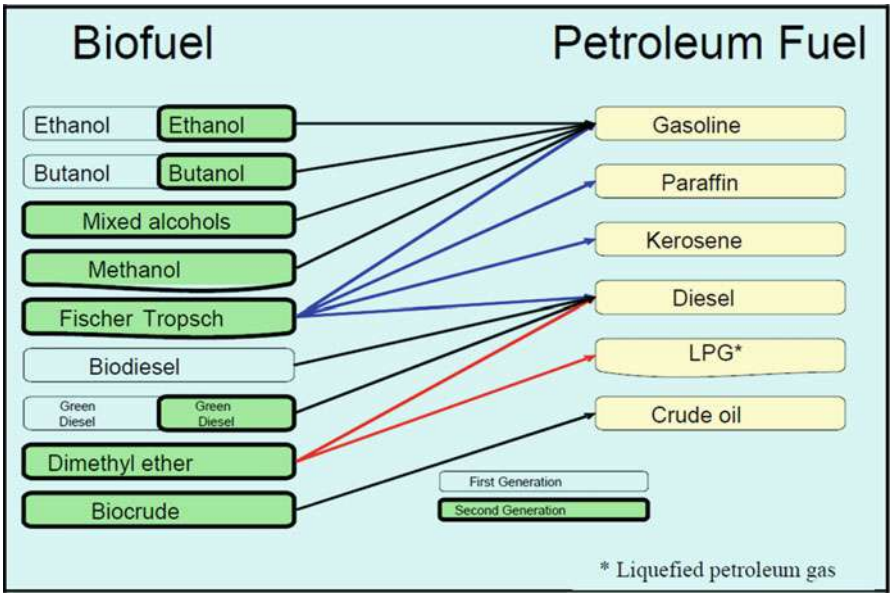

Fig. 2 Substitutability of biofuels with common petroleum-derived fuels (Source: http://unctad.org/en/docs/ditcted200710_en.pdf. Accessed 4 May 2015)

biofuel proliferation include biofuel blending obligations and fuel standards, duty exemptions, feedstock subsidies, and R&D and investment support.

Essentially, all fossil-based fuels can be replaced by biofuels, as Fig. 2 shows for the example of petroleum-derived fuels.

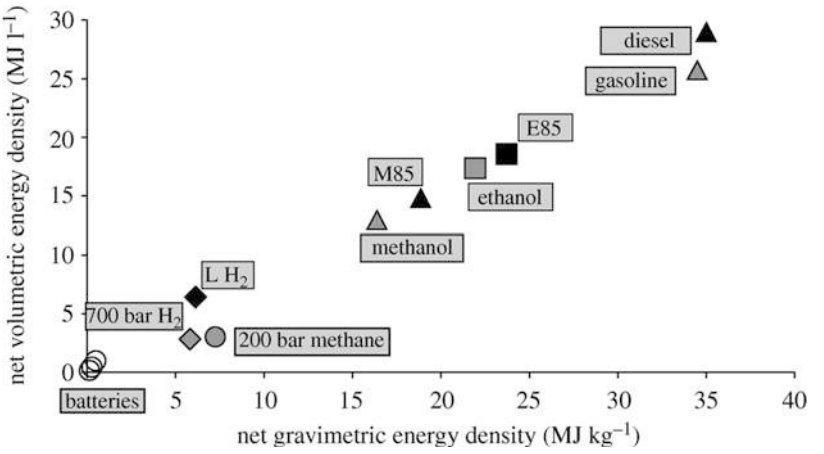

Fig. 3 Liquid fuels are particularly interesting because of their high energy densities. *L H_2* liquid hydrogen, *M85* 85 % methanol in gasoline, *E85* 85 % ethanol in gasoline (Source: Jiang et al. 2010)

Biofuels are solid, liquid, and gaseous fuels derived from renewable resources, suitable for energy production by combustion processes for light, heat and electricity generation, and propulsion. Combustion of fuels, which are predominantly fossil (e.g., coal, crude oil, natural gas), yields approx. 80 % of global primary energy production (Lackner et al. 2013). Traditional biomass burning, e.g., of wood, has been carried out for a long time (Miller 2013). Cheap coal and later crude oil have been increasingly used as of 1750, with the onset of the industrial revolution. Advantages of liquid fuels such as petrol (gasoline) and diesel are their high specific energy content (energy density), combined with ease of storage and handling (see Fig. 3).

Natural gas can be burnt with low emissions. With depleting conventional fossil fuel reserves, exploiting unconventional reserves has become profitable, e.g., of shale gas and tar sands. All of them contribute to climate change, as GHGs, predominantly CO_2 and CH_4, are being emitted into the atmosphere.

Generations of Biofuels

Based on their feedstock, biofuels can be grouped into families: 1st-generation, 2nd-generation, and 3rd-generation (or advanced) biofuels (see Fig. 4).

As Fig. 4 shows, there are many options for biofuels in terms of feedstocks and products. In Fig. 2, HVO stands for hydrotreated vegetable oil, also named "renewable diesel fuel," as opposed to "biodiesel," which is reserved for the fatty acid methyl esters (FAME) (Aatola et al. 2008). The process of HTU (hydrothermal upgrading) is described in Biofuels production via HTU and via pyrolysis; DMF (dimethylfuran) is a promising alternative biofuel (Tian et al. 2011), as is DME (dimethyl ether) (Wang et al. 2011).

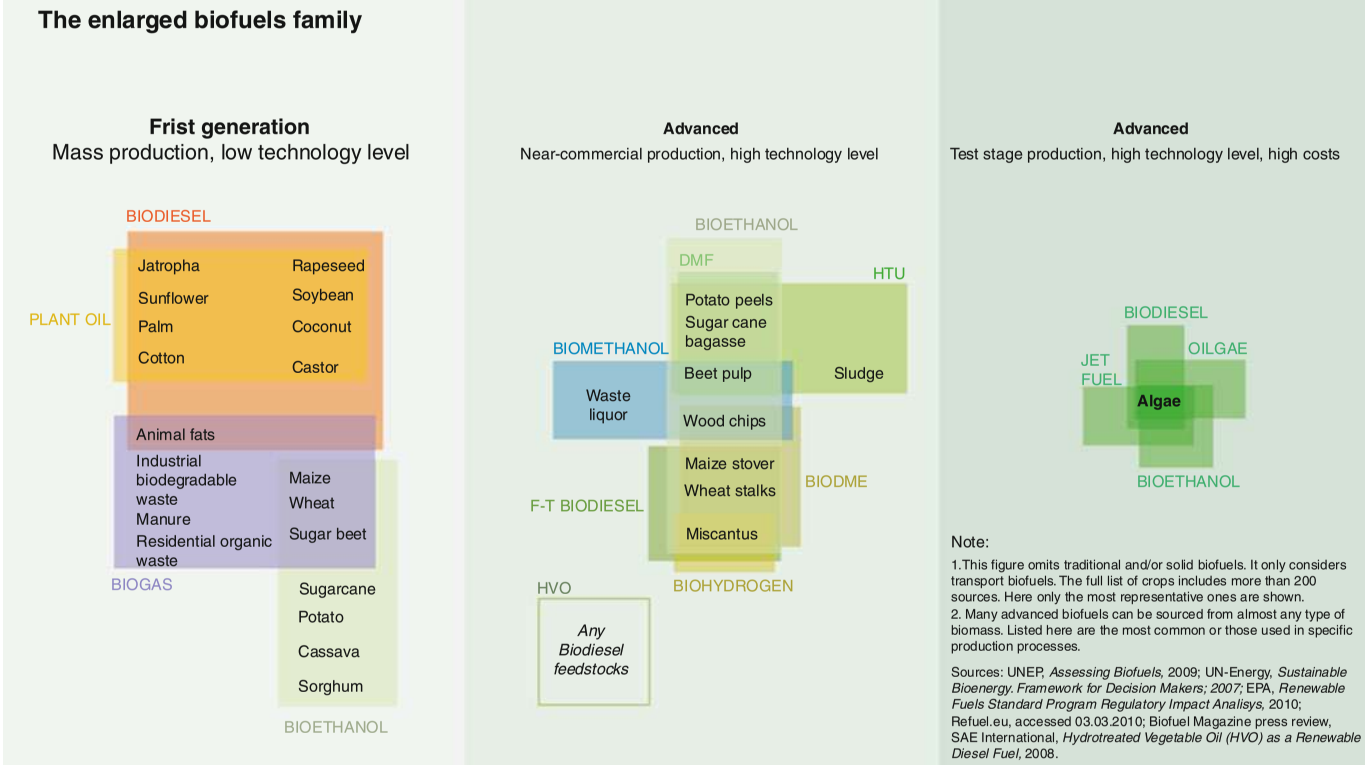

Fig. 4 The family of biofuels. *HVO* hydrotreated vegetable oil; *HTU* hydrothermal upgrading, *DMF* dimethylfuran, *DME* dimethyl ether, *FT* Fischer–Tropsch (Source: http://www.grida.no/publications/vg/biofuels/. Accessed 4 May 2015)

1st-generation biofuels use agricultural crops. The most prominent examples are biogas, biodiesel, and bioethanol. They are "drop in replacements," being compatible with their fossil fuel alternatives.

Biogas (synthetic natural gas (SNG), biomethane) is obtained from anaerobic digestion of sugar and starch (e.g., from sugar beets, maize, and wheat). It can also be collected from landfills (so-called landfill gas). Small-scale fermenters are used by farmers, who can be self-sufficient, or produce electricity and heat (cogeneration) with a gas engine. For details on biogas, see, e.g., Divya et al. (2015) and Deublein and Steinhauser (2010).

Bioethanol (BioEtOH, BioEt) is also obtained by fermentation of sugars, e.g., from corn, potatoes, or sugarcane. It can be admixed to conventional gasoline. The fuels E5 and E10 contain 5 % and 10 % ethanol, respectively. In Brazil and the USA, bioethanol fuel is extensively used. In 2010, US and Brazil's usage of corn and sugarcane, respectively, made 90 % of the world's bioethanol (Philbrook et al. 2013). Bioethanol can be made from brown algae (Fasahati et al. 2015). A recent book on advances in bioethanol is by Bajpai (2013).

Biodiesel is made by transesterification of plant oils (soybean, rapeseed, coconut, oil palm) with methanol, yielding FAMEs (fatty acid methyl esters) with glycerol as by-product. Straight vegetable oil (SVO), also called pure vegetable oils (PVOs) or pure plant oil (PPO), is produced through pressing or extraction, including refining (filtration), but without chemical modification. It has a too high viscosity for utilization in standard diesel engines; this is why the plant oils have to be further processed. The necessary methanol for transesterification can be obtained conventionally or from renewable resources. Depending on the source, biodiesel is called RME (rapeseed methyl ester), SME (soybean methyl ester), PME (palm methyl ester), etc. all subsumed under the generic term XME. Waste cooking oil or animal fat can also be used for biodiesel production. Higher alcohols can be used as a solvent for straight vegetable oil, the mixture being named BM. BM was mixed with diesel fuel (D) to yield biomix diesel (BMD) (Savvidis and Sitnik 2010). For a review on biodiesel, see, e.g., Demirbas (2010).

A major disadvantage of 1st-generation biofuels is their lack of sustainability. They are grown on arable land, where competition with food crops drives up food prices. In 2011, the World Bank and nine other international agencies produced a report advising governments to phase out biofuel subsidies as the use of food stock for 1G fuel production was linked to increasing food prices (Price volatility in food and agricultural markets: policy responses 2007).

Crop growth requires energy-intensive fertilizers, and sometimes, rainforests or other natural pieces of land are removed to create space for farming (land use change). 1st-generation (1G) biofuels are state-of-the-art; they are available in pure form or admixed to petroleum-based fuels. They are not considered sustainable any more. 1G biofuels are out of the scope of this chapter. Lessons learned from 1G biofuels are discussed in Mohr and Raman (2013).

The Role of Microorganisms

1G and 2G biofuels are made from plants and by/with microorganisms. Animals are not useful, since they are on a higher trophic state. However, microorganisms can be deployed for biofuel production in two ways:

1. Conversion of energetic compounds into biofuels (e.g., sugar to ethanol): 2G
2. Production of energetic compounds from sunlight (e.g., by algae): 3G

These two concepts are shown schematically in Fig. 5 below.

Leaving thermal methods aside, both 2G and 3G biofuels rely on microorganisms to convert the carbon feedstock into the desired hydrocarbon biofuels (Ruffing). Microorganisms can produce various biofuels, such as alcohols, hydrogen, biodiesel, and biogas, from multiple starting materials (Elshahed 2010). It is expected that microbially produced biofuels will eventually replace petroleum-based fuels as well as today's first-generation and second-generation biofuels (Singh et al. 2011). They are called "3rd-generation biofuels" in this chapter. Also for 2G biofuels, microorganisms (or their enzymes) are used. 2G biofuels focus on lignocellulosic material, which is challenging to break up into fermentable sugars (Faraco 2013). These 2G technologies utilize the full plant, for instance, dedicated energy crops. Lignocellulose, which forms the major part of plants, is composed of lignin, hemicellulose, and cellulose. In order to produce smaller fragment of these molecules, thermal methods or enzymatic methods have been proposed (Faraco 2013). Pretreatment and subsequent enzymatic hydrolysis are applied to produce fermentable sugars (saccharification). Fungi were also studied for the pretreatment of lignocellulose (see Table 1).

In Philbrook et al. (2013), different end products obtained from bacterial treatment of lignocellulose are presented.

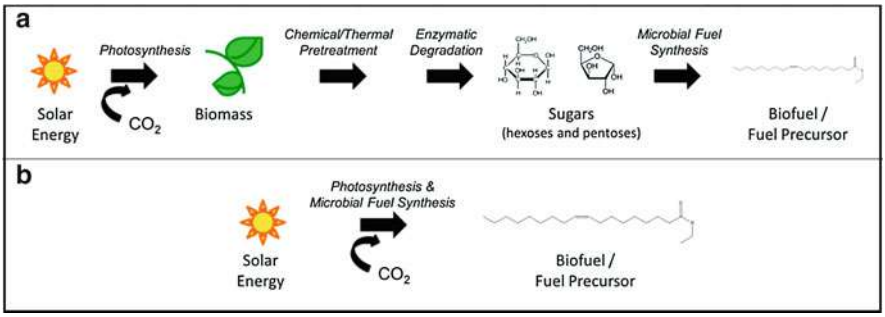

Fig. 5 Process steps for (**a**) 2G (biomass like lignocellulosic feedstock) and (**b**) 3G (i.e., inorganic carbon feedstock) biofuels (Source: Ruffing)

Table 1 Fungal strains studied for pretreatment of lignocellulosic biomass

Substrate	Species	Findings	Duration (days)
Bamboo	*Echinodontium taxodii*	29 % reduction in lignin	30
Bamboo	*Coriolus versicolor*	Enhanced saccharification rate of 37 %	2
Residues			
Bamboo	*Echinodontium taxodii*	5.15-fold increase in sugar yields	120
Culms			
Bamboo	*Trametes versicolor*	8.75-fold increase in sugar yields	120
Culms			
Cornstalk	*Phanerochaete chrysosporium*	34.3 % reduction in lignin with a maximum enzyme saccharification of 47.3 %	15
Corn stover	*Ceriporiopsis subvermispora*	Lignin degradation readied 45 %	30
Corn stover	*Irpex lacteus CD2*	66.4 % saccharification ratio	25
Corn stover	*Ceriporiopsis subvermispora*	31.59 % lignin degradation with less than 6 % cellulose loss	18
Corn stover	*Cyathus stercoreus*	3- to 5-fold improvement in enzymatic digestibility	29
Wheat straw	Basidiomycetous fungi Euc-1	4-fold increase in saccharification	46
Wheat straw	*Irpex lacteus*	3-fold increase in saccharification	46
Rice straw	*Dichomitus squalens*	58 % theoretical glucose yield for remaining glucan	15
Rice straw	*Pleurotus ostreatus*	39 % degradation of lignin with 79 % cellulose retention	48
Rice straw	*Phanerochaete chrysosporium*	64.9 % of maximum glucose yield from recovered glucan	15
Cotton	*Phanerochaete chrysosporium*	33.9 % lignin degradation with 18.4 % carbohydrate availability	14
Stalks			
Cotton	*Phanerochaete chrysosporium*	27.6 % lignin degradation	14
Stalks			
Sawdust	*Grifola frondosa*	21 % reduction in lignin and 90 % recovery of cellulose	2
Matrix			

Source: (Philbrook et al. 2013)

Table 2 1.5G biofuels are made from nonfood sugar/starch/oil crops

Fuel type[a]	Main product	Main feedstock	Status
1.0G biofuel	**Grain-based** ethanol	Corn, wheat	Industrialized (2004–)
	Waste oil-based diesel	Waste cooking oil	Industrialized (2006–)
1.5G biofuel	**Non-grain,** but sugar- or starch-based ethanol	**Cassava, sweet sorghum**	Industrialized (2008–)
	Nonedible oil-based biodiesel/ bio-jet fuel	Jatropha	Demonstration (2010–)
2.0G biofuel	**Cellulosic** ethanol	**Corn cob** Corn stalk	Demonstration (2010–); three scaled up (2013)
	BtL	Agricultural residue	Research stage

Source: (Kang 2014)
[a]It is not a standard but a conventional way to define biofuel types, 1.5 generation biofuels are produced by using nonfood sugar/starch/oil crops, to separate from the first-generation food-based fuels

The literature also describes "1.5G" biofuels, which are somewhere between 1G and 2G in terms of sustainability (see Table 2 for an example from China).

As Table 2 shows, Kang (2014) sees 1.0G biofuels as grain based and 2.0G biofuels as cellulose based. 1.5G biofuels are non-grain based, but still rely on sugar or starch, e.g., cassava or sweet sorghum in the case of bioethanol and nonedible oil (e.g., *Jatropha*) in the case of biodiesel. 3G biofuels are based on oleaginous material derived from microorganisms (algae, yeasts, bacteria). These can grow heterotrophically on organic waste/organic feedstock (e.g., sugar) or phototrophically, i.e., using only CO_2, sunlight, and nutrients. Photoautotrophic growth is considered the best mode, as sunlight is being used directly, whereas efficiency losses are encountered in case that energetic C-compounds such as sugars have to be produced first and are then fed to the microorganisms. Algae could be 200 times more productive per unit area than a land-based crop (http://www.cbd.int/doc/publications/cbd-ts-65-en.pdf. Accessed 4 May 2015).

Also, "4th-generation biofuels" (4G) are discussed in the literature (Lü et al. 2011), with varying definitions. 4G biofuels should be "carbon negative," e.g., by including CCS (carbon capture and storage). They are also based on microorganisms and seen as more "advanced" in terms of sustainability and yield than 2 and 3G biofuels, yet far from commercialization. Also, concepts for 4G biofuels are vague. 2G and 3G biofuels are where current research is focusing on.

Impact of Biofuels

When replacing fossil fuels by biofuels, one has to consider several dimensions of, e.g., farming, processing, and use of biofuels. The impact of biofuels is conceptualized in Fig. 6 below.

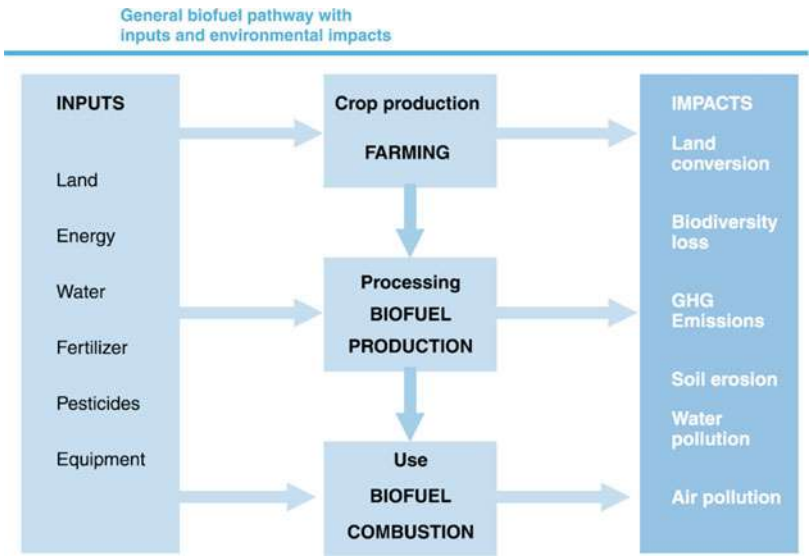

Fig. 6 Pathway to biofuels with inputs and environmental impact (Source: http://www.unep.org/pdf/Assessing_Biofuels-full_report-Web.pdf. Accessed 4 May 2015)

For instance, for crop production, land is needed, and land use change (LUC) can negatively affect the climate (Panichelli and Gnansounou 2015), as the N_2O emissions from fertilizer production and use (Crutzen et al. 2008). Air pollution from biofuel combustion, e.g., SO_x, NO_x, and dust, has to be taken into account as well (Lackner et al. 2013). Note: Apart from combustion, certain biofuels, after purification, can be used in **fuel cells**. Another aspect is water consumption (see the concept of virtual water). A valuable tool is life cycle assessment (LCA) or life cycle impact assessment (LCIA). Figure 7 below compares several biofuels in terms of GWP (greenhouse warming potential), smog formation, and eutrophication (i.e., excessive fertilizer usage).

It has to be noted that the different biofuels have not yet reached their maximum sustainability potential, as sometimes the technologies are not mature yet or economies of scale are missing. Nonetheless, a good indication can be derived, showing, e.g., that methane from manure has a high GWP reduction potential.

Growth Conditions of Microorganisms

Microorganisms are single-cell or multicell, microscopic living organisms. They include all bacteria and archaea and almost all protozoa, some fungi, algae, and certain animals, e.g., rotifers. Within this chapter, we focus on bacteria and algae.

Microorganisms have developed different strategies to obtain energy and carbon. Table 3 shows these growth conditions:

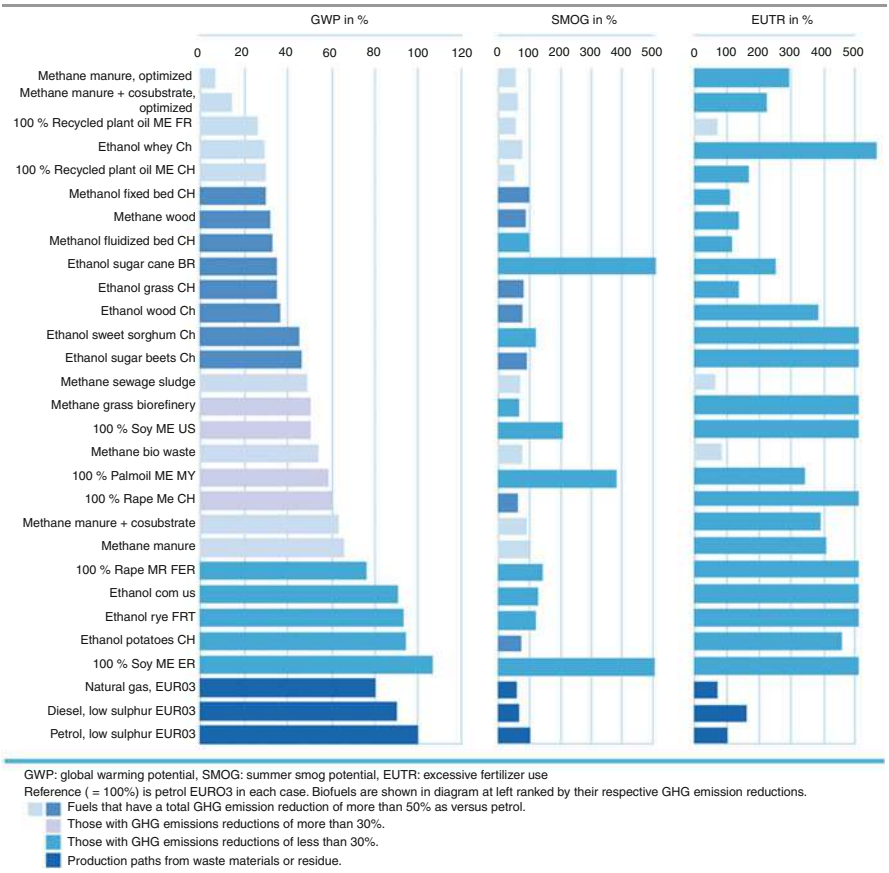

Fig. 7 Comparison of various biofuels in terms of global warming potential (*GWP*), smog and eutrophication (Source: http://www.unep.org/pdf/Assessing_Biofuels-full_report-Web.pdf. Accessed 4 May 2015)

The most common heterotrophic hosts for biofuel production are *Escherichia coli* (bacteria from the lower intestine of warm-blooded organisms, fecal indicator bacteria (Koschelnik et al. 2014)) and *Saccharomyces cerevisiae* (yeast for baking and brewing) (Gendy and El-Temtamy 2013). Advantages of these "model organisms" are the following:

- Fast growth rates
- Well-known genetics and regulation
- Availability of advanced molecular tools for genetic engineering
- Established use in the industrial setting (Gendy and El-Temtamy 2013)

Neither *E. coli* nor *S. cerevisiae* naturally produce hydrocarbon fuels, so metabolic engineering techniques (see further below in this chapter) are needed to express their production. For a discussion of genetically modified algae for biofuel production, see, e.g., Gendy and El-Temtamy (2013).

Table 3 Microorganisms can draw their energy from sunlight or organic compounds, or both. For details, see, e.g., (Cuellar-Bermudez et al. in press)

Mode	Description	Example
Photoautotrophic	Light is used as a sole energy source (autotrophic photosynthesis). CO_2 is converted into energetic compounds through photosynthetic reactions	Algae, e.g., microalgae, cyanobacteria
Heterotrophic	Only organic compounds are used as carbon and energy source (e.g., glucose, acetate, glycerol)	*Escherichia coli* and *Saccharomyces cerevisiae* (yeast)
Mixotrophic (bitroph)	Organisms may employ mixotrophy obligately or facultatively: Energy is derived from different modes. Combinations are photo- and chemotrophy, litho- and organotrophy, auto- and heterotrophy	Euglena
Photoheterotrophic	These organisms have a metabolism in which light is needed to use organic compounds as carbon source. The phenomenon is also known as photoorganotrophic, photoassimilation, or photometabolism	Purple non-sulfur bacteria, green non-sulfur bacteria, heliobacteria
Chemotrophic	Organisms that oxidize inorganic (chemolithotrophic) or organic (chemoorganotrophic) compounds as their principal energy source. Chemotrophs can be either autotrophic or heterotrophic	Bacteria in "black smokers" that feed on H_2S, iron- and manganese-oxidizing bacteria

Growth of Microalgae and Cyanobacteria

"Algae" encompass microalgae, cyanobacteria (the so-called blue-green algae), and macroalgae (or seaweed). Under certain conditions, some microalgae have the potential to accumulate significant amounts of lipids (more than 50 % of their ash-free cell dry weight) (http://www1.eere.energy.gov/bioenergy/pdfs/algal_biofuels_roadmap.pdf. Accessed 4 May 2015).

Microalgae (also called **microphytes**) are microscopic algae. Unicellular in nature, they exist individually, in chains and in groups, with sizes between 1 and several 100 μm. In contrast to higher plants, microalgae lack roots, stems, and leaves. They can be grown photoautotrophically, converting CO_2 into energetic compounds using sunlight.

Cyanobacteria is a phylum[1] of bacteria that obtain their energy by photosynthesis. Their name stems from the color of the bacteria, which are often called

[1] A taxonomic rank below kingdom and above class in biology.

blue-green algae. Cyanobacteria are no "true" algae, since cyanobacteria are prokaryotic and algae are eukaryotic cells.

Why Algae?

The biofuel yield varies geographically, with regions that provide optimum growth conditions having advantageous productivities. Also, the chosen type of crop plays an important role (see Table 4).

Using soybeans, 73 % of the global land area (!) would be needed to cover the global oil demand, whereas with algae, the space is significantly less, an estimated 0.3–2.7 % (Ullah et al. 2014). Considerations which make microalgae attractive for 3G biofuel production are the following:

1. High productivity per km^2
2. Nonfood-based feedstock resources
3. Use of otherwise nonproductive, nonarable land
4. Utilization of a wide variety of water sources (fresh, brackish, saline, marine, wastewater)
5. Production of both biofuels and valuable coproducts
6. Potential recycling of CO_2 and other nutrient waste streams (http://www1.eere.energy.gov/bioenergy/pdfs/algal_biofuels_roadmap.pdf. Accessed 4 May 2015.

The US DOE-supported Aquatic Species Program (ASP, 1978–1996) illustrated the potential of algae as biofuel feedstock.

Table 4 Comparison of crop-dependent biodiesel production efficiencies from plant oils. *TAGs* triacylglycerols (triglycerides). For the algae, two scenarios are shown

Plant source	Biodiesel L/ha/year	Area to produce global oil demand (10^6 ha)	Area required as % of global land mass	Area as % of arable land mass
Cotton	325	15,002	100.7	756.9
Soybean	446	10,932	73.4	551.6
Mustard seed	572	8,524	57.2	430.1
Sunflower	952	5,121	34.4	258.4
Rapeseed	1,190	4,097	27.5	206.7
Jatropha	1,892	2,577	17.3	130
Oil palm	5,950	819	5.5	41.3
Algae (10 g^{-2} day^{-1} at 30 % TAG)	12,000	406	2.7	20.5
Algae (50 g^{-2} day^{-1} at 50 % TAG)	98,500	49	0.3	2.5

Source: (Ullah et al. 2014)

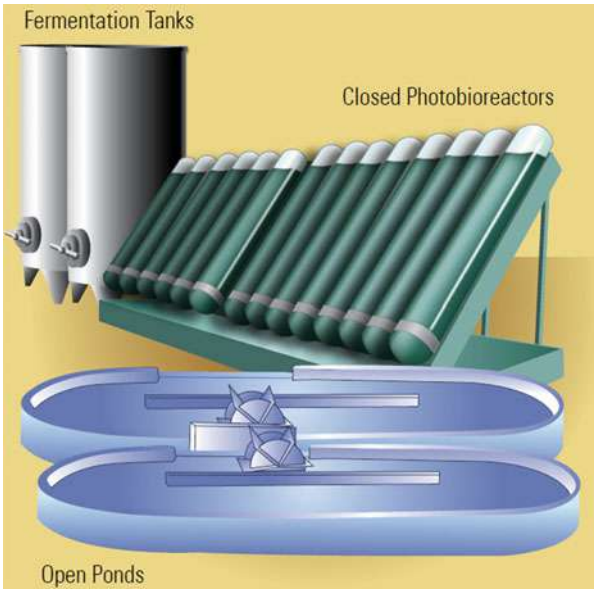

Fig. 8 Typical reactors to grow microalgae (Source: http://www1.eere.energy.gov/bioenergy/pdfs/algal_biofuels_roadmap.pdf. Accessed 4 May 2015)

In the ASP, over 3,000 species of microalgae from a diverse range of environmental habitats were isolated and screened. The focus of the program was on eukaryotic algae, as they naturally produce significant amounts of TAG (Ruffing).

Algae fuel, also called **oilgae**, is made from triglycerides (algal oil) within the algae. It is converted into biodiesel. The processing technology is essentially the same as that for biodiesel from 2G feedstocks (http://www.unep.org/pdf/Assessing_Biofuels-full_report-Web.pdf. Accessed 4 May 2015). Algae can also be fermented anaerobically to yield biogas, which eliminates the need for biomass drying.

Whereas chemotrophic organisms are cultured in fermenters, phototrophic ones have to be exposed to sunlight to harvest energy. This is achieved in various embodiments, the most common ones being open ponds (e.g., raceway ponds) and photobioreactors (PBRs). Figure 8 shows a figure of typical raceway ponds and PBRs.

Fermentation tanks and closed photobioreactors need to be fed with CO_2. Open ponds can take up CO_2 from the atmosphere. CO_2 fertilization will increase the yield, though. As light source, laboratory-scale photobioreactors often use artificial installations such as LED arrays, whereas large installations need to rely on sunlight. Energy efficiencies of the reactors shown in Fig. 8 above will be discussed in more details later.

In Table 5, the two systems “open raceway pond” and “photobioreactor” are compared.

In Table 6 below, the various cultivation approaches for microalgae are shown.

In heterotrophic cultivation, algae are grown without light and are fed a carbon source, such as sugars, to produce new, higher-value biomass. This approach

Table 5 Comparison between microalgae production in open and closed bioreactors

Factor	Open systems (raceway ponds)	Closed systems (photobioreactors)
Space required	High	Low
Area/volume ratio	Low (5–10 m^{-1})	High (20–200 m^{-1})
Evaporation	High	No evaporation
Water loss	Very high	Low
CO_2 loss	High	Low
Temperature	Highly variable	Required cooling
Weather dependence	High	Low
Process control	Difficult	Easy
Shear	Low	High
Cleaning	None	Required
Algal species	Restricted	Flexible
Biomass quality	Variable	Reproducible
Population density	Low	High
Harvesting efficiency	Low	High
Harvesting cost	High	Lower
Light utilization efficiency	Poor	Good
Most costly parameters	Mixing	Oxygen and temperature control
Contamination control	Difficult	Easy
Capital investments	Low	High
Productivity	Low	3–5 times more productive
Hydrodynamic stress on algae	Very low	Low–high
Gas transfer control	Low	High

Source: (Cuellar-Bermudez et al. in press)

capitalizes upon mature industrial fermentation technology (http://www1.eere.energy.gov/bioenergy/pdfs/algal_biofuels_roadmap.pdf. Accessed 4 May 2015).

Production cost is expected to be significantly lower in open ponds; however, PBRs are needed when pure cultures are to be grown. Open ponds are only suitable for extremophile organisms, such as halophiles, since else the pond would very fast become populated by other invading microorganisms. For "grazing" by ciliates, amoeba, rotifers, and other zooplankton taxa, see, e.g., Day et al. (2012).

In Table 7 below, the productivity of several microalgae species is shown, depending on growth scenarios.

3G biofuels based on algae and cyanobacteria are not yet commercially available yet. Today's plants producing microalgae focus on high-value products such as omega 3 fatty acids. Scale-up (Rogers et al. 2014) and downstream processing (algae harvesting and dewatering (http://www1.eere.energy.gov/bioenergy/pdfs/algal_biofuels_roadmap.pdf. Accessed 4 May 2015)) are major challenges that still need to be overcome.

Figures 9 and 10 below show simplified flowcharts on the two basic options of converting algae to biofuels: Using the entire organism or the extracted oil.

Table 6 Comparative features of microalgal cultivation approaches

		Advantages	Challenges
Photoautotrophic cultivation	Closed photobioreactors	Less loss of water than open ponds Superior long-term culture maintenance Higher surface to volume ratio can support higher volumetric cell densities	Scalability problems Require temperature maintenance as they do not have evaporative cooling May require periodic cleaning due to biofilm formation Need maximum light exposure
	Open ponds	Evaporative cooling maintains temperature Lower capital costs	Subject to daily and seasonal changes in temperature and humidity Inherently difficult to maintain monocultures Need maximum light exposure
Heterotrophic cultivation		Easier to maintain optimal conditions for production and contamination prevention Opportunity to utilize inexpensive lignocellulosic sugars for growth Achieves high biomass concentrations	Cost and availability of suitable feedstocks such as lignocellulosic sugars Competes for feedstocks with other biofuel technologies

Source: (http://www1.eere.energy.gov/bioenergy/pdfs/algal_biofuels_roadmap.pdf. Accessed 4 May 2015)

Table 7 Comparison of the growth characteristics and CO_2 fixation performance of microalgae strains under different CO_2 concentrations, temperature, and NO_x/SO_x contents. *N.S.* not specified

Microalgae specie	CO_2 (%)	Temperature (°C)	NO_x/So_x (mg L^{-1})	Biomass productivity (mg L^{-1} d^{-1})	CO_2 consumption rate (mg L^{-1} d^{-1})
Nannochloris sp.	15	25	0/50	350	658
Nannochloropsis sp.	15	25	0/50	300	564
Chlorella sp.	50	35	60/20	950	1,790
Chlorella sp.	20	40	N.S.	700	1,316
Chlorella sp.	50	25	N.S.	386	725
Chlorella sp.	15	25	0/60	1,000	1,880
Chlorella sp.	50	25	N.S.	500	940
Chlorogloeopsis sp.	5	50	N.S.	40	20.45
Chlorococcum littorale	50	22	N.S.	44	82

Source: (Elshahed 2010)

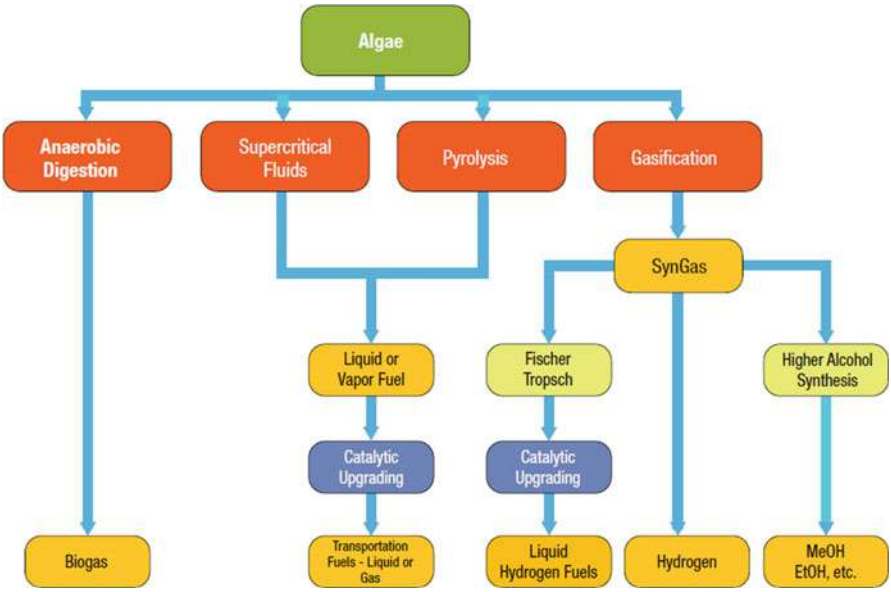

Fig. 9 Schematic of the potential conversion routes for whole algae into biofuels (Source: http://www1.eere.energy.gov/bioenergy/pdfs/algal_biofuels_roadmap.pdf. Accessed 4 May 2015)

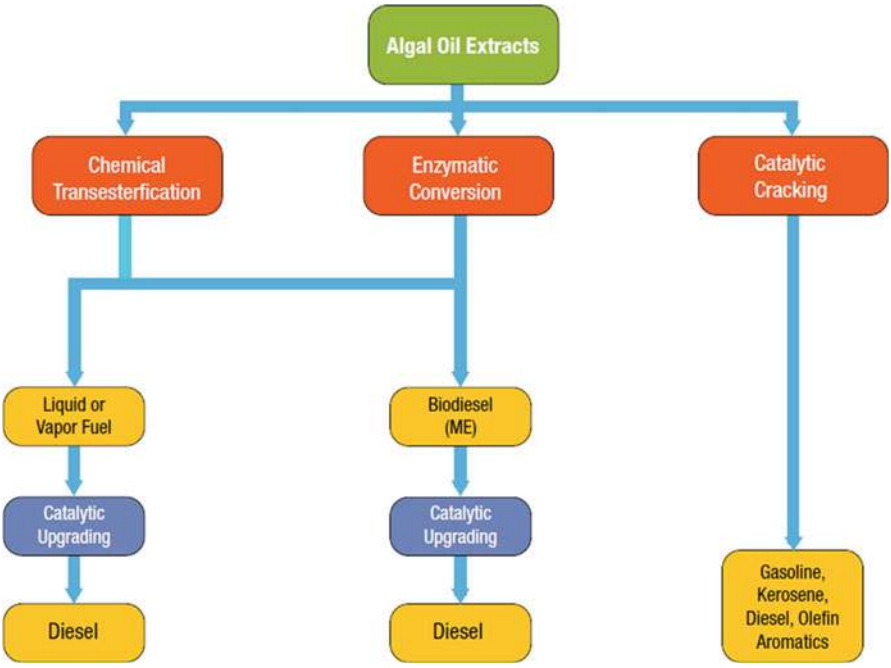

Fig. 10 Schematic of the various conversion strategies of algal extracts into biofuels (Source: http://www1.eere.energy.gov/bioenergy/pdfs/algal_biofuels_roadmap.pdf. Accessed 4 May 2015)

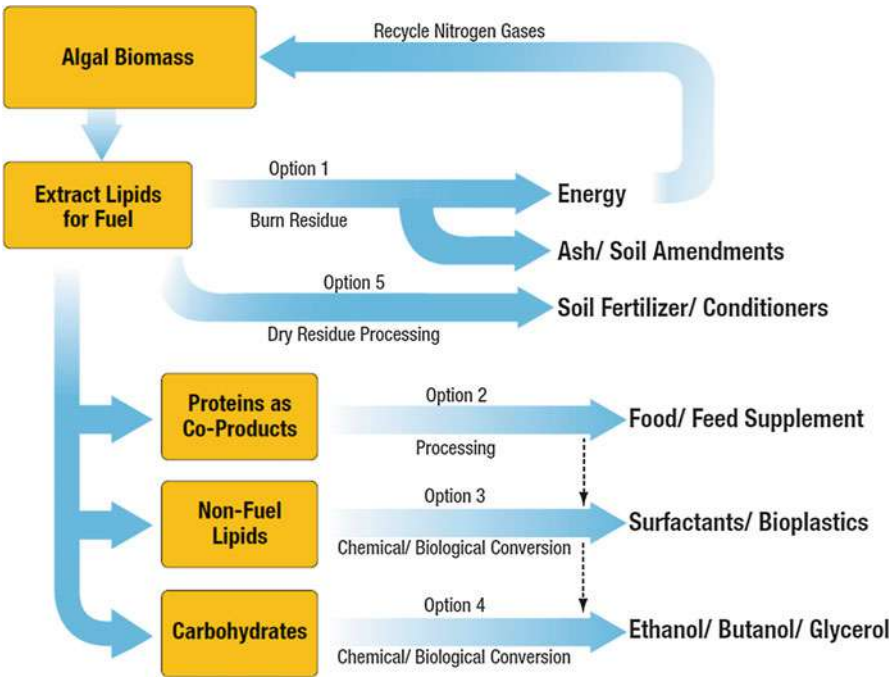

Fig. 11 Overview of the five potential options for the recovery and use of coproducts (Source: http://www1.eere.energy.gov/bioenergy/pdfs/algal_biofuels_roadmap.pdf. Accessed 4 May 2015)

The algae slurry can be anaerobically digested to biogas. Also, thermal methods such as pyrolysis and gasification are available.

The algae oil can be processed to biodiesel through transesterification. For an integrated, cost-optimized production of algae oil, the coproducts need to be utilized, too, which is depicted in terms of available options in Fig. 11 below.

Five concepts to recover and use coproducts have been devised:

Option 1: Combustion for maximum energy recovery from the leftovers of lipid extraction and use of the ash to fertilize and improve soil

Option 2: Production of food and feed supplements by recovering protein from the residues

Option 3: Recovery and utilization of nonfuel lipids and chemicals, e.g., for surfactants and bioplastics

Option 4: Recovery and utilization of carbohydrates in the algae residues and use in fermentation processes

Option 5: After extraction of (only) fuel lipids: use of the residue as soil fertilizer and conditioner (http://www1.eere.energy.gov/bioenergy/pdfs/algal_biofuels_roadmap.pdf. Accessed 4 May 2015.

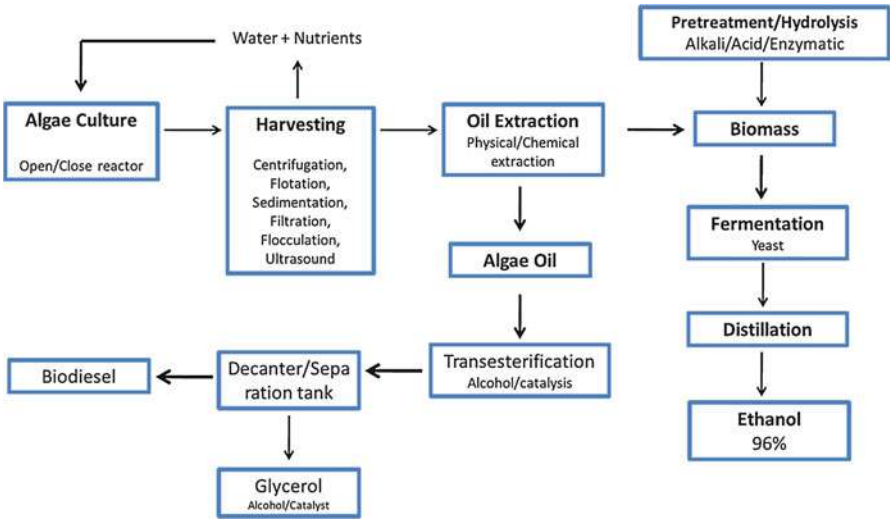

Fig. 12 Algae biofuels production approach. Biodiesel and bioethanol can be obtained from microalgal biomass, with glycerol as by-product (Source: Cuellar-Bermudez et al. in press)

In Kleinová et al. (2012), FAMEs prepared from algae oil TAG (*Nannochloropsis* and *Chlorella* microalgae) were found to meet the requirements of biodiesel standard EN 14 214. However, it was concluded that FAME from algae oil might show less oxidative stability due to higher level of unsaturation (Kleinová et al. 2012).

A simplified process flow diagram of how to obtain biodiesel and bioethanol from algae is shown below in Fig. 12.

Cyanobacteria

Cyanobacteria grow fast, do not need arable land, can use CO_2, and show genetic tractability; hence, they have a strong potential as a platform for biofuel production. They have been engineered to produce various biofuels and biofuel-related compounds, e.g., ethanol and lipids. Challenges for advancing cyanobacterial fuel production are improving genetic parts, carbon fixation, metabolic flux, nutrient requirements on a large scale, and photosynthetic efficiency using natural light (see Fig. 13).

Nozzi et al. (2013) writes: *"... despite years of research, eukaryotic algae have yet to realize their industrial potential andsynthetic biologytechniques for eukaryotic systems remain elusive ... Cyanobacteria, prokaryoticorganisms, combine of the advantages of both eukaryotic algae, as a photosynthetic microorganism, and E. coli, as a tractable and naturally transformable host."*

For more information on cyanobacteria for biofuel production, see, e.g., Nozzi et al. (2013), Parmar et al. (2011), Lu (2010), Savakis and Hellingwerf (2015),

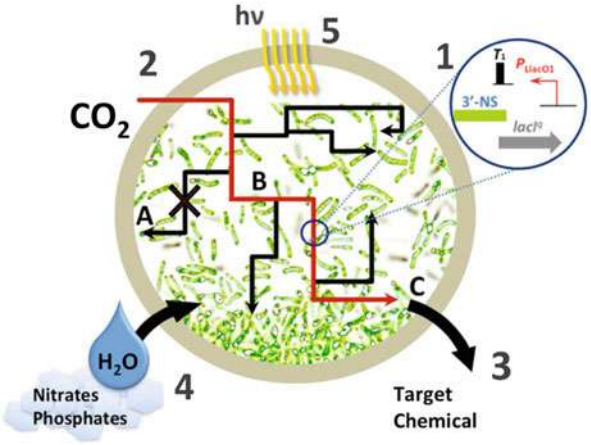

Fig. 13 Challenges in cyanobacterial chemical production. (*1*) Improving available biological parts at each level of the central dogma for engineering artificial pathways in cyanobacteria; (*2*) improving carbon fixation; (*3*) improving metabolic yield with various strategies, *A* –eliminating competing pathways, *B*–improving pathway flux, for example, via irreversible steps, *C*–improving tolerance to or continuous removal of the target chemical; (*4*) management of limited resources that may be stressed upon scale-up; (*5*) photosynthetic efficiency and bioreactor design. For details on the *insert*, see the source: (Nozzi et al. 2013)

Steinhoff et al. (2014), Leite and Hallenbeck (2014), and the section on metabolic engineering below.

Assessment of Biofuels

Energy Return Ratios (ERRs)

In order to compare the efficiencies of energy extraction and conversion systems, net energy analysis (NEA) is carried out, yielding energy return ratios (ERRs) such as the net energy ratio (NER) or energy return(ed) on investment (EROI) that are used (Brandt and Dale 2011). Key energy metrics are shown in Table 8 below.

NEB (net energy balance) is the difference between the total energy in the biofuel (and its coproducts) and the total primary energy necessary to produce it. A positive net energy balance is needed for sustainability. EROI and NER >1 correspond to a positive energy balance. FER and BF_{en} are variants, which refer the energy output to the amount of fossil or renewable energy input, respectively.

Table 9 below shows some energy ratios for common 1G and 2G biofuels relative to gasoline.

The comparison of NER of microalgae biomass production in raceway ponds and photobioreactors in a metastudy (Slade and Bauen 2013) has revealed strong differences (see Fig. 14 below).

Table 8 Key energy metrics

Name	Abbreviation	Formal definition
Net energy balance	NEB	$\sum \text{Energy}_{\text{output}} - \sum \text{Energy}_{\text{input}}$
Energy return on investment	EROI	$\frac{\sum \text{Energy Output}}{\sum \text{Energy Input}}$
Net energy ratio	NER	$\frac{\sum \text{Energy Output}}{\sum \text{Energy Input}}$
Fossil energy ratio	FER	$\frac{\sum \text{Energy Output}}{\sum \text{Fossil Energy Input}}$
Energy breeding factor	BF_{en}	$\frac{\sum \text{Energy Output}}{\sum \text{Nonrenewable Energy Input}}$

Source: (Gupta and Tuohy 2013)

Table 9 Energy ratios for gasoline and some first- and second-generation biofuels

	Overall energy ratio (OER)	Fossil energy ratio (FER)	Petroleum energy ratio (PER)
	Liquid fuel output	*Liquid fuel output*	*Liquid fuel output*
Liquid fuel	*Fossil + biomass input*	*Fossil input*	*Petroleum input*
Gasoline (USA)	0.81	0.81	0.91
Corn ethanol (USA)	0.57	1.4	5.0
Soy biodiesel (USA)	0.45	3.2	Not available
Cellulosic ethanol (USA)	0.45	5.0	5.0
Sugarcane ethanol (Brazil)	0.30	10	10

Source: (http://unctad.org/en/docs/ditcted200710_en.pdf. Accessed 4 May 2015)

NER is defined here as the sum of the energy used for cultivation, harvesting, and drying, divided by the energy content of the dry biomass. As it can be inferred from Fig. 14, six out of the eight reported raceway pond concepts have a NER <1, whereas the NER of all PBR was found to be >1. Likewise, this study has assessed the carbon emissions, expressed in CO_{2eq}, for different microalgae growth concepts (see Fig. 15 below).

In this study, the GHG emissions associated with algal biomass production were estimated by multiplying the external energy inputs (e.g., electricity for pumps, heat energy for drying) by the default emissions factors described in the EU renewable energy directive (RED) 2009/28/EC (European Union 2009). One can see that, based on today's growth technologies, the CO_{2eq} emissions associated with algal biomass production in raceway ponds are on the same level as emissions from the cultivation and production of RME (biodiesel). By contrast, production of microalgae in PBR yields emissions that are greater than those of conventional fossil diesel.

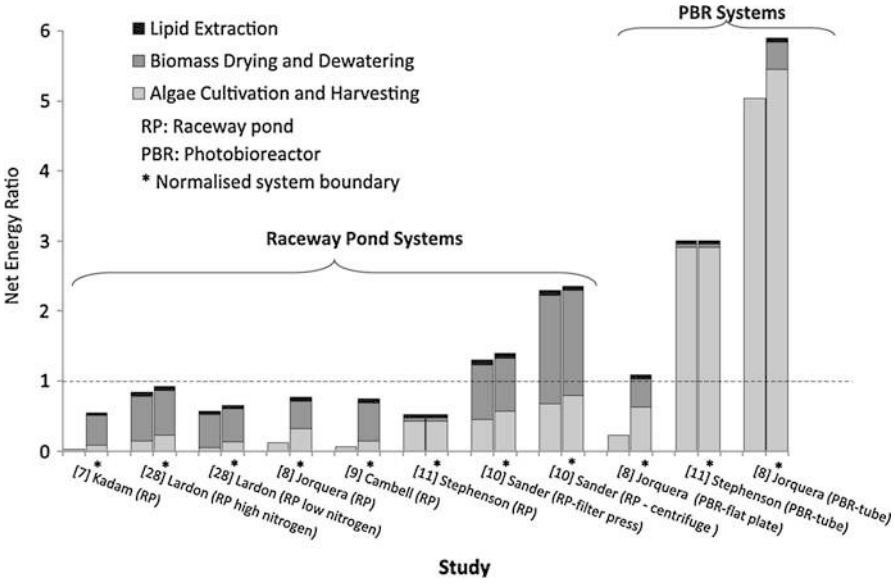

Fig. 14 Net energy ratio for microalgae biomass production: comparison of published values with normalized values (for direct comparison) (Source: Slade and Bauen 2013)

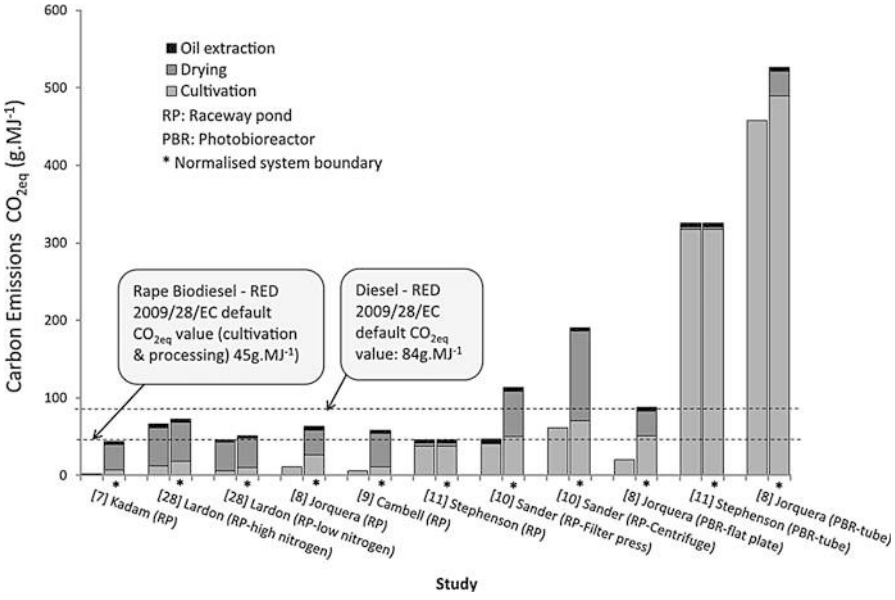

Fig. 15 Estimates for CO_2 emissions from algal biomass production in raceway ponds (The default emissions factors used to estimate carbon dioxide emissions were 83.80 g MJ/l (diesel), 91 g MJ/l (electricity), and 77 g MJ/l (heat). The emissions factor for the embodied energy in fertilizer and for production of PVC lining (in the case of raceway ponds) and PBR was assumed to be the same as for heat. Normalized system boundaries allow direct comparison of the original data (Source: Slade and Bauen 2013))

Biorefinery Concept

Petrochemical refineries are highly integrated, where the entire crude oil is being used. Cracking and other processes are used to shift the fractions of final product from fractionated distillation to the usage patterns. The biorefinery concept builds upon the same idea, where "green crude" (e.g., algae slurry) is processed into several products, high-value and low-value ones. A schematic concept is depicted below in Fig. 16.

For details on biorefineries, see, e.g., Kamm et al. (2010) and Fang (2013).

Gasoline Alternatives

In 2012, global petroleum consumption was estimated at 89 million barrels per day, and nearly half of it was for producing gasoline. Our energy demand is projected to increase by more than 50 % over the next 10 years (Arifin et al. 2014). It is estimated that in 2010, the number of 1 billion vehicles was surpassed. Today, an estimated 1.2 billion vehicles populate the world's roads, and by 2035, it will be 2 billion (Voelcker 2014). Most of them run on gasoline. The most common bio-based gasoline alternative is ethanol. Apart from ethanol, several alternative fuels can be used to replace petroleum-based gasoline and diesel; they are briefly described below (see also Table 10).

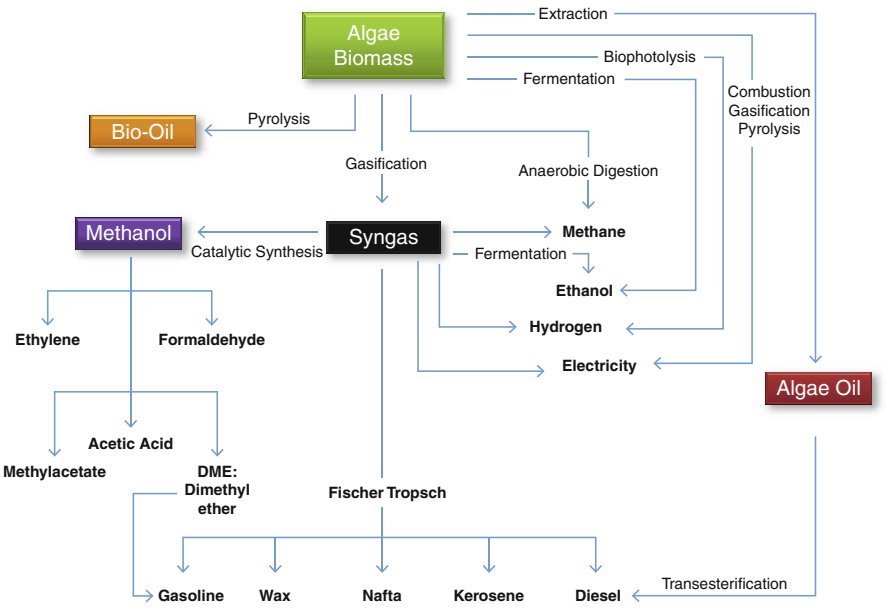

Fig. 16 Algae biorefinery concept (Source: Cuellar-Bermudez et al. in press)

Table 10 Fuel and physicochemical characteristics of petroleum-derived fuels and their potential substitutes

	Energy content (MJ/L)	Solubility[a] (g/L)	Cetane number[b]	Lubricity[c] (μm corrected wear scar)	Viscosity[d] cST	Density[a]	Autoignition temperature[b] (°C)	Boiling point[a] (°C)	Flash point[a] (°C)	Vapor pressure[a] (mmHg)	Freezing point[a] (°C)
Methanol	16	Miscible	2	1,100	0.6@40 °C	0.79	463	65	11	127	−98
Ethanol	19.6	Miscible	11	603	1.1 @40 °C	0.79	420	78	17	55	−114
1-Butanol	29.2	77	17	623	1.7@40 °C	0.81	343	117	29	7	−90
1-Hexanol	31.7	7.9	23	534	2.9@40 °C	0.81	285	158	59	1	−45
1-Octanol	33.7	0.59	39	404	4.4@40 °C	0.83	270	195	81	0.08	−16
1-Decanol	34.6	~0.04	50	406	6.5@40 °C	0.83	255	233	108	<0.1	6
1-Dodecanol	35.3	~0.004	64	345	9.0@40 °C	0.83	275	261	119	<0.1	24
Hydrogenated bisabolene[e]	~37	Immiscible	42	Unknown	2.91	0.82	Unknown	267	111	<0.01	<−78
Biodiesel	32.1	Immiscible	60	314	4–6@40 °C	0.87 (avg)	177–330	315–350	100–170	<1	−3 to −5
Petrodiesel[f]	40.3	Immiscible	45–50	315	1.8–5.8@40 °C	0.84 (avg)	210	150–350	52–96	0.4	−12
Petroleum[g]	32.1	Immiscible	13–17	711–1,064	0.4–0.8@20 °C	0.82 (avg)	246–280	27–225	−40	275–475	−60

Sources: Akhtar et al. (2015), with [a]Linstrom and Mallard (2015), [b]Harnisch et al. (2013), [c]Weinebeck and Murrenhoff (2013), [d]Viswanath et al. (2007), [e]Peralta-Yahya et al. (2011), [f]NREL (2009), [g]Louis and Arkoudeas (2012)

Production of these alternative fuels is possible from petrochemical and renewable resources; processes can be thermal (e.g., pyrolysis and gasification with subsequent Fischer–Tropsch synthesis: BTL, biomass to liquid or, alternatively, e.g., RTP, rapid thermal processing) or enzymatic (carried out in fermenters either with enzymes or with microorganisms).

Bioethanol

Ethanol can be obtained from various carbohydrates. Starch and sugar fermentation are used industrially (1G biofuels). Ethanol production via fermentation using glycerol as carbon source was carried out ethanologenic *Escherichia coli* bacterial (Adnan et al. 2014). This process is interesting, since glycerol is a by-product of biodiesel production. Bioethanol is widely used as renewable fuel, e.g., in Brazil. Disadvantages are its lower energy density compared to gasoline and its hygroscopic nature.

BioMTBE, BioETBE

The oxygenate additives MTBE (methyl tertiary-butyl ether) and ETBE (ethyl tertiary-butyl ether) can be added to gasoline in order to increase the octane rating, improve combustion efficiency, and reduce knocking. Both additives can also be made from renewable resources. Note that MTBE is banned in several states of the USA due to possible contamination of groundwater (What is MTBE? 2015). The reason for MTBE's contamination potential is its water solubility, which makes it more mobile than other gasoline constituents.

Biomethanol

Methanol is an attractive fuel; it can be burnt or be used in fuel cells. Conversion into higher hydrocarbons is also feasible (Olah et al. 2006). Using catalysts, methane can be chemically oxidized to methanol (Fei et al. 2014). It can also be made from glycerol (BioMCN produces biomethanol from by-product glycerol 2008). Renewably produced methanol can also be used for the production of biodiesel (transesterification) and dimethyl ether (DME). For the biochemical production of bioalcohols, see also Minteer (2011).

Biobutanol

Butanol (C_4H_{10}) is comparable to gasoline in its properties (Arifin et al. 2014). It is less corrosive than ethanol and not hygroscopic. Due to its lower heat of vaporization, butanol-fuelled cars are easier to start during cold weather than ones running on ethanol.

Butanol can be mixed with gasoline in any ratio, so the existing infrastructure such as pipelines and storage facilities can be used. Butanol can be obtained petrochemically. Also, it is accessible through carbohydrate fermentation by *Clostridium acetobutylicum* in a process known as acetone–butanol–ethanol (ABE) fermentation with a product ratio of 3:6:1 (Arifin et al. 2014; Gupta and Tuohy 2013).

Bio-Propanol

Propanol can be burnt in engines (Gong et al. 2015) and fuel cells (Markiewicz and Bergens 2010). It can be obtained via metabolically engineered microorganisms from lignocellulose (Deng and Fong 2011), glucose, or glycerol (Choi et al. 2012).

Biodiesel

Diesel is used in heavy engines (trucks, ships, locomotives, construction machinery). Kerosene, which is chemically similar to diesel fuel, is deployed for aircraft propulsion in jet turbines. Table 11 below compares conventional diesel ("summer diesel," according to the standard EN 590) to three bio-based diesel substitutes, HVO (hydrotreated vegetable oil), GTL (gas to liquid) fuel, and FAME (fatty acid methyl ester, or common biodiesel). HVO is sometimes termed "renewable diesel fuel" or "green diesel" to distinguish it from biodiesel. One can see that the three substitutes are comparable in properties.

Table 11 Typical properties of HVO, European EN 590:2004 diesel fuel, GTL, and FAME. *HFRR* high-frequency reciprocating rig

	HVO	EN 590 (summer grade)	GTL	FAME (from rapeseed oil)
Density at 15 °C (kg/m^3)	775...785	≈835	770...785	≈885
Viscosity at 40 °C (mm^2/s)	2.5...3.5	≈3.5	3.2...4.5	≈4.5
Cetane number	≈80...99	≈53	≈73...81	≈51
Distillation range (°C)	≈180...320	≈180...360	≈190...330	≈350...370
Cloud point (°C)	−5... − 25	≈ −5	−0... −25	≈ −5
Heating value, lower (MJ/kq)	≈44.0	=42.7	≈43.0	≈37.5
Heating value, lower (MJ/I)	≈34.4	≈35.7	≈34.0	≈33.2
Total aromatics (wt-%)	0	≈30	0	0
Polyaromatics (wt-%)[a]	0	≈4	0	0
Oxygen content (wt-%)	0	0	0	≈11
Sulfur content (mg/kg)	<10	<10	<10	<10
Lubricity HFRR at 60 °C (μm)	<460[b]	<460[b]	<460[b]	<460
Storage stability	Good	Good	Good	Very challenging

Source: (Aatola et al. 2008)
[a]European definition including di- and tri+ -aromatics
[b]With lubricity additive

Bio-Octanol

Another alternative fuel is 1-octanol (Akhtar et al. 2015). It is similar to diesel fuel (Akhtar et al. 2015). Traditional industrial production of octanol proceeds by the oligomerization of ethylene using triethylaluminium followed by oxidation. This route is known as the Ziegler alcohol synthesis. Production from renewable sources is feasible via microbial fermentation of organic compounds (Akhtar et al. 2015).

Bio-Jet Fuel

The global aviation industry aims to achieve carbon-neutral growth by 2020 and to cut its CO_2 emissions by 50 % relative to 2005 levels by 2050 (International Air Transport Association (IATA) 2009). Renewable jet fuel processes that are currently certified for use in commercial aviation include fuel produced from a hydroprocessed esters and fatty acids (HEFA) process (also known as hydrotreated renewable jet fuel) and biomass to liquid (BTL) via a Fischer–Tropsch (FT) process (Winchester et al. 2013).

For details on renewable aviation fuel, see, e.g., Cremonez et al. (2015).

Gaseous Biofuels

Apart from biogas and synthesis gas (out of the scope of this chapter), biohydrogen is an attractive option.

Biohydrogen

Hydrogen is needed by the chemical industry, e.g., for ammonia production (Haber–Bosch process) and methanol production (from CO). Today, approx. 95 % of H_2 is obtained from fossil fuels (steam reforming or partial oxidation of methane, coal gasification), with electrolysis playing a less important role.

Biohydrogen is H_2 that is produced biologically by algae, bacteria, and archaea. The carbon source can preferentially be waste. One can distinguish between dark fermentation and photofermentation. There is a great potential for improving hydrogen yield by metabolic engineering, i.e., the use of GMOs (genetically modified organisms) (see also below). Algae have been proposed for biohydrogen production (http://www1.eere.energy.gov/bioenergy/pdfs/algal_biofuels_roadmap.pdf. Accessed 4 May 2015). An advantage of biohydrogen production is energy efficiency (Kao et al. 2014). For details on biohydrogen, see, e.g., Demirbas (2011).

Gas to Liquids (GTL)

Biological Conversion of Natural Gas to Liquid Fuel (Bio-GTL)

Methane, which is the main constituent of biogas and natural gas, is the most common gaseous fuel. Attempts have been made to convert it into a liquid fuel, to meet the huge demand by the transportation sector. One approach uses certain

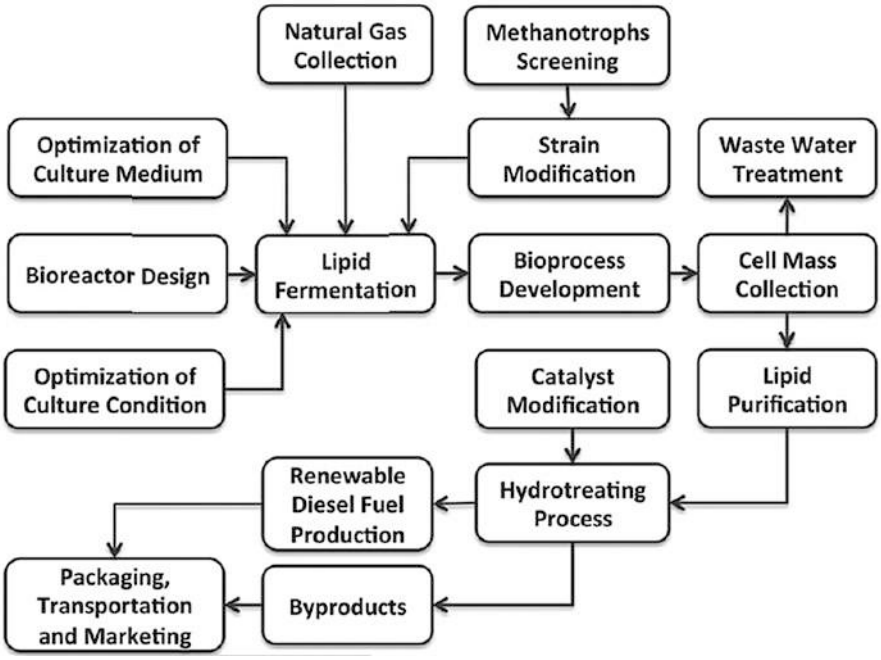

Fig. 17 Research and development map of Bio-GTL using methane as a substrate (Source: Fei et al. 2014)

bacteria, so-called **methanotrophs** (**methanophiles**). These bacteria can be grown aerobically or anaerobically, and they only feed on methane as carbon and energy source. Methanotrophs were considered for the production of vitamins, antibiotics, single-cell protein (SCP), and carboxylic acids (Fei et al. 2014). Also an important biopolymer, poly-β-hydroxybutyrate (PHB), which is a potential replacement for polypropylene (PP), can be produced by methanotrophs.

Methanotrophic bacteria are a promising concept for liquid fuel production, bypassing oil-rich crops such as rapeseed, soybean, and oil palms. A research and development roadmap for GTL with methanotrophs is shown in Fig. 17 below.

Biofuels from Biological Wastewater Treatment (BWWT) Plants

Wastewater from households or industry contains significant amounts of energetic carbon compounds. Processes in today's biological wastewater treatment (BWWT) plants are mainly based on the activated sludge process, where microorganisms oxidize organic molecules to CO_2. In municipal wastewater, lipids can represent more than 40 % of the total organic fraction, with the vast majority consisting of TAGs (triacylglycerols) (Arifin et al. 2014). Specialized oleaginous bacteria could either assimilate lipids from the wastewater or synthesize them *de novo* from other

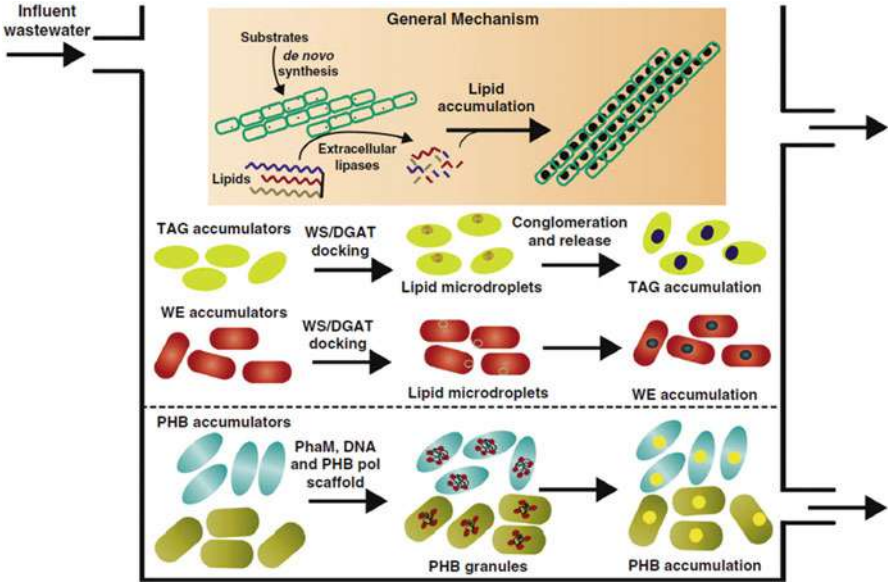

Fig. 18 Conceptual scheme of a "biorefinery column" for biofuel production from wastewater under anaerobic conditions using specifically enriched lipid accumulating bacterial populations. Abbreviations: *FAEE* fatty acid ethyl ester, *FAME* fatty acid methyl ester, *HAME* hydroxyalkanoate methyl ester, *PHB* polyhydroxybutyrate, *PHB pol* PHB polymerase, *TAG* triacylglycerol, *WE* wax ester (Source: Muller et al. 2014)

carbon sources and store them intracellularly as neutral lipids, for example, TAGs, wax esters (WEs), or polyhydroxyalkanoates (PHAs) (Arifin et al. 2014). Such a concept could be realized in a "biorefinery column" as part of a BWWT, see Fig. 18 below.

Other Technologies

Microbial Fuel Cells

A microbial fuel cell (MFC) is a device that converts chemical energy directly to electrical energy by the catalytic reaction of microorganisms (Yu et al. 2012). A configuration that derives energy directly from certain plants is known as a plant microbial fuel cell (PMFC). Potential applications for MFC lie in biosensors, bioremediation, and wastewater treatment with concurrent electricity production. **Electrohydrogenesis** can be used in microbial fuel cells.

Euglena

Euglena is a genus of single-celled flagellate protists. They live in freshwater and seawater. *Euglena* show properties like plants (photosynthesis) but also those of

animals (motion and digestion). *Euglena* were devised for jet fuel production in Japan (Alternative Jet Fuel 2015).

Archaea

Archaea are one of the three domains (kingdoms) of life, next to bacteria and eukaryota. They are single-celled microorganisms. These microbes are prokaryotes (like bacteria), meaning that they have no cell nucleus. Archaea were initially classified as bacteria, receiving the name archaebacterial. By contrast, eukaryotes are organisms whose cells contain a nucleus. Many unicellular organisms are eukaryotes, such as protozoa and algae. All multicellular organisms are eukaryotes, including animals, plants, and fungi.

Archaea could be interesting to provide special enzymes for biofuel synthesis, e.g., hyperthermophilic cellulose (Graham et al. 2011), or thermoacidophilic enzymes (Hess 2008) to break down lignocellulose.

Flue Gas Recycling

Large point sources such as power or cement plants (the latter release 8 % of anthropogenic CO_2 (Cuellar-Bermudez et al. in press)) end themselves for carbon capture and storage (CCS). For CO_2 capture from industrial sources, see, e.g., (Kuckshinrichs and Hake 2014; Romano et al. 2013). CO_2 can be captured from large point sources that burn fossil fuels, biomass can, or both. In carbon capture in processes using biomass (Bio-CCS), a negative CO_2 balance can be achieved (see Fig. 19 below).

Concepts for the integration of power plants with algae ponds are discussed in Schipper et al. (2013). For details on bio-CCS, see, e.g., Apel et al. (1994) and Zhao and Su (2014).

Metabolic Engineering

In metabolic engineering, genetic engineering is deployed to modify the metabolism of organisms. It can involve the optimization of existing biochemical pathways or the introduction of pathway components, mostly in bacteria, yeast, or plants. The goal is the high-yield production of certain metabolites (http://www.nature.com/subjects/metabolic-engineering) such as lipids for biofuel use. Anne M. Ruffing (http://cdn.intechopen.com/pdfs-wm/43693.pdf) writes: *"Metabolic engineering is a powerful tool to improve microbial fuel production, either through engineering the metabolic pathways within the native microorganism to encourage high fuel synthesis or though transferring the fuel production pathway into a model organism for optimization."*

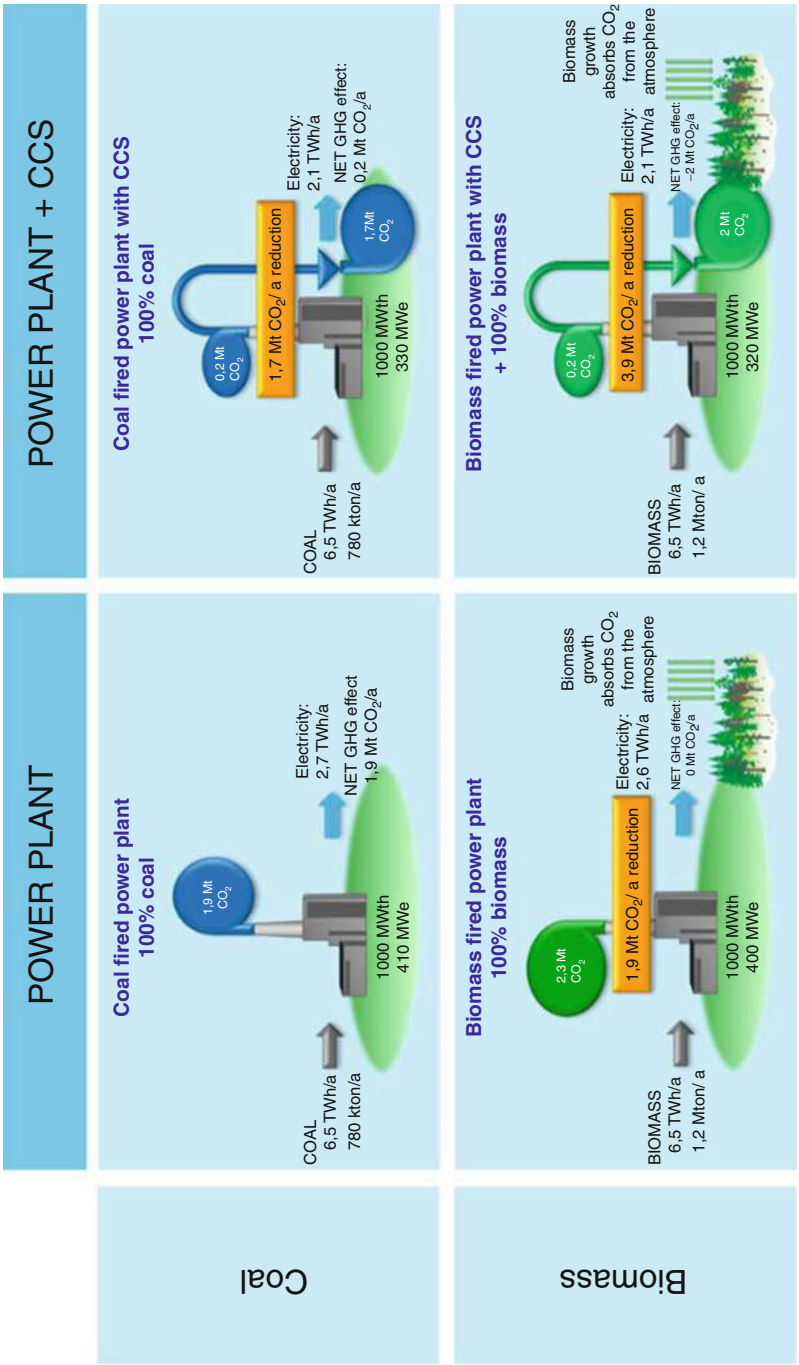

Fig. 19 Principle of carbon balance when applying Bio-CCS (Arasto et al. 2014)

Table 12 Hydrocarbon fuels and fuel precursors produced by genetically engineered microorganisms

Hydrocarbon fuel/fuel precursor	Concentration range	Microbial hosts
	Heterotrophic production	
FFA	0.5–7 g/L	*Escherichia coli*
	0.024–0.2 g/L	*Saccharomyces cerevisiae*
TAG	20–32.6 % dcw, 0.12 g/L	*Chlamydomonas reinhardtii*
	0.4–0.7 g/L	*Saccharomyces cerevisiae*
FAEE	0.07–1.5 g/L	*Escherichia coli*
	N/A	*Saccharomyces cerevisiae*
Fatty alcohols	0.001–1.67 g/L	*Escherichia coli*
Alkanes/alkenes	0.042–0.32 g/L	*Escherichia coli*
Other isoprenoids (lycopene, β-carotene, amorphadiene)	0.002–1 g/L	*Escherichia coli*
	0.01 g/L	*Saccharomyces cerevisiae*
	Autotrophic production	
FFA	0.11–0.20 g/L	*Synechocystis* sp. PCC 6803
	0.015–0.06 g/L	*Synechococcus elongatus* PCC 7942
	0.051 g/L	*Synechococcus* sp. PCC 7002
TAG	28.5 % dcw	*Chlamydomonas reinhardtii*
FAEE	0.077–0.086 g/L	*Synechococcus* sp. PCC 7002
Fatty alcohols	200 μg/L	*Synechocystis* sp. PCC 6803
Alkanes/alkenes	150 μg/L/OD730	*Synechocystis* sp. PCC 6803
	0.05 g/L	*Synechococcus* sp. PCC 7002
	N/A	*Thermosynechococcus elongatus* BP-1
Isoprene	0.5 mg/L	*Synechocystis* sp. PCC 6803

Source: (Ruffing 2013)

Genetic engineering has come under criticism for foodstuff. One can argue that for biofuel production crops, the risks are lower. Table 12 provides an exemplary overview of hydrocarbons and fuel precursors by genetically modified organisms (GMOs).

2G and 3G: Development of microorganisms for cellulose-biofuel consolidated bioprocessings: metabolic engineers' tricks (Mazzoli 2012).

For a review on microbiological aspects of biofuel production, see Elshahed (2010). For details on metabolic engineering for biofuel production, see, e.g., Ruffing (2013).

The production of biofuels by **in vitro synthetic biosystems** was suggested by Zhang (2014). The concept is to achieve a high product yield, coupled with fast reaction rate, easy product separation, open process control, broad reaction condition, and tolerance to toxic substrates (Zhang 2014), as opposed to living "cell factories" of engineered microorganisms.

Enzymes from (extremophile) microorganisms for biofuel processing and production are out of the scope of this chapter.

Discussion

Biofuels are one option for renewable energy; they cannot be the only one, as Fig. 20 below suggests.

Wind energy needs less space than biomass, and renewable electricity has proven to be very efficient. Hartmut Michel writes in (http://onlinelibrary.wiley.com/doi/10.1002/anie.201200218/pdf. Accessed 4 May 2015): *"Commercially available photovoltaic cells already possess a conversion efficiency for sunlight of more than 15 %, the electric energy produced can be stored in electric batteries without major losses. This is about 150 times better than the storage of the energy from sunlight in biofuels. In addition, 80 % of the energy stored in the battery is used for the propulsion of a car by an electric engine, whereas a combustion engine uses only around 20 % of the energy of the gasoline for driving the wheels. Both facts together lead to the conclusion that the combination photovoltaic cells/electric battery/electric engine uses the available land 600 times better than the combination biomass/biofuels/combustion engine."*

The author argues that the most sensible utilization of biomass is for the generation of base chemicals for syntheses purposes. He sees the future for car propulsion

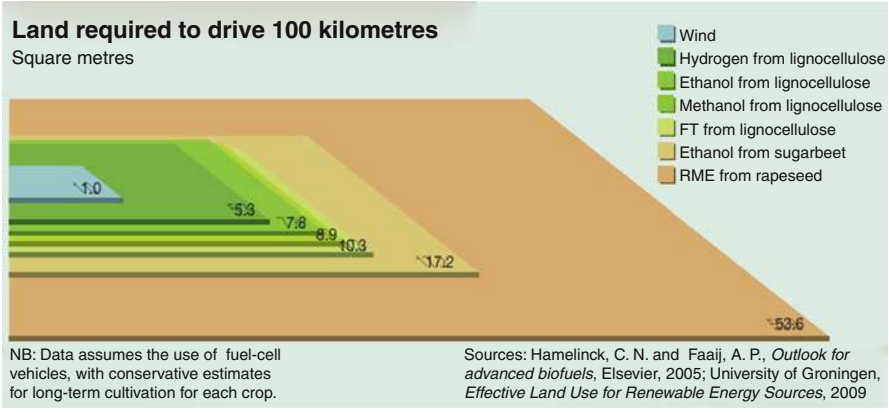

Fig. 20 Necessary land needed to generate the energy for a 100 km car trip (Source: http://www.grida.no/publications/vg/biofuels/. Accessed 4 May 2015)

in electricity. However, by replacing conventional fossil fuels with advanced biofuels in the short and medium terms, environmental benefits can be achieved.

Biofuels have their advantage in high energy densities and compatibility with existing (liquid) fuel handling systems. Hence, they are a viable option for the transportation sector, being an important "ingredient" in the mix of renewable technologies.

Conclusions

Due to rising oil prices and depleting fossil fuel reserves, interest in biofuels has increased over the last decades, with first-generation (1G) biofuels falling behind coal, oil, and gas in several performance dimensions. Advanced biofuels (2G, 3G) can contribute to sustainable transportation. Their manufacturing involves microorganisms, predominantly bacteria, yeasts, and algae. Such biofuels can replace liquid and gaseous transportation fuels. As this chapter has outlined, current challenges are the use of lignocellulosic biomass (2nd-generation biofuels), which is available abundantly, by thermal or enzymatic methods. Hopes are placed on 3rd-generation biofuels, i.e., energetic compounds obtained from microorganisms like algae or cyanobacteria from sunlight. These technologies have not yet reached commercial maturity, and metabolic engineering can support research efforts.

Outlook

Globally, biofuels now provide only 2 % of total transport fuel (http://www.cbd.int/doc/publications/cbd-ts-65-en.pdf. Accessed 4 May 2015). Most of the approx. $30*10^9$ l of biofuels that are used per year relies on 1G technologies (Ullah et al. 2014).

The IEA (International Energy Agency) predicts that biofuels will constitute approx. 27 % of the world transport fuel by 2050 (http://www.cbd.int/doc/publications/cbd-ts-65-en.pdf. Accessed 4 May 2015). In the long run, once electricity storage issues have been solved, vehicles might predominantly be powered electrically. In the meantime, replacing fossil fuels by renewable ones can help in climate change mitigation. Further research, particularly in 3G biofuel technology, is needed to bring promising concepts to commercial maturity.

References

(2007) Price volatility in food and agricultural markets: policy responses. FAO, IFAD, IMF,OECD, UNCTAD, WFP, the World Bank, the WTO, IFPRI and the UN HLTF, Rome, Italy. http://www.oecd.org/tad/agricultural-trade/48152638.pdf

(2008) BioMCN produces biomethanol from by-product glycerol. Focus Catal 2008(12):3. doi:10.1016/S1351-4180(08)70549-X

Aatola H, Larmi M, Sarjovaara T, Mikkonen S (2008) Hydrotreated vegetable oil (HVO) as a renewable diesel fuel: trade-off between NOx, particulate emission, and fuel consumption of a heavy duty engine, SAE paper 2008-01-2500. http://www.biofuelstp.eu/downloads/SAE_Study_Hydrotreated_Vegetable_Oil_HVO_as_a_Renewable_Diesel_Fuel.pdf

Adnan NAA, Suhaimi SN, Abd-Aziz S, Hassan MA, Phang L-Y (2014) Optimization of bioethanol production from glycerol by *Escherichia coli* SS1. Renew Energy 66:625–633

Akhtar MK, Dandapani H, Thiel K, Jones PR (2015) Microbial production of 1-octanol: a naturally excreted biofuel with diesel-like properties. Metab Eng Commun 2:1–5

Alternative Jet Fuel (2015) http://www.euglena.jp/en/solution/energy.html

Anne S, Ieva R, Martina O, Punjanit L Biofuels vital graphics - powering green economy. http://www.grida.no/publications/vg/biofuels/. Accessed 4 May 2015

Apel WA, Walton MR, Dugan PR (1994) An evaluation of autotrophic microbes for the removal of carbon dioxide from combustion gas streams. Fuel Process Technol 40(2–3):139–149

Arasto A, Onarheim K, Tsupari E, Kärki J (2014) Bio-CCS: feasibility comparison of large scale carbon-negative solutions. Energy Procedia 63:6756–6769

Arifin Y, Tanudjaja E, Dimyati A, Pinontoan R (2014) A second generation biofuel from cellulosic agricultural by-product fermentation using clostridium species for electricity generation. Energy Procedia 47:310–315

Bajpai P (2013) Advances in bioethanol. Springer. ISBN-13 978-8132215837

Biofuels and biodiversity, CBD technical series no. 65. http://www.cbd.int/doc/publications/cbd-ts-65-en.pdf. Accessed 4 May 2015

Biofuels production via HTU and via pyrolysis, report 2GAVE-05.07. http://english.rvo.nl/sites/default/files/2013/11/Report%20Biofuels%20production%20via%20HTU%20and%20pyrolysis%202GAVE-05-07.pdf

Brandt AR, Dale M (2011) A general mathematical framework for calculating systems-scale efficiency of energy extraction and conversion: energy return on investment (EROI) and other energy return ratios. Energies 4:1211–1245. doi:10.3390/en4081211

Choi YJ, Park JH, Kim TY, Lee SY (2012) Metabolic engineering of *Escherichia coli* for the production of 1-propanol. Metab Eng 14(5):477–486

Cremonez PA, Feroldi M, de Araújo AV, Negreiros Borges M, Weiser Meier T, Feiden A, Gustavo Teleken J (2015) Biofuels in Brazilian aviation: current scenario and prospects. Renew Sustain Energy Rev 43:1063–1072

Crutzen PJ, Mosier AR, Smith KA, Winiwarter W (2008) N_2O release from agro-biofuel production negates global warming reduction by replacing fossil fuels. Atmos Chem Phys 8:389–395. www.atmos-chem-phys.net/8/389/2008/

Cuellar-Bermudez SP, Garcia-Perez JS, Rittmann BE, Parra-Saldivar R (2015) Photosynthetic bioenergy utilizing CO_2: an approach on flue gases utilization for third generation biofuels. J Clean Prod 98:53–65

Daniel F, Rajita M, Joanne M, Ron P, Joyce Y, US department of energy, national algal biofuels technology roadmap. http://www1.eere.energy.gov/bioenergy/pdfs/algal_biofuels_roadmap.pdf. Accessed 4 May 2015

Day JG, Thomas NJ, Achilles-Day UEM, Leakey RJG (2012) Early detection of protozoan grazers in algal biofuel culture. Bioresour Technol 114:715–719

Demirbas A (2010) Biodiesel: a realistic fuel alternative for diesel engines. Springer. ISBN-13 978-1849966962

Demirbas A (2011) Biohydrogen: green energy and technology. Springer. ISBN 978-1447122869

Deng Y, Fong SS (2011) Metabolic engineering of Thermobifida fusca for direct aerobic bioconversion of untreated lignocellulosic biomass to 1-propanol. Metab Eng 13(5):570–577

Deublein D, Steinhauser A (2010) Biogas from waste and renewable resources: an introduction, 2nd edn. Wiley-VCH, Weinheim. ISBN 978-3527327980

Divya D, Gopinath LR, Merlin Christy P (2015) A review on current aspects and diverse prospects for enhancing biogas production in sustainable means. Renew Sustain Energy Rev 42:690–699

Elshahed MS (2010) Microbiological aspects of biofuel production: current status and future directions. J Adv Res 1(2):103–111
EPA (2015) What is sustainability? http://www.epa.gov/sustainability/basicinfo.htm. Accessed 4 May 2015
Eric DL Biofuel production technologies: status, prospects and implications for trade and development. http://unctad.org/en/docs/ditcted200710_en.pdf. Accessed 4 May 2015
European Union (2009) Directive 2009/28/EC of the European Parliament and of the Council on the promotion of the use of energy from renewable sources and amending and subsequently repealing Directives 2001/77/EC and 2003/30/EC. Off J Eur Union L 140:16–47. http://www.ecolex.org/ecolex/ledge/view/RecordDetails;jsessionid=81486EE7CA5E560409D392398C9539A0?id=LEX-FAOC088009&index=documents
Fang Z (2013) Pretreatment techniques for biofuels and biorefineries. Springer, Berlin. ISBN 978-3642327346
Faraco V (2013) Lignocellulose conversion: enzymatic and microbial tools for bioethanol production. Springer, Berlin. ISBN 978-3642378607
Fasahati P, Woo HC, Liu JJ (2015) Industrial-scale bioethanol production from brown algae: effects of pretreatment processes on plant economics. Appl Energy 139:175–187
Fei Q, Guarnieri MT, Tao L, Laurens LML, Dowe N, Pienkos PT (2014) Bioconversion of natural gas to liquid fuel: opportunities and challenges. Biotechnol Adv 32(3):596–614
Gendy TS, El-Temtamy SA (2013) Commercialization potential aspects of microalgae for biofuel production: an overview. Egypt J Pet 22(1):43–51
Gong J, Zhang S, Cheng Y, Huang Z, Tang C, Zhang J (2015) A comparative study of n-propanol, propanal, acetone, and propane combustion in laminar flames. Proc Combust Inst 35 (1):795–801
Graham JE, Clark ME, Nadler DC, Huffer S, Chokhawala HA, Rowland SE, Blanch HW, Clark DS, Robb FT (2011) Identification and characterization of a multidomain hyperthermophilic cellulase from an archaeal enrichment. Nat Commun 2:375. doi:10.1038/ncomms1373
Gupta VK, Tuohy MG (2013) Biofuel technologies: recent developments. Springer, Berlin. ISBN 978-3-642-34518-0
Harnisch F, Blei I, dos Santos TR, Möller M, Nilges P, Eilts P, Schröder U (2013) From the test-tube to the test-engine: assessing the suitability of prospective liquid biofuel compounds. RSC Adv 3:9594–9605
Hartmut M The nonsense of biofuels.http://onlinelibrary.wiley.com/doi/10.1002/anie.201200218/pdf. Accessed 4 May 2015
Hess M (2008) Thermoacidophilic proteins for biofuel production. Trends Microbiol 16 (9):414–419. doi:10.1016/j.tim.2008.06.001. Epub 6 Aug 2008
Inderwildi OR, King DA (2009) Quo vadis biofuels? Energy Environ Sci 2:343–346. doi:10.1039/b822951c
International Air Transport Association (IATA) (2009) A global approach to reducing aviation emissions. http://www.iata.org/SiteCollectionDocuments/Documents/Global_Approach_Reducing_Emissions_251109web.pdf
Jiang Z, Xiao T, Kuznetsov VL, Edwards PP (2010) Turning carbon dioxide into fuel. doi:10.1098/rsta.2010.0119Published, http://rsta.royalsocietypublishing.org/content/368/1923/3343
Kamm B, Gruber PR, Kamm M (2010) Biorefineries – industrial processes and products: status quo and future directions. Wiley-VCH. ISBN 978-3527329533
Kang L (2014) Biofuel experiences in China, Governance and Market Development Updates, the 6th Stakeholder Plenary Meeting of EBTP. European Biofuels Technology Platform, Brussels, 14–15 Oct 2014. http://www.biofuelstp.eu/spm6/docs/liping-kang.pdf
Kao P-M, Hsu B-M, Huang K-H, Tao C-W, Chang C-M, Ji W-T (2014) Biohydrogen production by immobilized co-culture of *Clostridium butyricum* and *Rhodopseudomonas palustris*. Energy Procedia 61:834–837
Kleinová A, Cvengrošová Z, Rimarcík J, Buzetzki E, Mikulec J, Cvengroš J (2012) Biofuels from algae. Procedia Eng 42:231–238

Koschelnik J, Epp M, Vogl W, Stadler P, Lackner M (2014) MFU/100ml: new measurement parameter for rapid enzymatic monitoring of fecal-associated indicator bacteria in water, 2014 water & health conference. UNC Water Institute

Kuckshinrichs W, Hake J-F (eds) (2014) Carbon capture, storage and use: technical, economic, environmental and societal perspectives. Springer, Cham. ISBN 978-3319119427

Lackner M, Winter F, Palotas A (2013) Combustion: from basics to applications. Wiley-VCH, Weinheim. ISBN 978-3-527-33376-9

Leite GB, Hallenbeck PC (2014) Chapter 22 – engineered cyanobacteria: research and application in bioenergy. In: Bioenergy research: advances and applications. pp 389–406

Linstrom PJ, Mallard WG (2015) NIST chemistry WebBook. NIST Standard Reference, Database Number 69, National Institute of Standards and Technology, Gaithersburg, 20899. http://webbook.nist.gov

Louis E, Arkoudeas P (2012) Lubricating aspects of automotive fuels In: Carmo JP, Ribeiro JE (eds) New advances in vehicular technology and automotive engineering. InTech. doi:10.5772/2617. ISBN 978-953-51-0698-2, 410 pp

Lu X (2010) A perspective: photosynthetic production of fatty acid-based biofuels in genetically engineered cyanobacteria. Biotechnol Adv 28(6):742–746

Lü J, Sheahan C, Fu P (2011) Metabolic engineering of algae for fourth generation biofuels production. Energy Environ Sci 4:2451–2466. doi:10.1039/C0EE00593B

Markiewicz MEP, Bergens SH (2010) A liquid electrolyte alkaline direct 2-propanol fuel cell. J Power Sources 195(21):7196–7201

Mazzoli R (2012) Development of microorganisms for cellulose-biofuel consolidated bioprocessings: metabolic engineers' tricks. Comput Struct Biotechnol J 3(4):1–9

Miller K (2013) Archaeologists find earliest evidence of humans cooking with fire, discover. http://discovermagazine.com/2013/may/09-archaeologists-find-earliest-evidence-of-humans-cooking-with-fire. Accessed 4 May 2015

Minteer SD (2011) 11 – Biochemical production of other bioalcohols: biomethanol, biopropanol, bioglycerol, and bioethylene glycol. In: Handbook of biofuels production. pp 258–265

Mohr A, Raman S (2013) Lessons from first generation biofuels and implications for the sustainability appraisal of second generation biofuels. Energy Policy 63:114–122

Muller EEL, Sheik AR, Wilmes P (2014) Lipid-based biofuel production from wastewater. Curr Opin Biotechnol 30:9–16

Nozzi NE, Oliver JWK, Atsumi S (2013) Cyanobacteria as a platform for biofuel production. Front Bioeng Biotechnol. doi:10.3389/fbioe.2013.00007

NREL (2009) Biodiesel handling and use guide, 4th edn. National Renewable Energy Laboratory, Golden

Olah GA, Goeppert A, Surya Prakash GK (2006) Beyond oil and gas: the methanol economy. Wiley-VCH, Weinheim. ISBN 978-3527312757

Panichelli L, Gnansounou E (2015) Impact of agricultural-based biofuel production on greenhouse gas emissions from land-use change: key modelling choices. Renew Sustain Energy Rev 42:344–360

Parmar A, Singh NK, Pandey A, Gnansounou E, Madamwar D (2011) Cyanobacteria and microalgae: a positive prospect for biofuels. Bioresour Technol 102(22):10163–10172

Peralta-Yahya PP, Ouellet M, Chan R, Mukhopadhyay A, Keasling JD, Lee TS (2011) Identification and microbial production of a terpene-based advanced biofuel. Nat Commun 2:483

Philbrook A, Alissandratos A, Easton CJ (2013) Biochemical processes for generating fuels and commodity chemicals from lignocellulosic biomass. http://cdn.intechopen.com/pdfs-wm/42494.pdf

Rogers JN, Rosenberg JN, Guzman BJ, Oh VH, Mimbela LE, Ghassemi A, Betenbaugh MJ, Oyler GA, Donohue MD (2014) A critical analysis of paddlewheel-driven raceway ponds for algal biofuel production at commercial scales. Algal Res 4:76–88

Romano MC, Anantharaman R, Arasto A, Ozcan DC, Ahn H, Dijkstra JW, Carbo M, Boavida D (2013) Application of advanced technologies for CO_2 capture from industrial sources. Energy Procedia 37:7176–7185

Ruffing AM (2013) Metabolic engineering of hydrocarbon biosynthesis for biofuel production. http://cdn.intechopen.com/pdfs-wm/43693.pdf. Accessed 4 May 2015
Savakis P, Hellingwerf KJ (2015) Engineering cyanobacteria for direct biofuel production from CO_2. Curr Opin Biotechnol 33:8–14
Savvidis D, Sitnik L (2010) Investigation of three different mixtures of ecofuels used on a Perkins engine on a test bed. SAE technical paper 2010-01-1970. doi:10.4271/2010-01-1970
Schipper K, van der Gijp S, van der Stel R, Goetheer E (2013) New methodologies for the integration of power plants with algae ponds. Energy Procedia 37:6687–6695
Singh A, Olsen SI, Nigam PS (2011) A viable technology to generate third-generation biofuel. J Chem Technol Biotechnol 86:1349–1353
Slade R, Bauen A (2013) Micro-algae cultivation for biofuels: cost, energy balance, environmental impacts and future prospects. Biomass Bioenergy 53:29–38
Stefan B, Helmut S, Meghan O, Lea K, Robert WH, Jeff M. UNEP, towards sustainable production and use of resources: assessing biofuels. http://www.unep.org/pdf/Assessing_Biofuels-full_report-Web.pdf. Accessed 4 May 2015
Steinhoff FS, Karlberg M, Graeve M, Wulff A (2014) Cyanobacteria in Scandinavian coastal waters – a potential source for biofuels and fatty acids? Algal Res 5:42–51
Subject areas, Macmillan Publishers Limited (2015) http://www.nature.com/subjects/metabolic-engineering
Tian G, Daniel R, Xu H (2011) DMF – a new biofuel candidate. http://cdn.intechopen.com/pdfs/20072/InTech-Dmf_a_new_biofuel_candidate.pdf
Ullah K, Ahmad M, Sofia, Sharma VK, Lu P, Harvey A, Zafar M, Sultana S, Anyanwu CN (2014) Algal biomass as a global source of transport fuels: overview and development perspectives. Prog Nat Sci Mater Int 24(4):329–339
Viswanath DS, Ghosh TK, Prasad DHL, Dutt NVK, Rani KY (2007) Viscosity of liquids: theory, estimation, experiment, and data. Springer, Dordrecht
Voelcker J (2014) 1.2 billion vehicles on world's roads now, 2 billion by 2035. http://www.greencarreports.com/news/1093560_1-2-billion-vehicles-on-worlds-roads-now-2-billion-by-2035-report
Wang T, Li Y, Ma L, Wu C (2011) Biomass to dimethyl ether by gasification/synthesis technology – an alternative biofuel production route. Front Energy 5(3):330–339. 8 Sept 2010
Weinebeck A, Murrenhoff H (2013) Lubricity of new tailor-made fuels from biomass. In: Proceedings of the 13th Scandinavian international conference on fluid power – SICFP2013, Linköping
What is MTBE? (2015) http://www.cancer.org/cancer/cancercauses/othercarcinogens/pollution/mtbe. Accessed 5 May 2015
Winchester N, McConnachie D, Wollersheim C, Waitz IA (2013) Economic and emissions impacts of renewable fuel goals for aviation in the US. Transp Res A Policy Pract 58:116–128
Yu D, Wang G, Xu F, Chen L (2012) Constitution and optimization on the performance of microbial fuel cell based on sulfate-reducing bacteria. Energy Procedia 16(Part C):1664–1670
Zhang YH (2014) Production of biofuels and biochemicals by in vitro synthetic biosystems: opportunities and challenges. Biotechnol Adv. doi:10.1016/j.biotechadv.2014.10.009. pii: S0734-9750(14)00158-X
Zhao B, Su Y (2014) Process effect of microalgal-carbon dioxide fixation and biomass production: a review. Renew Sustain Energy Rev 31:121–132

Biopolymers

Maximilian Lackner

Contents

Abstract

Synthetic polymers are used extensively. Approx. 98 % of the 300 million tons of polymers manufactured each year for packaging, construction, appliances, and other technical goods are made from fossil sources, predominantly crude oil. Combustion (thermal recycling) is a preferred route of disposal, at it removes waste, however, CO_2 emissions arise. Biobased polymers, by contrast, are made from renewable resources. A second class of biopolymers for technical applications is biodegradable, being produced from conventional or renewable feedstock. Common biobased plastics are drop-in materials such as biobased PE, biobased PP, and biobased PET, and frequently used biodegradable plastics are PLA (polylactic acid), TPS (thermoplastic starch), and PHA (polyhydroxyalkanoates). Also, composites can contain natural fibers such as sisal or

M. Lackner (✉)
Institute of Advanced Engineering Technologies, University of Applied Sciences FH Technikum Wien, Vienna, Austria
e-mail: maximilian.lackner@tuwien.ac.at

W.-Y. Chen et al. (eds.), *Handbook of Climate Change Mitigation and Adaptation*,
DOI 10.1007/978-3-319-14409-2_91

hemp. Biobased polymer additives, e.g., plasticizers, are also in use. Renewable feedstock reduces the carbon footprint of the plastics produced. Hence, biopolymers can contribute to climate change mitigation. Biodegradable bioplastics avoid accumulation of the material in the environment, which has detrimental effects, e.g., on marine wildlife. The degradation of bioplastics in general does not release pollutants, and mineralization of the polymer yields CO_2 and water in case of hydrogen, carbon, and oxygen compounds. In this chapter, biobased polymers, which have a substitution potential of up to 90 %, are briefly discussed with respect to climate change mitigation.

Introduction

Construction and building materials are produced on a large scale (Smil 2013), having significant environmental impacts. According to the Cement Association of Canada, the annual global production of concrete is approx. 3.8 billion m^3. Steel production also exceeds one billion tons/year. The annual plastic production, by comparison, has reached 300 million tons. Approx. 4 % of the world's oil production is used for plastic production (Chen 2014), which by 2020, is estimated to reach 400 million tons (Biron 2014). Figure 1 shows the historic development of plastic materials.

All these materials emit CO_2 during their manufacturing and also during other stages of their life cycles. The effect of plastics on the environment, however, is mixed and diverse: at the end of their useful lifetime, which can be 100 years (e.g., for pipes) and a few minutes (e.g., for shopping bags), plastics can become a carbon sink or release CO_2 in waste incineration plants. Toxic gases can be emitted, too, in case of uncontrolled combustion. Note that there are other issues, such as littering, particularly in the marine environment, where microplastics cause harm. Such effects are out of the scope of this chapter. During their useful life, plastics can also save fuel, e.g., by less weight in cars and airplanes, hence showing a better life cycle assessment (LCA) than other materials such as steel or aluminum. Cutting a modern car's weight by 100 kg lowers fuel consumption by roughly 0.4 l/100 km and reduces CO_2 emissions by approx. 10 g/km (PlasticsEurope 2013). A weight reduction of 5 % of the bodywork of a car through the use of plastics can yield an average 3 % reduction in fuel consumption (PlasticsEurope 2014a). As a rule of thumb, 1 kg of plastics in vehicles replaces 1.5 kg of conventional materials. In Europe, for instance, the average emissions of all car models sold by one manufacturer in 1 year needs to drop from approx. 140 g CO_2 per km (fleet average 2010) to 95 g in 2020 and to 75 g (or possibly less) in 2025 and afterwards (McKinsey & Company 2012).

On average, Europe produces 25 million tons of postconsumer plastic wastes. Its fate is shown below in Fig. 2.

One can see that recycling and energy recovery are higher in countries with a landfill ban. Only a fraction of the plastic materials are being truly recycled. The highest recycling rate is generally achieved for PET (bottle material), which has a high value.

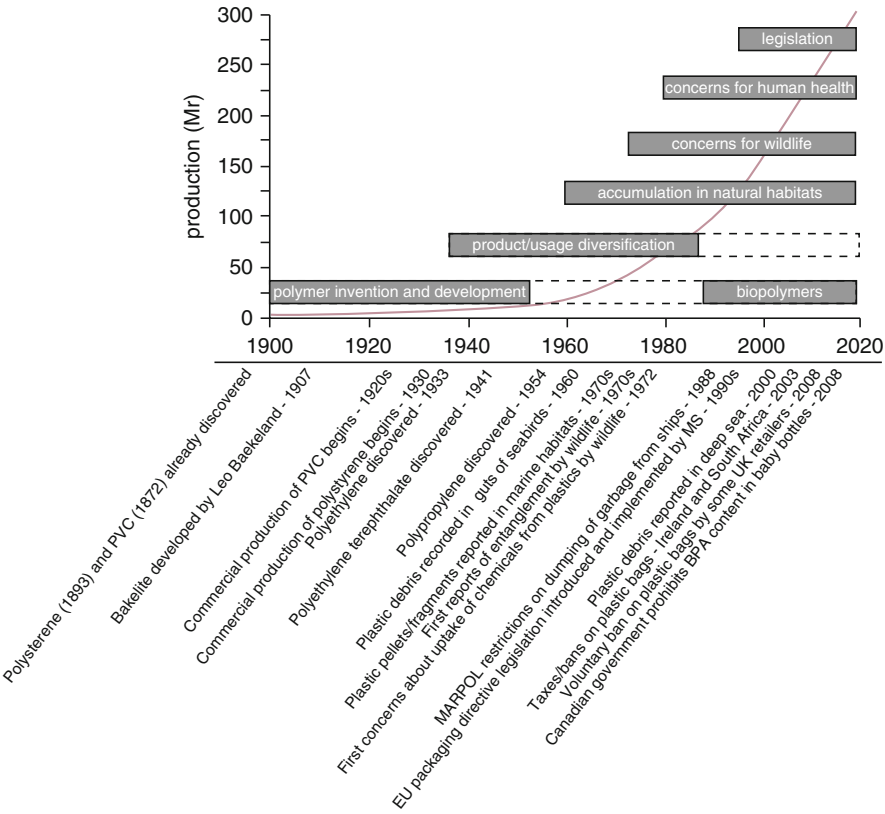

Fig. 1 Global plastic production with historical stages in the development, production, and use of plastics and associated concerns and legislative measures (Source: European Commission 2011)

Plastics in a usage cascade are also deployed in a more sustainable manner (compare Table 1).

Toxic additives in plastics can leach into the environment, which poses another concern. These general aspects are not covered here. This chapter discusses biopolymers compared to conventional plastics with a focus on climate change mitigation potential. In this chapter, the term "biopolymer" is used for technical biopolymers only (note that biopolymers are a broad, generic term).

Biobased Chemicals

Today, most chemicals are based on fossil resources. Technically, biomass can replace all fossil sources deployed for the production of materials and for generating low and medium temperature steam (Saygin et al. 2014). Cost-effective opportunities exist mainly for steam production from biomass residues and for

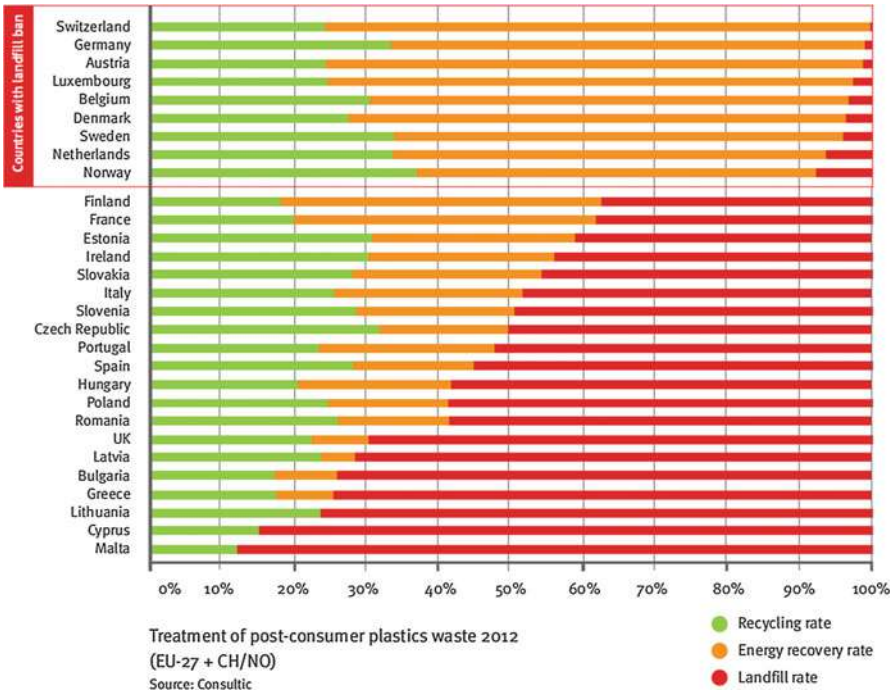

Fig. 2 Use of plastic wastes in Europe (Source: PlasticsEurope 2014b)

Table 1 "Cascade" terminology in plastic recycling (Source: European Commission 2011)

ASTM D7209 – 06 standard definitions	Equivalent ISO 15270 standard definitions	Other equivalent terms
Primary recycling	Mechanical recycling	Closed-loop recycling
Secondary recycling	Mechanical recycling	Downgrading
Tertiary recycling	Chemical recycling	Feedstock recycling
Quaternary recycling	Energy recovery	Valorization

substitution of high-value petrochemicals such as plastics (Saygin et al. 2014). Certain countries use coal (e.g., South Africa, Fischer-Tropsch synthesis) or natural gas (e.g., United Arab Emirates for PE and PP production) instead of crude oil. Natural resources are also used to some extent, with Brazil's bioethanol from sugarcane being a prominent example. In Fig. 3 below, the global organic chemical industry's mass balance and consumption of the renewable raw materials are shown (2007 data):

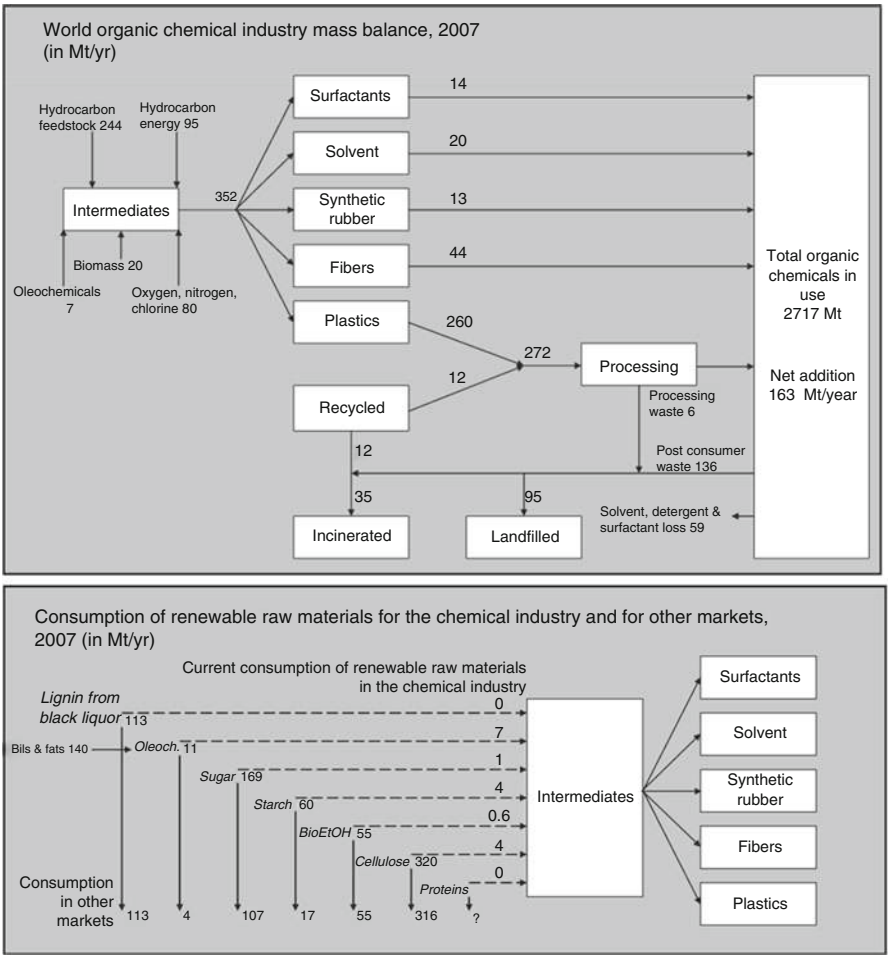

Fig. 3 World organic chemical industry mass balance and current consumption of the renewable raw materials for the chemical industry and for other markets (2007). Net addition is the total production of surfactants, solvents, synthetic rubber, fibers, and processed plastics minus the total of postconsumer waste and material loss. Total quantities of starch and sucrose consumed for bioethanol production are excluded (Source: Saygin et al. 2014)

According to a study by the US Department of Agriculture (USDA), the share of biobased chemicals in the global chemical industry will rise from currently 2 % to >22 % from 2008 (Philp et al. 2013a); see Fig. 4 below.

Biobased polymers, which currently account for approx. 1.5 % of global plastic production, are expected to gain significance in the coming years, as technology improves, consumers demand more "green products," and manufacturers want to appear "green," particularly in the area of plastics, which has a low environmental reputation.

a

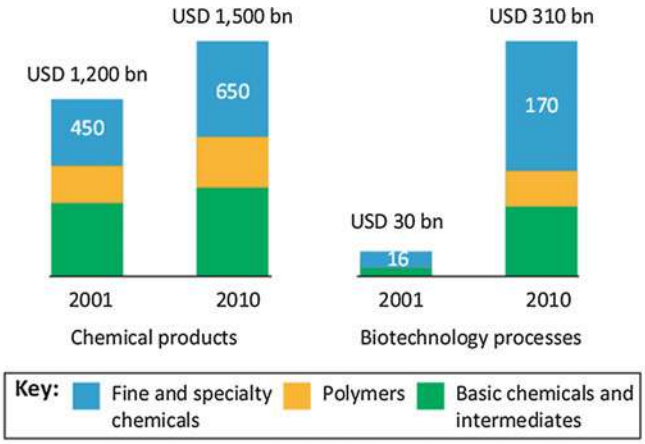

b

	2005		2010		2025	
Sector	Total	Biobased	Total	Biobased	Total	Biobased
Commodity	475	0.9	550	5-11	857	50-86
Specialty	375	5	435	87-110	679	300-340
Fine	100	15	125	25-32	195	88-98
Polymer	250	0.3	290	15-30	452	45-90
Total	1,200	21.2	1,400	132-183	2,183	483-614

Fig. 4 Trends in the production of biobased chemicals in relation to petrochemicals. (**a**) The global growth of the biobased chemicals and polymers between 2001 and 2010, (**b**) US predictions for growth of the biobased industry to 2025. All figures are in billion USD (Source: Philp et al. 2013a)

Biobased Polymers

Synthetic (synthesized) plastics are versatile, cost-effective, and durable materials. They consist of polymers and additives, and applications range from packaging, the automotive industry, and various appliances to the healthcare industry.

75 % of the volume of plastics is filled by polyethylene (PE), polypropylene (PP), polyvinylchloride (PVC), polystyrene (PS), and polyethylene terephthalate (PET) (Pei et al. 2011). Typical applications are highlighted in Fig. 5 below.

Biopolymers are polymers produced by living organisms, i.e., polymeric biomolecules, the most important ones being polysaccharides (e.g., cellulose), polynucleotides (e.g., DNA), and polypeptides. By contrast, **synthetic polymers** such as PE (polyethylene), PP (polypropylene), PVC (polyvinylchloride), and PET

Fig. 5 Typical applications of plastic materials in Europe (EU-27 + NO/CH) in 2013 (Source: Alvarenga and Dewulf 2013)

(polyethylene terephthalate) are used in technical applications as "plastics." Plastics contain polymers and additives such as plasticizers, UV stabilizers, and mineral fillers. Synthetic polymers are manufactured from fossil feedstocks: crude oil (e.g., cracked ethylene, propylene), coal (e.g., gasification and Fischer-Tropsch synthesis), or natural gas (e.g., methane dimerization and metathesis). **Biobased polymers**, or simply **biopolymers** or **bioplastics**, are plastics either made from renewable raw materials or being biodegradable (compare Fig. 6).

Hence, the definition of bioplastics is rather broad (only those plastics which are made from fossil sources and which are not biodegradable are excluded). Conventional polymers such as PE and PP can be made from renewable feedstock. For instance, sugarcane can be converted to ethanol, from which ethylene may be obtained. Such biobased PE, as manufactured by Brazilian company Braskem, is chemically identical to its petroleum-based counterpart. As "drop-in solution," such a material can most easily replace conventionally manufactured polymers. Other biopolymers are biodegradable. They can be made from both conventional and renewable feedstock.

Bioplastics like PHA can also be produced directly by plants "factories" (van Beilen and Poirier 2012) and microorganisms (Yu 2007), which can be metabolically engineered for higher yields.

The most common biobased plastics are biobased PET, bio-PE, starch blends and thermoplastic starch (TPS), polylactic acid (PLA) (Sin et al. 2013), and polyhydroxyalkanoates (PHA) (Chen et al. 2011); see Fig. 7 below. PET consists of 70 % terephthalic acid and 30 % monoethylene glycol (MEG). The latter can be made from renewable ethanol, so a partly renewable "drop-in polymer," which is identical to petrochemically produced PET, is obtained. Such bio-PET can be recycled normally. Research is ongoing for 100 % renewable PET (bottle) material.

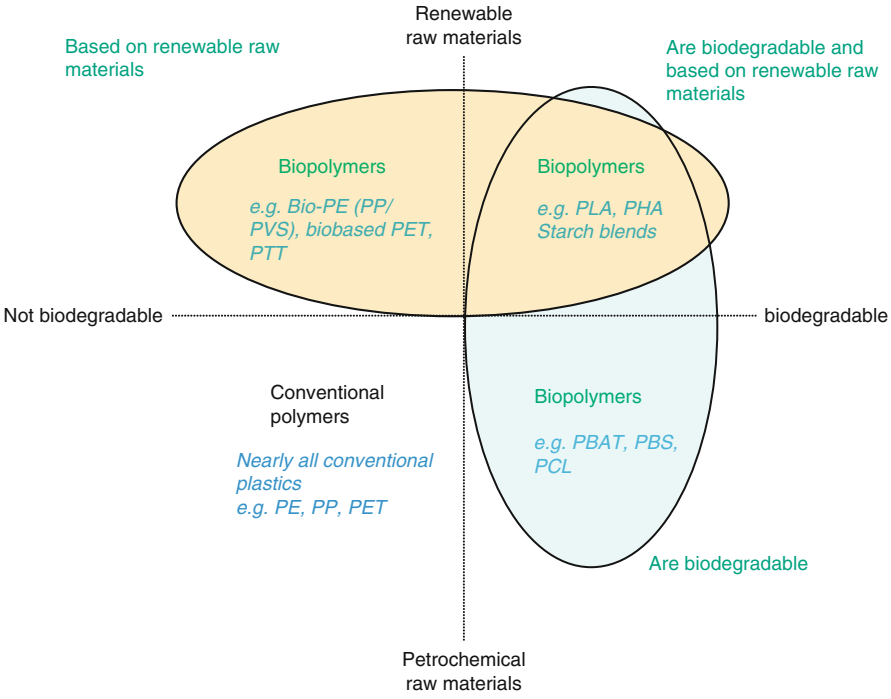

Fig. 6 Types of bioplastics, both biodegradable and nonbiodegradable (Source: Philp et al. 2013b)

The production capacity is approx. 2 % of current production volumes of conventional plastics. Compound annual growth rates for bioplastics are significantly above 10 % (PlasticsToday 2011; Globe Newswire 2013). The replacement potential for biobased polymers is estimated between 33 % and 90 % (OECD 2011). For a review on bioplastics, see, e.g., Lackner (2015), Ebnesajjad (2012), and Niaounakis (2013).

Lessons from First-Generation Biofuels

Sustainability is based in economic, social, and environmental aspects. When all three criteria are met, sustainable development is possible (compare "triple bottom line" of corporations). A balance between social and economic aspects alone is considered equitable, one between social and environmental aspects bearable and one between economic and environmental factors viable. As Fig. 8 below shows, the International Union for Conservation of Nature (IUCN) currently sees a strong imbalance toward environmental aspects of sustainable development, which is in line with common perception.

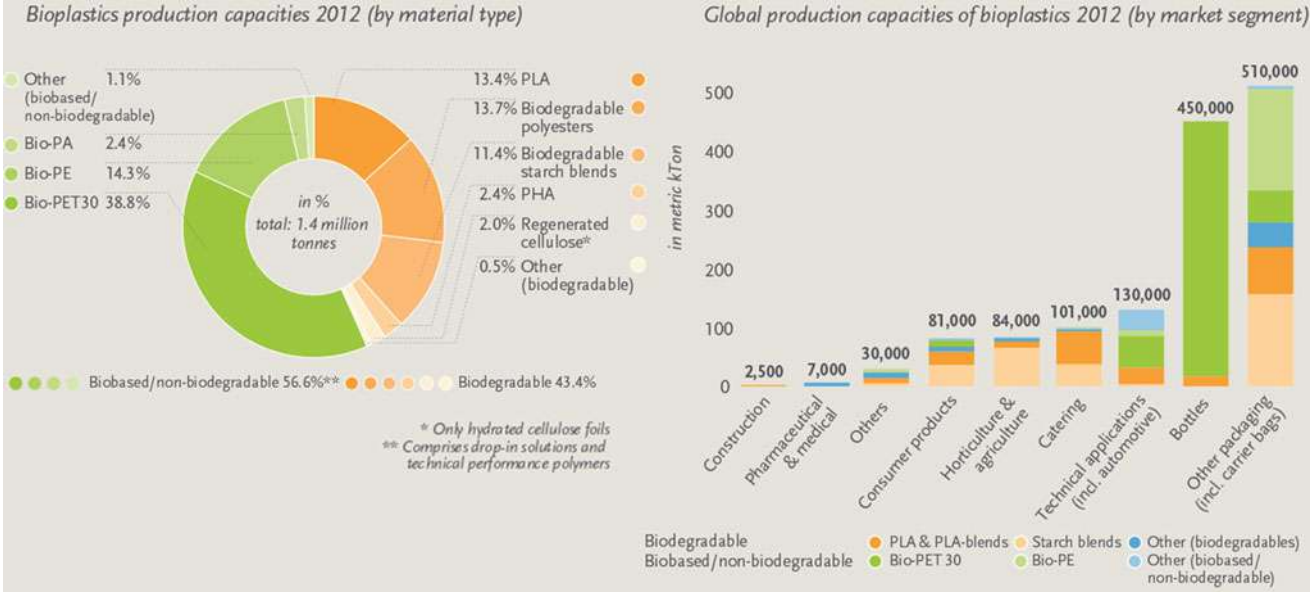

Fig. 7 Global bioplastics' production capacities in 2012 (*left*) and their use (*right*) (Source: European Bioplastics 2013)

Fig. 8 The three circles of sustainability. *Left*, theory; *middle*, current status; *right*, change needed for better balance (Source: Adams 2006)

Biofuels have been envisioned as sustainable solution for transportation, replacing petroleum-based fuels. First-generation (1G) biofuels such as sugarcane-based bioethanol or soybean-based biodiesel, however, have raised significant doubts. Lessons to be learned from 1G biofuels are discussed in Mohr and Raman (2013). Large-scale cultivation of dedicated biomass for biofuels and bioplastics is likely to affect global food prices and water scarcity (Popp et al. 2014). As agricultural commodities consume water during their production, the term "virtual water" was coined (Elena and Esther 2010). It has to be considered in environmental assessments, too.

Bioplastics or Biofuels?

Giving the limited quantity of high-value biomass available for either biofuel or bioplastic production, e.g., in case of Brazilian ethanol from sugarcane, one might ask the question which route is more environmentally sound. According to Alvarenga and Dewulf (2013), deploying ethanol to produce biobased ethylene (instead of fossil-based ethylene) for PE manufacturing would generate environmental gains in the order of 32.0 MJ of fossil energy and 1.87 kg CO_{2eq}, as opposed to the use of ethanol for transportation (instead of gasoline), where environmental gains in the order of 27.2 MJ of fossil energy and 1.82 kg CO_{2eq} were estimated. It was found that above a polymerization yield of 96 %, the bioplastics' route was better in terms of GHG emission reductions (Alvarenga and Dewulf 2013). "CO_{2eq}" stands for "CO_2 equivalent." It is that amount of CO_2 which would cause the same level of radiative forcing as a given type and amount of greenhouse gas (GHG).

According to the Bioplastics Council of the Society of the Plastics Industry (SPI), the widely held perception that the biobased plastics' industry is inextricably linked to and dependent on the emergence of a strong biorefining industry focused mainly on making biofuels is not correct (The Society of the Plastics Industry, Bioplastics Council 2013).

While conventional plastics draw their feedstock from refinery by-products, only a few selected raw materials for bioplastics such as glycerol are linked to biofuel production

(in this case, biodiesel). However, it is not necessary that bioplastics' feedstocks are coupled to biofuels (The Society of the Plastics Industry, Bioplastics Council 2013).

Biopolymers and Climate Change Mitigation

Greenhouse gases (GHG) such as CO_2, CH_4 and N_2O are emitted during feedstock production, transportation, bioplastic manufacturing, packaging, distribution, useful life, and at the end-of-life, which is considered in life cycle assessments (LCA). In a typical LCA of bioplastics, the GHG from land use change (LUC, the so-called carbon debt) for feedstock production is one of the most significant contributors to the environmental impacts (Pei et al. 2011), e.g., in case of rainforest destruction for plantations.

The system boundaries of LCA (the scope) may extend from cradle to gate, cradle to grave, or cradle to cradle; see Fig. 9 below. The cradle-to-gate (dashed lines) approach covers activities prior to usage, while cradle-to-grave approach (dashed and dotted lines) includes the product's use and end-of-life. Cradle to cradle (whole chart) is also used. Sometimes, the scope cradle to pellet is assessed.

Life cycle assessment allows the comparison of "like with like." A position paper on LCA of bioplastics by industry association European Bioplastics can be found in European Bioplastics (2008).

Guidelines for carrying out LCA are provided, e.g., by the International Organization for Standardization (ISO) 14040 series. Others were established by the US Environmental Protection Agency (EPA) and the Society for Environmental Toxicology and Chemistry (SETAC), an international NPO (Hottle et al. 2013).

In Kim and Dale (2008), it was estimated that corn-derived PHB (polyhydroxybutyrate, a potential replacement for PP) offers environmental advantages over fossil polymers, with lower nonrenewable energy consumption (95 % reduction) and lower greenhouse gas emissions (200 % reduction) compared to the petroleum-based plastics.

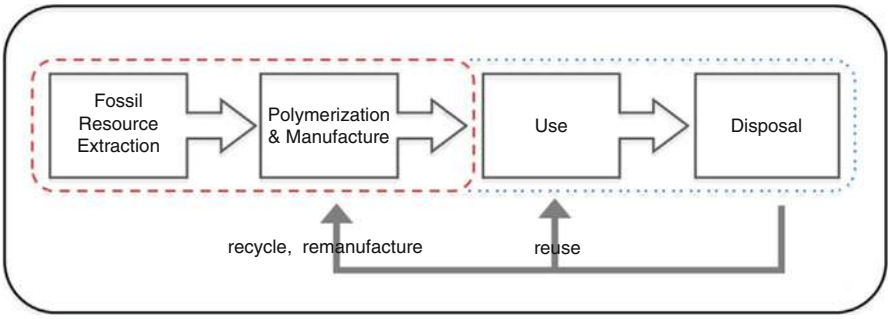

Fig. 9 Generic life cycle stages for polymers. The *dashed line* indicates a cradle-to-gate system boundaries, the dotted line is an extension of that system boundary to cradle to grave, and the entire figure is indicative of a cradle-to-cradle assessment (Source: Hottle et al. 2013)

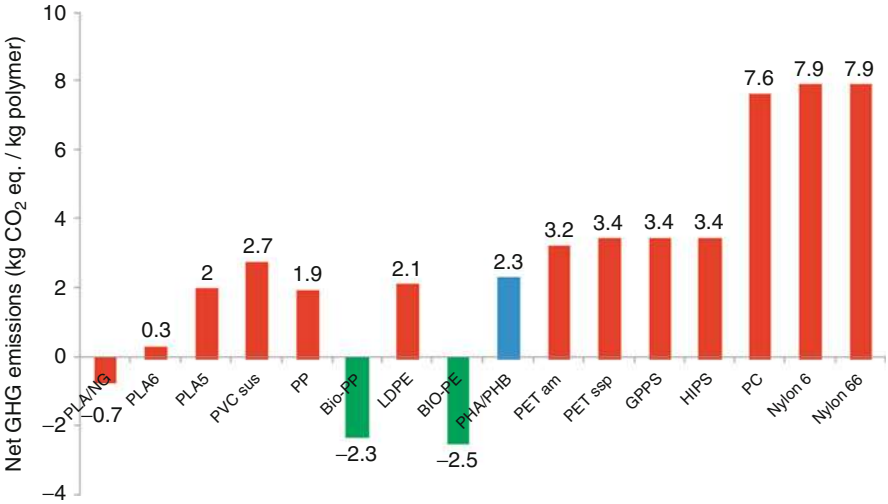

Fig. 10 GHG emissions in plastic production (From various sources: *PLA/NG* NatureWorks™ PLA next generation, *PLA5* NatureWorks™ PLA in 2005, *PLA6* NatureWorks™ in 2006, *PLA* polylactic acid, *PVC sus* PVC suspension, *HIPS* high impact polystyrene, *PC* polycarbonate, *GPPS* general purpose polystyrene, *PET am* PET amorph, *PET ssp* PET solid-state polycondensation, *Bio-PP* Braskem biobased polypropylene, *Bio-PE* Braskem biobased polyethylene (Source: Philp et al. 2013b)

Figure 10 below compares net GHG emissions, expressed in kg CO_{2eq} per kg of polymer, for conventional and biobased materials.

According to Tsiropoulos et al. (2014), a similar study, biobased polyethylene, results in greenhouse gas emissions of around 0.75 kg CO_{2eq}/kg polyethylene, i.e., 1.4 times lower than petrochemical PE, yet more than the −2.5 kg CO_{2eq}/kg found by Philp et al. (2013b). Savings of nonrenewable energy use for bio-PE were found to be roughly 65 % (Tsiropoulos et al. 2014). Such discrepancies in various studies will be discussed below.

PHB, which belongs to the class of PHA, is a biodegradable biopolymer which can be produced by bacteria and plants. Bio-PE and bio-PP are chemically identical to PE and PP, since they share the same feedstock, only of different provenience. They show significant CO_{2eq} savings compared to their traditional counterparts.

Yates and Barlow (2013) wrote that "*Biopolymers are generally considered an eco-friendly alternative to petrochemical polymers due to the renewable feedstock used to produce them and their biodegradability. However, the farming practices used to grow these feedstocks often carry significant environmental burdens, and the production energy can be higher than for petrochemical polymers.*"

They studied polylactic acid (PLA), polyhydroxyalkanoates (PHAs), and starch-based polymers, with some of the results shown in Figs. 11 (PLA) and 12 (PHA).

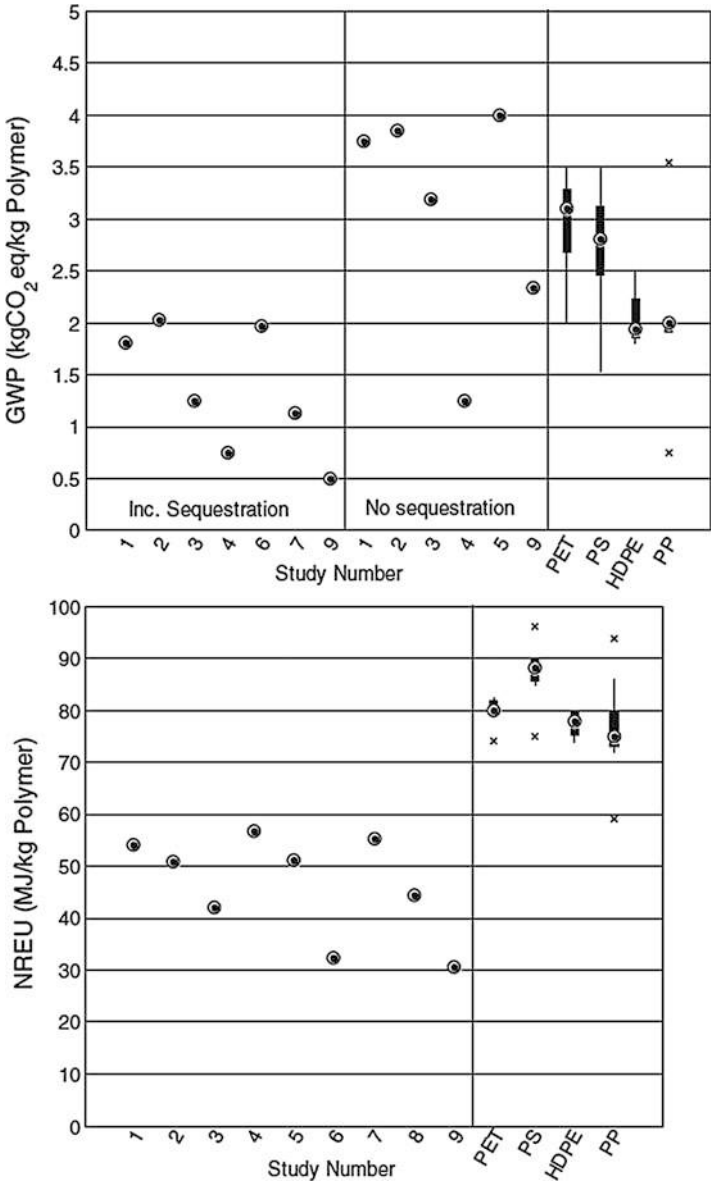

Fig. 11 GWP and NREU for **PLA** studies and petrochemical polymers. Sequestration refers to CO_2 uptake by plants used as the feedstock. Ranges for petrochemical polymers cover values reported in various comparative LCA studies and those provided by PlasticsEurope (Source: Yates and Barlow 2013)

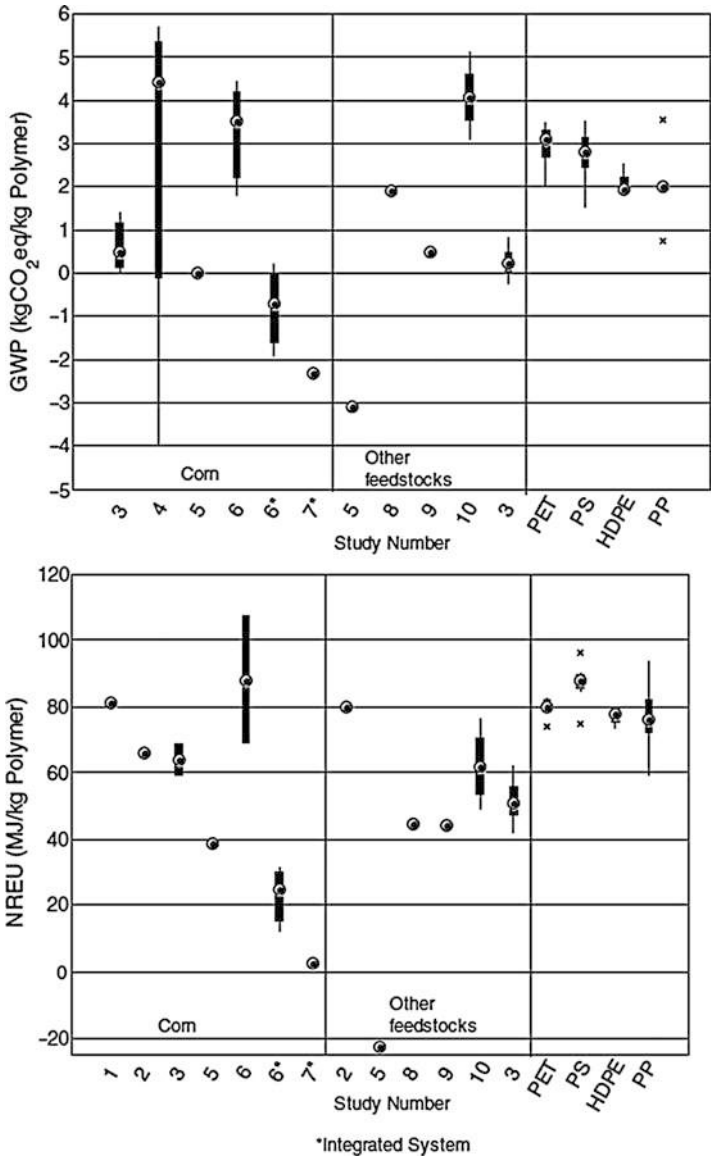

Fig. 12 GWP and NREU for **PHA** studies and petrochemical polymers. Ranges for petrochemical polymers cover values reported in various comparative LCA studies and those provided by PlasticsEurope (Source: Yates and Barlow 2013)

The LCA studies focused on nonrenewable energy use (NREU) and global warming potential (GWP). GWP is expressed in kg CO_{2eq} per kg of polymer.

As Fig. 11 shows, several studies found that GWP levels of PLA production are below those of competing conventional polymers, particularly in case of CO_2

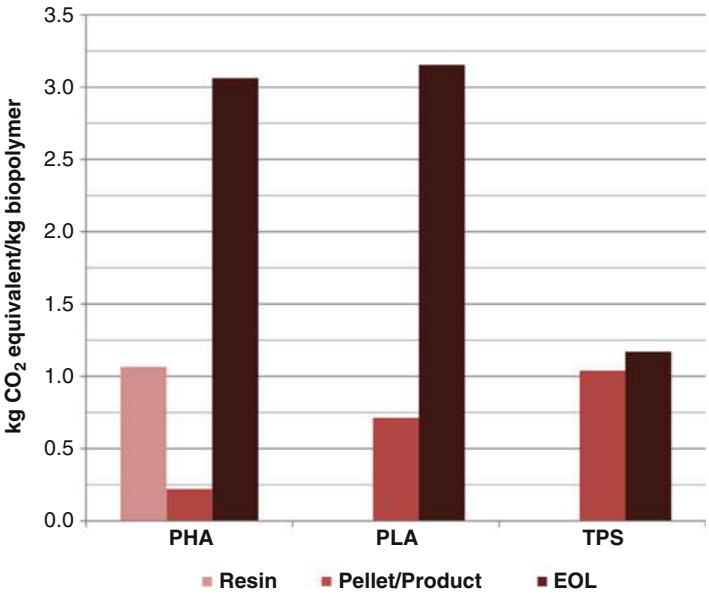

Fig. 13 Average global warming potential of biopolymers based on the extent of the system boundaries of fifteen different LCAs. *EOL* end of life (Source: Hottle et al. 2013)

sequestration, while other studies found just the opposite. Carbon sequestration stands for the long-term removal of CO_2 from the system, e.g., by landfilling.

In case of PHA, there is also disagreement in the literature on whether the biobased polymer has a lower GWP than its petrochemical counterparts. One needs to acknowledge that biobased plastics have not yet reached the same level of technological maturity as conventional plastics and that their currently smaller manufacturing units cannot be as efficient as a few 100,000 t/year standard polymerization plants. The higher GWP results, e.g., from energy consumption during production. Also, it needs to be highlighted that the outcome of life cycle assessments depends on the system boundaries as shown below in Fig. 13.

End-of-life assessment is more comprehensive. However, it depends on the chosen disposal route, which varies from country to country. For instance, in Europe incineration is used more than in the United States, where landfilling prevails, so other approaches such as "cradle to pellet" as mentioned above might be more meaningful.

Composite Materials

Apart from biobased polymers, additives and fillers can also be biobased (Lackner 2015). An example of biobased PVC plasticizers are glucose esters (Yin et al. 2014). Examples of compounds and composites with biobased fillers are

plastic wood composites (PWC), for which also recycled plastics can be used (Najafi 2013). Biobased fibers for use in plastics (both conventional and biobased) are, e.g., hemp fibers (Dhakal and Zhang 2015), cellulose fibers (González-Sánchez et al. 2014), flax fibers (El-Sabbagh et al. 2014), sisal, kenaf, jute, and coir (Wambua et al. 2003). Such fillers improve properties and can reduce both weight and costs. For a review on bionanocomposites, see, e.g., (Reddy et al. 2013).

Composite materials with biobased ingredients and recycling of bioplastics (Niaounakis 2013; Soroudi and Jakubowicz 2013) are not covered in this chapter. It only has to be stated that recycling of bioplastics would require a separate infrastructure, as some bioplastics are not compatible with regular recycling schemes (e.g., PHB in PET will degrade properties strongly; (Lackner 2015)).

Discussion

From what was depicted above, bioplastics are a "hot" topic for researchers, entrepreneurs, and customers/consumers alike, where the avoidance on crude oil dependency is a main driver and climate change mitigation a welcome side effect. Generally speaking, materials sell by properties (i.e., performance), not by price (only). The costs of bioplastics are typically higher than those of conventional polymers, which is partly due to more expensive feedstock and lack of economies of scale. Since the main barrier to market penetration of bioplastics is their price compared to that of oil-based plastics, a brief cost overview is shown here in Table 2.

Biobased plastics will play a vital role in a bioeconomy (Philp et al. 2013c). Some biobased plastics have a slightly higher density than petrochemical plastics

Table 2 Prices of bioplastics in 09/2012. Reference pellet prices (EUR per kg) – PE = 1.58; PP = 1.54; PET = 1.73 (Source: OECD 2014)

Product	Company	Location	Capacity (tones)	Price (EUR per kg)
PLA	Nature Works	United States	140,000	1.5–2.0
PLA	Hisun	China	5000	2.1
PHAs	Metabolix	United States	300/50,000	4.3–4.6
PHBV	Tianan	China	2000	4.1–4.3
Mater-Bi	Novamont	EU	75,000	3.4–5.1
Cereplast	Cereplast	United States	25,000	2.6–3.4
HDPE/LDPE/PP	Braskem	Brazil	200,000	1.3–1.7
Other	DuPont Plantic Innovia Arkema, others	Global	2000	2.5–6.9

such as PE and PP, so when being used in transportation applications, they will not result in the same fuel savings over the packagings' or vehicles' lifetime.

The IPCC writes in its Fourth Assessment Report (2007):

> It is theoretically possible to increase carbon storage in long-lived agricultural products (e.g., strawboards, wool, leather, bio-plastics) but the carbon held in these products has only increased from 37 to 83 MtC per year over the past 40 years. Assuming a first order decay rate of 10 to 20 % per year, this is estimated to be a global net annual removal of 3 to 7 $MtCO_2$ from the atmosphere, which is negligible compared to other mitigation measures. (IPCC Fourth Assessment Report: Climate Change 2007)

Hence, the main contribution to climate change mitigation of bioplastics comes from a reduction of fossil fuel use for their production.

Conclusions

Bioplastics were shown in this chapter to offer the potential for reduced GHG emissions compared to fossil plastics, rendering the same service level. Biopolymers show some unfavorable results in several LCA studies; however, the immature nature of these technologies needs to be considered (future optimization and efficiency improvements will come). Both drop-in replacements (e.g., biobased PE, biobased PP, bio-PET) and novel bioplastics (e.g., PLA, TPS, PHA) can contribute to climate change mitigation; however, a profound life cycle assessment including potential land use change has to be carried out to have a clear picture about the net effect. Further improvements in energy efficiency of feedstock production and reduction of fossil fuel use in the process are needed.

Gerngross and Slater wrote that "*any manufacturing process, not just those for plastics, would benefit from the use of renewable energy*" (Gerngross and Slater 2000), so it seems worthwhile to foster bioplastics from a climate change mitigation perspective.

The second major advantage of bioplastics, which is not related to climate change mitigation, is biodegradability as shown by some grades. Whereas the lifetime of conventional plastic materials can be hundreds of years (Harvey 2012), biodegradable plastics are mineralized to CO_2 and H_2O. They generally do not produce harmful pollutants during degradation. In landfills, nondegradable plastics act as carbon sink. However, a significant fraction of plastic wastes ends up in the oceans, where attrition leads to the formation of microplastics (Barboza and Gimenez 2015). There particles accumulate toxic substances and enter the food chain. Microplastics have become a major issue for the marine environment, and biodegradable materials can be a solution here.

Hence, it can be concluded that biobased polymers can contribute to climate change mitigation by avoiding fossil feedstock and, in case of nonbiodegradable grades, by acting as carbon sink.

Outlook

Plastics are a virtually impossible-to-replace class of materials, used from cost-effective packaging to high-end applications in health care. Biobased plastics, an emerging trend, can contribute to climate change mitigation with lower GHG emissions over their entire life cycle (Yates and Barlow 2013), European Bioplastics (2008) compared to conventional plastics. Sustainable feedstock production, alongside a decoupling from the biofuel industry, will be two major R&D topics for biobased plastics in the upcoming years. It is expected that the first huge market for biobased polymers is in packaging (Cooper 2013), which will gradually move toward higher-end applications, as performance increases (Chen 2014).

References

Adams WM (2006) The future of sustainability: re-thinking environment and development in the twenty-first century. Report of the IUCN renowned thinkers meeting, 29–31 Jan 2006. http://cmsdata.iucn.org/downloads/iucn_future_of_sustanability.pdf. Retrieved 16 Feb 2009

Alvarenga RAF, Dewulf J (2013) Plastic vs. fuel: which use of the Brazilian ethanol can bring more environmental gains? Renew Energy 59:49–52

Barboza LGA, Gimenez BCG (2015) Microplastics in the marine environment: current trends and future perspectives. Mar Pollut Bull 97(1–2):5–12

Biron M (2014) 2 – The plastics industry: economic overview, thermosets and composites, 2nd edn, William Andrew, Oxford. pp 25–104

Chen YJ (2014) Bioplastics and their role in achieving global sustainability. J Chem Pharm Res 6(1):226–231, http://jocpr.com/vol6-iss1-2014/JCPR-2014-6-1-226-231.pdf

Chen G-Q, Wu Q, Jung YK, Lee SY (2011) 3.21 – PHA/PHB, comprehensive biotechnology, 2nd edn, vol 3, Elsevier, Amsterdam, NL. pp 217–227

Cooper TA (2013) 5 – Developments in bioplastic materials for packaging food, beverages and other fast-moving consumer goods. In: Trends in packaging of food, beverages and other fast-moving consumer goods (FMCG), Woodhead Publishing, Sawston, USA, pp 108–152

Dhakal HN, Zhang Z (2015) 3 – The use of hemp fibres as reinforcements in composites. Biofiber Reinf Compos Mater 86–103

Ebnesajjad S (2012) Handbook of biopolymers and biodegradable plastics: properties, processing and applications. William Andrew Publishing, ISBN 978-1455728343

Elena G-d-C, Esther V (2010) From water to energy: the virtual water content and water footprint of biofuel consumption in Spain. Energy Policy 38(3):1345–1352

El-Sabbagh A, Steuernagel L, Ziegmann G, Meiners D, Toepfer O (2014) Processing parameters and characterisation of flax fibre reinforced engineering plastic composites with flame retardant fillers. Compos Part B 62:12–18

European Bioplastics (2008) Life cycle assessment of bioplastics, position paper. http://en.european-bioplastics.org/wpcontent/uploads/2011/04/pp/LCA_PositionsPaper.pdf

European Bioplastics (2013) Bioplastics, facts and figures. http://en.european-bioplastics.org/wp-content/uploads/2013/publications/EuBP_FactsFigures_bioplastics_2013.pdf

European Commission (2011) DG ENV, Plastic waste in the environment. http://ec.europa.eu/environment/waste/studies/pdf/plastics.pdf

Gerngross TU, Slater SC (2000) How green are green plastics? Sci Am 283:36–41. doi:10.1038/scientificamerican0800-36

Globe Newswire (2013) Bioplastics – a global market watch, 2011–2016, Friday, 11 Oct 2013| 10:39 AM ET. http://www.cnbc.com/id/101106035

González-Sánchez C, Martínez-Aguirre A, Pérez-García B, Martínez-Urreaga J, de la Orden MU, Fonseca-Valero C (2014) Use of residual agricultural plastics and cellulose fibers for obtaining sustainable eco-composites prevents waste generation. J Clean Prod 83(15):228–237

Harvey JA (2012) Lifetime predictions of plastics. In: Handbook of environmental degradation of materials, 2nd edn, William Andrew, Oxford, UK, pp 63–83

Hottle TA, Bilec MM, Landis AE (2013) Sustainability assessments of bio-based polymers. Polym Degrad Stab 98(9):1898–1907

IPCC Fourth Assessment Report: Climate Change (2007) Climate change 2007: working group III: mitigation of climate change. http://www.ipcc.ch/publications_and_data/ar4/wg3/en/ch8s8-1.html

Kim S, Dale BE (2008) Energy and greenhouse gas profiles of polyhydroxybutyrates derived from corn grain: a life cycle perspective. Environ Sci Technol 42:7690–7695

Lackner M (2015) Bioplastics. In: Baala E (ed) Kirk-Othmer encyclopedia of chemical technology. Wiley VCH, Weinheim. ISBN 978-0471484981

McKinsey & Company (2012) Advanced industries, lightweight, heavy impact, Berlin, Germany

Mohr A, Raman S (2013) Lessons from first generation biofuels and implications for the sustainability appraisal of second generation biofuels. Energy Policy 63:114–122

Najafi SK (2013) Use of recycled plastics in wood plastic composites – a review. Waste Manag 33(9):1898–1905

Niaounakis M (2013) Biopolymers reuse, recycling, and disposal. William Andrew. ISBN 978-1455731459

OECD (2011) Future prospects for industrial biotechnology. OECD Publishing, Paris. ISBN 978-9264119567

OECD (2014) Biobased chemicals and bioplastics: finding the right policy balance. OECD science, technology and industry policy papers, no 17. OECD Publishing. http://dx.doi.org/10.1787/5jxwwfjx0djf-en

Pei L, Schmidt M, Wei W (2011) Conversion of biomass into bioplastics and their potential environmental impacts. http://cdn.intechopen.com/pdfs-wm/16197.pdf

Philp JC, Ritchie RJ, Allan JEM (2013a) Biobased chemicals: the convergence of green chemistry with industrial biotechnology. Trends Biotechnol 31(4):219–222

Philp JC, Bartsev A, Ritchie RJ, Baucher M-A, Guy K (2013b) Bioplastics science from a policy vantage point. New Biotechnol 30(6):635–646

Philp JC, Ritchie RJ, Guy K (2013c) Biobased plastics in a bioeconomy. Trends Biotechnol 31(2):65–67

PlasticsEurope (2013) Automotive, the world moves with plastics. Brussels. www.plasticseurope.org/cust/documentrequest.aspx?DocID=58353

PlasticsEurope (2014a) The plastics industry (infographics). Brussels. http://www.plasticseurope.org/Document/the-plastics-industry-infographics.aspx?FolID=2

PlasticsEurope (2014b) Plastics – the facts 2014. Brussels. http://www.plasticseurope.org/Document/plastics-the-facts-2014.aspx?FolID=2

PlasticsToday (2011) Bioplastics demand will grow, but not all bioplastics are created equal. http://www.plasticstoday.com/articles/bioplastics-demand-will-grow-not-all-bioplastics-are-created-equal

Popp J, Lakner Z, Harangi-Rákos M, Fári M (2014) The effect of bioenergy expansion: food, energy, and environment. Renew Sustain Energy Rev 32:559–578

Reddy MM, Vivekanandhan S, Misra M, Bhatia SK, Mohanty AK (2013) Biobased plastics and bionanocomposites: current status and future opportunities. Prog Polym Sci 38(10–11):1653–1689

Saygin D, Gielen DJ, Draeck M, Worrell E, Patel MK (2014) Assessment of the technical and economic potentials of biomass use for the production of steam, chemicals and polymers. Renew Sustain Energy Rev 40:1153–1167

Sin LT, Rahmat AR, Wan Abdul Rahman WA (2013) 1 – Overview of poly(lactic acid), Polylactic Acid 1–70

Smil V (2013) Making the modern world: materials and dematerialization. Wiley, Hoboken. ISBN 978-1119942535

Soroudi A, Jakubowicz I (2013) Recycling of bioplastics, their blends and biocomposites: a review. Eur Polym J 49(10):2839–2858

The Society of the Plastics Industry, Bioplastics Council (2013) Development of biobased plastics independent of the future of biofuels. http://www.plasticsindustry.org/files/about/BPC/Development%20of%20Biobased%20Plastics%20-%20August%2026%202013%20-%20FINAL_1409082830062_1.pdf

Tsiropoulos I, Faaij APC, Lundquist L, Schenker U, Briois JF, Patel MK (2014) Life cycle impact assessment of bio-based plastics from sugarcane ethanol. J Clean Prod (in press) Corrected Proof, Available online. doi: dx.doi.org/10.1016/B978-1-4377-4459-0.00001-9

van Beilen JB, Poirier Y (2012) 30 – Plants as factories for bioplastics and other novel biomaterials. Plant Biotechnol Agric 481–494

Wambua P, Ivens J, Verpoest I (2003) Natural fibres: can they replace glass in fibre reinforced plastics? Compos Sci Technol 63(9):1259–1264

Yates MR, Barlow CY (2013) Life cycle assessments of biodegradable, commercial biopolymers – a critical review. Resour Conserv Recycl 78:54–66

Yin B, Aminlashgari N, Yang X, Hakkarainen M (2014) Glucose esters as biobased PVC plasticizers. Eur Polym J 58:34–40

Yu J (2007) Chapter 23 – Microbial production of bioplastics from renewable resources. In: Bioprocessing for value-added products from renewable resources, Elsevier, Amsterdam, pp 585–610

Glossary

Maximilian Lackner

This glossary is composed of entries based on terms supplied by the chapter authors of this Handbook and taken from the following sources:

- US Environmental Protection Agency (EPA)
- Intergovernmental Panel on Climate Change (IPCC)
- United Nations Framework Convention on Climate Change (UNFCCC)
- British Broadcasting Corporation (BBC)
- Agricultural Marketing Resource Center (AgMRC)
- National Oceanic and Atmospheric Administration (NOAA))

AAU See "Assigned amount unit"

Abatement Reduction of degree or intensity of greenhouse-gas emissions.

Abrupt Climate Change Sudden (on the order of decades), large change in some major component of the climate system, with rapid, widespread effects.

AC See "Adaptation Committee"

Accession An act whereby a state becomes a party to a treaty already negotiated and signed by other states; It has the same legal effect as ratification. See also "Ratification."

Acclimatization Adaptation by people to higher or lower ambient temperatures.

Acid Rain Program (ARP) A cap-and-trade emissions trading program undertaken in the USA in 1990 to control emissions of sulfur dioxide from electric utilities. This was the first significant regulatory use of the cap-and-trade mechanism for pollution control.

Active modes Walking and cycling. See also "Nonmotorized travel."

Activities implemented jointly (AIJ) Activities carried out under the Convention (UNFCCC) to mitigate climate change through partnerships between an investor from a developed country and a counterpart in a host country under a pilot phase

M. Lackner
Institute of Advanced Engineering Technologies, University of Applied Sciences FH Technikum Wien, Vienna, Austria
e-mail: maximilian.lackner@technikum-wien.at

W.-Y. Chen et al. (eds.), *Handbook of Climate Change Mitigation and Adaptation*,
DOI 10.1007/978-3-319-14409-2

that ended in the year 2000. The purpose was to involve private-sector money in the transfer of technology and know-how. See also "Joint Implementation and United Nations Framework Convention on Climate Change (UNFCCC)."

Adaptation Adjustment in natural or human systems in response to actual or expected climatic stimuli or their effects, which moderates harm or exploits beneficial opportunities.

Adaptive capacity The ability of a system to adjust to climate change (including climate variability and extremes) to moderate potential damages, to take advantage of opportunities, or to cope with the consequences.

Adaptation Committee (AC) A body that was established by the Conference of the Parties (COP) as part of the Cancun Agreements to promote the implementation of enhanced action on adaptation in a coherent manner under the Convention, inter alia, through various functions. See also "United Nations Framework Convention on Climate Change (UNFCCC) and Cancun Adaptation Framework."

Adaptation Fund Established to finance concrete adaptation projects and programs in developing countries that are particularly vulnerable and which are Parties to the Kyoto Protocol. The Fund is to be financed with a share of proceeds from clean development mechanism (CDM) project activities and receive funds from other sources. It is operated by the Adaptation Fund Board.

Additionality The property of a GHG reduction which ensures that it is surplus to regulation and beyond what would have happened in the absence of the project (or in the business-as-usual scenario).

Ad Hoc Working Group on Long-term Cooperative Action under the Convention (AWG-LCA) Established as a subsidiary body under the Convention by decision 1/CP.13 (the Bali Action Plan) to conduct a comprehensive process to enable the full, effective, and sustained implementation of the Convention through long-term cooperative action, now, up to and beyond 2012, in order to reach an agreed outcome to be presented to the COP for adoption.

Adjustment time See "Response time"

Aerosols Small particles or liquid droplets in the atmosphere that can absorb or reflect sunlight depending on their composition. Erroneously, the term has also become associated with the propellant used in "aerosol sprays."

Aerosol sprays Pressurized cans containing liquids and a propellant. Today, often propane, butane, air, nitrogen, or dimethylether are used as propellants. Previously, hydrofluorocarbons (strong GHG) were used.

Afforestation Planting of new forests on lands that historically have not contained forests. See also "Reforestation."

AGE See "Applied general equilibrium"

AIJ See "Activities implemented jointly"

Albedo The amount of solar radiation reflected from an object or surface, often expressed as a percentage.

Alternative energy Energy derived from nontraditional sources (e.g., compressed natural gas, solar, hydroelectric, wind). See also "Renewable energy" and "Unconventional oil."

Alliance of Small Island States (AOSIS) An ad hoc coalition of low-lying and island countries. These nations are particularly vulnerable to rising sea levels and share common positions on climate change. The 43 members and observers are American Samoa, Antigua and Barbuda, Bahamas, Barbados, Belize, Cape Verde, Comoros, Cook Islands, Cuba, Dominica, Dominican Republic, Federated States of Micronesia, Fiji, Grenada, Guam, Guinea-Bissau, Guyana, Haiti, Jamaica, Kiribati, Maldives, Marshall Islands, Mauritius, Nauru, Netherlands Antilles, Niue, Palau, Papua New Guinea, Samoa, Sao Tome and Principe, Seychelles, Singapore, Solomon Islands, St. Kitts & Nevis, St. Lucia, St. Vincent and the Grenadines, Suriname, Timor-Leste, Tonga, Trinidad and Tobago, Tuvalu, US Virgin Islands, and Vanuatu.

Amendment A modification by the COP to the text of the Convention. If consensus cannot be reached, an amendment must win three-quarters of the votes of all parties present and casting ballots.

Annex I Parties The industrialized countries listed in Annex I to the Convention, which committed to returning their greenhouse-gas emissions to 1990 levels by the year 2000 as per Article 4.2 (a) and (b). They have also accepted emissions targets for the period 2008–2012 as per Article 3 and Annex B of the Kyoto Protocol. They include the 24 original OECD members, the European Union, and 14 countries with economies in transition (Croatia, Liechtenstein, Monaco, and Slovenia joined Annex 1 at COP; the Czech Republic and Slovakia replaced Czechoslovakia.)

Annex II Parties The countries listed in Annex II to the Convention which have a special obligation to provide financial resources and facilitate technology transfer to developing countries. Annex II Parties include the 24 original OECD members plus the European Union.

Annex I Countries See "Annex I Parties"

Annex II Countries See "Annex II Parties"

Countries which have a special obligation under the Kyoto Protocol to provide financial resources and transfer technology to developing countries. This group is a subsection of the Annex I countries, excluding those that, in 1992, were in transition from centrally planned to a free market economy.

Anthropogenic Caused or produced by human activity, as opposed to natural. An example is the release of pollutants into the environment by human activities.

Anthropogenic greenhouse emissions Greenhouse-gas emissions resulting from human activities.

Anthropogenic climate change Man-made climate change, i.e., climate change caused by human activity as opposed to natural processes.

AOGCM See "Atmosphere-ocean General Circulation Model"

AOSIS See "Alliance of Small Island States"

Applied general equilibrium (AGE) Another term for computable general equilibrium (CGE), a class of economic models that use actual economic data to estimate how an economy might react to changes in policy, technology, or other external factors.

ARP See "Acid Rain Program"

AR4 IPCC Fourth Assessment Report (AR4). The Fourth Assessment Report produced by the Intergovernmental Panel on Climate Change (IPCC) published in 2007. The report assessed and summarized the climate change situation worldwide. It concluded that it was at least 90 % likely that the increase of the global average temperature since the mid-twentieth century was mainly due to man's activity. See also "IPCC" and "AR5."

AR5 See "IPCC Fifth Assessment Report"

Assigned amount unit (AAU) A Kyoto Protocol unit equal to 1 metric ton of CO_2 equivalent. Each Annex I Party issues AAUs up to the level of its assigned amount, established pursuant to Article 3, paragraphs 7 and 8, of the Kyoto Protocol. Assigned amount units may be exchanged through emissions trading.

Atmosphere The gaseous envelope surrounding the Earth. The dry atmosphere consists almost entirely of nitrogen (78.1 % by volume) and oxygen (20.9 % by volume), together with a number of trace gases, such as argon (0.93 % by volume), helium, radiatively active greenhouse gases such as carbon dioxide (0.04 % by volume), and ozone. In addition, the atmosphere contains water vapor, the amount of which is highly variable but typically 1 % by volume. The atmosphere also contains clouds and aerosols.

Atmosphere-ocean General Circulation Model (AOGCM) A numerical representation of the climate system based on the physical, chemical, and biological properties of its components, their interactions and feedback processes, and accounting for all or some of its known properties. The atmosphere and ocean general circulation model components are three-dimensional, time-dependent models that include a representation of the equations of motion on a sphere. In addition to atmosphere and ocean components, the term AOGCM is often applied to computer models that include land surface and sea ice model components. The model components are coupled, in the sense that fluxes are regularly exchanged between the different model components as they march forward in time. AOGCMs provide a relatively comprehensive representation of the climate system. AOGCM models are applied, as a research tool, to study and simulate the climate, but also for operational purposes, including monthly, seasonal, and interannual climate predictions.

Atmospheric lifetime The average time that a molecule resides in the atmosphere before it is removed by chemical reaction or deposition. This can also be thought of as the time that it takes after the human-caused emission of a gas for the concentrations of that gas in the atmosphere to return to natural levels. Greenhouse gas lifetimes can range from a few years to a few thousand years.

Atmospheric aerosols Microscopic particles suspended in the lower atmosphere that reflect sunlight back to space. They generally have a cooling effect on the planet and can mask global warming. They play a key role in the formation of clouds, fog, precipitation, and ozone depletion in the atmosphere.

AWG-LCA See "Ad Hoc Working Group on Long-term Cooperative Action under the Convention"

Backloading A measure undertaken by the EU ETS postponing the auctioning of allowances in order to give an opportunity for demand to increase.

Bali action plan (BAP) A plan drawn up at the UN Climate Change Conference in Bali, in December 2007, forming part of the Bali roadmap. The action plan established a working group to define a long-term global goal for reduction of greenhouse-gas emissions, and a "shared vision for long-term co-operative action" in the areas of mitigation, adaptation, finance, and technology. See also "Bali Road Map."

BAP See "Bali Action Plan"

Bali Road Map The Bali Road Map was adopted at the 13th Conference of the Parties and the 3rd Meeting of the Parties in Bali in December 2007. The Road Map is a set of forward-looking decisions that represent the work needed to be done under various negotiating "tracks" essential to reach a secure climate future. The roadmap gave deadlines to two working groups, one working on the Bali action plan and another discussing proposed emission reductions by Annex I countries after 2012.

Baseline-and-credit An emissions trading approach first introduced in the USA in the mid-1970s in which firms that reduced emissions below required command-and-control limits (i.e., the baseline) could earn "credits" that they could then sell to others who needed them in order to comply with regulations. Such schemes were subsequently adopted in the Kyoto Protocol under CDM and JI.

Baseline for cuts The year against which countries measure their target decrease of emissions. The Kyoto Protocol uses a baseline year of 1990. Some countries prefer to use later baselines. Climate change legislation in the USA, for example, uses a 2005 baseline.

BAU See "Business as usual"

BC See "Black carbon"

Berlin Mandate Adopted at COP-1, the mandate that launched negotiations leading to the adoption of the Kyoto Protocol.

BINGO Business and industry nongovernmental organizations. Civil society engages with the UNFCCC process through representative nongovernmental observer organizations. Since the early days of the UNFCCC, nongovernmental organizations (NGOs) have been actively involved, attending sessions and exchanging views with other participants, including government negotiators and delegates. There are currently nine NGO constituencies: BINGO (Business and Industry NGOs), ENGO (Environmental NGOs), TUNGO (Trade Union NGOs), IPO (Indigenous Peoples' Organizations), LGMA (Local Government and Municipal Authorities), RINGO (Research-oriented and Independent Organizations), YUNGO (Youth NGOs), Faith (Faith-based NGOs), Gender (Gender-based NGOs).

Biochar Slow-pyrolysis of biomass yields biochar, a stable carbon-rich solid product. See also "Hydrochar."

Biodiversity The existence of a wide variety of plant and animal species in their natural environments.

Biofuel A fuel derived from renewable sources, including crops such as maize and sugar cane, and some forms of waste. One can distinguish between 1st, 2nd, and 3rd generation (1G, 2G, and 3G) of biofuels, with increasing sustainability.

Biomass Materials of biological origin, including organic material (both living and dead) from above and below ground, for example, trees, crops, grasses, tree litter, roots, and animals and animal waste.

Biomass fuel See "Biofuel"

Biogeochemical cycle Movements through the Earth system of key chemical constituents essential to life, such as carbon, nitrogen, oxygen, and phosphorus.

Biome A naturally occurring community of flora and fauna (or the region occupied by such a community) adapted to the particular conditions in which they occur, e.g., tundra, grasslands, or deserts.
http://www.ucmp.berkeley.edu/glossary/gloss5/biome/

Biosphere The part of the Earth system comprising all ecosystems and living organisms, in the atmosphere, on land (terrestrial biosphere), or in the oceans (marine biosphere), including derived dead organic matter, such as soil organic matter and oceanic detritus.

Black carbon (BC) The soot that results from the incomplete combustion of fossil fuels, biofuels, and biomass (wood, animal dung, etc.). It is the most potent climate-warming aerosol. Unlike greenhouse gases, which trap infrared radiation that is already in the Earth's atmosphere, these particles absorb all wavelengths of sunlight and then reemit this energy as infrared radiation.

Black Carbon Aerosol See "Black carbon"

Bonn agreements Informal term for a political deal reached at COP-6 in Bonn, Germany, in 2001, by which governments agreed on the most politically controversial issues under the Buenos Aires Plan of Action. The Bonn agreements paved the way for the Marrakech Accords later in the same year.

Bonn convention See "Convention on the Conservation of Migratory Species of Wild Animals"

Bonn fund A special UNFCCC fund for contributions from the Government of Germany to cover costs of UNFCCC events held in Bonn.

Borehole Any exploratory hole drilled into the Earth or ice to gather geophysical data. Climate researchers often take ice core samples, a type of borehole, to predict atmospheric composition in earlier years. See also "Ice core."

bp-k Billion passenger-km, a unit deployed in the logistics industry.

Brazilian proposal A proposal by the delegation of Brazil made in May 1997 as part of the negotiations on the Kyoto Protocol. It included a formula to set differentiated emission reduction targets for parties based on the cumulative impact of parties' historic emissions on the global average surface temperature.

Bunker fuels Fuels consumed for international marine transport. Often, they are of inferior quality, containing higher amounts of sulphur than regular liquid transportation fuels.

Bureau A body responsible for directing the work of the COP. Its 10 members are delegates elected by each of five regional groups. The Bureau includes the COP President, six Vice Presidents, the Chairs of SBI and SBSTA, and a rapporteur. Each of the Convention's subsidiary bodies also has a Bureau.

Business as usual (BAU) A scenario used for projections of future emissions assuming no action, or no new action, is taken for mitigation. Some countries are pledging not to reduce their emissions but to make reductions compared to a business as usual scenario. Their emissions, therefore, would increase but to a lesser degree.

CACAM Negotiating coalition of countries of Central Asia and the Caucasus, Albania, and the Republic of Moldova.

Cancun Adaptation Framework (CAF) Parties adopted the Cancun Adaptation Framework (CAF) as part of the Cancun Agreements at the 2010 Climate Change Conference in Cancun, Mexico (COP 16/CMP 6). In the Agreements, Parties affirmed that adaptation must be addressed with the same level of priority as mitigation. The CAF is the result of 3 years of negotiations on adaptation under the AWG-LCA that had followed the adoption of the Bali Action Plan at the 2007 Climate Change Conference in Bali, Indonesia (COP 13/CMP 3).

Cap and trade An emission trading scheme whereby businesses or countries can buy or sell allowances to emit greenhouse gases via an exchange. The individual polluters can buy and/or sell these allowances in a market, thereby achieving the emissions target at lowest cost. The volume of allowances issued adds up to the limit, or cap, imposed by the authorities.

Capacity building In the context of climate change, the process of developing the technical skills and institutional capability in developing countries and economies in transition to enable them to address effectively the causes and results of climate change.

Carbonaceous Containing carbon.

Carbonaceous aerosol Aerosol consisting predominantly of organic substances and various forms of black carbon.

Carbon capture and sequestration (CCS) A set of technologies that can greatly reduce carbon dioxide emissions from new and existing coal- and gas-fired power plants, industrial processes, and other stationary sources of carbon dioxide. It is a three-step process that includes capture of carbon dioxide from power plants or industrial sources; transport of the captured and compressed carbon dioxide (usually in pipelines); and underground injection and geologic sequestration, or permanent storage, of that carbon dioxide in deep underground reservoirs such as rock formations that contain tiny openings or pores that trap and hold the carbon dioxide. Carbon capture is sometimes referred to as geological sequestration.

Carbon capture and storage See "Carbon capture and sequestration (CCS)"

Carbon cycle All parts (reservoirs) and fluxes of carbon. The cycle is usually thought of as four main reservoirs of carbon interconnected by pathways of exchange. The reservoirs are the atmosphere, terrestrial biosphere (usually includes freshwater systems), oceans, and sediments (includes fossil fuels). The annual movements of carbon, the carbon exchanges between reservoirs, occur because of various chemical, physical, geological, and biological processes. The ocean contains the largest pool of carbon near the surface of the Earth, but most of that pool is not involved with rapid exchange with the atmosphere.

Carbon dioxide (CO_2) A naturally occurring gas with approx. 400 ppm in the atmosphere and a by-product of burning carbonaceous fuels. It is the main anthropogenic greenhouse gas that affects Earth's radiative balance. It is the reference gas against which other greenhouse gases are measured and therefore it has a Global Warming Potential (GWP) of 1.

Carbon dioxide equivalent (CDE) A measure used to compare the effect of various greenhouse gases based upon their global warming potential (GWP). CDE is the quantity that describes, for a given amount of greenhouse gases, the amount of CO_2 that would have the same global warming potential (GWP), when measured over a specified timescale (generally, 100 years). Carbon dioxide equivalency thus reflects the time-integrated radiative forcing of a quantity of *emissions* or rate of greenhouse-gas emission – a *flow* into the atmosphere – rather than the instantaneous value of the radiative forcing of the *stock* (concentration) of greenhouse gases *in the atmosphere* described by equivalent CO_2 (CO_2e). The CDE for a gas is obtained by multiplying the mass and the GWP of the gas. The following units are commonly used:

- By the UN climate change panel IPCC: billion metric tons of CO_2 equivalent ($GtCO_2eq$)
- In industry: million metric tons of carbon dioxide equivalents (MMTCDE)
- For vehicles: g of carbon dioxide equivalents/km (gCDE/km)
- By contrast, equivalent CO_2 (CO_2e) is the concentration of CO_2 that would cause the same level of radiative forcing as a given type and concentration of greenhouse gas. Examples of such greenhouse gases are methane, perfluorocarbons, and nitrous oxide. CO_2e is expressed as parts per million by volume, ppmv.

Carbon dioxide fertilization The enhancement of the growth of plants by increasing the level of CO_2, e.g., in a greenhouse. Depending on their mechanism of photosynthesis, certain types of plants are more sensitive to changes in atmospheric CO_2 concentration.

Carbon dioxide removal (CDR) A set of concepts to moderate or retard global warming by removing CO_2 from the atmosphere on a large scale. See also "Climate engineering."

Carbon dioxide sequestration The process of removing carbon from the atmosphere and depositing it in a reservoir, also termed carbon sequestration.

Carbon equivalent See "Carbon dioxide equivalent (CDE)" and "Equivalent carbon dioxide (CO_2e)."

Carbon flux The rate of exchange of carbon between reservoirs.

Carbon footprint The total amount of greenhouse gases emitted into the atmosphere each year by a person, family, building, or organization. A person's carbon footprint includes greenhouse-gas emissions from fuel that an individual burns directly, such as by heating a home or riding in a car. It also includes greenhouse gases that come from producing the goods or services that the individual uses, including emissions from power plants that make electricity, factories that make

products, and landfills where trash is sent. For a product, the carbon footprint is the amount of carbon emitted during manufacturing.

Carbon intensity The relative amount of carbon emitted per unit of an underlying variable, often per unit of energy, quantity of fuel consumed, or per unit of GDP. See also "GDP."

Carbon leakage The part of emissions reductions that may be offset by an increase of the emissions in the nonconstrained countries above their baseline levels. See also "Emissions Trading."

Carbon market A popular (but misleading) term for a trading system through which countries may buy or sell units of greenhouse-gas emissions in an effort to meet their national limits on emissions, either under the Kyoto Protocol or under other agreements, such as that among member states of the European Union. The term comes from the fact that carbon dioxide is the predominant greenhouse gas, and other gases are measured in units called "carbon-dioxide equivalents."

Carbon negative A process where a net sink of CO_2 is realized. See also "Carbon neutral."

Carbon neutral A process where there is no net release of CO_2. For example, growing biomass removes CO_2 from the atmosphere, while burning it releases the CO_2 again. The process would be carbon neutral if the amount taken out and the amount released were identical. A company or country can also achieve carbon neutrality by means of carbon offsetting. See also "Carbon offsetting."

Carbon offset An investment in a project that will lead to the prevention or removal of carbon dioxide from the atmosphere (e.g., planting trees or building renewable energy power stations to avoid the construction of coal-fired ones).

Carbon offsetting A way of compensating for emissions of CO_2 by participating in, or funding, efforts to take CO_2 out of the atmosphere. Offsetting often involves paying another party, somewhere else, to save emissions equivalent to those produced by one's own activity.

Carbon pool Carbon pools are above-ground biomass, below-ground biomass, litter, dead wood, and soil organic carbon.

Carbon price The price placed on greenhouse-gas emissions to create a disincentive for their release (and incentive to capture or avoid them). A carbon price can be imposed, e.g., through a carbon tax, an emissions trading scheme (which fixes emission levels and allows prices to vary).

Carbon sequestration The process of storing carbon dioxide. Terrestrial, or biologic, carbon sequestration is the process by which trees and plants absorb carbon dioxide, release the oxygen, and store the carbon. Geologic sequestration is one step in the process of carbon capture and sequestration (CCS), and involves injecting carbon dioxide deep underground where it stays permanently. So one can distinguish between natural and industrial carbon sequestration.

Carbon sinks Carbon reservoirs and conditions that take-in and store more carbon (i.e., carbon sequestration) than they release. Carbon sinks can partially offset greenhouse-gas emissions. Forests and oceans are large carbon sinks.

Carboxylation A chemical reaction in which a carboxylic acid group is introduced in a substrate.

Cartagena Dialogue A collection of around 40 countries working towards an ambitious legally binding agreement under the UNFCCC, and who are committed to becoming or remaining low carbon domestically. Participates include: Antigua and Barbuda, Australia, Bangladesh, Barbados, Burundi, Chile, Colombia, Costa Rica, Denmark, Dominican Republic, Ethiopia, European Union, France, Gambia, Georgia, Germany, Ghana, Grenada, Guatemala, Indonesia, Kenya, Lebanon, Malawi, Maldives, Marshall Islands, México, Netherlands, New Zealand, Norway, Panama, Peru, Rwanda, Samoa, Spain, Swaziland, Sweden, Switzerland, Tajikistan, Tanzania, Uganda, UAE, and the UK.

Cartesian paradigm A world view in which Man is totally independent of his environment, where both body and mind are perceived as distinct and separate and not part of a unified whole. The name Cartesian is derived from the French philosopher Rene Descartes.

Cation Exchange Capacity (CEC) The capacity of soil to hold positively charged ions such as calcium (Ca^{2+}), magnesium (Mg^{2+}), and potassium (K^{+}).

Cavitation The formation of vapor cavities, consisting mainly of bubbles or voids in a liquid. As a consequence of cavitation, (strong) forces acting upon the liquid and vessel walls. It usually occurs when a liquid is subjected to rapid changes of pressure that cause the formation of cavities where the pressure is relatively low.

CBD Convention on Biological Diversity.

CCC See "UNFCCC"

CCERs See "Chinese certified emission reductions"

CC:TRAIN Training methodology for assessing vulnerability to climate change.

CDM Help Desk A support initiative for project participants, developers, coordinating and/or managing entities (CMEs), designated national authorities (DNAs), and designated operational entities (DOEs) to get reliable and timely information from the secretariat on issues regarding their CDM projects. It is only available to stakeholders in Africa, least developed countries (LDCs), small island developing states (SIDS), and countries that had 10 or fewer registered CDM projects as of 31 December 2010, as long as the project is in the process of validation or verification.

CDM Loan Scheme An interest-free loan initiative that provides funding to projects for development of PDD, validation, and first verification. It applies to projects located in host countries with less than 10 CDM project activities registered with the UNFCCC (as of 1 January of the year of submission), with a high probability of registration with the UNFCCC and generating at least 7,500 CERs/year for projects in least developed countries (LDCs), and 15,000 CERs/year in non-LDCs. Available at http://cdmloanscheme.org/

CCN See "Cloud condensation nuclei (CCN)"

CCS See "Carbon capture and sequestration"

CDM See "Clean Development Mechanism"

CDR See "Carbon dioxide removal"

CEC See "Cation Exchange Capacity"

CER See "Certified Emission Reduction"

Certified Emission Reduction (CER) A greenhouse gas trading credit, under the UN Clean Development Mechanism (CDMI) program. A CER may be earned by participating in emission reduction programs – installing green technology, or planting forests – in developing countries. Each CER is equivalent to one ton of carbon dioxide. Two special types of CERs called temporary certified emission reduction (tCERs) and long-term certified emission reductions (lCERs) are issued for emission removals from afforestation and reforestation CDM projects.

Central Group Formerly CG-11, a negotiating coalition of Central European Annex I Parties, now called the Central Group.

CFC Chlorofluorocarbon.

CFC See "Chlorofluorocarbons"

CGE See "Computable General Equilibrium"

CG-11 Central Group 11 (negotiating coalition of Central European Annex I Parties).

CH_4 Methane.

Chair National delegates elected by participating governments to lead the deliberations of the Convention's subsidiary bodies. Different chairs may be elected for other informal groups. The Chair is responsible for facilitating progress towards an agreement and serves during the intersessional period until the next COP.

Chairman See "Chair"

Chairperson See "Chair"

Chinese certified emission reductions (CCERs) Emission reduction credits certified for use in China's domestic emissions trading markets. Procedures for creating and using these credits closely follow those employed in the CDM.

Chlorofluorocarbons (CFC) Gases covered under the 1987 Montreal Protocol and used, e.g., for refrigeration, air conditioning, packaging, insulation, solvents, or aerosol propellants. Since they are not destroyed in the lower atmosphere, CFCs drift into the upper atmosphere where, given suitable conditions, they break down ozone. These gases are being replaced by other compounds: hydrochlorofluorocarbons, an interim replacement for CFCs that are also covered under the Montreal Protocol, and hydrofluorocarbons, which are covered under the Kyoto Protocol. All these substances are also greenhouse gases. See also "Hydrochlorofluorocarbons," "Hydrofluorocarbons," "Perfluorocarbons," and "Ozone depleting substance."

Clean coal technology Technology that enables coal to be burned without emitting CO_2. Some systems currently being developed remove the CO_2 before combustion, others remove it afterwards. Clean coal technology is unlikely to be widely available for at least a decade.

Clean Development Mechanism (CDM) A program that enables developed countries or companies to earn credits by investing in greenhouse-gas emission reduction or removal projects in developing countries. These credits can be used to offset emissions and bring the country or company below its mandatory target.

Clean Power Plan (CPP) A proposed rule introduced by the US EPA on June 2, 2014 to regulate GHG emissions from existing power plants in the USA.

Climate Climate in a narrow sense is usually defined as the "average weather," or more rigorously, as the statistical description in terms of the mean and variability of relevant quantities over a period of time ranging from months to thousands of years. The classical period is three decades, as defined by the World Meteorological Organization (WMO). These quantities are most often surface variables such as temperature, precipitation, and wind. Climate in a wider sense is the state, including a statistical description, of the climate system. See also "Weather."

Climate change

FCCC definition: A change of climate which is attributed directly or indirectly to human activity that alters the composition of the global atmosphere and which is in addition to natural climate variability observed over comparable time periods.

IPCC usage definition: Climate change as referred to in the observational record of climate occurs because of internal changes within the climate system or in the interaction between its components, or because of changes in external forcing either for natural reasons or because of human activities. It is generally not possible clearly to make attribution between these causes. Projections of future climate change reported by IPCC generally consider only the influence on climate of anthropogenic increases in greenhouse gases and other human-related factors.

Climate Change Convention See "UNFCCC"

Climate-carbon cycle coupling Future climate change induced by atmospheric emissions of greenhouse gases will impact on the global carbon cycle. Changes in the global carbon cycle in turn will influence the fraction of anthropogenic greenhouse gases that remains in the atmosphere, and hence the atmospheric concentrations of greenhouse gases, resulting in further climate change. This feedback is called climate-carbon cycle coupling. The first generation coupled climate-carbon cycle models indicates that global warming will increase the fraction of anthropogenic CO_2 that remains in the atmosphere.

Climate engineering Engineering the climate by means of carbon dioxide removal (CDR), earth radiation management (ERM), and/or solar radiation management (SRM) is a set of concepts and tools to deliberately, and on a large scale, moderate or retard global warming.

Climate feedback A process that acts to amplify or reduce direct warming or cooling effects.

Climate forcing See "Radiative forcing"

Climate lag The delay that occurs in climate change as a result of some factor that changes only very slowly. For example, the effects of releasing more carbon dioxide into the atmosphere occur gradually over time because the ocean takes a long time to warm up in response to a change in radiation. See "Climate and climate change."

Climate model A quantitative way of representing the interactions of the atmosphere, oceans, land surface, and ice. Models can range from relatively simple to quite comprehensive. See "General Circulation Model."

Climate sensitivity In IPCC reports, equilibrium climate sensitivity refers to the equilibrium change in global mean surface temperature following a doubling of the atmospheric (equivalent) CO_2 concentration. More generally, equilibrium climate sensitivity refers to the equilibrium change in surface air temperature following a unit change in radiative forcing (degrees Celsius, per watts per square meter, $^{\circ}CW^{-1}\ m^{-2}$). One method of evaluating the equilibrium climate sensitivity requires very long simulations with Coupled General Circulation Models (Climate model). The effective climate sensitivity is a related measure that circumvents this requirement. It is evaluated from model output for evolving nonequilibrium conditions. It is a measure of the strengths of the feedbacks at a particular time and may vary with forcing history and climate state. See also "Climate" and "Radiative forcing."

Climate system The five physical components (atmosphere, hydrosphere, cryosphere, lithosphere, and biosphere) that are responsible for the climate and its variations. Also called Earth system.

Cloud condensation nuclei (CCN) Airborne particles that serve as initial sites for the condensation of liquid water and which can lead to the formation of cloud droplets, e.g., soot or sea salt. Also known as cloud seeds.

Cloud seeds See "Cloud condensation nuclei"

Clean Development Mechanism (CDM) A mechanism under the Kyoto Protocol through which developed countries may finance greenhouse-gas emission reduction or removal projects in developing countries, and receive credits for doing so which they may apply towards meeting mandatory limits on their own emissions.

Clearing house A service which facilitates and simplifies transactions among multiple parties.

CMP See "Conference of the Parties serving as the Meeting of the Parties to the Kyoto Protocol."

CMS See "Convention on the Conservation of Migratory Species of Wild Animals."

CNG See "Compressed natural gas"

Coalbed methane Methane contained in coal seams. It is often referred to as virgin coalbed methane, or coal seam gas.

Coal mine methane Coal mine methane is the subset of coalbed methane that is released from the coal seams during the process of coal mining.

Coalition for Rainforest Nations A voluntary grouping of largely developing nations with rainforests which addresses issues surrounding environmental sustainability specific to tropical rainforests. Participation does not necessarily imply that countries adhere to any specific domestic policies or negotiating positions within the international context. In September 2011, the group included Argentina, Bangladesh, Belize, Cameroon, Central African Republic, Chile, Congo, Costa Rica, Cote d'Ivoire, DR Congo, Dominica, Dominican Republic, Ecuador, Equatorial Guinea, El Salvador, Fiji, Gabon, Ghana, Guatemala, Guyana, Honduras, Indonesia, Jamaica, Kenya, Lesotho, Liberia, Madagascar, Malaysia, Nicaragua, Nigeria, Pakistan, Panama, Papua New Guinea, Paraguay, Samoa, Sierra

Leone, Solomon Islands, Suriname, Thailand, Uruguay, Uganda, Vanuatu, and Vietnam. Countries participate on a voluntarily basis primarily through unified negotiating positions, workshops, and collaborative programs.

Co-Benefit The benefits of policies that are implemented for various reasons at the same time including climate change mitigation acknowledging that most policies designed to address greenhouse gas mitigation also have other, often at least equally important, rationales (e.g., related to objectives of development or sustainability).

Compressed natural gas (CNG) Methane stored at high pressure (typically 20–25 MPa or 2,900–3,600 psi) and used in place of gasoline (petrol), Diesel fuel and propane/LPG. The volumetric energy density of CNG is approx. 42 % that of liquefied natural gas (because it is not liquefied), and 25 % that of diesel fuel. See also "Liquefied natural gas (LNG)."

Computable General Equilibrium (CGE) A class of economic models that use actual economic data to estimate how an economy might react to changes in policy, technology, or other external factors. CGE models are also referred to as AGE (applied general equilibrium) models.

Concentration Amount of a chemical in a particular volume or weight of air, water, soil, or other medium. See also "Parts per billion (ppb)" and "Parts per million (ppm)."

Conference of the Parties (COP) The supreme body of the United Nations Framework Convention on Climate Change (UNFCCC). It comprises more than 180 nations that have ratified the Convention. Its first session was held in Berlin, Germany, in 1995 and it is expected to continue meeting on a yearly basis. The COP's role is to promote and review the implementation of the Convention. It will periodically review existing commitments in light of the Convention's objective, new scientific findings, and the effectiveness of national climate change programs. See also "United Nations Framework Convention on Climate Change (UNFCCC)."

Conference of the Parties serving as the Meeting of the Parties to the Kyoto Protocol (CMP) The UNFCCC's COP also serves as the meeting of the Parties to the Kyoto Protocol. The sessions of the COP and the CMP are held during the same period in order to reduce costs and improve coordination.

Consumerism The concept that an ever-expanding consumption of goods is advantageous to the economy.

Convention on the Conservation of Migratory Species of Wild Animals The Convention on Migratory Species, also known as the Bonn Convention, aims to conserve terrestrial, aquatic, and avian migratory species throughout their range. http://www.cms.int/

Convention See "United Nations Framework Convention on Climate Change"

COP See "Conference of the Parties"

Copenhagen Accord A political agreement reached at COP 15 which calls on participating countries to pledge specific actions they will undertake to mitigate

greenhouse-gas emissions. At the conclusion of the COP, however, delegates only voted to "take note of" the document.

Co-pollutant A pollutant that is produced by the same processes that produce carbon dioxide, and where changes in carbon dioxide emissions also influence emissions of the co-pollutant.

Coral bleaching The process in which a coral colony under environmental stress expels the microscopic algae (zooxanthellae) that live in symbiosis with their host organisms (polyps). The affected coral colony appears whitened.

Cost-benefit analysis A process by which you weigh expected costs against expected benefits to determine the best (or most profitable) course of action

Cost of Illness The total cost to society of a person's illness, including health care, lost worker productivity, additional insurance costs, and lost work days.

Coercive measures Policies which are not left to the discretion of the public, e.g., lower speed limits.

Commercialization The sequence of actions to achieve market entry and general market competitiveness of new innovative technologies, processes, and products.

Committee of the Whole Often created by a COP to aid in negotiating text. It consists of the same membership as the COP. When the Committee has finished its work, it turns the text over to the COP, which finalizes and then adopts the text during a plenary session.

Compliance Committee A committee that helps facilitate, promote and enforce compliance with the provisions of the Kyoto Protocol. It has 20 members with representation spread among various regions, small-island developing states, Annex I Parties, and non-Annex I Parties, and functions through a plenary, a bureau, a facilitative branch, and an enforcement branch.

Common Reporting Format (CRF) Standardized format for reporting estimates of greenhouse-gas emissions and removals and other relevant information by Annex I Parties.

Compliance Fulfillment by countries/businesses/individuals of emission reduction and reporting commitments under the UNFCCC and the Kyoto Protocol.

Conference of the Parties (COP) The supreme body of the Convention. It currently meets once a year to review the Convention's progress. The word "conference" is not used here in the sense of "meeting" but rather of "association." The "Conference" meets in sessional periods, for example, the "fourth session of the Conference of the Parties."

Conference of the Parties serving as the Meeting of the Parties to the Kyoto Protocol (CMP) The Convention's supreme body is the COP, which serves as the meeting of the Parties to the Kyoto Protocol. The sessions of the COP and the CMP are held during the same period to reduce costs and improve coordination between the Convention and the Protocol.

Conference room papers (CRPs) A category of in-session documents containing new proposals or outcomes of in-session work. CRPs are for use only during the session concerned.

Consultative Group of Experts on National Communications from non-Annex I Parties (CGE) A panel established to improve the preparation of national communications from developing countries. National communications are an obligation of Parties to the Climate Change Convention.

Contact group An open-ended meeting that may be established by the COP, a subsidiary body or a Committee of the Whole wherein Parties may negotiate before forwarding agreed text to a plenary for formal adoption. Observers generally may attend contact group sessions.

Convention on Biological Diversity (CBD) Signed by 150 government leaders at the 1992 Rio Earth Summit, the Convention on Biological Diversity is dedicated to promoting sustainable development. Conceived as a practical tool for translating the principles of Agenda 21 into reality, the Convention recognizes that biological diversity is about more than plants, animals, and microorganisms and their ecosystems – it is about people and our need for food security, medicines, fresh air and water, shelter, and a clean and healthy environment in which to live. https://www.cbd.int/

Countries with Economies in Transition (EIT) Central and East European countries and former republics of the Soviet Union in transition from state-controlled to market economies. At the time the Kyoto Protocol was adopted in 1997, these countries were on the path from a Communist planned economy to a market economy. Many of them would now be categorised as market economies. Countries in transition to a market economy are grouped with industrialized countries in Annex I of the Kyoto Protocol, so they have emission reduction commitments to meet in the 2008–2012 period. In some cases their industrial base collapsed to such a degree in the early 1990s that they will have no difficulty meeting these commitments.

Countries in transition See "Countries with Economies in Transition"

CO_2 See "Carbon dioxide."

CO_{2e} See "Equivalent CO_2"

CPP See "Clean Power Plan"

CRF See "Common Reporting Format"

Cross-sectional data Observations of units, such as households, firms, persons, or geographical units, at the same point in time.

Crop yield The amount of crop harvested per area unit of land, for instance tons of crop per hectare.

Cryotic soil See "Permafrost"

Cryosphere One of the interrelated components of the Earth's system. The cryosphere is frozen water in the form of snow, permanently frozen ground (permafrost), floating ice, and glaciers, i.e., all global snow, ice, and permafrost. Fluctuations in the volume of the cryosphere cause changes in ocean sea level, which directly impact the atmosphere and biosphere.

CSD See "United Nations Commission on Sustainable Development."

Currently realizable potential See "Market potential"

Damage function The relation between changes in the climate and reductions in economic activity relative to the rate that would be possible in an unaltered climate.

Dangerous climate change Severe climate change with a negative effect on societies, economies, and the environment as a whole. The phrase was introduced by the 1992 UN Framework Convention on Climate Change (UNFCCC), which aims at preventing "dangerous" human interference with the climate system.

Decadal-to-centennial variability See "Deccen"

Decarbonization The reduction in carbon dioxide emissions per unit GDP, thereby reducing the carbon intensity of the economy. See also "GDP" and "Carbon intensity."

Deccen (decadal-to-centennial variability) A term used to describe variations and changes in climatic elements occurring on time scale ranging from decades to centuries. These temporal variations may be induced by changes in forcing agents arising from either human activities (e.g., increasing levels of atmospheric greenhouse gases) or natural causes (e.g., volcanic aerosols or solar irradiance). Some deccen climate variability is unforced, in that it can be the product of internally generated climate system fluctuations.

Decoupling A process in which economic growth is created without increasing carbon dioxide emissions, so the economy and emissions can proceed along different paths.

Declaration A nonbinding political statement made by ministers attending a major meeting (e.g., the Marrakesh Ministerial Declaration of COP-7).

Deforestation The permanent removal of standing forests. Deforestation contributes to increasing carbon dioxide concentrations for two reasons: (1) the burning or decomposition of the wood releases carbon dioxide; and (2) trees that once removed carbon dioxide from the atmosphere in the process of photosynthesis are no longer present.

Desertification Land degradation in arid, semiarid, and dry subhumid areas resulting from various factors, including climatic variations and human activities.

Designated National Authority (DNA) An office, ministry, or other official entity appointed by a Party to the Kyoto Protocol to review and give national approval to projects proposed under the Clean Development Mechanism.

Designated operational entity (DOE) An entity designated by the CMP (based on a recommendation by the EB) as qualified to validate proposed CDM project activities and PoAs; thus DOEs serve as auditors in the CDM process.

Discounting A standard technique used for making intertemporal decisions in which the future costs and benefits are given less weight than the present. The process of converting monetary values backward in time to an equivalent amount is called discounting. The social discount rate is the rate at which society as a whole is willing to trade off present for future benefits.

Diurnal temperature range The difference between maximum and minimum temperature over a period of 24 h.

DNA See "Designated National Authority"

DNA Help Desk A support initiative for Designated National Authorities (DNAs) to provide advice, support, and assistance with the submission of proposals for standardized baselines, recommendations of microscale renewable energy technologies for automatic additionality, or grid emission factors. It targets DNAs from

least developed countries (LDCs), small island developing states (SIDS), African countries, or Parties with less than 10 registered projects as of 31 December 2010. It is possible for project participants and designated operational entities (DOEs) to liaise with a DNA to submit a request on their behalf.

Documents In this context, official documents are available to everyone and feature the logos of the United Nations and the Climate Change Convention. They carry a reference number, such as FCCC/CP/1998/1. Pre-session documents are available before a meeting, often in all six UN languages. In-session documents are distributed on-site (CRPs, L docs, Misc. docs, Inf. docs, and nonpapers).

DOE See "Designated operational entity"

Drafting group A smaller group established by the President or a Chair of a Convention body to meet separately and in private to prepare draft text (text that still has to be formally approved later in a plenary session). Observers generally may not attend drafting group meetings.

Dryland farming A technique that uses soil moisture conservation and seed selection to optimize production under dry conditions.

Dubinin-Radushkevich (DR) Model This model expressed in the DR equation is used to describe the adsorption of subcritical fluids in microporous solids such as activated carbon (biochar). The equation has the form

$$\frac{w}{w_0} = \exp\left[-\left(A/\beta E_o\right)^2\right], \qquad A = RTIn\left({}^{P}/_{P_o}\right)$$

where w and w_o are the amount of adsorption at a relative pressure (P/P_o) and the saturated amount of adsorption, respectively, E_o is a characteristic adsorption energy, and the parameter A is Polanyi's adsorption potential. The parameter β is the affinity coefficient, and is related to the adsorbate-adsorbent interaction. The equation provides macroscopic information of the fraction of the total microscopic volume occupied by the adsorbate.

Earth radiation management (ERM) A set of concepts to moderate or retard global warming by altering, on a large scale, the radiation sent back from Earth into space. See also "Climate engineering."

Earth Summit See "United Nations Conference on Environment and Development"

Earth system See "Climate system"

EB See "Executive Board of the CDM"

Eccentricity The extent to which the Earth's orbit around the Sun departs from a perfect circle.

Ecological economics A growing transdisciplinary field that aims to improve and expand economic theory to integrate the earth's natural systems, human values, and human health and well-being.

Ecology The study of the relationships between living organisms and their environment.

Economic growth An increase in the capacity of an economy to produce goods and services, compared from one period of time to another.

Economic potential The fraction of the technical potential for GHG emissions reductions or energy-efficiency improvements that could be achieved cost-effectively in the absence of market barriers. The achievement of the economic potential requires additional policies and measures to remove market barriers. See also "Market barriers."

Economic and Social Commission for Asia and the Pacific (ESCAP) The regional development arm of the United Nations for the Asia-Pacific region. Made up of 53 member states and 9 associate members, the region is home to 4.1 billion people, or two thirds of the world's population. This makes ESCAP the most comprehensive of the United Nations five regional commissions, and the largest United Nations body serving the Asia-Pacific region with over 600 staff. Established in 1947 with its headquarters in Bangkok, Thailand, ESCAP works to overcome some of the region's greatest challenges by providing results oriented projects, technical assistance, and capacity building to member states.
http://www.unescap.org/about

Economic and Social Council (ECOSOC) The United Nations' central platform for reflection, debate, and innovative thinking on sustainable development. It is one of the six main organs of the United Nations established by the UN Charter in 1946.
http://www.un.org/en/ecosoc/

Ecosystem Any natural unit or entity including living and nonliving parts that interact to produce a stable system through cyclic exchange of materials.

ECSOC See "Economic and Social Council"

Eddy mixing Mixing due to small scale turbulent processes (eddies). Such processes cannot be explicitly resolved by even the finest resolution Atmosphere-ocean General Circulation Models (AOGCM) currently in use. Therefore, their effects must be related to the larger scale conditions. See also "Atmosphere-ocean General Circulation Model (AOGCM)."

EGTT See "Expert Group on Technology Transfer"

EIA See "Energy Information Administration (US)"

EJ Exajoule (10^{18} J). Joule is the SI unit of energy. 1 J is the work required to produce one watt of power for one second, or one "watt second" (W · s) (compare kilowatt hour (kWh); 1 kWh = 3.6 MJ).

El Niño – Southern Oscillation (ENSO) El Niño, in its original sense, is a warm water current that periodically flows along the coast of Ecuador and Peru, disrupting the local fishery. This oceanic event is associated with a fluctuation of the intertropical surface pressure pattern and circulation in the Indian and Pacific Oceans, called the Southern Oscillation. This coupled atmosphere-ocean phenomenon is collectively known as El Niño-Southern Oscillation. During an El Niño event, the prevailing trade winds weaken and the equatorial countercurrent strengthens, causing warm surface waters in the Indonesian area to flow eastward to overlie the cold waters of the Peru current. This event has great impact on the wind, sea surface temperature, and precipitation patterns in the tropical Pacific. It has climatic effects throughout the Pacific region and in many other parts of the world. The opposite of an El Niño event is called La Niña.

Embodied energy The energy used to produce a material substance (such as processed metals or building materials), taking into account energy used at the manufacturing facility (zero order), energy used in producing the materials that are used in the manufacturing facility (first order), and so on.

Emissions The release of a substance (usually a gas when referring to the subject of climate change) into the atmosphere.

Emission Trading Scheme (ETS) A scheme set up to allow the trading of emissions permits between business and/or countries as part of a cap and trade approach to limiting greenhouse gas emissions. The best-developed example is the EU's trading scheme, launched in 2005. See "Cap and trade."

Emissions factor A unique value for scaling emissions to activity data in terms of a standard rate of emissions per unit of activity (e.g., grams of carbon dioxide emitted per barrel of fossil fuel consumed, or per gram of product produced).

Emission permit An allocation of entitlements by a government to an individual organization to emit a specified amount of a substance, e.g., CO_2. Emission permits can be nontransferable or tradable.

Emission quota The fractions of total allowable emissions assigned to a country or group of countries within a framework of maximum total emissions and mandatory allocations of resources or assessments.

Emission reduction unit (ERU) A Kyoto Protocol unit equal to 1 metric ton of CO_2 equivalent. ERUs are generated for emission reductions or emission removals from joint implementation projects.

Emission standard A level of emission that under the law must not be exceeded. An example is the EURO 6 emission standard for trucks.

Emissions trading One of the three Kyoto mechanisms, by which an Annex I Party may transfer Kyoto Protocol units to, or acquire units from, another Annex I Party. An Annex I Party must meet specific eligibility requirements to participate in emissions trading. The process allows market incumbents to either reduce emissions or pay for the right to pollute (with the money paid being used to reduce emissions elsewhere).

Emission trajectories These are projections of future emission pathways, or observed emission patterns.

Energy The amount of work or heat delivered. Energy is classified in a variety of types and becomes useful to human ends when it flows from one place to another or is converted from one type into another. The SI-derived unit of energy is Joule ($1\ \mathrm{J} = 1\ \mathrm{kg} \cdot \mathrm{m}^2/\mathrm{s}^2$).

Energy balance Averaged over the globe and over longer time periods, the energy budget of the climate system must be in balance. Because the climate system derives all its energy from the Sun, this balance implies that, globally, the amount of incoming solar radiation must on average be equal to the sum of the outgoing reflected solar radiation and the outgoing infrared radiation emitted by the climate system. A perturbation of this global radiation balance, be it human-induced or natural, is called radiative forcing. See also "Radiative forcing."

Energy efficiency Using less energy to provide the same service

Energy Information Administration (EIA) The US Energy Information Administration (EIA) collects, analyzes, and disseminates independent and impartial energy information to promote sound policymaking, efficient markets, and public understanding of energy and its interaction with the economy and the environment.
http://www.eia.gov/

Energy intensity Ratio of energy consumption to economic or physical output. At the national level, energy intensity is the ratio of total domestic primary energy consumption or final energy consumption to gross domestic product (GDP) or physical output.

Energy performance rating (EPR) A metric to assess the overall energy efficiency of a building (measured in kWh/m^2 per year), either using actual or modeled energy use data.

ENERGY STAR™ A US Environmental Protection Agency (EPA) voluntary program that helps businesses and individuals save money and protect our climate through superior energy efficiency.
https://www.energystar.gov/

Enhanced Greenhouse Effect The concept that the natural greenhouse effect has been enhanced by increased atmospheric concentrations of greenhouse gases (such as CO_2 and methane) emitted as a result of human activities. These added greenhouse gases cause the earth to warm.

Enteric fermentation Livestock, especially cattle, produce methane as part of their digestion. This process is called enteric fermentation, and it represents one third of the emissions from the agriculture sector.

Entry into force The point at which an intergovernmental agreement becomes legally binding – occurring at a prestated interval after a prestated and required number of ratifications by countries has been achieved. The Climate Change Convention required 50 ratifications to enter into force. It now enters into force for each new Party 90 days after that Party ratifies the Convention. See also "UNFCCC."

Environmental economics Environmental and natural resource economics is a subdiscipline of economics and deals with the study of how environmental and natural resources are developed and managed.

Environmental Integrity Group A coalition or negotiating alliance consisting of Mexico, the Republic of Korea, Switzerland, Lichtenstein, and Monaco.

Environmentally friendly modes Active travel modes plus public transport.

Environmental Protection Agency (EPA) An agency of the US federal government which was created for the purpose of protecting human health and the environment by writing and enforcing regulations based on laws passed by Congress. The EPA began operation in 1970.
http://www.epa.gov/

EPA See "Environmental Protection Agency"

EPR See "Energy performance rating"

Equilibrium response The steady state response of the climate system (or a climate model) to an imposed radiative forcing.

Equilibrium vapor pressure See "Vapor pressure"

Equivalent carbon dioxide See "Equivalent CO_2 (CO_2e)"

Equivalent CO_2 (CO_2e) The concentration of CO_2 that would cause the same level of radiative forcing as a given type and concentration of greenhouse gas. Examples of such greenhouse gases are methane, perfluorocarbons, and nitrous oxide. CO_{2e} is expressed as parts per million by volume, ppmv. See also "Carbon dioxide equivalent (CDE)."

ERM See "Earth radiation management"

ERU See "Emission reduction unit"

ESCAP See "Economic and Social Commission for Asia and the Pacific"

ETS See "Emission Trading Scheme"

EU See "European Union"

European Union (EU) As a regional economic integration organization, the EU is a Party to both the Convention and the Kyoto Protocol. However, it does not have a separate vote from its member states. Because the EU signed the Convention when it was known as the EEC (European Economic Community), the EU retains this name for all formal Convention-related purposes. Members are Austria, Belgium, Bulgaria, Cyprus, Czech Republic, Denmark, Estonia, Finland, France, Germany, Greece, Hungary, Ireland, Italy, Latvia, Lithuania, Luxembourg, Malta, the Netherlands, Poland, Portugal, Romania, Slovakia, Slovenia, Spain, Sweden, and the UK. http://europa.eu/index_en.htm

EUA See "European Union Allowances"

EU Burden-sharing agreement A political agreement that was reached to help the EU reach its emission reduction targets under the Kyoto Protocol (a reduction of 8 % during the period 2008–2012, on average, compared with 1990 levels). The 1998 agreement divided the burden unequally amongst member states, taking into account national conditions, including greenhouse-gas emissions at the time, the opportunity for reducing them, and countries' levels of economic development.

EU ETS (European Union Emissions Trading Scheme) An emissions trading scheme developed by the European Union, designed to help European countries meet their Kyoto Protocol commitments. The EU ETS has been the principal source of demand in the international carbon market.

European Union Allowances (EUA) Quantity-based emissions instruments employed within the EU ETS. Facilities included in the EU ETS must surrender an EUA for each ton of CO_2 emitted.

Evaporation The process by which water changes from a liquid to a gas or vapor.

Evapotranspiration The combined process of evaporation from the Earth's surface and transpiration from vegetation.

Executive Board of the CDM (EB) A 10-member panel which supervises the CDM (Clean Development Mechanism).
See also "CDM."

Exfoliation A chemical or thermal approach for individual separation of carbon sheets to produce single-layered graphene nanosheets.

Expert Group on Technology Transfer (EGTT) An expert group established at COP 7 with the objective of enhancing the implementation of Article 4.5 of the Convention, by analyzing and identifying ways to facilitate and advance technology transfer activities under the Convention. The EGTT completed its work in 2010.

Expert review teams Groups of experts, nominated by Parties, who review national reports submitted by Annex I Parties to the UNFCCC and the Kyoto Protocol.

External costs Costs, such as industrial air pollution, which are involuntarily imposed upon others.
See also "Externalities."

External impacts See "Externalities"

Externalities By-products of activities that affect the well-being of people or damage the environment, where those impacts are not reflected in market prices. The costs (or benefits) associated with externalities do not enter standard cost accounting schemes. For instance, car drivers do not need to pay for the damage caused by car emissions (e.g., acidic rain, climate change).

Falsifiability rule In science, there is no way to prove the absolute truth of any hypothesis or model, since it is always possible that a different explanation might account for the same observations. In this sense, even the most well established physical laws are "conditional." Hence, with scientific methodology it is never possible to prove conclusively that a hypothesis is true, it is only possible to prove that it is false.

Fast-start Finance (FSF) At COP 15 in Copenhagen in 2009, developed countries pledged to provide new and additional resources, including forestry and investments, approaching USD 30 billion for the period 2010–2012 and with balanced allocation between mitigation and adaptation. This collective commitment has come to be known as "Fast-start Finance."

FAR IPCC First Assessment Report (FAR), 1990. See also "IPCC" and "AR5."

FAO See "Food and Agriculture Organization of the United Nations."

FCCC See "United Nations Framework Convention on Climate Change"

Feedback When one variable in a system triggers changes in a second variable that in turn ultimately affects the original variable; a positive feedback intensifies the effect, and a negative feedback reduces the effect.

Feedback loop In a feedback loop, rising temperatures on the Earth change the environment in ways that affect the rate of warming. Feedback loops can be positive (adding to the rate of warming), or negative (reducing it). The melting of Arctic ice provides an example of a positive feedback process. As the ice on the surface of the Arctic Ocean melts away, there is a smaller area of white ice to reflect the Sun's heat back into space and more open, dark water to absorb it. The less ice there is, the more the water heats up, and the faster the remaining ice melts.

Feedback mechanisms Factors which increase or amplify (positive feedback) or decrease (negative feedback) the rate of a process. An example of positive climatic feedback is the ice-albedo feedback.

Final Energy Energy supplied that is available to the consumer to be converted into useful energy (e.g., electricity at the socket). See also "Primary energy."

Financial mechanism Developed country Parties (Annex II Parties) are required to provide financial resources to assist developing country Parties implement the Convention (UNFCCC). To facilitate this, the Convention established a financial mechanism to provide funds to developing country Parties. The Parties to the Convention assigned operation of the financial mechanism to the Global Environment Facility (GEF) on an on-going basis, subject to review every 4 years. The financial mechanism is accountable to the COP. See also "UNFCCC."

Flexible mechanism Instruments that help countries and companies meet emission reduction targets by paying others to reduce emissions for them. The mechanism in widest use is emissions trading, where companies or countries buy and sell permits to pollute. The Kyoto Protocol establishes two flexible mechanisms enabling rich countries to fund emission reduction projects in developing countries – Joint Implementation (JI) and the Clean Development Mechanism (CDM).

Fluorinated gases Powerful synthetic greenhouse gases such as hydrofluorocarbons, perfluorocarbons, and sulfur hexafluoride that are emitted from a variety of industrial processes. Fluorinated gases are sometimes used as substitutes for stratospheric ozone-depleting substances (e.g., chlorofluorocarbons, hydrochlorofluorocarbons, and halons) and are often used in coolants, foaming agents, fire extinguishers, solvents, pesticides, and aerosol propellants. These gases are emitted in small quantities compared to carbon dioxide (CO_2), methane (CH_4), or nitrous oxide (N_2O), but because they are potent greenhouse gases, they are sometimes referred to as High Global Warming Potential gases (High GWP gases).

Fluorocarbons Carbon-fluorine compounds that often contain other elements such as hydrogen, chlorine, or bromine. Common fluorocarbons include chlorofluorocarbons (CFCs), hydrochlorofluorocarbons (HCFCs), hydrofluorocarbons (HFCs), and perfluorocarbons (PFCs). See "Chlorofluorocarbons," "Hydrochlorofluorocarbons," "Hydrofluorocarbons," "Perfluorocarbons," and "Ozone depleting substance."

Food and Agriculture Organization of the United Nations (FAO) The FAO aims at "*achieving food security for all is at the heart of FAO's efforts – to make sure people have regular access to enough high-quality food to lead active, healthy lives. Our three main goals are: the eradication of hunger, food insecurity and malnutrition; the elimination of poverty and the driving forward of economic and social progress for all; and, the sustainable management and utilization of natural resources, including land, water, air, climate and genetic resources for the benefit of present and future generations*."
http://www.fao.org/

Food miles The distance an item of food travels from point of growth to point of final consumption.

Forcing mechanism A process that alters the energy balance of the climate system, i.e., changes the relative balance between incoming solar radiation and outgoing

infrared radiation from Earth. Such mechanisms include changes in solar irradiance, volcanic eruptions, and enhancement of the natural greenhouse effect by emissions of greenhouse gases. See "Radiation," "Infrared radiation," and "Radiative forcing."

Fossil fuel A general term for organic materials formed from decayed plants and animals that have been converted to crude oil, coal, natural gas, or heavy oils by exposure to heat and pressure in the earth's crust over hundreds of millions of years.

Fossil fuels Natural resources, such as coal, oil, and natural gas, containing hydrocarbons. These fuels are formed in the Earth over millions of years and produce carbon dioxide when burnt.

Fossil fuel reserves The quantity of a fossil fuel that is known to exist, based on geological and engineering evidence, and that can be recovered under current economic conditions and operating capabilities.

Fossil fuel resources See "Fossil fuel reserves"

Freundlich Model A model that expresses an empirical relationship between the concentration of a solute on the surface of an adsorbent and the concentration of the solute in the liquid with which it is in contact. The Freundlich Adsorption Isotherm is mathematically expressed as:

$$\frac{x}{m} = KP^{1/n}$$

It is also written as

$$\frac{x}{m} = Kc^{1/n},$$

where, x = mass of adsorbate
m = mass of adsorbent
p = equilibrium pressure of adsorbate
c = equilibrium concentration of adsorbate in solution
K and n are constants for a given adsorbate and adsorbent at a particular temperature

Friends of the Chair Delegates called upon by the Chair (who takes into account the need for political balance among various interests) to assist in carrying out specific tasks.

FSF See "Fast-start Finance"

Fuel switching In general, this is substituting one type of fuel for another. In the climate-change discussion it is implicit that the substituted fuel produces lower carbon emissions per unit of energy produced than the original fuel, e.g., natural gas for coal.

Fugitive fuel emissions Greenhouse-gas emissions as by-products or waste or loss in the process of fuel production, storage, or transport, such as methane given off during oil and gas drilling and refining, or leakage of natural gas from pipelines.

Full-cost pricing The pricing of commercial goods – such as electric power – that would include in the final prices faced by the end user not only the private costs of inputs, but also the costs of the externalities created by their production and use.

Gasification Noncombustion process of converting organic or fossil fuel based carbonaceous materials into carbon monoxide, hydrogen, and carbon dioxide at elevated temperatures under controlled addition of air/oxygen and/or steam.

GATT See "General Agreement on Tariffs and Trade"

GCF See "Green Climate Fund"

GCOS See "Global Climate Observing System"

GDP See "Gross domestic product"

GEF See "Global Environment Facility"

General Agreement on Tariffs and Trade (GATT) The GATT was a multilateral agreement regulating international trade with the purpose of a "substantial reduction of tariffs and other trade barriers and the elimination of preferences, on a reciprocal and mutually advantageous basis." It took effect on January 1, 1948 and lasted until April 14, 1994 (Uruguay Round Agreements, which established the World Trade Organization (WTO) on January 1, 1995). https://www.wto.org/english/docs_e/legal_e/gatt47_e.pdf

General circulation model (GCM) A general circulation model (GCM), a type of climate model, is a mathematical model of the general circulation of a planetary atmosphere or ocean and based on the Navier–Stokes equations on a rotating sphere with thermodynamic terms for various energy sources (radiation, latent heat). These equations are the basis for complex computer programs commonly used for simulating the atmosphere or ocean of the Earth. Atmospheric and oceanic GCMs (AGCM and OGCM) are key components of global climate models. Atmosphere-ocean General Circulation Models (AOGCM) encompass both land and sea masses. See also "Climate modeling."

Geoengineering See "Climate engineering"

Geosphere The soils, sediments, and rock layers of the Earth's crust, both continental and beneath the ocean floors.

Geological sequestration The injection of carbon dioxide into underground geological formations. When CO_2 is injected into declining oil fields it can help to recover more of the oil.

GHG See "Greenhouse gases"

GHG Reduction Potential Possible reductions in emissions of greenhouse gases (quantified in terms of absolute reductions or in percentages of baseline emissions) that can be achieved through the use of technologies and measures.

Glacier A multiyear surplus accumulation of snowfall in excess of snowmelt on land and resulting in a mass of ice at least 0.1 km^2 in area that shows some evidence of movement in response to gravity. A glacier may terminate on land or in water. Glacier ice is the largest reservoir of fresh water on Earth, and second only to the oceans as the largest reservoir of total water. Glaciers are found on every continent except Australia. See also "Snowpack."

Global Average Temperature The mean surface temperature of the Earth measured from three main sources: satellites, monthly readings from a network of over 3,000 surface temperature observation stations, and sea surface temperature measurements taken mainly from the fleet of merchant ships, naval ships, and data buoys.

GCOS See "Global Climate Observing System"

Global Climate Observing System (GCOS) A joint undertaking of the World Meteorological Organization (WMO), the Intergovernmental Oceanographic Commission (IOC) of the United Nations Educational Scientific and Cultural Organization (UNESCO), the United Nations Environment Programme (UNEP), and the International Council for Science (ICSU). Its goal is to provide comprehensive information on the total climate system, involving a multidisciplinary range of physical, chemical, and biological properties, and atmospheric, oceanic, hydrological, cryospheric, and terrestrial processes.
http://www.wmo.int/pages/prog/gcos/index.php?name=News

Global dimming An observed widespread reduction in sunlight at the surface of the Earth, which varies significantly between regions. The most likely cause of global dimming is an interaction between sunlight and microscopic aerosol particles from human activities. In some regions, such as Europe, global dimming no longer occurs, thanks to clean air regulations.

Global energy budget The balance between the Earth's incoming and outgoing energy. The current global climate system must adjust to rising greenhouse gas levels and, in the very long term, the Earth must get rid of energy at the same rate at which it receives energy from the sun.

Global Environment Facility (GEF) The GEF is an independent financial organization that provides grants to developing countries for projects that benefit the global environment and promote sustainable livelihoods in local communities. The Parties to the Convention assigned operation of the financial mechanism to the GEF on an on-going basis, subject to review every 4 years. The financial mechanism is accountable to the COP.
https://www.thegef.org/gef/

Global Ocean Observing System (GOOS) A permanent global system for observations, modelling, and analysis of marine and ocean variables to support operational ocean services worldwide. GOOS provides accurate descriptions of the present state of the oceans, including living resources; continuous forecasts of the future conditions of the sea for as far ahead as possible, and the basis for forecasts of climate change.
http://www.ioc-goos.org/

Global Trade Analysis Project (GTAP) A global network of researchers and policy makers conducting quantitative analysis of international policy issues. GTAP is coordinated by the Center for Global Trade Analysis in Purdue University's Department of Agricultural Economics.
https://www.gtap.agecon.purdue.edu/

Global Warming The recent and ongoing global average increase in temperature near the Earth's surface.

Global Warming Potential (GWP) A measure of the total energy that a gas absorbs over a particular period of time (usually 100 years), compared to carbon dioxide. The GWP depends on the absorption of infrared radiation spectrum by a given species and its atmospheric lifetime. For instance, the GWP of methane (AR5) is 34. See also "AR5."

GOOS See 'Global Ocean Observing System"

Greenhouse effect Trapping and build-up of heat in the atmosphere (troposphere) near the Earth's surface. Some of the heat flowing back toward space from the Earth's surface is absorbed by water vapor, carbon dioxide, ozone, and several other gases in the atmosphere and then reradiated back toward the Earth's surface. If the atmospheric concentrations of these greenhouse gases rise, the average temperature of the lower atmosphere will gradually increase. See also "Greenhouse gas," "Anthropogenic," "Climate," and "Global warming."

Green Climate Fund (GCF) At COP 16 in Cancun in 2010, Governments established a Green Climate Fund as an operating entity of the financial mechanism of the Convention under Article 11. The GCF will support projects, programs, policies, and other activities in developing country Parties. The Fund will be governed by the GCF Board.

Greenhouse effect The insulating effect of certain gases in the atmosphere, which allow solar radiation to warm the earth and then prevent some of the heat from escaping. See also "Natural greenhouse effect."

Greenhouse gases (GHGs) A gas that absorbs radiation at specific wavelengths within the spectrum of infrared radiation emitted by the Earth's surface. The gas in turn emits infrared radiation from a level where the temperature is colder than the surface. The net effect is a local trapping of part of the absorbed energy and a tendency to warm the planetary surface. Water vapour (H_2O), carbon dioxide (CO_2), nitrous oxide (N_2O), methane (CH_4), and ozone (O_3) are the primary greenhouse gases in the Earth's atmosphere.

The atmospheric gases (natural and industrial) responsible for causing global warming and climate change. The major GHGs, which are restricted by the Kyoto protocol, are carbon dioxide (CO_2), methane (CH_4), and nitrous oxide (N_2O). Less prevalent, but very powerful, greenhouse gases are hydrofluorocarbons (HFCs), perfluorocarbons (PFCs), and sulphur hexafluoride (SF_6).

Gross Domestic Product (GDP) The value of all goods and services produced (or consumed) within a nation's borders.

Group of 77 (G-77) and China A large negotiating alliance of developing countries that focuses on numerous international topics, including climate change. The G-77 was founded in 1967 under the auspices of the United Nations Conference on Trade and Development (UNCTAD). It seeks to harmonize the negotiating positions of its 131 member states.

Group of Mountain Landlocked Developing Countries Negotiating group formally established in June 2010 by the governments of Armenia, Kyrgyzstan, and

Tajikstan, focused issues faced by landlocked mountain developing countries specifically vulnerable to transportation costs and food insecurity, with a view towards expanding the group to include other interested countries.

GRULAC Group of Latin American and Caribbean States.

GTAP See "Global Trade Analysis Project"

GTOS Global Terrestrial Observing System.

GWP See "Global Warming Potential"

G77 The main negotiating bloc for developing countries, allied with China (G77 +China). The G77 comprises 130 countries, including India and Brazil, most African countries, the grouping of small island states (AOSIS), the Gulf states, and many others.

Habitat fragmentation A process during which larger areas of habitat are broken into a number of smaller patches of smaller total area, isolated from each other by a matrix of habitats unlike the original habitat.

Halocarbons Compounds containing chlorine, bromine or fluorine and carbon. The carbon backbone can be fully halogenated or contain hydrogen, too. Halocarbons can act as powerful greenhouse gases (GHG) in the atmosphere. The chlorine and bromine containing halocarbons are also involved in the depletion of the ozone layer.

HCT See "Hydrothermal carbonization"

Heat island An urban area characterized by temperatures higher than those of the surrounding nonurban area. As urban areas develop, buildings, roads, and other infrastructure replace open land and vegetation. These surfaces absorb more solar energy, which can create higher temperatures in urban areas.

Heat wave A prolonged period of excessive heat, often combined with excessive humidity.

HFC Hydrofluorocarbons.

High GWP gases See "Fluorinated gases"

Hockey stick The name given to a graph with characteristic pattern. In this context, a figure plotting the average temperature in the Northern hemisphere over the last 1,000 years. The line remains roughly flat until the last 100 years, when it bends sharply upwards. The graph has been cited as evidence to support the idea that global warming is a man-made phenomenon, but some scientists have challenged the data and methodology used to estimate historical temperatures. (It is also known as MBH98 after its creators, Michael E. Mann, Raymond S. Bradley and Malcolm K. Hughes, in 1998)

Holistic thinking See "Systems thinking"

"Hot air" Refers to the concern that some governments will be able to meet their targets for greenhouse-gas emissions under the Kyoto Protocol with minimal effort and could then flood the market with emissions credits, reducing the incentive for other countries to cut their own domestic emissions.

HOV High occupancy vehicle.

Hydrocarbons Substances containing only hydrogen and carbon. Fossil fuels are made up of hydrocarbons.

HTC See "Hydrothermal carbonization"

Hydrochar An alternative to slow-pyrolysis of biomass (which yields biochar) is a process called hydrothermal carbonization (HTC) of biomass, where the biomass is treated with hot compressed water instead of drying to yield hydrochar (HTC char). See also "Biochar."

Hydrochlorofluorocarbons (HCFCs) Compounds containing hydrogen, fluorine, chlorine, and carbon atoms. Although ozone depleting substances, they are less potent at destroying stratospheric ozone than chlorofluorocarbons (CFCs). They have been introduced as temporary replacements for CFCs and are also greenhouse gases. See also "Ozone depleting substance."

Hydrofluorocarbons (HFCs) Compounds containing only hydrogen, fluorine, and carbon atoms. They were introduced as alternatives to ozone depleting substances in serving many industrial, commercial, and personal needs. HFCs are emitted as by-products of industrial processes and are also used in manufacturing. They do not significantly deplete the stratospheric ozone layer, but they are powerful greenhouse gases with global warming potentials (GWP) ranging from approx. 140 (HFC-152a) to 11,700 (HFC-23). See also "Global Warming Potential."

Hydrogen bond Chemical bond formed by the electrostatic attraction between polar molecules that occurs when a hydrogen (H) atom bound to a highly electronegative atom such as nitrogen (N), oxygen (O), or fluorine (F) experiences attraction to some other nearby highly electronegative atom.

Hydrologic cycle The process of evaporation, vertical and horizontal transport of vapor, condensation, precipitation, and the flow of water from continents to oceans. It is a major factor in determining climate through its influence on surface vegetation, the clouds, snow and ice, and soil moisture. The hydrologic cycle is responsible for 25–30 % of the mid-latitudes' heat transport from the equatorial to polar regions.

Hydrophilic Surface A surface that has affinity for water.

Hydrophobic Surface A surface that repels water.

Hydrosphere The component of the climate system comprising liquid surface and subterranean water, such as: oceans, seas, rivers, fresh water lakes, underground water, etc.

Hydrothermal carbonization (HCT) An exothermic process in which wet biomass is converted in aqueous suspensions at moderate temperatures (180–250 °C) and medium pressure conditions into highly carbonaceous hydrochars. The HTC process offers several advantages over conventional pyrolysis, e.g., use of wet feedstock without the need for predrying. The obtained char (hydrochar) can be used for carbon sequestration, soil amelioration, bioenergy production, and wastewater pollution remediation. See also "Biochar" and "Hydrochar."

Hydrothermal carbonization (HTC) Biomass is treated with hot compressed water.

IAR See "Independent Assessment Report"

ICA See "International consultation and analysis"

ICAO See "International Civil Aviation Organization."

ICCP See "International Climate Change Partnership"

Ice Core A cylindrical section of ice removed from a glacier or an ice sheet in order to study climate patterns of the past. By performing chemical analyses on the air trapped in the ice, scientists can estimate the percentage of carbon dioxide and other trace gases in the atmosphere at a given time. Analysis of the ice itself can give some indication of historic temperatures.

ICLEI See "International Council of Local Environmental Initiatives"

International Council of Local Environmental Initiatives (ICLEI) An international association of local governments and national and regional local government organizations that have made a commitment to sustainable development. It was founded in 1990.
http://www.iclei.org/

IDR See "In-depth review"

IEA See "International Energy Agency"

IET See "International Emissions Trading"

IGO See "Intergovernmental organization"

IMF See "International Monetary Fund"

IMO See "International Maritime Organization"

Implementation Actions (legislation or regulations, judicial decrees, or other actions) that governments take to translate international accords into domestic law and policy.

INC Intergovernmental Negotiating Committee for the UNFCCC (1990–1995). A committee created to draft the Convention. The INC met in five sessions between February 1991 and May 1992. After the text of the Convention was adopted in 1992, the INC met six further times to prepare for COP-1. It completed its work in February 1995.

INDC See "Intended Nationally Determined Contributions"

Independent Assessment Report (IAR) The output of an independent assessment of each Annex I Party's International Transaction Log, which in turn is part of the Party's reporting requirements to the UNFCCC. IAR is forwarded to expert review teams for consideration as part of the review of national registries under Article 8 of the Kyoto Protocol. The procedure to produce the IAR is designed to provide independent assessment of each national registry.

In-depth review (IDR) A process by which an Annex I Party's implementation of the Convention and/or the Kyoto Protocol is technically assessed by international teams of experts.

Indirect emissions Indirect emissions from a building, home, or business are those emissions of greenhouse gases that occur as a result of the generation of electricity used in that building. These emissions are called "indirect" because the actual emissions occur at the power plant which generates the electricity, not at the building using the electricity.

Industrial revolution A period of rapid industrial growth with far-reaching social and economic consequences, beginning in England during the second half of the eighteenth century and spreading to Europe and later to other countries including

the USA. The industrial revolution marks the beginning of a strong increase in combustion of fossil fuels and related emissions of carbon dioxide.

Infrared radiation Infrared radiation consists of light whose wavelength is longer than the red color in the visible part of the spectrum, but shorter than microwave radiation. Infrared radiation can be perceived as heat. The Earth's surface, the atmosphere, and clouds all emit infrared radiation, which is also known as terrestrial or long-wave radiation. In contrast, solar radiation is mainly short-wave radiation because of the temperature of the Sun. See "Radiation," "Greenhouse effect," "Enhanced greenhouse effect," "Global warming."

INF document Denotes an Information document. These documents are not translated and are available in the original language of issue.

Informal contact group A group of delegates instructed by the President or a Chair to meet in private to discuss a specific matter in an effort to consolidate different views, reach a compromise, and produce an agreed proposal, often in the form of a written text.

Information and Education Measures Actions that provide information, training or encouragement, or help to develop understanding. Such measures may provide information about the availability, performance, and other characteristics of technologies, practices, and measures.

Infrared radiation Radiation between approx. 0.8 and 25 μm. In the context of climate change, it is emitted by the Earth's surface, the atmosphere, and by clouds and also known as terrestrial (long-wave) radiation. Infrared radiation has a distinctive spectrum (i.e., range of wavelengths) governed by the temperature of the Earth-atmosphere system (Planck's law).

Intended Nationally Determined Contributions (INDC) Established at COP 20 in Lima, Peru, INDCs identify the actions that individual countries will take (recognizing differences in national priorities, circumstances, and capabilities) in order to collectively limit the average global temperature rise to 2 °C.

Intergenerational equity/justice Intergenerational equity in economic, psychological, and sociological contexts, is the concept or idea of fairness or justice in relationships between children, youth, adults, and seniors, particularly in terms of treatment and interactions. It has been studied in environmental and sociological settings.

Intergovernmental organization (IGO) An organization composed primarily of sovereign states (referred to as member states), or of other intergovernmental organizations. They are often called international organizations, although that term may also include international nongovernmental organization such as international nonprofit organizations (NPO) or multinational corporations.

Integrated assessment A method of analysis that combines results and models from the physical, biological, economic, and social sciences, and the interactions between these components, in a consistent framework, to project the consequences of climate change and the policy responses to it.

Intergovernmental Oceanographic Commission (IOC) of UNESCO Established in 1960 as a body with functional autonomy within UNESCO, it is the only competent organization for marine science within the UN system.

The purpose of the Commission is to promote international cooperation and to coordinate programs in research, services, and capacity-building, in order to learn more about the nature and resources of the ocean and coastal areas and to apply that knowledge for the improvement of management, sustainable development, the protection of the marine environment, and the decision-making processes of its member states.
http://www.ioc-unesco.org/

Intergovernmental Panel on climate Change (IPCC) The leading international body for the assessment of climate change. The IPCC was established jointly by the United Nations Environment Programme (UNEP) and the World Meteorological Organization (WMO) in 1988. The purpose of the IPCC is to assess information in the scientific and technical literature related to all significant components of the issue of climate change. The IPCC draws upon hundreds of the world's expert scientists as authors and thousands as expert reviewers. Leading experts on climate change and environmental, social, and economic sciences from some 60 nations have helped the IPCC to prepare periodic assessments of the scientific underpinnings for understanding global climate change and its consequences. With its capacity for reporting on climate change, its consequences, and the viability of adaptation and mitigation measures, the IPCC is also looked to as the official advisory body to the world's governments on the state of the science of the climate change issue. For example, the IPCC organized the development of internationally accepted methods for conducting national greenhouse-gas emission inventories. The IPCC work is shared among three Working Groups, a Task Force and a Task Group. The activities of each Working Group and of the Task Force are coordinated and administrated by a Technical Support Unit (TSU). The IPCC was honored with the 2007 Nobel Peace Prize.
http://www.ipcc.ch/

International Civil Aviation Organization (ICAO) A UN specialized agency, created in 1944 upon the signing of the Convention on International Civil Aviation (Chicago Convention). ICAO works with the Convention's 191 member states and global aviation organizations to develop international Standards and Recommended Practices (SARPs) which states reference when developing their legally-enforceable national civil aviation regulations. Today, the global air transport operates close to 100,000 daily flights.
http://www.icao.int/

International Climate Change Partnership (ICCP) A global coalition of companies and trade associations committed to constructive participation in international policy making on climate change.

International consultation and analysis (ICA) A form of review currently being negotiated and designed in the UNFCCC intergovernmental process.

International Emissions Trading (IET) One of the three Kyoto Protocol flexibility mechanisms, by which an Annex I Party may transfer AAUs to (or acquire AAUs from) another Annex I Party.

International Energy Agency (IEA) The IEA is an autonomous organization which works to ensure reliable, affordable, and clean energy for its 29 member

countries and beyond. The IEA has four main areas of focus: energy security, economic development, environmental awareness, and engagement worldwide. The IEA was founded in 1974 to help countries coordinate a collective response to major disruptions in the supply of oil. While this remains a key aspect of its work, the IEA has evolved and expanded. It is at the heart of global dialogue on energy, providing authoritative statistics and analysis.
http://www.iea.org/

International governmental organization See "Intergovernmental organization (IGO)"

International Monetary Fund (IMF) An organization of 188 countries, working to foster global monetary cooperation, secure financial stability, facilitate international trade, promote high employment and sustainable economic growth, and reduce poverty around the world. The IMF was founded in 1945.
http://www.imf.org/

International Organization for Standardization See "International Standards Organization"

International Standards Organization (ISO) The International Organization for Standardization is an independent, nongovernmental membership organization and the world's largest developer of voluntary International Standards.
http://www.iso.org/iso/home.html

International Union for Conservation of Nature (IUCN) The world's oldest and largest global environmental organization, with more than 1,200 government and NGO Members and almost 11,000 volunteer experts in some 160 countries. IUCN's mission is to "*influence, encourage and assist societies throughout the world to conserve nature and to ensure that any use of natural resources is equitable and ecologically sustainable*."
http://www.iucn.org/

Inundation The submergence of land by water, particularly in a coastal setting.

Involuntary environmentalists People, usually from lower-income households, who have little choice but to consume less energy or nonrenewable materials.

IOC See "Intergovernmental Oceanographic Commission"

IOC-UNESCO See "Intergovernmental Oceanographic Commission (IOC)"

IPCC See "Intergovernmental Panel on Climate Change"

IPCC Fifth Assessment Report (AR5) The Fifth Assessment Report (AR5) is the most comprehensive assessment of scientific knowledge on climate change since 2007 when the Fourth Assessment Report (AR4) was released by IPCC in four parts between September 2013 and November 2014. AR5 is made up of the full reports prepared by the Working Groups (I, II, and III) and their Summaries for Policymakers as well as the Synthesis Report. The Fifth Assessment report says scientists are 95 % certain that humans are the "dominant cause" of global warming since the 1950s. See also "IPCC."

IPCC Working Group I (WG I) The IPCC Working Group I (WG I) assesses the physical scientific aspects of the climate system and climate change. The main topics assessed by WG I include: changes in greenhouse gases and aerosols in the

atmosphere; observed changes in air, land, and ocean temperatures, rainfall, glaciers and ice sheets, oceans and sea level; historical and paleoclimatic perspective on climate change; biogeochemistry, carbon cycle, gases, and aerosols; satellite data and other data; climate models; and climate projections, causes, and attribution of climate change.

IPCC Working Group II (WG II) The IPCC Working Group II (WG II) assesses the vulnerability of socioeconomic and natural systems to climate change, negative and positive consequences of climate change, and options for adapting to it. It also takes into consideration the interrelationship between vulnerability, adaptation, and sustainable development. The assessed information is considered by sectors (water resources, ecosystems, food and forests, coastal systems, industry, human health) and regions (Africa, Asia, Australia and New Zealand, Europe, Latin America, North America, Polar Regions, Small Islands).

IPCC Working Group III (WG III) The IPCC Working Group III (WG III) assesses options for mitigating climate change through limiting or preventing greenhouse-gas emissions and enhancing activities that remove them from the atmosphere. The main economic sectors are taken into account, both in a near-term and in a long-term perspective. The sectors include energy, transport, buildings, industry, agriculture, forestry, and waste management. The WG analyses the costs and benefits of the different approaches to mitigation, considering also the available instruments and policy measures. The approach is more and more solution-oriented.

ISO See "International Standards Organization"

IUCN See "International Union for Conservation of Nature"

Jevons paradox A paradox in ecological economics that occurs when technological progress increases the efficiency with which a resource is used (reducing the amount necessary for any one use), but the rate of consumption of that resource rises because of increasing demand. Also termed Jevons effect.

JI See "Joint implementation"

JISC See "Joint Implementation Supervisory Committee"

JLG See "Joint Liaison Group"

Joint Liaison Group (JLG) Group of representatives of UNFCCC, CBD, and UNCCD Secretariats set up to explore common activities to confront problems related to climate change, biodiversity and desertification. See also "UNFCCC," "BCD," and "UNCCD."

Joint implementation (JI) An agreement between two parties whereby one party struggling to meet its emission reductions under the Kyoto Protocol earns emission reduction units from another party's emission removal project. The JI is a flexible and cost-efficient way of fulfilling Kyoto agreements while also encouraging foreign investment and technology transfer. An Annex I Party must meet specific eligibility requirements to participate in joint implementation.

Joint Implementation Supervisory Committee (JISC) This body, under the authority and guidance of the CMP, inter alia, supervises the verification procedure for Joint Implementation projects.

JUSSCANNZ An acronym representing non-EU industrialized countries which occasionally meet to discuss various issues related to climate change. The members are Japan, the USA, Switzerland, Canada, Australia, Norway, and New Zealand. Iceland, Mexico, and the Republic of Korea may also attend JUSSCANZ meetings.

JWG Joint working group.

Karman-Gabreilli law The idea that the energy efficiency of a transport mode decreases with increasing travel speed.

KP See "Kyoto Protocol"

Kyoto "flexibility" mechanisms See "Kyoto mechanisms"

Kyoto mechanisms Three procedures established under the Kyoto Protocol to increase the flexibility and reduce the costs of making greenhouse-gas emissions cuts. They are the Clean Development Mechanism, Emissions Trading, and Joint Implementation.

Kyoto Protocol (KP) An international agreement standing on its own, and requiring separate ratification by governments, but linked to the UNFCCC. The Kyoto Protocol, among other things, sets binding targets for the reduction of greenhouse-gas emissions by industrialized countries. It has been ratified by 192 of the UNFCCC Parties. The ultimate objective of the treaty is to stabilize greenhouse gas concentrations in the atmosphere at a level that will prevent dangerous human interference with the climate system. Industrialized countries agreed to reduce their combined emissions to 5.2 % below 1990 levels during the 5-year period 2008–2012. It was agreed by governments at a 1997 UN conference in Kyoto, Japan, but did not legally come into force until 2005. A different set of countries agreed a second commitment period in 2013 that will run until 2020. See also "United Nations Framework Convention on Climate Change (UNFCCC)."

LAI See "Leaf Area Index"

Landfill Land waste disposal site in which waste is generally spread in thin layers, compacted, and covered with soil. An alternative to landfilling, depending on waste type, is waste incineration – or recycling.

Land use The total of arrangements, activities, and inputs undertaken in a certain land cover type (a set of human actions). The term land use is also used in the sense of the social and economic purposes for which land is managed (e.g., grazing, timber extraction, and conservation).

Land-use change A change in the use or management of land by humans, which may lead to a change in land cover. Land cover and landuse change may have an impact on the surface albedo, evapotranspiration, sources and sinks of greenhouse gases, or other properties of the climate system and may thus have a radiative forcing and/or other impacts on climate, locally or globally.

Land use, land-use change, and forestry (LULUCF) A greenhouse gas inventory sector that covers emissions and removals of greenhouse gases resulting from direct human-induced land use, land-use change, and forestry activities.

Langmuir Model A model that explains adsorption on the assumption that an adsorbate behaves as an ideal gas at isothermal conditions. At these conditions,

the adsorbate's partial pressure, P_A, is related to the volume of it, V, adsorbed onto a solid adsorbent. The adsorbate binding is treated as a chemical reaction between the adsorbate molecule A_g and an empty site, S. This reaction yields an adsorbed complex A_{ad} with an associated equilibrium constant K_{eq}:

$$A_g + S \longleftrightarrow A_{ad}$$

From these assumptions the Langmuir isotherm can be derived, which states that:

$$\theta_A = \frac{V}{V_m} = \frac{K_{eq}^A P_A}{1 + K_{eq}^A P_A}$$

Latent heat The heat that is either released or absorbed by a unit mass of a substance when it undergoes a change of state such as during evaporation, condensation, or sublimation. Energy released or absorbed when water changes state (melts, freezes, vaporizes, or condenses). The latent heat of evaporation is often represented by the symbol "LE".

Latitude The location north or south in reference to the equator, which is designated at zero (0) degrees. Lines of latitude are parallel to the equator and circle the globe. The North and South poles are at 90° North and South latitude.

LDC See "Least Developed Countries"

LDCF See "Least Developed Country Fund (LDCF)"

Leaf Area Index (LAI) The area of foliage per unit area of ground. Conventionally this refers to the ratio of the area of the upper side of the leaves in a canopy projected onto a flat surface to the area of the surface under the canopy. This has also been called single-sided LAI or projected LAI. Occasionally, LAI has been used in reference to the total surface area of leaves, sometimes referred to as double-sided LAI. If a leaf is flat, the double-sided LAI is about twice that of the single-sided LAI. If the leaf is cylindrical, the double-sided LAI will be more than twice the single-sided LAI.

Leakage That portion of cuts in greenhouse-gas emissions by developed countries – countries trying to meet mandatory limits under the Kyoto Protocol – that may reappear in other countries not bound by such limits. For example, multinational corporations may shift factories from developed countries to developing countries to escape restrictions on emissions.

Least Developed Countries (LDCs) The world's poorest countries. The criteria currently used by the Economic and Social Council (ECOSOC) for designation as an LDC include low income, human resource weakness, and economic vulnerability. Approximately 50 countries have been designated by the UN General Assembly as LDCs.

Least Developed Country Fund (LDCF) The LDCF is a fund established to support a work program to assist Least Developed Country Parties to carry out, inter alia, the preparation and implementation of national adaptation programs of action (NAPAs). The Global Environment Facility, as the entity that operates the financial mechanism of the Convention, has been entrusted to operate this fund.

Least Developed Countries Expert Group (LEG) A panel of 13 experts which provides advice to LDCs on the preparation and implementation of national adaptation programs of action (NAPAs) – plans for addressing the urgent and immediate needs of those countries to adapt to climate change.

LEG See "Least Developed Countries Expert Group"

Level of scientific understanding (LOSU) This is an index on a four-step scale (high, medium, low, and very low) designed to characterize the degree of scientific understanding of the radiative forcing agents that affect climate change. For each agent, the index represents a subjective judgment about the reliability of the estimate of its forcing, involving such factors as the assumptions necessary to evaluate the forcing, the degree of knowledge of the physical/chemical mechanisms determining the forcing, and the uncertainties surrounding the quantitative estimate.

L. docs In-session documents that contain draft reports and texts for adoption by the COP or its subsidiary bodies. Usually such documents are available in all six UN languages.

Lifetime The average length of time that an atom or molecule spends in a given reservoir, such as the atmosphere or oceans.

Lignin A structural substance in a plant that is very resistant to decomposition.

Linking Directive A 2004 Directive of the European Parliament linking the EU ETS with the flexibility mechanisms of the Kyoto Protocol.

Liquefied natural gas (LNG) Natural gas (predominantly methane, CH_4) that has been converted to liquid form for ease of storage or transport. See also "Compressed natural gas (CNG)."

Lithosphere The upper layer of the solid Earth, both continental and oceanic, which is composed of all crustal rocks and the cold, mainly elastic, part of the uppermost mantle. Volcanic activity, although part of the lithosphere, is not considered as part of the climate system, but acts as an external forcing factor.

Livelihood Main source of income or food for sustaining one's household.

LNG See "Liquefied natural gas"

Longwave radiation Radiation emitted in the spectral wavelength greater than about 4 μm, corresponding to the radiation emitted from the Earth and atmosphere. It is sometimes referred to as "terrestrial radiation" or "infrared radiation," although somewhat imprecisely. See also "Infrared radiation."

Loss and damage At COP 16 in Cancun in 2010, Governments established a work program in order to consider approaches to address loss and damage associated with climate change impacts in developing countries that are particularly vulnerable to the adverse effects of climate change as part of the Cancun Adaptation Framework.

LOSU See "Level of scientific understanding"

LULUCF See "Land Use, Land-Use Change, and Forestry"

MAC See "Marginal abatement cost"

MAGICC Climate model that calculates average atmospheric temperatures and sea levels. It is used by IPCC for the construction of the SRES (Special Report on Emissions Scenarios).

Maintenance Respiration Respiration in which energy is used to maintain living biomass.

Major Economies Forum on Energy and Climate A forum established in 2009 by US President Barack Obama to discuss elements of the agreement that will be negotiated at Copenhagen. Its members – Australia, Brazil, Canada, China, the European Union, France, Germany, India, Indonesia, Italy, Japan, Mexico, Russia, South Africa, South Korea, the UK, and the US – account for 80 % of greenhouse-gas emissions. The forum is a modification of the Major Economies Meeting started by the former President George Bush, which was seen by some countries as an attempt to undermine UN negotiations.

Marginal abatement cost (MAC) Marginal abatement costs identify the incremental (or "marginal") costs associated with taking the next step in pollution control.

Marginal cost The cost on one additional unit of effort. In terms of reducing emissions, it represents the cost of reducing emissions by one more unit.

Marginal social benefit (MSB) Marginal social benefits identify the incremental (or "marginal") benefits accruing to society when an incremental action (such as taking the next step in pollution control, or producing one more nonpolluting good) is undertaken.

Marine biosphere All living marine organisms.

Market barriers In this context, conditions that prevent or impede the diffusion of cost-effective technologies or practices that could mitigate GHG emissions.

Market-based incentives Measures intended to directly change relative prices of energy services and overcome market barriers.

Market damages The value of damages generated by climate change (or some other environmental change) and evaluated based on information available to and usable by a competitive market.

Market penetration The share of a given market that is provided by a particular good or service at a given time.

Market potential The portion of the economic potential for GHG emissions reductions or energy-efficiency improvements that could be achieved under existing market conditions, assuming no new policies and measures. Also termed currently realizable potential.

Market Stability Reserve (MSR) A mechanism employed by the EU ETS which triggers adjustments in annual auction volumes of allowances in situations where the total number of allowances in circulation is outside a certain predefined range.

Marrakesh Accords Agreements reached at COP-7 which set various rules for "operating" the more complex provisions of the Kyoto Protocol. Among other

things, the accords include details for establishing a greenhouse-gas emissions trading system, implementing and monitoring the Protocol's Clean Development Mechanism, and setting up and operating three funds to support efforts to adapt to climate change.

MBH98 See "Hockey stick"

Mean sea level (MSL) MSL is normally defined as the average relative sea level (RSL) over a period, such as a month or a year, long enough to average out transients such as waves.

Measures Actions that can be taken by a government or a group of governments, often in conjunction with the private sector, to accelerate the use of technologies or other practices that reduce GHG emissions.

Megacities Cities with populations over 10 million.

Methane (CH_4) A hydrocarbon that is a greenhouse gas with a global warming potential most recently (AR4) estimated at 25 times that of carbon dioxide (CO_2). Methane is produced through anaerobic (without oxygen) decomposition of waste in landfills, animal digestion, decomposition of animal wastes, production and distribution of natural gas and petroleum, coal production, and incomplete fossil fuel combustion. Methane is the second most important man-made greenhouse gas.

Metric Ton Common international measurement for the quantity of greenhouse-gas emissions. A metric ton is equal to 1000 kg, 2205 lbs, or 1.1 short tons. See also "Short ton."

MISC documents Denotes a Miscellaneous document. These documents are not translated and are issued on plain paper with no United Nations masthead. In the UNFCCC process, submissions by Parties are normally issued as miscellaneous documents. They generally contain views or comments published as received from a delegation without formal editing. See also "UNFCCC."

Mitigation In the context of climate change, a human intervention to reduce the sources or enhance the sinks of greenhouse gases. Examples include using fossil fuels more efficiently for industrial processes or electricity generation, switching to solar energy or wind power, improving the insulation of buildings, and expanding forests and other "sinks" to remove greater amounts of carbon dioxide from the atmosphere.

Mitigation marginal cost function The relation between the total quantity of emissions reduced and the marginal cost of the last unit reduced. The marginal cost of mitigation generally increases with the total quantity of emissions reduced.

Montreal Protocol The Montreal Protocol on Substances that Deplete the Ozone Layer, an international agreement adopted in Montreal in 1987.

Moral licensing In energy efficiency, the off-setting of energy-efficient behavior in one area by increased use in another. See also "Jevons paradox."

Mount Pinatubo A volcano in the Philippine Islands that erupted in 1991. The eruption of Mount Pinatubo ejected enough particulate and sulfate aerosol matter into the atmosphere to block some of the incoming solar radiation from reaching Earth's atmosphere. This effectively cooled the planet from 1992 to 1994, masking the warming that had been occurring for most of the 1980s and 1990s.

MRV (Monitoring, reporting, and verification) Measurable, reportable and verifiable. A process/concept that potentially supports greater transparency in the climate change regime.

MSB See "Marginal social benefit"

MSR See "Market Stability Reserve"

MSL See "Mean sea level"

MSW See "Municipal solid waste"

Municipal solid waste (MSW) Residential solid waste and some nonhazardous commercial, institutional, and industrial wastes. This material is generally sent to municipal landfills for disposal. See "Landfill."

Multifunctionalism (agriculture) The argument that in addition to food production, farming can also contribute to ecosystem management, landscape protection, rural employment, etc.

Multiplier The amount by which the impact of a climate policy or project changes the direct economic costs and benefits as a result of interconnections between sectors of an economy.

NAP See "National Allocation Plan"

NAPA See "National adaptation programs of action"

NAMAs See "Nationally appropriate mitigation actions"

National Allocation Plan (NAP) National plans developed in early stages of the EU ETS that specified the allocation of emissions reduction targets within individual countries, and the distribution of allowances for trading.

National adaptation programs of action (NAPAs) Documents prepared by least developed countries (LDCs) identifying urgent and immediate needs for adapting to climate change.

National communication A document submitted in accordance with the Convention (and the Protocol) by which a Party informs other Parties of activities undertaken to address climate change. Most developed countries have now submitted their fifth national communications; most developing countries have completed their first national communication and are in the process of preparing their second.

National delegation One or more officials empowered to represent and negotiate on behalf of a government.

Nationally appropriate mitigation actions (NAMAs) At COP 16 in Cancun in 2010, Governments decided to set up a registry to record nationally appropriate mitigation actions seeking international support, to facilitate the matching of finance, technology, and capacity-building support with these actions, and to recognize other NAMAs.

Natural capital The world's stocks of natural assets which include geology, soil, air, water, and all living things. It is from this Natural Capital that humans derive a wide range of services, often called ecosystem services, which make human life possible.

Natural Gas Underground deposits of gases consisting of 50–90 % of methane (CH_4) and small amounts of heavier gaseous hydrocarbon compounds such as

propane (C_3H_8) and butane (C_4H_{10}). It can be transported in pipelines or aboard ship as LNG (liquefied natural gas).

Natural greenhouse effect The natural level of greenhouse gases in our atmosphere, which keeps the planet about 30 °C warmer than it would otherwise be – essential for life as we know it. Water vapor is the most important component of the natural greenhouse effect.

Natural variability Variations in the mean state and other statistics (such as standard deviations or statistics of extremes) of the climate on all time and space scales beyond that of individual weather events. Natural variations in climate over time are caused by internal processes of the climate system, such as El Niño, as well as changes in external influences, such as volcanic activity and variations in the output of the sun.

New Market Mechanisms (NMM) New market-based mechanisms were defined in COP17/CMP7 at Durban to be those mechanisms operating under the guidance and authority of the COP to enhance the cost-effectiveness of, and to promote, mitigation actions, bearing in mind different circumstances of developed and developing countries.

NG See "Natural gas"

NGO See "Nongovernmental organization"

Nitrogen cycle The natural circulation of nitrogen among the atmosphere, plants, animals, and microorganisms that live in soil and water. Nitrogen takes on a variety of chemical forms throughout the nitrogen cycle, including nitrous oxide (N_2O) and nitrogen oxides (NOx).

Nitrogen fertilization Enhancement of plant growth through the deposition of nitrogen compounds. In IPCC reports, this typically refers to fertilization from anthropogenic sources of nitrogen such as man-made fertilizers and nitrogen oxides released from burning of fossil fuels.

Nitrogen oxides (NOx) Gases consisting of nitrogen and oxygen. Nitrogen oxides are produced in the emissions of vehicle exhausts and from power stations. In the atmosphere, nitrogen oxides can contribute to formation of photochemical ozone (smog), can impair visibility, and have health consequences; they are thus considered pollutants.

Nitrous oxide (N_2O) A powerful greenhouse gas with a global warming potential of 298 times that of carbon dioxide (CO_2) (AR4). Major sources of nitrous oxide include soil cultivation practices, especially the use of commercial and organic fertilizers, fossil fuel combustion, nitric acid production, and biomass burning. Natural emissions of N_2O are mainly from bacteria breaking down nitrogen in soils and the oceans. Nitrous oxide is mainly removed from the atmosphere through destruction in the stratosphere by ultraviolet radiation and associated chemical reactions, but it can also be consumed by certain types of bacteria in soils.

NMM See "New Market Mechanisms"

NMVOC See "Nonmethane Volatile Organic Compounds"

Non-Annex I Parties Refers to countries that have ratified or acceded to the United Nations Framework Convention on Climate Change that are not included in Annex I of the Convention.

Non-Annex I countries The group of developing countries that have signed and ratified the Kyoto Protocol. They do not have binding emission reduction targets.

Nongovernmental organizations (NGOs) Organizations that are not part of a governmental structure. They include environmental groups, research institutions, business groups, and associations of urban and local governments. Many NGOs attend climate talks as observers. To be accredited to attend meetings under the Convention, NGOs must be nonprofit.

Nonmotorized travel See "Active modes."

Nonmarket damages Damages generated by climate change (or some other environmental change) and that cannot be evaluated by a competitive market because of a lack of information and/or the inability to act on that information.

Nonmethane Volatile Organic Compounds (NMVOC) Organic compounds, other than methane, that participate in atmospheric photochemical reactions.

Nonpaper An in-session document issued informally to facilitate negotiations. A nonpaper does not have an official document symbol. It may have an identifying number or carry the name of its author.

Nonparty A state that has not ratified the Convention but attends meetings as an observer.

"No-regrets" mitigation options See "No-regrets options"

"No-regrets options" Technology for reducing greenhouse-gas emissions whose other benefits (in terms of efficiency or reduced energy costs) are so extensive that the investment is worth it for those reasons alone. For example, combined-cycle gas turbines – in which the heat from the burning fuel drives steam turbines while the thermal expansion of the exhaust gases drives gas turbines – may boost the efficiency of electricity generating plants by 70 %. They are sometimes known as "measures worth doing anyway."

NOx See "Nitrogen oxides"

N_2O See "Nitrous oxide"

Observers Agencies, nongovernmental organizations, and Governments not Parties to the Convention which are permitted to attend, but not vote, at meetings of the COP, the CMP, and the subsidiary bodies. Observers may include the United Nations and its specialized agencies, other intergovernmental organizations such as the International Atomic Energy Agency, and accredited nongovernmental organizations (NGOs).

Ocean acidification The ocean absorbs approximately one-fourth of man-made CO_2 from the atmosphere, which helps to reduce adverse climate change effects. However, when the CO_2 dissolves in seawater, carbonic acid is formed. Carbon emissions in the industrial era have already lowered the pH of seawater by 0.1. Ocean acidification can decrease the ability of calcifying marine organisms to build their shells and skeletal structures and kill off coral reefs, with serious

effects for people who rely on them as fishing grounds. Amongst others, corals, mollusks, algae, and crustaceans are affected.

ODS See "Ozone depleting substance"

OECD See "Organization for Economic Cooperation and Development"

Omitted variable bias Omitting one or more variables from an econometric model, where the omitted variable is both a determinant of the dependent variable and correlated with at least one independent variable in the model. This causes the ordinary least squares estimator to be biased and inconsistent.

OPEC See "Organization of Petroleum Exporting Countries"

Organization for Economic Cooperation and Development (OECD) An international economic organization of 34 countries, founded in 1961 to stimulate economic progress and world trade. Its mission is to "*to promote policies that will improve the economic and social well-being of people around the world.*" http://www.oecd.org/

Organization of the Petroleum Exporting Countries (OPEC) An intergovernmental organization of 14 nations which account for approx. 43% of global oil production (2015). OPEC was founded in 1960 and is headquartered in Vienna. OPEC's stated mission is "to coordinate and unify the petroleum policies of its member countries and ensure the stabilization of oil markets, in order to secure an efficient, economic and regular supply of petroleum to consumers, a steady income to producers, and a fair return on capital for those investing in the petroleum industry."

OPEC See "Organization of the Petroleum Exporting Countries"
An intergovernmental organization, created at the Baghdad Conference on September 10–14, 1960, by Iran, Iraq, Kuwait, Saudi Arabia, and Venezuela. The five Founding Members were later joined by nine other Members: Qatar (1961); Indonesia (1962) – suspended its membership from January 2009; Libya (1962); United Arab Emirates (1967); Algeria (1969); Nigeria (1971); Ecuador (1973) – suspended its membership from December 1992 to October 2007; Angola (2007); and Gabon (1975–1994). OPEC has its headquarters in Vienna, Austria. OPEC's objective is to coordinate and unify petroleum policies among Member Countries.
http://www.opec.org

Opportunity cost A benefit, profit, or value of something that must be given up to acquire or achieve something else. Since every resource (land, money, time, etc.) can be put to alternative uses, every action, choice, or decision has an associated opportunity cost.

Ozone Ozone, the triatomic form of oxygen (O_3), is a gaseous atmospheric constituent. In the troposphere, it is created by photochemical reactions involving gases resulting both from natural sources and from human activities (photochemical smog). In high concentrations, tropospheric ozone can be harmful to a wide range of living organisms. Tropospheric ozone acts as a greenhouse gas. In the stratosphere, ozone is created by the interaction between solar ultraviolet radiation and molecular oxygen (O_2). Stratospheric ozone plays a decisive role in the

stratospheric radiative balance. Depletion of stratospheric ozone, due to chemical reactions that may be enhanced by climate change, results in an increased ground-level flux of ultraviolet (UV-) B radiation. See also "Atmosphere" and "Ultraviolet radiation."

Ozone depleting substance (ODS) A family of man-made compounds that includes, but are not limited to, chlorofluorocarbons (CFCs), bromofluorocarbons (halons), methyl chloroform, carbon tetrachloride, methyl bromide, and hydrochlorofluorocarbons (HCFCs). These compounds have been shown to deplete stratospheric ozone, and therefore are typically referred to as ODSs. See "Ozone."

Ozone layer The layer of ozone that begins approximately 15 km above Earth and thins to an almost negligible amount at about 50 km, shields the Earth from harmful ultraviolet radiation from the sun. The highest natural concentration of ozone (approximately 10 parts per million by volume) occurs in the stratosphere at approximately 25 km above Earth. The stratospheric ozone concentration changes throughout the year as stratospheric circulation changes with the seasons. Natural events such as volcanoes and solar flares can produce changes in ozone concentration, but man-made changes are of the greatest concern. See also "Stratosphere" and "Ultraviolet radiation."

Ozone precursors Chemical compounds, such as carbon monoxide, methane, nonmethane hydrocarbons, and nitrogen oxides, which in the presence of solar radiation react with other chemical compounds to form ozone, mainly in the troposphere. See also "Troposphere."

PAH See "Polycyclic aromatic hydrocarbons"

PAM See "Policies and measures"

Panel data Repeated observations of the same units, such as households, firms, persons, or geographical units, over several periods of time

Parametrization In climate modeling, this term refers to the technique of representing processes that cannot be explicitly resolved at the resolution of the model (subgrid scale processes) by relationships between the area averaged effect of such subgrid scale processes and the larger scale flow.

Passive solar energy Use of the sun to heat, cool, or illuminate buildings, without the use of energy conversion devices such as solar cells.

Particulate matter (PM) Very small pieces of solid or liquid matter such as particles of soot, dust, fumes, mists, or aerosols. The physical characteristics of particles, and how they combine with other particles, are part of the feedback mechanisms of the atmosphere. See also "Aerosol" and "Sulfate aerosols."

Parts Per Billion (ppb) Number of parts of a chemical found in one billion parts of a particular gas, liquid, or solid mixture. See also "Concentration."

Parts Per Million by Volume (ppmv) Number of parts of a chemical found in one million parts of a particular gas, liquid, or solid. See also "Concentration."

Parts Per Trillion (ppt) Number of parts of a chemical found in one trillion parts of a particular gas, liquid, or solid. See also "Concentration."

Party A state (or regional economic integration organization such as the European Union) that agrees to be bound by a treaty and for which the treaty has entered into force.

PCT See "Personal carbon trading"

PDD See "Project design document"

PEB Pro-environmental behavior

Per-capita emissions The total amount of greenhouse gas emitted by a country per unit of population.

Permafrost Soil at or below the freezing point of water 0 °C (32 °F) for 2 or more years perennially (continually) frozen. Also known as cryotic soil.

Personal carbon trading (PCT) A proposed quantity-based policy instrument for reducing the carbon emissions emitted by individuals. The aim of the scheme would be to deliver guaranteed levels of carbon savings in successive years in an equitable way. A PCT scheme would set a total cap on all carbon emissions generated from the fossil fuel energy used by individuals. Individuals would use their allowance when purchasing fossil fuel based energy for home energy and transport. If an individual exceeds his or her allowance then additional carbon units would need to be bought from the market and if an individual has surplus carbon units these can be sold. The scheme would be mandatory and administered electronically.
http://www.eci.ox.ac.uk/research/energy/downloads/pct/pct-transport.pdf

Perfluorocarbons (PFCs) A group of chemicals composed of carbon and fluorine only. These chemicals (predominantly CF_4 and C_2F_6) were introduced as alternatives, along with hydrofluorocarbons, to the ozone depleting substances. In addition, PFCs are emitted as by-products of industrial processes and are also used in manufacturing. PFCs do not harm the stratospheric ozone layer, but they are powerful greenhouse gases: CF_4 has a global warming potential (GWP) of 7,390 and C_2F_6 has a GWP of 12,200. The GWP is from the IPCC's Fourth Assessment Report (AR4). These chemicals are predominantly human-made, though there is a small natural source of CF_4. See also "Ozone depleting substance."

Performance criteria See "Standards"

Petroleum A fossil hydrocarbon fuel. The name petroleum covers both naturally occurring unprocessed crude oil and petroleum products that are made up of refined crude oil.

PFC See "Perfluorocarbons"

Phenology The timing of natural events, such as flower blooms and animal migration, which is influenced by changes in climate. Phenology is the study of such important seasonal events. Phenological events are influenced by a combination of climate factors, including light, temperature, rainfall, and humidity.

Photosynthesis The process by which plants take CO_2 from the air (or bicarbonate in water) to build carbohydrates, releasing O_2 in the process. There are several pathways of photosynthesis with different responses to atmospheric CO_2 concentrations. See also "Carbon sequestration" and "Carbon dioxide fertilization."

Phytostabilization Inhibition of metal mobility by plant roots through absorption and accumulation process. Phytostabilization minimizes the metal availability to plants and metal leaching into ground water.

Plenary A formal meeting of the entire COP, CMP, or one of the subsidiary bodies. Formal decisions or conclusions may only be taken during plenary sessions.

PoA See "Program of Activities of CDM"

Point of Zero Charge (PZC) Concentration of charge determining ions corresponding to a neutral or zero-charged surface. When the pH is lower than the pzc value, the system is said to be "below the pzc." Below the pzc, acidic water donates more protons than hydroxide groups, and so the adsorbent surface is positively charged (attracting anions). Conversely, above pzc the surface is negatively charged (attracting cations/repelling anions).

Policies Procedures developed and implemented by government(s) regarding the goal of mitigating climate change through the use of technologies and measures.

Policies and measures (PAM) A frequently used phrase – sometimes abbreviated as PAMs – referring to the steps taken or to be taken by countries to reduce greenhouse-gas emissions under the UNFCCC and the Kyoto Protocol. Some possible policies and measures are listed in the Protocol and could offer opportunities for intergovernmental cooperation.

Polycyclic aromatic hydrocarbons (PAH) A diverse group of organic environmental pollutants consisting of two or more fused aromatic rings and are produced by natural and anthropogenic sources. Examples include acenapthene, acenaphthalene, napthalene, chrysene, phenanthrene, and benzo(a)pyrene.

Pool A component of the climate system that has the capacity to store, accumulate, or release a substance of concern, e.g., atmosphere, oceans, soils, and forests. See also "Reservoir."

ppm (350/450) An abbreviation for parts per million, usually used as short for ppmv (parts per million by volume). The Intergovernmental Panel on Climate Change (IPCC) suggested in 2007 that the world should aim to stabilise greenhouse gas levels at 450 ppm CO_2 equivalent in order to avert dangerous climate change. Some scientists, and many of the countries most vulnerable to climate change, argue that the safe upper limit is 350 ppm. Current levels of CO_2 only are about 400 ppm.

Preindustrial levels of carbon dioxide The levels of carbon dioxide in the atmosphere prior to the start of the Industrial Revolution. These levels are estimated to be about 280 parts per million (by volume). The current level is around 400 ppm.

President The official of a member government elected by the Parties to preside over the COP and the CMP. The President is often a senior official or minister from the state or region hosting the Conference. The President may not participate in the negotiations as a representative of the member government during the term of presidency.

Precautionary principle Avoiding a solution that is irreversible, because the assumptions on which the solution is based may prove incorrect, in favour of a seemingly inferior solution that can be reversed.

Precession The wobble over thousands of years of the tilt of the Earths axis with respect to the plane of the solar system.

Primary energy Energy embodied in natural resources (e.g., coal, crude oil, sunlight, uranium) that has not undergone any anthropogenic conversion or transformation. It is transformed into secondary energy by cleaning (natural gas), refining (oil in oil products), or by conversion into electricity or heat. When the secondary energy is delivered at the end-use facilities it is called final energy (e.g., electricity at the wall outlet), where it becomes usable energy (e.g., light). Primary energy is also referred to as energy sources. See also "Final energy."

Program of Activities of CDM (PoA) A voluntary coordinated action by a private or public entity which coordinates and implements any policy/measure or stated goal (i.e., incentive schemes and voluntary programs) reducing GHGs via an unlimited number of project activities, and meeting additionality requirements.

Project design document (PDD) The document prepared by the project participant of a CDM project activity which sets out in detail, in accordance with the CDM rules and requirements, the CDM project activity which is to be undertaken.

Protocol An international agreement linked to an existing convention, but as a separate and additional agreement which must be signed and ratified by the Parties to the convention concerned. Protocols typically strengthen a convention by adding new, more detailed commitments.

p-km Passenger-km

Pyrolysis A thermochemical decomposition of organic materials at high temperatures under no-oxygen or oxygen-limited conditions.

PZC See "Point of Zero Charge"

QELRO See "Quantified Emissions Limitation and Reduction Commitments"

Quantified Emissions Limitation and Reduction Commitments (QELRO) Legally binding targets and timetables under the Kyoto Protocol for the limitation or reduction of greenhouse-gas emissions by developed countries.

Radiation Energy transfer in the form of electromagnetic waves or particles that release energy when absorbed by an object. See also "Ultraviolet radiation," "Infrared radiation," "Solar radiation," and "Longwave radiation."

Radiative damping An imposed positive radiative forcing on the Earth-atmosphere system (e.g., through the addition of greenhouse gases) represents an energy surplus. The temperature of the surface and lower atmosphere will then increase and in turn increase the amount of infrared radiation being emitted to space, thus a new energy balance will be established. The amount that emissions of infrared radiation to space increase for a given increase in temperature is known as the radiative damping.

Radiative forcing A simple measure of the importance of a potential climate change mechanism. Radiative forcing is the perturbation to the energy balance of the Earth-atmosphere system (in W/m^2) following, for example, a change in the concentration of carbon dioxide or a change in the output of the Sun; the climate system responds to the radiative forcing so as to reestablish the energy

balance. A positive radiative forcing tends to warm the surface and a negative radiative forcing tends to cool the surface. The radiative forcing is normally quoted as a global and annual mean value. A more precise definition of radiative forcing, as used in IPCC reports, is the perturbation of the energy balance of the surface-troposphere system, after allowing for the stratosphere to readjust to a state of global mean radiative equilibrium. Sometimes called "climate forcing."

Rain-fed crops Crops that rely on natural rainfall for moisture, without access to irrigation.

Ratification Formal approval, often by a Parliament or other national legislature, of a convention, protocol, or treaty, enabling a country to become a Party. Ratification is a separate process that occurs after a country has signed an agreement. The instrument of ratification must be deposited with a "depositary" (in the case of the Climate Change Convention, the UN Secretary-General) to start the countdown to becoming a Party (in the case of the Convention, the countdown is 90 days). See also "Accession."

RCP See "Representative concentration pathway"

Rebound effects See "Spill-over effects"

Recommendation A formal act of the COP or the CMP which is weaker than a decision or a resolution, and is not binding on Parties to the Convention or the Kyoto Protocol.

RECs See "Renewable Energy Certificates"

Recycling Collecting and reprocessing a resource so it can be used again. An example is collecting aluminum cans, melting them down, and using the aluminum to make new cans or other aluminum products.

REDD See "Reducing Emissions from Deforestation and forest Degradation"

REDD+ REDD activities plus additional sustainable forestry management practices, including conservation and enhancement of forestry carbon stocks.

Reducing Emissions from Deforestation and forest Degradation (REDD) A UNFCCC mechanism whose objective is to mitigate climate change by reducing net emissions of greenhouse gases through enhanced forestry management in developing countries. It provides developing countries with financial incentives to preserve forests.

Reductionism An approach to understanding the nature of complex things by reducing them to the interactions of their parts, or to simpler or more fundamental things. It can also be described as the philosophical position that a complex system is nothing but the sum of its parts, and that an account of it can be reduced to accounts of individual constituents.

Reflectivity The ability of a surface material to reflect sunlight including the visible, infrared, and ultraviolet wavelengths.

Reforestation Direct human-induced conversion of nonforested land to forested land through planting, seeding, and/or the human-induced promotion of natural seed sources, on land that was previously forested but converted to nonforested land.

REG document Regular documents have a serial number following the year. They are translated into all six official languages of the United Nations.

Regional groups Alliances of countries, in most cases sharing the same geographic region, which meet privately to discuss issues and nominate bureau members and other officials for activities under the Convention. The five regional groups are Africa, Asia, Central and Eastern Europe (CEE), Latin America and the Caribbean (GRULAC), and the Western Europe and Others Group (WEOG).

Registries, registry systems Electronic databases that track and record all transactions under the Kyoto Protocol's greenhouse-gas emissions trading system (the "carbon market") and under mechanisms such as the Clean Development Mechanism. "Registry" may also refer to current discussions on a system for inscribing nationally appropriate mitigation actions.

Regulatory measures Rules or codes enacted by governments that mandate product specifications or process performance characteristics.

Relative Sea Level Rise The increase in ocean water levels at a specific location, taking into account both global sea level rise and local factors, such as local subsidence and uplift. Relative sea level rise is measured with respect to a specified vertical datum relative to the land, which may also be changing elevation over time.

Removal unit (RMU) A Kyoto Protocol unit equal to 1 metric ton of carbon dioxide equivalent. RMUs are generated in Annex I Parties by LULUCF activities that absorb carbon dioxide.

Renewable energy Energy created from sources that can be replenished in a short period of time. The five renewable sources used most often are: biomass (such as wood and biogas), the movement of water, geothermal (heat from within the earth), wind, and solar. See also "Alternative energy."

Renewable Energy Certificates (RECs) Renewable energy certificates represent the environmental attributes of power produced from renewable energy projects. They are sold separately from the electricity itself, in markets designed to increase renewable energy services, and are sometimes called renewable energy credits, green certificates, or green tags.

Research and systematic observation An obligation of Parties to the Climate Change Convention; they are called upon to promote and cooperate in research and systematic observation of the climate system, and called upon to aid developing countries to do so.

Research, Development, and Demonstration Scientific/technical research and development of new production processes or products, coupled with analysis and measures that provide information to potential users regarding the application of the new product or process; demonstration tests the feasibility of applying these products or processes via pilot plants and other precommercial applications.

Representative concentration pathways (RCPs) The radiative forcing scenarios used by the IPCC.

Reservation An exception or concern noted for the record by a Party in the course of accepting a decision of the COP or the CMP. No reservations are allowed to the Convention itself, or to the Protocol.

Reservoir A component of the climate system, other than the atmosphere, which has the capacity to store, accumulate, or release a substance of concern, e.g.,

carbon, a greenhouse gas or a precursor. Oceans, soils, and forests are examples of reservoirs of carbon. Pool is an equivalent term (note that the definition of pool often includes the atmosphere). The absolute quantity of substance of concern, held within a reservoir at a specified time, is called the stock.

Residence Time The average time spent in a reservoir by an individual atom or molecule. With respect to greenhouse gases, residence time usually refers to how long a particular molecule remains in the atmosphere. For most gases other than methane and carbon dioxide, the residence time is approximately equal to the atmospheric lifetime.

Resilience A capability to anticipate, prepare for, respond to, and recover from significant multihazard threats with minimum damage to social well-being, the economy, and the environment.

Resolution Directives that guide the work of the COP or the CMP – opinions rather than permanent legal acts. Unlike decisions, resolutions do not generally become part of the formal body of legislation enacted by the COP or the CMP.

Respiration The process whereby living organisms convert organic matter to CO_2, releasing energy and consuming O_2.

Response time The time needed for the climate system or its components to reequilibrate to a new state, following a forcing resulting from external and internal processes or feedbacks.

It is very different for various components of the climate system. The response time of the troposphere is relatively short, from days to weeks, whereas the stratosphere comes into equilibrium on a time scale of typically a few months. Due to their large heat capacity, the oceans have a much longer response time, typically decades, but up to centuries or millennia. The response time of the strongly coupled surface troposphere system is, therefore, slow compared to that of the stratosphere, and mainly determined by the oceans. The biosphere may respond fast (e.g., to droughts), but also very slowly to imposed changes. Also called adjustment time.

Retranslocation The transport of minerals and food from the leaves of a plant to storage when the leaves senesce. The addition of a substance of concern to a reservoir. The uptake of carbon containing substances, in particular carbon dioxide, is often called (carbon) sequestration.

Review of commitments Regular scrutiny by Convention Parties of the adequacy of the treaty's Article 4.2 (a) and (b) outlining developed country commitments to limit greenhouse-gas emissions. The first review took place at COP-1 and led to a finding that progress was not "adequate" – and so to negotiations that led to the Kyoto Protocol, which has more stringent commitments for developed countries.

Risk coefficient The amount of additional incidence or severity of disease in a population produced by a unit change in ambient air concentration of a pollutant.

Rio Conventions Three environmental conventions, two of which were adopted at the 1992 "Earth Summit" in Rio de Janeiro: the United Nations Framework Convention on Climate Change (UNFCCC), and the Convention on Biodiversity (CBD), while the third, the United Nations Convention to Combat Desertification (UNCCD), was adopted in 1994. The issues addressed by the three treaties are

related – in particular, climate change can have adverse effects on desertification and biodiversity – and through a Joint Liaison Group, the secretariats of the three conventions take steps to coordinate activities to achieve common progress.

Rio+20 The United Nations Conference on Sustainable Development, to be held in Rio de Janeiro, Brazil, on June 4–6, 2012. The first UN Conference on Sustainable Development was the "Earth Summit," held in 1992, and it spawned the three "Rio Conventions" – the UNFCCC, the UNCCD, and the UNCBD.

RMU See "Removal unit"

Roster of experts Experts nominated by Parties to the Climate Change Convention to aid the Secretariat in work related to review of national reports of Annex I Parties, preparation of reports on adaptation technology, the transfer of technology to developing countries, and the development of know-how on mitigating and adapting to climate change.

Rules of procedure The parliamentary rules that govern the procedures of the COP, the CMP, and the subsidiary bodies, covering such matters as decision-making and participation. The COP has not yet formally adopted rules of procedure, but all except one (on voting) are currently being "applied." As such, they are commonly referred to as the "draft rules of procedure being applied."

Salt water intrusion Displacement of fresh or ground water by the advance of salt water due to its greater density, usually in coastal and estuarine areas.

SAR IPCC Second Assessment Report (SAR), 1995. See also "IPCC" and "AR5."

SBI See "Subsidiary Body for Implementation"

SBSTA See "Subsidiary Body for Scientific and Technological Advice"

SCC See "Social cost of carbon"

SCCF See "Special Climate Change Fund"

SDGs See "Sustainable Development Goals"

Scenario A plausible description of how the future may develop, based on a coherent and internally consistent set of assumptions about key relationships and driving forces (e.g., rate of technology changes, prices). Note that scenarios are neither predictions nor forecasts.

SCM See "Sectoral crediting mechanism"

Sea Surface Temperature The temperature in the top several feet of the ocean, measured by ships, buoys, and drifters.

Second Assessment Report (SAR) An extensive review of worldwide research on climate change compiled by the IPCC and published in 1995. Some 2,000 scientists and experts participated. The report is also known as Climate Change 1995. The SAR concluded that "the balance of evidence suggests that there is a discernible human influence on global climate." It also said "no-regrets options" and other cost-effective strategies exist for combating climate change.

Secretariat The office staffed by international civil servants responsible for "servicing" the UNFCCC Convention and ensuring its smooth operation. The secretariat makes arrangements for meetings, compiles and prepares reports, and coordinates with other relevant international bodies. The Climate Change

Secretariat, which is based in Bonn, Germany, is institutionally linked to the United Nations. See also "UNFCCC."

Sectoral crediting mechanism (SCM) A baseline-and-credit scheme rewarding GHG emission reductions from a specific sector against a predetermined threshold.

Sectoral trading mechanism (STM) A sectoral GHG reduction mechanism based upon a cap-and-trade rather than baseline-and-credit approach; depending up the design, countries might receive sectoral allowances ex-ante for trading purposes.

Sensitivity The degree to which a system is affected, either adversely or beneficially, by climate variability or change. The effect may be direct (e.g., a change in crop yield in response to a change in the mean, range, or variability of temperature) or indirect (e.g., damages caused by an increase in the frequency of coastal flooding due to sea level rise).

SF_6 See "Sulphur hexafluoride."

Short ton Common measurement for a ton in the USA. A short ton is equal to 2,000 lbs or 0.907 metric tons or 907 kg. See "Metric ton."

SIDS Small island developing states.

Sink Any process, activity, or mechanism which removes a greenhouse gas, an aerosol, or a precursor of a greenhouse gas from the atmosphere. Forests and other vegetation are considered sinks because they remove carbon dioxide through photosynthesis.

Snowpack A seasonal accumulation of slow-melting snow. See also "Glacier."

Social cost of carbon (SCC) The marginal cost of emitting an additional ton of carbon (or carbon dioxide).

Social cost of carbon dioxide See "Social cost of carbon"

Social discount rate See "Discounting"

Social efficiency The use of nontechnical means to reduce energy consumption.

Soil carbon A major component of the terrestrial biosphere pool in the carbon cycle. The amount of carbon in the soil is a function of the historical vegetative cover and productivity, which in turn is dependent in part upon climatic variables.

Solar luminosity A measure of the brightness of (i.e., the amount of solar radiation being emitted by) the Sun.

Solar radiation Radiation emitted by the Sun. It is also referred to as short-wave radiation. Solar radiation has a distinctive range of wavelengths (spectrum) determined by the temperature of the Sun. See also "Ultraviolet radiation," "Infrared radiation," and "Radiation."

Solar radiation management (SRM) A set of concepts to moderate or retard global warming by shielding part of solar radiation from Earth. See also "Climate engineering."

Sonochemistry Chemistry of understanding the application of ultrasound to chemical reactions and processes. Ultrasound is the part of sonic spectrum which ranges from about 20 kHz to 10 MHz.

Sonoluminescence Initiation of bright flashes of light caused by imposing a loud, high frequency sound on a gas bubble contained within a liquid.

Sorption A physical or chemical process by which one substance becomes attached to another.

Spatial scales Continental: 10–100 million km^2
Regional: 100 thousand–10 million km^2
Local: less than 100 thousand km^2

Special Climate Change Fund (SCCF) The SCCF was established to finance projects relating to adaptation; technology transfer and capacity building; energy, transport, industry, agriculture, forestry, and waste management; and economic diversification. This fund should complement other funding mechanisms for the implementation of the Convention. The Global Environment Facility (GEF), as the entity that operates the financial mechanism of the Convention, has been entrusted to operate this fund.

Special Report on Emissions Scenarios (SRES) A report by the Intergovernmental Panel on Climate Change (IPCC) published in 2000.

Spill-over effects Reverberations in developing countries caused by actions taken by developed countries to cut greenhouse-gas emissions. For example, emissions reductions in developed countries could lower demand for oil and thus international oil prices, leading to more use of oil and greater emissions in developing nations, partially off-setting the original cuts. Current estimates are that full-scale implementation of the Kyoto Protocol may cause 5–20 % of emissions reductions in industrialized countries to "leak" into developing countries. Also known as "rebound effects" or "take-back effects."

Spin-up "Spin-up" is a technique used to initialize an AOGCM. At present it is not possible to diagnose accurately the state of the coupled atmosphere-ocean system and therefore it is not possible to prescribe observed starting conditions for an experiment with an AOGCM. Instead, the atmosphere and ocean components of the model are run separately, forced with "observed" boundary conditions, followed perhaps by a further period of "spin-up" when the atmosphere and ocean are coupled together, until the AOGCM is near to a steady state. See also "Atmosphere-ocean General Circulation Model (AOGCM)."

SRES See "Special Report on Emissions Scenarios"

SRM See "Solar radiation management"

Standards Set of rules or codes mandating or defining product performance (e.g., grades, dimensions, characteristics, test methods, rules for use). Also termed performance criteria.

STM See "Sectoral trading mechanism"

Stern review A report on the economics of climate change led by Lord Nicholas Stern, a former World Bank economist. It was published on 30 October 2006 and argued that the cost of dealing with the consequences of climate change in the future would be higher than taking action to mitigate the problem now. http://mudancasclimaticas.cptec.inpe.br/~rmclima/pdfs/destaques/sternreview_report_complete.pdf

Storm surge An abnormal rise in sea level accompanying a hurricane or other intense storm, whose height is the difference between the observed level of the sea surface and the level that would have occurred in the absence of the cyclone.

Stratosphere Region of the atmosphere between the troposphere and mesosphere, having a lower boundary of approximately 8 km at the poles to 15 km at the equator and an upper boundary of approximately 50 km. Depending upon latitude and season, the temperature in the lower stratosphere can increase, be isothermal, or even decrease with altitude, but the temperature in the upper stratosphere generally increases with height due to absorption of solar radiation by ozone.

Stratospheric ozone See "Ozone layer."

Streamflow The volume of water that moves over a designated point over a fixed period of time. It is often expressed as cubic feet per second (ft^3/s).

Structural changes Changes, for example, in the relative share of GDP produced by the industrial, agricultural, or services sectors of an economy; or, more generally, systems transformations whereby some components are either replaced or partially substituted by other ones.

Subsidence See "Subsiding"

Subsidiary body A committee that assists the Conference of the Parties. Two permanent subsidiary bodies are created by the Convention: the Subsidiary Body for Implementation (SBI) and the Subsidiary Body for Scientific and Technological Advice (SBSTA). Two major temporary bodies that exist currently are the Ad Hoc Working Group on Further Commitments for Annex I Parties under the Kyoto Protocol (AWG-KP), established at COP 11 in Montreal, and the Ad Hoc Working Group on Long-term Cooperative Action under the Convention (AWG-LCA), established at COP 13 in Bali. Additional subsidiary bodies may be established as needed.

Subsidiary Body for Implementation (SBI) The SBI makes recommendations on policy and implementation issues to the COP and, if requested, to other bodies.

Subsidiary Body for Scientific and Technological Advice (SBSTA) The SBSTA serves as a link between information and assessments provided by expert sources (such as the IPCC) and the COP, which focuses on setting policy.

Subsiding The downward settling of the Earth's crust relative to its surroundings.

Sulfate aerosols Particulate matter that consists of compounds of sulfur formed by the interaction of sulfur dioxide and sulfur trioxide with other compounds in the atmosphere. Sulfate aerosols are injected into the atmosphere from the combustion of fossil fuels and the eruption of volcanoes like Mt. Pinatubo. Sulfate aerosols can lower the Earth's temperature by reflecting away solar radiation (negative radiative forcing). General Circulation Models which incorporate the effects of sulfate aerosols more accurately predict global temperature variations. See "Particulate matter," "Aerosol," "General Circulation Models" (United Nations Framework Convention on Climate Change [UNFCCC]).

Sulfur hexafluoride (SF_6) A colorless gas soluble in alcohol and ether, slightly soluble in water. A very powerful greenhouse gas used primarily in electrical transmission and distribution systems and as a dielectric in electronics. The global warming potential (GWP) of SF_6 is 22,800 (AR4). See "Global Warming Potential."

Supertoxicants A special category of pollutants that includes dioxins, biphenyl, furans, etc., and are quite stable in the environment and are not subject to easy chemical and biological decomposition. Less than seven drops of supertoxic chemical if given in a liquid form to a 70-kg human could be lethal.

Sustainable development Development that meets the needs of the present without compromising the ability of future generations to meet their own needs.

Sustainable Development Goals (SDG) A post-2015 development agenda, launched at the Rio+20 Conference, to replace expiring Millennium Development Goals.

Systems thinking Systems thinking involves looking at the interconnections between parts of a whole rather than concentrating just on the parts. Systems thinking or holism acknowledges that complex systems are inherently irreducible, and more than the sum of their parts, and that a holistic approach is needed to understand them.

Take-back effects See "Spill-over effects"

TAR IPCC Third Assessment Report (TAR), 2001. See also "IPCC" and "AR5."

Technical potential The amount by which it is possible to reduce GHG emissions or improve energy efficiency by using a technology or practice in all applications in which it could technically be adopted, without consideration of its costs or practical feasibility.

Technology A piece of equipment or a technique for performing a particular activity.

Technology transfer (TT) The process whereby technological advances are shared between different countries. Developed countries could, for example, share up-to-date renewable energy technologies with developing countries, in an effort to lower global greenhouse-gas emissions.

Telecommuting Replacement of the work trip by working from home or in a neighborhood center using information technology.

Teleshopping Replacement of shopping trips by on-line purchasing.

Terrestrial biosphere All living organisms on land.

Thermal expansion The increase in volume (and decrease in density) that results from warming water. A warming of the ocean leads to an expansion of the ocean volume, which leads to an increase in sea level.

Thermocline The region in the world's ocean, typically at a depth of 1 km, where the temperature decreases rapidly with depth and which marks the boundary between the surface and deep ocean.

Thermohaline circulation Large-scale density-driven circulation in the ocean caused by differences in temperature and salinity. In the North Atlantic, the thermohaline circulation consists of warm surface water flowing northward and

cold deep water flowing southward, resulting in a net poleward transport of heat. The surface water sinks in highly restricted sinking regions located in high latitudes.

Third Assessment Report (TAR) The third extensive review of global scientific research on climate change, published by the IPCC in 2001. Among other things, the report stated that "The Earth's climate system has demonstrably changed on both global and regional scales since the pre-industrial era, with some of these changes attributable to human activities. There is new and stronger evidence that most of the warming observed over the last 50 years is attributable to human activities." The TAR also focused on the regional effects of climate change.

Tipping point A threshold for change, which, when reached, results in a process that is difficult to reverse. Scientists say it is urgent that policy makers halve global carbon dioxide emissions over the next 50 years or risk triggering changes that could be irreversible.

Trace gas Any one of the less common gases found in the Earth's atmosphere. Nitrogen, oxygen, and argon make up more than 99 % of the Earth's atmosphere. Other gases, such as carbon dioxide, water vapor, methane, oxides of nitrogen, ozone, and ammonia, are considered trace gases. Although relatively unimportant in terms of their absolute volume, they have significant effects on the Earth's weather and climate.

Track-two JI One of two approaches for verifying emission reductions or removals under joint implementation, whereby each JI project is subject to verification procedures established under the supervision of the Joint Implementation Supervisory Committee. Track-two procedures require that each project is reviewed by an accredited independent entity.

Transient climate response The time-dependent response of the climate system (or a climate model) to a time-varying change of forcing.

Transient climate simulation Mode of running a global climate model in which a period of time is simulated with continuously varying concentrations of greenhouse gases so that the climate of the model represents prospective changes already realized by the time of each future date in question, rather than the higher long-run equilibrium warming eventually resulting from atmospheric concentrations at each such date. The difference stems from ocean thermal lag.

Transpiration The process by which water vapor is lost from plants, evaporating from cell walls just below the surface of the leaf and diffusing into the air through small stomatal pores.

Travel demand management The attempt to reduce the volume of travel by measures such as car-pooling, lowering speed limits, parking control and pricing, etc.

Tropopause The atmospheric layer separating the stratosphere from the troposphere. It marks the transition from temperatures that decrease with increasing height within the troposphere to an atmospheric region that experiences increasing temperatures with height.

Troposphere The lowest part of the atmosphere from the surface to about 10 km in altitude in mid-latitudes (ranging from 9 km in high latitudes to 16 km in the tropics on average) where clouds and "weather" phenomena occur. In the troposphere, temperatures generally decrease with height.

Tropospheric Ozone (O_3) See "Ozone."

Tropospheric Ozone Precursors See "Ozone precursors."

Trust funds Funds earmarked for specific programs within the UN system.

TT See "Technology transfer"

TT:CLEAR Technology Transfer Information Clearing House.

Tundra A treeless, level or gently undulating plain characteristic of the Arctic and sub-Arctic regions characterized by low temperatures and short growing seasons.

TUNGO Trade related nongovernmental organizations.

Turn-over time The ratio between the mass of a reservoir (e.g., the mass of N_2O in the atmosphere) and the rate of removal from that reservoir (e.g., for N_2O, the rate of destruction by sunlight in the stratosphere).

Twenty-twenty-twenty (20-20-20) This refers to a pledge by the European Union to reach three targets by 2020: (a) a 20 % reduction in greenhouse-gas emissions from 1990 levels; (b) an increase in the use of renewable energy to 20 % of all energy consumed; and (c) a 20 % increase in energy efficiency. The EU says it will reduce emissions by 30 %, by 2020, if other developed countries also pledge tough action.

Ultraviolet (UV)-B radiation Solar radiation within a wavelength range of 280–320 nm, the greater part of which is absorbed by stratospheric ozone. Enhanced UV-B radiation suppresses the immune system and can have other adverse effects on living organisms.

Ultraviolet radiation (UV) The energy range just beyond the violet end of the visible spectrum. Although ultraviolet radiation constitutes only about 5 % of the total energy emitted from the sun, it is the major energy source for the stratosphere and mesosphere, playing a dominant role in both energy balance and chemical composition. Most ultraviolet radiation is blocked by Earth's atmosphere, but some solar ultraviolet penetrates and aids in plant photosynthesis and helps produce vitamin D in humans. Too much ultraviolet radiation can burn the skin, cause skin cancer and cataracts, and damage vegetation.

Umbrella group A loose coalition of non-European Union developed countries formed following the adoption of the Kyoto Protocol. Although there is no formal membership list, the group usually includes Australia, Canada, Iceland, Japan, New Zealand, Norway, the Russian Federation, Ukraine, and the USA.

Unconventional oil Petroleum produced or extracted using techniques other than the conventional (oil well) method. See also "Petroleum."

UN See "United Nations"

UNCCD See "United Nations Convention to Combat Desertification"

UNCED See "United Nations Conference on Environment and Development"

UN CSD See "United Nations Commission on Sustainable Development"

UNCTAD See "United Nations Conference on Trade and Development"

UNDP See "United Nations Development Programme"
UNECE See "United Nations Economic Commission for Europe"
UNEP See "United Nations Environment Programme"
UNESCAP See "Economic and Social Commission for Asia and the Pacific"
UNFCCC See "United Nations Framework Convention on Climate Change"
UNIDO See "United Nations Industrial Development Organization"
Uniform report format A standard format through which Parties submit information on activities implemented jointly under the Convention.
Unintended consequences Outcomes of an action not foreseen or intended.
United Nations An intergovernmental organization established in 1945 to promote international co-operation. It has 193 members. The headquarters of the United Nations is in Manhattan, New York City, and enjoys extraterritoriality. Further main offices are situated in Geneva, Nairobi, and Vienna. The organization is financed by assessed and voluntary contributions from its member states. Its objectives include maintaining international peace and security, promoting human rights, fostering social and economic development, protecting the environment, and providing humanitarian aid in cases of famine, natural disaster, and armed conflict.
http://www.un.org/
United Nations Commission on Sustainable Development (UN CSD) Established by the UN General Assembly in December 1992 to ensure effective follow-up of United Nations Conference on Environment and Development (UNCED), also known as the Earth Summit. From its inception, the CSD was highly participatory in structure and outlook, by engaging in its formal proceedings a wide range of official stakeholders and partners through innovative formulae. At its 11th session in 2003, the Commission decided on a multiyear work program consisting of review and policy years. Since its establishment in 1992, the Commission has greatly advanced the sustainable development agenda within the international community. At the United Nations Conference on Sustainable Development (Rio+20), member states agreed to establish a high level political forum that will subsequently replace the Commission on Sustainable Development.
https://sustainabledevelopment.un.org/csd.html
United Nations Conference on Environment and Development This was the 1992 Rio Conference (i.e., the "Earth Summit").
http://www.un.org/geninfo/bp/enviro.html
United Nations Conference on Trade and Development (UNCTAD) Governed by its 194 member states, it is the United Nations body responsible for dealing with development issues, particularly international trade – the main driver of development.
http://unctad.org/
United Nations Convention to Combat Desertification (UNCCD) Desertification, along with climate change and the loss of biodiversity, were identified as the greatest challenges to sustainable development during the 1992 Rio Earth Summit. Established in 1994, UNCCD is the sole legally binding international

agreement linking environment and development to sustainable land management. The Convention addresses specifically the arid, semiarid, and dry subhumid areas, known as the drylands, where some of the most vulnerable ecosystems and peoples can be found. In the 10-Year Strategy of the UNCCD (2008–2018) that was adopted in 2007, Parties to the Convention further specified their goals: "*to forge a global partnership to reverse and prevent desertification/land degradation and to mitigate the effects of drought in affected areas in order to support poverty reduction and environmental sustainability.*"
http://www.unccd.int

United Nations Development Programme (UNDP) The United Nations'global development network. Headquartered in New York City, UNDP advocates for change and connects countries to knowledge, experience, and resources to help people build a better life. It provides expert advice, training, and grant support to developing countries, with increasing emphasis on assistance to the least developed countries. The status of UNDP is that of an executive board within the United Nations General Assembly.
http://www.undp.org/

United Nations Economic Commission for Europe (UNECE) Set up in 1947 by ECOSOC, it is one of five regional commissions of the United Nations. The others are:

- Economic Commission for Africa (ECA)
- Economic and Social Commission for Asia and the Pacific (ESCAP)
- Economic Commission for Latin America and the Caribbean (ECLAC)
- Economic and Social Commission for Western Asia (ESCWA)

UNECE's major aim is to promote pan-European economic integration. To do so, it brings together 56 countries located in the European Union, non-EU Western and Eastern Europe, South-East Europe and Commonwealth of Independent States (CIS), and North America. All these countries dialogue and cooperate under the aegis of UNECE on economic and sectoral issues. However, all interested United Nations member states may participate in the work of UNECE. Over 70 international professional organizations and other nongovernmental organizations take part in UNECE activities. See also "ECOSOC."
http://www.unece.org/info/ece-homepage.html

United Nations Environment Programme (UNEP) The United Nations Environment Programme (UNEP) is a leading global environmental authority that promotes the coherent implementation of the environmental dimension of sustainable development within the United Nations system and serves as an authoritative advocate for the global environment. UNEP work encompasses:

- Assessing global, regional, and national environmental conditions and trends
- Developing international and national environmental instruments
- Strengthening institutions for the wise management of the environment

http://www.unep.org/

United Nations Framework Convention on Climate Change (UNFCCC) The Convention on Climate Change sets an overall framework for intergovernmental efforts to tackle the challenge posed by climate change. It recognizes that the climate system is a shared resource whose stability can be affected by industrial and other emissions of carbon dioxide and other greenhouse gases. The Convention enjoys near universal membership, with 196 countries having ratified.
Under the Convention, governments:
• Gather and share information on greenhouse-gas emissions, national policies, and best practices
• Launch national strategies for addressing greenhouse-gas emissions and adapting to expected impacts, including the provision of financial and technological support to developing countries
• Cooperate in preparing for adaptation to the impacts of climate change
The Convention entered into force on 21 March 1994.
http://newsroom.unfccc.int/

United Nations Industrial Development Organization (UNIDO) A specialized agency in the United Nations system, formed in 1966 and headquartered in Vienna, Austria. The Organization's primary objective is the promotion and acceleration of industrial development in developing countries and countries with economies in transition and the promotion of international industrial cooperation.
http://www.unido.org/

Uptake The addition of a substance of concern to a reservoir. The uptake of carbon containing substances, in particular carbon dioxide, is often called (carbon) sequestration.

Urban heat island The idea that many large cities are much warmer than the surrounding countryside because of urban heat release, impervious surfaces which restrict evaporation, etc.

USEPA See "Environmental Protection Agency"

Vapor pressure The pressure of a vapor in thermodynamic equilibrium with its condensed phases in a closed system. All liquids have a tendency to evaporate, and some solids can sublimate into a gaseous form. Vice versa, all gases have a tendency to condense back to their liquid form, or deposit back to solid form, as long as the temperature is below their critical temperature or decomposition temperature. In plain terms, a liquid evaporates at all pressures below its vapor pressure, while remaining stable at pressure above the vapor pressure. Also termed "equilibrium vapor pressure."

Vapor pressure deficit A measure of the "dryness" of the air. A high vapor pressure deficit corresponds to a low relative humidity and/or high temperature, while a low vapor pressure deficit corresponds to a high relative humidity and/or low air temperature.

VER See "Voluntary Emissions Reduction"

VOC See "Volatile Organic Compounds"

Volatile Organic Compounds (VOC) Any one of several organic compounds which are released to the atmosphere by plants or through vaporization of oil products, and which are chemically reactive and are involved in the chemistry of tropospheric ozone production. Methane, while strictly falling within the definition of a VOC, is usually considered separately.

Voluntary commitments A draft article considered during the negotiation of the Kyoto Protocol that would have permitted developing countries to voluntarily adhere to legally binding emissions targets. The proposed language was dropped in the final phase of the negotiations. The issue remains important for some delegations and continues to be discussed, currently in the context of the Bali Action Plan, in terms of what constitutes "voluntary."

Voluntary Emissions Reduction (VER) An emission reduction credit exchanged in voluntary (rather than compliance) emissions markets, and usually certified by a voluntary emission standard. VERs are sometimes referred to as verified emissions reductions.

Voluntary Measures Measures to reduce GHG emissions that are adopted by firms or other actors in the absence of government mandates. Voluntary measures help make climate-friendly products or processes more readily available or encourage consumers to incorporate environmental values in their market choices.

Vulnerability The degree to which a system is susceptible to, or unable to cope with, adverse effects of climate change, including climate variability and extremes. Vulnerability is a function of the character, magnitude, and rate of climate variation to which a system is exposed, its sensitivity, and its adaptive capacity.

Wastewater Water that has been used and contains dissolved or suspended waste materials.

Water Retention Capacity The maximum amount of water that a given soil can retain per unit quantity.

Water use efficiency (WUE) A higher water use efficiency in a plant means less water is lost while fixing a molecule of CO_2. C4 and CAM species have an enhanced ability to utilize light while restricting water loss. Although it may be defined in a number of ways, it is basically the amount of organic matter produced by a plant divided by the amount of water used by the plant in producing it.

Water vapor The most abundant greenhouse gas, it is the water present in the atmosphere in gaseous form. Water vapor is an important part of the natural greenhouse effect. While humans are not significantly increasing its concentration through direct emissions, it contributes to the enhanced greenhouse effect because the warming influence of greenhouse gases leads to a positive water vapor feedback. In addition to its role as a natural greenhouse gas, water vapor also affects the temperature of the planet because clouds form when excess water vapor in the atmosphere condenses to form ice and water droplets and precipitation. See "Greenhouse gas."

WBCSD See "World Business Council for Sustainable Development"

Wedge Theory The theory of opportunities for limiting or diminishing the greenhouse effect and global warming. Wedges include: decarbonized electricity,

decarbonized fuels, fuel displacement by alternative energy sources (e.g., solar energy, nuclear energy), methane management, and natural carbon sinks (e.g., forests).

WUE See "Water use efficiency"

Weather Atmospheric condition at any given time or place. It is measured in terms of wind, temperature, humidity, atmospheric pressure, cloudiness, and precipitation. In most places, weather can change from hour-to-hour, day-to-day, and season-to-season. Climate in a narrow sense is usually defined as the "average weather," or more rigorously, as the statistical description in terms of the mean and variability of relevant quantities over a period of time ranging from months to thousands or millions of years. The classical period is 30 years, as defined by the World Meteorological Organization (WMO). These quantities are most often surface variables such as temperature, precipitation, and wind. Climate in a wider sense is the state, including a statistical description, of the climate system. A simple way of remembering the difference is that climate is what you expect (e.g., cold winters) and "weather" is what you get (e.g., a blizzard).

Weber-Morris Model The model theorized that the rate of intraparticle diffusion varies proportionately with the half power of time (t) and is expressed as:

$$q_t = K_{id}\left(t^{1/2}\right) + c$$

where,

- q_t = adsorbate uptake at time t, (mg/g)
- K_{id} = the rate constant of intraparticle transport, (mg/g).$min^{-1/2}$
- c is the intercept and its value is related to the boundary layer thickness

WCC See "World Climate Conference"

Wedge Theory The theory of opportunities for limiting or diminishing the greenhouse effect and global warming. Wedges include: decarbonized electricity, decarbonized fuels, fuel displacement by alternative energy sources (e.g., solar energy, nuclear energy), methane management, and natural carbon sinks (e.g., forests).

WEOG Western European and Others Group (United Nations regional group).

Wet/dry deposition The removal of a substance from the atmosphere either through being washed out as rain falls (wet deposition) or through direct deposition on a surface (dry deposition).

WG I See "IPCC Working Group I"

WG II See "IPCC Working Group II"

WG III See "IPCC Working Group III"

"When" and "where" flexibility The ability to choose the time (when) or location (where) of a mitigation option or adaptation scheme in order to reduce the costs associated with climate change.

WHO World Health Organization.

WMO See "World Meteorological Organization"

World Business Council for Sustainable Development (WBCSD) The World Business Council for Sustainable Development (WBCSD) positions itself as "*a CEO-led organization of forward-thinking companies that galvanizes the global business community to create a sustainable future for business, society and the environment. Through its members, the Council applies its respected thought leadership and effective advocacy to generate constructive solutions and take shared action to drive business action on sustainability in the coming decade and beyond. The WBCSD aims to be the leading voice of business that will support companies in scaling up true value-added business solutions and in creating the conditions where more sustainable companies will succeed and be recognized. Member companies are represented on the Council by the CEO or a board level executive. Council Members drive the strategic direction of the WBCSD and of individual projects where they can join or lead Cluster boards*." http://www.wbcsd.org/

World Climate Conference (WCC) A series of international meetings, organized by the World Meteorological Organization (WMO). The First World Climate Conference was held on 12–23 February 1979 in Geneva.

World Meteorological Organization (WMO) The World Meteorological Organization (WMO) is a specialized agency of the United Nations. It is the UN system's authoritative voice on the state and behavior of the Earth's atmosphere, its interaction with the oceans, the climate it produces, and the resulting distribution of water resources. WMO has a membership of 191 member states and territories. It originated from the International Meteorological Organization (IMO), which was founded in 1873. Established in 1950, WMO became the specialized agency of the United Nations in 1951 for meteorology (weather and climate), operational hydrology, and related geophysical sciences. http://www.wmo.int

WSSD See "World Summit on Sustainable Development"

WTO See "World Trade Organization"

Zone Movement of wind or ocean waters in a direction that is roughly parallel to the lines of latitude

Zone of ablation Area of a glacier where losses of ice from melting, evaporation, and sublimation exceed additions of snow annually.

Zone of accumulation Area of a glacier where additions of snow exceed losses of ice from melting, evaporation, and sublimation.

100-Year Flood Levels Severe flood levels with a 1-in-100 likelihood of occurring in any given year.

References

US Environmental Protection Agency (EPA). http://www.epa.gov/climatechange/glossary.html. Accessed 25 July 2016

Intergovernmental Panel on Climate Change (IPCC). https://www.ipcc.ch/pdf/glossary/ipcc-glossary.pdf. Accessed 25 July 2016

United Nations Framework Convention on Climate Change (UNFCCC). http://unfccc.int/essential_background/glossary/items/3666.php. Accessed 25 July 2016
British Broadcasting Corporation (BBC). http://www.bbc.com/news/science-environment-11833685. Accessed 25 July 2016
Agricultural Marketing Resource Center (AgMRC). http://www.agmrc.org/media/cms/Glossary_of_Global_Warming_and_Clim_4314FBAC16B15.pdf. Accessed 25 July 2016
National Oceanic and Atmospheric Administration (NOAA). http://data1.gfdl.noaa.gov/nomads/forms/deccen/glossary/glossary.html. Accessed 25 July 2016